ISSN 1007-9327 (print)
ISSN 2219-2840 (online)

World Journal of *Gastroenterology*

World J Gastroenterol 2022 July 7; 28(25): 2782-3007



Published by Baishideng Publishing Group Inc

World Journal of Gastroenterology

Contents

Weekly Volume 28 Number 25 July 7, 2022

REVIEW

2782 Inflammation, microbiome and colorectal cancer disparity in African-Americans: Are there bugs in the genetics?

Ahmad S, Ashktorab H, Brim H, Housseau F

2802 Altered gut microbiota patterns in COVID-19: Markers for inflammation and disease severity

Chakraborty C, Sharma AR, Bhattacharya M, Dhama K, Lee SS

2823 Long noncoding RNAs in hepatitis B virus replication and oncogenesis

Li HC, Yang CH, Lo SY

MINIREVIEWS

2843 Characteristics of inflammatory bowel diseases in patients with concurrent immune-mediated inflammatory diseases

Akiyama S, Fukuda S, Steinberg JM, Suzuki H, Tsuchiya K

2854 Correlation of molecular alterations with pathological features in hepatocellular carcinoma: Literature review and experience of an Italian center

Maloberti T, De Leo A, Sanza V, Gruppioni E, Altimari A, Riefolo M, Visani M, Malvi D, D'Errico A, Tallini G, Vasuri F, de Biase D

2867 Micelles as potential drug delivery systems for colorectal cancer treatment

Fatfat Z, Fatfat M, Gali-Muhtasib H

2881 Incretin based therapy and pancreatic cancer: Realising the reality

Suryadevara V, Roy A, Sahoo J, Kamalanathan S, Naik D, Mohan P, Kalayarasan R

2890 Non-alcoholic fatty liver disease and the impact of genetic, epigenetic and environmental factors in the offspring

Wajsbrot NB, Leite NC, Salles GF, Villela-Nogueira CA

2900 Role of transcribed ultraconserved regions in gastric cancer and therapeutic perspectives

Gao SS, Zhang ZK, Wang XB, Ma Y, Yin GQ, Guo XB

2910 Multiple roles for cholinergic signaling in pancreatic diseases

Yang JM, Yang XY, Wan JH

ORIGINAL ARTICLE

Basic Study

2920 Fecal gene detection based on next generation sequencing for colorectal cancer diagnosis

He SY, Li YC, Wang Y, Peng HL, Zhou CL, Zhang CM, Chen SL, Yin JF, Lin M

World Journal of Gastroenterology

Weekly Volume 28 Number 25 July 7, 2022

Contents

2937 Mechanism and therapeutic strategy of hepatic *TM6SF2*-deficient non-alcoholic fatty liver diseases *via in vivo* and *in vitro* experiments

Li ZY, Wu G, Qiu C, Zhou ZJ, Wang YP, Song GH, Xiao C, Zhang X, Deng GL, Wang RT, Yang YL, Wang XL

2955 Upregulated adenosine 2A receptor accelerates post-infectious irritable bowel syndrome by promoting CD4+ T cells' T helper 17 polarization

Dong LW, Ma ZC, Fu J, Huang BL, Liu FJ, Sun D, Lan C

Retrospective Study

2968 Four-year experience with more than 1000 cases of total laparoscopic liver resection in a single center

Lan X, Zhang HL, Zhang H, Peng YF, Liu F, Li B, Wei YG

SCIENTOMETRICS

2981 Mapping the global research landscape on nutrition and the gut microbiota: Visualization and bibliometric analysis

Zyoud SH, Shakhshir M, Abushanab AS, Al-Jabi SW, Koni A, Shahwan M, Jairoun AA, Abu Taha A

CASE REPORT

2994 Early gastric cancer presenting as a typical submucosal tumor cured by endoscopic submucosal dissection: A case report

Cho JH, Lee SH

LETTER TO THE EDITOR

3001 Acupuncture and moxibustion for treatment of Crohn's disease: A brief review

Xie J, Huang Y, Wu HG, Li J

CORRECTION

3004 Correction to "Aberrant methylation of secreted protein acidic and rich in cysteine gene and its significance in gastric cancer"

Shao S, Zhou NM, Dai DQ

3006 Correction to "Gut microbiota dysbiosis in Chinese children with type 1 diabetes mellitus: An observational study"

Liu X, Cheng YW, Shao L, Sun SH, Wu J, Song QH, Zou HS, Ling ZX

World Journal of Gastroenterology

Weekly Volume 28 Number 25 July 7, 2022

Contents

ABOUT COVER

Editorial Board Member of *World Journal of Gastroenterology*, Hideyuki Chiba, MD, PhD, Director, Department of Gastroenterology, Omori Red Cross Hospital, 4-30-1, Chuo, Ota-Ku, Tokyo 143-8527, Japan. h.chiba04@gmail.com

AIMS AND SCOPE

The primary aim of *World Journal of Gastroenterology* (*WJG*, *World J Gastroenterol*) is to provide scholars and readers from various fields of gastroenterology and hepatology with a platform to publish high-quality basic and clinical research articles and communicate their research findings online. *WJG* mainly publishes articles reporting research results and findings obtained in the field of gastroenterology and hepatology and covering a wide range of topics including gastroenterology, hepatology, gastrointestinal endoscopy, gastrointestinal surgery, gastrointestinal oncology, and pediatric gastroenterology.

INDEXING/ABSTRACTING

The *WJG* is now abstracted and indexed in Science Citation Index Expanded (SCIE, also known as SciSearch®), Current Contents/Clinical Medicine, Journal Citation Reports, Index Medicus, MEDLINE, PubMed, PubMed Central, Scopus, Reference Citation Analysis, China National Knowledge Infrastructure, China Science and Technology Journal Database, and Superstar Journals Database. The 2022 edition of Journal Citation Reports® cites the 2021 impact factor (IF) for *WJG* as 5.374; IF without journal self cites: 5.187; 5-year IF: 5.715; Journal Citation Indicator: 0.84; Ranking: 31 among 93 journals in gastroenterology and hepatology; and Quartile category: Q2. The *WJG*'s CiteScore for 2021 is 8.1 and Scopus CiteScore rank 2021: Gastroenterology is 18/149.

RESPONSIBLE EDITORS FOR THIS ISSUE

Production Editor: *Ying-Yi Yuan*; **Production Department Director:** *Xiang Li*; **Editorial Office Director:** *Jia-Ru Fan*.

NAME OF JOURNAL
World Journal of Gastroenterology

ISSN
ISSN 1007-9327 (print) ISSN 2219-2840 (online)

LAUNCH DATE
October 1, 1995

FREQUENCY
Weekly

EDITORS-IN-CHIEF
Andrzej S Tarnawski

EDITORIAL BOARD MEMBERS
http://www.wjgnet.com/1007-9327/editorialboard.htm

PUBLICATION DATE
July 7, 2022

COPYRIGHT
© 2022 Baishideng Publishing Group Inc

INSTRUCTIONS TO AUTHORS
https://www.wjgnet.com/bpg/gerinfo/204

GUIDELINES FOR ETHICS DOCUMENTS
https://www.wjgnet.com/bpg/GerInfo/287

GUIDELINES FOR NON-NATIVE SPEAKERS OF ENGLISH
https://www.wjgnet.com/bpg/gerinfo/240

PUBLICATION ETHICS
https://www.wjgnet.com/bpg/GerInfo/288

PUBLICATION MISCONDUCT
https://www.wjgnet.com/bpg/gerinfo/208

ARTICLE PROCESSING CHARGE
https://www.wjgnet.com/bpg/gerinfo/242

STEPS FOR SUBMITTING MANUSCRIPTS
https://www.wjgnet.com/bpg/GerInfo/239

ONLINE SUBMISSION
https://www.f6publishing.com

© 2022 Baishideng Publishing Group Inc. All rights reserved. 7041 Koll Center Parkway, Suite 160, Pleasanton, CA 94566, USA

E-mail: bpgoffice@wjgnet.com https://www.wjgnet.com

World Journal of Gastroenterology

Submit a Manuscript: https://www.f6publishing.com

World J Gastroenterol 2022 July 7; 28(25): 2782-2801

DOI: 10.3748/wjg.v28.i25.2782

ISSN 1007-9327 (print) ISSN 2219-2840 (online)

REVIEW

Inflammation, microbiome and colorectal cancer disparity in African-Americans: Are there bugs in the genetics?

Sami Ahmad, Hassan Ashktorab, Hassan Brim, Franck Housseau

Specialty type: Gastroenterology and hepatology

Provenance and peer review: Unsolicited article; Externally peer reviewed.

Peer-review model: Single blind

Peer-review report's scientific quality classification
Grade A (Excellent): A
Grade B (Very good): 0
Grade C (Good): 0
Grade D (Fair): D
Grade E (Poor): 0

P-Reviewer: Dabravolski SA, Belarus; Ogino S, United States
A-Editor: Gao W, China

Received: October 28, 2021
Peer-review started: October 28, 2021
First decision: December 26, 2021
Revised: January 27, 2022
Accepted: May 26, 2022
Article in press: May 26, 2022
Published online: July 7, 2022

Sami Ahmad, Franck Housseau, Department of Oncology, Johns Hopkins University, Baltimore, MD 21231, United States

Hassan Ashktorab, Department of Medicine, Howard University, Washington, DC 20060, United States

Hassan Brim, Department of Pathology, Howard University, Washington, DC 20060, United States

Corresponding author: Franck Housseau, PharmD, PhD, Associate Professor, Department of Oncology, Johns Hopkins University, CRB1 4M59 1650 Orleans street, Baltimore, MD 21231, United States. fhousse1@jhmi.edu

Abstract

Dysregulated interactions between host inflammation and gut microbiota over the course of life increase the risk of colorectal cancer (CRC). While environmental factors and socio-economic realities of race remain predominant contributors to CRC disparities in African-Americans (AAs), this review focuses on the biological mediators of CRC disparity, namely the under-appreciated influence of inherited ancestral genetic regulation on mucosal innate immunity and its interaction with the microbiome. There remains a poor understanding of mechanisms linking immune-related genetic polymorphisms and microbiome diversity that could influence chronic inflammation and exacerbate CRC disparities in AAs. A better understanding of the relationship between host genetics, bacteria, and CRC pathogenesis will improve the prediction of cancer risk across race/ethnicity groups overall.

Key Words: Inflammation; African-American; Population-specific genome wide association studies; Minorities health; Microbiome; Colorectal cancer

©The Author(s) 2022. Published by Baishideng Publishing Group Inc. All rights reserved.

Core Tip: Studies largely examine either variations in microbiome composition or host immunity polymorphisms, often using genome-wide association studies comprised of populations mainly of European ancestry. There is, thus, a pressing need for studies that include, recruit, and account for more widely diverse cohorts. Identification of population-associated polymorphisms driving host/microbiome interactions linked to colorectal cancer (CRC) disparity may reveal genes or pathways that could be targeted for patient-specific CRC interception strategies.

Citation: Ahmad S, Ashktorab H, Brim H, Housseau F. Inflammation, microbiome and colorectal cancer disparity in African-Americans: Are there bugs in the genetics? *World J Gastroenterol* 2022; 28(25): 2782-2801
URL: https://www.wjgnet.com/1007-9327/full/v28/i25/2782.htm
DOI: https://dx.doi.org/10.3748/wjg.v28.i25.2782

INTRODUCTION

Colorectal cancer (CRC) is the second leading cause of death amongst cancer patients, an estimated 53000 of whom will die in the United States from CRC in 2021[1]. Strikingly, although total CRC mortality has decreased over the last two decades, particularly in older individuals (age 64 +), CRC incidence has increased in individuals under 50[1]. Recent studies showed early-onset CRC patients were more likely to be African-Americans (AAs), who bear the highest CRC incidence rate between 20-year-old and 44-year-old (7.9/100000) as compared to Caucasian Americans (CAs) (6.7/100000) and Asian-Pacific Islanders (6.3/100000)[2]. AAs commonly display more aggressive types of CRC as well, and are generally diagnosed at more advanced stages of the disease, exhibiting survival rates 7% below those of CAs (58% *vs* 65% 5-year survival)[3]. Such statistics must be interpreted cautiously, since the noted increase of early-onset CRC may result from recently recommended and adopted early colonoscopy (40-45 years old) screening campaigns. Nevertheless, there are multiple proposed influences on CRC disparities in AAs, including differences in health care and treatment access, comorbidities and tumor characteristics[4-8]. Socioeconomic status (SES) also weighs heavily on the late diagnoses and prevention campaign efficacy observed in AA populations[2,6,9]. Undoubtedly the source of CRC disparity is multifactorial, and a layered perspective is imperative to address the alarming rise of early onset CRC, an otherwise preventable disease when detected early.

Herein, we aim to elucidate novel biological factors that may also contribute to the AA disparities in CRC mortality. Specifically, in addition to the genetic influence on CRC pathogenesis, an accumulating body of evidence connects CRC to dysregulated interactions between mucosal innate immunity and the microbiome[10]. Indeed, sustained inflammation promoted by chronic colorectal dysbiosis is an established driver of CRC pathogenesis[11]. Related to this notion is a recent gut microbiome profiling study that found that, in addition to diminished overall species diversity, pro-inflammatory *Fusobacterium nucleatum (F. nucleatum)* and *Enterobacter* species were significantly more abundant in AA CRC patients as compared to a CA cohort[12]. The presence of *F. nucleatum* has also been linked to inflammation-associated microsatellite alterations found more prevalently in AA rectal tumors, a finding linked to worsened CRC prognosis[13-15]. Furthermore, genetic landscape and microbiome composition have been shown to influence the occurrence of proximal colorectal tumors[16], which are more difficult to detect and are diagnosed nearly four times more often in AA than in CA CRC patients[17]. Nearly 80% of sessile serrated polyps are found in the proximal colon, a phenomenon associated with microbial biofilms and *Fusobacteria*, plus the frequency of *BRAF* mutations, CpG island hypermethylation phenotype, and microsatellite instability that increases from the distal to the proximal region[16,18-22]. Altogether, there is emerging research on the genetically tuned relationships between mucosal innate immunity, the microbiome, and disparate CRC development, but a functional understanding of how said relationships impact CRC pathology remains incomplete[23]. Additionally, despite the evidence that mucosal innate immunity and the microbiome are intimately connected, this review highlights how minority health research currently evaluates their contribution to CRC risk in a largely separate fashion [24].

Accordingly, we propose an integrated concept whereby a differential mucosal inflammatory response to gut microbiota, influenced by host genetic ancestry, represents an underappreciated factor affecting population susceptibility to CRC. In support of this concept, a recent study found that the most differentially expressed genes (DEGs) between AA and CA CRC tumors were related to the regulation of inflammatory immunity[25]. More broadly, transcriptional regulation of inflammation was determined the most distinguishing DNA variation between African and European genetic ancestries[26]. Another study demonstrated that African genetic ancestry and level of African admixture (mixture with ancestral African genetic lineage) predicted a stronger inflammatory transcriptional response in macrophages infected with bacterial pathogens[27]. From this framework, one could theorize that in a CRC setting, the same bacterium or a community of bacteria may induce a differentially deleterious

inflammatory response based on a patient's immune-related genetic background. Positive ancestral selection of anti-pathogenic immunity providing survival benefit in endemic areas may, in a modern "westernized life style" context, exacerbate localized inflammation in the tumor micro-environment and, when compounded by SES and environmental factors, accelerate CRC progression into the more aggressive form seen in AA patients, whose self-reported race/ethnicity correlates with an elevated African admixture[28,29] (Figure 1).

Given that SES and a variety of environmental factors associated with CRC pathogenesis and disparities are commonly discussed elsewhere[2,9], we are limiting the scope of the present review to the nascent literature associating CRC first to genetic polymorphisms related to innate immunity, second to those related to the microbiome, and finally explore how they may conjointly contribute to CRC disparities in the AA population. We also emphasize that, by considering admixture and genetic ancestry rather than self-reported race, population-specific risk studies including microbiome genome-wide association studies (GWAS) can more accurately capture human genetic diversity, thereby increasing the likelihood of identifying clinically relevant CRC risk factors associated with African ancestry[30-34]. Furthermore, polymorphisms related to innate immunity as well as the microbiome and contributing to links between CRC risk and African ancestry may have been left undiscovered by the longstanding genetic homogeneity of genomic research cohorts, a problem we discuss in our closing remark. Although technically challenging, expanding GWAS to more diverse "multi-ancestry" cohorts will reveal novel linkages between the microbiome, inflammation, and CRC risk that can build predictive polygenic risk scores adaptable to an equally diverse patient base[35,36]. Crucially, functional evaluation of CRC risk variants associated with African ancestry may offer insights into the trend of aggressive, earlier onset CRC in AA patients, paving the way towards personalized prevention and precision medicine.

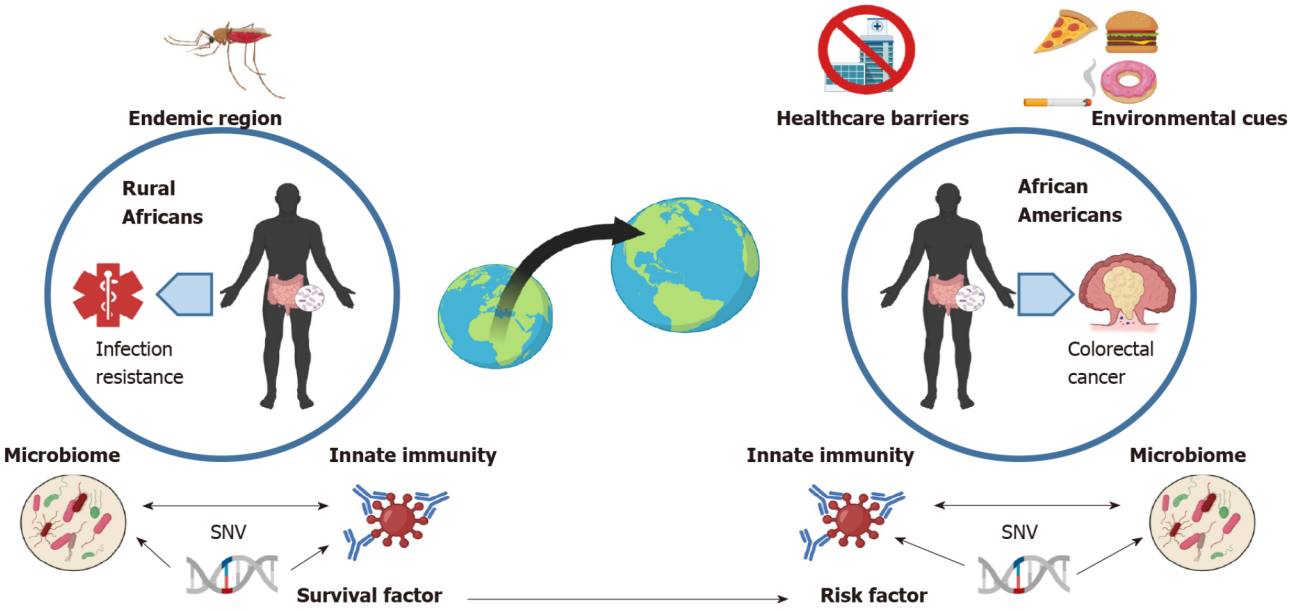
MUCOSAL INFLAMMATION, MICROBIOME, AND CRC

To better appreciate how host genetics may impact CRC risk between populations of different ancestral origins by modulating innate immunity or the microbiome, we will first highlight how mucosal inflammation and the gut microbiome interact to affect CRC pathogenesis. The human gut contains up to 10^{13} bacteria that play critical roles in immune, metabolic, cardiovascular, and neurological development [37]. The composition and functions of this bacterial community (microbiota) and its associated genome (microbiome) are highly dynamic and influenced by both environmental factors and host genetic background to maintain immunological and metabolic functionality[38]. Meanwhile, a tightly regulated physical separation between the immune system and commensal bacteria is necessary to limit a chronic inflammatory response to the microbiota[39,40]. The integrity of the intestinal barrier and its epithelium are therefore essential elements of healthy host-microbiota mutualism[40]. To establish a "demilitarized zone" and keep microbes at bay, the epithelium uses different mechanisms including tight junctions between epithelial cells, protective mucus production, and the expression of a complex arsenal of innate receptors that trigger bactericidal mediator secretion[41]. Nevertheless, a permissible level of contact or bacterial penetrance is necessary to facilitate metabolic exchanges and immunity maturation for homeostatic equilibrium between dense microbial flora and the host[39,40].

In the case of a high-fat diet, the cumulative alteration of bacterial metabolites can disrupt this equilibrium, thereby promoting carcinogenic dysbiosis and mucosal inflammation[42]. Diet is, thus, a critical environmental factor when connecting inflammation and the microbiome to CRC risk, especially when considering CRC disparities in AAs compared to Native Africans[43-45]. However, CRC as impacted by the genetic origins of host inflammatory response remains understudied. Inflammatory bowel disease (IBD), a model of perturbed micro-immune crosstalk and a known influencing factor of CRC etiology, can be a useful departure point for this line of inquiry[46]. In fact, multiple GWAS have linked higher risk of IBD, CRC[47-50], and microbiotic dysbiosis to host genetic variations, but surprisingly little is known about how CRC disparities may be compounded by the genetic regulation of host inflammatory response to gut bacteria[51].

There are, however, documented relationships between the genetic regulation of innate inflammatory immunity, the microbiome, and colon carcinogenesis. For example, adenomatous polyposis coli (Apc) $^{Min/+}$ mice knockout for toll-like receptor (TLR) 4 or its signaling adaptor partner myeloid differentiation primary response 88 demonstrated a decreased number of intestinal polyps[52]. Nucleotide-binding oligomerization domain leucine-rich repeat and pyrin domain containing 6 and nucleotide binding oligomerization domain containing protein 2 (NOD2) knockout mice were shown to develop colon tumors following colitis, and fecal microbiota transplantation from these mice into wild type recipients triggered similar tumorigenesis, which interestingly attributed carcinogenic causality to the microbiota [53,54]. In the case of lipocaline-2 knockout mice, *Alistipes spp.* commensals thrived and drove proximal colon tumorigenesis[55]. The nature of host genetic events can therefore drive different microbiome shifts impacting CRC and its anatomical pathogenesis (*i.e.*, distal *vs* proximal).

If inflammation is a mechanism connecting the microbiome and colorectal carcinogenesis, host genetic background, including immune-related single-nucleotide polymorphisms (irSNPs), could differ-



DOI: 10.3748/wjg.v28.i25.2782 **Copyright** ©The Author(s) 2022.

Figure 1 Immune-related variant may promote survival to pathogens in ancestral African environment but precipitate cancer in descendent African-Americans. Pathogens associated with endemic African regions (*e.g.*, malaria) are thought to pressure selection for specific immune-related genetic variants associated with pathogen resistance and survival of Native Africans (left). In the context of westernized diet and lifestyle, this genetic predisposition (represented herein by a single nucleotide variant), when associated with inflammatory regulation and inherited from African ancestors, may lead to altered interactions with bacteria or communities of bacteria of the gut microbiome, thereby precipitating the colon adenoma-carcinoma sequence in African-Americans (right). Higher inflammation associated with lack of exercise, high fat diet, and socio-economic status are thought to be predominant factors driving early colorectal cancer onset in African-Americans *via* their impact on shaping the gut microbiome and its interactions with the host genetic background. SNV: Single nucleotide variant. Created with Biorender.com.

entially regulate such associations based on ancestry. In humans, pattern recognition receptor polymorphisms are associated with both IBD and CRC risk[48]. GWAS have linked genetic loci to increased IBD risk and a variety of risk alleles affect immune response[56], including NOD2 or autophagy-related 16 like 1[57,58]. Such polymorphisms have been associated with microbial dysbiosis and an excessive inflammatory response[59,60]. Namely, Knights *et al*[59] found that among 474 individuals, NOD2 variants were associated with *Enterobacteriaceae* family enrichment, including *Escherichia coli*, a species notably enriched in IBD individuals. Also, Lavoie *et al*[60] described an increase of interleukin (IL)-17-producing CD4$^+$ T (*i.e.*, Th17) cells in the lamina propria of mice engineered to express the polymorphism T300A (rs2241880) in the *Atg16 L1* gene. Although Th17-based colitis was associated with an increase of *Bacteroides ovatus*, T300A did not directly induce the increase of *Bacteroides ovatus* but rather induced the increase of IL23p19, an important cytokine for maintaining the Th17 lineage[61]. Th17 cells and their canonical cytokine IL-17 are critical pro-inflammatory contributors to epithelial homeostasis and mucosal immunity by orchestrating anti-bacterial defense and epithelial repair and regeneration as well as regulating barrier permeability by controlling the expression of occludin proteins[62,63]. When dysregulated in a chronic setting, sustained IL-17 production may promote colon tumorigenesis[64,65]. Several studies have now identified IL-23/Th17 pathway-associated polymorphisms linked to IBD susceptibility and the gut microbiome profile[66-68]. Presumably, genetic regulation of Th17-driven inflammation may impact IBD and ensuing CRC risk *via* the extent or nature of colonic dysbiosis. In sum, these GWAS suggest that by influencing the extent or nature of colonic dysbiosis, genetic regulation of inflammation represents a risk factors for both IBD and CRC. Next, we review how genetic ancestry contributes to this phenomenon, and how it may exacerbate CRC disparity in AAs.

GEOGRAPHIC AND POPULATION-RELATED INNATE IMMUNITY DISPARITIES THAT MODULATE CRC RISK

The flow of genetic information across time and geography may contribute to current disparities in cancer incidence and progression[69]. Cancer is known to result from an accumulation of somatic genetic and epigenetic alterations that dysregulate the cell cycle but also depends on genetic background and polymorphisms that impact patient risk and predisposition[70,71]. Yet, few GWAS have implicated ancestral genetic variants in cancer predisposition amongst self-identified racial/ethnic

groups[72,73]. Many such polymorphisms regulate gene expression *via* epigenetic or post-translational modification mechanisms, which affect noncoding sequences like microRNA (miRNA) binding sites[74,75]. Yet, the biological and clinical significance of most polymorphisms associated with cancer disparities remains unknown[72]. Mechanistic associations between chronic inflammation and carcinogenesis could link ancestral genetic diversity to cancer, whereby immune-related genetic regulatory variants have the potential to differentially modulate CRC across populations[27].

In fact, a large fraction of population-associated polymorphisms impact gene expression related to inflammation and innate immunity, which, being likely essential for surviving life-threatening infections, evolved under stronger selection pressures than other traits[76,77]. For instance, human genome diversification *via* archaic human genome introgression (*i.e.*, admixture with Neanderthal genome) is a proposed adaptation of ancestral humans to infectious environments following "out of Africa" migration[77,78]. In non-African populations, Neanderthal-introgressed haplotypes reintroduced a splice variant (rs10774671) of the 2'-5'-oligoadenylate synthetase (*OAS*) *1* gene[79]. The *OAS* locus on chromosome 12 encodes three genes, *OAS1*, *OAS2* and *OAS3* that play an important role in virus defense. The elevated frequency of the Neanderthal-derived allele at the *OAS* locus was proposed to be the result of a positive selection in European and East Asian populations. This allele selection has a functional significance since it is associated with the production of a protein variant (OAS1 p46) characterized by higher enzymatic activity and improved resistance to West Nile virus and hepatitis virus C[80]. Therefore, the allele haplotype may provide a survival advantage to infectious agents in the non-African environment and represents an example of variety in baseline inflammation levels that may influence susceptibility to diseases like IBD and CRC in patients with insignificant African ancestry. Selection of genetic variants providing health and survival benefit in endemic areas may represent another means of adaptation and human genome diversification. In a cohort of 158 healthy individuals (distributed as European, Sub-Saharan African, and East-Asian), Barreiro *et al*[81] found that nucleotide diversity of the TLR family was shown to vary between African populations, suggesting pathogen-specific selection pressures. Specifically, the *TLR10/TLR1/TLR6* locus showed signs of recent positive selection amongst non-African populations. Furthermore, of all SNPs in this region, a high frequency *TLR1* single nucleotide variant (SNV) (non-synonymous T1805G variant) found in Europeans was the most significant population differentiator and was associated with a decrease in agonist-mediated nuclear factor-kappa B activation[81]. Although it is unclear if decreased TLR1-mediated immune response confers a selective advantage, it could potentially modulate otherwise harmful inflammatory responses to pathogens[82,83]. This finding suggested that a finely tuned balance between optimal defenses to pathogens and excessive inflammation may have been critical for evolutionary survival[78].

To investigate how ancestral immunity would impact pathogen response, Nédélec *et al*[27] studied interactions between macrophages and live bacteria (*Listeria* and *Salmonella*). Amongst the macrophages, they found that many of the DEGs; (30% of the 11914 genes analyzed) between AAs (n = 77) and CAs (n = 91) were involved in the regulation of the innate immunity. These results built off their previous findings that 9% of macrophage DEGs varied according to ancestry-associated regulation and that increased African ancestry could predict a stronger inflammatory response to infection[27]. Performing quantitative trait locus (QTL) analysis, the authors identified SNVs in 14% of DEGs or using alternative splicing between CA and AA individual-derived macrophages (either non-infected or infected with *Listeria* or *Salmonella*). A large fraction of DEGs were associated with expression QTL only in infected macrophages. In other words, SNVs in a significant fraction of inflammation-related genes were expressed in infected macrophages according to the level of African ancestry. Interestingly, the same authors also found that these DEGs included susceptibility genes previously reported by GWAS for rheumatoid arthritis, systemic sclerosis, or ulcerative colitis, all related to chronic inflammation and conditions with known AA disparity[78]. The interest of such a study, although performed on macrophages *in vitro*, is its illustration of the link between African genetic ancestry and inflammatory response to bacteria, one that could accelerate CRC by aggravating interactions between gut microbiota and the mucosal immune system. Reinforcing this concept is another GWAS that revealed that some of the most differentiating irSNPs between African and European populations were associated with genes regulating nuclear factor-kappa B or chemokine gene clusters[78]. Selected genetic variants may offer protection against infection in endemic regions for native/rural Africans but favor cancer development in descendants bearing the same variants in a western environment, a concept exemplifying the crossroad between host genetics and environmental factors that shapes cancer risk (Figure 1).

Regarding the possibility of a role of associations between irSNP and CRC risk into AA disparity, a recent study by Sanabria-Salas *et al*[33] studied links between pro-inflammatory *IL1B* haplotypes and CRC risk in patients from six Colombian cities. The authors associated the *IL1B* CGTC haplotype with CRC risk exclusively in patients from the coastal regions of Colombia who possessed the highest proportion of admixed African ancestry[33]. The same group has associated *IL1B* irSNPs (four SNPs -3737C/-1464G/-511T/-31C) with African ancestry and elevated cancer risk. The CGTC haplotype was most frequently found and highly expressed in AAs, establishing a functional link between *IL1B* irSNP and CRC risk[84]. Further studies, validating the connection between AA CRC patients and *IL1B* polymorphisms, will be required to confirm the *IL1B* SNP haplotype as a population-associated CRC risk marker; these findings nevertheless showcase a prime example of an exploitable connection

between ancestry-related inflammation and cancer risk disparity.

Next, a cancer genomic meta-analysis using 48 GWAS within the National Cancer Institute GAME-ON Network (64591 cancer and 74467 control patients) across five common cancer sites (ovarian, lung, breast, colorectal, and prostate) found that genetic variants associated with inflammation and innate immune response were relevant to CRC risk, including SH2B adapter protein 3 (*SH2B3*) (rs3184504, $P = 3.32 \times 10^{-5}$), a negative regulator of growth factors and cytokine-induced signaling (Table 1). Unfortunately, irSNP associations with race/ethnicity and geographic distributions were not evaluated[85]. In contrast, Wang *et al*[47] demonstrated the merit of accounting for population diversity in their analysis of associations between innate immunity pathways and CRC risk. In two large studies (discovery and validation cohorts) across five distinct ethnic groups (AA, CA, Japanese-American, Latino, and Native Hawaiian), they found that among more than 600 common variants associated with 37 innate immunity-related genes, a SNV in the second intron of peroxisome proliferator-activated receptor gamma (*PPARG*) (rs9858822) showed a statistically significant association with CRC in the AA population (Table 1). This variant, rare in other non-AA populations, was not previously reported. Importantly, a frequently reported *PPARG* variant rs1801282, inconsistently associated with CRC in other studies[86-88], was not detected in association with CRC in Wang *et al*[47]'s study that carefully controlled for population diversity, supporting the value of multi-ancestry SNP association studies. In another meta-analysis of 308 SNPs performed by Montazeri *et al*[89], 14 SNPs showed credible association with CRC including rs3802842, whose expression was associated with immune infiltration. Curiously, the *PPARG* rs9858822 polymorphism detected by Wang *et al*[47] failed as a positive SNP in this meta-analysis, a finding that warrants additional verification. However, such discrepancies between the multi-ethnic study of Wang *et al*[47] and European study of Montazeri *et al*[89] may highlight the issue of the underrepresented diversity when seeking genetic cancer risk. Population-associated risk may be missed, and alternatively discovered cancer risk may not be relevant for minorities.

Lastly, functional variants in the 3′-untranslated region (UTR) of inflammatory gene miRNA binding sites (miRSNPs) have been associated with CRC risk[75]. Four miRSNPs in the mannose binding lectin 2 (*MBL2*) gene 3′-UTR have been associated with increased CRC risk in the AA population. *MBL2* codes for mannose binding lactose protein, a pattern recognition receptor that binds a wide range of pathogen-expressed sugars, leading to their phagocytosis. Although not assessed in this study, the modulation of the interactions between the mucosal inflammation and the microbiome, *via* MBL2 expression, could be a mechanistic link between African ancestry and higher CRC risk[74]. irSNPs associated with CRC risk are summarized in Table 1.

Ultimately, linking chronic inflammation risk loci to positive selection *via* resistance to past infectious agents and population displacement should be done with caution, as the merits are still debated[78]. Physiological interfacing of the immune system with other biological systems (reproduction and organ development) may also explain positive selection in a manner distinct from past pathogen resistance [78]. Yet, considering the evidence of host innate immunity regulation by population-enriched irSNPS [27], it is reasonable to speculate that the mucosal inflammation associated with commensalism is differentially tuned according to the level of African ancestry and could therefore influence CRC disparities. This view is supported by disparity research in other cancers, such as the finding that *IL10* promoter SNPs enriched in AAs are also potential risk factors for prostate cancer development and progression [90]. Interestingly, one such *IL10* polymorphism (rs1800871) was associated with Proteobacteria load in the gut microbiome (Table 2), but a connection between rs1800871, proteobacteria, and prostate cancer remains to be established[90]. In breast cancer, Jenkins *et al*[91] demonstrated how the ancestral selection of immune variants in the African continent can predispose AA women to ancestry-related differences in tumor immunogenicity. Specifically, the status of a "Duffy-null" polymorphism-regulated atypical chemokine receptor 1 (*ACKR1*) allele linked West African genetic ancestry to tumor immune infiltration. Thus, for breast cancer, duffy antigen receptor for chemokines/ACKR1 polymorphism may serve as a biomarker for precision medicine and immunotherapy in patients bearing significant West African ancestry[91]. This result highlights the potential that ancestry-associated irSNPS have for cancer screening and clinical care when paired with functional analyses and elevating the importance of similar studies for CRC.

HOST GENETICS AND MICROBIOME INTERACTIONS' CONTRIBUTION TO CRC DISPARITY

While host genetics may impact mucosal inflammation and CRC risk, other factors, including environmental factors such as diet, lifestyle, and antibiotic exposure, undoubtedly influence CRC susceptibility and treatment response by shaping gut microbiome composition[51,92,93]. Notwithstanding such findings, we propose that the predominant reliance of the microbiome on environmental cues in healthy individuals may conceal host genetic contributions (including genetic ancestry and somatic mutations) in disease contexts (*e.g.*, CRC), driving the microbiome response to environmental fluctuations and defining, at least in part, differential susceptibility to cancer in AAs[94-96]. The numerous immune-related genetic variants that delineate chronic disease susceptibility between AAs and CAs (previously

Table 1 Immune-related single nucleotide polymorphism associated with colorectal cancer

Ref.	Size	Analysis	Gene	SNP	Function	Ethnicity	Comment
Montazeri *et al*[89], 2020	6149 CRC 7337 controls	Meta-analysis	*COLCA1/2*[1]	rs3802842 (11q23.1)	Immune infiltration of LP	Europeans	Confirmed by Lu *et al*[49], 2019[1]
			TGFB1, *SMAD7*, *SMAD7*	rs1800469, rs12953717, rs4464148	TGFB signaling inhibitor		
Law *et al*[50], 2019	34627 CRC 71379 controls	Meta-analysis	*HLA-C*	rs3131043 (6p21.33)	Adaptive immunity	Europeans	
			HLA-DRB1/DQA1	rs9271770 (6q21.33)	Adaptive immunity		
			COLCA1/2	rs3087967 (11q23.1)	Immune LP leukocytes		
			FUT2	rs12979278 (19q13.33)	Gut barrier		
Lu *et al*[49], 2019		GWAS	*NOD2*	rs2066847	Innate immunity	East Asians	Confirmed by Montazeri *et al*[89], 2020[2]
			GATA3	rs10795668 (10p14)	T cell transcription factor		
			SMAD7	rs7229639	TGFB signaling inhibitor		
			SMAD7	rs4939827	TGFB signaling inhibitor		
			COLCA1/2[2]	rs3802842 (11q23.1)	Immune infiltration of LP		
Sanabria-Salas *et al*[33], 2017	391 CRC	GWAS	*IL1B*	CGTC haplotype (2q14)	Inflammation	Columbian Africans	Association with AA admixture
Hung *et al*[85], 2015	15414 CRC 17688 controls	GWAS	*SH2B3*	rs3184504 (12q24)	Cytokine signaling	Europeans	Confirmed by Schumacher *et al*[135], 2015
Schumacher *et al*[135], 2015	18299 CRC, 19656 controls (Europeans), 2098 cases, 6172 controls (Asian 1), 2627 cases, 3797 controls (Asian 2)	Meta-analysis	*SH2B3*[3]	rs3184504 (12q24.12)	Cytokine signaling	Europeans/Asians	Confirmed by Hung *et al*[85], 2015[3]
			NOS1	rs73208120 (12q24.22)	ROS production		
Wang *et al*[47], 2013	2535 CRC, 3915 controls (discovery), 2153 CRC, 2630 controls (validation)	GWAS	*PPARG*	rs9858822	Monocyte activation	Multi-ethnic	High frequency in AA
Tsilidis *et al*[136], 2009	CLUE II cohort, 208 CRC, 381 controls	GWAS	*IL10*	rs1800896, rs1800890, rs3024496, rs3024498	Increased IL-10	ND	

[1]Confirmed by Lu *et al*[49].
[2]Confirmed by Montazeri *et al*[89].
[3]Confirmed by Hung *et al*[85].
AA: African-American; CRC: Colorectal cancer; GWAS: Genome-wide association studies; IL: Interleukin; LP: Lamina propria; ROS: Reactive oxygen species; SNP: Single nucleotide polymorphism; TGF: Transforming growth factor;

ND: Not determined; HLA: Human leukocyte antigen; FUT2: Fucosyltransferase 2; NOD2: Nucleotide binding oligomerization domain containing protein 2; GATA3: GATA binding protein 3; SH2B3: SH2B adapter protein 3; NOS1: Nitric oxide synthase 1; PPARG: Peroxisome proliferator-activated receptor gamma.

discussed) may then contribute to differential inflammatory responses to the microbiome dysbiosis and compound existing CRC disparities (Figure 2).

From this perspective, multiple metagenomic studies of fecal and mucosal samples have already found compositional and metabolomic differences between CRC and healthy patient microbiome[97-100]. Novel meta-analysis approaches combined these metagenome shotgun datasets across heterogeneous populations to explore relationships between the microbiome and CRC; associations were identified at both bacterial strain and gene levels[101-103]. A common core of 29 bacterial species was enriched in CRC cases, and choline metabolism was established as a reproducible biomarker of the CRC-associated microbiome[101,102]. While such findings are correlative and do not suggest causative links, several smaller studies have highlighted the role of specific bacteria[104-106] and microbial dysbiosis in triggering colorectal carcinogenesis in animal models[107]. However, microbiome GWAS (mGWAS) have not yet identified consistent associations between such carcinogenic bacteria and CRC risk[108]. Unfortunately, because population diversity was systematically underrepresented or not annotated in the metagenome datasets, it remains unknown how these results could translate into CRC risk factors or diagnostic biomarkers for specific racial/ethnic groups.

Meanwhile, several taxonomic and metagenomic studies have revealed an intriguing diversity in microbiome composition across racial/ethnic groups, but mechanistic understandings of associations between bacteria or groups of bacteria and race/ethnicity are sparse[34,109-113]. In particular, diversity of the microbiome is highly diet-driven. A study by O'Keefe *et al*[44] showed that a 2-wk food swap between AAs (received high fiber, low fat diet) and rural Africans (received low fiber, high fat diet) produced dramatic changes in mucosal biomarkers and a metabolome switch, illustrated by an increase in saccharolytic fermentation and anti-inflammatory butyrogenesis as well as suppression of secondary bile acid synthesis in AAs. In light of these results, it is critical that mGWAS take diet into consideration as a confounding factor, as its impact will inevitably interfere with the genetic/epigenetic influence on CRC risk[114]. Interestingly though, differences between CAs and AAs with respect to the mean alternate Healthy Eating Index (a measure of diet quality[115]) faded when adjusting for SES, implying that diet cannot entirely account for CRC disparities[116]. Multiple other factors besides diet are known to impact the composition and function of the microbiome, including smoking, alcohol consumption, as well as antibiotic exposure or metabolic condition such as diabetes or obesity, which are coincidentally also risk factors for CRC[117-119]. While these aspects of the microbiome biology have been extensively reviewed[120], we are paying much of our attention herein on the role of the host genetics and the ancestral genetic origin on the microbiome diversity and consequently CRC risk between ethnicities.

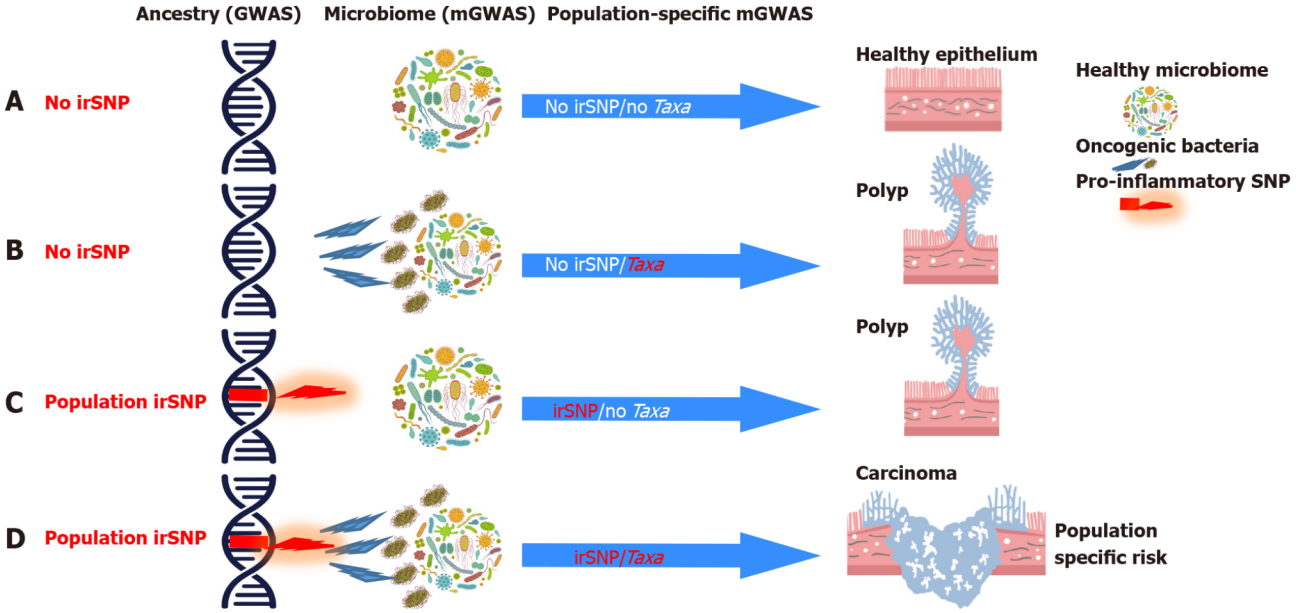
Interestingly, using the Healthy Life in an Urban Setting cohort and fecal 16S ribosomal RNA gene sequencing of over 2000 individuals, Deschasaux *et al*[110] found that microbiome diversity between racial/ethnic groups living in the same city was independent of metabolic health and only partially explained by SES, lifestyle, and diet factors. Yet, this finding was not always reproduced in other studies [45,111,121]. Overall, however, there is sufficient evidence to justify additional efforts to clarify if host genetics and population origins are taking part in shaping the microbiome[51,94]. The role of host genetic background has been suggested by mGWAS, which showed that SNPs such as rs4988235,

Table 2 Interactions of host genetics (metabolic and immune-related single nucleotide polymorphism) with gut bacteria

Ref.	Size	Analysis	Gene	SNP	Function	Bacteria	Ethnicity	Comment
Knights *et al*[59], 2014	474 IBD	16S RNA	*NOD2*	rs5743293, rs104895431, rs104895467, rs2068844, rs2068845, rs5743277, rs5743293	Innate immunity	*Enterobacteriaceae*	Europeans	IBD
Blekhman *et al*[122], 2015	93 (HMP)	Metagenomic	*LCT*	rs2304371, rs3754689	Metabolism	*Bifidobacterium*, *SMB53* (*Clostridiaceae*)	Multi-ethnic	NS
			GNA12	rs1182182	IBD			
Goodrich *et al*[123], 2016	1126	Fecal 16S rRNA	*CD36*	rs1360741	Immune-related	*Blautia*	Europeans	United Kingdom twins
Li *et al*[137], 2016	10523 IBD, 5726 IBD	Mucosal 16S rRNA	*SLC39A8*	rs13107325	Immune-related	*Composition*	ND	IBD
Bonder *et al*[68], 2016	1514	Metagenomic	*C11orf30-LRRC32*	rs2155219	IBD	*Coprococcus comes/Proteobacteria*		AA[1] PCa risk
			CCL2	rs3091315, rs3091316	Immune-related	*Methonobacteria*		
			DAP2	rs267939	Innate immunity	*Bifidobacterium*		
			IL23R	rs12141575	Immune-related	*Enterobacteriaceae/E. coli*		
			IL10	rs1800871[1]	Immune-related	*Proteobacteria/Sutterella*		
			MUC22	rs3873352	Barrier defense			
			NOD1	rs12669082	Innate immunity	*Enterobacteriaceae/E.coli*		
				rs41524946	Innate immunity	*Enteroba cteriaceae/E. coli*		
				rs55689059	Innate immunity	*Enterobacteriaceae/E. coli*		
				rs55841603	Innate immunity	*Enterobacteriaceae/E. coli*		
			NOD2	rs8056611, rs2357792,	Innate immunity	*Enterobacteriaceae/E. coli*		
			CD209	rs1010046	Innate immunity	*Bacteroidetes*		
Rühlemann *et al*[138], 2021	8956	16S rRNA/GWAS	*FUT2*	rs602662	Barrier defense	*Bacteroides* OTU97_27	Europeans	
			BLVRA	rs623108	Innate immunity	*Barnesiella spp*. OTU99_55		

[1]Studies include an analysis according to the population origins.

AA: African-American; GWAS: Genome-wide association studies; HMP: Human Microbiome Project; IBD: Inflammatory bowel disease; SNP: Single nucleotide polymorphism; ND: Not determined; NS: Not significant; PCa: Prostate cancer; rRNA: Ribosomal RNA; *E. coli*: *Escherichia coli*; FUT2: Fucosyltransferase 2; NOD2: Nucleotide binding oligomerization domain containing protein 2; LCT: Lactase; GNA12: Guanine nucleotide-binding protein alpha-12; CCL2: C-C motif chemokine ligand 2; IL: Interleukin; MUC22: Mucin 22; BLVRA: Biliverdin reductase.



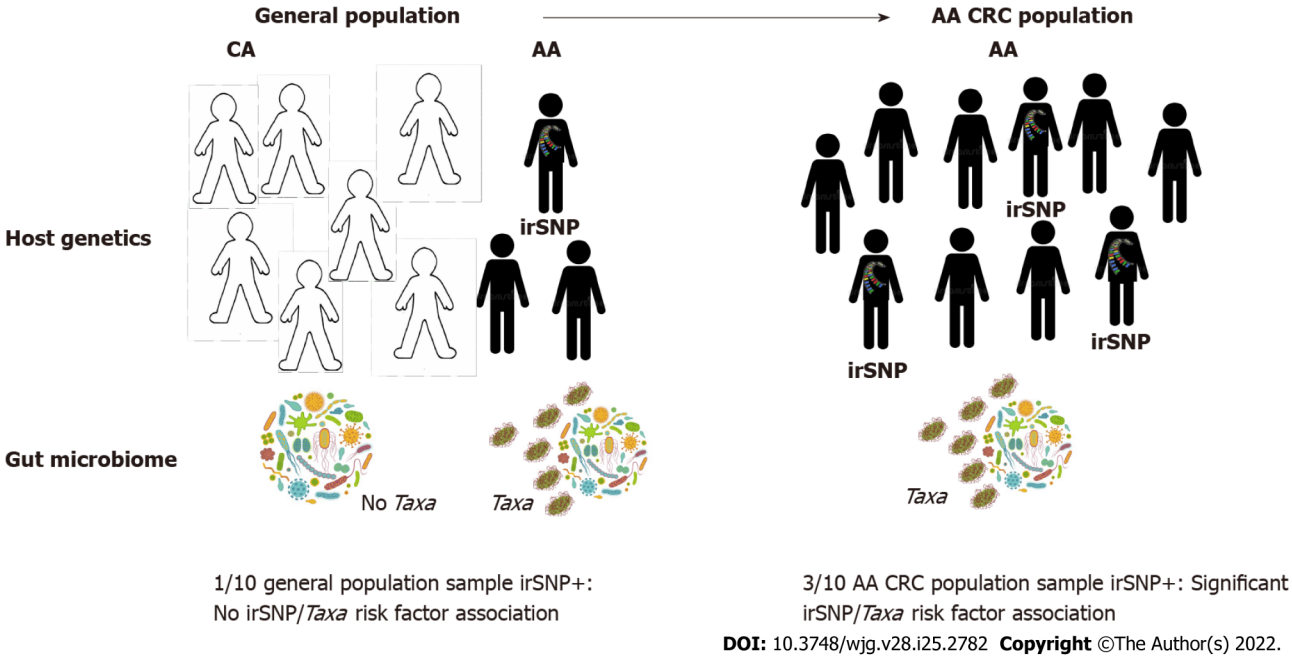
DOI: 10.3748/wjg.v28.i25.2782 **Copyright** ©The Author(s) 2022.

Figure 2 Interactions between host genetics and microbiome delineate colorectal cancer risk factors. Immune-related risk factors of colorectal cancer (CRC) may combine host genetics [including immune-related single-nucleotide polymorphisms (irSNPs)] and microbiome cues. The genetic regulation (irSNP) of bacteria (*Taxa*) recognition by the mucosal immunity may mediate the heterogeneity of CRC risk factors between populations which vary by the representation of irSNPs. A: Absence of irSNPs and pathogenic bacteria (no irSNPs/no *Taxa*) maintain healthy mucosal inflammation and gut barrier; B: Absence of irSNPs with enrichment of pathogenic bacteria (no irSNPs/*Taxa*) may lead to chronic inflammation that slowly promotes polyp formation; C: Presence of irSNP in absence of pathogenic bacteria may also lead to chronic inflammation that slowly promotes polyp formation; D: Combination of irSNP and pathogenic bacteria (dysbiosis) may trigger a smoldering chronic inflammatory response precipitating early progression of the adenoma-carcinoma sequence. Genome-wide association studies (GWAS) (irSNP as CRC risk) and microbiome GWAS (mGWAS) (bacteria as CRC risk) are poised to miss the association of the irSNP with CRC because of the necessity of a combined occurrence of irSNP and specific bacteria enrichment in the microbiota to increase the CRC risk. However, if the irSNP is linked to the genetic ancestry, population-specific microbiome GWAS will likely detect the association of irSNP and the bacteria as a CRC risk in the population carrying this genetic ancestry. CRC: Colorectal cancer; irSNPs: Immune-related single-nucleotide polymorphisms; GWAS: Genome-wide association studies; mGWAS: Microbiome genome-wide association studies.

associated with lactase persistence gene, contributed to microbiome composition[45,68,122,123]. A study performed with 416 twin pairs in the United Kingdom identified 26 "heritable" taxa, also suggesting that specific host genetic variants may participate in microbiome composition (Table 2)[124]. Notably, host genetic variants associated with microbiome composition were found to be enriched in immunity-related pathways[122]. Studies showing associations between metabolic and immune-related polymorphisms and microbiome composition are summarized in Table 2.

Finally, associations between the microbiome and somatic mutations in CRC have been described by Burns *et al*[95], who suggested that genetic determinants of the host and colon tumor mutations alter microbiome structure. The CRC mutanome could therefore help predict the composition and function of CRC-associated microbiomes and the clinical outcome or the response to therapies. To this end, of intrigue is the recent description by Ashktorab *et al*[125] and Brim *et al*[126] of genetic variation in tumor suppressor genes (*APC*), DNA mismatch repair genes, and other driver mutations (*KRAS* and *PIK3C*) in AAs with CRC, some of which were novel and not previously described in other populations. Loss of function mutations in *APC* were correlated with changes in 25 different microbial taxa, including an abundance of *Finegolia* or *Christensenellaceae*. Mutations in the zinc finger protein 717-coding gene were associated with an abundance of *Akkermansia* and *Verrucomicrobiaceae*, both colitis-associated species. Additionally, the same authors have isolated a novel *Streptococcus spp*. VT_162 from colon adenoma and CRC lesions in AAs[126]. Fecal *Streptococcus spp*. VT_162 was also confirmed in an advanced adenoma and CRC Chinese/Hong-Kong cohort[126]. An assessment of this bacterium's relative prevalence in CAs compared to AAs will be necessary. Whether CA genetic background is more restrictive, while AA genetic background is more permissive to this species is not yet established. It may be postulated that, as seen in IBD patients, host genetic background drives the nature of the microbiome and alters the CRC risk posed by procarcinogenic "driver" bacteria[48,51].

Although there is a lack of direct causative links between such bacteria and colon carcinogenesis or growth promotion, this evidence at least signals that CRC disparities in AAs may be related to differential host inflammatory responses to similar bacterial communities (inflammation-driven disparities) and/or the contribution of ancestry-related factors in shaping microbiome diversity (bacteria-driven disparities). The molecular pathological epidemiology (MPE) that aims at uncovering an interactive relationship between environmental features and disease subtypes to understand disease incidence and



DOI: 10.3748/wjg.v28.i25.2782 **Copyright** ©The Author(s) 2022.

Figure 3 Population-specific colorectal cancer microbiome genome-wide association studies to understand colorectal cancer disparities. Systemic underrepresentation of minorities in microbiome genome-wide association studies (mGWAS) may compromise the identification of microbiome-associated colorectal cancer (CRC) risks in African-Americans (AAs). Left: Associations between AA-enriched immune-related single-nucleotide polymorphisms (irSNPs) (pop-irSNPs) and gut bacteria (*Taxa*) may remain undetected in the global population if pop-irSNP and *Taxa* have too low frequency in the AA population and AAs are underrepresented. Right: If pop-irSNP and pathogenic bacteria are CRC risk factors in AA, they will be enriched in AA CRC patients compared to the general AA population (left), and mGWAS will detect the association between pop-irSNP and *Taxa* in AA CRC cohort. These features justify population-specific CRC mGWAS to detect additional CRC risk resulting from the interaction between ancestral irSNP and bacteria in minorities. CRC: Colorectal cancer; irSNPs: Immune-related single-nucleotide polymorphisms; mGWAS: Microbiome genome-wide association studies; AA: African-American; CA: Caucasian-American.

mortality will provide etiologic and pathogenic insights in CRC disparities[127,128]. However, discoveries made in healthy donors often remain inconsistent from one study to another, perhaps due to multiple confounding environmental factors between heterogeneous cohorts[45,129]. More likely culprits for the inconsistency seen in GWAS that seek to identify the impact of host genetics on microbiome diversity are the homogeneity in sampled cohorts and differences in experimental approaches including stool *vs* mucosa sampling, sequencing approaches, and annotations. Future GWAS must address such issues in order to identify associations between genetic background and the microbiome that can reliably be applied to the question of disparities.

CONCLUSION

CRC disparity is far from an exclusively biological phenomenon but rather involves a complex interplay of SES, environmental and genetic components that collectively impact CRC risk and prognostics. Although there is a growing understanding of this complexity, studies examining the influence on CRC pathogenesis from ancestry-specific interactions between host genetics and the commensal microbiome are lacking. Such work is nevertheless urgently needed to appropriately mitigate CRC on a population basis and especially to help address alarming new trends, such as early-onset CRC amongst AAs. To facilitate this line of investigation, we reviewed irSNPs identified in CRC mGWAS and proposed that some of such variants (and others yet to be discovered) may alter microbiome composition and/or differential inflammatory responses to bacteria, thereby impacting CRC risk in a manner associated with genetic ancestry. However, testing the functional significance of such variants will require systematic studies that can incorporate the microbiome, mucosal immunity, and host genetics. A recent investigation by DeStefano Shields *et al*[130], although not related to cancer disparity, offers a potential experimental blueprint. Researchers introduced the *BRAF*^{V600E} mutation to a Min$^{Apc\Delta716/+}$ murine model of distal colon polyposis, then colonized *BRAF* mutant and Min$^{Apc\Delta716/+}$ mice with *Enterotoxigenic Bacteroides fragilis*. Distal colon tumorigenesis was observed in Min$^{Apc\Delta716/+}$ mice following colonization, whereas *BRAF*^{V600E} Min$^{Apc\Delta716/+}$ mice developed proximal colon tumors associated with immune signature and microbiome alterations plus sensitivity to anti-programmed death ligand 1[130]. These results suggested that host gene/bacteria interactions may drive CRC risk and pathogenesis, and demonstrate how such interactions can be disentangled mechanistically using experimental models with clinical implications. In the nascent field of precision medicine and multidisciplinary big data integration, the rapidly

evolving MPE represents a successful model of integration of pathology, genomics, microbiome, immunology, epidemiology, and social science[127,128]. MPE will considerably improve precision medicine and prevention allowing, among other things, identifying SNPs that may impact microbiome and inflammation and serve as predictive markers. Genetic ancestry, however, remains to be integrated to this model to precisely address CRC disparities at the molecular level. Elucidating the mechanisms by which ancestry-associated variants impact CRC pathogenesis will be much more challenging, but models such as the one described by Lavoie *et al*[60], who used mice engineered to express the polymorphism T300A (rs2241880) in the *Atg16 L1* gene known to increase IBD risk in humans, represent a promising approach to identifying mechanisms that can lead to personalized interventions applicable to minorities.

Yet, without addressing biases in genomics science, the ability of GWAS to detect variants of significance for AAs (or other minorities in general) will remain stunted[131]. To date, cancer GWAS have examined cohorts predominantly composed of Caucasian individuals, an homogeneity that limits the appreciation of how genetic ancestry impacts cancer risk[101,102]. Critically, the lack of diverse representation in sampling cohorts results in the increased likelihood that, even if identified, cancer-associated variants may be of limited clinical significance for non-Caucasian populations. While commenting on this issue, Davis[131] recently argued that the current state of genomic medicine is inadequately equipped to confront current oncological trends of disparate incidence and mortality in inclusive fashion and advocated for a persistent push towards the prioritization of patient diversity. Such an agenda is not only more harmonious with the principles of ethical human subjects research but is also scientifically meritable, as studies that account for diversity have already revealed novel genomic data that may improve our understanding of cancer etiology[132]. Therefore, for powered GWAS to detect and discern associations between population-enriched irSNPs, the microbiome, and CRC, proper accounting of population diversity and sufficient cohort size (estimated at > 4000 individuals)[45], or even population-specific CRC studies will be essential (illustrated in Figure 3). Encouragingly, recent methodological frameworks for multi-ancestry cohort GWAS have already yielded ancestry-related cancer variant risk factors[133,134]. Moreover, the recent initiative of the National Cancer Institute: Genetic Association and Mechanism in Oncology (GAME-ON; https://epi.grants.cancer.gov), which regrouped genomic data from more than 33 GWAS across five different cancers (CRC, lung, breast, ovary, and oral), is an example of the benefit of data sharing that will help identifying through meta-analysis data cancer risk loci in understudied populations, especially since 40% of the samples are from African, Asian, and Hispanic backgrounds. However, our integrated concept for CRC genomic research proposes that to represent accurately and capture the contribution of irSNP/microbiome interactions to CRC disparities, such diversified host genomic data must be paired with microbiome data.

In sum, population-related irSNP that regulate mucosal inflammation may modify the microbiota and its interaction with colon epithelium. Alternatively, a population-related SNP not involved in immune regulation may also alter the microbiome and trigger procarcinogenic chronic inflammation. Finally, a combination of two SNPs impacting inflammation and the microbiome with minor effects on CRC pathogenesis may trigger a strong procarcinogenic bacteria/inflammation interaction when combined in an at-risk population (Figure 2). By hunting for and characterizing such genetic factors using the emerging genetic admixture and ancestry paradigms, we believe scientists and clinicians will have a precision tool that enables a clearer understanding of the association between CRC with AA populations and the increasing trend of early onset CRC, ultimately to better mitigate CRC outcome disparities.

FOOTNOTES

Author contributions: Ahmad S wrote the manuscript; Housseau F and Brim H contributed equally to the review's conception and oversight of the writing, with additional insight from Ashktorab H; and all authors have read and approve the final manuscript.

Conflict-of-interest statement: All the authors report no relevant conflicts of interest for this article.

Open-Access: This article is an open-access article that was selected by an in-house editor and fully peer-reviewed by external reviewers. It is distributed in accordance with the Creative Commons Attribution NonCommercial (CC BY-NC 4.0) license, which permits others to distribute, remix, adapt, build upon this work non-commercially, and license their derivative works on different terms, provided the original work is properly cited and the use is non-commercial. See: https://creativecommons.org/Licenses/by-nc/4.0/

Country/Territory of origin: United States

ORCID number: Sami Ahmad 0000-0001-5838-3137; Hassan Ashktorab 0000-0002-4048-4666; Hassan Brim 0000-0001-7055-2298; Franck Housseau 0000-0002-7028-3953.

S-Editor: Wang JJ

L-Editor: A
P-Editor: Wang JJ

REFERENCES

1 **Siegel RL**, Miller KD, Goding Sauer A, Fedewa SA, Butterly LF, Anderson JC, Cercek A, Smith RA, Jemal A. Colorectal cancer statistics, 2020. *CA Cancer J Clin* 2020; **70**: 145-164 [PMID: 32133645 DOI: 10.3322/caac.21601]
2 **Carethers JM**, Doubeni CA. Causes of Socioeconomic Disparities in Colorectal Cancer and Intervention Framework and Strategies. *Gastroenterology* 2020; **158**: 354-367 [PMID: 31682851 DOI: 10.1053/j.gastro.2019.10.029]
3 **Carethers JM**. Clinical and Genetic Factors to Inform Reducing Colorectal Cancer Disparitites in African Americans. *Front Oncol* 2018; **8**: 531 [PMID: 30524961 DOI: 10.3389/fonc.2018.00531]
4 **Polite BN**, Sing A, Sargent DJ, Grothey A, Berlin J, Kozloff M, Feng S. Exploring racial differences in outcome and treatment for metastatic colorectal cancer: results from a large prospective observational cohort study (BRiTE). *Cancer* 2012; **118**: 1083-1090 [PMID: 21800287 DOI: 10.1002/cncr.26394]
5 **Sanoff HK**, Sargent DJ, Green EM, McLeod HL, Goldberg RM. Racial differences in advanced colorectal cancer outcomes and pharmacogenetics: a subgroup analysis of a large randomized clinical trial. *J Clin Oncol* 2009; **27**: 4109-4115 [PMID: 19636001 DOI: 10.1200/JCO.2009.21.9527]
6 **Johnston FM**, Yeo HL, Clark C, Stewart JH 4th. Bias Issues in Colorectal Cancer Management: A Review. *Ann Surg Oncol* 2022; **29**: 2166-2173 [PMID: 34142287 DOI: 10.1245/s10434-021-10232-6]
7 **Ciccone G**, Prastaro C, Ivaldi C, Giacometti R, Vineis P. Access to hospital care, clinical stage and survival from colorectal cancer according to socio-economic status. *Ann Oncol* 2000; **11**: 1201-1204 [PMID: 11061620 DOI: 10.1023/a:1008352119907]
8 **Jepson C**, Kessler LG, Portnoy B, Gibbs T. Black-white differences in cancer prevention knowledge and behavior. *Am J Public Health* 1991; **81**: 501-504 [PMID: 2003635 DOI: 10.2105/ajph.81.4.501]
9 **Zavala VA**, Bracci PM, Carethers JM, Carvajal-Carmona L, Coggins NB, Cruz-Correa MR, Davis M, de Smith AJ, Dutil J, Figueiredo JC, Fox R, Graves KD, Gomez SL, Llera A, Neuhausen SL, Newman L, Nguyen T, Palmer JR, Palmer NR, Pérez-Stable EJ, Piawah S, Rodriquez EJ, Sanabria-Salas MC, Schmit SL, Serrano-Gomez SJ, Stern MC, Weitzel J, Yang JJ, Zabaleta J, Ziv E, Fejerman L. Cancer health disparities in racial/ethnic minorities in the United States. *Br J Cancer* 2021; **124**: 315-332 [PMID: 32901135 DOI: 10.1038/s41416-020-01038-6]
10 **Chen J**, Pitmon E, Wang K. Microbiome, inflammation and colorectal cancer. *Semin Immunol* 2017; **32**: 43-53 [PMID: 28982615 DOI: 10.1016/j.smim.2017.09.006]
11 **Dejea C**, Wick E, Sears CL. Bacterial oncogenesis in the colon. *Future Microbiol* 2013; **8**: 445-460 [PMID: 23534358 DOI: 10.2217/fmb.13.17]
12 **Farhana L**, Antaki F, Murshed F, Mahmud H, Judd SL, Nangia-Makker P, Levi E, Yu Y, Majumdar AP. Gut microbiome profiling and colorectal cancer in African Americans and Caucasian Americans. *World J Gastrointest Pathophysiol* 2018; **9**: 47-58 [PMID: 30283710 DOI: 10.4291/wjgp.v9.i2.47]
13 **Koi M**, Okita Y, Carethers JM. *Fusobacterium nucleatum* Infection in Colorectal Cancer: Linking Inflammation, DNA Mismatch Repair and Genetic and Epigenetic Alterations. *J Anus Rectum Colon* 2018; **2**: 37-46 [PMID: 30116794 DOI: 10.23922/jarc.2017-055]
14 **Devaraj B**, Lee A, Cabrera BL, Miyai K, Luo L, Ramamoorthy S, Keku T, Sandler RS, McGuire KL, Carethers JM. Relationship of EMAST and microsatellite instability among patients with rectal cancer. *J Gastrointest Surg* 2010; **14**: 1521-1528 [PMID: 20844976 DOI: 10.1007/s11605-010-1340-6]
15 **Carethers JM**, Koi M, Tseng-Rogenski SS. EMAST is a Form of Microsatellite Instability That is Initiated by Inflammation and Modulates Colorectal Cancer Progression. *Genes (Basel)* 2015; **6**: 185-205 [PMID: 25836926 DOI: 10.3390/genes6020185]
16 **Dejea CM**, Wick EC, Hechenbleikner EM, White JR, Mark Welch JL, Rossetti BJ, Peterson SN, Snesrud EC, Borisy GG, Lazarev M, Stein E, Vadivelu J, Roslani AC, Malik AA, Wanyiri JW, Goh KL, Thevambiga I, Fu K, Wan F, Llosa N, Housseau F, Romans K, Wu X, McAllister FM, Wu S, Vogelstein B, Kinzler KW, Pardoll DM, Sears CL. Microbiota organization is a distinct feature of proximal colorectal cancers. *Proc Natl Acad Sci U S A* 2014; **111**: 18321-18326 [PMID: 25489084 DOI: 10.1073/pnas.1406199111]
17 **Thornton JG**, Morris AM, Thornton JD, Flowers CR, McCashland TM. Racial variation in colorectal polyp and tumor location. *J Natl Med Assoc* 2007; **99**: 723-728 [PMID: 17668638]
18 **Park CH**, Han DS, Oh YH, Lee AR, Lee YR, Eun CS. Role of Fusobacteria in the serrated pathway of colorectal carcinogenesis. *Sci Rep* 2016; **6**: 25271 [PMID: 27125587 DOI: 10.1038/srep25271]
19 **Yu J**, Chen Y, Fu X, Zhou X, Peng Y, Shi L, Chen T, Wu Y. Invasive Fusobacterium nucleatum may play a role in the carcinogenesis of proximal colon cancer through the serrated neoplasia pathway. *Int J Cancer* 2016; **139**: 1318-1326 [PMID: 27130618 DOI: 10.1002/ijc.30168]
20 **DeDecker L**, Coppedge B, Avelar-Barragan J, Karnes W, Whiteson K. Microbiome distinctions between the CRC carcinogenic pathways. *Gut Microbes* 2021; **13**: 1854641 [PMID: 33446008 DOI: 10.1080/19490976.2020.1854641]
21 **Yang JF**, Tang SJ, Lash RH, Wu R, Yang Q. Anatomic distribution of sessile serrated adenoma/polyp with and without cytologic dysplasia. *Arch Pathol Lab Med* 2015; **139**: 388-393 [PMID: 25724036 DOI: 10.5858/arpa.2013-0523-OA]
22 **Yamauchi M**, Morikawa T, Kuchiba A, Imamura Y, Qian ZR, Nishihara R, Liao X, Waldron L, Hoshida Y, Huttenhower C, Chan AT, Giovannucci E, Fuchs C, Ogino S. Assessment of colorectal cancer molecular features along bowel subsites challenges the conception of distinct dichotomy of proximal *versus* distal colorectum. *Gut* 2012; **61**: 847-854 [PMID: 22427238 DOI: 10.1136/gutjnl-2011-300865]
23 **Polite BN**, Adams-Campbell LL, Brawley OW, Bickell N, Carethers JM, Flowers CR, Foti M, Gomez SL, Griggs JJ,

Lathan CS, Li CI, Lichtenfeld JL, McCaskill-Stevens W, Paskett ED. Charting the future of cancer health disparities research: A position statement from the American Association for Cancer Research, the American Cancer Society, the American Society of Clinical Oncology, and the National Cancer Institute. *CA Cancer J Clin* 2017; **67**: 353-361 [PMID: 28738442 DOI: 10.3322/caac.21404]

24 **Zheng D**, Liwinski T, Elinav E. Interaction between microbiota and immunity in health and disease. *Cell Res* 2020; **30**: 492-506 [PMID: 32433595 DOI: 10.1038/s41422-020-0332-7]

25 **Jovov B**, Araujo-Perez F, Sigel CS, Stratford JK, McCoy AN, Yeh JJ, Keku T. Differential gene expression between African American and European American colorectal cancer patients. *PLoS One* 2012; **7**: e30168 [PMID: 22276153 DOI: 10.1371/journal.pone.0030168]

26 **Quach H**, Rotival M, Pothlichet J, Loh YE, Dannemann M, Zidane N, Laval G, Patin E, Harmant C, Lopez M, Deschamps M, Naffakh N, Duffy D, Coen A, Leroux-Roels G, Clément F, Boland A, Deleuze JF, Kelso J, Albert ML, Quintana-Murci L. Genetic Adaptation and Neandertal Admixture Shaped the Immune System of Human Populations. *Cell* 2016; **167**: 643-656.e17 [PMID: 27768888 DOI: 10.1016/j.cell.2016.09.024]

27 **Nédélec Y**, Sanz J, Baharian G, Szpiech ZA, Pacis A, Dumaine A, Grenier JC, Freiman A, Sams AJ, Hebert S, Pagé Sabourin A, Luca F, Blekhman R, Hernandez RD, Pique-Regi R, Tung J, Yotova V, Barreiro LB. Genetic Ancestry and Natural Selection Drive Population Differences in Immune Responses to Pathogens. *Cell* 2016; **167**: 657-669.e21 [PMID: 27768889 DOI: 10.1016/j.cell.2016.09.025]

28 **Banda Y**, Kvale MN, Hoffmann TJ, Hesselson SE, Ranatunga D, Tang H, Sabatti C, Croen LA, Dispensa BP, Henderson M, Iribarren C, Jorgenson E, Kushi LH, Ludwig D, Olberg D, Quesenberry CP Jr, Rowell S, Sadler M, Sakoda LC, Sciortino S, Shen L, Smethurst D, Somkin CP, Van Den Eeden SK, Walter L, Whitmer RA, Kwok PY, Schaefer C, Risch N. Characterizing Race/Ethnicity and Genetic Ancestry for 100,000 Subjects in the Genetic Epidemiology Research on Adult Health and Aging (GERA) Cohort. *Genetics* 2015; **200**: 1285-1295 [PMID: 26092716 DOI: 10.1534/genetics.115.178616]

29 **Bryc K**, Durand EY, Macpherson JM, Reich D, Mountain JL. The genetic ancestry of African Americans, Latinos, and European Americans across the United States. *Am J Hum Genet* 2015; **96**: 37-53 [PMID: 25529636 DOI: 10.1016/j.ajhg.2014.11.010]

30 **Batai K**, Hooker S, Kittles RA. Leveraging genetic ancestry to study health disparities. *Am J Phys Anthropol* 2021; **175**: 363-375 [PMID: 32935870 DOI: 10.1002/ajpa.24144]

31 **Denny JC**. Chapter 13: Mining electronic health records in the genomics era. *PLoS Comput Biol* 2012; **8**: e1002823 [PMID: 23300414 DOI: 10.1371/journal.pcbi.1002823]

32 **Ruterbusch JJ**, Levin AM, Kittles R, Rybicki BA, Bock CH. Abstract A66: Admixture and fine mapping in African Americans identifies a susceptibility locus for prostate cancer on chromosome 7. *Cancer Epidemiol Biomarkers Prev* 2012; **21**: A66 [DOI: 10.1158/1055-9965.DISP12-A66]

33 **Sanabria-Salas MC**, Hernández-Suárez G, Umaña-Pérez A, Rawlik K, Tenesa A, Serrano-López ML, Sánchez de Gómez M, Rojas MP, Bravo LE, Albis R, Plata JL, Green H, Borgovan T, Li L, Majumdar S, Garai J, Lee E, Ashktorab H, Brim H, Margolin D, Fejerman L, Zabaleta J. IL1B-CGTC haplotype is associated with colorectal cancer in admixed individuals with increased African ancestry. *Sci Rep* 2017; **7**: 41920 [PMID: 28157220 DOI: 10.1038/srep41920]

34 **Nieves Delgado A**, Baedke J. Does the human microbiome tell us something about race? *Humanit Soc Sci Commun* 2021; **8**: 97 [DOI: 10.1057/s41599-021-00772-3]

35 **Gallagher S**, Hughes E, Wagner S, Tshiaba P, Rosenthal E, Roa BB, Kurian AW, Domchek SM, Garber J, Lancaster J, Weitzel JN, Gutin A, Lanchbury JS, Robson M. Association of a Polygenic Risk Score With Breast Cancer Among Women Carriers of High- and Moderate-Risk Breast Cancer Genes. *JAMA Netw Open* 2020; **3**: e208501 [PMID: 32609350 DOI: 10.1001/jamanetworkopen.2020.8501]

36 **Thomas M**, Sakoda LC, Hoffmeister M, Rosenthal EA, Lee JK, van Duijnhoven FJB, Platz EA, Wu AH, Dampier CH, de la Chapelle A, Wolk A, Joshi AD, Burnett-Hartman A, Gsur A, Lindblom A, Castells A, Win AK, Namjou B, Van Guelpen B, Tangen CM, He Q, Li CI, Schafmayer C, Joshu CE, Ulrich CM, Bishop DT, Buchanan DD, Schaid D, Drew DA, Muller DC, Duggan D, Crosslin DR, Albanes D, Giovannucci EL, Larson E, Qu F, Mentch F, Giles GG, Hakonarson H, Hampel H, Stanaway IB, Figueiredo JC, Huyghe JR, Minnier J, Chang-Claude J, Hampe J, Harley JB, Visvanathan K, Curtis KR, Offit K, Li L, Le Marchand L, Vodickova L, Gunter MJ, Jenkins MA, Slattery ML, Lemire M, Woods MO, Song M, Murphy N, Lindor NM, Dikilitas O, Pharoah PDP, Campbell PT, Newcomb PA, Milne RL, MacInnis RJ, Castellví-Bel S, Ogino S, Berndt SI, Bézieau S, Thibodeau SN, Gallinger SJ, Zaidi SH, Harrison TA, Keku TO, Hudson TJ, Vymetalkova V, Moreno V, Martín V, Arndt V, Wei WQ, Chung W, Su YR, Hayes RB, White E, Vodicka P, Casey G, Gruber SB, Schoen RE, Chan AT, Potter JD, Brenner H, Jarvik GP, Corley DA, Peters U, Hsu L. Genome-wide Modeling of Polygenic Risk Score in Colorectal Cancer Risk. *Am J Hum Genet* 2020; **107**: 432-444 [PMID: 32758450 DOI: 10.1016/j.ajhg.2020.07.006]

37 **Sommer F**, Bäckhed F. The gut microbiota--masters of host development and physiology. *Nat Rev Microbiol* 2013; **11**: 227-238 [PMID: 23435359 DOI: 10.1038/nrmicro2974]

38 **Sonnenburg ED**, Sonnenburg JL. The ancestral and industrialized gut microbiota and implications for human health. *Nat Rev Microbiol* 2019; **17**: 383-390 [PMID: 31089293 DOI: 10.1038/s41579-019-0191-8]

39 **Belkaid Y**, Harrison OJ. Homeostatic Immunity and the Microbiota. *Immunity* 2017; **46**: 562-576 [PMID: 28423337 DOI: 10.1016/j.immuni.2017.04.008]

40 **Hooper LV**, Littman DR, Macpherson AJ. Interactions between the microbiota and the immune system. *Science* 2012; **336**: 1268-1273 [PMID: 22674334 DOI: 10.1126/science.1223490]

41 **Johansson ME**, Phillipson M, Petersson J, Velcich A, Holm L, Hansson GC. The inner of the two Muc2 mucin-dependent mucus layers in colon is devoid of bacteria. *Proc Natl Acad Sci U S A* 2008; **105**: 15064-15069 [PMID: 18806221 DOI: 10.1073/pnas.0803124105]

42 **Louis P**, Hold GL, Flint HJ. The gut microbiota, bacterial metabolites and colorectal cancer. *Nat Rev Microbiol* 2014; **12**: 661-672 [PMID: 25198138 DOI: 10.1038/nrmicro3344]

43 **Ocvirk S**, Wilson AS, Posma JM, Li JV, Koller KR, Day GM, Flanagan CA, Otto JE, Sacco PE, Sacco FD, Sapp FR,

Newton K, Brouard F, DeLany JP, Behnning M, Appolonia CN, Soni D, Bhatti F, Methé B, Fitch A, Morris A, Gaskins HR, Kinross J, Nicholson JK, Thomas TK, O'Keefe SJD. A prospective cohort analysis of gut microbial co-metabolism in Alaska Native and rural African people at high and low risk of colorectal cancer. *Am J Clin Nutr* 2020; **111**: 406-419 [PMID: 31851298 DOI: 10.1093/ajcn/nqz301]

44 **O'Keefe SJ**, Li JV, Lahti L, Ou J, Carbonero F, Mohammed K, Posma JM, Kinross J, Wahl E, Ruder E, Vipperla K, Naidoo V, Mtshali L, Tims S, Puylaert PG, DeLany J, Krasinskas A, Benefiel AC, Kaseb HO, Newton K, Nicholson JK, de Vos WM, Gaskins HR, Zoetendal EG. Fat, fibre and cancer risk in African Americans and rural Africans. *Nat Commun* 2015; **6**: 6342 [PMID: 25919227 DOI: 10.1038/ncomms7342]

45 **Rothschild D**, Weissbrod O, Barkan E, Kurilshikov A, Korem T, Zeevi D, Costea PI, Godneva A, Kalka IN, Bar N, Shilo S, Lador D, Vila AV, Zmora N, Pevsner-Fischer M, Israeli D, Kosower N, Malka G, Wolf BC, Avnit-Sagi T, Lotan-Pompan M, Weinberger A, Halpern Z, Carmi S, Fu J, Wijmenga C, Zhernakova A, Elinav E, Segal E. Environment dominates over host genetics in shaping human gut microbiota. *Nature* 2018; **555**: 210-215 [PMID: 29489753 DOI: 10.1038/nature25973]

46 **Terzić J**, Grivennikov S, Karin E, Karin M. Inflammation and colon cancer. *Gastroenterology* 2010; **138**: 2101-2114.e5 [PMID: 20420949 DOI: 10.1053/j.gastro.2010.01.058]

47 **Wang H**, Taverna D, Stram DO, Fortini BK, Cheng I, Wilkens LR, Burnett T, Makar KW, Lindor NM, Hopper JL, Gallinger S, Baron JA, Haile R, Kolonel LN, Henderson BE, Newcomb PA, Casey G, Duggan D, Ulrich CM, Le Marchand L. Genetic variation in the inflammation and innate immunity pathways and colorectal cancer risk. *Cancer Epidemiol Biomarkers Prev* 2013; **22**: 2094-2101 [PMID: 24045924 DOI: 10.1158/1055-9965.EPI-13-0694]

48 **Turpin W**, Goethel A, Bedrani L, Croitoru Mdcm K. Determinants of IBD Heritability: Genes, Bugs, and More. *Inflamm Bowel Dis* 2018; **24**: 1133-1148 [PMID: 29701818 DOI: 10.1093/ibd/izy085]

49 **Lu Y**, Kweon SS, Tanikawa C, Jia WH, Xiang YB, Cai Q, Zeng C, Schmit SL, Shin A, Matsuo K, Jee SH, Kim DH, Kim J, Wen W, Shi J, Guo X, Li B, Wang N, Zhang B, Li X, Shin MH, Li HL, Ren Z, Oh JH, Oze I, Ahn YO, Jung KJ, Conti DV, Schumacher FR, Rennert G, Jenkins MA, Campbell PT, Hoffmeister M, Casey G, Gruber SB, Gao J, Gao YT, Pan ZZ, Kamatani Y, Zeng YX, Shu XO, Long J, Matsuda K, Zheng W. Large-Scale Genome-Wide Association Study of East Asians Identifies Loci Associated With Risk for Colorectal Cancer. *Gastroenterology* 2019; **156**: 1455-1466 [PMID: 30529582 DOI: 10.1053/j.gastro.2018.11.066]

50 **Law PJ**, Timofeeva M, Fernandez-Rozadilla C, Broderick P, Studd J, Fernandez-Tajes J, Farrington S, Svinti V, Palles C, Orlando G, Sud A, Holroyd A, Penegar S, Theodoratou E, Vaughan-Shaw P, Campbell H, Zgaga L, Hayward C, Campbell A, Harris S, Deary IJ, Starr J, Gatcombe L, Pinna M, Briggs S, Martin L, Jaeger E, Sharma-Oates A, East J, Leedham S, Arnold R, Johnstone E, Wang H, Kerr D, Kerr R, Maughan T, Kaplan R, Al-Tassan N, Palin K, Hänninen UA, Cajuso T, Tanskanen T, Kondelin J, Kaasinen E, Sarin AP, Eriksson JG, Rissanen H, Knekt P, Pukkala E, Jousilahti P, Salomaa V, Ripatti S, Palotie A, Renkonen-Sinisalo L, Lepistö A, Böhm J, Mecklin JP, Buchanan DD, Win AK, Hopper J, Jenkins ME, Lindor NM, Newcomb PA, Gallinger S, Duggan D, Casey G, Hoffmann P, Nöthen MM, Jöckel KH, Easton DF, Pharoah PDP, Peto J, Canzian F, Swerdlow A, Eeles RA, Kote-Jarai Z, Muir K, Pashayan N; PRACTICAL consortium, Harkin A, Allan K, McQueen J, Paul J, Iveson T, Saunders M, Butterbach K, Chang-Claude J, Hoffmeister M, Brenner H, Kirac I, Matošević P, Hofer P, Brezina S, Gsur A, Cheadle JP, Aaltonen LA, Tomlinson I, Houlston RS, Dunlop MG. Association analyses identify 31 new risk loci for colorectal cancer susceptibility. *Nat Commun* 2019; **10**: 2154 [PMID: 31089142 DOI: 10.1038/s41467-019-09775-w]

51 **Hall AB**, Tolonen AC, Xavier RJ. Human genetic variation and the gut microbiome in disease. *Nat Rev Genet* 2017; **18**: 690-699 [PMID: 28824167 DOI: 10.1038/nrg.2017.63]

52 **Rakoff-Nahoum S**, Medzhitov R. Regulation of spontaneous intestinal tumorigenesis through the adaptor protein MyD88. *Science* 2007; **317**: 124-127 [PMID: 17615359 DOI: 10.1126/science.1140488]

53 **Hu B**, Elinav E, Huber S, Strowig T, Hao L, Hafemann A, Jin C, Wunderlich C, Wunderlich T, Eisenbarth SC, Flavell RA. Microbiota-induced activation of epithelial IL-6 signaling links inflammasome-driven inflammation with transmissible cancer. *Proc Natl Acad Sci U S A* 2013; **110**: 9862-9867 [PMID: 23696660 DOI: 10.1073/pnas.1307575110]

54 **Couturier-Maillard A**, Secher T, Rehman A, Normand S, De Arcangelis A, Haesler R, Huot L, Grandjean T, Bressenot A, Delanoye-Crespin A, Gaillot O, Schreiber S, Lemoine Y, Ryffel B, Hot D, Nùñez G, Chen G, Rosenstiel P, Chamaillard M. NOD2-mediated dysbiosis predisposes mice to transmissible colitis and colorectal cancer. *J Clin Invest* 2013; **123**: 700-711 [PMID: 23281400 DOI: 10.1172/JCI62236]

55 **Moschen AR**, Gerner RR, Wang J, Klepsch V, Adolph TE, Reider SJ, Hackl H, Pfister A, Schilling J, Moser PL, Kempster SL, Swidsinski A, Orth Höller D, Weiss G, Baines JF, Kaser A, Tilg H. Lipocalin 2 Protects from Inflammation and Tumorigenesis Associated with Gut Microbiota Alterations. *Cell Host Microbe* 2016; **19**: 455-469 [PMID: 27078067 DOI: 10.1016/j.chom.2016.03.007]

56 **Davies JM**, Abreu MT. The innate immune system and inflammatory bowel disease. *Scand J Gastroenterol* 2015; **50**: 24-33 [PMID: 25523553 DOI: 10.3109/00365521.2014.966321]

57 **Hugot JP**, Chamaillard M, Zouali H, Lesage S, Cézard JP, Belaiche J, Almer S, Tysk C, O'Morain CA, Gassull M, Binder V, Finkel Y, Cortot A, Modigliani R, Laurent-Puig P, Gower-Rousseau C, Macry J, Colombel JF, Sahbatou M, Thomas G. Association of NOD2 Leucine-rich repeat variants with susceptibility to Crohn's disease. *Nature* 2001; **411**: 599-603 [PMID: 11385576 DOI: 10.1038/35079107]

58 **Ebbo M**, Crinier A, Vély F, Vivier E. Innate lymphoid cells: major players in inflammatory diseases. *Nat Rev Immunol* 2017; **17**: 665-678 [PMID: 28804130 DOI: 10.1038/nri.2017.86]

59 **Knights D**, Silverberg MS, Weersma RK, Gevers D, Dijkstra G, Huang H, Tyler AD, van Sommeren S, Imhann F, Stempak JM, Vangay P, Al-Ghalith GA, Russell C, Sauk J, Knight J, Daly MJ, Huttenhower C, Xavier RJ. Complex host genetics influence the microbiome in inflammatory bowel disease. *Genome Med* 2014; **6**: 107 [PMID: 25587358 DOI: 10.1186/s13073-014-0107-1]

60 **Lavoie S**, Conway KL, Lassen KG, Jijon HB, Pan H, Chun E, Michaud M, Lang JK, Gallini Comeau CA, Dreyfuss JM, Glickman JN, Vlamakis H, Ananthakrishnan A, Kostic A, Garrett WS, Xavier RJ. The Crohn's disease polymorphism, *ATG16L1* T300A, alters the gut microbiota and enhances the local Th1/Th17 response. *Elife* 2019; **8** [PMID: 30666959

DOI: 10.7554/eLife.39982]

61 **Harrington LE**, Hatton RD, Mangan PR, Turner H, Murphy TL, Murphy KM, Weaver CT. Interleukin 17-producing CD4+ effector T cells develop *via* a lineage distinct from the T helper type 1 and 2 lineages. *Nat Immunol* 2005; **6**: 1123-1132 [PMID: 16200070 DOI: 10.1038/ni1254]

62 **Lee JS**, Tato CM, Joyce-Shaikh B, Gulen MF, Cayatte C, Chen Y, Blumenschein WM, Judo M, Ayanoglu G, McClanahan TK, Li X, Cua DJ. Interleukin-23-Independent IL-17 Production Regulates Intestinal Epithelial Permeability. *Immunity* 2015; **43**: 727-738 [PMID: 26431948 DOI: 10.1016/j.immuni.2015.09.003]

63 **Stockinger B**, Veldhoen M. Differentiation and function of Th17 T cells. *Curr Opin Immunol* 2007; **19**: 281-286 [PMID: 17433650 DOI: 10.1016/j.coi.2007.04.005]

64 **Grivennikov SI**, Wang K, Mucida D, Stewart CA, Schnabl B, Jauch D, Taniguchi K, Yu GY, Osterreicher CH, Hung KE, Datz C, Feng Y, Fearon ER, Oukka M, Tessarollo L, Coppola V, Yarovinsky F, Cheroutre H, Eckmann L, Trinchieri G, Karin M. Adenoma-linked barrier defects and microbial products drive IL-23/IL-17-mediated tumour growth. *Nature* 2012; **491**: 254-258 [PMID: 23034650 DOI: 10.1038/nature11465]

65 **Wang K**, Kim MK, Di Caro G, Wong J, Shalapour S, Wan J, Zhang W, Zhong Z, Sanchez-Lopez E, Wu LW, Taniguchi K, Feng Y, Fearon E, Grivennikov SI, Karin M. Interleukin-17 receptor a signaling in transformed enterocytes promotes early colorectal tumorigenesis. *Immunity* 2014; **41**: 1052-1063 [PMID: 25526314 DOI: 10.1016/j.immuni.2014.11.009]

66 **Bank S**, Andersen PS, Burisch J, Pedersen N, Roug S, Galsgaard J, Ydegaard Turino S, Brodersen JB, Rashid S, Kaiser Rasmussen B, Avlund S, Bastholm Olesen T, Hoffmann HJ, Andersen Nexø B, Sode J, Vogel U, Andersen V. Polymorphisms in the Toll-Like Receptor and the IL-23/IL-17 Pathways Were Associated with Susceptibility to Inflammatory Bowel Disease in a Danish Cohort. *PLoS One* 2015; **10**: e0145302 [PMID: 26698117 DOI: 10.1371/journal.pone.0145302]

67 **Newman WG**, Zhang Q, Liu X, Amos CI, Siminovitch KA. Genetic variants in IL-23R and ATG16L1 independently predispose to increased susceptibility to Crohn's disease in a Canadian population. *J Clin Gastroenterol* 2009; **43**: 444-447 [PMID: 19276991 DOI: 10.1097/MCG.0b013e318168bdf0]

68 **Bonder MJ**, Kurilshikov A, Tigchelaar EF, Mujagic Z, Imhann F, Vila AV, Deelen P, Vatanen T, Schirmer M, Smeekens SP, Zhernakova DV, Jankipersadsing SA, Jaeger M, Oosting M, Cenit MC, Masclee AA, Swertz MA, Li Y, Kumar V, Joosten L, Harmsen H, Weersma RK, Franke L, Hofker MH, Xavier RJ, Jonkers D, Netea MG, Wijmenga C, Fu J, Zhernakova A. The effect of host genetics on the gut microbiome. *Nat Genet* 2016; **48**: 1407-1412 [PMID: 27694959 DOI: 10.1038/ng.3663]

69 **Yeyeodu ST**, Kidd LR, Kimbro KS. Protective Innate Immune Variants in Racial/Ethnic Disparities of Breast and Prostate Cancer. *Cancer Immunol Res* 2019; **7**: 1384-1389 [PMID: 31481520 DOI: 10.1158/2326-6066.CIR-18-0564]

70 **Quan B**, Qi X, Yu Z, Jiang Y, Liao M, Wang G, Feng R, Zhang L, Chen Z, Jiang Q, Liu G. Pathway analysis of genome-wide association study and transcriptome data highlights new biological pathways in colorectal cancer. *Mol Genet Genomics* 2015; **290**: 603-610 [PMID: 25362561 DOI: 10.1007/s00438-014-0945-y]

71 **Wallace TA**, Prueitt RL, Yi M, Howe TM, Gillespie JW, Yfantis HG, Stephens RM, Caporaso NE, Loffredo CA, Ambs S. Tumor immunobiological differences in prostate cancer between African-American and European-American men. *Cancer Res* 2008; **68**: 927-936 [PMID: 18245496 DOI: 10.1158/0008-5472.CAN-07-2608]

72 **Özdemir BC**, Dotto GP. Racial Differences in Cancer Susceptibility and Survival: More Than the Color of the Skin? *Trends Cancer* 2017; **3**: 181-197 [PMID: 28718431 DOI: 10.1016/j.trecan.2017.02.002]

73 **Yuan J**, Hu Z, Mahal BA, Zhao SD, Kensler KH, Pi J, Hu X, Zhang Y, Wang Y, Jiang J, Li C, Zhong X, Montone KT, Guan G, Tanyi JL, Fan Y, Xu X, Morgan MA, Long M, Zhang R, Sood AK, Rebbeck TR, Dang CV, Zhang L. Integrated Analysis of Genetic Ancestry and Genomic Alterations across Cancers. *Cancer Cell* 2018; **34**: 549-560.e9 [PMID: 30300578 DOI: 10.1016/j.ccell.2018.08.019]

74 **Zanetti KA**, Haznadar M, Welsh JA, Robles AI, Ryan BM, McClary AC, Bowman ED, Goodman JE, Bernig T, Chanock SJ, Harris CC. 3'-UTR and functional secretor haplotypes in mannose-binding lectin 2 are associated with increased colon cancer risk in African Americans. *Cancer Res* 2012; **72**: 1467-1477 [PMID: 22282660 DOI: 10.1158/0008-5472.CAN-11-3073]

75 **Karimzadeh MR**, Zarin M, Ehtesham N, Khosravi S, Soosanabadi M, Mosallaei M, Pourdavoud P. MicroRNA binding site polymorphism in inflammatory genes associated with colorectal cancer: literature review and bioinformatics analysis. *Cancer Gene Ther* 2020; **27**: 739-753 [PMID: 32203060 DOI: 10.1038/s41417-020-0172-0]

76 **Lazarus R**, Vercelli D, Palmer LJ, Klimecki WJ, Silverman EK, Richter B, Riva A, Ramoni M, Martinez FD, Weiss ST, Kwiatkowski DJ. Single nucleotide polymorphisms in innate immunity genes: abundant variation and potential role in complex human disease. *Immunol Rev* 2002; **190**: 9-25 [PMID: 12493003 DOI: 10.1034/j.1600-065x.2002.19002.x]

77 **Barreiro LB**, Quintana-Murci L. From evolutionary genetics to human immunology: how selection shapes host defence genes. *Nat Rev Genet* 2010; **11**: 17-30 [PMID: 19953080 DOI: 10.1038/nrg2698]

78 **Brinkworth JF**, Barreiro LB. The contribution of natural selection to present-day susceptibility to chronic inflammatory and autoimmune disease. *Curr Opin Immunol* 2014; **31**: 66-78 [PMID: 25458997 DOI: 10.1016/j.coi.2014.09.008]

79 **Sams AJ**, Dumaine A, Nédélec Y, Yotova V, Alfieri C, Tanner JE, Messer PW, Barreiro LB. Adaptively introgressed Neandertal haplotype at the OAS locus functionally impacts innate immune responses in humans. *Genome Biol* 2016; **17**: 246 [PMID: 27899133 DOI: 10.1186/s13059-016-1098-6]

80 **Green R**, Wilkins C, Thomas S, Sekine A, Hendrick DM, Voss K, Ireton RC, Mooney M, Go JT, Choonoo G, Jeng S, de Villena FP, Ferris MT, McWeeney S, Gale M Jr. Oas1b-dependent Immune Transcriptional Profiles of West Nile Virus Infection in the Collaborative Cross. *G3 (Bethesda)* 2017; **7**: 1665-1682 [PMID: 28592649 DOI: 10.1534/g3.117.041624]

81 **Barreiro LB**, Ben-Ali M, Quach H, Laval G, Patin E, Pickrell JK, Bouchier C, Tichit M, Neyrolles O, Gicquel B, Kidd JR, Kidd KK, Alcaïs A, Ragimbeau J, Pellegrini S, Abel L, Casanova JL, Quintana-Murci L. Evolutionary dynamics of human Toll-like receptors and their different contributions to host defense. *PLoS Genet* 2009; **5**: e1000562 [PMID: 19609346 DOI: 10.1371/journal.pgen.1000562]

82 **Ness RB**, Haggerty CL, Harger G, Ferrell R. Differential distribution of allelic variants in cytokine genes among African Americans and White Americans. *Am J Epidemiol* 2004; **160**: 1033-1038 [PMID: 15561982 DOI: 10.1093/aje/kwh325]

83 **Bidwell J**, Keen L, Gallagher G, Kimberly R, Huizinga T, McDermott MF, Oksenberg J, McNicholl J, Pociot F, Hardt C, D'Alfonso S. Cytokine gene polymorphism in human disease: on-line databases. *Genes Immun* 1999; **1**: 3-19 [PMID: 11197303 DOI: 10.1038/sj.gene.6363645]

84 **Chen H**, Wilkins LM, Aziz N, Cannings C, Wyllie DH, Bingle C, Rogus J, Beck JD, Offenbacher S, Cork MJ, Rafie-Kolpin M, Hsieh CM, Kornman KS, Duff GW. Single nucleotide polymorphisms in the human interleukin-1B gene affect transcription according to haplotype context. *Hum Mol Genet* 2006; **15**: 519-529 [PMID: 16399797 DOI: 10.1093/hmg/ddi469]

85 **Hung RJ**, Ulrich CM, Goode EL, Brhane Y, Muir K, Chan AT, Marchand LL, Schildkraut J, Witte JS, Eeles R, Boffetta P, Spitz MR, Poirier JG, Rider DN, Fridley BL, Chen Z, Haiman C, Schumacher F, Easton DF, Landi MT, Brennan P, Houlston R, Christiani DC, Field JK, Bickeböller H, Risch A, Kote-Jarai Z, Wiklund F, Grönberg H, Chanock S, Berndt SI, Kraft P, Lindström S, Al Olama AA, Song H, Phelan C, Wentzensen N, Peters U, Slattery ML; GECCO, Sellers TA; FOCI, Casey G, Gruber SB; CORECT, Hunter DJ; DRIVE, Amos CI, Henderson B; GAME-ON Network. Cross Cancer Genomic Investigation of Inflammation Pathway for Five Common Cancers: Lung, Ovary, Prostate, Breast, and Colorectal Cancer. *J Natl Cancer Inst* 2015; **107** [PMID: 26319099 DOI: 10.1093/jnci/djv246]

86 **Theodoropoulos G**, Papaconstantinou I, Felekouras E, Nikiteas N, Karakitsos P, Panoussopoulos D, Lazaris ACh, Patsouris E, Bramis J, Gazouli M. Relation between common polymorphisms in genes related to inflammatory response and colorectal cancer. *World J Gastroenterol* 2006; **12**: 5037-5043 [PMID: 16937502 DOI: 10.3748/wjg.v12.i31.5037]

87 **Landi S**, Moreno V, Gioia-Patricola L, Guino E, Navarro M, de Oca J, Capella G, Canzian F; Bellvitge Colorectal Cancer Study Group. Association of common polymorphisms in inflammatory genes interleukin (IL)6, IL8, tumor necrosis factor alpha, NFKB1, and peroxisome proliferator-activated receptor gamma with colorectal cancer. *Cancer Res* 2003; **63**: 3560-3566 [PMID: 12839942]

88 **Koh WP**, Yuan JM, Van Den Berg D, Ingles SA, Yu MC. Peroxisome proliferator-activated receptor (PPAR) gamma gene polymorphisms and colorectal cancer risk among Chinese in Singapore. *Carcinogenesis* 2006; **27**: 1797-1802 [PMID: 16513680 DOI: 10.1093/carcin/bgl001]

89 **Montazeri Z**, Li X, Nyiraneza C, Ma X, Timofeeva M, Svinti V, Meng X, He Y, Bo Y, Morgan S, Castellví-Bel S, Ruiz-Ponte C, Fernández-Rozadilla C, Carracedo Á, Castells A, Bishop T, Buchanan D, Jenkins MA, Keku TO, Lindblom A, van Duijnhoven FJB, Wu A, Farrington SM, Dunlop MG, Campbell H, Theodoratou E, Zheng W, Little J. Systematic meta-analyses, field synopsis and global assessment of the evidence of genetic association studies in colorectal cancer. *Gut* 2020; **69**: 1460-1471 [PMID: 31818908 DOI: 10.1136/gutjnl-2019-319313]

90 **Abbas M**, Mason T, Ibad A, Khraiwesh M, Apprey V, Kanaan Y, Wilson B, Dunston G, Ricks-Santi L, Brim H. Genetic Polymorphisms in IL-10 Promoter Are Associated With Smoking and Prostate Cancer Risk in African Americans. *Anticancer Res* 2020; **40**: 27-34 [PMID: 31892550 DOI: 10.21873/anticanres.13923]

91 **Jenkins BD**, Martini RN, Hire R, Brown A, Bennett B, Brown I, Howerth EW, Egan M, Hodgson J, Yates C, Kittles R, Chitale D, Ali H, Nathanson D, Nikolinakos P, Newman L, Monteil M, Davis MB. Atypical Chemokine Receptor 1 (*DARC/ACKR1*) in Breast Tumors Is Associated with Survival, Circulating Chemokines, Tumor-Infiltrating Immune Cells, and African Ancestry. *Cancer Epidemiol Biomarkers Prev* 2019; **28**: 690-700 [PMID: 30944146 DOI: 10.1158/1055-9965.EPI-18-0955]

92 **Cho I**, Blaser MJ. The human microbiome: at the interface of health and disease. *Nat Rev Genet* 2012; **13**: 260-270 [PMID: 22411464 DOI: 10.1038/nrg3182]

93 **Gopalakrishnan V**, Helmink BA, Spencer CN, Reuben A, Wargo JA. The Influence of the Gut Microbiome on Cancer, Immunity, and Cancer Immunotherapy. *Cancer Cell* 2018; **33**: 570-580 [PMID: 29634945 DOI: 10.1016/j.ccell.2018.03.015]

94 **Xu F**, Fu Y, Sun TY, Jiang Z, Miao Z, Shuai M, Gou W, Ling CW, Yang J, Wang J, Chen YM, Zheng JS. The interplay between host genetics and the gut microbiome reveals common and distinct microbiome features for complex human diseases. *Microbiome* 2020; **8**: 145 [PMID: 33032658 DOI: 10.1186/s40168-020-00923-9]

95 **Burns MB**, Montassier E, Abrahante J, Priya S, Niccum DE, Khoruts A, Starr TK, Knights D, Blekhman R. Colorectal cancer mutational profiles correlate with defined microbial communities in the tumor microenvironment. *PLoS Genet* 2018; **14**: e1007376 [PMID: 29924794 DOI: 10.1371/journal.pgen.1007376]

96 **Thyagarajan S**, Zhang Y, Thapa S, Allen MS, Phillips N, Chaudhary P, Kashyap MV, Vishwanatha JK. Comparative analysis of racial differences in breast tumor microbiome. *Sci Rep* 2020; **10**: 14116 [PMID: 32839514 DOI: 10.1038/s41598-020-71102-x]

97 **Yu J**, Feng Q, Wong SH, Zhang D, Liang QY, Qin Y, Tang L, Zhao H, Stenvang J, Li Y, Wang X, Xu X, Chen N, Wu WK, Al-Aama J, Nielsen HJ, Kiilerich P, Jensen BA, Yau TO, Lan Z, Jia H, Li J, Xiao L, Lam TY, Ng SC, Cheng AS, Wong VW, Chan FK, Yang H, Madsen L, Datz C, Tilg H, Wang J, Brünner N, Kristiansen K, Arumugam M, Sung JJ. Metagenomic analysis of faecal microbiome as a tool towards targeted non-invasive biomarkers for colorectal cancer. *Gut* 2017; **66**: 70-78 [PMID: 26408641 DOI: 10.1136/gutjnl-2015-309800]

98 **Zeller G**, Tap J, Voigt AY, Sunagawa S, Kultima JR, Costea PI, Amiot A, Böhm J, Brunetti F, Habermann N, Hercog R, Koch M, Luciani A, Mende DR, Schneider MA, Schrotz-King P, Tournigand C, Tran Van Nhieu J, Yamada T, Zimmermann J, Benes V, Kloor M, Ulrich CM, von Knebel Doeberitz M, Sobhani I, Bork P. Potential of fecal microbiota for early-stage detection of colorectal cancer. *Mol Syst Biol* 2014; **10**: 766 [PMID: 25432777 DOI: 10.15252/msb.20145645]

99 **Baxter NT**, Ruffin MT 4th, Rogers MA, Schloss PD. Microbiota-based model improves the sensitivity of fecal immunochemical test for detecting colonic lesions. *Genome Med* 2016; **8**: 37 [PMID: 27056827 DOI: 10.1186/s13073-016-0290-3]

100 **Zackular JP**, Rogers MA, Ruffin MT 4th, Schloss PD. The human gut microbiome as a screening tool for colorectal cancer. *Cancer Prev Res (Phila)* 2014; **7**: 1112-1121 [PMID: 25104642 DOI: 10.1158/1940-6207.CAPR-14-0129]

101 **Thomas AM**, Manghi P, Asnicar F, Pasolli E, Armanini F, Zolfo M, Beghini F, Manara S, Karcher N, Pozzi C, Gandini S, Serrano D, Tarallo S, Francavilla A, Gallo G, Trompetto M, Ferrero G, Mizutani S, Shiroma H, Shiba S, Shibata T, Yachida S, Yamada T, Wirbel J, Schrotz-King P, Ulrich CM, Brenner H, Arumugam M, Bork P, Zeller G, Cordero F,

Dias-Neto E, Setubal JC, Tett A, Pardini B, Rescigno M, Waldron L, Naccarati A, Segata N. Metagenomic analysis of colorectal cancer datasets identifies cross-cohort microbial diagnostic signatures and a link with choline degradation. *Nat Med* 2019; **25**: 667-678 [PMID: 30936548 DOI: 10.1038/s41591-019-0405-7]

102 **Wirbel J**, Pyl PT, Kartal E, Zych K, Kashani A, Milanese A, Fleck JS, Voigt AY, Palleja A, Ponnudurai R, Sunagawa S, Coelho LP, Schrotz-King P, Vogtmann E, Habermann N, Niméus E, Thomas AM, Manghi P, Gandini S, Serrano D, Mizutani S, Shiroma H, Shiba S, Shibata T, Yachida S, Yamada T, Waldron L, Naccarati A, Segata N, Sinha R, Ulrich CM, Brenner H, Arumugam M, Bork P, Zeller G. Meta-analysis of fecal metagenomes reveals global microbial signatures that are specific for colorectal cancer. *Nat Med* 2019; **25**: 679-689 [PMID: 30936547 DOI: 10.1038/s41591-019-0406-6]

103 **Dai Z**, Coker OO, Nakatsu G, Wu WKK, Zhao L, Chen Z, Chan FKL, Kristiansen K, Sung JJY, Wong SH, Yu J. Multi-cohort analysis of colorectal cancer metagenome identified altered bacteria across populations and universal bacterial markers. *Microbiome* 2018; **6**: 70 [PMID: 29642940 DOI: 10.1186/s40168-018-0451-2]

104 **Wu S**, Rhee KJ, Albesiano E, Rabizadeh S, Wu X, Yen HR, Huso DL, Brancati FL, Wick E, McAllister F, Housseau F, Pardoll DM, Sears CL. A human colonic commensal promotes colon tumorigenesis *via* activation of T helper type 17 T cell responses. *Nat Med* 2009; **15**: 1016-1022 [PMID: 19701202 DOI: 10.1038/nm.2015]

105 **Arthur JC**, Perez-Chanona E, Mühlbauer M, Tomkovich S, Uronis JM, Fan TJ, Campbell BJ, Abujamel T, Dogan B, Rogers AB, Rhodes JM, Stintzi A, Simpson KW, Hansen JJ, Keku TO, Fodor AA, Jobin C. Intestinal inflammation targets cancer-inducing activity of the microbiota. *Science* 2012; **338**: 120-123 [PMID: 22903521 DOI: 10.1126/science.1224820]

106 **Kostic AD**, Chun E, Robertson L, Glickman JN, Gallini CA, Michaud M, Clancy TE, Chung DC, Lochhead P, Hold GL, El-Omar EM, Brenner D, Fuchs CS, Meyerson M, Garrett WS. Fusobacterium nucleatum potentiates intestinal tumorigenesis and modulates the tumor-immune microenvironment. *Cell Host Microbe* 2013; **14**: 207-215 [PMID: 23954159 DOI: 10.1016/j.chom.2013.07.007]

107 **Tomkovich S**, Dejea CM, Winglee K, Drewes JL, Chung L, Housseau F, Pope JL, Gauthier J, Sun X, Mühlbauer M, Liu X, Fathi P, Anders RA, Besharati S, Perez-Chanona E, Yang Y, Ding H, Wu X, Wu S, White JR, Gharaibeh RZ, Fodor AA, Wang H, Pardoll DM, Jobin C, Sears CL. Human colon mucosal biofilms from healthy or colon cancer hosts are carcinogenic. *J Clin Invest* 2019; **129**: 1699-1712 [PMID: 30855275 DOI: 10.1172/JCI124196]

108 **Knippel RJ**, Drewes JL, Sears CL. The Cancer Microbiome: Recent Highlights and Knowledge Gaps. *Cancer Discov* 2021; **11**: 2378-2395 [PMID: 34400408 DOI: 10.1158/2159-8290.CD-21-0324]

109 **Brooks AW**, Priya S, Blekhman R, Bordenstein SR. Gut microbiota diversity across ethnicities in the United States. *PLoS Biol* 2018; **16**: e2006842 [PMID: 30513082 DOI: 10.1371/journal.pbio.2006842]

110 **Deschasaux M**, Bouter KE, Prodan A, Levin E, Groen AK, Herrema H, Tremaroli V, Bakker GJ, Attaye I, Pinto-Sietsma SJ, van Raalte DH, Snijder MB, Nicolaou M, Peters R, Zwinderman AH, Bäckhed F, Nieuwdorp M. Depicting the composition of gut microbiota in a population with varied ethnic origins but shared geography. *Nat Med* 2018; **24**: 1526-1531 [PMID: 30150717 DOI: 10.1038/s41591-018-0160-1]

111 **Gupta VK**, Paul S, Dutta C. Geography, Ethnicity or Subsistence-Specific Variations in Human Microbiome Composition and Diversity. *Front Microbiol* 2017; **8**: 1162 [PMID: 28690602 DOI: 10.3389/fmicb.2017.01162]

112 **Hester CM**, Jala VR, Langille MG, Umar S, Greiner KA, Haribabu B. Fecal microbes, short chain fatty acids, and colorectal cancer across racial/ethnic groups. *World J Gastroenterol* 2015; **21**: 2759-2769 [PMID: 25759547 DOI: 10.3748/wjg.v21.i9.2759]

113 **Ou J**, Carbonero F, Zoetendal EG, DeLany JP, Wang M, Newton K, Gaskins HR, O'Keefe SJ. Diet, microbiota, and microbial metabolites in colon cancer risk in rural Africans and African Americans. *Am J Clin Nutr* 2013; **98**: 111-120 [PMID: 23719549 DOI: 10.3945/ajcn.112.056689]

114 **Jung SY**, Papp JC, Sobel EM, Pellegrini M, Yu H, Zhang ZF. Pro-inflammatory cytokine polymorphisms in ONECUT2 and HNF4A and primary colorectal carcinoma: a post genome-wide gene-lifestyle interaction study. *Am J Cancer Res* 2020; **10**: 2955-2976 [PMID: 33042629]

115 **Chiuve SE**, Fung TT, Rimm EB, Hu FB, McCullough ML, Wang M, Stampfer MJ, Willett WC. Alternative dietary indices both strongly predict risk of chronic disease. *J Nutr* 2012; **142**: 1009-1018 [PMID: 22513989 DOI: 10.3945/jn.111.157222]

116 **Wang DD**, Leung CW, Li Y, Ding EL, Chiuve SE, Hu FB, Willett WC. Trends in dietary quality among adults in the United States, 1999 through 2010. *JAMA Intern Med* 2014; **174**: 1587-1595 [PMID: 25179639 DOI: 10.1001/jamainternmed.2014.3422]

117 **Lu SSM**, Mohammed Z, Häggström C, Myte R, Lindquist E, Gylfe Å, Van Guelpen B, Harlid S. Antibiotics Use and Subsequent Risk of Colorectal Cancer: A Swedish Nationwide Population-Based Study. *J Natl Cancer Inst* 2022; **114**: 38-46 [PMID: 34467395 DOI: 10.1093/jnci/djab125]

118 **Tsong WH**, Koh WP, Yuan JM, Wang R, Sun CL, Yu MC. Cigarettes and alcohol in relation to colorectal cancer: the Singapore Chinese Health Study. *Br J Cancer* 2007; **96**: 821-827 [PMID: 17311023 DOI: 10.1038/sj.bjc.6603623]

119 **Ali Khan U**, Fallah M, Sundquist K, Sundquist J, Brenner H, Kharazmi E. Risk of colorectal cancer in patients with diabetes mellitus: A Swedish nationwide cohort study. *PLoS Med* 2020; **17**: e1003431 [PMID: 33186354 DOI: 10.1371/journal.pmed.1003431]

120 **Rebersek M**. Gut microbiome and its role in colorectal cancer. *BMC Cancer* 2021; **21**: 1325 [PMID: 34895176 DOI: 10.1186/s12885-021-09054-2]

121 **Scepanovic P**, Hodel F, Mondot S, Partula V, Byrd A, Hammer C, Alanio C, Bergstedt J, Patin E, Touvier M, Lantz O, Albert ML, Duffy D, Quintana-Murci L, Fellay J; Milieu Intérieur Consortium. A comprehensive assessment of demographic, environmental, and host genetic associations with gut microbiome diversity in healthy individuals. *Microbiome* 2019; **7**: 130 [PMID: 31519223 DOI: 10.1186/s40168-019-0747-x]

122 **Blekhman R**, Goodrich JK, Huang K, Sun Q, Bukowski R, Bell JT, Spector TD, Keinan A, Ley RE, Gevers D, Clark AG. Host genetic variation impacts microbiome composition across human body sites. *Genome Biol* 2015; **16**: 191 [PMID: 26374288 DOI: 10.1186/s13059-015-0759-1]

123 **Goodrich JK**, Davenport ER, Beaumont M, Jackson MA, Knight R, Ober C, Spector TD, Bell JT, Clark AG, Ley RE.

Genetic Determinants of the Gut Microbiome in UK Twins. *Cell Host Microbe* 2016; **19**: 731-743 [PMID: 27173935 DOI: 10.1016/j.chom.2016.04.017]

124 **Goodrich JK**, Waters JL, Poole AC, Sutter JL, Koren O, Blekhman R, Beaumont M, Van Treuren W, Knight R, Bell JT, Spector TD, Clark AG, Ley RE. Human genetics shape the gut microbiome. *Cell* 2014; **159**: 789-799 [PMID: 25417156 DOI: 10.1016/j.cell.2014.09.053]

125 **Ashktorab H**, Azimi H, Varma S, Lee EL, Laiyemo AO, Nickerson ML, Brim H. Driver genes exome sequencing reveals distinct variants in African Americans with colorectal neoplasia. *Oncotarget* 2019; **10**: 2607-2624 [PMID: 31080553 DOI: 10.18632/oncotarget.26721]

126 **Brim H**, Yooseph S, Lee E, Sherif ZA, Abbas M, Laiyemo AO, Varma S, Torralba M, Dowd SE, Nelson KE, Pathmasiri W, Sumner S, de Vos W, Liang Q, Yu J, Zoetendal E, Ashktorab H. A Microbiomic Analysis in African Americans with Colonic Lesions Reveals Streptococcus sp.VT162 as a Marker of Neoplastic Transformation. *Genes (Basel)* 2017; **8** [PMID: 29120399 DOI: 10.3390/genes8110314]

127 **Ogino S**, Nowak JA, Hamada T, Milner DA Jr, Nishihara R. Insights into Pathogenic Interactions Among Environment, Host, and Tumor at the Crossroads of Molecular Pathology and Epidemiology. *Annu Rev Pathol* 2019; **14**: 83-103 [PMID: 30125150 DOI: 10.1146/annurev-pathmechdis-012418-012818]

128 **Nishi A**, Milner DA Jr, Giovannucci EL, Nishihara R, Tan AS, Kawachi I, Ogino S. Integration of molecular pathology, epidemiology and social science for global precision medicine. *Expert Rev Mol Diagn* 2016; **16**: 11-23 [PMID: 26636627 DOI: 10.1586/14737159.2016.1115346]

129 **Turpin W**, Espin-Garcia O, Xu W, Silverberg MS, Kevans D, Smith MI, Guttman DS, Griffiths A, Panaccione R, Otley A, Xu L, Shestopaloff K, Moreno-Hagelsieb G; GEM Project Research Consortium, Paterson AD, Croitoru K. Association of host genome with intestinal microbial composition in a large healthy cohort. *Nat Genet* 2016; **48**: 1413-1417 [PMID: 27694960 DOI: 10.1038/ng.3693]

130 **DeStefano Shields CE**, White JR, Chung L, Wenzel A, Hicks JL, Tam AJ, Chan JL, Dejea CM, Fan H, Michel J, Maiuri AR, Sriramkumar S, Podicheti R, Rusch DB, Wang H, De Marzo AM, Besharati S, Anders RA, Baylin SB, O'Hagan HM, Housseau F, Sears CL. Bacterial-Driven Inflammation and Mutant *BRAF* Expression Combine to Promote Murine Colon Tumorigenesis That Is Sensitive to Immune Checkpoint Therapy. *Cancer Discov* 2021; **11**: 1792-1807 [PMID: 33632774 DOI: 10.1158/2159-8290.CD-20-0770]

131 **Davis MB**. Genomics and Cancer Disparities: The Justice and Power of Inclusion. *Cancer Discov* 2021; **11**: 805-809 [PMID: 33811116 DOI: 10.1158/2159-8290.CD-21-0225]

132 **Sherman RM**, Forman J, Antonescu V, Puiu D, Daya M, Rafaels N, Boorgula MP, Chavan S, Vergara C, Ortega VE, Levin AM, Eng C, Yazdanbakhsh M, Wilson JG, Marrugo J, Lange LA, Williams LK, Watson H, Ware LB, Olopade CO, Olopade O, Oliveira RR, Ober C, Nicolae DL, Meyers DA, Mayorga A, Knight-Madden J, Hartert T, Hansel NN, Foreman MG, Ford JG, Faruque MU, Dunston GM, Caraballo L, Burchard EG, Bleecker ER, Araujo MI, Herrera-Paz EF, Campbell M, Foster C, Taub MA, Beaty TH, Ruczinski I, Mathias RA, Barnes KC, Salzberg SL. Assembly of a pan-genome from deep sequencing of 910 humans of African descent. *Nat Genet* 2019; **51**: 30-35 [PMID: 30455414 DOI: 10.1038/s41588-018-0273-y]

133 **Peterson RE**, Edwards AC, Bacanu SA, Dick DM, Kendler KS, Webb BT. The utility of empirically assigning ancestry groups in cross-population genetic studies of addiction. *Am J Addict* 2017; **26**: 494-501 [PMID: 28714599 DOI: 10.1111/ajad.12586]

134 **Adedokun B**, Du Z, Gao G, Ahearn TU, Lunetta KL, Zirpoli G, Figueroa J, John EM, Bernstein L, Zheng W, Hu JJ, Ziegler RG, Nyante S, Bandera EV, Ingles SA, Press MF, Deming-Halverson SL, Rodriguez-Gil JL, Yao S, Ogundiran TO, Ojengbede O, Blot W, Troester MA, Nathanson KL, Hennis A, Nemesure B, Ambs S, Fiorica PN, Sucheston-Campbell LE, Bensen JT, Kushi LH, Torres-Mejia G, Hu D, Fejerman L, Bolla MK, Dennis J, Dunning AM, Easton DF, Michailidou K, Pharoah PDP, Wang Q, Sandler DP, Taylor JA, O'Brien KM, Kitahara CM, Falusi AG, Babalola C, Yarney J, Awuah B, Addai-Wiafe B; GBHS Study Team, Chanock SJ, Olshan AF, Ambrosone CB, Conti DV, Ziv E, Olopade OI, Garcia-Closas M, Palmer JR, Haiman CA, Huo D. Cross-ancestry GWAS meta-analysis identifies six breast cancer loci in African and European ancestry women. *Nat Commun* 2021; **12**: 4198 [PMID: 34234117 DOI: 10.1038/s41467-021-24327-x]

135 **Schumacher FR**, Schmit SL, Jiao S, Edlund CK, Wang H, Zhang B, Hsu L, Huang SC, Fischer CP, Harju JF, Idos GE, Lejbkowicz F, Manion FJ, McDonnell K, McNeil CE, Melas M, Rennert HS, Shi W, Thomas DC, Van Den Berg DJ, Hutter CM, Aragaki AK, Butterbach K, Caan BJ, Carlson CS, Chanock SJ, Curtis KR, Fuchs CS, Gala M, Giovannucci EL, Gogarten SM, Hayes RB, Henderson B, Hunter DJ, Jackson RD, Kolonel LN, Kooperberg C, Küry S, LaCroix A, Laurie CC, Laurie CA, Lemire M, Levine D, Ma J, Makar KW, Qu C, Taverna D, Ulrich CM, Wu K, Kono S, West DW, Berndt SI, Bezieau S, Brenner H, Campbell PT, Chan AT, Chang-Claude J, Coetzee GA, Conti DV, Duggan D, Figueiredo JC, Fortini BK, Gallinger SJ, Gauderman WJ, Giles G, Green R, Haile R, Harrison TA, Hoffmeister M, Hopper JL, Hudson TJ, Jacobs E, Iwasaki M, Jee SH, Jenkins M, Jia WH, Joshi A, Li L, Lindor NM, Matsuo K, Moreno V, Mukherjee B, Newcomb PA, Potter JD, Raskin L, Rennert G, Rosse S, Severi G, Schoen RE, Seminara D, Shu XO, Slattery ML, Tsugane S, White E, Xiang YB, Zanke BW, Zheng W, Le Marchand L, Casey G, Gruber SB, Peters U. Genome-wide association study of colorectal cancer identifies six new susceptibility loci. *Nat Commun* 2015; **6**: 7138 [PMID: 26151821 DOI: 10.1038/ncomms8138]

136 **Tsilidis KK**, Helzlsouer KJ, Smith MW, Grinberg V, Hoffman-Bolton J, Clipp SL, Visvanathan K, Platz EA. Association of common polymorphisms in IL10, and in other genes related to inflammatory response and obesity with colorectal cancer. *Cancer Causes Control* 2009; **20**: 1739-1751 [PMID: 19760027 DOI: 10.1007/s10552-009-9427-7]

137 **Li D**, Achkar JP, Haritunians T, Jacobs JP, Hui KY, D'Amato M, Brand S, Radford-Smith G, Halfvarson J, Niess JH, Kugathasan S, Büning C, Schumm LP, Klei L, Ananthakrishnan A, Aumais G, Baidoo L, Dubinsky M, Fiocchi C, Glas J, Milgrom R, Proctor DD, Regueiro M, Simms LA, Stempak JM, Targan SR, Törkvist L, Sharma Y, Devlin B, Borneman J, Hakonarson H, Xavier RJ, Daly M, Brant SR, Rioux JD, Silverberg MS, Cho JH, Braun J, McGovern DP, Duerr RH. A Pleiotropic Missense Variant in SLC39A8 Is Associated With Crohn's Disease and Human Gut Microbiome Composition. *Gastroenterology* 2016; **151**: 724-732 [PMID: 27492617 DOI: 10.1053/j.gastro.2016.06.051]

138 **Rühlemann MC**, Hermes BM, Bang C, Doms S, Moitinho-Silva L, Thingholm LB, Frost F, Degenhardt F, Wittig M, Kässens J, Weiss FU, Peters A, Neuhaus K, Völker U, Völzke H, Homuth G, Weiss S, Grallert H, Laudes M, Lieb W, Haller D, Lerch MM, Baines JF, Franke A. Genome-wide association study in 8,956 German individuals identifies influence of ABO histo-blood groups on gut microbiome. *Nat Genet* 2021; **53**: 147-155 [PMID: 33462482 DOI: 10.1038/s41588-020-00747-1]

World Journal of Gastroenterology

Submit a Manuscript: https://www.f6publishing.com

World J Gastroenterol 2022 July 7; 28(25): 2802-2822

DOI: 10.3748/wjg.v28.i25.2802

ISSN 1007-9327 (print) ISSN 2219-2840 (online)

REVIEW

Altered gut microbiota patterns in COVID-19: Markers for inflammation and disease severity

Chiranjib Chakraborty, Ashish Ranjan Sharma, Manojit Bhattacharya, Kuldeep Dhama, Sang-Soo Lee

Specialty type: Biotechnology and applied microbiology

Provenance and peer review: Unsolicited article; Externally peer reviewed.

Peer-review model: Single blind

Peer-review report's scientific quality classification
Grade A (Excellent): A
Grade B (Very good): B, B
Grade C (Good): C, C
Grade D (Fair): 0
Grade E (Poor): 0

P-Reviewer: Gupta S, United States; Kamran M, Pakistan; Li S, China; Tan JK, Malaysia; Yu L, Singapore

Received: January 12, 2022
Peer-review started: January 12, 2022
First decision: March 10, 2022
Revised: March 19, 2022
Accepted: May 13, 2022
Article in press: May 13, 2022
Published online: July 7, 2022

Chiranjib Chakraborty, School of Life Science and Biotechnology, Adamas University, Kolkata 700126, India

Ashish Ranjan Sharma, Institute for Skeletal Aging & Orthopaedic Surgery, Hallym University, Chuncheon-si 24252, South Korea

Manojit Bhattacharya, Department of Zoology, Fakir Mohan University, Balasore 756020, India

Kuldeep Dhama, Division of Pathology, Indian Council of Agricultural Research (ICAR)-Indian Veterinary Research Institute (IVRI), Bareilly 243122, Uttar Pradesh, India

Sang-Soo Lee, Institute for Skeletal Aging & Orthopedic Surgery, Hallym University, Chuncheon-si 24252, South Korea

Corresponding author: Sang-Soo Lee, MD, PhD, Full Professor, Institute for Skeletal Aging & Orthopedic Surgery, Hallym University, Chuncheon-si 24252, South Korea.
123sslee@gmail.com

Abstract

The severe acute respiratory syndrome coronavirus 2 (SARS-CoV-2) infection leads to a severe respiratory illness and alters the gut microbiota, which dynamically interacts with the human immune system. Microbiota alterations include decreased levels of beneficial bacteria and augmentation of opportunistic pathogens. Here, we describe critical factors affecting the microbiota in coronavirus disease 2019 (COVID-19) patients. These include, such as gut microbiota imbalance and gastrointestinal symptoms, the pattern of altered gut microbiota composition in COVID-19 patients, and crosstalk between the microbiome and the gut-lung axis/gut-brain-lung axis. Moreover, we have illustrated the hypoxia state in COVID-19 associated gut microbiota alteration. The role of ACE2 in the digestive system, and control of its expression using the gut microbiota is discussed, highlighting the interactions between the lungs, the gut, and the brain during COVID-19 infection. Similarly, we address the gut microbiota in elderly or co-morbid patients as well as gut microbiota dysbiosis of in severe COVID-19. Several clinical trials to understand the role of probiotics in COVID-19 patients are listed in this review. Augmented inflammation is one of the major driving forces for COVID-19 symptoms and gut microbiome disruption and is associated with disease severity. However, understanding the role of the gut microbiota in immune modulation during SARS-CoV-2 infection may help improve therapeutic strategies for COVID-19 treatment.

Key Words: COVID-19; Inflammation; Gut microbiota; Therapeutic

©The Author(s) 2022. Published by Baishideng Publishing Group Inc. All rights reserved.

Core Tip: The gut microbiota of coronavirus disease 2019 (COVID-19) patients is altered compared to that of healthy individuals, with a reduction in the count of beneficial bacteria and an increase in the count of opportunistic fungi. In this review, we elucidate the components governing immune modulation. Additionally, we explore the effect of changes in the microbial ecosystem in COVID-19 patients, with an aim to help develop precise therapeutics and expand our knowledge regarding the pattern of changes in the gut microbiota of COVID-19 patients.

Citation: Chakraborty C, Sharma AR, Bhattacharya M, Dhama K, Lee SS. Altered gut microbiota patterns in COVID-19: Markers for inflammation and disease severity. *World J Gastroenterol* 2022; 28(25): 2802-2822
URL: https://www.wjgnet.com/1007-9327/full/v28/i25/2802.htm
DOI: https://dx.doi.org/10.3748/wjg.v28.i25.2802

INTRODUCTION

The coronavirus disease 2019 (COVID-19) pandemic has stimulated research on several medical conditions and on individual patient variations during severe acute respiratory syndrome coronavirus 2 (SARS-CoV-2) infection to unfold underlying disease mechanisms. Scientists have determined the inflammatory response and cellular injury mediated by acute SARS-CoV-2 infection. Moreover, several studies have revealed the involvement of the gastrointestinal (GI) tract and its associated gut microbiome during COVID-19, motivating research in this field. Increasing evidence has surfaced confirming the association of the GI tract and COVID-19, including[1,2] a severe state of gut dysbiosis in COVID-19 patients[3,4]. Similarly, GI symptoms such as vomiting, abdominal pain, and diarrhea have been noted in many COVID-19 patients[5-7]. Moreover, high expression of ACE2 receptor was reported in epithelial cells of the GI tract[8]. SARS-CoV-2 RNA has been identified in rectal and anal swabs, as well as stool specimens[7,9,10]. Finally, liver damage, loss of appetite, and irritable inflammatory diseases have been reported as post-COVID-19 illnesses[11]. These all data strongly indicate a correlation between the GI including the gut microbiome, and COVID-19.

The gut microbiota plays an important role in controlling gut health and acts as a health modulator (Figure 1)[12] aidings in different metabolic activities and extensively impacting health and disease[13,14]. Ongoing research aims to better understand the gut microbiota and provide insights into the mechanistic conditions required to implement normal health functions. The gut microbiota controls specific functions in the host, such as drug and xenobiotic metabolism and nutrient metabolism[15]. Simultaneously, it helps maintain the structural integrity of the gut mucosal barrier, protects against pathogens, and regulates immunomodulation, as well as health and disease conditions[16,17]. Several other studies suggest a possible link between COVID-19 and gut microbiota composition[18,19]. Additionally, an association has been shown between altered gut microbial composition and increased risk factors in COVID-19 patients (Figure 1)[20,21].

Inflammation is a major risk factor in COVID-19 patients[22-24]. During uncontrolled inflammation, abnormal levels of cytokines such as interleukin-1 beta (IL-1β), IL-6, IL-8, IL-10, IL-12, granulocyte-macrophage colony-stimulating factor (GM-CSF), tumor necrosis factor-alpha (TNF-α), and interferon-gamma (IFN-γ) are found in the patients[23,25-27]. Certain abnormal levels of cytokines are substantial related to the severity of COVID-19 and are probably responsible for the "cytokine storm" syndrome manifested during the disease[28-30]. Research has correlated the inflammation during COVID-19 with GI and hepatic manifestations of the disease[31].

Interactions between the gut microbiota and the lungs, known as the gut-lung axis, have sparked interest for gastroenterology studies focusing on COVID-19 as these interactions affect disease severity. Changes in the gut microbiome certainly affect homeostasis and may lead to increased infections[32,33]. Similarly, in addition to the gut, COVID-19 can also have a detrimental effect on the central nervous system (CNS) and the blood-brain barrier (BBB) and disrupt the gut-brain-lung axis. Studies have explored therapeutic options (nicotinic cholinergic agonists and vagus nerve stimulation) to minimize the damage caused to this axis[34].

Research is necessary to understand how the gut microbiome is altered during COVID-19 infection and the factors that influence the microbiome during mild to moderate and severe disease. Studies have been conducted to understand the GI symptoms during COVID-19 and to detect viral shedding using the fecal matter of SARS-CoV-2 patients. The gut microbiota of COVID-19 patients has been mapped to obtain evidence regarding inflammation, disease severity, and therapeutic development.

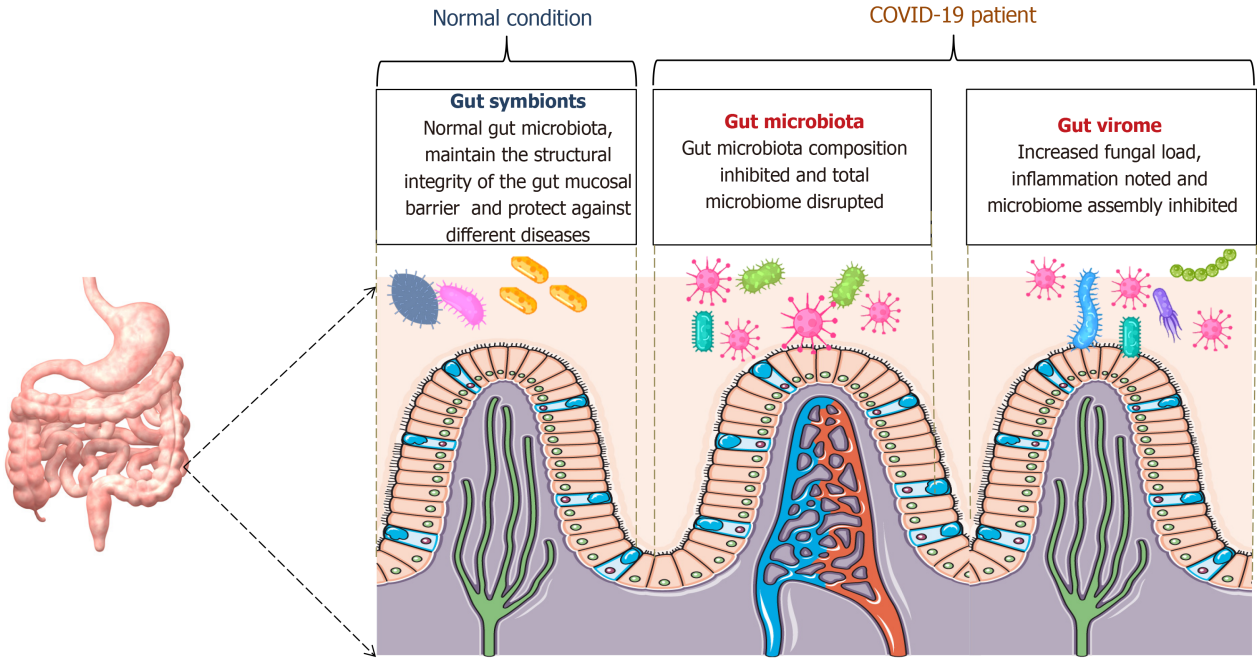


Figure 1 The schematic diagram shows normal healthy gut and the incidence in gut microbiota and gut virome in coronavirus disease 2019 patients. COVID-19: Coronavirus disease 2019.

Using these studies, we explore the following critical factors: (1) The gut microbiota imbalance and GI symptoms in COVID-19 patients; (2) fecal viral shedding in COVID-19 patients and restoration of the gut microbiota; (3) the pattern of altered gut microbiota composition in COVID-19 patients; (4) alterations in gut biosynthesis during COVID-19 infection; (5) the role of ACE2 in the digestive system and the gut microbiome; (6) crosstalk between the microbiome and the gut-lung axis during COVID-19 infection; (7) crosstalk between the microbiome and the gut-brain-lung axis during COVID-19 infection; and (8) hypoxia during COVID-19 associated with altered gut microbiota. We also discuss how immune responses and inflammation due to COVID-19 drive the changes in the microbial ecosystem and summarize therapeutic options currently in development.

GI SYMPTOMS IN COVID-19 PATIENTS

Along with respiratory symptoms and fever, GI symptoms have also been observed in COVID-19 patients (Table 1). A study by Redd *et al*[35] reported abdominal pain (14.5%), nausea (26.4%), diarrhea (33.7%), and vomiting (15.4%) in patients from the United States. Three hundred and eighteen hospitalized COVID-19 patients were evaluated to understand their symptoms. In another study with 204 COVID-19 patients, 50.5% (103 patients) exhibited GI symptoms. Among these 103 patients, 78.6% showed a lack of appetite, 34% had diarrhea, 3.9% vomited, and 1.9% complained of abdominal pain. The authors correlated patients describing GI symptoms with other measurements such as prothrombin time, monocyte count, and liver enzyme levels. Patients with GI symptoms had elevated mean liver enzyme levels, extended prothrombin times, and lower monocyte counts[36]. In a much larger cohort study involving 1099 COVID-19 patients from 552 different hospitals spread to over 30 provinces, only 3.8% of patients experienced diarrhea. The authors concluded that fever and cough are common symptoms, unlike diarrhea, among the COVID-19 patient population[37].

These findings suggest that the virus might be present for a period in the GI tract, which may cause a GI infection (Figure 2). Importantly, fecal viral shedding was noted after clearing SARS-CoV-2 from the respiratory tract, suggesting that the virus can persist for a long time in the GI tract, especially in patients who manifest GI symptoms. During COVID-19 infection, gut microbiota composition is altered, possibly explaining the GI imbalance and manifestations of the different GI symptoms such as abdominal pain, nausea, vomiting, and diarrhea, as described above. This change in the gut microbiota includes reduced levels of commensals microbes and is observed in patient samples even after 30 d of disease remission[38-40]. Additional studies addressed the imbalance of the gut microbiota and its association with different GI-related aspects of COVID-19[41]. The gut microbiota population in COVID-19 patients with low to moderate GI symptoms should also be analyzed. Evaluating these diverse patient populations will enable a thorough description of this phenomenon.

Table 1 Different gastrointestinal symptoms in coronavirus disease 2019 patients

Sl. No.	Total number of human subjects involved in study	Demographics of the study populations	Vomiting	Diarrhea	Nausea	Remarks/study summary	Ref.
1	191	Adults (46-67 years) hospitalised, Chinese peoples, 91 patients having comorbidity	7 (3.7%)	9 (4.7%)	7 (3.7%)	Identification of several risk factors and a detailed clinical course of illness for mortality of COVID-19 patients	[121]
2	171	Minor aged (1 d-15 years, hospitalised, Chinese children, no such comorbidity	11 (6.4%)	15 (8.8%)	NA	Report of a spectrum of illness from children infected with SARS-CoV-2 virus	[122]
3	1099	Median age group (35-58 years), hospitalised, Chinese patients without any comorbidity	55 (5.0%)	42 (3.8%)	55 (5.0%)	Identification and definition of clinical characteristics and disease severity of hospitalized COVID-19 patients	[37]
4	140	Adults (25-87 year), hospitalised Chinese patients with high comorbidity	7 (5.0%)	18 (12.9%)	24 (17.3%)	Report on hospitalized patients having COVID-19 with abnormal clinical manifestations (fever, fatigue, gastrointestinal symptoms, allergy)	[123]
5	73	Adults hospitalised Chinese patients, comorbidity reported	NA	26 (35.6%)	NA	Clinical significance of SARS-CoV-2 by examining viral RNA in feces of COVID-19 patients during hospitalizations	[124]
6	52	Adults (mean age 59.7 year), critically ill ICU- admitted Chinese patients, comorbidity reported	2 (3.8%)	NA	NA	Retrospective, single-centered, observational study on critically ill, ICU-admitted adult COVID-19 patients	[125]
7	138	Adult (median age 56 years), hospitalised Chinese patients with comorbidities	5 (3.6%)	14 (10.1%)	14 (10.1%)	Clinical characteristics of COVID-19 patients in hospitalized conditions	[126]
8	41	Middle age group (41-58 years) hospitalised Chinese patients with comorbidities	NA	1 (2.6%)	NA	Epidemiological, laboratory, clinical, and radiological features and treatment with clinical outcomes of hospitalized COVID-19 patients	[46]
9	62	Studied patients (median age 41 years) were hospitalised, Chinese ethnicity and comorbidity reported	NA	3 (4.8%)	NA	Most common symptoms at onset of illness with clinical data in confirmed COVID-19 patients	[127]
10	137	Studied patients (mean age 57-55) ware Chinese and hospitalised, comorbidity was also noted	NA	11 (8%)	NA	Investigation of epidemiological history, clinical characteristics, treatment, and prognosis of COVID-19 patients	[128]
11	81	Chinese patients (mean age was 49.5 years), hospitalised with high comorbidities	4 (4.9%)	3 (3.7%)	NA	Report of confirmed COVID-19 patients with chest computer tomography imaging anomalies	[129]
12	99	Hospitalised, Chinese patients (average age of the patients was 55.5 years), comorbidity was reported	1 (1%)	2 (2.0%)	1 (1%)	Inclusive exploration of epidemiology and clinical features of COVID-19 patients	[130]

NA: Not available; ICU: Intensive care unit; COVID-19: Coronavirus disease 2019; SARS-CoV-2: Severe acute respiratory syndrome coronavirus 2.

FECAL VIRAL SHEDDING IN COVID-19 PATIENTS

Table 2 lists various cohort studies reporting fecal viral shedding by COVID-19 patients and detecting SARS-CoV-2 RNA in the fecal matter[42,43]. SARS-CoV-2 RNA-positive fecal matter was detected in 66.67% of COVID-19 patients (42 patients) in China[43]. Researchers attempted to evaluate the viral shedding period in stool samples, and noted viral shedding in asymptomatic patients. For example, SARS-CoV-2 RNA was detected from a stool sample of an asymptomatic child 17 d after viral exposure [9].

Certain studies have reported that virus separation from stool samples is difficult. For example, Wölfel *et al*[44] detected viral RNA in stool samples but attempts to isolate the virus were unsuccessful, most likely due to the mild nature of the infection. A viral load below 10^6 copies per milliliter often hampers viral isolation[36]. The viral load also varies widely from one sample to another, including stool, serum, and respiratory samples[44-46]. However, understanding the correlation between the altered gut microbiota and the viral load in patient samples is essential for advancing therapeutic strategies centered around restoring the microbiota.

Additionally, efforts should focus on determining the possible correlation between fecal viral shedding and altered gut microbiota composition at different stages the infection, *i.e.*, mild to moderate

Table 2 Fecal viral shedding in coronavirus disease 2019 patients

Sl. No.	Total number of human subjects in study	Demographics of the study populations	Gastrointestinal symptoms	Confirmed cases of fecal shedding	Remarks/study summary	Ref.
1	205	Patients (mean age of 44 years) were hospitalised, Chinese without any comorbidities	No symptoms	44	Evidence-based study for gastrointestinal infection of SARS-CoV-2 virus and its possible fecal-oral transmission route in humans	[131]
2	73	Different age group (10 mo to 78 years old), hospitalised Chinese patients without report any comorbidities	Gastrointestinal bleeding, diarrhea	39	Description of epidemiological and clinical characteristics of COVID-19 patients	[124]
3	10	Chinese patients have aged 19-40 years, hospitalised and no such comorbidity was reported	Hemoptysis, diarrhea, cough	8	Report of median aged COVID-19 confirmed patients in ICU	[127]
4	14	Patients (18-87 years) were hospitalized, Chinese individuals without any comorbidities	No symptoms	5	Retrospective analysis of laboratory-confirmed COVID-19 cases in hospitalized conditions	[132]
5	66	Chinese patients (median age of 44 years) were hospitalised, comorbidity was not reported	No symptoms	11	Viral RNA detection was performed from throat swabs, stool, urine, and serum samples in different clinical conditions in COVID-19 patients	[133]
6	18	Adults patients (median age, 47 years) from Singapore were hospitalised and comorbidities was noted	No symptoms	4	COVID-19 patient case series using clinical, laboratory, and radiological data	[134]
7	74	Studied paients belonged from China and were hospitalised with comorbidities	No symptoms	41	Analysis of respiratory and fecal samples to determine clinical symptoms and medical treatments of COVID-19 patients	[135]
8	9	Adults Chinese patients were hospitalised without any comorbidities	Diarrhea and urinary irritation	2	Detection of SARS-CoV-2 RNA in urine and blood samples, and anal, oropharyngeal swabs of confirmed COVID-19 patients	[136]

ICU: Intensive care unit; COVID-19: Coronavirus disease 2019; SARS-CoV-2: Severe acute respiratory syndrome coronavirus 2.

or severe COVID-19.

ALTERED GUT MICROBIOTA COMPOSITION IN COVID-19 PATIENTS

SARS-CoV-2 infections have led to changes in the ecology of the gut microbiota in patients (compared to that seen in controls). These changes are influenced by the immune responses elicited during COVID-19 (Table 3). Different studies have revealed the growth of unusual microorganisms and depletion of common gut microbes (bacterial, viral, and fungal populations) in COVID-19 patients (Figure 3).

To understand the severity of disease in COVID-19 patients, the gut microbiota composition of 100 COVID-19 patients was analyzed in two hospital cohorts. Stool samples were collected from 27 of the 100 patients. The gut microbiome compositions were characterized using total DNA extracted from stool samples. The authors demonstrated that the number of gut commensals and Bifidobacteria was low and correlated with several factors of disease severity, such as high concentrations of inflammatory cytokines and C-reactive protein (CRP). These data suggests that the composition of the microbiota is associated with disease severity[38]. Another study carried out RNA and DNA profiling by sequencing of the virome using fecal matter from COVID-19 patients. The fecal matter of 98 COVID-19 patients was analyzed to understand COVID-19 severity and its association with the gut virome. The study showed that COVID-19 severity is inversely correlated with gut viruses, and older patients are more prone to severe COVID-19 outcomes[47]. Alterations in fungal microbiomes during COVID-19 have also been investigated. Analysis of the fecal mycobiome using the deep shotgun method showed heterogeneous microbial profiles, with enrichment of fungal genera such as Aspergillus and Candida. Two species of *Aspergillus* (*Aspergillus flavus* and *Aspergillus niger*) were identified in fecal samples after clearance of SARS-CoV-2 from nasopharyngeal samples[48]. Additionally, there is evidence of abundant symbionts among COVID-19 patients including *Clostridium ramosum*, *Coprobacillus*, and *Clostridium hathewayi*,

Table 3 Analysis of gut microbiota in coronavirus disease 2019 patients in different cohorts

Sl. No.	Cohort composition	No of Patients	Demographics of the study populations	Country	Significant gut microbiota found	Study conclusion	Reference
1	A pilot study with 15 healthy individuals (controls) and 15 patients with COVID-19	15	Study performed with hospitalised patients (median age 55 years), Chinese ethnicity and comorbidities were reported	Hong Kong	Abundance of *Clostridium hathewayi, Clostridium ramosum, Coprobacillus,* which are correlated with COVID-19 severity	Change in the fecal microbiome of COVID-19 patients during hospitalization, compared to healthy individuals (controls)	[48]
2	The two-hospitals cohort, serial stool samples collected from 27 COVID-19 patients among 100	27	Adults hospitalised Chinese patients, comorbidities were noted	Hong Kong	*Faecalibacterium prausnitzii, Eubacteriumrectale* and bifidobacteria	Gut microbiome involved in COVID-19 severity	[38]
3	United States cohort (majority African American)	50	Studied patients (mean age 62.3 years) were hospitalised with comorbidities, American ethnicity	United States	Some of the significant genera (*Corynebacterium Peptoniphilus, Campylobacter, etc.*)	No significant associations found between the composition microbiome and disease severity from COVID-19 patient gut microbiota	[50]
4	The study used 53 COVID-19 patients and 76 healthy individuals. 81 fecal samples collected during hospitalization	53	Adults Chinase hospitalised patients, no such comorbidities were noted	China	Elevated gut microbes such as *Rothia mucilaginosa, Granulicatella* spp, *etc.*	COVID-19 infection linked with change of the microbiome in COVID-19 patients	[137]
5	15 patients Cohort	15	Study performed adults hospitalised patients with comorbidities, Chinese ethnicity	Hong Kong	Elevated bacterial species *Collinsella tanakaei, Collinsella aerofaciens, Morganella morganii, Streptococcus infantis*	The study found fecal viral (SARS-CoV-2) activity	[54]
6	Two-hospital cohort with a total of 100 patients. Stool samples collected from 27 patients	27	Hospitalised adults patients were from China, comorbidities were noted	Hong Kong	Several gut microbiota such as *Faecalibacterium prausnitzii, Eubacterium rectale,* and bifidobacteria	Gut microbiota associated disease severity and inflammation in COVID-19 patients	[38]
7	98 COVID-19 patients (3 asymptomatic, 34 moderate, 53 mild, 3 critical, 5 severe), serial fecal samples collected from 37 COVID-19 patients	37	Adults (mean age 37 years) patients, hospitalised condition from Chinese ethnicity, comorbidities were reported	Hong Kong	A total of 10 virus species in fecal matter (9 DNA virus species and 1 RNA virus, pepper chlorotic spot virus)	Analysis of gut virome (RNA and DNA virome) in COVID-19 patients	[47]
8	Study of fecal samples from 30 COVID-19 patients	30	Patients (mean age 46 years) were hospitalised from Chinese groups, comorbidities were noted	Hong Kong	Increased proportions of fungal pathogens (*Candida albicans, Candida auris, Aspergillus flavus, Aspergillus niger*) in fecal samples	Analysis of fecal fungal microbiome of COVID-19 patients	[48]

COVID-19: Coronavirus disease 2019.

which directly correlated with disease severity. Conversely, *Faecalibacterium prausnitzii,* which was also abundant among the patients, was inversely correlated with disease severity[49].

Similarly, in a study by Yeoh *et al*[38], stool samples from 27 patients were correlated with blood markers and inflammatory cytokines. The study concluded that the scale of COVID-19 severity might be associated with the gut microbiome and linked it to COVID-19 inflammation[46]. In another study containing a greater number of African Americans, enriched genera (*Campylobacter, Corynebacterium,* and *Peptoniphilus)* were mapped in the COVID-19 patient population, the gut microbial composition was markedly different between positive and negative samples. However, the study did not identify any considerable association between COVID-19 severity and microbiome composition[50].

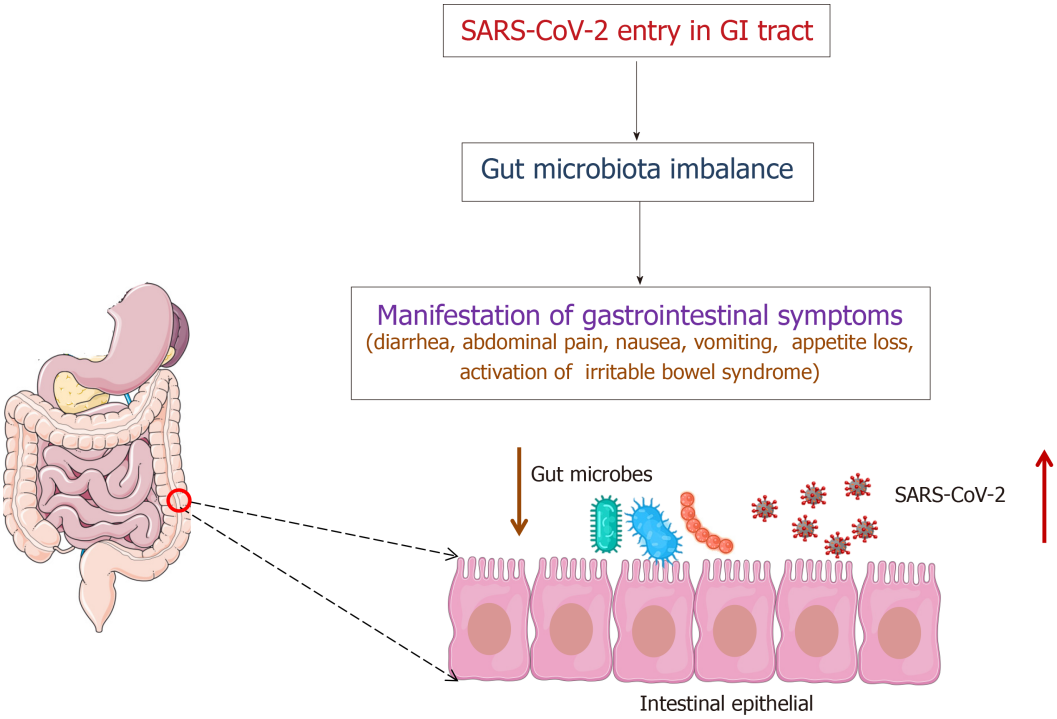


Figure 2 The schematic diagram illustrates the severe acute respiratory syndrome coronavirus 2 entry in the body, causes of gut microbiota imbalance which assists in manifesting the gastrointestinal symptoms in coronavirus disease 2019 patients. GI: Gastrointestinal; SARS-CoV-2: Severe acute respiratory syndrome coronavirus 2.

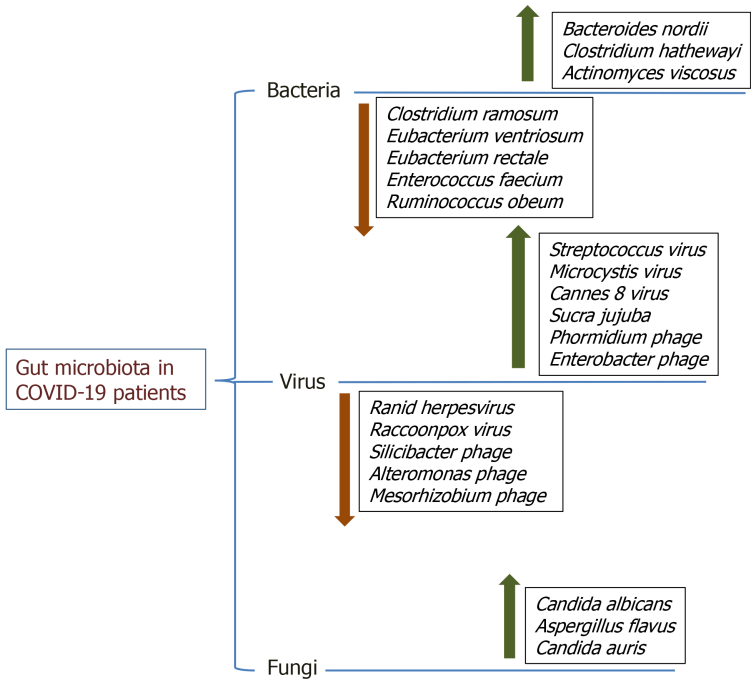


Figure 3 The diagram illustrates increased or decreased gut microbiota in coronavirus disease 2019 patients, including bacterial, viral, and fungal populations. COVID-19: Coronavirus disease 2019.

Certain studies even noted a reduction in fiber-utilizing bacteria such as *Prevotella*, *Bacteroides plebius*, and *Faecalibacterium prausnitzii* (*F. prausnitzii*), and a low Firmicute/Bacteroidetes ratio[51]. Poor outcomes were noted in special populations, such as hypertensive, diabetic, and elderly patients[52,53]. Research is still underway to ascertain the different types of gut microbial populations (pro-inflammatory, opportunistic, beneficial, or anti-inflammatory) present depending on COVID-19 severity (Figure 4).

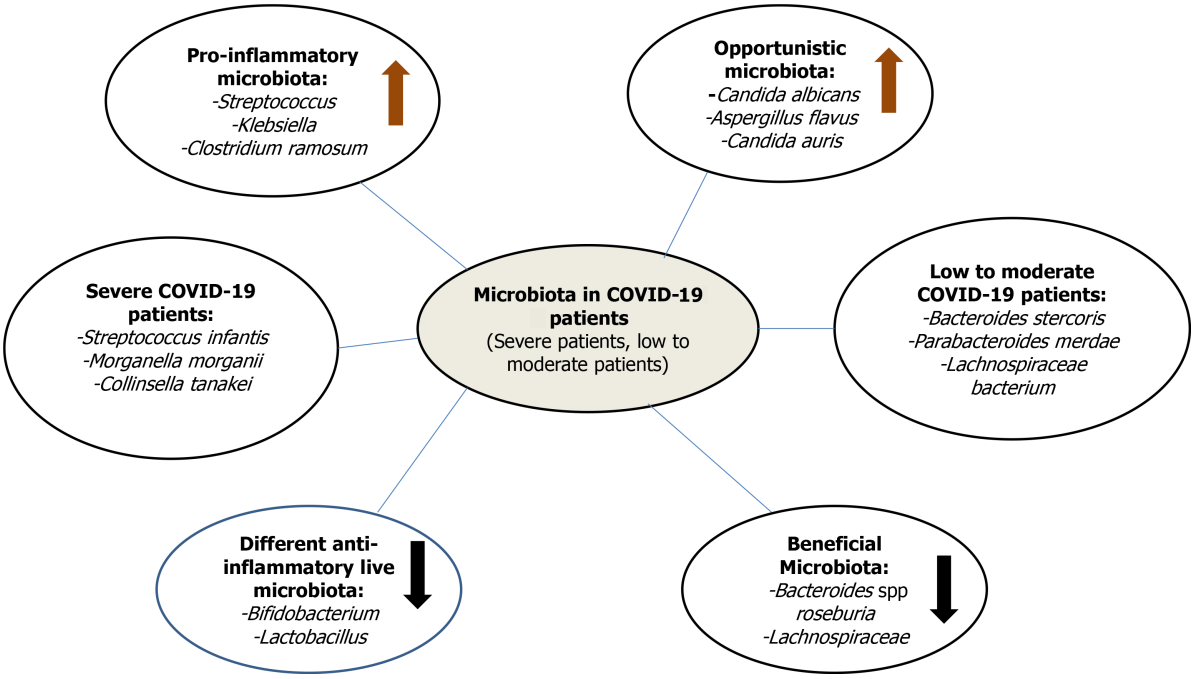


Figure 4 The diagram illustrates different types of mapped gut microbiota in coronavirus disease 2019 patients. Pro-inflammatory microbiota, opportunistic microbiota, the microbiome in severe coronavirus disease 2019 (COVID-19) patients, and the microbiome in low to moderate COVID-19 patients, anti-inflammatory microbiota, and beneficial microbiota. COVID-19: Coronavirus disease 2019.

These studies help us understand how gut microbiota composition affects patients with moderate to severe COVID-19 and how gut microbiota diversity might alter immunity in COVID-19 patients.

ALTERATIONS IN THE BIOSYNTHESIS OF BIOLOGICAL COMPOUNDS IN THE GUT DURING COVID-19 INFECTION

Other than compositional changes in gut microbiota, functional changes during SARS-CoV-2 infection were observed in some patients. The gut microbiota aids in different biosynthetic pathways, such as amino acid biosynthesis, carbohydrate metabolism, nucleotide de novo biosynthesis, and glycolysis. This might be due to the abundance of bacterial components such as *Collinsella tanakaei, Streptococcus infantis, Morganella morganii,* and *Collinsella aerofaciens*, *etc.* Apart from these microbes, many short-chain fatty acid (SCFA) synthesis bacteria, such as *Lachnospiraceae bacteria*, *Bacteroides stercoris*, *Alistipes onderdonkii,* and *Parabacteroides merdae* were present in COVID-19 samples with mild symptoms and in non-COVID-19 samples[54]. In a study using non-human primate models, β diversity analysis and 16S rRNA gene profiling were carried out to understand the gut microbiota composition during SARS-CoV-2 infection. The study revealed substantial changes in the gut microbiota composition and metabolism and a reduction in the concentration of SCFAs as well as a difference in the concentrations of bile acids. The study also found alterations in tryptophan metabolites during SARS-CoV-2 infection in the animal models[55].

Shotgun metagenomic sequencing using fecal samples has also been performed to profile the gut microbiome in SARS-CoV-2 infected patients. Researchers observed prolonged impairment of L-isoleucine biosynthesis and SCFAs due to alterations in the gut microbiome of patients with COVID-19 [56].

ROLE OF ACE2 IN THE DIGESTIVE SYSTEM AND THE GUT MICROBIOME

The ACE2 (angiotensin-converting enzyme 2) receptor acts as a binding site by which SARS-CoV-2 enters host cells[57,58]. A higher expression of ACE2 in the cell favors SARS-CoV-2 infection. Despite this, ACE2 deficiency can play a vital role in SARS-CoV-2 infection[59]. Increased ACE2 expression is found in the epithelial cells of the respiratory tract (nasal mucosa, nasopharynx, and lungs), in different parts of the intestine, and in different types of epithelial cells, including nasal, corneal, and intestinal epithelial cells in humans[60]. In addition, this protein is expressed in different parts of the digestive system, such as the small intestine, stomach, colon, and liver[61]. However, ACE2 expression is

controlled by distinct microbial communities in several body tissues. Mouse model studies suggest an association between certain microbial communities and overexpression of ACE2. This overexpression may prevent detrimental changes in hypoxia-induced gut pathophysiology and pulmonary pathophysiology[62]. ACE2 expression is controlled in the GI and respiratory tract[63]. Additionally, it can also be controlled by some bacterial species from important phyla. Downregulation of ACE2 expression was associated with the Bacteroidetes phylum. Among all species of this phylum, *Bacteroides dorei* has been shown to inhibit ACE2 expression in the colon, whereas the Firmicutes phylum plays a variable role in its modulation[20,49,64]. These findings are supported by other studies describing the modulation of ACE2 expression in the gut by the microbiota[65,66].

GUT-LUNG AXIS CROSSTALK DURING COVID-19 INFECTION

Several reports indicate that manipulation of the gut microbiota may be used to treat pulmonary diseases[67]. Therefore, the gut-lung axis crosstalk can help to elucidate these respiratory and digestive system interactions (Figure 5). Dysbiosis occurs when there are detrimental changes in the microbial composition of the gut or respiratory tract. It often leads to altered immune responses and the development of diseases, such as COVID-19. Nonetheless, of gut dysbiosis can be manipulated for treatment purposes[32,67-69]. Studies suggest that SARS-CoV-2 from the lungs travels to the gut *via* the lymphatic system leading to disrupted gut permeability[70,71]. Furthermore, the extent of dysbiosis is associated with COVID-19 severity[4,72]. Therefore, understanding the crosstalk between the microbiome and the gut-lung axis during COVID-19 infection may provide therapeutic approaches.

GUT-BRAIN-LUNG AXIS CROSSTALK DURING COVID-19 INFECTION

Like the gut-lung axis, crosstalk between the microbiome and the gut-brain axis has been recognized and remains the topic[73-75]. Several studies have illustrated the role of the microbiome-gut-brain axis in different neurological disorders[76,77].

The interaction between the brain and the gut (also called the gut-brain axis) is bidirectional, with several pathways involved, including bacterial metabolites, neuroanatomical communications, neurotransmitters, and hormones[78]. The vagus nerve is primarily involved in such communication, and these molecules (neurotransmitters/hormones) are produced in the GI tract. During communication between neurotransmitters and hormones, they might interact with the receptors on the vagus nerve, relaying information to the brain[78-81]. Many hormones can cross the BBB and affect the CNS directly. Additionally, neuroendocrine pathways which operate *via* the hypothalamic-pituitary-adrenal (HPA) axis associated with stress also affect the BBB. The stress-HPA axis is associated with the release of glucocorticoids such as cortisol from the adrenal cortex. Cortisol, is associated with augmented intestinal permeability and GI motility, affecting the gut microbiota[78,82-84]. The stress-HPA axis may also lead to inflammation and bacteria-derived impaired metabolite production, especially SCFAs[78,84]. Therefore, a thorough understanding of the gut-brain axis can help the development of therapeutic approaches *via* modulation of the gut microbial composition.

The gut microbiota might play a distinct role in controlling the host immune system, and research is underway to uncover more in this field[85,86]. The involvement of the lungs (gut-brain-lung axis) occurs when inflammation and neurodegeneration in the brain stem due to COVID-19 prevent cranial nerve signaling, disrupting anti-inflammatory pathways and normal respiratory and GI functions. Recently, the lungs have been associated in the crosstalk among the microbiota-gut-brain axis components, and this axis was also noted during COVID-19 (Figure 6)[34,78]. Moreover, in COVID-19 patients, alterations in the gut microbiota have been shown to reduce live microbes (Bifidobacterium and Lactobacillus) during intestinal microbial dysbiosis[87].

The microbial translocation to the gut and its subsequent damage may play a vital role in inferior clinical outcomes for the disease. The gut-brain-lung axis during COVID-19 infection can also offer clues indicate viable directions for therapeutic development[34].

HYPOXIA IN COVID-19 AND GUT MICROBIOTA

Abnormal cytokine release (cytokine storms) and inflammatory responses may be associated with hypoxia during severe COVID-19. Viral replication in the lungs leads to a cytokine storm, destroying normal lung function and causing hypoxemia, *i.e.*, low oxygen levels in the blood. Hypoxia-inducible factor-1α (HIF-1α) is a transcription factor that regulates cellular functions such as cell proliferation and angiogenesis. In hypoxic conditions, HIF-1α binds to the hypoxemic response element and induces the production of cytokines such as IL-6 and TNF-α, leading to hypoxia[88]. There are other collective causes of hypoxia, including pulmonary infiltration and thrombosis. The COVID-19 virus induces

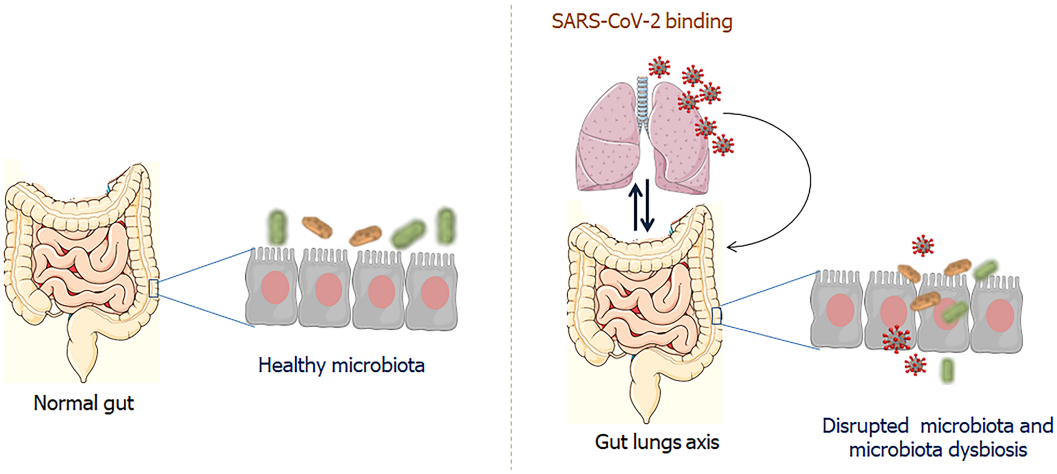


Figure 5 The diagram points out the normal gut and its microbial association. The figure also illustrates the crosstalk between the microbiome and gut-lung axis. SARS-CoV-2: Severe acute respiratory syndrome coronavirus 2.

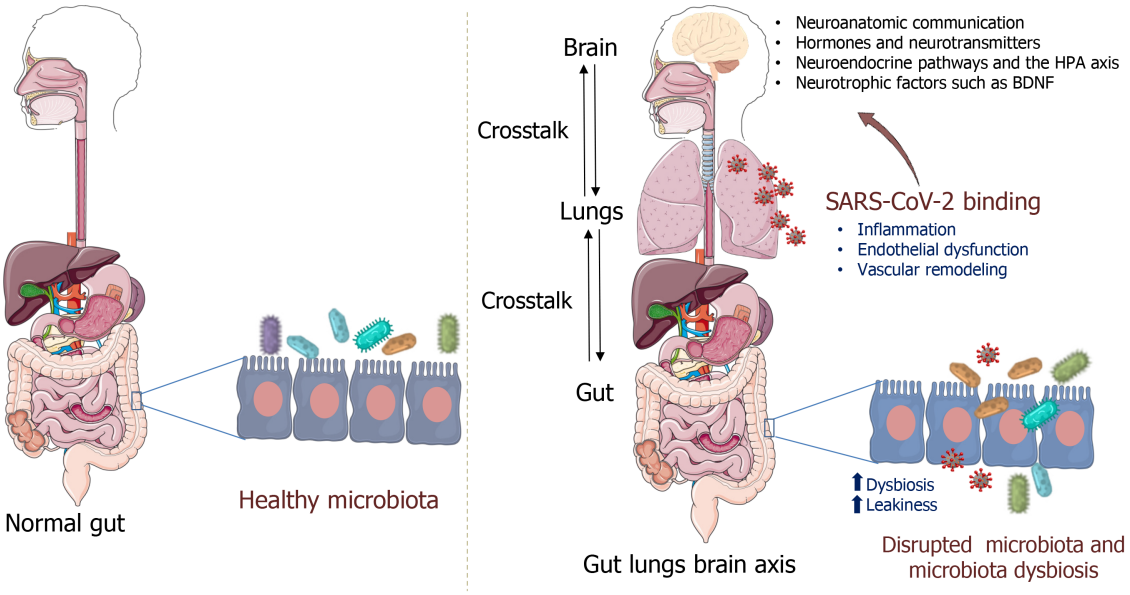


Figure 6 The diagram describes the normal gut and its microbial association. The figure also illustrates the crosstalk between the microbiome and gut-brain-lung axis. BDNF: Brain-derived neurotrophic factor; HPA: Hypothalamic-pituitary-adrenal; SARS-CoV-2: Severe acute respiratory syndrome coronavirus 2.

pneumonia that causes atelectasis (collapsing of air sacs), leading to low oxygen levels in the body[89]. Additionally, COVID-19 leads to mitochondrial damage, production of reactive oxygen species, and subsequently HIF-1α, further promoting viral infections and inflammation[90].

As part of its normal metabolic functions, the gut microbiota produces neurotropic metabolites, neurotransmitters, peptides, and SCFA, whose levels are disrupted due to COVID-19. SCFA such as butyrate confer neuroprotection. Modulation of gut microbes (responsible for such metabolite production) by SARS-CoV-2 alters hypoxia-sensing, negatively impacting the CNS[91]. Therefore, an association between gut microbiota and hypoxia in COVID-19 patients can be speculated, and may be linked to the CNS (Figure 7).

ALTERATION OF GUT MICROBIOTA IN COVID-19: EVIDENCE FOR INFLAMMATION OR DIEASE, SEVERITY?

Under normal conditions, colonization of the normal microbiota in the gut causes resistance to pathogen [92,93]. Much of the normal gut microbiota belongs to Clostridia., which produces butyric acid. This SCFA is produced during dietary fiber fermentation along with acetic acid and propionic acid, which

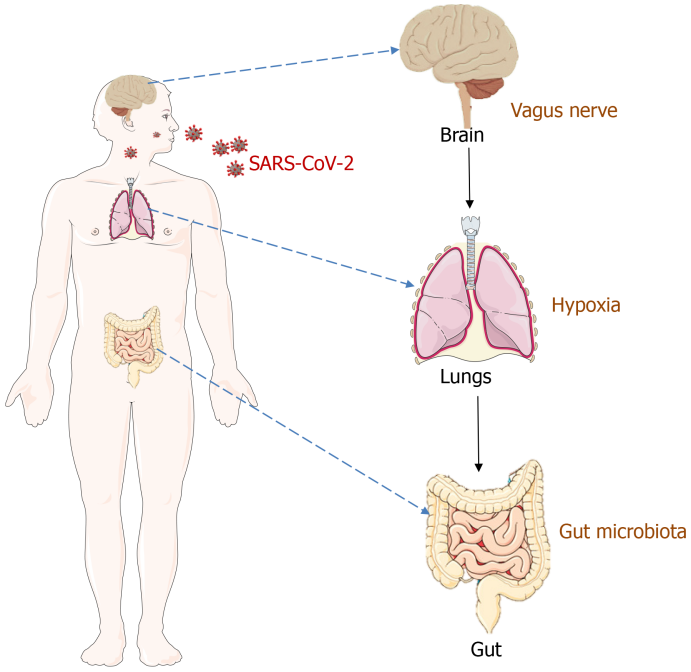


Figure 7 The figure illustrates an association between gut microbiota and hypoxia in coronavirus disease 2019 patients, and it is connected with central nervous system. SARS-CoV-2: Severe acute respiratory syndrome coronavirus 2.

play a critical role in gut health (Figure 8A)[94,95]. Butyric acid helps in maintain the integrity of the gut barrier by providing a vital energy resource for colonocytes. This SCFA also hinders histone deacetylase activity and inhibits the activation of the nuclear factor (NF)-κB signaling pathway activation. This phenomenon may activate the G protein-coupled receptor pair (GPR41 /GPR43). These events help exert an anti-inflammatory response in normal gut health and stimulate regulatory T cells (Treg cells) [96-100]. Treg cells play a central role in suppressing inflammatory responses[97,101]. However, in COVID-19 patients, typical microbiota dysbiosis causes an imbalance in all these events.

There is a distinct connection between dysbiosis of the gut microbiota and hyper-inflammatory responses, especially cytokine release, in some COVID-19 patients[102] (Figure 8). Researchers noted that gut microbiota composition is related to the COVID-19 severity of and observed an association between altered cytokine levels and gut microbiota composition[38]. Cytokines/inflammatory factors, such as IL-1β, IL-6, and TNF-α, are usually associated with inflammation during disease[103]. In the case of severe COVID-19, the levels of certain cytokines, such as IL-6, IL-10, TNF-α, and IFN-are raised abnormally, and in some cases, cytokine storms are observed (Figure 8B)[23]. In pilot study, the quality of gut microbial composition was associated with the severity COVID-19 in 15 patients at the time of hospitalization in Hong Kong. The study showed an abundance of microbes such as *Clostridium hathewayi*, *Clostridium ramosum*, and *Coprobacillus* in COVID-19 patients. Moreover, an anti-inflammatory bacteria, *Faecalibacterium prausnitzii*, was be inversely correlated with disease severity[49].

Nonetheless, more detailed studies are needed to understand the impaired gut health during COVID-19, especially in extreme forms of the disease. Another study confirmed microbiota dysbiosis in COVID-19 patients. This study found differential bacterial populations with a decrease in *F. prausnitzii* and *Clostridium* spp and an association of IL-21 in mild to severe COVID-19 patients[51].

A gut microbiota richness analysis in COVID-19 patients was conducted over through a six-month evaluation using 16S rDNA sequencing. This study showed that, patients with decreased post-convalescence richness in bacterial microbiota had high disease severity with increased CRP. Additionally, the authors observed increased incidence of intensive care unit admissions with worse pulmonary functions in these patients[104]. The study suggested an association between the hyper-inflammatory response in COVID-19 and gut dysbiosis. However, a greater number of studies testing patients well after recovery are required to fully illustrate gut dysbiosis, associated factors, and the hyper-inflammatory response during COVID-19.

GUT MICROBIOTA IN ELDERLY OR CO-MORBID COVID-19 PATIENTS

Researchers have attempted to understand the role of the gut microbiota in elderly or co-morbid COVID-19 patients. A recent study evaluated the association of the gut microbiota and its modulation in COVID-19 patients. In this study, the cohort comprised approximately 200 severe COVID-19 patients

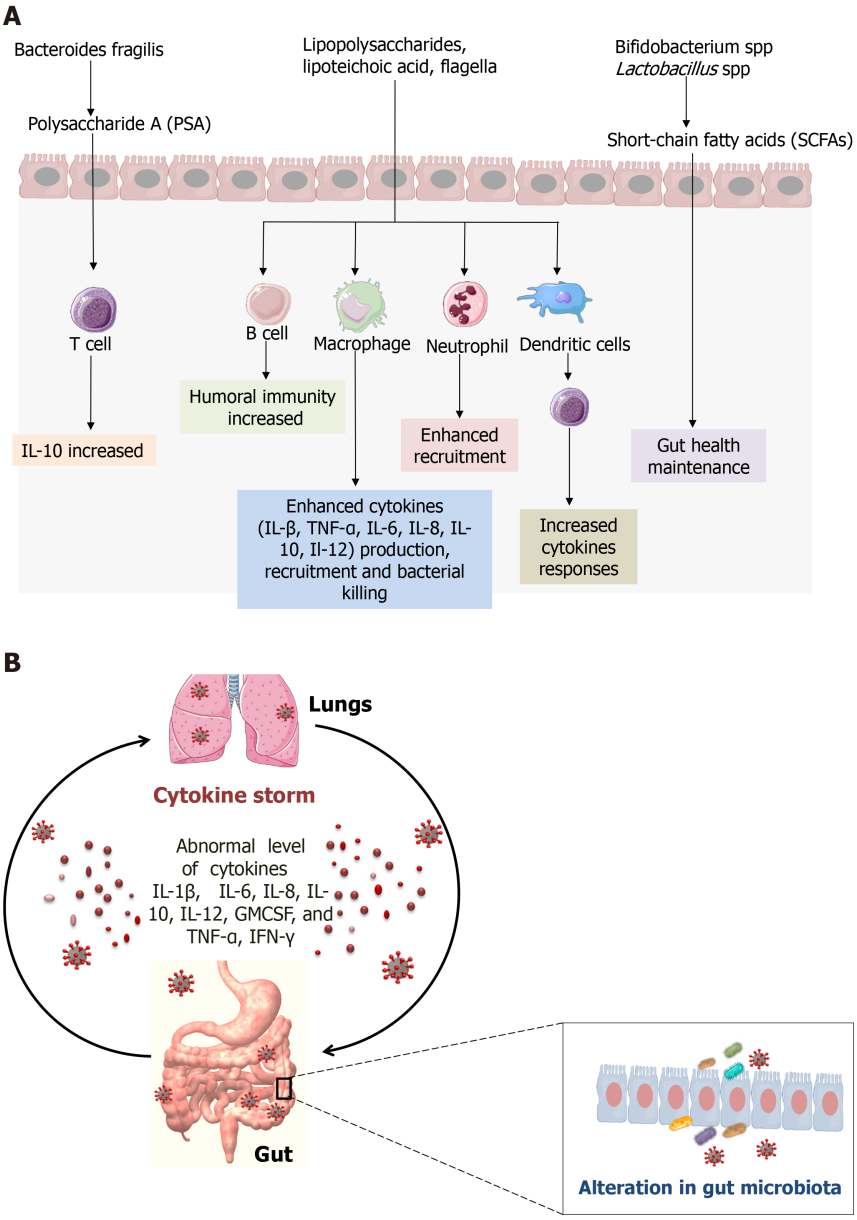


Figure 8 The figure illustrates normal gut microbiota and immunological consequences, and coronavirus disease 2019 related altered gut microbiota associated inflammation. A: Normal gut microbiota and immunological consequences for healthy gut; B: Coronavirus disease 2019 (COVID-19) related altered gut microbiota associated inflammation. The inflammatory condition in COVID-19 patients causes the abnormal release of different cytokines, such as interleukin-1 beta (IL-1β), IL-6, IL-8, IL-10, IL-12, granulocyte-macrophage colony-stimulating factor, tumor necrosis factor-alpha, and interferon-gamma. PSA: Polysaccharide A; SCFA: Short-chain fatty acid; IL-1β: Interleukin-1 beta; IL-6: Interleukin-6; GMCSF: Granulocyte-macrophage colony-stimulating factor; TNF-α: Tumor necrosis factor-alpha; IFN-γ: Interferon-gamma.

hospitalized with pneumonia. Researchers considered elderly patients (age 62 years to 64 years) and their comorbidity. Patients in this study received two types of treatments: one group was treated with only the best available therapy (BAT), and the other group was treated with oral bacteriotherapy and BAT. Researchers found a decline in mortality and decreased progress in severe disease. Finally, researchers concluded that oral bacteriotherapy might be helpful in the management of hospitalized COVID-19 patients[105]. Similarly, Rao *et al*[106] noted that people with the comorbidities are more prone to COVID-19-related complications. In this case, immune system deregulation and deaths were also noted. However, researchers used-glucan to enhance the immune system in COVID-19 patients. This glucan was used to augment the activity of macrophages, natural killer cells, and IL-8, implicating that it might enhance the defense mechanisms to combat the virus[106].

Recently, Liu *et al*[1] evaluated the role of the gut microbiota composition and its association with the post-acute COVID-19 syndrome (PACS). In this study, researchers considered the comorbidities and dietary patterns during patient selection compare gut microbiota compositions. However, no considerable differences were observed in age, comorbidities, gender, antibiotics, or antiviral drug use between patients with PACS or without PACS[1].

Therefore, in cases of elderly or co-morbid COVID-19 patients, the gut microbiota might play an important role in immune system deregulation, although further studies are required to validate the findings.

GUT MICROBIOTA BASED ON ANTIBIOTIC USAGE IN COVID-19 PATIENTS

In COVID-19 patients, the use of antibiotics is relatively common. The frequently used antibiotics in COVID-19 patients are Azithromycin, Amoxicillin Clavulanate, Cephalosporin, Tetracycline[49,107], *etc*. The composition of the gut microbiota is hampered in COVID-19 patients due to the usage of antibiotics, occasionally causing antibiotic-associated diarrhea (AAD)[108]. Antibiotics usages in COVID-19 patients were increased the number of opportunistic pathogens compared with that detected in an untreated control group. Zuo *et al*[49] reported that the gut of COVID-19 patients, using antibiotics contains opportunistic bacterial pathogens such as *Bacteroides nordii*, *Actinomyces viscosus*, and *Clostridium hathewayi*. Additional studies also reported this phenomenon[22,109]. An increase of opportunistic bacterial pathogens causes dysbiosis of the gut. Rafiqul Islam *et al*[110] also noted that the abundance of opportunistic pathogens in COVID-19 patients in Bangladesh could cause dysbiosis, with 46 genera of opportunistic bacteria being identified patient GI samples. However, a study demonstrated that particular strains of probiotics may be useful for AAD[111]. Scientists have shown that the administration of oral probiotics can recover gut health and have antiviral effects[112,53]. For probiotic strain identification, Mak *et al*[113] highlight the need for effective research to easily recognize the probiotic strains of therapeutic use. In this case, the probiotics should be specific for COVID-19, and help reduce the susceptibility to COVID-19 preventing severe COVID-19 disease.

GUT MICROBIOTA DYSBIOSIS DURING COVID-19 AND USE OF PROBIOTICS

Scientists identified an association between the gut microbiota dysbiosis and the severity of COVID-19. Magalhães *et al*[52] noted that gut microbiota dysbiosis causes poor outcomes in elderly COVID-19 patients with hypertension and diabetes. Additionally, co-morbid elderly COVID-19 patients were prone to increased inflammatory situations due to the dysbiosis. The elevated amount of bacterial products in the gut might translocate into the blood due to the increased permeability across the intestinal epithelium. Bacterial toxin products, such as lipopolysaccharides (LPS), may accumulate in blood, aggravating TLR4 and subsequent downstream signaling. This could contribute to the "cytokine storm", and result in complications in elderly COVID-19 patients[54]. Researchers also found a different route of activation of toll-like receptor (TLR4/TLR5) in COVID-19 patients[114-116]. Hung *et al*[53] also reported that gut microbiota dysbiosis increases COVID-19 severity in the elderly. However, the use of probiotics is a novel way to reduce COVID-19 severity in elderly populations.

THERAPEUTIC IMPLICATIONS AND CLINICAL TRIALS TO UNDERSTAND THE ROLE OF THE GUT MICROBIOTA DURING COVID-19

A careful analysis of the microbiome-gut-lung axis during COVID-19 infection can direct research towards therapeutic options for restoring gut health. As an altered gut microbiota is strongly associated with COVID-19 and its severity, supplementation of bacterial metabolites or commensals and prebiotics to enrich the microbial ecosystem is a path toward effective therapeutic options.

However, very few studies have explored this. A randomized clinical trial with 300 registered participants assessed the effectiveness of combination therapy using *Lactobacillus plantarum* (*L. plantarum*) CECT 7484, *L. plantarum* CECT 30292, *Pediococcus acidilactici* (*P. acidilactici*) CECT 7483, and *L. plantarum* CECT 7485, in adult COVID-19 patients (ClinicalTrials.gov; Clinical trial no. NCT04517422). Nonetheless, a deficiency of well-established data calls for more studies of this nature[41]. An open-label, randomized clinical trial with 350 participants conducted by Kaleido Biosciences sought to determine the effectiveness of a novel glycan molecule (KB109) in patients with mild to moderate COVID-19 (ClinicalTrials.gov; Clinical trial no. NCT04414124)[117]. The synthetic glycan molecule reduced the number of acute care visits by COVID-19 patients. Additionally, disease resolution in patients with comorbidities was improved, compared to that in patients relying solely on supportive self-care.

A similar study attempted to evaluate the glycan molecule's effectiveness (KB109) associated with gut microbiota function in COVID-19 patients. The same organization conducted the clinical study, an open-label, randomized clinical trial in 49 participants in the United States (ClinicalTrials.gov; Clinical trial no. NCT04486482)[118]. There were no conclusive results; however, more studies are likely to be conducted in this sense. A complete list of the clinical trials initiated to understand the role of the gut microbiota in COVID-19 and its therapeutic implications are shown in Table 4.

Table 4 List of clinical trials initiated to understand the role of gut microbiota in coronavirus disease 2019 and its therapeutic implications

Sl. No.	Objective of clinical trials	Clinical trials No.	Description of clinical trials	Remarks
1	Evaluate the combination of probiotics (*P. acidilactici* and *L. plantarum*) to reduce the viral load of moderate or severe COVID-19 patients	NCT04517422	It was a randomized controlled trial, 300 participants, treatment by dietary supplement (probiotics)	Observational study of adult and older adult, trial completed
2	To explore the natural history of mild-to-moderate COVID-19 illness and safety of a novel glycan (KB109) and self-supportive care	NCT04414124	It was a randomized, prospective, open-label, parallel-group controlled clinical study of 350 participants	Observational study of adults (both male and female), trial completed
3	Investigate the physiologic effects of the novel glycan (KB109) on patients with COVID-19 illness on gut microbiota structure and function in the outpatient	NCT04486482	It was a randomized, open-label clinical study of 49 participants	Observational study of adults patients with mild-to-moderate COVID-19 infections, trial completed
4	Evaluate the clinical contribution of the gut microbiota and its diversity on the COVID-19 disease severity and the viral load	NCT05107245	It was case-control, diagnostic study of 143 participants	Observational study on the diagnostic evaluation of the human intestinal microbiota, trial completed
5	Studied the effects of *Lactobacillus coryniformis* K8 intake on the prevalence and severity of COVID-19 in health professional	NCT04366180	A randomized, interventional study of 314 participants	Investigation of probiotic effects to healthcare personnel exposed to COVID-19 infection
6	Investigate to exploring the role of nutritional support by probiotics to COVID-19 outpatients (adult)	NCT04907877	Randomized, evidence based study of 300 participants	Used of probiotics as dietary supplement that enhance specific immune response of patients having COVID-19 respiratory infection
7	Use of dietary supplement (Omni-Biotic® 10 AAD) can decrease the intestinal inflammation and improves dysbiosis for COVID-19 patients	NCT04420676	It was a randomized Interventional study of 30 participants	This study performed as double blind, placebo-controlled study
8	Evaluate the probiotics efficacy to decrease the COVID-19 infection symptoms and duration of COVID-19 positive patients	NCT04621071	The double-blind, randomized, controlled trial of 17 participants	This study performed to explored the effects of dietary supplement: Probiotics (2 strains 10×10^9 UFC), trial completed
9	Impact analysis of probiotic strain *L. reuteri* DSM 17938 for specific Abs response against SARS-CoV-2 infection	NCT04734886	It was control, randomized trial of 161 participants	To assess the upon and after COVID-19 infection in healthy adults, trial completed
10	To evaluate the primary efficacy of live microbials (probiotics) for boosting up the immunity of SARS-CoV-2 infected persons (unvaccinated)	NCT04847349	It was double-blind, randomized, controlled trial of 54 participants	Efficacy analysis of dietary supplement (combination of live microbials) as anti COVID-19 infection, trial completed
11	Evaluate the follow -up of Symprove (probiotic) to COVID-19 positive patients	NCT04877704	The randomized clinical trial was performed with 60 patients	Observational study to supervision of hospitalized COVID-19 patients
12	Study was performed to evaluate the possible effect of a probiotic mixtures in the improvement of COVID-19 infection symptoms	NCT04390477	It was randomized case control, clinical trial of 41 participants	Observational study of dietary supplement: Probiotic to COVID-19 patients
13	The probiotic (Omni-Biotic Pro Vi 5) use for investigate the side effect of post-COVID syndrome	NCT04813718	It was a randomized trial of 20 participants	It was a therapeutic target study of probiotic for treatment of acute COVID-19 and prevention of post COVID infections
14	To evaluate the effect of a probiotic strain on the occurrence and severity of COVID-19 in hospitalised elderly population	NCT04756466	Randomized control trial of 201 participants	It was observational study, probiotic sued for improve the immune response of elderly patients
15	This study assesses the beneficial effects of the nutritional supplementation (ABBC1) to individuals taken the COVID-10 vaccine	NCT04798677	It was a double-blinded, placebo-controlled, randomized clinical study of 90 participants	Used as knowing the microbiome modulating properties, observational study
16	To investigate the consequence of *Ligilactobacillus salivarius* MP101 to hospitalised elderly individuals	NCT04922918	Non-randomised study of 25 participants	Observational study of aged patients having highly affected by COVID-19
17	Study was performed to explored the effect of the probiotic *Lactobacillus rhamnosus* GG	NCT04399252	It was a randomized double-blind, placebo-controlled trail of 182 participants	Observational study of individuals microbiome of household contacts exposed to COVID-19
18	Treatment approaches by probiotics to human gut microbiome and growing the anti-inflammatory response for COVID-19 infected patients	NCT04854941	It was a randomized controlled open-label study of 200 participants	The optimizing treatment approaches based observational study, trial completed
19	To evaluate the capability of the novel	NCT04666116	Randomized, single blind clinical	Used of dietary supplementation with

	nutritional supplement (probiotics and other vitamins) to COVID-19 infected and hospitalised patients		trial of 96 participants	probiotics aims to reduce the viral load
20	Using of probiotics for COVID 19 transmission reduction to health care professionals	NCT04462627	It was a non-randomized trial of 500 participants	Analysis and reduction of COVID-19 viral load to health care professionals

P. acidilactici: *Pediococcus acidilactici*; *L. plantarum*: *Lactobacillus plantarum*; COVID-19: Coronavirus disease 2019; SARS-CoV-2: Severe acute respiratory syndrome coronavirus 2.

As the pandemic persists, it is critical to assess the effect of next-generation probiotics, prebiotics, synbiotics, and increased fiber intake on changes in gut microbiota composition in patients with mild to moderate and severe COVID-19.

FUTURE PERSPECTIVE

In several cases, complex pathophysiological and immunological responses are reported in the host due to SARS-CoV-2 infection. However, very little is known regarding the changes in gut virome in the COVID-19 patients, and this should be explored in future studies should explore it further. Moreover, the possible role of the gut microbiota in COVID-19 should be explored in future research. Likewise, population-based cohorts should be generated to illustrate the function of the altered gut microbiota during COVID-19 in different populations. This will enable the design of diagnostics and therapeutics for COVID-19 in different population types. Simultaneously, population-specific changes need to be described as this can help resolve severe conditions in COVID-19 patients. In the future, researchers should attempt to understand population-specific gut microbiota alteration during COVID-19 to design therapeutic interventions as required. Moreover, research could focus on the population specific changes in the immune response generated against the two altered gut microbiota during COVID-19.

CONCLUSION

Presently, abundant research has described the marked changes in the gut microbiomes of COVID-19 patients. Therefore, an apparent association exsists between the overall health of the gut microbiome and the progression of COVID-19[119]. Furthermore, the altered gut microbiota has been shown to persist in patients even after several days of recovery from COVID-19.

However, poor outcome were observed in elderly or co-morbid patients[97,120]. Recently, several studies discussed the factors associated with the modified gut microbiota in COVID-19 patients manifesting GI symptoms. According to some reports, increased inflammation may lead to a leaky gut, which enables the translocation of bacterial metabolites and toxins into the systemic circulation[97,120]. This might cause further complications to the severe COVID-19 patients.

In this review, we have illustrated various GI aspects of COVID-19 patients including the gut microbiota imbalance and GI symptoms, the patterns of altered gut microbiota composition, the crosstalk between the microbiome and the gut-lung axis, the crosstalk between the microbiome and the gut-brain-lung axis, as well as hypoxia associated with altered gut microbiota. We also highlighted the association between the gut microbiota and elderly or co-morbid COVID-19 patients, as well as that of gut microbiota dysbiosis and COVID-19 severity. Additionally, we explored the correlation between, probiotics usage and the gut microbiota based on antibiotic usage in COVID-19 patients. Therefore, our review will provide a distinct outline for researchers working in the field. Also, it will provide valuable insight into the role of gut microbiomes in COVID-19 patients.

Currently, therapeutics are in development to combat COVID-19. In addition to antiviral therapeutics, probiotics might be effective for improving gut health through the gut-lung axis. Recently, several clinical trials have been initiated to understand the role of probiotics in COVID-19 patients. The ongoing clinical trials will elucidate the role of probiotic therapeutics or for COVID-19 patients, and offer new alternatives in COVID-19 treatment.

FOOTNOTES

Author contributions: Chakraborty C, Sharma AR, and Bhattacharya M contributed equally, Chakraborty C designed the research study and wrote the main manuscript draft; Sharma AR reviewed and edited the manuscript; Bhattacharya M developed the figures and tables; Dhama KD performed the English editing and validation; Lee SS did the funding acquisition; all authors have read and approved the final manuscript.

Supported by the Hallym University Research Fund and the Basic Science Research Program through the National Research Foundation of Korea (NRF) funded by the Ministry of Education (NRF-2020R1C1C1008694 & NRF-2020R1I1A3074575).

Conflict-of-interest statement: There are no conflicts of interest to report.

Open-Access: This article is an open-access article that was selected by an in-house editor and fully peer-reviewed by external reviewers. It is distributed in accordance with the Creative Commons Attribution Non Commercial (CC BY-NC 4.0) license, which permits others to distribute, remix, adapt, build upon this work non-commercially, and license their derivative works on different terms, provided the original work is properly cited and the use is non-commercial. See: https://creativecommons.org/Licenses/by-nc/4.0/

Country/Territory of origin: India

ORCID number: Chiranjib Chakraborty 0000-0002-3958-239X; Ashish Ranjan Sharma 0000-0003-3973-6755; Manojit Bhattacharya 0000-0001-9669-1835; Kuldeep Dhama 0000-0001-7469-4752.; Sang-Soo Lee 0000-0001-5074-7581.

S-Editor: Chen YL
L-Editor: A
P-Editor: Wu RR

REFERENCES

1 **Liu Q**, Mak JWY, Su Q, Yeoh YK, Lui GC, Ng SSS, Zhang F, Li AYL, Lu W, Hui DS, Chan PK, Chan FKL, Ng SC. Gut microbiota dynamics in a prospective cohort of patients with post-acute COVID-19 syndrome. *Gut* 2022; **71**: 544-552 [PMID: 35082169 DOI: 10.1136/gutjnl-2021-325989]
2 **Troisi J**, Venutolo G, Pujolassos Tanyà M, Delli Carri M, Landolfi A, Fasano A. COVID-19 and the gastrointestinal tract: Source of infection or merely a target of the inflammatory process following SARS-CoV-2 infection? *World J Gastroenterol* 2021; **27**: 1406-1418 [PMID: 33911464 DOI: 10.3748/wjg.v27.i14.1406]
3 **Al Kassaa I**, El Omari S, Abbas N, Papon N, Drider D, Kassem II, Osman M. High association of COVID-19 severity with poor gut health score in Lebanese patients. *PLoS One* 2021; **16**: e0258913 [PMID: 34673813 DOI: 10.1371/journal.pone.0258913]
4 **Donati Zeppa S**, Agostini D, Piccoli G, Stocchi V, Sestili P. Gut Microbiota Status in COVID-19: An Unrecognized Player? *Front Cell Infect Microbiol* 2020; **10**: 576551 [PMID: 33324572 DOI: 10.3389/fcimb.2020.576551]
5 **Gu J**, Han B, Wang J. COVID-19: Gastrointestinal Manifestations and Potential Fecal-Oral Transmission. *Gastroenterology* 2020; **158**: 1518-1519 [PMID: 32142785 DOI: 10.1053/j.gastro.2020.02.054]
6 **Ramachandran P**, Onukogu I, Ghanta S, Gajendran M, Perisetti A, Goyal H, Aggarwal A. Gastrointestinal Symptoms and Outcomes in Hospitalized Coronavirus Disease 2019 Patients. *Dig Dis* 2020; **38**: 373-379 [PMID: 32599601 DOI: 10.1159/000509774]
7 **Han C**, Duan C, Zhang S, Spiegel B, Shi H, Wang W, Zhang L, Lin R, Liu J, Ding Z, Hou X. Digestive Symptoms in COVID-19 Patients With Mild Disease Severity: Clinical Presentation, Stool Viral RNA Testing, and Outcomes. *Am J Gastroenterol* 2020; **115**: 916-923 [PMID: 32301761 DOI: 10.14309/ajg.0000000000000664]
8 **Ng SC**, Tilg H. COVID-19 and the gastrointestinal tract: more than meets the eye. *Gut* 2020; **69**: 973-974 [PMID: 32273292 DOI: 10.1136/gutjnl-2020-321195]
9 **Tang A**, Tong ZD, Wang HL, Dai YX, Li KF, Liu JN, Wu WJ, Yuan C, Yu ML, Li P, Yan JB. Detection of Novel Coronavirus by RT-PCR in Stool Specimen from Asymptomatic Child, China. *Emerg Infect Dis* 2020; **26**: 1337-1339 [PMID: 32150527 DOI: 10.3201/eid2606.200301]
10 **Wong SH**, Lui RN, Sung JJ. Covid-19 and the digestive system. *J Gastroenterol Hepatol* 2020; **35**: 744-748 [PMID: 32215956 DOI: 10.1111/jgh.15047]
11 **Mehandru S**, Merad M. Pathological sequelae of long-haul COVID. *Nat Immunol* 2022; **23**: 194-202 [PMID: 35105985 DOI: 10.1038/s41590-021-01104-y]
12 **Holmes E**, Li JV, Marchesi JR, Nicholson JK. Gut microbiota composition and activity in relation to host metabolic phenotype and disease risk. *Cell Metab* 2012; **16**: 559-564 [PMID: 23140640 DOI: 10.1016/j.cmet.2012.10.007]
13 **Nicholson JK**, Holmes E, Kinross J, Burcelin R, Gibson G, Jia W, Pettersson S. Host-gut microbiota metabolic interactions. *Science* 2012; **336**: 1262-1267 [PMID: 22674330 DOI: 10.1126/science.1223813]
14 **Joyce SA**, Gahan CG. The gut microbiota and the metabolic health of the host. *Curr Opin Gastroenterol* 2014; **30**: 120-127 [PMID: 24468803 DOI: 10.1097/MOG.0000000000000039]
15 **Jandhyala SM**, Talukdar R, Subramanyam C, Vuyyuru H, Sasikala M, Nageshwar Reddy D. Role of the normal gut microbiota. *World J Gastroenterol* 2015; **21**: 8787-8803 [PMID: 26269668 DOI: 10.3748/wjg.v21.i29.8787]
16 **Corfield AP**. The Interaction of the Gut Microbiota with the Mucus Barrier in Health and Disease in Human. *Microorganisms* 2018; **6** [PMID: 30072673 DOI: 10.3390/microorganisms6030078]
17 **Tang WH**, Kitai T, Hazen SL. Gut Microbiota in Cardiovascular Health and Disease. *Circ Res* 2017; **120**: 1183-1196 [PMID: 28360349 DOI: 10.1161/CIRCRESAHA.117.309715]
18 **Dhar D**, Mohanty A. Gut microbiota and Covid-19-possible link and implications. *Virus Res* 2020; **285**: 198018 [PMID: 32430279 DOI: 10.1016/j.virusres.2020.198018]

19 **Zuo T**, Wu X, Wen W, Lan P. Gut Microbiome Alterations in COVID-19. *Genomics Proteomics Bioinformatics* 2021 [PMID: 34560321 DOI: 10.1016/j.gpb.2021.09.004]

20 **Chen J**, Hall S, Vitetta L. Altered gut microbial metabolites could mediate the effects of risk factors in Covid-19. *Rev Med Virol* 2021; **31**: 1-13 [PMID: 34546607 DOI: 10.1002/rmv.2211]

21 **Yamamoto S**, Saito M, Tamura A, Prawisuda D, Mizutani T, Yotsuyanagi H. The human microbiome and COVID-19: A systematic review. *PLoS One* 2021; **16**: e0253293 [PMID: 34161373 DOI: 10.1371/journal.pone.0253293]

22 **Chiappetta S**, Sharma AM, Bottino V, Stier C. COVID-19 and the role of chronic inflammation in patients with obesity. *Int J Obes (Lond)* 2020; **44**: 1790-1792 [PMID: 32409680 DOI: 10.1038/s41366-020-0597-4]

23 **Del Valle DM**, Kim-Schulze S, Huang HH, Beckmann ND, Nirenberg S, Wang B, Lavin Y, Swartz TH, Madduri D, Stock A, Marron TU, Xie H, Patel M, Tuballes K, Van Oekelen O, Rahman A, Kovatch P, Aberg JA, Schadt E, Jagannath S, Mazumdar M, Charney AW, Firpo-Betancourt A, Mendu DR, Jhang J, Reich D, Sigel K, Cordon-Cardo C, Feldmann M, Parekh S, Merad M, Gnjatic S. An inflammatory cytokine signature predicts COVID-19 severity and survival. *Nat Med* 2020; **26**: 1636-1643 [PMID: 32839624 DOI: 10.1038/s41591-020-1051-9]

24 **Chen L**, Deng H, Cui H, Fang J, Zuo Z, Deng J, Li Y, Wang X, Zhao L. Inflammatory responses and inflammation-associated diseases in organs. *Oncotarget* 2018; **9**: 7204-7218 [PMID: 29467962 DOI: 10.18632/oncotarget.23208]

25 **Tang Y**, Liu J, Zhang D, Xu Z, Ji J, Wen C. Cytokine Storm in COVID-19: The Current Evidence and Treatment Strategies. *Front Immunol* 2020; **11**: 1708 [PMID: 32754163 DOI: 10.3389/fimmu.2020.01708]

26 **Costela-Ruiz VJ**, Illescas-Montes R, Puerta-Puerta JM, Ruiz C, Melguizo-Rodríguez L. SARS-CoV-2 infection: The role of cytokines in COVID-19 disease. *Cytokine Growth Factor Rev* 2020; **54**: 62-75 [PMID: 32513566 DOI: 10.1016/j.cytogfr.2020.06.001]

27 **García LF**. Immune Response, Inflammation, and the Clinical Spectrum of COVID-19. *Front Immunol* 2020; **11**: 1441 [PMID: 32612615 DOI: 10.3389/fimmu.2020.01441]

28 **Mehta P**, McAuley DF, Brown M, Sanchez E, Tattersall RS, Manson JJ; HLH Across Speciality Collaboration, UK. COVID-19: consider cytokine storm syndromes and immunosuppression. *Lancet* 2020; **395**: 1033-1034 [PMID: 32192578 DOI: 10.1016/S0140-6736(20)30628-0]

29 **Sinha P**, Matthay MA, Calfee CS. Is a "Cytokine Storm" Relevant to COVID-19? *JAMA Intern Med* 2020; **180**: 1152-1154 [PMID: 32602883 DOI: 10.1001/jamainternmed.2020.3313]

30 **Ragab D**, Salah Eldin H, Taeimah M, Khattab R, Salem R. The COVID-19 Cytokine Storm; What We Know So Far. *Front Immunol* 2020; **11**: 1446 [PMID: 32612617 DOI: 10.3389/fimmu.2020.01446]

31 **Perisetti A**, Gajendran M, Mann R, Elhanafi S, Goyal H. COVID-19 extrapulmonary illness -special gastrointestinal and hepatic considerations. *Dis Mon* 2020; **66**: 101064 [PMID: 32807535 DOI: 10.1016/j.disamonth.2020.101064]

32 **de Oliveira GLV**, Oliveira CNS, Pinzan CF, de Salis LVV, Cardoso CRB. Microbiota Modulation of the Gut-Lung Axis in COVID-19. *Front Immunol* 2021; **12**: 635471 [PMID: 33717181 DOI: 10.3389/fimmu.2021.635471]

33 **Zhou D**, Wang Q, Liu H. Coronavirus disease 2019 and the gut-lung axis. *Int J Infect Dis* 2021; **113**: 300-307 [PMID: 34517046 DOI: 10.1016/j.ijid.2021.09.013]

34 **Johnson SD**, Olwenyi OA, Bhyravbhatla N, Thurman M, Pandey K, Klug EA, Johnston M, Dyavar SR, Acharya A, Podany AT, Fletcher CV, Mohan M, Singh K, Byrareddy SN. Therapeutic implications of SARS-CoV-2 dysregulation of the gut-brain-lung axis. *World J Gastroenterol* 2021; **27**: 4763-4783 [PMID: 34447225 DOI: 10.3748/wjg.v27.i29.4763]

35 **Redd WD**, Zhou JC, Hathorn KE, McCarty TR, Bazarbashi AN, Thompson CC, Shen L, Chan WW. Prevalence and Characteristics of Gastrointestinal Symptoms in Patients With Severe Acute Respiratory Syndrome Coronavirus 2 Infection in the United States: A Multicenter Cohort Study. *Gastroenterology* 2020; **159**: 765-767.e2 [PMID: 32333911 DOI: 10.1053/j.gastro.2020.04.045]

36 **Pan L**, Mu M, Yang P, Sun Y, Wang R, Yan J, Li P, Hu B, Wang J, Hu C, Jin Y, Niu X, Ping R, Du Y, Li T, Xu G, Hu Q, Tu L. Clinical Characteristics of COVID-19 Patients With Digestive Symptoms in Hubei, China: A Descriptive, Cross-Sectional, Multicenter Study. *Am J Gastroenterol* 2020; **115**: 766-773 [PMID: 32287140 DOI: 10.14309/ajg.0000000000000620]

37 **Guan W-j**, Ni Z-y, Hu Y, Liang W-h, Ou C-q, He J-x, Liu L, Shan H, Lei C-l, Hui DS. Clinical characteristics of coronavirus disease 2019 in China. *New Engl J of Med* 2020; **382** (18): 1708-1720

38 **Yeoh YK**, Zuo T, Lui GC, Zhang F, Liu Q, Li AY, Chung AC, Cheung CP, Tso EY, Fung KS, Chan V, Ling L, Joynt G, Hui DS, Chow KM, Ng SSS, Li TC, Ng RW, Yip TC, Wong GL, Chan FK, Wong CK, Chan PK, Ng SC. Gut microbiota composition reflects disease severity and dysfunctional immune responses in patients with COVID-19. *Gut* 2021; **70**: 698-706 [PMID: 33431578 DOI: 10.1136/gutjnl-2020-323020]

39 **Shi J**, Sun J, Hu Y. Enteric involvement of SARS-CoV-2: Implications for the COVID-19 management, transmission, and infection control. *Virulence* 2020; **11**: 941-944 [PMID: 32715925 DOI: 10.1080/21505594.2020.1794410]

40 **Villapol S**. Gastrointestinal symptoms associated with COVID-19: impact on the gut microbiome. *Transl Res* 2020; **226**: 57-69 [PMID: 32827705 DOI: 10.1016/j.trsl.2020.08.004]

41 **Kaźmierczak-Siedlecka K**, Vitale E, Makarewicz W. COVID-19 -gastrointestinal and gut microbiota-related aspects. *Eur Rev Med Pharmacol Sci* 2020; **24**: 10853-10859 [PMID: 33155247 DOI: 10.26355/eurrev_202010_23448]

42 **Zhang T**, Cui X, Zhao X, Wang J, Zheng J, Zheng G, Guo W, Cai C, He S, Xu Y. Detectable SARS-CoV-2 viral RNA in feces of three children during recovery period of COVID-19 pneumonia. *J Med Virol* 2020; **92**: 909-914 [PMID: 32222992 DOI: 10.1002/jmv.25795]

43 **Chen Y**, Chen L, Deng Q, Zhang G, Wu K, Ni L, Yang Y, Liu B, Wang W, Wei C, Yang J, Ye G, Cheng Z. The presence of SARS-CoV-2 RNA in the feces of COVID-19 patients. *J Med Virol* 2020; **92**: 833-840 [PMID: 32243607 DOI: 10.1002/jmv.25825]

44 **Wölfel R**, Corman VM, Guggemos W, Seilmaier M, Zange S, Müller MA, Niemeyer D, Jones TC, Vollmar P, Rothe C, Hoelscher M, Bleicker T, Brünink S, Schneider J, Ehmann R, Zwirglmaier K, Drosten C, Wendtner C. Virological assessment of hospitalized patients with COVID-2019. *Nature* 2020; **581**: 465-469 [PMID: 32235945 DOI: 10.1038/s41586-020-2196-x]

45 **Kevadiya BD**, Machhi J, Herskovitz J, Oleynikov MD, Blomberg WR, Bajwa N, Soni D, Das S, Hasan M, Patel M,

Senan AM, Gorantla S, McMillan J, Edagwa B, Eisenberg R, Gurumurthy CB, Reid SPM, Punyadeera C, Chang L, Gendelman HE. Diagnostics for SARS-CoV-2 infections. *Nat Mater* 2021; **20**: 593-605 [PMID: 33589798 DOI: 10.1038/s41563-020-00906-z]

46 **Huang C**, Wang Y, Li X, Ren L, Zhao J, Hu Y, Zhang L, Fan G, Xu J, Gu X, Cheng Z, Yu T, Xia J, Wei Y, Wu W, Xie X, Yin W, Li H, Liu M, Xiao Y, Gao H, Guo L, Xie J, Wang G, Jiang R, Gao Z, Jin Q, Wang J, Cao B. Clinical features of patients infected with 2019 novel coronavirus in Wuhan, China. *Lancet* 2020; **395**: 497-506 [PMID: 31986264 DOI: 10.1016/S0140-6736(20)30183-5]

47 **Zuo T**, Liu Q, Zhang F, Yeoh YK, Wan Y, Zhan H, Lui GCY, Chen Z, Li AYL, Cheung CP, Chen N, Lv W, Ng RWY, Tso EYK, Fung KSC, Chan V, Ling L, Joynt G, Hui DSC, Chan FKL, Chan PKS, Ng SC. Temporal landscape of human gut RNA and DNA virome in SARS-CoV-2 infection and severity. *Microbiome* 2021; **9**: 91 [PMID: 33853691 DOI: 10.1186/s40168-021-01008-x]

48 **Zuo T**, Zhan H, Zhang F, Liu Q, Tso EYK, Lui GCY, Chen N, Li A, Lu W, Chan FKL, Chan PKS, Ng SC. Alterations in Fecal Fungal Microbiome of Patients With COVID-19 During Time of Hospitalization until Discharge. *Gastroenterology* 2020; **159**: 1302-1310.e5 [PMID: 32598884 DOI: 10.1053/j.gastro.2020.06.048]

49 **Zuo T**, Zhang F, Lui GCY, Yeoh YK, Li AYL, Zhan H, Wan Y, Chung ACK, Cheung CP, Chen N, Lai CKC, Chen Z, Tso EYK, Fung KSC, Chan V, Ling L, Joynt G, Hui DSC, Chan FKL, Chan PKS, Ng SC. Alterations in Gut Microbiota of Patients With COVID-19 During Time of Hospitalization. *Gastroenterology* 2020; **159**: 944-955.e8 [PMID: 32442562 DOI: 10.1053/j.gastro.2020.05.048]

50 **Newsome RC**, Gauthier J, Hernandez MC, Abraham GE, Robinson TO, Williams HB, Sloan M, Owings A, Laird H, Christian T, Pride Y, Wilson KJ, Hasan M, Parker A, Senitko M, Glover SC, Gharaibeh RZ, Jobin C. The gut microbiome of COVID-19 recovered patients returns to uninfected status in a minority-dominated United States cohort. *Gut Microbes* 2021; **13**: 1-15 [PMID: 34100340 DOI: 10.1080/19490976.2021.1926840]

51 **Khan M**, Mathew BJ, Gupta P, Garg G, Khadanga S, Vyas AK, Singh AK. Gut Dysbiosis and IL-21 Response in Patients with Severe COVID-19. *Microorganisms* 2021; **9** [PMID: 34199203 DOI: 10.3390/microorganisms9061292]

52 **Magalhães NS**, Savino W, Silva PMR, Martins MA, Carvalho VF. Gut Microbiota Dysbiosis Is a Crucial Player for the Poor Outcomes for COVID-19 in Elderly, Diabetic and Hypertensive Patients. *Front Med (Lausanne)* 2021; **8**: 644751 [PMID: 34458281 DOI: 10.3389/fmed.2021.644751]

53 **Hung YP**, Lee CC, Lee JC, Tsai PJ, Ko WC. Gut Dysbiosis during COVID-19 and Potential Effect of Probiotics. *Microorganisms* 2021; **9** [PMID: 34442684 DOI: 10.3390/microorganisms9081605]

54 **Zuo T**, Liu Q, Zhang F, Lui GC, Tso EY, Yeoh YK, Chen Z, Boon SS, Chan FK, Chan PK, Ng SC. Depicting SARS-CoV-2 faecal viral activity in association with gut microbiota composition in patients with COVID-19. *Gut* 2021; **70**: 276-284 [PMID: 32690600 DOI: 10.1136/gutjnl-2020-322294]

55 **Sokol H**, Contreras V, Maisonnasse P, Desmons A, Delache B, Sencio V, Machelart A, Brisebarre A, Humbert L, Deryuter L, Gauliard E, Heumel S, Rainteau D, Dereuddre-Bosquet N, Menu E, Ho Tsong Fang R, Lamaziere A, Brot L, Wahl C, Oeuvray C, Rolhion N, Van Der Werf S, Ferreira S, Le Grand R, Trottein F. SARS-CoV-2 infection in nonhuman primates alters the composition and functional activity of the gut microbiota. *Gut Microbes* 2021; **13**: 1-19 [PMID: 33685349 DOI: 10.1080/19490976.2021.1893113]

56 **Zhang F**, Wan Y, Zuo T, Yeoh YK, Liu Q, Zhang L, Zhan H, Lu W, Xu W, Lui GCY, Li AYL, Cheung CP, Wong CK, Chan PKS, Chan FKL, Ng SC. Prolonged Impairment of Short-Chain Fatty Acid and L-Isoleucine Biosynthesis in Gut Microbiome in Patients With COVID-19. *Gastroenterology* 2022; **162**: 548-561.e4 [PMID: 34687739 DOI: 10.1053/j.gastro.2021.10.013]

57 **Shang J**, Ye G, Shi K, Wan Y, Luo C, Aihara H, Geng Q, Auerbach A, Li F. Structural basis of receptor recognition by SARS-CoV-2. *Nature* 2020; **581**: 221-224 [PMID: 32225175 DOI: 10.1038/s41586-020-2179-y]

58 **Chakraborty C**, Sharma AR, Mallick B, Bhattacharya M, Sharma G, Lee SS. Evaluation of molecular interaction, physicochemical parameters and conserved pattern of SARS-CoV-2 Spike RBD and hACE2: in silico and molecular dynamics approach. *Eur Rev Med Pharmacol Sci* 2021; **25**: 1708-1723 [PMID: 33629340 DOI: 10.26355/eurrev_202102_24881]

59 **Verdecchia P**, Cavallini C, Spanevello A, Angeli F. The pivotal link between ACE2 deficiency and SARS-CoV-2 infection. *Eur J Intern Med* 2020; **76**: 14-20 [PMID: 32336612 DOI: 10.1016/j.ejim.2020.04.037]

60 **Sungnak W**, Huang N, Bécavin C, Berg M, Queen R, Litvinukova M, Talavera-López C, Maatz H, Reichart D, Sampaziotis F, Worlock KB, Yoshida M, Barnes JL; HCA Lung Biological Network. SARS-CoV-2 entry factors are highly expressed in nasal epithelial cells together with innate immune genes. *Nat Med* 2020; **26**: 681-687 [PMID: 32327758 DOI: 10.1038/s41591-020-0868-6]

61 **Hamming I**, Timens W, Bulthuis ML, Lely AT, Navis G, van Goor H. Tissue distribution of ACE2 protein, the functional receptor for SARS coronavirus. A first step in understanding SARS pathogenesis. *J Pathol* 2004; **203**: 631-637 [PMID: 15141377 DOI: 10.1002/path.1570]

62 **Sharma RK**, Oliveira AC, Yang T, Karas MM, Li J, Lobaton GO, Aquino VP, Robles-Vera I, de Kloet AD, Krause EG, Bryant AJ, Verma A, Li Q, Richards EM, Raizada MK. Gut Pathology and Its Rescue by ACE2 (Angiotensin-Converting Enzyme 2) in Hypoxia-Induced Pulmonary Hypertension. *Hypertension* 2020; **76**: 206-216 [PMID: 32418496 DOI: 10.1161/HYPERTENSIONAHA.120.14931]

63 **Koester ST**, Li N, Lachance DM, Morella NM, Dey N. Variability in digestive and respiratory tract Ace2 expression is associated with the microbiome. *PLoS One* 2021; **16**: e0248730 [PMID: 33725024 DOI: 10.1371/journal.pone.0248730]

64 **Geva-Zatorsky N**, Sefik E, Kua L, Pasman L, Tan TG, Ortiz-Lopez A, Yanortsang TB, Yang L, Jupp R, Mathis D, Benoist C, Kasper DL. Mining the Human Gut Microbiota for Immunomodulatory Organisms. *Cell* 2017; **168**: 928-943.e11 [PMID: 28215708 DOI: 10.1016/j.cell.2017.01.022]

65 **Penninger JM**, Grant MB, Sung JJY. The Role of Angiotensin Converting Enzyme 2 in Modulating Gut Microbiota, Intestinal Inflammation, and Coronavirus Infection. *Gastroenterology* 2021; **160**: 39-46 [PMID: 33130103 DOI: 10.1053/j.gastro.2020.07.067]

66 **Viana SD**, Nunes S, Reis F. ACE2 imbalance as a key player for the poor outcomes in COVID-19 patients with age-

related comorbidities -Role of gut microbiota dysbiosis. *Ageing Res Rev* 2020; **62**: 101123 [PMID: 32683039 DOI: 10.1016/j.arr.2020.101123]

67 **Budden KF**, Gellatly SL, Wood DL, Cooper MA, Morrison M, Hugenholtz P, Hansbro PM. Emerging pathogenic links between microbiota and the gut-lung axis. *Nat Rev Microbiol* 2017; **15**: 55-63 [PMID: 27694885 DOI: 10.1038/nrmicro.2016.142]

68 **Dumas A**, Bernard L, Poquet Y, Lugo-Villarino G, Neyrolles O. The role of the lung microbiota and the gut-lung axis in respiratory infectious diseases. *Cell Microbiol* 2018; **20**: e12966 [PMID: 30329198 DOI: 10.1111/cmi.12966]

69 **Enaud R**, Prevel R, Ciarlo E, Beaufils F, Wieërs G, Guery B, Delhaes L. The Gut-Lung Axis in Health and Respiratory Diseases: A Place for Inter-Organ and Inter-Kingdom Crosstalks. *Front Cell Infect Microbiol* 2020; **10**: 9 [PMID: 32140452 DOI: 10.3389/fcimb.2020.00009]

70 **S A**, K G, A AM. Intermodulation of gut-lung axis microbiome and the implications of biotics to combat COVID-19. *J Biomol Struct Dyn* 2021; 1-17 [PMID: 34699326 DOI: 10.1080/07391102.2021.1994875]

71 **Aktas B**, Aslim B. Gut-lung axis and dysbiosis in COVID-19. *Turk J Biol* 2020; **44**: 265-272 [PMID: 32595361 DOI: 10.3906/biy-2005-102]

72 **Hernández-Terán A**, Mejía-Nepomuceno F, Herrera MT, Barreto O, García E, Castillejos M, Boukadida C, Matias-Florentino M, Rincón-Rubio A, Avila-Rios S, Mújica-Sánchez M, Serna-Muñoz R, Becerril-Vargas E, Guadarrama-Pérez C, Ahumada-Topete VH, Rodríguez-Llamazares S, Martínez-Orozco JA, Salas-Hernández J, Pérez-Padilla R, Vázquez-Pérez JA. Dysbiosis and structural disruption of the respiratory microbiota in COVID-19 patients with severe and fatal outcomes. *Sci Rep* 2021; **11**: 21297 [PMID: 34716394 DOI: 10.1038/s41598-021-00851-0]

73 **Zhu X**, Han Y, Du J, Liu R, Jin K, Yi W. Microbiota-gut-brain axis and the central nervous system. *Oncotarget* 2017; **8**: 53829-53838 [PMID: 28881854 DOI: 10.18632/oncotarget.17754]

74 **Morais LH**, Schreiber HL 4th, Mazmanian SK. The gut microbiota-brain axis in behaviour and brain disorders. *Nat Rev Microbiol* 2021; **19**: 241-255 [PMID: 33093662 DOI: 10.1038/s41579-020-00460-0]

75 **Mayer EA**. Gut feelings: the emerging biology of gut-brain communication. *Nat Rev Neurosci* 2011; **12**: 453-466 [PMID: 21750565 DOI: 10.1038/nrn3071]

76 **Taché Y**, Saavedra JM. Introduction to the Special Issue "The Brain-Gut Axis". *Cell Mol Neurobiol* 2022; **42**: 311-313 [PMID: 34652580 DOI: 10.1007/s10571-021-01155-7]

77 **Dogra N**, Mani RJ, Katare DP. The Gut-Brain Axis: Two Ways Signaling in Parkinson's Disease. *Cell Mol Neurobiol* 2022; **42**: 315-332 [PMID: 33649989 DOI: 10.1007/s10571-021-01066-7]

78 **Manosso LM**, Arent CO, Borba LA, Ceretta LB, Quevedo J, Réus GZ. Microbiota-Gut-Brain Communication in the SARS-CoV-2 Infection. *Cells* 2021; **10** [PMID: 34440767 DOI: 10.3390/cells10081993]

79 **Strandwitz P**. Neurotransmitter modulation by the gut microbiota. *Brain Res* 2018; **1693**: 128-133 [PMID: 29903615 DOI: 10.1016/j.brainres.2018.03.015]

80 **O'Donnell MP**, Fox BW, Chao PH, Schroeder FC, Sengupta P. A neurotransmitter produced by gut bacteria modulates host sensory behaviour. *Nature* 2020; **583**: 415-420 [PMID: 32555456 DOI: 10.1038/s41586-020-2395-5]

81 **Mittal R**, Debs LH, Patel AP, Nguyen D, Patel K, O'Connor G, Grati M, Mittal J, Yan D, Eshraghi AA, Deo SK, Daunert S, Liu XZ. Neurotransmitters: The Critical Modulators Regulating Gut-Brain Axis. *J Cell Physiol* 2017; **232**: 2359-2372 [PMID: 27512962 DOI: 10.1002/jcp.25518]

82 **Konturek PC**, Brzozowski T, Konturek SJ. Stress and the gut: pathophysiology, clinical consequences, diagnostic approach and treatment options. *J Physiol Pharmacol* 2011; **62**: 591-599 [PMID: 22314561]

83 **Vodička M**, Ergang P, Hrnčíř T, Mikulecká A, Kvapilová P, Vagnerová K, Šestáková B, Fajstová A, Hermanová P, Hudcovic T, Kozáková H, Pácha J. Microbiota affects the expression of genes involved in HPA axis regulation and local metabolism of glucocorticoids in chronic psychosocial stress. *Brain Behav Immun* 2018; **73**: 615-624 [PMID: 29990567 DOI: 10.1016/j.bbi.2018.07.007]

84 **Ojeda J**, Ávila A, Vidal PM. Gut Microbiota Interaction with the Central Nervous System throughout Life. *J Clin Med* 2021; **10** [PMID: 33801153 DOI: 10.3390/jcm10061299]

85 **Zheng D**, Liwinski T, Elinav E. Interaction between microbiota and immunity in health and disease. *Cell Res* 2020; **30**: 492-506 [PMID: 32433595 DOI: 10.1038/s41422-020-0332-7]

86 **Cerf-Bensussan N**, Gaboriau-Routhiau V. The immune system and the gut microbiota: friends or foes? *Nat Rev Immunol* 2010; **10**: 735-744 [PMID: 20865020 DOI: 10.1038/nri2850]

87 **Xu K**, Cai H, Shen Y, Ni Q, Chen Y, Hu S, Li J, Wang H, Yu L, Huang H, Qiu Y, Wei G, Fang Q, Zhou J, Sheng J, Liang T, Li L. [Management of COVID-19: the Zhejiang experience]. *Zhejiang Da Xue Xue Bao Yi Xue Ban* 2020; **49**: 147-157 [PMID: 32391658 DOI: 10.3785/j.issn.1008-9292.2020.02.02]

88 **Jahani M**, Dokaneheifard S, Mansouri K. Hypoxia: A key feature of COVID-19 launching activation of HIF-1 and cytokine storm. *J Inflamm (Lond)* 2020; **17**: 33 [PMID: 33139969 DOI: 10.1186/s12950-020-00263-3]

89 **Rahman A**, Tabassum T, Araf Y, Al Nahid A, Ullah MA, Hosen MJ. Silent hypoxia in COVID-19: pathomechanism and possible management strategy. *Mol Biol Rep* 2021; **48**: 3863-3869 [PMID: 33891272 DOI: 10.1007/s11033-021-06358-1]

90 **Tian M**, Liu W, Li X, Zhao P, Shereen MA, Zhu C, Huang S, Liu S, Yu X, Yue M, Pan P, Wang W, Li Y, Chen X, Wu K, Luo Z, Zhang Q, Wu J. HIF-1α promotes SARS-CoV-2 infection and aggravates inflammatory responses to COVID-19. *Signal Transduct Target Ther* 2021; **6**: 308 [PMID: 34408131 DOI: 10.1038/s41392-021-00726-w]

91 **Gopal AB**, Chakraborty S, Padhan PK, Barik A, Dixit P, Chakraborty D, Poirah I, Samal S, Sarkar A, Bhattacharyya A. Silent hypoxia in COVID-19: a gut microbiota connection. *Curr Opin Physiol* 2021; **23**: 100456 [PMID: 34250324 DOI: 10.1016/j.cophys.2021.06.010]

92 **Belkaid Y**, Hand TW. Role of the microbiota in immunity and inflammation. *Cell* 2014; **157**: 121-141 [PMID: 24679531 DOI: 10.1016/j.cell.2014.03.011]

93 **von Rosenvinge EC**, O'May GA, Macfarlane S, Macfarlane GT, Shirtliff ME. Microbial biofilms and gastrointestinal diseases. *Pathog Dis* 2013; **67**: 25-38 [PMID: 23620117 DOI: 10.1111/2049-632X.12020]

94 **Ríos-Covián D**, Ruas-Madiedo P, Margolles A, Gueimonde M, de Los Reyes-Gavilán CG, Salazar N. Intestinal Short

Chain Fatty Acids and their Link with Diet and Human Health. *Front Microbiol* 2016; **7**: 185 [PMID: 26925050 DOI: 10.3389/fmicb.2016.00185]

95 **Parada Venegas D**, De la Fuente MK, Landskron G, González MJ, Quera R, Dijkstra G, Harmsen HJM, Faber KN, Hermoso MA. Short Chain Fatty Acids (SCFAs)-Mediated Gut Epithelial and Immune Regulation and Its Relevance for Inflammatory Bowel Diseases. *Front Immunol* 2019; **10**: 277 [PMID: 30915065 DOI: 10.3389/fimmu.2019.00277]

96 **Odenwald MA**, Turner JR. The intestinal epithelial barrier: a therapeutic target? *Nat Rev Gastroenterol Hepatol* 2017; **14**: 9-21 [PMID: 27848962 DOI: 10.1038/nrgastro.2016.169]

97 **Kim HS**. Do an Altered Gut Microbiota and an Associated Leaky Gut Affect COVID-19 Severity? *mBio* 2021; **12** [PMID: 33436436 DOI: 10.1128/mBio.03022-20]

98 **Inan MS**, Rasoulpour RJ, Yin L, Hubbard AK, Rosenberg DW, Giardina C. The luminal short-chain fatty acid butyrate modulates NF-kappaB activity in a human colonic epithelial cell line. *Gastroenterology* 2000; **118**: 724-734 [PMID: 10734024 DOI: 10.1016/s0016-5085(00)70142-9]

99 **Maslowski KM**, Vieira AT, Ng A, Kranich J, Sierro F, Yu D, Schilter HC, Rolph MS, Mackay F, Artis D, Xavier RJ, Teixeira MM, Mackay CR. Regulation of inflammatory responses by gut microbiota and chemoattractant receptor GPR43. *Nature* 2009; **461**: 1282-1286 [PMID: 19865172 DOI: 10.1038/nature08530]

100 **Samuel BS**, Shaito A, Motoike T, Rey FE, Backhed F, Manchester JK, Hammer RE, Williams SC, Crowley J, Yanagisawa M, Gordon JI. Effects of the gut microbiota on host adiposity are modulated by the short-chain fatty-acid binding G protein-coupled receptor, Gpr41. *Proc Natl Acad Sci U S A* 2008; **105**: 16767-16772 [PMID: 18931303 DOI: 10.1073/pnas.0808567105]

101 **Atarashi K**, Tanoue T, Oshima K, Suda W, Nagano Y, Nishikawa H, Fukuda S, Saito T, Narushima S, Hase K, Kim S, Fritz JV, Wilmes P, Ueha S, Matsushima K, Ohno H, Olle B, Sakaguchi S, Taniguchi T, Morita H, Hattori M, Honda K. Treg induction by a rationally selected mixture of Clostridia strains from the human microbiota. *Nature* 2013; **500**: 232-236 [PMID: 23842501 DOI: 10.1038/nature12331]

102 **Chhibber-Goel J**, Gopinathan S, Sharma A. Interplay between severities of COVID-19 and the gut microbiome: implications of bacterial co-infections? *Gut Pathog* 2021; **13**: 14 [PMID: 33632296 DOI: 10.1186/s13099-021-00407-7]

103 **Kany S**, Vollrath JT, Relja B. Cytokines in Inflammatory Disease. *Int J Mol Sci* 2019; **20** [PMID: 31795299 DOI: 10.3390/ijms20236008]

104 **Chen Y**, Gu S, Chen Y, Lu H, Shi D, Guo J, Wu WR, Yang Y, Li Y, Xu KJ, Ding C, Luo R, Huang C, Yu L, Xu M, Yi P, Liu J, Tao JJ, Zhang H, Lv L, Wang B, Sheng J, Li L. Six-month follow-up of gut microbiota richness in patients with COVID-19. *Gut* 2022; **71**: 222-225 [PMID: 33833065 DOI: 10.1136/gutjnl-2021-324090]

105 **Ceccarelli G**, Borrazzo C, Pinacchio C, Santinelli L, Innocenti GP, Cavallari EN, Celani L, Marazzato M, Alessandri F, Ruberto F, Pugliese F, Venditti M, Mastroianni CM, d'Ettorre G. Oral Bacteriotherapy in Patients With COVID-19: A Retrospective Cohort Study. *Front Nutr* 2020; **7**: 613928 [PMID: 33505983 DOI: 10.3389/fnut.2020.613928]

106 **Rao KS**, Suryaprakash V, Senthilkumar R, Preethy S, Katoh S, Ikewaki N, Abraham SJK. Role of Immune Dysregulation in Increased Mortality Among a Specific Subset of COVID-19 Patients and Immune-Enhancement Strategies for Combatting Through Nutritional Supplements. *Front Immunol* 2020; **11**: 1548 [PMID: 32733487 DOI: 10.3389/fimmu.2020.01548]

107 **Al-Hadidi SH**, Alhussain H, Abdel Hadi H, Johar A, Yassine HM, Al Thani AA, Eltai NO. The Spectrum of Antibiotic Prescribing During COVID-19 Pandemic: A Systematic Literature Review. *Microb Drug Resist* 2021; **27**: 1705-1725 [PMID: 34077290 DOI: 10.1089/mdr.2020.0619]

108 **Ramirez J**, Guarner F, Bustos Fernandez L, Maruy A, Sdepanian VL, Cohen H. Antibiotics as Major Disruptors of Gut Microbiota. *Front Cell Infect Microbiol* 2020; **10**: 572912 [PMID: 33330122 DOI: 10.3389/fcimb.2020.572912]

109 **Chattopadhyay I**, Shankar EM. SARS-CoV-2-Indigenous Microbiota Nexus: Does Gut Microbiota Contribute to Inflammation and Disease Severity in COVID-19? *Front Cell Infect Microbiol* 2021; **11**: 590874 [PMID: 33791231 DOI: 10.3389/fcimb.2021.590874]

110 **Rafiqul Islam SM**, Foysal MJ, Hoque MN, Mehedi HMH, Rob MA, Salauddin A, Tanzina AY, Biswas S, Noyon SH, Siddiki AMAMZ, Tay A, Mannan A. Dysbiosis of Oral and Gut Microbiomes in SARS-CoV-2 Infected Patients in Bangladesh: Elucidating the Role of Opportunistic Gut Microbes. *Front Med (Lausanne)* 2022; **9**: 821777 [PMID: 35237631 DOI: 10.3389/fmed.2022.821777]

111 **Baud D**, Dimopoulou Agri V, Gibson GR, Reid G, Giannoni E. Using Probiotics to Flatten the Curve of Coronavirus Disease COVID-2019 Pandemic. *Front Public Health* 2020; **8**: 186 [PMID: 32574290 DOI: 10.3389/fpubh.2020.00186]

112 **Xia Y**, Cao J, Wang M, Lu M, Chen G, Gao F, Liu Z, Zhang D, Ke X, Yi M. Effects of Lactococcus lactis subsp. lactis JCM5805 on colonization dynamics of gut microbiota and regulation of immunity in early ontogenetic stages of tilapia. *Fish Shellfish Immunol* 2019; **86**: 53-63 [PMID: 30428393 DOI: 10.1016/j.fsi.2018.11.022]

113 **Mak JW**, Chan FK, Ng SC. Probiotics and COVID-19-Authors' reply. *Lancet Gastroenterol Hepatol* 2020; **5** (8): 722-723

114 **Bhattacharya M**, Sharma AR, Mallick B, Sharma G, Lee SS, Chakraborty C. Immunoinformatics approach to understand molecular interaction between multi-epitopic regions of SARS-CoV-2 spike-protein with TLR4/MD-2 complex. *Infect Genet Evol* 2020; **85**: 104587 [PMID: 33039603 DOI: 10.1016/j.meegid.2020.104587]

115 **Petruk G**, Puthia M, Petrlova J, Samsudin F, Strömdahl AC, Cerps S, Uller L, Kjellström S, Bond PJ, Schmidtchen AA. SARS-CoV-2 spike protein binds to bacterial lipopolysaccharide and boosts proinflammatory activity. *J Mol Cell Biol* 2020; **12**: 916-932 [PMID: 33295606 DOI: 10.1093/jmcb/mjaa067]

116 **Chakraborty C**, Sharma AR, Bhattacharya M, Sharma G, Lee SS, Agoramoorthy G. Consider TLR5 for new therapeutic development against COVID-19. *J Med Virol* 2020; **92**: 2314-2315 [PMID: 32391920 DOI: 10.1002/jmv.25997]

117 **Haran JP**, Pinero JC, Zheng Y, Palma NA, Wingertzahn M. Virtualized clinical studies to assess the natural history and impact of gut microbiome modulation in non-hospitalized patients with mild to moderate COVID-19 a randomized, open-label, prospective study with a parallel group study evaluating the physiologic effects of KB109 on gut microbiota structure and function: a structured summary of a study protocol for a randomized controlled study. *Trials* 2021; **22**: 245 [PMID: 33810796 DOI: 10.1186/s13063-021-05157-0]

118 **van der Lelie D**, Taghavi S. COVID-19 and the Gut Microbiome: More than a Gut Feeling. *mSystems* 2020; **5** [PMID: 32694127 DOI: 10.1128/mSystems.00453-20]

119 **Buffie CG**, Pamer EG. Microbiota-mediated colonization resistance against intestinal pathogens. *Nat Rev Immunol* 2013; **13**: 790-801 [PMID: 24096337 DOI: 10.1038/nri3535]

120 **Vignesh R**, Swathirajan CR, Tun ZH, Rameshkumar MR, Solomon SS, Balakrishnan P. Could Perturbation of Gut Microbiota Possibly Exacerbate the Severity of COVID-19 *via* Cytokine Storm? *Front Immunol* 2020; **11**: 607734 [PMID: 33569053 DOI: 10.3389/fimmu.2020.607734]

121 **Zhou F**, Yu T, Du R, Fan G, Liu Y, Liu Z, Xiang J, Wang Y, Song B, Gu X, Guan L, Wei Y, Li H, Wu X, Xu J, Tu S, Zhang Y, Chen H, Cao B. Clinical course and risk factors for mortality of adult inpatients with COVID-19 in Wuhan, China: a retrospective cohort study. *Lancet* 2020; **395**: 1054-1062 [PMID: 32171076 DOI: 10.1016/S0140-6736(20)30566-3]

122 **Lu X**, Zhang L, Du H, Zhang J, Li YY, Qu J, Zhang W, Wang Y, Bao S, Li Y. SARS-CoV-2 infection in children. *New Engl J of Med* 2020; **382** (17): 1663-1665

123 **Zhang JJ**, Dong X, Cao YY, Yuan YD, Yang YB, Yan YQ, Akdis CA, Gao YD. Clinical characteristics of 140 patients infected with SARS-CoV-2 in Wuhan, China. *Allergy* 2020; **75**: 1730-1741 [PMID: 32077115 DOI: 10.1111/all.14238]

124 **Xiao F**, Tang M, Zheng X, Liu Y, Li X, Shan H. Evidence for Gastrointestinal Infection of SARS-CoV-2. *Gastroenterology* 2020; **158**: 1831-1833.e3 [PMID: 32142773 DOI: 10.1053/j.gastro.2020.02.055]

125 **Yang X**, Yu Y, Xu J, Shu H, Xia J, Liu H, Wu Y, Zhang L, Yu Z, Fang M, Yu T, Wang Y, Pan S, Zou X, Yuan S, Shang Y. Clinical course and outcomes of critically ill patients with SARS-CoV-2 pneumonia in Wuhan, China: a single-centered, retrospective, observational study. *Lancet Respir Med* 2020; **8**: 475-481 [PMID: 32105632 DOI: 10.1016/S2213-2600(20)30079-5]

126 **Wang D**, Hu B, Hu C, Zhu F, Liu X, Zhang J, Wang B, Xiang H, Cheng Z, Xiong Y, Zhao Y, Li Y, Wang X, Peng Z. Clinical Characteristics of 138 Hospitalized Patients With 2019 Novel Coronavirus-Infected Pneumonia in Wuhan, China. *JAMA* 2020; **323**: 1061-1069 [PMID: 32031570 DOI: 10.1001/jama.2020.1585]

127 **Xu XW**, Wu XX, Jiang XG, Xu KJ, Ying LJ, Ma CL, Li SB, Wang HY, Zhang S, Gao HN, Sheng JF, Cai HL, Qiu YQ, Li LJ. Clinical findings in a group of patients infected with the 2019 novel coronavirus (SARS-Cov-2) outside of Wuhan, China: retrospective case series. *BMJ* 2020; **368**: m606 [PMID: 32075786 DOI: 10.1136/bmj.m606]

128 **Liu K**, Fang YY, Deng Y, Liu W, Wang MF, Ma JP, Xiao W, Wang YN, Zhong MH, Li CH, Li GC, Liu HG. Clinical characteristics of novel coronavirus cases in tertiary hospitals in Hubei Province. *Chin Med J (Engl)* 2020; **133**: 1025-1031 [PMID: 32044814 DOI: 10.1097/CM9.0000000000000744]

129 **Shi H**, Han X, Jiang N, Cao Y, Alwalid O, Gu J, Fan Y, Zheng C. Radiological findings from 81 patients with COVID-19 pneumonia in Wuhan, China: a descriptive study. *Lancet Infect Dis* 2020; **20**: 425-434 [PMID: 32105637 DOI: 10.1016/S1473-3099(20)30086-4]

130 **Chen N**, Zhou M, Dong X, Qu J, Gong F, Han Y, Qiu Y, Wang J, Liu Y, Wei Y, Xia J, Yu T, Zhang X, Zhang L. Epidemiological and clinical characteristics of 99 cases of 2019 novel coronavirus pneumonia in Wuhan, China: a descriptive study. *Lancet* 2020; **395**: 507-513 [PMID: 32007143 DOI: 10.1016/S0140-6736(20)30211-7]

131 **Wang W**, Xu Y, Gao R, Lu R, Han K, Wu G, Tan W. Detection of SARS-CoV-2 in Different Types of Clinical Specimens. *JAMA* 2020; **323**: 1843-1844 [PMID: 32159775 DOI: 10.1001/jama.2020.3786]

132 **Zhang J**, Wang S, Xue Y. Fecal specimen diagnosis 2019 novel coronavirus-infected pneumonia. *J Med Virol* 2020; **92**: 680-682 [PMID: 32124995 DOI: 10.1002/jmv.25742]

133 **Ling Y**, Xu SB, Lin YX, Tian D, Zhu ZQ, Dai FH, Wu F, Song ZG, Huang W, Chen J, Hu BJ, Wang S, Mao EQ, Zhu L, Zhang WH, Lu HZ. Persistence and clearance of viral RNA in 2019 novel coronavirus disease rehabilitation patients. *Chin Med J (Engl)* 2020; **133**: 1039-1043 [PMID: 32118639 DOI: 10.1097/CM9.0000000000000774]

134 **Young BE**, Ong SWX, Kalimuddin S, Low JG, Tan SY, Loh J, Ng OT, Marimuthu K, Ang LW, Mak TM, Lau SK, Anderson DE, Chan KS, Tan TY, Ng TY, Cui L, Said Z, Kurupatham L, Chen MI, Chan M, Vasoo S, Wang LF, Tan BH, Lin RTP, Lee VJM, Leo YS, Lye DC; Singapore 2019 Novel Coronavirus Outbreak Research Team. Epidemiologic Features and Clinical Course of Patients Infected With SARS-CoV-2 in Singapore. *JAMA* 2020; **323**: 1488-1494 [PMID: 32125362 DOI: 10.1001/jama.2020.3204]

135 **Wu Y**, Guo C, Tang L, Hong Z, Zhou J, Dong X, Yin H, Xiao Q, Tang Y, Qu X, Kuang L, Fang X, Mishra N, Lu J, Shan H, Jiang G, Huang X. Prolonged presence of SARS-CoV-2 viral RNA in faecal samples. *Lancet Gastroenterol Hepatol* 2020; **5**: 434-435 [PMID: 32199469 DOI: 10.1016/S2468-1253(20)30083-2]

136 **Peng L**, Liu J, Xu W, Luo Q, Chen D, Lei Z, Huang Z, Li X, Deng K, Lin B, Gao Z. SARS-CoV-2 can be detected in urine, blood, anal swabs, and oropharyngeal swabs specimens. *J Med Virol* 2020; **92**: 1676-1680 [PMID: 32330305 DOI: 10.1002/jmv.25936]

137 **Wu Y**, Cheng X, Jiang G, Tang H, Ming S, Tang L, Lu J, Guo C, Shan H, Huang X. Altered oral and gut microbiota and its association with SARS-CoV-2 viral load in COVID-19 patients during hospitalization. *NPJ Biofilms Microbiomes* 2021; **7**: 61 [PMID: 34294722 DOI: 10.1038/s41522-021-00232-5]

World Journal of Gastroenterology

Submit a Manuscript: https://www.f6publishing.com

World J Gastroenterol 2022 July 7; 28(25): 2823-2842

DOI: 10.3748/wjg.v28.i25.2823

ISSN 1007-9327 (print) ISSN 2219-2840 (online)

REVIEW

Long noncoding RNAs in hepatitis B virus replication and oncogenesis

Hui-Chun Li, Chee-Hing Yang, Shih-Yen Lo

Specialty type: Gastroenterology and hepatology

Provenance and peer review: Invited article; Externally peer reviewed.

Peer-review model: Single blind

Peer-review report's scientific quality classification

Grade A (Excellent): 0
Grade B (Very good): B, B
Grade C (Good): 0
Grade D (Fair): 0
Grade E (Poor): 0

P-Reviewer: Elfayoumy KN, Egypt; Ghazy A, Egypt
A-Editor: Yao QG, China

Received: January 16, 2022
Peer-review started: January 16, 2022
First decision: April 11, 2022
Revised: April 16, 2022
Accepted: May 21, 2022
Article in press: May 21, 2022
Published online: July 7, 2022

Hui-Chun Li, Department of Biochemistry, Tzu Chi University, Hualien 97004, Taiwan

Chee-Hing Yang, Shih-Yen Lo, Department of Laboratory Medicine and Biotechnology, Tzu Chi University, Hualien 97004, Taiwan

Shih-Yen Lo, Department of Laboratory Medicine, Buddhist Tzu Chi General Hospital, Hualien 97004, Taiwan

Corresponding author: Shih-Yen Lo, PhD, Professor, Department of Laboratory Medicine and Biotechnology, Tzu Chi University, No. 701 Section 3, Chung Yang Road, Hualien 97004, Taiwan. losylo@mail.tcu.edu.tw

Abstract

Several diverse long noncoding RNAs (lncRNAs) have been identified to be involved in hepatitis B virus (HBV) replication and oncogenesis, especially those dysregulated in HBV-related hepatocellular carcinoma (HCC). Most of these dysregulated lncRNAs are modulated by the HBV X protein. The regulatory mechanisms of some lncRNAs in HBV replication and oncogenesis have been characterized. Genetic polymorphisms of several lncRNAs affecting HBV replication or oncogenesis have also been studied. The prognosis of HCC remains poor. It is important to identify novel tumor markers for early diagnosis and find more therapeutic targets for effective treatments of HCC. Some dysregulated lncRNAs in HBV-related HCC may become biomarkers for early diagnosis and/or the therapeutic targets of HCC. This mini-review summarizes these findings briefly, focusing on recent developments.

Key Words: Hepatitis B virus; Hepatocellular carcinoma; Long noncoding RNAs; Hepatitis B virus X protein; Biomarker

©The Author(s) 2022. Published by Baishideng Publishing Group Inc. All rights reserved.

Core Tip: The prognosis of hepatocellular carcinoma (HCC) remains poor. It is important to identify novel tumor markers for early diagnosis and find more therapeutic targets for effective treatments of HCC. Several diverse long noncoding RNAs (lncRNAs) have been identified to be involved in hepatitis B virus (HBV)-related HCC. A better understanding of the molecular mechanisms underlying lncRNA-mediated hepatocarcinogenesis may help for their use in early diagnosis and to identify appropriate targets for the prevention and treatment of HBV-related HCC.

Citation: Li HC, Yang CH, Lo SY. Long noncoding RNAs in hepatitis B virus replication and oncogenesis. *World J Gastroenterol* 2022; 28(25): 2823-2842
URL: https://www.wjgnet.com/1007-9327/full/v28/i25/2823.htm
DOI: https://dx.doi.org/10.3748/wjg.v28.i25.2823

INTRODUCTION

Majority of the human genome (70%–90%) is actively transcribed. Only approximately 2% of these transcribed RNAs translate into proteins, while more than 90% of them are noncoding RNAs (ncRNAs). Based on size, ncRNAs are classified into small ncRNAs [less than 200 nucleotides (nt)] and long noncoding RNAs (lncRNAs, more than 200 nt). Several kinds of small ncRNAs have been characterized, including transfer-, ribo-, small nucleolar-, piwi -and miRNAs. It is well known that miRNAs (generally 22–25 nt) can regulate gene expression by suppressing protein translation or by mRNA degradation through interacting with their target mRNA sequences, usually at the 3′-untranslated regions (3′UTR). Various miRNAs have been found to be dysregulated and play important roles in hepatitis B virus (HBV) infection and hepatocellular carcinoma (HCC) progression[1].

LncRNAs are mostly transcribed by RNA polymerase II, sometimes polyadenylated and located in nuclear and/or cytosolic fractions. LncRNAs are divided into intergenic, intronic, bidirectional, sense, and antisense lncRNAs based on their genomic location and strand orientation. These lncRNAs may function as signals, decoys, guides, or scaffolds to regulate the expression of their target genes through interacting with their partner molecules[2]. In this way, lncRNAs can modulate gene expression at different levels, including epigenetic silencing, transcriptional control, post-transcriptional regulation, and protein stability modulation[2]. Thus, they are involved in many biological processes such as cell proliferation, invasion and metastasis, autophagy, and apoptosis. Indeed, dysregulation of lncRNAs has now been implicated in numerous human diseases, especially cancers, *e.g.*, HCC[2].

Liver cancer was the sixth most common cancer and the third leading cause of cancer death in the world in 2020 (https://gco.iarc.fr/today/home). HCC represents approximately 90% of all cases of primary liver cancer. The leading cause of HCC is persistent HBV infection, which occurs in more than half of the HCC cases[3]. The management of HBV-related HCC has improved in the past decade. However, the outcome of HCC is still poor. Understanding more regarding the underlying mechanism of HBV-related HCC is required for improving the prevention, diagnosis, and treatment of HCC. The roles of lncRNAs in HBV-related HCC have received much more attention lately.

In this mini-review, we briefly outline the involvement of lncRNAs in HBV replication. We summarize the findings of dysregulated lncRNAs in HBV-related diseases, especially HCC, and discuss their roles and the potential clinical applications as diagnostic or therapeutic targets for HCC.

LNCRNAS IN HBV REPLICATION

HBV, belonging to the *Hepadnaviridae* family, is a small enveloped DNA virus. Ten HBV genotypes (A–J), which are based on eight percent or more sequence divergence across the viral genome, have been identified[4]. Even with the genotype differences, HBVs share the same pattern of replication cycle in the cells[5]. HBV infection begins with the attachment of virions to the surface proteoglycans on hepatocytes, followed by high affinity binding with more specific receptors (*e.g.*, sodium taurocholate cotransporting polypeptide; NTCP)[6]. After entry into the cell, the viral compact, partially double-stranded genome (*i.e.*, relaxed circular DNA) will form the stable covalently closed circular DNA (cccDNA) by viral and host factors[7]. Then, the viral RNAs [including sub-genomic mRNAs and pre-genomic RNA (pgRNA)] are transcribed from cccDNA using the cellular transcriptional machinery. The pgRNAs and the viral polymerase proteins (HBpAg) will be encapsidated by HBV core antigen (HBcAg) proteins. The newly formed nucleocapsids containing partially double-stranded HBV DNA made from pgRNA by HBpAg then either re-enter the nucleus to produce more cccDNA or release as mature virions following the assembly with HBV surface proteins (HBsAg)[5].

The 3.2 kilobases (kb) HBV genome contains four open reading frames (ORFs): Surface (S), precore (pre-C)/core (C), polymerase (P), and X. The S ORF encodes three viral envelope proteins initiated from different start codons: Large, middle, and small surface antigens (HBsAg). HBV e antigen and core antigen (HBcAg) are encoded in the pre-C/C ORF[5]. The P ORF encodes viral polymerase (HBpAg) possessing reverse transcriptase, RNase H, and DNA polymerase activities. HBV X protein (HBxAg, HBx) derived from X ORF can transactivate the expression of both cellular and viral genes required for viral replication[5].

Nearly 257 million people worldwide have been infected with HBV, resulting in 887000 people dying of liver cirrhosis or HCC annually. Therefore, identification of new therapeutic targets against HBV is urgently needed. LncRNAs could be potential targets as a growing number of them have been found to play a role in HBV replication[8] (Figure 1).

LncRNAs facilitating HBV replication

LncRNA deleted in lymphocytic leukemia 2 (DLEU2): HBx was found to bind the DLEU2 promoter to enhance its transcription. Nuclear DLEU2 could directly bind to HBx or the histone methyltransferase enhancer of zeste homolog 2 (EZH2). The interaction of HBx and DLEU2 on the viral cccDNA displaces EZH2 from the viral chromatin to boost viral transcription and replication[9].

HOX transcript antisense RNA (HOTAIR): HOTAIR was significantly upregulated in HBV-infected cells. HOTAIR promoted HBV transcription and replication by elevating the activities of HBV promoters *via* modulation of the levels of cccDNA-bound SP1[10].

LncRNA proliferating cell nuclear antigen (PCNA) pseudogene 1 (PCNAP1): The expression levels of PCNAP1 and PCNA were significantly elevated in the livers of HBV cccDNA-positive HCC patients. PCNA could interact with HBV cccDNA in a HBc-dependent manner. PCNAP1 enhanced PCNA through sponging miR-154, which targets the 3'UTR of PCNA mRNA. Moreover, PCNAP1 or PCNA enhanced HBV replication significantly both *in vitro* and *in vivo*. Thus, lncRNA PCNAP1 enhances HBV replication through the miR-154/PCNA/HBV cccDNA axis[11].

LncRNA highly upregulated in liver cancer (HULC): The HULC gene is located on chromosome 6p24.3 and contains two exons and one intron. HULC is an lncRNA of around 500 nt mainly localized in the cytoplasm. HULC was found to elevate HBx, which coactivated STAT3 to stimulate the miR-539 promoter. Elevated miR-539, which targets the 3'UTR of APOBEC3B mRNA, downregulated APOBEC3B and promoted HBV replication. Thus, HULC activates HBV through the HBx/STAT3/miR-539/APOBEC3B axis[12]. Another study demonstrated that lncRNA HULC enhanced HBV replication through the HAT1/HULC/HBc complex responsible for the accumulation on cccDNA minichromosome[13]. Moreover, the HULC genetic variant rs7763881 is associated with HBV infection[14].

LncRNA zinc ribbon domain containing 1-antisense RNA 1 (ZNRD1-AS1): A ZNRD1, cloned from the human leukocyte antigen region, should play an important role in immune response against HBV infection. ZNRD1-AS1 is an important regulator of ZNRD1. The variant allele of ZNRD1-AS1 (rs3757328) was reported to be associated with HBV clearance[15].

LncRNA HBx-long interspersed nuclear element 1 (HBx-LINE1): HBx-LINE1 suppresses miR-122 [16], a miRNA that has been demonstrated to inhibit HBV replication by directly targeting the HBV pgRNA sequence[17]. Thus, by depleting miR-122, HBx-LINE1 enhances HBV replication.

LncRNA AP000253: AP000253 was found to promote HBV transcription and replication in hepatoma cells[18]. However, the AP000253 expression in liver tissues and the molecular mechanism of its involvement in HBV infection are not clear yet.

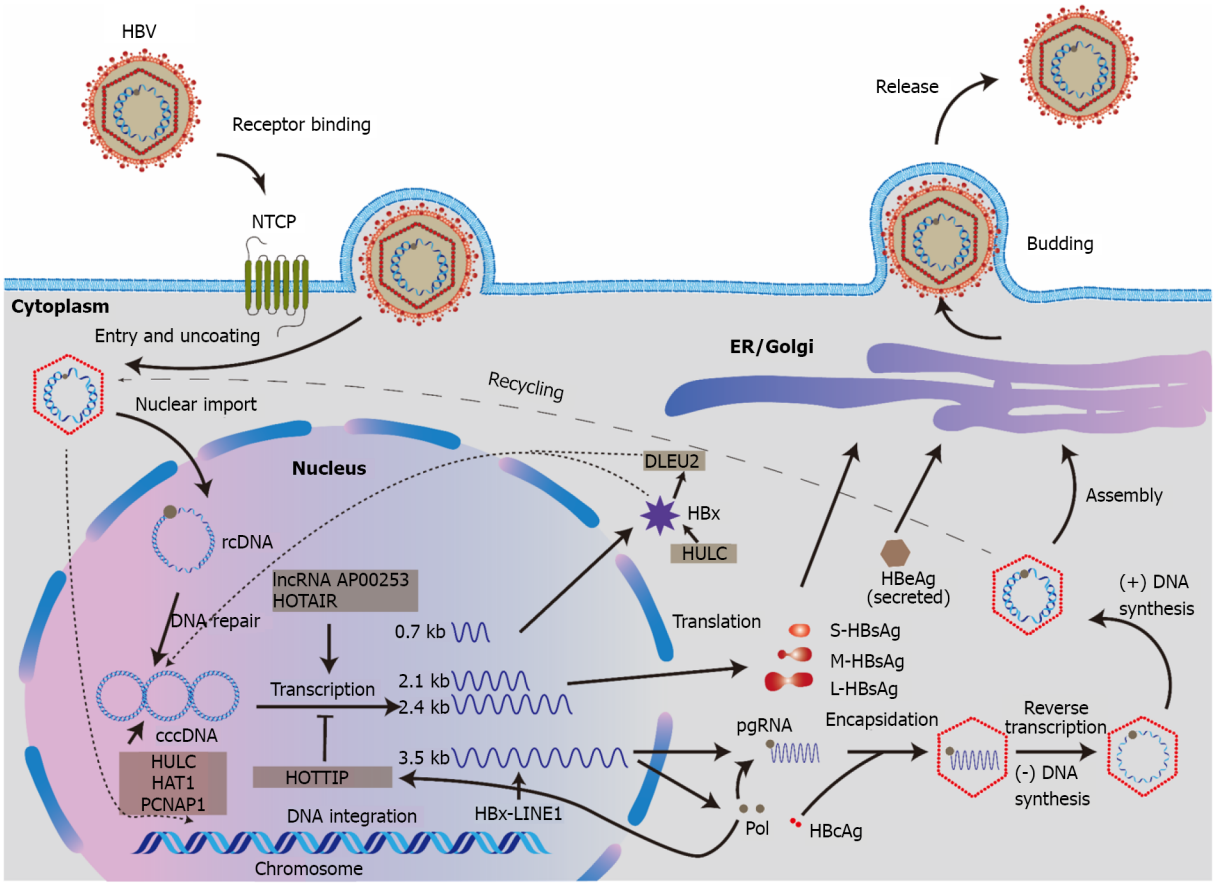
LncRNAs suppressing HBV replication

LncRNA HOXA transcript at the distal tip (HOTTIP): HOTTIP is a 3764 nt transcript mapped to the HOXA locus. HOTTIP was found to be induced by HBV in vitro. Further studies demonstrated that HBpAg could bind to and stabilize cAMP-responsive element-binding protein 1 (CREB1) mRNA to facilitate its translation. Then, the CREB1 protein would bind to the regulatory element of HOTTIP to promote its expression. HOTTIP significantly suppresses HBV replication through its downstream factor HOXA13, which was found to bind to HBV Enh I/Xp to reduce the production of pgRNA as well as HBV replication. Thus, HBpAg attenuates HBV replication *via* activation of the CREB1/HOTTIP/HOXA13 axis. In this way, lncRNA HOTTIP could restrain HBV replication and contribute to viral persistent infection[19].

Other lncRNAs involved in HBV replication

H11, a novel inhibitor of La protein, suppressed HBV replication by blocking the interaction between La protein and HBV RNA. Further studies have shown that 61 lncRNAs were upregulated and 74 lncRNAs were downregulated in an H11 treatment group when compared with the control group[20]. These lncRNAs should affect HBV replication though further verification is required.

The importance of lncRNAs in HBV replication has started to emerge. However, many unidentified lncRNAs critical for HBV replication should exist, such as those regulated by HBx (mentioned in the following sections). HBx is required for transcription from the viral cccDNA minichromosome. Thus, HBx modulates HBV replication. The lncRNAs affected by HBx may modulate HBV replication. The



DOI: 10.3748/wjg.v28.i25.2823 **Copyright** ©The Author(s) 2022.

Figure 1 Long noncoding RNAs involved in the lifecycle of the hepatitis B virus. Highly upregulated in liver cancer, HAT1, PCNAP1, and DLEU2 could enhance hepatitis B virus (HBV) replication[9,11,13]. LncRNA AP00253[18] and HOX transcript antisense RNA[10] promote, while HOXA transcript at the distal tip[19] inhibits, HBV transcription. HBV X protein-long interspersed nuclear elements 1 promotes HBV replication by suppressing miR-122, a miRNA directly targeting the HBV pgRNA sequence[16]. HULC: Highly upregulated in liver cancer; HBV: Hepatitis B virus; HBx: HBV X protein; LINE: Long interspersed nuclear elements; HOTTIP: HOXA transcript at the distal tip; HOTAIR: HOX transcript antisense RNA.

roles of these lncRNAs in HBV replication require further investigation.

LNCRNAS IN HBV-RELATED IMMUNE RESPONSES

The roles of lncRNAs in the host immune system during HBV infection have just started to emerge. LncRNA ENST00000519726 (lncRNA-HEIM) was highly expressed in monocytes and was further upregulated upon HBV infection. Elevated lncRNA-HEIM expression was remarkably correlated with the TGF- signaling pathway. Furthermore, altering the endogenous lncRNA-HEIM amount in monocytes significantly affected TGF- production[21].

LncRNA FTX downregulates the expression of tumor necrosis factor-α (TNF-α), interleukin (IL)-6, IL-1β, and nuclear factor kB (NF-kB) but upregulates the expression of Tim-3. This result demonstrated the effect of FTX on the expression of inflammatory cytokines through FTX-miR-545-TIM3 axis[22].

High lncRNA-CD160 expression level can inhibit interferon (IFN)-γ and TNF-α secretion in CD8+ T cells and decrease the immune response of CD8+ T cells. LncRNA-CD160 can interact with histone-modification enzyme gene histone deacetylase 11 (HDAC-11) to form a complex on the promoters of IFN-γ and TNF-α to inhibit their expression. Thus, lncRNA-CD160 acts as an immune suppressor. Indeed, knockdown of lncRNA-CD160 can block HBV infection[23].

Lnc-DC is a specific group of lncRNAs in dendritic cells. Lnc-DC could be activated by HBV infection. In addition, lnc-DC is important in regulating the growth, apoptosis, and immune response of dendritic cells mediated by TLR9/STAT3 signaling. Moreover, the regulation of lnc-DC controlled the immune response by reduction in secreted TNF-α, IL-6, IL-12, and IFN-γ, while increasing the IL-1β concentration in dendritic cells[24].

LncRNA#32 could positively regulate IFN-stimulated gene expression by interacting with activating transcription factor 2. Indeed, depletion of lncRNA#32 resulted in a significant increase in the replication of several viruses, including HBV. Thus, lncRNA#32 plays a role in host antiviral responses

[25].

The role of lncRNAs in the HBV-related immune responses remains unclear. There should be many unidentified lncRNAs important for HBV-related immune responses, such as those involved in HBV-related HCC.

LNCRNAS IN HBV-RELATED CHRONIC DISEASES

Progression of liver disease from chronic HBV infection to HCC may include several stages[26], such as fibrosis and cirrhosis (Figure 2). The roles of lncRNAs in these HBV-related chronic diseases are largely unknown.

Transforming growth factor-β (TGF-β) plays an important role in various pathogenic processes, from inflammation, fibrosis, and cirrhosis to cancer. LncRNA-ATB, which is activated by TGF-β, is a key regulator of the TGF-β signaling pathway. The plasma levels of lncRNA-ATB in HBV-related cirrhosis patients were significantly higher than those in healthy controls[27].

Serum lincRNA-p21 levels in CHB patients, those with hepatitis B cirrhosis, and HBV-related HCC, were higher than those in the control subjects. LincRNA-p21 level was negatively correlated with levels of HBV DNA, alanine aminotransferase, and aspartate aminotransferase in patients with liver diseases. Thus, serum lincRNA-p21 may serve as a potential biomarker for liver cell damage in patients with hepatitis virus infection, hepatitis B cirrhosis, and HBV-related HCC[28].

Compared with that in healthy controls, HBV carriers, and CHB patients, the expression of lnc-TCL6 was obviously upregulated in Child–Pugh A patients with liver cirrhosis. Thus, lnc-TCL6 was identified as a sensitive biomarker for early diagnosis of liver cirrhosis (Child–Pugh A)[29].

LncRNA metastasis associated in lung adenocarcinoma transcript 1 (MALAT1) expression in CHB group was significantly upregulated compared to the control group. Moreover, the thioredoxin interacting protein (TXNIP) was also significantly upregulated in the CHB group. Further studies indicate that the MALAT1/hsa-miR-20b-5p/TXNIP axis may mediate CHB-induced inflammatory damage in chronic HBV infection complicated with non-alcoholic fatty liver disease[30].

LncRNA-maternally expressed gene-3 (MEG3) was reported to be significantly downregulated in human HCC cell lines possibly due to the MEG3 promoter being hyper-methylated. Further studies indicated that the serum level of lncRNA-MEG3 was lower in CHB patients, which is negatively correlated to the liver fibrotic degree. In vitro experiments verified those results. Thus, lncRNA-MEG3 may serve as a diagnostic biomarker for CHB[31].

LncRNA growth arrest specific transcript 5 (GAS5) is significantly downregulated in CHB patients due to its promoter methylation. Compared with the sera of healthy controls, lower GAS5 levels were detected in the sera of CHB patients. Thus, lncRNA GAS5 is also reported as a biomarker for liver fibrosis in CHB patients[32].

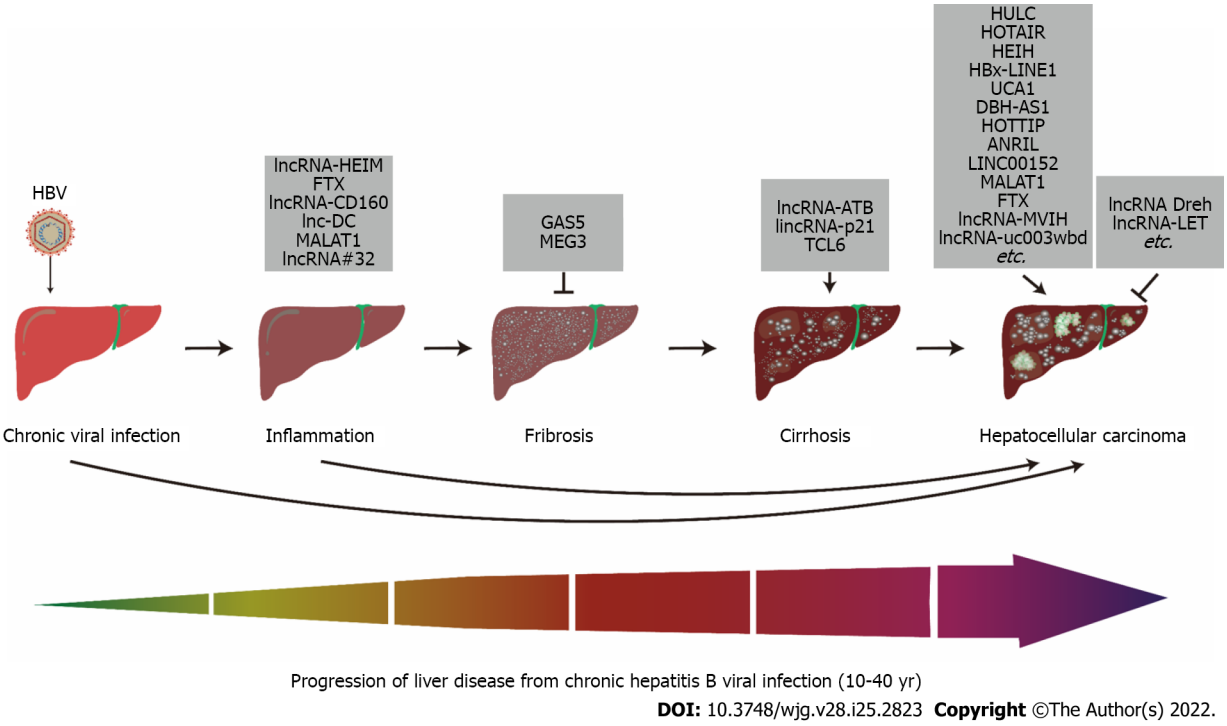
CHB patients might progress to acute-on-chronic liver failure (ACLF) with a high fatality rate. Four lncRNAs (RP11-25K21.6, THRB, RAB27A, and GNPTAB) were found to be differentially expressed between the ACLF and the control groups. Aberrant lncRNAs might be used to develop novel diagnostic biomarkers and/or therapeutic targets for ACLF[33].

The role of lncRNAs in the HBV-related chronic diseases is not clear yet. Those lncRNAs involved in HBV-related HCC (mentioned in the following section) may also play roles in HBV-related chronic diseases. This requires further investigation.

LNCRNAS DYSREGULATED IN HBV-RELATED HCC

HCC was the sixth most common cancer in world in 2020. Risk factors of HCC include external stimuli such as HBV or hepatitis C virus infection, intake of aflatoxin B1, alcohol consumption, smoking, and host factors such as age, gender, genetics, and comorbidities. Globally, approximately 2 billion people have been infected with HBV. Among them, more than 350 million people are chronic HBV carriers. Chronic HBV infection has been implicated in HCC development. In fact, persistent HBV infection occurs in more than half of HCC, particularly in developing countries. Comparing with other solid malignancies, HCC is characterized by its highly invasive and metastatic potential. Indeed, HCC is the third leading cause of cancer death in world. This is in part due to the fact that patients may not exhibit symptoms at early stages of HCC[34]. Therefore, comprehensive approaches are warranted to identify novel tumor markers and find more effective therapeutic targets to improve the diagnosis and treatment of HCC[8]. In recent years the idea has emerged that regulatory ncRNAs, such as miRNAs and lncRNAs, should play regulatory roles in cancers such as HCC[1]. Specifically, various lncRNAs were reported to regulate the expression of tumor suppressor genes or oncogenes involved in cancer development[2].

HCC caused by HBV infection is related to different HBV genotypes, the mutation status of viral genomes, integration of viral DNAs, and the dysregulation of signaling pathways affected by HBV. However, the detailed mechanisms of HBV-related HCC remain to be determined. The development of



DOI: 10.3748/wjg.v28.i25.2823 **Copyright** ©The Author(s) 2022.

Figure 2 Various long noncoding RNAs are involved in the progression of liver diseases caused by the hepatitis B virus[26]. HULC: Highly upregulated in liver cancer; HBV: Hepatitis B virus; HBx: HBV X protein; LINE: Long interspersed nuclear elements; HOTTIP: HOXA transcript at the distal tip; HOTAIR: HOX transcript antisense RNA; GAS5: Growth arrest specific transcript 5; MEG3: Maternally expressed gene-3; MALAT1: Metastasis associated in lung adenocarcinoma transcript 1.

the majority of HBV-related HCCs is associated with: (1) Chronic inflammation; (2) Insertion of viral sequences into the cellular chromosomes; (3) Transactivation of growth regulatory genes by HBx; and (4) Altered versions of the preS/S envelope proteins[35]. If the host immune system fails to clear HBV, the infection will become chronic. Then, HBV DNA may integrate into the cellular chromosome. Indeed, integrated viral DNA is found in 85%–90% of HBV-related HCCs. Insertion of the HBV DNA occurs preferentially at certain sites in the host genome, including repetitive elements such as LINEs and Alu repeats[36]. The HBx gene is the smallest ORF encoding a 154-amino acid regulatory protein. HBx is reported to contribute to the pathogenesis of HCC by trans-modulating many growth regulatory genes and activating various signaling pathways, including p53, NF-kB, and Wnt signaling. Diverse lncRNAs involved in the events of viral immune responses, viral integration, and HBx regulatory activities should play roles in HBV-related HCC[37]. Studies on lncRNAs which are differentially expressed in HBV-HCC tissue samples may elucidate oncogenic pathways and identify novel diagnostic and therapeutic targets[8]. When compared to normal and/or non-HBV HCC samples, hundreds of dysregulated lncRNAs in HBV-related HCC tissues have been detected[38-40]. It is also reported that HBx could alter the expression of 2002 lncRNA[41]. In this mini-review, the better characterized lncRNAs in HBV-related HCC will be discussed.

UPREGULATED LNCRNAS IN HBV-RELATED HCC

HULC

HULC was the first lncRNA reported to be specifically upregulated in HCC through microarray analysis and quantitative reverse transcriptase polymerase chain reaction (qRT-PCR). By interacting with CREB, HBx up-regulates the HULC expression in hepatoma cell lines and HBV-related HCC tissues. HULC downregulates the expression of p18, a tumor suppressor gene close to HULC, and thus promotes the proliferation of hepatoma cells[42]. Moreover, HULC can act as a molecular sponge for miR-107. By sponging miR-107, HULC upregulates E2F1 and then activates SPHK1 transcription in hepatoma cell lines and HBV-related HCC tissues. Thus, HULC promotes tumor angiogenesis through miR-107/E2F1/SPHK1 signaling[43]. Altogether, these studies indicate that HULC serves as an oncogene important for HBV-related HCC. HULC is also demonstrated to act as an endogenous 'sponge' for various other miRNAs (*e.g.*, miR-372, miR-186, miR-488, miR-200a-5p, miR-6825-5p, miR-6845-5p, and miR-6886-3p) in hepatoma cell lines and HCC tissues[44]. Those findings provide new insights into the mechanism of HULC in the HCC development (Table 1).

Table 1 Long noncoding RNAs up-regulated in hepatitis B virus-related hepatocellular carcinoma

LncRNA name	Regulatory mechanism	Biological function
HULC[43]	Sequesters microRNAs and decreases p18 expression	Promotes proliferation of hepatoma cells and tumor angiogenesis *in vitro* and *in vivo*
HOTAIR[45,47]	Suppresses miRNA-218 expression and inactivation of P14 and P16 signaling	Promotes migration and invasion of HCC cells
HEIH[48]	Binds to EZH2 and represses EZH2 targets	Promotes cell proliferation and tumor growth, modulates cell cycle
HBx-LINE1[16,49]	Sequesters miR-122 and activates Wnt signaling pathway	Promotes cell motility through EMT
UCA1[53,54]	Through the HBx/UCA1/EZH2/p27 axis in nucleus; sequesters miR-216b and miR-203 in cytoplasm	Promotes growth, metastasis, and EMT of HCC cell lines
DBH-AS1[56]	Activates the ERK/p38/JNK MAPK signaling pathway	Inhibits serum starvation-induced apoptosis of HCC cells, promotes tumor growth, proliferation, and cell-cycle progression of HCC cells
HOTTIP[57]	Upregulates the expression of HOXA genes (*e.g.*, HOXA 10, 11, and 13)	Inhibits proliferation and migration of HCC cells *in vitro* and reduces tumorigenesis and pulmonary metastasis *in vivo*
ANRIL[59,60]	Represses the KLF2 transcription through binding to PRC2; serves as a molecular sponge for miR-122-5p	Inhibits apoptosis of HCC cells *in vitro* and promotes proliferation, invasion, and migration of HCC cells *in vitro*
LINC00152[61]	Inhibits the expression of E-cadherin; activates the mTOR pathway	Promotes the proliferation and EMT of HCC cell lines and tumorigenesis
MALAT1[63,66]	Upregulates LTBP3 transcription	Promotes migration and invasion of HCC cells *in vitro* and tumor growth *in vivo*
Ftx[22]	Production of miR-545/374a	Promotes tumorigenesis and tumor progression
MVIH[68]	Activates angiogenesis through reducing the secretion of PGK1	Promotes tumor growth and metastasis
Unigene56159[69]	Sequesters miR-140-5p	Promotes EMT, migration, and invasion of hepatoma cells
LINC01232[70]	Downregulation of miR-708-5p	Promotes tumor progression *in vitro*
SAMD12-AS1[71]	Inhibition of p53	Promotes cell proliferation and inhibits apoptosis
lnc-HUR1[72]	Inhibition of p53	Promotes cell proliferation and tumorigenesis
n335586[73]	n335586/miR-924/CKMT1A axis	Contributes to cell migration and invasion
XIST[74]	XIST/miR-192/TRIM25 axis	Enhances the proliferation and migration of HCC cells
SNHG5[81]	SNHG5/miR-26a-5p/GSK3β signaling pathway	Promotes HCC progression
WEE2-AS1[76]	HBx/WEE2-AS1/FERMT3 pathway	Promotes HCC proliferation and invasion
MAFG-AS1[77]	HBx/ MAFG-AS1/MAFG	Promotes HCC proliferation and migration
lncRNA-ATB[78]	Induces autophagy	Promotes cell invasion and migration
TRERNA1[79]	TRERNA1/miR-22-3p/NRAS axis	Promotes cell proliferation in HCC
lncRNA IHS[80]	Regulates the ERK- and AKT/GSK-3β signaling pathways	Promotes tumor proliferation and metastasis in HCC
SNHG20[81]	Negatively regulated PTEN protein level	Facilitates the proliferation of HCC cells
AX800134[82]	Not known	Antiapoptosis

LncRNAs: Long noncoding RNAs; HCC: Hepatocellular carcinoma; EMT: Epithelial-to-mesenchymal transition; HULC: Highly upregulated in liver cancer; HBV: Hepatitis B virus; HBx: HBV X protein; LINE: Long interspersed nuclear elements; HOTTIP: HOXA transcript at the distal tip; HOTAIR: HOX transcript antisense RNA; GAS5: Growth arrest specific transcript 5; MEG3: Maternally expressed gene-3; MALAT1: Metastasis associated in lung adenocarcinoma transcript 1; PGK1: Phosphoglycerate kinase 1.

HOTAIR

The *HOTAIR* gene is on chromosome 12. LncRNA HOTAIR is a 2158 nt transcript derived from the *HOTAIR* gene. HOTAIR is involved in the occurrence of HBV-related HCC. HBV replication and, in particular, HBx production, stimulates expression of HOTAIR and Plk1. The combination of Plk1 and HOTAIR are involved in epigenetic reprogramming associated with oncogenic transformation[45]. *In vitro* studies have demonstrated that HOTAIR has sequence-specific effects and interacts with various chromatin modifying proteins, *e.g.*, Polycomb repressive complex 2 (PRC2)[46]. Another study showed

that HOTAIR might mediate hepatocarcinogenesis by down-regulating miR-218 and in-activating P14 and P16 signaling[47]. These findings suggest that lncRNA HOTAIR should play an important role in hepatocarcinogenesis (Table 1).

High expression in HCC

The *high expression in HCC* (*HEIH*) gene is on chromosome 5. LncRNA HEIH is a polyadenylated, approximately 1600 nt in length, lncRNA, whose expression is strongly linked to HBV-associated HCC. It is located both in the nucleus and cytoplasm. HEIH could promote cell proliferation by upregulating PCNA and decreasing the expression of p16, p21, and p27 in cells. Moreover, HEIH could promote tumor growth in nude mice. Mechanistically, HEIH is physiologically associated with EZH2, the catalytic subunit of the PRC2. The association of HEIH with EZH2 is needed to repress the EZH2 target genes[48]. These studies demonstrate that HEIH contributes to HBV-related HCC through the participation of epigenetic silencing (Table 1).

HBx-LINE1

Almost all HBV-related HCC tumors (85%–90%) have at least one HBV insertion site in the host genome. Thus, integration of HBV DNA should be important for the HCC development. LINEs appear to be a favored site for HBV DNA integration. To investigate the effect of HBV integration on genome disruption, HBx-LINE1, a viral-human chimeric fusion transcript derived from viral sequences containing HBx and cellular LINEs, was found functioning as an lncRNA. HBx-LINE1 was detected in 23.3% of HBV-related HCC patients[49,50]. HBx-LINE1, on chromosome 8p11.21, was transcribed from the HBx promoter. HBx-LINE1 contains six miR-122-binding sites and serves as a molecular sponge to sequester cellular miR-122. By downregulating miR-122, HBx-LINE1 activates the β-catenin signaling pathway, and in turn enhances HCC cell proliferation, invasion, and migration[16]. However, these findings were not consistent with those from other studies[51]. More studies with a larger sample size should help further clarify the role of HBx-LINE1 in the HBV-related HCC (Table 1).

Urothelial carcinoma associated 1

The *urothelial carcinoma associated 1* (*UCA1*) gene is approximately 7.3 kb in length on chromosome 19p13.12 and contains three exons. It has three transcriptional isoforms. UCA1, around 1400 nt in length, is the most abundant isoform of the *UCA1* gene[52]. UCA1 was originally identified in the bladder cancer cell line and also played an important role in HBV-related HCC. HBx could upregulate UCA1 expression[37,53]. UCA1, an lncRNA detected in both the cytoplasm and nucleus[53], has diverse functions. In nucleus, UCA1 recruits EZH2 to the p27 promoter, reduces the p27 expression, and enhances CDK2. Thus, UCA1 could promote the growth of hepatic and hepatoma cells through the HBx/UCA1/EZH2/p27 axis[53]. In cytoplasm, UCA1 serves as a molecular sponge for miR-216b and miR-203. Through sequestering miR-216b, UCA1 could promote the growth and metastasis of HCC cell lines by up-regulating the expression of fibroblast growth factor receptor 1 and activating the extracellular signal-regulated kinase signaling pathway[54]. In addition, sequestering miR-203 facilitates epithelial-to-mesenchymal transition (EMT) in HCC cells through Snail2 upregulation[55]. Thus, UCA1 could promote cell cycle progression, enhance cell proliferation, and decrease cell apoptosis in HBx-related HCC[37] (Table 1).

DBH-AS1

DBH-AS1 is an lncRNA of approximate 2 kb located on chromosome 9q34. HBx can upregulate the expression of DBH-AS1, which promotes HCC cell proliferation[37]. DBH-AS1 activates the ERK/p38/JNK MAPK signaling pathway. Once activated, ERK/p38/JNK MAPK can upregulate cyclin-dependent kinase 6 (CDK6), CCND1, and CCNE1 (members of cyclins) and downregulate p16, p21, and p27 (inhibitors of CDK). Thus, DBH-AS1 could induce the G1/S and G2/M transitions and promote cell proliferation. DBH-AS1 was also shown to protect HCC cells from serum starvation-induced apoptosis. These results suggested that DBH-AS1 acts as an oncogene[56]. However, a recent study showed contradicting results regarding the expression pattern of DBH-AS1[57]. To elucidate the exact role of DBH-AS1 in HBV-related HCC, more research is required (Table 1).

HOTTIP

LncRNA HOTTIP, a 3764 nt transcript, is located on chromosome 7p15.2 and encodes from a genomic region in the 5′tip of the HOXA locus. LncRNA-HOTTIP was significantly overexpressed in tumor tissues compared to adjacent non-tumor tissues of the HCC patients. Patients with high HOTTIP expression were associated with increased metastasis formation and decreased overall survival. HOTTIP has also been detected to be upregulated significantly in HBV-related HCC patients[57]. Elevated HOTTIP expression could enhance cell proliferation and migration and contribute to metastasis of HCC partly by upregulating its neighboring *HOXA* genes (*e.g.*, HOXA 10, 11 and 13), which are associated with various cancer types. These findings suggest that HOTTIP acts as an oncogene in HBV-related HCC (Table 1).

Antisense ncRNA in the INK4 locus

Antisense ncRNA in the INK4 locus (ANRIL), a 3800 nt lncRNA, is in the *INK4BARF-INK4A* gene cluster[58]. ANRIL is upregulated in several cancers including HBV-related HCC[57]. The ANRIL expression was associated with tumor size, histological grade, and overall survival in HCC patients[59]. These findings indicate that ANRIL plays a role in the HCC development, particularly HBV-related HCC. Knockdown of ANRIL expression in HCC cells *in vitro* could induce apoptosis and reduce the proliferation, invasion, and migration of these HCC cells[60]. Furthermore, inhibition of ANRIL led to slower tumor growth *in vivo*[59,60]. ANRIL represses the KLF2 transcription through binding with PRC2[59]. ANRIL also serves as a molecular sponge for miR-122-5p, whose overexpression significantly repressed the proliferation, migration, and invasion of HCC cells[60]. These findings indicate that ANRIL is also an oncogene in HBV-related HCC (Table 1).

LINC00152

LINC00152, an lncRNA of 828 nt, is mapped to chromosome 2p11.2 and contains four exons. It is mainly localized in the nucleus of HCC cells. The LINC00152 expression is associated with tumor size, HBV infection, and HBx amount[61]. Elevated LINC00152 expression also results in decreased overall survival[61]. LINC00152 is up-regulated by HBx protein and enhances proliferation and EMT of HCC cell lines *in vitro* and tumorigenesis *in vivo*[61]. LINC00152 has been shown to activate the mTOR pathway, which is a classic dysregulated pathway involved in the pathogenesis of HCC. In addition, LINC00152 promotes EMT by reducing the binding of EZH2 to the E-cadherin promoter and suppressing E-cadherin expression in HCC cell lines[61]. Ablation of E-cadherin will lose cell–cell contacts, resulting in EMT. These studies suggest that LINC00152 contributes to HBV-related HCC (Table 1).

Metastasis-associated lung adenocarcinoma transcript 1

Metastasis-associated lung adenocarcinoma transcript 1 (MALAT1) (also known as nuclear-enriched abundant transcript 2), an lncRNA of approximate 8000 nt in length, is mainly localized in the nucleus [62]. MALAT1 expression is elevated by HBx in HCC tissues and cell lines[63]. Sp1 and Sp3, also found upregulated, would bind to the proximal promoter region and enhance the transcription of MALAT1 [64]. MALAT1 affects alternative splicing and gene expression[62,65]. MALAT1 could promote tumor growth and metastasis by upregulating latent-transforming growth factor beta-binding protein 3 (LTBP3) expression. These results suggest that MALAT1 mediates the oncogenic effect of HBx through enhancing the LTBP3 expression, which promotes early metastatic events[63]. Moreover, a higher MALAT1 expression correlates to HCC recurrence after liver transplantation[66]. Additionally, knockdown of MALAT1 has been shown to reduce cell viability, motility, and invasiveness and increase sensitivity to apoptosis in HepG2 cells[66]. Therefore, MALAT1 is also an oncogene contributing to the risk of HBV-related HCC (Table 1).

Ftx

LncRNA Ftx is transcribed within the X-inactivation center[67]. Ftx encodes four miRNA clusters in its introns, among them, miR-545/374a located in intron b of Ftx has been implicated in HBV-associated HCC[22]. Expression of miR-374a and miR-545 was significantly higher in tumor tissues of HBV-related HCC. Further investigations suggested that miR-545/374a may contribute to poor prognosis by enhancing tumor invasion. This was supported by the observation that the proliferation of malignant cells was significantly suppressed in the presence of miR-545/374a inhibitors. On the other hand, overexpression of the miRNAs resulted in increased proliferation. miR-545/374a also enhanced migration and invasion abilities of HCC cells. Moreover, clinical samples positive for HBV DNA showed an increase in miR-545/374a. The upregulation of miR545 was also found to be HBx-dependent. Three targets for miR-545/374a were identified: Estrogen-related receptor alpha, estrogen-related receptor gamma (ESRRG), and arginine and glutamate rich. Experimental evidence demonstrated that miR-545 could downregulate ESRRG expression. Additionally, miR-374a had been shown to activate Wnt signaling pathway. In conclusion, lncRNA Ftx involves HBV-related HCC by serving as miRNAs precursor (Table 1).

Microvascular invasion in HCC

Microvascular invasion in HCC (MVIH) is situated within the intron of the *ribosomal protein S24* gene. The MVIH expression was significantly upregulated in HBV-related HCC. Highly expressed MVIH was associated with frequent microvascular invasion and decreased overall survival[68]. Further investigations found that MVIH could promote tumor growth and metastasis by enhancing angiogenesis through reducing the secretion of phosphoglycerate kinase 1 suppressing angiogenesis[68] (Table 1).

Unigene56159

Unigene56159, an lncRNA of 2653 nt, is in the second intron of ROBO1. Unigene56159 was elevated in HBV-related HCC and HBV-producing cell line. Further investigations have found that Unigene56159, induced by HBV, could promote the EMT, migration, and invasion of hepatoma cells through seques-

tering miR-140-5p and up-regulating the Slug expression[69].

In addition to the abovementioned lncRNAs, the expression of LINC01232[70], SAMD12-AS1[71], lncHUR1[72], n335586[73], XIST[74], and SNHG5[75] was found to be increased in HBV-related HCC. Moreover, the expression of WEE2-AS1[76], MAFG-AS1[77], lncRNA-ATB[78], TRERNA1[79], lncRNA-IHS[80], SNHG20[81], and AX800134[82] was upregulated by HBx.

Those upregulated lncRNAs by HBV and/or HBx may be involved in HCC progress through diverse mechanisms to enhance HCC cell proliferation, invasion, and metastasis, and/or prevent the death of HCC cells (*e.g.*, apoptosis)[83] (Table 1).

DOWNREGULATED LNCRNAS IN HBV RELATED HCC

Downregulated expression by HBx

Downregulated expression by HBx (Dreh), an lncRNA of approximate 700 nt in length, is mapped to chromosome 5. The Dreh expression was downregulated by HBx in HCC cell lines. Dreh is also significantly downregulated in HBV-related HCC tissues. Suppression of DREH facilitates proliferation of hepatoma cells *in vitro* and also tumor growth *in vivo*[84]. Lower Dreh expression is associated with the recurrence-free survival and overall survival of HCC patients[84]. Playing as a tumor suppressor in the development of HBV-related HCC, Dreh suppressed cell proliferation and cell migration *in vitro* and *in vivo*. By binding to the intermediate filament protein vimentin, lncRNA Dreh inhibits its expression and alters its filament structure to repress tumor cell migration. Therefore, HBx inhibits Dreh expression and in turn facilitates HCC (Table 2).

Low expression in tumor

LncRNA-low expression in tumor (LET) is an lncRNA identified to be decreased in HBV-related HCC. LncRNA-LET and nuclear factor 90 (NF90) are associated with each other. LncRNA-LET could downregulate NF90. NF90 has been implicated in the stabilization of many factors [*e.g.*, hypoxia induced factor 1-α (HIF-1α)] related to tumor growth and metastasis[85,86]. The LET/NF90/HIF-1α axis may be critical for HCC invasion in hypoxic environments. Under hypoxia conditions, induced HDAC-3 suppressed LET expression, which increased the expression of NF90 and HIF-1α, and, hence, enhanced the invasiveness of HCC and contributed to HCC progression[85].

In addition to the abovementioned lncRNAs, the expression of uc.306[87], UPAT[88], SEMA6A-AS1 [89], BANCR[90], and miR143HG[91] was found to be decreased in HBV-related HCC. Moreover, the expression of lncRNA-6195[92], LINC01352[93], and F11-AS1[94] was suppressed by HBx. These downregulated lncRNAs by HBV and/or HBx serve as tumor repressors and suppress HCC cell proliferation (Table 2).

OTHER LNCRNAS IN HBV-RELATED HCC

H19

The *H19* gene is located adjacent to the *insulin-like growth factor 2* gene on chromosome 11p15.5. This gene produces a 2.3 kb lncRNA, which is exclusively expressed from the maternal allele. Reports of H19 expression in HCC are controversial. Recently, lncRNA H19 was found to be upregulated in CHB patients[95]. On the other hand, lncRNA H19 could suppress the growth of hepatoblastoma cells by promoting their apoptosis[96].

Most of these dysregulated lncRNAs are modulated by HBx, it would help to know whether altered versions of the preS/S envelope proteins would modulate the expression of lncRNAs or not. The progress of research on the role of lncRNAs in HBV-related HCC is impressive. However, the functions of a large proportion of lncRNAs dysregulated in HBV-related HCC remain elusive. Future investigation on the function of lncRNAs in HBV-related HCC will shed the light on understanding the detailed mechanisms regarding the development of HBV-induced HCC. Understanding more regarding the molecular mechanisms underlying lncRNA-mediated oncogenesis should help for their use in diagnosis and to identify appropriate targets for prevention and treatment of HBV-related HCC.

GENETIC POLYMORPHISMS OF LNCRNAS IN HBV REPLICATION AND ONCOGENESIS

A number of dysregulated lncRNAs have been identified in HBV replication and oncogenesis[2,37]. Genetic polymorphisms affecting the expression (changes in the enhancer/promoter region) or activity (differences in the coding region) of these lncRNAs may also affect HBV replication and oncogenesis. Association studies are used to identify genetic variations of lncRNAs involved in HBV replication and oncogenesis[2].

Table 2 Long noncoding RNAs downregulated in hepatitis B virus-related hepatocellular carcinoma

LncRNA name	Regulatory mechanism	Biological function
Dreh[84]	Inhibits the vimentin expression and alters its structure	Inhibits proliferation of HCC cells *in vitro* and tumor growth *in vivo*
LET[85]	LET/NF90/HIF1-α axis	Inhibits HCC invasion
uc.306[87]	May participate in the Wnt pathway	Not known
UPAT[88]	Promotes ZEB1 degradation	Suppresses cellular migration, invasion, and EMT processes
SEMA6A-AS1[89]	Not known	Not known
BANCR[90]	Not known	Not known
miR143HG[91]	Suppresses the MAPK and Wnt signaling pathways	Inhibits tumor multiplication and metastasis
LncRNA-6195[92]	Represses the enzymatic activity of ENO1	Represses the growth of HCC
LINC01352[93]	LINC01352/miR-135b/APC axis	Facilitates HCC progression
F11-AS1[94]	lncRNA F11-AS1/miR-211-5p/NR1l3 axis	Inhibits HCC growth and metastasis

LncRNAs: Long noncoding RNAs; HCC: Hepatocellular carcinoma; EMT: Epithelial-to-mesenchymal transition; HIF-1α: Hypoxia induced factor 1-α.

GENETIC POLYMORPHISMS IN THE ENHANCER/PROMOTER OF LNCRNAS

The intronic enhancer of HOTAIR had significantly higher HOTAIR levels in the rs920778 TT genotype than in the CC genotype. By upregulating HOTAIR, the rs920778 TT genotype promotes the development of HBVrelated HCC and increases proliferation of HCC cells[97].

LncRNA GAS5 (growth arrest special 5) has been found to be downregulated in HCC patients[98]. A five-base-pair Ins/Del polymorphism (rs145204276) in the promoter region of GAS5 could affect the GAS5 expression. The deletion allele of rs145204276 increases the risk of HBV-related HCC significantly, though the detailed mechanism is unclear[99].

The sequence of RERT-lncRNA overlaps with those of the Ras-related GTP-binding protein 4b and prolyl hydroxylase 1 (EGLN2). An Ins/Del polymorphism (rs10680577) in the distal promoter of RERT-lncRNA may alter the structure of RERT-lncRNA and regulate the expression of RERT-lncRNA and EGLN2. A 4-bp deletion allele of rs10680577 in RERT-lncRNA increases expression of RERT-lncRNA and EGLN2 and promotes the occurrence of HBV-related HCC[100].

GENETIC POLYMORPHISMS IN THE CODING REGION OF LNCRNAS

A polymorphism in the coding region of KCNQ1-overlapping transcript 1 (KCNQ1OT1), *i.e.* rs35622507, may alter the structure of KCNQ1OT1 and modulate the expression of KCNQ1OT1 and cyclin-dependent kinase inhibitor 1C (CDKN1C). The homozygous 10-10 genotype with significantly lower expression of KCNQ1OT1 and higher expression of CDKN1C was shown to increase the risk of HBV-related HCC[101].

LINC01149 variant rs2844512 was identified to facilitate HBV spontaneous recovery but increase the risk of HCC. Further studies indicated this variant created a binding site for miR-128-3p and upregulated MICA expression by serving as a miRNA sponge[102].

OTHER GENETIC POLYMORPHISMS IN LNCRNAS

The variant allele of ZNRD1-AS1 (*i.e.*, rs3757328) is reported to associate with HBV clearance[15].

The SNPs in glutamate-ammonia ligase overlapping with LINC00272 were associated with increased risk of HBV-related HCC[103].

Caspase recruitment domain family, member 8 (CARD8) can coordinate innate and adaptive immune responses and may participate in HBV-related HCC. Several SNPs (rs7248320) within a new identified lncRNA AC008392.1, which is located in the upstream region of CARD8 in the long arm of the 9-chromosome, affect the CARD8 expression and may serve as a susceptibility marker for HBV-related HCC[104].

Three regulatory SNPs (rs3757328, rs6940552 and rs9261204) in the ZNRD1-AS1 and the HBV genotype significantly affected HCC susceptibility. The results indicate that ZNRD1-AS1 accompanied by HBV genotypes may influence HCC risk[15].

Tumor necrosis factor receptor superfamily member 10 (TNFRSF10) including TNFRSF10A and TNFRSF10B is a death domain-containing receptor for the apoptotic ligand TNFSF10. In the upstream region of TNFRSF10A and downstream region of TNFRSF10B, lncRNAs RP11-1149O23.3 and RP11-459E5.1 were identified, respectively. The two lncRNAs are possibly involved in the regulation of TNFRSF10A and TNFRSF10B. Several SNPs (*i.e.*, rs79037040-T and rs2055822-A) in RP11-1149O23.3 and RP11-459E5.1 may affect the expression of TNFRSF10A and TNFRSF10B and may be susceptibility markers for HCC and chronic HBV infection[105].

Paired-box family member PAX8 encodes a transcription factor that may participate in the prognosis of HCC. Several SNPs (rs4848320 and rs1110839) within AC016683.6 lncRNA may affect the PAX8 expression and affect the prognosis of HBV-related HCC[106].

The association of lnc-RP11-150O12.3 variants (rs2275959, rs1008547, and rs11776545) with HBV-related HCC risk and progression has been reported[107].

LncRNAs HULC and MALAT1 have been upregulated in HBV-related HCC. Genetic variants of lncRNA HULC (rs7763881) and lncRNA MALAT1 (rs619586) are associated with the decreased susceptibility to HCC[108].

These studies suggest that genetic polymorphisms in lncRNAs should affect the development and outcome of HBV-related HCC. This may help to identify appropriate targets for prevention and treatment of HCC in the age of personalized medicine.

REGULATORY MECHANISMS OF LNCRNAS IN HBV REPLICATION AND ONCOGENESIS

LncRNAs can function as signals, decoys, guides, or scaffolds through interacting with their partner molecules and regulate gene expression at different levels. Up to now, at least seven mechanisms have been found to affect HBV replication and oncogenesis by dysregulated lncRNAs: Epigenetic silencing, transcriptional control, splicing regulation, molecular sponge, production of miRNAs, protein stability modulation, and production of a small polypeptide (Figure 3)[2,109,110].

Epigenetic silencing: Polycomb group (PcG) proteins are epigenetic regulators of transcription. Through multiprotein complexes PRCs, PcGs could modify histones (and other proteins) and silence target genes. LncRNAs may decrease the expression of their target genes through epigenetic silencing either by altering the expression level of PcGs or by interacting with PcGs directly and then silencing their target genes. HOTAIR enhances the degradation of suppressor of Zeste 12 homolog, a key subunit of PRC2, through Plk1[45]. Several lncRNAs interact with EZH2, a component of PRC2 to modulate (repress in most cases) the expression of their target genes, *e.g.*, HEIH[48], UCA1[53], HOTAIR[47], LINC00152[61], and PVT1[111]. ANRIL can interact with PRC2[112].

Transcriptional control: LncRNAs can activate the transcription of their target genes in cis or in trans. HOTTIP could promote the expression of its neighboring homeobox A genes (*HOAX* genes) in HCC [57]. LINC00152 binds to the promoters of epithelial cell adhesion molecule and IL-23 to activate their transcription in HCC patients[113]. MALAT1 could up-regulate the expression of LTBP3[63].

Splicing regulation: LncRNAs could affect the expression of their target genes through alternative splicing regulation. MALAT1, a nuclear lncRNA, could interact with the SR proteins (serine/arginine-rich family of nuclear phosphoproteins) and change the cellular levels of the phosphorylated forms of SR proteins to modulate alternative splicing in HCC[62].

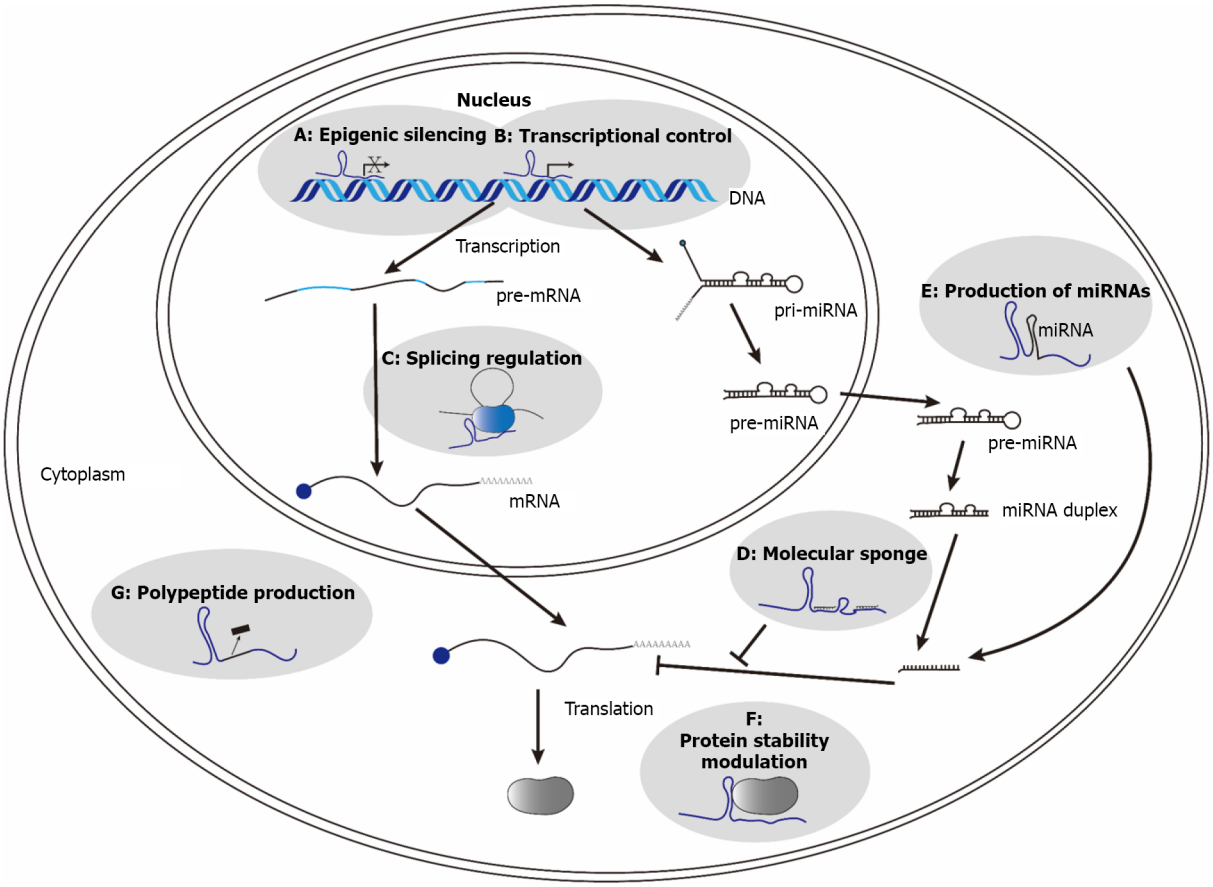
Molecular sponge: LncRNAs could exert their effects by acting as molecular sponges for miRNAs, *i.e.*, competitive endogenous RNA (ceRNA)[114]. Through molecular sponges, lncRNAs sequester miRNAs and then de-repress the expression of the miRNA target genes. Several lncRNAs, such as Unigene56159 [69], HULC[115], HBx-LINE1[16], UCA1[55], ANRIL[60], LINC01149 variant[102], LINC01352[93], F11-AS1[94], LINC01232[70], n335586[73], XIST[74], SNHG5[75], SSTR5-AS1[116], and TRERNA1[79] are involved in the development of HBV-related HCC by sequestering miRNAs.

Production of miRNAs: LncRNAs could produce miRNAs to regulate their target genes by serving as precursors of miRNAs. The Ftx transcript encodes two clusters of miRNAs (*i.e.*, miR-374a and miR-545) in its introns in HBV-related HCC[117].

Protein stability modulation: LncRNAs could stabilize their protein targets by direct interactions. LncRNA-Dreh could bind vimentin, a type III intermediate filament, and stabilize its filament structure [84]. LncRNAs could also stabilize their protein targets by reduced degradation of these proteins indirectly. By enhancing ubiquitin-specific peptidase 22, HULC suppresses ubiquitin-mediated degradation of cyclooxygenase-2 and silent information regulator 1 in HCC[118].

Production of a small polypeptide: A putative lncRNA HBVPTPAP could encode a small polypeptide to induce the apoptosis of HCC cells[110].

Through these different mechanisms, lncRNAs can regulate gene expression. As more lncRNAs are identified, more novel mechanisms will be revealed.



DOI: 10.3748/wjg.v28.i25.2823 **Copyright** ©The Author(s) 2022.

Figure 3 Regulatory mechanisms of various long noncoding RNAs in hepatitis B virus replication and oncogenesis[2]. A: HOX transcript antisense RNA (HOTAIR), high expression in hepatocellular carcinoma, urothelial carcinoma associated 1 (UCA1), HOTAIR, LINC00152, PVT1, and antisense noncoding RNA in the INK4 locus (ANRIL) could regulate gene expression through epigenetic silencing; B: HOXA transcript at the distal tip, LINC00152, and metastasis associated in lung adenocarcinoma transcript 1 (MALAT1) could increase the expression of their target genes through transcriptional control; C: MALAT1 could modulate alternative splicing; D: Unigene56159, highly upregulated in liver cancer (HULC), hepatitis B virus (HBV) X protein-long interspersed nuclear elements 1, UCA1, ANRIL, LINC01149 variant, LINC01352, F11-AS1, LINC01232, n335586, XIST, SNHG5, SSTR5-AS1, and TRERNA1 regulate the gene expression through molecular sponging to sequester miRNAs; E: Long noncoding RNAs (lncRNAs) Ftx could produce miRNAs to regulate their target genes; F: LncRNA-Dreh and HULC could modulate protein stability; G: LncRNA HBVPTPAP could encode a small polypeptide to exert its function.

LNCRNAS AS POTENTIAL BIOMARKERS FOR DIAGNOSIS AND THERAPY OF HBV-RELATED HCC

It is suggested that HOTAIR may potentially be a novel HBV diagnostic biomarker based on its ability to facilitate HBV transcription and replication. This may not be practical because the commercially available diagnostic kits for HBV infection already have high specificities and sensitivities. On the other hand, the specificity and sensitivity of currently available tumor markers for HBV-related HCC (*e.g.*, α-fetoprotein) are not sufficient. This results in the poor prognosis of HBV-related HCC. This has encouraged researchers to search for novel potential biomarkers of HCC. Various miRNAs have been accepted to be biomarkers for diagnosis and therapy for HCC[119]. As an increasing number of lncRNAs, as well as the genetic polymorphisms in lncRNAs, have been found to contribute in the development of HBV-related HCC, researchers have tried to study whether these lncRNAs could be used as novel biomarkers for HBV-related HCC[120]. To be tumor markers, lncRNAs have the advantage over proteins because they can be amplified easily, *e.g.*, by RT-PCR. A number of lncRNAs dysregulated in HBV-related HCC have been suggested to be potential markers for HCCs. If these lncRNAs can be secreted to biological fluids, *e.g.*, blood, they can be easily detected. Therefore, those secreted lncRNAs are suggested to be potential markers for HBV-related HCC, such as HULC[121], IGF2AS[122], Linc00152[121], lncRNA-uc003wbd[123], lncRNA-AF085935[123], uc001ncr[124], AX800134[124], and UCA1[53-55]. However, most of these circulating lncRNAs aberrantly expressed in HBV-related HCC are also dysregulated in other tumors. It is better to identify a circulating lncRNA specific for HBV-related HCC diagnosis[125]. Alternatively, detection of several lncRNAs together could be an option[126-130].

Gene therapies such as RNA interference may become a common treatment for HCC in the future. In this way, lncRNAs can be the new therapeutic targets for HBV-related HCC. It is reported that metformin can suppress the HULC expression and block the progression of HBV-related HCC[131]. Thus, HULC could be a potential therapeutic target for RNA interference in HBV-related HCC treatment. Other lncRNAs upregulated in HBV-related HCC are also reported to be potential therapeutic targets[8] , such as MVIH[68] and HBx-LINE1[16]. On the other hand, an effective way to deliver lncRNA MEG3 RNA using MS2 virus-like-particles to inhibit HCC cells has been developed [132]. Other lncRNAs downregulated in HBV-related HCC could use a similar approach to treat HBV-related HCC, such as DREH[84] and LET[85]. Other advances in gene and epigenetic editing will enable correcting the aberrations caused by the dysregulated lncRNAs in HBV-related HCC in the future.

CONCLUSION

The important roles of lncRNAs in HBV replication and oncogenesis have started to emerge in recent years. Growing evidence indicates that some lncRNAs are dysregulated in HBV-infected cells and/or HBV-related HCC. Functional characterization of these lncRNAs has led to a more comprehensive understanding of HBV replication and oncogenesis. These lncRNAs have diverse functions, which are now beginning to be revealed. Although the progress regarding the role of lncRNAs in HBV-related HCC has been impressive, their roles in HBV replication, host immune responses, and HBV-related chronic diseases need further characterization. Even in HBV-related HCC, only a small part of lncRNAs has been well characterized, and a large portion of lncRNAs remains to be further explored. Thus, more efforts are required to understand the detailed mechanisms of these lncRNAs in the progression of HCC. The growing studies on the roles of lncRNAs in hepatocarcinogenesis could result in designing LncRNAs as potential biomarkers for diagnosis and therapy of HBV-related HCC.

Several technologies such as chromatin immunoprecipitation (ChIP), RNA sequencing, ChIP sequencing, tiled RNA expression arrays, cap analysis of gene expression, and serial analysis of gene expression have been used to detect lncRNAs. Only recently, different types of post-transcriptional chemical modifications of RNAs have been detected and characterized through sequencing-based, transcriptome-wide studies, *e.g.*, pseudouridine (Ψ), N6–methyladenosine and 5-methylcytosine. These modifications have been shown to affect the fate of RNA, including lncRNAs[133]. Further details about the roles of these chemical modifications of lncRNAs in HBV replication and oncogenesis are expected in the near future.

FOOTNOTES

Author contributions: Li HC and Lo SY wrote the manuscript; Yang CH and Lo SY drew the figures.

Conflict-of-interest statement: All the authors report no relevant conflicts of interest for this article.

Open-Access: This article is an open-access article that was selected by an in-house editor and fully peer-reviewed by external reviewers. It is distributed in accordance with the Creative Commons Attribution NonCommercial (CC BY-NC 4.0) license, which permits others to distribute, remix, adapt, build upon this work non-commercially, and license their derivative works on different terms, provided the original work is properly cited and the use is non-commercial. See: https://creativecommons.org/Licenses/by-nc/4.0/

Country/Territory of origin: Taiwan

ORCID number: Hui-Chun Li 0000-0002-0969-5676; Chee-Hing Yang 0000-0001-6129-272X; Shih-Yen Lo 0000-0001-8651-0148.

S-Editor: Fan JR
L-Editor: A
P-Editor: Fan JR

REFERENCES

1 **Han TS**, Hur K, Cho HS, Ban HS. Epigenetic Associations between lncRNA/circRNA and miRNA in Hepatocellular Carcinoma. *Cancers (Basel)* 2020; **12** [PMID: 32937886 DOI: 10.3390/cancers12092622]
2 **Zhang H**, Chen X, Zhang J, Wang X, Chen H, Liu L, Liu S. Long noncoding RNAs in HBVrelated hepatocellular carcinoma (Review). *Int J Oncol* 2020; **56**: 18-32 [PMID: 31746420 DOI: 10.3892/ijo.2019.4909]
3 **Parkin DM**. The global health burden of infection-associated cancers in the year 2002. *Int J Cancer* 2006; **118**: 3030-3044 [PMID: 16404738 DOI: 10.1002/ijc.21731]

4 **Tong S**, Revill P. Overview of hepatitis B viral replication and genetic variability. *J Hepatol* 2016; **64**: S4-S16 [PMID: 27084035 DOI: 10.1016/j.jhep.2016.01.027]

5 **Tsukuda S**, Watashi K. Hepatitis B virus biology and life cycle. *Antiviral Res* 2020; **182**: 104925 [PMID: 32866519 DOI: 10.1016/j.antiviral.2020.104925]

6 **Herrscher C**, Roingeard P, Blanchard E. Hepatitis B Virus Entry into Cells. *Cells* 2020; **9** [PMID: 32570893 DOI: 10.3390/cells9061486]

7 **Wei L**, Ploss A. Hepatitis B virus cccDNA is formed through distinct repair processes of each strand. *Nat Commun* 2021; **12**: 1591 [PMID: 33707452 DOI: 10.1038/s41467-021-21850-9]

8 **Qiu L**, Tang Q, Li G, Chen K. Long non-coding RNAs as biomarkers and therapeutic targets: Recent insights into hepatocellular carcinoma. *Life Sci* 2017; **191**: 273-282 [PMID: 28987633 DOI: 10.1016/j.lfs.2017.10.007]

9 **Salerno D**, Chiodo L, Alfano V, Floriot O, Cottone G, Paturel A, Pallocca M, Plissonnier ML, Jeddari S, Belloni L, Zeisel M, Levrero M, Guerrieri F. Hepatitis B protein HBx binds the DLEU2 LncRNA to sustain cccDNA and host cancer-related gene transcription. *Gut* 2020; **69**: 2016-2024 [PMID: 32114505 DOI: 10.1136/gutjnl-2019-319637]

10 **Ren F**, Ren JH, Song CL, Tan M, Yu HB, Zhou YJ, Qin YP, Cheng ST, Zhang Y, Huang AL, Chen J, Yang X. LncRNA HOTAIR modulates hepatitis B virus transcription and replication by enhancing SP1 transcription factor. *Clin Sci (Lond)* 2020; **134**: 3007-3022 [PMID: 33103728 DOI: 10.1042/CS20200970]

11 **Feng J**, Yang G, Liu Y, Gao Y, Zhao M, Bu Y, Yuan H, Yuan Y, Yun H, Sun M, Gao H, Zhang S, Liu Z, Yin M, Song X, Miao Z, Lin Z, Zhang X. LncRNA PCNAP1 modulates hepatitis B virus replication and enhances tumor growth of liver cancer. *Theranostics* 2019; **9**: 5227-5245 [PMID: 31410212 DOI: 10.7150/thno.34273]

12 **Liu Y**, Feng J, Sun M, Yang G, Yuan H, Wang Y, Bu Y, Zhao M, Zhang S, Zhang X. Long non-coding RNA HULC activates HBV by modulating HBx/STAT3/miR-539/APOBEC3B signaling in HBV-related hepatocellular carcinoma. *Cancer Lett* 2019; **454**: 158-170 [PMID: 30981758 DOI: 10.1016/j.canlet.2019.04.008]

13 **Yang G**, Feng J, Liu Y, Zhao M, Yuan Y, Yuan H, Yun H, Sun M, Bu Y, Liu L, Liu Z, Niu JQ, Yin M, Song X, Miao Z, Lin Z, Zhang X. HAT1 signaling confers to assembly and epigenetic regulation of HBV cccDNA minichromosome. *Theranostics* 2019; **9**: 7345-7358 [PMID: 31695772 DOI: 10.7150/thno.37173]

14 **Shahen SM**, Elshenawy SZ, Mohamed SE, Talaat RM. Genetic polymorphisms in the miR-372 (rs12983273) and LncRNA HULC (rs7763881) genes and susceptibility to Hepatitis B virus (HBV) infection. *Mol Biol Rep* 2021; **48**: 7901-7906 [PMID: 34677712 DOI: 10.1007/s11033-021-06818-8]

15 **Wen J**, Liu Y, Liu J, Liu L, Song C, Han J, Zhu L, Wang C, Chen J, Zhai X, Shen H, Hu Z. Expression quantitative trait loci in long non-coding RNA ZNRD1-AS1 influence both HBV infection and hepatocellular carcinoma development. *Mol Carcinog* 2015; **54**: 1275-1282 [PMID: 25110835 DOI: 10.1002/mc.22200]

16 **Liang HW**, Wang N, Wang Y, Wang F, Fu Z, Yan X, Zhu H, Diao W, Ding Y, Chen X, Zhang CY, Zen K. Hepatitis B virus-human chimeric transcript HBx-LINE1 promotes hepatic injury *via* sequestering cellular microRNA-122. *J Hepatol* 2016; **64**: 278-291 [PMID: 26409216 DOI: 10.1016/j.jhep.2015.09.013]

17 **Li C**, Wang Y, Wang S, Wu B, Hao J, Fan H, Ju Y, Ding Y, Chen L, Chu X, Liu W, Ye X, Meng S. Hepatitis B virus mRNA-mediated miR-122 inhibition upregulates PTTG1-binding protein, which promotes hepatocellular carcinoma tumor growth and cell invasion. *J Virol* 2013; **87**: 2193-2205 [PMID: 23221562 DOI: 10.1128/JVI.02831-12]

18 **Hao Q**, Wang Z, Wang Q, Chen B, Qian H, Liu X, Cao H, Xia W, Jiang J, Lu Z. Identification and characterization of lncRNA AP000253 in occult hepatitis B virus infection. *Virol J* 2021; **18**: 125 [PMID: 34112188 DOI: 10.1186/s12985-021-01596-y]

19 **Zhao X**, Fan H, Chen X, Zhao X, Wang X, Feng Y, Liu M, Li S, Tang H. Hepatitis B Virus DNA Polymerase Restrains Viral Replication Through the CREB1/HOXA Distal Transcript Antisense RNA Homeobox A13 Axis. *Hepatology* 2021; **73**: 503-519 [PMID: 32314410 DOI: 10.1002/hep.31284]

20 **Pan J**, Tong S, Tang J. LncRNA expression profiles in HBV-transformed human hepatocellular carcinoma cells treated with a novel inhibitor of human La protein. *J Viral Hepat* 2018; **25**: 391-400 [PMID: 29091324 DOI: 10.1111/jvh.12821]

21 **Yao J**, Lin C, Jiang J, Zhang X, Li F, Liu T, Diao H. lncRNA-HEIM Facilitated Liver Fibrosis by Up-Regulating TGF-β Expression in Long-Term Outcome of Chronic Hepatitis B. *Front Immunol* 2021; **12**: 666370 [PMID: 34168644 DOI: 10.3389/fimmu.2021.666370]

22 **Liu X**, Li C, Zhu J, Li W, Zhu Q. Dysregulation of FTX/miR-545 signaling pathway downregulates Tim-3 and is responsible for the abnormal activation of macrophage in cirrhosis. *J Cell Biochem* 2018 [PMID: 30304545 DOI: 10.1002/jcb.27562]

23 **Wu J**, Niu Q, Yuan J, Xu X, Cao L. lncRNA-CD160 decreases the immunity of $CD8^+$ T cells through epigenetic mechanisms in hepatitis B virus infection. *Oncol Lett* 2020; **20**: 235-247 [PMID: 32565950 DOI: 10.3892/ol.2020.11534]

24 **Zhuang L**, Tian J, Zhang X, Wang H, Huang C. Lnc-DC regulates cellular turnover and the HBV-induced immune response by TLR9/STAT3 signaling in dendritic cells. *Cell Mol Biol Lett* 2018; **23**: 43 [PMID: 30202418 DOI: 10.1186/s11658-018-0108-y]

25 **Nishitsuji H**, Ujino S, Yoshio S, Sugiyama M, Mizokami M, Kanto T, Shimotohno K. Long noncoding RNA #32 contributes to antiviral responses by controlling interferon-stimulated gene expression. *Proc Natl Acad Sci U S A* 2016; **113**: 10388-10393 [PMID: 27582466 DOI: 10.1073/pnas.1525022113]

26 **D'souza S**, Lau KC, Coffin CS, Patel TR. Molecular mechanisms of viral hepatitis induced hepatocellular carcinoma. *World J Gastroenterol* 2020; **26**: 5759-5783 [PMID: 33132633 DOI: 10.3748/wjg.v26.i38.5759]

27 **Shoraka S**, Mohebbi SR, Hosseini SM, Asadzadeh Aghdaei H, Zali MR. Identification of plasma lncRNA-ATB levels in hepatitis B virus-related cirrhosis and non-cirrhotic chronic hepatitis B patients. *Virus Res* 2021; **303**: 198503 [PMID: 34331990 DOI: 10.1016/j.virusres.2021.198503]

28 **Wang S**, Jiang J, Zhang C, Zhang X, Wang C. Serum lincRNA-p21 expression in primary liver diseases and liver metastatic diseases. *Pathol Res Pract* 2019; **215**: 779-783 [PMID: 30704781 DOI: 10.1016/j.prp.2019.01.014]

29 **Li LJ**, Wu XY, Tan SW, Xie ZJ, Pan XM, Pan SW, Bai WR, Li HJ, Liu HL, Jiang J, Wu B. Lnc-TCL6 is a potential biomarker for early diagnosis and grade in liver-cirrhosis patients. *Gastroenterol Rep (Oxf)* 2019; **7**: 434-443 [PMID: 31857905 DOI: 10.1093/gastro/goz050]

30 **Li JZ**, Ye LH, Wang DH, Zhang HC, Li TY, Liu ZQ, Dai EH, Li MR. The identify role and molecular mechanism of the MALAT1/hsa-mir-20b-5p/TXNIP axis in liver inflammation caused by CHB in patients with chronic HBV infection complicated with NAFLD. *Virus Res* 2021; **298**: 198405 [PMID: 33775752 DOI: 10.1016/j.virusres.2021.198405]

31 **Chen MJ**, Wang XG, Sun ZX, Liu XC. Diagnostic value of LncRNA-MEG3 as a serum biomarker in patients with hepatitis B complicated with liver fibrosis. *Eur Rev Med Pharmacol Sci* 2019; **23**: 4360-4367 [PMID: 31173310 DOI: 10.26355/eurrev_201905_17943]

32 **Guo Y**, Li C, Zhang R, Zhan Y, Yu J, Tu J, Zheng J. Epigenetically-regulated serum GAS5 as a potential biomarker for patients with chronic hepatitis B virus infection. *Cancer Biomark* 2021; **32**: 137-146 [PMID: 34092613 DOI: 10.3233/CBM-203169]

33 **Fu X**, Cheng D, Ouyang Y, Li Y, Li R, Peng S, Fu L. Integrated Analysis of Long Noncoding RNA Expression Profiles in Acute-on-Chronic Liver Failure. *Biomed Res Int* 2021; **2021**: 5387856 [PMID: 34104647 DOI: 10.1155/2021/5387856]

34 **Kulik L**, El-Serag HB. Epidemiology and Management of Hepatocellular Carcinoma. *Gastroenterology* 2019; **156**: 477-491.e1 [PMID: 30367835 DOI: 10.1053/j.gastro.2018.08.065]

35 **Chaturvedi VK**, Singh A, Dubey SK, Hetta HF, John J, Singh MP. Molecular mechanistic insight of hepatitis B virus mediated hepatocellular carcinoma. *Microb Pathog* 2019; **128**: 184-194 [PMID: 30611768 DOI: 10.1016/j.micpath.2019.01.004]

36 **Bousali M**, Papatheodoridis G, Paraskevis D, Karamitros T. Hepatitis B Virus DNA Integration, Chronic Infections and Hepatocellular Carcinoma. *Microorganisms* 2021; **9** [PMID: 34442866 DOI: 10.3390/microorganisms9081787]

37 **Zhang B**, Han S, Feng B, Chu X, Chen L, Wang R. Hepatitis B virus X protein-mediated non-coding RNA aberrations in the development of human hepatocellular carcinoma. *Exp Mol Med* 2017; **49**: e293 [PMID: 28186085 DOI: 10.1038/emm.2016.177]

38 **Pan YF**, Qin T, Feng L, Yu ZJ. Expression profile of altered long non-coding RNAs in patients with HBV-associated hepatocellular carcinoma. *J Huazhong Univ Sci Technolog Med Sci* 2013; **33**: 96-101 [PMID: 23392715 DOI: 10.1007/s11596-013-1078-y]

39 **Yu TT**, Xu XM, Hu Y, Deng JJ, Ge W, Han NN, Zhang MX. Long noncoding RNAs in hepatitis B virus-related hepatocellular carcinoma. *World J Gastroenterol* 2015; **21**: 7208-7217 [PMID: 26109807 DOI: 10.3748/wjg.v21.i23.7208]

40 **Fang ZX**, Niu JJ, Liu PG, Lin Y. Genome-wide long noncoding RNA and mRNA expression profiles demonstrate associations between exposure to inorganic elements and the risk of developing hepatocellular carcinoma. *BMC Med Genomics* 2021; **14**: 85 [PMID: 33736645 DOI: 10.1186/s12920-021-00927-w]

41 **Jin Y**, Wu D, Yang W, Weng M, Li Y, Wang X, Zhang X, Jin X, Wang T. Hepatitis B virus x protein induces epithelial-mesenchymal transition of hepatocellular carcinoma cells by regulating long non-coding RNA. *Virol J* 2017; **14**: 238 [PMID: 29258558 DOI: 10.1186/s12985-017-0903-5]

42 **Du Y**, Kong G, You X, Zhang S, Zhang T, Gao Y, Ye L, Zhang X. Elevation of highly up-regulated in liver cancer (HULC) by hepatitis B virus X protein promotes hepatoma cell proliferation *via* down-regulating p18. *J Biol Chem* 2012; **287**: 26302-26311 [PMID: 22685290 DOI: 10.1074/jbc.M112.342113]

43 **Lu Z**, Xiao Z, Liu F, Cui M, Li W, Yang Z, Li J, Ye L, Zhang X. Long non-coding RNA HULC promotes tumor angiogenesis in liver cancer by up-regulating sphingosine kinase 1 (SPHK1). *Oncotarget* 2016; **7**: 241-254 [PMID: 26540633 DOI: 10.18632/oncotarget.6280]

44 **Yu X**, Zheng H, Chan MT, Wu WK. HULC: an oncogenic long non-coding RNA in human cancer. *J Cell Mol Med* 2017; **21**: 410-417 [PMID: 27781386 DOI: 10.1111/jcmm.12956]

45 **Zhang H**, Diab A, Fan H, Mani SK, Hullinger R, Merle P, Andrisani O. PLK1 and HOTAIR Accelerate Proteasomal Degradation of SUZ12 and ZNF198 during Hepatitis B Virus-Induced Liver Carcinogenesis. *Cancer Res* 2015; **75**: 2363-2374 [PMID: 25855382 DOI: 10.1158/0008-5472.CAN-14-2928]

46 **Balas MM**, Hartwick EW, Barrington C, Roberts JT, Wu SK, Bettcher R, Griffin AM, Kieft JS, Johnson AM. Establishing RNA-RNA interactions remodels lncRNA structure and promotes PRC2 activity. *Sci Adv* 2021; **7** [PMID: 33853770 DOI: 10.1126/sciadv.abc9191]

47 **Fu WM**, Zhu X, Wang WM, Lu YF, Hu BG, Wang H, Liang WC, Wang SS, Ko CH, Waye MM, Kung HF, Li G, Zhang JF. Hotair mediates hepatocarcinogenesis through suppressing miRNA-218 expression and activating P14 and P16 signaling. *J Hepatol* 2015; **63**: 886-895 [PMID: 26024833 DOI: 10.1016/j.jhep.2015.05.016]

48 **He Y**, Meng XM, Huang C, Wu BM, Zhang L, Lv XW, Li J. Long noncoding RNAs: Novel insights into hepatocelluar carcinoma. *Cancer Lett* 2014; **344**: 20-27 [PMID: 24183851 DOI: 10.1016/j.canlet.2013.10.021]

49 **Lau CC**, Sun T, Ching AK, He M, Li JW, Wong AM, Co NN, Chan AW, Li PS, Lung RW, Tong JH, Lai PB, Chan HL, To KF, Chan TF, Wong N. Viral-human chimeric transcript predisposes risk to liver cancer development and progression. *Cancer Cell* 2014; **25**: 335-349 [PMID: 24582836 DOI: 10.1016/j.ccr.2014.01.030]

50 Hepatitis B viral insertion generates an oncogenic long noncoding RNA. *Cancer Discov* 2014; **4**: OF13 [PMID: 24795017 DOI: 10.1158/2159-8290.CD-RW2014-058]

51 **Trung NT**, Hai LT, Giang DP, Hoan PQ, Binh MT, Hoan NX, Toan NL, Meyer CG, Velavan TP, Bang MH, Song LH. No expression of HBV-human chimeric fusion transcript (HBx-LINE1) among Vietnamese patients with HBV-associated hepatocellular carcinoma. *Ann Hepatol* 2019; **18**: 404-405 [PMID: 31036498 DOI: 10.1016/j.aohep.2019.02.002]

52 **Xue M**, Chen W, Li X. Urothelial cancer associated 1: a long noncoding RNA with a crucial role in cancer. *J Cancer Res Clin Oncol* 2016; **142**: 1407-1419 [PMID: 26341664 DOI: 10.1007/s00432-015-2042-y]

53 **Hu JJ**, Song W, Zhang SD, Shen XH, Qiu XM, Wu HZ, Gong PH, Lu S, Zhao ZJ, He ML, Fan H. HBx-upregulated lncRNA UCA1 promotes cell growth and tumorigenesis by recruiting EZH2 and repressing p27Kip1/CDK2 signaling. *Sci Rep* 2016; **6**: 23521 [PMID: 27009634 DOI: 10.1038/srep23521]

54 **Wang F**, Ying HQ, He BS, Pan YQ, Deng QW, Sun HL, Chen J, Liu X, Wang SK. Upregulated lncRNA-UCA1 contributes to progression of hepatocellular carcinoma through inhibition of miR-216b and activation of FGFR1/ERK signaling pathway. *Oncotarget* 2015; **6**: 7899-7917 [PMID: 25760077 DOI: 10.18632/oncotarget.3219]

55 **Xiao JN**, Yan TH, Yu RM, Gao Y, Zeng WL, Lu SW, Que HX, Liu ZP, Jiang JH. Long non-coding RNA UCA1

regulates the expression of Snail2 by miR-203 to promote hepatocellular carcinoma progression. *J Cancer Res Clin Oncol* 2017; **143**: 981-990 [PMID: 28271214 DOI: 10.1007/s00432-017-2370-1]

56 **Bao J**, Chen X, Hou Y, Kang G, Li Q, Xu Y. LncRNA DBH-AS1 facilitates the tumorigenesis of hepatocellular carcinoma by targeting miR-138 *via* FAK/Src/ERK pathway. *Biomed Pharmacother* 2018; **107**: 824-833 [PMID: 30142544 DOI: 10.1016/j.biopha.2018.08.079]

57 **Zhang Q**, Matsuura K, Kleiner DE, Zamboni F, Alter HJ, Farci P. Analysis of long noncoding RNA expression in hepatocellular carcinoma of different viral etiology. *J Transl Med* 2016; **14**: 328 [PMID: 27894309 DOI: 10.1186/s12967-016-1085-4]

58 **Pasmant E**, Laurendeau I, Héron D, Vidaud M, Vidaud D, Bièche I. Characterization of a germ-line deletion, including the entire INK4/ARF locus, in a melanoma-neural system tumor family: identification of ANRIL, an antisense noncoding RNA whose expression coclusters with ARF. *Cancer Res* 2007; **67**: 3963-3969 [PMID: 17440112 DOI: 10.1158/0008-5472.CAN-06-2004]

59 **Huang MD**, Chen WM, Qi FZ, Xia R, Sun M, Xu TP, Yin L, Zhang EB, De W, Shu YQ. Long non-coding RNA ANRIL is upregulated in hepatocellular carcinoma and regulates cell apoptosis by epigenetic silencing of KLF2. *J Hematol Oncol* 2015; **8**: 50 [PMID: 25966845 DOI: 10.1186/s13045-015-0146-0]

60 **Ma J**, Li T, Han X, Yuan H. Knockdown of LncRNA ANRIL suppresses cell proliferation, metastasis, and invasion *via* regulating miR-122-5p expression in hepatocellular carcinoma. *J Cancer Res Clin Oncol* 2018; **144**: 205-214 [PMID: 29127494 DOI: 10.1007/s00432-017-2543-y]

61 **Deng X**, Zhao XF, Liang XQ, Chen R, Pan YF, Liang J. Linc00152 promotes cancer progression in hepatitis B virus-associated hepatocellular carcinoma. *Biomed Pharmacother* 2017; **90**: 100-108 [PMID: 28343069 DOI: 10.1016/j.biopha.2017.03.031]

62 **Tripathi V**, Ellis JD, Shen Z, Song DY, Pan Q, Watt AT, Freier SM, Bennett CF, Sharma A, Bubulya PA, Blencowe BJ, Prasanth SG, Prasanth KV. The nuclear-retained noncoding RNA MALAT1 regulates alternative splicing by modulating SR splicing factor phosphorylation. *Mol Cell* 2010; **39**: 925-938 [PMID: 20797886 DOI: 10.1016/j.molcel.2010.08.011]

63 **Hou Z**, Xu X, Fu X, Tao S, Zhou J, Liu S, Tan D. HBx-related long non-coding RNA MALAT1 promotes cell metastasis *via* up-regulating LTBP3 in hepatocellular carcinoma. *Am J Cancer Res* 2017; **7**: 845-856 [PMID: 28469957]

64 **Huang Z**, Huang L, Shen S, Li J, Lu H, Mo W, Dang Y, Luo D, Chen G, Feng Z. Sp1 cooperates with Sp3 to upregulate MALAT1 expression in human hepatocellular carcinoma. *Oncol Rep* 2015; **34**: 2403-2412 [PMID: 26352013 DOI: 10.3892/or.2015.4259]

65 **Miyagawa R**, Tano K, Mizuno R, Nakamura Y, Ijiri K, Rakwal R, Shibato J, Masuo Y, Mayeda A, Hirose T, Akimitsu N. Identification of cis- and trans-acting factors involved in the localization of MALAT-1 noncoding RNA to nuclear speckles. *RNA* 2012; **18**: 738-751 [PMID: 22355166 DOI: 10.1261/rna.028639.111]

66 **Lai MC**, Yang Z, Zhou L, Zhu QQ, Xie HY, Zhang F, Wu LM, Chen LM, Zheng SS. Long non-coding RNA MALAT-1 overexpression predicts tumor recurrence of hepatocellular carcinoma after liver transplantation. *Med Oncol* 2012; **29**: 1810-1816 [PMID: 21678027 DOI: 10.1007/s12032-011-0004-z]

67 **Romito A**, Rougeulle C. Origin and evolution of the long non-coding genes in the X-inactivation center. *Biochimie* 2011; **93**: 1935-1942 [PMID: 21820484 DOI: 10.1016/j.biochi.2011.07.009]

68 **Yuan SX**, Yang F, Yang Y, Tao QF, Zhang J, Huang G, Wang RY, Yang S, Huo XS, Zhang L, Wang F, Sun SH, Zhou WP. Long noncoding RNA associated with microvascular invasion in hepatocellular carcinoma promotes angiogenesis and serves as a predictor for hepatocellular carcinoma patients' poor recurrence-free survival after hepatectomy. *Hepatology* 2012; **56**: 2231-2241 [PMID: 22706893 DOI: 10.1002/hep.25895]

69 **Lv J**, Fan HX, Zhao XP, Lv P, Fan JY, Zhang Y, Liu M, Tang H. Long non-coding RNA Unigene56159 promotes epithelial-mesenchymal transition by acting as a ceRNA of miR-140-5p in hepatocellular carcinoma cells. *Cancer Lett* 2016; **382**: 166-175 [PMID: 27597739 DOI: 10.1016/j.canlet.2016.08.029]

70 **Guo L**, Gao S, Sun W, Wang Y, Zhao J. Elevated LINC01232 is associated with poor prognosis and HBV infection in hepatocellular carcinoma patients and contributes to tumor progression in vitro. *Clin Res Hepatol Gastroenterol* 2022; **46**: 101813 [PMID: 34583064 DOI: 10.1016/j.clinre.2021.101813]

71 **Liu Q**, Liu N, Shangguan Q, Zhang F, Chai W, Tong X, Zhao X, Li Z, Qi D, Ye X. LncRNA SAMD12-AS1 promotes cell proliferation and inhibits apoptosis by interacting with NPM1. *Sci Rep* 2019; **9**: 11593 [PMID: 31406141 DOI: 10.1038/s41598-019-48116-1]

72 **Liu N**, Liu Q, Yang X, Zhang F, Li X, Ma Y, Guan F, Zhao X, Li Z, Zhang L, Ye X. Hepatitis B Virus-Upregulated LNC-HUR1 Promotes Cell Proliferation and Tumorigenesis by Blocking p53 Activity. *Hepatology* 2018; **68**: 2130-2144 [PMID: 29790592 DOI: 10.1002/hep.30098]

73 **Fan H**, Lv P, Mu T, Zhao X, Liu Y, Feng Y, Lv J, Liu M, Tang H. LncRNA n335586/miR-924/CKMT1A axis contributes to cell migration and invasion in hepatocellular carcinoma cells. *Cancer Lett* 2018; **429**: 89-99 [DOI: 10.1016/j.canlet.2018.05.010]

74 **Wang J**, Yin G, Bian H, Yang J, Zhou P, Yan K, Liu C, Chen P, Zhu J, Li Z, Xue T. LncRNA XIST upregulates TRIM25 *via* negatively regulating miR-192 in hepatitis B virus-related hepatocellular carcinoma. *Mol Med* 2021; **27**: 41 [PMID: 33858324 DOI: 10.1186/s10020-021-00278-3]

75 **Li Y**, Guo D, Zhao Y, Ren M, Lu G, Wang Y, Zhang J, Mi C, He S, Lu X. Long non-coding RNA SNHG5 promotes human hepatocellular carcinoma progression by regulating miR-26a-5p/GSK3β signal pathway. *Cell Death Dis* 2018; **9**: 888 [PMID: 30166525 DOI: 10.1038/s41419-018-0882-5]

76 **Hu Z**, Huang P, Yan Y, Zhou Z, Wang J, Wu G. Hepatitis B virus X protein related lncRNA WEE2-AS1 promotes hepatocellular carcinoma proliferation and invasion. *Biochem Biophys Res Commun* 2019; **508**: 79-86 [PMID: 30471857 DOI: 10.1016/j.bbrc.2018.11.091]

77 **Zhang F**, Li Y, Gan L, Tong X, Qi D, Wang Q, Ye X. HBx-upregulated MAFG-AS1 promotes cell proliferation and migration of hepatoma cells by enhancing MAFG expression and stabilizing nonmuscle myosin IIA. *FASEB J* 2021; **35**: e21529 [PMID: 33813778 DOI: 10.1096/fj.202002374R]

78 **Zhang Y**, Li J, Wang S, Yang F, Zhou Y, Liu Y, Zhu W, Shi X. HBxassociated long noncoding RNA activated by TGFβ

promotes cell invasion and migration by inducing autophagy in primary liver cancer. *Int J Oncol* 2020; **56**: 337-347 [PMID: 31746419 DOI: 10.3892/ijo.2019.4908]

79 **Song W**, Zheng C, Liu M, Xu Y, Qian Y, Zhang Z, Su H, Li X, Wu H, Gong P, Li Y, Fan H. TRERNA1 upregulation mediated by HBx promotes sorafenib resistance and cell proliferation in HCC *via* targeting NRAS by sponging miR-22-3p. *Mol Ther* 2021; **29**: 2601-2616 [PMID: 33839325 DOI: 10.1016/j.ymthe.2021.04.011]

80 **Chen Z**, Yu W, Zhou Q, Zhang J, Jiang H, Hao D, Wang J, Zhou Z, He C, Xiao Z. A Novel lncRNA IHS Promotes Tumor Proliferation and Metastasis in HCC by Regulating the ERK- and AKT/GSK-3β-Signaling Pathways. *Mol Ther Nucleic Acids* 2019; **16**: 707-720 [PMID: 31128422 DOI: 10.1016/j.omtn.2019.04.021]

81 **Tu W**, Yang Y, Song Y, Zhu W. Hepatitis B virus x protein accelerated the proliferation of hepatocellular carcinoma cell through lncRNA SNHG20/PTEN pathway. *J Biochem* 2019; **165**: 423-431 [PMID: 30690477 DOI: 10.1093/jb/mvy120]

82 **Zuo K**, Kong L, Xue D, Yang Y, Xie L. The expression and role of lncRNA AX800134 in hepatitis B virus-related hepatocellular carcinoma. *Virus Genes* 2018; **54**: 475-483 [PMID: 29789998 DOI: 10.1007/s11262-018-1564-1]

83 **Qiu L**, Wang T, Xu X, Wu Y, Tang Q, Chen K. Long Non-Coding RNAs in Hepatitis B Virus-Related Hepatocellular Carcinoma: Regulation, Functions, and Underlying Mechanisms. *Int J Mol Sci* 2017; **18** [PMID: 29168767 DOI: 10.3390/ijms18122505]

84 **Lv D**, Wang Y, Zhang Y, Cui P, Xu Y. Downregulated long non-coding RNA DREH promotes cell proliferation in hepatitis B virus-associated hepatocellular carcinoma. *Oncol Lett* 2017; **14**: 2025-2032 [PMID: 28789433 DOI: 10.3892/ol.2017.6436]

85 **Yang F**, Huo XS, Yuan SX, Zhang L, Zhou WP, Wang F, Sun SH. Repression of the long noncoding RNA-LET by histone deacetylase 3 contributes to hypoxia-mediated metastasis. *Mol Cell* 2013; **49**: 1083-1096 [PMID: 23395002 DOI: 10.1016/j.molcel.2013.01.010]

86 **Castella S**, Bernard R, Corno M, Fradin A, Larcher JC. Ilf3 and NF90 functions in RNA biology. *Wiley Interdiscip Rev RNA* 2015; **6**: 243-256 [PMID: 25327818 DOI: 10.1002/wrna.1270]

87 **Luo HL**, Chen J, Luo T, Wu FX, Liu JJ, Wang HF, Chen M, Li LQ, Li H. Downregulation of Macrophage-Derived T-UCR uc.306 Associates with Poor Prognosis in Hepatocellular Carcinoma. *Cell Physiol Biochem* 2017; **42**: 1526-1539 [PMID: 28723685 DOI: 10.1159/000479269]

88 **Xiang L**, Huang X, Wang S, Ou H, Chen Z, Hu Z, Huang Y, Li X, Yuan Y, Yang D. Deficiency of pseudogene UPAT leads to hepatocellular carcinoma progression and forms a positive feedback loop with ZEB1. *Cancer Sci* 2020; **111**: 4102-4117 [PMID: 32808348 DOI: 10.1111/cas.14620]

89 **Yu S**, Li N, Wang J, Fu Y, Huang Y, Yi P, Chen R, Tang D, Hu X, Fan X. Correlation of Long Noncoding RNA SEMA6A-AS1 Expression with Clinical Outcome in HBV-Related Hepatocellular Carcinoma. *Clin Ther* 2020; **42**: 439-447 [PMID: 32070484 DOI: 10.1016/j.clinthera.2020.01.012]

90 **Zhao NN**, Wang C, Lai CC, Cheng SJ, Yan J, Hong ZX, Yu LX, Zhu ZY, Zhang PR, Wang ZH, Wang XL, Zhang SG, Yang PH. Downregulation of BRAF-activated non-protein coding RNA in patients with hepatitis B virus-associated hepatocellular carcinoma. *Oncol Lett* 2018; **15**: 7794-7798 [PMID: 29725471 DOI: 10.3892/ol.2018.8327]

91 **Lin X**, Xiaoqin H, Jiayu C, Li F, Yue L, Ximing X. Long non-coding RNA miR143HG predicts good prognosis and inhibits tumor multiplication and metastasis by suppressing mitogen-activated protein kinase and Wnt signaling pathways in hepatocellular carcinoma. *Hepatol Res* 2019; **49**: 902-918 [PMID: 30945380 DOI: 10.1111/hepr.13344]

92 **Yu S**, Li N, Huang Z, Chen R, Yi P, Kang R, Tang D, Hu X, Fan X. A novel lncRNA, TCONS_00006195, represses hepatocellular carcinoma progression by inhibiting enzymatic activity of ENO1. *Cell Death Dis* 2018; **9**: 1184 [PMID: 30518748 DOI: 10.1038/s41419-018-1231-4]

93 **Huang P**, Xu Q, Yan Y, Lu Y, Hu Z, Ou B, Zhang H, Mao K, Zhang J, Wang J, Xiao Z. HBx/ERα complex-mediated LINC01352 downregulation promotes HBV-related hepatocellular carcinoma *via* the miR-135b-APC axis. *Oncogene* 2020; **39**: 3774-3789 [PMID: 32157216 DOI: 10.1038/s41388-020-1254-z]

94 **Deng Y**, Wei Z, Huang M, Xu G, Wei W, Peng B, Nong S, Qin H. Long non-coding RNA F11-AS1 inhibits HBV-related hepatocellular carcinoma progression by regulating NR1I3 *via* binding to microRNA-211-5p. *J Cell Mol Med* 2020; **24**: 1848-1865 [PMID: 31880390 DOI: 10.1111/jcmm.14881]

95 **Liu Y**, Xu L, Lu B, Zhao M, Li L, Sun W, Qiu Z, Zhang B. LncRNA H19/microRNA-675/PPARα axis regulates liver cell injury and energy metabolism remodelling induced by hepatitis B X protein *via* Akt/mTOR signalling. *Mol Immunol* 2019; **116**: 18-28 [PMID: 31574452 DOI: 10.1016/j.molimm.2019.09.006]

96 **Ge L**, Zhang X, Hu S, Song Y, Kong J, Zhang B, Yang X. H19 suppresses the growth of hepatoblastoma cells by promoting their apoptosis *via* the signaling pathways of miR-675/FADD and miR-138/PTK2. *J Cell Biochem* 2019; **120**: 5218-5231 [PMID: 30367502 DOI: 10.1002/jcb.27797]

97 **Li H**, Tang XM, Liu Y, Li W, Chen Q, Pan Y. Association of Functional Genetic Variants of HOTAIR with Hepatocellular Carcinoma (HCC) Susceptibility in a Chinese Population. *Cell Physiol Biochem* 2017; **44**: 447-454 [PMID: 29141248 DOI: 10.1159/000485011]

98 **Chang L**, Li C, Lan T, Wu L, Yuan Y, Liu Q, Liu Z. Decreased expression of long non-coding RNA GAS5 indicates a poor prognosis and promotes cell proliferation and invasion in hepatocellular carcinoma by regulating vimentin. *Mol Med Rep* 2016; **13**: 1541-1550 [PMID: 26707238 DOI: 10.3892/mmr.2015.4716]

99 **Tao R**, Hu S, Wang S, Zhou X, Zhang Q, Wang C, Zhao X, Zhou W, Zhang S, Li C, Zhao H, He Y, Zhu S, Xu J, Jiang Y, Li L, Gao Y. Association between indel polymorphism in the promoter region of lncRNA GAS5 and the risk of hepatocellular carcinoma. *Carcinogenesis* 2015; **36**: 1136-1143 [PMID: 26163879 DOI: 10.1093/carcin/bgv099]

100 **Zhu Z**, Gao X, He Y, Zhao H, Yu Q, Jiang D, Zhang P, Ma X, Huang H, Dong D, Wan J, Gu Z, Jiang X, Yu L, Gao Y. An insertion/deletion polymorphism within RERT-lncRNA modulates hepatocellular carcinoma risk. *Cancer Res* 2012; **72**: 6163-6172 [PMID: 23026137 DOI: 10.1158/0008-5472.CAN-12-0010]

101 **Wan J**, Huang M, Zhao H, Wang C, Zhao X, Jiang X, Bian S, He Y, Gao Y. A novel tetranucleotide repeat polymorphism within KCNQ1OT1 confers risk for hepatocellular carcinoma. *DNA Cell Biol* 2013; **32**: 628-634 [PMID: 23984860 DOI: 10.1089/dna.2013.2118]

102 **Zhong R**, Tian J, Fu M, Ma S, Liu L, Li J, Shen N, Ke J, Yang Y, Gong Y, Zhu Y, Wang Y, Gong J, Chang J, Lei P,

Cheng X, Huang K, Shen G, Miao X. LINC01149 variant modulates MICA expression that facilitates hepatitis B virus spontaneous recovery but increases hepatocellular carcinoma risk. *Oncogene* 2020; **39**: 1944-1956 [PMID: 31754211 DOI: 10.1038/s41388-019-1117-7]

103 **Lin YY**, Yu MW, Lin SM, Lee SD, Chen CL, Chen DS, Chen PJ. Genome-wide association analysis identifies a GLUL haplotype for familial hepatitis B virus-related hepatocellular carcinoma. *Cancer* 2017; **123**: 3966-3976 [PMID: 28662289 DOI: 10.1002/cncr.30851]

104 **Yin J**, Wen J, Hang D, Han J, Jiang J, Song C, Liu Y, Liu J, Liu L, Zhu L, Chen J, Zhai X, Xie S, Hu Z, Shen H, Dai M, Li N. Expression Quantitative Trait Loci for CARD8 Contributes to Risk of Two Infection-Related Cancers--Hepatocellular Carcinoma and Cervical Cancer. *PLoS One* 2015; **10**: e0132352 [PMID: 26147888 DOI: 10.1371/journal.pone.0132352]

105 **Wen J**, Song C, Liu J, Chen J, Zhai X, Hu Z. Expression quantitative trait loci for TNFRSF10 influence both HBV infection and hepatocellular carcinoma development. *J Med Virol* 2016; **88**: 474-480 [PMID: 26297860 DOI: 10.1002/jmv.24363]

106 **Ma S**, Yang J, Song C, Ge Z, Zhou J, Zhang G, Hu Z. Expression quantitative trait loci for PAX8 contributes to the prognosis of hepatocellular carcinoma. *PLoS One* 2017; **12**: e0173700 [PMID: 28339471 DOI: 10.1371/journal.pone.0173700]

107 **Liu Q**, Liu G, Lin Z, Tian N, Lin X, Tan J, Huang B, Ji X, Pi L, Yu X, Liu L, Gao Y. The association of lncRNA SNPs and SNPs-environment interactions based on GWAS with HBV-related HCC risk and progression. *Mol Genet Genomic Med* 2021; **9**: e1585 [PMID: 33432784 DOI: 10.1002/mgg3.1585]

108 **Huang X**, Zhang W, Shao Z. Association between long non-coding RNA polymorphisms and cancer risk: a meta-analysis. *Biosci Rep* 2018; **38** [PMID: 29802154 DOI: 10.1042/BSR20180365]

109 **Bhat SA**, Ahmad SM, Mumtaz PT, Malik AA, Dar MA, Urwat U, Shah RA, Ganai NA. Long non-coding RNAs: Mechanism of action and functional utility. *Noncoding RNA Res* 2016; **1**: 43-50 [PMID: 30159410 DOI: 10.1016/j.ncrna.2016.11.002]

110 **Lun YZ**, Pan ZP, Liu SA, Sun J, Han M, Liu B, Dong W, Pan LH, Cheng J. The peptide encoded by a novel putative lncRNA HBVPTPAP inducing the apoptosis of hepatocellular carcinoma cells by modulating JAK/STAT signaling pathways. *Virus Res* 2020; **287**: 198104 [PMID: 32755630 DOI: 10.1016/j.virusres.2020.198104]

111 **Jiang B**, Yang B, Wang Q, Zheng X, Guo Y, Lu W. lncRNA PVT1 promotes hepatitis B viruspositive liver cancer progression by disturbing histone methylation on the cMyc promoter. *Oncol Rep* 2020; **43**: 718-726 [PMID: 31894346 DOI: 10.3892/or.2019.7444]

112 **Kotake Y**, Nakagawa T, Kitagawa K, Suzuki S, Liu N, Kitagawa M, Xiong Y. Long non-coding RNA ANRIL is required for the PRC2 recruitment to and silencing of p15(INK4B) tumor suppressor gene. *Oncogene* 2011; **30**: 1956-1962 [PMID: 21151178 DOI: 10.1038/onc.2010.568]

113 **Chen T**, Pei J, Wang J, Luo R, Liu L, Wang L, Jia H. HBx-related long non-coding RNA 01152 promotes cell proliferation and survival by IL-23 in hepatocellular carcinoma. *Biomed Pharmacother* 2019; **115**: 108877 [PMID: 31054511 DOI: 10.1016/j.biopha.2019.108877]

114 **Salmena L**, Poliseno L, Tay Y, Kats L, Pandolfi PP. A ceRNA hypothesis: the Rosetta Stone of a hidden RNA language? *Cell* 2011; **146**: 353-358 [PMID: 21802130 DOI: 10.1016/j.cell.2011.07.014]

115 **Wang Y**, Chen F, Zhao M, Yang Z, Li J, Zhang S, Zhang W, Ye L, Zhang X. The long noncoding RNA HULC promotes liver cancer by increasing the expression of the HMGA2 oncogene *via* sequestration of the microRNA-186. *J Biol Chem* 2017; **292**: 15395-15407 [PMID: 28765279 DOI: 10.1074/jbc.M117.783738]

116 **Xu J**, Zhang J, Shan F, Wen J, Wang Y. SSTR5AS1 functions as a ceRNA to regulate CA2 by sponging miR15b5p for the development and prognosis of HBVrelated hepatocellular carcinoma. *Mol Med Rep* 2019; **20**: 5021-5031 [PMID: 31638225 DOI: 10.3892/mmr.2019.10736]

117 **Lin Y**, Shen Y, Chen J, Hu C, Zhou Z, Yuan C. The Function of LncRNA FTX in Several Common Cancers. *Curr Pharm Des* 2021; **27**: 2381-2386 [PMID: 33121404 DOI: 10.2174/1381612826666201029164036]

118 **Xiong H**, Li B, He J, Zeng Y, Zhang Y, He F. lncRNA HULC promotes the growth of hepatocellular carcinoma cells *via* stabilizing COX-2 protein. *Biochem Biophys Res Commun* 2017; **490**: 693-699 [PMID: 28634076 DOI: 10.1016/j.bbrc.2017.06.103]

119 **Nagy Á**, Lánczky A, Menyhárt O, Győrffy B. Author Correction: Validation of miRNA prognostic power in hepatocellular carcinoma using expression data of independent datasets. *Sci Rep* 2018; **8**: 11515 [PMID: 30046141 DOI: 10.1038/s41598-018-29514-3]

120 **Li H**, Zhao X, Li C, Sheng C, Bai Z. Integrated analysis of lncRNA-associated ceRNA network reveals potential biomarkers for the prognosis of hepatitis B virus-related hepatocellular carcinoma. *Cancer Manag Res* 2019; **11**: 877-897 [PMID: 30697079 DOI: 10.2147/CMAR.S186561]

121 **Li J**, Wang X, Tang J, Jiang R, Zhang W, Ji J, Sun B. HULC and Linc00152 Act as Novel Biomarkers in Predicting Diagnosis of Hepatocellular Carcinoma. *Cell Physiol Biochem* 2015; **37**: 687-696 [PMID: 26356260 DOI: 10.1159/000430387]

122 **Qi J**, Li J, Sun J, Li C. Long Non-Coding RNA IGF2AS in Serum may be a Biomarker for Diagnosis of Hepatitis B Virus-Related Hepatocellular Carcinoma. *Clin Lab* 2019; **65** [PMID: 31850718 DOI: 10.7754/Clin.Lab.2019.190442]

123 **Lu J**, Xie F, Geng L, Shen W, Sui C, Yang J. Investigation of serum lncRNA-uc003wbd and lncRNA-AF085935 expression profile in patients with hepatocellular carcinoma and HBV. *Tumour Biol* 2015; **36**: 3231-3236 [PMID: 25501706 DOI: 10.1007/s13277-014-2951-4]

124 **Wang K**, Guo WX, Li N, Gao CF, Shi J, Tang YF, Shen F, Wu MC, Liu SR, Cheng SQ. Serum LncRNAs Profiles Serve as Novel Potential Biomarkers for the Diagnosis of HBV-Positive Hepatocellular Carcinoma. *PLoS One* 2015; **10**: e0144934 [PMID: 26674525 DOI: 10.1371/journal.pone.0144934]

125 **Xie H**, Ma H, Zhou D. Plasma HULC as a promising novel biomarker for the detection of hepatocellular carcinoma. *Biomed Res Int* 2013; **2013**: 136106 [PMID: 23762823 DOI: 10.1155/2013/136106]

126 **Huang ZL**, Li W, Chen QF, Wu PH, Shen LJ. Eight key long non-coding RNAs predict hepatitis virus positive

hepatocellular carcinoma as prognostic targets. *World J Gastrointest Oncol* 2019; **11**: 983-997 [PMID: 31798779 DOI: 10.4251/wjgo.v11.i11.983]

127 **Xia Q**, Shu Z, Ye T, Zhang M. Identification and Analysis of the Blood lncRNA Signature for Liver Cirrhosis and Hepatocellular Carcinoma. *Front Genet* 2020; **11**: 595699 [PMID: 33365048 DOI: 10.3389/fgene.2020.595699]

128 **Liu H**, Zhao P, Jin X, Zhao Y, Chen Y, Yan T, Wang J, Wu L, Sun Y. A 9lncRNA risk score system for predicting the prognosis of patients with hepatitis B viruspositive hepatocellular carcinoma. *Mol Med Rep* 2019; **20**: 573-583 [PMID: 31115573 DOI: 10.3892/mmr.2019.10262]

129 **Bai Z**, Li H, Li C, Sheng C, Zhao X. Integrated analysis identifies a long non-coding RNAs-messenger RNAs signature for prediction of prognosis in hepatitis B virus-hepatocellular carcinoma patients. *Medicine (Baltimore)* 2020; **99**: e21503 [PMID: 33019382 DOI: 10.1097/MD.0000000000021503]

130 **Zhao X**, Bai Z, Li C, Sheng C, Li H. Identification of a Novel Eight-lncRNA Prognostic Signature for HBV-HCC and Analysis of Their Functions Based on Coexpression and ceRNA Networks. *Biomed Res Int* 2020; **2020**: 8765461 [PMID: 32382578 DOI: 10.1155/2020/8765461]

131 **Jiang Z**, Liu H. Metformin inhibits tumorigenesis in HBV-induced hepatocellular carcinoma by suppressing HULC overexpression caused by HBX. *J Cell Biochem* 2018; **119**: 4482-4495 [PMID: 29231260 DOI: 10.1002/jcb.26555]

132 **Chang L**, Wang G, Jia T, Zhang L, Li Y, Han Y, Zhang K, Lin G, Zhang R, Li J, Wang L. Armored long non-coding RNA MEG3 targeting EGFR based on recombinant MS2 bacteriophage virus-like particles against hepatocellular carcinoma. *Oncotarget* 2016; **7**: 23988-24004 [PMID: 26992211 DOI: 10.18632/oncotarget.8115]

133 **Jacob R**, Zander S, Gutschner T. The Dark Side of the Epitranscriptome: Chemical Modifications in Long Non-Coding RNAs. *Int J Mol Sci* 2017; **18** [PMID: 29125541 DOI: 10.3390/ijms18112387]

World Journal of Gastroenterology

Submit a Manuscript: https://www.f6publishing.com

World J Gastroenterol 2022 July 7; 28(25): 2843-2853

DOI: 10.3748/wjg.v28.i25.2843

ISSN 1007-9327 (print) ISSN 2219-2840 (online)

MINIREVIEWS

Characteristics of inflammatory bowel diseases in patients with concurrent immune-mediated inflammatory diseases

Shintaro Akiyama, Soma Fukuda, Joshua M Steinberg, Hideo Suzuki, Kiichiro Tsuchiya

Specialty type: Gastroenterology and hepatology

Provenance and peer review: Invited article; Externally peer reviewed.

Peer-review model: Single blind

Peer-review report's scientific quality classification

Grade A (Excellent): 0
Grade B (Very good): B
Grade C (Good): C, C
Grade D (Fair): 0
Grade E (Poor): 0

P-Reviewer: Aloi M, Italy; Bozkurt HS, Turkey; Knudsen T, Denmark
A-Editor: Gao W, China

Received: January 8, 2022
Peer-review started: January 8, 2022
First decision: March 9, 2022
Revised: March 10, 2022
Accepted: May 28, 2022
Article in press: May 28, 2022
Published online: July 7, 2022

Shintaro Akiyama, Soma Fukuda, Hideo Suzuki, Kiichiro Tsuchiya, Department of Gastroenterology, University of Tsukuba, Tsukuba 305-8575, Ibaraki, Japan

Joshua M Steinberg, Inflammatory Bowel Disease, Gastroenterology of the Rockies, Denver, CO 80218, United States

Corresponding author: Shintaro Akiyama, MD, MSc, PhD, Lecturer, Department of Gastroenterology, University of Tsukuba, 1-1-1 Tennodai, Tsukuba 305-8575, Ibaraki, Japan.
akiyama@md.tsukuba.ac.jp

Abstract

Patients with inflammatory bowel disease (IBD) are more likely to have concurrent immune-mediated inflammatory diseases (IMIDs) than those without IBD. IMIDs have been observed to alter the phenotype and outcomes of IBD in recent studies. Several studies have found that IBD patients with concurrent IMIDs may have more extensive or severe disease phenotypes, and are considered to be at increased risk of requiring biologics and IBD-related surgeries, suggesting that having multiple IMIDs is a poor prognostic factor for IBD. Furthermore, IBD patients with primary sclerosing cholangitis and Takayasu arteritis are reported to have unique endoscopic phenotypes, suggesting concurrent IMIDs can influence IBD phenotype with specific intestinal inflammatory distributions. In this review, we discuss the pathogenesis, disease phenotypes, and clinical outcomes in IBD patients with concomitant IMIDs.

Key Words: Inflammatory bowel disease; Phenotypes; Outcomes; Concurrent immune-mediated inflammatory diseases

©The Author(s) 2022. Published by Baishideng Publishing Group Inc. All rights reserved.

Core Tip: Patients with inflammatory bowel disease (IBD) are more likely to acquire other immune-mediated inflammatory diseases (IMIDs). IBD patients with concurrent IMIDs were more likely to require biologics and IBD-related surgeries than non-IBD patients due to extensive disease phenotypes according to recent studies. As a result, when treating IBD patients, we must be aware of the concurrence of other IMIDs and understand its pathogenesis to select biologic and small molecule therapies that treat multiple concomitant diseases.

Citation: Akiyama S, Fukuda S, Steinberg JM, Suzuki H, Tsuchiya K. Characteristics of inflammatory bowel diseases in patients with concurrent immune-mediated inflammatory diseases. *World J Gastroenterol* 2022; 28(25): 2843-2853
URL: https://www.wjgnet.com/1007-9327/full/v28/i25/2843.htm
DOI: https://dx.doi.org/10.3748/wjg.v28.i25.2843

INTRODUCTION

Inflammatory bowel disease (IBD), which includes ulcerative colitis (UC) and Crohn's disease (CD), is a chronic relapsing intestinal inflammatory disorder[1]. IBD is a complex disease that is linked to both hereditary and environmental variables, although the etiology is unknown[2-4]. Previous genome-wide association studies (GWASs) identified 99 loci associated with UC and revealed a minimum of 28 shared associations between UC and CD[5]. GWASs have revealed 71 unique loci related to CD and significant genetic overlap with loci related to other immune-mediated inflammatory diseases (IMIDs)[6].

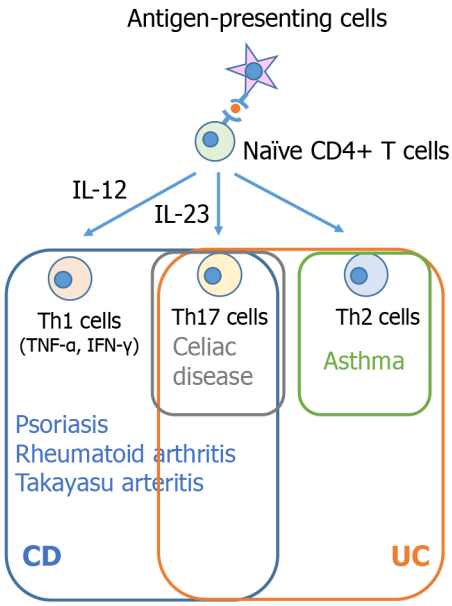
In the pathophysiology of intestinal inflammation in IBD, antigen-presenting cells (APCs) and effector T cells, such as T helper (Th) 1, Th2, and Th17 cells play a pathogenic role[4]. T-cell-mediated immune responses are triggered and modulated by APCs, such as dendritic cells and macrophages. Interleukin (IL)-12 activates Th1 cells that produce interferon-γ, tumor necrosis factor (TNF)-α, and IL-12 [7] (Figure 1). TNF-α is released from activated macrophages in response to interferon, leading to the differentiation of stromal cells into myofibroblasts and the synthesis of matrix metalloproteinases that destroy tissue[8]. While aberrant Th1 responses are thought to involve in CD intestinal inflammation, Th2 cell-mediated inflammation is suggested to be fundamental to the pathogenesis of UC[8]. Th17 cells are characterized by a distinct subset of $CD4^+$ T cells promoting the expression of IL-17 and maintained by IL-23[9,10] (Figure 1). Th17 cells and their cytokines play important roles in the inflammatory pathways of both UC and CD[11]. Innate lymphoid cells (ILCs), which do not exhibit antigen receptors to distinguish T cells from B cells, contribute to the pathogenesis in IBD as well, particularly in CD[12]. ILCs are divided into three groups based on the cytokine profiles of helper T-cell subsets, with ILC1, ILC2, and ILC3 serving as the counterparts of Th1, Th2, and Th17 cells, respectively[12].

Given that IBD patients are more likely to have additional IMIDs than nonIBD patients in various studies[13-15], multiple immune pathways may be shared between IBD and other IMIDs. Among recent cross-sectional research of members of a Northern California managed care organization, 17% of IBD patients had at least one IMID diagnosis, whereas the proportion of concurrent IMIDs was 10% in nonIBD individuals[13]. While another study found no significant differences in CD phenotype between individuals with and without IMID, UC patients with another IMID were more likely to have a pancolitis phenotype than those who did not. Furthermore, IBD patients with another IMID had a higher percentage of patients who needed TNF inhibitors or surgery than those without[14]. Of note, previous research found that IBD patients with primary sclerosing cholangitis (PSC) or Takayasu arteritis (TAK) have distinct endoscopic IBD phenotypes[16,17]. IBD can affect the phenotypes and disease courses of concurrent IMIDs as well, according to a recent meta-analysis[18]. All these studies reveal that the presence of other IMIDs in IBD patients can influence disease phenotypes and outcomes and vice versa.

We evaluate the pathogenesis, disease phenotypes, and clinical outcomes in IBD patients with concurrent IMIDs in this review, which includes IMIDs with a high prevalence among patients with IBD and IMIDs that alter IBD phenotypes and outcomes.

IMIDS WITH HIGH PREVALENCE AMONG IBD

Asthma, psoriasis, and rheumatoid arthritis (RA) were the most common IMIDs among IBD patients, according to the data from Northern California managed care organizations[13]. Another study based on prospective registry data found that 21% of IBD patients also had another IMID. Asthma (9.9%), psoriasis (6.1%), and RA (2.0%) were consistently reported to coexist with IBD[14].



DOI: 10.3748/wjg.v28.i25.2843 **Copyright** ©The Author(s) 2022.

Figure 1 The potential common immunological mechanisms shared between inflammatory bowel diseases and other immune-mediated inflammatory diseases. IFN-γ: Interferon-γ; TNF-α: Tumor necrosis factor-α; IL: Interleukin; Th17 cells: IL-17 producing T helper cells; Th1 cells: T helper 1 cells; Th2 cells: T helper 2 cells; CD: Crohn's disease; UC: Ulcerative colitis.

Asthma and IBD

Asthma is a prevalent chronic airway disease characterized by respiratory symptoms such as coughing and shortness of breath[19]. Asthma is a Th2 cell-mediated disease. Dendritic cells capture inhaled allergens and present them to naïve $CD4^+$ T cells, resulting in the polarization of Th2 cells. These cells produce IL-4, IL-5, and IL-13, promoting eosinophil migration to the airway, bronchial hyperresponsiveness, mucus overproduction, and immunoglobulin E synthesis[19]. ILC2 also plays a role in the pathogenesis of asthma. ILC2 is activated by IL-25 and IL-33 and can produce Th2 cell-associated cytokines, causing airway hypersensitivity and tissue remodeling[19]. Th2 cell-mediated inflammatory pathways are also implicated in IBD patients, particularly UC patients (Figure 1 and Table 1). Macrophages or dendritic cells acquire luminal antigens in the intestine and present them to naïve $CD4^+$ T cells, boosting their differentiation into Th2 cells in the immunological pathways involved in UC[20]. Given the high transcript levels of IL-17A that are detected in both of CD and UC, Th17 cells are also linked to the development of UC[11]. Although ILC1 and ILC3 are considered to be involved in the pathogenesis of CD, it is unclear if ILC2 contributes to the development of UC[12,21].

Psoriasis and IBD

Psoriasis is an immune-mediated skin disorder that affects the skin and/or joints[22] resulting in pruritic and painful skin plaques. Psoriasis is caused by the activation of plasmacytoid dendritic cells, which release various proinflammatory cytokines including TNF, interferon-γ, IL-12, and IL-23. IL-12 aids in the development of Th1 cells from naïve T cells, while IL-23 aids in the maintenance of IL-17-producing Th17 cells. Th17 cells generate IL-17A, IL-17F, and IL-22, while activated Th1 cells release interferon-γ and TNF-α, causing keratinocyte hyperproliferation and other psoriasis clinical features [23]. Similarly, Th1 and Th17 cells are involved in the major immunological mechanism of IBD, particularly CD[24]. ILC3, the counterpart of Th17 cells, is an important source of IL-17 in both psoriasis and CD[21]. Indeed, a systematic review and meta-analysis found that psoriasis patients had an increased risk of IBD, particularly CD[25]. A multicenter retrospective study found that 61% of IBD patients who started ustekinumab, an antagonist of the p40 subunit of IL-12 and IL-23, for concomitant active psoriasis achieved clinical remission of IBD[26]. Although TNF inhibitors are effective in the treatment of both psoriasis and IBD, they can also cause psoriasis[27]. TNF-α inhibition is speculated to cause uncontrolled production of interferon-γ by plasmacytoid dendritic cells, resulting in the recruitment of Th1 or Th17 cells into the dermis, which produces proinflammatory cytokines, such as IL-12 and IL-23 [28]. Thus, these data support the notion that the immune mechanism involving Th1 cells, Th17 cells, and ILC3 may be the common pathway between psoriasis and IBD (Figure 1 and Table 1).

RA and IBD

RA is a chronic inflammatory disease that affects the cartilage and bone[29] resulting in painful and disfiguring joint deformities. Dendritic cells or macrophages uptake antigens and present them to T cells in the pathogenesis of RA, resulting in Th1 or Th17 cell-mediated diseases in the synovial tissue.

Table 1 Characteristic and clinical outcomes in inflammatory bowel disease patients with concurrent immune-mediated inflammatory diseases

IMIDs with high prevalence among patients with IBD	Possible shared immune cells contributing to pathogenesis	IBD phenotypes	IBD outcomes	Possible shared therapies
Asthma	Th2 cells	Indefinite	Indefinite	Indefinite
Psoriasis	Th1 cells, Th17 cells, and ILC3	Indefinite	Indefinite	Ustekinumab; TNF inhibitors
Rheumatoid arthritis	Th1 cells, Th17 cells, ILC1, and ILC3	Indefinite	Indefinite	Tofacitinib; TNF inhibitors
IMIDs affecting phenotypes or outcomes of IBD				
PSC	Indefinite (leaky gut theory)	Severe right-sided colitis, rectal sparing, and backwash ileitis	PSC-IBD patients have fewer or no symptoms, and are less likely to require immunosuppressants, hospitalization, and surgery than IBD patients alone	Indefinite
Celiac disease	Th17 cells	CD patients with celiac disease are less likely to have ileocolonic involvement than CD patients alone	CD patients with celiac disease are less likely to require TNF inhibitors or azathioprine than CD patients alone. UC patients with celiac disease have an increased risk of colectomy	Indefinite
Takayasu arteritis	Th1 cells and Th17 cells	Discontinuous aphthous erosions/ulcers or focal mucosal inflammation	Indefinite	Tofacitinib; Ustekinumab; TNF inhibitors

IBD: Inflammatory bowel disease; PSC: Primary sclerosing cholangitis; IMIDs: Immune-mediated inflammatory diseases; TNF: Tumor necrosis factor; Th17 cells: Interleukin-17 producing T helper cells; Th1 cells: T helper 1 cells; Th2 cells: T helper 2 cells; CD: Crohn's disease; UC: Ulcerative colitis; ILC: Innate lymphoid cell.

Subsequently, the stimulated T cells activate macrophages, B cells, fibroblasts, and osteoclasts. TNF, IL-1, and IL-6 are secreted by the activated macrophages. Inflammatory mediators including matrix metalloproteinases are then produced by fibroblast-like synoviocytes, resulting in cartilage destruction. The activation of osteoclasts induces bone erosions as well[30]. A lymph node activation in RA patients is associated with an imbalance of ILCs, and ILC1 and ILC3 within the lymph node microenvironment can cause inflammation[21]. As a result, RA may have similar immune mechanisms with a CD rather than UC (Figure 1 and Table 1).

Ustekinumab was found to be ineffective in clinical trials of RA patients, whereas TNF, IL-6, and Janus kinase (JAK) inhibitors such as tofacitinib significantly improved RA disease activity when compared to placebo[31]. As a result, among medications approved for RA and IBD, TNF and JAK inhibitors may be effective for both IMIDs. Given that JAKs bind to cytokine receptors and transmit various extracellular cytokine signals such as IL-6, IL-12, IL-23, and interferons, JAK inhibitors are therefore expected to be effective for various IMIDs[28,32] (Table 1).

IMIDS AFFECTING IBD PHENOTYPES AND OUTCOMES

Several recent population-based studies and meta-analyses have shown that the presence of IMIDs may influence the disease course of IBD. According to a nationwide study of the Danish population, 22.5% of IBD patients had at least one concurrent IMID. This study found that risk factors such as older age and methotrexate use were associated with an increased risk of concurrent IMIDs, whereas male gender, a high socioeconomic status, and infliximab use were associated with a reduced risk of concurrent IMIDs. The impact of at least one concurrent IMID on the disease course of IBD was also investigated in this study. The occurrence of IMIDs increased the risk of surgery in CD patients but not in UC patients in the subgroup who developed IMIDs after the onset of IBD. Both UC and CD patients who had concurrent IMIDs were more likely to require biologics than those who did not[33]. IBD patients with concurrent IMIDs had an increased risk of extensive colitis/pancolitis and IBD-related surgeries compared with those without IMIDs, according to a recent systematic review and meta-analysis involving 16064 IBD patients with concurrent IMIDs and 3451414 IBD patients without IMIDs. Furthermore, those with concurrent IMIDs were at an increased risk of requiring immunomodulators and biologics[34]. Overall, these findings suggest that the coexistence of IMIDs is associated with severe IBD phenotypes.

Another recent systematic review and meta-analysis found that CD patients with concurrent IMIDs were more likely to have upper gastrointestinal involvement and nonstricturing and nonpenetrating phenotypes than those without IMIDs. Given that this meta-analysis suggests that CD patients with concurrent IMIDs may have a milder disease course, which contradicts the findings of the previous meta-analysis, more research is needed to better understand CD patients' behaviors if they develop other IMIDs and require medication[35].

While it is unclear how different IMIDs affect IBD phenotypes and outcomes, previous research has consistently suggested that IMIDs such as PSC or TAK can influence the endoscopic findings of IBD to specific phenotypes[16,17,36,37]. On the other hand, recent studies have shown that there is an association between celiac disease and IBD and that IBD patients with celiac disease can have distinct phenotypic characteristics and outcomes[38,39].

PSC and IBD

PSC is a chronic and progressive cholestatic disease that affects the intrahepatic and extrahepatic bile ducts[40]. PSC was found to be present in 2.2% of IBD patients. In one study, PSC was found to be present in 2.5% of UC patients and 0.96% of CD patients, respectively[41]. Patients with "extensive UC" had a higher prevalence of PSC than those with left-sided colitis. PSC was more common in CD patients with ileocolonic or colonic involvement than in those with ileal involvement[35,41]. PSC-IBD patients have a predilection for more severe right-sided colitis according to several studies[42,43]. Furthermore, patients with IBD who have PSC frequently develop a distinct IBD phenotype characterized by "rectal sparing" and "backwash ileitis"[16]. According to a systematic review of 11406 PSC-IBD patients, the pooled rate of rectal sparing and backwash ileitis was 9.9% and 12.3%, respectively[36]. Based on this systematic review, a meta-analysis found that the pooled event rate of pancolitis and rectal sparing was significantly higher in PSC-IBD patients than in IBD patients without PSC, but the rate of backwash ileitis was not statistically significant between the two groups[43].

Although PSC-IBD patients frequently develop pancolonic involvement with significant right-sided colitis, several studies have shown that their disease course was mild[43]. Previous studies found that PSC-IBD patients had fewer or no symptoms[44] and were less likely to require immunosuppressants such as steroids, thiopurines, hospitalization[45], and surgery than IBD patients without PSC[46]. In addition, patients with PSC-CD had a higher risk of nonstricturing and nonpenetrating behavior than those without PSC, as well as being less likely to undergo CD-related surgeries, according to a recent meta-analysis[35]. All of these findings suggest that PSC-IBD patients may have better IBD outcomes, suggesting that PSC-IBD is a distinct disease phenotype from IBD phenotypes in patients with other IMIDs (Table 1).

The cause of the disparity between endoscopic disease activity and clinical outcomes in patients with PSC-IBD is unknown. In a retrospective study, immunosuppressant use and colonic or ileal surgical resection were found to be less common in PSC-IBD patients than in IBD patients without PSC. However, this study discovered that a higher percentage of PSC-IBD patients used 5-aminosalicylates, suggesting that PSC-IBD patients are more likely to use 5-aminosalicylates to lower their risk of colorectal cancer or dysplasia and that their use can be associated with mild disease activity[46-48]. Meanwhile, a case-controlled study found that PSC-UC patients had a milder disease course than those with UC alone, even though the number of patients taking 5-aminosalicylates or sulfasalazine was the same[49]. Hence, more research is needed to understand if differences in the pathogenesis or medical therapies between PSC-IBD patients and patients with IBD alone can explain the unique disease phenotype of PSC-IBD.

Many studies have been carried out to better understand the mechanisms of PSC-IBD, and it has been discovered that there is less genetic overlap between PSC and IBD[50]. Thus, environmental factors such as the gut microbiome have been highlighted. According to the "leaky gut" theory, IBD-related mucosal injury allows the colonic bacteria to cross the gut barrier and into the liver, resulting in the development of PSC[43]. Although the exact mechanism is unknown, PSC-IBD patients were more likely to develop colorectal cancer than IBD patients without PSC[43], so UC guidelines recommend colorectal cancer screening at the time of PSC diagnosis[51].

Celiac disease and IBD

Celiac disease is a gluten-induced disease that frequently coexists in patients with IMIDs[52]. Patients with IBD have a higher risk of celiac disease compared to controls according to a systematic review and meta-analysis (risk ratio 3.96; 95% confidence interval: 2.23-7.02). Patients with celiac disease have a significantly increased risk of IBD compared to controls (risk ratio 9.88; 95% confidence interval: 4.03-24.2), suggesting the shared pathogenesis between both diseases[38]. A case–control study based on a national registry of pediatric IBD patients found that CD patients with celiac disease were less likely to have ileocolonic involvement and require medical therapies such as TNF inhibitors or azathioprine than CD patients alone. While disease distribution and medical treatments were not significantly different between UC patients with and without celiac disease, UC patients with celiac disease had a higher risk of colectomy[39], suggesting that CD patients with celiac disease may have better outcomes, whereas the concurrence of celiac disease can potentially worsen UC outcomes (Table 1).

Some genetic, environmental, and immunological factors are shared by celiac disease and IBD. GWASs revealed that celiac disease and CD share genetic risk loci including PTPN2, IL18RAP, TAGAP, and PUS10[53]. Both diseases have been linked to microbial factors[54,55]. Celiac disease is a $CD4^+$ T-cell-dependent disease associated with chronic intestinal inflammation, according to the immunological mechanism[56]. APCs present gliadin peptide to $CD4^+$ T cells, which then produce proinflammatory cytokines such as interferon-γ and IL-21, increasing intraepithelial lymphocytes (IELs)[56]. The IELs such as $CD8^+$ T cells carrying αβ T-cell receptor (TCR) or $CD4^-CD8^-$ γδ TCR^+ T cells cause cytolysis or apoptosis in intestinal epithelial cells[57,58]. Patients with celiac disease have mucosal Th17 cells, and an increased level of IL-17A expression is associated with villous atrophy, a hallmark pathologic feature of celiac disease[59,60]. Th17 cells produce IL-17, interferon-γ, and IL-21, which play a role in celiac disease pathogenesis[61]. In terms of ILCs, it remains unclear how these cells are associated with the disease initiation and progression[62]. These findings support that Th17 cells may be involved in both IBD and celiac disease (Figure 1 and Table 1).

TAK and IBD

TAK is a type of chronic large-vessel vasculitis that primarily affects the aorta, and its major branches, as well as pulmonary arteries[63]. The prevalence of UC and CD among TAK patients was reported to be 6.4% (30/470) and 9.0% (4/44), respectively[64,65]. Endoscopic features of IBD in TAK patients were found to be atypical for UC or CD in a previous retrospective study[17]. This study, which included 142 Japanese TAK patients, identified 13 TAK-IBD patients (9.2%), and their endoscopic findings at the initial time of IBD diagnosis were assessed. As a result, 7/8 (87.5%) of TAK patients had "discontinuous aphthous erosions/ulcers or focal mucosal inflammation" with only one patient having continuous inflammation typical of UC[17], suggesting that TAK-IBD patients have a distinct endoscopic IBD phenotype. This study also discovered that patients with TAK-IBD were more likely to have the HLA haplotype, which has a susceptible effect on UC, when compared with TAK patients without IBD, implying that TAK-IBD may have a similar immune mechanism to UC. A recent case study describing the evolution of colonic inflammation in a TAK-IBD patient during 10-year observation found that colonic inflammation was initially discontinuous and more severe in the proximal colon than in the remaining colon[37], supporting the presence of a distinct IBD phenotype in TAK-IBD patients (Table 1).

Th1 and Th17 cells are predominant in the pathophysiology of TAK just as they are in the pathogenesis of CD[66] (Figure 1 and Table 1). TAK patients' aorta expresses higher levels of IL-6, IL-12, IL-17, and interferon-γ[67], and a single nucleotide polymorphism encoding a common component of IL-12 and IL-23 is associated with the development of TAK[64]. In a previous study, ustekinumab was shown to reduce inflammatory markers and the dose of steroid needed in the treatment of TAK patients [68]. Many case studies have described TAK-IBD patients' therapeutic approaches to date. Tofacitinib, a JAK inhibitor that was recently approved for UC[69], was found to be effective for both inflammatory conditions[70,71], implying that it can inhibit multiple inflammatory signals involved in TAK and IBD, suggesting that JAK pathways could be a promising therapeutic target. To better understand the prognosis of IBD in such patients with TAK, further studies are needed.

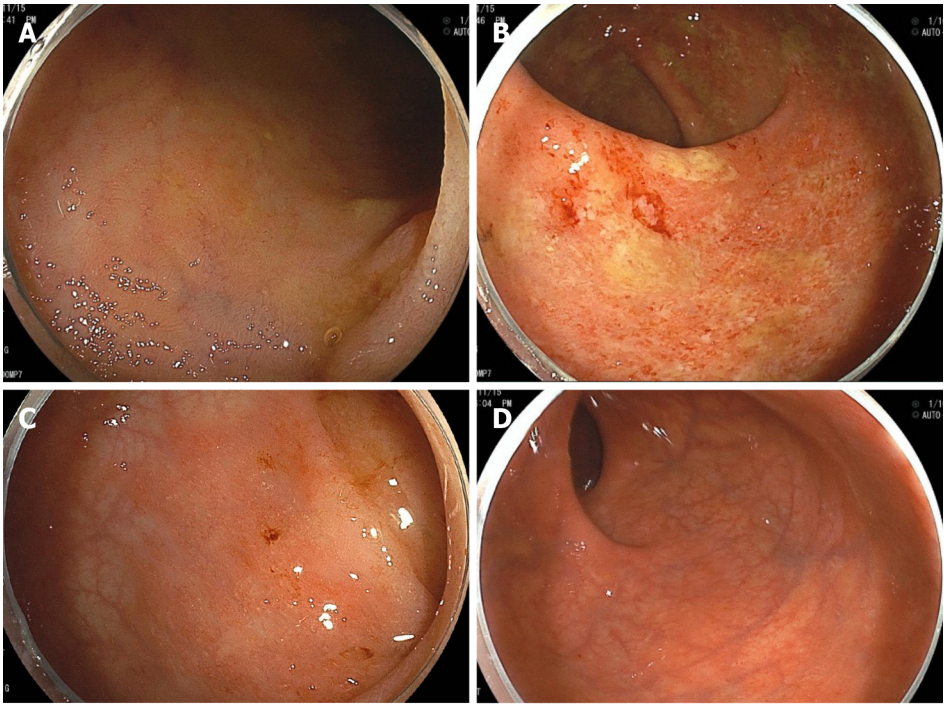
Figures 2 and 3 show representative endoscopic findings of PSC-IBD and TAK-IBD, respectively.

CONCLUSION

Recent research has revealed that IBD and other IMIDs share overlapping genetic and immunological etiologies. Indeed, IBD patients frequently develop concurrent IMIDs, and these patients have a higher risk of severe IBD phenotypes, implying that the presence of IMIDs is a poor prognostic factor for IBD. As a result, when treating IBD patients, we should be aware of the presence of other IMIDs, as biologics and small molecule therapies may be able to treat multiple disease states simultaneously. Multidisciplinary care with rheumatologists or dermatologists is also important when deciding the therapeutic strategy for IBD patients with concurrent IMIDs.

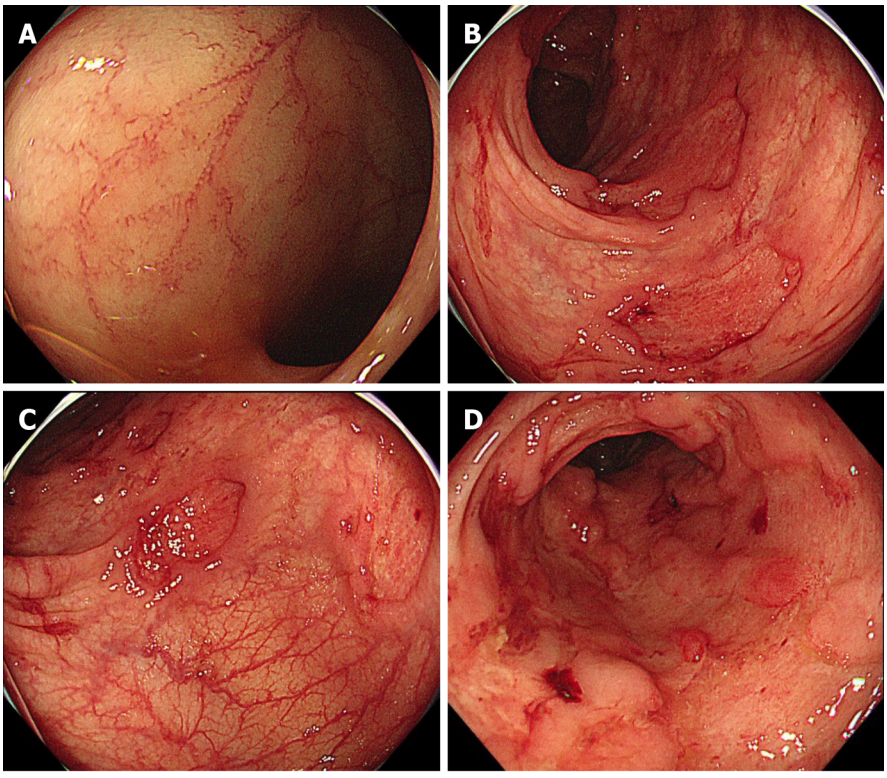
Furthermore, patients with IMIDs such as PSC or TAK can have distinct endoscopic phenotypes of IBD, suggesting that the immune mechanisms of these IMIDs may affect how intestinal inflammation is distributed. Even though IBD patients with concurrent IMIDs are more likely to require biologics or surgery, the disease course of PSC-IBD patients is not often associated with poor IBD outcomes, although these patients are more likely to develop pancolonic inflammation. Further research involving various concurrent IMIDs is needed in light of these findings to better understand how each IMID and its medication may affect the phenotype and natural history of IBD.

In the future, clinicians and researchers will face a challenge in identifying therapeutic targets to improve patient outcomes. Previous studies have shown that Th1 and Th17 cells (rather than Th2 cells) are more likely to be involved in the concurrence of other IMIDs in IBD patients, implying that these effector T cells and their cytokines could be promising therapeutic targets. Future research is needed to gain further insights into the shared immune mechanisms involved in the pathophysiology of IBD and other IMIDs to develop appropriate therapeutic targets to treat both diseases.



DOI: 10.3748/wjg.v28.i25.2843 **Copyright** ©The Author(s) 2022.

Figure 2 Colonoscopy showing representative endoscopic findings of a patient with primary sclerosing cholangitis and ulcerative colitis. Right-sided predominant colitis and rectal sparing. A: Terminal ileum with normal mucosa; B: Ascending colon, diffuse inflammation with erosions, loss of vascular pattern and friability; C: Sigmoid colon, with mild erythematous inflammation and decreased vascular pattern; D: Rectum, with normal mucosa.



DOI: 10.3748/wjg.v28.i25.2843 **Copyright** ©The Author(s) 2022.

Figure 3 Colonoscopy showing representative endoscopic findings of a patient with Takayasu arteritis and inflammatory bowel disease. A: Terminal ileum with normal mucosa; B and C: Sigmoid and rectosigmoid colon, respectively, with discontinuous round ulcers; D: Lower rectum, with deep and large longitudinal ulcers.

FOOTNOTES

Author contributions: Akiyama S designed the research; Akiyama S and Fukuda S performed the research and analyzed the data; Akiyama S, Fukuda S, Steinberg JM, Suzuki H, and Tsuchiya K wrote the paper.

Conflict-of-interest statement: Akiyama S, Fukuda S, and Suzuki H have no relevant disclosures; Steinberg JM was on Advisory Board for Pfizer; Tsuchiya K has received grant supports from Takeda Pharmaceutical Co., Ltd., Mitsubishi Tanabe Pharmaceutical Corp., and Hitachi Ltd.

Open-Access: This article is an open-access article that was selected by an in-house editor and fully peer-reviewed by external reviewers. It is distributed in accordance with the Creative Commons Attribution NonCommercial (CC BY-NC 4.0) license, which permits others to distribute, remix, adapt, build upon this work non-commercially, and license their derivative works on different terms, provided the original work is properly cited and the use is non-commercial. See: https://creativecommons.org/Licenses/by-nc/4.0/

Country/Territory of origin: Japan

ORCID number: Shintaro Akiyama 0000-0003-0727-7638; Soma Fukuda 0000-0003-2907-7776; Joshua M Steinberg 0000-0002-8809-3437; Hideo Suzuki 0000-0002-1469-7449; Kiichiro Tsuchiya 0000-0002-1977-8707.

S-Editor: Yan JP
L-Editor: A
P-Editor: Yan JP

REFERENCES

1 **Rosen MJ**, Dhawan A, Saeed SA. Inflammatory Bowel Disease in Children and Adolescents. *JAMA Pediatr* 2015; **169**: 1053-1060 [PMID: 26414706 DOI: 10.1001/jamapediatrics.2015.1982]
2 **Ananthakrishnan AN**, Bernstein CN, Iliopoulos D, Macpherson A, Neurath MF, Ali RAR, Vavricka SR, Fiocchi C. Environmental triggers in IBD: a review of progress and evidence. *Nat Rev Gastroenterol Hepatol* 2018; **15**: 39-49 [PMID: 29018271 DOI: 10.1038/nrgastro.2017.136]
3 **Younis N**, Zarif R, Mahfouz R. Inflammatory bowel disease: between genetics and microbiota. *Mol Biol Rep* 2020; **47**: 3053-3063 [PMID: 32086718 DOI: 10.1007/s11033-020-05318-5]
4 **Khor B**, Gardet A, Xavier RJ. Genetics and pathogenesis of inflammatory bowel disease. *Nature* 2011; **474**: 307-317 [PMID: 21677747 DOI: 10.1038/nature10209]
5 **Anderson CA**, Boucher G, Lees CW, Franke A, D'Amato M, Taylor KD, Lee JC, Goyette P, Imielinski M, Latiano A, Lagacé C, Scott R, Amininejad L, Bumpstead S, Baidoo L, Baldassano RN, Barclay M, Bayless TM, Brand S, Büning C, Colombel JF, Denson LA, De Vos M, Dubinsky M, Edwards C, Ellinghaus D, Fehrmann RS, Floyd JA, Florin T, Franchimont D, Franke L, Georges M, Glas J, Glazer NL, Guthery SL, Haritunians T, Hayward NK, Hugot JP, Jobin G, Laukens D, Lawrance I, Lémann M, Levine A, Libioulle C, Louis E, McGovern DP, Milla M, Montgomery GW, Morley KI, Mowat C, Ng A, Newman W, Ophoff RA, Papi L, Palmieri O, Peyrin-Biroulet L, Panés J, Phillips A, Prescott NJ, Proctor DD, Roberts R, Russell R, Rutgeerts P, Sanderson J, Sans M, Schumm P, Seibold F, Sharma Y, Simms LA, Seielstad M, Steinhart AH, Targan SR, van den Berg LH, Vatn M, Verspaget H, Walters T, Wijmenga C, Wilson DC, Westra HJ, Xavier RJ, Zhao ZZ, Ponsioen CY, Andersen V, Torkvist L, Gazouli M, Anagnou NP, Karlsen TH, Kupcinskas L, Sventoraityte J, Mansfield JC, Kugathasan S, Silverberg MS, Halfvarson J, Rotter JI, Mathew CG, Griffiths AM, Gearry R, Ahmad T, Brant SR, Chamaillard M, Satsangi J, Cho JH, Schreiber S, Daly MJ, Barrett JC, Parkes M, Annese V, Hakonarson H, Radford-Smith G, Duerr RH, Vermeire S, Weersma RK, Rioux JD. Meta-analysis identifies 29 additional ulcerative colitis risk loci, increasing the number of confirmed associations to 47. *Nat Genet* 2011; **43**: 246-252 [PMID: 21297633 DOI: 10.1038/ng.764]
6 **Franke A**, McGovern DP, Barrett JC, Wang K, Radford-Smith GL, Ahmad T, Lees CW, Balschun T, Lee J, Roberts R, Anderson CA, Bis JC, Bumpstead S, Ellinghaus D, Festen EM, Georges M, Green T, Haritunians T, Jostins L, Latiano A, Mathew CG, Montgomery GW, Prescott NJ, Raychaudhuri S, Rotter JI, Schumm P, Sharma Y, Simms LA, Taylor KD, Whiteman D, Wijmenga C, Baldassano RN, Barclay M, Bayless TM, Brand S, Büning C, Cohen A, Colombel JF, Cottone M, Stronati L, Denson T, De Vos M, D'Inca R, Dubinsky M, Edwards C, Florin T, Franchimont D, Gearry R, Glas J, Van Gossum A, Guthery SL, Halfvarson J, Verspaget HW, Hugot JP, Karban A, Laukens D, Lawrance I, Lemann M, Levine A, Libioulle C, Louis E, Mowat C, Newman W, Panés J, Phillips A, Proctor DD, Regueiro M, Russell R, Rutgeerts P, Sanderson J, Sans M, Seibold F, Steinhart AH, Stokkers PC, Torkvist L, Kullak-Ublick G, Wilson D, Walters T, Targan SR, Brant SR, Rioux JD, D'Amato M, Weersma RK, Kugathasan S, Griffiths AM, Mansfield JC, Vermeire S, Duerr RH, Silverberg MS, Satsangi J, Schreiber S, Cho JH, Annese V, Hakonarson H, Daly MJ, Parkes M. Genome-wide meta-analysis increases to 71 the number of confirmed Crohn's disease susceptibility loci. *Nat Genet* 2010; **42**: 1118-1125 [PMID: 21102463 DOI: 10.1038/ng.717]
7 **Monteleone G**, Biancone L, Marasco R, Morrone G, Marasco O, Luzza F, Pallone F. Interleukin 12 is expressed and actively released by Crohn's disease intestinal lamina propria mononuclear cells. *Gastroenterology* 1997; **112**: 1169-1178 [PMID: 9098000 DOI: 10.1016/s0016-5085(97)70128-8]
8 **Geremia A**, Biancheri P, Allan P, Corazza GR, Di Sabatino A. Innate and adaptive immunity in inflammatory bowel disease. *Autoimmun Rev* 2014; **13**: 3-10 [PMID: 23774107 DOI: 10.1016/j.autrev.2013.06.004]
9 **Akiyama S**, Sakuraba A. Distinct roles of interleukin-17 and T helper 17 cells among autoimmune diseases. *J Transl Autoimmun* 2021; **4**: 100104 [PMID: 34179741 DOI: 10.1016/j.jtauto.2021.100104]

10 **Yen D**, Cheung J, Scheerens H, Poulet F, McClanahan T, McKenzie B, Kleinschek MA, Owyang A, Mattson J, Blumenschein W, Murphy E, Sathe M, Cua DJ, Kastelein RA, Rennick D. IL-23 is essential for T cell-mediated colitis and promotes inflammation *via* IL-17 and IL-6. *J Clin Invest* 2006; **116**: 1310-1316 [PMID: 16670770 DOI: 10.1172/jci21404]

11 **Kobayashi T**, Okamoto S, Hisamatsu T, Kamada N, Chinen H, Saito R, Kitazume MT, Nakazawa A, Sugita A, Koganei K, Isobe K, Hibi T. IL23 differentially regulates the Th1/Th17 balance in ulcerative colitis and Crohn's disease. *Gut* 2008; **57**: 1682-1689 [PMID: 18653729 DOI: 10.1136/gut.2007.135053]

12 **Panda SK**, Colonna M. Innate Lymphoid Cells in Mucosal Immunity. *Front Immunol* 2019; **10**: 861 [PMID: 31134050 DOI: 10.3389/fimmu.2019.00861]

13 **Weng X**, Liu L, Barcellos LF, Allison JE, Herrinton LJ. Clustering of inflammatory bowel disease with immune mediated diseases among members of a northern california-managed care organization. *Am J Gastroenterol* 2007; **102**: 1429-1435 [PMID: 17437504 DOI: 10.1111/j.1572-0241.2007.01215.x]

14 **Conway G**, Velonias G, Andrews E, Garber JJ, Yajnik V, Ananthakrishnan AN. The impact of co-existing immune-mediated diseases on phenotype and outcomes in inflammatory bowel diseases. *Aliment Pharmacol Ther* 2017; **45**: 814-823 [PMID: 28105709 DOI: 10.1111/apt.13940]

15 **Halling ML**, Kjeldsen J, Knudsen T, Nielsen J, Hansen LK. Patients with inflammatory bowel disease have increased risk of autoimmune and inflammatory diseases. *World J Gastroenterol* 2017; **23**: 6137-6146 [PMID: 28970729 DOI: 10.3748/wjg.v23.i33.6137]

16 **Loftus EV Jr**, Harewood GC, Loftus CG, Tremaine WJ, Harmsen WS, Zinsmeister AR, Jewell DA, Sandborn WJ. PSC-IBD: a unique form of inflammatory bowel disease associated with primary sclerosing cholangitis. *Gut* 2005; **54**: 91-96 [PMID: 15591511 DOI: 10.1136/gut.2004.046615]

17 **Akiyama S**, Fujii T, Matsuoka K, Yusuke E, Negi M, Takenaka K, Nagahori M, Ohtsuka K, Isobe M, Watanabe M. Endoscopic features and genetic background of inflammatory bowel disease complicated with Takayasu arteritis. *J Gastroenterol Hepatol* 2017; **32**: 1011-1017 [PMID: 28449344 DOI: 10.1111/jgh.13640]

18 **Attauabi M**, Wewer MD, Bendtsen F, Seidelin JB, Burisch J. Inflammatory Bowel Diseases Affect the Phenotype and Disease Course of Coexisting Immune-Mediated Inflammatory Diseases: A Systematic Review With Meta-Analysis. *Inflamm Bowel Dis* 2022 [PMID: 35134921 DOI: 10.1093/ibd/izac003]

19 **Lambrecht BN**, Hammad H, Fahy JV. The Cytokines of Asthma. *Immunity* 2019; **50**: 975-991 [PMID: 30995510 DOI: 10.1016/j.immuni.2019.03.018]

20 **Ordás I**, Eckmann L, Talamini M, Baumgart DC, Sandborn WJ. Ulcerative colitis. *Lancet* 2012; **380**: 1606-1619 [PMID: 22914296 DOI: 10.1016/S0140-6736(12)60150-0]

21 **Mohammadi H**, Sharafkandi N, Hemmatzadeh M, Azizi G, Karimi M, Jadidi-Niaragh F, Baradaran B, Babaloo Z. The role of innate lymphoid cells in health and disease. *J Cell Physiol* 2018; **233**: 4512-4529 [PMID: 29058773 DOI: 10.1002/jcp.26250]

22 **Hoegler KM**, John AM, Handler MZ, Schwartz RA. Generalized pustular psoriasis: a review and update on treatment. *J Eur Acad Dermatol Venereol* 2018; **32**: 1645-1651 [PMID: 29573491 DOI: 10.1111/jdv.14949]

23 **Korman NJ**. Management of psoriasis as a systemic disease: what is the evidence? *Br J Dermatol* 2020; **182**: 840-848 [PMID: 31225638 DOI: 10.1111/bjd.18245]

24 **Torres J**, Mehandru S, Colombel JF, Peyrin-Biroulet L. Crohn's disease. *Lancet* 2017; **389**: 1741-1755 [PMID: 27914655 DOI: 10.1016/S0140-6736(16)31711-1]

25 **Fu Y**, Lee CH, Chi CC. Association of Psoriasis With Inflammatory Bowel Disease: A Systematic Review and Meta-analysis. *JAMA Dermatol* 2018; **154**: 1417-1423 [PMID: 30422277 DOI: 10.1001/jamadermatol.2018.3631]

26 **Pugliese D**, Daperno M, Fiorino G, Savarino E, Mosso E, Biancone L, Testa A, Sarpi L, Cappello M, Bodini G, Caprioli F, Festa S, Laino G, Maconi G, Mazzuoli S, Mocci G, Sartini A, D'Amore A, Alivernini S, Gremese E, Armuzzi A. Real-life effectiveness of ustekinumab in inflammatory bowel disease patients with concomitant psoriasis or psoriatic arthritis: An IG-IBD study. *Dig Liver Dis* 2019; **51**: 972-977 [PMID: 30992173 DOI: 10.1016/j.dld.2019.03.007]

27 **Pugliese D**, Guidi L, Ferraro PM, Marzo M, Felice C, Celleno L, Landi R, Andrisani G, Pizzolante F, De Vitis I, Papa A, Rapaccini GL, Armuzzi A. Paradoxical psoriasis in a large cohort of patients with inflammatory bowel disease receiving treatment with anti-TNF alpha: 5-year follow-up study. *Aliment Pharmacol Ther* 2015; **42**: 880-888 [PMID: 26235565 DOI: 10.1111/apt.13352]

28 **Akiyama S**, Lin A, Traboulsi C, Rubin DT. Treatment of Crohn's Disease and Concomitant Alopecia Areata With Tofacitinib. *ACG Case Rep J* 2021; **8**: e00690 [PMID: 34840997 DOI: 10.14309/crj.0000000000000690]

29 **McInnes IB**, Schett G. The pathogenesis of rheumatoid arthritis. *N Engl J Med* 2011; **365**: 2205-2219 [PMID: 22150039 DOI: 10.1056/NEJMra1004965]

30 **Smolen JS**, Aletaha D, Koeller M, Weisman MH, Emery P. New therapies for treatment of rheumatoid arthritis. *Lancet* 2007; **370**: 1861-1874 [PMID: 17570481 DOI: 10.1016/S0140-6736(07)60784-3]

31 **Kerschbaumer A**, Sepriano A, Smolen JS, van der Heijde D, Dougados M, van Vollenhoven R, McInnes IB, Bijlsma JWJ, Burmester GR, de Wit M, Falzon L, Landewé R. Efficacy of pharmacological treatment in rheumatoid arthritis: a systematic literature research informing the 2019 update of the EULAR recommendations for management of rheumatoid arthritis. *Ann Rheum Dis* 2020; **79**: 744-759 [PMID: 32033937 DOI: 10.1136/annrheumdis-2019-216656]

32 **Winthrop KL**. The emerging safety profile of JAK inhibitors in rheumatic disease. *Nat Rev Rheumatol* 2017; **13**: 234-243 [PMID: 28250461 DOI: 10.1038/nrrheum.2017.23]

33 **Burisch J**, Jess T, Egeberg A. Incidence of Immune-Mediated Inflammatory Diseases Among Patients With Inflammatory Bowel Diseases in Denmark. *Clin Gastroenterol Hepatol* 2019; **17**: 2704-2712.e3 [PMID: 30936024 DOI: 10.1016/j.cgh.2019.03.040]

34 **Attauabi M**, Zhao M, Bendtsen F, Burisch J. Systematic Review with Meta-analysis: The Impact of Co-occurring Immune-mediated Inflammatory Diseases on the Disease Course of Inflammatory Bowel Diseases. *Inflamm Bowel Dis* 2021; **27**: 927-939 [PMID: 32628745 DOI: 10.1093/ibd/izaa167]

35 **Attauabi M**, Zhao M, Bendtsen F, Burisch J. Systematic review and meta-analysis: the impact of co-occurring immune-mediated inflammatory diseases on the disease localization and behavior of Crohn's disease. *Therap Adv Gastroenterol*

2021; **14**: 17562848211004839 [PMID: 34234844 DOI: 10.1177/17562848211004839]
36 **de Vries AB**, Janse M, Blokzijl H, Weersma RK. Distinctive inflammatory bowel disease phenotype in primary sclerosing cholangitis. *World J Gastroenterol* 2015; **21**: 1956-1971 [PMID: 25684965 DOI: 10.3748/wjg.v21.i6.1956]
37 **Wada A**, Higashiyama M, Hirata D, Ito S, Tanemoto R, Nishii S, Mizoguchi A, Inaba K, Sugihara N, Hanawa Y, Horiuchi K, Akita Y, Narimatsu K, Komoto S, Tomita K, Hokari R. Changes in Colonic Inflammation Related with Takayasu Arteritis during a 10-year Observation Period. *Intern Med* 2022; **61**: 475-480 [PMID: 34393161 DOI: 10.2169/internalmedicine.7287-21]
38 **Pinto-Sanchez MI**, Seiler CL, Santesso N, Alaedini A, Semrad C, Lee AR, Bercik P, Lebwohl B, Leffler DA, Kelly CP, Moayyedi P, Green PH, Verdu EF. Association Between Inflammatory Bowel Diseases and Celiac Disease: A Systematic Review and Meta-Analysis. *Gastroenterology* 2020; **159**: 884-903.e31 [PMID: 32416141 DOI: 10.1053/j.gastro.2020.05.016]
39 **Bramuzzo M**, Lionetti P, Miele E, Romano C, Arrigo S, Cardile S, Di Nardo G, Illiceto MT, Pastore M, Felici E, Fuoti M, Banzato C, Citrano M, Congia M, Norsa L, Pozzi E, Zuin G, Agrusti A, Bianconi M, Grieco C, Giudici F, Aloi M, Alvisi P. Phenotype and Natural History of Children With Coexistent Inflammatory Bowel Disease and Celiac Disease. *Inflamm Bowel Dis* 2021; **27**: 1881-1888 [PMID: 33452803 DOI: 10.1093/ibd/izaa360]
40 **Beheshti-Maal A**, Tamimi A, Iravani S, Memarnejadian A, Sorouri M, Aghdaei HA, Zali MR, Hossein Khannazer N, Vosough M. PSC associated inflammatory bowel disease: a distinct entity. *Expert Rev Gastroenterol Hepatol* 2022; **16**: 129-139 [PMID: 35078376 DOI: 10.1080/17474124.2022.2031979]
41 **Barberio B**, Massimi D, Cazzagon N, Zingone F, Ford AC, Savarino EV. Prevalence of Primary Sclerosing Cholangitis in Patients With Inflammatory Bowel Disease: A Systematic Review and Meta-analysis. *Gastroenterology* 2021; **161**: 1865-1877 [PMID: 34425093 DOI: 10.1053/j.gastro.2021.08.032]
42 **Krugliak Cleveland N**, Rubin DT, Hart J, Weber CR, Meckel K, Tran AL, Aelvoet AS, Pan I, Gonsalves A, Gaetano JN, Williams KM, Wroblewski K, Jabri B, Pekow J. Patients With Ulcerative Colitis and Primary Sclerosing Cholangitis Frequently Have Subclinical Inflammation in the Proximal Colon. *Clin Gastroenterol Hepatol* 2018; **16**: 68-74 [PMID: 28756053 DOI: 10.1016/j.cgh.2017.07.023]
43 **Ricciuto A**, Kamath BM, Griffiths AM. The IBD and PSC Phenotypes of PSC-IBD. *Curr Gastroenterol Rep* 2018; **20**: 16 [PMID: 29594739 DOI: 10.1007/s11894-018-0620-2]
44 **Palmela C**, Peerani F, Castaneda D, Torres J, Itzkowitz SH. Inflammatory Bowel Disease and Primary Sclerosing Cholangitis: A Review of the Phenotype and Associated Specific Features. *Gut Liver* 2018; **12**: 17-29 [PMID: 28376583 DOI: 10.5009/gnl16510]
45 **Moayyeri A**, Daryani NE, Bahrami H, Haghpanah B, Nayyer-Habibi A, Sadatsafavi M. Clinical course of ulcerative colitis in patients with and without primary sclerosing cholangitis. *J Gastroenterol Hepatol* 2005; **20**: 366-370 [PMID: 15740478 DOI: 10.1111/j.1440-1746.2005.03727.x]
46 **Sokol H**, Cosnes J, Chazouilleres O, Beaugerie L, Tiret E, Poupon R, Seksik P. Disease activity and cancer risk in inflammatory bowel disease associated with primary sclerosing cholangitis. *World J Gastroenterol* 2008; **14**: 3497-3503 [PMID: 18567077 DOI: 10.3748/wjg.14.3497]
47 **van Staa TP**, Card T, Logan RF, Leufkens HG. 5-Aminosalicylate use and colorectal cancer risk in inflammatory bowel disease: a large epidemiological study. *Gut* 2005; **54**: 1573-1578 [PMID: 15994215 DOI: 10.1136/gut.2005.070896]
48 **Eaden J**, Abrams K, Ekbom A, Jackson E, Mayberry J. Colorectal cancer prevention in ulcerative colitis: a case-control study. *Aliment Pharmacol Ther* 2000; **14**: 145-153 [PMID: 10651654 DOI: 10.1046/j.1365-2036.2000.00698.x]
49 **Lundqvist K**, Broomé U. Differences in colonic disease activity in patients with ulcerative colitis with and without primary sclerosing cholangitis: a case control study. *Dis Colon Rectum* 1997; **40**: 451-456 [PMID: 9106695 DOI: 10.1007/BF02258391]
50 **Ellinghaus D**, Folseraas T, Holm K, Ellinghaus E, Melum E, Balschun T, Laerdahl JK, Shiryaev A, Gotthardt DN, Weismüller TJ, Schramm C, Wittig M, Bergquist A, Björnsson E, Marschall HU, Vatn M, Teufel A, Rust C, Gieger C, Wichmann HE, Runz H, Sterneck M, Rupp C, Braun F, Weersma RK, Wijmenga C, Ponsioen CY, Mathew CG, Rutgeerts P, Vermeire S, Schrumpf E, Hov JR, Manns MP, Boberg KM, Schreiber S, Franke A, Karlsen TH. Genome-wide association analysis in primary sclerosing cholangitis and ulcerative colitis identifies risk loci at GPR35 and TCF4. *Hepatology* 2013; **58**: 1074-1083 [PMID: 22821403 DOI: 10.1002/hep.25977]
51 **Rubin DT**, Ananthakrishnan AN, Siegel CA, Sauer BG, Long MD. ACG Clinical Guideline: Ulcerative Colitis in Adults. *Am J Gastroenterol* 2019; **114**: 384-413 [PMID: 30840605 DOI: 10.14309/ajg.0000000000000152]
52 **Lundin KE**, Wijmenga C. Coeliac disease and autoimmune disease-genetic overlap and screening. *Nat Rev Gastroenterol Hepatol* 2015; **12**: 507-515 [PMID: 26303674 DOI: 10.1038/nrgastro.2015.136]
53 **Festen EA**, Goyette P, Green T, Boucher G, Beauchamp C, Trynka G, Dubois PC, Lagacé C, Stokkers PC, Hommes DW, Barisani D, Palmieri O, Annese V, van Heel DA, Weersma RK, Daly MJ, Wijmenga C, Rioux JD. A meta-analysis of genome-wide association scans identifies IL18RAP, PTPN2, TAGAP, and PUS10 as shared risk loci for Crohn's disease and celiac disease. *PLoS Genet* 2011; **7**: e1001283 [PMID: 21298027 DOI: 10.1371/journal.pgen.1001283]
54 **Caminero A**, Meisel M, Jabri B, Verdu EF. Mechanisms by which gut microorganisms influence food sensitivities. *Nat Rev Gastroenterol Hepatol* 2019; **16**: 7-18 [PMID: 30214038 DOI: 10.1038/s41575-018-0064-z]
55 **Harris KG**, Chang EB. The intestinal microbiota in the pathogenesis of inflammatory bowel diseases: new insights into complex disease. *Clin Sci (Lond)* 2018; **132**: 2013-2028 [PMID: 30232239 DOI: 10.1042/CS20171110]
56 **Hisamatsu T**, Erben U, Kühl AA. The Role of T-Cell Subsets in Chronic Inflammation in Celiac Disease and Inflammatory Bowel Disease Patients: More Common Mechanisms or More Differences? *Inflamm Intest Dis* 2016; **1**: 52-62 [PMID: 29922658 DOI: 10.1159/000445133]
57 **Sollid LM**. Intraepithelial lymphocytes in celiac disease: license to kill revealed. *Immunity* 2004; **21**: 303-304 [PMID: 15357941 DOI: 10.1016/j.immuni.2004.08.002]
58 **Meresse B**, Chen Z, Ciszewski C, Tretiakova M, Bhagat G, Krausz TN, Raulet DH, Lanier LL, Groh V, Spies T, Ebert EC, Green PH, Jabri B. Coordinated induction by IL15 of a TCR-independent NKG2D signaling pathway converts CTL into lymphokine-activated killer cells in celiac disease. *Immunity* 2004; **21**: 357-366 [PMID: 15357947 DOI:

10.1016/j.immuni.2004.06.020]
59 **Fernández S**, Molina IJ, Romero P, González R, Peña J, Sánchez F, Reynoso FR, Pérez-Navero JL, Estevez O, Ortega C, Santamaría M. Characterization of gliadin-specific Th17 cells from the mucosa of celiac disease patients. *Am J Gastroenterol* 2011; **106**: 528-538 [PMID: 21206487 DOI: 10.1038/ajg.2010.465]
60 **Lahdenperä AI**, Fälth-Magnusson K, Högberg L, Ludvigsson J, Vaarala O. Expression pattern of T-helper 17 cell signaling pathway and mucosal inflammation in celiac disease. *Scand J Gastroenterol* 2014; **49**: 145-156 [PMID: 24325470 DOI: 10.3109/00365521.2013.863966]
61 **Monteleone I**, Sarra M, Del Vecchio Blanco G, Paoluzi OA, Franzè E, Fina D, Fabrizi A, MacDonald TT, Pallone F, Monteleone G. Characterization of IL-17A-producing cells in celiac disease mucosa. *J Immunol* 2010; **184**: 2211-2218 [PMID: 20061410 DOI: 10.4049/jimmunol.0901919]
62 **Yu X**, Vargas J, Green PHR, Bhagat G. Innate Lymphoid Cells and Celiac Disease: Current Perspective. *Cell Mol Gastroenterol Hepatol* 2021; **11**: 803-814 [PMID: 33309944 DOI: 10.1016/j.jcmgh.2020.12.002]
63 **Alibaz-Oner F**, Direskeneli H. Update on Takayasu's arteritis. *Presse Med* 2015; **44**: e259-e265 [PMID: 26033561 DOI: 10.1016/j.lpm.2015.01.015]
64 **Terao C**, Matsumura T, Yoshifuji H, Kirino Y, Maejima Y, Nakaoka Y, Takahashi M, Amiya E, Tamura N, Nakajima T, Origuchi T, Horita T, Matsukura M, Kochi Y, Ogimoto A, Yamamoto M, Takahashi H, Nakayamada S, Saito K, Wada Y, Narita I, Kawaguchi Y, Yamanaka H, Ohmura K, Atsumi T, Tanemoto K, Miyata T, Kuwana M, Komuro I, Tabara Y, Ueda A, Isobe M, Mimori T, Matsuda F. Takayasu arteritis and ulcerative colitis: high rate of co-occurrence and genetic overlap. *Arthritis Rheumatol* 2015; **67**: 2226-2232 [PMID: 25931203 DOI: 10.1002/art.39157]
65 **Reny JL**, Paul JF, Lefèbvre C, Champion K, Emmerich J, Blétry O, Piette JC, Fiessinger JN. Association of Takayasu's arteritis and Crohn's disease. Results of a study on 44 Takayasu patients and review of the literature. *Ann Med Interne (Paris)* 2003; **154**: 85-90 [PMID: 12746644 DOI: 10.1016/s0248-8663(97)80232-9]
66 **Saadoun D**, Garrido M, Comarmond C, Desbois AC, Domont F, Savey L, Terrier B, Geri G, Rosenzwajg M, Klatzmann D, Fourret P, Cluzel P, Chiche L, Gaudric J, Koskas F, Cacoub P. Th1 and Th17 cytokines drive inflammation in Takayasu arteritis. *Arthritis Rheumatol* 2015; **67**: 1353-1360 [PMID: 25604824 DOI: 10.1002/art.39037]
67 **Savioli B**, Abdulahad WH, Brouwer E, Kallenberg CGM, de Souza AWS. Are cytokines and chemokines suitable biomarkers for Takayasu arteritis? *Autoimmun Rev* 2017; **16**: 1071-1078 [PMID: 28778711 DOI: 10.1016/j.autrev.2017.07.023]
68 **Gon Y**, Yoshifuji H, Nakajima T, Murakami K, Nakashima R, Ohmura K, Mimori T, Terao C. Long-term outcomes of refractory Takayasu arteritis patients treated with biologics including ustekinumab. *Mod Rheumatol* 2021; **31**: 678-683 [PMID: 32700985 DOI: 10.1080/14397595.2020.1800560]
69 **Sandborn WJ**, Su C, Sands BE, D'Haens GR, Vermeire S, Schreiber S, Danese S, Feagan BG, Reinisch W, Niezychowski W, Friedman G, Lawendy N, Yu D, Woodworth D, Mukherjee A, Zhang H, Healey P, Panés J; OCTAVE Induction 1, OCTAVE Induction 2, and OCTAVE Sustain Investigators. Tofacitinib as Induction and Maintenance Therapy for Ulcerative Colitis. *N Engl J Med* 2017; **376**: 1723-1736 [PMID: 28467869 DOI: 10.1056/NEJMoa1606910]
70 **Kuwabara S**, Tanimura S, Matsumoto S, Nakamura H, Horita T. Successful remission with tofacitinib in a patient with refractory Takayasu arteritis complicated by ulcerative colitis. *Ann Rheum Dis* 2020; **79**: 1125-1126 [PMID: 32213500 DOI: 10.1136/annrheumdis-2019-216606]
71 **Sato S**, Matsumoto H, Temmoku J, Fujita Y, Matsuoka N, Furuya M, Gunji N, Fujiwara T, Asano T, Onizawa M, Kobayashi H, Watanabe H, Ohira H, Migita K. A case of Takayasu arteritis complicated by refractory ulcerative colitis successfully treated with tofacitinib. *Rheumatology (Oxford)* 2020; **59**: 1773-1775 [PMID: 31776552 DOI: 10.1093/rheumatology/kez580]

World Journal of Gastroenterology

Submit a Manuscript: https://www.f6publishing.com

World J Gastroenterol 2022 July 7; 28(25): 2854-2866

DOI: 10.3748/wjg.v28.i25.2854

ISSN 1007-9327 (print) ISSN 2219-2840 (online)

MINIREVIEWS

Correlation of molecular alterations with pathological features in hepatocellular carcinoma: Literature review and experience of an Italian center

Thais Maloberti, Antonio De Leo, Viviana Sanza, Elisa Gruppioni, Annalisa Altimari, Mattia Riefolo, Michela Visani, Deborah Malvi, Antonia D'Errico, Giovanni Tallini, Francesco Vasuri, Dario de Biase

Specialty type: Gastroenterology and hepatology

Provenance and peer review: Invited article; Externally peer reviewed.

Peer-review model: Single blind

Peer-review report's scientific quality classification

Grade A (Excellent): 0
Grade B (Very good): 0
Grade C (Good): C, C
Grade D (Fair): D
Grade E (Poor): 0

P-Reviewer: Castro-Gil M, Mexico; Citores MJ, Spain; Yang L, China
A-Editor: Zhou SM, China

Received: January 14, 2022
Peer-review started: January 14, 2022
First decision: March 9, 2022
Revised: March 23, 2022
Accepted: May 27, 2022
Article in press: May 27, 2022
Published online: July 7, 2022

Thais Maloberti, Antonio De Leo, Michela Visani, Giovanni Tallini, Department of Experimental, Diagnostic and Specialty Medicine, University of Bologna, Bologna 40138, Italy

Thais Maloberti, Antonio De Leo, Viviana Sanza, Elisa Gruppioni, Annalisa Altimari, Giovanni Tallini, Solid Tumor Molecular Pathology Laboratory, IRCCS Azienda Ospedaliero-Universitaria di Bologna, Bologna 40138, Italy

Mattia Riefolo, Deborah Malvi, Antonia D'Errico, Francesco Vasuri, Department of Pathology, IRCCS Azienda Ospedaliero-Universitaria di Bologna, Bologna 40138, Italy

Dario de Biase, Department of Pharmacy and biotechnology (FaBiT), University of Bologna, Bologna 40138, Italy

Corresponding author: Dario de Biase, MSc, PhD, Associate Professor, Department of Pharmacy and biotechnology (FaBiT), University of Bologna, Viale Ercolani 4/2, S. Orsola Hospital, Bologna 40138, Italy. dario.debiase@unibo.it

Abstract

Hepatocellular carcinoma (HCC) represents the primary carcinoma of the liver and the fourth leading cause of cancer-related deaths. The World Health Organization estimates an increase in cases in the coming years. The risk factors of HCC are multiple, and the incidence in different countries is closely related to the different risk factors to which the population is exposed. The molecular mechanisms that drive HCC tumorigenesis are extremely complex, but understanding this multistep process is essential for the identification of diagnostic, prognostic, and therapeutic markers. The development of multigenic next-generation sequencing panels through the parallel analysis of multiple markers can provide a landscape of the genomic status of the tumor. Considering the literature and our preliminary data based on 36 HCCs, the most frequently altered genes in HCCs are *TERT*, *CTNNB1*, and *TP53*. Over the years, many groups have attempted to classify HCCs on a molecular basis, but a univocal classification has never been achieved. Nevertheless, statistically significant correlations have been found in HCCs between the molecular signature and morphologic features, and this leads us to think that it would be desirable to integrate the approach between anatomic pathology and molecular laboratories.

Key Words: Hepatocarcinoma; Mutation; Next-generation sequencing; Review; *TP53*; *CTNNB1*; *TERT*

©The Author(s) 2022. Published by Baishideng Publishing Group Inc. All rights reserved.

Core Tip: The molecular mechanisms that drive hepatocellular carcinoma tumorigenesis are extremely complex, and a univocal classification based on molecular features has not been defined. In the age of precision medicine, the study of hepatocellular carcinoma mutations is still a field worth investigating. Based on this, we wanted to analyze the possible correlations between molecular alterations and pathological features. Considering both the literature data and our personal experience, about 80% of hepatocellular carcinomas harbor mutations in at least one of the following genes, *TERT*, *TP53*, or *CTNNB1*, with different biological and clinical implications.

Citation: Maloberti T, De Leo A, Sanza V, Gruppioni E, Altimari A, Riefolo M, Visani M, Malvi D, D'Errico A, Tallini G, Vasuri F, de Biase D. Correlation of molecular alterations with pathological features in hepatocellular carcinoma: Literature review and experience of an Italian center. *World J Gastroenterol* 2022; 28(25): 2854-2866
URL: https://www.wjgnet.com/1007-9327/full/v28/i25/2854.htm
DOI: https://dx.doi.org/10.3748/wjg.v28.i25.2854

INTRODUCTION

Hepatocellular carcinoma (HCC) is one of the world-leading cancers, representing approximately 80% of the primary carcinomas of the liver[1] and the fourth most common cause of cancer-related deaths. The World Health Organization (WHO) estimated more than 905500 new HCC cases in 2020 worldwide [2], and based on its projection an increase of 58% is evaluated by 2040 with a total of 1400000 new cases and 1000000 deaths in 2030[2].

The etiological factors for HCC development are: (1) Infections, including hepatitis B virus (HBV) and hepatitis C virus (HCV), with or without coinfection of hepatitis delta virus; (2) Lifestyle risk factors and behaviors, such as alcohol addiction and smoking; (3) Environment, such as dietary toxins (*e.g.*, aflatoxins, or aristolochic acid); (4) Underlying diseases, such as obesity, type 2 diabetes, nonalcoholic liver steatohepatitis/nonalcoholic fatty liver disease; and (5) Genetics, some single nucleotide polymorphisms are identified to be associated with HCC risk at different stages, from predisposition to risk factors to the severity of the chronic liver disease and its evolution to cirrhosis or to the malignant transformation and tumor progression[3,4]. For example, a single nucleotide polymorphism correlated with higher infection risk (MDM2 Promoter SNP309, MDM2 G-309T, rs2279744) has been associated with HCC patients with chronic hepatitis C[5].

The incidence of HCC in different countries varies considering the different risk factors mentioned above. In Eastern Asian countries and most African countries, the incidence of HCC is mostly due to aflatoxin exposure and HBV infection, except for Northern Africa where HCV infection is prevalent[6, 7]. In traditional Chinese herbal medicines, practiced particularly in China, Vietnam, and Southeast Asia, plants containing aristolochic acid are commonly used. In this area, next-generation sequencing studies underlined that a fraction of HCCs harbored high rates of mutations matching a distinctive mutational signature of aristolochic acid exposure[8-10]. Moving to Western countries, the incidence of HCC is usually associated with HCV infection, dietary habits, and related metabolic diseases, such as nonalcoholic liver steatohepatitis and nonalcoholic fatty liver disease. In this area, the low incidence of HCC due to HBV/HCV infections can be explained considering the use of the vaccine for HBV and anti-viral treatments against HCV in contrast with the increased incidence of metabolic syndrome[11].

All the aforementioned risk factors lead to liver disease (cirrhosis or chronic inflammation) that causes an accumulation of genomic alterations driving HCC. In general, HCC arises during the progression of pre-existing chronic hepatitis, and in the vast majority (80%) of patients, HCC occurs in the setting of cirrhosis[12]. The development of HCC is a process characterized by a specific sequence of lesions, from regenerative nodules in cirrhosis, low-grade dysplastic nodules and high-grade dysplastic nodules to early and progressed HCC[13,14].

The molecular mechanisms driving HCC tumorigenesis are extremely complex. Understanding this multistep process, with underlying genetic alteration, is essential for prevention, diagnostic, prognostic, and therapeutic purposes. Considering the future perspective, a better knowledge of molecular mechanisms involved in HCC tumorigenesis would help for a correct classification of HCC, for improving patient outcomes, and to develop new therapeutic targets. The advent of NGS technologies may help in the comprehensive study of genetic alteration and the different pathways involved in the initiation and progression of HCC. In fact, the development of NGS multi-gene panels allows the parallel analysis of multiple markers giving a broad view of the genomic situation[15,16]. To date, this

molecular landscape is crucial for therapeutic decision-making in other solid tumors[15]. The Cancer Genome Atlas Research Network investigated a total of 559 cases of HCC[17]. This study found that *TERT, TP53*, and *CTNNB1* are the most frequently altered genes in HCCs; 77% of HCCs showed a mutation in at least one of these three genes[17]. Correlation data between HCC molecular signatures and etiological agents are shown in Table 1.

Bearing in mind all this evidence, the present review will discuss the main molecular mutations in HCC, with particular emphasis on the influence that these alterations have on HCC morphology and biological aggressiveness.

MOLECULAR ALTERATIONS IN HCC

TERT

During cycles of genomic replication, the linear organization of chromosomes brings with it the problem of erosion of the 5'-terminus due to non-reproduction of the RNA primer binding site. Indeed, this erosion does not happen thanks to telomerase, constituted by telomerase reverse transcriptase (encoded by the *TERT* gene) and RNA template (encoded by the *TERC* gene). The telomerase complex adds nucleotides onto telomeres, preventing them from shortening. Telomeres are short tandem repeats of DNA (TTAGGG) coated by a protein complex known as Shelterin to protect the end of the chromosome where telomeres are located. Telomere synthesis is a controlled process activated in stem cells but deactivated in most somatic cells due to epigenetic silencing during the differentiation process. In the mature hepatocytes, the telomerase is not expressed[18,19]. The shortening of the telomeres exposes chromosomes to damage resulting in cellular senescence and is thought to be responsible for a sequence of events that drive to cancer[20].

Reactivation of *TERT* expression has been observed in several cancers (*e.g.*, melanomas, gliomas, poorly differentiated bladder cancer, anaplastic thyroid carcinomas, basal cell, squamous cell carcinomas) leading to a restoration of the telomerase activity[19] (Figure 1). This event avoids cellular senescence and leads cancer cells to acquire replicative immortality, a crucial feature in the progression of the neoplasm rather than in the transformation of the cells into malignant ones[21-24]. This upregulation of *TERT* in cancer can occur through several mechanisms, which are generally mutually exclusive: (1) Gene amplification, found in ovarian cancer, adrenocortical carcinoma, lung adenocarcinoma, and esophageal carcinoma[25]; (2) Gene rearrangements, found in high-risk neuroblastoma[26]; and (3) Gene mutations in hot-spot regions of the promoter region, found in melanomas, thyroid tumors, gliomas[19].

Alterations in the gene promoter region are the most common and most frequently detected, in particular C>T transition at chr5:1295228 (−124 or C228T) or chr5:1295250 (−146 or C250T). The C228T and C250T TERT mutations separately create an identical 11-base sequence that acts as a novel E-twenty-sis transcription factor binding site, causing *TERT* overexpression[21].

***TERT* and HCC:** Telomere length and telomere expression play a key role in the pathogenesis of HCC. Several studies have found telomere shortening in cirrhotic tissue, independently of the etiology of the liver disease (*e.g.*, alcohol abuse or viral hepatitis), suggesting that this event might represent a hallmark of liver senescence and chronic hepatitis[27-29]. In contrast to cirrhotic tissue, in 44%-59% of the HCC a reactivation of the *TERT* gene is observed[30]. Cellular senescence found in cirrhotic tissue followed by *TERT* reactivation is one of the mechanisms that may explain the development and progression of HCC in cirrhosis. In particular, with the accumulation of gene alterations senescence can induce neoplastic transformation, whereas subsequent telomerase activation can lead to a neoplastic progression (Figure 1).

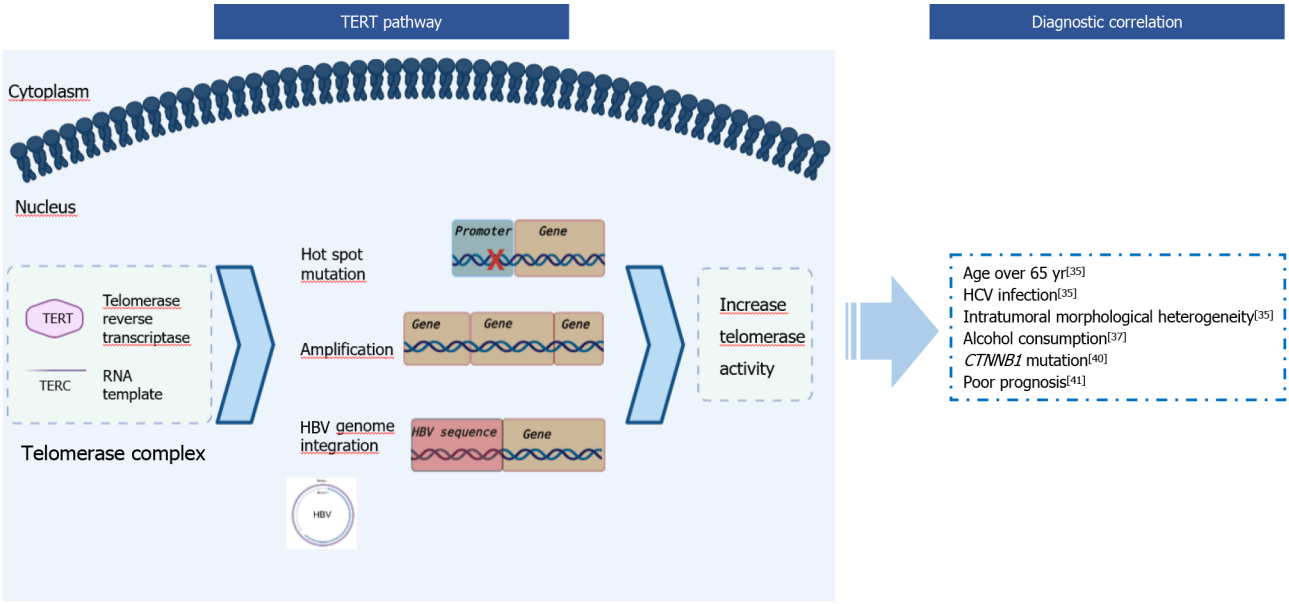
Reactivation of TERT can also be caused by HBV infection (Figure 1). HBV is an enveloped virus with partially double-stranded DNA with the capacity to integrate its own genome into that of the host, leading to the deregulation of the gene involved. *TERT* promoter is the most frequent site of integration (38.5%) in HBV-related cancers, and the viral integration leads to *TERT* overexpression[31,32]. Intriguingly, *TERT* mutations have never been described in hepatocellular adenoma (HCA) in contrast to *CTNNB1* (see "*CTNNB1* and HCC" paragraph)[13,32-34].

TERT mutations in HCC have been statistically correlated with: (1) Age over 65 years (P = 0.018), HCV infection more than HBV (P = 0.048), and intratumoral morphological heterogeneity (P = 0.0001) [35,36]. In a study performed on 97 HCCs by Kwa *et al*[35], the histological patterns in the tumor areas were classified into four groups: early, well, moderate, and poor. In particular, regarding the morphological aspect in *TERT* mutated HCC they observed two or more histological patterns as opposed to *TERT* wild-type HCCs, which showed only a single dominant pattern[35]; (2) Alcohol consumption[32, 37]. Schulze *et al*[32] performed a study on 243 surgically resected HCCs, and 60% of the alcohol-related HCCs had a mutation in the *TERT* gene promoter; (3) *CTNNB1* mutations. Several studies have shown the association between *CTNNB1* and *TERT*[38-40]. This correlation was demonstrated for the first time in a mice model in which it was observed that β-catenin binds the *TERT* promoter and participates in the control of its expression[40]; and (4) Poor prognosis, (P = 0.041). A study by Oh *et al*[41] on telomere length in HCC showed that telomere elongation was a poor prognostic factor, as it decreased overall

Table 1 Recurrent gene mutations in hepatocellular carcinoma related to risk factors

Frequency mutation		Etiological factor		
		HBV	HCV	Non-viral
Driver gene	*TERT*	50%	61%	65%
	CTNNB1	15%	30%	39%
	TP53	10%-65 %	24%	16%

HBV: Hepatitis B virus; HCV: Hepatitis C virus.



DOI: 10.3748/wjg.v28.i25.2854 **Copyright** ©The Author(s) 2022.

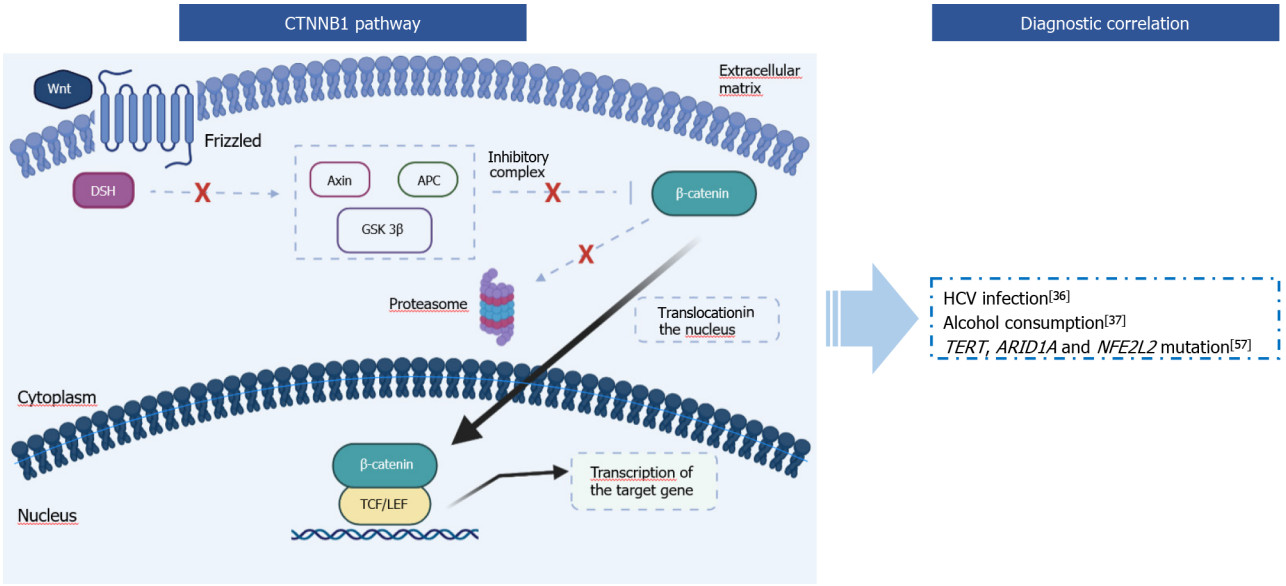
Figure 1 Main cellular pathways and clinical implications of *TERT* mutations in hepatocellular carcinoma. Created with BioRender.com. HBV: Hepatitis B virus; HCV: Hepatitis C virus.

survival (P = 0.044). Moreover, in the case of high telomerase activity the prognosis was unfavorable (P = 0.009)[41] (Figure 1).

CTNNB1

The *CTNNB1* gene encodes β-catenin, a protein that performs several cellular functions. When interacting with the cadherin protein complex, β-catenin is important for the stabilization of the cytoskeleton and intracellular adhesions, but it also plays a role as a transcription factor in the canonical Wnt/β-catenin pathway. This pathway is involved in embryonic development, cellular homeostasis, and several diseases[42]. The cytoplasmic concentration of β-catenin is tightly controlled through its ubiquitination and proteasomal degradation. The phosphorylation required for this degradation mechanism is performed by glycogen synthase kinase 3 alpha and beta through the action of axin and the protein adenomatous polyposis coli (APC)[43,44]. In the cytoplasmic membrane, there are receptors for the Wnt molecules, called frizzled. The ligand-receptor complex triggers a cascade of cytoplasmic reactions, leading to the activation of the disheveled protein. This protein binds axin, preventing the bond between axin and glycogen synthase kinase 3[45]. This mechanism inhibits the proteasomal degradation of β-catenin. Given that *CTNNB1* continues to be transcribed, the β-catenin cytoplasmic concentration increases.

Once all the β-catenin cytoplasmic binding sites are saturated, β-catenin protein is translocated into the nucleus. Here β-catenin interacts with many transcriptional factors, in particular with T-cell factor/lymphoid enhancing factor to promote the transcription of target genes, such as *c-Myc*, *CyclinD-1*, and *Jun* (Figure 2). Most of these gene targets encode for oncoproteins, leading to the activation of oncogenic mechanisms (*e.g.*, uncontrolled growth or escape from apoptosis)[46]. For this reason, β-catenin is a molecule that may be involved in carcinogenesis and tumor progression of several cancers: HCC, lung cancer, brain and cerebellum cancer, breast cancer, colon cancer, leukemia, and others[47-49].



DOI: 10.3748/wjg.v28.i25.2854 **Copyright** ©The Author(s) 2022.

Figure 2 Main cellular pathways and clinical implications of *CTNNB1* mutations in hepatocellular carcinoma. Created with BioRender.com. APC: Adenomatous polyposis coli; DSH: Disheveled; GSK: Glycogen synthase kinase; HCV: Hepatitis C virus; LEF: Lymphoid enhancing factor; TCF: T-cell factor.

The Wnt pathway can also be activated by transforming growth factor-β. Dysregulation of its signaling pathway is associated with an invasive phenotype and plays a central role in inflammation, fibrogenesis, and immunomodulation in the HCC microenvironment[50,51].

Activating mutations found in the *CTNNB1* gene are generally substitutions or in-frame deletions in hotspot regions that encode for the part of the protein that acts as a domain for the *APC/AXIN1/* glycogen synthase kinase 3B complex. Thus, β-catenin is not degraded by the proteosome and then uncontrollably activates the transcription of oncogenes[52].

CTNNB1 and HCC: In HCCs, *CTNNB1* mutations are among the most encountered genetic alterations, with a frequency of 20%-40%[32]. Regarding therapy, *CTNNB1* mutations induce resistance to immune checkpoint inhibitors (anti-PD-1/PD-L1 inhibitors and anti-CTLA4)[53]. Another important aspect concerns HCA. According to the literature, 5%-10% of HCA are subject to malignant transformation, but the most recent WHO guidelines considered CTNNB1-mutated HCAs as a specific subtype, with a higher risk for malignant transformation that could lead to the development of HCC. In HCA *CTNNB1* mutations are identified in 11%-43%[54-56].

CTNNB1 mutations are not the only alterations found in HCCs, regarding Wnt/β-catenin pathway. In fact, mutations in Axin and APC in HCCs have been detected in 6%-15% and 2%-4%, respectively[57]. Generally, mutations in *CTNNB1*, Axin, and *APC* are mutually exclusive[57].

HCCs with mutated *CTNNB1* are statistically correlated to: (1) HCV infection[36]. For example, in a study on 22 HCV-related HCCs, an association between HCV infection and activation of the Wnt signaling pathway caused by the β-catenin mutation was found in 41% of cases[36], while according to the WHO, 30% of HCCs caused by HCV harbors a mutation in the *CTNNB1* gene; (2) Alcohol consumption. Schulze *et al*[37] studied 243 surgically resected HCCs, and 37% of the alcohol-related HCCs harbored a mutation in the *CTNNB1* gene; (3) *TERT* mutation[38,39]. Correlations between *CTNNB1* and *TERT* have been described in the "*TERT* and HCC" paragraph; and (4) *ARID1A* mutations (P = 0.05) and *NFE2L2* mutation (P = 0.015) associations with *CTNNB1* were demonstrated in a study performed on 125 HCCs[57] (Figure 2).

TP53

The *TP53* gene encodes for the p53 protein, which owes its name to its molecular mass (53 kDa). p53 is called "the guardian of the genome" because it is an oncosuppressor that regulates the cell cycle, apoptosis, and genomic stability by preventing genomic mutations. The p53 pathway is crucial in cellular mechanisms as it interacts with other signal transduction pathways (*e.g.*, retinoblastoma pathway, Wnt-β-catenin, cyclin-cdk). Plenty of positive and negative autoregulatory feedback mechanisms act on p53 functions[58,59]. The activation of p53 occurs in response to many different stressors, both intrinsic and extrinsic to the cell (*e.g.*, gamma or UV radiation, oxidative stress, osmotic shock) that put faithful duplication of genetic material at risk[60]. The key event for p53 activation is the phosphorylation of the N-terminal domain by protein kinases. This event leads to the accumulation of p53 in the stressed cells through an increase in the half-life of the protein and an increase in efficiency as a transcription factor. After this activation, p53 initiates a program that blocks the cell cycle, leads the

cell to senescence, and then to apoptosis[61] (Figure 3).

In unstressed cells, cytoplasmic levels of p53 are kept in check through its degradation. The Mdm2 protein binds p53, transports it from the nucleus to the cytosol, and acts as a ubiquitin ligase so that ubiquitin binds to p53 leading to proteasome degradation[62]. If the *TP53* gene is altered, the p53 protein cannot function properly, driving tumorigenesis and tumor progression. As early as 1990, *TP53* was defined as the most frequently mutated gene in human cancers. *TP53* mutations remain among the most frequent and most significant in more common human cancers, although the frequency of mutations is highly variable depending on the type of cancer: from 90% in the ovary, 50%-80% in the lung up to less than 5% in the cervix[63]. Individuals affected by Li Fraumeni syndrome carry a mutated allele of *TP53*, and this syndrome predisposes to the development of several types of cancers[64].

***TP53* and HCC:** Approximately 15%-40% of HCCs carry mutations in the *TP53* gene, with a higher frequency in advanced tumors[65]. Intriguingly, a specific *TP53* mutation is significantly associated with dietary intake of aflatoxin B1, a mycotoxin produced by *Aspergillus* fungi. Exposure to aflatoxin B1 induces the transversion G → T at the *TP53* codon 249, leading to the p.R249S (c.747G>T) substitution. This mutation could then be considered a mutational signature of exposure to aflatoxin B1 in HCC[66-68].

HCCs with mutated *TP53* are statistically correlated to: (1) HBV infection and aflatoxin B1 exposure [68,69]. Lunn *et al*[69] conducted a population-based study on 110 HCCs. The relative risk (RR) that they obtained for HBV infection (RR=17.0), aflatoxin B1 exposure (RR=17.4), and the two risk agents together (RR=67.7) confirmed the correlation between these agents and HCC development. Exposure to aflatoxin B1 induces the p.R249S substitution in the *TP53* gene, and HBV infection causes integration of the viral genome into that of the host, promoting mutations in genes crucial for cellular regulation, such as *TP53*. For these reasons HBV infection and aflatoxin B1 promote a high rate of mutagenesis in HCC[68,69]; and (2) *TP53* alterations were usually exclusive from *CTNNB1* mutations (P = 0.0001) but not from *AXIN1* and *APC*[57] (Figure 3).

MOLECULAR HCC SUBTYPE CLASSIFICATION

Over the years, many groups have tried to classify HCCs according to a molecular basis, but a univocal classification has been never reached.

Kabashima *et al*[70] grouped different classifications, starting from that of Shimada *et al*[71], and grouped HCCs into three molecular subtypes (MS1, MS2, MS3). The groups identified by the different studies are only fairly overlapping with each other. These classifications were based on clinical, molecular, and immunological features[70,71].

Regarding gene alterations, some correlations were found between *TP53* and *CTNNB1*. *TP53*-mutated HCCs were classified into the MS1 group, which correlated with unfavorable prognosis, viral infection, high serum alpha-fetoprotein levels, vascular invasion and proliferation, extensive mitotic activity resulting in chromosomal instability, and stem cell-like properties.

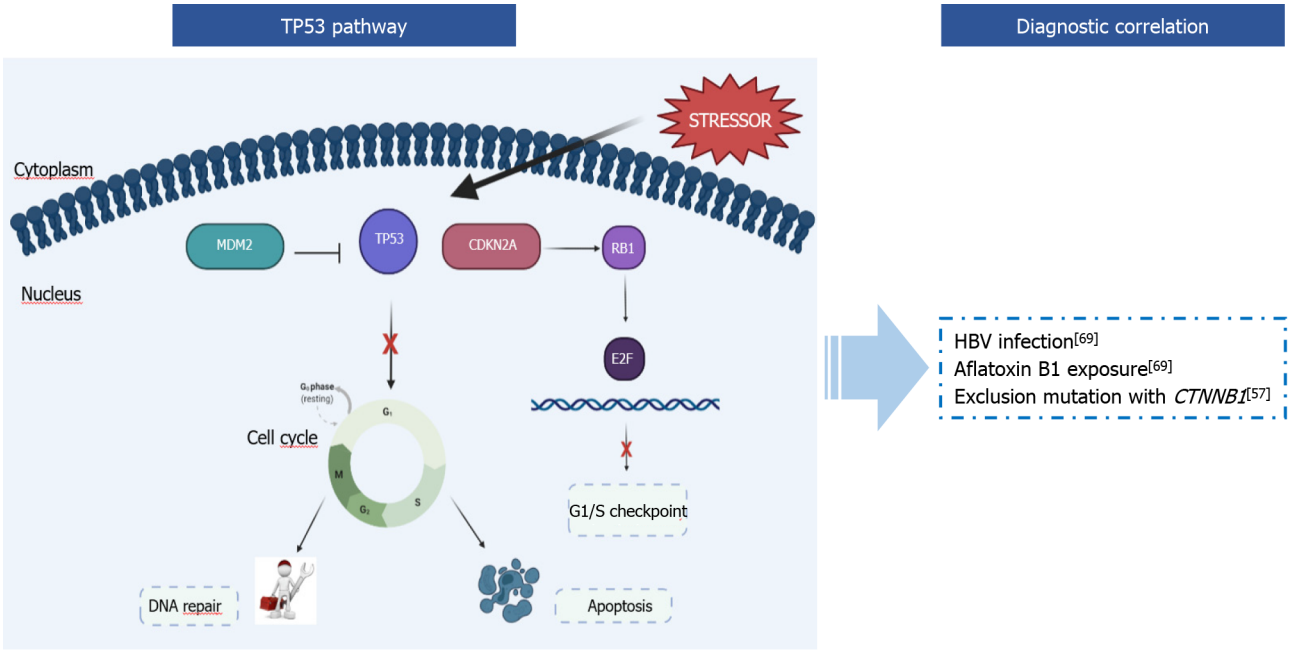
CTNNB1-mutated HCCs were placed into the MS2 group, correlating with aberrant activation of Wnt/ β-Catenin pathway, which could explain the high rate of methylation in CpG islands present in this group, as the constitutively active β-catenin protein recruits a DNMT1 methyltransferase. Another feature associated with the MS2 group is the immunosuppressive phenotype. Moreover, this class is considered non-proliferative/less progressive than others.

The MS3 group is not associated with molecular signatures, but only with metabolic disease-associated tumors[51,72-74].

The *TERT* gene is rarely found in these classifications. However, it should be considered that the most frequent mutations in *TERT* fall in a promoter region usually not covered by the exome sequencing studies. The Cancer Genome Atlas 2017 classification detected *TERT* mutations in HCC and included HCC-TERT samples in iCluster2 and iCluster3[17]. In 2019, further classification was drafted by Yang *et al*[75] that divides HCCs into 3 groups (C1, C2, C3), overlapping with a previous study performed by Hoshida *et al*[51]: C1→S3, C2→S1, C3→S2.

MOLECULAR HCC SUBTYPES AND PATHOLOGICAL FEATURES

In 2017, Calderaro *et al*[76] discriminated HCCs based on the presence of *TP53* or *CTNNB1* mutations, considering that these are two genes that mutate in a mutually exclusive manner and together comprise 57% of HCCs. In this study, CTNNB1-mutated HCCs were described as larger than the CTNNB1-wildtype HCCs but characterized by a lower tumor grade, with microtrabecular and pseudoglandular patterns of growth, without inflammatory infiltrates and with the presence of cholestasis[76]. Conversely, TP53-mutated HCCs were described as poorly differentiated tumors, with large multinucleated and pleomorphic cells, solid pattern of growth, frequent vascular invasion, and angiogenesis[76].



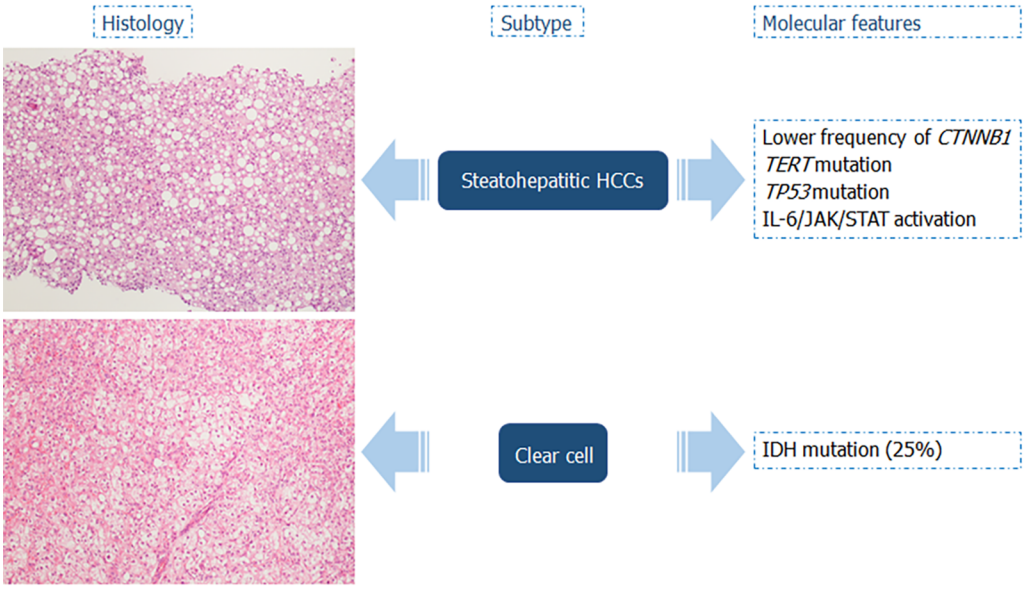
DOI: 10.3748/wjg.v28.i25.2854 **Copyright** ©The Author(s) 2022.

Figure 3 Main cellular pathways and clinical implications of *TP53* mutations in hepatocellular carcinoma. Created with BioRender.com. HBV: Hepatitis B virus.

Selected subtypes of HCCs recognized by the most recent WHO Classification of Tumors were described to have specific molecular alterations (Figures 4 and 5)[14]: (1) Up to 63% of steatohepatitic HCCs were associated with nonalcoholic fatty liver disease. This type of HCC is characterized by the following histologic features: macrovesicular steatosis, Mallory-Denk bodies, ballooning of tumoral hepatocytes, inflammation, and trabecular or pericellular fibrosis. With regard to key molecular features, steatohepatitic HCCs were significantly associated with a lower frequency of *CTNNB1* mutations, higher rate of mutations in *TERT* and *TP53*, IL-6/JAK/STAT activation, high level of C-reactive protein, and serum amyloid A positive at immunohistochemistry[14,77-80]; (2) Clear cell HCCs are considered a well-differentiated type, characterized by a cytoplasmic clearing, due to accumulation of glycogen, lipopolysaccharides, mucopolysaccharides, or cytoplasmic vesicles. *IDH* mutations were identified in 25% of clear cell HCCs, and these alterations were significantly associated with a worse prognosis. Moreover, *IDH* mutations are also found in intrahepatic cholangiocarcinoma, a tumor with a significantly worse prognosis than HCC[14,80-83]; (3) Macrotrabecular massive HCCs are frequently larger than 50 mm with vascular invasion, correlated high alpha-fetoprotein serum levels, high expression of angiopoietin 2, and vascular endothelial growth factor A. At the histological level, this subgroup is characterized by massive trabeculae surrounded by vascular spaces and coated by immature endothelial cells. On the molecular side, *TP53* mutations and *FGF19* amplifications have been detected. Macrotrabecular massive HCC is an aggressive phenotype associated with a worse prognosis [14,80,84,85]; and (5) Scirrhous HCCs develop in the non-cirrhotic liver, and they are characterized by hyaline stroma, intratumoral fibrosis with thin trabecular pattern growth (due to this characteristic is easily confusable radiologically to cholangiocarcinoma), or the lymphoepithelioma-like subtype, consisting of dense intratumor lymphocytic infiltration. Scirrhous HCCs may exhibit *TSC1*/*TSC2* mutations and transforming growth factor-β signaling activation. Regarding prognosis, scirrhous HCCs are an aggressive subgroup, often with invasion of the portal vein, but as far as long-term follow-up is concerned, the prognosis is similar or sometimes better to conventional HCCs[76,86,87].

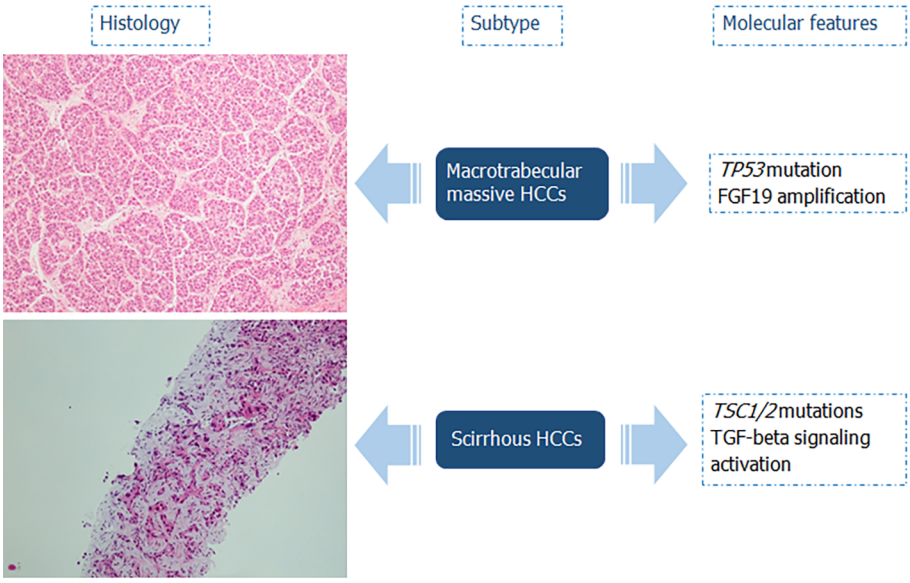
EXPERIENCE FROM OUR CENTER

Our preliminary results focused on 36 prospectively enrolled patients, all resected for HCC and selected for NGS by means of a laboratory-developed multi-gene panel Gene-Studio S5 sequencer, which comprises specific target regions including *TERT*[15]. We detected single mutations in the *TERT* promoter in 7 (19.4%) cases, in *TP53* in 4 (11.1%) cases, and in *CTNNB1* in 2 (5.6%) cases. *TERT* and *CTNNB1* coexistent mutations were observed in 8 (22.2%) cases, while *TERT* and *TP53* were in 8 (22.2%) cases. In 7 (19.4%) cases no mutations in these three genes were detected (Figure 6).



DOI: 10.3748/wjg.v28.i25.2854 **Copyright** ©The Author(s) 2022.

Figure 4 Steatohepatitic hepatocellular carcinomas and clear cell carcinoma and their molecular features. Hematoxylin-eosin stain (10 magnification). HCC: Hepatocellular carcinoma.



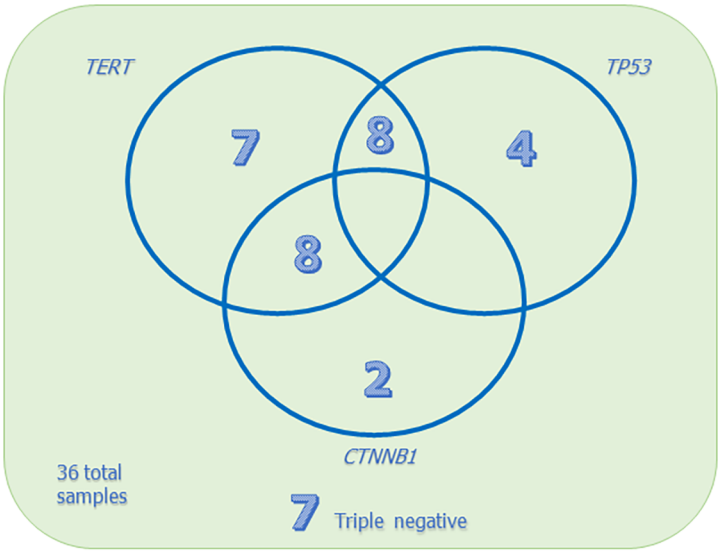
DOI: 10.3748/wjg.v28.i25.2854 **Copyright** ©The Author(s) 2022.

Figure 5 Macrotrabecular massive hepatocellular carcinomas and scirrhous hepatocellular carcinoma and their molecular features. Hematoxylin-eosin stain (10 magnification). HCC: Hepatocellular carcinoma; TGF: Transforming growth factor.

In line with a previous study by Calderaro *et al*[76], we observed a trend of *TERT*-mutated HCC towards a macrotrabecular or solid architecture. Moreover, the presence of *TERT* promoter mutations in combination with *TP53* mutation correlated with high-grade HCC ($P = 0.011$; Figure 7).

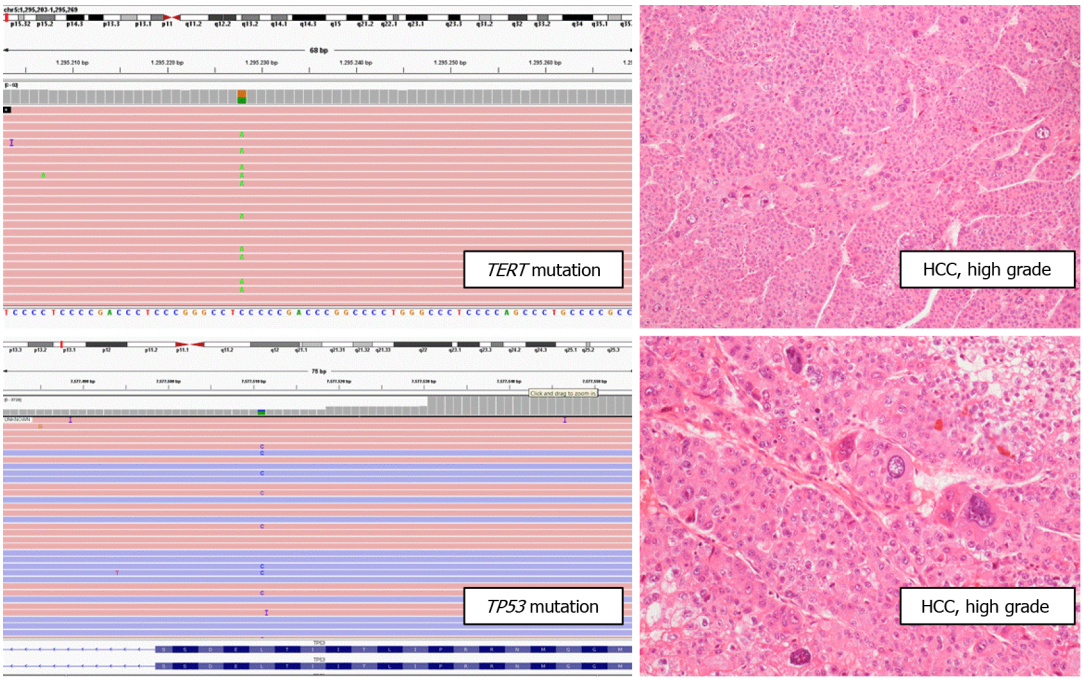
Interestingly, no correlations were found between mutations and tumor dimensions. This evidence leads us to hypothesize that the presence of *TERT* promoter mutations, alone or in combination with *TP53* alteration, correlates with a morphological progression in HCC, in terms of a higher tumor grade and an architecture more related to aggressive behavior (solid, macrotrabecular) but not of a dimensional evolution.

Most of the HCC in non-cirrhotic livers of our series showed no mutations or harbored only a *CTNNB1* mutation ($P = 0.031$), as a countercheck of the correlation between tumor progression and mutations. The validation of these results on a larger series as well as with post-surgical follow-up might indicate that small HCC may have an aggressive behavior from a molecular and morphological point of view, despite their dimensions.



DOI: 10.3748/wjg.v28.i25.2854 **Copyright** ©The Author(s) 2022.

Figure 6 Representation of our data based on the number of samples grouped according to their mutational status.



DOI: 10.3748/wjg.v28.i25.2854 **Copyright** ©The Author(s) 2022.

Figure 7 A case from our series of high-grade (Edmondson's 4) hepatocellular carcinoma, with tumor giant cells and macrotrabecular architecture. Left boxes: coexistent *TERT* and *TP53* mutations detected by next-generation sequencing analysis; Right boxes: Hematoxylin-eosin stain (10 and 20 magnification). HCC: Hepatocellular carcinoma.

CONCLUSION

The molecular signature of a tumor is becoming increasingly important in the approach of patients with different types of cancers, on diagnostic, prognostic, and predictive grounds. In the age of precision medicine, the study of HCC mutations is still a field that is worth investigating. Considering both the literature data and our personal experience, about 80% of HCCs harbor mutations in at least one gene among *TERT*, *TP53*, or *CTNNB1*, with different biological and clinical implications.

In the near future, a deeper analysis of these three genes is surely desirable since a molecular characterization of HCC would open up the possibility of personalized therapies, as has happened for other cancers (*e.g.*, lung adenocarcinomas, melanomas, gastrointestinal stromal tumors, colorectal adenocarcinomas). Moreover, the evidence of a tight correlation between the mutational profile and the HCC morphology is likely to imply an increasing integrative approach between anatomic pathology and

molecular laboratories.

FOOTNOTES

Author contributions: Vasuri F and de Biase D contributed equally to this paper; Maloberti T and Vasuri F designed the research study; Maloberti T, De Leo A, Sanza V, Gruppioni E, Altimari A, Riefolo M, Visani M, and Malvi D performed the research; Maloberti T and Vasuri F analyzed the data and wrote the manuscript; D'Errico A, Tallini G, and de Biase D supervised the manuscript preparation; All authors have read and approved the final manuscript.

Conflict-of-interest statement: Dario de Biase has received personal fees (as consultant and/or speaker bureau) from Boehringer Ingelheim and Eli Lilly, unrelated to the current work.

Open-Access: This article is an open-access article that was selected by an in-house editor and fully peer-reviewed by external reviewers. It is distributed in accordance with the Creative Commons Attribution NonCommercial (CC BY-NC 4.0) license, which permits others to distribute, remix, adapt, build upon this work non-commercially, and license their derivative works on different terms, provided the original work is properly cited and the use is non-commercial. See: https://creativecommons.org/Licenses/by-nc/4.0/

Country/Territory of origin: Italy

ORCID number: Thais Maloberti 0000-0002-8306-4653; Antonio De Leo 0000-0002-3761-5135; Viviana Sanza 0000-0001-9889-8776; Elisa Gruppioni 0000-0002-4334-6170; Annalisa Altimari 0000-0001-9944-2455; Mattia Riefolo 0000-0002-3673-532X; Michela Visani 0000-0002-9051-2231; Deborah Malvi 0000-0001-6109-3675; Antonia D'Errico 0000-0003-2747-3732; Giovanni Tallini 0000-0003-0113-6682; Francesco Vasuri 0000-0002-1145-6025; Dario de Biase 0000-0002-0609-8817.

S-Editor: Ma YJ
L-Editor: Filipodia
P-Editor: Ma YJ

REFERENCES

1 **Harris PS**, Hansen RM, Gray ME, Massoud OI, McGuire BM, Shoreibah MG. Hepatocellular carcinoma surveillance: An evidence-based approach. *World J Gastroenterol* 2019; **25**: 1550-1559 [PMID: 30983815 DOI: 10.3748/wjg.v25.i13.1550]
2 **World Health Organization**. Cancer Today. Available from: https://gco.iarc.fr/today/home
3 **Nahon P**, Zucman-Rossi J. Single nucleotide polymorphisms and risk of hepatocellular carcinoma in cirrhosis. *J Hepatol* 2012; **57**: 663-674 [PMID: 22609306 DOI: 10.1016/j.jhep.2012.02.035]
4 **Bidkhori G**, Benfeitas R, Klevstig M, Zhang C, Nielsen J, Uhlen M, Boren J, Mardinoglu A. Metabolic network-based stratification of hepatocellular carcinoma reveals three distinct tumor subtypes. *Proc Natl Acad Sci U S A* 2018; **115**: E11874-E11883 [PMID: 30482855 DOI: 10.1073/pnas.1807305115]
5 **Dharel N**, Kato N, Muroyama R, Moriyama M, Shao RX, Kawabe T, Omata M. MDM2 promoter SNP309 is associated with the risk of hepatocellular carcinoma in patients with chronic hepatitis C. *Clin Cancer Res* 2006; **12**: 4867-4871 [PMID: 16914573 DOI: 10.1158/1078-0432.CCR-06-0111]
6 **Park JW**, Chen M, Colombo M, Roberts LR, Schwartz M, Chen PJ, Kudo M, Johnson P, Wagner S, Orsini LS, Sherman M. Global patterns of hepatocellular carcinoma management from diagnosis to death: the BRIDGE Study. *Liver Int* 2015; **35**: 2155-2166 [PMID: 25752327 DOI: 10.1111/liv.12818]
7 **Wild CP**, Miller JD, Groopman JD. Mycotoxin Control in Low- And Middle-Income Countries. In: Wild CP, Miller JD, Groopman JD, editors. Mycotoxin Control in Low- and Middle-Income Countries. Lyon (FR), 2015
8 **Ng AWT**, Poon SL, Huang MN, Lim JQ, Boot A, Yu W, Suzuki Y, Thangaraju S, Ng CCY, Tan P, Pang ST, Huang HY, Yu MC, Lee PH, Hsieh SY, Chang AY, Teh BT, Rozen SG. Aristolochic acids and their derivatives are widely implicated in liver cancers in Taiwan and throughout Asia. *Sci Transl Med* 2017; **9** [PMID: 29046434 DOI: 10.1126/scitranslmed.aan6446]
9 **Arlt VM**, Stiborova M, Schmeiser HH. Aristolochic acid as a probable human cancer hazard in herbal remedies: a review. *Mutagenesis* 2002; **17**: 265-277 [PMID: 12110620 DOI: 10.1093/mutage/17.4.265]
10 **Yang JD**, Hainaut P, Gores GJ, Amadou A, Plymoth A, Roberts LR. A global view of hepatocellular carcinoma: trends, risk, prevention and management. *Nat Rev Gastroenterol Hepatol* 2019; **16**: 589-604 [PMID: 31439937 DOI: 10.1038/s41575-019-0186-y]
11 **Baecker A**, Liu X, La Vecchia C, Zhang ZF. Worldwide incidence of hepatocellular carcinoma cases attributable to major risk factors. *Eur J Cancer Prev* 2018; **27**: 205-212 [PMID: 29489473 DOI: 10.1097/CEJ.0000000000000428]
12 **Forner A**, Llovet JM, Bruix J. Hepatocellular carcinoma. *Lancet* 2012; **379**: 1245-1255 [PMID: 22353262 DOI: 10.1016/S0140-6736(11)61347-0]
13 **Zucman-Rossi J**, Villanueva A, Nault JC, Llovet JM. Genetic Landscape and Biomarkers of Hepatocellular Carcinoma. *Gastroenterology* 2015; **149**: 1226-1239.e4 [PMID: 26099527 DOI: 10.1053/j.gastro.2015.05.061]
14 **Tumours WCo**. Digestive System Tumours. 5th Edition. Lyon: IARC, 2019
15 **de Biase D**, Acquaviva G, Visani M, Sanza V, Argento CM, De Leo A, Maloberti T, Pession A, Tallini G. Molecular Diagnostic of Solid Tumor Using a Next Generation Sequencing Custom-Designed Multi-Gene Panel. *Diagnostics (Basel)*

2020; **10** [PMID: 32340363 DOI: 10.3390/diagnostics10040250]
16 **Malvi D**, de Biase D, Fittipaldi S, Grillini M, Visani M, Pession A, D'Errico A, Vasuri F. Immunomorphology and molecular biology of mixed primary liver cancers: is Nestin a marker of intermediate-cell carcinoma? *Histopathology* 2020; **76**: 265-274 [PMID: 31374137 DOI: 10.1111/his.13966]
17 **Cancer Genome Atlas Research Network**. ; Cancer Genome Atlas Research Network. Comprehensive and Integrative Genomic Characterization of Hepatocellular Carcinoma. *Cell* 2017; **169**: 1327-1341.e23 [PMID: 28622513 DOI: 10.1016/j.cell.2017.05.046]
18 **Nandakumar J**, Cech TR. Finding the end: recruitment of telomerase to telomeres. *Nat Rev Mol Cell Biol* 2013; **14**: 69-82 [PMID: 23299958 DOI: 10.1038/nrm3505]
19 **Heidenreich B**, Kumar R. TERT promoter mutations in telomere biology. *Mutat Res Rev Mutat Res* 2017; **771**: 15-31 [PMID: 28342451 DOI: 10.1016/j.mrrev.2016.11.002]
20 **Mason PJ**, Perdigones N. Telomere biology and translational research. *Transl Res* 2013; **162**: 333-342 [PMID: 24070997 DOI: 10.1016/j.trsl.2013.08.009]
21 **Colebatch AJ**, Dobrovic A, Cooper WA. *TERT* gene: its function and dysregulation in cancer. *J Clin Pathol* 2019; **72**: 281-284 [PMID: 30696697 DOI: 10.1136/jclinpath-2018-205653]
22 **Hanahan D**, Weinberg RA. Hallmarks of cancer: the next generation. *Cell* 2011; **144**: 646-674 [PMID: 21376230 DOI: 10.1016/j.cell.2011.02.013]
23 **Dratwa M**, Wysoczańska B, Łacina P, Kubik T, Bogunia-Kubik K. TERT-Regulation and Roles in Cancer Formation. *Front Immunol* 2020; **11**: 589929 [PMID: 33329574 DOI: 10.3389/fimmu.2020.589929]
24 **Esopi D**, Graham MK, Brosnan-Cashman JA, Meyers J, Vaghasia A, Gupta A, Kumar B, Haffner MC, Heaphy CM, De Marzo AM, Meeker AK, Nelson WG, Wheelan SJ, Yegnasubramanian S. Pervasive promoter hypermethylation of silenced TERT alleles in human cancers. *Cell Oncol (Dordr)* 2020; **43**: 847-861 [PMID: 32468444 DOI: 10.1007/s13402-020-00531-7]
25 **Barthel FP**, Wei W, Tang M, Martinez-Ledesma E, Hu X, Amin SB, Akdemir KC, Seth S, Song X, Wang Q, Lichtenberg T, Hu J, Zhang J, Zheng S, Verhaak RG. Systematic analysis of telomere length and somatic alterations in 31 cancer types. *Nat Genet* 2017; **49**: 349-357 [PMID: 28135248 DOI: 10.1038/ng.3781]
26 **Peifer M**, Hertwig F, Roels F, Dreidax D, Gartlgruber M, Menon R, Krämer A, Roncaioli JL, Sand F, Heuckmann JM, Ikram F, Schmidt R, Ackermann S, Engesser A, Kahlert Y, Vogel W, Altmüller J, Nürnberg P, Thierry-Mieg J, Thierry-Mieg D, Mariappan A, Heynck S, Mariotti E, Henrich KO, Gloeckner C, Bosco G, Leuschner I, Schweiger MR, Savelyeva L, Watkins SC, Shao C, Bell E, Höfer T, Achter V, Lang U, Theissen J, Volland R, Saadati M, Eggert A, de Wilde B, Berthold F, Peng Z, Zhao C, Shi L, Ortmann M, Büttner R, Perner S, Hero B, Schramm A, Schulte JH, Herrmann C, O'Sullivan RJ, Westermann F, Thomas RK, Fischer M. Telomerase activation by genomic rearrangements in high-risk neuroblastoma. *Nature* 2015; **526**: 700-704 [PMID: 26466568 DOI: 10.1038/nature14980]
27 **Kitada T**, Seki S, Kawakita N, Kuroki T, Monna T. Telomere shortening in chronic liver diseases. *Biochem Biophys Res Commun* 1995; **211**: 33-39 [PMID: 7779103 DOI: 10.1006/bbrc.1995.1774]
28 **Wiemann SU**, Satyanarayana A, Tsahuridu M, Tillmann HL, Zender L, Klempnauer J, Flemming P, Franco S, Blasco MA, Manns MP, Rudolph KL. Hepatocyte telomere shortening and senescence are general markers of human liver cirrhosis. *FASEB J* 2002; **16**: 935-942 [PMID: 12087054 DOI: 10.1096/fj.01-0977com]
29 **Carulli L**, Anzivino C. Telomere and telomerase in chronic liver disease and hepatocarcinoma. *World J Gastroenterol* 2014; **20**: 6287-6292 [PMID: 24876749 DOI: 10.3748/wjg.v20.i20.6287]
30 **Quaas A**, Oldopp T, Tharun L, Klingenfeld C, Krech T, Sauter G, Grob TJ. Frequency of TERT promoter mutations in primary tumors of the liver. *Virchows Arch* 2014; **465**: 673-677 [PMID: 25267585 DOI: 10.1007/s00428-014-1658-7]
31 **Jang JW**, Kim HS, Kim JS, Lee SK, Han JW, Sung PS, Bae SH, Choi JY, Yoon SK, Han DJ, Kim TM, Roberts LR. Distinct Patterns of HBV Integration and *TERT* Alterations between in Tumor and Non-Tumor Tissue in Patients with Hepatocellular Carcinoma. *Int J Mol Sci* 2021; **22** [PMID: 34209079 DOI: 10.3390/ijms22137056]
32 **Schulze K**, Nault JC, Villanueva A. Genetic profiling of hepatocellular carcinoma using next-generation sequencing. *J Hepatol* 2016; **65**: 1031-1042 [PMID: 27262756 DOI: 10.1016/j.jhep.2016.05.035]
33 **Lee SE**, Chang SH, Kim WY, Lim SD, Kim WS, Hwang TS, Han HS. Frequent somatic TERT promoter mutations and CTNNB1 mutations in hepatocellular carcinoma. *Oncotarget* 2016; **7**: 69267-69275 [PMID: 27661004 DOI: 10.18632/oncotarget.12121]
34 **Nault JC**, Zucman-Rossi J. TERT promoter mutations in primary liver tumors. *Clin Res Hepatol Gastroenterol* 2016; **40**: 9-14 [PMID: 26336998 DOI: 10.1016/j.clinre.2015.07.006]
35 **Kwa WT**, Effendi K, Yamazaki K, Kubota N, Hatano M, Ueno A, Masugi Y, Sakamoto M. Telomerase reverse transcriptase (TERT) promoter mutation correlated with intratumoral heterogeneity in hepatocellular carcinoma. *Pathol Int* 2020; **70**: 624-632 [PMID: 32559017 DOI: 10.1111/pin.12974]
36 **Huang H**, Fujii H, Sankila A, Mahler-Araujo BM, Matsuda M, Cathomas G, Ohgaki H. Beta-catenin mutations are frequent in human hepatocellular carcinomas associated with hepatitis C virus infection. *Am J Pathol* 1999; **155**: 1795-1801 [PMID: 10595907 DOI: 10.1016/s0002-9440(10)65496-x]
37 **Schulze K**, Imbeaud S, Letouzé E, Alexandrov LB, Calderaro J, Rebouissou S, Couchy G, Meiller C, Shinde J, Soysouvanh F, Calatayud AL, Pinyol R, Pelletier L, Balabaud C, Laurent A, Blanc JF, Mazzaferro V, Calvo F, Villanueva A, Nault JC, Bioulac-Sage P, Stratton MR, Llovet JM, Zucman-Rossi J. Exome sequencing of hepatocellular carcinomas identifies new mutational signatures and potential therapeutic targets. *Nat Genet* 2015; **47**: 505-511 [PMID: 25822088 DOI: 10.1038/ng.3252]
38 **Nault JC**, Mallet M, Pilati C, Calderaro J, Bioulac-Sage P, Laurent C, Laurent A, Cherqui D, Balabaud C, Zucman-Rossi J. High frequency of telomerase reverse-transcriptase promoter somatic mutations in hepatocellular carcinoma and preneoplastic lesions. *Nat Commun* 2013; **4**: 2218 [PMID: 23887712 DOI: 10.1038/ncomms3218]
39 **Pinyol R**, Tovar V, Llovet JM. TERT promoter mutations: gatekeeper and driver of hepatocellular carcinoma. *J Hepatol* 2014; **61**: 685-687 [PMID: 24859456 DOI: 10.1016/j.jhep.2014.05.028]
40 **Hoffmeyer K**, Raggioli A, Rudloff S, Anton R, Hierholzer A, Del Valle I, Hein K, Vogt R, Kemler R. Wnt/β-catenin

signaling regulates telomerase in stem cells and cancer cells. *Science* 2012; **336**: 1549-1554 [PMID: 22723415 DOI: 10.1126/science.1218370]

41 **Oh BK**, Kim H, Park YN, Yoo JE, Choi J, Kim KS, Lee JJ, Park C. High telomerase activity and long telomeres in advanced hepatocellular carcinomas with poor prognosis. *Lab Invest* 2008; **88**: 144-152 [PMID: 18158557 DOI: 10.1038/Labinvest.3700710]

42 **Shang S**, Hua F, Hu ZW. The regulation of β-catenin activity and function in cancer: therapeutic opportunities. *Oncotarget* 2017; **8**: 33972-33989 [PMID: 28430641 DOI: 10.18632/oncotarget.15687]

43 **Xing Y**, Clements WK, Kimelman D, Xu W. Crystal structure of a beta-catenin/axin complex suggests a mechanism for the beta-catenin destruction complex. *Genes Dev* 2003; **17**: 2753-2764 [PMID: 14600025 DOI: 10.1101/gad.1142603]

44 **Liu J**, Xing Y, Hinds TR, Zheng J, Xu W. The third 20 amino acid repeat is the tightest binding site of APC for beta-catenin. *J Mol Biol* 2006; **360**: 133-144 [PMID: 16753179 DOI: 10.1016/j.jmb.2006.04.064]

45 **Fiedler M**, Mendoza-Topaz C, Rutherford TJ, Mieszczanek J, Bienz M. Dishevelled interacts with the DIX domain polymerization interface of Axin to interfere with its function in down-regulating β-catenin. *Proc Natl Acad Sci U S A* 2011; **108**: 1937-1942 [PMID: 21245303 DOI: 10.1073/pnas.1017063108]

46 **Nishida N**, Goel A. Genetic and epigenetic signatures in human hepatocellular carcinoma: a systematic review. *Curr Genomics* 2011; **12**: 130-137 [PMID: 21966251 DOI: 10.2174/138920211795564359]

47 **Kobayashi M**, Honma T, Matsuda Y, Suzuki Y, Narisawa R, Ajioka Y, Asakura H. Nuclear translocation of beta-catenin in colorectal cancer. *Br J Cancer* 2000; **82**: 1689-1693 [PMID: 10817505 DOI: 10.1054/bjoc.1999.1112]

48 **Khramtsov AI**, Khramtsova GF, Tretiakova M, Huo D, Olopade OI, Goss KH. Wnt/beta-catenin pathway activation is enriched in basal-like breast cancers and predicts poor outcome. *Am J Pathol* 2010; **176**: 2911-2920 [PMID: 20395444 DOI: 10.2353/ajpath.2010.091125]

49 **Gekas C**, D'Altri T, Aligué R, González J, Espinosa L, Bigas A. β-Catenin is required for T-cell leukemia initiation and MYC transcription downstream of Notch1. *Leukemia* 2016; **30**: 2002-2010 [PMID: 27125305 DOI: 10.1038/leu.2016.106]

50 **Chen J**, Gingold JA, Su X. Immunomodulatory TGF-β Signaling in Hepatocellular Carcinoma. *Trends Mol Med* 2019; **25**: 1010-1023 [PMID: 31353124 DOI: 10.1016/j.molmed.2019.06.007]

51 **Hoshida Y**, Nijman SM, Kobayashi M, Chan JA, Brunet JP, Chiang DY, Villanueva A, Newell P, Ikeda K, Hashimoto M, Watanabe G, Gabriel S, Friedman SL, Kumada H, Llovet JM, Golub TR. Integrative transcriptome analysis reveals common molecular subclasses of human hepatocellular carcinoma. *Cancer Res* 2009; **69**: 7385-7392 [PMID: 19723656 DOI: 10.1158/0008-5472.CAN-09-1089]

52 **de La Coste A**, Romagnolo B, Billuart P, Renard CA, Buendia MA, Soubrane O, Fabre M, Chelly J, Beldjord C, Kahn A, Perret C. Somatic mutations of the beta-catenin gene are frequent in mouse and human hepatocellular carcinomas. *Proc Natl Acad Sci U S A* 1998; **95**: 8847-8851 [PMID: 9671767 DOI: 10.1073/pnas.95.15.8847]

53 **Pinyol R**, Sia D, Llovet JM. Immune Exclusion-Wnt/CTNNB1 Class Predicts Resistance to Immunotherapies in HCC. *Clin Cancer Res* 2019; **25**: 2021-2023 [PMID: 30617138 DOI: 10.1158/1078-0432.CCR-18-3778]

54 **Nault JC**, Couchy G, Balabaud C, Morcrette G, Caruso S, Blanc JF, Bacq Y, Calderaro J, Paradis V, Ramos J, Scoazec JY, Gnemmi V, Sturm N, Guettier C, Fabre M, Savier E, Chiche L, Labrune P, Selves J, Wendum D, Pilati C, Laurent A, De Muret A, Le Bail B, Rebouissou S, Imbeaud S; GENTHEP Investigators, Bioulac-Sage P, Letouzé E, Zucman-Rossi J. Molecular Classification of Hepatocellular Adenoma Associates With Risk Factors, Bleeding, and Malignant Transformation. *Gastroenterology* 2017; **152**: 880-894.e6 [PMID: 27939373 DOI: 10.1053/j.gastro.2016.11.042]

55 **Shen XY**, Hu XG, Kim YB, Kim MN, Hong SY, Kim BW, Wang HJ. Molecular classification of hepatocellular adenoma: A single-center experience. *Ann Hepatobiliary Pancreat Surg* 2019; **23**: 109-114 [PMID: 31225410 DOI: 10.14701/ahbps.2019.23.2.109]

56 **Rebouissou S**, Franconi A, Calderaro J, Letouzé E, Imbeaud S, Pilati C, Nault JC, Couchy G, Laurent A, Balabaud C, Bioulac-Sage P, Zucman-Rossi J. Genotype-phenotype correlation of CTNNB1 mutations reveals different ß-catenin activity associated with liver tumor progression. *Hepatology* 2016; **64**: 2047-2061 [PMID: 27177928 DOI: 10.1002/hep.28638]

57 **Guichard C**, Amaddeo G, Imbeaud S, Ladeiro Y, Pelletier L, Maad IB, Calderaro J, Bioulac-Sage P, Letexier M, Degos F, Clément B, Balabaud C, Chevet E, Laurent A, Couchy G, Letouzé E, Calvo F, Zucman-Rossi J. Integrated analysis of somatic mutations and focal copy-number changes identifies key genes and pathways in hepatocellular carcinoma. *Nat Genet* 2012; **44**: 694-698 [PMID: 22561517 DOI: 10.1038/ng.2256]

58 **Harris SL**, Levine AJ. The p53 pathway: positive and negative feedback loops. *Oncogene* 2005; **24**: 2899-2908 [PMID: 15838523 DOI: 10.1038/sj.onc.1208615]

59 **Toufektchan E**, Toledo F. The Guardian of the Genome Revisited: p53 Downregulates Genes Required for Telomere Maintenance, DNA Repair, and Centromere Structure. *Cancers (Basel)* 2018; **10** [PMID: 29734785 DOI: 10.3390/cancers10050135]

60 **Overholtzer M**, Rao PH, Favis R, Lu XY, Elowitz MB, Barany F, Ladanyi M, Gorlick R, Levine AJ. The presence of p53 mutations in human osteosarcomas correlates with high levels of genomic instability. *Proc Natl Acad Sci U S A* 2003; **100**: 11547-11552 [PMID: 12972634 DOI: 10.1073/pnas.1934852100]

61 **Jin S**, Levine AJ. The p53 functional circuit. *J Cell Sci* 2001; **114**: 4139-4140 [PMID: 11739646]

62 **Purvis JE**, Karhohs KW, Mock C, Batchelor E, Loewer A, Lahav G. p53 dynamics control cell fate. *Science* 2012; **336**: 1440-1444 [PMID: 22700930 DOI: 10.1126/science.1218351]

63 **Leroy B**, Anderson M, Soussi T. TP53 mutations in human cancer: database reassessment and prospects for the next decade. *Hum Mutat* 2014; **35**: 672-688 [PMID: 24665023 DOI: 10.1002/humu.22552]

64 **Gargallo P**, Yáñez Y, Segura V, Juan A, Torres B, Balaguer J, Oltra S, Castel V, Cañete A. Li-Fraumeni syndrome heterogeneity. *Clin Transl Oncol* 2020; **22**: 978-988 [PMID: 31691207 DOI: 10.1007/s12094-019-02236-2]

65 **Lombardo D**, Saitta C, Giosa D, Di Tocco FC, Musolino C, Caminiti G, Chines V, Franzè MS, Alibrandi A, Navarra G, Raimondo G, Pollicino T. Frequency of somatic mutations in *TERT* promoter, *TP53* and *CTNNB1* genes in patients with hepatocellular carcinoma from Southern Italy. *Oncol Lett* 2020; **19**: 2368-2374 [PMID: 32194736 DOI: 10.3892/ol.2020.11332]

66 **Bressac B**, Kew M, Wands J, Ozturk M. Selective G to T mutations of p53 gene in hepatocellular carcinoma from southern Africa. *Nature* 1991; **350**: 429-431 [PMID: 1672732 DOI: 10.1038/350429a0]

67 **Unsal H**, Yakicier C, Marçais C, Kew M, Volkmann M, Zentgraf H, Isselbacher KJ, Ozturk M. Genetic heterogeneity of hepatocellular carcinoma. *Proc Natl Acad Sci U S A* 1994; **91**: 822-826 [PMID: 8290606 DOI: 10.1073/pnas.91.2.822]

68 **Gouas D**, Shi H, Hainaut P. The aflatoxin-induced TP53 mutation at codon 249 (R249S): biomarker of exposure, early detection and target for therapy. *Cancer Lett* 2009; **286**: 29-37 [PMID: 19376640 DOI: 10.1016/j.canlet.2009.02.057]

69 **Lunn RM**, Zhang YJ, Wang LY, Chen CJ, Lee PH, Lee CS, Tsai WY, Santella RM. p53 mutations, chronic hepatitis B virus infection, and aflatoxin exposure in hepatocellular carcinoma in Taiwan. *Cancer Res* 1997; **57**: 3471-3477 [PMID: 9270015]

70 **Kabashima A**, Shimada S, Shimokawa M, Akiyama Y, Tanabe M, Tanaka S. Molecular and immunological paradigms of hepatocellular carcinoma: Special reference to therapeutic approaches. *J Hepatobiliary Pancreat Sci* 2021; **28**: 62-75 [PMID: 33259135 DOI: 10.1002/jhbp.874]

71 **Shimada S**, Mogushi K, Akiyama Y, Furuyama T, Watanabe S, Ogura T, Ogawa K, Ono H, Mitsunori Y, Ban D, Kudo A, Arii S, Tanabe M, Wands JR, Tanaka S. Comprehensive molecular and immunological characterization of hepatocellular carcinoma. *EBioMedicine* 2019; **40**: 457-470 [PMID: 30598371 DOI: 10.1016/j.ebiom.2018.12.058]

72 **Lee JS**, Chu IS, Heo J, Calvisi DF, Sun Z, Roskams T, Durnez A, Demetris AJ, Thorgeirsson SS. Classification and prediction of survival in hepatocellular carcinoma by gene expression profiling. *Hepatology* 2004; **40**: 667-676 [PMID: 15349906 DOI: 10.1002/hep.20375]

73 **Boyault S**, Rickman DS, de Reyniès A, Balabaud C, Rebouissou S, Jeannot E, Hérault A, Saric J, Belghiti J, Franco D, Bioulac-Sage P, Laurent-Puig P, Zucman-Rossi J. Transcriptome classification of HCC is related to gene alterations and to new therapeutic targets. *Hepatology* 2007; **45**: 42-52 [PMID: 17187432 DOI: 10.1002/hep.21467]

74 **Chiang DY**, Villanueva A, Hoshida Y, Peix J, Newell P, Minguez B, LeBlanc AC, Donovan DJ, Thung SN, Solé M, Tovar V, Alsinet C, Ramos AH, Barretina J, Roayaie S, Schwartz M, Waxman S, Bruix J, Mazzaferro V, Ligon AH, Najfeld V, Friedman SL, Sellers WR, Meyerson M, Llovet JM. Focal gains of VEGFA and molecular classification of hepatocellular carcinoma. *Cancer Res* 2008; **68**: 6779-6788 [PMID: 18701503 DOI: 10.1158/0008-5472.CAN-08-0742]

75 **Yang C**, Huang X, Liu Z, Qin W, Wang C. Metabolism-associated molecular classification of hepatocellular carcinoma. *Mol Oncol* 2020; **14**: 896-913 [PMID: 31955511 DOI: 10.1002/1878-0261.12639]

76 **Calderaro J**, Couchy G, Imbeaud S, Amaddeo G, Letouzé E, Blanc JF, Laurent C, Hajji Y, Azoulay D, Bioulac-Sage P, Nault JC, Zucman-Rossi J. Histological subtypes of hepatocellular carcinoma are related to gene mutations and molecular tumour classification. *J Hepatol* 2017; **67**: 727-738 [PMID: 28532995 DOI: 10.1016/j.jhep.2017.05.014]

77 **Salomao M**, Yu WM, Brown RS Jr, Emond JC, Lefkowitch JH. Steatohepatitic hepatocellular carcinoma (SH-HCC): a distinctive histological variant of HCC in hepatitis C virus-related cirrhosis with associated NAFLD/NASH. *Am J Surg Pathol* 2010; **34**: 1630-1636 [PMID: 20975341 DOI: 10.1097/PAS.0b013e3181f31caa]

78 **Ando S**, Shibahara J, Hayashi A, Fukayama M. β-catenin alteration is rare in hepatocellular carcinoma with steatohepatitic features: immunohistochemical and mutational study. *Virchows Arch* 2015; **467**: 535-542 [PMID: 26311355 DOI: 10.1007/s00428-015-1836-2]

79 **Taniai M**, Hashimoto E, Tobari M, Kodama K, Tokushige K, Yamamoto M, Takayama T, Sugitani M, Sano K, Kondo F, Fukusato T. Clinicopathological investigation of steatohepatitic hepatocellular carcinoma: A multicenter study using immunohistochemical analysis of adenoma-related markers. *Hepatol Res* 2018; **48**: 947-955 [PMID: 30058778 DOI: 10.1111/hepr.13203]

80 **El Jabbour T**, Lagana SM, Lee H. Update on hepatocellular carcinoma: Pathologists' review. *World J Gastroenterol* 2019; **25**: 1653-1665 [PMID: 31011252 DOI: 10.3748/wjg.v25.i14.1653]

81 **Lee WS**, Lee KW, Heo JS, Kim SJ, Choi SH, Kim YI, Joh JW. Comparison of combined hepatocellular and cholangiocarcinoma with hepatocellular carcinoma and intrahepatic cholangiocarcinoma. *Surg Today* 2006; **36**: 892-897 [PMID: 16998683 DOI: 10.1007/s00595-006-3276-8]

82 **Lee JH**, Shin DH, Park WY, Shin N, Kim A, Lee HJ, Kim YK, Choi KU, Kim JY, Yang YI, Lee CH, Sol MY. IDH1 R132C mutation is detected in clear cell hepatocellular carcinoma by pyrosequencing. *World J Surg Oncol* 2017; **15**: 82 [PMID: 28403884 DOI: 10.1186/s12957-017-1144-1]

83 **Bannasch P**, Ribback S, Su Q, Mayer D. Clear cell hepatocellular carcinoma: origin, metabolic traits and fate of glycogenotic clear and ground glass cells. *Hepatobiliary Pancreat Dis Int* 2017; **16**: 570-594 [PMID: 29291777 DOI: 10.1016/S1499-3872(17)60071-7]

84 **Vasuri F**, Fittipaldi S, Giunchi F, Monica M, Ravaioli M, Degiovanni A, Bonora S, Golfieri R, Bolondi L, Grigioni WF, Pasquinelli G, D'Errico-Grigioni A. Facing the enigma of the vascular network in hepatocellular carcinomas in cirrhotic and non-cirrhotic livers. *J Clin Pathol* 2016; **69**: 102-108 [PMID: 26243063 DOI: 10.1136/jclinpath-2015-203028]

85 **Ziol M**, Poté N, Amaddeo G, Laurent A, Nault JC, Oberti F, Costentin C, Michalak S, Bouattour M, Francoz C, Pageaux GP, Ramos J, Decaens T, Luciani A, Guiu B, Vilgrain V, Aubé C, Derman J, Charpy C, Zucman-Rossi J, Barget N, Seror O, Ganne-Carrié N, Paradis V, Calderaro J. Macrotrabecular-massive hepatocellular carcinoma: A distinctive histological subtype with clinical relevance. *Hepatology* 2018; **68**: 103-112 [PMID: 29281854 DOI: 10.1002/hep.29762]

86 **Matsuura S**, Aishima S, Taguchi K, Asayama Y, Terashi T, Honda H, Tsuneyoshi M. 'Scirrhous' type hepatocellular carcinomas: a special reference to expression of cytokeratin 7 and hepatocyte paraffin 1. *Histopathology* 2005; **47**: 382-390 [PMID: 16178893 DOI: 10.1111/j.1365-2559.2005.02230.x]

87 **Li W**, Gomez E, Zhang Z. Immunohistochemical expression of stromal cell-derived factor-1 (SDF-1) and CXCR4 ligand receptor system in hepatocellular carcinoma. *J Exp Clin Cancer Res* 2007; **26**: 527-533 [PMID: 18365549]

World Journal of Gastroenterology

Submit a Manuscript: https://www.f6publishing.com

World J Gastroenterol 2022 July 7; 28(25): 2867-2880

DOI: 10.3748/wjg.v28.i25.2867

ISSN 1007-9327 (print) ISSN 2219-2840 (online)

MINIREVIEWS

Micelles as potential drug delivery systems for colorectal cancer treatment

Zaynab Fatfat, Maamoun Fatfat, Hala Gali-Muhtasib

Specialty type: Oncology

Provenance and peer review: Invited article; Externally peer reviewed.

Peer-review model: Single blind

Peer-review report's scientific quality classification

Grade A (Excellent): 0
Grade B (Very good): B, B, B
Grade C (Good): 0
Grade D (Fair): 0
Grade E (Poor): 0

P-Reviewer: Diez-Alonso M, Spain; Manojlovic N, Serbia; Sun SY, China
A-Editor: Sato Y, Japan

Received: January 15, 2022
Peer-review started: January 15, 2022
First decision: March 8, 2022
Revised: March 22, 2022
Accepted: May 27, 2022
Article in press: May 27, 2022
Published online: July 7, 2022

Zaynab Fatfat, Maamoun Fatfat, Hala Gali-Muhtasib, Department of Biology, American University of Beirut, Beirut 1107 2020, Lebanon

Hala Gali-Muhtasib, Center for Drug Discovery, American University of Beirut, Beirut 1107 2020, Lebanon

Corresponding author: Hala Gali-Muhtasib, PhD, Professor, Department of Biology, and Center for Drug Discovery, American University of Beirut, Bliss street, Beirut 1107 2020, Lebanon. amro@aub.edu.lb

Abstract

Despite the significant progress in cancer therapy, colorectal cancer (CRC) remains one of the most fatal malignancies worldwide. Chemotherapy is currently the mainstay therapeutic modality adopted for CRC treatment. However, the long-term effectiveness of chemotherapeutic drugs has been hampered by their low bioavailability, non-selective tumor targeting mechanisms, non-specific biodistribution associated with low drug concentrations at the tumor site and undesirable side effects. Over the last decade, there has been increasing interest in using nanotechnology-based drug delivery systems to circumvent these limitations. Various nanoparticles have been developed for delivering chemotherapeutic drugs among which polymeric micelles are attractive candidates. Polymeric micelles are biocompatible nanocarriers that can bypass the biological barriers and preferentially accumulate in tumors *via* the enhanced permeability and retention effect. They can be easily engineered with stimuli-responsive and tumor targeting moieties to further ensure their selective uptake by cancer cells and controlled drug release at the desirable tumor site. They have been shown to effectively improve the pharmacokinetic properties of chemotherapeutic drugs and enhance their safety profile and anticancer efficacy in different types of cancer. Given that combination therapy is the new strategy implemented in cancer therapy, polymeric micelles are suitable for multidrug delivery and allow drugs to act concurrently at the action site to achieve synergistic therapeutic outcomes. They also allow the delivery of anticancer genetic material along with chemotherapy drugs offering a novel approach for CRC therapy. Here, we highlight the properties of polymeric micelles that make them promising drug delivery systems for CRC treatment. We also review their application in CRC chemotherapy and gene therapy as well as in combination cancer chemotherapy.

Key Words: Polymeric micelles; Drug delivery; Colorectal cancer; Chemotherapy; Gene

therapy; Combination cancer therapy

©The Author(s) 2022. Published by Baishideng Publishing Group Inc. All rights reserved.

Core Tip: Polymeric micelle-based drug delivery has demonstrated promising therapeutic outcomes against colorectal cancer. These safe nanocarriers exhibit high encapsulation efficiency of chemotherapeutic drugs, improve their water solubility and enhance the stability of nucleic acid-based therapeutics. They also accumulate preferentially at colorectal cancer sites, increase the anticancer effect of the delivered therapeutics and reduce their side effects. Incorporating stimuli-responsive and tumor targeting moieties to their structure further enhances their targeting and therapeutic efficacy. This platform also provides an opportunity to simultaneously deliver different chemotherapeutic drugs or nucleic acid-based therapeutics with chemotherapeutic drugs to the colorectal tumor to achieve an enhanced anticancer response.

Citation: Fatfat Z, Fatfat M, Gali-Muhtasib H. Micelles as potential drug delivery systems for colorectal cancer treatment. *World J Gastroenterol* 2022; 28(25): 2867-2880
URL: https://www.wjgnet.com/1007-9327/full/v28/i25/2867.htm
DOI: https://dx.doi.org/10.3748/wjg.v28.i25.2867

INTRODUCTION

Colorectal cancer (CRC) is the third most prevalent cancer and the second leading cause of cancer-related deaths in men and women globally with an estimated 1.9 million new cases and 0.9 million deaths in 2020[1]. These numbers are predicted to reach 3.1 million and 1.6 million, respectively, within the next two decades[2]. The majority of CRC patients present with localized tumors, and nearly 20%-30% of CRC patients have unresectable metastasis[3]. While the 5-year survival rate for localized CRCs is nearly 90%, it is reduced to about 12% for distant metastatic CRCs[4].

Surgery is the primary treatment for patients in early stages of CRC, whereas preoperative or postoperative radiotherapy and chemotherapy are added for patients in advanced stages[5]. Numerous chemotherapeutic drugs, approved by the Food and Drug Administration, have been used for CRC treatment including 5-fluorouracil (5-FU), irinotecan (IRI), oxaliplatin (OXA) and capecitabine[3]. However, their clinical efficacy has been constrained by the adverse side effects and drug resistance that causes cancer relapse and treatment failure[6-8]. To address these drawbacks, combination therapy has been used as an alternative therapeutic approach to cancer monotherapy. Combining therapeutic agents with different modes of action demonstrated great potential in achieving synergistic therapeutic outcomes with reduced side effects in addition to overcoming drug resistance[9]. Several combination chemotherapeutic regimens such as FOLFIRI (folinic acid, 5-FU and IRI), XELOX/CAPOX (OXA and capecitabine) and FOLFOX (folinic acid, 5-FU and OXA) are widely used in clinical treatment for CRC [10]. However, and despite the continued efforts devoted to advance CRC chemotherapy, the prognosis of this disease is still unsatisfactory, particularly for metastatic CRC patients[11].

The main concerns limiting the success of single agent or combination chemotherapy are poor solubility, short half-life, rapid metabolism of the anticancer drugs, lack of selectivity for the tumor sites, non-specific biodistribution and subsequent failure to achieve effective therapeutic concentrations at the action sites[12,13]. Over the past decades, nanotechnology-based drug delivery systems have emerged as a modern approach to overcome these limitations and improve drug performance. They enhance the pharmacokinetic proprieties of the drugs, ensure their delivery to the tumor, prevent toxicity to healthy tissues, increase drug concentration at the tumor site and therefore potentiate their anticancer activity while mitigating their associated side effects[14]. In combination therapy, they can effectively carry several drugs with dissimilar pharmacokinetic profiles and maintain the optimized synergistic drug ratio until they reach the target cancer cells[15]. Additionally, nanosized drug delivery systems opened up new opportunities for the delivery of novel therapeutics along with chemotherapeutic agents, such as genetic anticancer agents, which are considered to be innovative approaches in CRC management [15].

Among the broad range of nanocarriers, polymeric micelles have received particular attention for therapeutic applications in cancer. Many anticancer agents are polycyclic compounds with poor aqueous solubility[16], and polymeric micelles have proven to be powerful vehicles for loading and delivering hydrophobic drugs[17]. Besides being biocompatible and biodegradable, polymeric micelles provide distinct advantages including small size, low-cost, ease of preparation, high drug encapsulation capacity and structural stability[18-20]. They can be easily functionalized with stimuli-responsive and tumor targeting moieties to achieve site-specific delivery and controlled drug release[21]. They also allow the integration of multiple functions other than drug delivery including gene delivery and

imaging[21]. To date, two polymeric micelles, Genexol-PM loading paclitaxel (PTX) and Nanoxel loading docetaxel (DTX), have been approved in Korea and India, respectively, for the treatment of different types of cancer including breast and non-small cell lung cancers[22]. As these nanocarriers have shown therapeutic potential for these solid tumors, they could serve as drug delivery platforms to alleviate the current limitations of CRC chemotherapy and promote the introduction of gene therapy in the management of this disease. Here, we review the composition and characteristics of polymeric micelles in addition to the achievements in micelle-based drug delivery for CRC chemotherapy and gene therapy. Published studies included in this minireview were identified through searching PubMed and Google scholar using different permutations of these keywords "colorectal cancer" or "colon cancer," "chemotherapy" or "gene therapy," "combination" and "micelle." Clinical trials were identified through searching https://clinicaltrials.gov using two keywords "micelle" and "cancer".

COMPOSITION AND CHARACTERISTICS OF POLYMERIC MICELLES

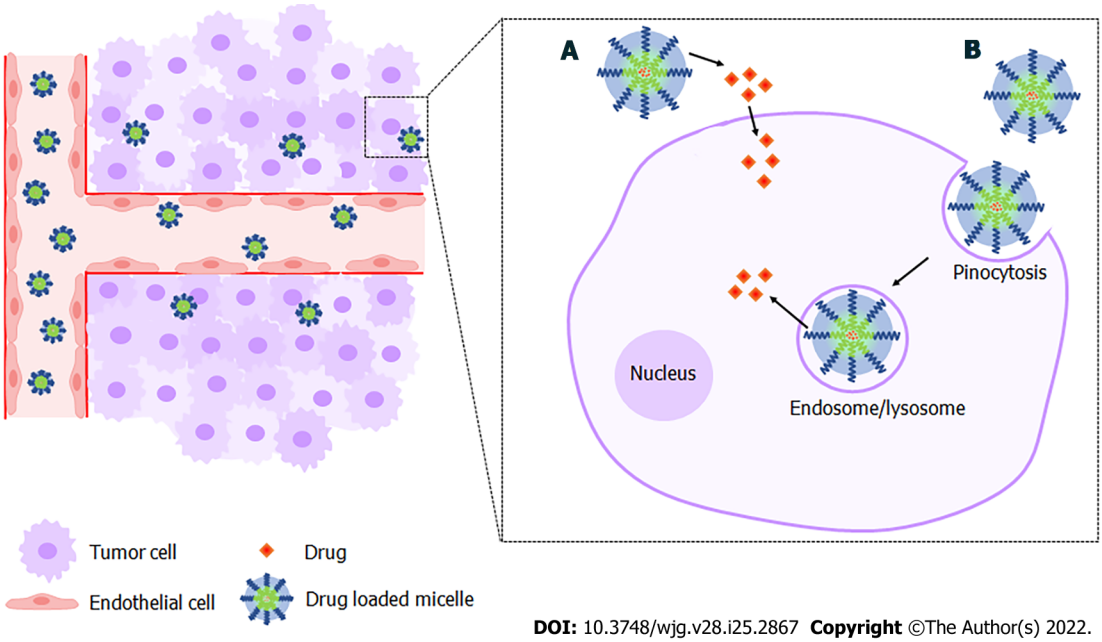
Polymeric micelles are formed by self-assembly of amphiphilic di-block, tri-block or grafted copolymers in aqueous solutions[23]. Micelles have a two-phase structure including an inner core composed of hydrophobic blocks surrounded by a corona of hydrophilic blocks[24,25]. The widely used core-forming polymers include polyesters, polyethers or polyamino acids, while the most used hydrophilic corona-forming polymer is polyethylene glycol (PEG)[26]. Alternatively, other hydrophilic polymers could be used including chitosan, dextran and hyaluronic acid (HA)[27]. The hydrophilic corona confers steric stability to the micelle, decreases its interactions with serum components and prevents its recognition and early elimination by the reticuloendothelial system, thus enhancing its retention in the systemic circulation[28,29]. The hydrophobic core forms a loading site for lipophilic drugs. It was reported that encapsulating drugs in micelles enhanced their water solubility by 10- to 500-fold[30]. Non-polar drugs can be loaded in micelles by physical entrapment or chemical conjugation[30]. Polymeric micelles used in gene delivery are known as micelleplexes and have cationic properties, which allow the association of nucleic acids *via* electrostatic interactions. The hydrophilic blocks of these micelles are usually composed of polycations including polyethyleneimine (PEI), poly (2-dimethylaminoethyl methacrylate) and polyamino acids[31].

The concentration of copolymers that is needed to form micelles is known as the critical micelle concentration. The critical micelle concentration should be low enough to prevent the dissociation of the micelles upon dilution in the bloodstream[32]. The size of polymeric micelles typically ranges from 10 to 100 nm[33]. Given that nanoparticles that are less than 10 nm can easily undergo renal clearance and those larger than 100 nm can be rapidly eliminated by the liver and spleen, the suitable size of micelles limits their rapid clearance from the circulation[34]. In addition, the nanosize of micelles allows them to passively accumulate in tumor tissues by the enhanced permeability and retention effect[27]. This passive targeting is due to the aberrant and leaky vascular architecture coupled with defective lymphatic drainage that uniquely characterize solid tumors[35]. Being unable to pass through the normal blood vessel walls, the micelles extravasate through the leaky tumor blood vessels, accumulate preferentially at the tumor site and consequently promote the retention of the delivered drug at the tumor tissue[36].

The polymeric micelles deliver the drug payload to the cancer cells by two mechanisms. The therapeutic agents can enter the cancer cell as free drugs after their release from the micelles or be internalized as drugs encapsulated within the micelles to be released within the cell[37]. Chemically conjugated drugs are released by bulk degradation or surface erosion of the micelles, while the physically entrapped drugs are mainly released by diffusion[38]. Intact drug-loaded micelles are internalized *via* cell- dependent pinocytosis, which includes macropinocytosis, clathrin-mediated endocytosis, caveolae-mediated endocytosis and clathrin- and caveolae-independent endocytosis[39-42] Internalized micelles have been shown to localize in acidic organelles, namely endosomes or lysosomes[40,43]. The loaded drugs were suggested to be released from the micelles in these organelles[40,43] and to subsequently exert their therapeutic effect at the action site[40] (Figure 1).

Active targeting can be used to complement passive targeting for enhanced tumor selectivity, improved cellular uptake and reduced off-target effects[21,23]. The surface of the micelles can be modified with ligands that can specifically recognize and bind to receptors or proteins overexpressed on the tumor cells but that are less expressed on normal cells[44]. Different types of ligands have been conjugated to micelles to ensure their active targeting to cancer cells including antibodies and antibody fragments, proteins including transferrin, peptides such as iRGD, nucleic acid-based ligands such as the AS1411 aptamer and small molecules including folic acid (FA) and HA[45].

Another interesting approach for active targeting is to achieve adequate drug release at the tumor site by designing stimuli-responsive micelles taking advantage of the unique features of the tumor microenvironment. The tumor tissues are characterized by a low pH, upregulation of specific enzymes and elevated levels of glutathione compared with the normal tissues[34]. Stimuli-sensitive polymeric micelles are developed by introducing pH-sensitive linkers in their structures, such as hydrazone bonds or pH-sensitive ionizable functional groups, enzyme-sensitive moieties or redox-sensitive linkers



DOI: 10.3748/wjg.v28.i25.2867 **Copyright** ©The Author(s) 2022.

Figure 1 Schematic illustration of the passive targeting of drug formulated micelles to the tumor tissue by enhanced permeability and retention effect and the proposed mechanisms of drug release in the cancer cell. A: The drug can enter the cancer cell in its free form after its release from the micelle; B: The drug can be internalized within the micelle after which it is released in the cancer cell.

including disulfide bonds[34]. When the micelles reach the tumor, the linker degrades in response to the internal stimulus leading to the disassembly of micelles and subsequent drug release[34]. In addition to internal stimuli, polymeric micelles responsive to external stimuli such as magnetic fields, ultrasound and light are designed to achieve a temporal and spatial controlled release of the drug in the desired tumor tissue[34]. After releasing the drug, micelles can dissociate into monomers that are excreted by the kidneys, therefore avoiding any long-term adverse effects[46]. All these properties make polymeric micelles an attractive platform for drug delivery against CRC.

APPLICATION OF POLYMERIC MICELLES IN CRC TREATMENT

The properties and the cellular and molecular mechanisms of action of polymeric micelles used for drug delivery in CRC treatment are presented in Table 1.

Chemotherapy

Numerous studies have demonstrated the potential of polymeric micelles to ensure the targeted delivery of chemotherapeutic drugs to colorectal tumor sites and enhance their therapeutic effectiveness.

IRI is a topoisomerase I inhibitor that is converted by enzymatic activation in the liver and tumors to 7-ethyl-10-hydroxy-camptothecin (SN-38). The latter is about 100-1000 times more potent than IRI against cancer cells[47]. However, only 2%-5% of the administered dose of IRI is converted to SN-38 in the clinic[48]. Although SN-38 demonstrated effective anticancer activity, its direct use as a free drug in the clinic was limited by its hydrophobicity[49]. To circumvent this problem, Koizumi *et al*[50] conjugated SN-38 to PEG-poly(glutamic acid) copolymer with a phenyl ester bond to develop SN-38-loaded polymeric micelles (NK012). The micelle formulation of SN-38 demonstrated extended blood circulation compared with free IRI in mice bearing CRC xenografts. It also prolonged and improved the distribution of SN-38 in the tumor and produced stronger antitumor activities compared to free IRI. To test the correlation between the efficacy of micellar drugs and tumor hypervascularity and hyperpermeability, the effect of NK012 and free IRI was tested in a vascular endothelial growth factor (VEGF)–secreting tumor model namely SBC-3/VEGF. Interestingly, NK012 was found to improve the accumulation and the antitumor activity of SN-38 in SBC-3/VEGF tumors compared to SBC-3/Neo tumors. This was due to the high vascular density and permeability induced by VEGF. However, treatment with free IRI neither significantly increased SN-38 concentration in SBC-3/VEGF tumors nor effectively suppressed tumor growth[50].

Doxorubicin (Dox) is an anthracycline antibiotic that is commonly used to treat several types of solid cancer. However, its clinical use is hampered by dose-dependent cardiotoxicity due to its nonspecific biodistribution[51]. Recently, Brunato *et al*[52] developed methoxyPEG (mPEG)-polyamino acid based

Table 1 Overview of micelles used for drug delivery in colorectal cancer treatment, their characteristics and cellular and molecular mechanisms of action

Block copolymer	CMC	Size in nm	Zeta potential in mV	Entrapment efficiency in %	Therapeutic agent	Cell line or animal model	Cellular and molecular mechanisms of action of micelles loaded with the therapeutic agents	Ref.
PEG-poly (glutamic acid)	N/A	20	N/A	N/A	SN-38	WiDR, SW480, Lovo and HT-29 human colon cancer cells; Female BALB/c nude mice subcutaneously injected with HT-29 cells		Koizumi *et al* [50]
mPEG5kDa-b-[(Dox-hydGlu)$_6$-r-Leu$_{10}$]	4.6 ± 0.2 μmol/L	29.2 ± 1.1	3.61 ± 0.28	N/A	Doxorubucin	CT26 murine colorectal cancer cells; BALB/c mice subcutaneously injected with CT26 cells	(1) Do not cause hemolysis; (2) Do not induce a significant increase of the levels of blood markers for organ toxicity AST, BUN and CPK; and (3) Induce a slight increase of ALT and LDH	Brunato *et al* [52]
PEG-poly (L-lactate-co-hexamethylene-co-adipate) (PEG-PLLHA) and FA-PEG-poly (hexamethylene adipate-co-hexamethylene 2-hydroxyl succinate)	3.65 μg/mL	215.6 ± 3.1	−2.4 ± 0.2	82.1 ± 0.6	Docetaxel	CT-26 cells; Female BALB/c mice subcutaneously injected with CT-26 cells	(1) Induce a more severe tumor necrosis compared to their non-targeted counterparts; (2) Do not cause hemolysis or erythrocyte agglutination; (3) Do not induce histological damage to the major organs of the treated mice; (4) Induce a slight increase of BUN levels; and (5) Do not affect the concentrations of ALT, AST, ALP, and CRE	Su *et al*[54]
PEG-poly (D,L lactate-co-hexamethylene-co-adipate) (PEG-PDLLHA) and FA-PEG-poly (hexamethylene adipate-co-hexamethylene 2-hydroxyl succinate)	3.50 μg/mL	245.5 ± 4.3	−2.8 ± 0.1	79.9 ± 1.0				
D-α-tocopherol succinate (TOS)-conjugated-hyaluronic acid	N/A	95.5 ± 13.7	N/A	90	Paclitaxel	CT26 mouse colon carcinoma cells; NIH-3T3 mouse embryo fibroblasts; HT29 and Lovo human colorectal adenocarcinoma cells; BALB/c mouse subcutaneously injected with CT26 cells	(1) Induce early and late apoptosis in HT29 and Lovo cancer cells *in vitro*; and (2) Induce apoptosis and decrease tumor cell proliferation *in vivo*	Zhu *et al*[58]
mPEG-PCL and DOTAP	N/A	144.8	46.4	N/A	Bcl-xl siRNA and Mcl1 siRNA	C26 cells; BALB/c mice inoculated with C26 cells		Lu *et al*[59]
mPEG-PCL and DOTAP	N/A	46.4 ± 3.7	44.1 ± 1.5	N/A	Plasmid pVAX1-mIL22BP expressing murine IL-22BP	C26 *Mus musculus* colon carcinoma cells; 293t human embryonic kidney cells; BALB/c mice intraperitoneally injected with C26 cells	(1) Induce apoptosis *in vitro*; (2) Decrease the microvessel density characterized by CD31 positive staining; and (3) Induce lymphocyte infiltration in tumor microenvironment as indicated by the detection of CD8+	Men *et al*[60]

							and CD4+ cells in the tumor tissues	
mPEG-PCL and DOTAP	N/A	46 ± 5.6	41.8 ± 0.5	N/A	Plasmid pcDNA-Survivin-T34A expressing Survivin-T34A	C-26 murine colon adenocarcinoma cells; BALB/c mice intraperitoneally injected with C-26 cells		Duan *et al*[61]
PEI-deoxycholic acid	N/A	88.4 ± 16	N/A	N/A	XIAP siRNA and paclitaxel	HCT-116 human colorectal cancer cells; Male BALB/c nu/nu mice subcutaneously injected with HCT-116 cells		Jang *et al*[63]
PEI-poly (DL-lactic acid)	0.1167 mg/mL	235 ± 25	−22	100	Survivin shRNA and camptothecin	C26 and CHO cells; Female BALB/c mice subcutaneously inoculated with C26 cells	(1) Induce a more pronounced apoptosis *in vitro* compared with their non-targeted counterparts; and (2) Have a lower accumulation in vital organs *in vivo* compared with their non-targeted counterparts	Sanati *et al*[64]
PDMA-b-PCL and mPEG-PCL	N/A	222.1	21.1	N/A	SN-38, USPIO and VEGF siRNA	LS174T human colon adenocarcinoma cells; Female BALB/c athymic nu+/nu+ mice subcutaneously injected with LS174T cells		Lee *et al*[66]
PEI-poly (D,L lactide) and 1,2-distearoyl-sn-glycero-3-phosphoethanolamine-N-mPEG	N/A	171.25 ± 4.70	15.12 ± 0.36	81.25 ± 3.12	miRNA-34a and irinotecan	CT-26 murine colon adenocarcinoma cells; Female BALB/c mice injected with CT-26 cells	(1) Upregulate miR-34a and reduce the expression of Bcl-2 and the phosphorylation level of mTOR; (2) Negligible hemolytic activity; and (3) Do not significantly alter the levels of ALP, ALT, ALB, AST, CK, LDH, BUN and CRE	Li *et al*[67]
PEG-lysyl-(α-fluorenylmethyl-oxycarbonyl-ε-Cbz-lysine)$_2$	2.6 μmol/L	25.4 ± 0.8	0.519 ± 0.730	N/A	Doxorubicin and dasatinib	HCT-116 human colon cancer cells		Zhang *et al*[69]
Poly {(*N*-methyl-diethenamine sebacate)-*co*-[(cholesteryl oxocarbonylamido ethyl) methyl bis (ethylene) ammonium bromide] sebacate}	N/A	230	70	N/A	Doxorubicin and TRAIL	SW480 human colorectal adenocarcinoma epithelial cells; WI38 human lung fibroblasts	Induce caspase-dependent apoptosis	Lee *et al*[70]
Cholesteryl-modified single strand DNA (Chl–ssDNA) and its complementary sequence	249 pmol/L	371.3 ± 3.1	-7.07 ± 2.3	84.9 ± 5.21	Doxorubicin and KLA peptide	C57/BL6 mice injected with C26 cells		Charbgoo *et al*[71]
FA-dextran-paclitaxel	3.1 μg/mL	76 ± 2	-11.2 ± 0.8	N/A	Adjudin and paclitaxel	HCT-8 and HCT-8/PTX cells; Mouse subcutaneously injected with HCT-8/PTX cells	(1) Reduce mitochondrial membrane potential and the levels of ATP; and (2) Do not cause hemolysis	Chen *et al*[72]
Poly-lactic-co-glycolic acid grafted branched PEI	1.32 ± 0.003 mg/mL	137.98 ± 2.13	12.3 ± 0.2	70.38 ± 2.34	5-fluorouracil and methotrexate	HCT 116 colon cancer cells		Ashwanikumar *et al*[73]
mPEG-PCL	56	167.5	-0.11	68.8	Doxifluridine	HT-29 human		Sawdon *et al*

	mg/L				and doxorubicin	colorectal adenocarcinoma cells	[74]
		267.5	1.01	86.3	Doxifluridine and SN-38		
Chitosan-PCL	40 mg/mL	163.7	38.8	N/A	Doxifluridine and SN-38	HT-29 human colorectal adenocarcinoma cells	Wang *et al*[75]

CMC: Critical micelle concentration; mPEG: Methoxypolyethylene glycol; Dox: Doxorubicin; hydGlu: Acid-γ-hydrazide; Leu: Leucine; AST: Aspartate aminotransferase; ALT: Alanine aminotransferase; BUN: Blood urea nitrogen; CPK: Creatine phosphokinase; CK: Creatine kinase; LDH: Lactate dehydrogenase; FA: Folic acid; ALP: Alkaline phosphatase; CRE: Creatinine; DOTAP: N-[1-(2, 3-dioleoyloxy) propyl]-N, N, N-trimethylammonium methyl sulfate; PEI: Polyethyleneimine; PCL: Poly(ε-caprolactone); ALB: Albumin; siRNA: Small interfering RNA; XIAP: X-linked inhibitor of apoptosis; shRNA: Short hairpin RNA; VEGF: Vascular endothelial growth factor; USPIO: Ultra-small superparamagnetic iron oxide nanoparticles; miR-34a: microRNA-34a; TRAIL: Tumor necrosis factor (TNF)-related apoptosis-inducing ligand; IL-22BP: Interleukin-22 binding protein; mTOR: Mammalian target of rapamycin; SN-38: 7-ethyl-10-hydroxy-camptothecin; N/A: Not available; PEG: Polyethylene glycol; TOS: D-α-tocopherol succinate; PTX: Paclitaxel.

micelles for the delivery and controlled release of Dox in CRC. The hydrophobic block of the copolymer included six glutamic acid-γ-hydrazide and ten leucines. Dox was conjugated to glutamic acid through pH-sensitive hydrazone bond to trigger its release in the acidic lysosomal microenvironment. The release of Dox was faster at pH 5.5, which mimics the lysosomal environment. In addition, the intracellular delivery of Dox by the micelles and its trafficking through the lysosomal compartment of CRC cells, where the acidic environment can induce the cleavage of the hydrazone bond, were confirmed by confocal microscopy. Therefore, encapsulating Dox in the formulated micelles may prevent its undesired release in the bloodstream. Interestingly, Dox-loaded micelles had good tolerability, produced a higher antitumor effect compared to the free drug and had limited toxicity in CRC bearing mice[52].

DTX is a microtubule inhibitor that is approved to treat numerous types of cancer. Due to its low water solubility, a mixture of Tween 80 and ethanol is required to solubilize DTX. Yet, Tween 80 used in the available marketed formulation of DTX Taxotere® was associated with adverse effects[53]. Recently, FA-targeted PEG-polyester micelles were formulated for the targeted delivery of DTX against colon cancer. The targeted formulation resulted in an accelerated internalization of the micelles by FA receptor-positive colon cancer cells *in vitro* and in a higher and preferential accumulation of the micelles in colon tumors *in vivo* compared to the non-targeted formulation. Besides being biocompatible and safe, the FA-targeted DTX-loaded micelles exhibited a remarkable 97% tumor-inhibiting efficiency, which was higher than that of non-targeted DTX-loaded micelles (85%) and free DTX (31%) in mice bearing colon tumor xenografts[54].

PTX is a microtubule stabilizing agent commonly used against a variety of cancers including CRC [55]. Because of its low aqueous solubility, Taxol®, the commercial formulation of PTX, uses a nonionic surfactant namely Cremophor® EL[56]. However, Cremophor® EL has been associated with serious side effects such as hypersensitivity, nephrotoxicity and neurotoxicity[57]. Zhu *et al*[58] developed smart micelles for the targeted delivery and controlled release of PTX in colon cancer. Micelles are made from the self-assembly of D-α-tocopherol succinate (TOS) conjugated to HA *via* a redox responsive disulfide bond. Their findings demonstrated that these micelles could specifically accumulate in orthotopic colon tumors and metastatic tumor cells rather than in normal intestinal tissue through binding of HA to CD44 receptors overexpressed on primary and metastatic colon tumor cells. They could also selectively release PTX in orthotopic colon tumors and metastatic tumor cells where the high levels of glutathione break disulfide bonds thus causing drug release. PTX-encapsulated micelles induced the highest survival rate (100%) in mice bearing orthotopic colon tumors compared to untreated group (60%) and free PTX (Taxol) treated group (40%). They also suppressed primary colon tumors and metastatic sites in the intestine and decreased metastasis to other organs and to the peritoneum[58].

Gene therapy

Polymeric micelles were also reported to successfully deliver anticancer genetic material to CRC. Cationic hybrid micelles composed of amphiphilic cationic lipid N-[1-(2,3-dioleoyloxy) propyl]-N, N, N-trimethylammonium methyl sulfate (DOTAP) and mPEG-poly (ε-caprolactone) (PCL) have been used to deliver genes or small interfering RNA (siRNA) for the treatment of colon cancer in preclinical studies. The cationic hydrophilic head of DOTAP ensures the adsorption of the anionic nucleic acid onto the surface of the micelles *via* electrostatic interaction. These hybrid micelles demonstrated an effective and safe delivery of siRNA targeting colon cancer cells. The micelle-based delivery of siRNA caused inhibition of the two anti-apoptotic genes *Bcl-xl* and *Mcl1*, which consequently induced apoptosis in colon cancer cells *in vitro* and suppressed the growth of colon tumors *in vivo*[59]. In another report, these hybrid micelles were used for the delivery of interleukin-22 binding protein (*IL-22BP*) gene, which is known to play a role in blocking the IL-22/IL-22R1 signal axis involved in tumor growth and

metastasis. The micelle-delivered *IL-22BP* gene was efficiently expressed in colon tumors *in vivo* leading to the inhibition of the growth of abdominal cavity metastases. Its anticancer mechanism involved blockage of IL-22, induction of apoptosis and anticancer immune response in addition to inhibition of angiogenesis[60]. In a study conducted by Duan *et al*[61], these hybrid micelles were found to efficiently deliver the classic suicide gene survivin-T34A that acts as a competitor in the survivin pathway involved in apoptosis inhibition[62]. The survivin-T34A gene-loaded micelles inhibited the proliferation of colon cancer cells *in vitro* and the growth of abdominal metastatic colon cancer and malignant ascites *in vivo* by inducing apoptosis[61]. Importantly, in all these studies, this micellar carrier did not induce any pathological changes in the vital organs of the mice with colon cancer.

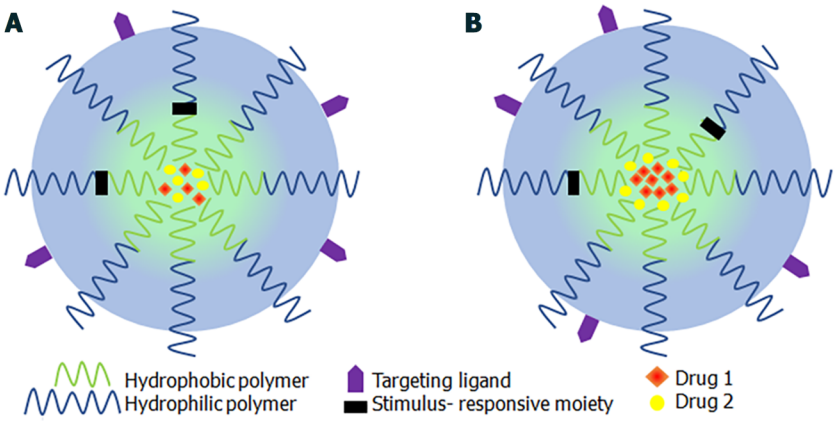
Combination of chemotherapy with gene therapy

The micellar dual delivery of chemotherapeutic drugs with agents targeted against specific genes have been shown to produce synergistic therapeutic responses against CRC. Cationic micelles based on PEI-deoxycholic acid conjugates have been used for the co-delivery of PTX and siRNA targeting the X-linked inhibitor of apoptosis gene to CRC. The micellar co-delivery of siRNA targeting X-linked inhibitor of apoptosis gene and PTX effectively decreased the expression of X-linked inhibitor of apoptosis at the mRNA and protein levels *in vitro* and *in vivo*. In addition, it was more potent than PTX-loaded micelles as it caused a greater reduction in cell viability of CRC cells and inhibited the growth of colorectal tumors *in vivo*[63]. In another study, Sanati *et al*[64] synthesized cationic micelles for the targeted dual delivery of camptothecin (CPN), a topoisomerase inhibitor, and short hairpin RNA targeting survivin to colon cancer. These micelles containing PEI-poly (D,L-lactic acid) copolymers were coated with polycarboxylic acid dextran and were subsequently modified with AS1411 aptamer that has high affinity for the nucleolin receptors expressed on the surface of colon cancer cells. Cell surface nucleolin expression is known to be more elevated in cancer cells than in normal cells[65]. The conjugation of AS1411 aptamer on the micelles improved their cellular internalization through nucleolin-mediated endocytosis *in vitro* and enhanced their accumulation in colon tumors *in vivo* in comparison with their non-targeted counterparts. While the non-targeted micellar formulation of each of CPN and short hairpin RNA targeting survivin exhibited 3% and 5% tumor inhibitory effect *in vivo*, the targeted and non-targeted formulations of the combination of CPN and short hairpin RNA targeting survivin exerted 93% and 87% tumor inhibitory effects, respectively. It is important to note that the free CPN did not have any anticancer effects *in vivo,* and its micellar formulation prevented the development of its associated systemic toxicity[64]. Moreover, Lee *et al*[66] designed theranostic micelles from cationic PDMA-b-PCL and mPEG-PCL polymers for the combined delivery of SN-38, siRNA targeting human VEGF in addition to a magnetic resonance imaging contrast agent namely ultra-small superparamagnetic iron oxide nanoparticles. The SN-38/ultra-small superparamagnetic iron oxide nanoparticles/siRNA-loaded mixed micelles were targeted passively to colorectal tumor regions *in vivo.* They induced a synergistic tumor growth suppression and allowed the tracking of anticancer effects by magnetic resonance imaging during the treatment[66]. Additionally, hybrid micelles co-self-assembled from PEI-poly (D,L lactide), and 1,2-distearoyl-sn-glycero-3-phosphoethanolamine-N-mPEG were used to deliver IRI and tumor suppressive microRNA-34a (miR-34a) to colon cancer. The micellar co-delivery of the two therapeutic agents showed higher efficacy in inducing apoptosis and inhibiting migration of colon cancer cells *in vitro* compared with free IRI and the single agent formulation. The micellar IRI and miR-34a combination also accumulated in colon tumors *in vivo* and showed superior tumor growth inhibition with low acute systemic toxicity compared with free IRI and the micellar formulation of individual agents[67].

Combination cancer chemotherapy

For dual combination therapy, the encapsulation of drugs in a micellar system could be performed in two ways (Figure 2). In the first method, both drugs are physically loaded in the micelles by hydrophobic interactions. Alternatively, one hydrophobic drug is conjugated to the amphiphilic copolymer, which self-assembles and forms prodrug micelles to subsequently encapsulate the second hydrophobic drug in its core[68].

The chemotherapeutic drug Dox and the tyrosine kinase inhibitor dasatinib were effectively co-encapsulated in the inner hydrophobic core of micelles formed by PEG-peptidic conjugate namely PEG-lysyl-(α-fluorenylmethyloxycarbonyl-ε-Cbz-lysine)$_2$. The dual drug-loaded micelles exhibited greater inhibition of colon cancer cell proliferation compared with the micellar formulation or the free form of individual drugs[69]. In another study, Dox was co-delivered with the tumor necrosis factor-related apoptosis-inducing ligand (TRAIL) in cationic micelles to CRC. The micelles were prepared with poly {(*N*-methyldietheneamine sebacate)-*co*-[(cholesteryl oxocarbonylamido ethyl) methyl bis(ethylene) ammonium bromide] sebacate. Dox was encapsulated in the micelles, whereas TRAIL was complexed onto their surface. The internalization of these micelles by CRC cells was mediated by the death receptors expressed on the cell surface. Compared to the formulation of single agents, Dox and TRAIL-loaded micelles enhanced the inhibition of CRC cell viability, the increase of sub-G1 population and the reduction of long-term survival and clonogenicity of cancer cells after the treatment. Interestingly, these remarkable anticancer effects were reported in both TRAIL sensitive and resistant CRC cells. In addition, the cytotoxic effect of the co-loaded micelles was selectively higher against cancer cells than



DOI: 10.3748/wjg.v28.i25.2867 **Copyright** ©The Author(s) 2022.

Figure 2 Polymeric micelles for dual drug delivery. A: Both drugs are physically loaded in the core of the micelle; B: One hydrophobic drug is conjugated to the amphiphilic copolymer forming the micelle and the second is encapsulated in its core.

normal cells. This was suggested to be due to the relative disparities in expression levels of decoy and death receptors between normal and cancer cells[70]. A third study reported the combined delivery of Dox and the proapoptotic cationic peptide KLA using DNA micelles. These micelles were made using cholesteryl-modified single strand DNA and its complementary sequence to which the KLA peptide was conjugated. The cationic peptides enhanced the stability of the micelles by protecting them from digestion by nucleases. Since oligonucleotides cannot cross cell membranes, DNA micelles were conjugated to a mucine1 aptamer to target mucine1 receptors overexpressed on the surface of cancer cells. These micelles were found to specifically bind to the mucine1 receptors overexpressing cells and to accumulate within them. The co-delivery of KLA and Dox using the targeted micelles potentiated the inhibition of colon tumor growth *in vivo* compared to free Dox in addition to attenuating its toxic effects [71]. A recent study reported the formulation of a folate receptor-targeted and redox-responsive micellar system for the co-delivery of PTX and adjudin (ADD), a mitochondrial inhibitor, to reverse multidrug resistance in colon cancer. In this drug delivery system, PTX was conjugated to dextran *via* a disulfide bond to form the PTX prodrug, and FA was conjugated to the side chain of dextran-PTX. The resulting PTX prodrug micelles were further used to encapsulate ADD in its hydrophobic core. *In vitro* studies showed that conjugation of FA to the surface of these micelles enhanced their internalization by PTX resistant CRC cells overexpressing the FA receptor. They also demonstrated that ADD inhibited PTX efflux, which consequently improved intracellular accumulation of PTX and therefore its cytotoxic activity. In addition, PTX and ADD-loaded micelles exhibited a prolonged circulation in the blood compared with free PTX *in vivo*. They also increased the concentrations of drugs in resistant colon tumors compared to their non-targeted counterparts and free PTX. Importantly, they demonstrated a strong tumor growth inhibition owing to the active tumor-targeting, the co-delivery of two therapeutic drugs and glutathione-responsive drug release[72]. In another study, micelles engineered with poly-lactic-co-glycolic acid grafted branched PEI were used to co-deliver 5-FU and methotrexate (MTX), which is an antagonist of FA and is known to have anticancer effects against different types of neoplasm. MTX was conjugated to the copolymer forming the prodrug micelles, which was further used to encapsulate 5-FU. In addition to its therapeutic potential, MTX has structural similarity with FA and can therefore act as an FA receptor targeting agent. The conjugation of MTX to the micelles improved their internalization by colon cancer cells compared to the non-conjugated micelles. The combined drug-loaded micelles were more effective in attenuating the viability of colon cancer cells compared to free 5-FU or the micellar MTX[73]. Doxifluridine, a prodrug of 5-FU, has been commonly used in cancer treatment to circumvent the toxicity of 5-FU. Doxifluridine is converted into toxic 5-FU by endogenous thymidine phosphorylase in cancer cells[74]. In a study conducted by Wang *et al*[75], doxifluridine was conjugated to PCL to form a hydrophobic segment that was grafted with hydrophilic chitosan. The produced polymeric prodrugs self-assembled into micelles used for SN-38 encapsulation. The dually loaded micelles were found to reduce the viability of colon cancer cells *in vitro* to a greater extent than doxifluridine-loaded micelles. In another study, doxifluridine-PCL hydrophobic segment was grafted with mPEG to form prodrug micelles serving as carriers to further encapsulate Dox or SN-38. The micellar co-delivery of doxifluridine with Dox or SN-38 exhibited superior inhibition of CRC cell viability with respect to doxifluridine-loaded micelles[74].

Polymeric micelles in clinical trials

Despite their promising potential in preclinical studies against colon cancer, few polymeric micelles have reached the clinical setting. A phase I clinical trial of NK012 was conducted in Japan with a total of 24 patients with solid tumors including 12 patients with CRC. NK012 was found to be well tolerated at

doses up to 28 mg/m^2 when administered every 3 wk. None of the CRC patients had a partial response. However, 5 CRC patients with a history of treatment with OXA and IRI had stable disease; 4 of them received the NK012 regimen for six cycles of treatment or more[76]. Subsequently, the efficacy and safety of NK012 was evaluated in a phase II clinical trial at an initial dose of 28 mg/m^2 in 58 Japanese patients with unresectable metastatic CRC who had been treated with OXA-based chemotherapy. Administration of NK012 resulted in a response rate similar to that of free IRI. In addition, febrile neutropenia and grade ≥ 3 neutropenia were reported in these patients suggesting that an initial dose of 28 mg/m^2 of NK012 may be too high. Further studies should be conducted to determine the optimal dose of NK012 and improve its efficacy and safety[77]. In another study, a phase I clinical trial of NK105, PTX-loaded micelles, was conducted with 19 patients with advanced solid tumors including 1 patient with colon cancer. NK105 was well tolerated, and the recommended phase II dose was determined to be 150 mg/m^2 every 3 wk. The colon cancer patient was reported to have a stable disease for longer than 4 weeks at the time of the completion of the study[78]. Two additional clinical trials on polymeric micelles in CRC were launched but their results have not been reported yet. The first is a phase I clinical trial that aims to determine the maximum tolerated dose/recommended phase II dose of the combination of NK012 with 5-FU and leucovorin in patients with CRC (NCT01238939)[79]. The second is a phase II clinical trial that aims to investigate the safety and the diagnostic performance of ONM-100, a polymer micelle covalently conjugated to an intraoperative fluorescence imaging agent indocyanine green, for the detection of cancer in patients with solid tumors including CRC patients undergoing routine surgery (NCT03735680)[80].

CONCLUSION

Polymeric micelles are potential candidates for delivery of chemotherapeutic drugs and therapeutic genetic material in single or combination treatment against CRC. Polymeric micelles exhibit a safe profile, help in solubilizing hydrophobic chemotherapeutic drugs and achieve prolonged and stabilized drug circulation in the blood. They also promote the passive accumulation of drugs at CRC sites, potentiate their anticancer activity and reduce their unwanted side effects. Conjugating polymeric micelles with stimuli-responsive and tumor targeting moieties further increases their internalization by cancer cells, thus achieving selective drug release at colorectal tumor sites and enhancing drug anticancer effects. In addition, polymeric micelles ensure an effective and safe delivery of genetic material to modulate the expression of apoptotic players in CRC. Co-delivering genetic anticancer agents with chemotherapeutic drugs using micellar systems is known to augment the therapeutic outcome of the latter and therefore represent a promising combination strategy for combating CRC.

This nanocarrier system also allows the incorporation of imaging agents with therapeutics and offers great potential to achieve tumor diagnosis, in addition to tracking the delivery and release of the therapeutic agent and evaluating its therapeutic performance. Although most of the studies evaluating polymeric micelle-mediated combination chemotherapy in CRC were performed *in vitro*, they yielded interesting results. The delivery of drug combinations using polymeric micelles could further intensify their inhibitory effects against CRC and help overcome drug resistance. However, further pharmacokinetic and pharmacodynamic studies are needed prior to the clinical translation of drug-loaded polymeric micelles. Few polymeric micelles have been used in the clinical setting for CRC treatment and diagnosis with promising outcomes, thus their application merits further investigation.

FOOTNOTES

Author contributions: Fatfat Z and Fatfat M reviewed the literature and drafted the manuscript; Gali-Muhtasib H initiated the idea and revised the manuscript; All authors have read and approved the final manuscript.

Conflict-of-interest statement: The authors declare that they have no conflict of interest.

Open-Access: This article is an open-access article that was selected by an in-house editor and fully peer-reviewed by external reviewers. It is distributed in accordance with the Creative Commons Attribution NonCommercial (CC BY-NC 4.0) license, which permits others to distribute, remix, adapt, build upon this work non-commercially, and license their derivative works on different terms, provided the original work is properly cited and the use is non-commercial. See: https://creativecommons.org/Licenses/by-nc/4.0/

Country/Territory of origin: Lebanon

ORCID number: Zaynab Fatfat 0000-0003-1254-0648; Maamoun Fatfat 0000-0001-9642-6708; Hala Gali-Muhtasib 0000-0001-6840-3015.

S-Editor: Ma YJ

L-Editor: Filipodia
P-Editor: Ma YJ

REFERENCES

1 **Xi Y**, Xu P. Global colorectal cancer burden in 2020 and projections to 2040. *Transl Oncol* 2021; **14**: 101174 [PMID: 34243011 DOI: 10.1016/j.tranon.2021.101174]
2 **World Health Organization**. International Agency for Research on Cancer: GLOBOCAN: Cancer tomorrow, 2022. Available from:https://gco.iarc.fr/tomorrow/en/dataviz/isotype?group_cancers=1&multiple_cancers=1&cancers=8_9_10&single_unit=50000 [DOI: 10.1002/food.19770210141]
3 **Matos AI**, Carreira B, Peres C, Moura LIF, Conniot J, Fourniols T, Scomparin A, Martínez-Barriocanal Á, Arango D, Conde JP, Préat V, Satchi-Fainaro R, Florindo HF. Nanotechnology is an important strategy for combinational innovative chemo-immunotherapies against colorectal cancer. *J Control Release* 2019; **307**: 108-138 [PMID: 31226355 DOI: 10.1016/j.jconrel.2019.06.017]
4 **Naeem M**, Awan UA, Subhan F, Cao J, Hlaing SP, Lee J, Im E, Jung Y, Yoo JW. Advances in colon-targeted nano-drug delivery systems: challenges and solutions. *Arch Pharm Res* 2020; **43**: 153-169 [PMID: 31989477 DOI: 10.1007/s12272-020-01219-0]
5 **Lei X**, He Q, Li Z, Zou Q, Xu P, Yu H, Ding Y, Zhu W. Cancer stem cells in colorectal cancer and the association with chemotherapy resistance. *Med Oncol* 2021; **38**: 43 [PMID: 33738588 DOI: 10.1007/s12032-021-01488-9]
6 **Rejhová A**, Opattová A, Čumová A, Slíva D, Vodička P. Natural compounds and combination therapy in colorectal cancer treatment. *Eur J Med Chem* 2018; **144**: 582-594 [PMID: 29289883 DOI: 10.1016/j.ejmech.2017.12.039]
7 **Hammond WA**, Swaika A, Mody K. Pharmacologic resistance in colorectal cancer: a review. *Ther Adv Med Oncol* 2016; **8**: 57-84 [PMID: 26753006 DOI: 10.1177/1758834015614530]
8 **Huang JR**, Lee MH, Li WS, Wu HC. Liposomal Irinotecan for Treatment of Colorectal Cancer in a Preclinical Model. *Cancers (Basel)* 2019; **11** [PMID: 30818855 DOI: 10.3390/cancers11030281]
9 **Bayat Mokhtari R**, Homayouni TS, Baluch N, Morgatskaya E, Kumar S, Das B, Yeger H. Combination therapy in combating cancer. *Oncotarget* 2017; **8**: 38022-38043 [PMID: 28410237 DOI: 10.18632/oncotarget.16723]
10 **Moradi-Marjaneh R**, Paseban M, Moradi Marjaneh M. Hsp70 inhibitors: Implications for the treatment of colorectal cancer. *IUBMB Life* 2019; **71**: 1834-1845 [PMID: 31441584 DOI: 10.1002/iub.2157]
11 **Ginghină O**, Hudiță A, Zaharia C, Tsatsakis A, Mezhuev Y, Costache M, Gălățeanu B. Current Landscape in Organic Nanosized Materials Advances for Improved Management of Colorectal Cancer Patients. *Materials (Basel)* 2021; **14** [PMID: 34066710 DOI: 10.3390/ma14092440]
12 **Entezar-Almahdi E**, Mohammadi-Samani S, Tayebi L, Farjadian F. Recent Advances in Designing 5-Fluorouracil Delivery Systems: A Stepping Stone in the Safe Treatment of Colorectal Cancer. *Int J Nanomedicine* 2020; **15**: 5445-5458 [PMID: 32801699 DOI: 10.2147/IJN.S257700]
13 **Arshad U**, Sutton PA, Ashford MB, Treacher KE, Liptrott NJ, Rannard SP, Goldring CE, Owen A. Critical considerations for targeting colorectal liver metastases with nanotechnology. *Wiley Interdiscip Rev Nanomed Nanobiotechnol* 2020; **12**: e1588 [PMID: 31566913 DOI: 10.1002/wnan.1588]
14 **Cabeza L**, Perazzoli G, Mesas C, Jiménez-Luna C, Prados J, Rama AR, Melguizo C. Nanoparticles in Colorectal Cancer Therapy: Latest In Vivo Assays, Clinical Trials, and Patents. *AAPS PharmSciTech* 2020; **21**: 178 [PMID: 32591920 DOI: 10.1208/s12249-020-01731-y]
15 **Gurunathan S**, Kang MH, Qasim M, Kim JH. Nanoparticle-Mediated Combination Therapy: Two-in-One Approach for Cancer. *Int J Mol Sci* 2018; **19** [PMID: 30347840 DOI: 10.3390/ijms19103264]
16 **Majumder N**, G Das N, Das SK. Polymeric micelles for anticancer drug delivery. *Ther Deliv* 2020; **11**: 613-635 [PMID: 32933425 DOI: 10.4155/tde-2020-0008]
17 **Deshmukh AS**, Chauhan PN, Noolvi MN, Chaturvedi K, Ganguly K, Shukla SS, Nadagouda MN, Aminabhavi TM. Polymeric micelles: Basic research to clinical practice. *Int J Pharm* 2017; **532**: 249-268 [PMID: 28882486 DOI: 10.1016/j.ijpharm.2017.09.005]
18 **Jhaveri AM**, Torchilin VP. Multifunctional polymeric micelles for delivery of drugs and siRNA. *Front Pharmacol* 2014; **5**: 77 [PMID: 24795633 DOI: 10.3389/fphar.2014.00077]
19 **Bholakant R**, Dong B, Zhou X, Huang X, Zhao C, Huang D, Zhong Y, Qian H, Chen W, Feijen J. Multi-functional polymeric micelles for chemotherapy-based combined cancer therapy. *J Mater Chem B* 2021; **9**: 8718-8738 [PMID: 34635905 DOI: 10.1039/d1tb01771c]
20 **Tawfik SM**, Azizov S, Elmasry MR, Sharipov M, Lee YI. Recent Advances in Nanomicelles Delivery Systems. *Nanomaterials (Basel)* 2020; **11** [PMID: 33396938 DOI: 10.3390/nano11010070]
21 **Raval N**, Maheshwari R, Shukla H, Kalia K, Torchilin VP, Tekade RK. Multifunctional polymeric micellar nanomedicine in the diagnosis and treatment of cancer. *Mater Sci Eng C Mater Biol Appl* 2021; **126**: 112186 [PMID: 34082985 DOI: 10.1016/j.msec.2021.112186]
22 **Mi P**, Miyata K, Kataoka K, Cabral H. Clinical translation of Self-Assembled cancer nanomedicines. *Adv Therap* 2021; **4**: 2000159 [DOI: 10.1002/adtp.202170001]
23 **Oerlemans C**, Bult W, Bos M, Storm G, Nijsen JF, Hennink WE. Polymeric micelles in anticancer therapy: targeting, imaging and triggered release. *Pharm Res* 2010; **27**: 2569-2589 [PMID: 20725771 DOI: 10.1007/s11095-010-0233-4]
24 **Yokoyama M**. Polymeric micelles as drug carriers: their lights and shadows. *J Drug Target* 2014; **22**: 576-583 [PMID: 25012065 DOI: 10.3109/1061186X.2014.934688]
25 **Torchilin VP**. Targeted polymeric micelles for delivery of poorly soluble drugs. *Cell Mol Life Sci* 2004; **61**: 2549-2559 [PMID: 15526161 DOI: 10.1007/s00018-004-4153-5]

26 **Morshed RA**, Cheng Y, Auffinger B, Wegscheid ML, Lesniak MS. The potential of polymeric micelles in the context of glioblastoma therapy. *Front Pharmacol* 2013; **4**: 157 [PMID: 24416018 DOI: 10.3389/fphar.2013.00157]

27 **Ghosh B**, Biswas S. Polymeric micelles in cancer therapy: State of the art. *J Control Release* 2021; **332**: 127-147 [PMID: 33609621 DOI: 10.1016/j.jconrel.2021.02.016]

28 **Yousefpour Marzbali M**, Yari Khosroushahi A. Polymeric micelles as mighty nanocarriers for cancer gene therapy: a review. *Cancer Chemother Pharmacol* 2017; **79**: 637-649 [PMID: 28314988 DOI: 10.1007/s00280-017-3273-1]

29 **Almeida M**, Magalhães M, Veiga F, Figueiras A. Poloxamers, poloxamines and polymeric micelles: Definition, structure and therapeutic applications in cancer. *J Polym Res* 2017; **25**: 1-14 [DOI: 10.1007/s10965-017-1426-x]

30 **Hanafy NAN**, El-Kemary M, Leporatti S. Micelles Structure Development as a Strategy to Improve Smart Cancer Therapy. *Cancers (Basel)* 2018; **10** [PMID: 30037052 DOI: 10.3390/cancers10070238]

31 **Pereira-Silva M**, Alvarez-Lorenzo C, Concheiro A, Santos AC, Veiga F, Figueiras A. Nanomedicine in osteosarcoma therapy: Micelleplexes for delivery of nucleic acids and drugs toward osteosarcoma-targeted therapies. *Eur J Pharm Biopharm* 2020; **148**: 88-106 [PMID: 31958514 DOI: 10.1016/j.ejpb.2019.10.013]

32 **Glavas L**, Olsén P, Odelius K, Albertsson AC. Achieving micelle control through core crystallinity. *Biomacromolecules* 2013; **14**: 4150-4156 [PMID: 24066701 DOI: 10.1021/bm401312j]

33 **Felber AE**, Dufresne MH, Leroux JC. pH-sensitive vesicles, polymeric micelles, and nanospheres prepared with polycarboxylates. *Adv Drug Deliv Rev* 2012; **64**: 979-992 [PMID: 21996056 DOI: 10.1016/j.addr.2011.09.006]

34 **Zhou Q**, Zhang L, Yang T, Wu H. Stimuli-responsive polymeric micelles for drug delivery and cancer therapy. *Int J Nanomedicine* 2018; **13**: 2921-2942 [PMID: 29849457 DOI: 10.2147/IJN.S158696]

35 **Kalyane D**, Raval N, Maheshwari R, Tambe V, Kalia K, Tekade RK. Employment of enhanced permeability and retention effect (EPR): Nanoparticle-based precision tools for targeting of therapeutic and diagnostic agent in cancer. *Mater Sci Eng C Mater Biol Appl* 2019; **98**: 1252-1276 [PMID: 30813007 DOI: 10.1016/j.msec.2019.01.066]

36 **Tan C**, Wang Y, Fan W. Exploring polymeric micelles for improved delivery of anticancer agents: recent developments in preclinical studies. *Pharmaceutics* 2013; **5**: 201-219 [PMID: 24300405 DOI: 10.3390/pharmaceutics5010201]

37 **Jarak I**, Varela CL, Tavares da Silva E, Roleira FFM, Veiga F, Figueiras A. Pluronic-based nanovehicles: Recent advances in anticancer therapeutic applications. *Eur J Med Chem* 2020; **206**: 112526 [PMID: 32971442 DOI: 10.1016/j.ejmech.2020.112526]

38 **Kedar U**, Phutane P, Shidhaye S, Kadam V. Advances in polymeric micelles for drug delivery and tumor targeting. *Nanomedicine* 2010; **6**: 714-729 [PMID: 20542144 DOI: 10.1016/j.nano.2010.05.005]

39 **Zhao Z**, Wang Y, Han J, Wang K, Yang D, Yang Y, Du Q, Song Y, Yin X. Self-assembled micelles of amphiphilic poly(L-phenylalanine)-b-poly(L-serine) polypeptides for tumor-targeted delivery. *Int J Nanomedicine* 2014; **9**: 5849-5862 [PMID: 25540585 DOI: 10.2147/IJN.S73111]

40 **Zhang C**, Jin S, Li S, Xue X, Liu J, Huang Y, Jiang Y, Chen WQ, Zou G, Liang XJ. Imaging intracellular anticancer drug delivery by self-assembly micelles with aggregation-induced emission (AIE micelles). *ACS Appl Mater Interfaces* 2014; **6**: 5212-5220 [PMID: 24606837 DOI: 10.1021/am5005267]

41 **Fang XB**, Zhang JM, Xie X, Liu D, He CW, Wan JB, Chen MW. pH-sensitive micelles based on acid-labile pluronic F68-curcumin conjugates for improved tumor intracellular drug delivery. *Int J Pharm* 2016; **502**: 28-37 [PMID: 26784981 DOI: 10.1016/j.ijpharm.2016.01.029]

42 **Qiu L**, Shan X, Long M, Ahmed KS, Zhao L, Mao J, Zhang H, Sun C, You C, Lv G, Chen J. Elucidation of cellular uptake and intracellular trafficking of heparosan polysaccharide-based micelles in various cancer cells. *Int J Biol Macromol* 2019; **130**: 755-764 [PMID: 30851320 DOI: 10.1016/j.ijbiomac.2019.02.133]

43 **Sakai-Kato K**, Un K, Nanjo K, Nishiyama N, Kusuhara H, Kataoka K, Kawanishi T, Goda Y, Okuda H. Elucidating the molecular mechanism for the intracellular trafficking and fate of block copolymer micelles and their components. *Biomaterials* 2014; **35**: 1347-1358 [PMID: 24290812 DOI: 10.1016/j.biomaterials.2013.11.027]

44 **Yu G**, Ning Q, Mo Z, Tang S. Intelligent polymeric micelles for multidrug co-delivery and cancer therapy. *Artif Cells Nanomed Biotechnol* 2019; **47**: 1476-1487 [PMID: 31070063 DOI: 10.1080/21691401.2019.1601104]

45 **Amjad MW**, Kesharwani P, Mohd Amin MCI, Iyer AK. Recent advances in the design, development, and targeting mechanisms of polymeric micelles for delivery of siRNA in cancer therapy. *Prog Polym Sci* 2017; **64**: 154-181 [DOI: 10.1016/j.progpolymsci.2016.09.008]

46 **Cabral H**, Kataoka K. Progress of drug-loaded polymeric micelles into clinical studies. *J Control Release* 2014; **190**: 465-476 [PMID: 24993430 DOI: 10.1016/j.jconrel.2014.06.042]

47 **Xu G**, Shi C, Guo D, Wang L, Ling Y, Han X, Luo J. Functional-segregated coumarin-containing telodendrimer nanocarriers for efficient delivery of SN-38 for colon cancer treatment. *Acta Biomater* 2015; **21**: 85-98 [PMID: 25910639 DOI: 10.1016/j.actbio.2015.04.021]

48 **Senter PD**, Beam KS, Mixan B, Wahl AF. Identification and activities of human carboxylesterases for the activation of CPT-11, a clinically approved anticancer drug. *Bioconjug Chem* 2001; **12**: 1074-1080 [PMID: 11716702 DOI: 10.1021/bc0155420]

49 **Carie A**, Rios-Doria J, Costich T, Burke B, Slama R, Skaff H, Sill K. IT-141, a Polymer Micelle Encapsulating SN-38, Induces Tumor Regression in Multiple Colorectal Cancer Models. *J Drug Deliv* 2011; **2011**: 869027 [PMID: 22187652 DOI: 10.1155/2011/869027]

50 **Koizumi F**, Kitagawa M, Negishi T, Onda T, Matsumoto S, Hamaguchi T, Matsumura Y. Novel SN-38-incorporating polymeric micelles, NK012, eradicate vascular endothelial growth factor-secreting bulky tumors. *Cancer Res* 2006; **66**: 10048-10056 [PMID: 17047068 DOI: 10.1158/0008-5472.CAN-06-1605]

51 **Kim TH**, Mount CW, Gombotz WR, Pun SH. The delivery of doxorubicin to 3-D multicellular spheroids and tumors in a murine xenograft model using tumor-penetrating triblock polymeric micelles. *Biomaterials* 2010; **31**: 7386-7397 [PMID: 20598741 DOI: 10.1016/j.biomaterials.2010.06.004]

52 **Brunato S**, Mastrotto F, Bellato F, Bastiancich C, Travanut A, Garofalo M, Mantovani G, Alexander C, Preat V, Salmaso S, Caliceti P. PEG-polyaminoacid based micelles for controlled release of doxorubicin: Rational design, safety and efficacy study. *J Control Release* 2021; **335**: 21-37 [PMID: 33989691 DOI: 10.1016/j.jconrel.2021.05.010]

53 **Repp L**, Unterberger CJ, Ye Z, Feltenberger JB, Swanson SM, Marker PC, Kwon GS. Oligo(Lactic Acid)$_8$-Docetaxel Prodrug-Loaded PEG-*b*-PLA Micelles for Prostate Cancer. *Nanomaterials (Basel)* 2021; **11** [PMID: 34685195 DOI: 10.3390/nano11102745]

54 **Su M**, Xie J, Zeng Q, Shu M, Liu J, Jiang Z. Enzymatic synthesis of PEGylated lactide-diester-diol copolyesters for highly efficient targeted anticancer drug delivery. *Mater Sci Eng C Mater Biol Appl* 2020; **115**: 111125 [PMID: 32600724 DOI: 10.1016/j.msec.2020.111125]

55 **Zhu L**, Chen L. Progress in research on paclitaxel and tumor immunotherapy. *Cell Mol Biol Lett* 2019; **24**: 40 [PMID: 31223315 DOI: 10.1186/s11658-019-0164-y]

56 **Repp L**, Rasoulianboroujeni M, Lee HJ, Kwon GS. Acyl and oligo(lactic acid) prodrugs for PEG-b-PLA and PEG-b-PCL nano-assemblies for injection. *J Control Release* 2021; **330**: 1004-1015 [PMID: 33166607 DOI: 10.1016/j.jconrel.2020.11.008]

57 **Yang T**, Cui FD, Choi MK, Cho JW, Chung SJ, Shim CK, Kim DD. Enhanced solubility and stability of PEGylated liposomal paclitaxel: in vitro and in vivo evaluation. *Int J Pharm* 2007; **338**: 317-326 [PMID: 17368984 DOI: 10.1016/j.ijpharm.2007.02.011]

58 **Zhu C**, Zhang H, Li W, Luo L, Guo X, Wang Z, Kong F, Li Q, Yang J, Du Y, You J. Suppress orthotopic colon cancer and its metastasis through exact targeting and highly selective drug release by a smart nanomicelle. *Biomaterials* 2018; **161**: 144-153 [PMID: 29421551 DOI: 10.1016/j.biomaterials.2018.01.043]

59 **Lu Y**, Zhong L, Jiang Z, Pan H, Zhang Y, Zhu G, Bai L, Tong R, Shi J, Duan X. Cationic micelle-based siRNA delivery for efficient colon cancer gene therapy. *Nanoscale Res Lett* 2019; **14**: 193 [PMID: 31165329 DOI: 10.1186/s11671-019-2985-z]

60 **Men K**, Huang R, Zhang X, Zhang R, Zhang Y, Peng Y, Tong R, Yang L, Wei Y, Duan X. Delivery of interleukin-22 binding protein (IL-22BP) gene by cationic micelle for colon cancer gene therapy. *RSC Adv* 2018; **8**: 16537-16548 [PMID: 35540501 DOI: 10.1039/c8ra02580k]

61 **Duan X**, Wang P, Men K, Gao X, Huang M, Gou M, Chen L, Qian Z, Wei Y. Treating colon cancer with a suicide gene delivered by self-assembled cationic MPEG-PCL micelles. *Nanoscale* 2012; **4**: 2400-2407 [PMID: 22388488 DOI: 10.1039/c2nr30079f]

62 **Martínez-García D**, Manero-Rupérez N, Quesada R, Korrodi-Gregório L, Soto-Cerrato V. Therapeutic strategies involving survivin inhibition in cancer. *Med Res Rev* 2019; **39**: 887-909 [PMID: 30421440 DOI: 10.1002/med.21547]

63 **Jang YL**, Yun UJ, Lee MS, Kim MG, Son S, Lee K, Chae SY, Lim DW, Kim HT, Kim SH, Jeong JH. Cell-penetrating peptide mimicking polymer-based combined delivery of paclitaxel and siRNA for enhanced tumor growth suppression. *Int J Pharm* 2012; **434**: 488-493 [PMID: 22613208 DOI: 10.1016/j.ijpharm.2012.04.083]

64 **Sanati S**, Taghavi S, Abnous K, Taghdisi SM, Babaei M, Ramezani M, Alibolandi M. Fabrication of anionic dextran-coated micelles for aptamer targeted delivery of camptothecin and survivin-shRNA to colon adenocarcinoma. *Gene Ther* 2022; **29**: 55-68 [PMID: 33633357 DOI: 10.1038/s41434-021-00234-0]

65 **Berger CM**, Gaume X, Bouvet P. The roles of nucleolin subcellular localization in cancer. *Biochimie* 2015; **113**: 78-85 [PMID: 25866190 DOI: 10.1016/j.biochi.2015.03.023]

66 **Lee SY**, Yang CY, Peng CL, Wei MF, Chen KC, Yao CJ, Shieh MJ. A theranostic micelleplex co-delivering SN-38 and VEGF siRNA for colorectal cancer therapy. *Biomaterials* 2016; **86**: 92-105 [PMID: 26896610 DOI: 10.1016/j.biomaterials.2016.01.068]

67 **Li Y**, Jia F, Deng X, Wang X, Lu J, Shao L, Cui X, Pan Z, Wu Y. Combinatorial miRNA-34a replenishment and irinotecan delivery *via* auto-fluorescent polymeric hybrid micelles for synchronous colorectal cancer theranostics. *Biomater Sci* 2020; **8**: 7132-7144 [PMID: 33150879 DOI: 10.1039/d0bm01579b]

68 **Yang T**, Lan Y, Cao M, Ma X, Cao A, Sun Y, Yang J, Li L, Liu Y. Glycyrrhetinic acid-conjugated polymeric prodrug micelles co-delivered with doxorubicin as combination therapy treatment for liver cancer. *Colloids Surf B Biointerfaces* 2019; **175**: 106-115 [PMID: 30529816 DOI: 10.1016/j.colsurfb.2018.11.082]

69 **Zhang P**, Li J, Ghazwani M, Zhao W, Huang Y, Zhang X, Venkataramanan R, Li S. Effective co-delivery of doxorubicin and dasatinib using a PEG-Fmoc nanocarrier for combination cancer chemotherapy. *Biomaterials* 2015; **67**: 104-114 [PMID: 26210177 DOI: 10.1016/j.biomaterials.2015.07.027]

70 **Lee AL**, Dhillon SH, Wang Y, Pervaiz S, Fan W, Yang YY. Synergistic anti-cancer effects *via* co-delivery of TNF-related apoptosis-inducing ligand (TRAIL/Apo2L) and doxorubicin using micellar nanoparticles. *Mol Biosyst* 2011; **7**: 1512-1522 [PMID: 21350763 DOI: 10.1039/c0mb00266f]

71 **Charbgoo F**, Alibolandi M, Taghdisi SM, Abnous K, Soltani F, Ramezani M. MUC1 aptamer-targeted DNA micelles for dual tumor therapy using doxorubicin and KLA peptide. *Nanomedicine* 2018; **14**: 685-697 [PMID: 29317345 DOI: 10.1016/j.nano.2017.12.010]

72 **Chen D**, Ge S, Zuo L, Wang S, Liu M, Li S. Adjudin-loaded redox-sensitive paclitaxel-prodrug micelles for overcoming multidrug resistance with efficient targeted Colon cancer therapy. *Drug Deliv* 2020; **27**: 1094-1105 [PMID: 32706289 DOI: 10.1080/10717544.2020.1797245]

73 **Ashwanikumar N**, Kumar NA, Nair SA, Kumar GSV. Dual drug delivery of 5-fluorouracil (5-FU) and methotrexate (MTX) through random copolymeric nanomicelles of PLGA and polyethylenimine demonstrating enhanced cell uptake and cytotoxicity. *Colloids Surf B Biointerfaces* 2014; **122**: 520-528 [PMID: 25108479 DOI: 10.1016/j.colsurfb.2014.07.024]

74 **Sawdon AJ**, Zhang J, Wang X, Peng CA. Enhanced Anticancer Activity of 5'-DFUR-PCL-MPEG Polymeric Prodrug Micelles Encapsulating Chemotherapeutic Drugs. *Nanomaterials (Basel)* 2018; **8** [PMID: 30551585 DOI: 10.3390/nano8121041]

75 **Wang J**, Peng CA. Anticancer effectiveness of polymeric drug nanocarriers on colorectal cancer cells. *Annu Int Conf IEEE Eng Med Biol Soc* 2011; **2011**: 3249-3252 [PMID: 22255032 DOI: 10.1109/IEMBS.2011.6090883]

76 **Hamaguchi T**, Doi T, Eguchi-Nakajima T, Kato K, Yamada Y, Shimada Y, Fuse N, Ohtsu A, Matsumoto S, Takanashi M, Matsumura Y. Phase I study of NK012, a novel SN-38-incorporating micellar nanoparticle, in adult patients with solid tumors. *Clin Cancer Res* 2010; **16**: 5058-5066 [PMID: 20943763 DOI: 10.1158/1078-0432.CCR-10-0387]

77 **Hamaguchi T**, Tsuji A, Yamaguchi K, Takeda K, Uetake H, Esaki T, Amagai K, Sakai D, Baba H, Kimura M, Matsumura

Y, Tsukamoto T. A phase II study of NK012, a polymeric micelle formulation of SN-38, in unresectable, metastatic or recurrent colorectal cancer patients. *Cancer Chemother Pharmacol* 2018; **82**: 1021-1029 [PMID: 30284603 DOI: 10.1007/s00280-018-3693-6]

78 **Hamaguchi T**, Kato K, Yasui H, Morizane C, Ikeda M, Ueno H, Muro K, Yamada Y, Okusaka T, Shirao K, Shimada Y, Nakahama H, Matsumura Y. A phase I and pharmacokinetic study of NK105, a paclitaxel-incorporating micellar nanoparticle formulation. *Br J Cancer* 2007; **97**: 170-176 [PMID: 17595665 DOI: 10.1038/sj.bjc.6603855]

79 **Kayaku N**. Study of NK012 and 5-FU/LV in Solid Tumors Followed by Dose Expansion in Colorectal Cancer. [accessed 2022 Mar 21]. In: ClinicalTrials.gov [Internet]. Nashville (TN): U.S. National Library of Medicine. Available from: https://clinicaltrials.gov/ct2/show/NCT01238939 ClinicalTrials.gov Identifier: NCT01238939

80 **OncoNano Medicine**. A Study to Evaluate ONM-100, an Intraoperative Fluorescence Imaging Agent for the Detection of Cancer. [accessed 2022 Mar 21]. In: ClinicalTrials.gov [Internet]. Philadelphia (PA): U.S. National Library of Medicine. Available from: https://clinicaltrials.gov/ct2/show/NCT03735680 ClinicalTrials.gov Identifier: NCT03735680

World Journal of Gastroenterology

Submit a Manuscript: https://www.f6publishing.com

World J Gastroenterol 2022 July 7; 28(25): 2881-2889

DOI: 10.3748/wjg.v28.i25.2881

ISSN 1007-9327 (print) ISSN 2219-2840 (online)

MINIREVIEWS

Incretin based therapy and pancreatic cancer: Realising the reality

Varun Suryadevara, Ayan Roy, Jayaprakash Sahoo, Sadishkumar Kamalanathan, Dukhabandhu Naik, Pazhanivel Mohan, Raja Kalayarasan

Specialty type: Gastroenterology and hepatology

Provenance and peer review: Invited article; Externally peer reviewed.

Peer-review model: Single blind

Peer-review report's scientific quality classification

Grade A (Excellent): A
Grade B (Very good): 0
Grade C (Good): C
Grade D (Fair): D
Grade E (Poor): 0

P-Reviewer: He Z, China; Herold Z, Hungary; Long P, China
A-Editor: Tung TH, China

Received: January 17, 2022
Peer-review started: January 17, 2022
First decision: March 9, 2022
Revised: March 23, 2022
Accepted: May 22, 2022
Article in press: May 22, 2022
Published online: July 7, 2022

Varun Suryadevara, Jayaprakash Sahoo, Sadishkumar Kamalanathan, Dukhabandhu Naik, Department of Endocrinology, Jawaharlal Institute of Postgraduate Medical Education and Research, Puducherry 605006, India

Ayan Roy, Department of Endocrinology, All India Institute of Medical Sciences, Kalyani 741245, West Bengal, India

Pazhanivel Mohan, Department of Medical Gastroenterology, Jawaharlal Institute of Postgraduate Medical Education and Research, Puducherry 605006, India

Raja Kalayarasan, Department of Surgical Gastroenterology, Jawaharlal Institute of Postgraduate Medical Education and Research, Puducherry 605006, India

Corresponding author: Jayaprakash Sahoo, MBBS, MD, Additional Professor, Department of Endocrinology, Jawaharlal Institute of Postgraduate Medical Education and Research, Room 5444, 4th Floor, Super Speciality Block, Puducherry 605006, India. jppgi@yahoo.com

Abstract

Incretin-based therapies like glucagon-like peptide-1 receptor agonists and dipeptidyl peptidase-4 inhibitors help maintain the glycaemic control in patients with type 2 diabetes mellitus with additional systemic benefits and little risk of hypoglycaemia. These medications are associated with low-grade chronic pancreatitis in animal models inconsistently. The incidence of acute pancreatitis was also reported in some human studies. This inflammation provides fertile ground for developing pancreatic carcinoma (PC). Although the data from clinical trials and population-based studies have established safety regarding PC, the pathophysiological possibility that low-grade chronic pancreatitis leads to PC remains. We review the existing literature and describe the relationship between incretin-based therapies and PC.

Key Words: Diabetes mellitus; Dipeptidyl peptidase-4 inhibitor; Glucagon-like peptide-1 receptor agonist; Incretin; Pancreatitis; Pancreatic Cancer

©The Author(s) 2022. Published by Baishideng Publishing Group Inc. All rights reserved.

Core Tip: Incretin-based therapies are increasingly being used to treat patients with type 2 diabetes mellitus . The early literature regarding pancreatic safety of incretin-based therapies was discordant. However, the follow-up data of various randomised trials have consistently shown that these medications are safe.

Citation: Suryadevara V, Roy A, Sahoo J, Kamalanathan S, Naik D, Mohan P, Kalayarasan R. Incretin based therapy and pancreatic cancer: Realising the reality. *World J Gastroenterol* 2022; 28(25): 2881-2889
URL: https://www.wjgnet.com/1007-9327/full/v28/i25/2881.htm
DOI: https://dx.doi.org/10.3748/wjg.v28.i25.2881

INTRODUCTION

Incretin-based therapies such as glucagon-like peptide-1 (GLP-1) receptor agonists (RAs) and dipeptidyl peptidase-4 inhibitors (DPP-4Is) are being increasingly used to treat patients with type 2 diabetes mellitus (T2DM). GLP-1 RAs mimic the action of endogenous GLP-1, whereas DPP-4Is prevent the degradation of GLP-1. These medications can control blood glucose levels without an increased risk of hypoglycemic episodes or weight gain. The initial clinical trials for GLP-1 RA and DPP-4I were conducted in 2003 and 2004, respectively[1,2]. The United States Food and Drug Administration (FDA) issued an alert regarding the potential risk of acute pancreatitis in 2007[3]. DPP-4Is have been widely used owing to the oral administration and low risk of hypoglycemia. However, the use of GLP-1 RA was limited until 2015. But the data from cardiovascular outcome trials (CVOTs) of GLP-1 RAs changed the scenario. The significant reduction in cardiovascular deaths with GLP-1 RAs such as liraglutide and semaglutide tilted the benefit-risk relationship. These therapies have become the next treatment choice after metformin in patients with or at high risk of atherosclerotic vascular disease[4]. Newer generation incretin-based therapies [coagonists of GLP-1 with gastric inhibitory peptide (GIP) or glucagon] are in the pipeline. They are presumed to have higher efficacy than GLP-1 RAs and DPP-4Is. Various incretin-based medications categorised according to their mechanism of action are shown in Table 1.

Incretin-based therapies are speculated to induce overstimulation of the GLP-1 receptor, leading to pancreatitis and pancreatic carcinoma (PC). However, the risk of both PC and pancreatitis is increased in DM compared to non-diabetic counterparts[5]. For PC, inflammation is relevant both as a risk factor and an effect of cancer. Patients with chronic pancreatitis carry a higher risk of developing PC. The initial postmarketing surveillance studies for incretin-based therapies revealed an increase in pancreatic adverse events[6]. Further observational studies of pancreatic adverse events showed conflicting results. Post hoc analyses of pertinent randomized controlled trials (RCTs) failed to distinguish pancreatic adverse events between controls and patients on incretin-based therapies[7]. However, the theoretical plausibility of PC in patients receiving incretin-based therapies still remains valid. It is worth reviewing the status of the incretin-based therapies now as an increasing number of therapies based on incretin are becoming available. The treating clinician must be aware of the benefit-risk ratio (RR) when prescribing incretin-based therapy.

SEARCH STRATEGY

Two authors (VS, AR) conducted the initial search in PubMed and Reference Citation Analysis (https://www.referencecitationanalysis.com/) database for relevant articles. The references of these articles were searched for additional relevant studies. The keywords used in the search were: 'Incretin'; 'pancreatic cancer'; glucagon-like peptide-1 receptor agonist'; 'dipeptidyl peptidase-4 inhibitor'; incretin and pancreatic cancer; 'GLP1-RA and pancreatic cancer'; 'DPP-4I and pancreatic cancer'. Only English language publications were included. SK, DN, and JS selected the appropriate articles to be included.

PATHOPHYSIOLOGY

The critical pathophysiologic mechanisms for developing PC in patients using incretin-based therapies are chronic low-grade inflammation and proliferative changes. A flowchart outlining the pathophysiology of pancreatic cancer is shown in Figure 1.

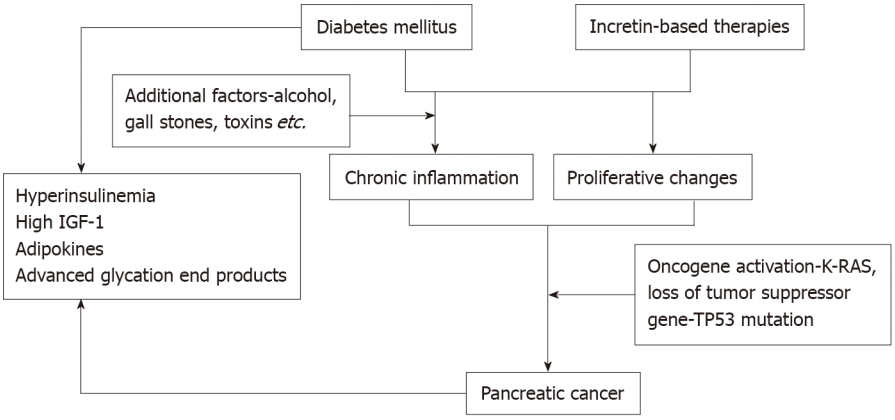
Role of inflammation

Even without any therapy, both PC and pancreatitis incidence is increased in T2DM[8,9]. Long term treatment of T2DM patients with DPP-4Is/GLP-1 RAs may exacerbate the pre-existing chronic inflammation. Any additional mutations in the background of inflammation can tilt the balance toward the

Table 1 Various incretin-based therapies

Class of drugs	Medications
GLP-1RA (oral/subcutaneous)	Subcutaneous-Exenatide, Albiglutide, Lixisenatide, Liraglutide, Semaglutide. Oral-Semaglutide
DPP-4I (oral)	Saxagliptin, Vildaglipitn, Sitagliptin, Aloglipitn, Linagliptin, Teneligliptin
Newer drugs/drugs in development	Tirzepatide (GLP1 + GIP co-agnoist)
	Cotadutide (GLP1 + glucagon co-agonist)
	Teduglutide (GLP-2 RA)
	Triple agnoists (GLP1 + Glucagon + GIP agnoists)

GLP-1RA: Glucagon like peptide receptor-1 receptor agonist; DPP-4I: Dipeptidyl peptidase-4 inhibitor; GIP: Gastric inhibitory peptide; GLP-2RA: Glucagon like peptide receptor-2 receptor agonist.



DOI: 10.3748/wjg.v28.i25.2881 **Copyright** ©The Author(s) 2022.

Figure 1 Flowchart explaining the mechanism of development of pancreatic cancer. IGF-1: Insulin-like growth factor-1; K-RAS: Kirsten rat sarcoma virus gene.

progression of neoplasia. Various researchers conducted animal studies to substantiate this hypothesis using rodents with mutant Kirsten rat sarcoma virus gene (K-RAS), leading to constitutive activation. The K-RAS gene is mutated in > 90% of human PC cases[10]. KC mice model has a single activating mutation (G12D) in the K-RAS gene. Prenatal expression of mutant K-RAS in all exocrine lineages of KC mice resulted in histological changes suggestive of pancreatitis, implying a cooperative relationship between K-RAS activation and inflammation. Treatment of KC mice with the pancreatitis-inducing agent caerulein (a cholecystokinin analog) dramatically accelerates the progression to pancreatic ductal adenocarcinoma (PDAC) within a few weeks[11]. Further animal experiments have shown that K-RAS mutation alone cannot reach the expected theoretical levels of activity required for the progression of carcinogenesis. Nevertheless, agents which cause inflammation can hyperstimulate K-RAS by modulating its activity above the putative threshold necessary for carcinogenesis. The constitutive activation of nuclear factor kappa B pathway in addition to K-RAS in acinar cells significantly accelerates carcinogenesis, whereas cyclooxygenase inhibition is associated with a reduced risk of PDAC. These findings highlight the importance of inflammation in the progression of PDAC[12].

Incretin-based medications induced pancreatitis in animal experiments[13-15]. However, most PDAC cases develop without clinically apparent acute or chronic pancreatitis[16]. This observation can be explained by low-grade subclinical inflammation being sufficient to promote carcinogenesis in the presence of additional drivers of carcinogenesis. On the other hand, it can also be a consequence of the earliest events in carcinogenesis.

Role of proliferative changes

In addition to low-grade asymptomatic chronic pancreatitis, incretin-based medications induce proliferative changes in the islets. Premalignant changes that precede the onset of PDAC are known as pancreatic intraepithelial neoplasia (PanIN) lesions. They herald the start of PDAC. PanINs can be found in up to 50% of the middle-aged population. However, only a few progress to PDAC[17]. As progression of PanINs to PDAC occurs *via* the accumulation of additional somatic mutations, any factor that increases cellular replication in PanINs is likely to increase the likelihood of PDAC. Both PanINs and PDAC express the human GLP-1 receptor. Acinar and duct cells proliferate in response to incretin-

based medications in the normal pancreas with an increase in pancreatic weight[18]. In the setting of chronic pancreatitis, as shown in animal models treated with incretin-based therapies, this proliferation may be sufficient to initiate carcinogenesis event sequences. Treatment with exenatide in KC mice resulted in the formation and growth of dysplastic PanIN lesions in addition to pancreatitis.

Histological changes following incretin-based therapies

The controversy about pancreatic adverse events due to incretin-based therapies was amplified by a publication by Butler *et al*[19]. The authors examined age-matched organ donor samples obtained from the Network for Pancreatic Organ Donation (nPOD). They included a total of 34 subjects with T2DM treated with incretin-based therapies (n = 8) or non-incretin-based therapies (n = 12) and nondiabetic control subjects (n = 14). The incretin group had an increase in pancreatic mass by 40% with increased exocrine cell proliferation and dysplasia. The authors also noticed alpha and beta-cell hyperplasia along with glucagon-expressing microadenomas in incretin-treated subjects. Islet cell costaining for insulin and glucagon was higher in DM subjects than non-DM control subjects and increased further with incretin therapy. The authors concluded that incretin therapy in humans results in the expansion of both exocrine and endocrine pancreatic compartments and that there is a potential for evolution into neuroendocrine tumors. However, this study was met with sharp criticism owing to methodological flaws. Harja *et al*[20], in a more detailed analysis of the nPOD database, found that the baseline characteristics were not comparable between the incretin group and the other two groups. Pancreatic weight data were missing for half of the subjects. The increase in PanINs can be explained by the nearly 20-year age difference between the incretin group and the other two groups. Bonner-Weir *et al*[21] and Kahn[22] also re-analyzed the data from nPOD and reached similar conclusions.

Despite the flaws in the study methodology, this study caught the attention of the FDA and the European Medicines Agency (EMA). Both agencies reviewed all available animal and human data for incretin-based therapies. Microscopic examinations from animal studies did not reveal pancreatic lesions or pancreatitis. Even at doses greater than human clinical exposure to incretin-based therapies, there were no tumours in rodents for up to 2 years (lifespan of rodents). The FDA studied the effect of exenatide in Zucker diabetic fatty rat, a chemical-induced pancreatitis model, and C57 black 6 (C57BL/6) high-fat diet mouse model. There was no identifiable pancreatic pathology in the pancreatitis mouse model and Zucker diabetic fatty rat model. After three months of exenatide in the C57BL/6 high-fat diet mouse, a minimal-to-moderate worsening of background findings was noted. Based on the available data, they could not draw any conclusions about the risk of pancreatic adverse events in patients using incretin-based therapies[23].

Ueberberg *et al*[24] conducted a study on cadaveric pancreata, similar to Butler *et al*[19]. They obtained pancreatic tissue during surgery from 13 diabetic patients (7 in the incretin group and 6 in the non-incretin group), 11 non-diabetic controls, and nine brain-dead organ donors. There were no differences between groups in the alpha cell area, beta and alpha cell replication, acinar, and ductal cell replication. Coexpression of insulin and glucagon has not been demonstrated. PanIN lesions were more common in the diabetic group, although the prevalence was low. Considering the small sample size and large interindividual variability, the authors advised caution on coming to any conclusion from such studies.

Chadwick *et al*[25] attempted to determine the background incidence of spontaneous pancreatic lesions in different rat strains fed a standard or high-fat diet over four months. They found that the pancreatic lesions previously thought to be due to incretins are common baseline findings. These lesions can be seen without any drug treatment. These lesions were independent of diet or glycaemic status. The authors concluded that we need to be cautious when interpreting patients' pancreatic findings on incretin-based therapies. Aston-Mourney *et al*[26] tried to characterize the amyloidogenic potential of sitagliptin in rodents. Human islet amyloid polypeptide transgenic mice, untreated nontransgenic mice, and those on treatment with sitagliptin, metformin, or the combination were followed up for one year. There was no increase in amyloid formation or ductal proliferation. However, there was an improvement in β-cell secretion, suggesting endocrine protective effects without associated toxicity to the exocrine compartment of the pancreas.

Effect of incretin-based therapies on cancer cells

The effect of incretin-based therapies on PC cells has also been studied *in vitro*. Lu *et al*[27] found that liraglutide in combination with metformin has synergistic anti-tumor effects *in vitro*. Yan *et al*[28] examined the effect of exendin-4 on a xenograft tumor model. Exendin-4 suppressed the PC cell proliferation by attenuating the function of pancreatic stellate cells (PSC) and suppressing extracellular matrix deposition. Zhao *et al*[29] examined the effect of liraglutide on PC cell line (PANC-1) cocultured with and without PSCs and found that liraglutide significantly reduced the migration and invasion of the PANC-1 cells. The authors hypothesized that the effect is probably mediated by calcium and calcium-binding proteins. In another study, Zhao *et al*[30] examined the effects of liraglutide on the chemosensitivity of PC cells to gemcitabine in PANC-1 and gemcitabine resistant cell lines (PANC-GR). Liraglutide inhibited proliferation and promoted apoptosis of the PANC-GR cells in a dose-dependent manner. It also increased GLP-1 receptor and protein kinase-A expression in the PANC-GR cells. In rodent studies, liraglutide treatment was observed to increase the chemosensitivity of PC cells to

gemcitabine.

DPP4 and cancer

DPP-4 cleaves many other polypeptides, such as chemokines, neuropeptides in addition to GLP-1. DPP-4, also known as cluster differentiation marker 26, plays a vital role in inflammation by modulating the inactivation of cytokines and chemokines. DPP-4 is expressed in various malignancies. The overexpression of DPP-4 exerts an antitumour effect predominantly through immunomodulation[31]. DPP-4 inhibition has been shown to improve antitumor immune response by preserving the function of a chemokine C-X-C motif ligand and through interleukin 33 (IL-33) mediated tumour control[32,33]. The effects of DPP-4 on cancer cells appear to be heterogeneous, depending on tumor types, stages, microenvironment, and host condition. In breast cancer and small cell lung cancers, decreased expression of DPP-4 is associated with more aggressiveness of the tumour. However, increased DPP-4 expression levels have been associated with poor prognosis in patients with PC[31].

INCRETIN-BASED THERAPIES AND PC-HUMAN STUDIES

Data from observational studies

Early case reports of pancreatitis following exenatide and sitagliptin led to the issue of FDA alert in 2007. These reports led to many database analyses to look for the prevalence of pancreas-related adverse events. Elashoff *et al*[6] raised concern regarding PDAC by studying the FDA adverse events reporting system (FDA AERS) during 2004-09. This study resulted in widespread coverage in media regarding the risk of PC. Elashoff *et al*[6] examined FDA AERS database for adverse events associated with exenatide and sitagliptin in this study. The odds ratio for reported pancreatitis was 6-fold higher for sitagliptin or exenatide users than other therapies. PC was also more frequent (approximately 3-fold) among patients who took sitagliptin or exenatide. However, we must understand that this was a retrospective, record-based study. The likelihood of reporting events is higher with new drugs than with the patients on older drugs. A series of observational studies followed this study and showed discordant results. Most of the observational studies were retrospective and record-based. Both the FDA and the EMA reviewed their clinical safety databases, and the pooled data did not reveal any compelling evidence of an increased risk of pancreatitis or PC.

The latest observational study from Montvida *et al*[34] used Centricity Electronic Medical Records from the United States. The authors assessed the time to pancreatic events for incretin-based and nonincretin therapies (sulfonylurea, thiazolidinedione, and insulin). This study surprisingly found that the group treated with insulin had higher pancreatitis events with a short time to event as compared to incretin-based therapies. For PC, the time to event rate was not significantly different between the groups. Among the older studies, few studies showed an increased risk of pancreatitis and PC, but most studies could not find any association between pancreatic adverse events and incretin-based therapies [34-38]. Although the sample size was adequate for these studies, we must keep in mind the unaccounted confounders. The baseline characteristics and the comparator drugs varied among different studies. A summary of these studies is compiled in Table 2.

Data from randomised controlled trials

Data from RCTs have conventionally been considered superior to data from observational studies. There have been many follow-up studies of the patients recruited for CVOT of the incretin-based therapies. Among the individual CVOT data, there was a non-significant trend for or against the development of PC for different incretin-based therapies. Many researchers also assessed the PC risk with incretin-based therapies using meta-analyses and systematic reviews. Alves *et al*[39] evaluated the association of liraglutide or exenatide with PC in a meta-analysis that included 25 longitudinal studies in 2012. Neither GLP-1 RAs nor DPP-4Is were associated with increased risk for PC.

The first meta-analysis evaluating PC association with all types of incretin-based therapies was published by Chen *et al*[40] in 2016. This meta-analysis included 24 RCTs enrolling 47904 patients. This meta-analysis also could not identify any increased risk of PC either as monotherapy (RR = 0.62, 95%CI: 0.38–1.01) or combination therapy (RR = 0.92, 95%CI: 0.45–1.90). This result was followed by a series of meta-analyses with a similar conclusion[41-43]. The latest meta-analysis is from Abd El Aziz *et al*[43], which evaluated 11 CVOTs studying 55921 patients. In the individual study data, lixisenatide and semaglutide were associated with nominally reduced RR, whereas liraglutide was associated with a slightly elevated RR. However, none of these RRs were statistically significant. In this meta-analysis, neither GLP-1 RAs nor DPP-4Is were associated with a significant increase or decrease in risk of PC [RR for PC- for GLP-1 RA 0.99 (95%CI: 0.9-1.08); DPP-4I 0.92 (95%CI: 0.83-1.01)]. The summary of the data from various meta-analyses is compiled in Table 3.

Newer incretin-based therapies

Tirzepatide is a dual agonist at GLP-1 and GIP receptors. It was formulated as a fatty acid-modified

Table 2 Important observational studies which evaluated the relationship between incretin-based therapies and pancreatic carcinoma

Ref.	Study design	Population	Findings
Elashoff *et al* [6], 2011	Retrospective study (Control drugs-rosiglitazone, glinides, glipizide), 2004-09	Database-FDA AERS. Patients of T2DM on exenatide and sitagliptin. *n* = 1541 events (exenatide). *n* = 322 (sitagliptin). *n* = 691 (controls)	PC was more common among patients who took sitagliptin (2.7-fold) or exenatide (2.9-fold) as compared with other therapies
Montvida *et al*[34], 2019	Retrospective record-based study. 2005 onwards. Follow-up duration 2.27-4.3 yr	Centricity electronic medical record, United States. DPP-4i *n* = 50095. GLP-1 RA *n* = 12654. SU *n* = 110747. TZD *n* = 17597. Insulin *n* = 34805	Compared with DPP-4i, the GLP-1 RA group developed PC 3 yr later (95%CI: 0.84-5.16). No other significant differences were observed between groups
Nagel *et al* [35], 2016	Retrospective study (Control drugs-rosiglitazone, glinides, glipizide), 1968-2013	Database-FDA AERS. Patients of T2DM on sitagliptin, saxagliptin, linagliptin, and alogliptin. *n* = 156 PC patients	EB05 was 10.3 for sitagliptin, 7.1 for saxagliptin, 4.9 for linagliptin, and 1.4 for alogliptin, compared with all other agents
Azoulay *et al* [36], 2016	Nested case control analysis (control drug- sulfonylureas), 2007-2014. Follow-up 1.3-2.8 yr	Database-CNODES (Canada, United States, United Kingdom). *n* = 972384	Compared with SUs, incretin-based drugs were not associated with an increased risk of PC-pooled aHR 1.02 (95%CI: 0.84-1.23)
Tseng *et al* [37], 2017	Retrospective population-based cohort study, 1997-2010. Follow up-till occurrence of adverse pancreatic event	Database-The Taiwan National Health Insurance Research Database. *n* = 13171 incretin. *n* = 13171 non-incretins	PC occurred in 6 (0.05%) and 10 (0.08%) patients in the incretin and non- incretin cohort, respectively
Boniol *et al* [38], 2018	Retrospective cohort study, 2008-2013. Follow-up 1.8-2.3 yr	Public health insurance databases of Belgium, Lombardy (Italy). *n* = 33292 incretin. *n* = 525733 control	The aHR for PC was 2.14 (95%CI: 1.71–2.67) for incretin group compared with control

FDA AERS: Food and drug administration adverse event reporting system; T2DM: Type 2 diabetes mellitus; PC: Pancreatic carcinoma; EB05: Empirical Bayesian fifty centile; aHR: Adjusted hazard ratio; CI: Confidence interval; CNODES: Canadian network for observational drug effect studies; SU: Sulfonylurea; OHA: Oral hypoglycemic agent; RR: Risk ratio; TZD: Thiazolidinedione.

Table 3 Important systematic reviews and meta-analyses which evaluated the relationship between incretin-based therapies and pancreatic cancer

Ref.	Description	Findings
Alves *et al* [39], 2012	All studies (25 RCT/longitudinal observational) assessing the estimate of pancreatitis/PC in patients with T2DM using exenatide or liraglutide	For PC risk, the OR of exenatide was 0.86 (95%CI: 0.29-2.60) and liraglutide was 1.35 (95%CI: 0.70-2.59)
Chen *et al* [40], 2016	All RCTs reporting PC with use of incretin-based therapies compared with placebo or non-incretin anti-diabetic drugs in patients with T2DM	Overall, no increased risk of PC was detected in association with incretin-based treatment (RR = 0.7, 95%CI: 0.37–1.05). The incidence of PC was even lower among incretin-based groups than controls (RR = 0.50, 95%CI: 0.29–0.87) in trials with duration more than 104 wk
Zhang *et al* [41], 2017	6 prospective randomized controlled trials (EXAMINE, SAVOR-TIMI 53, TECOS, ELIXA, LEADER and SUSTAIN-6)-3 trials for DPP-4is and 3 trials for GLP-1 RAs	Incretin-based agents did not significantly affect PC-OR: 0.71 (95%CI: 0.45–1.11)
Pinto *et al* [42], 2019	12 RCTs with GLP-1 RAs as an intervention, from database inception till 2017	GLP-1 RAs did not increase the risk for pancreatic cancer when compared to other treatments-OR: 1.06 (95%CI: 0.67-1.67)
Abd El Aziz *et al* [43], 2020	Meta-analysis of cases of acute pancreatitis and PC as well as any malignant neoplasm reported in 11 CVOTs with GLP-1 RAs and DPP-4i	Neither GLP-1 RAs nor DPP-4is were associated with a significantly elevated or reduced risk of PC. For GLP-1 RA OR was 1.14 (95%CI: 0.77-1.7) and for DPP4i OR was 0.94 (95%CI: 0.52-1.68)

PC: Pancreatic cancer; RCT: Randomised controlled trial; T2DM: Type 2 diabetes mellitus; OR: Odds ratio; RR: Risk ratio; CVOT: Cardiovascular outcome trial; GLP-1 RA: Glucagon like peptide-1 receptor agonists; DPP-4i: Dipeptidyl Peptidase-4 inhibitors; OHA: Oral hypoglycemic agent.

peptide based on the native GIP sequence. Tirzepatide demonstrated a more significant reduction in glycosylated hemoglobin, superior weight loss, and comparable adverse effects compared to semaglutide in a phase 3 trial. Pancreatitis was observed in four patients in the tirzepatide arm and three patients in the semaglutide arm during the study duration[44]. Cotadutide is a balanced GLP-1 and glucagon receptor dual agonist. Phase 2 clinical trials for cotadutide were published recently. The efficacy of cotadutide also appears to be better than that of semaglutide, although no head-to-head comparison is available. No case of pancreatitis has been reported in the phase 2a study of cotadutide, although the frequency of nausea and vomiting was increased in the cotadutide arm[45]. We must therefore wait until we have sufficient data on these new drugs. It is premature to make comment on the pancreatic safety of these drugs at present.

CONCLUSION

We have collected extensive data on the safety of incretin-based therapies over the past two decades. It seems that incretin-based therapies do not increase the risk for PC. Instead, new pre-clinical experimental data have shown beneficial effects on cancer cell lines that require further evaluation. The uncertain risks of PC appear to be smaller compared to the beneficial pleiotropic effects of incretin-based therapies. However, with newer incretin-based therapies, we should keep the theoretical possibility of PC in mind and be cautious until we obtain sufficient data.

FOOTNOTES

Author contributions: Suryadevara V and Roy A did the literature search and wrote the first draft; Sahoo J, Kamalanathan S and Naik D supervised the writing, gave intellectual inputs, and critically revised the manuscript; Mohan P and Kalayarasan R gave intellectual inputs and critically revised the manuscript; all of them approved the final version of the manuscript to be published.

Conflict-of-interest statement: All the authors report no relevant conflicts of interest for this article

Open-Access: This article is an open-access article that was selected by an in-house editor and fully peer-reviewed by external reviewers. It is distributed in accordance with the Creative Commons Attribution NonCommercial (CC BY-NC 4.0) license, which permits others to distribute, remix, adapt, build upon this work non-commercially, and license their derivative works on different terms, provided the original work is properly cited and the use is non-commercial. See: https://creativecommons.org/Licenses/by-nc/4.0/

Country/Territory of origin: India

ORCID number: Varun Suryadevara 0000-0002-9230-0734; Ayan Roy 0000-0003-4419-9376; Jayaprakash Sahoo 0000-0002-8805-143X; Sadishkumar Kamalanathan 0000-0002-2371-0625; Dukhabandhu Naik 0000-0003-4568-877X; Pazhanivel Mohan 0000-0003-1473-4382; Raja Kalayarasan 0000-0003-4056-8672.

S-Editor: Fan JR
L-Editor: A
P-Editor: Fan JR

REFERENCES

1 **Keating GM**. Exenatide. *Drugs* 2005; **65**: 1681-92; discussion 1693 [PMID: 16060703 DOI: 10.2165/00003495-200565120-00008]
2 **Ahrén B**, Landin-Olsson M, Jansson PA, Svensson M, Holmes D, Schweizer A. Inhibition of dipeptidyl peptidase-4 reduces glycemia, sustains insulin levels, and reduces glucagon levels in type 2 diabetes. *J Clin Endocrinol Metab* 2004; **89**: 2078-2084 [PMID: 15126524 DOI: 10.1210/jc.2003-031907]
3 **Butler PC**, Elashoff M, Elashoff R, Gale EA. A critical analysis of the clinical use of incretin-based therapies: Are the GLP-1 therapies safe? *Diabetes Care* 2013; **36**: 2118-2125 [PMID: 23645885 DOI: 10.2337/dc12-2713]
4 **American Diabetes Association**. 9. Pharmacologic Approaches to Glycemic Treatment: *Standards of Medical Care in Diabetes-2021*. *Diabetes Care* 2021; **44**: S111-S124 [PMID: 33298420 DOI: 10.2337/dc21-S009]
5 **Roy A**, Sahoo J, Kamalanathan S, Naik D, Mohan P, Kalayarasan R. Diabetes and pancreatic cancer: Exploring the two-way traffic. *World J Gastroenterol* 2021; **27**: 4939-4962 [PMID: 34497428 DOI: 10.3748/wjg.v27.i30.4939]
6 **Elashoff M**, Matveyenko AV, Gier B, Elashoff R, Butler PC. Pancreatitis, pancreatic, and thyroid cancer with glucagon-like peptide-1-based therapies. *Gastroenterology* 2011; **141**: 150-156 [PMID: 21334333 DOI: 10.1053/j.gastro.2011.02.018]
7 **Nauck MA**. The rollercoaster history of using physiological and pharmacological properties of incretin hormones to develop diabetes medications with a convincing benefit-risk relationship. *Metabolism* 2020; **103**: 154031 [PMID: 31785258 DOI: 10.1016/j.metabol.2019.154031]
8 **Méndez-Bailón M**, de Miguel Yanes JM, Jiménez-García R, Hernández-Barrera V, Pérez-Farinós N, López-de-Andrés A. National trends in incidence and outcomes of acute pancreatitis among type 2 diabetics and non-diabetics in Spain (2001-2011). *Pancreatology* 2015; **15**: 64-70 [PMID: 25500341 DOI: 10.1016/j.pan.2014.11.004]
9 **Koo DH**, Han KD, Park CY. The Incremental Risk of Pancreatic Cancer According to Fasting Glucose Levels: Nationwide Population-Based Cohort Study. *J Clin Endocrinol Metab* 2019; **104**: 4594-4599 [PMID: 31498870 DOI: 10.1210/jc.2019-00033]
10 **di Magliano MP**, Logsdon CD. Roles for KRAS in pancreatic tumor development and progression. *Gastroenterology* 2013; **144**: 1220-1229 [PMID: 23622131 DOI: 10.1053/j.gastro.2013.01.071]
11 **Carrière C**, Young AL, Gunn JR, Longnecker DS, Korc M. Acute pancreatitis markedly accelerates pancreatic cancer progression in mice expressing oncogenic Kras. *Biochem Biophys Res Commun* 2009; **382**: 561-565 [PMID: 19292977 DOI: 10.1016/j.bbrc.2009.03.068]
12 **Zambirinis CP**, Pushalkar S, Saxena D, Miller G. Pancreatic cancer, inflammation, and microbiome. *Cancer J* 2014; **20**:

195-202 [PMID: 24855007 DOI: 10.1097/PPO.0000000000000045]
13 **Rouse R**, Zhang L, Shea K, Zhou H, Xu L, Stewart S, Rosenzweig B, Zhang J. Extended exenatide administration enhances lipid metabolism and exacerbates pancreatic injury in mice on a high fat, high carbohydrate diet. *PLoS One* 2014; **9**: e109477 [PMID: 25291183 DOI: 10.1371/journal.pone.0109477]
14 **Bonner-Weir S**, Sullivan BA, Weir GC. Human Islet Morphology Revisited: Human and Rodent Islets Are Not So Different After All. *J Histochem Cytochem* 2015; **63**: 604-612 [PMID: 25604813 DOI: 10.1369/0022155415570969]
15 **Vrang N**, Jelsing J, Simonsen L, Jensen AE, Thorup I, Søeborg H, Knudsen LB. The effects of 13 wk of liraglutide treatment on endocrine and exocrine pancreas in male and female ZDF rats: a quantitative and qualitative analysis revealing no evidence of drug-induced pancreatitis. *Am J Physiol Endocrinol Metab* 2012; **303**: E253-E264 [PMID: 22589391 DOI: 10.1152/ajpendo.00182.2012]
16 **Ilic M**, Ilic I. Epidemiology of pancreatic cancer. *World J Gastroenterol* 2016; **22**: 9694-9705 [PMID: 27956793 DOI: 10.3748/wjg.v22.i44.9694]
17 **Sipos B**, Frank S, Gress T, Hahn S, Klöppel G. Pancreatic intraepithelial neoplasia revisited and updated. *Pancreatology* 2009; **9**: 45-54 [PMID: 19077454 DOI: 10.1159/000178874]
18 **Perfetti R**, Zhou J, Doyle ME, Egan JM. Glucagon-like peptide-1 induces cell proliferation and pancreatic-duodenum homeobox-1 expression and increases endocrine cell mass in the pancreas of old, glucose-intolerant rats. *Endocrinology* 2000; **141**: 4600-4605 [PMID: 11108273 DOI: 10.1210/endo.141.12.7806]
19 **Butler AE**, Campbell-Thompson M, Gurlo T, Dawson DW, Atkinson M, Butler PC. Marked expansion of exocrine and endocrine pancreas with incretin therapy in humans with increased exocrine pancreas dysplasia and the potential for glucagon-producing neuroendocrine tumors. *Diabetes* 2013; **62**: 2595-2604 [PMID: 23524641 DOI: 10.2337/db12-1686]
20 **Harja E**, Lord J, Skyler JS. An analysis of characteristics of subjects examined for incretin effects on pancreatic pathology. *Diabetes Technol Ther* 2013; **15**: 609-618 [PMID: 23927624 DOI: 10.1089/dia.2013.0177]
21 **Bonner-Weir S**, In't Veld PA, Weir GC. Reanalysis of study of pancreatic effects of incretin therapy: methodological deficiencies. *Diabetes Obes Metab***16**: 661-666 [PMID: 24400596 DOI: 10.1111/dom.12257]
22 **Kahn SE**. Incretin therapy and islet pathology: a time for caution. *Diabetes* 2013; **62**: 2178-2180 [PMID: 23596147 DOI: 10.2337/db13-0520]
23 **Egan AG**, Blind E, Dunder K, de Graeff PA, Hummer BT, Bourcier T, Rosebraugh C. Pancreatic safety of incretin-based drugs--FDA and EMA assessment. *N Engl J Med* 2014; **370**: 794-797 [PMID: 24571751 DOI: 10.1056/NEJMp1314078]
24 **Ueberberg S**, Jütte H, Uhl W, Schmidt W, Nauck M, Montanya E, Tannapfel A, Meier J. Histological changes in endocrine and exocrine pancreatic tissue from patients exposed to incretin-based therapies. *Diabetes Obes Metab* 2016; **18**: 1253-1262 [PMID: 27545110 DOI: 10.1111/dom.12766]
25 **Chadwick KD**, Fletcher AM, Parrula MC, Bonner-Weir S, Mangipudy RS, Janovitz E, Graziano MJ, Roy D, Reilly TP. Occurrence of spontaneous pancreatic lesions in normal and diabetic rats: a potential confounding factor in the nonclinical assessment of GLP-1-based therapies. *Diabetes* 2014; **63**: 1303-1314 [PMID: 24222349 DOI: 10.2337/db13-1268]
26 **Aston-Mourney K**, Subramanian SL, Zraika S, Samarasekera T, Meier DT, Goldstein LC, Hull RL. One year of sitagliptin treatment protects against islet amyloid-associated β-cell loss and does not induce pancreatitis or pancreatic neoplasia in mice. *Am J Physiol Endocrinol Metab* 2013; **305**: E475-E484 [PMID: 23736544 DOI: 10.1152/ajpendo.00025.2013]
27 **Lu R**, Yang J, Wei R, Ke J, Tian Q, Yu F, Liu J, Zhang J, Hong T. Synergistic anti-tumor effects of liraglutide with metformin on pancreatic cancer cells. *PLoS One* 2018; **13**: e0198938 [PMID: 29897998 DOI: 10.1371/journal.pone.0198938]
28 **Yan M**, Shen M, Xu L, Huang J, He G, An M, Li X, Gao Z, Meng X. Inactivation of Pancreatic Stellate Cells by Exendin-4 Inhibits the Migration and Invasion of Pancreatic Cancer Cells. *Onco Targets Ther* 2020; **13**: 9455-9463 [PMID: 33061431 DOI: 10.2147/OTT.S259853]
29 **Zhao H**, Jiang X, Duan L, Yang L, Wang W, Ren Z. Liraglutide suppresses the metastasis of PANC-1 co-cultured with pancreatic stellate cells through modulating intracellular calcium content. *Endocr J* 2019; **66**: 1053-1062 [PMID: 31474673 DOI: 10.1507/endocrj.EJ19-0215]
30 **Zhao HJ**, Jiang X, Hu LJ, Yang L, Deng LD, Wang YP, Ren ZP. Activation of GLP-1 receptor enhances the chemosensitivity of pancreatic cancer cells. *J Mol Endocrinol* 2020; **64**: 103-113 [PMID: 31855560 DOI: 10.1530/JME-19-0186]
31 **Kawakita E**, Koya D, Kanasaki K. CD26/DPP-4: Type 2 Diabetes Drug Target with Potential Influence on Cancer Biology. *Cancers (Basel)* 2021; **13** [PMID: 34063285 DOI: 10.3390/cancers13092191]
32 **Hollande C**, Boussier J, Ziai J, Nozawa T, Bondet V, Phung W, Lu B, Duffy D, Paradis V, Mallet V, Eberl G, Sandoval W, Schartner JM, Pol S, Barreira da Silva R, Albert ML. Inhibition of the dipeptidyl peptidase DPP4 (CD26) reveals IL-33-dependent eosinophil-mediated control of tumor growth. *Nat Immunol* 2019; **20**: 257-264 [PMID: 30778250 DOI: 10.1038/s41590-019-0321-5]
33 **Barreira da Silva R**, Laird ME, Yatim N, Fiette L, Ingersoll MA, Albert ML. Dipeptidylpeptidase 4 inhibition enhances lymphocyte trafficking, improving both naturally occurring tumor immunity and immunotherapy. *Nat Immunol* 2015; **16**: 850-858 [PMID: 26075911 DOI: 10.1038/ni.3201]
34 **Montvida O**, Green JB, Atherton J, Paul SK. Treatment with incretins does not increase the risk of pancreatic diseases compared to older anti-hyperglycaemic drugs, when added to metformin: real world evidence in people with Type 2 diabetes. *Diabet Med* 2019; **36**: 491-498 [PMID: 30306620 DOI: 10.1111/dme.13835]
35 **Nagel AK**, Ahmed-Sarwar N, Werner PM, Cipriano GC, Van Manen RP, Brown JE. Dipeptidyl Peptidase-4 Inhibitor-Associated Pancreatic Carcinoma: A Review of the FAERS Database. *Ann Pharmacother* 2016; **50**: 27-31 [PMID: 26497885 DOI: 10.1177/1060028015610123]
36 **Azoulay L**, Filion KB, Platt RW, Dahl M, Dormuth CR, Clemens KK, Durand M, Juurlink DN, Targownik LE, Turin TC, Paterson JM, Ernst P; Canadian Network for Observational Drug Effect Studies Investigators. Incretin based drugs and the risk of pancreatic cancer: international multicentre cohort study. *BMJ* 2016; **352**: i581 [PMID: 26888382 DOI: 10.1136/bmj.i581]
37 **Tseng CM**, Liao WC, Chang CY, Lee CT, Tseng CH, Hsu YC, Lin JT. Incretin-based pharmacotherapy and risk of adverse

pancreatic events in the ethnic Chinese with diabetes mellitus: A population-based study in Taiwan. *Pancreatology* 2017; **17**: 76-82 [PMID: 27743712 DOI: 10.1016/j.pan.2016.10.003]

38 **Boniol M**, Franchi M, Bota M, Leclercq A, Guillaume J, van Damme N, Corrao G, Autier P, Boyle P. Incretin-Based Therapies and the Short-term Risk of Pancreatic Cancer: Results From Two Retrospective Cohort Studies. *Diabetes Care* 2018; **41**: 286-292 [PMID: 29146599 DOI: 10.2337/dc17-0280]

39 **Alves C**, Batel-Marques F, Macedo AF. A meta-analysis of serious adverse events reported with exenatide and liraglutide: acute pancreatitis and cancer. *Diabetes Res Clin Pract* 2012; **98**: 271-284 [PMID: 23010561 DOI: 10.1016/j.diabres.2012.09.008]

40 **Chen H**, Zhou X, Chen T, Liu B, Jin W, Gu H, Hong T, Zhang G. Incretin-Based Therapy and Risk of Pancreatic Cancer in Patients with Type 2 Diabetes Mellitus: A Meta-analysis of Randomized Controlled Trials. *Diabetes Ther* 2016; **7**: 725-742 [PMID: 27655330 DOI: 10.1007/s13300-016-0198-3]

41 **Zhang Z**, Chen X, Lu P, Zhang J, Xu Y, He W, Li M, Zhang S, Jia J, Shao S, Xie J, Yang Y, Yu X. Incretin-based agents in type 2 diabetic patients at cardiovascular risk: compare the effect of GLP-1 agonists and DPP-4 inhibitors on cardiovascular and pancreatic outcomes. *Cardiovasc Diabetol* 2017; **16**: 31 [PMID: 28249585 DOI: 10.1186/s12933-017-0512-z]

42 **Pinto LC**, Falcetta MR, Rados DV, Leitão CB, Gross JL. Glucagon-like peptide-1 receptor agonists and pancreatic cancer: a meta-analysis with trial sequential analysis. *Sci Rep* 2019; **9**: 2375 [PMID: 30787365 DOI: 10.1038/s41598-019-38956-2]

43 **Abd El Aziz M**, Cahyadi O, Meier JJ, Schmidt WE, Nauck MA. Incretin-based glucose-lowering medications and the risk of acute pancreatitis and malignancies: a meta-analysis based on cardiovascular outcomes trials. *Diabetes Obes Metab* 2020; **22**: 699-704 [PMID: 31750601 DOI: 10.1111/dom.13924]

44 **Frías JP**, Davies MJ, Rosenstock J, Pérez Manghi FC, Fernández Landó L, Bergman BK, Liu B, Cui X, Brown K; SURPASS-2 Investigators. Tirzepatide *vs* Semaglutide Once Weekly in Patients with Type 2 Diabetes. *N Engl J Med* 2021; **385**: 503-515 [PMID: 34170647 DOI: 10.1056/NEJMoa2107519]

45 **Parker VER**, Robertson D, Wang T, Hornigold DC, Petrone M, Cooper AT, Posch MG, Heise T, Plum-Moerschel L, Schlichthaar H, Klaus B, Ambery PD, Meier JJ, Hirshberg B. Efficacy, Safety, and Mechanistic Insights of Cotadutide, a Dual Receptor Glucagon-Like Peptide-1 and Glucagon Agonist. *J Clin Endocrinol Metab* 2020; **105** [PMID: 31608926 DOI: 10.1210/clinem/dgz047]

World Journal of Gastroenterology

Submit a Manuscript: https://www.f6publishing.com

World J Gastroenterol 2022 July 7; 28(25): 2890-2899

DOI: 10.3748/wjg.v28.i25.2890

ISSN 1007-9327 (print) ISSN 2219-2840 (online)

MINIREVIEWS

Non-alcoholic fatty liver disease and the impact of genetic, epigenetic and environmental factors in the offspring

Natalia Balassiano Wajsbrot, Nathalie Carvalho Leite, Gil F Salles, Cristiane A Villela-Nogueira

Specialty type: Gastroenterology and hepatology

Provenance and peer review: Invited article; Externally peer reviewed.

Peer-review model: Single blind

Peer-review report's scientific quality classification

Grade A (Excellent): 0
Grade B (Very good): B, B
Grade C (Good): 0
Grade D (Fair): 0
Grade E (Poor): 0

P-Reviewer: Lara Riegos JC, Mexico; Sporea I, Romania
A-Editor: Maslennikov R

Received: January 17, 2022
Peer-review started: January 17, 2022
First decision: March 8, 2022
Revised: March 20, 2022
Accepted: May 14, 2022
Article in press: May 14, 2022
Published online: July 7, 2022

Natalia Balassiano Wajsbrot, Nathalie Carvalho Leite, Division of Hepatology, Clementino Fraga Filho University Hospital, Federal University of Rio de Janeiro, Rio de Janeiro 20941-913, Brazil

Gil F Salles, Cristiane A Villela-Nogueira, Department of Internal Medicine, Medical School, Federal University of Rio de Janeiro, Rio de Janeiro 22750-240, Brazil

Corresponding author: Cristiane A Villela-Nogueira, FAASLD, MD, PhD, Full Professor, Department of Internal Medicine, Medical School, Federal University of Rio de Janeiro, Rua Professor Rodolpho Paulo Rocco, 255 Room 9E16, Rio de Janeiro 22750-240, Brazil.
crisvillelanog@gmail.com

Abstract

Non-alcoholic fatty liver disease (NAFLD) is the most common chronic liver disease worldwide and is strongly associated with metabolic deregulation. More recently, a significant impact of parental NAFLD in the offspring was demonstrated and has been widely discussed. However, pathogenetic pathways implicated in the inheritance by the offspring and relatives are still under debate. Probably, multiple mechanisms are involved as well as in NAFLD pathogenesis itself. Among the multifactorial involved mechanisms, genetic, epigenetic and environmental backgrounds are strongly related to NAFLD development in the offspring. Thus, based on recent evidence from the available literature concerning genetic, epigenetic and environmental disease modifiers, this review aimed to discuss the relationship between parental NAFLD and its impact on the offspring.

Key Words: Steatosis; Genetic; Epigenetic; Environmental; Offspring; Non-alcoholic fatty liver disease

©The Author(s) 2022. Published by Baishideng Publishing Group Inc. All rights reserved.

Core Tip: Non-alcoholic fatty liver disease (NAFLD) is a multifactorial disease and familial clustering has been described, although there is still some debate about this association. Among the factors that contribute to the disease in the offspring of NAFLD patients, genetic, epigenetic and environmental factors are the most plausible ones. In this review we describe the main genetic, environmental and epigenetic factors linked to NAFLD and the studies investigating the relation of NAFLD in parents and its offspring. Although there are many experimental studies in animals, there is still much to be elucidated regarding studies and interventions in human beings.

Citation: Wajsbrot NB, Leite NC, Salles GF, Villela-Nogueira CA. Non-alcoholic fatty liver disease and the impact of genetic, epigenetic and environmental factors in the offspring. *World J Gastroenterol* 2022; 28(25): 2890-2899
URL: https://www.wjgnet.com/1007-9327/full/v28/i25/2890.htm
DOI: https://dx.doi.org/10.3748/wjg.v28.i25.2890

INTRODUCTION

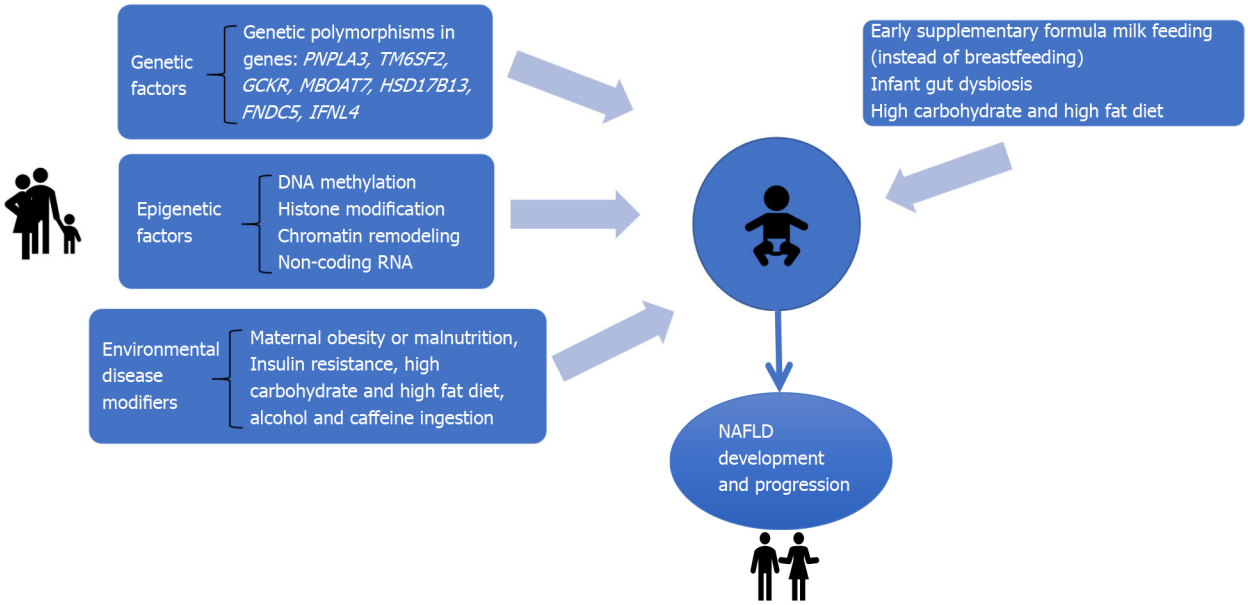
Although non-alcoholic fatty liver disease (NAFLD) is being replaced by metabolic dysfunction-associated fatty liver disease[1], studies concerning genetic and epigenetic factors in this new scenario are still scarce. This way, we will still adopt the nomenclature NAFLD when discussing the studies in this review.

NAFLD affects about 25% to 45% of the world's western population[2]. The spectrum of the disease includes simple steatosis, steatohepatitis with or without fibrosis, leading to cirrhosis, hepatic decompensation and hepatocellular carcinoma (HCC)[3]. NAFLD is currently the third indication for liver transplantation worldwide, and it will potentially be the leading indication in 2030[4].

Many cofactors have been recognized and related to NAFLD's high prevalence and severity. Metabolic syndrome, obesity and type 2 diabetes mellitus (T2DM) are the most relevant factors associated with progression from non-alcoholic fatty liver (NAFL) to non-alcoholic steatohepatitis (NASH) and fibrosis. Patients with T2DM have a higher prevalence of NAFLD, with a high prevalence of NASH and advanced fibrosis[5]. In a bidirectional relation, NAFLD also increases up to 5.5 times the risk of future development of T2DM and could be considered an early predictor of the disease[6]. Ethnicity also influences NAFLD prevalence, with Hispanics presenting a higher prevalence than Caucasians and African Americans, independently of metabolic factors. The genetic and environmental basis could be responsible for these findings in diverse ethnic groups[7]. Accordingly, the observation of NASH and cirrhosis familial clusters suggests a substantial hereditary influence on NAFLD progression [8]. Data from diverse epidemiological, familial aggregation and twin-cohorts studies, with a well-designed methodology, suggest that hepatic steatosis is highly heritable[9-12]. Some of these studies used magnetic resonance elastography to assess liver fibrosis or serum aminotransferase levels to infer hepatic steatosis. They demonstrated a high prevalence of NAFLD in family members of children with NAFLD, monozygotic and dizygotic twins, and first-degree family members of T2DM patients[11,13]. So far, the risk of hepatic steatosis and more severe disease in family members and children of patients with NAFLD is not fully understood, as well as the pathogenetic pathways involved in this process.

Genome-wide association studies have demonstrated the association of single nucleotide polymorphisms (SNP) with NAFLD. Patatin-like phospholipase-domain-containing 3 (rs738409 C>G encoding for PNPLA3 I148M), also known as adiponutrin gene, is located at chromosome 22 and was the first SNP described[14]. Although this is the most robust variant linked to NAFLD, additional genetic variants have been identified subsequently: Transmembrane 6 superfamily member 2 (TM6SF2) [15], glucokinase regulator (GCKR)[16], membrane-bound O-acyltransferase domain-containing 7 (MBOAT7)[17] and hydroxysteroid 17 β-dehydrogenase (HSD17B13)[18], among others. These variants have been associated with multiple pleiotropic effects, including a protective effect for NAFLD as seems to occur with the HSD17B13 polymorphism[18]. The different phenotypes resulting from these genes might partially explain the heritable component and metabolic profile of NAFLD patients and their offspring[9].

Although our understanding of genetic influence has exponentially increased in the past few years, it cannot thoroughly explain the high prevalence of NAFLD in family members of patients with the disease. Experimental studies have investigated different pathways related to NAFLD development in the offspring[9,19,20]. In this context, environmental and epigenetic mechanisms play an essential role in the occurrence and progression of NAFLD. Epigenetic factors involve mechanisms that affect and regulate gene expression without changes in DNA sequences[21]. Therefore, gene expression and cell phenotype related to NAFLD might depend on the genetic information encoded by DNA sequences and epigenetic factors[22]. Figure 1 shows the multifactorial mechanisms implicated in the offspring's NAFLD development. This review aims to discuss the impact of genetic, epigenetic and environment-related variables associated with NAFLD in the offspring.



DOI: 10.3748/wjg.v28.i25.2890 **Copyright** ©The Author(s) 2022.

Figure 1 The interplay among genetic, epigenetic and environmental factors in pre and postnatal periods that impact the development of non-alcoholic fatty liver disease in the offspring. NAFLD: Non-alcoholic fatty liver disease.

HERITAGE AND GENETIC FACTORS

Studies in familial clusters and twin cohorts

Several studies have shown a solid familial clustering of NAFLD, particularly in coexisting metabolic traits[23-25]. Familial combined hyperlipidemia is the most frequent genetic dyslipidemia with a high risk of premature atherothrombotic cardiovascular disease. To assess whether liver steatosis is involved in the pathogenetic pathway of familial combined hyperlipidemia, Brouwers *et al*[23] studied family members with steatosis and twenty spouses. Fatty liver diagnosed by ultrasound was significantly more prevalent in familial combined hyperlipidemia probands (40%) and relatives (35%) compared with their spouses[23]. Moreover, the authors evaluated the correlations between indicators of fatty liver with plasma lipid levels. Liver steatosis and alanine aminotransferase levels correlated with triglyceride levels in all familial combined hyperlipidemia family members[23].

In the multigenerational Framingham Heart Study, a community-based study, individuals with at least one parent presenting hepatic steatosis had two-fold increased odds of having liver steatosis themselves than those without a parental history. More participants without metabolic diseases had liver steatosis if they had at least one parent with liver steatosis than those without any parent with steatosis. On the other hand, there was no difference in the prevalence of steatosis in patients with high cardiometabolic risk among participants with or without a parental history of liver steatosis. Based on these findings, this study suggested that a family history of liver steatosis was a significant risk factor for liver steatosis, but only in metabolically healthy participants[26]. This study goes against the previous one, which showed a higher prevalence of steatosis in those with familial hyperlipidemia. There was no investigation if the genetic aspects of those patients with familial hyperlipidemia could have influenced the higher prevalence of steatosis.

Schwimmer *et al*[11] evaluated 33 overweight children with biopsy-proven NAFLD and 11 overweight children without; NAFLD was significantly more observed in siblings and parents of the NAFLD children group. The correlation of liver fat fraction to body mass index (BMI) was more substantial in overweight children with NAFLD than without NAFLD, showing that there is likely an interaction between BMI and genetic factors on steatosis severity in families of children with NAFLD [11].

Similar to steatosis, hepatic fibrosis in NAFLD is also a heritable trait. Familial aggregation studies revealed a marked coexistence of advanced fibrosis or NAFLD cirrhosis among index patients and their first-degree relatives[24,25]. A cross-sectional analysis demonstrated that first-degree relatives of probands with NAFLD cirrhosis present a 12 times higher risk of advanced fibrosis compared with the relatives of non-NAFLD controls[25]. Interestingly, in another recent cross-sectional study of a prospective cohort comprising 156 twins and their families, the same authors identified a metabolite (3-4-hydroxyphenyl lactate) related to the abundance of several gut microbiota species in individuals with advanced fibrosis. Then, in their conclusions, they propose a link between genetics and microbiota composition concerning NAFLD heritability[27].

The potential genetic link of NAFLD regarding steatosis and fibrosis inheritance triggered the development of studies in twins to evaluate if both steatosis and fibrosis had a significant shared gene. The first study on twins regarding NAFLD inheritance included 60 monozygotic and dizygotic twins [13]. Both liver steatosis and fibrosis were non-invasively quantified by magnetic resonance imaging. The presence of hepatic steatosis by proton-density fat fraction magnetic resonance imaging (MRI) and fibrosis by magnetic resonance elastography correlated between monozygotic twins but not between dizygotic twins, providing evidence that both hepatic steatosis and fibrosis might be heritable traits as well[13].

Following the same rationale, Cui *et al*[10] investigated a prospective cohort of community-dwelling monozygotic and dizygotic twin pairs living in Southern California, using non-invasive proton-density fat fraction MRI and magnetic resonance elastography to assess steatosis and fibrosis. They investigated if individuals prone to genetic susceptibilities to steatosis and fibrosis also had genetic susceptibilities to metabolic variables such as arterial hypertension, dyslipidemia, insulin resistance and diabetes mellitus. The authors have shown that hepatic steatosis and fibrosis have statistically and clinically significant shared genetic determination and metabolic traits such as high-density lipoprotein, triglycerides, insulin resistance, and glycosylated hemoglobin[10]. In another study, the same cohort of twins was evaluated regarding the metabolites of the gut microbiome and its effect on steatosis and liver fibrosis compared to a biopsy-proven NAFLD cohort. This proof of concept study provided a link between the gut-microbiome and 3-lactate that shared gene-effect with hepatic steatosis and fibrosis[27]. Hence, the heritage of NAFLD might relate to multiple factors like a genetic inheritance that could directly affect steatosis and fibrosis and heritable traits of the gut microbiome inherited, or even be influenced by a shared lifestyle in the probands and its parents.

Genetic polymorphisms

Genetic polymorphisms are involved in NAFLD expression regarding its relation with liver steatosis, advanced stages of fibrosis, and even a possible protective effect for disease progression[9,18,28]. However, studies evaluating their impact on the offspring of patients with NAFLD are scarce.

As previously described, PNPLA3 rs738409 C>G variant is associated with hepatic steatosis and severity of NAFLD, progression to cirrhosis and HCC, resulting in a worse prognosis[14]. PNPLA3 encodes a triacylglycerol lipase, and this variant promotes hepatic triglyceride accumulation by restricting substrate access to the catalytic dyad, thus inhibiting triglyceride hydrolysis in the cell[14].

TM6SF2 function is related to regulating cholesterol synthesis and secretion of lipoproteins. Individuals who carry the SNP rs58542926 C>T, which encodes the E167K amino acidic substitution, have a higher risk of NAFLD and histological disease severity. However, there is still a strong debate if it has a protective effect on coronary artery disease. A large study with 60801 patients with coronary artery disease compared to 123504 healthy individuals described a protective effect of the T variant of TM6SF2 on this disease and found an equivalent, although modest effect for the G variant of PNPLA3, that was more intense in the recessive model (genotype GG). At last, an exome study including more than 300000 individuals showed that both TM6SF2 and PNPLA3 polymorphisms induce a protective effect on coronary artery disease and an increased risk of NAFLD[29]. So far, there is no study regarding the evaluation of the impact of TM6SF2 in the offspring of NAFLD patients.

In young adolescents, the rs1260326 C>T variant in GCKR was significantly associated with de novo lipogenesis in those with TT genotype. Another variant in GCKR, the rs780094 A>G, was also associated with NAFLD in a meta-analysis involving 2091 cases and 3003 controls[30].

MBOAT7 was first studied in alcohol abusers and was related to a higher risk of cirrhosis. It encodes a protein involved in the re-acylation of phospholipids as a component of the phospholipid-remodeling pathway, known as the land cycle. Subsequently, the rs641738 C>T variant in this gene was associated with increased hepatic fat, more severe liver damage and fibrosis in NAFLD individuals of European descent; moreover, it has been demonstrated that the T allele may predispose to HCC in patients without cirrhosis[31].

Recently, three polymorphisms have been identified as protective against advanced stages of NAFLD. Results from exome-sequence data from 46455 individuals have shown an association of rs72613567:TA in HSD17B13, a variant with an adenine insertion, with lower levels of aminotransferases and reduced risk of chronic liver disease, including NASH[18]. Pirola *et al*[32] demonstrated the effect of this variant on a Hispanic population submitted to liver biopsy, investigating its association with histological parameters of NAFLD. They identified a lower risk of ballooning degeneration, lobular inflammation and liver fibrosis, mediated by reduced enzyme activity in converting retinol to retinoic acid, suggesting a protective effect in inflammation and fibrosis[32]. Di Sessa *et al*[33] evaluated 685 obese children (mean age 10.56 ± 2.94 years) and demonstrated that carriers of the HSD17B13 A allele had a lower percentage of liver steatosis on ultrasound imaging and lower serum aminotransferases levels[33].

Petta *et al*[34] evaluated the role of irisin, a myokine encoded by the fibronectin type III domain-containing protein 5 gene (FNDC5), in NAFLD patients. The variant rs3480 A>G was not associated with the severity of steatosis and NASH but was correlated with a lower prevalence of clinically significant fibrosis (F2-F4), showing a protective effect against fibrosis. They also found that irisin is expressed in human activated hepatic stellate cells, promoting profibrogenic actions and collagen

synthesis. Thus, the FNDC5 genotype might affect hepatic fibrogenesis by modulating irisin secretion [34].

The genetic polymorphisms associated with NAFLD, their functions and effects are summarized in Table 1.

Concerning NAFLD and family inheritance, the PNPLA3 polymorphism was the only one studied. Overweight and obese children with NAFLD confirmed by histology were evaluated regarding the role of lifetime exposures in association with a genetic predisposition, parental obesity, economic income, programming during fetal life, being breastfed or not, and later biomarkers of dietary habits and lifestyle, correlating with fibrosis. In this study, 75% of the children had fibrosis, independently associated with PNPLA3-GG genotype, parental obesity, not being breastfed, vitamin D levels (< 20 mg/dL) and fructose consumption. Notably, a high socioeconomic maternal occupation was related to less severe fibrosis[35]. These findings reinforce the multifactorial impact of NAFLD inheritance. Recently, Jain *et al*[36] studied 51 patients with NAFLD and their parents compared to 50 individuals without NAFLD and their parents as a control group. They observed that parents of the NAFLD group had a higher frequency of GG genotype when compared to parents of those without NAFLD (15% *vs* 5%)[36]. In this study, no other factors except for PNPLA3 polymorphism were evaluated.

ENVIRONMENTAL AND EPIGENETIC FACTORS: EVIDENCE IN EXPERIMENTAL AND CLINICAL STUDIES

In addition to the genetic information encoded by DNA sequences, epigenetic modifications increase or inhibit the expression of specific genes and affect chromatin structure without modifying nucleotide sequence. Epigenetics implies inheritable changes in the expression of genes, but they can also be acquired and may occur in response to environmental factors, such as nutrition, contributing to disease risk and severity[37]. These alterations can be transferred to the next generation and, in this way, may modify metabolic and NAFLD risk in the offspring. As epigenetic changes can be inheritable and modulated by environmental stimuli, they are considered reversible and could offer new individualized prevention and therapy[37]. So far, the impact of maternal and/or paternal risk factors on the clinical phenotypes of the offspring and the underlying epigenetic mechanisms has not been fully elucidated [37].

Epigenetic phenomena include four regulatory mechanisms: Modification in DNA methylation, covalent histone modification, chromatin remodeling, and RNA-based mechanisms, such as non-coding RNA. DNA methylation is the most studied[22,38].

Experimental studies

Some experimental studies, most of them in mice, tried to elucidate the mechanisms involved in the inheritance of NAFLD and the external factors that could modulate NAFLD development in the offspring through epigenetic factors. It has been shown that many factors during pregnancy may activate lipogenic and inflammatory pathways leading to NAFLD in the progeny[19]. Many authors have studied the impact of breastfeeding, maternal obesity and diet before or during pregnancy in animal models.

Oben *et al*[19] demonstrated that maternal obesity before and throughout pregnancy and lactation could be linked to dysmetabolism in the offspring of female mice. Offspring of obese dams showed a dysmetabolic pattern related to insulin resistance and NAFLD phenotype. Moreover, the offspring of lean dams fed by obese dams presented increased body weight and higher insulin levels and cytokines such as leptin, interleukin-6 and tumor necrosis factor-alpha. Raised levels of leptin were also observed in the breast milk of obese mice compared to lean ones. They proposed that a modified pathway over hypothalamic appetite nuclei signaling by maternal breast milk and neonatal adipose tissue-derived leptin in the early postnatal period was the mechanism behind these findings.

Considering the hypothesis that diet during and after pregnancy might also be involved in NAFLD in the post-weaning period, Pruis *et al*[39] observed that a maternal western-type diet during pregnancy could stimulate metabolic programming or phenotype induction, leading to NAFLD development.

Another study[40] suggested that modifying the diet during pregnancy could benefit the offspring by preventing a disrupted liver lipid profile[61]. When pregnant mice were fed either with a high fat-slow digestive diet or a rapid digestive diet, the offspring of the high fat-rapid digestive diet showed an abnormal liver lipid profile. However, it was not observed in their counterparts born from high fat-slow digestive diet fed-mice.

The relationship between obesity in pregnancy and circadian cycle deregulation might affect metabolic pathways related to NAFLD in adults. Mouralidarane *et al*[20] suggested that, in addition to an obesogenic post-weaning diet, obesity in the mother might lead to NAFLD by disrupting the liver's canonical metabolic rhythmicity gene expression. It implicates the role of abnormal circadian rhythm in the genesis of NAFLD, and alterations in this system during critical developmental periods might be responsible for the onset of the disease later in adulthood.

Table 1 Genetic polymorphisms involved in non-alcoholic fatty liver disease occurrence and related phenotypes

Gene	Variant (s)	Function	Phenotype
PNPLA3	rs738409 C>G	Triglyceride hydrolysis	↑ NAFLD, NASH, fibrosis, HCC
TM6SF2	rs58542926 C>T	Lipoproteins secretion	↑ NAFLD, NASH, fibrosis
GCKR	rs1260326 C>Trs780094 A>G	De novo lipogenesis regulation	↑ NAFLD, NASH, fibrosis
MBOAT7	rs641738 C>T	Phospholipid metabolism	↑ NAFLD and fibrosis
HSD17B13	rs72613567:TA	Conversion of retinol to retinoic acid	↓ NASH and fibrosis
FNDC5	rs3480 A>G	Hepatic fibrogenesis	↓ fibrosis

rs: Reference SNP; NAFLD: Non-alcoholic fatty liver disease; NASH: Non-alcoholic steatohepatitis; HCC: Hepatocellular carcinoma.

Another issue that might be considered regarding further development of NAFLD after birth is ethanol exposure[41]. Shen *et al*[41] developed a rat model of intrauterine growth retardation by prenatal ethanol exposure. These models were fed with normal and high-fat diets. Enhanced liver expression of the insulin growth factor-1 pathway, gluconeogenesis, lipid synthesis and diminished expression of lipid output were accompanied in prenatal ethanol exposure female offspring fed with a high-fat diet.

Oliveira *et al*[42] studied Wistar rats fed with a standard diet and a high-fat diet. Rats born from mice fed with a standard diet were not affected by changes in liver morphology, as did the offspring of high-fat-fed rats. Therefore, the study concluded that fructose intake during adolescence hastens NAFLD onset and reveals a differentiated hepatic response to metabolic insult, depending on the maternal diet. Notwithstanding, Nicolás-Toledo *et al*[43] showed that sucrose intake in adulthood increases fat content only in female rat offspring of dams fed with a low-protein diet during pregnancy, reinforcing the influence of maternal diet in the offspring[43]. Of note, regarding specific epigenetic mechanisms, Suter *et al*[44] have described that epigenetic changes to histones may act as a molecular memory of intrauterine exposure, rendering the risk of adult disease. The genome-wide epigenetic modifications in the fetal liver of susceptible offspring were analyzed, concluding that a maternal high-fat diet is associated with functional alterations to fetal hepatic histones, some of which may persist up to five weeks of age[44].

Another study by Wei *et al*[45] connected NAFLD with epigenetic methylation of specific genes in fathers that can be transmitted from gametes to embryos across generations. They have shown that even paternal diet patterns and prediabetes increase the risk of diabetes in the offspring through gametic epigenetic alterations such as different methylation of genes in the sperm of prediabetic fathers.

All these experimental studies in animal models have revealed that maternal obesity and parental diet during pregnancy or lactation may significantly influence NAFLD and lipid dysmetabolism in the offspring, either by environmental factors or through epigenetic factors, some yet to be better specified, mainly concerning environmental factors. Hence, cofactors as alcohol and fructose intake, among others not yet identified, may activate lipogenic and inflammatory pathways that can lead to NAFLD in the offspring.

Clinical studies

Studies in mothers and newborns: Animal studies confirmed that disruptions during early development could lead to increased susceptibility to metabolic dysfunctions later in life. Likewise, human data support that metabolic dysfunction and its contribution to NAFLD can be closely related to genetic and environmental predisposing factors. However, the precise mechanisms that link changes in pre and postnatal environments with NAFLD development risk in adolescence and adulthood remain poorly understood. These mechanisms involve shifts in lipid metabolism, mitochondrial dysfunction, altered gut microbiota, macrophage programming and activation of epigenetic changes.

In prior studies, it was demonstrated that low birth weight babies exhibit an altered postnatal metabolism after developing an adaptative response to a suboptimal fetal environment[46,47]. Although the mechanism is not entirely understood, exposure to excessive and deficient nutrition during the prenatal period may induce a nutritional mismatch between metabolic efficiency and energy expenditure, increasing the risk of future cardiometabolic diseases. If confirmed, an early and straightforward nutritional intervention might prevent the further development of metabolic diseases in adulthood.

Modi *et al*[48] evaluated 105 healthy mother-neonate pairs. They measured neonatal adipose tissue content by whole-body MRI and intrahepatic lipid content by a proton magnetic resonance spectroscopy. They have demonstrated that infant adiposity, particularly abdominal adipose tissue and intra hepatocellular lipid correlated with increased maternal BMI. Recently, Bedogni *et al*[49] studied the prevalence and risk factors associated with bright liver in 391 1-year-old toddlers born from healthy

mothers. The PNPLA3 I148M variant and maternal weight gain during pregnancy were related to the presence of bright liver in the ultrasonography[49]. Thus, interestingly, the authors suggested a potential gene-environment interchange between PNPLA3 and maternal environmental factors contributing to the risk of fatty liver disease at this earlier age, reinforcing the multifactorial inheritance of NAFLD.

In a large study, Ayonrinde *et al*[50] investigated the relation of maternal factors and infant nutrition with the future development of NAFLD in adolescents aged 17 years. They concluded that average pre-gestational BMI, breastfeeding for at least six months and avoiding early supplementary formula milk feeding reduce the risk of NAFLD diagnosis by liver ultrasound[50]. Additionally, more extended maintenance of breastfeeding resulted in multiple benefits on maternal metabolism and a lower risk of NAFLD in mid-life[51-53].

The Healthy Start study examined a cohort of 951 mothers from different ethnicities[54]. Similar to others, they found that maternal BMI was correlated to increased neonatal adiposity. It has also been demonstrated that increased maternal insulin resistance and fasting glucose levels contribute to this association. Excessive insulin resistance during pregnancy activates placental inflammatory pathways and affects the fetus indirectly by increasing placental nutrient transfer capacity[55].

Still regarding insulin-glucose metabolism, elevated blood glucose and insulin concentrations exacerbate de novo lipogenesis, resulting in increased intrahepatic lipids. Additionally, reduced glucose and pyruvate consumption in parallel with increased triglyceride concentrations and excess fatty acids incompletely oxidized can impair mitochondrial function and gene expression, limiting mitochondrial biogenesis and leading to NAFLD[55].

Peroxisome proliferator-activated receptor γcoactivator 1 (PGC1) gene is a transcriptional coactivator that participates in mitochondrial biogenesis and function and hypermethylation PGC1 promoter was associated with decreased mitochondrial DNA content and insulin resistance in NAFLD patients[56]. In a cross-sectional analysis, Gemma *et al*[57] noticed a positive correlation between maternal BMI and methylation of the PGC1 gene in the umbilical cord of their babies[57]. Based on their findings, the authors speculated that PGC1 might be a promising candidate gene involved in metabolic programming by epigenetic regulation[57]. DNA methylation in regulatory regions of different genes participates in NAFLD development and progression. Other epigenetic mechanisms affecting NAFLD pathogenesis include histone modification and microRNA (miRNA)-mediated processes. Notably, circulating miRNAs have been associated with the presence and heritability of NAFLD in a population study in 40 pairs of twins. Serum miR-331-3p and miR-30c were identified among the 21 miRs that differed between NAFLD and non-NAFLD individuals. These miRNAs are highly inheritable and correlate with each other suggesting a common pathway related to NAFLD[58].

Although shreds of evidence support that high pre-pregnancy BMI in the mothers may lead to significant modifications in the infant gut microbiome[59], few studies link maternal obesity and infant dysbiosis with NAFLD risk in later life. The neonatal gut microbiome can be essential for later homeostasis, and disruption of this early process may increase the risk of future metabolic diseases[60]. Emerging data provides evidence that the gut-liver axis is a fundamental element in the onset and progression of NAFLD. Gut microbiota dysbiosis may contribute to NAFLD by increasing concentrations of bacteria-derived endotoxins, pro-inflammatory cytokines, amino-acid metabolites, short-chain fatty acids and bile acids, all of which might exert effects that promote macrophage programming and activation, favoring liver injury[61].

CONCLUSION

The interplay among multiple genetic, epigenetic and environmental factors determine an individual's susceptibility to NAFLD. Current evidence points to genetic polymorphisms as pleiotropic tools that lead to diverse traits and phenotypes, including typical metabolic profiles in parents and their offspring. Importantly, epigenetic markers can also be transferred to successors by transgenerational epigenetic inheritance. Current studies in mothers and their offspring, although still small, show a direct effect of these factors and their related outcome, NAFLD. Future studies may clarify what interventions are essential for preventing this complex disease in the perinatal or postnatal period to reach the better liver and metabolic-related outcomes in the upcoming adult population.

FOOTNOTES

Author contributions: Leite NC, Salles GF and Villela-Nogueira CA contributed to study design and critical revision of the manuscript; all authors contributed to data analysis, wrote the initial draft and approved the final version.

Conflict-of-interest statement: The authors have nothing to declare.

Open-Access: This article is an open-access article that was selected by an in-house editor and fully peer-reviewed by

external reviewers. It is distributed in accordance with the Creative Commons Attribution NonCommercial (CC BY-NC 4.0) license, which permits others to distribute, remix, adapt, build upon this work non-commercially, and license their derivative works on different terms, provided the original work is properly cited and the use is non-commercial. See: https://creativecommons.org/Licenses/by-nc/4.0/

Country/Territory of origin: Brazil

ORCID number: Natalia Balassiano Wajsbrot 0000-0001-5780-4390; Nathalie Carvalho Leite 0000-0001-9066-0405; Gil F Salles 0000-0001-6318-7077; Cristiane A Villela-Nogueira 0000-0003-1355-2368.

Corresponding Author's Membership in Professional Societies: American Association for the Study of Liver Diseases, No. 114358; European Association for the study of Liver Diseases, No. 60371.

S-Editor: Fan JR
L-Editor: A
P-Editor: Fan JR

REFERENCES

1 **Kawaguchi T**, Tsutsumi T, Nakano D, Torimura T. MAFLD: Renovation of clinical practice and disease awareness of fatty liver. *Hepatol Res* 2021 [PMID: 34472683 DOI: 10.1111/hepr.13706]
2 **Bellentani S**, Marino M. Epidemiology and natural history of non-alcoholic fatty liver disease (NAFLD). *Ann Hepatol* 2009; **8** Suppl 1: S4-S8 [PMID: 19381118]
3 **Angulo P**. Nonalcoholic fatty liver disease. *N Engl J Med* 2002; **346**: 1221-1231 [PMID: 11961152]
4 **Shaker M**, Tabbaa A, Albeldawi M, Alkhouri N. Liver transplantation for nonalcoholic fatty liver disease: new challenges and new opportunities. *World J Gastroenterol* 2014; **20**: 5320-5330 [PMID: 24833862 DOI: 10.3748/wjg.v20.i18.5320]
5 **Leite NC**, Villela-Nogueira CA, Pannain VL, Bottino AC, Rezende GF, Cardoso CR, Salles GF. Histopathological stages of nonalcoholic fatty liver disease in type 2 diabetes: prevalences and correlated factors. *Liver Int* 2011; **31**: 700-706 [PMID: 21457442 DOI: 10.1111/j.1478-3231.2011.02482.x]
6 **Shibata M**, Kihara Y, Taguchi M, Tashiro M, Otsuki M. Nonalcoholic fatty liver disease is a risk factor for type 2 diabetes in middle-aged Japanese men. *Diabetes Care* 2007; **30**: 2940-2944 [PMID: 17666460 DOI: 10.2337/dc07-0792]
7 **Wagenknecht LE**, Scherzinger AL, Stamm ER, Hanley AJ, Norris JM, Chen YD, Bryer-Ash M, Haffner SM, Rotter JI. Correlates and heritability of nonalcoholic fatty liver disease in a minority cohort. *Obesity (Silver Spring)* 2009; **17**: 1240-1246 [PMID: 19584882 DOI: 10.1038/oby.2009.4]
8 **Adibi A**, Janghorbani M, Shayganfar S, Amini M. First-degree relatives of patients with type 2 diabetes mellitus and risk of non-alcoholic Fatty liver disease. *Rev Diabet Stud* 2007; **4**: 236-241 [PMID: 18338077 DOI: 10.1900/RDS.2007.4.236]
9 **Eslam M**, George J. Genetic contributions to NAFLD: leveraging shared genetics to uncover systems biology. *Nat Rev Gastroenterol Hepatol* 2020; **17**: 40-52 [PMID: 31641249 DOI: 10.1038/s41575-019-0212-0]
10 **Cui J**, Chen CH, Lo MT, Schork N, Bettencourt R, Gonzalez MP, Bhatt A, Hooker J, Shaffer K, Nelson KE, Long MT, Brenner DA, Sirlin CB, Loomba R; For The Genetics Of Nafld In Twins Consortium. Shared genetic effects between hepatic steatosis and fibrosis: A prospective twin study. *Hepatology* 2016; **64**: 1547-1558 [PMID: 27315352 DOI: 10.1002/hep.28674]
11 **Schwimmer JB**, Celedon MA, Lavine JE, Salem R, Campbell N, Schork NJ, Shiehmorteza M, Yokoo T, Chavez A, Middleton MS, Sirlin CB. Heritability of nonalcoholic fatty liver disease. *Gastroenterology* 2009; **136**: 1585-1592 [PMID: 19208353 DOI: 10.1053/j.gastro.2009.01.050]
12 **Dickson I**. NAFLD: Increased familial risk of fibrosis in NAFLD. *Nat Rev Gastroenterol Hepatol* 2017; **14**: 450 [PMID: 28676712 DOI: 10.1038/nrgastro.2017.95]
13 **Loomba R**, Schork N, Chen CH, Bettencourt R, Bhatt A, Ang B, Nguyen P, Hernandez C, Richards L, Salotti J, Lin S, Seki E, Nelson KE, Sirlin CB, Brenner D; Genetics of NAFLD in Twins Consortium. Heritability of Hepatic Fibrosis and Steatosis Based on a Prospective Twin Study. *Gastroenterology* 2015; **149**: 1784-1793 [PMID: 26299412 DOI: 10.1053/j.gastro.2015.08.011]
14 **Romeo S**, Kozlitina J, Xing C, Pertsemlidis A, Cox D, Pennacchio LA, Boerwinkle E, Cohen JC, Hobbs HH. Genetic variation in PNPLA3 confers susceptibility to nonalcoholic fatty liver disease. *Nat Genet* 2008; **40**: 1461-1465 [PMID: 18820647 DOI: 10.1038/ng.257]
15 **Kozlitina J**, Smagris E, Stender S, Nordestgaard BG, Zhou HH, Tybjærg-Hansen A, Vogt TF, Hobbs HH, Cohen JC. Exome-wide association study identifies a TM6SF2 variant that confers susceptibility to nonalcoholic fatty liver disease. *Nat Genet* 2014; **46**: 352-356 [PMID: 24531328 DOI: 10.1038/ng.2901]
16 **Yang J**, Trépo E, Nahon P, Cao Q, Moreno C, Letouzé E, Imbeaud S, Bayard Q, Gustot T, Deviere J, Bioulac-Sage P, Calderaro J, Ganne-Carrié N, Laurent A, Blanc JF, Guyot E, Sutton A, Ziol M, Zucman-Rossi J, Nault JC. A 17-Beta-Hydroxysteroid Dehydrogenase 13 Variant Protects From Hepatocellular Carcinoma Development in Alcoholic Liver Disease. *Hepatology* 2019; **70**: 231-240 [PMID: 30908678 DOI: 10.1002/hep.30623]
17 **Basyte-Bacevice V**, Skieceviciene J, Valantiene I, Sumskiene J, Petrenkiene V, Kondrackiene J, Petrauskas D, Lammert F, Kupcinskas J. *TM6SF2* and *MBOAT7* Gene Variants in Liver Fibrosis and Cirrhosis. *Int J Mol Sci* 2019; **20** [PMID: 30875804 DOI: 10.3390/ijms20061277]
18 **Abul-Husn NS**, Cheng X, Li AH, Xin Y, Schurmann C, Stevis P, Liu Y, Kozlitina J, Stender S, Wood GC, Stepanchick AN, Still MD, McCarthy S, O'Dushlaine C, Packer JS, Balasubramanian S, Gosalia N, Esopi D, Kim SY, Mukherjee S,

Lopez AE, Fuller ED, Penn J, Chu X, Luo JZ, Mirshahi UL, Carey DJ, Still CD, Feldman MD, Small A, Damrauer SM, Rader DJ, Zambrowicz B, Olson W, Murphy AJ, Borecki IB, Shuldiner AR, Reid JG, Overton JD, Yancopoulos GD, Hobbs HH, Cohen JC, Gottesman O, Teslovich TM, Baras A, Mirshahi T, Gromada J, Dewey FE. A Protein-Truncating HSD17B13 Variant and Protection from Chronic Liver Disease. *N Engl J Med* 2018; **378**: 1096-1106 [PMID: 29562163 DOI: 10.1056/NEJMoa1712191]

19 **Oben JA**, Mouralidarane A, Samuelsson AM, Matthews PJ, Morgan ML, McKee C, Soeda J, Fernandez-Twinn DS, Martin-Gronert MS, Ozanne SE, Sigala B, Novelli M, Poston L, Taylor PD. Maternal obesity during pregnancy and lactation programs the development of offspring non-alcoholic fatty liver disease in mice. *J Hepatol* 2010; **52**: 913-920 [PMID: 20413174 DOI: 10.1016/j.jhep.2009.12.042]

20 **Mouralidarane A**, Soeda J, Sugden D, Bocianowska A, Carter R, Ray S, Saraswati R, Cordero P, Novelli M, Fusai G, Vinciguerra M, Poston L, Taylor PD, Oben JA. Maternal obesity programs offspring non-alcoholic fatty liver disease through disruption of 24-h rhythms in mice. *Int J Obes (Lond)* 2015; **39**: 1339-1348 [PMID: 25971926 DOI: 10.1038/ijo.2015.85]

21 **Meaney MJ**. Epigenetics and the biological definition of gene x environment interactions. *Child Dev* 2010; **81**: 41-79 [PMID: 20331654 DOI: 10.1111/j.1467-8624.2009.01381.x]

22 **Chen L**, Huang W, Wang L, Zhang Z, Zhang F, Zheng S, Kong D. The effects of epigenetic modification on the occurrence and progression of liver diseases and the involved mechanism. *Expert Rev Gastroenterol Hepatol* 2020; **14**: 259-270 [PMID: 32124651 DOI: 10.1080/17474124.2020.1736042]

23 **Brouwers MC**, Cantor RM, Kono N, Yoon JL, van der Kallen CJ, Bilderbeek-Beckers MA, van Greevenbroek MM, Lusis AJ, de Bruin TW. Heritability and genetic loci of fatty liver in familial combined hyperlipidemia. *J Lipid Res* 2006; **47**: 2799-2807 [PMID: 16971732 DOI: 10.1194/jlr.M600312-JLR200]

24 **Struben VM**, Hespenheide EE, Caldwell SH. Nonalcoholic steatohepatitis and cryptogenic cirrhosis within kindreds. *Am J Med* 2000; **108**: 9-13 [PMID: 11059435 DOI: 10.1016/s0002-9343(99)00315-0]

25 **Caussy C**, Soni M, Cui J, Bettencourt R, Schork N, Chen CH, Ikhwan MA, Bassirian S, Cepin S, Gonzalez MP, Mendler M, Kono Y, Vodkin I, Mekeel K, Haldorson J, Hemming A, Andrews B, Salotti J, Richards L, Brenner DA, Sirlin CB, Loomba R; Familial NAFLD Cirrhosis Research Consortium. Nonalcoholic fatty liver disease with cirrhosis increases familial risk for advanced fibrosis. *J Clin Invest* 2017; **127**: 2697-2704 [PMID: 28628033 DOI: 10.1172/JCI93465]

26 **Long MT**, Gurary EB, Massaro JM, Ma J, Hoffmann U, Chung RT, Benjamin EJ, Loomba R. Parental non-alcoholic fatty liver disease increases risk of non-alcoholic fatty liver disease in offspring. *Liver Int* 2019; **39**: 740-747 [PMID: 30179294 DOI: 10.1111/liv.13956]

27 **Caussy C**, Hsu C, Lo MT, Liu A, Bettencourt R, Ajmera VH, Bassirian S, Hooker J, Sy E, Richards L, Schork N, Schnabl B, Brenner DA, Sirlin CB, Chen CH, Loomba R; Genetics of NAFLD in Twins Consortium. Link between gut-microbiome derived metabolite and shared gene-effects with hepatic steatosis and fibrosis in NAFLD. *Hepatology* 2018; **68**: 918-932 [PMID: 29572891 DOI: 10.1002/hep.29892]

28 **Anstee QM**, Day CP. The Genetics of Nonalcoholic Fatty Liver Disease: Spotlight on PNPLA3 and TM6SF2. *Semin Liver Dis* 2015; **35**: 270-290 [PMID: 26378644 DOI: 10.1055/s-0035-1562947]

29 **Simons N**, Isaacs A, Koek GH, Kuč S, Schaper NC, Brouwers MCGJ. PNPLA3, TM6SF2, and MBOAT7 Genotypes and Coronary Artery Disease. *Gastroenterology* 2017; **152**: 912-913 [PMID: 28157516 DOI: 10.1053/j.gastro.2016.12.020]

30 **Zain SM**, Mohamed Z, Mohamed R. Common variant in the glucokinase regulatory gene rs780094 and risk of nonalcoholic fatty liver disease: a meta-analysis. *J Gastroenterol Hepatol* 2015; **30**: 21-27 [PMID: 25167786 DOI: 10.1111/jgh.12714]

31 **Donati B**, Dongiovanni P, Romeo S, Meroni M, McCain M, Miele L, Petta S, Maier S, Rosso C, De Luca L, Vanni E, Grimaudo S, Romagnoli R, Colli F, Ferri F, Mancina RM, Iruzubieta P, Craxi A, Fracanzani AL, Grieco A, Corradini SG, Aghemo A, Colombo M, Soardo G, Bugianesi E, Reeves H, Anstee QM, Fargion S, Valenti L. MBOAT7 rs641738 variant and hepatocellular carcinoma in non-cirrhotic individuals. *Sci Rep* 2017; **7**: 4492 [PMID: 28674415 DOI: 10.1038/s41598-017-04991-0]

32 **Pirola CJ**, Garaycoechea M, Flichman D, Arrese M, San Martino J, Gazzi C, Castaño GO, Sookoian S. Splice variant rs72613567 prevents worst histologic outcomes in patients with nonalcoholic fatty liver disease. *J Lipid Res* 2019; **60**: 176-185 [PMID: 30323112 DOI: 10.1194/jlr.P089953]

33 **Di Sessa A**, Umano GR, Cirillo G, Passaro AP, Verde V, Cozzolino D, Guarino S, Marzuillo P, Miraglia Del Giudice E. Pediatric non-alcoholic fatty liver disease and kidney function: Effect of *HSD17B13* variant. *World J Gastroenterol* 2020; **26**: 5474-5483 [PMID: 33024398 DOI: 10.3748/wjg.v26.i36.5474]

34 **Petta S**, Valenti L, Svegliati-Baroni G, Ruscica M, Pipitone RM, Dongiovanni P, Rychlicki C, Ferri N, Cammà C, Fracanzani AL, Pierantonelli I, Di Marco V, Meroni M, Giordano D, Grimaudo S, Maggioni M, Cabibi D, Fargion S, Craxì A. Fibronectin Type III Domain-Containing Protein 5 rs3480 A>G Polymorphism, Irisin, and Liver Fibrosis in Patients With Nonalcoholic Fatty Liver Disease. *J Clin Endocrinol Metab* 2017; **102**: 2660-2669 [PMID: 28472477 DOI: 10.1210/jc.2017-00056]

35 **Mosca A**, De Cosmi V, Parazzini F, Raponi M, Alisi A, Agostoni C, Nobili V. The Role of Genetic Predisposition, Programing During Fetal Life, Family Conditions, and Post-natal Diet in the Development of Pediatric Fatty Liver Disease. *J Pediatr* 2019; **211**: 72-77.e4 [PMID: 31128886 DOI: 10.1016/j.jpeds.2019.04.018]

36 **Jain S**, Thanage R, Panchal F, Rathi PM, Munshi R, Udgirkar SS, Contractor QQ, Chandnani SJ, Sujit NP, Debnath P, Singh A. Screening of Family Members of Nonalcoholic Fatty Liver Disease Patients can Detect Undiagnosed Nonalcoholic Fatty Liver Disease Among Them: Is There a Genetic Link? *J Clin Exp Hepatol* 2021; **11**: 466-474 [PMID: 34276153 DOI: 10.1016/j.jceh.2020.10.003]

37 **Jonas W**, Schürmann A. Genetic and epigenetic factors determining NAFLD risk. *Mol Metab* 2021; **50**: 101111 [PMID: 33160101 DOI: 10.1016/j.molmet.2020.101111]

38 **Botello-Manilla AE**, Chávez-Tapia NC, Uribe M, Nuño-Lámbarri N. Genetics and epigenetics purpose in nonalcoholic fatty liver disease. *Expert Rev Gastroenterol Hepatol* 2020; **14**: 733-748 [PMID: 32552211 DOI: 10.1080/17474124.2020.1780915]

39 **Pruis MG**, Lendvai A, Bloks VW, Zwier MV, Baller JF, de Bruin A, Groen AK, Plösch T. Maternal western diet primes non-alcoholic fatty liver disease in adult mouse offspring. *Acta Physiol (Oxf)* 2014; **210**: 215-227 [PMID: 24224789 DOI: 10.1111/apha.12197]

40 **Salto R**, Manzano M, Girón MD, Cano A, Castro A, Vílchez JD, Cabrera E, López-Pedrosa JM. A Slow-Digesting Carbohydrate Diet during Rat Pregnancy Protects Offspring from Non-Alcoholic Fatty Liver Disease Risk through the Modulation of the Carbohydrate-Response Element and Sterol Regulatory Element Binding Proteins. *Nutrients* 2019; **11** [PMID: 31013988 DOI: 10.3390/nu11040844]

41 **Shen L**, Liu Z, Gong J, Zhang L, Wang L, Magdalou J, Chen L, Wang H. Prenatal ethanol exposure programs an increased susceptibility of non-alcoholic fatty liver disease in female adult offspring rats. *Toxicol Appl Pharmacol* 2014; **274**: 263-273 [PMID: 24275070 DOI: 10.1016/j.taap.2013.11.009]

42 **Oliveira LS**, Caetano B, Miranda RA, Souza AFP, Cordeiro A, Woyames J, Andrade CBV, Atella GC, Takiya CM, Fortunato RS, Trevenzoli IH, Souza LL, Pazos-Moura CC. Differentiated Hepatic Response to Fructose Intake during Adolescence Reveals the Increased Susceptibility to Non-Alcoholic Fatty Liver Disease of Maternal High-Fat Diet Male Rat Offspring. *Mol Nutr Food Res* 2020; **64**: e1900838 [PMID: 31916388 DOI: 10.1002/mnfr.201900838]

43 **Nicolás-Toledo L**, Cervantes-Rodríguez M, Cuevas-Romero E, Corona-Quintanilla DL, Pérez-Sánchez E, Zambrano E, Castelán F, Rodríguez-Antolín J. Hitting a triple in the non-alcoholic fatty liver disease field: sucrose intake in adulthood increases fat content in the female but not in the male rat offspring of dams fed a gestational low-protein diet. *J Dev Orig Health Dis* 2018; **9**: 151-159 [PMID: 29249214 DOI: 10.1017/S204017441700099X]

44 **Suter MA**, Ma J, Vuguin PM, Hartil K, Fiallo A, Harris RA, Charron MJ, Aagaard KM. In utero exposure to a maternal high-fat diet alters the epigenetic histone code in a murine model. *Am J Obstet Gynecol* 2014; **210**: 463.e1-463.e11 [PMID: 24793723 DOI: 10.1016/j.ajog.2014.01.045]

45 **Wei Y**, Yang CR, Wei YP, Zhao ZA, Hou Y, Schatten H, Sun QY. Paternally induced transgenerational inheritance of susceptibility to diabetes in mammals. *Proc Natl Acad Sci U S A* 2014; **111**: 1873-1878 [PMID: 24449870 DOI: 10.1073/pnas.1321195111]

46 **Barker DJ**, Hales CN, Fall CH, Osmond C, Phipps K, Clark PM. Type 2 (non-insulin-dependent) diabetes mellitus, hypertension and hyperlipidaemia (syndrome X): relation to reduced fetal growth. *Diabetologia* 1993; **36**: 62-67 [PMID: 8436255 DOI: 10.1007/BF00399095]

47 **Sarr O**, Yang K, Regnault TR. In utero programming of later adiposity: the role of fetal growth restriction. *J Pregnancy* 2012; **2012**: 134758 [PMID: 23251802 DOI: 10.1155/2012/134758]

48 **Modi N**, Murgasova D, Ruager-Martin R, Thomas EL, Hyde MJ, Gale C, Santhakumaran S, Doré CJ, Alavi A, Bell JD. The influence of maternal body mass index on infant adiposity and hepatic lipid content. *Pediatr Res* 2011; **70**: 287-291 [PMID: 21629154 DOI: 10.1203/PDR.0b013e318225f9b1]

49 **Bedogni G**, De Matteis G, Fabrizi M, Alisi A, Crudele A, Pizzolante F, Signore F, Dallapiccola B, Nobili V, Manco M. Association of Bright Liver With the PNPLA3 I148M Gene Variant in 1-Year-Old Toddlers. *J Clin Endocrinol Metab* 2019; **104**: 2163-2170 [PMID: 30649436 DOI: 10.1210/jc.2018-01998]

50 **Ayonrinde OT**, Oddy WH, Adams LA, Mori TA, Beilin LJ, de Klerk N, Olynyk JK. Infant nutrition and maternal obesity influence the risk of non-alcoholic fatty liver disease in adolescents. *J Hepatol* 2017; **67**: 568-576 [PMID: 28619255 DOI: 10.1016/j.jhep.2017.03.029]

51 **Gunderson EP**, Jacobs DR Jr, Chiang V, Lewis CE, Feng J, Quesenberry CP Jr, Sidney S. Duration of lactation and incidence of the metabolic syndrome in women of reproductive age according to gestational diabetes mellitus status: a 20-Year prospective study in CARDIA (Coronary Artery Risk Development in Young Adults). *Diabetes* 2010; **59**: 495-504 [PMID: 19959762 DOI: 10.2337/db09-1197]

52 **Stuebe AM**, Rich-Edwards JW, Willett WC, Manson JE, Michels KB. Duration of lactation and incidence of type 2 diabetes. *JAMA* 2005; **294**: 2601-2610 [PMID: 16304074 DOI: 10.1001/jama.294.20.2601]

53 **Ajmera V**, Liu A, Bettencourt R, Dhar D, Richards L, Loomba R. The impact of genetic risk on liver fibrosis in non-alcoholic fatty liver disease as assessed by magnetic resonance elastography. *Aliment Pharmacol Ther* 2021; **54**: 68-77 [PMID: 33975381 DOI: 10.1111/apt.16392]

54 **Shapiro AL**, Schmiege SJ, Brinton JT, Glueck D, Crume TL, Friedman JE, Dabelea D. Testing the fuel-mediated hypothesis: maternal insulin resistance and glucose mediate the association between maternal and neonatal adiposity, the Healthy Start study. *Diabetologia* 2015; **58**: 937-941 [PMID: 25628236 DOI: 10.1007/s00125-015-3505-z]

55 **Dimasuay KG**, Boeuf P, Powell TL, Jansson T. Placental Responses to Changes in the Maternal Environment Determine Fetal Growth. *Front Physiol* 2016; **7**: 12 [PMID: 26858656 DOI: 10.3389/fphys.2016.00012]

56 **Puigserver P**, Spiegelman BM. Peroxisome proliferator-activated receptor-gamma coactivator 1 alpha (PGC-1 alpha): transcriptional coactivator and metabolic regulator. *Endocr Rev* 2003; **24**: 78-90 [PMID: 12588810 DOI: 10.1210/er.2002-0012]

57 **Gemma C**, Sookoian S, Alvariñas J, García SI, Quintana L, Kanevsky D, González CD, Pirola CJ. Maternal pregestational BMI is associated with methylation of the PPARGC1A promoter in newborns. *Obesity (Silver Spring)* 2009; **17**: 1032-1039 [PMID: 19148128 DOI: 10.1038/oby.2008.605]

58 **Zarrinpar A**, Gupta S, Maurya MR, Subramaniam S, Loomba R. Serum microRNAs explain discordance of non-alcoholic fatty liver disease in monozygotic and dizygotic twins: a prospective study. *Gut* 2016; **65**: 1546-1554 [PMID: 26002934 DOI: 10.1136/gutjnl-2015-309456]

59 **Galley JD**, Bailey M, Kamp Dush C, Schoppe-Sullivan S, Christian LM. Maternal obesity is associated with alterations in the gut microbiome in toddlers. *PLoS One* 2014; **9**: e113026 [PMID: 25409177 DOI: 10.1371/journal.pone.0113026]

60 **Soderborg TK**, Clark SE, Mulligan CE, Janssen RC, Babcock L, Ir D, Young B, Krebs N, Lemas DJ, Johnson LK, Weir T, Lenz LL, Frank DN, Hernandez TL, Kuhn KA, D'Alessandro A, Barbour LA, El Kasmi KC, Friedman JE. The gut microbiota in infants of obese mothers increases inflammation and susceptibility to NAFLD. *Nat Commun* 2018; **9**: 4462 [PMID: 30367045 DOI: 10.1038/s41467-018-06929-0]

61 **Wesolowski SR**, Kasmi KC, Jonscher KR, Friedman JE. Developmental origins of NAFLD: a womb with a clue. *Nat Rev Gastroenterol Hepatol* 2017; **14**: 81-96 [PMID: 27780972 DOI: 10.1038/nrgastro.2016.160]

World Journal of Gastroenterology

Submit a Manuscript: https://www.f6publishing.com

World J Gastroenterol 2022 July 7; 28(25): 2900-2909

DOI: 10.3748/wjg.v28.i25.2900

ISSN 1007-9327 (print) ISSN 2219-2840 (online)

MINIREVIEWS

Role of transcribed ultraconserved regions in gastric cancer and therapeutic perspectives

Shen-Shuo Gao, Zhi-Kai Zhang, Xu-Bin Wang, Yan Ma, Guo-Qing Yin, Xiao-Bo Guo

Specialty type: Gastroenterology and hepatology

Provenance and peer review: Unsolicited article; Externally peer reviewed.

Peer-review model: Single blind

Peer-review report's scientific quality classification

Grade A (Excellent): 0
Grade B (Very good): B, B
Grade C (Good): 0
Grade D (Fair): 0
Grade E (Poor): 0

P-Reviewer: Kamran M, Pakistan; Senchukova M, Russia
A-Editor: Liu X, China

Received: February 21, 2022
Peer-review started: February 21, 2022
First decision: April 5, 2022
Revised: April 8, 2022
Accepted: May 28, 2022
Article in press: May 28, 2022
Published online: July 7, 2022

Shen-Shuo Gao, Zhi-Kai Zhang, Yan Ma, Xiao-Bo Guo, Department of Gastrointestinal Surgery, Shandong Provincial Hospital, Cheeloo College of Medicine, Shandong University, Jinan 250021, Shandong Province, China

Xu-Bin Wang, Yan Ma, Xiao-Bo Guo, Department of Gastrointestinal Surgery, Shandong Provincial Hospital Affiliated to Shandong First Medical University, Jinan 250021, Shandong Province, China

Guo-Qing Yin, Department of Anus and Intestine Surgery, Qingzhou Hospital Affiliated to Shandong First Medical University, Qingzhou 262500, Shandong Province, China

Corresponding author: Xiao-Bo Guo, PhD, Doctor, Department of Gastrointestinal Surgery, Shandong Provincial Hospital, Cheeloo College of Medicine, Shandong University, No. 324 Jingwu Road, Huaiyin District, Jinan 250021, Shandong Province, China.
guo992352@hotmail.com

Abstract

Gastric cancer (GC) is the fourth leading cause of cancer-related death. The occurrence and development of GC is a complex process involving multiple biological mechanisms. Although traditional regulation modulates molecular functions related to the occurrence and development of GC, the comprehensive mechanisms remain unclear. Ultraconserved region (UCR) refers to a genome sequence that is completely conserved in the homologous regions of the human, rat and mouse genomes, with 100% identity, without any insertions or deletions, and often located in fragile sites and tumour-related genes. The transcribed UCR (T-UCR) is transcribed from the UCR and is a new type of long noncoding RNA. Recent studies have found that the expression level of T-UCRs changes during the occurrence and development of GC, revealing a new mechanism underlying GC. Therefore, this article aims to review the relevant research on T-UCRs in GC, as well as the function of T-UCRs and their regulatory role in the occurrence and development of GC, to provide new strategies for GC diagnosis and treatment.

Key Words: Transcribed ultraconserved region; Gastric cancer; Development; Function; Therapeutic perspectives

©The Author(s) 2022. Published by Baishideng Publishing Group Inc. All rights reserved.

Core Tip: Transcribed ultraconserved region (T-UCR) is abnormally expressed in gastric cancer (GC) cells and tumors. It has been found that a variety of T-UCR affects downstream genes and related pathways, and plays a regulatory role in the proliferation, migration and invasion of GC. However, there are few relevant reviews, and this paper aims to review the related studies of T-UCR in GC. And the function of T-UCR and its regulatory role in the occurrence and development of GC, thus providing a new strategy for the diagnosis and treatment of GC.

Citation: Gao SS, Zhang ZK, Wang XB, Ma Y, Yin GQ, Guo XB. Role of transcribed ultraconserved regions in gastric cancer and therapeutic perspectives. *World J Gastroenterol* 2022; 28(25): 2900-2909
URL: https://www.wjgnet.com/1007-9327/full/v28/i25/2900.htm
DOI: https://dx.doi.org/10.3748/wjg.v28.i25.2900

INTRODUCTION

Gastric cancer (GC) is one of the most common malignant tumours in the world. Although the incidence of GC has decreased, GC ranks fourth in cancer-related deaths due to its high lethality[1,2]. Due to the limited specific biomarkers of GC, patients usually have advanced GC when they are diagnosed. The tumourigenesis and development of GC is a multistep process involving countless signal transduction pathways and gene regulation. Among them, oncogenic and tumour suppressor factors, such as the transcribed ultraconserved region (T-UCR), play a key role[3,4].

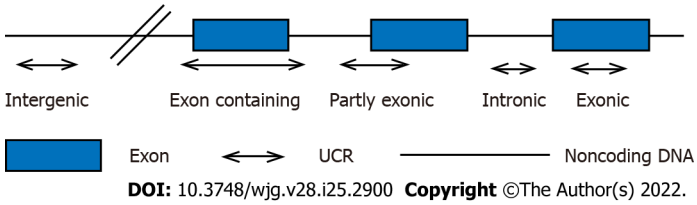
In the human genome, 93% of genes can be transcribed to produce RNA, but only 2% are translated to protein. This type of RNA that lacks the potential for translation into protein is called noncoding RNA[5-9]. According to the number of bases it contains, noncoding RNA is divided into long noncoding RNAs (lncRNAs, > 200 bp) and small noncoding RNAs (< 200 bp, including rRNA, miRNA, snRNA, snoRNA, siRNA and pi-RNA)[10-13]. T-UCRs are lncRNAs, transcribed from UCRs. Recent studies have found that the expression level of T-UCRs is altered and abnormally expressed in human GC[14-17], which reveals a new mechanism for the occurrence and development of GC. Therefore, this article aims to review the relevant research on T-UCRs in GC, to further understand the specific mechanism of T-UCRs in GC cells, which will facilitate preventive measures against GC, early diagnoses, and new treatments.

ULTRACONSERVED REGION AND T-UCR

In 2004, Bejerano *et al*[18] compared the genomes of humans, mice, and rats. They found highly conserved DNA sequences, which were subsequently renamed ultraconserved regions (UCRs)[19]. These regions were absolutely conserved in the three species (100% identical, no insertions or deletions) and were often located in fragile sites and genomic regions of tumour-related genes. UCRs are highly conserved in the evolutionary process, due to the long-distance enhancers and ultraconserved exons that originated from the short interspersed repetitive element retroposon family 400 million years ago. At present, such extreme conservation is still active in the Indonesian "coelacanth"[20].

UCRs represent a small part of the human genome, forming a subset of conserved sequences in intragenic and intergenic regions. UCRs are functional but do not encode proteins[21]. The length of UCRs is between 200 and 799 bp. To date, humans have found at least 481 UCR regions[18,22]. It is known that a large part of these regions can actively transcribe RNA, some of them overlap with known protein-coding sequences, and more than half are predicted to not contain any protein-coding sequences [23]. Based on their overlap with known protein-coding genes, these 481 ultraconserved elements were initially divided into three categories: Nonexons, exons and possibly exons[18,19]. However, based on the positional relationship between UCRs and genes, Mestdagh *et al*[24] reclassified them into 5 categories: Exon containing (4.2%), exonic (5%), partly exonic (5%), intergenic (38.7%) and intronic (42.6%) (Figure 1). The sense/antisense strand of each region produces two transcripts, resulting in a total of 962 possible transcripts: One corresponding to the sense genome sequence (named "+") and the other corresponding to the antisense sequence (named "+ A")[25].

T-UCRs are the transcripts of UCRs[26]. Due to their high degree of conservation, T-UCRs may have fundamental functional importance for the ontogeny and phylogeny of mammals and other vertebrates. Recent studies have shown that a T-UCR acts as a regulator in a variety of pathways (such as pri-miRNA processing, transcription regulation, translation and chromatin modification)[27-29]. It is speculated that T-UCRs may be candidate genes for cancer susceptibility because the transcription level of some UCRs is dysregulated in cancer[30,31].



DOI: 10.3748/wjg.v28.i25.2900 **Copyright** ©The Author(s) 2022.

Figure 1 Ultraconserved region classification based on the relationship between ultraconserved region and gene position. UCR: Ultraconserved region.

T-UCRS AND CANCER

Although transcribed T-UCRs are a type of lncRNA, transcribed by UCRs, they are completely different from lncRNA. T-UCRs are absolutely conserved, while lncRNAs are the least conserved among noncoding RNA[32]. The amazing evolutionary retention of T-UCRs strongly suggests their profound biological role in various physiological responses. As a type of evolutionarily conserved ncRNA, T-UCRs are regarded as essential for life by acting as an antisense transcription inhibitors for nearby protein coding RNA and other ncRNA. T-UCRs are thought to be involved in RNA processing or transcriptional regulation[18]. It has previously been demonstrated that T-UCRs act as regulators of gene expression[20,33]. In recent decades, increasing evidence has shown that T-UCRs are involved in carcinogenesis[23,30,31,34]. Recent studies have identified changes in T-UCR expression patterns associated with specific tumour phenotypes, such as hepatocellular carcinoma[35-37], pancreatic cancer [38,39], bladder cancer[40,41], colorectal cancer[22,26,42,43], prostate cancer[16,25,44,45], cervical cancer [46], neuroblastoma[24], breast cancer[47], lung cancer[22,48-50] and leukaemia[51], indicating a mechanism by which T-UCRs are involved in cancer development. Related studies in GC have also described changes in the expression pattern of T-UCRs[3,4,14-16], indicating that T-UCRs also play a regulatory role in the occurrence and development of GC.

T-UCRS IN GC

Uc.160+ is transcribed from the UCR on the 5q14.1 chromosome band. Honma *et al*[15] used real-time fluorescent quantitative polymerase chain reaction and in situ hybridization to detect Uc.160+. Compared with nontumour tissues, Uc.160+ expression is downregulated in GC and adenoma tissues. To further understand the biological mechanism of Uc.160+ in GC, the Uc.160+ overexpression vector was used to transfect GC cell lines MKN-1 and MKN-45, and then Western blotting was performed to detect the involvement of mitogens. Compared with the control group, the expression of phosphorylated-Akt and phosphorylated-ERK in the cell line transfected with the Uc.160+ overexpression vector decreased, while the expression of PTEN increased. These results suggest that Uc.160+ exclusively repressed the phosphorylation of Akt by regulating PTEN expression. In addition, Pang *et al* [17] found through a series of phenotypic experiments that the proliferation and activity of GC cells were inhibited after Uc.160 was overexpressed, and cell apoptosis was enhanced, which further proved the inhibitory effect of Uc.160 on GC. In conclusion, UC.160 plays an inhibitory role in the occurrence and development of GC.

Sakamoto *et al*[14] analysed the expression and distribution of Uc.63+ by using qRT-PCR and in situ hybridization, and they found that all GC tissues showed high Uc.63+ expression compared with normal tissues. The expression of Uc.63+ was also elevated in GC cell lines. After overexpression of Uc.63+ was induced by transfection of Uc.63+ expression vector, GC cell proliferation was significantly enhanced. After the expression of Uc.63+ was inhibited by siRNA, the proliferation of GC cells was inhibited. These results supported the possibility that Uc.63+ had a carcinogenic effect in GC. Additionally, they found that Uc.63+ had no effect on the survival rate of cancer patients, but Uc.63+ overexpression was associated with advanced cancer and GC classification. Uc.63+ was preferentially overexpressed in diffuse GC, but not in intestinal GC. In conclusion, Uc.63+ plays a key role in the classification and progression of GC.

Goto *et al*[16] found that UC.416+A is overexpressed in GC compared with normal tissues by in situ hybridization. The growth of GC cells was significantly inhibited after Uc.416+A was downregulated by siRNA. These results suggest that UC.416+A, as an oncogene, plays an important role in promoting the proliferation of GC cells. Global genetic analysis using Affymetrix GeneChips showed that the most upregulated gene was IGFBP1 (insulin-like growth factor binding protein 1) when Uc.416+A was overexpressed. Compared with the corresponding nontumour gastric mucosa, IGFBP6 was significantly downregulated in GC tissue, indicating that Uc.416+A might promote the proliferation of GC cells by inhibiting IGFBP6.

Table 1 Transcribed ultraconserved region in gastric cancer

T-UCR name	Location	Orientation	Expression in gastric cancer	Biological or molecular functions in gastric cancer	Ref.
Uc.63+	Chr.2	Sense	Downregulated	Associated with the classification and progression of gastric cancer	[14]
Uc.118	Chr.3	Antisense	Downregulated	-	[16]
Uc.158	Chr.5	Antisense	Downregulated	-	[16]
uc.160	Chr.5	Sense	Downregulated	Inhibits cell proliferation and promotes apoptosis in AGS and SGC-7901 cell lines, promoting gastric cancer tumourigenesis	[15, 17]
Uc.241	-	-	Downregulated	-	[16]
Uc.244	Chr.8	Sense	Down/upregulated	-	[16, 23]
Uc.249	Chr.9	Sense	Down/upregulated	-	[16, 23]
Uc.252	Chr.9	Antisense	Down/upregulated	-	[16, 23]
Uc.261	Chr.9	Sense	Down/upregulated	-	[16, 23]
Uc.282	Chr.9	Sense	Down/upregulated	-	[16, 23]
Uc.283	-	-	-	-	[16]
Uc.346	Chr.12	-	Downregulated	-	[23]
Uc.359	Chr.14	Antisense	Down/upregulated	-	[16, 23]
Uc.416	-	Antisense	Upregulated	Promotes proliferation in MKN-74 cell line, promoting gastric cancer tumourigenesis	[16]

T-UCR: Transcribed ultraconserved region.

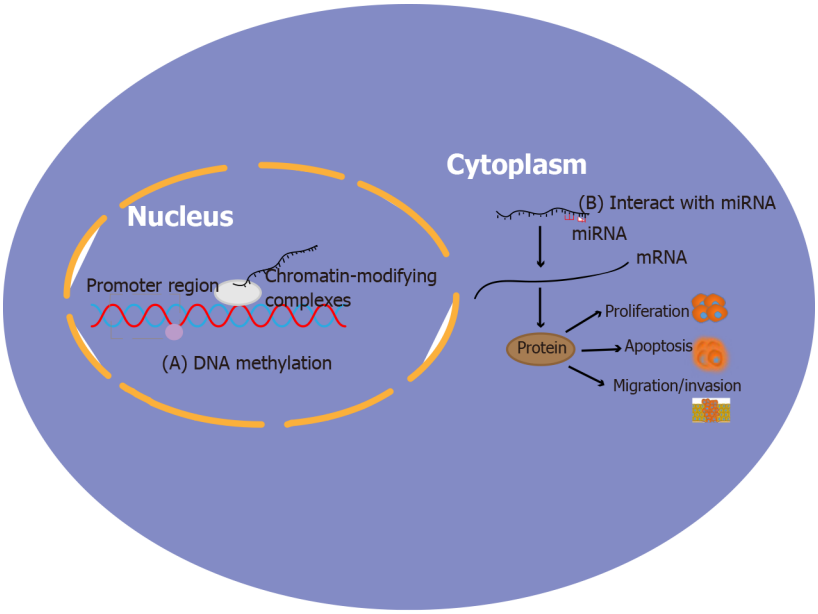
In addition, the expression levels of Uc.118, Uc.158, Uc.241 and Uc.346 were found to be significantly downregulated in GC; Uc.244, Uc.249, Uc.252, Uc.261, Uc.282, Uc.283 and Uc.359 Levels were undetermined (Table 1).

REGULATORY MECHANISM OF T-UCRS IN GC

The regulatory mechanism of T-UCRs in tumourigenesis and the development of cancer is largely unclear, but current studies have found that T-UCR are involved in three different regulatory mechanisms in tumours: CpG island methylation[52], interaction with miRNAs[53-55] and direct binding to the target mRNAs[27,43]. In GC related research, it was only found that T-UCRs participate in the occurrence and development of GC through the first two pathways (Figure 2).

CpG island methylation

The field of epigenetics describes the transmission of information through heritable changes in phenotypes that do not involve changes in DNA sequences during cell division[56]. CpG island methylation, histone modification and chromatin delivery structure are the potential mechanisms of epigenetic transmission, and CpG island methylation is a key component of the changes in gene expression associated with human cancer, especially the expression of GC related genes[57-60]. GC is the most susceptible of all cancers to epigenetic changes without any changes in DNA[59,61-63]. CpG islands are DNA fragments of at least 0.5 kb, that are rich in G:C and CpG content, and are present in approximately 70% of human gene promoters. In other words, CpG islands are tandem repeats of cytosine (C) and guanidine (G), where p is the phosphoric acid between C and G. In brief, the methylation of CpG occurs under the action of methylase whereby the hydrogen on the cytosine (C) 5 carbon atom is replaced by methyl (CH3)[60,64-66]. Demethylation is the opposite process. It has been found that more than 50% of human genes are regulated by promoters including CpG islands[67]. In normal cells, except for genes with inactive X chromosomes or genes related to imprinted genes, promoter CpG islands are usually unmethylated[68]. Although the aetiology is still unclear, promoter CpG island methylation may be related to cancer development and ageing[69]. It is a common feature of



DOI: 10.3748/wjg.v28.i25.2900 **Copyright** ©The Author(s) 2022.

Figure 2 The mechanism by which transcribed ultraconserved region affects gastric cancer. A: DNA methylation; B: Interaction with miRNAs.

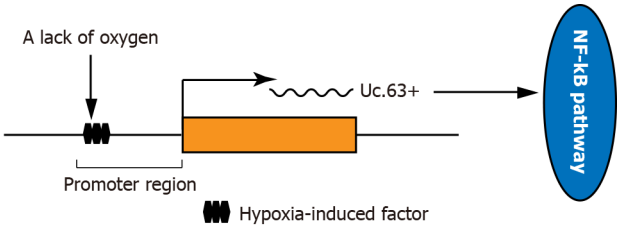
human cancers that low expression of tumour-suppressive ncRNA causes CpG island methylation and then affects epigenetic silencing. Promoter CpG island methylation has been found in almost all human cancer tissue types, and it is an important mechanism for the inactivation of tumour suppressor genes and tumour-related genes[70]. GC is the most common human cancer caused by methylation of the promoter CpG island. Interestingly, T-UCRs undergo DNA methylation-related silencing in cancer cells, and promoter CpG island methylation is now considered to be important for inactivating tumour suppressor genes or tumour-related genes. Previous studies have shown that T-UCR regulation in the occurrence and development of GC is closely related to the methylation of CpG islands of the host gene promoter[16].

Goto *et al*[16] discovered that there are CpG islands approximately 500bp upstream of the Uc.158+A transcription gene. Bisulfite genomic sequencing of GC cell lines and GC tissue samples showed specific DNA methylation of GC, which contained UCRs. The luciferase vector of the CpG island upstream of the Uc.158+A transcription gene proved that when the upstream sequence of the Uc.158+A transcription gene was methylated, reporter activity was significantly inhibited. Thus, this suggests that Uc.158+A expression is silenced by DNA methylation in the promoter region upstream of its transcription gene.

Interaction with miRNAs

Previous studies have shown that miRNAs affect the regulation of gene expression at both the transcriptional and posttranscriptional levels[71-73]. MiRNAs are also almost completely conserved[74,75]. Do T-UCRs interact with miRNAs to regulate the occurrence and development of cancer? In 2007, Calin and his collaborators demonstrated for the first time that certain T-UCRs are altered due to the direct regulation of high-level miRNAs in chronic lymphocytic leukaemia, and the expression of each T-UCR is negatively correlated with the corresponding microRNA level[19]. Recent studies have found that a T-UCR interacts with miR-596 and synergistically promotes the development of bladder cancer[28]. Terreri *et al*[55] found that the formation of T-UCR::miRNA pairs may have different effects, either targeting T-UCR or forming sponges that capture miRNAs. They also reported that the interaction between miRNAs and T-UCRs can act as a network to regulate the availability of certain lncRNAs in bladder urothelial carcinoma cells. These results indicated that miRNAs are involved in the process of T-UCR-mediated tumour regulation. In GC, we found that T-UCRs represent the possible targets of miRNAs[14-16], and these interactions may have biological and prognostic significance for cancer patients.

Goto *et al*[16] determined that the expression of miR-153 in GC cell lines with higher expression of Uc.416+A was significantly reduced, suggesting an inverse correlation between Uc.416+A and miR-153. The direct interaction between Uc.416+A and miR-153 was confirmed by a luciferase activity assay. This result showed that the overexpression of Uc.416+A is related to the downregulation of miR-153 in GC. Overexpression of UC.416+A caused changes in downstream related genes. The expression of insulin-like growth factor binding protein 6 (IGFBP6) was upregulated, and alcohol dehydrogenase 1C (ADH1C), homeobox B5 (HOXB5) and homeobox B6 (HOXB6) levels were downregulated. The expression of IGFBP6, HOXB5 and HOXB6 in GC and adjacent tissues showed statistically significant differences, indicating that the overexpression of UC.416+A is regulated by miR-153, which then affects



DOI: 10.3748/wjg.v28.i25.2900 **Copyright** ©The Author(s) 2022.

Figure 3 The mechanism of Uc.63 + in gastric cancer.

the gene changes of downstream coding proteins and plays a promoting role in the growth of GC.

CpG island methylation and miRNAs play a role together

Honma *et al*[15] found that the low expression of Uc.160+ in GC was caused by methylation of its upstream promoter region, and the low expression of Uc.160+ caused a decrease in PTEN expression, an increase in phosphatase activity and activation of the MAPK pathway. In addition, Pang *et al*[17]'s study found that UC.160 was also regulated by miR-155, which then regulated PTEN and affected the MAPK pathway. In other words, the low expression of UC.160 in GC is regulated by miR-155 and affected by methylation in the upstream promoter region of its transcriptional genes.

Other factors affecting T-UCR transcription

Sakamoto *et al*[14] found that the expression of UC.63+ is regulated by hypoxia. The promoter region located upstream of the Uc.63+ transcription gene is considered to have hypoxia-induced binding sites. Hypoxia induces overexpression of UC.63+, and the overexpression of UC.63+ upregulates its downstream target P65 and activates the NF-KB signalling pathway to promote the occurrence of GC (Figure 3).

CONCLUSION

In GC, T-UCRs change at the transcriptional level, and the abnormal expression of T-UCRs can lead to the occurrence and development of GC. Compared with normal cells, T-UCRs in GC cells have a unique expression profile, which indicates that changes in T-UCRs are involved in this malignant process. This study may provide new ideas and directions for GC diagnosis and prognosis. Compared with coding RNA, T-UCRs have incomparable advantages. Because T-UCRs do not code for proteins, they are relatively less regulated and more accurate. In addition, some T-UCR expression levels are completely different in different stages of cancer, and can also be used as one of the criteria for judging prognosis.

Despite the fact that this new type of dysregulated molecule seems to be useful in future clinical applications, further research is needed before it can be used as a valuable clinical biomarker for GC. First, although approximately 98% of the entire genome contains nonprotein coding genes, the proportion of T-UCRs is currently unclear. Second, current screening methods for T-UCRs (RT-qPCR, T-UCR chip) are useful, but simpler and more practical techniques will help in the identification and screening of disease-related T-UCRs. Third, it has been proven that T-UCRs are involved in the occurrence and development of GC, but their biological mechanism has not been fully elucidated. In addition, more powerful strategies are needed to clarify the regulatory role of T-UCR by constructing an interaction network, or to evaluate its function in typical signalling pathways. Since the knowledge of T-UCR is still in its infancy-especially when compared to other ncRNAs, further research is needed to convincingly incorporate these ncRNAs into the growing field of cancer therapeutics.

At present, there are few studies on T-UCR therapy, so there is still much room to explore treatment measures aimed at T-UCRs. Perhaps we can achieve a treatment purpose by changing the expression of T-UCRs. In the reference cell experiment, restoring the downregulated levels of T-UCRs or suppressing the overexpressed levels of T-UCRs *via* overexpression vectors or small interfering RNA methods can reverse the tumour phenotype. In clinical treatment, we can use the negative regulation between T-UCRs and miRNAs to inhibit the expression of T-UCRs, and methylation inhibitors can be used to restore the expression of T-UCRs with downregulated levels in tumours, thereby delaying or even reversing tumour progression.

Although these hypotheses have not been confirmed, we believe that as research on T-UCRs continues, the insight gained will definitely provide a novel strategy for the diagnosis, prognosis and treatment of tumours.

FOOTNOTES

Author contributions: Guo XB and Gao SS conceived of the presented idea and researched the background of the study; Zhang ZZ and Wang XB prepared the figures and tables; Ma Y and Yin GQ wrote the manuscript; all the authors read and approved the final manuscript.

Supported by National Natural Science Foundation of China, No. 81672379 and No. 81101858; and Natural Science Foundation of Shandong Province, China, No. ZR2016HM16.

Conflict-of-interest statement: There is no conflict of interest.

Open-Access: This article is an open-access article that was selected by an in-house editor and fully peer-reviewed by external reviewers. It is distributed in accordance with the Creative Commons Attribution NonCommercial (CC BY-NC 4.0) license, which permits others to distribute, remix, adapt, build upon this work non-commercially, and license their derivative works on different terms, provided the original work is properly cited and the use is non-commercial. See: https://creativecommons.org/Licenses/by-nc/4.0/

Country/Territory of origin: China

ORCID number: Shen-Shuo Gao 0000-0001-6883-4827; Xiao-Bo Guo 0000-0003-1746-9385.

S-Editor: Yan JP
L-Editor: A
P-Editor: Yan JP

REFERENCES

1 **Thrift AP**, El-Serag HB. Burden of Gastric Cancer. *Clin Gastroenterol Hepatol* 2020; **18**: 534-542 [PMID: 31362118 DOI: 10.1016/j.cgh.2019.07.045]
2 **Sung H**, Ferlay J, Siegel RL, Laversanne M, Soerjomataram I, Jemal A, Bray F. Global Cancer Statistics 2020: GLOBOCAN Estimates of Incidence and Mortality Worldwide for 36 Cancers in 185 Countries. *CA Cancer J Clin* 2021; **71**: 209-249 [PMID: 33538338 DOI: 10.3322/caac.21660]
3 **Ghafouri-Fard S**, Taheri M. Long non-coding RNA signature in gastric cancer. *Exp Mol Pathol* 2020; **113**: 104365 [PMID: 31899194 DOI: 10.1016/j.yexmp.2019.104365]
4 **Yu H**, Rong L. Emerging role of long non-coding RNA in the development of gastric cancer. *World J Gastrointest Oncol* 2018; **10**: 260-270 [PMID: 30254721 DOI: 10.4251/wjgo.v10.i9.260]
5 **ENCODE Project Consortium**. . An integrated encyclopedia of DNA elements in the human genome. *Nature* 2012; **489**: 57-74 [PMID: 22955616 DOI: 10.1038/nature11247]
6 **Oe S**, Kimura T, Yamada H. Regulatory non-coding RNAs in nervous system development and disease. *Front Biosci (Landmark Ed)* 2019; **24**: 1203-1240 [PMID: 31136976 DOI: 10.2741/4776]
7 **Tsagakis I**, Douka K, Birds I, Aspden JL. Long non-coding RNAs in development and disease: conservation to mechanisms. *J Pathol* 2020; **250**: 480-495 [PMID: 32100288 DOI: 10.1002/path.5405]
8 **Rederstorff M**, Hüttenhofer A. Small non-coding RNAs in disease development and host-pathogen interactions. *Curr Opin Mol Ther* 2010; **12**: 684-694 [PMID: 21154160 DOI: 10.2174/1566524107939377741]
9 **Dey BK**, Mueller AC, Dutta A. Long non-coding RNAs as emerging regulators of differentiation, development, and disease. *Transcription* 2014; **5**: e944014 [PMID: 25483404 DOI: 10.4161/21541272.2014.944014]
10 **Beermann J**, Piccoli MT, Viereck J, Thum T. Non-coding RNAs in Development and Disease: Background, Mechanisms, and Therapeutic Approaches. *Physiol Rev* 2016; **96**: 1297-1325 [PMID: 27535639 DOI: 10.1152/physrev.00041.2015]
11 **Zhang X**, Hamblin MH, Yin KJ. The long noncoding RNA Malat1: Its physiological and pathophysiological functions. *RNA Biol* 2017; **14**: 1705-1714 [PMID: 28837398 DOI: 10.1080/15476286.2017.1358347]
12 **Ransohoff JD**, Wei Y, Khavari PA. The functions and unique features of long intergenic non-coding RNA. *Nat Rev Mol Cell Biol* 2018; **19**: 143-157 [PMID: 29138516 DOI: 10.1038/nrm.2017.104]
13 **Romano G**, Veneziano D, Acunzo M, Croce CM. Small non-coding RNA and cancer. *Carcinogenesis* 2017; **38**: 485-491 [PMID: 28449079 DOI: 10.1093/carcin/bgx026]
14 **Sakamoto N**, Sekino Y, Fukada K, Pham QT, Honma R, Taniyama D, Ukai S, Takashima T, Hattori T, Naka K, Tanabe K, Ohdan H, Yasui W. Uc.63+ contributes to gastric cancer progression through regulation of NF-kB signaling. *Gastric Cancer* 2020; **23**: 863-873 [PMID: 32323025 DOI: 10.1007/s10120-020-01070-8]
15 **Honma R**, Goto K, Sakamoto N, Sekino Y, Sentani K, Oue N, Yasui W. Expression and function of Uc.160+, a transcribed ultraconserved region, in gastric cancer. *Gastric Cancer* 2017; **20**: 960-969 [PMID: 28382457 DOI: 10.1007/s10120-017-0714-9]
16 **Goto K**, Ishikawa S, Honma R, Tanimoto K, Sakamoto N, Sentani K, Oue N, Teishima J, Matsubara A, Yasui W. The transcribed-ultraconserved regions in prostate and gastric cancer: DNA hypermethylation and microRNA-associated regulation. *Oncogene* 2016; **35**: 3598-3606 [PMID: 26640143 DOI: 10.1038/onc.2015.445]
17 **Pang L**, Li Q, Zhang Y, Deng B, Wu F, Wang J, Wu K, Ding Y, Yu D. Transcribed ultraconserved noncoding RNA uc.160 acts as a negative regulator in gastric cancer. *Am J Transl Res* 2018; **10**: 2822-2833 [PMID: 30323869]
18 **Bejerano G**, Pheasant M, Makunin I, Stephen S, Kent WJ, Mattick JS, Haussler D. Ultraconserved elements in the human

genome. *Science* 2004; **304**: 1321-1325 [PMID: 15131266 DOI: 10.1126/science.1098119]

19 **Calin GA**, Liu CG, Ferracin M, Hyslop T, Spizzo R, Sevignani C, Fabbri M, Cimmino A, Lee EJ, Wojcik SE, Shimizu M, Tili E, Rossi S, Taccioli C, Pichiorri F, Liu X, Zupo S, Herlea V, Gramantieri L, Lanza G, Alder H, Rassenti L, Volinia S, Schmittgen TD, Kipps TJ, Negrini M, Croce CM. Ultraconserved regions encoding ncRNAs are altered in human leukemias and carcinomas. *Cancer Cell* 2007; **12**: 215-229 [PMID: 17785203 DOI: 10.1016/j.ccr.2007.07.027]

20 **Bejerano G**, Lowe CB, Ahituv N, King B, Siepel A, Salama SR, Rubin EM, Kent WJ, Haussler D. A distal enhancer and an ultraconserved exon are derived from a novel retroposon. *Nature* 2006; **441**: 87-90 [PMID: 16625209 DOI: 10.1038/nature04696]

21 **Qian XX**, Peng JC, Xu AT, Zhao D, Qiao YQ, Wang TR, Shen J, Ran ZH. Noncoding Transcribed Ultraconserved Region (T-UCR) uc.261 Participates in Intestinal Mucosa Barrier Damage in Crohn's Disease. *Inflamm Bowel Dis* 2016; **22**: 2840-2852 [PMID: 27846191 DOI: 10.1097/MIB.0000000000000945]

22 **Zhang Y**, Wang S, Qian W, Ji D, Wang Q, Zhang Z, Ji B, Fu Z, Sun Y. uc.338 targets p21 and cyclin D1 *via* PI3K/AKT pathway activation to promote cell proliferation in colorectal cancer. *Oncol Rep* 2018; **40**: 1119-1128 [PMID: 29901203 DOI: 10.3892/or.2018.6480]

23 **Pereira Zambalde E**, Mathias C, Rodrigues AC, de Souza Fonseca Ribeiro EM, Fiori Gradia D, Calin GA, Carvalho de Oliveira J. Highlighting transcribed ultraconserved regions in human diseases. *Wiley Interdiscip Rev RNA* 2020; **11**: e1567 [PMID: 31489780 DOI: 10.1002/wrna.1567]

24 **Mestdagh P**, Fredlund E, Pattyn F, Rihani A, Van Maerken T, Vermeulen J, Kumps C, Menten B, De Preter K, Schramm A, Schulte J, Noguera R, Schleiermacher G, Janoueix-Lerosey I, Laureys G, Powel R, Nittner D, Marine JC, Ringnér M, Speleman F, Vandesompele J. An integrative genomics screen uncovers ncRNA T-UCR functions in neuroblastoma tumours. *Oncogene* 2010; **29**: 3583-3592 [PMID: 20383195 DOI: 10.1038/onc.2010.106]

25 **Hudson RS**, Yi M, Volfovsky N, Prueitt RL, Esposito D, Volinia S, Liu CG, Schetter AJ, Van Roosbroeck K, Stephens RM, Calin GA, Croce CM, Ambs S. Transcription signatures encoded by ultraconserved genomic regions in human prostate cancer. *Mol Cancer* 2013; **12**: 13 [PMID: 23409773 DOI: 10.1186/1476-4598-12-13]

26 **Sana J**, Hankeova S, Svoboda M, Kiss I, Vyzula R, Slaby O. Expression levels of transcribed ultraconserved regions uc.73 and uc.388 are altered in colorectal cancer. *Oncology* 2012; **82**: 114-118 [PMID: 22328099 DOI: 10.1159/000336479]

27 **Liz J**, Portela A, Soler M, Gómez A, Ling H, Michlewski G, Calin GA, Guil S, Esteller M. Regulation of pri-miRNA processing by a long noncoding RNA transcribed from an ultraconserved region. *Mol Cell* 2014; **55**: 138-147 [PMID: 24910097 DOI: 10.1016/j.molcel.2014.05.005]

28 **Ding L**, Gong C, Zhao J, Liu X, Li T, Rao S, Wang S, Liu Y, Peng S, Xiao W, Xiong C, Wang R, Liang S, Xu H. Noncoding transcribed ultraconserved region (T-UCR) UC.48+ is a novel regulator of high-fat diet induced myocardial ischemia/reperfusion injury. *J Cell Physiol* 2019; **234**: 9849-9861 [PMID: 30417395 DOI: 10.1002/jcp.27674]

29 **Terracciano D**, Terreri S, de Nigris F, Costa V, Calin GA, Cimmino A. The role of a new class of long noncoding RNAs transcribed from ultraconserved regions in cancer. *Biochim Biophys Acta Rev Cancer* 2017; **1868**: 449-455 [PMID: 28916343 DOI: 10.1016/j.bbcan.2017.09.001]

30 **Fabris L**, Calin GA. Understanding the Genomic Ultraconservations: T-UCRs and Cancer. *Int Rev Cell Mol Biol* 2017; **333**: 159-172 [PMID: 28729024 DOI: 10.1016/bs.ircmb.2017.04.004]

31 **Peng JC**, Shen J, Ran ZH. Transcribed ultraconserved region in human cancers. *RNA Biol* 2013; **10**: 1771-1777 [PMID: 24384562 DOI: 10.4161/rna.26995]

32 **Johnsson P**, Lipovich L, Grandér D, Morris KV. Evolutionary conservation of long non-coding RNAs; sequence, structure, function. *Biochim Biophys Acta* 2014; **1840**: 1063-1071 [PMID: 24184936 DOI: 10.1016/j.bbagen.2013.10.035]

33 **Katzman S**, Kern AD, Bejerano G, Fewell G, Fulton L, Wilson RK, Salama SR, Haussler D. Human genome ultraconserved elements are ultraselected. *Science* 2007; **317**: 915 [PMID: 17702936 DOI: 10.1126/science.1142430]

34 **Scaruffi P**. The transcribed-ultraconserved regions: a novel class of long noncoding RNAs involved in cancer susceptibility. *ScientificWorldJournal* 2011; **11**: 340-352 [PMID: 21298224 DOI: 10.1100/tsw.2011.35]

35 **Luo HL**, Chen J, Luo T, Wu FX, Liu JJ, Wang HF, Chen M, Li LQ, Li H. Downregulation of Macrophage-Derived T-UCR uc.306 Associates with Poor Prognosis in Hepatocellular Carcinoma. *Cell Physiol Biochem* 2017; **42**: 1526-1539 [PMID: 28723685 DOI: 10.1159/000479269]

36 **Carotenuto P**, Fassan M, Pandolfo R, Lampis A, Vicentini C, Cascione L, Paulus-Hock V, Boulter L, Guest R, Quagliata L, Hahne JC, Ridgway R, Jamieson T, Athineos D, Veronese A, Visone R, Murgia C, Ferrari G, Guzzardo V, Evans TRJ, MacLeod M, Feng GJ, Dale T, Negrini M, Forbes SJ, Terracciano L, Scarpa A, Patel T, Valeri N, Workman P, Sansom O, Braconi C. Wnt signalling modulates transcribed-ultraconserved regions in hepatobiliary cancers. *Gut* 2017; **66**: 1268-1277 [PMID: 27618837 DOI: 10.1136/gutjnl-2016-312278]

37 **Kogure T**, Yan IK, Lin WL, Patel T. Extracellular Vesicle-Mediated Transfer of a Novel Long Noncoding RNA TUC339: A Mechanism of Intercellular Signaling in Human Hepatocellular Cancer. *Genes Cancer* 2013; **4**: 261-272 [PMID: 24167654 DOI: 10.1177/1947601913499020]

38 **Jiang J**, Azevedo-Pouly AC, Redis RS, Lee EJ, Gusev Y, Allard D, Sutaria DS, Badawi M, Elgamal OA, Lerner MR, Brackett DJ, Calin GA, Schmittgen TD. Globally increased ultraconserved noncoding RNA expression in pancreatic adenocarcinoma. *Oncotarget* 2016; **7**: 53165-53177 [PMID: 27363020 DOI: 10.18632/oncotarget.10242]

39 **Liu C**, Wang J, Yuan X, Qian W, Zhang B, Shi M, Xie J, Shen B, Xu H, Hou Z, Chen H. Long noncoding RNA uc.345 promotes tumorigenesis of pancreatic cancer by upregulation of hnRNPL expression. *Oncotarget* 2016; **7**: 71556-71566 [PMID: 27689400 DOI: 10.18632/oncotarget.12253]

40 **Terreri S**, Mancinelli S, Ferro M, Vitale MC, Perdonà S, Castaldo L, Gigantino V, Mercadante V, De Cecio R, Aquino G, Montella M, Angelini C, Del Prete E, Aprile M, Ciaramella A, Liguori GL, Costa V, Calin GA, La Civita E, Terracciano D, Febbraio F, Cimmino A. Subcellular Localization of uc.8+ as a Prognostic Biomarker in Bladder Cancer Tissue. *Cancers (Basel)* 2021; **13** [PMID: 33567603 DOI: 10.3390/cancers13040681]

41 **Sekino Y**, Sakamoto N, Ishikawa A, Honma R, Shigematsu Y, Hayashi T, Sentani K, Oue N, Teishima J, Matsubara A, Yasui W. Transcribed ultraconserved region Uc.63+ promotes resistance to cisplatin through regulation of androgen

receptor signaling in bladder cancer. *Oncol Rep* 2019; **41**: 3111-3118 [PMID: 30864720 DOI: 10.3892/or.2019.7039]

42 **Zheng Z**, Hong D, Zhang X, Chang Y, Sun N, Lin Z, Li H, Huang S, Zhang R, Xie Q, Huang H, Jin H. uc.77-Downregulation Promotes Colorectal Cancer Cell Proliferation by Inhibiting FBXW8-Mediated CDK4 Protein Degradation. *Front Oncol* 2021; **11**: 673223 [PMID: 34094975 DOI: 10.3389/fonc.2021.673223]

43 **Wang C**, Wang Z, Zhou J, Liu S, Wu C, Huang C, Ding Y. TUC.338 promotes invasion and metastasis in colorectal cancer. *Int J Cancer* 2017; **140**: 1457-1464 [PMID: 27914101 DOI: 10.1002/ijc.30542]

44 **Sekino Y**, Sakamoto N, Goto K, Honma R, Shigematsu Y, Sentani K, Oue N, Teishima J, Matsubara A, Yasui W. Transcribed ultraconserved region Uc.63+ promotes resistance to docetaxel through regulation of androgen receptor signaling in prostate cancer. *Oncotarget* 2017; **8**: 94259-94270 [PMID: 29212226 DOI: 10.18632/oncotarget.21688]

45 **Bao BY**, Lin VC, Yu CC, Yin HL, Chang TY, Lu TL, Lee HZ, Pao JB, Huang CY, Huang SP. Genetic variants in ultraconserved regions associate with prostate cancer recurrence and survival. *Sci Rep* 2016; **6**: 22124 [PMID: 26902966 DOI: 10.1038/srep22124]

46 **Li Q**, Li X, Wang C. Uc.206 regulates cell proliferation and apoptosis by targeting P53 in cervical cancer cells. *Neoplasma* 2016; **63**: 411-418 [PMID: 26925787 DOI: 10.4149/310_151017N538]

47 **Pereira Zambalde E**, Bayraktar R, Schultz Jucoski T, Ivan C, Rodrigues AC, Mathias C, Knutsen E, Silveira de Lima R, Fiori Gradia D, de Souza Fonseca Ribeiro EM, Hannash S, Adrian Calin G, Carvalhode Oliveira J. A novel lncRNA derived from an ultraconserved region: lnc-*uc.147*, a potential biomarker in luminal A breast cancer. *RNA Biol* 2021; **18**: 416-429 [PMID: 34387142 DOI: 10.1080/15476286.2021.1952757]

48 **Liu X**, Zhou X, Deng CJ, Zhao Y, Shen J, Wang Y, Zhang YL. Comprehensive analyses of T-UCR expression profiles and exploration of the efficacy of uc.63- and uc.280+ as biomarkers for lung cancer in Xuanwei, China. *Pathol Res Pract* 2020; **216**: 152978 [PMID: 32360249 DOI: 10.1016/j.prp.2020.152978]

49 **Gao X**, Gao X, Li C, Zhang Y, Gao L. Knockdown of Long Noncoding RNA uc.338 by siRNA Inhibits Cellular Migration and Invasion in Human Lung Cancer Cells. *Oncol Res* 2016; **24**: 337-343 [PMID: 27712590 DOI: 10.3727/096504016X14666990347671]

50 **Tian Y**, Feng Y. Up-regulation of long noncoding RNA uc.338 predicts poor survival in non-small cell lung cancer. *Cancer Biomark* 2018; **22**: 781-785 [PMID: 29843223 DOI: 10.3233/CBM-181331]

51 **das Chagas PF**, de Sousa GR, Kodama MH, de Biagi Junior CAO, Yunes JA, Brandalise SR, Calin GA, Tone LG, Scrideli CA, de Oliveira JC. Ultraconserved long non-coding RNA uc.112 is highly expressed in childhood T versus B-cell acute lymphoblastic leukemia. *Hematol Transfus Cell Ther* 2021; **43**: 28-34 [PMID: 32014474 DOI: 10.1016/j.htct.2019.12.003]

52 **Lujambio A**, Portela A, Liz J, Melo SA, Rossi S, Spizzo R, Croce CM, Calin GA, Esteller M. CpG island hypermethylation-associated silencing of non-coding RNAs transcribed from ultraconserved regions in human cancer. *Oncogene* 2010; **29**: 6390-6401 [PMID: 20802525 DOI: 10.1038/onc.2010.361]

53 **Xiao L**, Wu J, Wang JY, Chung HK, Kalakonda S, Rao JN, Gorospe M. Long Noncoding RNA uc.173 Promotes Renewal of the Intestinal Mucosa by Inducing Degradation of MicroRNA 195. *Gastroenterology* 2018; **154**: 599-611 [PMID: 29042220 DOI: 10.1053/j.gastro.2017.10.009]

54 **Wang JY**, Cui YH, Xiao L, Chung HK, Zhang Y, Rao JN, Gorospe M, Wang JY. Regulation of Intestinal Epithelial Barrier Function by Long Noncoding RNA *uc.173* through Interaction with MicroRNA 29b. *Mol Cell Biol* 2018; **38** [PMID: 29632078 DOI: 10.1128/MCB.00010-18]

55 **Terreri S**, Durso M, Colonna V, Romanelli A, Terracciano D, Ferro M, Perdonà S, Castaldo L, Febbraio F, de Nigris F, Cimmino A. New Cross-Talk Layer between Ultraconserved Non-Coding RNAs, MicroRNAs and Polycomb Protein YY1 in Bladder Cancer. *Genes (Basel)* 2016; **7** [PMID: 27983635 DOI: 10.3390/genes7120127]

56 **Bhol CS**, Panigrahi DP, Praharaj PP, Mahapatra KK, Patra S, Mishra SR, Behera BP, Bhutia SK. Epigenetic modifications of autophagy in cancer and cancer therapeutics. *Semin Cancer Biol* 2020; **66**: 22-33 [PMID: 31158463 DOI: 10.1016/j.semcancer.2019.05.020]

57 **Patel TN**, Roy S, Ravi R. Gastric cancer and related epigenetic alterations. *Ecancermedicalscience* 2017; **11**: 714 [PMID: 28144288 DOI: 10.3332/ecancer.2017.714]

58 **Choi SJ**, Jung SW, Huh S, Chung YS, Cho H, Kang H. Alteration of DNA Methylation in Gastric Cancer with Chemotherapy. *J Microbiol Biotechnol* 2017; **27**: 1367-1378 [PMID: 28621113 DOI: 10.4014/jmb.1704.04035]

59 **Song Y**, Tu J, Cheng Y, Zhou F, Liu P, Zhou S, Gu Y, Sun Y. HHIP Overexpression Suppresses Human Gastric Cancer Progression and Metastasis by Reducing Its CpG Island Methylation. *Front Oncol* 2020; **10**: 1667 [PMID: 33415068 DOI: 10.3389/fonc.2020.01667]

60 **Issa JP**. CpG-island methylation in aging and cancer. *Curr Top Microbiol Immunol* 2000; **249**: 101-118 [PMID: 10802941 DOI: 10.1007/978-3-642-59696-4_7]

61 **Shigeyasu K**, Nagasaka T, Mori Y, Yokomichi N, Kawai T, Fuji T, Kimura K, Umeda Y, Kagawa S, Goel A, Fujiwara T. Clinical Significance of MLH1 Methylation and CpG Island Methylator Phenotype as Prognostic Markers in Patients with Gastric Cancer. *PLoS One* 2015; **10**: e0130409 [PMID: 26121593 DOI: 10.1371/journal.pone.0130409]

62 **Tedaldi G**, Molinari C, São José C, Barbosa-Matos R, André A, Danesi R, Arcangeli V, Ravegnani M, Saragoni L, Morgagni P, Rebuzzi F, Canale M, Pignatta S, Ferracci E, Martinelli G, Ranzani GN, Oliveira C, Calistri D, Ulivi P. Genetic and Epigenetic Alterations of *CDH1* Regulatory Regions in Hereditary and Sporadic Gastric Cancer. *Pharmaceuticals (Basel)* 2021; **14** [PMID: 34066170 DOI: 10.3390/ph14050457]

63 **Loh M**, Liem N, Vaithilingam A, Lim PL, Sapari NS, Elahi E, Mok ZY, Cheng CL, Yan B, Pang B, Salto-Tellez M, Yong WP, Iacopetta B, Soong R. DNA methylation subgroups and the CpG island methylator phenotype in gastric cancer: a comprehensive profiling approach. *BMC Gastroenterol* 2014; **14**: 55 [PMID: 24674026 DOI: 10.1186/1471-230X-14-55]

64 **Curtin K**, Slattery ML, Samowitz WS. CpG island methylation in colorectal cancer: past, present and future. *Patholog Res Int* 2011; **2011**: 902674 [PMID: 21559209 DOI: 10.4061/2011/902674]

65 **Draht MX**, Riedl RR, Niessen H, Carvalho B, Meijer GA, Herman JG, van Engeland M, Melotte V, Smits KM. Promoter CpG island methylation markers in colorectal cancer: the road ahead. *Epigenomics* 2012; **4**: 179-194 [PMID: 22449189 DOI: 10.2217/epi.12.9]

66 **Toyota M**, Ahuja N, Suzuki H, Itoh F, Ohe-Toyota M, Imai K, Baylin SB, Issa JP. Aberrant methylation in gastric cancer associated with the CpG island methylator phenotype. *Cancer Res* 1999; **59**: 5438-5442 [PMID: 10554013]

67 **Nazemalhosseini Mojarad E**, Kuppen PJ, Aghdaei HA, Zali MR. The CpG island methylator phenotype (CIMP) in colorectal cancer. *Gastroenterol Hepatol Bed Bench* 2013; **6**: 120-128 [PMID: 24834258]

68 **De Carvalho DD**, You JS, Jones PA. DNA methylation and cellular reprogramming. *Trends Cell Biol* 2010; **20**: 609-617 [PMID: 20810283 DOI: 10.1016/j.tcb.2010.08.003]

69 **Ehrlich M**. DNA hypermethylation in disease: mechanisms and clinical relevance. *Epigenetics* 2019; **14**: 1141-1163 [PMID: 31284823 DOI: 10.1080/15592294.2019.1638701]

70 **Malta TM**, de Souza CF, Sabedot TS, Silva TC, Mosella MS, Kalkanis SN, Snyder J, Castro AVB, Noushmehr H. Glioma CpG island methylator phenotype (G-CIMP): biological and clinical implications. *Neuro Oncol* 2018; **20**: 608-620 [PMID: 29036500 DOI: 10.1093/neuonc/nox183]

71 **Kang BW**, Chau I. Current status and future potential of predictive biomarkers for immune checkpoint inhibitors in gastric cancer. *ESMO Open* 2020; **5** [PMID: 32817133 DOI: 10.1136/esmoopen-2020-000791]

72 **Gu H**, Zhong Y, Liu J, Shen Q, Wei R, Zhu H, Zhang X, Xia X, Yao M, Ni M. The Role of miR-4256/HOXC8 Signaling Axis in the Gastric Cancer Progression: Evidence From lncRNA-miRNA-mRNA Network Analysis. *Front Oncol* 2021; **11**: 793678 [PMID: 35111675 DOI: 10.3389/fonc.2021.793678]

73 **Liu J**, Wang H, Liao X. MicroRNA-223-5p targets long non-coding RNA TP73 antisense RNA1 to promote the invasion of gastric cancer. *Hum Cell* 2020; **33**: 676-682 [PMID: 32248369 DOI: 10.1007/s13577-020-00349-3]

74 **Mohr AM**, Mott JL. Overview of microRNA biology. *Semin Liver Dis* 2015; **35**: 3-11 [PMID: 25632930 DOI: 10.1055/s-0034-1397344]

75 **Andrés-León E**, Cases I, Alonso S, Rojas AM. Novel miRNA-mRNA interactions conserved in essential cancer pathways. *Sci Rep* 2017; **7**: 46101 [PMID: 28387377 DOI: 10.1038/srep46101]

World Journal of Gastroenterology

Submit a Manuscript: https://www.f6publishing.com

World J Gastroenterol 2022 July 7; 28(25): 2910-2919

DOI: 10.3748/wjg.v28.i25.2910

ISSN 1007-9327 (print) ISSN 2219-2840 (online)

MINIREVIEWS

Multiple roles for cholinergic signaling in pancreatic diseases

Jun-Min Yang, Xiao-Yu Yang, Jian-Hua Wan

Specialty type: Gastroenterology and hepatology

Provenance and peer review: Unsolicited article; Externally peer reviewed.

Peer-review model: Single blind

Peer-review report's scientific quality classification

Grade A (Excellent): 0
Grade B (Very good): B, B, B
Grade C (Good): C, C
Grade D (Fair): 0
Grade E (Poor): 0

P-Reviewer: Aktekin A, Turkey; Kitamura K, Japan; Luyer MDP, Netherlands; Matsuo Y, Japan; Susak YM, Ukraine

Received: February 20, 2022
Peer-review started: February 20, 2022
First decision: May 9, 2022
Revised: May 18, 2022
Accepted: June 13, 2022
Article in press: June 13, 2022
Published online: July 7, 2022

Jun-Min Yang, Xiao-Yu Yang, Jian-Hua Wan, Department of Gastroenterology, The First Affiliated Hospital of Nanchang University, Nanchang 330006, Jiangxi Province, China

Corresponding author: Jian-Hua Wan, MD, PhD, Doctor, Department of Gastroenterology, The First Affiliated Hospital of Nanchang University, No. 17 Yongwaizheng Street, Nanchang 330006, Jiangxi Province, China. 18942337437@163.com

Abstract

Cholinergic nerves are widely distributed throughout the human body and participate in various physiological activities, including sensory, motor, and visceral activities, through cholinergic signaling. Cholinergic signaling plays an important role in pancreatic exocrine secretion. A large number of studies have found that cholinergic signaling overstimulates pancreatic acinar cells through muscarinic receptors, participates in the onset of pancreatic diseases such as acute pancreatitis and chronic pancreatitis, and can also inhibit the progression of pancreatic cancer. However, cholinergic signaling plays a role in reducing pain and inflammation through nicotinic receptors, but enhances the proliferation and invasion of pancreatic tumor cells. This review focuses on the progression of cholinergic signaling and pancreatic diseases in recent years and reveals the role of cholinergic signaling in pancreatic diseases.

Key Words: Acetylcholine; Muscarinic receptors; Nicotinic receptors; Pancreatic exocrine; Pancreatitis; Pancreatic cancer

©The Author(s) 2022. Published by Baishideng Publishing Group Inc. All rights reserved.

Core Tip: The pancreas is a nerve-rich organ that lies behind the peritoneum and is surrounded by many nerve plexuses. Studies have found that cholinergic signaling is involved in the physiological function of the pancreas and the pathological process of pancreatic diseases due to its action on different receptors. Perhaps starting with cholinergic receptors could uncover potential therapeutic targets for pancreatic diseases.

Citation: Yang JM, Yang XY, Wan JH. Multiple roles for cholinergic signaling in pancreatic diseases. *World J Gastroenterol* 2022; 28(25): 2910-2919
URL: https://www.wjgnet.com/1007-9327/full/v28/i25/2910.htm
DOI: https://dx.doi.org/10.3748/wjg.v28.i25.2910

INTRODUCTION

Acetylcholine is a neurotransmitter released by all cholinergic neurons that plays an important role in the peripheral and central nervous systems. The vagus nerve is the longest nerve in the human body and provides innervation to most organs, especially the organs of the digestive system. Cholinergic signaling released by vagus nerve activation mainly acts on cholinergic receptors. According to pharmacological properties, cholinergic receptors are divided into muscarinic receptors (M receptors) and nicotinic receptors (N receptors). Among them, M receptors are widely distributed in smooth muscles and glands and participate in the secretion of glands. M receptors are divided into 5 subtypes of M1-M5, among which M1, M3, and M5 receptors are coupled to Gq protein and M2 and M4 receptors are coupled to Gi protein[1,2]. Each of these five subtypes of M receptors has a unique distribution pattern and is expressed in many areas of the central nervous system and peripheral tissues[1,3-5]. N receptors are ligand-gated ion channels, a pentamer made up of 5 identical homologous subunits (including α1-10, β1-β5, γ, δ, and ε) and retain the potential to be activated by the appropriate agonist[6-8].

The pancreas is an important digestive organ of the human body and plays an important role in the digestion and absorption of food. Pancreatic diseases include acute pancreatitis (AP), chronic pancreatitis (CP), and pancreatic cancer (PCa). Recently, the incidence of pancreatic disease has been increasing year by year, posing a serious threat to human life and health[9-11]. Recent studies have found that cholinergic neuromodulation is involved in the occurrence and development of pancreatic diseases[12-14]. This article reviews the relationship between the three main types of pancreatic diseases (AP, CP, PCa) and cholinergic signaling.

CHOLINERGIC SIGNALING AND PANCREATIC EXOCRINE FUNCTION

The exocrine system of the pancreas includes three different stages, namely, the cephalic stage, the stomach stage, and the intestinal stage[15]. The total amount of daily exocrine activity of the human pancreas is 1-2 L, and approximately 20% occurs in the cephalic stage, which is under the control of the vagus nerve[16-18]. Studies on humans and animals have shown that the cholinergic system regulates pancreatic exocrine secretion through the vagus nerve reflex. These reflexes originate in the dorsal motor nucleus of the vagus nerve in the medulla oblongata. The cranial preganglionic nerve fibers exit the vagus nerve and terminate at the intrapancreatic ganglia to form synapses through cholinergic preganglionic fibers[19,20].

The intrapancreatic ganglion are the integration center of pancreatic exocrine secretion, and terminal axons from these ganglia innervate approximately every acinar artery. Although preganglionic neurotransmission is mediated by acetylcholine through nicotinic and muscarinic receptors, postpancreatic innervation can be mediated by a variety of neurotransmitters, including acetylcholine, which acts on muscarinic receptors in pancreatic acinar cells[21,22]. Cholinergic agonists produce a pancreatic secretory response similar to that of cephalic stimulation, whereas cholinergic antagonists or resection of the vagus nerve can block the cephalic response. These results show that the acetylcholine released by the efferents of the vagus nerve is the primary mechanism by which sensory input leads to the regulation of pancreatic exocrine secretion[23-26]. The cholinergic system also plays an important role in the gastric and intestinal stages of pancreatic secretion regulation[27,28], which are regulated by nerves and bodily fluids. In the intestinal phase, exocrine secretion of the pancreas is mainly regulated by cholecystokinin (CCK) and other gastrointestinal hormones. However, the cholinergic system also plays a role in the secretion of human pancreatic enzymes stimulated by CCK[21,29]. The postprandial physiological dose of CCK mainly acts on the afferent pathway of the vagus nerve in the gastric and duodenal mucosa and stimulates pancreatic exocrine secretion through the cholinergic efferent nerve [19].

Studies have found that human pancreatic acinar cells preferentially express the M3 receptor[30] and are highly expressed in acinar cells[31]. Acetylcholine acts on the M3 receptor and couples to the Gq protein to activate phospholipase C and promote the release of intracellular calcium ions by initiating the phosphatidyl C-inositol triphosphate cascade and promoting the secretion of pancreatic acinar cells [2,32,33]. According to drug blocking studies, the M3 receptor is a muscarinic receptor that stimulates exocrine secretion form the pancreas[34-36]. However, some studies have shown that the M1 receptor can also control pancreatic exocrine secretion[37,38]. The inhibitory effect of drugs blocking the M1 receptor on the secretion of amylase in isolated pancreatic acinar cells was significantly greater than that of drugs blocking the M3 receptor[39]. Carbachol-induced amylase secretion was significantly impaired in the isolated acinars with M1 and M3 muscarinic receptor single knockout (KO) mice, and amylase secretion was eliminated in the acinar preparation of M1 and M3 muscarinic receptor double KO mice. Therefore, it is proposed that cholinergic signaling stimulates the secretion of pancreatic amylase and is mediated by the combination of M1 and M3 receptors[40].

CHOLINERGIC SIGNALING AND AP

AP is a common pancreatic disease in clinical practice. AP has a rapid onset and progress, and high morbidity and mortality worldwide[11]. There are many causes of AP, such as biliary, hypertriglyceridemia, and chronic alcohol consumption, among which biliary is the most common factor[41]. However, the specific mechanism underlying the cause of pancreatitis is not clear. When the human body is exposed to cholinergic agonists, such as scorpion stings or organophosphorus pesticide poisoning, some patients will develop AP. This is direct evidence that cholinergic signaling stimulation is associated with the occurrence of human AP[42-45]. Organophosphorus pesticides can inhibit cholinesterase activity and cause a large amount of acetylcholine to accumulate in nerve endings. Similarly, scorpion toxin is a neurotoxic protein that can cause AP by activating the nerve pathway that releases acetylcholine[46,47].

Pancreatic duct ligation in the rat model is often used to simulate clinical AP caused by gallstone obstruction[48], but the severity of experimental pancreatitis is low except when used in the possum model. However, some researchers have found in a pancreatic duct ligation rat model that cholinergic signaling stimulation can aggravate AP inflammation, suggesting that cholinergic signaling may be involved in the pathogenesis of AP caused by cholangiopancreatic duct obstruction[49]. This may be due to an increase in M3 receptor expression induced by rat pancreatic duct ligation, which amplifies the overstimulation of cholinergic signaling on acinar cells and aggravates the intracellular stress response[50]. Before the first clinical onset of acute alcoholic pancreatitis, patients usually have a history of alcohol abuse for many years. Chronic alcohol intake can affect the exocrine regulation of the pancreas by interfering with the cholinergic and trypsin pathways[51]. Long-term use of ethanol feeding can significantly reduce pancreatic acetylcholinesterase activity in rats, while the expression level of pancreatic cholinergic M receptors has not changed, which increases the level and duration of acetylcholine in the pancreas and leads to excessive cholinergic signaling stimulation and damage to pancreatic acinar cells[52,53]. Ethanol-treated pancreatic acinar cells can aggravate the pancreatic injury response caused by the cholinergic agonist carbachol, and its effect may be mediated by protein kinase C downstream signaling of cholinergic receptors[54]. The cholinergic receptor antagonist atropine can improve pancreatitis induced by the combination of alcohol and cerulein suggesting that the cholinergic signaling pathway is involved in the pathogenesis of pancreatitis[52]. Therefore, acetylcholine may play a key role in the pathogenesis of acute alcoholic pancreatitis[12].

The M3 receptor is highly expressed in human pancreatic acinar cells[31]. Wan *et al*[55] used chemical genetic technology, in which designer receptors are exclusively activated by designer drugs, to express mutant M3 receptors in mouse acinar cells, causing them to lose their response to acetylcholine but can be activated by the specific drug clozapine-N-oxide (CNO). CNO can induce AP in mutant M3 receptor mice and cause more extensive acinar cell necrosis and inflammation. In addition, the use of M3 receptor antagonists can improve the severity of AP induced by cerulein in wild-type mice (Figure 1)[55].

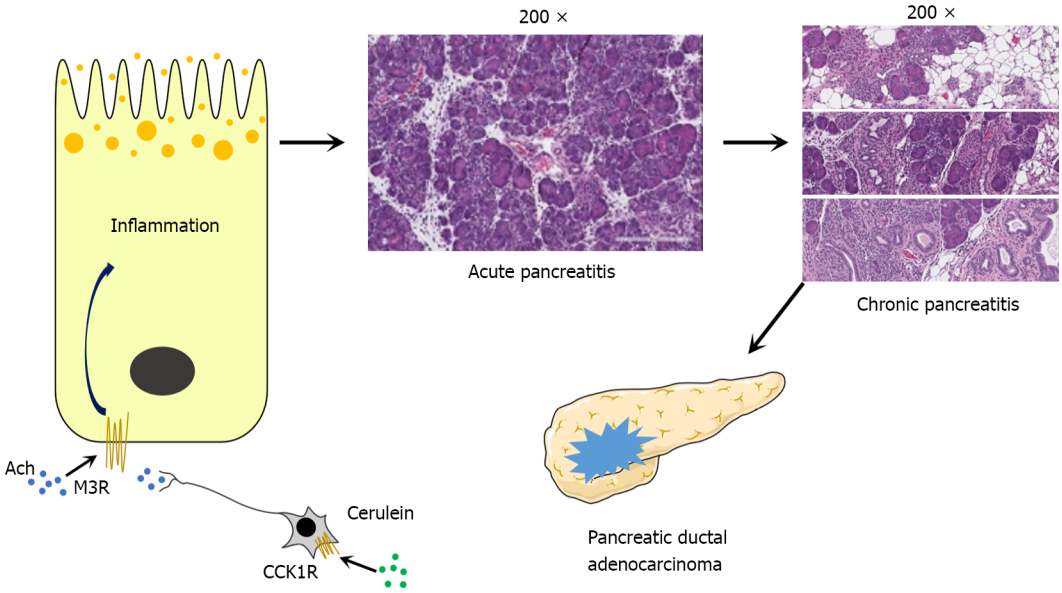
These results indicate that the activation of the M3 receptor by cholinergic nerve terminals releasing acetylcholine may be one of the pathogeneses of AP. Muscarinic receptor agonists stimulate the activation of trypsinogen and nuclear factor-kappaB, which are two key signaling pathways in the pathogenesis of pancreatitis[56]. Reducing inflammation has always been a major goal in the treatment of AP, and many anti-inflammatory drugs have shown beneficial responses in experimental pancreatitis[57]. However, due to the lack of an in-depth understanding of its pathogenesis, there is currently no effective prevention and treatment strategy[58]. Through in-depth research on the cholinergic signaling pathway, it may be possible to block cholinergic signaling early to treat AP, especially in the prevention of pancreatitis after endoscopic retrograde cholangiopancreatography.

CHOLINERGIC SIGNALING AND CP

CP is characterized by chronic inflammation and fibrosis of the pancreas caused by multiple factors. The incidence and prevalence of CP are increasing each year, but there is no current specific treatment[10]. The most common causes of CP are excessive drinking, smoking or genetic mutations[59]. Alcohol is considered to be one of the main risk factors for CP. A total of 40%-70% of CP patients become sick due to excessive alcohol consumption[10]. At the same time, excessive alcohol consumption increases the risk of PCa in individuals[60].

Recurrent episodes of AP have been associated with the progression of CP, which is more common in patients with alcoholism. It has been reported that a certain extent of chronic pancreatic damage was already present at the time of AP episodes[41]. The dose-response relationship between alcohol consumption for AP and CP is linear in males[61]. Alcohol-induced pancreatitis may be caused by the alcohol-induced increased viscosity of pancreatic secretions, which blocks the pancreatic duct, and by premature activation of trypsinogen in acinar cells[62].

The hypertonicity of intrapancreatic cholinergic neurons caused by chronic alcoholism may be involved in the pathogenesis of CP[13]. In CP patients, ethanol can cause excessive sensitivity of the



DOI: 10.3748/wjg.v28.i25.2910 **Copyright** ©The Author(s) 2022.

Figure 1 M3 receptor activation on pancreatic acinar cells causes acute and chronic pancreatitis. Ach: Acetylcholine; CCK: Cholecystokinin.

pancreatic parasympathetic nerve pathways after a meal[63]. This may be due to chronic alcoholism interrupting the autonomic nerve suppression reflex, leading to the decentralization of the intermediate autonomic nerve (located in the gastric antrum and duodenum) and the intrapancreatic ganglia. Due to an increase in the activity of these autonomic nerves, cholinergic signaling in the pancreas increases, resulting in excessive protein secretion and obstruction of pancreatic juice flow[64,65]. Histopathological analysis of pancreatic tissue samples from patients with CP (including alcoholic pancreatitis) demonstrated that the density of cholinergic fibers in the pancreas of patients with CP was slightly increased compared with normal pancreatic tissue samples[66]. Therefore, the impaired interaction between cholinergic signaling and their receptors on pancreatic acinar cells may be a mechanism of the pathogenesis of alcoholic pancreatitis.

Compared with AP, few CP models use injury mechanisms that may be related to the pathogenesis of human diseases, and the clinical relevance of the pathogenesis of most CP models is unclear[48]. However, Wan *et al*[55] used a mutant M3 receptor mouse-induced CP model and observed typical CP features, such as extensive chronic inflammation, fibrosis, adipose tissue infiltration, and pancreatic atrophy (Figure 1)[55]. The use of this M3 receptor model may increase our understanding of the pathophysiological process of human CP and identify specific treatments.

Long-term and recurrent pain is a common characteristic of CP[10,67]. A large number of studies have shown that cholinergic nerves have a significant analgesic effect on chronic neuropathic pain, inflammatory pain, and visceral pain[68-70]. Choline transporter (CHT1) is considered to be the rate-limiting step of neuronal acetylcholine synthesis and is essential for the effective recovery of acetylcholine[71,72]. CHT1 is upregulated in CP-induced pain models. CHT1 specific inhibitor, hemicholinium-3, can significantly enhance CP-induced hyperalgesia and reduce the amount of acetylcholine in the dorsal root ganglia of the pancreas in a dose-dependent manner[73]. Further research found that acetylcholine reduces pain and inflammation through α7 nicotinic acetylcholine receptors (α7 nAChRs)[70,74-77]. The activation of α7 nAChRs enhances the autophagic flux of acinar cells mediated by the transcription factor EB pathway and promotes lysosomal degradation to inhibit acinar cell damage, thereby protecting experimental pancreatitis. It has been suggested that cholinergic signaling activation of endogenous α7 nAChRs in the pancreas may be an endogenous protective mechanism in the process of pancreatitis[78]. Therefore, the use of α7 nAChRs to develop analgesic and anti-inflammatory drugs will be a promising target, especially for the treatment of CP.

CHOLINERGIC SIGNALING AND PCa

PCa is a gastrointestinal tumor with a poor prognosis, and more than 90% of PCa are pancreatic ductal adenocarcinoma (PDAC). According to reports, the 5-year survival rate for PCa patients in the United States from 2009 to 2015 was only 9%[79]. With the continuous increase in morbidity and mortality, PCa is expected to become the second leading cause of cancer-related deaths by 2030[80].

CP has been identified as a risk factor for PCa[81,82]. A meta-analysis found that CP increases the risk of PCa, and five years after the diagnosis of CP the risk of PCa increased nearly eightfold[83]. Pain is a characteristic feature of CP and PCa. Studies have found that increased nerve fiber density and hypertrophy are typical features of CP and PCa, and this pathological change appears to enhance and produce pancreatic neuropathic pain[84]. In vitro, myenteric plexus and dorsal root ganglia neurons were isolated from neonatal rats with CP and PCa, and they exhibited strong neurite outgrowth, more complex branching patterns, and somatic hypertrophy. They findings suggest that the intrapancreatic microenvironment in CP and PCa appears to be a key factor in the generation of pancreatic neuropathy and neural plasticity[85].

In-depth research on the tumor microenvironment found that perineural invasion is an important feature of PCa, which can lead to local tumor recurrence and poor prognosis[86]. As the degree of invasion increases, the survival rate of PCa patients is significantly reduced[87]. However, cholinergic signaling appears to play a tumor-suppressing role in PCa[14,88]. Regarding the relationship between heart rate variability (HRV) as an indicator of vagus nerve activity and the overall survival of patients with advanced PCa, it was found that higher vagus nerve activity represented by a higher initial HRV was significantly associated with a lower risk of death from PCa and was not affected by confounding factors such as age and cancer treatment[89]. The activation of M receptors by cholinergic signals can inhibit the progression of pancreatic tumors. Inhibition of the downstream EGFR/MAPK and PI3K/AKT signaling pathways of PCa cells through the M1 receptor signaling pathway inhibits tumor stem cells, $CD11b^+$ cells, tumor necrosis factor-α levels, and liver metastasis[14].

However, M3 receptor expression seems to be a biomarker for the poor prognosis of PDAC. Compared with patients with low M3 expression, patients with high M3 expression have a worse prognosis and shorter survival time, but the study did not find a statistically significant relationship between M3 receptor expression and peripheral nerve infiltration in PCa[90]. The presence of nonneuronal acetylcholine secreted by fibroblasts and pancreatic stellate cells in the microenvironment of pancreatic tumors activates the M3 receptor, leading to further tumor progression[91].

Oxidative stress and inflammatory signaling contribute to the development of pancreatitis. Español *et al*[92] reported that long-term inflammatory stimulation by LPS plus interferon-γ (IFN-γ) could induce muscarinic receptor expression which mainly involved the M3 and M5 receptors. It could also upregulate the expression of NOS and COX-2 to enhance the effect of carbachol on NO and PGE_2 production[92]. Transgenic overexpression of COX-2 in the pancreas induces CP and the formation of preinvasive ductal tumors[93,94]. Muscarinic receptors could serve as promising therapeutic targets for pancreatic inflammation and could prevent the transformation of CP to PCa.

The increase in acetylcholine levels by nAChRs can inhibit histone deacetylase 1-mediated CCL5 chemokines. This could weaken the ability of PDAC cells to recruit $CD8^+$ T cells and directly inhibit the production of IFN-γ by $CD8^+$ T cells. This effect is conducive to Th2 differentiation and could thereby promot tumor growth[86]. Smoking is one of the main causes of PCa[95], and approximately 21% of PCa deaths are attributed to smoking[96]. Studies have shown that nicotine (nAChR agonist) can increase the proliferation activity and self-renewal ability of PCa stem cells by activating the sonic hedgehog signaling pathway[97]. α7 nAChRs have also been shown to upregulate mucin-4 by coactivating the JAK2/STAT3 downstream signaling cascade *via* the MEK/ERK1/2 pathway, thereby increasing the migration and invasion capabilities of PCa cells[98]. Because the pancreas is widely innervated by many different neurons, the relationship between PCa and the nervous system is complicated[99]. Cholinergic signaling produces different effects based on the different receptor mechanisms involved and may become a potential therapeutic target for PCa in the future.

CONCLUSION

Cholinergic signaling participates in the physiological function of the pancreas and the pathological process of pancreatic diseases. Although the mechanism by which cholinergic signaling regulates pancreatic diseases is still unclear, an increasing number of studies have shown that cholinergic signaling plays a key role in the occurrence and development of pancreatic diseases. There are many animal models of pancreatitis that can be used to help us study the pathogenesis and pathophysiological process of pancreatitis. Among them, rodent models are most commonly used to study acute and CP, but experimental pancreatitis is not necessarily the most relevant to human diseases[48]. Due to the lack of an in-depth understanding of its pathogenesis, there is no effective prevention and treatment strategy at present. Activation of the M3 receptor may be one of the causes of pancreatitis since muscarinic receptors are widely expressed in various glands and smooth muscles throughout the body. The mutant M3 receptor model provides an alternative method for the study of pancreatitis[55]. The pancreas is an organ rich in nervous tissue and lies behind the peritoneum and is surrounded by many nerve plexus. Cholinergic signaling has different effects due to its action on different receptors, which leads to a complicated pathogenesis of pancreatic diseases such as AP, CP, and pancreatic tumors (Table 1). Reducing or enhancing the signal downstream of the receptor may provide a potential therapeutic target in the future.

Table 1 Role of different cholinergic receptors in pancreatic diseases

Pancreatic diseases	Receptor type	Relevant mechanism	Effect	Ref.
Acute pancreatitis	M3	Receptor overexpression	Acinar cell hypersecretion	[49,50,52,55]
Chronic pancreatitis	M3	Cholinergic signaling increases	Acinar cell hypersecretion	[13,64-66]
	M3/M5	Receptor overexpression	Induce fibroblast proliferation	[92]
	α7	Enhances the autophagic flux of acinar cells	Inhibit acinar cell damage	[70,74-77]
Pancreatic cancer	M1	Inhibition of the EGFR/MAPK and PI3K/AKT signaling pathways	Inhibit the progression of pancreatic tumors	[14]
	M3	Receptor overexpression	Induction of preinvasive ductal tumor formation	[90,92-94]
	α7	Activating the JAK2/STAT3 signaling pathway	Increasing the migration and invasion capabilities of tumor cells	[86,97,98]

FOOTNOTES

Author contributions: Yang JM and Yang XY conceived the study, participated in the design, and drafted the manuscript; Wan JH edited and checked the manuscript; all of the authors have read and approved the final manuscript.

Supported by National Natural Science Foundation of China, No. 82100686.

Conflict-of-interest statement: All the authors report no relevant conflicts of interest for this article.

Open-Access: This article is an open-access article that was selected by an in-house editor and fully peer-reviewed by external reviewers. It is distributed in accordance with the Creative Commons Attribution NonCommercial (CC BY-NC 4.0) license, which permits others to distribute, remix, adapt, build upon this work non-commercially, and license their derivative works on different terms, provided the original work is properly cited and the use is non-commercial. See: https://creativecommons.org/Licenses/by-nc/4.0/

Country/Territory of origin: China

ORCID number: Jian-Hua Wan 0000-0002-1364-3844.

S-Editor: Fan JR
L-Editor: A
P-Editor: Fan JR

REFERENCES

1 **Caulfield MP**, Birdsall NJ. International Union of Pharmacology. XVII. Classification of muscarinic acetylcholine receptors. *Pharmacol Rev* 1998; **50**: 279-290 [PMID: 9647869]
2 **Qin K**, Dong C, Wu G, Lambert NA. Inactive-state preassembly of G(q)-coupled receptors and G(q) heterotrimers. *Nat Chem Biol* 2011; **7**: 740-747 [PMID: 21873996 DOI: 10.1038/nchembio.642]
3 **Wess J**. Molecular biology of muscarinic acetylcholine receptors. *Crit Rev Neurobiol* 1996; **10**: 69-99 [PMID: 8853955 DOI: 10.1615/critrevneurobiol.v10.i1.40]
4 **Volpicelli LA**, Levey AI. Muscarinic acetylcholine receptor subtypes in cerebral cortex and hippocampus. *Prog Brain Res* 2004; **145**: 59-66 [PMID: 14650906 DOI: 10.1016/S0079-6123(03)45003-6]
5 **Abrams P**, Andersson KE, Buccafusco JJ, Chapple C, de Groat WC, Fryer AD, Kay G, Laties A, Nathanson NM, Pasricha PJ, Wein AJ. Muscarinic receptors: their distribution and function in body systems, and the implications for treating overactive bladder. *Br J Pharmacol* 2006; **148**: 565-578 [PMID: 16751797 DOI: 10.1038/sj.bjp.0706780]
6 **Wang J**, Lindstrom J. Orthosteric and allosteric potentiation of heteromeric neuronal nicotinic acetylcholine receptors. *Br J Pharmacol* 2018; **175**: 1805-1821 [PMID: 28199738 DOI: 10.1111/bph.13745]
7 **Wonnacott S**, Bermudez I, Millar NS, Tzartos SJ. Nicotinic acetylcholine receptors. *Br J Pharmacol* 2018; **175**: 1785-1788 [PMID: 29878346 DOI: 10.1111/bph.14209]
8 **Hurst R**, Rollema H, Bertrand D. Nicotinic acetylcholine receptors: from basic science to therapeutics. *Pharmacol Ther* 2013; **137**: 22-54 [PMID: 22925690 DOI: 10.1016/j.pharmthera.2012.08.012]
9 **Mizrahi JD**, Surana R, Valle JW, Shroff RT. Pancreatic cancer. *Lancet* 2020; **395**: 2008-2020 [PMID: 32593337 DOI: 10.1016/S0140-6736(20)30974-0]
10 **Beyer G**, Habtezion A, Werner J, Lerch MM, Mayerle J. Chronic pancreatitis. *Lancet* 2020; **396**: 499-512 [PMID:

32798493 DOI: 10.1016/S0140-6736(20)31318-0]
11 **Petrov MS**, Yadav D. Global epidemiology and holistic prevention of pancreatitis. *Nat Rev Gastroenterol Hepatol* 2019; **16**: 175-184 [PMID: 30482911 DOI: 10.1038/s41575-018-0087-5]
12 **Grönroos JM**, Kaila T, Aho HJ, Nevalainen TJ. Decrease in the number of muscarinic receptors in rat pancreas after chronic alcohol intake. *Pharmacol Toxicol* 1989; **64**: 356-359 [PMID: 2748543 DOI: 10.1111/j.1600-0773.1989.tb00664.x]
13 **Tiscornia OM**, Dreiling DA. Physiopathogenic hypothesis of alcoholic pancreatitis: supranormal ecbolic stimulation of the "pancreon" units secondary to the loss of the negative component of pancreas innervation. *Pancreas* 1987; **2**: 604-612 [PMID: 3313381]
14 **Renz BW**, Tanaka T, Sunagawa M, Takahashi R, Jiang Z, Macchini M, Dantes Z, Valenti G, White RA, Middelhoff MA, Ilmer M, Oberstein PE, Angele MK, Deng H, Hayakawa Y, Westphalen CB, Werner J, Remotti H, Reichert M, Tailor YH, Nagar K, Friedman RA, Iuga AC, Olive KP, Wang TC. Cholinergic Signaling *via* Muscarinic Receptors Directly and Indirectly Suppresses Pancreatic Tumorigenesis and Cancer Stemness. *Cancer Discov* 2018; **8**: 1458-1473 [PMID: 30185628 DOI: 10.1158/2159-8290.CD-18-0046]
15 **Konturek SJ**, Pepera J, Zabielski K, Konturek PC, Pawlik T, Szlachcic A, Hahn EG. Brain-gut axis in pancreatic secretion and appetite control. *J Physiol Pharmacol* 2003; **54**: 293-317 [PMID: 14566070]
16 **Anagnostides A**, Chadwick VS, Selden AC, Maton PN. Sham feeding and pancreatic secretion. Evidence for direct vagal stimulation of enzyme output. *Gastroenterology* 1984; **87**: 109-114 [PMID: 6724252]
17 **Konturek SJ**, Zabielski R, Konturek JW, Czarnecki J. Neuroendocrinology of the pancreas; role of brain-gut axis in pancreatic secretion. *Eur J Pharmacol* 2003; **481**: 1-14 [PMID: 14637169 DOI: 10.1016/j.ejphar.2003.08.042]
18 **Defilippi C**, Solomon TE, Valenzuela JE. Pancreatic secretory response to sham feeding in humans. *Digestion* 1982; **23**: 217-223 [PMID: 6183160 DOI: 10.1159/000198753]
19 **Owyang C**. Physiological mechanisms of cholecystokinin action on pancreatic secretion. *Am J Physiol* 1996; **271**: G1-G7 [PMID: 8760100 DOI: 10.1152/ajpgi.1996.271.1.G1]
20 **Owyang C**, Logsdon CD. New insights into neurohormonal regulation of pancreatic secretion. *Gastroenterology* 2004; **127**: 957-969 [PMID: 15362050 DOI: 10.1053/j.gastro.2004.05.002]
21 **Niebergall-Roth E**, Singer MV. Central and peripheral neural control of pancreatic exocrine secretion. *J Physiol Pharmacol* 2001; **52**: 523-538 [PMID: 11787756]
22 **Singer MV**, Niebergall-Roth E. Secretion from acinar cells of the exocrine pancreas: role of enteropancreatic reflexes and cholecystokinin. *Cell Biol Int* 2009; **33**: 1-9 [PMID: 18948215 DOI: 10.1016/j.cellbi.2008.09.008]
23 **Becker S**, Niebel W, Singer MV. Nervous control of gastric and pancreatic secretory response to 2-deoxy-D-glucose in the dog. *Digestion* 1988; **39**: 187-196 [PMID: 3209002 DOI: 10.1159/000199624]
24 **Holtmann G**, Singer MV, Kriebel R, Stäcker KH, Goebell H. Differential effects of acute mental stress on interdigestive secretion of gastric acid, pancreatic enzymes, and gastroduodenal motility. *Dig Dis Sci* 1989; **34**: 1701-1707 [PMID: 2582983 DOI: 10.1007/BF01540047]
25 **Chariot J**, de la Tour J, Anglade P, Rozé C. Cholinergic mechanisms in the pancreas after extrinsic denervation in the rat. *Am J Physiol* 1987; **252**: G755-G761 [PMID: 3591943 DOI: 10.1152/ajpgi.1987.252.6.G755]
26 **Park HS**, Lee YL, Kwon HY, Chey WY, Park HJ. Significant cholinergic role in secretin-stimulated exocrine secretion in isolated rat pancreas. *Am J Physiol* 1998; **274**: G413-G418 [PMID: 9486197 DOI: 10.1152/ajpgi.1998.274.2.G413]
27 **You CH**, Rominger JM, Chey WY. Effects of atropine on the action and release of secretin in humans. *Am J Physiol* 1982; **242**: G608-G611 [PMID: 7091334 DOI: 10.1152/ajpgi.1982.242.6.G608]
28 **Blair EL**, Brown JC, Harper AA, Scratcherd T. A gastric phase of pancreatic secretion. *J Physiol* 1966; **184**: 812-824 [PMID: 5912208 DOI: 10.1113/jphysiol.1966.sp007949]
29 **Gabryelewicz A**, Kulesza E, Konturek SJ. Comparison of loxiglumide, a cholecystokinin receptor antagonist, and atropine on hormonal and meal-stimulated pancreatic secretion in man. *Scand J Gastroenterol* 1990; **25**: 731-738 [PMID: 2396088 DOI: 10.3109/00365529008997600]
30 **Lugea A**, Waldron RT, Mareninova OA, Shalbueva N, Deng N, Su HY, Thomas DD, Jones EK, Messenger SW, Yang J, Hu C, Gukovsky I, Liu Z, Groblewski GE, Gukovskaya AS, Gorelick FS, Pandol SJ. Human Pancreatic Acinar Cells: Proteomic Characterization, Physiologic Responses, and Organellar Disorders in ex Vivo Pancreatitis. *Am J Pathol* 2017; **187**: 2726-2743 [PMID: 28935577 DOI: 10.1016/j.ajpath.2017.08.017]
31 **Ji B**, Bi Y, Simeone D, Mortensen RM, Logsdon CD. Human pancreatic acinar cells lack functional responses to cholecystokinin and gastrin. *Gastroenterology* 2001; **121**: 1380-1390 [PMID: 11729117 DOI: 10.1053/gast.2001.29557]
32 **Futatsugi A**, Nakamura T, Yamada MK, Ebisui E, Nakamura K, Uchida K, Kitaguchi T, Takahashi-Iwanaga H, Noda T, Aruga J, Mikoshiba K. IP3 receptor types 2 and 3 mediate exocrine secretion underlying energy metabolism. *Science* 2005; **309**: 2232-2234 [PMID: 16195467 DOI: 10.1126/science.1114110]
33 **Wakui M**, Osipchuk YV, Petersen OH. Receptor-activated cytoplasmic Ca2+ spiking mediated by inositol trisphosphate is due to Ca2(+)-induced Ca2+ release. *Cell* 1990; **63**: 1025-1032 [PMID: 1701691 DOI: 10.1016/0092-8674(90)90505-9]
34 **Louie DS**, Owyang C. Muscarinic receptor subtypes on rat pancreatic acini: secretion and binding studies. *Am J Physiol* 1986; **251**: G275-G279 [PMID: 2426974 DOI: 10.1152/ajpgi.1986.251.2.G275]
35 **Iwatsuki K**, Horiuchi A, Yonekura H, Homma N, Haruta K, Chiba S. Subtypes of muscarinic receptors in pancreatic exocrine secretion in anesthetized dog. *Pancreas* 1989; **4**: 339-345 [PMID: 2734277 DOI: 10.1097/00006676-198906000-00011]
36 **van Zwam AJ**, Willems PH, Rodrigues de Miranda JF, de Pont JJ, van Ginneken CA. Binding characteristics of the muscarinic receptor subtype in rabbit pancreas. *J Recept Res* 1990; **10**: 119-135 [PMID: 2262932 DOI: 10.3109/10799899009064661]
37 **Singer MV**, Teyssen S, Küppers U. Influence of the M1-receptor antagonists telenzepine and pirenzepine on pancreatic secretory response to intraduodenal tryptophan in dogs. *Digestion* 1991; **48**: 34-42 [PMID: 1868967 DOI: 10.1159/000200661]
38 **Teyssen S**, Niebergall E, Chari ST, Singer MV. Comparison of two dose-response techniques to study the pancreatic

secretory response to intraduodenal tryptophan in the absence and presence of the M1-receptor antagonist telenzepine. *Pancreas* 1995; **10**: 368-373 [PMID: 7792293 DOI: 10.1097/00006676-199505000-00008]
39 **Schmid SW**, Modlin IM, Tang LH, Stoch A, Rhee S, Nathanson MH, Scheele GA, Gorelick FS. Telenzepine-sensitive muscarinic receptors on rat pancreatic acinar cells. *Am J Physiol* 1998; **274**: G734-G741 [PMID: 9575856 DOI: 10.1152/ajpgi.1998.274.4.G734]
40 **Gautam D**, Han SJ, Heard TS, Cui Y, Miller G, Bloodworth L, Wess J. Cholinergic stimulation of amylase secretion from pancreatic acinar cells studied with muscarinic acetylcholine receptor mutant mice. *J Pharmacol Exp Ther* 2005; **313**: 995-1002 [PMID: 15764735 DOI: 10.1124/jpet.105.084855]
41 **Lankisch PG**, Apte M, Banks PA. Acute pancreatitis. *Lancet* 2015; **386**: 85-96 [PMID: 25616312 DOI: 10.1016/S0140-6736(14)60649-8]
42 **Bartholomew C**. Acute scorpion pancreatitis in Trinidad. *Br Med J* 1970; **1**: 666-668 [PMID: 5443968 DOI: 10.1136/bmj.1.5697.666]
43 **Singh S**, Bhardwaj U, Verma SK, Bhalla A, Gill K. Hyperamylasemia and acute pancreatitis following anticholinesterase poisoning. *Hum Exp Toxicol* 2007; **26**: 467-471 [PMID: 17698941 DOI: 10.1177/0960327107076814]
44 **Roeyen G**, Chapelle T, Jorens P, de Beeck BO, Ysebaert D. Necrotizing pancreatitis due to poisoning with organophosphate pesticides. *Acta Gastroenterol Belg* 2008; **71**: 27-29 [PMID: 18396746]
45 **Marsh WH**, Vukov GA, Conradi EC. Acute pancreatitis after cutaneous exposure to an organophosphate insecticide. *Am J Gastroenterol* 1988; **83**: 1158-1160 [PMID: 3421227]
46 **Becerril B**, Marangoni S, Possani LD. Toxins and genes isolated from scorpions of the genus Tityus. *Toxicon* 1997; **35**: 821-835 [PMID: 9241777 DOI: 10.1016/s0041-0101(96)00198-5]
47 **Fletcher PL Jr**, Fletcher MD, Possani LD. Characteristics of pancreatic exocrine secretion produced by venom from the Brazilian scorpion, Tityus serrulatus. *Eur J Cell Biol* 1992; **58**: 259-270 [PMID: 1385124]
48 **Lerch MM**, Gorelick FS. Models of acute and chronic pancreatitis. *Gastroenterology* 2013; **144**: 1180-1193 [PMID: 23622127 DOI: 10.1053/j.gastro.2012.12.043]
49 **Samuel I**, Chaudhary A, Fisher RA, Joehl RJ. Exacerbation of acute pancreatitis by combined cholinergic stimulation and duct obstruction. *Am J Surg* 2005; **190**: 721-724 [PMID: 16226947 DOI: 10.1016/j.amjsurg.2005.07.010]
50 **Samuel I**, Zaheer S, Fisher RA, Zaheer A. Cholinergic receptor induction and JNK activation in acute pancreatitis. *Am J Surg* 2003; **186**: 569-574 [PMID: 14599627 DOI: 10.1016/j.amjsurg.2003.07.016]
51 **Grönroos JM**, Aho HJ, Nevalainen TJ. Cholinergic hypothesis of alcoholic pancreatitis. *Dig Dis* 1992; **10**: 38-45 [PMID: 1551245 DOI: 10.1159/000171342]
52 **Lugea A**, Gong J, Nguyen J, Nieto J, French SW, Pandol SJ. Cholinergic mediation of alcohol-induced experimental pancreatitis. *Alcohol Clin Exp Res* 2010; **34**: 1768-1781 [PMID: 20626730 DOI: 10.1111/j.1530-0277.2010.01264.x]
53 **Grönroos JM**, Kaila T, Hietaranta AJ. Alcohol, pancreatic muscarinic receptors and acute pancreatitis. *Exp Toxicol Pathol* 1994; **45**: 503-505 [PMID: 8054828 DOI: 10.1016/S0940-2993(11)80513-0]
54 **Satoh A**, Gukovskaya AS, Reeve JR Jr, Shimosegawa T, Pandol SJ. Ethanol sensitizes NF-kappaB activation in pancreatic acinar cells through effects on protein kinase C-epsilon. *Am J Physiol Gastrointest Liver Physiol* 2006; **291**: G432-G438 [PMID: 16574982 DOI: 10.1152/ajpgi.00579.2005]
55 **Wan J**, Wang J, Wagner LE 2nd, Wang OH, Gui F, Chen J, Zhu X, Haddock AN, Edenfield BH, Haight B, Mukhopadhyay D, Wang Y, Yule DI, Bi Y, Ji B. Pancreas-specific CHRM3 activation causes pancreatitis in mice. *JCI Insight* 2021; **6** [PMID: 34314386 DOI: 10.1172/jci.insight.132585]
56 **Zhan X**, Wang F, Bi Y, Ji B. Animal models of gastrointestinal and liver diseases. Animal models of acute and chronic pancreatitis. *Am J Physiol Gastrointest Liver Physiol* 2016; **311**: G343-G355 [PMID: 27418683 DOI: 10.1152/ajpgi.00372.2015]
57 **Sah RP**, Saluja A. Molecular mechanisms of pancreatic injury. *Curr Opin Gastroenterol* 2011; **27**: 444-451 [PMID: 21844752 DOI: 10.1097/MOG.0b013e328349e346]
58 **Kambhampati S**, Park W, Habtezion A. Pharmacologic therapy for acute pancreatitis. *World J Gastroenterol* 2014; **20**: 16868-16880 [PMID: 25493000 DOI: 10.3748/wjg.v20.i45.16868]
59 **Singh VK**, Yadav D, Garg PK. Diagnosis and Management of Chronic Pancreatitis: A Review. *JAMA* 2019; **322**: 2422-2434 [PMID: 31860051 DOI: 10.1001/jama.2019.19411]
60 **Wang YT**, Gou YW, Jin WW, Xiao M, Fang HY. Association between alcohol intake and the risk of pancreatic cancer: a dose-response meta-analysis of cohort studies. *BMC Cancer* 2016; **16**: 212 [PMID: 26968702 DOI: 10.1186/s12885-016-2241-1]
61 **Samokhvalov AV**, Rehm J, Roerecke M. Alcohol Consumption as a Risk Factor for Acute and Chronic Pancreatitis: A Systematic Review and a Series of Meta-analyses. *EBioMedicine* 2015; **2**: 1996-2002 [PMID: 26844279 DOI: 10.1016/j.ebiom.2015.11.023]
62 **Klochkov A**, Kudaravalli P, Lim Y, Sun Y. Alcoholic Pancreatitis. StatPearls. Treasure Island (FL), 2021
63 **Hirano H**, Shimosegawa T, Meguro T, Shiga N, Koizumi M, Toyota T. Effects of ethanol on meal-stimulated secretion of pancreatic polypeptide and cholecystokinin: comparison of healthy volunteers, heavy drinkers, and patients with chronic pancreatitis. *J Gastroenterol* 1996; **31**: 86-93 [PMID: 8808434 DOI: 10.1007/BF01211192]
64 **Gregg JA**, Sharma MM. Endoscopic measurement of pancreatic juice secretory flow rates and pancreatic secretory pressures after secretin administration in human controls and in patients with acute relapsing pancreatitis, chronic pancreatitis, and pancreatic cancer. *Am J Surg* 1978; **136**: 569-574 [PMID: 707739 DOI: 10.1016/0002-9610(78)90312-4]
65 **Renner IG**, Rinderknecht H, Valenzuela JE, Douglas AP. Studies of pure pancreatic secretions in chronic alcoholic subjects without pancreatic insufficiency. *Scand J Gastroenterol* 1980; **15**: 241-244 [PMID: 7384747 DOI: 10.3109/00365528009181462]
66 **Ceyhan GO**, Demir IE, Rauch U, Bergmann F, Müller MW, Büchler MW, Friess H, Schäfer KH. Pancreatic neuropathy results in "neural remodeling" and altered pancreatic innervation in chronic pancreatitis and pancreatic cancer. *Am J Gastroenterol* 2009; **104**: 2555-2565 [PMID: 19568227 DOI: 10.1038/ajg.2009.380]
67 **Di Sebastiano P**, di Mola FF, Bockman DE, Friess H, Büchler MW. Chronic pancreatitis: the perspective of pain

generation by neuroimmune interaction. *Gut* 2003; **52**: 907-911 [PMID: 12740353 DOI: 10.1136/gut.52.6.907]
68 **Zhang XL**, Albers KM, Gold MS. Inflammation-induced increase in nicotinic acetylcholine receptor current in cutaneous nociceptive DRG neurons from the adult rat. *Neuroscience* 2015; **284**: 483-499 [PMID: 25453771 DOI: 10.1016/j.neuroscience.2014.10.018]
69 **Joshi SK**, Mikusa JP, Weaver B, Honore P. Morphine and ABT-594 (a nicotinic acetylcholine agonist) exert centrally mediated antinociception in the rat cyclophosphamide cystitis model of visceral pain. *J Pain* 2008; **9**: 146-156 [PMID: 18088559 DOI: 10.1016/j.jpain.2007.09.004]
70 **Freitas K**, Ghosh S, Ivy Carroll F, Lichtman AH, Imad Damaj M. Effects of α7 positive allosteric modulators in murine inflammatory and chronic neuropathic pain models. *Neuropharmacology* 2013; **65**: 156-164 [PMID: 23079470 DOI: 10.1016/j.neuropharm.2012.08.022]
71 **Okuda T**, Haga T. High-affinity choline transporter. *Neurochem Res* 2003; **28**: 483-488 [PMID: 12675135 DOI: 10.1023/a:1022809003997]
72 **Yamamura HI**, Snyder SH. Choline: high-affinity uptake by rat brain synaptosomes. *Science* 1972; **178**: 626-628 [PMID: 5086398 DOI: 10.1126/science.178.4061.626]
73 **Luo D**, Chen L, Yu B. Inhibition of the high affinity choline transporter enhances hyperalgesia in a rat model of chronic pancreatitis. *Biochem Biophys Res Commun* 2017; **488**: 204-210 [PMID: 28483526 DOI: 10.1016/j.bbrc.2017.05.036]
74 **van Westerloo DJ**, Giebelen IA, Florquin S, Bruno MJ, Larosa GJ, Ulloa L, Tracey KJ, van der Poll T. The vagus nerve and nicotinic receptors modulate experimental pancreatitis severity in mice. *Gastroenterology* 2006; **130**: 1822-1830 [PMID: 16697744 DOI: 10.1053/j.gastro.2006.02.022]
75 **Schneider L**, Jabrailova B, Soliman H, Hofer S, Strobel O, Hackert T, Büchler MW, Werner J. Pharmacological cholinergic stimulation as a therapeutic tool in experimental necrotizing pancreatitis. *Pancreas* 2014; **43**: 41-46 [PMID: 24212240 DOI: 10.1097/MPA.0b013e3182a85c21]
76 **Damaj MI**, Meyer EM, Martin BR. The antinociceptive effects of alpha7 nicotinic agonists in an acute pain model. *Neuropharmacology* 2000; **39**: 2785-2791 [PMID: 11044748 DOI: 10.1016/s0028-3908(00)00139-8]
77 **Rowley TJ**, McKinstry A, Greenidge E, Smith W, Flood P. Antinociceptive and anti-inflammatory effects of choline in a mouse model of postoperative pain. *Br J Anaesth* 2010; **105**: 201-207 [PMID: 20511332 DOI: 10.1093/bja/aeq113]
78 **Li B**, Wu J, Bao J, Han X, Shen S, Ye X, Dai J, Wu Z, Niu M, He Y, Ni J, Wen L, Wang X, Hu G. Activation of α7nACh receptor protects against acute pancreatitis through enhancing TFEB-regulated autophagy. *Biochim Biophys Acta Mol Basis Dis* 2020; **1866**: 165971 [PMID: 32950676 DOI: 10.1016/j.bbadis.2020.165971]
79 **Siegel RL**, Miller KD, Jemal A. Cancer statistics, 2020. *CA Cancer J Clin* 2020; **70**: 7-30 [PMID: 31912902 DOI: 10.3322/caac.21590]
80 **Rahib L**, Smith BD, Aizenberg R, Rosenzweig AB, Fleshman JM, Matrisian LM. Projecting cancer incidence and deaths to 2030: the unexpected burden of thyroid, liver, and pancreas cancers in the United States. *Cancer Res* 2014; **74**: 2913-2921 [PMID: 24840647 DOI: 10.1158/0008-5472.CAN-14-0155]
81 **Lowenfels AB**, Maisonneuve P, Cavallini G, Ammann RW, Lankisch PG, Andersen JR, Dimagno EP, Andrén-Sandberg A, Domellöf L. Pancreatitis and the risk of pancreatic cancer. International Pancreatitis Study Group. *N Engl J Med* 1993; **328**: 1433-1437 [PMID: 8479461 DOI: 10.1056/NEJM199305203282001]
82 **Malka D**, Hammel P, Maire F, Rufat P, Madeira I, Pessione F, Lévy P, Ruszniewski P. Risk of pancreatic adenocarcinoma in chronic pancreatitis. *Gut* 2002; **51**: 849-852 [PMID: 12427788 DOI: 10.1136/gut.51.6.849]
83 **Kirkegård J**, Mortensen FV, Cronin-Fenton D. Chronic Pancreatitis and Pancreatic Cancer Risk: A Systematic Review and Meta-analysis. *Am J Gastroenterol* 2017; **112**: 1366-1372 [PMID: 28762376 DOI: 10.1038/ajg.2017.218]
84 **Ceyhan GO**, Bergmann F, Kadihasanoglu M, Altintas B, Demir IE, Hinz U, Müller MW, Giese T, Büchler MW, Giese NA, Friess H. Pancreatic neuropathy and neuropathic pain--a comprehensive pathomorphological study of 546 cases. *Gastroenterology* 2009; **136**: 177-186.e1 [PMID: 18992743 DOI: 10.1053/j.gastro.2008.09.029]
85 **Demir IE**, Ceyhan GO, Rauch U, Altintas B, Klotz M, Müller MW, Büchler MW, Friess H, Schäfer KH. The microenvironment in chronic pancreatitis and pancreatic cancer induces neuronal plasticity. *Neurogastroenterol Motil* 2010; **22**: 480-490, e112 [PMID: 19912545 DOI: 10.1111/j.1365-2982.2009.01428.x]
86 **Yang MW**, Tao LY, Jiang YS, Yang JY, Huo YM, Liu DJ, Li J, Fu XL, He R, Lin C, Liu W, Zhang JF, Hua R, Li Q, Jiang SH, Hu LP, Tian GA, Zhang XX, Niu N, Lu P, Shi J, Xiao GG, Wang LW, Xue J, Zhang ZG, Sun YW. Perineural Invasion Reprograms the Immune Microenvironment through Cholinergic Signaling in Pancreatic Ductal Adenocarcinoma. *Cancer Res* 2020; **80**: 1991-2003 [PMID: 32098780 DOI: 10.1158/0008-5472.CAN-19-2689]
87 **Liebl F**, Demir IE, Mayer K, Schuster T, D'Haese JG, Becker K, Langer R, Bergmann F, Wang K, Rosenberg R, Novotny AR, Feith M, Reim D, Friess H, Ceyhan GO. The impact of neural invasion severity in gastrointestinal malignancies: a clinicopathological study. *Ann Surg* 2014; **260**: 900-7; discussion 907 [PMID: 25379860 DOI: 10.1097/SLA.0000000000000968]
88 **Kamiya A**, Hiyama T, Fujimura A, Yoshikawa S. Sympathetic and parasympathetic innervation in cancer: therapeutic implications. *Clin Auton Res* 2021; **31**: 165-178 [PMID: 32926324 DOI: 10.1007/s10286-020-00724-y]
89 **De Couck M**, Maréchal R, Moorthamers S, Van Laethem JL, Gidron Y. Vagal nerve activity predicts overall survival in metastatic pancreatic cancer, mediated by inflammation. *Cancer Epidemiol* 2016; **40**: 47-51 [PMID: 26618335 DOI: 10.1016/j.canep.2015.11.007]
90 **Zhang L**, Xiu D, Zhan J, He X, Guo L, Wang J, Tao M, Fu W, Zhang H. High expression of muscarinic acetylcholine receptor 3 predicts poor prognosis in patients with pancreatic ductal adenocarcinoma. *Onco Targets Ther* 2016; **9**: 6719-6726 [PMID: 27826198 DOI: 10.2147/OTT.S111382]
91 **Pfitzinger PL**, Fangmann L, Wang K, Demir E, Gürlevik E, Fleischmann-Mundt B, Brooks J, D'Haese JG, Teller S, Hecker A, Jesinghaus M, Jäger C, Ren L, Istvanffy R, Kühnel F, Friess H, Ceyhan GO, Demir IE. Indirect cholinergic activation slows down pancreatic cancer growth and tumor-associated inflammation. *J Exp Clin Cancer Res* 2020; **39**: 289 [PMID: 33357230 DOI: 10.1186/s13046-020-01796-4]
92 **Español AJ**, Maddaleno MO, Lombardi MG, Cella M, Martínez Pulido P, Sales ME. Treatment with LPS plus INF-γ induces the expression and function of muscarinic acetylcholine receptors, modulating NIH3T3 cell proliferation:

participation of NOS and COX. *Br J Pharmacol* 2014; **171**: 5154-5167 [PMID: 24990429 DOI: 10.1111/bph.12834]

93 **Colby JK**, Klein RD, McArthur MJ, Conti CJ, Kiguchi K, Kawamoto T, Riggs PK, Pavone AI, Sawicki J, Fischer SM. Progressive metaplastic and dysplastic changes in mouse pancreas induced by cyclooxygenase-2 overexpression. *Neoplasia* 2008; **10**: 782-796 [PMID: 18670639 DOI: 10.1593/neo.08330]

94 **Müller-Decker K**, Fürstenberger G, Annan N, Kucher D, Pohl-Arnold A, Steinbauer B, Esposito I, Chiblak S, Friess H, Schirmacher P, Berger I. Preinvasive duct-derived neoplasms in pancreas of keratin 5-promoter cyclooxygenase-2 transgenic mice. *Gastroenterology* 2006; **130**: 2165-2178 [PMID: 16762637 DOI: 10.1053/j.gastro.2006.03.053]

95 **Vincent A**, Herman J, Schulick R, Hruban RH, Goggins M. Pancreatic cancer. *Lancet* 2011; **378**: 607-620 [PMID: 21620466 DOI: 10.1016/S0140-6736(10)62307-0]

96 **GBD 2017 Pancreatic Cancer Collaborators**. . The global, regional, and national burden of pancreatic cancer and its attributable risk factors in 195 countries and territories, 1990-2017: a systematic analysis for the Global Burden of Disease Study 2017. *Lancet Gastroenterol Hepatol* 2019; **4**: 934-947 [PMID: 31648972 DOI: 10.1016/S2468-1253(19)30347-4]

97 **Al-Wadei MH**, Banerjee J, Al-Wadei HA, Schuller HM. Nicotine induces self-renewal of pancreatic cancer stem cells *via* neurotransmitter-driven activation of sonic hedgehog signalling. *Eur J Cancer* 2016; **52**: 188-196 [PMID: 26689865 DOI: 10.1016/j.ejca.2015.10.003]

98 **Momi N**, Ponnusamy MP, Kaur S, Rachagani S, Kunigal SS, Chellappan S, Ouellette MM, Batra SK. Nicotine/cigarette smoke promotes metastasis of pancreatic cancer through α7nAChR-mediated MUC4 upregulation. *Oncogene* 2013; **32**: 1384-1395 [PMID: 22614008 DOI: 10.1038/onc.2012.163]

99 **Hutchings C**, Phillips JA, Djamgoz MBA. Nerve input to tumours: Pathophysiological consequences of a dynamic relationship. *Biochim Biophys Acta Rev Cancer* 2020; **1874**: 188411 [PMID: 32828885 DOI: 10.1016/j.bbcan.2020.188411]

World Journal of Gastroenterology

Submit a Manuscript: https://www.f6publishing.com

World J Gastroenterol 2022 July 7; 28(25): 2920-2936

DOI: 10.3748/wjg.v28.i25.2920

ISSN 1007-9327 (print) ISSN 2219-2840 (online)

ORIGINAL ARTICLE

Basic Study

Fecal gene detection based on next generation sequencing for colorectal cancer diagnosis

Si-Yu He, Ying-Chun Li, Yong Wang, Hai-Lin Peng, Cheng-Lin Zhou, Chuan-Meng Zhang, Sheng-Lan Chen, Jian-Feng Yin, Mei Lin

Specialty type: Gastroenterology and hepatology

Provenance and peer review: Invited article; Externally peer reviewed.

Peer-review model: Single blind

Peer-review report's scientific quality classification
Grade A (Excellent): A
Grade B (Very good): B
Grade C (Good): C
Grade D (Fair): 0
Grade E (Poor): 0

P-Reviewer: Beenet L, United States; Kołat D, Poland
A-Editor: Sahin TT, Turkey

Received: January 16, 2022
Peer-review started: January 16, 2022
First decision: March 8, 2022
Revised: March 18, 2022
Accepted: May 27, 2022
Article in press: May 27, 2022
Published online: July 7, 2022

Si-Yu He, Hai-Lin Peng, Cheng-Lin Zhou, Mei Lin, Department of Clinical Laboratory, Taizhou People's Hospital (Postgraduate Training Base of Dalian Medical University), Taizhou 225300, Jiangsu Province, China

Si-Yu He, Department of Clinical Laboratory, The First People's Hospital of Tianmen City, Tianmen 431700, Hubei Province, China

Ying-Chun Li, Yong Wang, Department of General Surgery, Taizhou People's Hospital (Postgraduate Training Base of Dalian Medical University), Taizhou 225300, Jiangsu Province, China

Chuan-Meng Zhang, Central Laboratory, Taizhou People's Hospital (Postgraduate training base of Dalian Medical University), Taizhou 225300, Jiangsu Province, China

Sheng-Lan Chen, Department of Laboratory, Taizhou Genewill Medical Laboratory Company Limited, Taizhou 225300, Jiangsu Province, China

Jian-Feng Yin, Department of Laboratory, Jiangsu CoWin Biotech Co., Ltd., Taizhou 225300, Jiangsu Province, China

Corresponding author: Mei Lin, MD, PhD, Senior Scientist, Department of Clinical Laboratory, Taizhou People's Hospital (Postgraduate Training Base of Dalian Medical University), No. 366 Taihu Road, Taizhou 225300, Jiangsu Province, China. l_mei@163.com

Abstract

BACKGROUND

Colorectal cancer (CRC) is one of the most common malignancies worldwide. Given its insidious onset, the condition often already progresses to advanced stage when symptoms occur. Thus, early diagnosis is of great significance for timely clinical intervention, efficacy enhancement, and prognostic improvement. Featuring high throughput, fastness, and rich information, next generation sequencing (NGS) can greatly shorten the detection time, which is a widely used detection technique at present.

AIM

To screen specific genes or gene combinations in fecal DNA that are suitable for diagnosis and prognostic prediction of CRC, and to establish a technological

platform for CRC screening, diagnosis, and efficacy monitoring through fecal DNA detection.

METHODS

NGS was used to sequence the stool DNA of patients with CRC, which were then compared with the genetic testing results of the stool samples of normal controls and patients with benign intestinal disease, as well as the tumor tissues of CRC patients. Specific genes or gene combinations in fecal DNA suitable for diagnosis and prognostic prediction of CRC were screened, and their significances in diagnosing CRC and predicting patients' prognosis were comprehensively evaluated.

RESULTS

High mutation frequencies of *TP53*, *APC,* and *KRAS* were detected in the stools and tumor tissues of CRC patients prior to surgery. Contrastively, no pathogenic mutations of the above three genes were noted in the postoperative stools, the normal controls, or the benign intestinal disease group. This indicates that tumor-specific DNA was detectable in the preoperative stools of CRC patients. The preoperative fecal expression of tumor-associated genes can reflect the gene mutations in tumor tissues to some extent. Compared to the postoperative stools and the stools in the two control groups, the pathogenic mutation frequencies of *TP53* and *KRAS* were significantly higher for the preoperative stools ($\chi^2 = 7.328$, $P < 0.05$; $\chi^2 = 4.219$, $P < 0.05$), suggesting that fecal *TP53* and *KRAS* genes can be used for CRC screening, diagnosis, and prognostic prediction. No significant difference in the pathogenic mutation frequency of the *APC* gene was found from the postoperative stools or the two control groups ($\chi^2 = 0.878$, $P > 0.05$), so further analysis with larger sample size is required. Among CRC patients, the pathogenic mutation sites of *TP53* occurred in 16 of 27 preoperative stools, with a true positive rate of 59.26%, while the pathogenic mutation sites of *KRAS* occurred in 10 stools, with a true positive rate of 37.04%. The sensitivity and negative predictive values of the combined genetic testing of *TP53* and *KRAS* were 66.67% (18/27) and 68.97%, respectively, both of which were higher than those of *TP53* or *KRAS* mutation detection alone, suggesting that the combined genetic testing can improve the CRC detection rate. The mutation sites *TP53* exon 4 A84G and *EGFR* exon 20 I821T (mutation start and stop positions were both 7579436 for the former, while 55249164 for the latter) were found in the preoperative stools and tumor tissues. These "undetected" mutation sites may be new types of mutations occurring during the CRC carcinogenesis and progression, which needs to be confirmed through further research. Some mutations of "unknown clinical significance" were found in such genes as *TP53*, *PTEN*, *KRAS*, *BRAF*, *AKT1*, and *PIK3CA*, whose clinical values is worthy of further exploration.

CONCLUSION

NGS-based fecal genetic testing can be used as a complementary technique for the CRC diagnosis. Fecal *TP53* and *KRAS* can be used as specific genes for the screening, diagnosis, prognostic prediction, and recurrence monitoring of CRC. Moreover, the combined testing of *TP53* and *KRAS* genes can improve the CRC detection rate.

Key Words: Colorectal cancer; Feces; Next generation sequencing; Diagnosis; Gene

©The Author(s) 2022. Published by Baishideng Publishing Group Inc. All rights reserved.

Core Tip: Colorectal cancer (CRC) is characterized by high morbidity and mortality, as well as low early diagnosis rate. The development of current gold standard for clinical diagnosis of CRC is restricted due to its invasiveness. The purpose of this study is to explore the potential value of fecal gene detection based on next generation sequencing in the diagnosis of CRC, to screen specific genes or gene combinations suitable for CRC diagnosis and prognosis prediction in fecal DNA, and to establish a technical platform for fecal DNA detection for CRC screening, diagnosis, and efficacy monitoring.

Citation: He SY, Li YC, Wang Y, Peng HL, Zhou CL, Zhang CM, Chen SL, Yin JF, Lin M. Fecal gene detection based on next generation sequencing for colorectal cancer diagnosis. *World J Gastroenterol* 2022; 28(25): 2920-2936

URL: https://www.wjgnet.com/1007-9327/full/v28/i25/2920.htm

DOI: https://dx.doi.org/10.3748/wjg.v28.i25.2920

INTRODUCTION

Colorectal cancer (CRC), as a health issue of great concern worldwide, poses a serious threat to human health. According to the latest data released by the International Agency for Research on Cancer, there were approximately 19.3 million new cancer cases and nearly 10 million cancer deaths globally in 2020. Among them, new CRC cases amounted to about 1.93 million (10%), ranking third, while CRC deaths amounted to about 0.94 million (9.4%), ranking second. For female patients, there were approximately 860000 new cases of CRC (9.4%), second only to breast cancer, and nearly 870000 CRC deaths (9.5%), ranking third. As for male population, the numbers of new cases and deaths both ranked third for CRC, which were 930000 (10.6%) and 50000 (9.3%), respectively[1].

In recent years, the morbidity and mortality of CRC have been on the rise in China, and the onset age of patients has gradually become younger. Early detection of CRC is difficult due to the insidious onset, long progressive course, and unobvious symptoms and signs of patients at the onset stage. As the tumor grows and gradually compresses the intestinal cavity, such symptoms as altered bowel habit and abnormal stool color or traits may occur. At this time, the condition often already progresses to advanced stage. Studies have shown that the 5-year survival of patients with early CRC can reach 90%, while is only about 12.5% for advanced stage patients[2]. Thus, early diagnosis is conducive to early intervention and treatment of CRC, which is of great significance for improving the efficacy and prognosis[3,4]. In response, the American Cancer Society recommended the CRC screening since the age of 45 for adults in 2018, which is 5 years earlier than the previously recommended age[5].

The occurrence and progression are a multi-factor, multi-stage complex process[6-8]. It is generally believed that CRC is caused by the mutations and malignant proliferation of colorectal mucosal epithelial cells. Other studies have shown that CRC can develop from inflammatory bowel disease (IBD). IBD is mainly characterized by intestinal mucosal barrier dysfunction, because the changes of cytokines aggravate tissue damage and eventually lead to tumorigenesis. It is reported that patients with ulcerative colitis have a higher risk of developing CRC than the general population[9]. In addition, microRNA and tumor microenvironment also have potential pathogenic effects on CRC[10,11]. Currently, the clinically recognized gold standard for CRC detection remains endoscopy combined with histopathological analysis. Given the heterogeneity of tumor tissues and the invasiveness of endoscopy, the same patient cannot be sampled multiple times, so that the genetic testing results cannot fully display the mutation spectrum of oncogenic genes[12]. According to the Chinese *Expert Consensus on Early Diagnosis and Screening Strategies for Colorectal Tumors* published in October 2018, fecal detection is a promising method for early diagnosis[13]. Its theoretical basis is that the tumor cells in the intestinal cavity of CRC patients adhere less to the base and can be continuously exfoliated from the colorectal mucosa. Studies have shown that tumor-associated DNA can stably exist in the stools, which has high specificity for the detection of CRC and is the most suitable biomarker in fecal detection[14-16]. By extracting the DNA of shed tumor cells in stools and analyzing their mutations, the traits of intestinal tumor cells can be reflected. Fecal DNA detection, as an emerging, noninvasive technique for screening CRC, has attracted great attention in recent years, which has the advantages of noninvasiveness, convenient access to materials, good patient compliance, and continuous dynamic monitoring. It is in line with the concept and conforms to the trend of "precision medicine", which is an exceptionally promising detection method.

With the continuous development of molecular biotechnology, next generation sequencing (NGS) has emerged to gradually become a hot research topic worldwide. It is also known as high-throughput sequencing, which operates on the following principles: Four different deoxynucleotide triphosphates (dNTPs) are labeled with different fluorescent colors. Conforming to the complementary base pairing rule, the bound base releases the corresponding fluorescence by the action of DNA polymerase every time a dNTP is added. Finally, the base is identified according to the fluorescent signal. Compared to the first-generation Sanger sequencing, NGS is a set of technologies that completely change the standard concept of nucleic acid sequencing. Capable of detecting millions of DNA molecules simultaneously, it achieves concurrent synthesis and sequencing, which can greatly shorten the detection time, and has the advantages of high throughput, high efficiency, and rich information[17,18]. NGS can more comprehensively display the full spectrum of tumor-associated genes, which can reflect the changes in tumor-specific genes, expand the understanding of tumor-specific genes, and improve the predictability of targeted therapy, suggesting its significance in achieving personalized tumor treatment and developing new therapeutic strategies[19-21]. Currently, NGS has been widely applied in the research of various solid tumors, including CRC. Kraus and his colleagues performed NGS analysis on the tissue paraffin sections and blood samples of 152 CRC patients based on 18 CRC-related genes. Their results showed that NGS had a high detection rate and could effectively identify the high-risk patients with hereditary CRC[22]. In a study by Li *et al*[23], the NGS (Ion Torrent PGM platform) technology was applied to analyze 22 tumor-associated mutation hotspots in 526 CRC patients, finding that *TP53* and *KRAS* mutations were the most common in tumor tissues, and confirming that NGS was a highly sensitive detection technique.

This study performed NGS-based genetic testing of 50 tumor-associated mutation hotspots in the stools of CRC patients, and compared them with the genetic testing results of corresponding tumor tissues, with an aim to find the fecal genes or gene combinations with high specificity and sensitivity,

and to establish a technological platform for CRC screening, diagnosis, and efficacy monitoring through fecal DNA detection. The findings herein will provide support and basis for personalized diagnosis and treatment of CRC.

MATERIALS AND METHODS

Subjects

Fifty tumor tissues, 27 preoperative stools, and 19 postoperative stools (stools formed over 7 d postoperatively) collected from patients with CRC were included in an experimental group. Twenty stool samples collected from healthy subjects were included in a normal control group. Seventeen stool samples of patients with benign intestinal polyps confirmed by digestive endoscopy were collected, as well as three stool samples from patients with ulcerative colitis, totaling 20 samples, were included in a benign control group. Postoperative pathological reports of polyp patients revealed inflammatory or adenomatous polyps, none of which had progressed to the CRC stage.

This study was approved by the Ethics Committee of Taizhou People's Hospital in Jiangsu, and the patients provided signed informed consent for sample collection.

Main reagents

Fecal DNA sample preservation tubes, tissue nucleic acid preservation tubes, fecal DNA extraction kit (immunomagnetic bead method), universal columnar genomic nucleic acid extraction kit, fast DNA library preparation kit were provided by Cowin Bio., Jiangsu, while high-throughput kit (MGISEQ-2000RS) was provided by MGI, Shenzhen.

Samples sources

The subjects of this project are patients who were diagnosed with CRC for the first time and underwent surgery at Taizhou People's Hospital from January 2019 to January 2021. A total of 54 tumor tissue samples, 45 preoperative stool samples, and 41 postoperative stool samples were collected. The normal control group consisted of healthy physical examination takers without malignancies (including CRC), intestinal polyps, or IBD, from whom 20 stool samples were collected. The benign control group comprised 20 patients who were diagnosed with intestinal polyps or IBD by digestive endoscopy, and admitted to the Department of Gastroenterology, Taizhou People's Hospital for polypectomy or anti-inflammatory treatment. Twenty formed stool samples were collected from patients who had not taken laxatives preoperatively or from patients before receiving anti-inflammatory therapies. The above samples were tested by NGS, unreliable results were filtered during analysis of genetic testing results based on biological information, and poor quality samples were eliminated (heterogeneous tumor tissues, atypical fecal specimens, and little or degraded DNA in stools). Finally, effectively detected samples included 50 tumor tissues, 27 preoperative stools, 19 postoperative stools, 20 stools in the normal control group, and 20 stools in the benign control group.

Sample collection and processing

Stool samples: Patients were instructed to use the fecal DNA preservation tube correctly (tubes contained protective solution to prevent the degradation of nucleic acid, while steel beads played a mixing role). They were asked to take samples immediately after natural defecation. Using sampling spoon located on the tube cap, typical formed stool about the size of soybean was excavated while avoiding spillover of protective solution and steel beads in the tube. After tightening the tube cap, the patients were asked to shake the tubes for approximately 30 s for uniform mixing. The samples were stored in a -80 °C refrigerator for subsequent testing.

Tissue samples: The freshly isolated tumor tissues were quickly cut into pieces (< 0.5 cm in thickness) using sterile tissue scissors, and then the tissue pieces were soaked in the protective solution of preservation tubes (if the volume was excessively large, the protective solution would not easily penetrate the tissues, which could not protect the nucleic acid from degradation). After tightening the tube caps, the samples were stored in a 4–8 °C refrigerator for subsequent testing.

DNA extraction from stool samples

The DNA in stool samples should be extracted strictly in accordance with the kit instructions (immunomagnetic bead method). Initially, the samples were homogenized, and then the precipitates (fecal particles) were removed, and the supernatants were retained for subsequent use. Different reagents were added to the corresponding wells of deep 96-well plates as *per* the instruction procedures, and then the deep well plates and magnetic sleeves containing the reagents were placed at the corresponding positions of nucleic acid extractor, followed by running of the stool extraction program. Under high salinity condition, DNA can bind to the surfaces of silica-coated Magbeads. After rinsing, high-purity DNA was eluted and stored in Buffer GE. The DNA-containing Buffer GE was transferred to an EP tube and stored under refrigeration for subsequent testing.

Table 1 details the reaction system. Relevant reagents were added to the corresponding wells of deep 96-well plates (wells 1–6 corresponded to one sample, wells 7–12 corresponded to another sample, and so forth).

The deep 96-well plates and corresponding magnetic sleeves were placed into the corresponding positions of an automatic nucleic acid extractor, and then the fecal DNA extraction program was initiated. After running for about 20 min, the program was paused, and each 220 μL of pre-prepared mixture (Magbeads PN 20 μL, isopropanol 200 μL) was added to the first well of each sample, followed by continuation of the program. The product in the last well of each sample was transferred to the centrifuge tube and stored at low temperature for subsequent testing.

DNA extraction from tissue samples

DNA was extracted from tissue samples strictly following the instructions of universal columnar genomic nucleic acid extraction kit. Initially, fresh tumor tissues were ground to small pieces and added with lysis buffer and proteinase K for complete digestion and lysis. Then, RNase was added to remove RNA. Since DNA was insoluble in absolute ethanol, the samples added with absolute ethanol were centrifuged to adsorb the DNA on the column. The residual impurities dissolved in absolute ethanol were discarded along with the liquid waste in the collection tube. Next, the collection tube was replaced with a new one, and the centrifugation was repeated several times. The DNA-containing adsorption column was placed at room temperature, and let stand to dry the absolute ethanol. The elution buffer was suspended, added to the adsorption column with a new collection tube, and centrifuged, and then the DNA-containing eluate in the collection tube was collected and refrigerated for subsequent testing.

The nucleic acid extraction was carried out in Cowin Bio., Jiangsu.

Library construction and NGS detection

In accordance with the instructions of fast DNA library preparation kit, the hotspot mutation panels of 50 tumor-associated genes designed for specific genomic regions or targets were added initially based on the multiplex polymerase chain reaction (PCR) library construction technology, and then multiplex PCR enrichment was performed on specific gene region fragments. Next, the obtained target gene fragments were subjected to end repair, barcode adapter ligation, and PCR amplification (Eastwin Scientific Equipment, Suzhou) to prepare a library. Afterwards, the library was quantified with Qubit 3.0 fluorescence quantifier (Thermo Fisher Scientific, Shanghai), and the fragment size of the library was analyzed with the Bioptic Qsep 100 automatic nucleic acid analyzer (Bioptic Inc., Jiangsu) to evaluate the library quality. Finally, a high-throughput sequencer (MGI, Shenzhen) was used for sequencing, and the data splitting, denoising, and comparison were accomplished in the Linux system to obtain the gene mutation results of various samples.

The library construction and NGS were carried out in Cowin Bio., Jiangsu.

Statistical analysis

Data were analyzed using SPSS 26.0 software. The gene mutation frequencies are expressed as the numbers of cases or percentages. Inter-group differences were examined by χ^2 and Fisher exact tests. $P < 0.05$ was considered statistically significant.

RESULTS

Clinical data analysis of CRC patients

Among the CRC patients corresponding to 50 tumor tissue samples, 24 were female (48.00%) and 26 were male (52.00%). The age span was large (35–84 years), and the median age was 59.5 years. According to the histopathological results of tumor tissues, there were 29 cases of rectal cancer (58.00%), 11 cases of left colon cancer + sigmoid colon cancer (22.00%), and 10 cases of right colon cancer (20.00%). Twelve cases (24.00%) were well-differentiated + well-to-moderately differentiated, 25 (50.00%) were moderately differentiated, and 12 (24.00%) were moderately-to-poorly differentiated + poorly differentiated (the degree of differentiation was not determined in 1 of 50 colorectal cancer tumor tissues). Among 19 cases (38.00%) of lymph node metastasis, only 1 had distant metastasis (metastasis to the liver). Regarding pathological staging (according to eighth edition of AJCC TNM staging system), 33 cases (66.00%) were at stages I + II, and 17 (34.00%) were at stages III + IV (Table 2).

Gene mutations in various samples

As is clear from the NGS testing results of CRC specimens in Table 3, genes like *TP53*, *APC*, *KRAS*, *PTEN*, *MET*, *HRAS*, and *PDGFRA* had high incidences of mutations in tumor tissues and preoperative stools, while in postoperative stools, the mutation frequencies of *TP53*, *HRAS*, and *PDGFRA* were high. Despite high mutation frequencies of *HRAS* and *PDGFRA* in the three groups of samples, their mutations were mostly same sense mutations, meaning that there were only base mutations, without changes in amino acids, which had no clinical significance.

Table 1 The reaction system

Position	Reagent
Wells 1 and 7	Proteinase K: 20 μL
	Lysate: 200 μL
Wells 2 and 8	Buffer KCL: 750 μL
Wells 3 and 9	Buffer GW1: 750 μL
Wells 4 and 10	Buffer GW2: 750 μL
Wells 5 and 11	Buffer MW3: 750 μL
Wells 6 and 12	Buffer GE: 100 μL

Table 2 Clinical data analysis of colorectal cancer patients

Clinical feature	Stratification	Number of people (%)
Age (years old)	≥ 60	30 (60.00)
	< 60	20 (40.00)
Sex	Male	26 (52.00)
	Female	24 (48.00)
Tumor location	Sigmoid colon + left hemicolon	11 (22.00)
	Right hemicolon	10 (20.00)
	Rectum	29 (58.00)
Tumor size (cm)	≥ 6	12 (24.00)
	< 6	38 (76.00)
Degree of tumor differentiation	High + medium high	12 (24.00)
	Moderately	25 (50.00)
	Low medium + low	12 (24.00)
TNM classification	I + II	33 (66.00)
	III + IV	17 (34.00)

As shown in Table 4, the *PDGFRA*, *HRAS*, and *KIT* mutations occurred in only 3 of 20 stool samples in the normal control group. In the benign control group, only 4 stool samples had *PDGFRA*, *HRAS*, *KIT*, or *STK11* mutations.

Since every gene has numerous mutation sites, different site mutations have different meanings. We classified and summarized the results of gene sequencing, and queried them online (https://www.ncbi.nlm.nih.gov/clinvar/). After combining the start and stop positions of each gene mutation site, various gene mutation sites were classified into four types depending on their pathogenicity: "Pathogenic", "benign", "unknown clinical significance", and "undetected in the system" (hereinafter referred to as "undetected"). "Benign" gene mutation sites imply a large number of mutations that can occur multiple times in the normal population, albeit less than 1% incidences. Mutation sites of "unknown clinical significance" indicate that such mutations are neither pathogenic nor benign, on whom the experimental conclusions in the literature reports are inconsistent. There is insufficient evidence to clearly classify them, and further exploration is required. "Undetected" mutation sites are identified by comprehensively checking multiple items such as the exons, the types of amino acid mutations, and the start and end positions of mutations. In the case of non-conformity of any item, the corresponding mutation site is regarded as "undetected". In Table 3, the mutations of the *PTEN* gene in tumor tissues were quite frequent, all of which were mutation sites of "unknown clinical significance". Among the 27 cases of preoperative stools, 1 had pathogenic mutation. Given the small case number, the possible cause of tumor heterogeneity was not ruled out. The *MET* gene exhibited high mutation frequencies in both tumor tissues and preoperative stools, all of which were "benign" mutations upon query. The four *MET* mutations in the postoperative stools were all "undetected" mutations. In Table 4, the mutation sites of *KIT* and *STK11* in the benign control group were benign mutation sites, while the rest were all same sense mutations and had no clinical significance.

Table 3 Summary of gene mutations in colorectal cancer patients

Gene	Tumor tissue		Preoperative feces		Postoperative stools	
	Total number of mutations	Mutation frequency	Total number of mutations	Mutation frequency	Total number of mutations	Mutation frequency
TP53	40	62.00% (31/50)	27	59.26% (16/27)	7	31.58% (6/19)
APC	15	24.00% (12/50)	3	11.11% (3/27)	0	0
KRAS	30	58.00% (29/50)	11	37.04% (10/27)	0	0
PIK3CA	13	22.00% (11/50)	1	3.70% (1/27)	2	10.53% (2/19)
FBXW7	5	10.00% (5/50)	1	3.70% (1/27)	0	0
GNAS	2	4.00% (2/50)	1	3.70% (1/27)	0	0
PTEN	11	22.00% (11/50)	1	3.70% (1/27)	0	0
ABL1	0	0	1	3.70% (1/27)	0	0
PDGFRA	12	24.00% (12/50)	8	29.63% (8/27)	6	31.58% (6/19)
ATM	1	2.00% (1/50)	0	0	0	0
SMAD4	1	2.00% (1/50)	0	0	0	0
BRAF	2	4.00% (2/50)	0	0	2	10.53% (2/19)
PTPN11	1	2.00% (1/50)	0	0	0	0
NRAS	1	2.00% (1/50)	0	0	0	0
CTNNB1	3	6.00% (3/50)	1	3.70% (1/27)	0	0
STK11	2	4.00% (2/50)	1	3.70% (1/27)	0	0
AKT1	1	2.00% (1/50)	1	3.70% (1/27)	0	0
CDKN2A	3	6.00% (3/50)	4	7.41% (2/27)	3	5.26% (1/19)
HRAS	21	42.00% (21/50)	12	40.74% (11/27)	8	42.11% (8/19)
EGFR	2	4.00% (2/50)	2	7.41% (2/27)	1	5.26% (1/19)
IDH1	2	4.00% (2/50)	2	7.41% (2/27)	1	5.26% (1/19)
NOTCH1	2	4.00% (2/50)	0	0	2	5.26% (1/19)
VHL	0	0	1	3.70% (1/27)	0	0
KIT	7	14.00% (7/50)	2	7.41% (2/27)	4	21.05% (4/19)
MET	9	18.00% (9/50)	5	18.52% (5/27)	4	21.05% (4/19)
MLH1	3	6.00% (3/50)	2	7.41% (2/27)	2	10.53% (2/19)
MPL	0	0	0	0	1	5.26% (1/19)

Total number of mutations: The overall number of mutations of any gene in various samples. Mutation frequency: The number of people with mutations in various samples/total number of people.

This study focused on analyzing the pathogenic mutation sites of various genes.

Comparison between preoperative stool and tumor tissue results in CRC patients

As shown in Table 5, the *TP53*, *APC*, and *KRAS* genes had high incidences of pathogenic mutations in tumor tissues and preoperative stools among CRC patients. Despite high mutation frequency of *PIK3CA* in tumor tissues, its pathogenic mutation frequency in preoperative stools was only 3.70% (1/27). The possible causes of tumor heterogeneity or individual disparity could not be ruled out. Although other genes had pathogenic mutations, their mutation frequencies were rather low.

Comparison between preoperative/postoperative stool results of CRC patients and control stool results

For CRC patients, the pathogenic mutation incidences of *APC*, *TP53*, and *KRAS* in the preoperative stools were 11.11% (3/27), 37.04% (10/27), and 25.93% (7/27), respectively. There were mutations of *PIK3CA*, *BRAF*, and *MPL* genes in the postoperative stools. Although they were pathogenic, only one

Table 4 Fecal gene mutation results in the control groups

Group	Genes	Location	Amino acid mutation	Mutation frequency
Normal control	*PDGFRA*	Exon 19	V824V	2
	KIT	Exon 10	K546K	1
	HRAS	Exon 2	H27H	1
Intestinal benign disease	*PDGFRA*	Exon 19	V824V	3
	HRAS	Exon 2	H27H	1
	KIT	Exon 10	M541L	1
	STK11	Exon 8	F354L	1

Table 5 Comparison of pathogenic mutation sites in preoperative stools *vs* tumor tissues

Gene	Positive rate of pathogenic gene mutation sites	
	Preoperative feces	Tumor tissues
TP53	37.04% (10/27)	46.00% (23/50)
APC	11.11% (3/27)	18.00% (9/50)
KRAS	25.93% (7/27)	54.00% (27/50)
PIK3CA	3.70% (1/27)	22.00% (11/50)
FBXW7	3.70% (1/27)	6.00% (3/50)
GNAS	3.70% (1/27)	4.00% (2/50)
PTEN	3.70% (1/27)	0
ABL1	3.70% (1/27)	0
PDGFRA	3.70% (1/27)	0
ATM	0	2.00% (1/50)
SMAD4	0	2.00% (1/50)
BRAF	0	2.00% (1/50)
PTPN11	0	2.00% (1/50)
NRAS	0	2.00% (1/50)
CTNNB1	0	2.00% (1/50)
VHL	3.70% (1/27)	0

Positive rate of pathogenic gene mutation site: The number of people with mutations corresponding to the pathogenic mutation sites of any gene/total number of samples.

case was found for each gene. The possible cause of tumor heterogeneity could not be ruled out. No pathogenic gene mutation sites were detected in stool samples from the normal and benign control groups (Tables 6–8).

According to a combination of Tables 5–8, the *TP53*, *APC*, and *KRAS* genes all had high mutation frequencies in the preoperative stools and tumor tissues of CRC patients, while exhibiting no pathogenic mutations in the postoperative stools, or in the stool samples of the normal or benign control group. This indicates that tumor-specific DNA can be detected in the preoperative stools of CRC patients, and that the preoperative fecal expression of tumor-associated genes can reflect the gene mutations in tumor tissue to some extent. Compared to the postoperative stools and the stool samples of the two control groups, the pathogenic mutation frequencies of *TP53* and *KRAS* were significantly higher in the preoperative stools ($P < 0.05$), suggesting that fecal *TP53* and *KRAS* genes can be used for the screening, diagnosis, and prognostic prediction of CRC. Contrastively, the pathogenic mutation frequency of the *APC* gene in the preoperative stools differed insignificantly from that in the postoperative stool or the two control groups ($P > 0.05$), which was probably associated with the excessively small sample size.

Table 6 Comparison of pathogenic mutation sites in preoperative stools *vs* normal control stools

Gene	Positive rate of pathogenic gene mutation sites		χ^2	*P* value
	Preoperative feces	Normal control group		
TP53	37.04% (10/27)	0	7.328	0.007
APC	11.11% (3/27)	0	0.878	0.349
KRAS	25.93% (7/27)	0	4.219	0.040
PIK3CA	3.70% (1/27)	0	Fisher exact test	1
FBXW7	3.70% (1/27)	0	Fisher exact test	1
GNAS	3.70% (1/27)	0	Fisher exact test	1
PTEN	3.70% (1/27)	0	Fisher exact test	1
ABL1	3.70% (1/27)	0	Fisher exact test	1
PDGFRA	3.70% (1/27)	0	Fisher exact test	1

Positive rate of pathogenic gene mutation site: The number of people with mutations corresponding to the pathogenic mutation sites of any gene/total number of samples.

Mutation site analysis for TP53, KRAS, and APC genes

As shown in Table 9, *TP53* mutations occurred in 31 of 50 tumor tissues, and the total mutation frequency was 40 times, of which pathogenic mutation sites accounted for 60.00% (24/40), with exon 5 R175H, exon 7 R248Q/W, and exon 8 R273H/C being the most common. The proportion of pathogenic mutation sites in 29 tumor tissues with *KRAS* mutations was 90.00% (27/30), most of which were located in exon 2, with G12D/V/S being predominant, followed by G13D/C. Additionally, there was 1 case of exon 3 Q61H mutation. As for the *APC* gene, all its pathogenic mutation sites were located in exon 17.

The 12 of 27 *TP53* mutations in preoperative stools were pathogenic mutations, which were mostly exon 7 R248Q and exon 8 R273H/C. The pathogenic mutation sites of the *KRAS* gene were primarily exon 2 G12D/V. As for the *APC* gene, all its pathogenic mutation sites were located in exon 17 (Table 10).

As are clear from Tables 9 and 10, the aforementioned pathogenic mutation sites occurred in both preoperative stools and tumor tissues, suggesting the possible correlation between preoperative stool and tumor tissue in CRC patients.

Combined TP53–KRAS detection

Among the 27 preoperative stools of CRC patients, 16 had pathogenic mutations of the *TP53* gene, with a true positive rate of 59.26%, and 10 had pathogenic mutations of the *KRAS* gene, with a true positive rate of 37.04%. Pathogenic mutations of *TP53* or *KRAS* occurred in 18 preoperative stools, showing a true positive rate of 66.67% (18/27). According to Table 11, the sensitivity and negative predictive value of the combined TP53–KRAS detection were 66.67% and 68.97%, respectively, which were higher than that those of *TP53* or *KRAS* mutation detection alone. This suggests that the combined testing of *TP53* and *KRAS* genes can improve the detection rate.

Distribution of mutation sites of "unknown clinical significance"

Mutation sites of "unknown clinical significance" occurred for such genes as TP53, *PTEN*, *KRAS*, *BRAF*, and *AKT1* in the tumor tissues of CRC patients. The five mutation sites of "unknown clinical significance" for *TP53* were respectively exon 5 A159V/V172G/G154D/P153S and exon 7 S241T. In the case of *PTEN*, 9 of 11 mutations were of "unknown clinical significance", all of which were exon 6 V133I. For the *KRAS* gene, the mutation sites of "unknown clinical significance" accounted for 10.00% (3/30), all of which were exon 4 A146T. In preoperative stools, the mutation sites of "unknown clinical significance" were scattered in *TP53*, *KRAS*, *AKT1*, and *STK11*. In the case of *TP53*, such mutation sites were exon 5 V172G and exon 7 I251T/S241T, which were identical to the mutation locations in tumor tissues. For the *KRAS* gene, the mutation site of "unknown clinical significance" was exon 4 A146T. As for *AKT1* and *STK11*, such mutation sites were located separately in exon 3 E17K and exon 4 E199K.

Distribution of "undetected" mutation sites

As shown in Table 12, genes like *TP53*, *APC*, *EGFR*, *FBXW7*, and *NOTCH1* in tumor tissues all had "undetected" mutation sites, among which exon 4 A84G of *TP53* occurred more frequently (4/40). For the *APC* gene, "undetected" mutation sites were all found in exon 17. The pathogenic mutation sites of *APC* in Tables 9 and 10 were also located in exon 17, suggesting that the "undetected" mutation sites of

Table 7 Comparison of pathogenic mutation sites in preoperative stools *vs* benign control group

Gene	Positive rate of pathogenic gene mutation sites		χ^2	*P* value
	Preoperative feces	Benign control group		
TP53	37.04% (10/27)	0	7.328	0.007
APC	11.11% (3/27)	0	0.878	0.349
KRAS	25.93% (7/27)	0	4.219	0.040
PIK3CA	3.70% (1/27)	0	Fisher exact test	1
FBXW7	3.70% (1/27)	0	Fisher exact test	1
GNAS	3.70% (1/27)	0	Fisher exact test	1
PTEN	3.70% (1/27)	0	Fisher exact test	1
ABL1	3.70% (1/27)	0	Fisher exact test	1
PDGFRA	3.70% (1/27)	0	Fisher exact test	1

Positive rate of pathogenic gene mutation site: The number of people with mutations corresponding to the pathogenic mutation sites of any gene/total number of samples.

Table 8 Comparison of pathogenic mutation sites in preoperative stools *vs* postoperative stools

Gene	Positive rate of pathogenic gene mutation sites		χ^2	*P* value
	Preoperative feces	Postoperative stools		
TP53	37.04% (10/27)	0	6.947	0.008
APC	11.11% (3/27)	0	0.804	0.370
KRAS	25.93% (7/27)	0	3.974	0.046
PIK3CA	3.70% (1/27)	5.26% (1/19)	Fisher exact test	1
FBXW7	3.70% (1/27)	0	Fisher exact test	1
GNAS	3.70% (1/27)	0	Fisher exact test	1
PTEN	3.70% (1/27)	0	Fisher exact test	1
ABL1	3.70% (1/27)	0	Fisher exact test	1
PDGFRA	3.70% (1/27)	0	Fisher exact test	1
BRAF	0	5.26% (1/19)	Fisher exact test	1
MPL	0	5.26% (1/19)	Fisher exact test	1

Positive rate of pathogenic gene mutation site: The number of people with mutations corresponding to the pathogenic mutation sites of any gene/total number of sample.

APC in Table 12 may be unreported new sites. They are probably associated with the carcinogenesis and progression of CRC, which require further exploration. Table 13 shows that 6 of 27 *TP53* mutation sites in the preoperative stools were "undetected" sites. They were distributed in exon 4, exon 5, exon 7, and exon 8, among which there were three exon 7 N247D (mutation start and stop positions were both 7577542). Additionally, genes like *CDKN2A*, *HRAS*, *EGFR*, *IDH1*, and *PDGFRA* also had "undetected" mutations sites.

DISCUSSION

Studies have shown that the genetic factors coupled with prolonged unfavorable external factors induce the disturbance of homeostasis, which leads to a series of changes including angiogenesis, cell hyperproliferation, apoptosis evasion, and enhanced invasion capacity, ultimately resulting in the occurrence of malignancies. It is generally believed that CRC often develops slowly from adenomas, during which multiple steps are involved, including the activation of proto-oncogenes and the

Table 9 Analysis of pathogenic mutation sites in tumor tissues

Gene	Location	Amino acid mutation	Mutation frequency	N	M
TP53	Exon 4	R110L	1		
	Exon 5	R175H	4		
		Y163C	1		
		C176Y	1		
	Exon 6	R196[1]	2		
		Y220C	2		
	Exon 7	R248Q/W	3		
		G245S/C	2		
	Exon 8	R273H/C	4		
		R282W	2		
		R306[1]	1		
	Exon 10	R342[1]	1	24/40	23/31
KRAS	Exon 2	G12D/V/S	22		
		G13D/C	4		
	Exon 3	Q61H	1	27/30	27/29
APC	Exon 17	Q886[1]	1		
		S1483fs	1		
		R876[1]	2		
		R1450[1]	2		
		E1306[1]	1		
		Q1294[1]	1		
		G1312[1]	1	9/15	9/12

[1]Indicates stop codon.

N: Pathogenic sites/total mutation sites; M: Number of pathogenic cases/total number of mutation cases.

inactivation of tumor suppressor genes. The mutation statuses of genes like *TP53*, *APC*, and *KRAS* have been reported to be closely associated with the carcinogenesis and progression of CRC[24,25]. With the introduction of the concept of "precision medicine", molecular targeted therapy has become a hot research topic in recent years. This NGS-based study investigated the value of fecal genetic testing in the CRC diagnosis.

As a tumor suppressor gene, *TP53* regulates downstream genes when cells are under stress, which induces apoptosis and cell cycle arrest *via* a series of processes, thereby preventing the growth of tumor cells[26,27]. Its mutation is a key step in facilitating the adenoma–adenocarcinoma transition. In malignancies, the p53 protein encoded by *TP53* is mutant. The mutant p53 protein can lose its tumor suppressor effect and acquire new oncogenic functions to promote the invasion and metastasis of tumor cells[28]. In this study, *TP53* had 60.00% (24/40) and 59.26% (16/27) of mutations in the tumor tissues and preoperative stools of CRC patients, respectively, among which pathogenic mutation sites accounted for 60.00% (24/40) and 40.74% (11/27) of total mutation sites. Such pathogenic mutation sites as exon 5 C176Y, exon 6 R196*, exon 7 R248Q, exon 7 G245C/S, and exon 8 R273H/C existed in both types of samples, showing consistency. Such mutation hotspots as *R273H*, *R248Q*, and *R282W* have been reported as typical "hotspots" in the DNA binding domain. Over 95% of missense *TP53* mutations occur in the DNA binding domain, which can affect the ability of proteins to bind to their target DNA sequences[29-31]. Lo *et al*[32] screened a patient with CRC lymphatic metastasis for tumor infiltrating lymphocytes. Since some tumor patients had TP53 R175H mutations during genetic testing, and HLA-A *0201 could limit the recognition of mutant TP53 R175H, they identified the T cell receptors capable of recognizing the TP53 R175H mutation hotspots, thereby finding patients with different tumor types who shared the same mutation hotspots. In their opinion, the mutant *TP53* could serve as an ideal common antigen target, and these specific hotspot mutations had potential as valuable therapeutic targets for a variety of tumor cells. A study by Olszewski *et al*[33] suggested that changes in the

Table 10 Analysis of pathogenic mutation sites in preoperative feces

Gene	Location	Amino acid mutation	Mutation frequency	N	M
TP53	Exon 5	C176Y	1		
		F134V	1		
	Exon 6	R196[1]	1		
	Exon 7	N235D	1		
		R248Q	3		
		G245C/S	2		
	Exon 8	R273H/C	3	12/27	10/16
KRAS	Exon 2	G12D/V	5		
		G13D	1		
	Exon 3	Q61H	1		
		A59T	1	8/11	7/10
APC	Exon 17	R1450[1]	1		
		Q886[1]	1		
		Q1294[1]	1	3/3	3/3

[1]Indicates stop codon.
N: Pathogenic sites/total mutation sites; M: Number of pathogenic cases/total number of mutation cases.

Table 11 Colorectal cancer diagnosis results by *TP53* and *KRAS* mutations in preoperative stools, *n* (%)

Gene	TP	FP	FN	TN	Sensitivity	Specificity	PPV	NPV
TP53	16	0	11	20	59.26	100.00	100.00	64.52
KRAS	10	0	17	20	37.04	100.00	100.00	54.05
TP53 or *KRAS*	18	0	9	20	66.67	100.00	100.00	68.97

TP: True positive; FP: False positive; FN: False negative; TN: True negative; PPV: Positive predictive value; NPV: Negative predictive value.

oncogenic activity of TP53 led to acquisition of new functions for the mutated tumor suppressor p53 protein, and that the overexpression of such mutation hotspots as codons 175, 248, or 273 might be associated with the chemotherapeutic resistance or invasive changes. Their analysis of *TP53* mutation database in human somatic cells revealed that patients carrying TP53 R248Q allele had earlier tumor onsets, but lower frequencies of metastasis.

The 21 kDa protein encoded by *KRAS*, a member of the ras proto-oncogene family, can participate in the G protein signaling pathway and regulate the proliferation and differentiation of cells. *KRAS* mutations can continuously activate the RAS-RAF-MAPK pathway, causing uncontrolled cellular proliferation and differentiation, thereby inducing CRC[14]. Research has demonstrated that the patients' resistance to EGFR-targeted drugs was closely associated with the activation of the *KRAS* gene[34]. In the present study, the incidences of *KRAS* mutations in tumor tissue and preoperative stools of CRC patients were 58.00% (29/50) and 37.04% (10/27), respectively. Among them, pathogenic mutation sites existed in 27 tissues and 7 preoperative stools, with the most common ones being G12D/V and G13D located in exon 2. Armengol *et al*[35] explored the gene mutations in stool samples of 52 CRC patients. They found 12 cases of *KRAS* gene mutations, of which 58.3% (7/12) were located in codons 12 and 13 of exon 2. Knight argued that when there was a KRAS G12D carcinogenic mutation in the body, the formation or growth of intestinal adenomas was not inhibited by rapamycin[36]. Compared to KRAS G12D, patients with KRAS A146T mutation could have stronger resistance to EGFR tolerance, and better survival rates[37]. Mulla *et al*[38] analyzed the RAS mutations in 51 CRC patients, finding that 43% of them had RAS mutations, 91% of which were *KRAS* mutations. The majority of *KRAS* mutations were located in G12D, followed by G13D. They also found that the incidence of *KRAS* mutations was slightly higher among individuals under 50 years of age than that of the elderly (> 50 years). Ottaiano *et al*[39] reported that mutant *KRAS* was a negative influencing factor of prognosis in CRC patients. Among these patients, those with G12C/S mutation showed the shortest survival and the worst prognosis.

Table 12 "Undetected" gene mutation sites in tumor tissues

Gene	Location	Amino acid mutation	Mutation start position	Mutation end position	Number of cases	Undetected sites/total mutation sites
TP53	Exon 4	A84G	7579436	7579436	4	
	Exon 5	P152A	7578476	7578476	1	
	Exon 8	L289P	7577072	7577072	1	6/40
APC	Exon 17	S1346[1]	112175328	112175328	1	
		K1573fs	112175953	112175954	1	
		E1327fs	112175213	112175217	1	3/15
FBXW7	Exon 7	R278[1]	153258983	153258983	1	
	Exon 12	R266C	153247289	153247289	1	2/5
NOTCH1	Exon 26	R1599P	139399350	139399350	2	2/2
EGFR	Exon 20	I821T	55249164	55249164	1	1/2

[1]Indicates stop codon.
fs: Frameshift mutation.

Table 13 "Undetected" gene mutation sites in preoperative feces

Gene	Location	Amino acid mutation	Mutation start position	Mutation end position	Number of cases	Undetected sites/total mutation sites
TP53	Exon 4	A84G	7579436	7579436	1	
	Exon 5	S166P	7578434	7578434	1	
	Exon 7	N247D	7577542	7577542	3	
	Exon 8	L289P	7577072	7577072	1	6/27
CDKN2A	Exon 2	V51A	21971206	21971206	2	
		L63P	21971170	21971170	1	3/4
HRAS	Exon 2	G12R	534289	534289	1	1/10
EGFR	Exon 20	I821T	55249164	55249164	1	1/2
IDH1	Exon 4	R119Q	209113151	209113151	1	1/2
PDGFRA	Exon 13	G594fs	55141059	55141059	1	1/8

fs: Frameshift mutation.

Varshavi *et al*[40] investigated how *KRAS* mutations in different codons affected the metabolic pathways. According to their findings, metabolic differences existed between various *KRAS* mutation sites, which might be one of the reasons for the varying efficacies of anti-cancer therapies across patients. Hence, more effective, individualized molecular targeted drugs can be searched based on such metabolic differences.

Mutations of *APC* were linked to familial adenomatous polyposis, and its inactivation and the activation of Wnt signaling pathway also played pivotal roles in the occurrence of CRC, which could affect the adhesion between tumor cells to accelerate the cellular migration[41,42]. It has been reported that in sporadic CRC, most of the *APC* mutations occurred around the mutation cluster region, especially between codons 1286 and 1513[43]. In this study, the incidences of *APC* mutations in tumor tissues and preoperative stools were 24.00% (12/50) and 11.11% (3/27), respectively. As shown in Tables 5 and 6, the pathogenic mutation frequency of the *APC* gene in preoperative stools differed insignificantly from that in control stools (P = 0.370), which thus cannot serve as a specific gene for CRC screening and diagnosis. This may be attributed to the small sample size of this study, which remains further exploration. We found that all the pathogenic mutation sites of *APC* were located in exon 17, most of which used the mutations of certain amino acids as stop codons, thus allowing premature termination of mRNA translation (Tables 8 and 9). Luo's team performed NGS-based gene sequencing

on the blood and tissue samples of 22 CRC patients and 21 patients with intestinal polyps, in order to understand gene mutations. Through screening, they found that the *APC* mutations were most common in both types of samples, which were mostly pathogenic mutation sites. These pathogenic mutation sites of the *APC* gene accounted for 77.3% (17/22) of the total pathogenic mutation sites in all samples[44].

In addition to the pathogenic mutation sites of various samples, this study also found multiple mutation sites of "unknown clinical significance", which were scattered in such genes as *TP53*, *PTEN*, *KRAS*, *BRAF*, *AKT1*, and *PIK3CA*. There were also some gene mutation sites that had not been found in the Clinvar database. *TP53* exon4 A84G and *EGFR* exon20 I821T were present in both the preoperative stools and tumor tissues of CRC patients. The mutation start and stop positions were both 7579436 for the former, while 55249164 for the latter.

CONCLUSION

Conclusively, NGS-based fecal DNA detection can be used as a complementary technique for the CRC diagnosis. Fecal *TP53* and *KRAS* can serve as a specific gene combination for the screening, diagnosis, prognostic prediction, and recurrence monitoring of CRC. Moreover, the combined TP53–KRAS testing can improve the CRC detection rate, which provides a molecular reference for developing personalized treatment programs. The mutation sites of "unknown clinical significance" and the "undetected" mutation sites may be unreported new mutation sites associated with CRC. Whether these genes are linked to the CRC diagnosis and prognosis remains to be further explored and researched.

ARTICLE HIGHLIGHTS

Research background

Colorectal cancer (CRC) is currently a health problem of global concern. In recent years, the incidence of CRC presents a trend of gradual increase. Most patients have unobvious early symptoms, and they are commonly in mid and advanced stages when the symptoms become evident, with rather high mortalities. Featuring high throughput, fastness, and rich information, next generation sequencing (NGS) can greatly shorten the detection time, which is a research hotspot at home and abroad at present.

Research motivation

As we all know, histopathological examination is the gold standard of diagnosis, but its invasiveness limits its development. Therefore, it is imperative to explore the screening, diagnosis, and prognosis of CRC by strong specificity, high sensitivity, and non-invasive methods.

Research objectives

In this study, NGS technology was used to conduct genetic testing on stool samples of CRC patients, and the results were compared with the corresponding tumor tissue genetic testing results. The aim was to find genes or gene combinations with high specificity and sensitivity in the stool and establish a technical platform for CRC screening and diagnosis and curative effect monitoring through fecal DNA detection, providing a strong basis and support for personalized diagnosis and treatment of CRC.

Research methods

NGS was used to sequence the DNA in stools of patients with CRC, which were then compared with the genetic testing results of the stool samples of normal control and benign intestinal disease groups, as well as the tumor tissues of CRC patients. Specific genes or gene combinations in fecal DNA suitable for diagnosis and prognostic prediction of CRC were screened, and their significance in diagnosing CRC and predicting patients' prognosis was comprehensively evaluated.

Research results

High mutation frequencies of *TP53*, *APC,* and *KRAS* were detected in the stools and tumor tissues of CRC patients prior to surgery. Contrastively, no pathogenic mutations of the above three genes were noted in the postoperative stools, or two control groups. This indicates that the tumor-specific DNA was detectable in the preoperative stools of CRC patients. Compared to the postoperative stools and the stools in the two control groups, the pathogenic mutation frequencies of *TP53* and *KRAS* were significantly higher for the preoperative stools ($P < 0.05$), suggesting that fecal *TP53* and *KRAS* genes can be used for CRC screening, diagnosis, and prognostic prediction. No significant difference in the pathogenic mutation frequency of the *APC* gene was found from the postoperative stools or the two control groups ($P > 0.05$), so further analysis with larger sample size is required. In 27 preoperative stools of CRC patients, the sensitivity and negative predictive value of *TP53*- *KRAS* gene combination detection were higher than those of *TP53* mutation or *KRAS* mutation alone, suggesting that *TP53*-*KRAS*

gene combination detection can improve the detection rate of CRC. The "undetected" mutation sites found in preoperative stools and tumor tissues may be new mutation types in the occurrence and development of CRC, which need to be further studied. In addition, some mutations of "unknown clinical significance" were found, and their clinical value is worth further study.

Research conclusions

NGS-based fecal genetic testing can be used as a complementary technique for the CRC diagnosis. Fecal *TP53* and *KRAS* can be used as specific genes for the screening, diagnosis, prognostic prediction, and recurrence monitoring of CRC. Moreover, the combined testing of *TP53* and *KRAS* genes can improve the CRC detection rate.

Research perspectives

Fecal genetic detection is a new method for CRC diagnosis, which has the advantages of non-invasiveness, convenient sampling, and dynamic monitoring. Although the sensitivity of fecal genetic test in CRC screening is low, it is certain that it has great potential and broad prospects in the diagnosis and prognosis assessment of CRC. In addition, the "undetected" mutation sites in preoperative stools of CRC patients and the "unknown clinical significance" mutation sites are related to the occurrence and development of CRC, which requires further research and exploration.

FOOTNOTES

Author contributions: He SY performed most of the experiments, analyzed some data, and drafted the manuscript; Li YC and Wang Y provided specimens for the study; Peng HL and Zhou CL gave constructive guidance on the study; Zhang CM contributed to the statistics; Chen SL and Yin JF performed some of the experiments; Lin M designed and supervised the study and edited the manuscript; all authors approved the final version of the article.

Supported by Taizhou Social Development Plan, No. TS202004; Natural Science Foundation of Nanjing University of Chinese Medicine China, No. XZR2020093; and Taizhou People's Hospital Medical Innovation Team Foundation, No. CXTDA201901.

Institutional review board statement: This study was reviewed and approved by the Ethics Committee of Taizhou people's Hospital in Jiangsu Province (No. KY201912501).

Conflict-of-interest statement: All the authors report no relevant conflicts of interest for this article.

Data sharing statement: No additional data are available.

Open-Access: This article is an open-access article that was selected by an in-house editor and fully peer-reviewed by external reviewers. It is distributed in accordance with the Creative Commons Attribution NonCommercial (CC BY-NC 4.0) license, which permits others to distribute, remix, adapt, build upon this work non-commercially, and license their derivative works on different terms, provided the original work is properly cited and the use is non-commercial. See: https://creativecommons.org/Licenses/by-nc/4.0/

Country/Territory of origin: China

ORCID number: Si-Yu He 0000-0003-3411-8616; Ying-Chun Li 0000-0003-0650-531X; Yong Wang 0000-0002-6348-4562; Hai-Lin Peng 0000-0001-8332-1704; Cheng-Lin Zhou 0000-0003-2661-2067; Chuan-Meng Zhang 0000-0002-5642-1512; Sheng-Lan Chen 0000-0002-8366-451X; Jian-Feng Yin 0000-0002-5638-263X; Mei Lin 0000-0001-9815-2966.

S-Editor: Fan JR
L-Editor: Wang TQ
P-Editor: Fan JR

REFERENCES

1 **Sung H**, Ferlay J, Siegel RL, Laversanne M, Soerjomataram I, Jemal A, Bray F. Global Cancer Statistics 2020: GLOBOCAN Estimates of Incidence and Mortality Worldwide for 36 Cancers in 185 Countries. *CA Cancer J Clin* 2021; **71**: 209-249 [PMID: 33538338 DOI: 10.3322/caac.21660]
2 **Siegel R**, Desantis C, Jemal A. Colorectal cancer statistics, 2014. *CA Cancer J Clin* 2014; **64**: 104-117 [PMID: 24639052 DOI: 10.3322/caac.21220]
3 **Huang GW**. Clinical Value of Combined Examination of Fecal Occult Blood and Tumor Markers in the Diagnosis of Colorectal Cancer. [cited 10 January 2022]. Available from: http://en.cnki.com.cn/Article_en/CJFDTotal-HZZZ201907062.htm
4 **Chen WQ**, Li XQ, Zhang XM, Wu JN, Zhao XH, Gu HG, Ren J, Wang DQ. Expression and clinical significance of C-

terminal tensin-like protein in colorectal cancer. *Zhonghua Xiaohua Waike Zazhi* 2016; **15**: 809-814 [DOI: 10.21767/2172-0479.100116]
5 **Croke L**. Colorectal Cancer Screening: ACS Updates Guideline for Adults with Average Risk. *Am Fam Physician* 2019; **99**: 129-130 [PMID: 30633474]
6 **van Lanschot MC**, Carvalho B, Coupé VM, van Engeland M, Dekker E, Meijer GA. Molecular stool testing as an alternative for surveillance colonoscopy: a cross-sectional cohort study. *BMC Cancer* 2017; **17**: 116 [PMID: 28173852 DOI: 10.1186/s12885-017-3078-y]
7 **Sun Y**, Yang B, Lin M, Yu H, Chen H, Zhang Z. Identification of serum miR-30a-5p as a diagnostic and prognostic biomarker in colorectal cancer. *Cancer Biomark* 2019; **24**: 299-305 [PMID: 30829615 DOI: 10.3233/CBM-182129]
8 **Loktionov A**. Biomarkers for detecting colorectal cancer non-invasively: DNA, RNA or proteins? *World J Gastrointest Oncol* 2020; **12**: 124-148 [PMID: 32104546 DOI: 10.4251/wjgo.v12.i2.124]
9 **Al Buthi SA**, Bin Gheshayan SF, Al Samaani I, Al Ahmadi B, Al Selaim NA. A Mixed Neuroendocrine/Non-Neuroendocrine Neoplasm Arising in the Background of Ulcerative Colitis: A Case Report and Review of the Literature. *Am J Case Rep* 2022; **23**: e934396 [PMID: 35236818 DOI: 10.12659/AJCR.934396]
10 **Yan F**, Tu Z, Duan L, Wang D, Lin F. MicroRNA-383 suppresses cell proliferation and invasion in colorectal cancer by directly targeting paired box 6. *Mol Med Rep* 2018; **17**: 6893-6901 [PMID: 29512711 DOI: 10.3892/mmr.2018.8682]
11 **Yu CT**, Chen T, Lu S, Hu W, Zhang Q, Tan J, Sun D, Li L, Sun X, Xu C, Lai Y, Fan M, Shen Z, Shen W, Cheng H. Identification of Significant Modules and Targets of Xian-Lian-Jie-Du Decoction Based on the Analysis of Transcriptomics, Proteomics and Single-Cell Transcriptomics in Colorectal Tumor. *J Inflamm Res* 2022; **15**: 1483-1499 [PMID: 35256851 DOI: 10.2147/JIR.S344861]
12 **Wang B**, Wu S, Huang F, Shen M, Jiang H, Yu Y, Yu Q, Yang Y, Zhao Y, Zhou Y, Pan B, Liu T, Guo W. Analytical and clinical validation of a novel amplicon-based NGS assay for the evaluation of circulating tumor DNA in metastatic colorectal cancer patients. *Clin Chem Lab Med* 2019; **57**: 1501-1510 [PMID: 31339850 DOI: 10.1515/cclm-2019-0142]
13 **Ma CX**, Guan X, Wang S, Liu Z, Jiang Z, Wang XS. [Application and prospect of fecal DNA test in colorectal cancer screening]. *Zhonghua Wei Chang Wai Ke Za Zhi* 2019; **22**: 491-494 [PMID: 31104434 DOI: 10.3760/cma.j.issn.1671-0274.2019.05.018]
14 **Mahasneh A**, Al-Shaheri F, Jamal E. Molecular biomarkers for an early diagnosis, effective treatment and prognosis of colorectal cancer: Current updates. *Exp Mol Pathol* 2017; **102**: 475-483 [PMID: 28506769 DOI: 10.1016/j.yexmp.2017.05.005]
15 **Carethers JM**. Fecal DNA Testing for Colorectal Cancer Screening. *Annu Rev Med* 2020; **71**: 59-69 [PMID: 31451044 DOI: 10.1146/annurev-med-103018-123125]
16 **Anderson BW**, Ahlquist DA. Molecular Detection of Gastrointestinal Neoplasia: Innovations in Early Detection and Screening. *Gastroenterol Clin North Am* 2016; **45**: 529-542 [PMID: 27546847 DOI: 10.1016/j.gtc.2016.04.009]
17 **Wakai T**, Prasoon P, Hirose Y, Shimada Y, Ichikawa H, Nagahashi M. Next-generation sequencing-based clinical sequencing: toward precision medicine in solid tumors. *Int J Clin Oncol* 2019; **24**: 115-122 [PMID: 30515675 DOI: 10.1007/s10147-018-1375-3]
18 **Del Vecchio F**, Mastroiaco V, Di Marco A, Compagnoni C, Capece D, Zazzeroni F, Capalbo C, Alesse E, Tessitore A. Next-generation sequencing: recent applications to the analysis of colorectal cancer. *J Transl Med* 2017; **15**: 246 [PMID: 29221448 DOI: 10.1186/s12967-017-1353-y]
19 **Hinrichs JW**, van Blokland WT, Moons MJ, Radersma RD, Radersma-van Loon JH, de Voijs CM, Rappel SB, Koudijs MJ, Besselink NJ, Willems SM, de Weger RA. Comparison of next-generation sequencing and mutation-specific platforms in clinical practice. *Am J Clin Pathol* 2015; **143**: 573-578 [PMID: 25780010 DOI: 10.1309/AJCP40XETVYAMJPY]
20 **Nagahashi M**, Shimada Y, Ichikawa H, Kameyama H, Takabe K, Okuda S, Wakai T. Next generation sequencing-based gene panel tests for the management of solid tumors. *Cancer Sci* 2019; **110**: 6-15 [PMID: 30338623 DOI: 10.1111/cas.13837]
21 **Xuan J**, Yu Y, Qing T, Guo L, Shi L. Next-generation sequencing in the clinic: promises and challenges. *Cancer Lett* 2013; **340**: 284-295 [PMID: 23174106 DOI: 10.1016/j.canlet.2012.11.025]
22 **Kraus C**, Rau TT, Lux P, Erlenbach-Wünsch K, Löhr S, Krumbiegel M, Thiel CT, Stöhr R, Agaimy A, Croner RS, Stürzl M, Hohenberger W, Hartmann A, Reis A. Comprehensive screening for mutations associated with colorectal cancer in unselected cases reveals penetrant and nonpenetrant mutations. *Int J Cancer* 2015; **136**: E559-E568 [PMID: 25142776 DOI: 10.1002/ijc.29149]
23 **Li W**, Qiu T, Guo L, Ying J, Zhou A. NGS-based oncogenic mutations analysis in advanced colorectal cancer patients improves targeted therapy prediction. *Pathol Res Pract* 2019; **215**: 483-489 [PMID: 30611619 DOI: 10.1016/j.prp.2018.12.037]
24 **Fearon ER**, Vogelstein B. A genetic model for colorectal tumorigenesis. *Cell* 1990; **61**: 759-767 [PMID: 2188735 DOI: 10.1016/0092-8674(90)90186-i]
25 **Kronborg O**, Fenger C, Olsen J, Jørgensen OD, Søndergaard O. Randomised study of screening for colorectal cancer with faecal-occult-blood test. *Lancet* 1996; **348**: 1467-1471 [PMID: 8942774 DOI: 10.1016/S0140-6736(96)03430-7]
26 **Soussi T**, Wiman KG. Shaping genetic alterations in human cancer: the p53 mutation paradigm. *Cancer Cell* 2007; **12**: 303-312 [PMID: 17936556 DOI: 10.1016/j.ccr.2007.10.001]
27 **Li XL**, Zhou J, Chen ZR, Chng WJ. P53 mutations in colorectal cancer - molecular pathogenesis and pharmacological reactivation. *World J Gastroenterol* 2015; **21**: 84-93 [PMID: 25574081 DOI: 10.3748/wjg.v21.i1.84]
28 **Tong X**, Xu D, Mishra RK, Jones RD, Sun L, Schiltz GE, Liao J, Yang GY. Identification of a druggable protein-protein interaction site between mutant p53 and its stabilizing chaperone DNAJA1. *J Biol Chem* 2021; **296**: 100098 [PMID: 33208462 DOI: 10.1074/jbc.RA120.014749]
29 **Shah HD**, Saranath D, Murthy V. A molecular dynamics and docking study to screen anti-cancer compounds targeting mutated p53. *J Biomol Struct Dyn* 2022; **40**: 2407-2416 [PMID: 33111621 DOI: 10.1080/07391102.2020.1839559]
30 **Navalkar A**, Ghosh S, Pandey S, Paul A, Datta D, Maji SK. Prion-like p53 Amyloids in Cancer. *Biochemistry* 2020; **59**: 146-155 [PMID: 31603660 DOI: 10.1021/acs.biochem.9b00796]

31 **Cho Y**, Gorina S, Jeffrey PD, Pavletich NP. Crystal structure of a p53 tumor suppressor-DNA complex: understanding tumorigenic mutations. *Science* 1994; **265**: 346-355 [PMID: 8023157 DOI: 10.1126/science.8023157]

32 **Lo W**, Parkhurst M, Robbins PF, Tran E, Lu YC, Jia L, Gartner JJ, Pasetto A, Deniger D, Malekzadeh P, Shelton TE, Prickett T, Ray S, Kivitz S, Paria BC, Kriley I, Schrump DS, Rosenberg SA. Immunologic Recognition of a Shared p53 Mutated Neoantigen in a Patient with Metastatic Colorectal Cancer. *Cancer Immunol Res* 2019; **7**: 534-543 [PMID: 30709841 DOI: 10.1158/2326-6066.CIR-18-0686]

33 **Olszewski MB**, Pruszko M, Snaar-Jagalska E, Zylicz A, Zylicz M. Diverse and cancer typespecific roles of the p53 R248Q gainoffunction mutation in cancer migration and invasiveness. *Int J Oncol* 2019; **54**: 1168-1182 [PMID: 30968154 DOI: 10.3892/ijo.2019.4723]

34 **Yun J**, Mullarky E, Lu C, Bosch KN, Kavalier A, Rivera K, Roper J, Chio II, Giannopoulou EG, Rago C, Muley A, Asara JM, Paik J, Elemento O, Chen Z, Pappin DJ, Dow LE, Papadopoulos N, Gross SS, Cantley LC. Vitamin C selectively kills KRAS and BRAF mutant colorectal cancer cells by targeting GAPDH. *Science* 2015; **350**: 1391-1396 [PMID: 26541605 DOI: 10.1126/science.aaa5004]

35 **Armengol G**, Sarhadi VK, Ghanbari R, Doghaei-Moghaddam M, Ansari R, Sotoudeh M, Puolakkainen P, Kokkola A, Malekzadeh R, Knuutila S. Driver Gene Mutations in Stools of Colorectal Carcinoma Patients Detected by Targeted Next-Generation Sequencing. *J Mol Diagn* 2016; **18**: 471-479 [PMID: 27155048 DOI: 10.1016/j.jmoldx.2016.01.008]

36 **Knight JRP**, Alexandrou C, Skalka GL, Vlahov N, Pennel K, Officer L, Teodosio A, Kanellos G, Gay DM, May-Wilson S, Smith EM, Najumudeen AK, Gilroy K, Ridgway RA, Flanagan DJ, Smith RCL, McDonald L, MacKay C, Cheasty A, McArthur K, Stanway E, Leach JD, Jackstadt R, Waldron JA, Campbell AD, Vlachogiannis G, Valeri N, Haigis KM, Sonenberg N, Proud CG, Jones NP, Swarbrick ME, McKinnon HJ, Faller WJ, Le Quesne J, Edwards J, Willis AE, Bushell M, Sansom OJ. MNK Inhibition Sensitizes *KRAS*-Mutant Colorectal Cancer to mTORC1 Inhibition by Reducing eIF4E Phosphorylation and c-MYC Expression. *Cancer Discov* 2021; **11**: 1228-1247 [PMID: 33328217 DOI: 10.1158/2159-8290.CD-20-0652]

37 **Poulin EJ**, Bera AK, Lu J, Lin YJ, Strasser SD, Paulo JA, Huang TQ, Morales C, Yan W, Cook J, Nowak JA, Brubaker DK, Joughin BA, Johnson CW, DeStefanis RA, Ghazi PC, Gondi S, Wales TE, Iacob RE, Bogdanova L, Gierut JJ, Li Y, Engen JR, Perez-Mancera PA, Braun BS, Gygi SP, Lauffenburger DA, Westover KD, Haigis KM. Tissue-Specific Oncogenic Activity of $KRAS^{A146T}$. *Cancer Discov* 2019; **9**: 738-755 [PMID: 30952657 DOI: 10.1158/2159-8290.CD-18-1220]

38 **Mulla N**, Alshareef A, Syed AR, Al-Jahel M. Clinico-Pathological Study of K-ras Mutations in Colorectal Tumors: A Single-Center Retrospective Study of 51 Patients in Madinah, Saudi Arabia. *Cureus* 2020; **12**: e9978 [PMID: 32983680 DOI: 10.7759/cureus.9978]

39 **Ottaiano A**, Normanno N, Facchini S, Cassata A, Nappi A, Romano C, Silvestro L, De Stefano A, Rachiglio AM, Roma C, Maiello MR, Scala S, Delrio P, Tatangelo F, Di Mauro A, Botti G, Avallone A, Nasti G. Study of Ras Mutations' Prognostic Value in Metastatic Colorectal Cancer: STORIA Analysis. *Cancers (Basel)* 2020; **12** [PMID: 32708575 DOI: 10.3390/cancers12071919]

40 **Varshavi D**, Varshavi D, McCarthy N, Veselkov K, Keun HC, Everett JR. Metabolic characterization of colorectal cancer cells harbouring different KRAS mutations in codon 12, 13, 61 and 146 using human SW48 isogenic cell lines. *Metabolomics* 2020; **16**: 51 [PMID: 32300895 DOI: 10.1007/s11306-020-01674-2]

41 **Phull MS**, Jadav SS, Gundla R, Mainkar PS. A perspective on medicinal chemistry approaches towards adenomatous polyposis coli and Wnt signal based colorectal cancer inhibitors. *Eur J Med Chem* 2021; **212**: 113149 [PMID: 33445154 DOI: 10.1016/j.ejmech.2020.113149]

42 **Caspi M**, Wittenstein A, Kazelnik M, Shor-Nareznoy Y, Rosin-Arbesfeld R. Therapeutic targeting of the oncogenic Wnt signaling pathway for treating colorectal cancer and other colonic disorders. *Adv Drug Deliv Rev* 2021; **169**: 118-136 [PMID: 33346022 DOI: 10.1016/j.addr.2020.12.010]

43 **Aitchison A**, Hakkaart C, Day RC, Morrin HR, Frizelle FA, Keenan JI. *APC* Mutations Are Not Confined to Hotspot Regions in Early-Onset Colorectal Cancer. *Cancers (Basel)* 2020; **12** [PMID: 33352971 DOI: 10.3390/cancers12123829]

44 **Luo J**. Mutation analysis of sporadic colorectal cancer and polypby next-generation of sequencing. M.M. Thesis, Fujian Medical University. 2015. [cited 10 January 2022]. Available from: https://kns.cnki.net/kns8/defaultresult/index

World Journal of Gastroenterology

Submit a Manuscript: https://www.f6publishing.com

World J Gastroenterol 2022 July 7; 28(25): 2937-2954

DOI: 10.3748/wjg.v28.i25.2937

ISSN 1007-9327 (print) ISSN 2219-2840 (online)

ORIGINAL ARTICLE

Basic Study

Mechanism and therapeutic strategy of hepatic *TM6SF2*-deficient non-alcoholic fatty liver diseases *via in vivo* and *in vitro* experiments

Zu-Yin Li, Gang Wu, Chen Qiu, Zhi-Jie Zhou, Yu-Peng Wang, Guo-He Song, Chao Xiao, Xin Zhang, Gui-Long Deng, Rui-Tao Wang, Yu-Long Yang, Xiao-Liang Wang

Specialty type: Gastroenterology and hepatology

Provenance and peer review: Unsolicited article; Externally peer reviewed.

Peer-review model: Single blind

Peer-review report's scientific quality classification
Grade A (Excellent): 0
Grade B (Very good): 0
Grade C (Good): C, C
Grade D (Fair): 0
Grade E (Poor): 0

P-Reviewer: Di Leo A, Italy; Sasikala M, India
A-Editor: Liu X, China

Received: December 21, 2021
Peer-review started: December 21, 2021
First decision: March 10, 2022
Revised: April 15, 2022
Accepted: May 22, 2022
Article in press: May 22, 2022
Published online: July 7, 2022

Zu-Yin Li, Department of Hepatobiliary Surgery, Peking University People's Hospital, Beijing 100034, China

Gang Wu, Department of Gastrointestinal Surgery, Henan Provincial People's Hospital, Zhengzhou 450003, Henan Province, China

Chen Qiu, Institute of Gallstone Disease, Shanghai East Hospital, Shanghai 200120, China

Zhi-Jie Zhou, Department of General Surgery, Huashan Hospital North, Shanghai 201907, China

Yu-Peng Wang, Guo-He Song, Department of Liver Surgery and Transplantation, Liver Cancer Institute, Zhongshan Hospital, Fudan University, Shanghai 200032, China

Chao Xiao, Department of General Surgery, Huashan Hospital, Fudan University, Shanghai 200041, China

Xin Zhang, Xiao-Liang Wang, Department of General Surgery, Qingpu Branch of Zhongshan Hospital Affiliated to Fudan University, Shanghai 201700, China

Gui-Long Deng, Rui-Tao Wang, Department of General Surgery, Shanghai General Hospital, Shanghai 201600, China

Yu-Long Yang, Institute of Gallstone Disease, Center of Gallbladder Disease, Shanghai East Hospital, Tongji University School of Medicine, Shanghai 200120, China

Xiao-Liang Wang, Department of Hepatobiliary Surgery, Shanghai Pudong Hospital, Fudan University Pudong Medical Center, Shanghai 201399, China

Corresponding author: Xiao-Liang Wang, PhD, Chief Doctor, Department of Hepatobiliary Surgery, Shanghai Pudong Hospital, Fudan University Pudong Medical Center, No. 2800 Gongwei Road, Huinan Town, Pudong New Area, Shanghai 201399, China.
xiaoliangwang2018@163.com

Abstract

BACKGROUND

The lack of effective pharmacotherapies for nonalcoholic fatty liver disease (NAFLD) is mainly attributed to insufficient research on its pathogenesis. The

pathogenesis of TM6SF2-efficient NAFLD remains unclear, resulting in a lack of therapeutic strategies for TM6SF2-deficient patients.

AIM

To investigate the role of TM6SF2 in fatty acid metabolism in the context of fatty liver and propose possible therapeutic strategies for NAFLD caused by TM6SF2 deficiency.

METHODS

Liver samples collected from both NAFLD mouse models and human participants (80 cases) were used to evaluate the expression of TM6SF2 by using western blotting, immunohistochemistry, and quantitative polymerase chain reaction. RNA-seq data retrieved from the Gene Expression Omnibus database were used to confirm the over-expression of TM6SF2. Knockdown and overexpression of TM6SF2 were performed to clarify the mechanistic basis of hepatic lipid accumulation in NAFLD. MK-4074 administration was used as a therapeutic intervention to evaluate its effect on NAFLD caused by TM6SF2 deficiency.

RESULTS

Hepatic TM6SF2 levels were elevated in patients with NAFLD and NAFLD mouse models. TM6SF2 overexpression can reduce hepatic lipid accumulation, suggesting a protective role for TM6SF2 in a high-fat diet (HFD). Downregulation of TM6SF2, simulating the TM6SF2 E167K mutation condition, increases intracellular lipid deposition due to dysregulated fatty acid metabolism and is characterized by enhanced fatty acid uptake and synthesis, accompanied by impaired fatty acid oxidation. Owing to the potential effect of TM6SF2 deficiency on lipid metabolism, the application of an acetyl-CoA carboxylase inhibitor (MK-4074) could reverse the NAFLD phenotypes caused by TM6SF2 deficiency.

CONCLUSION

TM6SF2 plays a protective role in the HFD condition; its deficiency enhanced hepatic lipid accumulation through dysregulated fatty acid metabolism, and MK-4074 treatment could alleviate the NAFLD phenotypes caused by TM6SF2 deficiency.

Key Words: TM6SF2; Nonalcoholic fatty liver disease; Fatty acid metabolism; Treatment; MK-4074

©The Author(s) 2022. Published by Baishideng Publishing Group Inc. All rights reserved.

Core Tip: In this study, we observed TM6SF2 overexpression in nonalcoholic fatty liver disease (NAFLD) cases. TM6SF2 overexpression can reduce hepatic lipid accumulation, suggesting a protective role for TM6SF2 in a high-fat diet. Meanwhile, there is an imbalance in the processes of uptake, synthesis, and intracellular expense of fatty acids in TM6SF2-deficient mouse models. Therefore, we propose possible therapeutic strategies for NAFLD caused by TM6SF2 deficiency.

Citation: Li ZY, Wu G, Qiu C, Zhou ZJ, Wang YP, Song GH, Xiao C, Zhang X, Deng GL, Wang RT, Yang YL, Wang XL. Mechanism and therapeutic strategy of hepatic *TM6SF2*-deficient non-alcoholic fatty liver diseases *via in vivo* and *in vitro* experiments. *World J Gastroenterol* 2022; 28(25): 2937-2954
URL: https://www.wjgnet.com/1007-9327/full/v28/i25/2937.htm
DOI: https://dx.doi.org/10.3748/wjg.v28.i25.2937

INTRODUCTION

The prevalence of nonalcoholic fatty liver disease (NAFLD) is rapidly increasing and is now more than one-quarter of the global population[1]. Approximately 6%–30% of patients with NAFLD evolve from simple steatosis (SS) to steatohepatitis, characterized by excessive hepatic lipid accumulation, inflammation, and hepatocyte damage[2,3]. Long-term steatohepatitis can cause liver fibrosis, and its adverse outcome may include liver dysfunction and hepatocellular carcinoma[4,5]. The prognosis of NAFLD and its related complications varies among individuals, given that genetic variants affect the occurrence and progression of NAFLD[6]. The development of genome-wide association studies and high-throughput technologies has allowed for in-depth analysis of genetic risk factors for NAFLD[7,8]. Identification of genes with high-risk single nucleotide polymorphisms (SNPs) has allowed the screening of individuals with a genetic predisposition to NAFLD[9], and several studies have reported some potential SNP loci (*e.g.*, PNPLA3 rs738409, MBOAT7 rs641738, and PPARGC1A rs2290602)

associated with the susceptibility and progression of fatty liver[10-12]. To further elucidate the mechanistic basis of the link between potential SNPs and susceptibility to NAFLD, the functions of many candidate genes have been thoroughly investigated, including *TM6SF2*.

TM6SF2 is a multi-transmembrane protein expressed predominantly in the intestine and liver, implying a metabolism-related function[13]. Our previous study and others have demonstrated that the rs58542926 locus of TM6SF2 confers susceptibility to NAFLD[14-16]. The nonsynonymous variant of TM6SF2, rs58542926 (E167K), leads to protein misfolding, acceleration of protein degradation, and, therefore, a reduction in TM6SF2 protein levels and gene function[15]. Recently, several studies have focused on the influence of TM6SF2 deficiency or its E167K mutant on cholesterol metabolism and its association with reduced very low-density lipoproteins (VLDL) content that causes a decrease in hepatic triglyceride (TG) output[17-19]. Considering that the liver is the central hub for lipid metabolism, there is a balance among the processes of uptake, synthesis, and intracellular expense of fatty acids under normal circumstances. Hepatic lipid accumulation may occur when this balance is disrupted[20]. However, the regulatory role of TM6SF2 in fatty acid metabolism in the context of NAFLD remains largely unknown. Therefore, our study aimed to elucidate the influence of TM6SF2 on fatty acid metabolism in experimental NAFLD models.

The present study revealed that hepatic TM6SF2 expression was elevated in patients with NAFLD and mouse models. Our results suggest that TM6SF2 elevation is a compensatory response to NAFLD. Physiologically, the reactive overexpression of TM6SF2 can protect the liver and reduce hepatic lipid accumulation under the condition of a high-fat diet (HFD). Loss of TM6SF2 exacerbates hepatic lipid accumulation. Further investigation revealed that the enhanced processes of uptake and synthesis of fatty acids and impaired oxidation processes were observed in hepatic TM6SF2 deficiency, suggesting that TM6SF2 deficiency caused a pathogenic link between the metabolic dysfunction of fatty acids and hepatic steatosis in NAFLD. The elucidation of metabolic alterations suggested the way of therapeutic intervention, and our results showed that liver-specific acetyl-CoA carboxylase (ACC) inhibitor (MK-4074) would block the enhanced synthesis of fatty acid, improve fatty acid β-oxidation, and then reverse the NAFLD phenotypes caused by TM6SF2 deficiency. Collectively, this study suggested a protective role of TM6SF2 in HFD conditions, revealed a pivotal role of TM6SF2 in fatty acid metabolism, and suggested a therapeutic intervention for TM6SF2-deficient exacerbated NAFLD.

MATERIALS AND METHODS

Cell culture

Knockdown of the *TM6SF2* gene was mediated by the lentiviral vectors pLenti6.3-MCS-TM6SF2-EGFP (sh-TM6SF2) or pLenti6.3-MCS-EGFP (sh-Ctrl). Target sequence for sh-TM6SF2: TGACCTGGCCCT-TGTCATATA. After two or three generations of antibiotic screening, the expression of TM6SF2 was evaluated by immunoblotting. All cells were cultured in DMEM containing 10% fetal bovine serum (FBS) and 1% penicillin-streptomycin (Cat. No. C125C5, NCM Biotech, Suzhou, China) at 37 ℃ and 5% CO_2. The cells were cultured under 1% O_2 and 5% CO_2 for 24 h to simulate hypoxic conditions. For starvation, cells were cultured in DMEM containing 0.1% FBS for 24 h.

Western blot

Cells in a 6-cm dish at 80% confluence were lysed with 250 μL of RIPA lysis buffer and centrifuged at 13000 rpm. The quantification of the supernatant collected was assessed using the BCA method (Beyotime, Jiangsu, China). Proteins were transferred to a 0.45 μm PVDF membrane according to the standard immunoblotting protocol after electrophoresis. The membrane was blocked in 5% fat-free milk and then maintained in primary antibodies for 12 h at 4 ℃. After washing, the membrane was incubated with HRP-labeled goat anti-rabbit (mouse) antibody at 25 ℃ for 60 min and visualized using an ECL reagent (Millipore, MA, United States). Supplementary Table 1 lists the antibodies used in this study.

Clinical specimens

Liver specimens were collected from the Shanghai General Hospital. Parts of the specimens were snap frozen in liquid nitrogen and then transferred to a -80℃ refrigerator to detect mRNA levels, and some were stored in formaldehyde solution for later pathological examination. When ≥ 5% of hepatocytes had steatosis, NAFLD diagnosis was confirmed. The diagnosis of the tissue sections was independently reviewed by two pathologists. This study was approved by the Ethics Committee of the Shanghai General Hospital and was performed strictly in accordance with the Declaration of Helsinki. All patients or their family members were fully informed of the study and signed written consent forms.

Immunohistochemistry

Paraffin-embedded liver tissues were deparaffinized using standard protocols and rehydrated. After antigen retrieval, the tissue was blocked and incubated with an anti-TM6SF2 (1:200) antibody overnight at 4 ℃. Then the slides were washed and incubated with biotin-labeled goat anti-mouse IgG (H + L) at

37 ℃ for 15 min and developed with a DAB work solution. Images were obtained using a microscope (Leica, Germany).

Real-time polymerase chain reaction assay

A total of 50 mg of liver samples from mice or humans was lysed with RNAiso Plus reagent (Takara Biotechnology, Otsu, Japan), and total RNA was extracted according to the standard protocol. Reverse transcription of 500ng of RNA was performed using the RNA polymerase chain reaction (PCR) Kit (Takara Biotechnology), and the resulting cDNA was used as the PCR template. Quantification of target gene expression was performed using a LightCycler® 96 (Roche, Switzerland) and a Hieff® quantitative PCR SYBR Green Master Mix (No Rox) kit (Yeasen Biotechnology Co., Ltd, China). The mRNA level of *β-actin* was used as the endogenous control. We chose the TM6SF2 level of one patient as the reference, and the TM6SF2 levels of all other patients were presented several times of this reference. The primers used are listed in Supplementary Table 1.

Experimental animals

The AAV system (type 8) expressing TM6SF2 short hairpin RNA (shRNA) (AAV-shTm6sf2) or overexpressing human TM6SF2 (AAV8-TM6SF2) was used to regulate the levels of TM6SF2 in C57BL/6 mice. The corresponding controls were AAV-shNC and AAV8-vector, respectively. All mice were fed a normal chow diet (NCD) for three days, and then 100 μL of AAV8 virus (2×10^{11}) was injected into the tail vein. Transfection efficiency was determined by immunoblotting. Male mice weighing 19–22 g (aged 4–6 wk) were housed in a 23 ± 2°C environment with a 12 h light/dark cycle. All mice were allowed water ad libitum and were continuously fed an HFD or NCD for 16 wk. For MK-4074 treatment, the mice were primarily fed an 8-wk HFD to induce NAFLD phenotypes and then administered MK4074 (10 mg/kg/day) or placebo (normal saline) for an additional eight weeks on the same diets.

Evaluation of serum parameters and hepatic lipid content

The concentrations of cytokines, metabolites, and hepatic enzymes in serum were determined using commercial kits [ab208348 for tumor necrosis factor (TNF), ab197742 for interleukin (IL)-1β, ab222503 for IL-6, JLC049 for CCL2, JLC5800 for CXCL10, ab180875 for acetoacetate, ab180876 for β-hydroxybutyrate (β-OH), C010-2-1 for aspartate transaminase (AST), and C009-2-1 for alanine aminotransferase (ALT)] according to the manufacturer's instructions. The hepatic lipid content and malonyl-CoA levels were also measured using commercial kits [A110-1-1 for TG, A111-1-1 for total cholesterol (TC), A042-2-1 for non-esterified fatty acids (NEFA), and JL47416 for malonyl-CoA], and normalized by the total protein. The details of all the commercial kits used are listed in Supplementary Table 1.

Microarrays

After palmitic acid (PA, 150 μmol/L) stimulation for 24 h, total RNA was extracted from both TM6SF2-knockdown L02 cells and the corresponding controls using RNAiso Plus (Takara Biotechnology). Microarray gene expression analysis was performed by Illumina sequencing. We analyzed differentially expressed genes (DEGs) between sh-Ctrl and sh-TM6SF2 cells by using the "edgeR" package based on the R platform[21]. Fold change > 1.2 and adjusted *P*-value < 0.05 were set as the screening cutoffs for the upregulated DEGs. These DEGs were further analyzed *via* DAVID 6.8 (https://david.ncifcrf.gov/) for Kyoto Encyclopedia of Genes and Genomes (KEGG) pathway analyses. The "ggplot2" package in R is used for result visualization.

Preparation of fatty acid solution

A 5 mmol/L stock solution of PA (Sigma-Aldrich) was obtained by dissolving PA in 3% of bovine serum albumin (BSA, Sigma-Aldrich) medium by continuous stirring for approximately 4 h in a 60 °C water bath. The stock solution was then diluted in DMEM to achieve the designated concentration, and 3% of BSA was used as a control. The concentrations of free fatty acids range from 0.1 to 0.7 mmol/L[22-24].

Glucose and insulin tolerance test

Glucose tolerance test (GTT) and insulin tolerance test (ITT) were performed as previously described [25]. After the above steps were completed, the glucose concentrations of the blood collected from the tail vein at the indicated points were analyzed immediately using a glucose meter (Yuwell, China).

Nile red staining

After sh-ctrl and sh-TM6SF2 L02 cells were constructed, they were incubated in DMEM containing 150 μmol/L of PA for 24 h to generate a steatosis cell model. Cells were then fixed with 4% paraformaldehyde and incubated with 0.1 μg/mL Nile Red for 15 min. After washing with PBS, the cells were incubated with DAPI (Solarbio) for 5 min. Images were taken with a Leica microscope (Leica, Germany) and quantified using the ImageJ software.

Magnetic resonance imaging

Magnetic resonance imaging (MRI) imaging was performed using a 7.0 T Bruker BioSpec MRI scanner (Bruker, United States). Before imaging, the mice were fasted overnight to avoid disturbance of stomach contents during liver imaging. The mice were first anesthetized with oxygen containing 2%–3% isoflurane and then placed in a prone position with their heads facing inward. Throughout the imaging process, the mice were continuously provided with oxygen mixed with 1%-3% isoflurane through the nosecone to maintain the respiratory rate at 50-70 breaths/minute. All mice underwent abdominal MRI to determine the maximum cross-sectional area of the liver. The region of interest was analyzed using ImageJ software, and the size of the cross-sectional area was represented by the number of pixels.

Histological analysis

Liver sections were embedded in paraffin and stained with hematoxylin and eosin (H&E), and frozen liver sections were stained with Oil Red O (O8010-5g; Solarbio) for lipid visualization. Images were obtained using a light microscope (Leica). Oil Red O- stained sections were quantified using ImageJ software.

FAO measurement

A total of 6000 cells were seeded in an XF96 cell culture microplate, and each group was assayed in five or six replicate wells. After cell adherence (about 8 h), the growth medium was changed to a substrate-limited growth medium (0.5 mmol/L of glucose, 1 mmol/L of GlutaMAX, 0.5 mmol/L of XF L-carnitine, 1% FBS, pH 7.4) for overnight incubation. Before the Seahorse Bioscience XF96 instrument (Agilent, United States) was started, the medium was changed to a PA measurement medium. Different inhibitors (oligomycin 2 μmol/L, FCCP 2 μmol/L, and R/A 1.2 μmol/L) were added to each chamber when the instrument began to measure the oxygen change rate. The difference in each group's oxygen consumption rate (OCR) revealed the level of fatty acid oxidation (FAO) based on palmitate substrates. The basal respiration, maximal respiration, spare respiratory capacity, and ATP production were calculated.

Cell viability assay

Cell viability was assessed using the CCK-8 assay (NCM Biotech, China). Sh-ctrl and sh-TM6SF2 cells were seeded in a 96-well plate at a density of 5000 cells *per* well, and a cell viability assay was performed after PA or fatty acid-free BSA treatment for 24 h. Absorbance (450 nm) was measured using a microplate reader (BioTek, United States). Each sample was assayed in five replicate wells, and the experiment was independently performed three times.

Quantitation of intracellular TG levels in cell lines

After PA or BSA treatment for 24 h, cells were lysed on ice with RIPA buffer (Beyotime, Beijing, China) for 20 min and centrifuged at 13000 rpm for 20 min at 4 °C. Then the supernatant was transferred to a new tube. TG levels were evaluated using a TG detection kit (Nanjing Jiancheng, Jiangsu, China) and normalized to the total protein level. The experiment was independently performed three times.

Bioinformatic analyses

Expression profiles of TM6SF2 in NAFLD cases were retrieved from the Gene Expression Omnibus (GEO; www.ncbi.nlm.nih.gov/geo) database. The accession numbers are GSE130970, GSE48452, GSE83452, and GSE89632. The details of the cohorts are presented in Supplementary Table 2.

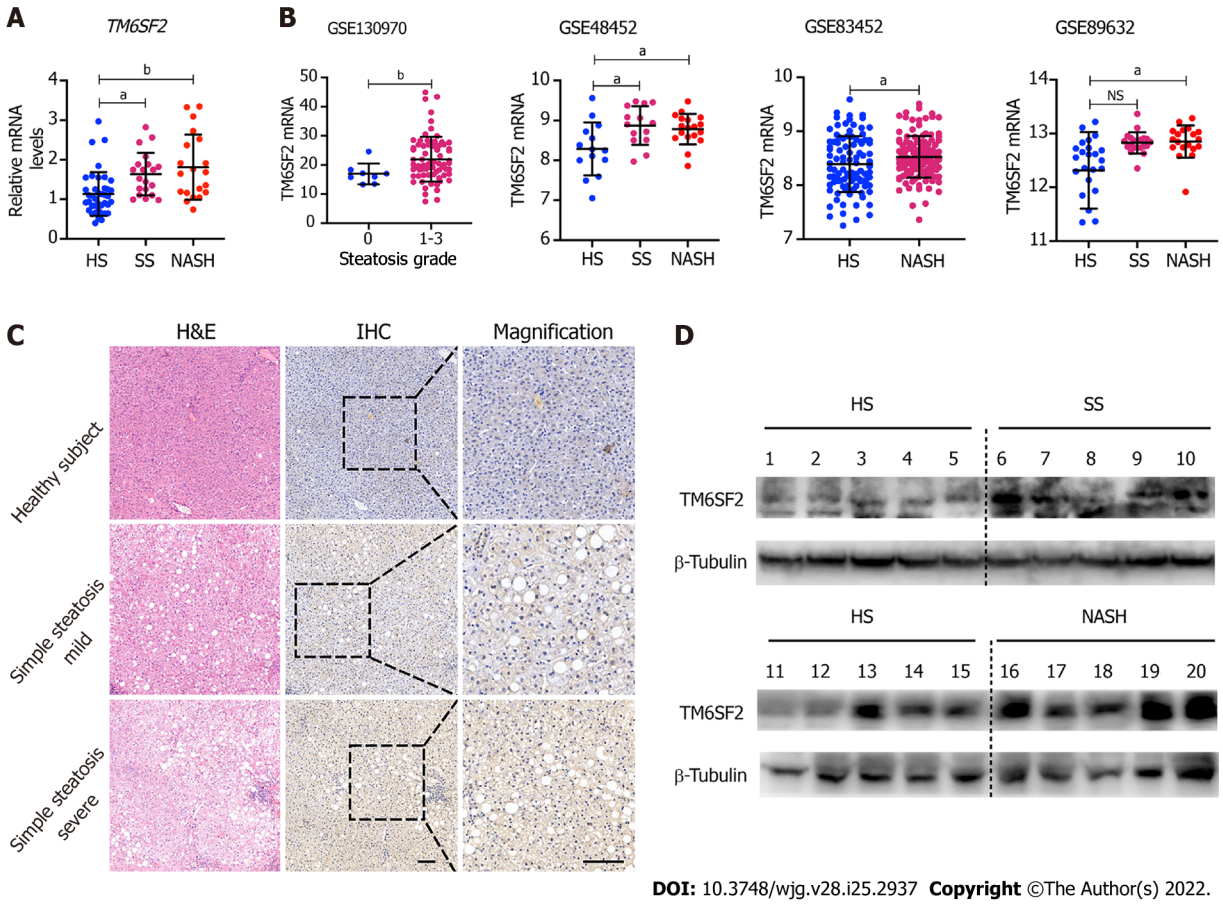
Statistical analysis

All data are presented as the mean ± SD. Student's t-test was used to evaluate the differences between the two groups. Differences between more than two groups were compared using one-way analysis of variance followed by Tukey's multiple comparisons test. *In vitro* studies, all experiments were independently performed three times in vitro. The SPSS software (version 25.0) was used for all statistical analyses. $P < 0.05$ was considered statistically significant and denoted as $^{a}P < 0.05$, $^{b}P < 0.01$, and $^{c}P < 0.001$; NS: Not significant.

RESULTS

Hepatic TM6SF2 expression is upregulated in patients with NAFLD and HFD-induced mice models

The mRNA levels of TM6SF2 were examined in 80 liver samples of patients with NAFLD and healthy subjects ($n = 40$), which showed that the transcriptional levels of TM6SF2 were both elevated in patients with SS or nonalcoholic steatohepatitis (NASH) (Figure 1A, SS: $n = 20$; NASH: $n = 20$). Additionally, we retrospectively analyzed another four transcriptomic datasets retrieved from the GEO database (GSE13970, GSE48452, GSE83452, and GSE89632, Figure 1B), which contained transcriptional profiles of both healthy participants and patients with NAFLD. Patients with SS or NASH displayed higher hepatic



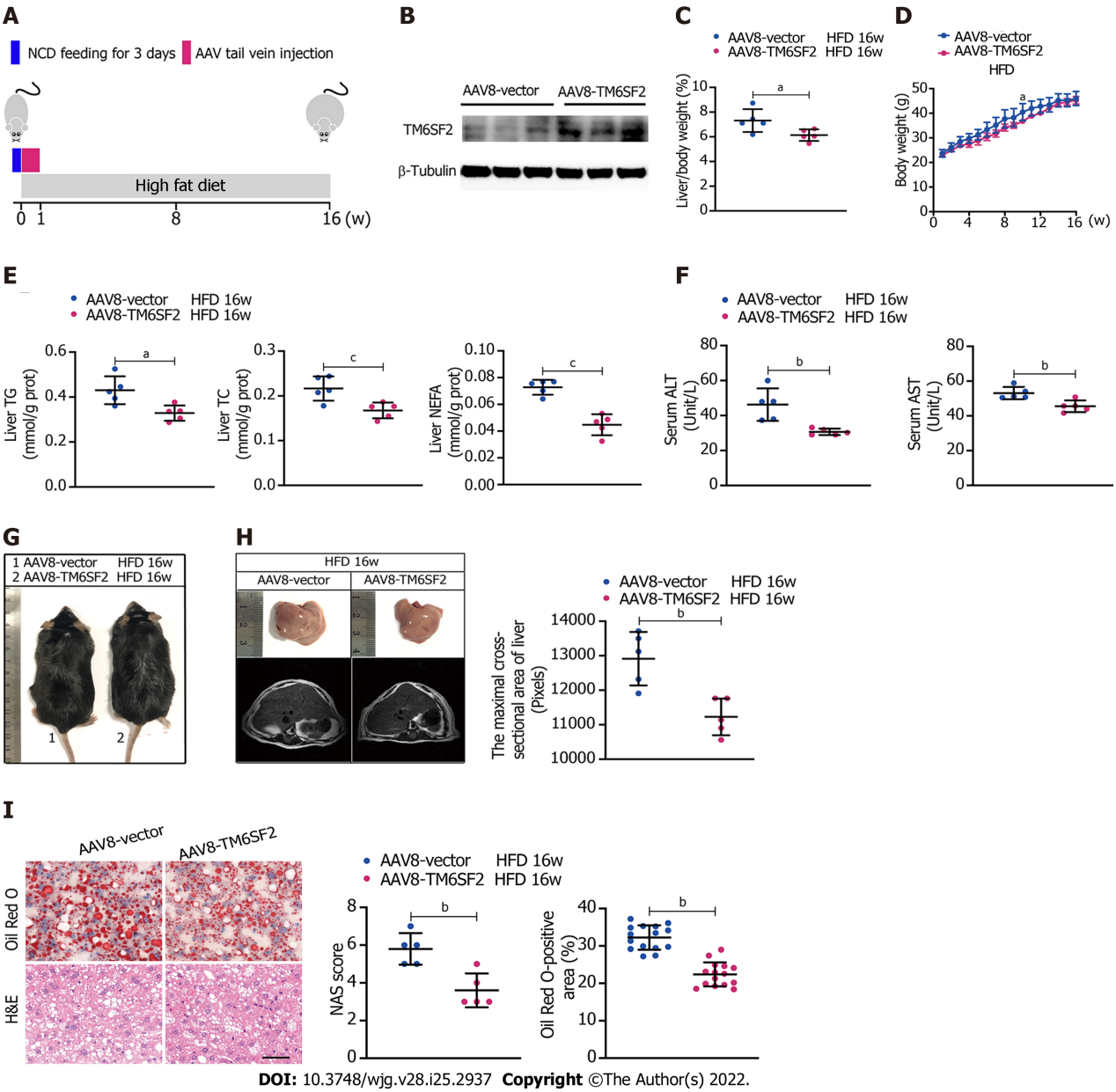
DOI: 10.3748/wjg.v28.i25.2937 **Copyright** ©The Author(s) 2022.

Figure 1 Hepatic TM6SF2 expression is upregulated in nonalcoholic fatty liver disease patients. A: Hepatic mRNA levels of TM6SF2 in liver specimens, including healthy subjects (HS, *n* = 40) and patients with simple steatosis (SS, *n* = 20) or nonalcoholic steatohepatitis (NASH, *n* = 20); B: Hepatic mRNA levels of TM6SF2 in individuals with or without nonalcoholic fatty liver disease (NAFLD) from four expression microarray series retracted from Gene Expression Omnibus database; C: Immunohistochemical staining with TM6SF2 was performed on individuals with or without NAFLD. Representative images of normal liver tissues *vs* tissues of SS were shown. Scale bars: 50 μm; D: Immunoblot analysis of TM6SF2 expression in liver specimens. HS (*n* = 10), SS (*n* = 5) and NASH (*n* = 5). $^{a}P < 0.05$; $^{b}P < 0.01$, NS: Not significant; HS: Healthy subjects; SS: Simple steatosis; NASH: Nonalcoholic steatohepatitis; IHC: Immunohistochemistry; H&E: Hematoxylin and eosin.

TM6SF2 mRNA levels than healthy participants. Immunohistochemistry staining indicated that TM6SF2 tended to upregulate TM6SF2 expression from normal liver to severe SS (Figure 1C). We also noted upregulation of TM6SF2 protein in the liver samples of patients with SS or NASH (Figure 1D). To further confirm TM6SF2 overexpression under overnutrition, we evaluated the changes in TM6SF2 expression in and *in vitro* NAFLD cell model and stimulated two cell lines, L02 and HepG2, with PA, as it was reported that this *in vitro* model mimics steatosis *in vivo*[22-24]. The results showed that PA stimulation increased the protein levels of TM6SF2 in a time- and dose-dependent manner (Supplementary Figure 1A). Further, whether in protein or mRNA levels, the augmented TM6SF2 expression was also demonstrated in HFD-fed mice for 12 wk (Supplementary Figure 1B). These results revealed that hepatic TM6SF2 levels were upregulated in patients with NAFLD and HFD-induced mouse models.

TM6SF2 overexpression mitigates hepatic lipid accumulation in HFD-induced mice models

As we had found that the levels of TM6SF2 were increased in participants with NAFLD and HFD-induced models, we wanted to determine the physiological significance of TM6SF2 elevation when NAFLD phenotypes occur. To this end, we used the AAV8 vector to deliver human TM6SF2 (AAV8-TM6SF2) in the livers of mice (AAV8-vector was used as a control) and fed them HFD for 16 wk (Figure 2A and B). The results showed that TM6SF2 overexpression in the liver significantly reduced the liver/body weight ratio, and its impact on body weight was limited (Figure 2C and D). Hepatic TM6SF2 overexpression in mice resulted in lower levels of hepatic lipid content as well as lower serum ALT and AST levels (Figure 2E and F). TM6SF2-overexpression groups relative to controls displayed equal body size (Figure 2G) but demonstrated a minor fatty liver and a smaller cross-sectional area of the fatty liver (Figure 2H). Hepatic lipid accumulation was also ameliorated in AAV8-TM6SF2 mice, as indicated by the pathological examination (Figure 2I). We also observed that TM6SF2 knocked-down cells reconstituted with wild-type TM6SF2 exhibited decreased intracellular lipid accumulation and



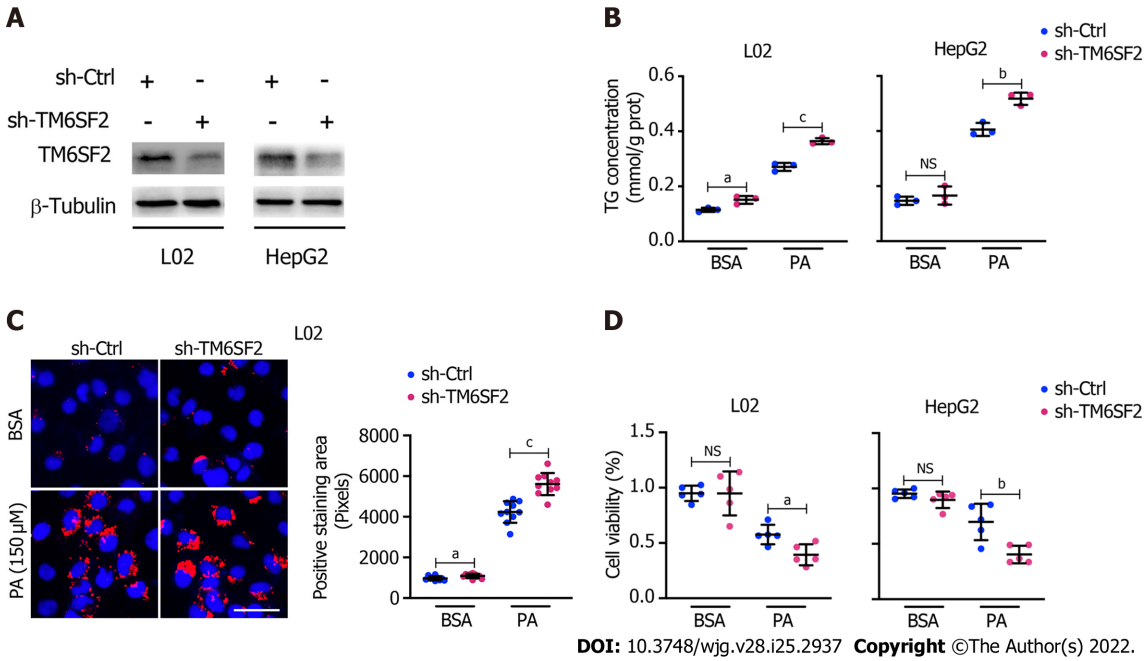
DOI: 10.3748/wjg.v28.i25.2937 **Copyright** ©The Author(s) 2022.

Figure 2 Overexpression of TM6SF2 improves hepatic lipid accumulation in high-fat diet-induced mice models. A: Schematic representation of animal experiments. Mice were injected with AAV8-vector or AAV8-TM6SF2 virus *via* the tail vein and fed a high-fat diet for 16 wk (n = 5 mice *per* group); B: The efficiency of TM6SF2 overexpression in liver were shown; C-F: The liver/body weight ratio (C), the body weight (D), hepatic lipid content (E), and serum levels of alanine aminotransferase and aspartate transaminase (F) were shown; G: Representative images of gross morphology; H: Left, representative photos of fatty livers (top) and livers subjected to magnetic resonance imaging scanning (bottom) were shown. Right, the maximal cross-sectional area of livers is quantified by the number of pixels; I: Left, representative images of hematoxylin and eosin-staining (left) and Oil Red O-staining (right) of liver sections. Right, the nonalcoholic fatty liver disease activity score (left) and quantification of lipid (right, 8 fields of each mouse were examined) were performed. $^{a}P < 0.05$; $^{b}P < 0.01$; $^{c}P < 0.001$. H&E: Hematoxylin and eosin; NCD: Normal chow diet; HFD: High-fat diet; NAS: Nonalcoholic fatty liver disease activity score.

improved PA-induced cell death (Supplementary Figure 2). This evidence suggests that the elevation of TM6SF2 is a potential reaction to antagonize NAFLD phenotypes and serves a protective role during NAFLD.

Knockdown of TM6SF2 promotes hepatic lipid accumulation and inflammation in the HFD-induced mice model

Pathologically, there exists a genetic E167K mutation in the TM6SF2 protein in humans, and those with the TM6SF2 E167K mutation are associated with an increased risk of NAFLD[26]. Ehrhardt *et al*[27] reported that the E167K mutation causes downregulation of TM6SF2 at the protein level. To simulate the E167K condition and explore the influence of TM6SF2 on lipid accumulation, we generated TM6SF2-knockdown cells in both the L02 and HepG2 cell lines (Figure 3A), which were incubated with PA (150 μmol/L) or BSA (fatty acid free) for 24 h. We found that TM6SF2-knockdown cells demonstrated higher levels of intracellular TG (Figure 3B) and more severe lipid accumulation (Figure 3C). Lipid overload



DOI: 10.3748/wjg.v28.i25.2937 **Copyright** ©The Author(s) 2022.

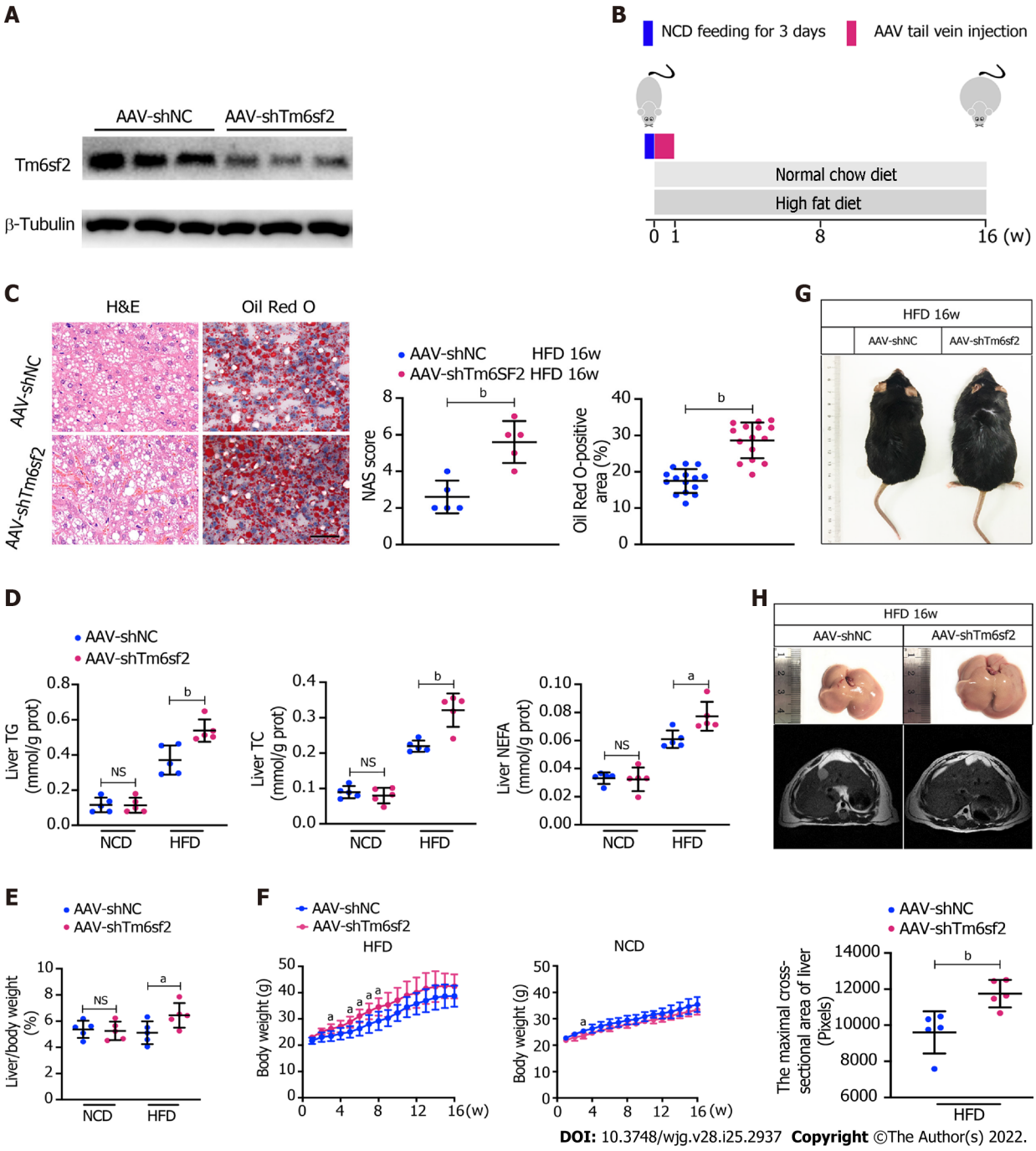
Figure 3 Knockdown of TM6SF2 promotes intracellular lipid accumulation and lipid-overload induced cell death. A: The efficiency of TM6SF2 knockdown in two cell lines; B: Intracellular triglyceride levels (n = 3) in TM6SF2-knockdown cells were examined after palmitic acid (PA) (150 μmol/L) or bovine serum albumin (BSA) (fatty acid free) treatment for 24 h; C: Nile red staining (left, nuclei labeled with DAPI, blue) and quantification of lipid accumulation (right) of sh-Ctrl or sh-TM6SF2 L02 cells after PA or BSA treatment. Scale bars: 50 μm; D: TM6SF2-knockdown cells were incubated with PA (150 μmol/L) or BSA for 24 h. The cellular viability was examined (n = 5). $^{a}P < 0.05$; $^{b}P < 0.01$; $^{c}P < 0.001$. NS: Not significant; BSA: Bovine serum albumin; PA: Palmitic acid; TG: Triglyceride; μM: μmol/L.

induces endoplasmic reticulum stress (ERS) and causes cell death[28,29]. The cell viability assay results proved that TM6SF2 knockdown markedly exacerbated PA-induced cell death (Figure 3D), which reflected the increase in lipid content in the TM6SF2-knockdown group. To determine whether TM6SF2 deficiency exacerbated hepatic steatosis *in vivo*, we generated hepatic TM6SF2-knockdown (hereafter referred to as AAV-shTm6sf2, AAV-shNC was used as a control) mice by injecting AAV vectors carrying TM6SF2-targeting shRNA, and mice were fed an HFD or NCD for 16 wk (Figure 4A and B). Compared to the control mice, the HFD-fed AAV-shTm6sf2 mice displayed severe hepatocellular ballooning degeneration and lipid accumulation, as shown by H&E and Oil Red O staining (Figure 4C); these mice had higher levels of hepatic TG, TC, and NEFA (Figure 4D). Similarly, AAV-shTm6sf2 mice had a higher liver/body weight ratio (Figure 4E) but exhibited a slightly higher body weight (Figure 4F) only at the initiation of feeding. In addition, hepatic TM6SF2-knockdown mice relative to controls displayed a modest increase in size (Figure 4G) but a significantly enlarged liver and a larger maximal cross-sectional area of the liver (Figure 4H). However, these parameters did not differ between the two groups when placed in a NCD environment (Figures 4D–F).

It is noteworthy that hepatic steatosis is often accompanied by inflammation, and the boundary between the two phases (SS and NASH) of NAFLD is blurred[30]. The hepatic TM6SF2-knockdown group displayed higher serum levels of inflammatory cytokines, such as TNF, IL-6, IL-1β, CCL2, and CXCL10 than control mice after 16 wk of HFD feeding (Supplementary Figure 3A). Consistently, hepatic expression of inflammation-related genes was also augmented in the AAV-shTm6sf2 group (Supplementary Figure 3B). Meanwhile, the AAV-shTm6sf2 group showed higher serum levels of ALT and AST (Supplementary Figure 3C) and more infiltrated neutrophils and macrophages than the AAV-shNC group (Supplementary Figure 3D). These results show that TM6SF2 knockdown promotes hepatic lipid accumulation and inflammation in an HFD-induced mouse model.

Hepatic knockdown of TM6SF2 enhances de novo lipogenesis

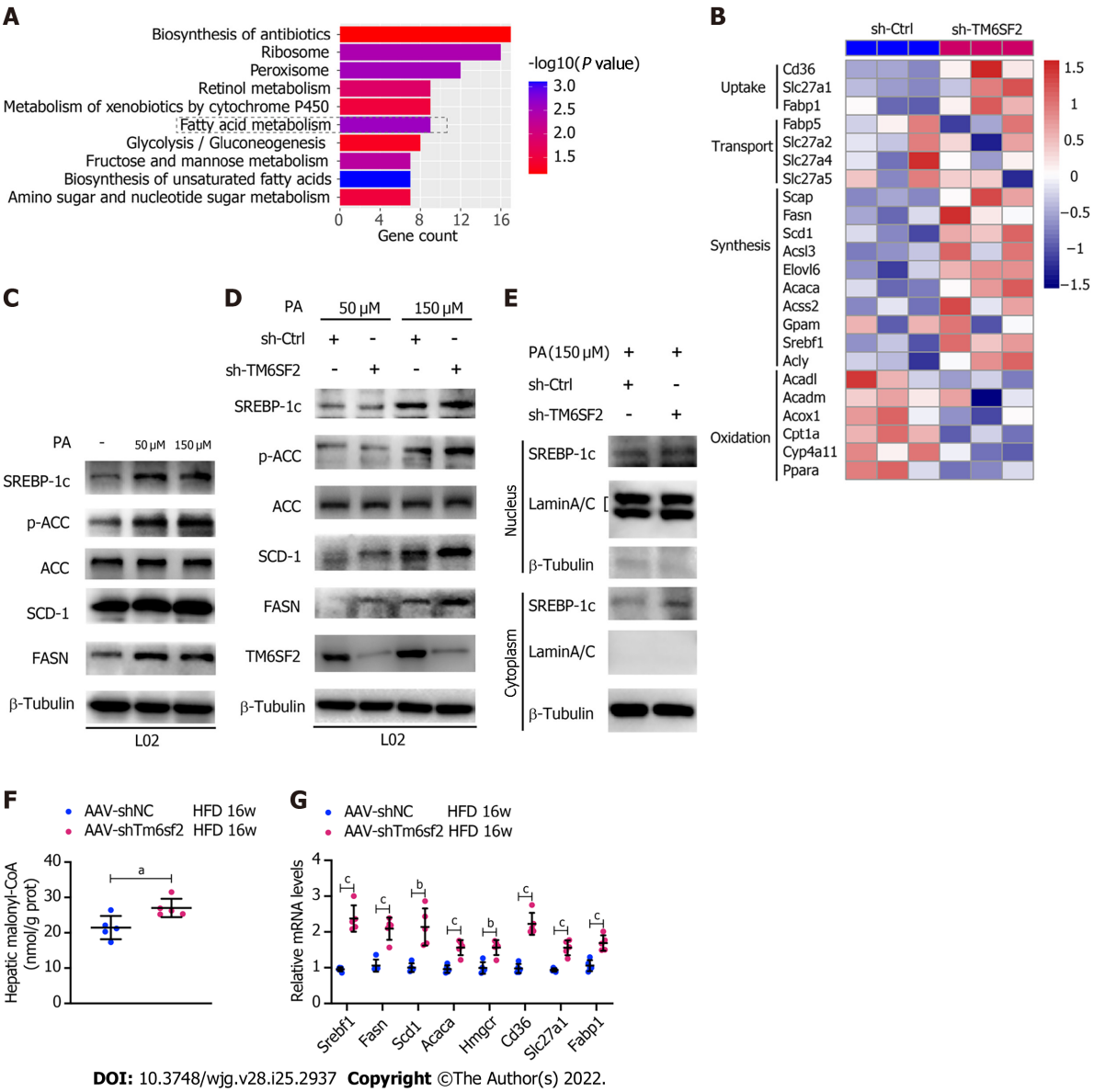
Triplicate samples of PA-treated TM6SF2-knockdown L02 cells and their controls were used for transcriptome analysis to explore the changes in biological processes in TM6SF2 knockdown and identify upregulated DEGs. KEGG pathway enrichment analysis was applied to explore the function of these DEGs, which highlighted that fatty acid metabolism was the key process that changed in TM6SF2-knockdown cells (Figure 5A), and genes associated with fatty acid synthesis were found to be upregulated (Figure 5B). To confirm this, *in vitro* NAFLD models were used to verify our findings. PA is a potent agonist of fatty acid synthesis[31]. PA administration activated fatty acid synthesis *in vitro*, as indicated by increased protein levels of p-ACC, FASN, SCD-1, and sterol regulatory element-binding protein 1c (SREBP-1c) (Figure 5C). When comparing the levels of these proteins between TM6SF2-



DOI: 10.3748/wjg.v28.i25.2937 **Copyright** ©The Author(s) 2022.

Figure 4 TM6SF2 deficiency exacerbates hepatic lipid accumulation and inflammation. A: Mice were injected with AAV-shNC and AAV-shTm6sf2 viruses *via* the tail vein and fed a high-fat diet or normal chow diet for 16 wk (n = 5 mice *per* group). The efficiency of TM6SF2 knockdown in liver were shown; B: Schematic representation of animal experiments; C: Left, representative images of hematoxylin and eosin-staining (left) and Oil Red O-staining (right) of liver sections. Right, the Nonalcoholic fatty liver disease activity score (left) and quantification of lipid (right, 8 fields of each mouse were examined) were performed; D-F: Hepatic lipid contents (triglyceride, total cholesterol and non-esterified fatty acids) (D), liver/body weight ratio (E) and body weight (F) were measured; G: Representative images of mice morphology; H: Top, representative photos of fatty livers (top) and livers subjected to magnetic resonance imaging scanning (bottom) of mice were shown. Bottom, the maximal cross-sectional area of livers is quantified by the number of pixels. $^{a}P < 0.05$; $^{b}P < 0.01$. NS: Not significant; H&E: Hematoxylin and eosin; NCD: Normal chow diet; HFD: High-fat diet; TG: Triglyceride; TC: Total cholesterol; NEFA: Non-esterified fatty acids.

knockdown cells and the corresponding controls, the results showed that these proteins were upregulated in TM6SF2-knockdown cells, suggesting that PA-induced fatty acid synthesis was enhanced by the knockdown of TM6SF2 (Figure 5D). *De novo* lipogenesis is mainly mediated by SREBP-1c on the transcriptional regulation of ACC and fatty acid synthase. The mature form of SREBP-1c translocates to the nucleus and activates its target genes, such as *Acaca* and *Fasn*[32]. This translocation-to-nucleus phenomenon was also enhanced in the TM6SF2-knockdown cells (Figure 5E). In addition, TM6SF2 knockdown increased hepatic malonyl-CoA, a metabolite of ACC[33], in HFD-fed AAV-shTm6sf2 mice (Figure 5F), which indicated that ACC activity was enhanced due to TM6SF2 deficiency. It is noteworthy that the transcriptional activity of hepatic SREBP-1c is also influenced by circulating



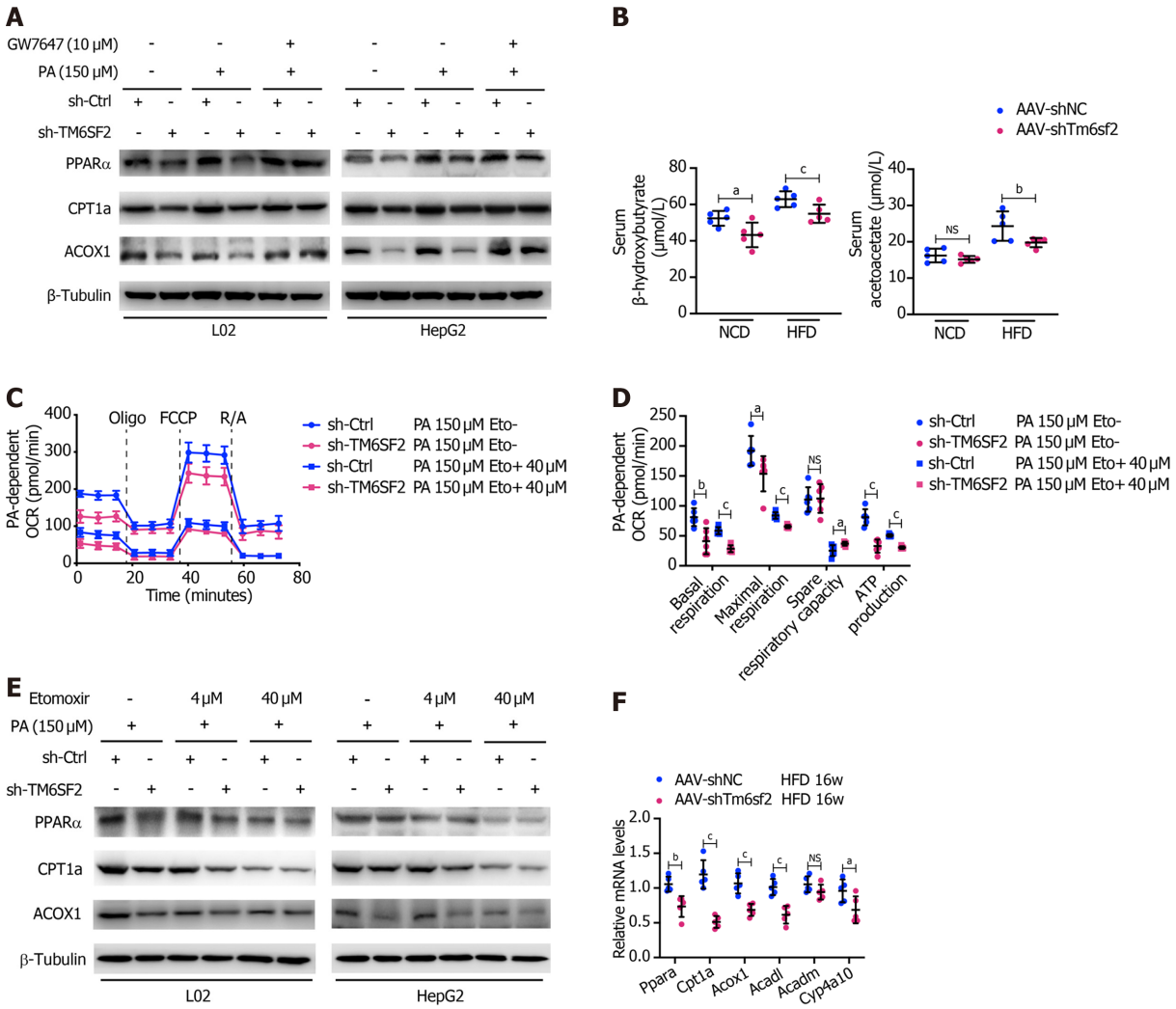
DOI: 10.3748/wjg.v28.i25.2937 **Copyright** ©The Author(s) 2022.

Figure 5 The activity of fatty acid synthesis was enhanced in TM6SF2 knockdown group. A: Pathway enrichment of the up-regulated differentially expressed genes by Kyoto Encyclopedia of Genes and Genomes analysis; B: Microarray heatmap of genes involved in fatty acid metabolism in TM6SF2-knockdown cells; C: The SREBP-1c target protein levels in L02 and HepG2 cells after palmitic acid (PA) treatment; D: The SREBP-1c target protein levels in TM6SF2-knockdown cells after PA treatment; E: Immunoblot analysis of SREBP-1c in cytoplasmic and nuclear extracts; F: Hepatic malonyl-CoA contents of mice in two groups (n = 5 mice *per* group); G: The mRNA levels of genes involved in fatty acid synthesis (*Srebf1*, *Fasn*, *Scd1*, *Acaca* and *Hmgcr*) and uptake (*Cd36*, *Slc27a1* and *Fabp1*). $^{a}P < 0.05$; $^{b}P < 0.01$; $^{c}P < 0.001$. HFD: High-fat diet; PA: Palmitic acid; ACC: Acetyl-CoA carboxylase; μM: μmol/L.

insulin status. We evaluated the mice's blood glucose and insulin levels and found no differences between the two groups with or without HFD feeding (Supplementary Figure 4A). In addition, no obvious differences were noted in the GTT and ITT (Supplementary Figure 4B). These results suggest that the enhanced steatosis in hepatic TM6SF2-knockdown mice is unlikely to be induced by altering insulin sensitivity. Moreover, we also noted that TM6SF2 knockdown did not affect the fatty acid transport process but caused an increase in the mRNA levels of molecules involved in fatty acid uptake (*e.g.*, CD36 and FABP1) (Figure 5B). This increase was augmented when the TM6SF2-knockdown cells were under starvation or hypoxic conditions (Supplementary Figure 4C), as hypoxia and starvation have been reported to enhance lipid uptake[34-36]. In parallel, the levels of fatty acid synthesis- and uptake-related genes were elevated in the livers of AAV-shTm6sf2 mice compared to control mice (Figure 5G). This evidence suggests that the unfavorable fatty liver in hepatic TM6SF2-knowndown mice may be associated with enhanced *de novo* lipogenesis and lipid uptake.

TM6SF2 deficiency could lead to impaired FAO

It was previously reported that NAFLD caused by TM6SF2 deficiency was partially due to impaired VLDL secretion, which is detrimental to the liver, as VLDL secretion is considered a significant pathway of lipid export in the liver[18]. FAO, another method of energy expenditure[37], has rarely been



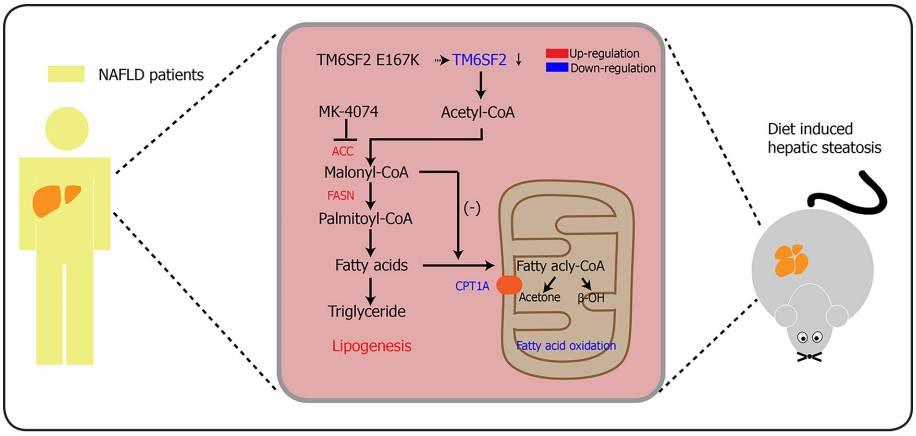
DOI: 10.3748/wjg.v28.i25.2937 **Copyright** ©The Author(s) 2022.

Figure 6 TM6SF2 deficiency caused the downregulation of fatty acid oxidation in liver. A: Protein levels of PPARα, CPT1A and ACOX1 was analyzed in TM6SF2-knockdown cells after palmitic acid (PA) stimulation and their response to GW7647 (10 μmol/L) treatment; B: Serum levels of β-hydroxybutyrate and acetoacetate in normal chow diet- or high-fat diet-fed AAV-shNC or AAV-shTm6sf2 mice (n = 5 mice *per* group); C and D: PA-dependent oxygen consumption rate in sh-Ctrl and sh-TM6SF2 L02 cells with or without etomoxir (ETO, 40 μmol/L) administration (C, n = 6). The basal respiration, maximal respiration, spare respiratory capacity, and ATP production were calculated (D); E: Protein levels of PPARα, CPT1A and ACOX1 were determined in TM6SF2-knockdown cells with or without ETO treatment under PA (150 μmol/L) stimulation; F: The hepatic mRNA levels of fatty acid oxidation-related genes in the indicated mice. $^{a}P < 0.05$; $^{b}P < 0.01$; $^{c}P < 0.001$. PA: Palmitic acid; NS: Not significant; NCD: Normal chow diet; HFD: High-fat diet; OCR: Oxygen consumption rate; μM: μmol/L.

reported in the absence of the TM6SF2 protein. Therefore, we evaluated and compared the expression of the key molecules involved in FAO. The results showed that TM6SF2-knockdown cells exhibited decreased levels of FAO-related proteins[38], including PPARα, CPT1A, and ACOX1, with or without PA stimulation (Figure 6A), which is consistent with the results of transcriptomic data (Figure 5B). Furthermore, PPARα signaling has been reported to function as a key factor in regulating FAO[39], and we found that the downregulated levels of FAO-related proteins in TM6SF2-knockdown cells could be reversed by PPARα activation through PPARα agonist (GW7647) stimulation (Figure 6A). We next tested hepatic FAO *in vivo* by evaluating the levels of serum ketone bodies, β-OH, and acetoacetate in both AAV-shTm6sf2 mice and control groups after a 16 h fast. The results showed that the levels of ketone bodies were significantly lower in the TM6SF2-knockdown group (Figure 6B), suggesting that TM6SF2 deficiency reduces FAO. In addition, compared to the control group, TM6SF2-knockdown L02 cells had a lower OCR with PA as the only substrate (Figures 6C and D). Meanwhile, the CPT1A inhibitor etomoxir inhibited the FAO process and diminished the difference in both groups, as well as the FAO-related proteins (Figure 6C-E). AAV-shTm6sf2 mice also showed a lower expression of FAO-related genes in the liver (Figure 6F). Together, these data indicate that TM6SF2 deficiency impairs cellular FAO.

MK4074 is effective in treating NAFLD exacerbated by TM6SF2 deficiency

These results showed that TM6SF2 deficiency could lead to abnormal fatty acid metabolism within cells,



DOI: 10.3748/wjg.v28.i25.2937 **Copyright** ©The Author(s) 2022.

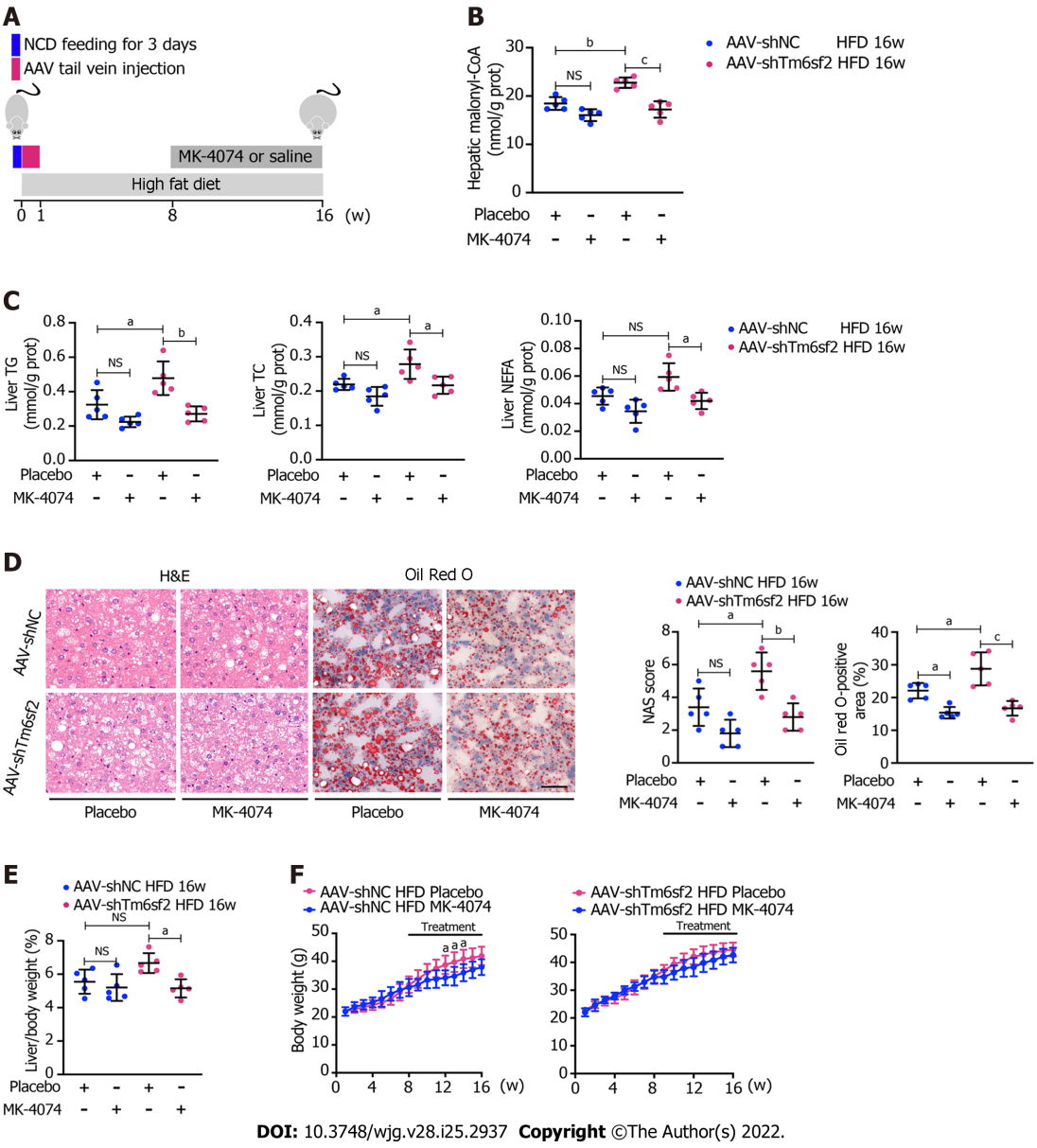
Figure 7 Schematic diagram of MK-4074 blocking acetyl-CoA carboxylase pathway and alleviating nonalcoholic fatty liver disease in TM6SF2-deficient mice. ACC: Acetyl-CoA carboxylase; NAFLD: Nonalcoholic fatty liver disease.

characterized by enhanced lipogenesis and uptake, accompanied by impaired fatty acid β-oxidation (Figure 7). It is worth noting that the suppressed β-oxidation process may be associated with the increased malonyl-CoA content due to the enhanced activity of ACC in this situation. Malonyl-CoA is a natural CPT1A inhibitor, which causes a decrease in β-oxidation in mitochondria[40]. Therefore, inhibiting the activity of ACC may be a promising method to alleviate fatty liver disease in mice with hepatic TM6SF2 deficiency. To test this idea and rectify this metabolic abnormality, we thought of a way of inhibiting ACC, this rate-limiting enzyme, by using a previously reported ACC inhibitor, MK-4074, which could simultaneously limit the *de novo* lipid synthesis pathway and increase the level of intracellular lipid oxidation, to explore whether the drug has therapeutic effect on TM6SF2-deficient cases. To this end, both AAV-shTm6sf2 and control mice were first subjected to 8-wk HFD feeding to induce NAFLD phenotypes, and then two groups of mice received MK-4074 (MK-4074, 10 mg/kg/day) or placebo (normal saline) treatment and were fed with HFD for an additional eight weeks (Figure 8A). The results showed that MK-4074 treatment could diminish the increase in the levels of malonyl-CoA (Figure 8B), as well as hepatic TG, TC, and NEFA caused by TM6SF2 deficiency (Figure 8C), suggesting the success of blocking the SPREBP-1c/ACC pathway. Compared to placebo treatment, the HFD-fed AAV sh-Tm6sf2- mice under MK-4074 treatment exhibited mild hepatic ballooning degeneration and steatosis (Figure 8D). At the same time, MK-4074 treatment improved the liver/body weight ratio (Figure 8E), although the body weight improvement was rather limited (Figure 8F). In addition, the beneficial effect is also manifested *in vitro* experiments that MK-4074 could reduce lipid accumulation (Figure 9A and B) and improve PA-induced cell death in TM6SF2 knocked-down groups (Figure 9C). Meanwhile, MK-4074 inhibited malonyl-CoA production (Figure 8B) and improved the decrease in FAO caused by TM6SF2 deficiency, as evidenced by the increased FAO-related protein and ketone body levels in the TM6SF2-knockdown group (Figure 9D and E), which renders MK-4074 the prime option for treating this condition.

DISCUSSION

The present study revealed that hepatic TM6SF2 expression was upregulated in both NAFLD mouse models and patients. TM6SF2 overexpression alleviated NAFLD phenotypes in HFD-induced models, suggesting a protective role for reactive TM6SF2 elevation under NAFLD conditions. Simulating the situation in patients with the E167K mutation, TM6SF2 knockdown exacerbated hepatic steatosis and inflammation. We noted a dysregulated fatty acid metabolism process under TM6SF2 deficiency, characterized by enhanced fatty acid uptake and fatty acid synthesis, accompanied by an impaired FAO process and insufficient ketone body production. Given the potential impact of TM6SF2 on fatty acid metabolism in NAFLD, exploring the effects of targeted NAFLD therapeutics on fatty liver is of the utmost importance, inspiring us to consider the impact of genetic variation on fatty liver. We used a previously reported liver-specific ACC inhibitor, MK-4074, which could reduce hepatic lipogenesis while increasing FAO, to explore the therapeutic effect on fatty liver caused by TM6SF2 deficiency (Figure 7). Our results show that MK-4074 has an encouraging effect on treating TM6SF2 knockdown-induced NAFLD, as indicated by the reduced hepatic lipid content, lower liver/body ratio, and alleviated PA-induced cell death suggesting the effectiveness of MK-4074 in treating this condition.

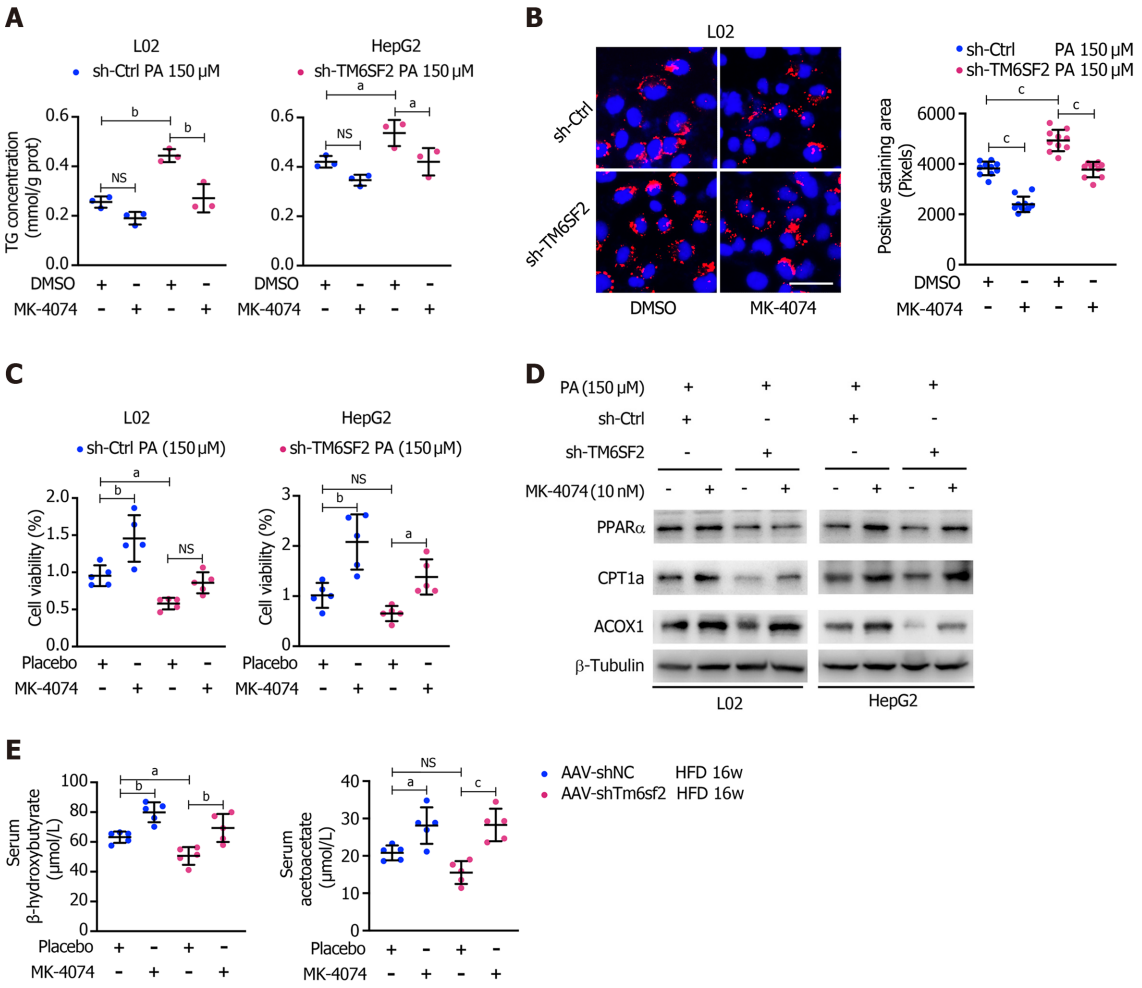
Previous studies have considered TM6SF2 as a pivotal molecule in hepatic lipid output in the form of VLDL-TG, and a majority of studies have focused on the association between the export of accumulated



DOI: 10.3748/wjg.v28.i25.2937 **Copyright** ©The Author(s) 2022.

Figure 8 Therapeutic potential of MK-4074 on nonalcoholic fatty liver disease caused by TM6SF2 deficiency. A: Schematic representation of animal experiments; B-D: Two groups (AAV-shNC and AAV-shTm6sf2) of mice were fed a high-fat diet (HFD) for 8 wk to induce nonalcoholic fatty liver disease phenotypes and then each subgroup was dosed with MK-4074 (10 mg/kg/day) or placebo orally for additional 8 wk. The hepatic malonyl-CoA levels (B) and lipid content (C) as well as results of hematoxylin and eosin-staining and Oil Red O-staining of liver sections (D) were shown; E and F: The liver/body weight ratio (E) and the body weight (F) of HFD-fed AAV-shNC and AAV-shTm6sf2 mice with or without MK-4074 treatment (n = 5 mice *per* group) were shown. $^{a}P < 0.05$; $^{b}P < 0.01$; $^{c}P < 0.001$. NS: Not significant; H&E: Hematoxylin and eosin; NCD: Normal chow diet; HFD: High-fat diet; TG: Triglyceride; TC: Total cholesterol; NEFA: Non-esterified fatty acids.

lipids and the TM6SF2 E167K mutant[15,18,41]. The TM6SF2 E167K mutant may result in a misfolded protein easily degraded within the cells, resulting in decreased TM6SF2 levels[42]. The liver is a pivotal hub for lipid metabolism, and its dysregulation could be a significant cause of NAFLD[43]. Therefore, we investigated the cause of TM6SF2 deficiency-induced NAFLD from another perspective, dysregulated fatty acid metabolism. Our results revealed that TM6SF2 knockdown significantly increased the expression of SREBP-1c and its target genes both *in vivo* and *in vitro*, suggesting abnormally enhanced *de novo* lipogenesis (DNL). Meanwhile, the results showed that the levels of OCR were decreased in the TM6SF2-knockdown groups, indicating that the FAO process was impaired under these circumstances. We further tested the transcriptional levels of FAO-related genes in hepatic TM6SF2-knockdown mice fed an HFD and showed lower levels of genes involving FAO than the control mice on the same diet for 16 wk. Previous studies showed that elevated levels of malonyl-CoA would suppress FAO by inhibiting CPT1A activity[44]. In our study, the malonyl-CoA content was higher in AAV-shTm6sf2 mice than in the control mice, which implies that the decreased FAO process is related to the enhanced DNL due to TM6SF2 knockdown.



DOI: 10.3748/wjg.v28.i25.2937 **Copyright** ©The Author(s) 2022.

Figure 9 MK-4074 can improve intracellular lipid accumulation, lipid overload-induced cell death, and fatty acids β-oxidation. A: Intracellular triglyceride levels (n = 3) in TM6SF2-knockdown cells with palmitic acid (PA) (150 μmol/L) stimulation were examined after MK-4074 (10 nM) treatment for 24 h; B: Representative nile red staining images (left) and lipid droplet quantification (right) of sh-Ctrl or sh-TM6SF2 L02 cells after PA stimulation in response to MK-4074 (10 nM) treatment (10 fields of each sample were examined). Scale bars: 50 μm; C: The cellular viability was examined in TM6SF2-knockdown cells with or without MK-4074 treatment in response to PA-induced cell death (n = 5); D: The sh-Ctrl and sh-TM6SF2 cells were cultured with PA (150 μmol/L) for 24 h. Cells were then treated with MK-4074 (10 nM) for 12 h. The expression of fatty acid oxidation-related proteins was determined; E: Serum levels of β-hydroxybutyrate and acetoacetate in the indicated mice with or without MK-4074 treatment. $^{a}P < 0.05$; $^{b}P < 0.01$; $^{c}P < 0.001$. NS: Not significant; HFD: High-fat diet; TG: Triglyceride; PA: Palmitic acid; μM: μmol/L.

Currently, genetic technologies have already allowed for the identification of a subgroup of people with an increased risk of NAFLD or NAFLD-related complications associated with specific pathophysiological characteristics[45]. Unfortunately, there is no precise treatment for metabolic diseases with specific congenital genetic variations in NAFLD. However, much effort has been made to elucidate the mechanism of NAFLD caused by genetic mutations and implement precision medicine. For example, human genetics of NAFLD offers the opportunity to apply targeted therapy with the PNPLA3 I148M variant. This locus is the strongest genetic factor that increases susceptibility to NAFLD[10]. Recently, researchers used mice with the PNPLA3 variant knock-in and tried to improve NAFLD phenotypes through antisense oligonucleotides to downregulate the PNPLA3 mutant protein[46]. Although the mechanisms are not fully understood, accumulating evidence reveals that PNPLA3 I148M impairs lipid droplet remodeling in hepatocytes due to the loss of lipase activity[47]. Inhibition of PNPLA3 148M expression reduced liver fat content in these engineered mice and, specifically, had a beneficial effect in mitigating inflammation and fibrosis. If these applications are translated into humans, after safety and reliability examinations, downregulation of PNPLA3 148M may be the first case of human genetics-based targeted therapy. The importance of this method is to treat not only the phenotype of the disease but also the cause.

As described in the PNPLA3 mutant protein case, this evidence proved the possibility of targeted therapy to eliminate the cause of fatty liver in patients carrying a specific risk allele. However, there have been no reports of attempts to treat fatty liver caused by TM6SF2 deficiency or its E167K mutant. Based on our data, mice with TM6SF2 deficiency show enhanced DNL. Among the TM6SF2/SREBP-1c/ACC axis, ACC acts as the rate-limiting enzyme for converting acetyl-CoA to malonyl-CoA[48]. The

product, malonyl-CoA, was further catalyzed by FASN to form palmitate. TGs are one of the many lipid species that are integrated with DNL-derived palmitate. ACC inhibitors have the potential to mitigate hepatic steatosis in NAFLD, given that ACC is essential and pivotal in hepatic fatty acid metabolism. Independent studies have revealed that blocking DNL by ACC inhibition has a beneficial effect in reducing liver fat, steatosis, and inflammation in NAFLD models[44,49]. Among ACC inhibitors, MK-4074 has recently been tested for NAFLD treatment, and its effects have been encouraging. MK-4074 treatment decreased DNL and enhanced FAO in participants under overnutrition. Based on its function, we hypothesized that it could be used to treat fatty liver caused by the reduction of TM6SF2, and *in vivo* and *in vitro* experiments confirmed this hypothesis. ACC inhibitors have recently been shown to effectively mitigate liver fibrosis in NASH patients[49,50]. The accumulating evidence has shown that TM6SF2 E167K is also associated with NASH and fibrosis[18,51]. Whether ACC inhibitors can be applied to mitigate liver fibrosis in NASH models with TM6SF2 deficiency or the E167K mutant is unknown. This indicates the direction of our future work.

CONCLUSION

This study showed that dysregulated fatty acid metabolism occurs in the context of TM6SF2 deficiency under overnutrition. Therapeutics aimed at abnormal fatty acid metabolism may be a promising strategy for improving the hepatic lipid profile of patients with the TM6SF2 E167K variant in the clinical setting. Furthermore, our study suggests that MK-4074 could be a potential drug to lower hepatic lipid content in a TM6SF2-knockdown NAFLD mouse model. Further investigations are required to test whether this approach would lower hepatic lipid levels in NAFLD patients with the E167K mutation.

ARTICLE HIGHLIGHTS

Research background

Previously, we found that the TM6SF2 E167K mutation was associated with susceptibility to nonalcoholic fatty liver disease (NAFLD) in a Chinese cohort, but the underlying mechanism is poorly understood.

Research motivation

Because existing evidence has shown that *TM6SF2* gene mutation would reduce its expression at the protein level, we used NAFLD mouse models to explore the causes of NAFLD caused by TM6SF2 deficiency in the context of high-fat feeding and test possible treatment strategies. This would benefit our understanding of the mechanisms underlying NAFLD in humans.

Research objectives

Mechanism and therapeutic strategy of hepatic TM6SF2-deficient NAFLD *via in vivo* and *in vitro* experiments.

Research methods

This study mainly involved the knockdown and overexpression of the hepatic *TM6SF2* gene in NAFLD mice and cell models to explore its effects on pathological changes in the liver. In addition, RNA-seq, oxygen consumption rate technology, western blotting, and pathological examination were performed to investigate the underlying mechanisms of NALFD caused by TM6SF2 deficiency.

Research results

Hepatic TM6SF2 expression was upregulated in patients with NAFLD and high-fat diet (HFD)-fed mice. Overexpression of TM6SF2 mitigated hepatic lipid accumulation in HFD-fed mouse models. Knockdown of TM6SF2 promoted hepatic lipid accumulation and inflammation. TM6SF2 deficiency promotes hepatic lipid accumulation through the dysregulation of fatty acid metabolism. MK-4074 administration may serve as a potential drug to improve NAFLD caused by TM6SF2 deficiency.

Research conclusions

In this study, we found that the reactive overexpression of TM6SF2 under HFD conditions could alleviate hepatic lipid accumulation, the loss of which accelerated the NALFD phenotypes under HFD feeding. We also found that dysregulated fatty acid metabolism occurs in the context of TM6SF2 deficiency under overnutrition conditions. Therapeutics aimed at abnormal fatty acid metabolism may be a promising strategy for improving the hepatic lipid profile of patients with the TM6SF2 E167K variant in the clinical setting. Our study suggests that MK-4074 could be a potential drug for lowering hepatic lipid content in a TM6SF2-knockdown NAFLD mouse model.

Research perspectives

TM6SF2 plays a protective role in the HFD condition; its deficiency enhanced hepatic lipid accumulation through dysregulated fatty acid metabolism, and MK-4074 treatment could alleviate the NAFLD phenotypes caused by TM6SF2 deficiency. The next step was to investigate whether MK-4074 has a therapeutic effect in patients with NAFLD harboring the TM6SF2 E167K mutation.

FOOTNOTES

Author contributions: Li ZY and Wu G contributed equally to the work, Li ZY and Wu G performed the *in vitro* and *in vivo* experiments; Qiu C, Zhou ZJ, Wang YP, Song GH and Xiao C performed the analysis of GEO data; Deng GL and Wang RT provided the technical supports; Zhang X interpreted the data; Li ZY wrote the manuscript; Wang XL and Yang YL contributed equally, Wang XL and Yang YL conceived and supervised the study; all authors critically reviewed and edited the manuscript.

Supported by National Natural Science Foundation of China, No. 81670514 and No. 81702337; Scientific Research Project of Shanghai Municipal Health Commission, No. 202040065; and Natural Science Foundation of Shanghai Scientific and Technological Project of Innovative Action, No. 20ZR1411900.

Institutional review board statement: The study was reviewed and approved by the Shanghai First People's Hospital Institutional Review Board, No. 2016KY074.

Institutional animal care and use committee statement: All procedures involving animals were reviewed and approved by the Institutional Animal Care and Use Committee of the Shanghai First People's Hospital, No. 2020-A0072-01.

Conflict-of-interest statement: All the authors report no relevant conflicts of interest for this article.

Data sharing statement: The data used and analyzed during the current study are available from the corresponding author on reasonable request.

ARRIVE guidelines statement: The authors have read the ARRIVE guidelines, and the manuscript was prepared and revised according to the ARRIVE guidelines.

Open-Access: This article is an open-access article that was selected by an in-house editor and fully peer-reviewed by external reviewers. It is distributed in accordance with the Creative Commons Attribution NonCommercial (CC BY-NC 4.0) license, which permits others to distribute, remix, adapt, build upon this work non-commercially, and license their derivative works on different terms, provided the original work is properly cited and the use is non-commercial. See: https://creativecommons.org/Licenses/by-nc/4.0/

Country/Territory of origin: China

ORCID number: Zu-Yin Li 0000-0002-3804-0994; Gang Wu 0000-0002-3211-688X; Qiu Chen 0000-0002-5414-1672; Zhi-Jie Zhou 0000-0001-7414-411X; Yu-Peng Wang 0000-0002-9891-2141; Guo-He Song 0000-0002-1452-6316; Chao Xiao 0000-0002-9202-0863; Xin Zhang 0000-0002-8097-4061; Gui-Long Deng 0000-0003-4353-8452; Rui-Tao Wang 0000-0002-3210-8396; Yu-Long Yang 0000-0002-5783-6381; Xiao-Liang Wang 0000-0001-9851-0436.

S-Editor: Fan JR
L-Editor: A
P-Editor: Li X

REFERENCES

1 **Younossi Z**, Anstee QM, Marietti M, Hardy T, Henry L, Eslam M, George J, Bugianesi E. Global burden of NAFLD and NASH: trends, predictions, risk factors and prevention. *Nat Rev Gastroenterol Hepatol* 2018; **15**: 11-20 [PMID: 28930295 DOI: 10.1038/nrgastro.2017.109]
2 **Marengo A**, Jouness RI, Bugianesi E. Progression and Natural History of Nonalcoholic Fatty Liver Disease in Adults. *Clin Liver Dis* 2016; **20**: 313-324 [PMID: 27063271 DOI: 10.1016/j.cld.2015.10.010]
3 **Enomoto H**, Bando Y, Nakamura H, Nishiguchi S, Koga M. Liver fibrosis markers of nonalcoholic steatohepatitis. *World J Gastroenterol* 2015; **21**: 7427-7435 [PMID: 26139988 DOI: 10.3748/wjg.v21.i24.7427]
4 **Younossi ZM**. Long-Term Outcomes of Nonalcoholic Fatty Liver Disease: From Nonalcoholic Steatohepatitis to Nonalcoholic Steatofibrosis. *Clin Gastroenterol Hepatol* 2017; **15**: 1144-1147 [PMID: 28549675 DOI: 10.1016/j.cgh.2017.05.029]
5 **Wong VW**, Chitturi S, Wong GL, Yu J, Chan HL, Farrell GC. Pathogenesis and novel treatment options for non-alcoholic steatohepatitis. *Lancet Gastroenterol Hepatol* 2016; **1**: 56-67 [PMID: 28404113 DOI: 10.1016/S2468-1253(16)30011-5]

6 **Carlsson B**, Lindén D, Brolén G, Liljeblad M, Bjursell M, Romeo S, Loomba R. Review article: the emerging role of genetics in precision medicine for patients with non-alcoholic steatohepatitis. *Aliment Pharmacol Ther* 2020; **51**: 1305-1320 [PMID: 32383295 DOI: 10.1111/apt.15738]

7 **Kahali B**, Halligan B, Speliotes EK. Insights from Genome-Wide Association Analyses of Nonalcoholic Fatty Liver Disease. *Semin Liver Dis* 2015; **35**: 375-391 [PMID: 26676813 DOI: 10.1055/s-0035-1567870]

8 **Namjou B**, Lingren T, Huang Y, Parameswaran S, Cobb BL, Stanaway IB, Connolly JJ, Mentch FD, Benoit B, Niu X, Wei WQ, Carroll RJ, Pacheco JA, Harley ITW, Divanovic S, Carrell DS, Larson EB, Carey DJ, Verma S, Ritchie MD, Gharavi AG, Murphy S, Williams MS, Crosslin DR, Jarvik GP, Kullo IJ, Hakonarson H, Li R; eMERGE Network, Xanthakos SA, Harley JB. GWAS and enrichment analyses of non-alcoholic fatty liver disease identify new trait-associated genes and pathways across eMERGE Network. *BMC Med* 2019; **17**: 135 [PMID: 31311600 DOI: 10.1186/s12916-019-1364-z]

9 **Li YY**. Genetic and epigenetic variants influencing the development of nonalcoholic fatty liver disease. *World J Gastroenterol* 2012; **18**: 6546-6551 [PMID: 23236228 DOI: 10.3748/wjg.v18.i45.6546]

10 **Romeo S**, Kozlitina J, Xing C, Pertsemlidis A, Cox D, Pennacchio LA, Boerwinkle E, Cohen JC, Hobbs HH. Genetic variation in PNPLA3 confers susceptibility to nonalcoholic fatty liver disease. *Nat Genet* 2008; **40**: 1461-1465 [PMID: 18820647 DOI: 10.1038/ng.257]

11 **Thangapandi VR**, Knittelfelder O, Brosch M, Patsenker E, Vvedenskaya O, Buch S, Hinz S, Hendricks A, Nati M, Herrmann A, Rekhade DR, Berg T, Matz-Soja M, Huse K, Klipp E, Pauling JK, Wodke JA, Miranda Ackerman J, Bonin MV, Aigner E, Datz C, von Schönfels W, Nehring S, Zeissig S, Röcken C, Dahl A, Chavakis T, Stickel F, Shevchenko A, Schafmayer C, Hampe J, Subramanian P. Loss of hepatic Mboat7 leads to liver fibrosis. *Gut* 2021; **70**: 940-950 [PMID: 32591434 DOI: 10.1136/gutjnl-2020-320853]

12 **Yoneda M**, Hotta K, Nozaki Y, Endo H, Uchiyama T, Mawatari H, Iida H, Kato S, Hosono K, Fujita K, Yoneda K, Takahashi H, Kirikoshi H, Kobayashi N, Inamori M, Abe Y, Kubota K, Saito S, Maeyama S, Wada K, Nakajima A. Association between PPARGC1A polymorphisms and the occurrence of nonalcoholic fatty liver disease (NAFLD). *BMC Gastroenterol* 2008; **8**: 27 [PMID: 18588668 DOI: 10.1186/1471-230X-8-27]

13 **Mahdessian H**, Taxiarchis A, Popov S, Silveira A, Franco-Cereceda A, Hamsten A, Eriksson P, van't Hooft F. TM6SF2 is a regulator of liver fat metabolism influencing triglyceride secretion and hepatic lipid droplet content. *Proc Natl Acad Sci U S A* 2014; **111**: 8913-8918 [PMID: 24927523 DOI: 10.1073/pnas.1323785111]

14 **Wang X**, Liu Z, Peng Z, Liu W. The TM6SF2 rs58542926 T allele is significantly associated with non-alcoholic fatty liver disease in Chinese. *J Hepatol* 2015; **62**: 1438-1439 [PMID: 25687425 DOI: 10.1016/j.jhep.2015.01.040]

15 **Kozlitina J**, Smagris E, Stender S, Nordestgaard BG, Zhou HH, Tybjærg-Hansen A, Vogt TF, Hobbs HH, Cohen JC. Exome-wide association study identifies a TM6SF2 variant that confers susceptibility to nonalcoholic fatty liver disease. *Nat Genet* 2014; **46**: 352-356 [PMID: 24531328 DOI: 10.1038/ng.2901]

16 **Roh YS**, Loomba R, Seki E. The TM6SF2 variants, novel genetic predictors for nonalcoholic steatohepatitis. *Gastroenterology* 2015; **148**: 252-254 [PMID: 25451657 DOI: 10.1053/j.gastro.2014.11.014]

17 **Fan Y**, Lu H, Guo Y, Zhu T, Garcia-Barrio MT, Jiang Z, Willer CJ, Zhang J, Chen YE. Hepatic Transmembrane 6 Superfamily Member 2 Regulates Cholesterol Metabolism in Mice. *Gastroenterology* 2016; **150**: 1208-1218 [PMID: 26774178 DOI: 10.1053/j.gastro.2016.01.005]

18 **Dongiovanni P**, Petta S, Maglio C, Fracanzani AL, Pipitone R, Mozzi E, Motta BM, Kaminska D, Rametta R, Grimaudo S, Pelusi S, Montalcini T, Alisi A, Maggioni M, Kärjä V, Borén J, Käkelä P, Di Marco V, Xing C, Nobili V, Dallapiccola B, Craxi A, Pihlajamäki J, Fargion S, Sjöström L, Carlsson LM, Romeo S, Valenti L. Transmembrane 6 superfamily member 2 gene variant disentangles nonalcoholic steatohepatitis from cardiovascular disease. *Hepatology* 2015; **61**: 506-514 [PMID: 25251399 DOI: 10.1002/hep.27490]

19 **Li BT**, Sun M, Li YF, Wang JQ, Zhou ZM, Song BL, Luo J. Disruption of the ERLIN-TM6SF2-APOB complex destabilizes APOB and contributes to non-alcoholic fatty liver disease. *PLoS Genet* 2020; **16**: e1008955 [PMID: 32776921 DOI: 10.1371/journal.pgen.1008955]

20 **Hodson L**, Gunn PJ. The regulation of hepatic fatty acid synthesis and partitioning: the effect of nutritional state. *Nat Rev Endocrinol* 2019; **15**: 689-700 [PMID: 31554932 DOI: 10.1038/s41574-019-0256-9]

21 **Robinson MD**, McCarthy DJ, Smyth GK. edgeR: a Bioconductor package for differential expression analysis of digital gene expression data. *Bioinformatics* 2010; **26**: 139-140 [PMID: 19910308 DOI: 10.1093/bioinformatics/btp616]

22 **Gómez-Lechón MJ**, Donato MT, Martínez-Romero A, Jiménez N, Castell JV, O'Connor JE. A human hepatocellular in vitro model to investigate steatosis. *Chem Biol Interact* 2007; **165**: 106-116 [PMID: 17188672 DOI: 10.1016/j.cbi.2006.11.004]

23 **Ricchi M**, Odoardi MR, Carulli L, Anzivino C, Ballestri S, Pinetti A, Fantoni LI, Marra F, Bertolotti M, Banni S, Lonardo A, Carulli N, Loria P. Differential effect of oleic and palmitic acid on lipid accumulation and apoptosis in cultured hepatocytes. *J Gastroenterol Hepatol* 2009; **24**: 830-840 [PMID: 19207680 DOI: 10.1111/j.1440-1746.2008.05733.x]

24 **Alsabeeh N**, Chausse B, Kakimoto PA, Kowaltowski AJ, Shirihai O. Cell culture models of fatty acid overload: Problems and solutions. *Biochim Biophys Acta Mol Cell Biol Lipids* 2018; **1863**: 143-151 [PMID: 29155055 DOI: 10.1016/j.bbalip.2017.11.006]

25 **Aji G**, Huang Y, Ng ML, Wang W, Lan T, Li M, Li Y, Chen Q, Li R, Yan S, Tran C, Burchfield JG, Couttas TA, Chen J, Chung LH, Liu D, Wadham C, Hogg PJ, Gao X, Vadas MA, Gamble JR, Don AS, Xia P, Qi Y. Regulation of hepatic insulin signaling and glucose homeostasis by sphingosine kinase 2. *Proc Natl Acad Sci U S A* 2020; **117**: 24434-24442 [PMID: 32917816 DOI: 10.1073/pnas.2007856117]

26 **Xu M**, Li Y, Zhang S, Wang X, Shen J. Interaction of TM6SF2 E167K and PNPLA3 I148M variants in NAFLD in northeast China. *Ann Hepatol* 2019; **18**: 456-460 [PMID: 31054977 DOI: 10.1016/j.aohep.2018.10.005]

27 **Ehrhardt N**, Doche ME, Chen S, Mao HZ, Walsh MT, Bedoya C, Guindi M, Xiong W, Ignatius Irudayam J, Iqbal J, Fuchs S, French SW, Mahmood Hussain M, Arditi M, Arumugaswami V, Péterfy M. Hepatic Tm6sf2 overexpression affects cellular ApoB-trafficking, plasma lipid levels, hepatic steatosis and atherosclerosis. *Hum Mol Genet* 2017; **26**: 2719-2731 [PMID: 28449094 DOI: 10.1093/hmg/ddx159]

28 **Zou Y**, Qi Z. Understanding the Role of Exercise in Nonalcoholic Fatty Liver Disease: ERS-Linked Molecular Pathways.

Mediators Inflamm 2020; **2020**: 6412916 [PMID: 32774148 DOI: 10.1155/2020/6412916]
29 **Yang WS**, Stockwell BR. Ferroptosis: Death by Lipid Peroxidation. *Trends Cell Biol* 2016; **26**: 165-176 [PMID: 26653790 DOI: 10.1016/j.tcb.2015.10.014]
30 **Anstee QM**, Reeves HL, Kotsiliti E, Govaere O, Heikenwalder M. From NASH to HCC: current concepts and future challenges. *Nat Rev Gastroenterol Hepatol* 2019; **16**: 411-428 [PMID: 31028350 DOI: 10.1038/s41575-019-0145-7]
31 **Chen X**, Li L, Liu X, Luo R, Liao G, Liu J, Cheng J, Lu Y, Chen Y. Oleic acid protects saturated fatty acid mediated lipotoxicity in hepatocytes and rat of non-alcoholic steatohepatitis. *Life Sci* 2018; **203**: 291-304 [PMID: 29709653 DOI: 10.1016/j.lfs.2018.04.022]
32 **Li Y**, Xu S, Mihaylova MM, Zheng B, Hou X, Jiang B, Park O, Luo Z, Lefai E, Shyy JY, Gao B, Wierzbicki M, Verbeuren TJ, Shaw RJ, Cohen RA, Zang M. AMPK phosphorylates and inhibits SREBP activity to attenuate hepatic steatosis and atherosclerosis in diet-induced insulin-resistant mice. *Cell Metab* 2011; **13**: 376-388 [PMID: 21459323 DOI: 10.1016/j.cmet.2011.03.009]
33 **Fadó R**, Rodríguez-Rodríguez R, Casals N. The return of malonyl-CoA to the brain: Cognition and other stories. *Prog Lipid Res* 2021; **81**: 101071 [PMID: 33186641 DOI: 10.1016/j.plipres.2020.101071]
34 **Tian Y**, Yang B, Qiu W, Hao Y, Zhang Z, Li N, Cheng S, Lin Z, Rui YC, Cheung OKW, Yang W, Wu WKK, Cheung YS, Lai PBS, Luo J, Sung JJY, Chen R, Wang HY, Cheng ASL, Yang P. ER-residential Nogo-B accelerates NAFLD-associated HCC mediated by metabolic reprogramming of oxLDL lipophagy. *Nat Commun* 2019; **10**: 3391 [PMID: 31358770 DOI: 10.1038/s41467-019-11274-x]
35 **Tomašić N**, Kotarsky H, de Oliveira Figueiredo R, Hansson E, Mörgelin M, Tomašić I, Kallijärvi J, Elmér E, Jauhiainen M, Eklund EA, Fellman V. Fasting reveals largely intact systemic lipid mobilization mechanisms in respiratory chain complex III deficient mice. *Biochim Biophys Acta Mol Basis Dis* 2020; **1866**: 165573 [PMID: 31672551 DOI: 10.1016/j.bbadis.2019.165573]
36 **Chen X**, Gao Y, Wu G, Gu J, Cai Y, Xu J, Cheng H. Molecular cloning, tissue expression, and transcriptional regulation of fabp1 and fabp2 in javelin goby (Synechogobius hasta) in response to starvation stress. *Comp Biochem Physiol B Biochem Mol Biol* 2020; **250**: 110484 [PMID: 32745520 DOI: 10.1016/j.cbpb.2020.110484]
37 **Wang J**, Zhang Y, Zhuo Q, Tseng Y, Wang J, Ma Y, Zhang J, Liu J. TET1 promotes fatty acid oxidation and inhibits NAFLD progression by hydroxymethylation of PPARα promoter. *Nutr Metab (Lond)* 2020; **17**: 46 [PMID: 32577122 DOI: 10.1186/s12986-020-00466-8]
38 **Xu J**, Xiao G, Trujillo C, Chang V, Blanco L, Joseph SB, Bassilian S, Saad MF, Tontonoz P, Lee WN, Kurland IJ. Peroxisome proliferator-activated receptor alpha (PPARalpha) influences substrate utilization for hepatic glucose production. *J Biol Chem* 2002; **277**: 50237-50244 [PMID: 12176975 DOI: 10.1074/jbc.M201208200]
39 **Wang Y**, Nakajima T, Gonzalez FJ, Tanaka N. PPARs as Metabolic Regulators in the Liver: Lessons from Liver-Specific PPAR-Null Mice. *Int J Mol Sci* 2020; **21** [PMID: 32192216 DOI: 10.3390/ijms21062061]
40 **Foster DW**. Malonyl-CoA: the regulator of fatty acid synthesis and oxidation. *J Clin Invest* 2012; **122**: 1958-1959 [PMID: 22833869 DOI: 10.1172/jci63967]
41 **Borén J**, Adiels M, Björnson E, Matikainen N, Söderlund S, Rämö J, Ståhlman M, Ripatti P, Ripatti S, Palotie A, Mancina RM, Hakkarainen A, Romeo S, Packard CJ, Taskinen MR. Effects of TM6SF2 E167K on hepatic lipid and very low-density lipoprotein metabolism in humans. *JCI Insight* 2020; **5** [PMID: 33170809 DOI: 10.1172/jci.insight.144079]
42 **Prill S**, Caddeo A, Baselli G, Jamialahmadi O, Dongiovanni P, Rametta R, Kanebratt KP, Pujia A, Pingitore P, Mancina RM, Lindén D, Whatling C, Janefeldt A, Kozyra M, Ingelman-Sundberg M, Valenti L, Andersson TB, Romeo S. The TM6SF2 E167K genetic variant induces lipid biosynthesis and reduces apolipoprotein B secretion in human hepatic 3D spheroids. *Sci Rep* 2019; **9**: 11585 [PMID: 31406127 DOI: 10.1038/s41598-019-47737-w]
43 **Alves-Bezerra M**, Cohen DE. Triglyceride Metabolism in the Liver. *Compr Physiol* 2017; **8**: 1-8 [PMID: 29357123 DOI: 10.1002/cphy.c170012]
44 **Wu X**, Huang T. Recent development in acetyl-CoA carboxylase inhibitors and their potential as novel drugs. *Future Med Chem* 2020; **12**: 533-561 [PMID: 32048880 DOI: 10.4155/fmc-2019-0312]
45 **Trépo E**, Valenti L. Update on NAFLD genetics: From new variants to the clinic. *J Hepatol* 2020; **72**: 1196-1209 [PMID: 32145256 DOI: 10.1016/j.jhep.2020.02.020]
46 **Lindén D**, Ahnmark A, Pingitore P, Ciociola E, Ahlstedt I, Andréasson AC, Sasidharan K, Madeyski-Bengtson K, Zurek M, Mancina RM, Lindblom A, Bjursell M, Böttcher G, Ståhlman M, Bohlooly-Y M, Haynes WG, Carlsson B, Graham M, Lee R, Murray S, Valenti L, Bhanot S, Åkerblad P, Romeo S. Pnpla3 silencing with antisense oligonucleotides ameliorates nonalcoholic steatohepatitis and fibrosis in Pnpla3 I148M knock-in mice. *Mol Metab* 2019; **22**: 49-61 [PMID: 30772256 DOI: 10.1016/j.molmet.2019.01.013]
47 **Wang Y**, Kory N, BasuRay S, Cohen JC, Hobbs HH. PNPLA3, CGI-58, and Inhibition of Hepatic Triglyceride Hydrolysis in Mice. *Hepatology* 2019; **69**: 2427-2441 [PMID: 30802989 DOI: 10.1002/hep.30583]
48 **Brownsey RW**, Zhande R, Boone AN. Isoforms of acetyl-CoA carboxylase: structures, regulatory properties and metabolic functions. *Biochem Soc Trans* 1997; **25**: 1232-1238 [PMID: 9449982 DOI: 10.1042/bst0251232]
49 **Gao YS**, Qian MY, Wei QQ, Duan XB, Wang SL, Hu HY, Liu J, Pan CY, Zhang SQ, Qi LW, Zhou JP, Zhang HB, Wang LR. WZ66, a novel acetyl-CoA carboxylase inhibitor, alleviates nonalcoholic steatohepatitis (NASH) in mice. *Acta Pharmacol Sin* 2020; **41**: 336-347 [PMID: 31645659 DOI: 10.1038/s41401-019-0310-0]
50 **Bates J**, Vijayakumar A, Ghoshal S, Marchand B, Yi S, Kornyeyev D, Zagorska A, Hollenback D, Walker K, Liu K, Pendem S, Newstrom D, Brockett R, Mikaelian I, Kusam S, Ramirez R, Lopez D, Li L, Fuchs BC, Breckenridge DG. Acetyl-CoA carboxylase inhibition disrupts metabolic reprogramming during hepatic stellate cell activation. *J Hepatol* 2020; **73**: 896-905 [PMID: 32376414 DOI: 10.1016/j.jhep.2020.04.037]
51 **Liu Z**, Que S, Zhou L, Zheng S, Romeo S, Mardinoglu A, Valenti L. The effect of the TM6SF2 E167K variant on liver steatosis and fibrosis in patients with chronic hepatitis C: a meta-analysis. *Sci Rep* 2017; **7**: 9273 [PMID: 28839198 DOI: 10.1038/s41598-017-09548-9]

World Journal of Gastroenterology

Submit a Manuscript: https://www.f6publishing.com

World J Gastroenterol 2022 July 7; 28(25): 2955-2967

DOI: 10.3748/wjg.v28.i25.2955

ISSN 1007-9327 (print) ISSN 2219-2840 (online)

ORIGINAL ARTICLE

Basic Study

Upregulated adenosine 2A receptor accelerates post-infectious irritable bowel syndrome by promoting CD4+ T cells' T helper 17 polarization

Li-Wei Dong, Zhi-Chao Ma, Jiao Fu, Bai-Li Huang, Fu-Jin Liu, Deming Sun, Cheng Lan

Specialty type: Gastroenterology and hepatology

Provenance and peer review: Unsolicited article; Externally peer reviewed.

Peer-review model: Single blind

Peer-review report's scientific quality classification

Grade A (Excellent): 0
Grade B (Very good): B, B
Grade C (Good): C
Grade D (Fair): 0
Grade E (Poor): 0

P-Reviewer: Curro G, Italy; Imam S, United States; Lin TY, Taiwan
A-Editor: Zhu JQ, China

Received: February 14, 2022
Peer-review started: February 14, 2022
First decision: April 12, 2022
Revised: April 26, 2022
Accepted: June 13, 2022
Article in press: June 13, 2022
Published online: July 7, 2022

Li-Wei Dong, Zhi-Chao Ma, Jiao Fu, Bai-Li Huang, Fu-Jin Liu, Cheng Lan, Department of Gastroenterology, Hainan General Hospital, Affiliated Hainan Hospital, Hainan Medical University, Haikou 570311, Hainan Province, China

Deming Sun, Doheny Eye Institute, Department of Ophthalmology, David Geffen School of Medicine, University of California Los Angeles, Los Angeles, CA 90033, United States

Corresponding author: Cheng Lan, MD, PhD, Chief Doctor, Professor, Department of Gastroenterology, Hainan General Hospital, Affiliated Hainan Hospital, Hainan Medical University, No. 19 Xiuhua Road, Xiuying District, Haikou 570311, Hainan Province, China. lancheng71@163.com

Abstract

BACKGROUND

Post-infectious irritable bowel syndrome (PI-IBS) is generally regarded as a functional disease. Several recent studies have reported the involvement of low-grade inflammation and immunological dysfunction in PI-IBS. T helper 17 (Th17) polarization occurs in IBS. Adenosine and its receptors participate in intestinal inflammation and immune regulation.

AIM

To investigate the role of Th17 polarization of CD4+ T cells regulated by adenosine 2A receptor (A2AR) in PI-IBS.

METHODS

A PI-IBS model was established by infecting mice with *Trichinella spiralis*. The intestinal A2AR and CD4+ T lymphocytes were detected by immunohistochemistry, and the inflammatory cytokines were detected by enzyme-linked immunoassay. CD4+ T lymphocytes present in the animal's spleen were separated and cultured with or without A2AR agonist and antagonist. Western blotting and real-time quantitative polymerase chain reaction were performed to determine the effect of A2AR on the cells and intestinal tissue. Cytokine production was determined. The protein and mRNA levels of A2AR associated signaling pathway molecules were also evaluated. Furthermore, A2AR agonist and antagonist were injected into the mouse model and the clinical features were observed.

RESULTS

The PI-IBS mouse model showed increased expression of ATP and A2AR ($P < 0.05$), and inhibition of A2AR improved the clinical features in PI-IBS, including the abdominal withdrawal reflex and colon transportation test ($P < 0.05$). The number of intestinal CD4+ T cells and interleukin-17 (IL-17) protein levels increased during PI-IBS, which was reversed by administration of the A2AR antagonist ($P < 0.05$). CD4+ T cells expressed A2AR and produced IL-17 *in vitro*, which was regulated by the A2AR agonist and antagonist. The A2AR antagonist increased the production of IL-17 by CD4+ T cells *via* the Janus kinase-signal transducer and activator of transcription-receptor-related orphan receptor γ signaling pathway.

CONCLUSION

The results of the present study suggested that the upregulation of A2AR increases PI-IBS by promoting the Th17 polarization of CD4+ T cells.

Key Words: Adenosine 2A receptor; CD4+ T cells; T helper 17 polarization; Post-infectious irritable bowel syndrome; Regulation

©The Author(s) 2022. Published by Baishideng Publishing Group Inc. All rights reserved.

Core Tip: T helper 17 (Th17) polarization occurs during the development of irritable bowel syndrome (IBS). Adenosine and its receptors participate in the development of intestinal inflammation and immune regulation. Here, we found that the intestinal levels of ATP, adenosine 2A receptor (A2AR), and interleukin-17 (IL-17) and the number of CD4+ T cells increased in post-infectious IBS (PI-IBS) mice. In addition, A2AR promoted CD4+ T cells' IL-17 production. Upregulated A2AR accelerated PI-IBS by promoting CD4+ T cells' Th17 polarization, which was reversed by the A2AR antagonist. Thus, our results prove that the regulation of CD4+ T cells' Th17 polarization by A2AR plays a pathogenetic role in the development of PI-IBS.

Citation: Dong LW, Ma ZC, Fu J, Huang BL, Liu FJ, Sun D, Lan C. Upregulated adenosine 2A receptor accelerates post-infectious irritable bowel syndrome by promoting CD4+ T cells' T helper 17 polarization. *World J Gastroenterol* 2022; 28(25): 2955-2967

URL: https://www.wjgnet.com/1007-9327/full/v28/i25/2955.htm

DOI: https://dx.doi.org/10.3748/wjg.v28.i25.2955

INTRODUCTION

The predominant clinical features of irritable bowel syndrome (IBS) include abdominal pain, abnormal bowel habit, and stool changes. IBS occurs predominantly in developed countries. The incidence rate is about 10%-60%. During the past three decades, the incidence of IBS has rapidly increased in underdeveloped countries[1]. IBS can occur after an acute gastrointestinal infection, which is defined as post-infectious IBS (PI-IBS)[2]. The patients suffer from refractory discomfort, live with problems, and have to undergo high medical costs for their treatment. The laboratory reports of these patients do not show morphological findings, which leads to a shortage of time in targeting treatment[3]. Low-grade inflammation and immune activation in the colonic mucosa are observed during IBS[4]. PI-IBS might be alleviated due to regulation of the inflammatory response[5]. Upregulated ephrin type-A receptor 2 and activated nuclear factor kappa-light-chain-enhancer of activated B cells signaling pathway can alleviate PI-IBS[6]. Moreover, non-coding RNAs such as microRNA can modulate inflammation and immune response by targeting peroxiredoxin-1 in PI-IBS[7].

Recently, interleukin-17 (IL-17) raised concerns in PI-IBS. For instance, rifaximin protects mice against PI-IBS by suppressing the production of IL-17[8]. Our previous studies reported that heat shock protein 70 alleviated PI-IBS by upregulating T helper 17 (Th17) response in γδ T cells[9,10].

Adenosine originates from ATP in the local tissue during inflammation and regulates tissue blood flow[11]. As an endogenous molecule, adenosine exhibits anti-inflammatory and immunosuppressive effects by binding to the adenosine receptors (ARs), which are located on some immune and tissue cells and function as a G-protein coupled receptor[12-14]. ARs consist of the following four subtypes: A1R, adenosine A2a receptor, adenosine A2b receptor, and A3R, which are expressed at various locations in the intestine[15]. Different receptors induce different pathophysiological roles. A2BR inhibits the release of inflammatory cytokines, tumor necrosis factor-α, IL-6, and IL-12[16-18]. We previously reported that ARs contribute to the modulation of immune response by γ δ T cells[19,20]. In the intestine, adenosine

and its receptors regulate the enteric nervous system and visceral hypersensitivity. Endogenous adenosine affects the secretion of hydrocarbon by duodenum, whereas extracellular ATP induces the apoptosis of intestinal epithelial cells[21,22]. Adenosine inhibits inflammatory damage in the intestine, protects the intestine against ischemia, and reduces lesions in chronic septic mice by A1AR, A2AR, and A2BR[23,24]. A3R regulates distal colonic neuro-muscle function in rats with colitis[25]. Adenosine receptors also contribute to the inhibition of visceral pain by electroacupuncture in IBS[26]. The role of ARs in intestinal functions shows that they can be a potential target for intestinal inflammatory diseases. However, ARs are not widely studied in IBS, especially in PI-IBS. A2AR is reported to protect the enteric Glia barrier function against intestinal injury induced by hypoxia[27].

The relationship between A2AR, CD4+ T cells, and IL-17 is unknown. Whether A2AR is expressed in CD4+ T cells is not known. Whether A2AR affects IL-17 production directly or through other indirect pathways is unknown. Furthermore, the relationship between A2AR, IL-17, and CD4+ T cells in PI-IBS is unknown. Therefore, we investigated the role of Th17 polarization of CD4+ T cells regulated by A2AR in PI-IBS.

MATERIALS AND METHODS

Animal grouping

57BL/6 mice (female, mean age: 56 d, average weight: 15 g) were provided by the Hainan Provincial Experimental Animal Center and fed in pathogen-free, room temperature conditions under a normal 12-h light/dark diurnal rhythm. The animals were provided with a standard diet and water *ad libitum*. Four groups of mice were formed: Control, PI-IBS, PI-IBS+Sch58261, and PI-IBS+CGS21680 (n = 24 in each group). Twelve mice were processed for the measurement of A2AR, cytokines, and signaling molecules protein and mRNA levels. Six mice were sacrificed in order to isolate, purify, and culture their CD4+ T cells. Visceral hypersensitivity and intestinal motility were evaluated in the remaining 6 animals.

PI-IBS modeling

Infection with *Trichinella spiralis* (Lanzhou Veterinary Research Institute, Lanzhou, China) was performed to establish the PI-IBS model[28]. After 60 d of infection, the parasite larvae were digested from Sprague–Dawley rats with 1.5% gastric pepsin (Invitrogen, Carlsbad, CA, United States) and suspended in 0.2 mL of saline. The mice were fed the larvae (300 larvae/mouse).

Histopathological examination

On the 56th day after infection, the animals' ileum was fixed in 10% formalin and embedded in paraffin wax. The tissues were mounted on slides after creating 5-μm-thick sections, followed by dewaxing and dehydration. The slides were stained with hematoxylin-eosin and used for further evaluation of the inflammatory score following previous scoring standards[29].

Abdominal withdrawal reflex

Visceral hypersensitivity was evaluated with the abdominal withdrawal reflex (AWR)[30]. A gasbag was inserted into the anesthetized animal's anus, which was distended in volume from 0.25 mL to 0.65 mL for 15 min, thrice, followed by a recording of the animal's behavior. The AWR score was found to be in accordance with the standard from 0 to 4 points, as described previously[30]. The AWR scoring standard: when stimulated, the animals are in stable mood, 0 point; if the animals are in unstable mood, twisting their heads once in a while, 1 point; slightly contracting their abdominal and back muscles, 2 points; intensively contracting their abdominal muscles and uplifting the abdomen from the ground, 3 points; intensively contracting abdominal muscles, bowing the abdomen and uplifting the abdomen and perineum, 4 points.

Colon transportation test

Intestinal motility was evaluated with the colon transportation test (CTT); 0.4 mL of activated carbon was placed in the animal's stomach, and the animal's initial time to black stool elimination was recorded. After 8 h, the Bristol stool scoring system was used to assess the total stool's characteristics [31]. Normal shaped stool, 1 point; soft or deformed stool, 2 points; water-like stool, 3 points.

Cellular immunohistochemistry

Cellular immunohistochemistry was performed as reported elsewhere[32]. The suspended cells were fixed in 4% paraformaldehyde and uniformly placed onto slides. The sections were then incubated with primary antibody rabbit anti-mouse A2AR monoclonal antibody and a secondary antibody goat anti-rabbit HRP antibody (ab60032 and ab6721; Abcam, Cambridge, United Kingdom). DAB reagent sets (Beijing Sequoia Jinqiao, Beijing, China) were used to determine the reactivity. The quantitative expression of A2AR in the cellular membrane was calculated using a semi-quantitative integral method.

The staining intensity was scored on a scale of 0-3. The percentage area of positively stained cells was classified as 0-4 corresponding to the values of < 5% to > 75%. The evaluation with a score of ≥ 6 was expressed as a positive expression. The stain was analyzed by Nikon DR-Si2 cell count software and digital image analysis; two senior pathologists verified the results.

Western blotting

Western blotting (Wuhan Boster Corporation, Wuhan, China) was performed to evaluate the protein level. RIPA (R0278; Sigma-Aldrich, Saint Louis, MO, United States) buffer was used to extract the protein from the ground ileum tissue samples. The Bradford assay was performed to determine the protein concentration. After separation on SDS-PAGE gel electrophoresis, 40 μg of the sample was transferred onto a polyvinylidene fluoride membrane. The following transmembrane conditions were set during the assay: (1) β-actin and A2AR: running at 200 mA for 90 min; (2) Janus kinase (JAK) and p-JAK: running at 200 mA for 120 min, followed by running at 300 mA for 30 min; (3) Signal transducer and activator of transcription (STAT3) and p-STAT3: running at 200 mA for 20 min, followed by running at 300 mA for 15 min; and (4) Receptor-related orphan receptor-γt (RORγt): running at 200 mA for 120 min.

The dilution rate of the primary antibodies rabbit anti-mouse multiple-clone antibodies is shown in Table 1.

Blotted in TBST for 60 min, the membrane was incubated with rabbit anti-mouse protein antibodies (ab2787; Abcam, United States) as the primary antibodies and with goat anti-rabbit antibodies as the secondary antibodies (ab8226; Abcam) at 4 °C for 12 h. ECL chemiluminescent assay was performed to autograph the membrane. The detected gray-scale ratio of protein/β-actin represented the relative protein level.

Real-time quantitative PCR

Total RNA in the ileum tissues was extracted with the Trizol reagent set (Invitrogen). The primers were designed by Invitrogen (Table 2). β-actin served as an internal control.

RT-PCR was performed under the following protocol conditions: The samples were run by a pre-denaturation program (5 min at 94 °C), followed by a denaturation program (1 min at 94 °C). The amplification and qualification program was repeated for 30 cycles (50 s at 57 °C, 20 s at 60 °C), followed by an extension program (7 min at 72 °C).

The relative expression was expressed as the ratio of the target gene to the control.

Determination of ATP

The ileum tissue sample was treated ultrasonically and centrifuged at 4 °C for 15 min, followed by the addition of double-distilled water (1:9). The 10% homogenate was heated in a boiling water bath for 10 min and then centrifuged at 3000 rpm for 10 min. The supernatant was collected for enumeration.

The concentration of ATP was measured by a colorimetric method. Briefly, the OD of the tube was measured at the wavelength of 636 nm. The ATP concentration in the sample μmol/gprot) = (measured OD - Control OD)/(Standard OD - OD) × standard concentration (1000 μmol/mL)/sample concentration (gprot/L).

Isolation and purification of CD4+ T cells

CD4+ T cells were isolated from the animals' spleen[33]. Briefly, the animals were sacrificed and their spleens were collected and washed with PBS. The red blood cells were rinsed with red blood cell lysis buffer. The lymphocytes liquid overflowing from the cleaned spleen was repeatedly washed with PBS, centrifuged at 1960 rpm, and incubated with CD4 (FITC) 0.25 μg/test; the CD4+ T cells were selected by fluorescence-activated cell sorting (FACS).

Evaluation of CD4+ T cells' function

The effect of A2AR on CD4 T cell function, including proliferation, apoptosis, ATP production, and Th17 polarization response was evaluated by the CCK8 assay, Annexin V staining assay, and ELISA. Furthermore, the intra-cellular signaling pathway was investigated by Western blotting and RT-PCR.

Proliferation

The CCK8 assay was performed to determine proliferation of the isolated CD4+ T cells. The cell density was set to 5×10^5/mL. The cells were added to a 96 well culture plate at the concentration of 100 μL (5×10^4 cells), followed by treatment with 100 nmol/L of CGS-21680 and 1 μmol/L Sch58261, cultured for 0.5 h at 37°C under 5% CO_2 atmosphere. Then, 20 μL/well of CCK8 was added into the system and continuously cultured for 2 h at 37°C under 5% CO_2 atmosphere. The OD_{450} of the cultured cells was measured with an enzyme-labeled instrument.

Apoptosis

The rate of apoptosis of CD4+ T cells was measured by Annexin V staining assay. Briefly, the collected CD4+ T cells were incubated in a 6-well plate (5×10^5 cells/well), to which 100 nmol/L of CGS-21680

Table 1 The dilution rate of primary antibodies

Primary antibodies	Dilution rate
β-actin	1:1000
A2AR	1:500
RORγt	1:2000
STAT3	1:1000
p-STAT3	1:2000
JAK2	1:1000
p-JAK2	1:1000

Table 2 Primers used in the present study

Name	Primer	Sequence	Size
mus β-actin	Forward	5′-CACGATGGAGGGGCCGGACTCATC-3′	240 bp
	Reverse	5′-TAAAGACCTCTATGCCAACACAGT-3′	
musRORγt	Forward	5′-CGCACCAACCTCTTTTCA-3′	274 bp
	Reverse	5′-GCTCCACACCACCGTATTT-3′	
mus JAK	Forward	5′-AGTGGCGGCATGATTTTGTT-3′	181 bp
	Reverse	5′-GCTCGAACGCACTTTGGTAA-3′	
mus STAT3	Forward	5′-GTAGAGCCATACACCAAGCAGCAG-3′	123 bp
	Reverse	5′-AATGTCGGGGTAGAGGTAGACAAGT-3′	
mus A2AR	Forward	5′-GCCTCTTCTTCGCCTGCTTTGTCC-3′	140 bp
	Reverse	5′-GCCCTTCGCCCTCATACCCGTCAC-3′	

and 1 μmol/L of Sch58261 were added and cultured at 37°C under 5% CO_2 for 0.5 h. Then, 5 μL of Annexin V-APC and 5 μL of 7-AAD staining liquid were added to the wells. FACS was performed to detect the rate of apoptosis.

Th17 polarization

ELISA was performed to determine the concentration of cytokines in the supernatant of CD4+ T cells. A high-sensitivity (sensitivity range: 0.25-16 pg/mL) ELISA kit (R&D Systems, Minneapolis, MI, United States) was used to analyze the IL-17 and IFNγ protein concentrations according to the manufacturer's protocol.

Signaling pathway

The protein and mRNA of the signaling-associated molecules were determined by Western blotting and RT-qPCR, as described previously.

Statistical analysis

The Kolmogorov–Smirnov test was performed using SPSS 22.0 software to indicate normal distribution of the data. Data were expressed as the mean ±standard error of the mean. The differences between the two groups were analyzed by the Student's *t*-test. Values in the same row with different superscripts indicate significance ($P < 0.05$), otherwise no significance ($P > 0.05$).

Ethical considerations

The experimental protocol was approved by the Animal Care and Use Committee of Hainan Province and conducted in accordance with the Chinese guidelines for animal welfare.

Table 3 The effect of adenosine 2A receptor on the abdominal withdrawal reflex score in the post-infectious irritable bowel syndrome mouse

Distending air volume (mL)	AWR			
	0.25	0.35	0.5	0.65
Control (n = 6)	0.00 ± 0.00	1.67 ± 0.53	2.56 ± 0.62	3.67 ± 0.57
PI-IBS (n = 6)	0.00 ± 0.00	2.11 ± 0.49[a]	3.22 ± 0.58	3.89 ± 0.46
IBS + Sch58261 (n = 6)	0.00 ± 0.00	1.89 ± 0.40[c]	2.89 ± 0.45	3.67 ± 0.52
IBS + CGS21680 (n = 6)	0.00 ± 0.00	2.00 ± 0.41	3.11 ± 0.54	3.78 ± 0.57

[a]P < 0.05 *vs* control group.
[c]P < 0.05 *vs* post-infectious irritable bowel syndrome group. AWR: Abdominal withdrawal reflex; PI-IBS: Post-infectious irritable bowel syndrome.

Table 4 The effect of adenosine 2A receptor on intestinal mobility in the post-infectious irritable bowel syndrome mouse

Group	Time to first black stool (min)	Bristol stool grade
Control (n = 6)	105.39 ± 15.16	1.01 ± 0.12
PI-IBS (n = 6)	69.45 ± 8.72[a]	2.54 ± 0.48[a]
IBS + Sch58261 (n = 6)	94.70 ± 14.56[c]	1.29 ± 0.35[c]
IBS + CGS21680 (n = 6)	78.91 ± 9.74	3.11 ± 0.54

[a]P < 0.05 *vs* control group.
[c]P < 0.05 *vs* post-infectious irritable bowel syndrome group. PI-IBS: Post-infectious irritable bowel syndrome.

RESULTS

PI-IBS mouse model and the effect of A2AR on the clinical features of PI-IBS

On the 56th day of infection with *T. spiralis*, the experimental mice showed no significant colonic inflammation (Figure 1), accompanied by a higher AWR score, longer CTT, and higher Bristol stool grade (Tables 3 and 4), suggesting that the PI-IBS mouse model was successfully established. Injection of the A2AR agonist CGS21680 significantly increased the clinical features and slightly accelerated intestinal inflammation. On the other hand, the A2AR antagonist Sch58261 markedly improved the model animal's clinical manifestations. These results confirm the important role of A2AR in the development of PI-IBS. However, the underlying mechanism behind this role warrants further investigation.

Changes in intestinal ATP and A2AR in the PI-IBS mouse

When compared with the control group, intestinal ATP significantly increased in the PI-IBS mouse (P < 0.05; Figure 2) along with an increase in A2AR protein expression (P < 0.05; Figure 3A and B). The A2AR antagonist Sch58261 significantly decreased intestinal ATP and A2AR protein levels, while the A2AR antagonist CGS21680 significantly increased these protein levels (P < 0.05; Figure 2, Figure 3A and B). These results suggest that adenosine and A2AR are involved in the development of PI-IBS.

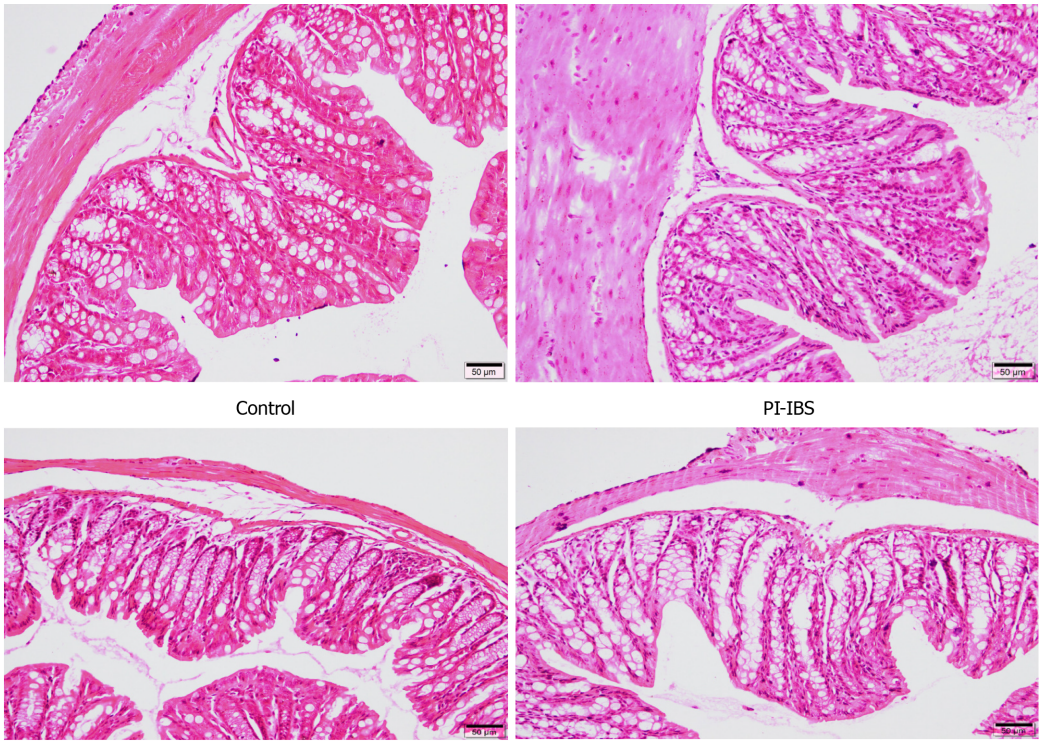
CD4+ T cells' isolation and A2AR expression

CD4+ T cells were isolated and purified from PI-IBS mice spleens by FACS (Figure 3A) for further functional evaluation *in vitro*. Cellular immunohistochemistry results revealed that the CD4+ T cells from PI-IBS mice obviously increased their A2AR protein and mRNA expression, which could have been regulated by the A2AR antagonist and agonist, respectively (P < 0.05; Figure 3C-E). These results suggest that CD4+ T cells could express A2AR, and their expression was regulated by A2AR.

CD4+ T cells from PI-IBS mice showed obvious proliferation, decreased apoptosis, and increased ATP and IL-17 production, which could have been regulated by the A2AR antagonist and agonist, respectively (P < 0.05; Figure 4A-D). These results suggest that CD4+ T cell function, especially Th17 polarization was regulated by A2AR.

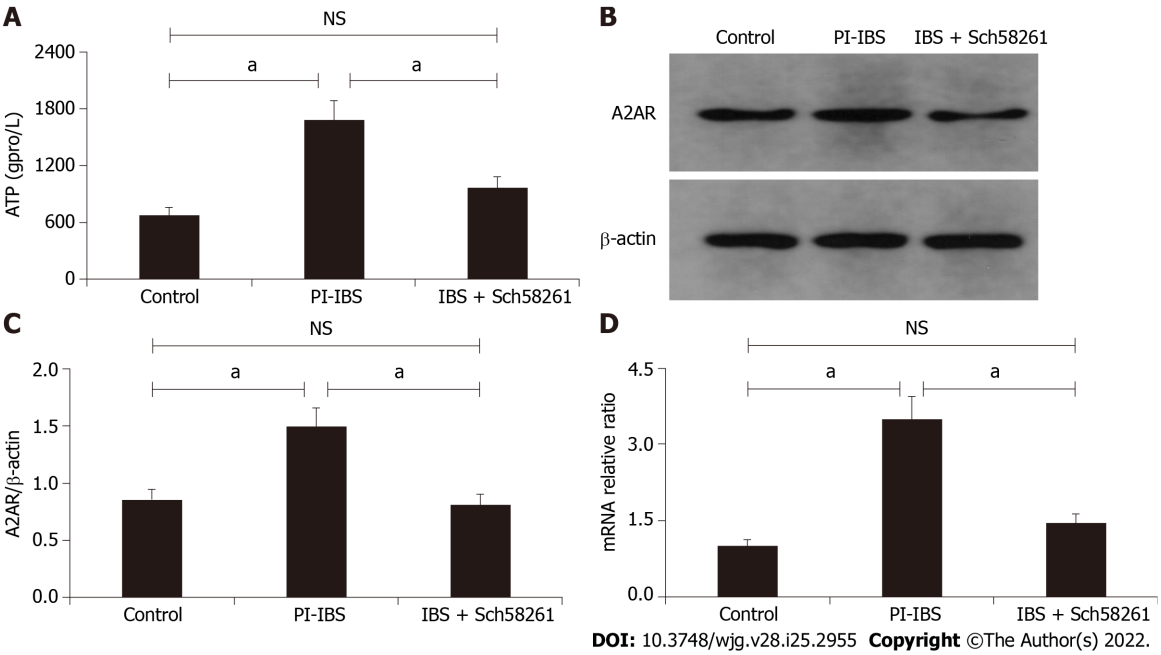
CD4+ T cells signaling pathway

The JAK/p-JAK protein and mRNA expression in CD4+ T cells from PI-IBS mice were detected by Western blotting and RT-PCR. The A2AR antagonist Sch58261 decreased JAK/p-JAK protein and mRNA expression, while the A2AR agonist CGS21680 increased JAK/p-JAK protein and mRNA



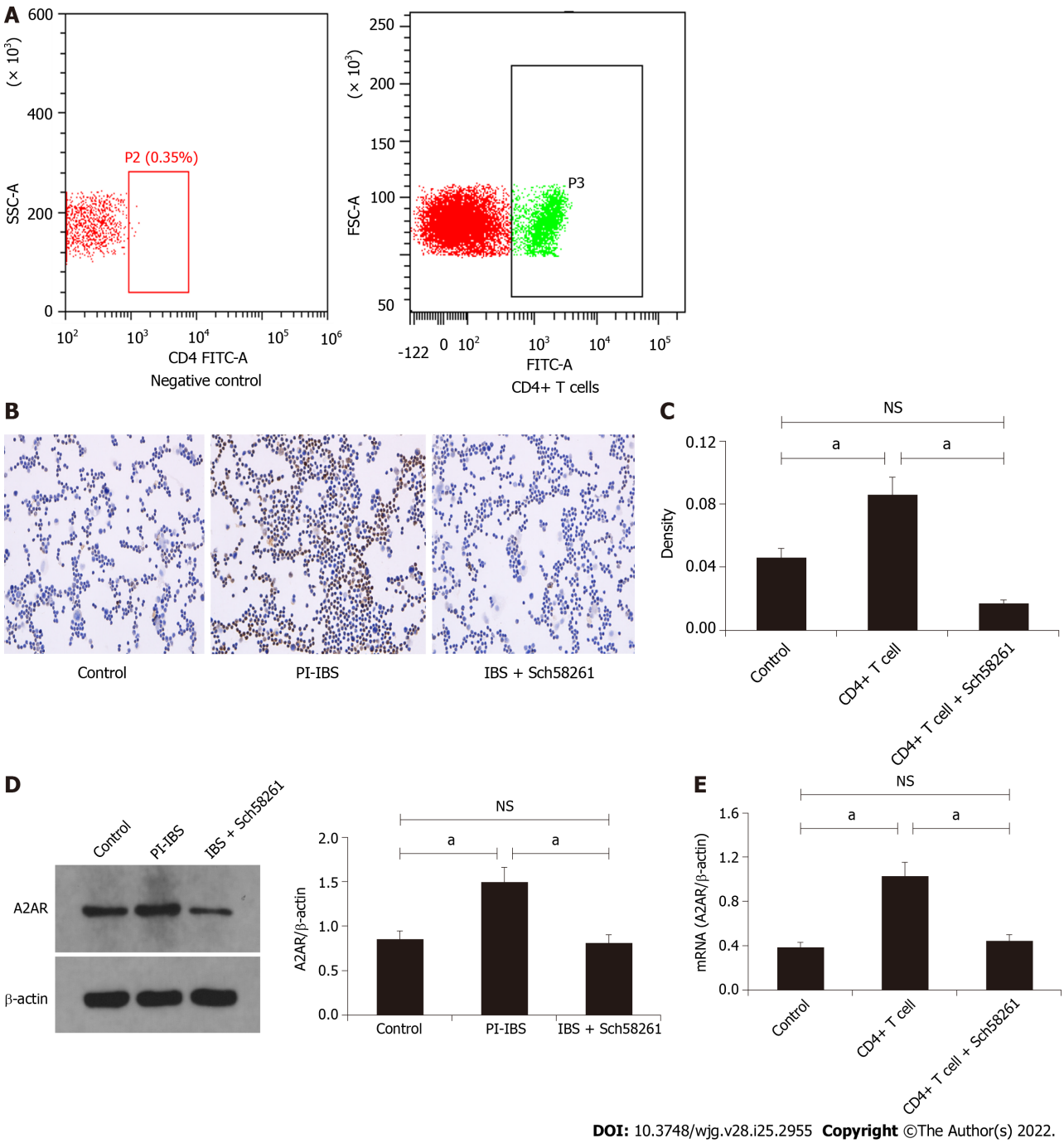
DOI: 10.3748/wjg.v28.i25.2955 **Copyright** ©The Author(s) 2022.

Figure 1 The effect of adenosine 2A receptor on the histopathological changes in the post-infectious irritable bowel syndrome mouse. On the 56th day of infection with *T. spiralis*, colon tissues from the infected mice were collected, fixed, sectioned, stained with hematoxylin-eosin, and evaluated by light microscopy. Compared with the control mouse, the post-infectious irritable bowel syndrome (PI-IBS) mouse model showed no significant inflammatory changes in colon tissues. CGS21680, an agonist of adenosine 2A receptor, induced subtle inflammatory changes in the colon tissues of the PI-IBS model mouse, such as slight infiltration of inflammatory cells. IBS: Irritable bowel syndrome.



DOI: 10.3748/wjg.v28.i25.2955 **Copyright** ©The Author(s) 2022.

Figure 2 The expression of intestinal ATP and adenosine 2A receptor in the post-infectious irritable bowel syndrome mouse. A: The expression level of ATP in different groups; B and C: Western blot analysis showed the expression level of adenosine 2A receptor (A2AR) in the three different groups; D: Relative intestinal A2AR mRNA level in the three groups. $^{a}P < 0.05$. A2AR: Adenosine 2A receptor; PI-IBS: Post-infectious irritable bowel syndrome; NS: Not significant.



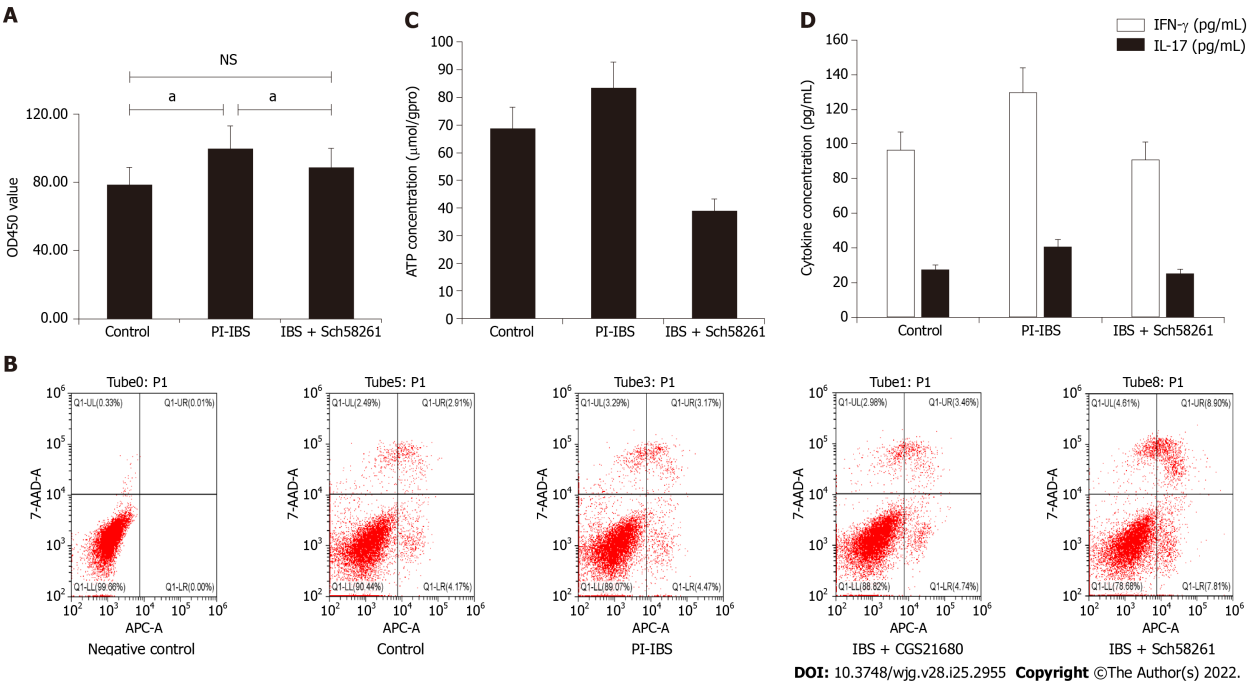
DOI: 10.3748/wjg.v28.i25.2955 **Copyright** ©The Author(s) 2022.

Figure 3 Adenosine 2A receptor expression level in CD4+ T cells isolated and purified from the post-infectious irritable bowel syndrome mouse. A: Fluorescence-activated cell sorting results showed that CD4+ T cells (P3) were successfully isolated and purified; B-C: Immunohistochemistry staining of adenosine 2A receptor (A2AR) in CD4+ T cells; D: Western blot assay evaluated A2AR expression levels in CD4+ T cells isolated from different groups; E: Relative A2AR mRNA levels in the three groups. $^{a}P < 0.05$. A2AR: Adenosine 2A receptor; PI-IBS: Post-infectious irritable bowel syndrome; NS: Not significant.

expression. These results suggest that, during PI-IBS, the JAK pathway participates in CD4+ T cell A2AR-associated biological behavior (Figure 5A and B).

The STAT3/P-STAT3 protein and mRNA expression in CD4+ T cells from PI-IBS mice were detected by Western blotting and RT-PCR. The A2AR antagonist Sch58261 decreased STAT3/P-STAT3 protein and mRNA expression, while the A2AR agonist CGS21680 increased STAT3/P-STAT3 protein and mRNA expression. These results suggest that, during PI-IBS, the STAT3 pathway participated in CD4+ T-cell A2AR-associated biological behavior (Figure 5A and B).

The RORγt protein and mRNA expression in CD4+ T cells from PI-IBS mice were detected by Western blotting and RT-PCR. The A2AR antagonist Sch58261 decreased RORγt protein and mRNA expression, while the A2AR agonist CGS21680 increased RORγt protein and mRNA expression. These results suggest that, during PI-IBS, the RORγt pathway participated in CD4+ T cell A2AR-associated biological behavior (Figure 5A and B).



DOI: 10.3748/wjg.v28.i25.2955 **Copyright** ©The Author(s) 2022.

Figure 4 Functional evaluation of CD4+ T cells *in vitro*. A: CCK-8 assay indicated that CD4+ T cells from post-infectious irritable bowel syndrome mice showed increased proliferation ability; B: Apoptosis analysis of CD4+ T cells between the three groups; C: ATP expression in CD4+ T cells between the three groups; D: Expression level of IFN-γ and IL-17 in the three groups. [a]$P < 0.05$. A2AR: Adenosine 2A receptor; PI-IBS: Post-infectious irritable bowel syndrome; NS: Not significant.

DISCUSSION

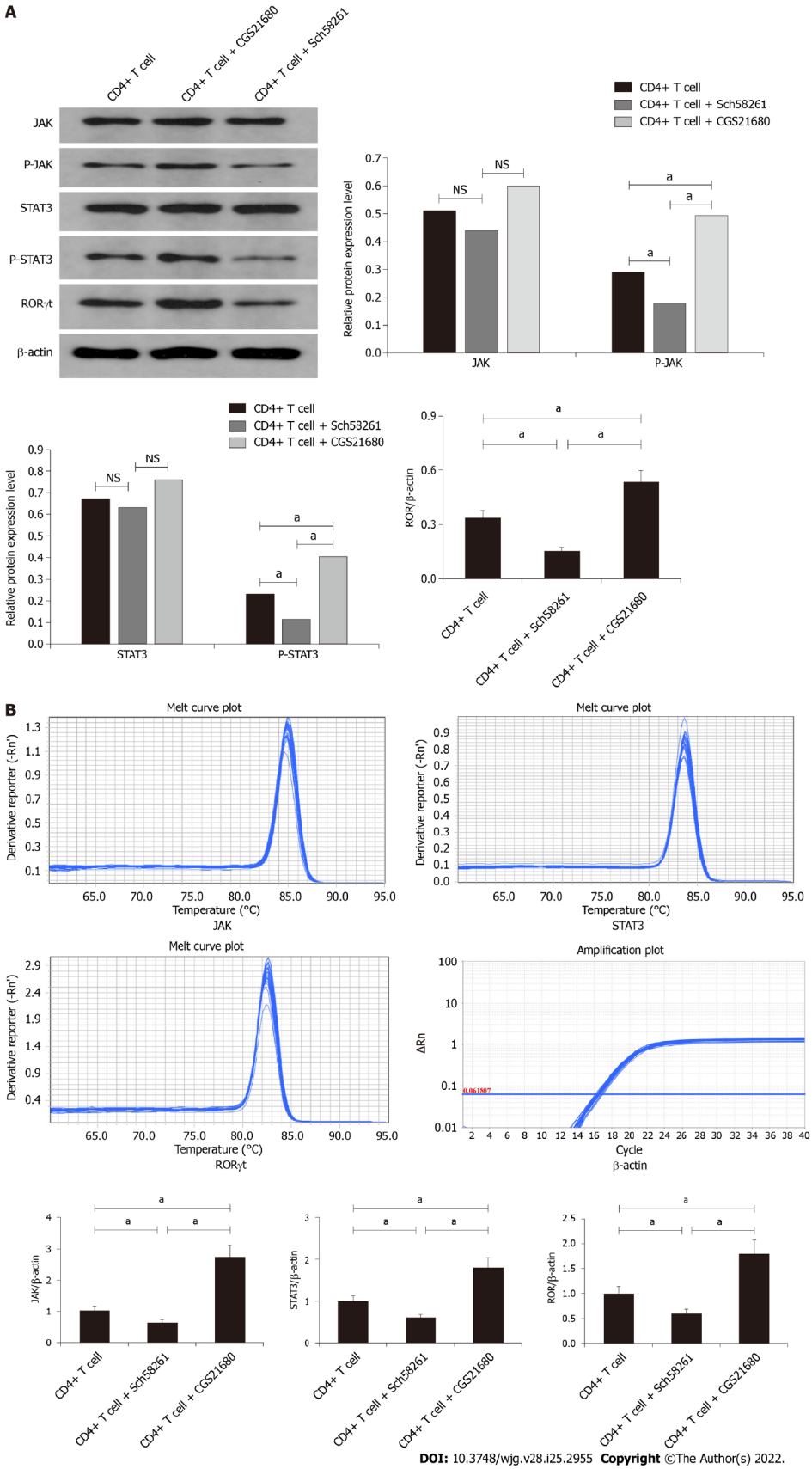
Lasting low level inflammation occurs in the intestine in IBS and especially in PI-IBS due to complex immune abnormalities. Therefore, patients show continuous clinical symptoms and not distinct biochemical and pathological changes. However, the precise mechanism underlying immune regulation in PI-IBS is unclear. Therefore, the relationship between ARs and IL-17 response in the inflammation and immune response in PI-IBS should be investigated.

Our results showed that increasing intestinal ATP level in PI-IBS was accompanied by increasing intestinal A2AR level, which suggested that ATP and A2AR could participate in the pathogenesis of PI-IBS. The quantitative changes that lead to the development of PI-IBS, resulted from PI-IBS, or increased PI-IBS is not known. The animal's intestinal tissue remained unchanged following injection of the A2AR antagonist, but the clinical symptoms improved. This result was contradictory to the previous hypotheses which state that adenosine and its receptors play a protective role in inflammation. During the inflammatory process, adenosine and its receptors could trigger another unknown pathway to maintain the balance of inflammation and the immune response, otherwise, a prolonged presence of increased concentrations of adenosine can be harmful and can induce an immunosuppressed environment that is ideal for the onset and development of neoplasia[34]. Our study reports the complex condition in PI-IBS.

We elucidated the mechanism underlying the role of A2AR in PI-IBS. CD4+ T cells act as an important regulator in inflammation and immune response. Th17 polarization is one of the most important pathways of the immune event associated with CD4+ T cells. We first found that the number of CD4+ T cells distinctly increased, accompanied by an increase in the expression of A2AR on these cells. We then found that the agonist of A2AR increased the number of CD4+ T cells accompanied by an increase in the expression of A2AR on these cells. The A2AR agonist increased the proliferation of CD4+ T cells and inhibited their apoptosis. On the contrary, the A2AR antagonist decreased the number of CD4+ T cells and inhibited their function. These results suggested that CD4+ T cells participate in A2AR-induced intestinal inflammation.

Th17 polarization was associated with A2AR. IL-17 plays a dual role in inflammation and the immune response. IL-17 can improve inflammation in some conditions. For instance, HSP70 induces γ δ T cells to produce IL-17 that protects mice against PI-IBS[10]. IL-17 protects mice against colitis induced by adherent-invasive *Escherichia coli*[35]. In other conditions, IL-17 can increase inflammation. For instance, Th17 cells and IL-17 promotes skin and lung inflammation and fibrosis in the bleomycin-induced murine model of systemic sclerosis[36].

Unfortunately, the studies involving animal models have not determined the efficacy of anti-IL-17 antibodies in improving intestinal inflammation[37]. Our results showed that the increase in A2AR expression and chronic inflammation is associated with the Th17 polarization of CD4+ T cells, which



DOI: 10.3748/wjg.v28.i25.2955 **Copyright** ©The Author(s) 2022.

Figure 5 Signaling pathway analysis by Western blot assay. A: Western blot results indicate that the expression level of p-JAK, p-STAT3, and receptor-related orphan receptor (ROR) were significantly increased in the CD4+ T cell + CGS21680 group and decreased in CD4+ T cell + Sch58261 group; B: The mRNA expression level of p-JAK, p-STAT3, and ROR between the different groups. [a]*P* < 0.05. A2AR: Adenosine 2A receptor; PI-IBS: Post-infectious irritable bowel syndrome; NS: Not significant.

suggested that the A2AR-CD4+ T cells-IL-17 polarization pathway is present in PI-IBS.

We investigated the intracellular signaling pathway of the Th17 polarization of CD4+ T cells induced by A2AR. We found that JAK and STAT3 protein and their phosphorylated products were significantly increased in CD4+ T cells from the PI-IBS mouse model. The A2AR antagonist reduced the protein and mRNA level of JAK and STAT3, which was increased by the A2AR agonist. Our results suggested that the JAK-STAT3 pathway is an important intracellular signaling pathway in the A2AR-induced Th17 polarization of CD4+ T cells in PI-IBS.

The present study has some limitations. The type of visceral hypersensitivity in the PI-IBS mouse model was not investigated. The water content in the Bristol stool grade was not analyzed. The direct isolation of CD4+ T cells from the intestine is difficult. Therefore, we used CD4+ T cells isolated from the spleen, which might have resulted in some variation compared with CD4+ T cells from the intestine.

CONCLUSION

In the present study, we established a mouse model of PI-IBS and the mice were administered an A2AR agonist and antagonist. Interestingly, we found that A2AR increased in PI-IBS accompanied by CD4+ T cell activation, proliferation and production of IL-17. A2AR antagonist improved the clinical symptoms and the cellular and molecular events during PI-IBS. This study showed that the upregulation of A2AR increases PI-IBS by promoting the Th17 polarization of CD4+ T cells.

ARTICLE HIGHLIGHTS

Research background

It has been proved that low-grade inflammation and immunological dysfunction are involved in post-infectious irritable bowel syndrome (PI-IBS). T helper 17 (Th17) polarization occurs in IBS. Adenosine and its receptors participate in intestinal inflammation and immune regulation.

Research motivation

To elucidate the pathogenesis of PI-IBS and identify a potential target for the treatment of this disease.

Research objectives

This study aims to explore the role of adenosine 2A receptor (A2AR) in PI-IBS and its underlying mechanism, especially the relationship between A2AR and Th17 response.

Research methods

A PI-IBS model was established by infecting mice with *Trichinella spiralis*. The expression and function of A2AR and CD4+ T lymphocytes were examined. Furthermore, the effect of A2AR on CD4+ T lymphocyte Th17 polarization was observed and the clinical features of PI-IBS were evaluated.

Research results

The main results can be summarized as follow: (1) expression of ATP and A2AR and inhibition of A2AR improved the clinical features in PI-IBS; (2) CD4+ T cells expressed A2AR and produced IL-17 *in vitro*, which was regulated by the A2AR agonist and antagonist; and (3) The A2AR antagonist increased the production of IL-17 by CD4+ T cells *via* the Janus kinase-signal transducer and activator of transcription-receptor-related orphan receptor γ signaling pathway.

Research conclusions

The upregulation of A2AR increases PI-IBS by promoting the Th17 polarization of CD4+ T cells.

Research perspectives

The present study could provide a new pathway to elucidate the pathogenesis of PI-IBS and identify a novel therapy target for this disease.

FOOTNOTES

Author contributions: Dong LW and Lan C designed the study and interpreted the findings; Dong LW and Ma ZC performed the experiments, analyzed the data, and drafted the manuscript; Fu J, Huang BL and Liu FJ helped collect and analyze the data; Sun D and Lan C critically revised the manuscript for important intellectual content and reviewed the article; all authors have read and approved the final manuscript.

Supported by National Natural Science Foundation of China, No. 81160057, No. 81860102, and No. 82060102.

Institutional animal care and use committee statement: The experimental protocol was approved by the Animal Care and Use Committee of Hainan General Hospital.

Conflict-of-interest statement: All the authors report no relevant conflicts of interest for this article.

Data sharing statement: No additional data are available.

ARRIVE guidelines statement: The authors have read the ARRIVE guidelines, and the manuscript was prepared and revised according to the ARRIVE guidelines.

Open-Access: This article is an open-access article that was selected by an in-house editor and fully peer-reviewed by external reviewers. It is distributed in accordance with the Creative Commons Attribution NonCommercial (CC BY-NC 4.0) license, which permits others to distribute, remix, adapt, build upon this work non-commercially, and license their derivative works on different terms, provided the original work is properly cited and the use is non-commercial. See: https://creativecommons.org/Licenses/by-nc/4.0/

Country/Territory of origin: China

ORCID number: Cheng Lan 0000-0002-1435-5510.

S-Editor: Gong ZM
L-Editor: Webster JR
P-Editor: Gong ZM

REFERENCES

1 **Mayer EA**, Labus JS, Tillisch K, Cole SW, Baldi P. Towards a systems view of IBS. *Nat Rev Gastroenterol Hepatol* 2015; **12**: 592-605 [PMID: 26303675 DOI: 10.1038/nrgastro.2015.121]
2 **Chey WD**, Kurlander J, Eswaran S. Irritable bowel syndrome: a clinical review. *JAMA* 2015; **313**: 949-958 [PMID: 25734736 DOI: 10.1001/jama.2015.0954]
3 **Hellström PM**. Pathophysiology of the irritable bowel syndrome - Reflections of today. *Best Pract Res Clin Gastroenterol* 2019; **40-41**: 101620 [PMID: 31594651 DOI: 10.1016/j.bpg.2019.05.007]
4 **Barbara G**, Grover M, Bercik P, Corsetti M, Ghoshal UC, Ohman L, Rajilić-Stojanović M. Rome Foundation Working Team Report on Post-Infection Irritable Bowel Syndrome. *Gastroenterology* 2019; **156**: 46-58.e7 [PMID: 30009817 DOI: 10.1053/j.gastro.2018.07.011]
5 **Balemans D**, Mondelaers SU, Cibert-Goton V, Stakenborg N, Aguilera-Lizarraga J, Dooley J, Liston A, Bulmer DC, Vanden Berghe P, Boeckxstaens GE, Wouters MM. Evidence for long-term sensitization of the bowel in patients with post-infectious-IBS. *Sci Rep* 2017; **7**: 13606 [PMID: 29051514 DOI: 10.1038/s41598-017-12618-7]
6 **Zeng L**, Li K, Wei H, Hu J, Jiao L, Yu S, Xiong Y. A Novel EphA2 Inhibitor Exerts Beneficial Effects in PI-IBS *in Vivo* and *in Vitro* Models *via* Nrf2 and NF-κB Signaling Pathways. *Front Pharmacol* 2018; **9**: 272 [PMID: 29662452 DOI: 10.3389/fphar.2018.00272]
7 **Zhang Y**, Wu X, Wu J, Li S, Han S, Lin Z, Ding S, Jia X, Gong W. Decreased expression of microRNA-510 in intestinal tissue contributes to post-infectious irritable bowel syndrome *via* targeting PRDX1. *Am J Transl Res* 2019; **11**: 7385-7397 [PMID: 31934286]
8 **Xu D**, Gao J, Gillilland M 3rd, Wu X, Song I, Kao JY, Owyang C. Rifaximin alters intestinal bacteria and prevents stress-induced gut inflammation and visceral hyperalgesia in rats. *Gastroenterology* 2014; **146**: 484-96.e4 [PMID: 24161699 DOI: 10.1053/j.gastro.2013.10.026]
9 **Yang B**, Zhou X, Lan C. Changes of cytokine levels in a mouse model of post-infectious irritable bowel syndrome. *BMC Gastroenterol* 2015; **15**: 43 [PMID: 25886744 DOI: 10.1186/s12876-015-0272-8]
10 **He Z**, Sun X, Ma Z, Fu J, Huang B, Liu F, Chen Y, Deng T, Han X, Sun D, Lan C. Heat shock protein 70 protects mouse against post-infection irritable bowel syndrome *via* up-regulating intestinal γδ T cell's Th17 response. *Cell Biosci* 2018; **8**: 38 [PMID: 29928498 DOI: 10.1186/s13578-018-0237-z]
11 **Aslam M**, Gündüz D, Troidl C, Heger J, Hamm CW, Schulz R. Purinergic Regulation of Endothelial Barrier Function. *Int J Mol Sci* 2021; **22** [PMID: 33530557 DOI: 10.3390/ijms22031207]
12 **Effendi WI**, Nagano T, Kobayashi K, Nishimura Y. Focusing on Adenosine Receptors as a Potential Targeted Therapy in Human Diseases. *Cells* 2020; **9** [PMID: 32213945 DOI: 10.3390/cells9030785]
13 **Burnstock G**. Purinergic Signalling: Therapeutic Developments. *Front Pharmacol* 2017; **8**: 661 [PMID: 28993732 DOI: 10.3389/fphar.2017.00661]
14 **Colgan SP**, Fennimore B, Ehrentraut SF. Adenosine and gastrointestinal inflammation. *J Mol Med (Berl)* 2013; **91**: 157-164 [PMID: 23296303 DOI: 10.1007/s00109-012-0990-0]
15 **Fredholm BB**, IJzerman AP, Jacobson KA, Klotz KN, Linden J. International Union of Pharmacology. XXV. Nomenclature and classification of adenosine receptors. *Pharmacol Rev* 2001; **53**: 527-552 [PMID: 11734617]
16 **Kolachala VL**, Bajaj R, Chalasani M, Sitaraman SV. Purinergic receptors in gastrointestinal inflammation. *Am J Physiol Gastrointest Liver Physiol* 2008; **294**: G401-G410 [PMID: 18063703 DOI: 10.1152/ajpgi.00454.2007]

17 **Antonioli L**, Colucci R, Pellegrini C, Giustarini G, Tuccori M, Blandizzi C, Fornai M. The role of purinergic pathways in the pathophysiology of gut diseases: pharmacological modulation and potential therapeutic applications. *Pharmacol Ther* 2013; **139**: 157-188 [PMID: 23588157 DOI: 10.1016/j.pharmthera.2013.04.002]

18 **Belikoff BG**, Hatfield S, Georgiev P, Ohta A, Lukashev D, Buras JA, Remick DG, Sitkovsky M. A2B adenosine receptor blockade enhances macrophage-mediated bacterial phagocytosis and improves polymicrobial sepsis survival in mice. *J Immunol* 2011; **186**: 2444-2453 [PMID: 21242513 DOI: 10.4049/jimmunol.1001567]

19 **Liang D**, Zuo A, Shao H, Chen M, Kaplan HJ, Sun D. A2B adenosine receptor activation switches differentiation of bone marrow cells to a CD11c(+)Gr-1(+) dendritic cell subset that promotes the Th17 response. *Immun Inflamm Dis* 2015; **3**: 360-373 [PMID: 26734458 DOI: 10.1002/iid3.74]

20 **Chen M**, Liang D, Zuo A, Shao H, Kaplan HJ, Sun D. An A2B Adenosine Receptor Agonist Promotes Th17 Autoimmune Responses in Experimental Autoimmune Uveitis (EAU) *via* Dendritic Cell Activation. *PLoS One* 2015; **10**: e0132348 [PMID: 26147733 DOI: 10.1371/journal.pone.0132348]

21 **Vuerich M**, Mukherjee S, Robson SC, Longhi MS. Control of Gut Inflammation by Modulation of Purinergic Signaling. *Front Immunol* 2020; **11**: 1882 [PMID: 33072065 DOI: 10.3389/fimmu.2020.01882]

22 **Longhi MS**, Moss A, Jiang ZG, Robson SC. Purinergic signaling during intestinal inflammation. *J Mol Med (Berl)* 2017; **95**: 915-925 [PMID: 28547076 DOI: 10.1007/s00109-017-1545-1]

23 **Sitaraman SV**, Merlin D, Wang L, Wong M, Gewirtz AT, Si-Tahar M, Madara JL. Neutrophil-epithelial crosstalk at the intestinal lumenal surface mediated by reciprocal secretion of adenosine and IL-6. *J Clin Invest* 2001; **107**: 861-869 [PMID: 11285305 DOI: 10.1172/JCI11783]

24 **Belikoff B**, Hatfield S, Sitkovsky M, Remick DG. Adenosine negative feedback on A2A adenosine receptors mediates hyporesponsiveness in chronically septic mice. *Shock* 2011; **35**: 382-387 [PMID: 21192284 DOI: 10.1097/SHK.0b013e3182085f12]

25 **Guzman J**, Yu JG, Suntres Z, Bozarov A, Cooke H, Javed N, Auer H, Palatini J, Hassanain HH, Cardounel AJ, Javed A, Grants I, Wunderlich JE, Christofi FL. ADOA3R as a therapeutic target in experimental colitis: proof by validated high-density oligonucleotide microarray analysis. *Inflamm Bowel Dis* 2006; **12**: 766-789 [PMID: 16917233 DOI: 10.1097/00054725-200608000-00014]

26 **Hou T**, Xiang H, Yu L, Su W, Shu Y, Li H, Zhu H, Lin L, Hu X, Liang S, Zhang H, Li M. Electroacupuncture inhibits visceral pain *via* adenosine receptors in mice with inflammatory bowel disease. *Purinergic Signal* 2019; **15**: 193-204 [PMID: 31187350 DOI: 10.1007/s11302-019-09655-4]

27 **Sun L**, Li X, Guan H, Chen S, Fan X, Zhou C, Yang H, Xiao W. A Novel Role of $A_{2A}R$ in the Maintenance of Intestinal Barrier Function of Enteric Glia from Hypoxia-Induced Injury by Combining with mGluR5. *Front Pharmacol* 2021; **12**: 633403 [PMID: 34093180 DOI: 10.3389/fphar.2021.633403]

28 **Zhou X**, Dong L, Yang B, He Z, Chen Y, Deng T, Huang B, Lan C. Preinduction of heat shock protein 70 protects mice against post-infection irritable bowel syndrome *via* NF-κB and NOS/NO signaling pathways. *Amino Acids* 2015; **47**: 2635-2645 [PMID: 26215736 DOI: 10.1007/s00726-015-2056-4]

29 **Suzuki R**, Kohno H, Sugie S, Tanaka T. Dose-dependent promoting effect of dextran sodium sulfate on mouse colon carcinogenesis initiated with azoxymethane. *Histol Histopathol* 2005; **20**: 483-492 [PMID: 15736053 DOI: 10.14670/HH-20.483]

30 **Lan C**, Sun XN, Zhou XC, Yang B, Huang BL, Deng TZ, He ZT, Han XY. Preinduced intestinal HSP70 improves visceral hypersensitivity and abnormal intestinal motility in PI-IBS mouse model. *Asian Pac J Trop Med* 2016; **9**: 302-305 [PMID: 26972407 DOI: 10.1016/j.apjtm.2016.01.022]

31 **Vork L**, Wilms E, Penders J, Jonkers DMAE. Stool Consistency: Looking Beyond the Bristol Stool Form Scale. *J Neurogastroenterol Motil* 2019; **25**: 625 [PMID: 31587553 DOI: 10.5056/jnm19086]

32 **Wu Z**, Yang L, Shi L, Song H, Shi P, Yang T, Fan R, Jiang T, Song J. Prognostic Impact of Adenosine Receptor 2 (A2aR) and Programmed Cell Death Ligand 1 (PD-L1) Expression in Colorectal Cancer. *Biomed Res Int* 2019; **2019**: 8014627 [PMID: 31275983 DOI: 10.1155/2019/8014627]

33 **Sauer KA**, Scholtes P, Karwot R, Finotto S. Isolation of CD4+ T cells from murine lungs: a method to analyze ongoing immune responses in the lung. *Nat Protoc* 2006; **1**: 2870-2875 [PMID: 17406546 DOI: 10.1038/nprot.2006.435]

34 **D'Antongiovanni V**, Fornai M, Pellegrini C, Benvenuti L, Blandizzi C, Antonioli L. The Adenosine System at the Crossroads of Intestinal Inflammation and Neoplasia. *Int J Mol Sci* 2020; **21** [PMID: 32708507 DOI: 10.3390/ijms21145089]

35 **Zhang HJ**, Xu B, Wang H, Wang GD, Jiang MZ, Lei C, Ding ML, Yu PF, Nie YZ, Wu KC, Sha SM, Li MB. IL-17 is a protection effector against the adherent-invasive Escherichia coli in murine colitis. *Mol Immunol* 2018; **93**: 166-172 [PMID: 29195141 DOI: 10.1016/j.molimm.2017.11.020]

36 **Lei L**, Zhao C, Qin F, He ZY, Wang X, Zhong XN. Th17 cells and IL-17 promote the skin and lung inflammation and fibrosis process in a bleomycin-induced murine model of systemic sclerosis. *Clin Exp Rheumatol* 2016; **34** Suppl 100: 14-22 [PMID: 26750756]

37 **Fauny M**, Moulin D, D'Amico F, Netter P, Petitpain N, Arnone D, Jouzeau JY, Loeuille D, Peyrin-Biroulet L. Paradoxical gastrointestinal effects of interleukin-17 blockers. *Ann Rheum Dis* 2020; **79**: 1132-1138 [PMID: 32719044 DOI: 10.1136/annrheumdis-2020-217927]

World Journal of Gastroenterology

Submit a Manuscript: https://www.f6publishing.com

World J Gastroenterol 2022 July 7; 28(25): 2968-2980

DOI: 10.3748/wjg.v28.i25.2968

ISSN 1007-9327 (print) ISSN 2219-2840 (online)

ORIGINAL ARTICLE

Retrospective Study

Four-year experience with more than 1000 cases of total laparoscopic liver resection in a single center

Xiang Lan, Hai-Li Zhang, Hua Zhang, Yu-Fu Peng, Fei Liu, Bo Li, Yong-Gang Wei

Specialty type: Surgery

Provenance and peer review: Unsolicited article; Externally peer reviewed.

Peer-review model: Single blind

Peer-review report's scientific quality classification

Grade A (Excellent): 0
Grade B (Very good): B, B, B
Grade C (Good): C, C, C
Grade D (Fair): 0
Grade E (Poor): 0

P-Reviewer: Labori KJ, Norway; Morise Z, Japan; Rakić M, Croatia; Tsoulfas G, Greece
A-Editor: Soldera J, Brazil

Received: January 4, 2022
Peer-review started: January 4, 2022
First decision: March 9, 2022
Revised: April 1, 2022
Accepted: May 27, 2022
Article in press: May 27, 2022
Published online: July 7, 2022

Xiang Lan, Department of Hepatobiliary Surgery, The First Affiliated Hospital, Chongqing Medical University, Chongqing 400016, China

Hai-Li Zhang, Hua Zhang, Yu-Fu Peng, Fei Liu, Bo Li, Yong-Gang Wei, Department of Liver Surgery & Liver Transplantation Center, Sichuan University West China Hospital, Chengdu 610041, Sichuan Province, China

Corresponding author: Yong-Gang Wei, MD, PhD, Professor, Surgeon, Department of Liver Surgery & Liver Transplantation Center, Sichuan University West China Hospital, No. 37 Guo Xue Road, Wuhou District, Chengdu 610041, Sichuan Province, China.
docweiyonggang@163.com

Abstract

BACKGROUND

Laparoscopic liver resection (LLR) has become a safe surgical procedure that needs additional summarization.

AIM

To review 4 years of total LLR surgeries, exceeding 1000 cases, which were performed at a single center.

METHODS

Patients who underwent LLR at West China Hospital of Sichuan University between January 2015 and December 2018 were identified. Surgical details, including the interventional year, category of liver disease, and malignant liver tumors prognosis, were evaluated. The learning curve for LLR was evaluated using the cumulative sum method. The Kaplan-Meier method was used to perform survival analysis.

RESULTS

Ultimately, 1098 patients were identified. Hepatocellular carcinoma (HCC) was the most common disease that led to the need for LLR at the center (n = 462, 42.08%). The average operation time was 216.94 ± 98.51 min. The conversion rate was 1.82% (20/1098). The complication rate was 9.20% (from grade II to V). The 1-year and 3-year overall survival rates of HCC patients were 89.7% and 81.9%, respectively. The learning curve was grouped into two phases for local resection (cases 1-106 and 107-373), three phases for anatomical segmentectomy (cases 1-44, 45-74 and 75-120), and three phases for hemihepatectomy (cases 1-17, 18-48 and

49-88).

CONCLUSION
LLR may be considered a first-line surgical intervention for liver resection that can be performed safely for a variety of primary, secondary, and recurrent liver tumors and for benign diseases once technical competence is proficiently attained.

Key Words: Laparoscopic liver resection; Single-center experience; Learning curve; Liver

©The Author(s) 2022. Published by Baishideng Publishing Group Inc. All rights reserved.

Core Tip: West China Hospital of Sichuan University is the biggest and most advanced one in the western region of China. About 1500-2500 cases of liver resection have been performed in our center every year. Since the first laparoscopic liver resection (LLR) was performed in 2015, we have accumulated more than 1000 cases rapidly, including hemi-hepatectomy, mesohepatectomy, anatomical segmentectomy from segment I to VIII and even the first case of laparoscopic donor hepatectomy in Mainland China. In this study, we want to share our experiences and introduce technical innovation of LLR.

Citation: Lan X, Zhang HL, Zhang H, Peng YF, Liu F, Li B, Wei YG. Four-year experience with more than 1000 cases of total laparoscopic liver resection in a single center. *World J Gastroenterol* 2022; 28(25): 2968-2980
URL: https://www.wjgnet.com/1007-9327/full/v28/i25/2968.htm
DOI: https://dx.doi.org/10.3748/wjg.v28.i25.2968

INTRODUCTION

Laparoscopic liver resection (LLR) has become a safe approach for liver resection, following advances in surgical techniques, anesthesiology, and perioperative care. Since its first use was reported in 1996 by Azagra *et al*[1], LLR has evolved to become a primary choice of intervention for many patients with liver tumors[2-6]. Experience with laparoscopic procedures has allowed for the development of complex liver resection techniques using laparoscopy, including mesohepatectomy, caudate lobectomy, and even combined resection of several hepatic segments[7-9].

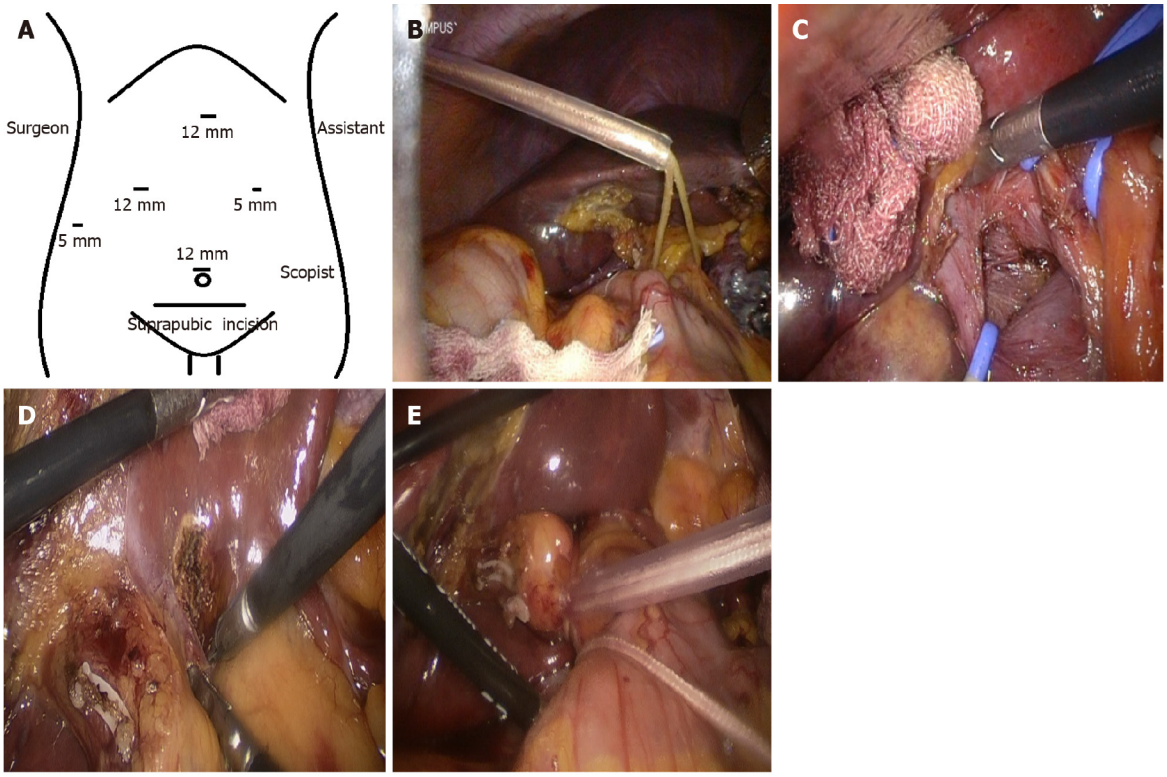
Total LLR has been performed since 2015 at the West China Hospital of Sichuan University. Although total LLR has been performed for a shorter period of time at the West China Hospital of Sichuan University compared to other centers, a large number of clinical patients in the western region of China have been treated with LLR at the West China Hospital of Sichuan University, conveying a rich experience in performing open liver resection to surgeons at the center. Over the past 4 years, LLR, including hemihepatectomy, mesohepatectomy, anatomical segmentectomy from segment I to VIII, and even the first case of laparoscopic donor hepatectomy in mainland China, has been performed successfully at the center[10]. The present study reviews the single center's 4-year experience with LLR in more than 1000 patients and discusses its safety and feasibility, the learning curve for performing laparoscopic surgery, LLR technical innovations, and patient outcomes.

MATERIALS AND METHODS

Patient characteristics

Patients who underwent LLR between January 2015 and December 2018 at the West China Hospital of Sichuan University were studied retrospectively. Inclusion criteria were as follows: patients who had undergone LLR due to liver disease; patients with hemangioma who met the following criteria: (1) Symptomatic hemangioma; (2) Increasing tumor size; (3) Heavy psychological burden and anxiety symptoms that affect daily life and require surgical treatment; (4) Tumor located in special segments (*e.g.*, the caudate lobe or the porta hepatis) that are difficult to treat as tumor size increases; and (5) Unclear diagnosis in which the possibility of a malignant tumor cannot be completely ruled out; and patients with hepatocellular carcinoma (HCC) who met the following criteria: Barcelona Clinic Liver Cancer 0-B stage HCC[11]; A3 stage with normal liver function after conservative treatment; and A4 or B stage with a tumor located in the same hemiliver. Exclusion criteria were as follows: patients who only received laparoscopic surgery without hepatectomy.

Patient data (age, sex, liver function before and after the operation, complications, hospital stay after the operation, operation time, hemorrhage, ascites, and perioperative mortality) were collected. All



DOI: 10.3748/wjg.v28.i25.2968 **Copyright** ©The Author(s) 2022.

Figure 1 Hepatic inflow occlusion methods. A: Trocar position; B: Extracorporeal intermittent pringle maneuver; C: Anatomical continuous hemihepatic vascular inflow occlusion (CHVIO; intro-Glissonian methods); D and E: Extra-Glissonian CHVIO.

patients provided written informed consent for surgery, and this study was approved by the Ethical Review Board of West China Hospital of Sichuan University.

Surgical technique

Surgical procedures were described in our previous study[12]. A five-trocar approach was used at the tumor location (Figure 1A). Two hepatic inflow occlusion methods were adopted at the center[12]. Intermittent pringle (IP): During the operation, hepatic inflow was blocked for 15 min and released for 5 min (Figure 1B) and continuous hemihepatic vascular inflow occlusion (CHVIO) (Figure 1C-E).

Histopathology

Liver capsule invasion and tumor location: Liver capsule invasion was determined by the histopathological report. In this study, "central tumor" was defined as a tumor within the main hepatic body, located in segments I/IV/V/VIII; otherwise, the tumor was considered a "marginal tumor". If the tumor spanned across regions I/IV/V/VIII and another region, it was considered a "central tumor".

Diagnosis of cirrhosis: Liver cirrhosis was diagnosed by histological examination of hepatic tissues by two experienced pathologists. The histopathology diagnostic standard used to diagnose chronic hepatitis was previously described by Desmet *et al*[13]. G0-4/S1-3 was not considered liver cirrhosis, whereas G0-4/S4 was diagnosed as liver cirrhosis.

HCC differentiation: HCC differentiation was classified according to the World Health Organization Classification of Tumors of the Digestive System[14], with grade 1 being well differentiated, grade 2 moderately differentiated, and grade 3 poorly differentiated. At the center, pathological reports sometimes describe grade 1-2 or grade 2-3 HCC in a single patient. Patients with grades 1, 2 and 1-2 were allocated to the "well-to-moderately differentiated" group, and patients with grades 2-3 and 3 were allocated to the "poorly differentiated" group in this study.

Classification of complications: The Clavien–Dindo classification of surgical complications was adopted[15]. Grade I was regarded as the absence of complications, while Grades II-V were regarded as the presence of complications.

The learning curve

The learning curve of LLR was evaluated using the cumulative sum (CUSUM) method. The CUSUM procedure is a well-established method that detects data changes and monitors surgical performance. In

Table 1 The demographic data of all 1098 patients

Demographic data	Frequencies	Range/percentage
Sex		
Male	655	59.65%
Female	443	40.35%
Age (yr)	50.28 ± 13.01	15-86
Disease		
HCC	462	42.08%
ICC	58	5.28%
HCC and ICC mixed carcinoma	5	0.46%
Metastasis	92	8.38%
Hepatolithiasis	59	5.37%
Hemangioma	213	19.40%
FNH and hyperplastic disease	88	8.01%
Parasitic disease	30	2.73%
Living donors	15	1.37%
Liver abscess	11	1.00%
Caroli disease	5	0.46%
Hepatic cyst	6	0.55%
Trauma	2	0.18%
Other benign liver occupancy	52	4.73%

ICC: Intrahepatic cholangiocarcinoma; FNH: Focal nodular hyperplasia; HCC: Hepatocellular carcinoma.

this study, the operation time of each case was ordered chronologically (date of surgery). The formulation of the CUSUM was defined as: Where was an individual operation time, and was the mean of the overall operation time[16]. The learning curve is presented as a broken line graph according to the above formulation.

Follow-up

Patients were followed up 1, 3, 6, 12, 24 and 36 mo postoperatively and assessed by computerized tomography or magnetic resonance imaging, liver function testing, and serum tumor marker measurement. All patients were followed until confirmation of death. If a patient lost contact during follow-up, the survival time was divided into the former interval of follow-up and was included in the censored data.

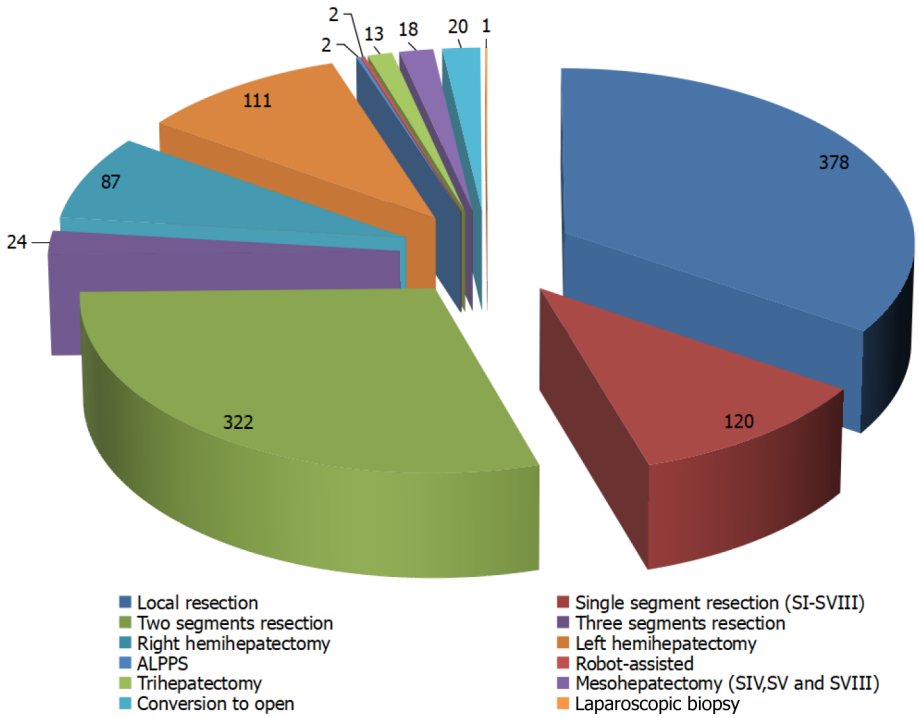
Statistical analysis

Measurement data between 2 comparative intervals were evaluated by independent-samples *t* test. Pearson's chi-square test and Fisher's exact test (when expected cell frequencies were less than 5) were used to determine significant differences in categorical parameters. The Kaplan-Meier method was used to perform survival analysis. Multiple regression analysis was used to assess risk factors determining the patient's disease prognosis. A P value < 0.05 was considered to represent a statistically significant difference.

RESULTS

Demographic data

A total of 1148 consecutive patients who received laparoscopic surgery (except laparoscopic cholecystectomy) between January 2015 and December 2018 were identified. Fifty patients did not meet the inclusion criteria. The remaining 1098 patients underwent LLR, and their demographic data were collected (Table 1).



DOI: 10.3748/wjg.v28.i25.2968 **Copyright** ©The Author(s) 2022.

Figure 2 The details of different types of liver resection at the center. ALPPS: Associating liver partition and portal vein ligation for staged hepatectomy.

The average operation time was 216.95 ± 98.51 min (range, 31-650 min). The longest operation time was observed in LLR in which resection of a tumor in segments I, IV, V and VIII was combined with resection in the caudate lobe invading the middle hepatic vein[9]. The average blood loss was 242.51 ± 143.23 mL (range, 5-4000 mL). The greatest blood loss, 4000 mL was observed in a patient who had liver paragonimiasis and that underwent conversion to open left hemihepatectomy with a splenectomy. A total of 22 patients (2.00%) underwent blood transfusion. The rate of conversion to open surgery was 1.82% (20/1098). With regard to methods of hepatic inflow occlusion, the IP maneuver was employed in 77.14% of patients (847/1098), and CHVIO was used in 21.58% of patients (237/1098). Local resection, 2 segmental resections and anatomical hepatectomy of a single segment represented the top 3 categories of LLR at the center (Figure 2).

Compared with preoperative data, alanine transaminase and aspartate aminotransferase levels peaked at postoperative day (POD) 1 and then gradually decreased ($P < 0.01$, Figure 3A and B). However, the average total bilirubin level tended to increase postoperatively and peaked at POD 5 ($P < 0.01$, Figure 3C). Albumin (ALB) levels and drainage decreased quickly following operation, and ALB levels were maintained at a lower level for a longer period of time ($P < 0.01$, Figure 3D and E).

The progression of surgical outcomes each year

Since the first LLR case in 2015, surgical procedures at the center have been continuously improved according to accumulated experiences. For example, the method of hepatic inflow occlusion was changed from CHVIO to IP, as the latter resulted in less blood loss and a clearer view of the operation site[12].

To further examine technique progression, surgical outcomes, including intraoperative data, mortality on POD 90, and surgical complications, were analyzed by year (Table 2). The inpatient time, postoperative inpatient time, operative time, postoperative liver function, mortality, complications, and drainage significantly decreased from year to year. Although some data (hospitalization expenses and blood loss) did not change significantly, the data trended toward decreasing over time. These results imply that surgeons at the center conquered the LLR learning curve, resulting in the LLR technique advancements.

The learning curves for different types of LLR

Considering that the surgical difficulty of different types of LLR is distinct, 3 representative LLR techniques were selected for investigation of their learning curves: local resection, anatomical resection, and right hemihepatectomy.

For local resection, there was one peak point observed in the 106th case. Therefore, 2 phases were initially differentiated on the graph: Phase I, cases 1-106, and phase II, cases 107-373 (Figure 4A). For anatomical resection, 2 peak points were observed at the 44th and 74th cases. Therefore, 3 phases were

Table 2 Main operation-related data for different years

Index/year	2015 (*n* = 88)	2016 (*n* = 279)	2017 (*n* = 351)	2018 (*n* = 380)	*F*/x^2	*P* value
Age (yr)	51.97 ± 11.35	49.34 ± 12.60	49.88 ± 13.05	50.95 ± 13.58	1.415	-
Sex (M/F)	55/34	159/120	203/148	239/141	3.134	-
LLR types						
Local resection	2.27% (2/88)	35.13% (98/279)	39.60% (139/351)	36.58% (139/380)	45.306	< 0.01[b]
Anatomical resection	23.86% (21/88)	8.24% (23/279)	11.40% (40/351)	9.47% (36/380)	18.096	< 0.01[b]
Right hemi-hepatectomy	14.77% (13/88)	9.32% (26/279)	7.41% (26/351)	5.79% (22/380)	8.903	< 0.05[a]
Pre-operative ALT (U/L)	36.82 ± 28.17	36.67 ± 20.05	35.71 ± 25.37	43.58 ± 33.39	1.667	-
Pre-operative TBL (umol/L)	14.76 ± 5.81	13.55 ± 5.83	13.51 ± 6.21	14.63 ± 7.78	2.519	-
Inpatient time (d)	12.48 ± 6.23	11.77 ± 6.67	9.53± 5.04	8.03 ± 3.20	37.583	< 0.01[b]
Post operative inpatient time (d)	7.98 ± 5.00	6.87 ± 4.82	5.39 ± 3.70	4.70 ± 2.22	29.781	< 0.01[b]
Hospitalization expense (RMB, Yuan)	48708.55 ± 20939.76	47280.53 ± 17249.26	46468.97 ± 35172.25	43016.31 ± 14509.30	2.448	-
Operation time (min)	257.98 ± 114.25	236.85 ± 100.40	203.81 ± 85.83	205.61 ± 99.54	12.596	< 0.01[b]
Blood loss (mL)	275.65 ± 39.19	245.53 ± 19.10	232.54 ± 12.34	241.84 ± 20.32	0.413	-
Post operative ALT (U/L)	355.19 ± 44.44	288.22 ± 19.17	237.16 ± 10.66	251.93 ± 16.03	5.262	< 0.01[b]
Post operative TBL (umol/L)	36.07 ± 3.49	27.86 ± 1.01	28.31 ± 0.92	24.61 ± 1.02	7.443	< 0.01[b]
Mortality of 90 d	2.27% (2/88)	0.36% (1/279)	0 (0/351)	0 (0/380)	14.989	< 0.01[b]
Complications	13.64% (12/88)	13.98% (39/279)	7.98% (28/351)	5.79% (22/380)	15.621	< 0.01[b]
Drainage (mL)	133.12 ± 20.44	111.88 ± 7.62	103.10 ± 6.63	82.44 ± 8.27	3.433	< 0.05[a]
Conversion rate	0 (0/88)	2.15% (6/279)	2.56% (9/351)	1.32% (5/380)	3.427	-

[a]$P < 0.05$.
[b]$P < 0.01$.
ALT: Alanine transaminase; LLR: Laparoscopic liver resection; TBL: Total bilirubin.

initially differentiated on the graph: Phase I, cases 1-44; phase II, cases 45-74; and phase III, cases 75-120 (Figure 4B). For right hemihepatectomy, there were 2 peak points observed at the 17th and 48th cases. Therefore, 3 phases were initially differentiated on the graph: Phase I, cases 1-17; phase II, cases 18-48; and phase III, cases 49-88 (Figure 4C).

These results indicate that the learning processes of anatomical resection and right hemihepatectomy were more complicated than the learning process of local resection and involved an initial period, increased competence in LLR, and then mastery and the challenging period.

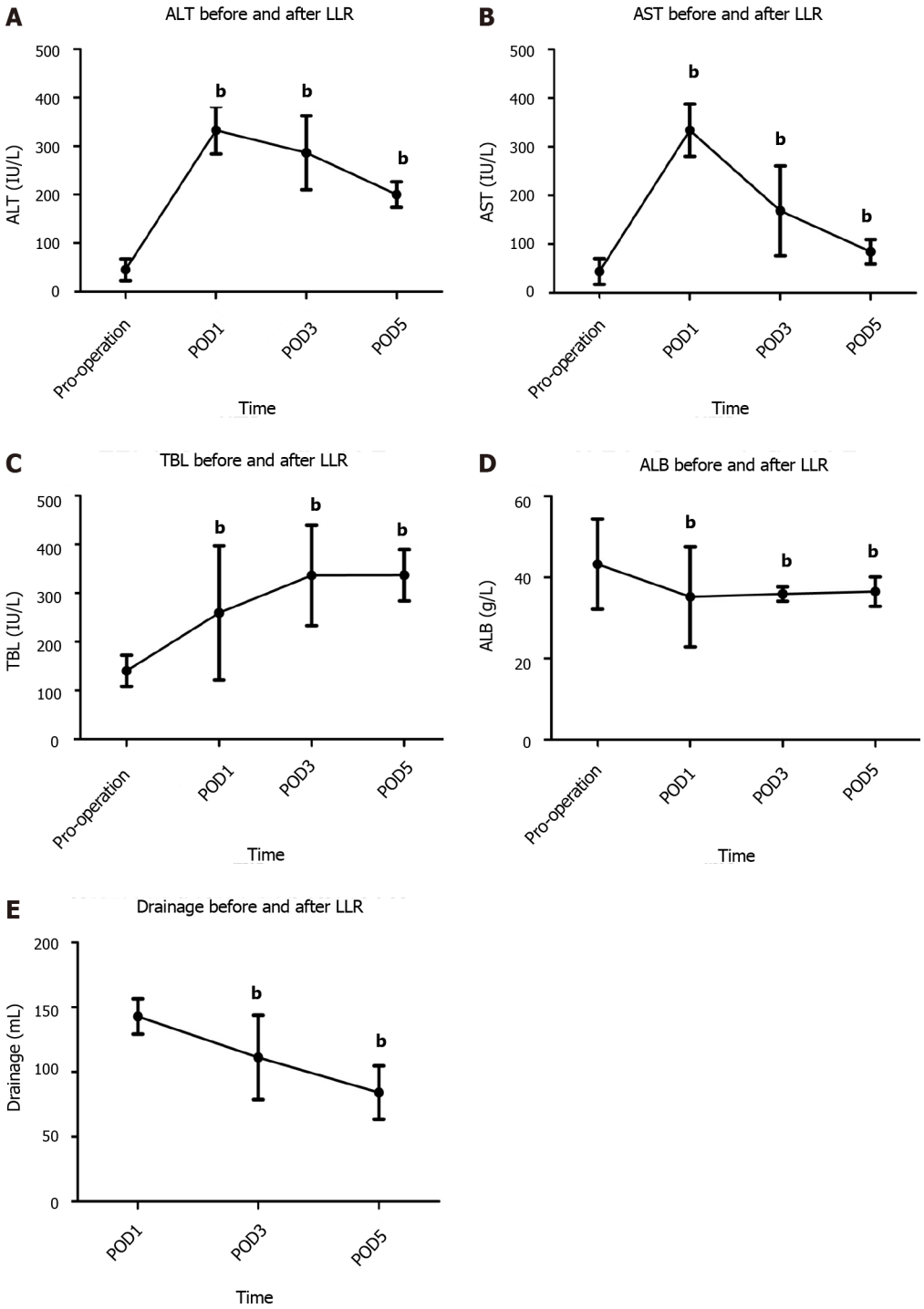
HCC patient characteristics and disease prognosis

Among the 1098 patients enrolled in the study, 462 patients suffered from HCC, and 5 patients suffered from mixed carcinoma (Table 1). The details of all 467 patients with HCC-related disease are shown in Table 3.

Follow-up data were obtained for 438 patients, and disease-free survival (DFS) and overall survival (OS) were assessed. The 3-year DFS and OS rates were 69.4% and 81.9%, respectively. The 1-year DFS and OS rates were 76.3% and 89.7%, respectively (Figure 5).

DISCUSSION

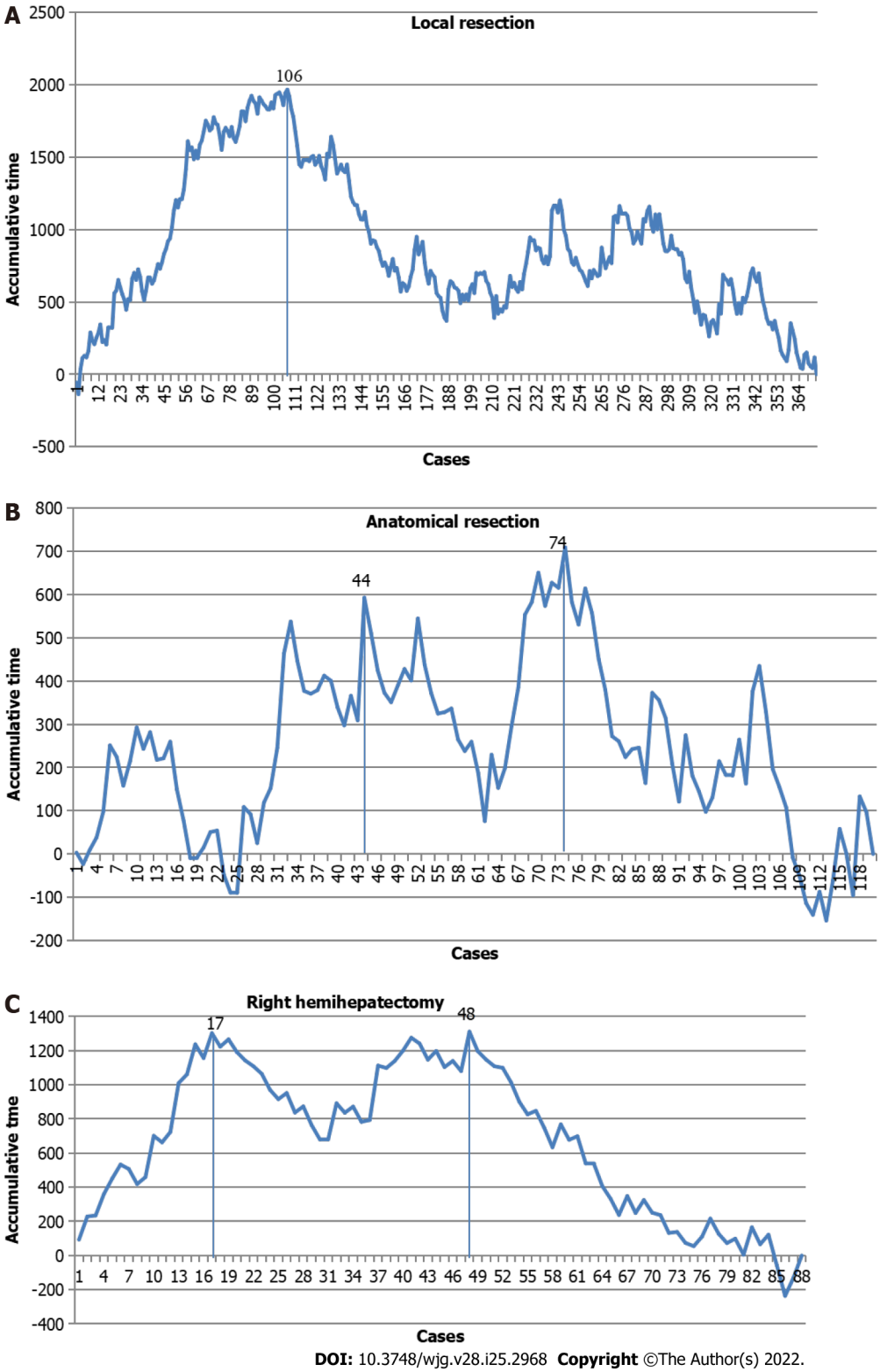
The present study shows that LLR is a safe and efficient treatment for a variety of primary, secondary, and recurrent liver tumors and for benign diseases. LLR has several advantages, including minimal damage to the abdominal wall, faster postoperative recovery, and fewer patient complaints[17,18]. Currently, LLR is widely performed in many liver surgery centers. The College of Medicine, Zhejiang University, was one of the first medical centers to perform LLR in China. They reported a 14-year, single-center experience with 365 cases and claimed that LLR has several advantages: lower economic burden, time saving, less blood loss, minimal harm, and improved safety[19]. Researchers also found that surgeons who use LLR must have extensive experience in performing open hepatectomy and that



DOI: 10.3748/wjg.v28.i25.2968 **Copyright** ©The Author(s) 2022.

Figure 3 Liver function and drainage trends in the perioperative period ($^{b}P < 0.01$). A: Alanine transaminase before and after laparoscopic liver resection (LLR); B: Aspartate aminotransferase before and after LLR; C: Total bilirubin before and after LLR; D: Albumin before and after LLR; E: Drainage before and after LLR. ALT: Alanine transaminase; AST: Aspartate aminotransferase; LLR: Laparoscopic liver resection; ALB: Albumin; TBL: Total bilirubin; POD: Postoperative day.

these surgeons will experience a learning curve when performing LLR. The need for a stepwise progression through the learning curve to minimize morbidity and mortality has been highlighted by many centers[20-22]. Furthermore, using laparoscopic surgery for major liver resections and liver resections for lesions adjacent to major vessels has been confirmed to be both feasible and safe[23-25]. Previous researchers have claimed that the use of LLR for major liver resection has similar morbidity and mortality rates as open surgery. Moreover, tumor recurrence rates following LLR for lesions adjacent to major vessels was not increased[24]. Recent studies support the consensus that LLR is feasible, safe, and minimally invasive. Once surgeons progress through the learning curve, this procedure can offer benefits to patients. Halls *et al*[26] and Ban *et al*[27] established a difficulty score



DOI: 10.3748/wjg.v28.i25.2968 **Copyright** ©The Author(s) 2022.

Figure 4 The learning curves for different types of laparoscopic liver resection. A: The learning curve for local resection; B: The learning curve for anatomical resection; C: The learning curve for right hemihepatectomy.

model to predict intraoperative complications during LLR. Patient characteristics such as neoadjuvant chemotherapy, lesion type and size, classification of resection, and previous open liver resection were associated with a higher risk of surgery-related complications after LLR when compared to surgery-related complications after open liver resection. These findings may provide insight for surgeons when making treatment decisions to obtain better patient outcomes following LLR.

The large Chinese population, especially in Sichuan Province, allowed the center in the present study to accumulate over 1000 LLR cases in a 4-year period. These cases involved all types of LLR, including laparoscopic living donor resection. As reported, the increase in the volume of LLRs performed in 2009-

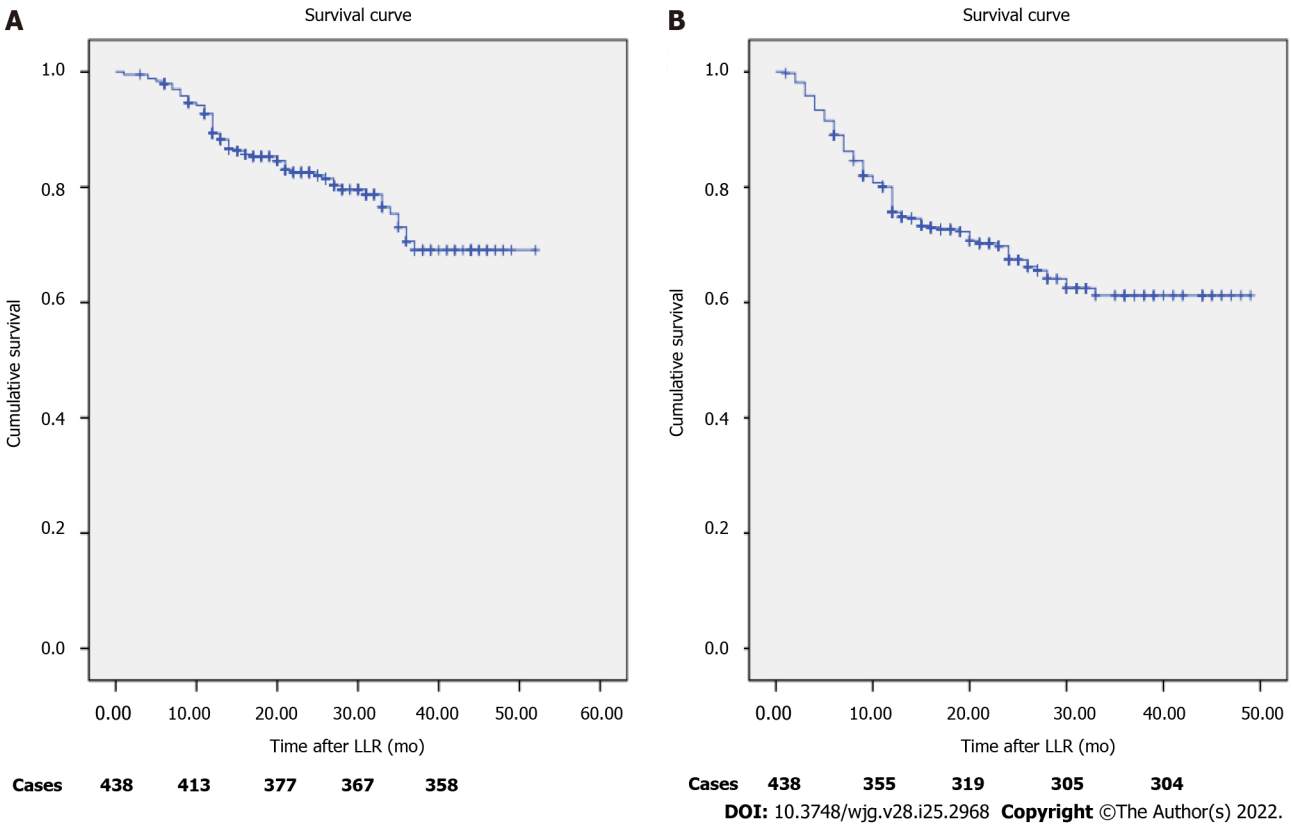
Table 3 Characteristics of patients with hepatocellular carcinoma and mixed carcinoma

	Frequencies	Range/percentage
Incision margin (cm)	1.18 ± 1.0	0-20
Liver cirrhosis		
Cirrhosis	201	43.04%
Non	266	56.96%
Tumor location		
Central	229	49.03%
Marginal	238	50.97%
BCLC stage		
0	81	17.34%
A1	245	52.46%
A2	40	8.57%
A3	22	4.71%
A4	14	3.00%
B	48	10.27%
C	17	3.64%
D	0	0
TNM stage		
Ia	302	64.66%
Ib	99	21.20%
IIa	43	9.21%
IIb	15	3.21%
IIIa	7	1.50%
IIIb	1	0.21%
IV	0	0
Liver capsule invasion		
Positive	156	33.40%
Differentiation	311	66.60%
Well-moderate	275	58.87%
Poor	192	41.13%

BCLC: Barcelona Clinic Liver Cancer; TNM: Tumor-node-metastasis.

2012 *vs* 2000-2008 may be partially attributed to the Louisville 2009 Consensus[28]. Therefore, approximately 22 out of the total of 160 cases were necessary to overcome the learning curve[22,29,30]. A decrease in blood loss during LLR was observed after a minimum of performing 50 cases[29]; and at least 25 cases were needed to master laparoscopic living donor resection[31]. At the center, 106 cases were needed to optimize local resection *via* LLR. However, for complex LLR, 2 peak points were observed in the learning curve. Repetitive training (an initial period, increased competence in LLR, and then mastery and the challenging period) was necessary for surgeons to master hemihepatectomy and anatomical resection *via* LLR. Furthermore, an increase in the conversion rate in 2016/2017 was noted. This time period corresponded to the second and third years of performing LLR at the center when surgeons were overcoming the second peak of the LLR learning curve and at which time there was a huge increase in the number of LLR cases requiring more complex surgeries. After the LLR technology was mastered, the conversion rate at the center decreased significantly in 2018.

Some studies have claimed that continuous hemi-hepatic vascular inflow occlusion is associated with similar outcomes as IP[32,33]. However, at the center in the present study, the IP method was adopted instead of hemihepatic vascular inflow occlusion once the LLR learning curve was overcome, as the IP



DOI: 10.3748/wjg.v28.i25.2968 **Copyright** ©The Author(s) 2022.

Figure 5 Survival rates of patients with hepatocellular carcinoma. A: Overall survival rates; B: Disease-free survival rates. LLR: Laparoscopic liver resection.

method resulted in less blood loss than the hemihepatic vascular inflow occlusion method[12]. Additionally, the intrahepatic Glissonian approach was adopted to replace the extra-Glissonian approach.

The morbidity and mortality rates at the center are similar to those in other centers. One study reviewed 2804 patients who received LLR and found a cumulative mortality rate of 0.3% and a morbidity rate of 10.5%. Liver-specific complications included bile leaks (1.5%), transient liver ascites (1%), and abscesses (2%)[34]. At the center in the present study, in addition to observing these common complications, 4 patients who underwent right anterior lobectomy suffered from right posterior branch injury. One of these 4 patients suffered from liver failure and ultimately died. Due to this complication the LLR technique was improved so that a longer right anterior pedicle is now exposed prior to transection. Similarly, for patients who undergo right hemihepatectomy, the right anterior and posterior pedicle must be transected to prevent left pedicle injury. For patients who undergo left hemihepatectomy, the presence of ischemia in the right lobe following ligation of the left Glissonian sheath must be determined. The cause of death in the other 2 patients was refractory hypernatremia and ascites with liver failure. The most common postoperative complications at the center were pneumonia, hypohepatia, ascites, and bile leakage. Postoperative bleeding requiring a second operation was rare in these cases. Once the LLR learning curve was conquered and the LLR technique advanced and was optimized, postoperative complications significantly decreased from year to year.

CONCLUSION

In conclusion, LLR may be performed safely for a variety of primary, secondary and recurrent liver tumors and for benign diseases. Once the learning curve is overcome, LLR can offer short-term benefits for patients.

ARTICLE HIGHLIGHTS

Research background

Laparoscopic liver resection (LLR) has become a safe approach but still need to be further summarized.

Research motivation
The present study reviews the 4-year experience of total LLR in a single center, which exceeded 1000 cases.

Research objectives
Summarize the past, in order to obtain better progress in this technology in the future.

Research methods
Patients who underwent LLR at West China Hospital of Sichuan University between January 2015 and December 2018 were identified. Surgical details in different years, categories of liver disease and prognosis of malignant liver tumors were evaluated. The learning curve for LLR was evaluated using the cumulative sum method. The Kaplan-Meier method was used to perform survival analysis.

Research results
Ultimately, 1098 patients were identified. Hepatocellular carcinoma (HCC) was the most common disease that led to the need for LLR in our center (n = 462, 42.08%). The average operation time was 216.94 min ± 98.51 min. The conversion rate was 1.82% (20/1098). The complication rate was 9.20% (from grade II to V). The 1-year and 3-year overall survival rates of HCC patients were 89.7% and 81.9%, respectively. The learning curve was grouped into two phases for local resection (cases 1-106 and 107-373), three phases for anatomical segmentectomy (cases 1-44, 45-74 and 75-120) and three phases for hemi-hepatectomy (cases 1-17, 18-48 and 49-88).

Research conclusions
LLR may be considered a first-line surgical intervention for liver resection that can be performed safely for a variety of primary, secondary, and recurrent liver tumors and for benign diseases once technical competence is proficiently attained.

Research perspectives
It is a very promising surgical procedure that can give patients a faster recovery time.

ACKNOWLEDGEMENTS

We thank Dr. Chen YF (Department of Liver Surgery & Liver Transplantation Center, West China Hospital of Sichuan University) for the assistance of data collection.

FOOTNOTES

Author contributions: Lan X and Zhang HL contributed equally to this study and participated in the research design and preparation of the paper; Liu F, Zhang H and Zhang HL performed the statistical analysis; Li B revised this article and Wei YG performed the operation; all the authors contributed to this study.

Supported by Sichuan Provincial Key Project-Science and Technology Project Plan, No. 2019yfs0372.

Institutional review board statement: All clinical investigations were in accordance with the ethical guidelines of the Declaration of Helsinki. Ethical approval was obtained from the Committee of Ethics in West China Hospital of Sichuan University.

Informed consent statement: Written informed consent for surgery was obtained from both patient and her family in this study.

Conflict-of-interest statement: All the authors have no conflicts of interest or financial ties to disclose.

Data sharing statement: No additional data are available.

Open-Access: This article is an open-access article that was selected by an in-house editor and fully peer-reviewed by external reviewers. It is distributed in accordance with the Creative Commons Attribution NonCommercial (CC BY-NC 4.0) license, which permits others to distribute, remix, adapt, build upon this work non-commercially, and license their derivative works on different terms, provided the original work is properly cited and the use is non-commercial. See: https://creativecommons.org/Licenses/by-nc/4.0/

Country/Territory of origin: China

ORCID number: Xiang Lan 0000-0002-5626-0106; Hai-Li Zhang 0000-0002-7291-7446; Hua Zhang 0000-0001-7277-1283;

Yu-Fu Peng 0000-0002-0030-1714; Fei Liu 0000-0002-9650-1576; Bo Li 0000-0002-1411-3722; Yong-Gang Wei 0000-0002-0395-1691.

S-Editor: Yan JP
L-Editor: A
P-Editor: Yuan YY

REFERENCES

1 **Azagra JS**, Goergen M, Gilbart E, Jacobs D. Laparoscopic anatomical (hepatic) left lateral segmentectomy-technical aspects. *Surg Endosc* 1996; **10**: 758-761 [PMID: 8662435 DOI: 10.1007/BF00193052]
2 **Feldbrügge L**, Wabitsch S, Benzing C, Krenzien F, Kästner A, Haber PK, Atanasov G, Andreou A, Öllinger R, Pratschke J, Schmelzle M. Safety and feasibility of laparoscopic liver resection in patients with a history of abdominal surgeries. *HPB (Oxford)* 2020; **22**: 1191-1196 [PMID: 31831317 DOI: 10.1016/j.hpb.2019.11.006]
3 **Schmelzle M**, Krenzien F, Schöning W, Pratschke J. Laparoscopic liver resection: indications, limitations, and economic aspects. *Langenbecks Arch Surg* 2020; **405**: 725-735 [PMID: 32607841 DOI: 10.1007/s00423-020-01918-8]
4 **Kaibori M**, Ichihara N, Miyata H, Kakeji Y, Nanashima A, Kitagawa Y, Yamaue H, Yamamoto M, Endo I. Surgical outcomes of laparoscopic versus open repeat liver resection for liver cancers: A report from a nationwide surgical database in Japan. *J Hepatobiliary Pancreat Sci* 2022 [PMID: 35445565 DOI: 10.1002/jhbp.1156]
5 **Cai LX**, Tong YF, Yu H, Liang X, Liang YL, Cai XJ. Is Laparoscopic Hepatectomy a Safe, Feasible Procedure in Patients with a Previous Upper Abdominal Surgery? *Chin Med J (Engl)* 2016; **129**: 399-404 [PMID: 26879012 DOI: 10.4103/0366-6999.176068]
6 **Monden K**, Sadamori H, Hioki M, Ohno S, Takakura N. Short-term outcomes of laparoscopic versus open liver resection for hepatocellular carcinoma in older patients: a propensity score matching analysis. *BMC Surg* 2022; **22**: 63 [PMID: 35197022 DOI: 10.1186/s12893-022-01518-x]
7 **Coelho FF**, Kruger JA, Fonseca GM, Araújo RL, Jeismann VB, Perini MV, Lupinacci RM, Cecconello I, Herman P. Laparoscopic liver resection: Experience based guidelines. *World J Gastrointest Surg* 2016; **8**: 5-26 [PMID: 26843910 DOI: 10.4240/wjgs.v8.i1.5]
8 **Ho KM**, Han HS, Yoon YS, Cho JY, Choi YR, Jang JS, Kwon SU, Kim S, Choi JK. Laparoscopic Total Caudate Lobectomy for Hepatocellular Carcinoma. *J Laparoendosc Adv Surg Tech A* 2017; **27**: 1074-1078 [PMID: 27855267 DOI: 10.1089/lap.2016.0459]
9 **Li H**, Wei Y, Li B, Peng B. Laparoscopic hepatectomy for segments I, IV, V and VIII. *Surg Endosc* 2017; **31**: 3028-3029 [PMID: 27822585 DOI: 10.1007/s00464-016-5319-6]
10 **Li H**, Wei Y, Li B, Peng B. The First Case of Total Laparoscopic Living Donor Right Hemihepatectomy in Mainland China and Literature Review. *Surg Laparosc Endosc Percutan Tech* 2016; **26**: 172-175 [PMID: 26974531 DOI: 10.1097/SLE.0000000000000256]
11 **Marrero JA**, Kudo M, Bronowicki JP. The challenge of prognosis and staging for hepatocellular carcinoma. *Oncologist* 2010; **15** Suppl 4: 23-33 [PMID: 21115578 DOI: 10.1634/theoncologist.2010-S4-23]
12 **Lan X**, Li H, Liu F, Li B, Wei Y, Zhang H, Xu H. Does liver cirrhosis have an impact on the results of different hepatic inflow occlusion methods in laparoscopic liver resection? *HPB (Oxford)* 2019; **21**: 531-538 [PMID: 30342833 DOI: 10.1016/j.hpb.2018.09.009]
13 **Desmet VJ**, Gerber M, Hoofnagle JH, Manns M, Scheuer PJ. Classification of chronic hepatitis: diagnosis, grading and staging. *Hepatology* 1994; **19**: 1513-1520 [PMID: 8188183]
14 **Li ZS**, Li Q. [The latest 2010 WHO classification of tumors of digestive system]. *Zhonghua Bing Li Xue Za Zhi* 2011; **40**: 351-354 [PMID: 21756837]
15 **Dindo D**, Demartines N, Clavien PA. Classification of surgical complications: a new proposal with evaluation in a cohort of 6336 patients and results of a survey. *Ann Surg* 2004; **240**: 205-213 [PMID: 15273542 DOI: 10.1097/01.sla.0000133083.54934.ae]
16 **Steiner SH**, Cook RJ, Farewell VT, Treasure T. Monitoring surgical performance using risk-adjusted cumulative sum charts. *Biostatistics* 2000; **1**: 441-452 [PMID: 12933566 DOI: 10.1093/biostatistics/1.4.441]
17 **Chen J**, Li H, Liu F, Li B, Wei Y. Surgical outcomes of laparoscopic versus open liver resection for hepatocellular carcinoma for various resection extent. *Medicine (Baltimore)* 2017; **96**: e6460 [PMID: 28328863 DOI: 10.1097/MD.0000000000006460]
18 **Morise Z**, Ciria R, Cherqui D, Chen KH, Belli G, Wakabayashi G. Can we expand the indications for laparoscopic liver resection? *J Hepatobiliary Pancreat Sci* 2015; **22**: 342-352 [PMID: 25663288 DOI: 10.1002/jhbp.215]
19 **Cai X**, Li Z, Zhang Y, Yu H, Liang X, Jin R, Luo F. Laparoscopic liver resection and the learning curve: a 14-year, single-center experience. *Surg Endosc* 2014; **28**: 1334-1341 [PMID: 24399518 DOI: 10.1007/s00464-013-3333-5]
20 **Ibuki S**, Hibi T, Tanabe M, Geller DA, Cherqui D, Wakabayashi G; INSTALL-2 Collaborative Study Group. Short-term Outcomes of "Difficult" Laparoscopic Liver Resection at Specialized Centers: Report From INSTALL (International Survey on Technical Aspects of Laparoscopic Liver Resection)-2 on 4478 Patients. *Ann Surg* 2022; **275**: 940-946 [PMID: 32889884 DOI: 10.1097/SLA.0000000000004434]
21 **Sultana A**, Nightingale P, Marudanayagam R, Sutcliffe RP. Evaluating the learning curve for laparoscopic liver resection: a comparative study between standard and learning curve CUSUM. *HPB (Oxford)* 2019; **21**: 1505-1512 [PMID: 30992198 DOI: 10.1016/j.hpb.2019.03.362]
22 **Shanti H**, Raman R, Chakravartty S, Belgaumkar AP, Patel AG. Effect of the learning curve on survival after laparoscopic liver resection for colorectal metastases. *BJS Open* 2022; **6** [PMID: 35380619 DOI: 10.1093/bjsopen/zrac020]

23 **Wang ZY**, Chen QL, Sun LL, He SP, Luo XF, Huang LS, Huang JH, Xiong CM, Zhong C. Laparoscopic versus open major liver resection for hepatocellular carcinoma: systematic review and meta-analysis of comparative cohort studies. *BMC Cancer* 2019; **19**: 1047 [PMID: 31694596 DOI: 10.1186/s12885-019-6240-x]

24 **Abu Hilal M**, van der Poel MJ, Samim M, Besselink MG, Flowers D, Stedman B, Pearce NW. Laparoscopic liver resection for lesions adjacent to major vasculature: feasibility, safety and oncological efficiency. *J Gastrointest Surg* 2015; **19**: 692-698 [PMID: 25564324 DOI: 10.1007/s11605-014-2739-2]

25 **Morise Z**, Kawabe N, Tomishige H, Nagata H, Kawase J, Arakawa S, Isetani M. How Far Can We Go with Laparoscopic Liver Resection for Hepatocellular Carcinoma? *Biomed Res Int* 2015; **2015**: 960752 [PMID: 26448949 DOI: 10.1155/2015/960752]

26 **Halls MC**, Berardi G, Cipriani F, Barkhatov L, Lainas P, Harris S, D'Hondt M, Rotellar F, Dagher I, Aldrighetti L, Troisi RI, Edwin B, Abu Hilal M. Development and validation of a difficulty score to predict intraoperative complications during laparoscopic liver resection. *Br J Surg* 2018; **105**: 1182-1191 [PMID: 29737513 DOI: 10.1002/bjs.10821]

27 **Ban D**, Tanabe M, Ito H, Otsuka Y, Nitta H, Abe Y, Hasegawa Y, Katagiri T, Takagi C, Itano O, Kaneko H, Wakabayashi G. A novel difficulty scoring system for laparoscopic liver resection. *J Hepatobiliary Pancreat Sci* 2014; **21**: 745-753 [PMID: 25242563 DOI: 10.1002/jhbp.166]

28 **Chen TH**, Yang HR, Jeng LB, Hsu SC, Hsu CH, Yeh CC, Yang MD, Chen WT. Laparoscopic Liver Resection: Experience of 436 Cases in One Center. *J Gastrointest Surg* 2019; **23**: 1949-1956 [PMID: 30421118 DOI: 10.1007/s11605-018-4023-3]

29 **Tomassini F**, Scuderi V, Colman R, Vivarelli M, Montalti R, Troisi RI. The single surgeon learning curve of laparoscopic liver resection: A continuous evolving process through stepwise difficulties. *Medicine (Baltimore)* 2016; **95**: e5138 [PMID: 27787369 DOI: 10.1097/MD.0000000000005138]

30 **Efanov M**, Alikhanov R, Tsvirkun V, Kazakov I, Melekhina O, Kim P, Vankovich A, Grendal K, Berelavichus S, Khatkov I. Comparative analysis of learning curve in complex robot-assisted and laparoscopic liver resection. *HPB (Oxford)* 2017; **19**: 818-824 [PMID: 28599892 DOI: 10.1016/j.hpb.2017.05.003]

31 **Broering DC**, Berardi G, El Sheikh Y, Spagnoli A, Troisi RI. Learning Curve Under Proctorship of Pure Laparoscopic Living Donor Left Lateral Sectionectomy for Pediatric Transplantation. *Ann Surg* 2020; **271**: 542-548 [PMID: 29995683 DOI: 10.1097/SLA.0000000000002948]

32 **Ni JS**, Lau WY, Yang Y, Pan ZY, Wang ZG, Liu H, Wu MC, Zhou WP. A prospective randomized controlled trial to compare pringle manoeuvre with hemi-hepatic vascular inflow occlusion in liver resection for hepatocellular carcinoma with cirrhosis. *J Gastrointest Surg* 2013; **17**: 1414-1421 [PMID: 23715650 DOI: 10.1007/s11605-013-2236-z]

33 **Fu SY**, Lau WY, Li GG, Tang QH, Li AJ, Pan ZY, Huang G, Yin L, Wu MC, Lai EC, Zhou WP. A prospective randomized controlled trial to compare Pringle maneuver, hemihepatic vascular inflow occlusion, and main portal vein inflow occlusion in partial hepatectomy. *Am J Surg* 2011; **201**: 62-69 [PMID: 20409520 DOI: 10.1016/j.amjsurg.2009.09.029]

34 **Nguyen KT**, Gamblin TC, Geller DA. World review of laparoscopic liver resection-2,804 patients. *Ann Surg* 2009; **250**: 831-841 [PMID: 19801936 DOI: 10.1097/SLA.0b013e3181b0c4df]

World Journal of Gastroenterology

Submit a Manuscript: https://www.f6publishing.com

World J Gastroenterol 2022 July 7; 28(25): 2981-2993

DOI: 10.3748/wjg.v28.i25.2981

ISSN 1007-9327 (print) ISSN 2219-2840 (online)

SCIENTOMETRICS

Mapping the global research landscape on nutrition and the gut microbiota: Visualization and bibliometric analysis

Sa'ed H Zyoud, Muna Shakhshir, Amani S Abushanab, Samah W Al-Jabi, Amer Koni, Moyad Shahwan, Ammar Abdulrahman Jairoun, Adham Abu Taha

Specialty type: Gastroenterology and hepatology

Provenance and peer review: Invited article; Externally peer reviewed.

Peer-review model: Single blind

Peer-review report's scientific quality classification

Grade A (Excellent): 0
Grade B (Very good): 0
Grade C (Good): C, C, C
Grade D (Fair): 0
Grade E (Poor): 0

P-Reviewer: Sato H, Japan; Wang JH, South Korea; Yang M, United States

A-Editor: Liu X, China

Received: January 18, 2022
Peer-review started: January 18, 2022
First decision: April 11, 2022
Revised: April 30, 2022
Accepted: May 28, 2022
Article in press: May 28, 2022
Published online: July 7, 2022

Sa'ed H Zyoud, Amani S Abushanab, Samah W Al-Jabi, Amer Koni, Department of Clinical and Community Pharmacy, College of Medicine and Health Sciences, An-Najah National University, Nablus 44839, Palestine

Sa'ed H Zyoud, Poison Control and Drug Information Center, College of Medicine and Health Sciences, An-Najah National University, Nablus 44839, Palestine

Sa'ed H Zyoud, Clinical Research Centre, An-Najah National University Hospital, Nablus 44839, Palestine

Muna Shakhshir, Department of Nutrition, An-Najah National University Hospital, Nablus 44839, Palestine

Amer Koni, Division of Clinical Pharmacy, Hematology and Oncology Pharmacy Department, An-Najah National University Hospital, Nablus 44839, Palestine

Moyad Shahwan, Department of Pharmacy, Ajman University, Ajman 346, United Arab Emirates

Moyad Shahwan, Centre of Medical and Bio-allied Health Sciences Research, Ajman University, Ajman 346, United Arab Emirates

Ammar Abdulrahman Jairoun, Department of Health and Safety, Dubai Municipality, Dubai 67, United Arab Emirates

Adham Abu Taha, Department of Biomedical Sciences, College of Medicine and Health Sciences, An-Najah National University, Nablus 44839, Palestine

Adham Abu Taha, Department of Medicine, College of Medicine and Health Sciences, An-Najah National University, Nablus 44839, Palestine

Corresponding author: Sa'ed H Zyoud, PhD, Associate Professor, Department of Clinical and Community Pharmacy, College of Medicine and Health Sciences, An-Najah National University, Academic Street, Nablus 44839, Palestine. saedzyoud@yahoo.com

Abstract

BACKGROUND

Nutrition is a significant modifiable element that influences the composition of the gastrointestinal microbiota, implying the possibility of therapeutic diet

methods that manipulate the composition and diversity of the microbial.

AIM
To overview research papers on nutrition and gut microbiota and determines the hotspots in this field at the global level.

METHODS
Scopus and Reference Citation Analysis were used to construct a bibliometric technique. It was decided to create bibliometric indicators and mapping as in most previous studies. 2012 through 2021 served as the study's timeframe.

RESULTS
A total of 5378 documents from the Scopus database were selected for analysis. Of all retrieved studies, 78.52% were research papers (n = 4223), followed by reviews (n = 820; 15.25%). China ranked first with a total number of articles of 1634 (30.38%), followed by the United States in second place with a total number of articles of 1307 (24.3%). In the last decade, emerging hotspots for gut microbiota and nutrition research included "gut microbiota metabolism and interaction with dietary components", "connection between the gut microbiota and weight gain", and "the influence of high-fat diet and gut microbiota on metabolic disorders".

CONCLUSION
This is the first thorough bibliometric analysis of nutrition and gut microbiota publications conducted on a global level. Investigation of the association between nutrition/diet and the gut microbiota is still in its infancy and will be expanded in the future. However, according to recent trends, the “effect of gut microbiota and high-fat diet on metabolic disorders" will be an increasing concern in the future.

Key Words: Gut microbiota; Microbiome; Nutrition; Diet; Bibliometric; Scopus; VOSviewer

©The Author(s) 2022. Published by Baishideng Publishing Group Inc. All rights reserved.

Core Tip: The number of publications on the gut microbiota has progressively expanded as the potential clinical implications of the gut microbiota have become better known, and this has become an emerging research subject. Therefore, this comprehensive bibliometric study intends to provide an overview of the current state of worldwide nutrition and gut microbiota research and to stay ahead of emerging trends and important turns in the field's evolution. Investigation on the association between nutrition/diet and the gut microbiota is still in its infancy and will be expanded in the future. However, according to recent trends, the “effect of gut microbiota and high-fat diet on metabolic disorders" will be a bigger worry in the future.

Citation: Zyoud SH, Shakhshir M, Abushanab AS, Al-Jabi SW, Koni A, Shahwan M, Jairoun AA, Abu Taha A. Mapping the global research landscape on nutrition and the gut microbiota: Visualization and bibliometric analysis. *World J Gastroenterol* 2022; 28(25): 2981-2993
URL: https://www.wjgnet.com/1007-9327/full/v28/i25/2981.htm
DOI: https://dx.doi.org/10.3748/wjg.v28.i25.2981

INTRODUCTION

The microbiome is a term that refers to the collective genomes of microorganisms living in a certain habitat, and the gut microbiota is a complex collection of microorganisms that includes archaea, bacteria, fungus, viruses, and protozoa, among others[1]. These communities interact with each other and their host, with the majority of them being bacteria that reside mainly in the colon of the gastrointestinal tract and interact with them. The human genome has thousands of genes; however, the microbiome contains millions of genes that produce a large number of metabolites that alter host activities, resulting in a substantial impact on the host at the physiological level[2]. Different levels of evidence show that functional or compositional changes in the microbiota present in the human gut contribute to human disease and health, including metabolic, immunological and neuro-behavioral traits that support the role of the microbiota in human health[3,4].

The composition of the gut microbiota varies greatly between individuals. Several studies have found that dietary variations between people are one of the external variables that influence and define the gut microbiota structure[5-8]. Studies in recent years have shown that diet or food as the main source of

energy for gut microbes can greatly affect the diversity and components of the gut microbiota, which affects host health[9-12]. In addition to diet, the gut microbiota is affected by different external variables, such as lifestyle and medication (*e.g.*, antibiotics), which mainly affect the microbiota. There are also intrinsic factors that can affect the gut microbiota, such as host genetics, immune and metabolic regulations[13]. Dietary modifications can account for more than 50% of the changes in the gut microbiota changes; however, host genes account for only 10%[14].

Research showed that disturbances in the interaction between nutrients in food and the microbiome affect its structure, which has been shown to be linked to the development of a variety of diseases[15, 16]. Long-term or, to a lesser extent, short-term dietary intake modifications could determine each human's stable microbiota profile. For example, regardless of the stage of life, the intake of protein, fat, fermentable or non-fermentable carbs, probiotic, and polyphenol effectively modulates the host's gut microbiota, metabolic, and immunological parameters. Compared to high animal protein consumption and low carbohydrate intake, high consumption increases the risk of various health conditions, such as diabetes, cancer, cardiovascular disease, and irritable bowel syndrome[7,10]. Another evidence on the diversity of bacterial content in the gastrointestinal tract of humans revealed that lower bacterial diversity has been found in individuals with various diseases such as arthritis, inflammatory bowel disease, type 1 and type 2 diabetes, eczema, and obesity than in healthy individuals who support the role of the microbiota in human health and diseases[17-21]. Accordingly, diversity appears as a positive indicator of a healthy gastrointestinal tract[22,23].

The results have been applied to numerous domains connected to the gut microbiota over the last years[24-28]. However, there are no bibliometric analyses of nutrition/diet and gut microbiota publications. As a result, the objective of the present study was to carefully review publications related to nutrition and gut microbiota to assess the current state and hotspots in this field. Therefore, this comprehensive bibliometric study intends to provide an overview of the current state of worldwide nutrition and gut microbiota research and to stay ahead of emerging trends and important turns in the field's evolution.

MATERIALS AND METHODS

Data sources

We performed this bibliometric analysis using the Scopus bibliographic database, which Elsevier B.V. owns. In bibliometric research, only one database is used because bibliometric indicators and literature mapping are difficult to execute on documents acquired from several databases. Furthermore, the grey literature cannot be included in the data retrieved[29,30]. The current analysis was conducted using the SciVerse Scopus database for numerous reasons. First, Scopus has a much larger number and diversity of indexed publications compared to other databases like PubMed or Web of Science. Scopus has nearly the same number of journals indexed as PubMed and Web of Science combined[31]. Second, because all articles listed in PubMed are simultaneously indexed in Scopus, PubMed is completely comprehensive in Scopus. As a result, Scopus is considered to be comprehensive, as it includes papers from both PubMed and Web of Science[29,30]. Third, Scopus publishes publications in a wide range of disciplines, including science, technology, medicine, social science, and the arts and humanities. Fourth, Scopus enables academics to create sophisticated and extensive search queries by combining various Boolean operators. Finally, Scopus enables the researcher to export and examine the data that have been retrieved. This comprises mapping and statistical analysis. Due to the rapid update of the database, the literature retrieval was carried out on a single day (January 7, 2022). Therefore, it was decided that the publication period for this study would be between 2012 and 2021.

Goal definition

The primary goal of this study is to assess the current state and hotspots in the field of nutrition and gut microbiota by examining the scientific production data set related to nutrition and gut microbiota with the goal of characterisation and understanding it in terms of scientometric indices. Based on bibliometric and/or scientometric indicators, the mapping and analysis of scientific knowledge allow the identification of the dynamics and/or expansion of a specific field of study and the support of strategic decisions related to various research institutions[32].

Search strategy

We used the key terms "microbiome or microbiota" and "nutrition or diet" and its synonyms because we are interested in nutrition and gut microbiota *per se* as a novel concept in scientific research rather than related subjects. The current study focuses on research papers containing "nutrt* or nutrient* or diet* or eat* or feeding" and "microbiome or microbiota or *flora" to recognize items based on their search in the fields topic and the time was ten years between 2012 and 2021. The asterisk (*) was used in search query to retrieve documents with keywords such as diet or dietary.

Validation of the search strategy

The search query was repeatedly fine-tuned in the current study until the top 100 cited publications in the retrieved literature were free of false-positive results. Furthermore, the search query was checked for missing data (false-negative) using a previously published method that depends on the association between the retrieved research output and the actual research output in this field[29,30]. Instead of a title/abstract search, keywords were used in the title search. As a result, the title search will produce the fewest false positive documents, making it a reliable method[29,33-35]. However, a title/abstract search will show many false positives in which the main focus is not on nutrition and the microbiota *per se*.

Bibliometric analysis

The Scopus advanced search tool was used to implement the method. Using the "analyze" function, the retrieved documents were examined. The abstained findings were saved as.csv files in Microsoft Excel. Annual growth, document types, journal names with impact factor (IF), funding agencies, country names, institution names, and document citations were all included in the exported findings. This data was displayed as a linear graph of the annual growth of publication and tables for the core of (top 10 active) journals, funding agencies, countries, institutions, and cited documents in the results section.

The *Impact Index Per Article* for the top 10 high-cited papers collected from Reference Citation Analysis (RCA) is presented. RCA is an open multidisciplinary citation analysis database owned by Baishideng Publishing Group Inc. (Pleasanton, CA 94566, United States)[36].

Visualized analysis

Data on terms in titles and abstracts and cross-country collaboration were visualized using the free Web tool VOSviewer 1.6.17 to determine a worldwide scientific cooperation network across countries/regions and examine hotspots and research trends. Nodes in VOSviewer maps are colored and sized differently. The size is related to the number of times it occurs. The node's color shows its relationship to other nodes with similar colors[37].

RESULTS

Number of publications and evolution over time

A total of 5378 documents from the Scopus database were selected for analysis. The documents retrieved were of 11 types, mainly research articles (n = 4223; 78.52%), followed by reviews (n = 820; 15.25%). Our findings revealed that the scientific advancement of articles on nutrition and gut microbiota has grown in the past ten years. For example, we found 1295 documents in 2021, compared to only 120 documents in 2012 (Figure 1). Of the 5378 documents retrieved, 89 were clinical trials. Fifteen publications on nutrition and gut microbiota were case reports or case series.

Contributions of countries to global publications

Table 1 Lists the contributions of the top 10 countries in publications related to nutrition and gut microbiota from 2012 to 2021. Topping the list was China, with 1634 items (30.38% of the total), followed by the United States, with 1307 items (second place) (24.3%). Italy (n = 346, 6.43%) and Spain (n = 313, 5.82%) ranked third and fourth positions, respectively. An examination of countries with more than 20 publications on nutrition and gut microbiota was conducted. Using data from 44 eligible nations, five VOSviewer clusters were used to examine their centrality and connections to other countries (Figure 2). The United States and China had the highest number of publications in the clusters (green cluster). There is a direct correlation between the number and width of the lines on this map with the degree of interaction and strength between countries.

Analysis of affiliations

As shown in Table 2, the top ten affiliations with the highest number of publications relevant to nutritional science and the gut microbiota were identified. The country with the highest number of affiliations was China. The *Chinese Academy of Sciences* had the highest number of publications (n = 138; 2.57%), followed by the *China Agricultural University* (n = 111; 2.06%), the *Chinese Academy of Agricultural Sciences* (n = 95; 1.77%), and the *University College Cork* (n = 81; 1.51%).

Analysis of funding agencies

Of the documents retrieved 3271 (60.82%) were publications that were part of funded projects. Again, *Chinese funding agencies* were the most active in this field, the *National Natural Science Foundation of China* (n = 711; 13.22%) being the most active, followed by the *National Institutes of Health* (n = 327; 6.08%), and the *National Institute of Diabetes and Digestive and Kidney Diseases* (n = 190; 3.53%) (Table 3).

Table 1 List of the top ten countries publishing research on nutrition and the gut microbiota from 2012 to 2021

Ranking	Country	Number of documents	%
1st	China	1634	30.38
2nd	United States	1307	24.30
3rd	Italy	346	6.43
4th	Spain	313	5.82
5th	United Kingdom	259	4.82
6th	Canada	246	4.57
7th	Germany	240	4.46
8th	Australia	227	4.22
9th	France	216	4.02
10th	South Korea	204	3.79

Table 2 The top 10 productive affiliations publishing research on nutrition and the gut microbiota from 2012 to 2021

Ranking	Institute	Country	*n*	%
1st	*Chinese Academy of Sciences*	China	138	2.57
2nd	*China Agricultural University*	China	111	2.06
3rd	*Chinese Academy of Agricultural Sciences*	China	95	1.77
4th	*University College Cork*	Ireland	81	1.51
5th	*APC Microbiome Ireland*	Ireland	80	1.49
6th	*Nanjing Agricultural University*	China	74	1.38
7th	*Københavns Universitet*	Denmark	73	1.36
8th	*Wageningen University & Research*	Netherlands	62	1.15
9th	*Consejo Superior de Investigaciones Cientificas*	Spain	55	1.02
10th	*Dankook University*	South Korea	54	1.00

Table 3 The top ten funding agencies having the most publications on nutrition and the gut microbiota from 2012 to 2021

Ranking	Funding agencies	Country	No. of publication	%
1st	*National Natural Science Foundation of China*	China	711	13.22
2nd	*National Institutes of Health*	United States	327	6.08
3rd	*National Institute of Diabetes and Digestive and Kidney Diseases*	United States	190	3.53
4th	*National Key Research and Development Program of China*	China	184	3.42
5th	*European Commission*	European Union	102	1.90
6th	*Ministry of Science and Technology of the People's Republic of China*	China	86	1.60
6th	*National Institute of General Medical Sciences*	China	86	1.60
8th	*European Regional Development Fund*	European Union	80	1.49
9th	*National Institute of Allergy and Infectious Diseases*	United States	75	1.39
10th	*Horizon 2020 Framework Programme*	European Union	74	1.38

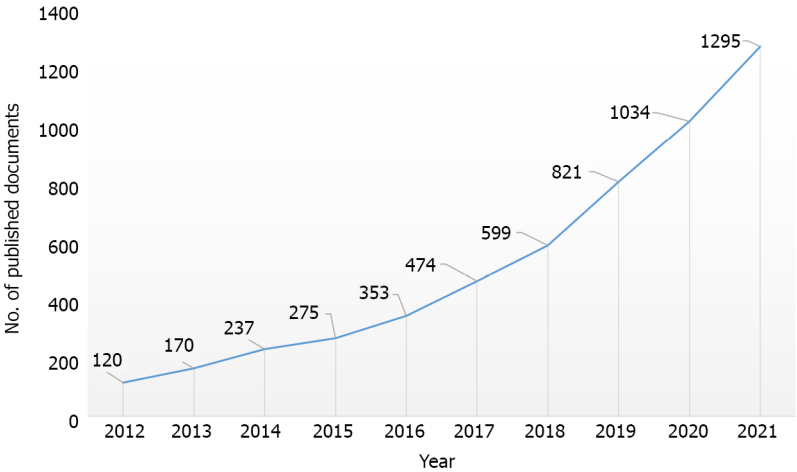
Journal analysis

As presented in Table 4, *Nutrients* (*n* = 271 publications, IF: 5.717) published the most papers on nutrition and the gut microbiota, followed by *Frontiers in Microbiology* (*n* = 167 publications, IF: 5.64), and *Scientific Reports* (*n* = 136 publications, IF: 4.379). The top ten academic journals published approx-

Table 4 The top 10 most active journals publishing research on nutrition and the gut microbiota from 2012 to 2021

Ranking	Journal	*n*	%	IF[1]
1st	*Nutrients*	271	5.04	5.717
2nd	*Frontiers in Microbiology*	167	3.11	5.64
3rd	*Scientific Reports*	136	2.53	4.379
4th	*Plos One*	124	2.31	3.24
5th	*Food and Function*	116	2.16	5.396
6th	*Journal of Functional Foods*	87	1.62	4.451
7th	*Molecular Nutrition and Food Research*	82	1.52	5.914
8th	*Poultry Science*	78	1.45	3.352
9th	*Animals*	70	1.30	2.752
10th	*Journal of Agricultural and Food Chemistry*	68	1.26	5.279

[1]Impact factor (IF) was extracted from Journal Citation Reports (Source Clarivate, 2021).



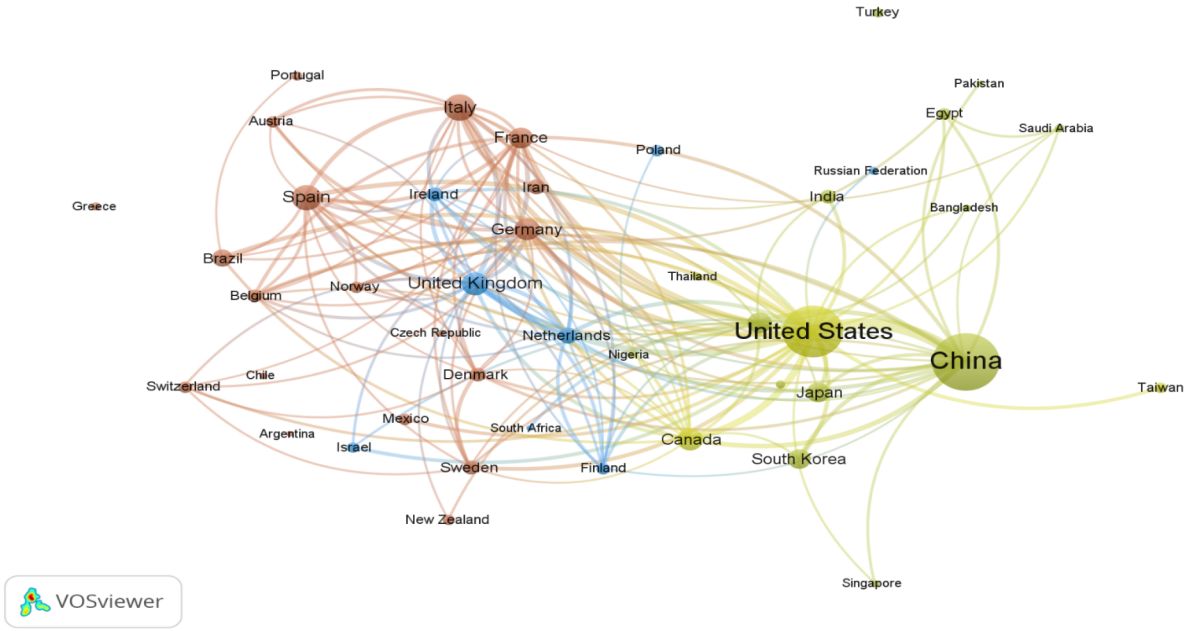
DOI: 10.3748/wjg.v28.i25.2981 **Copyright** ©The Author(s) 2022.

Figure 1 Growth trends of publications on the nutrition and the gut microbiota from 2012 to 2021.

imately 22.3% of the publications.

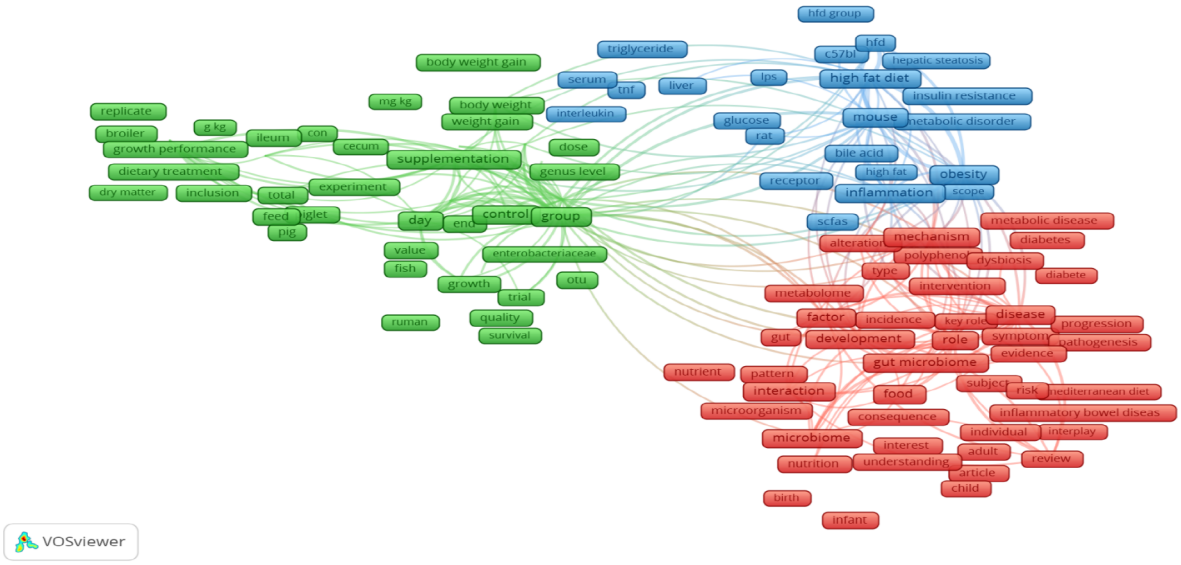
Analysis of research hotspots

To detect trends and topics in most articles on nutrition and gut microbiota, we used VOSviewer software to look at the distribution of cooccurrence terms in the titles and abstracts of 5378 papers. By mapping terms in titles and abstracts with a minimum frequency of 100 occurrences, three major clusters emerged, highlighting three remarkable research themes. For example, in Figure 3, of the 85327 terms, 293 terms appeared at least 100 times, distributed in three clusters. Cluster 1, indicated by red frames, includes those terms commonly seen in publications related to interaction of the gut microbiota with dietary components; Cluster 2, shown by green frames, contains terms commonly seen in publications related tothe correlation between weight gain and the gut microbiota; and Cluster 3, marked by green frames, includes terms commonly observed in studies related to the effect of the gut microbiota and a high-fat diet and on metabolic syndromes. Figure 4 illustrates an overlay visualization in which the VOSviewer was used to color the terms based on their publication year. The blue and green colors indicate that the terminology appeared first, while the yellow colors indicate that they appeared later. Most studies before 2019 focused on the "connection between the gut microbiota and weight gain" and the "interaction of the gut microbiota with dietary components". However, according to recent trends, the "effect of high-fat diet and the gut microbiota on metabolic syndromes" will be a bigger concern in the future.



DOI: 10.3748/wjg.v28.i25.2981 **Copyright** ©The Author(s) 2022.

Figure 2 A network visualization map depicting international collaboration in nutrition and gut microbiota research during 2012-2021. This visualized map of collaborations was created after each country had at least 20 publications. Of 154 countries active in this field, 44 countries meet this threshold. The node's size indicates the number of publications for that country.



DOI: 10.3748/wjg.v28.i25.2981 **Copyright** ©The Author(s) 2022.

Figure 3 Network visualization map of terms in the title/abstract fields of publications relevant to nutrition and gut microbiota research from 2012 to 2021. When the minimum-term occurrences were put 100 times, this graphical map of terms was created. Of the 85327 terms in this field, 293 achieve this threshold, which were grouped into three clusters and colored differently. The size of the frame shows the number of publications that contain that term.

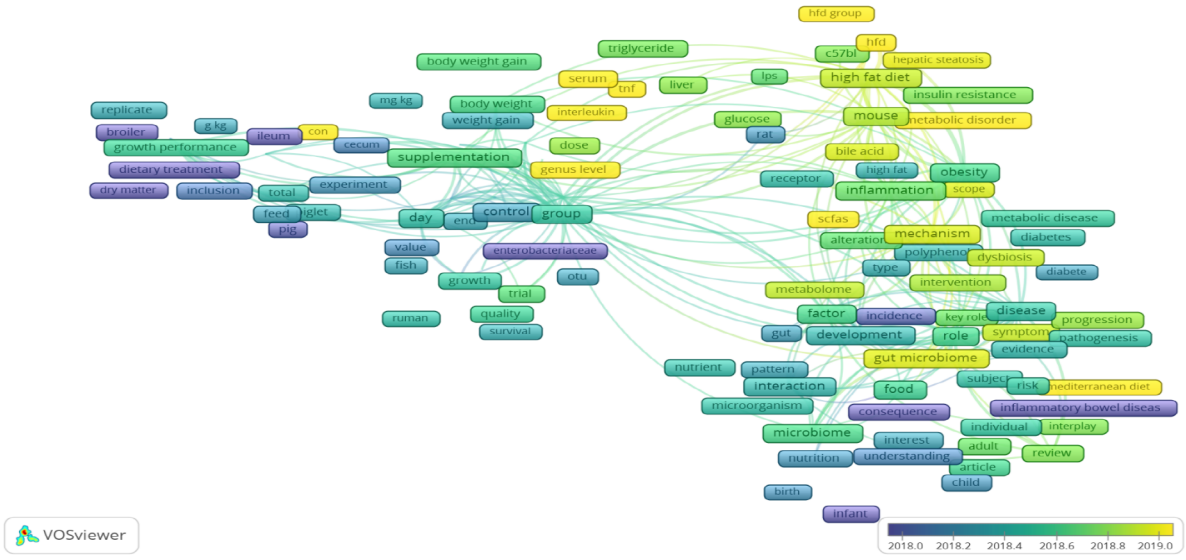
Analysis of citations

According to citation analysis, the retrieved articles garnered 146101 citations, averaging 27.17 *per* document, and an h-index of 154. Citations ranged from 0 to 4588. Two thousand four hundred forty-two items were indexed with ten or more citations, while 852 were indexed without citations. Table 5 lists the top ten articles with the highest number of articles on research related to nutrition and gut microbiota from 2012 to 2021. The 10 highest citations ranged from 4588 to 796. The impact index *per* article of the 10 most cited articles ranged from 96.3 to 506.2 (Table 5).

Table 5 The top 10 high cited papers on research related to nutrition and the gut microbiota from 2012 to 2021

Ranking	Ref.	Year	Source title	IF[1]	Impact index *per* article[2]	Cited by
1st	David *et al*[56]	2014	*Nature*	49.962	506.2	4588
2nd	Koeth *et al*[57]	2013	*Nature Medicine*	53.44	242.8	2294
3rd	Den Besten *et al*[58]	2013	*Journal of Lipid Research*	5.922	202.2	1921
4th	Claesson *et al*[59]	2012	*Nature*	49.962	168.0	1793
5th	Trompette *et al*[60]	2014	*Nature Medicine*	53.44	165.6	1368
6th	Flint *et al*[61]	2012	*Nature Reviews Gastroenterology and Hepatology*	46.802	96.3	1011
7th	Desai *et al*[62]	2016	*Cell*	41.582	182.0	948
8th	Sonnenburg and Bäckhed[63]	2016	*Nature*	49.962	150.3	914
9th	Chassaing *et al*[64]	2015	*Nature*	49.962	122.1	889
10th	Dao *et al*[65]	2016	*Gut*	23.059	111.3	796
10th	Singh *et al*[10]	2017	*Journal of Translational Medicine*	5.531	148.0	796

[1]Impact factor (IF) was extracted from Journal Citation Reports (Source Clarivate, 2021).
[2]The impact index *per* article is presented based on Reference Citation Analysis [Source: Baishideng Publishing Group Inc. (Pleasanton, CA 94566, United States)].



DOI: 10.3748/wjg.v28.i25.2981 **Copyright** ©The Author(s) 2022.

Figure 4 Network visualization map of terms in the title/abstract and their frequency of appearance of keywords is distributed according to the mean frequency of appearance. Blue-colored and green-colored terms first showed, and then yellow terms appeared later.

DISCUSSION

This study has developed research techniques to thoroughly analyze the current status and direction of development of studies related to nutrition and the gut microbiota from 2012 to 2021 using a bibliometric and visualization analysis. The number of publications on the gut microbiota has progressively expanded as the potential clinical implications of the gut microbiota have become better known, and this has become an emerging research subject. Our review of research on global nutrition and gut microbiota found that relevant publications have expanded in the last ten years. A possible explanation for this finding might be that our understanding of the role of the gut microbiota has advanced significantly due to the advancement of scientific tools.

The examination of collaboration networks can provide rich data for evaluating research collaborations and characterizing essential collaborators. China and the United States had a clear advantage in this field, possibly due to their superior economics and investment in the scientific field; for example, in 2013, a notable research project from the United States was launched on the intestinal microbiota-brain

axis[38], which resulted in a positive impact on the quality and productivity. In addition, Chinese scientists have made significant advances in the field of gut microbiota[39]. Fecal microbiota transplantation (FMT) has attracted remarkable interest in the treatment of extraintestinal health problems. China registered 84 (24%) of the 367 clinical investigations employing FMT[40]. This is a significant contribution by Chinese researchers to this field and the clinical transformation of studies on the gut microbiota. In addition to FMT research, Chinese researchers are also interested in the development and clinical application of probiotics[41]. Furthermore, one possible reason for the increase in Chinese publication numbers, the *National Natural Science Foundation of China* launched a fund for the role and mechanism of the 'Gut-Liver Axis' in gastrointestinal diseases (H03)[42]. This research should focus on the gut microbiota and metabolites, nutrition, neurotransmitters, gastrointestinal hormones, and bile acid, particularly their interactions with the gastrointestinal tract or liver-localized immune cells/factors to mediate a variety of functional roles. Expand on the "gut-liver axis" and its role in the mechanisms of gastrointestinal disease mechanisms to develop novel diagnostic and therapeutic strategies[42].

Furthermore, the increase in publications on the microbiota and nutrition can be attributed to the fact that numerous hot topics were published during this period of time, exposing new theories and establishing new research fields such as the "interaction of the gut microbiota with dietary components", "connection between the gut microbiota and weight gain", and "the impact of a high-fat diet and the gut microbiota on metabolic syndrome". The effect of diet on the gut microbiota and, consequently, on human health suggests new therapeutic and diagnostic concepts and guides to develop probiotic and prebiotic strategies and functional nutrition[43-47].

The 'effect of a high-fat diet and the gut microbiota on metabolic syndromes' as a theme was among the main hot topics in the current study. Most publications on nutrition and gut microbiota before 2019 used words such as "connection between the gut microbiota and weight gain" and "interaction of the gut microbiota with dietary components". This was in the early stages of this research area. The "effect of a high-fat diet and gut microbiota on metabolic syndrome" as a theme was one of the main hot topics in this work and was considered the current trend after 2019. As a result, the evidence that emerges proposes that the gut microbiota may play a role in maintaining body weight and energy balance. It is assumed to be fueled, at least in part, by changes in gut microbiota composition caused by high-fat diets (HFDs); HFDs have been correlated with changes in gut microbial profile as well as decreased diversity [48,49]. Furthermore, metabolic syndrome and its associated disorders have been linked to increasing evidence suggesting that the gut microbiota in the digestive tract plays a significant role. Numerous studies in animals and humans have shown that high-fat and high-sugar (fructose) diets are responsible for the three hallmarks of metabolic syndrome: Obesity, dyslipidemia, and insulin resistance by altering the composition and diversity of the gut microbiota[50-53]. Furthermore, there is evidence that HFD is associated with cardiovascular disease[54] because the intestinal microbiota converts dietary choline to trimethylamine, which is absorbed in the gut and converted to trimethylamine N-oxygen. This metabolite causes atherosclerosis in the liver[55].

Strengths and limitations

This is the first thorough bibliometric analysis of nutrition and gut microbiota research conducted on a global level. Research on the relationship between nutrition/diet and gut microbiota is still in its infancy and will expand in the future. The aforementioned growing hotspots serve as a foundation and guide for the development of new projects by scientific researchers, physicians, and medical educators.

Our study has several limitations. First, although Scopus is indeed the largest database available, the search for studies was carried out only from the Scopus database, which could have limited the generalizability of the findings due to the loss of certain documents published in unindexed journals. Second, the accuracy and comprehensiveness of the keywords have a significant impact on the reliability of the data retrieved in our study. As a result, some important and influential articles may be omitted from a representative list due to the use of other terms in their titles. Third, the current study only looked for terms such as "nutrition", "gut microbiota" and other related terms in the title search only. Papers with these terms in the abstract or text may have been missed in this study. Furthermore, while most publications were published and indexed in 2021, the amount of scientific research productivity this year could be higher because new journal issues are still being published and indexed.

CONCLUSION

To our knowledge, this is the first bibliometric study of trends in publications on microbiota and nutrition. We are entering an era in which we can more easily alter our health through diet and track results using our microbiota or their metabolites. Over the last decade, there has been an increase in the number of publications on the microbiota and nutrition. The top three contributors to microbiota and nutrition research were China, the United States, and Italy. China is the leading country in this area of study, achieving some significant research findings and playing a key role in the progress of the field. "Connection between the gut microbiota and weight gain', 'interaction with dietary components" and

"the effect of a high-fat diet and the gut microbiota on metabolic syndromes' were hotspots for gut microbiota and nutrition research in the last 10 years. As a result, our timely examination and analysis of hotspots and research trends may aid in the growth of this discipline. Furthermore, these findings offer a fresh perspective on the study of the microbiota and nutrition/diet, which could help with future etiological research, diagnosis, and treatment of metabolic syndromes.

ARTICLE HIGHLIGHTS

Research background

Dietary composition is crucial in regulating the gut microbiota and, as a result, in the prevention, management, and treatment of diseases including diabetes and cancer.

Research motivation

According to a growing body of evidence, the gut microbiota appears to considerably impact human health. Intestinal homeostasis, physiology, gut microbiome, immune system, and host metabolic pathways are all affected by changes in the gut microbiota. However, there are no bibliometric analyses of nutrition/diet and gut microbiota publications.

Research objectives

The current study gives an overview of research publications on nutrition and gut microbiota and identifies global hotspots on this topic.

Research methods

A comprehensive, validated search query was used to find relevant publications on nutrition and gut microbiota. SciVerse Scopus was the database used.

Research results

This is the first bibliometric analysis of trends in microbiota and nutrition publications. The number of publications on microbiota and nutrition has increased over the last decade. China, the United States, and Italy were the top three contributors to microbiota and nutrition research.

Research conclusions

In conclusion with our timely examination and analysis of hotspots and research trends, we believe that this discipline will grow. Furthermore, these findings shed new light on the study of the microbiota and nutrition/diet, which could aid in future etiological research, diagnosis, and treatment of metabolic syndromes.

Research perspectives

This comprehensive bibliometric study aims to provide an overview of the current state of global nutrition and gut microbiota research and stay ahead of emerging trends and critical turns in the field's evolution.

FOOTNOTES

Author contributions: Zyoud SH designed the study, collected the data, analyzed the data, made major contributions to the manuscript's existing literature search and interpretation, and drafted the manuscript; Shakhshir M, Abushanab AS, Al-Jabi SW, Jairoun AA, Shahwan M, Koni A and Abu Taha A were involved in the interpretation of the data, and made revisions to the initial draft; all authors provided a critical review and approved the final manuscript before submission.

Conflict-of-interest statement: All the authors report no relevant conflicts of interest for this article.

PRISMA 2009 Checklist statement: The authors have read the PRISMA 2009 Checklist, and the manuscript was prepared and revised according to the PRISMA 2009 Checklist.

Open-Access: This article is an open-access article that was selected by an in-house editor and fully peer-reviewed by external reviewers. It is distributed in accordance with the Creative Commons Attribution NonCommercial (CC BY-NC 4.0) license, which permits others to distribute, remix, adapt, build upon this work non-commercially, and license their derivative works on different terms, provided the original work is properly cited and the use is non-commercial. See: https://creativecommons.org/Licenses/by-nc/4.0/

Country/Territory of origin: Palestine

ORCID number: Sa'ed H Zyoud 0000-0002-7369-2058; Muna Shakhshir 0000-0002-6213-8457; Amani S Abushanab 0000-0001-6290-787X; Samah W Al-Jabi 0000-0002-4414-9427; Amer Koni 0000-0002-0514-9352; Moyad Shahwan 0000-0001-8367-4841; Ammar Abdulrahman Jairoun 0000-0002-4471-0878; Adham Abu Taha 0000-0002-2889-1138.

S-Editor: Fan JR
L-Editor: A
P-Editor: Fan JR

REFERENCES

1 **Berg G**, Rybakova D, Fischer D, Cernava T, Vergès MC, Charles T, Chen X, Cocolin L, Eversole K, Corral GH, Kazou M, Kinkel L, Lange L, Lima N, Loy A, Macklin JA, Maguin E, Mauchline T, McClure R, Mitter B, Ryan M, Sarand I, Smidt H, Schelkle B, Roume H, Kiran GS, Selvin J, Souza RSC, van Overbeek L, Singh BK, Wagner M, Walsh A, Sessitsch A, Schloter M. Microbiome definition re-visited: old concepts and new challenges. *Microbiome* 2020; **8**: 103 [PMID: 32605663 DOI: 10.1186/s40168-020-00875-0]

2 **Rath CM**, Dorrestein PC. The bacterial chemical repertoire mediates metabolic exchange within gut microbiomes. *Curr Opin Microbiol* 2012; **15**: 147-154 [PMID: 22209085 DOI: 10.1016/j.mib.2011.12.009]

3 **Jackson MA**, Verdi S, Maxan ME, Shin CM, Zierer J, Bowyer RCE, Martin T, Williams FMK, Menni C, Bell JT, Spector TD, Steves CJ. Gut microbiota associations with common diseases and prescription medications in a population-based cohort. *Nat Commun* 2018; **9**: 2655 [PMID: 29985401 DOI: 10.1038/s41467-018-05184-7]

4 **Valdes AM**, Walter J, Segal E, Spector TD. Role of the gut microbiota in nutrition and health. *BMJ* 2018; **361**: k2179 [PMID: 29899036 DOI: 10.1136/bmj.k2179]

5 **Zhang C**, Zhang M, Wang S, Han R, Cao Y, Hua W, Mao Y, Zhang X, Pang X, Wei C, Zhao G, Chen Y, Zhao L. Interactions between gut microbiota, host genetics and diet relevant to development of metabolic syndromes in mice. *ISME J* 2010; **4**: 232-241 [PMID: 19865183 DOI: 10.1038/ismej.2009.112]

6 **Kolodziejczyk AA**, Zheng D, Elinav E. Diet-microbiota interactions and personalized nutrition. *Nat Rev Microbiol* 2019; **17**: 742-753 [PMID: 31541197 DOI: 10.1038/s41579-019-0256-8]

7 **Mills S**, Stanton C, Lane JA, Smith GJ, Ross RP. Precision Nutrition and the Microbiome, Part I: Current State of the Science. *Nutrients* 2019; **11** [PMID: 31022973 DOI: 10.3390/nu11040923]

8 **Donovan SM**. Introduction to the special focus issue on the impact of diet on gut microbiota composition and function and future opportunities for nutritional modulation of the gut microbiome to improve human health. *Gut Microbes* 2017; **8**: 75-81 [PMID: 28282253 DOI: 10.1080/19490976.2017.1299309]

9 **McKenney PT**, Pamer EG. From Hype to Hope: The Gut Microbiota in Enteric Infectious Disease. *Cell* 2015; **163**: 1326-1332 [PMID: 26638069 DOI: 10.1016/j.cell.2015.11.032]

10 **Singh RK**, Chang HW, Yan D, Lee KM, Ucmak D, Wong K, Abrouk M, Farahnik B, Nakamura M, Zhu TH, Bhutani T, Liao W. Influence of diet on the gut microbiome and implications for human health. *J Transl Med* 2017; **15**: 73 [PMID: 28388917 DOI: 10.1186/s12967-017-1175-y]

11 **Conlon MA**, Bird AR. The impact of diet and lifestyle on gut microbiota and human health. *Nutrients* 2014; **7**: 17-44 [PMID: 25545101 DOI: 10.3390/nu7010017]

12 **Li YD**, Liu BN, Zhao SH, Zhou YL, Bai L, Liu EQ. Changes in gut microbiota composition and diversity associated with post-cholecystectomy diarrhea. *World J Gastroenterol* 2021; **27**: 391-403 [PMID: 33584071 DOI: 10.3748/wjg.v27.i5.391]

13 **Rothschild D**, Weissbrod O, Barkan E, Kurilshikov A, Korem T, Zeevi D, Costea PI, Godneva A, Kalka IN, Bar N, Shilo S, Lador D, Vila AV, Zmora N, Pevsner-Fischer M, Israeli D, Kosower N, Malka G, Wolf BC, Avnit-Sagi T, Lotan-Pompan M, Weinberger A, Halpern Z, Carmi S, Fu J, Wijmenga C, Zhernakova A, Elinav E, Segal E. Environment dominates over host genetics in shaping human gut microbiota. *Nature* 2018; **555**: 210-215 [PMID: 29489753 DOI: 10.1038/nature25973]

14 **Clark A**, Mach N. Exercise-induced stress behavior, gut-microbiota-brain axis and diet: a systematic review for athletes. *J Int Soc Sports Nutr* 2016; **13**: 43 [PMID: 27924137 DOI: 10.1186/s12970-016-0155-6]

15 **Sommer F**, Bäckhed F. The gut microbiota--masters of host development and physiology. *Nat Rev Microbiol* 2013; **11**: 227-238 [PMID: 23435359 DOI: 10.1038/nrmicro2974]

16 **Garn H**, Neves JF, Blumberg RS, Renz H. Effect of barrier microbes on organ-based inflammation. *J Allergy Clin Immunol* 2013; **131**: 1465-1478 [PMID: 23726530 DOI: 10.1016/j.jaci.2013.04.031]

17 **Vijay A**, Valdes AM. Role of the gut microbiome in chronic diseases: a narrative review. *Eur J Clin Nutr* 2022; **76**: 489-501 [PMID: 34584224 DOI: 10.1038/s41430-021-00991-6]

18 **Zheng L**, Wen XL. Gut microbiota and inflammatory bowel disease: The current status and perspectives. *World J Clin Cases* 2021; **9**: 321-333 [PMID: 33521100 DOI: 10.12998/wjcc.v9.i2.321]

19 **Xia F**, Wen LP, Ge BC, Li YX, Li FP, Zhou BJ. Gut microbiota as a target for prevention and treatment of type 2 diabetes: Mechanisms and dietary natural products. *World J Diabetes* 2021; **12**: 1146-1163 [PMID: 34512884 DOI: 10.4239/wjd.v12.i8.1146]

20 **Li WZ**, Stirling K, Yang JJ, Zhang L. Gut microbiota and diabetes: From correlation to causality and mechanism. *World J Diabetes* 2020; **11**: 293-308 [PMID: 32843932 DOI: 10.4239/wjd.v11.i7.293]

21 **LaCourse KD**, Johnston CD, Bullman S. The relationship between gastrointestinal cancers and the microbiota. *Lancet Gastroenterol Hepatol* 2021; **6**: 498-509 [PMID: 33743198 DOI: 10.1016/S2468-1253(20)30362-9]

22 **Dogra SK**, Doré J, Damak S. Gut Microbiota Resilience: Definition, Link to Health and Strategies for Intervention. *Front Microbiol* 2020; **11**: 572921 [PMID: 33042082 DOI: 10.3389/fmicb.2020.572921]

23 **Voigt RM**, Bishehsari F. The intestinal microbiota: determinants of resiliency? *Lancet Healthy Longev* 2021; **2**: e2-e3 [DOI: 10.1016/s2666-7568(20)30048-9]

24 **Yuan X**, Chang C, Chen X, Li K. Emerging trends and focus of human gastrointestinal microbiome research from 2010-2021: a visualized study. *J Transl Med* 2021; **19**: 327 [PMID: 34332587 DOI: 10.1186/s12967-021-03009-8]

25 **Zhu X**, Hu J, Deng S, Tan Y, Qiu C, Zhang M, Ni X, Lu H, Wang Z, Li L, Luo Y, Huang S, Xiao T, Liu S, Li X, Shang D, Wen Y. Comprehensive Bibliometric Analysis of the Kynurenine Pathway in Mood Disorders: Focus on Gut Microbiota Research. *Front Pharmacol* 2021; **12**: 687757 [PMID: 34239441 DOI: 10.3389/fphar.2021.687757]

26 **Xavier-Santos D**, Padilha M, Fabiano GA, Vinderola G, Gomes Cruz A, Sivieri K, Costa Antunes AE. Evidences and perspectives of the use of probiotics, prebiotics, synbiotics, and postbiotics as adjuvants for prevention and treatment of COVID-19: A bibliometric analysis and systematic review. *Trends Food Sci Technol* 2022; **120**: 174-192 [PMID: 35002079 DOI: 10.1016/j.tifs.2021.12.033]

27 **Yue YY**, Fan XY, Zhang Q, Lu YP, Wu S, Wang S, Yu M, Cui CW, Sun ZR. Bibliometric analysis of subject trends and knowledge structures of gut microbiota. *World J Clin Cases* 2020; **8**: 2817-2832 [PMID: 32742991 DOI: 10.12998/wjcc.v8.i13.2817]

28 **Zyoud SH**, Smale S, Waring WS, Sweileh W, Al-Jabi SW. Global research trends in the microbiome related to irritable bowel syndrome: A bibliometric and visualized study. *World J Gastroenterol* 2021; **27**: 1341-1353 [PMID: 33833487 DOI: 10.3748/wjg.v27.i13.1341]

29 **Sweileh WM**. Bibliometric analysis of peer-reviewed literature on antimicrobial stewardship from 1990 to 2019. *Global Health* 2021; **17**: 1 [PMID: 33397377 DOI: 10.1186/s12992-020-00651-7]

30 **Sweileh WM**. Bibliometric analysis of global scientific literature on vaccine hesitancy in peer-reviewed journals (1990-2019). *BMC Public Health* 2020; **20**: 1252 [PMID: 32807154 DOI: 10.1186/s12889-020-09368-z]

31 **Falagas ME**, Pitsouni EI, Malietzis GA, Pappas G. Comparison of PubMed, Scopus, Web of Science, and Google Scholar: strengths and weaknesses. *FASEB J* 2008; **22**: 338-342 [PMID: 17884971 DOI: 10.1096/fj.07-9492LSF]

32 **Santos BS**, Silva I, Lima L, Endo PT, Alves G, Ribeiro-Dantas MDC. Discovering temporal scientometric knowledge in COVID-19 scholarly production. *Scientometrics* 2022; **127**: 1609-1642 [PMID: 35068619 DOI: 10.1007/s11192-021-04260-y]

33 **Sweileh WM**. Global research activity on antimicrobial resistance in food-producing animals. *Arch Public Health* 2021; **79**: 49 [PMID: 33849636 DOI: 10.1186/s13690-021-00572-w]

34 **Sweileh WM**. Global research publications on systemic use of off-label and unlicensed drugs: A bibliometric analysis (1990-2020). *Int J Risk Saf Med* 2022; **33**: 77-89 [PMID: 34275912 DOI: 10.3233/JRS-210012]

35 **Sweileh WM**. Global Research Activity on Elder Abuse: A Bibliometric Analysis (1950-2017). *J Immigr Minor Health* 2021; **23**: 79-87 [PMID: 32488667 DOI: 10.1007/s10903-020-01034-1]

36 **Baishideng Publishing Group Inc**. Reference Citation Analysis. 2022. [cited 29 April 2022]. Available from: https://www.referencecitationanalysis.com/

37 **van Eck NJ**, Waltman L. Software survey: VOSviewer, a computer program for bibliometric mapping. *Scientometrics* 2010; **84**: 523-538 [PMID: 20585380 DOI: 10.1007/s11192-009-0146-3]

38 **Schmidt C**. Mental health: thinking from the gut. *Nature* 2015; **518**: S12-S15 [PMID: 25715275 DOI: 10.1038/518S13a]

39 **Wang H**, Yang X. China's contribution to gut microbiota research. *Arch Community Med Public Health* 2020; **6**: 049-052

40 **Olesen SW**, Panchal P, Chen J, Budree S, Osman M. Global disparities in faecal microbiota transplantation research. *Lancet Gastroenterol Hepatol* 2020; **5**: 241 [PMID: 32061326 DOI: 10.1016/S2468-1253(19)30452-2]

41 **Zhang B**, Wang Y, Tan Z, Li Z, Jiao Z, Huang Q. Screening of Probiotic Activities of Lactobacilli Strains Isolated from Traditional Tibetan Qula, A Raw Yak Milk Cheese. *Asian-Australas J Anim Sci* 2016; **29**: 1490-1499 [PMID: 26954218 DOI: 10.5713/ajas.15.0849]

42 **National Natural Science Foundation of China**. National Natural Science Fund Guide to Programs 2020. [cited 15 January 2022]. Available from: https://www.nsfc.gov.cn/english/site_1/pdf/NationalNaturalScienceFundGuidetoPrograms2020.pdf

43 **Rowland I**, Gibson G, Heinken A, Scott K, Swann J, Thiele I, Tuohy K. Gut microbiota functions: metabolism of nutrients and other food components. *Eur J Nutr* 2018; **57**: 1-24 [PMID: 28393285 DOI: 10.1007/s00394-017-1445-8]

44 **Kim KA**, Gu W, Lee IA, Joh EH, Kim DH. High fat diet-induced gut microbiota exacerbates inflammation and obesity in mice *via* the TLR4 signaling pathway. *PLoS One* 2012; **7**: e47713 [PMID: 23091640 DOI: 10.1371/journal.pone.0047713]

45 **Makki K**, Deehan EC, Walter J, Bäckhed F. The Impact of Dietary Fiber on Gut Microbiota in Host Health and Disease. *Cell Host Microbe* 2018; **23**: 705-715 [PMID: 29902436 DOI: 10.1016/j.chom.2018.05.012]

46 **Rinninella E**, Raoul P, Cintoni M, Franceschi F, Miggiano GAD, Gasbarrini A, Mele MC. What is the Healthy Gut Microbiota Composition? *Microorganisms* 2019; **7** [PMID: 30634578 DOI: 10.3390/microorganisms7010014]

47 **Wu WC**, Inui A, Chen CY. Weight loss induced by whole grain-rich diet is through a gut microbiota-independent mechanism. *World J Diabetes* 2020; **11**: 26-32 [PMID: 32064033 DOI: 10.4239/wjd.v11.i2.26]

48 **Murphy EA**, Velazquez KT, Herbert KM. Influence of high-fat diet on gut microbiota: a driving force for chronic disease risk. *Curr Opin Clin Nutr Metab Care* 2015; **18**: 515-520 [PMID: 26154278 DOI: 10.1097/MCO.0000000000000209]

49 **He C**, Cheng D, Peng C, Li Y, Zhu Y, Lu N. High-Fat Diet Induces Dysbiosis of Gastric Microbiota Prior to Gut Microbiota in Association With Metabolic Disorders in Mice. *Front Microbiol* 2018; **9**: 639 [PMID: 29686654 DOI: 10.3389/fmicb.2018.00639]

50 **O'Donovan AN**, Herisson FM, Fouhy F, Ryan PM, Whelan D, Johnson CN, Cluzel G, Ross RP, Stanton C, Caplice NM. Gut microbiome of a porcine model of metabolic syndrome and HF-pEF. *Am J Physiol Heart Circ Physiol* 2020; **318**: H590-H603 [PMID: 32031871 DOI: 10.1152/ajpheart.00512.2019]

51 **Velasquez MT**. Altered Gut Microbiota: A Link Between Diet and the Metabolic Syndrome. *Metab Syndr Relat Disord* 2018; **16**: 321-328 [PMID: 29957105 DOI: 10.1089/met.2017.0163]

52 **Guevara-Cruz M**, Flores-López AG, Aguilar-López M, Sánchez-Tapia M, Medina-Vera I, Díaz D, Tovar AR, Torres N. Improvement of Lipoprotein Profile and Metabolic Endotoxemia by a Lifestyle Intervention That Modifies the Gut

Microbiota in Subjects With Metabolic Syndrome. *J Am Heart Assoc* 2019; **8**: e012401 [PMID: 31451009 DOI: 10.1161/JAHA.119.012401]

53 **Cândido FG**, Valente FX, Grześkowiak ŁM, Moreira APB, Rocha DMUP, Alfenas RCG. Impact of dietary fat on gut microbiota and low-grade systemic inflammation: mechanisms and clinical implications on obesity. *Int J Food Sci Nutr* 2018; **69**: 125-143 [PMID: 28675945 DOI: 10.1080/09637486.2017.1343286]

54 **Novakovic M**, Rout A, Kingsley T, Kirchoff R, Singh A, Verma V, Kant R, Chaudhary R. Role of gut microbiota in cardiovascular diseases. *World J Cardiol* 2020; **12**: 110-122 [PMID: 32431782 DOI: 10.4330/wjc.v12.i4.110]

55 **Yoo W**, Zieba JK, Foegeding NJ, Torres TP, Shelton CD, Shealy NG, Byndloss AJ, Cevallos SA, Gertz E, Tiffany CR, Thomas JD, Litvak Y, Nguyen H, Olsan EE, Bennett BJ, Rathmell JC, Major AS, Bäumler AJ, Byndloss MX. High-fat diet-induced colonocyte dysfunction escalates microbiota-derived trimethylamine *N*-oxide. *Science* 2021; **373**: 813-818 [PMID: 34385401 DOI: 10.1126/science.aba3683]

56 **David LA**, Maurice CF, Carmody RN, Gootenberg DB, Button JE, Wolfe BE, Ling AV, Devlin AS, Varma Y, Fischbach MA, Biddinger SB, Dutton RJ, Turnbaugh PJ. Diet rapidly and reproducibly alters the human gut microbiome. *Nature* 2014; **505**: 559-563 [PMID: 24336217 DOI: 10.1038/nature12820]

57 **Koeth RA**, Wang Z, Levison BS, Buffa JA, Org E, Sheehy BT, Britt EB, Fu X, Wu Y, Li L, Smith JD, DiDonato JA, Chen J, Li H, Wu GD, Lewis JD, Warrier M, Brown JM, Krauss RM, Tang WH, Bushman FD, Lusis AJ, Hazen SL. Intestinal microbiota metabolism of L-carnitine, a nutrient in red meat, promotes atherosclerosis. *Nat Med* 2013; **19**: 576-585 [PMID: 23563705 DOI: 10.1038/nm.3145]

58 **den Besten G**, van Eunen K, Groen AK, Venema K, Reijngoud DJ, Bakker BM. The role of short-chain fatty acids in the interplay between diet, gut microbiota, and host energy metabolism. *J Lipid Res* 2013; **54**: 2325-2340 [PMID: 23821742 DOI: 10.1194/jlr.R036012]

59 **Claesson MJ**, Jeffery IB, Conde S, Power SE, O'Connor EM, Cusack S, Harris HM, Coakley M, Lakshminarayanan B, O'Sullivan O, Fitzgerald GF, Deane J, O'Connor M, Harnedy N, O'Connor K, O'Mahony D, van Sinderen D, Wallace M, Brennan L, Stanton C, Marchesi JR, Fitzgerald AP, Shanahan F, Hill C, Ross RP, O'Toole PW. Gut microbiota composition correlates with diet and health in the elderly. *Nature* 2012; **488**: 178-184 [PMID: 22797518 DOI: 10.1038/nature11319]

60 **Trompette A**, Gollwitzer ES, Yadava K, Sichelstiel AK, Sprenger N, Ngom-Bru C, Blanchard C, Junt T, Nicod LP, Harris NL, Marsland BJ. Gut microbiota metabolism of dietary fiber influences allergic airway disease and hematopoiesis. *Nat Med* 2014; **20**: 159-166 [PMID: 24390308 DOI: 10.1038/nm.3444]

61 **Flint HJ**, Scott KP, Louis P, Duncan SH. The role of the gut microbiota in nutrition and health. *Nat Rev Gastroenterol Hepatol* 2012; **9**: 577-589 [PMID: 22945443 DOI: 10.1038/nrgastro.2012.156]

62 **Desai MS**, Seekatz AM, Koropatkin NM, Kamada N, Hickey CA, Wolter M, Pudlo NA, Kitamoto S, Terrapon N, Muller A, Young VB, Henrissat B, Wilmes P, Stappenbeck TS, Núñez G, Martens EC. A Dietary Fiber-Deprived Gut Microbiota Degrades the Colonic Mucus Barrier and Enhances Pathogen Susceptibility. *Cell* 2016; **167**: 1339-1353.e21 [PMID: 27863247 DOI: 10.1016/j.cell.2016.10.043]

63 **Sonnenburg JL**, Bäckhed F. Diet-microbiota interactions as moderators of human metabolism. *Nature* 2016; **535**: 56-64 [PMID: 27383980 DOI: 10.1038/nature18846]

64 **Chassaing B**, Koren O, Goodrich JK, Poole AC, Srinivasan S, Ley RE, Gewirtz AT. Dietary emulsifiers impact the mouse gut microbiota promoting colitis and metabolic syndrome. *Nature* 2015; **519**: 92-96 [PMID: 25731162 DOI: 10.1038/nature14232]

65 **Dao MC**, Everard A, Aron-Wisnewsky J, Sokolovska N, Prifti E, Verger EO, Kayser BD, Levenez F, Chilloux J, Hoyles L; MICRO-Obes Consortium, Dumas ME, Rizkalla SW, Doré J, Cani PD, Clément K. Akkermansia muciniphila and improved metabolic health during a dietary intervention in obesity: relationship with gut microbiome richness and ecology. *Gut* 2016; **65**: 426-436 [PMID: 26100928 DOI: 10.1136/gutjnl-2014-308778]

World Journal of Gastroenterology

Submit a Manuscript: https://www.f6publishing.com

World J Gastroenterol 2022 July 7; 28(25): 2994-3000

DOI: 10.3748/wjg.v28.i25.2994

ISSN 1007-9327 (print) ISSN 2219-2840 (online)

CASE REPORT

Early gastric cancer presenting as a typical submucosal tumor cured by endoscopic submucosal dissection: A case report

Joon Hyun Cho, Si Hyung Lee

Specialty type: Gastroenterology and hepatology

Provenance and peer review: Unsolicited article; Externally peer reviewed.

Peer-review model: Single blind

Peer-review report's scientific quality classification

Grade A (Excellent): 0
Grade B (Very good): B
Grade C (Good): C, C
Grade D (Fair): 0
Grade E (Poor): 0

P-Reviewer: Jin X, China; Kawabata H, Japan; Zhang H, China
A-Editor: Yao QG, China

Received: December 18, 2021
Peer-review started: December 18, 2021
First decision: March 10, 2022
Revised: March 12, 2022
Accepted: May 27, 2022
Article in press: May 27, 2022
Published online: July 7, 2022

Joon Hyun Cho, Si Hyung Lee, Division of Gastroenterology and Hepatology, Department of Internal Medicine, Yeungnam University College of Medicine, Daegu 42415, South Korea

Corresponding author: Si Hyung Lee, MD, Professor, Division of Gastroenterology and Hepatology, Department of Internal Medicine, Yeungnam University College of Medicine, 170 Hyeonchung-ro, Nam-gu, Daegu 42415, South Korea. dr9696@gmail.com

Abstract

BACKGROUND

Submucosal tumor (SMT)-like gastric cancer is rare, and almost all cases undergo curative surgical treatment because the submucosal layer is usually deeply invaded by tumor cells or because histopathologic types of SMT-like gastric cancer are undifferentiated or poorly differentiated. No report has been issued on an SMT-like gastric cancer cured by endoscopic resection alone or on changes in the endoscopic features of this type of tumor over several years.

CASE SUMMARY

We describe an exceptional case of a 53-year-old male with a 1.5 cm-sized SMT-like lesion covered by normal-appearing mucosa discovered by esophagogastroduodenoscopy (EGD) at the gastric antrum. Endoscopic ultrasound (EUS) visualized a homogeneous, well-circumscribed hypoechogenic lesion arising from the second sonographic layer with associated subtle obliteration of the third sonographic layer. Initial endoscopic biopsy was negative for neoplasm. The patient refused to undergo an invasive procedure and was subsequently lost to follow-up. Three years after initial detection, EGD revealed the lesion had become markedly erythematous, and at 4 years after initial EGD it had increased in size to 1.8 cm and developed a central ulcer and a heterogeneous EUS echo. Finally, endoscopic submucosal dissection (ESD) was performed, and histopathologic examination revealed a moderately differentiated adenocarcinoma had minutely invaded the submucosal layer (invasion depth 169 μm) but without lymphovascular invasion and with negative resection margins. Fortunately, no additional surgical treatment was required. He has been followed for 4 years after ESD without any evidence of local or distant recurrence.

CONCLUSION

This report describes an extremely rare case of early gastric cancer presenting as SMT that was cured by ESD after a treatment delay of 4 years and the endoscopic changes that occurred during this period. The report highlights the importance of

considering the possibility of gastric cancer when SMT is encountered in clinical practice.

Key Words: Subepithelial lesion; Submucosal tumor; Early gastric cancer; Adenocarcinoma; Endoscopic mucosal dissection; Case report

©The Author(s) 2022. Published by Baishideng Publishing Group Inc. All rights reserved.

Core Tip: We experienced an exceptionally rare case of early gastric cancer presenting as submucosal tumor (SMT) that was successfully treated by endoscopic submucosal dissection (ESD) alone, although the procedure was performed four years after first detection due to patient refusal and follow-up loss. The present case cautions that SMT-like gastric cancer should be included in the differential diagnosis when a hypoechogenic mass is detected in the 2nd or 3rd layer by endoscopic ultrasound, regardless of size and the absence of findings suggesting malignancy. When diagnosis is uncertain, invasive techniques such as diagnostic endoscopic mucosal resection or ESD, which can potentially be used for therapeutic purposes, should be considered and close follow-up is recommended.

Citation: Cho JH, Lee SH. Early gastric cancer presenting as a typical submucosal tumor cured by endoscopic submucosal dissection: A case report. *World J Gastroenterol* 2022; 28(25): 2994-3000
URL: https://www.wjgnet.com/1007-9327/full/v28/i25/2994.htm
DOI: https://dx.doi.org/10.3748/wjg.v28.i25.2994

INTRODUCTION

Gastric carcinoma is an epithelial tumor exposed to the mucosal surface that occurs in lamina propria with variable gross findings. However, cases of gastric carcinoma with features of submucosal tumor (SMT) are rarely encountered in routine clinical settings and reportedly account for only 0.2% to 0.62% of all resected gastric cancers[1]. The majority of patients with gastric adenocarcinoma resembling SMT are not indicated for endoscopic resection or offered non-curative resection after endoscopic resection. Submucosal layer is deeply invaded by tumor cells, even in cases of early gastric cancer (EGC)[2], and histopathologically, most adenocarcinomas presenting as SMTs are undifferentiated or poorly differentiated[3,4], and as a result, almost all undergo curative surgical treatment. Accordingly, no case has been reported on SMT-like gastric cancer cured by endoscopic resection alone. In addition, no report has been issued on changes in the endoscopic features of this type of tumor over several years. Here, we report an exceptionally rare case of EGC presenting as SMT that was cured by endoscopic submucosal dissection (ESD) and describe changes in the endoscopic features of this tumor over a period of 4 years.

CASE PRESENTATION

Chief complaints

A 53-year-old male Korean patient was referred to our institution for further evaluation and treatment of a gastric SMT discovered by esophagogastroduodenoscopy (EGD) during a routine medical check-up.

History of present illness

The patient had no abdominal pain or related discomfort.

History of past illness

He had a history of abdominal surgery due to duodenal ulcer perforation 30 years previously.

Personal and family history

The patient had diabetes that was being treated with oral hypoglycemic agents. He was a smoker (30 pack-years) and social-alcohol drinker and had no significant family history.

Physical examination

Physical examination was unremarkable, and his abdomen was soft, nontender, and nondistended with no palpable mass.

Laboratory examinations

Laboratory tests, which included tests for common serum tumor markers such as CEA and CA 19-9, revealed no abnormalities.

Imaging examinations

At initial EGD, an SMT-like elevated lesion of diameter 15-mm was observed at the great curvature side of the proximal part of the gastric antrum (Figure 1A). The lesion was covered with normal-appearing mucosa without any erosion, ulcer, or mucosal erythema. Mild-atrophic gastritis, confined to antrum, was observed in background mucosa. Endoscopic ultrasound (EUS; GF-UM2000, Olympus, Tokyo, Japan) demonstrated a 15 mm × 7 mm homogeneous, well-circumscribed hypoechogenic lesion arising from the second sonographic layer with associated subtle obliteration of the third sonographic layer (Figure 2A). The EUS appearance of the lesion was suggestive of a gastric neuroendocrine tumor (NET) or ectopic pancreas. Initial biopsy specimens were negative for neoplasm. Computed tomography (CT) of the abdomen showed a 15 mm protruding intraluminal mass at the gastric antrum and no evidence of lymph node enlargement or distant metastasis (Figure 3). After this initial work-up, endoscopic resection of the lesion was planned for definitive histopathologic examination and treatment. However, the patient declined any invasive procedure and was subsequently lost to follow-up.

Further diagnostic work-up

About 3 years after initial EGD, he underwent a national health screening examination at our hospital, and the previously noted gastric SMT was detected again by EGD. The lesion showed no change in size as compared with its size 3 years previously, but marked erythema of overlying mucosa was observed (Figure 1B). Endoscopic biopsy was performed, but specimens were negative for neoplasm. During consultation regarding his health examination results, he was recommended for further evaluation and treatment at the gastroenterology department but again refused and was lost to follow-up.

About a year later, he revisited our hospital with mild indigestion. Follow-up EGD then revealed the SMT-like lesion had enlarged (to a greatest diameter of approximately 18 mm) and that a 5 mm central ulcer had developed on the top of the lesion (Figure 1C). EUS also demonstrated an 18 mm × 9 mm homogeneous, well-circumscribed hypoechogenic mass arising from the second sonographic layer with associated subtle obliteration of the third sonographic layer (Figure 2B). Echogenicity at this time was slightly more heterogeneous than that observed by initial EUS. CT of the abdomen showed no evidence of lymph node enlargement or distant metastasis, and endoscopic biopsy specimens taken from the lesion revealed tubular adenoma with high-grade dysplasia.

FINAL DIAGNOSIS

The patient was then admitted for further endoscopic treatment. A serum anti-*Helicobacter pylori* (*H. pylori*) IgG assay was negative on the day of endoscopic examination. ESD of the lesion was performed, and histopathologic examination of the resected specimen revealed moderately differentiated adenocarcinoma that invaded the submucosal layer (depth of invasion 169 μm) with no lymphovascular invasion (Figure 4).

TREATMENT

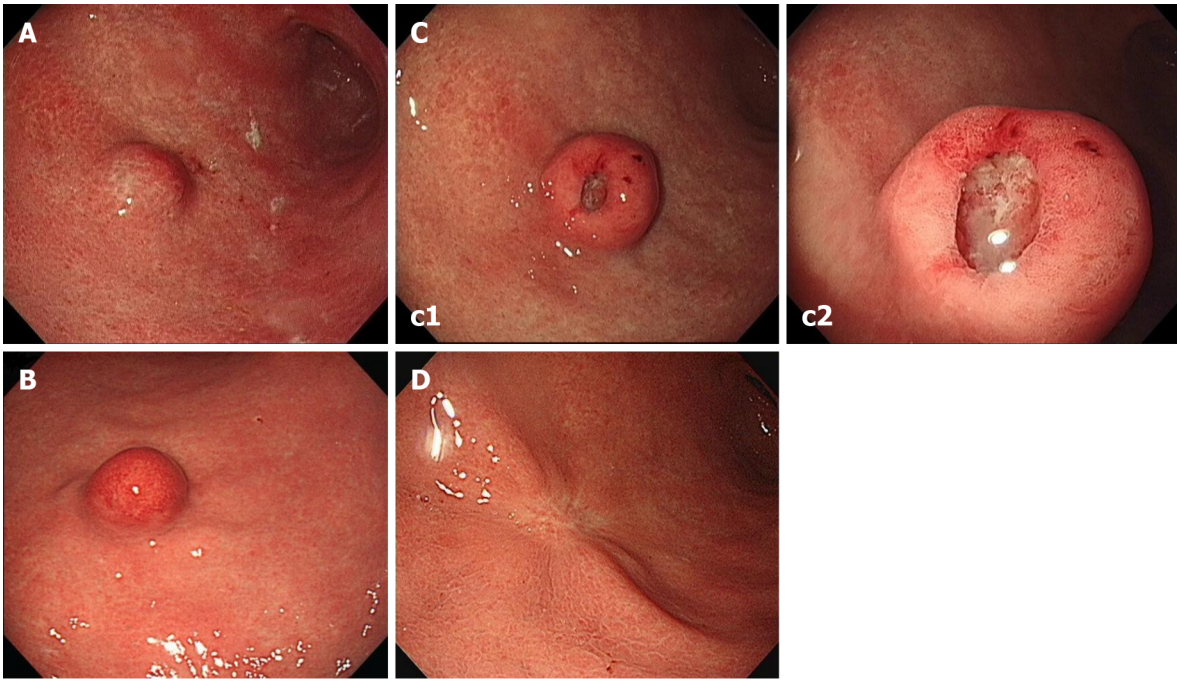
Furthermore, resection margins were all negative for cancer. Also, rapid urease test and Giemsa staining were negative for *H. pylori* infection.

OUTCOME AND FOLLOW-UP

His post-ESD course was uneventful, and he has since been followed up at our outpatient department for 4 years without any evidence of local or distant recurrence. The latest follow-up EGD performed (approximately 3.5 years after ESD) showed only post-ESD scarring (Figure 1D).

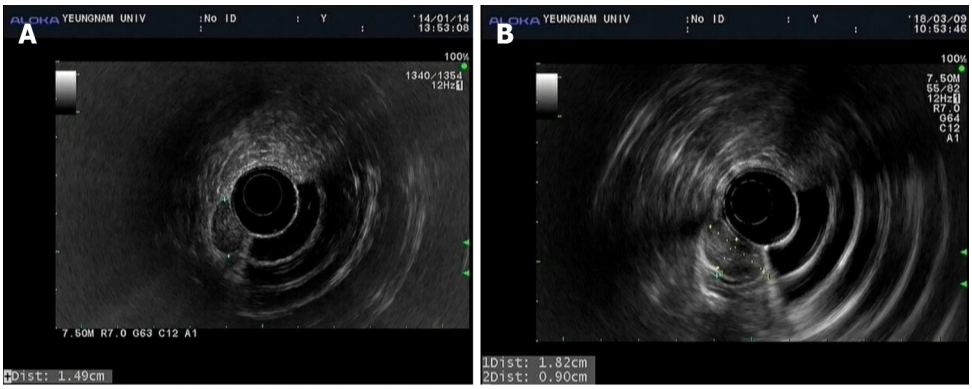
DISCUSSION

This case report is meaningful for the following reasons. First, to the best of our knowledge, this is the first case report of SMT-like gastric cancer cured by ESD alone, and this result was obtained even though ESD was performed four years after initial detection. Second, this case report describes the natural course of SMT-like gastric cancer and the endoscopic changes that occurred after a treatment



DOI: 10.3748/wjg.v28.i25.2994 **Copyright** ©The Author(s) 2022.

Figure 1 Endoscopy images. A: Initial endoscopic image showing a 15 mm-sized submucosal tumor-like elevated lesion with normally appearing mucosa at the great curvature side of the proximal part of gastric antrum; B: Endoscopic image obtained 3 years later showing the tumor had not changed in size but that marked erythema had developed on overlying mucosa; C: Endoscopic image (c2 shows a higher magnification image of the mass) obtained 4 years after initial examination [immediately before endoscopic submucosal dissection (ESD)] showing the tumor had increased in size to 18 mm and developed a 5-mm-sized central ulcer and overlying reddish mucosa of fine granularity; D: Endoscopic image obtained approximately 2.5 years after ESD showing post-ESD scarring.



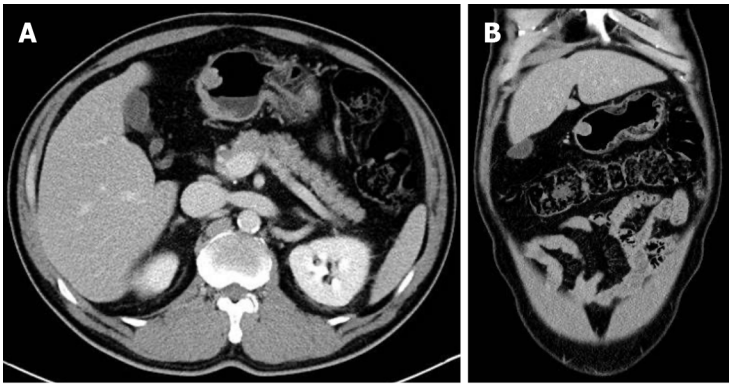
DOI: 10.3748/wjg.v28.i25.2994 **Copyright** ©The Author(s) 2022.

Figure 2 Endoscopic ultrasound images. A: Initial endoscopic ultrasound (EUS) image showing a well-circumscribed homogeneous and hypoechogenic mass measuring about 15 mm × 7 mm originating from the second sonographic layer with associated subtle obliteration of the third sonographic layer; B: EUS image obtained 4 years after the initial examination showing a well-circumscribed, hypoechogenic mass of greater size (18 mm × 9 mm) with slightly more heterogeneous echogenicity, and that the mass originated from the second sonographic layer with associated subtle obliteration of the third sonographic layer.

delay of 4 years. Furthermore, unlike previous reports, mucosa overlying the SMT appeared completely normal when the tumor was first detected.

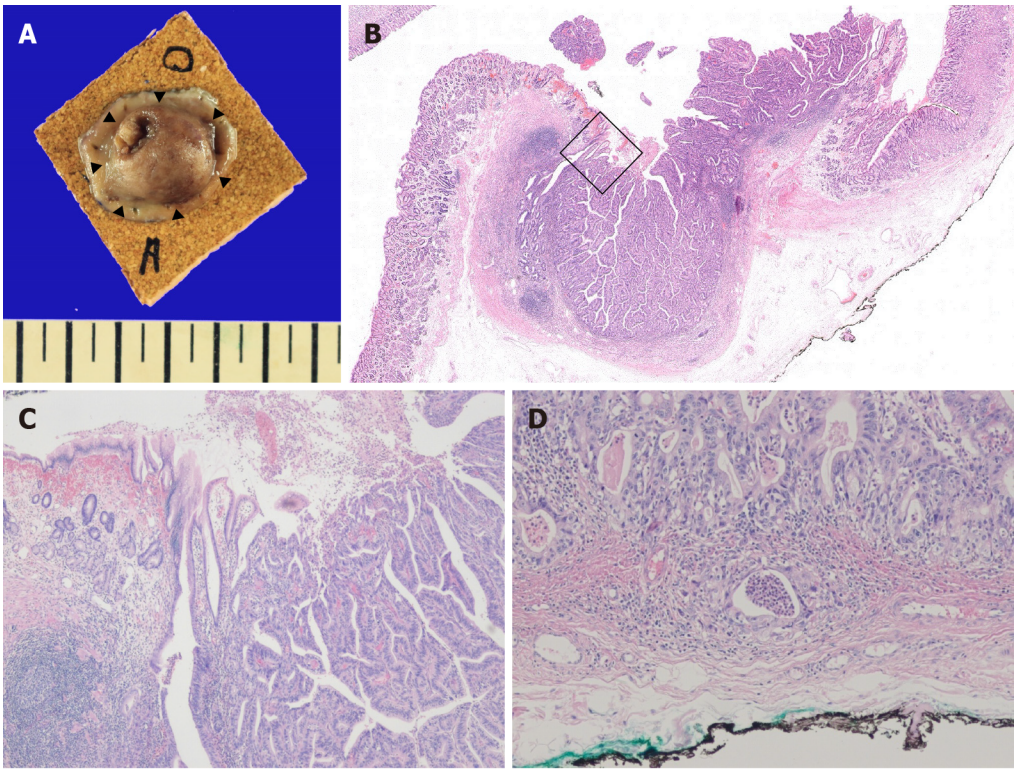
Gastric cancer usually derives from the lamina propria layer and has macroscopic appearances ranging from well-defined protuberant to diffuse infiltrating. Approximately 95% of gastric cancers are adenocarcinomas[5] but only rarely appear in the form of SMT. According to the literature[2], fewer than 0.5% of gastric cancer cases present as SMT. However, when an SMT-like lesion is encountered in clinical practice, the possibility of gastric cancer should be carefully considered and the lesion differentiated from other submucosal lesions, such as gastric NET[6], leiomyoma, lymphoma, gastrointestinal stromal tumor (GIST), lipoma, ectopic pancreas, and other unusual manifestations, such as metastatic carcinoma[7] and gastric glomus tumor[8], which require completely different treatment strategies.

Pathologic diagnoses of reported cases of gastric cancer presenting as SMT include gastric adenocarcinoma[9], gastric mucinous adenocarcinoma[10,11], and gastric lymphoepithelioma-like carcinoma



DOI: 10.3748/wjg.v28.i25.2994 **Copyright** ©The Author(s) 2022.

Figure 3 Abdominal computed tomography images. Initial axial (A) and coronal (B) computed tomography images showing a 15 mm protruding intraluminal mass at gastric antrum.



DOI: 10.3748/wjg.v28.i25.2994 **Copyright** ©The Author(s) 2022.

Figure 4 Pathology of the endoscopically resected lesion. A: Gross appearance of the resected lesion, which had negative lateral margins. The black triangles indicate the border of the cancerous region; B: Hematoxylin & eosin stained section showing gastric wall mucosal layer elevation by the adenocarcinoma, central erosion, and exposed tumor cells (original magnification × 10); C: Microscopic finding of the boxed area in Figure B showing the periphery of the tumor mass, which demonstrated moderately differentiated adenocarcinoma (original magnification × 40); D: Microscopic finding of the vertical resection margin showing penetration of the muscularis mucosa and minute invasion of submucosa (depth of invasion 169 μm) by tumor cells (original magnification × 100).

[12]. The most common histopathologic type is undifferentiated to poorly differentiated adenocarcinoma, which constitutes 68.8% to 71.4% of these cancers[3,4]. The mechanism of SMT-like gastric cancer development is obscure, but several pathologic mechanisms have been suggested. These mechanisms include the biologic tendencies of poorly differentiated adenocarcinomas to exhibit invasion of a deeper layer at an early stage, marked lymphocyte infiltration around tumors[1], the production of large amounts of mucin by mucinous adenocarcinoma[10,11], substantial amounts of surrounding fibrosis due to repetitive inflammation, abundant edematous fibrosis[13], and adenocarcinomas arising from a submucosal heterotopic gastric gland[9,14], which have been recognized as aberrant lamina propria components associated with repeated erosion and regeneration. These factors may facilitate a predominance of submucosal growth and penetration of muscularis mucosa during the early stage of carcinogenesis and contribute to a macroscopic appearance indistinguishable from SMT.

However, the tumor in our case had a moderately differentiated histology, which was not in line with any of these mechanisms.

Although the diagnosis of SMT-like gastric cancer is usually difficult due to a deep tumor location and non-specific and overlapping imaging features, some EGD characteristics of SMT-like gastric cancer have been reported. In particular, SMT with central ulceration or depression has been described as common for SMT-like gastric cancer[10,14-16]. Erythematous surface change is another reported characteristic[14,15]. Fujiyoshi *et al*[16] concluded that a small SMT (3-5 cm) with a central ulcer or irregular erythematous change should raise suspicion of malignancy. However, since our case originally appeared as SMT with completely normal overlying mucosa, we suspected SMT originating from the second or third layer rather than cancer. However, EGD at 3 and 4 years after initial detection of the SMT-like lesion, showed erythematous change and central ulceration. Interestingly, definite changes were observed in the endoscopic features of the tumor 4 years after initial detection, but it was not possible to determine when these morphologic changes occurred precisely due to follow-up loss.

Histological diagnosis of gastric SMT by endoscopic biopsy is often difficult and detailed imaging usually fails to provide sufficient evidence to differentiate benign and malignant tumors. Furthermore, endoscopic biopsy specimens, even those taken from a central ulcer, may be unhelpful[17], and when a tumor is completely covered with normal mucosa, it is extremely difficult to obtain an adequate sample of the underlying lesion. In the present case, negative results for neoplasm were reported for biopsies performed during EGD on overlying normal mucosa at initial presentation and on overlying erythematous mucosa 3 years later.

EUS is useful for evaluating gastric SMT. Findings that suggest malignant SMT include[18] a size > 3 cm or > 5 cm, rapid growth, heterogeneous echogenicity, and irregular margins, whereas GIST or leiomyoma may present as a homogeneous, well-demarcated, submucosal mass with smooth margins. However, these imaging characteristics are non-specific, and EUS images alone are insufficient for accurate diagnosis. More invasive techniques such as EUS-guided fine-needle aspiration or biopsy and endoscopic mucosal resection may aid differential diagnoses[18]. In our patient, initial EUS depicted a 15 mm-sized well-circumscribed homogeneous mass, which did not suggest malignant SMT. However, EUS performed 4 years later showed the mass had increased in size to 18 mm and had slightly more heterogeneous echogenicity.

Gastric cancers resembling SMT are characterized by a predominance of submucosal or sometimes deeper invasion into the gastric wall[2], which suggests they are likely to be more advanced and pose a greater risk of metastasis than ordinary gastric cancers of similar size[13]. Furthermore, most adenocarcinomas presenting as SMTs are of the undifferentiated or poorly differentiated histopathologic types[3,4], and thus, in almost all case reports, SMT-like gastric cancer, even when small, has been treated in the same way as advanced gastric cancer. Although ESD can potentially be used for therapeutic purposes, the pathologic results of most specimens resected by ESD indicate non-curative resection, and thus, additional gastrectomy with lymphadenectomy is required[19]. To date, no case report of cure by endoscopic resection has been published in the English literature. However, in the present case, ESD was performed to provide a definitive histopathologic diagnosis and a treatment strategy, and additional surgery was not needed, based on a final pathologic report that the tumor was not poorly differentiated, did not invade deep submucosa, and had negative lateral and deep margins.

CONCLUSION

The present case emphasizes that although SMT-like gastric cancer is rare, it should be included in the differential diagnosis when a hypoechogenic mass is visualized in the 2nd or 3rd layer by EUS, regardless of lesion size and the absence of findings suggesting malignancy. In addition, if diagnosis is uncertain, the use of techniques more aggressive than EUS alone, such as diagnostic endoscopic mucosal resection or ESD, which can potentially be used for therapeutic purposes, should be considered and close follow-up is recommended.

FOOTNOTES

Author contributions: Cho JH and Lee SH were responsible for the design of this report, the acquisition of clinical data, and writing and revision of the manuscript.

Informed consent statement: Informed written consent was obtained from the patient regarding the publication of this report and accompanying images.

Conflict-of-interest statement: The authors have no conflict of interest to declare.

CARE Checklist (2016) statement: The authors have read the CARE Checklist (2016), and the manuscript was prepared and revised according to the CARE Checklist (2016).

Open-Access: This article is an open-access article that was selected by an in-house editor and fully peer-reviewed by external reviewers. It is distributed in accordance with the Creative Commons Attribution NonCommercial (CC BY-NC 4.0) license, which permits others to distribute, remix, adapt, build upon this work non-commercially, and license their derivative works on different terms, provided the original work is properly cited and the use is non-commercial. See: https://creativecommons.org/Licenses/by-nc/4.0/

Country/Territory of origin: South Korea

ORCID number: Joon Hyun Cho 0000-0002-3584-6300; Si Hyung Lee 0000-0001-7221-7506.

S-Editor: Yan JP
L-Editor: A
P-Editor: Yan JP

REFERENCES

1 **Umehara Y**, Kimura T, Okubo T, Sano Y, Nakai K, Oi S, Higashi Y, Funai K. Gastric carcinoma resembling submucosal tumor. *Gastric Cancer* 1999; **2**: 191-193 [PMID: 11957095 DOI: 10.1007/s101200050045]
2 **Ishiguro S**, Tsukamoto Y, Kasugai T, Yasuhara Y, Tsuji N, Fujii Y, Nishizawa Y, Yamato N. Characteristic feature of the gastric carcinoma with submucosal tumor like appearance. *Stomach Intest* 2003; **38**: 1519-1526
3 **Takemoto N**, Baba T. Kaku Y, Takekoshi T, Maruyama M, Takahashi T, Kato H, Yanagisawa A. Radiologic diagnosis of gastric cancer morphologically mimicking submucosal tumor. *Stomach Intest* 1995; **30**: 759-768 [DOI: 10.11641/pdensks.53.0_156]
4 **Mitsunaga A**, Futami S, Murata Y, Suzuki A. Uchida KJ, Nemoto Y, Ikeda I, Nakamura S, Murata Y, Suzuki H. Endoscopic diagnosis of the gastric cancer showing the features of a submucosal tumor. *tomach Intest* 1995; **30**: 769-776 [DOI: 10.1055/s-2007-1001465]
5 **Nagini S**. Carcinoma of the stomach: A review of epidemiology, pathogenesis, molecular genetics and chemoprevention. *World J Gastrointest Oncol* 2012; **4**: 156-169 [PMID: 22844547 DOI: 10.4251/wjgo.v4.i7.156]
6 **Gheorghe AV**, Rimbas M, Ginghina O, Spanu A, Voiosu TA. An atypical type I gastric neuroendocrine tumor. *Rom J Intern Med* 2017; **55**: 253-256 [PMID: 28710883 DOI: 10.1515/rjim-2017-0029]
7 **Inagaki C**, Suzuki T, Kitagawa Y, Hara T, Yamaguchi T. A case report of prostate cancer metastasis to the stomach resembling undifferentiated-type early gastric cancer. *BMC Gastroenterol* 2017; **17**: 93 [PMID: 28784100 DOI: 10.1186/s12876-017-0655-0]
8 **Handa Y**, Kano M, Kaneko M, Hirabayashi N. Gastric Glomus Tumor: A Rare Cause of Upper Gastrointestinal Bleeding. *Case Rep Surg* 2015; **2015**: 193684 [PMID: 26697255 DOI: 10.1155/2015/193684]
9 **Manabe S**, Mukaisho KI, Yasuoka T, Usui F, Matsuyama T, Hirata I, Boku Y, Takahashi S. Gastric adenocarcinoma of fundic gland type spreading to heterotopic gastric glands. *World J Gastroenterol* 2017; **23**: 7047-7053 [PMID: 29097877 DOI: 10.3748/wjg.v23.i38.7047]
10 **Yu BC**, Lee WK. Two cases of mucinous adenocarcinoma of the stomach mistaken as submucosal tumor. *J Korean Surg Soc* 2013; **84**: 118-122 [PMID: 23396274 DOI: 10.4174/jkss.2013.84.2.118]
11 **Yoo CH**, Park SJ, Park MI, Moon W, Kim HH, Lee JS, Song JY, Jang HK. Submucosal tumor-like early-stage mucinous gastric carcinoma: a case study. *Korean J Gastroenterol* 2013; **62**: 122-125 [PMID: 23981947 DOI: 10.4166/kjg.2013.62.2.122]
12 **Takahashi T**, Otani Y, Yoshida M, Furukawa T, Kameyama K, Akiba Y, Saikawa Y, Kubota T, Kumai K, Kuramochi S, Mukai M, Ishii H, Kitajima M. Gastric cancer mimicking a submucosal tumor diagnosed by laparoscopic excision biopsy. *J Laparoendosc Adv Surg Tech A* 2005; **15**: 51-56 [PMID: 15772477 DOI: 10.1089/Lap.2005.15.51]
13 **Ohara N**, Tominaga O, Uchiyama M, Nakano H. A case of advanced gastric cancer resembling submucosal tumor of the stomach. *Jpn J Clin Oncol* 1997; **27**: 423-426 [PMID: 9438007 DOI: 10.1093/jjco/27.6.423]
14 **Hashimoto R**, Hamamoto H, Omori Y, Tanuma T. Early gastric cancer on submucosal heterotopic gastric glands. *Gastrointest Endosc* 2017; **85**: 851-852 [PMID: 27179691 DOI: 10.1016/j.gie.2016.05.002]
15 **Teraishi F**, Uno F, Kagawa S, Fujiwara T, Gouchi A, Tanaka N. Advanced gastric adenocarcinoma mimicking a submucosal tumor. *Endoscopy* 2007; **39** Suppl 1: E191-E192 [PMID: 17614044 DOI: 10.1055/s-2007-966403]
16 **Fujiyoshi A**, Kawamura M, Ishitsuka S. Gastric adenocarcinoma mimicking a submucosal tumor: case report. *Gastrointest Endosc* 2003; **58**: 633-635 [PMID: 14560759]
17 **Tio TL**, Tytgat GN, den Hartog Jager FC. Endoscopic ultrasonography for the evaluation of smooth muscle tumors in the upper gastrointestinal tract: an experience with 42 cases. *Gastrointest Endosc* 1990; **36**: 342-350 [PMID: 2210274 DOI: 10.1016/s0016-5107(90)71061-9]
18 **Papanikolaou IS**, Triantafyllou K, Kourikou A, Rösch T. Endoscopic ultrasonography for gastric submucosal lesions. *World J Gastrointest Endosc* 2011; **3**: 86-94 [PMID: 21772939 DOI: 10.4253/wjge.v3.i5.86]
19 **Kim HI**, Shim KN, Yoon SY, Song EM, Cho WY, Kim SE, Jung HK, Jung SA. A case of early gastric adenocarcinoma resembling subepithelial tumor. *Korean J Helicobacter Up Gastrointest Res* 2013; **13**: 60-63 [DOI: 10.7704/kjhugr.2013.13.1.60]

World Journal of Gastroenterology

Submit a Manuscript: https://www.f6publishing.com

World J Gastroenterol 2022 July 7; 28(25): 3001-3003

DOI: 10.3748/wjg.v28.i25.3001

ISSN 1007-9327 (print) ISSN 2219-2840 (online)

LETTER TO THE EDITOR

Acupuncture and moxibustion for treatment of Crohn's disease: A brief review

Jing Xie, Yan Huang, Huan-Gan Wu, Jing Li

Specialty type: Gastroenterology and hepatology

Provenance and peer review: Unsolicited article; Externally peer reviewed.

Peer-review model: Single blind

Peer-review report's scientific quality classification

Grade A (Excellent): 0
Grade B (Very good): B
Grade C (Good): C
Grade D (Fair): 0
Grade E (Poor): 0

P-Reviewer: Sitkin S, Russia; Tao M, China
A-Editor: Chen KM, Taiwan

Received: September 5, 2021
Peer-review started: September 5, 2021
First decision: November 8, 2021
Revised: November 18, 2021
Accepted: May 26, 2022
Article in press: May 26, 2022
Published online: July 7, 2022

Jing Xie, Jing Li, Department of Acupuncture, Yueyang Hospital of Integrated Traditional Chinese and Western Medicine, Shanghai University of Traditional Chinese Medicine, Shanghai 200437, China

Yan Huang, Huan-Gan Wu, Shanghai Research Institute of Acupuncture and Meridian, Shanghai University of Traditional Chinese Medicine, Shanghai 200030, China

Corresponding author: Jing Li, MD, PhD, Chief Physician, Department of Acupuncture, Yueyang Hospital of Integrated Traditional Chinese and Western Medicine, Shanghai University of Traditional Chinese Medicine, No. 110 Ganhe Road, Shanghai 200437, China. lj0806@hotmail.com

Abstract

Crohn's disease (CD) is a kind of intestinal inflammatory disease that can affect any part of the gastrointestinal tract and the incidence rate of CD is gradually increasing worldwide. Acupuncture and moxibustion have unique curative effects on gastrointestinal diseases and can be new options for the treatment of CD.

Key Words: Crohn's disease; Acupuncture; Moxibustion; Treatment; Review

©The Author(s) 2022. Published by Baishideng Publishing Group Inc. All rights reserved.

Core Tip: Crohn's disease (CD) can affect any part of the gastrointestinal tract, especially the terminal ileum and the ascending colon, and is collectively known as inflammatory bowel disease with ulcerative colitis. The incidence rate of CD is gradually increasing worldwide. This letter mainly introduces that acupuncture has a unique curative effect on CD and can provide a new research direction for the treatment of CD.

Citation: Xie J, Huang Y, Wu HG, Li J. Acupuncture and moxibustion for treatment of Crohn's disease: A brief review. *World J Gastroenterol* 2022; 28(25): 3001-3003
URL: https://www.wjgnet.com/1007-9327/full/v28/i25/3001.htm
DOI: https://dx.doi.org/10.3748/wjg.v28.i25.3001

TO THE EDITOR

Crohn's disease (CD) can affect any part of the gastrointestinal tract, especially the terminal ileum and the ascending colon, and is collectively known as inflammatory bowel disease (IBD) with ulcerative colitis. The main symptoms include abdominal pain, diarrhea, fistula, intestinal obstruction, fever, emaciation, and nutritional disorders. In the past three decades, the incidence rate of CD has gradually increased worldwide at an annual growth rate between 4%-15%, which warrants our attention[1]. Currently, biological therapy is the preferred treatment for CD, and the commonly used biological agents such as infliximab and adalimumab have brought significant benefits to the patients. With multiple biological agents at their disposal, clinicians can, according to different symptoms, choose drugs with different anti-inflammatory mechanisms. However, despite the undisputed efficacy of these agents, a significant proportion of patients fail to receive effective treatments. For example, many patients do not respond to induction therapy or lose the response after initial improvements. As traditional Chinese medicine therapies, acupuncture and moxibustion have a long history in treating gastrointestinal diseases and significant advantages against symptoms such as abdominal pain, diarrhea, fatigue, and anorexia. Therefore, we summarize articles about clinical acupuncture and moxibustion treatment for CD to explore their unique advantages.

Using keywords such as acupuncture, CD, and clinical trials, we searched PubMed for clinical trials of acupuncture and moxibustion in the treatment of CD up to February 28, 2020, and found four articles that met the criteria. The four articles that we found and retrieved showed that acupuncture and moxibustion had curative effects on CD. Joos *et al*'s randomized controlled trial confirmed that after 4 wk of treatment, the CD activity index (CDAI) of the acupuncture group showed a significantly larger ($P = 0.003$) decrease (from 250 ± 51 to 163 ± 56) than that of the groups without acupuncture (from 220 ± 42 to 181 ± 46)[2]. Bao *et al*'s 12-wk trial with the treatment group undergoing herb-partitioned moxibustion combined with acupuncture (HMA) and the control group receiving wheat bran partitioned moxibustion combined with superficial acupuncture showed a significantly higher ($P = 0.000$) total treatment efficacy of the treatment group at 83.72% compared to 40.48% of the control group and a significantly lower ($P = 0.000$) CDAI in the treatment group than that of the control group[3]. Both clinical trials demonstrated that acupuncture combined with moxibustion significantly reduced the CDAI in the patients and significantly improved their quality of life. Shang *et al*[4] conducted a clinical trial with one group receiving HMA and the other group treated with mesalazine (MESA). After 12 wk of treatment, the expression of *ZO-1* mRNA in the HMA group was significantly improved compared with the MESA group (2378.17 ± 308.77 *vs* 2200.56 ± 281.88; $P = 0.023$), confirming that HMA can repair the intestinal epithelial barrier by up-regulating the expression of tight junction protein and its mRNA, thus reducing the intestinal inflammatory response in CD patients. Horta *et al*[5] investigated whether electroacupuncture (EAc) therapy could relieve fatigue in patients with IBD by allocating 52 patients into the EAc, sham EAc (ShEAc), and waitlist (WL) groups. Evaluation with the IBD-validated Functional Assessment of Chronic Illness Therapy-Fatigue Scale showed reduced fatigue scores in patients of the EAc and ShEAc groups after 8 wk of treatment and significantly better curative effects in the two groups than that in the WL group.

According to these four clinical trials, acupuncture treatment tends to attenuate symptoms such as abdominal pain, diarrhea, and fatigue in patients with CD. Therefore, acupuncture and moxibustion therapy may potentially improve the physical and mental health of CD patients. Unfortunately, clinical trials of acupuncture for CD with relatively long-term observation and a large sample are still lacking. Except those conducted by Chinese researchers, there are few studies on treating CD with acupuncture, and more evidence is required to support the application of acupuncture and moxibustion therapies in treating CD and verify their potential benefits.

FOOTNOTES

Author contributions: Xie J wrote the manuscript; Yan H, Wu HG, and Li J edited the manuscript.

Supported by the National Nature Science Foundation of China, No. 81774405 and No. 81873372.

Conflict-of-interest statement: All the authors report no relevant conflicts of interest for this article.

Open-Access: This article is an open-access article that was selected by an in-house editor and fully peer-reviewed by external reviewers. It is distributed in accordance with the Creative Commons Attribution NonCommercial (CC BY-NC 4.0) license, which permits others to distribute, remix, adapt, build upon this work non-commercially, and license their derivative works on different terms, provided the original work is properly cited and the use is non-commercial. See: https://creativecommons.org/Licenses/by-nc/4.0/

Country/Territory of origin: China

ORCID number: Jing Xie 0000-0001-8982-5452; Yan Huang 0000-0002-5588-0274; Huan-Gan Wu 0000-0003-0563-1560;

Jing Li 0000-0001-9388-5036.

S-Editor: Wang JJ
L-Editor: Wang TQ
P-Editor: Wang JJ

REFERENCES

1 **Adamina M**, Bonovas S, Raine T, Spinelli A, Warusavitarne J, Armuzzi A, Bachmann O, Bager P, Biancone L, Bokemeyer B, Bossuyt P, Burisch J, Collins P, Doherty G, El-Hussuna A, Ellul P, Fiorino G, Frei-Lanter C, Furfaro F, Gingert C, Gionchetti P, Gisbert JP, Gomollon F, González Lorenzo M, Gordon H, Hlavaty T, Juillerat P, Katsanos K, Kopylov U, Krustins E, Kucharzik T, Lytras T, Maaser C, Magro F, Marshall JK, Myrelid P, Pellino G, Rosa I, Sabino J, Savarino E, Stassen L, Torres J, Uzzan M, Vavricka S, Verstockt B, Zmora O. ECCO Guidelines on Therapeutics in Crohn's Disease: Surgical Treatment. *J Crohns Colitis* 2020; **14**: 155-168 [PMID: 31742338 DOI: 10.1093/ecco-jcc/jjz187]

2 **Joos S**, Brinkhaus B, Maluche C, Maupai N, Kohnen R, Kraehmer N, Hahn EG, Schuppan D. Acupuncture and moxibustion in the treatment of active Crohn's disease: a randomized controlled study. *Digestion* 2004; **69**: 131-139 [PMID: 15114043 DOI: 10.1159/000078151]

3 **Bao CH**, Zhao JM, Liu HR, Lu Y, Zhu YF, Shi Y, Weng ZJ, Feng H, Guan X, Li J, Chen WF, Wu LY, Jin XM, Dou CZ, Wu HG. Randomized controlled trial: moxibustion and acupuncture for the treatment of Crohn's disease. *World J Gastroenterol* 2014; **20**: 11000-11011 [PMID: 25152604 DOI: 10.3748/wjg.v20.i31.11000]

4 **Shang HX**, Wang AQ, Bao CH, Wu HG, Chen WF, Wu LY, Ji R, Zhao JM, Shi Y. Moxibustion combined with acupuncture increases tight junction protein expression in Crohn's disease patients. *World J Gastroenterol* 2015; **21**: 4986-4996 [PMID: 25945013 DOI: 10.3748/wjg.v21.i16.4986]

5 **Horta D**, Lira A, Sanchez-Lloansi M, Villoria A, Teggiachi M, García-Rojo D, García-Molina S, Figuerola A, Esteve M, Calvet X. A Prospective Pilot Randomized Study: Electroacupuncture vs. Sham Procedure for the Treatment of Fatigue in Patients With Quiescent Inflammatory Bowel Disease. *Inflamm Bowel Dis* 2020; **26**: 484-492 [PMID: 31091322 DOI: 10.1093/ibd/izz091]

World Journal of Gastroenterology

Submit a Manuscript: https://www.f6publishing.com

World J Gastroenterol 2022 July 7; 28(25): 3004-3005

DOI: 10.3748/wjg.v28.i25.3004

ISSN 1007-9327 (print) ISSN 2219-2840 (online)

CORRECTION

Correction to "Aberrant methylation of secreted protein acidic and rich in cysteine gene and its significance in gastric cancer"

Shuai Shao, Nuo-Ming Zhou, Dong-Qiu Dai

Specialty type: Oncology

Provenance and peer review: Unsolicited article; Externally peer reviewed.

Peer-review model: Single blind

Peer-review report's scientific quality classification

Grade A (Excellent): 0
Grade B (Very good): 0
Grade C (Good): C
Grade D (Fair): 0
Grade E (Poor): 0

P-Reviewer: Shahini E, Italy
A-Editor: Zhu JQ, China

Received: October 23, 2021
Peer-review started: October 23, 2021
First decision: April 16, 2022
Revised: April 26, 2022
Accepted: May 28, 2022
Article in press: May 28, 2022
Published online: July 7, 2022

Shuai Shao, Nuo-Ming Zhou, Dong-Qiu Dai, Department of Gastroenterological Surgery, The Fourth Affiliated Hospital of China Medical University, Shenyang 110032, Liaoning Province, China

Corresponding author: Dong-Qiu Dai, MD, PhD, Chief Doctor, Professor, Surgical Oncologist, Department of Gastrointestinal Surgery and Cancer Center, The Fourth Affiliated Hospital of China Medical University, No. 4 Chongshan East Road, Shenyang 110032, Liaoning Province, China. daidq63@163.com

Abstract

We have replaced the misapplied images and the revised Figure 6C is provided.

Key Words: Correction

©The Author(s) 2022. Published by Baishideng Publishing Group Inc. All rights reserved.

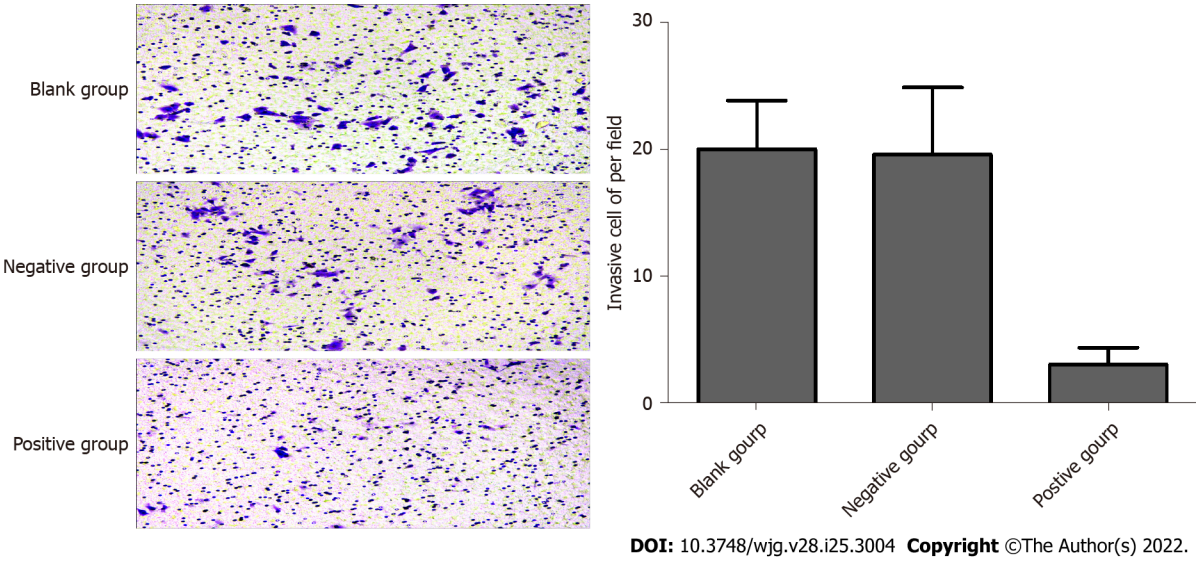
Core Tip: This is a correction to "Aberrant methylation of secreted protein acidic and rich in cysteine gene and its significance in gastric cancer".

Citation: Shao S, Zhou NM, Dai DQ. Correction to "Aberrant methylation of secreted protein acidic and rich in cysteine gene and its significance in gastric cancer". *World J Gastroenterol* 2022; 28(25): 3004-3005
URL: https://www.wjgnet.com/1007-9327/full/v28/i25/3004.htm
DOI: https://dx.doi.org/10.3748/wjg.v28.i25.3004

CORRECTION

Correction to: Shao S, Zhou NM, Dai DQ. Aberrant methylation of secreted protein acidic and rich in cysteine gene and its significance in gastric cancer. *World J Gastroenterol* 2019; 25: 6713-6727 PMID: 31857774 DOI: 10.3748/wjg.v25.i46.6713.

We are deeply regretful that we have misapplied one inappropriate image in this article. We have replaced the misapplied image and the corrected pictures are shown in Figure 1. This correction will have no influence on the interpretation of the entire results and conclusion in this study. We apologize for any inconvenience this may



DOI: 10.3748/wjg.v28.i25.3004 **Copyright** ©The Author(s) 2022.

Figure 1 Modification of the Figure 6C in original manuscript.

cause.

We have provided the correction document, and we would like to express our sincere apologies to the editors and readers for our mistakes. We are looking forward to hearing from you at your earliest convenience.

FOOTNOTES

Author contributions: Shao S, Zhou NM and Dai DQ contributed to this paper.

Open-Access: This article is an open-access article that was selected by an in-house editor and fully peer-reviewed by external reviewers. It is distributed in accordance with the Creative Commons Attribution NonCommercial (CC BY-NC 4.0) license, which permits others to distribute, remix, adapt, build upon this work non-commercially, and license their derivative works on different terms, provided the original work is properly cited and the use is non-commercial. See: https://creativecommons.org/Licenses/by-nc/4.0/

Country/Territory of origin: China

ORCID number: Shuai Shao 0000-0003-3454-5845; Nuo-Ming Zhou 0000-0001-7718-2197; Dong-Qiu Dai 0000-0002-1154-3276.

S-Editor: Zhang H
L-Editor: A
P-Editor: Zhang H

REFERENCES

1 **Shao S**, Zhou NM, Dai DQ. Aberrant methylation of secreted protein acidic and rich in cysteine gene and its significance in gastric cancer. *World J Gastroenterol* 2019; **25**: 6713-6727 [PMID: 31857774 DOI: 10.3748/wjg.v25.i46.6713]

World Journal of Gastroenterology

Submit a Manuscript: https://www.f6publishing.com

World J Gastroenterol 2022 July 7; 28(25): 3006-3007

DOI: 10.3748/wjg.v28.i25.3006

ISSN 1007-9327 (print) ISSN 2219-2840 (online)

CORRECTION

Correction to "Gut microbiota dysbiosis in Chinese children with type 1 diabetes mellitus: An observational study"

Xia Liu, Yi-Wen Cheng, Li Shao, Shu-Hong Sun, Jian Wu, Qing-Hai Song, Hong-Sheng Zou, Zong-Xin Ling

Specialty type: Gastroenterology and hepatology

Provenance and peer review: Unsolicited article; Externally peer reviewed.

Peer-review model: Single blind

Peer-review report's scientific quality classification

Grade A (Excellent): A
Grade B (Very good): 0
Grade C (Good): C
Grade D (Fair): 0
Grade E (Poor): 0

P-Reviewer: Herraiz JL, Spain; Moreno-Gómez-Toledano R, Spain

Received: March 21, 2022
Peer-review started: March 21, 2022
First decision: May 29, 2022
Revised: May 31, 2022
Accepted: June 13, 2022
Article in press: June 13, 2022
Published online: July 7, 2022

Xia Liu, Department of Intensive Care Unit, The First Affiliated Hospital, School of Medicine, Zhejiang University, Hangzhou 310003, Zhejiang Province, China

Yi-Wen Cheng, Jian Wu, Zong-Xin Ling, Collaborative Innovation Center for Diagnosis and Treatment of Infectious Diseases, State Key Laboratory for Diagnosis and Treatment of Infectious Diseases, National Clinical Research Center for Infectious Diseases, The First Affiliated Hospital, School of Medicine, Zhejiang University, Hangzhou 310003, Zhejiang Province, China

Li Shao, Institute of Hepatology and Metabolic Diseases, Hangzhou Normal University, Hangzhou 311121, Zhejiang Province, China

Shu-Hong Sun, Department of Laboratory Medicine, Linyi People's Hospital, Linyi 276000, Shandong Province, China

Qing-Hai Song, Department of Geriatrics, Lishui Second People's Hospital, Lishui 323000, Zhejiang Province, China

Hong-Sheng Zou, Department of Intensive Care Unit, People's Hospital of Rongcheng, Rongcheng 264300, Shandong Province, China

Corresponding author: Zong-Xin Ling, PhD, Professor, Collaborative Innovation Center for Diagnosis and Treatment of Infectious Diseases, State Key Laboratory for Diagnosis and Treatment of Infectious Diseases, National Clinical Research Center for Infectious Diseases, the First Affiliated Hospital, School of Medicine, Zhejiang University, No. 79 Qingchun Road, Hangzhou 310003, Zhejiang Province, China. lingzongxin_lzx@163.com

Abstract

Liu X, Cheng YW, Shao L, Sun SH, Wu J, Song QH, Zou HS, Ling ZX. Gut microbiota dysbiosis in Chinese children with type 1 diabetes mellitus: An observational study. *World J Gastroenterol* 2021; 27(19): 2394-2414 [PMID: 34040330 DOI: 10.3748/wjg.v27.i19.2394]. In this article, the affiliation of the first author was wrong. Xia Liu, the first author, belonged to Department of Intensive Care Unit, The First Affiliated Hospital, School of Medicine, Zhejiang University, Hangzhou, 310003, China.

Key Words: Correction

©The Author(s) 2022. Published by Baishideng Publishing Group Inc. All rights reserved.

Core Tip: This manuscript is an author's affiliation correction for Gut microbiota dysbiosis in Chinese children with type 1 diabetes mellitus: An observational study. *World J Gastroenterol* 2021; 27: 2394-2414.

Citation: Liu X, Cheng YW, Shao L, Sun SH, Wu J, Song QH, Zou HS, Ling ZX. Correction to "Gut microbiota dysbiosis in Chinese children with type 1 diabetes mellitus: An observational study". *World J Gastroenterol* 2022; 28(25): 3006-3007
URL: https://www.wjgnet.com/1007-9327/full/v28/i25/3006.htm
DOI: https://dx.doi.org/10.3748/wjg.v28.i25.3006

CORRECTION

Correction to: Liu X, Cheng YW, Shao L, Sun SH, Wu J, Song QH, Zou HS, Ling ZX. Gut microbiota dysbiosis in Chinese children with type 1 diabetes mellitus: An observational study. *World J Gastroenterol* 2021; 27(19): 2394-2414. PMID: 34040330 DOI: 10.3748/wjg.v27.i19.2394.

In this article[1], the affiliation of the first author was wrong. Xia Liu, the first author, belonged to Department of Intensive Care Unit, The First Affiliated Hospital, School of Medicine, Zhejiang University, Hangzhou, 310003, China.

FOOTNOTES

Author contributions: Liu X and Ling ZX contributed to this correction; all authors approved this correction.

Conflict-of-interest statement: All authors declare that they have no known competing financial interests or personal relationships that could have appeared to influence the work reported in this paper.

Open-Access: This article is an open-access article that was selected by an in-house editor and fully peer-reviewed by external reviewers. It is distributed in accordance with the Creative Commons Attribution NonCommercial (CC BY-NC 4.0) license, which permits others to distribute, remix, adapt, build upon this work non-commercially, and license their derivative works on different terms, provided the original work is properly cited and the use is non-commercial. See: https://creativecommons.org/Licenses/by-nc/4.0/

Country/Territory of origin: China

ORCID number: Xia Liu 0000-0002-9987-3332; Yi-Wen Cheng 0000-0003-3095-9311; Li Shao 0000-0003-4006-0641; Shu-Hong Sun 0000-0002-8694-308X; Jian Wu 0000-0003-0087-3744; Qing-Hai Song 0000-0002-8749-313X; Hong-Sheng Zou 0000-0002-1854-5741; Zong-Xin Ling 0000-0001-9662-099X.

S-Editor: Wang LL
L-Editor: A
P-Editor: Wang LL

REFERENCES

1 **Liu X**, Cheng YW, Shao L, Sun SH, Wu J, Song QH, Zou HS, Ling ZX. Gut microbiota dysbiosis in Chinese children with type 1 diabetes mellitus: An observational study. *World J Gastroenterol* 2021; **27**: 2394-2414 [PMID: 34040330 DOI: 10.3748/wjg.v27.i19.2394]



Published by **Baishideng Publishing Group Inc**
7041 Koll Center Parkway, Suite 160, Pleasanton, CA 94566, USA
Telephone: +1-925-3991568
E-mail: bpgoffice@wjgnet.com
Help Desk: https://www.f6publishing.com/helpdesk
https://www.wjgnet.com



© 2022 Baishideng Publishing Group Inc. All rights reserved.

ISSN 1007-9327 (print)
ISSN 2219-2840 (online)

World Journal of *Gastroenterology*

World J Gastroenterol 2022 July 14; 28(26): 3008-3281



Published by Baishideng Publishing Group Inc

World Journal of Gastroenterology

Contents

Weekly Volume 28 Number 26 July 14, 2022

REVIEW

3008 Advances in the imaging of gastroenteropancreatic neuroendocrine neoplasms

Ramachandran A, Madhusudhan KS

3027 Tumor microenvironment involvement in colorectal cancer progression *via* Wnt/β-catenin pathway: Providing understanding of the complex mechanisms of chemoresistance

Novoa Díaz MB, Martín MJ, Gentili C

3047 Role of baicalin as a potential therapeutic agent in hepatobiliary and gastrointestinal disorders: A review

Ganguly R, Gupta A, Pandey AK

MINIREVIEWS

3063 Alterations of autophagic and innate immune responses by the Crohn's disease-associated *ATG16L1* mutation

Okai N, Watanabe T, Minaga K, Kamata K, Honjo H, Kudo M

3071 Anabolic androgenic steroid-induced liver injury: An update

Petrovic A, Vukadin S, Sikora R, Bojanic K, Smolic R, Plavec D, Wu GY, Smolic M

3081 Epidemiological and clinical aspects of hepatitis B virus infection in Italy over the last 50 years

Sagnelli C, Sica A, Creta M, Calogero A, Ciccozzi M, Sagnelli E

3092 Shared decision-making in the management of patients with inflammatory bowel disease

Song K, Wu D

3101 Clinical implications and mechanism of histopathological growth pattern in colorectal cancer liver metastases

Kong BT, Fan QS, Wang XM, Zhang Q, Zhang GL

3116 Role of gadoxetic acid-enhanced liver magnetic resonance imaging in the evaluation of hepatocellular carcinoma after locoregional treatment

Gatti M, Maino C, Darvizeh F, Serafini A, Tricarico E, Guarneri A, Inchingolo R, Ippolito D, Ricardi U, Fonio P, Faletti R

ORIGINAL ARTICLE

Basic Study

3132 Neutrophil extracellular traps participate in the development of cancer-associated thrombosis in patients with gastric cancer

Li JC, Zou XM, Yang SF, Jin JQ, Zhu L, Li CJ, Yang H, Zhang AG, Zhao TQ, Chen CY

3150 Activation of natural killer T cells contributes to Th1 bias in the murine liver after 14 d of ethinylestradiol exposure

Zou MZ, Kong WC, Cai H, Xing MT, Yu ZX, Chen X, Zhang LY, Wang XZ

World Journal of Gastroenterology

Weekly Volume 28 Number 26 July 14, 2022

Contents

3164 *Bifidobacterium infantis* regulates the programmed cell death 1 pathway and immune response in mice with inflammatory bowel disease

Zhou LY, Xie Y, Li Y

3177 Involvement of Met receptor pathway in aggressive behavior of colorectal cancer cells induced by parathyroid hormone-related peptide

Novoa Díaz MB, Carriere P, Gigola G, Zwenger AO, Calvo N, Gentili C

3201 Intracellular alpha-fetoprotein mitigates hepatocyte apoptosis and necroptosis by inhibiting endoplasmic reticulum stress

Chen YF, Liu SY, Cheng QJ, Wang YJ, Chen S, Zhou YY, Liu X, Jiang ZG, Zhong WW, He YH

Retrospective Cohort Study

3218 Divergent trajectories of lean *vs* obese non-alcoholic steatohepatitis patients from listing to post-transplant: A retrospective cohort study

Qazi-Arisar FA, Uchila R, Chen C, Yang C, Chen SY, Karnam RS, Azhie A, Xu W, Galvin Z, Selzner N, Lilly L, Bhat M

Retrospective Study

3232 Tumor-feeding artery diameter reduction is associated with improved short-term effect of hepatic arterial infusion chemotherapy plus lenvatinib treatment

Wu DD, He XF, Tian C, Peng P, Chen CL, Liu XH, Pang HJ

Observational Study

3243 Impact of sodium glucose cotransporter-2 inhibitors on liver steatosis/fibrosis/inflammation and redox balance in non-alcoholic fatty liver disease

Bellanti F, Lo Buglio A, Dobrakowski M, Kasperczyk A, Kasperczyk S, Aich P, Singh SP, Serviddio G, Vendemiale G

SYSTEMATIC REVIEWS

3258 Endoscopic techniques for diagnosis and treatment of gastro-entero-pancreatic neuroendocrine neoplasms: Where we are

Rossi RE, Elvevi A, Gallo C, Palermo A, Invernizzi P, Massironi S

LETTER TO THE EDITOR

3274 Intestinal inflammation and the microbiota: Beyond diversity

Alberca GGF, Cardoso NSS, Solis-Castro RL, Nakano V, Alberca RW

3279 Intestinal virome: An important research direction for alcoholic and nonalcoholic liver diseases

Li Y, Liu WC, Chang B

Contents

ABOUT COVER

Editorial Board Member of *World Journal of Gastroenterology*, Koichi Suda, MD, PhD, FACS, Professor and Head, Divisions of GI and HPB Surgery, Department of Surgery, Fujita Health University, Rm C908, 1-98 Dengakugakubo, Kutsukake, Toyoake, Aichi 470-1192, Japan. ko-suda@fujita-hu.ac.jp

AIMS AND SCOPE

The primary aim of *World Journal of Gastroenterology* (*WJG*, *World J Gastroenterol*) is to provide scholars and readers from various fields of gastroenterology and hepatology with a platform to publish high-quality basic and clinical research articles and communicate their research findings online. *WJG* mainly publishes articles reporting research results and findings obtained in the field of gastroenterology and hepatology and covering a wide range of topics including gastroenterology, hepatology, gastrointestinal endoscopy, gastrointestinal surgery, gastrointestinal oncology, and pediatric gastroenterology.

INDEXING/ABSTRACTING

The *WJG* is now abstracted and indexed in Science Citation Index Expanded (SCIE, also known as SciSearch®), Current Contents/Clinical Medicine, Journal Citation Reports, Index Medicus, MEDLINE, PubMed, PubMed Central, Scopus, Reference Citation Analysis, China National Knowledge Infrastructure, China Science and Technology Journal Database, and Superstar Journals Database. The 2022 edition of Journal Citation Reports® cites the 2021 impact factor (IF) for *WJG* as 5.374; IF without journal self cites: 5.187; 5-year IF: 5.715; Journal Citation Indicator: 0.84; Ranking: 31 among 93 journals in gastroenterology and hepatology; and Quartile category: Q2. The *WJG*'s CiteScore for 2021 is 8.1 and Scopus CiteScore rank 2021: Gastroenterology is 18/149.

RESPONSIBLE EDITORS FOR THIS ISSUE

Production Editor: *Hua-Ge Yu*; **Production Department Director:** *Xu Guo*; **Editorial Office Director:** *Jia-Ru Fan*.

NAME OF JOURNAL
World Journal of Gastroenterology

ISSN
ISSN 1007-9327 (print) ISSN 2219-2840 (online)

LAUNCH DATE
October 1, 1995

FREQUENCY
Weekly

EDITORS-IN-CHIEF
Andrzej S Tarnawski

EDITORIAL BOARD MEMBERS
http://www.wjgnet.com/1007-9327/editorialboard.htm

PUBLICATION DATE
July 14, 2022

COPYRIGHT
© 2022 Baishideng Publishing Group Inc

INSTRUCTIONS TO AUTHORS
https://www.wjgnet.com/bpg/gerinfo/204

GUIDELINES FOR ETHICS DOCUMENTS
https://www.wjgnet.com/bpg/GerInfo/287

GUIDELINES FOR NON-NATIVE SPEAKERS OF ENGLISH
https://www.wjgnet.com/bpg/gerinfo/240

PUBLICATION ETHICS
https://www.wjgnet.com/bpg/GerInfo/288

PUBLICATION MISCONDUCT
https://www.wjgnet.com/bpg/gerinfo/208

ARTICLE PROCESSING CHARGE
https://www.wjgnet.com/bpg/gerinfo/242

STEPS FOR SUBMITTING MANUSCRIPTS
https://www.wjgnet.com/bpg/GerInfo/239

ONLINE SUBMISSION
https://www.f6publishing.com

© 2022 Baishideng Publishing Group Inc. All rights reserved. 7041 Koll Center Parkway, Suite 160, Pleasanton, CA 94566, USA
E-mail: bpgoffice@wjgnet.com https://www.wjgnet.com

World Journal of Gastroenterology

Submit a Manuscript: https://www.f6publishing.com

World J Gastroenterol 2022 July 14; 28(26): 3008-3026

DOI: 10.3748/wjg.v28.i26.3008

ISSN 1007-9327 (print) ISSN 2219-2840 (online)

REVIEW

Advances in the imaging of gastroenteropancreatic neuroendocrine neoplasms

Anupama Ramachandran, Kumble Seetharama Madhusudhan

Specialty type: Radiology, nuclear medicine and medical imaging

Provenance and peer review: Invited article; Externally peer reviewed.

Peer-review model: Single blind

Peer-review report's scientific quality classification

Grade A (Excellent): A
Grade B (Very good): B
Grade C (Good): C, C
Grade D (Fair): 0
Grade E (Poor): 0

P-Reviewer: Cerwenka H, Austria; Wang WQ, China

Received: October 11, 2021
Peer-review started: October 11, 2021
First decision: November 15, 2021
Revised: November 30, 2021
Accepted: June 19, 2022
Article in press: June 19, 2022
Published online: July 14, 2022

Anupama Ramachandran, Kumble Seetharama Madhusudhan, Department of Radiodiagnosis and Interventional Radiology, All India Institute of Medical Sciences, New Delhi 110029, India

Corresponding author: Kumble Seetharama Madhusudhan, MD, Additional Professor, Department of Radiodiagnosis and Interventional Radiology, All India Institute of Medical Sciences, Ansari Nagar, New Delhi 110029, India. drmadhuks@gmail.com

Abstract

Gastroenteropancreatic neuroendocrine neoplasms comprise a heterogeneous group of tumors that differ in their pathogenesis, hormonal syndromes produced, biological behavior and consequently, in their requirement for and/or response to specific chemotherapeutic agents and molecular targeted therapies. Various imaging techniques are available for functional and morphological evaluation of these neoplasms and the selection of investigations performed in each patient should be customized to the clinical question. Also, with the increased availability of cross sectional imaging, these neoplasms are increasingly being detected incidentally in routine radiology practice. This article is a review of the various imaging modalities currently used in the evaluation of neuroendocrine neoplasms, along with a discussion of the role of advanced imaging techniques and a glimpse into the newer imaging horizons, mostly in the research stage.

Key Words: Neuroendocrine tumor; Gastroenteropancreatic; Intravoxel incoherent motion; Diffusion weighted imaging; Perfusion imaging; Dual energy computed tomography

©The Author(s) 2022. Published by Baishideng Publishing Group Inc. All rights reserved.

Core Tip: The prognosis of gastroenteropancreatic neuroendocrine neoplasms (GEPNENs) depends on the stage of the disease and tumor grade. Traditional imaging techniques like multiphase contrast-enhanced computed tomography perform well at disease staging. For tumor grading, histopathological examination, with determination of number of mitoses and Ki-67 index is considered optimal. Advances in imaging techniques have enabled detection of smaller neuroendocrine neoplasms (< 2 cm). By analysing functional information like diffusion, perfusion and tumor heterogeneity, quantitative imaging is currently focused on noninvasive prediction of the grade of GEPNENs preoperatively.

Citation: Ramachandran A, Madhusudhan KS. Advances in the imaging of gastroenteropancreatic neuroendocrine neoplasms. *World J Gastroenterol* 2022; 28(26): 3008-3026
URL: https://www.wjgnet.com/1007-9327/full/v28/i26/3008.htm
DOI: https://dx.doi.org/10.3748/wjg.v28.i26.3008

INTRODUCTION

Gastroenteropancreatic neuroendocrine neoplasms (GEPNENs) are a rare and heterogeneous group of tumors that originate from the gastrointestinal and pancreatic neuroendocrine cells[1,2]. They may be benign or malignant and may or may not secrete hormones. Use of the previous terminology - carcinoid tumor - is no longer encouraged. The gastrointestinal tract (GIT), having the highest density of neuroendocrine cells in the body, is the most common site of involvement of neuroendocrine neoplasms (NENs), comprising nearly 60% of all NENs[3]. Pancreatic NENs (PNENs) account for about 7% of all GEPNENs [4]. Most PNENs are sporadic. However, association with four familial syndromes (in up to 25%) is well described: multiple endocrine neoplasia type I, von Hippel Lindau syndrome, neurofibromatosis type I and tuberous sclerosis[5,6].

Classification based on histological differentiation and grade is desirable as it provides insight into tumor biology, clinical course and helps in planning management. In 2019, the 5th edition of the World Health Organization (WHO) classification of tumors series published the latest NEN classification (Table 1)[7]. The latest WHO classification recognizes that well-differentiated NENs may be high grade, but they are distinct from the poorly differentiated neuroendocrine carcinomas (NECs). Most GEPNENs are well-differentiated and slowly growing. Grade 3 NENs are most common in the pancreas, but can occur throughout the GIT[7]. Given the differences in prognosis, tumor grade is the most important factor determining the treatment of GEPNENs. The treatment of GEPNENs depends on grade, differentiation, site of origin, and stage of tumor, and the opinion about the best treatment strategy is evolving. Surgical resection remains the cornerstone and is the only curative treatment. For patients with small (< 2 cm), low-grade NENs, decisions on surgery *vs* active surveillance need to be individualized based on tumor size, morphology (homogeneous, well circumscribed tumor < 1 cm correlate with low malignant potential) and patient characteristics like age and presence of comorbidities[8].

The commonly used imaging modalities include ultrasonography (US), computed tomography (CT), magnetic resonance imaging (MRI) and positron emission tomography (PET)-CT. Imaging is primarily aimed at accurate detection, characterization and staging of these neoplasms and also at assessment of response to treatment. Sensitivity of common imaging modalities used in the evaluation of GEPNENs are summarized in Table 2.

Improvements and advances in the imaging techniques have mainly focused on the noninvasive prediction of the grade of the NENs. The European Neuroendocrine Tumor Society (ENETS) has also recommended that preoperative assessment of the grade of the NENs is essential for prognosis prediction and management planning[9]. In addition, with the improvements in the imaging technologies, the detection rates of small NENs have significantly improved, with many often being detected incidentally.

US

Transabdominal ultrasonography (USG) often is the commonest initial modality used for patients with gastrointestinal symptoms. It has value in the detection of liver metastases (sensitivity reaching 85%-90%). PNENs in general appear as hypoechoic masses with a hyperechoic halo on USG[10].

However, transabdominal USG has limitations. It has a poor sensitivity (13%-27%) for the detection of GEPNENs[11]. The technique is dependent on the experience of the operator. Presence of bowel gas and increased subcutaneous fat can obscure adequate visualization.

The advent of harmonic imaging, pulse inversion sequence, low mechanical index techniques and ultrasound contrast agents (UCAs) has enabled routine application of contrast-enhanced ultrasound (CEUS) to overcome the limitations of conventional B mode USG. The inherent advantage of CEUS is its ability to assess tumor-enhancement patterns in real time during transabdominal USG[12]. The enhancement patterns are described during arterial, portal venous and late phases. UCAs are gas microbubbles stabilized by a shell, the composition of which varies depending on the type of contrast agent. UCAs are blood pool agents and increase the back scatter of US, enhancing the echogenicity of flowing blood[12]. Harmonic imaging detects harmonic signals from the microbubbles and CEUS specific US modes filter signals from the background tissue, thereby showing even very slow blood flow without Doppler related artifacts. UCAs, unlike CT and MRI contrast agents, are excreted by the lungs and hence can be used safely in patients with deranged renal function.

Table 1 World Health Organization Classification and grading criteria for neuroendocrine neoplasms of the gastrointestinal tract and hepatopancreatobiliary organs (7)

Terminology	Differentiation	Grade	Mitoses/2 mm^2	Ki-67 index
NEN grade 1	Well differentiated	Low	< 2	< 3%
NEN grade 2		Intermediate	2-20	3%-20%
NEN grade 3		High	> 20	> 20%
SCNEC	Poorly differentiated	High[1]	> 20	> 20%
LCNEC			> 20	> 20%
MiNEN	Well or poorly differentiated	Variable	Variable	Variable

[1]Poorly differentiated neuroendocrine carcinomas are not formally graded, but are considered high-grade by definition.
LCNEC: Large cell neuroendocrine carcinoma; MiNEN: Mixed neuroendocrine non-neuroendocrine neoplasm; NEN: Neuroendocrine neoplasm; SCNEC: Small-cell neuroendocrine carcinoma.

Table 2 Sensitivity of common imaging modalities used in the evaluation of gastroenteropancreatic neuroendocrine neoplasms

Imaging modality	Sensitivity
Transabdominal USG	13%-27% for GEPNEN
Contrast enhanced ultrasound	99% in detecting liver metastases
Endoscopic ultrasonography	82%-93% for PNEN
CECT	63%-82% for PNEN
CE MRI	79% for PNEN
DWI	83% for liver metastases

USG: Ultrasonography; GEPNEN: Gastroenteropancreatic neuroendocrine neoplasms; CECT: Contrast enhanced computed tomography; CE MRI: Contrast-enhanced magnetic resonance imaging; DWI: Diffusion-weighted imaging.

The differential perfusion on CEUS has been shown to identify and diagnose pancreatic tumors. Pancreatic adenocarcinomas are in general hypovascular, while NENs are hypervascular. Takeda *et al* [13] found three patterns of hyperenhancement of PNENs and found that CEUS was useful in the differentiation of PNENs from pancreatic adenocarcinomas. Malagò *et al*[14] also showed that the enhancement patterns of nonfunctioning PNENs on CEUS (hyper-, iso- or hypovascular) correlated well with Ki-67 index and CEUS improved the detection of hepatic metastases. Hypervascular lesions had lower Ki-67 index. Another study showed that the enhancement patterns of NENs on CEUS correlated significantly with CT enhancement pattern and histological Ki-67 index and CEUS was a good predictor of response of tumors to somatostatin analogues[15].

Elastography

Elastography is an advancement in USG that enables real-time measurement of tissue stiffness along with display in colors superimposed on the grey scale images[16]. In general, elastography helps with the differentiation of benign and malignant lesions based on stiffness, as malignant lesions are usually hard. Only a few studies have reported the usefulness of transabdominal shear wave elastography (SWE) in the evaluation of pancreatic tumors. Park *et al*[17] showed that elastography can differentiate benign and malignant solid pancreatic lesions based on the difference in the shear wave velocity values (relative stiffness) between the tumor and the normal parenchyma. An early study by Uchida *et al*[18] found that NENs were homogeneous and soft on elastography, comparable to the normal pancreas. They also reported that a combination of elastography and B mode USG, improved the diagnostic accuracy to 90%, from 70%-80 % when B mode USG was used alone. However, if the visualization on the baseline B mode USG is suboptimal, the results of CEUS and elastography are also often unsatisfactory. These limitations have been overcome by the use of endoscopic ultrasound (EUS).

EUS

EUS is considered the most accurate test for the diagnosis of pancreatic masses[19]. EUS uses higher frequency (7.5-12 MHz) probes, placed in proximity to the area of interest and hence performs better at detection of tumors < 2 cm for which CT and MRI have poor sensitivity[20]. Overall, EUS has a sensitivity of 82%-93% and a specificity of 92%-95% for localizing PNENs. EUS is particularly useful in the detection of benign insulinomas that lack somatostatin receptors and consequently are not detected on somatostatin receptor scintigraphy/single photon emission computed tomography (SPECT)/PET [21]. EUS also plays an important role in the detection of functional pancreatic and extrapancreatic (duodenal) gastrinomas[22]; both of which generally have a small size (average 1 cm) at diagnosis. The additional benefit of EUS is its ability to guide accurate tissue sampling *via* fine needle aspiration and core biopsy[23]. CEUS can also be performed through EUS with the use of second generation UCAs (*e.g*, Sonovue), which produce harmonic signals at low acoustic powers. A recent study showed that the time intensity curve analysis during CEUS showed high diagnostic accuracy in grading PNENs, and could differentiate grade 1/2 tumors from grade 3 tumors/carcinomas[24].

EUS elastography

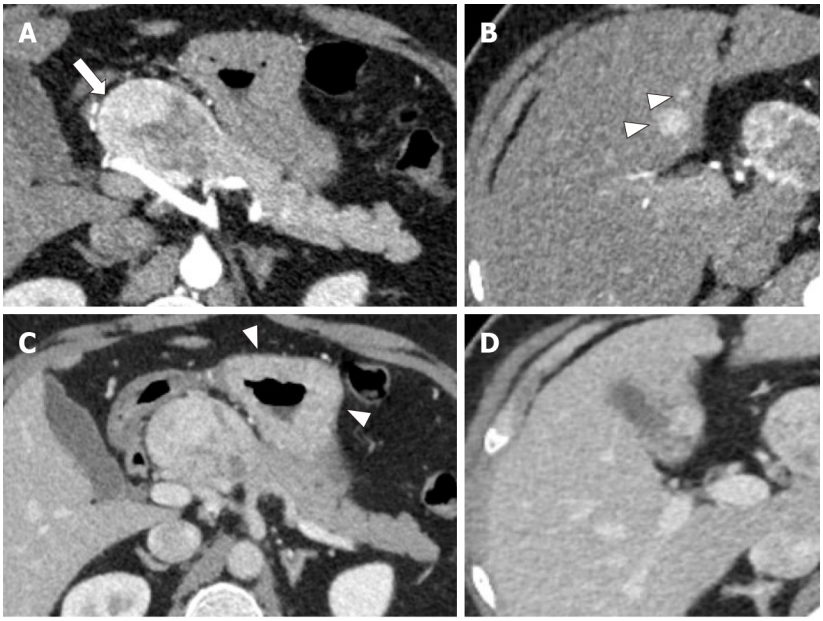
EUS elastography of the pancreas has been shown to be a promising imaging technique in several studies[25-27]. However, a prospective study by Hirche *et al*[28] including 70 patients with undifferentiated pancreatic masses showed an overall lower sensitivity (41%), specificity (53%) and accuracy (45%) for the detection of malignancy. One of the early studies evaluating conventional strain elastography for pancreatic lesions showed significant strain difference between benign and malignant masses[29]. The major utility of EUS elastography is in increasing the yield of sampling by aiding better tumor targeting, especially in the background of pancreatic parenchymal fibrosis[30]. SWE EUS is a recent development and studies evaluating its utility in the pancreas are just emerging[31,32]. A recent comparative study suggested that conventional strain elastography was superior to SWE in the characterization of pancreatic lesions[33].

CT

CT is the cornerstone and the most commonly performed imaging modality for the diagnosis and preoperative staging of GEPNEN. Standard CT scan has low sensitivity (~60%) for the detection of GIT NENs[34]. Dynamic dual-phase protocol, which includes the arterial and portal venous phases, is recommended in patients with suspected NEN[35,36] (Figure 1). For PNEN, the late arterial phase acquired at 40-45 s (pancreatic phase) suits best. For detection of small bowel NENs, CT enterography (oral administration of neutral contrast agent like mannitol for bowel distension) or CT enteroclysis (administration of neutral contrast *via* nasojejunal tube) is required. CT enteroclysis combines the advantages of enteroclysis with imaging capabilities of multidetector computed tomography (MDCT). Study by Kamaoui *et al*[37] showed that CT enteroclysis had 100% sensitivity and 96.2% specificity for the detection of small bowel NEN. A comparative study from Mayo Clinic found that CT enterography was better than capsule endoscopy in detecting small bowel tumors, with a sensitivity of up to 93%[38]. This ability of CT enterography to detect small bowel tumors remains high (sensitivity of 88%) even in the presence of gastrointestinal bleeding[39].

The characteristic imaging feature on CT scan suggesting the diagnosis of NENs is their intense enhancement in the late arterial phase, owing to the hypervascular nature of the tumor. The arterial phase also helps in outlining the relationship of the tumor with the adjacent arteries. Using the maximum intensity projection technique, virtual angiographic images can be obtained. Volume rendering techniques applied to the arterial phase provide easily explainable images to the surgeon. Portal venous phase helps to draw the relationship of the tumor with major veins, especially the splenic vein and the superior mesenteric vein for PNENs. Dual-phase imaging is also crucial for the evaluation of hepatic metastases. The classic liver metastases from NEN, being hypervascular, are most evident on the arterial phase images. About 6%-15% of NEN liver metastases are appreciated only in the arterial phase[40,41]. However up to 16% are hypovascular and show delayed enhancement[40].

One of the early studies suggested that the size of the tumor is an important prognostic factor, with tumors < 1 cm showing lesser incidence of liver metastasis (20%–30%) compared to those with > 1 cm (> 40% risk)[42]. Studies have shown that up to 42% of PNENs may not show arterial phase hyperenhancement[43,44]. Such arterial phase hypoenhancing tumors were associated with a significantly lower 5-year survival (54%) compared to the lesions which were isoenhancing (89%) or hyperenhancing (93%) [45]. Rodallec *et al*[46] found that tumor enhancement on CT scan correlated with microvascular density (MVD) evaluated on histology and that hypoenhancing PNENs correlated with poorly differentiated tumors and a decrease in overall survival rate. These studies showed that the CT enhancement characteristics of NENs have a prognostic value. Gallotti *et al*[6] found that incidentally detected PNENs, size > 3 cm, complex enhancement pattern and, presence of calcification, vascular invasion, main pancreatic duct dilatation, and peripancreatic lymph nodes were associated with nonbenign tumors and required



DOI: 10.3748/wjg.v28.i26.3008 **Copyright** ©The Author(s) 2022.

Figure 1 49-year-old man with epigastric pain and raised serum gastrin levels. A and B: Axial contrast enhanced pancreatic phase computed tomography (CT) images show a well-defined hyperenhancing mass (arrow in A) in the head and neck of pancreas, abutting the proper hepatic artery along with two hyperenhancing focal lesions in the liver (arrowheads in B), indicating hepatic metastases; C and D: Axial portal venous phase CT images show retention of contrast in the lesions in both locations. Thickened gastric mucosal folds is also noted (arrowheads in C).

more aggressive course of management.

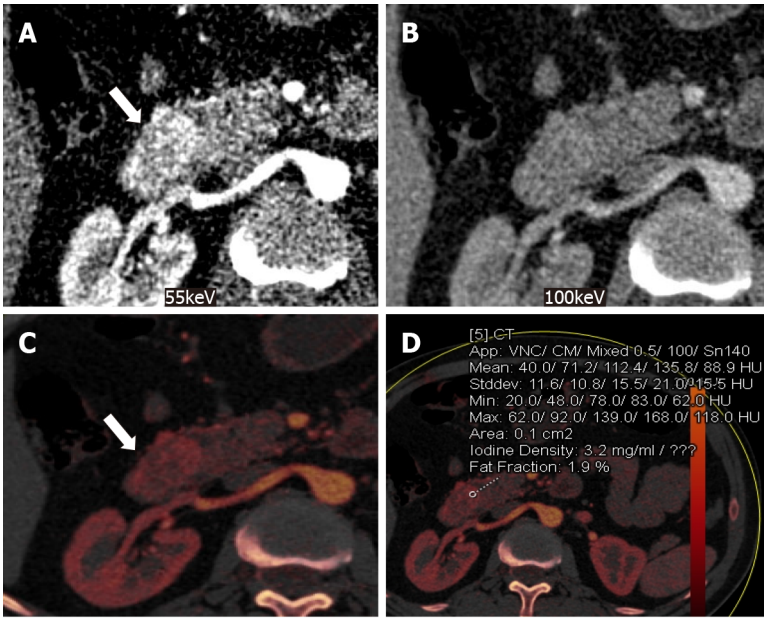
The role of various CT quantitative parameters based on enhancement of the NEN in the arterial or pancreatic and the venous phases has been evaluated in the prediction of tumor grade. Kim *et al*[47] found that portal enhancement ratio (HU value of the tumor divided by the HU value of pancreatic parenchyma on portal phase images) had the best odds ratio (49.6) and a cutoff value of < 1.1 had a sensitivity of 92% and specificity of 81% in differentiating grade 3 PNENs from grade 1 and 2. This high sensitivity and specificity of portal enhancement ratio in differentiating neuroendocrine carcinomas from well-differentiated NENs was also confirmed by another study[48]. Yamada *et al*[49] showed that corrected true enhancement values in the pancreatic phase had a sensitivity of 92%, specificity of 84% and area under the curve of 0.897 in the differentiation of grade 1 from grade 2 PNENs. D'Onofrio *et al*[50] showed that various tumor enhancement parameters (tumor permeability ratios, tumor parenchyma ratios, tumor arterial ratio and tumor venous ratio) were significantly different between grade 1 and grade 3 and between grade 2 and grade 3 PNENs. However, these values could not differentiate grade 1 from grade 2 tumors.

Dual-energy CT

Dual-energy CT (DECT) is an advancement in CT, which allows acquisition of images at two energy levels, with lower energy being 80-100 kVp and higher being 140 kVp. Using DECT, material decomposition of images and generation of iodine maps, virtual noncontrast images, and monochromatic images at different energy levels is possible (Figures 2 and 3). Monoenergetic images at low keV (55 keV) in the pancreatic phase of DECT show improved image contrast for evaluation of pancreatic masses[51]. Monochromatic spectral images improve the sensitivity of detection of NENs like insulinomas, particularly the hypovascular and isoattenuating tumors and the sensitivity is comparable to MRI[52]. One study showed that iodine uptake obtained from DECT is useful in the differentiation of hepatocellular carcinoma from liver metastases arising from NENs, with the former showing significantly higher iodine uptake (3.8 ± 1.2 *vs* 2.3 ± 0.6)[53]. This iodine uptake parameter on DECT may also be used in assessing the response to treatment of NENs.

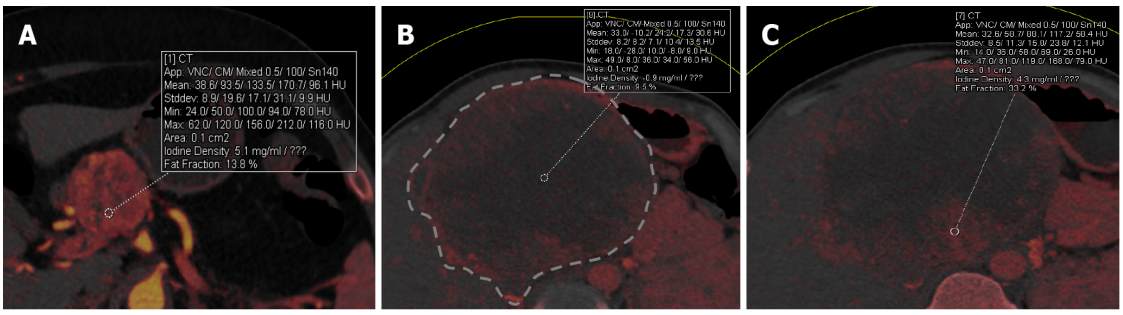
Perfusion CT

Perfusion CT is a technique that measures the dynamic changes in the attenuation of the tissues after contrast administration. It allows quantitative measurement of tissue perfusion, thereby assisting in the assessment of tumor viability and biological behavior[54]. The commonly used quantitative parameters of perfusion CT in oncoimaging are blood flow, blood volume, vascular permeability-surface area product and mean transit time (Figures 4 and 5). These parameters serve as imaging biomarkers of tumor angiogenesis, which is ideally assessed histologically by calculating the MVD[55]. NENs are among the tumors with significant angiogenesis. Unlike majority of the cancers, where increased tumor



DOI: 10.3748/wjg.v28.i26.3008 **Copyright** ©The Author(s) 2022.

Figure 2 Dual-energy computed tomography images of a 46-year-old man presenting with melena. A: Axial monochromatic computed tomography (CT) image at 55 keV in pancreatic phase shows a hyperenhancing well-defined mass (arrow) arising from the duodenal wall; B: Enhancement of the same lesion (arrow) appears subtle on the axial 100 keV monochromatic CT image; C and D: Iodine overlay maps show bright areas (arrow) suggesting contrast uptake (C), with iodine concentration of 3.2 mg/mL in areas of uptake (D). Iodine concentration of normal pancreas was 0.5 mg/mL.

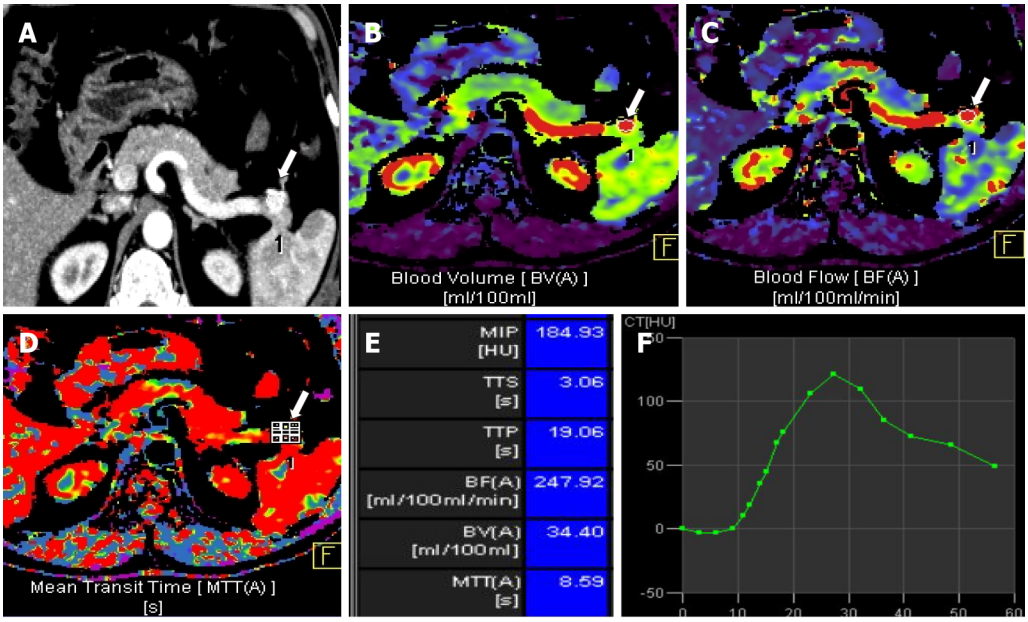


DOI: 10.3748/wjg.v28.i26.3008 **Copyright** ©The Author(s) 2022.

Figure 3 Dual-energy computed tomography in grading the pancreatic neuroendocrine neoplasms. A: Iodine overlay dual-energy computed tomography (CT) map of a 40-year-old woman with low-grade (grade 2) pancreatic neuroendocrine neoplasms (PNEN) in head of pancreas shows hyperenhancement of the tumor with an iodine concentration of 5.1 mg/mL; B and C: Iodine overlay dual energy CT maps of a 29-year-old man with grade 3 PNEN (outlined in B) shows large hypoenhancing areas with low iodine concentration (0.9 mg/mL) and peripheral bright areas with iodine concentration of 4.3 mg/mL (C). Measuring iodine concentration helps in objectively assessing the grade of the tumor.

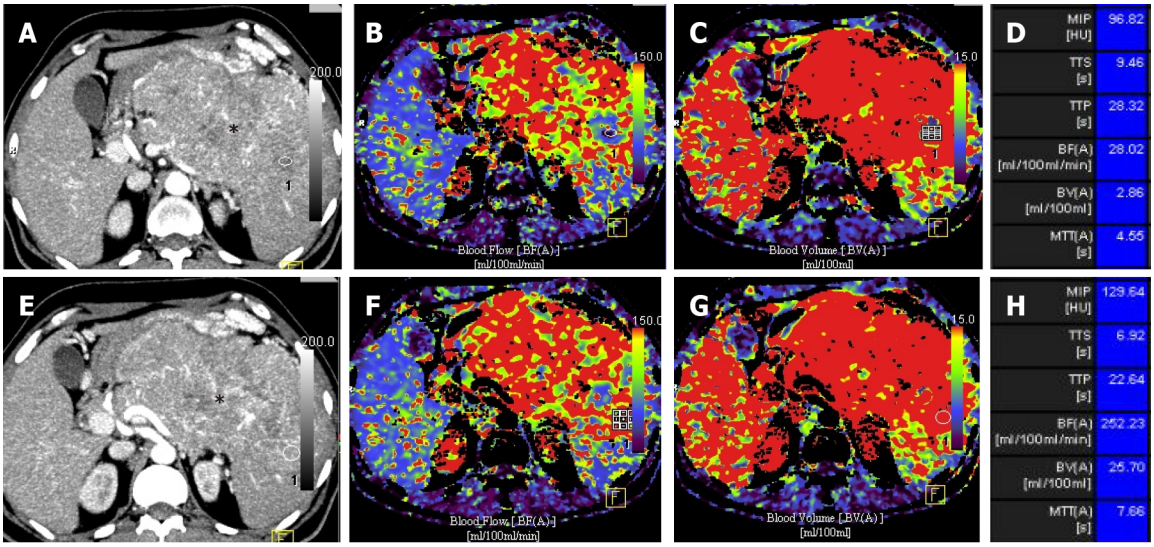
vascularity is associated with aggressive behavior, higher microvascular density in NENs is associated with a low tumor grade[54]. Low MVD was found to be an unfavorable prognostic factor for PNENs in several studies despite the presence of other favorable conventional histoprognostic factors, and call for a more aggressive treatment approach[56-58]. A study by d'Assignies *et al*[59] on 36 patients with PNENs found a significant correlation between MVD and blood flow assessed by using perfusion CT. In their study, the authors found that tumors that are small (< 2 cm), benign (grade 1), with a proliferation index of ≤ 2%, and without histological signs of microvascular involvement had a significantly higher blood flow. Volume perfusion CT has been shown to improve the detection of pancreatic insulinomas, particularly the ones which have transient hyperenhancement (comprising 30% cases)[60,61]. A recent study demonstrated that addition of low dose perfusion CT to contrast enhanced CT improved the detection rate of PNENs from 83.6% to 89.1% and found that blood flow parameters were significantly different between grade 1 and grade 2 tumors[62].

Perfusion CT has also been shown to have a role in monitoring response to treatment with antiangiogenic drugs. Few studies have shown that the perfusion parameters of PNENs and liver metastases decrease as early as 48 h after treatment with anti-angiogenic drugs and perfusion CT offers a significant role in an early noninvasive assessment[63,64]. A major limitation of perfusion CT is the higher radiation dose, resulting in an additional dose of approximately 7 mSv[65].



DOI: 10.3748/wjg.v28.i26.3008 **Copyright** ©The Author(s) 2022.

Figure 4 Volume perfusion computed tomography images of a 56-year-old man with recurrent hyperinsulinemic hypoglycemia. A: Axial pancreatic phase computed tomography image shows a hyperenhancing lesion in the pancreatic tail (arrow); B-D: Color-coded parametric maps for blood volume (B), blood flow (C) and mean transit time (D) of the tumor (arrow) and normal pancreatic tissue; E: Chart shows mean value of each perfusion parameter of the tumor. Blood flow in the tumor was higher (247 mL/100 mL/min) compared to normal pancreatic parenchyma (72 mL/100 mL/min); F: Time attenuation curve shows dynamic enhancement pattern of the tumor corresponding to transient hyperenhancement. Histopathology after enucleation proved the tumor to be grade 1 insulinoma.



DOI: 10.3748/wjg.v28.i26.3008 **Copyright** ©The Author(s) 2022.

Figure 5 Volume perfusion computed tomography images of a 67-year-old man with a large grade 3 neuroendocrine neoplasm involving body and tail of pancreas. A and B: Axial arterial phase computed tomography images with circular regions of interest placed at two different locations in the lesion (*); C-H: Parametric maps for blood flow (C and D) and blood volume (E and F) with mean value of each perfusion parameter (G and H) are shown. Lower values of mean blood flow, mean blood volume and mean transit time are features of high grade neuroendocrine neoplasm.

MRI

MRI is best performed as a problem-solving tool when CT scan findings are equivocal or negative, and is aimed at acquiring images of the lesion and organ with better soft tissue contrast. For instance, MRI has shown better sensitivity for the detection of liver metastases compared to CT and somatostatin receptor scintigraphy[66]. The absence of exposure to ionizing radiation makes MRI the apt modality for screening young individuals suspected of having NEN and those with syndromic association who require multiple follow up imaging[67]. Most NENs are hypointense on T1-weighted and hyperintense on T2-weighted images[10]. Contrast enhancement pattern and morphologic appearances are similar to

that seen in CT scan (Figure 6). For the detection of PNENs, the sensitivity of MRI ranges from 85% to 100% and specificity from 75% to 100%[68].

Diffusion-weighted imaging

Diffusion-weighted imaging (DWI) is a widely used technique in clinical imaging as it reflects the microscopic environment of the neoplasm including tumor cellularity and extracellular matrix. The application of DWI in oncology is mainly in tumor detection and assessing response to chemotherapy and radiotherapy. Wang *et al*[69] demonstrated that the apparent diffusion coefficient (ADC) values of PNEN correlated well with Ki-67 labelling index, thus indicating that DWI has a prognostic value (Figure 6). Another study showed that the ADC values were significantly different between benign and non-benign PNENs (1.48×10^{-3} mm^2/s *vs* 1.04×10^{-3} mm^2/s, respectively)[70]. Lotfalizadeh *et al*[71] showed that DWI has the additional value in identification of high grade tumors (grade 3) and can accurately differentiate grade 3 from grade 1/2 tumors (AUROC-0.96). The ADC values showed an inverse relation with the grade of the tumor.

Another major utility of DWI is in the detection and characterization of liver metastases. Several studies have shown that DWI is more sensitive for the detection of liver metastases than T2-weighted and multiphase gadolinium-enhanced MRI, especially for smaller lesions[72-74]. Besa *et al*[75] showed that the ADC of liver metastases from NEN weakly and significantly correlated negatively with tumor grade and Ki-67 and that the mean ADC and the minimum ADC values were significantly different between the three grades (1.6, 1.35 and 0.9×10^3 mm^2/s and 0.84, 0.5 and 0.27×10^3 mm^2/s for grades 1, 2 and 3, respectively). DWI is hence recommended in routine MRI abdomen protocol for the detection of liver metastases from NEN.

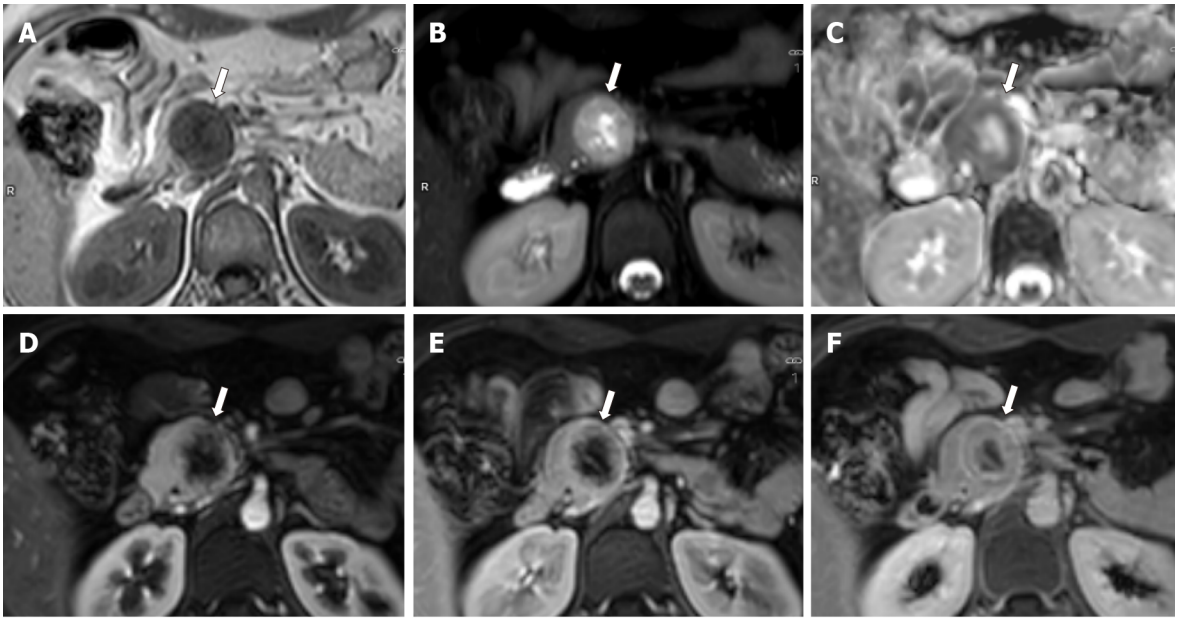
Histogram analysis of the ADC of the whole tumor has also been shown to predict tumor grade and aggressiveness. Pereira *et al*[76] found that whole tumor histogram analysis of the ADC, including the skewness and kurtosis can reliably differentiate grade 1 from grade 2/3 tumors. Another study also showed that this histogram analysis of ADC was useful in predicting tumor grade, vascular invasion and metastasis (node, liver) in PNENs and that $ADC_{entropy}$ and $ADC_{kurtosis}$ were the best markers in identifying tumor aggressiveness[77].

DWI is also useful in predicting and assessing response to various medical treatments for NENs. A recent study by Le Bihan *et al*[78] showed that the change in the ADC values of liver metastases from NENs after transarterial radioembolization was significantly different between the partial response and progressive disease groups, thus concluding that ADC can be used as an additional marker for treatment response evaluation.

While DWI investigates diffusion of water molecules in tissues, it does not detect perfusion of blood. Intravoxel incoherent motion (IVIM) DWI detects translational motion of water molecules in a voxel and can simultaneously quantify their diffusion and microcirculation in tissue capillary network[79]. IVIM images are quantified by ADC, which integrates the effects of both diffusion and perfusion. IVIM therefore enables evaluation of tissue perfusion without the requirement of a contrast agent. The quantitative parameters in IVIM include the pure diffusion coefficient (D_{slow}), which reflects the diffusion of water molecules, the pseudodiffusion coefficient (D_{fast}), which reflects the diffusion movement of capillary microcirculation perfusion, and the perfusion fraction (f), which represents the volume ratio between the perfusion effect of local microcirculation and the overall molecular diffusion (Figures 7 and 8). IVIM-DWI is a useful method to assess true tumor cellularity of PNEN, represented by tissue diffusion, as increased microcirculation of hypervascular PNENs may cause the pseudodiffusion effect and thus leads to the overestimation of ADC values[79]. Hwang *et al*[80] observed that IVIM DWI can differentiate grade 1 from grade 2 or 3 PNENs. They found that pure diffusion coefficient is a better marker of tumor cellularity than ADC, and was significantly higher in grade 1 PNENs, thereby enabling prediction of tumor grade on imaging. A recent study showed that D_{slow} and D_{fast} parameters help in the differentiation of high grade PNENs from pancreatic adenocarcinoma with high diagnostic accuracy (0.460 *vs* 0.579×10^3 mm^2/s and 13.361 *vs* 4.985×10^3 mm^2/s, respectively)[81].

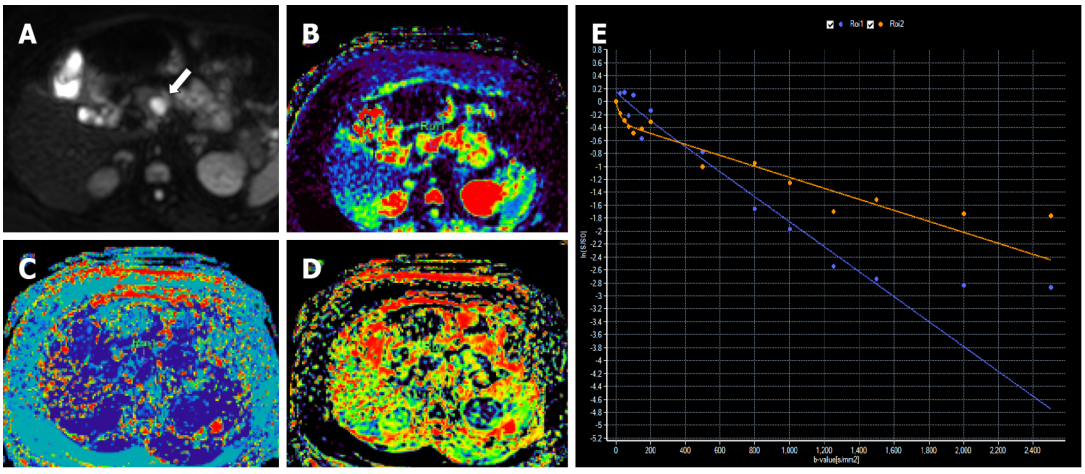
Diffusion kurtosis imaging

Diffusion kurtosis imaging (DKI) is a new rapidly advancing MRI technique based on the concept that water molecules in biological environment have non Gaussian properties. This is in contrast to standard DWI that calculates ADC using monoexponential analysis, assuming that diffusion of water in tissues follows Gaussian behavior[82]. At higher b values (> 1000 s/mm^2), due to the barriers encountered by water molecules in tissues, there is deviation from Gaussian distribution. The deviation when quantified, in fact represents the tissue microenvironment. Two quantitative parameters, diffusion coefficient (D) and kurtosis (K), representing deviation from Gaussian distribution, can be extracted from DKI. DKI thus provides a more accurate model of diffusion and quantifies tissue heterogeneity, and irregularity of cellular microstructure by capturing non Gaussian diffusion parameters (Figure 9)[82,83]. A drawback which hampers its use in routine practice is the long acquisition time due to scan acquisition at multiple b values. There are studies showing application of DKI for the assessment of the pancreas[84,85]. Shi *et al*[83] found that the radiomics model of DKI and T2 weighted imaging could improve the diagnostic accuracy for PNENs.



DOI: 10.3748/wjg.v28.i26.3008 **Copyright** ©The Author(s) 2022.

Figure 6 Magnetic resonance images of a 24-year-old woman with multiple endocrine neoplasia-type 1 syndrome and pancreatic neuroendocrine neoplasm. A-C: Axial magnetic resonance images through the head of pancreas show a round heterogeneous mass (arrow) which appears hypointense on T1-weighted image (A), hyperintense on T2-weighted image with central cystic / necrotic change (B) and shows peripheral hypointensity on apparent diffusion coefficient (ADC) image (C) suggesting diffusion restriction along the periphery (ADC = 0.93 × 10^3 mm^2/s); D-F: Axial dynamic contrast enhanced T1-weighted images show hyperenhancement of the tumor along the periphery in pancreatic phase (D), with contrast retention in venous (E) and delayed (F) phase images. The patient also had bilateral inferior parathyroid and left superior parathyroid adenomas.

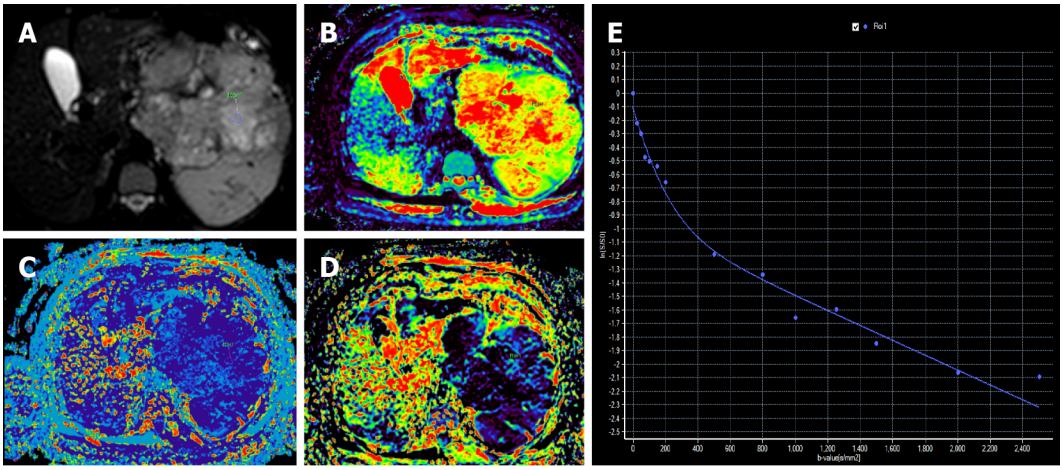


DOI: 10.3748/wjg.v28.i26.3008 **Copyright** ©The Author(s) 2022.

Figure 7 Intravoxel incoherent motion diffusion-weighted imaging in a 46-year-old woman with proven grade 1 pancreatic neuroendocrine neoplasm. A: Axial diffusion weighted image (b = 800 s/mm^2) shows a small pancreatic lesion with diffusion restriction (arrow); B: Color-coded diffusion map shows true diffusion coefficient, D = 2.33 × 10^3 mm^2/s; C: Color-coded perfusion map shows pseudodiffusion coefficient, D* = 5.37 × 10^3 mm^2/s); D: Color-coded perfusion fraction map shows a value, f = 3.2%; E: Signal decay curve of the tumor (purple) shows fall in signal at lower b values with plateau at higher b values. In comparison, normal pancreas (orange) shows lesser diffusion restriction than the tumor.

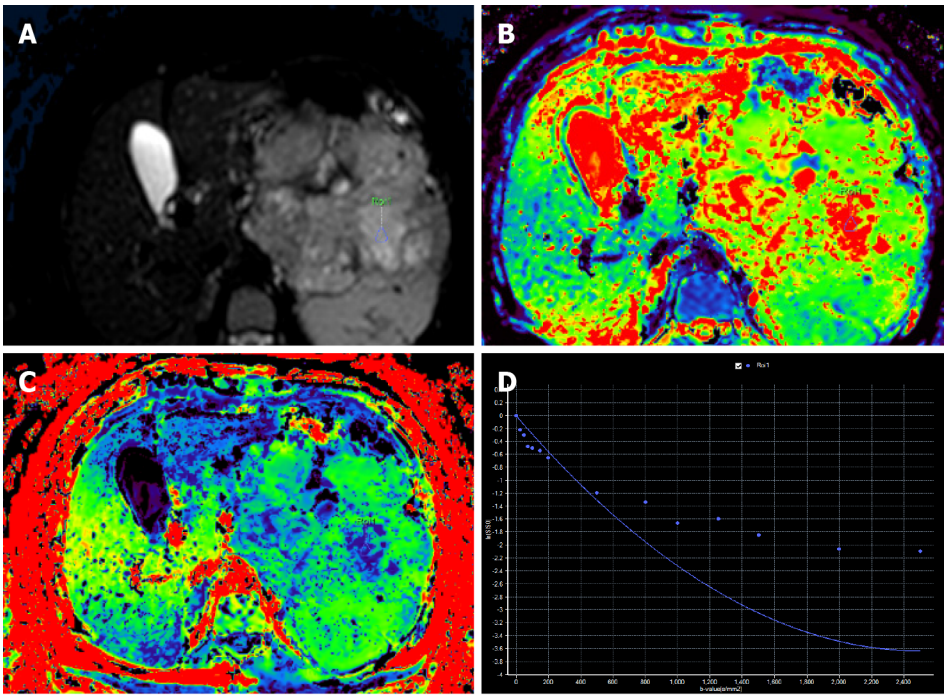
MR elastography

MR elastography (MRE) is a phase-contrast-based MRI technique for the evaluation of mechanical tissue properties noninvasively, *e.g.,* tissue stiffness. MRE of pancreas is at an early stage. Recent studies have used MRE to differentiate healthy from pathological pancreatic tissue[86]. The normal pancreatic stiffness in adults measured by MRE is 1.1–1.21 kPa[86]. Shi *et al*[87] used MRE for the characterization of solid pancreatic masses. They found that malignant masses had significantly higher stiffness (3.27 kPa) than benign masses (1.96 kPa). PNENs had a median stiffness of 2.32 kPa. They also suggested that stiffness ratio (ratio of stiffness of mass to normal parenchyma) may perform better in the differentiation of benign from malignant pancreatic masses.



DOI: 10.3748/wjg.v28.i26.3008 **Copyright** ©The Author(s) 2022.

Figure 8 Intravoxel incoherent motion diffusion-weighted imaging in a 67-year-old man with grade 3 pancreatic neuroendocrine neoplasm. A: Axial diffusion weighted image (b = 200 s/mm^2) with circular region of interest in the tumor; B: Color-coded diffusion map shows true diffusion coefficient, D = 0.84 × 10^3 mm^2/s; C: Color-coded perfusion map shows pseudodiffusion coefficient, D* = 5.01 × 10^3 mm^2/s); D: Color-coded perfusion fraction map shows a value, f = 4.5%; E: Signal decay curve shows steeper decay at low b values and continued fall at higher b values [in comparison to grade 1 pancreatic neuroendocrine neoplasm (PNEN) (Figure 7), true diffusion coefficient is lower in grade 3 PNENs].



DOI: 10.3748/wjg.v28.i26.3008 **Copyright** ©The Author(s) 2022.

Figure 9 Diffusion kurtosis of the lesion same as in Figure 8. A: Axial diffusion-weighted image (b = 200 s/mm^2) with region of interest marked; B: Diffusion map (D = 3 × 10^3 mm^2/s); C: Kurtosis map (k = 0.40); D: Signal decay curve shows non-Gaussian diffusion.

MRI perfusion

MRI perfusion techniques for the assessment of tumor perfusion have the major advantage that they lack adverse effects of radiation compared to the radiation-intensive CT perfusion. T1-weighted dynamic contrast enhanced (DCE) MRI is the technique applied in the evaluation of tumors in the abdomen[88]. This provides both semiquantitative and quantitative information on the microvascular perfusion of the tissue. The semiquantitative analysis is based on the time-signal intensity curve and the quantitative analysis is based on the Tofts two-compartment pharmacokinetic model (intravascular and extravascular-extracellular compartments) with the parameters evaluated being Ktrans (volume transfer constant, wash in), Kep (reverse efflux rate constant, wash out) and Ve (extravascular extracellular space volume fraction)[89]. This technique has shown promising results in the evaluation of PNENs. A study by Donati *et al*[90] showed that Ktrans and Kep values were higher in NENs (2.709 ± 0.110/min; 5.957 ±

0.371/min) compared to other focal lesions and healthy pancreatic parenchyma. This in fact reflects the wash in (Ktrans) and wash out (Kep) of the contrast agent from the hypervascular NENs. Also, well differentiated and poorly differentiated NENs showed different perfusion characteristics. In the study by Kim *et al*[91], Ktrans value of NENs were significantly higher than that of neuroendocrine carcinomas (0.339 ± 0.187/min *vs* 0.077 ± 0.036/min). Ductal adenocarcinomas being hypovascular, show significantly lower average values of Ktrans and Kep[90-92]. The role of DCE MRI in the evaluation of response to systemic chemotherapy and targeted molecular therapy by assessing the changes in the values of MRI perfusion parameters reflecting good or poor response to treatment is a direction for future studies.

PET CT AND PET MRI

Hybrid anatomical and functional imaging using PET/CT is a valuable tool in the current practice of grading and management of NENs. In general, in dual tracer PET/CT (somatostatin receptor imaging with Ga^{68} DOTATATE/TOC/NOC PET/CT and glucose metabolism with FDG PET/CT), low-grade tumors, which express somatostatin receptors, bind to somatostatin analog, but not to FDG[93]. In contrast, poorly differentiated GEPNENs with high Ki-67 index would be negative on somatostatin PET/CT but FDG avid[94]. Zhang *et al*[95] suggested that dual tracer PET /CT may be used as an alternative to tissue sampling, as it reflects both cellular somatostatin receptor expression and glucose metabolism. The authors also found a positive correlation between SUVmax (standardized uptake value) and Ki-67 index with respect to FDG PET/CT and negative correlation with respect to Ga^{68} DOTATATE PET/CT. However, low-grade insulinomas show low expression of somatostatin receptors in contrast to other secreting and nonsecreting NENs and are frequently not detected on Ga^{68} DOTATATE PET/CT[96]. Since virtually all benign insulinomas express glucagon-like peptide 1 (GLP-1) receptors (incretin receptors), these receptors can be targeted by PET/CT for preoperative localization of occult benign insulinomas. GLP-1R PET/CT had higher sensitivity than MRI and SPECT/CT for localization of benign insulinomas in a study by Antwi *et al*[97]. Glucose dependent insulinotropic polypeptide receptor (GIPR) is another incretin receptor overexpressed in GEPNENs. It is a potential target for imaging the small percentage (~10%) of GEPNENs which do not express SSTR and GLP1R, as confirmed by studies in animal models[98].

With technical advances, simultaneous PET and MRI acquisition in an integrated scanner is now possible. The first study in 2013 by Beiderwellen *et al*[99] showed that every lesion detected on PET/CT was identified on PET/MRI. Hope *et al*[100] evaluated hepatic lesions in patients with NENs using Ga^{68} DOTATOC PET/CT and PET/MRI and found that there was a strong correlation between SUVmax obtained in PET/CT and PET/MRI. However, due to the high cost, the routine use of PET/MRI is limited.

RADIOMICS, TEXTURE ANALYSIS AND MACHINE LEARNING

Radiomics is the process of conversion of digital biomedical images to mineable data and the subsequent analysis of this data[101]. Texture analysis is an imaging technique under the wider arena of radiomics, that extracts, analyzes and interprets quantitative imaging features, and enables objective assessment of tumor heterogeneity beyond what is possible to human eyes[102]. In statistical-based model of texture analysis, from each voxel in a region of interest, various first order (*e.g.*, first-order entropy, kurtosis, skewness, standard deviation, mean intensity) and second order (*e.g.*, contrast, uniformity, second order entropy, *etc.*), or higher order features are extracted and analyzed using post processing software. As mentioned previously, tumor grade is an important prognostic factor of NENs and their prediction noninvasively is valuable.

CT radiomics is increasingly finding its place in the grading of NENs. Canellas *et al*[103], evaluating PNENs on CT scan, found that tumors with high entropy (a texture parameter reflecting tissue heterogeneity) values had 3.7 times higher odds of being aggressive (grades 2 and 3). In this study, entropy was a better predictor of tumor grade than the size of the lesion. Choi *et al*[104] found that lower kurtosis, lower sphericity and higher skewness correlated to grade 2 or 3 PNENs. A study on 3D texture analysis of PNENs in 100 patients showed that kurtosis was significantly different between all the three grades and entropy could differentiate grade 1 from grade 3 and grade 2 from grade 3, but not grade 1 from grade 2 tumors[50]. These results of CT texture analysis were confirmed in other recent studies [105,106] thus emphasizing its role in the prediction of tumor grade.

MRI radiomics also help in characterizing PNENs. MRI texture analysis was found to be useful in differentiating nonfunctioning PNEN from solid pseudopapillary neoplasm in a study by Li *et al*[107]. Nonlinear discriminant analysis was found to have the lowest misclassification rate of all the types of analyses performed in their study. Shindo *et al*[108] studied ADC histogram for differentiation of pancreatic adenocarcinoma from PNENs. In their study, ADC entropy had the highest area under the curve (AUC) for differentiating adenocarcinoma from NEN. De Robertis *et al*[77] found that ADC

Table 3 Summary of important research studies on imaging of gastroenteropancreatic neuroendocrine neoplasms

	Ref.	Number (*n*)	Modality	Results	Conclusion
Ultrasonography	Takada *et al* [25], 2019	30	Contrast-enhanced harmonic EUS	Three parameters in TIC showed high diagnostic accuracy: Echo intensity change - 87%; Rate of enhancement - 87%; Enhancement ratio for node/pancreatic parenchyma - 88.5%	Contrast-enhanced EUS and TIC analysis show high diagnostic accuracy for grading of PNEN
CT	Worhunsky *et al*[45], 2014	118	APCT	5-year overall survival: Hypoenhancing - 54%; Isoenhancing - 89%; Hyperenhancin - 93%. On multivariate analysis only hypoenhancement (HR 2.32, P = 0.02) was independently associated with survival	Hypoenhancement of PNEN on APCT (22% of well-differentiated PNEN) was an independent predictor of poor outcome
	Rodallec *et al*[46], 2006	37	Dual-phase contrast-enhanced CT	Poorly differentiated NEC: Hypoattenuating - 71%; Isoattenuating or weakly hyperattenuating - 29%; Well-differentiated NECmoderately or strongly hyperattenuating - 53%. Poor enhancement at pancreatic phase and less vascularized tumors were associated with decreased survival rate	Enhancement of PNEN at CT correlated with microscopic tumor vascularity. Low-enhancing PNEN correlated with poor differentiation and lower overall survival
	Park *et al* [48], 2020	69	Dynamic CT	NEC (compared to well-differentiated NEN): Significantly higher frequencies of main pancreatic ductal dilatation, bile duct dilatation, vascular invasion; Significantly lower conspicuity of interface between tumor and parenchyma, AER and PER. PER < 0.8 showed 94.1% sensitivity, 88.5% specificity for differentiation of NEC from well-differentiated NEN. On combining 3 significant CT features, the sensitivity and specificity for diagnosing NEC were 88.2% and 88.5% respectively	Tumor parenchyma enhancement ratio in portal phase is useful to distinguish NECs from well differentiated NENs. Combining qualitative and quantitative CT features aid in achieving good diagnostic accuracy in differentiation between NEC and well-differentiated NEN
	d'Assignies *et al*[59], 2009	36	MDCT perfusion	Tumor blood flow and intratumoral MVD showed high correlation (r = 0.620, P < 0.001). Blood flow was significantly higher in: Grade 1 than grade 2/3 tumors; Tumors with proliferation index ≤ 2% (P = 0.005); Tumors without histological signs of microscopic vascular involvement (P = 0.008). Mean transit time was longer in tumors with lymph node (P = 0.02) or liver (P = 0.05) metastasis	Perfusion CT is feasible in patients with pancreatic NENs and reflects MVD. Perfusion CT measurements correlated with histoprognostic factors, such as proliferation index and WHO grading
MRI	Canellas *et al*[103], 2018	80	MRI	MRI features associated with aggressive tumors: Size > 2 cm (OR = 4.8); T2 non-bright lesions (OR = 4.6); Presence of pancreatic ductal dilatation (OR = 4.9); Diffusion restriction (OR = 4.9)	MRI can assess aggressiveness of PNEN and identify patients at risk for early disease progression after surgical resection
	d'Assignies *et al*[74], 2013	59	MRI	DWI (71%-71.6%) was more sensitive than T2 weighted images (55.6%) and dynamic CEMRI (47.5%-48.1%). Combination of these sequences improved detection of liver metastases. Specificity of each sequence was comparable (89%-100%)	DWI is more sensitive for detection and characterization of liver metastases from NENs than T2-weighted and dynamic gadolinium-enhanced MRI
Radiomics, texture analysis and machine learning	Canellas *et al*[103], 2018	101	CECT with texture analysis	CT features predictive of a more aggressive tumor: Size > 2 cm (OR = 3.3); Vascular involvement (OR = 25.2); Pancreatic ductal dilatation (OR = 6); Lymphadenopathy (OR = 6.8); Entropy (OR = 3.7); Differences (P < 0.05) in progression free survival were found for: Grade 1 *vs* grade 2 *vs* grade 3 tumors; PNEN with vascular involvement; Tumors with entropy values > 4.65	CT texture analysis and CT features are predictive of aggressiveness and can be used to identify patients at risk of early disease progression after surgical resection
	De Robertis *et al*[77], 2018	42	MRI and histogram analysis	ADC entropy is significantly higher in grade 2/3 tumors (sensitivity: 83.3%, specificity: 61.1%). ADC kurtosis is higher in PNENs with vascular involvement, nodal and hepatic metastases (sensitivity: 85.7%, specificity: 74.3%)	Whole tumor ADC histogram analysis can predict aggressiveness in PNENs. ADC entropy and ADC kurtosis are the most accurate parameters for identification of PNEN with malignant behavior
	Luo *et al* [112], 2020	93	CECT with application of a CNN based DL algorithm	AUC = 0.81 of arterial phase in validation set was significantly higher than those of venous (AUC = 0.57, P = 0.03) and arterial/venous phase (AUC = 0.70, P = 0.03) in predicting the pathological grading of PNENs. The AUC and accuracy of DL algorithm for diagnosing grade 3 PNEN were 0.80% and 79.1%. There was significant difference in OS and PFS between the predicted G1/2 and G3 groups	The CNN-based DL method showed a relatively robust performance in predicting pathological grading of PNENs from CECT images
	Gao *et al*	96	CEMRI with	The average accuracy of the five trained CNNs	With the help of GAN, the CNN

	[114], 2019	application of deep learning algorithm on images	ranged between 79.08% and 82.35%, and the range of micro- average AUC was between 0.8825 and 0.8932. The average accuracy and micro-average AUC of the averaged CNN were 81.05% and 0.8847 respectively	showed the potential to predict the grades of PNENs on CEMRI

EUS: Enhanced ultrasonography; TIC: Time-signal intensity curve; APCT: Arterial phase computed tomography; ADC: Apparent diffusion coefficient; CECT: Contrast enhanced computed tomography; CEMRI: Contrast enhanced magnetic resonance imaging; CNN: Convolutional neural network; DWI: Diffusion weighted imaging; NEC: Neuroendocrine carcinoma; NEN: Neuroendocrine neoplasm; AER: Annual equivalent ratio; PER: Portal enhancement ratio; MVD: Microvascular density; WHO: World Health Organization; MDCT: Multidetector row computed tomography; OS: Overall survival; PFS: Progression free survival; AUC: Area under the curve; PNEN: Pancreatic neuroendocrine neoplasm; GAN: Generative Adversarial Network.

histogram analysis of DWI, using radiomics, could predict aggressiveness of PNENs. They found high ADC kurtosis values in tumors with vascular invasion (AUC of 0.763 for a cut off value of 4.13) and distant metastases (AUC of 0.820 for a cut off of 3.642)[77]. The future prospects of radiomics are in the direction of development of a robust predictive model combining qualitative and quantitative imaging parameters.

Machine learning is increasingly being used in medicine and has various applications including detection of disease, classification of images, identifying treatment and monitoring adherence to therapy [109,110]. The standard radiomics analysis on CT or MRI requires marking of the tumor margins for analysis. However, deep learning using convolutional neural network (CNN) performs analysis automatically and provides better results[111]. A few recent preliminary studies have shown the promising role of deep learning using CNN in the prediction of grade of PNEN and survival using contrast enhanced CT[112-114]. Clinical trials for translation of these imaging techniques into clinical practice and validation for routine use are ongoing.

In short, the quantitative parameters derived from imaging, relevant for prognostication of GEPNENs include tumor size, enhancement ratios derived from HU values, iodine uptake on DECT, entropy on CT texture analysis, tumor blood flow, tumor blood volume, and mean transit time on perfusion CT, ADC and ADC histogram analysis of DWI, true and pseudodiffusion coefficients and perfusion fraction on IVIM DWI, Ktrans and Kep on perfusion MRI and SUVmax on dual tracer PET/CT. A combination of qualitative features and quantitative factors with the newer functional imaging techniques enables better tumor classification based on their prognosis. A summary of important studies on advanced imaging in GEPNENs is shown in Table 3.

CONCLUSION

With the recent advances in CT, MRI, USG and hybrid imaging techniques like PET/CT and PET/MRI using dual tracers, smaller pancreatic and bowel NENs are now being increasingly detected and staged. In addition to tumor detection and staging, their non-invasive grading, prognostication and monitoring response to treatment are shown to be feasible and reliable with the emerging studies using quantitative imaging techniques like CT and MR perfusion studies, DWI, IVIM and texture analysis with radiomics. Standardization of these techniques with more large scale studies would be an important future prospect. These advances in imaging will help in making the right treatment choice, contributing to an overall improvement in patient outcome.

FOOTNOTES

Author contributions: Ramachandran A contributed to initial draft and revision; Madhusudhan KS contributed to review of draft and revision.

Conflict-of-interest statement: No conflict of interests.

Open-Access: This article is an open-access article that was selected by an in-house editor and fully peer-reviewed by external reviewers. It is distributed in accordance with the Creative Commons Attribution NonCommercial (CC BY-NC 4.0) license, which permits others to distribute, remix, adapt, build upon this work non-commercially, and license their derivative works on different terms, provided the original work is properly cited and the use is non-commercial. See: https://creativecommons.org/Licenses/by-nc/4.0/

Country/Territory of origin: India

ORCID number: Anupama Ramachandran 0000-0002-5808-6076; Kumble Seetharama Madhusudhan 0000-0001-8806-2625.

Corresponding Author's Membership in Professional Societies: Indian Radiological and Imaging Association, No.

501LM/D-285A.

S-Editor: Zhang H
L-Editor: Kerr C
P-Editor: Zhang H

REFERENCES

1 **Lawrence B**, Gustafsson BI, Chan A, Svejda B, Kidd M, Modlin IM. The epidemiology of gastroenteropancreatic neuroendocrine tumors. *Endocrinol Metab Clin North Am* 2011; **40**: 1-18, vii [PMID: 21349409 DOI: 10.1016/j.ecl.2010.12.005]
2 **Turaga KK**, Kvols LK. Recent progress in the understanding, diagnosis, and treatment of gastroenteropancreatic neuroendocrine tumors. *CA Cancer J Clin* 2011; **61**: 113-132 [PMID: 21388967 DOI: 10.3322/caac.20097]
3 **Modlin IM**, Lye KD, Kidd M. A 5-decade analysis of 13,715 carcinoid tumors. *Cancer* 2003; **97**: 934-959 [PMID: 12569593 DOI: 10.1002/cncr.11105]
4 **Sahani DV**, Bonaffini PA, Fernández-Del Castillo C, Blake MA. Gastroenteropancreatic neuroendocrine tumors: role of imaging in diagnosis and management. *Radiology* 2013; **266**: 38-61 [PMID: 23264526 DOI: 10.1148/radiol.12112512]
5 **Toumpanakis CG**, Caplin ME. Molecular genetics of gastroenteropancreatic neuroendocrine tumors. *Am J Gastroenterol* 2008; **103**: 729-732 [PMID: 18341492 DOI: 10.1111/j.1572-0241.2007.01777.x]
6 **Gallotti A**, Johnston RP, Bonaffini PA, Ingkakul T, Deshpande V, Fernández-del Castillo C, Sahani DV. Incidental neuroendocrine tumors of the pancreas: MDCT findings and features of malignancy. *AJR Am J Roentgenol* 2013; **200**: 355-362 [PMID: 23345357 DOI: 10.2214/AJR.11.8037]
7 **Nagtegaal ID**, Odze RD, Klimstra D, Paradis V, Rugge M, Schirmacher P, Washington KM, Carneiro F, Cree IA; WHO Classification of Tumours Editorial Board. The 2019 WHO classification of tumours of the digestive system. *Histopathology* 2020; **76**: 182-188 [PMID: 31433515 DOI: 10.1111/his.13975]
8 **Kunz PL**, Reidy-Lagunes D, Anthony LB, Bertino EM, Brendtro K, Chan JA, Chen H, Jensen RT, Kim MK, Klimstra DS, Kulke MH, Liu EH, Metz DC, Phan AT, Sippel RS, Strosberg JR, Yao JC; North American Neuroendocrine Tumor Society. Consensus guidelines for the management and treatment of neuroendocrine tumors. *Pancreas* 2013; **42**: 557-577 [PMID: 23591432 DOI: 10.1097/MPA.0b013e31828e34a4]
9 **Falconi M**, Eriksson B, Kaltsas G, Bartsch DK, Capdevila J, Caplin M, Kos-Kudla B, Kwekkeboom D, Rindi G, Klöppel G, Reed N, Kianmanesh R, Jensen RT; Vienna Consensus Conference participants. ENETS Consensus Guidelines Update for the Management of Patients with Functional Pancreatic Neuroendocrine Tumors and Non-Functional Pancreatic Neuroendocrine Tumors. *Neuroendocrinology* 2016; **103**: 153-171 [PMID: 26742109 DOI: 10.1159/000443171]
10 **Tan EH**, Tan CH. Imaging of gastroenteropancreatic neuroendocrine tumors. *World J Clin Oncol* 2011; **2**: 28-43 [PMID: 21603312 DOI: 10.5306/wjco.v2.i1.28]
11 **Modlin IM**, Oberg K, Chung DC, Jensen RT, de Herder WW, Thakker RV, Caplin M, Delle Fave G, Kaltsas GA, Krenning EP, Moss SF, Nilsson O, Rindi G, Salazar R, Ruszniewski P, Sundin A. Gastroenteropancreatic neuroendocrine tumours. *Lancet Oncol* 2008; **9**: 61-72 [PMID: 18177818 DOI: 10.1016/S1470-2045(07)70410-2]
12 **Giovannini M**. Contrast-enhanced and 3-dimensional endoscopic ultrasonography. *Gastroenterol Clin North Am* 2010; **39**: 845-858 [PMID: 21093759 DOI: 10.1016/j.gtc.2010.08.027]
13 **Takeda K**, Goto H, Hirooka Y, Itoh A, Hashimoto S, Niwa K, Hayakawa T. Contrast-enhanced transabdominal ultrasonography in the diagnosis of pancreatic mass lesions. *Acta Radiol* 2003; **44**: 103-106 [PMID: 12631008]
14 **Malagò R**, D'Onofrio M, Zamboni GA, Faccioli N, Falconi M, Boninsegna L, Mucelli RP. Contrast-enhanced sonography of nonfunctioning pancreatic neuroendocrine tumors. *AJR Am J Roentgenol* 2009; **192**: 424-430 [PMID: 19155405 DOI: 10.2214/AJR.07.4043]
15 **Del Prete M**, Di Sarno A, Modica R, Lassandro F, Giorgio A, Bianco A, Muto M, Gasperi M, Del Prete F, Colao A, Montesarchio V, Faggiano A; ENETS Centre of Excellence Multidisciplinary Group for Neuroendocrine Tumors in Naples (Italy). Role of contrast-enhanced ultrasound to define prognosis and predict response to biotherapy in pancreatic neuroendocrine tumors. *J Endocrinol Invest* 2017; **40**: 1373-1380 [PMID: 28667452 DOI: 10.1007/s40618-017-0723-x]
16 **Giovannini M**, Hookey LC, Bories E, Pesenti C, Monges G, Delpero JR. Endoscopic ultrasound elastography: the first step towards virtual biopsy? *Endoscopy* 2006; **38**: 344-348 [PMID: 16680632 DOI: 10.1055/s-2006-925158]
17 **Park MK**, Jo J, Kwon H, Cho JH, Oh JY, Noh MH, Nam KJ. Usefulness of acoustic radiation force impulse elastography in the differential diagnosis of benign and malignant solid pancreatic lesions. *Ultrasonography* 2014; **33**: 26-33 [PMID: 24936492 DOI: 10.14366/usg.13017]
18 **Uchida H**, Hirooka Y, Itoh A, Kawashima H, Hara K, Nonogaki K, Kasugai T, Ohno E, Ohmiya N, Niwa Y, Katano Y, Ishigami M, Goto H. Feasibility of tissue elastography using transcutaneous ultrasonography for the diagnosis of pancreatic diseases. *Pancreas* 2009; **38**: 17-22 [PMID: 18695627 DOI: 10.1097/MPA.0b013e318184db78]
19 **Hunt GC**, Faigel DO. Assessment of EUS for diagnosing, staging, and determining resectability of pancreatic cancer: a review. *Gastrointest Endosc* 2002; **55**: 232-237 [PMID: 11818928 DOI: 10.1067/mge.2002.121342]
20 **Legmann P**, Vignaux O, Dousset B, Baraza AJ, Palazzo L, Dumontier I, Coste J, Louvel A, Roseau G, Couturier D, Bonnin A. Pancreatic tumors: comparison of dual-phase helical CT and endoscopic sonography. *AJR Am J Roentgenol* 1998; **170**: 1315-1322 [PMID: 9574609 DOI: 10.2214/ajr.170.5.9574609]
21 **Rösch T**, Lightdale CJ, Botet JF, Boyce GA, Sivak MV Jr, Yasuda K, Heyder N, Palazzo L, Dancygier H, Schusdziarra V. Localization of pancreatic endocrine tumors by endoscopic ultrasonography. *N Engl J Med* 1992; **326**: 1721-1726 [PMID: 1317506 DOI: 10.1056/NEJM199206253262601]
22 **Kim MK**. Endoscopic ultrasound in gastroenteropancreatic neuroendocrine tumors. *Gut Liver* 2012; **6**: 405-410 [PMID:

23170141 DOI: 10.5009/gnl.2012.6.4.405]
23 **Anderson MA**, Carpenter S, Thompson NW, Nostrant TT, Elta GH, Scheiman JM. Endoscopic ultrasound is highly accurate and directs management in patients with neuroendocrine tumors of the pancreas. *Am J Gastroenterol* 2000; **95**: 2271-2277 [PMID: 11007228 DOI: 10.1111/j.1572-0241.2000.02480.x]
24 **Guo J**, Sahai AV, Teoh A, Arcidiacono PG, Larghi A, Saftoiu A, Siddiqui AA, Arturo Arias BL, Jenssen C, Adler DG, Lakhtakia S, Seo DW, Itokawa F, Giovannini M, Mishra G, Sabbagh L, Irisawa A, Iglesias-Garcia J, Poley JW, Vila JJ, Jesse L, Kubota K, Kalaitzakis E, Kida M, El-Nady M, Mukai SU, Ogura T, Fusaroli P, Vilmann P, Rai P, Nguyen NQ, Ponnudurai R, Achanta CR, Baron TH, Yasuda I, Wang HP, Hu J, Duan B, Bhutani MS, Sun S. An international, multi-institution survey on performing EUS-FNA and fine needle biopsy. *Endosc Ultrasound* 2020; **9**: 319-328 [PMID: 32883921 DOI: 10.4103/eus.eus_56_20]
25 **Takada S**, Kato H, Saragai Y, Muro S, Uchida D, Tomoda T, Matsumoto K, Horiguchi S, Tanaka N, Okada H. Contrast-enhanced harmonic endoscopic ultrasound using time-intensity curve analysis predicts pathological grade of pancreatic neuroendocrine neoplasm. *J Med Ultrason (2001)* 2019; **46**: 449-458 [PMID: 31377939 DOI: 10.1007/s10396-019-00967-x]
26 **Janssen J**, Schlörer E, Greiner L. EUS elastography of the pancreas: feasibility and pattern description of the normal pancreas, chronic pancreatitis, and focal pancreatic lesions. *Gastrointest Endosc* 2007; **65**: 971-978 [PMID: 17531630 DOI: 10.1016/j.gie.2006.12.057]
27 **Săftoiu A**, Vilmann P, Gorunescu F, Gheonea DI, Gorunescu M, Ciurea T, Popescu GL, Iordache A, Hassan H, Iordache S. Neural network analysis of dynamic sequences of EUS elastography used for the differential diagnosis of chronic pancreatitis and pancreatic cancer. *Gastrointest Endosc* 2008; **68**: 1086-1094 [PMID: 18656186 DOI: 10.1016/j.gie.2008.04.031]
28 **Hirche TO**, Ignee A, Barreiros AP, Schreiber-Dietrich D, Jungblut S, Ott M, Hirche H, Dietrich CF. Indications and limitations of endoscopic ultrasound elastography for evaluation of focal pancreatic lesions. *Endoscopy* 2008; **40**: 910-917 [PMID: 19009483 DOI: 10.1055/s-2008-1077726]
29 **Havre RF**, Ødegaard S, Gilja OH, Nesje LB. Characterization of solid focal pancreatic lesions using endoscopic ultrasonography with real-time elastography. *Scand J Gastroenterol* 2014; **49**: 742-751 [PMID: 24713038 DOI: 10.3109/00365521.2014.905627]
30 **Micames CG**, Gress FG. EUS elastography: a step ahead? *Gastrointest Endosc* 2007; **65**: 979-981 [PMID: 17531631 DOI: 10.1016/j.gie.2007.02.059]
31 **Ohno E**, Hirooka Y, Kawashima H, Ishikawa T. Feasibility of EUS-guided shear-wave measurement: A preliminary clinical study. *Endosc Ultrasound* 2019; **8**: 215-216 [PMID: 30924448 DOI: 10.4103/eus.eus_6_19]
32 **Yamashita Y**, Tanioka K, Kawaji Y, Tamura T, Nuta J, Hatamaru K, Itonaga M, Yoshida T, Ida Y, Maekita T, Iguchi M, Kitano M. Utility of Elastography with Endoscopic Ultrasonography Shear-Wave Measurement for Diagnosing Chronic Pancreatitis. *Gut Liver* 2020; **14**: 659-664 [PMID: 31722469 DOI: 10.5009/gnl19170]
33 **Ohno E**, Kawashima H, Ishikawa T, Iida T, Suzuki H, Uetsuki K, Yashika J, Yamada K, Yoshikawa M, Gibo N, Aoki T, Kataoka K, Mori H, Yamamura T, Furukawa K, Nakamura M, Hirooka Y, Fujishiro M. Diagnostic performance of endoscopic ultrasonography-guided elastography for solid pancreatic lesions: Shear-wave measurements versus strain elastography with histogram analysis. *Dig Endosc* 2021; **33**: 629-638 [PMID: 32662150 DOI: 10.1111/den.13791]
34 **Manguso N**, Gangi A, Johnson J, Harit A, Nissen N, Jamil L, Lo S, Wachsman A, Hendifar A, Amersi F. The role of pre-operative imaging and double balloon enteroscopy in the surgical management of small bowel neuroendocrine tumors: Is it necessary? *J Surg Oncol* 2018; **117**: 207-212 [PMID: 28940412 DOI: 10.1002/jso.24825]
35 **Malla S**, Kumar P, Madhusudhan KS. Radiology of the neuroendocrine neoplasms of the gastrointestinal tract: a comprehensive review. *Abdom Radiol (NY)* 2021; **46**: 919-935 [PMID: 32960304 DOI: 10.1007/s00261-020-02773-3]
36 **Bonekamp D**, Raman SP, Horton KM, Fishman EK. Role of computed tomography angiography in detection and staging of small bowel carcinoid tumors. *World J Radiol* 2015; **7**: 220-235 [PMID: 26435774 DOI: 10.4329/wjr.v7.i9.220]
37 **Kamaoui I**, De-Luca V, Ficarelli S, Mennesson N, Lombard-Bohas C, Pilleul F. Value of CT enteroclysis in suspected small-bowel carcinoid tumors. *AJR Am J Roentgenol* 2010; **194**: 629-633 [PMID: 20173138 DOI: 10.2214/AJR.09.2760]
38 **Hakim FA**, Alexander JA, Huprich JE, Grover M, Enders FT. CT-enterography may identify small bowel tumors not detected by capsule endoscopy: eight years experience at Mayo Clinic Rochester. *Dig Dis Sci* 2011; **56**: 2914-2919 [PMID: 21735085 DOI: 10.1007/s10620-011-1773-0]
39 **Huprich JE**, Fletcher JG, Fidler JL, Alexander JA, Guimarães LS, Siddiki HA, McCollough CH. Prospective blinded comparison of wireless capsule endoscopy and multiphase CT enterography in obscure gastrointestinal bleeding. *Radiology* 2011; **260**: 744-751 [PMID: 21642417 DOI: 10.1148/radiol.11110143]
40 **Dromain C**, de Baere T, Baudin E, Galline J, Ducreux M, Boige V, Duvillard P, Laplanche A, Caillet H, Lasser P, Schlumberger M, Sigal R. MR imaging of hepatic metastases caused by neuroendocrine tumors: comparing four techniques. *AJR Am J Roentgenol* 2003; **180**: 121-128 [PMID: 12490490 DOI: 10.2214/ajr.180.1.1800121]
41 **Paulson EK**, McDermott VG, Keogan MT, DeLong DM, Frederick MG, Nelson RC. Carcinoid metastases to the liver: role of triple-phase helical CT. *Radiology* 1998; **206**: 143-150 [PMID: 9423664 DOI: 10.1148/radiology.206.1.9423664]
42 **Horton KM**, Kamel I, Hofmann L, Fishman EK. Carcinoid tumors of the small bowel: a multitechnique imaging approach. *AJR Am J Roentgenol* 2004; **182**: 559-567 [PMID: 14975946 DOI: 10.2214/ajr.182.3.1820559]
43 **Manfredi R**, Bonatti M, Mantovani W, Graziani R, Segala D, Capelli P, Butturini G, Mucelli RP. Non-hyperfunctioning neuroendocrine tumours of the pancreas: MR imaging appearance and correlation with their biological behaviour. *Eur Radiol* 2013; **23**: 3029-3039 [PMID: 23793519 DOI: 10.1007/s00330-013-2929-4]
44 **Humphrey PE**, Alessandrino F, Bellizzi AM, Mortele KJ. Non-hyperfunctioning pancreatic endocrine tumors: multimodality imaging features with histopathological correlation. *Abdom Imaging* 2015; **40**: 2398-2410 [PMID: 25989932 DOI: 10.1007/s00261-015-0458-0]
45 **Worhunsky DJ**, Krampitz GW, Poullos PD, Visser BC, Kunz PL, Fisher GA, Norton JA, Poultsides GA. Pancreatic neuroendocrine tumours: hypoenhancement on arterial phase computed tomography predicts biological aggressiveness. *HPB (Oxford)* 2014; **16**: 304-311 [PMID: 23991643 DOI: 10.1111/hpb.12139]

46 **Rodallec M**, Vilgrain V, Couvelard A, Rufat P, O'Toole D, Barrau V, Sauvanet A, Ruszniewski P, Menu Y. Endocrine pancreatic tumours and helical CT: contrast enhancement is correlated with microvascular density, histoprognostic factors and survival. *Pancreatology* 2006; **6**: 77-85 [PMID: 16327283 DOI: 10.1159/000090026]

47 **Kim DW**, Kim HJ, Kim KW, Byun JH, Song KB, Kim JH, Hong SM. Neuroendocrine neoplasms of the pancreas at dynamic enhanced CT: comparison between grade 3 neuroendocrine carcinoma and grade 1/2 neuroendocrine tumour. *Eur Radiol* 2015; **25**: 1375-1383 [PMID: 25465713 DOI: 10.1007/s00330-014-3532-z]

48 **Park HJ**, Kim HJ, Kim KW, Kim SY, Choi SH, You MW, Hwang HS, Hong SM. Comparison between neuroendocrine carcinomas and well-differentiated neuroendocrine tumors of the pancreas using dynamic enhanced CT. *Eur Radiol* 2020; **30**: 4772-4782 [PMID: 32346794 DOI: 10.1007/s00330-020-06867-w]

49 **Yamada S**, Fujii T, Suzuki K, Inokawa Y, Kanda M, Nakayama G, Sugimoto H, Koike M, Nomoto S, Fujiwara M, Nakao A, Kodera Y. Preoperative Identification of a Prognostic Factor for Pancreatic Neuroendocrine Tumors Using Multiphase Contrast-Enhanced Computed Tomography. *Pancreas* 2016; **45**: 198-203 [PMID: 26390421 DOI: 10.1097/MPA.0000000000000443]

50 **D'Onofrio M**, Ciaravino V, Cardobi N, De Robertis R, Cingarlini S, Landoni L, Capelli P, Bassi C, Scarpa A. CT Enhancement and 3D Texture Analysis of Pancreatic Neuroendocrine Neoplasms. *Sci Rep* 2019; **9**: 2176 [PMID: 30778137 DOI: 10.1038/s41598-018-38459-6]

51 **Hardie AD**, Picard MM, Camp ER, Perry JD, Suranyi P, De Cecco CN, Schoepf UJ, Wichmann JL. Application of an Advanced Image-Based Virtual Monoenergetic Reconstruction of Dual Source Dual-Energy CT Data at Low keV Increases Image Quality for Routine Pancreas Imaging. *J Comput Assist Tomogr* 2015; **39**: 716-720 [PMID: 26196343 DOI: 10.1097/RCT.0000000000000276]

52 **Lin XZ**, Wu ZY, Tao R, Guo Y, Li JY, Zhang J, Chen KM. Dual energy spectral CT imaging of insulinoma-Value in preoperative diagnosis compared with conventional multi-detector CT. *Eur J Radiol* 2012; **81**: 2487-2494 [PMID: 22153746 DOI: 10.1016/j.ejrad.2011.10.028]

53 **Kaltenbach B**, Wichmann JL, Pfeifer S, Albrecht MH, Booz C, Lenga L, Hammerstingl R, D'Angelo T, Vogl TJ, Martin SS. Iodine quantification to distinguish hepatic neuroendocrine tumor metastasis from hepatocellular carcinoma at dual-source dual-energy liver CT. *Eur J Radiol* 2018; **105**: 20-24 [PMID: 30017280 DOI: 10.1016/j.ejrad.2018.05.019]

54 **Kambadakone AR**, Sahani DV. Body perfusion CT: technique, clinical applications, and advances. *Radiol Clin North Am* 2009; **47**: 161-178 [PMID: 19195541 DOI: 10.1016/j.rcl.2008.11.003]

55 **Sinitsyn V**. Analysis and Interpretation of Perfusion CT in Oncology: Type of Cancer Matters. *Radiology* 2019; **292**: 636-637 [PMID: 31287775 DOI: 10.1148/radiol.2019191265]

56 **Marion-Audibert AM**, Barel C, Gouysse G, Dumortier J, Pilleul F, Pourreyron C, Hervieu V, Poncet G, Lombard-Bohas C, Chayvialle JA, Partensky C, Scoazec JY. Low microvessel density is an unfavorable histoprognostic factor in pancreatic endocrine tumors. *Gastroenterology* 2003; **125**: 1094-1104 [PMID: 14517793 DOI: 10.1016/s0016-5085(03)01198-3]

57 **Couvelard A**, O'Toole D, Turley H, Leek R, Sauvanet A, Degott C, Ruszniewski P, Belghiti J, Harris AL, Gatter K, Pezzella F. Microvascular density and hypoxia-inducible factor pathway in pancreatic endocrine tumours: negative correlation of microvascular density and VEGF expression with tumour progression. *Br J Cancer* 2005; **92**: 94-101 [PMID: 15558070 DOI: 10.1038/sj.bjc.6602245]

58 **Takahashi Y**, Akishima-Fukasawa Y, Kobayashi N, Sano T, Kosuge T, Nimura Y, Kanai Y, Hiraoka N. Prognostic value of tumor architecture, tumor-associated vascular characteristics, and expression of angiogenic molecules in pancreatic endocrine tumors. *Clin Cancer Res* 2007; **13**: 187-196 [PMID: 17200354 DOI: 10.1158/1078-0432.CCR-06-1408]

59 **d'Assignies G**, Couvelard A, Bahrami S, Vullierme MP, Hammel P, Hentic O, Sauvanet A, Bedossa P, Ruszniewski P, Vilgrain V. Pancreatic endocrine tumors: tumor blood flow assessed with perfusion CT reflects angiogenesis and correlates with prognostic factors. *Radiology* 2009; **250**: 407-416 [PMID: 19095784 DOI: 10.1148/radiol.2501080291]

60 **Zhu L**, Wu WM, Xue HD, Liu W, Wang X, Sun H, Li P, Zhao YP, Jin ZY. Sporadic insulinomas on volume perfusion CT: dynamic enhancement patterns and timing of optimal tumour-parenchyma contrast. *Eur Radiol* 2017; **27**: 3491-3498 [PMID: 28108839 DOI: 10.1007/s00330-016-4709-4]

61 **Zhu L**, Xue H, Sun H, Wang X, Wu W, Jin Z, Zhao Y. Insulinoma Detection With MDCT: Is There a Role for Whole-Pancreas Perfusion? *AJR Am J Roentgenol* 2017; **208**: 306-314 [PMID: 27929662 DOI: 10.2214/AJR.16.16351]

62 **Wan Y**, Hao H, Meng S, Li Z, Yu F, Meng Chi, Chao Q, Gao J. Application of low dose pancreas perfusion CT combined with enhancement scanning in diagnosis of pancreatic neuroendocrine tumors. *Pancreatology* 2021; **21**: 240-245 [PMID: 33191144 DOI: 10.1016/j.pan.2020.10.046]

63 **Ng CS**, Charnsangavej C, Wei W, Yao JC. Perfusion CT findings in patients with metastatic carcinoid tumors undergoing bevacizumab and interferon therapy. *AJR Am J Roentgenol* 2011; **196**: 569-576 [PMID: 21343498 DOI: 10.2214/AJR.10.4455]

64 **Ng CS**, Wei W, Duran C, Ghosh P, Anderson EF, Chandler AG, Yao JC. CT perfusion in normal liver and liver metastases from neuroendocrine tumors treated with targeted antivascular agents. *Abdom Radiol (NY)* 2018; **43**: 1661-1669 [PMID: 29075824 DOI: 10.1007/s00261-017-1367-1]

65 **Ketelsen D**, Horger M, Buchgeister M, Fenchel M, Thomas C, Boehringer N, Schulze M, Tsiflikas I, Claussen CD, Heuschmid M. Estimation of radiation exposure of 128-slice 4D-perfusion CT for the assessment of tumor vascularity. *Korean J Radiol* 2010; **11**: 547-552 [PMID: 20808699 DOI: 10.3348/kjr.2010.11.5.547]

66 **Dromain C**, de Baere T, Lumbroso J, Caillet H, Laplanche A, Boige V, Ducreux M, Duvillard P, Elias D, Schlumberger M, Sigal R, Baudin E. Detection of liver metastases from endocrine tumors: a prospective comparison of somatostatin receptor scintigraphy, computed tomography, and magnetic resonance imaging. *J Clin Oncol* 2005; **23**: 70-78 [PMID: 15625361 DOI: 10.1200/JCO.2005.01.013]

67 **Waldmann J**, Fendrich V, Habbe N, Bartsch DK, Slater EP, Kann PH, Rothmund M, Langer P. Screening of patients with multiple endocrine neoplasia type 1 (MEN-1): a critical analysis of its value. *World J Surg* 2009; **33**: 1208-1218 [PMID: 19350320 DOI: 10.1007/s00268-009-9983-8]

68 **Sundin A**, Vullierme MP, Kaltsas G, Plöckinger U; Mallorca Consensus Conference participants; European

Neuroendocrine Tumor Society. ENETS Consensus Guidelines for the Standards of Care in Neuroendocrine Tumors: radiological examinations. *Neuroendocrinology* 2009; **90**: 167-183 [PMID: 19077417 DOI: 10.1159/000184855]

69 **Wang Y**, Chen ZE, Yaghmai V, Nikolaidis P, McCarthy RJ, Merrick L, Miller FH. Diffusion-weighted MR imaging in pancreatic endocrine tumors correlated with histopathologic characteristics. *J Magn Reson Imaging* 2011; **33**: 1071-1079 [PMID: 21509863 DOI: 10.1002/jmri.22541]

70 **Jang KM**, Kim SH, Lee SJ, Choi D. The value of gadoxetic acid-enhanced and diffusion-weighted MRI for prediction of grading of pancreatic neuroendocrine tumors. *Acta Radiol* 2014; **55**: 140-148 [PMID: 23897307 DOI: 10.1177/0284185113494982]

71 **Lotfalizadeh E**, Ronot M, Wagner M, Cros J, Couvelard A, Vullierme MP, Allaham W, Hentic O, Ruzniewski P, Vilgrain V. Prediction of pancreatic neuroendocrine tumour grade with MR imaging features: added value of diffusion-weighted imaging. *Eur Radiol* 2017; **27**: 1748-1759 [PMID: 27543074 DOI: 10.1007/s00330-016-4539-4]

72 **Parikh T**, Drew SJ, Lee VS, Wong S, Hecht EM, Babb JS, Taouli B. Focal liver lesion detection and characterization with diffusion-weighted MR imaging: comparison with standard breath-hold T2-weighted imaging. *Radiology* 2008; **246**: 812-822 [PMID: 18223123 DOI: 10.1148/radiol.2463070432]

73 **Soyer P**, Boudiaf M, Placé V, Sirol M, Pautrat K, Vignaud A, Staub F, Tiah D, Hamzi L, Duchat F, Fargeaudou Y, Pocard M. Preoperative detection of hepatic metastases: comparison of diffusion-weighted, T2-weighted fast spin echo and gadolinium-enhanced MR imaging using surgical and histopathologic findings as standard of reference. *Eur J Radiol* 2011; **80**: 245-252 [PMID: 20650588 DOI: 10.1016/j.ejrad.2010.06.027]

74 **d'Assignies G**, Fina P, Bruno O, Vullierme MP, Tubach F, Paradis V, Sauvanet A, Ruszniewski P, Vilgrain V. High sensitivity of diffusion-weighted MR imaging for the detection of liver metastases from neuroendocrine tumors: comparison with T2-weighted and dynamic gadolinium-enhanced MR imaging. *Radiology* 2013; **268**: 390-399 [PMID: 23533288 DOI: 10.1148/radiol.13121628]

75 **Besa C**, Ward S, Cui Y, Jajamovich G, Kim M, Taouli B. Neuroendocrine liver metastases: Value of apparent diffusion coefficient and enhancement ratios for characterization of histopathologic grade. *J Magn Reson Imaging* 2016; **44**: 1432-1441 [PMID: 27227756 DOI: 10.1002/jmri.25320]

76 **Pereira JA**, Rosado E, Bali M, Metens T, Chao SL. Pancreatic neuroendocrine tumors: correlation between histogram analysis of apparent diffusion coefficient maps and tumor grade. *Abdom Imaging* 2015; **40**: 3122-3128 [PMID: 26280127 DOI: 10.1007/s00261-015-0524-7]

77 **De Robertis R**, Maris B, Cardobi N, Tinazzi Martini P, Gobbo S, Capelli P, Ortolani S, Cingarlini S, Paiella S, Landoni L, Butturini G, Regi P, Scarpa A, Tortora G, D'Onofrio M. Can histogram analysis of MR images predict aggressiveness in pancreatic neuroendocrine tumors? *Eur Radiol* 2018; **28**: 2582-2591 [PMID: 29352378 DOI: 10.1007/s00330-017-5236-7]

78 **Le Bihan D**, Breton E, Lallemand D, Grenier P, Cabanis E, Laval-Jeantet M. MR imaging of intravoxel incoherent motions: application to diffusion and perfusion in neurologic disorders. *Radiology* 1986; **161**: 401-407 [PMID: 3763909 DOI: 10.1148/radiology.161.2.3763909]

79 **Katharina Ingenerf M**, Karim H, Fink N, Ilhan H, Ricke J, Treitl KM, Schmid-Tannwald C. Apparent diffusion coefficients (ADC) in response assessment of transarterial radioembolization (TARE) for liver metastases of neuroendocrine tumors (NET): a feasibility study. *Acta Radiol* 2021; 2841851211024004 [PMID: 34225464 DOI: 10.1177/02841851211024004]

80 **Hwang EJ**, Lee JM, Yoon JH, Kim JH, Han JK, Choi BI, Lee KB, Jang JY, Kim SW, Nickel MD, Kiefer B. Intravoxel incoherent motion diffusion-weighted imaging of pancreatic neuroendocrine tumors: prediction of the histologic grade using pure diffusion coefficient and tumor size. *Invest Radiol* 2014; **49**: 396-402 [PMID: 24500090 DOI: 10.1097/RLI.0000000000000028]

81 **Ma W**, Wei M, Han Z, Tang Y, Pan Q, Zhang G, Ren J, Huan Y, Li N. The added value of intravoxel incoherent motion diffusion weighted imaging parameters in differentiating high-grade pancreatic neuroendocrine neoplasms from pancreatic ductal adenocarcinoma. *Oncol Lett* 2019; **18**: 5448-5458 [PMID: 31612053 DOI: 10.3892/ol.2019.10863]

82 **Rosenkrantz AB**, Padhani AR, Chenevert TL, Koh DM, De Keyzer F, Taouli B, Le Bihan D. Body diffusion kurtosis imaging: Basic principles, applications, and considerations for clinical practice. *J Magn Reson Imaging* 2015; **42**: 1190-1202 [PMID: 26119267 DOI: 10.1002/jmri.24985]

83 **Shi YJ**, Zhu HT, Liu YL, Wei YY, Qin XB, Zhang XY, Li XT, Sun YS. Radiomics Analysis Based on Diffusion Kurtosis Imaging and T2 Weighted Imaging for Differentiation of Pancreatic Neuroendocrine Tumors From Solid Pseudopapillary Tumors. *Front Oncol* 2020; **10**: 1624 [PMID: 32974201 DOI: 10.3389/fonc.2020.01624]

84 **Kartalis N**, Manikis GC, Loizou L, Albiin N, Zöllner FG, Del Chiaro M, Marias K, Papanikolaou N. Diffusion-weighted MR imaging of pancreatic cancer: A comparison of mono-exponential, bi-exponential and non-Gaussian kurtosis models. *Eur J Radiol Open* 2016; **3**: 79-85 [PMID: 27957518 DOI: 10.1016/j.ejro.2016.04.002]

85 **Pasicz K**, Podgórska J, Jasieniak J, Fabiszewska E, Skrzyński W, Anysz-Grodzicka A, Cieszanowski A, Kukołowicz P, Grabska I. Optimal b-values for diffusion kurtosis imaging of the liver and pancreas in MR examinations. *Phys Med* 2019; **66**: 119-123 [PMID: 31600671 DOI: 10.1016/j.ejmp.2019.09.238]

86 **Steinkohl E**, Bertoli D, Hansen TM, Olesen SS, Drewes AM, Frøkjær JB. Practical and clinical applications of pancreatic magnetic resonance elastography: a systematic review. *Abdom Radiol (NY)* 2021; **46**: 4744-4764 [PMID: 34076721 DOI: 10.1007/s00261-021-03143-3]

87 **Shi Y**, Gao F, Li Y, Tao S, Yu B, Liu Z, Liu Y, Glaser KJ, Ehman RL, Guo Q. Differentiation of benign and malignant solid pancreatic masses using magnetic resonance elastography with spin-echo echo planar imaging and three-dimensional inversion reconstruction: a prospective study. *Eur Radiol* 2018; **28**: 936-945 [PMID: 28986646 DOI: 10.1007/s00330-017-5062-y]

88 **Madhuranthakam AJ**, Yuan Q, Pedrosa I. Quantitative Methods in Abdominal MRI: Perfusion Imaging. *Top Magn Reson Imaging* 2017; **26**: 251-258 [PMID: 29176470 DOI: 10.1097/RMR.0000000000000145]

89 **Tofts PS**, Brix G, Buckley DL, Evelhoch JL, Henderson E, Knopp MV, Larsson HB, Lee TY, Mayr NA, Parker GJ, Port RE, Taylor J, Weisskoff RM. Estimating kinetic parameters from dynamic contrast-enhanced T(1)-weighted MRI of a

diffusable tracer: standardized quantities and symbols. *J Magn Reson Imaging* 1999; **10**: 223-232 [PMID: 10508281 DOI: 10.1002/(sici)1522-2586(199909)10:3<223::aid-jmri2>3.0.co;2-s]

90 **Donati F**, Boraschi P, Cervelli R, Pacciardi F, Lombardo C, Boggi U, Falaschi F, Caramella D. 3 T MR perfusion of solid pancreatic lesions using dynamic contrast-enhanced DISCO sequence: Usefulness of qualitative and quantitative analyses in a pilot study. *Magn Reson Imaging* 2019; **59**: 105-113 [PMID: 30878601 DOI: 10.1016/j.mri.2019.03.001]

91 **Kim JH**, Lee JM, Park JH, Kim SC, Joo I, Han JK, Choi BI. Solid pancreatic lesions: characterization by using timing bolus dynamic contrast-enhanced MR imaging assessment--a preliminary study. *Radiology* 2013; **266**: 185-196 [PMID: 23192779 DOI: 10.1148/radiol.12120111]

92 **Huh J**, Choi Y, Woo DC, Seo N, Kim B, Lee CK, Kim IS, Nickel D, Kim KW. Feasibility of test-bolus DCE-MRI using CAIPIRINHA-VIBE for the evaluation of pancreatic malignancies. *Eur Radiol* 2016; **26**: 3949-3956 [PMID: 26809293 DOI: 10.1007/s00330-016-4209-6]

93 **Basu B**, Basu S. Correlating and Combining Genomic and Proteomic Assessment with In Vivo Molecular Functional Imaging: Will This Be the Future Roadmap for Personalized Cancer Management? *Cancer Biother Radiopharm* 2016; **31**: 75-84 [PMID: 27093341 DOI: 10.1089/cbr.2015.1922]

94 **Binderup T**, Knigge U, Loft A, Federspiel B, Kjaer A. 18F-fluorodeoxyglucose positron emission tomography predicts survival of patients with neuroendocrine tumors. *Clin Cancer Res* 2010; **16**: 978-985 [PMID: 20103666 DOI: 10.1158/1078-0432.CCR-09-1759]

95 **Zhang P**, Yu J, Li J, Shen L, Li N, Zhu H, Zhai S, Zhang Y, Yang Z, Lu M. Clinical and Prognostic Value of PET/CT Imaging with Combination of ^{68}Ga-DOTATATE and ^{18}F-FDG in Gastroenteropancreatic Neuroendocrine Neoplasms. *Contrast Media Mol Imaging* 2018; **2018**: 2340389 [PMID: 29681780 DOI: 10.1155/2018/2340389]

96 **Reubi JC**, Waser B. Concomitant expression of several peptide receptors in neuroendocrine tumours: molecular basis for in vivo multireceptor tumour targeting. *Eur J Nucl Med Mol Imaging* 2003; **30**: 781-793 [PMID: 12707737 DOI: 10.1007/s00259-003-1184-3]

97 **Antwi K**, Fani M, Heye T, Nicolas G, Rottenburger C, Kaul F, Merkle E, Zech CJ, Boll D, Vogt DR, Gloor B, Christ E, Wild D. Comparison of glucagon-like peptide-1 receptor (GLP-1R) PET/CT, SPECT/CT and 3T MRI for the localisation of occult insulinomas: evaluation of diagnostic accuracy in a prospective crossover imaging study. *Eur J Nucl Med Mol Imaging* 2018; **45**: 2318-2327 [PMID: 30054698 DOI: 10.1007/s00259-018-4101-5]

98 **Regazzo D**, Barbot M, Scaroni C, Albiger N, Occhi G. The pathogenic role of the GIP/GIPR axis in human endocrine tumors: emerging clinical mechanisms beyond diabetes. *Rev Endocr Metab Disord* 2020; **21**: 165-183 [PMID: 31933128 DOI: 10.1007/s11154-019-09536-6]

99 **Beiderwellen KJ**, Poeppel TD, Hartung-Knemeyer V, Buchbender C, Kuehl H, Bockisch A, Lauenstein TC. Simultaneous 68Ga-DOTATOC PET/MRI in patients with gastroenteropancreatic neuroendocrine tumors: initial results. *Invest Radiol* 2013; **48**: 273-279 [PMID: 23493121 DOI: 10.1097/RLI.0b013e3182871a7f]

100 **Hope TA**, Pampaloni MH, Nakakura E, VanBrocklin H, Slater J, Jivan S, Aparici CM, Yee J, Bergsland E. Simultaneous (68)Ga-DOTA-TOC PET/MRI with gadoxetate disodium in patients with neuroendocrine tumor. *Abdom Imaging* 2015; **40**: 1432-1440 [PMID: 25820755 DOI: 10.1007/s00261-015-0409-9]

101 **Gillies RJ**, Kinahan PE, Hricak H. Radiomics: Images Are More than Pictures, They Are Data. *Radiology* 2016; **278**: 563-577 [PMID: 26579733 DOI: 10.1148/radiol.2015151169]

102 **Lubner MG**, Smith AD, Sandrasegaran K, Sahani DV, Pickhardt PJ. CT Texture Analysis: Definitions, Applications, Biologic Correlates, and Challenges. *Radiographics* 2017; **37**: 1483-1503 [PMID: 28898189 DOI: 10.1148/rg.2017170056]

103 **Canellas R**, Burk KS, Parakh A, Sahani DV. Prediction of Pancreatic Neuroendocrine Tumor Grade Based on CT Features and Texture Analysis. *AJR Am J Roentgenol* 2018; **210**: 341-346 [PMID: 29140113 DOI: 10.2214/AJR.17.18417]

104 **Choi TW**, Kim JH, Yu MH, Park SJ, Han JK. Pancreatic neuroendocrine tumor: prediction of the tumor grade using CT findings and computerized texture analysis. *Acta Radiol* 2018; **59**: 383-392 [PMID: 28766979 DOI: 10.1177/0284185117725367]

105 **Guo C**, Zhuge X, Wang Z, Wang Q, Sun K, Feng Z, Chen X. Textural analysis on contrast-enhanced CT in pancreatic neuroendocrine neoplasms: association with WHO grade. *Abdom Radiol (NY)* 2019; **44**: 576-585 [PMID: 30182253 DOI: 10.1007/s00261-018-1763-1]

106 **Reinert CP**, Baumgartner K, Hepp T, Bitzer M, Horger M. Complementary role of computed tomography texture analysis for differentiation of pancreatic ductal adenocarcinoma from pancreatic neuroendocrine tumors in the portal-venous enhancement phase. *Abdom Radiol (NY)* 2020; **45**: 750-758 [PMID: 31953587 DOI: 10.1007/s00261-020-02406-9]

107 **Li X**, Zhu H, Qian X, Chen N, Lin X. MRI Texture Analysis for Differentiating Nonfunctional Pancreatic Neuroendocrine Neoplasms From Solid Pseudopapillary Neoplasms of the Pancreas. *Acad Radiol* 2020; **27**: 815-823 [PMID: 31444110 DOI: 10.1016/j.acra.2019.07.012]

108 **Shindo T**, Fukukura Y, Umanodan T, Takumi K, Hakamada H, Nakajo M, Umanodan A, Ideue J, Kamimura K, Yoshiura T. Histogram Analysis of Apparent Diffusion Coefficient in Differentiating Pancreatic Adenocarcinoma and Neuroendocrine Tumor. *Medicine (Baltimore)* 2016; **95**: e2574 [PMID: 26825900 DOI: 10.1097/MD.0000000000002574]

109 **Jordan MI**, Mitchell TM. Machine learning: Trends, perspectives, and prospects. *Science* 2015; **349**: 255-260 [PMID: 26185243 DOI: 10.1126/science.aaa8415]

110 **Briganti G**, Le Moine O. Artificial Intelligence in Medicine: Today and Tomorrow. *Front Med (Lausanne)* 2020; **7**: 27 [PMID: 32118012 DOI: 10.3389/fmed.2020.00027]

111 **Yasaka K**, Akai H, Abe O, Kiryu S. Deep Learning with Convolutional Neural Network for Differentiation of Liver Masses at Dynamic Contrast-enhanced CT: A Preliminary Study. *Radiology* 2018; **286**: 887-896 [PMID: 29059036 DOI: 10.1148/radiol.2017170706]

112 **Luo Y**, Chen X, Chen J, Song C, Shen J, Xiao H, Chen M, Li ZP, Huang B, Feng ST. Preoperative Prediction of Pancreatic Neuroendocrine Neoplasms Grading Based on Enhanced Computed Tomography Imaging: Validation of Deep Learning with a Convolutional Neural Network. *Neuroendocrinology* 2020; **110**: 338-350 [PMID: 31525737 DOI:

10.1159/000503291]

113 **Zhou RQ**, Ji HC, Liu Q, Zhu CY, Liu R. Leveraging machine learning techniques for predicting pancreatic neuroendocrine tumor grades using biochemical and tumor markers. *World J Clin Cases* 2019; **7**: 1611-1622 [PMID: 31367620 DOI: 10.12998/wjcc.v7.i13.1611]

114 **Gao X**, Wang X. Deep learning for World Health Organization grades of pancreatic neuroendocrine tumors on contrast-enhanced magnetic resonance images: a preliminary study. *Int J Comput Assist Radiol Surg* 2019; **14**: 1981-1991 [PMID: 31555998 DOI: 10.1007/s11548-019-02070-5]

World Journal of Gastroenterology

Submit a Manuscript: https://www.f6publishing.com

World J Gastroenterol 2022 July 14; 28(26): 3027-3046

DOI: 10.3748/wjg.v28.i26.3027

ISSN 1007-9327 (print) ISSN 2219-2840 (online)

REVIEW

Tumor microenvironment involvement in colorectal cancer progression *via* Wnt/β-catenin pathway: Providing understanding of the complex mechanisms of chemoresistance

María Belén Novoa Díaz, María Julia Martín, Claudia Gentili

Specialty type: Gastroenterology and hepatology

Provenance and peer review: Invited article; Externally peer reviewed.

Peer-review model: Single blind

Peer-review report's scientific quality classification

Grade A (Excellent): 0
Grade B (Very good): B, B, B, B
Grade C (Good): C
Grade D (Fair): 0
Grade E (Poor): 0

P-Reviewer: Koustas E, Greece; Pan JS, China; Rahimi-Movaghar E, Iran; Scurtu RR, Romania; Ying HQ, China

Received: December 21, 2021
Peer-review started: December 21, 2021
First decision: March 10, 2022
Revised: April 29, 2022
Accepted: June 20, 2022
Article in press: June 20, 2022
Published online: July 14, 2022

María Belén Novoa Díaz, María Julia Martín, Claudia Gentili, Departamento de Biología, Bioquímica y Farmacia, Universidad Nacional del Sur (UNS)-INBIOSUR (CONICET-UNS), Bahía Blanca 8000, Argentina

María Julia Martín, Departamento de Química, Universidad Nacional del Sur (UNS)-INQUISUR (CONICET-UNS), Bahía Blanca 8000, Argentina

Corresponding author: María Julia Martín, PhD, Research Assistant, Departamento de Biología, Bioquímica y Farmacia, Universidad Nacional del Sur (UNS)-INBIOSUR (CONICET-UNS), San Juan 670, Bahía Blanca 8000, Argentina. julia.martin@uns.edu.ar

Abstract

Colorectal cancer (CRC) continues to be one of the main causes of death from cancer because patients progress unfavorably due to resistance to current therapies. Dysregulation of the Wnt/β-catenin pathway plays a fundamental role in the genesis and progression of several types of cancer, including CRC. In many subtypes of CRC, hyperactivation of the β-catenin pathway is associated with mutations of the *adenomatous polyposis coli* gene. However, it can also be associated with other causes. In recent years, studies of the tumor microenvironment (TME) have demonstrated its importance in the development and progression of CRC. In this tumor nest, several cell types, structures, and biomolecules interact with neoplastic cells to pave the way for the spread of the disease. Cross-communications between tumor cells and the TME are then established primarily through paracrine factors, which trigger the activation of numerous signaling pathways. Crucial advances in the field of oncology have been made in the last decade. This Minireview aims to actualize what is known about the central role of the Wnt/β-catenin pathway in CRC chemoresistance and aggressiveness, focusing on cross-communication between CRC cells and the TME. Through this analysis, our main objective was to increase the understanding of this complex disease considering a more global context. Since many treatments for advanced CRC fail due to mechanisms involving chemoresistance, the data here exposed and analyzed are of great interest for the development of novel and effective therapies.

Key Words: Colorectal cancer; β-catenin pathway; Tumor stroma; Tumor microenvironment factors; Cancer progression; Drug resistance

©The Author(s) 2022. Published by Baishideng Publishing Group Inc. All rights reserved.

Core Tip: Currently, there is a high probability of failure in treatments for the advanced stages of colorectal cancer (CRC). For this reason, it is necessary to obtain a better understanding of CRC biology in a more global context for the future design of novel therapeutic approaches. The effects of the Wnt/β-catenin signaling pathway and the tumor microenvironment (TME) on the progression and chemoresistance of this disease were separately described in several review articles. Therefore, herein we comprehensively analyze the complex mechanisms of CRC chemoresistance triggered by TME factors that impact Wnt/β-catenin signaling.

Citation: Novoa Díaz MB, Martín MJ, Gentili C. Tumor microenvironment involvement in colorectal cancer progression *via* Wnt/β-catenin pathway: Providing understanding of the complex mechanisms of chemoresistance. *World J Gastroenterol* 2022; 28(26): 3027-3046
URL: https://www.wjgnet.com/1007-9327/full/v28/i26/3027.htm
DOI: https://dx.doi.org/10.3748/wjg.v28.i26.3027

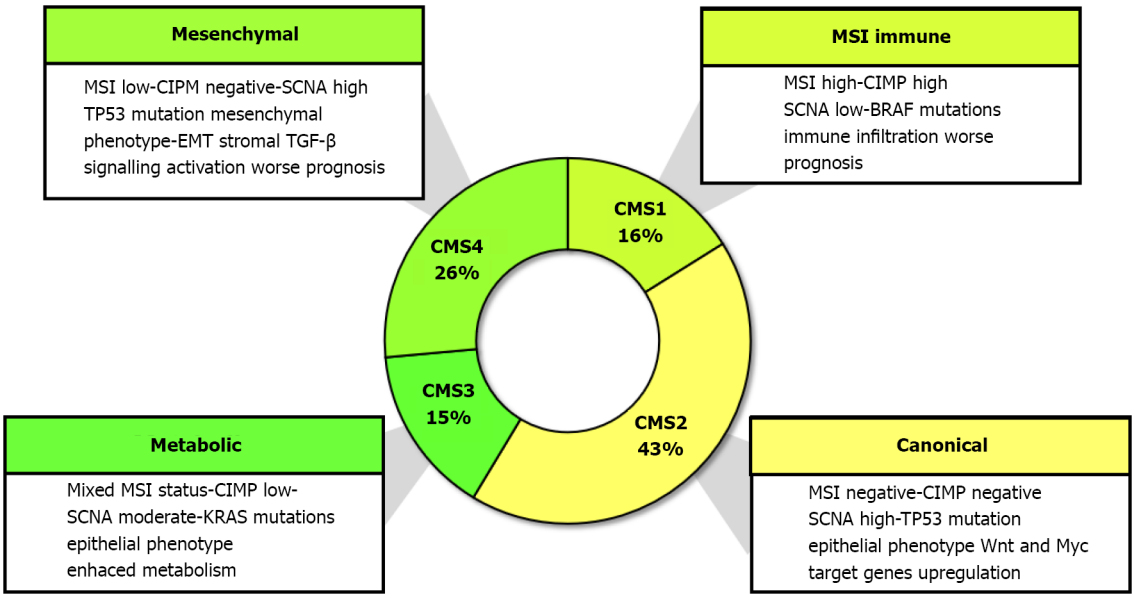
INTRODUCTION

Colorectal cancer (CRC) is the third most frequent malignant disease worldwide in both men and women[1,2]. Data provided by the World Cancer Research Fund International indicate that CRC incidence is growing, and the prevalence of this pathology is expected to increase by 60% in the next 15 years[3]. Among all cancer-induced deaths, the ones associated with CRC reach values of 8%-9%[4,5]. These statistics rely mainly on the fact that 20% of patients show metastasis (stage IV) at the time of diagnosis and the overall survival in these patients is low due to failure in the treatments[5,6]. To improve the response of these patients to therapy, it is necessary to expand the knowledge about the mechanisms that play a critical role in the development, progression and chemoresistance of CRC.

In 2015, Guinney *et al*[7] proposed a classification of colorectal tumors based on four consensus molecular subtypes (CMSs). Groups were defined according to certain parameters such as clinical, genetic and molecular characteristics (Figure 1): The CMS1 group, also designated microsatellite instability immune, is characterized by high microsatellite instability and immune response. The canonical subtype (CMS2) represents 37% of cases and presents hyperactivation of the Wnt and Myc signaling pathways. The CMS3 (metabolic subtype) is characterized by a marked dysregulation of metabolic pathways. Finally, the CMS4 (mesenchymal subtype) group exhibits hyperactivation of the transforming growth factor-β (TGF-β) pathway and a marked switch from the epithelial to mesenchymal transition (EMT)[7,8]. Remarkably, 90% of CRC cases present with aberrant activation of the canonical Wnt/β-catenin signaling pathway[9-11]. This pathway is strictly regulated in physiological conditions and modulates fetal development and homeostasis in adult tissues[11]. Briefly, in the absence of Wnt ligand, β-catenin is continuously phosphorylated in the cytoplasm by a destruction complex comprised of adenomatous polyposis coli (APC), axis inhibition protein (Axin), glycogen synthase kinase 3 (GSK3), and casein kinase 1. Once phosphorylated, β-catenin is ubiquitinated and degraded by the proteasome. When Wnt ligand binds to its receptor, the destruction of β-catenin stops, so this protein accumulates in the cytosol and then translocates to the nucleus. Finally, β-catenin binds to transcription factors from the T-cell factor/lymphoid enhancer factor (TCF/LEF) family and promotes the transcription of several genes[12]. There are several published research as well as review articles on the involvement of the Wnt/β-catenin pathway in CRC development, progression, and chemoresistance[10,13,14]. Furthermore, this pathway became an unquestionable target for novel therapies for CRC. Despite this, to date, there are no approved treatments or clinical trials for CRC based on targeting the Wnt/β-catenin pathway[15].

As extensively described in the open literature, hyperactivation of the Wnt/β-catenin pathway in CRC is directly associated with intrinsic causes such as mutations in the *APC* gene. This results in the nuclear accumulation of β-catenin and the induction of Wnt target genes that promote tumor progression[16]. In this contribution, we intend to analyze how Wnt/β-catenin aberrant activation can be induced or exacerbated by external causes.

In the last decade, the tumor microenvironment (TME) or tumor stroma has become relevant in the progression of CRC[17]. The TME is a niche composed of the extracellular matrix (ECM), a great variety of modified stromal cells and aberrant vasculature[9]. Intercellular communications between the tumor cells and the TME are mainly established through paracrine signaling[9,18]. These communications and factors are extrinsic and may directly affect CRC progression through the Wnt/β-catenin pathway. In this way, a wide range of novel therapeutic targets appears, expanding the possibilities of achieving effective treatments for CRC.



DOI: 10.3748/wjg.v28.i26.3027 **Copyright** ©The Author(s) 2022.

Figure 1 Consensus molecular subtypes classification for colorectal tumors. BRAF: B-Raf proto-oncogene; CIMP: CpG island methylator phenotype; CNAs: Copy number alterations; EMT: Epithelial to mesenchymal transition; KRAS: Kirsten rat sarcoma 2 viral oncogene homolog; MSI: Microsatellite instability; TGF-β: Transforming growth factor-β; TP53: Tumor protein 53.

This work analyzed the available literature regarding the biomolecules associated with the TME that can modulate the Wnt/β-catenin signaling pathway in CRC cells, which allows a better understanding of the biological causes of the high morbidity and mortality of this pathology in a global context. Although antecedents of this particular analysis are registered in 2008[19], the enormous amount of information collected in recent years results in the emergence of new biomolecules, structures, and even processes related to the TME and the CRC cells that were previously unknown or unrelated. The comprehension of this information enables countless new possibilities for the development of new therapies for CRC.

DYNAMICS ESTABLISHED BETWEEN THE TME AND CRC CELLS

During CRC genesis, the TME and its associated signaling play a key role in tumor fate, since they facilitate the proliferation, invasion, metastasis, and chemoresistance processes. Specifically, the TME is composed of ECM proteins, mesenchymal stem cells, fibroblasts, cancer-associated fibroblasts (CAFs), endothelial cells (ECs), and tumor-infiltrating immune cells, with the last group comprising tumor-associated macrophages (TAMs), tumor-associated neutrophils, natural killer (NK) cells, regulatory T cells, myeloid-derived suppressor cells, and cytotoxic T lymphocytes (also known as CD8+ T cells), among others[5,20].

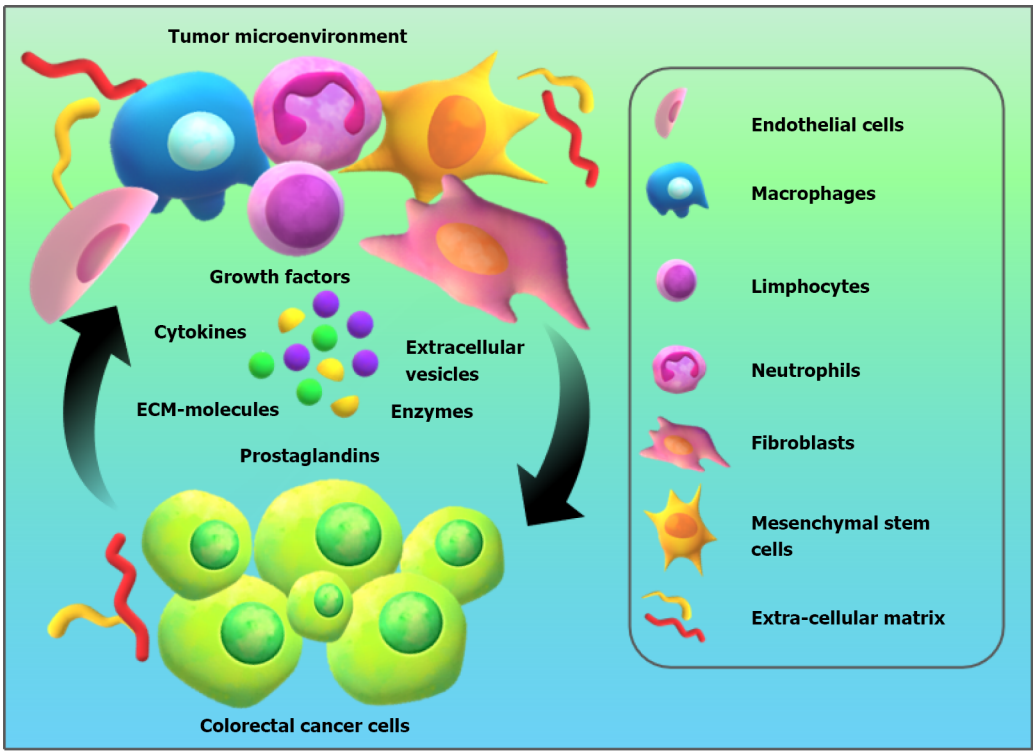
The TME cells and neoplastic cells continuously secrete and internalize factors that modulate the CRC development and contribute to the maintenance of the tumor ecosystem. These extracellular signals are schematized in Figure 2 and involve soluble proteins, insoluble proteins from the ECM, or compounds of variable nature loaded in vesicles[21]. Table 1 compiles the biomolecules well described in the literature that can be secreted by the TME cells and that allow communication with CRC cells. Some of these factors can travel freely through the tumor stroma space, whereas others are transported through membrane-bound vesicles known as extracellular vesicles (EVs)[22,23]. The EVs structure includes a lipid bilayer composed mainly of ceramide, cholesterol, sphingomyelin, phosphoglycerides, glycosphingolipids, phosphatidyl serine, phosphatidylethanolamine, mannose, N-linked glycans, polylactosamine, and sialic acid[22]. In recent years, EVs have acquired relevance as biological mediators in the communication between the TME and tumor cells. Concerning EVs related to CRC, their loads are considered prognostic factors or indicative of response to therapies. Recent studies have shown that EVs can carry large amounts of biomolecules from the TME cells to cancer cells and vice versa. Usual cargoes include cytokines/chemokines, angiogenic factors, ECM remodeling factors, and nucleic acids such as microRNAs (miRs), long non-coding RNAs (lncRNAs), and circular RNAs (cRNAs)[24-27]. Fluids from CRC patients such as plasma, saliva, and urine contain large amounts of secreted EVs. These molecules can stimulate or inhibit the expression of oncogenes and oncoproteins, thus affecting the phenotype of the neoplastic cells or altering the secretory profile of the TME cells[22,25,28]. Unlike cytokines and growth factors that act in the nearby cells, the EVs can influence both the primary colorectal tumor and

Table 1 Factors secreted by the tumor microenvironment and their role in colorectal cancer progression

Released/secreted components	Source, TME cell	Known effects in CRC	Ref.
Growth factors			
TGF-β	CAFs; TIICs[1]; MSCs[1]	Proliferation on tumor and stromal cells in late stages of tumorigenesis. EMT program and CSC-like traits. Metastasis, vasculogenesis and angiogenesis	[5,21,136]
BMPs	CAFs	Anti-tumor activity. Or pro-tumor activity, induce CSCs phenotype, EMT program and chemoresistance. Differentiation of colon CSCs	[5,137,138]
HGF	CAFs; TIICs; MSCs[1]	Invasion, metastasis and stemness	[21,54,139,140]
VEGF	ECs; CAFs; TIICs	Angiogenesis, invasiveness, metastasis	[104,140,141]
FGF	CAFs; MSCs	CAFs profiles. Tumor growth and metastasis	[142,143]
PDGF	CAFs	Tumor growth and metastasis	[144]
TNF-α	TIICs	Proliferation. Growth arrest and cancer cell death, angiogenesis and metastasis	[141,145]
Cytokines			
IL-1	TIICs	Angiogenesis and metastasis	[141,146]
IL-2	TIICs	Anti-tumor activity	[1,147]
IL-6	TIICs; MSCs; CAFs	Proliferation, angiogenesis and metastasis	[1,141]
IL-8	TIICs; MSCs	Tumor growth, angiogenesis and chemoresistance	[1,148]
IL-17	CAFs; TIICs	Anti-tumor or pro-tumor activity. Invasion and self-renewal of CSCs	[1,104,149]
IL-18	TIICs	Anti-tumor activity	[150]
IL-22	TIICs	Proliferation, invasion and stemness	[1,104]
IL-33	ECs; TIICs	Anti-tumor activity Suppresses tumorigenesis. Or pro-tumor activity. Angiogenesis and metastasis. Tumor growth through immunosuppressive microenvironment favoring	[1,104,151]
CCL2	TIICs; MCS	Tumor progression	[152]
CCL5	TIICs	Tumor progression. Acts on tumor cells and TAMs	[153]
CCL7	CAFs	Proliferation, invasion, and migration	[154]
CXCL12	CAFs; MSCs	Proliferation and invasion	[142,155]
PTHrP	Undefined TME cells	Proliferation, invasion, angiogenesis, migration and chemoresistance	[34,35,66,156,157]
Osteopontin	TIICs	Metastasis, stemness and chemoresistance	[85]
Prostaglandins			
PGs (like PGE2)	CAFs; TIICs; MSCs	Resistance to apoptosis, increased proliferation, angiogenesis and metastasis	[21,32]
Signaling pathways ligands			
NOTCH ligands (Jagged-1; Jagged-2; DLL4)	ECs	CSCs phenotype, EMT program and metastasis	[104,158]
WNT ligands (Wnt2, Wnt5)	CAFs	Invasion, metastasis and angiogenesis	[44,45,54]
Enzymes			
Serine proteinases (like MMPs)	TAMs; TANs	Invasion and angiogenesis	[140,145]
Immunosuppressive enzymes (like iNOS)	TIICs	Tumor progression. Inhibitory effect on the immune system, apoptosis of immune cells	[39]
Receptors			
TLRs	CAFs, ECs	Inflammatory-mediated tumorigenesis	[41,43]
RNA molecules			

miR-92a-3p	CAFs	CSCs phenotype, EMT program and chemoresistance	[24]
lncRNA H19	CAFs	Stemness and chemoresistance	[25]
miR-155	MSCs[1]	Migration	[21,159]
miR-375	MSCs[1]	Chemoresistance	[21,160]
cRNA	CAFs	Tumor progression or anti-tumor activity	[26,27]

[1]Factor's actions demonstrated for colorectal cancer (CRC). Their source from the tumor microenvironment (TME) has been identified for other types of cancer, but not for CRC. BMP: Bone morphogenetic CAFs: Cancer-associated fibroblasts; CCL: C-C motif chemokine ligand; cRNA: Circular RNA; CSCs: Cancer stem cells; CXCL: C-X-C motif chemokine ligand; ECs: Endothelial cells; EMT: Epithelial to mesenchymal transition; FGF: Fibroblast growth factor; HGF: Hepatocyte growth factor; IL: Interleukin; iNOS: Inducible nitric oxide synthase; lncRNA: Long non-coding RNA; miR: MicroRNA; MMPs: Matrix metalloproteinases; MSCs: Mesenchymal stem cells; PDGF: Platelet-derived growth factor; PGs: Prostaglandins; PTHrP: Parathyroid Hormone-related Peptide; TAMs: Tumor-associated macrophages; TANs: Tumor-associated neutrophils; TGF-β: Transforming growth factor-β; TIICs: Tumor-infiltrating immune cells; TLRs: Toll-like receptors; TNF-α: Tumor necrosis factor-α; VEGF: Vascular endothelial growth factor.



DOI: 10.3748/wjg.v28.i26.3027 **Copyright** ©The Author(s) 2022.

Figure 2 Extracellular signal molecules secreted by the tumor microenvironment and neoplastic cells. The traffic of soluble and insoluble factors allows crosstalk between tumor cells and their environment modulating colorectal cancer development and progression.

metastatic niche remotely[22,29]. For instance, analysis of the plasma from CRC patients revealed that EVs are directly linked to the establishment of liver proinflammatory phenotype and liver metastasis, with this effect mediated by the modulation of macrophages by EVs[30]. The correlation between CD8+ T cell activation and high EVs concentrations in plasma has also been demonstrated, thus showing the role of EVs in the modulation of the immune response in CRC[31]. In conclusion, EVs have become a new source of therapeutic targets for CRC[22].

On the other hand, the soluble molecules that are directly secreted to the biological fluids exert their actions locally and participate in the communication between the tumor and the microenvironment. These factors are prostaglandins, cytokines, and other paracrine factors, which have distinctive modes of action. Prostaglandins and cytokines act especially as immunomodulators, by promoting or inhibiting the progression of CRC[1,32,33]. Growth factors such as TGF-β, vascular endothelial growth factor (VEGF), and EGF promote the transformation and development of neoplastic cells by inducing proliferation, invasion, and migration responses and also by affecting the TME[21]. In previous works *in vitro* using two CRC cell lines with different grades of aggressiveness, we demonstrated that parathyroid hormone-related peptide (PTHrP) acts as a paracrine factor by inducing the survival, proliferation, migration, cell cycle progression, angiogenesis, and EMT program. Moreover, our *in vivo* studies in CRC

tumor xenografts revealed that the intratumor administration of PTHrP modulates the expression of several tumorigenic markers, which are involved in the same cell responses observed *in vitro*[5,34-37].

Other proteins with different functions were studied in relation to CRC and the TME. In recent years, it has been reported that both neoplastic cells and TME cells can synthesize and secrete enzymes that participate in tumorigenesis. Muñoz-Galván *et al*[38] demonstrated that phospholipase D2 (PLD2) enzyme is overexpressed and secreted by CRC cells. PLD2 in the extracellular space modulates the phenotype and secretory profile of CAFs, thus contributing to promote stemness in tumor cells[38]. Other enzymes such as nitric oxide synthase are capable of inducing immunomodulatory effects[39]. Moreover, enzymes present in the TME, such as metalloproteases, enable the invasion and migration of cancer cells[39]. These enzymes act mainly by altering the structure and function of the ECM, thus allowing the activation of other factors that amplify the pro-tumor signals[40]. Receptor proteins such as Toll-like receptors (TLRs) play a fundamental role in maintaining epithelial barrier homeostasis in the gut and mediating inflammatory and immune responses[41]. TLRs are also expressed in fibroblasts and ECs in the TME and in CRC cells. The dysregulation in TLR pathways is associated with inflammation-driven carcinogenesis[42]. In response to this evidence, currently, there are clinical trials that include TLRs agonists for the treatment of CRC (www.clinicaltrials.gov)[41,43].

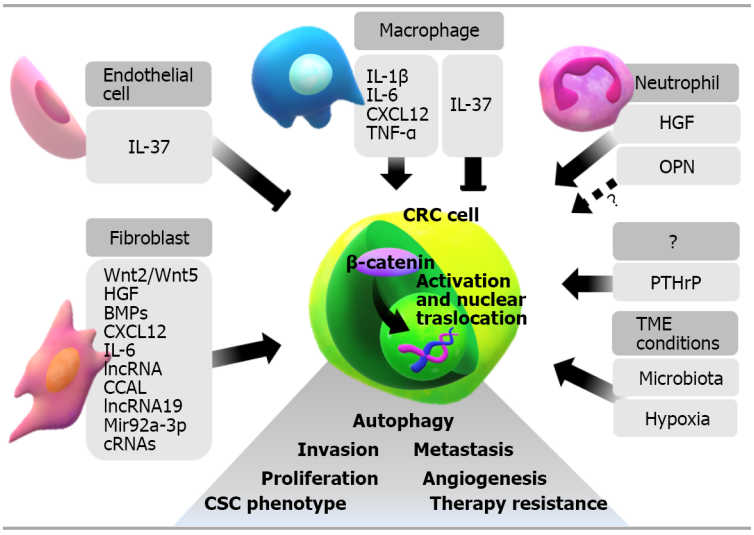
The abovementioned factors generally exert their effects by modulating several signaling pathways in the tumor[1,44-46]. In accordance with the focus of this contribution, in the next sections, we further discuss which of these biomolecules participate in aberrant activation of the β-catenin signaling pathway in CRC, and how these findings have provided new opportunities for the development of more efficient therapies.

TME FACTORS AND CONDITIONS THAT MODULATE THE WNT/β-CATENIN PATHWAY IN CRC

It is clear that the signaling triggered by factors that mediate the communication between TME and CRC cells is of great importance. Since Wnt/β-catenin is involved in most of the processes related to CRC genesis and progression[8,47], in this section we focus on the factors from the TME able to modulate this pathway. Figure 3 schematizes the complex interrelationships between the TME and CRC cells that lead to the activation of β-catenin and the consequent effects on disease progression.

Other β-catenin regulation, independently of the destruction complex actions described in the introduction section, involves phosphorylation by other kinases in different amino acids, such as Ser-552 and Ser-675, resulting in the stabilization and nuclear accumulation of this protein[48]. Mutations in the gene that encodes the β-catenin protein (*CTNNB1* gene) will produce structural alterations and its consequent hyperactivation and nuclear accumulation, events directly associated with CRC genesis and progression[7,49]. Voorneveld and collaborators[50] demonstrated that nuclear β-catenin is found predominantly in cells at the invasive front of CRC tumors. Other investigations have proven that the signals that exacerbate aberrant β-catenin function independently of others than those produced by the tumor can come from the TME[44,51].

Activation of the Wnt pathway by TME factors was initially studied a decade ago. Vermeulen and colleagues showed that CAF-derived hepatocyte growth factor (HGF) activates Wnt/β-catenin signaling and subsequently the clonogenicity in cancer stem cells (CSCs) isolated from CRC patients that were transiently transfected with TCF/LEF luciferase reporter vector. Moreover, HGF restored the CSC phenotype in more differentiated tumor cells both *in vitro* and *in vivo*[52]. Essex and collaborators recently replicated these studies, emphasizing the relevance of this pathway and the interaction of tumor cells with their stroma, and in the promotion and development of CRC[53]. As stated in Table 1, various Wnt ligands are secreted mostly by CAFs[44,45,54,55]. A recent study confirmed that Wnt2 acts in an autocrine manner, generating morphogenetic changes in fibroblasts and contributing to the invasive and metastatic capacity of CRC-derived cells[44]. *In vitro* experiments revealed that the treatment of DLD1 and HCT116 cells (both derived from CRC) with conditioned medium obtained from CAFs transfected with small interfering RNA targeting Wnt2, significantly decreased cell invasion and migration[45]. It is of clinical relevance that these ligands are overexpressed in the tumor stroma of CRC patients[45,53]. Moreover, the aberrant expression of Wnt ligand is correlated with a worse prognosis [44]. EVs play a key role in activating Wnt signaling in CRC. On the one hand, EVs can transport mutant β-catenin and activate the Wnt signaling pathway in the recipient cells, thus promoting CRC progression[56]. Regarding the effects of EVs on TME cells, Hu and colleagues demonstrated *in vitro* that fibroblast-derived exosomes (one type of EVs) promote the tumor growth of CSCs upon treatment with 5-fluorouracil (5-FU) or oxaliplatin (OXA)[57]. Further investigations of the same group in subcutaneous xenografts achieved through HT-29 CRC-derived cells and fibroblast co-implantation demonstrated that stromal fibroblasts can secrete exosomes loaded with Wnt ligands. Once these exosomes interact with differentiated CRC cells, Wnt ligands induce the phenotypic reversion of CRC cells to CSCs, which includes features such as the expression of CSCs markers and elevated Wnt activity [57].



DOI: 10.3748/wjg.v28.i26.3027 **Copyright** ©The Author(s) 2022.

Figure 3 Influence of tumor microenvironment-derived factors in the activation of β-catenin pathways. Several cytokines, growth factors, and small nuclei acid molecules secreted by stromal cells induce aberrantly activation of β-catenin and its nuclear translocation in colorectal cancer (CRC) cells promoting events associated with an aggressive phenotype of the tumor cells. Il-37 represses the expression of β-catenin and its transcriptional activity. Osteopontin is statistically associated with the expression of β-catenin in CRC and is known to induce its activation in other types of cancer. More studies are necessary to confirm positive feedback between the secretion of this tumor microenvironment (TME) factor and β-catenin signaling pathways in CRC. In addition to these factors, the microbiota and the hypoxia in the TME, also participate in the modulation of β-catenin activation. This figure is original for this work. BMP: Bone morphogenic protein; CCAL: Colorectal cancer-associated lncRNA; cRNA: Circular RNA; CXCL: C-X-C motif chemokine ligand; HGF: Hepatocyte growth factor; IL: Interleukin; lncRNA: Long non-coding RNA; OPN: Osteopontin; PTHrP: Parathyroid Hormone-related Peptide; TNF-α: Tumor necrosis factor-α; Wnt: Wingless protein.

Hypoxia is a prevalent condition in the solid tumor TME, which involves oxygen pressures of less than 5-10 mmHg. The hypoxic TME can deeply influence CRC, and these effects may be mediated by β-catenin. For instance, it was found *in vitro* that Wnt/β-catenin signaling is responsible for the hypoxia-induced self-renewal of colorectal stem cells[58]. Furthermore, Huang and collaborators observed that hypoxic CRC cells can secrete exosomes enriched with Wnt4 Ligands. These exosomes can activate β-catenin signaling in normoxic CRC cells and stimulate prometastatic behaviors such as cell migration and invasion[59]. In another work, the authors demonstrated that Wnt4-loaded exosomes secreted by the tumor cells promoted angiogenesis through the proliferation and migration of ECs. These effects were induced in conditions of hypoxia and mediated by the activation of Wnt/β-catenin signaling[60].

Autophagy is a physiological process through which normal cells degrade intracellular components to maintain cellular homeostasis. It is postulated as an alternative to cell death when the apoptotic machinery fails and is associated with both CRC and the TME, with controversial findings[61-63]. TME hypoxia induces autophagy and also activates several tumor escape mechanisms[62]. Some of the molecular mechanisms involved in the modulation of autophagy are phosphoinositide 3-kinases (PI3K)/protein kinase B (also known as Akt)/mammalian target of rapamycin, TGF-β, Notch, and Wnt/β-catenin signaling[63]. According to evidence, autophagy induced in the early stages of tumor development prevents the infiltration of immune cells as well as tumor cell death. Autophagy can also promote tumor progression in the advanced stages of the disease[63]. On the other hand, it has been reported that the relationship between autophagy and increased lymphocytic infiltration in the TME is mediated by the autophagy-related protein Vps34 in CRC. The modulation of this autophagy-related protein would improve the efficacy of immunotherapies[64]. However, it is still necessary to conduct additional studies on the interrelationship between the Wnt/β-catenin signaling pathway and autophagy, and which TME factors can mediate these events in CRC.

Because about 90% of patients with CRC present with mutations in genes associated with the Wnt pathway[65], more efforts have been made to identify other molecules with the ability to regulate β-catenin. In line with this evidence, our research group also reported interesting results regarding the participation of PTHrP in the activation of signaling pathways associated with β-catenin. Our published data showed that the exposition of cells derived from colorectal adenocarcinoma, to exogenous PTHrP increases β-catenin expression and upregulates cyclin D1 and c-Myc oncogenes with the concomitant cell proliferation induction[66]. Regarding the role of this cytokine in the TME, we demonstrated *in vitro* that tumor conditioned media from PTHrP-exposed CRC cells promotes pro-angiogenic characteristics in the stromal EC line HMEC-1 through VEGF modulation[35]. In addition, we recently found that PTHrP modulates the protein expression and secretion from the HMEC-1 cells of secreted protein acidic and cysteine-rich, a TME factor involved in the EMT program. This event promotes molecular and morphological changes associated with EMT in cells derived from CRC[36]. In this context, we believe that cross-communication may be initially established through overexpression and secretion of PTHrP

by the tumor, which in turn affects the behavior of neoplastic cells and TME cells inducing the subsequent release from them of this cytokine and other factors. More studies are needed to elucidate which stromal cells can secrete PTHrP and participate in the modulation of the β-catenin pathway. Several authors have also described the relationship between PTHrP and activation of the β-catenin signaling pathway in other types of cancer. In prostate cancer-derived cells, PTHrP downregulates the Wnt inhibitor, DKK1, promoting aberrant activation of this pathway[67]. Other research has shown that PTHrP modulates activation of the canonical Wnt/β-catenin signaling in the mammary mesenchyme [68]. Moreover, Johnson and collaborators reported that Wnt activation promotes PTHrP expression in breast and lung tumor cells[69].

Tumor small and long non-coding RNAs are other factors transported by EVs, which are also involved in the modulation of β-catenin signaling. Colorectal cancer-associated lncRNA (CCAL) and H19 (lncRNA19) expressed by CAFs are capable of stimulating aberrant activation of β-catenin in tumor cells[9,25]. Besides, the overexpression of miR-103 and miR-107 has been detected in the plasma and tumor tissue of patients with CRC[70]. In HCT116 and HT29 cell lines, miR-103/107 overexpression enhanced β-catenin activity and its nuclear translocation. These molecules act by inhibiting Axin2, a negative regulator of the Wnt/β-catenin pathway, and in this way, β-catenin is stabilized and its activation is prolonged[70]. Another study showed that miR-92a-3p secreted by CAFs, induces β-catenin nuclear translocation and the expression of target genes related to stemness, the EMT program, and chemoresistance in the human CRC cell lines SW480, SW620, and LOVO. Moreover, the high expression of exosomal miR-92a-3p in serum predicts metastasis and chemotherapy resistance in CRC patients[24]. The overexpression of miR-100, miR-125b, miR-27a, miR-135, and MIR100HG in CRC tumors modulates the canonical Wnt pathway, promoting events such as proliferation and invasion[71,72].

In the last decade, research on small non-coding RNA molecules has focused on cRNAs. Increasing studies have shown that these molecules intervene in the development and progression of various types of tumors including CRC[73]. Results obtained by Zhang *et al*[73] show that circAGFG1 activates the Wnt/β-catenin pathway in SW480 and HCT116 cells promoting the transcription of the CTNNB1 gene. Two years earlier, Fang and his group revealed that circ_100290 promotes CRC progression through activation of the Wnt/β-catenin pathway[74]. Other cRNAs involved in the activation of this signaling pathway in CRC are Hsa_circ_0005075[75], circMTO1[76] and Circ-PRKDC[72]. On the other hand, cRNAs such as circPRKDC and cirITCH act by inhibiting the activity of the β-catenin pathway[77,78]. The action of most of these molecules is mediated by miRNAs[26,79].

HGF and its receptor RTK Met are associated with β-catenin-related pathways in CRC cells, promoting a CSC phenotype, metastasis, and drug resistance[46,51,80,81]. Other factors including tumor necrosis factor-α (TNF-α) also stimulate the main regulatory mechanism of β-catenin activation in CRC cells. Wei and colleagues demonstrated that under TNF-α action, the CSCs derived from the HT29 cell line increase the survival rate and their invasive capacity *via* the Wnt pathway. These actions are mediated by the modulation of β-catenin related proteins expression, such as c-Myc, cyclin D1, E-cadherin, and vimentin, which are cell cycle regulators associated with the stimulation of cell proliferation and/or the progress of the EMT program[82]. Molecules released from tumor cells including PLD2, modify the secretome of CAFs by promoting the release of the following factors: Macrophage migration inhibitory factor (MIF), HGF, and CCL2. The results shown in this article confirm that the treatment of CRC-derived cells (HCT116 and LS180) with these three factors induces the activation of the Wnt/β-catenin signaling pathway. The authors of this work observed a reduction of β-catenin phosphorylation together with an increase in its total expression after treatment with CCL2, HGF, and MIF, as well as a decrease and an increase in the expression of Axin1 and c-Myc, respectively, consistent with Wnt activation. This research also demonstrated that gene transcription induced by the Wnt signaling pathway correlates with high expression of PLD2 and CAFs-derived factors in CRC patients [38].

Osteopontin (OPN) is another factor that plays an important role in the regulatory mechanism of β-catenin. It is a glycoprotein synthesized by a great variety of cells and is overexpressed in CRC. This protein is capable of activating β-catenin *via* Akt and subsequently GSK3β, or by recruiting and activating mitogen-activated protein kinase (MAPK)[83,84]. Youssef and Osman analyzed tumor samples and found an association between the expression of nuclear OPN/β-catenin and markers related to poor prognosis in CRC[85]. In the last decade, an association has also been established between OPN expression and the activation and nuclear translocation of β-catenin in other types of cancer[83,84]. Recent research has shown that this protein is a target gene of the Wnt pathway[86] and in these cases, positive feedback from the system can be generated. Based on the evidence analyzed in the previous lines, positive feedback is highly probable between OPN secretion and the modulation of the Wnt/β-catenin pathway in CRC.

Other cytokines and growth factors released by the TME cells promote activation of the canonical Wnt pathway in cells derived from human CRC[87]. Bone morphogenetic proteins (BMPs) are cytokines closely linked to angiogenesis, EMT program, and induction of CSCs[88]. Voorneveld and colleagues transfected HCT116, HT29, LS174T, RKO, and SW480 cells with the BMPR2 plasmid, increasing BMP signaling. Hyperactivation of this pathway only downregulated Wnt signaling in HCT116 and LS174T cells, both were SMAD4-positive and had wild type p53. In the remaining cell lines, the Wnt pathway was activated by BMP signaling. This work demonstrated that modulation of Wnt/β-catenin signaling

by the BMP pathway is dependent on SMAD4 and p53 status[5,50]. Regarding the role of interleukins (ILs), neoplastic cells promote the release of IL-1β, mainly from TME macrophages. In HCT116 cells, this cytokine induces β-catenin activation and consequently the expression of target genes, through nuclear factor kappa B (NF-KB)/Akt signaling pathway[87,89]. IL-6 secreted by TME cells induces activation of the Wnt/β-catenin pathway through the signal transducer and activator of transcription 3/extracellular signal-related kinase (ERK) pathway favoring the promotion of the aggressive phenotype of SW48 cells [90]. Chemokines such as C-X-C Motif Chemokine Ligand 12 (CXCL12) are overexpressed in CRC. Song *et al*[91] showed that the increased expression of this cytokine and its receptor (CXCR4) in tumor cells induces activation of the canonical Wnt pathway, possibly mediating the processes of proliferation, survival, and invasion[91]. However, not all cytokines act by promoting aberrant activation of the Wnt pathway. IL-37 mainly expressed by TAMs[92] has been observed to inhibit the proliferation, migration, and CSC phenotype by directly repressing the expression of β-catenin and consequently its translocation to the nucleus[49].

Bacteria, fungi, and viruses constitute the microbiota residing within the gastrointestinal tract. However, the gut microbiota and their metabolites can be altered in the TME and directly influence CRC progression[93,94]. Various bacteria have been implicated in these processes by modulating the β-catenin pathway. *Fusobacterium nucleatum* is a CRC inductor and suppressor of NK cell activity[93,95] Recently, it was reported that *F. nucleatum* can stimulate annexin A1 protein, specifically expressed in CRC cells. Then annexin A1 can induce β-catenin nuclear accumulation and finally the exacerbation of CRC cell proliferation[96]. On the opposite side, as extensively analyzed by Li *et al*[93] in their review article, other bacteria could be beneficial for CRC treatment or its prevention. For example, *Lactobacillus* and *Clostridium butyricum* are probiotics that have inhibitory effects on CRC progression *via* modulation of the β-catenin pathway[93]. This background shows that the complex interrelations between tumor cells and their microenvironment (including the microbiota) involve the participation of one of the most outstanding signaling pathways in the promotion and development of CRC, the β-catenin pathway. Therefore, it is important to consider these phenomena in the development of new treatments that focus on inhibiting or silencing the activators/exacerbators of this pathway.

ROLE OF β-CATENIN AND THE TME IN THE CHEMORESISTANCE OF CRC

Among the most used chemotherapeutic drugs, approved as first- and second-line adjuvants in CRC, are 5-FU, irinotecan (CPT-11), OXA, capecitabine, and leucovorin[97,98]. Depending on the CRC subtype, these drugs are also used in combination with monoclonal antibodies, such as bevacizumab or cetuximab[5]. On certain occasions, signs of a poor prognosis appear. Therefore, neoadjuvant or adjuvant chemotherapy must be implemented[99]. Despite this, patients with advanced grades of metastatic disease continue to lag far behind in successful treatment. One of the main causes of failure in treatment is the chemoresistance observed in about half of patients with CRC[99,100]. In this regard, the cell responses that mediate drug resistance are associated with hypoxic conditions, autophagy, induction of the CSC phenotype, and the EMT program[101,102]. At the molecular level, the development of drug-resistant tumors involves alterations of Wnt/β-catenin among other important signaling pathways such as Hedgehog and Notch. It also includes disturbances in the expression of anti-apoptotic proteins, the overexpression of drug transporters of the ATP-binding cassette (ABC) family, increased aldehyde dehydrogenase 1 enzyme activity and also the release of factors from the TME[99, 103]. Regarding the Wnt pathway, its aberrant activation involves induction of the CSC phenotype, the EMT program, the expression of proteins from the ABC family and factors from the TME, all of these events being related to drug resistance[99]. Furthermore, various biological mediators released by stromal cells are capable of inducing chemoresistance through the Wnt/β-catenin pathway in tumor cells[9,25,104]. In this regard, *in vitro* studies made by Hu and colleagues revealed that miR-92a-3p secreted from CAFs activates the Wnt/β-catenin signaling, decreasing the sensitivity to the combination of 5-FU/OXA in SW480, SW620, and Lovo CRC-derived cells[24]. Moreover, *in vivo* studies have demonstrated that exosomes secreted by fibroblasts can load Wnt ligands, thus promoting CSC features and resistance to 5-FU or OXA. On the contrary, the inhibition of Wnt release reverted the observed effects[57]. CAFs are capable of inducing drug resistance by transferring small nucleic acid molecules such as H19 or CCAL lncRNA and activating β-catenin in neighboring cells[25]. H19 lncRNA can also trigger autophagy *via* SIRT1 and consequently induce resistance to 5-FU in CRC cells[105]. Other miRNAs such as miR-27[106], miR-103, and miR-107 decrease the sensitivity of HCT116 cells to 5-FU and OXA, through hyperactivation of the β-catenin pathway[9]. Zhou and colleagues reported that the inhibition of the Wnt/β-catenin signaling pathway by the overexpression of miR-506 decreases the chemoresistance response of HCT116 cells to OXA. The mechanism that explains this effect is that the gene and protein expression of the transporter of the ABC family and multidrug resistance protein 1/P-glycoprotein are blocked[107]. Several cRNAs are also involved in the acquisition of drug resistance by CRC cells through modulation of the β-catenin axis. For instance, circ-PRKDC participates in the development of chemoresistance to 5-FU in SW620 and SW480 cell lines by regulation of miR-375 and the Wnt/β-catenin pathway[77]. These molecules constitute a novel target for the development of

alternative therapies for CRC, given their role in the communication between tumor cells and the TME and their participation in the regulation of Wnt/β-catenin[26,108].

Macrophages also play a crucial role in the development of resistance to drugs. IL-1β released by TAMs activates the canonical Wnt pathway through NF-κB/Akt and subsequently induces the expression of genes associated with chemoresistance. This has been observed in several cell lines derived from CRC such as HCT116, Hke-3, SW480, and RKO[109,110].

In our laboratory, we previously reported that PTHrP, acting as a cytokine, induces chemoresistance to CPT-11 through ERK MAPK and Akt pathways in the CRC cell lines Caco-2 and HCT116[34]. Moreover, as described in previous sections, we also registered nuclear β-catenin nuclear-increased expression after PTHrP treatment in CRC cells[37]. In view of these data, we hypothesize that this protein also participates in the resistance to CPT-11. This is our current research focus.

Growth factors are also involved in the therapy resistance mediated by β-catenin. Activation of the c-MET pathway through HGF signaling is related to drug resistance in many types of tumors[111]. Several works have already shown that HGF is associated with both Met and β-catenin pathways[52,54]. Studies published by Woo and collaborators showed that this factor is related to resistance to CPT-11 in CRC cells[112]. Since the HGF/Met axis plays an important role in CRC, molecules such as inhibitors, neutralizing antibodies, and antagonists of this pathway have been designed. To date, preclinical trials have failed and demonstrated poor efficacy[111,113]. One of the possible causes of the resistance of CRC cells to HGF pathway inhibitors is the activation of the Wnt/β-catenin signaling pathway[113]. All of these data highlight the need for consideration of the mitogenic pathways and paracrine factors released by both the tumor and the TME as targets to revert the chemoresistance.

Li *et al*[114] made a relevant contribution in the field of basic sciences related to CRC therapy and TME cells. They observed that the pharmacological treatment of CAFs inhibits their recruitment and increases the sensitivity of tumor cells to OXA[114]. Chemotherapy combined with treatments that inhibit CAFs recruitment and/or their activity may represent a novel method for the improvement of tumor response to chemotherapy[114]. This area of research is practically vacant and needs to be further explored since other unknown factors derived from TME may be able to stimulate the nuclear translocation of β-catenin and modulate the events related to the chemoresistance of CRC cells.

THE TME AND β-CATENIN PATHWAY: FUTURE PERSPECTIVES FOR CRC MANAGEMENT

In the last decade, therapeutic inhibition of the β-catenin pathway has been considered an invaluable tool for developing new therapy regimens for patients with CRC[115-117]. Despite this, as previously stated, there are still no approved drugs for the treatment of CRC or clinical trials based on the targeting of this signaling pathway[15,117]. For these reasons, comprehension of the regulatory mechanisms of the Wnt/β-catenin signaling pathway will not only expand the knowledge about the pathogenesis and evolution of CRC but also improve the treatment with the implementation of new targeted therapies. Many small molecules with β-catenin inhibitory effects have been developed such as tankyrase inhibitors (TNKSi), R-spondin inhibitors, and porcupine enzyme inhibitors. tankyrases (TNKSs) favor Wnt signaling by inducing Axin degradation. Therefore, TNKSi including XAV939 (XAV), JW55, NVP-TNKS656, and GOO7-LK are effective approaches for inhibiting this pathway in the preclinical stage of validation[118,119]. Moon and collaborators recently discovered that β-catenin expression influences the response of CRC-derived cells to MEK inhibitors, and that TNKSi allows the resistance to this treatment to be exceeded in CRC cell lines with mutant KRAS and PI3K. These results demonstrate the possible efficacy of combined treatments with inhibitors of MEK and β-catenin signaling pathways. However, this kind of therapeutic strategy is not yet in the clinical trial phase[118], and there is even controversy on the implementation of this type of scheme[116]. Drugs that disable enzymes related to Wnt secretion are another possibility to inhibit the Wnt/β-catenin. These compounds are denominated IWP-2, LGK974, or ETC-159 and inhibit porcupine enzyme actions. Some R-spondin inhibitors, such as OMP-131R10 (rosmantuzumab), are also currently under investigation for the treatment of CRC. When this ligand binds to the receptor leucine rich repeat containing G protein-coupled receptor 4 (LGR4) or LGR5, it enhances Wnt signaling, so blocking this point would consequently decrease the transcriptional activity of β-catenin[119].

One of the therapeutic targets that is being studied for CRC treatment is the use of antibodies or small molecules for the inhibition of Wnt ligands, like OMP-54F28, OMP-18R5, and OTSA101[116]; the disruption of the transcriptional activity of β-catenin using small molecules that prevent the binding of this protein with the nuclear transcription factors TCF and LEF, such as LF3 and 2,4-diaminoquinazoline; or pharmacological drugs that stimulate β-catenin proteasomal degradation as MSAB[119,120].

In addition to the hyper-activating mutations affecting the β-catenin pathway in CRC, as previously mentioned, cross-communication through paracrine signals between tumor cells and TME cells amplify these effects. The Wnt/β-catenin pathway is key for immune cells differentiation and functioning[120], the aberrant activation of this signaling alters the activation and downregulation of the immune

response, especially related to dendritic cells (DCs) and T cells[119]. In the TME, the β-catenin pathway-dependent production of cytokines, such as IL-10, by DCs has been shown to induce immune tolerance through CD4+ and CD8+ T cells[121]. Moreover, it was reported that β-catenin signaling is activated in tumors with an inflammatory microenvironment, immune evasion and poor infiltration of CD8+ T cells [119,122,123]. In CRC, this immune response is favored by the activation of β-catenin, Myc, and RAS[7, 124,125]. Currently known mechanisms that mediate immune exclusion and evasion through the Wnt/β -catenin pathway are: Modulating the production and release of cytokines from DCs and consequently diminishing CD8+ T cells infiltration; stimulating the production and release of soluble factors like Snail and IL-1β from tumor cells and TAMs, respectively; and increasing regulatory T cells survival, which are also effective inhibitors of CD8+ T cells[120,126]. To date, there are some inhibitors related to the immune response that are approved for clinical use, one of them is programmed death-1[127]. However, although immunomodulation can be effective in the treatment of CRC, resistance often occurs. Given that several of these drugs target CD8+ T cells, one of the explanations for the failure of these therapies may be the hyperactivation of the β-catenin pathway in the TME[128]. From this point of view, the current research focuses on the importance of the development of anticancer therapies that target the Wnt/β-catenin pathway as a checkpoint to improve the efficacy of immunotherapies, mainly by restoring T-cell infiltration[119,120,122].

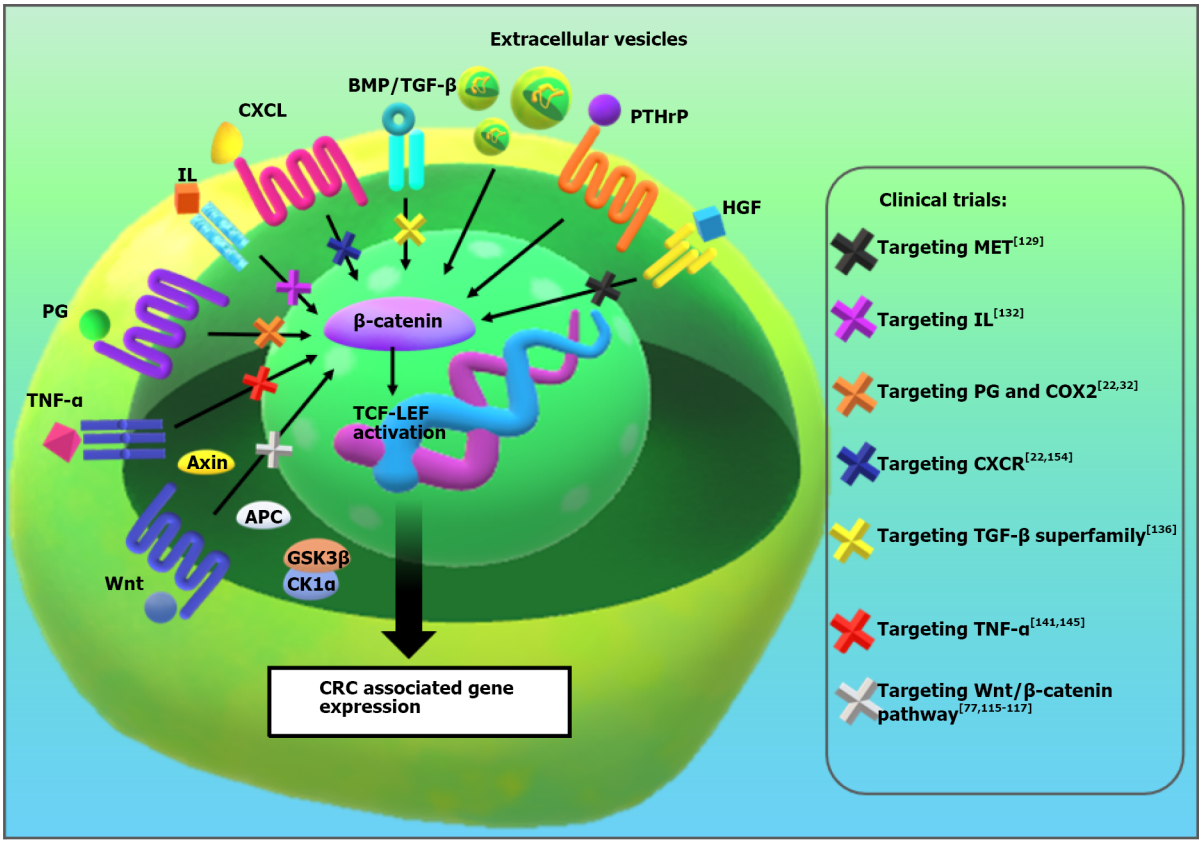
In previous sections, we described the role of several TME-derived factors that activates the β-catenin signaling pathway. Currently, clinical research is aimed at blocking or inhibiting the effects of these molecules on CRC. In our laboratory, we have found that the selective inhibition of the HGF receptor, the RTK Met, suppresses β-catenin phosphorylation at domains that favor its nuclear translocation induced by PTHrP. Concerning this, Rimassa and his research group[129] explored in a clinical phase II study the effect of an oral selective Met inhibitor (tivantinib) and found that, in combination with another drug, at least 10% of patients with CRC respond better to the therapy. This drug is a possible emerging treatment that is already in phase III study in other types of tumors[130]. Another drug that inhibits the activity of the Met receptor by inducing the degradation of β-catenin is celecoxib[116]. However, recent evidence indicates that the combined treatment of celecoxib with the usual chemotherapy did not improve overall survival or progression-free time in patients with CRC[131].

On the other hand, a large number of clinical trials have been developed using cytokine-based immunotherapy for CRC. Different drugs targeting IL, prostaglandins, CXCL, TNF-α and TGF-β superfamily factors are in clinical trials. Although it has not yet been proven that they generate an effect as monotherapy or in combined treatments with commonly used drugs, future expectations are very optimistic[132,133].

Employing non-coding RNA such as miRNAs or cRNAs is a promising solution to overcome CRC drug resistance. It has been seen that miR505, miR199a/b and miR320 decreased sensitivity to cisplatin and OXA by modulating the activity of the Wnt/β-catenin pathway. Others, such as miR30-5p, favor chemosensitivity in CRC cells[134]. In this work, we have also described the role of TME-derived cRNAs in activating the β-catenin signaling pathway and its influence on CRC development and progression. Nevertheless, there is still a lot to explore about its potential role in future therapies for CRC. In this regard, recent research indicates that knockdown circ-PRKDC decreases the resistance of CRC-derived cells to 5-FU by modulating the Wnt/β-catenin pathway[77]. These results could postulate a new strategy to deal with multidrug resistance in CRC. Additionally, Viralippurath and collaborators propose that gene therapy could be aimed at silencing these oncogenic cRNAs or increasing the effects of those molecules that act as tumor suppressors[26]. Despite these findings, to date, there are no available therapies that use these small molecules to evade the strategies of tumor cells against chemotherapeutic drugs. More studies are needed regarding the role of non-coding RNAs in CRC chemoresistance as well as for the development of delivery strategies for these molecules in new targeted therapies. Figure 4 schematizes current studies related to the disruption of the interrelationships between TME and CRC cells that trigger β-catenin activation and are involved in treatment failure.

As previously mentioned, autophagy is a mechanism associated with chemoresistance in CRC[105]. Recent investigations aim to find drugs that help reverse the autophagy process and overcome chemoresistance in CRC[135]. According to Pérez-Plasencia *et al*[62], the involvement of Wnt/β-catenin signaling in the regulation of autophagy was demonstrated in several types of cancer, such as leukemia, hepatocarcinoma, squamous cell carcinoma, lung cancer and prostate cancer[62]. However, it is just a matter of time before the relationship between these two pathways in CRC will be considered crucial for future pharmacological treatments. In their work, the authors postulate several therapeutic approaches based on drugs that are capable of simultaneously disrupting components of β-catenin and autophagy pathways[61].

From what we have analyzed in this work, it is important to highlight that concerning CRC, the achievement of successful future therapies will involve the use of combined pharmacological compounds that inhibit not only the canonical β-catenin signaling pathway but also the TME- derived signaling.



DOI: 10.3748/wjg.v28.i26.3027 **Copyright** ©The Author(s) 2022.

Figure 4 Pharmacological targeting of the tumor microenvironment factors involved in the activation of β-catenin signaling in colorectal cancer. Several therapeutic strategies to block or inhibit the induction of the β-catenin pathway by tumor microenvironment factors in colorectal cancer (CRC) are currently under clinical study. This figure is original for this work. APC: Adenomatous polyposis coli; BMP: Bone morphogenic protein; CK1α: Casein kinase 1 alpha; CXCL: C-X-C motif chemokine ligand; GSK3β: Glycogen Synthase Kinase 3 Beta; HGF: Hepatocyte growth factor; IL: Interleukin; PTHrP: Parathyroid Hormone-related Peptide; PG: prostaglandin; TCF/LEF: T-cell factor/lymphoid enhancer factor; TGF-β: Transforming growth factor-beta; TNF-α: Tumor necrosis factor-α; Wnt: Wingless protein.

CONCLUSION

The cells of the TME are mainly responsible for triggering the mechanisms that determine a worse prognosis of cancer disease. These cells and the biological mediators released in the neoplastic context regulate the expression of ligands and modulate the activity of pro-tumor signaling pathways. TME cells control the fate of the tumor cells through permanent bidirectional communication. It is known that a considerable proportion of CRC patients evolve unfavorably due to chemoresistance. To improve CRC therapies, it is necessary to expand the knowledge about the mechanisms that play a critical role in the development, progression and chemoresistance of CRC.

Given that the factors associated with the TME activate the β-catenin signaling pathway, it will be possible in the future to improve the response of CRC patients to treatment. This goal could be achieved through new therapeutic interventions based on interrupting the crosstalk between the stroma and the tumor that control the β-catenin pathway activation. From the exhaustive search of the bibliography made by the authors of this work, it is concluded that there are multiple vacant areas in the research related to chemoresistance induced by cells from the tumor environment. Even to date, new types of biomarkers are continuously identified and related to a worse prognosis and aggressiveness of CRC. For this reason, it is imperative to strengthen *in vitro* and preclinical studies to support clinical trials in order to achieve novel therapeutic approaches considering the background of each patient and personalized medicine.

ACKNOWLEDGEMENTS

The authors would like to thank Antonela Rossi Bertone for her helpful advice. Being a teacher of English graduated from Instituto Superior Juan XXIII (from Bahia Blanca city, Argentina) and currently working at San Cayetano school (in the same city), she revised the paper and made useful comments as

regards the spelling, grammar and punctuation of this manuscript. MBND and MJM thanks CONICET for the fellowships.

FOOTNOTES

Author contributions: Novoa Díaz MB, Martín MJ, and Gentili C contributed to the conceptualization, methodology, investigation, formal analysis, and visualization, wrote the original draft, and edited the manuscript; Gentili C obtained the resources and oversaw the project administration and funding acquisition.

Supported by Agencia Nacional de Promoción Científica y Tecnológica, No. PICT-2013-1441; Consejo Nacional de Investigaciones Científicas y Técnicas, No. PIP11220150100350; Instituto Nacional del Cáncer Asistencia Financiera II, RESOL 493/14, No. 2002-4395-14-1; Instituto Nacional del Cáncer Asistencia Financiera III-2016-2017, RESOL-2016-1006-E-APN-MS, No. 2002-3862-16-1; and Universidad Nacional del Sur (PGI), Argentina, No. 24/B230 and No. 24/B303.

Conflict-of-interest statement: All the authors report no relevant conflicts of interest for this article.

Open-Access: This article is an open-access article that was selected by an in-house editor and fully peer-reviewed by external reviewers. It is distributed in accordance with the Creative Commons Attribution NonCommercial (CC BY-NC 4.0) license, which permits others to distribute, remix, adapt, build upon this work non-commercially, and license their derivative works on different terms, provided the original work is properly cited and the use is non-commercial. See: https://creativecommons.org/Licenses/by-nc/4.0/

Country/Territory of origin: Argentina

ORCID number: María Belén Novoa Díaz 0000-0002-6684-4076; María Julia Martín 0000-0001-5046-7686; Claudia Gentili 0000-0002-9957-7824.

S-Editor: Fan JR
L-Editor: Filipodia
P-Editor: Fan JR

REFERENCES

1 **Li J**, Huang L, Zhao H, Yan Y, Lu J. The Role of Interleukins in Colorectal Cancer. *Int J Biol Sci* 2020; **16**: 2323-2339 [PMID: 32760201 DOI: 10.7150/ijbs.46651]
2 **Siegel RL**, Miller KD, Jemal A. Cancer statistics, 2020. *CA Cancer J Clin* 2020; **70**: 7-30 [PMID: 31912902 DOI: 10.3322/caac.21590]
3 Erratum: Global cancer statistics 2018: GLOBOCAN estimates of incidence and mortality worldwide for 36 cancers in 185 countries. *CA Cancer J Clin* 2020; **70**: 313 [PMID: 32767693 DOI: 10.3322/caac.21609]
4 **Siegel RL**, Miller KD, Fedewa SA, Ahnen DJ, Meester RGS, Barzi A, Jemal A. Colorectal cancer statistics, 2017. *CA Cancer J Clin* 2017; **67**: 177-193 [PMID: 28248415 DOI: 10.3322/caac.21395]
5 **Villalba M**, Evans SR, Vidal-Vanaclocha F, Calvo A. Role of TGF-β in metastatic colon cancer: it is finally time for targeted therapy. *Cell Tissue Res* 2017; **370**: 29-39 [PMID: 28560691 DOI: 10.1007/s00441-017-2633-9]
6 **Martín MJ**, Gentili C, Lassalle V. In vitro Biological Tests as the First Tools To Validate Magnetic Nanotheranostics for Colorectal Cancer Models. *ChemMedChem* 2020; **15**: 1003-1017 [PMID: 32365271 DOI: 10.1002/cmdc.202000119]
7 **Guinney J**, Dienstmann R, Wang X, de Reyniès A, Schlicker A, Soneson C, Marisa L, Roepman P, Nyamundanda G, Angelino P, Bot BM, Morris JS, Simon IM, Gerster S, Fessler E, De Sousa E Melo F, Missiaglia E, Ramay H, Barras D, Homicsko K, Maru D, Manyam GC, Broom B, Boige V, Perez-Villamil B, Laderas T, Salazar R, Gray JW, Hanahan D, Tabernero J, Bernards R, Friend SH, Laurent-Puig P, Medema JP, Sadanandam A, Wessels L, Delorenzi M, Kopetz S, Vermeulen L, Tejpar S. The consensus molecular subtypes of colorectal cancer. *Nat Med* 2015; **21**: 1350-1356 [PMID: 26457759 DOI: 10.1038/nm.3967]
8 **Stastna M**, Janeckova L, Hrckulak D, Kriz V, Korinek V. Human Colorectal Cancer from the Perspective of Mouse Models. *Genes (Basel)* 2019; **10** [PMID: 31614493 DOI: 10.3390/genes10100788]
9 **Yuan S**, Tao F, Zhang X, Zhang Y, Sun X, Wu D. Role of Wnt/*β*-Catenin Signaling in the Chemoresistance Modulation of Colorectal Cancer. *Biomed Res Int* 2020; **2020**: 9390878 [PMID: 32258160 DOI: 10.1155/2020/9390878]
10 **Flores-Hernández E**, Velázquez DM, Castañeda-Patlán MC, Fuentes-García G, Fonseca-Camarillo G, Yamamoto-Furusho JK, Romero-Avila MT, García-Sáinz JA, Robles-Flores M. Canonical and non-canonical Wnt signaling are simultaneously activated by Wnts in colon cancer cells. *Cell Signal* 2020; **72**: 109636 [PMID: 32283254 DOI: 10.1016/j.cellsig.2020.109636]
11 **Bian J**, Dannappel M, Wan C, Firestein R. Transcriptional Regulation of Wnt/β-Catenin Pathway in Colorectal Cancer. *Cells* 2020; **9** [PMID: 32961708 DOI: 10.3390/cells9092125]
12 **Anthony CC**, Robbins DJ, Ahmed Y, Lee E. Nuclear Regulation of Wnt/β-Catenin Signaling: It's a Complex Situation. *Genes (Basel)* 2020; **11** [PMID: 32759724 DOI: 10.3390/genes11080886]

13 **Chatterjee A**, Paul S, Bisht B, Bhattacharya S, Sivasubramaniam S, Paul MK. Advances in targeting the WNT/β-catenin signaling pathway in cancer. *Drug Discov Today* 2022; **27**: 82-101 [PMID: 34252612 DOI: 10.1016/j.drudis.2021.07.007]

14 **Voloshanenko O**, Schwartz U, Kranz D, Rauscher B, Linnebacher M, Augustin I, Boutros M. β-catenin-independent regulation of Wnt target genes by RoR2 and ATF2/ATF4 in colon cancer cells. *Sci Rep* 2018; **8**: 3178 [PMID: 29453334 DOI: 10.1038/s41598-018-20641-5]

15 **Disoma C**, Zhou Y, Li S, Peng J, Xia Z. Wnt/β-catenin signaling in colorectal cancer: Is therapeutic targeting even possible? *Biochimie* 2022; **195**: 39-53 [PMID: 35066101 DOI: 10.1016/j.biochi.2022.01.009]

16 **Krishnamurthy N**, Kurzrock R. Targeting the Wnt/beta-catenin pathway in cancer: Update on effectors and inhibitors. *Cancer Treat Rev* 2018; **62**: 50-60 [PMID: 29169144 DOI: 10.1016/j.ctrv.2017.11.002]

17 **Li J**, Chen D, Shen M. Tumor Microenvironment Shapes Colorectal Cancer Progression, Metastasis, and Treatment Responses. *Front Med (Lausanne)* 2022; **9**: 869010 [PMID: 35402443 DOI: 10.3389/fmed.2022.869010]

18 **van Pelt GW**, Sandberg TP, Morreau H, Gelderblom H, van Krieken JHJM, Tollenaar RAEM, Mesker WE. The tumour-stroma ratio in colon cancer: the biological role and its prognostic impact. *Histopathology* 2018; **73**: 197-206 [PMID: 29457843 DOI: 10.1111/his.13489]

19 **Huang D**, Du X. Crosstalk between tumor cells and microenvironment *via* Wnt pathway in colorectal cancer dissemination. *World J Gastroenterol* 2008; **14**: 1823-1827 [PMID: 18350618 DOI: 10.3748/wjg.14.1823]

20 **Sandberg TP**, Stuart MPME, Oosting J, Tollenaar RAEM, Sier CFM, Mesker WE. Increased expression of cancer-associated fibroblast markers at the invasive front and its association with tumor-stroma ratio in colorectal cancer. *BMC Cancer* 2019; **19**: 284 [PMID: 30922247 DOI: 10.1186/s12885-019-5462-2]

21 **Laplagne C**, Domagala M, Le Naour A, Quemerais C, Hamel D, Fournié JJ, Couderc B, Bousquet C, Ferrand A, Poupot M. Latest Advances in Targeting the Tumor Microenvironment for Tumor Suppression. *Int J Mol Sci* 2019; **20** [PMID: 31547627 DOI: 10.3390/ijms20194719]

22 **Siveen KS**, Raza A, Ahmed EI, Khan AQ, Prabhu KS, Kuttikrishnan S, Mateo JM, Zayed H, Rasul K, Azizi F, Dermime S, Steinhoff M, Uddin S. The Role of Extracellular Vesicles as Modulators of the Tumor Microenvironment, Metastasis and Drug Resistance in Colorectal Cancer. *Cancers (Basel)* 2019; **11** [PMID: 31146452 DOI: 10.3390/cancers11060746]

23 **Gonda A**, Kabagwira J, Senthil GN, Wall NR. Internalization of Exosomes through Receptor-Mediated Endocytosis. *Mol Cancer Res* 2019; **17**: 337-347 [PMID: 30487244 DOI: 10.1158/1541-7786.MCR-18-0891]

24 **Hu JL**, Wang W, Lan XL, Zeng ZC, Liang YS, Yan YR, Song FY, Wang FF, Zhu XH, Liao WJ, Liao WT, Ding YQ, Liang L. CAFs secreted exosomes promote metastasis and chemotherapy resistance by enhancing cell stemness and epithelial-mesenchymal transition in colorectal cancer. *Mol Cancer* 2019; **18**: 91 [PMID: 31064356 DOI: 10.1186/s12943-019-1019-x]

25 **Ren J**, Ding L, Zhang D, Shi G, Xu Q, Shen S, Wang Y, Wang T, Hou Y. Carcinoma-associated fibroblasts promote the stemness and chemoresistance of colorectal cancer by transferring exosomal lncRNA H19. *Theranostics* 2018; **8**: 3932-3948 [PMID: 30083271 DOI: 10.7150/thno.25541]

26 **Viralippurath Ashraf J**, Sasidharan Nair V, Saleh R, Elkord E. Role of circular RNAs in colorectal tumor microenvironment. *Biomed Pharmacother* 2021; **137**: 111351 [PMID: 33550046 DOI: 10.1016/j.biopha.2021.111351]

27 **Gu C**, Lu H, Qian Z. Matrine reduces the secretion of exosomal circSLC7A6 from cancer-associated fibroblast to inhibit tumorigenesis of colorectal cancer by regulating CXCR5. *Biochem Biophys Res Commun* 2020; **527**: 638-645 [PMID: 32423804 DOI: 10.1016/j.bbrc.2020.04.142]

28 **Herrera M**, Llorens C, Rodríguez M, Herrera A, Ramos R, Gil B, Candia A, Larriba MJ, Garre P, Earl J, Rodríguez-Garrote M, Caldés T, Bonilla F, Carrato A, García-Barberán V, Peña C. Differential distribution and enrichment of non-coding RNAs in exosomes from normal and Cancer-associated fibroblasts in colorectal cancer. *Mol Cancer* 2018; **17**: 114 [PMID: 30075793 DOI: 10.1186/s12943-018-0863-4]

29 **Wortzel I**, Dror S, Kenific CM, Lyden D. Exosome-Mediated Metastasis: Communication from a Distance. *Dev Cell* 2019; **49**: 347-360 [PMID: 31063754 DOI: 10.1016/j.devcel.2019.04.011]

30 **Shao Y**, Chen T, Zheng X, Yang S, Xu K, Chen X, Xu F, Wang L, Shen Y, Wang T, Zhang M, Hu W, Ye C, Yu X, Shao J, Zheng S. Colorectal cancer-derived small extracellular vesicles establish an inflammatory premetastatic niche in liver metastasis. *Carcinogenesis* 2018; **39**: 1368-1379 [PMID: 30184100 DOI: 10.1093/carcin/bgy115]

31 **Abu N**, Othman N, Ab Razak NS, Bakarurraini NAAR, Nasir SN, Soh JEC, Mazlan L, Azman ZAM, Jamal R. Extracellular Vesicles Derived From Colorectal Cancer Affects CD8 T Cells: An Analysis Based on Body Mass Index. *Front Cell Dev Biol* 2020; **8**: 564648 [PMID: 33324632 DOI: 10.3389/fcell.2020.564648]

32 **Karpisheh V**, Nikkhoo A, Hojjat-Farsangi M, Namdar A, Azizi G, Ghalamfarsa G, Sabz G, Yousefi M, Yousefi B, Jadidi-Niaragh F. Prostaglandin E2 as a potent therapeutic target for treatment of colon cancer. *Prostaglandins Other Lipid Mediat* 2019; **144**: 106338 [PMID: 31100474 DOI: 10.1016/j.prostaglandins.2019.106338]

33 **Landskron G**, De la Fuente López M, Dubois-Camacho K, Díaz-Jiménez D, Orellana-Serradell O, Romero D, Sepúlveda SA, Salazar C, Parada-Venegas D, Quera R, Simian D, González MJ, López-Köstner F, Kronberg U, Abedrapo M, Gallegos I, Contreras HR, Peña C, Díaz-Araya G, Roa JC, Hermoso MA. Interleukin 33/ST2 Axis Components Are Associated to Desmoplasia, a Metastasis-Related Factor in Colorectal Cancer. *Front Immunol* 2019; **10**: 1394 [PMID: 31281317 DOI: 10.3389/fimmu.2019.01394]

34 **Martín MJ**, Gigola G, Zwenger A, Carriquiriborde M, Gentil F, Gentili C. Potential therapeutic targets for growth arrest of colorectal cancer cells exposed to PTHrP. *Mol Cell Endocrinol* 2018; **478**: 32-44 [PMID: 30009852 DOI: 10.1016/j.mce.2018.07.005]

35 **Calvo N**, Carriere P, Martín MJ, Gigola G, Gentili C. PTHrP treatment of colon cancer cells promotes tumor associated-angiogenesis by the effect of VEGF. *Mol Cell Endocrinol* 2019; **483**: 50-63 [PMID: 30639585 DOI: 10.1016/j.mce.2019.01.005]

36 **Carriere P**, Calvo N, Novoa Díaz MB, Lopez-Moncada F, Herrera A, Torres MJ, Alonso E, Gandini NA, Gigola G, Contreras HR, Gentili C. Role of SPARC in the epithelial-mesenchymal transition induced by PTHrP in human colon cancer cells. *Mol Cell Endocrinol* 2021; **530**: 111253 [PMID: 33781836 DOI: 10.1016/j.mce.2021.111253]

37 **Novoa Díaz MB**, Carriere PM, Martín MJ, Calvo N, Gentili C. Involvement of parathyroid hormone-related peptide in the

aggressive phenotype of colorectal cancer cells. *World J Gastroenterol* 2021; **27**: 7025-7040 [PMID: 34887626 DOI: 10.3748/wjg.v27.i41.7025]

38 **Muñoz-Galván S**, Lucena-Cacace A, Perez M, Otero-Albiol D, Gomez-Cambronero J, Carnero A. Tumor cell-secreted PLD increases tumor stemness by senescence-mediated communication with microenvironment. *Oncogene* 2019; **38**: 1309-1323 [PMID: 30305726 DOI: 10.1038/s41388-018-0527-2]

39 **Molinier-Frenkel V**, Castellano F. Immunosuppressive enzymes in the tumor microenvironment. *FEBS Lett* 2017; **591**: 3135-3157 [PMID: 28792588 DOI: 10.1002/1873-3468.12784]

40 **Cox TR**. The matrix in cancer. *Nat Rev Cancer* 2021; **21**: 217-238 [PMID: 33589810 DOI: 10.1038/s41568-020-00329-7]

41 **Sameer AS**, Nissar S. Toll-Like Receptors (TLRs): Structure, Functions, Signaling, and Role of Their Polymorphisms in Colorectal Cancer Susceptibility. *Biomed Res Int* 2021; **2021**: 1157023 [PMID: 34552981 DOI: 10.1155/2021/1157023]

42 **Angrini M**, Varthaman A, Cremer I. Toll-Like Receptors (TLRs) in the Tumor Microenvironment (TME): A Dragon-Like Weapon in a Non-fantasy Game of Thrones. *Adv Exp Med Biol* 2020; **1263**: 145-173 [PMID: 32588327 DOI: 10.1007/978-3-030-44518-8_9]

43 **Kamal Y**, Schmit SL, Frost HR, Amos CI. The tumor microenvironment of colorectal cancer metastases: opportunities in cancer immunotherapy. *Immunotherapy* 2020; **12**: 1083-1100 [PMID: 32787587 DOI: 10.2217/imt-2020-0026]

44 **Unterleuthner D**, Neuhold P, Schwarz K, Janker L, Neuditschko B, Nivarthi H, Crncec I, Kramer N, Unger C, Hengstschläger M, Eferl R, Moriggl R, Sommergruber W, Gerner C, Dolznig H. Cancer-associated fibroblast-derived WNT2 increases tumor angiogenesis in colon cancer. *Angiogenesis* 2020; **23**: 159-177 [PMID: 31667643 DOI: 10.1007/s10456-019-09688-8]

45 **Aizawa T**, Karasawa H, Funayama R, Shirota M, Suzuki T, Maeda S, Suzuki H, Yamamura A, Naitoh T, Nakayama K, Unno M. Cancer-associated fibroblasts secrete Wnt2 to promote cancer progression in colorectal cancer. *Cancer Med* 2019; **8**: 6370-6382 [PMID: 31468733 DOI: 10.1002/cam4.2523]

46 **Matsumoto K**, Umitsu M, De Silva DM, Roy A, Bottaro DP. Hepatocyte growth factor/MET in cancer progression and biomarker discovery. *Cancer Sci* 2017; **108**: 296-307 [PMID: 28064454 DOI: 10.1111/cas.13156]

47 **Goïta AA**, Guenot D. Colorectal Cancer: The Contribution of CXCL12 and Its Receptors CXCR4 and CXCR7. *Cancers (Basel)* 2022; **14** [PMID: 35406582 DOI: 10.3390/cancers14071810]

48 **Martín MJ**, Calvo N, de Boland AR, Gentili C. Molecular mechanisms associated with PTHrP-induced proliferation of colon cancer cells. *J Cell Biochem* 2014; **115**: 2133-2145 [PMID: 25053227 DOI: 10.1002/jcb.24890]

49 **Amable G**, Martínez-León E, Picco ME, Di Siervi N, Davio C, Rozengurt E, Rey O. Metformin inhibits β-catenin phosphorylation on Ser-552 through an AMPK/PI3K/Akt pathway in colorectal cancer cells. *Int J Biochem Cell Biol* 2019; **112**: 88-94 [PMID: 31082618 DOI: 10.1016/j.biocel.2019.05.004]

50 **Yan X**, Zhao J, Zhang R. Interleukin-37 mediates the antitumor activity in colon cancer through β-catenin suppression. *Oncotarget* 2017; **8**: 49064-49075 [PMID: 28467774 DOI: 10.18632/oncotarget.17093]

51 **Voorneveld PW**, Kodach LL, Jacobs RJ, van Noesel CJ, Peppelenbosch MP, Korkmaz KS, Molendijk I, Dekker E, Morreau H, van Pelt GW, Tollenaar RA, Mesker W, Hawinkels LJ, Paauwe M, Verspaget HW, Geraets DT, Hommes DW, Offerhaus GJ, van den Brink GR, Ten Dijke P, Hardwick JC. The BMP pathway either enhances or inhibits the Wnt pathway depending on the SMAD4 and p53 status in CRC. *Br J Cancer* 2015; **112**: 122-130 [PMID: 25393365 DOI: 10.1038/bjc.2014.560]

52 **Essex A**, Pineda J, Acharya G, Xin H, Evans J; Reproducibility Project: Cancer Biology. Replication Study: Wnt activity defines colon cancer stem cells and is regulated by the microenvironment. *Elife* 2019; **8** [PMID: 31215867 DOI: 10.7554/eLife.45426]

53 **Vermeulen L**, De Sousa E Melo F, van der Heijden M, Cameron K, de Jong JH, Borovski T, Tuynman JB, Todaro M, Merz C, Rodermond H, Sprick MR, Kemper K, Richel DJ, Stassi G, Medema JP. Wnt activity defines colon cancer stem cells and is regulated by the microenvironment. *Nat Cell Biol* 2010; **12**: 468-476 [PMID: 20418870 DOI: 10.1038/ncb2048]

54 **Zhang L**, Jiang X, Li Y, Fan Q, Li H, Jin L, Li L, Jin Y, Zhang T, Mao Y, Hua D. Clinical Correlation of Wnt2 and COL8A1 With Colon Adenocarcinoma Prognosis. *Front Oncol* 2020; **10**: 1504 [PMID: 32983993 DOI: 10.3389/fonc.2020.01504]

55 **Koliaraki V**, Pallangyo CK, Greten FR, Kollias G. Mesenchymal Cells in Colon Cancer. *Gastroenterology* 2017; **152**: 964-979 [PMID: 28111227 DOI: 10.1053/j.gastro.2016.11.049]

56 **Kalra H**, Gangoda L, Fonseka P, Chitti SV, Liem M, Keerthikumar S, Samuel M, Boukouris S, Al Saffar H, Collins C, Adda CG, Ang CS, Mathivanan S. Extracellular vesicles containing oncogenic mutant β-catenin activate Wnt signalling pathway in the recipient cells. *J Extracell Vesicles* 2019; **8**: 1690217 [PMID: 31819794 DOI: 10.1080/20013078.2019.1690217]

57 **Hu Y**, Yan C, Mu L, Huang K, Li X, Tao D, Wu Y, Qin J. Fibroblast-Derived Exosomes Contribute to Chemoresistance through Priming Cancer Stem Cells in Colorectal Cancer. *PLoS One* 2015; **10**: e0125625 [PMID: 25938772 DOI: 10.1371/journal.pone.0125625]

58 **Hu YB**, Yan C, Mu L, Mi YL, Zhao H, Hu H, Li XL, Tao DD, Wu YQ, Gong JP, Qin JC. Exosomal Wnt-induced dedifferentiation of colorectal cancer cells contributes to chemotherapy resistance. *Oncogene* 2019; **38**: 1951-1965 [PMID: 30390075 DOI: 10.1038/s41388-018-0557-9]

59 **Dong HJ**, Jang GB, Lee HY, Park SR, Kim JY, Nam JS, Hong IS. The Wnt/β-catenin signaling/Id2 cascade mediates the effects of hypoxia on the hierarchy of colorectal-cancer stem cells. *Sci Rep* 2016; **6**: 22966 [PMID: 26965643 DOI: 10.1038/srep22966]

60 **Huang Z**, Yang M, Li Y, Yang F, Feng Y. Exosomes Derived from Hypoxic Colorectal Cancer Cells Transfer Wnt4 to Normoxic Cells to Elicit a Prometastatic Phenotype. *Int J Biol Sci* 2018; **14**: 2094-2102 [PMID: 30585272 DOI: 10.7150/ijbs.28288]

61 **Huang Z**, Feng Y. Exosomes Derived From Hypoxic Colorectal Cancer Cells Promote Angiogenesis Through Wnt4-Induced β-Catenin Signaling in Endothelial Cells. *Oncol Res* 2017; **25**: 651-661 [PMID: 27712599 DOI: 10.3727/096504016X14752792816791]

62 **Pérez-Plasencia C**, López-Urrutia E, García-Castillo V, Trujano-Camacho S, López-Camarillo C, Campos-Parra AD. Interplay Between Autophagy and Wnt/β-Catenin Signaling in Cancer: Therapeutic Potential Through Drug Repositioning. *Front Oncol* 2020; **10**: 1037 [PMID: 33014767 DOI: 10.3389/fonc.2020.01037]

63 **Janji B**, Berchem G, Chouaib S. Targeting Autophagy in the Tumor Microenvironment: New Challenges and Opportunities for Regulating Tumor Immunity. *Front Immunol* 2018; **9**: 887 [PMID: 29922284 DOI: 10.3389/fimmu.2018.00887]

64 **Pandurangan AK**, Divya T, Kumar K, Dineshbabu V, Velavan B, Sudhandiran G. Colorectal carcinogenesis: Insights into the cell death and signal transduction pathways: A review. *World J Gastrointest Oncol* 2018; **10**: 244-259 [PMID: 30254720 DOI: 10.4251/wjgo.v10.i9.244]

65 **Janji B**, Hasmim M, Parpal S, Berchem G, Noman MZ. Firing up the cold tumors by targeting Vps34. *Oncoimmunology* 2020; **9**: 1809936 [PMID: 32939326 DOI: 10.1080/2162402X.2020.1809936]

66 **Rahmani F**, Avan A, Hashemy SI, Hassanian SM. Role of Wnt/β-catenin signaling regulatory microRNAs in the pathogenesis of colorectal cancer. *J Cell Physiol* 2018; **233**: 811-817 [PMID: 28266708 DOI: 10.1002/jcp.25897]

67 **Zhang H**, Yu C, Dai J, Keller JM, Hua A, Sottnik JL, Shelley G, Hall CL, Park SI, Yao Z, Zhang J, McCauley LK, Keller ET. Parathyroid hormone-related protein inhibits DKK1 expression through c-Jun-mediated inhibition of β-catenin activation of the DKK1 promoter in prostate cancer. *Oncogene* 2014; **33**: 2464-2477 [PMID: 23752183 DOI: 10.1038/onc.2013.203]

68 **Hiremath M**, Dann P, Fischer J, Butterworth D, Boras-Granic K, Hens J, Van Houten J, Shi W, Wysolmerski J. Parathyroid hormone-related protein activates Wnt signaling to specify the embryonic mammary mesenchyme. *Development* 2012; **139**: 4239-4249 [PMID: 23034629 DOI: 10.1242/dev.080671]

69 **Johnson RW**, Merkel AR, Page JM, Ruppender NS, Guelcher SA, Sterling JA. Wnt signaling induces gene expression of factors associated with bone destruction in lung and breast cancer. *Clin Exp Metastasis* 2014; **31**: 945-959 [PMID: 25359619 DOI: 10.1007/s10585-014-9682-1]

70 **Chen HY**, Lang YD, Lin HN, Liu YR, Liao CC, Nana AW, Yen Y, Chen RH. miR-103/107 prolong Wnt/β-catenin signaling and colorectal cancer stemness by targeting Axin2. *Sci Rep* 2019; **9**: 9687 [PMID: 31273221 DOI: 10.1038/s41598-019-41053-z]

71 **Ba S**, Xuan Y, Long ZW, Chen HY, Zheng SS. MicroRNA-27a Promotes the Proliferation and Invasiveness of Colon Cancer Cells by Targeting SFRP1 through the Wnt/β-Catenin Signaling Pathway. *Cell Physiol Biochem* 2017; **42**: 1920-1933 [PMID: 28772260 DOI: 10.1159/000479610]

72 **Chu J**, Fang X, Sun Z, Gai L, Dai W, Li H, Yan X, Du J, Zhang L, Zhao L, Xu D, Yan S. Non-Coding RNAs Regulate the Resistance to Anti-EGFR Therapy in Colorectal Cancer. *Front Oncol* 2021; **11**: 801319 [PMID: 35111681 DOI: 10.3389/fonc.2021.801319]

73 **Zhang L**, Dong X, Yan B, Yu W, Shan L. CircAGFG1 drives metastasis and stemness in colorectal cancer by modulating YY1/CTNNB1. *Cell Death Dis* 2020; **11**: 542 [PMID: 32681092 DOI: 10.1038/s41419-020-2707-6]

74 **Fang G**, Ye BL, Hu BR, Ruan XJ, Shi YX. CircRNA_100290 promotes colorectal cancer progression through miR-516b-induced downregulation of FZD4 expression and Wnt/β-catenin signaling. *Biochem Biophys Res Commun* 2018; **504**: 184-189 [PMID: 30173892 DOI: 10.1016/j.bbrc.2018.08.152]

75 **Jin YD**, Ren YR, Gao YX, Zhang L, Ding Z. Hsa_circ_0005075 predicts a poor prognosis and acts as an oncogene in colorectal cancer *via* activating Wnt/β-catenin pathway. *Eur Rev Med Pharmacol Sci* 2019; **23**: 3311-3319 [PMID: 31081084 DOI: 10.26355/eurrev_201904_17693]

76 **Ge Z**, Li LF, Wang CY, Wang Y, Ma WL. CircMTO1 inhibits cell proliferation and invasion by regulating Wnt/β-catenin signaling pathway in colorectal cancer. *Eur Rev Med Pharmacol Sci* 2018; **22**: 8203-8209 [PMID: 30556859 DOI: 10.26355/eurrev_201812_16513]

77 **Chen H**, Pei L, Xie P, Guo G. Circ-PRKDC Contributes to 5-Fluorouracil Resistance of Colorectal Cancer Cells by Regulating miR-375/FOXM1 Axis and Wnt/β-Catenin Pathway. *Onco Targets Ther* 2020; **13**: 5939-5953 [PMID: 32606803 DOI: 10.2147/OTT.S253468]

78 **Su K**, Yi Q, Dai X, Liu O. Circular RNA ITCH: An Emerging Multifunctional Regulator. *Biomolecules* 2022; **12** [PMID: 35327551 DOI: 10.3390/biom12030359]

79 **Geng Y**, Zheng X, Hu W, Wang Q, Xu Y, He W, Wu C, Zhu D, Jiang J. Hsa_circ_0009361 acts as the sponge of miR-582 to suppress colorectal cancer progression by regulating APC2 expression. *Clin Sci (Lond)* 2019; **133**: 1197-1213 [PMID: 31109967 DOI: 10.1042/CS20190286]

80 **Wang J**, Du Y, Liu X, Cho WC, Yang Y. MicroRNAs as Regulator of Signaling Networks in Metastatic Colon Cancer. *Biomed Res Int* 2015; **2015**: 823620 [PMID: 26064956 DOI: 10.1155/2015/823620]

81 **Tomida C**, Yamagishi N, Nagano H, Uchida T, Ohno A, Hirasaka K, Nikawa T, Teshima-Kondo S. VEGF pathway-targeting drugs induce evasive adaptation by activation of neuropilin-1/cMet in colon cancer cells. *Int J Oncol* 2018; **52**: 1350-1362 [PMID: 29532881 DOI: 10.3892/ijo.2018.4291]

82 **Wei X**, Li X, Kong F, Ma L, Sui Y, Chen D, Xu F. [TNF-α activates Wnt signaling pathway to promote the invasion of human colon cancer stem cells]. *Xi Bao Yu Fen Zi Mian Yi Xue Za Zhi* 2018; **34**: 982-988 [PMID: 30591106]

83 **Zheng Y**, Zhou C, Yu XX, Wu C, Jia HL, Gao XM, Yang JM, Wang CQ, Luo Q, Zhu Y, Zhang Y, Wei JW, Sheng YY, Dong QZ, Qin LX. Osteopontin promotes metastasis of intrahepatic cholangiocarcinoma through recruiting MAPK1 and mediating Ser675 phosphorylation of β-Catenin. *Cell Death Dis* 2018; **9**: 179 [PMID: 29415992 DOI: 10.1038/s41419-017-0226-x]

84 **Yi J**, Liu Y, Zhang L, Fang C. Secreted phosphoprotein-1 accelerates the progression of human colorectal cancer through activating β-catenin signaling. *Oncol Lett* 2021; **21**: 372 [PMID: 33777196 DOI: 10.3892/ol.2021.12633]

85 **Youssef NS**, Osman WM. Relationship between osteopontin and β-catenin immunohistochemical expression and prognostic parameters of colorectal carcinoma. *Int J Clin Exp Pathol* 2015; **8**: 1503-1514 [PMID: 25973035]

86 **Ishigamori R**, Komiya M, Takasu S, Mutoh M, Imai T, Takahashi M. Osteopontin Deficiency Suppresses Intestinal Tumor Development in Apc-Deficient Min Mice. *Int J Mol Sci* 2017; **18** [PMID: 28505114 DOI: 10.3390/ijms18051058]

87 **Kaler P**, Augenlicht L, Klampfer L. Macrophage-derived IL-1beta stimulates Wnt signaling and growth of colon cancer

cells: a crosstalk interrupted by vitamin D3. *Oncogene* 2009; **28**: 3892-3902 [PMID: 19701245 DOI: 10.1038/onc.2009.247]

88 **Bach DH**, Park HJ, Lee SK. The Dual Role of Bone Morphogenetic Proteins in Cancer. *Mol Ther Oncolytics* 2018; **8**: 1-13 [PMID: 29234727 DOI: 10.1016/j.omto.2017.10.002]

89 **Kaler P**, Galea V, Augenlicht L, Klampfer L. Tumor associated macrophages protect colon cancer cells from TRAIL-induced apoptosis through IL-1beta-dependent stabilization of Snail in tumor cells. *PLoS One* 2010; **5**: e11700 [PMID: 20661477 DOI: 10.1371/journal.pone.0011700]

90 **Gao S**, Hu J, Wu X, Liang Z. PMA treated THP-1-derived-IL-6 promotes EMT of SW48 through STAT3/ERK-dependent activation of Wnt/β-catenin signaling pathway. *Biomed Pharmacother* 2018; **108**: 618-624 [PMID: 30243096 DOI: 10.1016/j.biopha.2018.09.067]

91 **Song ZY**, Gao ZH, Chu JH, Han XZ, Qu XJ. Downregulation of the CXCR4/CXCL12 axis blocks the activation of the Wnt/β-catenin pathway in human colon cancer cells. *Biomed Pharmacother* 2015; **71**: 46-52 [PMID: 25960214 DOI: 10.1016/j.biopha.2015.01.020]

92 **La Fleur L**, Botling J, He F, Pelicano C, Zhou C, He C, Palano G, Mezheyeuski A, Micke P, Ravetch JV, Karlsson MCI, Sarhan D. Targeting MARCO and IL37R on Immunosuppressive Macrophages in Lung Cancer Blocks Regulatory T Cells and Supports Cytotoxic Lymphocyte Function. *Cancer Res* 2021; **81**: 956-967 [PMID: 33293426 DOI: 10.1158/0008-5472.CAN-20-1885]

93 **Li J**, Zhang AH, Wu FF, Wang XJ. Alterations in the Gut Microbiota and Their Metabolites in Colorectal Cancer: Recent Progress and Future Prospects. *Front Oncol* 2022; **12**: 841552 [PMID: 35223525 DOI: 10.3389/fonc.2022.841552]

94 **Yachida S**, Mizutani S, Shiroma H, Shiba S, Nakajima T, Sakamoto T, Watanabe H, Masuda K, Nishimoto Y, Kubo M, Hosoda F, Rokutan H, Matsumoto M, Takamaru H, Yamada M, Matsuda T, Iwasaki M, Yamaji T, Yachida T, Soga T, Kurokawa K, Toyoda A, Ogura Y, Hayashi T, Hatakeyama M, Nakagama H, Saito Y, Fukuda S, Shibata T, Yamada T. Metagenomic and metabolomic analyses reveal distinct stage-specific phenotypes of the gut microbiota in colorectal cancer. *Nat Med* 2019; **25**: 968-976 [PMID: 31171880 DOI: 10.1038/s41591-019-0458-7]

95 **Kim YJ**, Kim BK, Park SJ, Kim JH. Impact of *Fusobacterium nucleatum* in the gastrointestinal tract on natural killer cells. *World J Gastroenterol* 2021; **27**: 4879-4889 [PMID: 34447232 DOI: 10.3748/wjg.v27.i29.4879]

96 **Rubinstein MR**, Baik JE, Lagana SM, Han RP, Raab WJ, Sahoo D, Dalerba P, Wang TC, Han YW. *Fusobacterium nucleatum* promotes colorectal cancer by inducing Wnt/β-catenin modulator Annexin A1. *EMBO Rep* 2019; **20** [PMID: 30833345 DOI: 10.15252/embr.201847638]

97 **Parsons S**, Maldonado EB, Prasad V. Comparison of Drugs Used for Adjuvant and Metastatic Therapy of Colon, Breast, and Non-Small Cell Lung Cancers. *JAMA Netw Open* 2020; **3**: e202488 [PMID: 32275321 DOI: 10.1001/jamanetworkopen.2020.2488]

98 **Chang CL**, Yuan KS, Wu ATH, Wu SY. Adjuvant Therapy for High-Risk Stage II or III Colon Adenocarcinoma: A Propensity Score-Matched, Nationwide, Population-Based Cohort Study. *Cancers (Basel)* 2019; **11** [PMID: 31842371 DOI: 10.3390/cancers11122003]

99 **Hu T**, Li Z, Gao CY, Cho CH. Mechanisms of drug resistance in colon cancer and its therapeutic strategies. *World J Gastroenterol* 2016; **22**: 6876-6889 [PMID: 27570424 DOI: 10.3748/wjg.v22.i30.6876]

100 **Meyers BM**, Cosby R, Quereshy F, Jonker D. Adjuvant Chemotherapy for Stage II and III Colon Cancer Following Complete Resection: A Cancer Care Ontario Systematic Review. *Clin Oncol (R Coll Radiol)* 2017; **29**: 459-465 [PMID: 28341242 DOI: 10.1016/j.clon.2017.03.001]

101 **Shibue T**, Weinberg RA. EMT, CSCs, and drug resistance: the mechanistic link and clinical implications. *Nat Rev Clin Oncol* 2017; **14**: 611-629 [PMID: 28397828 DOI: 10.1038/nrclinonc.2017.44]

102 **Erin N**, Grahovac J, Brozovic A, Efferth T. Tumor microenvironment and epithelial mesenchymal transition as targets to overcome tumor multidrug resistance. *Drug Resist Updat* 2020; **53**: 100715 [PMID: 32679188 DOI: 10.1016/j.drup.2020.100715]

103 **Gupta R**, Bhatt LK, Johnston TP, Prabhavalkar KS. Colon cancer stem cells: Potential target for the treatment of colorectal cancer. *Cancer Biol Ther* 2019; **20**: 1068-1082 [PMID: 31050577 DOI: 10.1080/15384047.2019.1599660]

104 **Tauriello DV**, Calon A, Lonardo E, Batlle E. Determinants of metastatic competency in colorectal cancer. *Mol Oncol* 2017; **11**: 97-119 [PMID: 28085225 DOI: 10.1002/1878-0261.12018]

105 **Wang M**, Han D, Yuan Z, Hu H, Zhao Z, Yang R, Jin Y, Zou C, Chen Y, Wang G, Gao X, Wang X. Long non-coding RNA H19 confers 5-Fu resistance in colorectal cancer by promoting SIRT1-mediated autophagy. *Cell Death Dis* 2018; **9**: 1149 [PMID: 30451820 DOI: 10.1038/s41419-018-1187-4]

106 **Barisciano G**, Colangelo T, Rosato V, Muccillo L, Taddei ML, Ippolito L, Chiarugi P, Galgani M, Bruzzaniti S, Matarese G, Fassan M, Agostini M, Bergamo F, Pucciarelli S, Carbone A, Mazzoccoli G, Colantuoni V, Bianchi F, Sabatino L. miR-27a is a master regulator of metabolic reprogramming and chemoresistance in colorectal cancer. *Br J Cancer* 2020; **122**: 1354-1366 [PMID: 32132656 DOI: 10.1038/s41416-020-0773-2]

107 **Zhou H**, Lin C, Zhang Y, Zhang X, Zhang C, Zhang P, Xie X, Ren Z. miR-506 enhances the sensitivity of human colorectal cancer cells to oxaliplatin by suppressing MDR1/P-gp expression. *Cell Prolif* 2017; **50** [PMID: 28217977 DOI: 10.1111/cpr.12341]

108 **Zhang Q**, Wang W, Zhou Q, Chen C, Yuan W, Liu J, Li X, Sun Z. Roles of circRNAs in the tumour microenvironment. *Mol Cancer* 2020; **19**: 14 [PMID: 31973726 DOI: 10.1186/s12943-019-1125-9]

109 **Kaler P**, Godasi BN, Augenlicht L, Klampfer L. The NF-κB/AKT-dependent Induction of Wnt Signaling in Colon Cancer Cells by Macrophages and IL-1β. *Cancer Microenviron* 2009; **2**: 69-80 [PMID: 19779850 DOI: 10.1007/s12307-009-0030-y]

110 **Yoshida GJ**. Regulation of heterogeneous cancer-associated fibroblasts: the molecular pathology of activated signaling pathways. *J Exp Clin Cancer Res* 2020; **39**: 112 [PMID: 32546182 DOI: 10.1186/s13046-020-01611-0]

111 **Kim KH**, Kim H. Progress of antibody-based inhibitors of the HGF-cMET axis in cancer therapy. *Exp Mol Med* 2017; **49**: e307 [PMID: 28336955 DOI: 10.1038/emm.2017.17]

112 **Hwang K**, Yoon JH, Lee JH, Lee S. Recent Advances in Monoclonal Antibody Therapy for Colorectal Cancers.

Biomedicines 2021; **9** [PMID: 33466394 DOI: 10.3390/biomedicines9010039]

113 **Huang X**, Li E, Shen H, Wang X, Tang T, Zhang X, Xu J, Tang Z, Guo C, Bai X, Liang T. Targeting the HGF/MET Axis in Cancer Therapy: Challenges in Resistance and Opportunities for Improvement. *Front Cell Dev Biol* 2020; **8**: 152 [PMID: 32435640 DOI: 10.3389/fcell.2020.00152]

114 **Li M**, Li M, Yin T, Shi H, Wen Y, Zhang B, Chen M, Xu G, Ren K, Wei Y. Targeting of cancerassociated fibroblasts enhances the efficacy of cancer chemotherapy by regulating the tumor microenvironment. *Mol Med Rep* 2016; **13**: 2476-2484 [PMID: 26846566 DOI: 10.3892/mmr.2016.4868]

115 **Novellasdemunt L**, Antas P, Li VS. Targeting Wnt signaling in colorectal cancer. A Review in the Theme: Cell Signaling: Proteins, Pathways and Mechanisms. *Am J Physiol Cell Physiol* 2015; **309**: C511-C521 [PMID: 26289750 DOI: 10.1152/ajpcell.00117.2015]

116 **Shang S**, Hua F, Hu ZW. The regulation of β-catenin activity and function in cancer: therapeutic opportunities. *Oncotarget* 2017; **8**: 33972-33989 [PMID: 28430641 DOI: 10.18632/oncotarget.15687]

117 **de Assis JV**, Coutinho LA, Oyeyemi IT, Oyeyemi OT, Grenfell RFEQ. Diagnostic and therapeutic biomarkers in colorectal cancer: a review. *Am J Cancer Res* 2022; **12**: 661-680 [PMID: 35261794]

118 **Moon JH**, Hong SW, Kim JE, Shin JS, Kim JS, Jung SA, Ha SH, Lee S, Kim J, Lee DH, Park YS, Kim DM, Park SS, Hong JK, Kim DY, Kim EH, Jung J, Kim MJ, Kim SM, Deming DA, Kim K, Kim TW, Jin DH. Targeting β-catenin overcomes MEK inhibition resistance in colon cancer with KRAS and PIK3CA mutations. *Br J Cancer* 2019; **120**: 941-951 [PMID: 30944457 DOI: 10.1038/s41416-019-0434-5]

119 **Haseeb M**, Pirzada RH, Ain QU, Choi S. Wnt Signaling in the Regulation of Immune Cell and Cancer Therapeutics. *Cells* 2019; **8** [PMID: 31684152 DOI: 10.3390/cells8111380]

120 **Li X**, Xiang Y, Li F, Yin C, Li B, Ke X. WNT/β-Catenin Signaling Pathway Regulating T Cell-Inflammation in the Tumor Microenvironment. *Front Immunol* 2019; **10**: 2293 [PMID: 31616443 DOI: 10.3389/fimmu.2019.02293]

121 **Hong Y**, Manoharan I, Suryawanshi A, Majumdar T, Angus-Hill ML, Koni PA, Manicassamy B, Mellor AL, Munn DH, Manicassamy S. β-catenin promotes regulatory T-cell responses in tumors by inducing vitamin A metabolism in dendritic cells. *Cancer Res* 2015; **75**: 656-665 [PMID: 25568183 DOI: 10.1158/0008-5472.CAN-14-2377]

122 **Luke JJ**, Bao R, Sweis RF, Spranger S, Gajewski TF. WNT/β-catenin Pathway Activation Correlates with Immune Exclusion across Human Cancers. *Clin Cancer Res* 2019; **25**: 3074-3083 [PMID: 30635339 DOI: 10.1158/1078-0432.CCR-18-1942]

123 **Spranger S**, Bao R, Gajewski TF. Melanoma-intrinsic β-catenin signalling prevents anti-tumour immunity. *Nature* 2015; **523**: 231-235 [PMID: 25970248 DOI: 10.1038/nature14404]

124 **Lal N**, White BS, Goussous G, Pickles O, Mason MJ, Beggs AD, Taniere P, Willcox BE, Guinney J, Middleton GW. KRAS Mutation and Consensus Molecular Subtypes 2 and 3 Are Independently Associated with Reduced Immune Infiltration and Reactivity in Colorectal Cancer. *Clin Cancer Res* 2018; **24**: 224-233 [PMID: 29061646 DOI: 10.1158/1078-0432.CCR-17-1090]

125 **Grasso CS**, Giannakis M, Wells DK, Hamada T, Mu XJ, Quist M, Nowak JA, Nishihara R, Qian ZR, Inamura K, Morikawa T, Nosho K, Abril-Rodriguez G, Connolly C, Escuin-Ordinas H, Geybels MS, Grady WM, Hsu L, Hu-Lieskovan S, Huyghe JR, Kim YJ, Krystofinski P, Leiserson MDM, Montoya DJ, Nadel BB, Pellegrini M, Pritchard CC, Puig-Saus C, Quist EH, Raphael BJ, Salipante SJ, Shin DS, Shinbrot E, Shirts B, Shukla S, Stanford JL, Sun W, Tsoi J, Upfill-Brown A, Wheeler DA, Wu CJ, Yu M, Zaidi SH, Zaretsky JM, Gabriel SB, Lander ES, Garraway LA, Hudson TJ, Fuchs CS, Ribas A, Ogino S, Peters U. Genetic Mechanisms of Immune Evasion in Colorectal Cancer. *Cancer Discov* 2018; **8**: 730-749 [PMID: 29510987 DOI: 10.1158/2159-8290.CD-17-1327]

126 **Pai SG**, Carneiro BA, Mota JM, Costa R, Leite CA, Barroso-Sousa R, Kaplan JB, Chae YK, Giles FJ. Wnt/beta-catenin pathway: modulating anticancer immune response. *J Hematol Oncol* 2017; **10**: 101 [PMID: 28476164 DOI: 10.1186/s13045-017-0471-6]

127 **Payandeh Z**, Khalili S, Somi MH, Mard-Soltani M, Baghbanzadeh A, Hajiasgharzadeh K, Samadi N, Baradaran B. PD-1/PD-L1-dependent immune response in colorectal cancer. *J Cell Physiol* 2020; **235**: 5461-5475 [PMID: 31960962 DOI: 10.1002/jcp.29494]

128 **Spranger S**, Dai D, Horton B, Gajewski TF. Tumor-Residing Batf3 Dendritic Cells Are Required for Effector T Cell Trafficking and Adoptive T Cell Therapy. *Cancer Cell* 2017; **31**: 711-723.e4 [PMID: 28486109 DOI: 10.1016/j.ccell.2017.04.003]

129 **Rimassa L**, Bozzarelli S, Pietrantonio F, Cordio S, Lonardi S, Toppo L, Zaniboni A, Bordonaro R, Di Bartolomeo M, Tomasello G, Dadduzio V, Tronconi MC, Piombo C, Giordano L, Gloghini A, Di Tommaso L, Santoro A. Phase II Study of Tivantinib and Cetuximab in Patients With KRAS Wild-type Metastatic Colorectal Cancer With Acquired Resistance to EGFR Inhibitors and Emergence of MET Overexpression: Lesson Learned for Future Trials With EGFR/MET Dual Inhibition. *Clin Colorectal Cancer* 2019; **18**: 125-132.e2 [PMID: 30846365 DOI: 10.1016/j.clcc.2019.02.004]

130 **Wu ZX**, Yang Y, Teng QX, Wang JQ, Lei ZN, Lusvarghi S, Ambudkar SV, Yang DH, Chen ZS. Tivantinib, A c-Met Inhibitor in Clinical Trials, Is Susceptible to ABCG2-Mediated Drug Resistance. *Cancers (Basel)* 2020; **12** [PMID: 31940916 DOI: 10.3390/cancers12010186]

131 **Meyerhardt JA**, Shi Q, Fuchs CS, Meyer J, Niedzwiecki D, Zemla T, Kumthekar P, Guthrie KA, Couture F, Kuebler P, Bendell JC, Kumar P, Lewis D, Tan B, Bertagnolli M, Grothey A, Hochster HS, Goldberg RM, Venook A, Blanke C, O'Reilly EM, Shields AF. Effect of Celecoxib *vs* Placebo Added to Standard Adjuvant Therapy on Disease-Free Survival Among Patients With Stage III Colon Cancer: The CALGB/SWOG 80702 (Alliance) Randomized Clinical Trial. *JAMA* 2021; **325**: 1277-1286 [PMID: 33821899 DOI: 10.1001/jama.2021.2454]

132 **Turano M**, Cammarota F, Duraturo F, Izzo P, De Rosa M. A Potential Role of IL-6/IL-6R in the Development and Management of Colon Cancer. *Membranes (Basel)* 2021; **11** [PMID: 33923292 DOI: 10.3390/membranes11050312]

133 **Zhao H**, Wu L, Yan G, Chen Y, Zhou M, Wu Y, Li Y. Inflammation and tumor progression: signaling pathways and targeted intervention. *Signal Transduct Target Ther* 2021; **6**: 263 [PMID: 34248142 DOI: 10.1038/s41392-021-00658-5]

134 **Vaghari-Tabari M**, Majidinia M, Moein S, Qujeq D, Asemi Z, Alemi F, Mohamadzadeh R, Targhazeh N, Safa A, Yousefi B. MicroRNAs and colorectal cancer chemoresistance: New solution for old problem. *Life Sci* 2020; **259**: 118255

[PMID: 32818543 DOI: 10.1016/j.lfs.2020.118255]

135 **Azwar S**, Seow HF, Abdullah M, Faisal Jabar M, Mohtarrudin N. Recent Updates on Mechanisms of Resistance to 5-Fluorouracil and Reversal Strategies in Colon Cancer Treatment. *Biology (Basel)* 2021; **10** [PMID: 34571731 DOI: 10.3390/biology10090854]

136 **van Meeteren LA**, Thorikay M, Bergqvist S, Pardali E, Stampino CG, Hu-Lowe D, Goumans MJ, ten Dijke P. Anti-human activin receptor-like kinase 1 (ALK1) antibody attenuates bone morphogenetic protein 9 (BMP9)-induced ALK1 signaling and interferes with endothelial cell sprouting. *J Biol Chem* 2012; **287**: 18551-18561 [PMID: 22493445 DOI: 10.1074/jbc.M111.338103]

137 **Panda PK**, Naik PP, Praharaj PP, Meher BR, Gupta PK, Verma RS, Maiti TK, Shanmugam MK, Chinnathambi A, Alharbi SA, Sethi G, Agarwal R, Bhutia SK. Abrus agglutinin stimulates BMP-2-dependent differentiation through autophagic degradation of β-catenin in colon cancer stem cells. *Mol Carcinog* 2018; **57**: 664-677 [PMID: 29457276 DOI: 10.1002/mc.22791]

138 **Kim BR**, Oh SC, Lee DH, Kim JL, Lee SY, Kang MH, Lee SI, Kang S, Joung SY, Min BW. BMP-2 induces motility and invasiveness by promoting colon cancer stemness through STAT3 activation. *Tumour Biol* 2015; **36**: 9475-9486 [PMID: 26124007 DOI: 10.1007/s13277-015-3681-y]

139 **Todaro M**, Gaggianesi M, Catalano V, Benfante A, Iovino F, Biffoni M, Apuzzo T, Sperduti I, Volpe S, Cocorullo G, Gulotta G, Dieli F, De Maria R, Stassi G. CD44v6 is a marker of constitutive and reprogrammed cancer stem cells driving colon cancer metastasis. *Cell Stem Cell* 2014; **14**: 342-356 [PMID: 24607406 DOI: 10.1016/j.stem.2014.01.009]

140 **Mizuno R**, Kawada K, Itatani Y, Ogawa R, Kiyasu Y, Sakai Y. The Role of Tumor-Associated Neutrophils in Colorectal Cancer. *Int J Mol Sci* 2019; **20** [PMID: 30691207 DOI: 10.3390/ijms20030529]

141 **Yahaya MAF**, Lila MAM, Ismail S, Zainol M, Afizan NARNM. Tumour-Associated Macrophages (TAMs) in Colon Cancer and How to Reeducate Them. *J Immunol Res* 2019; **2019**: 2368249 [PMID: 30931335 DOI: 10.1155/2019/2368249]

142 **Wang S**, Miao Z, Yang Q, Wang Y, Zhang J. The Dynamic Roles of Mesenchymal Stem Cells in Colon Cancer. *Can J Gastroenterol Hepatol* 2018; **2018**: 7628763 [PMID: 30533404 DOI: 10.1155/2018/7628763]

143 **Yu Z**, Lou L, Zhao Y. Fibroblast growth factor 18 promotes the growth, migration and invasion of MDAMB231 cells. *Oncol Rep* 2018; **40**: 704-714 [PMID: 29901199 DOI: 10.3892/or.2018.6482]

144 **Gonzalez-Zubeldia I**, Dotor J, Redrado M, Bleau AM, Manrique I, de Aberasturi AL, Villalba M, Calvo A. Co-migration of colon cancer cells and CAFs induced by TGFβ$_1$ enhances liver metastasis. *Cell Tissue Res* 2015; **359**: 829-839 [PMID: 25557989 DOI: 10.1007/s00441-014-2075-6]

145 **Vinnakota K**, Zhang Y, Selvanesan BC, Topi G, Salim T, Sand-Dejmek J, Jönsson G, Sjölander A. M2-like macrophages induce colon cancer cell invasion *via* matrix metalloproteinases. *J Cell Physiol* 2017; **232**: 3468-3480 [PMID: 28098359 DOI: 10.1002/jcp.25808]

146 **Wu D**, Ding Y, Wang T, Cui P, Huang L, Min Z, Xu M. Significance of Tumor-Infiltrating Immune Cells in the Prognosis of Colon Cancer. *Onco Targets Ther* 2020; **13**: 4581-4589 [PMID: 32547088 DOI: 10.2147/OTT.S250416]

147 **Silva DA**, Yu S, Ulge UY, Spangler JB, Jude KM, Labão-Almeida C, Ali LR, Quijano-Rubio A, Ruterbusch M, Leung I, Biary T, Crowley SJ, Marcos E, Walkey CD, Weitzner BD, Pardo-Avila F, Castellanos J, Carter L, Stewart L, Riddell SR, Pepper M, Bernardes GJL, Dougan M, Garcia KC, Baker D. De novo design of potent and selective mimics of IL-2 and IL-15. *Nature* 2019; **565**: 186-191 [PMID: 30626941 DOI: 10.1038/s41586-018-0830-7]

148 **Fisher RC**, Bellamkonda K, Alex Molina L, Xiang S, Liska D, Sarvestani SK, Chakrabarti S, Berg A, Jorgensen ML, Hatala D, Chen S, Aiello A, Appelman HD, Scott EW, Huang EH. Disrupting Inflammation-Associated CXCL8-CXCR1 Signaling Inhibits Tumorigenicity Initiated by Sporadic- and Colitis-Colon Cancer Stem Cells. *Neoplasia* 2019; **21**: 269-281 [PMID: 30738331 DOI: 10.1016/j.neo.2018.12.007]

149 **Wang X**, Yang L, Huang F, Zhang Q, Liu S, Ma L, You Z. Inflammatory cytokines IL-17 and TNF-α up-regulate PD-L1 expression in human prostate and colon cancer cells. *Immunol Lett* 2017; **184**: 7-14 [PMID: 28223102 DOI: 10.1016/j.imlet.2017.02.006]

150 **Feng X**, Zhang Z, Sun P, Song G, Wang L, Sun Z, Yuan N, Wang Q, Lun L. Interleukin-18 Is a Prognostic Marker and Plays a Tumor Suppressive Role in Colon Cancer. *Dis Markers* 2020; **2020**: 6439614 [PMID: 33294056 DOI: 10.1155/2020/6439614]

151 **Pastille E**, Wasmer MH, Adamczyk A, Vu VP, Mager LF, Phuong NNT, Palmieri V, Simillion C, Hansen W, Kasper S, Schuler M, Muggli B, McCoy KD, Buer J, Zlobec I, Westendorf AM, Krebs P. The IL-33/ST2 pathway shapes the regulatory T cell phenotype to promote intestinal cancer. *Mucosal Immunol* 2019; **12**: 990-1003 [PMID: 31165767 DOI: 10.1038/s41385-019-0176-y]

152 **De la Fuente López M**, Landskron G, Parada D, Dubois-Camacho K, Simian D, Martinez M, Romero D, Roa JC, Chahuán I, Gutiérrez R, Lopez-K F, Alvarez K, Kronberg U, López S, Sanguinetti A, Moreno N, Abedrapo M, González MJ, Quera R, Hermoso-R MA. The relationship between chemokines CCL2, CCL3, and CCL4 with the tumor microenvironment and tumor-associated macrophage markers in colorectal cancer. *Tumour Biol* 2018; **40**: 1010428318810059 [PMID: 30419802 DOI: 10.1177/1010428318810059]

153 **Halama N**, Zoernig I, Berthel A, Kahlert C, Klupp F, Suarez-Carmona M, Suetterlin T, Brand K, Krauss J, Lasitschka F, Lerchl T, Luckner-Minden C, Ulrich A, Koch M, Weitz J, Schneider M, Buechler MW, Zitvogel L, Herrmann T, Benner A, Kunz C, Luecke S, Springfeld C, Grabe N, Falk CS, Jaeger D. Tumoral Immune Cell Exploitation in Colorectal Cancer Metastases Can Be Targeted Effectively by Anti-CCR5 Therapy in Cancer Patients. *Cancer Cell* 2016; **29**: 587-601 [PMID: 27070705 DOI: 10.1016/j.ccell.2016.03.005]

154 **Noh GT**, Kwon J, Kim J, Park M, Choi DW, Cho KA, Woo SY, Oh BY, Lee KY, Lee RA. Verification of the role of exosomal microRNA in colorectal tumorigenesis using human colorectal cancer cell lines. *PLoS One* 2020; **15**: e0242057 [PMID: 33175885 DOI: 10.1371/journal.pone.0242057]

155 **Ma J**, Sun X, Wang Y, Chen B, Qian L. Fibroblast-derived CXCL12 regulates PTEN expression and is associated with the proliferation and invasion of colon cancer cells *via* PI3k/Akt signaling. *Cell Commun Signal* 2019; **17**: 119 [PMID: 31500630 DOI: 10.1186/s12964-019-0432-5]

156 **Calvo N**, Martín MJ, de Boland AR, Gentili C. Involvement of ERK1/2, p38 MAPK, and PI3K/Akt signaling pathways in the regulation of cell cycle progression by PTHrP in colon adenocarcinoma cells. *Biochem Cell Biol* 2014; **92**: 305-315 [PMID: 25051885 DOI: 10.1139/bcb-2013-0106]

157 **Calvo N**, Carriere P, Martin MJ, Gentili C. RSK activation *via* ERK modulates human colon cancer cells response to PTHrP. *J Mol Endocrinol* 2017; **59**: 13-27 [PMID: 28385776 DOI: 10.1530/JME-16-0216]

158 **Meurette O**, Mehlen P. Notch Signaling in the Tumor Microenvironment. *Cancer Cell* 2018; **34**: 536-548 [PMID: 30146333 DOI: 10.1016/j.ccell.2018.07.009]

159 **Al-Haidari A**, Algaber A, Madhi R, Syk I, Thorlacius H. MiR-155-5p controls colon cancer cell migration *via* post-transcriptional regulation of Human Antigen R (HuR). *Cancer Lett* 2018; **421**: 145-151 [PMID: 29471005 DOI: 10.1016/j.canlet.2018.02.026]

160 **Mussnich P**, Rosa R, Bianco R, Fusco A, D'Angelo D. MiR-199a-5p and miR-375 affect colon cancer cell sensitivity to cetuximab by targeting PHLPP1. *Expert Opin Ther Targets* 2015; **19**: 1017-1026 [PMID: 26107137 DOI: 10.1517/14728222.2015.1057569]

World Journal of Gastroenterology

Submit a Manuscript: https://www.f6publishing.com

World J Gastroenterol 2022 July 14; 28(26): 3047-3062

DOI: 10.3748/wjg.v28.i26.3047

ISSN 1007-9327 (print) ISSN 2219-2840 (online)

REVIEW

Role of baicalin as a potential therapeutic agent in hepatobiliary and gastrointestinal disorders: A review

Risha Ganguly, Ashutosh Gupta, Abhay K Pandey

Specialty type: Gastroenterology and hepatology

Provenance and peer review: Invited article; Externally peer reviewed.

Peer-review model: Single blind

Peer-review report's scientific quality classification

Grade A (Excellent): 0
Grade B (Very good): B
Grade C (Good): C
Grade D (Fair): 0
Grade E (Poor): 0

P-Reviewer: Sitkin S, Russia; Wan XH, China
A-Editor: Ribeiro IB, Brazil

Received: January 16, 2022
Peer-review started: January 16, 2022
First decision: March 8, 2022
Revised: March 21, 2022
Accepted: May 21, 2022
Article in press: May 21 2022
Published online: July 14, 2022

Risha Ganguly, Ashutosh Gupta, Abhay K Pandey, Department of Biochemistry, University of Allahabad, Allahabad (Prayagraj) 211002, Uttar Pradesh, India

Corresponding author: Abhay K Pandey, PhD, Full Professor, Department of Biochemistry, University of Allahabad, Faculty of Science, Katra, Allahabad (Prayagraj) 211002, Uttar Pradesh, India. akpandey23@rediffmail.com

Abstract

Baicalin is a natural bioactive compound derived from *Scutellaria baicalensis*, which is extensively used in traditional Chinese medicine. A literature survey demonstrated the broad spectrum of health benefits of baicalin such as antioxidant, anticancer, anti-inflammatory, antimicrobial, cardio-protective, hepatoprotective, renal protective, and neuroprotective properties. Baicalin is hydrolyzed to its metabolite baicalein by the action of gut microbiota, which is further reconverted to baicalin *via* phase 2 metabolism in the liver. Many studies have suggested that baicalin exhibits therapeutic potential against several types of hepatic disorders including hepatic fibrosis, xenobiotic-induced liver injury, fatty liver disease, viral hepatitis, cholestasis, ulcerative colitis, hepatocellular and colorectal cancer. During *in vitro* and *in vivo* examinations, it has been observed that baicalin showed a protective role against liver and gut-associated abnormalities by modifying several signaling pathways such as nuclear factor-kappa B, transforming growth factor beta 1/SMAD3, sirtuin 1, p38/mitogen-activated protein kinase/Janus kinase, and calcium/calmodulin-dependent protein kinase kinaseβ/adenosine monophosphate-activated protein kinase/acetyl-coenzyme A carboxylase pathways. Furthermore, baicalin also regulates the expression of fibrotic genes such as smooth muscle actin, connective tissue growth factor, β-catenin, and inflammatory cytokines such as interferon gamma, interleukin-6 (IL-6), tumor necrosis factor-alpha, and IL-1β, and attenuates the production of apoptotic proteins such as caspase-3, caspase-9 and B-cell lymphoma 2. However, due to its low solubility and poor bioavailability, widespread therapeutic applications of baicalin still remain a challenge. This review summarized the hepatic and gastrointestinal protective attributes of baicalin with an emphasis on the molecular mechanisms that regulate the interaction of baicalin with the gut microbiota.

Key Words: Baicalin; Biotransformation; Gut microbiota; Hepatobiliary and gastrointestinal disorders; Signaling pathways

©The Author(s) 2022. Published by Baishideng Publishing Group Inc. All rights reserved.

Core Tip: Baicalin possesses therapeutic efficacy against hepatic and gastrointestinal diseases including hepatic fibrosis, xenobiotic-induced liver injury, fatty liver disease, viral hepatitis, cholestasis, ulcerative colitis, hepatocellular and colorectal cancer. The drug action is mediated through its interaction with the gut microbiota, modulation of several signaling pathways, and inflammatory factors. The limitations of low solubility, permeability, and bioavailability pose challenges in the therapeutic applications. The different modes of drug delivery used in the transport of baicalin for ready absorption have paved the way for its use as a pharmacological agent against hepato-intestinal disorders.

Citation: Ganguly R, Gupta A, Pandey AK. Role of baicalin as a potential therapeutic agent in hepatobiliary and gastrointestinal disorders: A review. *World J Gastroenterol* 2022; 28(26): 3047-3062
URL: https://www.wjgnet.com/1007-9327/full/v28/i26/3047.htm
DOI: https://dx.doi.org/10.3748/wjg.v28.i26.3047

INTRODUCTION

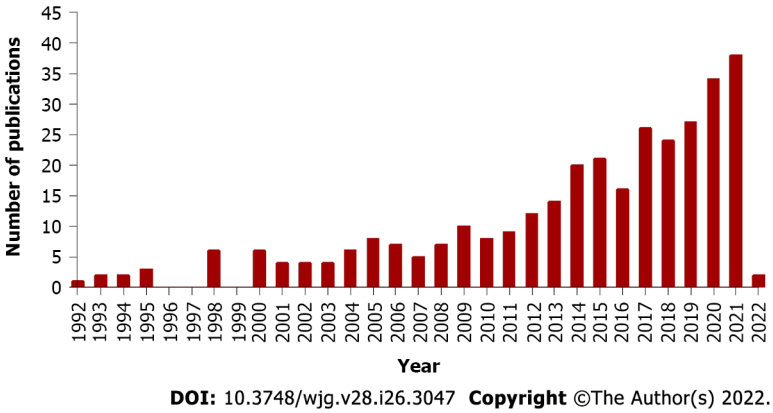
The liver is the largest and central digestive organ in the body, which plays a vital role in several physiological processes including growth, nutrition, immunity, and metabolism of xenobiotics[1-3]. The hepatobiliary system mainly consists of the liver, and intra-hepatic and extra-hepatic bile ducts including the gall bladder. The liver in association with the intestine plays an essential role in digestion with the help of digestive enzymes, which facilitate the breakdown of larger biomolecules into simpler forms such as monosaccharides, amino acids, fatty acids, and glycerol. The intestinal microbiota also interacts with bile and other digestive juices, aiding the process of digestion. The complex network of molecular pathways and signal molecules that are involved in the functioning of the hepatobiliary system are also part of the immune cascade[4-6]. Therefore, any disruption in the gastrointestinal (GI) tract or gut microbiota results in the generation of an inflammatory response. Hepatic disorders such as fibrosis, viral hepatitis, non-alcoholic fatty liver, cirrhosis, cholestasis, and hepatocellular carcinoma (HCC) can be identified by alteration in the levels of inflammatory cytokines such as tumor necrosis factor-alpha (TNF-α), interleukin-6 (IL-6), IL-1β, and nuclear factor-kappa B (NF-κB)[7,8]. Researchers in the past two decades have found numerous natural compounds, which have the ability to interact with the gut microbiome and aid in the treatment of diseases of the hepatobiliary system[9,10]. Natural products and their derivatives form a group of compounds known as secondary metabolites produced by the plants. Several such metabolites such as silymarin, ellagic acid, phyllanthin, rutin, and glycyrrhizin have been used to treat hepatic fibrosis, viral hepatitis, fatty liver disease, and cirrhosis[11, 12].

Baicalin (5, 6-dihydroxy-7-O-glucuronide) is a flavonoid isolated predominantly from the roots of *Scutellaria baicalensis* (*S. baicalensis*), a Chinese medicinal herb that belongs to the family Lamiaceae and is widely known as Chinese skullcap[13]. The roots of *S. baicalensis* also contain several other significant bioactive molecules such as baicalein and wogonin[14]. Numerous *in vitro* and *in vivo* studies have indicated different pharmacological properties of baicalin, which include anti-oxidative, antiviral, anti-inflammatory, cardioprotective, hepatoprotective, neuroprotective, and pro-apoptotic properties. These biological activities can be attributed to the ability of baicalin to target multiple pathways and bind with several signaling molecules[15-18]. In addition, baicalin possesses anti-obese, antidyslipidemia, and pro-apoptotic effects, which help to improve hepatic function after injury, alleviate liver diseases due to alcohol abuse, and promote apoptosis of proliferating hepatocytes[19].

In the last two decades, there has been growing interest and research on the hepatoprotective and anticancer properties of baicalin indicated by the increasing number of publications on PubMed. In recent years (2017 to present), there has been a remarkable rise in the number of research and review articles on the biological potential of baicalin as shown in Figure 1. This review gives an account of the therapeutic effects of baicalin exerted on the hepatobiliary system and the mitigation of GI and liver-associated disorders. The use of baicalin alone or in combination with drugs in several *in vitro* and *in vivo* experiments in the last two decades, impact of baicalin on the gut microbiota, its interaction with molecules and receptors at different molecular pathways, and the range of doses at which baicalin has shown maximum activity have also been discussed.

SOURCES OF BAICALIN

Baicalin is the most abundant and important bioactive ingredient obtained from the roots of the



DOI: 10.3748/wjg.v28.i26.3047 **Copyright** ©The Author(s) 2022.

Figure 1 Increasing trend of publications on "hepatoprotective and anticancer properties of baicalin" indexed by PubMed.

medicinal plant *S. baicalensis*[20]. The roots of *S. baicalensis* possess baicalin in the range of 8% to 15%. Baicalin is also the main component of other species of *Scutellaria* such as *S. rivularia*, *S. galericulata*, and *S. lateriflora*[21,22]. Baicalin, chrysin, and its glucoside derivatives have also been obtained from various other parts of the popular Asian medicinal plant *Oroxylum indicum*, belonging to the family Bignoniaceae[23]. Baicalin, and its aglycone baicalein, are gaining increasing importance in the pharmaceutical, food, and cosmetics industries due to their remarkable biological properties. Baicalin and baicalein, in particular, have shown anti-inflammatory effects and the potential to ameliorate mitochondrial dysfunction[24], and combination strategies with baicalin or baicalein as chemotherapy adjuncts have been shown to be effective in various cancers and associated signaling pathways[25]. Due to growing interest in the properties of baicalin as a potential therapeutic agent, many studies in last few years have focused on developing appropriate techniques for the identification and quantification of baicalin in raw drug formulations including simple thin layer chromatography, and different modifications of the sophisticated technique of high-performance liquid chromatography[26,27].

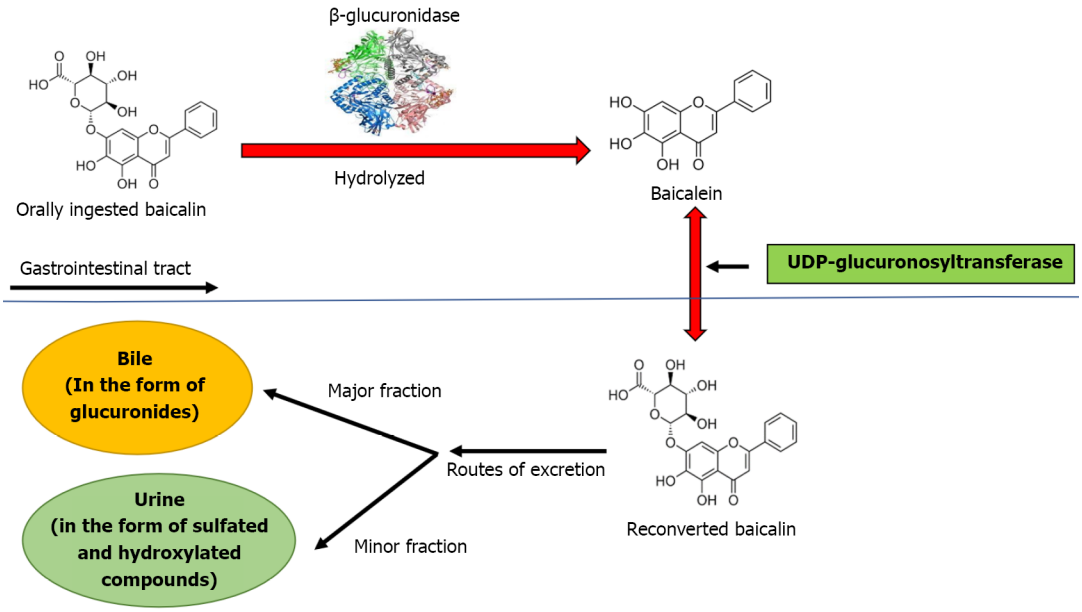
CHEMISTRY AND BIOAVAILABILITY

Baicalin is a flavone glycoside (molecular mass = 446.4 g/moL; melting point = 202-205 °C), which is hydrolyzed to its aglycone baicalein in the stomach after ingestion. Baicalin is hydrolyzed to baicalein immediately after administration with the help of β-glucuronidase from gut bacteria. Baicalein is reconverted to baicalin in the systemic circulation by uridine 5'-diphospho(UDP)-glucuronosyltransferase-glucuronosyl transferase *via* phase 2 metabolism[21]. It is noteworthy that the circulating baicalin in the system is not the parent molecule but the conjugated metabolite of baicalein. Circulating baicalin returns to the GI system primarily by bile excretion in the form of glucuronides. The bile excretion of baicalin is mainly mediated by the multidrug resistance (MDR) protein 2 transporter. When baicalin and baicalein are given orally, the conjugated metabolites actually contribute to the *in vivo* effect because the glucuronide/sulfate of baicalin circulates predominantly in plasma[25]. Baicalin is moderately absorbed in the stomach and poorly absorbed in the small and large intestines (Figure 2).

PHARMACOKINETICS OF BAICALIN IN THE GI SYSTEM

The pharmacokinetic profile of baicalin in the GI system involves hydrolysis, enterohepatic recycling, carrier-mediated transport, and complex routes of metabolism with the interaction of gut microbiota. Baicalin administration is safe and endurable, and no evidence of liver or kidney toxicity has been recorded. The main obstacles to the clinical use of baicalin are its low water solubility (approximately 67.0 μg/mL) and bioavailability. Several nano-techniques such as solid nanocrystals, nanoemulsions, and lipid-based solid nanoparticles have been used to improve baicalin lysis, thus improving bioavailability[28-30]. Incomplete absorption in the GI system has emerged as the main barrier to bioavailability [31]. MDR protein 2 is the most important transporter of baicalin, which mediates bile outflow to hepatocytes[32]. In fact, biliary excretion of baicalin in rats with MDR protein 2 deficiency is significantly reduced with a significant increase in plasma baicalin levels[33]. Baicalin is also capable of crossing the blood-brain barrier and may be protective against a variety of neurodegenerative diseases [34,35].

β-glucuronidase and UDP-glucuronosyltransferase are important metabolic enzymes involved in the *in vivo* transformation of baicalin. In fact, five bile metabolites have been identified in rat liver after



DOI: 10.3748/wjg.v28.i26.3047 **Copyright** ©The Author(s) 2022.

Figure 2 Biotransformation of baicalin after oral ingestion. Orally administered baicalin is hydrolyzed to baicalein by β-glucuronidase. Further, baicalein is reconverted to baicalin by uridine 5'-diphospho-glucuronosyltransferase in intestine. The major part of baicalin excretion takes place *via* the biliary route in the form of glucuronides, and a small fraction of baicalin is excreted *via* urine in the form of sulfated and hydroxylated compounds. UDP: Uridine 5'-diphospho.

baicalin administration. The main metabolites include baicalein 6,7diβ-glucopyranuloside and 6oβ-glucopyranuronosyl baicalein-7 sulfate. These conjugated metabolites are hydrolyzed to baicalein in the GI tract by β-glucuronidase/sulfatase. Thirty-two baicalin metabolites have been reported in plasma, urine, and other rat tissues using more efficient approaches[36,37]. In terms of tissue distribution, liver and kidney contain most of the metabolites, indicating that these are the major sites of baicalin metabolism. Baicalin undergoes multiple chemical transformations *in vivo* including hydrolysis, methylation, hydroxylation, methoxylation, glucuronide conjugates, sulfate conjugates, and their combined reactions[37]. The pharmacokinetics of baicalin may help to understand its therapeutic implications in the liver. As a result of enterohepatic circulation, baicalin remains particularly concentrated in the liver and is thus beneficial in the treatment of hepatic anomalies. Baicalein also plays a crucial role in the treatment of hepatic diseases, indicating that the mechanism of baicalin's emphasis on liver-associated disorders may include the ameliorative effects of the metabolites as well. The major part of baicalin excretion takes place *via* the biliary route in the form of glucuronides, and a small fraction of baicalin is excreted *via* urine in the form of sulfated and hydroxylated compounds[38,39].

AMELIORATING EFFECTS OF BAICALIN AGAINST HEPATIC AND COLORECTAL DISEASES

Fatty liver syndrome

Fatty liver syndrome (FLS) occurs due to excess accumulation of non-esterified fatty acids in the hepatocytes. FLS accounts for approximately one-fourth of all liver-related anomalies in the world[40]. FLS causes several hepatic anomalies such as non-alcoholic fatty liver disease, non-alcoholic steatohepatitis (NASH), and advanced FLS may also lead to cirrhosis and ultimately hepatic failure[17,41]. Due to its antioxidant and hepatoprotective potential, baicalin is effective against FLS and associated diseases. Baicalin improves lipid metabolism and suppresses hepatic lipid production by inhibiting the calcium/calmodulin-dependent protein kinase kinase-β/adenosine monophosphate-activated protein kinase (AMPK)/acetyl-coenzyme A (CoA) carboxylase pathway[42,43]. Additionally, baicalin binds directly to carnitine palmitoyl-transferase-1α (CPT-1α) and promotes the influx of lipid into mitochondria, where it is oxidized[44]. Baicalin also downregulates lipid-producing genes such as fatty acid synthase (FASN), peroxisome proliferator-activated receptor-α (PPAR-α), and sterol regulatory element-binding protein-1c (SREBP-1c) to inhibit lipid accumulation in the liver[42,45]. Baicalin (200 mg/kg) has been found to reduce the expression of TNF-α, monocyte chemoattractant protein (MCP-1) and IL-1β, downregulate caspase-3 to alleviate NASH induced by a methionine- and choline-deficient (MCD) diet. In addition, treatment with baicalin can partially lessen the accumulation of lipids induced by the MCD diet in the liver by modulating the expression of SREBP-1c, FASN, PPAR-α, and CPT-1α

[46]. Moreover, baicalin (50 mg/kg) also reduces the synthesis of inflammatory cytokines including TNF-α, IL-6, and IL-1β, and suppresses the Toll-like receptor 4 (TLR-4) signaling pathways in MCD diet fed mice to inhibit fat accumulation in liver. Thus, baicalin also acts as an anti-inflammatory compound in the attenuation of non-alcoholic FLS[47]. In a study of high-fat diet induced FLS, it was found that baicalin (25-100 mg/kg) exerted a substantial ameliorating effect on FLS by activating the expression of hepatic PPAR-γ receptors[48]. In addition, baicalin (5 g/kg) also alleviates FLS by reducing the levels of serum hepatic enzymes such as aspartate aminotransferase (AST) and alanine aminotransferase (ALT), and inflammatory mediators such as TNF-α and MCP-1. Moreover, baicalin also inhibited the phosphorylation of Janus kinase (JNK), and suppressed the production of inflammatory enzyme cyclooxygenase-2 and pro-oxidative enzyme CYP-2E1 in the liver of a mouse model[49]. In another study of orotic acid-induced FLS, baicalin (12.5-50 mg/kg) downregulated SREBP-1c and upregulated AMPK to reduce the toxic effects of free fatty acids, subsequently inhibiting fat accumulation in the liver [45]. In an *in vitro* study of palmitic acid-induced FLS in AML-12 hepatocytes, baicalin (6.25-25 μM) alleviated FLS by reducing endoplasmic reticulum stress and suppression of the thioredoxin-interacting protein/Nod-like receptor protein 3 pathway[50].

Liver injury

The liver is the most important organ for the metabolism and elimination of toxins from the human body. Normal liver function can be deterred with excessive hepatic injuries, which occur due to a variety of factors including alcohol intake, chemical contaminants, hepatocellular ischemia, and drug damage[50,51]. Liver damage is a complex process that can manifest extensive hepatocellular apoptosis [52]. Baicalin (120 mg/kg) has been shown to alleviate alcohol-induced liver injury in a rat model *via* the reduced expression of inflammatory cytokines such as TNF-α, IL-6 and IL-1β and enhances the activity of antioxidant enzymes such as superoxide dismutase (SOD) and glutathione peroxidase (GSH-Px), which is further regulated by blocking the sonic-hedgehog signaling pathway[19]. Similarly, baicalin (30 mg/kg) has been shown to produce anti-inflammatory effects by downregulating the expression of IL-17 in a rat model with acetaminophen-induced liver injury[53]. Baicalin (80 and 200 mg/kg) activates heme oxygenase-1 *via* the nuclear respiratory factor (NRF)-2 antioxidant pathway and inhibits the activity of reactive oxygen species (ROS) generating enzymes in a liver injury model. Baicalin plays an important role in blocking the combination of NRF-2 and Kelch-like ECH-associated protein 1 (Keap-1) that causes phosphorylation of NRF-2, thus reversing liver damage[54,55]. Furthermore, baicalin (60 mg/kg) also downregulates extracellular signal-regulated kinase (ERK) in acetaminophen-induced liver injury[56]. In addition, baicalin (100 mg/kg) downregulates caspase-3 and caspase-9 and also increases the expression of the anti-apoptotic protein B-cell lymphoma 2 (Bcl-2). This helps to significantly reduce NG-nitro-L-arginine methyl ester-induced liver injury in rats[57].

The therapeutic effect of baicalin on reducing liver damage *via* the apoptotic pathway has also been demonstrated *via in vitro* experiments (Table 1). Baicalin at 100 μmol/L regulates apoptotic proteins such as caspase-3, caspase-9, and Bcl-2 associated X (Bax), and has a considerable therapeutic impact on the hypoxic model of L02 human hepatocytes[58]. Another *in vitro* study with L02 hepatocytes and acetaldehyde-treated HepG2 cells were used to identify the adverse effects of baicalin (20-100 mmol/L) on progression of the epithelial-mesenchymal transition (EMT) in the liver, which is an indicator of liver fibrosis and inflammation. This study demonstrated that baicalin considerably suppressed the progression of EMT by downregulating the transforming growth factor-β (TGF-β)/Smad signaling pathway, thus ameliorating liver damage[59]. Studies have shown that baicalin (60 μM) can repair liver injury in nanosecond pulse electric field (ns-PEF)-induced damage to L02 hepatocytes by stabilizing mitochondrial transmembrane potential and prevent excess ROS production[60]. Furthermore, baicalin (5 and 25 μM) can suppress the oxidation and nitrification of the hemin/nitrite/hydrogen peroxide system and protect HepG2 cells by inhibiting lipid peroxidation and GSH depletion[61]. Another study emphasized that baicalin administration (74 mg/kg) can restore the metabolism of amino acids to normal, improve the tricarboxylic acid cycle and ameliorate acute lipopolysaccharide (LPS)-induced sepsis in mice model[62].

Liver fibrosis

Liver fibrosis occurs due to excess deposition of extracellular matrix proteins and collagen. It is characterized by hepatic tissue degeneration, inflammatory cell infiltration and hepatic cell necrosis[63,64]. It has also been confirmed that activation of hepatic stellate cells (HSCs) plays a central role in liver fibrosis[65]. In the absence of appropriate treatment, advanced liver fibrosis causes chronic hepatitis subsequently leading to liver cancer or cirrhosis[66,67]. In a recent study, it was shown that baicalin (200 mg/kg) decreased the expression of fibrotic genes such as α-smooth muscle actin (SMA) and connective tissue growth factor and inflammatory cytokines such as TNF-α, macrophage inflammatory protein-1α (MIP-1α), IL-1β, MIP-2, thereby effectively suppressing liver fibrosis induced by bile duct ligation (BDL) in mice. In addition, an *in vitro* study also showed the efficacy of baicalin in reducing the activation of HSCs and downregulating the expression of SMA, fibronectin, tissue inhibitor of metalloproteinase-1 (TIMP1) protein andcollagen-1[68]. Similarly, baicalin (150 μM) reduced microRNA (miR)-3595 expression and increased the activity of the enzyme long-chain fatty acid CoA ligase 4, significantly inhibiting the activity of HSCs leading to a reduction in fibrosis in HSCT6 hepatocyte cell lines caused

Table 1 *In vitro* hepatoprotective effects of baicalin on different cell lines

Disease/type of study	Cell line	Dose	Mechanism/target pathways	Ref.
Palmitic acid-induced fatty liver	AML-12 hepatocytes	6.25-25 μM	ER stress↓; TXNIP/NLRP-3 pathway ↓	[50]
Hypoxic liver injury	L02 human hepatocytes	100 μmol/L	Caspase-3, caspase-9, and Bax↓	[58]
Acetaldehyde induced EMT	HepG2 cells	20-100 mmol/L	TGF-β/Smad pathway↓	[59]
ns-PEF induced liver injury	L02 hepatocytes	60 μM	MTP stabilization, ROS↓	[60]
Hemin-nitrite-H_2O_2 induced liver injury	HepG2 cells	5 μM and 25 μM	Lipid peroxidation↓; GSH depletion↓	[61]
PDGF-BB induced fibrosis	HSCT6 hepatocytes	150 μM	miR-3595↓; ACSL-4↑	[69]
BDL-induced fibrosis	HSCs	67.5-270 μM	Wnt pathway↓; PPAR-γ↓	[70]
LPS-induced hepatitis	L20, THLE cell lines	25-100 μM	TUG-1↑; p38-MAPK↓; JNK pathway↓	[82]
Viral hepatitis	HuH7, HepG2 cells	75 μg/mL	NF-κB pathway↓	[83]
	pHBV1.2HepG2 cells	10 μM	HNF-4α/HNF-1α↓	[84]
	HepG2.2.15 cells	10 μg/kg	HBsAg, HBeAg↓	[85]
	PBMCs	50-200 mg/mL	Mitochondrial pathway↑; Caspase 3↑	[87]
HCC	HepG2-HCC	100 μmol/L	ER-mediated TF-6↑; S-2P protein↑	[94]
	SMMC7721-HCC cells	160 μM	CD47↓	[95]
	SMMC7721, HepG2-HCC cells	40 μM	STAT3, IFN-γ↓; Block PDL-1/PD-1 pathway	[96,97]

ACSL-4: Long chain fatty acid CoA ligase 4; AML: Alpha mouse liver; BDL: Bile duct ligation; EMT: Epithelial-mesenchymal transition; ER: Endoplasmic reticulum; GSH: Reduced glutathione; HCC: Hepatocellular carcinoma; HSCs: Hepatic stellate cells; LPS: Lipopolysaccharide; MAPK: Mitogen-activated protein kinase; MTP: Mitochondrial transmembrane potential; NLRP-3: Nod-like receptor protein 3; nsPEF: Nanosecond-pulse electric field; PBMCs: Peripheral blood mononuclear cells; PDGF-BB: Platelet-derived growth factor BB; PPAR-γ: Peroxisome proliferator-activated receptor-γ; ROS: Reactive oxygen species; THLE: Transformed human liver epithelial; TUG-1: Taurine upregulated-1; TXNIP: Thioredoxin-interacting protein.

by platelet-derived growth factor BB[69]. Moreover, baicalin (67.5-270 μM) helps in the reduction of BDL-induced activity of HSCs by inhibiting PPAR-γ *via* Wnt signaling, leading to alleviation of liver fibrosis[70]. Baicalin (100 mg/kg) attenuated carbon tetrachloride-induced hepatic fibrosis in mice by regulating the rise in TGF-β1, hydroxyproline, type III collagen, and hyaluronic acid laminin (Table 2). In addition, baicalin also attenuates liver fibrosis by suppressing the activity of antioxidant enzymes SOD and GSH-Px[71]. Similarly, baicalin (25-100 mg/kg) evidently reduces the level of PPAR-γ, suppresses the activity of HSCs, and downregulates the expression of TGF-β1, causing inhibition of hepatic fibrosis[72].

Cholestasis

Cholestasis is a condition that occurs due to the obstruction or complete blockage of bile secretion through the intrahepatic or extrahepatic bile ducts[73]. Consequently, there is excess accumulation of conjugated bilirubin, bile salts, and cholesterol in the liver, which leads to hepatic injury and damage to the human body[74]. Baicalin plays an important role at several stages to mitigate cholestasis and related hepatic damage. Baicalin specifically targets nuclear factor-erythroid factor 2-related factor 2 (NRF-2) in reversing cholestasis. Recent studies in a mouse model indicate that the interaction of baicalin (50 mg/kg) with NRF-2, inflammatory cytokines, and oxidative stress regulatory elements forms the central pathway of reducing cholestasis induced hepatic damage. Baicalin is capable of activating SMA, TIMP1, and collagen, resulting in amelioration of liver fibrosis due to BDL-induced cholestasis[68]. Another pharmacokinetic study in a rat model indicated that administration of baicalin (50-200 mg/kg) has therapeutic potential for cholestasis. It significantly increases bile excretion rates, which lead to a decline in serum levels of total bile acids as well as hepatic enzymes such as AST, ALT, and alkaline phosphatase in 17α-ethinyl estradiol-induced cholestasis[75,76]. In estrogen-induced cholestasis, it has been shown that baicalin targets NF-κB and inhibits the expression of inflammatory markers such as TNF-α, IL-6, and IL-1β, thereby increasing the activity of hepatic bile acid-metabolizing enzymes. Reports have also shown that baicalin alleviates 17α-ethinyl estradiol-induced cholestasis in mice by suppressing the expression of multidrug resistance protein 2 and bile salt export pump genes *via* the sirtuin 1/nuclear hepatic receptor 1α (HNF-1α)/farnesoid X receptor (FXR) pathway[77].

Table 2 *In vivo* protective effects of baicalin on various hepatobiliary and colorectal disorders

Disease/type of study	Dose	Mechanism/target pathway	Ref.
MCD induced NASH	200 mg/kg	TNF-α, MCP-1, IL-1β↓; Caspase-3↓; SREBP-1c, FASN, PPAR-α, CPT-1α↓	[46]
	50 mg/kg	TNF-α, IL-6, IL-1β↓; TLR-4 pathway↓	[47]
High fat diet induced non- alcoholic FLS	25-100 mg/kg	PPAR-γ receptors↑	[48]
	5 g/kg	AST, ALT↓; TNF-α, MCP-1↓; JNK-P↓; COX-2, CYP-2E1↓	[49]
Orotic acid induced FLS	12.5-50 mg/kg	SREBP-1c↓; AMPK↑	[45]
Alcohol-induced liver injury	120 mg/kg	TNF-α, IL-6, IL-1β↓; SOD, GSH-Px↑; Block sonic-hedgehog pathway	[19]
	200 mg/kg	HO-1, NRF-2 pathway↑	[54]
Acetaminophen-induced liver injury	30 mg/kg	IL-17↓	[53]
	80 mg/kg	NRF-2, Keap-1↓	[55]
	60 mg/kg	ERK↓	[56]
NG-nitro-L-arginine methyl ester induced liver injury	100 mg/kg	Caspases-3 and 9↓; Bcl-2↑	[57]
LPS-induced sepsis	74 mg/kg	Amino acid metabolism↑; TCA cycle↑	[62]
BDL-induced liver fibrosis	200 mg/kg	SMA, CTGF↓; TNF-α, MIP-1α, IL-1β, MIP-2↓	[68]
CCl_4-induced fibrosis	100 mg/kg	TGF-β1, hydroxyproline, type III collagen, hyaluronic acid laminin↑; SOD, GSH-Px↓	[71]
	25-100 mg/kg	PPAR-γ↓; TGF-β1↓	[72]
17α- ethinyl estradiol-induced cholestasis	50-200 mg/kg	TBA, AST, ALT, ALP↓; TNF-α, IL-6 and IL-1β↓	[75,76]
		Sirt1/HNF-1α/FXR pathway↓	[77]
Hepatitis B in young duck model	10 μg/kg	HBsAg, HBeAg↓; HNF-4α/HNF-1α↓	[85]
Hepatitis in male BALB/c mouse model	100-200 mg/kg	TNF-α, IL-6 and IFN-γ↓	[86]
Hepatitis in male Sprague-Dawley rat model	0.5-5.0 mg/kg	ALT, AST↓	[86]
HCC	50 mg/kg	RelB/p52 pathway↑	[93]
CRC in mice	100, 200 mg/kg	TGF-β/Smad pathway↓	[100]
TNBS-induced UC	30-90 mg/kg	IL-1β, TNF-α↓; Caspase 9, Bcl-2↓; IKK/IKB/NF-κB pathway↓	[107]
	5-20 mg	IL-1β, TNF-α, IL-6↓; TLR4/NF-κB pathway↓	[108]
	30-120 mg/kg	Catalase, GSH-PX, SOD↑; Bcl-2↑; MDA↓; TGF-β, Bax↓	[109]
HTHE-induced UC	100 mg/kg	NF-κB, MAPK pathways↓	[110]
DSS-induced UC	50-150 mg/kg	MPO, NO↓; IL-1β, TNF-α and IL-6↑	[111]
	100 mg/kg	TLR-4/NF-κB-p65/IL-6 pathway↓; TNF-α, IL-6, IL-13↓	[112]
TNBS-induced UC	10 mg/kg	MIF, MCP-1, MIP-3a↓	[113]
	20-100mg/kg	Maintain Th17/Treg balance	[114]

ALP: Alkaline phosphatase; ALT: Alanine transaminase; AST: Aspartate transaminase; AMPK; AMP-activated protein kinase; Bcl-2: B-cell lymphoma 2; CCL_4: Carbon tetrachloride; COX-2: Cyclooxygenase-2; CPT-1α: Carnitine palmitoyl-transferase-1α; CRC: Colorectal cancer; CTGF: Connective tissue growth factor; CYP-2E1: Cytochrome P450 2E1; DSS: Dextran sulfate sodium; ERK: Extracellular signal-regulated kinase; FASN: Fatty acid synthase; FLS: Fatty liver syndrome; FXR: Farnesoid X receptor; GSH-Px: Glutathione peroxidase; HBsAg: Hepatitis B surface antigen; HBeAg: Hepatitis B e antigen; HNF: hepatic nuclear factor; HO-1: Heme oxygenase 1; HTHE: High temperature and humid environment; IL-1: Interleukin-1; JNK: c-Jun N-terminal kinase; Keap-1: Kelch-like ECH-associated protein 1; MCD: Methionine- and choline-deficient; MCP-1: Monocyte chemoattractant protein-1; MIP-1α: Macrophage inflammatory protein-1 alpha; NASH: Non-alcoholic steatohepatitis; NF-κB: Nuclear factor-kappa B; NRF2: Nuclear factor-erythroid factor 2-related factor 2; PPAR-γ: Peroxisome proliferator-activated receptor-γ; Sirt: Sirtuin; SMA: Smooth muscle actin; SOD: Superoxide dismutase; SREBP: Sterol

regulatory element-binding protein; TBA: Total bile acid; TCA: Tricarboxylic acid cycle; Th17: T helper 17 cells; TLR-4: Toll-like receptor 4; TNBS: 2,4,6-trinitrobenzenesulfonic acid; TNF-α: Tumor necrosis factor-alpha; Treg: Regulatory T cells; UC: Ulcerative colitis.

Hepatitis

Hepatitis caused by hepatitis A virus (HAV), hepatitis B virus (HBV), and other viral hepatitis are prevalent infectious diseases worldwide[78,79]. Liver-specific proteins and immune complex hypersensitivity have multiple roles in hepatitis[80]. Subsequent studies have proven that baicalin plays a key role in the attenuation of hepatitis by lowering the levels of hepatitis B surface antigen (HBsAg), viral antigen protein hepatitis B e-antigen (HBeAg), and hepatitis B virus (HBV)-DNA, and regulating oxidative stress, inflammation, and apoptosis in hepatic cells[80,81]. It has been found that baicalin (25-100 μM) significantly increases *taurine upregulated 1* gene expression to suppress inflammation and apoptosis by downregulating the p38-mitogen activated protein kinase (MAPK) and JNK signaling pathways in L20 and transformed human liver epithelial cell lines to thwart LPS-induced hepatitis[82]. Another recent study showed that baicalin (75 μg/mL) significantly suppressed HBV replication and inflammation by downregulating the NF-κB signaling pathway in HepG2 and HuH7 cells[83]. Furthermore, it has also been confirmed that baicalin (10 μM) strongly suppresses the transcription of HBV by downregulating the liver-specific HNF-4α/HNF-1α axis in pHBV1.2 HepG2 cells[84]. In another experiment, baicalin (10 μg/kg) significantly reduced HBsAg and HBeAg levels in HepG2 cells, wild-type HBV cells, and young duck models infected with HBV by downregulating the HNF-4α/HNF-1α axis[85]. In addition, baicalin pre-treatment (100-200 mg/kg) attenuated elevated levels of plasma cytokines such as TNF-α, IL-6, and interferon-γ (IFN-γ) in male BALB/c mouse models, resulting in alleviation of hepatocyte necrosis and apoptosis[86]. Similarly in an *in vivo* study, pre-treatment with baicalin (0.5-5.0 mg/kg) considerably reduced serum levels of ALT and AST and lowered hepatic oxidative stress in a male Sprague-Dawley rat model[86]. Another study demonstrated the pro-oxidant properties of baicalin (50-200 mg/mL) by upregulating the mitochondrial signaling pathway in human peripheral blood mononuclear cells, thereby inducing the activation of caspase-3 and apoptosis[87]. Furthermore, baicalin has often been co-administered with other bioactive flavonoids in combination studies, to yield better results at prevention of hepatitis. For instance, combination of the alkaloid oxymatrine (1 g/L) with baicalin showed more efficacy against HBV than oxymatrine alone[88]. Below 31.50 μg/mL, the baicalin-phospholipid complex exhibits direct anti-duck HAV-1 activity by preventing the adsorption, replication, and release of duck HAV-1 and indirectly by promoting immunity in ducklings[89]. Baicalin (20 μg/mL) regulates the immunomodulatory effects and anti-HAV-1 reproduction by reducing the adsorption and release of HAV-1 in duck-suppressed embryonic hepatocytes[90].

HCC

HCC ranks sixth amongst the most common malignant tumors worldwide, and is the fourth highest cause of mortality due to malignancies[91]. The present modes of treatment for HCC include radiation therapy, local resection therapy, surgery, and liver transplantation. However, these treatments typically cause several side effects and have adverse consequences[91,92]. Several studies have reported that baicalin can effectively ameliorate HCC by indirectly inducing autophagy in liver tumor cells. Studies have revealed that baicalin (50 mg/kg) promotes the polarization of tumor-related macrophages into M1-like macrophages, subsequently increasing autophagy in cancerous cells to make them non-proliferating. Additionally, baicalin mediated anti-cancer effects may also be closely associated with activation of the RelB/p52 signaling pathway[93]. Similarly, baicalin (100 μmol/L) promotes apoptosis in HepG2-HCC cells by activating the ER-mediated TF-6 signaling cascade combined with S-2P protein [94]. Moreover, baicalin (160 μM) suppresses cluster of differentiation 47 and activates apoptosis and autophagy in SMMC7721-HCC cells[95]. Although nsPEFs have been developed as a new mode of treatment for cancer, they also result in the elimination of normal hepatocytes. Therefore, a study was designed combining nsPEF and baicalin for the treatment of HCC, which revealed that baicalin suppresses the proliferation of HCC cells, and protects normal liver cells by increasing mitochondrial membrane potential and reducing ROS production[59]. In recent times, cancer immunotherapy has emerged as a significant line of treatment for HCC. Baicalin (40 μM) is capable of reducing the activity of signal transducer and activator of transcription 3 protein and IFN-γ, thereby blocking the programmed death-ligand 1/programmed cell death protein 1 pathway. This increases the sensitivity of the immune system to hepatic cancerous cells and thus further activates T cells against hepatic cancer cells[96,97]. Based on several *in vitro* and *in vivo* studies, the protective effect of baicalin on many hepatic disorders is summarized in Tables 1 and 2.

Colorectal cancer

Colorectal cancer (CRC) is also a common malignant tumor worldwide, and is primarily due to genetic inheritance, colon polyps, and ulcerative colitis (UC)[98,99]. Baicalin, due to its pro-apoptotic properties, results in the killing of CRC cells. Researchers have used the human colon cancer cell line (HCT-166)

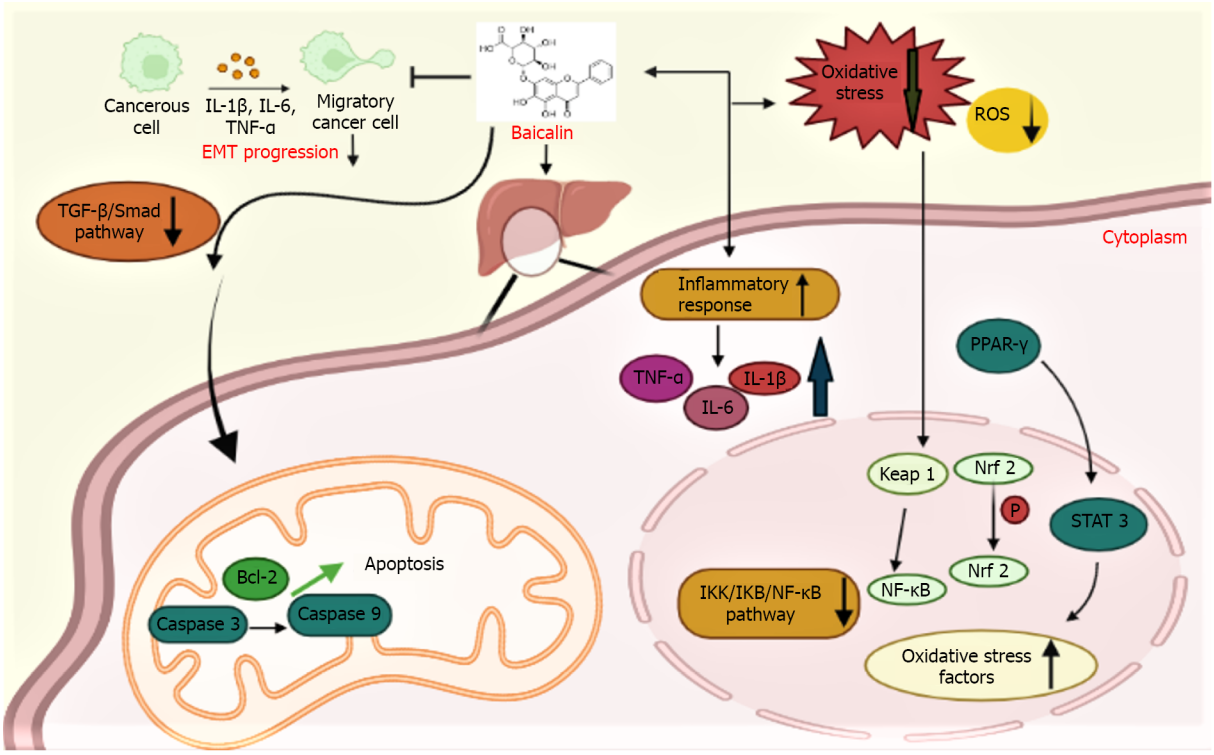
and transplanted colon tumors into mice to conduct simultaneous *in vivo* and *in vitro* experiments to examine the antitumor mechanism of baicalin (100 and 200 mg/kg). Baicalin induces apoptosis in colon tumors by inhibiting the cells at the G1 stage and arresting EMT protein expression by blocking the TGF-β/Smad pathway[100]. Baicalin (40 mmol/L) promotes Dickkopf protein expression, suppresses the expression of proteins β-catenin and c-Myc, and inhibits miR-217 expression, thereby leading to the apoptosis of HCT-166 cancer cells by inhibition of the Wnt signaling pathway[101]. Another similar study demonstrated that apoptosis of HT-29 colon cancer cells was induced by baicalin (50-200 μM) *via* inhibition of c-Myc expression and regulation of the miR-10a, miR-23a, miR-31, miR-151a, and miR-205 mechanism[14]. Similarly, it has been reported that the antioxidant properties of baicalin (40 μM) increase progesterone expression in the intestine and leads to the apoptosis of HCT-116 colon cancer cells by activating the Ras/Raf/MEK/ERK pathways[102]. Reports have also shown that the antitumor activity of baicalin can be further enhanced by glycosidase pre-treatment[103]. Several studies have revealed that the development of CRC is closely associated with genetic mutations. In a study on colon cancer cells SW-480, baicalin (50-400 μg/mL) inhibited the expression of the transcription factor SP-1, leading to the apoptosis of cancer cells[104].

Inflammatory bowel disease

Inflammatory bowel disease (IBD) is a collective term that refers to the chronic inflammation of GI tract. The two major types of IBD are Crohn's disease (CD) and UC. CD and UC are nonspecific chronic IBDs that cause inflammation and ulcers on the inner lining of the large intestine[105-107]. Baicalin plays an important role in the treatment of IBD, as it is capable of suppressing oxidative stress, immune regulation, and its anti-inflammatory properties. In addition, baicalin is capable of regulating NF-κB activation, which modulates both autophagic and inflammatory processes in intestinal epithelial cells, subsequently leading to enhancement in paracellular permeability. Baicalin alleviates dextran sulfate sodium (DSS)-induced UC by modulating the polarization of M1 macrophages to the M2 phenotype [107]. Dose-dependent administration of baicalin (30-90 mg/kg) has been found to largely downregulate the inflammatory cytokines IL-1β and TNF-α, and apoptotic genes Bcl-2 and caspase-9 in the colon tissue of rats affected by 2,4,6-trinitrobenzenesulfonic acid (TNBS)-induced UC. In addition, baicalin also inhibits the inhibitory κB (IKB) kinase (IKK)/IKB/NF-κB signaling pathway, leading to the alleviation of IBD[107,108]. Likewise, in another study, rats with TNBS-induced UC were given baicalin (5-20 mg) which resulted in the downregulation of inflammatory factors TNF-α, IL-6 and IL-1β in rat intestine and inhibition of the TLR4/NF-κB signaling pathway, leading to alleviation of UC[109]. Furthermore, baicalin (30-120 mg/kg) has also been effective in the treatment of TNBS-induced UC by promoting antioxidant enzymes such as catalase, SOD and GSH-PX, and reducing malondialdehyde (MDA). Baicalin also suppresses the regulation of apoptosis by upregulating Bcl-2 and downregulating TGF-β and Bax[110]. In a UC model generated by high temperature and humid environment, baicalin (100 mg/kg) significantly reduced the serum levels of IL-6, IL-1β, and IL-17, and inhibited SOD, GSH-PX, and MDA. That study attributed the anti-inflammatory effect of baicalin to suppression of the NF-κB and MAPK pathways[111]. In an *in vivo* study, baicalin (50-150 mg/kg) reduced myeloperoxidase activity, nitric oxide content, and elevated IL-1β, TNF-α and IL-6 levels in the colon of DSS-induced UC rats[112]. Another study revealed that baicalin (100 mg/kg) attenuated DSS-induced UC by blocking the TLR-4/NF-κB-p65/IL-6 signaling pathway and suppressing TNF-α, IL-6, and IL-13 mRNA expression [113]. Furthermore, baicalin (10 mg/kg) downregulated the expression of macrophage migration inhibitory factor, MCP-1 and MIP-3a in the colon tissue of TNBS-induced UC rat model[114]. Several reports have suggested the association of T helper 16 cell (Th17)/regulatory T cell (Treg) equilibrium with UC. Baicalin (20-100 mg/kg) regulates the Th17/Treg balance by inhibiting the rise in ROS and MDA, whereas simultaneously reducing GSH and SOD levels and regulating the expression of Th17-related factors IL-6 and IL-17 in TNBS-induced UC rats[115,116]. In a clinical study of UC patients, baicalin promoted the production of immune cells like CD4+ and CD29+ and induced immunomodulation to alleviate UC[117] (Figure 3).

INTERACTION OF BAICALIN WITH THE INTESTINAL MICROBIOTA

In the past decade, the intestinal microbiota has become an emerging aspect of research for the evaluation of several diseases. Besides playing an important role in the metabolism and breakdown of biomolecules into simpler molecules like fatty acids, amino acids, vitamins and bile salts, the gut microbiota is also capable of interacting with the host and affect the functioning of various organs including the liver and kidney to regulate homeostasis and disease development[5,118]. Baicalin, a flavonoid, exerts many therapeutic effects by modulating gut microbiota homeostasis. Intake of high fat diet causes imbalance of the gut microbiota, leading to several metabolic syndromes. Baicalin administered (200 mg/kg/d) to mice with high fat diet induced metabolic syndrome led to an increase in short-chain fatty acid (SCFA)-producing gut bacteria, thereby effectively reducing the metabolic syndrome in mice[119]. Baicalin also reduces damage to the intestinal barrier caused due to hypertension. A study reported that baicalin (100 mg/kg) significantly increased the number of SCFA-



DOI: 10.3748/wjg.v28.i26.3047 **Copyright** ©The Author(s) 2022.

Figure 3 Mechanism of baicalin action against hepatobiliary diseases. Baicalin downregulated peroxisome proliferator-activated receptor-α and activated the nuclear respiratory factor-2 antioxidant pathway to reduce oxidative stress in the hepatocytes. Baicalin suppressed epithelial-mesenchymal transition progression by downregulating the transforming growth factor-β/Smad pathway, inhibited the inhibitory κB (IKB) kinase/IKB/nuclear factor-kappa B pathway, reduced the elevated levels of inflammatory factors such as tumor necrosis factor-α, interleukin-6 (IL-6) and IL-1β, and attenuated the apoptotic proteins caspase-3, caspase-9, B-cell lymphoma 2, which led to the alleviation of liver diseases. ROS: Reactive oxygen species; STAT: Signal transducer and activator of transcription; PPAR-γ: Peroxisome proliferator-activated receptor-γ; IL: Interleukin; Nrf2: Nuclear respiratory factor-2; TGF-β: Transforming growth factor-β; NF-κB: Nuclear factor-kappa B; TNF-α: Tumor necrosis factor-alpha; Bcl-2: B-cell lymphoma 2; EMT: Epithelial-mesenchymal transition; IKK: Inhibitory κB kinase; IKB: Inhibitory κB.

producing bacteria and altered the intestinal microflora, leading to a reduction in damage of the intestinal barrier in rats caused by hypertension[120]. Another study revealed that baicalin (25-100 mg/kg) helped increase SCFA-producing bacteria such as *Eubacterium* spp, *Subdoligranulum* spp, and *Butyricimonas* spp, thereby ameliorating TNBS-induced UC[114]. In some cases, the gut microbiome can also downregulate the therapeutic efficacy of baicalin[121]. The gut microbiota regulates hepatobiliary homeostasis *via* the gut-hepatic axis, and although it can regulate baicalin activity, baicalin can also modulate the gut microbiota[122]. Consequently, baicalin has the potential to exert a therapeutic role in liver and gut diseases by modulating FXR and TGR5-mediated crosstalk involving bile acids associated with the gut microbiome.

DRUG DELIVERY, CLINICAL TRIAL, AND FUTURE PROSPECTS

The clinical application of baicalin in pharmacology has been challenging, due to its low solubility and bioavailability. In the last decade, many researchers have designed novel delivery strategies for baicalin that include phospholipid complex, liposomes, solid baicalin nanocrystals, and micelle formation[123]. The dissolution and solubility of baicalin is considerably enhanced when administered in combination with other molecules in complex form. For instance, baicalin has exhibited improved oral bioavailability, distribution, targeting, and therapeutic efficacy when combined with polyethylene glycol and folic acid in the form of liposomes. β-Cyclodextrin complex has also been used as an effective formulation to facilitate the effective delivery of baicalin with wide range of therapeutic outcomes[123, 124]. Moreover, baicalin is commonly used as adjuvant therapy for hepatitis. In a clinical study, single dose baicalin (500 mg/kg) in combination with cyclosporin A was found to be safe and well tolerated in adult human subjects without any severe adverse effects[125]. However, the co-administration of baicalin with other herbal formulations or drugs might impede baicalin's *in vivo* actions and consequently its efficacy. Therefore, it is important to thoroughly study the clinically approved doses of baicalin which can be administered in combination with other compounds that help to improve the absorption and effectiveness of baicalin.

CONCLUSION

GI disorders have emerged as the leading cause of mortality in the recent years across the world. Baicalin, a major flavone obtained from *S. baicalensis*, exerts protective effect against hepatobiliary and colorectal disorders by modulating signaling pathways. Further, novel delivery strategies that are used in the transport of baicalin for ready absorption including phospholipid complex, liposomes, solid baicalin nanocrystals, and β-cyclodextrin complex have paved way for its widespread use as a pharmacological alternative in hepatic and GI disorders.

ACKNOWLEDGEMENTS

All of the authors acknowledge DST-FIST and UGC-SAP facilities of the Department of Biochemistry, University of Allahabad, Prayagraj, India.

FOOTNOTES

Author contributions: Ganguly R performed the literature review and wrote the manuscript; Ganguly R and Gupta A made the tables and figures; Pandey AK conceptualized the idea, critically reviewed and revised the manuscript; All authors have read and approved the final manuscript.

Supported by University Grants Commission, New Delhi, India in The Form of UGC-Junior and Senior Research Fellowships.

Conflict-of-interest statement: All the authors report no relevant conflicts of interest for this article.

Open-Access: This article is an open-access article that was selected by an in-house editor and fully peer-reviewed by external reviewers. It is distributed in accordance with the Creative Commons Attribution NonCommercial (CC BY-NC 4.0) license, which permits others to distribute, remix, adapt, build upon this work non-commercially, and license their derivative works on different terms, provided the original work is properly cited and the use is non-commercial. See: https://creativecommons.org/Licenses/by-nc/4.0/

Country/Territory of origin: India

ORCID number: Risha Ganguly 0000-0002-6190-8923; Ashutosh Gupta 0000-0002-6547-6312; Abhay K Pandey 0000-0002-4774-3085.

S-Editor: Fan JR
L-Editor: Filipodia
P-Editor: Fan JR

REFERENCES

1 **Gupta A**, Pandey AK. Aceclofenac-induced hepatotoxicity: An ameliorative effect of *Terminalia bellirica* fruit and ellagic acid. *World J Hepatol* 2020; **12**: 949-964 [PMID: 33312421 DOI: 10.4254/wjh.v12.i11.949]
2 **Sharma UK**, Kumar R, Ganguly R, Gupta A, Pandey AK. Cinnamaldehyde, an active component of cinnamon provides protection against food color induced oxidative stress and hepatotoxicity in albino wistar rats. *Vegetos* 2018; **31**: 123-129 [DOI: 10.5958/2229-4473.2018.00063.0]
3 **Gupta A**, Kumar R, Ganguly R, Singh AK, Rana HK, Pandey AK. Antioxidant, anti-inflammatory and hepatoprotective activities of *Terminalia bellirica* and its bioactive component ellagic acid against diclofenac induced oxidative stress and hepatotoxicity. *Toxicol Rep* 2021; **8**: 44-52 [PMID: 33391996 DOI: 10.1016/j.toxrep.2020.12.010]
4 **Björkholm B**, Bok CM, Lundin A, Rafter J, Hibberd ML, Pettersson S. Intestinal microbiota regulate xenobiotic metabolism in the liver. *PLoS One* 2009; **4**: e6958 [PMID: 19742318 DOI: 10.1371/journal.pone.0006958]
5 **Kumar S**, Kumar R, Dwivedi A, Pandey AK. In vitro antioxidant, antibacterial, and cytotoxic activity and in vivo effect of *Syngonium podophyllum* and *Eichhornia crassipes* leaf extracts on isoniazid induced oxidative stress and hepatic markers. *Biomed Res Int* 2014; **2014**: 459452 [PMID: 25162013 DOI: 10.1155/2014/459452]
6 **Hu Q**, Zhang W, Wu Z, Tian X, Xiang J, Li L, Li Z, Peng X, Wei S, Ma X, Zhao Y. Baicalin and the liver-gut system: Pharmacological bases explaining its therapeutic effects. *Pharmacol Res* 2021; **165**: 105444 [PMID: 33493657 DOI: 10.1016/j.phrs.2021.105444]
7 **Xiong F**, Guan YS. Cautiously using natural medicine to treat liver problems. *World J Gastroenterol* 2017; **23**: 3388-3395 [PMID: 28596675 DOI: 10.3748/wjg.v23.i19.3388]
8 **Rajaratnam M**, Prystupa A, Lachowska-Kotowska P, Załuska W, Filip R. Herbal medicine for treatment and prevention of liver diseases. *J Pre Clin Clin Res* 2014; **8**: 55-60

9 **Kumar Singh A**, Cabral C, Kumar R, Ganguly R, Kumar Rana H, Gupta A, Rosaria Lauro M, Carbone C, Reis F, Pandey AK. Beneficial Effects of Dietary Polyphenols on Gut Microbiota and Strategies to Improve Delivery Efficiency. *Nutrients* 2019; **11**: 2216 [PMID: 31540270 DOI: 10.3390/nu11092216]

10 **Sharma UK**, Kumar R, Gupta A, Ganguly R, Singh AK, Ojha AK, Pandey AK. Ameliorating efficacy of eugenol against metanil yellow induced toxicity in albino Wistar rats. *Food Chem Toxicol* 2019; **126**: 34-40 [PMID: 30738991 DOI: 10.1016/j.fct.2019.01.032]

11 **Sharma AK**, Kumar S, Chashoo G, Saxena AK, Pandey AK. Cell cycle inhibitory activity of *Piper longum* against A549 cell line and its protective effect against metal-induced toxicity in rats. *Indian J Biochem Biophys* 2014; **51**: 358-364 [PMID: 25630105]

12 **Sharma UK**, Sharma AK, Gupta A, Kumar R, Pandey A, Pandey AK. Pharmacological activities of cinnamaldehyde and eugenol: antioxidant, cytotoxic and anti-leishmanial studies. *Cell Mol Biol (Noisy-le-grand)* 2017; **63**: 73-78 [PMID: 28968213 DOI: 10.14715/cmb/2017.63.6.15]

13 **Waisundara VY**, Hsu A, Tan BK, Huang D. Baicalin reduces mitochondrial damage in streptozotocin-induced diabetic Wistar rats. *Diabetes Metab Res Rev* 2009; **25**: 671-677 [PMID: 19688721 DOI: 10.1002/dmrr.1005]

14 **Tao Y**, Zhan S, Wang Y, Zhou G, Liang H, Chen X, Shen H. Baicalin, the major component of traditional Chinese medicine *Scutellaria baicalensis* induces colon cancer cell apoptosis through inhibition of oncomiRNAs. *Sci Rep* 2018; **8**: 14477 [PMID: 30262902 DOI: 10.1038/s41598-018-32734-2]

15 **Zheng WX**, Wang F, Cao XL, Pan HY, Liu XY, Hu XM, Sun YY. Baicalin protects PC-12 cells from oxidative stress induced by hydrogen peroxide *via* anti-apoptotic effects. *Brain Inj* 2014; **28**: 227-234 [PMID: 24456060 DOI: 10.3109/02699052.2013.860469]

16 **Chen H**, Xu Y, Wang J, Zhao W, Ruan H. Baicalin ameliorates isoproterenol-induced acute myocardial infarction through iNOS, inflammation and oxidative stress in rat. *Int J Clin Exp Pathol* 2015; **8**: 10139-10147 [PMID: 26617721]

17 **Zhong X**, Liu H. Baicalin attenuates diet induced nonalcoholic steatohepatitis by inhibiting inflammation and oxidative stress *via* suppressing JNK signaling pathways. *Biomed Pharmacother* 2018; **98**: 111-117 [PMID: 29247950 DOI: 10.1016/j.biopha.2017.12.026]

18 **Lei K**, Shen Y, He Y, Zhang L, Zhang J, Tong W, Xu Y, Jin L. Baicalin represses C/EBP*β via* its antioxidative effect in Parkinson's Disease. *Oxid Med Cell Longev* 2020; **2020**: 8951907 [PMID: 32566108 DOI: 10.1155/2020/8951907]

19 **Wang H**, Zhang Y, Bai R, Wang M, Du S. Baicalin attenuates alcoholic liver injury through modulation of hepatic oxidative stress, inflammation and sonic hedgehog pathway in rats. *Cell Physiol Biochem* 2016; **39**: 1129-1140 [PMID: 27576501 DOI: 10.1159/000447820]

20 **Li-Weber M**. New therapeutic aspects of flavones: the anticancer properties of *Scutellaria* and its main active constituents wogonin, baicalein and baicalin. *Cancer Treat Rev* 2009; **35**: 57-68 [PMID: 19004559 DOI: 10.1016/j.ctrv.2008.09.005]

21 **Noh K**, Kang Y, Nepal MR, Jeong KS, Oh DG, Kang MJ, Lee S, Kang W, Jeong HG, Jeong TC. Role of Intestinal Microbiota in Baicalin-Induced Drug Interaction and its pharmacokinetics. *Molecules* 2016; **21**: 337 [PMID: 26978333 DOI: 10.3390/molecules21030337]

22 **Sowndhararajan K**, Deepa P, Kim M, Park SJ, Kim S. Neuroprotective and cognitive enhancement potentials of baicalin: a review. *Brain Sci* 2018; **8** [PMID: 29891783 DOI: 10.3390/brainsci8060104]

23 **Dinda B**, SilSarma I, Dinda M, Rudrapaul P. *Oroxylum indicum* (L.) Kurz, an important Asian traditional medicine: from traditional uses to scientific data for its commercial exploitation. *J Ethnopharmacol* 2015; **161**: 255-278 [PMID: 25543018 DOI: 10.1016/j.jep.2014.12.027]

24 **Mu X**, He G, Cheng Y, Li X, Xu B, Du G. Baicalein exerts neuroprotective effects in 6-hydroxydopamine-induced experimental parkinsonism in vivo and in vitro. *Pharmacol Biochem Behav* 2009; **92**: 642-648 [PMID: 19327378 DOI: 10.1016/j.pbb.2009.03.008]

25 **Chen H**, Gao Y, Wu J, Chen Y, Chen B, Hu J, Zhou J. Exploring therapeutic potentials of baicalin and its aglycone baicalein for hematological malignancies. *Cancer Lett* 2014; **354**: 5-11 [PMID: 25128647 DOI: 10.1016/j.canlet.2014.08.003]

26 **Lin M**, Tsai MJ, Wen KC. Supercritical fluid extraction of flavonoids from *Scutellariae* Radix. *J Chromatogr A* 1999; **830**: 387-395 [DOI: 10.1016/S0021-9673(98)00906-6]

27 **Yang R**, Zeng HJ, Wang QW, Guo C, Li JJ, Qu LB. Simultaneous determination of eight active components in Chinese medicine 'JiangYaBiFeng' tablet by HPLC coupled with diode array detection. *J Pharm Biomed Anal* 2011; **55**: 552-556 [PMID: 21376498 DOI: 10.1016/j.jpba.2011.01.021]

28 **Taiming L**, Xuehua J. Investigation of the absorption mechanisms of baicalin and baicalein in rats. *J Pharm Sci* 2006; **95**: 1326-1333 [PMID: 16628739 DOI: 10.1002/jps.20593]

29 **Hao J**, Wang F, Wang X, Zhang D, Bi Y, Gao Y, Zhao X, Zhang Q. Development and optimization of baicalin-loaded solid lipid nanoparticles prepared by coacervation method using central composite design. *Eur J Pharm Sci* 2012; **47**: 497-505 [PMID: 22820033 DOI: 10.1016/j.ejps.2012.07.006]

30 **Zhao L**, Wei Y, Huang Y, He B, Zhou Y, Fu J. Nanoemulsion improves the oral bioavailability of baicalin in rats: in vitro and in vivo evaluation. *Int J Nanomedicine* 2013; **8**: 3769-3779 [PMID: 24124365 DOI: 10.2147/IJN.S51578]

31 **Moore OA**, Gao Y, Chen AY, Brittain R, Chen YC. The extraction, anticancer effect, bioavailability, and nanotechnology of baicalin. *J Nutr Med Diet Care* 2016; **2** [PMID: 27790646 DOI: 10.23937/2572-3278.1510011]

32 **Kalapos-Kovács B**, Magda B, Jani M, Fekete Z, Szabó PT, Antal I, Krajcsi P, Klebovich I. Multiple ABC transporters efflux baicalin. *Phytother Res* 2015; **29**: 1987-1990 [PMID: 26400418 DOI: 10.1002/ptr.5477]

33 **Akao T**, Sato K, Hanada M. Hepatic contribution to a marked increase in the plasma concentration of baicalin after oral administration of its aglycone, baicalein, in multidrug resistance-associated protein 2-deficient rat. *Biol Pharm Bull* 2009; **32**: 2079-2082 [PMID: 19952434 DOI: 10.1248/bpb.32.2079]

34 **Tang Y**, Zhu H, Zhang Y, Huang C. Determination of human plasma protein binding of baicalin by ultrafiltration and high-performance liquid chromatography. *Biomed Chromatogr* 2006; **20**: 1116-1119 [PMID: 16708379 DOI: 10.1002/bmc.655]

35 **Liang W**, Huang X, Chen W. The effects of baicalin and baicalein on cerebral ischemia: a review. *Aging Dis* 2017; **8**:

850-867 [PMID: 29344420 DOI: 10.14336/AD.2017.0829]
36 **Abe K**, Inoue O, Yumioka E. Biliary excretion of metabolites of baicalin and baicalein in rats. *Chem Pharm Bull (Tokyo)* 1990; **38**: 209-211 [PMID: 2337942 DOI: 10.1248/CPB.38.208]
37 **Zhang J**, Cai W, Zhou Y, Liu Y, Wu X, Li Y, Lu J, Qiao Y. Profiling and identification of the metabolites of baicalin and study on their tissue distribution in rats by ultra-high-performance liquid chromatography with linear ion trap-Orbitrap mass spectrometer. *J Chromatogr B Analyt Technol Biomed Life Sci* 2015; **985**: 91-102 [PMID: 25661005 DOI: 10.1016/j.jchromb.2015.01.018]
38 **Lai CC**, Huang PH, Yang AH, Chiang SC, Tang CY, Tseng KW, Huang CH. Baicalein reduces liver injury induced by myocardial ischemia and reperfusion. *Am J Chin Med* 2016; **44**: 531-550 [PMID: 27109160 DOI: 10.1142/S0192415X16500294]
39 **Dong Y**, Xing Y, Sun J, Sun W, Xu Y, Quan C. Baicalein alleviates liver oxidative stress and apoptosis induced by high-level glucose through the activation of the PERK/Nrf2 signaling pathway. *Molecules* 2020; **25** [PMID: 32019168 DOI: 10.3390/molecules25030599]
40 **Akuta N**, Kawamura Y, Suzuki F, Saitoh S, Arase Y, Fujiyama S, Sezaki H, Hosaka T, Kobayashi M, Suzuki Y, Ikeda K, Kumada H. Analysis of association between circulating miR-122 and histopathological features of nonalcoholic fatty liver disease in patients free of hepatocellular carcinoma. *BMC Gastroenterol* 2016; **16**: 141 [PMID: 27955628 DOI: 10.1186/s12876-016-0557-6]
41 **Xi Y**, Wu M, Li H, Dong S, Luo E, Gu M, Shen X, Jiang Y, Liu Y, Liu H. Baicalin attenuates high fat diet-induced obesity and liver dysfunction: dose-response and potential role of CaMKKβ/AMPK/ACC pathway. *Cell Physiol Biochem* 2015; **35**: 2349-2359 [PMID: 25896320 DOI: 10.1159/000374037]
42 **Guo HX**, Liu DH, Ma Y, Liu JF, Wang Y, Du ZY, Wang X, Shen JK, Peng HL. Long-term baicalin administration ameliorates metabolic disorders and hepatic steatosis in rats given a high-fat diet. *Acta Pharmacol Sin* 2009; **30**: 1505-1512 [PMID: 19890358 DOI: 10.1038/aps.2009.150]
43 **Ma Y**, Yang F, Wang Y, Du Z, Liu D, Guo H, Shen J, Peng H. CaMKKβ is involved in AMP-activated protein kinase activation by baicalin in LKB1 deficient cell lines. *PLoS One* 2012; **7**: e47900 [PMID: 23110126 DOI: 10.1371/journal.pone.0047900]
44 **Dai J**, Liang K, Zhao S, Jia W, Liu Y, Wu H, Lv J, Cao C, Chen T, Zhuang S, Hou X, Zhou S, Zhang X, Chen XW, Huang Y, Xiao RP, Wang YL, Luo T, Xiao J, Wang C. Chemoproteomics reveals baicalin activates hepatic CPT1 to ameliorate diet-induced obesity and hepatic steatosis. *Proc Natl Acad Sci U S A* 2018; **115**: E5896-E5905 [PMID: 29891721 DOI: 10.1073/pnas.1801745115]
45 **Chen Q**, Liu M, Yu H, Li J, Wang S, Zhang Y, Qiu F, Wang T. *Scutellaria baicalensis* regulates FFA metabolism to ameliorate NAFLD through the AMPK-mediated SREBP signaling pathway. *J Nat Med* 2018; **72**: 655-666 [PMID: 29542003 DOI: 10.1007/s11418-018-1199-5]
46 **Zhang J**, Zhang H, Deng X, Zhang N, Liu B, Xin S, Li G, Xu K. Baicalin attenuates non-alcoholic steatohepatitis by suppressing key regulators of lipid metabolism, inflammation and fibrosis in mice. *Life Sci* 2018; **192**: 46-54 [PMID: 29158052 DOI: 10.1016/j.lfs.2017.11.027]
47 **Liu J**, Yuan Y, Gong X, Zhang L, Zhou Q, Wu S, Zhang X, Hu J, Kuang G, Yin X, Wan J. Baicalin and its nanoliposomes ameliorates nonalcoholic fatty liver disease *via* suppression of TLR4 signaling cascade in mice. *Int Immunopharmacol* 2020; **80**: 106208 [PMID: 31955065 DOI: 10.1016/j.intimp.2020.106208]
48 **Zhao W**, Liu L, Wang Y, Mao T, Li J. Effects of a combination of puerarin, baicalin and berberine on the expression of proliferator-activated receptor-γ and insulin receptor in a rat model of nonalcoholic fatty liver disease. *Exp Ther Med* 2016; **11**: 183-190 [PMID: 26889237 DOI: 10.3892/etm.2015.2846]
49 **Zhang J**, Zhang H, Deng X, Zhang Y, Xu K. Baicalin protects AML-12 cells from lipotoxicity *via* the suppression of ER stress and TXNIP/NLRP3 inflammasome activation. *Chem Biol Interact* 2017; **278**: 189-196 [PMID: 29031535 DOI: 10.1016/j.cbi.2017.10.010]
50 **Zhang HY**, Wang HL, Zhong GY, Zhu JX. Molecular mechanism and research progress on pharmacology of traditional Chinese medicine in liver injury. *Pharm Biol* 2018; **56**: 594-611 [PMID: 31070528 DOI: 10.1080/13880209.2018.1517185]
51 **Real M**, Barnhill MS, Higley C, Rosenberg J, Lewis JH. Drug-induced liver injury: highlights of the recent literature. *Drug Saf* 2019; **42**: 365-387 [PMID: 30343418 DOI: 10.1007/s40264-018-0743-2]
52 **Brenner C**, Galluzzi L, Kepp O, Kroemer G. Decoding cell death signals in liver inflammation. *J Hepatol* 2013; **59**: 583-594 [PMID: 23567086 DOI: 10.1016/j.jhep.2013.03.033]
53 **Liao CC**, Day YJ, Lee HC, Liou JT, Chou AH, Liu FC. Baicalin attenuates IL-17-mediated acetaminophen-induced liver injury in a mouse model. *PLoS One* 2016; **11**: e0166856 [PMID: 27855209 DOI: 10.1371/journal.pone.0166856]
54 **He P**, Wu Y, Shun J, Liang Y, Cheng M, Wang Y. Baicalin ameliorates liver injury induced by chronic plus binge ethanol feeding by modulating oxidative stress and inflammation *via* CYP2E1 and NRF2 in mice. *Oxid Med Cell Longev* 2017; **2017**: 4820414 [PMID: 28951767 DOI: 10.1155/2017/4820414]
55 **Shi L**, Hao Z, Zhang S, Wei M, Lu B, Wang Z, Ji L. Baicalein and baicalin alleviate acetaminophen-induced liver injury by activating Nrf2 antioxidative pathway: The involvement of ERK1/2 and PKC. *Biochem Pharmacol* 2018; **150**: 9-23 [PMID: 29338970 DOI: 10.1016/j.bcp.2018.01.026]
56 **Liao CC**, Day YJ, Lee HC, Liou JT, Chou AH, Liu FC. ERK signaling pathway plays a key role in baicalin protection against acetaminophen-induced liver injury. *Am J Chin Med* 2017; **45**: 105-121 [PMID: 28081632 DOI: 10.1142/S0192415X17500082]
57 **Wang Y**, Jia Y, Yang X, Liang B, Gao H, Yang T. A potential role of Baicalin to inhibit apoptosis and protect against acute liver and kidney injury in rat preeclampsia model. *Biomed Pharmacother* 2018; **108**: 1546-1552 [PMID: 30372856 DOI: 10.1016/j.biopha.2018.09.107]
58 **Liu F**, Zhang J, Qian J, Wu G, Ma Z. Baicalin attenuates liver hypoxia/reoxygenation injury by inducing autophagy. *Exp Ther Med* 2018; **16**: 657-664 [PMID: 30116320 DOI: 10.3892/etm.2018.6284]
59 **Wu T**, Liu T, Xing L, Ji G. Baicalin and puerarin reverse epithelial-mesenchymal transition *via* the TGF-β1/Smad3

pathway *in vitro*. *Exp Ther Med* 2018; **16**: 1968-1974 [PMID: 30186426 DOI: 10.3892/etm.2018.6400]
60 **Wang Y**, Yin S, Zhou Y, Zhou W, Chen T, Wu Q, Zhou L, Zheng S. Dual-function of Baicalin in nsPEFs-treated hepatocytes and hepatocellular carcinoma cells for different death pathway and mitochondrial response. *Int J Med Sci* 2019; **16**: 1271-1282 [PMID: 31588193 DOI: 10.7150/ijms.34876]
61 **Zhao Y**, Li H, Gao Z, Gong Y, Xu H. Effects of flavonoids extracted from *Scutellaria baicalensis* Georgi on hemin-nitrite-H2O2 induced liver injury. *Eur J Pharmacol* 2006; **536**: 192-199 [PMID: 16574098 DOI: 10.1016/j.ejphar.2006.02.045]
62 **Liao S**, Li P, Wang J, Zhang Q, Xu D, Yang M, Kong L. Protection of baicalin against lipopolysaccharide induced liver and kidney injuries based on ^{1}H NMR metabolomic profiling. *Toxicol Res (Camb)* 2016; **5**: 1148-1159 [PMID: 30090421 DOI: 10.1039/c6tx00082g]
63 **Seki E**, Brenner DA. Recent advancement of molecular mechanisms of liver fibrosis. *J Hepatobiliary Pancreat Sci* 2015; **22**: 512-518 [PMID: 25869468 DOI: 10.1002/jhbp.245]
64 **Klingenberg M**, Groß M, Goyal A, Polycarpou-Schwarz M, Miersch T, Ernst AS, Leupold J, Patil N, Warnken U, Allgayer H, Longerich T, Schirmacher P, Boutros M, Diederichs S. The long noncoding RNA cancer susceptibility 9 and RNA binding protein heterogeneous nuclear ribonucleoprotein L form a complex and coregulate genes linked to AKT signaling. *Hepatology* 2018; **68**: 1817-1832 [PMID: 29790588 DOI: 10.1002/hep.30102]
65 **Dawood RM**, El-Meguid MA, Salum GM, El Awady MK. Key players of hepatic fibrosis. *J Interferon Cytokine Res* 2020; **40**: 472-489 [PMID: 32845785 DOI: 10.1089/jir.2020.0059]
66 **Lin L**, Zhou F, Shen S, Zhang T. Fighting liver fibrosis with naturally occurring antioxidants. *Planta Med* 2018; **84**: 1318-1333 [PMID: 30312974 DOI: 10.1055/a-0757-0008]
67 **Zhao Z**, Lin CY, Cheng K. siRNA- and miRNA-based therapeutics for liver fibrosis. *Transl Res* 2019; **214**: 17-29 [PMID: 31476281 DOI: 10.1016/j.trsl.2019.07.007]
68 **Shen K**, Feng X, Pan H, Zhang F, Xie H, Zheng S. Baicalin ameliorates experimental liver cholestasis in mice by modulation of oxidative stress, inflammation, and NRF2 transcription factor. *Oxid Med Cell Longev* 2017; **2017**: 6169128 [PMID: 28757911 DOI: 10.1155/2017/6169128]
69 **Wu X**, Zhi F, Lun W, Deng Q, Zhang W. Baicalin inhibits PDGF-BB-induced hepatic stellate cell proliferation, apoptosis, invasion, migration and activation *via* the miR-3595/ACSL4 axis. *Int J Mol Med* 2018; **41**: 1992-2002 [PMID: 29393361 DOI: 10.3892/ijmm.2018.3427]
70 **Yang MD**, Chiang YM, Higashiyama R, Asahina K, Mann DA, Mann J, Wang CC, Tsukamoto H. Rosmarinic acid and baicalin epigenetically derepress peroxisomal proliferator-activated receptor γ in hepatic stellate cells for their antifibrotic effect. *Hepatology* 2012; **55**: 1271-1281 [PMID: 22095555 DOI: 10.1002/hep.24792]
71 **Wei XL**, Fang RT, Yang YH, Bi XY, Ren GX, Luo AL, Zhao M, Zang WJ. Protective effects of extracts from Pomegranate peels and seeds on liver fibrosis induced by carbon tetrachloride in rats. *BMC Complement Altern Med* 2015; **15**: 389 [PMID: 26508316 DOI: 10.1186/s12906-015-0916-9]
72 **Qiao H**, Han H, Hong D, Ren Z, Chen Y, Zhou C. Protective effects of baicalin on carbon tetrachloride induced liver injury by activating PPARγ and inhibiting TGFβ1. *Pharm Biol* 2011; **49**: 38-45 [PMID: 20687787 DOI: 10.3109/13880209.2010.493179]
73 **de Vries E**, Bolier R, Goet J, Parés A, Verbeek J, de Vree M, Drenth J, van Erpecum K, van Nieuwkerk K, van der Heide F, Mostafavi N, Helder J, Ponsioen C, Oude Elferink R, van Buuren H, Beuers U; Netherlands association for the study of the liver-cholestasis working group. Fibrates for Itch (FITCH) in fibrosing cholangiopathies: a double-blind, randomized, placebo-controlled trial. *Gastroenterology* 2021; **160**: 734-743.e6 [PMID: 33031833 DOI: 10.1053/j.gastro.2020.10.001]
74 **Salas-Silva S**, Simoni-Nieves A, Razori MV, López-Ramirez J, Barrera-Chimal J, Lazzarini R, Bello O, Souza V, Miranda-Labra RU, Gutiérrez-Ruiz MC, Gomez-Quiroz LE, Roma MG, Bucio-Ortiz L. HGF induces protective effects in α-naphthylisothiocyanate-induced intrahepatic cholestasis by counteracting oxidative stress. *Biochem Pharmacol* 2020; **174**: 113812 [PMID: 31954718 DOI: 10.1016/j.bcp.2020.113812]
75 **Zhang CL**, Xu YJ, Xiang D, Yang JY, Lei K, Liu D. Pharmacokinetic characteristics of baicalin in rats with 17α-ethynyl-estradiol-induced intrahepatic cholestasis. *Curr Med Sci* 2018; **38**: 167-173 [PMID: 30074167 DOI: 10.1007/s11596-018-1861-x]
76 **Gupta A**, Kumar R, Bhattacharyya P, Bishayee A, Pandey AK. *Terminalia bellirica* (Gaertn.) roxb. (Bahera) in health and disease: A systematic and comprehensive review. *Phytomedicine* 2020; **77**: 153278 [PMID: 32781393 DOI: 10.1016/j.phymed.2020.153278]
77 **Yang J**, Xiang D, He W, Liu Y, Lan L, Li G, Jiang C, Ren X, Liu D, Zhang C. Baicalin protects against 17α-ethinylestradiol-induced cholestasis *via* the sirtuin1/hepatic nuclear receptor-1α/farnesoid X receptor pathway. *Front Pharmacol* 2019; **10**: 1685 [PMID: 32116682 DOI: 10.3389/fphar.2019.01685]
78 **Lanini S**, Ustianowski A, Pisapia R, Zumla A, Ippolito G. Viral hepatitis: etiology, epidemiology, transmission, diagnostics, treatment, and prevention. *Infect Dis Clin North Am* 2019; **33**: 1045-1062 [PMID: 31668190 DOI: 10.1016/j.idc.2019.08.004]
79 **Suzuki K**, Suda G, Yamamoto Y, Furuya K, Baba M, Nakamura A, Miyoshi H, Kimura M, Maehara O, Yamada R, Kitagataya T, Yamamoto K, Shigesawa T, Ohara M, Kawagishi N, Nakai M, Sho T, Natsuizaka M, Morikawa K, Ogawa K, Ohnishi S, Sakamoto N; NORTE Study Group. Tenofovir-disoproxil-fumarate modulates lipid metabolism *via* hepatic CD36/PPAR-alpha activation in hepatitis B virus infection. *J Gastroenterol* 2021; **56**: 168-180 [PMID: 33211179 DOI: 10.1007/s00535-020-01750-3]
80 **Lim HK**, Jeffrey GP, Ramm GA, Soekmadji C. Pathogenesis of viral hepatitis-induced chronic liver disease: role of extracellular vesicles. *Front Cell Infect Microbiol* 2020; **10**: 587628 [PMID: 33240824 DOI: 10.3389/fcimb.2020.587628]
81 **Robertson BH**. Viral hepatitis and primates: historical and molecular analysis of human and nonhuman primate hepatitis A, B, and the GB-related viruses. *J Viral Hepat* 2001; **8**: 233-242 [PMID: 11454173 DOI: 10.1046/j.1365-2893.2001.00295.x]
82 **Huang Y**, Sun M, Yang X, Ma A, Ma Y, Zhao A. Baicalin relieves inflammation stimulated by lipopolysaccharide *via* upregulating TUG1 in liver cells. *J Physiol Biochem* 2019; **75**: 463-473 [PMID: 31396818 DOI:

10.1007/s13105-019-00698-0]
83 **Pollicino T**, Musolino C, Irrera N, Bitto A, Lombardo D, Timmoneri M, Minutoli L, Raimondo G, Squadrito G, Squadrito F, Altavilla D. Flavocoxid exerts a potent antiviral effect against hepatitis B virus. *Inflamm Res* 2018; **67**: 89-103 [PMID: 29018874 DOI: 10.1007/s00011-017-1099-2]
84 **Xia C**, Tang W, Geng P, Zhu H, Zhou W, Huang H, Zhou P, Shi X. Baicalin down-regulating hepatitis B virus transcription depends on the liver-specific HNF4α-HNF1α axis. *Toxicol Appl Pharmacol* 2020; **403**: 115131 [PMID: 32687838 DOI: 10.1016/j.taap.2020.115131]
85 **Huang H**, Zhou W, Zhu H, Zhou P, Shi X. Baicalin benefits the anti-HBV therapy *via* inhibiting HBV viral RNAs. *Toxicol Appl Pharmacol* 2017; **323**: 36-43 [PMID: 28322895 DOI: 10.1016/j.taap.2017.03.016]
86 **Hwang JM**, Tseng TH, Tsai YY, Lee HJ, Chou FP, Wang CJ, Chu CY. Protective effects of baicalein on tert-butyl hydroperoxide-induced hepatic toxicity in rat hepatocytes. *J Biomed Sci* 2005; **12**: 389-397 [PMID: 15917992 DOI: 10.1007/s11373-005-1572-8]
87 **Ueda S**, Nakamura H, Masutani H, Sasada T, Takabayashi A, Yamaoka Y, Yodoi J. Baicalin induces apoptosis *via* mitochondrial pathway as prooxidant. *Mol Immunol* 2002; **38**: 781-791 [PMID: 11841838 DOI: 10.1016/s0161-5890(01)00115-8]
88 **Cheng Y**, Ping J, Xu HD, Fu HJ, Zhou ZH. Synergistic effect of a novel oxymatrine-baicalin combination against hepatitis B virus replication, alpha smooth muscle actin expression and type I collagen synthesis in vitro. *World J Gastroenterol* 2006; **12**: 5153-5159 [PMID: 16937525 DOI: 10.3748/wjg.v12.i32.5153]
89 **Wan JY**, Gong X, Zhang L, Li HZ, Zhou YF, Zhou QX. Protective effect of baicalin against lipopolysaccharide/D-galactosamine-induced liver injury in mice by up-regulation of heme oxygenase-1. *Eur J Pharmacol* 2008; **587**: 302-308 [PMID: 18420187 DOI: 10.1016/j.ejphar.2008.02.081]
90 **Chen Y**, Zeng L, Yang J, Wang Y, Yao F, Wu Y, Wang D, Hu Y, Liu J. Anti-DHAV-1 reproduction and immuno-regulatory effects of a flavonoid prescription on duck virus hepatitis. *Pharm Biol* 2017; **55**: 1545-1552 [PMID: 28385083 DOI: 10.1080/13880209.2017.1309554]
91 **Singh AK**, Kumar R, Pandey AK. Hepatocellular carcinoma: causes, mechanism of progression and biomarkers. *Curr Chem Genom Transl Med* 2018; **12**: 9-26 [PMID: 30069430 DOI: 10.2174/2213988501812010009]
92 **Su L**, Zhou T, Zhang Z, Zhang X, Zhi X, Li C, Wang Q, Jia C, Shi W, Yue Y, Gao Y, Cheng B. Optimal staging system for predicting the prognosis of patients with hepatocellular carcinoma in China: a retrospective study. *BMC Cancer* 2016; **16**: 424 [PMID: 27387757 DOI: 10.1186/s12885-016-2420-0]
93 **Tan HY**, Wang N, Man K, Tsao SW, Che CM, Feng Y. Autophagy-induced RelB/p52 activation mediates tumour-associated macrophage repolarisation and suppression of hepatocellular carcinoma by natural compound baicalin. *Cell Death Dis* 2015; **6**: e1942 [PMID: 26492375 DOI: 10.1038/cddis.2015.271]
94 **Yu Z**, Luo X, Wang C, Ye J, Liu S, Xie L, Wang F, Bao J. Baicalin promoted site-2 protease and not site-1 protease in endoplasmic reticulum stress-induced apoptosis of human hepatocellular carcinoma cells. *FEBS Open Bio* 2016; **6**: 1093-1101 [PMID: 27833850 DOI: 10.1002/2211-5463.12130]
95 **Zhang X**, Tang X, Liu H, Li L, Hou Q, Gao J. Autophagy induced by baicalin involves downregulation of CD147 in SMMC-7721 cells in vitro. *Oncol Rep* 2012; **27**: 1128-1134 [PMID: 22200845 DOI: 10.3892/or.2011.1599]
96 **Giraud J**, Chalopin D, Blanc JF, Saleh M. Hepatocellular carcinoma immune landscape and the potential of immunotherapies. *Front Immunol* 2021; **12**: 655697 [PMID: 33815418 DOI: 10.3389/fimmu.2021.655697]
97 **Gupta A**, Singh AK, Kumar R, Ganguly R, Rana HK, Pandey PK, Sethi G, Bishayee A, Pandey AK. Corilagin in cancer: a critical evaluation of anticancer activities and molecular mechanisms. *Molecules* 2019; **24** [PMID: 31546767 DOI: 10.3390/molecules24183399]
98 **Kurilova I**, Bendet A, Petre EN, Boas FE, Kaye E, Gonen M, Covey A, Brody LA, Brown KT, Kemeny NE, Yarmohammadi H, Ziv E, D'Angelica MI, Kingham TP, Cercek A, Solomon SB, Beets-Tan RGH, Sofocleous CT. Factors associated with local tumor control and complications after thermal ablation of colorectal cancer liver metastases: a 15-year retrospective cohort study. *Clin Colorectal Cancer* 2021; **20**: e82-e95 [PMID: 33246789 DOI: 10.1016/j.clcc.2020.09.005]
99 **Singh AK**, Bishayee A, Pandey AK. Targeting histone deacetylases with natural and synthetic agents: an emerging anticancer strategy. *Nutrients* 2018; **10** [PMID: 29882797 DOI: 10.3390/nu10060731]
100 **Yang B**, Bai H, Sa Y, Zhu P, Liu P. Inhibiting EMT, stemness and cell cycle involved in baicalin-induced growth inhibition and apoptosis in colorectal cancer cells. *J Cancer* 2020; **11**: 2303-2317 [PMID: 32127957 DOI: 10.7150/jca.37242]
101 **Jia Y**, Chen L, Guo S, Li Y. Baicalin induced colon cancer cells apoptosis through miR-217/DKK1-mediated inhibition of Wnt signaling pathway. *Mol Biol Rep* 2019; **46**: 1693-1700 [PMID: 30737617 DOI: 10.1007/s11033-019-04618-9]
102 **Wang Z**, Ma L, Su M, Zhou Y, Mao K, Li C, Peng G, Zhou C, Shen B, Dou J. Baicalin induces cellular senescence in human colon cancer cells *via* upregulation of DEPP and the activation of Ras/Raf/MEK/ERK signaling. *Cell Death Dis* 2018; **9**: 217 [PMID: 29440765 DOI: 10.1038/s41419-017-0223-0]
103 **Yu C**, Zhang Z, Zhang H, Zhen Z, Calway T, Wang Y, Yuan CS, Wang CZ. Pretreatment of baicalin and wogonoside with glycoside hydrolase: a promising approach to enhance anticancer potential. *Oncol Rep* 2013; **30**: 2411-2418 [PMID: 24026776 DOI: 10.3892/or.2013.2726]
104 **Ma W**, Liu X, Du W. Baicalin induces apoptosis in SW480 cells through downregulation of the SP1 transcription factor. *Anticancer Drugs* 2019; **30**: 153-158 [PMID: 30362980 DOI: 10.1097/CAD.0000000000000708]
105 **Neurath MF**, Leppkes M. Resolution of ulcerative colitis. *Semin Immunopathol* 2019; **41**: 747-756 [PMID: 31278430 DOI: 10.1007/s00281-019-00751-6]
106 **Ungaro R**, Mehandru S, Allen PB, Peyrin-Biroulet L, Colombel JF. Ulcerative colitis. *Lancet* 2017; **389**: 1756-1770 [PMID: 27914657 DOI: 10.1016/S0140-6736(16)32126-2]
107 **Rizzo V**, Ferlazzo N, Currò M, Isola G, Matarese M, Bertuccio MP, Caccamo D, Matarese G, Ientile R. Baicalin-induced autophagy preserved LPS-stimulated intestinal cells from inflammation and alterations of paracellular permeability. *Int J Mol Sci* 2021; **22** [PMID: 33652555 DOI: 10.3390/ijms22052315]

108 **Shen J**, Cheng J, Zhu S, Zhao J, Ye Q, Xu Y, Dong H, Zheng X. Regulating effect of baicalin on IKK/IKB/NF-kB signaling pathway and apoptosis-related proteins in rats with ulcerative colitis. *Int Immunopharmacol* 2019; **73**: 193-200 [PMID: 31103874 DOI: 10.1016/j.intimp.2019.04.052]

109 **Cui L**, Feng L, Zhang ZH, Jia XB. The anti-inflammation effect of baicalin on experimental colitis through inhibiting TLR4/NF-κB pathway activation. *Int Immunopharmacol* 2014; **23**: 294-303 [PMID: 25239813 DOI: 10.1016/j.intimp.2014.09.005]

110 **Yao J**, Cao X, Zhang R, Li YX, Xu ZL, Zhang DG, Wang LS, Wang JY. Protective effect of baicalin against experimental colitis *via* suppression of oxidant stress and apoptosis. *Pharmacogn Mag* 2016; **12**: 225-234 [PMID: 27601854 DOI: 10.4103/0973-1296.186342]

111 **Liang S**, Deng X, Lei L, Zheng Y, Ai J, Chen L, Xiong H, Mei Z, Cheng YC, Ren Y. The comparative study of the therapeutic effects and mechanism of baicalin, baicalein, and their combination on ulcerative colitis rat. *Front Pharmacol* 2019; **10**: 1466 [PMID: 31920656 DOI: 10.3389/fphar.2019.01466]

112 **Zhang CL**, Zhang S, He WX, Lu JL, Xu YJ, Yang JY, Liu D. Baicalin may alleviate inflammatory infiltration in dextran sodium sulfate-induced chronic ulcerative colitis *via* inhibiting IL-33 expression. *Life Sci* 2017; **186**: 125-132 [PMID: 28802904 DOI: 10.1016/j.lfs.2017.08.010]

113 **Feng J**, Guo C, Zhu Y, Pang L, Yang Z, Zou Y, Zheng X. Baicalin down regulates the expression of TLR4 and NFkB-p65 in colon tissue in mice with colitis induced by dextran sulfate sodium. *Int J Clin Exp Med* 2014; **7**: 4063-4072 [PMID: 25550915]

114 **Dai SX**, Zou Y, Feng YL, Liu HB, Zheng XB. Baicalin down-regulates the expression of macrophage migration inhibitory factor (MIF) effectively for rats with ulcerative colitis. *Phytother Res* 2012; **26**: 498-504 [PMID: 21887805 DOI: 10.1002/ptr.3581]

115 **Zhu L**, Xu LZ, Zhao S, Shen ZF, Shen H, Zhan LB. Protective effect of baicalin on the regulation of Treg/Th17 balance, gut microbiota and short-chain fatty acids in rats with ulcerative colitis. *Appl Microbiol Biotechnol* 2020; **104**: 5449-5460 [PMID: 32322944 DOI: 10.1007/s00253-020-10527-w]

116 **Zou Y**, Dai SX, Chi HG, Li T, He ZW, Wang J, Ye CG, Huang GL, Zhao B, Li WY, Wan Z, Feng JS, Zheng XB. Baicalin attenuates TNBS-induced colitis in rats by modulating the Th17/Treg paradigm. *Arch Pharm Res* 2015; **38**: 1873-1887 [PMID: 25269538 DOI: 10.1007/s12272-014-0486-2]

117 **Yu FY**, Huang SG, Zhang HY, Ye H, Chi HG, Zou Y, Lv RX, Zheng XB. Effects of baicalin in CD4 + CD29 + T cell subsets of ulcerative colitis patients. *World J Gastroenterol* 2014; **20**: 15299-15309 [PMID: 25386078 DOI: 10.3748/wjg.v20.i41.15299]

118 **Feng W**, Ao H, Peng C, Yan D. Gut microbiota, a new frontier to understand traditional Chinese medicines. *Pharmacol Res* 2019; **142**: 176-191 [PMID: 30818043 DOI: 10.1016/j.phrs.2019.02.024]

119 **Ju M**, Liu Y, Li M, Cheng M, Zhang Y, Deng G, Kang X, Liu H. Baicalin improves intestinal microecology and abnormal metabolism induced by high-fat diet. *Eur J Pharmacol* 2019; **857**: 172457 [PMID: 31202804 DOI: 10.1016/j.ejphar.2019.172457]

120 **Wu D**, Ding L, Tang X, Wang W, Chen Y, Zhang T. Baicalin protects against hypertension-associated intestinal barrier impairment in part through enhanced microbial production of short-chain fatty acids. *Front Pharmacol* 2019; **10**: 1271 [PMID: 31719823 DOI: 10.3389/fphar.2019.01271]

121 **Dey P**. Gut microbiota in phytopharmacology: A comprehensive overview of concepts, reciprocal interactions, biotransformations and mode of actions. *Pharmacol Res* 2019; **147**: 104367 [PMID: 31344423 DOI: 10.1016/j.phrs.2019.104367]

122 **Chopyk DM**, Grakoui A. Contribution of the intestinal microbiome and gut barrier to hepatic disorders. *Gastroenterology* 2020; **159**: 849-863 [PMID: 32569766 DOI: 10.1053/j.gastro.2020.04.077]

123 **Ganguly R**, Kumar R, Pandey AK. Baicalin provides protection against fluoxetine-induced hepatotoxicity by modulation of oxidative stress and inflammation. *World J Hepatol* 2022; **14**: 729-743 [DOI: 10.4254/wjh.v14.i4.729]

124 **Li J**, Jiang Q, Deng P, Chen Q, Yu M, Shang J, Li W. The formation of a host-guest inclusion complex system between β-cyclodextrin and baicalin and its dissolution characteristics. *J Pharm Pharmacol* 2017; **69**: 663-674 [PMID: 28299800 DOI: 10.1111/jphp.12708]

125 **Ibrahim A**, Nasr M, El-Sherbiny IM. Baicalin as an emerging magical nutraceutical molecule: Emphasis on pharmacological properties and advances in pharmaceutical delivery. *J Drug Deliv Sci Technol* 2022; **70**: 1773-2247 [DOI: 10.1016/j.jddst.2022.103269]

World Journal of Gastroenterology

Submit a Manuscript: https://www.f6publishing.com

World J Gastroenterol 2022 July 14; 28(26): 3063-3070

DOI: 10.3748/wjg.v28.i26.3063

ISSN 1007-9327 (print) ISSN 2219-2840 (online)

MINIREVIEWS

Alterations of autophagic and innate immune responses by the Crohn's disease-associated *ATG16L1* mutation

Natsuki Okai, Tomohiro Watanabe, Kosuke Minaga, Ken Kamata, Hajime Honjo, Masatoshi Kudo

Specialty type: Immunology

Provenance and peer review: Invited article; Externally peer reviewed.

Peer-review model: Single blind

Peer-review report's scientific quality classification

Grade A (Excellent): 0
Grade B (Very good): B, B
Grade C (Good): 0
Grade D (Fair): 0
Grade E (Poor): 0

P-Reviewer: Huang X, China; Kaczmarek-Ryś M

Received: January 10, 2022
Peer-review started: January 10, 2022
First decision: April 16, 2022
Revised: April 21, 2022
Accepted: June 16, 2022
Article in press: June 16, 2022
Published online: July 14, 2022

Natsuki Okai, Tomohiro Watanabe, Kosuke Minaga, Ken Kamata, Hajime Honjo, Masatoshi Kudo, Department of Gastroenterology and Hepatology, Kindai University Faculty of Medicine, Osaka-Sayama 589-8511, Osaka, Japan

Corresponding author: Tomohiro Watanabe, MD, PhD, Associate Professor, Department of Gastroenterology and Hepatology, Kindai University Faculty of Medicine, 377-2 Ohno-Higashi, Osaka-Sayama 589-8511, Osaka, Japan. tomohiro@med.kindai.ac.jp

Abstract

Crohn's disease (CD) is driven by the loss of tolerance to intestinal microbiota and excessive production of pro-inflammatory cytokines. These pro-inflammatory cytokines are produced by macrophages and dendritic cells (DCs) upon sensing the intestinal microbiota by the pattern recognition receptors (PRRs). Impaired activation of PRR-mediated signaling pathways is associated with chronic gastrointestinal inflammation, as shown by the fact that loss-of-function mutations in the nucleotide-binding oligomerization domain 2 gene increase the risk of CD development. Autophagy is an intracellular degradation process, during which cytoplasmic nutrients and intracellular pathogens are digested. Given that impaired reaction to intestinal microbiota alters signaling pathways mediated by PRRs, it is likely that dysfunction of the autophagic machinery is involved in the development of CD. Indeed, the loss-of-function mutation T300A in the autophagy related 16 like 1 (ATG16L1) protein, a critical regulator of autophagy, increases susceptibility to CD. Recent studies have provided evidence that ATG16L1 is involved not only in autophagy, but also in PRR-mediated signaling pathways. ATG16L1 negatively regulates pro-inflammatory cytokine responses of macrophages and DCs after these cells sense the intestinal microbiota by PRRs. Here, we discuss the molecular mechanisms underlying the development of CD in the T300A *ATG16L1* mutation by focusing on PRR-mediated signaling pathways.

Key Words: ATG16L1; Crohn's disease; Autophagy; Innate immunity; Cytokine; Pattern recognition receptors

©The Author(s) 2022. Published by Baishideng Publishing Group Inc. All rights reserved.

Core Tip: The loss-of-function mutation T300A in autophagy related 16 like 1 (*ATG16L1*) increases the risk of Crohn's disease (CD). ATG16L1 is a multifunctional protein involved in autophagy and innate immunity. The CD-associated *ATG16L1* mutation T300A leads to overgrowth of intestinal microbiota and enhanced pro-inflammatory cytokine responses, which disrupt intestinal immune homeostasis. In this minireview article, we have summarized the immunopathogenesis of CD in the presence of *ATG16L1* mutation.

Citation: Okai N, Watanabe T, Minaga K, Kamata K, Honjo H, Kudo M. Alterations of autophagic and innate immune responses by the Crohn's disease-associated *ATG16L1* mutation. *World J Gastroenterol* 2022; 28(26): 3063-3070
URL: https://www.wjgnet.com/1007-9327/full/v28/i26/3063.htm
DOI: https://dx.doi.org/10.3748/wjg.v28.i26.3063

INTRODUCTION

Pro-inflammatory cytokines, such as tumor necrosis factor (TNF)-α, interleukin (IL)-6, IL-12, and IL-23, underlie the immunopathogenesis of Crohn's disease (CD), as evidenced by the clinical efficacy of targeting these cytokines for the treatment of patients[1,2]. These colitogenic cytokines are produced by macrophages and dendritic cells (DCs) upon sensing the intestinal microbiota by the pattern recognition receptors (PRRs), which are classified into Toll-like receptors (TLRs), nucleotide-binding oligomerization domain (NOD)-like receptors (NLRs), and retinoic acid-inducible gene I (RIG-I)-like receptors (RLRs)[3-6]. Thus, excessive pro-inflammatory cytokine responses caused by PRR activation play critical roles in the development of CD. This notion is fully supported by the identification of loss-of-function mutations in *NOD2* as one of the strongest risk factors for CD. NOD2 is an intracellular PRR that senses muramyl dipeptide (MDP) derived from bacterial cell wall components and negatively regulates TLR-mediated pro-inflammatory cytokine responses[5,6].

Autophagy refers to the process during which cytoplasmic components and intracellular pathogens are delivered to the lysosome for degradation in the form of double-membrane-bound autophagosomes [7]. The autophagy related 16 like 1 (ATG16L1) protein plays an indispensable role in the initiation and completion of the autophagic process. In addition to its role in autophagy, ATG16L1 has been shown to be involved in PRR-mediated innate immunity. ATG16L1 negatively regulates pro-inflammatory and type I interferon (IFN-I) responses mediated by TLRs, NLRs, and RLRs[8]. More importantly, the loss-of-function mutation T300A in *ATG16L1* has been identified as a risk factor for CD in parallel with mutations in *NOD2*[6]. In this minireview article, we summarize the molecular mechanisms by which the T300A mutation in *ATG16L1* predisposes the host to CD development by focusing on the regulatory role of ATG16L1 in PRR-mediated signaling pathways.

INDUCTION OF AUTOPHAGY BY ATG16L1

ATG16L1 is an indispensable molecule for autophagic responses (Table 1). The autophagy process includes vesicle nucleation, vesicle elongation, vesicle completion, fusion with lysosome, degradation, and recycling[9]. Autophagy dysfunction is associated with neurodegenerative diseases, microbial infections, and aging[7]. Although autophagy has been identified as the primary cell response to the lack of nutrients, recent studies have highlighted the importance of autophagy in microbial infection and immune responses[9]. The autophagy process is negatively regulated by growth factors, which activate the mechanistic target of rapamycin (mTOR) and the phosphoinositide 3-kinase (PI3K)-AKT pathways[7,9]. On the contrary, nutrient starvation or rapamycin treatment promotes the autophagic process through the inhibition of mTOR. Thus, the PI3K–AKT–mTOR pathway negatively regulates autophagic process. On the molecular level, mTOR activation controls the initiation of autophagy by suppressing the activation of the primary initiation complex of autophagy, called Unc-51 Like autophagy activating kinase 1 (ULK1) complex, composed of ULK1/2, ATG101, ATG13, and RB1CC1/FIP200[9]. The formed ULK1 complex translocates to the site of the second complex, called the PI3K complex[9]. The latter PI3K complex recruits a number of ATG proteins to promote elongation and expansion of the autophagosome.

Two ubiquitin-like conjugation systems, the ATG5–ATG12–ATG16L1 conjugation system and the microtubule-associated protein 1 Light chain 3 (LC3) conjugation system, play important roles in the elongation and expansion of the autophagosome[7,9]. The conjugation of the membrane lipid phosphatidylethanolamine with the soluble form of LC3 and formation of the ATG5–ATG12–ATG16L1 complex is necessary for the maturation of autophagosomes[7,9,10]. Matured autophagosomes are fused with lysosomes for the degradation of cellular materials. Vesicles containing ATG16L1 are necessary for

Table 1 Physiological functions of autophagy related 16 like 1

Function	Cell type	Ref.
Positive regulation		
Autophagy	ECs, DCs, macrophages	[9,10]
Regulatory T cell responses	DCs	[22]
Negative regulation		
IFN-I production by RLRs	MEFs	[11,12]
IFN-I production by TLR3 and TLR4	Macrophages	[13]
IL-1β production by TLR4	Macrophages	[16,17,19]
IL-6 and IL-12 production by TLR2	DCs	[27]

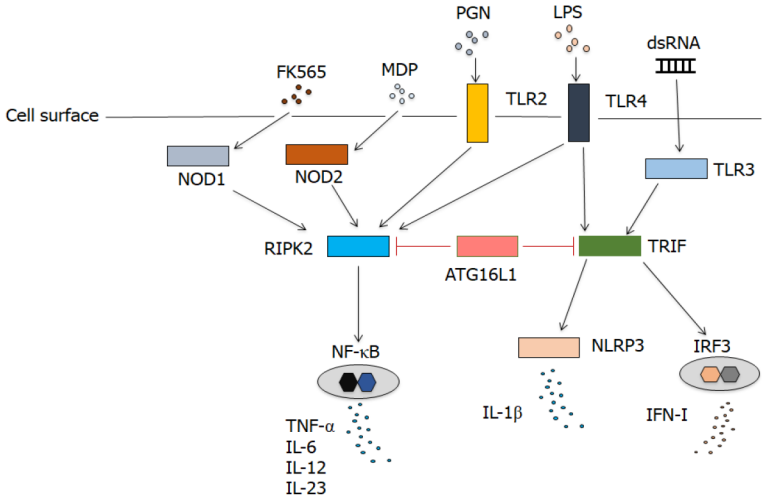
EC: Epithelial cell; DC: Dendritic cell; IFN-I: Type I interferon; RLR: Retinoic acid-inducible gene I-like receptors; MEF: Mouse embryonic fibroblast; TLR: Toll-like receptor; IL: Interleukin.

membrane trafficking and autophagosome formation[7,9,10]. Thus, ATG16L1 is an essential protein for the induction and completion of autophagic responses.

ATG16L1 AND INNATE IMMUNITY

ATG16L1 has been shown to attenuate proinflammatory cytokine responses in innate immunity (Table 1)[8]. RLRs, including RIG-I and melanoma differentiation-associated gene 5 (MDA5), are sensors for RNA viruses[3]. IFN-I, which is produced after viral RNA is sensed by RLRs, plays a protective role in host defense[3]. Mouse embryonic fibroblasts deficient in ATG5 displayed enhanced production of IFN-I after exposure to vesicular stomatitis virus due to enhanced activation of IFN regulatory factor 3 [11]. Enhanced production of IFN-I is associated with reduced viral load[11]. ATG16L1 is involved in the regulation of IFN-I mediated by RLRs. Two mitochondrial proteins, NLRX1 and its binding partner, Tu translation elongation factor, interact with ATG5, ATG12, and ATG16L1, and suppress RLR-induced IFN-I production and thereby promoting autophagy[12]. In addition, ATG16L1 has been shown to regulate IFN-I production by interacting with TLR3 and TLR4[13]. Samie *et al*[13] have provided evidence that macrophages deficient in ATG16L1 produced large amounts of IFN-I after stimulation with TLR3 and TLR4 Ligands (Figure 1). Mechanistically, the loss of ATG16L1 resulted in the accumulation of the toll-IL-1 receptor domain-containing adaptor inducing IFN-β protein (TRIF), leading to the excessive activation of TLR3- and TLR4-mediated signaling pathways. Interestingly, macrophages isolated from individuals bearing the CD-associated ATG16L1 T300A variant also exhibited enhanced IFN-I production upon stimulation with TLR3 and TLR4 Ligands[13]. Thus, ATG16L1 functions as a negative regulator of IFN-I production induced by TLR activation. Excessive activation of IFN-I signaling caused by ATG16L1 deficiency may protect against microbial infection. In fact, ATG16L1 hypomorphic mice displayed enhanced IFN-I signaling upon challenge with *Citrobacter rodentium*, which conferred protection from enteric pathogen infection[14]. This protection was mediated by mitochondrial antiviral signaling (MAVS) and stimulator of interferon genes (STING) proteins, because mice with hypomorphic ATG16L1 expression and deficient in MAVS or STING were not protected from the *C. rodentium* infection. Similarly, the clearance of *Salmonella typhimurium* from the intestine was augmented in mice with myeloid cell-specific ATG16L1 deficiency in an IFN-I-dependent manner[13]. IL-22 is a barrier protective cytokine that stimulates antimicrobial responses in the intestine[15]. IL-22 induces STING-dependent IFN-I signaling, which is augmented in the absence of ATG16L1[15]. Such enhanced IFN-I signaling promotes TNF-α production, leading to ileal inflammation, suggesting that ATG16L1 deficiency mediates pro-inflammatory TNF-α responses through cooperative interaction between IL-22 and IFN-I[15]. Taken together, these studies suggest that ATG16L1 dampens IFN-I production mediated by RLRs and TLRs. In turn, the lack of negative regulation of IFN-I signaling owing to the absence of ATG16L1 or the presence of ATG16L1 T300A variant mediates protection from microbial infection in the gastrointestinal tract in an IFN-I-dependent manner.

In addition to attenuating IFN-I production, ATG16L1 also suppresses IL-1β production by macrophages[16,17]. Macrophages expressing ATG16L1 that lacks the coiled-coil domain produced large amounts of IL-1β upon stimulation with lipopolysaccharide (LPS) (Figure 1)[17]. Pro-IL-1β is processed into the mature form of IL-1β by caspase-1[18]. Accumulation of TRIF is involved in enhanced IFN-I production in the absence of *ATG16L1* or presence of the *ATG16L1* T300A mutation[13]. Similarly, TRIF-dependent activation of caspase-1 leads to increased production of IL-1β in macrophages lacking ATG16L1[17]. In a murine model of urinary tract infection, ATG16L1 deficiency promoted clearance of



DOI: 10.3748/wjg.v28.i26.3063 **Copyright** ©The Author(s) 2022.

Figure 1 Negative effect of autophagy related 16 like 1 on pattern recognition receptor signaling pathways. Autophagy related 16 like 1 (ATG16L1) negatively regulates pro-inflammatory and type I interferon (IFN-I) responses by toll-like receptors (TLRs) and nucleotide-binding oligomerization domain (NOD)-like receptors (NLRs). Production of pro-inflammatory cytokines such as tumor necrosis factor (TNF)-α, interleukin (IL)-6, IL-12, and IL-23 mediated by TLRs is suppressed by ATG16L1 through the inhibition of activation of receptor-interacting serine/threonine-protein kinase 2 and nuclear factor-kB. Production of IL-1β and IFN-I mediated by TLRs is suppressed by ATG16L1 through the inhibition of toll-IL-1 receptor domain-containing adaptor inducing IFN-β, NOD-, LRR-, and pyrin domain-containing protein 3, and interferon regulatory factor 3. MDP: Muramyl dipeptide; PGN: Peptidoglycan; TLR: Toll-like receptor; LPS: Lipopolysaccharide; NOD: Nucleotide-binding oligomerization domain; RIPK2: Receptor-interacting serine/threonine-protein kinase 2; ATG16L1: Autophagy related 16 like 1; IL: Interleukin; IFN: Interferon; TRIF: Toll-IL-1 receptor domain-containing adaptor inducing IFN-β protein; NF-κB: Nuclear factor-κB; NLRP3: NOD-, LRR-, and pyrin domain-containing protein 3; IRF3: Interferon regulatory factor 3; TNF: Tumor necrosis factor.

uropathogenic *Escherichia coli* through excessive production of IL-1β[19]. Thus, ATG16L1 negatively regulates pro-inflammatory pathways mediated not only by IFN-I, but also by IL-1β.

Regulatory T cells (Tregs) expressing forkhead box P3 (FOXP3) are a specialized T cell population that is indispensable for the establishment and maintenance of immunological self-tolerance[20]. Impaired activation of Tregs leads to the development of autoimmune disorders. *Bacteroides fragilis* (*B. fragilis*) has been considered to stimulate beneficial immunoregulatory functions through induction of Tregs[21]. Chu *et al*[22] provided evidence that ATG16L1 expressed in DCs was required for the induction of Tregs expressing FOXP3 upon exposure to outer membrane vesicles (OMVs) of *B. fragilis*. Oral administration of OMVs from *B. fragilis* protected wild-type mice from experimental colitis[22], and this effect was accompanied by increased proportions of Tregs expressing FOXP3 and IL-10. Such protective effect of oral administration of OMVs was not seen in mice with DC-specific ATG16L1 deficiency. Thus, ATG16L1 is involved in the maintenance of immune homeostasis through induction of Tregs expressing FOXP3.

Mutations in *NOD2* are the strongest risk factor for the development of CD[5,6]. MDP, a bacterial component derived from intestinal bacteria, is a prototypical NOD2 ligand[23,24]. Activation of NOD2 by MDP induces autophagy in macrophages, DCs, and fibroblasts, but not in cells harboring CD-associated *NOD2* mutations[25]. Physical interaction between NOD2 and ATG16L1 is induced by the stimulation with MDP[25,26]. Thus, MDP activation of NOD2 mediates bactericidal effects in an ATG16L1-dependent manner, and the presence of CD-associated *NOD2* mutations promotes overgrowth of intestinal bacteria, leading to excessive production of pro-inflammatory cytokines.

Receptor-interacting serine/threonine-protein kinase 2 (RIPK2) is a signaling molecule downstream of NOD2 and TLRs[23,24]. It remains unclear whether ATG16L1 binds to RIPK2 after activation of NOD2. In this regard, we confirmed that ATG16L1 binds to the kinase domain of RIPK2 in overexpression studies[26,27]. In human DCs, ATG16L1 interacted with RIPK2 after the stimulation with MDP and this interaction suppressed NF-κB-dependent proinflammatory responses mediated by TLRs[26,27]. Transfection of intact *ATG16L1*, but not of *ATG16L1* with the T300A mutation, reduced TLR2-mediated NF-κB activation in human embryonic kidney cells. In the physiological setting, NF-κB activation, as assessed by the degradation of IκBα and expression of phospho-IκBα, was markedly suppressed in human DCs stimulated with TLR2 and NOD2 ligands as compared to the effect of stimulation with a TLR2 ligand alone[26,27]. Furthermore, knockdown of *ATG16L1* by its specific siRNA increased IL-6 and IL-12p40 production by human DCs upon exposure to TLR2 and NOD2 ligands as compared to the levels of those cytokines in cells transfected with control siRNA[26,27]. These studies strongly suggest that ATG16L1 functions as a negative regulator of TLR2-mediated pro-inflammatory cytokine responses (Figure 1).

NF-κB activation mediated by TLRs and NOD2 is tightly regulated by Lys (K63)- linked polyubiquitination of RIPK2[23,24,27,28]. As for the molecular mechanisms accounting for the suppression of TLR2-mediated NF-κB activation and pro-inflammatory cytokine production, ATG16L1 has been shown to inhibit polyubiquitination of RIPK2[26,28]. NOD2 activation by MDP also inhibited polyubiquitination of RIPK2 through the induction of interferon regulatory factor 4 (IRF4)[23,24]. Overexpression studies revealed that ATG16L1 and IRF4 act cooperatively to suppress K63-linked polyubiquitination of RIPK2 [27]. Given that physical interaction between RIPK2 and IRF4 or ATG16L1 is induced after NOD2 activation by MDP, it is likely that NOD2 downregulates TLR-mediated proinflammatory cytokine responses through binding of ATG16L1 and IRF4 to RIPK2. This idea is fully supported by the fact that RIPK2 expression level is markedly elevated in the colonic mucosa of patients with CD and ulcerative colitis (UC), and it corelates with the levels of pro-inflammatory cytokines, such as TNF-α and IL-6[29]. Furthermore, the percentages of lamina propria DCs expressing ATG16L1 and IRF4 in the colon inversely correlate with the expression levels of TNF-α and IL-6[27]. Collectively, these studies support the idea that ATG16L1 acts in concert with NOD2 to suppress excessive pro-inflammatory cytokine responses mediated by TLRs and thereby maintains intestinal homeostasis.

ATG16L1 AND CD

The polymorphism Thr300Ala (or T300A) in the coding region of the *ATG16L1* gene confers increased risk for the development of CD[6,10,16]. This polymorphism is a loss-of-function mutation, which affects the induction of autophagy against invading bacteria and is associated with gut bacterial overgrowth and pro-inflammatory cytokine responses[6,10,16]. Recent studies have successfully elucidated some of the molecular mechanisms accounting for the development of CD in the presence of the ATG16L1 T300A variant. Given that ATG16L1 is constitutively expressed in epithelial cells, especially Paneth cells and myeloid cells, these studies have highlighted the importance of ATG16L1-mediated signaling pathways in innate immune cells for the immunopathogenesis of CD[17,25,28,30,31].

Paneth cells are localized at the base of the crypts in the ileum, and they contribute to the maintenance of intestinal homeostasis through the secretion of antimicrobial peptides (AMPs) and inhibition of intestinal bacterial overgrowth[32]. Mice with hypomorphic expression of ATG16L1 and ATG16L1 T300A-knockin (KI) mice exhibit increased proportions of Paneth cells with abnormal phenotypes, as assessed by lysozyme localization and granule morphology[30-32]. Moreover, Paneth cells from patients with CD carrying ATG16L1 T300A have unusual granule morphology and accumulation of AMPs, with both having been observed also in mice deficient in ATG16L1 or expressing ATG16L1 T300A[32]. Furthermore, defective function of Paneth cells in the absence of ATG16L1 or the presence of the *ATG16L1* T300A mutation led to higher susceptibility to TNF-α-mediated necroptosis and accumulation of the endoplasmic reticulum stress sensor IRE1a, indicating that necroptosis and endoplasmic reticulum stress are involved in the pathogenesis of CD[33]. Thus, the ileal mucosa of patients and mice bearing ATG16L1 T300A is characterized by the defective function of Paneth cells, which results in the overgrowth of intestinal bacteria. This notion is supported by the fact that CD patients bearing the *ATG16L1* T300A mutation display impaired clearance of pathogenic bacteria in the ileal mucosa[34]. It is well established that CD occurs as a result of the interplay between genetic susceptibility and environmental factors. Cigarette smoking is a risk factor for developing CD[35]. Interestingly, cigarette smoking has been suggested to amplify effects of the *ATG16L1* T300A mutation, triggering Paneth cell defects, thereby causing chronic intestinal inflammation[31].

Pro-inflammatory cytokine responses play an important role in the development of CD[1]. The *ATG16L1* T300A mutation has been shown to enhance pro-inflammatory cytokine responses in the intestine. Mice lacking ATG16L1 in hematopoietic cells were susceptible to dextran sodium sulfate (DSS)-induced colitis[17]. Aggravated DSS-induced colitis in mice lacking ATG16L1 was alleviated by blocking IL-1β-mediated signaling pathways[17]. Furthermore, macrophages lacking ATG16L1 produced more IL-1β upon stimulation with LPS[17]. As for the molecular mechanisms accounting for enhanced production of IL-1β in the absence of ATG16L1, Saitoh *et al*[17] showed that ATG16L1 deficiency resulted in increased production of this cytokine through the TRIF-dependent activation of caspase-1. Thus, ATG16L1 deficiency predisposed mice to DSS-induced colitis by activating IL-1β-mediated signaling pathways. In line with these data obtained in mice lacking ATG16L1 in hematopoietic cells, ATG16L1 T300A-KI mice displayed enhanced production of IL-1β upon exposure to LPS[16]. These studies, which utilized ATG16L1-deficient and ATG16L1 T300A-KI mice, support the idea that intact ATG16L1-medaited signaling pathways limit pro-inflammatory cytokine responses triggered by activation of TLRs. In this regard, we and others have reported that ATG16L1 negatively regulates pro-inflammatory cytokine responses mediated by RIPK2, a downstream signaling molecule of TLRs and NLRs[27,28]. Binding of ATG16L1 to the kinase domain of RIPK2 inhibits polyubiquitination of RIPK2, followed by suppression of NF-κB activation[27,28]. These studies strongly suggest that ATG16L1 activation maintains intestinal homeostasis and attenuates reactions against microbiota by inhibiting TLR-mediated pro-inflammatory cytokine responses in macrophages and DCs. Strong support for this idea also comes from the observations that colonic pro-inflammatory cytokine

expression inversely correlates with the percentage of $CD11c^+$ DCs expressing ATG16L1 in patients with CD and that induction of remission is accompanied by accumulation of $CD11c^+$ DCs expressing ATG16L1 in the gastrointestinal tract of patients with CD[27].

ATG16L1 negatively regulates IFN-I responses mediated by RLRs and TLRs[11-14]. Isolated macrophages from patients with CD bearing the *ATG16L1* T300A mutation produced more IFN-I upon stimulation with TLR3 and TLR4 ligands than macrophages from patients with intact ATG16L1[13,36]. Excessive production of IFN-I is involved in the immunopathogenesis of CD and UC. Expression levels of the IFN-stimulated genes was shown to be higher in the inflamed colonic mucosa of patients with CD or UC than in healthy controls[13]. Moreover, expression levels of IFN-stimulated genes rapidly declined in response to infliximab treatment. Although the presence of the *ATG16L1* T300A variant is associated with colitogenic IFN-I responses, the enhanced production of IFN-I may improve survival of patients with colorectal cancer[36].

Similar to the molecular mechanisms of chronic inflammation in the presence of CD-associated mutations in *NOD2*, the *ATG16L1* T300A mutation promotes the development of CD by causing impaired production of AMPs in Paneth cells and excessive secretion of TLR-mediated pro-inflammatory cytokines by macrophages and DCs. MDP activation of NOD2 induces robust production of AMPs from Paneth cells, thereby preventing bacterial overgrowth in the intestine[5]. Paneth cells deficient in NOD2 or bearing CD-associated *NOD2* mutations fail to produce AMPs[5]. With regard to the pro-inflammatory cytokine responses, activation of intact NOD2 by MDP negatively regulates the production of TLR-mediated pro-inflammatory cytokines through the induction of IRF4[23,24]. In the absence of intact *NOD2* or the presence of CD-associated *NOD2* mutations, pro-inflammatory cytokine responses by DCs are markedly enhanced upon exposure to TLR ligands derived from the intestinal microbiota[5]. Thus, impaired function of Paneth cells and excessive pro-inflammatory cytokine responses by TLRs underlie the immunopathogenesis of CD in the presence of *ATG16L1* and *NOD2* mutations.

CONCLUSION

The autophagic protein ATG16L1 plays an indispensable role in the maintenance of intestinal homeostasis. The *ATG16L1* T300A mutation confers an increased risk for the development of CD as it is associated with increased bacterial burden and excessive pro-inflammatory cytokine responses in the gastrointestinal tract. Elucidation of the molecular mechanisms by which the *ATG16L1* T300A variant leads to the development of CD has provided new insights into the immunopathogenesis of CD induced by impaired induction of autophagy.

ACKNOWLEDGEMENTS

We appreciate Ms. Yukiko Ueno for her secretarial support.

FOOTNOTES

Author contributions: Okai N and Watanabe T drafted the manuscript; Watanabe T, Minaga K, Kamata K, Honjo H, and Kudo M revised the manuscript; OKai N, Watanabe T, Minaga K, Kamata K, Honjo H and Kudo M have read and approved the final manuscript.

Conflict-of-interest statement: The authors declare that they have no conflicts of interest to disclose.

Open-Access: This article is an open-access article that was selected by an in-house editor and fully peer-reviewed by external reviewers. It is distributed in accordance with the Creative Commons Attribution NonCommercial (CC BY-NC 4.0) license, which permits others to distribute, remix, adapt, build upon this work non-commercially, and license their derivative works on different terms, provided the original work is properly cited and the use is non-commercial. See: https://creativecommons.org/Licenses/by-nc/4.0/

Country/Territory of origin: Japan

ORCID number: Natsuki Okai 0000-0002-3167-4927; Tomohiro Watanabe 0000-0001-7781-6305; Kosuke Minaga 0000-0001-5407-7925; Ken Kamata 0000-0003-1568-0769; Hajime Honjo 0000-0002-0888-3384; Masatoshi Kudo 0000-0002-4102-3474.

Corresponding Author's Membership in Professional Societies: The Japanese Society of Gastroenterology, No. 34410.

S-Editor: Ma YJ
L-Editor: A

P-Editor: Ma YJ

REFERENCES

1 **Strober W**, Fuss IJ. Proinflammatory cytokines in the pathogenesis of inflammatory bowel diseases. *Gastroenterology* 2011; **140**: 1756-1767 [PMID: 21530742 DOI: 10.1053/j.gastro.2011.02.016]

2 **Neurath MF**. Current and emerging therapeutic targets for IBD. *Nat Rev Gastroenterol Hepatol* 2017; **14**: 269-278 [PMID: 28144028 DOI: 10.1038/nrgastro.2016.208]

3 **Kawai T**, Akira S. Toll-like receptor and RIG-I-like receptor signaling. *Ann N Y Acad Sci* 2008; **1143**: 1-20 [PMID: 19076341 DOI: 10.1196/annals.1443.020]

4 **Takeda K**, Akira S. Toll-like receptors in innate immunity. *Int Immunol* 2005; **17**: 1-14 [PMID: 15585605 DOI: 10.1093/intimm/dxh186]

5 **Strober W**, Asano N, Fuss I, Kitani A, Watanabe T. Cellular and molecular mechanisms underlying NOD2 risk-associated polymorphisms in Crohn's disease. *Immunol Rev* 2014; **260**: 249-260 [PMID: 24942694 DOI: 10.1111/imr.12193]

6 **Cho JH**. The genetics and immunopathogenesis of inflammatory bowel disease. *Nat Rev Immunol* 2008; **8**: 458-466 [PMID: 18500230 DOI: 10.1038/nri2340]

7 **Klionsky DJ**, Petroni G, Amaravadi RK, Baehrecke EH, Ballabio A, Boya P, Bravo-San Pedro JM, Cadwell K, Cecconi F, Choi AMK, Choi ME, Chu CT, Codogno P, Colombo MI, Cuervo AM, Deretic V, Dikic I, Elazar Z, Eskelinen EL, Fimia GM, Gewirtz DA, Green DR, Hansen M, Jäättelä M, Johansen T, Juhász G, Karantza V, Kraft C, Kroemer G, Ktistakis NT, Kumar S, Lopez-Otin C, Macleod KF, Madeo F, Martinez J, Meléndez A, Mizushima N, Münz C, Penninger JM, Perera RM, Piacentini M, Reggiori F, Rubinsztein DC, Ryan KM, Sadoshima J, Santambrogio L, Scorrano L, Simon HU, Simon AK, Simonsen A, Stolz A, Tavernarakis N, Tooze SA, Yoshimori T, Yuan J, Yue Z, Zhong Q, Galluzzi L, Pietrocola F. Autophagy in major human diseases. *EMBO J* 2021; **40**: e108863 [PMID: 34459017 DOI: 10.15252/embj.2021108863]

8 **Hamaoui D**, Subtil A. ATG16L1 functions in cell homeostasis beyond autophagy. *FEBS J* 2022; **289**: 1779-1800 [PMID: 33752267 DOI: 10.1111/febs.15833]

9 **Kabat AM**, Pott J, Maloy KJ. The Mucosal Immune System and Its Regulation by Autophagy. *Front Immunol* 2016; **7**: 240 [PMID: 27446072 DOI: 10.3389/fimmu.2016.00240]

10 **Salem M**, Ammitzboell M, Nys K, Seidelin JB, Nielsen OH. ATG16L1: A multifunctional susceptibility factor in Crohn disease. *Autophagy* 2015; **11**: 585-594 [PMID: 25906181 DOI: 10.1080/15548627.2015.1017187]

11 **Jounai N**, Takeshita F, Kobiyama K, Sawano A, Miyawaki A, Xin KQ, Ishii KJ, Kawai T, Akira S, Suzuki K, Okuda K. The Atg5 Atg12 conjugate associates with innate antiviral immune responses. *Proc Natl Acad Sci U S A* 2007; **104**: 14050-14055 [PMID: 17709747 DOI: 10.1073/pnas.0704014104]

12 **Lei Y**, Wen H, Yu Y, Taxman DJ, Zhang L, Widman DG, Swanson KV, Wen KW, Damania B, Moore CB, Giguère PM, Siderovski DP, Hiscott J, Razani B, Semenkovich CF, Chen X, Ting JP. The mitochondrial proteins NLRX1 and TUFM form a complex that regulates type I interferon and autophagy. *Immunity* 2012; **36**: 933-946 [PMID: 22749352 DOI: 10.1016/j.immuni.2012.03.025]

13 **Samie M**, Lim J, Verschueren E, Baughman JM, Peng I, Wong A, Kwon Y, Senbabaoglu Y, Hackney JA, Keir M, Mckenzie B, Kirkpatrick DS, van Lookeren Campagne M, Murthy A. Selective autophagy of the adaptor TRIF regulates innate inflammatory signaling. *Nat Immunol* 2018; **19**: 246-254 [PMID: 29358708 DOI: 10.1038/s41590-017-0042-6]

14 **Martin PK**, Marchiando A, Xu R, Rudensky E, Yeung F, Schuster SL, Kernbauer E, Cadwell K. Autophagy proteins suppress protective type I interferon signalling in response to the murine gut microbiota. *Nat Microbiol* 2018; **3**: 1131-1141 [PMID: 30202015 DOI: 10.1038/s41564-018-0229-0]

15 **Aden K**, Tran F, Ito G, Sheibani-Tezerji R, Lipinski S, Kuiper JW, Tschurtschenthaler M, Saveljeva S, Bhattacharyya J, Häsler R, Bartsch K, Luzius A, Jentzsch M, Falk-Paulsen M, Stengel ST, Welz L, Schwarzer R, Rabe B, Barchet W, Krautwald S, Hartmann G, Pasparakis M, Blumberg RS, Schreiber S, Kaser A, Rosenstiel P. ATG16L1 orchestrates interleukin-22 signaling in the intestinal epithelium *via* cGAS-STING. *J Exp Med* 2018; **215**: 2868-2886 [PMID: 30254094 DOI: 10.1084/jem.20171029]

16 **Lassen KG**, Kuballa P, Conway KL, Patel KK, Becker CE, Peloquin JM, Villablanca EJ, Norman JM, Liu TC, Heath RJ, Becker ML, Fagbami L, Horn H, Mercer J, Yilmaz OH, Jaffe JD, Shamji AF, Bhan AK, Carr SA, Daly MJ, Virgin HW, Schreiber SL, Stappenbeck TS, Xavier RJ. Atg16L1 T300A variant decreases selective autophagy resulting in altered cytokine signaling and decreased antibacterial defense. *Proc Natl Acad Sci U S A* 2014; **111**: 7741-7746 [PMID: 24821797 DOI: 10.1073/pnas.1407001111]

17 **Saitoh T**, Fujita N, Jang MH, Uematsu S, Yang BG, Satoh T, Omori H, Noda T, Yamamoto N, Komatsu M, Tanaka K, Kawai T, Tsujimura T, Takeuchi O, Yoshimori T, Akira S. Loss of the autophagy protein Atg16L1 enhances endotoxin-induced IL-1beta production. *Nature* 2008; **456**: 264-268 [PMID: 18849965 DOI: 10.1038/nature07383]

18 **Place DE**, Kanneganti TD. Recent advances in inflammasome biology. *Curr Opin Immunol* 2018; **50**: 32-38 [PMID: 29128729 DOI: 10.1016/j.coi.2017.10.011]

19 **Symington JW**, Wang C, Twentyman J, Owusu-Boaitey N, Schwendener R, Núñez G, Schilling JD, Mysorekar IU. ATG16L1 deficiency in macrophages drives clearance of uropathogenic E. coli in an IL-1β-dependent manner. *Mucosal Immunol* 2015; **8**: 1388-1399 [PMID: 25669147 DOI: 10.1038/mi.2015.7]

20 **Kitagawa Y**, Sakaguchi S. Molecular control of regulatory T cell development and function. *Curr Opin Immunol* 2017; **49**: 64-70 [PMID: 29065384 DOI: 10.1016/j.coi.2017.10.002]

21 **Caruso R**, Lo BC, Núñez G. Host-microbiota interactions in inflammatory bowel disease. *Nat Rev Immunol* 2020; **20**: 411-426 [PMID: 32005980 DOI: 10.1038/s41577-019-0268-7]

22 **Chu H**, Khosravi A, Kusumawardhani IP, Kwon AH, Vasconcelos AC, Cunha LD, Mayer AE, Shen Y, Wu WL, Kambal A, Targan SR, Xavier RJ, Ernst PB, Green DR, McGovern DP, Virgin HW, Mazmanian SK. Gene-microbiota interactions

contribute to the pathogenesis of inflammatory bowel disease. *Science* 2016; **352**: 1116-1120 [PMID: 27230380 DOI: 10.1126/science.aad9948]

23 **Watanabe T**, Asano N, Murray PJ, Ozato K, Tailor P, Fuss IJ, Kitani A, Strober W. Muramyl dipeptide activation of nucleotide-binding oligomerization domain 2 protects mice from experimental colitis. *J Clin Invest* 2008; **118**: 545-559 [PMID: 18188453 DOI: 10.1172/JCI33145]

24 **Watanabe T**, Asano N, Meng G, Yamashita K, Arai Y, Sakurai T, Kudo M, Fuss IJ, Kitani A, Shimosegawa T, Chiba T, Strober W. NOD2 downregulates colonic inflammation by IRF4-mediated inhibition of K63-linked polyubiquitination of RICK and TRAF6. *Mucosal Immunol* 2014; **7**: 1312-1325 [PMID: 24670424 DOI: 10.1038/mi.2014.19]

25 **Cooney R**, Baker J, Brain O, Danis B, Pichulik T, Allan P, Ferguson DJ, Campbell BJ, Jewell D, Simmons A. NOD2 stimulation induces autophagy in dendritic cells influencing bacterial handling and antigen presentation. *Nat Med* 2010; **16**: 90-97 [PMID: 19966812 DOI: 10.1038/nm.2069]

26 **Honjo H**, Watanabe T, Kamata K, Minaga K, Kudo M. RIPK2 as a New Therapeutic Target in Inflammatory Bowel Diseases. *Front Pharmacol* 2021; **12**: 650403 [PMID: 33935757 DOI: 10.3389/fphar.2021.650403]

27 **Honjo H**, Watanabe T, Arai Y, Kamata K, Minaga K, Komeda Y, Yamashita K, Kudo M. ATG16L1 negatively regulates RICK/RIP2-mediated innate immune responses. *Int Immunol* 2021; **33**: 91-105 [PMID: 32909611 DOI: 10.1093/intimm/dxaa062]

28 **Sorbara MT**, Ellison LK, Ramjeet M, Travassos LH, Jones NL, Girardin SE, Philpott DJ. The protein ATG16L1 suppresses inflammatory cytokines induced by the intracellular sensors Nod1 and Nod2 in an autophagy-independent manner. *Immunity* 2013; **39**: 858-873 [PMID: 24238340 DOI: 10.1016/j.immuni.2013.10.013]

29 **Watanabe T**, Minaga K, Kamata K, Sakurai T, Komeda Y, Nagai T, Kitani A, Tajima M, Fuss IJ, Kudo M, Strober W. RICK/RIP2 is a NOD2-independent nodal point of gut inflammation. *Int Immunol* 2019; **31**: 669-683 [PMID: 31132297 DOI: 10.1093/intimm/dxz045]

30 **Cadwell K**, Liu JY, Brown SL, Miyoshi H, Loh J, Lennerz JK, Kishi C, Kc W, Carrero JA, Hunt S, Stone CD, Brunt EM, Xavier RJ, Sleckman BP, Li E, Mizushima N, Stappenbeck TS, Virgin HW 4th. A key role for autophagy and the autophagy gene Atg16l1 in mouse and human intestinal Paneth cells. *Nature* 2008; **456**: 259-263 [PMID: 18849966 DOI: 10.1038/nature07416]

31 **Liu TC**, Kern JT, VanDussen KL, Xiong S, Kaiko GE, Wilen CB, Rajala MW, Caruso R, Holtzman MJ, Gao F, McGovern DP, Nunez G, Head RD, Stappenbeck TS. Interaction between smoking and ATG16L1T300A triggers Paneth cell defects in Crohn's disease. *J Clin Invest* 2018; **128**: 5110-5122 [PMID: 30137026 DOI: 10.1172/JCI120453]

32 **Stappenbeck TS**, McGovern DPB. Paneth Cell Alterations in the Development and Phenotype of Crohn's Disease. *Gastroenterology* 2017; **152**: 322-326 [PMID: 27729212 DOI: 10.1053/j.gastro.2016.10.003]

33 **Tschurtschenthaler M**, Adolph TE, Ashcroft JW, Niederreiter L, Bharti R, Saveljeva S, Bhattacharyya J, Flak MB, Shih DQ, Fuhler GM, Parkes M, Kohno K, Iwawaki T, Janneke van der Woude C, Harding HP, Smith AM, Peppelenbosch MP, Targan SR, Ron D, Rosenstiel P, Blumberg RS, Kaser A. Defective ATG16L1-mediated removal of IRE1α drives Crohn's disease-like ileitis. *J Exp Med* 2017; **214**: 401-422 [PMID: 28082357 DOI: 10.1084/jem.20160791]

34 **Sadaghian Sadabad M**, Regeling A, de Goffau MC, Blokzijl T, Weersma RK, Penders J, Faber KN, Harmsen HJ, Dijkstra G. The ATG16L1-T300A allele impairs clearance of pathosymbionts in the inflamed ileal mucosa of Crohn's disease patients. *Gut* 2015; **64**: 1546-1552 [PMID: 25253126 DOI: 10.1136/gutjnl-2014-307289]

35 **Georgiou AN**, Ntritsos G, Papadimitriou N, Dimou N, Evangelou E. Cigarette Smoking, Coffee Consumption, Alcohol Intake, and Risk of Crohn's Disease and Ulcerative Colitis: A Mendelian Randomization Study. *Inflamm Bowel Dis* 2021; **27**: 162-168 [PMID: 32628751 DOI: 10.1093/ibd/izaa152]

36 **Grimm WA**, Messer JS, Murphy SF, Nero T, Lodolce JP, Weber CR, Logsdon MF, Bartulis S, Sylvester BE, Springer A, Dougherty U, Niewold TB, Kupfer SS, Ellis N, Huo D, Bissonnette M, Boone DL. The Thr300Ala variant in ATG16L1 is associated with improved survival in human colorectal cancer and enhanced production of type I interferon. *Gut* 2016; **65**: 456-464 [PMID: 25645662 DOI: 10.1136/gutjnl-2014-308735]

World Journal of Gastroenterology

Submit a Manuscript: https://www.f6publishing.com

World J Gastroenterol 2022 July 14; 28(26): 3071-3080

DOI: 10.3748/wjg.v28.i26.3071

ISSN 1007-9327 (print) ISSN 2219-2840 (online)

MINIREVIEWS

Anabolic androgenic steroid-induced liver injury: An update

Ana Petrovic, Sonja Vukadin, Renata Sikora, Kristina Bojanic, Robert Smolic, Davor Plavec, George Y Wu, Martina Smolic

Specialty type: Gastroenterology and hepatology

Provenance and peer review: Invited article; Externally peer reviewed.

Peer-review model: Single blind

Peer-review report's scientific quality classification

Grade A (Excellent): 0
Grade B (Very good): B, B
Grade C (Good): C
Grade D (Fair): D
Grade E (Poor): 0

P-Reviewer: He F, China; Kreisel W, Germany; Liu P, China

Received: January 11, 2022
Peer-review started: January 11, 2022
First decision: March 8, 2022
Revised: March 22, 2022
Accepted: June 18, 2022
Article in press: June 18, 2022
Published online: July 14, 2022

Ana Petrovic, Sonja Vukadin, Robert Smolic, Martina Smolic, Department of Pharmacology and Biochemistry, Faculty of Dental Medicine and Health Osijek, J. J. Strossmayer University of Osijek, Osijek 31000, Croatia

Ana Petrovic, Sonja Vukadin, Martina Smolic, Department of Pharmacology, Faculty of Medicine Osijek, J. J. Strossmayer University of Osijek, Osijek 31000, Croatia

Renata Sikora, Department of Dental Medicine, Faculty of Dental Medicine and Health Osijek, J. J. Strossmayer University of Osijek, Osijek 31000, Croatia

Renata Sikora, Department of Dental Medicine, Health Center Osijek-Baranja County, Osijek 31000, Croatia

Kristina Bojanic, Department of Otorhinolaryngology, Neurosurgery and Radiology, Faculty of Dental Medicine and Health Osijek, J. J. Strossmayer University of Osijek, Osijek 31000, Croatia

Kristina Bojanic, Department of Biophysics and Radiology, Faculty of Medicine Osijek, J. J. Strossmayer University of Osijek, Osijek 31000, Croatia

Kristina Bojanic, Department of Radiology, Health Center Osijek-Baranja County, Osijek 31000, Croatia

Davor Plavec, Research Department, Srebrnjak Children's Hospital, Zagreb 10000, Croatia

George Y Wu, Department of Medicine, Division of Gastrenterology/Hepatology, University of Connecticut Health Center, Farmington, CT 06030, United States

Corresponding author: Martina Smolic, MD, PhD, Professor, Department of Pharmacology and Biochemistry, Faculty of Dental Medicine and Health Osijek, J. J. Strossmayer University of Osijek, 10E Cara Hadrijana, Osijek 31000, Croatia. martina.smolic@mefos.hr

Abstract

Anabolic androgenic steroids (AASs) are a group of molecules including endogenous testosterone and synthetic derivatives that have both androgenic and anabolic effects. These properties make them therapeutically beneficial in medical conditions such as hypogonadism. However, they are commonly bought illegally and misused for their anabolic, skeletal muscle building, and performance-enhancing effects. Supraphysiologic and long-term use of AASs affects all organs, leading to cardiovascular, neurological, endocrine, gastrointestinal, renal, and hematologic disorders. Hepatotoxicity is one of the major concerns regarding

AASs treatment and abuse. Testosterone and its derivatives have been most often shown to induce a specific form of cholestasis, peliosis hepatis, and hepatic benign and malignant tumors. It is currently believed that mechanisms of pathogenesis of these disorders include disturbance of antioxidative factors, upregulation of bile acid synthesis, and induction of hepatocyte hyperplasia. Most toxicity cases are treated with supportive measures and liver function normalizes with discontinuation of AAS. However, some long-term consequences are irreversible. AAS-induced liver injury should be taken in consideration in patients with liver disorders, especially with the increasing unintentional ingestion of supplements containing AAS. In this paper, we review the most current knowledge about AAS-associated adverse effects on the liver, and their clinical presentations, prevalence, and pathophysiological mechanisms.

Key Words: Androgens; Steroids; Cholestasis; Fibrosis; Liver; Chemical and drug induced liver injury

©The Author(s) 2022. Published by Baishideng Publishing Group Inc. All rights reserved.

Core Tip: There is a great deal of literature on the prevalence, pathophysiology, and therapeutic options for anabolic androgenic steroid (AAS)-associated adverse effects. However, AAS-induced liver injury is perhaps still underreported and poorly understood. In this paper, we review the latest knowledge obtained about molecular mechanisms of AAS-associated liver injury from most recent *in vitro* and animal studies, as well as the latest case reports regarding adverse effects of AASs in dietary supplements.

Citation: Petrovic A, Vukadin S, Sikora R, Bojanic K, Smolic R, Plavec D, Wu GY, Smolic M. Anabolic androgenic steroid-induced liver injury: An update. *World J Gastroenterol* 2022; 28(26): 3071-3080
URL: https://www.wjgnet.com/1007-9327/full/v28/i26/3071.htm
DOI: https://dx.doi.org/10.3748/wjg.v28.i26.3071

INTRODUCTION

Anabolic androgenic steroids (AASs) are group of compounds that include endogenous androgens, most importantly testosterone, and their synthetic derivatives[1]. Testosterone and synthetic AASs have been commonly used for their androgenic masculinizing effects resulting in male secondary characteristics, as well as anabolic skeletal muscle building effects due to enhanced protein utilization and synthesis mechanisms[2,3]. AASs are medically indicated in conditions such as male primary and secondary hypogonadism, aplastic anemia, muscle wasting in human immunodeficiency virus-infected patients, osteoporosis, libido dysfunction, chronic kidney disease, and breast cancer[4]. However, they are often misused because of their performance-enhancing and anabolic effects resulting in increased fat-free mass and improved muscle fiber size and strength. Abuse of AASs for aesthetic purposes and athletic performance improvement has surged as a public health problem in the past few decades among both professional and recreational athletes and bodybuilders[5,6]. Unmodified testosterone is rapidly metabolized when administered orally or parenterally and exerts a similar proportion of anabolic and androgenic effects. Chemical modifications of testosterone allow prolonged effective blood concentrations and changes to its pharmacodynamic properties, therefore enhancing desired anabolic or androgenic effects. In its synthetic derivatives used for aestethic and performance-enhancing purposes, testosterone is altered mainly through alkylation and esterification to enhance bioavailability by reducing hepatic metabolism, prolong duration of action, and maximize anabolic properties, though all of the synthetic compounds still exert significant androgenic effects. Supraphysiologic doses and prolonged unsupervised use of AASs have major impacts on users, affecting all organs and causing cardiovascular, neuroendocrine, neuropsychiatric, renal, gastrointestinal, musculoskeletal, dermatologic, immune, and hematologic disorders. Testosterone has a major impact on homeostasis of electrolytes, macromolecules, and micromolecules, including alterations in systemic iron balance and erythropoiesis. It has been established that AAS-induced erythropoiesis is mediated by erythropoietin [7]. Most recent studies also imply suppression of hepcidin (a negative regulator of the iron transporter ferroportin) as a mechanism of androgen-induced enhanced iron absorbtion and incorporation into red blood cells[8]. Some of the most common adverse effects related to AASs are dyslipidemia, hypertension, hypogonadism and infertility, aggression and mood disorders, addiction, and liver and kidney injury[9-11]. This has led to stricter laws regarding availability of AASs, mainly in professional sports organizations which ban anabolic steroid use, and test competitors for the presence of illegal steroids not only because of the unfair advantage in performance, but also because of their potentially dangerous side effects. In legal terms, AASs are classified in the United States as schedule 3 drugs by the

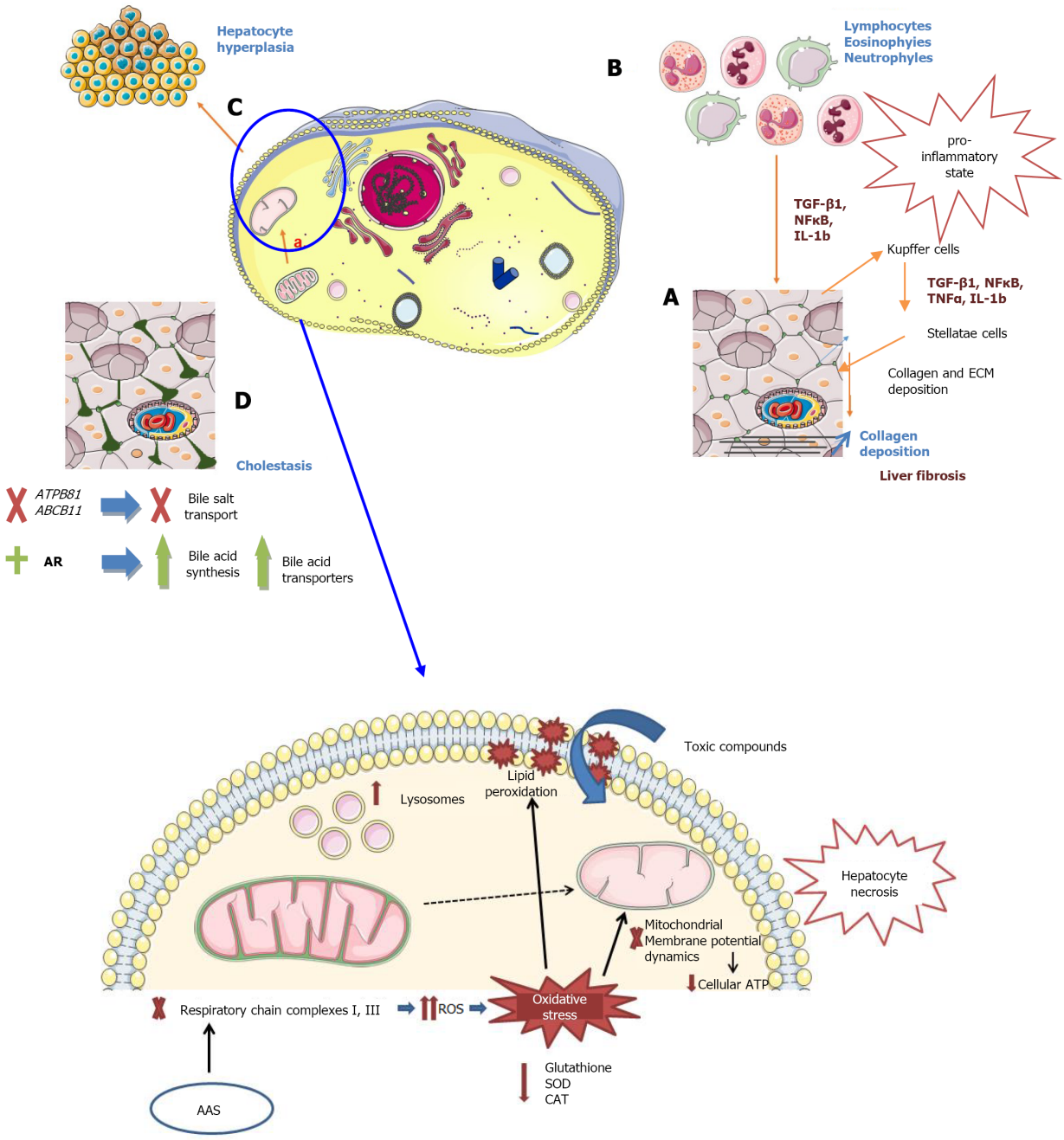
Drug Enforcement Agency, meaning that they can be legally obtained as prescription-only drugs. However, they are illegally sold among teammates, trainers, and fitness centers, through black market or counterfeit prescriptions. Furthermore, many AASs are legally bought and consumed unknowingly in over-the-counter dietary supplements advertised as energy, virility, and muscle strength enhancers [12-14]. Although the precise number of AAS users is difficult to determine, it is estimated that the prevalence across the world is 1%-5%[15]. A study in 2013 found that the prevalence of AAS use among male elite college students in the United States during their lifetime is about 20%[16]. In Norway high school population, a prevalence of 4% was found[17]. While it is difficult to establish a true prevalence of AAS use due to underreporting of this socially undesirable behavior, all the surveys nevertheless found significantly higher AAS use in male compared to female persons and the majority of AAS users are or were professional or near professional athletes[15]. With the liver being the main site of steroid clearance, hepatotoxicity is one of the major adverse effects of chronic AAS use. The aim of this paper is to focus on the most recent studies and knowledge obtained regarding AAS-induced liver injury.

HEPATOTOXICITY

Since the 1950s, a significant number of studies and case reports have raised concerns regarding hepatotoxic effects including cholestasis, hepatic neoplasms, hepatocyte toxicity, and peliosis hepatis related to use of AASs[11,18]. Correlation between steroids and these effects has been attributed to the role of the liver as the primary clearance site for AASs. As mentioned before, synthetic steroids are usually modified to prevent first-pass hepatic metabolism, preventing their clearance by the liver and, therefore, elevating their risk of hepatotoxicity[19]. Most studies of long-term use have not identified exact dosages and concentrations, administration paths, and types of steroid compounds often used simultaneously. Prospective studies with supraphysiologic doses are difficult to gain institutional review board (IRB) approval due to ethical and legal considerations[20], therefore randomized controlled trials are lacking and in this minireview we discuss data from case reports, *in vitro* studies, and studies on animal models.

Proposed mechanisms of liver injury include anabolic steroid-induced infiltration of inflammatory cells in the hepatic tissue, and Kupffer cell activation resulting in production of inflammatory cytokines and collagen deposition, increased oxidative stress and reactive oxygen species with subsequent mitochondrial degeneration in liver cells, and stimulation of intracellular androgenic steroid receptors inducing unregulated growth of hepatocytes. An *in vitro* study in 2021 reported that disruption of mitochondrial respiratory chain reactions occurs early in the pathogenesis of liver injury caused by supraphysiologic doses of nandrolone, a synthetic AAS commonly used for performance enhancement. It specifically inhibits respiratory chain complexes I and III, which causes accumulation of reactive oxygen species and oxidative stress[21]. Indeed, earlier animal studies detected a reduced amount of glutathione and enzymes that serve as free radical scavengers (superoxide dismutase and catalase) as well as increasing thiobarbituric acid-reactive substances indicating impaired redox homeostasis[22,23]. Furthermore, oxidative stress interfered with mitochondrial membrane potential dynamics[24] and altogether resulted in reduced cell energy supply leading to malfunction and necrosis of hepatocytes. Apart from disturbance in cellular function, distortion in mitochondrial morphology and increased number of lysosomes in hepatocytes were observed by electron microscopy[25]. Another process observed after prolonged administration of nandrolone in animal studies was excess collagen deposition in liver parenchyma. It is known that AASs induce infiltration of the liver with inflammatory cells, which together with activated Kupffer cells, favor a pro-inflammatory state by releasing nuclear factor-κB (NF-κB) and inflammatory cytokines transforming growth factor beta1 (TGF-β1), tumor necrosis factor alpha (TNFα), and interleukin-1B (IL-1B). Such conditions also lead to activation of liver stellate cells, resulting in excessive collagen synthesis and deposition[26]. Interestingly, AASs can also promote collagen synthesis by activating their intracellular receptor and activation of transcription factors involved in collagen synthesis[27]. A recent study also gave convincing evidence for a role of testosterone in the pathophysiology of liver diseases with higher occurrences in males than in females. It demonstrated that the susceptibility of the mouse liver to injury was correlated with excessive inflammatory response mediated by androgen receptors (ARs) and testosterone-induced NOD-like receptor family pyrin domain containing 3 (NLRP3) inflammasome activation associated with a variety of chronic diseases[28]. Hepatotoxicity of AASs may also vary due to individual susceptibility, pre-existing liver conditions, and genetic factors. Most frequently reported liver disorders related to AASs are cholestasis, peliosis hepatis, and development of liver tumors[11,29-32]. Figure 1 shows an overview of proposed mechanisms of hepatotoxicity caused by AAS.

AAS drug-induced liver injury (AAS DILI) has also been frequently reported to cause serum liver enzyme elevations in AAS users. Elevated aspartate aminotransferase (AST), alanine aminotransferase (ALT), and lactate dehydrogenase (LDH) activities are, in general, regarded as indicators of hepatocellular damage. Transient elevation of AST and ALT in plasma has been largely reported in AAS users [33], but liver damage may not be the cause of the elevations because of the possible contribution of heavy and intense workouts with consequent muscle damage and rhabdomyolysis. Thus, liver enzymes



DOI: 10.3748/wjg.v28.i26.3071 **Copyright** ©The Author(s) 2022.

Figure 1 Proposed mechanisms of anabolic androgen steroid-induced liver injury. A: Oxidative stress in the mitochondria. Anabolic androgenic steroids (AASs) impair mitochondrial respiratory function, which leads to reactive oxygen species (ROS) accumulation. Cell membrane is damaged due to lipid peroxidation and intracellular ATP depletion occurs due to mitochondrial impairment. This results in cellular dysfunction at many levels (*e.g.*, toxic compounds can enter the cell). Mitochondrial morphology is also changed, with reduced cristae and swelling. In addition, there is an increase in lysosome number. Lack of energy supply eventually leads to hepatocyte necrosis; B: Immune cell infiltration of liver parenchyma. Long-term treatment with AASs like nandrolone is associated with immune cell infiltration which maintains proinflammatory state in liver tissue. Under such conditions, Kupffer cells release transforming growth factor beta1 (TGF-β1), tumor necrosis factor alpha (TNFα), and interleukin-1B (IL-1B) which mediate hepatic stellate cell activation: Extracellular matrix and collagen deposition leading to liver fibrosis; C: Hepatocyte hyperplasia causes formation of hepatic tumors. In rats treated with high-dose nandrolone, it was observed that it supported the viability of hepatic stem cells, which are potential reservoir of cancer stem cells. Nodular hepatocyte hyperplasia causes parenchyma distortion and mechanical blockage of vasculature which forms cystic lesions filled with blood, known as peliosis hepatic; D: "Bland cholestasis". Activation of androgen receptors (ARs) by AASs interferes with bile transporters, mediates intrahepatic microfilament damage, and increases expression of genes for acid bile and bile transporter synthesis, and these changes result in bile acid accumulation, cholestasis, and cholestatic jaundice. SOD: Superoxide dismutase; CAT: Catalase; AR: Androgene receptor; AAS: Anabolic androgenic steroid; AR: Androgen receptor. Figure created with Servier Medical Art, https://smart.servier.com/.

can be elevated independent of androgenic steroid use. Studies showing elevations of creatine kinase (CK) and AST, with no ALT and gamma glutamyl transferase (GGT) elevations, support this concept and suggest that hepatotoxicity related to AASs may be over-estimated if serum ALT, AST, and GGT concentrations are the sole criteria used[34]. Furthermore, a recent multi-center prospective study regarding the incidence of liver injury in transgender patients treated with hormone therapy including AASs showed no significant ALT, AST, alkaline phosphatase (ALP), or GGT elevations[35]. Most of the hepatotoxic effects, cholestasis, peliosis, and liver tumors are associated with orally administered AASs such as testosterone cypionate, enanthate, propionate, methyltestosterone, oxymetholone, danazol, stanozolol, formebolone, and methandienone[36,37], but intramuscular preparations were also linked to hepatotoxic effects[38]. Patil *et al*[38] reported three cases of AAS-induced hepatotoxicity which all manifested differently. The first case was a 31-year-old man who developed cholestatic liver injury after 2 mo of oxymetholone use, the second case was a 24-year-old man who developed well-differentiated hepatocellular carcinomas (HCC) and multiple hepatic adenomas after 3 years of intramuscular testosterone decanoate and daily oral stanozolol use, and the third case was a 36-year-old man with steatohepatitis after 2 mo of intramuscular nandrolone decanoate use[38]. The exact incidence of AAS DILI is difficult to establish due to both underreporting and lack of awareness. On the other hand, even when a history of AAS use is known, it may be difficult to establish the causality, particularly when multiple agents are used concomitantly or if there is an underlying liver condition. However, there has been a trend of increased AAS DILI reporting in recent years which may lead to new insights into pathophysiology and disease course. According to currently available data, AAS DILI has a good prognosis as the majority of cases recover completely and only a very small number of cases develop hepatic failure or die[39].

CHOLESTASIS

Although cholestasis is unlikely in patients treated with parenterally administered unmodified testosterone, 17α-alkyl-substituted steroids, which are designed to decrease hepatic metabolism, directly contribute to a highly characteristic form of acute cholestasis, ranging from very mild to severe. Some characteristic clinical manifestations are nausea, pruritus, fatigue, jaundice, and dark urine with elevated bilirubin and ALP, but without significant elevations of AST, ALT, and GGT. Such characteristics are indicative of cholestasis with minimal inflammation of the liver or bile duct. Resolution usually occurs upon discontinuation of anabolic steroids, although some case reports indicate benefits of hydrocortisone and ursodeoxycholic acid treatment[13,39-42].

Some animal model studies have suggested AAS-induced disruption of intrahepatic microfilaments and interference with bile transporter proteins as a pathophysiological mechanism of this syndrome rather than inflammation and injury to the liver and bile duct[29,43]. El-Sherrif *et al*[13] reported two cases of cholestatic DILI caused by the short-term use of AAS-containing dietary supplement Mass-Drol. The authors found that inhibition of expression of genes *ATPB81* and *ABCB11* by AAS may play a crucial role as the underlying mechanism of cholestatic injury. This leads to impaired bile salt transport and also reduced excretion of different hepatic ectoenzymes. Indeed, both patients presented with cholestasis with marked hyperbilirubinemia, but lack of GGT rise. The authors postulated that individuals who are carriers of c.2093G >A mutation in *ABCB11* may be specifically susceptible to cholestatic hepatic injury caused by AASs due to this mechanism[13]. Additionally, the role of multidrug-related proteins (MRP2, MRP3, and MRP4) is important in bile acid transfer as a complimentary mechanism. It was shown that testosterone metabolites are substrates of MRP2 protein, which has reduced activity in Dubin-Johnson syndrome (DJS). The effect of AAS in DJS has not been investigated to our knowledge, whereas it was found that pregnancy and oral contraceptives increase bilirubin levels in women with DJS[44]. Different underlying mechanism was proposed by Petrov *et al*[45], who used an *in vitro* model to demonstrate that AR activation may upregulate the expression of bile acid synthesis genes as well as bile acid transporters. Most recent studies have reported that the patterns of "bland" cholestasis in AAS users are so specific that this picture can be virtually sufficient to make a diagnosis of AAS-induced cholestasis[46]. Many reports refer to these phenomena as AAS DILI[39,47].

PELIOSIS HEPATIS

Peliosis hepatis is a rare condition characterized by hypervascular liver parenchyma and blood-filled cysts that is known to be associated with use of AASs and several other drugs like estrogens, corticosteroids, and azathioprine. So far, disruption of hepatic extracellular matrix and direct endothelial cell injury have been suggested as generating mechanisms for liver peliosis. It has also been proposed that steroid-induced hepatocyte hyperplasia results in mechanical obstruction of hepatic vascular system, causing dilatation and loss of endothelial barrier function[11,30,48]. Molecular mechanisms in pathophysiology of peliosis remain poorly understood; however, an important role of vascular

endothelial growth factor (VEGF) has been suggested in recent studies. VEGF induces angiogenesis, capillary permeability, and proliferation of endothelial cells in liver and other tissues. Tzirogiannis *et al* [49] found a major protective effect of VEGF which almost totally reversed the extent of peliosis in a model of cadmium-induced toxic liver injury and peliosis, implying that it preserves endothelial cell function. However, a study of peliosis hepatis in a patient with follicular lymphoma found elevated VEGF and suggested that lesions could be caused by elevation of VEGF and its angiogenic effects[50]. An animal model study of peliosis hepatis associated with melanoma supports a concept that a tumor-derived factor such as VEGF could induce development of peliosis due to its endothelial cell proliferation effect[51]. These conclusions indicate a need for further research of pathophysiology in peliosis hepatis as well as AASs and their impact on growth factors. Peliosis hepatis is commonly asymptomatic, but case reports described presentation characterized by sharp abdominal pain and hemoperitoneum in cases of cyst rupture[52]. Peliosis is usually treated with supportive care and the condition has shown to regress with discontinuation of AASs[53,54]. The condition has been reported not only in use of 17-alpha-alkylated steroids, but also in patients treated with unmodified testosterone[19]. Given its benign nature, most cases of peliosis hepatis are incidentally found and the most appropriate diagnostic modalities are magnetic resonance imaging[55] and histological examination. Once diagnosed, the offending drug should be discontinued and the condition closely monitored to reduce the risk of rupture, especially with larger lesions.

NEOPLASMS

Hepatic tumors, ranging from benign adenomas to malignant hepatocellular carcinoma, have been reported in patients with long-term anabolic steroid therapy[56-58]. Studies have suggested a higher hepatic cancer prevalence in males than in females. Higher endogenous concentrations of androgens may be a major factor in the development of liver carcinomas. Having both the estrogen and ARs, the liver is a hormone sensitive organ. The use of AASs is highly associated with hepatocyte proliferation and liver tumors[59]. An i*n vitro* study on HepG2 cells showed that a supraphysiologic dose of nandrolone changed their phenotype to be stem-like, but the mechanism of this transformation remains to be elucidated. In the same study, nandrolone administered *in vivo* in a mouse model promoted "stemness" in healthy organs, primarily ones naturally rich in stem cells such as the liver. Cell "stemness" phenotype is a metabolically latent state in which there is a lower oxygen consumption in the mitochondria. Expression of *Nanog*, *Lin28*, *Myc*, and *Klf4* genes and CD133 membrane protein is also considered to be markers of cell stemness. This led to a hypothesis that long-term supraphysiologic doses of nandrolone in young healthy individuals possibly increase the risk of malignancy in stem-cell rich organs by increasing the reservoir of stem cells which over a period of time under additional toxic stimuli may turn into cancer stem cells[21]. Studies to date indicate that most of AAS-induced tumors occur with use of agents containing a 17-alpha-alkyl group, but it has also been reported in patients treated with unmodified testosterone[56,60,61]. Histologically, these tumors are most commonly hepatic adenomas or HCC, but cholangiocarcinomas and angiosarcomas have also been reported with long-term AAS use[20]. Given the possibility of malignant transformation of hepatic adenoma, which occurs 10 times more commonly in men than in women, it is recommended that surgical resection be the most appropriate approach in men. In women, estrogen-containing oral contraceptives are a common cause, so their cessation, together with periodic surveillance, is an acceptable approach[62,63]. Solimini *et al*[11] reviewed case reports regarding liver tumors as well as cholestatic hepatitis associated with AASs and reported that several different AAS agents were associated with such liver pathology. Notably, chronic AAS use of several years is linked to development of HCC, while benign neoplasms were mostly linked to short-term use of AAS[11].

ADDITIONAL CONCERNS REGARDING AASS AND THE LIVER

Other hepatic disorders associated with AASs include toxicant-associated fatty liver disease (TAFLD), and possible increased risk of hepatitis B and C infections due to unsafe administration of AASs[64]. In addition, a negative effect on lipoproteins with reduced HDL-cholesterol and increased LDL-cholesterol concentrations has been reported mostly in long-term steroid users[65,66], which contribute to increased risk of coronary disease with AAS use.

Another concerning issue is the increasing number of mislabeled over-the-counter dietary supplements sold legally and containing significant amount of AASs. This has also been associated with adverse effects, but remains underreported and poorly understood. However, new case reports have been published on DILI with jaundice, cholestasis, dyslipidemia, and elevated serum liver enzyme panels in patients directly associated with dietary supplement use. After discontinuation of supplements, liver function commonly returned to normal[67,68]. Consumers may unknowingly use AASs which can result in acute, but also chronic, health problems that are difficult to link to these products and lead to re-exposure[69-71].

CONCLUSION

AAS use is closely linked to hepatotoxicity and serious hepatic conditions such as cholestasis, peliosis hepatis, and benign and malignant hepatic tumors, as well as steatohepatitis and dyslipidemia with multiple studies supporting a causal association. Several pathophysiological mechanisms have been proposed including AR receptor-mediated inflammatory response, disturbance of hepatic antioxidant factors, promotion of hepatocyte hyperplasia, and upregulation of bile acid synthesis. Most of these conditions have been reported with 17-alpha-alkylated steroids. Liver function usually returns to normal with discontinuation of use, but a higher HCC prevalence with AASs is concerning. Another important fact is the increasing number of case reports presenting patients with dietary supplements-associated liver conditions that are still underreported. Given all of the above, screening for liver pathology in known AAS users should be considered in order to possibly reverse the condition. Also, if certain liver pathology is diagnosed incidentally, a history of AAS as potential causal agent should be actively sought, and if found, addressed promptly.

FOOTNOTES

Author contributions: Petrovic A, Smolic R, Smolic M, and Wu GY designed the research study; Petrovic A, Vukadin S, Sikora R, Bojanic K, Plavec D, and Smolic M performed the research; Petrovic A and Vukadin S analyzed the data and wrote the manuscript; all authors have read and approved the final manuscript.

Conflict-of-interest statement: There are no conflicts of interest to report.

Open-Access: This article is an open-access article that was selected by an in-house editor and fully peer-reviewed by external reviewers. It is distributed in accordance with the Creative Commons Attribution NonCommercial (CC BY-NC 4.0) license, which permits others to distribute, remix, adapt, build upon this work non-commercially, and license their derivative works on different terms, provided the original work is properly cited and the use is non-commercial. See: https://creativecommons.org/Licenses/by-nc/4.0/

Country/Territory of origin: Croatia

ORCID number: Ana Petrovic 0000-0001-5585-3121; Sonja Vukadin 0000-0002-1636-2538; Renata Sikora 0000-0001-8594-549X; Kristina Bojanic 0000-0003-4473-5706; Robert Smolic 0000-0003-4614-4344; Davor Plavec 0000-0003-2020-8119; George Y. Wu 0000-0003-0068-1072; Martina Smolic 0000-0002-6867-826X.

S-Editor: Chen YL
L-Editor: Wang TQ
P-Editor: Chen YL

REFERENCES

1 **Roman M**, Roman DL, Ostafe V, Ciorsac A, Isvoran A. Computational Assessment of Pharmacokinetics and Biological Effects of Some Anabolic and Androgen Steroids. *Pharm Res* 2018; **35**: 41 [PMID: 29404794 DOI: 10.1007/s11095-018-2353-1]
2 **Mullen C**, Whalley BJ, Schifano F, Baker JS. Anabolic androgenic steroid abuse in the United Kingdom: An update. *Br J Pharmacol* 2020; **177**: 2180-2198 [PMID: 31989581 DOI: 10.1111/bph.14995]
3 **Barceloux DG**, Palmer RB. Anabolic-androgenic steroids. *Dis Mon* 2013; **59**: 226-248 [PMID: 23719201 DOI: 10.1016/j.disamonth.2013.03.010]
4 **Margo K**, Winn R. Testosterone treatments: why, when, and how? *Am Fam Physician* 2006; **73**: 1591-1598 [PMID: 16719252]
5 **Basaria S**. Androgen abuse in athletes: detection and consequences. *J Clin Endocrinol Metab* 2010; **95**: 1533-1543 [PMID: 20139230 DOI: 10.1210/jc.2009-1579]
6 **Bhasin S**, Storer TW, Berman N, Callegari C, Clevenger B, Phillips J, Bunnell TJ, Tricker R, Shirazi A, Casaburi R. The effects of supraphysiologic doses of testosterone on muscle size and strength in normal men. *N Engl J Med* 1996; **335**: 1-7 [PMID: 8637535 DOI: 10.1056/NEJM199607043350101]
7 **Shahidi NT**. Androgens and erythropoiesis. *N Engl J Med* 1973; **289**: 72-80 [PMID: 4575719 DOI: 10.1056/NEJM197307122890205]
8 **Beggs LA**, Yarrow JF, Conover CF, Meuleman JR, Beck DT, Morrow M, Zou B, Shuster JJ, Borst SE. Testosterone alters iron metabolism and stimulates red blood cell production independently of dihydrotestosterone. *Am J Physiol Endocrinol Metab* 2014; **307**: E456-E461 [PMID: 25074984 DOI: 10.1152/ajpendo.00184.2014]
9 **Hoffman JR**, Ratamess NA. Medical issues associated with anabolic steroid use: are they exaggerated? *J Sports Sci Med* 2006; **5**: 182-193 [PMID: 24259990]
10 **Pope HG Jr**, Wood RI, Rogol A, Nyberg F, Bowers L, Bhasin S. Adverse health consequences of performance-enhancing drugs: an Endocrine Society scientific statement. *Endocr Rev* 2014; **35**: 341-375 [PMID: 24423981 DOI: 10.1210/er.2013-1058]

11 **Solimini R**, Rotolo MC, Mastrobattista L, Mortali C, Minutillo A, Pichini S, Pacifici R, Palmi I. Hepatotoxicity associated with illicit use of anabolic androgenic steroids in doping. *Eur Rev Med Pharmacol Sci* 2017; **21**: 7-16 [PMID: 28379599]

12 **Rahnema CD**, Crosnoe LE, Kim ED. Designer steroids - over-the-counter supplements and their androgenic component: review of an increasing problem. *Andrology* 2015; **3**: 150-155 [PMID: 25684733 DOI: 10.1111/andr.307]

13 **El Sherrif Y**, Potts JR, Howard MR, Barnardo A, Cairns S, Knisely AS, Verma S. Hepatotoxicity from anabolic androgenic steroids marketed as dietary supplements: contribution from ATP8B1/ABCB11 mutations? *Liver Int* 2013; **33**: 1266-1270 [PMID: 23750872 DOI: 10.1111/liv.12216]

14 **DEA**. Drugs of abuse. In: Administration. United States department of justice, 2020

15 **Anawalt BD**. Diagnosis and Management of Anabolic Androgenic Steroid Use. *J Clin Endocrinol Metab* 2019; **104**: 2490-2500 [PMID: 30753550 DOI: 10.1210/jc.2018-01882]

16 **Buckman JF**, Farris SG, Yusko DA. A national study of substance use behaviors among NCAA male athletes who use banned performance enhancing substances. *Drug Alcohol Depend* 2013; **131**: 50-55 [PMID: 23688842 DOI: 10.1016/j.drugalcdep.2013.04.023]

17 **Jenssen IH**, Johannessen KB. Aggression and body image concerns among anabolic androgenic steroid users, contemplators, and controls in Norway. *Body Image* 2015; **12**: 6-13 [PMID: 25261635 DOI: 10.1016/j.bodyim.2014.08.009]

18 **Quaglio G**, Fornasiero A, Mezzelani P, Moreschini S, Lugoboni F, Lechi A. Anabolic steroids: dependence and complications of chronic use. *Intern Emerg Med* 2009; **4**: 289-296 [PMID: 19468827 DOI: 10.1007/s11739-009-0260-5]

19 **Shahidi NT**. A review of the chemistry, biological action, and clinical applications of anabolic-androgenic steroids. *Clin Ther* 2001; **23**: 1355-1390 [PMID: 11589254 DOI: 10.1016/s0149-2918(01)80114-4]

20 **Niedfeldt MW**. Anabolic Steroid Effect on the Liver. *Curr Sports Med Rep* 2018; **17**: 97-102 [PMID: 29521706 DOI: 10.1249/JSR.0000000000000467]

21 **Agriesti F**, Tataranni T, Pacelli C, Scrima R, Laurenzana I, Ruggieri V, Cela O, Mazzoccoli C, Salerno M, Sessa F, Sani G, Pomara C, Capitanio N, Piccoli C. Nandrolone induces a stem cell-like phenotype in human hepatocarcinoma-derived cell line inhibiting mitochondrial respiratory activity. *Sci Rep* 2020; **10**: 2287 [PMID: 32041983 DOI: 10.1038/s41598-020-58871-1]

22 **Sadowska-Krępa E**, Kłapcińska B, Nowara A, Jagsz S, Szołtysek-Bołdys I, Chalimoniuk M, Langfort J, Chrapusta SJ. High-dose testosterone supplementation disturbs liver pro-oxidant/antioxidant balance and function in adolescent male Wistar rats undergoing moderate-intensity endurance training. *PeerJ* 2020; **8**: e10228 [PMID: 33240609 DOI: 10.7717/peerj.10228]

23 **Lima EM**, Cassaro KODS, Silva CLD, Silva MA, Poltronieri MP, Nascimento AMD, Andrade TU, Bissoli NS, Brasil GA. Eight weeks of treatment with nandrolone decanoate in female rats promotes disruption in the redox homeostasis and impaired renal function. *Life Sci* 2020; **242**: 117227 [PMID: 31881226 DOI: 10.1016/j.lfs.2019.117227]

24 **Carteri RB**, Kopczynski A, Rodolphi MS, Strogulski NR, Wannmacher CMD, Franceschi ID, Hammerschmitt ME, Driemeier D, Portela LV. Anabolic-androgenic steroids impair mitochondrial function and redox status in the heart and liver of mice. *Steroids* 2021; **172**: 108861 [PMID: 33984388 DOI: 10.1016/j.steroids.2021.108861]

25 **Gragera R**, Saborido A, Molano F, Jiménez L, Muñiz E, Megías A. Ultrastructural changes induced by anabolic steroids in liver of trained rats. *Histol Histopathol* 1993; **8**: 449-455 [PMID: 8358156]

26 **Shalaby AM**, Bahey NG. Reversal of the hepatic damage induced by the supraphysiological dose of nandrolone decanoate after its withdrawal in the adult male rat. *Tissue Cell* 2018; **53**: 44-52 [PMID: 30060826 DOI: 10.1016/j.tice.2018.05.013]

27 **Markova MS**, Zeskand J, McEntee B, Rothstein J, Jimenez SA, Siracusa LD. A role for the androgen receptor in collagen content of the skin. *J Invest Dermatol* 2004; **123**: 1052-1056 [PMID: 15610513 DOI: 10.1111/j.0022-202X.2004.23494.x]

28 **Ma X**, Zhou Y, Qiao B, Jiang S, Shen Q, Han Y, Liu A, Chen X, Wei L, Zhou L, Zhao J. Androgen aggravates liver fibrosis by activation of NLRP3 inflammasome in CCl_4-induced liver injury mouse model. *Am J Physiol Endocrinol Metab* 2020; **318**: E817-E829 [PMID: 32182125 DOI: 10.1152/ajpendo.00427.2019]

29 **Neri M**, Bello S, Bonsignore A, Cantatore S, Riezzo I, Turillazzi E, Fineschi V. Anabolic androgenic steroids abuse and liver toxicity. *Mini Rev Med Chem* 2011; **11**: 430-437 [PMID: 21443508 DOI: 10.2174/138955711795445916]

30 **Vieira RP**, França RF, Damaceno-Rodrigues NR, Dolhnikoff M, Caldini EG, Carvalho CR, Ribeiro W. Dose-dependent hepatic response to subchronic administration of nandrolone decanoate. *Med Sci Sports Exerc* 2008; **40**: 842-847 [PMID: 18408615 DOI: 10.1249/MSS.0b013e3181666f1c]

31 **Schwingel PA**, Cotrim HP, Salles BR, Almeida CE, dos Santos CR Jr, Nachef B, Andrade AR, Zoppi CC. Anabolic-androgenic steroids: a possible new risk factor of toxicant-associated fatty liver disease. *Liver Int* 2011; **31**: 348-353 [PMID: 21040407 DOI: 10.1111/j.1478-3231.2010.02346.x]

32 **Riezzo I**, Turillazzi E, Bello S, Cantatore S, Cerretani D, Di Paolo M, Fiaschi AI, Frati P, Neri M, Pedretti M, Fineschi V. Chronic nandrolone administration promotes oxidative stress, induction of pro-inflammatory cytokine and TNF-α mediated apoptosis in the kidneys of CD1 treated mice. *Toxicol Appl Pharmacol* 2014; **280**: 97-106 [PMID: 25065671 DOI: 10.1016/j.taap.2014.06.031]

33 **Hartgens F**, Kuipers H. Effects of androgenic-anabolic steroids in athletes. *Sports Med* 2004; **34**: 513-554 [PMID: 15248788 DOI: 10.2165/00007256-200434080-00003]

34 **Dickerman RD**, Pertusi RM, Zachariah NY, Dufour DR, McConathy WJ. Anabolic steroid-induced hepatotoxicity: is it overstated? *Clin J Sport Med* 1999; **9**: 34-39 [PMID: 10336050 DOI: 10.1097/00042752-199901000-00007]

35 **A Stangl T**, M Wiepjes C, Defreyne J, Conemans E, D Fisher A, Schreiner T, T'Sjoen G, den Heijer M. Is there a need for liver enzyme monitoring in people using gender-affirming hormone therapy? *Eur J Endocrinol* 2021; **184**: 513-520 [PMID: 33524005 DOI: 10.1530/EJE-20-1064]

36 **Büttner A**, Thieme D. Side effects of anabolic androgenic steroids: pathological findings and structure-activity relationships. *Handb Exp Pharmacol* 2010; 459-484 [PMID: 20020376 DOI: 10.1007/978-3-540-79088-4_19]

37 **Maravelias C**, Dona A, Stefanidou M, Spiliopoulou C. Adverse effects of anabolic steroids in athletes. A constant threat. *Toxicol Lett* 2005; **158**: 167-175 [PMID: 16005168 DOI: 10.1016/j.toxlet.2005.06.005]

38 **Patil V**, Jothimani D, Harika K, Hakeem AR, Sachan D, Vij M, Rela M. Versatility of Anabolic Androgenic Steroid-

Induced Hepatotoxicity. *J Clin Exp Hepatol* 2022; **12**: 216-221 [PMID: 35068803 DOI: 10.1016/j.jceh.2021.03.003]

39 **Abeles RD**, Foxton M, Khan S, Goldin R, Smith B, Thursz MR, Verma S. Androgenic anabolic steroid-induced liver injury: two case reports assessed for causality by the updated Roussel Uclaf Causality Assessment Method (RUCAM) score and a comprehensive review of the literature. *BMJ Open Gastroenterol* 2020; **7** [PMID: 33214235 DOI: 10.1136/bmjgast-2020-000549]

40 **Robles-Diaz M**, Gonzalez-Jimenez A, Medina-Caliz I, Stephens C, García-Cortes M, García-Muñoz B, Ortega-Alonso A, Blanco-Reina E, Gonzalez-Grande R, Jimenez-Perez M, Rendón P, Navarro JM, Gines P, Prieto M, Garcia-Eliz M, Bessone F, Brahm JR, Paraná R, Lucena MI, Andrade RJ; Spanish DILI Registry; SLatinDILI Network. Distinct phenotype of hepatotoxicity associated with illicit use of anabolic androgenic steroids. *Aliment Pharmacol Ther* 2015; **41**: 116-125 [PMID: 25394890 DOI: 10.1111/apt.13023]

41 **Kafrouni MI**, Anders RA, Verma S. Hepatotoxicity associated with dietary supplements containing anabolic steroids. *Clin Gastroenterol Hepatol* 2007; **5**: 809-812 [PMID: 17509944 DOI: 10.1016/j.cgh.2007.02.036]

42 **Stępień PM**, Reczko K, Wieczorek A, Zarębska-Michaluk D, Pabjan P, Król T, Kryczka W. Severe intrahepatic cholestasis and liver failure after stanozolol usage - case report and review of the literature. *Clin Exp Hepatol* 2015; **1**: 30-33 [PMID: 28856252 DOI: 10.5114/ceh.2015.51376]

43 **Modlinski R**, Fields KB. The effect of anabolic steroids on the gastrointestinal system, kidneys, and adrenal glands. *Curr Sports Med Rep* 2006; **5**: 104-109 [PMID: 16529682 DOI: 10.1097/01.csmr.0000306529.74500.f6]

44 **Erlinger S**, Arias IM, Dhumeaux D. Inherited disorders of bilirubin transport and conjugation: new insights into molecular mechanisms and consequences. *Gastroenterology* 2014; **146**: 1625-1638 [PMID: 24704527 DOI: 10.1053/j.gastro.2014.03.047]

45 **Petrov PD**, Fernández-Murga L, Conde I, Martínez-Sena T, Guzmán C, Castell JV, Jover R. Epistane, an anabolic steroid used for recreational purposes, causes cholestasis with elevated levels of cholic acid conjugates, by upregulating bile acid synthesis (CYP8B1) and cross-talking with nuclear receptors in human hepatocytes. *Arch Toxicol* 2020; **94**: 589-607 [PMID: 31894354 DOI: 10.1007/s00204-019-02643-y]

46 **Chopra S**, Gawrieh S, Vuppalanchi R, Saxena R. Role of the Surgical Pathologist in Diagnosis of Drug-induced Liver Injury: Recognizing Specific Patterns of Drug Injury. *Adv Anat Pathol* 2021; **28**: 383-395 [PMID: 34050060 DOI: 10.1097/PAP.0000000000000307]

47 **Goh HG**, Lee YJ, Kim TH. Severe Persistent Jaundice after the Abuse of an Anabolic Androgenic Steroid Analogue. *Korean J Gastroenterol* 2020; **76**: 167-170 [PMID: 32969366 DOI: 10.4166/kjg.2020.76.3.167]

48 **Tsirigotis P**, Sella T, Shapira MY, Bitan M, Bloom A, Kiselgoff D, Levin M, Libster D, Abdul Hai A, Gesundheit B, Or R, Slavin S, Resnick I. Peliosis hepatis following treatment with androgen-steroids in patients with bone marrow failure syndromes. *Haematologica* 2007; **92**: e106-e110 [PMID: 18024386 DOI: 10.3324/haematol.11343]

49 **Tzirogiannis KN**, Papadimas GK, Kondyli VG, Kourentzi KT, Demonakou MD, Kyriakou LG, Mykoniatis MG, Hereti RI, Panoutsopoulos GI. Peliosis hepatis: microscopic and macroscopic type, time pattern, and correlation with liver cell apoptosis in a model of toxic liver injury. *Dig Dis Sci* 2006; **51**: 1998-2006 [PMID: 17053957 DOI: 10.1007/s10620-006-9242-x]

50 **de la Mano EP**, Martín-Sánchez G, López RL, Galán MAF, Ríos ST, Jiménez MJM, de Morales JMGR, Santos MAC, Núñez GM. Peliosis hepatis associated with follicular lymphoma with a rise in vascular endothelial growth factor and anaemia of inflammation. *Ecancermedicalscience* 2018; **12**: 882 [PMID: 30679949 DOI: 10.3332/ecancer.2018.882]

51 **Edwards R**, Colombo T, Greaves P. "Have you seen this? *Toxicol Pathol* 2002; **30**: 521-523 [PMID: 12187943 DOI: 10.1080/01926230290105686]

52 **Choi SK**, Jin JS, Cho SG, Choi SJ, Kim CS, Choe YM, Lee KY. Spontaneous liver rupture in a patient with peliosis hepatis: a case report. *World J Gastroenterol* 2009; **15**: 5493-5497 [PMID: 19916182 DOI: 10.3748/wjg.15.5493]

53 **Nadell J**, Kosek J. Peliosis hepatis. Twelve cases associated with oral androgen therapy. *Arch Pathol Lab Med* 1977; **101**: 405-410 [PMID: 577673]

54 **Fidelman N**, LaBerge JM, Kerlan RK Jr. SCVIR 2002 Film Panel case 4: massive intraperitoneal hemorrhage caused by peliosis hepatis. *J Vasc Interv Radiol* 2002; **13**: 542-545 [PMID: 11997366 DOI: 10.1016/s1051-0443(07)61539-5]

55 **Hui CL**, Lee ZJ. Hepatic disorders associated with exogenous sex steroids: MR imaging findings. *Abdom Radiol (NY)* 2019; **44**: 2436-2447 [PMID: 30955069 DOI: 10.1007/s00261-019-01941-4]

56 **Nakao A**, Sakagami K, Nakata Y, Komazawa K, Amimoto T, Nakashima K, Isozaki H, Takakura N, Tanaka N. Multiple hepatic adenomas caused by long-term administration of androgenic steroids for aplastic anemia in association with familial adenomatous polyposis. *J Gastroenterol* 2000; **35**: 557-562 [PMID: 10905366 DOI: 10.1007/s005350070081]

57 **Evert M**, Dombrowski F. [Hepatocellular carcinoma in the non-cirrhotic liver]. *Pathologe* 2008; **29**: 47-52 [PMID: 18057936 DOI: 10.1007/s00292-007-0953-3]

58 **Socas L**, Zumbado M, Pérez-Luzardo O, Ramos A, Pérez C, Hernández JR, Boada LD. Hepatocellular adenomas associated with anabolic androgenic steroid abuse in bodybuilders: a report of two cases and a review of the literature. *Br J Sports Med* 2005; **39**: e27 [PMID: 15849280 DOI: 10.1136/bjsm.2004.013599]

59 **Velazquez I**, Alter BP. Androgens and liver tumors: Fanconi's anemia and non-Fanconi's conditions. *Am J Hematol* 2004; **77**: 257-267 [PMID: 15495253 DOI: 10.1002/ajh.20183]

60 **El-Serag HB**. Hepatocellular carcinoma: recent trends in the United States. *Gastroenterology* 2004; **127**: S27-S34 [PMID: 15508094 DOI: 10.1053/j.gastro.2004.09.013]

61 **Tanaka K**, Sakai H, Hashizume M, Hirohata T. Serum testosterone:estradiol ratio and the development of hepatocellular carcinoma among male cirrhotic patients. *Cancer Res* 2000; **60**: 5106-5110 [PMID: 11016636]

62 **Farges O**, Ferreira N, Dokmak S, Belghiti J, Bedossa P, Paradis V. Changing trends in malignant transformation of hepatocellular adenoma. *Gut* 2011; **60**: 85-89 [PMID: 21148580 DOI: 10.1136/gut.2010.222109]

63 **European Association for the Study of the Liver (EASL)**. EASL Clinical Practice Guidelines on the management of benign liver tumours. *J Hepatol* 2016; **65**: 386-398 [PMID: 27085809 DOI: 10.1016/j.jhep.2016.04.001]

64 **Aitken C**, Delalande C, Stanton K. Pumping iron, risking infection? *Drug Alcohol Depend* 2002; **65**: 303-308 [PMID: 11841901 DOI: 10.1016/s0376-8716(01)00174-0]

65 **Hartgens F**, Rietjens G, Keizer HA, Kuipers H, Wolffenbuttel BH. Effects of androgenic-anabolic steroids on apolipoproteins and lipoprotein (a). *Br J Sports Med* 2004; **38**: 253-259 [PMID: 15155420 DOI: 10.1136/bjsm.2003.000199]

66 **Kouri EM**, Pope HG Jr, Oliva PS. Changes in lipoprotein-lipid levels in normal men following administration of increasing doses of testosterone cypionate. *Clin J Sport Med* 1996; **6**: 152-157 [PMID: 8792045 DOI: 10.1097/00042752-199607000-00003]

67 **Magee CD**, Witte S, Kwok RM, Deuster PA. Mission Compromised? *Mil Med* 2016; **181**: e1169-e1171 [PMID: 27612377 DOI: 10.7205/MILMED-D-15-00502]

68 **Cabb E**, Baltar S, Powers DW, Mohan K, Martinez A, Pitts E. The Diagnosis and Manifestations of Liver Injury Secondary to Off-Label Androgenic Anabolic Steroid Use. *Case Rep Gastroenterol* 2016; **10**: 499-505 [PMID: 27721739 DOI: 10.1159/000448883]

69 **García-Cortés M**, Robles-Díaz M, Ortega-Alonso A, Medina-Caliz I, Andrade RJ. Hepatotoxicity by Dietary Supplements: A Tabular Listing and Clinical Characteristics. *Int J Mol Sci* 2016; **17**: 537 [PMID: 27070596 DOI: 10.3390/ijms17040537]

70 **Pascale B**, Steele C, Attipoe S, O'Connor FG, Deuster PA. Dietary Supplements: Knowledge and Adverse Event Reporting Among American Medical Society for Sports Medicine Physicians. *Clin J Sport Med* 2016; **26**: 139-144 [PMID: 26035683 DOI: 10.1097/JSM.0000000000000213]

71 **Medina-Caliz I**, Garcia-Cortes M, Gonzalez-Jimenez A, Cabello MR, Robles-Diaz M, Sanabria-Cabrera J, Sanjuan-Jimenez R, Ortega-Alonso A, García-Muñoz B, Moreno I, Jimenez-Perez M, Fernandez MC, Ginés P, Prieto M, Conde I, Hallal H, Soriano G, Roman E, Castiella A, Blanco-Reina E, Montes MR, Quiros-Cano M, Martin-Reyes F, Lucena MI, Andrade RJ; Spanish DILI Registry. Herbal and Dietary Supplement-Induced Liver Injuries in the Spanish DILI Registry. *Clin Gastroenterol Hepatol* 2018; **16**: 1495-1502 [PMID: 29307848 DOI: 10.1016/j.cgh.2017.12.051]

World Journal of Gastroenterology

Submit a Manuscript: https://www.f6publishing.com

World J Gastroenterol 2022 July 14; 28(26): 3081-3091

DOI: 10.3748/wjg.v28.i26.3081

ISSN 1007-9327 (print) ISSN 2219-2840 (online)

MINIREVIEWS

Epidemiological and clinical aspects of hepatitis B virus infection in Italy over the last 50 years

Caterina Sagnelli, Antonello Sica, Massimiliano Creta, Armando Calogero, Massimo Ciccozzi, Evangelista Sagnelli

Specialty type: Gastroenterology and hepatology

Provenance and peer review: Invited article; Externally peer reviewed.

Peer-review model: Single blind

Peer-review report's scientific quality classification

Grade A (Excellent): 0
Grade B (Very good): B
Grade C (Good): C, C
Grade D (Fair): D
Grade E (Poor): 0

P-Reviewer: Dang SS, China; Gu JY, China; Inoue J, Japan; Biswas S, Ireland

A-Editor: Liu X, China

Received: January 12, 2022
Peer-review started: January 12, 2022
First decision: March 8, 2022
Revised: March 16, 2022
Accepted: June 18, 2022
Article in press: June 18, 2022
Published online: July 14, 2022

Caterina Sagnelli, Evangelista Sagnelli, Department of Mental Health and Public Medicine, Section of Infectious Diseases, University of Campania "Luigi Vanvitelli", Naples 80138, Italy

Antonello Sica, Department of Precision Medicine, University of Campania "Luigi Vanvitelli", Naples 80131, Italy

Massimiliano Creta, Department of Neurosciences, Reproductive Sciences and Odontostomatology, University of Naples Federico II, Naples 80138, Italy

Armando Calogero, Department of Advanced Biomedical Sciences-UO General Surgery, University Federico II of Naples, Naples 80127, Italy

Massimo Ciccozzi, Medical Statistics and Molecular Epidemiology Unit, Campus Bio-Medico University, Rome 80138, Italy

Corresponding author: Caterina Sagnelli, Doctor, MD, PhD, Doctor, Postdoc, Professor, Research Scientist, Department of Mental Health and Public Medicine, Section of Infectious Diseases, University of Campania "Luigi Vanvitelli", 5 Via L. Armanni, Naples 80138, Italy. caterina.sagnelli@unicampania.it

Abstract

A relevant gradual reduction of both the incidence rate of acute hepatitis B (AHB) and prevalence of chronic hepatitis B has occurred in Italy in the last 50 years, due to substantial epidemiological changes: Improvement in socioeconomic and hygienic conditions, reduction of the family unit, accurate screening of blood donations, abolition of re-usable glass syringes, hepatitis B virus (HBV)-universal vaccination started in 1991, use of effective well tolerated nucleo(t)side analogues able to suppress HBV replication available from 1998, and educational mediatic campaigns against human immunodeficiency virus infection focusing on the prevention of sexual and parenteral transmission of infections. As an example, AHB incidence has gradually decreased from 10/100000 inhabitants in 1985 to 0.21 in 2020. Unfortunately, the coronavirus disease 2019 (COVID-19) pandemic has interrupted the trend towards HBV eradication. In fact, several HBV chronic carriers living in the countryside have become unable to access healthcare facilities for screening, diagnosis, clinical management, and nucleo(t)side analogue therapy in the COVID-19 pandemic, mainly for anxiety of becoming infected with severe acute respiratory syndrome coronavirus 2 (SARS-CoV-2), movement restrictions, and reduced gains from job loss. In addition, one-third of

healthcare facilities and personnel for HBV patients have been devolved to the COVID-19 assistance.

Key Words: Hepatitis B virus; Hepatitis B virus epidemiology; Acute hepatitis B; COVID-19

©The Author(s) 2022. Published by Baishideng Publishing Group Inc. All rights reserved.

Core Tip: An impressive reduction in the spread of hepatitis B virus (HBV) infection has been observed over the past 5 decades in Italy. This review article analyzes, in Italy, the effects of various events on HBV endemicity: Reduction of the impact of several risk factors, HBV-universal vaccination started in 1991, the nucleo(t)side analogue therapy started in 1996, the increased immigration flows from countries at high HBV endemicity, and the restrictions generated by the coronavirus disease 2019 (COVID-19) pandemic. Particular attention has been directed at the negative effects of the COVID-19 pandemic that threaten to interrupt the favorable trend towards HBV eradication.

Citation: Sagnelli C, Sica A, Creta M, Calogero A, Ciccozzi M, Sagnelli E. Epidemiological and clinical aspects of hepatitis B virus infection in Italy over the last 50 years. *World J Gastroenterol* 2022; 28(26): 3081-3091
URL: https://www.wjgnet.com/1007-9327/full/v28/i26/3081.htm
DOI: https://dx.doi.org/10.3748/wjg.v28.i26.3081

INTRODUCTION

Hepatitis B virus (HBV) infection is a global health problem with 3.61% of the world population chronically infected and 890000 deaths per year for cirrhosis, liver failure, or hepatocellular carcinoma (HCC)[1,2]. Despite the availability of an effective recombinant HBV vaccine from 1991[3] and of effective well-tolerated nucleo(t)side analogues since 1998, the rate of individuals persistently infected with HBV does not decrease worldwide and, unfortunately, it is increasing in some developing countries[4]. Several factors support the level of endemicity of HBV infection: (1) Most patients with chronic infections are asymptomatic and undiagnosed for years[5]; (2) 70% of the individuals with chronic HBV infections live in developing areas where HBV vaccination does not have the character of universality, with 95.3 million in Western Pacific areas and 75.6 million in Africa, where there is a prevalence of hepatitis B surface antigen (HBsAg) chronic carriers of 5.26% and 8.83%, respectively[6]; and (3) Nucleo(t)side analogues suppress but do not eradicate chronic HBV infection. Instead, in the last 30 years, a trend to HBV eradication has been observed in northern America, western Europe, and Japan [7].

As far as Italy, HBV endemicity has progressively decreased over the last 50 years, due to universal HBV vaccination since 1991, the improvement in socioeconomic conditions correlated to better standard of hygiene, substantial reduction of the family unit, and continuous mediatic human immunodeficiency virus (HIV) campaigns organized and financed by the Italian government[8].

Italy is experiencing a continuous migratory flow, more frequently from eastern Europe and sub-Saharan Africa for 20 years and today migrants represent about 9% of the resident population. As an effect of immigration, some HBV genotypes previously rare in Italy are currently responsible for about 40% of acute hepatitis B (AHB) cases[9-12]. There is the fear that the continuous immigrant flows from countries with high or intermediated HBV endemicity will adversely affect the low endemicity level of Italy. As an example, of 882 asymptomatic undocumented migrants or refugees observed in southern Italy in 2015, 78 (9%) were HBsAg positive. This rate was 14% in 444 sub-Saharan Africa subjects, 6% in 198 eastern Europe subjects, and 2%-3% in the 240 migrants from northern Africa, Bangladesh, India, Pakistan, or Sri Lanka, percentages much higher than the 0.8% registered in the people born and living in Italy[13]. The regional office of the World Health Organization (WHO) for Europe reported that a high percentage of immigrants are not vaccinated against HBV upon their arrival in host countries[14] and therefore at risk of becoming infected even in geographic areas with a low HBV endemicity level; accordingly, in Italy one fifth of the new AHB cases are represented by the immigrant population.

Like for numerous other sectors of medicine, the severe acute respiratory syndrome coronavirus 2 (SARS-CoV-2) pandemic reduced care levels also for HBV-related diseases. A recent web-based survey performed in Italy registered that a quarter of healthcare centers and personnel dedicated to liver diseases had been intended for coronavirus disease 2019 (COVID-19) and that 23% of cases with chronic hepatitis B (CHB) undergoing HBV suppression with nuclo(t)side analogues have suffered interruptions of therapeutic plans[15]. There is therefore a suggestion for the healthcare institutions of Italy not to neglect the need of patients with HBV infection throughout this long terrible COVID-19 pandemic, not to lose in short time the advantages obtained with decades of considerable efforts and economic

commitment.

EPIDEMIOLOGICAL AND CLINICAL CHANGES OF AHB IN ITALY OVER LAST FIVE DECADES

HBV is a non-cytopathic virus that induces liver cell necrosis through cytolytic action of human cytotoxic T cells made able to recognize the viral antigens expressed on the surface of infected hepatocytes from a previous pre-sensitization to HBV. The degree of immune response depends on the age of the host at the acquisition of HBV infection, being absent or low in infants and young children who often develop an asymptomatic acute hepatitis frequently progressing to an HBsAg chronic carriage, but high in young adults and adults who usually develop a self-limiting symptomatic acute hepatitis, progressing to chronicity in only 2%-5% of cases. Fulminant hepatitis occurs in only 1%-3% of cases, more frequently in adolescents and young adults, with a mortality rate of 70%, and in most cases requiring liver transplantation[16-19]. In its classic form, AHB begins with generic symptoms such as fever, malaise, headache, nausea, anorexia, vomiting, and diarrhea, followed by jaundice common in adults and rare in children. The aminotransferases serum levels are usually normal or moderately increased in children and high in adults, reflecting the extension of liver damage. High serum titers of IgM to hepatitis B core antigen identify HBV as the etiological factor, simultaneously with serum HBsAg positivity. Hepatitis B e antigen (HBeAg) and serum HBV DNA are signs of high infectivity; they can be found in the early stage of the disease and are no more detectable in the elimination phase of the virus, event accompanied by seroconversion to anti-HBe. A Cochrane's review of seven randomized controlled trials involving a total number of 597 participants found that antiviral treatment has no benefit for AHB[20], since any evolution to chronicity is strongly determined by the reactivity of the patient's immune system. Some more severe cases, however, may require supportive therapy.

All yearly AHB cases occurred in Italy in the sixties were registered by the Italian Institute of Statistic (ISTAT) under one single entry, with an incidence rate of 98 cases per 100000 inhabitants, followed by a subsequent gradual decline to 20 cases per 100000 inhabitants until 1987[8]. Reliable data on AHB incidence in Italy are reported since 1985, when the surveillance of the integrate epidemiological system of acute viral hepatitis (SEIEVA) registered 12 cases per 100000 inhabitants. This incidence gradually decreased in subsequent years, driven by two important events: (1) The beginning in 1985 of mediatic HIV educational campaigns that advised the condoms for sexual intercourses at risk and to avoid syringe sharing[21]; and (2) since 1991, the national universal HBV vaccination continued so far without interruption; currently all Italian people aged 0 to 41 have been vaccinated[22]. The AHB incidence in 1987 decreased to 10.4 cases per 100000 inhabitants, 5.4 in 1990, 0.9 in 2012, 0.6 in 2016, and 0.21 in 2020 (Table 1).

These data testify the strong contribution of the HBV vaccination to reduction of AHB incidence, but it is equally evident that this reduction had already begun before the universal HBV vaccination campaign had started in 1991. The reason for this is that other factors have contributed to the decrease of AHB incidence in Italy, such as the obligation to test blood donations for HBV markers and not to transfuse the samples testing positive, improvement of socioeconomic and hygienic conditions, and some behavioral changes that have led to the reduction of domestic contacts with a chronic HBsAg carrier and not to use non-disposable or improperly sterilized instruments for medical and surgical practice, piercings, tattoos, manicures, pedicures, acupuncture, and barber's shop[23-25]. Vertical transmission of HBV is no longer a route of HBV transmission in Italy from 1991, due to the mandatory screening for HBV infection among women in pregnancy or at delivery, and to the mandatory, in babies born of HBsAg-positive mothers, active and passive immune prophylaxis. Two routes of HBV transmission remain active, the parenteral one because of the exchange of syringes or other objects between intravenous drug users and the sexual one because of the unusual use of condom in sexual intercourses. It should also be underlined that the impact of these two risk factors on HBV endemicity has progressively lowered, due to the positive effect of universal HBV vaccination which currently covers the Italian population aged 0-41.

Analyzed by the age classes, 0-14 years, 15-24 years, and 25 years or more, the data registered by SEIEVA in 1985 showed 6 subjects with AHB per 100000 inhabitants in age class 0-14, 41 in age class 15-24, and 7 in age class 25 or more. The progressive decline was observed in subsequent years in all the three age classes: (1) In 1990: 1, 17, and 4 cases per 100000 inhabitants, respectively; (2) in 1995: 1, 6, and 3 cases, respectively; (3) in 2000: 0.1, 2, and 2 cases, respectively; (4) in 2005: 0, 5, and 1.8 cases, respectively; and (5) in 2011: 0, 0.5, and 1.2 cases per 100000 inhabitants, respectively[26] (Table 1).

Patients with acute viral hepatitis B registered by SEIEVA from 2009 to 2020 were allocated in five age classes (0-14, 15-24, 25-34, 35-54, and 55 or more), with an incidence close to zero in age classes 0-14 and 15-24 and with a continuous downtrend in older age classes up to 2020[26] (Table 1). The cases of AHB in SEIEVA in the period 1991-2019 have been also analyzed by their geographical distribution[26,27], northern + central Italy *vs* southern Italy + main islands (Sicily and Sardinia), a distribution reflecting historical events and the behaviors of the respective inhabitants (Figure 1).

Table 1 Incidence rate of acute hepatitis B in Italy: Cases per 100000 inhabitants per year, according to age classes

Age classes	1985	1990	1995	2000	2005	2009	2010	2011	2012	2013	2014	2015	2016	2017	2018	2019	2020
0-14	6.00	1.00	1.00	0.10	0.00	0.00	0.00	0.00	0.04	0.10	0.03	0.05	0.00	0.00	0.03	0.03	0.00
15-24	41.00	17.00	6.00	2.00	5.00	0.50	0.50	0.45	0.40	0.30	0.28	0.30	0.20	0.15	0.32	0.08	0.08
> 25	7.00	4.00	3.00	2.00	1.80	-	-	-	-	-	-	-	-	-	-	-	-
25-34	-	-	-	-	-	1.20	1.20	1.20	0.80	0.70	0.46	0.33	0.30	0.23	0.34	0.26	0.26
35-54	-	-	-	-	-	1.90	1.80	2.00	1.70	1.90	1.76	1.40	1.10	1.04	0.76	0.69	0.34
> 55	-	-	-	-	-	0.70	0.50	0.50	0.60	0.70	0.51	0.46	0.60	0.48	0.39	0.38	0.20
Total	12.00	5.00	3.00	2.00	1.30	1.00	0.90	1.00	0.85	0.90	0.80	0.70	0.60	0.51	0.44	0.38	0.21

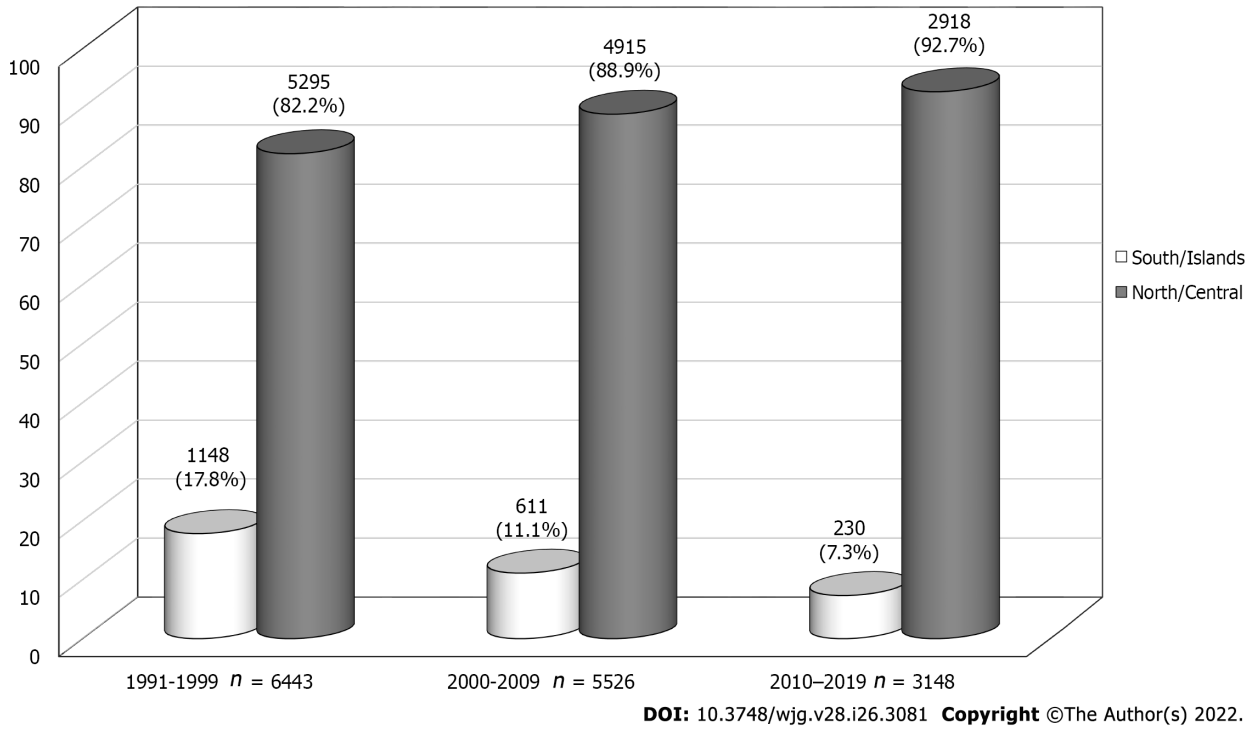
Figure 1 shows a clear trend towards an overtime reduction of the total number of cases in Italy, and moderate changes in cases distribution, increased in northern and central regions and decreased in southern and island areas[26,27].

In Italy, the uninterrupted flux of migrants over the last 20 years brought that about 9% of resident population are composed of immigrants, more frequently from eastern Europe and sub-Saharan Africa. Out of the 4981 AHB cases reported to SEIEVA from 2004 to 2019 by 10 of the 20 Italian regions, 849 (17.0%) occurred in immigrants, of whom 53.4% had come from eastern Europe, 14.6% from Asia, 21.6% from Africa, 8.9% from central/southern America, 0.1% from North America, and 0.1% from Oceania. The comparison between the AHB incidence rates among people born in Italy and foreigners, reported by the "Strong Migratory Pressure Countries", report among foreigners values up to 4 times higher until 2008, a difference progressively decreased from 2009 to 2019, when the standardized rates were 0.4 per 100000 for Italians, and 0.6 for foreigners[26,27].

In Italy, the uninterrupted flux of migrants modified the AHB molecular evolution, where, for decades, genotype D was observed in 95% of patients. Coppola *et al*[28] showed that in 123 AHB-patients, a significant increase in HBV genotypes non-D, from 11% in 1999-2003 to 41.1% in 2004-2008, associated with unsafe sexual habits. In good agreement, Ferraro *et al*[10] showed a high rate of cases with acute hepatitis B due to HBV genotypes non-D in Sicily in 2012 (44% genotype A, 3% genotype E), infected mainly through unsafe sexual intercourses.

In 2015, Zuccaro *et al*[11] reported that HBV genotypes non-D were responsible of nearly half of 103 consecutive cases of acute hepatitis B, mainly HBV genotypes A and F, associated with unsafe sexual exposure. In addition, mutations of antiviral resistance or viral mutants in the antigenic determinant "a" of HBsAg have been reported in AHB-patients[28].

Even clinical presentation and outcome of AHB have changed over time in Italy since, in abolishing the circulation of the virus in subjects aged 0-41, the universal HBV vaccination has confined acute hepatitis B to older ages when the disease is more severe[28,29].



DOI: 10.3748/wjg.v28.i26.3081 **Copyright** ©The Author(s) 2022.

Figure 1 Geographic distribution of 15117 new cases of acute hepatitis B registered in the surveillance of the integrate epidemiological system of acute viral hepatitis (SEIEVA) system from 1991 to 2019, according to the time of occurrence.

EPIDEMIOLOGICAL AND CLINICAL CHANGES OF CHB IN ITALY IN THE LAST 50 YEARS

The worldwide prevalence of subjects with chronic HBV infection is estimated at around 5%, with wide differences from a geographic area to another, 0.1%-2.0% in northern America and northwestern Europe, 1.0%-8.0% Japan and African countries overlooking the Mediterranean sea, and 8.0%-20.0% in Southeast Asia/sub-Saharan regions[16,17]. HBV genotype A prevails in northern America and northwestern Europe, HBV genotypes B and C in Asia, genotype D in southern Europe, northern Africa, India, and Middle East, HBV genotype E in western Africa, HBV genotype F in southern/central America, HBV genotype G in the USA and France, and genotype H in Mexico and some countries of South America[30]. CHB, defined as the persistence of HBsAg in serum for more than 6 mo, is a dynamic process which develops through five main phases: (1) "Immune tolerant" phase with mild/absent necroinflammation with normal/low aminotransferase levels, high HBV DNA levels, and HBeAg positivity, with no/slow evolution to fibrosis; (2) "immune reactive phase" characterized by liver necroinflammation, increased or fluctuating aminotransferase serum values, low or intermediate HBV-DNA level, HBeAg positivity, and progression to liver fibrosis or cirrhosis; (3) "inactive HBV carrier state" with low/absent necroinflammation, low/normal aminotransferase serum levels and with very low or undetectable serum HBV DNA, commonly, seroconversion to anti-HBe; (4) "HBeAg-negative CHB" characterized by mild to severe necroinflammation, fluctuating serum levels of aminotransferases and HBV-DNA, linked to e-minus HBV variant unable to express HBeAg[31]; and (5) "occult HBV infection" with HBsAg negativity and low HBV replication with detection of HBV DNA in the liver cells and also in serum (some cases) which clinical impact needs further investigation[32,33].

A complete clinical history should always be the first approach to patients with chronic hepatitis B, including family history, alcohol consumption analysis, metabolic risk assessment, and vaccinations performed. Physical examination should be complete and especially directed at identifying signs indicative of cirrhosis[1]. The laboratory tests useful to define the degree of viral replication and the stage of chronic hepatitis include the search for HBeAg/anti-HBe in serum, HBV DNA load, the blood count, the detection of aminotransferases, total bilirubin, and alkaline phosphatase serum values, and any other tests eventually necessary for the patient under examination[1].

For untreated adult patients, the 5-year cumulative incidence of developing cirrhosis varies between 8% to 20% across studies, and the risk of HCC from 2% to 5%[1]. Among the instrumental investigations, liver biopsy is needed to evaluate the degree of inflammation and fibrosis, a technique, however, sometimes burdened by serious complications, while transient elastography is considered sufficient for the evaluation of fibrosis alone; hepatic ultrasound is of great use for monitoring the clinical course of liver cirrhosis and, in particular, for the early identification of intrahepatic nodules of HCC. Better definition of HCC can be obtained with computed tomography and magnetic resonance imaging.

Drugs recommended and most frequently used to treat CHB are nucleus(t)side analogues tenofovir disoproxil fumarate or tenofovir alafenamide and entecavir, chosen in relation to their high genetic barrier, antiviral potency, and excellent profiles of resistance, tolerability, and safety[1,34]. The duration of treatment remains indefinite because these drugs suppress HBV replication but do not eradicate viral infection and reactivation of both viral replication and chronic disease occurs frequently upon treatment suspension, sometimes with a serious clinical impact[1,34].

At the end of 1970s, the HBV endemicity was considered intermediate, with a prevalence of HBsAg chronic carriers nearly 3%[35,36] and with an increasing gradient from North to South of Italy, where 5% of people were HBsAg positive[37,38]. At that time, the main routes of transmission were vertical transmission at delivery, intravenous drug use (IVDU), and living with an HBsAg chronic carrier, mainly between siblings.

As a result of the reduced HBV circulation, the percentage of HBsAg chronic carriers has decreased overtime in Italy. An impressive decline in HBsAg prevalence in children and teenagers has been observed even before the universal HBV vaccination had been introduced. As an example, the rate of HBsAg positivity decreased from 2.2% in 1980 to 0.8% in 1988 in schoolchildren aged 7-12 years in the city of Naples[39]. This decline has been confirmed in subsequent studies in pregnant women tested at the delivery[40], and in young adults at their enrolment in the army[41].

The rate of HBsAg positivity in patients with chronic hepatitis of all etiologies, either inpatients or outpatients of numerous Italian liver units, was: 61% in 1975[42], 44% in 1980, 34% in 1989[43], and 12.2% in 2001[43-45]. At present, only 0.8% of subjects born in Italy are HBsAg positive, also thanks to the universal HBV vaccination. Additional evidence of efficacy of HBV vaccination in Italy was the increase in the mean age of patients with CHB, from 30.8 years in 1980-1989[42] to 57.3 years in 2019[46].

The positive effects of HBV vaccination to reduce levels of HBV endemicity were also observed in countries with a high level of endemicity. About that, it seems interesting to evaluate the data reported by some authors from China, a nation that like Italy has achieved a remarkable socio-economic improvement in the last decades, where an extensive vaccination campaign against HBV infection has been conducted. A national cross-sectional epidemiological study performed in China in 1992 reported a 9.8% rate of HBsAg chronic carriers[47]. A reduction of this prevalence to 7.2%, due also to a series of measures implemented by the Chinese government, has been reported by Tedder *et al*[48] in 2006. A tendency to a further decline has been shown by a meta-analysis by Wang *et al*[49] who, analyzing the data published in 27 studies from January 2013 to December 2017, estimated a 6.89 HBsAg prevalence in the Chinese population, with more than 90% of HBV infected subjects aging more than 20 years[49]. The data reported by the above-mentioned studies indicate that even starting from very high level of endemicity, the correct application of general and special prophylactic measures, including a wide vaccination campaign against HBV, can yield significant results.

Italy, as mentioned above, has now a country of migration from geographical areas with high or intermediate HBV endemicity in the last two decades. Currently, nearly 9% of the 60 million of inhabitants are immigrants, of whom the major part has not received HBV vaccination and 250000 are estimated to be HBsAg chronic carriers with a 30% rate of HBeAg positivity[50]. The integration of immigrants is proceeding slowly, and it is unlikely that their continuous flow could not impair the favorable results obtained in Italy in the last five decades. El-Hamad *et al*[23] observed 3.728 migrants, mainly undocumented, 12.4% from northern Africa, 21.4% from sub-Saharan Africa, 16.8% from Asia, 44% from eastern Europe, and 5.4% from Central/South America, have come to Italy from 2006 to 2010. The mean rate of HBsAg positivity was 6%, different in the various geographic groups as well as the prevailing HBV genotype, both reflecting those of the country of origin. Coppola *et al*[13] studied 882 undocumented migrants/refugees who lived in the South Italy (period of study January 2012-June 2013), of whom 9% were HBsAg positive. This percentage was 14% in 444 individuals from sub-Saharan Africa, 6% in 198 individuals from Eastern Europe, and 2%-3% in the remaining 240 migrants from other geographic areas[13]. Zermiani *et al*[51] found a 3.5% HBsAg positive rate in migrant female sex workers. A cross-sectional Italy study[50] carried out in 3760 HBV chronic carriers from February to July 2008, reported that 37.1% (932 cases) were migrants from Far East, 35.4% from eastern Europe, 17.5% from sub-Saharan Africa, 5.5% from northern Africa, and 4.5% from other sites. HBV genotype D was detected in 40% of migrants and in 87% of subjects born in Italy. Migrants more frequently than subjects born in Italy were HBV-inactive carriers and less frequently showed CHB, cirrhosis, and HCC.

Sagnelli *et al*[52] evaluated 53 HBsAg chronic carriers with genotype E, immigrated in Southern Italy, of whom 47 (88.7%) were from sub-Saharan Africa, 4 (7.5%) from eastern Europe, and 1 (1.9%) from Asia. The molecular epidemiology study disclosed four statistically supported clusters and traced the genetic evolution and phylogenesis. In addition, phylogenetic analysis on a time scale considering the year of arrival in Italy showed that 52 immigrants had contracted genotype E infection in their country of origin before they arrived in Italy[52].

CONCLUSION

In Italy, the level of HBV endemicity has progressively decreased over the last 50 years. The main

contribution to the downward trend of AHB incidence and of the prevalence of their chronic sequelae is mainly attributable to improvement in socioeconomic and hygienic conditions, the effective educational HIV infection campaigns, and the HBV vaccination since 1991 continued without interruptions until now[43]. There was a consequent strong reduction in the impact of major risk factors for HBV infection acquisition. Vertical transmission from HBsAg positive mother to their newborn babies is just a memory, due to mandatory determination of serum HBsAg in pregnant women, and to passive and active immunization of babies born of HBsAg positive mothers. Besides, the impressive reduction in size of families, particularly in the South Italy regions and islands, has strongly impaired HBV transmission through household contacts with HBsAg-positive chronic carriers. A strong contribution to the significant reduction of HBV endemicity in Italy has been also given by the mandatory screening of blood donations for HBV markers and by the remarkable reduction or abolition of improperly sterilized instruments for medical, surgical, and cosmetic procedures. Also, the role of IVDU has progressively reduced by extension of vaccination to persons aged up to 41. Currently, sexual transmission plays the major role in HBV transmission in Italy, due to infrequent use of condom in unsafe sexual activity[53].

As a consequence of the reduced impact of risk factors for HBV infection acquisition, the prevalence of HBV chronic carriers in the general population has undergone an impressive continuous decrease and to date is 0.8%; similarly, the current AHB incidence B has been reduced to 0.21 per 100000 inhabitants, higher in males than in females, most of cases occurring in Italian citizens with unsafe sexual habits aged over 41 and in unvaccinated migrants[27]. In this regard, most immigrants who come to Italy are not vaccinated against hepatitis B and are three times more likely to acquire HBV infection than Italian citizens[13,26,52,53]. The WHO Regional Office for Europe strongly motivated the national health authorities of the host countries to set up national hepatitis B vaccination protocols for all unvaccinated migrants and instruct local health authorities how to apply them[14]. It should be also emphasized that HBsAg positive migrants should be entrusted to local healthcare facilities for further diagnostic information and clinical therapeutic follow-up.

Like for numerous other sectors of medicine, SARS-CoV2 pandemic has reduced care level also for HBV related diseases. In this period, nearly half people worldwide have not been able to enter clinical center for HBV prevention, diagnosis, and treatment due to breakdowns or other restrictions on the movement imposed by individual governments, absence, or reduction of earnings due to loss of work activities and for the subject' fear to acquire SARS-CoV-2 infection in clinical environments[54]. Furthermore, the activity of clinical structures dedicated to HBsAg positive patients has been greatly reduced, with a sharp contraction in the number of beds for hospitalization, day hospital facilities and healthcare personnel, devolved to assistance for SARS-CoV-2 patients. In Italy, recent web-based survey performed by the Italian Association for the Study of the Liver (AISF) registered that a quarter of hepatology centers have been transformed into divisions for the management of COVID-19 patients and also a quarter of other health services for liver outpatients have been suspended[15]. A continuous clinical/therapeutic follow up has been provided only to 32.5% of patients with decompensated cirrhosis and to 18% of those with HCC; in addition, 23% of CHB patients treated with nuclo(t)side analogues have undergone temporary interruptions of therapy[15]. In this regard international guidelines give clear indications on how to apply therapy with entecavir or tenofovir for an effective long-term suppression of viral replication in CHB patients: Start therapy at first diagnosis, and then continue without interruption to avoid serious and sometimes life-threatening virus reactivations[55,56].

The percentage of subjects vaccinated against COVID-19 in developing countries is decidedly low. In addition, many children have not yet been vaccinated and a minority of adults has refused vaccination in countries with a high socioeconomic level. All this has favored the development of viral variants more and more infectious that is leading the pandemic to its fifth wave. Nevertheless, by reducing SARS-CoV-2 circulation, COVID-19 vaccination is exerting a favorable effect on CHB management, whose consistency, however, is not yet fully assessable because liver units and transplant centers are still suffering severe limitations. Furthermore, most of the damages produced by COVID-19 to patients with liver diseases will come both from the delays in screening, diagnosis and start of treatment and from the interruptions of clinical activities for outpatients, damages not yet calculable. However, the consequences of the first 3 waves of the COVID-19 pandemic have been analysed by Tapper *et al*[57] who reported that all screening procedures were significantly delayed and that this has resulted in a substantial increase in early diagnoses in the advanced stages of liver diseases or at the onset of complications. Analysing the events following the pandemic waves, these Authors identified three phases: The first one taking place in lockdown and other social distances, characterized by high priority for the needs of COVID-19 patients and a strong delay for elective and routine activities regarding other pathologies; the second one following abolition of physical distancing, with a rapid increase in morbidity and decompensation of non-COVID-19 diseases and by a crowding of health facilities forced to solve old and new problems; a long third stage heavily burdened by consequences of delays in diagnosis and start of treatment and by the interruptions of clinical-therapeutic follow-up[57]. More tuned with the problems of HBsAg positive subjects, Mandel *et al*[58] analysed the effect of three waves of COVID-19 pandemic on HBV testing volume in Ontario, a state of Canada with a high socioeconomic level. Test volume for HBV DNA decreased by 37% during the first pandemic wave, by 27% in second one and by 20% in the third one, reflecting reduction in HBsAg testing, 33%, 18% and 15%, respectively. These reductions are most likely due to both an adaptation of citizens to subsequent pandemic waves,

and a favorable effect of an overtime increase in COVID-19 vaccination coverage.

In numerous developing countries, the COVID-19 pandemic is also severely damaging the programs of the HBV-vaccination, as demonstrated by an analysis by the Institute for Health Metrics and Evaluation which showed in 2020 a dropped of vaccination activity to 1990s levels[59].

In clinical practice, telemedicine was increased over the past 20 years[60], with a sharp increase in 2020 and 2021 due to social distancing measures mandatory to curb COVID-19. Consent to the use of telemedicine was expressed by American Association for the Study of Liver Diseases and EASL-ESCMID experts who recommended it in COVID-19 emergency for the care of chronic hepatitis patients, those on waiting for liver transplantation, and those already transplanted[61,62]. On the strength of the experiences gained in waves of COVID-19, telemedicine can usefully be introduced in programs of prevention and screening, diagnosis, clinical, and therapeutic follow-up of HBV patients, with particular advantage for those living in rural areas and for those who have serious trouble getting to a liver unit.

The COVID-19 has caused quickly significant damage to hepatitis B setting that has lost some of the beneficial impact of several scientific research on clinical practice and on technological application, and huge economic investments. Local health authorities should monitor the damages inflicted to HBV patients by COVID-19 pandemic and work to reduce and, when possible, abolish them. Also, a greater spread of telemedicine could reduce the impact of COVID-19 pandemic.

To prevent onset of new SARS-CoV-2 variants highly infectious, nations with high economic levels should contribute to increase the coverage of COVID-19 vaccination in low- or moderate-income nations; the development of new low-cost vaccines suitable for countries with limited health resources will be of help in solving this problem. As far HBV infection, the HBV-universal vaccination must continue worldwide without interruption and health authorities should extend their HBV vaccination protocols to all unvaccinated migrants.

FOOTNOTES

Author contributions: Sagnelli C, Sica A, and Creta M contributed to conceptualization, methodology, validation, formal analysis, investigation, data curation, and original draft preparation; Calogero A and Ciccozzi M contributed to validation and data curation; Sagnelli E contributed to manuscript writing, review, and editing, visualization, and supervision; all authors have read and agreed to the published version of the manuscript.

Conflict-of-interest statement: There are no conflicts of interest to report.

Open-Access: This article is an open-access article that was selected by an in-house editor and fully peer-reviewed by external reviewers. It is distributed in accordance with the Creative Commons Attribution NonCommercial (CC BY-NC 4.0) license, which permits others to distribute, remix, adapt, build upon this work non-commercially, and license their derivative works on different terms, provided the original work is properly cited and the use is non-commercial. See: https://creativecommons.org/Licenses/by-nc/4.0/

Country/Territory of origin: Italy

ORCID number: Caterina Sagnelli 0000-0002-6413-7810; Antonello Sica 0000-0002-8676-4620; Massimiliano Creta 0000-0003-2082-3330; Armando Calogero 0000-0003-2315-0610; Massimo Ciccozzi 0000-0003-3866-9239; Evangelista Sagnelli 0000-0003-2817-8436.

S-Editor: Chen YL
L-Editor: Wang TQ
P-Editor: Chen YL

REFERENCES

1 **Terrault NA**, Bzowej NH, Chang KM, Hwang JP, Jonas MM, Murad MH; American Association for the Study of Liver Diseases. AASLD guidelines for treatment of chronic hepatitis B. *Hepatology* 2016; **63**: 261-283 [PMID: 26566064 DOI: 10.1002/hep.28156]

2 **Goldstein ST**, Zhou F, Hadler SC, Bell BP, Mast EE, Margolis HS. A mathematical model to estimate global hepatitis B disease burden and vaccination impact. *Int J Epidemiol* 2005; **34**: 1329-1339 [PMID: 16249217 DOI: 10.1093/ije/dyi206]

3 **Huzair F**, Sturdy S. Biotechnology and the transformation of vaccine innovation: The case of the hepatitis B vaccines 1968-2000. *Stud Hist Philos Biol Biomed Sci* 2017; **64**: 11-21 [PMID: 28511068 DOI: 10.1016/j.shpsc.2017.05.004]

4 **Thomas DL**. Global Elimination of Chronic Hepatitis. *N Engl J Med* 2019; **380**: 2041-2050 [PMID: 31116920 DOI: 10.1056/NEJMra1810477]

5 **Global Burden of Disease Study 2013 Collaborators**. Global, regional, and national incidence, prevalence, and years lived with disability for 301 acute and chronic diseases and injuries in 188 countries, 1990-2013: a systematic analysis for the Global Burden of Disease Study 2013. *Lancet* 2015; **386**: 743-800 [PMID: 26063472 DOI:

10.1016/S0140-6736(15)60692-4]
6 **World Health Organization (WHO)**. Hepatitis B; WHO fact sheet. July 27, 2021. [cited 10 January 2022]. Available from: https://www.who.int/news-room/fact-sheets/detail/hepatitis-b
7 **Chen DS**. Toward elimination and eradication of hepatitis B. *J Gastroenterol Hepatol* 2010; **25**: 19-25 [PMID: 20136972 DOI: 10.1111/j.1440-1746.2009.06165.x]
8 **Crovari P**. Epidemiology of viral hepatitis B in Italy. *Vaccine* 1995; **13** Suppl 1: S26-S30 [PMID: 7571823 DOI: 10.1016/0264-410x(95)80043-d]
9 **Sagnelli E**, Sagnelli C, Pisaturo M, Macera M, Coppola N. Epidemiology of acute and chronic hepatitis B and delta over the last 5 decades in Italy. *World J Gastroenterol* 2014; **20**: 7635-7643 [PMID: 24976701 DOI: 10.3748/wjg.v20.i24.7635]
10 **Ferraro D**, Urone N, Pizzillo P, Gussio M, Magliocco S, Cacopardo B, Craxì A, Di Marco V, Di Stefano R. Phylogenetic analysis of isolates from new cases of HBV infection in Southern Italy. *Infect Genet Evol* 2012; **12**: 1591-1596 [PMID: 22824417 DOI: 10.1016/j.meegid.2012.07.006]
11 **Zuccaro O**, Romanò L, Mele A, Mariano A, Clementi M, Tosti ME, Taliani G, Galli C, Zanetti AR, Spada E; Study Group. Clinical, epidemiological and virological features of acute hepatitis B in Italy. *Infection* 2015; **43**: 431-441 [PMID: 25697541 DOI: 10.1007/s15010-015-0747-0]
12 **Romanò L**, Paladini S, Zanetti AR. Twenty years of universal vaccination against hepatitis B in Italy: achievements and challenges. *J Public Health Res* 2012; **1**: 126-129 [PMID: 25170454 DOI: 10.4081/jphr.2012.e18]
13 **Coppola N**, Alessio L, Gualdieri L, Pisaturo M, Sagnelli C, Caprio N, Maffei R, Starace M, Angelillo IF, Pasquale G, Sagnelli E. Hepatitis B virus, hepatitis C virus and human immunodeficiency virus infection in undocumented migrants and refugees in southern Italy, January 2012 to June 2013. *Euro Surveill* 2015; **20**: 30009 [PMID: 26530499 DOI: 10.2807/1560-7917.ES.2015.20.35.30009]
14 **World Health Organization Regional Office for Europe (WHO-EURO)**. Health of Refugees and Migrants Regional Situation Analysis, Practices, Experiences, Lessons Learned and Ways Forward, WHO European Region. 2018. [cited 10 January 2022]. Available from: https://www.euro.who.int/en/publications/abstracts/report-on-the-health-of-refugees-and-migrants-in-the-who european-region-no-public- health-without-refugee-and-migrant
15 **Aghemo A**, Masarone M, Montagnese S, Petta S, Ponziani FR, Russo FP; Associazione Italiana Studio Fegato (AISF). Assessing the impact of COVID-19 on the management of patients with liver diseases: A national survey by the Italian association for the study of the Liver. *Dig Liver Dis* 2020; **52**: 937-941 [PMID: 32703730 DOI: 10.1016/j.dld.2020.07.008]
16 **Lavanchy D**. Worldwide epidemiology of HBV infection, disease burden, and vaccine prevention. *J Clin Virol* 2005; **34** Suppl 1: S1-S3 [PMID: 16461208 DOI: 10.1016/S1386-6532(05)00384-7]
17 **Liaw YF**, Chu CM. Hepatitis B virus infection. *Lancet* 2009; **373**: 582-592 [PMID: 19217993 DOI: 10.1016/S0140-6736(09)60207-5]
18 **McMahon BJ**, Alward WL, Hall DB, Heyward WL, Bender TR, Francis DP, Maynard JE. Acute hepatitis B virus infection: relation of age to the clinical expression of disease and subsequent development of the carrier state. *J Infect Dis* 1985; **151**: 599-603 [PMID: 3973412 DOI: 10.1093/infdis/151.4.599]
19 **Coppola N**, Sagnelli C, Pisaturo M, Minichini C, Messina V, Alessio L, Starace M, Signoriello G, Gentile I, Filippini P, Sagnelli E. Clinical and virological characteristics associated with severe acute hepatitis B. *Clin Microbiol Infect* 2014; **20**: O991-O997 [PMID: 24930916 DOI: 10.1111/1469-0691.12720]
20 **Mantzoukis K**, Rodríguez-Perálvarez M, Buzzetti E, Thorburn D, Davidson BR, Tsochatzis E, Gurusamy KS. Pharmacological interventions for acute hepatitis B infection: an attempted network meta-analysis. *Cochrane Database Syst Rev* 2017; **3**: CD011645 [PMID: 28321877 DOI: 10.1002/14651858.CD011645.pub2]
21 **Stroffolini T**. The changing pattern of hepatitis B virus infection over the past three decades in Italy. *Dig Liver Dis* 2005; **37**: 622-627 [PMID: 15996630 DOI: 10.1016/j.dld.2005.02.010]
22 **Romanò L**, Paladini S, Tagliacarne C, Zappa A, Zanetti AR. The changing face of the epidemiology of type A, B, and D viral hepatitis in Italy, following the implementation of vaccination. *Vaccine* 2009; **27**: 3439-3442 [PMID: 19200848 DOI: 10.1016/j.vaccine.2009.01.056]
23 **El-Hamad I**, Pezzoli MC, Chiari E, Scarcella C, Vassallo F, Puoti M, Ciccaglione A, Ciccozzi M, Scalzini A, Castelli F; ad-hoc Working Group for Hepatitis B in migrants. Point-of-care screening, prevalence, and risk factors for hepatitis B infection among 3,728 mainly undocumented migrants from non-EU countries in northern Italy. *J Travel Med* 2015; **22**: 78-86 [PMID: 25424439 DOI: 10.1111/jtm.12176]
24 **Lai A**, Sagnelli C, Presti AL, Cella E, Angeletti S, Spoto S, Costantino S, Sagnelli E, Ciccozzi M. What is changed in HBV molecular epidemiology in Italy? *J Med Virol* 2018; **90**: 786-795 [PMID: 29315661 DOI: 10.1002/jmv.25027]
25 **Sagnelli C**, Ciccozzi M, Alessio L, Cella E, Gualdieri L, Pisaturo M, Minichini C, Di Caprio G, Starace M, Onorato L, Capoprese M, Occhiello L, Angeletti S, Scotto G, Macera M, Sagnelli E, Coppola N. HBV molecular epidemiology and clinical condition of immigrants living in Italy. *Infection* 2018; **46**: 523-531 [PMID: 29796738 DOI: 10.1007/s15010-018-1153-1]
26 **L'epidemiologia per la sanità pubblica**, Istituto Superiore di Sanità. Sistema epidemiologico integrato dell'epatite virale acuta (SEIEVA). December 22, 2017. Available from: https://www.epicentro.iss.it/epatite/dati-seieva
27 **Stroffolini T**, Morisco F, Ferrigno L, Pontillo G, Iantosca G, Cossiga V, Crateri S, Tosti ME; The Seieva Collaborating Group. Effectiveness of Hepatitis B Vaccination Campaign in Italy: Towards the Control of HBV Infection for the First Time in a European Country. *Viruses* 2022; **14** [PMID: 35215839 DOI: 10.3390/v14020245]
28 **Coppola N**, Tonziello G, Colombatto P, Pisaturo M, Messina V, Moriconi F, Alessio L, Sagnelli C, Cavallone D, Brunetto M, Sagnelli E. Lamivudine-resistant HBV strain rtM204V/I in acute hepatitis B. *J Infect* 2013; **67**: 322-328 [PMID: 23796869 DOI: 10.1016/j.jinf.2013.06.006]
29 **Zanetti AR**, Mariano A, Romanò L, D'Amelio R, Chironna M, Coppola RC, Cuccia M, Mangione R, Marrone F, Negrone FS, Parlato A, Zamparo E, Zotti C, Stroffolini T, Mele A; Study Group. Long-term immunogenicity of hepatitis B vaccination and policy for booster: an Italian multicentre study. *Lancet* 2005; **366**: 1379-1384 [PMID: 16226616 DOI: 10.1016/S0140-6736(05)67568-X]
30 **Kao JH**. Role of viral factors in the natural course and therapy of chronic hepatitis B. *Hepatol Int* 2007; **1**: 415-430 [PMID:

19669337 DOI: 10.1007/s12072-007-9033-2]
31 **Lok AS**, McMahon BJ. Chronic hepatitis B. *Hepatology* 2007; **45**: 507-539 [PMID: 17256718 DOI: 10.1002/hep.21513]
32 **Raimondo G**, Allain JP, Brunetto MR, Buendia MA, Chen DS, Colombo M, Craxì A, Donato F, Ferrari C, Gaeta GB, Gerlich WH, Levrero M, Locarnini S, Michalak T, Mondelli MU, Pawlotsky JM, Pollicino T, Prati D, Puoti M, Samuel D, Shouval D, Smedile A, Squadrito G, Trépo C, Villa E, Will H, Zanetti AR, Zoulim F. Statements from the Taormina expert meeting on occult hepatitis B virus infection. *J Hepatol* 2008; **49**: 652-657 [PMID: 18715666 DOI: 10.1016/j.jhep.2008.07.014]
33 **Coppola N**, Gentile I, Pasquale G, Buonomo AR, Capoluongo N, D'Armiento M, Borgia G, Sagnelli E. Anti-HBc positivity was associated with histological cirrhosis in patients with chronic hepatitis C. *Ann Hepatol* 2013; **13**: 20-26 [PMID: 24378262 DOI: 10.1016/S1665-2681(19)30900-7]
34 **Ghany MG**. Current treatment guidelines of chronic hepatitis B: The role of nucleos(t)ide analogues and peginterferon. *Best Pract Res Clin Gastroenterol* 2017; **31**: 299-309 [PMID: 28774412 DOI: 10.1016/j.bpg.2017.04.012]
35 **Dardanoni L**, Mele A, Polizzi MC. Epidemiology of hepatitis B in Italy. *Ann Ist Super Sanita* 1987; **24**: 235-243 [PMID: 3453605]
36 **Stroffolini T**. Epidemiologia dell'epatite B in Italia. In: La vaccinazione contro l'Epatite da virus B: una scelta prioritaria di politica sanitaria ed economica. Milan: Franco Angelini, 1990: 17-28
37 **Giusti G**, Galanti B, Gaeta GB, Piccinino F, Ruggiero G. HBsAg carriers among blood donors in Italy; a retrospective survey of data from 189 blood banks. *Hepatogastroenterology* 1981; **28**: 96-98 [PMID: 7216155]
38 **Pasquini P**, Kahn HA, Pileggi D, Panà A, Terzi J, Guzzanti E. Prevalence of hepatitis B markers in Italy. *Am J Epidemiol* 1983; **118**: 699-709 [PMID: 6637996 DOI: 10.1093/oxfordjournals.aje.a113680]
39 **D'Argenio P**, Esposito D, Mele A, Ortolani G, Adamo B, Rapicetta M, Forte P, Pisani A, Soldo L, Sarrecchia B. Decline in the exposure to hepatitis A and B infections in children in Naples, Italy. *Public Health* 1989; **103**: 385-389 [PMID: 2798751 DOI: 10.1016/s0033-3506(89)80009-5]
40 **Stroffolini T**, Bianco E, Szklo A, Bernacchia R, Bove C, Colucci M, Cristina Coppola R, D'Argenio P, Lopalco P, Parlato A, Ragni P, Simonetti A, Zotti C, Mele A. Factors affecting the compliance of the antenatal hepatitis B screening programme in Italy. *Vaccine* 2003; **21**: 1246-1249 [PMID: 12559805 DOI: 10.1016/S0264-410X(02)00439-5]
41 **D'Amelio R**, Stroffolini T, Nisini R, Matricardi PM, Rapicetta M, Spada E, Napoli A, Pasquini P. Incidence of hepatitis B virus infection among an Italian military population: evidence of low infection spread. *Eur J Epidemiol* 1994; **10**: 105-107 [PMID: 7957780 DOI: 10.1007/BF01717462]
42 **Giusti G**, Sagnelli E, Gallo C, Piccinino F, Galanti B, Gaeta GB. The etiology of chronic hepatitis in Italy: a multicenter study. *Hepatogastroenterology* 1994; **41**: 397-400 [PMID: 7959581]
43 **Stroffolini T**, Sagnelli E, Mele A, Craxì A, Almasio P; Italian Hospitals Collaborating Group. The aetiology of chronic hepatitis in Italy: results from a multicentre national study. *Dig Liver Dis* 2004; **36**: 829-833 [PMID: 15646431 DOI: 10.1016/j.dld.2004.07.013]
44 **Sagnelli E**, Pasquale G, Coppola N, Marrocco C, Scarano F, Imparato M, Sagnelli C, Scolastico C, Piccinino F. Liver histology in patients with HBsAg negative anti-HBc and anti-HCV positive chronic hepatitis. *J Med Virol* 2005; **75**: 222-226 [PMID: 15602732 DOI: 10.1002/jmv.20260]
45 **Sagnelli E**, Stroffolini T, Mele A, Imparato M, Sagnelli C, Coppola N, Almasio PL. Impact of comorbidities on the severity of chronic hepatitis B at presentation. *World J Gastroenterol* 2012; **18**: 1616-1621 [PMID: 22529690 DOI: 10.3748/wjg.v18.i14.1616]
46 **Stroffolini T**, Ciancio A, Furlan C, Vinci M, Niro GA, Russello M, Colloredo G, Morisco F, Coppola N, Babudieri S, Ferrigno L, Sagnelli C, Sagnelli E; Collaborating group. Chronic hepatitis B virus infection in Italy during the twenty-first century: an updated survey in 2019. *Eur J Clin Microbiol Infect Dis* 2021; **40**: 607-614 [PMID: 33029767 DOI: 10.1007/s10096-020-04065-6]
47 **Xia GL**, Liu CB, Cao HL, Bi SL, Zhan MY, Su CA, Nanc JH, Qic XQ. Prevalence of hepatitis B and C virus infections in the general Chinese population. Results from a nationwide cross-sectional seroepidemiologic study of hepatitis A, B, C, D, and E virus infections in China, 1992. *Int Hepatol Comm* 1996; **5**: 62-73 [DOI: 10.1016/S0928-4346(96)82012-3]
48 **Tedder RS**, Rodger AJ, Fries L, Ijaz S, Thursz M, Rosenberg W, Naoumov N, Banatvala J, Williams R, Dusheiko G, Chokshi S, Wong T, Rosenberg G, Moreea S, Bassendine M, Jacobs M, Mills PR, Mutimer D, Ryder SD, Bathgate A, Hussaini H, Dillon JF, Wright M, Bird G, Collier J, Anderson M, Johnson AM; Collaborative UK Study of Chronic Hepatitis B Infection (CUSHI-B) Study Group. The diversity and management of chronic hepatitis B virus infections in the United Kingdom: a wake-up call. *Clin Infect Dis* 2013; **56**: 951-960 [PMID: 23223601 DOI: 10.1093/cid/cis1013]
49 **Wang H**, Men P, Xiao Y, Gao P, Lv M, Yuan Q, Chen W, Bai S, Wu J. Hepatitis B infection in the general population of China: a systematic review and meta-analysis. *BMC Infect Dis* 2019; **19**: 811 [PMID: 31533643 DOI: 10.1186/s12879-019-4428-y]
50 **Fasano M**, Saracino A, Carosi G, Mazzotta F, Marino N, Sagnelli E, Gaeta GB, Angarano G, Verucchi G, Bellissima P, Angeletti C, Santantonio T. Hepatitis B and immigrants: a SIMIT multicenter cross-sectional study. *Infection* 2013; **41**: 53-59 [PMID: 23264094 DOI: 10.1007/s15010-012-0384-9].]
51 **Zermiani M**, Mengoli C, Rimondo C, Galvan U, Cruciani M, Serpelloni G. Prevalence of sexually transmitted diseases and hepatitis C in a survey of female sex workers in the north-East of Italy. *Open AIDS J* 2012; **6**: 60-64 [PMID: 22833775 DOI: 10.2174/1874613601206010060]
52 **Sagnelli C**, Ciccozzi M, Coppola N, Minichini C, Lo Presti A, Starace M, Alessio L, Macera M, Cella E, Gualdieri L, Caprio N, Pasquale G, Sagnelli E. Molecular diversity in irregular or refugee immigrant patients with HBV-genotype-E infection living in the metropolitan area of Naples. *J Med Virol* 2017; **89**: 1015-1024 [PMID: 27805272 DOI: 10.1002/jmv.24724]
53 **Mele A**, Catapano R, Ferrigno L, Marzolini A, Stazi MA, Martelli A, Pasquini P. Sistema Epidemiologico Integrato dell'epatite Virale Acuta. Rapporto. annuale 1991. Roma: Rapporti Istituto Superiore di sanità, 1993: 16
54 **Wingrove C**, Ferrier L, James C, Wang S. The impact of COVID-19 on hepatitis elimination. *Lancet Gastroenterol Hepatol* 2020; **5**: 792-794 [PMID: 32730783 DOI: 10.1016/S2468-1253(20)30238-7]

55 **Reddy KR**. SARS-CoV-2 and the Liver: Considerations in Hepatitis B and Hepatitis C Infections. *Clin Liver Dis (Hoboken)* 2020; **15**: 191-194 [PMID: 32489654 DOI: 10.1002/cld.970]

56 **Terrault NA**, Lok ASF, McMahon BJ, Chang KM, Hwang JP, Jonas MM, Brown RS Jr, Bzowej NH, Wong JB. Update on prevention, diagnosis, and treatment of chronic hepatitis B: AASLD 2018 hepatitis B guidance. *Hepatology* 2018; **67**: 1560-1599 [PMID: 29405329 DOI: 10.1002/hep.29800]

57 **Tapper EB**, Asrani SK. The COVID-19 pandemic will have a long-lasting impact on the quality of cirrhosis care. *J Hepatol* 2020; **73**: 441-445 [PMID: 32298769 DOI: 10.1016/j.jhep.2020.04.005]

58 **Mandel E**, Peci A, Cronin K, Capraru CI, Shah H, Janssen HLA, Tran V, Biondi MJ, Feld JJ. The impact of the first, second and third waves of covid-19 on hepatitis B and C testing in Ontario, Canada. *J Viral Hepat* 2022; **29**: 205-208 [PMID: 34820967 DOI: 10.1111/jvh.13637]

59 **Gates B**, Gates M. Covid-19 a global perspective 2020 golakeepers report. 2020. [cited 10 January 2022]. Available from: https://www.gatesfoundation.org/goalkeepers/downloads/2020-report/report_a4_en.pdf

60 **Kahn EN**, La Marca F, Mazzola CA. Neurosurgery and Telemedicine in the United States: Assessment of the Risks and Opportunities. *World Neurosurg* 2016; **89**: 133-138 [PMID: 26852710 DOI: 10.1016/j.wneu.2016.01.075]

61 **Fix OK**, Hameed B, Fontana RJ, Kwok RM, McGuire BM, Mulligan DC, Pratt DS, Russo MW, Schilsky ML, Verna EC, Loomba R, Cohen DE, Bezerra JA, Reddy KR, Chung RT. Clinical Best Practice Advice for Hepatology and Liver Transplant Providers During the COVID-19 Pandemic: AASLD Expert Panel Consensus Statement. *Hepatology* 2020; **72**: 287-304 [PMID: 32298473 DOI: 10.1002/hep.31281]

62 **Boettler T**, Newsome PN, Mondelli MU, Maticic M, Cordero E, Cornberg M, Berg T. Care of patients with liver disease during the COVID-19 pandemic: EASL-ESCMID position paper. *JHEP Rep* 2020; **2**: 100113 [PMID: 32289115 DOI: 10.1016/j.jhepr.2020.100113]

World Journal of Gastroenterology

Submit a Manuscript: https://www.f6publishing.com

World J Gastroenterol 2022 July 14; 28(26): 3092-3100

DOI: 10.3748/wjg.v28.i26.3092

ISSN 1007-9327 (print) ISSN 2219-2840 (online)

MINIREVIEWS

Shared decision-making in the management of patients with inflammatory bowel disease

Kai Song, Dong Wu

Specialty type: Gastroenterology and hepatology

Provenance and peer review: Invited article; Externally peer reviewed.

Peer-review model: Single blind

Peer-review report's scientific quality classification

Grade A (Excellent): A
Grade B (Very good): 0
Grade C (Good): C
Grade D (Fair): 0
Grade E (Poor): 0

P-Reviewer: Kaur M, United States; Razzaque MS, United States

Received: January 16, 2022
Peer-review started: January 16, 2022
First decision: April 11, 2022
Revised: April 21, 2022
Accepted: June 19, 2022
Article in press: June 19, 2022
Published online: July 14, 2022

Kai Song, Dong Wu, Department of Gastroenterology, State Key Laboratory of Complex Severe and Rare Diseases, Peking Union Medical College Hospital, Chinese Academy of Medical Sciences, Peking Union Medical College, Beijing 100730, China

Corresponding author: Dong Wu, MD, Professor, Department of Gastroenterology, State Key Laboratory of Complex Severe and Rare Diseases, Peking Union Medical College Hospital, Chinese Academy of Medical Sciences, Peking Union Medical College, No. 1 Shuaifuyuan, Dongcheng District, Beijing 100730, China. wudong@pumch.cn

Abstract

The rapid progress of research into inflammatory bowel disease (IBD) has resulted in increasingly more treatment options. Different options have different advantages and disadvantages, and the preferences of patients may also differ. If patients can be invited to the formulation of medical decision-making, their compliance and satisfaction would be improved, thus possibly achieving better therapeutic results. The present review aims to summarize the current literature on shared decision-making (SDM) in the management of IBD, with the goal of promoting the application of SDM.

Key Words: Inflammatory bowel diseases; Decision making; Shared; Therapeutics

©The Author(s) 2022. Published by Baishideng Publishing Group Inc. All rights reserved.

Core Tip: It is often challenging to make therapeutic decisions for patients with inflammatory bowel disease (IBD), given the uncertainty of therapeutic options and diverse patient values. Shared decision-making (SDM) is a process to formulate treatment with patients, trying to clarify and take account of the preferences of patients, increasing their compliance and satisfaction. We summarize current evidence and illustrate the necessity of applying SDM in IBD management.

Citation: Song K, Wu D. Shared decision-making in the management of patients with inflammatory bowel disease. *World J Gastroenterol* 2022; 28(26): 3092-3100
URL: https://www.wjgnet.com/1007-9327/full/v28/i26/3092.htm
DOI: https://dx.doi.org/10.3748/wjg.v28.i26.3092

INTRODUCTION

Inflammatory bowel disease (IBD) refers to a group of chronic inflammatory diseases of the gastrointestinal tract, mainly including Crohn's disease (CD) and ulcerative colitis (UC), which are lifelong diseases that tend to affect individuals aged 20–40 years[1,2]. IBD affects nearly all aspects of living, including patients' private, occupational and social lives. In total, 50%–80% of UC patients and about 67% of CD patients suffer from relapses and remissions, which is a clinical feature of IBD. Around 15%–30% of UC patients fail to achieve sustained remission, while only 13% of CD patients have a relapse-free course[3,4]. Therefore, IBD has a large socioeconomic burden, and direct and indirect costs caused by UC reach 0.81–1.49 billion dollars per year in the United States[5].

Previous research on the mechanism of IBD suggests that genetic susceptibility, intestinal microbiota, environmental factors (such as diet and stress), and the association between proinflammatory and anti-inflammatory cells and factors are involved in the occurrence and development of IBD[6,7]. An increasing number of therapeutic agents have been investigated, including the tumor necrosis factor (TNF)-α antagonist infliximab, and the effectiveness of these agents has been confirmed[8]. Although the large number of treatment options available for IBD is a positive aspect, it complicates the choice of optimal treatment for individual patients.

TRADITIONAL THERAPEUTIC STRATEGIES

The primary therapeutic aim for IBD is to induce and maintain remission[9], of which mucosal healing is the most important target[10]. Besides clinical remission, the most important objective is to achieve mucosal healing under endoscopy[1,2,9,11], which is associated with reduction in recurrence, surgical interventions, intestinal damage and steroid dependence[12,13]. The current treatment regimens for UC and CD are stratified according to severity. A step-up strategy is usually used to treat mild-to-moderate IBD[1,2,14]. For example, mild-to-moderate UC would be first subjected to 5-aminosalicylic acid (5-ASA). When efficacy is unsatisfactory, treatments are escalated to glucocorticoid and/or immunosuppressants, while biologicals are usually used as the final resort. By contrast, for severe IBD or steroid-refractory IBD, immunosuppressants or biologicals may be considered in the earlier stage.

Although the majority of patients with mild-to-moderate UC who receive 5-ASA achieved symptomatic relief within 8 wk, 41% of patients who achieve induced remission eventually experience relapse[15,16]. Thus, daily medication over a longer period of time is necessary to maintain remission. In addition, multiple daily doses of 5-ASA are required in the stage of induced remission, which may impair compliance, particularly for outpatients without regular medication reminders. Additionally, when 5-ASA administration is reduced to once daily during the induction or maintenance of remission stage[16,17], patient compliance may drop to 40%[18]. Poor compliance is a key obstacle for the induction and maintenance of remission[19].

Glucocorticoids constitute an important treatment for the induction of remission in active disease, particularly in CD. However, about 16% of CD patients do not respond to glucocorticoids after treatment for 30 d[20]. In addition, glucocorticoid therapy is often accompanied by a variety of side effects, including diabetes, hypertension, opportunistic infections, and osteoporosis[21,22]. More than 28% of patients with CD develop steroid dependence[20]. Glucocorticoids are not effective in maintaining remission, and the risks associated with long-term use are marked; thus, the dose of glucocorticoids needs to be tapered at the onset of clinical remission[9,16]. When mucosal remission is not achieved, complications such as fistula and stenosis can easily occur[23,24].

Contrary to traditional step-up therapy, the TOP-DOWN trial[25] confirmed that early combination of immunosuppressants led to a higher remission rate than standard step-up therapy in patients without steroids. Evidence has confirmed that the early use of biologicals may benefit certain patients with mild-to-moderate IBD[26]. The CHARM[27], SONIC[24], PRECISE 2[28] and GEMINI 2[29] trials demonstrated the advantages of early biological treatment over step-up therapy in patients with CD, involving anti-TNFα (infliximab and certolizumab) and anti-integrins (vedolizumab). Without sufficient evidence in patients with UC, previous studies showed lower remission rates in patients who had a shorter course of the disease[30], while other studies suggested that early use of vedolizumab increased remission in patients with UC[31].

However, no consensus has formed regarding the early use of biologicals for patients with mild-to-moderate IBD. The Pharmaceutical Benefits Scheme (PBS) of Australia specifies that biologicals should be considered only when the disease remains clinically active after 6 wk of steroids and 3 mo of immunosuppressants[9]. Despite current evidence supporting early use of biologicals, particularly for patients with CD, clinical decision-making needs to involve patients when treatment is economically demanding. It would be improper for clinicians to use biologicals at an early stage solely relying on the personal opinion of the physician, as it could generate conflicts between physicians and patients.

Refractory IBD patients with severe complications (uncontrolled hemorrhage, perforation, abscesses or malignancy) are candidates for surgery[1,2]. However, a previous study showed that gastroenterologists might differ from IBD patients in the willingness to surgery. Patients were more willing than

gastroenterologists to take risks to undergo surgery, and surgeons agreed with patients in the majority of cases[32]. The differences in perceptions among physicians and surgeons have a marked impact on patients, including the timing of referral for surgery.

Due to the convenience of wide access to information, patients may have their own ideas about treatment. Ignoring patients' values or preferences may lead to patient dissatisfaction, poor compliance, and eventually reduced treatment efficacy. Therefore, it is advisable to involve patients in decision-making and to discuss patients' preference after they have been fully informed about the treatment options, which can share the risks and improve patients' compliance. This is called shared decision-making (SDM).

SDM

SDM is an approach where clinicians and patients share the best available evidence when faced with decision-making, and that patients are supported to consider options to achieve informed preferences [33]. Different from traditional diagnosis and treatment procedures, SDM requires that clinicians provide alternative choices of examinations and treatments, and describe the associated risks and benefits, while patients express their preferences and values, and both sides ultimately make decisions that are appropriate and are consistent with patients' best interests[34].

SDM consists of three key steps: (1) Clinicians inform patients of alternative decisions and provide relevant, high-quality, accessible information; (2) Clinicians consider the patients' values and preferences, particularly the most desired therapeutic targets; and (3) Physicians integrate the patients' preferences and values into the decisions to be made[34-36]. The three-talk model is practical to distribute the aforementioned three steps into three conversations, including team talk, option talk and decision talk[37,38]. In the team talk, physicians first actively promote patient participation, inform patients of the current options available for consideration, help patients realize that this is a bidirectional treatment requiring their own participation, and allow patients to think about the primary therapeutic target. In the options talk, physicians introduce each choice to the patients in detail, including the associated advantages and disadvantages, so that patients can compare each option based on their values. For example, for patients with CD, it is necessary to discuss treatment options, such as medical, surgical, and endoscopic therapy, and evidence-based information should be used to explain the remission rate, risks, and costs of each option, so as to objectively demonstrate the advantages and disadvantages of each choice to allow the patients to balance the pros and cons of each approach according to their own preferences and values. In the decision talk, physicians should elicit the patients' preferences and values; thus, the physicians need to understand what is most important to the patients, and make the appropriate decision together with the patients based on the patients' preferences and values. It should be emphasized that it is a course of patients' deliberation, from the stage of being aware of the options to that of understanding those options and having sufficient time to think about what is most important to them with the support of the physicians.

Decision aids can be used for patient education during SDM[39,40]. Decision aids are tools based on evidence-driven medical information. For example, patients can be intuitively told of the clinical remission rate of CD under infliximab monotherapy, and the approximate increased infection rate as well. These tools can be accessed online, on paper, or in video form[34,41,42], and aim to help patients to make deliberate choices among various treatment alternatives[43]. These tools can help patients to obtain relevant clinical evidence, include patients' preferences when medical decision-making dilemmas occur, allow patients to understand the possible long- and short-term results, and promote high-quality decision-making. In terms of decision aids for biological agents, Almario *et al*[44] designed the online decision aid tool IBD and me, which covers the commonly used cetuzumab, viduzumab, adalimumab, infliximab, galimumab and eutecumab; and introduces the timing and frequency of biological use, route of administration, side effects (mainly infectious and oncogenic risks), and common adverse effects of hormones and immunosuppressants. A personalized decision preference report can be obtained after finishing the questionnaire online.

SDM IN IBD

Surveys have shown that the majority of IBD patients agree to be involved in decision-making, and want to be informed about alternative treatments[45-48]. The majority of patients who participate in SDM experience improved clinical satisfaction, higher trust in doctors, and better compliance[49-51]. However, SDM is not suitable for all cases. Medical decisions include effective decisions and preference-sensitive decisions[52]. For effective decisions, it has been demonstrated that the benefits outweigh the risks, so the decisions are undoubtedly the best strategy. For example, coloproctectomy is required in UC patients with complicated colorectal cancer. However, for preference-sensitive decisions, there is no sufficient evidence to demonstrate which treatment is the best, as there may be multiple reasonable treatment options (even including follow-up observation); thus, the judgement of the benefit/risk ratio

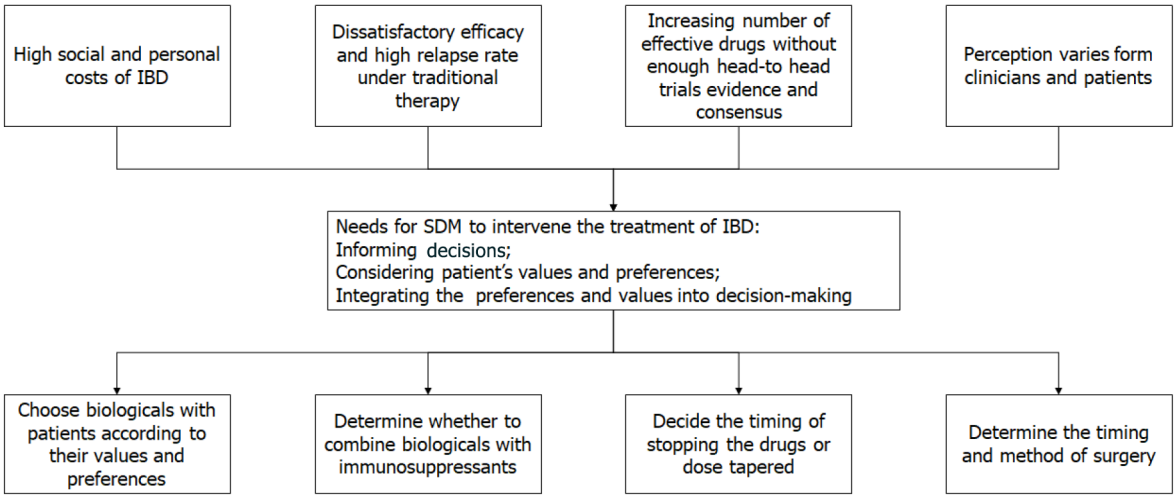
falls upon patients, such as whether the treatment target they value has been achieved, or whether the side effects they are concerned about have occurred in the past. Of the two decision types, SDM only fits in the preference-sensitive decisions, which is often present in the management of IBD. IBD is a complex disease with large individual variation, and each treatment has particular advantages and disadvantages. Therefore, SDM is suitable for the management of IBD.

In addition to the aforementioned selection of step up therapy or top-down early intervention treatment strategy, SDM can be used for choosing biologicals. A number of biologicals are currently available for the treatment of IBD, including infliximab, adalimumab, certolizumab, golimumab, natalizumab, vedolizumab and ustekinumab, with differences in the mechanism, route of administration, and side effects[53]. However, it was not until 2019 that the first head-to-head VARSITY trial[54] compared the efficacy and safety of intravenous vedolizumab to subcutaneous adalimumab. Other head-to-head trials of different biologicals are still awaited[55]. Clinicians' selection of biologicals especially for CD patients is varied, because the majority of real-world data on CD show no significant differences in clinical remission rate[56]. Under these circumstances, it is a preference-sensitive decision to choose biologicals. For example, infliximab is administered intravenously, while adalimumab is administered subcutaneously, thus the length of hospital stay varies. While infliximab is administered at intervals of 0, 2 and 6 wk to induce remission, and then administered every 8 wk, adalimumab is administered every 2 wk. In such a case, some patients may be more concerned with the frequency or route of administration due to the distance to the hospital, and therefore may choose infliximab treatment at longer intervals, whereas other patients may give priority to side effects. In a study involving 640 patients with IBD[44], factors that influenced the choice of biologicals for patients with UC were in the following order: long-term remission rate, route/frequency of administration, and risk of lymphoma. For patients with CD, these factors were short-term remission rate, risk of lymphoma, and route/frequency of administration. Of note, a small percentage of patients (3.6%) cited the mechanism of action as the primary factor for their selection of a given biological. At the same time, physicians' assumption of patients' acceptance of biologicals and their preferred route of administration differs from the patients' opinion[57]. If doctors impose on their patients what they think is universally applicable instead of incorporating the patients' preference into the decision-making process, patients may be forced to agree to a treatment plan against their own values. Patients who do not trust their doctors may develop a self-protective mechanism of rejection, thus leading to poor compliance. This awkward situation can be avoided to a large extent by involving patients in the decision-making process.

For the past 20 years, it has been discussed whether biologicals alone or in combination with immunosuppressants should be used for the treatment of IBD. The results of the SONIC study showed the advantages of the combination treatment[58]. Infliximab combined with immunosuppressants achieved higher rates of clinical remission and mucosal healing compared with infliximab or azathioprine alone in corticosteroid-free patients with CD. This may be associated with the fact that immunosuppressants reduce the generation of antidrug antibodies and increase the blood concentration of biological agents[58,59]. Although there is increasing evidence that combination treatment is superior to single-drug treatment[59-61], and the early use of infliximab with azathioprine or methotrexate for ≥ 1 year has been recommended[62], to date, not all the studies support the use of combination treatment, particularly in the case of biologicals other than infliximab[63-67]. In terms of safety, previous studies have shown that biologicals combined with immunosuppressants can increase the incidence of infection and malignancy[68-72]. Therefore, the benefit/risk ratio remains unclear regarding the combination of biological agents with immunosuppressants; thus, clinicians need to explain the benefits and risks to patients. More importantly, the preferences of the patients need to be considered to determine whether the patients would be willing to accept the risk of increased infection and tumor incidence to achieve an increase in remission rate. By involving patients in the decision-making process, the risk of increased side effects can be shared by both doctors and patients.

IBD patients have a risk of relapse after reduction or withdrawal of 5-ASA, glucocorticoids, immunosuppressants, biologicals, or combination therapy. Approximately 30% of patients with CD or UC who stop immunosuppressant monotherapy relapse within 2 years, while 50%–75% relapse within 5 years. By contrast, the risk of relapse after stopping anti-TNF therapy is 30%–40% at 1 year and > 50% at 2 years[73]. The therapeutic cost associated with the long-term use of aforementioned drugs is high, and some side effects may be related to the duration of use, such as the risk of cancer after the use of biologicals. Therefore, whether the treatment should be stopped or the dose tapered needs to be weighed with regard to the possible benefits, costs and risks, and decisions must be made individually. Given the high recurrence rate of IBD and the uncertainty about the optimal timing for clinical, biochemical and endoscopic follow-up, follow-up plans after drug withdrawal or dose reduction should also be made together with patients, taking their preferences into account[73].

As mentioned above, in addition to requiring informed consent, whether patients with IBD should undergo surgery also requires SDM. Controversies exist regarding the choice of surgery[74]. Ileal pouch–anal anastomosis (IPAA) has become the standard surgical option offered to patients with UC, with endoanal mucosal resection being the second choice. IPAA preserves the anal transition zone, which improves fecal continence. However, the elimination of colonic mucosa is the goal of surgical intervention; thus, what IPAA preserves will put the patient at risk of developing dysplasia and



DOI: 10.3748/wjg.v28.i26.3092 **Copyright** ©The Author(s) 2022.

Figure 1 The reasons and fields of application for shared decision making in inflammatory bowel disease treatments. IBD: Inflammatory bowel disease; SDM: Shared decision making.

residual disease in the remaining anal canal epithelium, while mucosectomy can decrease dysplasia risk. Therefore, doctors and patients should balance the benefits against potential relapse and malignant change in the retained mucosa.

DISCUSSION

In multiple aspects of IBD management, SDM has shown potential. We believe that SDM can and should be used in IBD therapy (Figure 1). As mentioned, the treatment of IBD is a preference-sensitive choice; the advantages and disadvantages of which need to be weighed by the patients. Clinicians need to invite patients to the decision-making process, even though not all situations are suitable for SDM. For example, when perforation occurs in a UC patient with toxic megacolon, there is no doubt about the choice of treatment, but patients still need to be aware of the need to undergo surgery. Therefore, clinicians must determine whether it is a preference-sensitive decision and whether SDM is required. If patients decline to participate in the SDM even after multiple invitations by doctors, clinicians may not have to continue spending their time on persuading patients.

SDM is a type of informed consent based on evidence-based medicine, putting forward certain requirements for doctors and patients. Challenges inevitably exist in the implementation of SDM. From the aspect of clinicians, as mentioned above, it is important to consider whether doctors are fully aware of the pros and cons of the drugs they choose as new treatments emerge and research advances rapidly. Although it can be resolved with the help of decision aids tools, the tools also should be updated continually. In addition, clinicians should have the awareness and techniques of SDM, and need to receive professional education. With the SDM skills, physicians' willingness to impart relevant knowledge to patients should be emphasized. In addition, different perceptions of IBD between physicians and surgeons may influence patients' perceptions. However, it is worth mentioning that diagnosis and treatment after discussion with a multidisciplinary team is a model that will help bridge the cognitive gap between physicians and surgeons. IBD patients' preferences and disease patterns vary [44], meaning that no SDM plan fits all patients once and for all. Doctors need to be flexible, and patients need to have unlimited access to information and they should be actively invited to the decision-making process. The implementation of SDM undoubtedly needs policy support. For example, biologicals obtained in a first-tier city may not be available in other less-developed cities, which is a restriction for SDM. Unfortunately, SDM is not adequately addressed in current medical education, leading to less awareness of what it is and how to implement it. Therefore, we can't emphasize it too much that the healthcare providers should be trained in their early stage of career to increase the benefits of implementing of SDM. And the early stage training hopefully will cultivate physicians' habit unconsciously to take advantage of SDM in the medical practice.

These challenges need to be carefully considered before SDM can be implemented. Although SDM is theoretically suitable for patients with IBD, studies comparing SDM with traditional decision-making methods remain sparse and are eagerly awaited in the future. We hope that this review will promote the use of SDM in the management of IBD.

CONCLUSION

The investigations delineated in the present article revealed the dilemma of choosing individualized treatments for patients with IBD. We also discussed the advantages of SDM and the aspects in which SDM can be used. Current evidence showed the limitations of conventional step-up therapy for IBD. However, lack of head-to-head clinical trials and diverse treatment preferences of patients lead to difficulty of individualized decision-making. We demonstrate the latest advance of SDM with the support of clinical data, hoping that SDM will be better used by physicians caring for IBD patients.

ACKNOWLEDGEMENTS

We thank Pro. Ji Li for his comment upon this article.

FOOTNOTES

Author contributions: Song K proposed the article framework and performed the majority of the writing; and Wu D settled down the outline and revised the article

Supported by Peking Union Medical College, No. 2019zlgc0503.

Conflict-of-interest statement: All authors report no relevant conflicts of interest for this article.

Open-Access: This article is an open-access article that was selected by an in-house editor and fully peer-reviewed by external reviewers. It is distributed in accordance with the Creative Commons Attribution NonCommercial (CC BY-NC 4.0) license, which permits others to distribute, remix, adapt, build upon this work non-commercially, and license their derivative works on different terms, provided the original work is properly cited and the use is non-commercial. See: https://creativecommons.org/Licenses/by-nc/4.0/

Country/Territory of origin: China

ORCID number: Kai Song 0000-0003-4459-7059; Dong Wu 0000-0001-9430-9874.

S-Editor: Ma YJ
L-Editor: A
P-Editor: Ma YJ

REFERENCES

1 **Torres J**, Mehandru S, Colombel JF, Peyrin-Biroulet L. Crohn's disease. *Lancet* 2017; **389**: 1741-1755 [PMID: 27914655 DOI: 10.1016/S0140-6736(16)31711-1]
2 **Ungaro R**, Mehandru S, Allen PB, Peyrin-Biroulet L, Colombel JF. Ulcerative colitis. *Lancet* 2017; **389**: 1756-1770 [PMID: 27914657 DOI: 10.1016/S0140-6736(16)32126-2]
3 **Holtmann MH**, Galle PR. Current concept of pathophysiological understanding and natural course of ulcerative colitis. *Langenbecks Arch Surg* 2004; **389**: 341-349 [PMID: 14760536 DOI: 10.1007/s00423-003-0448-5]
4 **Gajendran M**, Loganathan P, Catinella AP, Hashash JG. A comprehensive review and update on Crohn's disease. *Dis Mon* 2018; **64**: 20-57 [PMID: 28826742 DOI: 10.1016/j.disamonth.2017.07.001]
5 **Cohen RD**, Yu AP, Wu EQ, Xie J, Mulani PM, Chao J. Systematic review: the costs of ulcerative colitis in Western countries. *Aliment Pharmacol Ther* 2010; **31**: 693-707 [PMID: 20064142 DOI: 10.1111/j.1365-2036.2010.04234.x]
6 **Guan Q**. A Comprehensive Review and Update on the Pathogenesis of Inflammatory Bowel Disease. *J Immunol Res* 2019; **2019**: 7247238 [PMID: 31886308 DOI: 10.1155/2019/7247238]
7 **Khor B**, Gardet A, Xavier RJ. Genetics and pathogenesis of inflammatory bowel disease. *Nature* 2011; **474**: 307-317 [PMID: 21677747 DOI: 10.1038/nature10209]
8 **Ngo B**, Farrell CP, Barr M, Wolov K, Bailey R, Mullin JM, Thornton JJ. Tumor necrosis factor blockade for treatment of inflammatory bowel disease: efficacy and safety. *Curr Mol Pharmacol* 2010; **3**: 145-152 [PMID: 20799925 DOI: 10.2174/1874467211003030145]
9 **Wright EK**, Ding NS, Niewiadomski O. Management of inflammatory bowel disease. *Med J Aust* 2018; **209**: 318-323 [PMID: 30257634 DOI: 10.5694/mja17.01001]
10 **Jeong DY**, Kim S, Son MJ, Son CY, Kim JY, Kronbichler A, Lee KH, Shin JI. Induction and maintenance treatment of inflammatory bowel disease: A comprehensive review. *Autoimmun Rev* 2019; **18**: 439-454 [PMID: 30844556 DOI: 10.1016/j.autrev.2019.03.002]
11 **Siegel CA**, Whitman CB, Spiegel BMR, Feagan B, Sands B, Loftus EV Jr, Panaccione R, D'Haens G, Bernstein CN, Gearry R, Ng SC, Mantzaris GJ, Sartor B, Silverberg MS, Riddell R, Koutroubakis IE, O'Morain C, Lakatos PL, McGovern DPB, Halfvarson J, Reinisch W, Rogler G, Kruis W, Tysk C, Schreiber S, Danese S, Sandborn W, Griffiths A, Moum B,

Gasche C, Pallone F, Travis S, Panes J, Colombel JF, Hanauer S, Peyrin-Biroulet L. Development of an index to define overall disease severity in IBD. *Gut* 2018; **67**: 244-254 [PMID: 27780886 DOI: 10.1136/gutjnl-2016-312648]

12 **Shah SC**, Colombel JF, Sands BE, Narula N. Systematic review with meta-analysis: mucosal healing is associated with improved long-term outcomes in Crohn's disease. *Aliment Pharmacol Ther* 2016; **43**: 317-333 [PMID: 26607562 DOI: 10.1111/apt.13475]

13 **Shah SC**, Colombel JF, Sands BE, Narula N. Mucosal Healing Is Associated With Improved Long-term Outcomes of Patients With Ulcerative Colitis: A Systematic Review and Meta-analysis. *Clin Gastroenterol Hepatol* 2016; **14**: 1245-1255.e8 [PMID: 26829025 DOI: 10.1016/j.cgh.2016.01.015]

14 **Seyedian SS**, Nokhostin F, Malamir MD. A review of the diagnosis, prevention, and treatment methods of inflammatory bowel disease. *J Med Life* 2019; **12**: 113-122 [PMID: 31406511 DOI: 10.25122/jml-2018-0075]

15 **Feagan BG**, Macdonald JK. Oral 5-aminosalicylic acid for maintenance of remission in ulcerative colitis. *Cochrane Database Syst Rev* 2012; **10**: CD000544 [PMID: 23076890 DOI: 10.1002/14651858.CD000544.pub3]

16 **Bressler B**, Marshall JK, Bernstein CN, Bitton A, Jones J, Leontiadis GI, Panaccione R, Steinhart AH, Tse F, Feagan B; Toronto Ulcerative Colitis Consensus Group. Clinical practice guidelines for the medical management of nonhospitalized ulcerative colitis: the Toronto consensus. *Gastroenterology* 2015; **148**: 1035-1058.e3 [PMID: 25747596 DOI: 10.1053/j.gastro.2015.03.001]

17 **Feagan BG**, Macdonald JK. Oral 5-aminosalicylic acid for induction of remission in ulcerative colitis. *Cochrane Database Syst Rev* 2012; **10**: CD000543 [PMID: 23076889 DOI: 10.1002/14651858.CD000543.pub3]

18 **Kane SV**, Cohen RD, Aikens JE, Hanauer SB. Prevalence of nonadherence with maintenance mesalamine in quiescent ulcerative colitis. *Am J Gastroenterol* 2001; **96**: 2929-2933 [PMID: 11693328 DOI: 10.1111/j.1572-0241.2001.04683.x]

19 **Jackson B**, De Cruz P. Algorithms to facilitate shared decision-making for the management of mild-to-moderate ulcerative colitis. *Expert Rev Gastroenterol Hepatol* 2018; **12**: 1079-1100 [PMID: 30284911 DOI: 10.1080/17474124.2018.1530109]

20 **Faubion WA Jr**, Loftus EV Jr, Harmsen WS, Zinsmeister AR, Sandborn WJ. The natural history of corticosteroid therapy for inflammatory bowel disease: a population-based study. *Gastroenterology* 2001; **121**: 255-260 [PMID: 11487534 DOI: 10.1053/gast.2001.26279]

21 **Rezaie A**, Kuenzig ME, Benchimol EI, Griffiths AM, Otley AR, Steinhart AH, Kaplan GG, Seow CH. Budesonide for induction of remission in Crohn's disease. *Cochrane Database Syst Rev* 2015; CD000296 [PMID: 26039678 DOI: 10.1002/14651858.CD000296.pub4]

22 **Benchimol EI**, Seow CH, Steinhart AH, Griffiths AM. Traditional corticosteroids for induction of remission in Crohn's disease. *Cochrane Database Syst Rev* 2008; CD006792 [PMID: 18425970 DOI: 10.1002/14651858.CD006792.pub2]

23 **Bouguen G**, Peyrin-Biroulet L. Surgery for adult Crohn's disease: what is the actual risk? *Gut* 2011; **60**: 1178-1181 [PMID: 21610273 DOI: 10.1136/gut.2010.234617]

24 **Peyrin-Biroulet L**, Reinisch W, Colombel JF, Mantzaris GJ, Kornbluth A, Diamond R, Rutgeerts P, Tang LK, Cornillie FJ, Sandborn WJ. Clinical disease activity, C-reactive protein normalisation and mucosal healing in Crohn's disease in the SONIC trial. *Gut* 2014; **63**: 88-95 [PMID: 23974954 DOI: 10.1136/gutjnl-2013-304984]

25 **D'Haens G**, Baert F, van Assche G, Caenepeel P, Vergauwe P, Tuynman H, De Vos M, van Deventer S, Stitt L, Donner A, Vermeire S, Van De Mierop FJ, Coche JR, van der Woude J, Ochsenkühn T, van Bodegraven AA, Van Hootegem PP, Lambrecht GL, Mana F, Rutgeerts P, Feagan BG, Hommes D; Belgian Inflammatory Bowel Disease Research Group; North-Holland Gut Club. Early combined immunosuppression or conventional management in patients with newly diagnosed Crohn's disease: an open randomised trial. *Lancet* 2008; **371**: 660-667 [PMID: 18295023 DOI: 10.1016/S0140-6736(08)60304-9]

26 **Berg DR**, Colombel JF, Ungaro R. The Role of Early Biologic Therapy in Inflammatory Bowel Disease. *Inflamm Bowel Dis* 2019; **25**: 1896-1905 [PMID: 30934053 DOI: 10.1093/ibd/izz059]

27 **Schreiber S**, Reinisch W, Colombel JF, Sandborn WJ, Hommes DW, Robinson AM, Huang B, Lomax KG, Pollack PF. Subgroup analysis of the placebo-controlled CHARM trial: increased remission rates through 3 years for adalimumab-treated patients with early Crohn's disease. *J Crohns Colitis* 2013; **7**: 213-221 [PMID: 22704916 DOI: 10.1016/j.crohns.2012.05.015]

28 **Schreiber S**, Colombel JF, Bloomfield R, Nikolaus S, Schölmerich J, Panés J, Sandborn WJ; PRECiSE 2 Study Investigators. Increased response and remission rates in short-duration Crohn's disease with subcutaneous certolizumab pegol: an analysis of PRECiSE 2 randomized maintenance trial data. *Am J Gastroenterol* 2010; **105**: 1574-1582 [PMID: 20234346 DOI: 10.1038/ajg.2010.78]

29 **Sandborn WJ**, Feagan BG, Rutgeerts P, Hanauer S, Colombel JF, Sands BE, Lukas M, Fedorak RN, Lee S, Bressler B, Fox I, Rosario M, Sankoh S, Xu J, Stephens K, Milch C, Parikh A; GEMINI 2 Study Group. Vedolizumab as induction and maintenance therapy for Crohn's disease. *N Engl J Med* 2013; **369**: 711-721 [PMID: 23964933 DOI: 10.1056/NEJMoa1215739]

30 **Murthy SK**, Greenberg GR, Croitoru K, Nguyen GC, Silverberg MS, Steinhart AH. Extent of Early Clinical Response to Infliximab Predicts Long-term Treatment Success in Active Ulcerative Colitis. *Inflamm Bowel Dis* 2015; **21**: 2090-2096 [PMID: 26099066 DOI: 10.1097/MIB.0000000000000474]

31 **Feagan BG**, Rubin DT, Danese S, Vermeire S, Abhyankar B, Sankoh S, James A, Smyth M. Efficacy of Vedolizumab Induction and Maintenance Therapy in Patients With Ulcerative Colitis, Regardless of Prior Exposure to Tumor Necrosis Factor Antagonists. *Clin Gastroenterol Hepatol* 2017; **15**: 229-239.e5 [PMID: 27639327 DOI: 10.1016/j.cgh.2016.08.044]

32 **Byrne CM**, Solomon MJ, Young JM, Selby W, Harrison JD. Patient preferences between surgical and medical treatment in Crohn's disease. *Dis Colon Rectum* 2007; **50**: 586-597 [PMID: 17380368 DOI: 10.1007/s10350-006-0847-0]

33 **Elwyn G**, Laitner S, Coulter A, Walker E, Watson P, Thomson R. Implementing shared decision making in the NHS. *BMJ* 2010; **341**: c5146 [PMID: 20947577 DOI: 10.1136/bmj.c5146]

34 **Barry MJ**, Edgman-Levitan S. Shared decision making--pinnacle of patient-centered care. *N Engl J Med* 2012; **366**: 780-781 [PMID: 22375967 DOI: 10.1056/NEJMp1109283]

35 **Barratt A**. Evidence Based Medicine and Shared Decision Making: the challenge of getting both evidence and preferences into health care. *Patient Educ Couns* 2008; **73**: 407-412 [PMID: 18845414 DOI: 10.1016/j.pec.2008.07.054]

36 **Elwyn G**, Tsulukidze M, Edwards A, Légaré F, Newcombe R. Using a 'talk' model of shared decision making to propose an observation-based measure: Observer OPTION 5 Item. *Patient Educ Couns* 2013; **93**: 265-271 [PMID: 24029581 DOI: 10.1016/j.pec.2013.08.005]

37 **Elwyn G**, Frosch D, Thomson R, Joseph-Williams N, Lloyd A, Kinnersley P, Cording E, Tomson D, Dodd C, Rollnick S, Edwards A, Barry M. Shared decision making: a model for clinical practice. *J Gen Intern Med* 2012; **27**: 1361-1367 [PMID: 22618581 DOI: 10.1007/s11606-012-2077-6]

38 **Elwyn G**, Durand MA, Song J, Aarts J, Barr PJ, Berger Z, Cochran N, Frosch D, Galasiński D, Gulbrandsen P, Han PKJ, Härter M, Kinnersley P, Lloyd A, Mishra M, Perestelo-Perez L, Scholl I, Tomori K, Trevena L, Witteman HO, Van der Weijden T. A three-talk model for shared decision making: multistage consultation process. *BMJ* 2017; **359**: j4891 [PMID: 29109079 DOI: 10.1136/bmj.j4891]

39 **Stacey D**, Légaré F, Lewis K, Barry MJ, Bennett CL, Eden KB, Holmes-Rovner M, Llewellyn-Thomas H, Lyddiatt A, Thomson R, Trevena L. Decision aids for people facing health treatment or screening decisions. *Cochrane Database Syst Rev* 2017; **4**: CD001431 [PMID: 28402085 DOI: 10.1002/14651858.CD001431.pub5]

40 **Trevena LJ**, Zikmund-Fisher BJ, Edwards A, Gaissmaier W, Galesic M, Han PK, King J, Lawson ML, Linder SK, Lipkus I, Ozanne E, Peters E, Timmermans D, Woloshin S. Presenting quantitative information about decision outcomes: a risk communication primer for patient decision aid developers. *BMC Med Inform Decis Mak* 2013; **13** Suppl 2: S7 [PMID: 24625237 DOI: 10.1186/1472-6947-13-S2-S7]

41 **Allen LA**, McIlvennan CK, Thompson JS, Dunlay SM, LaRue SJ, Lewis EF, Patel CB, Blue L, Fairclough DL, Leister EC, Glasgow RE, Cleveland JC Jr, Phillips C, Baldridge V, Walsh MN, Matlock DD. Effectiveness of an Intervention Supporting Shared Decision Making for Destination Therapy Left Ventricular Assist Device: The DECIDE-LVAD Randomized Clinical Trial. *JAMA Intern Med* 2018; **178**: 520-529 [PMID: 29482225 DOI: 10.1001/jamainternmed.2017.8713]

42 **Staszewska A**, Zaki P, Lee J. Computerized Decision Aids for Shared Decision Making in Serious Illness: Systematic Review. *JMIR Med Inform* 2017; **5**: e36 [PMID: 28986341 DOI: 10.2196/medinform.6405]

43 **Chenel V**, Mortenson WB, Guay M, Jutai JW, Auger C. Cultural adaptation and validation of patient decision aids: a scoping review. *Patient Prefer Adherence* 2018; **12**: 321-332 [PMID: 29535507 DOI: 10.2147/PPA.S151833]

44 **Almario CV**, Keller MS, Chen M, Lasch K, Ursos L, Shklovskaya J, Melmed GY, Spiegel BMR. Optimizing Selection of Biologics in Inflammatory Bowel Disease: Development of an Online Patient Decision Aid Using Conjoint Analysis. *Am J Gastroenterol* 2018; **113**: 58-71 [PMID: 29206816 DOI: 10.1038/ajg.2017.470]

45 **Conrad S**, Hüppe A, Raspe H. [Preference of patients with inflammatory bowel disease regarding information and shared decision-making: results from a cross-sectional survey in Germany]. *Z Gastroenterol* 2012; **50**: 364-372 [PMID: 22467539 DOI: 10.1055/s-0031-1281949]

46 **Baars JE**, Markus T, Kuipers EJ, van der Woude CJ. Patients' preferences regarding shared decision-making in the treatment of inflammatory bowel disease: results from a patient-empowerment study. *Digestion* 2010; **81**: 113-119 [PMID: 20093836 DOI: 10.1159/000253862]

47 **Mahlich J**, Matsuoka K, Sruamsiri R. Shared Decision Making and Treatment Satisfaction in Japanese Patients with Inflammatory Bowel Disease. *Dig Dis* 2017; **35**: 454-462 [PMID: 28380481 DOI: 10.1159/000471795]

48 **Morishige R**, Nakajima H, Yoshizawa K, Mahlich J, Sruamsiri R. Preferences Regarding Shared Decision-Making in Japanese Inflammatory Bowel Disease Patients. *Adv Ther* 2017; **33**: 2242-2256 [PMID: 27807816 DOI: 10.1007/s12325-016-0436-0]

49 **Siegel CA**, Lofland JH, Naim A, Gollins J, Walls DM, Rudder LE, Reynolds C. Novel Statistical Approach to Determine Inflammatory Bowel Disease: Patients' Perspectives on Shared Decision Making. *Patient* 2016; **9**: 79-89 [PMID: 25963447 DOI: 10.1007/s40271-015-0126-z]

50 **Lofland JH**, Johnson PT, Ingham MP, Rosemas SC, White JC, Ellis L. Shared decision-making for biologic treatment of autoimmune disease: influence on adherence, persistence, satisfaction, and health care costs. *Patient Prefer Adherence* 2017; **11**: 947-958 [PMID: 28572722 DOI: 10.2147/PPA.S133222]

51 **Veilleux S**, Noiseux I, Lachapelle N, Kohen R, Vachon L, Guay BW, Bitton A, Rioux JD; iGenoMed Consortium. Patients' perception of their involvement in shared treatment decision making: Key factors in the treatment of inflammatory bowel disease. *Patient Educ Couns* 2018; **101**: 331-339 [PMID: 28760459 DOI: 10.1016/j.pec.2017.07.028]

52 **O'Connor AM**, Légaré F, Stacey D. Risk communication in practice: the contribution of decision aids. *BMJ* 2003; **327**: 736-740 [PMID: 14512487 DOI: 10.1136/bmj.327.7417.736]

53 **Patel DB**, van Deen WK, Almario CV, Khalil C, Warui E, Bonthala N, Melmed GY, Spiegel BMR. Assessing Patient Decision-Making on Biologic and Small-Molecule Therapies in Inflammatory Bowel Diseases: Insights From a Conjoint Analysis in the United States, Canada, and the United Kingdom. *Inflamm Bowel Dis* 2021; **27**: 1593-1601 [PMID: 33300555 DOI: 10.1093/ibd/izaa311]

54 **Sands BE**, Peyrin-Biroulet L, Loftus EV Jr, Danese S, Colombel JF, Törüner M, Jonaitis L, Abhyankar B, Chen J, Rogers R, Lirio RA, Bornstein JD, Schreiber S; VARSITY Study Group. Vedolizumab versus Adalimumab for Moderate-to-Severe Ulcerative Colitis. *N Engl J Med* 2019; **381**: 1215-1226 [PMID: 31553834 DOI: 10.1056/NEJMoa1905725]

55 **Pouillon L**, Travis S, Bossuyt P, Danese S, Peyrin-Biroulet L. Head-to-head trials in inflammatory bowel disease: past, present and future. *Nat Rev Gastroenterol Hepatol* 2020; **17**: 365-376 [PMID: 32303700 DOI: 10.1038/s41575-020-0293-9]

56 **Meserve J**, Barsky M, Dulai PS. In the absence of head-to-head trials, what do real world studies tell us about the comparative effectiveness of biologics in Crohn's disease. *Best Pract Res Clin Gastroenterol* 2019; **38-39**: 101619 [PMID: 31327408 DOI: 10.1016/j.bpg.2019.05.006]

57 **Kariburyo MF**, Xie L, Teeple A, Tan H, Ingham M. Predicting Pre-emptive Discussions of Biologic Treatment: Results from an Openness and Preference Survey of Inflammatory Bowel Disease Patients and Their Prescribers. *Adv Ther* 2017; **34**: 1398-1410 [PMID: 28484953 DOI: 10.1007/s12325-017-0545-4]

58 **Colombel JF**, Sandborn WJ, Reinisch W, Mantzaris GJ, Kornbluth A, Rachmilewitz D, Lichtiger S, D'Haens G, Diamond RH, Broussard DL, Tang KL, van der Woude CJ, Rutgeerts P; SONIC Study Group. Infliximab, azathioprine, or

combination therapy for Crohn's disease. *N Engl J Med* 2010; **362**: 1383-1395 [PMID: 20393175 DOI: 10.1056/NEJMoa0904492]

59 **Panaccione R**, Ghosh S, Middleton S, Márquez JR, Scott BB, Flint L, van Hoogstraten HJ, Chen AC, Zheng H, Danese S, Rutgeerts P. Combination therapy with infliximab and azathioprine is superior to monotherapy with either agent in ulcerative colitis. *Gastroenterology* 2014; **146**: 392-400.e3 [PMID: 24512909 DOI: 10.1053/j.gastro.2013.10.052]

60 **Christophorou D**, Funakoshi N, Duny Y, Valats JC, Bismuth M, Pineton De Chambrun G, Daures JP, Blanc P. Systematic review with meta-analysis: infliximab and immunosuppressant therapy vs. infliximab alone for active ulcerative colitis. *Aliment Pharmacol Ther* 2015; **41**: 603-612 [PMID: 25678223 DOI: 10.1111/apt.13102]

61 **Targownik LE**, Benchimol EI, Bernstein CN, Singh H, Tennakoon A, Zubieta AA, Coward S, Jones J, Kaplan GG, Kuenzig ME, Murthy SK, Nguyen GC, Peña-Sánchez JN. Combined Biologic and Immunomodulatory Therapy is Superior to Monotherapy for Decreasing the Risk of Inflammatory Bowel Disease-Related Complications. *J Crohns Colitis* 2020; **14**: 1354-1363 [PMID: 32648579 DOI: 10.1093/ecco-jcc/jjaa050]

62 **Bots S**, Gecse K, Barclay M, D'Haens G. Combination Immunosuppression in IBD. *Inflamm Bowel Dis* 2018; **24**: 539-545 [PMID: 29462391 DOI: 10.1093/ibd/izx065]

63 **Chalhoub JM**, Rimmani HH, Gumaste VV, Sharara AI. Systematic Review and Meta-analysis: Adalimumab Monotherapy Versus Combination Therapy with Immunomodulators for Induction and Maintenance of Remission and Response in Patients with Crohn's Disease. *Inflamm Bowel Dis* 2017; **23**: 1316-1327 [PMID: 28719541 DOI: 10.1097/MIB.0000000000001203]

64 **Reinisch W**, Sandborn WJ, Hommes DW, D'Haens G, Hanauer S, Schreiber S, Panaccione R, Fedorak RN, Tighe MB, Huang B, Kampman W, Lazar A, Thakkar R. Adalimumab for induction of clinical remission in moderately to severely active ulcerative colitis: results of a randomised controlled trial. *Gut* 2011; **60**: 780-787 [PMID: 21209123 DOI: 10.1136/gut.2010.221127]

65 **Colombel JF**, Sandborn WJ, Rutgeerts P, Enns R, Hanauer SB, Panaccione R, Schreiber S, Byczkowski D, Li J, Kent JD, Pollack PF. Adalimumab for maintenance of clinical response and remission in patients with Crohn's disease: the CHARM trial. *Gastroenterology* 2007; **132**: 52-65 [PMID: 17241859 DOI: 10.1053/j.gastro.2006.11.041]

66 **Feagan BG**, McDonald JW, Panaccione R, Enns RA, Bernstein CN, Ponich TP, Bourdages R, Macintosh DG, Dallaire C, Cohen A, Fedorak RN, Paré P, Bitton A, Saibil F, Anderson F, Donner A, Wong CJ, Zou G, Vandervoort MK, Hopkins M, Greenberg GR. Methotrexate in combination with infliximab is no more effective than infliximab alone in patients with Crohn's disease. *Gastroenterology* 2014; **146**: 681-688.e1 [PMID: 24269926 DOI: 10.1053/j.gastro.2013.11.024]

67 **Hu A**, Kotze PG, Burgevin A, Tan W, Jess A, Li PS, Kroeker K, Halloran B, Panaccione R, Peyrin-Biroulet L, Ma C, Ananthakrishnan AN. Combination Therapy Does Not Improve Rate of Clinical or Endoscopic Remission in Patients with Inflammatory Bowel Diseases Treated With Vedolizumab or Ustekinumab. *Clin Gastroenterol Hepatol* 2021; **19**: 1366-1376.e2 [PMID: 32668338 DOI: 10.1016/j.cgh.2020.07.012]

68 **Toruner M**, Loftus EV Jr, Harmsen WS, Zinsmeister AR, Orenstein R, Sandborn WJ, Colombel JF, Egan LJ. Risk factors for opportunistic infections in patients with inflammatory bowel disease. *Gastroenterology* 2008; **134**: 929-936 [PMID: 18294633 DOI: 10.1053/j.gastro.2008.01.012]

69 **D'haens G**, Reinisch W, Satsangi J, Loftus E, Panaccione R, Alperovich G, Kalabic J, Bereswill M, Arikan D, Petersson J, Robinson A. P353 Long-term safety of adalimumab in patients with Crohn's disease: final data from PYRAMID registry. *J Crohns Colitis* 2017; **11**: S256-257 [DOI: 10.1093/ecco-jcc/jjx002.478]

70 **Osterman MT**, Sandborn WJ, Colombel JF, Robinson AM, Lau W, Huang B, Pollack PF, Thakkar RB, Lewis JD. Increased risk of malignancy with adalimumab combination therapy, compared with monotherapy, for Crohn's disease. *Gastroenterology* 2014; **146**: 941-949 [PMID: 24361468 DOI: 10.1053/j.gastro.2013.12.025]

71 **Lichtenstein GR**, Rutgeerts P, Sandborn WJ, Sands BE, Diamond RH, Blank M, Montello J, Tang L, Cornillie F, Colombel JF. A pooled analysis of infections, malignancy, and mortality in infliximab- and immunomodulator-treated adult patients with inflammatory bowel disease. *Am J Gastroenterol* 2012; **107**: 1051-1063 [PMID: 22613901 DOI: 10.1038/ajg.2012.89]

72 **Lemaitre M**, Kirchgesner J, Rudnichi A, Carrat F, Zureik M, Carbonnel F, Dray-Spira R. Association Between Use of Thiopurines or Tumor Necrosis Factor Antagonists Alone or in Combination and Risk of Lymphoma in Patients With Inflammatory Bowel Disease. *JAMA* 2017; **318**: 1679-1686 [PMID: 29114832 DOI: 10.1001/jama.2017.16071]

73 **Doherty G**, Katsanos KH, Burisch J, Allez M, Papamichael K, Stallmach A, Mao R, Berset IP, Gisbert JP, Sebastian S, Kierkus J, Lopetuso L, Szymanska E, Louis E. European Crohn's and Colitis Organisation Topical Review on Treatment Withdrawal ['Exit Strategies'] in Inflammatory Bowel Disease. *J Crohns Colitis* 2018; **12**: 17-31 [PMID: 28981623 DOI: 10.1093/ecco-jcc/jjx101]

74 **Larson DW**, Pemberton JH. Current concepts and controversies in surgery for IBD. *Gastroenterology* 2004; **126**: 1611-1619 [PMID: 15168371 DOI: 10.1053/j.gastro.2004.03.063]

World Journal of Gastroenterology

Submit a Manuscript: https://www.f6publishing.com

World J Gastroenterol 2022 July 14; 28(26): 3101-3115

DOI: 10.3748/wjg.v28.i26.3101

ISSN 1007-9327 (print) ISSN 2219-2840 (online)

MINIREVIEWS

Clinical implications and mechanism of histopathological growth pattern in colorectal cancer liver metastases

Bing-Tan Kong, Qing-Sheng Fan, Xiao-Min Wang, Qing Zhang, Gan-Lin Zhang

Specialty type: Oncology

Provenance and peer review: Invited article; Externally peer reviewed.

Peer-review model: Single blind

Peer-review report's scientific quality classification
Grade A (Excellent): 0
Grade B (Very good): 0
Grade C (Good): C, C, C
Grade D (Fair): 0
Grade E (Poor): 0

P-Reviewer: Arigami T, Japan; Cassese G, Italy; Morera-Ocon FJ, Spain

Received: January 17, 2022
Peer-review started: January 17, 2022
First decision: April 11, 2022
Revised: April 21, 2022
Accepted: June 16, 2022
Article in press: June 16, 2022
Published online: July 14, 2022

Bing-Tan Kong, Qing-Sheng Fan, Xiao-Min Wang, Qing Zhang, Gan-Lin Zhang, Department of Oncology, Beijing Hospital of Traditional Chinese Medicine, Capital Medical University, Beijing 100010, China

Bing-Tan Kong, School of Graduates, Beijing University of Chinese Medicine, Beijing 100029, China

Corresponding author: Gan-Lin Zhang, PhD, Associate Research Scientist, Department of Oncology, Beijing Hospital of Traditional Chinese Medicine, Capital Medical University, No. 23 Back Road of Art Gallery, Dongcheng District, Beijing 100010, China.
kalinezhang@163.com

Abstract

Liver is the most common site of metastases of colorectal cancer, and liver metastases present with distinct histopathological growth patterns (HGPs), including desmoplastic, pushing and replacement HGPs and two rare HGPs. HGP is a miniature of tumor-host reaction and reflects tumor biology and pathological features as well as host immune dynamics. Many studies have revealed the association of HGPs with carcinogenesis, angiogenesis, and clinical outcomes and indicates HGP functions as bond between microscopic characteristics and clinical implications. These findings make HGP a candidate marker in risk stratification and guiding treatment decision-making, and a target of imaging observation for patient screening. Of note, it is crucial to determine the underlying mechanism shaping HGP, for instance, immune infiltration and extracellular matrix remodeling in desmoplastic HGP, and aggressive characteristics and special vascularization in replacement HGP (rHGP). We highlight the importance of aggressive features, vascularization, host immune and organ structure in formation of HGP, hence propose a novel "advance under camouflage" hypothesis to explain the formation of rHGP.

Key Words: Colorectal cancer liver metastases; Histopathological growth pattern; Desmoplastic histopathological growth pattern; Replacement histopathological growth pattern; Prognostic value; Vessel co-option

©The Author(s) 2022. Published by Baishideng Publishing Group Inc. All rights reserved.

Core Tip: Histopathological growth pattern (HGP) reflects tumor–host interaction, vascularization, aggressiveness and immune infiltration. Remarkable performance on predicting survival and recurrence and distinct response to therapies makes HGP a promising prognostic biomarker and stratification parameter in pretreatment decision-making. Exploiting on mechanism of HGP would provide potential therapeutic targets. In this context, we propose one novel "advance under camouflage" hypothesis to interpret formation of replacement HGP.

Citation: Kong BT, Fan QS, Wang XM, Zhang Q, Zhang GL. Clinical implications and mechanism of histopathological growth pattern in colorectal cancer liver metastases. *World J Gastroenterol* 2022; 28(26): 3101-3115
URL: https://www.wjgnet.com/1007-9327/full/v28/i26/3101.htm
DOI: https://dx.doi.org/10.3748/wjg.v28.i26.3101

INTRODUCTION

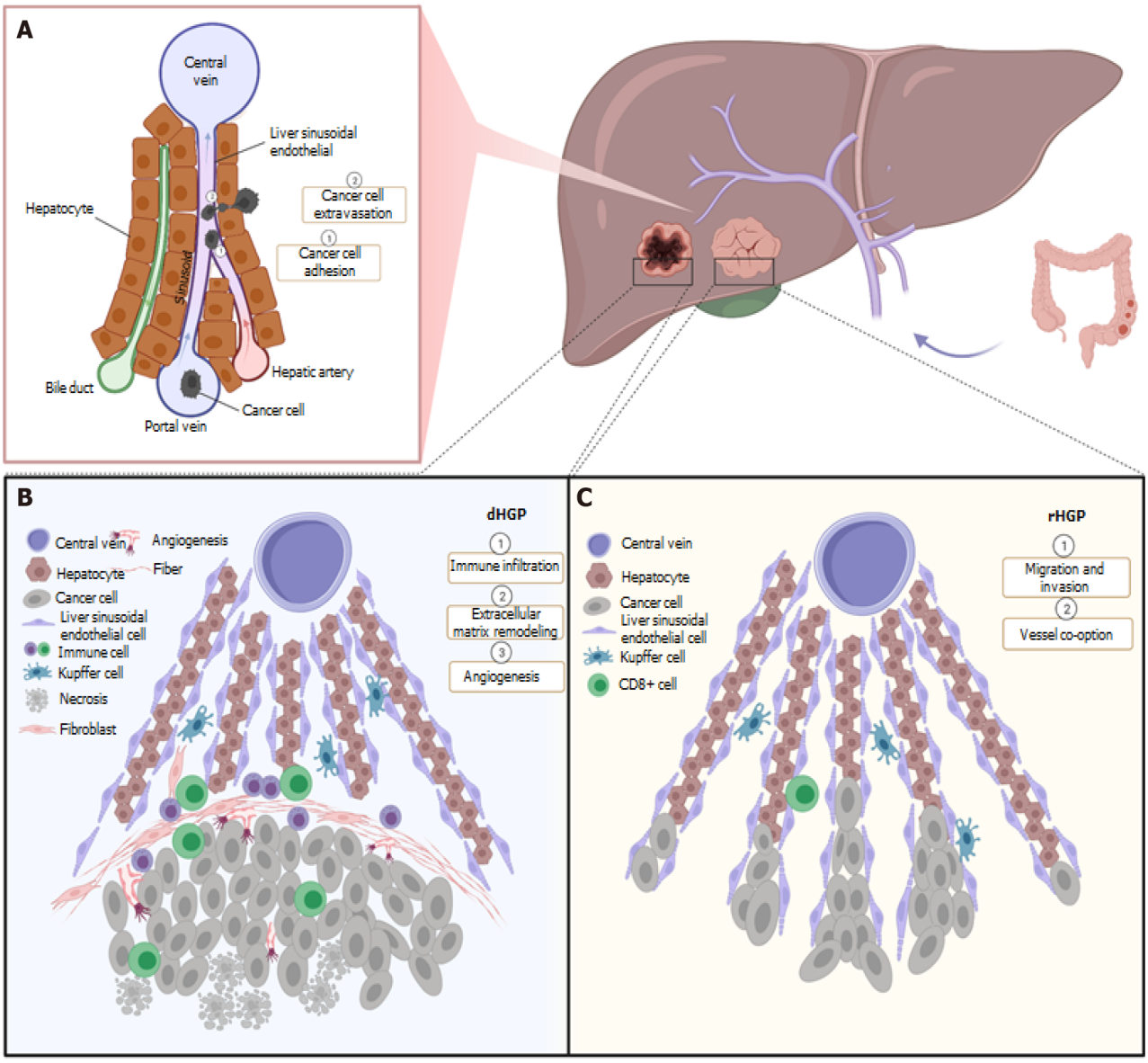
Colorectal cancer (CRC) is the third most frequent tumor worldwide and the second most common in Europe. In diagnosed CRC, 20%–25% of patients are classified as stage IV and 15%–25% of those develop liver metastases[1]. For these whose metastases are confined to the liver, the only opportunity to cure is radical surgical resection. However, not all patients are fit for surgery and there is still a high rate of intrahepatic recurrence after curative resection. Therefore, the attempt on seeking for more comprehensive prognostic and stratification markers is of utmost importance. Deriving from this aim, the invasive margin as one pathological variable was selected to construct a prognostic system for rectal cancer patients[2]. There, tumor margin was classified into expanding type (pushing or well circumscribed) and infiltrating type. Based on these studies, the histopathological growth pattern (HGP) initially came into shape.

In 2016, international consensus guidelines[3] for scoring HGPs of liver metastasis were produced. Three common HGPs, *i.e.*, desmoplastic HGP (dHGP), pushing HGP (pHGP) and replacement HGP (rHGP), and two rare HGPs, *i.e.*, sinusoidal HGP and portal HGP are described in these consensus guidelines. In principle, HGPs could be distinguished according to the character of the invasive margin and morphology of the tumor, which is usually observed in light microscopy on standard hematoxylin and eosin (H&E)-stained tissue sections. Distinct biological and invasive patterns are presented in different HGPs. The key histopathological characteristic of dHGP is that there is a broad desmoplastic rim at the tumor periphery, which separates tumor cells from normal liver tissue. rHGP tumor cells mimic the liver architecture and replace the hepatocytes within liver plates, and the tumor displays an infiltrative border and irregular contours. pHGP tumor expands in a pushing way and the adjacent liver is compressed. Its interface is as sharp as that of dHGP but without a desmoplastic rim[3]. Figurative knowledge of dHGP and rHGP is presented in Figure 1.

PROGNOSTIC VALUE OF HGPS

Frequently, HGP predicts overall survival and recurrence in patients resected for CRC liver metastasis (CRCLM). HGPs have been extensively characterized not only in liver metastases but also in the primary cancer and metastases in lung, brain and skin; therefore, there are different categorization about HGPs in different tissues. They are ordinarily classified into dHGP and non-dHGP or expanding and infiltrative HGP[2] when used as prognostic biomarkers. In this fashion, dHGP refers to pure dHGP with a 100% desmoplastic interface on every section, while non-dHGP actually includes pushing, replacement and a mixed (pushing-replacement) pattern. As the major form in most cases, rHGP represents non-dHGPs and infiltrative HGP. One of the most important findings from studies on predictive value of HGP is that CRCLM patients with dHGP, especially pure dHGP, are prone to longer overall survival. dHGP is verified as an independent factor for superior overall survival (OS) and progression-free survival (PFS)[4-8], while non-dHGPs are strong prognostic indicators of worse survival[8-14]. More than in CRCLM, a similar trend has been observed in liver metastases from cutaneous melanoma[15], which implies that the prognostic value of HGP is generally applied in various liver metastases.

For CRCLM patients who have undergone hepatectomy, high recurrence rate may cause repeat resection and impair their survival. Non-dHGP might be responsible for this damage from intrahepatic as well as overall recurrences[12]. Compared with dHGP, rHGP and pHGP more frequently experience multiorgan recurrence, while dHGP has more liver-limited disease recurrence[16-18]. Evidence supports that dHGP predicts good outcomes, but the infiltrative pattern or rHGP indicates poorer outcomes and higher recurrence. In this context, we provide an overview of studies focusing on prognostic and strati-



DOI: 10.3748/wjg.v28.i26.3101 **Copyright** ©The Author(s) 2022.

Figure 1 Formation and mechanism of desmoplastic histopathological growth pattern and replacement histopathological growth pattern.
A: Cancer cells originating from colorectal cancer arrive in the liver *via* portal vein, adhere to lumen of liver sinusoid and migrate with extravasation through fenestrae on liver sinusoidal endothelial cells (LSECs); B: There is a desmoplastic rim in interface of tumor with desmoplastic histopathological growth pattern, with tumor cells destroying liver plate, causing immune infiltration and extracellular matrix remodeling induced by activated fibroblasts and deposited fiber. Both angiogenesis and necrosis are presented in the tumor; C: In replacement histopathological growth pattern, tumor cells with highly migration and invasion replace hepatocytes and co-opt LSECs but without disturbing the liver structure and extensive immune infiltration. dHGP: Desmoplastic histopathological growth pattern; rHGP: Replacement histopathological growth pattern.

fication value of HGPs in Table 1.

Apart from predicting survival, the growth pattern of primary CRC was also found to predict the HGP of liver metastases. The primary CRCs with expanding growth pattern significantly tend to form dHGP liver metastasis, while CRC patients presenting with infiltrating growth pattern are more likely to have rHGP liver metastasis[19]. It seems that some invasive characteristics are inherited from primary tumor to secondary metastases. However, there are few reports about this. Wu *et al*[19] found several specific gene mutations, among which representative gene mutation *PIK3CA* appearing in 40% of primary CRC patients with dHGP liver metastasis was speculated to mediate vascular development and angiogenesis through the vascular endothelial growth factor (VEGF) signaling pathway, further supporting dHGP. Nevertheless, these findings have not revealed the genomic correlation between growth pattern in primary CRC and HGP in liver metastases.

Some relevant factors such as surgical margin, immunoscore[20] and glucose uptake[21,22] were also widely investigated as predictor in outcomes of CRC. The combination of HGP with resection margin, parameters of immune status, genes and metabolism also paves the way for creating comprehensive and accurate predictive models. Surgical margin in tumorectomy is a critical but controversial issue as

Table 1 Studies on stratification value of histopathological growth pattern in colorectal cancer liver metastasis

Year	Factors	Prediction	Distribution of HGPs	Ref.
Survival stratification				
2018-2019	dHGP and rHGP (based on radiomics)	dHGP *vs* rHGP and mixed HGP: longer PFS (no detail)	119 patients: dHGP (206 lesions), rHGP (140 lesions)	Wei *et al* [43]
2004-2019	Pushing GP and infiltrative GP	Infiltrative GP *vs* pushing GP: Worse OS (50.2 mo *vs* 92 mo) and DFS (10.5 mo *vs* 21.5 mo), higher intrahepatic recurrence (75% *vs* 20%)	266 patients: Infiltrative (n = 182, 68.4%) and pushing (n = 84, 31.6%)	Jayme *et al* [16]
2005-2017	dHGP and non-dHGP group; metabolic-clinical risk score	dHGP *vs* non-dHGP: Longer 5 yr OS (83.3% *vs* 34.3%) and 10 yr OS (62.5% *vs* 22.8%) and DFS (14.4 mo *vs* 8.3 mo)	108 patients: dHGP (26, 20%), non-dHGP (38, 35%)	Bohlok *et al* [23]
2000-2015	dHGP and non-dHGP; positive resection margins (R1) and negative resection margins(R0)	Non-dHGP *vs* dHGP: worse OS (50 mo *vs* 80 mo), higher risk of positive resection margins (76.6% *vs* 23.4%)	1302 patients: dHGP (305, 23%) and non-dHGP (997, 77%); R1 (170, 13%) and R0 (1132, 87%)	Nierop *et al* [9]
2004-2017	dHGP and non-dHGP, clinical risk score, the immunoscore	dHGP *vs* non-dHGP: Higher immunoscore (51.9% *vs* 33%), longer relapse free survival (32 mo *vs* 12 mo) and OS (not reached *vs* 40 mo)	166 patients: dHGP (54, 32.5%), non-dHGP (112, 67.5%)	Liang *et al* [4]
2012-2017	Expanding GP, infiltrating GP; low tumor budding score, and Crohn's disease-like response	Expanding GP in primary CRC: dHGP liver metastasis and better OS (no detail); infiltrating GP in primary carcinoma: rHGP liver metastasis and worse OS (no detail)	29 patients; primary CRC: expanding GP (11, 37.9%) and infiltrating GP (18, 62.1%); liver metastasis: dHGP (15, 51.7%) and rHGP (14, 48.2%)	Wu *et al*[19]
2000-2015	dHGP and non-dHGP	dHGP *vs* non-dHGP: More liver-limited disease recurrence (43% *vs* 31%); less frequently experience multi-organ recurrence (19% *vs* 34%)	690 patients: dHGP (173, 25%) and non-dHGP (517, 75%)	Nierop *et al* [17]
2000-2009	Infiltrative and pushing tumor margin	Infiltrative margin *vs* pushing margin: poorer 5 yr DFS (20.2% *vs* 40.5%)	91 patients: infiltrative margin (54, 59.3%) and pushing margin (37, 40.7%)	Pinheiro *et al*[12]
2007-2011	dHGP, rHGP, pHGP, mixed HGP	rHGP *vs* dHGP, pHGP and mixed HGP: Poorer OS (22.8 mo *vs* > 60 mo, 44.2 mo and 40.3 mo)	217 patients: pHGP(33%), dHGP(32%), rHGP(11%) and mixed HGP(24%)	Nielsen *et al* [8]
1997-2005	dHGP, rHGP, pHGP, mixed HGP	pHGP *vs* dHGP, rHGP and mixed HGP: Poorer 2 yr OS (43.8% *vs* 72.5%, 70.2%, and 54.3%)	205 patients: pHGP (15.6%), dHGP (34.6%), rHGP (27.8%) and mixed HGP (17.6 %)	Van den Eynden *et al* [13]
Therapy response stratification				
2000-2016	dHGP and non-dHGP	Non-dHGP: Superior response to adjuvant systemic chemotherapy on improving OS and DFS but only in patients that were not treated with chemotherapy	1236 patients; 580 not pretreated patients (46.9%): dHGP (91, 15.6%) and non-dHGP (489, 84.4%); 656 pretreated patients (53.1%), dHGP (189, 28.8%) and non-dHGP (467, 71.2%).	Buisman *et al*[27]
2000-2015	dHGP and non-dHGP	dHGP *vs* non-dHGP: Better 5-year PFS (50% *vs* 19%) and 5 yr OS (70% *vs* 37%) but only in chemo-naive patients with resecting CRCLM	732 patients; in the chemo-naive patient cohort (n = 367), dHGP (68, 19%) and non-dHGP (299, 81%); in the neoadjuvantly treated patient cohort (n = 365), dHGP (109, 30%) and non-dHGP (256, 70%)	Galjart *et al* [6]
2010-2013	dHGP, rHGP, pHGP, mixed HGP	pHGP: Worse OS and DFS; significantly associated with Oxaliplatin-based chemotherapy	110 patients: pHGP (33, 30%), dHGP (23, 21%), rHGP (19, 18%) and mixed HGP (34, 31%)	Falcao *et al* [11]

HGP: Histopathological growth pattern; GP: Growth pattern; dHGP: Desmoplastic histopathological growth pattern; rHGP: Replacement histopathological growth pattern; pHGP: Pushing histopathological growth pattern; OS: Overall survival; DFS: Disease-free survival; PFS: Progression-free survival.

biologic factors driving margin-based differences may lead to the need for larger surgical margins, which indicate less chance of residual tumor cells and recurrence. Nierop *et al*[9] found that patients with non-dHGP are at higher risk of positive resection margins. It seems to be necessary to enlarge resection margin size when tumors present more aggressive borders or worse HGPs. Partly answering this question, Jayme *et al*[16] found that those with infiltrative-type borders indeed presented with worse overall and disease-free survival, and had a 2.32 higher risk of hepatic recurrence than patients with pushing borders. However, a larger resection margin (> 10 mm) in patients with infiltrative borders did not affect the prognosis. It could be pointed out that what really counts is tumor biology rather than tumor size. In parallel with HGPs, high preoperative glucose uptake representing high metabolism rate is associated with poor prognosis in CRCLM[21,22]. When integrating preoperative metabolic parameters with HGPs, the postoperative prognostic value could be improved[23]. As

expected, similar results appeared in studies on correlation between HGPs and immunophenotype and genomic mutation[19,24].

HGPS AND THERAPIES

HGP is also a useful tool to stratify patients for their response to therapy. For both resectable and unresectable patients, additional chemotherapy and angiogenesis inhibitors (AIs) are regarded as essential adjuvant therapy, however, their timing of administration and effect remains a matter of debate. Previous studies showed perioperative chemotherapy was not that beneficial as expected[25,26]. Retrospective analysis on long-term outcomes of 236 resectable CRCLMs suggested that there were no measurable differences between groups receiving adjuvant and perioperative chemotherapy[26]. Whereas an interesting phenomenon is that the effectiveness of adjuvant therapies varies with different HGP subgroups. For patients who were not pretreated with chemotherapy, non-dHGP subgroup have longer OS and disease-free survival (DFS) after adjuvant chemotherapy[27]. dHGP and pHGP are more sensitive to triplets + cetuximab and triplets + bevacizumab, respectively, while rHGP has poor response to the both therapies[28]. In other words, HGPs may determine the sensitivity to chemotherapy and AIs. Besides, chemotherapy somehow changes the component of HGPs. One study found more than half (55%) of chemonaive resected CRCLMs showed rHGP, while patients with neoadjuvant therapy presented the opposite phenomenon, in which dHGP comprised the major proportion (66%)[6]. Chemotherapy as an independent relevant factor induced an HGP phenotypic change with an increase of dHGP. A similar trend was shown in another study in which Nierop *et al*[29] evaluated the effect of preoperative systemic chemotherapy on the HGPs of CRCLM, and obtained multiple verification in three independent cohorts. Conclusively, HGP could be a stratification factor when considering the effectiveness of adjuvant chemotherapy after resection.

The remarkable results with AIs in preclinical studies brought hope to patients; however, with passing decades, AIs have failed to demonstrate a survival advantage. Increasing findings strongly imply that rHGP is insensitive to AIs and increasing proportion of rHGP furtherly drives reactive resistance after AIs therapy, all of which is mainly due to vessel co-option being as predominant vascularization. Serial clinical studies in patients with liver metastases verified that rHGP is prevalent in post-treatment patients and rHGP subgroup poorly responds to AI therapy[30]. Whereas, supplementary inhibition of rHGP through suppressing cancer cell motility and migration facilitated effectiveness of AIs *in vivo*. Other direct evidence supporting vessel co-option (rHGP) as a mechanism of acquiring resistance to AI therapy was obtained from an orthotopic human hepatocellular carcinoma (HCC) model[31]. The researchers paid more attention to vascularization within the tumor instead of the interface between the tumor and liver, and found the number of co-option vessels was elevated from 23.3% in untreated controls to 75% in resistant tumors, along with a shift from angiogenesis (dHGP) to vessel co-option (rHGP)[31]. These observations make it clear that rHGP induces resistance to AI therapy in *in vivo* and *in vitro*.

Collectively, HGPs determine the sensitivity to therapy, and both chemotherapy and AIs somehow change the components of HGPs. Chemotherapy tends to the change with increase of dHGP, while AIs make a shift from angiogenesis (dHGP) to vessel co-option (rHGP). Considering prognostic significance and drug response of HGP in liver metastases, HGP could be used to guide treatment for CRCLM patients, select out ideal subgroup, design precision therapy for individual patient, even develop approaches to transform HGP of drug-resistant group to one sensitive type so that they can benefit from current therapy.

HGPS AND VASCULARIZATION

Tumors adopt various forms of vascularization, among which, angiogenesis occupies a dominant position. Yet, increasing evidence shows that vessel co-option is a crucially alternative nonangiogenic strategy by which tumor cells hijack the pre-existing vessels instead of creating new vessels and gain access to nutrients to support tumor survival, growth and metastasis. Different HGPs correspond with distinct vascularization patterns, which also vary with metastatic organs. In CRCLM, rHGP and dHGP obtain blood supply *via* different routes, *i.e.*, the former is vessel co-option while the latter is sprouting angiogenesis. This difference of vascularization contributes to distinct therapy response.

For a long time, dHGP has been known to represent an angiogenic growth pattern. Different from rHGP, tumors with dHGP completely destroy liver architecture and form neovascularization. Chemotherapy and antiangiogenic agents caused 100% necrosis and few surviving carcinoma cells left under the desmoplastic rim[32]. It is believed that leakiness of immature vascular allows cytotoxic agents sufficient interaction with malignant cells contributing to more efficient of chemotherapy on dHGP. In the process of sprouting angiogenesis, with extracellular matrix (ECM) and basement membrane degrading, endothelial cells and pericytes proliferate, migrate and eventually form immature vasculature[33,34]. Like a double-edged sword, abnormal basement and loose pericytes of new vessels

lead to leakiness and heavily impair blood supply to the whole tumor which causes hypoxia and acidosis[35]. This leakiness may affect drug delivery and only after normalizing the abnormal tumor vasculature can chemotherapy as well as oxygen efficiently penetrate throughout tumor[35]. AIs has been verified with the ability to prune proliferating vessels, render tumor vasculature normalized and enhance the delivery and efficacy of cytotoxic agents[36,37]. Collectively, sprouting angiogenic vascularization contributes to favorable effect of chemotherapy on dHGP.

In contrast, rHGP tumors expand in a "conventional way" by replacing liver cells, attaching liver sinusoidal endothelial cells (LSECs) and co-opting liver vessels with liver structure preserved. The data from Frentzas and colleagues[30] provide direct evidence supporting cancer cells utilizing pre-existing sinusoidal blood vessels in rHGP liver tumors. They found invading tumor cells followed the "RR" rule that tumor cells replaced hepatocytes in the liver parenchyma but respected the sinusoidal blood vessels, leaving the sinusoidal space complete. Sinusoidal vessels with one end embedded in the tumors were frequently observed, with the other end originating from normal liver. Different from dHGP, there were more mature vessels in continuity with the sinusoidal network in rHGP. rHGP lesions preserve more viable carcinoma cells, more microvascular density (MVD) and showed no necrosis after chemotherapy and antiangiogenic agents[32].

These vascularization characteristics could partly explain why rHGP tumors initiate less response to chemotherapy and antiangiogenic therapy than dHGP tumors do, and even resistance to antiangiogenic therapy. Tumor with rHGP lacks proliferating vasculature, while the co-opted liver sinusoidal capillary network as a mature and endogenous vascular network does not respond to AIs. Current studies on vascularization of HGPs extensively pay attention to tumor periphery other than central region, and particularly co-option vessels were only observed in interface. In this case, what the vascularization in central region of rHGP tumor requires further investigation.

IDENTIFYING HGPS IN NONINVASIVE METHODS

In spite of strong prognostic and stratification value, HGP has not been put into clinical decision-making, which is mainly because of its limitation of requiring histopathological assessment of surgical resection specimens. Thus, a noninvasive method identifying HGP is urgently needed, especially when selecting optimal therapies for patients with untreated and unresectable liver metastasis and predicting their survival for long-term healthcare. Rim enhancement as a hotspot topic has attracted much attention. Radiomics stands out with a remarkable performance in identifying HGPs and predicting outcomes and several novel predictive models combining morphological score or not have superior ability to conventional response evaluation criteria.

Over the years, several noninvasive approaches, such as computed tomography (CT), magnetic resonance imaging (MRI) and ultrasound, were used to identify HGP and explore their correlation with response to therapy and even survival forecasting. There are some common imaging features of HGPs, *e.g.*, a significantly enhanced rim and clear tumor–liver interface in dHGP, compared with an indefinite margin and no rim enhancement in rHGP. Earlier studies on the correlation between radiology images and morphological features concentrated on rim enhancement since knowledge on HGP was insufficient. In the 1990s, scientists studied the enhancing rim through comparing radiology images with histopathological slides, attributed this phenomenon to blood flow and perfusion and believed that the morphological substrate of rim enhancement of colorectal metastases seen by CT was compressed liver parenchyma[38]. The compressed liver parenchyma lacked a portal blood supply but was compensated by an increase in the arterial blood supply, and the rim enhancement of metastases could only be seen during hepatic arteriography. Similarly, Terayama *et al*[39] found two-way blood flow between the tumor and the adjacent liver tissues contributed to peritumoral enhancement. This abnormal blood circulation and occlusion in the tumoral–peritumoral area caused sinusoidal congestion, the thickness of which reflected thickness the perilesional hyperintense rim[40]. The findings from Semelka *et al*[41] implied that the level of compression of hepatic parenchyma was not positively correlated with the degree of perilesional enhancement. The concomitant reactions such as peritumoral desmoplastic reaction, vascular proliferation and peritumoral inflammation contributed a lot to the increase in rim enhancement. Above all, these findings on the mechanism of rim enhancement focusing on inflammatory infiltration and reactive vascularization step forward to comprehensive knowledge on HGP.

Nevertheless, in some cases, it is difficult to recognize some minor differences in rim enhancement because distinct vascularization for HGPs cannot be exactly and quantitatively identified visually. Current studies have focused on the correlation between HGPs and radiomics. Radiomics is a promising tool to predict HGPs but still faces great challenges. Radiomics containing pre- and post-contrast (arterial and portal venous phase) multidetector CT images were demonstrated to improve distinguishing accuracy on HGPs in the training cohort[42]. Importantly, the performance predicting HGPs of radiomics models alone did not differ from combining clinical and qualitative imaging factors[42]. Given the diagnostic performance of this model with area under the curve > 0.9, another study verified its potential for predicting survival[43]. In unresected patients additionally treated with bevacizumab-

containing chemotherapy, the dHGP subgroup had > 1-year PFS, which was in line with HGP prediction on resected specimens[43].

CT criteria based on morphological forecast outcomes superior to Response Evaluation Criteria In Solid Tumors (RECIST) based on tumor size and number[44,45]. A radiomics model based on tumor-liver interface exhibited better predictive value compared with a model based on tumor zone; nevertheless, combination of the two models was superior to any single one, even clinical model[46]. Some evaluative and predictive models, *e.g.*, SPECTRA-score[47] based on a radiomic nomogram, displayed superior sensitivity and accuracy to standard evaluation with RECIST 1.1. Even though CT, MRI and positron emission tomography/CT have comparative diagnostic value in detecting CRCLM, gadoxetate-disodium-enhanced MRI was found to have greater accuracy in a systemic review[48]. These imply that the combined prediction model of morphological characteristics and imaging studies perform better than the mono-model.

UNDERLYING MECHANISM OF HGPS

dHGP: Immune infiltration and ECM remodeling

Immune infiltration: The tumor microenvironment not only carries out major tumor-relevant activities including antitumor response and stromal remodeling but also involves in formation of distinct pathological phenotypes. The immunoscore of patients with dHGP remains high, which implies that dHGP is an abundant immune status. As unique marker of dHGP tumor, the desmoplastic rim usually indicates active antitumor response meanwhile rim itself is a product of matrix deposition and immune infiltration. Here, adaptive lymphocytes participate in both cytotoxic and immunosuppressive effects. In dHGP, there was an increase of $CD3^+$ T cells, $CD8^+$ T cells, $CD20^+$ B cells and CD8/CD4 ratio; all of which enhance antitumor immunity, while decrease of $CD4^+$ T cells[4,5]. That this phenomenon appeared in peritumoral and intratumoral regions and even distant tumor-free liver but not peripheral blood suggested local immune situation instead of systemic immunity drove and determined the HGP phenotype. In dHGP, Eefsen *et al*[49] observed macrophages accumulating at the tumor border in patients given neoadjuvant chemotherapy and higher level of urokinase-type plasminogen activation receptor in chemonaive patients. As part of the plasminogen activation system, urokinase-type plasminogen activation receptor is mainly expressed in macrophages and myofibroblasts and some cancer cells[50], and induces changes in the macrophages during tumor invasion. Therefore, higher urokinase-type plasminogen activation receptor expression in desmoplastic metastases may be a secondary reaction of the tumor cells to the desmoplasia.

ECM remodeling: Desmoplasia is also a host-specific reaction to protect against malignant cells invasion of adjacent parenchyma and plays a protective role in tumor progression. On formation of desmoplasia, cancer-associated fibroblasts (CAFs) play a pivotal role through producing collagen and fiber, coupled with the role of self-produced cytokines and growth factors, thereby remodeling the ECM [51]. When stromal content automatically decreases within tumor microenvironment or inducing stromal depletion with medication, *e.g.*, type I collagen, the tumor will become more aggressive, with lower tissue stiffness and rapid growth, leading to poorer overall survival of the host[52]. This desmoplastic capsule mainly consists of collagen fibers originating from activated myofibroblasts. Capsule formation typically occurs when there is a high level of infiltration by $CD4^+$, $CD45RO^+$ and $CD8^+$ T cells in the near stromal region[53]. However, the distant stromal area with low density of immune cells hardly ever forms a capsule. The desmoplastic rim may be a complicated collection of several components, *e.g.*, fibers, blood vessels, fibroblasts and immune cells. This rim originates from the antitumor response, and functions as a barrier separating malignant cells from normal tissues.

rHGP: Aggressive characteristics and special vascularization

Metastatic capability: Cell motility, invasion and migration: To our knowledge, rHGP was initially described as infiltrating growth pattern[2] other than replacement growth pattern, implying that this type of tumor has aggressive biology and is prone to adopt an infiltrative growth patten. Tumor cells with rHGP present a highly motile, invasive and adhesive phenotype, which accelerates infiltration of the adjacent liver and utilizes the pre-existing vasculature.

For molecules involved in cancer cell motility supporting rHGP, the actin-related protein 2/3 (ARP2/3) complex is indispensable. It has been demonstrated ARP2/3 mediates the nucleation of actin filaments at the frontier cells to drive cell movement and facilitate the motility and invasion of breast and colorectal cancer cells[54]. ARP2/3 subunit ARPC3 is highly expressed in rHGP human CRCLM specimens, and its knockdown results in a significant decrease of rHGP in animal models[30]. *In vitro* data have shown that ARPC3 silencing suppresses migration other than proliferation of CRC cells. Apart from ARP2/3, Runt-related transcription factor (RUNX)1 also regulates motility and epithelial–mesenchymal transition (EMT) in cancer cells. As a key upstream transcriptional regulator of ARP2/3, RUNX1 is overexpressed in rHGP CRCLM lesions[55], and its inhibition could suppress tumor cell motility and EMT. Downstream proteins ARP2/3 and thrombospondin 1 are also reported to

facilitate cancer cell motility; however, whether RUNX1 support of rHGP is ARP2/3 dependent needs more investigation.

Tumor with strong adhesion to hepatocytes has potential to develop rHGP. Claudins as critical components of tight-junctional complexes that modulate carcinogenesis and metastasis[56]. Claudin-2 acts as an essential determinant in the formation of rHGP liver metastases from either CRC or breast cancer[57]. During tumor metastasis to the liver, there is functional shift in claudin-2 from tight-junctional complex to adhesion molecule between cancer cells and hepatocytes[58,59]. Claudin-2 promotes tumor cell adhesion to hepatocytes and is specifically expressed at high levels in rHGP; at the same time, claudin-8 is specifically expressed at high levels in dHGP[57].

Co-opting vessels: Different HGPs are associated with different types of tumor vascularization. In rHGP, tumor cells replace hepatocytes to spread and co-opt liver vessels to obtain blood. Since rHGP corresponds with vessel co-option, those regulating vascular factors should be paid attention. Angiopoietin (Ang)1 and Ang2 are vascular growth factors that act as agonists to active their ligand Tie2, which then together induce endothelial cell (EC) formation, survival, proliferation and migration. Ang1 has a distinct vascular-relevant effect, protects against EC apoptosis, and mediates vessel maturation by enhancing pericyte recruitment. Ang2 has a proangiogenic function through mediating pericyte detachment and blood vessel destabilization[60]. In human resected CRCLM specimens with rHGP, Ang1 supporting vessel co-option displays higher expression in the liver adjacent to tumor[61]. To demonstrate the critical role of Ang1, an animal model of Ang1 knockout was established and showed a change from rHGP to dHGP along with a decrease of liver metastases[61]. This verified that high expression of Ang1 in the host liver supported rHGP. Additionally, some inflammatory molecules partly participated in rHGP. RNA sequencing showed that two genes, *CXCL6* and *LOXL4*, were significantly upregulated in rHGP tumors *vs* dHGP tumors, and were involved in cell migration and wound healing[62]. Neutrophils expressing *LOXL4* concentrated at the tumor–liver interface and in areas of inflammation in rHGP lesions, and circulating neutrophil expression of LOXL4 protein is increased in CRCLM patients. It indicates that the chemoattraction and subsequent activation of neutrophils may be vital in promoting rHGP in CRCLM[62].

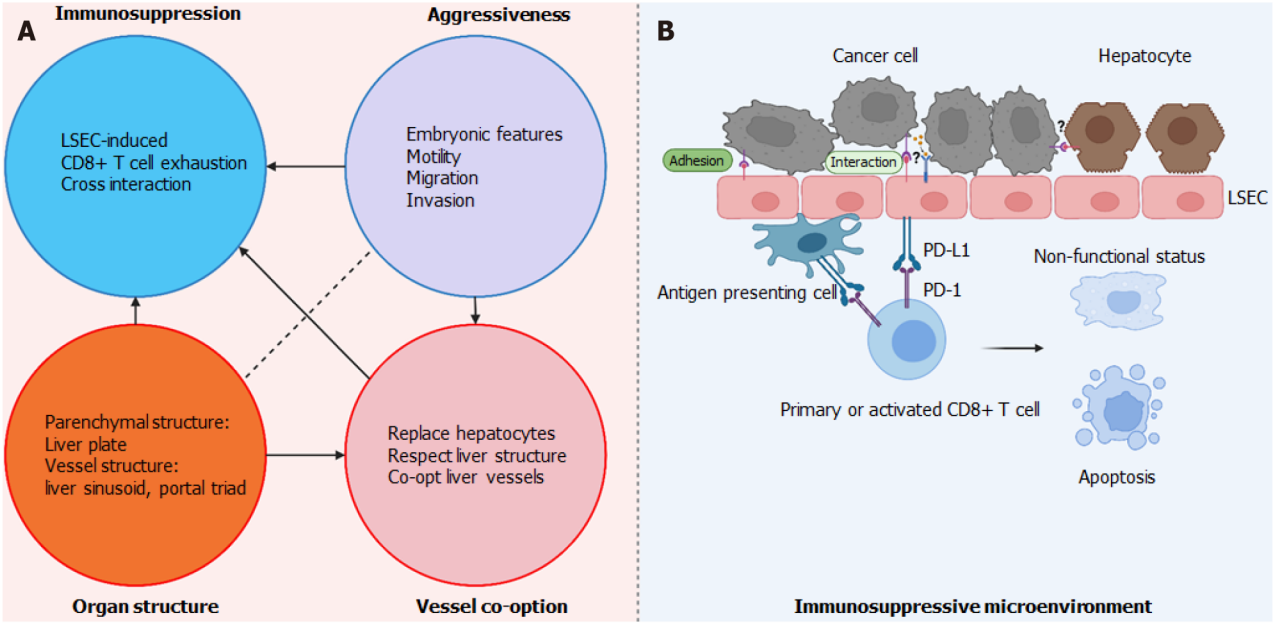
Hypothesis for HGPs

Liver injury hypothesis: When coping with exogenous or endogenous injuries, the liver has both the potential for healthy regeneration following acute injury and the potential for repair toward fibrosis under persistent damage[63]. Given malignant cells proliferate within the liver, causing injury and activating host reactions, van Dam *et al*[64] proposed the hypothesis that HGPs represent the response patterns of the liver to injury.

Development of liver metastases has similar pathological changes to those in liver injury. In liver fibrosis, portal fibroblasts and hepatic stellate cells transform to activated myofibroblasts, binding with components of ECM (crosslinking collagen), and together induce fibrogenic activation and support fibrogenic units based on activation and reorganization of cholangiocytes, accounting for fibrotic progression[65]. For dHGP, the peripheral desmoplastic rim shares one common ECM remodeling and ductular reaction with liver fibrosis, among which the activated cholangiocytes proliferate and form small nonfunctional bile ducts. Differently, rHGP adopts an analogous pattern with liver regeneration where the process of new cells replacing older hepatocytes takes place. In the context of vascularization, in liver regeneration, regenerating liver cells co-opt pre-existing sinusoidal capillaries instead of sprouting angiogenesis which is akin to rHGP. Even though it is far from reaching a certain conclusion that dHGP and rHGP exemplify liver fibrosis and regeneration, but there is still similarity between formation of liver metastasis and liver development and regeneration; knowledge of which would enable us to determine the underlying mechanism of HGPs.

Advance under camouflage hypothesis: Researchers have detailed knowledge of the mechanism of dHGP, but there is little ideal explanation for the formation of rHGP. Except for some tumoral phenotypic and molecular drivers observed in rHGP, there is still no systematic model to support the explanation. We put forward a hypothesis that malignant cells benumb and educate the immune system, and advance by an unknown path under camouflage (Figure 2).

The tumor cells with an infiltrative pattern paralyze or tame the local immune system *via* interaction with LSECs and induce immune tolerance. LSECs are a major group of hepatic cells that specialize in detection and capture of pathogens from the blood. However, in some cases, this group also downregulates T-cell response through crosstalk with immune cell subsets, leading to immune escape[64,66]. Through programmed death (PD) ligand 1 on T cells binding to PD-1 on LSECs, $CD8^+$ T cells are activated to a dynamic but nonlicensed type, which fails to produce effector cytokines (*e.g.*, interferon-γ) and have decreased cellular cytotoxicity[67]. Similar suppressive immune activity takes place with mediation of another specific surface protein LSECtin, through which LSECs directly identify activated T cells and inhibit immune-response-mediated T cells[68]. These strongly imply that LSECs are important players in immune tolerance, which enhances invasive and metastatic potential of tumor cells. Taking advantage of this point, tumor cells obtain sufficient interaction with LSECs and hepatocytes, so that tumor cells educate these normal liver cells and remodel the immune microenvir-



DOI: 10.3748/wjg.v28.i26.3101 **Copyright** ©The Author(s) 2022.

Figure 2 "Advance under camouflage" hypothesis for replacement histopathological growth pattern. A: "Advance under camouflage" hypothesis of replacement histopathological growth pattern (rHGP) includes four elements. Embryonic features, motility, migration and adhesion contributes to aggressiveness of tumor, which drives tumor progression as an intrinsic factor. Tumor cells interact with liver sinusoidal endothelial cells (LSECs) and hepatocytes, so that tumor cells educate these normal liver cells and remodel the immune microenvironment into a tolerance state *via* CD8+ T cells. In this manner, under camouflage of LSECs, tumor cells are able to survive and slowly progress. Co-opting LSECs enable the tumor to obtain sufficient blood supply and less chance of exposure to immune system. With its unique parenchymal and vessel structure, organ architecture of liver supports the whole advance process; B: Immunosuppressive microenvironment in tumor with rHGP. Under cross interaction of cancer cells and LSECs and other immune cells (unknown mechanism), programmed death (PD) ligand 1 on LSECs and antigen presenting cells binds to PD-1 on T cells making CD8+ T cells activated to a dynamic but nonfunctional type which fails to produce effector cytokines and has decreased cellular cytotoxicity, or is apoptostic. LSEC: Liver sinusoidal endothelial cell; PD: Programmed death.

onment into a state of tolerance. In this manner, under camouflage of LSECs, tumor cells are able to survive and slowly advance. To expand further, the leading cells at the tumor border also initiate adaptive changes, *e.g.*, enhanced metastatic capacity including cell motility, adhesion and migration. Many of them are driven by some embryonic features that are relevant to co-option-type metastases[69,70]. As a whole, embryonic characteristics, interaction between tumor and normal liver cells, and immunological inertia allows efficient and safe advance of tumor cells. Two other factors must be paid attention: (1) Co-opting normal hepatic vasculature reduces the chance of direct exposure of the tumor to the immune system and achieves normalization of the blood supply. In this case, the intratumoral microvessel keep their normal structure and evenly perfuse the whole nodule, which reduces hypoxia and necrosis and is conducive to overall development of the tumor; and (2) Organ structure is another essential aspect. In an organ with a clear and distinct architecture such as the lungs and liver, the metastatic foci can often expand and develop along with its structure[71,72], which implies that organ architecture sometimes directs how tumor cells expand. We propose a complex axis that 'embryonic characteristics playing a primitive driving role - tumor hepatic sinusoidal endothelial cell interaction as the mediator - organ structure as the support' and advance under camouflage hypothesis to explain the underlying mechanism of rHGP.

CONCLUSION

We proposed a novel hypothesis to explain the mechanism of rHGP formation. We denoted four elements, *i.e.*, intrinsic features of cancer cells, tumor vascularization, immunosuppressive microenvironment and host organ structure in the HGP formation. Vascularization and tumor microenvironment have been emphasized in previous studies while the pivotal role of organ structure is addressed for the first time in this review. Common features in angiogenic HGP, for instance, desmoplastic reaction, immune infiltration and sprouting angiogenesis, have been shown. Organ specific morphology was only observed in non-angiogenic HGP, exhibiting angio-tropism and structure-dependent properties. It was observed that non-angiogenic HGP metastases in brain[73] and skin[74] adopted pericytic mimicry and extravascular migratory behavior to get access to the blood. Similarly, metastatic cells remained the mesenchymal structure (pulmonary alveoli and hepatic plate) and presented with alveolar HGP, interstitial HGP and perivascular cuffing HGP in the lung[75], as well as rHGP in the liver. Thus, it

Table 2 Characteristics of desmoplastic histopathological growth pattern and replacement histopathological growth pattern in colorectal cancer liver metastasis

Aspects	dHGP	rHGP
Morphology	Sharp desmoplastic rim separating tumor cells from adjacent liver	Ill-defined border; Tumor cells replace normal hepatocytes along with the architecture of liver plate
Invasion pattern	Expanding and mild	Infiltrative and aggressive
Immune phenotype	Abundant	Desert
Vascularization	Angiogenesis	Non-angiogenesis (vessel co-option)
Organ-specific	No, widely appears in brain, lung and liver	Yes, only appears in liver
Therapy response	Superior response	Inferior response and drug resistance
Clinical outcome	Longer OS, DFS and PFS	Poorer survival and high recurrence

dHGP: Desmoplastic histopathological growth pattern; rHGP: Replacement histopathological growth pattern; OS: Overall survival; DFS: Disease-free survival; PFS: Progression-free survival.

could be hypothesized that the organ architecture provides metastatic tumor cells with attachment and support for their growth. We also highlight the specific interaction of tumor cells with LSECs in rHGP which might indirectly contribute to tumor progress. However, it is still a pure conceptual idea and it remains to be verified.

Clinical implications of HGP are as follows: (1) The association of HGP with clinical outcomes suggests that HGP can be used to stratify patients by survival risk. Early risk stratification helps provide individualized care and guide long-term follow-up; (2) Patients with dHGP are more likely to benefit from systematic therapy, those with rHGP are prone to acquire resistance to AIs and those with non-dHGP are at high risk of positive surgical margin, indicating that HGP can serve as a biomarker for therapy. Based on pre-treatment prediction of HGP, stratification of patients may help clinicians in treatment decision-making and surgical planning for CRCLM patients. The patients with non-dHGP tumor are at higher risk of hepatic recurrence, therefore radical surgery may be of utmost importance. Furthermore, combination therapy would be an inevitable choice for the subgroup with rHGP. Nevertheless, the above benefit from HGP is on the premise of identifying HGP by a non-interventional method. In this regard, radiomics aiming to distinguish HGP in combination with other markers may be a powerful tool in classification of patients; and (3) Studies of mechanism of HGP favor development of therapeutic approaches, and it is encouraging that there have been relevant preliminary trails. For instance, vessel co-option was found to be inhibited through suppressing cancer cell motility and migration in rHGP tumor, and inhibitors targeting both angiogenesis and vessel co-option were more effective *in vivo*[30]. Considering the enrichment of fibrotic and angiogenic reaction of dHGP tumors, anti-angiogenic and anti-fibrotic therapies may be effective for these tumors. However, even though both anti-fibrotic[76,77] and anti-VEGF[78] treatment could restore the immune response, these treatments should be used with caution due to the unsatisfying results shown in trials[79].

In addition, we put forward our perspectives on some hot topics. HGP is a miniature of tumor-host reaction and reflects tumor biology and pathological features as well as host immune dynamics. In this sense, HGP builds a bridge between microscopic characteristics and clinical implications. Is HGP plastic? With existence of spatial and temporal heterogeneity, tumors utilize different vascularization at different stages, and their HGP also changes with development of tumor, but knowledge about this is still lacking. What is the key motivation shaping HGP? In addition to motility, invasion and migration giving rise to formation of HGP, the association between HGP and other biological characteristics such as embryonic features, stemness, and spontaneous mutation should be explored. In summary, HGP is a paradox involving several dimensions: malignant and normal cells, central and peripheral sites, angiogenesis and non-angiogenesis, and aggressive and mild characteristics (the summary on characteristics of dHGP and rHGP is listed out in Table 2). Combination of AIs with immune checkpoint inhibitors and AIs with vessel co-option inhibitors showed better effects, suggesting that complex targeted treatment would be a direction for the precision therapy in the future.

FOOTNOTES

Author contributions: Kong BT performed the majority of the writing, and prepared the figures and tables; Fan QS, Wang XM and Zhang Q conceptualized the manuscript; Zhang GL revised the manuscript, provided guidance on the overall concept and execution of the manuscript; and All authors have read and approved the final manuscript.

Supported by National Nature Science Foundation, No. 81873111, No. 82174454, and No. 82074182; Natural Science Foundation of Beijing, No. 7202066.

Conflict-of-interest statement: All authors report no relevant conflicts of interest for this article.

Open-Access: This article is an open-access article that was selected by an in-house editor and fully peer-reviewed by external reviewers. It is distributed in accordance with the Creative Commons Attribution NonCommercial (CC BY-NC 4.0) license, which permits others to distribute, remix, adapt, build upon this work non-commercially, and license their derivative works on different terms, provided the original work is properly cited and the use is non-commercial. See: https://creativecommons.org/Licenses/by-nc/4.0/

Country/Territory of origin: China

ORCID number: Bing-Tan Kong 0000-0001-5352-1406; Qing-Sheng Fan 0000-0002-5648-2833; Xiao-Min Wang 0000-0003-1274-224X; Qing Zhang 0000-0003-3713-4785; Gan-Lin Zhang 0000-0003-3674-3060.

S-Editor: Ma YJ
L-Editor: A
P-Editor: Ma YJ

REFERENCES

1 **Adam R**, de Gramont A, Figueras J, Kokudo N, Kunstlinger F, Loyer E, Poston G, Rougier P, Rubbia-Brandt L, Sobrero A, Teh C, Tejpar S, Van Cutsem E, Vauthey JN, Påhlman L; of the EGOSLIM (Expert Group on OncoSurgery management of LIver Metastases) group. Managing synchronous liver metastases from colorectal cancer: a multidisciplinary international consensus. *Cancer Treat Rev* 2015; **41**: 729-741 [PMID: 26417845 DOI: 10.1016/j.ctrv.2015.06.006]

2 **Jass JR**, Love SB, Northover JM. A new prognostic classification of rectal cancer. *Lancet* 1987; **1**: 1303-1306 [PMID: 2884421 DOI: 10.1016/s0140-6736(87)90552-6]

3 **van Dam PJ**, van der Stok EP, Teuwen LA, Van den Eynden GG, Illemann M, Frentzas S, Majeed AW, Eefsen RL, Coebergh van den Braak RRJ, Lazaris A, Fernandez MC, Galjart B, Laerum OD, Rayes R, Grünhagen DJ, Van de Paer M, Sucaet Y, Mudhar HS, Schvimer M, Nyström H, Kockx M, Bird NC, Vidal-Vanaclocha F, Metrakos P, Simoneau E, Verhoef C, Dirix LY, Van Laere S, Gao ZH, Brodt P, Reynolds AR, Vermeulen PB. International consensus guidelines for scoring the histopathological growth patterns of liver metastasis. *Br J Cancer* 2017; **117**: 1427-1441 [PMID: 28982110 DOI: 10.1038/bjc.2017.334]

4 **Liang JY**, Xi SY, Shao Q, Yuan YF, Li BK, Zheng Y, Wang DS, Wu XJ, Ding PR, Chen G, Li LR, Wang FH, Wang ZQ, Pan ZZ, Xu RH, Li YH. Histopathological growth patterns correlate with the immunoscore in colorectal cancer liver metastasis patients after hepatectomy. *Cancer Immunol Immunother* 2020; **69**: 2623-2634 [PMID: 32601799 DOI: 10.1007/s00262-020-02632-6]

5 **Höppener DJ**, Nierop PMH, Hof J, Sideras K, Zhou G, Visser L, Gouw ASH, de Jong KP, Sprengers D, Kwekkeboom J, Vermeulen PB, Grünhagen DJ, Verhoef C. Enrichment of the tumour immune microenvironment in patients with desmoplastic colorectal liver metastasis. *Br J Cancer* 2020; **123**: 196-206 [PMID: 32418992 DOI: 10.1038/s41416-020-0881-z]

6 **Galjart B**, Nierop PMH, van der Stok EP, van den Braak RRJC, Höppener DJ, Daelemans S, Dirix LY, Verhoef C, Vermeulen PB, Grünhagen DJ. Angiogenic desmoplastic histopathological growth pattern as a prognostic marker of good outcome in patients with colorectal liver metastases. *Angiogenesis* 2019; **22**: 355-368 [PMID: 30637550 DOI: 10.1007/s10456-019-09661-5]

7 **Siriwardana PN**, Luong TV, Watkins J, Turley H, Ghazaley M, Gatter K, Harris AL, Hochhauser D, Davidson BR. Biological and Prognostic Significance of the Morphological Types and Vascular Patterns in Colorectal Liver Metastases (CRLM): Looking Beyond the Tumor Margin. *Medicine (Baltimore)* 2016; **95**: e2924 [PMID: 26937938 DOI: 10.1097/MD.0000000000002924]

8 **Nielsen K**, Rolff HC, Eefsen RL, Vainer B. The morphological growth patterns of colorectal liver metastases are prognostic for overall survival. *Mod Pathol* 2014; **27**: 1641-1648 [PMID: 24851832 DOI: 10.1038/modpathol.2014.4]

9 **Nierop PMH**, Höppener DJ, van der Stok EP, Galjart B, Buisman FE, Balachandran VP, Jarnagin WR, Kingham TP, Allen PJ, Shia J, Vermeulen PB, Groot Koerkamp B, Grünhagen DJ, Verhoef C, D'Angelica MI. Histopathological growth patterns and positive margins after resection of colorectal liver metastases. *HPB (Oxford)* 2020; **22**: 911-919 [PMID: 31735649 DOI: 10.1016/j.hpb.2019.10.015]

10 **Li X**, Zhao Q, An B, Qi J, Wang W, Zhang D, Li Z, Qin C. Prognostic and predictive value of the macroscopic growth pattern in patients undergoing curative resection of colorectal cancer: a single-institution retrospective cohort study of 4,080 Chinese patients. *Cancer Manag Res* 2018; **10**: 1875-1887 [PMID: 30013394 DOI: 10.2147/CMAR.S165279]

11 **Falcão D**, Alexandrino H, Caetano Oliveira R, Martins J, Ferreira L, Martins R, Serôdio M, Martins M, Tralhão JG, Cipriano MA, Castro E Sousa F. Histopathologic patterns as markers of prognosis in patients undergoing hepatectomy for colorectal cancer liver metastases - Pushing growth as an independent risk factor for decreased survival. *Eur J Surg Oncol* 2018; **44**: 1212-1219 [PMID: 29691114 DOI: 10.1016/j.ejso.2018.03.023]

12 **Pinheiro RS**, Herman P, Lupinacci RM, Lai Q, Mello ES, Coelho FF, Perini MV, Pugliese V, Andraus W, Cecconello I, D'Albuquerque LC. Tumor growth pattern as predictor of colorectal liver metastasis recurrence. *Am J Surg* 2014; **207**: 493-

498 [PMID: 24112674 DOI: 10.1016/j.amjsurg.2013.05.015]
13 **Van den Eynden GG**, Bird NC, Majeed AW, Van Laere S, Dirix LY, Vermeulen PB. The histological growth pattern of colorectal cancer liver metastases has prognostic value. *Clin Exp Metastasis* 2012; **29**: 541-549 [PMID: 22476470 DOI: 10.1007/s10585-012-9469-1]
14 **Rajaganeshan R**, Prasad R, Guillou PJ, Scott N, Poston G, Jayne DG. Expression patterns of hypoxic markers at the invasive margin of colorectal cancers and liver metastases. *Eur J Surg Oncol* 2009; **35**: 1286-1294 [PMID: 19540709 DOI: 10.1016/j.ejso.2009.05.008]
15 **Barnhill R**, van Dam PJ, Vermeulen P, Champenois G, Nicolas A, Rawson RV, Wilmott JS, Thompson JF, Long GV, Cassoux N, Roman-Roman S, Busam KJ, Scolyer RA, Lazar AJ, Lugassy C. Replacement and desmoplastic histopathological growth patterns in cutaneous melanoma liver metastases: frequency, characteristics, and robust prognostic value. *J Pathol Clin Res* 2020; **6**: 195-206 [PMID: 32304183 DOI: 10.1002/cjp2.161]
16 **Jayme VR**, Fonseca GM, Amaral IMA, Coelho FF, Kruger JAP, Jeismann VB, Pinheiro RSN, de Mello ES, Herman P. Infiltrative Tumor Borders in Colorectal Liver Metastasis: Should We Enlarge Margin Size? *Ann Surg Oncol* 2021; **28**: 7636-7646 [PMID: 33834322 DOI: 10.1245/s10434-021-09916-w]
17 **Nierop PMH**, Galjart B, Höppener DJ, van der Stok EP, Coebergh van den Braak RRJ, Vermeulen PB, Grünhagen DJ, Verhoef C. Salvage treatment for recurrences after first resection of colorectal liver metastases: the impact of histopathological growth patterns. *Clin Exp Metastasis* 2019; **36**: 109-118 [PMID: 30843120 DOI: 10.1007/s10585-019-09960-7]
18 **Nyström H**, Naredi P, Berglund A, Palmqvist R, Tavelin B, Sund M. Liver-metastatic potential of colorectal cancer is related to the stromal composition of the tumour. *Anticancer Res* 2012; **32**: 5183-5191 [PMID: 23225415 DOI: 10.1016/j.ejso.2012.06.187]
19 **Wu JB**, Sarmiento AL, Fiset PO, Lazaris A, Metrakos P, Petrillo S, Gao ZH. Histologic features and genomic alterations of primary colorectal adenocarcinoma predict growth patterns of liver metastasis. *World J Gastroenterol* 2019; **25**: 3408-3425 [PMID: 31341365 DOI: 10.3748/wjg.v25.i26.3408]
20 **Mlecnik B**, Van den Eynde M, Bindea G, Church SE, Vasaturo A, Fredriksen T, Lafontaine L, Haicheur N, Marliot F, Debetancourt D, Pairet G, Jouret-Mourin A, Gigot JF, Hubert C, Danse E, Dragean C, Carrasco J, Humblet Y, Valge-Archer V, Berger A, Pagès F, Machiels JP, Galon J. Comprehensive Intrametastatic Immune Quantification and Major Impact of Immunoscore on Survival. *J Natl Cancer Inst* 2018; **110** [PMID: 28922789 DOI: 10.1093/jnci/djx123]
21 **Shim JR**, Lee SD, Han SS, Lee SJ, Lee DE, Kim SK, Kim SH, Park SJ, Oh JH. Prognostic significance of ^{18}F-FDG PET/CT in patients with colorectal cancer liver metastases after hepatectomy. *Eur J Surg Oncol* 2018; **44**: 670-676 [PMID: 29459018 DOI: 10.1016/j.ejso.2018.01.243]
22 **Nemeth Z**, Wijker W, Lengyel Z, Hitre E, Borbely K. Metabolic Parameters as Predictors for Progression Free and Overall Survival of Patients with Metastatic Colorectal Cancer. *Pathol Oncol Res* 2020; **26**: 2683-2691 [PMID: 32661836 DOI: 10.1007/s12253-020-00865-5]
23 **Bohlok A**, Duran Derijckere I, Azema H, Lucidi V, Vankerckhove S, Hendlisz A, Van Laethem JL, Vierasu I, Goldman S, Flamen P, Larsimont D, Demetter P, Dirix L, Vermeulen P, Donckier V. Clinico-metabolic characterization improves the prognostic value of histological growth patterns in patients undergoing surgery for colorectal liver metastases. *J Surg Oncol* 2021; **123**: 1773-1783 [PMID: 33751583 DOI: 10.1002/jso.26466]
24 **Baldin P**, Van den Eynde M, Mlecnik B, Bindea G, Beniuga G, Carrasco J, Haicheur N, Marliot F, Lafontaine L, Fredriksen T, Lanthier N, Hubert C, Navez B, Huyghe N, Pagès F, Jouret-Mourin A, Galon J, Komuta M. Prognostic assessment of resected colorectal liver metastases integrating pathological features, RAS mutation and Immunoscore. *J Pathol Clin Res* 2021; **7**: 27-41 [PMID: 32902189 DOI: 10.1002/cjp2.178]
25 **Allard MA**, Nishioka Y, Beghdadi N, Imai K, Gelli M, Yamashita S, Kitano Y, Kokudo T, Yamashita YI, Sa Cunha A, Vibert E, Elias D, Cherqui D, Goere D, Adam R, Baba H, Hasegawa K. Multicentre study of perioperative *versus* adjuvant chemotherapy for resectable colorectal liver metastases. *BJS Open* 2019; **3**: 678-686 [PMID: 31592094 DOI: 10.1002/bjs5.50174]
26 **Araujo R**, Gonen M, Allen P, Blumgart L, DeMatteo R, Fong Y, Kemeny N, Jarnagin W, D'Angelica M. Comparison between perioperative and postoperative chemotherapy after potentially curative hepatic resection for metastatic colorectal cancer. *Ann Surg Oncol* 2013; **20**: 4312-4321 [PMID: 23897009 DOI: 10.1245/s10434-013-3162-8]
27 **Buisman FE**, van der Stok EP, Galjart B, Vermeulen PB, Balachandran VP, Coebergh van den Braak RRJ, Creasy JM, Höppener DJ, Jarnagin WR, Kingham TP, Nierop PMH, Sadot E, Shia J, Groot Koerkamp B, Grünhagen DJ, D'Angelica M, Verhoef C. Histopathological growth patterns as biomarker for adjuvant systemic chemotherapy in patients with resected colorectal liver metastases. *Clin Exp Metastasis* 2020; **37**: 593-605 [PMID: 32691187 DOI: 10.1007/s10585-020-10048-w]
28 **Cremolini C**, Milione M, Marmorino F, Morano F, Zucchelli G, Mennitto A, Prisciandaro M, Lonardi S, Pellegrinelli A, Rossini D, Bergamo F, Aprile G, Urbani L, Morelli L, Schirripa M, Cardellino GG, Fassan M, Fontanini G, de Braud F, Mazzaferro V, Falcone A, Pietrantonio F. Differential histopathologic parameters in colorectal cancer liver metastases resected after triplets plus bevacizumab or cetuximab: a pooled analysis of five prospective trials. *Br J Cancer* 2018; **118**: 955-965 [PMID: 29531324 DOI: 10.1038/s41416-018-0015-z]
29 **Nierop PM**, Höppener DJ, Buisman FE, van der Stok EP, Galjart B, Balachandran VP, Jarnagin WR, Kingham TP, Shia J, Mauer M, Nordlinger B, Julié C, Groot Koerkamp B, Doukas M, Vermeulen PB, Grünhagen DJ, D'Angelica MI, Verhoef C. Preoperative systemic chemotherapy alters the histopathological growth patterns of colorectal liver metastases. *J Pathol Clin Res* 2022; **8**: 48-64 [PMID: 34480530 DOI: 10.1002/cjp2.235]
30 **Frentzas S**, Simoneau E, Bridgeman VL, Vermeulen PB, Foo S, Kostaras E, Nathan M, Wotherspoon A, Gao ZH, Shi Y, Van den Eynden G, Daley F, Peckitt C, Tan X, Salman A, Lazaris A, Gazinska P, Berg TJ, Eltahir Z, Ritsma L, Van Rheenen J, Khashper A, Brown G, Nystrom H, Sund M, Van Laere S, Loyer E, Dirix L, Cunningham D, Metrakos P, Reynolds AR. Vessel co-option mediates resistance to anti-angiogenic therapy in liver metastases. *Nat Med* 2016; **22**: 1294-1302 [PMID: 27748747 DOI: 10.1038/nm.4197]
31 **Kuczynski EA**, Yin M, Bar-Zion A, Lee CR, Butz H, Man S, Daley F, Vermeulen PB, Yousef GM, Foster FS, Reynolds

AR, Kerbel RS. Co-option of Liver Vessels and Not Sprouting Angiogenesis Drives Acquired Sorafenib Resistance in Hepatocellular Carcinoma. *J Natl Cancer Inst* 2016; **108** [PMID: 27059374 DOI: 10.1093/jnci/djw030]

32 **Lazaris A**, Amri A, Petrillo SK, Zoroquiain P, Ibrahim N, Salman A, Gao ZH, Vermeulen PB, Metrakos P. Vascularization of colorectal carcinoma liver metastasis: insight into stratification of patients for anti-angiogenic therapies. *J Pathol Clin Res* 2018; **4**: 184-192 [PMID: 29654716 DOI: 10.1002/cjp2.100]

33 **Hillen F**, Griffioen AW. Tumour vascularization: sprouting angiogenesis and beyond. *Cancer Metastasis Rev* 2007; **26**: 489-502 [PMID: 17717633 DOI: 10.1007/s10555-007-9094-7]

34 **Paku S**, Paweletz N. First steps of tumor-related angiogenesis. *Lab Invest* 1991; **65**: 334-346 [PMID: 1716330]

35 **Jain RK**. Normalization of tumor vasculature: an emerging concept in antiangiogenic therapy. *Science* 2005; **307**: 58-62 [PMID: 15637262 DOI: 10.1126/science.1104819]

36 **Batchelor TT**, Sorensen AG, di Tomaso E, Zhang WT, Duda DG, Cohen KS, Kozak KR, Cahill DP, Chen PJ, Zhu M, Ancukiewicz M, Mrugala MM, Plotkin S, Drappatz J, Louis DN, Ivy P, Scadden DT, Benner T, Loeffler JS, Wen PY, Jain RK. AZD2171, a pan-VEGF receptor tyrosine kinase inhibitor, normalizes tumor vasculature and alleviates edema in glioblastoma patients. *Cancer Cell* 2007; **11**: 83-95 [PMID: 17222792 DOI: 10.1016/j.ccr.2006.11.021]

37 **Tolaney SM**, Boucher Y, Duda DG, Martin JD, Seano G, Ancukiewicz M, Barry WT, Goel S, Lahdenrata J, Isakoff SJ, Yeh ED, Jain SR, Golshan M, Brock J, Snuderl M, Winer EP, Krop IE, Jain RK. Role of vascular density and normalization in response to neoadjuvant bevacizumab and chemotherapy in breast cancer patients. *Proc Natl Acad Sci U S A* 2015; **112**: 14325-14330 [PMID: 26578779 DOI: 10.1073/pnas.1518808112]

38 **Irie T**, Tsushima Y, Terahata S, Hatsuse K, Kusano S. Rim enhancement in colorectal metastases at CT during infusion hepatic arteriography. Does it represent liver parenchyma or live tumor cell zone? *Acta Radiol* 1997; **38**: 416-421 [PMID: 9191433 DOI: 10.1080/02841859709172093]

39 **Terayama N**, Matsui O, Ueda K, Kobayashi S, Sanada J, Gabata T, Kawamori Y, Kadoya M. Peritumoral rim enhancement of liver metastasis: hemodynamics observed on single-level dynamic CT during hepatic arteriography and histopathologic correlation. *J Comput Assist Tomogr* 2002; **26**: 975-980 [PMID: 12488746 DOI: 10.1097/00004728-200211000-00021]

40 **Kanematsu M**, Matsuo M, Yamada Y, Semelka RC, Kondo H, Goshima S, Hoshi H, Moriyama N. Perilesional hyperintense rim of malignant hepatic tumors on ferumoxide-enhanced T1-weighted gradient-echo MR images: correlation between MR imaging and histopathologic findings. *J Magn Reson Imaging* 2003; **18**: 40-48 [PMID: 12815638 DOI: 10.1002/jmri.10328]

41 **Semelka RC**, Hussain SM, Marcos HB, Woosley JT. Perilesional enhancement of hepatic metastases: correlation between MR imaging and histopathologic findings-initial observations. *Radiology* 2000; **215**: 89-94 [PMID: 10751472 DOI: 10.1148/radiology.215.1.r00mr2989]

42 **Cheng J**, Wei J, Tong T, Sheng W, Zhang Y, Han Y, Gu D, Hong N, Ye Y, Tian J, Wang Y. Prediction of Histopathologic Growth Patterns of Colorectal Liver Metastases with a Noninvasive Imaging Method. *Ann Surg Oncol* 2019; **26**: 4587-4598 [PMID: 31605342 DOI: 10.1245/s10434-019-07910-x]

43 **Wei S**, Han Y, Zeng H, Ye S, Cheng J, Chai F, Wei J, Zhang J, Hong N, Bao Y, Zhou J, Ye Y, Meng X, Zhou Y, Deng Y, Qiu M, Tian J, Wang Y. Radiomics diagnosed histopathological growth pattern in prediction of response and 1-year progression free survival for colorectal liver metastases patients treated with bevacizumab containing chemotherapy. *Eur J Radiol* 2021; **142**: 109863 [PMID: 34343846 DOI: 10.1016/j.ejrad.2021.109863]

44 **Chun YS**, Vauthey JN, Boonsirikamchai P, Maru DM, Kopetz S, Palavecino M, Curley SA, Abdalla EK, Kaur H, Charnsangavej C, Loyer EM. Association of computed tomography morphologic criteria with pathologic response and survival in patients treated with bevacizumab for colorectal liver metastases. *JAMA* 2009; **302**: 2338-2344 [PMID: 19952320 DOI: 10.1001/jama.2009.1755]

45 **Shindoh J**, Loyer EM, Kopetz S, Boonsirikamchai P, Maru DM, Chun YS, Zimmitti G, Curley SA, Charnsangavej C, Aloia TA, Vauthey JN. Optimal morphologic response to preoperative chemotherapy: an alternate outcome end point before resection of hepatic colorectal metastases. *J Clin Oncol* 2012; **30**: 4566-4572 [PMID: 23150701 DOI: 10.1200/JCO.2012.45.2854]

46 **Han Y**, Chai F, Wei J, Yue Y, Cheng J, Gu D, Zhang Y, Tong T, Sheng W, Hong N, Ye Y, Wang Y, Tian J. Identification of Predominant Histopathological Growth Patterns of Colorectal Liver Metastasis by Multi-Habitat and Multi-Sequence Based Radiomics Analysis. *Front Oncol* 2020; **10**: 1363 [PMID: 32923388 DOI: 10.3389/fonc.2020.01363]

47 **Dohan A**, Gallix B, Guiu B, Le Malicot K, Reinhold C, Soyer P, Bennouna J, Ghiringhelli F, Barbier E, Boige V, Taieb J, Bouché O, François E, Phelip JM, Borel C, Faroux R, Seitz JF, Jacquot S, Ben Abdelghani M, Khemissa-Akouz F, Genet D, Jouve JL, Rinaldi Y, Desseigne F, Texereau P, Suc E, Lepage C, Aparicio T, Hoeffel C; PRODIGE 9 Investigators and PRODIGE 20 Investigators. Early evaluation using a radiomic signature of unresectable hepatic metastases to predict outcome in patients with colorectal cancer treated with FOLFIRI and bevacizumab. *Gut* 2020; **69**: 531-539 [PMID: 31101691 DOI: 10.1136/gutjnl-2018-316407]

48 **Choi SH**, Kim SY, Park SH, Kim KW, Lee JY, Lee SS, Lee MG. Diagnostic performance of CT, gadoxetate disodium-enhanced MRI, and PET/CT for the diagnosis of colorectal liver metastasis: Systematic review and meta-analysis. *J Magn Reson Imaging* 2018; **47**: 1237-1250 [PMID: 28901685 DOI: 10.1002/jmri.25852]

49 **Eefsen RL**, Engelholm L, Alpizar-Alpizar W, Van den Eynden GG, Vermeulen PB, Christensen IJ, Laerum OD, Rolff HC, Høyer-Hansen G, Vainer B, Osterlind K, Illemann M. Inflammation and uPAR-Expression in Colorectal Liver Metastases in Relation to Growth Pattern and Neo-adjuvant Therapy. *Cancer Microenviron* 2015; **8**: 93-100 [PMID: 26268716 DOI: 10.1007/s12307-015-0172-z]

50 **Illemann M**, Bird N, Majeed A, Laerum OD, Lund LR, Danø K, Nielsen BS. Two distinct expression patterns of urokinase, urokinase receptor and plasminogen activator inhibitor-1 in colon cancer liver metastases. *Int J Cancer* 2009; **124**: 1860-1870 [PMID: 19123477 DOI: 10.1002/ijc.24166]

51 **Garcia-Vicién G**, Mezheyeuski A, Bañuls M, Ruiz-Roig N, Molleví DG. The Tumor Microenvironment in Liver Metastases from Colorectal Carcinoma in the Context of the Histologic Growth Patterns. *Int J Mol Sci* 2021; **22** [PMID: 33546502 DOI: 10.3390/ijms22041544]

52 **Jiang H**, Torphy RJ, Steiger K, Hongo H, Ritchie AJ, Kriegsmann M, Horst D, Umetsu SE, Joseph NM, McGregor K, Pishvaian MJ, Blais EM, Lu B, Li M, Hollingsworth M, Stashko C, Volmar K, Yeh JJ, Weaver VM, Wang ZJ, Tempero MA, Weichert W, Collisson EA. Pancreatic ductal adenocarcinoma progression is restrained by stromal matrix. *J Clin Invest* 2020; **130**: 4704-4709 [PMID: 32749238 DOI: 10.1172/JCI136760]

53 **Brunner SM**, Kesselring R, Rubner C, Martin M, Jeiter T, Boerner T, Ruemmele P, Schlitt HJ, Fichtner-Feigl S. Prognosis according to histochemical analysis of liver metastases removed at liver resection. *Br J Surg* 2014; **101**: 1681-1691 [PMID: 25331841 DOI: 10.1002/bjs.9627]

54 **Iwaya K**, Oikawa K, Semba S, Tsuchiya B, Mukai Y, Otsubo T, Nagao T, Izumi M, Kuroda M, Domoto H, Mukai K. Correlation between liver metastasis of the colocalization of actin-related protein 2 and 3 complex and WAVE2 in colorectal carcinoma. *Cancer Sci* 2007; **98**: 992-999 [PMID: 17459058 DOI: 10.1111/j.1349-7006.2007.00488.x]

55 **Rada M**, Kapelanski-Lamoureux A, Petrillo S, Tabariès S, Siegel P, Reynolds AR, Lazaris A, Metrakos P. Runt related transcription factor-1 plays a central role in vessel co-option of colorectal cancer liver metastases. *Commun Biol* 2021; **4**: 950 [PMID: 34376784 DOI: 10.1038/s42003-021-02481-8]

56 **Tabariès S**, Siegel PM. The role of claudins in cancer metastasis. *Oncogene* 2017; **36**: 1176-1190 [PMID: 27524421 DOI: 10.1038/onc.2016.289]

57 **Tabariès S**, Annis MG, Lazaris A, Petrillo SK, Huxham J, Abdellatif A, Palmieri V, Chabot J, Johnson RM, Van Laere S, Verhoef C, Hachem Y, Yumeen S, Meti N, Omeroglu A, Altinel G, Gao ZH, Yu ASL, Grünhagen DJ, Vermeulen P, Metrakos P, Siegel PM. Claudin-2 promotes colorectal cancer liver metastasis and is a biomarker of the replacement type growth pattern. *Commun Biol* 2021; **4**: 657 [PMID: 34079064 DOI: 10.1038/s42003-021-02189-9]

58 **Tabariès S**, Dupuy F, Dong Z, Monast A, Annis MG, Spicer J, Ferri LE, Omeroglu A, Basik M, Amir E, Clemons M, Siegel PM. Claudin-2 promotes breast cancer liver metastasis by facilitating tumor cell interactions with hepatocytes. *Mol Cell Biol* 2012; **32**: 2979-2991 [PMID: 22645303 DOI: 10.1128/MCB.00299-12]

59 **Tabariès S**, McNulty A, Ouellet V, Annis MG, Dessureault M, Vinette M, Hachem Y, Lavoie B, Omeroglu A, Simon HG, Walsh LA, Kimbung S, Hedenfalk I, Siegel PM. Afadin cooperates with Claudin-2 to promote breast cancer metastasis. *Genes Dev* 2019; **33**: 180-193 [PMID: 30692208 DOI: 10.1101/gad.319194.118]

60 **Ahmad SA**, Liu W, Jung YD, Fan F, Wilson M, Reinmuth N, Shaheen RM, Bucana CD, Ellis LM. The effects of angiopoietin-1 and -2 on tumor growth and angiogenesis in human colon cancer. *Cancer Res* 2001; **61**: 1255-1259 [PMID: 11245414 DOI: 10.1002/1097-0142(20010215)91:4<874::AID-CNCR1076>3.0.CO;2-O]

61 **Ibrahim NS**, Lazaris A, Rada M, Petrillo SK, Huck L, Hussain S, Ouladan S, Gao ZH, Gregorieff A, Essalmani R, Seidah NG, Metrakos P. Angiopoietin1 Deficiency in Hepatocytes Affects the Growth of Colorectal Cancer Liver Metastases (CRCLM). *Cancers (Basel)* 2019; **12** [PMID: 31877668 DOI: 10.3390/cancers12010035]

62 **Palmieri V**, Lazaris A, Mayer TZ, Petrillo SK, Alamri H, Rada M, Jarrouj G, Park WY, Gao ZH, McDonald PP, Metrakos P. Neutrophils expressing lysyl oxidase-like 4 protein are present in colorectal cancer liver metastases resistant to anti-angiogenic therapy. *J Pathol* 2020; **251**: 213-223 [PMID: 32297656 DOI: 10.1002/path.5449]

63 **Cordero-Espinoza L**, Huch M. The balancing act of the liver: tissue regeneration versus fibrosis. *J Clin Invest* 2018; **128**: 85-96 [PMID: 29293095 DOI: 10.1172/JCI93562]

64 **van Dam PJ**, Daelemans S, Ross E, Waumans Y, Van Laere S, Latacz E, Van Steen R, De Pooter C, Kockx M, Dirix L, Vermeulen PB. Histopathological growth patterns as a candidate biomarker for immunomodulatory therapy. *Semin Cancer Biol* 2018; **52**: 86-93 [PMID: 29355613 DOI: 10.1016/j.semcancer.2018.01.009]

65 **Schuppan D**, Kim YO. Evolving therapies for liver fibrosis. *J Clin Invest* 2013; **123**: 1887-1901 [PMID: 23635787 DOI: 10.1172/JCI66028]

66 **Arteta B**, Lasuen N, Lopategi A, Sveinbjörnsson B, Smedsrød B, Vidal-Vanaclocha F. Colon carcinoma cell interaction with liver sinusoidal endothelium inhibits organ-specific antitumor immunity through interleukin-1-induced mannose receptor in mice. *Hepatology* 2010; **51**: 2172-2182 [PMID: 20513002 DOI: 10.1002/hep.23590]

67 **Kubes P**, Jenne C. Immune Responses in the Liver. *Annu Rev Immunol* 2018; **36**: 247-277 [PMID: 29328785 DOI: 10.1146/annurev-immunol-051116-052415]

68 **Tang L**, Yang J, Liu W, Tang X, Chen J, Zhao D, Wang M, Xu F, Lu Y, Liu B, Sun Q, Zhang L, He F. Liver sinusoidal endothelial cell lectin, LSECtin, negatively regulates hepatic T-cell immune response. *Gastroenterology* 2009; **137**: 1498-508.e1 [PMID: 19632227 DOI: 10.1053/j.gastro.2009.07.051]

69 **Lugassy C**, Kleinman HK, Vermeulen PB, Barnhill RL. Angiotropism, pericytic mimicry and extravascular migratory metastasis: an embryogenesis-derived program of tumor spread. *Angiogenesis* 2020; **23**: 27-41 [PMID: 31720876 DOI: 10.1007/s10456-019-09695-9]

70 **Sakariassen PØ**, Prestegarden L, Wang J, Skaftnesmo KO, Mahesparan R, Molthoff C, Sminia P, Sundlisaeter E, Misra A, Tysnes BB, Chekenya M, Peters H, Lende G, Kalland KH, Øyan AM, Petersen K, Jonassen I, van der Kogel A, Feuerstein BG, Terzis AJ, Bjerkvig R, Enger PØ. Angiogenesis-independent tumor growth mediated by stem-like cancer cells. *Proc Natl Acad Sci U S A* 2006; **103**: 16466-16471 [PMID: 17056721 DOI: 10.1073/pnas.0607668103]

71 **Donnem T**, Reynolds AR, Kuczynski EA, Gatter K, Vermeulen PB, Kerbel RS, Harris AL, Pezzella F. Non-angiogenic tumours and their influence on cancer biology. *Nat Rev Cancer* 2018; **18**: 323-336 [PMID: 29520090 DOI: 10.1038/nrc.2018.14]

72 **Kuczynski EA**, Vermeulen PB, Pezzella F, Kerbel RS, Reynolds AR. Vessel co-option in cancer. *Nat Rev Clin Oncol* 2019; **16**: 469-493 [PMID: 30816337 DOI: 10.1038/s41571-019-0181-9]

73 **Berghoff AS**, Rajky O, Winkler F, Bartsch R, Furtner J, Hainfellner JA, Goodman SL, Weller M, Schittenhelm J, Preusser M. Invasion patterns in brain metastases of solid cancers. *Neuro Oncol* 2013; **15**: 1664-1672 [PMID: 24084410 DOI: 10.1093/neuonc/not112]

74 **Lugassy C**, Zadran S, Bentolila LA, Wadehra M, Prakash R, Carmichael ST, Kleinman HK, Péault B, Larue L, Barnhill RL. Angiotropism, pericytic mimicry and extravascular migratory metastasis in melanoma: an alternative to intravascular cancer dissemination. *Cancer Microenviron* 2014; **7**: 139-152 [PMID: 25304454 DOI: 10.1007/s12307-014-0156-4]

75 **Bridgeman VL**, Vermeulen PB, Foo S, Bilecz A, Daley F, Kostaras E, Nathan MR, Wan E, Frentzas S, Schweiger T, Hegedus B, Hoetzenecker K, Renyi-Vamos F, Kuczynski EA, Vasudev NS, Larkin J, Gore M, Dvorak HF, Paku S, Kerbel

RS, Dome B, Reynolds AR. Vessel co-option is common in human lung metastases and mediates resistance to anti-angiogenic therapy in preclinical lung metastasis models. *J Pathol* 2017; **241**: 362-374 [PMID: 27859259 DOI: 10.1002/path.4845]

76 **Feig C**, Jones JO, Kraman M, Wells RJ, Deonarine A, Chan DS, Connell CM, Roberts EW, Zhao Q, Caballero OL, Teichmann SA, Janowitz T, Jodrell DI, Tuveson DA, Fearon DT. Targeting CXCL12 from FAP-expressing carcinoma-associated fibroblasts synergizes with anti-PD-L1 immunotherapy in pancreatic cancer. *Proc Natl Acad Sci U S A* 2013; **110**: 20212-20217 [PMID: 24277834 DOI: 10.1073/pnas.1320318110]

77 **Kraman M**, Bambrough PJ, Arnold JN, Roberts EW, Magiera L, Jones JO, Gopinathan A, Tuveson DA, Fearon DT. Suppression of antitumor immunity by stromal cells expressing fibroblast activation protein-alpha. *Science* 2010; **330**: 827-830 [PMID: 21051638 DOI: 10.1126/science.1195300]

78 **Wallin JJ**, Bendell JC, Funke R, Sznol M, Korski K, Jones S, Hernandez G, Mier J, He X, Hodi FS, Denker M, Leveque V, Cañamero M, Babitski G, Koeppen H, Ziai J, Sharma N, Gaire F, Chen DS, Waterkamp D, Hegde PS, McDermott DF. Atezolizumab in combination with bevacizumab enhances antigen-specific T-cell migration in metastatic renal cell carcinoma. *Nat Commun* 2016; **7**: 12624 [PMID: 27571927 DOI: 10.1038/ncomms12624]

79 **Özdemir BC**, Pentcheva-Hoang T, Carstens JL, Zheng X, Wu CC, Simpson TR, Laklai H, Sugimoto H, Kahlert C, Novitskiy SV, De Jesus-Acosta A, Sharma P, Heidari P, Mahmood U, Chin L, Moses HL, Weaver VM, Maitra A, Allison JP, LeBleu VS, Kalluri R. Depletion of carcinoma-associated fibroblasts and fibrosis induces immunosuppression and accelerates pancreas cancer with reduced survival. *Cancer Cell* 2014; **25**: 719-734 [PMID: 24856586 DOI: 10.1016/j.ccr.2014.04.005]

World Journal of Gastroenterology

Submit a Manuscript: https://www.f6publishing.com

World J Gastroenterol 2022 July 14; 28(26): 3116-3131

DOI: 10.3748/wjg.v28.i26.3116

ISSN 1007-9327 (print) ISSN 2219-2840 (online)

MINIREVIEWS

Role of gadoxetic acid-enhanced liver magnetic resonance imaging in the evaluation of hepatocellular carcinoma after locoregional treatment

Marco Gatti, Cesare Maino, Fatemeh Darvizeh, Alessandro Serafini, Eleonora Tricarico, Alessia Guarneri, Riccardo Inchingolo, Davide Ippolito, Umberto Ricardi, Paolo Fonio, Riccardo Faletti

Specialty type: Gastroenterology and hepatology

Provenance and peer review: Invited article; Externally peer reviewed.

Peer-review model: Single blind

Peer-review report's scientific quality classification

Grade A (Excellent): 0
Grade B (Very good): B
Grade C (Good): C
Grade D (Fair): 0
Grade E (Poor): 0

P-Reviewer: Chai RM, China; Hu Q, China
A-Editor: Dong QJ, China

Received: February 25, 2022
Peer-review started: February 25, 2022
First decision: April 5, 2022
Revised: April 25, 2022
Accepted: June 16, 2022
Article in press: June 16, 2022
Published online: July 14, 2022

Marco Gatti, Alessandro Serafini, Paolo Fonio, Riccardo Faletti, Department of Surgical Sciences, University of Turin, Turin 10126, Italy

Cesare Maino, Davide Ippolito, Department of Diagnostic Radiology, University of Milano-Bicocca, Monza 20900, Italy

Cesare Maino, Davide Ippolito, Department of Diagnostic Radiology, Ospedale San Gerardo, Monza 20900, Italy

Fatemeh Darvizeh, School of Medicine, Vita-Salute San Raffaele University, Milan 20121, Italy

Eleonora Tricarico, Department of Radiology, "F. Perinei" Hospital, Altamura (BA) 70022, Italy

Alessia Guarneri, Umberto Ricardi, Department of Oncology, University of Turin, Turin 10126, Italy

Riccardo Inchingolo, Interventional Radiology Unit, "F. Miulli" Regional General Hospital, Acquaviva delle Fonti (BA) 70021, Italy

Corresponding author: Marco Gatti, MD, Research Fellow, Department of Surgical Sciences, University of Turin, Via Genova 3, Turin 10126, Italy. marcogatti17@gmail.com

Abstract

Locoregional treatments, as alternatives to surgery, play a key role in the management of hepatocellular carcinoma (HCC). Liver magnetic resonance imaging (MRI) enables a multiparametric assessment, going beyond the traditional dynamic computed tomography approach. Moreover, the use of hepatobiliary agents can improve diagnostic accuracy and are becoming important in the diagnosis and follow-up of HCC. However, the main challenge is to quickly identify classical responses to loco-regional treatments in order to determine the most suitable management strategy for each patient. The aim of this review is to provide a summary of the most common and uncommon liver MRI findings in patients who underwent loco-regional treatments for HCC, with a special focus on ablative therapies (radiofrequency, microwaves and cryoablation), trans-arterial chemoembolization, trans-arterial radio-embolization and stereotactic ablative radiotherapy techniques, considering the usefulness of gadoxetate

disodium (Gd-EOB-DTPA) contrast agent.

Key Words: Carcinoma; Hepatocellular; Magnetic resonance imaging; Gd-EOB-DTPA; Radiofrequency ablation; Catheter ablation; Ablation techniques

©The Author(s) 2022. Published by Baishideng Publishing Group Inc. All rights reserved.

Core Tip: Ablation techniques are useful tools in the treatment of patients with hepatocellular carcinoma, both in case with a small lesion and as a bridging option prior to surgical resection or liver transplantation and in addition to palliative treatment in advanced disease. In clinical practice it is of utmost importance to acquire a specific skill to identify classical magnetic resonance imaging appearance of the treated lesion and for early detection of tumor recurrence, to guarantee the best possible management for each patient.

Citation: Gatti M, Maino C, Darvizeh F, Serafini A, Tricarico E, Guarneri A, Inchingolo R, Ippolito D, Ricardi U, Fonio P, Faletti R. Role of gadoxetic acid-enhanced liver magnetic resonance imaging in the evaluation of hepatocellular carcinoma after locoregional treatment. *World J Gastroenterol* 2022; 28(26): 3116-3131
URL: https://www.wjgnet.com/1007-9327/full/v28/i26/3116.htm
DOI: https://dx.doi.org/10.3748/wjg.v28.i26.3116

INTRODUCTION

Hepatocellular carcinoma (HCC) is the most common primary liver cancer and represents a major public health issue worldwide[1]. Treatment of patients with HCC is closely related to Barcelona Clinic Liver Cancer (BCLC) stage. Locoregional treatments, as alternatives to surgery, play a key role in the management of HCC. Percutaneous thermoablation strategies are considered as an alternative to surgery in patients with BCLC 0-A, transcatheter embolization therapies are essential in patients with more advanced disease (*i.e.*, BCLC B) and both together with Stereotactic Body Radiation Therapy (SBRT) are useful in patients who are not a surgical candidate[2].

The evaluation of both short- and long-term treatment outcomes is crucial for patient management. According to the guidelines, this evaluation should be performed using either dynamic computed tomography (CT) or magnetic resonance imaging (MRI)[2].

Liver MRI enables a multiparametric assessment, going beyond the vascularity assessment provided by traditional dynamic CT[3,4]. In recent years, liver MRI has made significant advances in the evaluation of HCC thanks to the introduction of new sequences for non-contrast evaluation (*e.g.*, diffusion-weighted sequences), the high temporal resolution sequences for optimal contrast enhancement assessment[5,6] and finally, the use of hepatobiliary contrast agents (gadoxetate disodium: Gd-EOB-DTPA, Eovist/Primovist; gadobenate disodium: Gd-BOPTA, Multihance). Gd-EOB–DTPA combines the properties of an extracellular agent, allowing for conventional contrast-enhanced multiphasic imaging, and a hepatocyte agent, allowing for hepatocyte uptake and biliary excretion evaluation, with the added benefit of tumor assessment in the transitional phase (TP) and delayed hepatobiliary phase (HBP) (20-min)[4,7,8]. This contrast agent improves the diagnostic accuracy and is becoming increasingly important in the detection of HCC[9].

The use of liver MRI with hepatobiliary contrast agents has become critical in patients with HCC. Therefore, understanding the typical and atypical features of treatment outcomes and recurrences is of paramount importance for proper treatment strategy.

The purpose of this review is to provide a comprehensive overview of locoregional therapies and to describe how to assess treatment outcomes using contrast-enhanced hepatobiliary MRI.

ABLATIVE THERAPIES

There are several ablation techniques available for the treatment of HCC as reported in a recent literature review by Makary *et al*[10], such as radiofrequency ablation (RFA), microwaves (MWA), cryoablation (CA), irreversible electroporation (IRE), laser-induced interstitial thermotherapy (LITT), and high-intensity focused ultrasound (HIFU). The process of choosing among alternative techniques is principally based on institutional expertise and should be fitted to each patient. The main target for the abovementioned treatment methods is an early-stage HCC with a maximum axial diameter of 3 cm with BCLC class 0 or A. Moreover, this approach may lead to better clinical outcomes in patients with larger HCC lesions (axial diameter of 3 cm to 5 cm), when combined with trans-arterial chemoembolization

(TACE)[10].

Even though the ablation techniques are widely performed, they are not risk-free: it is important to underline that the treated patients can present post-ablation syndrome, loco-regional bleeding, and adjacent organs injuries. The ablative therapy shows similar outcomes to surgical resection in the treatment of HCC with a maximum diameter of 3 cm, with a remarkable advantage of no pre-and post-surgical complications[10].

Most published studies on electronic medical databases including PubMed and Web of Science are strictly linked to RFA and MWA, while CA, IRE, LITT, and HIFU are not deeply evaluated and consequently data regarding response to therapy are lacking. On this basis, we'll present the most common MR imaging findings regarding RFA, MWA and CA therapies.

RFA

RFA technique relies on the destruction of tumoral tissue by producing frictional heat using rapidly alternating electrical current thanks to the application of at least one electrode inside the region of treatment. The ablation zone includes a wider region than the tumor itself, of at least 5 mm to 10 mm[8]. The use of RFA results in hyperthermia-induced coagulation necrosis and represents a heterogeneous low or mixed signal intensity on T1-weighted (T1w) and homogeneously low signal intensity on T2-weighted (T2w) images.

After contrast media administration (extracellular or hepatobiliary agents), the RFA zone manifests as a well-demarcated hypointense area with the absence of contrast enhancement[8]. The presence of slight rim signal intensity on T2w images and contrast enhancement especially in the equilibrium phase should be considered as a physiological response to thermal injury, mainly during early follow-up[11]. The typical appearance of HCC recurrence is the hypervascularity on arterial phase [arterial phase hyperenhancement (APHE)], hypointensity on portal-venous and HBPs. However, in clinical practice, the discrimination between hyperemia and residual HCC might be difficult. This aspect was demonstrated by Mikami *et al*[12], who reported a typical enhancement pattern in only 17.5% of recurrent HCCs, while 40.6% with APHE without washout in the portal venous phase and 11.9% with portal venous phase washout without APHE.

In this setting, the use of Gd-EOB-DTPA can help to distinguish vascular pseudolesions from hypervascular tumors including recurrent HCC[13]. Since 2013, it has been reported[14] the efficacy of EOB-MRI in the decision-making of curative treatment for HCC: it was demonstrated that the HBP improves the diagnostic accuracy and treatment decision making in the early-stage HCC and these results can perfectly fit candidates to RFA. Imai *et al*[15], by enrolling 97 patients who underwent RFA, revealed that EOB-MRI had higher diagnostic accuracy and sensitivity for detection of recurrent hypervascular HCC (44 *vs* 24, $P < 0.001$) in comparison to CT. They also reported a good inter-observer agreement between the 2 readers, underlying the effectiveness of EOB-MRI.

As known, the main advantage of EOB-MRI is the HBP, where the radiologist can face a hypointense nodule without significant hypervascular appearance. On this basis, it is important to determine the risk of non-hypervascular HCC recurrence after loco-regional treatment. The systematic review and meta-analysis by Kim *et al*[16] demonstrated the post-ablation recurrence of HCC: they showed that hypointense nodules in the HBP represent a high-risk factor for recurrence (hazard ratio = 1.74-3.07), underlying the importance of EOB-MRI in the detection of HCC recurrence post-RFA.

More recently, a retrospective study by Bae *et al*[17] on 183 patients who underwent different treatments including RFA, showed that satellite nodules and peritumoral hypointensity on HBP images were associated with poor disease-free survival and overall survival ($P = 0.018$ and $P = 0.016$, respectively).

On the other hand, the study by Rimola *et al*[18], on 49 patients who underwent locoregional treatment, determined that MRI with extracellular agents has a similar specificity in detecting viable HCC in comparison to EOB-MRI (84% *vs* 85%, respectively), with a higher AUROC (0.80 *vs* 0.72, respectively). These findings are not in line with most studies, however, should be carefully considered due to the small sample size and the remarkable risk of bias, since different ablation techniques were evaluated.

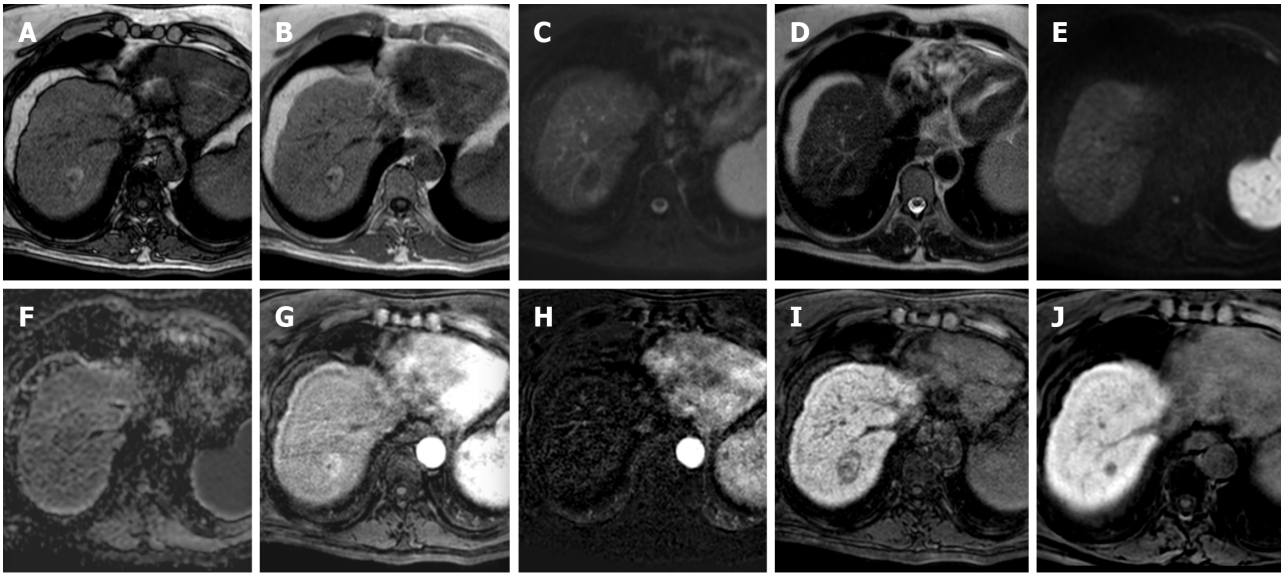
Finally, EOB-MRI was found efficient not only in the evaluation of treatment response but also in the feasibility of ablative margin grading before RFA. Koda *et al*[19] by enrolling 124 HCCs, showed that EOB-MRI enables an early assessment of RFA effectiveness in the majority of HCC nodules with the tumor size as an independent predictor factor for local tumor progression.

To conclude, EOB-MRI can be considered as a useful tool in the detection of HCC recurrence after RFA treatment, however, large prospective studies are needed to determine a more accurate evaluation of diagnostic performance.

Figure 1 depicts a liver MRI after RF treatment with no evidence of disease persistence or relapse, and Figure 2 depicts its evolution. Figure 3 depicts a case of HCC recurrence after RF treatment.

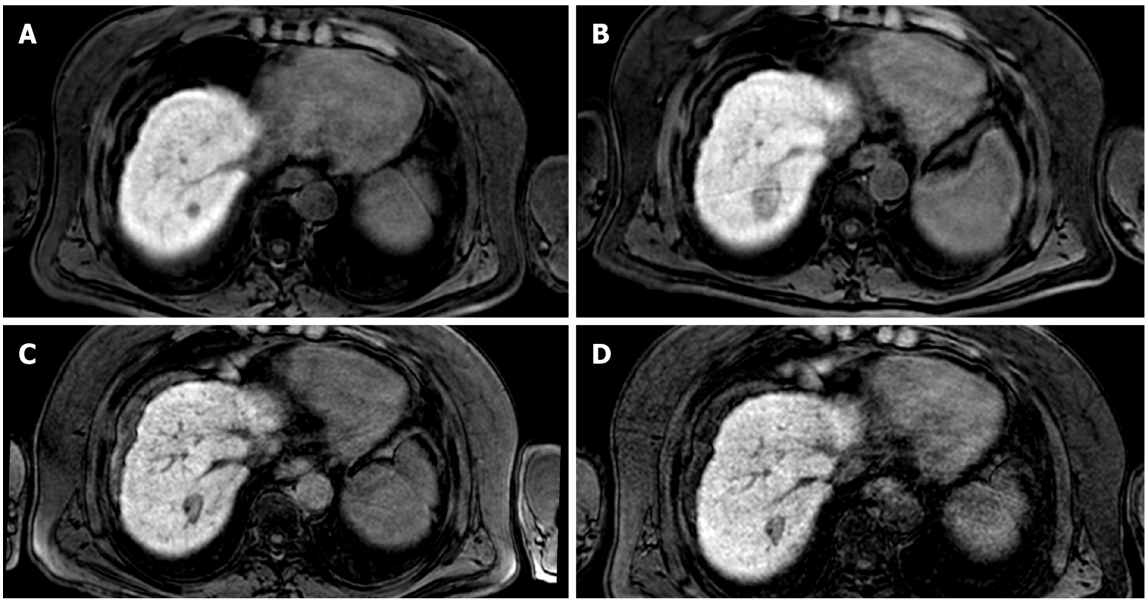
Microwave ablation

MWA technique is based on analogous physical principles of RFA, however, it employs an antenna that produces electromagnetic waves which can interact with water molecules and, consequently, raises the temperature[20].



DOI: 10.3748/wjg.v28.i26.3116 **Copyright** ©The Author(s) 2022.

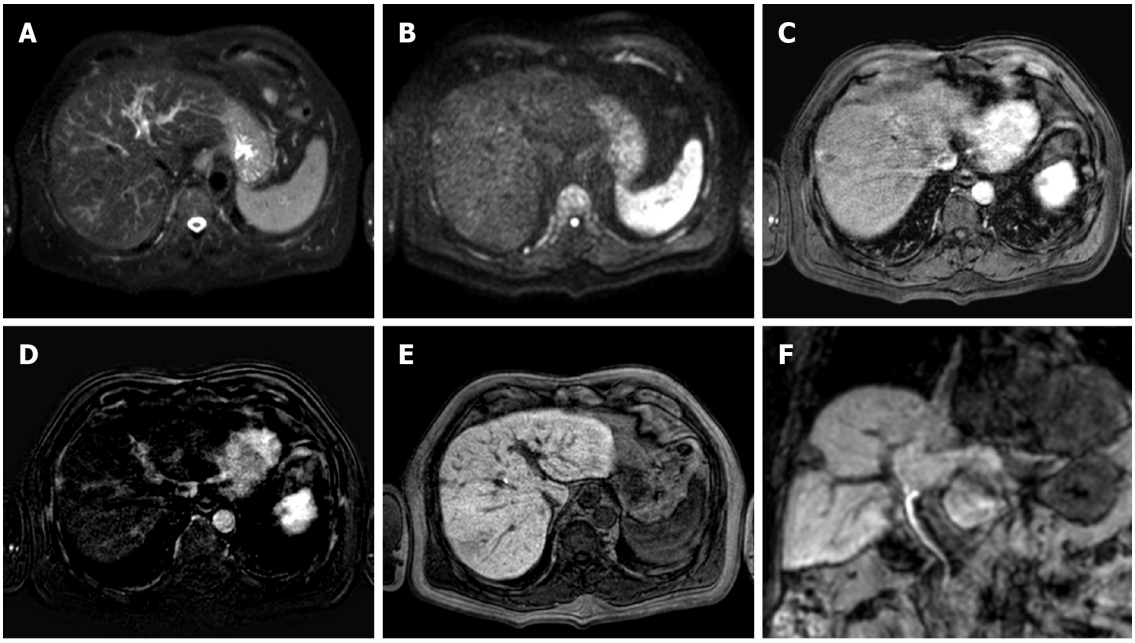
Figure 1 hree-month follow-up liver magnetic resonance imaging of a 69-yr-old male post radiofrequency ablation of right hepatic lobe hepatocellular carcinoma (segment VII). A: Out-phase T1-weighted image; B: In-phase T1-weighted image; C: T2-spectral attenuated inversion recovery; D: T2-weighted image; E: High b-value diffusion weighted imaging; F: Apparent diffusion coefficient map; G: Arterial phase magnetic resonance imaging (MRI); H: Arterial phase MRI with image subtraction technique; I and J: Hepatobiliary phase MRI. Follow-up MRI (A-I) after 3 mo post treatment revealed a good outcome characterized by inhomogeneous high signal hyperintensity in T1 sequences due to the presence of coagulative necrosis with associated signal hypointensity in T2 weighted sequences and the absence signal hyperintensity in diffusion weighted imaging. Dynamic study showed no enhancement in arterial phase with inhomogeneous hypointensity during hepatobiliary excretion. Findings are suggestive of complete tumor ablation also when compared to the similar pre-treatment sequences (J).



DOI: 10.3748/wjg.v28.i26.3116 **Copyright** ©The Author(s) 2022.

Figure 2 The evolution of the ablation zone shown in Figure 1. A: Hepatobiliary phase (HBP) phase magnetic resonance imaging (MRI) prior to radiofrequency ablation (RFA); B: HBP MRI 3 mo after RFA; C: HBP MRI 9 mo after RFA; D: HBP MRI 19 mo after RFA. Liver MRIs demonstrate a progressive reduction of ablation zone together with fibrotic changes.

MR findings after MWA are like those reported for RFA. On unenhanced T1w images, the ablated lesion shows a target-like appearance: linear hypointensity in the center of the ablation zone surrounded by hyperintense region due to coagulative necrosis, and outer hypointense areas of signal intensity corresponding to a slight to high signal intensity on T2w images due to inflammation[21]. After injection of contrast media, no APHE should be seen to consider a complete response. However, only a few studies evaluated the usefulness of EOB-MRI in the detection of HCC recurrence after MWA. Imai *et al*[15] reported that the diagnostic value of EOB-MRI is better than CT to evaluate HCC after



DOI: 10.3748/wjg.v28.i26.3116 **Copyright** ©The Author(s) 2022.

Figure 3 Two-years liver magnetic resonance imaging follow-up of a 71-yr-old male with liver cirrhosis and previous subcapsular hepatocellular carcinoma in segment VIII underwent radiofrequency ablation. A: T2-spectral attenuated inversion recovery; B: High b-value diffusion weighted imaging; C: Arterial phase magnetic resonance imaging (MRI); D: Arterial phase MRI with image subtraction technique; E and F: Hepatobiliary phase MRI. Liver MRI showed recurrent hepatocellular carcinoma (8 mm) located infero-lateral to the radiofrequency scar, characterized by moderate to high signal hyperintensity in T2, hyperintensity in high b-value diffusion sequences, with arterial "wash in" and hypointensity in hepatobiliary excretion phase.

treatment by image-guided tumor procedures, including patients who underwent both ablation and chemoembolization.

CA

As reported by Song[22], CA should be included in the family of thermal ablation in HCC patients. The physical bases are like RFA and MWA, however, the employed temperature is not hot but cold, thanks to chemical agents such as liquid nitrogen. According to a recent meta-analysis[23], the effects of MWA and CA appeared to be similar to those of RFA, but there were lower rates of local tumor progression and higher rates of complete thermal ablation in large tumors compared to RFA ($P < 0.05$). MR imaging findings after the CA procedure are similar to RFA and MWA, as reported above: the ablation zone at 24h appears hypointense and heterogeneously hyperintense on T1w and T2w images, respectively[24]. Foci of inhomogeneous signal intensities on T1w and T2w images should be principally due to blood products and can be present in further follow-up examinations[24]. The peripheral zone shows a slight to hyper- signal intensity on T2w images, due to inflammation and granulation tissue formation. The residual tumor presents analogous imaging features to the treated lesion, while the recurrence can be seen as an area of APHE with consequent hypointensity on portal-venous and HBP. Even if not fully reported in the literature, a focal hypointense area of HBP images without APHE might be referred to a suspected recurrence.

TACE AND TRANS-ARTERIAL RADIOEMBOLIZATION

Treatment options for HCC depend on tumor burden and extent, patient's performance status, liver function, extra-hepatic disease, and co-morbidities, according to the BCLC system[10]. Intra-arterial therapies, including TACE and trans-arterial radio-embolization (TARE), come into play to improve survival and quality of life where curative treatments like ablation, liver resection, or liver transplantation are not applicable[10,25]. TACE and TARE are regarded as a standard of care for a patient with intermediate-stage HCC (BCLC class B, Child-Pugh A-B) not eligible for surgical resection or transplantation and without portal vein thrombosis or extrahepatic spread. Moreover, the application of these techniques range from curative-intent for small tumors, to downstaging or bridging to resection and transplantation for early and intermediate disease, and locoregional control and palliation for advanced disease[26].

The main contraindications to TACE and TARE are decompensated liver cirrhosis, bilobar liver involvement, and technical infeasibility; absolute contraindication specific to TARE is the presence of

hepato-pulmonary shunt or hepato-enteric shunts[10].

In the case of portal vein thrombosis, in clinical practice, TACE is contraindicated, even if Patidar *et al* [27] described a good outcome of patients with segmental-branch or first-border branch portal vein thrombosis treated with TACE. On the contrary, TARE may have applications even if there is portal vein thrombosis because of the reduced embolic effect of the technique[10].

TACE

TACE is performed by cannulation of the arteries that feed the HCC through a catheter or a microcatheter and releasing both the chemotherapeutic agent and embolic particles. The treatment may be performed in two ways, conventional TACE that uses lipiodol, an oily radiopaque material mixed with one or more chemotherapeutics agents, followed by administration of an embolic agent and drug-eluting beads TACE (DEB-TACE) with slowing releasing of chemotherapy by particles[26].

Multiphasic MRI is performed to evaluate the response to treatment and to detect new HCCs from 1 mo to 3 mo after treatment for the first imaging study, followed by every 3 mo for 2 years[28]. As previously mentioned, MRI may use gadolinium-based extracellular contrast agents, or gadolinium-based hepatobiliary agents[28,29].

MRI imaging after TACE is related to tumor necrosis caused by ischemic injury from arterial embolization and chemotoxic injury from the administered chemotherapy[28]. Gd-EOB-DTPA allows similar dynamic acquisition of extracellular agents in arterial and portal phases, essential in detection of a viable tumor. If the treatment is successful the expected findings are: absence of APHE, associated with surrounding perfusion changes related to edema and arterial embolization, a thin APHE phase due to inflammatory, that may persist up to a year, and a volumetric reduction of the treated lesion over time[28]. The HBP contributes to the diagnosis of complete response to treatment, showing a corresponding hypointensity of the lesion if complete necrosis occurs. A thin, continuous, and smooth APHE rim associated with a corresponding isointense area in the HBP defines a benign finding[30].

After treatment, the damage of the liver parenchyma around the treated lesion may cause geographic perfusion changes and corresponding hypointensity on the HBP, a feature that needs careful evaluation and examination of additional sequences to avoid diagnostic mistakes of infiltrative disease[31]. If pseudolesions related to treatment occur (arterial-venous shunt and portal vein obstruction), they usually don't show hypointensity on the HBP, an element that helps in the diagnosis of benignity, although hypointense pseudolesions on the HBP mimicking malignancy have been described by Motosugi *et al*[32].

The sign of residual and/or recurrent disease is represented by the presence of thick, peripheral, irregular, eccentric, nodular APHE with or without washout within the treated lesion, or enhancement similar to pre-treatment tumor. Aslam *et al*[30] showed findings suggestive of the presence of viable tumor after thermoablation, applicable for TACE too: the presence of thick, nodular and eccentric hypointense signal on HBP or a discontinuous hypointense rim. Considering these findings on the HBP-like viable tumor is much more important when there is equivocal APHE, consisting of viable isoenhance or hypoenhance tumor in arterial phase[33].

Figure 4 depicts a pre-treatment CT images and subsequent TACE treatment of an HCC nodule, the results of which are illustrated in Figure 5.

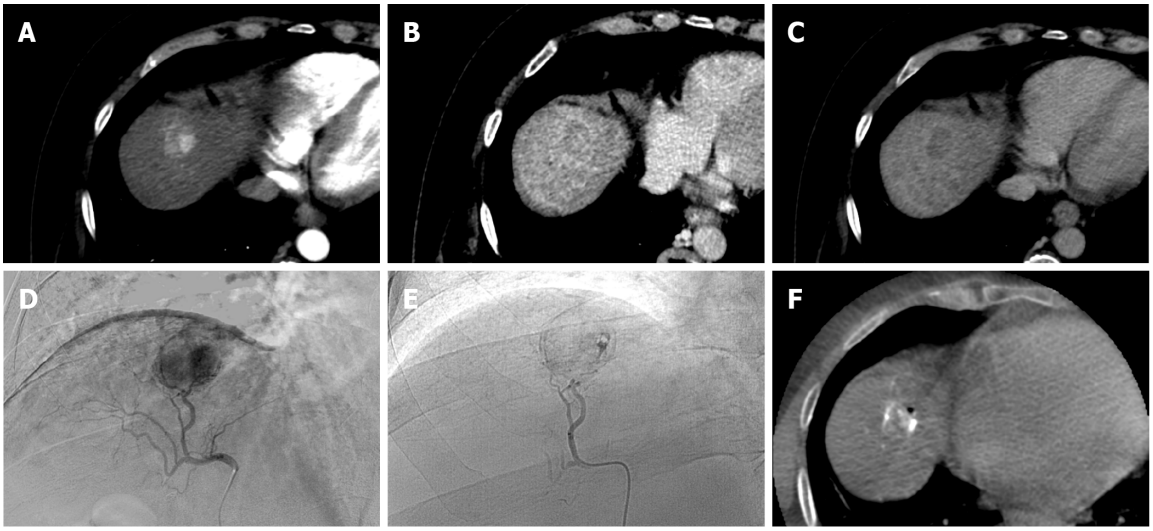
TARE

TARE is a trans-arterial catheter treatment based on delivering microspheres (glass or resin) coated with ^{90}Y. ^{90}Y is an unstable isotope that releases a beta particle during its decay into a stable element, zirconium 90, inducing destruction of the target tumor with a limited depth of penetration to minimize radiation exposure of surrounding parenchyma[33].

^{90}Y microspheres have a main radiant effect and a small microembolic effect due to the little diameter of microspheres; therefore, tumor necrosis related to TARE is mostly radiation-induced and the arterial flow to adjacent parenchyma is largely conserved, which is an important advantage in the case of portal venous thrombosis (*i.e.*, contraindication for TACE)[33].

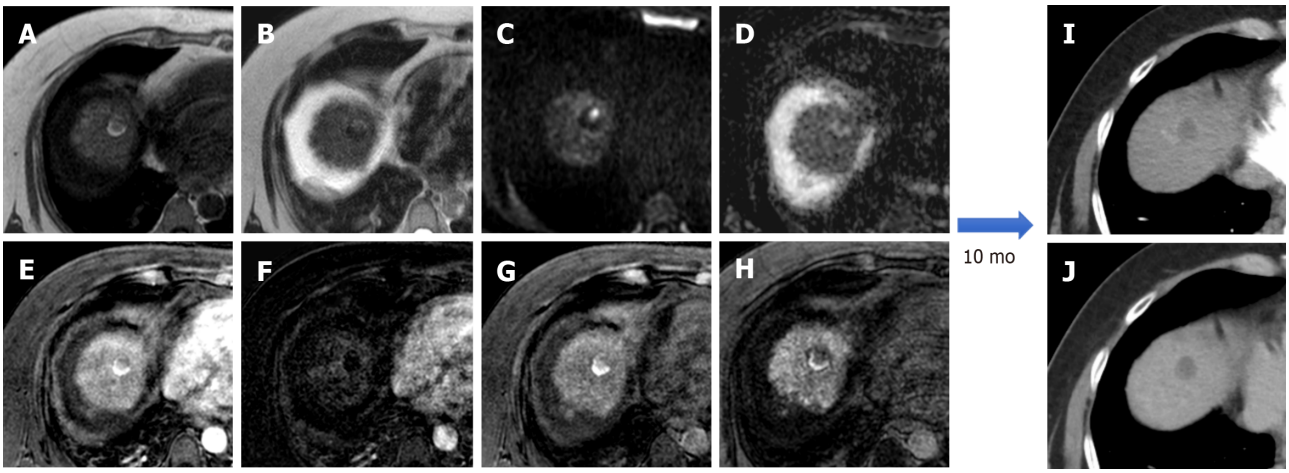
Multiphasic MRI after TARE is performed at 3-mo intervals even for the first examination, because imaging performed earlier may show exuberant arterial phase involving the treated lesion and the surrounding parenchyma with consequently difficult interpretation[29]. MRI imaging findings in TACE and TARE are not similar because of the different mechanisms of action: TARE induces modifications that evolve because of the impact of radiation on the liver parenchyma surrounding the lesion[28,30].

The expected Gd-EOB-DTPA imaging findings of TARE-treated HCC are persistent APHE or portal washout that can persist for at least one year, geographic peri-tumoral APHE, complete loss of APHE, thin rim of peripheral APHE, transitory growth in the size of the tumor due to edema, and cytostatic effect of radiation, a delay in tumor decreasing size. In TARE, in the immediate post-treatment setting, the penetration of beta particles in the surrounding liver parenchyma causing inflammation, edema, hemorrhage, leads to a heterogeneous enhancement, more accentuated than TACE. Even in this case, Gd-EOB-DTPA may show a related hypointensity on the HBP, an important element to be assessed since it can be misdiagnosed with an infiltrative disease. This finding may usually resolve after 6 mo, so in the early phase is very important to consider other sequences to make the differential diagnosis, especially T2w and DWI images. The changes in the lesion diameter should be characterized with



DOI: 10.3748/wjg.v28.i26.3116 **Copyright** ©The Author(s) 2022.

Figure 4 A 62-yr-old male with typical hepatocellular carcinoma in segment IVa who underwent trans-arterial chemoembolization with microparticles (Lifepearl 100 +/- 25 microns) preloaded with 50 mg of Farmorubicin and later with non-loadable Hydropearl 400 +/- 75 microns microparticles. A: Pre-treatment computed tomography (CT) images: arterial phase; B: Pre-treatment CT images: portal phase; C: Pre-treatment CT images: delayed phase; D: Pre-trans-arterial chemoembolization (TACE) angiographic image; E: Post-TACE angiographic image; F: Post-TACE cone beam CT.



DOI: 10.3748/wjg.v28.i26.3116 **Copyright** ©The Author(s) 2022.

Figure 5 Post-trans-arterial chemoembolization follow-up magnetic resonance imaging with hepatospecific contrast agent in the same patient described in Figure 4. A: In-phase T1-weighted image; B: T2-weighted image C: High b-value diffusion weighted imaging (DWI); D: Apparent diffusion coefficient map; E: Arterial phase magnetic resonance imaging (MRI); F: Arterial phase MRI with image subtraction technique; G: Portal venous phase MRI; H: Hepatobiliary phase MRI; I: Ten-month computed tomography (CT) follow-up: arterial phase; J: Ten-month CT follow-up: delayed phase. Liver MRI shows an inhomogeneously hyperintense nodule in T1WI in its right posterior portion, coexisting with a more hyperintense area in T2WI with high signal intensity in high b-value DWI in the left anterior portion. Dynamic study showed no arterial enhancement confirmed with the subtraction technique image, absence of vascularization in the portal phase and inhomogeneous hypointensity in the hepatobiliary phase. The findings are suggestive of good treatment outcome with presence of both coagulative and colliquative necrosis and no residual disease and CT scans control after 10 mo confirmed the outcome.

caution based on the persistent APHE and typical washout of the lesion after TARE. Viable tumor manifests itself with an increase in the size of the treated nodule with new or growing nodular enhancement within or beyond the margin of the post-radiation zone with hypointense signal on the HBP[28,30].

For both TARE and TACE techniques the use of Gd-EOB-DTPA implies knowledge of some technical concerns. An optimal arterial phase may be more difficult to obtain compared to extracellular-contrast agents because of acute transient severe motion artifacts affecting EOB-MRI. Several approaches have been applied to reduce motion artifacts: (1) Lowering thecontrast injection rate; (2) Using multiple arterial phasetechnique; (3) Shortening the scanning time; and (4) Using a modified breathing command, and dilutingcontrast medium[5,34]. Moreover, "washout" evaluation of the nodule has to be assessed in the portal phase because hypointensity during the TP could be related to true washout or

pseudo-washout resulting from the hyperintensity of the surrounding parenchyma[34]. Another element to be considered is the adequacy of the HBP, strictly linked to the assessment of the degree of contrast uptake in the liver parenchyma relative to the hepatic vessels and of the presence of contrast excretion into the biliary system. A signal intensity ratio of 1.8 between liver and vein, with the maximal enhancement of liver parenchyma and hypointensity of the veins, is the best predictor of the ideal phase. In a functional liver, this ideal condition is achieved at 15-20 min after contrast injection[35]. In this setting, the main limitation of Gd-EOB-DTPA is the necessity of a functional liver for an optimal HBP; the cirrhotic liver may have diminished or delayed parenchymal enhancement leading to failure of the mechanism of contrast uptake and excretion. Therefore, in a situation with deeply compromised liver function (Child-Pugh B-C) acquisition of delayed HBP beyond the 20 min is necessary.

At present, the treatment response algorithms used in the clinical practice, such as Modified Response Evaluation Criteria in Solid Tumors (mRECIST), European Association for the Study of the Liver Disease Criteria, and Liver Imaging and Reporting Data System Treatment Response Algorithm are enhancement-based classification systems that don't include transitional or HBP obtained by Gd-EOB-DTPA[28-30]. However, many authors have analyzed the contribution of EOB-MRI in follow-up after TACE and TARE with promising results. To the best of our knowledge the actual studies published in the literature, have analyzed the impact of Gd-EOB-DTPA in the follow-up of loco-regional therapy group (for example both ablation and TACE) without examination of the single procedure, therefore next considerations are almost effective for both TACE and TARE.

In a recent study, Kim *et al*[33] showed an increased sensitivity in the detection of viable tumor considering all ancillary features (HBP hypointensity, restricted diffusion, and intermediate signal on T2w) with growing sensitivity into the LI-RADS-TR viable category of 57%-87% *vs* 39%-65% without changing in specificity. Park *et al*[36] obtained similar results for TACE and ablation, with increased sensitivity of 84% *vs* 76%.

Kim *et al*[37] first, in a recent retrospective study, analyzed the impact of the incorporation of the individual ancillary feature instead of multiple ancillary features on the diagnostic performance of the LI-RADS-TR for viable tumor. They found that hypointense signal during the transition and/or HBP can improve the sensitivity than contrast dynamic assessment alone.

Conversely, Rimola *et al*[18] show a small contribution of HBP in the evaluation of tumor response after loco-regional therapy, with greater accuracy, sensitivity, and inter-reader agreement using extracellular agents in comparison with Gd-EOB-DTPA[37]. These results may depend on better conspicuity of the APHE with extracellular agents and to the misdiagnosis of viable tumor for hypointense areas on the HBP related to damaged liver parenchyma, an avoidable mistake considering additional sequences[18,30].

Another important fact is that EOB-MRI in follow-up after TACE and TARE significantly contributes not only to determination of viable tumors on the treated cavity but also for detection of new HCC lesions, that may be disguised by the post-treatment changes of the surrounding hepatic parenchyma [30].

The use of EOB-MRI after TACE and TARE is widespread in the clinical practice and its contribution with transitional and HBP to identify the viable tumor, necrotic cavity, damaged liver tissue, and new HCC has been shown in the literature, although it still has not been included in treatment response algorithms.

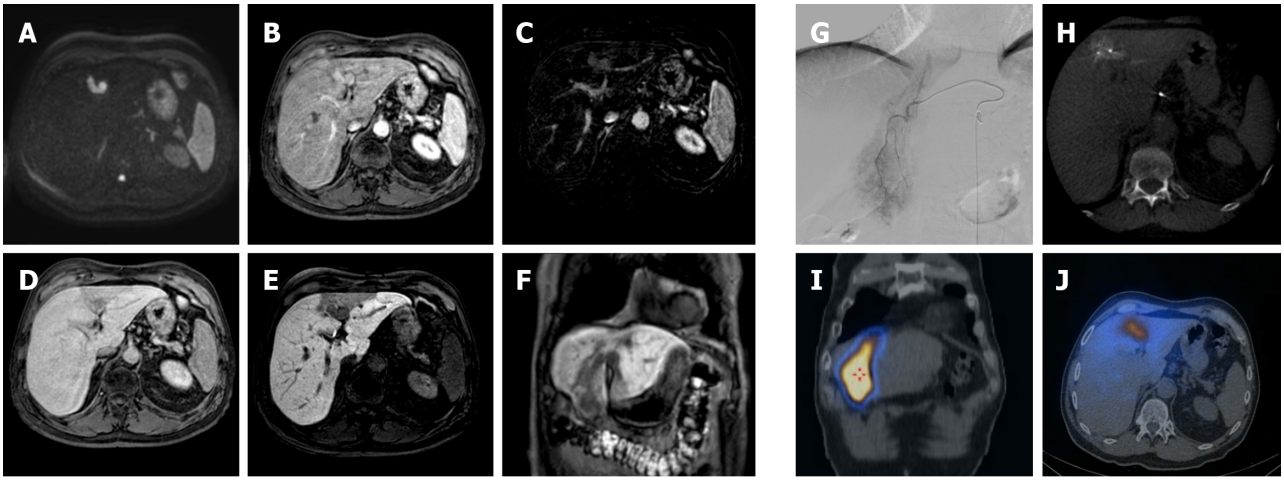
Figure 6 depicts the pre-treatment liver MRI and preoperative planning for TARE of a patient with voluminous infiltrating HCC. Figure 7 illustrates the outcome of treatment.

STEREOTACTIC ABLATIVE RADIOTHERAPY

Recent improvements in image guidance and conformal radiation techniques have made it possible to administer high doses of radiation to liver tumors with minimal damage to adjacent parenchymal tissue [38]. Although SBRT is not part of the current BCLC system, it is included as a treatment option in the most recent version of the National Comprehensive Cancer Network (NCCN) for primary liver cancer for unresectable disease or medically inoperable patients[38,39].

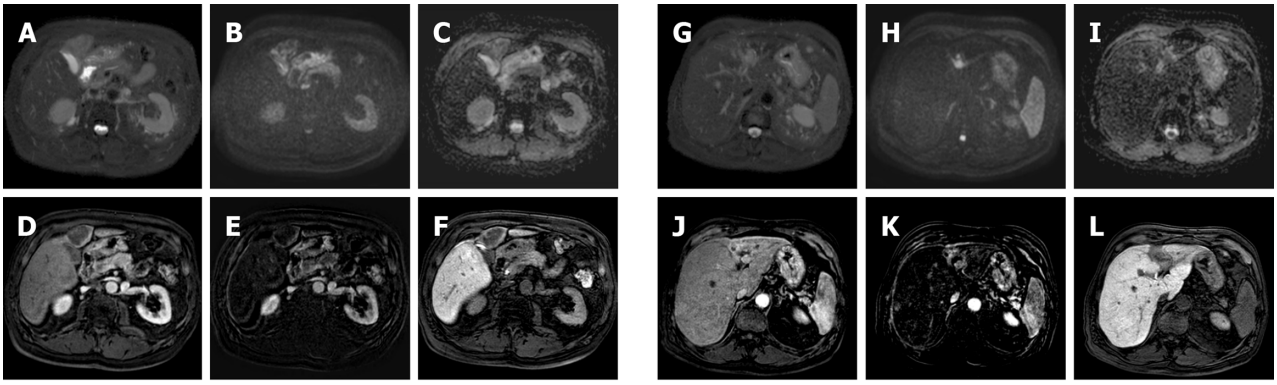
Indications for SBRT are applicable in the following cases: (1) Early-stage HCC, not eligible for surgical resection, liver transplantation, or local ablation; (2) Intermediate or advance stage HCC not eligible or not responsive to TACE; (3) Palliative purpose for symptomatic end-stage HCC; and (4) Bridging or downstaging therapy for liver transplantation in patients not eligible for other locoregional therapies[40].

Factors that generally hinder percutaneous ablative therapies, such as proximity of the tumor to vascular structures, bile ducts or the diaphragmatic surface are not contraindication to treatment[41]. SBRT is most appropriate in patients with cirrhotic disease in Child-Pugh class A. Treatment is available for patients up to Child-Pugh B7, for whom close clinical monitoring and dose reduction are recommended due to the increased risk of radiation-induced liver disease (RILD). From a technical point of view, the number of target lesions, together with their intraparenchymal location, are potential limitations during treatment planning and dose delivery.



DOI: 10.3748/wjg.v28.i26.3116 **Copyright** ©The Author(s) 2022.

Figure 6 A 62-yr-old patient with infiltrative hepatocellular carcinoma with associated neoplastic portal vein thrombosis. A: High-b-value diffusion-weighted image; B: Arterial phase magnetic resonance imaging (MRI); C: Arterial phase MRI with image subtraction technique; D: Portal venous phase MRI; E and F: Hepatobiliary phase MRI; G: Pre-treatment arteriography; H: Pre-treatment cone beam computed tomography (CT); I and J: Post trans-arterial radio-embolization single photon emission computed tomography (SPECT) images. Left panel shows pre-treatment liver MRI, illustrating the cranial portion of the lesion with portal branch infiltration; whereas the right panel shows pre-treatment arteriography, the cone beam CT of the cranial portion of the lesion with the portal vein infiltration, and preoperative planning with SPECT images post administration of Tc-99m-labeled albumin macroaggregates with hyperfixation at both lesion site and portal thrombosis.



DOI: 10.3748/wjg.v28.i26.3116 **Copyright** ©The Author(s) 2022.

Figure 7 Post-trans-arterial radio-embolization images in the patient mentioned in Figure 6. A: T2-spectral attenuated inversion recovery; B: High b-value diffusion weighted imaging; C: Apparent diffusion coefficient (ADC) map; D: Arterial phase magnetic resonance imaging (MRI); E: Arterial phase MRI with image subtraction technique; F: Hepatobiliary phase (HBP) MRI; G: T2-spectral attenuated inversion recovery; H: High b-value diffusion weighted imaging; I: ADC map; J: Arterial phase MRI; K: Arterial phase MRI with image subtraction technique; L: HBP MRI. The liver MRIs reveal almost no signal restriction in DWI and no enhancement in dynamic study in the caudal portion of the lesion (left panel) which are suggestive of a good outcome. Whereas in the cranial infiltrating part of the lesion (right panel) at portal branch level, the high signal in DWI with arterial enhancement is suspected for residual disease.

Ionizing radiations directly impairs the DNA replication process by causing breaks and thus preventing cancer cells from replicating, most powerfully on tissues with a high cell turnover. After radiotherapy, centrilobular hepatocytes die by a hypoxic process secondary to vascular congestion, which does not recover until several months later[42]. Furthermore, proinflammatory mechanisms will be set on the treated region. These histological changes initially lead to an acute reduction in cellular vascular supply, with peripheral hypervascularization induced by the proinflammatory mechanisms, while over time, fibrosis leads to a reduction of tumor size and vascular supply[43]. Damage also occurs in the surrounding liver parenchyma with the evolution of the chronic inflammatory context, characterized initially by edema and subsequently by fibrosis, leading to capsular retraction[42].

Acute, subacute and chronic stages can be distinguished by assessing the evolution of histological changes. In the acute stage (1-3 mo) typical peripheral hyperarterialization, defined as a ring-like enhancement during the arterial and portal venous phases, can be observed. In the subacute stage (3-6 mo), the involved parenchyma shows relative hypointensity before and after contrast media injection especially on the portal-venous phase, with progressive enhancement in the late phases, concerning the occlusion of the centrilobular veins and to the reduced clearance of intravenous contrast. In the chronic

stage (> 6 mo), imaging will reveal changes caused by radio-induced fibrosis. The subcapsular location of the target lesions also correlates with the progressive occurrence of capsular retraction. This reaction typically appears as a band-like finding, a typical appearance that can help the differential diagnosis with residual or recurrent tumor[44]. Finally, the classic RILD generally occurs within 4 mo of total or subtotal hepatic irradiation, and manifests with hepatomegaly, ascites, and increased alkaline phosphatase levels, without a radiological intrahepatic progression disease. Nowadays, this complication is effectively prevented by sparing a sufficient portion of the parenchyma during therapy.

Patients with pre-existing chronic liver disease undergoing this type of treatment tend to experience a different spectrum of toxicity than with classic RILD, including a general decline in liver function, a marked increase in transaminases or jaundice within 3 mo of the end of therapy, collectively referred as "non-classic" RILD[44].

The radiological findings of SBRT treated lesions differ from the imaging of other locoregional therapies. Indeed, while the latter results in immediate tumor devascularization, SBRT leads to gradual histological changes in the lesion and surrounding parenchyma over time, which may lead to the incorrect assumption of a lack of efficacy.

As previously mentioned, different algorithms are employed to determine the response evaluation, such as mRECIST, applied to CT and MRI[45]. The intensity of arterial enhancement may appear quite early (15-45 d after SBRT) and may persist over time. Therefore, lesions dimensionally stable over time with a reduced arterial hypervascularization should be considered as a responder. The decrease in size occurs more slowly, over 22-24 mo, due to progressive necrosis up to 12 mo after treatment, which results in a slower evolution of structural changes.

In post-SBRT MRI examinations it is common to find a hyperintense perilesional halo on T2w due to the inflammatory reaction and venous congestion induced by veno-occlusive disease or, in subsequent follow-ups, a slight signal hyperintensity on T2w in the whole irradiated field, a direct sign of parenchymal fibrosis. Moreover, the application of DWI sequences can provide information on tissue cellularity and the integrity of cell membranes. In fact, during the early phase after treatment, hepatic edema occurs due to decreased venous outflow secondary to centrilobular obstruction, and there may be mild restricted diffusion and a slight increase in apparent diffusion coefficient (ADC).

Finally, tumor response after SBRT can be challenging, as described above: tumor shrinkage may not happen in the immediate months after SBRT. Even in the absence of volumetric reduction, progressive reduction in tumor enhancement is consistent with treatment response. This is typically accompanied by a corresponding increase in ADC. An increment in ADC of 20%-25% was found to be an indicator of SBRT response in a few small retrospective studies[46,47]. Thus, in stereotactic radiotherapy, a statistically significant increase in ADC values measured in HCC undergoing radiofrequency was found to be the most important independent factor in recurrence and survival rates.

The use of hepatobiliary contrast agents allows the assessment of both lesion and the adjacent hepatocytes: The presence of a hypointense nodular lesion during HBP nearby an SBRT-treated HCC may signify either the presence of neoplastic cells or a scar. The picture is further complicated by the manifestation in such sequences of the focal hepatic reaction induced by radiotherapy. This alteration can be demarcated as a band-like area of signal hypointensity, such as hyperintensity on T2w, related to altered hepatocyte function in the irradiated field[48].

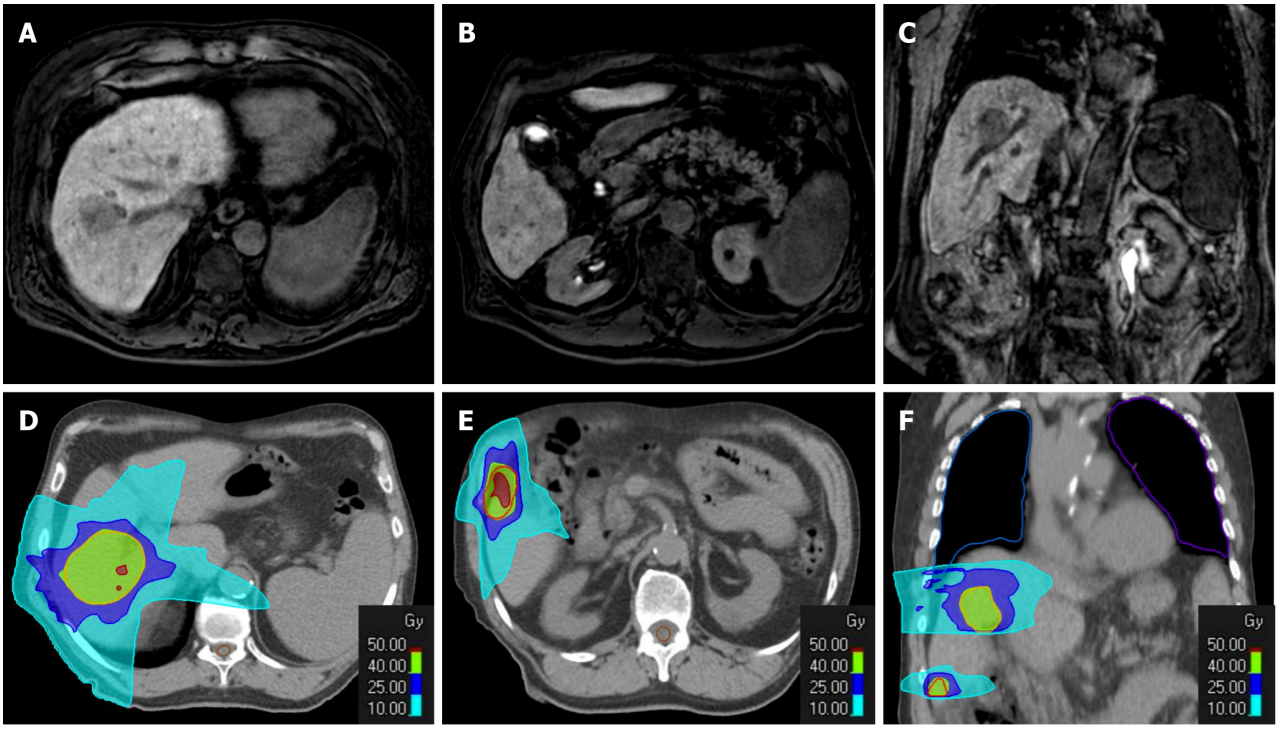
Figure 8 depicts the radiotherapy treatment plan; Figure 9 shows the SBRT treatment outcomes; Figure 10 depicts the treated zone's evolution; and Figure 11 illustrates the outcome 20 mo after treatment.

LIVER MRI ACCURACY AND LIMITATIONS

Although MRI is notably known as a highly sensitive and accurate imaging technique in detection and characterization of focal liver lesions, there is still no consensus regarding the best imaging follow-up modality for patients affected with HCC after locoregional treatments. Moreover, to date, only few studies have conducted a comparison among imaging techniques after locoregional treatments, and this raises the scientific interest in further investigations.

Kubota *et al*[49], by evaluating 84 HCCs underwent TACE treatment, showed the superiority of MRI to CT for early detection of lesion. Authors reported 76.0% sensitivity, 67.6% specificity and 72.6% accuracy for lipiodol-CT in comparison to 100% sensitivity, specificity and accuracy for dynamic MRI. Moreover, DWI and ADC values can help identify the early HCC recurrence: the presence of pathological tissues results in a higher signal intensity on DWI relative to normal liver parenchyma and a low signal on ADC maps, differentiating it from treated lesion (necrotic/edematous area) which manifests as high ADC values[50]. In these settings, the use of Gd-EOB-DTPA can maintain the highest diagnostic values, as mentioned above.

MRI was demonstrated to be useful also prior to treatment, especially by evaluating the HBP. Kim *et al*[16] found that HBP hypointense nodules without APHE are risk factors for intrahepatic distant recurrence in HCC patients treated with RFA or hepatectomy in a meta-analysis of 842 patients. In patients with HCC who have these nodules on pretreatment gadoxetic acid-enhanced MRI, stratification



DOI: 10.3748/wjg.v28.i26.3116 **Copyright** ©The Author(s) 2022.

Figure 8 Radiotherapy treatment planning of a 70-yr-old male patient with two hypovascular hepatocellular carcinomas in segment VIII (4.3 cm) and segment VI (1.3 cm). A-C: Hepatobiliary phase magnetic resonance imaging (MRI); D-F: Computed tomography (CT) simulation for radiation therapy planning. In the upper panel from A to C are reported hepatobiliary phase MRI images prior to stereotactic ablative radiotherapy treatment. In the bottom panel from D to F are reported CT images from radiotherapy treatment plan with isodose curve distributions.

of patient management in terms of performing additional tests or treatment for these nodules, as well as modification of proper follow-up strategies, may be required.

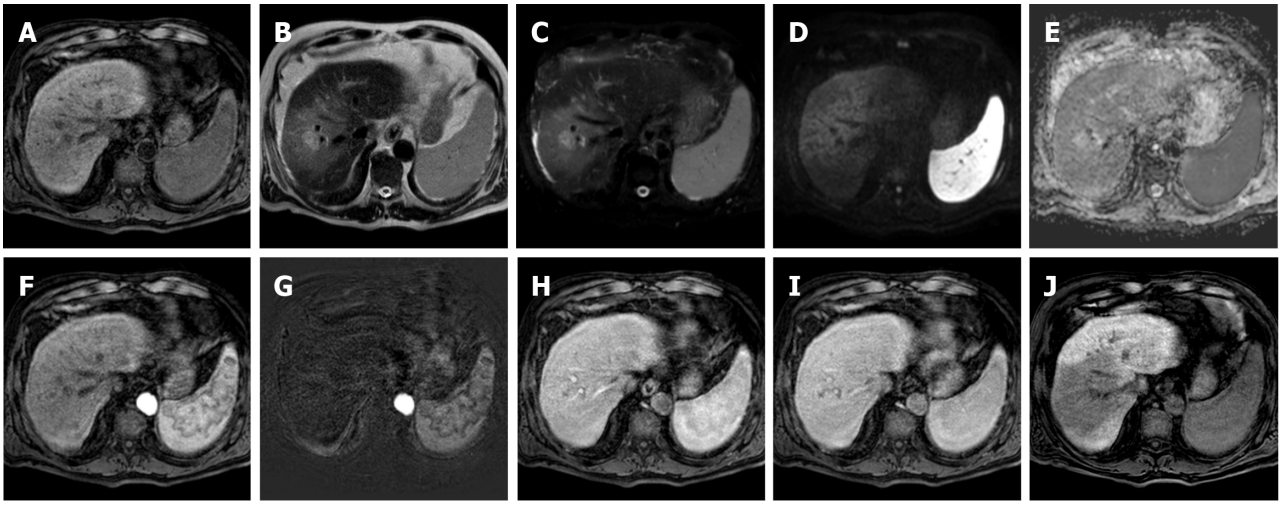
Considering the therapeutic response to RFA, literature may not be much of a help since the two most important studies in this field were published in the early 2000s[51]. Both studies reported that MRI may have an edge over CT in the early detection of local regrowth in particular after 4 mo of treatment [51]. This aspect should be carefully considered according to readers' experience, MR image quality, and the scattered use of hepatobiliary contrast agents, which was not widely used 20 years ago.

Regarding therapeutic response to TACE, it is important to underline that beam hardening artifacts can lead to the underestimation of hyperenhancement during the CT arterial phase and thus reducing the sensitivity and accuracy dramatically[49,52]. On the other hand, the wider use of DEB-TACE can partially solve this issue due to the lack of beam hardening artifacts[53]. The abovementioned issues can be partially left out when using MR to detect recurrence. On the other hand, the use of dual-energy CT can help increase diagnostic accuracy, even if not widely available[54]. CT and MR diagnostic accuracy can be considered completely superimposable after TARE[26], although the added value of HBP imaging was not deeply evaluated.

In the recent years, perfusion techniques, both with CT and MR, were used to diagnose HCC and determine different treatment responses, especially after medical therapy: in this setting CT perfusion can be considered a reliable tool in the early detection of recurrence, as reported by Choi *et al*[55]. More recently the effectiveness of CT perfusion was evaluated by Ruff *et al*[56], demonstrating that residual tumor perfusion parameters are linked to HCC recurrence. However, both CT and MR perfusion imaging need an extra time, added costs and are not widely available to be considered convenient tool in daily clinical practice[57].

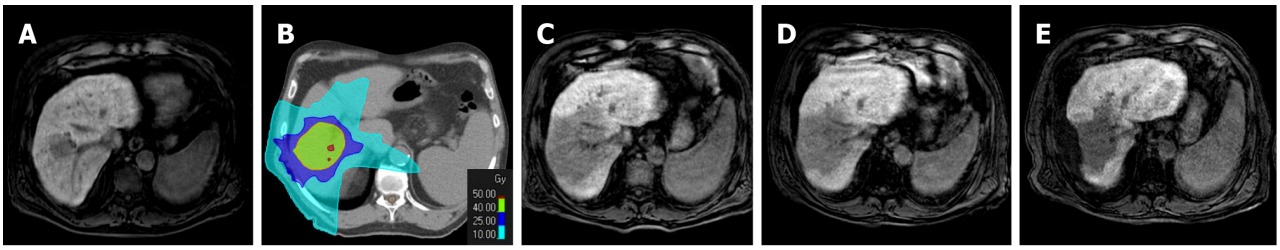
In the recent years, radiomics models based especially on texture analysis are showing promising results[58]. Zhang *et al*[59], by enrolling 132 patients who underwent locoregional therapies, demonstrated that radiomic features extracted from Gd-EOB-DTPA MR imaging associated with clinical data can predict the early tumor recurrence. Even if pioneering, radiomics analyses should be carefully evaluated, especially due to different types of software and MR techniques used which vary between centers. However, further studies should focus on these aspects to validate its potential values[60].

Overall, it is important to underline the presence of artifacts during MR acquisition, especially in the arterial phase when using Gd-EOB-DTPA studies. As previously reported and demonstrated[61], flow rate and acquisition protocol[5] can lead to the degradation of the arterial phase and should be carefully managed to avoid the leak of important data, linked to the risk of early recurrence.



DOI: 10.3748/wjg.v28.i26.3116 **Copyright** ©The Author(s) 2022.

Figure 9 Four-months follow-up post stereotactic body radiation therapy liver magnetic resonance imaging of the hepatocellular carcinoma in segment VIII shown in the Figure 8. A: Non contrast T1-weighted high resolution isotropic volume examination; B: T2-weighted image; C: T2-spectral attenuated inversion recovery; D: High b-value diffusion weighted imaging (DWI); E: Apparent diffusion coefficient (ADC) map; F: Arterial phase magnetic resonance imaging (MRI); G: Arterial phase MRI with image subtraction technique; H: Portal venous phase MRI; I: Delayed phase MRI; J: Hepatobiliary phase MRI. The liver MRI shows an ill-defined area of signal hypointensity in T1 in the treatment zone with a blurred and inhomogeneous signal hyperintensity with evidence of increased signal hyperintensity in the residual nodule. A shaded signal hyperintensity on DWI without signal hyperintensity of the previous lesion, with higher ADC values relative to the surrounding liver parenchyma. No areas of enhancement are shown, and a coarse hypointense signal in the hepatobiliary phase due to the initial fibrotic evolution of the treated zone is evident.



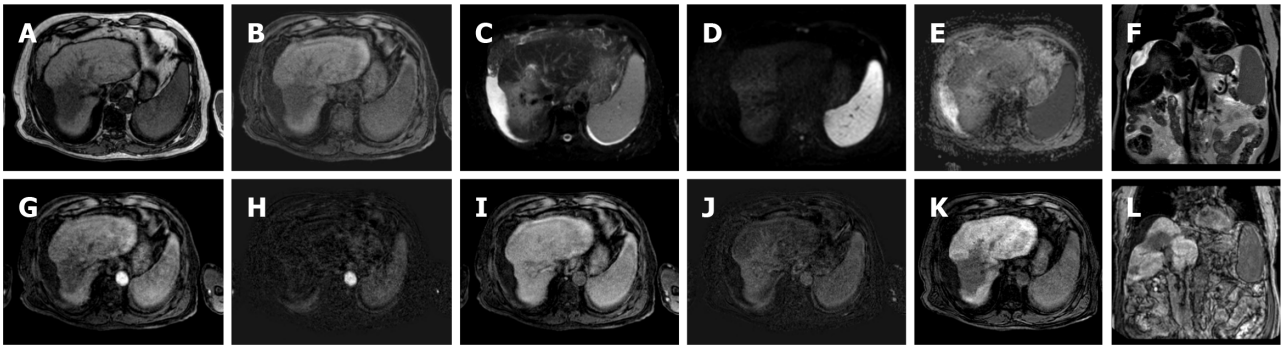
DOI: 10.3748/wjg.v28.i26.3116 **Copyright** ©The Author(s) 2022.

Figure 10 The evolution of the hepatocellular carcinoma stereotactic body radiation therapy treatment zone in patient shown in Figures 8 and 9. A: Hepatobiliary phase (HBP) magnetic resonance imaging (MRI) prior to stereotactic body radiation therapy (SBRT); B: SBRT plan with isodose curve distributions; C: HBP MRI 4 mo after treatment; D: HBP MRI 8 mo after treatment; E: HBP MRI 20 mo after treatment. The MRIs demonstrated the progressive fibrotic evolution of the treatment area.

Finally, the use of CT or MRI is strictly linked to each institution's flow charts: it is important to underline the low CT associated costs, the need for less patient cooperation, and its usefulness when ascites is present[62]. Also in these settings, a direct comparison with MR with HBP imaging is lacking and further studies are needed to validate the abovementioned data.

CONCLUSION

Locoregional therapy is critical in the treatment of patients with HCC. The accurate evaluation of tumor response using imaging modalities is essential for optimal management. Gadoxetic acid-enhanced liver MRI is an important radiological tool in these patients because it allows for optimal non-invasive tissue characterization using a multiparametric approach. For HCC patients to get proper therapeutic management, radiologists must know the usual post-treatment imaging findings associated with locoregional therapy, as well as a thorough comparison of imaging before and after therapy. Overall, gadoxetic acid-enhanced liver MRI is a critical modality in the assessment of results following locoregional HCC therapy, having a significant impact on patient management.



DOI: 10.3748/wjg.v28.i26.3116 **Copyright** ©The Author(s) 2022.

Figure 11 Follow-up liver magnetic resonance imaging of abovementioned patient (Figures 8-10), 20 mo after stereotactic body radiation therapy. A: Out-phase T1-weighted image; B: Non contrast T1-weighted high resolution isotropic volume examination; C: T2-spectral attenuated inversion recovery; D: High b-value diffusion weighted imaging; E: Apparent diffusion coefficient map; F: T2-weighted image; G: Arterial phase magnetic resonance imaging (MRI); H: Arterial phase MRI with image subtraction technique; I: Portal venous phase MRI; J: Portal venous phase MRI with image subtraction technique; K and L: Hepatobiliary phase MRI. MRI revealed parenchymal retraction with signal hypointensity on T1-weighted images corresponding to inhomogeneous hyperintensity in axial and coronal T2 sequences, with no significant increase in diffusion signal. Dynamic perfusion study after contrast medium administration: no enhancement in arterial phase and a progressive enhancement in delayed phase with corresponding hypointense signal in the hepatobiliary excretion phase testifying the fibrotic evolution of the treated liver and the absence of locoregional recurrence.

FOOTNOTES

Author contributions: Gatti M was involved in conception and design of the study; Gatti M, Maino C, Serafini A and Tricarico E were involved in literature review, analysis and writing of the original draft; Darvizeh F was involved in writing of the original draft; Guarneri A, Inchingolo R, Ippolito D, Ricardi U and Fonio P took part in supervision of the study; Faletti R took part in supervision of the study and is the guarantor of the study; all the authors worked together to editing, reviewing and final approval of article.

Conflict-of-interest statement: All the authors report no relevant conflicts of interest for this article.

Open-Access: This article is an open-access article that was selected by an in-house editor and fully peer-reviewed by external reviewers. It is distributed in accordance with the Creative Commons Attribution NonCommercial (CC BY-NC 4.0) license, which permits others to distribute, remix, adapt, build upon this work non-commercially, and license their derivative works on different terms, provided the original work is properly cited and the use is non-commercial. See: https://creativecommons.org/Licenses/by-nc/4.0/

Country/Territory of origin: Italy

ORCID number: Marco Gatti 0000-0001-8168-5280; Cesare Maino 0000-0002-5742-802X; Fatemeh Darvizeh 0000-0002-3735-0472; Alessandro Serafini 0000-0002-4992-4824; Eleonora Tricarico 0000-0001-9805-2551; Alessia Guarneri 0000-0003-1711-3645; Riccardo Inchingolo 0000-0002-0253-5936; Davide Ippolito 0000-0002-2696-7047; Umberto Ricardi 0000-0003-4406-7621; Paolo Fonio 0000-0002-1106-2990; Riccardo Faletti 0000-0002-8865-8637.

S-Editor: Gao CC
L-Editor: A
P-Editor: Chen YX

REFERENCES

1 **Yang J**, Pan G, Guan L, Liu Z, Wu Y, Lu W, Li S, Xu H, Ouyang G. The burden of primary liver cancer caused by specific etiologies from 1990 to 2019 at the global, regional, and national levels. *Cancer Med* 2022; **11**: 1357-1370 [PMID: 34989144 DOI: 10.1002/cam4.4530]
2 **Vogel A**, Cervantes A, Chau I, Daniele B, Llovet JM, Meyer T, Nault JC, Neumann U, Ricke J, Sangro B, Schirmacher P, Verslype C, Zech CJ, Arnold D, Martinelli E; ESMO Guidelines Committee. Hepatocellular carcinoma: ESMO Clinical Practice Guidelines for diagnosis, treatment and follow-up. *Ann Oncol* 2018; **29**: iv238-iv255 [PMID: 30285213 DOI: 10.1093/annonc/mdy308]
3 **Ippolito D**, Inchingolo R, Grazioli L, Drago SG, Nardella M, Gatti M, Faletti R. Recent advances in non-invasive magnetic resonance imaging assessment of hepatocellular carcinoma. *World J Gastroenterol* 2018; **24**: 2413-2426 [PMID: 29930464 DOI: 10.3748/wjg.v24.i23.2413]
4 **Inchingolo R**, Faletti R, Grazioli L, Tricarico E, Gatti M, Pecorelli A, Ippolito D. MR with Gd-EOB-DTPA in assessment of liver nodules in cirrhotic patients. *World J Hepatol* 2018; **10**: 462-473 [PMID: 30079132 DOI: 10.4254/wjh.v10.i7.462]
5 **Grazioli L**, Faletti R, Frittoli B, Battisti G, Ambrosini R, Romanini L, Gatti M, Fonio P. Evaluation of incidence of acute

transient dyspnea and related artifacts after administration of gadoxetate disodium: a prospective observational study. *Radiol Med* 2018; **123**: 910-917 [PMID: 30084108 DOI: 10.1007/s11547-018-0927-y]

6 **Gatti M**, Calandri M, Bergamasco L, Darvizeh F, Grazioli L, Inchingolo R, Ippolito D, Rousset S, Veltri A, Fonio P, Faletti R. Characterization of the arterial enhancement pattern of focal liver lesions by multiple arterial phase magnetic resonance imaging: comparison between hepatocellular carcinoma and focal nodular hyperplasia. *Radiol Med* 2020; **125**: 348-355 [PMID: 31916102 DOI: 10.1007/s11547-019-01127-4]

7 **Inchingolo R**, Maino C, Gatti M, Tricarico E, Nardella M, Grazioli L, Sironi S, Ippolito D, Faletti R. Gadoxetic acid magnetic-enhanced resonance imaging in the diagnosis of cholangiocarcinoma. *World J Gastroenterol* 2020; **26**: 4261-4271 [PMID: 32848332 DOI: 10.3748/wjg.v26.i29.4261]

8 **Granata V**, Grassi R, Fusco R, Belli A, Cutolo C, Pradella S, Grazzini G, La Porta M, Brunese MC, De Muzio F, Ottaiano A, Avallone A, Izzo F, Petrillo A. Diagnostic evaluation and ablation treatments assessment in hepatocellular carcinoma. *Infect Agent Cancer* 2021; **16**: 53 [PMID: 34281580 DOI: 10.1186/s13027-021-00393-0]

9 **Yinzhong W**, Xiaoxue T, Jinhui T, Pengcheng Y, Xiaoying L, Junqiang L. Is Gadoxetic Acid Disodium (Gd-EOB-DTPA)-Enhanced Magnetic Resonance Imaging an Accurate Diagnostic Method for Hepatocellular Carcinoma? *Curr Med Imaging* 2022; **18**: 633-647 [PMID: 34533447 DOI: 10.2174/1573405617666210917124404]

10 **Makary MS**, Khandpur U, Cloyd JM, Mumtaz K, Dowell JD. Locoregional Therapy Approaches for Hepatocellular Carcinoma: Recent Advances and Management Strategies. *Cancers (Basel)* 2020; **12** [PMID: 32679897 DOI: 10.3390/cancers12071914]

11 **Minami Y**, Nishida N, Kudo M. Therapeutic response assessment of RFA for HCC: contrast-enhanced US, CT and MRI. *World J Gastroenterol* 2014; **20**: 4160-4166 [PMID: 24764654 DOI: 10.3748/wjg.v20.i15.4160]

12 **Mikami S**, Tateishi R, Akahane M, Asaoka Y, Kondo Y, Goto T, Shiina S, Yoshida H, Koike K. Computed tomography follow-up for the detection of hepatocellular carcinoma recurrence after initial radiofrequency ablation: a single-center experience. *J Vasc Interv Radiol* 2012; **23**: 1269-1275 [PMID: 22999746 DOI: 10.1016/j.jvir.2012.06.032]

13 **Yoon JH**, Lee EJ, Cha SS, Han SS, Choi SJ, Juhn JR, Kim MH, Lee YJ, Park SJ. Comparison of gadoxetic acid-enhanced MR imaging *vs* four-phase multi-detector row computed tomography in assessing tumor regression after radiofrequency ablation in subjects with hepatocellular carcinomas. *J Vasc Interv Radiol* 2010; **21**: 348-356 [PMID: 20116285 DOI: 10.1016/j.jvir.2009.11.014]

14 **Yoo SH**, Choi JY, Jang JW, Bae SH, Yoon SK, Kim DG, Yoo YK, Rha SE, Lee YJ, Jung ES. Gd-EOB-DTPA-enhanced MRI is better than MDCT in decision making of curative treatment for hepatocellular carcinoma. *Ann Surg Oncol* 2013; **20**: 2893-2900 [PMID: 23649931 DOI: 10.1245/s10434-013-3001-y]

15 **Imai Y**, Katayama K, Hori M, Yakushijin T, Fujimoto K, Itoh T, Igura T, Sakakibara M, Takamura M, Tsurusaki M, Takahashi H, Nakanishi K, Usuki N, Tsuji K, Ohashi H, Kim T, Takehara T, Murakami T. Prospective Comparison of Gd-EOB-DTPA-Enhanced MRI with Dynamic CT for Detecting Recurrence of HCC after Radiofrequency Ablation. *Liver Cancer* 2017; **6**: 349-359 [PMID: 29234638 DOI: 10.1159/000481416]

16 **Kim TH**, Woo S, Han S, Suh CH, Lee DH, Lee JM. Hepatobiliary phase hypointense nodule without arterial phase hyperenhancement: are they at risk of HCC recurrence after ablation or surgery? *Eur Radiol* 2020; **30**: 1624-1633 [PMID: 31776747 DOI: 10.1007/s00330-019-06499-9]

17 **Bae JS**, Kim JH, Lee DH, Han JK. Hepatobiliary phase of gadoxetic acid-enhanced MRI in patients with HCC: prognostic features before resection, ablation, or TACE. *Eur Radiol* 2021; **31**: 3627-3637 [PMID: 33211146 DOI: 10.1007/s00330-020-07499-w]

18 **Rimola J**, Davenport MS, Liu PS, Brown T, Marrero JA, McKenna BJ, Hussain HK. Diagnostic accuracy of MRI with extracellular vs. hepatobiliary contrast material for detection of residual hepatocellular carcinoma after locoregional treatment. *Abdom Radiol (NY)* 2019; **44**: 549-558 [PMID: 30218239 DOI: 10.1007/s00261-018-1775-x]

19 **Koda M**, Tokunaga S, Okamoto T, Hodozuka M, Miyoshi K, Kishina M, Fujise Y, Kato J, Matono T, Sugihara T, Oyama K, Hosho K, Okano J, Murawaki Y, Kakite S, Yamashita E. Clinical usefulness of the ablative margin assessed by magnetic resonance imaging with Gd-EOB-DTPA for radiofrequency ablation of hepatocellular carcinoma. *J Hepatol* 2015; **63**: 1360-1367 [PMID: 26232269 DOI: 10.1016/j.jhep.2015.07.023]

20 **Vogl TJ**, Nour-Eldin NA, Hammerstingl RM, Panahi B, Naguib NNN. Microwave Ablation (MWA): Basics, Technique and Results in Primary and Metastatic Liver Neoplasms - Review Article. *Rofo* 2017; **189**: 1055-1066 [PMID: 28834968 DOI: 10.1055/s-0043-117410]

21 **Bouda D**, Lagadec M, Alba CG, Barrau V, Dioguardi Burgio M, Moussa N, Vilgrain V, Ronot M. Imaging review of hepatocellular carcinoma after thermal ablation: The good, the bad, and the ugly. *J Magn Reson Imaging* 2016; **44**: 1070-1090 [PMID: 27505619 DOI: 10.1002/jmri.25369]

22 **Song KD**. Percutaneous cryoablation for hepatocellular carcinoma. *Clin Mol Hepatol* 2016; **22**: 509-515 [PMID: 28081593 DOI: 10.3350/cmh.2016.0079]

23 **Luo W**, Zhang Y, He G, Yu M, Zheng M, Liu L, Zhou X. Effects of radiofrequency ablation *vs* other ablating techniques on hepatocellular carcinomas: a systematic review and meta-analysis. *World J Surg Oncol* 2017; **15**: 126 [PMID: 28693505 DOI: 10.1186/s12957-017-1196-2]

24 **Ratanaprasatporn L**, Sainani N, Duda JB, Aghayev A, Tatli S, Silverman SG, Shyn PB. Imaging findings during and after percutaneous cryoablation of hepatic tumors. *Abdom Radiol (NY)* 2019; **44**: 2602-2626 [PMID: 31004203 DOI: 10.1007/s00261-019-01999-0]

25 **Couri T**, Pillai A. Goals and targets for personalized therapy for HCC. *Hepatol Int* 2019; **13**: 125-137 [PMID: 30600478 DOI: 10.1007/s12072-018-9919-1]

26 **Young S**, Taylor AJ, Sanghvi T. Post Locoregional Therapy Treatment Imaging in Hepatocellular Carcinoma Patients: A Literature-based Review. *J Clin Transl Hepatol* 2018; **6**: 189-197 [PMID: 29951364 DOI: 10.14218/JCTH.2017.00059]

27 **Patidar Y**, Basavaraj 1, Mukund A, Sarin SK. Transarterial Chemoembolization in Unresectable Hepatocellular Carcinoma with Portal Vein Tumor Thrombosis: A Tertiary Care Center Experience. *Indian J Radiol Imaging* 2021; **31**: 270-276 [PMID: 34556907 DOI: 10.1055/s-0041-1734367]

28 **Mendiratta-Lala M**, Masch WR, Shampain K, Zhang A, Jo AS, Moorman S, Aslam A, Maturen KE, Davenport MS. MRI

Assessment of Hepatocellular Carcinoma after Local-Regional Therapy: A Comprehensive Review. *Radiol Imaging Cancer* 2020; **2**: e190024 [PMID: 33778692 DOI: 10.1148/rycan.2020190024]

29 **American College of Radiology**. CT/MRI LI-RADS v2018. [cited 15 February 2022]. In: American College of Radiology [Internet]. Available from: https://www.acr.org/Clinical-Resources/Reporting-and-Data-Systems/LI-RADS/CT-MRI-LI-RADS-v2018

30 **Aslam A**, Kamath A, Spieler B, Maschiocchi M, Sabottke CF, Chernyak V, Lewis SC. Assessing locoregional treatment response to Hepatocellular Carcinoma: comparison of hepatobiliary contrast agents to extracellular contrast agents. *Abdom Radiol (NY)* 2021; **46**: 3565-3578 [PMID: 33856509 DOI: 10.1007/s00261-021-03076-x]

31 **Yaghmai V**, Besa C, Kim E, Gatlin JL, Siddiqui NA, Taouli B. Imaging assessment of hepatocellular carcinoma response to locoregional and systemic therapy. *AJR Am J Roentgenol* 2013; **201**: 80-96 [PMID: 23789661 DOI: 10.2214/AJR.13.10706]

32 **Motosugi U**, Ichikawa T, Sou H, Sano K, Tominaga L, Muhi A, Araki T. Distinguishing hypervascular pseudolesions of the liver from hypervascular hepatocellular carcinomas with gadoxetic acid-enhanced MR imaging. *Radiology* 2010; **256**: 151-158 [PMID: 20574092 DOI: 10.1148/radiol.10091885]

33 **Kim SW**, Joo I, Kim HC, Ahn SJ, Kang HJ, Jeon SK, Lee JM. LI-RADS treatment response categorization on gadoxetic acid-enhanced MRI: diagnostic performance compared to mRECIST and added value of ancillary features. *Eur Radiol* 2020; **30**: 2861-2870 [PMID: 32006170 DOI: 10.1007/s00330-019-06623-9]

34 **Chernyak V**, Fowler KJ, Heiken JP, Sirlin CB. Use of gadoxetate disodium in patients with chronic liver disease and its implications for liver imaging reporting and data system (LI-RADS). *J Magn Reson Imaging* 2019; **49**: 1236-1252 [PMID: 30609194 DOI: 10.1002/jmri.26540]

35 **Bashir MR**, Breault SR, Braun R, Do RK, Nelson RC, Reeder SB. Optimal timing and diagnostic adequacy of hepatocyte phase imaging with gadoxetate-enhanced liver MRI. *Acad Radiol* 2014; **21**: 726-732 [PMID: 24717550 DOI: 10.1016/j.acra.2014.02.005]

36 **Park S**, Joo I, Lee DH, Bae JS, Yoo J, Kim SW, Lee JM. Diagnostic Performance of LI-RADS Treatment Response Algorithm for Hepatocellular Carcinoma: Adding Ancillary Features to MRI Compared with Enhancement Patterns at CT and MRI. *Radiology* 2020; **296**: 554-561 [PMID: 32692297 DOI: 10.1148/radiol.2020192797]

37 **Kim YY**, Kim MJ, Yoon JK, Shin J, Roh YH. Incorporation of Ancillary MRI Features Into the LI-RADS Treatment Response Algorithm: Impact on Diagnostic Performance After Locoregional Treatment of Hepatocellular Carcinoma. *AJR Am J Roentgenol* 2022; **218**: 484-493 [PMID: 34585608 DOI: 10.2214/AJR.21.26677]

38 **Schaub SK**, Hartvigson PE, Lock MI, Høyer M, Brunner TB, Cardenes HR, Dawson LA, Kim EY, Mayr NA, Lo SS, Apisarnthanarax S. Stereotactic Body Radiation Therapy for Hepatocellular Carcinoma: Current Trends and Controversies. *Technol Cancer Res Treat* 2018; **17**: 1533033818790217 [PMID: 30068240 DOI: 10.1177/1533033818790217]

39 **Benson AB 3rd**, D'Angelica MI, Abbott DE, Abrams TA, Alberts SR, Saenz DA, Are C, Brown DB, Chang DT, Covey AM, Hawkins W, Iyer R, Jacob R, Karachristos A, Kelley RK, Kim R, Palta M, Park JO, Sahai V, Schefter T, Schmidt C, Sicklick JK, Singh G, Sohal D, Stein S, Tian GG, Vauthey JN, Venook AP, Zhu AX, Hoffmann KG, Darlow S. NCCN Guidelines Insights: Hepatobiliary Cancers, Version 1.2017. *J Natl Compr Canc Netw* 2017; **15**: 563-573 [PMID: 28476736 DOI: 10.6004/jnccn.2017.0059]

40 **European Association for Study of Liver**. European Organisation for Research and Treatment of Cancer. EASL-EORTC clinical practice guidelines: management of hepatocellular carcinoma. *Eur J Cancer* 2012; **48**: 599-641 [PMID: 22424278 DOI: 10.1016/j.ejca.2011.12.021]

41 **Sapisochin G**, Barry A, Doherty M, Fischer S, Goldaracena N, Rosales R, Russo M, Beecroft R, Ghanekar A, Bhat M, Brierley J, Greig PD, Knox JJ, Dawson LA, Grant DR. Stereotactic body radiotherapy vs. TACE or RFA as a bridge to transplant in patients with hepatocellular carcinoma. An intention-to-treat analysis. *J Hepatol* 2017; **67**: 92-99 [PMID: 28257902 DOI: 10.1016/j.jhep.2017.02.022]

42 **Olsen CC**, Welsh J, Kavanagh BD, Franklin W, McCarter M, Cardenes HR, Gaspar LE, Schefter TE. Microscopic and macroscopic tumor and parenchymal effects of liver stereotactic body radiotherapy. *Int J Radiat Oncol Biol Phys* 2009; **73**: 1414-1424 [PMID: 18990508 DOI: 10.1016/j.ijrobp.2008.07.032]

43 **Macià I Garau M**. Radiobiology of stereotactic body radiation therapy (SBRT). *Rep Pract Oncol Radiother* 2017; **22**: 86-95 [PMID: 28490978 DOI: 10.1016/j.rpor.2017.02.010]

44 **Velec M**, Haddad CR, Craig T, Wang L, Lindsay P, Brierley J, Brade A, Ringash J, Wong R, Kim J, Dawson LA. Predictors of Liver Toxicity Following Stereotactic Body Radiation Therapy for Hepatocellular Carcinoma. *Int J Radiat Oncol Biol Phys* 2017; **97**: 939-946 [PMID: 28333016 DOI: 10.1016/j.ijrobp.2017.01.221]

45 **Kudo M**, Ikeda M, Ueshima K, Sakamoto M, Shiina S, Tateishi R, Nouso K, Hasegawa K, Furuse J, Miyayama S, Murakami T, Yamashita T, Kokudo N. Response Evaluation Criteria in Cancer of the liver version 6 (Response Evaluation Criteria in Cancer of the Liver 2021 revised version). *Hepatol Res* 2022; **52**: 329-336 [PMID: 35077590 DOI: 10.1111/hepr.13746]

46 **Lall C**, Bhargava P, Sandrasegaran K, Shanbhogue AK, Ramsinghani N, Koh YW, Choi JY, Choi JI. Three-dimensional conformal radiation therapy in the liver: MRI findings along a time continuum. *J Comput Assist Tomogr* 2015; **39**: 356-364 [PMID: 25700224 DOI: 10.1097/RCT.0000000000000219]

47 **Yip C**, Cook GJR, Owczarczyk K, Goh V. Challenges in imaging assessment following liver stereotactic body radiotherapy: pitfalls to avoid in clinical practice. *Chin Clin Oncol* 2017; **6**: S11 [PMID: 28917249 DOI: 10.21037/cco.2017.06.06]

48 **Mendiratta-Lala M**, Gu E, Owen D, Cuneo KC, Bazzi L, Lawrence TS, Hussain HK, Davenport MS. Imaging Findings Within the First 12 Months of Hepatocellular Carcinoma Treated With Stereotactic Body Radiation Therapy. *Int J Radiat Oncol Biol Phys* 2018; **102**: 1063-1069 [PMID: 29029891 DOI: 10.1016/j.ijrobp.2017.08.022]

49 **Kubota K**, Hisa N, Nishikawa T, Fujiwara Y, Murata Y, Itoh S, Yoshida D, Yoshida S. Evaluation of hepatocellular carcinoma after treatment with transcatheter arterial chemoembolization: comparison of Lipiodol-CT, power Doppler sonography, and dynamic MRI. *Abdom Imaging* 2001; **26**: 184-190 [PMID: 11178697 DOI: 10.1007/s002610000139]

50 **Gluskin JS**, Chegai F, Monti S, Squillaci E, Mannelli L. Hepatocellular Carcinoma and Diffusion-Weighted MRI:

Detection and Evaluation of Treatment Response. *J Cancer* 2016; **7**: 1565-1570 [PMID: 27471573 DOI: 10.7150/jca.14582]

51 **Dromain C**, de Baere T, Elias D, Kuoch V, Ducreux M, Boige V, Petrow P, Roche A, Sigal R. Hepatic tumors treated with percutaneous radio-frequency ablation: CT and MR imaging follow-up. *Radiology* 2002; **223**: 255-262 [PMID: 11930075 DOI: 10.1148/radiol.2231010780]

52 **Takayasu K**, Arii S, Matsuo N, Yoshikawa M, Ryu M, Takasaki K, Sato M, Yamanaka N, Shimamura Y, Ohto M. Comparison of CT findings with resected specimens after chemoembolization with iodized oil for hepatocellular carcinoma. *AJR Am J Roentgenol* 2000; **175**: 699-704 [PMID: 10954453 DOI: 10.2214/ajr.175.3.1750699]

53 **Lee JM**, Yoon JH, Joo I, Woo HS. Recent Advances in CT and MR Imaging for Evaluation of Hepatocellular Carcinoma. *Liver Cancer* 2012; **1**: 22-40 [PMID: 24159569 DOI: 10.1159/000339018]

54 **Yue X**, Jiang Q, Hu X, Cen C, Song S, Qian K, Lu Y, Yang M, Li Q, Han P. Quantitative dual-energy CT for evaluating hepatocellular carcinoma after transarterial chemoembolization. *Sci Rep* 2021; **11**: 11127 [PMID: 34045528 DOI: 10.1038/s41598-021-90508-9]

55 **Choi SH**, Chung JW, Kim HC, Baek JH, Park CM, Jun S, Kim MU, Lee ES, Cho HR, Jae HJ, Lee W, Park JH. The role of perfusion CT as a follow-up modality after transcatheter arterial chemoembolization: an experimental study in a rabbit model. *Invest Radiol* 2010; **45**: 427-436 [PMID: 20440211 DOI: 10.1097/RLI.0b013e3181e07516]

56 **Ruff C**, Artzner C, Syha R, Grosse U, Hoffmann R, Bitzer M, Partovi S, Horger M, Nikolaou K, Grözinger G. Transarterial Chemoembolization of Hepatocellular Carcinoma Using Radiopaque Drug-Eluting Embolics: Impact of Embolic Density and Residual Tumor Perfusion on Tumor Recurrence and Survival. *Cardiovasc Intervent Radiol* 2021; **44**: 1403-1413 [PMID: 34021375 DOI: 10.1007/s00270-021-02858-6]

57 **Chen X**, Xiao E, Shu D, Yang C, Liang B, He Z, Bian D. Evaluating the therapeutic effect of hepatocellular carcinoma treated with transcatheter arterial chemoembolization by magnetic resonance perfusion imaging. *Eur J Gastroenterol Hepatol* 2014; **26**: 109-113 [PMID: 24284371 DOI: 10.1097/MEG.0b013e328363716e]

58 **Castaldo A**, De Lucia DR, Pontillo G, Gatti M, Cocozza S, Ugga L, Cuocolo R. State of the Art in Artificial Intelligence and Radiomics in Hepatocellular Carcinoma. *Diagnostics (Basel)* 2021; **11** [PMID: 34209197 DOI: 10.3390/diagnostics11071194]

59 **Zhang L**, Cai P, Hou J, Luo M, Li Y, Jiang X. Radiomics Model Based on Gadoxetic Acid Disodium-Enhanced MR Imaging to Predict Hepatocellular Carcinoma Recurrence After Curative Ablation. *Cancer Manag Res* 2021; **13**: 2785-2796 [PMID: 33790652 DOI: 10.2147/CMAR.S300627]

60 **van Timmeren JE**, Cester D, Tanadini-Lang S, Alkadhi H, Baessler B. Radiomics in medical imaging-"how-to" guide and critical reflection. *Insights Imaging* 2020; **11**: 91 [PMID: 32785796 DOI: 10.1186/s13244-020-00887-2]

61 **Ichikawa S**, Motosugi U, Sato K, Shimizu T, Wakayama T, Onishi H. Transient Respiratory-motion Artifact and Scan Timing during the Arterial Phase of Gadoxetate Disodium-enhanced MR Imaging: The Benefit of Shortened Acquisition and Multiple Arterial Phase Acquisition. *Magn Reson Med Sci* 2021; **20**: 280-289 [PMID: 32863326 DOI: 10.2463/mrms.mp.2020-0064]

62 **Westwood M**, Joore M, Grutters J, Redekop K, Armstrong N, Lee K, Gloy V, Raatz H, Misso K, Severens J, Kleijnen J. Contrast-enhanced ultrasound using SonoVue® (sulphur hexafluoride microbubbles) compared with contrast-enhanced computed tomography and contrast-enhanced magnetic resonance imaging for the characterisation of focal liver lesions and detection of liver metastases: a systematic review and cost-effectiveness analysis. *Health Technol Assess* 2013; **17**: 1-243 [PMID: 23611316 DOI: 10.3310/hta17160]

World Journal of Gastroenterology

Submit a Manuscript: https://www.f6publishing.com

World J Gastroenterol 2022 July 14; 28(26): 3132-3149

DOI: 10.3748/wjg.v28.i26.3132

ISSN 1007-9327 (print) ISSN 2219-2840 (online)

ORIGINAL ARTICLE

Basic Study

Neutrophil extracellular traps participate in the development of cancer-associated thrombosis in patients with gastric cancer

Jia-Cheng Li, Xiao-Ming Zou, Shi-Feng Yang, Jia-Qi Jin, Lei Zhu, Chang-Jian Li, Hao Yang, An-Ge Zhang, Tian-Qi Zhao, Chong-Yan Chen

Specialty type: Gastroenterology and hepatology

Provenance and peer review: Unsolicited article; Externally peer reviewed.

Peer-review model: Single blind

Peer-review report's scientific quality classification
Grade A (Excellent): 0
Grade B (Very good): B, B, B
Grade C (Good): C
Grade D (Fair): 0
Grade E (Poor): 0

P-Reviewer: Ferreira GSA, Brazil; Mohamed SY, Egypt; Morozov S, Russia; Singh I, United States

Received: October 19, 2021
Peer-review started: October 19, 2021
First decision: January 11, 2022
Revised: January 20, 2022
Accepted: March 16, 2022
Article in press: March 16, 2022
Published online: July 14, 2022

Jia-Cheng Li, Xiao-Ming Zou, Shi-Feng Yang, Lei Zhu, Chang-Jian Li, Hao Yang, An-Ge Zhang, Tian-Qi Zhao, Chong-Yan Chen, Department of Gastrointestinal Surgery, The Second Affiliated Hospital of Harbin Medical University, Harbin 150001, Heilongjiang Province, China

Jia-Cheng Li, Shi-Feng Yang, Jia-Qi Jin, Lei Zhu, Hao Yang, An-Ge Zhang, The Key Laboratory of Myocardial Ischemia, Harbin Medical University, Harbin 150001, Heilongjiang Province, China

Jia-Qi Jin, Department of Neurosurgery, The Second Affiliated Hospital of Harbin Medical University, Harbin 150001, Heilongjiang Province, China

Corresponding author: Xiao-Ming Zou, MD, PhD, Chief Doctor, Professor, Surgeon, Department of Gastrointestinal Surgery, The Second Affiliated Hospital of Harbin Medical University, No. 246 Xuefu Road, Nangang District, Harbin 150001, Heilongjiang Province, China. zou4930@163.com

Abstract

BACKGROUND

The development of venous thromboembolism (VTE) is associated with high mortality among gastric cancer (GC) patients. Neutrophil extracellular traps (NETs) have been reported to correlate with the prothrombotic state in some diseases, but are rarely reported in GC patients.

AIM

To investigate the effect of NETs on the development of cancer-associated thrombosis in GC patients.

METHODS

The levels of NETs in blood and tissue samples of patients were analyzed by ELISA, flow cytometry, and immunofluorescence staining. NET generation and hypercoagulation of platelets and endothelial cells (ECs) *in vitro* were observed by immunofluorescence staining. NET procoagulant activity (PCA) was determined by fibrin formation and thrombin–antithrombin complex (TAT) assays. Thrombosis *in vivo* was measured in a murine model induced by flow stenosis in the inferior vena cava (IVC).

RESULTS

NETs were likely to form in blood and tissue samples of GC patients compared with healthy individuals. *In vitro* studies showed that GC cells and their conditioned medium, but not gastric mucosal epithelial cells, stimulated NET release from neutrophils. In addition, NETs induced a hypercoagulable state of platelets by upregulating the expression of phosphatidylserine and P-selectin on the cells. Furthermore, NETs stimulated the adhesion of normal platelets on glass surfaces. Similarly, NETs triggered the conversion of ECs to hypercoagulable phenotypes by downregulating the expression of their intercellular tight junctions but upregulating that of tissue factor. Treatment of normal platelets or ECs with NETs augmented the level of plasma fibrin formation and the TAT complex. In the models of IVC stenosis, tumor-bearing mice showed a stronger ability to form thrombi, and NETs abundantly accumulated in the thrombi of tumor-bearing mice compared with control mice. Notably, the combination of deoxyribonuclease I, activated protein C, and sivelestat markedly abolished the PCA of NETs.

CONCLUSION

GC-induced NETs strongly increased the risk of VTE development both *in vitro* and *in vivo*. NETs are potential therapeutic targets in the prevention and treatment of VTE in GC patients.

Key Words: Neutrophil extracellular traps; Gastric cancer; Platelet; Endothelial cells; Venous thromboembolism

©The Author(s) 2022. Published by Baishideng Publishing Group Inc. All rights reserved.

Core tip: We found that gastric cancer (GC)-induced neutrophil extracellular traps (NETs) strongly increase the risk of venous thromboembolism (VTE) development in GC patients. NETs are potential therapeutic targets in the prevention and treatment of VTE in GC patients.

Citation: Li JC, Zou XM, Yang SF, Jin JQ, Zhu L, Li CJ, Yang H, Zhang AG, Zhao TQ, Chen CY. Neutrophil extracellular traps participate in the development of cancer-associated thrombosis in patients with gastric cancer. *World J Gastroenterol* 2022; 28(26): 3132-3149

URL: https://www.wjgnet.com/1007-9327/full/v28/i26/3132.htm

DOI: https://dx.doi.org/10.3748/wjg.v28.i26.3132

INTRODUCTION

Gastric cancer (GC) is one of the most prevalent gastrointestinal tumors and the third most fatal cancer in the world[1,2]. Additionally, venous thromboembolism (VTE) is a more common complication among GC patients when compared to healthy individuals[3-5]. Notably, VTE is associated with a high mortality in GC patients[6,7]. Several factors, such as tumor stage, neoadjuvant chemotherapy, and surgery, contribute to the development of VTE in GC patients[8,9]. Cancer cells exert a procoagulant activity (PCA) in their microenvironment, which is related to activation of the coagulation system[10]. However, the molecular mechanism underlying PCA in GC patients is poorly understood. Uncovering molecular targets associated with VTE in GC patients can help in the development of appropriate therapy, which can improve the clinical outcomes of these patients.

Neutrophil extracellular traps (NETs) are web-like structures composed of filamentous DNA and histones, decorated with antimicrobial protein granules and enzymes, including neutrophil elastase (NE), myeloperoxidase (MPO), matrix metalloproteinase-9 (MMP-9), and cathepsin G (CatG)[11,12]. They result from interactions between neutrophils and bacterial or other stimulating factors[13,14]. Overall, they protect the host from pathogen-related damage. NETs were initially described as an antimicrobial reaction, but some undesirable effects of NETs have been reported in autoimmune diseases[15-17]. Citrullinated histone H3 (citH3) is proposed as a biomarker reflecting NETs formation. Recent studies have linked NETs to the development of metastasis and cancer-associated thrombosis[18,19]. In particular, NETs result in arterial and venous thrombosis, both of which are mediated by neutrophils[20]. Furthermore, using mouse models, it has been shown that thrombosis in breast cancer tissues is closely linked to the formation of NETs[21]. This finding suggests the potential relationship between NETs and cancer-associated thrombosis.

A recent study revealed that priming metastatic pancreatic cancer cells with platelets stimulates neutrophils to release NETs, which promotes thrombosis in both static and dynamic states[22]. We first reported that platelets derived from GC can stimulate neutrophils to release NETs. NETs enhance PCA in GC patients, which is positively correlated with the expression of the thrombin–antithrombin (TAT)

complex and the level of serum D-dimers[23]. Moreover, both human and animal studies suggest that enhanced thrombosis may result from increased activated platelets[24,25]. Nevertheless, little is known about the interaction between NETs and platelet activation in GC patients. Venous endothelial cell (EC) injury in cancer patients is also closely related to venous thrombosis[26,27]. Interestingly, the cytotoxicity of NETs against ECs enhances PCA in oral squamous cancer, even in patients with obstructive jaundice and inflammatory bowel disease[28-30]. Even so, the potential mechanism underlying EC injury in GC patients is poorly understood.

Our central hypothesis is that GC-induced NETs participate in VTE responses by platelet activation and endothelial injury. Therefore, we first explored the complex relationship between NET formation and platelet activation as well as EC injury. Furthermore, we showed the effect of NETs on thrombosis in an inferior vena cava (IVC) stenosis mouse model. In general, our results may indicate that NETs are potential therapeutic targets in the prevention and treatment of VTE in GC patients.

MATERIALS AND METHODS

Patients and tissue samples

Sixty-three patients newly diagnosed with primary GC and 13 healthy donors (HDs) attending the Second Affiliated Hospital of Harbin Medical University between October 2019 and April 2021 were enrolled in this study. GC diagnoses were performed based on pathological examinations. Pathological tumor-node-metastasis (TNM) staging and histological classification of GC were performed according to the 7th American Joint Committee on Cancer (AJCC) guidelines[31]. Patients who were < 18 years old or pregnant, those on antitumor or anticoagulant treatment before surgical treatment, or those with underlying complications such as endocrine, cardiovascular, hematological and other cancers or infectious disease were all excluded. The main clinical characteristics of the patients with GC and HDs are shown in Table 1. We extracted tumor and adjacent normal tissues from GC patients who consented to this study in writing. Blood samples of preoperative patients were obtained at first diagnosis before any clinical treatment, and blood samples of postoperative patients were obtained from 1 mo after surgery before adjuvant therapy to avoid errors caused by postoperative stress. The protocol for this study was approved by the Ethics Committee of the Second Affiliated Hospital of Harbin Medical University (No. KY2016-032).

Isolation of human plasma, platelets, and neutrophils

Fresh whole venous blood was collected into tubes containing 3.2% sodium citrate using 21-gauge needles. The patients underwent overnight fasting before blood collection. The blood was centrifuged at 150 *g* for 20 min at room temperature (RT) to obtain platelet-rich plasma (PRP), within 1 h of collection. Clean top PRP layer was collected in a new tube, diluted with platelet wash buffer (TBD, Tianjin, China), and centrifuged at 460 *g* for 20 min at RT to obtain clean platelets and platelet-free plasma (PFP) [32]. The platelets were resuspended in prewarmed modified Tyrode's buffer (137 mmoL/L NaCl, 2.8 mmoL/L KCl, 1.0 mmoL/L $MgCl_2$, 12 mmoL/L $NaHCO_3$, 0.4 mmoL/L Na_2HPO_4, 5.5 mmoL/L glucose, pH 7.4; Solarbio, Beijing, China). Neutrophils were isolated based on the density gradient centrifugation, using the whole blood neutrophil isolation kit (TBD). After lysing erythrocytes based on the red blood cell lysis buffer (150 mmoL/L NH_4CL, 10 mmoL/L $KHCO_3$, 0.2 mmoL/L Na_2EDTA, pH 7.4; TBD), the purity (> 96%) and viability (> 96%) of neutrophils were assessed using Wright–Giemsa staining and Trypan blue staining, respectively.

Cell lines and conditioned medium

The human metastatic GC KATO-III and MKN-45 cell lines, human primary GC AGS cell line, human gastric mucosal epithelial cell (GES-1) line, human umbilical cord endothelial cell (HUVEC) line, and mouse forestomach squamous carcinoma (MFC) cell line were purchased from PROCELL (Wuhan, China). All cell lines were characterized using short tandem repeat (STR) profiling. The GES-1, AGS, MKN-45 and MFC cells were cultured in RPMI 1640 (Gibco, USA), KATO-III cells were cultured in IMDM (Gibco), and HUVECs were cultured in DME/F12 (HyClone, Logan, UT, USA). All media were supplemented with 10% fetal bovine serum (FBS; Gibco) and 1% penicillin–streptomycin solution (Beyotime, Beijing, China). Incubation was performed at 37°C under 5% CO_2in a humidified environment. To prepare conditioned medium (CM), the cells were cultured to 90% confluence in medium supplemented with 10% FBS, washed three times using 1 × PBS, and recultured for 48 h in medium without FBS. The supernatant was centrifuged at 1500 *g* for 10 min at 4°C to remove cell debris. The CM was collected and stored at -80°C until use.

Animal models

The animal protocol was designed to minimize pain or discomfort to the animals. Wild-type male C57BL/6 mice (7–9 wk old, weighing 20–26 g) were purchased from the Animal Experimental Center of Harbin Medical University, and all procedures were approved by the Animal Care and Use Committee

Table 1 Main clinical and laboratory features of 13 healthy subjects and 63 patients diagnosed with gastric cancer

Characteristics (n = 76, DF = 4)	Control (n = 13)	Stage I (n = 14)	Stage II (n = 15)	Stage III (n = 22)	Stage IV (n = 12)
Male (%)	61.5	50	53.3	72.7	66.6
Age(yr)	58.46 ± 5.43	57.0 ± 10.07	63.07 ± 9.12	60.32 ± 11.54	63.64 ± 9.68
Erythrocytes (× 10^{12}/L)	4.70 ± 0.57	4.46 ± 0.32	4.12 ± 0.83	4.13 ± 0.69	4.03 ± 0.81
Leukocytes (× 10^{9}/L)	6.87 ± 2.86	6.57 ± 2.04	8.60 ± 2.54[a]	8.58 ± 4.66[a]	10.60 ± 5.25[b]
Neutrophils (× 10^{9}/L)	4.36 ± 3.0	4.62 ± 2.54	6.36 ± 2.82[a]	6.75 ± 4.92[a]	8.53 ± 5.46[c]
Hb (g/L)	140.84 ± 20.31	137.23 ± 10.76	121.29 ± 26.65	121.23 ± 29.72	111 ± 33.23[a]
PLT (× 10^{9})	259.15 ± 59.0	242.69 ± 52.19	293.29 ± 83.74	250.64 ± 104.63	302.0 ± 156.9
ALB (g/L)	44.84 ± 3.27	43.33 ± 4.84	38.06 ± 6.29	37.39 ± 9.23	35.59 ± 4.08[a]
PT (s)	11.24 ± 1.03	12.66 ± 4.16	12.42 ± 2.03	12.05 ± 0.86	12.24 ± 1.57
APTT (s)	35.06 ± 2.71	36.03 ± 7.54	34.52 ± 3.46	33.49±3.81	35.08±4.68
D-dimer (mg/L)	53.30 ± 48.16	238.46 ± 265.28[c]	280.21 ± 269.55[c]	291.23 ± 262.88[c]	950.0 ± 743.72[d]
Fibrinogen (g/L)	2.46 ± 0.43	2.69 ± 0.58	3.67 ± 0.98[a]	3.19 ± 0.61[a]	4.68 ± 2.61[b]

[a]P < 0.05 *vs* healthy control.
[b]P < 0.01 *vs* healthy control.
[c]P < 0.001 *vs* healthy control.
[d]P < 0.0001 *vs* healthy control.
Data are presented as numbers (percentages) or the mean ± SD. DF: Degree of freedom; Hb: Hemoglobin; PLT: Platelets; ALB: Albumin; PT: Prothrombin time; APTT: Activated partial thromboplastin time.

of the Second Affiliated Hospital of Harbin Medical University (No. KY2016-032). The animals were individually housed and maintained under standard conditions (12 h/12 h light/dark cycle, 22 ± 1 °C, 50% humidity) and provided with a conventional laboratory diet and an unrestricted supply of drinking water. In the subcutaneous tumor models, mice were injected with MFC cells (2 × 10^{7} cells/mL) subcutaneously into the right axilla, and the tumor volumes were measured every 3 d from 7 d after injection with MFC cells and allowed to reach 1000 mm^{3} (usually 28–35 d). The volume was calculated by measuring the length (L) and width (W) of the tumor: Tumor volume = π/6 × L × W^{2}. Thereafter, a murine model of deep vein thrombosis (DVT) was developed as previously described[33]. The mice were anesthetized by intraperitoneal injection of 2,2,2-tribromoethanol (Sigma, St . Louis, MO, USA), and the intestines were removed to expose the IVC after entering the abdominal cavity through a median abdominal incision. The IVC was carefully separated below the left renal vein plane. After 5-0 (1 mm) sutures passed through the IVC, 3-0 (2 mm) sutures were placed at the parallel part of the IVC as the blocking line. The IVC was ligated and 3-0 sutures were carefully extracted. This procedure has been shown to decrease the vascular lumen by approximately 90%. The other branches of the IVC were ligated to the level of the iliac vein. Thereafter, the abdominal incision was closed, mice were sacrificed after 6 or 48 h, and thrombi that had formed in the IVC were harvested. The IVC stenosis mice in the treatment groups were injected with DNase I (50 μg/mouse; Roche, Switzerland) intraperitoneally every 12 h until the time of death. All animals were killed for tissue collection. Blood (300 μL/mouse) was drawn from the periorbital eye plexus and stabilized with 0.5 mmoL/L EDTA. Plasma was obtained as described above. Thrombi of control and tumor-bearing mice were fixed in 4% paraformaldehyde for 24 h, embedded in Optimal Cutting Temperature (OCT) compound (SAKURA, Torrance, CA, USA), and cryosectioned at a thickness of 4 μm for immunofluorescence staining.

Quantification of plasma NETs marker

Plasma cell-free DNA (cf-DNA), MPO-DNA and citH3-DNA complexes were quantified using capture ELISA as previously described[34]. The quantification of cf-DNA was performed using the Quant-iT PicoGreen dsDNA assay kit (Invitrogen, Carlsbad, CA, USA). For detection of NET-DNA complexes, 5 μg/mL anti-MPO (ab90810; Abcam, Cambridge, UK) or anti-citH3 antibody (ab5103; Abcam) was coated onto 96-well plates overnight at 4°C. After blocking in 1% bovine serum albumin (BSA), the plasma from GC patients or healthy individuals was added per well and incubated at RT for 2 h. After washing five times with PBST, Quant-iT PicoGreen dsDNA Reagent was added. The values were then read with a fluorometer with a filter setting of 480 nm/520 nm excitation/emission wavelengths.

Fibrin formation and TAT complex assay

Fibrin formation of platelets and ECs was detected by turbidity as previously described[35]. To assess

the fibrin formation in the setting of platelet or EC monolayers, cell monolayers in 96-well plates were stimulated by NETs with or without DNase I, activated protein C (APC), and sivelestat treatment alone or together for 4 h, followed by two washes with Hank's balanced salt solution (137 mmoL/L NaCl, 5.3 mmoL/L KCl, 4.17 mmoL/L $NaHCO_3$, 0.33 mmoL/L Na_2HPO_4, 5.5 mmoL/L glucose, pH 7.4) and then 150 μL PFP from HDs was cocultured with cells at 37°C for 2 min, followed by the addition of 50 μL prewarmed 25 mmoL/L $CaCl_2$. The fibrin formation was tested using turbidity measurements and quantified as the maximum value by measuring the OD at 405 nm every 10 s for 30 min on a SpectraMax 340 PC plate reader. To assess the fibrin formation in the plasma of mice, 150 μL PFP from control, tumor-bearing mice, or DNase I infused tumor-bearing mice was cultured at 37°C for 2 min, followed by addition of 50 μL prewarmed 25 mmoL/L $CaCl_2$. To detect the level of TAT complex, a human and mouse TAT complex ELISA kit (Jingkbio, Shanghai, China) was used as previously described[36].

Flow cytometry

Circulating NETs were measured using flow cytometry. Here, whole blood from HDs and GC patients was diluted with 1 × PBS and incubated in the dark at RT for 30 min with FITC-conjugated-citH3 (eBioscience, San Diego, CA, USA) and PE-conjugated MPO (eBioscience) antibodies. For the assessment of phosphatidylserine (PS) and P-selectin expression on platelets, platelets (2×10^6 cells) isolated from the blood of HDs and GC patients were incubated with FITC-conjugated lactadherin (Haematologic, Essex Junction, VT, USA), APC-conjugated CD62P (Biolegend, San Diego, CA, USA), and PerCP-conjugated CD41 (Biolegend) antibodies.

Immunofluorescence staining of NETs

Tumor and paratumor tissues of GC patients were fixed in 4% paraformaldehyde for 24 h, embedded in OCT compound (SAKURA), and cryosectioned into slices of 4-μm thickness. The samples were cultured overnight at 4°C with primary rabbit anti-histone H3 (1:500, ab5103; Abcam) and mouse anti-MPO (1:500, ab90810; Abcam) antibodies, and washed three times with PBS before incubation for 1 h at RT with Alexa Fluor 594-conjugated goat anti-rabbit (1:200; Proteintech, China) and Alexa Fluor 488-conjugated goat anti-mouse (1:200; Proteintech) secondary antibodies. The tissues were stained for 5 min at RT in the dark with 4',6-diamidino-2-phenylindole (DAPI) and anti-fade mounting medium (Solarbio, Beijing, China). Thrombi in the IVC of tumor models or control mice were stained with primary rabbit anti-histone H3 (1:500, ab5103; Abcam) and rat anti-Ly6G (1:500, Novus, St. Charles, MO, USA), and the specimens were incubated with the Alexa Fluor 488-conjugated goat anti-rabbit (1:200; Proteintech) and Alexa Fluor 594-conjugated goat anti-rat (1:200; Proteintech) secondary antibodies as previously described[37]. The tissue images were captured using a confocal microscope (LSM 800; Zeiss, Germany).

Neutrophils (5×10^5 cells) isolated from HDs were seeded and incubated in glass-based poly-L-lysine-coated 24-well plates for 1 h at 37°C under 5% CO_2. Thereafter, cell suspensions of KATO-III, MKN-45, AGS, and GES-1 (2×10^5 cells) or CM from GC cells were cocultured with neutrophils for 4 h at 37°C under 5% CO_2. To detect and quantify NETs, the samples of the CM group were incubated with primary rabbit anti-histone H3 and mouse anti-MPO antibodies and then fluorescent secondary antibodies. For the samples of cell-cell contact groups, NETs were stained with Sytox Green (Solarbio) for 10 min in the dark at RT. All images were captured using a confocal microscope (LSM 800; Zeiss) and analyzed with ImageJ software (National Institutes of Health, Bethesda, MD, USA).

Preparation of cell-free NETs

Cell-free NETs were isolated from neutrophils of GC patients as previously described, with modifications[38]. Neutrophils (10^7 cells/mL) were cultured for 4 h at 37°C under 5% CO_2 in medium supplemented with 500 nM PMA (HY-18739; MedChemExpress, Monmouth Junction, NJ, USA). The supernatant was discarded, and ice-cold 1 × PBS was added to wash down the cell layer of neutrophils to obtain the NET medium and centrifuged at 1500 *g* for 10 min at 4°C to remove cell debris. Thereafter, 1.5 mL supernatant (sterile DNA–protein complex) was centrifuged at 15 000 *g* for 15 min at 4°C. The resultant pellets were suspended in ice-cold 1 × PBS, followed by DNA concentration measurement in the medium obtained using spectrophotometry (Biospec-nano, Japan). An adequate DNA concentration in the medium should range between 50 and 100 μg/mL. The medium containing the NETs was stored at -80°C for subsequent experiments.

Platelet activation and adhesion assays

Platelet activation and adhesion assays were performed as previously described[22]. Glass-based wells of 24-well plates were coated with cell-free NETs after overnight incubation in the corresponding medium at 4°C in a humidified chamber. For controls, 1% denatured BSA was used. Denatured BSA was prepared by heating the solution in PBS without calcium or magnesium to 80°C for 3 min and immediately placing it on ice until cool; it was then stored at 20°C until use. Platelet suspensions (10^7 cells/mL) were then seeded in the wells, cultured for 1 h at 37°C under 5% CO_2, fixed for 15 min at RT with 4% paraformaldehyde, and washed three times using 1 × PBS before 20 min permeabilization

using 0.1% Triton-X 100. The platelets were then incubated for 30 min with Alexa Fluor 594-conjugated phalloidin primary antibody (1:300; Thermo Fisher, Waltham, MA, USA). To assess PS and P-selectin expression, the platelet suspension was incubated for 1 h at 37°C under 5% CO_2, and the cells were stimulated with NETs for 1 h, followed by FITC-conjugated lactadherin (Hematologic) staining for 30 min. Platelets were washed twice with PBS before fixation for 15 min at RT with 4% paraformaldehyde, permeabilized using 0.1% Triton-X 100 for 20 min, and then stained with primary rabbit anti-P-selectin (1:200; Proteintech) and mouse anti-CD41 (1:500; Novus) antibodies. Images were captured using a confocal microscope (LSM 800; Zeiss) and analyzed with ImageJ software (National Institutes of Health).

HUVECs stimulation assay

HUVECs were incubated with cell-free NETs or PBS in 24-well plates for 4 h when the cells grew to a confluent monolayer. The cells were fixed in 4% paraformaldehyde for 15 min at RT, washed three times using 1 × PBS, and blocked for 1 h using 10% goat serum with 1% BSA solution in PBS. For detection of tissue factor (TF) expression, ECs were incubated overnight at 4 °C with rabbit anti-TF (1:500, ab228968; Abcam) and mouse anti-CD31 (1:500, ab9498; Abcam) primary antibodies. The cells were washed with PBS and reincubated for 1 h at RT with Alexa Fluor 594-conjugated (Proteintech) goat anti-rabbit and Alexa Fluor 488-conjugated (Proteintech) goat anti-mouse secondary antibodies. For detection of intercellular junctions of cells, cells were incubated overnight at 4°C with rabbit anti-VE-cadherin (1:500, ab33168; Abcam) primary antibody, followed by Alexa Fluor 488-conjugated (Proteintech) goat anti-rabbit secondary antibody, and were further incubated with Alexa Fluor 594-conjugated phalloidin primary antibody (1:300; Thermo Fisher, Waltham, MA, USA). They were stained with DAPI and fixed with mounting medium (Solarbio) for 5 min at RT in the dark. The cells were observed and photographed using a confocal microscope. The photos were analyzed with ImageJ software.

Platelet and HUVEC inhibition assays

For inhibition assays, platelets and HUVECs were cocultured with cell-free NETs for 1 h at 37°C in a humidifier chamber in the presence of DNase I (100 U/mL, Roche), APC (100 nM, HY-P1918; MedChemExpress), and sivelestat (100 nM, HY-17443; MedChemExpress) alone or together. DNase I cleaves NET DNA, whereas APC and sivelestat disrupt histones and NE functions, respectively.

Statistical analysis

Data are expressed as the mean ± SD. Data were analyzed to assess distribution normality. For normally distributed data, statistical significance was analyzed using Student's *t*-tests and one-way analysis of variance. For non-normally distributed data, statistical significance was analyzed using the Mann–Whitney test and Kruskal–Wallis test. All analyses were performed using GraphPad Prism version 8.0 and SPSS 16.0 statistical software. Spearman's correlation was used to evaluate the association between two variables. $P < 0.05$ was considered statistically significant.

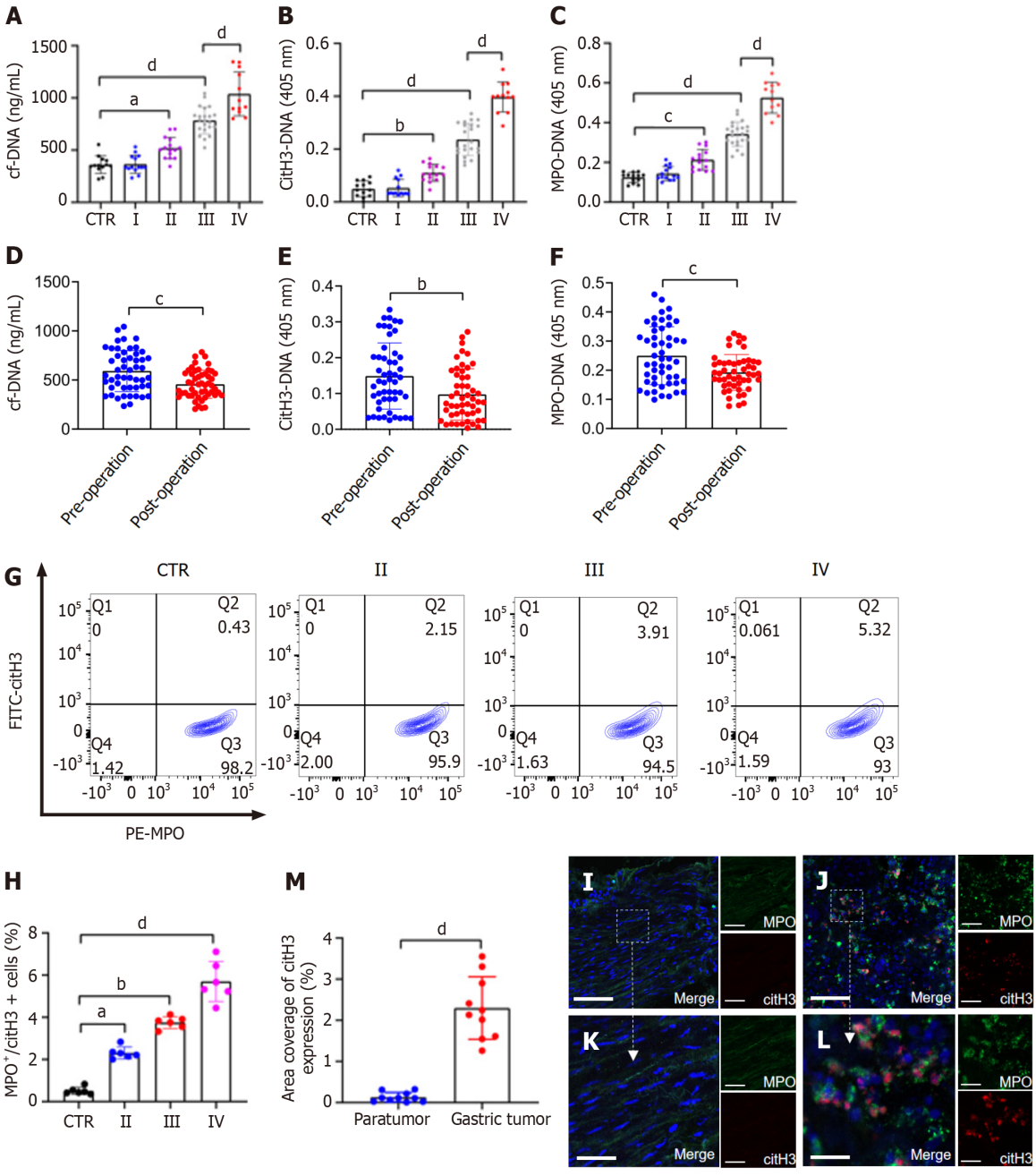
RESULTS

GC patients display greater NET formation

The levels of plasma cf-DNA, citH3-DNA,and MPO-DNA complexes in GC patients ($n = 63$) and HDs ($n = 13$), which reflect the concentration of NETs, were measured using capture ELISA. The levels of NET markers were significantly higher in patients with stage II/III/IV GC than in HDs (Figure 1A–C). There was also a significant difference in preoperative and postoperative plasma NET marker levels in GC patients (Figure 1D–F). The levels of NET markers positively correlated with those of serum D-dimer (cf-DNA: $r = 0.5595$, $P < 0.0001$; citH3-DNA: $r = 0.5469$, $P < 0.0001$; MPO-DNA: $r = 0.5479$, $P < 0.0001$), suggesting that NETs were associated with hypercoagulation and VTE development in GC patients. The levels of NETs ($MPO^+/citH3^+$ neutrophils) in the circulation in GC patients and HDs were measured using flow cytometry. Circulating NETs were higher in the blood of patients with either GC stage (II–IV) than in their HD counterparts (Figure 1G and H). Furthermore, based on MPO and citH3 levels, immunofluorescence staining revealed that NETs were significantly higher in the tumor microenvironment than in the paratumor tissue of the same patients (Figure 1I–M).

GC cells stimulate formation of NETs by neutrophils

To assess whether GC cells directly stimulated NET formation, we analyzed the expression of NETs in a coculture of GC cell lines and neutrophils. Immunofluorescence analysis revealed that compared with GES-1 cells, the rate of NET formation was significantly higher in GC cells (Figure 2A). However, the formation of NETs was greater in the metastatic GC cell line than in the nonmetastatic GC cell line (Figure 2B). We measured NET formation when normal neutrophils were cocultured with CM from KATO-III, MKN-45, AGS and GES-1 cells. Immunofluorescence analysis further revealed that the CM of KATO-III and MKN-45 cells exerted greater neutrophil activation for NET formation than the CM of



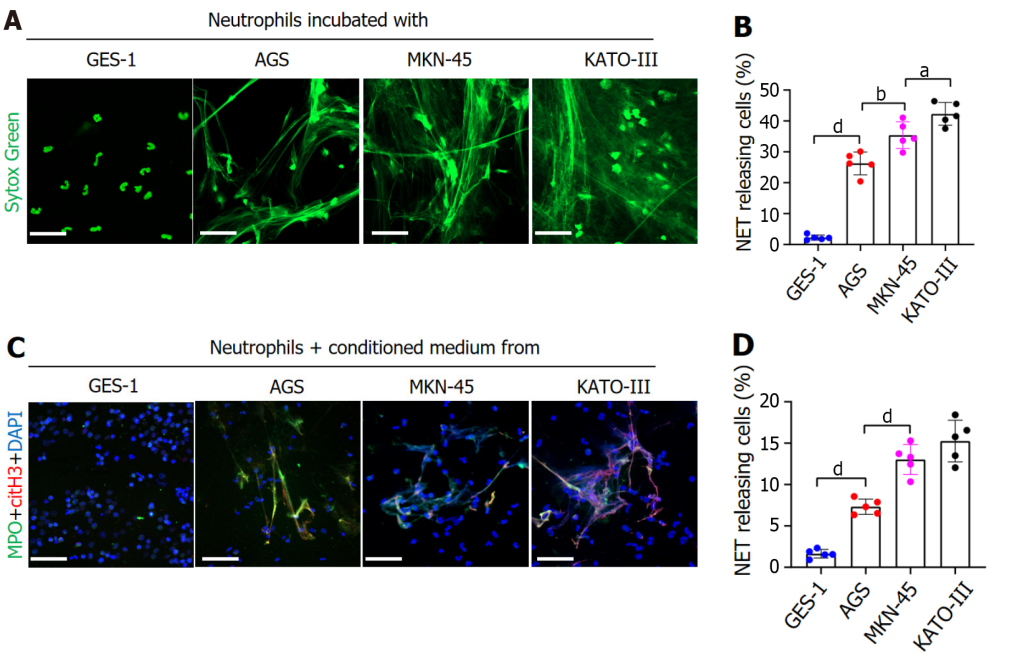
DOI: 10.3748/wjg.v28.i26.3132 **Copyright** ©The Author(s) 2022.

Figure 1 NETs are accumulated in samples of GC patients. A–C: Plasma levels of NET markers cf-DNA, citH3-DNA, and MPO-DNA in GC patients and healthy individuals were measured by ELISA. Healthy individuals, *n* = 13; stage I, *n* = 14; II, *n* = 15; III, *n* = 22; IV, *n* = 12; D-F: Comparison of cf-DNA, citH3-DNA and MPO-DNA in the plasma of patients with GC preoperatively and postoperatively by ELISA. *n* = 51; G and H: The rate of activated neutrophils in the circulating environment of GC patients and healthy individuals was measured by flow cytometry with APC-MPO and FITC-citH3 staining. Each group: *n* = 6; I and J: NET accumulation was detected by confocal microscopy with MPO and citH3 staining in paratumor and tumor samples from the same GC patient. Magnification 20×; scale bars: 50 μm. Red-citH3, Green-MPO and Blue-DAPI; K and L: Magnified (40×) part of MPO and citH3 colocation in paratumor and tumor samples from the same patient. Scale bars: 10 μm. Red-citH3, Green-MPO and Blue-DAPI; M: The percentage of area coverage of citH3 expression was defined as the rate of red area in total area and analyzed with ImageJ software; all values are the mean ± SD. $^{a}P < 0.05$; $^{b}P < 0.01$; $^{c}P < 0.001$; $^{d}P < 0.0001$. NET: Neutrophil extracellular trap; GC: Gastric cancer; cf-DNA: Cell-free DNA; MPO: Myeloperoxidase; citH3: Citrullinated histone H3.

AGS cells. However, the CM of GES-1 cells had no effect on NET formation (Figure 2C and D). Overall, these findings demonstrate that GC cells stimulate NET formation through both intercellular contact and noncontact mechanisms.

NETs contribute to hypercoagulation of platelets

To examine the effect of NETs on platelet activation, we measured the levels of PS and P-selectin expression in these cells. Flow cytometry revealed that compared to HDs, the expression of PS and P-selectin was significantly higher on platelets of patients with GC (Figure 3). In addition, platelets



DOI: 10.3748/wjg.v28.26.3132 **Copyright** ©The Author(s) 2022.

Figure 2 GC cells can stimulate neutrophils to form NETs. A and B: Control neutrophils were cocultured with normal gastric mucosal epithelial cells (GES-1) or GC cells (AGS, MKN-45 and KATO-III) and NET formation was measured by confocal microscopy with cell-impermeable Sytox-Green staining. Magnification 20×; scale bars: 50 μm. Green: Neutrophils; C and D: Control neutrophils were cocultured with CM from GES-1 or GC cells, and stained with MPO and citH3. The percentage of NET-releasing cells was defined as the ratio of the calculated NET releasing neutrophils to the total number of neutrophils. Magnification 20×; scale bars: 50 μm. Red-citH3, Green-MPO, and Blue-DAPI. All values are the mean ± SD. $^{a}P < 0.05$; $^{b}P < 0.01$; $^{c}P < 0.001$; $^{d}P < 0.0001$. GC: Gastric cancer; GES-1: Gastric mucosal epithelial cells; NET: Neutrophil extracellular trap; CM: Conditioned medium; MPO: Myeloperoxidase; citH3: Citrullinated histone H3.

isolated from HDs were cocultured with NET medium or PBS before analyzing PS and P-selectin expression. We found that NETs stimulated PS and P-selectin expression on platelets by confocal microscopy (Figure 4A–C). Flow cytometry also demonstrated this hypercoagulable phenotype of platelets which was stimulated by NETs (Figure 4D and E). In the inhibition assay, we added DNase I, APC and sivelestat alone or together to cleave DNA, histones and NE, which were the most functional factors of NETs. At the highest concentration of NETs (0.5 μg DNA/mL), flow cytometry revealed that DNase I, APC, sivelestat, or a combination of the three inhibited 60.2%, 47.1%, 41.9% and 83.2% of PS expression, respectively (Figure 4D), and 55.2%, 47.0%, 41.0%, and 91.76% of P-selectin expression on platelets, respectively (Figure 4E).

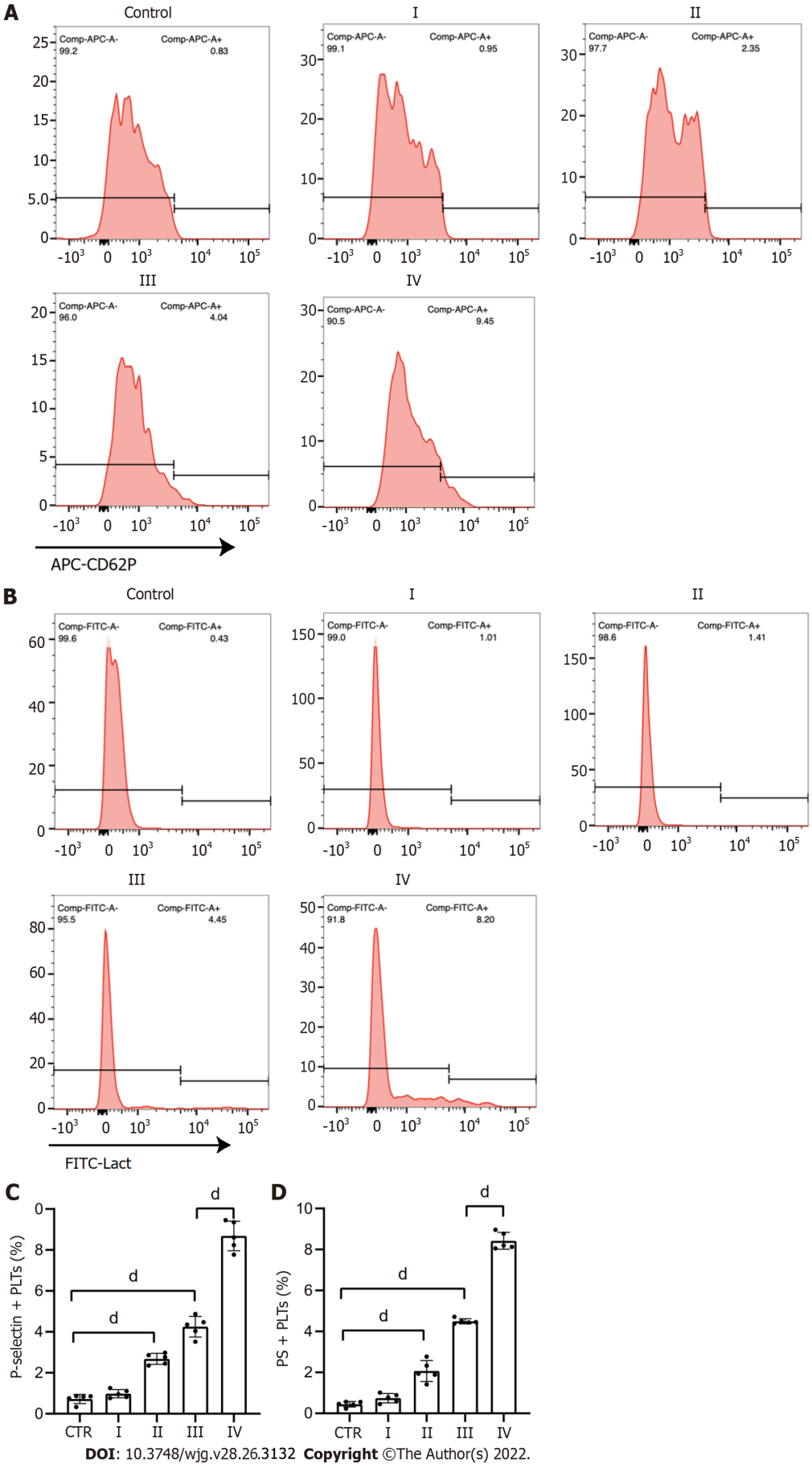
NETs promote platelet adhesion and prothrombotic state

Previous studies have shown that NETs promote thrombosis in murine late-stage breast cancer models and DVT models[19,39]. However, whether NETs derived from GC neutrophils have the ability to stimulate platelet adhesion under static conditions is unknown. To determine the effect of NETs on platelet adhesion, platelets isolated from HDs were seeded in NET-coated wells to measure the effects of NETs on the adherence of platelets to blood vessels. Confocal microscopy revealed that NETs enhanced adherence of platelets to glass slides (Figure 5A and B), indicating that NETs induce the development of thrombosis. Moreover, the results revealed that fibrin formation and TAT complex levels were increased when control plasma was cocultured with platelets activated by NETs (Figure 5C and D).

Inhibition assays revealed that digestion of NET DNA using DNase I modulated the adhesion of platelets on glass surfaces. Even so, a few platelets still adhered to the NET-coated well pretreated with DNase I (Figure 5A). This suggested that other protein components other than NET-DNA participated in the adhesion of platelets. NETs treated with DNase I, APC, sivelestat, or a combination of the three inhibited 67.1%, 56.6%, 38.9%, and 91.8% of platelet adhesion, respectively (Figure 5B). The degree of platelet adhesion in the combination group was comparable to that of the controls. We found that DNase I, APC, sivelestat, or a combination of the three reduced fibrin formation by 81.1%, 73.9%, 64.3%, and 90.7%, respectively (Figure 5C), and inhibited 78.9%, 57.4%, 51.2%, and 91.9% of TAT complex level, respectively (Figure 5D), at the highest concentration of NETs. Taken together, these findings demonstrate that NETs play a role in the development of thrombosis.

NETs drive hypercoagulation of ECs

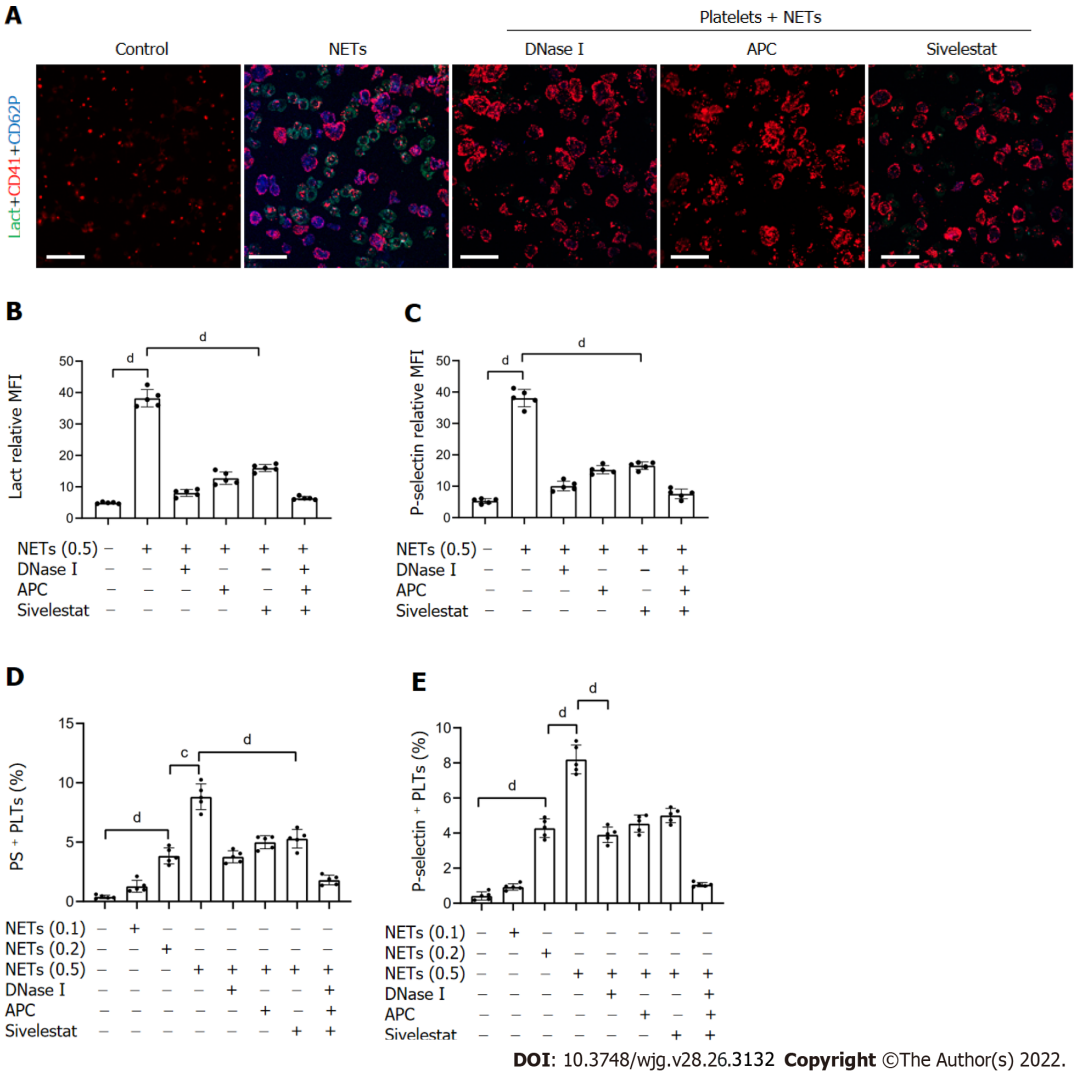
To detect the effect of NETs on EC thrombogenicity, HUVECs were cocultured with NET medium. Confocal microscopy revealed that NETs destroyed the normal intercellular junctions between ECs



DOI: 10.3748/wjg.v28.26.3132 **Copyright** ©The Author(s) 2022.

Figure 3 Platelets are activated in patients with GC. A and C: Flow cytometry showed the rate of P-selectin-positive platelets from each stage GC patients

and healthy individuals; B and D: Rate of phosphatidylserine-positive platelets from each stage GC patients and healthy individuals. All values are the mean ± SD. $^{d}P < 0.0001$. PS: Phosphatidylserine; GC: Gastric cancer. CD62P: P-selectin; Lact: Lactadherin.



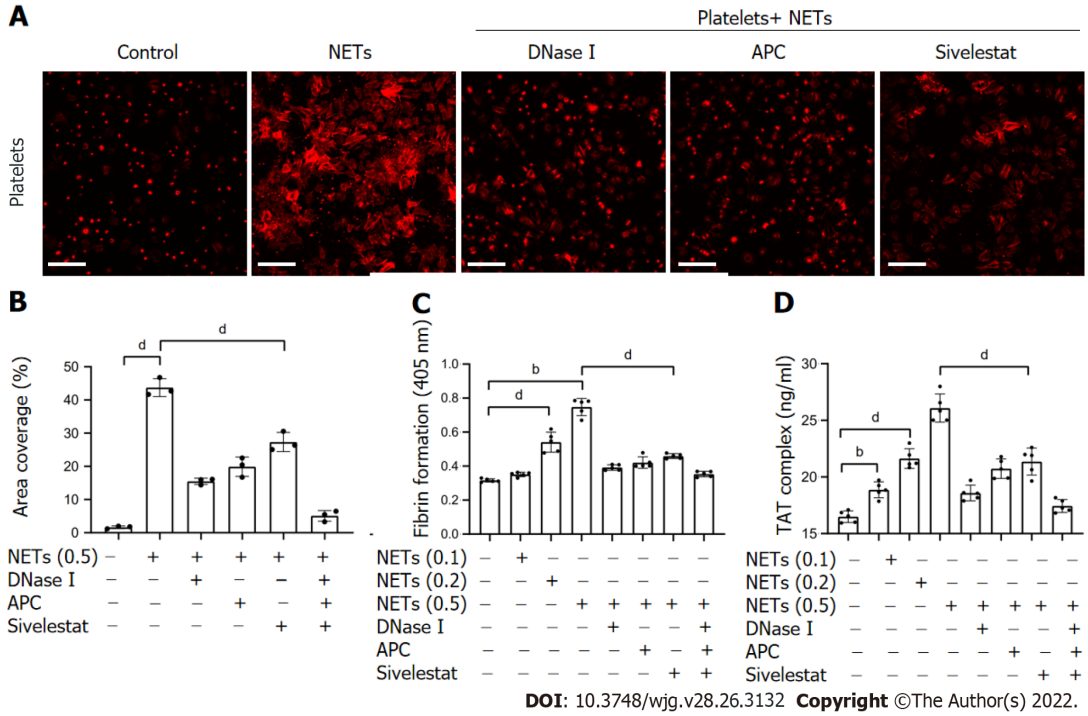
DOI: 10.3748/wjg.v28.26.3132 **Copyright** ©The Author(s) 2022.

Figure 4 NETs contribute to hypercoagulation of platelets. A: PS exposure and P-selectin expression were measured when isolated platelets were cocultured with BETs (μg, DNA/mL) or in the presence of DNase I, activated protein C, and sivelestat alone or together by confocal microscopy. Magnification 63×; scale bars: 10 μm. Red-platelets, Green-Lactadherin, and Blue-P-selectin; B and C: PS exposure and P-selectin expression are indicated as MFI. MFI was defined as the ratio of total fluorescence intensity to the area; D and E: The rates of PS-positive platelets and P-selectin-positive platelets were detected by flow cytometry. All values are the mean ± SD. $^{c}P < 0.001$; $^{d}P < 0.0001$. PS: Phosphatidylserine; GC: Gastric cancer; DNase I: Deoxyribonuclease I; APC: Activated protein C; MFI: Mean fluorescence intensity; Lact: Lactadherin; CD41: Platelet; NET: Neutrophil extracellular trap.

(Figure 6A and C). NET treatment upregulated expression of TF on the surface membrane of ECs (Figure 6B and D). In addition, plasma fibrin formation and TAT complex levels were significantly increased when control plasma was incubated with EC monolayers activated by NETs (Figure 6E and F). Further inhibition assays were performed to assess the effect of NETs on ECs after pretreatment with DNase I, APC, sivelestat, or a combination of the three. We found that NET treatment after incubation with DNase I, APC, sivelestat, or all three drugs returned 47.5%, 36.3%, 33.4%, and 86.5%, respectively, of VE expression on ECs (Figure 6C), whereas similar treatment inhibited 60.4%, 44.8%, 38.6%, and 95.5%, respectively, of TF expression (Figure 6D). Additionally, we found that NET treat-ment after incubation with the above inhibitors inhibited 59.7%, 54.4%, 54.0%, and 91.5% of fibrin formation level, respectively (Figure 6E), and inhibited 51.2%, 35.6%, 25.9%, and 84.3% of TAT complex level, respectively (Figure 6F). Taken together, these findings suggest that NETs promote hypercoagulation of ECs; thus, inhibiting NET function can protect against venous injury.

NETs promote formation of thrombi in tumor-bearing IVC flow restriction mice

Based on these findings *in vitro* and the pivotal role of NETs in thrombosis, we hypothesized that GC-



DOI: 10.3748/wjg.v28.26.3132 **Copyright** ©The Author(s) 2022.

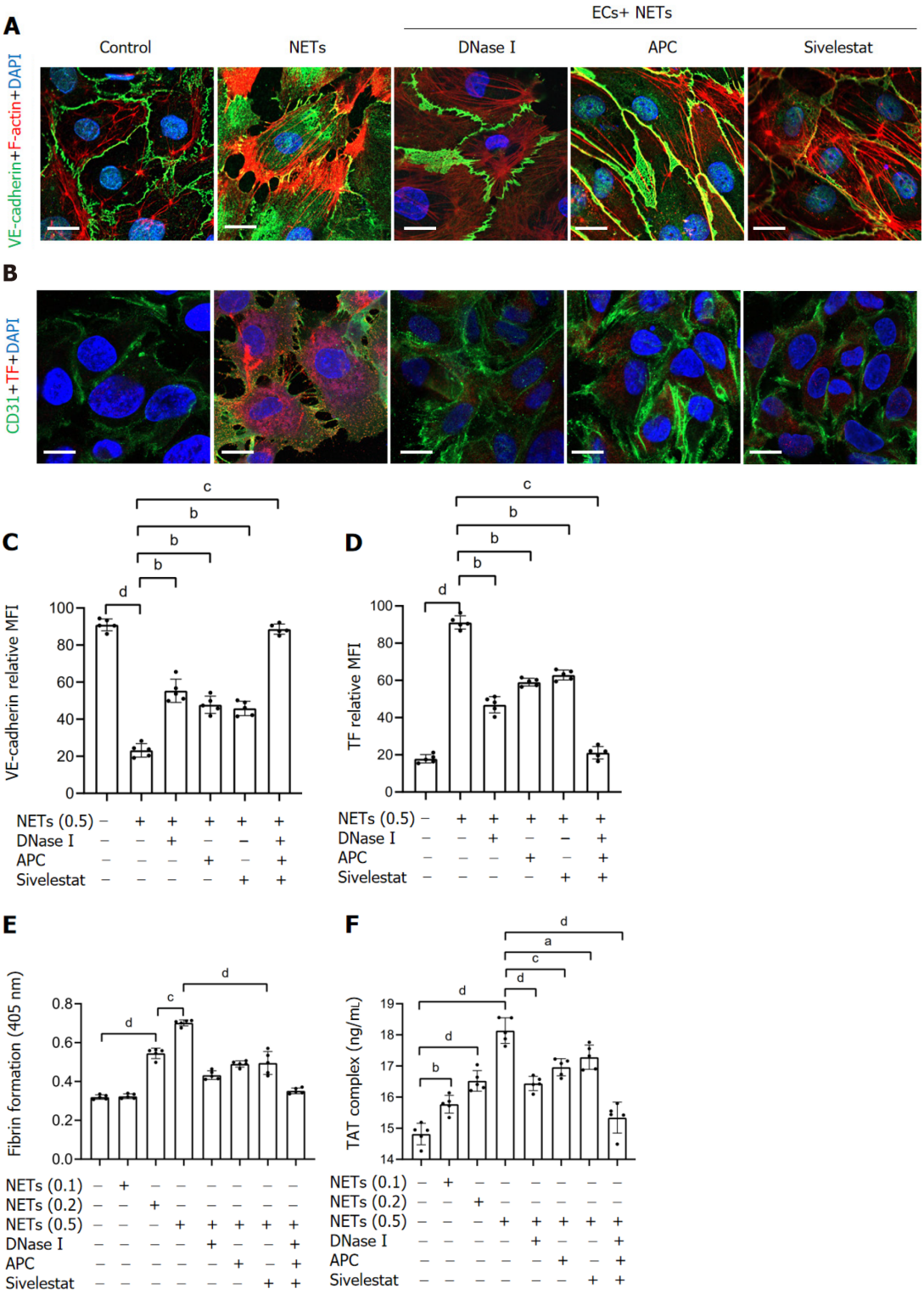
Figure 5 NETs promote platelet adhesion and prothrombotic state. A: Isolated platelets were incubated on glass slides which were coated with 1% dBSA, NETs (μg DNA/mL), or NETs pretreated with DNase I, APC, and sivelestat alone or together, followed by the F-actin components of platelets with 594-phalloidin staining. Magnification 63×; scale bars: 10 μm. Red-platelets; B: The percentage of area coverage of platelet adhesion was defined as the rate of red area in the total area and analyzed with ImageJ software; C: Isolated platelets were cocultured with different concentrations of NETs for 30 min with or without DNase I, APC and sivelestat treatment alone or together, and plasma fibrin formation was tested using turbidity measurements and monitored OD at 405 nm; D: TAT complex level of activated platelets was analyzed by ELISA. All values are the mean ± SD. $^{a}P < 0.05$; $^{b}P < 0.01$; $^{c}P < 0.001$; $^{d}P < 0.0001$. dBSA: Denatured bovine serum albumin; NETs: Neutrophil extracellular traps; DNase I: Deoxyribonuclease I; APC: Activated protein C; TAT: Thrombin–antithrombin.

induced NETs can also promote thrombosis *in vivo*. Here, in a mouse IVC flow stenosis model, tumor-bearing mice demonstrated more capacity to form thrombi and showed heavier weight and longer length of thrombi compared to control mice (Figure 7A–D). In the 6 h models, three of nine of control mice showed thrombi, whereas seven of nine of tumor-bearing mice formed thrombi. In the 48 h models, all mice demonstrated thrombi in the IVC. In addition, confocal images of thrombi formed in the tumor-bearing mice after 48 h of IVC stenosis showed that NETs were significantly accumulated compared to control mice (Figure 7E–H). The thrombi of control mice included some neutrophils (Ly6G+) but were not activated to form NETs (Figure 7E and G). Furthermore, tumor-bearing mice showed higher fibrin formation and TAT complex levels than control mice (Figure 7I and J).

In the inhibition assay, we infused DNase I into mice immediately after IVC stenosis and examined thrombosis after 6 or 48 h of surgery. We found that treatment with DNase I significantly inhibited thrombi formation in tumor-bearing IVC stenosis mice (Figure 7A–D). Furthermore, fibrin formation and TAT complex levels in tumor-bearing mice were significantly decreased by DNase I treatment (Figure 7I and J). These data suggest that NETs play a role in thrombosis *in vivo*, which was induced by GC, and inhibiting NETs by DNase I had a protective effect on thrombosis in this mouse model.

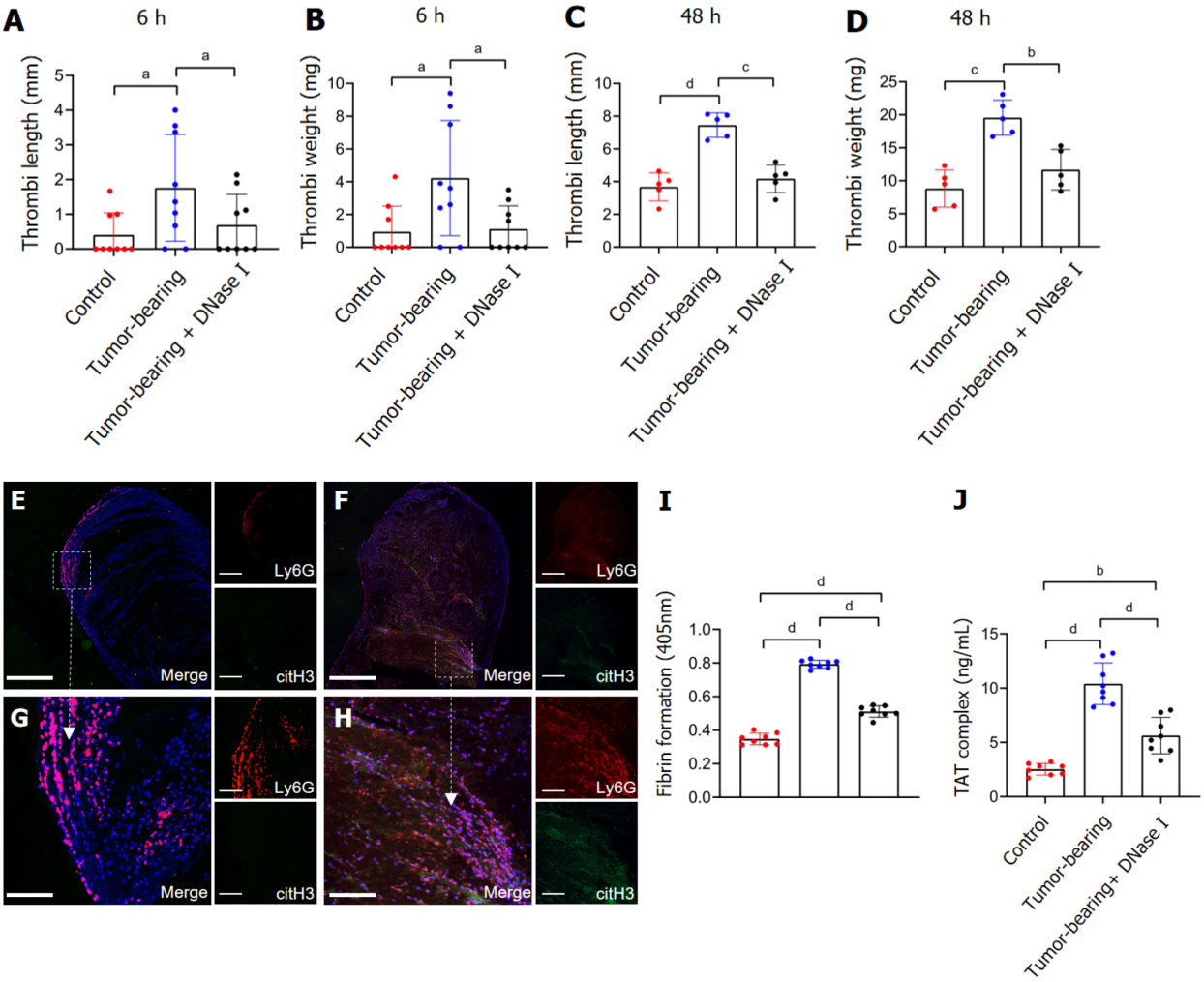
DISCUSSION

Inflammation is one of the hallmarks of cancer. Additionally, neutrophils are among the most important immune cells implicated in promoting tumor progression[40,41]. NETs participate in cancer progression by promoting the proliferation, invasion, metastasis and angiogenesis of cancer cells as well as thrombosis in numerous tumor types[42-44]. A recent study using mouse models with Jak^{2V617F} knock-in revealed that most myeloproliferative neoplasms display NET formation and DVT[45]. Our previous studies revealed that NETs promote the migration and metastasis of GC cells both *in vitro* and *in vivo* through epithelial mesenchymal transition[46]. Intriguingly, inhibition of NETs promotes apoptosis and inhibits the invasion of GC cells by regulating the expression of Bcl-2, Bax and nuclear factor-κB proteins[47]. Our initial studies revealed that NETs released by neutrophils in GC patients promoted the conversion of thrombin and fibrin[23]. Accordingly, we hypothesized that NETs promote thrombosis in GC patients. We investigated the interactions between GC cells, neutrophils, platelets and ECs, with a keen focus on their role in cancer-associated thrombosis.



DOI: 10.3748/wjg.v28.26.3132 **Copyright** ©The Author(s) 2022.

Figure 6 NETs drive hypercoagulation of ECs. A: ECs were cocultured with NETs (μg DNA/mL) or PBS in the presence of DNase I, APC, or sivelestat alone or together for 4 h and analyzed by confocal microscopy. The intercellular junctions of ECs were stained with VE–cadherin and phalloidin. Magnification 63×; scale bars: 10 μm. Red-phalloidin, Green-VE, and Blue-DAPI; B: EC activation was stained with CD31 and TF. Magnification 63×; scale bars: 10 μm. Red-TF, Green-CD31, and Blue-DAPI; C and D: VE–cadherin expression and TF expression on ECs were detected by confocal microscopy and analyzed with ImageJ software (expression indicated as MFI). MFI was defined as the ratio of total fluorescence intensity to the area; E and F: EC monolayers were stimulated with various concentrations of NETs for 4 h, followed by determination of fibrin formation by turbidity measurement at 405 nm, and the TAT complex level was detected by ELISA. All values are the mean ± SD. $^{a}P < 0.05$; $^{b}P < 0.01$; $^{c}P < 0.001$; $^{d}P < 0.0001$. NETs: Neutrophil extracellular traps; ECs: Endothelial cells; DNase I: Deoxyribonuclease I; APC: Activated protein C; TF: Tissue factor; TAT: Thrombin–antithrombin; MFI: Mean fluorescence intensity.



DOI: 10.3748/wjg.v28.i26.3132 **Copyright** ©The Author(s) 2022.

Figure 7 Tumor-bearing mice show a greater ability to form thrombi by inferior vena cava flow restriction. A and B: The values for weight and length of thrombi present in control, tumor-bearing mice, DNase I infused tumor-bearing mice at 6 h after surgery. Each group, *n* = 9; C and D: Values for weight and length of thrombi present in mice at 48 h after surgery. Each group, *n* = 5; E and F: Confocal imaging of thrombi derived from control mice and tumor-bearing mice with Ly6G and citH3 staining. Magnification 10×; scale bars: 200 μm. Red-Ly6G, Green-citH3, and Blue-DAPI; G and H: Magnified (40×) part of thrombi derived from control mice and tumor-bearing mice. Scale bars: 50 μm. Red-Ly6G, Green-citH3, and Blue-DAPI; I and J: Fibrin formation levels in the plasma of control, tumor-bearing mice, or DNase-I-infused tumor-bearing mice were detected by turbidity measurement at 405 nm, and TAT complex levels were detected by ELISA. Each group, *n* = 8. All values are the mean ± SD. $^{a}P < 0.05$; $^{b}P < 0.01$; $^{c}P < 0.001$; $^{d}P < 0.0001$. DNase I: Deoxyribonuclease I; TAT: Thrombin–antithrombin.

In this study, we found that the levels of plasma NET markers and citH3-positive neutrophils were significantly higher in GC patients than in HDs. Expression of NETs decreased significantly after resection of GC tissues. Neutrophil infiltration and NET formation were upregulated in tumor tissues, relative to adjacent paratumor tissues of the same GC patient. The levels of serum D-dimer were positively correlated with tumor TNM stage, consistent with previous findings[48]. These findings suggest that the expression of NETs promotes GC development and thrombosis in the same group of patients.

It has been reported that hepatocellular cancer and hypoxic CM stimulate the production of NETs by neutrophils[44]. However, the relationship between GC cells and neutrophils is poorly understood. Our experiments demonstrated that both metastatic and nonmetastatic GC cancer cells directly stimulated production of NETs from neutrophils, contrary to GES-1 cells. CM of GC cells, but not that of GES-1, also induced the formation of neutrophil-related NETs. This suggests that NET formation is also mediated by factors secreted by GC cells. Inflammatory cytokines, such as interleukin (IL)-1β, IL-6, IL-8, and tumor necrosis factor-, as well as damage-associated molecular patterns, all overexpressed in tumor microenvironments, stimulate neutrophils to release NETs[49,50]. Although IL-8 is the cytokine with the highest overexpression in GC patients, whether it is the main mediator of NET formation and the subsequent underlying mechanism in GC remain to be validated.

A recent study showed that NETs promote thrombosis by activating and promoting the adhesion of platelets in the venous walls of pancreatic cancer patients[22]. Activated platelets express PS on their surface membranes[51]. Additionally, P-selectin expression on the surface membrane of platelets is also

associated with thrombosis[52]. In this study, we found that compared to HDs, PS and P-selectin expression on platelets was significantly higher in GC patients, particularly those with stage III/IV GC. NET treatment upregulated PS and P-selectin expression on platelets. Additionally, NETs stimulated the adhesion of normal platelets on glass slides. However, even though DNase I treatment modulated this phenomenon, some platelets still adhered to the glass slides, suggesting that other secretory factors participated in the adhesion property.

Previous studies have shown that histones in NETs promote thrombosis in colorectal cancer patients [53]. NE is another most abundant protein that binds NETs. Although this potent protein stimulates tumor progression both *in vitro* and *in vivo*, the mechanisms underlying NE-mediated cancer-associated thrombosis remain to be clarified. A recent study on DVT using mouse models showed that NE deficiency or NE inhibition alone does not completely inhibit DVT[54]. In this study, we found that hypercoagulation of platelets was not completely mediated by NET DNA, but also by other secretory proteins in the NETs, such as histones and NE. Consequently, DNase I treatment of NETs had no complete effect on hypercoagulation of platelets. However, a combination of DNase I, APC and sivelestat treatment almost completely inhibited hypercoagulation of platelets. Although sivelestat did not show a strong antihypercoagulation effect similar to DNase I, it nonetheless modulated the activation and adhesion of platelets. This demonstrated that histones and NE also participate in the activation and adhesion of platelets.

DVT can be triggered by injury to vascular ECs. Previous studies have shown that under certain malignancies, NETs can induce dysfunction and apoptosis of ECs[35]. In patients with chronic pancreatic disease and pancreatic cancer, NETs exert their cytotoxicity against ECs *via* intercellular cell adhesion molecule-1 and vascular cell adhesion molecule-1 expression[26]. Recent studies have shown that treatment of ECs with NETs derived from patients with colorectal cancer promotes and enhances the production of fibrin and the corresponding coagulation[53]. In this study, we found that NET treatment inhibited the secretion of intercellular junctions in ECs and promoted hypercoagulation of platelets by upregulating TF expression. Moreover, NET treatment upregulated the expression of PS on ECs. ECs activated by NETs significantly increased the level of TAT complexes and fibrin generation in the plasma of HDs. Given that a combination of DNase I, APC and sivelestat treatment completely inhibited hypercoagulation, the process was regulated through numerous mechanisms. These findings strongly suggest that NETs contribute to GC-associated thrombosis.

In the late stage of murine mammary tumor models, thrombi were found in lung vessels, and NETs accumulated, indicating that cancer-induced NETs contribute to the cancer-associated thrombosis[19]. Here, we demonstrated that GC-bearing mice have a greater ability to form thrombi than control mice have and that NETs were abundantly present in the thrombi of tumor-bearing mouse IVC stenosis models. Most of this response can be blocked by DNase I treatment, which was similar to previous studies. In DVT models, flow restriction of the IVC may result in a hypoxic microenvironment to recruit neutrophils and stimulate NET release. In addition, cancer cells often secrete more inflammatory factors, which aggravate the recruitment of neutrophils to form NETs under a hypoxic conditions[50]. Therefore, neutrophils are exposed to two major triggers of NET release: A tumor hypoxic environment and IVC flow restriction, which then participate in the development of thrombi in GC.

CONCLUSION

Our findings demonstrate that GC cells can directly induce NET formation, which in turn strongly increases the risks of VTE development both *in vitro* and *in vivo*. In addition, we found that not only NET DNA but also histones and NE participate in the development of cancer-associated thrombosis. Accordingly, NETs are potential therapeutic targets against VTE in GC patients.

ARTICLE HIGHLIGHTS

Research background

The development of venous thromboembolism (VTE) is associated with high mortality among gastric cancer (GC) patients. Neutrophil extracellular traps (NETs) have been reported to correlate with the prothrombotic state in some diseases, but it was rarely reported in GC patients.

Research motivation

Cancer cells exert a procoagulant activity (PCA) in their microenvironment, which is related to activation of the coagulation system. However, the molecular mechanism underlying PCA in GC patients is poorly understood.

Research objectives

The present study aimed to investigate the effect of NETs on the development of cancer-associated thrombosis in GC patients.

Research methods

The levels of NETs in blood and tissue samples of patients were analyzed by ELISA, flow cytometry, and immunofluorescence staining. NET generation and hypercoagulation of platelets and endothelial cells (ECs) *in vitro* were observed by immunofluorescence staining. NET PCA was determined by fibrin formation and thrombin–antithrombin complex assays. Thrombosis *in vivo* was measured in a murine model induced by flow stenosis in the inferior vena cava (IVC).

Research results

NETs were likely to form in blood and tissue samples of GC patients compared with healthy individuals. *In vitro* studies showed that GC cells and their conditioned medium, but not gastric mucosal epithelial cells, can stimulate NET release from neutrophils. Furthermore, NETs induced hypercoagulable state of platelets and ECs. In a model of IVC stenosis, tumor-bearing mice showed a stronger ability to form thrombi, and NETs abundantly accumulated in the thrombi of tumor-bearing mice compared with control mice. Notably, the combination of deoxyribonuclease, activated protein C, and sivelestat markedly abolished the PCA of NETs.

Research conclusions

Our findings demonstrate that GC-induced NETs strongly increase the risk of VTE development both *in vitro* and *in vivo*. NETs are potential therapeutic targets in the prevention and treatment of VTE in GC patients.

Research perspectives

The treatment strategies can consider the combination of traditional anticoagulant drugs and NETs inhibiting drugs, so as to reduce the risk of cancer associated thrombosis in patients with GC and improve the clinical treatment effect.

FOOTNOTES

Author contributions: Zou XM and Li JC designed the study, completed the experiments, and drafted the manuscript; Yang SF, Zhao TQ, and Jin JQ collected the patient clinical data and performed part of the experiments; Zhu L, Li CJ, and Chen CY participated in the animal experiments; Yang H and Zhang AG performed the statistical analysis; all authors have read and approved the final manuscript.

Supported by National Natural Science Foundation of China, No. 81672355.

Institutional review board statement: The study was reviewed and approved by the ethics committee of the Second Affiliated Hospital of Harbin Medical University (No. KY2016-032).

Institutional animal care and use committee statement: All animal experiments in this study were approved by the ethics committee of the Second Affiliated Hospital of Harbin Medical University (No. KY2016-032).

Conflict-of-interest statement: The authors declare no conflict of interest for this manuscript.

Data sharing statement: No additional data are available.

ARRIVE guidelines statement: The authors have read the ARRIVE guidelines, and the manuscript was prepared and revised according to the ARRIVE guidelines.

Open-Access: This article is an open-access article that was selected by an in-house editor and fully peer-reviewed by external reviewers. It is distributed in accordance with the Creative Commons Attribution NonCommercial (CC BY-NC 4.0) license, which permits others to distribute, remix, adapt, build upon this work non-commercially, and license their derivative works on different terms, provided the original work is properly cited and the use is non-commercial. See: https://creativecommons.org/Licenses/by-nc/4.0/

Country/Territory of origin: China

ORCID number: Jia-Cheng Li 0000-0002-0467-7225; Xiao-Ming Zou 0000-0002-9689-5026; Shi-Feng Yang 0000-0002-4395-6753; Jia-Qi Jin 0000-0002-7635-5452; Lei Zhu 0000-0002-7495-606X; Chang-Jian Li 0000-0003-0441-0368; Hao Yang 0000-0003-0952-3345; An-Ge Zhang 0000-0003-4772-1254; Tian-Qi Zhao 0000-0002-1938-1419; Chong-Yan Chen 0000-0003-2749-4891.

S-Editor: Fan JR
L-Editor: Kerr C Wang TQ
P-Editor: Fan JR

REFERENCES

1 **Sung H**, Ferlay J, Siegel RL, Laversanne M, Soerjomataram I, Jemal A, Bray F. Global Cancer Statistics 2020: GLOBOCAN Estimates of Incidence and Mortality Worldwide for 36 Cancers in 185 Countries. *CA Cancer J Clin* 2021; **71**: 209-249 [PMID: 33538338 DOI: 10.3322/caac.21660]
2 **Banks M**, Graham D, Jansen M, Gotoda T, Coda S, di Pietro M, Uedo N, Bhandari P, Pritchard DM, Kuipers EJ, Rodriguez-Justo M, Novelli MR, Ragunath K, Shepherd N, Dinis-Ribeiro M. British Society of Gastroenterology guidelines on the diagnosis and management of patients at risk of gastric adenocarcinoma. *Gut* 2019; **68**: 1545-1575 [PMID: 31278206 DOI: 10.1136/gutjnl-2018-318126]
3 **Farge D**, Bounameaux H, Brenner B, Cajfinger F, Debourdeau P, Khorana AA, Pabinger I, Solymoss S, Douketis J, Kakkar A. International clinical practice guidelines including guidance for direct oral anticoagulants in the treatment and prophylaxis of venous thromboembolism in patients with cancer. *Lancet Oncol* 2016; **17**: e452-e466 [PMID: 27733271 DOI: 10.1016/S1470-2045(16)30369-2]
4 **Kang MJ**, Ryoo BY, Ryu MH, Koo DH, Chang HM, Lee JL, Kim TW, Kang YK. Venous thromboembolism (VTE) in patients with advanced gastric cancer: an Asian experience. *Eur J Cancer* 2012; **48**: 492-500 [PMID: 22169121 DOI: 10.1016/j.ejca.2011.11.016]
5 **Khan F**, Tritschler T, Kahn SR, Rodger MA. Venous thromboembolism. *Lancet* 2021; **398**: 64-77 [PMID: 33984268 DOI: 10.1016/S0140-6736(20)32658-1]
6 **Tanizawa Y**, Bando E, Kawamura T, Tokunaga M, Makuuchi R, Iida K, Nanri K, Yoneyama M, Terashima M. Prevalence of deep venous thrombosis detected by ultrasonography before surgery in patients with gastric cancer: a retrospective study of 1140 consecutive patients. *Gastric Cancer* 2017; **20**: 878-886 [PMID: 27987041 DOI: 10.1007/s10120-016-0677-2]
7 **Jung YJ**, Seo HS, Park CH, Jeon HM, Kim JI, Yim HW, Song KY. Venous Thromboembolism Incidence and Prophylaxis Use After Gastrectomy Among Korean Patients With Gastric Adenocarcinoma: The PROTECTOR Randomized Clinical Trial. *JAMA Surg* 2018; **153**: 939-946 [PMID: 30027281 DOI: 10.1001/jamasurg.2018.2081]
8 **Wada T**, Fujiwara H, Morita S, Fukagawa T, Katai H. Incidence of and risk factors for preoperative deep venous thrombosis in patients undergoing gastric cancer surgery. *Gastric Cancer* 2017; **20**: 872-877 [PMID: 28120128 DOI: 10.1007/s10120-017-0690-0]
9 **Osaki T**, Saito H, Fukumoto Y, Kono Y, Murakami Y, Shishido Y, Kuroda H, Matsunaga T, Sato K, Hirooka Y, Fujiwara Y. Risk and incidence of perioperative deep vein thrombosis in patients undergoing gastric cancer surgery. *Surg Today* 2018; **48**: 525-533 [PMID: 29234961 DOI: 10.1007/s00595-017-1617-4]
10 **Varki A**. Trousseau's syndrome: multiple definitions and multiple mechanisms. *Blood* 2007; **110**: 1723-1729 [PMID: 17496204 DOI: 10.1182/blood-2006-10-053736]
11 **Brinkmann V**, Reichard U, Goosmann C, Fauler B, Uhlemann Y, Weiss DS, Weinrauch Y, Zychlinsky A. Neutrophil extracellular traps kill bacteria. *Science* 2004; **303**: 1532-1535 [PMID: 15001782 DOI: 10.1126/science.1092385]
12 **Brinkmann V**, Zychlinsky A. Beneficial suicide: why neutrophils die to make NETs. *Nat Rev Microbiol* 2007; **5**: 577-582 [PMID: 17632569 DOI: 10.1038/nrmicro1710]
13 **McDonald B**, Urrutia R, Yipp BG, Jenne CN, Kubes P. Intravascular neutrophil extracellular traps capture bacteria from the bloodstream during sepsis. *Cell Host Microbe* 2012; **12**: 324-333 [PMID: 22980329 DOI: 10.1016/j.chom.2012.06.011]
14 **Zeng H**, Fu X, Cai J, Sun C, Yu M, Peng Y, Zhuang J, Chen J, Chen H, Yu Q, Xu C, Zhou H, Cao Y, Hu L, Li J, Cao S, Gu C, Yan F, Chen G. Neutrophil Extracellular Traps may be a Potential Target for Treating Early Brain Injury in Subarachnoid Hemorrhage. *Transl Stroke Res* 2022; **13**: 112-131 [PMID: 33852132 DOI: 10.1007/s12975-021-00909-1]
15 **Zuo Y**, Yalavarthi S, Gockman K, Madison JA, Gudjonsson JE, Kahlenberg JM, Joseph McCune W, Bockenstedt PL, Karp DR, Knight JS. Anti-Neutrophil Extracellular Trap Antibodies and Impaired Neutrophil Extracellular Trap Degradation in Antiphospholipid Syndrome. *Arthritis Rheumatol* 2020; **72**: 2130-2135 [PMID: 32729667 DOI: 10.1002/art.41460]
16 **Cichon I**, Ortmann W, Bednarz A, Lenartowicz M, Kolaczkowska E. Reduced Neutrophil Extracellular Trap (NET) Formation During Systemic Inflammation in Mice With Menkes Disease and Wilson Disease: Copper Requirement for NET Release. *Front Immunol* 2019; **10**: 3021 [PMID: 32010131 DOI: 10.3389/fimmu.2019.03021]
17 **Marcos V**, Zhou Z, Yildirim AO, Bohla A, Hector A, Vitkov L, Wiedenbauer EM, Krautgartner WD, Stoiber W, Belohradsky BH, Rieber N, Kormann M, Koller B, Roscher A, Roos D, Griese M, Eickelberg O, Döring G, Mall MA, Hartl D. CXCR2 mediates NADPH oxidase-independent neutrophil extracellular trap formation in cystic fibrosis airway inflammation. *Nat Med* 2010; **16**: 1018-1023 [PMID: 20818377 DOI: 10.1038/nm.2209]
18 **Martins-Cardoso K**, Almeida VH, Bagri KM, Rossi MID, Mermelstein CS, König S, Monteiro RQ. Neutrophil Extracellular Traps (NETs) Promote Pro-Metastatic Phenotype in Human Breast Cancer Cells through Epithelial-Mesenchymal Transition. *Cancers (Basel)* 2020; **12** [PMID: 32545405 DOI: 10.3390/cancers12061542]
19 **Demers M**, Krause DS, Schatzberg D, Martinod K, Voorhees JR, Fuchs TA, Scadden DT, Wagner DD. Cancers predispose neutrophils to release extracellular DNA traps that contribute to cancer-associated thrombosis. *Proc Natl Acad Sci U S A* 2012; **109**: 13076-13081 [PMID: 22826226 DOI: 10.1073/pnas.1200419109]
20 **Thålin C**, Hisada Y, Lundström S, Mackman N, Wallén H. Neutrophil Extracellular Traps: Villains and Targets in Arterial, Venous, and Cancer-Associated Thrombosis. *Arterioscler Thromb Vasc Biol* 2019; **39**: 1724-1738 [PMID: 31315434 DOI: 10.1161/ATVBAHA.119.312463]
21 **Gomes T**, Várady CBS, Lourenço AL, Mizurini DM, Rondon AMR, Leal AC, Gonçalves BS, Bou-Habib DC, Medei E, Monteiro RQ. IL-1β Blockade Attenuates Thrombosis in a Neutrophil Extracellular Trap-Dependent Breast Cancer Model.

Front Immunol 2019; **10**: 2088 [PMID: 31552036 DOI: 10.3389/fimmu.2019.02088]
22 **Abdol Razak N**, Elaskalani O, Metharom P. Pancreatic Cancer-Induced Neutrophil Extracellular Traps: A Potential Contributor to Cancer-Associated Thrombosis. *Int J Mol Sci* 2017; **18** [PMID: 28245569 DOI: 10.3390/ijms18030487]
23 **Yang C**, Sun W, Cui W, Li X, Yao J, Jia X, Li C, Wu H, Hu Z, Zou X. Procoagulant role of neutrophil extracellular traps in patients with gastric cancer. *Int J Clin Exp Pathol* 2015; **8**: 14075-14086 [PMID: 26823721]
24 **Zhao L**, Bi Y, Kou J, Shi J, Piao D. Phosphatidylserine exposing-platelets and microparticles promote procoagulant activity in colon cancer patients. *J Exp Clin Cancer Res* 2016; **35**: 54 [PMID: 27015840 DOI: 10.1186/s13046-016-0328-9]
25 **Suzuki-Inoue K**. Platelets and cancer-associated thrombosis: focusing on the platelet activation receptor CLEC-2 and podoplanin. *Blood* 2019; **134**: 1912-1918 [PMID: 31778548 DOI: 10.1182/blood.2019001388]
26 **Gasiorowska A**, Talar-Wojnarowska R, Kaczka A, Borkowska A, Czupryniak L, Małecka-Panas E. Subclinical Inflammation and Endothelial Dysfunction in Patients with Chronic Pancreatitis and Newly Diagnosed Pancreatic Cancer. *Dig Dis Sci* 2016; **61**: 1121-1129 [PMID: 26597191 DOI: 10.1007/s10620-015-3972-6]
27 **Chang Z**, Zhang Y, Liu J, Zheng Y, Li H, Kong Y, Li P, Peng H, Shi Y, Cao B, Ran F, Chen Y, Song Y, Ye Q, Ding L. Snail promotes the generation of vascular endothelium by breast cancer cells. *Cell Death Dis* 2020; **11**: 457 [PMID: 32541667 DOI: 10.1038/s41419-020-2651-5]
28 **Li B**, Liu Y, Hu T, Zhang Y, Zhang C, Li T, Wang C, Dong Z, Novakovic VA, Shi J. Neutrophil extracellular traps enhance procoagulant activity in patients with oral squamous cell carcinoma. *J Cancer Res Clin Oncol* 2019; **145**: 1695-1707 [PMID: 31020419 DOI: 10.1007/s00432-019-02922-2]
29 **Zhang J**, Yu M, Liu B, Zhou P, Zuo N, Wang Y, Feng Y, Zhang Y, Wang J, He Y, Wu Y, Dong Z, Hong L, Shi J. Neutrophil extracellular traps enhance procoagulant activity and thrombotic tendency in patients with obstructive jaundice. *Liver Int* 2021; **41**: 333-347 [PMID: 33159371 DOI: 10.1111/liv.14725]
30 **Li T**, Wang C, Liu Y, Li B, Zhang W, Wang L, Yu M, Zhao X, Du J, Zhang J, Dong Z, Jiang T, Xie R, Ma R, Fang S, Zhou J, Shi J. Neutrophil Extracellular Traps Induce Intestinal Damage and Thrombotic Tendency in Inflammatory Bowel Disease. *J Crohns Colitis* 2020; **14**: 240-253 [PMID: 31325355 DOI: 10.1093/ecco-jcc/jjz132]
31 **Edge SB**, Compton CC. The American Joint Committee on Cancer: the 7th edition of the AJCC cancer staging manual and the future of TNM. *Ann Surg Oncol* 2010; **17**: 1471-1474 [PMID: 20180029 DOI: 10.1245/s10434-010-0985-4]
32 **Koupenova M**, Corkrey HA, Vitseva O, Manni G, Pang CJ, Clancy L, Yao C, Rade J, Levy D, Wang JP, Finberg RW, Kurt-Jones EA, Freedman JE. The role of platelets in mediating a response to human influenza infection. *Nat Commun* 2019; **10**: 1780 [PMID: 30992428 DOI: 10.1038/s41467-019-09607-x]
33 **Brill A**, Fuchs TA, Chauhan AK, Yang JJ, De Meyer SF, Köllnberger M, Wakefield TW, Lämmle B, Massberg S, Wagner DD. von Willebrand factor-mediated platelet adhesion is critical for deep vein thrombosis in mouse models. *Blood* 2011; **117**: 1400-1407 [PMID: 20959603 DOI: 10.1182/blood-2010-05-287623]
34 **Yang LY**, Luo Q, Lu L, Zhu WW, Sun HT, Wei R, Lin ZF, Wang XY, Wang CQ, Lu M, Jia HL, Chen JH, Zhang JB, Qin LX. Increased neutrophil extracellular traps promote metastasis potential of hepatocellular carcinoma *via* provoking tumorous inflammatory response. *J Hematol Oncol* 2020; **13**: 3 [PMID: 31907001 DOI: 10.1186/s13045-019-0836-0]
35 **Folco EJ**, Mawson TL, Vromman A, Bernardes-Souza B, Franck G, Persson O, Nakamura M, Newton G, Luscinskas FW, Libby P. Neutrophil Extracellular Traps Induce Endothelial Cell Activation and Tissue Factor Production Through Interleukin-1α and Cathepsin G. *Arterioscler Thromb Vasc Biol* 2018; **38**: 1901-1912 [PMID: 29976772 DOI: 10.1161/ATVBAHA.118.311150]
36 **Zhou P**, Li T, Jin J, Liu Y, Li B, Sun Q, Tian J, Zhao H, Liu Z, Ma S, Zhang S, Novakovic VA, Shi J, Hu S. Interactions between neutrophil extracellular traps and activated platelets enhance procoagulant activity in acute stroke patients with ICA occlusion. *EBioMedicine* 2020; **53**: 102671 [PMID: 32114386 DOI: 10.1016/j.ebiom.2020.102671]
37 **Brill A**, Fuchs TA, Savchenko AS, Thomas GM, Martinod K, De Meyer SF, Bhandari AA, Wagner DD. Neutrophil extracellular traps promote deep vein thrombosis in mice. *J Thromb Haemost* 2012; **10**: 136-144 [PMID: 22044575 DOI: 10.1111/j.1538-7836.2011.04544.x]
38 **Najmeh S**, Cools-Lartigue J, Giannias B, Spicer J, Ferri LE. Simplified Human Neutrophil Extracellular Traps (NETs) Isolation and Handling. *J Vis Exp* 2015 [PMID: 25938591 DOI: 10.3791/52687]
39 **Fuchs TA**, Brill A, Duerschmied D, Schatzberg D, Monestier M, Myers DD Jr, Wrobleski SK, Wakefield TW, Hartwig JH, Wagner DD. Extracellular DNA traps promote thrombosis. *Proc Natl Acad Sci U S A* 2010; **107**: 15880-15885 [PMID: 20798043 DOI: 10.1073/pnas.1005743107]
40 **Bodac A**, Meylan E. Neutrophil metabolism in the cancer context. *Semin Immunol* 2021; 101583 [PMID: 34963565 DOI: 10.1016/j.smim.2021.101583]
41 **Ustyanovska Avtenyuk N**, Visser N, Bremer E, Wiersma VR. The Neutrophil: The Underdog That Packs a Punch in the Fight against Cancer. *Int J Mol Sci* 2020; **21** [PMID: 33105656 DOI: 10.3390/ijms21217820]
42 **Zha C**, Meng X, Li L, Mi S, Qian D, Li Z, Wu P, Hu S, Zhao S, Cai J, Liu Y. Neutrophil extracellular traps mediate the crosstalk between glioma progression and the tumor microenvironment **via** the HMGB1/RAGE/IL-8 axis. *Cancer Biol Med* 2020; **17**: 154-168 [PMID: 32296583 DOI: 10.20892/j.issn.2095-3941.2019.0353]
43 **Itatani Y**, Yamamoto T, Zhong C, Molinolo AA, Ruppel J, Hegde P, Taketo MM, Ferrara N. Suppressing neutrophil-dependent angiogenesis abrogates resistance to anti-VEGF antibody in a genetic model of colorectal cancer. *Proc Natl Acad Sci U S A* 2020; **117**: 21598-21608 [PMID: 32817421 DOI: 10.1073/pnas.2008112117]
44 **Tohme S**, Yazdani HO, Al-Khafaji AB, Chidi AP, Loughran P, Mowen K, Wang Y, Simmons RL, Huang H, Tsung A. Neutrophil Extracellular Traps Promote the Development and Progression of Liver Metastases after Surgical Stress. *Cancer Res* 2016; **76**: 1367-1380 [PMID: 26759232 DOI: 10.1158/0008-5472.CAN-15-1591]
45 **Wolach O**, Sellar RS, Martinod K, Cherpokova D, McConkey M, Chappell RJ, Silver AJ, Adams D, Castellano CA, Schneider RK, Padera RF, DeAngelo DJ, Wadleigh M, Steensma DP, Galinsky I, Stone RM, Genovese G, McCarroll SA, Iliadou B, Hultman C, Neuberg D, Mullally A, Wagner DD, Ebert BL. Increased neutrophil extracellular trap formation promotes thrombosis in myeloproliferative neoplasms. *Sci Transl Med* 2018; **10** [PMID: 29643232 DOI: 10.1126/scitranslmed.aan8292]
46 **Zhu T**, Zou X, Yang C, Li L, Wang B, Li R, Li H, Xu Z, Huang D, Wu Q. Neutrophil extracellular traps promote gastric

cancer metastasis by inducing epithelialmesenchymal transition. *Int J Mol Med* 2021; **48** [PMID: 34013374 DOI: 10.3892/ijmm.2021.4960]

47 **Li R**, Zou X, Zhu T, Xu H, Li X, Zhu L. Destruction of Neutrophil Extracellular Traps Promotes the Apoptosis and Inhibits the Invasion of Gastric Cancer Cells by Regulating the Expression of Bcl-2, Bax and NF-κB. *Onco Targets Ther* 2020; **13**: 5271-5281 [PMID: 32606746 DOI: 10.2147/OTT.S227331]

48 **Zhang Y**, Hu Y, Ma C, Sun H, Wei X, Li M, Wei W, Zhang F, Yang F, Wang H, Gu K. Diagnostic, Therapeutic Predictive, and Prognostic Value of Neutrophil Extracellular Traps in Patients With Gastric Adenocarcinoma. *Front Oncol* 2020; **10**: 1036 [PMID: 32714865 DOI: 10.3389/fonc.2020.01036]

49 **Keshari RS**, Jyoti A, Dubey M, Kothari N, Kohli M, Bogra J, Barthwal MK, Dikshit M. Cytokines induced neutrophil extracellular traps formation: implication for the inflammatory disease condition. *PLoS One* 2012; **7**: e48111 [PMID: 23110185 DOI: 10.1371/journal.pone.0048111]

50 **Liu Y**, Yan W, Tohme S, Chen M, Fu Y, Tian D, Lotze M, Tang D, Tsung A. Hypoxia induced HMGB1 and mitochondrial DNA interactions mediate tumor growth in hepatocellular carcinoma through Toll-like receptor 9. *J Hepatol* 2015; **63**: 114-121 [PMID: 25681553 DOI: 10.1016/j.jhep.2015.02.009]

51 **Harper MT**, Poole AW. Chloride channels are necessary for full platelet phosphatidylserine exposure and procoagulant activity. *Cell Death Dis* 2013; **4**: e969 [PMID: 24357800 DOI: 10.1038/cddis.2013.495]

52 **Cleary SJ**, Hobbs C, Amison RT, Arnold S, O'Shaughnessy BG, Lefrançais E, Mallavia B, Looney MR, Page CP, Pitchford SC. LPS-induced Lung Platelet Recruitment Occurs Independently from Neutrophils, PSGL-1, and P-Selectin. *Am J Respir Cell Mol Biol* 2019; **61**: 232-243 [PMID: 30768917 DOI: 10.1165/rcmb.2018-0182OC]

53 **Zhang Y**, Wang C, Yu M, Zhao X, Du J, Li Y, Jing H, Dong Z, Kou J, Bi Y, Novakovic VA, Zhou J, Shi J. Neutrophil extracellular traps induced by activated platelets contribute to procoagulant activity in patients with colorectal cancer. *Thromb Res* 2019; **180**: 87-97 [PMID: 31271975 DOI: 10.1016/j.thromres.2019.06.005]

54 **Martinod K**, Witsch T, Farley K, Gallant M, Remold-O'Donnell E, Wagner DD. Neutrophil elastase-deficient mice form neutrophil extracellular traps in an experimental model of deep vein thrombosis. *J Thromb Haemost* 2016; **14**: 551-558 [PMID: 26712312 DOI: 10.1111/jth.13239]

World Journal of Gastroenterology

Submit a Manuscript: https://www.f6publishing.com

World J Gastroenterol 2022 July 14; 28(26): 3150-3163

DOI: 10.3748/wjg.v28.i26.3150

ISSN 1007-9327 (print) ISSN 2219-2840 (online)

ORIGINAL ARTICLE

Basic Study

Activation of natural killer T cells contributes to Th1 bias in the murine liver after 14 d of ethinylestradiol exposure

Meng-Zhi Zou, Wei-Chao Kong, Heng Cai, Meng-Tao Xing, Zi-Xun Yu, Xin Chen, Lu-Yong Zhang, Xin-Zhi Wang

Specialty type: Toxicology

Provenance and peer review: Invited article; Externally peer reviewed.

Peer-review model: Single blind

Peer-review report's scientific quality classification

Grade A (Excellent): 0
Grade B (Very good): B
Grade C (Good): 0
Grade D (Fair): 0
Grade E (Poor): 0

P-Reviewer: Imai Y, Japan
A-Editor: Lin FY, China

Received: October 26, 2021
Peer-review started: October 26, 2021
First decision: April 16, 2022
Revised: April 25, 2022
Accepted: May 22, 2022
Article in press: May 22, 2022
Published online: July 14, 2022

Meng-Zhi Zou, Wei-Chao Kong, Heng Cai, Zi-Xun Yu, Xin Chen, Lu-Yong Zhang, Xin-Zhi Wang, New Drug Screening Center, China Pharmaceutical University, Nanjing 210009, Jiangsu Province, China

Meng-Tao Xing, Department of Pharmacology, China Pharmaceutical University, Nanjing 210009, Jiangsu Province, China

Lu-Yong Zhang, Center for Drug Research and Development, Guangdong Pharmaceutical University, Guangzhou 510006, Guangdong Province, China

Corresponding author: Xin-Zhi Wang, PhD, Associate Research Scientist, New Drug Screening Center, China Pharmaceutical University, No. 24 Tongjiaxiang, Nanjing 210009, Jiangsu Province, China. wangxz@cpu.edu.cn

Abstract

BACKGROUND

As the main component of oral contraceptives (OCs), ethinylestradiol (EE) has been widely applied as a model drug to induce murine intrahepatic cholestasis. The clinical counterpart of EE-induced cholestasis includes women who are taking OCs, sex hormone replacement therapy, and susceptible pregnant women. Taking intrahepatic cholestasis of pregnancy (ICP) as an example, ICP consumes the medical system due to its high-risk fetal burden and the impotency of ursodeoxycholic acid in reducing adverse perinatal outcomes.

AIM

To explore the mechanisms and therapeutic strategies of EE-induced cholestasis based on the liver immune microenvironment.

METHODS

Male C57BL/6J mice or invariant natural killer T (iNKT) cell deficiency (Jα18$^{-/-}$ mice) were administered with EE (10 mg/kg, subcutaneous) for 14 d.

RESULTS

Both Th1 and Th2 cytokines produced by NKT cells increased in the liver skewing toward a Th1 bias. The expression of the chemokine/chemokine receptor Cxcr6/Cxcl16, toll-like receptors, Ras/Rad, and PI3K/Bad signaling was upregulated after EE administration. EE also influenced bile acid synthase

Cyp7a1, Cyp8b1, and tight junctions ZO-1 and Occludin, which might be associated with EE-induced cholestasis. iNKT cell deficiency (Jα18$^{-/-}$ mice) robustly alleviated cholestatic liver damage and lowered the expression of the abovementioned signaling pathways.

CONCLUSION

Hepatic NKT cells play a pathogenic role in EE-induced intrahepatic cholestasis. Our research improves the understanding of intrahepatic cholestasis by revealing the hepatic immune microenvironment and also provides a potential clinical treatment by regulating iNKT cells.

Key Words: Natural killer T cell; Th1/Th2; IFN-γ; Estrogen; Cholestasis

©The Author(s) 2022. Published by Baishideng Publishing Group Inc. All rights reserved.

Core Tip: In this study, we observed the production of both Th1 and Th2 cytokines by natural killer T (NKT) cells in the liver after 14 d of exposure to ethinylestradiol-induced cholestasis. The liver immune microenvironment was also skewed toward a Th1 bias mainly contributed by NKT cells. Invariant NKT cell deficiency robustly alleviated cholestatic liver damage and downregulated the associated signaling pathways, highlighting the pathogenic role and therapeutic potential of hepatic NKT cells in cholestatic liver diseases.

Citation: Zou MZ, Kong WC, Cai H, Xing MT, Yu ZX, Chen X, Zhang LY, Wang XZ. Activation of natural killer T cells contributes to Th1 bias in the murine liver after 14 d of ethinylestradiol exposure. *World J Gastroenterol* 2022; 28(26): 3150-3163

URL: https://www.wjgnet.com/1007-9327/full/v28/i26/3150.htm

DOI: https://dx.doi.org/10.3748/wjg.v28.i26.3150

INTRODUCTION

Cholestasis is a mild and common phenomenon during liver diseases but also a crucial triggering element of severe hepatopathy, such as fibrosis, cirrhosis, and hepatic venous thrombosis[1]. Both estrogen and oral contraceptives (OCs) can elicit intrahepatic cholestasis (IHC), whose effects manifest as retention of toxic bile acids in the liver and circulation[2]. 17α-ethinylestradiol (EE) is used as a model drug to induce murine IHC. As the predominant component of OCs and hormone replacement therapy, the clinical counterpart of EE-induced IHC includes women who are taking OCs, postmenopausal replacement therapy and susceptible pregnant women. Sex steroids may lead to alterations in bile components and the elevation of total bile acids (TBAs), which may induce apoptosis and oxidative stress and thus have harmful effects on hepatocytes and other organs[3]. In clinical studies, administration of EE to both males and females leads to increased serum TBA levels and decreased clearance of sulfobromophthalein[4]. In murine studies, the mechanisms involve the activation of AMP-activated protein kinase[5] and estrogen receptor α[6], the inhibition of farnesoid X receptor (FXR), bile acid transporters, bile acid synthase and metabolism enzymes, and inflammatory reactions[7-9]. The first-line therapy ursodeoxycholic acid (UDCA) for cholestatic diseases is a naturally hydrophilic bile acid, although its potency is limited, as approximately 40% of patients are not responsive to UDCA treatment [10].

Among these predisposing factors, the significance of the local immune microenvironment in the liver has been emphasized because sex hormones are immunomodulators that are metabolized in the liver. In a murine model of EE-induced cholestasis, hepatic expression of TNF-α and IL-6 was greatly upregulated[8]. Proinflammatory mediators can affect nuclear receptors and transporters and then cause bile acid equilibrium disorder, increased cytokine secretion, and further exacerbated cholestasis, forming a positive regulation loop[8]. In patients with intrahepatic cholestasis of pregnancy (ICP), an increase in Th1-type cytokines and a decrease in Th2-type cytokines suggest the involvement of proinflammatory and cytotoxic Th1 biases in ICP[11]. However, the impotency of corticosteroids in the treatment of cholestasis indicates that promising therapies or active agents are in heavy demand[12].

Natural killer T (NKT) cells are one of the most abundant lymphocytes in the liver, and their role in cholestasis is noteworthy[13]. NKT cells behave similarly to conventional T cells and function as both effector and regulatory immune cells. Jα18$^{-/-}$ mice are not prone to developing cholestatic liver injury after alpha-naphthylisothiocyanate (ANIT) administration due to the invariant NKT-cell (iNKT cell) knockout-related reduction in cytokines and the restored expression of transporters and bile acid metabolism enzymes[14]. Recent work also demonstrated that IL-4 secreted by type 1 NKT cells (iNKT cells) may inhibit type 2 NKT cells and upregulate immunoregulators, affecting the expression of bile

acid nuclear receptors, transporters, and CYP450 enzymes, thus exacerbating triptolide-induced cholestatic liver damage[15]. However, Jα18$^{-/-}$ mice showed aggravation of liver damage after bile duct ligation (BDL) surgery compared with wild-type mice due to the increase in neutrophils, chemokines and cytokines[16]. Moreover, knockout of the bile acid sensor FXR gene increases liver NKT cells and aggravates liver damage, indicating that FXR can regulate the activation of liver NKT cells[17]. Certain antigens that can activate NKT cells exist in the bile of patients with chronic liver diseases[18]. Thus, the aim of the present study was to investigate the effects and mechanisms of NKT cells in a murine model of EE-induced cholestatic hepatotoxicity.

MATERIALS AND METHODS

Reagents

17α-EE (CAS:57-63-6, batch number: E0037, contents > 98.0% (T) high performance liquid chromatography) was purchased from tcichemicals (Shanghai, China). EE was dissolved in an 80% 1,2-propylene glycol solution and diluted with physiological saline to a dosing concentration of 10 mg/kg before the experiment. Anti-CD16/32 antibody (clone: 2.4G2), which was used for blocking before staining, anti-CD3e-FITC antibody (clone: 145-2C11), anti-CD49b-APC antibody (clone: DX5), leukocyte activation cocktail with BD GolgiPlug™, anti-IFN-γ-PE antibody (clone: XMG1.2), and anti-IL-4-PE antibody (clone: 11B11) were purchased from BD Pharmingen (San Diego, CA, United States).

Animals and treatment

Male C57BL/6J mice (6-8 wk of age and 18-20 g of weight) were obtained from SLAC Laboratory Animal Co., Ltd. (Shanghai, China). iNKT cell-deficient Jα18$^{-/-}$ mice on a C57BL/6 background (6 to 8 wk old) were kindly provided by Dr. Li Bai (University of Science and Technology of China). All mice were administered physiological saline or EE (10 mg/kg) subcutaneously (s.c.) for 14 continuous d. Each group contained 6 mice. All mice were maintained and bred under controlled conditions (pathogen-free, 22 ± 2 °C, 12:12-h light-dark regular photoperiod) with ad libitum mouse chow and water access. The animals were housed in the laboratory for 1 wk prior to experiments to acclimate. All procedures involved in this study were performed under the Ethical Committee of China Pharmaceutical University and the Laboratory Animal Management Committee of Jiangsu Province guidelines (Approval No.: 2021-10-003).

Nonparenchymal cell isolation and labeling

After perfusing saline solution into the heart to eliminate blood, the mouse liver was minced through a 200-gauge nylon mesh and washed with cold PBS. After centrifugation at 50 × g for 2 min in the crude solution, the separated supernatant was centrifuged for another 10 min at 800 × g. The cell pellets were resuspended in 40% Percoll for centrifugation at 1250 × g for 15 min. After nonparenchymal cell (NPC) isolation from the cell pellets by red blood cell lysis solution (0.15 M NH4Cl and 0.1 mmol/L Na2EDTA) treatment and 2 washes, NPCs were stimulated with leukocyte activation cocktail for 4-5 h (BD Pharmingen).

After stimulation, NPCs were blocked with anti-CD16/32 and then surface-labeled with FITC-conjugated anti-mouse CD3e and APC-CD49b antibodies. NPCs were permeabilized with Cytofix/Cytoperm (Becton Dickinson) following the manufacturer's instructions, and intracellular staining was performed by incubation with IFN-γ or IL-4 antibodies. After each step, unbound antibodies were excluded from the system by centrifugation. Then, the cells were analyzed using a FACSCalibur flow cytometer (Becton Dickinson, Palo Alto, CA, United States), with 50000 events recorded per tube. The results were processed using FlowJo version 10 software (FlowJo, Ashland, OR, United States). The gating strategy was as follows: first, NPCs were gated by FSC and SSC, followed by the gating of CD3e$^+$ or CD3e$^-$ cells. CD49b$^+$ IFN-γ$^+$, CD49b$^+$ IL-4$^+$ or CD49b$^-$ IFN-γ$^+$, and CD49b$^-$ IL-4$^+$ cells were then gated and analyzed.

Blood biochemical analysis

Anticoagulant-free serum was collected and then analyzed for the levels of alkaline phosphatase (ALP), total bile acid (TBA), alanine transaminase (ALT), and aspartate transaminase (AST) using the ALP, ALT, and AST quantification kit (Whitman Biotech, Nanjing, China) and TBA quantification kit (Jiancheng Bioengineering Institute, Nanjing, China).

Histopathology and immunohistochemistry

The liver lobules were fixed, paraffin embedded, sectioned, and stained with hematoxylin and eosin for histopathological examination. Slides were coded, randomized, and assessed by pathologists who, during the evaluation of the slides, were blinded to the treatment groups. Scoring for liver injury was conducted according to the following criteria: no hepatocellular necrosis, proliferation of pseudocholangiolar duct, or inflammatory cell infiltration, 0; mild, 1; moderate, 2; severe, 3. The other sections were

Table 1 The primer sequence used for real-time polymerase chain reaction in mice

Name	Forward (5' to 3')	Reserve (5' to 3')
Gapdh	CATCACTGCCACCCAGAAGACTG	ATGCCAGTGAGCTTCCCGTTCAG
Tlr2	TGCTCCTGCGAACTCCTATC	CAGACTCCAGACACCAGTGC
Tlr4	AGCTTCTCCAATTTTTCAGAACTTC	TGAGAGGTGGTGTAAGCCATGC
Tlr6	AGCCAAGACAGAAAACCCATC	GGGGTCATGCTTCCGACTAT
Tlr7	CACCACCAATCTTACCCTTACC	CAGATGGTTCAGCCTACGGAA
Tlr9	GCTGTCAATGGCTCTCAGTTCC	CCTGCAACTGTGGTAGCTCACT
Cxcr6	GGTTCTTCCTGCCATTGCTCAC	GCAGGAACACAGCCACTACAAG
Cxcl16	GCAGGGTACTTTGGATCACATCC	AGTTCACGGACCCACTGGTCTT
Ras	TCGCACTGTTGAGTCTCGGCAG	TATGCTGCCGAATCTCACGGAC
Raf	CGCCAAGTCAATCATCCACAGAG	CACCGAGATTTCACTGTGGCTAG
Pi3k	CACCTGAACAGACAAGTAGAGGC	GCAAAGCATCCATGAAGTCTGGC
Bad	GGGAGCAACATTCATCAGCAGG	CGTCCTCGAAAAGGGCTAAGCT

subjected to IHC for semiquantification of the expression of toll-like receptor (TLR) 9 (Novus, 26C593.2, dilution percentage: 1:200).

RNA extraction and real-time polymerase chain reaction

RNA was extracted from liver sections by TRIzol reagent (Vazyme Biotech, Nanjing, China). Isolated RNA was processed by the HiScript™ Q RT SuperMix for quantitative polymerase chain reaction (qPCR) (+ gDNA wiper) kit (Vazyme Biotech) for cDNA synthesis. A 20 μL real-time PCR system was prepared according to the manufacturer's instructions. The mRNA levels were normalized to the housekeeping gene *Gapdh*. The primer sequences used are shown in Table 1.

Statistical analysis

Values are expressed as the means ± SE. The groups were evaluated using Student's *t* test. A P value < 0.05 was considered statistically significant.

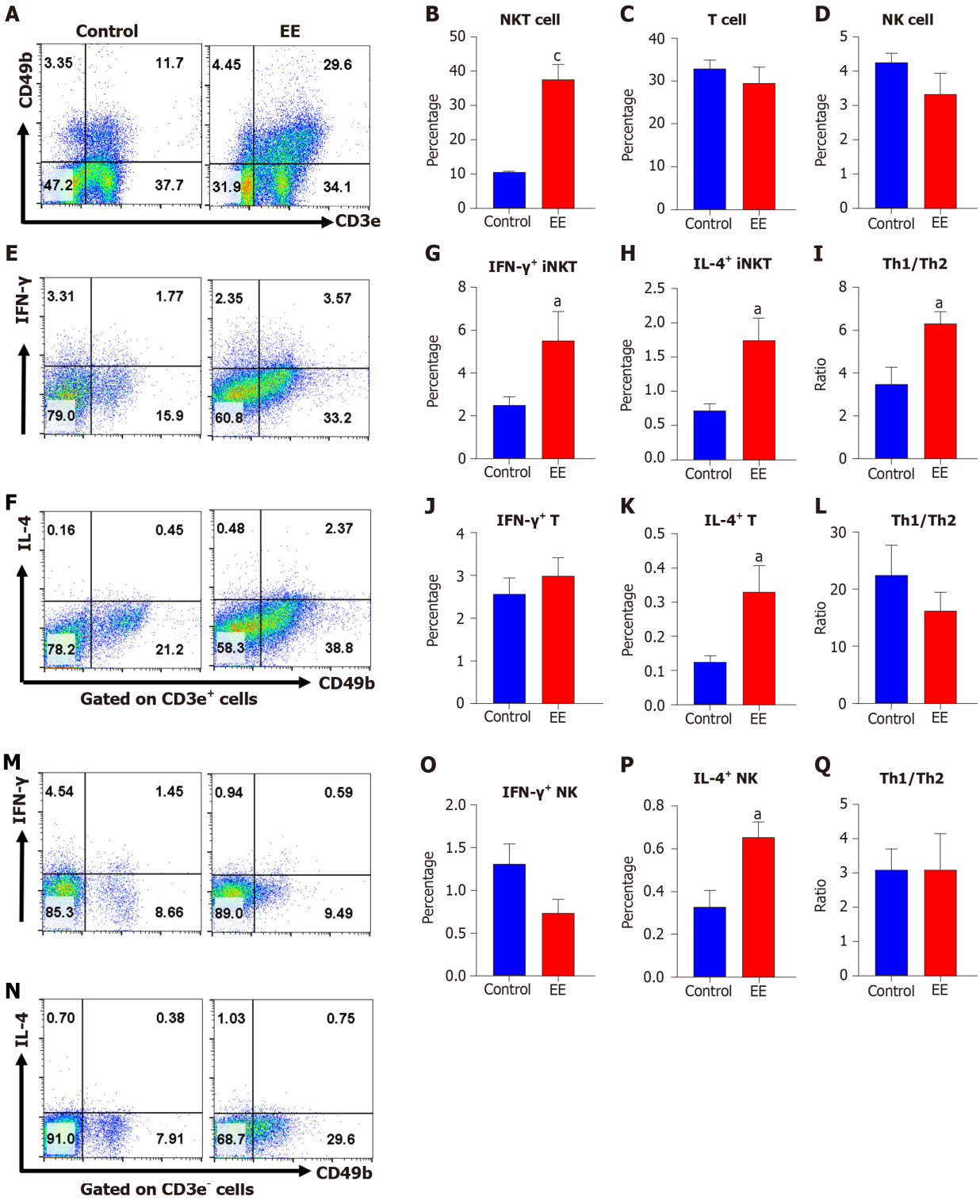
RESULTS

EE promotes hepatic NKT-cell proliferation along with biased Th1 cytokine production

Increased activation of NKT cells, T cells, or NK cells has been reported to contribute to the pathophysiology of cholestasis[15,19,20]. Here, we measured and analyzed their percentages and Th1/Th2 cytokine production to evaluate their activation. Hepatic NKT cells, $CD3^+$ T cells (excluding NKT cells) and NK cells were defined as $CD3e^+CD49b^+$ (Figure 1A upper right), $CD3e^+CD49b^-$ (Figure 1A lower right), and $CD3e^-CD49b^+$ (Figure 1A upper left), respectively. After EE administration, the percentage of hepatic NKT cells expanded more than 3-fold compared with the control group, while the frequencies of $CD3^+$ T cells and NK cells showed no significant changes (Figure 1A-D). Both IFN-γ and IL-4 secreted from NKT cells increased, which further indicated NKT-cell activation. Moreover, the upregulated Th1/Th2 ratios indicated that a skewed hepatic Th1 immune response was due to NKT cells (Figure 1E–I). Compared with the control group, IL-4 secreted by $CD3^+$ T cells and NK cells increased, and their IFN-γ secretion and Th1/Th2 ratios remained unaltered (Figure 1J–Q).

iNKT cells exacerbate EE-induced cholestatic liver damage

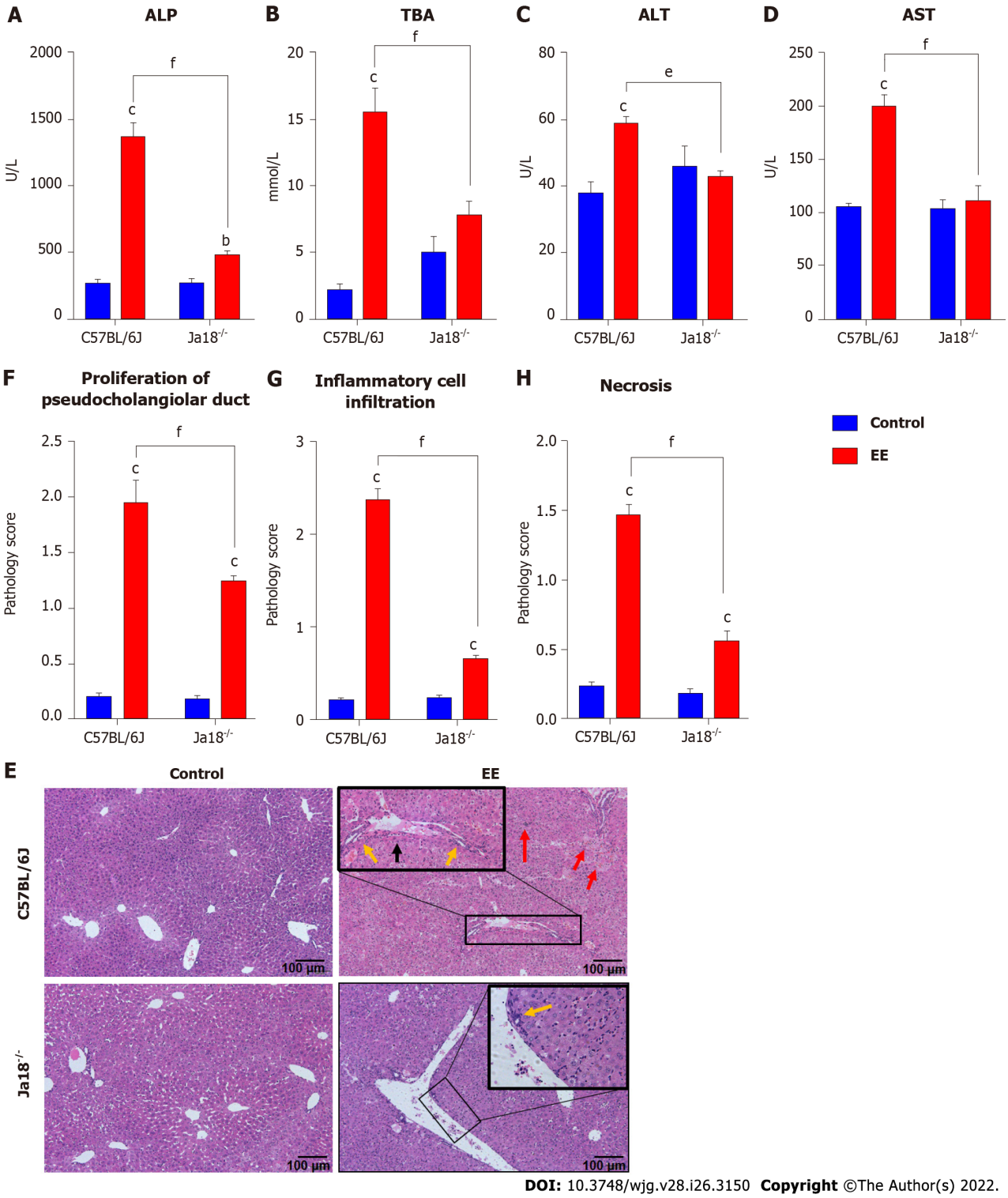
For further investigation of the NKT-cell effect, cholestatic liver injury was compared between iNKT cell knockout mice ($J\alpha18^{-/-}$ mice) and C57BL/6J mice after EE administration. Compared with the control group, EE induced increased levels of ALP, TBA, ALT, and AST in C57BL/6J mice. Compared with C57BL/6J mice, $J\alpha18^{-/-}$ mice demonstrated significantly lower levels of ALP, TBA, ALT, and AST (Figure 2A-D). Based on the scoring criteria[21], the histopathological and hepatic injury score results showed proliferation of pseudocholangiolar duct (yellow arrows), inflammatory cell infiltration (red arrows) and hepatocyte necrosis (black arrows) after EE treatment, whereas $J\alpha18^{-/-}$ mice exhibited reduced proliferation of the pseudocholangiolar duct, inflammatory cell infiltration, and necrosis (Figure 2E-G). These results showed that iNKT cell-deficient mice can inhibit the development of cholestatic hepatotoxicity induced by EE, indicating a pathogenic effect exerted by iNKT cells on EE-



DOI: 10.3748/wjg.v28.i26.3150 **Copyright** ©The Author(s) 2022.

Figure 1 Ethinylestradiol promotes hepatic natural killer T cell proliferation along with biased Th1 cytokine production. A: The percentage of hepatic natural killer T (NKT) cells, T cells and NK cells were detected and defined as $CD3e^+CD49b^+$ (upper right), $CD3e^+CD49b^-$ (lower right), $CD3e^-CD49b^+$ (upper left), respectively; B: Proportion analysis and comparison of NKT cells; C: Proportion analysis and comparison of T cells; D: Proportion analysis and comparison of NK cells; E and F: Th1 cytokine (IFN-γ) (E) and Th2 cytokine (IL-4) (F) produced by NKT cells and T cells were detected, respectively; G: IFN-γ produced by NKT cells; H: IL-4 produced by NKT cells; I: The ratio of Th1/Th2 by NKT cells; J: IFN-γ produced by T cells; K: IL-4 produced by T cells; L: The ratio of Th1/Th2 by T cells; M and N: Th1 cytokine (IFN-γ) (M) and Th2 cytokine (IL-4) (N) produced by NK cells were detected; O: IFN-γ produced by NK cells; P: IL-4 produced by NK cells; Q: The ratio of Th1/Th2 by NK cells. All values are the means ± SE (n = 4-6). $^aP < 0.05$, $^cP < 0.001$ *vs* control.

induced cholestatic liver damage.

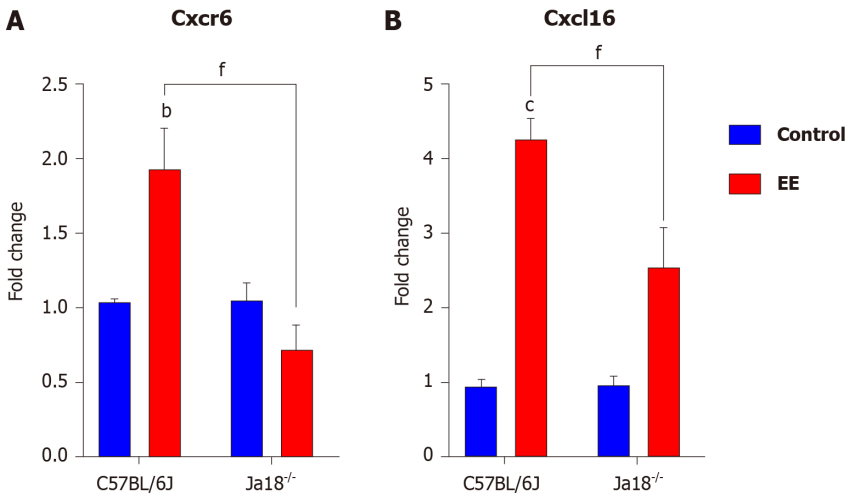


DOI: 10.3748/wjg.v28.i26.3150 **Copyright** ©The Author(s) 2022.

Figure 2 Invariant natural killer T cells exacerbate ethinylestradiol-induced cholestatic liver damage. A-D: The serum levels of ALP (A), TBA (B), ALT (C) and AST (D); E: Liver sections stained with hematoxylin and eosin (10×); F: Proliferation of pseudocholangiolar duct (yellow arrows); G and H: Inflammatory cell infiltration (G, red arrows) and hepatocyte necrosis (H, black arrows) were compared as pathology scores. All values are the means ± SE (n = 4-6). $^{b}P < 0.01$, $^{c}P < 0.001$ *vs* control; $^{e}P < 0.01$, $^{f}P < 0.001$ *vs* C57BL/6J group.

iNKT cell deficiency lowers the hepatic expression of chemokine/chemokine receptors

CXCR6, the receptor for chemokine CXCL16, is expressed on the surface of several hepatic lymphocytes, including NKT cells. The CXCR6-dependent infiltration of NKT cells into the liver induces enhanced inflammation in a murine model of chronic hepatic damage[22]. The qPCR results showed that EE promoted the hepatic mRNA expression of Cxcr6/Cxcl16 in C57BL/6J mice. Compared with C57BL/6J mice, iNKT cell deficiency significantly suppressed the mRNA expression of Cxcr6/Cxcl16, which may be related to the absence of the need for hepatic recruitment of NKT cells (Figure 3).



DOI: 10.3748/wjg.v28.i26.3150 **Copyright** ©The Author(s) 2022.

Figure 3 Invariant natural killer T cell deficiency lowers the hepatic expression of chemokine/chemokine receptors. A and B: Hepatic mRNA expressions of Cxcr6 (A) and Cxcl16 (B) were determined and compared. All values are the means ± SE (n = 4-6). $^{b}P < 0.01$, $^{c}P < 0.001$ *vs* control; $^{f}P < 0.001$ *vs* C57BL/6J group.

Absence of iNKT cells alters the expression of TLRs and associated signaling pathways

Accumulating evidence suggests that TLRs contribute to the development of hepatobiliary damage[23]. TLRs have also been reported to contribute to the activation and subsequent cytokine production of NKT cells[24]. Intriguingly, iNKT cells have been reported to express certain TLRs, some of which are functional[25]. In the present study, TLRs associated with NKT-cell activation or liver disease were measured and analyzed. The results showed that the mRNA expression levels of Tlr2, Tlr4, Tlr6, Tlr7, and Tlr9 were significantly upregulated after EE administration. Deficiency of iNKT cells significantly downregulated the expression of the above TLRs compared with that in C57BL/6J mice (Figure 4), which suggested that the absence of iNKT cells may influence the expression of TLRs. The hepatic immunohistochemistry results of TLR9 showed a trend similar to that of mRNA (Figure 4F).

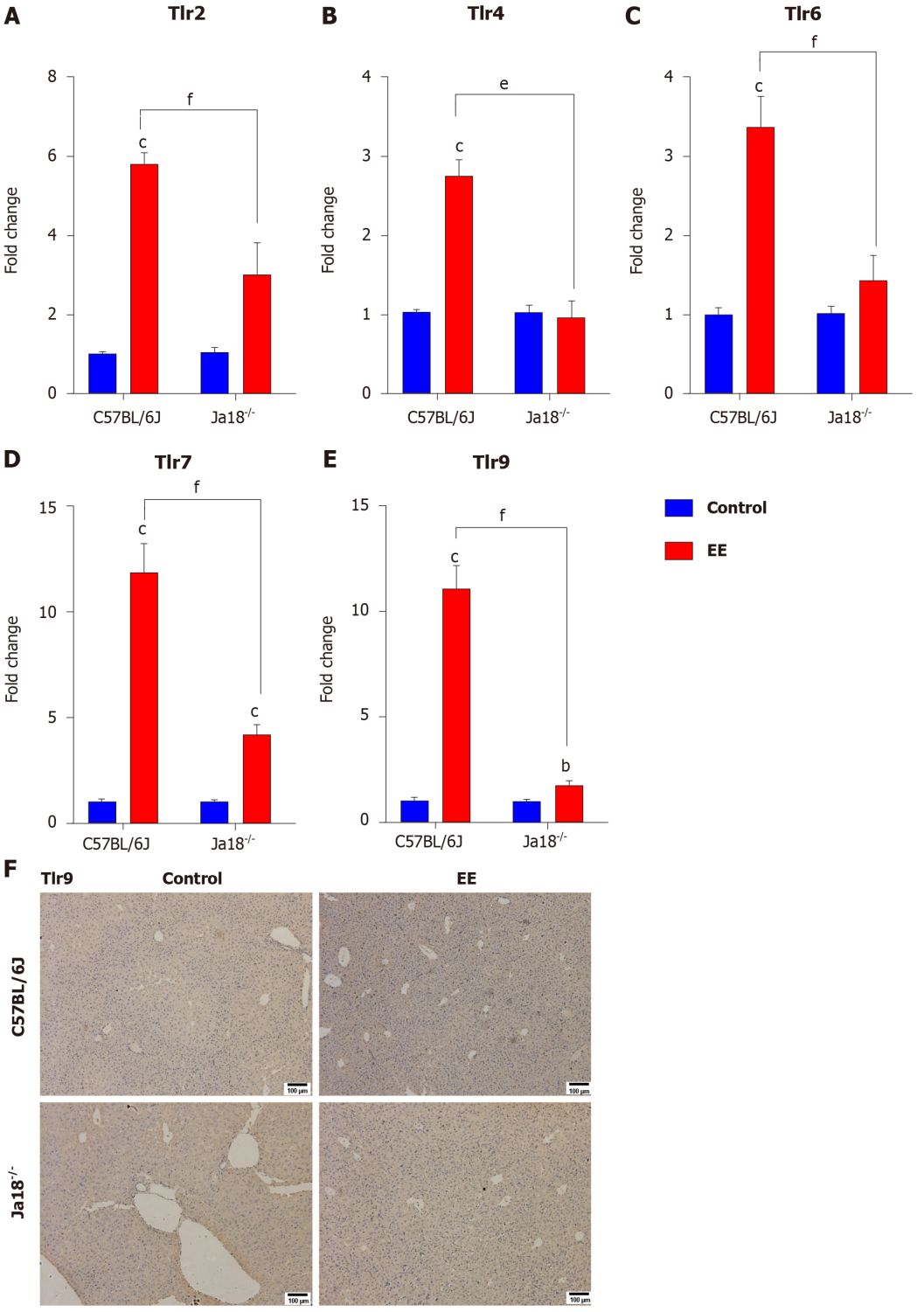
TLRs or T cell receptors (TCRs) can stimulate T cells, leading to MAPK signaling pathway activation, which is required for the effects of T cells[26]. iNKT cell activation by TCR stimulation has also been reported to be mediated by ERK and p38 MAPK[27]. In the present study, the expression of both MAPK and PI3K signaling was investigated after EE administration in C57BL/6J and Jα18$^{-/-}$ mice. The hepatic mRNA expression levels of MAPK upstream Ras and Raf as well as Pi3k and its downstream Bad, which might be associated with TLR activation, were increased in C57BL/6J mice after EE administration. The above mRNA levels were remarkably inhibited in Jα18$^{-/-}$ mice compared with C57BL/6J mice, which suggested that the absence of iNKT cells changes the expression of MAPK and PI3K signaling pathways (Figure 5).

Knockout of iNKT cells may inhibit the synthesis of bile acid and weaken the inhibition of hepatocyte polarity

Dysregulated bile acid homeostasis may be attributed to the disorder of bile acid synthesis/metabolism and/or the dysfunction of tight junctions (TJs)[28]. To investigate the possible mechanism of the alleviation of cholestatic liver injury in NKT-cell knockout mice, the levels of CYP450 synthase and TJs were detected. The mRNA levels of Cyp7a1 and Cyp8b1 were upregulated after EE administration in C57BL/6J mice, whereas a nonsignificant difference was shown in Jα18$^{-/-}$ mice. In comparison to C57BL/6J mice, the mRNA expression of Cyp7a1 and Cyp8b1 was inhibited in Jα18$^{-/-}$ mice after EE administration, indicating the relatively reduced synthesis of bile acid (Figure 6A and B). The IHC results showed that, in comparison to the control group, fewer cells positively stained for ZO-1 or Occludin after EE treatment in C57BL/6J mice, and positive cells remained unaltered between the control and EE groups in Jα18$^{-/-}$ mice (Figure 6C and D). These data suggested that knockout of iNKT cells can inhibit bile acid synthase and weaken the inhibition of hepatocyte polarity, thereby reducing cholestatic liver injury.

DISCUSSION

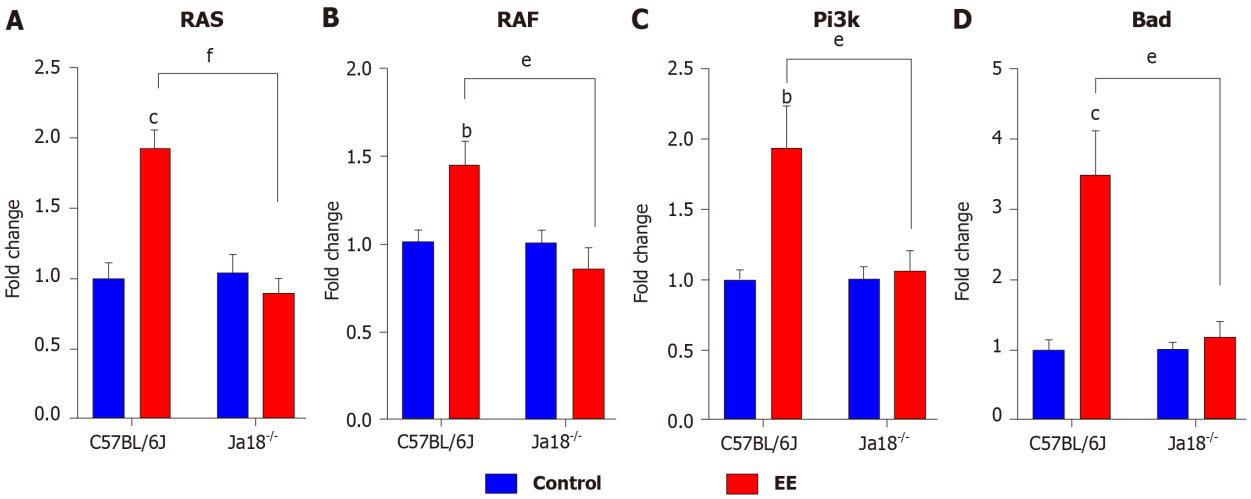
As the most common hepatic disorder, the principal pathogenic factors of EE-induced IHC include estrogen and toxic bile acid, both of which are correlated with immune imbalance. Increased activation



DOI: 10.3748/wjg.v28.i26.3150 **Copyright** ©The Author(s) 2022.

Figure 4 Absence of invariant natural killer T cells alters the expression of toll-like receptors. A-E: Hepatic mRNA levels of Tlr2 (A), Tlr4 (B), Tlr6 (C), Tlr7 (D) and Tlr9 (E) were determined and compared; F: Changes in the protein level of TLR9 were determined by immunohistochemistry. All values are the means ± SE (n = 4-6). $^{b}P < 0.01$, $^{c}P < 0.001$ *vs* control; $^{e}P < 0.01$, $^{f}P < 0.001$ *vs* C57BL/6J group.

status of NKT cells, T cells, or NK cells has been reported to contribute to the pathophysiology of cholestatic diseases[15,19,20]. Therefore, the percentages of hepatic NKT cells, $CD3^+$ T cells, and NK cells along with their Th1/Th2 cytokine secretion and bias were compared in the present study. Surprisingly, in EE-induced cholestasis, only the NKT-cell percentage and its Th1/Th2 cytokine secretion and ratio significantly increased, indicating their activation and Th1-biased immune response. The percentage of $CD3^+$ T cells and NK cells, along with their secretion of Th1 cytokines, remained unaltered. Th2 cytokines from $CD3^+$ T cells and NK cells showed a rising trend, which did not seem to affect the Th1/Th2 balance (Figure 1). Our results revealed that both Th1 and Th2 cytokines existed in the liver,



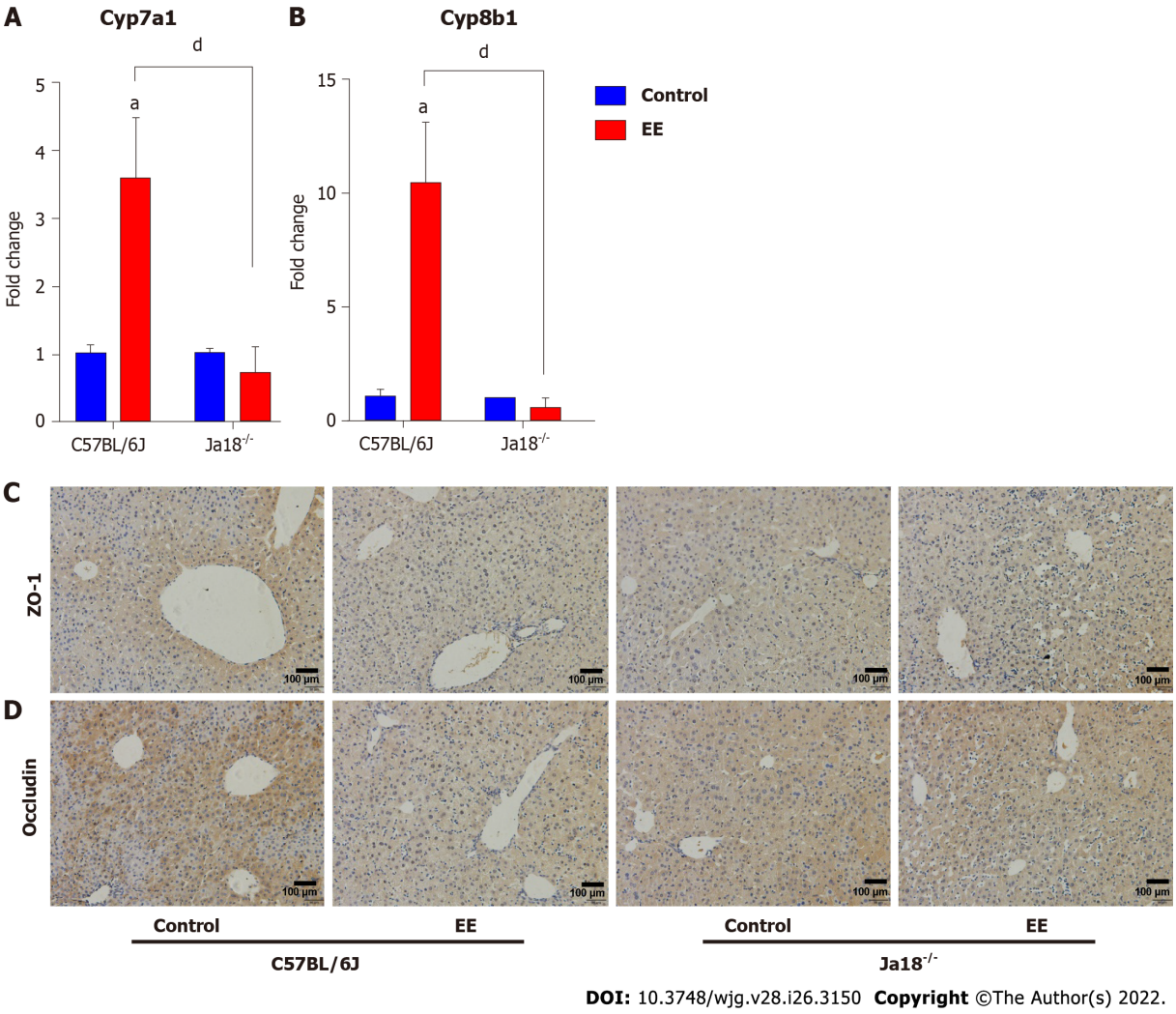
DOI: 10.3748/wjg.v28.i26.3150 Copyright ©The Author(s) 2022.

Figure 5 Absence of invariant natural killer T cells alters the expression of Ras/Raf and PI3K/Bad signaling pathways. A-D: Hepatic gene expressions of Ras (A), Raf (B), Pi3k (C) and Bad (D) were determined and compared. All values are the means ± SE (n = 4-6), $^{b}P < 0.01$, $^{c}P < 0.001$ *vs* control; $^{e}P < 0.01$, $^{f}P < 0.001$ *vs* C57BL/6J group.

consistent with previous studies[14,29], and the Th1 bias was mainly contributed by NKT cells. To further confirm the effect of NKT cells in EE-induced cholestasis, cholestatic liver damage was compared between iNKT cell-deficient mice and C57BL/6J mice after EE administration. Jα18$^{-/-}$ mice showed significantly reduced blood biochemistry parameters, including levels of ALP, TBA, ALT, and AST, and alleviated liver histopathological changes, suggesting that NKT cells have a harmful effect on EE-induced cholestasis. NKT cells have been accepted as a key connection between innate and adaptive immunity. Upon activation, NKT cells can activate and influence most innate and adaptive immune cells by rapid and abundant cytokine production[30,31]. NKT cells, whose role is noteworthy in cholestasis, are mostly abundant in the liver rather than other organs. In the PBC mouse model, NKT cells are highly activated and secrete enormous amounts of IFN-γ. In comparison to mice with PBC, cholangitis and liver inflammation are significantly alleviated in mice with NKT-cell deficiency[32]. Our previous investigations also found that iNKT cells and their cytokines aggravate ANIT- and triptolide-induced cholestasis by disrupting bile acid homeostasis[14,15]. Although NKT cells can be protective by suppressing neutrophils in an extrahepatic cholestasis model[16], our research data suggest the harmful effects of NKT cells in EE-induced cholestasis. The above studies indicate that the role of NKT cells may vary in different diseases and models.

Under physiological conditions, CXCR6/CXCL16 regulate the migration of NKT cells in hepatic sinusoids[33]. Under the early pathologic states of chronic liver damage, they specifically mediate the hepatic accumulation of NKT cells, exacerbating hepatic inflammation and promoting fibrogenesis[22]. CXCL16 can be expressed in hepatobiliary tissues of patients with hepatopathy[34] but also in mouse liver sinusoidal endothelial cells triggered by intestinal microorganism-induced bile acids, indicating that its expression is related to hepatobiliary damage[33,35]. Our results showed that the hepatic gene levels of Cxcr6 and Cxcl16 were upregulated (Figure 3). Inflammatory cytokines, such as IFN-γ, which was increased in the present model, are capable of further inducing CXCL16 expression, forming a positive regulation loop[36]. In the present study, iNKT cell deficiency inhibited the mRNA levels of Cxcr6 and Cxcl16, which may be linked to the absence of hepatic infiltration of NKT cells (Figure 3).

Activation of iNKT cells can be caused by direct interaction with TCR or indirect effects of TLR agonists and/or IL-12[37]. TLRs, which are widely expressed in the liver, can stimulate hepatic inflammation and actively participate in the initiation and development of liver damage under pathological conditions[38,39]. Lipopolysaccharide (LPS), a specific TLR4 Ligand, activates hepatic iNKT cells and leads to their secretion of IL-4 within 2 h *in vivo* or in vitro, demonstrating that TLR4 is expressed and functional in iNKT cells[40]. In alcoholic liver disease, TLR4 inhibition results in drastically reduced levels of hepatic proinflammatory mediators[41]. TLR4 deletion nearly eliminates inflammatory cell infiltration in the liver and hepatocyte injury in a murine model of ischemia reperfusion[42]. In EE-induced cholestatic liver injury, hepatic mRNA levels of Tlr2, 4, 6, 7, and 9 were markedly increased (Figure 4). CD1d knockout mice (lacking NKT cells) exhibit enhanced (> 4-fold) proinflammatory cytokine secretion and higher mRNA levels of TLR4 in the kidney of a nonalcoholic fatty liver disease model[43]. In the present study, iNKT cell deficiency significantly downregulated the expression of the above TLRs compared with C57BL/6J mice (Figure 4), suggesting the effect of iNKT cells on the expression of TLRs. NKT cells have been found to express certain functional TLRs[24]. The IHC results of TLR9 showed a similar trend as the mRNA levels (Figure 4F). In a murine autoimmune hepatitis model induced by concanavalin A, NKT cells infiltrate and are activated, promoted by TLR9



DOI: 10.3748/wjg.v28.i26.3150 **Copyright** ©The Author(s) 2022.

Figure 6 Knockout of invariant natural killer T cells may inhibit the synthesis of bile acid and weaken the inhibition of hepatocyte polarity. A and B: Hepatic gene levels of bile acid synthase Cyp7a1 (A) and Cyp8b1 (B) were determined and compared; C and D: Changes in the protein expressions of tight junction Zo-1 (C) and Occludin (D) were determined by immunohistochemistry. All values are the means ± SE (n = 6), $^{a}P < 0.05$ *vs* control; $^{d}P < 0.05$ *vs* C57BL/6J group.

stimulation, thereby leading to aggravated hepatotoxicity[44]. The PI3K/Akt and Ras/Raf/MEK/ERK signaling pathways are considered to be activated and function following inflammation[45], which further upregulates proinflammatory mediators in cholestasis[46]. Our data demonstrated that the mRNA levels of the downstream pathways Ras/Raf and Pi3k/Bad were also upregulated, while iNKT cell deficiency suppressed their upregulation (Figure 5). These results indicated that iNKT cell deletion affected TLRs and their downstream Ras/Raf and PI3K/Bad signaling.

Growing numbers of studies have reported that hepatocyte TJs, constituting hepatocyte polarization, play a pivotal role in the maintenance of the epithelial barrier and permeability; therefore, their structural disruption can lead to the leakage of bile components into blood circulation, bile acid homeostasis disorder, and cholestatic liver injury[47]. TJ damage can be found in obstructive jaundice patients[48] and murine cholestatic models of ANIT[28], carbon tetrachloride[49], BDL[50], and EE[51]. Inflammation has been associated with structural and functional alterations of hepatic TJs[52]. In the present study, the results showed that iNKT cell-deficient mice ameliorated disorders of bile acid synthesis and TJs (Figure 6) and restored previously deteriorated bile acid homeostasis and hepatocyte barrier function, contributing to the mitigation of EE-induced cholestatic hepatotoxicity.

CONCLUSION

In EE-induced cholestatic hepatotoxicity, EE promoted hepatic NKT-cell proliferation and activation, which contributed to Th1 cytokine bias and influenced the liver immune microenvironment. EE also upregulated the expression of Cxcr6/Cxcl16, TLRs, and downstream Ras/Rad and PI3K/Bad signaling. Moreover, EE influenced the levels of the bile acid synthase Cyp7a1 and Cyp8b1 and the TJs ZO-1 and

Occludin. iNKT cell deficiency significantly alleviated cholestatic liver damage and downregulated the abovementioned signaling pathways, indicating the pathogenic effects of hepatic iNKT cells in EE-induced cholestatic liver damage. It is noteworthy that mouse and human NKT cells share similar functions, including the killing of tumor/infected cells by cytotoxicity and their crucial role in autoimmunity[53]. Therefore, regulation of NKT-cell activation may serve as a potential therapeutic strategy with clinical implications for cholestatic diseases.

ARTICLE HIGHLIGHTS

Research background

Cholestasis is mild and common during liver diseases but is also a crucial triggering element of severe hepatopathy. As the predominant component of oral contraceptives (OCs) and hormone replacement therapy, 17α-ethinylestradiol (EE) is used as a model drug to induce murine intrahepatic cholestasis (IHC). The clinical counterpart of EE-induced IHC includes women who are taking OCs, postmenopausal replacement therapy, and susceptible pregnant women.

Research motivation

The significance of the local immune microenvironment in the liver has been emphasized because estrogens are immunomodulators that are metabolized in the liver.

Research objectives

The aim of the present study was to investigate the effects and mechanisms of natural killer T (NKT) cells in a murine model of EE-induced cholestatic hepatotoxicity.

Research methods

Male C57BL/6J mice or invariant NKT (iNKT) cell deficiency (Jα18$^{-/-}$ mice) were administered with EE (10 mg/kg, subcutaneous) for 14 d.

Research results

Both Th1 and Th2 cytokines produced by NKT cells increased in the liver skewing toward a Th1 bias. The expression of the chemokine/chemokine receptor Cxcr6/Cxcl16, toll-like receptors, Ras/Rad, and PI3K/Bad signaling was upregulated after EE administration. EE also influenced bile acid synthase Cyp7a1, Cyp8b1, and tight junctions ZO-1 and Occludin, which might be associated with EE-induced cholestasis. iNKT cell deficiency (Jα18$^{-/-}$ mice) robustly alleviated cholestatic liver damage and lowered the expression of the abovementioned signaling pathways.

Research conclusions

The present study demonstrated that hepatic NKT cells play a pathogenic role in EE-induced intrahepatic cholestasis, contributing to the development of the IHC mechanisms and the potential treatment targeting NKT cells.

Research perspectives

Hepatic NKT cells and their Th1 cytokine production play a pathogenic role in a 14-d murine model of EE-induced intrahepatic cholestasis.

ACKNOWLEDGEMENTS

The authors would like to acknowledge Li Bai (University of Science and Technology of China) for kindly providing iNKT cell-deficient (Jα18$^{-/-}$ mice).

FOOTNOTES

Author contributions: Zou MZ and Kong WC contributed equally to the work; Zou MZ, Kong WC, Yu ZX, and Chen X performed the experiments, collected data, and analyzed the data; Xing MT, Zhang LY, and Wang XZ contributed to the guidance of experiments and the final manuscript; Wang XZ and Xing MT designed the study; Wang XZ, Xing MT, Zou MZ and Cai H wrote the manuscript; All the authors have reviewed and approved the final version of the manuscript.

Supported by the National Natural Science Foundation of China, No. 82073948 and 81703626; and National Innovation and Entrepreneurship Training Program for Undergraduate, No. 202210316040Z.

Institutional animal care and use committee statement: All animal experiments involved in this study were performed under the Ethical Committee of China Pharmaceutical University and the Laboratory Animal Management Committee of Jiangsu Province guidelines (Approval No.: 2021-10-003).

Conflict-of-interest statement: All authors have nothing to disclose.

Data sharing statement: No additional data are available.

ARRIVE guidelines statement: The authors have read the ARRIVE guidelines, and the manuscript was prepared and revised according to the ARRIVE guidelines.

Open-Access: This article is an open-access article that was selected by an in-house editor and fully peer-reviewed by external reviewers. It is distributed in accordance with the Creative Commons Attribution NonCommercial (CC BY-NC 4.0) license, which permits others to distribute, remix, adapt, build upon this work non-commercially, and license their derivative works on different terms, provided the original work is properly cited and the use is non-commercial. See: https://creativecommons.org/Licenses/by-nc/4.0/

Country/Territory of origin: China

ORCID number: Meng-Zhi Zou 0000-0001-5303-7550; Wei-Chao Kong 0000-0001-9083-2609; Heng Cai 0000-0001-6544-2414; Meng-Tao Xing 0000-0003-3816-4214; Zi-Xun Yu 0000-0002-7272-7394; Xin Chen 0000-0002-5330-6543; Lu-Yong Zhang 0000-0003-1164-7371; Xin-Zhi Wang 0000-0001-9624-0102.

S-Editor: Zhang H
L-Editor: A
P-Editor: Guo X

REFERENCES

1 **Xiang D**, Xu Y, He W, Yang J, Zhang C, Liu D. Bioinformatics-based identification of key pathways and candidate genes for estrogeninduced intrahepatic cholestasis using DNA microarray analysis. *Mol Med Rep* 2019; **20**: 303-311 [PMID: 31115536 DOI: 10.3892/mmr.2019.10256]
2 LiverTox: Clinical and Research Information on Drug-Induced Liver Injury [Internet]. Bethesda (MD): National Institute of Diabetes and Digestive and Kidney Diseases; 2012–. Estrogens and Oral Contraceptives. [PMID: 31643857]
3 **McIlvride S**, Dixon PH, Williamson C. Bile acids and gestation. *Mol Aspects Med* 2017; **56**: 90-100 [PMID: 28506676 DOI: 10.1016/j.mam.2017.05.003]
4 **Reyes H**, Ribalta J, González MC, Segovia N, Oberhauser E. Sulfobromophthalein clearance tests before and after ethinyl estradiol administration, in women and men with familial history of intrahepatic cholestasis of pregnancy. *Gastroenterology* 1981; **81**: 226-231 [PMID: 7195358]
5 **Li X**, Liu R, Luo L, Yu L, Chen X, Sun L, Wang T, Hylemon PB, Zhou H, Jiang Z, Zhang L. Role of AMP-activated protein kinase α1 in 17α-ethinylestradiol-induced cholestasis in rats. *Arch Toxicol* 2017; **91**: 481-494 [PMID: 27090119 DOI: 10.1007/s00204-016-1697-8]
6 **Yamamoto Y**, Moore R, Hess HA, Guo GL, Gonzalez FJ, Korach KS, Maronpot RR, Negishi M. Estrogen receptor alpha mediates 17alpha-ethynylestradiol causing hepatotoxicity. *J Biol Chem* 2006; **281**: 16625-16631 [PMID: 16606610 DOI: 10.1074/jbc.M602723200]
7 **Wang J**, Fu T, Dong R, Wang C, Liu K, Sun H, Huo X, Ma X, Yang X, Meng Q. Hepatoprotection of auraptene from the peels of citrus fruits against 17α-ethinylestradiol-induced cholestasis in mice by activating farnesoid X receptor. *Food Funct* 2019; **10**: 3839-3850 [PMID: 31210195 DOI: 10.1039/c9fo00318e]
8 **Yu L**, Liu X, Li X, Yuan Z, Yang H, Zhang L, Jiang Z. Protective effects of SRT1720 *via* the HNF1α/FXR signalling pathway and anti-inflammatory mechanisms in mice with estrogen-induced cholestatic liver injury. *Toxicol Lett* 2016; **264**: 1-11 [PMID: 27818225 DOI: 10.1016/j.toxlet.2016.10.016]
9 **Milona A**, Owen BM, Cobbold JF, Willemsen EC, Cox IJ, Boudjelal M, Cairns W, Schoonjans K, Taylor-Robinson SD, Klomp LW, Parker MG, White R, van Mil SW, Williamson C. Raised hepatic bile acid concentrations during pregnancy in mice are associated with reduced farnesoid X receptor function. *Hepatology* 2010; **52**: 1341-1349 [PMID: 20842631 DOI: 10.1002/hep.23849]
10 **Jansen PL**, Ghallab A, Vartak N, Reif R, Schaap FG, Hampe J, Hengstler JG. The ascending pathophysiology of cholestatic liver disease. *Hepatology* 2017; **65**: 722-738 [PMID: 27981592 DOI: 10.1002/hep.28965]
11 **Peng B**, Liu S. [Study of relationship between T helper cell type-1 and type-2 cytokines and intrahepatic cholestasis of pregnancy]. *Zhonghua Fu Chan Ke Za Zhi* 2002; **37**: 516-518 [PMID: 12411008]
12 **Jin F**, Cheng D, Tao JY, Zhang SL, Pang R, Guo YJ, Ye P, Dong JH, Zhao L. Anti-inflammatory and anti-oxidative effects of corilagin in a rat model of acute cholestasis. *BMC Gastroenterol* 2013; **13**: 79 [PMID: 23641818 DOI: 10.1186/1471-230X-13-79]
13 **Zou M**, Wang A, Wei J, Cai H, Yu Z, Zhang L, Wang X. An insight into the mechanism and molecular basis of dysfunctional immune response involved in cholestasis. *Int Immunopharmacol* 2021; **92**: 107328 [PMID: 33412394 DOI: 10.1016/j.intimp.2020.107328]

14 **Nong C**, Zou M, Xue R, Bai L, Liu L, Jiang Z, Sun L, Huang X, Zhang L, Wang X. The role of invariant natural killer T cells in experimental xenobiotic-induced cholestatic hepatotoxicity. *Biomed Pharmacother* 2020; **122**: 109579 [PMID: 31794947 DOI: 10.1016/j.biopha.2019.109579]

15 **Zou M**, Nong C, Yu Z, Cai H, Jiang Z, Xue R, Huang X, Sun L, Zhang L, Wang X. The role of invariant natural killer T cells and associated immunoregulatory factors in triptolide-induced cholestatic liver injury. *Food Chem Toxicol* 2020; **146**: 111777 [PMID: 32987112 DOI: 10.1016/j.fct.2020.111777]

16 **Duwaerts CC**, Sun EP, Cheng CW, van Rooijen N, Gregory SH. Cross-activating invariant NKT cells and kupffer cells suppress cholestatic liver injury in a mouse model of biliary obstruction. *PLoS One* 2013; **8**: e79702 [PMID: 24260285 DOI: 10.1371/journal.pone.0079702]

17 **Mencarelli A**, Renga B, Migliorati M, Cipriani S, Distrutti E, Santucci L, Fiorucci S. The bile acid sensor farnesoid X receptor is a modulator of liver immunity in a rodent model of acute hepatitis. *J Immunol* 2009; **183**: 6657-6666 [PMID: 19880446 DOI: 10.4049/jimmunol.0901347]

18 **Valestrand L**, Berntsen NL, Zheng F, Schrumpf E, Hansen SH, Karlsen TH, Blumberg RS, Hov JR, Jiang X, Melum E. Lipid antigens in bile from patients with chronic liver diseases activate natural killer T cells. *Clin Exp Immunol* 2021; **203**: 304-314 [PMID: 33089489 DOI: 10.1111/cei.13541]

19 **Sun K**, Ma S, Tian S, Zhang M, Liu Y, Li B, Zhou X, Zheng X, Wang L, Han Y. An enhanced level of LAMP-2A participates in $CD4^+$T cell hyperactivity in patients with primary biliary cholangitis. *Ann Transl Med* 2021; **9**: 101 [PMID: 33569403 DOI: 10.21037/atm-20-2427]

20 **Hydes TJ**, Blunt MD, Naftel J, Vallejo AF, Seumois G, Wang A, Vijayanand P, Polak ME, Khakoo SI. Constitutive Activation of Natural Killer Cells in Primary Biliary Cholangitis. *Front Immunol* 2019; **10**: 2633 [PMID: 31803181 DOI: 10.3389/fimmu.2019.02633]

21 **Zhang YY**, Zhang CX, Li Y, Jiang X, Wang YF, Sun Y, Wang J, Ji WY, Liu Y. Development of a novel rat model of heterogeneous hepatic injury by injection with colchicine *via* the splenic vein. *World J Gastroenterol* 2018; **24**: 5005-5012 [PMID: 30510375 DOI: 10.3748/wjg.v24.i44.5005]

22 **Wehr A**, Baeck C, Heymann F, Niemietz PM, Hammerich L, Martin C, Zimmermann HW, Pack O, Gassler N, Hittatiya K, Ludwig A, Luedde T, Trautwein C, Tacke F. Chemokine receptor CXCR6-dependent hepatic NK T Cell accumulation promotes inflammation and liver fibrosis. *J Immunol* 2013; **190**: 5226-5236 [PMID: 23596313 DOI: 10.4049/jimmunol.1202909]

23 **Liu W**, Jing ZT, Xue CR, Wu SX, Chen WN, Lin XJ, Lin X. PI3K/AKT inhibitors aggravate death receptor-mediated hepatocyte apoptosis and liver injury. *Toxicol Appl Pharmacol* 2019; **381**: 114729 [PMID: 31445927 DOI: 10.1016/j.taap.2019.114729]

24 **Kulkarni RR**, Villanueva AI, Read LR, Brisbin JT, Bhaumik SK, LaMarre J, Murali-Krishna K, Sharif S. CpG oligonucleotide-mediated co-stimulation of mouse invariant natural killer T cells negatively regulates their activation status. *Cell Tissue Res* 2017; **369**: 541-554 [PMID: 28550425 DOI: 10.1007/s00441-017-2631-y]

25 **Kulkarni R**, Behboudi S, Sharif S. Insights into the role of Toll-like receptors in modulation of T cell responses. *Cell Tissue Res* 2011; **343**: 141-152 [PMID: 20680345 DOI: 10.1007/s00441-010-1017-1]

26 **Dong C**, Davis RJ, Flavell RA. MAP kinases in the immune response. *Annu Rev Immunol* 2002; **20**: 55-72 [PMID: 11861597 DOI: 10.1146/annurev.immunol.20.091301.131133]

27 **Stuart JK**, Bisch SP, Leon-Ponte M, Hayatsu J, Mazzuca DM, Maleki Vareki S, Haeryfar SM. Negative modulation of invariant natural killer T cell responses to glycolipid antigens by p38 MAP kinase. *Int Immunopharmacol* 2010; **10**: 1068-1076 [PMID: 20584631 DOI: 10.1016/j.intimp.2010.06.007]

28 **Yang T**, Wang X, Zhou Y, Yu Q, Heng C, Yang H, Yuan Z, Miao Y, Chai Y, Wu Z, Sun L, Huang X, Liu B, Jiang Z, Zhang L. SEW2871 attenuates ANIT-induced hepatotoxicity by protecting liver barrier function *via* sphingosine 1-phosphate receptor-1-mediated AMPK signaling pathway. *Cell Biol Toxicol* 2021; **37**: 595-609 [PMID: 33400020 DOI: 10.1007/s10565-020-09567-9]

29 **Caielli S**, Conforti-Andreoni C, Di Pietro C, Usuelli V, Badami E, Malosio ML, Falcone M. On/off TLR signaling decides proinflammatory or tolerogenic dendritic cell maturation upon CD1d-mediated interaction with invariant NKT cells. *J Immunol* 2010; **185**: 7317-7329 [PMID: 21078913 DOI: 10.4049/jimmunol.1000400]

30 **Zeissig S**, Blumberg RS. Analyzing Antigen Recognition by Natural Killer T Cells. *Methods Mol Biol* 2019; **1988**: 439-453 [PMID: 31147957 DOI: 10.1007/978-1-4939-9450-2_30]

31 **Terabe M**, Berzofsky JA. The immunoregulatory role of type I and type II NKT cells in cancer and other diseases. *Cancer Immunol Immunother* 2014; **63**: 199-213 [PMID: 24384834 DOI: 10.1007/s00262-013-1509-4]

32 **Chuang YH**, Lian ZX, Yang GX, Shu SA, Moritoki Y, Ridgway WM, Ansari AA, Kronenberg M, Flavell RA, Gao B, Gershwin ME. Natural killer T cells exacerbate liver injury in a transforming growth factor beta receptor II dominant-negative mouse model of primary biliary cirrhosis. *Hepatology* 2008; **47**: 571-580 [PMID: 18098320 DOI: 10.1002/hep.22052]

33 **Geissmann F**, Cameron TO, Sidobre S, Manlongat N, Kronenberg M, Briskin MJ, Dustin ML, Littman DR. Intravascular immune surveillance by CXCR6+ NKT cells patrolling liver sinusoids. *PLoS Biol* 2005; **3**: e113 [PMID: 15799695 DOI: 10.1371/journal.pbio.0030113]

34 **Heydtmann M**, Lalor PF, Eksteen JA, Hübscher SG, Briskin M, Adams DH. CXC chemokine ligand 16 promotes integrin-mediated adhesion of liver-infiltrating lymphocytes to cholangiocytes and hepatocytes within the inflamed human liver. *J Immunol* 2005; **174**: 1055-1062 [PMID: 15634930 DOI: 10.4049/jimmunol.174.2.1055]

35 **Ma C**, Han M, Heinrich B, Fu Q, Zhang Q, Sandhu M, Agdashian D, Terabe M, Berzofsky JA, Fako V, Ritz T, Longerich T, Theriot CM, McCulloch JA, Roy S, Yuan W, Thovarai V, Sen SK, Ruchirawat M, Korangy F, Wang XW, Trinchieri G, Greten TF. Gut microbiome-mediated bile acid metabolism regulates liver cancer *via* NKT cells. *Science* 2018; **360** [PMID: 29798856 DOI: 10.1126/science.aan5931]

36 **Abel S**, Hundhausen C, Mentlein R, Schulte A, Berkhout TA, Broadway N, Hartmann D, Sedlacek R, Dietrich S, Muetze B, Schuster B, Kallen KJ, Saftig P, Rose-John S, Ludwig A. The transmembrane CXC-chemokine ligand 16 is induced by IFN-gamma and TNF-alpha and shed by the activity of the disintegrin-like metalloproteinase ADAM10. *J Immunol* 2004;

172: 6362-6372 [PMID: 15128827 DOI: 10.4049/jimmunol.172.10.6362]
37 **Anderson CK**, Reilly SP, Brossay L. The Invariant NKT Cell Response Has Differential Signaling Requirements during Antigen-Dependent and Antigen-Independent Activation. *J Immunol* 2021; **206**: 132-140 [PMID: 33229442 DOI: 10.4049/jimmunol.2000870]
38 **Kiziltas S**. Toll-like receptors in pathophysiology of liver diseases. *World J Hepatol* 2016; **8**: 1354-1369 [PMID: 27917262 DOI: 10.4254/wjh.v8.i32.1354]
39 **Chu AJ**. Antagonism by bioactive polyphenols against inflammation: a systematic view. *Inflamm Allergy Drug Targets* 2014; **13**: 34-64 [PMID: 24251781 DOI: 10.2174/1871528112666131119211002]
40 **Askenase PW**, Itakura A, Leite-de-Moraes MC, Lisbonne M, Roongapinun S, Goldstein DR, Szczepanik M. TLR-dependent IL-4 production by invariant Valpha14+Jalpha18+ NKT cells to initiate contact sensitivity in vivo. *J Immunol* 2005; **175**: 6390-6401 [PMID: 16272291 DOI: 10.4049/jimmunol.175.10.6390]
41 **Ishida K**, Kaji K, Sato S, Ogawa H, Takagi H, Takaya H, Kawaratani H, Moriya K, Namisaki T, Akahane T, Yoshiji H. Sulforaphane ameliorates ethanol plus carbon tetrachloride-induced liver fibrosis in mice through the Nrf2-mediated antioxidant response and acetaldehyde metabolization with inhibition of the LPS/TLR4 signaling pathway. *J Nutr Biochem* 2021; **89**: 108573 [PMID: 33388347 DOI: 10.1016/j.jnutbio.2020.108573]
42 **Uchida Y**, Ke B, Freitas MC, Yagita H, Akiba H, Busuttil RW, Najafian N, Kupiec-Weglinski JW. T-cell immunoglobulin mucin-3 determines severity of liver ischemia/reperfusion injury in mice in a TLR4-dependent manner. *Gastroenterology* 2010; **139**: 2195-2206 [PMID: 20637206 DOI: 10.1053/j.gastro.2010.07.003]
43 **Alhasson F**, Dattaroy D, Das S, Chandrashekaran V, Seth RK, Schnellmann RG, Chatterjee S. NKT cell modulates NAFLD potentiation of metabolic oxidative stress-induced mesangial cell activation and proximal tubular toxicity. *Am J Physiol Renal Physiol* 2016; **310**: F85-F101 [PMID: 26447219 DOI: 10.1152/ajprenal.00243.2015]
44 **Jiang W**, Sun R, Zhou R, Wei H, Tian Z. TLR-9 activation aggravates concanavalin A-induced hepatitis *via* promoting accumulation and activation of liver CD4+ NKT cells. *J Immunol* 2009; **182**: 3768-3774 [PMID: 19265155 DOI: 10.4049/jimmunol.0800973]
45 **Choi SH**, Harkewicz R, Lee JH, Boullier A, Almazan F, Li AC, Witztum JL, Bae YS, Miller YI. Lipoprotein accumulation in macrophages *via* toll-like receptor-4-dependent fluid phase uptake. *Circ Res* 2009; **104**: 1355-1363 [PMID: 19461045 DOI: 10.1161/CIRCRESAHA.108.192880]
46 **Xiang D**, Yang J, Xu Y, Lan L, Li G, Zhang C, Liu D. Estrogen cholestasis induces gut and liver injury in rats involving in activating PI3K/Akt and MAPK signaling pathways. *Life Sci* 2021; **276**: 119367 [PMID: 33775691 DOI: 10.1016/j.lfs.2021.119367]
47 **Gissen P**, Arias IM. Structural and functional hepatocyte polarity and liver disease. *J Hepatol* 2015; **63**: 1023-1037 [PMID: 26116792 DOI: 10.1016/j.jhep.2015.06.015]
48 **Assimakopoulos SF**, Tsamandas AC, Louvros E, Vagianos CE, Nikolopoulou VN, Thomopoulos KC, Charonis A, Scopa CD. Intestinal epithelial cell proliferation, apoptosis and expression of tight junction proteins in patients with obstructive jaundice. *Eur J Clin Invest* 2011; **41**: 117-125 [PMID: 20840373 DOI: 10.1111/j.1365-2362.2010.02379.x]
49 **Horikoshi Y**, Kitatani K, Toriumi K, Fukunishi N, Itoh Y, Nakamura N, Ohno S, Matsura T, Takekoshi S. Aberrant activation of atypical protein kinase C in carbon tetrachloride-induced oxidative stress provokes a disturbance of cell polarity and sealing of bile canalicular lumen. *Am J Pathol* 2015; **185**: 958-968 [PMID: 25688837 DOI: 10.1016/j.ajpath.2014.12.015]
50 **Fallon MB**, Mennone A, Anderson JM. Altered expression and localization of the tight junction protein ZO-1 after common bile duct ligation. *Am J Physiol* 1993; **264**: C1439-C1447 [PMID: 8333499 DOI: 10.1152/ajpcell.1993.264.6.C1439]
51 **Landmann L**. Cholestasis-induced alterations of the trans- and paracellular pathways in rat hepatocytes. *Histochem Cell Biol* 1995; **103**: 3-9 [PMID: 7736278 DOI: 10.1007/BF01464469]
52 **Han X**, Fink MP, Uchiyama T, Yang R, Delude RL. Increased iNOS activity is essential for hepatic epithelial tight junction dysfunction in endotoxemic mice. *Am J Physiol Gastrointest Liver Physiol* 2004; **286**: G126-G136 [PMID: 12946943 DOI: 10.1152/ajpgi.00231.2003]
53 **Takahashi T**, Chiba S, Nieda M, Azuma T, Ishihara S, Shibata Y, Juji T, Hirai H. Cutting edge: analysis of human V alpha 24+CD8+ NK T cells activated by alpha-galactosylceramide-pulsed monocyte-derived dendritic cells. *J Immunol* 2002; **168**: 3140-3144 [PMID: 11907064 DOI: 10.4049/jimmunol.168.7.3140]

World Journal of Gastroenterology

Submit a Manuscript: https://www.f6publishing.com

World J Gastroenterol 2022 July 14; 28(26): 3164-3176

DOI: 10.3748/wjg.v28.i26.3164

ISSN 1007-9327 (print) ISSN 2219-2840 (online)

ORIGINAL ARTICLE

Basic Study

Bifidobacterium infantis regulates the programmed cell death 1 pathway and immune response in mice with inflammatory bowel disease

Lin-Yan Zhou, Ying Xie, Yan Li

Specialty type: Gastroenterology and hepatology

Provenance and peer review: Unsolicited article; Externally peer reviewed.

Peer-review model: Single blind

Peer-review report's scientific quality classification

Grade A (Excellent): A
Grade B (Very good): B, B
Grade C (Good): 0
Grade D (Fair): 0
Grade E (Poor): 0

P-Reviewer: Bozkurt HS, Turkey; Rodrigues AT, Brazil; Serban ED, Romania

Received: December 6, 2021
Peer-review started: December 6, 2021
First decision: January 8, 2022
Revised: January 12, 2022
Accepted: June 16, 2022
Article in press: June 16, 2022
Published online: July 14, 2022

Lin-Yan Zhou, Ying Xie, Yan Li, Department of Gastroenterology, Shengjing Hospital of China Medical University, Shenyang 110004, Liaoning Province, China

Corresponding author: Yan Li, PhD, Chief Doctor, Professor, Department of Gastroenterology, Shengjing Hospital of China Medical University, No. 36 Sanhao Road, Heping District, Shenyang 110004, Liaoning Province, China. liy@sj-hospital.org

Abstract

BACKGROUND

Inflammatory bowel disease (IBD) is caused by an abnormal immune response. Programmed cell death 1 (PD-1) is an immunostimulatory molecule, which interacts with PD ligand (PD-L1) playing a prime important role among autoimmune diseases. *Bifidobacterium infantis* (*B. infantis*) can promote the differentiation of CD (cluster of differentiation) 4^+ T cells into regulatory T cells (Tregs). Tregs participate in the development of IBD and may be related to disease activity. *B. infantis* amplify the expression level of PD-1, PD-L1 and Tregs' nuclear transcription factor forkhead box protein 3 (Foxp3). But the mechanism of *B. infantis* on PD-1/PD-L1 signaling remains unclear.

AIM

To explore the mechanism of *B. infantis* regulating the immune response in IBD.

METHODS

Forty-eight-week-old BALB/c mice were randomly divided into five groups: The control group, dextran sulphate sodium (DSS) model group, DSS + *B. infantis* group, DSS + *B. infantis* + anti-PD-L1 group, and DSS + anti-PD-L1 group. The control group mice were given drinking water freely, the other four groups were given drinking water containing 5% DSS freely. The control group, DSS model group, and DSS + anti-PD-L1 group were given normal saline (NS) 400 μL daily by gastric lavage, and the DSS + *B. infantis* group and DSS + *B. infantis* + anti-PD-L1 group were given NS and 1×10^9 colony-forming unit of *B. infantis* daily by gastric lavage. The DSS + *B. infantis* + anti-PD-L1 group and DSS + anti-PD-L1 group were given 200 μg of PD-L1 blocker intraperitoneally at days 0, 3, 5, and 7; the control group, DSS + anti-PD-L1 group, and DSS + *B. infantis* group were given an intraperitoneal injection of an equal volume of phosphate buffered saline

(PBS). Changes in PD-L1, PD-1, Foxp3, interleukin (IL)-10, and transforming growth factor β (TGF-β) 1 protein and gene expression were observed. Flow cytometry was used to observe changes in $CD4^+$, $CD25^+$, $Foxp3^+$ cell numbers in the blood and spleen.

RESULTS

Compared to the control group, the expression of PD-1, Foxp3, IL-10, and TGF-β1 was significantly decreased in the intestinal tract of the DSS mice ($P < 0.05$). Compared to the control group, the proportion of $CD4^+$, $CD25^+$, $Foxp3^+$ cells in spleen and blood of DSS group was visibly katabatic ($P < 0.05$). *B. infantis* upgraded the express of PD-L1, PD-1, Foxp3, IL-10, and TGF-β1 ($P < 0.05$) and increased the proportion of $CD4^+$, $CD25^+$, $Foxp3^+$ cells both in spleen and blood ($P < 0.05$). After blocking PD-L1, the increase in Foxp3, IL-10, and TGF-β1 protein and gene by *B. infantis* was inhibited ($P < 0.05$), and the proliferation of $CD4^+$, $CD25^+$, $Foxp3^+$ cells in the spleen and blood was also inhibited ($P < 0.05$). After blocking PD-L1, the messenger ribonucleic acid and protein expression of PD-1 were invariant.

CONCLUSION

It is potential that *B. infantis* boost the proliferation of $CD4^+$, $CD25^+$, $Foxp3^+$ T cells in both spleen and blood, as well as the expression of Foxp3 in the intestinal tract by activating the PD-1/PD-L1 pathway.

Key Words: *Bifidobacterium infantis*; Enteritis; Programmed cell death ligand; T-Lymphocytes

©The Author(s) 2022. Published by Baishideng Publishing Group Inc. All rights reserved.

Core Tip: *Bifidobacterium infantis* (*B. infantis*) can be used as a therapeutic agent to treat inflammatory bowel disease. It regulates the intestinal microbiota, alleviates inflammation, and regulates the immune response. We found that *B. infantis* increases the expression of forkhead box protein 3 (Foxp3) and the proliferation of $Foxp3^+$ T cells, and activates the programmed cell death 1 (PD-1)/ PD ligand 1 pathway.

Citation: Zhou LY, Xie Y, Li Y. *Bifidobacterium infantis* regulates the programmed cell death 1 pathway and immune response in mice with inflammatory bowel disease. *World J Gastroenterol* 2022; 28(26): 3164-3176
URL: https://www.wjgnet.com/1007-9327/full/v28/i26/3164.htm
DOI: https://dx.doi.org/10.3748/wjg.v28.i26.3164

INTRODUCTION

Inflammatory bowel disease (IBD) results from the aberrant immune responses or the disruption of immune tolerance to intestinal antigens. Several factors, including the immune system, infections, and genetic and environmental factors, may remarkably contribute to the development of IBD[1-4]. To maintain immune tolerance to the intestinal environment, the intestinal immune system monitors changes in the bacterial microbiota and the expression of antigens on the surface of the intestinal mucosa[5,6]. Antigen-presenting cells, including dendritic cells and intestinal epithelial cells, present intestinal antigens to $CD4^+$ T cells and induce their differentiation into regulatory T cells (Tregs), which maintain tolerance to the intestinal microbiota. Hyperactive T cell responses to the intestinal microbiota contribute to the inflammatory response observed in IBD[7].

Programmed cell death protein 1 (PD-1) and PD-ligand 1 (PD-L1), belong to the CD28/B7 super-family, which primarily functions in T cell-mediated immune responses and is closely related to several diseases and disease states, including autoimmune diseases, tumors, chronic viral infections, and chronic inflammation[8-10]. The role of the PD-1/PD-L1 signaling pathway in glomerulonephritis, systemic lupus erythematosus, rheumatoid arthritis, dilated cardiomyopathy, autoimmune diabetes, and other autoimmune diseases has been widely studied[11,12]; however, few studies have examined the role of the PD-1/PD-L1 signaling pathway in IBD[13].

Tregs are a subpopulation of T lymphocytes with immunoregulatory functions[14]. They can inhibit the activation and proliferation of autoreactive T cells by secreting cytokines such as interleukin (IL)-10 and transforming growth factor β (TGF-β), downregulating the function of auxiliary T cells, and maintaining intestinal homeostasis and immune tolerance[15,16]. Tregs are divided into two categories: Natural Tregs (nTregs) and induced Tregs (iTregs). The nTregs mature in the thymus and are positive for CD4, CD25, and Foxp3. The iTregs are induced by specific antigen stimulation of $CD4^+$ T cells in the presence of IL-2 and TGF-β1, in the intestine, spleen, and other peripheral sites[17]. Animal studies have shown that injecting T cells with no CD4 and Tregs expressing CD25 into T cell-deficient mice can

induce the development of autoimmune colitis, whereas the injection of T cells expressing CD4 with that of $CD25^+$ Tregs can inhibit colitis development. These results suggest that $CD4^+$ and $CD25^+$ Tregs are vital for the inhibition of the intestinal immune response[18]. Maul *et al*[19] found that the percentage of Tregs in the peripheral blood of patients with IBD decreased in the active phase and increased in the remission phase of the disease; however, the number of Tregs in the intestinal epithelium increased in the active phase of the disease but was still significantly lower than that observed in patients with diverticulitis. This suggests a role of Tregs in IBD development.

The adoptive transfer of immature $CD4^+$ T cells into wild-type $rag^{-/-}$ mice and PD-$L1^{-/-}rag^{-/-}$ mice significantly decreases the number of Tregs in PD-$L1^{-/-}rag^{-/-}$ mice, suggesting a dominant role of PD-L1 in Treg differentiation[20]. PD-L1 can enhance Treg function and promote the production of IL-10 by Tregs[21]. Treg differentiation depends on the PD-L1 signaling pathway. Higher levels of PD-L1 expression in hepatodendritic cells result in greater induction of Tregs which maintain the tolerance toward transplanted organs.

We have previously found that *Bifidobacterium infantis* (*B. infantis*) can alleviate intestinal epithelial injury and maintain intestinal immune tolerance in a mouse model of IBD and may have therapeutic implications for the immunological injuries observed in IBD**.** *Bifidobacterium infantis* notably increased the expression levels of PD-L1 and PD-1 in the intestine and promoted the expression of nuclear transcription factors and of anti-inflammatory factors (IL-10 and TGF-β1) in Tregs[22,23]. Therefore, this study aimed to explore the mechanism of action of *B. infantis* in the PD-1/PD-L1 signaling pathway and the differentiation and function of Tregs.

MATERIALS AND METHODS

Reagents and antibodies

Dextran sulfate sodium (DSS; molecular weight 36000-50000) was purchased from MP Biomedicals (Irvine, CA, United States). *B. infantis* freeze-dried powder, containing 1.6×10^{11} colony-forming units (CFU)/g, was provided by Shandong Kexing Biological Products Co., Ltd. (Batch No. 2017012, Shandong Province, China). Invivomab anti-mouse PD-L1 was purchased from BIOX Cell (Lebanon, NH, United States). BALB/c mice were purchased from Huafukang Biotechnology (Beijing, China). Allophycocyanin (APC) rat anti-mouse Cd4, Bb515 rat anti-mouse, P-phycoerythrin (PE) rat anti-mouse Foxp3, and a transcription factor buffer set were purchased from BD Biosciences (Franklin Lakes, NJ, United States). Antibodies against PD-L1, PD-1, and Foxp3 were purchased from Proteintech Group (Rosemont, IL, United States). Antibodies against IL-10 and TGF-β1 were purchased from Abcam (Cambridge, United Kingdom). Real-time quantitative PCR was performed using the following reagents: TRIzol (Invitrogen, Thermo Fisher, Waltham, MA, United States), Primescript™ RT Regent kit with gDNA eraser, quick response training (qRT) PCR kit SYBR® premier ex taq™ II (Tli RNaseH Plus, Takara, Japan), and the specific primers (Biotechnology Co., Ltd., China).

Animals

Forty-eight-week-old BALB/c mice, male and female, weighing 20 g ± 2 g, were raised under pathogen-free conditions in the standalone animal experimental center affiliated with the Shengjing Hospital of China Medical University. The mice were kept at 20 °C-26 °C and in an atmosphere with a relative humidity of 40%-70%, with a 12 h light/dark cycle. Sterilized water and standard feed were provided for free consumption by the animals. The experimental protocol was approved by the ethics committee of the hospital (No. 2017PS353K). The operators ensured that suitable measures were taken to reduce malaise and injury to the animals during experiments.

Experimental grouping and modeling

Forty mice were randomly divided into five groups: Control, DSS, DSS + *B. infantis*, DSS + *B. infantis* + anti-PD-L1, and DSS + anti-PD-L1. Mice in the control group were given free access drinking water for 7 d. The other four groups were administered sterilized water containing 5% DSS for 7 d. The drinking. Drinking water was changed daily. The control, DSS, and DSS + anti-PD-L1 groups were administered 400 μL normal saline (NS) *via* gavage daily, and the DSS + *B. infantis* and DSS + *B. infantis* + anti-PD-L1 groups were administered 400 μL NS *via* gavage and *B. infantis* (1×10^9 CFU) daily. The DSS + *B. infantis* + anti-PD-L1 and DSS + anti-PD-L1 groups were administered an intraperitoneal injection of PD-L1 blocker (200 μg), and the control, DSS model, and DSS + *B. infantis* groups were intraperitoneally injected with phosphate-buffered phosphate buffered saline (PBS) on days 0, 3, 5, and 7.

Specimen collection

General characteristics of the mice: During the experimental period, temperament, reactivity, activity, hair color, weight, eating, and defecation of each mouse were observed seriatim and recorded in detail daily.

Peripheral blood collection: On day 8, all animals were anesthetized *via* isoflurane inhalation, and the beards were removed. Blood was collected through retro-orbital bleeding and placed in blood collection vessels containing EDTA. The blood and EDTA were mixed and stored on ice.

Extraction of single cells from mouse spleen: After blood collection, the sacrificed mice were dissected along the midline, and the spleen was fully exposed. After blunt dissection, the spleen was removed, placed in PBS, and transported on ice. The spleen was then transferred to a glass dish containing RPMI 1640 medium and mashed with ground glass. The cells were then transferred to a centrifuge tube and centrifuged at 1200 rpm for 5 min, and the supernatant was discarded. Next, 2 mL of RBC lysate was added to each sample. PBS (3 mL) was added to dilute and stop the lysis, and the samples were centrifuged again at 400 × *g* for 5 min at 4 °C. The supernatant was discarded and 3 mL of PBS was added. The cells were filtered and centrifuged for 10 min. The supernatant was discarded, and PBS was added to obtain a single-cell suspension. All the procedures were performed at 4 °C to ensure cell viability.

Acquisition of mouse colon: After splenectomy, the colon was exposed and the colon from the blind part to the anus was removed, washed with pre-cooled NS, and divided into four parts. The samples were then transferred to a -80 °C ultra-low-temperature refrigerator in liquid nitrogen for long-term preservation.

Detection of $CD4^+$, $CD25^+$, $Foxp3^+$ T cells by flow cytometry

Spleen: Splenic $CD4^+$, $CD25^+$, and $Foxp3^+$ T cells were detected using flow cytometry. The prepared single-cell spleen suspension (100 μL) was aliquoted into labeled flow tubes. Anti-$CD4^+$ and anti-$CD25^+$ antibodies were then added to the tubes and the tubes were incubated at 4 °C in the dark for 30 min. Next, 1 mL of 1X fix/perm working solution was added to each sample and the samples were incubated at 4 °C in the dark for 40 min to permeabilize the nucleus. Anti-Foxp3 antibody was then added and the resulting solution was incubated at 4 °C in the dark for 40 min. Excess antibodies were removed, and the samples were run on a flow cytometer (FACSCalibur, BD Bioscience).

Peripheral blood: After RBC lysis, flow cytometry was performed on the peripheral blood samples using the protocol described above.

Western blotting

Total protein was extracted from the colon, and the protein concentration was determined. The samples were subjected to electrophoresis at 60 V. After marker separation, the voltage was adjusted to 80 V. After 30 min, the voltage was adjusted to 100 V. Electrophoresis was terminated when the target protein with the lowest molecular weight reached the end of the gel. A voltage of 100 V was used to transfer proteins to the membrane. Proteins with a molecular weight < 25 kDa were transferred for 25 min, and proteins weighing 26-70 kDa were transferred for 70 min. The membrane was blocked with 2.5% bovine serum albumin (BSA) at room temperature for 1.5 h. Primary antibodies against PD-L1 (1:750), PD-1 (1:500), Foxp3 (1:1000), IL-10 (1:800), TGF-β1 (1:500), and GAPDH (1:10000) were added and the membrane was incubated at 4 °C overnight. Then, goat anti-rabbit IgG secondary antibody labeled with horseradish peroxidase was added to the membrane, followed by incubation at room temperature for 1.5 h. In a dark room, a chemiluminescence imaging analysis system was used to visualize the membranes. GelPro software was used to analyze the images and to perform quantitative analysis using the following formula: Protein content = grey value of the target protein of the sample/grey value of the same sample.

Real time qPCR

The experiment consists of 5 steps: (1) Ribonucleic acid (RNA) purification: DSS can reduce the purity of RNA, so extra purification of the colon RNA was necessary. RNA purification was performed as follows: 30 μL lithium chloride (8 mol/L) + 270 μL ddH_2O was added to 10 μL RNA and placed on ice for 2 h. The samples were then centrifuged at 14000 × g for 30 min. The supernatant was then discarded, and the RNA was dissolved in 90 μL ddH_2O. Next, 10 μL sodium acetate (3 mol/L) + 200 μL anhydrous ethanol was added to the RNA and incubated at -20 °C for 30 min to precipitate the RNA. The samples were then centrifuged at 14000 × g for 30 min at 4 °C. The supernatant was then discarded, 500 μL 75% ethanol was added, and the samples were gently blown with a pipette to clean the RNA. Next, the samples were centrifuged at 800 × g for 10 min at 4 °C. The supernatant was discarded, and the RNA was dissolved with 10 μL ddH_2O. Finally, the samples were transferred to -80 °C on ice for preservation; (2) detection of RNA concentration: The ratio of A260/A280 was eligible for all of the samples, which indicates that the purity of the RNA was high and suitable for further experiments; (3) preparation of cDNA by RNA reverse transcription: The gDNA was removed, and the specimens were heated to 42 °C for 2 min. For reverse transcription, the reaction solution was prepared according to Table 1. The samples were heated at 37 °C for 15 min and 85 °C for 5 s. The reaction was then stopped and cooled down to 4 °C; (4) concentration and purity of cDNA: After zero adjustment, 1 μL of the cDNA sample to

Table 1 Preparation of reverse transcription system

Reagent	Dose (μL)
5 × prime script buffer	4
Prime sript RT enzyme mix	1
RT primer xix	1
ddH_2O	4

RT: Real time; dd: Double distilled.

be tested was dropped onto the detection probe to determine the concentration and purity. The probe was washed with ddH2O between the evaluation of the two samples; and (5) qRT-PCR: qRT-PCR was carried out as follows: PCR amplification reaction, denaturation at 95 °C for 5 min, PCR reaction at 95 °C for 10 s, and 60 °C for 30 s for 45 cycles.

Statistical analysis

Data are presented as mean ± SD. Differences among the groups were analyzed using the analysis of variance. SPSS (version 23.0; IBM, Armonk, NY, United States) and GraphPad 7.0 (Software, CA, United States) statistical software were used to perform statistical analyses. Two-tailed *P* values were calculated, and statistical significance was set as $P < 0.05$.

RESULTS

The effect of B. infantis on the expression of PD-1 after PD-L1 blockade

Western blot results: Compared to the DSS + *B. infantis* group, PD-1 protein in the DSS + *B. infantis* + anti-PD-L1 group decreased, but the difference was not statistically significant ($P = 0.07$). Compared to DSS model group, the expression of PD-1 was no significant distinction in DSS + anti-PD-L1 group ($P = 0.62$) (Figure 1A-C).

qRT-PCR results: In contrast to control group, PD-1 messenger ribonucleic acid (mRNA) in DSS group decreased significantly ($P < 0.05$). In constrast to DSS group, the expression of DSS + *B. infantis* group increased, but the difference was not statistically significant ($P = 0.36$). Compared to the *B. infantis* group, PD-1 RNA decreased significantly in the DSS + *B. infantis* + anti-PD-L1 group ($P < 0.05$) (Figure 1A-C).

Effect of B. infantis on Tregs and Foxp3 expression after PD-L1 blockade

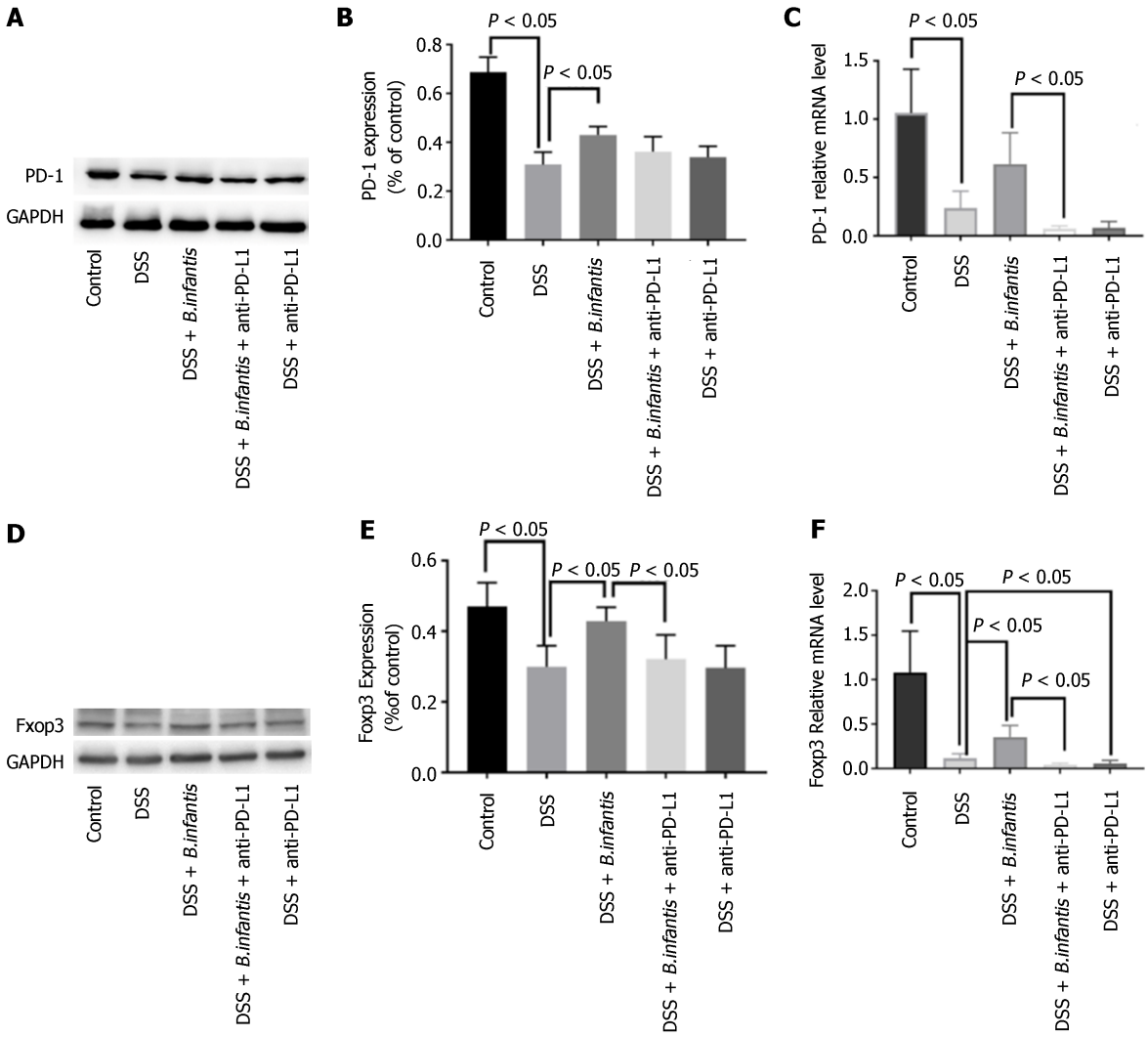
Western blot results: Compared to the DSS + *B. infantis* group, Foxp3 protein decreased in DSS + *B. infantis* + anti-PD-L1 group, and the difference was statistically significant ($P < 0.05$). There was no significant difference in Foxp3 protein expression between the DSS model group and DSS + anti-PD-L1 group ($P = 0.99$) (Figure 1D-F).

RT-qPCR results: In contrast to control group, Foxp3 mRNA in DSS model group decreased significantly ($P < 0.05$); Foxp3 mRNA in DSS + *B. infantis* group was significantly higher than that in DSS model group ($P < 0.05$). Compared to the *B. infantis* group, the expression of Foxp3 mRNA decreased significantly in the DSS + *B. infantis* + anti-PD-L1 group ($P < 0.05$). In comparison with DSS model group, Foxp3 mRNA in DSS + anti-PD-L1 group was also visible distinction ($P < 0.05$) (Figure 1D -F).

Flow cytometry results

Flow cytometry of peripheral blood: Compared to control group, the proportion of peripheral $CD4^+$, $CD25^+$, $Foxp3^+$ cells decreased visibly ($P < 0.05$) of DSS group and increased visibly in the blood of the DSS + *B. infantis* group ($P < 0.05$). Compared to the DSS + *B. infantis* group, the proportion of $CD4^+$, $CD25^+$, $Foxp3^+$ cells in the peripheral blood of DSS + *B. infantis* + anti-PD-L1 group was significantly lower ($P < 0.05$). The proportion of $CD4^+$, $CD25^+$, $Foxp3^+$ cells in the blood of the DSS + anti-PD-L1 group was also distinctly lower compared to the DSS group ($P < 0.05$) (Figure 2).

Flow cytometry of splenocytes: The ratio of splenic $CD4^+$, $CD25^+$, $Foxp3^+$ cells in DSS model group was significantly lower ($P < 0.05$), comparing to control group. The ratio of $CD4^+$, $CD25^+$, $Foxp3^+$ cells in the DSS + *B. infantis* group was significantly higher than that in the DSS model group ($P < 0.05$). Compared to the DSS + *B. infantis* group, the proportion of $CD4^+$, $CD25^+$, $Foxp3^+$ cells in the DSS + *B. infantis* + anti-



DOI: 10.3748/wjg.v28.i26.3164 **Copyright** ©The Author(s) 2022.

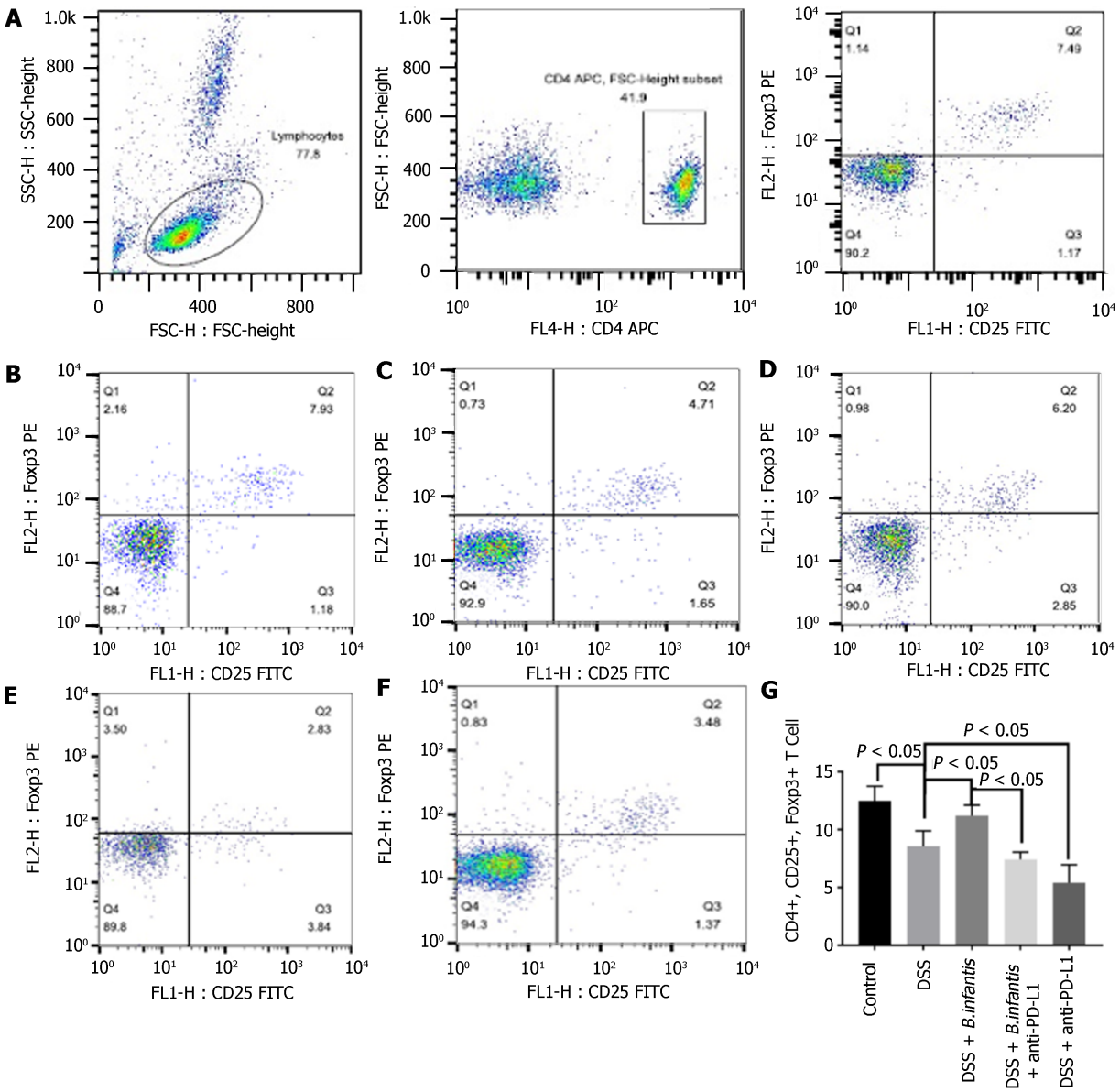
Figure 1 The effects of blocking programmed cell death ligand. A: Expression of programmed cell death 1 (PD-1) protein; B: Statistical chart showing the differences in PD-1 protein expression; C: Statistical map showing the differences in PD-1 mRNA expression; D: Western blot showing forkhead box protein 3 protein (Foxp3) expression; E: Statistical chart showing the differences in Foxp3 expression; F: Statistical map showing the differences in Foxp3 mRNA levels. Data are presented as mean ± SD, and comparisons between groups were analyzed by one-way analysis of variance. Statistical significance was set as $P < 0.05$. PD-1: Programmed cell death 1; PD-L1: Programmed cell death ligand; GAPDH: Glyceraldehyde-3-phosphate dehydrogenase; DSS: Dextran sulfate sodium; *B. infantis*: *Bifidobacterium infantis*; Foxp3: Forkhead box protein 3.

PD-L1 group decreased significantly ($P < 0.05$). The proportion of $CD4^+$, $CD25^+$, $Foxp3^+$ cells in the DSS + anti-PD-L1 group also decreased significantly compared to the DSS group ($P < 0.05$) (Figure 3).

The effect of B. infantis on the expression of IL-10 and TGF-β1 after PD-L1 blockade

Western blot results: The expression of IL-10 and TGF-β1 protein in the DSS + *B. infantis* group was lower than that in DSS + *B. infantis* + anti-PD-L1 group ($P < 0.05$). Compared to the DSS model group, there was no apparent distinction in the express of IL-10 ($P = 0.99$) or TGF-β1 in the DSS + anti-PD-L1 group ($P < 0.05$) (Figure 4).

Real time PCR results: In comparison with control group, mRNA of IL-10 and TGF-β1 in the DSS model group decreased ($P < 0.05$), and mRNA of IL-10 and TGF-β1 in the DSS + *B. infantis* group increased clearly ($P < 0.05$). IL-10 and TGF-β1 mRNA expression in DSS + *B. infantis* + anti-PD-L1 group decreased clearly ($P < 0.05$) contrsating to DSS + *B. infantis* group. Compared to the DSS model group, IL-10 and TGF-β1 mRNA in DSS + anti-PD-L1 group were also statistically distinction ($P < 0.05$) (Figure 4).



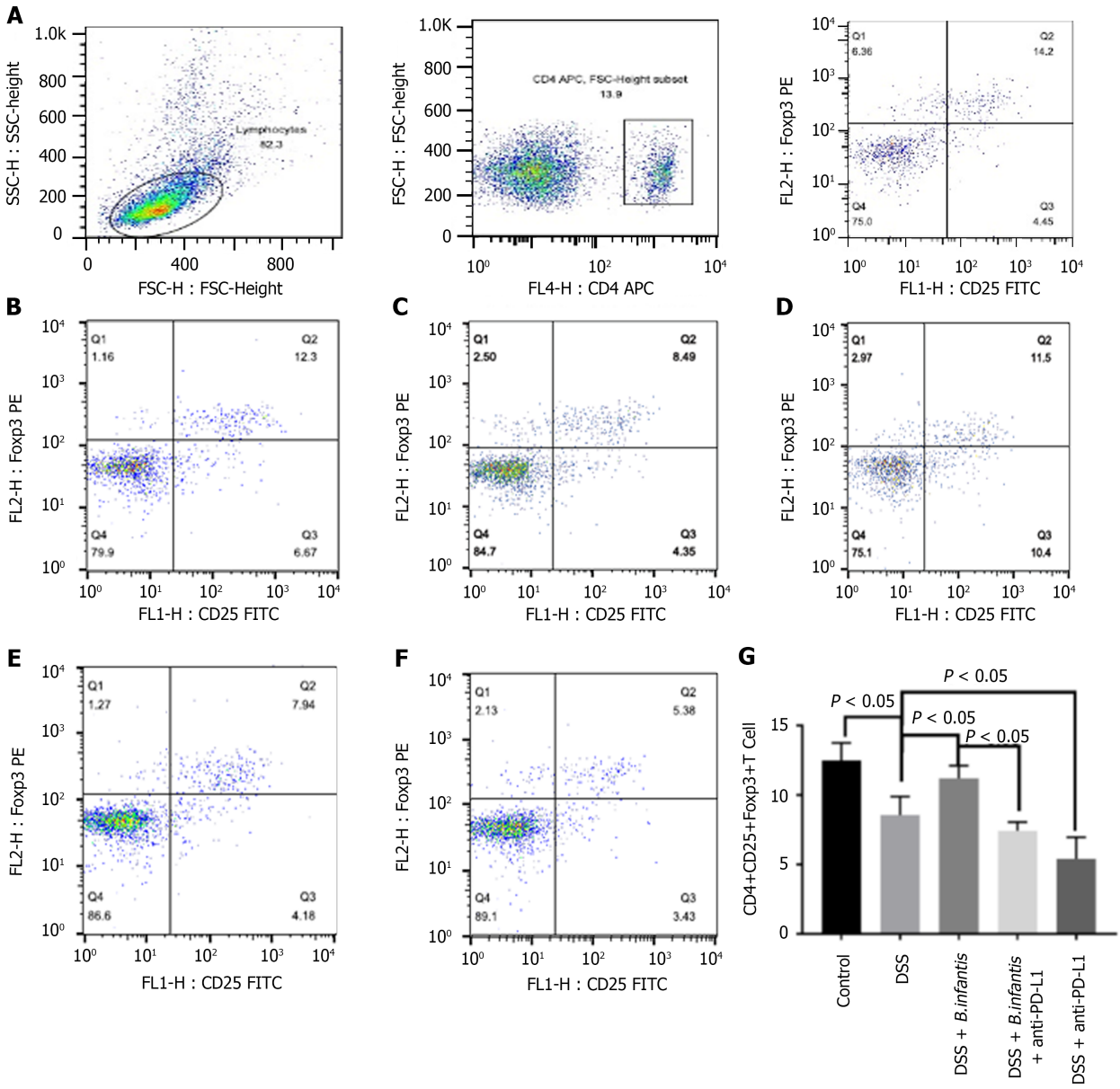
DOI: 10.3748/wjg.v28.i26.3164 **Copyright** ©The Author(s) 2022.

Figure 2 Effects of *Bifidobacterium infantis* and programmed cell death ligand inhibition on the proportion of CD4⁺, CD25⁺, and forkhead box protein 3⁺ cells in the blood. A: The strategy of CD4⁺, CD25⁺, and forkhead box protein (Foxp) 3⁺ cells; B-F: Flow cytometry results for the control group (B), the DSS model group (C), the DSS + *B. infantis* group (D), the DSS + *B. infantis* + anti-PD-L1 group (E), the DSS + anti-PD-L1 group (F); G: Statistical chart of the numbers of CD4⁺, CD25⁺, and Foxp3⁺ cells. Data are presented as mean ± SD, and the comparisons among each group were analyzed by one-way analysis of variance. Statistical significance was set as $P < 0.05$. PD-1: Programmed cell death 1; PD-L1: Programmed cell death ligand; DSS: Dextran sulfate sodium; *B. infantis: Bifidobacterium infantis*; Foxp3⁺: Forkhead box protein 3⁺; CD: Cluster of differentiation; SSC: Side scatter; FSC: Forward scatter; FL: Fluorescence; APC: Allophycocyanin; FITC: Fluorescein isothiocyanate; H: Height.

DISCUSSION

The specific pathogenesis of IBD remains unclear; however, abnormal inflammatory responses and continuous inflammatory damage to the intestine are recognized as the basic mechanisms of IBD pathogenesis[24,25]. Intestinal immunity is a complex and interactive process, involving several immune factors such as intestinal mucosal immunity, T cells, cytokines, and intestinal microecology [26]. The intestinal mucosal immune system is responsible for monitoring the intestinal microbiota and surface antigens[27], presenting antigens to CD4⁺ T cells, promoting the interaction between PD-1 and PD-L1, establishing immune tolerance, and preventing the occurrence of autoimmunity. Several inflammatory mediators including interferon γ, tumor necrosis factor α, IL-10, and other cytokines, are involved in the pathogenesis of DSS colitis, suggesting that inflammatory immune responses play a critical role in the pathogenesis of IBD[28-30].

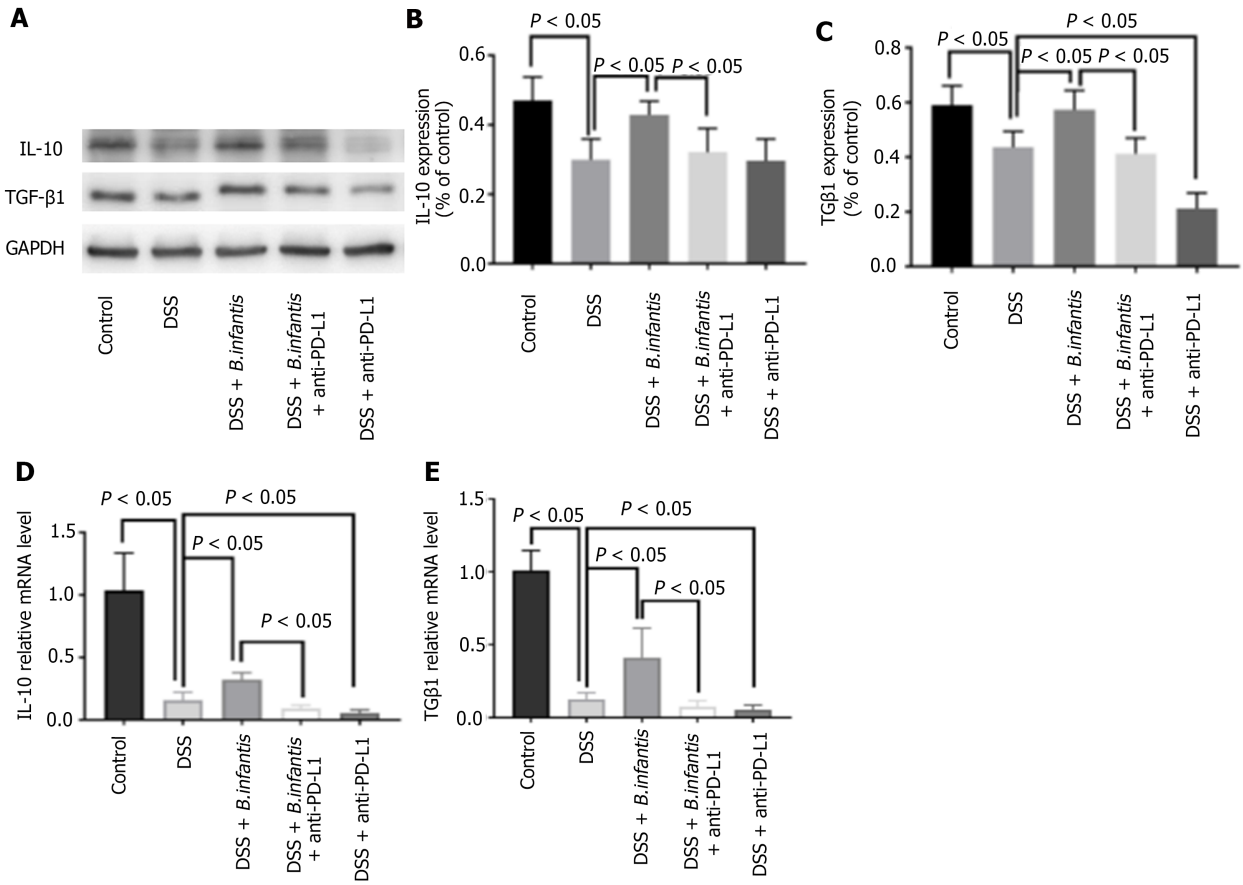
A recently discovered immunostimulatory molecule, PD-1 interacts with its ligand PD-L1 to regulate T cell-mediated immunity and induce immune tolerance, thereby playing a critical role in autoimmune



DOI: 10.3748/wjg.v28.i26.3164 **Copyright** ©The Author(s) 2022.

Figure 3 Effects of *Bifidobacterium infantis* and programmed cell death ligand inhibition on the proportion of splenic CD4⁺, CD25⁺, and forkhead box protein 3⁺ cells. A: The strategy of CD4⁺, CD25⁺, and forkhead box protein (Foxp) 3⁺ cells; B-F: Flow cytometry results for the the control group (B), the DSS model group (C), the DSS + *B. infantis* group (D), the DSS + *B. infantis* + anti-PD-L1 group (E); and the DSS + anti-PD-L1 group (F); G: Statistical chart of the numbers of CD4⁺, CD25⁺, and Foxp3⁺ cells. Data are presented as mean ± SD, and the comparisons among each group were analyzed by one-way analysis of variance. Statistical significance was set as $P < 0.05$. PD-1: Programmed cell death 1; PD-L1: Programmed cell death ligand; DSS: Dextran sulfate sodium; *B. infantis* : *Bifidobacterium infantis*; Foxp3⁺: Forkhead box protein 3⁺; CD: Cluster of differentiation; SSC: Side scatter; FSC: Forward scatter; FL: Fluorescence; APC: Allophycocyanin; FITC: Fluorescein isothiocyanate; H: Height.

diseases (such as IBD), tumor immunity, and the acceptance of transplanted organs. Studies have shown that PD-1 knockout results in autoimmune diseases in animal models[31-33]. Activation of the PD-1/PD-L1 signaling pathway can induce the differentiation of Tregs[34] and the release of cytokines, such as IL-10 and TGF-β1, to inhibit the activation and proliferation of reactive T cells, thus maintaining intestinal immune tolerance. Additionally, the inhibition of the PD-1/PD-L1 pathway may reduce the proportion of Tregs[35]. These findings indicate that PD-1/PD-L1 signaling plays a critical role in immune tolerance[36]. In this study, we found that PD-L1 inhibition did not alter the PD-1 protein and mRNA levels in the intestine of DSS-induced mice, suggesting that PD-L1 did not affect the transcription or translation of PD-1 in the intestine of the IBD mouse model. However, although the expression of PD-1 mRNA in the intestinal tracts of DSS mice significantly decreased, the expression of PD-1 protein did not change after *B. infantis* administration. We, therefore, speculate that PD-L1 inhibition may indirectly inhibit the *B. infantis*-induced PD-1 gene transcription, but not the post-transcriptional modification and translation of PD-1 protein. This transcriptional inhibition of PD-1 may be due to a negative feedback mechanism caused by the high PD-1 protein levels. Further studies are



DOI: 10.3748/wjg.v28.i26.3164 **Copyright** ©The Author(s) 2022.

Figure 4 Effects of programmed cell death ligand inhibition on the expression of interleukin-10 and transforming growth factor β 1. A: Western blot showing interleukin (IL)-10 and transforming growth factor β (TGF-β) 1 protein expression; B-E: Statistical maps of the differences in IL-10 protein expression (B), TGF-β1 protein expression (C), IL-10 mRNA expression (D), and TGF-β1 expression (E). Data are presented as mean ± SD, and the comparisons among each group were analyzed by one-way analysis of variance. Statistical significance was set as $P < 0.05$. PD-1: Programmed cell death 1; PD-L1: Programmed cell death ligand; DSS: Dextran sulfate sodium; *B. infantis: Bifidobacterium infantis*; IL: Interleukin; TGF-β: Transforming growth factor β; GAPDH: Glyceraldehyde-3-phosphate dehydrogenase; mRNA: Messenger ribonucleic acid.

needed to determine how PD-L1 inhibition suppresses the transcription and translation of PD-1 and the underlying mechanism of action of the effect of *B. infantis* on PD-1 after PD-L1 inhibition.

B. infantis can be used to treat IBD by regulating the intestinal microbiota, alleviating inflammation, and regulating the immune response. *B. infantis* can reduce the intestinal wall permeability, edema, and neutrophil infiltration in IBD mice, and alleviate intestinal inflammatory responses[37]. We have previously shown that a combined administration of *B. infantis* with *Clostridium butyricum* increases the abundance of probiotic bacteria (such as members of the genera *Bifidobacterium* and *Lactobacillus)* in the intestinal microbiota of patients with IBD, reduces the prevalence of enterococci, improves clinical symptoms, and promotes the healing of colonic mucosa[38]. *B. infantis* also plays an important role in immune regulation by promoting the proliferation of Tregs[39] and increasing the expression of IL-10 and TGF-β1. *In vivo* and *in vitro* experiments have revealed that *B. infantis* can significantly accelerate the differentiation of $CD4^+$ T cells into Tregs by inducing the maturation of resistant dendritic cells and further inhibiting the inflammatory response induced by reactive T cell activation. Furthermore, we have previously revealed that, compared to the observations in normal mice, the number of $CD4^+$, $CD25^+$, and $Foxp3^+$ T cells in the blood and spleen of DSS mice and the expression of Foxp3 mRNA in their intestines showed a decrease, suggesting that the differentiation and proliferation of Tregs may be correlated to the pathogenesis of IBD[40]. The number of Tregs in the colon was reported to be related to the intestinal microbiota. Treg populations in the colons of sterile mice are significantly low; however, feeding sterile mice with feces collected from specific pathogen-free mice significantly increases the number of Tregs in the colon[41], indicating that Treg population is dependent on the intestinal microbiota. In patients with IBD, the proportion of normal intestinal bacteria decreases, resulting in intestinal microbiota-associated disorders[42]. Therefore, improving the composition of the intestinal microbiota can help increase the number of Tregs; however, further studies are needed for the elucidation of the underlying mechanism. In the present study, we found that *B. infantis* promotes the proliferation of $CD4^+$, $CD25^+$, and $Foxp3^+$ T cells in the blood and spleen, as well as the expression of Foxp3 mRNA in the intestine. PD-L1 inhibition significantly reduced the numbers of $CD4^+$, $CD25^+$, and

Foxp3$^+$ T cells in the blood and spleen, and decreased the expression of Foxp3 protein and mRNA in the intestine. Therefore, *B. infantis* promotes Treg proliferation by activating the PD-L1/PD-1 pathway.

In addition, our results indicate that *B. infantis* promoted the mRNA expression of IL-10 and TGF-β1 in the mouse intestine. PD-L1 inhibition significantly reduced the protein and mRNA expression levels of IL-10 and TGF-β1 in the intestine. These results further indicate that *B. infantis* affected IL-10 and TGF-β1 expression through the PD-1/PD-L1 pathway. Notably, Tregs mainly secrete TGF-β1 and IL-10 to inhibit inflammatory responses. Further studies are needed to confirm the immunosuppressive effects of *B. infantis* in patients with IBD. Additionally, Francisco *et al*[20] found that PD-L1 can downregulate Protein kinase B (Akt), mammalian target of rapamycin (mTOR), and extracellular regulated protein kinases (ERK2), while upregulating phosphatase and tensin homolog deleted on chromosome ten (PTEN) expression in Tregs; however, whether *B. infantis* can accelerate the differentiation and proliferation of Tregs by activating the PD-1/PD-L1 pathway and regulating Akt, mTOR, or PTEN expression requires further investigation.

CONCLUSION

In conclusion, *B. infantis* may accelerate the proliferation of CD4$^+$, CD25$^+$, and Foxp3$^+$ T cells in the spleen and peripheral blood, and the expression of Foxp3 in the intestine by activating the PD-1/PD-L1 signaling pathway. It can also promote the expression of IL-10 and TGF-β1 to reduce the intestinal inflammatory response, which has a therapeutic effect on IBD mice. We aim to further investigate the role of the PD-1/PD-L1 pathway in IBD and the possible therapeutic effect of *B. infantis* on patients with IBD in future studies.

ARTICLE HIGHLIGHTS

Research background

The immune-inflammatory response plays an important role in the pathogenesis and development of inflammatory bowel disease (IBD). *Bifidobacterium infantis* (*B. infantis*) can repair the acute intestinal mucosal injury and maintain autoimmune tolerance in mice with IBD.

Research motivation

The specific mechanism of action of *B. infantis* in the treatment of IBD is unclear. Understanding this underlying mechanism will help in the treatment of IBD.

Research objectives

To explore if *B. infantis* can promote regulatory T cell Treg differentiation through the programmed cell death 1 (PD-1)/PD ligand (PD-L1) pathway to promote the expression of forkhead box protein 3 (Foxp3), interleukin (IL)-10 and transforming growth factor β (TGF-β) 1, and reduce the inflammatory response.

Research methods

We blocked the expression of PD-L1 in the intestine and performed western blotting and real-time qPCR to observe the effects of *B. infantis* on PD-1, Foxp3, IL-10, and TGF-β1. Flow cytometry was used to examine the changes in the differentiation of CD4$^+$, CD25$^+$, and Foxp3$^+$ cells in the blood and spleen after blocking PD-L1.

Research results

PD-L1 inhibition reduced the promoting effects of *B. infantis* on intestinal PD-1, Foxp3, IL-10, and TGF-β 1. The promoting effect of *B. infantis* on the differentiation of CD4$^+$, CD25$^+$, and Foxp3$^+$ cells was also reduced.

Research conclusions

B. infantis mediates Foxp3 expression through the PD-1/PD-L1 pathway, thereby promoting Treg differentiation and improving IL-10 and TGF-β1 expression to reduce the immune and inflammatory response in IBD. *B. infantis* may act as a therapeutic agent for IBD.

Research perspectives

To explore the mechanism of action of *B. infantis* in the treatment of IBD at the cellular level. Further experiments are essential to determine whether *B. infantis* inhibits the immune response through the PD-1/PD-L1 pathway in the patients with IBD.

ACKNOWLEDGEMENTS

The authors thank Professor Liu DY for her guidance during the experiments.

FOOTNOTES

Author contributions: Zhou LY obtained funding, processed the samples, analyzed the raw data, and wrote manuscript; Xie Y processed the samples, obtained and managed data; Li Y conceived the study protocol, critically revised the manuscript, and approved the final version.

Supported by the Doctoral Start-up Foundation of Liaoning Province, No. 2021-BS-114.

Institutional review board statement: The study was reviewed and approved by the Institutional Review Board at Shengjing Hospital of China Medical University.

Institutional animal care and use committee statement: All animal experiments conformed to the internationally accepted principles for the care and use of laboratory animals, No. 2017PS353K.

Conflict-of-interest statement: The authors declare that they have no conflict of interest.

Data sharing statement: No additional data are available.

ARRIVE guidelines statement: The authors have read the ARRIVE guidelines, and the manuscript was prepared and revised according to the ARRIVE guidelines.

Open-Access: This article is an open-access article that was selected by an in-house editor and fully peer-reviewed by external reviewers. It is distributed in accordance with the Creative Commons Attribution NonCommercial (CC BY-NC 4.0) license, which permits others to distribute, remix, adapt, build upon this work non-commercially, and license their derivative works on different terms, provided the original work is properly cited and the use is non-commercial. See: https://creativecommons.org/Licenses/by-nc/4.0/

Country/Territory of origin: China

ORCID number: Lin-Yan Zhou 0000-0002-9403-2809; Ying Xie 0000-0001-8226-4242; Yan Li 0000000276903324.

S-Editor: Chen YL
L-Editor: A
P-Editor: Cai YX

REFERENCES

1 **Burisch J**, Zammit SC, Ellul P, Turcan S, Duricova D, Bortlik M, Andersen KW, Andersen V, Kaimakliotis IP, Fumery M, Gower-Rousseau C, Girardin G, Valpiani D, Goldis A, Brinar M, Čuković-Čavka S, Oksanen P, Collin P, Barros L, Magro F, Misra R, Arebi N, Eriksson C, Halfvarson J, Kievit HAL, Pedersen N, Kjeldsen J, Myers S, Sebastian S, Katsanos KH, Christodoulou DK, Midjord J, Nielsen KR, Kiudelis G, Kupcinskas L, Nikulina I, Belousova E, Schwartz D, Odes S, Salupere R, Carmona A, Pineda JR, Vegh Z, Lakatos PL, Langholz E, Munkholm P; Epi-IBD group. Disease course of inflammatory bowel disease unclassified in a European population-based inception cohort: An Epi-IBD study. *J Gastroenterol Hepatol* 2019; **34**: 996-1003 [PMID: 30562421 DOI: 10.1111/jgh.14563]

2 **Olendzki B**, Bucci V, Cawley C, Maserati R, McManus M, Olednzki E, Madziar C, Chiang D, Ward DV, Pellish R, Foley C, Bhattarai S, McCormick BA, Maldonado-Contreras A. Dietary manipulation of the gut microbiome in inflammatory bowel disease patients: Pilot study. *Gut Microbes* 2022; **14**: 2046244 [PMID: 35311458 DOI: 10.1080/19490976.2022.2046244]

3 **Lo Sasso G**, Phillips BW, Sewer A, Battey JND, Kondylis A, Talikka M, Titz B, Guedj E, Peric D, Bornand D, Dulize R, Merg C, Corciulo M, Ouadi S, Yanuar R, Tung CK, Ivanov NV, Peitsch MC, Hoeng J. The reduction of DSS-induced colitis severity in mice exposed to cigarette smoke is linked to immune modulation and microbial shifts. *Sci Rep* 2020; **10**: 3829 [PMID: 32123204 DOI: 10.1038/s41598-020-60175-3]

4 **Algethmi W**, Baumann C, Alnajjar W, Sroji A, Alsahafi M, Jawa H, Qari Y, Peyrin-Biroulet L, Saadah OI, Mosli M. Environmental exposures and the risk of inflammatory bowel disease: a case-control study from Saudi Arabia. *Eur J Gastroenterol Hepatol* 2020; **32**: 358-364 [PMID: 31851095 DOI: 10.1097/MEG.0000000000001619]

5 **Illiano P**, Brambilla R, Parolini C. The mutual interplay of gut microbiota, diet and human disease. *FEBS J* 2020; **287**: 833-855 [PMID: 31955527 DOI: 10.1111/febs.15217]

6 **Lavelle A**, Sokol H. Gut microbiota-derived metabolites as key actors in inflammatory bowel disease. *Nat Rev Gastroenterol Hepatol* 2020; **17**: 223-237 [PMID: 32076145 DOI: 10.1038/s41575-019-0258-z]

7 **Sartor RB**. Mechanisms of disease: pathogenesis of Crohn's disease and ulcerative colitis. *Nat Clin Pract Gastroenterol Hepatol* 2006; **3**: 390-407 [PMID: 16819502 DOI: 10.1038/ncpgasthep0528]

8 **Li J**, Jie HB, Lei Y, Gildener-Leapman N, Trivedi S, Green T, Kane LP, Ferris RL. PD-1/SHP-2 inhibits Tc1/Th1 phenotypic responses and the activation of T cells in the tumor microenvironment. *Cancer Res* 2015; **75**: 508-518 [PMID: 25480946 DOI: 10.1158/0008-5472.CAN-14-1215]

9 **Pauken KE**, Sammons MA, Odorizzi PM, Manne S, Godec J, Khan O, Drake AM, Chen Z, Sen DR, Kurachi M, Barnitz RA, Bartman C, Bengsch B, Huang AC, Schenkel JM, Vahedi G, Haining WN, Berger SL, Wherry EJ. Epigenetic stability of exhausted T cells limits durability of reinvigoration by PD-1 blockade. *Science* 2016; **354**: 1160-1165 [PMID: 27789795 DOI: 10.1126/science.aaf2807]

10 **Garcia-Bates TM**, Palma ML, Shen C, Gambotto A, Macatangay BJC, Ferris RL, Rinaldo CR, Mailliard RB. Contrasting Roles of the PD-1 Signaling Pathway in Dendritic Cell-Mediated Induction and Regulation of HIV-1-Specific Effector T Cell Functions. *J Virol* 2019; **93** [PMID: 30541848 DOI: 10.1128/JVI.02035-18]

11 **Zamani MR**, Aslani S, Salmaninejad A, Javan MR, Rezaei N. PD-1/PD-L and autoimmunity: A growing relationship. *Cell Immunol* 2016; **310**: 27-41 [PMID: 27660198 DOI: 10.1016/j.cellimm.2016.09.009]

12 **Kuol N**, Stojanovska L, Nurgali K, Apostolopoulos V. PD-1/PD-L1 in disease. *Immunotherapy* 2018; **10**: 149-160 [PMID: 29260623 DOI: 10.2217/imt-2017-0120]

13 **Long Y**, Xia C, Sun Y, Ma Y, Xu L, Song Y, Liu C. Increased circulating PD-1^{hi}CXCR5- peripheral helper T cells are associated with disease severity of active ulcerative colitis patients. *Immunol Lett* 2021; **233**: 2-10 [PMID: 33675861 DOI: 10.1016/j.imlet.2021.03.001]

14 **Li JY**, Yu M, Pal S, Tyagi AM, Dar H, Adams J, Weitzmann MN, Jones RM, Pacifici R. Parathyroid hormone-dependent bone formation requires butyrate production by intestinal microbiota. *J Clin Invest* 2020; **130**: 1767-1781 [PMID: 31917685 DOI: 10.1172/JCI133473]

15 **Hartwig T**, Zwicky P, Schreiner B, Yawalkar N, Cheng P, Navarini A, Dummer R, Flatz L, Conrad C, Schlapbach C, Becher B. Regulatory T Cells Restrain Pathogenic T Helper Cells during Skin Inflammation. *Cell Rep* 2018; **25**: 3564-3572.e4 [PMID: 30590032 DOI: 10.1016/j.celrep.2018.12.012]

16 **Barbi J**, Pardoll D, Pan F. Treg functional stability and its responsiveness to the microenvironment. *Immunol Rev* 2014; **259**: 115-139 [PMID: 24712463 DOI: 10.1111/imr.12172]

17 **Vitale A**, Strisciuglio C, Vitale S, Santopaolo M, Bruzzese D, Micillo T, Scarpato E, Miele E, Staiano A, Troncone R, Matarese G, Gianfrani C. Increased frequency of regulatory T cells in pediatric inflammatory bowel disease at diagnosis: a compensative role? *Pediatr Res* 2020; **87**: 853-861 [PMID: 31715619 DOI: 10.1038/s41390-019-0662-7]

18 **O'Garra A**, Vieira P. Regulatory T cells and mechanisms of immune system control. *Nat Med* 2004; **10**: 801-805 [PMID: 15286781 DOI: 10.1038/nm0804-801]

19 **Maul J**, Loddenkemper C, Mundt P, Berg E, Giese T, Stallmach A, Zeitz M, Duchmann R. Peripheral and intestinal regulatory CD4+ CD25(high) T cells in inflammatory bowel disease. *Gastroenterology* 2005; **128**: 1868-1878 [PMID: 15940622 DOI: 10.1053/j.gastro.2005.03.043]

20 **Francisco LM**, Salinas VH, Brown KE, Vanguri VK, Freeman GJ, Kuchroo VK, Sharpe AH. PD-L1 regulates the development, maintenance, and function of induced regulatory T cells. *J Exp Med* 2009; **206**: 3015-3029 [PMID: 20008522 DOI: 10.1084/jem.20090847]

21 **Ding Q**, Lu L, Zhou X, Zhou Y, Chou KY. Human PD-L1-overexpressing porcine vascular endothelial cells induce functionally suppressive human CD4+CD25hiFoxp3+ Treg cells. *J Leukoc Biol* 2011; **90**: 77-86 [PMID: 21498584 DOI: 10.1189/jlb.1210691]

22 **Zhou L**, Liu D, Xie Y, Yao X, Li Y. *Bifidobacterium infantis* Induces Protective Colonic PD-L1 and Foxp3 Regulatory T Cells in an Acute Murine Experimental Model of Inflammatory Bowel Disease. *Gut Liver* 2019; **13**: 430-439 [PMID: 30600673 DOI: 10.5009/gnl18316]

23 **Chaudhary CL**, Gurung P, Jang S, Banskota S, Nam TG, Kim JA, Jeong BS. Synthesis, activity and mechanism of alkoxy-, carbamato-, sulfonamido-, thioureido-, and ureido-derivatives of 2,4,5-trimethylpyridin-3-ol against inflammatory bowel disease. *J Enzyme Inhib Med Chem* 2020; **35**: 1-20 [PMID: 31619080 DOI: 10.1080/14756366.2019.1677637]

24 **Lee KH**, Ahn BS, Cha D, Jang WW, Choi E, Park S, Park JH, Oh J, Jung DE, Park H, Suh Y, Jin D, Lee S, Jang YH, Yoon T, Park MK, Seong Y, Pyo J, Yang S, Kwon Y, Jung H, Lim CK, Hong JB, Park Y, Shin JI, Kronbichler A. Understanding the immunopathogenesis of autoimmune diseases by animal studies using gene modulation: A comprehensive review. *Autoimmun Rev* 2020; **19**: 102469 [PMID: 31918027 DOI: 10.1016/j.autrev.2020.102469]

25 **Eichele DD**, Kharbanda KK. Dextran sodium sulfate colitis murine model: An indispensable tool for advancing our understanding of inflammatory bowel diseases pathogenesis. *World J Gastroenterol* 2017; **23**: 6016-6029 [PMID: 28970718 DOI: 10.3748/wjg.v23.i33.6016]

26 **Yan PG**, Li JN. Advances in the understanding of the intestinal micro-environment and inflammatory bowel disease. *Chin Med J (Engl)* 2020; **133**: 834-841 [PMID: 32106123 DOI: 10.1097/CM9.0000000000000718]

27 **Aden K**, Rehman A, Waschina S, Pan WH, Walker A, Lucio M, Nunez AM, Bharti R, Zimmerman J, Bethge J, Schulte B, Schulte D, Franke A, Nikolaus S, Schroeder JO, Vandeputte D, Raes J, Szymczak S, Waetzig GH, Zeuner R, Schmitt-Kopplin P, Kaleta C, Schreiber S, Rosenstiel P. Metabolic Functions of Gut Microbes Associate With Efficacy of Tumor Necrosis Factor Antagonists in Patients With Inflammatory Bowel Diseases. *Gastroenterology* 2019; **157**: 1279-1292.e11 [PMID: 31326413 DOI: 10.1053/j.gastro.2019.07.025]

28 **Yan Y**, Kolachala V, Dalmasso G, Nguyen H, Laroui H, Sitaraman SV, Merlin D. Temporal and spatial analysis of clinical and molecular parameters in dextran sodium sulfate induced colitis. *PLoS One* 2009; **4**: e6073 [PMID: 19562033 DOI: 10.1371/journal.pone.0006073]

29 **Hall LJ**, Faivre E, Quinlan A, Shanahan F, Nally K, Melgar S. Induction and activation of adaptive immune populations during acute and chronic phases of a murine model of experimental colitis. *Dig Dis Sci* 2011; **56**: 79-89 [PMID: 20467900 DOI: 10.1007/s10620-010-1240-3]

30 **Fukata M**, Michelsen KS, Eri R, Thomas LS, Hu B, Lukasek K, Nast CC, Lechago J, Xu R, Naiki Y, Soliman A, Arditi M, Abreu MT. Toll-like receptor-4 is required for intestinal response to epithelial injury and limiting bacterial translocation in a murine model of acute colitis. *Am J Physiol Gastrointest Liver Physiol* 2005; **288**: G1055-G1065 [PMID: 15826931 DOI: 10.1152/ajpgi.00328.2004]

31 **Chen L**, Pai V, Levinson R, Sharpe AH, Freeman GJ, Braun J, Gordon LK. Constitutive neuronal expression of the immune regulator, programmed death 1 (PD-1), identified during experimental autoimmune uveitis. *Ocul Immunol Inflamm* 2009; **17**: 47-55 [PMID: 19294574 DOI: 10.1080/09273940802491884]

32 **Roosenboom B**, Horjus Talabur Horje CS, Smids C, Leeuwis JW, van Koolwijk E, Groenen MJM, Wahab PJ, van Lochem EG. Distribution of mucosal PD-1 expressing T cells in patients with colitis of different etiologies. *Scand J Gastroenterol* 2021; **56**: 671-679 [PMID: 33779456 DOI: 10.1080/00365521.2021.1906316]

33 **Bodhankar S**, Galipeau D, Vandenbark AA, Offner H. PD-1 Interaction with PD-L1 but not PD-L2 on B-cells Mediates Protective Effects of Estrogen against EAE. *J Clin Cell Immunol* 2013; **4**: 143 [PMID: 24009988 DOI: 10.4172/2155-9899.1000143]

34 **Gianchecchi E**, Fierabracci A. Inhibitory Receptors and Pathways of Lymphocytes: The Role of PD-1 in Treg Development and Their Involvement in Autoimmunity Onset and Cancer Progression. *Front Immunol* 2018; **9**: 2374 [PMID: 30386337 DOI: 10.3389/fimmu.2018.02374]

35 **O'Shaughnessy MJ**, Murray KS, La Rosa SP, Budhu S, Merghoub T, Somma A, Monette S, Kim K, Corradi RB, Scherz A, Coleman JA. Systemic Antitumor Immunity by PD-1/PD-L1 Inhibition Is Potentiated by Vascular-Targeted Photodynamic Therapy of Primary Tumors. *Clin Cancer Res* 2018; **24**: 592-599 [PMID: 28954788 DOI: 10.1158/1078-0432.CCR-17-0186]

36 **Lo YC**, Price C, Blenman K, Patil P, Zhang X, Robert ME. Checkpoint Inhibitor Colitis Shows Drug-Specific Differences in Immune Cell Reaction That Overlap With Inflammatory Bowel Disease and Predict Response to Colitis Therapy. *Am J Clin Pathol* 2021; **156**: 214-228 [PMID: 33555016 DOI: 10.1093/ajcp/aqaa217]

37 **Elian SD**, Souza EL, Vieira AT, Teixeira MM, Arantes RM, Nicoli JR, Martins FS. Bifidobacterium longum subsp. infantis BB-02 attenuates acute murine experimental model of inflammatory bowel disease. *Benef Microbes* 2015; **6**: 277-286 [PMID: 25391346 DOI: 10.3920/BM2014.0070]

38 **Li Hui**, Gong Yi, Li Yan. Clinical efficacy of mesalazine combined with Clostridium butyricum in the treatment of active mild to moderate ulcerative colitis. *Shiyong Yaowu Yu Linchuang* 2016; **19**: 1389-1393 [DOI: 10.14053/j.cnki.ppcr.201611017]

39 **Mi H**, Dong Y, Zhang B, Wang H, Peter CCK, Gao P, Fu H, Gao Y. Bifidobacterium Infantis Ameliorates Chemotherapy-Induced Intestinal Mucositis Via Regulating T Cell Immunity in Colorectal Cancer Rats. *Cell Physiol Biochem* 2017; **42**: 2330-2341 [PMID: 28848081 DOI: 10.1159/000480005]

40 **Fu L**, Song J, Wang C, Fu S, Wang Y. *Bifidobacterium infantis* Potentially Alleviates Shrimp Tropomyosin-Induced Allergy by Tolerogenic Dendritic Cell-Dependent Induction of Regulatory T Cells and Alterations in Gut Microbiota. *Front Immunol* 2017; **8**: 1536 [PMID: 29176981 DOI: 10.3389/fimmu.2017.01536]

41 **Bozkurt HS**, Kara B. A new treatment for ulcerative colitis: Intracolonic Bifidobacterium and xyloglucan application. *Eur J Inflamm* 2020; **18**: 1-7 [DOI: 10.1177/2058739220942626]

42 **Zuo T**, Ng SC. The Gut Microbiota in the Pathogenesis and Therapeutics of Inflammatory Bowel Disease. *Front Microbiol* 2018; **9**: 2247 [PMID: 30319571 DOI: 10.3389/fmicb.2018.02247]

World Journal of Gastroenterology

Submit a Manuscript: https://www.f6publishing.com

World J Gastroenterol 2022 July 14; 28(26): 3177-3200

DOI: 10.3748/wjg.v28.i26.3177

ISSN 1007-9327 (print) ISSN 2219-2840 (online)

ORIGINAL ARTICLE

Basic Study

Involvement of Met receptor pathway in aggressive behavior of colorectal cancer cells induced by parathyroid hormone-related peptide

María Belén Novoa Díaz, Pedro Carriere, Graciela Gigola, Ariel Osvaldo Zwenger, Natalia Calvo, Claudia Gentili

Specialty type: Biochemistry and molecular biology

Provenance and peer review: Invited article; Externally peer reviewed.

Peer-review model: Single blind

Peer-review report's scientific quality classification

Grade A (Excellent): 0
Grade B (Very good): B, B
Grade C (Good): C
Grade D (Fair): D
Grade E (Poor): 0

P-Reviewer: Ding L, China; Gao W, China; Xu HC, China; Wan XH, China
A-Editor: Soldera J, Brazil

Received: January 13, 2022
Peer-review started: January 13, 2022
First decision: March 8, 2022
Revised: March 21, 2022
Accepted: May 27, 2022
Article in press: May 27, 2022
Published online: July 14, 2022

María Belén Novoa Díaz, Pedro Carriere, Graciela Gigola, Natalia Calvo, Claudia Gentili, Departamento de Biología, Bioquímica y Farmacia, Universidad Nacional del Sur (UNS)-INBIOSUR (CONICET-UNS), Bahía Blanca 8000, Buenos Aires, Argentina

Ariel Osvaldo Zwenger, Centro de Estudios Clínicos SAGA, CEC SAGA, Santiago de Chile 8320000, Chile

Corresponding author: Claudia Gentili, PhD, Professor, Research Scientist, Departamento de Biología, Bioquímica y Farmacia, Universidad Nacional del Sur (UNS)- INBIOSUR (CONICET-UNS), 670 San Juan, Bahía Blanca 8000, Buenos Aires, Argentina.
cgentili@criba.edu.ar

Abstract

BACKGROUND

Parathyroid hormone-related peptide (PTHrP) plays a key role in the development and progression of many tumors. We found that in colorectal cancer (CRC) HCT116 cells, the binding of PTHrP to its receptor PTHR type 1 (PTHR1) activates events associated with an aggressive phenotype. In HCT116 cell xenografts, PTHrP modulates the expression of molecular markers linked to tumor progression. Empirical evidence suggests that the Met receptor is involved in the development and evolution of CRC. Based on these data, we hypothesized that the signaling pathway trigged by PTHrP could be involved in the transactivation of Met and consequently in the aggressive behavior of CRC cells.

AIM

To elucidate the relationship among PTHR1, PTHrP, and Met in CRC models.

METHODS

For *in vitro* assays, HCT116 and Caco-2 cells derived from human CRC were incubated in the absence or presence of PTHrP (1-34) (10^{-8} M). Where indicated, cells were pre-incubated with specific kinase inhibitors or dimethylsulfoxide, the vehicle of the inhibitors. The protein levels were evaluated by Western blot technique. Real-time polymerase chain reaction (RT-qPCR) was carried out to determine the changes in gene expression. Wound healing assay and morpho-

logical monitoring were performed to evaluate cell migration and changes related to the epithelial-mesenchymal transition (EMT), respectively. The number of viable HCT116 cells was counted by trypan blue dye exclusion test to evaluate the effects of irinotecan (CPT-11), oxaliplatin (OXA), or doxorubicin (DOXO) with or without PTHrP. For *in vivo* tests, HCT116 cell xenografts on 6-wk-old male N:NIH (S)_nu mice received daily intratumoral injections of PTHrP (40 μg/kg) in 100 μL phosphate-buffered saline (PBS) or the vehicle (PBS) as a control during 20 d. Humanitarian slaughter was carried out and the tumors were removed, weighed, and fixed in a 4% formaldehyde solution for subsequent treatment by immunoassays. To evaluate the expression of molecular markers in human tumor samples, we studied 23 specimens obtained from CRC patients which were treated at the Hospital Interzonal de Graves y Agudos Dr. José Penna (Bahía Blanca, Buenos Aires, Argentina) and the Hospital Provincial de Neuquén (Neuquén, Neuquén, Argentina) from January 1990 to December 2007. Seven cases with normal colorectal tissues were assigned to the control group. Tumor tissue samples and clinical histories of patients were analyzed. Paraffin-embedded blocks from primary tumors were reviewed by hematoxylin-eosin staining technique; subsequently, representative histological samples were selected from each patient. From each paraffin block, tumor sections were stained for immunohistochemical detection. The statistical significance of differences was analyzed using proper statistical analysis. The results were considered statistically significant at $P < 0.05$.

RESULTS

By Western blot analysis and using total Met antibody, we found that PTHrP regulated Met expression in HCT116 cells but not in Caco-2 cells. In HCT116 cells, Met protein levels increased at 30 min ($P < 0.01$) and at 20 h ($P < 0.01$) whereas the levels diminished at 3 min ($P < 0.05$), 10 min ($P < 0.01$), and 1 h to 5 h ($P < 0.01$) of PTHrP treatment. Using an active Met antibody, we found that where the protein levels of total Met decreased (3 min, 10 min, and 60 min of PTHrP exposure), the status of phosphorylated/activated Met increased ($P < 0.01$) at the same time, suggesting that Met undergoes proteasomal degradation after its phosphorylation/activation by PTHrP. The increment of its protein level after these decreases (at 30 min and 20 h) suggests a modulation of Met expression by PTHrP in order to improve Met levels and this idea is supported by our observation that the cytokine increased *Met* mRNA levels at least at 15 min in HCT116 cells as revealed by RT-qPCR analysis ($P < 0.05$). We then proceeded to evaluate the signaling pathways that mediate the phosphorylation/ activation of Met induced by PTHrP in HCT116 cells. By Western blot technique, we observed that PP1, a specific inhibitor of the activation of the proto-oncogene protein tyrosine kinase Src, blocked the effect of PTHrP on Met phosphorylation ($P < 0.05$). Furthermore, the selective inhibition of the ERK 1/2 mitogen-activated protein kinase (ERK 1/2 MAPK) using PD98059 and the p38 MAPK using SB203580 diminished the effect of PTHrP on Met phosphorylation/activation ($P < 0.05$). Using SU11274, the specific inhibitor of Met activation, and trypan blue dye exclusion test, Western blot, wound healing assay, and morphological analysis with a microscope, we observed the reversal of cell events induced by PTHrP such as cell proliferation ($P < 0.05$), migration ($P < 0.05$), and the EMT program ($P < 0.01$) in HCT116 cells. Also, PTHrP favored the chemoresistance to CPT-11 ($P < 0.001$), OXA ($P < 0.01$), and DOXO ($P < 0.01$) through the Met pathway. Taken together, these findings suggest that Met activated by PTHrP participates in events associated with the aggressive phenotype of CRC cells. By immunohistochemical analysis, we found that PTHrP in HCT116 cell xenografts enhanced the protein expression of Met (0.190 ± 0.014) compared to tumors from control mice (0.110 ± 0.012; $P < 0.05$) and of its own receptor (2.27 ± 0.20) compared to tumors from control mice (1.98 ± 0.14; $P < 0.01$). Finally, assuming that the changes in the expression of PTHrP and its receptor are directly correlated, we investigated the expression of both Met and PTHR1 in biopsies of CRC patients by immunohistochemical analysis. Comparing histologically differentiated tumors with respect to those less differentiated, we found that the labeling intensity for Met and PTHR1 increased and diminished in a gradual manner, respectively ($P < 0.05$).

CONCLUSION

PTHrP acts through the Met pathway in CRC cells and regulates Met expression in a CRC animal model. More basic and clinical studies are needed to further evaluate the PTHrP/Met relationship.

Key Words: PTHrP; MET receptor tyrosine kinase; Parathyroid hormone receptor type 1; Colorectal cancer; Drug resistance

©The Author(s) 2022. Published by Baishideng Publishing Group Inc. All rights reserved.

Core Tip: Colorectal cancer (CRC) is one of the leading causes of cancer death, and chemoresistance is common in the treatment of CRC patients. Parathyroid hormone-related peptide (PTHrP) and the receptor tyrosine kinase Met are involved in the aggressive behavior of CRC cells. However, to date it is unknown whether PTHrP and Met are related to promoting events associated with the progression and chemoresistance of CRC. Herein we showed, for the first time, a PTHrP/Met axis that could have a positive impact on the knowledge of CRC biology and on the development of new targeted therapies.

Citation: Novoa Díaz MB, Carriere P, Gigola G, Zwenger AO, Calvo N, Gentili C. Involvement of Met receptor pathway in aggressive behavior of colorectal cancer cells induced by parathyroid hormone-related peptide. *World J Gastroenterol* 2022; 28(26): 3177-3200
URL: https://www.wjgnet.com/1007-9327/full/v28/i26/3177.htm
DOI: https://dx.doi.org/10.3748/wjg.v28.i26.3177

INTRODUCTION

Colorectal cancer (CRC) is one of the most frequent tumors of the digestive system and represents the third type of cancer with the highest incidence worldwide[1]. According to statistics, the development of metastasis and resistance to chemotherapeutic drugs causes 90% of deaths in patients with CRC[2]. Although treatment strategies have been improved in the past years, the mortality associated with this oncological disease is still around 50%[1,3]. In this line, the World Cancer Research Fund International indicates that CRC incidence is still increasing and that its prevalence is expected to augment by 60% in the next few years[4]. This is mainly due to the emergence of CRC patients under 50 years old and the appearance of new tumors subtypes that have a refractory response to the usual therapy[5]. Currently, two of the chemotherapeutic agents approved as first and second-line palliative drugs in CRC are oxaliplatin (OXA) and irinotecan (CPT-11)[6,7]. However, more than half of patients with stage II/III disease who underwent surgery and were treated with these drugs relapsed and died[8]. Thus, all these facts evidence an urgent need to elucidate the molecular mechanisms associated with two key aspects of therapy: Effectiveness and resistance.

Parathyroid hormone-related peptide (PTHrP) is a cytokine-like protein that is normally produced in many adult and fetal tissues[9,10]. The N-terminal 13 amino acid residues of PTHrP exhibit high structural homology with the PTH[11]. This allows the binding of both ligands to the same G-protein-coupled receptor, PTH/PTHrP type 1 (PTHR1)[12,13]. It is known that PTHrP and its receptor are expressed in the same cells or neighboring cells. This juxtaposition is directly related to its activity as an autocrine and paracrine factor[14,15].

Regarding the expression of this protein in neoplastic disease, studies in patients show its overexpression in tissues of breast, prostate, lung, and colon cancers[16,17]. Moreover, 95% of colorectal adenocarcinomas have elevated expression of this protein[18-20]. Although PTHrP was initially identified as a major contributor to hypercalcemia in paraneoplastic syndromes, it is known that this peptide also plays a key role in the development and progression of many tumors [10,16,21-23]. In this concern, in CRC-derived cells we found that PTHrP stimulated cell proliferation, survival, and migration, the epithelial-mesenchymal transition (EMT), the release of pro-angiogenic factors, and the resistance to CPT-11[13,24-26]. In xenografts of CRC cells, we have observed that PTHrP also modulates the expression of molecular markers linked to tumor progression[24-27]. Despite these contributions, relevant aspects from the action of this peptide are still unknown, specifically, whether PTHrP could promote resistance to other forms of chemotherapy and the validation of our previous observations using human samples.

Met is a receptor with tyrosine kinase (RTK) activity, and it is expressed in normal tissues and participates in various physiological processes such as embryonic development and wound repair[28]. Only hepatocyte growth factor (HGF) is known as a necessary ligand for its activation. However, cross-communications between this RTK and G-protein-coupled receptors were reported to promote its aberrant activation[29-31]. Met overexpression or its dysregulation can lead to malignant cell transformation and contributes to the development and progression of different types of cancer including colorectal tumors[28,32-35]. Moreover, Met dysregulation is also associated with drug resistance in colon cancer cells[32,35,36]. Several studies demonstrated the overexpression of this RTK in tumor tissue of CRC patients; in this regard, its inhibition is being widely investigated as a complementary treatment to usual therapies[37,38]. Despite this, the value of Met as a prognostic marker or in treatment strategies has not been established yet.

Although empirical evidence suggests that Met and PTHrP play a key role in the development and evolution of CRC, it is still unknown whether PTHrP and Met act cooperatively to promote events associated with the progression and chemoresistance in CRC. Based on our previous studies, we hypothesized that the signaling pathway trigged by PTHR1 after binding to PTHrP could be involved in

the transactivation of the RTK Met and consequently in the aggressive behavior of CRC cells. For this reason, the present work aimed to elucidate the relationship among PTHR1, PTHrP, and Met.

MATERIALS AND METHODS

Reagents and antibodies

Human PTHrP (1-34) and trypan blue dye were obtained from Sigma-Aldrich Chemical Co (St. Louis, MO, United States). Antibodies were purchased from the following sources: Anti-Met and anti-phospho Met (Tyr 1234/1235) and anti-E-cadherin were provided by Cell Signaling Technology (Beverly, MA, United States); anti-PTH/PTHrP receptor type 1, anti-GAPDH, goat anti-rabbit peroxidase conjugated secondary antibody, and goat anti-mouse peroxidase conjugated secondary antibody were from Santa Cruz Biotechnology (Santa Cruz, CA, United States). PD98059, SB203580, and PP1 were obtained from Calbiochem (San Diego, CA, United States) and SU11274 from Sigma-Aldrich Chemical Co. RNase CocktailTM Enzime Mix was from Applied Biosystems (Carlsbad, CA, United States). Protein size markers were from Amersham Biosciences (Piscataway, NJ, United States). Immobilonpolyvinylidene difluoride (PVDF) membranes and electrochemiluminescence (ECL) detection kit were from Amersham (Little Chalfont, Buckinghamshire, England). The chemotherapeutic drugs CPT-11, OXA, and doxorubicin (DOXO) were generously provided by Dr. Ariel Zwenger.

Cell culture and treatment

Human colon cancer cells Caco-2 and HCT116 (American Type Culture Collection, Manassas, VA, United States) were grown at 37 °C in an atmosphere containing 5.5% CO_2 in Dulbecco's Modified Eagle Culture Medium (DMEM) containing 10% heat-inactivated and irradiated fetal bovine serum (FBS), 1% non-essential amino acids, penicillin (100 IU/mL), streptomycin (100 mg/mL), and gentamicin (50 mg/mL). The cells were cultured until reaching 80% confluence and then they were deprived of FBS for 2 h. Treatments were performed by incubating cells with 2.5% FBS-DMEM in the absence or presence of PTHrP (1-34) (10^{-8} M) at different times. This dose was selected based on previous studies[39,40]. Where indicated, cells were pre-incubated for 30 min with PD-98059 (20 μM), an inhibitor of the mitogen-activated protein kinase (MAPK) kinases (MEKs), the upstream kinases of ERK1/2; SB203580 (20 μM), an inhibitor of p38 MAPK; PP1 (10 μM), an inhibitor of Src; or SU11274 (0.5 μM), a Met inhibitor. In previous works, we confirmed the effectiveness of the inhibitors PD98059, SB203580, and PP1[26,27], whereas SU11274 dose was chosen in accordance with the literature[41]. Controls were run by the addition of an equivalent volume of dimethylsulfoxide (DMSO), the vehicle of the inhibitors.

Western blot analysis

Cells were washed with phosphate buffered saline (PBS) with 25 mmol/L NaF and 1 mmol/L Na_3VO_4 and lysed in buffer containing 50 mmol/L Tris-HCl (pH 7.4), 150 mmol/L NaCl, 3 mmol/L KCl, 1 mmol/L ethylenediaminetetraacetic acid (EDTA), 1% Tween 20, 1% Nonidet P-40, 20 μg/mL aprotinin, 20 μg/mL leupeptin, 1 mmol/L phenylmethylsulfonyl fluoride (PMSF), 25 mmol/L NaF, and 1 mmol/L Na_3VO_4. Lysates were vortexed for 45 s, incubated on ice for 10 min, and then centrifuged at 14000 *g* and 4 °C for 15 min. The supernatant was collected and protein quantification was performed by the Bradford method[42]. The proteins present in the samples were separated (30 μg/lane) using sodium dodecyl sulfate (SDS)-polyacrylamide gels (8%-10% acrylamide) and electrotransferred to hydrophilic polyvinylidene fluoride (PVDF) membranes. The membranes were blocked with 5% skim milk in Tris buffered saline-Tween (TBS-T) buffer (50 mmol/L Tris, pH 7.2-7.4, 200 mmol/L NaCl, 0.1% Tween-20), and then incubated overnight with the appropriate dilution of primary antibody (Met #8198 1:3000, p-Met #3077 1:500, E-cadherin #3195 1:1000; GAPDH sc-32233 1:5000) in TBS-T with 2.5% bovine serum albumin. After washing, the membranes were incubated with the appropriate dilution of horseradish peroxidase conjugated secondary antibody in TBS-T with 2.5% skim milk. Finally, proteins were revealed using a commercial electrochemiluminescence kit, and the bands obtained were digitized densitometrically and quantified with Image J program.

Stripping and reprobing membranes

To remove primary and secondary antibodies, membranes were incubated in stripping buffer (62.5 mmol/LTris-HCl pH 6.8, 2% SDS, and 50 mmol/L β-mercaptoethanol) at 55 °C for 30 min in agitation, washed for 10 min in TBS-T (1% Tween-20), and then blocked, as indicated above. After this procedure, it is possible to re-test antibodies in the membranes.

RNA isolation and cDNA synthesis

HCT116 cells were incubated in serum-free DMEM for 2 h and then treated with or without PTHrP (10^{-8} mol/L, in DMEM 2.5% FBS) for 15 min. Total RNA from all samples was isolated using the High Pure RNA Isolation Kit (Roche Diagnostics, Mannheim, Germany) according to the manufacturer's instructions. Total RNA (1 g) from each sample was used for first-strand cDNA synthesis using High

Capacity cDNA Reverse Transcription Kits following the manufacturer's instructions (Applied Biosystems, United States). The cDNA product was quantified and then stored at -20 °C for real-time polymerase chain reaction (RT-qPCR).

RT-qPCR

PCR reactions were carried out on a real-time PCR system (Applied Biosystems, model 7500). The primers used are the following: 5'-GGAAACACCCATCCAGAATGTCATT-3' (forward) and 5'-TGATATCGAATGCAATGGATGATCT-3' (reverse) for *Met*; 5'-ACCACAGTCCATGCCATCA-3' (forward) and 5'-TCCACCACCCTGTTGCTGTA-3' (reverse) for *GAPDH*. The PCR reactions were prepared using SYBR green master mix (No. 4309159, Applied Biosystems). On ice, the following was added: 5 μL of 2 × SYBR green, 0.8 μL of forward primer (400 nmol/L), 0.8 μL of reverse primer (400 nmol/L), 2 μL of template cDNA (12 ng), and 1.4 μL of Milli Q sterile water. *GAPDH* cDNA was amplified in parallel for all genes to provide an appropriate internal PCR control. For each experiment, water was added as a sample without a template (negative control). Mean Ct of the gene of interest (Met) was calculated from triplicate measurements using the following equation: Ct =Ct of the gene of interest -Ct of *GAPDH*. mRNA levels were calculated by the $2^{-\Delta CT}$ method.

Wound healing assay and morphological monitoring

Once confluence was reached, a cross-shaped wound was made manually in the cell monolayer with a tip and two washes were performed with sterile 1 × PBS to remove debris from the procedure. Then, the treatments were performed in DMEM without FBS as detailed above. Finally, the wounds were visualized under an inverted microscope and each of them was photographed at 0 h, 5 h, and 24 h, where the same fields were photographed. For each condition, the closure of the wound concerning the control was analyzed using ImageJ-NIH program, which allows for quantifying the area that remains cell-free.

To evaluate morphological changes potentially associated with the EMT, cells were treated with PTHrP as detailed above and the same fields were observed with a microscope and photographed during the times when significant molecular changes were observed.

Measurements of drug effects of chemotherapeutics

CPT-11, OXA, and DOXO cytotoxicities were assessed by trypan blue dye exclusion test. HCT116 cells were seeded in a 24-well plate until 80% confluence and then treated with or without PTHrP 10^{-8} M and/or CPT-11(10 μM)/OXA (10 μM)/DOXO (5 μM) in triplicate for 24 h. The doses of these drugs were chosen according to previous works[26,43-45]. Where indicated, HCT116 cells were pre-incubated with SU11274 (0.5 μM)[41] or DMSO, the vehicle of the inhibitor. After the treatment, cells were washed with PBS and then incubated with trypsin-EDTA to separate them from the culture substrate. The cell suspension was diluted in equal volume with trypan blue stain (1:1). The number of cells per field was counted in a Neubauer chamber; cells that exclude the dye were considered viable cells. The number of viable cells was calculated according to the following formula: Total number of viable cells = average number of viable cells × dilution factor × 10^4[46].

Xenograft in nude mice

Xenografts on 6-wk old male N:NIH (S)_nu mice (body weight 20-25 g) were generated through a subcutaneous injection of 1 × 10^6 HCT116 cells in their left dorsal flanks[47]. Four days after this procedure, the animals were randomly separated into treated and control groups (n = 6/group). Mice received a daily intratumoral injection of PTHrP (40 μg/kg) in 100 μL PBS, or PBS as a control. This manner of administration was in order to keep the compound level constant in the tumor area. The dose of PTHrP was selected according to previous studies performed by us and by other investigators with PTH and/or PTHrP in rodents[27,48-50]. Throughout the experiment, animals were kept under strict sanitary barriers in insulated cabins and had access to sterilized food and water *ad libitum*. Besides, they were exposed to 12 h cycles of light and darkness (200 Lux/1 m from the floor), atmospheric pressure, 25 °C, and humidity of 40%-60%. Humanitarian slaughter was carried out after 20 d of treatment by inhalation of the chemical agent CO_2. The tumors were removed, weighed, and fixed in a 4% formaldehyde solution and included in a paraffin block for subsequent treatment in immunoassays. At the end of the trial, the average weights were 0.30 g ± 0.11 g (standard deviation) and 0.40 g ± 0.10 g for control tumors and treated tumors, respectively. Whereas the average volumes were 0.21 mm^3 ± 0.08 mm^3 (standard deviation) and 0.26 mm^3 ± 0.08 mm^3 for control tumors and treated tumors, respectively. The present animal protocol was approved by the Institutional Committee for the Care and Use of Experimental Animals from the Universidad Nacional del Sur (CICUAE-UNS, institutional endorsement updated to 2021) and it was executed in accordance with the National Institutes of Health guide for the care and use of laboratory animals (NIH 1996) in order to minimize pain or discomfort for the animals.

Patients and clinical specimens

The following research protocol (File number 8610-017183/2018, Registry of Investigations in Health (RIS) number N° 11.00.18) has the endorsement of the Advisory Commission on Biomedical Research in

Beings Human Rights (CAIBSH) and the approval of the Health Ministry of the Province of Neuquén, Argentina (provision 0088-18-1-19) and was authorized by the Ethical Committee of the Hospital Interzonal de Graves y Agudos Dr. José Penna, Buenos Aires, Argentina in accordance with article 23 of Law 11044 of the Ministry of Health and the Central Research Ethics Committee (CECI) on research with biological samples from Argentina.

We performed an analysis of specimens obtained from patients with colorectal adenocarcinoma which were admitted to the Hospital Interzonal de Graves y Agudos Dr. José Penna (Bahía Blanca, Buenos Aires, Argentina) and the Hospital Provincial de Neuquén (Neuquén, Neuquén, Argentina) from January 1990 to December 2007. Normal colorectal tissue samples were assigned to a control group. The medical record of each patient was analyzed for the information as follows: Sex; age; primary tumor location; histological grade; and initial stage (according to the TNM staging system issued by the American Joint Committee on Cancer-AJCC and International Union for Cancer Control-UICC). The exclusion criteria were: Patients under 18 years of age due to the low prevalence of this cancer in the child and youth population[51]; pregnant patients due to the fact that high levels of PTHrP have been observed in the placenta and fetal tissues[52]; lactating patients because high levels of PTHrP have been detected in breast tissue and in breast milk and correlate with serum PTHrP levels in these women[53]; patients who have previously developed other types of tumors (liver, lung, and bone) since CRC commonly metastasizes to these sites. These considerations are necessary to exclude cases where the cytokine derived from other tissues may interfere with the analysis of the results from this study. All are exclusion criteria at the time of diagnosis. The confidentiality criteria were based on the regulatory provisions referring to confidentiality in clinical investigations, including Law 11044 and Law 25326 on data protection, from Argentina, the Guide for Health Research of the National Ministry of Health, the UNESCO Declaration on the Protection of Genetic Data and the Declaration of Helsinki of the World Medical Association (version 2008), and the Council for International Organizations of Medical Sciences (CIOMS) Guidelines. This study respected the dignity and rights of the patients. All data derived from the clinical history was treated under strict confidentiality to protect and preserve the patient's identities.

Paraffin-embedded archival blocks from primary tumors were reviewed by hematoxylin-eosin staining technique; subsequently, representative histological samples of each patient were selected for immunoassays.

Immunohistochemistry

From each paraffin block, tumor sections were sliced and prepared for immunohistochemical detection using the primary monoclonal antibody anti-Met (#8198, 1:2000) or anti-PTHR1 antibody (sc-12722-3D1.1, 1:50) according to the manufacturer's protocol. The sections were deparaffinized with xylol for 15 min and subsequently rehydrated in decreasing concentrations of alcohol. Antigenic retrieval was carried out using a pressure cooker with sodium citrate buffer (10 mmol/L, pH 6) for 15 min at 1 atm. The sections were washed twice with PBS and we proceeded to block endogenous peroxidase with 30% $H_2O_2$for 10 min. After two washes with PBS, the corresponding antibody was added to each sample and incubated overnight at 4 °C. Immunohistochemical staining was carried out manually using ABCAM Detection IHC Kit (Abcam, Cambridge, MA, United States) according to the manufacturer's instructions. The images obtained under an optical microscope were analyzed using an open-source image processing package based on ImageJ-NIH program[54,55].

Statistical analysis

To obtain statistical data, three experiments were carried out independently and the results are expressed as the mean ± SD. To determine significant differences between two groups of data, Student's *t*-test (two-tailed, equal variance) was carried out. A P value < 0.05 was considered statistically significant.

For the statistical analysis of human tumor samples, the correlation coefficient between the expression of Met and PTHR1 was evaluated by the Spearman test. Then, the patients were grouped according to clinicopathological characteristics such as age, sex, TNM stage (II, III, and IV), location of the primary tumor (right colon, left colon, and rectum), and histological grade (G1, G2, and G3). The Fisher's exact test was used to evaluate the association of Met or PTHR1 expression with each variable. These statistical analyses were performed using the R programming language version 4.1.1[56]. A P value < 0.05 was considered statistically significant.

RESULTS

PTHrP modulates the expression of the RTK Met in human HCT116 cells

Met is a heterodimeric receptor that is composed of two chains, alpha and beta. Initially, this RTK is synthesized as a single-chain precursor (pro-Met), and it then undergoes posttranslational modifications to produce the mature form[57]. The binding of the HGF to the beta subunit of Met induces its dimerization and the phosphorylation of tyrosine domains in the intracellular portion of the receptor

(Y1234 and Y1235). These events promote the kinase activity of Met and its autophosphorylation (Y1349 and Y1356). Then, various proteins are recruited to these phosphorylated sites, triggering different signaling pathways[33,58].

In CRC cells, Met signaling is activated by various mechanisms to promote tumor development and progression[28,59]. Gene amplification or mutations (that lead to receptor overexpression) and increased activity due to ligand-mediated stimulation induce the aberrant activation of Met[28]. As mentioned earlier, another mechanism that favors its abnormal activation involves the phosphorylation in Met activator domains and is indirectly due to the previous activation of cell-surface receptors like G-protein-coupled receptors[29,31].

In the past years, several authors have reported a correlation between the overexpression of PTHrP and tumor progression in lung, breast, and prostate cancers[16,21,60]. Our research group has shown that this cytokine also promotes the aggressive phenotype of intestinal tumor cells[13,24-26]. This pro-tumor factor exerts its action on CRC cells through several mitogenic signaling pathways[13]. In view of this background, in this work we decided to investigate whether the molecular mechanisms trigged by PTHR1 after binding of PTHrP are capable of modulating the expression of the mature form of the RTK Met and/or its activation in CRC-derived cells. To that end, we initially treated Caco-2 cells and HCT116 cells with PTHrP for different times and then the cell lysates were immunoblotted with an anti-Met antibody. We selected these cell lines from CRC with different aggressive phenotypes because both express the receptor PTHR1 and we had previously verified that their cell responses are mediated exclusively by this receptor[26,40,61]. Met did not change its protein expression when Caco-2 cells were treated with PTHrP over a wide interval of exposure times (data not shown). However, the response of the HCT116 cell line, which is more aggressive than Caco-2 cell line, was different. As seen in Figure 1 (top and middle panels), PTHrP treatment for 30 min increased Met protein levels. However, the protein expression diminished at 3 min and 10 min, and at 1 h to 3 h of exposure to the peptide. Figure 1 (lower panel) shows that at 5 h of treatment, Met protein levels continued to decrease. However, PTHrP increased Met protein expression at 20 h of treatment.

As it happens with other RTKs on the cell surface, after its phosphorylation/activation, Met is internalized with the subsequent decrease in its protein levels due to the proteasomal degradation[62,63]. In this regard, the reduction of Met protein levels observed in HCT116 cells suggested a previous activation of this receptor by PTHrP, and the increment of its protein level after these decreases (at 30 min and 20 h) suggested a modulation of Met expression by PTHrP in order to improve Met levels.

PTHrP promotes Met phosphorylation and activation through Src kinase in human HCT116 cells

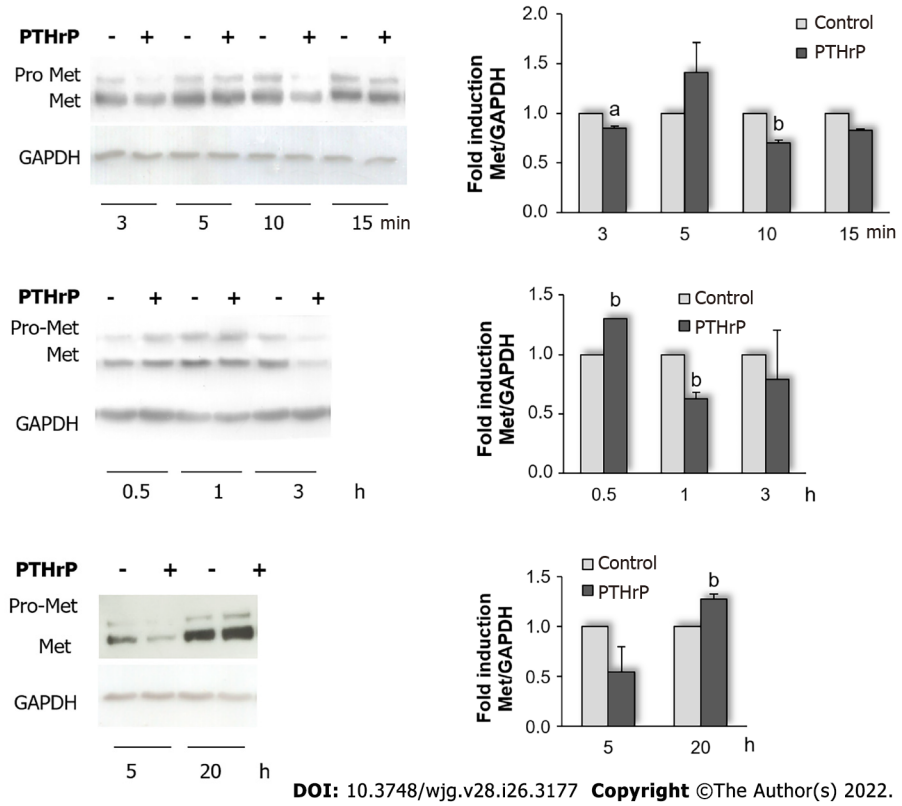
Our next goal was to elucidate if the decrease in Met protein levels observed in HCT116 cell line and mediated by exogenous PTHrP could be due to its previous phosphorylation/activation. Thus, we proceeded to evaluate the status of phosphorylated Met under PTHrP action. As shown in Figure 2A, Western blot analysis using a specific antibody that recognizes active Met, revealed that PTHrP treatment for 3 min and 10 min increased the phosphorylation of Met at the residues Tyr 1234 and Tyr 1235. These phosphorylation sites constitute activating domains of the receptor. The decrease in total Met protein levels (showed in Figure 1 and pointed in Figure 2A with arrows) ruled out the possibility that an increase in phosphorylated Met levels at the same time was due to the up-regulation of Met protein expression.

Src is a cytosolic tyrosine kinase deregulated in 80% of CRC patients[64-66]. Previously, we reported the activation of Src in the HCT116 cell line induced by PTHrP at 3 min of treatment[26]. As we mentioned above and taking into account that we observed phosphorylation of Met by PTHrP on specific tyrosine residues that are needed for its activation, we decided to evaluate whether Src is involved in this process induced by the cytokine PTHrP in intestinal tumor cells. For this purpose, the cells were pre-treated with PP1, a specific inhibitor of Src activation, and then with PTHrP for 3 min. As shown in Figure 2B, we observed that PP1 decreased PTHrP-induced phosphorylation of Met at Tyr1234/1235. These findings suggested that in the HCT116 cell line, PTHrP rapidly activate the Src signaling pathway, leading to the phosphorylation and activation of Met.

PTHrP promotes the phosphorylation/activation of Met through the MAPK signaling pathway in human HCT116 cells

It has been described that MAPK signaling pathway activation is very common in CRC and is related to an aggressive phenotype of intestinal tumor cells[67]. Due to its relevance in cancer, in recent decades the possibility of employing MAPK pathway inhibitors has been studied for the treatment of this disease[68,69]. In our laboratory, we found that PTHrP induces the activation of the ERK 1/2 MAPK and p38 MAPK and that the activity of Src converges in the phosphorylation/activation of MAPK in CRC-derived cells [26,27].

Based on our previous results, we next decided to investigate in our model if ERK 1/2 MAPK and p38 MAPK are also involved in the effects of PTHrP on the Met signaling pathway. To that end, the cells were pre-incubated with PD-98059 (a selective inhibitor of MEK, the upstream kinases of ERK 1/2) or with SB-203580 (a specific p38 MAPK inhibitor) and then exposed to PTHrP for 1 h. This time point was selected because the phosphorylation/activation of ERK 1/2 MAPK and p38 MAPK significantly



DOI: 10.3748/wjg.v28.i26.3177 **Copyright** ©The Author(s) 2022.

Figure 1 Parathyroid hormone-related peptide modulates the protein expression of Met receptor in HCT116 cells. Cells were treated with or without 10^{-8} mol/L parathyroid hormone-related peptide (PTHrP) for different times. The protein levels of pro-Met (Met precursor) and Met [tyrosine kinase receptor (RTK) mature form] were analyzed by Western blot to investigate whether the molecular mechanisms trigged by PTHR type 1 (PTHR1) after binding of PTHrP are capable of modulating the expression of the mature form of the RTK Met in HCT116 cells. GAPDH protein levels were determined as a control of the amount of proteins present in the membrane, since this protein is not substantially modified with the treatment by the cytokine. Graph bars represent the average of the results obtained from three independent experiments. GAPDH: Glyceraldehyde 3-phosphate dehydrogenase; Met: Receptor tyrosine kinase Met; PTHrP: Parathyroid hormone-related peptide. $^{a}P < 0.05$; $^{b}P < 0.01$.

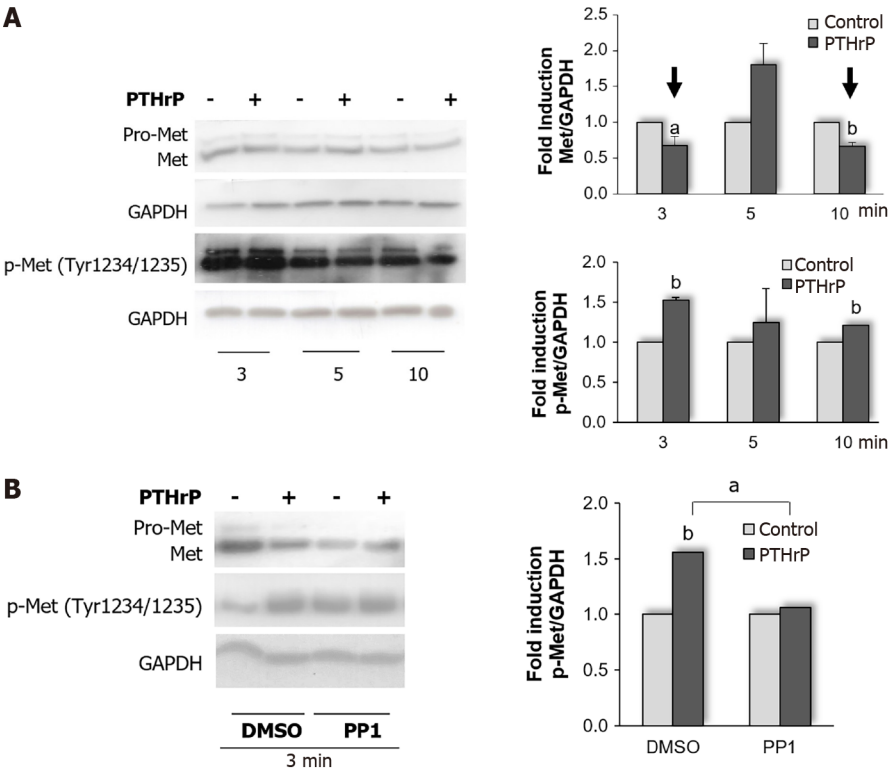
increased at 60 min after PTHrP treatment in HCT116 cells[26,27]. Regarding the cell response when tumor cells were exposed to PTHrP for 1 h (Figure 1), Figure 3 shows an increase in the phosphorylated Met levels, suggesting that the treatment with the cytokine for 1 h also induces the phosphorylation/activation of Met with the subsequent reduction in its protein levels due to its proteasomal degradation. Moreover, Figure 3 reveals that the selective inhibition of MEK MAPK and p38 MAPK averted the effect on Met phosphorylation, suggesting that Met activation is regulated by the ERK 1/2 MAPK and p38 MAPK signaling pathways in HCT116 cells under PTHrP action.

PTHrP increases Met gene expression in human HCT116 cells

As it was commented earlier, the fact that Met, like other RTKs, undergoes proteasomal degradation after its phosphorylation/activation[62,63] explains that at the same time points of PTHrP exposure (3 min, 10 min, and 60 min), the levels of phosphorylated Met increased while the protein levels of total Met decreased. Furthermore, in this work we elucidated that Met is phosphorylated by PTHrP through the Src and MAPK signaling pathways. In view of the results shown in Figure 1, we selected a time before 30 min with the purpose to evaluate whether the increase in Met protein levels initially observed by PTHrP treatment is related to the modulation of gene expression. By real-time PCR, we analyzed the *Met* mRNA levels and found that PTHrP increased *Met* gene expression at 15 min (Figure 4). This result suggested that in HCT116 cells, PTHrP at least at this time promotes the transcription of the *Met* gene and its translation, correlating with the increase of the protein levels observed at 30 min of PTHrP exposure.

Met signaling pathway induced by PTHrP participates in cell events related to the aggressive behavior of human HCT116 cells

Our studies in CRC cell models have demonstrated that PTHrP favors several events associated with the progression of the disease, such as cell proliferation, migration, and the EMT program[13,24,26,27,39]. Based on these previous findings and since Met is modulated by PTHrP in HCT116 cells, we decided to evaluate whether the Met signaling pathway participates in events induced by the cytokine and associated with an aggressive phenotype of CRC-derived cells. For this purpose, cells were incubated



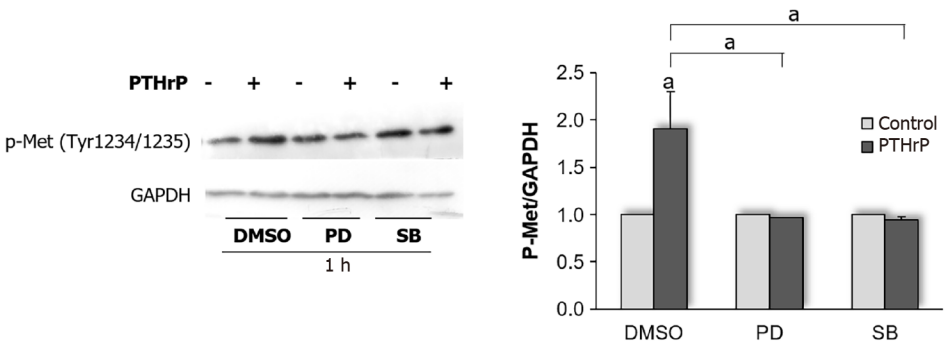
DOI: 10.3748/wjg.v28.i26.3177 **Copyright** ©The Author(s) 2022.

Figure 2 Parathyroid hormone-related peptide increases Met phosphorylation and activation through Src kinase in HCT116 cells. A: Cells were exposed to 10^{-8} mol/L parathyroid hormone-related peptide (PTHrP) 10^{-8} mol/L for 3 min, 5 min, and 10 min. The protein levels of Met and p-Met (phosphorylated in the residues Tyr1234 and Tyr1235) were assessed by Western blot to investigate whether PTHrP is capable of modulating Met phosphorylation and activation in HCT116 cells. Graph bars represent the average of the results obtained from three independent experiments; B: Cells were pre-treated with PP1, a selective Src inhibitor, for 30 min and then exposed to 10^{-8} mol/L PTHrP for 3 min to evaluate whether Src kinase mediates the effect of PTHrP on Met activation in HCT116 cells. Controls were run by adding an equivalent volume of DMSO, the vehicle of the inhibitor. The protein levels of p-Met and Met were evaluated by Western blot. Graph bars represent the average of the results obtained from three independent experiments. In all experiments, GAPDH protein levels were determined as a control of the amount of proteins present in the membrane, since this protein is not substantially modified with the treatment by the cytokine. DMSO: Dimethylsulfoxide; GAPDH: Glyceraldehyde 3-phosphate dehydrogenase; Met: Receptor tyrosine kinase Met; p-Me: Phospho-Met (Tyr1234/1235); PTHrP: Parathyroid hormone-related peptide. $^{a}P < 0.05$; $^{b}P < 0.01$.

with SU11274, an ATP competitive inhibitor of the catalytic activity of the Met kinase[70], followed by the treatment with or without PTHrP for different times, and then we performed different procedures as described below. The times of PTHrP exposure were selected based on our previous findings[24,26,27]. As shown in Figure 5A, PTHrP or PTHrP plus DMSO (the vehicle of the inhibitor) at 24 h increased the number of HCT116 cells. However, the treatment with the Met inhibitor significantly decreased the number of viable cells concerning the control. As the Met signaling pathway is involved in the proliferation and survival of intestinal tumor cells[41,71-73], this descent in the cell viability suggests that both cell responses are affected.

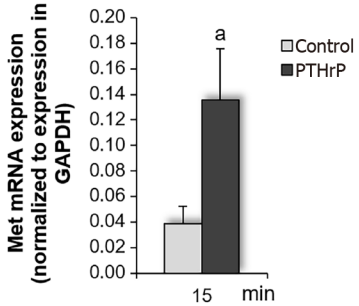
By the wound healing assay, we evaluated whether Met signaling is also involved in the migration of HCT116 cells induced by PTHrP. We observed the wound healing in the culture of confluent HCT116 cells to compare the migration between untreated cells and cells treated with PTHrP in the presence or absence of SU11274. Representative photographs, taken at time points 0 h, 5 h, and 24 h of the identical location and the quantification of the results of two separate experiments are shown in Figure 5B. A significant enhancement in wound closure was detected in cells exposed to PTHrP or PTHrP plus DMSO compared to the control at 5 h and 24 h. However, this effect was not observed in cells that had been pre-treated with the Met inhibitor.

We recently published results revealing that PTHrP is able to induce the EMT in HCT116 cells[24]. The EMT is a key program of CRC that participates in the invasion, angiogenesis, and chemoresistance associated with metastasis[74,75]. Based on this previous work, herein we analyzed if PTHrP also induces this program through the Met pathway. To that end, HCT116 cells were incubated with SU11274 and then treated with or without PTHrP. The cells were observed under an inverted microscope after treatment with PTHrP for 5 h and 24 h to analyze the morphological changes associated with the EMT. The arrows in Figure 5C point to morphological changes corresponding to the transition from a polygonal structure to spindle-like structure in cells treated for 24 h with PTHrP or PTHrP plus DMSO. These findings revealed an effective transition to the mesenchymal phenotype and are consistent with our previous work in HCT116 cells[24]. There were no changes between SU 11274



DOI: 10.3748/wjg.v28.i26.3177 **Copyright** ©The Author(s) 2022.

Figure 3 Parathyroid hormone-related peptide modulates Met activation through the mitogen-activated protein kinase signaling pathway in HCT116 cells. Cells were treated with PD-98059 or SB-203580, a selective mitogen-activated protein kinase (MAPK) kinase (MEK) or P38 MAPK inhibitor, respectively, for 30 min and then exposed to 10^{-8} mol/L PTHrP for 1 h to evaluate whether ERK1/2 MAPK and/or p38 MAPK mediate the effect of PTHrP on Met activation in HCT116 cells. Controls were run by adding an equivalent volume of dimethylsulfoxide, the vehicle of the inhibitors. The protein levels of Met phosphorylated in the residues Tyr1234 and Tyr1235 were assessed by Western blot. These phosphorylation sites constitute activating domains of the receptor. GAPDH protein levels were determined as a control of the amount of proteins present in the membrane, since this protein is not substantially modified with the treatment by the cytokine. Graph bars represent the average of the results obtained from three independent experiments. DMSO: Dimethylsulfoxide; GAPDH: Glyceraldehyde 3-phosphate dehydrogenase; Met: Receptor tyrosine kinase Met; p-Met: Phospho-Met (Tyr1234/1235); PTHrP: Parathyroid hormone-related peptide. $^{a}P < 0.05$.



DOI: 10.3748/wjg.v28.i26.3177 **Copyright** ©The Author(s) 2022.

Figure 4 Parathyroid hormone-related peptide increases mRNA levels of *Met* in HCT116 cells. Colon cancer cells were exposed to parathyroid hormone-related peptide (PTHrP) for 15 min, followed by real-time polymerase chain reaction analysis to detect *Met* mRNA levels as described in Materials and Methods to evaluate whether PTHrP modulates *Met* mRNA levels in HCT116 cells. Graph bars represent the average of the results obtained from three independent experiments. GAPDH: Glyceraldehyde 3-phosphate dehydrogenase; Met: Receptor tyrosine kinase Met; PTHrP: Parathyroid hormone-related peptide. $^{a}P < 0.05$.

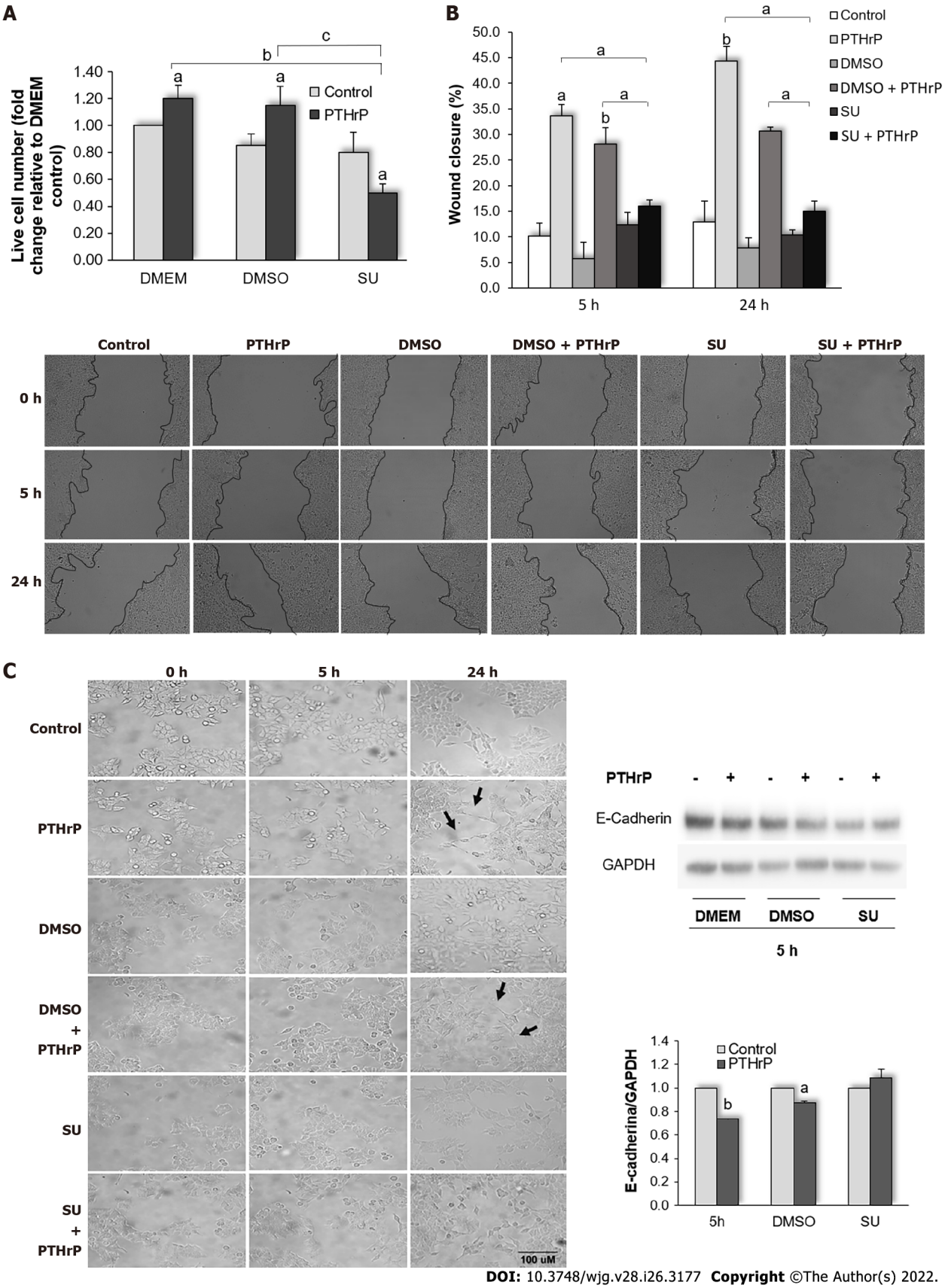
control cells and those treated with the inhibitor of Met plus PTHrP. To further evaluate the phenotype related to a mesenchymal shape, we measured the minor and major axes in the photomicrographs using the Image J-NIH program. Figure 6 reveal that under PTHrP action, the cells lost their epithelial characteristics. The increase of the relation between the major and minor axes indicated that the exposure to PTHrP for 24 h significantly increased the degree of HCT116 cell elongation, a typical feature of the mesenchymal shape. However, when the cells were pre-incubated with SU11274, the effects of the cytokine were reverted.

It has been shown that the loss of the expression of the epithelial marker E-cadherin is associated with EMT progress in CRC[76,77]. In our recent work[24], we showed that in HCT116 cells, PTHrP at 5 h modulated the expression of E-cadherin and other epithelial markers as well as certain mesenchymal markers. Based on these morphological changes related to the EMT and mediated through Met, we then explored by Western blot analysis whether Met is involved in the modulation of E-cadherin protein expression by the cytokine. As seen in Figure 5C, the effects of the cytokine on E-cadherin protein levels were reverted when the cells were pre-incubated with SU11274. Taken together, these findings suggest that PTHrP induces the EMT program in HCT116 cells through the Met signaling pathway.

In agreement with other works published[78], our findings suggest that the Met signaling pathway induced by PTHrP is involved in cell events related to tumor aggressive behavior in the HCT116 cells.

PTHrP attenuates the cytotoxic effect of CPT-11, OXA, and DOXO in human HCT116 cells through the Met signaling pathway

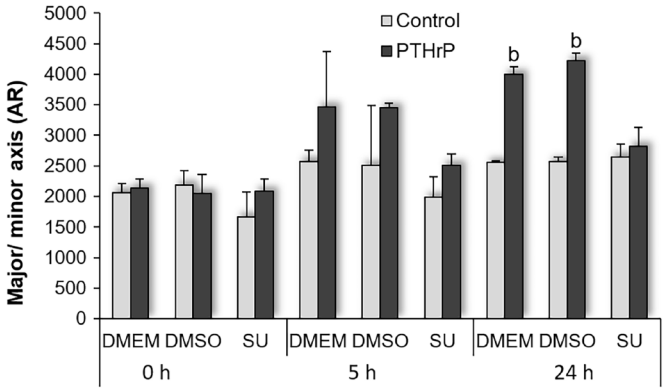
In CRC-derived cells, our group has previously described a role of PTHrP in the resistance to CPT-11, the most widely used chemotherapeutic drug today[26]. In the treatment of CRC, many pharmaco-



DOI: 10.3748/wjg.v28.i26.3177 **Copyright** ©The Author(s) 2022.

Figure 5 Parathyroid hormone-related peptide promotes events related to the aggressive behavior of HCT116 cells through the Met signaling pathway. HCT116 cells were pre-incubated with SU11274, a specific Met inhibitor, for 30 min and then treated with or without parathyroid hormone-related peptide (PTHrP; 10^{-8}M). A: Trypan blue technique showed that Met inhibition decreased the cell proliferation induced by PTHrP at 24 h; B: Images from wound healing assay show that Met inhibition reverted the wound closure promoted by PTHrP at 5 h and 24 h; C: E-cadherin protein levels analyzed by Western blot to investigate whether Met is involved in the decrease of this epithelial-mesenchymal transition (EMT) program marker induced by PTHrP in HCT116 cells. Using the

Image J-NIH program, we performed the analysis of the parameters related to cell morphology. The arrows indicate the morphological changes corresponding to the transition from a polygonal structure to spindle-like structure related to EMT program progress observed when the cells were treated for 24 h with PTHrP or PTHrP plus dimethylsulfoxide (DMSO). In all experiments, a control with DMSO, the vehicle of the inhibitor, was performed. Graph bars represent the average of the results obtained from two independent experiments. DMEM: Dulbecco's Modified Eagle Culture Medium; DMSO: Dimethylsulfoxide; EMT: Epithelial to mesenchymal transition; PTHrP: Parathyroid hormone-related peptide. [a]*P* < 0.05; [b]*P* < 0.01; [c]*P* < 0.001.



Time	Image J analysis of cells aspect radio (AR)	Area	Perimeter	Major	Minor	AR	Round
0 h	Control	371608.35	83700.44	29714.67	15072.84	2.06	0.51
	PTHrP	445243.58	95072.71	32963.65	16999.08	2.12	0.55
	DMSO	401221.98	90350.81	31896.07	16001.69	2.19	0.53
	DMSO + PTHrP	507695.83	102479.62	35812.26	18038.25	2.02	0.53
	SU	540780.15	104863.69	33247.98	17729.93	1.87	0.53
	SU+ PTHrP	502373.55	104550.15	35027.30	18751.45	2.10	0.57
5 h	Control	549152.49	114728.86	40994.62	20538.01	2.00	0.50
	PTHrP	572497.91	134398.89	48988.78	15197.87	3.47	0.34
	DMSO	459528.84	104492.96	36189.49	16991.24	2.51	0.53
	DMSO + PTHrP	540958.38	132183.13	47145.72	15112.32	3.45	0.36
	SU	433503.43	91961.62	32499.24	17279.31	2.00	0.56
	SU+ PTHrP	474989.59	107135.04	37739.83	16617.10	2.51	0.48
24 h	Control	487973.50	108293.98	37998.97	16948.69	2.55	0.48
	PTHrP	440312.67	134882.49	44247.08	13044.18	3.70	0.32
	DMSO	453802.96	117009.26	37199.63	16191.98	2.57	0.47
	DMSO + PTHrP	492995.40	132117.10	44167.20	13864.80	3.20	0.31
	SU	453382.04	118630.81	37624.58	15650.04	2.50	0.45
	SU+ PTHrP	508934.37	124074.22	41166.22	16517.61	2.80	0.44

DOI: 10.3748/wjg.v28.i26.3177 **Copyright** ©The Author(s) 2022.

Figure 6 Analysis of the aspect ratio (major/minor axis) of HCT116 cells, obtained using the Image J-NIH program. The table shows values of parameters associated to cell morphology: Area; perimeter; round; major axis; minor axis; and aspect radio, relation between major axis and minor axis (AR). Graph bars show the AR for each condition. The increase of the degree of cell elongation at 24 h of exposure to parathyroid hormone-related peptide was significantly reversed in the presence of the Met inhibitor. DMSO: Dimethylsulfoxide; PTHrP: Parathyroid hormone-related peptide; SU: SU11274. [b]*P* < 0.01.

logical strategies have been implemented. OXA is another drug commonly employed for this purpose and it exerts its cytotoxic action through different mechanisms with respect to CPT-11. Thereby, the combination of CPT-11 and OXA is generally used to improve the effectiveness of the adjuvant therapy [79,80]. DOXO is another chemotherapeutic agent that has been effective in the treatment of advanced CRC; however, the side effects associated with its use at high doses and the development of chemores-

istance constitute a great challenge to the effective treatment[43,81,82]. Since the greatest problem in CRC treatment is the development of chemoresistance, we proceeded to evaluate if PTHrP affects the cytotoxicity promoted by these other drugs. Trypan blue dye exclusion test revealed that PTHrP not only decreased the sensitivity of intestinal tumor cells to CPT-11 but also to OXA and DOXO (Figure 7).

Studies carried out by colleagues demonstrated the correlation between overexpression and/or hyper-activation of Met in tumor tissues with a poor prognosis of cancer patients and with a chemoresistant phenotype[32,83,84]. These findings support the interest in Met inhibitors as new therapeutic strategies. Since herein we found that Met inhibition substantially reverts the effects of PTHrP on events associated with the malignant behavior such as cell proliferation, migration, and the EMT program, we set out to assess if the signaling pathway trigged by this RTK also promotes chemoresistance in our experimental system. Counting live cells by means of trypan blue dye exclusion test revealed that Met inhibition restored the sensitivity of HCT116 cells to CPT-11 (Figure 7A), OXA (Figure 7B), and DOXO (Figure 7C) even in the presence of PTHrP, suggesting that this cytokine attenuates the cytotoxic effect of these drugs in CRC cells through the Met signaling pathway.

PTHrP enhances the protein expression of Met and its receptor in HCT116 cells tumor xenografts

In a murine model, we have previously observed that the administration of PTHrP in HCT116 cell xenografts changed the protein expression of markers linked to CRC progression, such as Ki67, cyclin D1, ERK1/2 MAPK, CREB/ATF-1[26], RSK[27], VEGF[25], SPARC, and E-cadherin[24]. As Met overexpression promotes events related to tumor progression like proliferation, invasion, and migration[63,70] and taking into account our previous finding in the animal model, in this work we evaluated whether the administration of PTHrP in the same murine model (HCT116 cell xenografts in nude mice N: NIH(S)_nu) also changes the protein levels of Met in tumor tissues. To that end, 12 male mice, between 4 and 6 wk of age and with a body weight between 20 g and 25 g, were randomly divided into two groups (n = 6 each), after an acclimatization period of 4 d. Group 1 received the cytokine vehicle (100 μL PBS), while group 2 received PTHrP at a concentration of 40 μg/kg body weight in 100 μL PBS[49]. The treatment was intra-tumoral daily and until the end of the experiment to maintain the level of the compound constant in the tumor area. The mice were kept throughout the protocol in sterile conditions (see Materials and Methods). The immunohistochemical analysis with the quantification of Met immunoreactivity revealed that Met levels were elevated in tumors from mice treated with PTHrP (0.190 ± 0.014) compared to tumors from control mice (0.110 ± 0.012; $P < 0.05$) (Figure 8, top images). As the present work was aimed to elucidate the relationship between PTHR1, PTHrP, and Met, we also analyzed the immunoreactivity of PTHR1 using an anti-PTHR1 antibody in HCT116 cell xenografts from untreated nude mice (control) and mice treated with PTHrP. Interestingly, as seen in Figure 8 (lower images), PTHrP increased the protein expression of its receptor in the tumor of these animals (2.27 ± 0.20) compared to tumors from control mice (1.98 ± 0.14; $P < 0.01$). The data shown in this section together with those in the first and fourth sections of results indicate that PTHrP modulates the expression of Met both *in vitro* and *in vivo*. Perhaps the cytokine modulates the expression of its own receptor in this animal model in order to amplify its signaling within the cell and thus makes its effects more effective in CRC. More studies are necessary to confirm this hypothesis.

Evaluation of Met and PTHR1 expressions in CRC human samples

As we mentioned before, the Met receptor has the HGF as its only known ligand. However, it could be aberrantly activated by G-protein-coupled receptors[29,31]. The results reported herein in the previous sections suggest that PTHR1 activation (after its binding with PTHrP) is able to trigger the activation of the Met signaling pathway through a cross-talk between both receptors that is mediated by cytosolic kinases like Src. In this context, and taking into account the findings obtained by *in vitro* and *in vivo* assays, we decided to validate our observations and therefore our ultimate objective was to assess the expression of both receptors in CRC human tumor samples with the aim to elucidate if there is a relation between them and with the tumor characteristics. So, we analyzed 23 specimens obtained from patients with colorectal adenocarcinoma. Seven cases with normal colorectal tissues were assigned to the control group. Table 1 shows the patients' characteristics. The average age was 62 years; 48% (n = 11) were male, and 52% (n = 12) were female. Regarding the primary tumor location, 39% (n = 9) presented right-colon cancer, 30.5% (n = 7) presented left-colon cancer, while in 30.5% (n = 7) of patients the location was in the rectum; 61% (n = 14) of the tumors presented a high grade of histological differentiation, while 39% (n = 9) were moderately or poorly differentiated; 48% (n = 11) of the patients with CRC presented stage II, 39% (n = 9) stage III, and 13% (n = 3) stage IV.

The expression of Met and PTHR1 was evaluated in biopsies of patients with well (G1), moderately (G2), and poorly differentiated (G3) colon adenocarcinomas, as well as in normal colon tissue using the immunohistochemical technique. Figure 9A shows the comparison between both quantifications, Met and PTHR1, for each histological grade of differentiation. As shown in Figure 9B, in normal tissue Met receptor labeling is homogeneous throughout the cytoplasm of the epithelial cell. However, in tumor cells, we observed that the intensity of the immunostaining in the membrane increased as tumor differentiation declined. Concerning PTHR1, the intensity of the staining gradually decreased in histologically less differentiated tumors and the receptor seemed to relocate from the plasma membrane of the epithelial cell in G1 to the cytoplasm and the perinuclear zone in G3. Based on these observations, we

Table 1 Clinicopathological characteristics of the patients

Variable	Value
Sex, *n* (%)	
Male	11 (48)
Female	12 (52)
Age, median (range)	62 (58-74)
Primary tumor site, *n* (%)	
Right-side	9 (39)
Left-side	7 (30.5)
Rectum	7 (30.5)
Tumor differentiation, *n* (%)	
Well differentiated	14 (61)
Moderately or poorly differentiated	9 (39)
Initial stage, *n* (%)	
II	11 (48)
III	9 (39)
IV	3 (13)

Data are presented as *n* (%) except where otherwise stated.

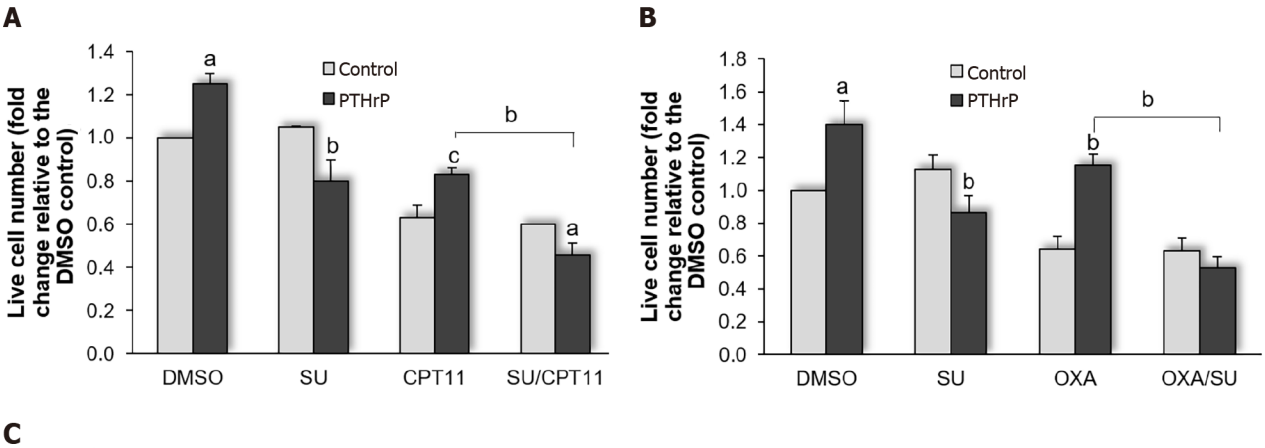
decided to investigate whether there is a correlation between the expression of Met and PTHR1. No statistical significance was found between the expression of both receptors in the tumor samples. Additionally, we studied if there is a statistically significant association between the clinicopathological characteristics and the immunohistochemical staining for Met or PTHR1. For this purpose, we dichotomized the specimens into low, medium, and high expression levels of Met or PTHR1. We found that in less differentiated tumors, Met expression increased (P = 0.035), while PTHR1 expression was statistically lower (P = 0.0496). However, we did not find a statistically significant association of Met or PTHR1 with age, sex, primary tumor location, and TNM stage. These results indicate that the expression of PTHR1 is more marked in well-differentiated tumors, while Met showed a higher expression level in poorly differentiated tumors.

DISCUSSION

Resistance to chemotherapeutic drugs constitutes an obstacle in the therapy of CRC[2]. In this context, it is crucial to identify the molecular mechanisms related to the aggressive phenotype of CRC to develop more effective therapeutic strategies and find new prognostic and predictive markers.

PTHrP is expressed in various types of cancer, including CRC[16]. In fact, 95% of colorectal tumors present elevated levels of this protein[18-20,85]. Our research group found that this cytokine modulates different signaling pathways and events associated with the aggressive phenotype in CRC-derived cells [13,24-26].

Several studies have demonstrated the participation of the Met signaling pathway in the evolution of different types of cancer[28,33-35,83]. Moreover, this receptor is overexpressed and/or can be aberrantly activated by several mechanisms in CRC cells, triggering tumor development and progression[28,36,38,59]. A recent study addresses the relationship between the HGF/Met axis and cytokines such as PTHrP in bone metastasis and renal cell cancer progression[86]. In agreement with these observations, the results from this work suggest that the expression and activity of Met are regulated by signaling pathways trigged by the binding of PTHrP to PTHR1. We observed that exogenous PTHrP treatment modulates Met protein and gene expression in HCT116 cells. Despite that the cytokine regulates Met expression in HCT116 cells, our initial observations in Caco-2 cells reveal that PTHrP is not able to modulate its protein levels. In line with these findings, we previously reported that PTHrP modulates the protein levels of SPARC (an invasion marker) and E-cadherin (a marker related with EMT program) in HCT116 cells but not in Caco-2 cells[24]. The fact that the cytokine can modulate the expression of markers associated with the malignant behavior in a more aggressive cell line (HCT116) but not in a less aggressive cell line (Caco-2) may be because these CRC cells have different mutations[87,88] and



DOI: 10.3748/wjg.v28.i26.3177 **Copyright** ©The Author(s) 2022.

Figure 7 Parathyroid hormone-related peptide attenuates the cytotoxicity of CPT11, oxaliplatin, and doxorubicin through the Met signaling pathway. A-C: HCT116 cells were pre-incubated with SU11274, a specific Met inhibitor, and then treated with PTHrP (10^{-8} M) and/or irinotecan (CPT-11, 10 μM) (A), oxaliplatin (OXA, 10 μM) (B), or doxorubicin (DOXO, 5 μM) (C) for 24 h. The number of viable cells was quantified by Trypan blue technique. In each experiment, a control with DOXO, the vehicle of the inhibitor, was performed. Graph bars represent the average of the results obtained from two independent experiments. CPT-11: Irinotecan; DMSO: Dimethylsulfoxide; DOXO: Doxorubicin; OXA: Oxaliplatin; PTHrP: Parathyroid hormone-related peptide; SU: SU11274. $^{a}P < 0.05$; $^{b}P < 0.01$; $^{c}P < 0.001$.

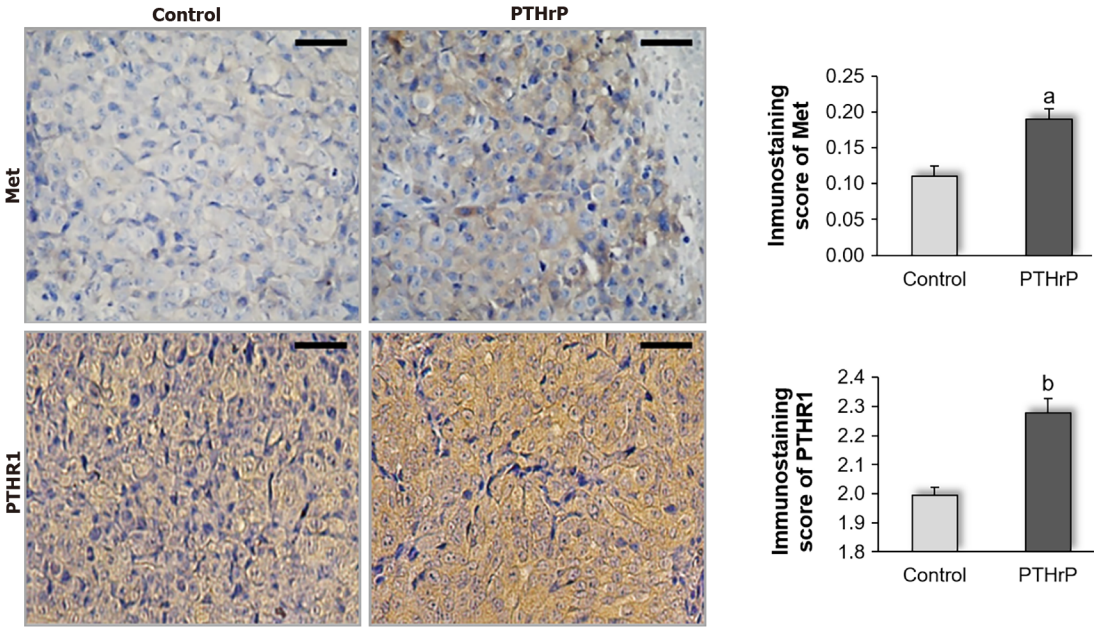
perhaps several events triggered by PTHrP in these two cell lines may be dependent on these mutations explaining the different response between Caco-2 and HCT116 cells.

We found in HCT116 cells that the peptide promotes the activation of Met by phosphorylation on Tyr residues. Bradley and colleagues and later Critchley and his research group, demonstrated that, like other RTKs, Met after its activation is degraded by the proteasomal pathway[62,63]. Consistent with these data, our results suggest that Met protein levels decline after PTHrP-induced phosphorylation.

Previous studies by our research group established that PTHrP in the HCT116 cell line promotes phosphorylation and activation of Src; then this kinase acts upstream of ERK 1/2 MAPK to induce their phosphorylation/activation, though the mechanisms that lead to the phosphorylation/activation of p38 MAPK by the cytokine is still unknown[13,26]. Herein, we demonstrated that PTHrP induces the phosphorylation and activation of Met through Src. Furthermore, PTHrP modulates the phosphorylation/activation of Met through ERK 1/2 and p38 MAPK. The fact that the cytokine diminishes Met protein levels in a range of time between 1 h to 5 h suggests that Met is activated by PTHrP (with its subsequent degradation) not only by the MAPKs but also by some pathway/s that is/are effector/s of the action of these MAPKs. This idea is supported by our finding that the effects of PTHrP is mediated by these MAPKs in HCT116 cells at longer exposure times[26]. More studies are needed to confirm this hypothesis.

Given these observations, the results obtained in this work suggest that at least the Src-ERK 1/2 MAPK and p38 MAPK axis is required for the phosphorylation/activation of Met induced by PTHrP in our model. Since MAPKs are serine-threonine kinases and Met requires phosphorylation on tyrosine residues for its activation, further studies are necessary to determine the link between these molecules.

As we previously mentioned, in CRC, the Met signaling pathway is associated with tumor evolution and also with resistance to chemotherapeutic drugs[32]. Currently, the inhibition of this RTK is being widely studied as a complementary therapy to conventional CRC treatments[37,38]. SU11274 prevents Met activation because it is an ATP competitive inhibitor of Met catalytic activity[70]. We previously showed that PTHrP has several effects on CRC derived cells such as proliferation, survival, migration, and induction of EMT program, among others[13,26,39]; the fact that we found a significant reduction in the viability and migration of HCT116 cells in the presence of an Met inhibitor as well as the reversal of the mesenchymal phenotype induction, even in the presence of PTHrP, indicates that Met mainly



DOI: 10.3748/wjg.v28.i26.3177 **Copyright** ©The Author(s) 2022.

Figure 8 Parathyroid hormone-related peptide increases the protein expression of Met and parathyroid hormone receptor type 1 in tumor xenografts. Met and parathyroid hormone-related peptide receptor type 1 (PTHR1) protein levels were evaluated by the immunohistochemistry technique in the HCT116 cell tumor-bearing nude mouse model. Tumor sections were stained with an anti-Met antibody or anti-PTHR1 antibody. Images (400 ×) are from the tumor treated with saline solution (left) or with PTHrP (right). The immunostaining was quantified with the Fiji image processing package of the Image J-NIH program. Scale bar: 50 μM. Met: Receptor tyrosine kinase Met; PTHR1: Parathyroid hormone receptor type 1; PTHrP: Parathyroid hormone-related peptide. $^{a}P < 0.05$; $^{b}P < 0.01$.

participates in the molecular mechanisms that are involved in these cell responses to PTHrP action.

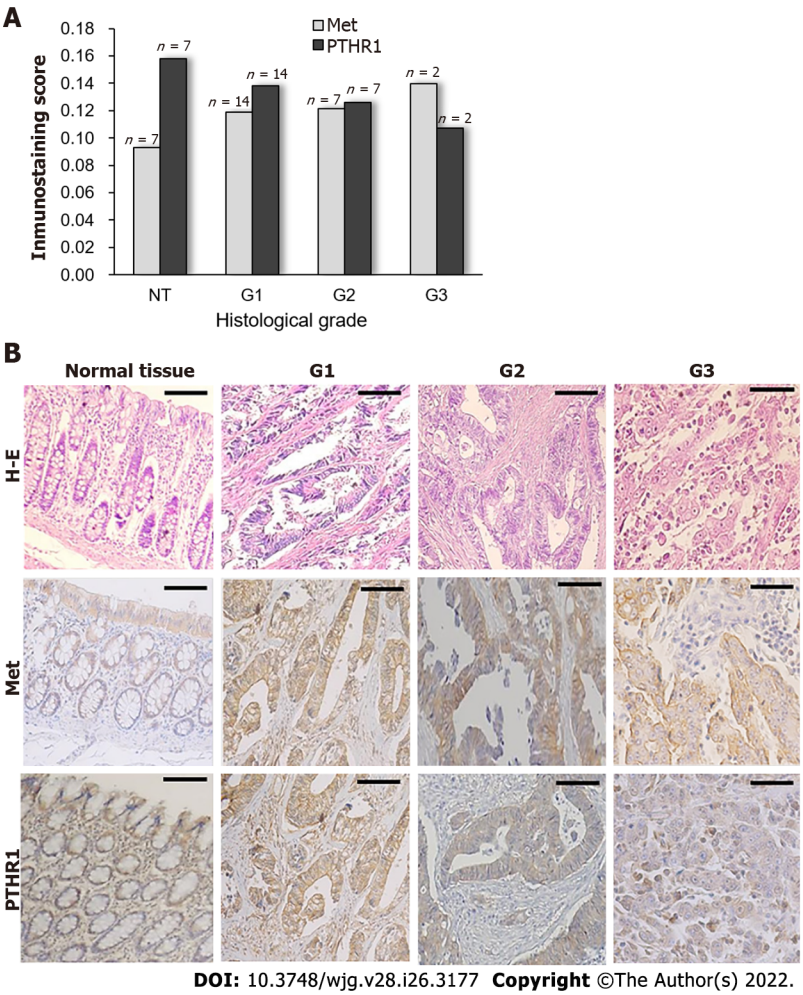
PTHrP favors the aggressive behavior of CRC cells, inducing other events related to the malignant phenotype such as chemoresistance to CPT-11. The tumor cell response to this drug under PTHrP action involves the ERK signaling pathway[26]. Other investigations carried out by Paillas and colleagues demonstrated that the p38 MAPK pathway also modulates the sensitivity of CRC cells to CPT-11[89]. Given the data obtained previously by us and by other researchers and taking into account the link in CRC between Met signaling and the MAPKs pathway showed in this work and by other authors[41], our next motivation was to further investigate the chemoresistance of CRC-derived cells induced by PTHrP by analyzing two key aspects: Whether the cytokine affects the sensitivity of CRC cells to other chemotherapeutic drugs and whether the Met signaling pathway participates in PTHrP-trigged chemoresistance.

Our work shows that the treatment with this cytokine also attenuates the cytotoxicity induced by OXA and DOXO. This is an interesting result as it indicates that PTHrP promotes resistance to different types of cytotoxic agents. Perhaps the mechanisms trigged by this cytokine alter specific targets or the signaling of these drugs. Tumor cells develop different strategies to avoid chemotherapeutic drug effects. To improve the efficacy of the treatment, combinations of multiple agents are usually used[90]. Given that these drugs present different modes of action, pharmacological doses, and side effects[91-93], in the future it will be necessary to continue this research by testing new drugs and combinations thereof as well as elucidating the specific targets of PTHrP for each one.

Besides, the use of SU11274 together with CPT-11, OXA, or DOXO increases the sensitivity of CRC cells to these drugs, suggesting that Met participates in the chemoresistance induced by PTHrP. The inhibitors of markers/pathways related to cancer progression are still under investigation and like all anti-cancer approaches, their applications have challenges in the therapy of the disease[78,94]. With respect to the inhibition of the Met signaling pathway, a recent publication by Du and colleagues proposes to target the HGF/Met axis as a possible strategy for patients with metastatic CRC[94].

So far, our *in vitro* observations have allowed us to suppose the existence of a mechanism based on the action of PTHrP on the regulation of *Met* gene expression and also on its activation through Src kinase and the MAPKs pathway. Once activated, Met signaling leads to molecular changes in the tumor cell to promote chemoresistance to CPT-11, OXA, and DOXO. Probably, the up-regulation of Met expression also collaborates in the induction of events associated with the aggressive behavior of CRC cells (Figure 10). Besides, our results support those studies that suggest the incorporation of Met inhibitors combined with adjuvant drugs as new therapeutic strategies in CRC treatment and establish the need to further investigate whether PTHrP is a predictive and/or prognostic marker of CRC.

In this work, we also performed *in vivo* assays with the aim to evaluate the effects of PTHrP in a different context for tumor cells. As we expected, in agreement with our *in vitro* observations, HCT116

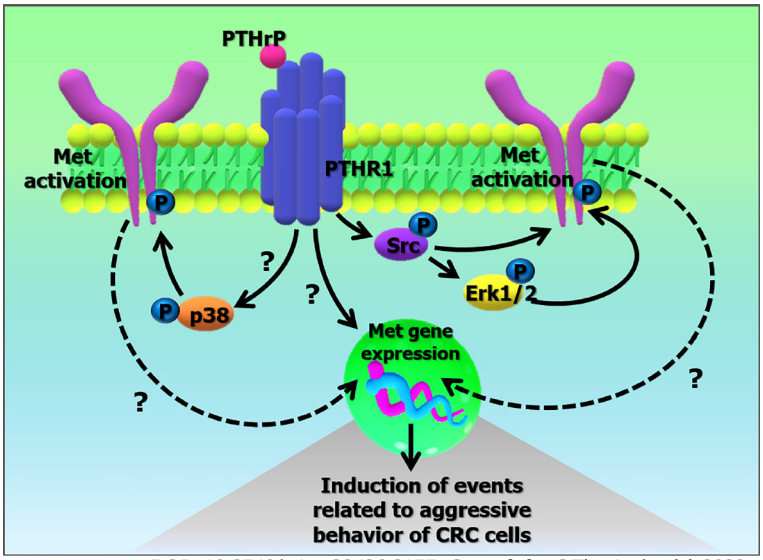


DOI: 10.3748/wjg.v28.i26.3177 **Copyright** ©The Author(s) 2022.

Figure 9 Relation of Met and parathyroid hormone receptor type 1 staining intensity with tumor histological differentiation. A: Quantification of the immunostaining by optical density analysis using the FIJI plug-in from the Image J program; B: Representative images (200 ×) obtained by hematoxylin-eosin staining and by the immunohistochemistry technique performed for Met and PTHR1 for normal colorectal tissue and colorectal cancer tissue, with histological grades G1, G2, and G3. Scale bar: 10 μM. H-E: Hematoxylin-eosin staining; Met: Receptor tyrosine kinase Met; NT: Normal tissue; PTHR1: Parathyroid hormone receptor type 1.

cell tumor xenografts treated with the peptide exhibited an increase in Met protein expression concerning the control. PTHrP increases the levels of its own receptor, perhaps to amplify its signaling within the cell, and thus makes its effects more effective in CRC. Despite the limitations of the N:NIH (S)_nu model regarding the interaction of tumor cells with the stroma[13,24], these results allow us to presume a relationship between the aberrant expression of Met already observed in the tumor tissue of CRC patients[38] and PTHrP/PTHR1.

As we previously stated, although HGF is the only known ligand capable of inducing Met phosphorylation and activation, studies have shown that the cross-communication with G-coupled protein receptors transactivates this RTK. Concerning this, it was demonstrated that the prostaglandin E2 receptor EP1 can induce an aberrant activation of RTKs like Met in hepatocellular carcinoma cells [30]. Similar results had previously been obtained by Fischer and colleagues in pancreatic and hepatocellular carcinoma cells[29]. As we previously mentioned, PTHrP has intracrine, autocrine, endocrine, and mainly paracrine actions through the binding to a G-coupled protein receptor, PTHR1[9,10]. For this reason, the peptide and its receptor are expressed in the same cells or adjacent cells and changes in their expression are directly correlated[14,15]. Considering the previously described background, we evaluated Met and PTHR1 expression in normal colorectal tissues and in biopsies from patients with colon adenocarcinoma. Although Lee and colleagues did not find a statistical relevance between Met overexpression and the clinicopathological characteristics of patients with CRC, they demonstrated that it is associated with a lower overall survival and progression-free survival[38]. In contrast, Kim and his research group concluded that Met expression in patients with CRC is not a prognostic indicator for overall survival[95]. Despite these data, there was no information about the association between Met and PTHR1 expression and its impact on the evolution of CRC. As we expected, given that both receptors have a physiological role, Met and the PTHrP receptor are expressed in normal colon tissue. We found a statistically significant result when we compared the staining of tumors with high



DOI: 10.3748/wjg.v28.i26.3177 **Copyright** ©The Author(s) 2022.

Figure 10 Possible mechanism based on the action of parathyroid hormone-related peptide in the regulation of Met gene expression and its activation. The binding of parathyroid hormone-related peptide (PTHrP) to PTHR type 1 (PTHR1) in HCT116 cells promotes the up-regulation of *Met* gene expression. PTHrP also induces the activation of Met through Src kinase and the mitogen-activated protein kinases (MAPKs) pathway (Erk 1/2 MAPK and p38 MAPK). Once activated, Met signaling leads to molecular changes in the tumor cell that promote events related to the aggressive behavior of colorectal cancer cells. CRC: Colorectal cancer; Erk 1/2: Extracellular signal-regulated kinases 1/2; Met: Receptor tyrosine kinase Met; P: Activators domains phosphorylated; PTHR1: Parathyroid hormone receptor type 1; PTHrP: Parathyroid hormone-related peptide.

histological differentiation compared to those more undifferentiated with regard to the immunoreactivity for Met and PTHR1 that gradually increase and diminish, respectively.

Interestingly, García and colleagues showed that in neuroblastoma, PTHrP acts as a growth factor promoting tumor progression and high levels of its receptor are associated with less aggressive tumor characteristics; also, the intracrine and paracrine actions of the cytokine promote phenotypes with different levels of aggressiveness in their experimental models. These researchers found that PTHR1 is poorly expressed in neuroblastoma cell lines that are not well differentiated; however, in those cells with a high degree of differentiation, PTHR1 has greater expression. Furthermore, they observed that the receptor knockdown promotes a much more aggressive phenotype in more differentiated cells[96]. These data support our observations and could be related with the role of PTHrP and PTHR1 in the promotion of an aggressive phenotype of CRC.

We observed that the intensity of Met immunostaining in tumor cell plasma membrane increases as tumor differentiation declines. Concerning the location of PTHR1 in the plasma membrane, the intensity of the staining gradually decreases in histologically less differentiated tumors; also, it is located in the cytoplasm and the perinuclear region of the tumor cell, with immunoreactivity more predominant in samples with histological degree G3. This could be related to an intracrine role of the cytokine most preponderant in less differentiated CRC cells. More studies are necessary to confirm this.

Based on the above, it is presumed that in the early stages of tumor development, PTHrP would act by binding to its receptor in the tumor cell, possibly inducing Met receptor expression. The secretion of this cytokine from tumor stromal cells has also been reported[97] and we have previously demonstrated its influence on the synthesis and release of tumor microenvironment factors that favor an aggressive CRC phenotype[24,25]. Considering that in less differentiated tumors, we observed lower expression of PTHR1, we hypothesize that in this instance the tumor stromal cells adopt a leading role by secreting (perhaps in response to PTHrP) other cytokines that promote the expression and activation of molecular markers related to a worse prognosis of the disease. The high levels of Met in more advanced stages could be mediated not only by the action of PTHrP but also by other cytokines as other researchers have previously demonstrated[63,98]. It is known that the loss of cellular identity, characteristic of an advanced undifferentiated state, is evidenced by changes in the expression of surface molecules including receptors on tumor cells[99]. The high levels of PTHR1 observed in normal samples and primary neoplasms, and its decrease in undifferentiated histological grades could respond to this effect. On the other hand, high expression of Met in tumor samples is observed in association with a low degree of cellular differentiation. In this context, perhaps PTHR1 and Met could act as markers of cellular dedifferentiation. However, more studies are needed to verify this hypothesis.

CONCLUSION

Here we have demonstrated using an *in vitro* model that the PTHrP pathway promotes events that are associated with a worse evolution of CRC through Met activation. We also provide evidence for the association between PTHrP action and Met expression *in vivo*. Given all this information, it will be of great interest to ascertain the participation of Met in other molecular events related to CRC progression trigged by PTHrP and its translational relevance. More studies are needed in the areas of basic and clinical oncology to confirm this.

ARTICLE HIGHLIGHTS

Research background

Colorectal cancer (CRC) patients usually relapse and die due to the development of metastasis and resistance to chemotherapeutic drugs employed in the treatment. Parathyroid hormone-related peptide (PTHrP) is a cytokine that has a key role in the carcinogenesis and the progression of several tumors. Our research group found that the binding of PTHrP to its receptor, the parathyroid hormone receptor type 1 (PTHR1), promotes events associated with the aggressive phenotype of colorectal cancer cells. The receptor tyrosine kinase Met is associated with metastasis and chemoresistance in CRC.

Research motivation

The mechanisms that lead to an aggressive tumor behavior and a worse response to CRC treatment are still unknown. To date, it has not been studied whether there is a cross-talk between the PTHrP and Met signaling pathways to trigger molecular mechanisms associated with CRC progression.

Research objectives

To investigate the relationship between PTHR1, PTHrP, and Met in the aggressive behavior of CRC cells. These findings could have implications for the future diagnosis, prognosis, and treatment of patients with CRC.

Research methods

By RT-PCR and Western blot analysis, we studied whether PTHrP modulates the expression of Met and its activation in CRC cells. By Western blot and using specific inhibitors, we also evaluated the signaling pathways involved in Met activation induced by PTHrP. By Trypan blue technique, Wound healing assay, Western blot, and morphological analysis, we evaluated whether the Met signaling pathway mediates the effects induced by PTHrP in HCT116 cells. By the immunohistochemistry technique, we evaluated the expression of Met and the PTHrP receptor, PTHR1, in HCT116 cell xenografts of nude mice in response to the treatment with or without PTHrP. An observational analysis of human samples was performed to validate the findings obtained by *in vitro* and *in vivo* assays.

Research results

PTHrP modulated the expression of Met and promoted its activation through Src kinase and the mitogen-activated protein kinase (MAPK) signaling pathway in human HCT116 cells. The Met signaling pathway triggered by PTHrP participated in cellular events related to the aggressive behavior of human HCT116 cells such as proliferation, morphological changes associated with epithelial to mesenchymal transition, and migration and in the decrease of the sensitivity to chemotherapy drugs. PTHrP increased the protein expression of its receptor, PTHR1, and of Met in HCT116 cell tumor xenografts. PTHR1 was highly expressed in well-differentiated human CRC samples. In contrast, Met showed an expression pattern that was increased in poorly differentiated CRC tumors.

Research conclusions

PTHrP promotes events associated with a worse behavior of CRC cells through Met activation. To date, our *in vitro* observations suggest that the binding of PTHrP to its receptor, PTHR1, promotes the regulation of *Met* gene expression and also its activation through the Src kinase and the MAPKs pathway. Once activated, Met signaling leads to molecular changes in the tumor cell to promote events associated with the aggressive behavior of CRC cells. Our previous data together with the findings shown herein reveal that PTHrP *in vivo* modulates the expression of markers linked to tumor progression (including Met) and also of its own receptor. These events could favor the tumor phenotype in the CRC animal model studied in this work.

Research perspectives

In the future, it will be of great interest to evaluate whether Met mediates other molecular mechanisms and events triggered by PTHrP that are involved in CRC progression. Concerning translational

relevance, more studies are needed in the areas of basic and clinical oncology.

FOOTNOTES

Author contributions: Novoa Díaz MB and Carriere P contributed to conceptualization, methodology, investigation, formal analysis, visualization, and manuscript drafting, review, and editing; Gigola G and Zwenger AO contributed to conceptualization, methodology, and investigation; Calvo N contributed to conceptualization, methodology, investigation, formal analysis, visualization, supervision, and manuscript drafting, review, and editing; Gentili C contributed to conceptualization, methodology, resources, investigation, formal analysis, visualization, supervision, manuscript drafting, review, and editing, project administration, and funding acquisition.

Supported by the Agencia Nacional de Promoción Científica y Tecnológica, No. PICT-2013-1441; Consejo Nacional de Investigaciones Científicas y Técnicas, No. PIP11220150100350; Instituto Nacional del Cáncer Asistencia Financiera II, RESOL 493/14, No. 2002-4395-14-1; Instituto Nacional del Cáncer Asistencia Financiera III-2016-2017, RESOL-2016-1006-E-APN-MS, No. 2002-3862-16-1 CANCER; Universidad Nacional del Sur, No. PGI: 24/B230 and No. PGI: 24/B303; and Fundación Alberto J. Roemmers of Argentina.

Institutional review board statement: The study was reviewed and approved by the committee of experts on the subject conformed by members of the Department of Biology, Biochemistry and Pharmacy of the National University of the South.

Institutional animal care and use committee statement: All applicable international, national, and/or institutional guidelines for the care and use of animals were followed. All experiments with animals were approved by a local animal committee for ethics (CICUAE-UNS, institutional endorsement updated to 2021), and were carried out in accordance with the National Institutes of Health guide for the care and use of Laboratory animals (NIH 1996).

Conflict-of-interest statement: There are no conflicts of interest to report.

Data sharing statement: No additional data are available.

ARRIVE guidelines statement: The authors have read the ARRIVE Guidelines, and the manuscript was prepared and revised according to the ARRIVE Guidelines.

Open-Access: This article is an open-access article that was selected by an in-house editor and fully peer-reviewed by external reviewers. It is distributed in accordance with the Creative Commons Attribution NonCommercial (CC BY-NC 4.0) license, which permits others to distribute, remix, adapt, build upon this work non-commercially, and license their derivative works on different terms, provided the original work is properly cited and the use is non-commercial. See: https://creativecommons.org/Licenses/by-nc/4.0/

Country/Territory of origin: Argentina

ORCID number: María Belén Novoa Díaz 0000-0002-6684-4076; Pedro Carriere 0000-0002-5751-8850; Graciela Gigola 0000-0001-7362-3178; Ariel Osvaldo Zwenger 0000-0002-4407-5413; Natalia Calvo 0000-0003-3627-6749; Claudia Gentili 0000-0002-9957-7824.

S-Editor: Chen YL
L-Editor: Wang TQ
P-Editor: Yu HG

REFERENCES

1 **Wang J**, Dong X, Zhu X, Zhao H, Mao D, Zhao X. [Expression of interleukin-9 in colon cancer tissues and its clinical significance]. *Nan Fang Yi Ke Da Xue Xue Bao* 2018; **38**: 943-948 [PMID: 30187869 DOI: 10.3969/j.issn.1673-4254.2018.08.07]
2 **Arnold M**, Sierra MS, Laversanne M, Soerjomataram I, Jemal A, Bray F. Global patterns and trends in colorectal cancer incidence and mortality. *Gut* 2017; **66**: 683-691 [PMID: 26818619 DOI: 10.1136/gutjnl-2015-310912]
3 **Hatano Y**, Fukuda S, Hisamatsu K, Hirata A, Hara A, Tomita H. Multifaceted Interpretation of Colon Cancer Stem Cells. *Int J Mol Sci* 2017; **18** [PMID: 28678194 DOI: 10.3390/ijms18071446]
4 Erratum: Global cancer statistics 2018: GLOBOCAN estimates of incidence and mortality worldwide for 36 cancers in 185 countries. *CA Cancer J Clin* 2020; **70**: 313 [PMID: 32767693 DOI: 10.3322/caac.21609]
5 **Li J**, Huang L, Zhao H, Yan Y, Lu J. The Role of Interleukins in Colorectal Cancer. *Int J Biol Sci* 2020; **16**: 2323-2339 [PMID: 32760201 DOI: 10.7150/ijbs.46651]
6 **Parsons S**, Maldonado EB, Prasad V. Comparison of Drugs Used for Adjuvant and Metastatic Therapy of Colon, Breast, and Non-Small Cell Lung Cancers. *JAMA Netw Open* 2020; **3**: e202488 [PMID: 32275321 DOI:

10.1001/jamanetworkopen.2020.2488]
7 **Chang CL**, Yuan KS, Wu ATH, Wu SY. Adjuvant Therapy for High-Risk Stage II or III Colon Adenocarcinoma: A Propensity Score-Matched, Nationwide, Population-Based Cohort Study. *Cancers (Basel)* 2019; **11** [PMID: 31842371 DOI: 10.3390/cancers11122003]
8 **Meyers BM**, Cosby R, Quereshy F, Jonker D. Adjuvant Chemotherapy for Stage II and III Colon Cancer Following Complete Resection: A Cancer Care Ontario Systematic Review. *Clin Oncol (R Coll Radiol)* 2017; **29**: 459-465 [PMID: 28341242 DOI: 10.1016/j.clon.2017.03.001]
9 **Maioli E**, Fortino V. PTHrP on MCF-7 breast cancer cells: a growth factor or an antimitogenic peptide? *Br J Cancer* 2004; **90**: 1293-4; author reply 1295 [PMID: 15026815 DOI: 10.1038/sj.bjc.6601689]
10 **McCauley LK**, Martin TJ. Twenty-five years of PTHrP progress: from cancer hormone to multifunctional cytokine. *J Bone Miner Res* 2012; **27**: 1231-1239 [PMID: 22549910 DOI: 10.1002/jbmr.1617]
11 **Goltzman D**. Nonparathyroid Hypercalcemia. *Front Horm Res* 2019; **51**: 77-90 [PMID: 30641526 DOI: 10.1159/000491040]
12 **He S**, Tang J, Diao N, Liao Y, Shi J, Xu X, Xie F, Bai L. Parathyroid hormone-related protein activates HSCs *via* hedgehog signalling during liver fibrosis development. *Artif Cells Nanomed Biotechnol* 2019; **47**: 1984-1994 [PMID: 31311343 DOI: 10.1080/21691401.2019.1615931]
13 **Novoa Díaz MB**, Carriere PM, Martín MJ, Calvo N, Gentili C. Involvement of parathyroid hormone-related peptide in the aggressive phenotype of colorectal cancer cells. *World J Gastroenterol* 2021; **27**: 7025-7040 [PMID: 34887626 DOI: 10.3748/wjg.v27.i41.7025]
14 **Martin TJ**. Parathyroid Hormone-Related Protein, Its Regulation of Cartilage and Bone Development, and Role in Treating Bone Diseases. *Physiol Rev* 2016; **96**: 831-871 [PMID: 27142453 DOI: 10.1152/physrev.00031.2015]
15 **Kim MR**, Choi SH, Lee BN, Min KS, Hwang YC. Effect of parathyroid hormone-related protein on odontogenic differentiation in human dental pulp cells. *BMC Oral Health* 2020; **20**: 101 [PMID: 32276610 DOI: 10.1186/s12903-020-01085-8]
16 **Zhang R**, Li J, Assaker G, Camirand A, Sabri S, Karaplis AC, Kremer R. Parathyroid Hormone-Related Protein (PTHrP): An Emerging Target in Cancer Progression and Metastasis. *Adv Exp Med Biol* 2019; **1164**: 161-178 [PMID: 31576548 DOI: 10.1007/978-3-030-22254-3_13]
17 **Kremer R**, Li J, Camirand A, Karaplis AC. Parathyroid hormone related protein (PTHrP) in tumor progression. *Adv Exp Med Biol* 2011; **720**: 145-160 [PMID: 21901625 DOI: 10.1007/978-1-4614-0254-1_12]
18 **Nishihara M**, Kanematsu T, Taguchi T, Razzaque MS. PTHrP and tumorigenesis: is there a role in prognosis? *Ann N Y Acad Sci* 2007; **1117**: 385-392 [PMID: 18056053 DOI: 10.1196/annals.1402.046]
19 **Nishihara M**, Ito M, Tomioka T, Ohtsuru A, Taguchi T, Kanematsu T. Clinicopathological implications of parathyroid hormone-related protein in human colorectal tumours. *J Pathol* 1999; **187**: 217-222 [PMID: 10365097 DOI: 10.1002/(SICI)1096-9896(199901)187:2<217:AID-PATH210>3.0.CO;2-0]
20 **Malakouti S**, Asadi FK, Kukreja SC, Abcarian HA, Cintron JR. Parathyroid hormone-related protein expression in the human colon: immunohistochemical evaluation. *Am Surg* 1996; **62**: 540-4; discussion 544 [PMID: 8651548]
21 **Ongkeko WM**, Burton D, Kiang A, Abhold E, Kuo SZ, Rahimy E, Yang M, Hoffman RM, Wang-Rodriguez J, Deftos LJ. Parathyroid hormone related-protein promotes epithelial-to-mesenchymal transition in prostate cancer. *PLoS One* 2014; **9**: e85803 [PMID: 24465715 DOI: 10.1371/journal.pone.0085803]
22 **Sen S**, Dasgupta P, Kamath G, Srikanth HS. Paratharmone related protein (peptide): A novel prognostic, diagnostic and therapeutic marker in Head & Neck cancer. *J Stomatol Oral Maxillofac Surg* 2018; **119**: 33-36 [PMID: 29081380 DOI: 10.1016/j.jormas.2017.10.016]
23 **Hong N**, Yoon HJ, Lee YH, Kim HR, Lee BW, Rhee Y, Kang ES, Cha BS, Lee HC. Serum PTHrP Predicts Weight Loss in Cancer Patients Independent of Hypercalcemia, Inflammation, and Tumor Burden. *J Clin Endocrinol Metab* 2016; **101**: 1207-1214 [PMID: 26765580 DOI: 10.1210/jc.2015-3785]
24 **Carriere P**, Calvo N, Novoa Díaz MB, Lopez-Moncada F, Herrera A, Torres MJ, Alonso E, Gandini NA, Gigola G, Contreras HR, Gentili C. Role of SPARC in the epithelial-mesenchymal transition induced by PTHrP in human colon cancer cells. *Mol Cell Endocrinol* 2021; **530**: 111253 [PMID: 33781836 DOI: 10.1016/j.mce.2021.111253]
25 **Calvo N**, Carriere P, Martín MJ, Gigola G, Gentili C. PTHrP treatment of colon cancer cells promotes tumor associated-angiogenesis by the effect of VEGF. *Mol Cell Endocrinol* 2019; **483**: 50-63 [PMID: 30639585 DOI: 10.1016/j.mce.2019.01.005]
26 **Martín MJ**, Gigola G, Zwenger A, Carriquiriborde M, Gentil F, Gentili C. Potential therapeutic targets for growth arrest of colorectal cancer cells exposed to PTHrP. *Mol Cell Endocrinol* 2018; **478**: 32-44 [PMID: 30009852 DOI: 10.1016/j.mce.2018.07.005]
27 **Calvo N**, Carriere P, Martin MJ, Gentili C. RSK activation *via* ERK modulates human colon cancer cells response to PTHrP. *J Mol Endocrinol* 2017; **59**: 13-27 [PMID: 28385776 DOI: 10.1530/JME-16-0216]
28 **Choi YJ**, Kim JH, Rho JK, Kim JS, Choi CM, Kim WS, Son J, Lee JC. AXL and MET receptor tyrosine kinases are essential for lung cancer metastasis. *Oncol Rep* 2017; **37**: 2201-2208 [PMID: 28260071 DOI: 10.3892/or.2017.5482]
29 **Fischer OM**, Giordano S, Comoglio PM, Ullrich A. Reactive oxygen species mediate Met receptor transactivation by G protein-coupled receptors and the epidermal growth factor receptor in human carcinoma cells. *J Biol Chem* 2004; **279**: 28970-28978 [PMID: 15123705 DOI: 10.1074/jbc.M402508200]
30 **Han C**, Michalopoulos GK, Wu T. Prostaglandin E2 receptor EP1 transactivates EGFR/MET receptor tyrosine kinases and enhances invasiveness in human hepatocellular carcinoma cells. *J Cell Physiol* 2006; **207**: 261-270 [PMID: 16331686 DOI: 10.1002/jcp.20560]
31 **Cattaneo F**, Guerra G, Parisi M, De Marinis M, Tafuri D, Cinelli M, Ammendola R. Cell-surface receptors transactivation mediated by g protein-coupled receptors. *Int J Mol Sci* 2014; **15**: 19700-19728 [PMID: 25356505 DOI: 10.3390/ijms151119700]
32 **Mezquita B**, Pineda E, Mezquita J, Mezquita P, Pau M, Codony-Servat J, Martínez-Balibrea E, Mora C, Maurel J, Mezquita C. LoVo colon cancer cells resistant to oxaliplatin overexpress c-MET and VEGFR-1 and respond to VEGF with

dephosphorylation of c-MET. *Mol Carcinog* 2016; **55**: 411-419 [PMID: 25647613 DOI: 10.1002/mc.22289]
33 **Mulcahy EQX**, Colón RR, Abounader R. HGF/MET Signaling in Malignant Brain Tumors. *Int J Mol Sci* 2020; **21** [PMID: 33066121 DOI: 10.3390/ijms21207546]
34 **Huang L**, Xie K, Li H, Wang R, Xu X, Chen K, Gu H, Fang J. Suppression of c-Met-Overexpressing Tumors by a Novel c-Met/CD3 Bispecific Antibody. *Drug Des Devel Ther* 2020; **14**: 3201-3214 [PMID: 32982167 DOI: 10.2147/DDDT.S254117]
35 **Wang S**, Qiu J, Liu L, Su C, Qi L, Huang C, Chen X, Zhang Y, Ye Y, Ding Y, Liang L, Liao W. CREB5 promotes invasiveness and metastasis in colorectal cancer by directly activating MET. *J Exp Clin Cancer Res* 2020; **39**: 168 [PMID: 32843066 DOI: 10.1186/s13046-020-01673-0]
36 **Cai P**, Xie Y, Dong M, Zhu Q. Inhibition of *MEIS3* Generates Cetuximab Resistance through c-Met and Akt. *Biomed Res Int* 2020; **2020**: 2046248 [PMID: 33376716 DOI: 10.1155/2020/2046248]
37 **Shali H**, Ahmadi M, Kafil HS, Dorosti A, Yousefi M. IGF1R and c-met as therapeutic targets for colorectal cancer. *Biomed Pharmacother* 2016; **82**: 528-536 [PMID: 27470393 DOI: 10.1016/j.biopha.2016.05.034]
38 **Lee SJ**, Lee J, Park SH, Park JO, Lim HY, Kang WK, Park YS, Kim ST. c-MET Overexpression in Colorectal Cancer: A Poor Prognostic Factor for Survival. *Clin Colorectal Cancer* 2018; **17**: 165-169 [PMID: 29576428 DOI: 10.1016/j.clcc.2018.02.013]
39 **Martín MJ**, Calvo N, de Boland AR, Gentili C. Molecular mechanisms associated with PTHrP-induced proliferation of colon cancer cells. *J Cell Biochem* 2014; **115**: 2133-2145 [PMID: 25053227 DOI: 10.1002/jcb.24890]
40 **Calvo N**, Martín MJ, de Boland AR, Gentili C. Involvement of ERK1/2, p38 MAPK, and PI3K/Akt signaling pathways in the regulation of cell cycle progression by PTHrP in colon adenocarcinoma cells. *Biochem Cell Biol* 2014; **92**: 305-315 [PMID: 25051885 DOI: 10.1139/bcb-2013-0106]
41 **Larsen CA**, Dashwood RH. (-)-Epigallocatechin-3-gallate inhibits Met signaling, proliferation, and invasiveness in human colon cancer cells. *Arch Biochem Biophys* 2010; **501**: 52-57 [PMID: 20361925 DOI: 10.1016/j.abb.2010.03.017]
42 **Bradford MM**. A rapid and sensitive method for the quantitation of microgram quantities of protein utilizing the principle of protein-dye binding. *Anal Biochem* 1976; **72**: 248-254 [PMID: 942051 DOI: 10.1006/abio.1976.9999]
43 **Naba NM**, Tolay N, Erman B, Sayi Yazgan A. Doxorubicin inhibits miR-140 expression and upregulates PD-L1 expression in HCT116 cells, opposite to its effects on MDA-MB-231 cells. *Turk J Biol* 2020; **44**: 15-23 [PMID: 32123492 DOI: 10.3906/biy-1909-12]
44 **Attoub S**, Arafat K, Khalaf T, Sulaiman S, Iratni R. Frondoside A Enhances the Anti-Cancer Effects of Oxaliplatin and 5-Fluorouracil on Colon Cancer Cells. *Nutrients* 2018; **10** [PMID: 29724012 DOI: 10.3390/nu10050560]
45 **Lu X**, Wei H, Zhang X, Zheng W, Chang C, Gu J. Rapamycin synergizes with low-dose oxaliplatin in the HCT116 colon cancer cell line by inducing enhanced apoptosis. *Oncol Lett* 2011; **2**: 643-647 [PMID: 22848242 DOI: 10.3892/ol.2011.299]
46 **Sabit H**, Samy MB, Said OA, El-Zawahri MM. Procaine Induces Epigenetic Changes in HCT116 Colon Cancer Cells. *Genet Res Int* 2016; **2016**: 8348450 [PMID: 27843649 DOI: 10.1155/2016/8348450]
47 **Dunn EF**, Iida M, Myers RA, Campbell DA, Hintz KA, Armstrong EA, Li C, Wheeler DL. Dasatinib sensitizes KRAS mutant colorectal tumors to cetuximab. *Oncogene* 2011; **30**: 561-574 [PMID: 20956938 DOI: 10.1038/onc.2010.430]
48 **Zhou H**, Iida-Klein A, Lu SS, Ducayen-Knowles M, Levine LR, Dempster DW, Lindsay R. Anabolic action of parathyroid hormone on cortical and cancellous bone differs between axial and appendicular skeletal sites in mice. *Bone* 2003; **32**: 513-520 [PMID: 12753867 DOI: 10.1016/s8756-3282(03)00057-7]
49 **Stewart AF**, Cain RL, Burr DB, Jacob D, Turner CH, Hock JM. Six-month daily administration of parathyroid hormone and parathyroid hormone-related protein peptides to adult ovariectomized rats markedly enhances bone mass and biomechanical properties: a comparison of human parathyroid hormone 1-34, parathyroid hormone-related protein 1-36, and SDZ-parathyroid hormone 893. *J Bone Miner Res* 2000; **15**: 1517-1525 [PMID: 10934650 DOI: 10.1359/jbmr.2000.15.8.1517]
50 **Frolik CA**, Cain RL, Sato M, Harvey AK, Chandrasekhar S, Black EC, Tashjian AH Jr, Hock JM. Comparison of recombinant human PTH(1-34) (LY333334) with a C-terminally substituted analog of human PTH-related protein(1-34) (RS-66271): In vitro activity and in vivo pharmacological effects in rats. *J Bone Miner Res* 1999; **14**: 163-172 [PMID: 9933468 DOI: 10.1359/jbmr.1999.14.2.163]
51 **Sierrasesµmaga L**. Tumores sólidos más frecuentes en la infancia. *AnPediatriContin* 2004; 153
52 **Farrugia W**, de Gooyer T, Rice GE, Moseley JM, Wlodek ME. Parathyroid hormone(1-34) and parathyroid hormone-related protein(1-34) stimulate calcium release from human syncytiotrophoblast basal membranes *via* a common receptor. *J Endocrinol* 2000; **166**: 689-695 [PMID: 10974662 DOI: 10.1677/joe.0.1660689]
53 **Lassoued S**, Caulier M, Poey C, Fournié B, Fournié A. [Lumbago-sciatica disclosing a spinal lipoma. A case report]. *Rev Rhum Mal Osteoartic* 1990; **57**: 563-565 [PMID: 2149201 DOI: 10.1089/bfm.2010.0101]
54 **Crowe AR**, Yue W. Semi-quantitative Determination of Protein Expression using Immunohistochemistry Staining and Analysis: An Integrated Protocol. *Bio Protoc* 2019; **9** [PMID: 31867411 DOI: 10.21769/BioProtoc.3465]
55 **Schindelin J**, Arganda-Carreras I, Frise E, Kaynig V, Longair M, Pietzsch T, Preibisch S, Rueden C, Saalfeld S, Schmid B, Tinevez JY, White DJ, Hartenstein V, Eliceiri K, Tomancak P, Cardona A. Fiji: an open-source platform for biological-image analysis. *Nat Methods* 2012; **9**: 676-682 [PMID: 22743772 DOI: 10.1038/nmeth.2019]
56 **R Core Team**. A language and environment for statistical computing. 2020. [cited 20 March 2022]. Available from: https://www.R-project.org/
57 **Chen R**, Li J, Feng CH, Chen SK, Liu YP, Duan CY, Li H, Xia XM, He T, Wei M, Dai RY. c-Met function requires N-linked glycosylation modification of pro-Met. *J Cell Biochem* 2013; **114**: 816-822 [PMID: 23060267 DOI: 10.1002/jcb.24420]
58 **Zhang J**, Wang Z, Zhang S, Chen Y, Xiong X, Li X, Tonks NK, Fan G. Spatial regulation of signaling by the coordinated action of the protein tyrosine kinases MET and FER. *Cell Signal* 2018; **50**: 100-110 [PMID: 29920310 DOI: 10.1016/j.cellsig.2018.06.006]
59 **Ma DJ**, Cao Z, Wang BS, Sun YL. [Effect of silencing hepatocyte growth factor receptor c-Met expression on biological

characteristics of colon cancer cells]. *Zhonghua Zhong Liu Za Zhi* 2020; **42**: 362-368 [PMID: 32482024 DOI: 10.3760/cma.j.cn112152-112152-20191106-00714]

60 **Hastings RH**, Montgrain PR, Quintana RA, Chobrutskiy B, Davani A, Miyanohara A, Mahooti S. Lung carcinoma progression and survival versus amino- and carboxyl-parathyroid hormone-related protein expression. *J Cancer Res Clin Oncol* 2017; **143**: 1395-1407 [PMID: 28342003 DOI: 10.1007/s00432-017-2396-4]

61 **Calvo N**, German O, Russo de Boland A, Gentili C. Pro-apoptotic effects of parathyroid hormone in intestinal cells. *Biochem Cell Biol* 2009; **87**: 389-400 [PMID: 19370057 DOI: 10.1139/O08-143]

62 **Critchley WR**, Pellet-Many C, Ringham-Terry B, Harrison MA, Zachary IC, Ponnambalam S. Receptor Tyrosine Kinase Ubiquitination and De-Ubiquitination in Signal Transduction and Receptor Trafficking. *Cells* 2018; **7** [PMID: 29543760 DOI: 10.3390/cells7030022]

63 **Bradley CA**, Dunne PD, Bingham V, McQuaid S, Khawaja H, Craig S, James J, Moore WL, McArt DG, Lawler M, Dasgupta S, Johnston PG, Van Schaeybroeck S. Transcriptional upregulation of c-MET is associated with invasion and tumor budding in colorectal cancer. *Oncotarget* 2016; **7**: 78932-78945 [PMID: 27793046 DOI: 10.18632/oncotarget.12933]

64 **Martínez-Pérez J**, Lopez-Calderero I, Saez C, Benavent M, Limon ML, Gonzalez-Exposito R, Soldevilla B, Riesco-Martínez MC, Salamanca J, Carnero A, Garcia-Carbonero R. Prognostic relevance of Src activation in stage II-III colon cancer. *Hum Pathol* 2017; **67**: 119-125 [PMID: 28601656 DOI: 10.1016/j.humpath.2017.05.025]

65 **Steeg PS**. Targeting metastasis. *Nat Rev Cancer* 2016; **16**: 201-218 [PMID: 27009393 DOI: 10.1038/nrc.2016.25]

66 **Chen J**, Elfiky A, Han M, Chen C, Saif MW. The role of Src in colon cancer and its therapeutic implications. *Clin Colorectal Cancer* 2014; **13**: 5-13 [PMID: 24361441 DOI: 10.1016/j.clcc.2013.10.003]

67 **Braicu C**, Buse M, Busuioc C, Drula R, Gulei D, Raduly L, Rusu A, Irimie A, Atanasov AG, Slaby O, Ionescu C, Berindan-Neagoe I. A Comprehensive Review on MAPK: A Promising Therapeutic Target in Cancer. *Cancers (Basel)* 2019; **11** [PMID: 31652660 DOI: 10.3390/cancers11101618]

68 **Yuan J**, Dong X, Yap J, Hu J. The MAPK and AMPK signalings: interplay and implication in targeted cancer therapy. *J Hematol Oncol* 2020; **13**: 113 [PMID: 32807225 DOI: 10.1186/s13045-020-00949-4]

69 **Degirmenci U**, Wang M, Hu J. Targeting Aberrant RAS/RAF/MEK/ERK Signaling for Cancer Therapy. *Cells* 2020; **9** [PMID: 31941155 DOI: 10.3390/cells9010198]

70 **Gao W**, Bing X, Li M, Yang Z, Li Y, Chen H. Study of critical role of c-Met and its inhibitor SU11274 in colorectal carcinoma. *Med Oncol* 2013; **30**: 546 [PMID: 23536000 DOI: 10.1007/s12032-013-0546-3]

71 **Matsumoto K**, Umitsu M, De Silva DM, Roy A, Bottaro DP. Hepatocyte growth factor/MET in cancer progression and biomarker discovery. *Cancer Sci* 2017; **108**: 296-307 [PMID: 28064454 DOI: 10.1111/cas.13156]

72 **Gao SH**, Liu C, Wei J, Feng Y. Effect of c-Met inhibitor SU11274 on human colon cancer cell growth. *Chin Med J (Engl)* 2013; **126**: 2705-2709 [PMID: 23876900]

73 **Troiani T**, Martinelli E, Napolitano S, Vitagliano D, Ciuffreda LP, Costantino S, Morgillo F, Capasso A, Sforza V, Nappi A, De Palma R, D'Aiuto E, Berrino L, Bianco R, Ciardiello F. Increased TGF-α as a mechanism of acquired resistance to the anti-EGFR inhibitor cetuximab through EGFR-MET interaction and activation of MET signaling in colon cancer cells. *Clin Cancer Res* 2013; **19**: 6751-6765 [PMID: 24122793 DOI: 10.1158/1078-0432.CCR-13-0423]

74 **Loboda A**, Nebozhyn MV, Watters JW, Buser CA, Shaw PM, Huang PS, Van't Veer L, Tollenaar RA, Jackson DB, Agrawal D, Dai H, Yeatman TJ. EMT is the dominant program in human colon cancer. *BMC Med Genomics* 2011; **4**: 9 [PMID: 21251323 DOI: 10.1186/1755-8794-4-9]

75 **Tsoumas D**, Nikou S, Giannopoulou E, Champeris Tsaniras S, Sirinian C, Maroulis I, Taraviras S, Zolota V, Kalofonos HP, Bravou V. ILK Expression in Colorectal Cancer Is Associated with EMT, Cancer Stem Cell Markers and Chemoresistance. *Cancer Genomics Proteomics* 2018; **15**: 127-141 [PMID: 29496692 DOI: 10.21873/cgp.20071]

76 **Gurzu S**, Silveanu C, Fetyko A, Butiurca V, Kovacs Z, Jung I. Systematic review of the old and new concepts in the epithelial-mesenchymal transition of colorectal cancer. *World J Gastroenterol* 2016; **22**: 6764-6775 [PMID: 27570416 DOI: 10.3748/wjg.v22.i30.6764]

77 **Druzhkova I**, Ignatova N, Prodanets N, Kiselev N, Zhukov I, Shirmanova M, Zagainov V, Zagaynova E. E-Cadherin in Colorectal Cancer: Relation to Chemosensitivity. *Clin Colorectal Cancer* 2019; **18**: e74-e86 [PMID: 30415989 DOI: 10.1016/j.clcc.2018.10.003]

78 **Jeon HM**, Lee J. MET: roles in epithelial-mesenchymal transition and cancer stemness. *Ann Transl Med* 2017; **5**: 5 [PMID: 28164090 DOI: 10.21037/atm.2016.12.67]

79 **Mocellin S**, Baretta Z, Roqué I Figuls M, Solà I, Martin-Richard M, Hallum S, Bonfill Cosp X. Second-line systemic therapy for metastatic colorectal cancer. *Cochrane Database Syst Rev* 2017; **1**: CD006875 [PMID: 28128439 DOI: 10.1002/14651858.CD006875.pub3]

80 **Goldberg RM**, Sargent DJ, Morton RF, Fuchs CS, Ramanathan RK, Williamson SK, Findlay BP, Pitot HC, Alberts SR. A randomized controlled trial of fluorouracil plus leucovorin, irinotecan, and oxaliplatin combinations in patients with previously untreated metastatic colorectal cancer. *J Clin Oncol* 2004; **22**: 23-30 [PMID: 14665611 DOI: 10.1200/JCO.2004.09.046]

81 **Zhou X**, Xiao D. Long non-coding RNA GAS5 is critical for maintaining stemness and induces chemoresistance in cancer stem-like cells derived from HCT116. *Oncol Lett* 2020; **19**: 3431-3438 [PMID: 32269616 DOI: 10.3892/ol.2020.11471]

82 **Yang C**, Ran Q, Zhou Y, Liu S, Zhao C, Yu X, Zhu F, Ji Y, Du Q, Yang T, Zhang W, He S. Doxorubicin sensitizes cancer cells to Smac mimetic *via* synergistic activation of the CYLD/RIPK1/FADD/caspase-8-dependent apoptosis. *Apoptosis* 2020; **25**: 441-455 [PMID: 32418059 DOI: 10.1007/s10495-020-01604-6]

83 **Delitto D**, Vertes-George E, Hughes SJ, Behrns KE, Trevino JG. c-Met signaling in the development of tumorigenesis and chemoresistance: potential applications in pancreatic cancer. *World J Gastroenterol* 2014; **20**: 8458-8470 [PMID: 25024602 DOI: 10.3748/wjg.v20.i26.8458]

84 **Cañadas I**, Rojo F, Taus Á, Arpí O, Arumí-Uría M, Pijuan L, Menéndez S, Zazo S, Dómine M, Salido M, Mojal S, García de Herreros A, Rovira A, Albanell J, Arriola E. Targeting epithelial-to-mesenchymal transition with Met inhibitors reverts chemoresistance in small cell lung cancer. *Clin Cancer Res* 2014; **20**: 938-950 [PMID: 24284055 DOI: 10.1158/1078-0432.CCR-13-1330]

85 **Soki FN**, Park SI, McCauley LK. The multifaceted actions of PTHrP in skeletal metastasis. *Future Oncol* 2012; **8**: 803-817 [PMID: 22830401 DOI: 10.2217/fon.12.76]

86 **Silva Paiva R**, Gomes I, Casimiro S, Fernandes I, Costa L. c-Met expression in renal cell carcinoma with bone metastases. *J Bone Oncol* 2020; **25**: 100315 [PMID: 33024658 DOI: 10.1016/j.jbo.2020.100315]

87 **Ahmed D**, Eide PW, Eilertsen IA, Danielsen SA, Eknæs M, Hektoen M, Lind GE, Lothe RA. Epigenetic and genetic features of 24 colon cancer cell lines. *Oncogenesis* 2013; **2**: e71 [PMID: 24042735 DOI: 10.1038/oncsis.2013.35]

88 **Ilyas M**, Tomlinson IP, Rowan A, Pignatelli M, Bodmer WF. Beta-catenin mutations in cell lines established from human colorectal cancers. *Proc Natl Acad Sci U S A* 1997; **94**: 10330-10334 [PMID: 9294210 DOI: 10.1073/pnas.94.19.10330]

89 **Paillas S**, Boissière F, Bibeau F, Denouel A, Mollevi C, Causse A, Denis V, Vezzio-Vié N, Marzi L, Cortijo C, Ait-Arsa I, Askari N, Pourquier P, Martineau P, Del Rio M, Gongora C. Targeting the p38 MAPK pathway inhibits irinotecan resistance in colon adenocarcinoma. *Cancer Res* 2011; **71**: 1041-1049 [PMID: 21159664 DOI: 10.1158/0008-5472.CAN-10-2726]

90 **Gelibter AJ**, Caponnetto S, Urbano F, Emiliani A, Scagnoli S, Sirgiovanni G, Napoli VM, Cortesi E. Adjuvant chemotherapy in resected colon cancer: When, how and how long? *Surg Oncol* 2019; **30**: 100-107 [PMID: 31500770 DOI: 10.1016/j.suronc.2019.06.003]

91 **Murai J**, Thomas A, Miettinen M, Pommier Y. Schlafen 11 (SLFN11), a restriction factor for replicative stress induced by DNA-targeting anti-cancer therapies. *Pharmacol Ther* 2019; **201**: 94-102 [PMID: 31128155 DOI: 10.1016/j.pharmthera.2019.05.009]

92 **Riddell IA**. Cisplatin and Oxaliplatin: Our Current Understanding of Their Actions. *Met Ions Life Sci* 2018; **18** [PMID: 29394020 DOI: 10.1515/9783110470734-007]

93 **Dasari S**, Tchounwou PB. Cisplatin in cancer therapy: molecular mechanisms of action. *Eur J Pharmacol* 2014; **740**: 364-378 [PMID: 25058905 DOI: 10.1016/j.ejphar.2014.07.025]

94 **Du F**, Li X, Feng W, Qiao C, Chen J, Jiang M, Qiu Z, Qian M, Tian D, Nie Y, Fan D, Wu K, Xia L. SOX13 promotes colorectal cancer metastasis by transactivating SNAI2 and c-MET. *Oncogene* 2020; **39**: 3522-3540 [PMID: 32111984 DOI: 10.1038/s41388-020-1233-4]

95 **Kim HJ**, Baek MJ, Kang DH, Lee SC, Bae SB, Lee KT, Lee N, Kim H, Jeong D, Ahn TS, Lee MS, Hong DS, Won JH. Association Between c-Met and Lymphangiogenic Factors in Patients With Colorectal Cancer. *Ann Coloproctol* 2018; **34**: 88-93 [PMID: 29742856 DOI: 10.3393/ac.2017.10.10]

96 **García M**, Rodríguez-Hernández CJ, Mateo-Lozano S, Pérez-Jaume S, Gonçalves-Alves E, Lavarino C, Mora J, de Torres C. Parathyroid hormone-like hormone plays a dual role in neuroblastoma depending on PTH1R expression. *Mol Oncol* 2019; **13**: 1959-1975 [PMID: 31293052 DOI: 10.1002/1878-0261.12542]

97 **Cowan RW**, Singh G, Ghert M. PTHrP increases RANKL expression by stromal cells from giant cell tumor of bone. *J Orthop Res* 2012; **30**: 877-884 [PMID: 22102368 DOI: 10.1002/jor.22020]

98 **Takeuchi H**, Bilchik A, Saha S, Turner R, Wiese D, Tanaka M, Kuo C, Wang HJ, Hoon DS. c-MET expression level in primary colon cancer: a predictor of tumor invasion and lymph node metastases. *Clin Cancer Res* 2003; **9**: 1480-1488 [PMID: 12684423]

99 **Kim WT**, Ryu CJ. Cancer stem cell surface markers on normal stem cells. *BMB Rep* 2017; **50**: 285-298 [PMID: 28270302 DOI: 10.5483/BMBRep.2017.50.6.039]

World Journal of Gastroenterology

Submit a Manuscript: https://www.f6publishing.com

World J Gastroenterol 2022 July 14; 28(26): 3201-3217

DOI: 10.3748/wjg.v28.i26.3201

ISSN 1007-9327 (print) ISSN 2219-2840 (online)

ORIGINAL ARTICLE

Basic Study

Intracellular alpha-fetoprotein mitigates hepatocyte apoptosis and necroptosis by inhibiting endoplasmic reticulum stress

Yun-Fen Chen, Si-Ying Liu, Qi-Jiao Cheng, Yu-Jiao Wang, Shuang Chen, Yi-Yang Zhou, Xia Liu, Zhi-Gang Jiang, Wei-Wei Zhong, Yi-Huai He

Specialty type: Gastroenterology and hepatology

Provenance and peer review: Unsolicited article; Externally peer reviewed.

Peer-review model: Single blind

Peer-review report's scientific quality classification

Grade A (Excellent): A
Grade B (Very good): 0
Grade C (Good): C
Grade D (Fair): 0
Grade E (Poor): 0

P-Reviewer: Kai K, Japan; Salgado LP, United States

Received: January 13, 2022
Peer-review started: January 13, 2022
First decision: March 8, 2022
Revised: March 22, 2022
Accepted: May 13, 2022
Article in press: May 13, 2022
Published online: July 14, 2022

Yun-Fen Chen, Si-Ying Liu, Qi-Jiao Cheng, Shuang Chen, Yi-Yang Zhou, Xia Liu, Yi-Huai He, Department of Infectious Diseases, The Affiliated Hospital of Zunyi Medical University, Zunyi 563000, Guizhou Province, China

Yu-Jiao Wang, Department of General Medicine, The Affiliated Hospital of Zunyi Medical University, Zunyi 563000, Guizhou Province, China

Zhi-Gang Jiang, School of Public Health, Zunyi Medical University, Zunyi 563099, Guizhou Province, China

Wei-Wei Zhong, Department of Endoscopy, Jingmen No.1 People's Hospital, Jingmen 448000, Hubei Province, China

Corresponding author: Yi-Huai He, MM, Director, Department of Infectious Diseases, The Affiliated Hospital of Zunyi Medical University, No. 201 Dalian Street, Zunyi 563000, Guizhou Province, China. 993565989@qq.com

Abstract

BACKGROUND

Endoplasmic reticulum (ER) stress contributes to the pathogenesis of chronic liver diseases, but how hepatocytes respond to ER stress has not been clarified. Alpha-fetoprotein (AFP) is secreted by hepatoma cells and elevated levels of serum AFP are associated with development of liver malignancies.

AIM

To investigate whether and how AFP could regulate ER stress and hepatocyte injury.

METHODS

The distribution of AFP and the degrees of ER stress in liver tissues and liver injury were characterized by histology, immunohistochemistry, and Western blot in biopsied human liver specimens, two mouse models of liver injury and a cellular model. The levels of AFP in sera and the supernatants of cultured cells were quantified by chemiluminescence.

RESULTS

High levels of intracellular AFP were detected in liver tissues, particularly in the

necrotic areas, from patients with chronic liver diseases and mice after carbon tetrachloride (CCl_4) administration or induction of ER stress, but not from the controls. The induced intracellular AFP was accompanied by elevated activating transcription factor-6 (ATF6) expression and protein kinase R-like ER kinase (PERK) phosphorylation in mouse livers. ER stress induced AFP expression in LO2 cells and decreased their viability. ATF6, but not PERK, silencing mitigated the ER-stress-induced AFP expression in LO2 cells. Conversely, AFP silencing deteriorated the ER stress-mediated LO2 cell injury and CCl_4 administration-induced liver damages by increasing levels of cleaved caspase-3, the C/enhancer binding protein homologous protein expression, mixed lineage kinase domain-like pseudokinase and PERK phosphorylation, but decreasing ATF6 expression.

CONCLUSION

ER stress upregulated intra-hepatocyte AFP expression by activating ATF6 during the process of liver injury and intracellular AFP attenuated hepatocyte apoptosis and necroptosis by alleviating ER stress.

Key Words: Alpha-fetoprotein; Endoplasmic reticulum stress; Necroptosis; Apoptosis; Liver injury

©The Author(s) 2022. Published by Baishideng Publishing Group Inc. All rights reserved.

Core Tip: During the process of liver injury, alpha-fetoprotein (AFP) expression was up-regulated in hepatocytes, especially in the necrotic areas, but it did not increase the serum AFP level. Endoplasmic reticulum (ER) stress induced intracellular AFP expression through activating activating transcription factor-6 and the up-regulated intracellular AFP expression attenuated hepatocyte apoptosis and necroptosis by feedback-down-regulating ER stress.

Citation: Chen YF, Liu SY, Cheng QJ, Wang YJ, Chen S, Zhou YY, Liu X, Jiang ZG, Zhong WW, He YH. Intracellular alpha-fetoprotein mitigates hepatocyte apoptosis and necroptosis by inhibiting endoplasmic reticulum stress. *World J Gastroenterol* 2022; 28(26): 3201-3217
URL: https://www.wjgnet.com/1007-9327/full/v28/i26/3201.htm
DOI: https://dx.doi.org/10.3748/wjg.v28.i26.3201

INTRODUCTION

Chronic liver diseases, such as chronic hepatitis B (CHB), affect many patients, especially in East Asia, such as China. However, the pathogenesis of chronic liver diseases remains unclear. Although human liver has powerful capacity to compensate the disease-related liver injury, how hepatocytes respond and defense against these diseases has not been clarified. Hence, it is of great significance to clarify it for the management of patients with chronic liver diseases.

Alpha-fetoprotein (AFP) is a protein with similar biological function to albumin and secreted mainly by embryonic tissue cells physiologically and malignant hepatocytes pathologically after birth. Elevated levels of serum AFP have been considered as a reliable biomarker for prediction of birth defect and diagnosis of liver cancer, teratoma, renal cell carcinoma, and pancreatic cancer[1] although moderate serum AFP levels can be temporarily detected in individuals with aberrant liver regeneration, hepatitis, and chronic liver disease. Furthermore, low levels of serum AFP have been continually observed in patients with liver cirrhosis and positively correlated with the degrees of liver inflammation and fibrosis [2,3]. The low and moderate levels of serum AFP are likely from the activation and proliferation of liver precursor cells, including oval cells, hepatic progenitor cells, in response to severe liver damages, particularly in liver failure[4-6]. While hepatocyte proliferation usually compensates for mild and moderate liver injury, liver precursor cells can differentiate into hepatocytes and bile duct cells, promoting liver regeneration. The activated liver precursor cells can secrete AFP and high levels of serum AFP have been suggested to be a biomarker of better prognosis of liver failure[7,8]. However, it is unclear whether chronic liver injury can induce AFP expression and secretion in differentiated mature hepatocytes, and how the induced AFP modulates the pathogenic process of chronic liver diseases.

It is notable that endoplasmic reticulum (ER) stress contributes to the pathogenesis of chronic liver diseases[9,10] and is regulated by inositol requiring enzyme-1 and activating transcription factor-6 (ATF6) and protein kinase R-like ER kinase (PERK)/eukaryotic translational initiation factor 2 alpha (eIF2α) signaling[11,12]. Aberrant ER stress can activate cell injury reactions, such as apoptosis and necroptosis by activating the C/enhancer binding protein (EBP)-homologous protein (CHOP) pathway,

caspase-3 cleavage and mixed lineage kinase domain-like pseudokinase (MLKL) phosphorylation[13, 14]. Our previous study has shown that ER stress inhibits the AFP secretion in hepatoma cells and the increase in the levels of intracellular AFP feedback attenuates the ER stress-related apoptosis and necroptosis in hepatoma cells[15]. However, it is unknown how ER stress can regulate AFP expression and secretion, and how intracellular AFP can modulate the ER stress-induced liver injury during the pathogenic process of chronic liver diseases.

In this research, we focus on whether intracellular AFP exists in hepatocytes during the liver injury, its regulatory relationship with ER stress, and its role in hepatocyte injury through clinical research, *in vivo* and *in vitro* experiments.

MATERIALS AND METHODS

Clinical samples

A total of 34 biopsied liver specimens were collected from CHB patients, eight surgical liver specimens were obtained from patients with hepatic trauma, and another eight surgical liver specimens were obtained from patients with hepatocellular carcinoma (HCC) in the Department of Infectious Diseases, or Hepatobiliary Surgery, the Affiliated Hospital of Zunyi Medical University since 2012. The patients with CHB were diagnosed, according to the Guidelines for Prevention and Treatment of Chronic Hepatitis B revised in 2019[16]. Individual patients were excluded if she/he had current infectious disease, autoimmune liver disease, liver malignant tumor, alcoholic liver disease, drug-induced liver disease, multiple organ dysfunction syndrome, obvious bleeding tendency, deep jaundice, obvious ascites, or another situation not suitable for liver biopsy. Their demographic and clinical data are shown in Table 1. The experimental protocol was approved by the Ethics Committee of Affiliated Hospital of Zunyi Medical University (ZYFYLS[2018] 28).

Establishment of liver injury in mice

Male BALB/c mice (25.0 g ± 3.0 g) were purchased from the Animal Center of Zunyi Medical University (Guizhou Province, China; SYXK[Qin] 2021-0004). The mice were maintained in a specific pathogen-free facility with a controlled temperature (20 °C-24 °C), a 12-h light/dark cycle and allowed free access to food and water *ad libitum*. The experimental protocol was established, according to the Animal Care and Research guidelines[17] and approved by the Animal Experiment Ethics Committee of Zunyi Medical University (LS[2020] 2-231).

To induce liver injury by carbon tetrachloride (CCl_4) administration, the mice were randomized using a random number table into the healthy control group (NC; untreated), solvent control group (olive oil, 5 mL/kg, intraperitoneally, *i.p.*) and CCl_4 group (1 mL/kg mixed with 4 mL of olive oil, *i.p.*) (n = 12 per group). The mice in the solvent and CCl_4 group were administrated with solvent or CCl_4 once or twice per week for 8 wk. Their peripheral blood samples were collected 24 h after the last dose, euthanized and their liver tissues were dissected.

To induce ER stress-related liver injury, the mice were randomized into the healthy NC (untreated), solvent control (phosphate buffer saline, PBS, 10 mL/kg) and tunicamycin (TM; an inhibitor of protein glycosylation) groups (2 mg/kg in the same volume of PBS, *i.p.*; Sigma) once (n = 12 per time point group). One or two days later, their peripheral blood samples were collected, euthanized and their liver tissues were dissected.

To test the role of AFP in the CCl_4-induced liver injury, the mice were randomized and treated intravenously with 1×10^{10} recombinant serotype 8 adeno-associated virus (rAAV8) for expression of control short hairpin RNA (shRNA) or *Afp*-specific shRNA (Table 2, Genechem, Beijing, China). Six weeks after infection, the levels of AFP expression in the livers of mice were analyzed by Western blot to confirm *Afp* silencing. The mice with control shRNA or *Afp*-specific shRNA were administrated with olive oil or CCl_4 as the control shRNA + olive oil, CCl_4 (control shRNA + CCl_4), *Afp* shRNA + olive oil, or *Afp* shRNA + CCl_4 (*Afp* shRNA + CCl_4). Their peripheral blood samples were collected, euthanized and their livers were dissected at 36 h (n = 12 per group) post CCl_4 administration, based on our preliminary studies.

Cell lines and culture

Human hepatocyte LO2 and hepatoma HepG2 cell lines were obtained from the Type Culture Collection of the Chinese Academy of Sciences (Shanghai, China) and identified by STR. The cells were cultured in RPMI-1640 containing 10% fetal bovine serum, 100 Units/mL of penicillin and 100 μg/mL of streptomycin at 37 °C in a 5% CO_2 incubator. To induce ER stress, LO2 cells were treated with, or without (NC group), solvent control group (dimethyl sulfoxide, DMSO) and 0.5 μmol/L thapsigargin (TG; an inhibitor of intracellular calcium balance) in DMSO (Sigma, TG group) for 12 h, 24 h and 48 h, respectively.

In addition, LO2 cells (1.2×10^6 cell/well) were cultured in 6-well plates overnight and transfected with plasmids for control shRNA, *PERK*-specific shRNA and *ATF6*-specific shRNA (Beijing Genechem) using lipofectamine 3000 (Fisher). Two days later, the cells were treated with vehicle DMSO or TG for 24

Table 1 The demographic and clinical data of subjects

Group	CHB	Control	HCC
n	34	8	8
Age (years; 25%, 75%)	41.00 (35.00, 48.75)	32.50 (28.25, 41.85)	47.00 (40.25, 53.42)
ALT (U/L; 25%, 75%)	137.50 (59.00, 221.50)	31.5000 (14.5000, 63.1725)	48.50 (39.00, 65.25)
TBil (μmol/L; 25%, 75%)	16.300 (11.500, 24.225)	10.80 (9.42, 20.58)	20.6 (14.5, 32.5)
AFP (ng/mL; 25%, 75%)	4.5400 (2.9850, 13.1725)	2.02 (1.05, 4.75)	179.80 (14.65, 207.53)

CHB: Chronic hepatitis B; HCC: Hepatocellular carcinoma; AFP: Alpha-fetoprotein; ALT: Serum alanine aminotransferase; TBil: Total bilirubin.

Table 2 The sequences of short hairpin RNAs

Insert content			5'-3'
Mouse	*Afp* shRNA	Target sequence	GCATCCATTGCAAAGGAATTA
		shRNA sequence	GCATCCATTGCAAAGGAATTACGAA*TAATTCCTTTGCAATGGATGC*
	Control shRNA	shRNA sequence	AAACGTGACACGTTCGGAGAACGAATTCTCCGAACGTGTCACGTTT
Human	*PERK* shRNA	Target sequence	GCACTTTAGATGGGAGAATTG
		shRNA sequence	GCACTTTAGATGGGAGAATTGCGAA*CAATTCTCCCATCTAAAGTGC*
	Control shRNA	shRNA sequence	AAACGTGACACGTTCGGAGAACGAATTCTCCGAACGTGTCACGTTT
	ATF6 shRNA	Target sequence	GCAGGTCCTCCTGTTATTAGA
		shRNA sequence	GCAGGTCCTCCTGTTATTAGACGAA*TCTAATAACAGGAGGACCTGC*
	Control shRNA	shRNA sequence	AAACGTGACACGTTCGGAGAA CGAATTCTCCGAACGTGTCACGTTT
	AFP shRNA	Target sequence	GCTTCCATATTGGATTCTTAC
		shRNA sequence	GCTTCCATATTGGATTCTTAC CGAA*GTAAGAATCCAATATGGAAGC*
	Control shRNA	shRNA sequence	AAACGTGACACGTTCGGAGAA CGAATTCTCCGAACGTGTCACGTTT

AFP: Alpha-fetoprotein; ATF6: Activating transcription factor-6; PERK: Protein kinase R-like ER kinase; shRNA: Short hairpin RNA.

h. Additionally, LO2 cells were transfected with plasmid for the expression of control shRNA or *AFP*-specific shRNA (Beijing Genechem) for 48 h and treated with DMSO or TG for 36 h, respectively.

Western blot analysis

LO2, HepG2 cells, or individual liver samples were homogenized in immunoprecipitation assay lysis buffer (R0010, Solarbio, Beijing, China). After centrifugation, individual liver lysates (40 μg) were separated in sodium dodecyl sulfate polyacrylamide gel on 10% gels and transferred to polyvinylidene fluoride membranes (Millipore, Billerica, MA, United States). The membranes were blocked with 5% skim dry milk in TBST (Tris-HCl buffer salt solution + Tween 20) and probed with mouse monoclonal antibodies (mAb) against AFP (sc-130302; Santa Cruz Biotechnology, Santa Cruz, CA, United States), ATF6 (sc-166659, 1:1000, Santa Cruz Biotechnology), GAPDH (sc-166545, 1:10000, Santa Cruz Biotechnology), CHOP (GADD153, sc-71136, 1:10000, Santa Cruz Biotechnology), eIF2α (sc-133132, 1:10000, Santa Cruz Biotechnology), phosphorylated PERK (p-PERK, MA5-15033, 1:1000, Thermofisher Scientific, United States), and PERK (sc-377400, 1:10000, Santa Cruz Biotechnology), or rabbit monoclonal antibodies against cleaved caspase-3 (9664, 1:10000, Cell Signaling Technology), and phosphorylated eIF2α (p-eIF2α, 3398, 1:10000, Cell Signaling Technology), or rabbit polyclonal antibodies against phosphorylated MLKL (p-MLKL, PA5-105677, 1:2000, Thermofisher Scientific), and MLKL (PA5-34733, 1:3000, Thermofisher Scientific). After reaction with horseradish peroxidase (HRP)-conjugated anti-mouse or anti-rabbit IgG, the immunocomplexes were visualized with enhanced chemiluminescent reagents. Quantity One software (Bio-Rad, Hercules, CA, United States) was used to determine the relative levels of each targeted protein to the control (standardized as 1)[18].

Pathological analysis of liver tissue

Fresh liver tissues (5 mm × 5 mm in size from each mouse or 1 mm × 30 mm in size from one patient)

were fixed in 4% paraformaldehyde for ≥ 24 h, paraffin-embedded and cut. The liver tissue sections (5 μm) were dewaxed, rehydrated and routine-stained with hematoxylin and eosin (H&E). The sections were examined under a light microscope (OLYMPUS CX31) using CaseViewer 2.4 software (3DHISTECH, Hungary). The necrotic areas in the liver were analyzed by Image-Pro Plus 6.0 (Media Cybernetics, United States)[19]. The Histology Activity Index-Knodell scores were determined by two pathologists blindly[20].

Immunohistochemistry

The liver tissue sections were dewaxed, rehydrated and blocked with 3% of bovine serum albumin for 20 min. The sections were incubated with mAb against AFP (sc-130302, 1:250) at 4 °C overnight and the bound antibodies were detected with HRP-conjugated anti-mouse IgG, followed by visualizing with diaminobenzidine. The intensity of anti-AFP staining was evaluated by Image Pro Plus 6.0[19].

TUNEL assay

The effect of *Afp* silencing on the frequency of apoptotic hepatocytes in liver sections was determined by terminal deoxynucleotidyl transferase (TdT)-mediated deoxyribonucleotide derivative digoxigenin (dUTP) nick end labeling (TUNEL) using a specific kit (Roche, 11684817910), according to the manufacturer's instruction. Briefly, the paraffin-embedded liver sections were dehydrated, permeabilized, and incubated with a mixture of TdT and dUTP at 1:14 in a humidified chamber for 2 h at 37 °C. The labeled cells were detected with detection solution and after being washed, the sections were counterstained with 4′, 6-diamidino-2-phenylindole. The TUNEL signals were examined under a fluorescent microscope. The apoptotic cells were defined by nuclear green staining while non-apoptotic cells with blue nuclear staining. Five visual fields in each section were randomly selected and the percentages of apoptotic cells in each section were calculated using the formula of positive cells/total cells × 100%.

Analysis of AFP levels

AFP levels in the supernatant of cultured cells and mouse serum samples were measured by chemiluminescence immunoassay on the Beckman Coulter Auto Analyzer (Model DX1800; 04481798190, Roche Diagnostics GmbH) as previously described[21]. Samples were centrifuged to remove the remaining cells and possible cell debris before testing the AFP concentration.

Alanine aminotransferase and total bilirubin levels

The levels of serum alanine aminotransferase (ALT), total bilirubin (TBil) were two commonly used measures of liver injury, and analyzed by an auto-analyzer (AU5800, Beckman Coulter, United States)[22].

Cell viability assay

The impact of specific gene silencing or ER stress on LO2 cell viability was determined using the cell counting kit-8 (CCK-8; Cat. No. 40203ES60; Yeasen Biotechnology, Shanghai, China), per the product instruction. Briefly, LO2 cells (5000 cells/100 μL medium/well in 96-well plates) were treated with, or without, TG for 48 h (5 replicates per sample). During the last one-hour culture, the cells were exposed to CCK-8 and the absorbance of individual wells was detected at a wavelength of 450 nm (Bio-Rad, CA, United States). The relative cell viability (%) = (OD value of the treatment group-OD value of the blank group)/(OD value of the control group-OD value of the blank group) × 100.

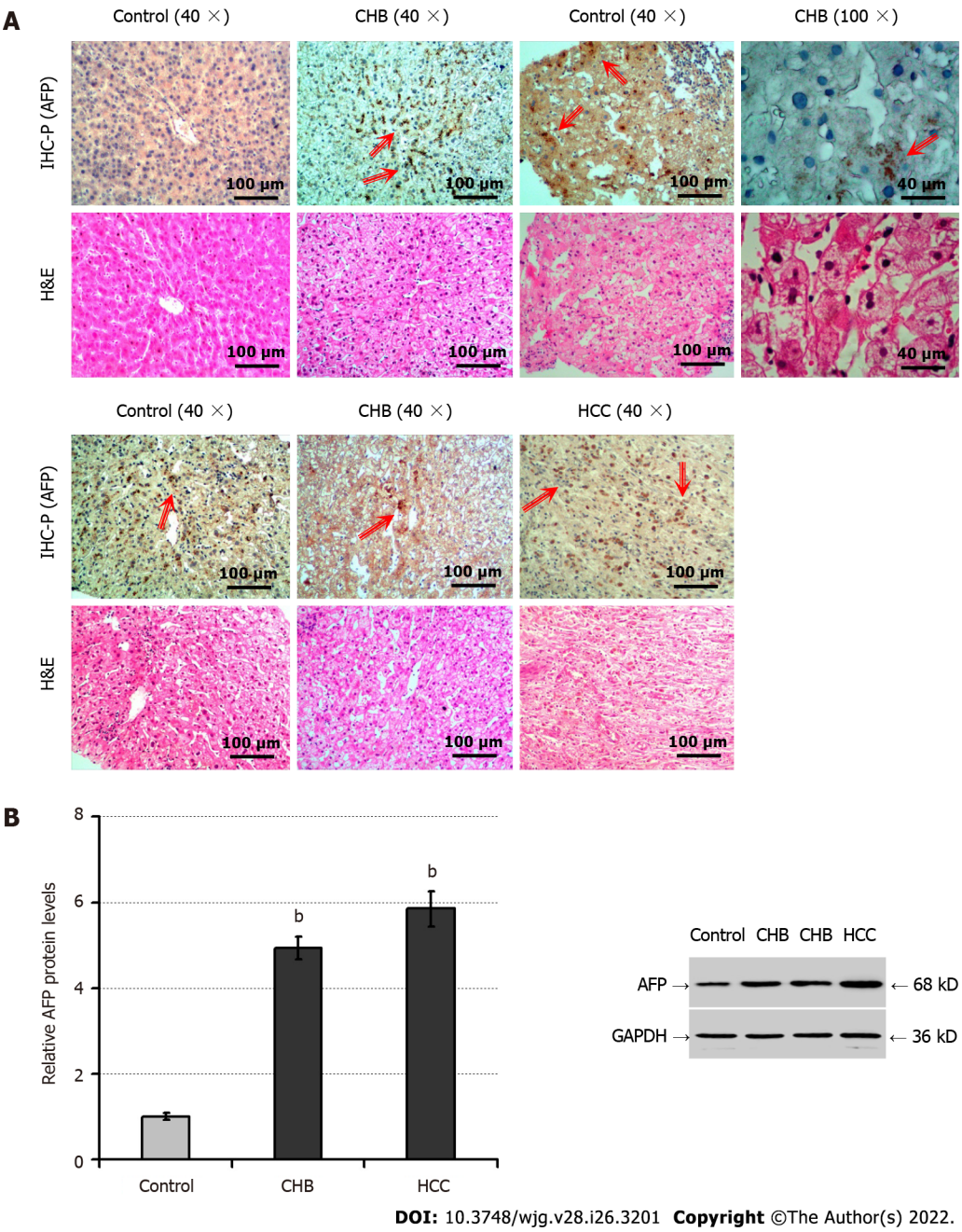
Statistical analysis

Data are representative images or expressed as the mean ± SD of each group from 3 separate experiments. The difference of normally distributed values among groups was analyzed by one-way ANOVA and post hoc Tukey's method. The difference between groups was analyzed by Student's *t*-test. Survival rates were estimated using the Kaplan-Meier method and analyzed by the log-rank test. A *P*-value less than 0.05 was considered statistically significant.

RESULTS

AFP expression is induced in the liver of patients with chronic liver injury

To explore the potential role of AFP in the progression of chronic hepatocyte injury, we analyzed AFP expression in liver tissues of patients with CHB (n = 34), controls (liver trauma; n = 8), and those with HCC (positive controls, n = 8). While there were healthy hepatocytes without degeneration and necrosis in the control liver tissues there were many hepatocytes undergoing degeneration and necrosis (Figure 1A). Immunohistochemistry indicated positive anti-AFP staining in the liver tissues from patients with HCC or CHB, but little in the controls. Interestingly, the positively stained anti-AFP was particularly in the regions with hepatocyte degeneration and necrosis of the liver tissues from CHB



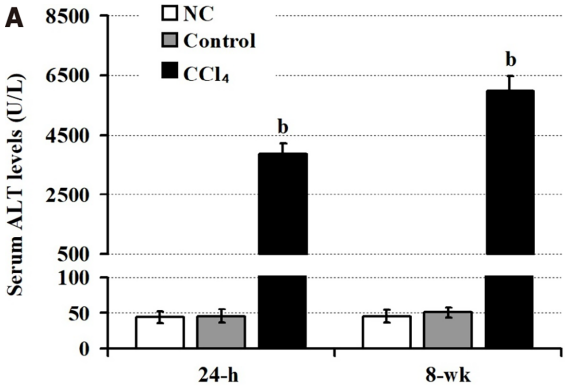
DOI: 10.3748/wjg.v28.i26.3201 **Copyright** ©The Author(s) 2022.

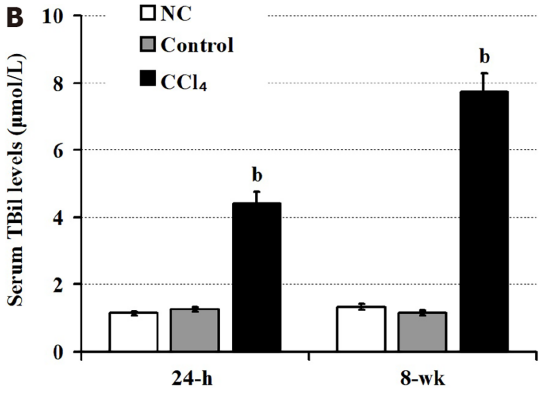
Figure 1 The intrahepatic levels of alpha-fetoprotein protein are elevated in injured livers. A: Immunohistochemistry and hematoxylin and eosin (H&E) staining analyzed alpha-fetoprotein (AFP) expression and pathological changes, respectively, in liver tissues of patients with chronic hepatitis B (CHB, n = 34), trauma (n = 8) or hepatocellular carcinoma (HCC, the positive control group, n = 8). The upper panels display immunohistochemical staining, and the lower panels exhibit H&E staining in sequential tissue sections. The positive expression of AFP was stained with brownish yellow by immunohistochemistry and indicated by the arrows; B: The relative levels of AFP protein expression were analyzed by Western blot in the liver specimens indicated. H&E: Hematoxylin and eosin; IHC-P: Immunohistochemistry-paraffin; AFP: Alpha-fetoprotein; HCC: Hepatocellular carcinoma; CHB: Chronic hepatitis B. $^{b}P < 0.01$, compared with the control group.

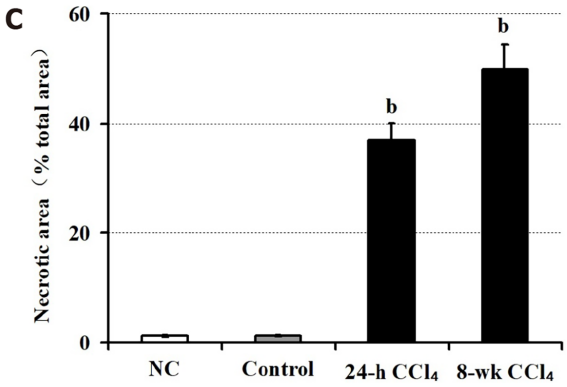
patients. Further Western blot displayed significantly increased levels of AFP expression in the livers from HCC or CHB patients, relative to that in the controls ($P < 0.01$, Figure 1B). Such data indicated that AFP expression was induced in hepatocytes, associated with hepatocyte degeneration and necrosis in humans during the process of hepatocyte injury.

Induction of liver injury enhances AFP expression and ER stress in the liver of mice following CCl_4 administration

Next, we tested whether AFP expression could be induced in the liver of mouse model of CCl_4-induced hepatocyte injury. As expected, CCl_4 administration significantly elevated serum ALT ($P < 0.05$; Figure 2A), TBil ($P < 0.05$; Figure 2B) levels, accompanied by increased areas of liver tissue necrosis in mice, relative to the NC and the control groups (olive oil) of mice ($P < 0.05$; Figure 2C), particularly in the livers of mice following administration with CCl_4 for 8 wk. There were similarly low levels of serum



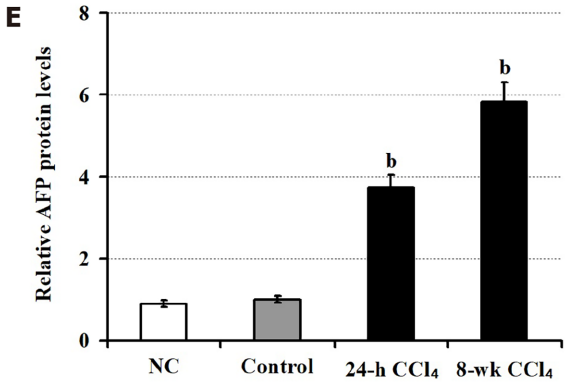


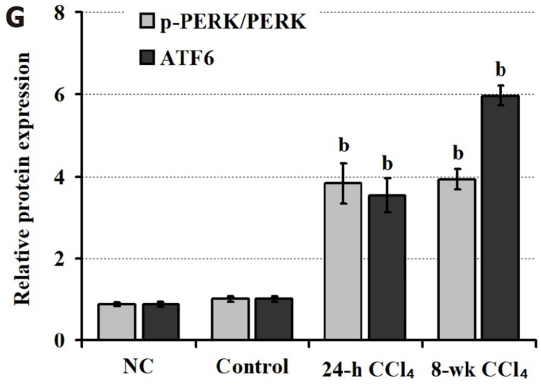


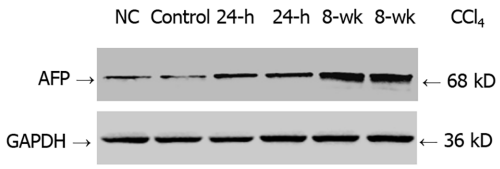
D

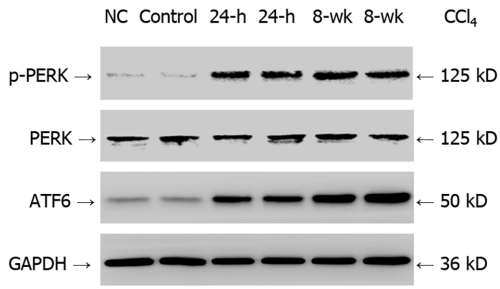
Serum AFP levels (ng/mL)

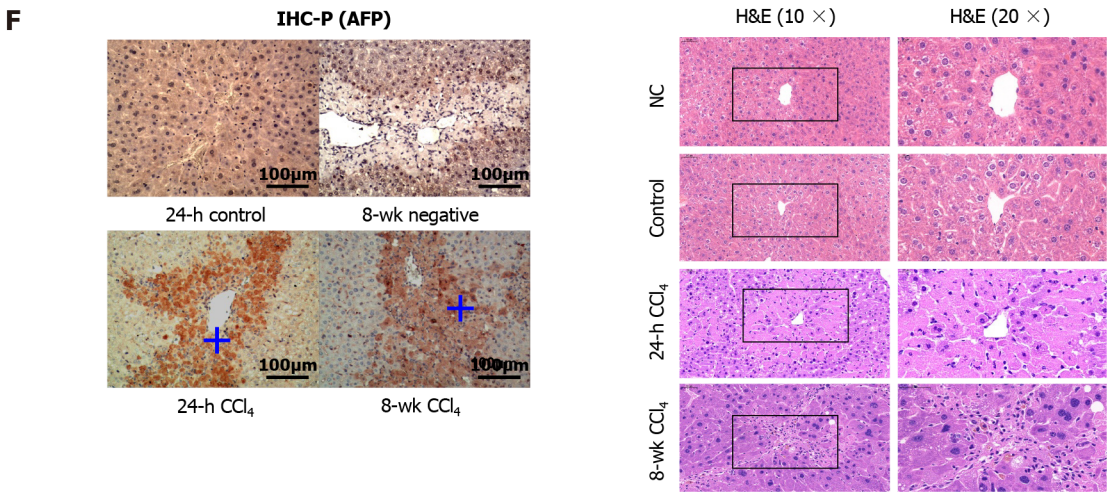
Groups	Untreated	Control	CCl_4
24-h	< 0.61	< 0.61	< 0.61
8-wk	< 0.61	< 0.61	< 0.61











DOI: 10.3748/wjg.v28.i26.3201 **Copyright** ©The Author(s) 2022.

Figure 2 Administration with carbon tetrachloride induces alpha-fetoprotein expression, endoplasmic reticulum stress and liver injury in mice. Male BALB/c mice were untreated (NC), or administrated with olive oil (control) or carbon tetrachloride (CCl_4) for 24 h, or 8 wk. A: Serum alanine aminotransferase levels; B: Serum total bilirubin levels; C: Hematoxylin and eosin staining analysis of pathological changes in mouse liver tissues at 24-h and 8-wk post CCl_4; D: Chemiluminescence immunoassay of serum alpha-fetoprotein (AFP) levels; E: Western blot analysis of the relative levels of AFP expression in liver tissues of mice; F: Immunohistochemical staining of AFP expression in liver tissue of mice at 24-h post CCl_4, the positive expression of AFP was stained with brownish yellow and indicated by a plus sign; G: Western blot analysis of the relative levels of protein kinase R-like endoplasmic reticulum kinase phosphorylation and activating transcription factor-6 expression in liver tissues of mice. AFP: Alpha-fetoprotein; ALT: Alanine aminotransferase; ATF6: Activating transcription factor-6; CCl_4: Carbon tetrachloride; H&E: Hematoxylin and eosin; PERK: Protein kinase R-like endoplasmic reticulum kinase; TBil: Total bilirubin. $^bP < 0.01$ compared with the control group.

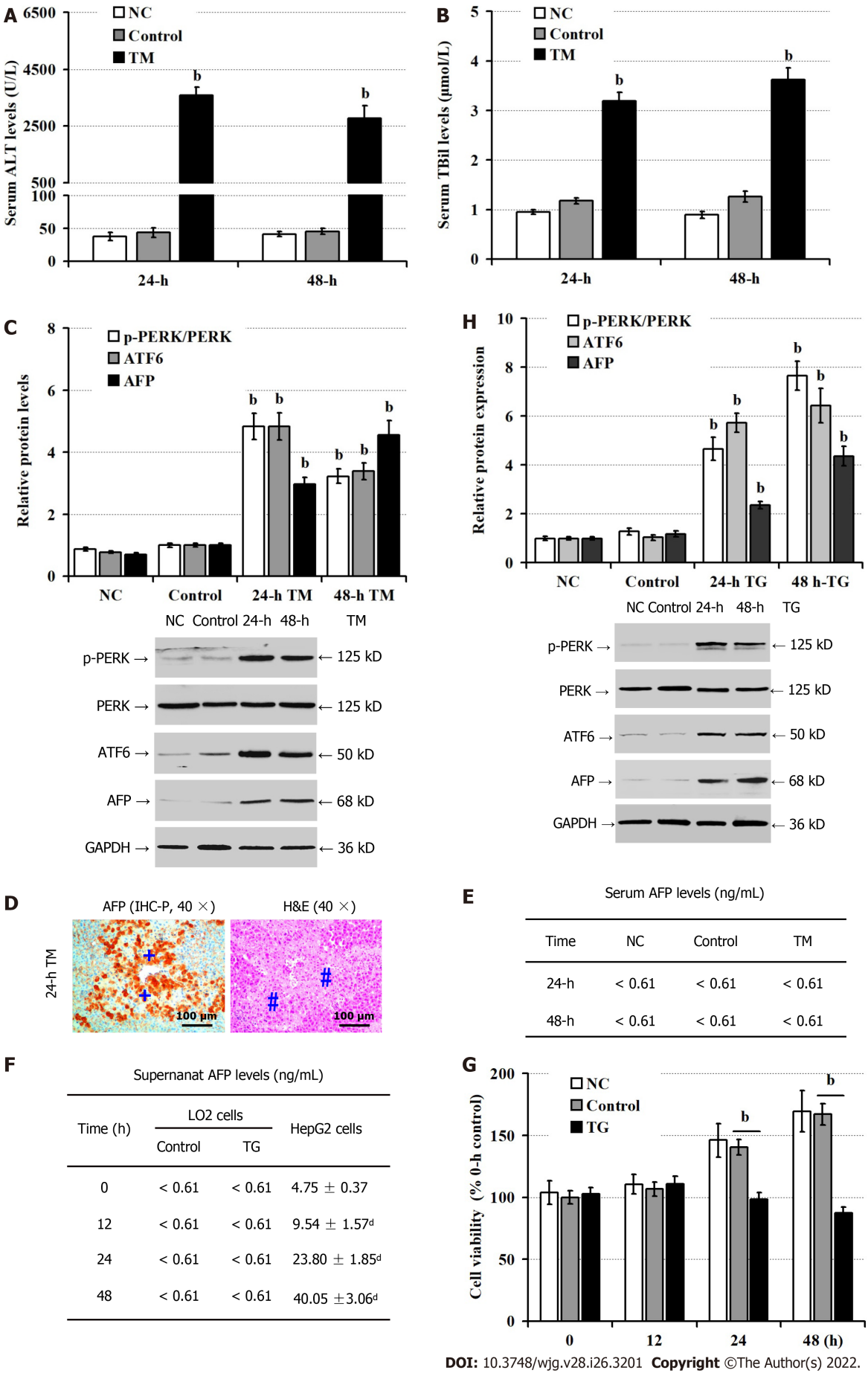
AFP detected in the different groups of mice (about 0.61 ng/mL, Figure 2D). In contrast, Western blot revealed that CCl_4 administration obviously up-regulated AFP expression in the livers of mice in a trend of time-dependence ($P < 0.05$; Figure 2E). Further immunohistochemistry exhibited that the up-regulated AFP expression was mainly accumulated in the injured liver areas (Figure 2F). Finally, CCl_4 administration significantly enhanced the relative levels of PERK phosphorylation and ATF6 expression ($P < 0.05$; Figure 2G), the hallmarks of enhancing ER stress in the livers of mice. Collectively, CCl_4 administration induced hepatocyte injury and ER stress, and up-regulated AFP expression, but not its secretion in mice.

ER stress up-regulates AFP expression in hepatocytes

Given that up-regulated AFP expression was associated with enhanced ER stress, we tested whether induction of ER stress could up-regulate AFP expression in TM-injected mice. Compared with the NC and vehicle controls, significantly elevated levels of serum ALT ($P < 0.05$; Figure 3A) and TBil ($P < 0.05$; Figure 3B) were detected in mice at 24 h and 48 h post TM injection, implicating that induction of ER stress induced liver damages in mice. Consistently, Western blot revealed that TM injection obviously up-regulated ATF6, and AFP expression and PERK phosphorylation in the livers of mice, relative to that of the controls ($P < 0.05$; Figure 3C). Interestingly, there were damaged liver areas with strong anti-AFP staining in the mice with TM injection (Figure 3D). However, there were similar levels of serum AFP in the different groups of mice (< 0.61 ng/mL, Figure 3E). Furthermore, while there was no detectable AFP in the supernatants of cultured human non-tumor hepatocyte LO2 cells, even after treatment with TG, the levels of AFP in the supernatants of cultured HepG2 cells increased in a time-dependent manner (Figure 3F). Moreover, TG treatment significantly decreased the viability of LO2 cells at 24 h and 48 h post treatment ($P < 0.05$, Figure 3G), but TG treatment significantly enhanced the relative levels of AFP and ATF6 expression and PERK phosphorylation in LO2 cells ($P < 0.05$, Figure 3H). Thus, induction of ER stress induced hepatocyte injury and AFP expression.

ATF6 silencing mitigates the TG-induced AFP expression in LO2 cells

To understand how ER stress promoted AFP expression, we transfected LO2 cells with *PERK* or *ATF6*-specific shRNA. We found that *PERK* silencing significantly reduced the viability of LO2 cells ($P < 0.05$), and deteriorated the TG-induced damages in LO2 cells ($P < 0.01$; Figure 4A). While *PERK* silencing significantly reduced the levels of PERK protein expression in both regular cultures and TG-treated LO2 cells, and mitigated the relative levels of TG-enhanced eIF2α phosphorylation in LO2 cells, *PERK* silencing failed to significantly alter AFP protein expression in LO2 cells regardless of TG treatment (Figure 4B). In contrast, *ATF6* silencing significantly reduced the viability of LO2 cells, but enhanced the TG-induced damages in LO2 cells ($P < 0.01$; Figure 4C). Moreover, transfection with *ATF6* shRNA not



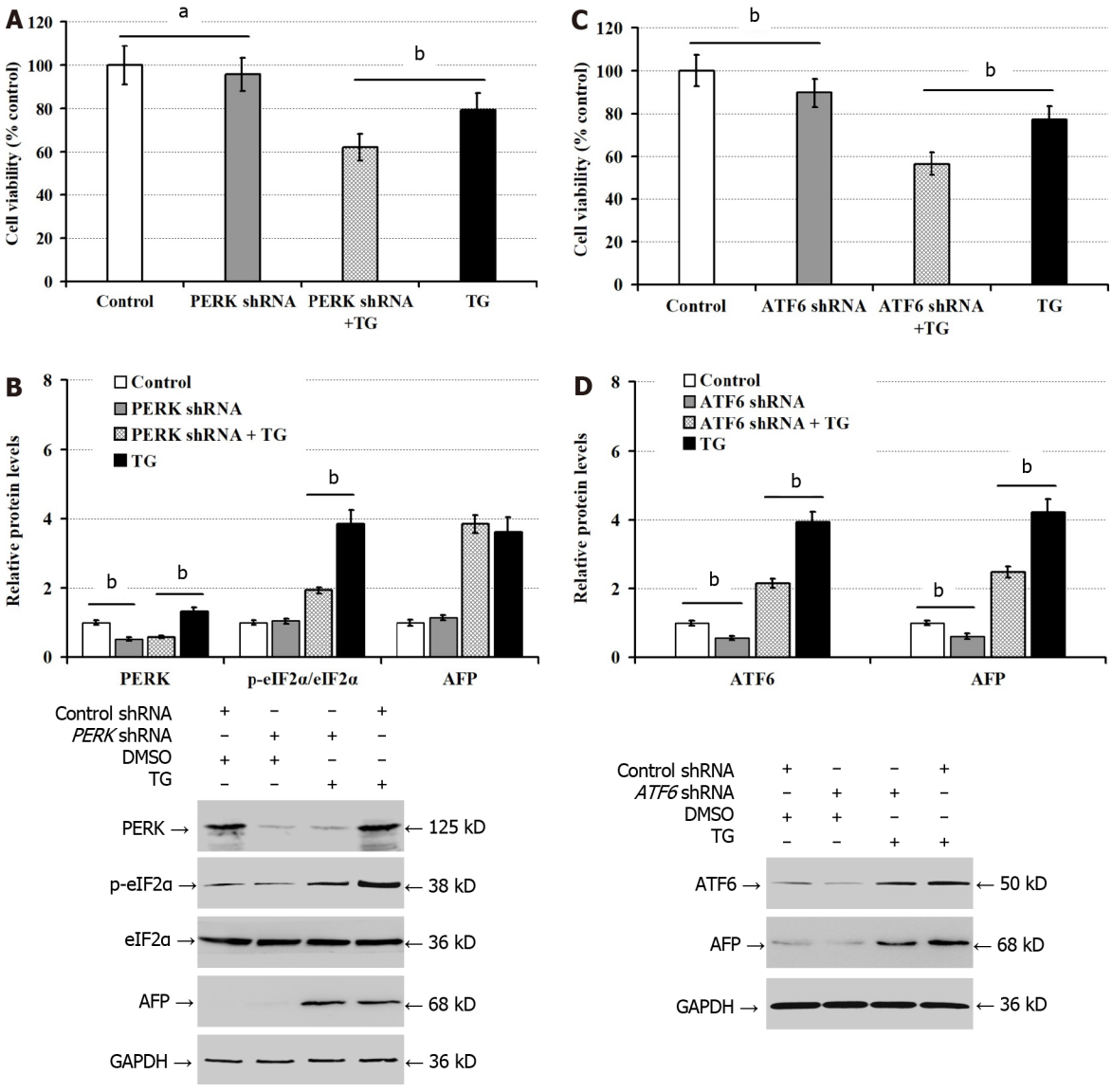
Time	NC	Control	TM
24-h	< 0.61	< 0.61	< 0.61
48-h	< 0.61	< 0.61	< 0.61

Time (h)	LO2 cells		HepG2 cells
	Control	TG	
0	< 0.61	< 0.61	4.75 ± 0.37
12	< 0.61	< 0.61	9.54 ± 1.57[d]
24	< 0.61	< 0.61	23.80 ± 1.85[d]
48	< 0.61	< 0.61	40.05 ±3.06[d]

DOI: 10.3748/wjg.v28.i26.3201 **Copyright** ©The Author(s) 2022.

Figure 3 Endoplasmic reticulum stress up-regulates alpha-fetoprotein expression in hepatocytes. Male BALB/c mice were untreated (NC), or

treated with phosphate buffer saline (control) or TM for 24 h or 48 h. LO2 cells were untreated (NC), or treated with dimethyl sulfoxide (control) or thapsigargin (TG) for 24 h, and 48 h. A: Serum alanine aminotransferase levels; B: Serum total bilirubin levels; C: Western blot analysis of the relative levels of proteins; D: Immunohistochemical analysis of alpha-fetoprotein (AFP) expression and hematoxylin and eosin staining analysis of liver injury in mice at 24 h post endoplasmic reticulum stress. The positive expression of AFP was stained with brownish yellow and indicated by a plus sign. Hash sign indicates the area of necrosis; E: Chemiluminescence immunoassay of serum AFP levels in mice; F: The levels of AFP in the supernatants of cultured cells; G: Cell counting kit-8 analysis of the cell viability; H: Western blot analysis of the relative levels of p-protein kinase R-like endoplasmic reticulum kinase, ATF6 and AFP expression in LO2 cells. AFP: Alpha-fetoprotein; ALT: Alanine aminotransferase; ATF6: Activating transcription factor-6; CCl_4: Carbon tetrachloride; CCK-8: Cell counting kit-8; DMSO: Dimethyl sulfoxide; H&E: Hematoxylin and eosin; IHC-P: Immunohistochemistry-paraffin; PBS: Phosphate buffer saline; p-PERK: Phosphorylated protein kinase R-like endoplasmic reticulum kinase; TBil: Total Bilirubin; TM: Tunicamycin; TG: Thapsigargin. $^{b}P < 0.01$, compared with the control group; $^{d}P < 0.01$, compared with the 0 h group in HepG2 cells.



DOI: 10.3748/wjg.v28.i26.3201 **Copyright** ©The Author(s) 2022.

Figure 4 Activating transcription factor-6 silencing inhibits the expression of alpha-fetoprotein induced by thapsigargin *in vitro*. LO2 cells were transfected with control shRNA, *protein kinase R-like endoplasmic reticulum kinase* (*PERK*)-shRNA, or *activating transcription factor-6* (*ATF6*)-shRNA for 48 h, and treated with dimethyl sulfoxide (control) or thapsigargin for 24 h. A: Cell counting kit-8 (CCK-8) analysis of cell viability; B: Western blot analysis of p-PERK, phosphorylated eukaryotic translational initiation factor 2 alpha, and alpha-fetoprotein expression; C: CCK-8 analysis of cell viability; D: Western blot analysis of the relative levels of ATF6 and AFP protein expression. AFP: Alpha-fetoprotein; ATF6: Activating transcription factor-6; CCK-8: Cell counting kit-8; DMSO: Dimethyl sulfoxide; p-eIF2α: Phosphorylated eukaryotic translational initiation factor 2 alpha; p-PERK: Phosphorylated protein kinase R-like endoplasmic reticulum kinase; TG: Thapsigargin. $^{a}P < 0.05$, $^{b}P < 0.01$, compared with these two groups.

only significantly inhibited ATF6 expression, but also attenuated the relative levels of AFP expression in both regular cultures and TG-treated LO2 cells ($P < 0.01$; Figure 4D). Hence, *ATF6* silencing mitigated the TG-induced AFP expression in LO2 cells.

AFP silencing increases the TG-induced hepatocyte apoptosis and necroptosis in LO2 cells

To understand the importance of AFP in ER stress-induced hepatocyte injury, we further explored the impact of *AFP* silencing on the ER stress-induced hepatocyte injury *in vitro*. Compared with the control LO2 cells, transfection with *AFP*-specific shRNA, but not the control shRNA, dramatically reduced AFP expression in LO2 cells ($P < 0.01$; Figure 5A), and deteriorated the TG-induced damages ($P < 0.01$), but it did not significantly alter the viability of LO2 cells ($P > 0.05$, Figure 5B). Furthermore, the *AFP* silencing significantly increased the levels of cleaved caspase-3 and MLKL phosphorylation regardless of TG treatment ($P < 0.05$, Figure 5C). Consistently, *AFP* silencing also significantly increased CHOP expression and PERK phosphorylation, but decreased ATF6 expression in LO2 cells ($P < 0.01$, Figure 5D). These results clearly indicated that *AFP* silencing enhanced spontaneous and TG-induced ER stress, apoptosis and necroptosis in LO2 cells.

AFP silencing deteriorates the CCl_4-induced liver injury in mice

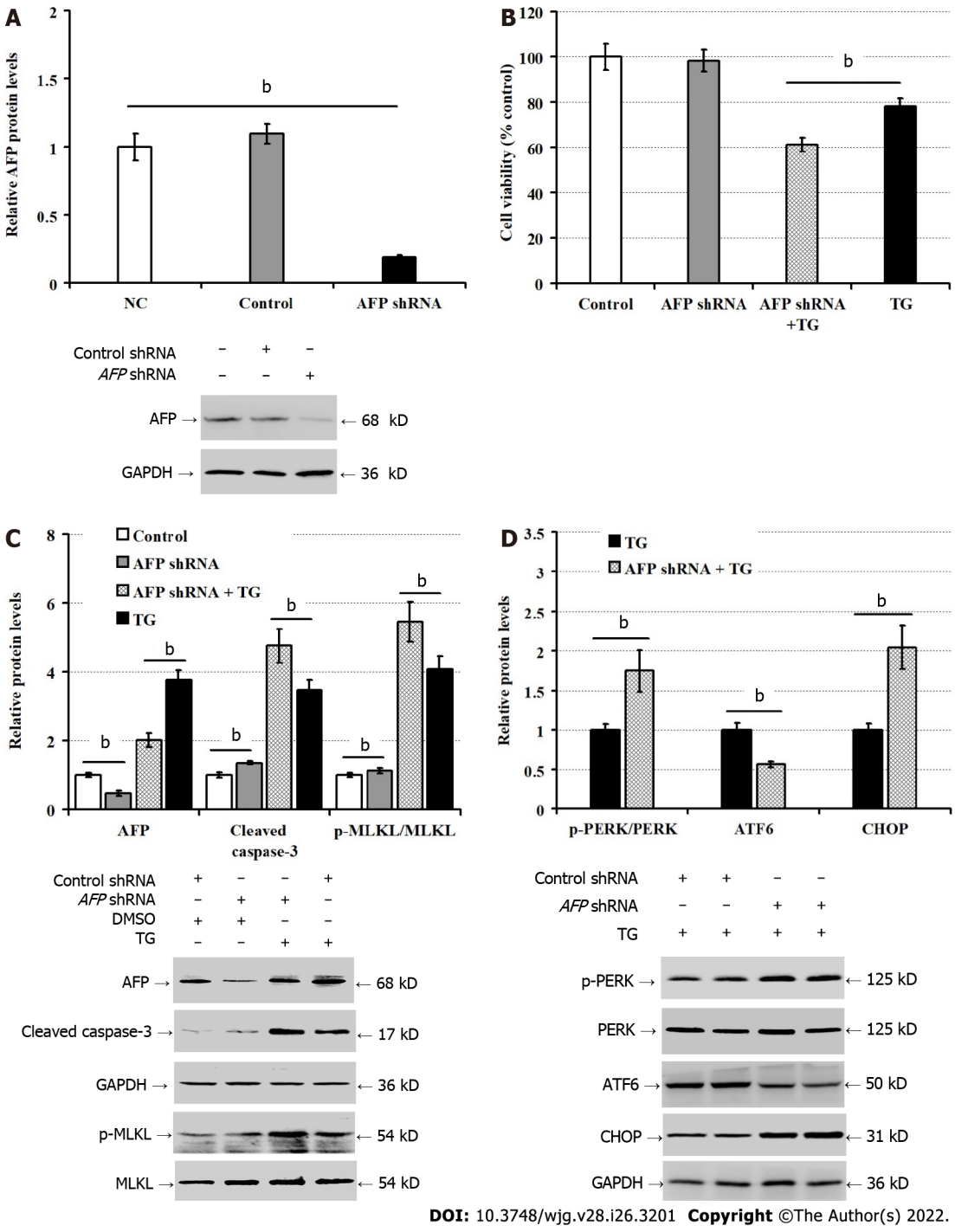
Finally, we tested whether induction of *Afp* silencing could modulate the CCl_4-induced liver injury in mice. After intravenous administration with rAAV8 virus for the expression of control or *Afp*-specific shRNA for 6 wk, the levels of AFP expression in the liver tissues were reduced dramatically, confirming the *Afp* silencing ($P < 0.01$, Figure 6A). Both groups of mice were administrated with vehicle olive oil or CCl_4 and 36 h later, we found that *Afp* silencing increased serum ALT ($P < 0.01$, Figure 6B), and TBil levels ($P < 0.01$, Figure 6C), regardless of CCl_4 administration. Compared with the control mice, *Afp* silencing increased the percentages of necrotic areas in the livers of mice ($P < 0.01$, Figure 6D). Furthermore, *Afp* silencing decreased AFP expression, but remarkably increased the relative levels of cleaved caspase-3 expression, MLKL phosphorylation ($P < 0.01$, Figure 6E) and the percentages of apoptotic hepatocytes in the livers of both vehicle and CCl_4-treated mice ($P < 0.01$, Figure 6F). Finally, *Afp* silencing significantly increased CHOP expression and PERK phosphorylation, but decreased ATF6 expression in the livers of CCl_4-treated mice ($P < 0.01$; Figure 6G). Therefore, *Afp* silencing enhanced ER stress and liver injury induced by CCl4 in mice.

DISCUSSION

In this study, we investigated AFP expression, its regulatory mechanism, and its effect on hepatocyte injury during the process of liver injury. We detected high levels of AFP expression in the livers, particularly in the areas of hepatocyte necrosis, of patients with CHB, but not in those with hepatic trauma. Similarly, high levels of AFP expression were observed in the livers of mice following CCl_4 administration and ER stress induction. The induced AFP expression was accompanied by liver injury in those patients and mice. Interestingly, there was no significant difference in the levels of serum AFP in those experimental patients and mice, compared to the controls. Moreover, induction of ER stress in human non-tumor hepatocyte LO2 cells also induced AFP expression, hepatocyte apoptosis and necroptosis, but failed to detect AFP in the supernatants of cultured cells. These indicated that during chronic liver diseases, ER stress and other inducers triggered hepatocyte apoptosis and necroptosis and stimulated AFP expression, but limited its secretion, leading to increased levels of intracellular AFP in hepatocytes. These novel data extended our previous study on hepatoma cells[15], and support the notion that AFP can be induced during the process of chronic liver diseases[7,23]. Our findings may shed light on the liver responses to ER stress in the pathogenic process of chronic liver diseases.

Low levels of serum AFP are detected in patients with chronic liver disease, and are positively correlated with the degrees of liver damages[8,24]. Although high levels of AFP expression were detected in mouse livers, we did not detect abnormally high levels of serum AFP in liver-injured mice, consistent with our observation in hepatoma cells[15]. These indicated that ER stress induced intracellular AFP expression by limiting its secretion. Given that healthy hepatocytes do not express AFP in adults it is possible that ER stress-induced hepatocyte injury may also induce compensative hepatocyte proliferation to repair liver damages in these models. However, the induced intracellular AFP is unlikely from the proliferation and differentiation of liver precursor cells. We are interested in further investigating how ER stress limits the secretion of AFP in hepatocytes during the process of chronic liver diseases.

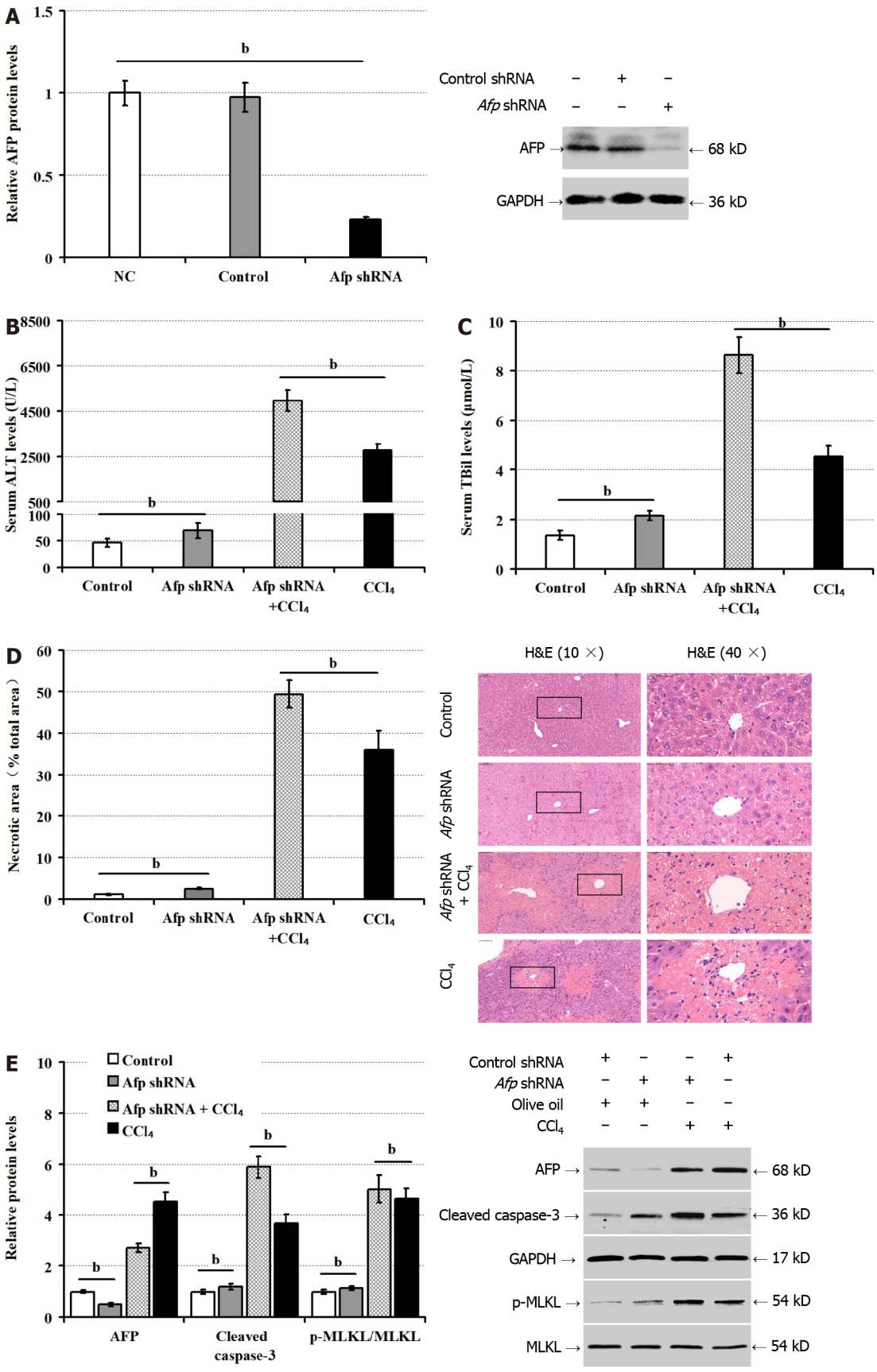
AFP expression is regulated in a manner of tissue-specific and time-restriction[25]. Previous studies have shown that AFP expression is regulated by transcription factors, such as hepatocyte nuclear factor-1 (HNF1), ACCAAT-enhancer binding protein (C/EBP) and NF-1 and their enhancers[26-28]. Furthermore, the mutation in the AFP promoter region can increase the binding affinity of HNF1, leading to sustained increase in the levels of AFP expression[29]. Moreover, the AFP promoter activity is also regulated by the competitive modulation of these transcription factors, activators and inhibitors [30]. In this study, we explored how ER stress induced AFP expression in hepatocytes. ER stress mainly enhances eIF2α activation and regulates the expression of target molecules through ATF4, ATF6, and XBP1 to enhance cell ability to eliminate and degrade misfolded proteins[11]. We found that *ATF6*, but not *PERK*, silencing significantly mitigated the ER stress-induced AFP expression in LO2 cells. These data suggest that ATF6 may promote AFP expression in hepatocytes under an ER stress condition.

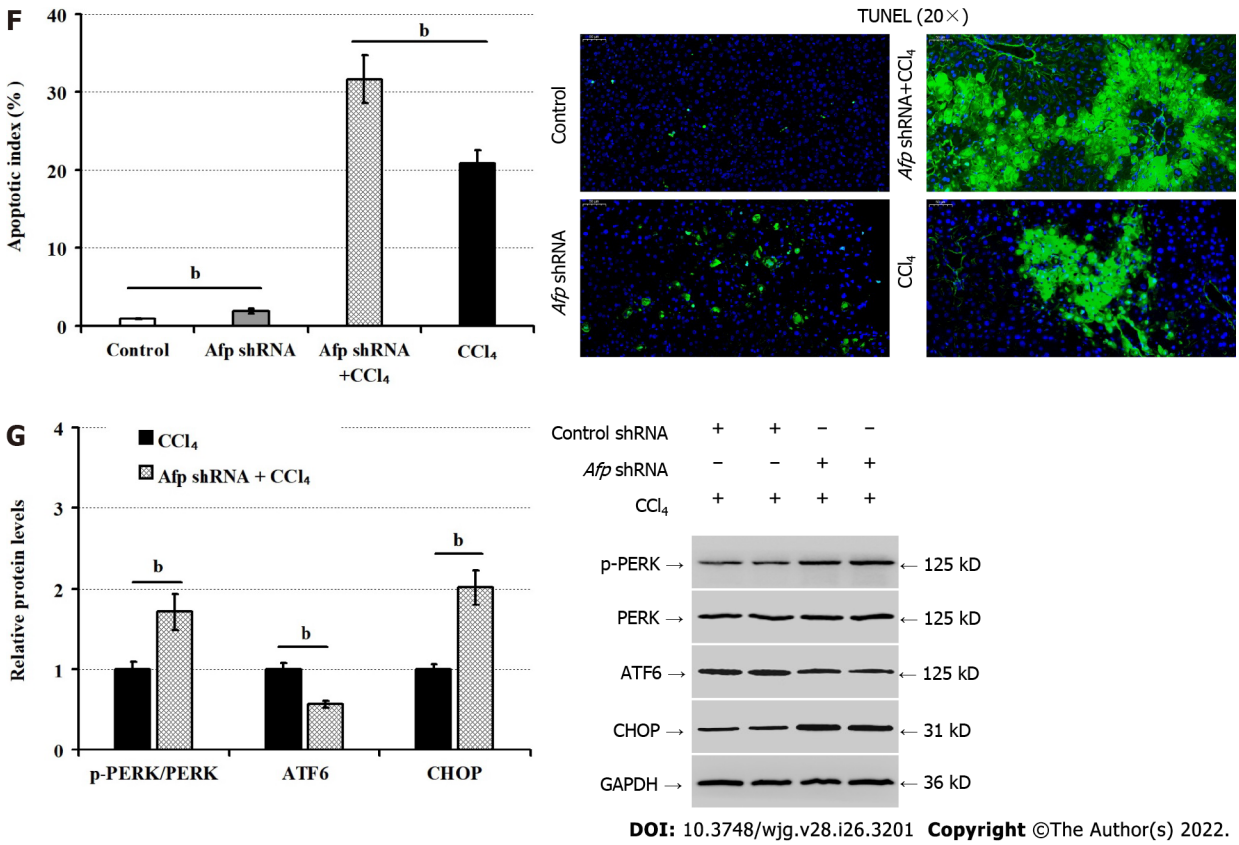


DOI: 10.3748/wjg.v28.i26.3201 **Copyright** ©The Author(s) 2022.

Figure 5 Silencing of *alpha-fetoprotein* exacerbates the thapsigargin-induced LO2 cell injury. A: Western blot determined alpha-fetoprotein silencing in LO2 cells; B: Cell counting kit-8 analysis of LO2 cell viability; C: Western blot for the relative levels of indicated protein expression in LO2 cells; D: Western blot for the relative levels of endoplasmic reticulum stress-related protein. AFP: Alpha-fetoprotein; CCK-8: Cell counting kit-8; ER: Endoplasmic reticulum; TG: Thapsigargin; p-MLKL: Phosphorylated mixed lineage kinase domain-like pseudokinase; p-PERK: Phosphorylated protein kinase R-like endoplasmic reticulum kinase. Data are typical images or expressed as the mean ± SD of each group from 3 separate experiments. $^{b}P < 0.01$ compared with these two groups.

Functionally, AFP can act as a carrier to maintain plasma colloidal osmotic pressure and transport bilirubin, estrogen, fatty acids, retinoids, steroids and progesterone to regulate hormone homeostasis [31]. Second, AFP can induce immune cell apoptosis and down-regulates the gene expression of a variety of inflammatory factors, inhibiting autoimmunity and aberrant inflammation by protecting the fetus from maternal immune attack and attenuating the immune clearance of tumors[32,33]. Furthermore, AFP can enhance the malignant behavior of hepatoma cells by inhibiting their apoptosis and autophagy[34,35]. Accordingly, AFP can promote the survival and growth of a variety of tumor and non-tumor cells[36,37]. AFP can reduce the tumor necrosis factor alpha (TNF-α)-mediated damages of liver cancer cells or hepatocytes, and promotes their proliferation[38,39]. Studies have found that AFP can enhance the expression of p53, c-fos, c-jun, N-ras and hepatocyte growth factor receptor by binding


A
Relative AFP protein levels
1.5
1
0.5
0
b
NC
Control
Afp shRNA
Control shRNA − + −
Afp shRNA − − +
AFP → ← 68 kD
GAPDH → ← 36 kD
B
Serum ALT levels (U/L)
8500
6500
4500
2500
500
100
50
0
b
b
Control
Afp shRNA
Afp shRNA +CCl4
CCl4
C
Serum TBil levels (μmol/L)
10
8
6
4
2
0
b
b
Control
Afp shRNA
Afp shRNA +CCl4
CCl4
D
Necrotic area （% total area）
60
50
40
30
20
10
0
b
b
Control
Afp shRNA
Afp shRNA +CCl4
CCl4
H&E (10 ×)
H&E (40 ×)
Control
Afp shRNA
Afp shRNA + CCl4
CCl4
E
Relative protein levels
10
8
6
4
2
0
Control
Afp shRNA
Afp shRNA + CCl4
CCl4
b
b
b
b
b
b
AFP
Cleaved caspase-3
p-MLKL/MLKL
Control shRNA + − − +
Afp shRNA − + + −
Olive oil + + − −
CCl4 − − + +
AFP → ← 68 kD
Cleaved caspase-3 → ← 36 kD
GAPDH → ← 17 kD
p-MLKL → ← 54 kD
MLKL → ← 54 kD



DOI: 10.3748/wjg.v28.i26.3201 **Copyright** ©The Author(s) 2022.

Figure 6 Silencing of *alpha-fetoprotein* increases liver injury in mice following CCl_4 administration. A: Western blot for the protein levels of alpha-fetoprotein (AFP) in the liver tissues of mice; B: Serum alanine aminotransferase levels; C: Serum levels of total bilirubin; D: Liver sections stained by hematoxylin and eosin and measurements of necrotic areas in mice; E: Western blot for the relative levels of AFP, cleaved caspase-3, and phosphorylated mixed lineage kinase domain-like pseudokinase expression in the liver tissues; F: TUNEL analysis of hepatocyte apoptosis; G: The relative levels of phosphorylated protein kinase R-like ER kinase, activating transcription factor-6 and C/enhancer binding protein homologous protein protein in liver tissues. AFP: Alpha-fetoprotein; ALT: Alanine aminotransferase; ATF6: Activating transcription factor-6; CCl_4: Carbon tetrachloride; CHOP: C/enhancer binding protein homologous protein; H&E: Hematoxylin and eosin; p-MLKL: Phosphorylated mixed lineage kinase domain-like pseudokinase; p-PERK: Phosphorylated protein kinase R-like ER kinase; TBil: Total bilirubin; TUNEL: Terminal deoxynucleotidyl transferase-mediated dUTP nick end labeling. $^bP < 0.01$ compared with these two groups.

to its receptors to activate the cyclic adenosine 3′, 5′-monophosphate (cAMP)-protein kinase A (PKA) pathway and induce Ca^{2+} influx. This process increases intracellular cAMP and PKA, and promotes the proliferation, differentiation and regeneration of hepatocytes. In this study, *Afp* silencing deteriorated the ER stress-mediated apoptosis and necroptosis of LO2 cells *in vitro*. Preferable liver *Afp* silencing also aggravated the CCl_4-induced liver damages, hepatocyte apoptosis, and necroptosis in mice. The results suggest that the induced AFP expression in the liver by ER stress may enhance the resistance of hepatocytes to apoptosis and necroptosis stimulators, alleviating liver injury. Interestingly, we found that AFP silencing also exacerbated the ER stress, but lowed ATF6 expression in LO2 cells and in hepatocytes of liver tissues in mice, consistent with our previous observation[15]. These findings suggest that intracellular AFP induced by the ATF6 signaling may feedback-attenuate the ER stress-induced hepatocyte apoptosis and necroptosis, partially by up-regulating ATF6 expression. Given that AFP is not a transcription factor for the ATF6 expression the ER stress-induced AFP expression may through signal-crosstalk induce the ATF6-specific transcription factor and activator expression, indirectly inducing ATF6 expression in hepatocytes in a condition of ER stress.

We have reported that ATF6 is important for hepatocyte apoptosis and programmed necrosis[40]. It is possible that intracellular AFP may interact with intracellular proteins, transcription factors, kinases, co-activators and cell cycle regulators, such as PTEN to activate the PI3K/AKT/mTOR signaling to support the hepatocyte survival[41]. In addition, intracellular AFP may also interact with the apoptosis-related signaling to enhance apoptosis resistance by up-regulating Bcl-2 expression[35]. However, how intracellular AFP mitigates the ER stress-induced hepatocyte injury remains to be further examined.

CONCLUSION

ER stress induced intracellular AFP expression through activating ATF6 and the induced intracellular AFP feedback-attenuated the ER stress-induced hepatocyte injury. Thus, our findings may shed lights

on the molecular regulation by which hepatocytes respond to ER stress, promoting compensative liver repair following ER stress-induced liver injury.

ARTICLE HIGHLIGHTS

Research background

Endoplasmic reticulum (ER) stress plays an important role in the pathogenesis of chronic liver diseases, but how hepatocytes respond to ER stress has not been clarified. Alpha-fetoprotein (AFP) is secreted by hepatoma cells and elevated levels of serum AFP are associated with development of liver malignancies.

Research motivation

Anti-injury response is an important force for hepatocytes to resist liver injury mediated by various reasons, which has a close relationship to the progress and prognosis of liver injury. Studying the anti-injury mechanism of hepatocytes is important for the diagnosis and treatment of liver injury in the clinic.

Research objectives

To investigate whether and how AFP could regulate ER stress and hepatocyte injury.

Research methods

The distribution of AFP and the degrees of ER stress in liver tissues were characterized by histology, immunohistochemistry, and Western blot in biopsied human liver specimens, two mouse models of liver injury and a cellular model. The levels of AFP in sera and the supernatants of cultured cells were quantified by chemiluminescence.

Research results

ER stress induces liver injury and increases intracellular AFP expression in hepatocytes. ER stress up-regulates intracellular AFP expression by up-regulating activating transcription factor-6 (ATF6). Upregulated AFP feedback attenuates ER stress, forming a regulatory loop. Upregulated AFP mitigates the ER stress-induced hepatocyte apoptosis and necroptosis.

Research conclusions

ER stress upregulated intracellular AFP expression in hepatocytes by up-regulating ATF6 during the process of liver injury and intracellular AFP feedback-attenuated hepatocyte apoptosis and necroptosis by alleviating ER stress.

Research perspectives

Intracellular AFP induced by ER stress alleviates hepatocyte apoptosis and necroptosis by activating ATF6.

FOOTNOTES

Author contributions: Chen YF, Liu SY, and Cheng QJ contributed equally to this work; Chen YF, Liu SY, Cheng QJ, and He YH conceived and designed research; Chen YF, Liu SY, Wang YJ, Chen S, Zhou YY, and Liu X collected data and conducted research; Jiang ZG, Chen YF, and Zhong WW analyzed and interpreted data; Chen YF, Liu SY, and Cheng QJ wrote the initial paper; He YH and Zhong WW revised the paper; He YH had primary responsibility for final content; all authors read and approved the final manuscript.

Supported by the National Natural Science Foundation of China, No. 81560110; Tian Qing Liver Disease Research Fund Project of the Chinese Foundation for Hepatitis Prevention and Control, No. TQGB20200001; and the Science and Technology Planning Projects of Guizhou Province and Zunyi City, No. QKH·ZC[2019] 2803, No. QKHJC-ZK[2022]YB642, No. QKH·PTRC[2017]5733-013, No. gzwjkj2020-1-041, No. ZSKHSZ[2020]230, and No. ZMC·YZ[2018]38.

Institutional review board statement: The study was reviewed and approved by the Ethics Committee of Affiliated Hospital of Zunyi Medical University (ZYFYLS[2018] 28).

Institutional animal care and use committee statement: All procedures involving animals were reviewed and approved by the Animal Experiment Ethics Committee of Zunyi Medical University (LS[2020] 2-231).

Conflict-of-interest statement: There are no conflicts of interest to report.

Data sharing statement: The datasets generated and analyzed during the current study are available from the corresponding author on reasonable request.

ARRIVE guidelines statement: The authors have read the ARRIVE guidelines, and the manuscript was prepared and revised according to the ARRIVE guidelines.

Open-Access: This article is an open-access article that was selected by an in-house editor and fully peer-reviewed by external reviewers. It is distributed in accordance with the Creative Commons Attribution NonCommercial (CC BY-NC 4.0) license, which permits others to distribute, remix, adapt, build upon this work non-commercially, and license their derivative works on different terms, provided the original work is properly cited and the use is non-commercial. See: https://creativecommons.org/Licenses/by-nc/4.0/

Country/Territory of origin: China

ORCID number: Yun-Fen Chen 0000-0002-7940-7481; Si-Ying Liu 0000-0001-9938-4232; Qi-Jiao Cheng 0000-0002-3746-5923; Yu-Jiao Wang 0000-0002-9077-4979; Shuang Chen 0000-0001-9879-7529; Yi-Yang Zhou 0000-0002-1549-1821; Xia Liu 0000-0003-4140-184X; Zhi-Gang Jiang 0000-0003-4539-6988; Wei-Wei Zhong 0000-0002-9736-8148; Yi-Huai He 0000-0002-8639-3436.

S-Editor: Chen YL
L-Editor: A
P-Editor: Yuan YY

REFERENCES

1 **Galle PR**, Foerster F, Kudo M, Chan SL, Llovet JM, Qin S, Schelman WR, Chintharlapalli S, Abada PB, Sherman M, Zhu AX. Biology and significance of alpha-fetoprotein in hepatocellular carcinoma. *Liver Int* 2019; **39**: 2214-2229 [PMID: 31436873 DOI: 10.1111/liv.14223]
2 **Fouad R**, Elsharkawy A, Abdel Alem S, El Kassas M, Alboraie M, Sweedy A, Afify S, Abdellatif Z, Khairy M, Esmat G. Clinical impact of serum α-fetoprotein and its relation on changes in liver fibrosis in hepatitis C virus patients receiving direct-acting antivirals. *Eur J Gastroenterol Hepatol* 2019; **31**: 1129-1134 [PMID: 30896550 DOI: 10.1097/MEG.0000000000001400]
3 **Tai WC**, Hu TH, Wang JH, Hung CH, Lu SN, Changchien CS, Lee CM. Clinical implications of alpha-fetoprotein in chronic hepatitis C. *J Formos Med Assoc* 2009; **108**: 210-218 [PMID: 19293036 DOI: 10.1016/S0929-6646(09)60054-1]
4 **Fausto N**, Campbell JS. The role of hepatocytes and oval cells in liver regeneration and repopulation. *Mech Dev* 2003; **120**: 117-130 [PMID: 12490302 DOI: 10.1016/s0925-4773(02)00338-6]
5 **Vessey CJ**, de la Hall PM. Hepatic stem cells: a review. *Pathology* 2001; **33**: 130-141 [PMID: 11358043]
6 **Kuhlmann WD**, Peschke P. Hepatic progenitor cells, stem cells, and AFP expression in models of liver injury. *Int J Exp Pathol* 2006; **87**: 343-359 [PMID: 16965562 DOI: 10.1111/j.1365-2613.2006.00485.x]
7 **Wang X**, Shen C, Yang J, Yang X, Qin S, Zeng H, Wu X, Tang S, Zeng W. Alpha-Fetoprotein as a Predictive Marker for Patients with Hepatitis B-Related Acute-on-Chronic Liver Failure. *Can J Gastroenterol Hepatol* 2018; **2018**: 1232785 [PMID: 29854714 DOI: 10.1155/2018/1232785]
8 **Huang GQ**, Xie YY, Zhu PW, Wang XD, Lin Z, Wang Y, Ye JP, Wang YM, Chen YX, Jin XZ, Van Poucke S, Chen YP, Zheng MH. Stratified alpha-fetoprotein pattern accurately predicts mortality in patients with acute-on-chronic hepatitis B liver failure. *Expert Rev Gastroenterol Hepatol* 2018; **12**: 295-302 [PMID: 29300103 DOI: 10.1080/17474124.2018.1424540]
9 **Malhi H**, Kaufman RJ. Endoplasmic reticulum stress in liver disease. *J Hepatol* 2011; **54**: 795-809 [PMID: 21145844 DOI: 10.1016/j.jhep.2010.11.005]
10 **Zhong W**, Wang X, Rao Z, Pan X, Sun Y, Jiang T, Wang P, Zhou H. Aging aggravated liver ischemia and reperfusion injury by promoting hepatocyte necroptosis in an endoplasmic reticulum stress-dependent manner. *Ann Transl Med* 2020; **8**: 869 [PMID: 32793713 DOI: 10.21037/atm-20-2822]
11 **Hetz C**. The unfolded protein response: controlling cell fate decisions under ER stress and beyond. *Nat Rev Mol Cell Biol* 2012; **13**: 89-102 [PMID: 22251901 DOI: 10.1038/nrm3270]
12 **Jäger R**, Bertrand MJ, Gorman AM, Vandenabeele P, Samali A. The unfolded protein response at the crossroads of cellular life and death during endoplasmic reticulum stress. *Biol Cell* 2012; **104**: 259-270 [PMID: 22268789 DOI: 10.1111/boc.201100055]
13 **Zhao XC**, Livingston MJ, Liang XL, Dong Z. Cell Apoptosis and Autophagy in Renal Fibrosis. *Adv Exp Med Biol* 2019; **1165**: 557-584 [PMID: 31399985 DOI: 10.1007/978-981-13-8871-2_28]
14 **Grootjans S**, Vanden Berghe T, Vandenabeele P. Initiation and execution mechanisms of necroptosis: an overview. *Cell Death Differ* 2017; **24**: 1184-1195 [PMID: 28498367 DOI: 10.1038/cdd.2017.65]
15 **Chen H**, Chen GM, Liu YJ, Rao JX, Zhou SZ, Chen S, Chen PT, Yang FW, Cheng QJ, He YH. Alpha-fetoprotein/endoplasmic reticulum stress signaling mitigates injury in hepatoma cells. *Neoplasma* 2021; **68**: 983-993 [PMID: 34374292 DOI: 10.4149/neo_2021_210205N180]
16 **Chinese Society of Infectious Diseases**; Chinese Medical Association; Chinese Society of Hepatology, Chinese Medical Association. The guidelines of prevention and treatment for chronic hepatitis B (2019 version). *Zhonghua Gan Zang Bing*

Za Zhi 2019; **27**: 938-961 [PMID: 31941257 DOI: 10.3760/cma.j.issn.1007-3418.2019.12.007]
17 **Simmonds RC**. Bioethics and Animal Use in Programs of Research, Teaching, and Testing. In: Weichbrod RH, Thompson GAH, Norton JN, editors. Management of Animal Care and Use Programs in Research, Education, and Testing. Boca Raton (FL), 2018: 35-62
18 **Chen G**, Yang X, He Y, Tang Y, Tian R, Huang W, Chen H, Yang F, Li Y, Lin S. Inhibiting alpha subunit of eukaryotic initiation factor 2 dephosphorylation protects injured hepatocytes and reduces hepatocyte proliferation in acute liver injury. *Croat Med J* 2019; **60**: 532-544 [PMID: 31894919 DOI: 10.3325/cmj.2019.60.532]
19 **Tian RD**, Chen YQ, He YH, Tang YJ, Chen GM, Yang FW, Li Y, Huang WG, Chen H, Liu X, Lin SD. Phosphorylation of eIF2α mitigates endoplasmic reticulum stress and hepatocyte necroptosis in acute liver injury. *Ann Hepatol* 2020; **19**: 79-87 [PMID: 31548168 DOI: 10.1016/j.aohep.2019.05.008]
20 **Knodell RG**, Ishak KG, Black WC, Chen TS, Craig R, Kaplowitz N, Kiernan TW, Wollman J. Formulation and application of a numerical scoring system for assessing histological activity in asymptomatic chronic active hepatitis. *Hepatology* 1981; **1**: 431-435 [PMID: 7308988 DOI: 10.1002/hep.1840010511]
21 **Huang H**, Zheng XL, Zheng JS, Pan J, Pu XY. Rapid analysis of alpha-fetoprotein by chemiluminescence microfluidic immunoassay system based on super-paramagnetic microbeads. *Biomed Microdevices* 2009; **11**: 213-216 [PMID: 18923903 DOI: 10.1007/s10544-008-9226-z]
22 **Lippi G**, Dipalo M, Musa R, Avanzini P, Ferrarini C, Pattini A, Aloe R. Evaluation of the analytical performances of the novel Beckman Coulter AU5800. *Clin Biochem* 2012; **45**: 502-504 [PMID: 22296728 DOI: 10.1016/j.clinbiochem.2012.01.015]
23 **Kakisaka K**, Kataoka K, Onodera M, Suzuki A, Endo K, Tatemichi Y, Kuroda H, Ishida K, Takikawa Y. Alpha-fetoprotein: A biomarker for the recruitment of progenitor cells in the liver in patients with acute liver injury or failure. *Hepatol Res* 2015; **45**: E12-E20 [PMID: 25376981 DOI: 10.1111/hepr.12448]
24 **Yang N**, Li Z, Yan M, Xiao W, Zhang W, Long Y, Cheng Y, Ming K, Xu B. Evaluation of Serum Alpha-Fetoprotein Level in Chronic Hepatitis C Patients. *Clin Lab* 2019; **65** [PMID: 30775893 DOI: 10.7754/Clin.Lab.2018.180607]
25 **Zhang H**, Cao D, Zhou L, Zhang Y, Guo X, Li H, Chen Y, Spear BT, Wu JW, Xie Z, Zhang WJ. ZBTB20 is a sequence-specific transcriptional repressor of alpha-fetoprotein gene. *Sci Rep* 2015; **5**: 11979 [PMID: 26173901 DOI: 10.1038/srep11979]
26 **Lee K**. [Regulation of human alpha-fetoprotein gene by C/EBPalpha]. *Hokkaido Igaku Zasshi* 2004; **79**: 377-387 [PMID: 15373210]
27 **Jose-Estanyol M**, Danan JL. A liver-specific factor and nuclear factor I bind to the rat alpha-fetoprotein promoter. *J Biol Chem* 1988; **263**: 10865-10871 [PMID: 2455718]
28 **Sakata N**, Kaneko S, Ikeno S, Miura Y, Nakabayashi H, Dong XY, Dong JT, Tamaoki T, Nakano N, Itoh S. TGF- β Signaling Cooperates with AT Motif-Binding Factor-1 for Repression of the α -Fetoprotein Promoter. *J Signal Transduct* 2014; **2014**: 970346 [PMID: 25105025 DOI: 10.1155/2014/970346]
29 **Jeon Y**, Choi YS, Jang ES, Kim JW, Jeong SH. Persistent α-Fetoprotein Elevation in Healthy Adults and Mutational Analysis of α-Fetoprotein Promoter, Enhancer, and Silencer Regions. *Gut Liver* 2017; **11**: 136-141 [PMID: 27609486 DOI: 10.5009/gnl16069]
30 **Bois-Joyeux B**, Danan JL. Members of the CAAT/enhancer-binding protein, hepatocyte nuclear factor-1 and nuclear factor-1 families can differentially modulate the activities of the rat alpha-fetoprotein promoter and enhancer. *Biochem J* 1994; **301** (Pt 1): 49-55 [PMID: 7518671 DOI: 10.1042/bj3010049]
31 **Terentiev AA**, Moldogazieva NT. Structural and functional mapping of alpha-fetoprotein. *Biochemistry (Mosc)* 2006; **71**: 120-132 [PMID: 16489915 DOI: 10.1134/s0006297906020027]
32 **Wang X**, Wang Q. Alpha-Fetoprotein and Hepatocellular Carcinoma Immunity. *Can J Gastroenterol Hepatol* 2018; **2018**: 9049252 [PMID: 29805966 DOI: 10.1155/2018/9049252]
33 **Meng W**, Bai B, Bai Z, Li Y, Yue P, Li X, Qiao L. The immunosuppression role of alpha-fetoprotein in human hepatocellular carcinoma. *Discov Med* 2016; **21**: 489-494 [PMID: 27448785]
34 **Wang S**, Zhu M, Wang Q, Hou Y, Li L, Weng H, Zhao Y, Chen D, Ding H, Guo J, Li M. Alpha-fetoprotein inhibits autophagy to promote malignant behaviour in hepatocellular carcinoma cells by activating PI3K/AKT/mTOR signalling. *Cell Death Dis* 2018; **9**: 1027 [PMID: 30301886 DOI: 10.1038/s41419-018-1036-5]
35 **Li M**, Li H, Li C, Zhou S, Guo L, Liu H, Jiang W, Liu X, Li P, McNutt MA, Li G. Alpha fetoprotein is a novel protein-binding partner for caspase-3 and blocks the apoptotic signaling pathway in human hepatoma cells. *Int J Cancer* 2009; **124**: 2845-2854 [PMID: 19267404 DOI: 10.1002/ijc.24272]
36 **Terentiev AA**, Moldogazieva NT. Alpha-fetoprotein: a renaissance. *Tumour Biol* 2013; **34**: 2075-2091 [PMID: 23765762 DOI: 10.1007/s13277-013-0904-y]
37 **Yang X**, Zhang Y, Zhang L, Mao J. Silencing alpha-fetoprotein expression induces growth arrest and apoptosis in human hepatocellular cancer cell. *Cancer Lett* 2008; **271**: 281-293 [PMID: 18657899 DOI: 10.1016/j.canlet.2008.06.017]
38 **Semenkova LN**, Dudich EI, Dudich IV, Shingarova LN, Korobko VG. Alpha-fetoprotein as a TNF resistance factor for the human hepatocarcinoma cell line HepG2. *Tumour Biol* 1997; **18**: 30-40 [PMID: 8989923 DOI: 10.1159/000218013]
39 **Cavin LG**, Venkatraman M, Factor VM, Kaur S, Schroeder I, Mercurio F, Beg AA, Thorgeirsson SS, Arsura M. Regulation of alpha-fetoprotein by nuclear factor-kappaB protects hepatocytes from tumor necrosis factor-alpha cytotoxicity during fetal liver development and hepatic oncogenesis. *Cancer Res* 2004; **64**: 7030-7038 [PMID: 15466196 DOI: 10.1158/0008-5472.CAN-04-1647]
40 **Huang MY**, Wan DW, Deng J, Guo WJ, Huang Y, Chen H, Xu DL, Jiang ZG, Xue Y, He YH. Downregulation of RIP3 Improves the Protective Effect of ATF an Acute Liver Injury Model. *Biomed Res Int* 2021; **2021**: 8717565 [PMID: 34778458 DOI: 10.1155/2021/8717565]
41 **Mizejewski GJ**. Alpha-fetoprotein structure and function: relevance to isoforms, epitopes, and conformational variants. *Exp Biol Med (Maywood)* 2001; **226**: 377-408 [PMID: 11393167 DOI: 10.1177/153537020122600503]

World Journal of Gastroenterology

Submit a Manuscript: https://www.f6publishing.com

World J Gastroenterol 2022 July 14; 28(26): 3218-3231

DOI: 10.3748/wjg.v28.i26.3218

ISSN 1007-9327 (print) ISSN 2219-2840 (online)

ORIGINAL ARTICLE

Retrospective Cohort Study

Divergent trajectories of lean *vs* obese non-alcoholic steatohepatitis patients from listing to post-transplant: A retrospective cohort study

Fakhar Ali Qazi-Arisar, Raj Uchila, Catherine Chen, Cathy Yang, Shi-Yi Chen, Ravikiran Sindhuvalada Karnam, Amirhossein Azhie, Wei Xu, Zita Galvin, Nazia Selzner, Leslie Lilly, Mamatha Bhat

Specialty type: Gastroenterology and hepatology

Provenance and peer review: Unsolicited article; Externally peer reviewed.

Peer-review model: Single blind

Peer-review report's scientific quality classification

Grade A (Excellent): 0
Grade B (Very good): B
Grade C (Good): C, C
Grade D (Fair): 0
Grade E (Poor): 0

P-Reviewer: Gluvic Z, Serbia; Sibulesky L, United States; Tiejun W, China

Received: February 3, 2022
Peer-review started: February 3, 2022
First decision: April 10, 2022
Revised: April 22, 2022
Accepted: June 15, 2022
Article in press: June 15, 2022
Published online: July 14, 2022

Fakhar Ali Qazi-Arisar, Raj Uchila, Catherine Chen, Cathy Yang, Ravikiran Sindhuvalada Karnam, Amirhossein Azhie, Zita Galvin, Nazia Selzner, Leslie Lilly, Mamatha Bhat, Ajmera Transplant Program, Toronto General Hospital, University Health Network, Toronto M5G 2N2, Ontario, Canada

Fakhar Ali Qazi-Arisar, Raj Uchila, Ravikiran Sindhuvalada Karnam, Zita Galvin, Nazia Selzner, Leslie Lilly, Mamatha Bhat, Division of Gastroenterology and Hepatology, Department of Medicine, University of Toronto, Toronto M5G 2N2, Ontario, Canada

Fakhar Ali Qazi-Arisar, National Institute of Liver and GI Diseases, Dow University of Health Sciences, Karachi 75330, Pakistan

Shi-Yi Chen, Wei Xu, Department of Biostatistics, Princess Margaret Cancer Center, University Health Network, Toronto M5G 2C1, Ontario, Canada

Wei Xu, Division of Biostatistics, Dalla Lana School of Public Health, University of Toronto, Toronto M5G 2C1, Ontario, Canada

Corresponding author: Mamatha Bhat, FRCP (C), MD, PhD, Assistant Professor, Ajmera Transplant Program, Toronto General Hospital, University Health Network, 585 University Ave, 11th Floor, Room 183, Toronto M5G 2N2, Ontario, Canada. mbhat33@gmail.com

Abstract

BACKGROUND

Non-alcoholic steatohepatitis (NASH) cirrhosis is the second most common indication for liver transplantation (LT). The role of body mass index (BMI) on outcomes of NASH cirrhosis has been conflicting.

AIM

To compare the longitudinal trajectories of patients with lean *vs* obese NASH cirrhosis, from listing up to post-transplant, having adjusted their BMI for ascites.

METHODS

We retrospectively reviewed all adult NASH patients listed for LT in our program from 2012 to 2019. Fine-Gray Competing Risk analyses and Cox Proportional-Hazard Models were performed to examine the cumulative incidence of transplant and survival outcomes respectively.

RESULTS

Out of 265 NASH cirrhosis listed patients, 176 were included. Median age was 61.0 years; 46% were females. 111 patients underwent LT. Obese robust patients had better waitlist survival [hazard ratio (HR): 0.12; 95%CI: 0.05–0.29, $P < 0.0001$] with higher instantaneous rate of transplant (HR: 5.71; 95%CI: 1.26–25.9, $P = 0.02$). Lean NASH patients had a substantially higher risk of graft loss within 90 d post-LT (1.2% *vs* 13.8%, $P = 0.032$) and death post-LT (2.4% *vs* 17.2%, $P = 0.029$). 1-3- and 5-year graft survival was poor for lean NASH (78.6%, 77.3% and 41.7% *vs* 98.6%, 96% and 85% respectively). Overall patient survival post-LT was significantly worse in lean NASH (HR: 0.17; 95%CI: 0.03–0.86, $P = 0.0142$) with 83% lower instantaneous rate of death in obese group.

CONCLUSION

Although lean NASH is considered to be more benign than obese NASH, our study suggests a paradoxical correlation of lean NASH with waitlist outcomes, and graft and patient survival post-LT.

Key Words: Outcomes; Frailty; Waitlist; Liver transplant; Survival

©The Author(s) 2022. Published by Baishideng Publishing Group Inc. All rights reserved.

Core Tip: Non-alcoholic steatohepatitis continues to rise as an indication for liver transplantation (LT). In this study, we analyzed our single-center data of adult patients listed for LT between 2012 and 2019 and reported their outcomes on the waitlist as well as post-LT based on their body mass index.

Citation: Qazi-Arisar FA, Uchila R, Chen C, Yang C, Chen SY, Karnam RS, Azhie A, Xu W, Galvin Z, Selzner N, Lilly L, Bhat M. Divergent trajectories of lean *vs* obese non-alcoholic steatohepatitis patients from listing to post-transplant: A retrospective cohort study. *World J Gastroenterol* 2022; 28(26): 3218-3231

URL: https://www.wjgnet.com/1007-9327/full/v28/i26/3218.htm

DOI: https://dx.doi.org/10.3748/wjg.v28.i26.3218

INTRODUCTION

Non-alcoholic steatohepatitis (NASH) cirrhosis is currently the second most common indication for liver transplantation (LT) and is on track to become the leading indication by 2030 in the United States[1,2]. The ability to cure hepatitis C with antivirals and the twin epidemics of diabetes and obesity have fueled the rise of NASH as an indication for LT worldwide.

NASH patients are often older at presentation and have some or all the components of metabolic syndrome such as diabetes, hypertension, dyslipidemia, and obesity. Non-alcoholic fatty liver disease (NAFLD) and NASH have also been described in the absence of obesity[3]. About 25% of all NAFLD patients exhibit this lean phenotype[4]. However, the role of body mass index (BMI) on outcomes of NASH cirrhosis has been conflicting. Several studies have disproved the perception of NAFLD being a 'milder' condition in lean individuals. In fact, lean patients with NASH have been shown to have more severe liver disease, more advanced fibrosis, shorter waitlist survival, and poorer post-transplant graft and patient survival[5-8].

However, these retrospective studies have been limited by their ability to accurately interpret BMI and the paucity of specific details regarding waitlist and post-transplant outcomes such as cardiometabolic disease, recurrent NASH, and graft fibrosis. Previous attempts to correct BMI for ascites have been shown to move at least 20% of patients to a lower BMI group[9]. Therefore, our study's objective is to compare the longitudinal trajectories of patients with lean *vs* obese NASH cirrhosis, from listing up to post-transplant, having adjusted their BMI for ascites.

MATERIALS AND METHODS

The study was approved by the Research Ethics Board of the University Health Network (Toronto, Canada).

Patients

This was a single-centre retrospective study of all NASH cirrhosis patients listed for LT between November 12, 2012, and May 31, 2019, in the Multi-Organ Transplant Program at the University Health

Network in Toronto, Canada. The study's start date was decided as November 13, 2012, as our program transitioned to the model for end stage liver disease (MELD)-Na system for listing on that day. All patients were followed until May 31, 2020, yielding a minimum follow-up of 1 year. In our program, NASH cirrhosis was diagnosed either based on findings of significant steatosis on histopathology (pre-transplant liver biopsy or explant pathology), or the presence of risk factors (diabetes, obesity, and metabolic syndrome) in the absence of significant alcohol consumption and evidence of other etiology on serology or histopathology.

We excluded candidates listed for hepatocellular carcinoma with exception points, all other candidates listed with exception points, patients with fulminant liver failure, NASH concomitant with a secondary etiology of chronic liver disease (such as alcohol, viral, autoimmune hepatitis, or cryptogenic cirrhosis), multiorgan transplants and those relisted for transplantation.

Data collected from the database on each recipient at the time of listing included age, gender, height, weight, BMI, Na MELD, Creatinine, estimated glomerular filtration rate (eGFR), biochemical parameters (bilirubin, albumin, international normalized ratio), frailty using clinical frailty scale, complications of cirrhosis including the severity of ascites and associated comorbidities were collected. The severity of ascites (mild, moderate, or severe) is graded according to what was recorded in the patient's clinical notes as determined either by physical or more often by radiological examination. Duration on the waitlist, intensive care unit (ICU) stay, sepsis, outcomes on the waitlist, reasons for delisting, and cause of death were also collected. Post-transplant data includes the type of transplant, re-hospitalization within 90 d, recurrence of NAFLD and NASH, time to recurrent NAFLD or NASH, metabolic, cardiovascular, and biliary complications, BMI at 1 and 5 years, patient, and graft survival details.

The above data was collected from the Organ Transplant Tracking Registry software, an internal transplant database linked to the electronic medical record of all patients evaluated at the University Health Network.

Our primary outcomes included patient and graft survival at 90 d, 1- 3- and 5 years.

Dry-weight BMI or adjusted BMI

The adjusted BMI was calculated by evaluating the patient's dry weight, which is estimated by post-paracentesis body weight, or weight recorded before fluid retention if available, or by subtracting a percentage of weight based upon the severity of ascites (mild 5%; moderate 10%; severe 15%) as performed in several studies. The dry-weight BMI or adjusted BMI was then calculated by dividing the patient's estimated dry weight (kg) by the square of the patient's height (m) as performed in several studies[10,11]. We categorized the variable of calculated adjusted BMI at listing into two groups: Group 1 comprising of overweight (BMI ≥ 25 and < 30 kg/m^2) or obese group (BMI ≥ 30 kg/m^2) and Group 2 comprising of underweight (< 18.5 kg/m^2) or normal (≥ 18.5 and < 25 kg/m^2) BMI group.

Adjusted BMI was determined for all the listed patients. The cohort of patients was analyzed according to their weight category.

Statistical analysis

A two-sided test with an overall sample size of 153 subjects (51 in the underweight or normal group, and 102 in the overweight or obese group) achieved 80% power at a 0.05 significance level when the estimated hazard ratio (HR) for the overall survival was 0.5 with the null hypothesis of HR = 1. To account for drop-offs, final sample size was increased to 54 and 122. These results assume that the HR was constant throughout the study and that Cox proportional hazards (PH) regression was used to analyze the data.

Descriptive statistics were performed for demographic and clinical variables. Counts and proportions were calculated for categorical variables and the differences between patients with lean *vs* obese NASH were compared using the Chi-squared test or Fisher's exact test. Mean ± SD and median (range) were calculated for continuous variables and the differences between the two groups were compared using two-sample t-tests or Wilcoxon tests, depending on the distribution of the data.

Cumulative incidence of transplant by lean *vs* obese NASH was plotted and group differences were compared using Gray k-sample test and Fine-Gray Competing risk models. Kaplan-Meier plots for waitlist survival and post-transplant survival were also plotted and differences between patients with lean and obese NASH were compared using log-rank tests and Cox PH models. Complete-case analyses were performed on observations with complete sets of data while the data for observations that has one or more missing values were removed.

Sample size was calculated using PASS (Power Analysis and Sample Size Software) 2021. (NCSS, LLC. Kaysville, Utah, United States, ncss.com/software/pass). SAS 9.4 (SAS Institute, Cary NC) was used to perform statistical analyses. Statistical significance was defined as a P value of ≤ 0.05.

RESULTS

Patient characteristics

Out of 265 patients listed for NASH cirrhosis, 176 met the eligibility criteria. The median age was 61 (32–71.4) years; 46% were females. A total of 111 patients underwent LT, 78 deceased donor LT (DDLT), and 33 living donor LT (LDLT). Table 1 describes the pre-LT clinical and laboratory variables.

Impact of ascites on BMI

Correcting for ascites volume resulted in patients moving into a lower BMI classification among all groups except the underweight group (BMI < 18 kg/m^2). The change was larger among patients in the higher BMI groups with 72.2%, 62.9%, and 78.1% of patients moved to a lower BMI group from Obesity classes 3, 2, and 1, respectively as shown in Table 2.

Waitlist parameters and outcomes

Patients in lean NASH group were elderly at time of listing (median age 61.6 years *vs* 60.3 years, P = 0.048), had worse renal functions at end of listing (median eGFR 48 mL/min/1.73 m^2 *vs* 57 mL/min/1.73 m^2, P = 0.017), carried more severe ascites (66.6% *vs* 45%, P = 0.03) and were more paracentesis dependent (72.2% *vs* 52.9%, P = 0.016). Other characteristics such as sex, clinical frailty scale, and frequency of complications were similar between the two groups.

Patients in the overweight/obese group spent a median of 139.5 d on the waitlist which was not dissimilar to the 117 d spent by their counterparts in the lean group. Waitlist events such as episodes of sepsis and ICU stay were similar in the two groups. With regards to waitlist outcomes, a similar number of patients were de-listed or transplanted in both groups. More patients belonging to the lean NASH group compared to the obese group died (31.5% *vs* 20.5%, P = 0.26); however, the difference was not significant. Time to death or delisting was similar in both obese and lean groups (HR: 0.83; 95%CI: 0.46–1.50, P = 0.53). However, when sub-grouped based on BMI and frailty, patients with obese NASH and none/mild frailty had better survival than lean NASH with moderate to severe frailty (HR: 0.12; 95%CI: 0.05–0.29, P < 0.0001) (Figure 1).

With regards to transplant data, a comparable number of patients underwent DDLT and LDLT in both obese and lean groups (DDLT: 69.5% in overweight/obese group and 72.4% in the lean group; P = 0.77). The cumulative incidence of transplant was equal in both groups (HR: 1.33; 95%CI: 0.87–2.05, P = 0.16). However, obese NASH patients with none/mild frailty had a significantly better instantaneous rate of transplant than lean NASH with moderate to severe frailty (HR: 5.71; 95%CI: 1.26–25.9, P = 0.02) (Figure 2). The Median cold ischemia time in obese patients undergoing DDLT was significantly longer than that of lean patients (465 min *vs* 330.5 min, P = 0.024).

Post-transplant outcomes

Compared to listing, the obese group had a significant reduction in BMI 1 year post-transplant (β = -2.08, SE = 0.87, P = 0.006). At 5-year post-transplant, the overweight or obese group's BMI returned to the same level as listing time (β = 1.80, SE = 1.54, P = 0.52). No change in BMI was observed in the underweight or normal group (overall P = 0.3) (Figure 3). There was no difference in post-transplant parameters such as 90-d rehospitalization, biliary complications or recurrence of NASH in lean *vs* obese groups. However, renal function was significantly better in lean NASH patients at 5 years (median creatinine 111 μmol/L *vs* 153.5 μmol/L, P = 0.019) (Table 3).

The graft loss within 90 d post-transplant (1.2% *vs* 13.8%, P = 0.032) and death following transplant (2.4% *vs* 17.2%, P = 0.029) were significantly higher in lean patients compared to obese patients. The 1- 3- and 5-year graft survivals were significantly worse for lean patients 98.6%, 96% and 85% *vs* 78.6%, 77.3% and 41.7% respectively, all P < 0.05) (Table 3). There was a trend toward worse 1- 3- and 5-year patient survival (98.7%, 96% and 90% *vs* 89.7%, 81.8% and 58.3%; P = 0.06, 0.07 and 0.07 respectively). The two groups were analysed to compare patient survival using Kaplan Meier Survival Plots and Cox PH models, which noted a statistically significant difference in overall survival between the two groups (HR: 0.17; 95%CI: 0.03–0.86, P = 0.0142). The instantaneous rate of death in the overweight/obese group was 83% lower than those in the underweight/normal weight group (Figure 4).

DISCUSSION

Our study highlights the paradoxical impact of pretransplant BMI on the survival of NASH patients post-liver transplant, with lean NASH patients demonstrating inferior 90-d, 1- 3- and 5-year graft survival, and overall patient survival.

Lean NAFLD prevalence varies from 12% to 20% depending on the population. The presence of comorbid conditions such as components of metabolic syndrome along with older age increases the morbidity and mortality of NASH cirrhotic patients. However, it is unclear if the same applies to lean NASH. The prevalence of metabolic syndrome is less common in lean NAFLD patients as compared to

Table 1 Pre-liver transplant clinical and laboratory variables

	Total (*n* = 176)	BMI groups after ascites correction		*P* value
		Overweight or obese (*n* = 122)	Underweight or normal (*n* = 54)	
Age at listing, median (range) years	61.0 (32.0–71.4)	60.3 (32.0–71.4)	61.6 (45.2–71.0)	0.048[a]
Age at end of listing, median (range) years	61.0 (32.0–72.0)	61.0 (32.0–71.0)	62.0 (48.0–72.0)	0.09
Female sex, *n* (%)	81 (46.02)	53 (43.44)	28 (51.85)	0.30
Height at listing, median (range) cm	168.0 (148.0–193.0)	168.0 (148.0–188.0)	168.0 (150.0–193.0)	0.23
Weight at listing, median (range) kg	88.3 (39.6–146.5)	94.9 (69.0–146.5)	72.0 (39.6–94.2)	< 0.001[c]
Ascites adjusted weight at listing, median (range) kg	77.4 (33.7–140.0)	85.1 (60.5–140.0)	64.4 (33.7–80.1)	< 0.001[c]
Weight at end of listing, median (range) kg	86.9 (39.6–161.8)	92.9 (50.7–161.8)	73.9 (39.6–94.2)	< 0.001[c]
BMI at listing, median (range) kg/m^2	31.0 (17.6–48.9)	33.7 (25.6–48.9)	25.4 (17.6–30.8)	< 0.001[c]
Ascites adjusted BMI at listing, median (range) kg/m^2	27.4 (15.0–45.3)	29.2 (25.0–45.3)	22.6 (15.0–24.9)	< 0.001[c]
Na MELD (at listing), median (range)	22.0 (10.0–48.0)	21.0 (11.0–48.0)	22.0 (10.0–43.0)	0.34
Na MELD at end of listing, median (range)	23.0 (6.0–45.0)	23.0 (6.0–44.0)	23.0 (10.0–45.0)	0.41
Creatinine at listing, median (range) μmol/L	98.5 (51.0–564.0)	96.5 (55.0–564.0)	103.0 (51.0–399.0)	0.50
Creatinine at end of listing, median (range) μmol/L	112.5 (44.0–719.0)	115.0 (44.0–719.0)	109.0 (49.0–483.0)	0.50
eGFR at listing, median (range) mL/min/1.73 m^2	63.0 (17.0–120.0)	65.5 (18.0–117.0)	56.0 (17.0–120.0)	0.11
eGFR at end of listing, median (range) mL/min/1.73 m^2	52.5 (17.0–116.0)	57.0 (17.0–116.0)	48.0 (20.0–98.0)	0.017[a]
Bilirubin at listing, median (range) μmol/L	49.0 (8.0–955.0)	51.0 (8.0–755.0)	45.5 (14.0–955.0)	0.11
Bilirubin at end of listing, median (range) μmol/L	56.5 (3.0–927.0)	58.0 (8.0–927.0)	50.0 (3.0–802.0)	0.19
INR at listing, median (range)	1.5 (1.1–4.7)	1.5 (1.1–4.7)	1.5 (1.1–3.9)	0.05
INR at end of listing, median (range)	1.7 (1.1–7.6)	1.7 (1.1–7.6)	1.8 (1.1–5.0)	0.46
Na at listing, median (range) mEq/L	134.0 (116.0–147.0)	135.0 (120.0–147.0)	133.0 (116.0–142.0)	0.014[a]
Na at end of listing, median (range) mEq/L	135.0 (116.0–159.0)	135.0 (116.0–159.0)	134.0 (120.0–152.0)	0.10
Albumin at listing, median (range) g/L	30.5 (9.0 – 47.0)	29.5 (20.0–47.0)	31.0 (9.0–42.0)	0.08
Albumin at end of listing, median (range) g/L	30.0 (10.0–54.0)	30.0 (12.0–54.0)	30.0 (10.0–50.0)	0.28
Frailty score (*n* = 159), median (range)	4.0 (2.0–8.0)	4.0 (2.0–8.0)	5.0 (3.0–8.0)	0.25
None to mild, *n* (%)	116 (72.96)	78 (71.56)	38 (76)	0.56
Moderate to severe, *n* (%)	43 (27.04)	31 (28.44)	12 (24)	
Missing, *n* (%)	17 (9.66)	13 (10.66)	4 (7.41)	
Encephalopathy, *n* (%)	141 (80.11)	99 (81.15)	42 (77.78)	0.61
Ascites, *n* (%)	161 (91.48)	109 (089.34)	052 (096.30)	0.15
Degree of ascites, *n* (%)				
None	14 (07.95)	13 (10.66)	1 (1.85)	0.030[a]
Mild	41 (23.30)	30 (24.59)	11 (20.37)	
Moderate	30 (17.05)	24 (019.67)	6 (11.11)	
Severe	91 (51.70)	55 (45.08)	36 (66.67)	
Need for LVP, *n* (%)	103 (58.86)	64 (52.89)	39 (72.22)	0.016[a]

SBP, *n* (%)	46 (26.44)	33 (27.05)	13 (25.00)	0.78
Variceal bleed, *n* (%)	53 (30.11)	34 (27.87)	19 (35.19)	0.33
Hepatorenal syndrome, *n* (%)	48 (27.27)	30 (24.59)	18 (33.33)	0.23
Hypertension, *n* (%)	80 (45.45)	58 (47.54)	22 (40.74)	0.40
Diabetes, *n* (%)	104 (59.09)	68 (55.74)	36 (66.67)	0.17
Hyperlipidemia, *n* (%)	57 (32.39)	35 (28.69)	22 (40.74)	0.12
CKD, *n* (%)	18 (10.23)	12 (9.84)	6 (11.11)	0.80
CAD, *n* (%)	29 (16.48)	22 (18.03)	7 (12.96)	0.40
Time on waiting list, median (range) days	136.0 (1.0–1566.0)	139.5 (1.0–1497.0)	117.0 (1.0–1566.0)	0.42
ICU stay within 90 d before end of listing, *n* (%)	30 (17.05)	21 (17.21)	9 (16.67)	0.93
No of hospitalizations within 90 d before end of listing, median (range), *n* (%)	1.0 (0.0–5.0)	1.0 (0.0–5.0)	1.0 (0.0–5.0)	0.42
< 2	151 (85.80)	105 (86.07)	46 (85.19)	0.88
≥ 2	25 (14.20)	17 (13.93)	8 (14.81)	
Bacteraemia/sepsis within 90 d before end of listing, *n* (%)	19 (11.66)	12 (10.62)	7 (14.00)	0.54
Outcome, *n* (%)				
Active living	1 (0.57)	1 (0.82)	0 (00)	0.26
De-listed	22 (12.50)	14 (11.48)	8 (14.81)	
Died	42 (23.86)	25 (20.49)	17 (31.48)	
Transplanted	111 (63.07)	82 (67.21)	29 (53.70)	
Type of LT received, *n* (%)				
DDLT	78 (70.27)	57 (69.51)	21 (72.41)	0.77
LDLT	33 (29.73)	25 (30.49)	8 (27.59)	

[a]$P < 0.05$.

[c]$P < 0.001$.

BMI: Body mass index; CAD: Coronary artery disease; CKD: Chronic kidney disease; DDLT: Deceased donor liver transplant; eGFR: Estimated glomerular filtration rate; ICU: Intensive care unit; INR: International normalized ratio; LT: Liver transplant; LDLT: Living donor liver transplant; LVP: Large volume paracentesis; MELD: Model for end stage liver disease; Na: Sodium; SBP: Spontaneous bacterial peritonitis.

obese[4,12-14]. A long-term follow-up study showed that biopsy-proven lean NAFLD patients are more likely to develop severe liver disease (F3/F4) than overweight patients[5]. Literature is scant about the outcomes of lean NASH while on the waiting list for LT. A study comprising of 1090 patients revealed shorter cumulative survival in lean NAFLD compared to non-lean NAFLD (log-rank test = 5.6; $P < 0.02$) [6] In a recent study, morbid obesity and diabetes were related to an increased risk of drop out of NASH patients from the waiting list[15].

Frailty, a common complication of cirrhosis, is seen more frequently in NASH cirrhosis patients as compared to other etiologies such as alcoholic liver disease[16]. Frailty has previously been shown to determine a patient's overall health, the number of hospitalizations, length of hospital stay, delisting, and waitlist mortality[17-21]. especially in patients older than 65 years of age[22] independent of portosystemic encephalopathy or ascites[23]. However, the impact of frailty in the NASH cohort was not assessed. In a multicentre study, frailty was associated with a 2-fold higher risk of wait-list mortality among nonobese/class 1 obese patients, while more than 3-fold higher risk of wait-list mortality among class 2 or greater obese liver transplant candidates[24]. However, NASH comprised only 17.5% of their patient population, while BMI was not corrected for ascites which was present in 37.1% of their patients. In a retrospective analysis, a higher frailty score was associated with an increased risk of delisting in NASH patients (HR: 1.46; 95%CI: 1.06–2.03, $P = 0.02$)[16]. In our study, lean NASH patients with frailty had poor survival (HR: 0.12; 95%CI: 0.05–0.29, $P < 0.0001$) with lower instantaneous rate of transplant (HR: 5.71; 95%CI: 1.26–25.9, $P = 0.02$). Therefore, the convergence of frailty with lean NASH led to significantly worse outcomes on the waitlist as well as in the early period post-transplant.

Though lean NAFLD is considered to be benign, the dysfunctional adipose tissue, in particular, visceral adiposity is related with increase cardiometabolic risk in lean NAFLD. Further, alterations in

Table 2 Percentage of patients who changed body mass index groups after ascites correction

Reduction in BMI after ascites correction					Original/uncorrected	Unchanged
Underweight	Normal	Overweight	Obesity 1	Obesity 2		
					Underweight, 2 (1.1%)	2 (100%)
5 (22.73%)					Normal, 22 (12.5%)	17 (77.27%)
	29 (55.77%)				Overweight, 52 (29.55%)	23 (44.23%)
	1 (1.82%)	42 (76.36%)			Obesity 1, 55 (31.25%)	12 (21.82%)
			17 (62.96%)		Obesity 2, 27 (15.34%)	10 (37.04%)
			2 (11.11%)	11 (61.11%)	Obesity 3, 18 (10.23%)	5 (27.78%)
All BMI group had some level of decrease after correction			Especially higher BMI groups have more % reduction		Total (n = 176)	% of unchanged are higher among low BMI groups

BMI: Body mass index.

TM6SF2, a gene conferring susceptibility to NASH and fibrosis, are shown to be increased in lean NAFLD than obese NAFLD patients. However, there is a paucity of data on post-transplant outcomes in lean patients specifically[25]. In the post-transplant setting, a pivotal study looking at the patients on the UNOS database revealed that both short- and long-term survivals were low in patients who were morbidly obese before transplantation, owing to adverse cardiovascular events[26]. However, none of the patients in this study belonged to the NASH group. On the contrary, obesity was noted to paradoxically favour the NASH patients compared to their non-NASH counterparts. A recent study found that lean patients have both poorer graft and patient survival than their obese counterparts[7]. However, they did not adjust the BMI for ascites, whereas elevated BMI might have reflected fluid overload instead of true obesity. There is still much that is not known or understood, and hence it is challenging to explain the underlying molecular mechanisms linking lean NASH with worse outcomes post LT. Nonetheless, our study also confirms the enigmatic effect of obesity in the NASH subset. This study also highlighted the importance of correcting BMI for ascites. Despite correcting BMI for ascites, 69% of NASH patients belong to the overweight/obese group.

NASH has been associated with metabolic syndrome-related complications such as cardiovascular disease and chronic kidney disease (CKD)[27]. Post-transplant the risk of metabolic complications increases further owing to the immunosuppressive medications. Furthermore, calcineurin inhibitors carry direct nephrotoxic effects. In general, obese NAFLD patients appear to have a higher risk of developing CKD than non-obese[28]. In post-LT patients, obesity has been identified as a risk for post-operative severe acute kidney injury[29] as well as renal disease progression needing a kidney transplant after LT[30]. We further augmented this data by showing that median creatinine in our obese patients was significantly higher than in lean patients at 5 years (153.5 μmol/L *vs* 111 μmol/L, P = 0.019). The incidence of diabetes and hypertension were numerically higher in the obese group at 1 and 5 years, however, this difference was statistically insignificant. Further, the incidence of cardiovascular events was also not significantly different among the two groups. Further expansion of follow-up to 10 years might show a statistically meaningful difference. However, this analysis was not possible in the current study. Given the selection criteria with the start of the study from November 2012, none of the patients has achieved the 10-year benchmark yet.

This study has been limited by its retrospective design, smaller sample size, and lack of a comparison group from a non-NASH subset. We also acknowledge the limitation of missing data given the retrospective design, transfer of care to other local centres post-transplant, and a limited number of patients achieving the 5-year benchmark. The results of this study should be interpreted cautiously as it does not suggest the listing of all morbidly obese NASH cirrhotic patients for liver transplant. Nonetheless, under current practice, outcomes of carefully selected NASH patients with higher BMI are better than their lean counterparts. This conundrum could have been explained by improvement in patient selection protocols, post-transplant critical care support, and immunosuppressive treatment. Future larger studies would be required to validate the generalizability of our findings. Moreover, there is need of identifying the factors such as genetic variants, and body fat distribution/visceral adiposity, which can play role in this paradox.

CONCLUSION

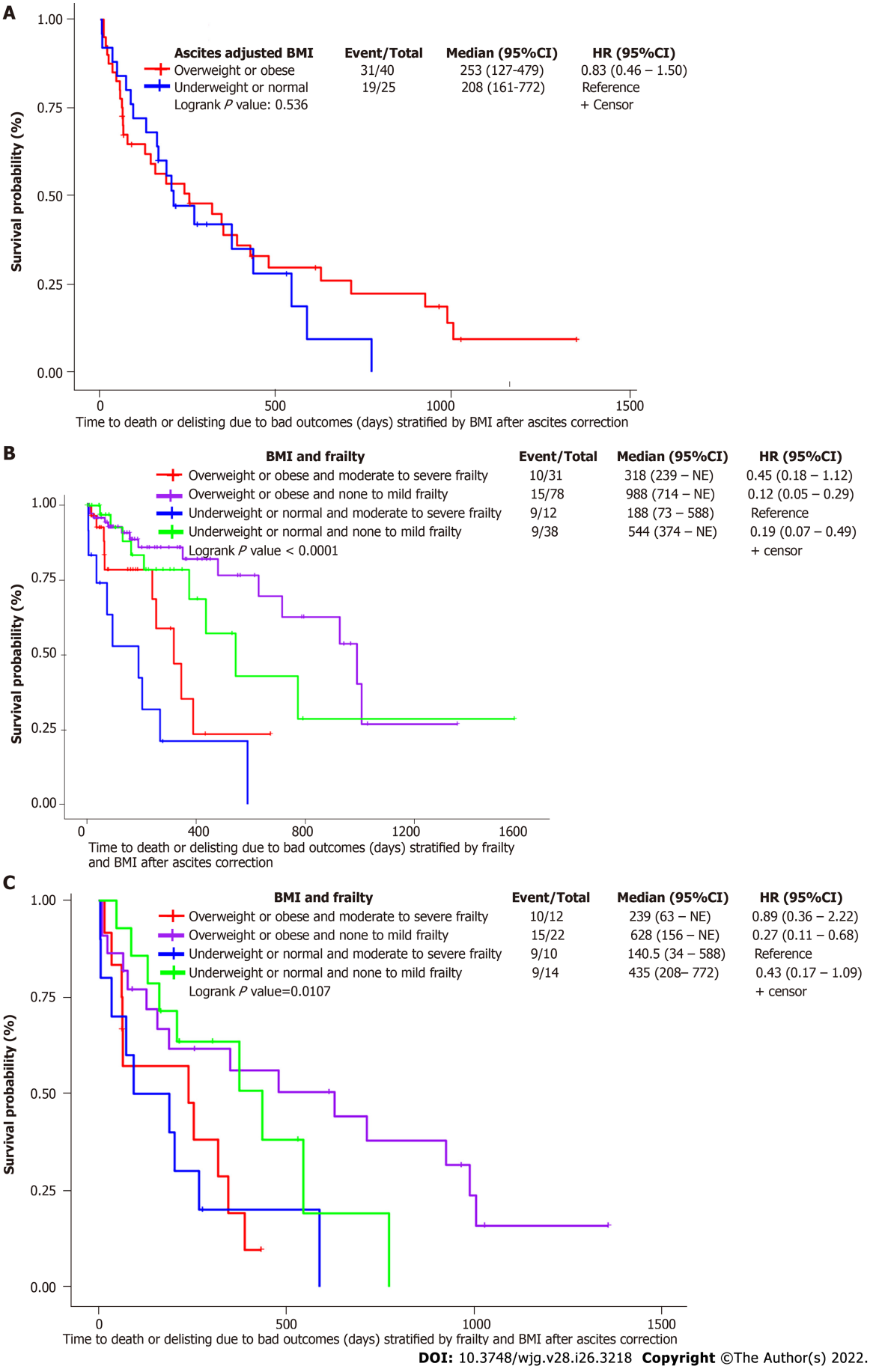
Lean NASH is associated with adverse outcomes on the waiting list as well as early post-transplant, in

Table 3 Post transplant outcomes

	Total (n = 111)	BMI after ascites correction		P value
		Overweight or obese (n = 82)	Underweight or normal (n = 29)	
Biliary stricture, n (%)	22 (19.8)	16 (19.5)	6 (20.7)	0.97
Biliary leak, n (%)	10 (9)	7 (8.5)	3 (10.3)	1.0
Hepatic artery thrombosis, n (%)	2 (1.8)	0 (0)	2 (6.9)	0.07
90-d re-hospitalization (n = 103), n (%)	23 (22.3)	17 (22.6)	6 (21.4)	0.89
Recurrent NAFLD, n (%)	57 (51.4)	44 (53.7)	13 (44.8)	0.59
Time to recurrent NAFLD, median (range) days	568 (13–2135)	489 (13–1821)	757 (80–2135)	0.21
Recurrent NASH, n (%)	7 (6.3)	5 (6.1)	2 (6.9)	1.0
Time to recurrent NASH, median (range) days	812 (363–1119)	802 (363–1119)	957.5 (812–1103)	0.28
BMI at 1 yr (n = 83), median (range) kg/m^2	30.3 (19.2–44.0)	31.7 (23.2–44.0)	26.1 (19.2–34.2)	< 0.001[c]
BMI at 5 yr (n = 17), median (range) kg/m^2	33.9 (20.3–47.9)	35.1 (26.6 – 47.9)	27.0 (20.3–31.5)	0.004[b]
Creatinine at 1 yr (n = 70), median (range) μmol/L	114.0 (54.0–279.0)	117.5 (63.0–279.0)	106.0 (54.0–178.0)	0.21
Creatinine at 5 yr (n = 19), median (range) μmol/L	143.0 (67.0-257.0)	153.5 (78.0–257.0)	111.0 (67.0–127.0)	0.019[a]
Diabetes at 1 yr (n = 82), n (%)	36 (43.9)	27 (45.8)	9 (39.1)	0.59
Diabetes at 5 yr (n = 20), n (%)	10 (50)	8 (53.3)	2 (40)	0.72
Hypertension at 1 yr (n = 83), n (%)	44 (53)	33 (55)	11 (47.8)	0.56
Hypertension at 5 yr (n = 20), n (%)	12 (60)	10 (66.7)	2 (40)	0.35
Cardiovascular events post LT, n (%)	22 (19.8)	14 (17)	8 (27.6)	0.45
Fibroscan Elastography (n = 48), median (range) kPa	6.4 (2.3–21.8)	6.8 (3.5–21.8)	4.8 (2.3–14.5)	0.011[a]
Fibroscan CAP (n = 48), median (range) dB/m	286.5 (181.0–400.0)	298.0 (198.0–400.0)	283.5 (181.0–400.0)	0.26
Graft loss within 90 d post LT, n (%)	5 (4.5)	1 (1.2)	4 (13.8)	0.032[a]
Graft survival post LT 1 yr (n = 101), n (%)	94 (93.1)	72 (98.6)	22 (78.6)	0.002[b]
Graft survival post LT 3 yr (n = 72), n (%)	65 (90.3)	48 (96)	17 (77.3)	0.025[a]
Graft survival post LT 5 yr (n = 32), n (%)	22 (68.8)	17 (85)	5 (41.7)	0.018[a]
Deaths post LT, n (%)	7 (6.3)	2 (2.4)	5 (17.2)	0.029[a]
Time to death post LT (n = 7), median (range) days	224 (13–1176)	192.5 (20–365)	224 (13–1176)	0.42
Death within 90 d post-LT, n (%)	2 (1.8)	1 (1.2)	1 (3.4)	0.38
Patient survival at 1 yr (n = 108), n (%)	104 (96.3)	78 (98.7)	26 (89.7)	0.06
Patient survival at 3 yr (n = 97), n (%)	66 (91.7)	48 (96)	18 (81.8)	0.07
Patient survival at 5 yr (n = 32), n (%)	25 (78.1)	18 (90)	7 (58.3)	0.07

[a]P < 0.05.
[b]P < 0.01.
[c]P < 0.001.
BMI: Body mass index; CAP: Controlled attenuation parameter; LT: Liver transplant; NAFLD: Non-alcoholic fatty liver disease; NASH: Non-alcoholic steatohepatitis.

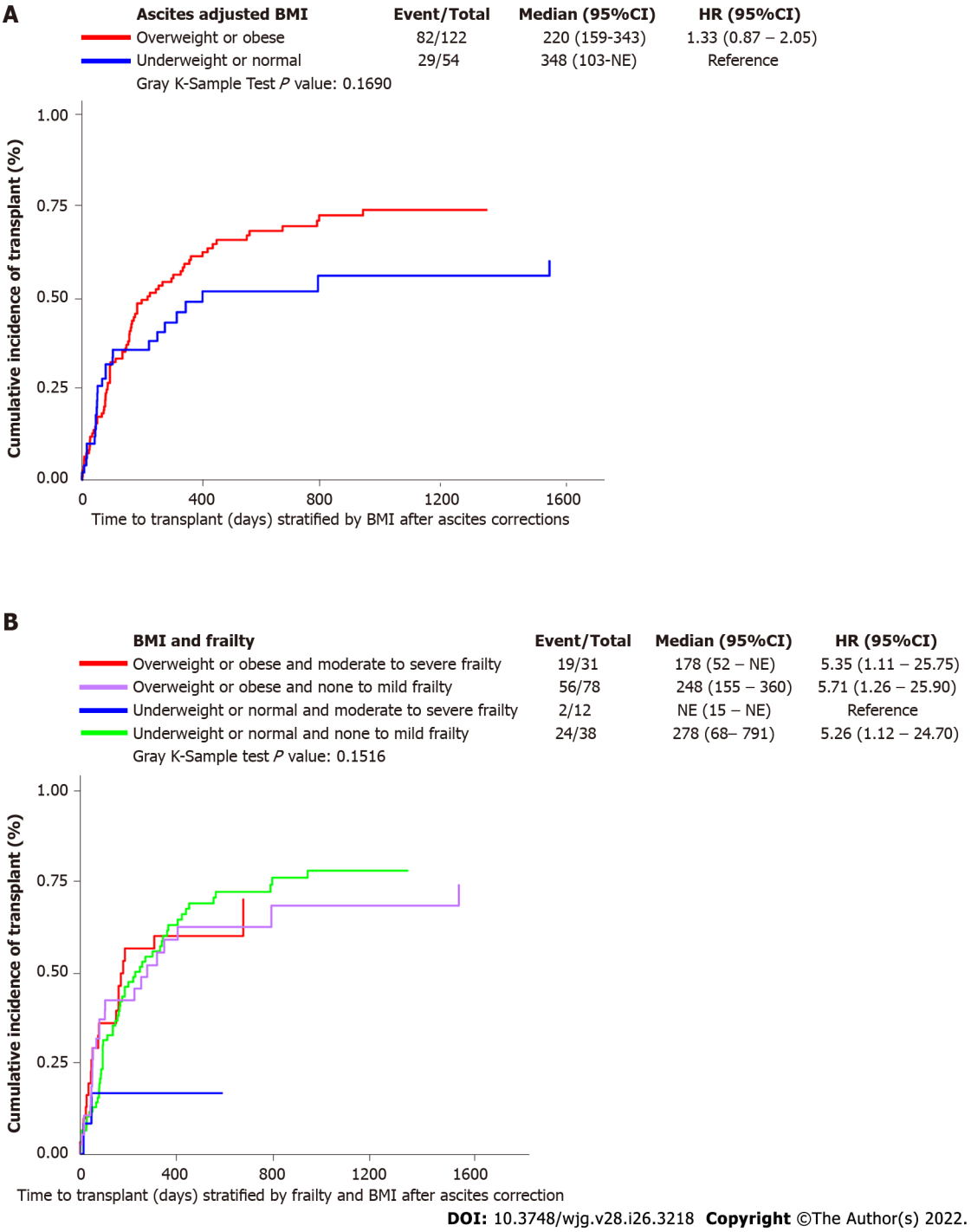
conjunction with often comorbid frailty. Our study emphasizes the need to actively support the nutritional and physical functional status of lean NASH patients on the waiting list. Post-transplant, all NASH patients should have active lifestyle counselling regarding a healthy diet and regular exercise to improve long-term cardiometabolic outcomes.



DOI: 10.3748/wjg.v28.i26.3218 **Copyright** ©The Author(s) 2022.

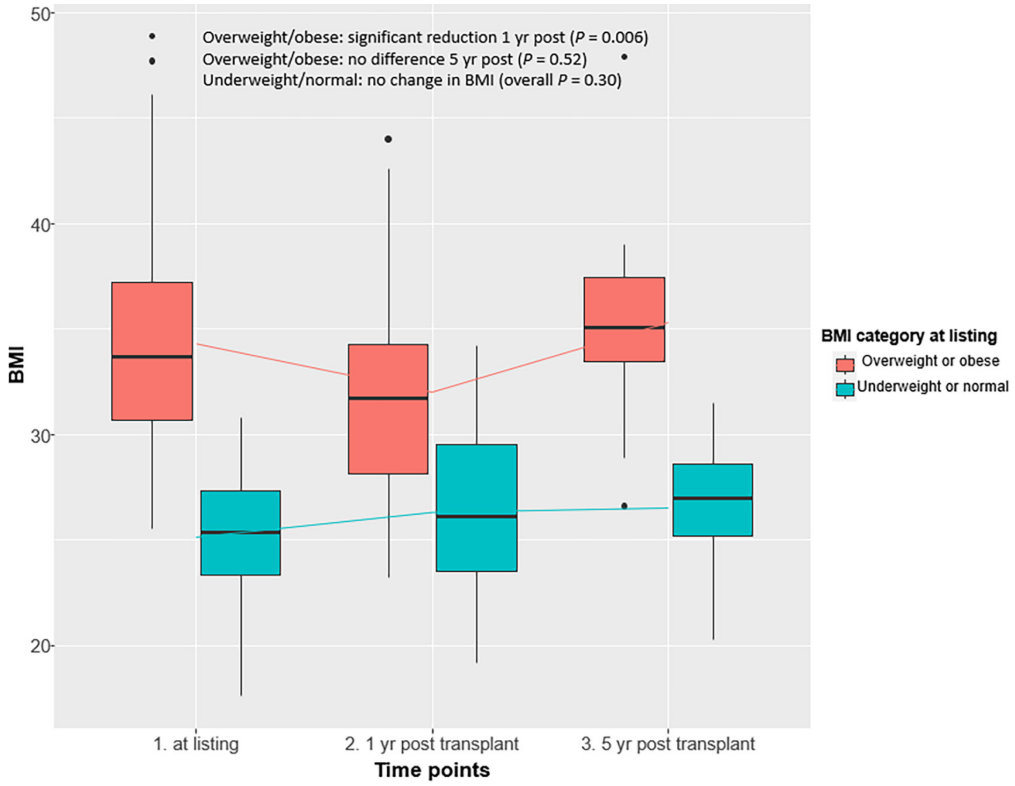
Figure 1 Kaplan-Meier–overall survival: Time to delisting or death on waitlist. A: Ascites adjusted body mass index (BMI) groups (non-transplanted

patients only); B: Ascites adjusted BMI and frailty (full cohort); C: Ascites adjusted BMI and frailty (non-transplanted patients only). HR: Hazard ratio; BMI: Body mass index.



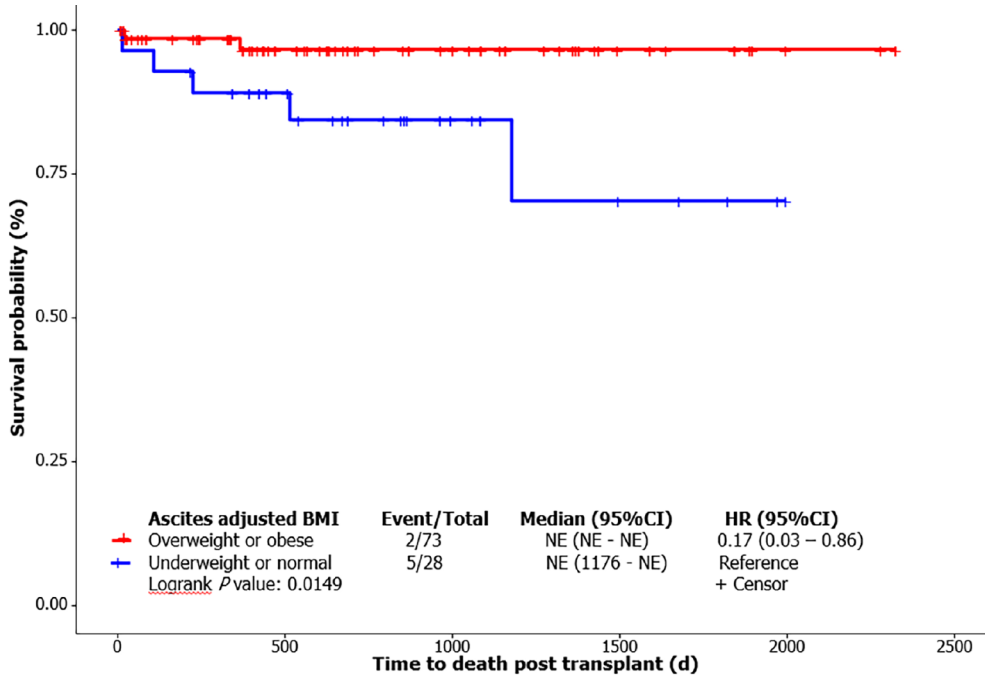
DOI: 10.3748/wjg.v28.i26.3218 **Copyright** ©The Author(s) 2022.

Figure 2 Competing risk analysis for time to transplant. A: Ascites adjusted body mass index (BMI) groups; B: Ascites adjusted BMI and frailty. HR: Hazard ratio; BMI: Body mass index.



DOI: 10.3748/wjg.v28.i26.3218 **Copyright** ©The Author(s) 2022.

Figure 3 Change in body mass index from time of listing to post liver transplant at 1 and 5 yr. BMI: Body mass index.



Survival estimations (95%CI)	Overweight or obese	Underweight or normal	*P* value
1 yr	96.7% (92.2% - 100%)	89.1% (78.3% - 100%)	0.13
5 yr	96.7% (92.2% - 100%)	70.4% (47.4% - 100%)	0.01

DOI: 10.3748/wjg.v28.i26.3218 **Copyright** ©The Author(s) 2022.

Figure 4 Kaplan-Meier–overall survival: Time to death post liver transplant stratified by ascites adjusted body mass index groups. Lower panel shows the 1- and 5-yr survival estimates. HR: Hazard ratio; BMI: Body mass index.

ARTICLE HIGHLIGHTS

Research background

Non-alcoholic steatohepatitis (NASH) cirrhosis is the second leading indication for liver transplantation (LT). There is a conflicted role of body mass index (BMI) on outcomes of NASH cirrhosis while on waitlist and post liver transplant.

Research motivation

There are few reports on the waitlist and post liver transplant outcomes of lean *vs* obese NASH patients, and the impact of ascites adjusted BMI have not been fully clarified.

Research objectives

The objective of this study was to compare the longitudinal trajectories of patients with lean *vs* obese NASH cirrhosis, from listing up to post-transplant, having adjusted their BMI for ascites.

Research methods

A retrospective analysis of all adult NASH patients listed for LT at the University Health Network, Toronto between November 2012 and May 2019 was performed. We summarized the clinical characteristics of patients with lean and obese NASH. Competing risk analyses and Cox Proportional Hazard models were used to assess the cumulative incidence of transplant and survival outcomes.

Research results

Out of 265 patients listed for NASH cirrhosis, 176 were included. The median age was 61 (32–71.4) years; 46% were females. 111 patients underwent LT. Lean NASH patients were elderly at time of listing (median age 61.6 years *vs* 60.3 years, P = 0.048), worse renal functions at end of listing (median estimated glomerular filtration 48 mL/min/1.73 m^2 *vs* 57 mL/min/1.73 m^2, P = 0.017), carried more severe ascites (66.6% *vs* 45%, P = 0.03) and were more paracentesis dependent (72.2% *vs* 52.9%, P = 0.016). Obese robust patients had better waitlist survival [hazard ratio (HR): 0.12; 95%CI: 0.05–0.29, P < 0.0001] with higher instantaneous rate of transplant (HR: 5.71; 95%CI: 1.26–25.9, P = 0.02). Lean NASH patients had a substantially higher risk of graft loss within 90 d post-LT (1.2% *vs* 13.8%, P = 0.032) and death post-LT (2.4% *vs* 17.2%, P = 0.029). 1- 3- and 5-year graft survival was poor for lean NASH (78.6%, 77.3% and 41.7% *vs* 98.6%, 96% and 85% respectively). Overall patient survival post-LT was significantly worse in lean NASH (HR: 0.17; 95%CI: 0.03–0.86, P = 0.0142) with 83% lower instantaneous rate of death in obese group. Post-transplant renal function was significantly better in lean NASH patients at 5 years (median creatinine 111 μmol/L *vs* 153.5 μmol/L, P = 0.019).

Research conclusions

Although lean NASH was thought to be more benign than obese NASH, our study suggests a paradoxical correlation of lean NASH with waitlist outcomes, and graft and patient survival post-LT, in conjunction with often comorbid frailty.

Research perspectives

To understand the underlying molecular mechanisms linking lean NASH with worse outcomes, there is need of identifying the factors such as genetic variants, body fat distribution/visceral adiposity, which can play role in this paradox.

FOOTNOTES

Author contributions: Qazi-Arisar FA and Uchila R given their equal contribution in the manuscript; Bhat M was the guarantor and designed the study; Qazi-Arisar FA, Uchila R, Chen C, Yang C, Chen SY, Karnam RS and Azhie A participated in the acquisition, analysis, and interpretation of the data, and drafted the initial manuscript; Qazi-Arisar FA, Xu W, Galvin Z, Selzner N, Lilly L and Bhat M revised the article critically for important intellectual content.

Institutional review board statement: The study was reviewed and approved by the Research Ethics board of the University Health Network (Toronto, Canada).

Informed consent statement: Given retrospective nature of study from chart review, written informed consent was not required.

Conflict-of-interest statement: Dr. Bhat reports other from Novo Nordisk, other from Ipsen, grants from Paladin, grants from Natera, grants from Oncoustics, grants from MedoAI, grants from Lallemand, personal fees from Novartis, personal fees from Lupin, outside the submitted work.

Data sharing statement: No additional data are available.

STROBE statement: The authors have read the STROBE Statement—checklist of items, and the manuscript was prepared and revised according to the STROBE Statement—checklist of items.

Open-Access: This article is an open-access article that was selected by an in-house editor and fully peer-reviewed by external reviewers. It is distributed in accordance with the Creative Commons Attribution NonCommercial (CC BY-NC 4.0) license, which permits others to distribute, remix, adapt, build upon this work non-commercially, and license their derivative works on different terms, provided the original work is properly cited and the use is non-commercial. See: https://creativecommons.org/Licenses/by-nc/4.0/

Country/Territory of origin: Canada

ORCID number: Mamatha Bhat 0000-0003-1960-8449.

Corresponding Author's Membership in Professional Societies: American Association for the Study of Liver Diseases.

S-Editor: Fan JR
L-Editor: A
P-Editor: Yu HG

REFERENCES

1 **Parikh ND**, Marrero WJ, Wang J, Steuer J, Tapper EB, Konerman M, Singal AG, Hutton DW, Byon E, Lavieri MS. Projected increase in obesity and non-alcoholic-steatohepatitis-related liver transplantation waitlist additions in the United States. *Hepatology* 2019; **70**: 487-495 [PMID: 28833326 DOI: 10.1002/hep.29473]
2 **Vernon G**, Baranova A, Younossi ZM. Systematic review: the epidemiology and natural history of non-alcoholic fatty liver disease and non-alcoholic steatohepatitis in adults. *Aliment Pharmacol Ther* 2011; **34**: 274-285 [PMID: 21623852 DOI: 10.1111/j.1365-2036.2011.04724.x]
3 **Non-alcoholic Fatty Liver Disease Study Group**, Lonardo A, Bellentani S, Argo CK, Ballestri S, Byrne CD, Caldwell SH, Cortez-Pinto H, Grieco A, Machado MV, Miele L, Targher G. Epidemiological modifiers of non-alcoholic fatty liver disease: Focus on high-risk groups. *Dig Liver Dis* 2015; **47**: 997-1006 [PMID: 26454786 DOI: 10.1016/j.dld.2015.08.004]
4 **Young S**, Tariq R, Provenza J, Satapathy SK, Faisal K, Choudhry A, Friedman SL, Singal AK. Prevalence and Profile of Nonalcoholic Fatty Liver Disease in Lean Adults: Systematic Review and Meta-Analysis. *Hepatol Commun* 2020; **4**: 953-972 [PMID: 32626829 DOI: 10.1002/hep4.1519]
5 **Hagström H**, Nasr P, Ekstedt M, Hammar U, Stål P, Hultcrantz R, Kechagias S. Risk for development of severe liver disease in lean patients with nonalcoholic fatty liver disease: A long-term follow-up study. *Hepatol Commun* 2018; **2**: 48-57 [PMID: 29404512 DOI: 10.1002/hep4.1124]
6 **Cruz ACD**, Bugianesi E, George J, Day CP, Liaquat H, Charatcharoenwitthaya P, Mills PR, Dam-Larsen S, Bjornsson ES, Haflidadottir S, Adams LA, Bendtsen F, Angulo P. Characteristics and Long-Term Prognosis of Lean Patients With Nonalcoholic Fatty Liver Disease. *Gastroenterology* 2014; **146**: S-909 [DOI: 10.1016/s0016-5085(14)63307-2]
7 **Satapathy SK**, Jiang Y, Agbim U, Wu C, Bernstein DE, Teperman LW, Kedia SK, Aithal GP, Bhamidimarri KR, Duseja A, Maiwall R, Maliakkal B, Jalal P, Patel K, Puri P, Ravinuthala R, Wong VW, Abdelmalek MF, Ahmed A, Thuluvath PJ, Singal AK; Global NAFLD Consortium. Posttransplant Outcome of Lean Compared With Obese Nonalcoholic Steatohepatitis in the United States: The Obesity Paradox. *Liver Transpl* 2020; **26**: 68-79 [PMID: 31665561 DOI: 10.1002/lt.25672]
8 **Wang Q**, You H, Ou X, Zhao X, Sun Y, Wang M, Wang P, Wang Y, Duan W, Wang X, Wu S, Kong Y, Saxena R, Gouw ASH, Jia J. Non-obese histologically confirmed NASH patients with abnormal liver biochemistry have more advanced fibrosis. *Hepatol Int* 2019; **13**: 766-776 [PMID: 31559605 DOI: 10.1007/s12072-019-09982-z]
9 **Leonard J**, Heimbach JK, Malinchoc M, Watt K, Charlton M. The impact of obesity on long-term outcomes in liver transplant recipients-results of the NIDDK liver transplant database. *Am J Transplant* 2008; **8**: 667-672 [PMID: 18294163 DOI: 10.1111/j.1600-6143.2007.02100.x]
10 **European Association for the Study of the Liver**. EASL Clinical Practice Guidelines on nutrition in chronic liver disease. *J Hepatol* 2019; **70**: 172-193 [PMID: 30144956 DOI: 10.1016/j.jhep.2018.06.024]
11 **Tandon P**, Low G, Mourtzakis M, Zenith L, Myers RP, Abraldes JG, Shaheen AA, Qamar H, Mansoor N, Carbonneau M, Ismond K, Mann S, Alaboudy A, Ma M. A Model to Identify Sarcopenia in Patients With Cirrhosis. *Clin Gastroenterol Hepatol* 2016; **14**: 1473-1480.e3 [PMID: 27189915 DOI: 10.1016/j.cgh.2016.04.040]
12 **Fracanzani AL**, Petta S, Lombardi R, Pisano G, Russello M, Consonni D, Di Marco V, Cammà C, Mensi L, Dongiovanni P, Valenti L, Craxì A, Fargion S. Liver and Cardiovascular Damage in Patients With Lean Nonalcoholic Fatty Liver Disease, and Association With Visceral Obesity. *Clin Gastroenterol Hepatol* 2017; **15**: 1604-1611.e1 [PMID: 28554682 DOI: 10.1016/j.cgh.2017.04.045]
13 **Akyuz U**, Yesil A, Yilmaz Y. Characterization of lean patients with nonalcoholic fatty liver disease: potential role of high hemoglobin levels. *Scand J Gastroenterol* 2015; **50**: 341-346 [PMID: 25540973 DOI: 10.3109/00365521.2014.983160]
14 **Margariti A**, Deutsch M, Manolakopoulos S, Tiniakos D, Papatheodoridis GV. The severity of histologic liver lesions is independent of body mass index in patients with nonalcoholic fatty liver disease. *J Clin Gastroenterol* 2013; **47**: 280-286

[PMID: 23391869 DOI: 10.1097/MCG.0b013e31826be328]

15 **Kardashian AA**, Dodge JL, Roberts J, Brandman D. Weighing the risks: Morbid obesity and diabetes are associated with increased risk of death on the liver transplant waiting list. *Liver Int* 2018; **38**: 553-563 [PMID: 28727287 DOI: 10.1111/liv.13523]

16 **Bhanji RA**, Narayanan P, Moynagh MR, Takahashi N, Angirekula M, Kennedy CC, Mara KC, Dierkhising RA, Watt KD. Differing Impact of Sarcopenia and Frailty in Nonalcoholic Steatohepatitis and Alcoholic Liver Disease. *Liver Transpl* 2019; **25**: 14-24 [PMID: 30257063 DOI: 10.1002/lt.25346]

17 **Dolgin NH**, Smith AJ, Harrington SG, Movahedi B, Martins PNA, Bozorgzadeh A. Association Between Sarcopenia and Functional Status in Liver Transplant Patients. *Exp Clin Transplant* 2019; **17**: 653-664 [PMID: 30295589 DOI: 10.6002/ect.2018.0018]

18 **Kahn J**, Wagner D, Homfeld N, Müller H, Kniepeiss D, Schemmer P. Both sarcopenia and frailty determine suitability of patients for liver transplantation-A systematic review and meta-analysis of the literature. *Clin Transplant* 2018; **32**: e13226 [PMID: 29478305 DOI: 10.1111/ctr.13226]

19 **Van Jacobs AC**. Frailty Assessment in Patients with Liver Cirrhosis. *Clin Liver Dis (Hoboken)* 2019; **14**: 121-125 [PMID: 31632663 DOI: 10.1002/cld.825]

20 **Lai JC**, Feng S, Terrault NA, Lizaola B, Hayssen H, Covinsky K. Frailty predicts waitlist mortality in liver transplant candidates. *Am J Transplant* 2014; **14**: 1870-1879 [PMID: 24935609 DOI: 10.1111/ajt.12762]

21 **Lai JC**, Dodge JL, Sen S, Covinsky K, Feng S. Functional decline in patients with cirrhosis awaiting liver transplantation: Results from the functional assessment in liver transplantation (FrAILT) study. *Hepatology* 2016; **63**: 574-580 [PMID: 26517301 DOI: 10.1002/hep.28316]

22 **Wang CW**, Covinsky KE, Feng S, Hayssen H, Segev DL, Lai JC. Functional impairment in older liver transplantation candidates: From the functional assessment in liver transplantation study. *Liver Transpl* 2015; **21**: 1465-1470 [PMID: 26359787 DOI: 10.1002/lt.24334]

23 **Lai JC**, Rahimi RS, Verna EC, Kappus MR, Dunn MA, McAdams-DeMarco M, Haugen CE, Volk ML, Duarte-Rojo A, Ganger DR, O'Leary JG, Dodge JL, Ladner D, Segev DL. Frailty Associated With Waitlist Mortality Independent of Ascites and Hepatic Encephalopathy in a Multicenter Study. *Gastroenterology* 2019; **156**: 1675-1682 [PMID: 30668935 DOI: 10.1053/j.gastro.2019.01.028]

24 **Haugen CE**, McAdams-DeMarco M, Verna EC, Rahimi RS, Kappus MR, Dunn MA, Volk ML, Gurakar A, Duarte-Rojo A, Ganger DR, O'Leary JG, Ladner D, Garonzik-Wang J, Segev DL, Lai JC. Association Between Liver Transplant Wait-list Mortality and Frailty Based on Body Mass Index. *JAMA Surg* 2019; **154**: 1103-1109 [PMID: 31509169 DOI: 10.1001/jamasurg.2019.2845]

25 **VanWagner LB**, Armstrong MJ. Lean NAFLD: A not so benign condition? *Hepatol Commun* 2018; **2**: 5-8 [PMID: 29404505 DOI: 10.1002/hep4.1143]

26 **Nair S**, Verma S, Thuluvath PJ. Obesity and its effect on survival in patients undergoing orthotopic liver transplantation in the United States. *Hepatology* 2002; **35**: 105-109 [PMID: 11786965 DOI: 10.1053/jhep.2002.30318]

27 **Kovalic AJ**, Cholankeril G, Satapathy SK. Nonalcoholic fatty liver disease and alcoholic liver disease: metabolic diseases with systemic manifestations. *Transl Gastroenterol Hepatol* 2019; **4**: 65 [PMID: 31620647 DOI: 10.21037/tgh.2019.08.09]

28 **Chon YE**, Kim HJ, Choi YB, Hwang SG, Rim KS, Kim MN, Lee JH, Ha Y, Lee MJ. Decrease in waist-to-hip ratio reduced the development of chronic kidney disease in non-obese non-alcoholic fatty liver disease. *Sci Rep* 2020; **10**: 8996 [PMID: 32488147 DOI: 10.1038/s41598-020-65940-y]

29 **Zhou J**, Lyu L, Zhu L, Liang Y, Dong H, Chu H. Association of overweight with postoperative acute kidney injury among patients receiving orthotopic liver transplantation: an observational cohort study. *BMC Nephrol* 2020; **21**: 223 [PMID: 32527305 DOI: 10.1186/s12882-020-01871-0]

30 **Locke JE**, Shelton B, Orandi B, Olthoff K, Pomfret E, Forde KA, Sawinski D, Gray M, Ascher N. Obesity is a risk factor for progression to kidney transplant waitlisting after liver transplantation. *Clin Transplant* 2021; **35**: e14317 [PMID: 33866616 DOI: 10.1111/ctr.14317]

World Journal of Gastroenterology

Submit a Manuscript: https://www.f6publishing.com

World J Gastroenterol 2022 July 14; 28(26): 3232-3242

DOI: 10.3748/wjg.v28.i26.3232

ISSN 1007-9327 (print) ISSN 2219-2840 (online)

ORIGINAL ARTICLE

Retrospective Study

Tumor-feeding artery diameter reduction is associated with improved short-term effect of hepatic arterial infusion chemotherapy plus lenvatinib treatment

De-Di Wu, Xiao-Feng He, Chen Tian, Peng Peng, Chuan-Li Chen, Xue-Han Liu, Hua-Jin Pang

Specialty type: Gastroenterology and hepatology

Provenance and peer review: Unsolicited article; Externally peer reviewed.

Peer-review model: Single blind

Peer-review report's scientific quality classification

Grade A (Excellent): 0
Grade B (Very good): B
Grade C (Good): C
Grade D (Fair): 0
Grade E (Poor): 0

P-Reviewer: Dilek ON, Turkey; Tsoulfas G, Greece

Received: January 22, 2022
Peer-review started: January 22, 2022
First decision: March 8, 2022
Revised: March 17, 2022
Accepted: June 18, 2022
Article in press: June 18, 2022
Published online: July 14, 2022

De-Di Wu, Xiao-Feng He, Chen Tian, Peng Peng, Hua-Jin Pang, Division of Vascular and Interventional Radiology, Department of General Surgery, Nanfang Hospital, Southern Medical University, Guangzhou 510515, Guangdong Province, China

Chuan-Li Chen, Medical Imaging Center, Nanfang Hospital, Southern Medical University, Guangzhou 510515, Guangdong Province, China

Xue-Han Liu, Department of Statistics, Huazhong University of Science and Technology, Wuhan 430000, Hubei Province, China

Corresponding author: Hua-Jin Pang, PhD, Associate Chief Physician, Associate Professor, Division of Vascular and Interventional Radiology, Department of General Surgery, Nanfang Hospital, Southern Medical University, No. 1838 North Baiyun Avenue, Guangzhou 510515, Guangdong Province, China. nfyyphj@163.com

Abstract

BACKGROUND

Recently, hepatic arterial infusion chemotherapy (HAIC) plus lenvatinib has been frequently used to treat unresectable hepatocellular carcinoma (uHCC) in China. In the clinic, the hepatic arteries of some patients shrink significantly during this treatment, leading to improved short-term efficacy.

AIM

To investigate the relationship between the shrinkage of hepatic arteries and the short-term effect of HAIC plus lenvatinib treatment.

METHODS

Sixty-seven participants with uHCC were enrolled in this retrospective study. The patients received HAIC every 3 wk, followed by oral lenvatinib after the first HAIC course. Hepatic artery diameters were measured on CT before treatment and after 1 and 2 mo of treatment. Meanwhile, the changes in tumor capillaries were also examined on pathological specimens before and after 1 mo of treatment. The antitumor response after 1, 3, and 6 mo of treatment was assessed using the modified Response Evaluation Criteria in Solid Tumors (mRECIST). The relationship between the changes in vessel diameters and the short-term effect of the combination treatment was evaluated by receiver-operating characteristic and

logistic regression analyses.

RESULTS

The hepatic artery diameters were all significantly decreased after 1 and 2 mo of treatment ($P < 0.001$), but there was no difference in the vessel diameters between 1 and 2 mo ($P > 0.05$). The microvessel density in the tumor lesions decreased significantly after 1 mo of combination treatment ($P < 0.001$). According to mRECIST, 46, 41, and 24 patients had complete or partial responses after 1, 3, and 6 mo of treatment, respectively, whereas 21, 21, and 32 patients had a stable or progressive disease at these times, respectively. Shrinkage of the tumor-feeding artery was significantly associated with the tumor response after 1, 3, and 6 mo of treatment ($P < 0.001$, $P = 0.004$, and $P = 0.023$, respectively); however, changes in other hepatic arteries were not significantly associated with the tumor response. Furthermore, shrinkage of the tumor-feeding artery was an independent factor for treatment efficacy ($P = 0.001$, $P = 0.001$, and $P = 0.002$ and 1, 3, and 6 mo, respectively).

CONCLUSION

The hepatic arteries shrank rapidly after treatment with HAIC plus lenvatinib, and shrinkage of the tumor-feeding artery diameter was closely related to improved short-term efficacy.

Key Words: Hepatocellular carcinoma; Hepatic arterial infusion chemotherapy; Lenvatinib; Short-term effect; Hepatic artery; Vessel diameter

©The Author(s) 2022. Published by Baishideng Publishing Group Inc. All rights reserved.

Core Tip: In this study, it was observed for the first time that the hepatic arteries shrank rapidly after hepatic arterial infusion chemotherapy plus lenvatinib therapy, and the close relationship between shrinkage of the tumor-feeding artery and improved short-term effect in patients with unresectable hepatocellular carcinoma was also confirmed. These findings would be of great significance to physicians for evaluating the effectiveness of this combination therapy earlier in the course of treatment and altering the treatment plan as needed.

Citation: Wu DD, He XF, Tian C, Peng P, Chen CL, Liu XH, Pang HJ. Tumor-feeding artery diameter reduction is associated with improved short-term effect of hepatic arterial infusion chemotherapy plus lenvatinib treatment. *World J Gastroenterol* 2022; 28(26): 3232-3242

URL: https://www.wjgnet.com/1007-9327/full/v28/i26/3232.htm

DOI: https://dx.doi.org/10.3748/wjg.v28.i26.3232

INTRODUCTION

Hepatocellular carcinoma (HCC) is one of the most common malignant tumors, with 850000 new cases reported per year worldwide[1,2]. In total, 70%-80% of patients with HCC in China are ineligible for surgical resection at the time of onset[3]. Recently, hepatic arterial infusion chemotherapy (HAIC) has been increasingly used to treat patients with unresectable HCC (uHCC) in Asian countries[4,5]. HAIC is recommended as a major treatment option in patients with intermediate and advanced HCC by current Japanese and Chinese guidelines[6].

Lenvatinib is an oral multi-target tyrosine kinase inhibitor (TKI) with antiangiogenic effects. Previous studies demonstrated the survival benefit of lenvatinib plus HAIC *vs* lenvatinib alone in patients with advanced HCC[7]. This combination therapy often requires 6-8 cycles, and early assessment of the antitumor response appears essential for both patients and physicians[8].

Recently, a clinical study demonstrated that the diameters of hepatic arteries are significantly reduced after TKI therapy[9]. Since the early imaging response is often associated with survival benefits, it should be clarified whether the changes in hepatic vessel diameters are related to the efficacy of HAIC combined with lenvatinib. As a result, we conducted a retrospective study of patients with uHCC treated with HAIC plus lenvatinib. The aim of this study was to: (1) Explore the changes in hepatic arteries after combination treatment; and (2) Determine the relationship between the hepatic artery changes and early therapeutic effects.

MATERIALS AND METHODS

Patient eligibility

This was a single-center, retrospective analysis of data from 67 patients with uHCC treated at our institution from January 2019 to October 2020. Approval for the study was obtained from the local ethics committee on human research. The HCC diagnosis was based on the findings of pathological, imaging, and clinical assessments using the European Association for the Study of the Liver criteria[10]. Eligible patients were those aged 18 years or older with uHCC (including patients with large/multifocal HCC and/or with vascular invasion and extrahepatic spread) who received HAIC plus lenvatinib as an initial treatment. Patients who underwent transcatheter arterial chemoembolization or received other TKIs before combination therapy were excluded. Enrolled patients who discontinued treatment during the follow-up period were also excluded.

Treatments

HAIC was repeated at an interval of 3 wk in enrolled patients in our hospital. A catheter was initially advanced into the celiac or superior mesenteric artery for digital subtraction angiography from the femoral artery; then, a microcatheter was left in the tumor-feeding artery (TFA) for subsequent treatment.

The patients received the following regimen for HAIC through the indwelling microcatheter connected to an artery infusion pump in the ward: oxaliplatin 85 mg/m^2 administered intraarterially for 2 h, leucovorin 400 mg/m^2 administered intraarterially for 1 h, and 5FU 400 mg/m^2 intra-arterial bolus injection on day 1, followed by 5FU 2400 mg/m^2 continuous arterial infusion for 46 h. Three days after the first HAIC course, patients began to take lenvatinib (Eisai, Tokyo, Japan) orally at the recommended doses of 12 mg/day for patients weighing ≥ 60 kg and 8 mg/day for patients weighing < 60 kg[11]. Dose adjustment or termination of lenvatinib therapy was allowed when drug-related adverse events (AEs) occurred. Discontinuation of the combination treatment was also allowed for potentially fatal AEs, clinical tumor progression, or the need for conversion therapy.

Evaluations and measurement

Therapeutic responses after 1, 3, and 6 mo of combination treatment were assessed according to the modified Response Evaluation Criteria in Solid Tumors using CT (Philips Brilliance iCT; Philips Medical Systems, Best, the Netherlands) images. Treatment responders were defined as patients with a complete response (CR) or partial response (PR). Non-responders were defined as patients with stable disease (SD) or progressive disease (PD). AEs were assessed using the Common Terminology Criteria for Adverse Events (CTCAE) version 5.0[12].

Epigastric enhanced CT Digital Imaging and Communication of Medicine (DICOM) data were collected before treatment and after 1 and 2 mo of treatment and introduced into an image post-processing workstation (Philips IntelliSpace Portal; Koninklijke Philips N.V., Eindhoven, the Netherlands) for three-dimensional reconstruction. On the image post-processing workstation, multiplanar reconstruction images centered on the contrast-enhanced hepatic arteries and the centerline (CLL) of the blood vessels were generated by the software to straighten the curved arteries. The trunk or the thickest branch of the TFA was selected as the object of measurement. The CLL was adjusted manually to measure the largest diameter of the arteries. The diameters of the opening of the common hepatic artery (CHA), proper hepatic artery (PHA), left hepatic artery (LHA), right hepatic artery (RHA), and TFA were further measured by manually drawing the region of interest (Figure 1)[13]. The change in vessel diameters was defined and calculated using the following formula: $\Delta_{artery} = (D_{post} - \Delta_{pre}) / \Delta_{pre}$ (Δ_{artery}: The rate of change in the diameter of CHA, PHA, LHA, RHA, or TFA; D_{pre}: The vessel diameter before combination treatment; D_{post}: The vessel diameter after combination treatment).

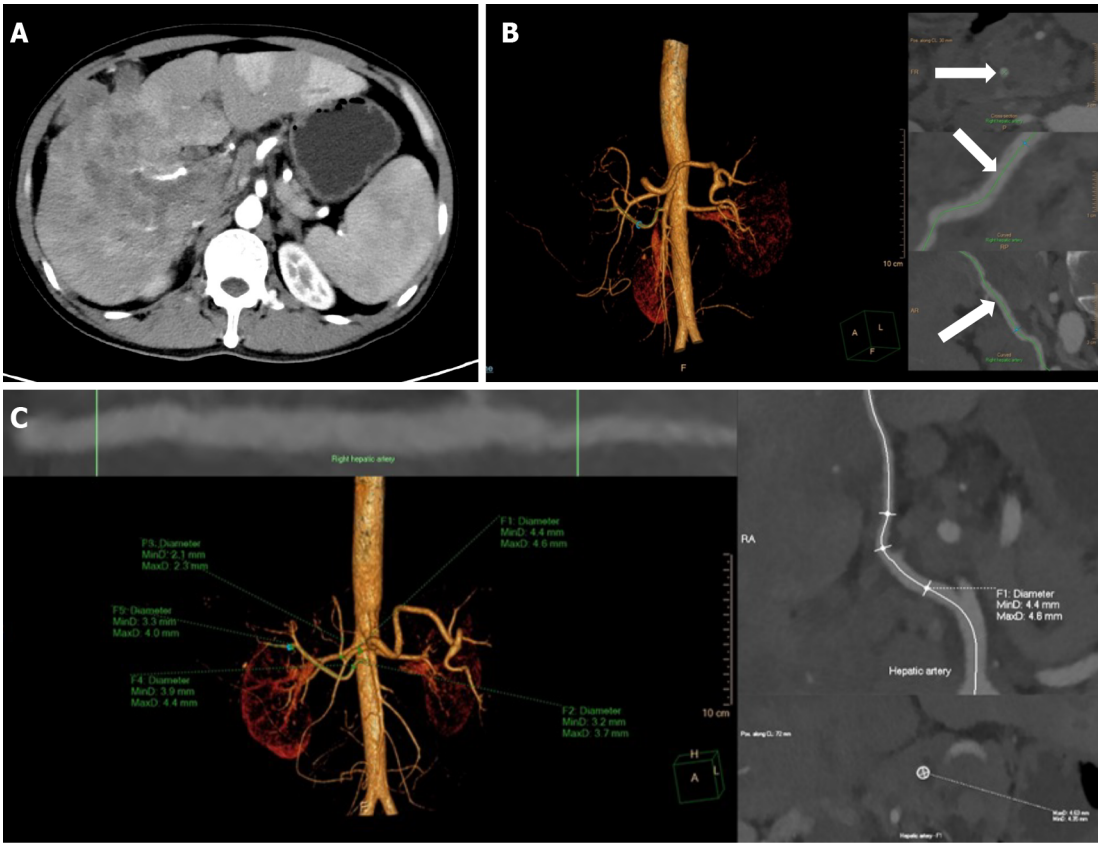
Both the measurement of artery diameters and the evaluation of therapeutic efficacy were individually conducted by two physicians with experience in gastroenterological diagnostics, and differences were resolved by a more experienced physician.

Immunohistochemistry

Tumor angiogenesis was evaluated by measuring microvessel density (MVD) after staining using an anti-CD34 antibody. Punch biopsy samples were obtained from tumor lesions before and 1 mo after the start of HAIC plus lenvatinib therapy. The tumor samples were fixed in 10% formalin and embedded in paraffin. After routine laboratory procedures, immunohistochemistry was performed to detect the expression of CD34 (endothelial cell marker) through the avidin–biotin–peroxidase complex[14,15]. MVD was measured at × 100 magnification in five regions of interest using a light microscope. All endothelial cells, including individual cells and grouped cells, were counted as a single vessel if they were separated from the surrounding tumor and other connective tissues[16].

Statistical analysis

Statistical analyses were performed using IBM SPSS Statistics 26.0. The measurement data were presented as the mean ± SD, and $P < 0.05$ indicated statistical significance. Considering the loss to



DOI: 10.3748/wjg.v28.i26.3232 **Copyright** ©The Author(s) 2022.

Figure 1 Reconstruction and measurement of the hepatic arteries. A: The thickest branch of tumor-feeding arteries generated from the right hepatic artery; B: Three-dimensional reconstruction of hepatic arteries in an image post-processing workstation and the adjustment of center line (arrows) on multiple layers; C: The hepatic artery diameters are measured automatically by drawing the region of interest. F1-5, the opening of the common hepatic artery, the proper hepatic artery, the left hepatic artery, the right hepatic artery and the tumor-feeding artery.

follow-up, the changes in the artery diameters were compared using the mixed linear model for repeated measured data, and follow-up pairwise comparison was conducted among the three periods. The independent-samples *t*-test was used to analyze the changes in MVD. Receiver-operating characteristic (ROC) analysis was used to evaluate the changes in the diameter of all hepatic arteries to differentiate between responders and non-responders and identify the cutoff values. The cutoff was calculated for any factors that were statistically significant in the ROC analysis, which were candidates for univariate and multivariable logistic regression analyses with baseline data.

RESULTS

Participant characteristics

During the study period, patients meeting the inclusion criteria were followed up for 6 mo after the start of the combination treatment. The study population was predominantly male (59/67, 88.1%), and most of the enrolled patients were infected with hepatitis B virus (53/67, 79.1%). In total, 45 (67.2%) patients were estimated to have Child–Pugh stage A liver function, and 22 (32.8%) patients were categorized as Child–Pugh stage B. Portal vein tumor thrombosis was diagnosed in 44 (65.7%) patients, hepatic vein tumor thrombus in 17 (25.4%) patients, and extrahepatic spread occurred in 13 (19.4%) patients. The characteristics of the patients are summarized in Table 1.

Treatment-related AEs

There were no treatment-related deaths in our study. According to CTCAE, grade 1-2 events were observed in 37 patients (55.2%) and grade 3 events in 2 (3.0%) patients, whereas no grade ≥ 4 AEs occurred. The most common grade 1-2 events were abdominal pain (17/67, 25.4%), fever (8/67, 11.9%), and transient nausea and vomiting (8/67, 11.9%). The grade 3 events were liver dysfunction and decreased leukocyte counts, both of which normalized after treatment.

Table 1 The baseline characteristics of patients

Characteristics	*n* (%)
Age	
≤ 60	52 (77.6)
> 60	15 (22.4)
Gender	
Male	59 (88.1)
Female	8 (11.9)
ECOG PS	
0	52 (77.6)
1	15 (22.4)
HBsAg	
Positive	53 (79.1)
Negative	14 (20.9)
Child-Pugh Class	
Class A	45 (67.2)
Class B	22 (32.8)
Tumor size, cm	
≤ 10	43 (64.2)
> 10	24 (35.8)
No. of intrahepatic tumors	
≤ 3	32 (47.8)
> 3	35 (52.2)
Baseline AFP level, ng/mL	
≤ 400	29 (43.3)
> 400	38 (56.7)
PVTT	
Absent	23 (34.3)
Present	44 (65.7)
HVTT	
Absent	50 (74.6)
Present	17 (25.4)
Metastasis	
Absent	54 (80.6)
Present	13 (19.4)

ECOG PS: Eastern Cooperative Oncology Group performance status; HBsAg: Hepatitis B surface antigen; AFP: Alfa-fetoprotein; PVTT: Portal vein tumor thrombus; HVTT: Hepatic vein tumor thrombus.

Efficacy

Five patients missed the 3-mo imaging evaluation, and 11 patients missed the 6-mo evaluation because of loss to follow-up. In total, 46, 41, and 24 patients were classified as responders (CR + PR) after 1, 3, and 6 mo of treatment, respectively, whereas the numbers of non-responders (SD + PD) at these time points were 21, 21, and 32, respectively. The overall response rates (ORR) in this study at 1, 3, and 6 mo were 68.7%, 66.1%, and 42.9%, respectively. Eight patients received downstaging therapy within 1 year after treatment, of which six patients underwent hepatectomy and the other two patients underwent radiofrequency ablation.

Artery diameters

Vessel diameters were measured in all patients before treatment and after 1 mo of treatment, whereas six patients missed the 2-month measurement. After 1 and 2 mo of treatment, all vessel diameters had gradually decreased compared with the baseline ($P < 0.001$), but the difference in vessel diameters between 1 and 2 mo was not significant ($P > 0.05$, Figure 2). According to the ROC analysis, the change in the TFA diameter was significantly different between the responders and non-responders at 1, 3, and 6 mo ($P < 0.001$, $P = 0.004$, and $P = 0.023$, respectively), and the corresponding cutoff values were -0.169, -0.169, and -0.264, respectively. Meanwhile, there were no significant differences in the diameters of other hepatic arteries between the groups (Table 2). Considering the unclear clinical meaning of continuous changes in vessel diameters, the change in the TFA diameter was classified as reduced or unchanged based on the cutoff values.

The results of the univariate and multivariable logistic regression analyses of tumor response are listed in Table 3. According to the multivariable analysis, the change in the TFA diameter was an independent factor for the efficacy of HAIC plus lenvatinib after 1 [odds ratio (OR) = 0.12; 95% confidence interval (CI): 0.03-0.43; $P = 0.001$], 3 (OR = 0.06; 95%CI: 0.01-0.29; $P = 0.001$), and 6 mo (OR = 0.14; 95%CI: 0.04-0.47; $P = 0.002$) of treatment. Other independent factors included the alpha-fetoprotein level (OR = 0.17; 95%CI: 0.04-0.73; $P = 0.018$) at 1 mo and tumor size (OR = 7.65; 95%CI: 1.36-42.88; $P = 0.021$) at 3 mo.

MVD

The MVD of tumor lesions after the administration of lenvatinib was robustly smaller than that before treatment, suggesting that angiogenesis was strongly suppressed by lenvatinib ($P < 0.001$, Figure 3).

DISCUSSION

In the present study, significant shrinkage of hepatic arteries was observed in patients with uHCC after 1 mo of HAIC plus lenvatinib therapy for the first time. We also confirmed that the morphological change in the TFA was closely related to the tumor response after 1, 3, and 6 mo of combination treatment, and this change was an independent factor for improved short-term therapeutic efficacy. These findings would be of great significance to physicians for evaluating the effectiveness of this combination therapy earlier in the course of treatment and altering the treatment plan as needed.

Hepatic arteries were shown to be markedly thin following TKI treatment, and Chen *et al*[17] attributed these morphological changes to the anti-angiogenic effect of targeted drugs. Notably, lenvatinib more effectively suppresses angiogenesis and inhibits tumor growth than sorafenib by targeting both vascular endothelial growth factor (VEGF) and fibroblast growth factor[18,19]. In our study, shrinkage of hepatic vessels was observed early after the start of HAIC plus lenvatinib therapy, and the powerful antiangiogenic effect of lenvatinib was proven by the decrease in the MVD of the tumor lesions. Meanwhile, anti-VEGF therapies can reverse vessel abnormalities and improve the tumor microenvironment[20]. The decline in local tumor perfusion secondary to the decrease in tumor capillaries and the "normalization hypothesis" may be the main reasons for the conspicuous reduction of hepatic arteries with the combination regimen.

The efficiency of HAIC combined with lenvatinib for intermediate and advanced HCC has been confirmed in previous studies[21,22]. In this study, the ORR reached 68.7%, 66.1%, and 42.9% at 1, 3, and 6 mo, and conversion therapy was achieved in eight patients, which further verified the effectiveness of the combination therapy. Thus, it was necessary to explore the mechanism of action of this combination therapy. A reduction in hepatic artery diameters was observed in most patients in the present study. Kuorda *et al*[23] also reported that local tumor perfusion declined significantly after oral lenvatinib administration. These findings illustrated that lenvatinib reduces the tumor blood supply after combination therapy. Meanwhile, HAIC has the advantage of achieving high local concentrations in the tumor during arterial infusion[24]. According to the pharmacokinetic characteristics of the intra-arterial infusion[25], a decrease in tumor blood flow can increase the dose of the drug in the target organ, thus enhancing the antitumor effect of HAIC. Furthermore, the normalization and improved functionality of tumor vessels including reduced hypoxia, reduced vascular leakage, and improved vascular permeability can improve the delivery of local chemotherapeutic drugs in tumors[26,27]. The increased drug accumulation in the target organ often results in improved therapeutic efficacy. Since the combined therapy could improve the therapeutic effect, it may also expand the scope of HAIC, which is limited to patients with HCC and multinodule lesions or vascular invasion.

In clinical practice, HAIC often requires 6-8 courses. Moreover, repetitive and inefficient treatment is harmful to patients with uHCC. Therefore, early evaluation of the treatment response is of great significance. In this study, we found that the reduction in the TFA diameter after combination therapy was an independent factor for improved therapeutic efficacy within 6 mo. The morphological change in the TFA is easy to observe during HAIC, and it can help in estimating the early therapeutic effect. Since an improved short-term effect often results in a good prognosis, the observation on thinning of the TFA is significant and more practical for patients with uHCC who are receiving HAIC plus lenvatinib.

Table 2 Receiver-operating characteristic analysis for antitumor response

Δ_{artery}	1 mo			3 mo			6 mo		
	Responder	Non-responder	*P* value	Responder	Non-responder	*P* value	Responder	Non-responder	*P* value
CHA	- (0.17 ± 0.17)	- (0.14 ± 0.18)	0.25	- (0.15 ± 0.16)	- (0.18 ± 0.19)	1.00	- (0.18 ± 0.16)	- (0.15 ± 0.18)	0.51
PHA	- (0.21 ± 0.14)	- (0.13 ± 0.25)	0.15	- (0.20 ± 0.15)	- (0.16 ± 0.20)	0.35	- (0.16 ± 0.16)	- (0.22 ± 0.17)	0.30
LHA	- (0.27 ± 0.17)	- (0.21 ± 0.28)	0.59	(0.28 ± 0.18)	(0.20 ± 0.27)	0.43	- (0.22 ± 0.24)	- (0.30 ± 0.17)	0.18
RHA	- (0.22 ± 0.17)	- (0.16 ± 0.23)	0.26	- (0.20 ± 0.19)	- (0.22 ± 0.20)	0.58	- (0.16 ± 0.23)	- (0.24 ± 0.17)	0.44
TFA	- (0.33 ± 0.20)	- (0.16 ± 0.19)	< 0.001	- (0.32 ± 0.19)	- (0.18 ± 0.22)	0.004	- (0.36 ± 0.16)	- (0.25± 0.23)	0.023

Δ_{artery}: The rate of change in vessel diameters of hepatic arteries; CHA: Common hepatic artery; PHA: Proper hepatic artery; LHA: Left hepatic artery; RHA: Right hepatic artery; TFA: Tumor-feeding artery.

Table 3 Univariate and multivariate logistic regression analysis for efficacy of treatment with hepatic arterial infusion chemotherapy plus lenvatinib

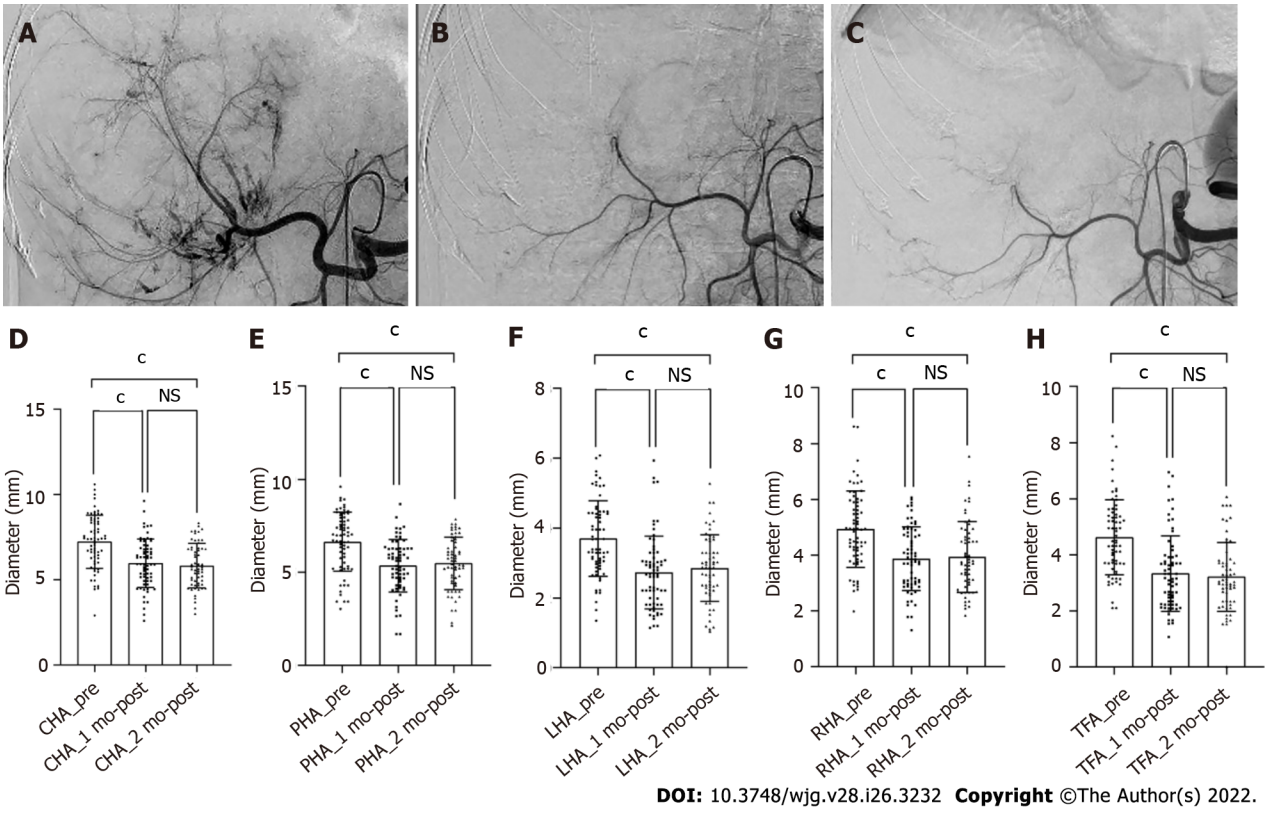
	1 mo			3 mo			6 mo		
	Univariate	Multivariate		Univariate	Multivariate		Univariate	Multivariate	
	P1 value	*P2* value	OR (95%CI)	*P1* value	*P2* value	OR (95%CI)	*P1* value	*P2* value	OR (95%CI)
TFA (reduced/basically unchanged)	< 0.001	0.001	0.12 (0.03-0.43)	< 0.001	0.001	0.06 (0.01-0.29)	0.002	0.002	0.14 (0.04-0.47)
Sex (male/female)	0.680	-	-	0.349	-	-	0.892	-	-
Age (≤ 60/> 60)	0.850	-	-	0.868	-	-	0.573	-	-
ECOG (0/1)	0.412	-	-	0.147	-	-	0.365	-	-
HBsAg (positive/negative)	0.122	-	-	0.113	-	-	0.784	-	-
AFP, ng/mL (≤ 400/> 400)	0.003	0.018	0.17 (0.04-0.73)	0.089	0.546	-	0.040	0.122	-
Child-Pugh (A/B)	0.384	-	-	0.897	-	-	0.869	-	-
Tumor size, cm (≤ 10/> 10)	0.166	-	-	0.053	0.021	7.65 (1.36-42.88)	0.625	-	-
Tumor number (≤ 3/> 3)	0.609	-	-	0.533	-	-	0.280	-	-
PVTT (absent/present)	0.220	-	-	0.169	-	-	0.577	-	-
HVTT (absent/present)	0.842	-	-	0.455	-	-	1.000	-	-
Metastasis (absent/present)	0.960	-	-	0.694	-	-	0.615	-	-

Any factors that were statistically significant at $P < 0.10$ in the univariate logistic regression analysis were candidates for entry into the multivariate logistic regression analysis. TFA: The tumor-feeding artery; ECOG PS: Eastern Cooperative Oncology Group performance status; HBsAg: Hepatitis B surface antigen; AFP: Alfa-fetoprotein; PVTT: Portal vein tumor thrombus; HVTT: Hepatic vein tumor thrombus; OR: Odds ratio; CI: Confidence interval.

The present study had some limitations. This was a single-center retrospective study, and the sample size was small.

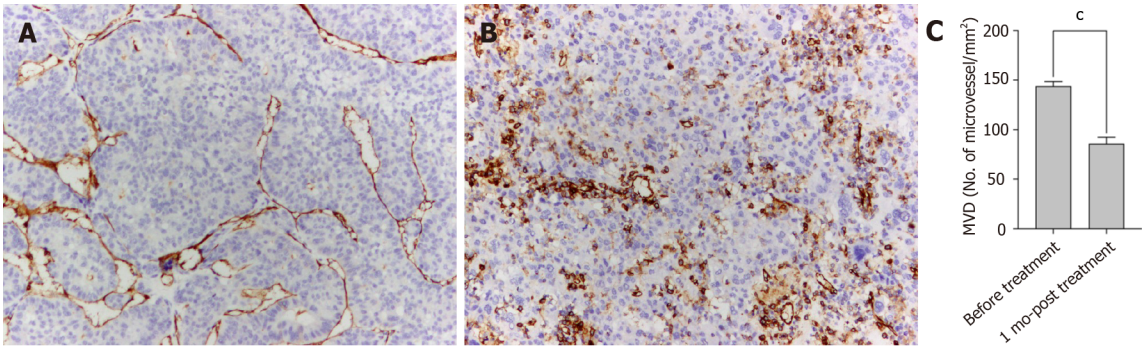
CONCLUSION

In conclusion, lenvatinib can reduce the diameters of hepatic arteries and thus enhance the effect of HAIC. Shrinkage of the TFA after HAIC plus lenvatinib therapy was linked to improved short-term outcomes in patients with uHCC.



DOI: 10.3748/wjg.v28.i26.3232 **Copyright** ©The Author(s) 2022.

Figure 2 Shrinkage of the hepatic artery diameters in patient with unresectable hepatocellular carcinoma after treatment with hepatic arterial infusion chemotherapy plus lenvatinib. A-C: Digital subtraction angiography performed before treatment (A), after 1 (B) and 2 (C) mo of treatment; D-H: Bars represent the vessel diameters before treatment, at 1 and 2 mo after treatment. *P*-values are calculated using the mixed linear model for repeated measured data. °*P* < 0.001. NS: Not significant (*P* > 0.05); CHA: Common hepatic artery; PHA: Proper hepatic artery; LHA: Left hepatic artery; RHA: Right hepatic artery; TFA: Tumor-feeding artery.



DOI: 10.3748/wjg.v28.i26.3232 **Copyright** ©The Author(s) 2022.

Figure 3 Anti-angiogenic activities of lenvatinib in tumor lesions. A and B: The microvessels in the tumor lesion collected before (A) and after 1 mo (B) of treatment with lenvatinib are stained with anti-CD34 antibody (× 100); C: Bars represent the microvessel density that decreased sharply after administration of lenvatinib. Data are presented as means ± SD. °*P* < 0.001 *vs* before treatment. MVD: Micro-vessel density.

ARTICLE HIGHLIGHTS

Research background

Combination of hepatic arterial infusion chemotherapy (HAIC) and lenvatinib has been frequently used to treat unresectable hepatocellular carcinoma (uHCC) in China.

Research motivation

Shrinkage of hepatic arteries after the combination therapy is a common phenomenon and may early reflect the antitumor response, the relationship between which needs further exploration.

Research objectives

To investigate the relationship between hepatic artery diameters reduction and the short-term efficacy of HAIC plus lenvatinib.

Research methods

Sixty-seven patients with uHCC receiving HAIC plus lenvatinib were analyzed retrospectively. The modified Response Evaluation Criteria in Solid Tumors was used to assess the antitumor response after 1, 3, and 6 mo of treatment. The measurement of hepatic artery diameters before treatment and after 1 and 2 mo of treatment were conducted in a computed tomography image post-processing workstation. Meanwhile, the changes in tumor capillaries were also examined on pathological specimens before and after 1 mo of treatment.

Research results

All the hepatic artery diameters and the microvessel density in the tumor lesions were significantly decreased after the combination treatment (all $P < 0.001$). Shrinkage of the tumor-feeding artery (TFA) was significantly associated with the antitumor response after 1, 3, and 6 mo of treatment ($P < 0.001$, $P = 0.004$, and $P = 0.023$, respectively) and an independent factor for treatment efficacy ($P = 0.001$, $P = 0.001$, and $P = 0.002$ and 1, 3, and 6 mo, respectively).

Research conclusions

The retrospective study demonstrated that the shrinkage of the TFA diameter was closely related to improved short-term efficacy of treatment with HAIC plus lenvatinib for the first time.

Research perspectives

We believe the findings in this paper will be of interest to the researchers in uHCC. Further, prospective randomized multicenter trials are needed to confirm the relationship between the morphological change in TFA and the early therapeutic effect of uHCC treatment.

ACKNOWLEDGEMENTS

All authors are grateful to Dr. Fan XY for assisting with the reconstruction of the CT images.

FOOTNOTES

Author contributions: Wu DD and Pang HJ designed this study; Wu DD, Tian C, and Chen CL performed the reconstruction and measurement; Wu DD, Liu XH, and Pang HJ analyzed the data; Peng P collected the clinical data; Wu DD wrote the paper; He XF and Pang HJ made critical revisions to the paper; all authors approved the publication of the paper.

Institutional review board statement: The research was conducted in accordance with the 1975 Declaration of Helsinki and approved by the medical ethics committee of Nanfang Hospital, Southern Medical University.

Informed consent statement: The requirement for informed consent was waived owing to the retrospective nature of the study.

Conflict-of-interest statement: There was no conflict of interest to disclose.

Data sharing statement: No additional data are available.

Open-Access: This article is an open-access article that was selected by an in-house editor and fully peer-reviewed by external reviewers. It is distributed in accordance with the Creative Commons Attribution NonCommercial (CC BY-NC 4.0) license, which permits others to distribute, remix, adapt, build upon this work non-commercially, and license their derivative works on different terms, provided the original work is properly cited and the use is non-commercial. See: https://creativecommons.org/Licenses/by-nc/4.0/

Country/Territory of origin: China

ORCID number: De-Di Wu 0000-0001-8409-9770; Xiao-Feng He 0000-0001-8255-1874; Chen Tian 0000-0003-4260-290X; Peng Peng 0000-0001-9864-0580; Chuan-Li Chen 0000-0001-7610-5966; Xue-Han Liu 0000-0002-8966-7172; Hua-Jin Pang 0000-0001-7367-5701.

S-Editor: Yan JP
L-Editor: A

P-Editor: Yan JP

REFERENCES

1 **Torre LA**, Bray F, Siegel RL, Ferlay J, Lortet-Tieulent J, Jemal A. Global cancer statistics, 2012. *CA Cancer J Clin* 2015; **65**: 87-108 [PMID: 25651787 DOI: 10.3322/caac.21262]

2 **Llovet JM**, Zucman-Rossi J, Pikarsky E, Sangro B, Schwartz M, Sherman M, Gores G. Hepatocellular carcinoma. *Nat Rev Dis Primers* 2016; **2**: 16018 [PMID: 27158749 DOI: 10.1038/nrdp.2016.18]

3 **European Association for the Study of the Liver**. Corrigendum to "EASL Clinical Practice Guidelines: Management of hepatocellular carcinoma" [J Hepatol 69 (2018) 182-236]. *J Hepatol* 2019; **70**: 817 [PMID: 30739718 DOI: 10.1016/j.jhep.2019.01.020]

4 **Kudo M**, Trevisani F, Abou-Alfa GK, Rimassa L. Hepatocellular Carcinoma: Therapeutic Guidelines and Medical Treatment. *Liver Cancer* 2016; **6**: 16-26 [PMID: 27995084 DOI: 10.1159/000449343]

5 **Ikeda M**, Morizane C, Ueno M, Okusaka T, Ishii H, Furuse J. Chemotherapy for hepatocellular carcinoma: current status and future perspectives. *Jpn J Clin Oncol* 2018; **48**: 103-114 [PMID: 29253194 DOI: 10.1093/jjco/hyx180]

6 **Kudo M**, Matsui O, Izumi N, Iijima H, Kadoya M, Imai Y, Okusaka T, Miyayama S, Tsuchiya K, Ueshima K, Hiraoka A, Ikeda M, Ogasawara S, Yamashita T, Minami T, Yamakado K; Liver Cancer Study Group of Japan. JSH Consensus-Based Clinical Practice Guidelines for the Management of Hepatocellular Carcinoma: 2014 Update by the Liver Cancer Study Group of Japan. *Liver Cancer* 2014; **3**: 458-468 [PMID: 26280007 DOI: 10.1159/000343875]

7 **He MK**, Liang RB, Zhao Y, Xu YJ, Chen HW, Zhou YM, Lai ZC, Xu L, Wei W, Zhang YJ, Chen MS, Guo RP, Li QJ, Shi M. Lenvatinib, toripalimab, plus hepatic arterial infusion chemotherapy *versus* lenvatinib alone for advanced hepatocellular carcinoma. *Ther Adv Med Oncol* 2021; **13**: 17588359211002720 [PMID: 33854567 DOI: 10.1177/17588359211002720]

8 **Obi S**, Sato S, Kawai T. Current Status of Hepatic Arterial Infusion Chemotherapy. *Liver Cancer* 2015; **4**: 188-199 [PMID: 26674592 DOI: 10.1159/000367746]

9 **Matsuda N**, Imai N, Kuzuya T, Yamamoto K, Ito T, Ishizu Y, Honda T, Ishigami M, Fujishiro M. Progression After Molecular Targeted Agents: Hepatic Arterial Changes and Transarterial Chemoembolization in Hepatocellular Carcinoma. *In Vivo* 2021; **35**: 1185-1189 [PMID: 33622919 DOI: 10.21873/invivo.12367]

10 **Jiang H**, Liu X, Chen J, Wei Y, Lee JM, Cao L, Wu Y, Duan T, Li X, Ma L, Song B. Man or machine? *Cancer Imaging* 2019; **19**: 84 [PMID: 31806050 DOI: 10.1186/s40644-019-0266-9]

11 **Okusaka T**, Ikeda K, Kudo M, Finn R, Qin S, Han KH, Cheng AL, Piscaglia F, Kobayashi M, Sung M, Chen M, Wyrwicz L, Yoon JH, Ren Z, Mody K, Dutcus C, Tamai T, Ren M, Hayato S, Kumada H. Safety and efficacy of lenvatinib by starting dose based on body weight in patients with unresectable hepatocellular carcinoma in REFLECT. *J Gastroenterol* 2021; **56**: 570-580 [PMID: 33948712 DOI: 10.1007/s00535-021-01785-0]

12 **Freites-Martinez A**, Santana N, Arias-Santiago S, Viera A. Using the Common Terminology Criteria for Adverse Events (CTCAE - Version 5.0) to Evaluate the Severity of Adverse Events of Anticancer Therapies. *Actas Dermosifiliogr (Engl Ed)* 2021; **112**: 90-92 [PMID: 32891586 DOI: 10.1016/j.ad.2019.05.009]

13 **Pang H**, Chen Y, He X, Tan X, Wang J, Yao Q, Liu X. Twelve-Month Computed Tomography Follow-Up after Thoracic Endovascular Repair for Acute Complicated Aortic Dissection. *Ann Vasc Surg* 2021; **71**: 444-450 [PMID: 32891743 DOI: 10.1016/j.avsg.2020.08.125]

14 **Matsuki M**, Adachi Y, Ozawa Y, Kimura T, Hoshi T, Okamoto K, Tohyama O, Mitsuhashi K, Yamaguchi A, Matsui J, Funahashi Y. Targeting of tumor growth and angiogenesis underlies the enhanced antitumor activity of lenvatinib in combination with everolimus. *Cancer Sci* 2017; **108**: 763-771 [PMID: 28107584 DOI: 10.1111/cas.13169]

15 **Matsuki M**, Hoshi T, Yamamoto Y, Ikemori-Kawada M, Minoshima Y, Funahashi Y, Matsui J. Lenvatinib inhibits angiogenesis and tumor fibroblast growth factor signaling pathways in human hepatocellular carcinoma models. *Cancer Med* 2018; **7**: 2641-2653 [PMID: 29733511 DOI: 10.1002/cam4.1517]

16 **Mohamed A**, Chenna A, Abdelfatah M, Sanjay J, Mohammad MK, Saber I, Kauh J, Elhammali B, Kaseb A. Microvessel density analysis in patients with viral hepatitis-related hepatocellular carcinoma. *J Gastrointest Cancer* 2015; **46**: 104-108 [PMID: 25645584 DOI: 10.1007/s12029-015-9684-5]

17 **Chen L**, Zheng Y, Zhang H, Pan H, Liu Q, Zhou X, Wei W, Liu Y, Zhen M, Wang J, Zhou J, Zhao Y. Comparative analysis of tumor-associated vascular changes following TACE alone or in combination with sorafenib treatment in HCC: A retrospective study. *Oncol Lett* 2018; **16**: 3690-3698 [PMID: 30127979 DOI: 10.3892/ol.2018.9055]

18 **Yamamoto Y**, Matsui J, Matsushima T, Obaishi H, Miyazaki K, Nakamura K, Tohyama O, Semba T, Yamaguchi A, Hoshi SS, Mimura F, Haneda T, Fukuda Y, Kamata JI, Takahashi K, Matsukura M, Wakabayashi T, Asada M, Nomoto KI, Watanabe T, Dezso Z, Yoshimatsu K, Funahashi Y, Tsuruoka A. Lenvatinib, an angiogenesis inhibitor targeting VEGFR/FGFR, shows broad antitumor activity in human tumor xenograft models associated with microvessel density and pericyte coverage. *Vasc Cell* 2014; **6**: 18 [PMID: 25197551 DOI: 10.1186/2045-824X-6-18]

19 **Perera S**, Kelly D, O'Kane GM. Non-immunotherapy options for the first-line management of hepatocellular carcinoma: exploring the evolving role of sorafenib and lenvatinib in advanced disease. *Curr Oncol* 2020; **27**: S165-S172 [PMID: 33343210 DOI: 10.3747/co.27.7159]

20 **Liu K**, Zhang X, Xu W, Chen J, Yu J, Gamble JR, McCaughan GW. Targeting the vasculature in hepatocellular carcinoma treatment: Starving *vs* normalizing blood supply. *Clin Transl Gastroenterol* 2017; **8**: e98 [PMID: 28617447 DOI: 10.1038/ctg.2017.28]

21 **Shimose S**, Iwamoto H, Tanaka M, Niizeki T, Shirono T, Noda Y, Kamachi N, Okamura S, Nakano M, Suga H, Yamaguchi T, Kawaguchi T, Kuromatsu R, Noguchi K, Koga H, Torimura T. Alternating Lenvatinib and Trans-Arterial Therapy Prolongs Overall Survival in Patients with Inter-Mediate Stage HepatoCellular Carcinoma: A Propensity Score Matching Study. *Cancers (Basel)* 2021; **13** [PMID: 33466496 DOI: 10.3390/cancers13010160]

22 **Mai QC**, Mo ZQ, Shi F, Chen XM. Lenvatinib plus hepatic arterial infusion of modified FOLFOX regime in patients with advanced hepatocellular carcinoma. *J Clin Oncol* 2020; **38** [DOI: 10.1200/jco.2020.38.15_suppl.e16603]

23 **Kuorda H**, Abe T, Fujiwara Y, Okamoto T, Yonezawa M, Sato H, Endo K, Oikawa T, Sawara K, Takikawa Y. Change in arterial tumor perfusion is an early biomarker of lenvatinib efficacy in patients with unresectable hepatocellular carcinoma. *World J Gastroenterol* 2019; **25**: 2365-2372 [PMID: 31148907 DOI: 10.3748/wjg.v25.i19.2365]

24 **Kondo Y**, Fukuda R. [Cutting Edge of Hepatic Artery Infusion Chemotherapy for Hepatocellular Carcinoma]. *Gan To Kagaku Ryoho* 2020; **47**: 1-5 [PMID: 32381852]

25 **Chen HS**, Gross JF. Intra-arterial infusion of anticancer drugs: theoretic aspects of drug delivery and review of responses. *Cancer Treat Rep* 1980; **64**: 31-40 [PMID: 6155210 DOI: 10.1016/0304-3835(80)90154-8]

26 **Jain RK**. Normalizing tumor vasculature with anti-angiogenic therapy: a new paradigm for combination therapy. *Nat Med* 2001; **7**: 987-989 [PMID: 11533692 DOI: 10.1038/nm0901-987]

27 **Willett CG**, Boucher Y, di Tomaso E, Duda DG, Munn LL, Tong RT, Chung DC, Sahani DV, Kalva SP, Kozin SV, Mino M, Cohen KS, Scadden DT, Hartford AC, Fischman AJ, Clark JW, Ryan DP, Zhu AX, Blaszkowsky LS, Chen HX, Shellito PC, Lauwers GY, Jain RK. Direct evidence that the VEGF-specific antibody bevacizumab has antivascular effects in human rectal cancer. *Nat Med* 2004; **10**: 145-147 [PMID: 14745444 DOI: 10.1038/nm988]

World Journal of Gastroenterology

Submit a Manuscript: https://www.f6publishing.com

World J Gastroenterol 2022 July 14; 28(26): 3243-3257

DOI: 10.3748/wjg.v28.i26.3243

ISSN 1007-9327 (print) ISSN 2219-2840 (online)

ORIGINAL ARTICLE

Observational Study

Impact of sodium glucose cotransporter-2 inhibitors on liver steatosis/fibrosis/inflammation and redox balance in non-alcoholic fatty liver disease

Francesco Bellanti, Aurelio Lo Buglio, Michał Dobrakowski, Aleksandra Kasperczyk, Sławomir Kasperczyk, Palok Aich, Shivaram P Singh, Gaetano Serviddio, Gianluigi Vendemiale

Specialty type: Gastroenterology and hepatology

Provenance and peer review: Invited article; Externally peer reviewed.

Peer-review model: Single blind

Peer-review report's scientific quality classification

Grade A (Excellent): 0
Grade B (Very good): B
Grade C (Good): C
Grade D (Fair): 0
Grade E (Poor): 0

P-Reviewer: Boscá L , Spain; Zhao XK, China

Received: January 10, 2022
Peer-review started: January 10, 2022
First decision: March 8, 2022
Revised: March 18, 2022
Accepted: June 18, 2022
Article in press: June 18, 2022
Published online: July 14, 2022

Francesco Bellanti, Aurelio Lo Buglio, Gaetano Serviddio, Gianluigi Vendemiale, Department of Medical and Surgical Sciences, University of Foggia, Foggia 71122, Italy

Michał Dobrakowski, Aleksandra Kasperczyk, Sławomir Kasperczyk, Department of Biochemistry, Medical University of Silesia in Katowice, Zabrze 41-808, Poland

Palok Aich, School of Biological Sciences, National Institute of Science Education and Research, Khurdha 752050, India

Shivaram P Singh, Department of Gastroenterology, SCB Medical College, Cuttack 753007, India

Corresponding author: Francesco Bellanti, MD, PhD, Associate Professor, Department of Medical and Surgical Sciences, University of Foggia, viale Pinto, 1, Foggia 71122, Italy. francesco.bellanti@unifg.it

Abstract

BACKGROUND

Sodium glucose cotransporter-2 inhibitors (SGLT2-I) are the most recently approved drugs for type 2 diabetes (T2D). Recent clinical trials of these compounds reported beneficial cardiovascular (CV) and renal outcomes. A major cause of vascular dysfunction and CV disease in diabetes is hyperglycemia associated with inflammation and oxidative stress. Pre-clinical studies demonstrated that SGLT2-I reduce glucotoxicity and promote anti-inflammatory effects by lowering oxidative stress.

AIM

To investigate the effects of SGLT2-I on markers of oxidative stress, inflammation, liver steatosis, and fibrosis in patients of T2D with non-alcoholic fatty liver disease (NAFLD).

METHODS

We referred fifty-two consecutive outpatients treated with metformin monotherapy and exhibiting poor glycemic control to our centre. We introduced the outpatients to an SGLT2-I (dapagliflozin, empagliflozin, or canagliflozin; n = 26)

or a different hypoglycemic drug [other glucose-lowering drugs (OTHER), *n* = 26]. We evaluated circulating interleukins and serum hydroxynonenal (HNE)- or malondialdehyde (MDA)-protein adducts, fatty liver index (FLI), NAFLD fibrosis score, aspartate aminotransferase (AST)/alanine aminotransferase (ALT) ratio, AST-to-platelet-ratio index (APRI), and fibrosis-4 on the day before (T0) and following treatment for six months (T1). We also performed transient elastography at T0 and T1.

RESULTS

Add-on therapy resulted in improved glycemic control and reduced fasting blood glucose in both groups. Of note, following treatment for six months, a reduction of FLI and APRI, as well as of the FibroScan result, was reported in patients treated with SGLT2-I, but not in the OTHER group; furthermore, in the SGLT2-I group, we reported lower circulating levels of interleukin (IL)-1β, IL-6, tumor necrosis factor, vascular endothelial growth factor, and monocyte chemoattractant protein-1, and higher levels of IL-4 and IL-10. We did not observe any modification in circulating interleukins in the OTHER group. Finally, serum HNE- and MDA-protein adducts decreased significantly in SGLT2-I rather than OTHER patients and correlated with liver steatosis and fibrosis scores.

CONCLUSION

The present data indicate that treatment with SGLT2-I in patients with T2D and NAFLD is associated with improvement of liver steatosis and fibrosis markers and circulating pro-inflammatory and redox status, more than optimizing glycemic control.

Key Words: Sodium glucose cotransporter-2 inhibitors; Non-alcoholic fatty liver disease; Oxidative stress; Type 2 diabetes; Liver fibrosis; Inflammation

©The Author(s) 2022. Published by Baishideng Publishing Group Inc. All rights reserved.

Core Tip: Non-alcoholic fatty liver disease (NAFLD) is the most common hepatic disorder, and it is often associated with type 2 diabetes mellitus (T2DM). Diabetic patients often suffer from advanced NAFLD and are keen on progressing toward severe fibrosis and end-stage liver disease. There is no approved treatment for NAFLD, but new drug classes introduced to treat T2DM can exert favorable effects beyond glucose control. This pilot study demonstrates that treatment with sodium glucose cotransporter-2 inhibitors in patients with T2DM and NAFLD is associated with improving liver steatosis and fibrosis markers and circulating pro-inflammatory and redox status.

Citation: Bellanti F, Lo Buglio A, Dobrakowski M, Kasperczyk A, Kasperczyk S, Aich P, Singh SP, Serviddio G, Vendemiale G. Impact of sodium glucose cotransporter-2 inhibitors on liver steatosis/fibrosis/inflammation and redox balance in non-alcoholic fatty liver disease. *World J Gastroenterol* 2022; 28(26): 3243-3257
URL: https://www.wjgnet.com/1007-9327/full/v28/i26/3243.htm
DOI: https://dx.doi.org/10.3748/wjg.v28.i26.3243

INTRODUCTION

Patients affected by type 2 diabetes mellitus (T2DM) present with an increased risk of cardiovascular (CV) disease, which is associated with a high mortality rate and low quality of life[1,2]. T2DM is strongly associated with non-alcoholic fatty liver disease (NAFLD), whose prevalence in diabetic patients is over 60%[3,4]. NAFLD is the most common chronic liver disease, characterized by a broad spectrum of hepatic disorders, ranging from simple steatosis to steatohepatitis (non-alcoholic steatohepatitis), fibrosis, and cirrhosis[5]. The co-existence of NAFLD and T2DM pushes the progression of liver damage, increasing the risk of advanced fibrosis[6]. Besides, NAFLD is an independent risk factor of CV disease. Patients with T2DM and NAFLD present a higher CV risk than diabetic patients without NAFLD, suggesting that these conditions share common pathophysiological mechanisms, including low-grade systemic inflammation and oxidative stress[7].

Studies using new classes of antidiabetic drugs, such as sodium-glucose co-transporter-2 inhibitors (SGLT2-I) and glucagon-like peptide-1 receptor agonists (GLP1-RA), demonstrated definite CV advantage in patients with T2D[8]. Several clinical trials suggest that both classes also ameliorate liver steatosis and inflammation, potentially reversing fibrosis in NAFLD[9]. The currently approved SGLT2-I are dapagliflozin, canagliflozin, empagliflozin, and ertugliflozin, which increase urinary glucose

excretion and improve glycemic control independent of insulin. Furthermore, these drugs reduce body weight, visceral adiposity, blood pressure, and arterial stiffness[10]. Real-world CVD-REAL and CVD-REAL 2 studies have demonstrated that the benefits of SGLT2-I on CV outcomes observed in clinical trials may be attributed to a class effect and may be extended to a broad range of patients[11,12]. Despite clinical evidence on the efficacy of SGLT2-I in both the reduction of CV events and the improvement of hepatic damage in NAFLD, human mechanistic trials remain elusive.

Pre-clinical studies demonstrated that dapagliflozin, empagliflozin, and canagliflozin attenuate inflammation in apolipoprotein E knockout mice[13-15], reduce oxidative stress and improve mitochondrial function through direct pleiotropic and epigenetic effects[16,17]. Furthermore, these compounds may also exert antifibrotic effects in diabetic and non-diabetic cardiopathy or nephropathy [18-20]. Such results strongly encourage clinical studies to clarify the impact of SGLT2-I on systemic inflammation, oxidative stress, and liver fibrosis in diabetic patients with NAFLD. Thus, the present investigation was aimed to evaluate the effects of SGLT2-I addition to metformin on circulating markers of inflammation and oxidative protein damage in patients affected by uncontrolled T2DM and NAFLD and compare these outcomes with other glucose-lowering drugs (OTHER).

MATERIALS AND METHODS

Study design

We collected and analyzed data from 204 patients affected by T2DM who underwent outpatient consultation between June 2017 and June 2018 at the University Internal Medicine clinic of the "Policlinico Riuniti" in Foggia (Italy). We designed the investigation as an observational pilot study considering the problematic setting, the limited scale, and the multiple outcome parameters. Patients aged > 18 years old who were: (1) Diagnosed with NAFLD; and (2) Presented with glycated hemoglobin equal to or greater than 7% after at least three months of treatment with metformin monotherapy at the maximal tolerated dosage were assessed for eligibility. NAFLD was suspected on previous ultrasound imaging and/or altered liver function tests[21]. We did not consider subjects diagnosed with viral or autoimmune hepatitis, atherosclerotic CV disease, chronic inflammatory disorders, or those diagnosed with active cancer for the study. Further exclusion criteria were alcohol consumption > 20 g/d (women) or > 30 g/d (men), anemia, severe hepatic failure, glomerular filtration rate < 60 mg/min/m^2, use of drugs affecting redox balance, use of anti-inflammatory medications or corticosteroids during the observational period, use of medications associated with fatty liver (amiodarone, tamoxifen, sodium valproate, methotrexate), current smoker status, and prescription of a glucagon-like peptide-1 agonist (Supplementary Figure 1).

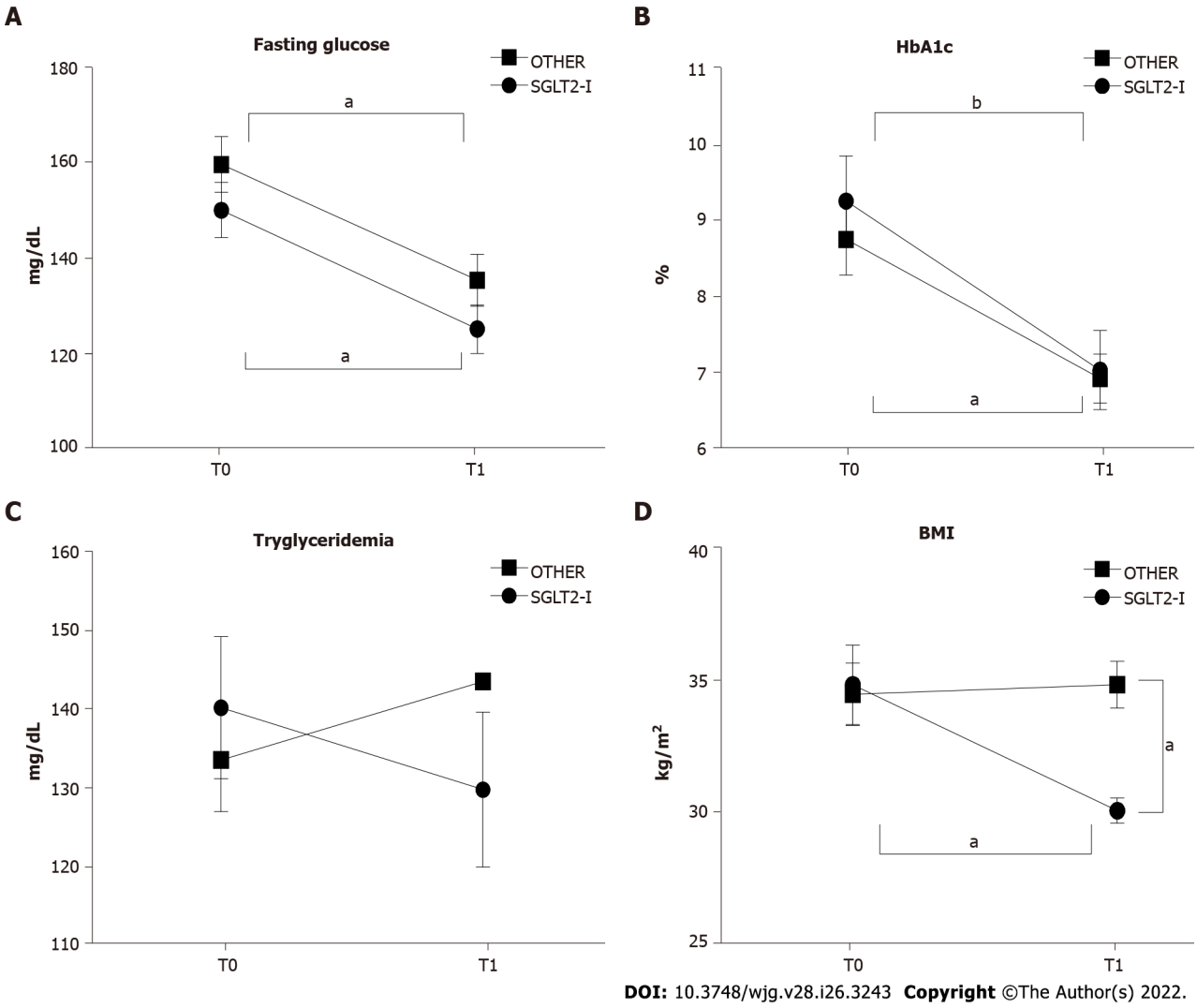
52 patients were finally referred to a combination therapy; of these, 26 patients were treated with an SGLT2-I, while 26 patients were treated with OTHER. The combination therapy was not randomized, and the second compound was chosen according to the standard of medical care in diabetes - 2017, considering the clinical characteristics of patients to maximize therapeutic advantages and minimize risks and side effects[22]. Compliance and adverse events were assessed by a verbal questionnaire. The frequency and distribution of the different compounds prescribed are reported in the Supplementary Table 1. For the study purposes, patients enrolled were assessed at baseline (T0) and after six months (T1). Our Institutional Review Board approved the study at the Policlinico Riuniti in Foggia (reference number 2325/2018) and performed it according to the Declaration of Helsinki. All patients gave written informed consent.

Laboratory measurements

Blood samples were obtained from a brachial vein between 8:00 and 9:00 AM, after an overnight fast, and immediately processed. Standard laboratory measurements included glycated hemoglobin A1c (HbA1c), fasting serum glucose, serum triglycerides, serum aspartate aminotransferase (AST), alanine aminotransferase (ALT) and gamma-glutamyl transpeptidase (gamma-GT) activities, platelet count, and serum albumin. The concentrations of serum cytokines and growth factors, including several interleukins (IL), such as IL-1α, IL-1β, IL-2, IL-4, IL-6, IL-8, IL-10, tumor necrosis factor (TNF), interferon-γ (IFN-γ), monocyte chemoattractant protein-1 (MCP-1), epidermal growth factor (EGF), and vascular endothelial growth factor (VEGF), were measured using the EV 3513 cytokine biochip array and competitive chemiluminescence immunoassays (Randox Laboratories Ltd, Crumlin, United Kingdom), according to the manufacturer's instructions, using the Randox Evidence Investigator[23]. As previously reported, serum fluorescent adducts formed between peroxidation-derived aldehydes [hydroxynonenal (HNE) and malondialdehyde (MDA)] and proteins were measured by spectrofluorimetry[24].

Non-invasive markers of liver steatosis and fibrosis

Patients were assessed at baseline and after six months of treatment for the following parameters: Fatty liver index (FLI), calculated according to the formula e^y / (1 + e^y) × 100, where "y" = 0.953 × ln(triglycerides, mg/dL) + 0.139 × body mass index (BMI), kg/m^2 + 0.718 × ln (gamma-GT, U/L) + 0.053 × waist circumference, cm - 15.745[25]; AST-to-platelet ratio index (APRI), calculated according to the formula



DOI: 10.3748/wjg.v28.i26.3243 **Copyright** ©The Author(s) 2022.

Figure 1 Glycemic control and body weight in patients enrolled in the study and included in groups treated with the sodium-glucose co-transporter-2 inhibitors or other glucose-lowering drugs before (T0) and after 1 wk of treatment (T1). A: Serum fasting glucose; B: Serum hemoglobin A1c; C: Serum triglycerides; D: Body mass index in patients observed in the study, grouped according to the assigned treatment. Data in the graphs are represented as mean ± SEM. Two-way analysis of variance and Tukey assessed statistical differences as post hoc test. $^{a}P < 0.05$, $^{b}P < 0.001$. HbA1c: Hemoglobin A1c; SGLT2-I: Sodium-glucose co-transporter-2 inhibitor; OTHER: Other glucose lowering drug; BMI: Body mass index.

AST, IU/L/AST upper limit of normal, IU/L/platelets, 10^9/L[26]; NAFLD fibrosis score, calculated according to the formula - 1.675 + 0.037 × age, years + 0.094 × BMI, kg/m^2 + 1.13 × impaired fasting glucose or diabetes (yes = 1, no = 0) + 0.99 × AST/ALT ratio - 0.013 × platelets, 10^9/L - 0.66 × albumin, g/dL[27]. The cut-off values chosen to categorize fibrosis grades F0-F2 or F3-F4 were < -1.455 and > 0.675, respectively; fibrosis-4 (FIB-4), calculated according to the formula (age, years × AST, IU/L)/(platelets, 10^9/L × rad ALT, IU/L)[28]. The cut-off values chosen to categorize fibrosis grades F0-F1 or F3-F4 were < -1.30 and > 2.67, respectively; AST/ALT ratio, whose cut-off value > 0.8 is associated with advanced disease[29].

Transient elastography

Transient elastography (TE) was performed by a Fibroscan (Echosense, Paris) on supine patients with the right arm elevated. The probe tip was put on the intercostal space at the level of the right liver lobe. The Fibroscan probe contains an ultrasound transducer and a mechanical device that provides a controlled vibrating external shot on the body surface to generate shear waves. TE measures liver stiffness (LS) in 1 cm cylindric volume (width: 25-65 mm, M probe; 35-75 mm, XL probe) below the skin surface. Criteria for a valid examination were as follows: (1) At least 10 valid measurements; (2) A success rate [(valid + invalid measurements)/total measurements] > 70%; and (3) An interquartile range < 30% of the median value. Measurements were expressed as KPa[30].

Statistical analysis

Data were expressed as count and percentages for categorical variables and as mean ± SDM for

Table 1 Baseline characteristics of patients observed in the study (*n* = 52) and included in groups treated with the sodium-glucose co-transporter-2 inhibitors or other glucose lowering drugs

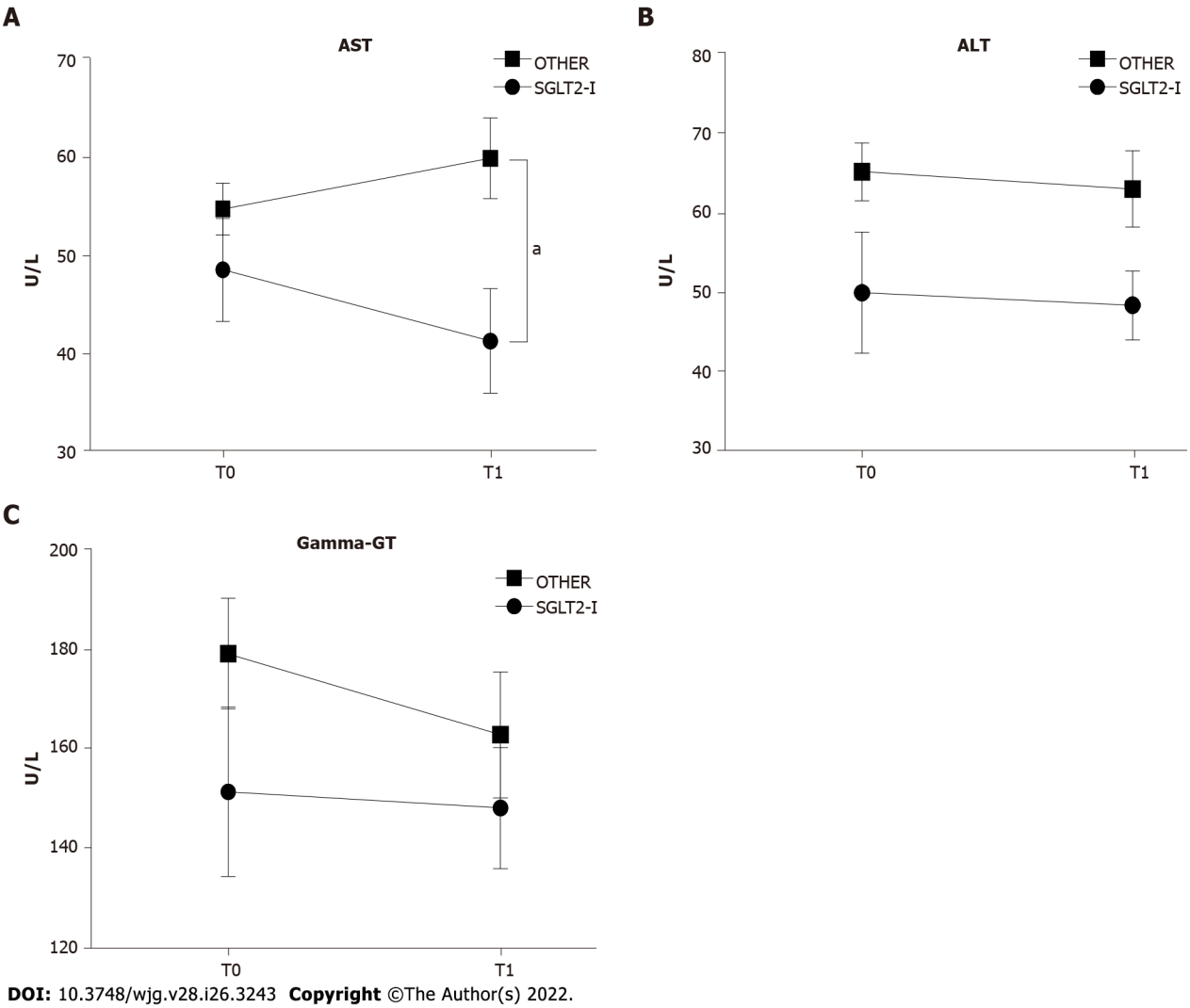
Variable	SGLT2-I (*n* = 26)	OTHER (*n* = 26)	*P* value
Age (yr)	60.6 ± 6.78	63.4 ± 10.4	0.246
Sex (male/female)	15/11	15/11	1.000
BMI (kg/m^2)	34.8 ± 7.7	34.5 ± 5.9	0.875
No comorbidities, *n* (%)	2 (7.7)	2 (7.7)	1.000
Dyslipidemia, *n* (%)	13 (50.0)	15 (57.7)	0.578
Hypertension, *n* (%)	10 (38.5)	15 (57.7)	0.165
Chronic heart failure, *n* (%)	8 (30.8)	3 (11.5)	0.089
Chronic kidney disease, *n* (%)	9 (34.6)	4 (15.4)	0.109
AST (U/L)	48.5 ± 26.6	54.7 ± 13.3	0.293
ALT (U/L)	49.6 ± 39.2	65.0 ± 18.7	0.077
Gamma-GT (U/L)	151.3 ± 87.2	179.2 ± 56.9	0.178
Tryglycerides (mg/dL)	140.2 ± 45.9	133.5 ± 33.2	0.549
Fasting glucose (mg/dL)	150.1 ± 45.9	159.7 ± 49.8	0.473
HbA1c (%)	9.24 ± 3.01	8.73 ± 2.31	0.496
Creatininemia (mg/dL)	1.01 ± 0.44	0.88 ± 0.32	0.229
eGFR (mL/min/1.73 m^2)	61.4 ± 38.9	73.2 ± 24.6	0.197
Albuminemia (g/dL)	3.91 ± 0.44	4.08 ± 0.47	0.184
Platelets (*n*, × 10^3/mm^3)	175.7 ± 113.1	179.7 ± 76.7	0.882

BMI: Body mass index; AST: Aspartate aminotransferase; ALT: Alanine aminotransferase; Gamma-GT: Gamma-glutamyl transpeptidase; HbA1c: Hemoglobin A1c; eGFR: Epidermal growth factor receptor; SGLT2-I: Sodium-glucose co-transporter-2 inhibitor; OTHER: Other glucose lowering drug.

quantitative variables. Gaussian distribution of the samples was evaluated by Kolgomorov-Smirnov test. The significance of differences between the 2 treatment groups (SGLT2-I *vs* OTHER) at baseline was assessed by student's *t*-test (continuous variables) or in contingency tables by Pearson's Chi-squared test and Fisher's exact test (categorical variables). The significance of differences between the 2 treatment groups between the beginning (T0) and the end of the observational period (T1) was assessed by the two-way analysis of variance to test the main effects of time and treatment as a between-subject factor; the interaction time × treatment was studied, and a Tukey test was applied as post hoc test for multiple comparisons. The correlation analysis between changes in non-invasive markers of hepatic steatosis and fibrosis with fasting serum glucose or HbA1c, serum interleukins, or serum HNE- and MDA-protein adducts was performed using Pearson correlation test followed by linear regression. All tests were 2-sided, and $P < 0.05$ were considered statistically significant. Statistical analysis was performed with the Statistical Package for Social Sciences version 23.0 (SPSS, Inc., Chicago, IL) and Graph-Pad Prism 6.0 for Windows (GraphPad Software, Inc., San Diego, CA).

RESULTS

Baseline characteristics of the subjects included in the SGLT2-I or the OTHER group are represented in Table 1. The two groups were comparable in terms of clinical and biochemical features. No side effects in both groups were reported. After six months of treatment, a lowering effect on both fasting serum glucose (time factor: $F_{(1, 100)} = 16.04$, $P < 0.0001$) and HbA1c (time factor: $F_{(1, 100)} = 14.83$, $P < 0.0001$) was observed, with a significant reduction from T0 to T1 in both groups (Figures 1A and B). No significant variations were reported as regards serum triglycerides after 6 mo of treatment (Figure 1C). Interestingly, we observed an impact of time, treatment and interaction on body mass index (time factor: $F_{(1, 100)} = 4.146$, $P = 0.0444$; treatment factor: $F_{(1, 100)} = 4.169$, $P = 0.0438$; interaction factor: $F_{(1, 100)} = 5.650$, $P = 0.0194$), and the post hoc analysis resulted in significant differences between the two treatment groups at T1, and between T0 and T1 in the SGLT2-I group (Figure 1D). These data suggest that 6 mo of add-on treatment to metformin improves glycemic control compared to baseline; nevertheless, this improvement is not related to a particular drug class. Furthermore, a beneficial impact on weight loss is



DOI: 10.3748/wjg.v28.i26.3243 **Copyright** ©The Author(s) 2022.

Figure 2 Serum liver enzyme activities in patients enrolled in the study and included in groups treated with the sodium-glucose co-transporter-2 inhibitors or other glucose-lowering drugs before (T0) and after 1 wk of treatment (T1). A: Serum aspartate aminotransferase; B: Serum alanine aminotransferase; C: Serum gamma-glutamyl transpeptidase activities in patients observed in the study, grouped according to the assigned treatment. Data in the graphs are represented as mean ± SEM. Two-way analysis of variance and Tukey assessed statistical differences as posthoc test. $^{a}P < 0.05$. AST: Aspartate aminotransferase; ALT: Alanine aminotransferase; Gamma-GT: Gamma-glutamyl transpeptidase; SGLT2-I: Sodium-glucose co-transporter-2 inhibitor; OTHER: Other glucose lowering drug.

exerted by SGLT2-I but not by other glucose-lowering agents.

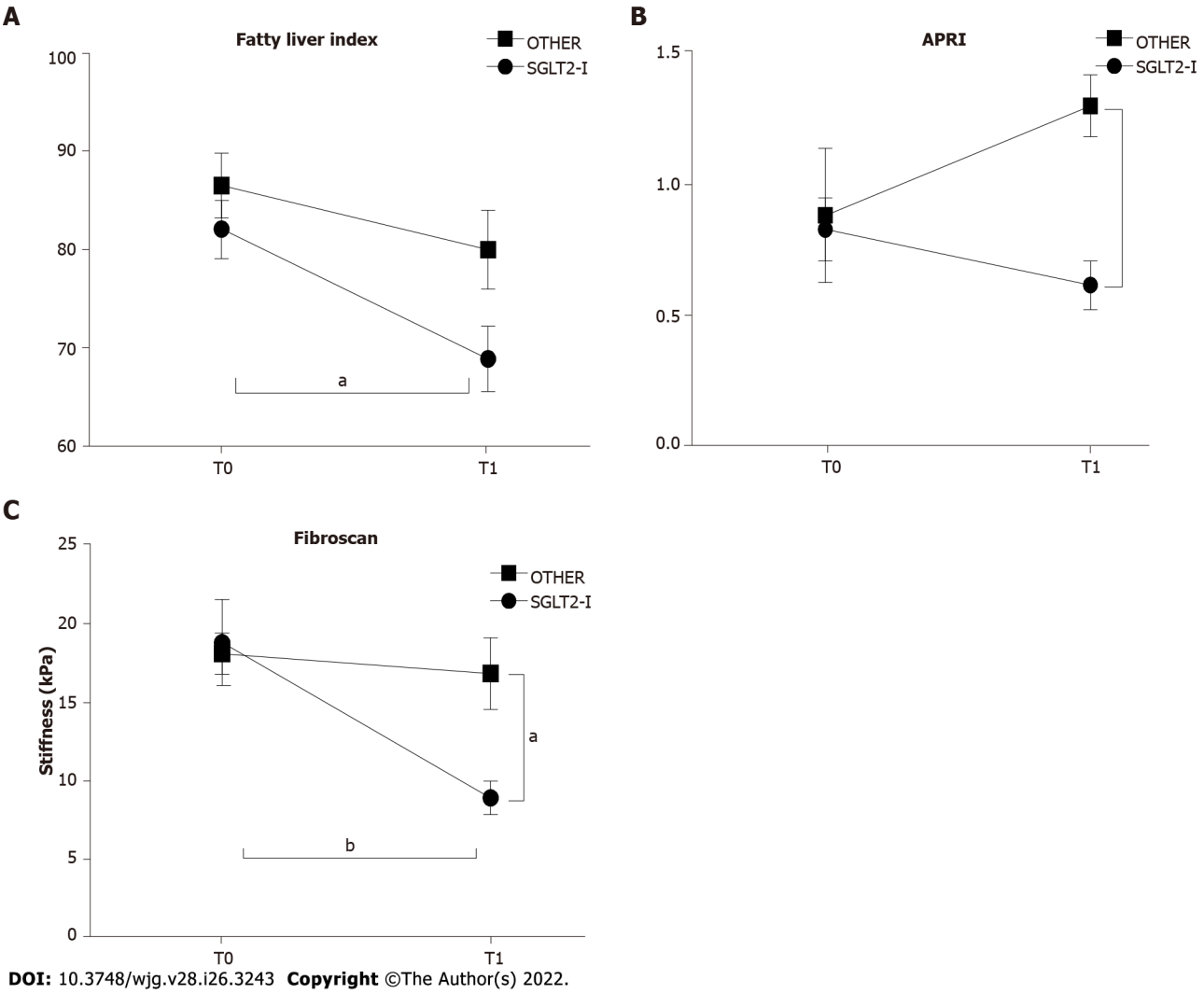
Effect of different add-on therapies on liver function tests and non-invasive markers of hepatic steatosis/fibrosis

We then compared the impact of combined treatment with SGLT2-I *vs* OTHER on circulating liver enzymes. The effect of treatment was significant for serum AST level ($F_{(1, 100)} = 7.703$, $P = 0.0066$), and the post hoc analysis showed lower values in SGLT2-I rather than the OTHER group at T1 (Figure 2A). No significant variations were reported for serum ALT and gamma-GT activities (Figures 2B and C). Non-invasive liver steatosis and fibrosis markers were further evaluated at baseline and after 6 mo of therapy in both groups. We observed the effect of both time and treatment on FLI (time factor: $F_{(1, 100)} = 8.279$, $P = 0.0049$ and treatment factor: $F_{(1, 100)} = 5.113$, $P = 0.0259$), but after 6 mo it decreased only in the SGLT2-I group - and not in OTHER patients - with respect to baseline (Figure 3A). A significant effect of treatment was also observed for the APRI ($F_{(1, 100)} = 5.309$, $P = 0.0233$), with a lower value in SGLT2-I rather than OTHER group at T1 (Figure 3B). The proportion of patients affected by a fibrotic form of liver disease according to NAFLD fibrosis score, FIB-4, and AST/ALT ratio reduced significantly after 6 mo of therapy in the SGLT2-I group rather than in the OTHER group (Table 2). Finally, we observed a significant effect of time ($F_{(1, 100)} = 7.996$, $P = 0.0057$) and interaction ($F_{(1, 100)} = 4.772$, $P = 0.0313$) on hepatic elastometry, and LS in patients treated with SGLT2-I for six months was lower with respect to baseline and to the OTHER group (Figure 3C).

Table 2 Non-invasive markers of hepatic fibrosis in patients observed in the study (*n* = 52) and included in groups treated with the sodium-glucose co-transporter-2 inhibitors or other glucose lowering drugs at baseline (T0) and after 6 mo of therapy (T1)

		T0	T1	*P* value
NAFLD fibrosis score (F3/4), *n* (%)	SGLT2-I (*n* = 26)	9 (34.6)	4 (15.4)	0.042
	OTHER (*n* = 26)	7 (26.9)	7 (26.9)	
FIB-4 (F3/4), *n* (%)	SGLT2-I (*n* = 26)	11 (42.3)	6 (23.1)	0.036
	OTHER (*n* = 26)	7 (26.9)	7 (26.9)	
AST/ALT ≥ 0.8, *n* (%)	SGLT2-I (*n* = 26)	15 (57.7)	6 (23.1)	0.001
	OTHER (*n* = 26)	10 (38.5)	11 (42.3)	

NAFLD: Non-alcoholic fatty liver disease; FIB-4: Fibrosis-4; AST: Aspartate aminotransferase; ALT: Alanine aminotransferase; SGLT2-I: Sodium-glucose co-transporter-2 inhibitor; OTHER: Other glucose lowering drug.



DOI: 10.3748/wjg.v28.i26.3243 **Copyright** ©The Author(s) 2022.

Figure 3 Non-invasive markers of liver steatosis and fibrosis in patients enrolled in the study and included in groups treated with the sodium-glucose co-transporter-2 inhibitors or other glucose glucose-lowering before (T0) and after 1 wk of treatment (T1). A: Fatty liver index; B: Aspartate aminotransferase-to-platelet ratio index; C: Hepatic elastometry in patients observed in the study grouped according to the assigned treatment. Data in the graphs are represented as mean ± SEM. Two-way analysis of variance and Tukey assessed statistical differences as posthoc test. $^{a}P < 0.05$, $^{b}P < 0.01$. SGLT2-I: Sodium-glucose co-transporter-2 inhibitor; OTHER: Other glucose lowering drug; APRI: Aspartate aminotransferase-to-platelet ratio index.

Effect of different add-on therapies on circulating markers of inflammation and oxidative stress

We further analyzed markers of systemic inflammation, such as circulating interleukins and growth factors. Table 3 summarizes the results related to serum levels of 12 different cytokines and growth

Table 3 Circulating interleukin levels in patients enrolled in the study and included in groups treated with the sodium-glucose co-transporter-2 inhibitors or other glucose lowering drugs before (T0) and after 1 wk of treatment (T1)

Variable	SGLT2-I (*n* = 26)		OTHER (*n* = 26)		Fisher's test (1, 100)		
	T0	T1	T0	T1	Time	Treatment	Interaction
IL-1α (pg/mL)	1.35 ± 1.64	1.58 ± 1.30	1.44 ± 1.88	1.59 ± 1.56	0.373	0.026	0.016
IL-1β (pg/mL)	9.90 ± 2.39	7.31 ± 3.51[e]	8.84 ± 2.54	9.15 ± 2.42	4.455[a]	0.521	7.207[b]
IL-2 (U/mL)	≤ 0.5	≤ 0.5	≤ 0.5	≤ 0.5	-	-	-
IL-4 (pg/mL)	5.39 ± 4.20	8.54 ± 3.51[d]	4.89 ± 3.54	5.94 ± 3.66	8.207[b]	4.471[a]	2.052
IL-6 (pg/mL)	9.41 ± 4.21	6.92 ± 1.98	11.4 ± 5.41	13.7 ± 9.01[h]	0.007	15.4[c]	4.516[a]
IL-8 (pg/mL)	428 ± 216	409 ± 271	412 ± 296	449 ± 204	0.338	0.060	0.327
IL-10 (pg/mL)	1.33 ± 1.02	2.31 ± 1.12[e]	1.29 ± 1.06	1.32 ± 1.04[g]	5.894[a]	6.130[a]	5.214[a]
TNF (pg/mL)	6.82 ± 3.02	4.61 ± 2.01[d]	7.94 ± 3.14	7.81 ± 3.56[g]	3.989[a]	13.59[c]	3.151
VEGF (pg/mL)	262 ± 162	142 ± 109[d]	244 ± 201	268 ± 147[f]	2.393	3.029	5.384[a]
IFN-γ (pg/mL)	0.53 ± 0.23	0.57 ± 0.57	0.50 ± 0.39	0.61 ± 0.44	0.809	0.004	0.176
MCP-1 (pg/mL)	411 ± 168	291 ± 156	389 ± 154	414 ± 184[f]	2.131	2.408	4.964[a]
EGF (pg/mL)	25.7 ± 13.7	22.2 ± 12.1	24.9 ± 20.1	23.6 ± 18.6	0.553	0.009	0.116

[a]$P < 0.05$.
[b]$P < 0.01$.
[c]$P < 0.001$.
[d]$P < 0.05$ *vs* sodium-glucose co-transporter-2 inhibitor T0.
[e]$P < 0.01$ *vs* sodium-glucose co-transporter-2 inhibitor T0.
[f]$P < 0.05$ *vs* sodium-glucose co-transporter-2 inhibitor T1.
[g]$P < 0.01$ *vs* sodium-glucose co-transporter-2 inhibitor T1.
[h]$P < 0.001$ *vs* sodium-glucose co-transporter-2 inhibitor T1.
Data are expressed as mean ± SD. Statistical differences were assessed by two-way analysis of variance. VEGF: Vascular endothelial growth factor; MCP-1: Monocyte chemoattractant protein-1; EGF: Epidermal growth factor; SGLT2-I: Sodium-glucose co-transporter-2 inhibitor; OTHER: Other glucose lowering drug; IL: Interleukin; TNF: Tumor necrosis factor; IFN: Interferon.

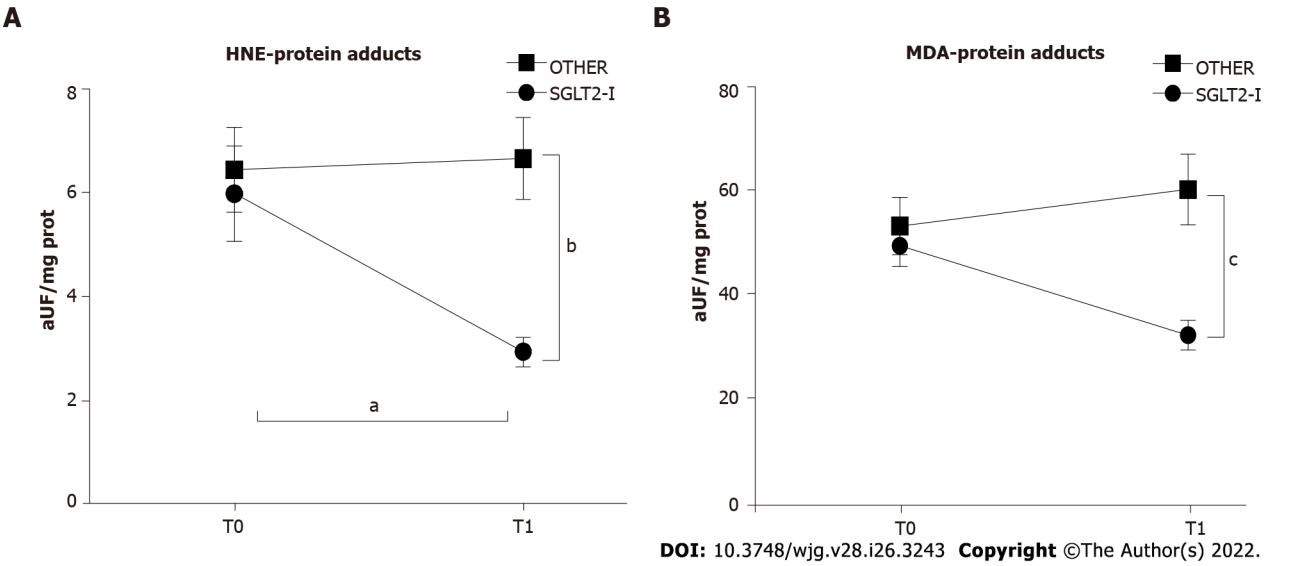
factors evaluated at baseline (T0) and after 6 mo of therapy (T1) in both treatment groups. We could not observe any significant impact of time, treatment, or interaction on IL-1α, IL-2, IL-8, IFN-γ, and EGF. On the contrary, the time effect was observed for IL-1β, IL-4, IL-10, and TNF; the treatment effect was reported for IL-4, IL-6, IL-10, and TNF; the interaction effect was described for IL-1β, IL-6, IL-10, VEGF, and MCP-1. According to the post-hoc analysis, SGLT2-I patients at T1 showed: (1) Lower values of the pro-inflammatory cytokines IL-1β and TNF, and VEGF than T0; (2) Lower values of the pro-inflammatory cytokines IL-6 and TNF, VEGF, and MCP-1 than OTHER patients at T1; and (3) Higher values of the anti-inflammatory cytokines IL-4 and IL-10 as compared to SGLT2-I at T0 and OTHER at T1.

We evaluated systemic oxidative stress markers changes by measuring serum HNE- and MDA-protein adducts. A significant effect of treatment and interaction was observed for both HNE-protein adducts (treatment factor: $F_{(1, 100)} = 7.924$, $P = 0.0059$; interaction factor: $F_{(1, 100)} = 4.820$, $P = 0.0305$) and MDA-protein adducts (treatment factor: $F_{(1, 100)} = 10.17$, $P = 0.0019$; interaction factor: $F_{(1, 100)} = 5.844$, $P = 0.0174$). The post hoc analysis showed that, after 6 mo of therapy, circulating markers of oxidative stress were lower in the SGLT2-I group rather than OTHER patients; furthermore, HNE-protein adducts were significantly reduced from T0 to T1 in SGLT2-I patients (Figures 4A and B).

Reduction of liver steatosis and fibrosis markers is associated with decreased circulating oxidative stress in patients treated with SGLT2-I

We then focused on patients treated with SGLT2-I. We performed a Pearson's correlation analysis on non-invasive markers of hepatic steatosis and fibrosis, circulating parameters of glucose metabolism, inflammation, and oxidative stress after 6 mo of therapy. Of note, the FLI, the APRI, and LS showed: (1) A positive bivariate relationship with pro-inflammatory cytokines (IL-1β, IL6, TNF); and (2) A negative correlation with the anti-inflammatory cytokines (IL-4 and IL-10). Interestingly, all the non-invasive liver steatosis and fibrosis markers were strongly related to HNE- and MDA-protein adducts (Supplementary Table 2).

To verify whether the improvement of non-invasive markers of liver steatosis and fibrosis reported in patients treated with SGLT2-I after 6 mo of therapy was associated with the observed reduction of serum HNE- and MDA-protein adducts, a linear regression analysis on T1-T0 difference values was



DOI: 10.3748/wjg.v28.i26.3243 **Copyright** ©The Author(s) 2022.

Figure 4 Circulating markers of oxidative stress in patients enrolled in the study and included in groups treated with the sodium-glucose co-transporter-2 inhibitors or other glucose-lowering drugs before (T0) and after 1 wk of treatment (T1). Data in the graphs are represented as mean ± SEM. Two-way analysis of variance and Tukey assessed statistical differences as a post hoc test. $^{a}P < 0.05$, $^{b}P < 0.01$, $^{c}P < 0.001$. HNE: Hydroxynonenal; MDA: Malondialdehyde; SGLT2-I: Sodium-glucose co-transporter-2 inhibitor; OTHER: Other glucose lowering drug.

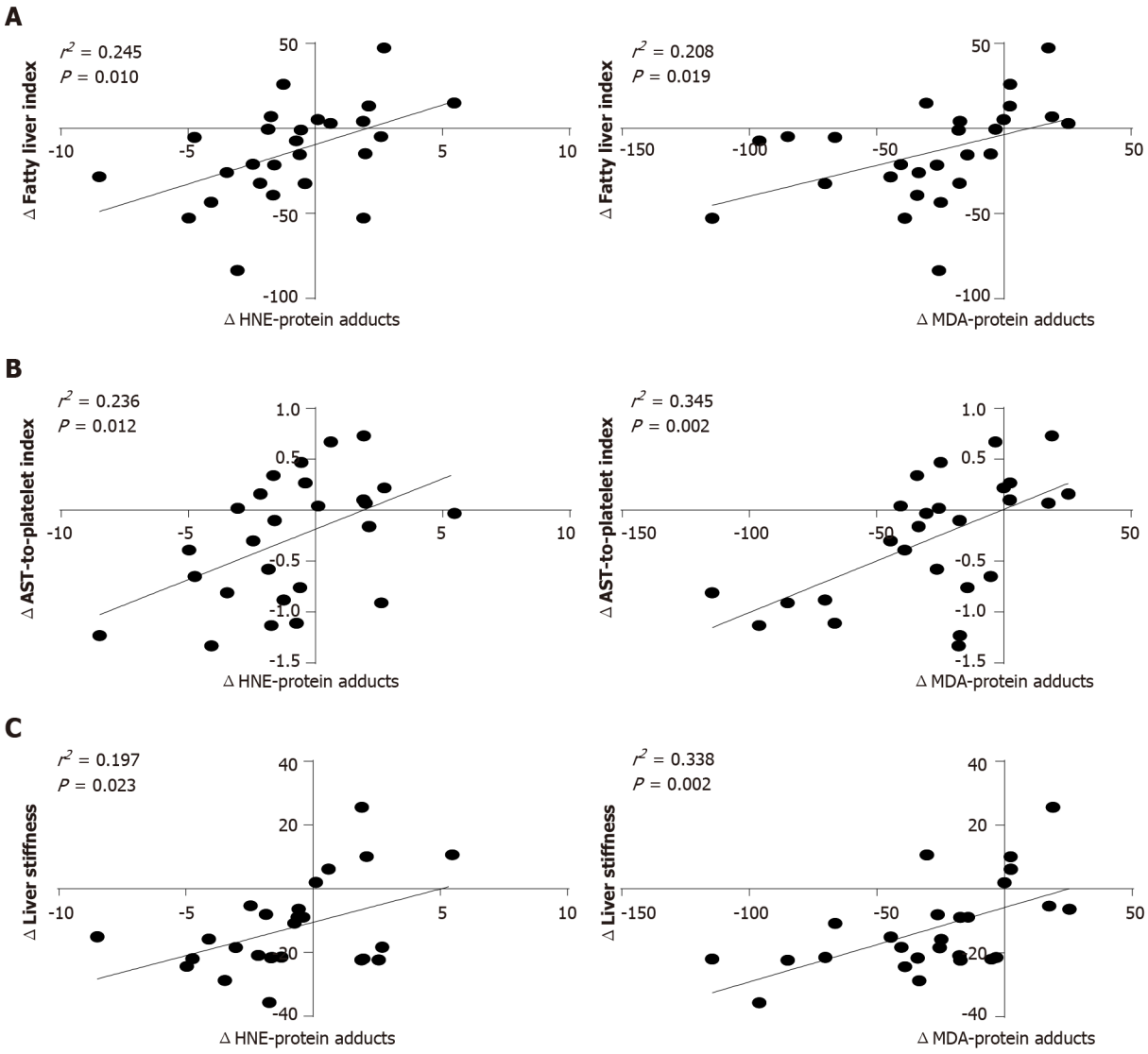
performed. Further, SGLT2-I treatment related alterations in both markers of circulating oxidative stress were directly related to variations in FLI, APRI, and LS (Figures 5A-C).

DISCUSSION

The present study demonstrates that the addition of an SGLT2-I - as compared to dipeptidyl peptidase-4 inhibitors (DPP4-I) or pioglitazone - to metformin monotherapy exerts a positive impact on systemic inflammation and circulating oxidative stress in patients with T2DM and NAFLD. It is associated with favorable changes in the non-invasive hepatic steatosis and fibrosis markers. The incidence of T2DM is exponentially increasing worldwide[31]. T2DM often presents associated with NAFLD since insulin resistance accounts for the alteration of lipid homeostasis, favoring hepatic fat accumulation by induction of lipogenesis and inhibition of very-low-density lipoprotein secretion[32,33]. Furthermore, hyperglycemia in diabetic patients worsens insulin resistance through mechanisms induced by glucose toxicity[34]. In addition, the efficacy of several antidiabetic drugs is lost during the time, leading to the progression of T2DM, which could worsen NAFLD[35]. There are currently no approved therapies for the treatment for NAFLD. Several compounds tested in phase 2 and phase 3 clinical trials target metabolic stress as a critical factor for the initiation and progression of hepatic injury. Data on the effects of antidiabetic drugs in NAFLD are limited although pioglitazone and GLP1-RA have demonstrated some protective effects[36]. SGLT2-I are molecules with direct action on the kidney, reduce the reabsorption of filtered glucose and significantly decrease blood glucose levels both in fasting and post-prandial conditions, with consequent decline of glucose toxicity and improvement of insulin resistance [37]. Moreover, these drugs may interfere with several mechanisms involved in the progression of T2DM, such as dysfunction or apoptosis of pancreatic β-cells[38].

Clinical studies testing the efficacy of SGLT2-I on NAFLD demonstrated that this class of drugs reduces both hepatic steatosis, as evaluated by several imaging techniques, and serum liver enzymes [39]. Our study confirms these observations since we report that the addition of SGLT2-I to metformin reduces both the FLI and serum AST after 6 mo; this effect is not observed when pioglitazone or DPP4-I are added to metformin. Furthermore, our data show that six months of therapy with an SGLT2-I are associated with reducing hepatic fibrosis - which occurs mainly in NAFLD patients with higher fibrosis grade - as suggested by decrease in NAFLD fibrosis score, FIB-4, as well as LS measured by TE. These results are comparable to the reported outcome in a similar study, suggesting that SGLT2-I are superior to other oral hypoglycemic agents in reducing hepatic steatosis and fibrosis[40].

Among other glucose-lowering agents, pioglitazone and GLP1-RA were demonstrated to reduce hepatic steatosis, inflammation, and fibrosis[41,42]. We designed this study by excluding patients treated with GLP1-RA, even though 38.5% of patients of the OTHER group were treated with pioglitazone added to metformin. Despite this subgroup of patients in the comparison group, SGLT2-I improved non-invasive liver steatosis and fibrosis markers. A previous randomized trial compared the SGLT2-I ipragliflozin against pioglitazone, showing that both treatments were equivalent in reducing



DOI: 10.3748/wjg.v28.i26.3243 **Copyright** ©The Author(s) 2022.

Figure 5 Linear regression analysis between the variation of circulating oxidative stress parameters and non-invasive markers of hepatic steatosis or fibrosis in patients treated with the sodium-glucose co-transporter-2 inhibitors. Data in the graphs represent scatterplots of hydroxynonenal- or malondialdehyde-protein adducts A: Fatty liver index; B: Aspartate aminotransferase-to-platelet ratio index; C: Liver stiffness. HNE: Hydroxynonenal; AST: Aspartate aminotransferase; MDA: Malondialdehyd.

liver fat infiltration and serum aminotransferase levels, even though ipragliflozin effected a reduction in body weight and abdominal fat area[43]. However, it is worth noting that more than one-third of patients included in our study showed a high grade of steatosis and fibrosis as assessed by non-invasive markers. In contrast, previous studies using pioglitazone enrolled patients with milder hepatic injury. More than potentially explaining differences between the present results and those of different studies, our results suggest that SGLT2-I treatment would be more beneficial in T2DM patients with advanced NAFLD.

Mechanisms explaining the benefits of SGLT2-I therapy in T2DM and NAFLD are primarily undefined, but the results of this study lead to several speculations. Even though SGLT2-I significantly controls blood glucose, an improvement in glucose metabolism was described in all patients treated with additional drugs. However, other studies could not demonstrate that amelioration of NAFLD after SGLT2-I treatment was dependent on improved circulating glucose concentration[44-46]. Weight loss induced by non-pharmacological interventions such as diet, exercise, or bariatric surgery, may ameliorate liver damage in NAFLD[47]. SGLT2-I decreases body weight and fat mass, reducing hepatic steatosis and serum liver enzymes[48]. Our data show that SGLT2-I effectively promoted weight loss after 6 mo of therapy in patients with T2DM and NAFLD. However, there was no relationship between BMI reduction and the improvement of non-invasive markers of hepatic steatosis and fibrosis.

Besides, previous studies have also shown improved liver function tests, and steatosis irrespective of weight loss in patients affected by T2DM and NAFLD treated with SGLT2-I[49,50]. The evidence so far indicated that SGLT2-I would induce different beneficial mechanisms than glucose control and weight

loss in NAFLD. The present results further revealed that SGLT2-I - and not pioglitazone or DPP4-I - favorably modulate circulating cytokines, switching from pro-inflammatory to anti-inflammatory patterns, and reducing systemic markers of oxidative stress. These results are further buttressed by pre-clinical studies providing proving2-I inhibits pro-inflammatory cytokine secretion and reduces oxidative stress[16,51,52]. Our study clearly demonstrates a significant association between improving hepatic steatosis/fibrosis markers and reducing circulating oxidative stress in patients treated with SGLT2-I for 6 mo. On the other hand, we could not find any relationship between changes in circulating cytokines and reduction of liver injury markers. Reactive oxygen species (ROS) and reactive nitrogen species (RNS) represent physiological products of cellular metabolism, which are normally counteracted by endogenous antioxidants. When ROS/RNS production overwhelms the antioxidant defense, oxidative stress occurs with consequent injury of macromolecules such as nucleic acids (DNA oxidation), lipids (lipoperoxidation), and proteins, which in turn leads to an impairment of normal cellular functions[53]. Oxidative stress promotes the generation of HNE and MDA, lipid peroxidation products which are able to generate adducts with cellular and circulating proteins, which may be used as systemic markers of injury. Oxidative stress is considered one of the main determinants of NAFLD pathogenesis and progression[54]. For the first time, our study provides evidence that the reduction of circulating oxidative stress induced by SGLT2-I is related to improved markers of hepatic damage in T2DM patients with NAFLD, suggesting a potential protective mechanism by this drug class. Studies to define how SGLT2-I modulate molecular pathways that impact redox balance need to be designed.

This study suffers from the following limitations: (1) It was not designed as a randomized placebo-controlled trial since the type of combined treatment was decided according to a patient-centered approach (of note, the newest Standards of Medical Care in Diabetes were not available at the time of enrolment); (2) Patients treated with GLP-1 agonists were not included; (3) Since this study was performed at a single-center, it may have presented some bias, resulting in slightly larger intervention effects than multicenter studies; (4) Our small pilot study was not designed to determine the impact of single compounds; and (5) Liver histology was not performed to evaluate steatosis, inflammation, and fibrosis.

CONCLUSION

In conclusion, treatment with SGLT2-I in T2DM patients affected by NAFLD is associated with a rapid improvement of non-invasive markers of hepatic steatosis and fibrosis, providing insights into the mechanisms by which such class of antidiabetic drugs may reduce liver damage in humans. More extensive randomized controlled trials are encouraged to confirm these preliminary observations, and fundamental studies are needed to define the molecular mechanisms underlying the effects of SGLT2-I in NAFLD.

ARTICLE HIGHLIGHTS

Research background

Clinical trials of sodium glucose cotransporter-2 inhibitors (SGLT2-I), recently approved drugs for type 2 diabetes (T2D), reported beneficial cardiovascular (CV) and renal outcomes.

Research motivation

Inflammation and oxidative stress are major causes of vascular dysfunction and CV disease in diabetes and pre-clinical studies demonstrated that SGLT2-I promote anti-inflammatory effects by lowering oxidative stress.

Research objectives

To investigate the effects of SGLT2-I on markers of oxidative stress, inflammation, liver steatosis, and fibrosis in patients of T2D with non-alcoholic fatty liver disease (NAFLD).

Research methods

Observational prospective study enrolling 52 consecutive outpatients treated with metformin monotherapy and exhibiting poor glycemic control, which were introduced to an SGLT2-I (n = 26) or a different hypoglycemic drug (n = 26). Circulating interleukins and serum hydroxynonenal (HNE)- or malondialdehyde (MDA)-protein adducts, fatty liver index (FLI), NAFLD fibrosis score, aspartate aminotransferase (AST)/alanine aminotransferase (ALT) ratio ratio, AST-to-platelet-ratio index (APRI), and fibrosis-4, as well as transient elastography (FibroScan) on the day before (T0) and following treatment for six months (T1) were evaluated.

Research results

With respect to other hypoglycemic drugs, treatment with SGLT2-I resulted in a reduction of FLI and APRI, as well as of the FibroScan result, as well as lower circulating levels of interleukins (IL)-1β, IL-6, tumor necrosis factor, vascular endothelial growth factor, and monocyte chemoattractant protein-1, higher levels of IL-4 and IL-10, decreased serum HNE- and MDA-protein adducts. Markers of circulating oxidative stress correlated with liver steatosis and fibrosis scores.

Research conclusions

This study indicates that, more than optimizing glucose control, treatment with SGLT2-I in patients with T2D and NAFLD is associated with improvement of liver steatosis and fibrosis markers and circulating pro-inflammatory and redox status.

Research perspectives

This study encourages extensive randomized controlled trials to confirm these preliminary observations, and basic investigations to define the molecular mechanisms underlying the effects of SGLT2-I in NAFLD.

FOOTNOTES

Author contributions: Bellanti F and Vendemiale G designed and coordinated the study; Bellanti, F, Lo Buglio A, Dobrakowsky M, and Kasperczyk A performed the experiments, acquired and analyzed data; Bellanti F, Lo Buglio A, Dobrakowsky M, Kasperczyk A, Kasperczyk S, Serviddio G, Singh SP, Aich P, and Vendemiale G interpreted the data; Bellanti F wrote the manuscript; Kasperczyk S, Serviddio G, Singh SP, Aich P, and Vendemiale G supervised the manuscript; and all authors approved the final version of the article.

Institutional review board statement: The study was reviewed and approved by the Institutional Review Board at the University of Foggia.

Informed consent statement: All study participants, or their legal guardian, provided informed written consent prior to study enrollment.

Conflict-of-interest statement: All the authors report no relevant conflicts of interest for this article.

Data sharing statement: No additional data are available.

STROBE statement: The Authors have read the STROBE statement - checklist of items, and the manuscript was prepared and revised according to the STROBE statement - checklist of items.

Open-Access: This article is an open-access article that was selected by an in-house editor and fully peer-reviewed by external reviewers. It is distributed in accordance with the Creative Commons Attribution NonCommercial (CC BY-NC 4.0) license, which permits others to distribute, remix, adapt, build upon this work non-commercially, and license their derivative works on different terms, provided the original work is properly cited and the use is non-commercial. See: https://creativecommons.org/Licenses/by-nc/4.0/

Country/Territory of origin: Italy

ORCID number: Francesco Bellanti 0000-0002-8196-7373; Aurelio Lo Buglio 0000-0003-1569-3658; Michał Dobrakowski 0000-0001-8399-7624; Aleksandra Kasperczyk 0000-0002-2035-0388; Sławomir Kasperczyk 0000-0001-8974-5786; Palok Aich 0000-0003-4927-7812; Shivaram P Singh 0000-0002-8197-2674; Gaetano Serviddio 0000-0002-6424-7841; Gianluigi Vendemiale 0000-0002-7951-0219.

S-Editor: Wang JJ
L-Editor: A
P-Editor: Wang JJ

REFERENCES

1 **Redekop WK**, Koopmanschap MA, Stolk RP, Rutten GE, Wolffenbuttel BH, Niessen LW. Health-related quality of life and treatment satisfaction in Dutch patients with type 2 diabetes. *Diabetes Care* 2002; **25**: 458-463 [PMID: 11874930 DOI: 10.2337/diacare.25.3.458]

2 **Rao Kondapally Seshasai S**, Kaptoge S, Thompson A, Di Angelantonio E, Gao P, Sarwar N, Whincup PH, Mukamal KJ, Gillum RF, Holme I, Njølstad I, Fletcher A, Nilsson P, Lewington S, Collins R, Gudnason V, Thompson SG, Sattar N, Selvin E, Hu FB, Danesh J; Emerging Risk Factors Collaboration. Diabetes mellitus, fasting glucose, and risk of cause-specific death. *N Engl J Med* 2011; **364**: 829-841 [PMID: 21366474 DOI: 10.1056/NEJMoa1008862]

3 **Younossi ZM**, Loomba R, Rinella ME, Bugianesi E, Marchesini G, Neuschwander-Tetri BA, Serfaty L, Negro F, Caldwell SH, Ratziu V, Corey KE, Friedman SL, Abdelmalek MF, Harrison SA, Sanyal AJ, Lavine JE, Mathurin P, Charlton MR, Chalasani NP, Anstee QM, Kowdley KV, George J, Goodman ZD, Lindor K. Current and future therapeutic regimens for nonalcoholic fatty liver disease and nonalcoholic steatohepatitis. *Hepatology* 2018; **68**: 361-371 [PMID: 29222911 DOI: 10.1002/hep.29724]

4 **Younossi Z**, Tacke F, Arrese M, Chander Sharma B, Mostafa I, Bugianesi E, Wai-Sun Wong V, Yilmaz Y, George J, Fan J, Vos MB. Global Perspectives on Nonalcoholic Fatty Liver Disease and Nonalcoholic Steatohepatitis. *Hepatology* 2019; **69**: 2672-2682 [PMID: 30179269 DOI: 10.1002/hep.30251]

5 **Hardy T**, Oakley F, Anstee QM, Day CP. Nonalcoholic Fatty Liver Disease: Pathogenesis and Disease Spectrum. *Annu Rev Pathol* 2016; **11**: 451-496 [PMID: 26980160 DOI: 10.1146/annurev-pathol-012615-044224]

6 **Younossi Z**, Anstee QM, Marietti M, Hardy T, Henry L, Eslam M, George J, Bugianesi E. Global burden of NAFLD and NASH: trends, predictions, risk factors and prevention. *Nat Rev Gastroenterol Hepatol* 2018; **15**: 11-20 [PMID: 28930295 DOI: 10.1038/nrgastro.2017.109]

7 **Caussy C**, Aubin A, Loomba R. The Relationship Between Type 2 Diabetes, NAFLD, and Cardiovascular Risk. *Curr Diab Rep* 2021; **21**: 15 [PMID: 33742318 DOI: 10.1007/s11892-021-01383-7]

8 **Sajja AP**, Dey AK, Guha A, Elnabawi Y, Joshi AA, Kalra A. SGLT-2 Inhibitors and GLP-1 Agonists: First-Line Therapy for Diabetes With Established Cardiovascular Disease. *J Cardiovasc Pharmacol Ther* 2019; **24**: 422-427 [PMID: 31064213 DOI: 10.1177/1074248419838511]

9 **Dougherty JA**, Guirguis E, Thornby KA. A Systematic Review of Newer Antidiabetic Agents in the Treatment of Nonalcoholic Fatty Liver Disease. *Ann Pharmacother* 2021; **55**: 65-79 [PMID: 32571083 DOI: 10.1177/1060028020935105]

10 **Wu JH**, Foote C, Blomster J, Toyama T, Perkovic V, Sundström J, Neal B. Effects of sodium-glucose cotransporter-2 inhibitors on cardiovascular events, death, and major safety outcomes in adults with type 2 diabetes: a systematic review and meta-analysis. *Lancet Diabetes Endocrinol* 2016; **4**: 411-419 [PMID: 27009625 DOI: 10.1016/S2213-8587(16)00052-8]

11 **Kosiborod M**, Cavender MA, Fu AZ, Wilding JP, Khunti K, Holl RW, Norhammar A, Birkeland KI, Jørgensen ME, Thuresson M, Arya N, Bodegård J, Hammar N, Fenici P; CVD-REAL Investigators and Study Group*. Lower Risk of Heart Failure and Death in Patients Initiated on Sodium-Glucose Cotransporter-2 Inhibitors Versus Other Glucose-Lowering Drugs: The CVD-REAL Study (Comparative Effectiveness of Cardiovascular Outcomes in New Users of Sodium-Glucose Cotransporter-2 Inhibitors). *Circulation* 2017; **136**: 249-259 [PMID: 28522450 DOI: 10.1161/CIRCULATIONAHA.117.029190]

12 **Kosiborod M**, Lam CSP, Kohsaka S, Kim DJ, Karasik A, Shaw J, Tangri N, Goh SY, Thuresson M, Chen H, Surmont F, Hammar N, Fenici P; CVD-REAL Investigators and Study Group. Cardiovascular Events Associated With SGLT-2 Inhibitors Versus Other Glucose-Lowering Drugs: The CVD-REAL 2 Study. *J Am Coll Cardiol* 2018; **71**: 2628-2639 [PMID: 29540325 DOI: 10.1016/j.jacc.2018.03.009]

13 **Leng W**, Ouyang X, Lei X, Wu M, Chen L, Wu Q, Deng W, Liang Z. The SGLT-2 Inhibitor Dapagliflozin Has a Therapeutic Effect on Atherosclerosis in Diabetic ApoE$^{-/-}$ Mice. *Mediators Inflamm* 2016; **2016**: 6305735 [PMID: 28104929 DOI: 10.1155/2016/6305735]

14 **Han JH**, Oh TJ, Lee G, Maeng HJ, Lee DH, Kim KM, Choi SH, Jang HC, Lee HS, Park KS, Kim YB, Lim S. The beneficial effects of empagliflozin, an SGLT2 inhibitor, on atherosclerosis in ApoE $^{-/-}$ mice fed a western diet. *Diabetologia* 2017; **60**: 364-376 [PMID: 27866224 DOI: 10.1007/s00125-016-4158-2]

15 **Nasiri-Ansari N**, Dimitriadis GK, Agrogiannis G, Perrea D, Kostakis ID, Kaltsas G, Papavassiliou AG, Randeva HS, Kassi E. Canagliflozin attenuates the progression of atherosclerosis and inflammation process in APOE knockout mice. *Cardiovasc Diabetol* 2018; **17**: 106 [PMID: 30049285 DOI: 10.1186/s12933-018-0749-1]

16 **Steven S**, Oelze M, Hanf A, Kröller-Schön S, Kashani F, Roohani S, Welschof P, Kopp M, Gödtel-Armbrust U, Xia N, Li H, Schulz E, Lackner KJ, Wojnowski L, Bottari SP, Wenzel P, Mayoux E, Münzel T, Daiber A. The SGLT2 inhibitor empagliflozin improves the primary diabetic complications in ZDF rats. *Redox Biol* 2017; **13**: 370-385 [PMID: 28667906 DOI: 10.1016/j.redox.2017.06.009]

17 **Lahnwong S**, Chattipakorn SC, Chattipakorn N. Potential mechanisms responsible for cardioprotective effects of sodium-glucose co-transporter 2 inhibitors. *Cardiovasc Diabetol* 2018; **17**: 101 [PMID: 29991346 DOI: 10.1186/s12933-018-0745-5]

18 **Das NA**, Carpenter AJ, Belenchia A, Aroor AR, Noda M, Siebenlist U, Chandrasekar B, DeMarco VG. Empagliflozin reduces high glucose-induced oxidative stress and miR-21-dependent TRAF3IP2 induction and RECK suppression, and inhibits human renal proximal tubular epithelial cell migration and epithelial-to-mesenchymal transition. *Cell Signal* 2020; **68**: 109506 [PMID: 31862399 DOI: 10.1016/j.cellsig.2019.109506]

19 **Quagliariello V**, De Laurentiis M, Rea D, Barbieri A, Monti MG, Carbone A, Paccone A, Altucci L, Conte M, Canale ML, Botti G, Maurea N. The SGLT-2 inhibitor empagliflozin improves myocardial strain, reduces cardiac fibrosis and pro-inflammatory cytokines in non-diabetic mice treated with doxorubicin. *Cardiovasc Diabetol* 2021; **20**: 150 [PMID: 34301253 DOI: 10.1186/s12933-021-01346-y]

20 **Zeng S**, Delic D, Chu C, Xiong Y, Luo T, Chen X, Gaballa MMS, Xue Y, Cao Y, Hasan AA, Stadermann K, Frankenreiter S, Yin L, Krämer BK, Klein T, Hocher B. Antifibrotic effects of low dose SGLT2 Inhibition with empagliflozin in comparison to Ang II receptor blockade with telmisartan in 5/6 nephrectomised rats on high salt diet. *Biomed Pharmacother* 2022; **146**: 112606 [PMID: 34968924 DOI: 10.1016/j.biopha.2021.112606]

21 **European Association for the Study of the Liver (EASL)**; European Association for the Study of Diabetes (EASD); European Association for the Study of Obesity (EASO). EASL-EASD-EASO Clinical Practice Guidelines for the management of non-alcoholic fatty liver disease. *J Hepatol* 2016; **64**: 1388-1402 [PMID: 27062661 DOI: 10.1016/j.jhep.2015.11.004]

22 Standards of Medical Care in Diabetes-2017: Summary of Revisions. *Diabetes Care* 2017; **40**: S4-S5 [PMID: 27979887 DOI: 10.2337/dc17-S003]

23 **Molloy RM**, Mc Connell RI, Lamont JV, FitzGerald SP. Automation of biochip array technology for quality results. *Clin Chem Lab Med* 2005; **43**: 1303-1313 [PMID: 16309365 DOI: 10.1515/CCLM.2005.224]

24 **Bellanti F**, Romano AD, Lo Buglio A, Castriotta V, Guglielmi G, Greco A, Serviddio G, Vendemiale G. Oxidative stress is increased in sarcopenia and associated with cardiovascular disease risk in sarcopenic obesity. *Maturitas* 2018; **109**: 6-12 [PMID: 29452783 DOI: 10.1016/j.maturitas.2017.12.002]

25 **Koehler EM**, Schouten JN, Hansen BE, Hofman A, Stricker BH, Janssen HL. External validation of the fatty liver index for identifying nonalcoholic fatty liver disease in a population-based study. *Clin Gastroenterol Hepatol* 2013; **11**: 1201-1204 [PMID: 23353640 DOI: 10.1016/j.cgh.2012.12.031]

26 **Tapper EB**. The aspartate aminotransferase-to-platelet ratio and the evaluation of non-alcoholic fatty liver disease. *Gastroenterol Rep (Oxf)* 2014; **2**: 326-327 [PMID: 25371483 DOI: 10.1093/gastro/gou080]

27 **Angulo P**, Hui JM, Marchesini G, Bugianesi E, George J, Farrell GC, Enders F, Saksena S, Burt AD, Bida JP, Lindor K, Sanderson SO, Lenzi M, Adams LA, Kench J, Therneau TM, Day CP. The NAFLD fibrosis score: a noninvasive system that identifies liver fibrosis in patients with NAFLD. *Hepatology* 2007; **45**: 846-854 [PMID: 17393509 DOI: 10.1002/hep.21496]

28 **Shah AG**, Lydecker A, Murray K, Tetri BN, Contos MJ, Sanyal AJ; Nash Clinical Research Network. Comparison of noninvasive markers of fibrosis in patients with nonalcoholic fatty liver disease. *Clin Gastroenterol Hepatol* 2009; **7**: 1104-1112 [PMID: 19523535 DOI: 10.1016/j.cgh.2009.05.033]

29 **McPherson S**, Stewart SF, Henderson E, Burt AD, Day CP. Simple non-invasive fibrosis scoring systems can reliably exclude advanced fibrosis in patients with non-alcoholic fatty liver disease. *Gut* 2010; **59**: 1265-1269 [PMID: 20801772 DOI: 10.1136/gut.2010.216077]

30 **Wong VW**, Vergniol J, Wong GL, Foucher J, Chan HL, Le Bail B, Choi PC, Kowo M, Chan AW, Merrouche W, Sung JJ, de Lédinghen V. Diagnosis of fibrosis and cirrhosis using liver stiffness measurement in nonalcoholic fatty liver disease. *Hepatology* 2010; **51**: 454-462 [PMID: 20101745 DOI: 10.1002/hep.23312]

31 **Chatterjee S**, Khunti K, Davies MJ. Type 2 diabetes. *Lancet* 2017; **389**: 2239-2251 [PMID: 28190580 DOI: 10.1016/S0140-6736(17)30058-2]

32 **Poulsen MK**, Nellemann B, Stødkilde-Jørgensen H, Pedersen SB, Grønbæk H, Nielsen S. Impaired Insulin Suppression of VLDL-Triglyceride Kinetics in Nonalcoholic Fatty Liver Disease. *J Clin Endocrinol Metab* 2016; **101**: 1637-1646 [PMID: 26829441 DOI: 10.1210/jc.2015-3476]

33 **Smith GI**, Shankaran M, Yoshino M, Schweitzer GG, Chondronikola M, Beals JW, Okunade AL, Patterson BW, Nyangau E, Field T, Sirlin CB, Talukdar S, Hellerstein MK, Klein S. Insulin resistance drives hepatic de novo lipogenesis in nonalcoholic fatty liver disease. *J Clin Invest* 2020; **130**: 1453-1460 [PMID: 31805015 DOI: 10.1172/JCI134165]

34 **Luo W**, Ai L, Wang BF, Zhou Y. High glucose inhibits myogenesis and induces insulin resistance by down-regulating AKT signaling. *Biomed Pharmacother* 2019; **120**: 109498 [PMID: 31634780 DOI: 10.1016/j.biopha.2019.109498]

35 **Evans JL**, Goldfine ID. Aging and insulin resistance: just say iNOS. *Diabetes* 2013; **62**: 346-348 [PMID: 23349542 DOI: 10.2337/db12-1239]

36 **Snyder HS**, Sakaan SA, March KL, Siddique O, Cholankeril R, Cummings CD, Gadiparthi C, Satapathy SK, Ahmed A, Cholankeril G. Non-alcoholic Fatty Liver Disease: A Review of Anti-diabetic Pharmacologic Therapies. *J Clin Transl Hepatol* 2018; **6**: 168-174 [PMID: 29951362 DOI: 10.14218/JCTH.2017.00050]

37 **Chao EC**. SGLT-2 Inhibitors: A New Mechanism for Glycemic Control. *Clin Diabetes* 2014; **32**: 4-11 [PMID: 26246672 DOI: 10.2337/diaclin.32.1.4]

38 **Terami N**, Ogawa D, Tachibana H, Hatanaka T, Wada J, Nakatsuka A, Eguchi J, Horiguchi CS, Nishii N, Yamada H, Takei K, Makino H. Long-term treatment with the sodium glucose cotransporter 2 inhibitor, dapagliflozin, ameliorates glucose homeostasis and diabetic nephropathy in db/db mice. *PLoS One* 2014; **9**: e100777 [PMID: 24960177 DOI: 10.1371/journal.pone.0100777]

39 **Scheen AJ**. Effect of sodium-glucose cotransporter type 2 inhibitors on liver fat in patients with type 2 diabetes: hepatic beyond cardiovascular and renal protection? *Ann Transl Med* 2018; **6**: S68 [PMID: 30613643 DOI: 10.21037/atm.2018.10.39]

40 **Arai T**, Atsukawa M, Tsubota A, Mikami S, Ono H, Kawano T, Yoshida Y, Tanabe T, Okubo T, Hayama K, Nakagawa-Iwashita A, Itokawa N, Kondo C, Kaneko K, Emoto N, Nagao M, Inagaki K, Fukuda I, Sugihara H, Iwakiri K. Effect of sodium-glucose cotransporter 2 inhibitor in patients with non-alcoholic fatty liver disease and type 2 diabetes mellitus: a propensity score-matched analysis of real-world data. *Ther Adv Endocrinol Metab* 2021; **12**: 20420188211000243 [PMID: 33815743 DOI: 10.1177/20420188211000243]

41 **Musso G**, Cassader M, Paschetta E, Gambino R. Thiazolidinediones and Advanced Liver Fibrosis in Nonalcoholic Steatohepatitis: A Meta-analysis. *JAMA Intern Med* 2017; **177**: 633-640 [PMID: 28241279 DOI: 10.1001/jamainternmed.2016.9607]

42 **Lv X**, Dong Y, Hu L, Lu F, Zhou C, Qin S. Glucagon-like peptide-1 receptor agonists (GLP-1 RAs) for the management of nonalcoholic fatty liver disease (NAFLD): A systematic review. *Endocrinol Diabetes Metab* 2020; **3**: e00163 [PMID: 32704576 DOI: 10.1002/edm2.163]

43 **Ito D**, Shimizu S, Inoue K, Saito D, Yanagisawa M, Inukai K, Akiyama Y, Morimoto Y, Noda M, Shimada A. Comparison of Ipragliflozin and Pioglitazone Effects on Nonalcoholic Fatty Liver Disease in Patients With Type 2 Diabetes: A Randomized, 24-Week, Open-Label, Active-Controlled Trial. *Diabetes Care* 2017; **40**: 1364-1372 [PMID: 28751548 DOI: 10.2337/dc17-0518]

44 **Cefalu WT**, Leiter LA, Yoon KH, Arias P, Niskanen L, Xie J, Balis DA, Canovatchel W, Meininger G. Efficacy and safety of canagliflozin *vs* glimepiride in patients with type 2 diabetes inadequately controlled with metformin (CANTATA-SU): 52 wk results from a randomised, double-blind, phase 3 non-inferiority trial. *Lancet* 2013; **382**: 941-950 [PMID: 23850055 DOI: 10.1016/S0140-6736(13)60683-2]

45 **Kuchay MS**, Krishan S, Mishra SK, Farooqui KJ, Singh MK, Wasir JS, Bansal B, Kaur P, Jevalikar G, Gill HK, Choudhary NS, Mithal A. Effect of Empagliflozin on Liver Fat in Patients With Type 2 Diabetes and Nonalcoholic Fatty Liver Disease: A Randomized Controlled Trial (E-LIFT Trial). *Diabetes Care* 2018; **41**: 1801-1808 [PMID: 29895557

DOI: 10.2337/dc18-0165]
46 **Lee PCH**, Gu Y, Yeung MY, Fong CHY, Woo YC, Chow WS, Tan K, Lam KSL. Dapagliflozin and Empagliflozin Ameliorate Hepatic Dysfunction Among Chinese Subjects with Diabetes in Part Through Glycemic Improvement: A Single-Center, Retrospective, Observational Study. *Diabetes Ther* 2018; **9**: 285-295 [PMID: 29322486 DOI: 10.1007/s13300-017-0355-3]
47 **Hannah WN Jr**, Harrison SA. Effect of Weight Loss, Diet, Exercise, and Bariatric Surgery on Nonalcoholic Fatty Liver Disease. *Clin Liver Dis* 2016; **20**: 339-350 [PMID: 27063273 DOI: 10.1016/j.cld.2015.10.008]
48 **Koutoukidis DA**, Koshiaris C, Henry JA, Noreik M, Morris E, Manoharan I, Tudor K, Bodenham E, Dunnigan A, Jebb SA, Aveyard P. The effect of the magnitude of weight loss on non-alcoholic fatty liver disease: A systematic review and meta-analysis. *Metabolism* 2021; **115**: 154455 [PMID: 33259835 DOI: 10.1016/j.metabol.2020.154455]
49 **Komiya C**, Tsuchiya K, Shiba K, Miyachi Y, Furuke S, Shimazu N, Yamaguchi S, Kanno K, Ogawa Y. Ipragliflozin Improves Hepatic Steatosis in Obese Mice and Liver Dysfunction in Type 2 Diabetic Patients Irrespective of Body Weight Reduction. *PLoS One* 2016; **11**: e0151511 [PMID: 26977813 DOI: 10.1371/journal.pone.0151511]
50 **Sattar N**, Fitchett D, Hantel S, George JT, Zinman B. Empagliflozin is associated with improvements in liver enzymes potentially consistent with reductions in liver fat: results from randomised trials including the EMPA-REG OUTCOME® trial. *Diabetologia* 2018; **61**: 2155-2163 [PMID: 30066148 DOI: 10.1007/s00125-018-4702-3]
51 **Mancini SJ**, Boyd D, Katwan OJ, Strembitska A, Almabrouk TA, Kennedy S, Palmer TM, Salt IP. Canagliflozin inhibits interleukin-1β-stimulated cytokine and chemokine secretion in vascular endothelial cells by AMP-activated protein kinase-dependent and -independent mechanisms. *Sci Rep* 2018; **8**: 5276 [PMID: 29588466 DOI: 10.1038/s41598-018-23420-4]
52 **Lee DM**, Battson ML, Jarrell DK, Hou S, Ecton KE, Weir TL, Gentile CL. SGLT2 inhibition *via* dapagliflozin improves generalized vascular dysfunction and alters the gut microbiota in type 2 diabetic mice. *Cardiovasc Diabetol* 2018; **17**: 62 [PMID: 29703207 DOI: 10.1186/s12933-018-0708-x]
53 **Sies H**. Oxidative stress: a concept in redox biology and medicine. *Redox Biol* 2015; **4**: 180-183 [PMID: 25588755 DOI: 10.1016/j.redox.2015.01.002]
54 **Chen Z**, Tian R, She Z, Cai J, Li H. Role of oxidative stress in the pathogenesis of nonalcoholic fatty liver disease. *Free Radic Biol Med* 2020; **152**: 116-141 [PMID: 32156524 DOI: 10.1016/j.freeradbiomed.2020.02.025]

World Journal of Gastroenterology

Submit a Manuscript: https://www.f6publishing.com

World J Gastroenterol 2022 July 14; 28(26): 3258-3273

DOI: 10.3748/wjg.v28.i26.3258

ISSN 1007-9327 (print) ISSN 2219-2840 (online)

SYSTEMATIC REVIEWS

Endoscopic techniques for diagnosis and treatment of gastro-entero-pancreatic neuroendocrine neoplasms: Where we are

Roberta Elisa Rossi, Alessandra Elvevi, Camilla Gallo, Andrea Palermo, Pietro Invernizzi, Sara Massironi

Specialty type: Gastroenterology and hepatology

Provenance and peer review: Invited article; Externally peer reviewed.

Peer-review model: Single blind

Peer-review report's scientific quality classification

Grade A (Excellent): A
Grade B (Very good): B
Grade C (Good): 0
Grade D (Fair): 0
Grade E (Poor): 0

P-Reviewer: Batyrbekov K, Kazakhstan; Poddymova AV, Russia

Received: October 27, 2021
Peer-review started: October 27, 2021
First decision: December 27, 2021
Revised: January 4, 2022
Accepted: April 15, 2022
Article in press: April 15, 2022
Published online: July 14, 2022

Roberta Elisa Rossi, HPB Surgery, Hepatology and Liver Transplantation, ENETS Center of Excellence, Fondazione IRCCS Istituto Nazionale Tumori (INT, National Cancer Institute), Milan 20133, Italy

Alessandra Elvevi, Camilla Gallo, Andrea Palermo, Pietro Invernizzi, Sara Massironi, Division of Gastroenterology and Center for Autoimmune Liver Diseases, Department of Medicine and Surgery, University of Milano-Bicocca, Monza 20900, Italy

Corresponding author: Roberta Elisa Rossi, MD, PhD, Doctor, HPB Surgery, Hepatology and Liver Transplantation, ENETS Center of Excellence, Fondazione IRCCS Istituto Nazionale Tumori (INT, National Cancer Institute), Via G. Venezian 1, Milan 20133, Italy.
robertaelisa.rossi@gmail.com

Abstract

BACKGROUND

The correct localization of the primary tumor site and a complete histological diagnosis represent the milestones for the proper management of gastro-entero-pancreatic neuroendocrine neoplasms (GEP-NENs).

AIM

To analyze current evidence on the role of endoscopy in the diagnosis/treatment of GEP-NENs.

METHODS

An extensive bibliographical search was performed in PubMed to identify guidelines and primary literature (retrospective and prospective studies, systematic reviews, case series) published in the last 15 years, using both medical subject heading (MeSH) terms and free-language keywords: gastro-entero-pancreatic neuroendocrine neoplasms; endoscopy; ultrasound endoscopy; capsule endoscopy; double-balloon enteroscopy; diagnosis; therapy; staging.

RESULTS

In the diagnostic setting, endoscopic ultrasonography (EUS) represents the diagnostic gold standard for pancreatic NENs and the technique of choice for the locoregional staging of gastric, duodenal and rectal NENs. The diagnosis of small bowel NENs (sbNENs) has been improved with the advent of video capsule endoscopy and double-balloon enteroscopy, which allow for direct visualization of the entire small bowel; however, data regarding the efficacy/safety of these techniques in the detection of sbNENs are scanty and often inconclusive. From a

therapeutic point of view, endoscopic removal is the treatment of choice for the majority of gastric NENs (type 1/2), for well-differentiated localized nonmetastatic duodenal NENs < 1 cm, confined to the submucosa layer and for < 10 mm, stage T1–T2, rectal NENs. EUS-guided pancreatic locoregional ablative treatments have been proposed in recent studies with promising results in order to control symptoms or reduce tumor burden in selected patients.

CONCLUSION

Standard axial endoscopy and EUS still play a pivotal role in several GEP-NENs. Advanced techniques for increasing the rate of R0 resection should be reserved for high-volume referral centers.

Key Words: Gastro-entero-pancreatic neuroendocrine neoplasms; Endoscopy; Ultrasound endoscopy; Capsule endoscopy; Double-balloon enteroscopy; Diagnosis; Therapy; Staging

©The Author(s) 2022. Published by Baishideng Publishing Group Inc. All rights reserved.

Core tip: Standard axial endoscopy and endoscopic ultrasonography (EUS) play a pivotal role in gastro-entero-pancreatic neuroendocrine neoplasms (GEP-NENs). Upper/lower gastrointestinal endoscopy is essential for the detection of gastrointestinal NENs. EUS represents the diagnostic gold standard for pancreatic NENs and the technique of choice for the locoregional staging of gastric, duodenal and rectal NENs. The diagnosis of small bowel NENs has been improved with the advent of capsule endoscopy and double-balloon enteroscopy, however, their use is limited in clinical practice. In selected localized GEP-NENs, endoscopic therapy is appropriate with radical intent. The multidisciplinary management and the referral to high-volume tertiary centers remain fundamental.

Citation: Rossi RE, Elvevi A, Gallo C, Palermo A, Invernizzi P, Massironi S. Endoscopic techniques for diagnosis and treatment of gastro-entero-pancreatic neuroendocrine neoplasms: Where we are. *World J Gastroenterol* 2022; 28(26): 3258-3273

URL: https://www.wjgnet.com/1007-9327/full/v28/i26/3258.htm

DOI: https://dx.doi.org/10.3748/wjg.v28.i26.3258

INTRODUCTION

Gastro-entero-pancreatic neuroendocrine neoplasms (GEP-NENs) represent heterogeneous and rare tumors, whose incidence has been progressively increased in the last decades[1]. The prognosis of these neoplasms is widely variable depending on several factors including the site of the primary tumor, the grading as assessed by the specific WHO classification, and the stage as classified in a specific TNM system[2]. It is therefore clear that the correct localization of the primary tumor site, as well as a complete histologic diagnosis, represent the milestones for the proper management and the prognosis of these tumors[3-5].

In this scenario, despite advances in radiological and metabolic imaging, standard axial endoscopy and endoscopic ultrasonography (EUS) still play a pivotal role in several GEP-NENs. Upper gastrointestinal (GI) endoscopy is essential for the detection and characterization of esophageal, gastric, and duodenal NENs. Ileocolonoscopy allows the assessing and diagnosing of rectal, colonic and rarely distal ileal lesions. Small bowel NENs have proven difficult to diagnose, given their nonspecific presentation and poor accessibility of the distal small bowel to common endoscopic techniques. The diagnosis of small bowel NENs (sbNENs) has been largely improved with the advent of video capsule endoscopy (CE) in 2000 and double-balloon enteroscopy (DBE), the most promising device-assisted enteroscopy (DAE) system, in 2001, which allow for direct visualization of the entire Sb[6]. Finally, EUS is the modality of choice for both diagnosing pancreatic NENs and for the locoregional staging of several NENs, including gastric, duodenal, pancreatic and rectal NENs; of note, in the setting of pancreatic NENs (panNENs), it has demonstrated higher accuracy in tumor detection than other imaging modalities[7].

The present review is aimed at analyzing current evidence on the role of endoscopy in the management of GEP-NENs, with a specific focus on CE and DBE for sbNENs and EUS for the diagnosis and staging of panNENs and other NENs. Furthermore, we summarized available evidence on the role of endoscopy in the radical treatment of selected GEP-NENs.

MATERIALS AND METHODS

An extensive bibliographical search was performed in PubMed to identify guidelines and primary literature (retrospective and prospective studies, systematic reviews, case series) published in the last 15 years, using both medical subject heading (MeSH) terms and free-language keywords: gastro-entero-pancreatic neuroendocrine neoplasms; endoscopy; ultrasound endoscopy; capsule endoscopy; double-balloon enteroscopy; diagnosis; therapy; staging. The reference lists from the studies returned by the electronic search were manually searched to identify further relevant reports. The reference lists from all available review articles, primary studies, and proceedings of major meetings were also considered. Articles published as abstracts were included, whereas non-English language papers were excluded.

RESULTS

A total of 448 records were reviewed and 84 were defined as fulfilling the criteria for final consideration. Figure 1 presents the flow chart showing the process of study selection.

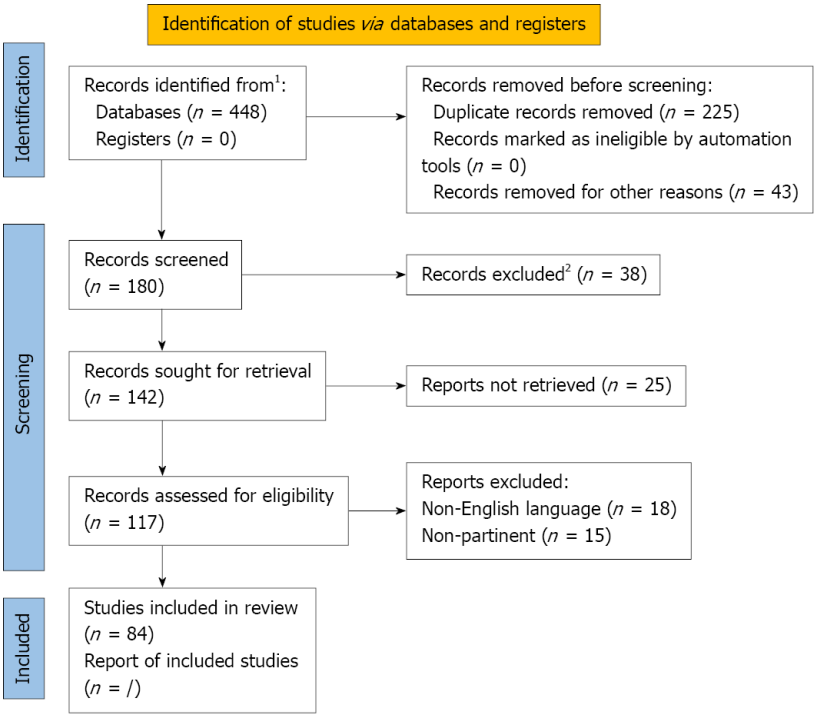
DIAGNOSIS

Ultrasound endoscopy (EUS)

EUS represents the diagnostic gold standard for panNENs and the technique of choice for the locoregional staging of gastric, duodenal and rectal NENs. According to the latest European Neuroendocrine Tumor Society (ENETS) Consensus guidelines, EUS proved to be the most accurate diagnostic technique in panNENs detection, leading to an up-to-94% sensitivity[8]; PanNENs usually appear rounded and homogeneously hypoechoic at EUS examination (Figure 2). EUS sensitivity in detecting panNENs is even higher than noninvasive computed tomography (CT)-scan or magnetic resonance imaging (MRI) pancreatic lesion detection rate[9]. EUS is also extremely accurate in locating the lesions, even very small ones, within the pancreatic parenchyma, and it can describe the distance between the lesion and the main pancreatic duct, which represents an independent predictor of aggressive tumor behavior and of developing pancreatic fistulas[10]. EUS overall complication rate is about 1%–2%, higher for pancreatic cysts rather than for solid masses[11].

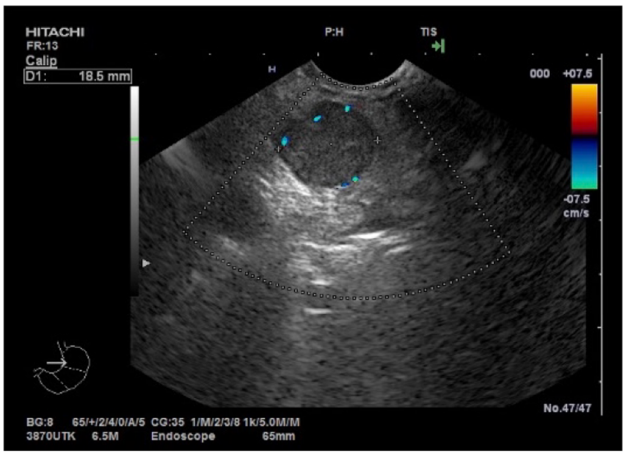
Advanced EUS techniques allow to study specific morphological and histological details of the detected lesions that may be helpful in the differential diagnosis of panNENs and in the choice of the corresponding best-suited treatment[7]. Contrast-enhanced harmonic EUS (CH-EUS) allows real-time visualization of parenchymal perfusion and, thus, helps in distinguishing hypovascular carcinomas from hypervascular less aggressive lesions. It consists of harmonic detectors that register microbubbles produced by contrast agents administrated intravenously; this method allows the identification of microvessels even with slow blood flow[12]. As demonstrated for nonfunctioning panNENs, the CH-EUS vascular pattern of neuroendocrine lesions represents an indirect reliable surrogate predictor of their aggressiveness and, thus, of their prognosis; a statistically significant positive correlation was, in fact, proven between the inhomogeneous sonographic pattern of the lesions and their Ki67 proliferative index, which in turn represents the most reliable independent predictor of malignancy. Sonographic heterogeneity at CH-EUS, and especially hypoenhancement in the early arterial phase, corresponds to lower intratumoral microvascular density and to a greater degree of fibrosis on pathological specimens, which were demonstrated to be typical features of tumor aggressiveness on a par with tumor grading [13]. According to a Japanese retrospective study[14], hypoenhancement at CH-EUS proved to be a reliable predictor of tumor aggressiveness and poor prognosis also for G1 and G2 panNENs, with sensitivity, specificity, positive predictive value, negative predictive value and accuracy of 94.7%, 100%, 100%, 96.6% and 97.9%, respectively.

EUS-fine needle aspiration (FNA) is another diagnostic advanced EUS technique, which represents the gold standard least invasive option to obtain the histological identification of a suspected pancreatic neoplasm or peripancreatic lymph nodes, with a sensitivity ranging between 80% and 90% and a specificity of nearly 96%[15] (Figure 3). It is also the operative technique of choice to aspirate the contents of cystic lesions for serological analysis and for the tumor marker dosage, which might help in the differential diagnosis of pancreatic cystic lesions. It can be performed with different diameter needles, mainly depending on the type and site of the lesion, its consistency, and echogenicity. There are several techniques described, which make different use of the suction: some of them suggest not to apply any suction due to the high risk of contaminating the specimen with blood (especially in case of highly vascularized lesions), some others apply wet or dry negative-pressure suction to guarantee sufficient material for histological diagnosis, and others again proposed a slow-pull fanning technique to ensure at the same time a greater collection of pathological cells and a low blood contamination risk [16]; to date, even if still no consensus has been reached on the optimal strategy, overall FNA–EUS sampling adequacy rates up to 94%[17,18] and its diagnostic sensitivity proved to be significantly higher



DOI: 10.3748/wjg.v28.i26.3258 **Copyright** ©The Author(s) 2022.

Figure 1 The flow chart showing the process of study selection.



DOI: 10.3748/wjg.v28.i26.3258 **Copyright** ©The Author(s) 2022.

Figure 2 Endoscopic appearance at endoscopic ultrasound of a pancreatic neuroendocrine neoplasm with marginal vascularization.

than CT and/or MRI specifically in case of solid, cystic and combined solid-cystic panNENs (84% *vs* 42%, 70% *vs* 10% and 81% *vs* 36% respectively)[19].

The Ki-67 index histological expression of the suspected pancreatic lesion plays a fundamental role in defining the aggressiveness of the tumor, together with its radiological aspect, its localization and distance from the pancreatic duct, and its CH-EUS vascular behavior. Therefore, the Ki-67 index also drives the choice of the best-suited therapeutic approach. Data about the concordance rate between EUS–FNA and surgical specimens in terms of G1, G2 or G3 panNEN and G3 pan-neuroendocrine carcinoma differentiation based on the Ki-67 index are discordant, ranging from a 78% of accordance rate (k-statistic: 0.65)[10], to a relatively significant discrepancy, especially for G2 lesions[20]. This discordance may be first attributed to the fact that endoscopic sampling of large lesions > 20 mm, often included in the studies available to date, may not be representative of the area with the highest concentration of malignant cells and, thus, that the measured Ki-67 index might be not indicative of the most proliferative area of the neoplasm. There is a strong necessity for further studies that subclassify more accurately the included lesions depending on their size.



DOI: 10.3748/wjg.v28.i26.3258 **Copyright** ©The Author(s) 2022.

Figure 3 Endoscopic appearance at endoscopic ultrasound of a pancreatic neuroendocrine neoplasm located at the tail of the pancreas during fine needle aspiration/biopsy procedure.

New EUS needle acquisition techniques (*i.e.*, 19/22/25- G ProCoreTM needle, Cook Endoscopy, Winston-Salem, NC, USA; 19-G fine-needle biopsy, Cook Endoscopy Inc., Limerick, Ireland; Acquire® Endoscopic Ultrasound Fine Needle Biopsy (FNB) Device 22/25-G, Boston Scientific, Natick, MA, USA; SharkCoreTM, Covidien, Dublin, Ireland) have been proposed to overcome the rare cases of EUS–FNA inadequate tissue sampling; these devices are designed to maximize tissue capture and minimize bleeding and tissue fragmentation and some of them are thought to provide both cytological and histological sampling[21]. However, further studies are needed to validate these approaches in the specific setting of NENs.

EUS real-time elastography (EUS–RTE) allows not only a qualitative but also a quantitative assessment of the elasticity of the suspected pancreatic lesion compared to the one of the normal surrounding pancreatic parenchyma. Based on the evidence of higher tissue stiffness in the case of malignant lesions when compared to the normal parenchyma[22], some authors have proposed different quantitative elastography cutoffs to stratify the risk of malignancy. Havre *et al*[23] observed a EUS–RTE sensitivity of 67% and specificity of 71% in detecting pancreatic malignant lesions with a strain ratio cutoff of 4.4. Iglesias-García *et al*[24] showed an EUS–RTE sensitivity of 100% and specificity of 88% in differentiating specifically pancreatic adenocarcinomas from panNENs with a 26.6 strain ratio cutoff value. Even if, according to the European Federation of Societies for Ultrasound in Medicine and Biology (EFSUMB) guidelines, EUS–RTE cannot yet replace the histo-cytopathological diagnosis of carcinoma[25], this technique may facilitate the differentiation from benign to malignant pancreatic lesions.

Another advanced technique in EUS that can drive in the diagnostic orientation is represented by the needle-based confocal laser endomicroscopy, which allows the real-time direct *in vivo* visualization of the histological aspect of the GI mucosa overlying pancreatic NENs, which is traditionally described as clusters of compact cells on a dark background surrounded by numerous small and irregular vessels and fibrotic areas[26]. Giovannini *et al*[27], observed a negative predictive value of 100% for the characterization of pancreatic NENs in EUS needle-based confocal laser endomicroscopy; therefore supporting the concept that it cannot be considered as an alternative to the histological diagnosis, but that it may help to rule out malignancy.

Further applications of EUS in panNENs is represented by the preoperative EUS-guided fine-needle tattooing and EUS-guided fiducial implantation, which may help surgeons find little pancreatic lesions during laparoscopic surgery, limiting the laparoscopic resection to the lesion itself, sparing the normal surrounding parenchyma, and reducing the operating time[28].

As regards GI-NENs, EUS mainly plays a diagnostic and staging role; its sensitivity in detecting GI-NENs is up to 94%[29]; they usually appear as submucosal rounded, hypoechoic, well-demarcated lesions and can be detected when smaller than 10 mm, especially rectal NENs thanks to the growing sensibility to colorectal carcinoma screening. According to the ENETS most recent guidelines, in case of the endoscopic identification of a GI lesion that is compatible with a GI-NEN, EUS is recommended in case of lesions > 10 mm in order to study the depth of the lesion, to stage the hypothetical presence of locoregional lymph nodes and, thus, to drive the choice of the most appropriate endoscopic or surgical treatment[30]. Less than 10 mm GI-NENs, in fact, have a low risk of both lymphatic invasion and distant metastases, which is reported to be 1%–2%[31]. GI-NENs measuring 10–19 mm at their first endoscopic diagnosis deserve more accurate EUS evaluation because of the reported higher incidence rate of lymph node invasion or distant metastases, leading up to 5%–15%[32]. If the GI-NEN is limited to the submucosa and does not invade the muscularis mucosae (which corresponds to a T1 lesion), regardless of its lateral spreading, a simple *en bloc* endoscopic resection treatment has proved to be effective in

guaranteeing a radical resection and a very limited recurrence rate during the follow-up[33], otherwise, a surgical approach is suggested. T2 or N+ stage lesions should be accurately studied with total body imaging such as 68-Ga-DOTATATE positron emission tomography (PET) and a CT scan in order to plan the best therapeutic approach.

Capsule Endoscopy (CE) and Double-balloon enteroscopy (DBE)

The small intestine is the most common NEN site in humans. Historically, sbNENs have proved difficult to diagnose because of both the lack of specific symptoms at presentation and the poor accessibility of the distal small bowel[34]. Conventional radiology (both CT and MRI either in the standard technique or in combination with enteroclysis) are often not accurate enough in the detection of sbNENs [35], whereas PET/CT with 68Ga-DOTA peptides remains the most sensitive modality in the detection of well-differentiated NENs, although it does not allow to get a histological diagnosis and might not be fully accurate in the anatomical location of the primary tumor being, for instance, unable to differentiate between intestinal and mesenteric localization[36]. Furthermore, in the case of metastatic disease, the detection of the primary tumor is recommended in both resectable and non resectable diseases. However, in up to 10% of the cases after the discovery of liver or lymph node metastases, the primary tumor site remains unknown despite an extensive workup[35].

With the advent of CE and DBE the diagnosis of sbNENs has improved, even if data regarding the efficacy and safety of these techniques in the detection of sbNENs are scanty and mainly based on small retrospective series, given the rarity of the disease and the still-limited use of these techniques in routine clinical practice. Most of the available studies are focused on small bowel tumors in general and only a small percentage of included patients displayed an sbNEN[37-39]. In a study comparing CT, enteroclysis, nuclear imaging, and CE of the small bowel[34], CE showed a high diagnostic yield (45%) in identifying primary tumors. Of note, in 12 of 20 patients (60%), CE showed small-intestinal lesions that were then confirmed histologically as NEN in six of seven patients who underwent surgery.

When considering the few studies specifically focused on NENs, the results came back to be inconclusive. In a retrospective study by Frilling *et al*[40], including 390 patients with metastatic NENs of whom 11 with unknown primary tumor, CE identified lesions suggestive of small bowel primary in 8/10 patients in whom it was successful, and these tumors were all histologically confirmed. In a recent prospective study[41], the diagnostic yield of CE was reported to be limited. In 24 patients with a histological diagnosis of metastatic NEN of unknown origin, CE, which was preferred to DBE as less invasive and less expensive, was requested before explorative laparotomy and its diagnostic yield was compared to the surgical exploration. CE identified a primary sbNEN in 11 subjects. However, diagnosis of sbNEN was confirmed only in five (41%) cases after surgical and ultrasound exploration were performed. The high number of false-positive results could have been related to small bowel contractions, extrinsic compression, lymph stasis, or submucosal lesion of another type.

Although CE is less invasive, DBE is necessary for determining the precise location, number of tumors, and pathological diagnosis; it can be carried out through the oral (antegrade) or the anal (retrograde) route and with a combined oral and anal approach[42]. Bellutti *et al*[43], in a study involving 12 consecutive patients with suspected sbNEN or with liver NEN metastases, who underwent DBE, found a diagnostic yield of DBE for primary tumor of 33%. In a case series by Scherubl *et al*[44], five consecutive patients with metastatic midgut carcinoids underwent DBE and an NEN of the ileum was detected in four of the five patients; the histopathological evaluation of their biopsy specimens confirmed the diagnosis revealing well-differentiated NENs. Conversely, conventional radiological imaging did not visualize any of the primary tumors.

In our recent prospective study[45], we reported sensitivity and specificity of 60% and 100%, respectively for DBE in detecting sbNEN in six patients with unknown primary, showing that DBE is a safe and effective procedure in diagnosing sbNENs. We suggested that when a sbNEN is suspected, DBE should be taken into account as an accurate diagnostic tool in order both to collect biopsies for final diagnosis and to make tattoos before surgery; of note, DBE should be preferred over CE in the presurgical setting given the high specificity. Considering the limited available data, further studies are needed to better define the actual role of CE and DBE in the diagnosis of sbNENs.

TREATMENT

Gastric NENs

Gastric NENs (gNENs) are usually subclassified into three types, according to their pathophysiology and behavior[29,46]. Type I tumors correspond to the majority of gNENs (~80%) and are associated with autoimmune atrophic gastritis. Histologically, type I gNENs are composed of enterochromaffin-like cells. The diagnosis is made by upper digestive endoscopy with biopsy. The majority of type I gNENs present as small, multiple tumors, located in the gastric body or fundus, and limited to the mucosal or submucosal layers of the stomach wall[46,47]. Since the risk of metastasis is < 5% in type I gNENs, a conservative approach based on endoscopic follow-up with lesion resection is advised for this kind of tumor. The treatment of choice for type I gNENs is endoscopic resection for lesions > 0.5 cm and

endoscopic surveillance for lesions < 0.5 cm[46,48,49]. This approach has been shown to be safe and effective in a prospective series of 33 type I gNENs, with no significant procedure-related complications, no development of metastases, and a 100% long-term survival rate[50].

The ENETS guidelines[29] suggest performing EUS in case of lesions > 1 cm. Staging EUS is frequently performed to confirm the appropriateness of endoscopic resection, which applies to lesions not infiltrating beyond the muscularis propria[7]. For lesions > 1 cm, EUS is excellent for determining the exact tumor size and for excluding infiltration of the type I gNENs into the muscularis propria (T2) or enlarged regional lymph nodes[47,51].

Type II gNENs correspond to 5%–10% of gNENs; they usually develop when multiple endocrine neoplasia type 1 is present and are often associated with Zollinger–Ellison syndrome[46,48]. Like type I gNENs, type II gNENs originate from enterochromaffin-like cells. They are small, multiple, and relatively benign tumors, even though about 10%–30% of patients present as metastatic at the diagnosis [52]. For type II gNENs local excision is recommended, preferentially by endoscopy; as well as for type I gNENs, EUS plays a pivotal role in determining the tumor size, lymph node involvement, and depth of invasion; endoscopic treatment is again reserved for lesions not infiltrating beyond the muscularis propria, without lymph node involvement[7,53].

Type III gastric NENs are usually larger sporadic tumors with an infiltrative and metastatic tendency and account for 15% of all gNENs. They are generally characterized by being single lesions, > 1 cm and with a greater likelihood of evolving to regional and systemic metastases, as more than half of patients with type III gNENs are metastatic at diagnosis, mainly to the liver[46,48]. From a therapeutic point of view, surgery is the standard treatment, *i.e.*, total or subtotal gastrectomy together with lymphadenectomy, as recommended in gastric adenocarcinoma. For patients with any surgical contraindication, endoscopic resection may be an alternative, but the risk of regional lymph node spread remains high [46]. Of note, in selected cases of small (< 1 cm) type III G1/G2 (Ki-67 < 5%) gNENs fully resected (R0) by endoscopy with no risk factors for metastatic disease, endoscopic resection might be sufficient[54]. As for other gNENs, EUS is a useful tool for locoregional staging, particularly to stage the disease by assessing the presence of regional lymph node involvement.

Conventional polypectomy with a snare for flat mucosal lesions should be avoided because complete resection is often not achieved. Early gNENs are generally removed by endoscopic mucosal resection (EMR) or endoscopic submucosal dissection (ESD)[47,54]. In EMR, snare resection is preceded by the submucosal injection of saline in order to raise the tumor and cut into the submucosa below the tumor [47]. ESD is preferred over EMR in case of suspicion of limited submucosal invasion or a tumor > 2 cm [55]. After submucosal injection of saline, the submucosa is dissected with specific knives in order to achieve endoscopic *en bloc* resection of the whole neoplasm.

The resected specimen has to be carefully evaluated regarding grade, angioinvasion, and infiltration of the deep resection margin. In case of angioinvasion, histological infiltration of the muscularis propria (T2), or grade G2/G3, radicalization with surgery with lymph node dissection is the therapy of choice in localized neuroendocrine disease[47].

Duodenal NENs

Duodenal NENs (dNENs) are rare, usually small well-differentiated tumors in most of the cases; however, according to a recent multicenter retrospective study[56], dNENs' prognosis may be highly variable as these tumors can be metastatic in up to 50% of the cases at the time of first diagnosis and can develop metastases thereafter. Upper GI endoscopy with biopsy is necessary for dNEN diagnosis and EUS should be performed to assess the local extent of tumor depth.

In view of this heterogeneous behavior, surgical resection has been suggested as the preferred treatment modality over endoscopic treatment, and surgery is generally recommended for ampullary dNENs and lesions > 2 cm in size[38]. Endoscopic resection is the treatment of choice for well-differentiated localized nonmetastatic tumors with a diameter < 1 cm and confined to the submucosa layer and the rationale for preferring the endoscopic treatment for tumors < 1 cm relies on the fact that they seem to have a low rate of nodal disease[57]. In this setting, there is no current evidence to prefer an endoscopic approach over another as prospective studies comparing the available techniques (*i.e.*, ESD *vs* EMR) are lacking.

However, there is still controversy regarding the management of tumors between 1 and 2 cm, which is mainly based on the tumor location and the presence of nodal involvement on imaging. According to some authors, > 10% of patients with dNENs < 1 cm in size develop lymph node metastases, thus suggesting the need for a radical surgical approach for all dNENs despite the size of the primary tumor [58-60]. Another issue to be taken into account is the high risk of conventional and functional imaging of understaging mainly due to the presence of nodal and distant micrometastases[60]. These results represent a sign of warning for conservative approaches including endoscopy, suggesting as a possible strategy, the inclusion of EUS in the preoperative phase, although prospective studies are necessary to draw solid conclusions.

In summary, all considered, endoscopic resection either EMR or ESD should be reserved for dNENs < 10 mm, limited to the submucosal layer without evidence of lymph node or distant metastases, whereas surgery might be advised for dNENs > 10 mm with evidence of muscular layer invasion or nodal involvement. EUS should be encouraged for all dNENs in order to plan the best therapeutic approach.

Rectal NENs

Endoscopic treatment for rectal NENs (rNENs) is indicated if there is no evidence of invasion beyond submucosa and presence of locoregional disease since it aims to achieve a complete oncological resection[61].

The ENETS guidelines[30] suggest that well-differentiated (G1/G2) rNENs that are < 10 mm in stage T1 and T2 and rNENs between 10 and 20 mm in stage T1 without lymph node metastasis should be removed endoscopically. On the contrary, surgical resection is indicated in cases of G3 rNENs, 10–19 mm with muscolaris propria invasion (stage T2) and for tumors > 20 mm and/or in presence of lymph node metastases.

Endoscopic techniques for treating rNENs include standard polypectomy, EMR, modified EMR, ESD, and endoscopic full-thickness resection (EFTR). Standard polypectomy does not offer an adequate and complete resection of the lesion; therefore, it is not indicated in rNEN treatment[62]. Of note, a large number of rNENs is still removed by an improper method, such as routine snare polypectomy, during colorectal cancer screening making management more complex and putting patients at risk of metastatic spread[63].

EMR is largely used in the resection of small and superficial neoplasia confined to the mucosa and submucosal layer, but its application in rNENs is still debated since modified EMR and ESD are superior in terms of *en bloc* resection rate and histological complete resection rate (defined as *en bloc* resection with no margin involved)[64,65].

Recently, Park *et al*[66] observed that when EMR is performed underwater, the histological complete resection rate of NENs < 10 mm is similar to that for ESD (86.1% *vs* 86.1%, respectively) but with a shorter procedure time (5.8 ± 2.9 *vs* 26.6 ±13.4 min, respectively).

EMR performed with a dual-channel endoscope allows deeper resection compared to conventional EMR by lifting the lesion with forceps. Lee *et al*[67] observed that dual-channel EMR reaches a complete histological resection rate similar to that of ESD for rNENs < 16 mm (86.3 *vs* 88.4 %, respectively), but with a shorter procedure time (9.75 ± 7.11 *vs* 22.38 ± 7.56 min, respectively) and fewer complications.

Modified EMR techniques include the use of special devices that allow better resection of the tumor. EMR after circumferential precutting (EMR-P) is performed by lifting the submucosal with saline injection, precutting using the tip of the snare or special endoknife and resecting the tumor with a snare. Cap-assisted EMR (EMR-C) is performed by lifting the mucosa with saline injection, suctioning the lesion with a transparent cap fitted to the scope and then removing it with a snare looped along the ridge of the cap. EMR with a ligation device (EMR-L) is conducted by lifting the lesion with saline injection, deploying an elastic band around its base, and resecting with a snare. Histological complete resection rate for EMR-P is superior to EMR and no difference was found between EMR-P and the other modified EMR techniques, even if it required a longer procedure time[68]. Park *et al*[69] demonstrated that EMR-C is a safe and effective technique for rNENs, with a histological complete resection rate even better than that of ESD (92.3% *vs* 78.4%, respectively).

EMR-L is only applicable for tumors of < 10 mm due to the short diameter of the caps fitted to colonoscopes, but it is significantly superior to EMR in terms of complete resection of rNENs (93.3% *vs* 65.5%, respectively), regardless of the tumor location[70]. Histological complete resection rate is similar between EMR-C and EMR-L. However, Lee *et al*[71] demonstrated that EMR-L might be preferable for achieving a higher rate of *en bloc* resection (100% *vs* 92.9%, respectively), but this could be due to the fact that the band thickness used in EMR-L is larger than the snare thickness of EMR-C.

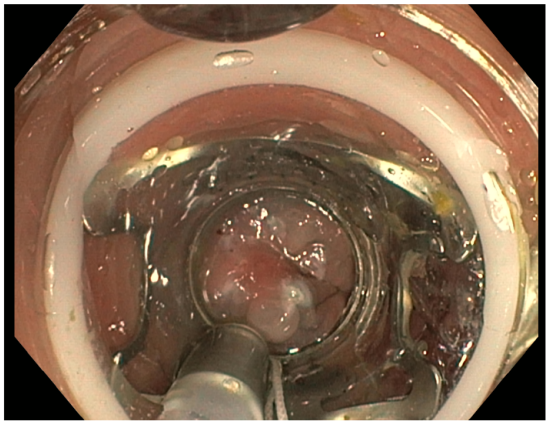
ESD is an interventional procedure suitable for *en bloc* resection of slightly invasive GI lesions. After injection of the submucosal with a viscous solution, an endoknife is used to incise the mucosa surrounding the lesion and to dissect it from the submucosal layer. ESD is an effective technique to treat rectal lesions, even if it is associated with a high risk of complications and a long procedure time. As it concerns rNENs, ESD has been demonstrated to be superior to EMR in terms of histological complete resection rate, but there are no significant differences between ESD and modified EMR[70].

Niimi *et al*[72] observed that ESD is associated with a longer procedure time and hospitalization period compared with EMR-L, with a similar complete resection rate. In order to reduce procedure time, Wang *et al*[73] proposed a hybrid ESD, in which the mucosal incision is performed with a polypectomy snare instead of an endoknife. This technique showed a similar *en bloc* resection rate (99.2% *vs* 98.2) and complete resection rate (94.1% *vs* 90.9%) to ESD but with a shorter procedure time (13.2 ± 8.3 *vs* 18.1 ± 9.7 min).

EFTR is a technique mainly used in lesions that are difficult to resect and its application in rNENs has recently been proposed. A full-thickness resection device is fitted over the scope and, after placement of a modified over-the-scope-clip, allows a single step EFTR (Figure 4).

Meier *et al*[74] collected data on 40 EFTRs in rNENs and observed that resection was macroscopically and histologically complete in all cases without major events, but prospective comparative studies between different resection techniques are still missing.

To conclude, rNENs < 10 mm should be treated endoscopically, and EMR-L should be considered as the first-line treatment; ESD can be used as second-line therapy when EMR-L is not applicable. EFTR can be an effective and safe technique in lesions that are difficult to treat. Treatment of rNENs with a size of 10-19 mm should be chosen after assessing the stage and the grade of differentiation.



DOI: 10.3748/wjg.v28.i26.3258 **Copyright** ©The Author(s) 2022.

Figure 4 Over-the-scope clipping system for endoscopic full-thickness resection of a rectal neuroendocrine neoplasm.

pancreatic NENs

In recent years there has been a great development of EUS techniques, not only used as diagnostic, but also as therapeutic tools. These methods find application in the management of panNENs, given the direct approach to the pancreas through the echoendoscope. The incidentally discovered small panNENs, mainly nonfunctional, represent a therapeutic challenge because surgery could be very complex in the face of neoplasms with indolent biological behavior, and active surveillance may represent an option for G1 or low G2 neoplasms, asymptomatic, mainly localized in the head of the pancreas, without radiological signs suspicious for malignancy[8,75]. In this setting, however, EUS-guided pancreatic locoregional ablative treatments, using either ethanol injection or radiofrequency ablation, have been proposed in recent studies with promising results in order to control symptoms or reduce tumor burden in selected patients[76]. The thermoablative techniques are the most used, mainly the radiofrequency methods. EUS-guided radiofrequency ablation (RFA) is reported to be a potentially effective and safe treatment for Pan-NENs[77].

Several RFA devices for EUS-guided applications are currently available. The Habib EUS-guided RFA probe (EndoHPB, EMcision UK, London, UK) is a 1 Fr (0.33 mm), monopolar catheter, which can be inserted through a regular 19- or 22-gauge FNA needle and connected to a standard radiofrequency generator. The other systems are needle-electrodes, and the most commonly used in literature is the one from Taewoong Medical (EUSRA, Taewoong Medical Co. Ltd., Gimpo-si, Geyonggi-do, South Korea), an 18- or 19-gauge needle with a long electrode lacking insulation over the terminal tip, connected to a dedicated RF current source, and an inner cooling system that circulates chilled saline inside the needle to avoid tissue charring. Under the EUS guide, the needle is inserted into the target lesion that is being treated by using high-frequency alternating current, and the energy release is applied when the needle tip of the electrode is within the lesion, while maintaining a distance of at least 2 mm from the pancreatic and bile ducts and vessels, to avoid injury or duct strictures. A recent systematic literature review explored the feasibility, effectiveness, and safety of EUS–RFA in the treatment of panNENs[94]: 12 articles describing 61 patients and 73 panNENs were analyzed and the overall effectiveness of EUS–RFA resulted in 96% (75%–100%) without any difference between functional and nonfunctional panNENs and without relevant side effects (mild adverse events, AEs 13.7%)[78-81].

The same conclusions were also confirmed by a further systematic review which included 14 studies with a total of 158 patients with solid pancreatic tumors[82]. However, even if the results of these studies are encouraging, especially for nonfunctioning panNENs and insulinomas < 2 cm, EUS–RFA is a recent technique and long-term data are thus lacking[82]. Larger studies with longer follow-up are needed to evaluate the long-term effectiveness of EUS–RFA. The specific setting of patients and the actual indication for the radiofrequency has not been standardized.

As concerned EUS-guided ethanol injection for small panNENs, this option has been proposed and studied for the treatment of patients with small panNENs not suitable for surgery or who refused surgical approach. Using pure ethanol or ethanol–lipiodol emulsion, the complete ablation rate has been reported to be ~50% up to 80% by performing more sessions[83].

In view of these results, a study protocol for a multicenter prospective study has been published[84] and the results will become available in due time.

Finally, possible future intriguing perspectives can be represented by the application, also in panNENs, of the novel techniques of locoregional delivery of drugs, such as LOcal Drug EluteR [LODER(TM)] which is a novel biodegradable polymeric matrix that shields drugs. panNENs may be considered as a possible future field of application of locoregional radiotherapy by using fiducial markers implantation, similarly to other pancreatic cancers.

Table 1 Available endoscopic treatment options for gastro-entero-pancreatic neuroendocrine neoplasms

Primary site	Tumor characteristics	Endoscopic management
Stomach	Type I < 5 mm	Surveillance
	Type I ≥ 5 mm	Resection (EMR, ESD)
	Type II	
	Type III	Resection (EMR, ESD)[1]
	G1-G2	
	< 10 mm	
Duodenum	< 10 mm[2]	Resection (EMR, ESD)
	G1	
	No muscularis mucosae invasion	
	No periampullary	
Pancreas	≤ 20 mm	Surveillance; EUS-guided RFA; EUS-guided ethanol injection
	G1-low G2	
	Non-functioning	
	No bile/pancreatic duct compression	
	Functioning tumors, not suitable for surgery	EUS-guided ethanol injection
	The patient refuses the surgical approach	
Rectum	< 10 mm[3]	Resection (EMR, mEMR, ESD, EFTR)
	G1-G2	
	No muscularis mucosae invasion	

[1]Endoscopic resection of type III gastric NENs can be considered curative only in case of histological complete resection.
[2]There is still controversy regarding the management of duodenal NENs between 10 and 20 mm.
[3]Treatment of rectal NENs with a size of 10–19 mm should be chosen after assessing the stage and the grade of differentiation.
G: Grading according to WHO classification; EMR: Endoscopic mucosal resection; mEMR: Modified endoscopic mucosal resection; ESD: Endoscopic submucosal dissection; EFTR: Endoscopic full-thickness resection; EUS: Endoscopic ultrasound.

DISCUSSION

The incidence of GEP-NENs has hugely increased over the last decades mainly due to better disease knowledge and to an improvement in diagnostic techniques, including endoscopy. Standard axial endoscopy and EUS still play a pivotal role in several GEP-NENs. Upper GI endoscopy is essential for the detection and characterization of esophageal, gastric and duodenal NENs. EUS represents the diagnostic gold standard for panNENs and the technique of choice for the locoregional staging of gastric, duodenal and rectal NENs. Ileocolonoscopy allows the assessing and diagnosing of rectal, colonic and rarely distal ileal lesions. However, the diagnosis of sbNENs has been largely improved with the advent of CE and DBE, although data regarding the safety and efficacy of these techniques in the neuroendocrine setting are still scanty and their use is still limited in clinical practice. In terms of treatment, in selected localized GI-NENs with the absence of features associated with lymph node metastases, endoscopic therapy is generally an appropriate treatment with radical intent. In highly selected G1 or low G2 small neoplasms without radiological signs suspicious for malignancy EUS-guided pancreatic locoregional ablative treatments, using either ethanol injection or radiofrequency ablation, have been proposed in recent studies with promising results in order to control symptoms or reduce tumor burden. Table 1 summarizes available endoscopic treatment options for GEP-NENs.

CONCLUSION

In summary, endoscopy plays a key role for diagnosis and treatment of GEP-NENs. In selected localized GEP-NENs, endoscopic therapy is appropriate with radical intent. Advanced resection techniques aimed at increasing the rate of R0 resection should be reserved to high-volume referral centers. The multidisciplinary management remains the gold standard to offer the patient the best therapeutic

approach.

ARTICLE HIGHLIGHTS

Research background

The prognosis of gastro-entero-pancreatic neuroendocrine neoplasms (GEP-NENs) is widely variable depending on several factors including the site of the primary tumor, the grading, and the stage. The correct localization of the primary tumor site, as well as a complete histologic diagnosis, represent the milestones for the proper management and the prognosis of these tumors. Standard axial endoscopy and endoscopic ultrasonography (EUS) still play a pivotal role in several GEP-NENs.

Research motivation

The incidence of GEP-NENs has hugely increased over the last decades; given the well-known heterogeneity of these tumors and the lack of large prospective studies, there is an urgent need to standardize their management.

Research objectives

To analyze current evidence on the role of endoscopy in the management of GEP-NENs (both diagnosis and potential treatment). A specific focus will be reserved to capsule endoscopy, double-balloon enteroscopy and ultrasound endoscopy.

Research methods

An extensive bibliographical search was performed in PubMed to identify guidelines and primary literature (retrospective and prospective studies, systematic reviews, case series) published in the last 15 years, using both medical subject heading (MeSH) terms and free-language keywords: gastro-entero-pancreatic neuroendocrine neoplasms; endoscopy; ultrasound endoscopy; capsule endoscopy; double-balloon enteroscopy; diagnosis; therapy; staging.

Research results

EUS represents the diagnostic gold standard for pancreatic NENs (panNENs) and the technique of choice for the locoregional staging of gastric, duodenal and rectal NENs. EUS proved to be the most accurate diagnostic technique in panNEN detection. EUS–fine needle aspiration is a diagnostic advanced EUS technique, which represents the gold standard least invasive option to obtain the histological identification of a suspected pancreatic neoplasm or peripancreatic lymph node. The diagnosis of small bowel NENs (sbNENs) has been improved with the advent of capsule endoscopy (CE) and double-balloon enteroscopy (DBE), even if data regarding the efficacy and safety of these techniques in the detection of sbNENs are scanty and mainly based on small retrospective series, given the rarity of the disease and the still-limited use of these techniques in routine clinical practice. In selected localized gastrointestinal NENs with the absence of features associated with lymph node metastases, endoscopic therapy is generally an appropriate treatment with radical intent. In highly selected G1 or low G2 small neoplasms without radiological signs suspicious for malignancy EUS-guided pancreatic locoregional ablative treatments, using either ethanol injection or radiofrequency ablation, have been proposed in recent studies with promising results in order to control symptoms or reduce tumor burden.

Research conclusions

Endoscopy plays a key role in GEP-NENs for both the diagnosis and the treatment. In selected localized GEP-NENs, endoscopic therapy is appropriate with radical intent. The multidisciplinary management and the referral to high-volume tertiary centers remain fundamental.

Research perspectives

Further studies are needed: (1) To better define the actual role of CE and DBE in the diagnosis of sbNENs; and (2) To better analyze the possible role of endoscopic confocal laser endomicroscopy in the diagnosis of panNENs and radiofrequency ablation as a potential treatment. Possible future intriguing perspectives can be represented by the application, also in panNENs, of the novel techniques of locoregional delivery of drugs.

FOOTNOTES

Author contributions: Rossi RE designed the research; Rossi RE, Elvevi A, Gallo C, Palermo A, and Massironi S performed the literature search and wrote the first draft of the paper; Rossi RE, Invernizzi P and Massironi S

reviewed for important intellectual content; Rossi RE and Massironi S wrote the final version of the paper; all the authors approved it.

Conflict-of-interest statement: None.

PRISMA 2009 Checklist statement: The authors have read the PRISMA 2009 Checklist, and the manuscript was prepared and revised according to the PRISMA 2009 Checklist.

Open-Access: This article is an open-access article that was selected by an in-house editor and fully peer-reviewed by external reviewers. It is distributed in accordance with the Creative Commons Attribution NonCommercial (CC BY-NC 4.0) license, which permits others to distribute, remix, adapt, build upon this work non-commercially, and license their derivative works on different terms, provided the original work is properly cited and the use is non-commercial. See: https://creativecommons.org/Licenses/by-nc/4.0/

Country/Territory of origin: Italy

ORCID number: Roberta Elisa Rossi 0000-0003-4208-4372; Alessandra Elvevi 0000-0001-9841-2051; Camilla Gallo 0000-0002-7598-7220; Andrea Palermo 0000-0001-8057-9398; Pietro Invernizzi 0000-0003-3262-1998; Sara Massironi 0000-0003-3214-8192.

S-Editor: Wu YXJ
L-Editor: Kerr C
P-Editor: Wu YXJ

REFERENCES

1 **Dasari A**, Shen C, Halperin D, Zhao B, Zhou S, Xu Y, Shih T, Yao JC. Trends in the Incidence, Prevalence, and Survival Outcomes in Patients With Neuroendocrine Tumors in the United States. *JAMA Oncol* 2017; **3**: 1335-1342 [PMID: 28448665 DOI: 10.1001/jamaoncol.2017.0589]

2 **Rindi G**, Bordi C, La Rosa S, Solcia E, Delle Fave G; Gruppo Italiano Patologi Apparato Digerente (GIPAD); Società Italiana di Anatomia Patologica e Citopatologia Diagnostica/International Academy of Pathology, Italian division (SIAPEC/IAP). Gastroenteropancreatic (neuro)endocrine neoplasms: the histology report. *Dig Liver Dis* 2011; **43** Suppl 4: S356-S360 [PMID: 21459341 DOI: 10.1016/S1590-8658(11)60591-4]

3 **Rindi G**, Falconi M, Klersy C, Albarello L, Boninsegna L, Buchler MW, Capella C, Caplin M, Couvelard A, Doglioni C, Delle Fave G, Fischer L, Fusai G, de Herder WW, Jann H, Komminoth P, de Krijger RR, La Rosa S, Luong TV, Pape U, Perren A, Ruszniewski P, Scarpa A, Schmitt A, Solcia E, Wiedenmann B. TNM staging of neoplasms of the endocrine pancreas: results from a large international cohort study. *J Natl Cancer Inst* 2012; **104**: 764-777 [PMID: 22525418 DOI: 10.1093/jnci/djs208]

4 **Boninsegna L**, Panzuto F, Partelli S, Capelli P, Delle Fave G, Bettini R, Pederzoli P, Scarpa A, Falconi M. Malignant pancreatic neuroendocrine tumour: lymph node ratio and Ki67 are predictors of recurrence after curative resections. *Eur J Cancer* 2012; **48**: 1608-1615 [PMID: 22129889 DOI: 10.1016/j.ejca.2011.10.030]

5 **Panzuto F**, Boninsegna L, Fazio N, Campana D, Pia Brizzi M, Capurso G, Scarpa A, De Braud F, Dogliotti L, Tomassetti P, Delle Fave G, Falconi M. Metastatic and locally advanced pancreatic endocrine carcinomas: analysis of factors associated with disease progression. *J Clin Oncol* 2011; **29**: 2372-2377 [PMID: 21555696 DOI: 10.1200/JCO.2010.33.0688]

6 **Rossi RE**, Conte D, Elli L, Branchi F, Massironi S. Endoscopic techniques to detect small-bowel neuroendocrine tumors: A literature review. *United European Gastroenterol J* 2017; **5**: 5-12 [PMID: 28405316 DOI: 10.1177/2050640616658220]

7 **Zilli A**, Arcidiacono PG, Conte D, Massironi S. Clinical impact of endoscopic ultrasonography on the management of neuroendocrine tumors: lights and shadows. *Dig Liver Dis* 2018; **50**: 6-14 [PMID: 29102525 DOI: 10.1016/j.dld.2017.10.007]

8 **Falconi M**, Eriksson B, Kaltsas G, Bartsch DK, Capdevila J, Caplin M, Kos-Kudla B, Kwekkeboom D, Rindi G, Klöppel G, Reed N, Kianmanesh R, Jensen RT; Vienna Consensus Conference participants. ENETS Consensus Guidelines Update for the Management of Patients with Functional Pancreatic Neuroendocrine Tumors and Non-Functional Pancreatic Neuroendocrine Tumors. *Neuroendocrinology* 2016; **103**: 153-171 [PMID: 26742109 DOI: 10.1159/000443171]

9 **Manta R**, Nardi E, Pagano N, Ricci C, Sica M, Castellani D, Bertani H, Piccoli M, Mullineris B, Tringali A, Marini F, Germani U, Villanacci V, Casadei R, Mutignani M, Conigliaro R, Bassotti G, Zullo A. Pre-operative Diagnosis of Pancreatic Neuroendocrine Tumors with Endoscopic Ultrasonography and Computed Tomography in a Large Series. *J Gastrointestin Liver Dis* 2016; **25**: 317-321 [PMID: 27689195 DOI: 10.15403/jgld.2014.1121.253.ned]

10 **Fujimori N**, Osoegawa T, Lee L, Tachibana Y, Aso A, Kubo H, Kawabe K, Igarashi H, Nakamura K, Oda Y, Ito T. Efficacy of endoscopic ultrasonography and endoscopic ultrasonography-guided fine-needle aspiration for the diagnosis and grading of pancreatic neuroendocrine tumors. *Scand J Gastroenterol* 2016; **51**: 245-252 [PMID: 26513346 DOI: 10.3109/00365521.2015.1083050]

11 **Atiq M**, Bhutani MS, Bektas M, Lee JE, Gong Y, Tamm EP, Shah CP, Ross WA, Yao J, Raju GS, Wang X, Lee JH. EUS-FNA for pancreatic neuroendocrine tumors: a tertiary cancer center experience. *Dig Dis Sci* 2012; **57**: 791-800 [PMID: 21964743 DOI: 10.1007/s10620-011-1912-7]

12 **Dietrich CF**, Ignee A, Braden B, Barreiros AP, Ott M, Hocke M. Improved differentiation of pancreatic tumors using contrast-enhanced endoscopic ultrasound. *Clin Gastroenterol Hepatol* 2008; **6**: 590-597.e1 [PMID: 18455699 DOI:

10.1016/j.cgh.2008.02.030]
13 **Malagò R**, D'Onofrio M, Zamboni GA, Faccioli N, Falconi M, Boninsegna L, Mucelli RP. Contrast-enhanced sonography of nonfunctioning pancreatic neuroendocrine tumors. *AJR Am J Roentgenol* 2009; **192**: 424-430 [PMID: 19155405 DOI: 10.2214/AJR.07.4043]
14 **Ishikawa R**, Kamata K, Hara A, Tanaka H, Okamoto A, Yamazaki T, Nakai A, Omoto S, 4inaga K, Yamao K, Takenaka M, Minami Y, Watanabe T, Chiba Y, Chikugo T, Matsumoto I, Takeyama Y, Matsukubo Y, Hyodo T, Kudo M. Utility of contrast-enhanced harmonic endoscopic ultrasonography for predicting the prognosis of pancreatic neuroendocrine neoplasms. *Dig Endosc* 2021; **33**: 829-839 [PMID: 33020955 DOI: 10.1111/den.13862]
15 **Leiman G**. My approach to pancreatic fine needle aspiration. *J Clin Pathol* 2007; **60**: 43-49 [PMID: 16698956 DOI: 10.1136/jcp.2005.034959]
16 **Matsubayashi H**, Matsui T, Yabuuchi Y, Imai K, Tanaka M, Kakushima N, Sasaki K, Ono H. Endoscopic ultrasonography guided-fine needle aspiration for the diagnosis of solid pancreaticobiliary lesions: Clinical aspects to improve the diagnosis. *World J Gastroenterol* 2016; **22**: 628-640 [PMID: 26811612 DOI: 10.3748/wjg.v22.i2.628]
17 **Chen S**, Lin J, Wang X, Wu HH, Cramer H. EUS-guided FNA cytology of pancreatic neuroendocrine tumour (PanNET): a retrospective study of 132 cases over an 18-year period in a single institution. *Cytopathology* 2014; **25**: 396-403 [PMID: 24635775 DOI: 10.1111/cyt.12137]
18 **Gornals J**, Varas M, Catalá I, Maisterra S, Pons C, Bargalló D, Serrano T, Fabregat J. Definitive diagnosis of neuroendocrine tumors using fine-needle aspiration-puncture guided by endoscopic ultrasonography. *Rev Esp Enferm Dig* 2011; **103**: 123-128 [PMID: 21434714 DOI: 10.4321/s1130-01082011000300003]
19 **Mitra V**, Nayar MK, Leeds JS, Wadehra V, Haugk B, Scott J, Charnley RM, Oppong KW. Diagnostic performance of endoscopic ultrasound (EUS)/endoscopic ultrasound--fine needle aspiration (EUS-FNA) cytology in solid and cystic pancreatic neuroendocrine tumours. *J Gastrointestin Liver Dis* 2015; **24**: 69-75 [PMID: 25822436 DOI: 10.15403/jgld.2014.1121.vmi]
20 **Weynand B**, Borbath I, Bernard V, Sempoux C, Gigot JF, Hubert C, Lannoy V, Deprez PH, Jouret-Mourin A. Pancreatic neuroendocrine tumour grading on endoscopic ultrasound-guided fine needle aspiration: high reproducibility and inter-observer agreement of the Ki-67 labelling index. *Cytopathology* 2014; **25**: 389-395 [PMID: 24750272 DOI: 10.1111/cyt.12111]
21 **Delconte G**, Cavalcoli F, Magarotto A, Centonze G, Bezzio C, Cattaneo L, Rausa E, Kelly ME, Bonitta G, Milione M, Enzo M. Does ProCore Fine-Needle Biopsy Really Improve the Clinical Outcome of Endoscopic Ultrasound-Guided Sampling of Pancreatic Masses? *Dig Dis* 2022; **40**: 78-84 [PMID: 33780932 DOI: 10.1159/000516177]
22 **Dietrich CF**, Săftoiu A, Jenssen C. Real time elastography endoscopic ultrasound (RTE-EUS), a comprehensive review. *Eur J Radiol* 2014; **83**: 405-414 [PMID: 23643030 DOI: 10.1016/j.ejrad.2013.03.023]
23 **Havre RF**, Ødegaard S, Gilja OH, Nesje LB. Characterization of solid focal pancreatic lesions using endoscopic ultrasonography with real-time elastography. *Scand J Gastroenterol* 2014; **49**: 742-751 [PMID: 24713038 DOI: 10.3109/00365521.2014.905627]
24 **Iglesias-Garcia J**, Larino-Noia J, Abdulkader I, Forteza J, Dominguez-Munoz JE. Quantitative endoscopic ultrasound elastography: an accurate method for the differentiation of solid pancreatic masses. *Gastroenterology* 2010; **139**: 1172-1180 [PMID: 20600020 DOI: 10.1053/j.gastro.2010.06.059]
25 **Cosgrove D**, Piscaglia F, Bamber J, Bojunga J, Correas JM, Gilja OH, Klauser AS, Sporea I, Calliada F, Cantisani V, D'Onofrio M, Drakonaki EE, Fink M, Friedrich-Rust M, Fromageau J, Havre RF, Jenssen C, Ohlinger R, Săftoiu A, Schaefer F, Dietrich CF; EFSUMB. EFSUMB guidelines and recommendations on the clinical use of ultrasound elastography. Part 2: Clinical applications. *Ultraschall Med* 2013; **34**: 238-253 [PMID: 23605169 DOI: 10.1055/s-0033-1335375]
26 **Napoleon B**, Lemaistre AI, Pujol B, Caillol F, Lucidarme D, Bourdariat R, Morellon-Mialhe B, Fumex F, Lefort C, Lepilliez V, Palazzo L, Monges G, Poizat F, Giovannini M. In vivo characterization of pancreatic cystic lesions by needle-based confocal laser endomicroscopy (nCLE): proposition of a comprehensive nCLE classification confirmed by an external retrospective evaluation. *Surg Endosc* 2016; **30**: 2603-2612 [PMID: 26428198 DOI: 10.1007/s00464-015-4510-5]
27 French comment on article: Endoscopic ultrasound-guided needle-based confocal laser endomicroscopy in solid pancreatic masses. *Endoscopy* 2016; **48**: 961 [PMID: 27669477 DOI: 10.1055/s-0042-116197]
28 **Varas MJ**, Gornals JB, Pons C, Espinós JC, Abad R, Lorente FJ, Bargalló D. Usefulness of endoscopic ultrasonography (EUS) for selecting carcinoid tumors as candidates to endoscopic resection. *Rev Esp Enferm Dig* 2010; **102**: 577-582 [PMID: 21039065 DOI: 10.4321/s1130-01082010001000002]
29 **Delle Fave G**, O'Toole D, Sundin A, Taal B, Ferolla P, Ramage JK, Ferone D, Ito T, Weber W, Zheng-Pei Z, De Herder WW, Pascher A, Ruszniewski P; Vienna Consensus Conference participants. ENETS Consensus Guidelines Update for Gastroduodenal Neuroendocrine Neoplasms. *Neuroendocrinology* 2016; **103**: 119-124 [PMID: 26784901 DOI: 10.1159/000443168]
30 **Ramage JK**, De Herder WW, Delle Fave G, Ferolla P, Ferone D, Ito T, Ruszniewski P, Sundin A, Weber W, Zheng-Pei Z, Taal B, Pascher A; Vienna Consensus Conference participants. ENETS Consensus Guidelines Update for Colorectal Neuroendocrine Neoplasms. *Neuroendocrinology* 2016; **103**: 139-143 [PMID: 26730835 DOI: 10.1159/000443166]
31 **Cangemi DJ**, Patel MK, Gomez V, Cangemi JR, Stark ME, Lukens FJ. Small bowel tumors discovered during double-balloon enteroscopy: analysis of a large prospectively collected single-center database. *J Clin Gastroenterol* 2013; **47**: 769-772 [PMID: 23426457 DOI: 10.1097/MCG.0b013e318281a44e]
32 **Bader TR**, Semelka RC, Chiu VC, Armao DM, Woosley JT. MRI of carcinoid tumors: spectrum of appearances in the gastrointestinal tract and liver. *J Magn Reson Imaging* 2001; **14**: 261-269 [PMID: 11536403 DOI: 10.1002/jmri.1182]
33 **Frilling A**, Sotiropoulos GC, Radtke A, Malago M, Bockisch A, Kuehl H, Li J, Broelsch CE. The impact of 68Ga-DOTATOC positron emission tomography/computed tomography on the multimodal management of patients with neuroendocrine tumors. *Ann Surg* 2010; **252**: 850-856 [PMID: 21037441 DOI: 10.1097/SLA.0b013e3181fd37e8]
34 **van Tuyl SA**, van Noorden JT, Timmer R, Stolk MF, Kuipers EJ, Taal BG. Detection of small-bowel neuroendocrine tumors by video capsule endoscopy. *Gastrointest Endosc* 2006; **64**: 66-72 [PMID: 16813805 DOI:

10.1016/j.gie.2006.01.054]
35 **Prasad V**, Ambrosini V, Hommann M, Hoersch D, Fanti S, Baum RP. Detection of unknown primary neuroendocrine tumours (CUP-NET) using (68)Ga-DOTA-NOC receptor PET/CT. *Eur J Nucl Med Mol Imaging* 2010; **37**: 67-77 [PMID: 19618183 DOI: 10.1007/s00259-009-1205-y]
36 **Sharma P**, Arora S, Mukherjee A, Pal S, Sahni P, Garg P, Khadgawat R, Thulkar S, Bal C, Kumar R. Predictive value of 68Ga-DOTANOC PET/CT in patients with suspicion of neuroendocrine tumors: is its routine use justified? *Clin Nucl Med* 2014; **39**: 37-43 [PMID: 24152621 DOI: 10.1097/RLU.0000000000000257]
37 **Cobrin GM**, Pittman RH, Lewis BS. Increased diagnostic yield of small bowel tumors with capsule endoscopy. *Cancer* 2006; **107**: 22-27 [PMID: 16736516 DOI: 10.1002/cncr.21975]
38 **McEwen BS**. Protective and damaging effects of stress mediators. *N Engl J Med* 1998; **338**: 171-179 [PMID: 9428819 DOI: 10.1056/NEJM199801153380307]
39 **Sidhu R**, McAlindon ME. The use of capsule endoscopy for the investigation of small bowel tumors: experience from a United Kingdom single center. *Dig Dis Sci* 2011; **56**: 2763 [PMID: 21750932 DOI: 10.1007/s10620-011-1813-9]
40 **Frilling A**, Smith G, Clift AK, Martin J. Capsule endoscopy to detect primary tumour site in metastatic neuroendocrine tumours. *Dig Liver Dis* 2014; **46**: 1038-1042 [PMID: 25086997 DOI: 10.1016/j.dld.2014.07.004]
41 **Furnari M**, Buda A, Delconte G, Citterio D, Voiosu T, Ballardini G, Cavallaro F, Savarino E, Mazzaferro V, Meroni E. The role of wireless capsule endoscopy (WCE) in the detection of occult primary neuroendocrine tumors. *J Gastrointestin Liver Dis* 2017; **26**: 151-156 [PMID: 28617885 DOI: 10.15403/jgld.2014.1121.262.wce]
42 **Tominaga K**, Kamimura K, Yokoyama J, Terai S. Usefulness of Capsule Endoscopy and Double-balloon Enteroscopy for the Diagnosis of Multiple Carcinoid Tumors in the Small Intestine: Case Reports and a Literature Review. *Intern Med* 2019; **58**: 655-659 [PMID: 30333421 DOI: 10.2169/internalmedicine.1700-18]
43 **Bellutti M**, Fry LC, Schmitt J, Seemann M, Klose S, Malfertheiner P, Mönkemüller K. Detection of neuroendocrine tumors of the small bowel by double balloon enteroscopy. *Dig Dis Sci* 2009; **54**: 1050-1058 [PMID: 18770038 DOI: 10.1007/s10620-008-0456-y]
44 **Scherübl H**, Faiss S, Tschöpe R, Zeitz M. Double-balloon enteroscopy for the detection of midgut carcinoids. *Gastrointest Endosc* 2005; **62**: 994; author reply 994-994; author reply 995 [PMID: 16301062 DOI: 10.1016/j.gie.2005.08.012]
45 **Rossi RE**, Elli L, Branchi F, Conte D, Massironi S. Double-Balloon Enteroscopy in Detecting Small-Bowel Neuroendocrine Neoplasms: A Single-Center Prospective Study. *Digestion* 2021; **102**: 722-730 [PMID: 33361694 DOI: 10.1159/000511850]
46 **Roberto GA**, Rodrigues CMB, Peixoto RD, Younes RN. Gastric neuroendocrine tumor: A practical literature review. *World J Gastrointest Oncol* 2020; **12**: 850-856 [PMID: 32879663 DOI: 10.4251/wjgo.v12.i8.850]
47 **Scherübl H**, Cadiot G. Early Gastroenteropancreatic Neuroendocrine Tumors: Endoscopic Therapy and Surveillance. *Visc Med* 2017; **33**: 332-338 [PMID: 29177161 DOI: 10.1159/000459404]
48 **Putzer D**, Schullian P, Jaschke W, Bale R. NEN: Advancement in Diagnosis and Minimally Invasive Therapy. *Rofo* 2020; **192**: 422-430 [PMID: 31747704 DOI: 10.1055/a-1030-4631]
49 **Panzuto F**, Massironi S, Partelli S, Campana D, Rinzivillo M, Invernizzi P, Andreasi V, Lamberti G, Falconi M. Gastro-entero-pancreatic neuroendocrine neoplasia: The rules for non-operative management. *Surg Oncol* 2020; **35**: 141-148 [PMID: 32877883 DOI: 10.1016/j.suronc.2020.08.015]
50 **Merola E**, Sbrozzi-Vanni A, Panzuto F, D'Ambra G, Di Giulio E, Pilozzi E, Capurso G, Lahner E, Bordi C, Annibale B, Delle Fave G. Type I gastric carcinoids: a prospective study on endoscopic management and recurrence rate. *Neuroendocrinology* 2012; **95**: 207-213 [PMID: 21811050 DOI: 10.1159/000329043]
51 **Manfredi S**, Walter T, Baudin E, Coriat R, Ruszniewski P, Lecomte T, Laurenty AP, Goichot B, Rohmer V, Roquin G, Cojocarasu OZ, Lombard-Bohas C, Lepage C, Morcet J, Cadiot G. Management of gastric neuro-endocrine tumours in a large French national cohort (GTE). *Endocrine* 2017; **57**: 504-511 [PMID: 28664309 DOI: 10.1007/s12020-017-1355-9]
52 **Kwon YH**, Jeon SW, Kim GH, Kim JI, Chung IK, Jee SR, Kim HU, Seo GS, Baik GH, Choi KD, Moon JS. Long-term follow up of endoscopic resection for type 3 gastric NET. *World J Gastroenterol* 2013; **19**: 8703-8708 [PMID: 24379589 DOI: 10.3748/wjg.v19.i46.8703]
53 **Scherübl H**, Jensen RT, Cadiot G, Stölzel U, Klöppel G. Management of early gastrointestinal neuroendocrine neoplasms. *World J Gastrointest Endosc* 2011; **3**: 133-139 [PMID: 21860682 DOI: 10.4253/wjge.v3.i7.133]
54 **Pimentel-Nunes P**, Dinis-Ribeiro M, Ponchon T, Repici A, Vieth M, De Ceglie A, Amato A, Berr F, Bhandari P, Bialek A, Conio M, Haringsma J, Langner C, Meisner S, Messmann H, Morino M, Neuhaus H, Piessevaux H, Rugge M, Saunders BP, Robaszkiewicz M, Seewald S, Kashin S, Dumonceau JM, Hassan C, Deprez PH. Endoscopic submucosal dissection: European Society of Gastrointestinal Endoscopy (ESGE) Guideline. *Endoscopy* 2015; **47**: 829-854 [PMID: 26317585 DOI: 10.1055/s-0034-1392882]
55 **Massironi S**, Campana D, Partelli S, Panzuto F, Rossi RE, Faggiano A, Brighi N, Falconi M, Rinzivillo M, Delle Fave G, Colao AM, Conte D. Heterogeneity of Duodenal Neuroendocrine Tumors: An Italian Multi-center Experience. *Ann Surg Oncol* 2018; **25**: 3200-3206 [PMID: 30054824 DOI: 10.1245/s10434-018-6673-5]
56 **Kim GH**, Kim JI, Jeon SW, Moon JS, Chung IK, Jee SR, Kim HU, Seo GS, Baik GH, Lee YC; Korean College of Helicobacter and Upper Gastrointestinal Research. Endoscopic resection for duodenal carcinoid tumors: a multicenter, retrospective study. *J Gastroenterol Hepatol* 2014; **29**: 318-324 [PMID: 24117946 DOI: 10.1111/jgh.12390]
57 **Untch BR**, Bonner KP, Roggin KK, Reidy-Lagunes D, Klimstra DS, Schattner MA, Fong Y, Allen PJ, D'Angelica MI, DeMatteo RP, Jarnagin WR, Kingham TP, Tang LH. Pathologic grade and tumor size are associated with recurrence-free survival in patients with duodenal neuroendocrine tumors. *J Gastrointest Surg* 2014; **18**: 457-62; discussion 462 [PMID: 24448999 DOI: 10.1007/s11605-014-2456-x]
58 **Gamboa AC**, Liu Y, Lee RM, Zaidi MY, Staley CA, Kooby DA, Winer JH, Shah MM, Russell MC, Cardona K, Maithel SK. Duodenal neuroendocrine tumors: Somewhere between the pancreas and small bowel? *J Surg Oncol* 2019; **120**: 1293-1301 [PMID: 31621090 DOI: 10.1002/jso.25731]
59 **Hatta W**, Koike T, Iijima K, Asanuma K, Asano N, Musha H, Inomata Y, Sano T, Endo H, Ikehata A, Horii T, Ohyauchi

M, Yokosawa S, Kasajima A, Fujishima F, Sasano H, Nakaya N, Nakamura T, Shimosegawa T. The Risk Factors for Metastasis in Non-Ampullary Duodenal Neuroendocrine Tumors Measuring 20 mm or Less in Diameter. *Digestion* 2017; **95**: 201-209 [PMID: 28315861 DOI: 10.1159/000459619]

60 **Rossi RE**, Milanetto AC, Andreasi V, Campana D, Coppa J, Nappo G, Rinzivillo M, Invernizzi P, Modica R, David A, Partelli S, Lamberti G, Mazzaferro V, Zerbi A, Panzuto F, Pasquali C, Falconi M, Massironi S; ItaNet (Italian Association for Neuroendocrine Tumours) study group. Risk of preoperative understaging of duodenal neuroendocrine neoplasms: a plea for caution in the treatment strategy. *J Endocrinol Invest* 2021; **44**: 2227-2234 [PMID: 33651317 DOI: 10.1007/s40618-021-01528-1]

61 **Basuroy R**, Haji A, Ramage JK, Quaglia A, Srirajaskanthan R. Review article: the investigation and management of rectal neuroendocrine tumours. *Aliment Pharmacol Ther* 2016; **44**: 332-345 [PMID: 27302838 DOI: 10.1111/apt.13697]

62 **Son HJ**, Sohn DK, Hong CW, Han KS, Kim BC, Park JW, Choi HS, Chang HJ, Oh JH. Factors associated with complete local excision of small rectal carcinoid tumor. *Int J Colorectal Dis* 2013; **28**: 57-61 [PMID: 22821140 DOI: 10.1007/s00384-012-1538-z]

63 **Dąbkowski K**, Szczepkowski M, Kos-Kudła B, Starzynska T. Endoscopic management of rectal neuroendocrine tumours. How to avoid a mistake and what to do when one is made? *Endokrynol Pol* 2020; **71**: 343-349 [PMID: 32852049 DOI: 10.5603/EP.a2020.0045]

64 **He L**, Deng T, Luo H. Efficacy and safety of endoscopic resection therapies for rectal carcinoid tumors: a meta-analysis. *Yonsei Med J* 2015; **56**: 72-81 [PMID: 25510749 DOI: 10.3349/ymj.2015.56.1.72]

65 **Zhou X**, Xie H, Xie L, Li J, Cao W, Fu W. Endoscopic resection therapies for rectal neuroendocrine tumors: a systematic review and meta-analysis. *J Gastroenterol Hepatol* 2014; **29**: 259-268 [PMID: 24118068 DOI: 10.1111/jgh.12395]

66 **Park SS**, Han KS, Kim B, Chang Kim B, Hong CW, Sohn DK, Chang HJ. Comparison of underwater endoscopic mucosal resection and endoscopic submucosal dissection of rectal neuroendocrine tumors (with videos). *Gastrointest Endosc* 2020; **91**: 1164-1171.e2 [PMID: 31904380 DOI: 10.1016/j.gie.2019.12.039]

67 **Lee WH**, Kim SW, Lim CH, Kim JS, Cho YK, Lee IS, Choi MG, Choi KY. Efficacy of endoscopic mucosal resection using a dual-channel endoscope compared with endoscopic submucosal dissection in the treatment of rectal neuroendocrine tumors. *Surg Endosc* 2013; **27**: 4313-4318 [PMID: 23807754 DOI: 10.1007/s00464-013-3050-0]

68 **Lee HS**, Moon HS, Kwon IS, Park JH, Kim JS, Kang SH, Lee ES, Kim SH, Sung JK, Lee BS, Jeong HY. Comparison of conventional and modified endoscopic mucosal resection methods for the treatment of rectal neuroendocrine tumors. *Surg Endosc* 2021; **35**: 6055-6065 [PMID: 33094828 DOI: 10.1007/s00464-020-08097-z]

69 **Park SB**, Kim HW, Kang DH, Choi CW, Kim SJ, Nam HS. Advantage of endoscopic mucosal resection with a cap for rectal neuroendocrine tumors. *World J Gastroenterol* 2015; **21**: 9387-9393 [PMID: 26309365 DOI: 10.3748/wjg.v21.i31.9387]

70 **Kim HH**, Park SJ, Lee SH, Park HU, Song CS, Park MI, Moon W. Efficacy of endoscopic submucosal resection with a ligation device for removing small rectal carcinoid tumor compared with endoscopic mucosal resection: analysis of 100 cases. *Dig Endosc* 2012; **24**: 159-163 [PMID: 22507089 DOI: 10.1111/j.1443-1661.2011.01190.x]

71 **Lee J**, Park YE, Choi JH, Heo NY, Park J, Park SH, Moon YS, Nam KH, Kim TO. Comparison between cap-assisted and ligation-assisted endoscopic mucosal resection for rectal neuroendocrine tumors. *Ann Gastroenterol* 2020; **33**: 385-390 [PMID: 32624659 DOI: 10.20524/aog.2020.0485]

72 **Niimi K**, Goto O, Fujishiro M, Kodashima S, Ono S, Mochizuki S, Asada-Hirayama I, Konno-Shimizu M, Mikami-Matsuda R, Minatsuki C, Yamamichi N, Koike K. Endoscopic mucosal resection with a ligation device or endoscopic submucosal dissection for rectal carcinoid tumors: an analysis of 24 consecutive cases. *Dig Endosc* 2012; **24**: 443-447 [PMID: 23078437 DOI: 10.1111/j.1443-1661.2012.01303.x]

73 **Wang XY**, Chai NL, Linghu EQ, Li HK, Zhai YQ, Feng XX, Zhang WG, Zou JL, Li LS, Xiang JY. Efficacy and safety of hybrid endoscopic submucosal dissection compared with endoscopic submucosal dissection for rectal neuroendocrine tumors and risk factors associated with incomplete endoscopic resection. *Ann Transl Med* 2020; **8**: 368 [PMID: 32355812 DOI: 10.21037/atm.2020.02.25]

74 **Meier B**, Albrecht H, Wiedbrauck T, Schmidt A, Caca K. Full-thickness resection of neuroendocrine tumors in the rectum. *Endoscopy* 2020; **52**: 68-72 [PMID: 31614372 DOI: 10.1055/a-1008-9077]

75 **Partelli S**, Ramage JK, Massironi S, Zerbi A, Kim HB, Niccoli P, Panzuto F, Landoni L, Tomazic A, Ibrahim T, Kaltsas G, Bertani E, Sauvanet A, Segelov E, Caplin M, Coppa J, Armstrong T, Weickert MO, Butturini G, Staettner S, Boesch F, Cives M, Moulton CA, He J, Selberherr A, Twito O, Castaldi A, De Angelis CG, Gaujoux S, Almeamar H, Frilling A, Vigia E, Wilson C, Muffatti F, Srirajaskanthan R, Invernizzi P, Lania A, Kwon W, Ewald J, Rinzivillo M, Nessi C, Smid LM, Gardini A, Tsoli M, Picardi EE, Hentic O, Croagh D, Toumpanakis C, Citterio D, Ramsey E, Mosterman B, Regi P, Gasteiger S, Rossi RE, Smiroldo V, Jang JY, Falconi M. Management of Asymptomatic Sporadic Nonfunctioning Pancreatic Neuroendocrine Neoplasms (ASPEN) ≤2 cm: Study Protocol for a Prospective Observational Study. *Front Med (Lausanne)* 2020; **7**: 598438 [PMID: 33425946 DOI: 10.3389/fmed.2020.598438]

76 **Melita G**, Pallio S, Tortora A, Crinò SF, Macrì A, Dionigi G. Diagnostic and Interventional Role of Endoscopic Ultrasonography for the Management of Pancreatic Neuroendocrine Neoplasms. *J Clin Med* 2021; **10** [PMID: 34203922 DOI: 10.3390/jcm10122638]

77 **Imperatore N**, de Nucci G, Mandelli ED, de Leone A, Zito FP, Lombardi G, Manes G. Endoscopic ultrasound-guided radiofrequency ablation of pancreatic neuroendocrine tumors: a systematic review of the literature. *Endosc Int Open* 2020; **8**: E1759-E1764 [PMID: 33269308 DOI: 10.1055/a-1261-9605]

78 **Rossi S**, Viera FT, Ghittoni G, Cobianchi L, Rosa LL, Siciliani L, Bortolotto C, Veronese L, Vercelli A, Gallotti A, Ravetta V. Radiofrequency ablation of pancreatic neuroendocrine tumors: a pilot study of feasibility, efficacy, and safety. *Pancreas* 2014; **43**: 938-945 [PMID: 24717825 DOI: 10.1097/MPA.0000000000000133]

79 **Pai M**, Habib N, Senturk H, Lakhtakia S, Reddy N, Cicinnati VR, Kaba I, Beckebaum S, Drymousis P, Kahaleh M, Brugge W. Endoscopic ultrasound guided radiofrequency ablation, for pancreatic cystic neoplasms and neuroendocrine tumors. *World J Gastrointest Surg* 2015; **7**: 52-59 [PMID: 25914783 DOI: 10.4240/wjgs.v7.i4.52]

80 **Oleinikov K**, Dancour A, Epshtein J, Benson A, Mazeh H, Tal I, Matalon S, Benbassat CA, Livovsky DM, Goldin E,

Gross DJ, Jacob H, Grozinsky-Glasberg S. Endoscopic Ultrasound-Guided Radiofrequency Ablation: A New Therapeutic Approach for Pancreatic Neuroendocrine Tumors. *J Clin Endocrinol Metab* 2019; **104**: 2637-2647 [PMID: 31102458 DOI: 10.1210/jc.2019-00282]

81 **de Nucci G**, Imperatore N, Mandelli ED, di Nuovo F, d'Urbano C, Manes G. Endoscopic ultrasound-guided radiofrequency ablation of pancreatic neuroendocrine tumors: a case series. *Endosc Int Open* 2020; **8**: E1754-E1758 [PMID: 33269307 DOI: 10.1055/a-1261-9359]

82 **Zhang L**, Tan S, Huang S, Zhong C, Lü M, Peng Y, Tang X. The safety and efficacy of endoscopic ultrasound-guided ablation therapy for solid pancreatic tumors: a systematic review. *Scand J Gastroenterol* 2020; **55**: 1121-1131 [PMID: 32730715 DOI: 10.1080/00365521.2020.1797870]

83 **Park DH**, Choi JH, Oh D, Lee SS, Seo DW, Lee SK, Kim MH. Endoscopic ultrasonography-guided ethanol ablation for small pancreatic neuroendocrine tumors: results of a pilot study. *Clin Endosc* 2015; **48**: 158-164 [PMID: 25844345 DOI: 10.5946/ce.2015.48.2.158]

84 **Matsumoto K**, Kato H, Kitano M, Hara K, Kuwatani M, Ashida R, Takenaka M, Yamazaki T, Sakurai J, Yoshida M, Okada H. Study protocol for endoscopic ultrasonography-guided ethanol injection therapy for patients with pancreatic neuroendocrine neoplasm: a multicentre prospective study. *BMJ Open* 2021; **11**: e046505 [PMID: 34253667 DOI: 10.1136/bmjopen-2020-046505]

World Journal of Gastroenterology

Submit a Manuscript: https://www.f6publishing.com

World J Gastroenterol 2022 July 14; 28(26): 3274-3278

DOI: 10.3748/wjg.v28.i26.3274

ISSN 1007-9327 (print) ISSN 2219-2840 (online)

LETTER TO THE EDITOR

Intestinal inflammation and the microbiota: Beyond diversity

Gabriela Gama Freire Alberca, Naiane Samira Souza Cardoso, Rosa Liliana Solis-Castro, Viviane Nakano, Ricardo Wesley Alberca

Specialty type: Gastroenterology and hepatology

Provenance and peer review: Invited article; Externally peer reviewed.

Peer-review model: Single blind

Peer-review report's scientific quality classification
Grade A (Excellent): 0
Grade B (Very good): B, B, B, B
Grade C (Good): C
Grade D (Fair): 0
Grade E (Poor): 0

P-Reviewer: Carannante F, Italy; Gao W, China; Suzuki T, Japan; Xu PF, United States; Zhao G, China

Received: August 6, 2021
Peer-review started: August 6, 2021
First decision: September 4, 2021
Revised: September 5, 2021
Accepted: June 23, 2022
Article in press: June 23, 2022
Published online: July 14, 2022

Gabriela Gama Freire Alberca, Naiane Samira Souza Cardoso, Viviane Nakano, Department of Microbiology, Institute of Biomedical Sciences, University of São Paulo, São Paulo 05508-000, Brazil

Rosa Liliana Solis-Castro, Departamento Académico de Biología Bioquímica, Facultad de Ciencias de la Salud, Universidad Nacional de Tumbes, Pampa Grande 24000, Tumbes, Peru

Ricardo Wesley Alberca, Laboratorio de Dermatologia e Imunodeficiencias, Departamento de Dermatologia, Faculdade de Medicina FMUSP, Universidade de São Paulo, São Paulo 01246-903, Brazil

Corresponding author: Ricardo Wesley Alberca, PhD, Academic Research, Research Fellow, Laboratorio de Dermatologia e Imunodeficiencias, Departamento de Dermatologia, Faculdade de Medicina FMUSP, Universidade de São Paulo, 455-Cerqueira César, São Paulo 01246-903, Brazil. ricardowesley@gmail.com

Abstract

The recent manuscript entitled "Relationship between clinical features and intestinal microbiota in Chinese patients with ulcerative colitis" reported a difference in the intestinal microbiota of patients with ulcerative colitis according to the severity of the colitis. The influence of the intestinal microbiota on the development and progress of gastrointestinal disorders is well established. Besides the diversity in the microbiome, the presence of virulence factors and toxins by commensal bacteria may affect an extensive variety of cellular processes, contributing to the induction of a proinflammatory environment.

Key Words: Inflammation; Microbiota; Toxins; Intestinal; Ulcerative; Colitis; Cancer

©The Author(s) 2022. Published by Baishideng Publishing Group Inc. All rights reserved.

Core Tip: The manuscript entitled "Relationship between clinical features and intestinal microbiota in Chinese patients with ulcerative colitis" and previous investigations have identified alterations in the intestinal microbiome of patients with inflammatory bowel disease, ulcerative colitis, and colorectal cancer. The microbiota composition impacts the development of inflammatory disorders. Nevertheless, investigations should focus on identifying alterations not only on the diversity of the microbiota but the presence of the toxin-producing bacteria. Further investigations should investigate alterations in the microbiota composition and the production of toxins by commensal bacteria such as *Escherichia coli*, *Clostridium perfringens*, and *Bacteroides fragilis*.

Citation: Alberca GGF, Cardoso NSS, Solis-Castro RL, Nakano V, Alberca RW. Intestinal inflammation and the microbiota: Beyond diversity. *World J Gastroenterol* 2022; 28(26): 3274-3278
URL: https://www.wjgnet.com/1007-9327/full/v28/i26/3274.htm
DOI: https://dx.doi.org/10.3748/wjg.v28.i26.3274

TO THE EDITOR

We read with great interest the manuscript entitled "Relationship between clinical features and intestinal microbiota in Chinese patients with ulcerative colitis" published by He *et al*[1] in the World Journal Gastroenterology. He *et al*[1] performed an investigation on the microbiota composition on the fecal and mucosa samples from patients with ulcerative colitis. Their work reinforces the importance of the microbiota on the inflammatory process and gastrointestinal disorders. Importantly, the manuscript provided information on the composition of the gastrointestinal microbiota of patients with ulcerative colitis of various severity and patients without ulcerative colitis[1]. We would like to raise a few considerations regarding the microbiota and gastrointestinal inflammatory disorders.

The microbiota is an ecosystem in constant regulation, influenced by the diet, antibiotics, sanitary conditions, environmental stimulus, and the host's immune system[2]. The gastrointestinal tract is the largest reservoir of bacteria in the human body and shapes both the local and systemic immune responses[3-5]. The microbiome influences the maturation and development of the host's immune system[6], regulating the development of food tolerance, response to inflammation, infections, vaccination, and metabolism[7,8]. Importantly, the microbiota directly influences the development of the inflammatory process independent of dietary intake[9], and abrupt alterations in the microbiota composition can result in an inflammatory insult[10]. He *et al*[1] identified an increase in *Escherichia* and *Shigella* in patients with ulcerative colitis in comparison to patients without ulcerative colitis[1]. *Escherichia* and *Shigella* has been implicated in a reduction in the response to anticoagulation therapy and could impact the treatment of patients with gastrointestinal disorders and under anticoagulation therapy such as coronavirus disease 2019 patients[11-14].

Shiga toxin-producing *Shigella* species and *Escherichia coli* are considered pathogenic, associated with diarrhea and colitis[15]. These toxins can induce the activation of the NOD-like receptor protein 3 inflammasome, inducing the production of interleukin (IL)-1β and IL-18 and cellular death by pyroptosis[16]. The virulence of Shiga-toxin-producing *Escherichia coli* can lead to diarrheal sicknesses and death[17,18]. Shiga-toxins can be encapsulated within microvesicles and influence the inflammatory response in other organs, such as the kidneys[19]. Shiga toxin-producing *Escherichia coli* (O26:H11 strain 97-3250 and O145:H28 strain 4865/96) induces a greater production of chemokines and cytokines, such as IL-8 and IL-1β, in comparison to *Escherichia coli* (O9:H4 strain HS)[20].

The complex symbiotic interaction between the microbiota and the host is mediated by an equilibrium in the tolerance and inflammatory response to microbial products in the gut[6]. He *et al*[1] did not identify an increase in other strains in patients with ulcerative colitis. Nevertheless, in addition to the microbiota composition, certain commensal bacteria, such as *Clostridium perfringens* and *Bacteroides fragilis*, can express a wide range of toxins and metabolic compounds to induce inflammation [21-23]. *Clostridium perfringens* is a gram-positive anaerobic bacteria, commonly in the environment and is part of the resident microbiota but can become virulent by the expression of toxin genes[24,25]. *Clostridium perfringens* can produce over 20 toxins including alpha (α), beta (β), epsilon (e), enterotoxins, and hydrolytic enzymes[26-29]. These toxins can damage and kill intestinal cells, disturb the epithelial barrier, and induce proinflammatory and propathogenic milieu[26,30,31].

The alpha toxin produced by *Clostridium perfringens* is a zinc-dependent metalloenzyme, is able to rupture the plasma membrane of the host's cells[25,32], induces an immature profile in the host's innate immune response (neutrophils), and is involved in the formation of myonecrosis in animals, including humans[33,34]. The β toxin is a pore-forming toxin associated with hemorrhagic diarrhea[35]. *Clostridium perfringens* with the expression of α and β toxins is associated with necrotic enteritis in animals and humans[36-38]. The e toxin is also pore-forming and is involved in intestinal and neurological diseases in humans[39-43].

In addition, *Clostridium perfringens* is able to produce several other toxins such as enterotoxins[44-46], NetB[47,48], and TpeL[49,50], which can induce inflammatory responses, biofilm formation, and chronically disrupt the intestinal epithelium[44,47,50]. *Bacteroides fragilis,* another resident bacteria, can produce a zinc-dependent metalloprotease called fragilisyn[51]. Fragilisyn-producing *Bacteroides fragilis* are named *Enterotoxigenic Bacteroides Fragilis* (ETBF)[52]. ETBF toxin is coded by the *bft* gene and is highly correlated with diarrhea in humans[53,54]. ETBF can cleave E-cadherin in the epithelial cells, allowing bacterial translocation[55,56]. ETBF induces an IL-17-mediated immune response with the infiltration of lymphocytes and neutrophils and damages the DNA *via* the formation of microadenoma [4,53,54]. In addition, the inflammatory process may be mediated by several bacteria. For example, in the "driver-passenger" model, the colonization by one bacteria may facilitate the expansion and proinflammatory action of another microorganism[55].

A recent manuscript by Avril and DePaolo[56], identified that the co-colonization of ETBF and *Escherichia coli* strains, harboring the pks island, promotes the development of intestinal cancer. ETBF promotes the degradation of the intestinal mucus and induction of IL-17-mediated inflammation by the host's immune cells. This process enables the adherence of *Escherichia coli* to the intestinal wall, releases colibactin, and promotes cancer development[56]. Therefore, quantitative analyses are important to characterize the composition of the microbiota in several diseases and aid in the design of possible interventions to modulate the immune response of the host in microbiota-mediated inflammatory disorders[1]. Nevertheless, due to the potential pathobiont role of several resident bacteria, investigations on toxin-producing bacteria are crucial for an overall interpretation of the role of the microbiota on gastrointestinal disorders.

FOOTNOTES

Author contributions: All authors wrote and reviewed the manuscript.

Conflict-of-interest statement: All the authors report no relevant conflicts of interest for this article.

Open-Access: This article is an open-access article that was selected by an in-house editor and fully peer-reviewed by external reviewers. It is distributed in accordance with the Creative Commons Attribution NonCommercial (CC BY-NC 4.0) license, which permits others to distribute, remix, adapt, build upon this work non-commercially, and license their derivative works on different terms, provided the original work is properly cited and the use is non-commercial. See: https://creativecommons.org/Licenses/by-nc/4.0/

Country/Territory of origin: Brazil

ORCID number: Gabriela Gama Freire Alberca 0000-0002-3467-5562; Naiane Samira Souza Cardoso 0000-0002-3305-6567; Rosa Liliana Solis-Castro 0000-0002-1813-8644; Viviane Nakano 0000-0002-7005-3701; Ricardo Wesley Alberca 0000-0002-3602-3306.

S-Editor: Wang JJ
L-Editor: Filipodia
P-Editor: Wang JJ

REFERENCES

1 **He XX**, Li YH, Yan PG, Meng XC, Chen CY, Li KM, Li JN. Relationship between clinical features and intestinal microbiota in Chinese patients with ulcerative colitis. *World J Gastroenterol* 2021; **27**: 4722-4737 [PMID: 34366632 DOI: 10.3748/wjg.v27.i28.4722]
2 **Voreades N**, Kozil A, Weir TL. Diet and the development of the human intestinal microbiome. *Front Microbiol* 2014; **5**: 494 [PMID: 25295033 DOI: 10.3389/fmicb.2014.00494]
3 **Jandhyala SM**, Talukdar R, Subramanyam C, Vuyyuru H, Sasikala M, Nageshwar Reddy D. Role of the normal gut microbiota. *World J Gastroenterol* 2015; **21**: 8787-8803 [PMID: 26269668 DOI: 10.3748/wjg.v21.i29.8787]
4 **Lucas C**, Barnich N, Nguyen HTT. Microbiota, Inflammation and Colorectal Cancer. *Int J Mol Sci* 2017; **18** [PMID: 28632155 DOI: 10.3390/ijms18061310]
5 **Chiu CY**, Chan YL, Tsai MH, Wang CJ, Chiang MH, Chiu CC. Gut microbial dysbiosis is associated with allergen-specific IgE responses in young children with airway allergies. *World Allergy Organ J* 2019; **12**: 100021 [PMID: 30937143 DOI: 10.1016/j.waojou.2019.100021]
6 **Pandiyan P**, Bhaskaran N, Zou M, Schneider E, Jayaraman S, Huehn J. Microbiome Dependent Regulation of T_{regs} and Th17 Cells in Mucosa. *Front Immunol* 2019; **10**: 426 [PMID: 30906299 DOI: 10.3389/fimmu.2019.00426]
7 **Round JL**, Mazmanian SK. The gut microbiota shapes intestinal immune responses during health and disease. *Nat Rev Immunol* 2009; **9**: 313-323 [PMID: 19343057 DOI: 10.1038/nri2515]
8 **Fonseca DM**, Hand TW, Han SJ, Gerner MY, Glatman Zaretsky A, Byrd AL, Harrison OJ, Ortiz AM, Quinones M, Trinchieri G, Brenchley JM, Brodsky IE, Germain RN, Randolph GJ, Belkaid Y. Microbiota-Dependent Sequelae of Acute

Infection Compromise Tissue-Specific Immunity. *Cell* 2015; **163**: 354-366 [PMID: 26451485 DOI: 10.1016/j.cell.2015.08.030]

9 **Battson ML**, Lee DM, Li Puma LC, Ecton KE, Thomas KN, Febvre HP, Chicco AJ, Weir TL, Gentile CL. Gut microbiota regulates cardiac ischemic tolerance and aortic stiffness in obesity. *Am J Physiol Heart Circ Physiol* 2019; **317**: H1210-H1220 [PMID: 31559829 DOI: 10.1152/ajpheart.00346.2019]

10 **Saltzman ET**, Palacios T, Thomsen M, Vitetta L. Intestinal Microbiome Shifts, Dysbiosis, Inflammation, and Non-alcoholic Fatty Liver Disease. *Front Microbiol* 2018; **9**: 61 [PMID: 29441049 DOI: 10.3389/fmicb.2018.00061]

11 **Wang L**, Liu L, Liu X, Xiang M, Zhou L, Huang C, Shen Z, Miao L. The gut microbes, Enterococcus and Escherichia-Shigella, affect the responses of heart valve replacement patients to the anticoagulant warfarin. *Pharmacol Res* 2020; **159**: 104979 [PMID: 32505835 DOI: 10.1016/j.phrs.2020.104979]

12 **Gu S**, Chen Y, Wu Z, Gao H, Lv L, Guo F, Zhang X, Luo R, Huang C, Lu H, Zheng B, Zhang J, Yan R, Zhang H, Jiang H, Xu Q, Guo J, Gong Y, Tang L, Li L. Alterations of the Gut Microbiota in Patients With Coronavirus Disease 2019 or H1N1 Influenza. *Clin Infect Dis* 2020; **71**: 2669-2678 [PMID: 32497191 DOI: 10.1093/cid/ciaa709]

13 **Alberca GGF**, Solis-Castro RL, Solis-Castro ME, Alberca RW. Coronavirus disease-2019 and the intestinal tract: An overview. *World J Gastroenterol* 2021; **27**: 1255-1266 [PMID: 33833480 DOI: 10.3748/wjg.v27.i13.1255]

14 **Giannis D**, Ziogas IA, Gianni P. Coagulation disorders in coronavirus infected patients: COVID-19, SARS-CoV-1, MERS-CoV and lessons from the past. *J Clin Virol* 2020; **127**: 104362 [PMID: 32305883 DOI: 10.1016/j.jcv.2020.104362]

15 **Wang X**, Sun J, Wan L, Yang X, Lin H, Zhang Y, He X, Zhong H, Guan K, Min M, Sun Z, Wang B, Dong M, Wei C. The *Shigella* Type III Secretion Effector IpaH4.5 Targets NLRP3 to Activate Inflammasome Signaling. *Front Cell Infect Microbiol* 2020; **10**: 511798 [PMID: 33117724 DOI: 10.3389/fcimb.2020.511798]

16 **Hauser JR**, Atitkar RR, Petro CD, Lindsey RL, Strockbine N, O'Brien AD, Melton-Celsa AR. The Virulence of *Escherichia coli* O157:H7 Isolates in Mice Depends on Shiga Toxin Type 2a (Stx2a)-Induction and High Levels of Stx2a in Stool. *Front Cell Infect Microbiol* 2020; **10**: 62 [PMID: 32175286 DOI: 10.3389/fcimb.2020.00062]

17 **Harrison LM**, Lacher DW, Mammel MK, Leonard SR. Comparative Transcriptomics of Shiga Toxin-Producing and Commensal *Escherichia coli* and Cytokine Responses in Colonic Epithelial Cell Culture Infections. *Front Cell Infect Microbiol* 2020; **10**: 575630 [PMID: 33194815 DOI: 10.3389/fcimb.2020.575630]

18 **Huycke MM**, Gaskins HR. Commensal bacteria, redox stress, and colorectal cancer: mechanisms and models. *Exp Biol Med (Maywood)* 2004; **229**: 586-597 [PMID: 15229352 DOI: 10.1177/153537020422900702]

19 **Blacher E**, Levy M, Tatirovsky E, Elinav E. Microbiome-Modulated Metabolites at the Interface of Host Immunity. *J Immunol* 2017; **198**: 572-580 [PMID: 28069752 DOI: 10.4049/jimmunol.1601247]

20 **Louis P**, Hold GL, Flint HJ. The gut microbiota, bacterial metabolites and colorectal cancer. *Nat Rev Microbiol* 2014; **12**: 661-672 [PMID: 25198138 DOI: 10.1038/nrmicro3344]

21 **Uzal FA**, Vidal JE, McClane BA, Gurjar AA. *Clostridium Perfringens* Toxins Involved in Mammalian Veterinary Diseases. *Open Toxinology J* 2010; **2**: 24-42 [PMID: 24511335]

22 **Kiu R**, Hall LJ. An update on the human and animal enteric pathogen Clostridium perfringens. *Emerg Microbes Infect* 2018; **7**: 141 [PMID: 30082713 DOI: 10.1038/s41426-018-0144-8]

23 **Revitt-Mills SA**, Rood JI, Adams V. Clostridium perfringens extracellular toxins and enzymes: 20 and counting. *Microbiol Aust* 2015; **36** [DOI: 10.1071/MA15039]

24 **Liu F**, Li J, Guan Y, Lou Y, Chen H, Xu M, Deng D, Chen J, Ni B, Zhao L, Li H, Sang H, Cai X. Dysbiosis of the Gut Microbiome is associated with Tumor Biomarkers in Lung Cancer. *Int J Biol Sci* 2019; **15**: 2381-2392 [PMID: 31595156 DOI: 10.7150/ijbs.35980]

25 **Rood JI**, Adams V, Lacey J, Lyras D, McClane BA, Melville SB, Moore RJ, Popoff MR, Sarker MR, Songer JG, Uzal FA, Van Immerseel F. Expansion of the Clostridium perfringens toxin-based typing scheme. *Anaerobe* 2018; **53**: 5-10 [PMID: 29866424 DOI: 10.1016/j.anaerobe.2018.04.011]

26 **Hotze EM**, Tweten RK. Membrane assembly of the cholesterol-dependent cytolysin pore complex. *Biochim Biophys Acta* 2012; **1818**: 1028-1038 [PMID: 21835159 DOI: 10.1016/j.bbamem.2011.07.036]

27 **Schwabe RF**, Jobin C. The microbiome and cancer. *Nat Rev Cancer* 2013; **13**: 800-812 [PMID: 24132111 DOI: 10.1038/nrc3610]

28 **Jewell SA**, Titball RW, Huyet J, Naylor CE, Basak AK, Gologan P, Winlove CP, Petrov PG. Clostridium perfringensα-toxin interaction with red cells and model membranes. *Soft Matter* 2015; **11**: 7748-7761 [PMID: 26303814 DOI: 10.1039/c5sm00876j]

29 **Junior CAO**, Silva ROS, Lobato FCF, Navarro MA, Uzal FA. Gas gangrene in mammals: a review. *J Vet Diagn Invest* 2020; **32**: 175-183 [PMID: 32081096 DOI: 10.1177/1040638720905830]

30 **Takehara M**, Takagishi T, Seike S, Ohtani K, Kobayashi K, Miyamoto K, Shimizu T, Nagahama M. Clostridium perfringens α-Toxin Impairs Innate Immunity *via* Inhibition of Neutrophil Differentiation. *Sci Rep* 2016; **6**: 28192 [PMID: 27306065 DOI: 10.1038/srep28192]

31 **Hunter SE**, Brown JE, Oyston PC, Sakurai J, Titball RW. Molecular genetic analysis of beta-toxin of Clostridium perfringens reveals sequence homology with alpha-toxin, gamma-toxin, and leukocidin of Staphylococcus aureus. *Infect Immun* 1993; **61**: 3958-3965 [PMID: 8359918 DOI: 10.1128/iai.61.9.3958-3965.1993]

32 **Matsuda T**, Okada Y, Inagi E, Tanabe Y, Shimizu Y, Nagashima K, Sakurai J, Nagahama M, Tanaka S. Enteritis necroticans 'pigbel' in a Japanese diabetic adult. *Pathol Int* 2007; **57**: 622-626 [PMID: 17685936 DOI: 10.1111/j.1440-1827.2007.02149.x]

33 **Posthaus H**, Kittl S, Tarek B, Bruggisser J. *Clostridium perfringens* type C necrotic enteritis in pigs: diagnosis, pathogenesis, and prevention. *J Vet Diagn Invest* 2020; **32**: 203-212 [PMID: 31955664 DOI: 10.1177/1040638719900180]

34 **Thiel A**, Mogel H, Bruggisser J, Baumann A, Wyder M, Stoffel MH, Summerfield A, Posthaus H. Effect of Clostridium perfringens β-Toxin on Platelets. *Toxins (Basel)* 2017; **9** [PMID: 29064418 DOI: 10.3390/toxins9100336]

35 **Wagley S**, Bokori-Brown M, Morcrette H, Malaspina A, D'Arcy C, Gnanapavan S, Lewis N, Popoff MR, Raciborska D, Nicholas R, Turner B, Titball RW. Evidence of Clostridium perfringens epsilon toxin associated with multiple sclerosis.

Mult Scler 2019; **25**: 653-660 [PMID: 29681209 DOI: 10.1177/1352458518767327]
36 **Savva CG**, Clark AR, Naylor CE, Popoff MR, Moss DS, Basak AK, Titball RW, Bokori-Brown M. The pore structure of Clostridium perfringens epsilon toxin. *Nat Commun* 2019; **10**: 2641 [PMID: 31201325 DOI: 10.1038/s41467-019-10645-8]
37 **Popoff MR**. Epsilon toxin: a fascinating pore-forming toxin. *FEBS J* 2011; **278**: 4602-4615 [PMID: 21535407 DOI: 10.1111/j.1742-4658.2011.08145.x]
38 **Freedman JC**, McClane BA, Uzal FA. New insights into Clostridium perfringens epsilon toxin activation and action on the brain during enterotoxemia. *Anaerobe* 2016; **41**: 27-31 [PMID: 27321761 DOI: 10.1016/j.anaerobe.2016.06.006]
39 **Harkness JM**, Li J, McClane BA. Identification of a lambda toxin-negative Clostridium perfringens strain that processes and activates epsilon prototoxin intracellularly. *Anaerobe* 2012; **18**: 546-552 [PMID: 22982043 DOI: 10.1016/j.anaerobe.2012.09.001]
40 **Freedman JC**, Shrestha A, McClane BA. Clostridium perfringens Enterotoxin: Action, Genetics, and Translational Applications. *Toxins (Basel)* 2016; **8** [PMID: 26999202 DOI: 10.3390/toxins8030073]
41 **Grass JE**, Gould LH, Mahon BE. Epidemiology of foodborne disease outbreaks caused by Clostridium perfringens, United States, 1998-2010. *Foodborne Pathog Dis* 2013; **10**: 131-136 [PMID: 23379281 DOI: 10.1089/fpd.2012.1316]
42 **Li J**, Miyamoto K, Sayeed S, McClane BA. Organization of the cpe locus in CPE-positive clostridium perfringens type C and D isolates. *PLoS One* 2010; **5**: e10932 [PMID: 20532170 DOI: 10.1371/journal.pone.0010932]
43 **Rood JI**, Keyburn AL, Moore RJ. NetB and necrotic enteritis: the hole movable story. *Avian Pathol* 2016; **45**: 295-301 [PMID: 27009522 DOI: 10.1080/03079457.2016.1158781]
44 **Keyburn AL**, Bannam TL, Moore RJ, Rood JI. NetB, a pore-forming toxin from necrotic enteritis strains of Clostridium perfringens. *Toxins (Basel)* 2010; **2**: 1913-1927 [PMID: 22069665 DOI: 10.3390/toxins2071913]
45 **Chen J**, McClane BA. Characterization of Clostridium perfringens TpeL toxin gene carriage, production, cytotoxic contributions, and trypsin sensitivity. *Infect Immun* 2015; **83**: 2369-2381 [PMID: 25824828 DOI: 10.1128/IAI.03136-14]
46 **Schorch B**, Heni H, Zahaf NI, Brummer T, Mione M, Schmidt G, Papatheodorou P, Aktories K. Targeting oncogenic Ras by the *Clostridium perfringens* toxin TpeL. *Oncotarget* 2018; **9**: 16489-16500 [PMID: 29662661 DOI: 10.18632/oncotarget.24740]
47 **Pierce JV**, Bernstein HD. Genomic Diversity of Enterotoxigenic Strains of Bacteroides fragilis. *PLoS One* 2016; **11**: e0158171 [PMID: 27348220 DOI: 10.1371/journal.pone.0158171]
48 **Shah N**, Osmon D, Tande AJ, Steckelberg J, Sierra R, Walker R, Berbari EF. Clinical and Microbiological Characteristics of *Bacteroides* Prosthetic Joint Infections. *J Bone Jt Infect* 2017; **2**: 122-126 [PMID: 28540148 DOI: 10.7150/jbji.17129]
49 **Zhang G**, Svenungsson B, Kärnell A, Weintraub A. Prevalence of enterotoxigenic Bacteroides fragilis in adult patients with diarrhea and healthy controls. *Clin Infect Dis* 1999; **29**: 590-594 [PMID: 10530453 DOI: 10.1086/598639]
50 **Sears CL**. Enterotoxigenic Bacteroides fragilis: a rogue among symbiotes. *Clin Microbiol Rev* 2009; **22**: 349-369, Table of Contents [PMID: 19366918 DOI: 10.1128/CMR.00053-08]
51 **Wu S**, Rhee KJ, Zhang M, Franco A, Sears CL. Bacteroides fragilis toxin stimulates intestinal epithelial cell shedding and gamma-secretase-dependent E-cadherin cleavage. *J Cell Sci* 2007; **120**: 1944-1952 [PMID: 17504810 DOI: 10.1242/jcs.03455]
52 **Deng H**, Li Z, Tan Y, Guo Z, Liu Y, Wang Y, Yuan Y, Yang R, Bi Y, Bai Y, Zhi F. A novel strain of Bacteroides fragilis enhances phagocytosis and polarises M1 macrophages. *Sci Rep* 2016; **6**: 29401 [PMID: 27381366 DOI: 10.1038/srep29401]
53 **DeStefano Shields CE**, Van Meerbeke SW, Housseau F, Wang H, Huso DL, Casero RA Jr, O'Hagan HM, Sears CL. Reduction of Murine Colon Tumorigenesis Driven by Enterotoxigenic Bacteroides fragilis Using Cefoxitin Treatment. *J Infect Dis* 2016; **214**: 122-129 [PMID: 26908749 DOI: 10.1093/infdis/jiw069]
54 **Chung L**, Thiele Orberg E, Geis AL, Chan JL, Fu K, DeStefano Shields CE, Dejea CM, Fathi P, Chen J, Finard BB, Tam AJ, McAllister F, Fan H, Wu X, Ganguly S, Lebid A, Metz P, Van Meerbeke SW, Huso DL, Wick EC, Pardoll DM, Wan F, Wu S, Sears CL, Housseau F. Bacteroides fragilis Toxin Coordinates a Pro-carcinogenic Inflammatory Cascade *via* Targeting of Colonic Epithelial Cells. *Cell Host Microbe* 2018; **23**: 203-214.e5 [PMID: 29398651 DOI: 10.1016/j.chom.2018.01.007]
55 **Tjalsma H**, Boleij A, Marchesi JR, Dutilh BE. A bacterial driver-passenger model for colorectal cancer: beyond the usual suspects. *Nat Rev Microbiol* 2012; **10**: 575-582 [PMID: 22728587 DOI: 10.1038/nrmicro2819]
56 **Avril M**, DePaolo RW. "Driver-passenger" bacteria and their metabolites in the pathogenesis of colorectal cancer. *Gut Microbes* 2021; **13**: 1941710 [PMID: 34225577 DOI: 10.1080/19490976.2021.1941710]

World Journal of Gastroenterology

Submit a Manuscript: https://www.f6publishing.com

World J Gastroenterol 2022 July 14; 28(26): 3279-3281

DOI: 10.3748/wjg.v28.i26.3279

ISSN 1007-9327 (print) ISSN 2219-2840 (online)

LETTER TO THE EDITOR

Intestinal virome: An important research direction for alcoholic and nonalcoholic liver diseases

Yan Li, Wen-Cheng Liu, Bing Chang

Specialty type: Gastroenterology and hepatology

Provenance and peer review: Unsolicited article; Externally peer reviewed.

Peer-review model: Single blind

Peer-review report's scientific quality classification

Grade A (Excellent): A
Grade B (Very good): B
Grade C (Good): 0
Grade D (Fair): 0
Grade E (Poor): 0

P-Reviewer: AbdEl-Wahab EW, Ghoneim S

Received: November 3, 2021
Peer-review started: November 3, 2021
First decision: November 29, 2021
Revised: December 7, 2021
Accepted: June 13, 2022
Article in press: June 13, 2022
Published online: July 14, 2022

Yan Li, Wen-Cheng Liu, Bing Chang, Department of Gastroenterology, The First Affiliated Hospital of China Medical University, Shenyang 110001, Liaoning Province, China

Corresponding author: Bing Chang, MD, Associate Professor, Department of Gastroenterology, The First Affiliated Hospital of China Medical University, No. 155 Nanjing North Street, Heping District, Shenyang 110001, Liaoning Province, China. cb000216@163.com

Abstract

In recent years, the interaction between the gut microflora and liver diseases has attracted much attention. The intestinal microflora is composed of bacteria, archaea, fungi and viruses. There are few studies on the intestinal virome, and whether it has a causal relationship with bacterial changes in the gut is still unclear. However, it is undeniable that the intestinal virome is also a very important portion of the blueprint for the development of liver diseases and the diagnosis and therapeutic modalities in the future.

Key Words: Alcoholic fatty liver disease; Nonalcoholic fatty liver disease; Fatty liver disease; Gut microbiome; Intestinal virome

©The Author(s) 2022. Published by Baishideng Publishing Group Inc. All rights reserved.

Core Tip: As of the study of the gut microflora expands, the interaction between the intestinal virome and liver diseases has been gradually revealed. In this letter to the editor, we discuss the changes in the intestinal virome in patients with alcoholic liver disease and nonalcoholic liver disease, and provide suggestions for developing future diagnosis and treatment methods.

Citation: Li Y, Liu WC, Chang B. Intestinal virome: An important research direction for alcoholic and nonalcoholic liver diseases. *World J Gastroenterol* 2022; 28(26): 3279-3281
URL: https://www.wjgnet.com/1007-9327/full/v28/i26/3279.htm
DOI: https://dx.doi.org/10.3748/wjg.v28.i26.3279

TO THE EDITOR

We have carefully studied the reviews recently written by Sharma *et al*[1], titled "Significance of gut microbiota in alcoholic and nonalcoholic fatty liver diseases". The authors elaborated the intestinal microecological changes in both alcoholic and nonalcoholic liver diseases, and the important effects of intestinal microorganisms on the development of fatty liver diseases. These findings could provide new ideas for the future diagnosis and treatment of fatty liver disease.

In addition to bacteria, archaea and a small amount of fungi, viruses are also an indispensable part of the intestinal microflora in human[2] . In 2020, a multicenter observational study on the enteroviruses from 89 patients with alcoholic hepatitis, 36 patients with alcohol use disorder and 17 patients without alcohol use disorder was concluded[3]. The results showed that in stool samples from patients with alcoholic liver disease, bacterial and fungal diversity decreased and virus diversity increased, which mainly manifested as a large increase in the number of *Myoviridae*, *Lactobacillus* phages, *Streptococcus* phages, *Podoviridae*, *Geobacillus* phages, *Escherichia* phages, and *Herpesviridae*[3]. This trend was positively correlated with the severity of the disease. The changes in the intestinal microecology of people with alcohol use disorder are mainly characterized by an increase in *Parvoviridae* and *Lactococcus* phages[3]. Another study of the intestinal virome in patients with nonalcoholic fatty liver disease (NAFLD) showed that the average relative abundance and viral diversity of phages in patients with NAFLD and severe hepatic fibrosis were significantly lower than those in patients with NAFLD and no or mild hepatic fibrosis[4]. Hence viruses also have positive implications in the diagnosis, severity classification, treatment and prognosis of alcoholic and nonalcoholic liver diseases. However, as an easily neglected part of gut microecology, the impact of viruses was not mentioned in Sharma *et al*[1]'s article.

Bacteria and fungi in the gut microflora have large individual variability and are susceptible to various factors such as age, drugs[5], environment[6], and diet[7]. Likewise, the same is true for viruses. A shotgun metagenome sequencing analysis of DNA viruses in fecal samples from cynomolgus monkeys of different ages showed that the abundance of DNA viruses was inversely proportional to age; that is, the DNA virus group in fecal samples of elderly individuals decreased significantly[8]. However, Lang *et al*[4] found that after the use of proton pump inhibitors, enteroviruses in the feces of patients with nonalcoholic liver disease were also changed. In addition, in high-fat diet-fed mice, the structural composition and β-diversity of enteroviruses were changed. There was a significant decrease in the expression of *Siphoviridae* and a significant increase in the expression of the eukaryotic viruses *Phycodnaviridae* and *Mimivirdae*, and these changes were accompanied by changes in intestinal bacteria [9]. Therefore, considering the original proposal that gut microorganisms should be included in future liver disease diagnosis and treatment, we suggest that in addition to performing a horizontal comparison and finding representative biological markers, it is indispensable to have a methodological design and vertical comparison. However, the effects of confounding factors should also be considered, and individualized diagnosis and treatment plans should be developed for different patients.

ACKNOWLEDGEMENTS

We would like to thank the Department of Gastroenterology of the First Affiliated Hospital of China Medical University for technical assistance.

FOOTNOTES

Author contributions: Li Y and Liu WC wrote this manuscript; Li Y and Chang B revised this manuscript; and all the authors contributed to the writing of this manuscript.

Conflict-of-interest statement: All the authors report no relevant conflicts of interest for this article.

Open-Access: This article is an open-access article that was selected by an in-house editor and fully peer-reviewed by external reviewers. It is distributed in accordance with the Creative Commons Attribution NonCommercial (CC BY-NC 4.0) license, which permits others to distribute, remix, adapt, build upon this work non-commercially, and license their derivative works on different terms, provided the original work is properly cited and the use is non-commercial. See: https://creativecommons.org/Licenses/by-nc/4.0/

Country/Territory of origin: China

ORCID number: Yan Li 0000-0002-1749-0283; Wen-Cheng Liu 0000-0002-7721-6892; Bing Chang 0000-0003-1965-5827.

S-Editor: Antwi SO, United States S-Editor
L-Editor: A

P-Editor: Wang JJ

REFERENCES

1 **Sharma SP**, Suk KT, Kim DJ. Significance of gut microbiota in alcoholic and non-alcoholic fatty liver diseases. *World J Gastroenterol* 2021; **27**: 6161-6179 [PMID: 34712025 DOI: 10.3748/wjg.v27.i37.6161]

2 **Whon TW**, Shin NR, Kim JY, Roh SW. Omics in gut microbiome analysis. *J Microbiol* 2021; **59**: 292-297 [PMID: 33624266 DOI: 10.1007/s12275-021-1004-0]

3 **Jiang L**, Lang S, Duan Y, Zhang X, Gao B, Chopyk J, Schwanemann LK, Ventura-Cots M, Bataller R, Bosques-Padilla F, Verna EC, Abraldes JG, Brown RS Jr, Vargas V, Altamirano J, Caballería J, Shawcross DL, Ho SB, Louvet A, Lucey MR, Mathurin P, Garcia-Tsao G, Kisseleva T, Brenner DA, Tu XM, Stärkel P, Pride D, Fouts DE, Schnabl B. Intestinal Virome in Patients With Alcoholic Hepatitis. *Hepatology* 2020; **72**: 2182-2196 [PMID: 32654263 DOI: 10.1002/hep.31459]

4 **Lang S**, Demir M, Martin A, Jiang L, Zhang X, Duan Y, Gao B, Wisplinghoff H, Kasper P, Roderburg C, Tacke F, Steffen HM, Goeser T, Abraldes JG, Tu XM, Loomba R, Stärkel P, Pride D, Fouts DE, Schnabl B. Intestinal Virome Signature Associated With Severity of Nonalcoholic Fatty Liver Disease. *Gastroenterology* 2020; **159**: 1839-1852 [PMID: 32652145 DOI: 10.1053/j.gastro.2020.07.005]

5 **Fasullo M**, Rau P, Liu DQ, Holzwanger E, Mathew JP, Guilarte-Walker Y, Szabo G. Proton pump inhibitors increase the severity of hepatic encephalopathy in cirrhotic patients. *World J Hepatol* 2019; **11**: 522-530 [PMID: 31293720 DOI: 10.4254/wjh.v11.i6.522]

6 **Ng KM**, Aranda-Díaz A, Tropini C, Frankel MR, Van Treuren W, O'Loughlin CT, Merrill BD, Yu FB, Pruss KM, Oliveira RA, Higginbottom SK, Neff NF, Fischbach MA, Xavier KB, Sonnenburg JL, Huang KC. Recovery of the Gut Microbiota after Antibiotics Depends on Host Diet, Community Context, and Environmental Reservoirs. *Cell Host Microbe* 2019; **26**: 650-665.e4 [PMID: 31726029 DOI: 10.1016/j.chom.2019.10.011]

7 **González Olmo BM**, Butler MJ, Barrientos RM. Evolution of the Human Diet and Its Impact on Gut Microbiota, Immune Responses, and Brain Health. *Nutrients* 2021; **13** [PMID: 33435203 DOI: 10.3390/nu13010196]

8 **Tan X**, Chai T, Duan J, Wu J, Zhang H, Li Y, Huang Y, Hu X, Zheng P, Song J, Ji P, Jin X, Xie P. Dynamic changes occur in the DNA gut virome of female cynomolgus macaques during aging. *Microbiologyopen* 2021; **10**: e1186 [PMID: 33970533 DOI: 10.1002/mbo3.1186]

9 **Schulfer A**, Santiago-Rodriguez TM, Ly M, Borin JM, Chopyk J, Blaser MJ, Pride DT. Fecal Viral Community Responses to High-Fat Diet in Mice. *mSphere* 2020; **5** [PMID: 32102942 DOI: 10.1128/msphere.00833-19]



Published by **Baishideng Publishing Group Inc**
7041 Koll Center Parkway, Suite 160, Pleasanton, CA 94566, USA
Telephone: +1-925-3991568
E-mail: bpgoffice@wjgnet.com
Help Desk: https://www.f6publishing.com/helpdesk
https://www.wjgnet.com



© 2022 Baishideng Publishing Group Inc. All rights reserved.

ISSN 1007-9327 (print)
ISSN 2219-2840 (online)

World Journal of *Gastroenterology*

World J Gastroenterol 2022 July 21; 28(27): 3282-3534



Published by Baishideng Publishing Group Inc

World Journal of Gastroenterology

Contents

Weekly Volume 28 Number 27 July 21, 2022

REVIEW

3282 Hepatitis B and circadian rhythm of the liver

Skrlec I, Talapko J

3297 Tumor microenvironment in pancreatic ductal adenocarcinoma: Implications in immunotherapy

Smith C, Zheng W, Dong J, Wang Y, Lai J, Liu X, Yin F

3314 Crosstalk between dietary patterns, obesity and nonalcoholic fatty liver disease

Ristic-Medic D, Bajerska J, Vucic V

MINIREVIEWS

3334 Application of intravoxel incoherent motion diffusion-weighted imaging in hepatocellular carcinoma

Zhou Y, Zheng J, Yang C, Peng J, Liu N, Yang L, Zhang XM

3346 Regulatory T cells and their associated factors in hepatocellular carcinoma development and therapy

Zhang CY, Liu S, Yang M

3359 Single-incision laparoscopic surgery to treat hepatopancreatobiliary cancer: A technical review

Chuang SH, Chuang SC

3370 Probiotics and postbiotics in colorectal cancer: Prevention and complementary therapy

Kvakova M, Kamlarova A, Stofilova J, Benetinova V, Bertkova I

3383 Interventional strategies in infected necrotizing pancreatitis: Indications, timing, and outcomes

Purschke B, Bolm L, Meyer MN, Sato H

3398 Artificial intelligence in liver ultrasound

Cao LL, Peng M, Xie X, Chen GQ, Huang SY, Wang JY, Jiang F, Cui XW, Dietrich CF

3410 Risk factors and diagnostic biomarkers for nonalcoholic fatty liver disease-associated hepatocellular carcinoma: Current evidence and future perspectives

Ueno M, Takeda H, Takai A, Seno H

ORIGINAL ARTICLE

Basic Study

3422 Accumulation of poly (adenosine diphosphate-ribose) by sustained supply of calcium inducing mitochondrial stress in pancreatic cancer cells

Jeong KY, Sim JJ, Park M, Kim HM

World Journal of Gastroenterology

Weekly Volume 28 Number 27 July 21, 2022

Contents

3435 RING finger and WD repeat domain 3 regulates proliferation and metastasis through the Wnt/β-catenin signalling pathways in hepatocellular carcinoma

Liang RP, Zhang XX, Zhao J, Lu QW, Zhu RT, Wang WJ, Li J, Bo K, Zhang CX, Sun YL

3455 Associations of gut microbiota with dyslipidemia based on sex differences in subjects from Northwestern China

Guo L, Wang YY, Wang JH, Zhao HP, Yu Y, Wang GD, Dai K, Yan YZ, Yang YJ, Lv J

Retrospective Cohort Study

3476 Prognostic significance of hemoglobin, albumin, lymphocyte, platelet in gastrointestinal stromal tumors: A propensity matched retrospective cohort study

Zhao Z, Yin XN, Wang J, Chen X, Cai ZL, Zhang B

Retrospective Study

3488 Contrast-enhanced ultrasound Liver Imaging Reporting and Data System: Lights and shadows in hepatocellular carcinoma and cholangiocellular carcinoma diagnosis

Vidili G, Arru M, Solinas G, Calvisi DF, Meloni P, Sauchella A, Turilli D, Fabio C, Cossu A, Madeddu G, Babudieri S, Zocco MA, Iannetti G, Di Lembo E, Delitala AP, Manetti R

3503 Novel index for the prediction of significant liver fibrosis and cirrhosis in chronic hepatitis B patients in China

Liao MJ, Li J, Dang W, Chen DB, Qin WY, Chen P, Zhao BG, Ren LY, Xu TF, Chen HS, Liao WJ

SYSTEMATIC REVIEWS

3514 Percutaneous transhepatic cholangiography *vs* endoscopic ultrasound-guided biliary drainage: A systematic review

Hassan Z, Gadour E

CASE REPORT

3524 Isolated gastric variceal bleeding related to non-cirrhotic portal hypertension following oxaliplatin-based chemotherapy: A case report

Zhang X, Gao YY, Song DZ, Qian BX

LETTER TO THE EDITOR

3532 Hepatitis B core-related antigen: Are we near a treatment endpoint?

Gupta T

Contents

ABOUT COVER

Editorial Board Member of *World Journal of Gastroenterology*, Govind K Makharia, MD, DM,DNB, Professor, Department of Gastroenterology and Human Nutrition, All India Institute of Medical Sciences, Ansari Nagar, New Delhi 110029, India. govindmakharia@aiims.edu

AIMS AND SCOPE

The primary aim of *World Journal of Gastroenterology* (*WJG*, *World J Gastroenterol*) is to provide scholars and readers from various fields of gastroenterology and hepatology with a platform to publish high-quality basic and clinical research articles and communicate their research findings online. *WJG* mainly publishes articles reporting research results and findings obtained in the field of gastroenterology and hepatology and covering a wide range of topics including gastroenterology, hepatology, gastrointestinal endoscopy, gastrointestinal surgery, gastrointestinal oncology, and pediatric gastroenterology.

INDEXING/ABSTRACTING

The *WJG* is now abstracted and indexed in Science Citation Index Expanded (SCIE, also known as SciSearch®), Current Contents/Clinical Medicine, Journal Citation Reports, Index Medicus, MEDLINE, PubMed, PubMed Central, Scopus, Reference Citation Analysis, China National Knowledge Infrastructure, China Science and Technology Journal Database, and Superstar Journals Database. The 2022 edition of Journal Citation Reports® cites the 2021 impact factor (IF) for *WJG* as 5.374; IF without journal self cites: 5.187; 5-year IF: 5.715; Journal Citation Indicator: 0.84; Ranking: 31 among 93 journals in gastroenterology and hepatology; and Quartile category: Q2. The *WJG*'s CiteScore for 2021 is 8.1 and Scopus CiteScore rank 2021: Gastroenterology is 18/149.

RESPONSIBLE EDITORS FOR THIS ISSUE

Production Editor: *Wen-Wen Qi*; **Production Department Director:** *Xiang Li*; **Editorial Office Director:** *Jia-Ru Fan.*

NAME OF JOURNAL
World Journal of Gastroenterology

ISSN
ISSN 1007-9327 (print) ISSN 2219-2840 (online)

LAUNCH DATE
October 1, 1995

FREQUENCY
Weekly

EDITORS-IN-CHIEF
Andrzej S Tarnawski

EDITORIAL BOARD MEMBERS
http://www.wjgnet.com/1007-9327/editorialboard.htm

PUBLICATION DATE
July 21, 2022

COPYRIGHT
© 2022 Baishideng Publishing Group Inc

INSTRUCTIONS TO AUTHORS
https://www.wjgnet.com/bpg/gerinfo/204

GUIDELINES FOR ETHICS DOCUMENTS
https://www.wjgnet.com/bpg/GerInfo/287

GUIDELINES FOR NON-NATIVE SPEAKERS OF ENGLISH
https://www.wjgnet.com/bpg/gerinfo/240

PUBLICATION ETHICS
https://www.wjgnet.com/bpg/GerInfo/288

PUBLICATION MISCONDUCT
https://www.wjgnet.com/bpg/gerinfo/208

ARTICLE PROCESSING CHARGE
https://www.wjgnet.com/bpg/gerinfo/242

STEPS FOR SUBMITTING MANUSCRIPTS
https://www.wjgnet.com/bpg/GerInfo/239

ONLINE SUBMISSION
https://www.f6publishing.com

© 2022 Baishideng Publishing Group Inc. All rights reserved. 7041 Koll Center Parkway, Suite 160, Pleasanton, CA 94566, USA
E-mail: bpgoffice@wjgnet.com https://www.wjgnet.com

World Journal of Gastroenterology

Submit a Manuscript: https://www.f6publishing.com

World J Gastroenterol 2022 July 21; 28(27): 3282-3296

DOI: 10.3748/wjg.v28.i27.3282

ISSN 1007-9327 (print) ISSN 2219-2840 (online)

REVIEW

Hepatitis B and circadian rhythm of the liver

Ivana Skrlec, Jasminka Talapko

Specialty type: Gastroenterology and hepatology

Provenance and peer review: Invited article; Externally peer reviewed.

Peer-review model: Single blind

Peer-review report's scientific quality classification

Grade A (Excellent): A, A
Grade B (Very good): B
Grade C (Good): C
Grade D (Fair): 0
Grade E (Poor): 0

P-Reviewer: Jiang W, China; Miyoshi E, Japan; Shkodina A, Ukraine
A-Editor: de Melo FF, Brazil

Received: January 11, 2022
Peer-review started: January 11, 2022
First decision: March 8, 2022
Revised: March 15, 2022
Accepted: June 13, 2022
Article in press: June 13, 2022
Published online: July 21, 2022

Ivana Skrlec, Department of Biophysics, Biology, and Chemistry, Faculty of Dental Medicine and Health, J. J. Strossmayer University of Osijek, Osijek 31000, Croatia

Jasminka Talapko, Department of Anatomy Histology, Embryology, Pathology Anatomy and Pathology Histology, Faculty of Dental Medicine and Health, Osijek 31000, Croatia

Corresponding author: Ivana Skrlec, MSc, PhD, Assistant Professor, Department of Biophysics, Biology, and Chemistry, Faculty of Dental Medicine and Health, J. J. Strossmayer University of Osijek, 21 Crkvena, Osijek 31000, Croatia. iskrlec@fdmz.hr

Abstract

The circadian rhythm in humans is determined by the central clock located in the hypothalamus's suprachiasmatic nucleus, and it synchronizes the peripheral clocks in other tissues. Circadian clock genes and clock-controlled genes exist in almost all cell types. They have an essential role in many physiological processes, including lipid metabolism in the liver, regulation of the immune system, and the severity of infections. In addition, circadian rhythm genes can stimulate the immune response of host cells to virus infection. Hepatitis B virus (HBV) infection is the leading cause of liver disease and liver cancer globally. HBV infection depends on the host cell, and hepatocyte circadian rhythm genes are associated with HBV replication, survival, and spread. The core circadian rhythm proteins, REV-ERB and brain and muscle ARNTL-like protein 1, have a crucial role in HBV replication in hepatocytes. In addition to influencing the virus's life cycle, the circadian rhythm also affects the pharmacokinetics and efficacy of antiviral vaccines. Therefore, it is vital to apply antiviral therapy at the appropriate time of day to reduce toxicity and improve the effectiveness of antiviral treatment. For these reasons, understanding the role of the circadian rhythm in the regulation of HBV infection and host responses to the virus provides us with a new perspective of the interplay of the circadian rhythm and anti-HBV therapy. Therefore, this review emphasizes the importance of the circadian rhythm in HBV infection and the optimization of antiviral treatment based on the circadian rhythm-dependent immune response.

Key Words: Circadian rhythm; Clock genes; Hepatitis B virus; Immune system; Liver

©The Author(s) 2022. Published by Baishideng Publishing Group Inc. All rights reserved.

Core Tip: Some studies in the literature contribute to the association of the circadian rhythm and liver pathophysiology associated with hepatitis B virus (HBV) infection. However, this is the first review to report the latest molecular mechanisms of HBV infection, including cellular circadian rhythm disorders, circadian clock-related immune response, therapeutic strategies in improving health outcomes, and the significance of personalized medicine and chronotherapy in treating chronic HBV infections.

Citation: Skrlec I, Talapko J. Hepatitis B and circadian rhythm of the liver. *World J Gastroenterol* 2022; 28(27): 3282-3296
URL: https://www.wjgnet.com/1007-9327/full/v28/i27/3282.htm
DOI: https://dx.doi.org/10.3748/wjg.v28.i27.3282

INTRODUCTION

The circadian rhythm in humans is determined by the central clock found in the hypothalamus's suprachiasmatic nucleus (SCN) which receives light signals from the retina[1]. Endogenous functional circadian rhythms are active in peripheral tissues. For example, the circadian clock in humans, expressed in almost every cell, consists of a whole range of transcription-translation feedback loops[2]. Furthermore, all peripheral clocks in every tissue are synchronized by the central clock in the SCN[3]. Therefore, circadian clock genes and clock-controlled genes (CCG) exist in almost all cell types. Approximately 10%-40% of the genome is encoded in a circadian manner[4]. Furthermore, most physiological processes, such as lipid metabolism, immune system regulation, and infection severity, are under circadian control, and therefore circadian rhythm disorders can result in pathophysiological changes downstream[4,5].

The liver has a vital role in maintaining energy homeostasis within the body. The primary biochemical reactions within the liver are involved in the breakdown and generation of glucose, which is associated with fatty acid metabolism[6]. In addition, the metabolic functions of the liver show rhythmic fluctuations with a periodicity of 24 h[6]. Hepatitis-causing viruses depend closely on hepatocytes for replication, survival, and spread[6]. In addition, viral infection can disrupt the hepatocytes' circadian rhythm[5]. Circadian rhythm transcription factors alter liver metabolism and are linked with various conditions, including viral infection, fatty liver disease, diabetes, and hepatocellular carcinoma (HCC)[1].

What makes the hepatitis B virus (HBV) significantly different from other hepatotropic viruses is its global impact on human health[7], namely, infections caused by this virus result in liver disease, which is a growing global problem[8]. According to the World Health Organization (WHO), it is estimated that 296 million people lived with chronic hepatitis B in 2019, and that 1.5 million new infections are detected each year[9]. Furthermore, due to HBV infection in 2019, mainly from cirrhosis and HCC, about 820000 people died[10]. Hepatitis B can develop in an acute or chronic form[11]. Most infected people do not have any symptoms, which does not mean that there is no disease. Symptoms of acute infection usually occur 2 mo to 3 mo after infection and are nonspecific[12,13].

The HBV begins to multiply within the first 3 d of infection[14]. Whether and to what extent liver damage occurs depends on the infected person's immune system, the infectious dose, and the site of virus entry. Tissue compatibility antigens and interferon promote the viral antigens' [hepatitis B surface antigen (HBsAg), hepatitis B envelope antigen (HbeAg), and hepatitis B core antigen (HBcAg)] exposure to cytotoxic T lymphocytes[15]. If there is no adequate response by these cells, milder signs of the disease occur, which may progress to the development of chronic hepatitis[16]. About 10% of acute HBV infections progress to a chronic form[17]. Chronic HBV can be clinically manifested as mild conditions to severe chronic hepatitis[18], which, in untreated cases, results in 8%-20% of cases with cirrhosis and HCC[19]. Persistent hepatitis is a mild disease that occurs in 8%-10% of patients, occasionally causing elevated aminotransferases, but generally does not progress toward cirrhosis and has a favorable prognosis[20]. HBV plays a significant role in the development of HCC, which can occur many years after chronic infection[21]. Still, typically the HBV is not a cytopathogen, and cell damage is thought to be mediated by a persistently unproductive immune response[17].

Therefore, this mini-review highlights the significance of the circadian rhythm in HBV infection, and the effectiveness of therapy in relation to the circadian rhythm-dependent immune response.

HBV

The epidemiological model of the spread of HBV and human immunodeficiency virus (HIV) is the same, but HBV is 50-100 times more infectious than HIV[22]. The source of infection is people with HBV infection[23]. However, the geographical prevalence of HBV infection varies[24]. In addition, it depends

on several factors, such as different modes of transmission in the population and the age at which the infection originated, which relates to the likelihood of progression to chronic infection[25].

HBV is mainly transmitted by percutaneous or mucosal exposure to infected blood or body fluids [26]. Perinatal transmission is the primary route of infection in endemic regions[27], while the most direct route in the low-endemic regions is sexual transmission[28]. Globally, the epidemiology of HBV infection is changing, influenced by infant vaccination programs and migration between low- and high-prevalence populations[29]. On the basis of the available data, it is estimated that the prevalence of new chronic HBV cases is 70% in developing countries[30].

On the basis of the prevalence of the HBsAg, the epidemiology of HBV in certain areas of the world can be classified into one of three categories (Table 1)[31]: Low prevalence areas (< 2%), medium prevalence areas (2%-7%), and high prevalence areas (> 8% HBsAg prevalence)[32]. These categories are important for understanding the transmission and outcome of infection, and the consequences of chronic hepatitis B[25].

Biology and life cycle of HBV

HBV is a DNA virus with ten known genotypes, labeled A-J. HBV belongs to the group of hepatotropic viruses from the family Hepadnaviridae, genus Orthohepadnavirus[33]. It is a small round virus of a very complex structure, 42 nm in diameter, with a double shell (Dane particle) (Table 2)[33]. Genotypes are divided into subgenotypes due to the significant variability of the nucleotide sequences[34]. They are based on a more than 4% difference along the entire genome. In addition, HBV genotypes and subgenotypes are related by geographical distribution, and also related to the pathogenesis and outcome of HBV infection (Table 3)[35].

The HBV genome has 3.2 kb long, relaxed circular, partially double-stranded DNA (rcDNA)[36]. The minus strand is complete, while the plus strand is regularly incomplete with a stable 5′ end, but an inconsistent 3′ end. The 5′ end of the plus strand is covalently linked to the RNA with a 5′ cap formation. In addition, the viral polymerase (reverse transcriptase) is covalently bound to the 5′ end of the minus strand[36,37].

Linear DNA is the direct precursor of viral DNA that is randomly incorporated into the hepatocytes' DNA throughout infection. Incorporated DNA has no role in virus replication[37,38]. The HBV genome is highly compact, with four open reading frames (ORFs) overlapping multiple times and encoding seven proteins[39]. All ORFs are identical orientations and encoded by the negative strand of DNA[40]. Thanks to the ORFs, the coding capacity increases, and DNA is transcribed one and a half to two times because there is no stop codon[41]. In addition to ORF, there are six start codons, four promoters, and two transcription enhancers[42].

ORF C encodes the nuclear core antigen HBc and envelope E antigen (HBe)[39]. The precore protein in serum indicates active virus replication[43]. The presence of HBeAg in serum suggests prevented or decreased virus replication. HBeAg can repress the cellular immune response to HBsAg, thereby reducing perinatal transmission and promoting chronic infection[37,44]. The longest ORF is the P gene, encoding most of the virus genome (80%) and viral polymerase (reverse transcriptase)[45]. The ORF X encoding hepatitis B protein X (HBx) activates viral RNA transcription[37,38]. HBx causes the progression of the cell cycle and is essential for activating the transcription of covalently closed circular DNA (cccDNA) and pregenomic RNA (pgRNA) after infection[37]. ORF S codes three different sizes of the surface S antigen (S-small, M-medium, and L-large HBs)[46]. The M- and L-HBs have additional PreS2 and PreS1 domains[39]. The PreS1 region, present in L-HBsAg, possesses a binding domain for the sodium taurocholate co-transporting polypeptide (NTCP) receptors, essential for viral internalization[37,47]. HBsAg are embedded in the outer lipid envelope, and the inner nucleocapsid structure contains the DNA genome, HBcAg, and viral polymerase (reverse transcriptase)[48]. In addition, HbeAg is between the nucleus and the outer shell[49].

HBV replicates in hepatocytes *via* pgRNA (Figure 1)[35]. The entry of the virus into the hepatocyte is the first step in its life cycle[50]. After the virus enters the liver, S-HBsAg recognizes heparan sulfate proteoglycans (HSPG) on the hepatocytes, and binds them with low affinity[51]. A high-affinity interaction between the PreS1 region of the L-HBs protein and NTCP follows[52]. Later, the virus envelope and the hepatocytes' membrane merge, releasing the nucleocapsid into the cytoplasm[53]. After the capsid shell is removed, the viral genome is transferred to the nucleus. As a result, viral DNA enters the nucleus of the hepatocytes. The relaxed circular (rc) genome is restored, resulting in cccDNA [54]. Viral DNA can be integrated into the hepatocytes' DNA, and is a constant HBsAg source[55]. The cccDNA is a template for pgRNA production and the transcription of all viral mRNAs[37]. On this basis, cccDNA in the hepatocytes can stimulate virus replication[56]. The cccDNA is associated with cellular histones and forms a minichromosome. Each viral protein has a promoter and mRNA, except for reverse transcriptase, translated from the same pgRNA as the virus core protein[37,44]. The onset of infection is indicated by the expression of core proteins and polymerase from pgRNA. HBc is a phosphoprotein and a subunit of the viral nucleocapsid. The core proteins are constructed into nucleocapsids, icosahedral shells of 120 dimers[57]. They merge with RNA and are assembled into core particles. Viral DNA synthesis takes place in the core particles, followed by packaging of pgRNA and polymerase[37,47]. Upon completing viral DNA synthesis by reverse transcription, viral particles can exit the hepatocytes in two ways. First, while envelope protein levels are low, core particles recycle and

Table 1 Prevalence of hepatitis B surface antigen

	Low prevalence area (< 2%)	Area of medium prevalence (2%-7%)	Area of high prevalence (> 8%)
Geographical areas	United states, Canada, and Western European countries	Parts of Russia, border Eurasian, and Asian-African areas	Asia, sub-Saharan Africa, South, and Central America
% of the world population	12%	43%	45%

Table 2 Classification of hepatitis B virus

Genus	Orthohepadnavirus
Family	Hepadnaviridae
Species	HBV
Genotypes	A-J
Virion	42 nm, spherical
Envelope	Yes (HBs)
Genome	Circular ds/ssDNA
Genome size	3.2 kb
Sensitivity	Acid-sensitive
Virus antigens	HBsAg, HBcAg, HBeAg, polymerase

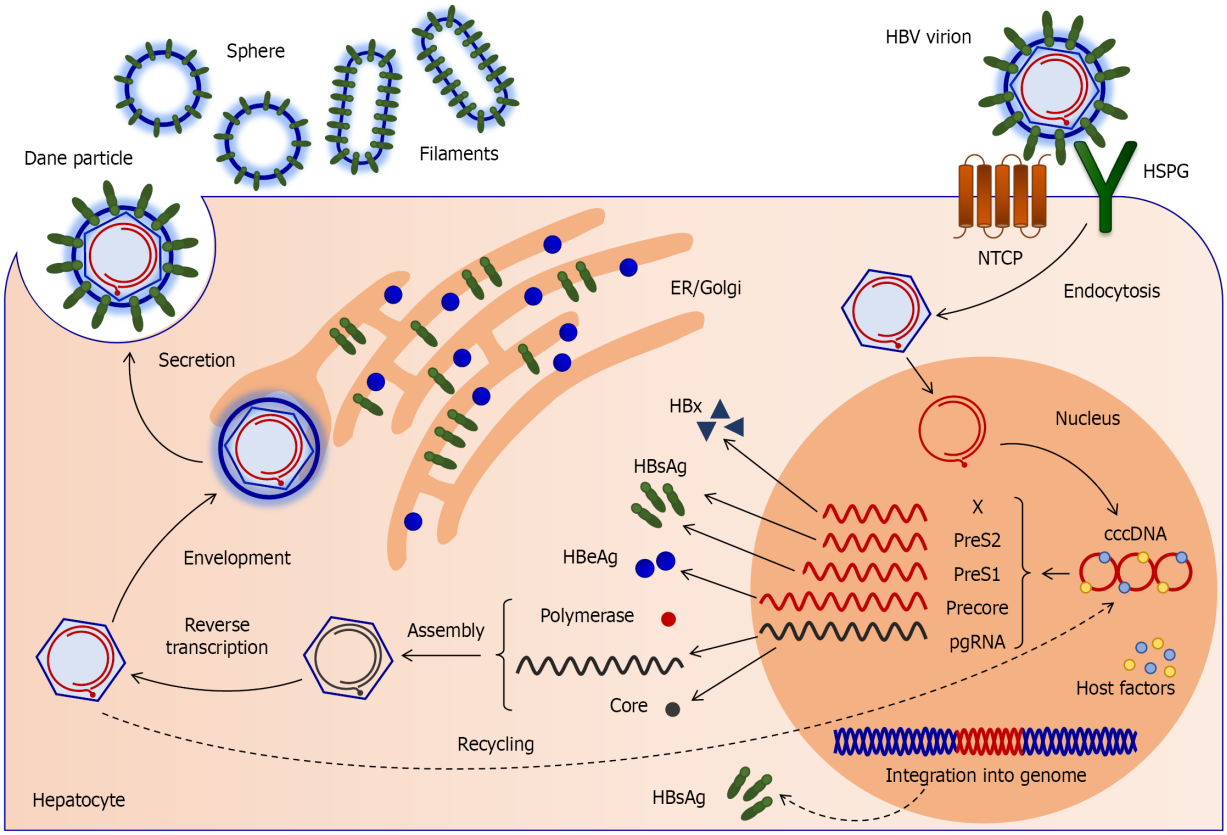
HBV: Hepatitis B virus; HBs: Hepatitis B surface protein; ds/ssDNA: Double-stranded/single-stranded DNA; HBsAg: Hepatitis B surface antigen; HBcAg: Hepatitis B nuclear core antigen; HBeAg: Hepatitis B envelope E antigen.

Table 3 Prevalence of hepatitis B virus genotypes and subgenotypes

Genotype	Subgenotype	Prevalence
A	A1 -A6	Africa, India, Northern Europe, USA
B	B1-B8	Asia, USA
C	C1-C14	Asia, USA
D	D1-D9	India, Middle East, Southern Europe, USA
E	F1-F4	West and South Africa
F		Central and South America
G		Europe, USA
H		Central and South America, California (USA)
I	I1-12	Vietnam
J		Japan

USA: United States.

enter the nucleus, resulting in the replenishment of cccDNA[37,39]. Later, the core particles gather with the envelope proteins in the endoplasmic reticulum, enter the secretory pathway, and are discharged from hepatocytes into the blood[58]. In addition to infectious virions (Dane particles), incomplete subviral particles are secreted by secretory pathways (such as spheres and filaments lacking nucleocapsid proteins and naked nucleocapsids)[59]. The virus emerges on the surface of the hepatocytes by budding, and can thus infect another cell[52]. Once created in the cell nucleus, the cccDNA minichromosome is very difficult to eliminate from infected cells, where it can survive until the death of the host cell[56].



DOI: 10.3748/wjg.v28.i27.3282 **Copyright** ©The Author(s) 2022.

Figure 1 Hepatitis B virus life cycle. Hepatitis B virus (HBV) enters hepatocytes *via* interaction with the heparan sulfate proteoglycan (HSPG), followed by the sodium taurocholate co-transporting polypeptide (NTCP) receptor. The virus envelope and the hepatocytes' membrane merge, releasing the nucleocapsid into the cytoplasm. The viral genome is transferred to the nucleus after the capsid is removed. The relaxed circular genome is restored in the nucleus, resulting in covalently closed circular DNA (cccDNA), and viral DNA could be integrated into the host DNA. Integrated viral DNA is a constant source of hepatitis B surface antigen (dashed line). The cccDNA is a template for pregenomic RNA (pgRNA) production and the transcription of all viral mRNAs. In addition, the cccDNA is associated with host factors and cellular histones, and forms a minichromosome. The core proteins are constructed into nucleocapsids together with pgRNA. Viral polymerase converts the pgRNA to relax circular DNA, resulting in a mature nucleocapsid. The core particles can recycle and replenish cccDNA (dashed line), or gather with the envelope proteins in the endoplasmic reticulum and Golgi, and enter the secretory pathway. Through the secretory process, virions gain surface antigens and are secreted as infectious virions-Dane particles. Also, incomplete subviral particles are secreted, such as spheres and filaments lacking nucleocapsid proteins. HSP: Heparan sulfate proteoglycan; NTCP: Sodium taurocholate co-transporting polypeptide receptor; cccDNA: Covalently closed circular DNA; pgRNA: Pregenomic RNA; HBx: Hepatitis B protein X; HBsAg: Hepatitis B surface antigen; HBe: E antigen; ER: Endoplasmatic reticulum.

CIRCADIAN RHYTHM

The molecular basis of the circadian rhythm includes transcriptional and translocation feedback loops. In addition, the circadian rhythm is driven by the circadian locomotor output cycles kaput (CLOCK), and brain and muscle ARNTL-like protein 1 (BMAL1 or ARNTL) transcription factors. In contrast, transcription repressors are period (PER) and cryptochrome (CRY) transcription factors. The central transcription factors that make up the activation and positive part of the molecular clock are BMAL1 and CLOCK. The heterodimer CLOCK-BMAL1 enters the nucleus, where it initiates transcription by binding to a specific sequence, the E-box, in promoters of the target genes. CLOCK's main downstream goals include *BMAL1* and its repressors, cryptochrome (*CRY1*, *CRY2*), and period (*PER1*, *PER2*, and *PER3*) and multiple CCG[60]. CRYs and PERs accumulate during the positive loop in the cytoplasm. They are controlled by F-box/LRR-repeat protein 3 (FBXL3) and casein kinase 1 (CK1) ε and CK1δ[4,61]. CK1ε and CK1δ phosphorylate PERs for degradation, while FBXL3 stimulates CRYs degradation. If CK1ε phosphorylates heterodimer PER-CRY, it enters the nucleus and suppresses the CLOCK-BMAL1 heterodimer. By suppressing their activator, CRYs and PERs suppress their own expression[62]. Posttranslational phosphorylation of CRYs and PERs promotes their degradation, which triggers a new circadian cycle, with increased binding of the CLOCK-BMAL1 heterodimer to the E-box of CCG[2,63].

The second regulatory loop includes the retinoic acid receptor-related orphan receptor (*ROR*) α and *RORγ*, and the *REV-ERBα* and *REV-ERBβ* genes. The CLOCK-BMAL1 heterodimer initiates their transcription by binding to the E-box elements of their promoters. RORs and REV-ERBs receptors bind to the ROR element (RORE). REV-ERBα and β inhibit transcription, while RORα and γ stimulate expression of target genes. RORs and REV-ERBs together create cyclic fluctuations in the expression of

many CCG, including the regulation of *BMAL1* transcription[6,64]. REV-ERBα accumulates rapidly and prevents *BMAL1* transcription, while RORα accumulates more slowly and promotes *BMAL1* transcription. In this way, the stability and robustness of the rhythmicity of the internal clock system are enhanced[2,63].

An additional independent feedback loop includes the helix-loop-helix e40 family (DEC1 or BHLHE40) and DEC2 (BHLHE41) that prevent CLOCK-BMAL1 activity[65]. The CLOCK-BMAL1 heterodimer stimulates the expression of *DEC1* and *DEC2* by binding to the E-box of their promoters. Conversely, DECs suppress transcription of genes with E-box elements in the promoter, including transcription of itself and CRYs and PERs, due to its binding to the E-box[66]. In addition, the CLOCK-BMAL1 heterodimer affects the expression of other CCG by stimulating D-box binding protein (DBP) transcription, by binding to E-box elements on the promoter[67]. DBP rhythmically triggers genes with D-box elements in the promoter[2,4].

The transcriptional and translational feedback loop creates rhythms in the expression and levels of downstream CCG[4]. All of these connected feedback loops create a circadian rhythm. For example, CCGs containing RORE elements in promoters are transcribed during the active phase. In contrast, the genes' promoters containing E-box and D-box elements are transcribed during the resting phase[63].

The circadian rhythm is controlled at the transcriptional and posttranslational levels, including cellular pathways, transcription factors, epigenetic changes, and posttranslational modifications[68]. Many posttranslational modifications of clock elements include acetylation, phosphorylation, ubiquitylation, and sumoylation[4,63]. Epigenetic modifications, such as DNA methylation, histone modifications, and non-coding RNAs, interfere with the target genes' transcription and post-transcriptional expression, including clock genes[69]. Different patterns of histone modifications, such as histone deacetylase sirtuin 1 (SIRT1), or microRNA, can be direct and indirect modulators in maintaining different aspects of circadian rhythm function[53,70].

Liver physiology and circadian rhythm

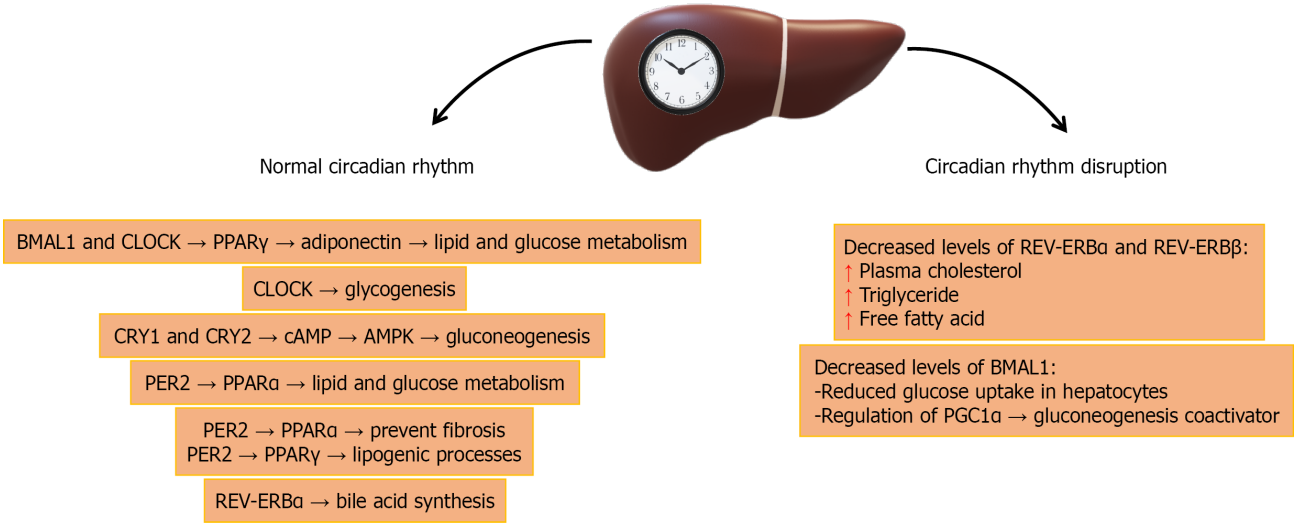
With a lack of environmental signs, such as the alternation of light and dark, food intake affects the circadian rhythm of the liver[6]. Circadian rhythms largely control different genes, levels of proteins, and the enzymes in the liver[2]. The circadian rhythm and liver metabolism are connected through the peroxisome proliferator-activated receptors (PPARs) α and γ[6,71]. PPARα controls the transcription of genes participating in lipid and glucose metabolism, while PPARγ is involved in lipogenic processes because it binds eicosanoids from omega-3 or omega-6 fatty acids[4,72]. Both genes are rhythmically expressed, and their expression is controlled by PER2, which directly regulates *BMAL1* transcription (Figure 2). The binding of PPARα to PPAR response elements (PPRE) in the *BMAL1* promoter leads to its transcription. Also, PPARα interacts with PER2 in the liver to impact the expression of target genes [73]. In the positive feedback loop in the liver, BMAL1 and CLOCK control the circadian oscillations of *PPARα*[4], and thus the expression of enzymes participating in glucose and lipid homeostasis, and the biosynthesis of bile acids and apolipoproteins[6]. REV-ERBα is implicated in the control of bile acid synthesis[74]. Adiponectin, triggered by BMAL1 and CLOCK *via* the transcription of *PPARγ* and its coactivator 1α (PGC-1α), is involved in glucose and lipid metabolism[75].

In addition, gluconeogenesis is controlled in a circadian manner in the liver *via* CRY1 and CRY2, which prevent signaling *via* the secondary messenger cyclic adenosine monophosphate (cAMP)[76]. Moreover, AMP-activated protein kinase (AMPK) can influence circadian cycle length by phosphorylating CRYs and directing it to degradation[4]. Activation of RORα in the liver may impact lipid metabolism and control hepatic steatosis by triggering AMPK[77]. Furthermore, CLOCK controls glycogenesis in the liver by acting on glycogen synthase 2 expression[78]. Disorders of the *CLOCK* and *BMAL1* genes lead to impaired glucose homeostasis[6]. Histone deacetylase SIRT1 prevents hepatic steatosis by controlling lipid homeostasis by positive binding of PPARα and PGC1α coactivators, or by direct action on BMAL1[70].

Circadian rhythm and HBV

There is a functional association between virus replication and circadian dysfunction in the pathogenesis of liver disease[79]. HBV has been revealed to impact the liver clock genes and disrupt the internal molecular clock in order to make better use of hepatocytes for self-replication[80]. HBV is randomly incorporated into the human genome, yet there are sites where it is incorporated more frequently, such as circadian rhythm-related elements, *CLOCK*, and *BMAL1*. Those elements are one way that the circadian rhythm is associated with diseases caused by HBV infection[81]. HBV replicates in the liver where around 20% of genes exhibit a rhythmic expression pattern, implying that the virus has successfully evolved to persist in the liver[5,50]. Integrated copies of HBV, which have regulatory elements similar to circadian rhythm genes, present additional circadian rhythm motifs in the infected cell, resulting in undesirable oscillations of specific genes, or disrupted circadian rhythms of the hepatocytes, and are a risk factor for cancer[50].

The circadian rhythm impacts gene expression in the liver and thus HBV replication[50]. In patients with HBV infection, a reduction in *BMAL1* and an increase in *REV-ERBα* and *REV-ERBβ* transcription have been observed compared to healthy subjects, which indicates that circadian rhythm gene transcription is impaired in HBV infection[50]. In hepatocytes, decreased expression or deletion of *REV-*



DOI: 10.3748/wjg.v28.i27.3282 **Copyright** ©The Author(s) 2022.

Figure 2 Role of circadian rhythm genes in liver metabolism. BMAL1: Brain and muscle ARNTL-like protein 1; CLOCK: Circadian locomotor output cycles kaput; PPAR: Peroxisome proliferator-activated receptors; CRY: Cryptochrome; PER: Period; ROR: Retinoic acid receptor-related orphan receptor; cAMP: Cyclic adenosine monophosphate; AMPK: AMP-activated protein kinase; PGC1α: PPAR coactivator 1α.

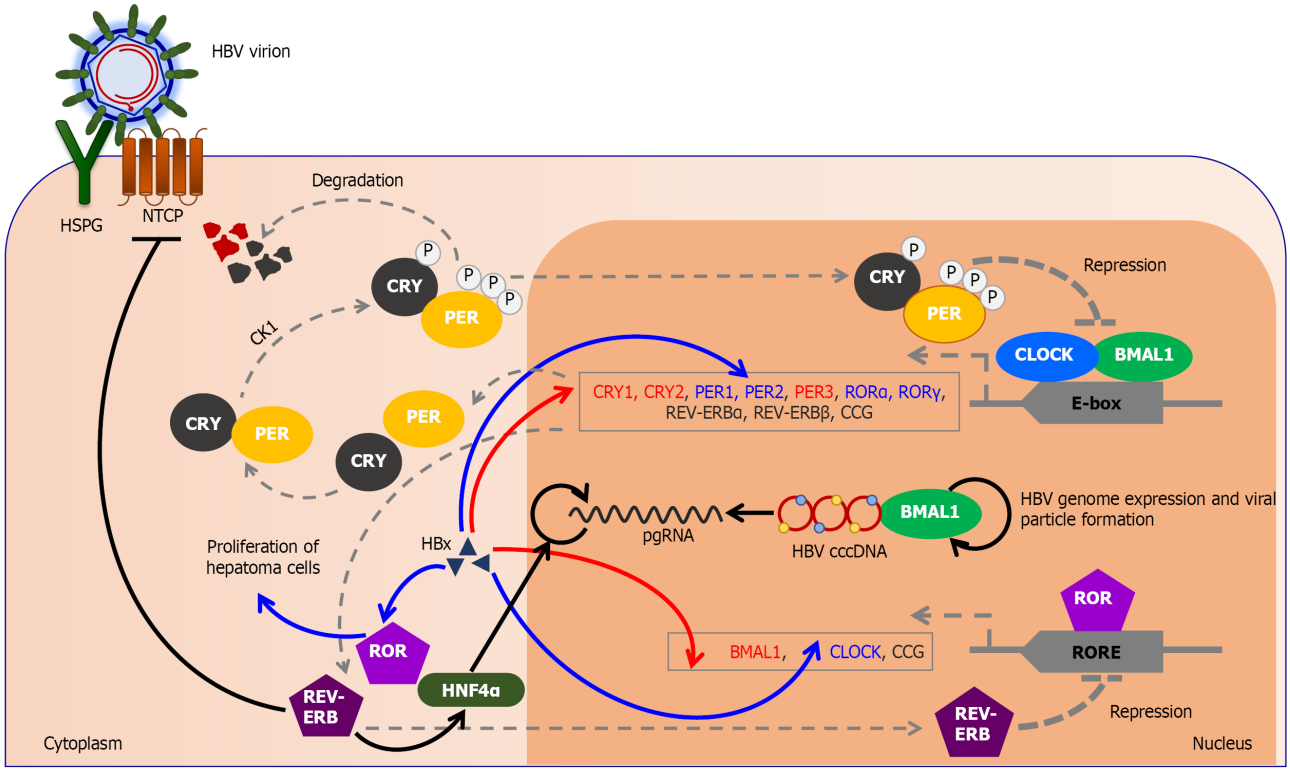
ERBα and *REV-ERBβ* in hepatocytes increases plasma cholesterol, triglycerides, and free fatty acid levels [63]. In addition, REV-ERB binds and controls NTCP expression, and stimulation of *REV-ERB* prevents HBV from entering the hepatocytes[50]. The NTCP receptor has a circadian pattern in hepatocytes[82]. Decreased expression of *BMAL1* in hepatocytes leads to reduced glucose uptake. In addition, BMAL1 regulates the transcription of the *PGC1α* gene, a coactivator of gluconeogenesis[63]. Thus, PPARα can prevent the development of fibrosis[63], and it is known that HBV dysregulates PPARα and PPARγ[6]. Also, BMAL1 binds HBV DNA, and controls viral genome expression and new viral particle formation [50].

The impaired circadian rhythm in HCC may favor the selective survival of cancer cells and facilitate carcinogenesis[83]. An increased risk of developing HCC is linked with chronic HBV infection. The HBx protein is linked with HCC due to the disturbance of cell proliferation[19]. It is a possible cause of significantly reduced transcription levels of the *BMAL1*, *PER3*, *CRY1*, *CRY2*, and *CK1ε* genes in HCC [84]. At the same time, elevated HBx expression in HCC results in increased *CLOCK*, *PER1*, and *PER2* expression[1,85]. In addition, abnormal expression of *REV-ERBα* was observed in a cell line that stably expressed HBV[86]. The circadian rhythm acts *via* REV-ERBα in the liver on hepatocyte nuclear factor 4 alpha (HNF4α), and thus directs the action of glucocorticoid receptors on energy metabolism (Figure 3). Consequently, the interactions between CRY and glucocorticoid receptors affect carbohydrate metabolism, hence transacting *PER2*[87]. HNF4α increases the transcription of pgRNA in hepatoma cells and thus affects HBV biosynthesis[88]. In addition, P2-HNF4α inhibits the expression of *BMAL1*, leading to the localization of P1-HNF4α from the nucleus to the cytoplasm. *BMAL1* is expressed in healthy hepatocytes, but tumor growth is prevented if *BMAL1* expression is induced in HNF4α-positive tumor cells[89]. The possible reason for the inhibition of tumor growth is that BMAL1 mediates the transcription of *P53* pathway genes, a well-known tumor-suppressor gene[90]. DNA viruses rely more on host transcription for gene expression; however, *BMAL1* deficiency increases virus replication. REV-ERBα has a protective effect because it reduces the inflammatory response, thus decreasing the severity of the disease. Thus, REV-ERBα agonists inhibit HBV replication, while BMAL1 promotes virus replication. Nevertheless, as BMAL1 stimulates oscillations in genes that metabolize drugs and sensitivity to toxicity, it also promotes HBV infection in hepatocytes[91].

HBV infection leads to overexpression of *RORα* and *RORγ*[92]. *RORγ* overexpression is associated with promoter methylation and HBx protein. Furthermore, HBx-induced *RORγ* may facilitate the proliferation and migration of hepatoma cells[93], and RORα may be a possible diagnostic and prognostic biomarker for disease severity[94]. Overexpression of *RORα*, *CRY2*, and *PER1* is associated with a better survival of HCC patients, and regulating the circadian rhythm gene may help in the chronotherapy of such patients[94]. HBV infection leads to disruptions of the *CLOCK* gene and its downstream circadian genes and other CCGs[2]. All the above indicates that circadian rhythm disorders caused by a virus may contribute to the pathogenesis of cancer.

Immunopathogenesis of chronic HBV infection and circadian rhythm

Clinical manifestations of chronic hepatitis B result from a cellular and humoral immune response to the recognized target antigenic viral epitopes, HBcAg and HBsAg[21]. Integration of HBV into the



DOI: 10.3748/wjg.v28.i27.3282 **Copyright** ©The Author(s) 2022.

Figure 3 Relationship between circadian rhythm genes and hepatitis B virus replication. Gray dashed lines indicate normal circadian rhythm in hepatocytes. Black arrows show the association between core clock proteins and hepatitis B virus (HBV) entry into hepatocytes and its replication. Increased levels of REV-ERB protein prevent the entry of HBV into hepatocytes by impaired action on the sodium taurocholate co-transporting polypeptide (NTCP) receptor. Brain and muscle ARNTL-like protein 1 (BMAL1) protein binds HBV DNA and thus controls viral genome expression and the formation of new viral particles. In infected hepatocytes, REV-ERB through HNF4α mediator increases pregenomic RNA (pgRNA) transcription, while HNF4α inhibits BMAL1 expression, promoting HBV replication. Red arrows indicate circadian rhythm genes inhibited by hepatitis B protein X (HBx) protein (BMAL1, CRY1, CRY2, and PER3). Conversely, HBx increases *CLOCK*, *PER1*, *PER2*, and *RORγ* gene expression (indicated by blue arrows). Increased expression of *RORγ* leads to the proliferation of hepatoma cells. BMAL1: Brain and muscle ARNTL-like protein 1; cccDNA: Covalently closed circular DNA; CCG: Clock-controlled genes; CLOCK: Circadian locomotor output cycles kaput; CK1: Casein kinase 1; CRY: Cryptochrome; HBx: Hepatitis B protein X; HNF4α: Hepatocyte nuclear factor 4 alpha; HSP: Heparan sulfate proteoglycan; NTCP: Sodium taurocholate co-transporting polypeptide receptor; PER: Period; pgRNA: Pregenomic RNA; ROR: Retinoic acid receptor-related orphan receptor; RORE: ROR element.

hepatocytes' genome serves as a constant source of HBsAg during chronic infection. It may induce dysfunctional T-cell responses, and favor harmful immunopathology and disease progression to fibrosis and cirrhosis[95]. Hepatocytes expressing HBcAg are recognized and attacked by cytotoxic $CD8^+$ lymphocytes (CTL)[96]. The increase in alanine aminotransferase is the result of hepatocyte lysis[97]. HBcAg has strong immunogenicity and can cause the antigen-specific T-cell responses necessary for controlling HBV infection. HBcAg stimulates the production of interleukin 6 (IL)-6, IL-10, IL-17A, IL-22, IL-23, and transforming growth factor β (TGFβ) by peripheral blood mononuclear cells[98]. In addition, the immunosuppressive cytokine IL-10 negatively controls the expansion of Th17 cells, which plays a part in the existence and promotion of HBV infection[46]. Persistent HBV infection is marked by a poor immune response due to the poor response of $CD4^+$ lymphocytes in the early phases of infection. This results in qualitatively and quantitatively weaker $CD8^+$ T cell responses[21].

In addition to other viral proteins, HBeAg is also important for the persistence of infection, as it suppresses the humoral and cellular immune response to HbcAg, weakens the action of CTL on HBcAg, and allows the maintenance of the infection[99]. The predominance of Th-1 over the Th-2 cytokine response, with the production of IL-2, interferon-alpha (IFN-α), and lymphotoxin-β receptor (LT-βR), is responsible for virus elimination during acute and chronic HBV infections[100]. Conversely, the predominance of Th-2 cytokine response is responsible for maintaining chronic infection, with IL-4, IL-5, and IL-10, which enhance the humoral immune response[98].

Many innate and adaptive immune system elements are under circadian regulation[1], and the adaptive immune response mediates virus removal and liver disease[95]. Cellular immune rhythms are synchronized with the central clock in the SCN[6]. Innate and adaptive immune system cells have a molecular clock that controls their rhythmic activity over 24 h[101]. Certain functions of the innate immune system rely on the hepatocytes' circadian rhythm[5,65]. Increased amounts of pro-inflammatory hormones such as growth hormone, prolactin, and melatonin and cytokines such as IL-1 and TNF-α are present during the rest period. In addition, immune rhythms are affected by hormonal

rhythms, so cortisol regulates the number of naive T cells. Epinephrine influences the number of CTL cells over 24 h[102].

Furthermore, the transcription factor CRY2 links the circadian rhythm and the innate immune system [103]. Moreover, CLOCK and BMAL1 control transcription of the pattern recognition receptor, which is involved in nucleic acid detection during viral infections[104]. RORγ regulates the differentiation of Th17 cells, which secrete IL-17, an essential regulator of pro-inflammatory signaling[93]. REV-ERBα has a protective effect in various inflammatory processes[105]. Additionally, the suppression of REV-ERB receptors elevates virus-associated mortality by promoting the inflammatory response[106]. The circadian hormone melatonin has protective and antiviral actions and a role in the inflammatory response[105]. Melatonin increased IFN-γ levels during viral infection, decreased Venezuelan equine encephalomyelitis virus (VEE) levels, and reduced mortality rates in mice infected with VEE. The protective impact of melatonin is associated with increased IL-1β production because it acts as a cytokine modulator and antioxidant[107]. This shows the positive role of the circadian rhythm in regulating antiviral immunity[91].

ANTIVIRAL THERAPY

There are two main drugs for HBV infection therapy: Nucleoside/nucleotide analogs (NAs), which interfere with viral DNA synthesis during reverse transcription, and IFN-α[108,109]. NAs effectively inhibit virus replication and may suppress the generation of new cccDNA[109]. Existing drugs can suppress virus replication, slow fibrosis progression, and decrease infectivity, but rarely remove the cccDNA responsible for HBV persistence[108]. Therefore, the development of therapy aims to achieve a "functional healing" state, *i.e.*, the removal of cccDNA from hepatocytes[110,111]. However, in the treatment of HBV infection, NAs rarely eliminate the virus, that is, they do not eradicate HBV from the liver[95]. This is because each HBV surface protein (S, M, and L) has an HBsAg determinant. Therefore, HBsAg circulates in the bloodstream of HBV patients, mainly in non-infectious subviral spheres and filaments[95].

Alternative therapeutic strategies are based on silencing viral genes using RNA interference (RNAi) [108] and antisense oligonucleotide (ASO) technology[110]. Both approaches are based on the effective suppression of HBV replication in patients with chronic HBV infection[108,110]. RNAi is a mechanism for silencing genes after transcription, and can be used in mammalian cells against viral infections[108]. ASO technology prevents HBV antigen production by targeting all HBV genome transcripts in infected hepatocytes[10,110]. It is based on NAs that act on viral polymerase but do not influence the cccDNA transcription[110]. ASO and other nucleic acid-based therapies may potentially decrease the tolerogenic outcome of the high HBsAg levels characteristic of chronic infection[63,110].

Role of circadian rhythm in antiviral therapy

One of the principles of personalized medicine is to optimize the time of day for administration of drugs whose action is affected by the circadian rhythm[5,112]. Circadian oscillations can affect vaccine responses to viral pathogens[91]. The direct impact of the circadian rhythm on the cellular and humoral immune reaction is mediated by melatonin and cortisol. Research on the severe acute respiratory syndrome coronavirus 2 (SARS-CoV-2) has shown that melatonin can affect circadian clocks and modulate the immune response during viral infections and thus impact virus replication[113]. Therefore, vaccination in the morning or evening may impact the immune response to the vaccine[114]. Thus, it was observed that patients vaccinated against the SARS-CoV-2 in the morning had significantly lower C-reactive protein levels compared to patients vaccinated in the evening[115]. Making a simple effort to determine the appropriate time for administration of drugs or vaccine can improve the drug's effectiveness and reduce side effects[5]. However, studying the interaction of the circadian rhythm and virus replication may lead to a better knowledge of viral infections and the associated immune response, discovery of new antiviral targets, improvement of existing treatments, and therapy for chronic infections[5]. Chronic infection is linked with a weakened immune response, and poor T-cell responses that fail to control HBV replication[50]. The effectiveness of current antiviral therapies could be enhanced by modulating the timing of vaccine administration. For example, the engineered T cell receptor activity showed a circadian pattern upon antigen activation. However, this daily effect was attenuated in *CLOCK* mutant mice, emphasizing the importance of timing T cell therapy to maximize antiviral immunity[1].

Many studies show that the efficacy or toxicity of treatment depends on the dosing time in many diseases. Also, inter-individual variations in the circadian rhythm resulting from lifestyle differences should be considered[116]. The efficiency of the DNA virus vaccine can be enhanced by specifying the time of day for vaccination. For example, some studies have found that patients immunized in the morning produce a more significant antibody response to hepatitis A and influenza vaccines[1,117]. In addition, morning vaccination is considered to significantly increase responses to viral-specific antibodies, compared to afternoon vaccination[1]. As viruses are intracellular pathogens that replicate within host cells, given the high association of circadian rhythm transcription factors with cell

transcription, the circadian rhythm plays a vital role in determining host susceptibility to viral infections and the immune response[1].

Circadian clock-modulating small molecules may help inhibit or activate circadian rhythm proteins and enzymes in viral infections. Thus, the small molecule SRT2183 modulates the circadian clock that inhibits SARS-CoV-2 replication[118] because it modulates physiological and circadian rhythm gene expression[119]. Inhibiting *BMAL1* expression and overexpression of *REV-ERB via* circadian rhythm-modulating small molecules may prevent dengue virus, hepatitis C virus, Zika virus, and HIV1 virus replication. In addition, clock genes have antiviral abilities that can be applied to HBV[120]. One of the effective circadian clock-modulating small molecules in treating HBV infections is GSK4112, a synthetic ligand for REV-ERB, but it is not suitable for *in vivo* use due to its poor pharmacokinetic properties. In contrast, ARN5187 is a REV-ERBβ agonist with dual function, an inhibitor of REV-ERB and autophagy [121]. SR9009 is a REV-ERBα agonist based on the chemical structure of GSK4112. It has better pharmacokinetic properties than GSK4112 and affects many oncogenes. In addition, REV-ERBα is known to regulate cancer development by inhibiting proliferation[121], and hence SR9009 inhibits *BMAL1* and prevents the entry and replication of HBV into hepatocytes[50].

Challenges associated with antiviral drug development, including circadian clock-modulating small molecules, may be adverse effects or suboptimal pharmacokinetics. Therefore, for an antiviral agent to succeed, the target drug should be distributed locally to avoid unfavorable consequences on other tissues.

CONCLUSION

Interaction exists between viruses and the circadian rhythm of hepatocytes. Infection susceptibility depends on the infectivity of the inoculum, the mode of transmission, the length of exposure to the virus, and the time of the day infection occurs[1]. Understanding how HBV interacts with the circadian rhythm of hepatocytes may influence the treatment of infections[1]. Viruses are among the most critical human carcinogens[6], and pharmacotherapy and chronotherapy should be united to treat or prevent viral infections[1]. Research on the impact of viral infections on the circadian rhythm may help detect new antiviral targets and optimize the timing of immune-based therapies[1]. The main challenge in treating HBV infection is eradicating or silencing the cccDNA[50]. By acting on specific components of the circadian rhythm, such as REV-ERB and BMAL1, HBV can be prevented from entering hepatocytes and producing new virions. In addition to lifestyle changes, circadian rhythm-focused approaches may provide new therapeutic options in treating HBV infections[63].

FOOTNOTES

Author contributions: Škrlec I did the majority of the writing and prepared the figures; Talapko J did some writing and prepared the tables; all authors have read and approved the final manuscript.

Conflict-of-interest statement: There are no conflicts of interest to report.

Open-Access: This article is an open-access article that was selected by an in-house editor and fully peer-reviewed by external reviewers. It is distributed in accordance with the Creative Commons Attribution NonCommercial (CC BY-NC 4.0) license, which permits others to distribute, remix, adapt, build upon this work non-commercially, and license their derivative works on different terms, provided the original work is properly cited and the use is non-commercial. See: https://creativecommons.org/Licenses/by-nc/4.0/

Country/Territory of origin: Croatia

ORCID number: Ivana Skrlec 0000-0003-1842-930X; Jasminka Talapko 0000-0001-5957-0807.

S-Editor: Chen YL
L-Editor: Wang TQ
P-Editor: Chen YL

REFERENCES

1 **Zhuang X**, Rambhatla SB, Lai AG, McKeating JA. Interplay between circadian clock and viral infection. *J Mol Med (Berl)* 2017; **95**: 1283-1289 [PMID: 28963570 DOI: 10.1007/s00109-017-1592-7]

2 **Zhou D**, Wang Y, Chen L, Jia L, Yuan J, Sun M, Zhang W, Wang P, Zuo J, Xu Z, Luan J. Evolving roles of circadian rhythms in liver homeostasis and pathology. *Oncotarget* 2016; **7**: 8625-8639 [PMID: 26843619 DOI: 10.18632/oncotarget.7065]

3 **Škrlec I**, Milic J, Heffer M, Peterlin B, Wagner J. Genetic variations in circadian rhythm genes and susceptibility for myocardial infarction. *Genet Mol Biol* 2018; **41**: 403-409 [PMID: 29767668 DOI: 10.1590/1678-4685-GMB-2017-0147]

4 **Saran AR**, Dave S, Zarrinpar A. Circadian Rhythms in the Pathogenesis and Treatment of Fatty Liver Disease. *Gastroenterology* 2020; **158**: 1948-1966.e1 [PMID: 32061597 DOI: 10.1053/j.gastro.2020.01.050]

5 **Borrmann H**, McKeating JA, Zhuang X. The Circadian Clock and Viral Infections. *J Biol Rhythms* 2021; **36**: 9-22 [PMID: 33161818 DOI: 10.1177/0748730420967768]

6 **Vinciguerra M**, Mazzoccoli G, Piccoli C, Tataranni T, Andriulli A, Pazienza V. Exploitation of host clock gene machinery by hepatitis viruses B and C. *World J Gastroenterol* 2013; **19**: 8902-8909 [PMID: 24379614 DOI: 10.3748/wjg.v19.i47.8902]

7 **Cheng Z**, Lin P, Cheng N. HBV/HIV Coinfection: Impact on the Development and Clinical Treatment of Liver Diseases. *Front Med (Lausanne)* 2021; **8**: 713981 [PMID: 34676223 DOI: 10.3389/fmed.2021.713981]

8 **Al-Sadeq DW**, Taleb SA, Zaied RE, Fahad SM, Smatti MK, Rizeq BR, Al Thani AA, Yassine HM, Nasrallah GK. Hepatitis B Virus Molecular Epidemiology, Host-Virus Interaction, Coinfection, and Laboratory Diagnosis in the MENA Region: An Update. *Pathogens* 2019; **8** [PMID: 31083509 DOI: 10.3390/PATHOGENS8020063]

9 **Liang Y**, Bai X, Liu X, Zhang Z, Pang X, Nie L, Qiu W, Zhao W, Hu G. Hepatitis B Vaccination Coverage Rates and Associated Factors: A Community-Based, Cross-Sectional Study Conducted in Beijing, 2019-2020. *Vaccines (Basel)* 2021; **9** [PMID: 34696178 DOI: 10.3390/VACCINES9101070]

10 **Yuen MF**, Heo J, Jang JW, Yoon JH, Kweon YO, Park SJ, Tami Y, You S, Yates P, Tao Y, Cremer J, Campbell F, Elston R, Theodore D, Paff M, Bennett CF, Kwoh TJ. Safety, tolerability and antiviral activity of the antisense oligonucleotide bepirovirsen in patients with chronic hepatitis B: a phase 2 randomized controlled trial. *Nat Med* 2021; **27**: 1725-1734 [PMID: 34642494 DOI: 10.1038/s41591-021-01513-4]

11 **Splawn LM**, Bailey CA, Medina JP, Cho JC. Heplisav-B vaccination for the prevention of hepatitis B virus infection in adults in the United States. *Drugs Today (Barc)* 2018; **54**: 399-405 [PMID: 30090877 DOI: 10.1358/dot.2018.54.7.2833984]

12 **Kappus MR**, Sterling RK. Extrahepatic manifestations of acute hepatitis B virus infection. *Gastroenterol Hepatol (N Y)* 2013; **9**: 123-126 [PMID: 23983659 DOI: 10.1016/s0976-0016(11)60191-9]

13 **Chen L**, Bao D, Gu L, Gu Y, Zhou L, Gao Z, Huang Y. Co-infection with hepatitis B virus among tuberculosis patients is associated with poor outcomes during anti-tuberculosis treatment. *BMC Infect Dis* 2018; **18**: 295 [PMID: 29970037 DOI: 10.1186/s12879-018-3192-8]

14 **Yue L**, Li C, Xu M, Wu M, Ding J, Liu J, Zhang X, Yuan Z. Probing the spatiotemporal patterns of HBV multiplication reveals novel features of its subcellular processes. *PLoS Pathog* 2021; **17**: e1009838 [PMID: 34370796 DOI: 10.1371/journal.ppat.1009838]

15 **Le Bert N**, Gill US, Hong M, Kunasegaran K, Tan DZM, Ahmad R, Cheng Y, Dutertre CA, Heinecke A, Rivino L, Tan A, Hansi NK, Zhang M, Xi S, Chong Y, Pflanz S, Newell EW, Kennedy PTF, Bertoletti A. Effects of Hepatitis B Surface Antigen on Virus-Specific and Global T Cells in Patients With Chronic Hepatitis B Virus infection. *Gastroenterology* 2020; **159**: 652-664 [PMID: 32302614 DOI: 10.1053/j.gastro.2020.04.019]

16 **Terrault NA**, Lok ASF, McMahon BJ, Chang KM, Hwang JP, Jonas MM, Brown RS Jr, Bzowej NH, Wong JB. Update on prevention, diagnosis, and treatment of chronic hepatitis B: AASLD 2018 hepatitis B guidance. *Hepatology* 2018; **67**: 1560-1599 [PMID: 29405329 DOI: 10.1002/hep.29800]

17 **Lim HK**, Jeffrey GP, Ramm GA, Soekmadji C. Pathogenesis of Viral Hepatitis-Induced Chronic Liver Disease: Role of Extracellular Vesicles. *Front Cell Infect Microbiol* 2020; **10**: 587628 [PMID: 33240824 DOI: 10.3389/fcimb.2020.587628]

18 **Peng L**, Gao ZL, Wang YM, He DM, Zhao JM, Bai XF, Wang XJ, Peng L. Clinical Manifestations and Laboratory Tests of AECHB and Severe Hepatitis (Liver Failure). In: Ning Q. Acute Exacerbation of Chronic Hepatitis B. Dordrecht: Springer, 2019:1-89

19 **Alqahtani SA**, Colombo M. Viral hepatitis as a risk factor for the development of hepatocellular carcinoma. *Hepatoma Res* 2020; **6**: 58 [DOI: 10.20517/2394-5079.2020.49]

20 **Wu J**, Han M, Li J, Yang X, Yang D. Immunopathogenesis of HBV Infection. *Adv Exp Med Biol* 2020; **1179**: 71-107 [PMID: 31741334 DOI: 10.1007/978-981-13-9151-4_4]

21 **Cai Y**, Yin W. The Multiple Functions of B Cells in Chronic HBV Infection. *Front Immunol* 2020; **11**: 582292 [PMID: 33381113 DOI: 10.3389/fimmu.2020.582292]

22 **Kafeero HM**, Ndagire D, Ocama P, Kudamba A, Walusansa A, Sendagire H. Prevalence and predictors of hepatitis B virus (HBV) infection in east Africa: evidence from a systematic review and meta-analysis of epidemiological studies published from 2005 to 2020. *Arch Public Health* 2021; **79**: 167 [PMID: 34537079 DOI: 10.1186/s13690-021-00686-1]

23 **Nelson NP**, Easterbrook PJ, McMahon BJ. Epidemiology of Hepatitis B Virus Infection and Impact of Vaccination on Disease. *Clin Liver Dis* 2016; **20**: 607-628 [PMID: 27742003 DOI: 10.1016/j.cld.2016.06.006]

24 **MacLachlan JH**, Cowie BC. Hepatitis B virus epidemiology. *Cold Spring Harb Perspect Med* 2015; **5**: a021410 [PMID: 25934461 DOI: 10.1101/cshperspect.a021410]

25 **Nguyen MH**, Wong G, Gane E, Kao JH, Dusheiko G. Hepatitis B Virus: Advances in Prevention, Diagnosis, and Therapy. *Clin Microbiol Rev* 2020; **33** [PMID: 32102898 DOI: 10.1128/CMR.00046-19]

26 **Schillie S**, Vellozzi C, Reingold A, Harris A, Haber P, Ward JW, Nelson NP. Prevention of Hepatitis B Virus Infection in the United States: Recommendations of the Advisory Committee on Immunization Practices. *MMWR Recomm Rep* 2018; **67**: 1-31 [PMID: 29939980 DOI: 10.15585/mmwr.rr6701a1]

27 **Drazilova S**, Kristian P, Janicko M, Halanova M, Safcak D, Dorcakova PD, Marekova M, Pella D, Madarasova-Geckova A, Jarcuska P, HepaMeta Team. What is the Role of the Horizontal Transmission of Hepatitis B Virus Infection in Young Adult and Middle-Aged Roma Population Living in the Settlements in East Slovakia? *Int J Environ Res Public Health* 2020; **17** [PMID: 32397342 DOI: 10.3390/IJERPH17093293]

28 **Weis-Torres SMDS**, Fitts SMF, Cardoso WM, Higa Junior MG, Lima LA, Bandeira LM, Castro VOL, Carneiro FA, Iglecias LMM, Cesar GA, Tanaka TSO, Puga MAM, Rezende GR, Croda J, Lago BV, Motta-Castro ARC. High level of

exposure to hepatitis B virus infection in a vulnerable population of a low endemic area: A challenge for vaccination coverage. *Int J Infect Dis* 2020; **90**: 46-52 [PMID: 31589921 DOI: 10.1016/j.ijid.2019.09.029]

29 **de Villiers MJ**, Nayagam S, Hallett TB. The impact of the timely birth dose vaccine on the global elimination of hepatitis B. *Nat Commun* 2021; **12**: 6223 [PMID: 34711822 DOI: 10.1038/s41467-021-26475-6]

30 **Guimarães LCDC**, Brunini S, Guimarães RA, Galdino-Júnior H, Minamisava R, da Cunha VE, Santos JRS, Silveira-Lacerda EP, Souza CM, de Oliveira VLB, Albernaz GC, de Menezes TG, Rezza G. Epidemiology of hepatitis B virus infection in people living in poverty in the central-west region of Brazil. *BMC Public Health* 2019; **19**: 443 [PMID: 31035990 DOI: 10.1186/s12889-019-6828-8]

31 **Makuza JD**, Rwema JOT, Ntihabose CK, Dushimiyimana D, Umutesi J, Nisingizwe MP, Serumondo J, Semakula M, Riedel DJ, Nsanzimana S. Prevalence of hepatitis B surface antigen (HBsAg) positivity and its associated factors in Rwanda. *BMC Infect Dis* 2019; **19**: 381 [PMID: 31053097 DOI: 10.1186/s12879-019-4013-4]

32 **Fattahi MR**, Mehrabani D, Mehvarz S, Jaliani NZ, Alipour A, Davarpanah MA. The Seroprevalence of Hepatitis B in Akbar Abad Village, Kavar, Southern Iran. *Int J Prev Med* 2014; **5**: S223-S230 [PMID: 26622994]

33 **McNaughton AL**, D'Arienzo V, Ansari MA, Lumley SF, Littlejohn M, Revill P, McKeating JA, Matthews PC. Insights From Deep Sequencing of the HBV Genome-Unique, Tiny, and Misunderstood. *Gastroenterology* 2019; **156**: 384-399 [PMID: 30268787 DOI: 10.1053/j.gastro.2018.07.058]

34 **Locarnini SA**, Littlejohn M, Yuen LKW. Origins and Evolution of the Primate Hepatitis B Virus. *Front Microbiol* 2021; **12**: 653684 [PMID: 34108947 DOI: 10.3389/fmicb.2021.653684]

35 **Zhang ZH**, Wu CC, Chen XW, Li X, Li J, Lu MJ. Genetic variation of hepatitis B virus and its significance for pathogenesis. *World J Gastroenterol* 2016; **22**: 126-144 [PMID: 26755865 DOI: 10.3748/wjg.v22.i1.126]

36 **Tsukuda S**, Watashi K. Hepatitis B virus biology and life cycle. *Antiviral Res* 2020; **182**: 104925 [PMID: 32866519 DOI: 10.1016/j.antiviral.2020.104925]

37 **Seeger C**, Mason WS, Lai MMC. Molecular Biology of Hepatitis Viruses. In: Arias IM, Alter HJ, Boyer JL, Cohen DE, Shafritz DA, Thorgeirsson SS, Wolkoff AW. The Liver: Biology and Pathobiology. Oxford, UK: John Wiley & Sons, Ltd, 2020: 793-820

38 **Mohebbi A**, Lorestani N, Tahamtan A, Kargar NL, Tabarraei A. An Overview of Hepatitis B Virus Surface Antigen Secretion Inhibitors. *Front Microbiol* 2018; **9**: 662 [PMID: 29675010 DOI: 10.3389/fmicb.2018.00662]

39 **Seeger C**, Mason WS. Molecular biology of hepatitis B virus infection. *Virology* 2015; **479-480**: 672-686 [PMID: 25759099 DOI: 10.1016/j.virol.2015.02.031]

40 **Patel N**, White SJ, Thompson RF, Bingham R, Weiß EU, Maskell DP, Zlotnick A, Dykeman E, Tuma R, Twarock R, Ranson NA, Stockley PG. HBV RNA pre-genome encodes specific motifs that mediate interactions with the viral core protein that promote nucleocapsid assembly. *Nat Microbiol* 2017; **2**: 17098 [PMID: 28628133 DOI: 10.1038/nmicrobiol.2017.98]

41 **Ko C**, Su J, Festag J, Bester R, Kosinska AD, Protzer U. Intramolecular recombination enables the formation of hepatitis B virus (HBV) cccDNA in mice after HBV genome transfer using recombinant AAV vectors. *Antiviral Res* 2021; **194**: 105140 [PMID: 34284057 DOI: 10.1016/j.antiviral.2021.105140]

42 **Altinel K**, Hashimoto K, Wei Y, Neuveut C, Gupta I, Suzuki AM, Dos Santos A, Moreau P, Xia T, Kojima S, Kato S, Takikawa Y, Hidaka I, Shimizu M, Matsuura T, Tsubota A, Ikeda H, Nagoshi S, Suzuki H, Michel ML, Samuel D, Buendia MA, Faivre J, Carninci P. Single-Nucleotide Resolution Mapping of Hepatitis B Virus Promoters in Infected Human Livers and Hepatocellular Carcinoma. *J Virol* 2016; **90**: 10811-10822 [PMID: 27681123 DOI: 10.1128/JVI.01625-16]

43 **Watanabe T**, Inoue T, Tanaka Y. Hepatitis B Core-Related Antigen and New Therapies for Hepatitis B. *Microorganisms* 2021; **9** [PMID: 34683404 DOI: 10.3390/MICROORGANISMS9102083]

44 **Philips CA**, Ahamed R, Abduljaleel JK, Rajesh S, Augustine P. Critical Updates on Chronic Hepatitis B Virus Infection in 2021. *Cureus* 2021; **13**: e19152 [PMID: 34733599 DOI: 10.7759/cureus.19152]

45 **Pavesi A**. Origin, Evolution and Stability of Overlapping Genes in Viruses: A Systematic Review. *Genes (Basel)* 2021; **12** [PMID: 34073395 DOI: 10.3390/genes12060809]

46 **Zhao F**, Xie X, Tan X, Yu H, Tian M, Lv H, Qin C, Qi J, Zhu Q. The Functions of Hepatitis B Virus Encoding Proteins: Viral Persistence and Liver Pathogenesis. *Front Immunol* 2021; **12**: 691766 [PMID: 34456908 DOI: 10.3389/fimmu.2021.691766]

47 **Pazienza V**, Niro GA, Fontana R, Vinciguerra M, Andriulli A. Advance in molecular diagnostic tools for hepatitis B virus detection. *Clin Chem Lab Med* 2013; **51**: 1707-1717 [PMID: 23612658 DOI: 10.1515/cclm-2013-0136]

48 **Hu J**, Liu K. Complete and Incomplete Hepatitis B Virus Particles: Formation, Function, and Application. *Viruses* 2017; **9** [PMID: 28335554 DOI: 10.3390/V9030056]

49 **Pastor F**, Herrscher C, Patient R, Eymieux S, Moreau A, Burlaud-Gaillard J, Seigneuret F, de Rocquigny H, Roingeard P, Hourioux C. Direct interaction between the hepatitis B virus core and envelope proteins analyzed in a cellular context. *Sci Rep* 2019; **9**: 16178 [PMID: 31700077 DOI: 10.1038/s41598-019-52824-z]

50 **Zhuang X**, Forde D, Tsukuda S, D'Arienzo V, Mailly L, Harris JM, Wing PAC, Borrmann H, Schilling M, Magri A, Rubio CO, Maidstone RJ, Iqbal M, Garzon M, Minisini R, Pirisi M, Butterworth S, Balfe P, Ray DW, Watashi K, Baumert TF, McKeating JA. Circadian control of hepatitis B virus replication. *Nat Commun* 2021; **12**: 1658 [PMID: 33712578 DOI: 10.1038/s41467-021-21821-0]

51 **Watashi K**, Wakita T. Hepatitis B Virus and Hepatitis D Virus Entry, Species Specificity, and Tissue Tropism. *Cold Spring Harb Perspect Med* 2015; **5**: a021378 [PMID: 26238794 DOI: 10.1101/cshperspect.a021378]

52 **Zeyen L**, Prange R. Host Cell Rab GTPases in Hepatitis B Virus Infection. *Front Cell Dev Biol* 2018; **6**: 154 [PMID: 30510928 DOI: 10.3389/fcell.2018.00154]

53 **Lamontagne RJ**, Bagga S, Bouchard MJ. Hepatitis B virus molecular biology and pathogenesis. *Hepatoma Res* 2016; **2**: 163-186 [PMID: 28042609 DOI: 10.20517/2394-5079.2016.05]

54 **Marchetti AL**, Guo H. New Insights on Molecular Mechanism of Hepatitis B Virus Covalently Closed Circular DNA Formation. *Cells* 2020; **9** [PMID: 33172220 DOI: 10.3390/CELLS9112430]

55 **Tu T**, Zhang H, Urban S. Hepatitis B Virus DNA Integration: In Vitro Models for Investigating Viral Pathogenesis and Persistence. *Viruses* 2021; **13** [PMID: 33530322 DOI: 10.3390/V13020180]

56 **Wang G**, Guan J, Khan NU, Li G, Shao J, Zhou Q, Xu L, Huang C, Deng J, Zhu H, Chen Z. Potential capacity of interferon-α to eliminate covalently closed circular DNA (cccDNA) in hepatocytes infected with hepatitis B virus. *Gut Pathog* 2021; **13**: 22 [PMID: 33845868 DOI: 10.1186/s13099-021-00421-9]

57 **Karayiannis P**. Hepatitis B virus: virology, molecular biology, life cycle and intrahepatic spread. *Hepatol Int* 2017; **11**: 500-508 [PMID: 29098564 DOI: 10.1007/s12072-017-9829-7]

58 **Jiang B**, Hildt E. Intracellular Trafficking of HBV Particles. *Cells* 2020; **9** [PMID: 32887393 DOI: 10.3390/CELLS9092023]

59 **Inan N**, Tabak F. Hepatitis B Virus: Biology and Life Cycle. *Viral Hepat J* 2015; **21**: 1-7 [DOI: 10.4274/vhd.36036]

60 **Škrlec I**, Milić J, Cilenšek I, Petrovič D, Wagner J, Peterlin B. Circadian clock genes and myocardial infarction in patients with type 2 diabetes mellitus. *Gene* 2019; **701**: 98-103 [PMID: 30905809 DOI: 10.1016/j.gene.2019.03.038]

61 **Zhao M**, Xing H, Chen M, Dong D, Wu B. Circadian clock-controlled drug metabolism and transport. *Xenobiotica* 2020; **50**: 495-505 [PMID: 31544568 DOI: 10.1080/00498254.2019.1672120]

62 **Škrlec I**, Milić J, Steiner R. The Impact of the Circadian Genes *CLOCK* and *ARNTL* on Myocardial Infarction. *J Clin Med* 2020; **9** [PMID: 32050674 DOI: 10.3390/JCM9020484]

63 **Mukherji A**, Bailey SM, Staels B, Baumert TF. The circadian clock and liver function in health and disease. *J Hepatol* 2019; **71**: 200-211 [PMID: 30930223 DOI: 10.1016/j.jhep.2019.03.020]

64 **Škrlec I**. Circadian rhythm and myocardial infarction. *Med Flum* 2019; **55**: 32-42 [DOI: 10.21860/medflum2019_216321]

65 **Haspel JA**, Anafi R, Brown MK, Cermakian N, Depner C, Desplats P, Gelman AE, Haack M, Jelic S, Kim BS, Laposky AD, Lee YC, Mongodin E, Prather AA, Prendergast BJ, Reardon C, Shaw AC, Sengupta S, Szentirmai É, Thakkar M, Walker WE, Solt LA. Perfect timing: circadian rhythms, sleep, and immunity - an NIH workshop summary. *JCI Insight* 2020; **5** [PMID: 31941836 DOI: 10.1172/JCI.INSIGHT.131487]

66 **Shi D**, Chen J, Wang J, Yao J, Huang Y, Zhang G, Bao Z. Circadian Clock Genes in the Metabolism of Non-alcoholic Fatty Liver Disease. *Front Physiol* 2019; **10**: 423 [PMID: 31139087 DOI: 10.3389/fphys.2019.00423]

67 **Mukherji A**, Dachraoui M, Baumert TF. Perturbation of the circadian clock and pathogenesis of NAFLD. *Metabolism* 2020; **111S**: 154337 [PMID: 32795560 DOI: 10.1016/j.metabol.2020.154337]

68 **Kim YH**, Lazar MA. Transcriptional Control of Circadian Rhythms and Metabolism: A Matter of Time and Space. *Endocr Rev* 2020; **41** [PMID: 32392281 DOI: 10.1210/ENDREV/BNAA014]

69 **Dandri M**. Epigenetic modulation in chronic hepatitis B virus infection. *Semin Immunopathol* 2020; **42**: 173-185 [PMID: 32185454 DOI: 10.1007/s00281-020-00780-6]

70 **Kong F**, Li Q, Zhang F, Li X, You H, Pan X, Zheng K, Tang R. Sirtuins as Potential Therapeutic Targets for Hepatitis B Virus Infection. *Front Med (Lausanne)* 2021; **8**: 751516 [PMID: 34708060 DOI: 10.3389/fmed.2021.751516]

71 **Du L**, Ma Y, Liu M, Yan L, Tang H. Peroxisome Proliferators Activated Receptor (PPAR) agonists activate hepatitis B virus replication in vivo. *Virol J* 2017; **14**: 96 [PMID: 28545573 DOI: 10.1186/s12985-017-0765-x]

72 **Dubuquoy L**, Louvet A, Hollebecque A, Mathurin P, Dharancy S. Peroxisome proliferator-activated receptors in HBV-related infection. *PPAR Res* 2009; **2009**: 145124 [PMID: 19365584 DOI: 10.1155/2009/145124]

73 **Charoensuksai P**, Xu W. PPARs in Rhythmic Metabolic Regulation and Implications in Health and Disease. *PPAR Res* 2010; **2010** [PMID: 20871864 DOI: 10.1155/2010/243643]

74 **Le Martelot G**, Claudel T, Gatfield D, Schaad O, Kornmann B, Lo Sasso G, Moschetta A, Schibler U. REV-ERBalpha participates in circadian SREBP signaling and bile acid homeostasis. *PLoS Biol* 2009; **7**: e1000181 [PMID: 19721697 DOI: 10.1371/journal.pbio.1000181]

75 **Kawai M**, Rosen CJ. PPARγ: a circadian transcription factor in adipogenesis and osteogenesis. *Nat Rev Endocrinol* 2010; **6**: 629-636 [PMID: 20820194 DOI: 10.1038/nrendo.2010.155]

76 **Zhang EE**, Liu Y, Dentin R, Pongsawakul PY, Liu AC, Hirota T, Nusinow DA, Sun X, Landais S, Kodama Y, Brenner DA, Montminy M, Kay SA. Cryptochrome mediates circadian regulation of cAMP signaling and hepatic gluconeogenesis. *Nat Med* 2010; **16**: 1152-1156 [PMID: 20852621 DOI: 10.1038/nm.2214]

77 **Kim EJ**, Yoon YS, Hong S, Son HY, Na TY, Lee MH, Kang HJ, Park J, Cho WJ, Kim SG, Koo SH, Park HG, Lee MO. Retinoic acid receptor-related orphan receptor α-induced activation of adenosine monophosphate-activated protein kinase results in attenuation of hepatic steatosis. *Hepatology* 2012; **55**: 1379-1388 [PMID: 22183856 DOI: 10.1002/hep.25529]

78 **Kalsbeek A**, la Fleur S, Fliers E. Circadian control of glucose metabolism. *Mol Metab* 2014; **3**: 372-383 [PMID: 24944897 DOI: 10.1016/j.molmet.2014.03.002]

79 **Diallo AB**, Coiffard B, Leone M, Mezouar S, Mege JL. For Whom the Clock Ticks: Clinical Chronobiology for Infectious Diseases. *Front Immunol* 2020; **11**: 1457 [PMID: 32733482 DOI: 10.3389/fimmu.2020.01457]

80 **Mazzoccoli G**, Vinciguerra M, Carbone A, Relógio A. The Circadian Clock, the Immune System, and Viral Infections: The Intricate Relationship Between Biological Time and Host-Virus Interaction. *Pathogens* 2020; **9** [PMID: 32012758 DOI: 10.3390/PATHOGENS9020083]

81 **Wu C**, Guo X, Li M, Shen J, Fu X, Xie Q, Hou Z, Zhai M, Qiu X, Cui Z, Xie H, Qin P, Weng X, Hu Z, Liang J. DeepHBV: a deep learning model to predict hepatitis B virus (HBV) integration sites. *BMC Ecol Evol* 2021; **21**: 138 [PMID: 34233610 DOI: 10.1186/s12862-021-01869-8]

82 **Zhuang X**, Edgar RS, McKeating JA. The role of circadian clock pathways in viral replication. *Semin Immunopathol* 2022; **44**: 175-182 [PMID: 35192001 DOI: 10.1007/s00281-021-00908-2]

83 **Sulli G**, Lam MTY, Panda S. Interplay between Circadian Clock and Cancer: New Frontiers for Cancer Treatment. *Trends Cancer* 2019; **5**: 475-494 [PMID: 31421905 DOI: 10.1016/j.trecan.2019.07.002]

84 **Jiang Y**, Shen X, Fasae MB, Zhi F, Chai L, Ou Y, Feng H, Liu S, Liu Y, Yang S. The Expression and Function of Circadian Rhythm Genes in Hepatocellular Carcinoma. *Oxid Med Cell Longev* 2021; **2021**: 4044606 [PMID: 34697563 DOI: 10.1155/2021/4044606]

85 **Yang SL**, Yu C, Jiang JX, Liu LP, Fang X, Wu C. Hepatitis B virus X protein disrupts the balance of the expression of circadian rhythm genes in hepatocellular carcinoma. *Oncol Lett* 2014; **8**: 2715-2720 [PMID: 25360177 DOI: 10.3892/OL.2014.2570]

86 **Li H**, Lu YF, Chen H, Liu J. Dysregulation of metallothionein and circadian genes in human hepatocellular carcinoma. *Chronobiol Int* 2017; **34**: 192-202 [PMID: 27997226 DOI: 10.1080/07420528.2016.1256300]

87 **Caratti G**, Iqbal M, Hunter L, Kim D, Wang P, Vonslow RM, Begley N, Tetley AJ, Woodburn JL, Pariollaud M, Maidstone R, Donaldson IJ, Zhang Z, Ince LM, Kitchen G, Baxter M, Poolman TM, Daniels DA, Stirling DR, Brocker C, Gonzalez F, Loudon AS, Bechtold DA, Rattray M, Matthews LC, Ray DW. REVERBa couples the circadian clock to hepatic glucocorticoid action. *J Clin Invest* 2018; **128**: 4454-4471 [PMID: 30179226 DOI: 10.1172/JCI96138]

88 **Li M**, Wang Y, Xia X, Mo P, Xu J, Yu C, Li W. Steroid receptor coactivator 3 inhibits hepatitis B virus gene expression through activating Akt signaling to prevent HNF4α nuclear translocation. *Cell Biosci* 2019; **9**: 64 [PMID: 31417670 DOI: 10.1186/s13578-019-0328-5]

89 **Fekry B**, Ribas-Latre A, Baumgartner C, Deans JR, Kwok C, Patel P, Fu L, Berdeaux R, Sun K, Kolonin MG, Wang SH, Yoo SH, Sladek FM, Eckel-Mahan K. Incompatibility of the circadian protein BMAL1 and HNF4α in hepatocellular carcinoma. *Nat Commun* 2018; **9**: 4349 [PMID: 30341289 DOI: 10.1038/s41467-018-06648-6]

90 **Shkodina AD**, Tan SC, Hasan MM, Abdelgawad M, Chopra H, Bilal M, Boiko DI, Tarianyk KA, Alexiou A. Roles of clock genes in the pathogenesis of Parkinson's disease. *Ageing Res Rev* 2022; **74**: 101554 [DOI: 10.1016/J.ARR.2021.101554]

91 **Pearson JA**, Voisey AC, Boest-Bjerg K, Wong FS, Wen L. Circadian Rhythm Modulation of Microbes During Health and Infection. *Front Microbiol* 2021; **12**: 721004 [PMID: 34512600 DOI: 10.3389/fmicb.2021.721004]

92 **Qi ZX**, Wang LY, Fan YC, Zhang JJ, Li T, Wang K. Increased peripheral RORα and RORγt mRNA expression is associated with acute-on-chronic hepatitis B liver failure. *J Viral Hepat* 2012; **19**: 811-822 [PMID: 23043388 DOI: 10.1111/j.1365-2893.2012.01603.x]

93 **Huang Y**, Liang H, He C, Peng F. Hepatitis B Virus X Protein-Induced RORγ Expression to Promote the Migration and Proliferation of Hepatocellular Carcinoma. *Biomed Res Int* 2019; **2019**: 5407126 [PMID: 31781621 DOI: 10.1155/2019/5407126]

94 **Liang Y**, Wang S, Huang X, Chai R, Tang Q, Yang R, Wang X, Zheng K. Dysregulation of Circadian Clock Genes as Significant Clinic Factor in the Tumorigenesis of Hepatocellular Carcinoma. *Comput Math Methods Med* 2021; **2021**: 8238833 [PMID: 34745328 DOI: 10.1155/2021/8238833]

95 **Iannacone M**, Guidotti LG. Immunobiology and pathogenesis of hepatitis B virus infection. *Nat Rev Immunol* 2022; **22**: 19-32 [PMID: 34002067 DOI: 10.1038/s41577-021-00549-4]

96 **Tan A**, Koh S, Bertoletti A. Immune Response in Hepatitis B Virus Infection. *Cold Spring Harb Perspect Med* 2015; **5**: a021428 [PMID: 26134480 DOI: 10.1101/cshperspect.a021428]

97 **Ghosh A**, Onsager C, Mason A, Arriola L, Lee W, Mubayi A. The role of oxygen intake and liver enzyme on the dynamics of damaged hepatocytes: Implications to ischaemic liver injury *via* a mathematical model. *PLoS One* 2021; **16**: e0230833 [PMID: 33886563 DOI: 10.1371/journal.pone.0230833]

98 **Gu Y**, Lian Y, Gu L, Chen L, Li X, Zhou L, Huang Y, Wang J. Correlations between cytokines produced by T cells and clinical-virological characteristics in untreated chronic hepatitis B patients. *BMC Infect Dis* 2019; **19**: 216 [PMID: 30832595 DOI: 10.1186/s12879-019-3853-2]

99 **Matsumura S**, Yamamoto K, Shimada N, Okano N, Okamoto R, Suzuki T, Hakoda T, Mizuno M, Higashi T, Tsuji T. High frequency of circulating HBcAg-specific CD8 T cells in hepatitis B infection: a flow cytometric analysis. *Clin Exp Immunol* 2001; **124**: 435-444 [PMID: 11472405 DOI: 10.1046/J.1365-2249.2001.01561.X]

100 **Meier MA**, Suslov A, Ketterer S, Heim MH, Wieland SF. Hepatitis B virus covalently closed circular DNA homeostasis is independent of the lymphotoxin pathway during chronic HBV infection. *J Viral Hepat* 2017; **24**: 662-671 [PMID: 28182305 DOI: 10.1111/jvh.12689]

101 **Pick R**, He W, Chen CS, Scheiermann C. Time-of-Day-Dependent Trafficking and Function of Leukocyte Subsets. *Trends Immunol* 2019; **40**: 524-537 [PMID: 31109762 DOI: 10.1016/j.it.2019.03.010]

102 **Dimitrov S**, Benedict C, Heutling D, Westermann J, Born J, Lange T. Cortisol and epinephrine control opposing circadian rhythms in T cell subsets. *Blood* 2009; **113**: 5134-5143 [PMID: 19293427 DOI: 10.1182/blood-2008-11-190769]

103 **Narasimamurthy R**, Hatori M, Nayak SK, Liu F, Panda S, Verma IM. Circadian clock protein cryptochrome regulates the expression of proinflammatory cytokines. *Proc Natl Acad Sci U S A* 2012; **109**: 12662-12667 [PMID: 22778400 DOI: 10.1073/pnas.1209965109]

104 **Silver AC**, Arjona A, Walker WE, Fikrig E. The circadian clock controls toll-like receptor 9-mediated innate and adaptive immunity. *Immunity* 2012; **36**: 251-261 [PMID: 22342842 DOI: 10.1016/j.immuni.2011.12.017]

105 **Crespo I**, Fernández-Palanca P, San-Miguel B, Álvarez M, González-Gallego J, Tuñón MJ. Melatonin modulates mitophagy, innate immunity and circadian clocks in a model of viral-induced fulminant hepatic failure. *J Cell Mol Med* 2020; **24**: 7625-7636 [PMID: 32468679 DOI: 10.1111/jcmm.15398]

106 **Griffett K**, Bedia-Diaz G, Elgendy B, Burris TP. REV-ERB agonism improves liver pathology in a mouse model of NASH. *PLoS One* 2020; **15**: e0236000 [PMID: 33002003 DOI: 10.1371/journal.pone.0236000]

107 **Srinivasan V**, Mohamed M, Kato H. Melatonin in bacterial and viral infections with focus on sepsis: a review. *Recent Pat Endocr Metab Immune Drug Discov* 2012; **6**: 30-39 [PMID: 22264213 DOI: 10.2174/187221412799015317]

108 **van den Berg F**, Limani SW, Mnyandu N, Maepa MB, Ely A, Arbuthnot P. Advances with RNAi-Based Therapy for Hepatitis B Virus Infection. *Viruses* 2020; **12** [PMID: 32759756 DOI: 10.3390/V12080851]

109 **Pierra Rouviere C**, Dousson CB, Tavis JE. HBV replication inhibitors. *Antiviral Res* 2020; **179**: 104815 [PMID: 32380149 DOI: 10.1016/j.antiviral.2020.104815]

110 **Liang TJ**. Hepatitis B: a new weapon against an old enemy. *Nat Med* 2021; **27**: 1672-1673 [PMID: 34642493 DOI: 10.1038/s41591-021-01512-5]

111 **Raimondo G**, Locarnini S, Pollicino T, Levrero M, Zoulim F, Lok AS; Taormina Workshop on Occult HBV Infection Faculty Members. Update of the statements on biology and clinical impact of occult hepatitis B virus infection. *J Hepatol*

2019; **71**: 397-408 [PMID: 31004683 DOI: 10.1016/j.jhep.2019.03.034]

112 **Greco CM**, Sassone-Corsi P. Personalized medicine and circadian rhythms: Opportunities for modern society. *J Exp Med* 2020; **217** [PMID: 32433754 DOI: 10.1084/JEM.20200702]

113 **Maiese K**. Circadian Clock Genes: Targeting Innate Immunity for Antiviral Strategies Against COVID-19. *Curr Neurovasc Res* 2020; **17**: 531-533 [PMID: 33272180 DOI: 10.2174/1567202617666201203110008]

114 **Karabay O**, Temel A, Koker AG, Tokel M, Ceyhan M, Kocoglu E. Influence of circadian rhythm on the efficacy of the hepatitis B vaccination. *Vaccine* 2008; **26**: 1143-1144 [PMID: 18255201 DOI: 10.1016/j.vaccine.2007.12.046]

115 **De Giorgi A**, Fabbian F, Di Simone E, Greco S, De Giorgio R, Zuliani G, Passaro A, Caselli E, Manfredini R; OUTCOME-INTMED-COV19 Study Collaborators. Morning vs. evening administration of antiviral therapy in COVID-19 patients. A preliminary retrospective study in Ferrara, Italy. *Eur Rev Med Pharmacol Sci* 2020; **24**: 8219-8225 [PMID: 32767353 DOI: 10.26355/eurrev_202008_22511]

116 **Ruben MD**, Smith DF, FitzGerald GA, Hogenesch JB. Dosing time matters. *Science* 2019; **365**: 547-549 [PMID: 31395773 DOI: 10.1126/science.aax7621]

117 **Kurupati RK**, Kossenkoff A, Kannan S, Haut LH, Doyle S, Yin X, Schmader KE, Liu Q, Showe L, Ertl HCJ. The effect of timing of influenza vaccination and sample collection on antibody titers and responses in the aged. *Vaccine* 2017; **35**: 3700-3708 [PMID: 28583307 DOI: 10.1016/j.vaccine.2017.05.074]

118 **Sultan A**, Ali R, Sultan T, Ali S, Khan NJ, Parganiha A. Circadian clock modulating small molecules repurposing as inhibitors of SARS-CoV-2 M^{pro} for pharmacological interventions in COVID-19 pandemic. *Chronobiol Int* 2021; **38**: 971-985 [PMID: 33820462 DOI: 10.1080/07420528.2021.1903027]

119 **Sultan A**. Identification and development of clock-modulating small molecules-an emerging approach to fine-tune the disrupted circadian clocks. *Biol Rhythm Res* 2018; **50**: 769-786 [DOI: 10.1080/09291016.2018.1498197]

120 **Borrmann H**, Davies R, Dickinson M, Pedroza-Pacheco I, Schilling M, Vaughan-Jackson A, Magri A, James W, Balfe P, Borrow P, McKeating JA, Zhuang X. Pharmacological activation of the circadian component REV-ERB inhibits HIV-1 replication. *Sci Rep* 2020; **10**: 13271 [PMID: 32764708 DOI: 10.1038/s41598-020-70170-3]

121 **Wang S**, Li F, Lin Y, Wu B. Targeting REV-ERBα for therapeutic purposes: promises and challenges. *Theranostics* 2020; **10**: 4168-4182 [PMID: 32226546 DOI: 10.7150/thno.43834]

World Journal of Gastroenterology

Submit a Manuscript: https://www.f6publishing.com

World J Gastroenterol 2022 July 21; 28(27): 3297-3313

DOI: 10.3748/wjg.v28.i27.3297

ISSN 1007-9327 (print) ISSN 2219-2840 (online)

REVIEW

Tumor microenvironment in pancreatic ductal adenocarcinoma: Implications in immunotherapy

Caitlyn Smith, Wei Zheng, Jixin Dong, Yaohong Wang, Jinping Lai, Xiuli Liu, Feng Yin

Specialty type: Gastroenterology and hepatology

Provenance and peer review: Invited article; Externally peer reviewed.

Peer-review model: Single blind

Peer-review report's scientific quality classification

Grade A (Excellent): 0
Grade B (Very good): B
Grade C (Good): C, C
Grade D (Fair): 0
Grade E (Poor): 0

P-Reviewer: Plougmann JI, Denmark; Tantau AI, Romania; Zhao CF, China

Received: January 16, 2022
Peer-review started: January 16, 2022
First decision: April 11, 2022
Revised: April 22, 2022
Accepted: June 19, 2022
Article in press: June 19, 2022
Published online: July 21, 2022

Caitlyn Smith, Department of Pathology and Anatomical Sciences, University of Missouri School of Medicine, Columbia, MO 65212, United States

Wei Zheng, Department of Pathology, Emory University School of Medicine, Atlanta, GA 30322, United States

Jixin Dong, Eppley Institute for Research in Cancer and Allied Diseases, Fred and Pamela Buffett Cancer Center, University of Nebraska Medical Center, Omaha, NE 68198, United States

Yaohong Wang, Department of Pathology, Microbiology and Immunology, Vanderbilt University Medical Center, Nashville, TN 37232, United States

Jinping Lai, Department of Pathology and Laboratory Medicine, Kaiser Permanente Sacramento Medical Center, Sacramento, CA 95825, United States

Xiuli Liu, Department of Pathology and Immunology, Washington University, St. Louis, MO 63110, United States

Feng Yin, Department of Pathology and Anatomical Sciences, University of Missouri, Columbia, MO 65212, United States

Corresponding author: Feng Yin, MD, PhD, Assistant Professor, Department of Pathology and Anatomical Sciences, University of Missouri, One Hospital Drive, MSB M263, Columbia, MO 65212, United States. fengyin@health.missouri.edu

Abstract

Pancreatic ductal adenocarcinoma is one of the most aggressive and lethal cancers. Surgical resection is the only curable treatment option, but it is available for only a small fraction of patients at the time of diagnosis. With current therapeutic regimens, the average 5-year survival rate is less than 10% in pancreatic cancer patients. Immunotherapy has emerged as one of the most promising treatment options for multiple solid tumors of advanced stage. However, its clinical efficacy is suboptimal in most clinical trials on pancreatic cancer. Current studies have suggested that the tumor microenvironment is likely the underlying barrier affecting immunotherapy drug efficacy in pancreatic cancer. In this review, we discuss the role of the tumor microenvironment in pancreatic cancer and the latest advances in immunotherapy on pancreatic cancer.

Key Words: Pancreatic ductal adenocarcinoma; Tumor microenvironment; Immunotherapy; Clinical trial; Chemotherapy; Treatment

©The Author(s) 2022. Published by Baishideng Publishing Group Inc. All rights reserved.

Core Tip: Despite advances in basic and translational research, pancreatic cancer remains one of the most lethal cancers. Recent breakthroughs in immunotherapy have revolutionized cancer therapy and have shown great potential to transform pancreatic cancer treatment. However, due to the barrier related to the tumor microenvironment, pancreatic cancer has shown inferior treatment outcomes toward various immunotherapy regimens. Further efforts, such as combinatory immunotherapy or molecular tumor subtyping, are warranted to overcome immunotherapy resistance in pancreatic cancer.

Citation: Smith C, Zheng W, Dong J, Wang Y, Lai J, Liu X, Yin F. Tumor microenvironment in pancreatic ductal adenocarcinoma: Implications in immunotherapy. *World J Gastroenterol* 2022; 28(27): 3297-3313
URL: https://www.wjgnet.com/1007-9327/full/v28/i27/3297.htm
DOI: https://dx.doi.org/10.3748/wjg.v28.i27.3297

INTRODUCTION

Pancreatic ductal adenocarcinoma (PDAC) develops in the exocrine compartment of the pancreas and accounts for approximately 90% of pancreatic malignancies, making it the most common pancreatic neoplasm. Due to the lack of early diagnosis and limited treatment response, PDAC remains a highly aggressive and lethal malignancy and is the fourth leading cause of cancer-related death worldwide[1]. Although there has been notable progress in understanding tumor biology and the development of novel therapeutic regimens, the average 5-year survival rate is still less than 5%-10% in PDAC patients [1,2]. The clinical manifestations of pancreatic cancers are generally nonspecific, including weight loss, abdominal pain, thromboembolic disease, and type 2 diabetes[3,4]. In approximately 60%-70% of PDAC cases, the tumor arises from the head of the pancreas and could present as pancreatitis and obstructive jaundice[5]. Tumors of the pancreatic body and tail frequently have a poor prognosis due to their late presentation and associated advanced tumor stage[6].

The standard of care for resectable PDAC is surgical resection followed by adjuvant chemotherapy. Surgical resection remains the only curative therapy, but it is available for merely 10%-20% of patients at the time of diagnosis. Moreover, even with curative surgical resection, local recurrence and distal metastasis of PDAC are still quite common[7]. Advanced-stage PDAC is routinely treated with neoadjuvant chemotherapy, and the current first-line therapy regimens include gemcitabine, gemcitabine plus nab-paclitaxel, and FOLFIRINOX (the combination of oxaliplatin, leucovorin, fluorouracil, and irinotecan) [8]. Recently, the poly(adenosine diphosphate-ribose) polymerase inhibitor (PARPi) olaparib (Lynparza) has been approved for patients with germline BRCA-mutated metastatic pancreatic cancer[9]. The development of these neoadjuvant chemotherapy regimens has greatly improved patient survival and quality of life. However, a significant portion of PDAC eventually relapses despite surgical resection and/or neoadjuvant chemotherapy and leads to patient death[10,11].

The difficulties in treating pancreatic cancer lie at the cellular and genetic levels[12]. Mutational changes in pancreatic tumors lead to gene instability, tumor growth, and resistance to treatments[13]. In addition to the characteristic molecular landmarks, including oncogenic *KRAS* mutation and inactivation of the tumor suppressor genes *CDKN2A/P16*, *TP53,* and *SMAD4*, PDAC also frequently harbors mutations involving diverse cell signaling pathways[14]. The molecular heterogeneity likely accounts for its drug resistance in chemotherapy[15]. In addition, pancreatic cancer stem cells, accounting for approximately 1% of all pancreatic cancer cells, have the capacity for self-renewal and exhibit chemoresistance properties[16].

Immunotherapy has emerged as one of the most promising treatment options for advanced solid tumors, including lung, kidney, bladder, liver, and colorectal cancers[17]. Unfortunately, PDAC is notoriously resistant to immunotherapy, and thus far, most phase I/II clinical trials on PDAC have failed to demonstrate the desirable clinical efficacy of immunotherapy[18]. Of note, microsatellite instability (MSI), one of the predictive biomarkers for immune checkpoint blockade therapy, is only detected in a rare small portion of PDAC patients (less than 1%)[19,20]. On the other hand, emerging evidence has pinpointed the tumor microenvironment (TME) in PDAC as a critical component of treatment resistance toward immunotherapy[21,22].

In this review, we discuss the role of the tumor microenvironment and the latest advances in immunotherapy on pancreatic cancer through the search of peer-reviewed clinical and basic research articles related to this topic on PubMed, as well as the publicly accessible information on relevant

clinical trials through ClinicalTrials.gov.

TUMOR MICROENVIRONMENT IN PANCREATIC CANCER

PDAC is a type of stromal-rich cancer that frequently presents with a prominent desmoplastic reaction and is characterized by fibrogenic connective stromal tissue surrounding invasive carcinoma[23] (Figure 1). Desmoplastic reaction, or desmoplasia, is considered as the morphological basis of the TME. In general, the TME in PDAC demonstrates extensive desmoplasia, decreased stromal vascularization, and altered immune cell infiltration that lead to reduced drug activity and advancement of tumor progression. This process is characterized by an increase in the deposition of noncellular components, such as extracellular matrix (ECM), as well as an increase in the proliferation of cellular components, such as cancer-associated fibroblasts (CAFs) and immune cells[24,25]. Various cytokines, including interferons, interleukins, tumor necrosis factor (TNF), and transforming growth factor β (TGF-β), also play essential roles linking the TME cellular and noncellular components to regulate tumor growth, metastases, and drug resistance. Of note, the overall stroma is responsible for most of the tumor mass, but the stromal cellular components make up a relatively small fraction, approximately 10%-30%, of the tumor mass[26].

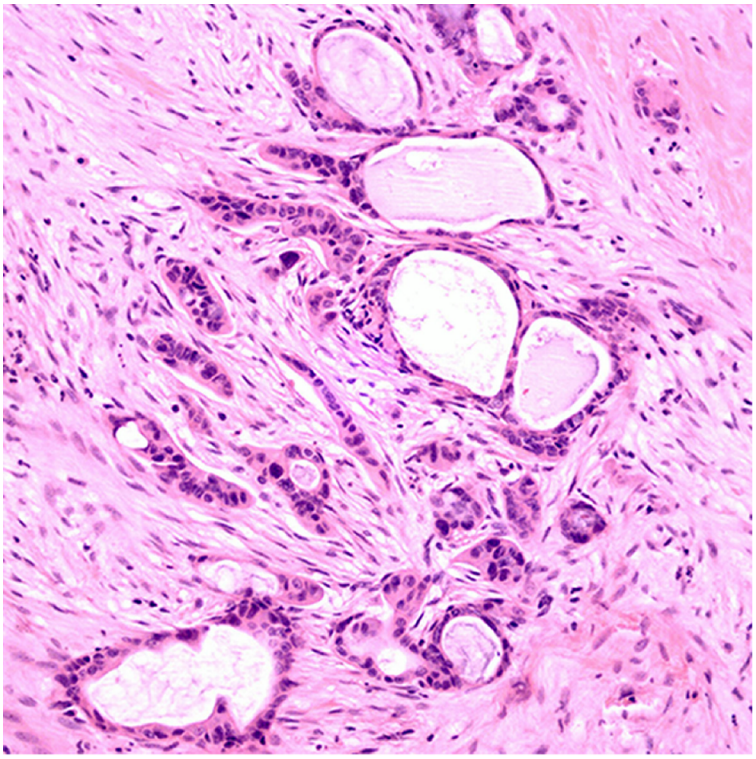
Noncellular components of the tumor microenvironment

The ECM is a significant factor in the initiation and progression of PDAC, and its deposition is associated with tumor migration, invasion, and poor prognosis[27]. The ECM is predominantly produced by cancer-associated pancreatic stellate cells (PSCs), a subtype of CAFs[28]. In PDAC, the ECM comprises most of the tumor mass and various matrix proteins, including collagen, fibronectin, proteoglycans, hyaluronan, proteolytic matrix metalloproteinases (MMPs), and tissue inhibitors of MMP [29]. Among ECM components of particular interest are hyaluronan and MMPs in tumor progression and prognosis in PDAC.

In general, ECM provides a rigid barrier leading to increased tumor pressure, decreased vascularization, and reduced drug delivery. A significant cause of drug resistance is the inability of conventional chemotherapeutic drugs such as gemcitabine to penetrate the thick stromal layer[30]. Therefore, it is rational to propose a combinatory therapeutic strategy for PDAC by targeting the tumor ECM. Hyaluronan, or hyaluronic acid (HA), is a glycosaminoglycan polymer and a major component of the ECM. Increased deposition of HA is associated with tumor metastases, drug resistance, and poor prognosis in PDAC[27,31]. Since stromal HA levels are dynamically regulated by synthases (to produce HA) and hyaluronidases (to degrade HA), hyaluronidase-based drug development has been a promising field in targeted therapy against the TME. The enzymatic depletion of hyaluronan through recombinant hyaluronidase (PEGPH20) has led to significantly increased overall survival when combined with neoadjuvant chemotherapy[32]. This is attributed mainly to improved delivery of systemic therapy through degradation of HA and remodeling of the TME. However, a recent phase IB/II randomized study (NCT01959139) of FOLFIRINOX plus pegylated recombinant PEGPH20 showed increased toxicity with this combination therapy and decreased overall survival (OS) (7.7 mo *vs* 14.4 mo) compared with FOLFIRINOX monotherapy[33]. Moreover, despite promising results of PEGPH20 in phase I-II studies, in a recent phase III randomized study (HALO 109-301), the addition of PEGPH20 to nab-paclitaxel/gemcitabine did not improve OS and progression-free survival (PFS) in patients with hyaluronan-high metastatic PDAC, and additional development of PEHPH20 in metastatic PDAC was halted[34].

MMPs are calcium-dependent metalloproteinases responsible for ECM protein degradation and are implicated in cancer initiation, growth, and metastasis. Clinical trial results with broad-spectrum MMP inhibitors were discouraging due to lack of specificity, associated toxicity, and insufficient clinical benefit[35], warranting further basic and translational studies to classify the role of individual MMPs in PDAC. Among MMP family members, the expression levels of MMP-2, MMP-7, MMP-9, and MMP-11 were significantly elevated in PDAC tumor tissues compared with normal pancreas samples[36,37]. Increased MMP-2 expression in PDAC leads to tumor invasion and progression[38-40]. MMP-7 expression is also associated with PDAC initiation and progression[41] and has been shown to be an independent prognostic factor for PDAC in a multivariate analysis. MMP-9 is significantly associated with pancreatic cancer progression and poor prognosis[37] and has emerged as a prognostic biomarker and potential therapeutic target. Highly selective and potent MMP-9 inhibitory antibodies have been developed for ulcerative colitis and colorectal cancer[42]. However, in a preclinical study, systemic ablation of MMP-9 facilitated pancreatic cancer growth and metastasis by creating a tumor-promoting TME[43]. This study has suggested a controversial role for MMP-9 in pancreatic cancer progression.

Additional studies have also demonstrated conflicting results in drugs targeting the tumor stroma. Olive *et al*[44] demonstrated that depletion of ECM in PDAC, through inhibition of the Sonic Hedgehog signaling pathway, promoted gemcitabine efficacy and improved survival. However, the involvement of the Sonic Hedgehog-dependent tumor stroma in PDAC has been controversial, as evidence shows that some components of the tumor stroma could actually act to restrain, rather than support, tumor



DOI: 10.3748/wjg.v28.i27.3297 **Copyright** ©The Author(s) 2022.

Figure 1 Pancreatic ductal adenocarcinoma with an associated tumor microenvironment. Please note the desmoplastic stromal reaction surrounding the tumor glands, decreased stromal vascularization, and scattered infiltrating inflammatory cells (HE stain, 200 x).

growth[45]. All these failures indicate that targeting desmoplasia alone is insufficient for treating advanced PDAC. The tumor stroma has both tumor-promoting and tumor-suppressing functions, which are probably context dependent. The stromal heterogeneity should be considered for the development of targeted therapy.

Cellular components of the tumor microenvironment

PDAC displays unique immunologic hallmarks. The TME in PDAC consists of diverse cellular components, including CAFs, regulatory and cytotoxic lymphocytes, macrophages, and endothelial cells [46]. CAFs are the major TME cellular component responsible for the production and deposition of ECM proteins. The involvement of CAFs in the progression of PDAC has been a hot and controversial topic. Similar to the observations made with tumor stroma, CAFs also play dual functions in regulating PDAC progression. On the one hand, CAFs promote cancer progression and drug resistance through the deposition of dense ECM, the release of exosomes (extracellular vesicles), and metabolic support[47-49]. On the other hand, depletion of CAFs leads to accelerated PDAC progression and reduced survival in multiple preclinical studies[50,51]. These discrepancies are likely associated with the heterogeneity of CAFs[52,53], a concept supported by recent studies demonstrating the existence of multiple distinct and mutually exclusive CAF subtypes in pancreatic cancer[54,55]. CAF subtypes with diverse biomarkers, including α-smooth muscle actin (αSMA), fibroblast activation protein (FAP), S100A4, and platelet-derived growth factor receptor-β (PDGFRβ), have been identified[56]. Specifically, FAP-positive active CAFs have been linked to tumor-promoting functions by maintaining an immunosuppressive TME[57]. FAP is a type-II transmembrane serine protease, and its expression has been detected in both the tumor stroma and cancer cells in PDAC, with the highest expression in the tumor stroma at the tumor front [58]. FAP-positive CAFs potently shape the immune landscape in the TME by secreting TGF-β, VEGF, and multiple matrix processing enzymes[59,60], recruiting circulating myeloid-derived suppressor cells (MDSCs) into the tumor stroma[57], and inhibiting natural killer cell (NK) cytotoxicity and cytokine production[61]. FAP has been suggested as an ideal target for the TME, and its specific therapeutic reagents are in development[62].

In addition to CAFs, the TME also consists of multiple types of immunosuppressive cells, including regulatory T cells (Tregs), MDSCs, and tumor-associated macrophages (TAMs)[63]. These cells correlate to provide an immunosuppressive TME and have been under extensive preclinical and clinical investigation.

Tregs, defined as CD4+/CD25+/FOXP3+ T cells, are a subtype of repressive T cells that play an essential role in maintaining immune tolerance and preventing autoimmune disorders. Tregs can be found in PDAC and premalignant lesion intraductal papillary mucinous neoplasms (IPMNs). The

prevalence of Tregs in CD4+ T lymphocytes correlates significantly with the progression and invasion of IPMNs and is associated with poor prognosis in PDAC. The immunosuppressive function of Tregs has been attributed to the secretion of suppressive cytokines, including IL-10 and TGF-β1, and the induction of CD4+ T-cell death[64,65]. Preoperative chemoradiation therapy has been shown to decrease Tregs in PDAC[66]. However, in a recent study, depletion of Tregs in a mouse model caused accelerated tumor progression due to unexpected crosstalk between Tregs and CAFs in PDAC[67]. This study has challenged the current view and posed uncertainties in developing Treg-based targeted therapy.

MDSCs and TAMs have also been suggested as potential therapeutic targets against the TME. Even though these two cell types are considered as separate entities, they have no demarcated boundaries and share many common characteristics[68]. MDSCs are a group of heterogeneous immature myeloid cells and can potently suppress T-cell function in tumors[69]. The levels of MDSCs correlate with the progression of PDAC and have been proposed as a predictive biomarker of chemotherapy failure[70,71]. TAMs are circulating monocyte-derived macrophages in the tumor stroma and represent a significant population of immune cells within the TME. TAMs can be further subclassified into the M1 and M2 subtypes, with M1 being proinflammatory (antitumorigenic) and M2 being anti-inflammatory (protumorigenic)[72]. M2-polarized TAMs are associated with an unfavorable prognosis in PDAC[73]. Liu *et al*[74] revealed progressive accumulations of MDSCs and M2-polarized TAMs accompanied by dynamic reductions in cytotoxic T cells (CTLs) and helper T cells (Ths) in PDAC progression. Gemcitabine affects the TME by inhibiting the expansion of MDSCs and the induction of Th2 cells while promoting M2-polarized TAMs[74]. M2-polarized TAMs can also be induced by other chemotherapeutic agents, such as carboplatin and cisplatin, leading to increased secretion of interleukin-6 (IL-6), IL-10, and prostaglandin E2[75]. In addition, interferon-γ upregulates the expression of programmed death-ligand 1 (PD-L1) in MDSCs, resulting in an immunosuppressive environment[76]. Further investigations and clinical trials are needed to test the efficacy of targeting MDSCs and TAMs in pancreatic cancer.

IMMUNOTHERAPY IN PANCREATIC CANCER

Current treatment options for PDAC have limited effects on patient survival. The recent development of immunotherapy has improved clinical outcomes for various types of solid tumors[17] and can revolutionize cancer treatment in PDAC. Activating the patient's T cells is the principal basis for cancer immunotherapy. This is accomplished through multiple mechanisms, such as decreased tumor-specific antigen presentation, T-cell activation, T-cell infiltration into the pancreatic tumor, and elimination of cancer cells by T cells[77]. Multiple cancer immunotherapies have been introduced, including immune checkpoint inhibitors, cancer vaccines, and adoptive cell transfer.

Immune checkpoint inhibitors

Immune checkpoint molecules are a group of surface receptors expressed on various immune cells that transduce inhibitory signals to T cells upon ligand binding. These molecules play an important role in preventing an autoimmune attack against self-antigens. Due to strong immune selective pressure, cancer cells frequently adopt the power of immune checkpoint molecules to avoid immune destruction. Initially approved for the treatment of metastatic melanoma, immune checkpoint inhibitors (ICIs) have been cleared to treat various solid tumors, including advanced or metastatic urothelial carcinoma, non-small-cell lung cancer, colorectal cancer, triple-negative breast cancer, and head and neck squamous cell carcinoma[78,79]. Currently, FDA-approved immune checkpoint inhibitors (ICIs) include anti-CTLA-4 agents (ipilimumab), anti-PD-1 agents (nivolumab, pembrolizumab, cemiplimab) and anti-PD-L1 agents (atezolizumab, avelumab, durvalumab)[79].

ICIs have emerged as a new therapeutic option for pancreatic cancer. Unfortunately, most phase I and II clinical trials on ICI treatment have failed to show the desired beneficial effect in PDAC. Two independent phase II clinical trials have demonstrated unsatisfactory clinical outcomes on monotherapy with anti-CTLA-4 mAb (Table 1). Single-agent ipilimumab, an anti-CTLA-4 mAb, was ineffective for the treatment of advanced PDAC (NCT00112580) (https://clinicaltrials.gov/ct2/show/NCT00112580)[80,81]. Monotherapy with tremelimumab, another anti-CTLA-4 mAb, also yielded poor clinical outcomes in PDAC, with 18 out of 20 patients demonstrating progressive disease and a poor median OS of 4 mo (95%CI: 2.83-5.42 mo) (NCT02527434) (https://clinicaltrials.gov/ct2/show/NCT02527434).

Combination therapy with ipilimumab and gemcitabine, on the other hand, has demonstrated promising results due to the increased immune response by enhancing naïve T-cell activation[82]. In a phase 1b clinical trial (NCT01473940) (https://clinicaltrials.gov/ct2/show/NCT01473940), initial results on combination therapy with ipilimumab and gemcitabine showed that the treatment was tolerable, with a median PFS of 2.5 mo (95%CI: 0.8-4.8 mo) and a median OS of 8.5 mo (95%CI: 2.2-10.3 mo). In this study, five out of the 11 patients had stable disease, while two had a partial response. An ongoing clinical trial (NCT01928394) (https://clinicaltrials.gov/ct2/show/NCT01928394) is comparing nivolumab (anti-PD-1 mAb) monotherapy and combination therapy with nivolumab plus ipilimumab in patients with advanced or metastatic PDAC, and the results will be released in 2023.

Table 1 Complete immune checkpoint inhibitor-based clinical trials in pancreatic ductal adenocarcinoma

Strategy	Treatment	Phase	Number	Cancer stage	Outcomes
Immune checkpoint inhibitor (target) monotherapy	Tremelimumab (CTLA-4)	II	NCT02527434	Advanced/metastatic PDAC	Tremelimumab monotherapy is ineffective for metastatic PDAC.
	Ipilimumab (CTLA-4)	II	NCT00112580	Advanced PDAC	Ipilimumab monotherapy is ineffective for advanced PDAC.
	Atezolizumab (PD-L1)	I/II	NCT03829501	Advanced PDAC	No results reported yet
Immune checkpoint inhibitor (target) + immune checkpoint inhibitor(target)	Tremelimumab (CTLA-4) + Durvalumab (PD-L1)	II	NCT02558894	Metastatic PDAC	ORR 3.1% for combination therapy. (ORR 0% for monotherapy).
	Nivolumab (PD-1) + Ipilimumab (CTLA-4)	I/II	NCT01928394	Advanced/metastatic PDAC	No results reported yet
Immune checkpoint inhibitor (target) + chemotherapy	Tremelimumab (CTLA-4) + Gemcitabine	I	NCT00556023	Advanced PDAC	Median OS 7.4 mo (95%CI: 5.8-9.4 mo)
	Ipilimumab(CTLA-4) + Gemcitabine	Ib	NCT01473940	Advanced/metastatic PDAC	Median OS 6.90 mo (95%CI: 2.63–9.57 mo)
	Pembrolizumab (PD-1) + Gemcitabine and Nab-paclitaxel	Ib/II	NCT02331251	Advanced/metastatic PDAC	Median OS 15.0 mo (95%CI: 6.8–22.6 mo)
Immune Checkpoint Inhibitor (Target) + Target therapy	Durvalumab (PD-L1) + Galunisertib	I	NCT02734160	Metastatic PDAC	Median PFS 1.9 mo (95%CI: 1.5-2.2 mo); median OS was NR (95%CI: 3.6 mo, NR)
	Durvalumab (PD-L1) + Pexidartinib	I	NCT02777710	Advanced/metastatic PDAC	No results reported yet
Immune Checkpoint Inhibitor (Target) + Radiation Therapy	Tremelimumab (CTLA-4) + Durvalumab (PD-1) + SBRT	I/II	NCT02311361	Advanced/metastatic PDAC	ORR of 9.6% including 2 patients who achieved a durable partial response lasting over 12 mo

https://clinicaltrials.gov/. PDAC: Pancreatic ductal adenocarcinoma; CTLA-4: Cytotoxic T lymphocyte-associated antigen-4; PD-1: Programmed cell death protein 1; PD-L1: Programmed cell death ligand 1; OS: Overall survival; PFS: Progression-free survival; ORR: Overall response rate; NR: Not reached.

Notably, in a phase I clinical trial (NCT00556023) (https://clinicaltrials.gov/ct2/show/NCT00556023), a tolerable and safe profile was demonstrated by combination therapy with tremelimumab plus gemcitabine, warranting further study in patients with metastatic PDAC. Thirty-four patients were enrolled in the study, and the median OS was 7.4 mo (95%CI: 5.8-9.4 mo). Two patients achieved a partial response at the end of treatment[83]. A phase Ib/II study (NCT02331251) (https://clinicaltrials.gov/ct2/show/NCT02331251) was performed to evaluate the safety and efficacy of pembrolizumab, an anti-PD-1 mAb, in combination with gemcitabine plus nab-paclitaxel chemotherapy. The median PFS and OS were 9.1 and 15.0 mo for chemotherapy naïve-treated patients, respectively, and changes in tumor cell-free DNA copy number instability were considered to be a potential prognostic factor for OS[84].

A phase I study on atezolizumab, an engineered IgG1 mAb targeting PD-L1, showed tolerability at doses up to 20 mg/kg every three weeks in a Japanese cohort[85]. In a phase II randomized clinical trial (NCT02558894) (https://clinicaltrials.gov/ct2/show/NCT02558894), evaluation of durvalumab, an anti-PD-L1 agent, with or without tremelimumab in patients with metastatic PDAC was evaluated following the failure of 5-FU and gemcitabine-based chemotherapy[86]. No patients in the study responded to durvalumab monotherapy, and the efficacy analysis demonstrated an objective response rate (ORR) of 3.1% (95%CI: 0.08-16.22) with the combination therapy of durvalumab plus tremelimumab [86].

A high tumor mutational burden (TMB) in cancer cells tends to produce more immunogenic neoantigens and may predict immunotherapy response[87]. A phase II clinical trial (NCT05093231) (https://clinicaltrials.gov/ct2/show/NCT05093231) investigating the efficacy of pembrolizumab plus olaparib in metastatic pancreatic adenocarcinoma patients exhibiting high tumor mutation burden is ongoing, and the results will be released in 2026.

Based on the results from current clinical trials, further studies need to focus on the combined approaches using ICIs with different therapeutic approaches, including chemotherapy, radiotherapy, or additional innovative platforms of immunotherapy, such as cancer vaccine and adoptive cell transfer.

Therapeutic cancer vaccines

Therapeutic cancer vaccines include whole-cell vaccines, dendritic cells, DNA, and peptide vaccines that activate cancer antigen-specific cytotoxic T lymphocytes (CTLs), eliciting immunogenic antigen presentation and leading to an anticancer response[88]. One such pancreatic cancer vaccine is GVAX,

which is generated from irradiated pancreatic cancer cells expressing granulocyte-macrophage colony-stimulating factor (GM-CSF)[89] (Table 2). Upon vaccination, GVAX secretes GM-CSF, induces subsequent activation of antigen-presenting cell and T-cell priming, and stimulates the patient's immune system against pancreatic cancer cells[90]. GVAX was tolerable even at high doses, and the vaccination-induced increased delayed-type hypersensitivity response to autologous tumor cells[91]. In a phase II clinical trial on GVAX (NCT00084383) (https://clinicaltrials.gov/ct2/show/NCT00084383), sixty patients received GVAX 8-10 wk after surgical intervention, followed by adjuvant 5-FU-based chemoradiotherapy. The median PFS was 17.3 mo (95%CI: 14.6-22.8 mo), with a median OS of 24.8 mo (95%CI: 21.2-31.6 mo), which compares favorably with published data for resected PDAC[92]. Combinatory immunotherapy has aimed to induce a much more sustained antitumor T-cell response [93]. In a phase Ib trial for locally advanced, unresectable or metastatic PDAC (NCT00836407) (https://clinicaltrials.gov/ct2/show/NCT00836407), thirty patients received either ipilimumab monotherapy or ipilimumab plus GVAX cancer vaccine, and the median OS was 3.6 mo for the ipilimumab monotherapy group, compared to 5.7 mo in the group with combination therapy[94]. Although combinatory immunotherapy has shown its potential for advanced PDAC, more studies are needed to fully explore this novel therapeutic strategy's capability.

Few human leukocyte antigen (HLA)-A(*)2402-restricted tumor-associated antigens, including the KIF20A-10-66 peptide, have been identified in PDAC[95]. A phase I/II clinical trial in Japan showed a better prognosis in patients with metastatic PDAC and HLA-A*2402-positive status who received KIF20A-10-66 peptide vaccination as second-line treatment after failure of gemcitabine chemotherapy [96]. In two separate phase II clinical trials, KIF20A-derived peptide was evaluated in combination with two antiangiogenic cancer vaccines targeting vascular endothelial growth factor receptor 1 (VEGFR1) and VEGFR2. In the HLA-A*2402-matched group, patients with peptide-specific CTL induction had improved prognosis and increased OS[97,98]. Another HLA-A24-restricted antigenic peptide, SVN-2B, also functions as an immunogenic molecule. A vaccination protocol of SVN-2B in combination with interferon-α has demonstrated effective clinical and immunological responses for advanced PDAC[99].

Algenpantucel-L is a whole-cell pancreatic cancer vaccine with two irradiated allogenic human pancreatic cell lines (HAPa-1 and HAPa-2) expressing the murine enzyme (1,3)-galactosyltransferase (α GT)[100]. Of note, the αGT enzyme is the critical barrier to xenotransplantation due to hyperacute rejection[101]. As a result, Algenpantucel-L will induce a hyperacute rejection of the allograft cells through rapid activation of antibody-dependent cell-mediated cytotoxicity (ADCC), leading to a response against the patient's pancreatic cancer cells through epitope spreading[102]. A phase II, open-label trial (NCT00569387) (https://clinicaltrials.gov/ct2/show/NCT00569387) evaluated the use of the Algenpantucel-L tumor vaccine in combination with gemcitabine plus 5-FU chemoradiotherapy in patients with resected PDAC. Seventy patients were recruited in the study, and the 12-mo disease-free survival (DFS) and OS were 63% and 86%, respectively, suggesting that the Algenpantucel-L tumor vaccine could be administered with standard chemotherapy following surgical resection of pancreatic cancer[101]. Unfortunately, in a recent phase 3, open-label, randomized clinical trial (NCT01836432) (https://clinicaltrials.gov/ct2/show/NCT01836432), Algenpantucel-L failed to improve survival on borderline resectable or locally advanced PDAC receiving neoadjuvant chemoradiation therapy[103].

Overexpression of Mucin 1 (MUC-1), a type I transmembrane protein with O-linked glycosylation, plays a crucial role in oncogenic signaling to promote metastasis, angiogenesis, and invasion[104]. MUC-1 has served as a target for cancer vaccine immunotherapy[105]. Following surgical resection, a phase I/II study of a MUC1 peptide-loaded dendritic cell vaccine was conducted in 12 pancreaticobiliary cancer patients. Four out of twelve (33.3%) patients who received this MUC-1-based tumor vaccine were alive after four years without evidence of recurrence[106]. An optimized construct with MUC-1-variable number tandem repeats has been designed with much more potent immunogenicity [107].

Dendritic cell vaccines have been introduced to enhance the antitumor immune response through the stimulation of naïve T cells[108]. In a study evaluating the effectiveness of a dendritic cell vaccine in patients with advanced PDAC (NCT01410968) (https://clinicaltrials.gov/ct2/show/NCT01410968), autologous dendritic cells were isolated in HLA-A2-positive patients, loaded with three A-2 restricted peptides, and readministered as a cellular vaccine. The results were promising with the generation of antigen-specific T cells in three patients, as well as tolerable adverse effects[109]. In a phase I study in Japan, a Wilms' tumor 1 (WT1)-pulsed dendritic cell vaccine combined with chemotherapy showed safety and potential acquisition of immunity in resected PDAC[110]. Multiple associated studies have further supported the clinical benefits of dendritic cell-based vaccines in PDAC[111-113].

Approximately 95% of PDAC patients have mutations in the *KRAS* oncogene. Despite an early study suggesting an unproven efficacy by targeting mutated KRAS in PDAC[114], multiple subsequent clinical studies have demonstrated the clinical potential for such a therapeutic approach. A phase I/II clinical trial (NCT02261714) (https://clinicaltrials.gov/ct2/show/NCT02261714) evaluated the efficacy of a synthetic mutant RAS peptide vaccine with GM-CSF in PDAC. TG01, a mixture of 7 synthetic RAS peptides representing the most common *KRAS* mutations, combined with GM-CSF and gemcitabine was well tolerated with a robust immune response and improved clinical outcome[115]. One study demonstrated a long-term immune response and improved survival in patients with resected PDAC after KRAS vaccination[116]. An alternative KRAS-based tumor vaccine is GI-4000, a recombinant heat-

Table 2 Complete vaccine immunotherapy-based clinical trials in pancreatic ductal adenocarcinoma

Treatment	Phase	Number	Cancer stage	Outcomes
GVAX, 5-FU, chemoradiation	II	NCT00084383	Resected stage I/II PDAC	Median OS 24.8 mo (95%CI: 21.2-31.6 mo)
GVAX, cyclophosphamide, CRS-207	II	NCT01417000	Metastatic PDAC	Cy/GVAX and CRS-207 extended OS for PDAC patients, with minimal toxicity
GVAX, cyclophosphamide, CRS-207	II	NCT02004262	Metastatic PDAC	Cy/GVAX and CRS-207 did not show survival benefit over chemotherapy in patients with previously treated metastatic PDAC
GVAX, Ipilimumab, FOLFIRINOX	II	NCT01896869	Metastatic PDAC	Ipilimumab + GVAX group did not show survival benefit over chemotherapy [median OS 9.38 mo (95% CI, 5.0-12.2 mo) *vs* 14.7 mo (95%CI: 11.6-20.0 mo)]
Algenpantucel-L	II	NCT00569387	Surgically resected PDAC	The addition of algenpantucel-L to standard adjuvant therapy for resected pancreatic cancer may improve survival (12-mo DFS 62%, 12-mo OS 86%)
Gemcitabine, 5FU Chemoradiation, Algenpantucel-L	III	NCT01072981	Surgically Resected PDAC	No results reported yet
Dendritic cells pulsed with MUC-1/WT-1	I/II	NCT03114631	PDAC	Dendritic cells immunotherapy provided a favorable outcome in PDAC patents (12-mo OS 78.2% *vs* 33.8%)
GI-4000 (KRAS), Gemcitabine	II	NCT00300950	Non-metastatic, Post-resection PDAC	Overall, GI-4000 group showed a similar pattern of recurrence-free survival and OS compared with the placebo group. For stratified R1 resection subgroup, there was a trend in 1 year OS (72% *vs* 56%), an improvement in OS (523.5 *vs* 443.5 d (hazard ratio: 1.06; 95%CI: 0.53–2.13, P = 0.872), and increased frequency of immune responders (40% *vs* 8%; P = 0.062) for GI-4000 *vs* placebo.
Ras-peptide vaccine, IL-2, GM-CSF	II	NCT00019331	Metastatic PDAC	No results reported yet
GV1001 (telomerase peptide vaccine), Gemcitabine, Capecitabine	III	NCT00425360	Locally Advanced or Metastatic PDAC	Adding GV1001 vaccination to chemotherapy did not improve OS.

https://clinicaltrials.gov/. PDAC: Pancreatic ductal adenocarcinoma; Cy: cyclophosphamide; DFS: Disease-free survival; OS: Overall survival.

inactivated Saccharomyces cerevisiae yeast-derived vaccine expressing mutated KRAS proteins. A phase I trial revealed a favorable safety profile and immunogenicity of the GI-4000 cancer vaccine[117]. A subsequent phase II trial (NCT00300950) (https://clinicaltrials.gov/ct2/show/NCT00300950) compared GI-4000 plus gemcitabine with placebo plus gemcitabine alone in patients with resected PDAC carrying *KRAS* mutation. GI-4000 was well tolerated. It led to a similar median OS compared with placebo. However, compared with the placebo group, the GI-4000 group had a trend of improved OS (523.5 *vs* 443.5 d) and an increased frequency of immune responders (40% *vs* 8%) in the stratified R1 resection subgroup[118].

The GV1001 tumor vaccine consists of a fragment (16 amino acids) of human telomerase reverse transcriptase (hTERT) found in a high proportion in PDAC cancer cells and has been introduced as a novel therapeutic regimen[119]. In a phase I/II clinical trial evaluating the clinical outcomes in patients with unresectable PDAC, GV1001 plus GM-CSF elicited an immune response in 63% of patients, resulting in a median OS of 7.2 mo for immune responders compared to 2.9 mo for nonimmune responders[120]. However, in a randomized phase III study of patients with locally advanced and metastatic PDAC, combination therapy consisting of GV1001, gemcitabine, and capecitabine chemotherapy showed no improvement in OS compared to chemotherapy alone [6.9 mo (95%CI: 6.4–7.6 mo) *vs* 7.9 mo (95%CI: 7.1–8.8 mo)] (NCT00425360) (https://clinicaltrials.gov/ct2/show/NCT00425360) [121]. Another GV1001-based phase III clinical trial (NCT00358566) (https://clinicaltrials.gov/ct2/show/NCT00358566) was terminated early because of a lack of survival advantage.

Adoptive cell transfer

Adoptive cell transfer, also known as cellular immunotherapy, includes chimeric antigen receptor T-cell (CAR T cell) therapy and tumor-infiltrating lymphocyte (TIL) therapy[122,123]. CAR T-cell therapy is the most common type of adoptive cell transfer. Generally, it involves harvesting the patient's T cells, genetic modification to express surface chimeric antigen receptor, *ex vivo* expansion, and then transferring the cells back to enhance tumor immunity. In forty-three patients with PDAC who underwent radical pancreatectomy, gemcitabine plus adoptive cell transfer with T cells stimulated by the MUC1-expressing human pancreatic cancer cell line demonstrated a median OS of 14.7 mo[124]. Mesothelin is a tumor antigen highly expressed in PDAC[125]. In a preclinical study, CAR T-cell therapy targeting mesothelin demonstrated promising tumor-suppressive effects[126]. Amatuximab

Table 3 Complete adoptive cell transfer-based clinical trials in pancreatic ductal adenocarcinoma

Treatment	Phase	Number	Cancer stage	Outcomes
MORAb-009, Gemcitabine	II	NCT00570713	Advanced PDAC	MORAb-009 did not show survival benefit over placebo group [median OS 6.5 mo, 95%CI: 4.5–8.10 mo *vs* 6.9 mo 95%CI: 5.4–8.8 mo]
MORAb-009	I	NCT00325494	PDAC	No results reported yet
Radiolabeled Amatuximab (MORAb-009)	I	NCT01521325	PDAC	No results reported yet
Autologous Redirected RNA Mesothelin CAR T cells	I	NCT01897415	PDAC	No results reported yet
CART-133 T cells	I/II	NCT02541370	Relapsed and/or Chemotherapy Refractory Advanced PDAC	No results reported yet

https://clinicaltrials.gov/. PDAC: Pancreatic ductal adenocarcinoma; OS: Overall survival.

(MORab-009), a chimeric mAb targeting mesothelin, also led to reduced growth of mesothelin-expressing tumors, including PDAC[127]. In a phase I trial, the efficacy of MORAb-009 was tested in seven PDAC patients, and one patient had disease control for greater than six months[128]. However, in a phase II randomized placebo-controlled clinical trial (NCT00570713) (https://clinicaltrials.gov/show/NCT00570713) evaluating the efficacy of MORAb-009 plus gemcitabine, no significantly improved clinical outcome was observed [median OS: 6.5 mo (95%CI: 4.5–8.10 mo) *vs* 6.9 mo (95%CI: 5.4–8.8 mo)]. Compared with the development of ICIs and cancer vaccines, adoptive cell transfer therapy is still in the early development phase against pancreatic cancer (Table 3); more preclinical and clinical studies are needed to further explore its full clinical potential.

IMMUNOTHERAPY AND THE TUMOR MICROENVIRONMENT

Immunotherapy has thus far failed to fulfill its promise in PDAC. The underlying mechanisms appear to be complex and multifactorial primarily due to their unique genetic signatures, metabolic features, and immunosuppressive TME. Pancreatic cancers carry unique molecular genetic backgrounds. MSI in pancreatic cancer is extremely rare (approximately 1%). Oncogenic *KRAS* mutations, the most common mutation in PDAC, have also contributed to PDAC initiation and maintenance by producing an immunosuppressive TME[129].

Furthermore, altered metabolism of glucose, amino acids, and lipids and their crosstalk with the TME play essential roles in PDAC tumor progression[130]. Multiple lines of evidence have pinpointed the TME as one of the significant barriers to developing effective immunotherapy for PDAC. It is of great clinical interest to sensitize PDAC to immunotherapy through modification of the TME.

One such effort has been focused on CAFs in the TME. As an immunosuppressive component of the TME, FAP-positive CAFs potentially account for the ineffectiveness of immunotherapy in PDAC[131]. Another subtype of CAFs, characterized by the expression of the leucine-rich repeat-containing 15 (LRRC15) protein, could only be detected in pancreatic cancer tissue and is associated with poor response to anti-PD-L1 therapy[132]. Notably, FAP-positive CAFs are the only CAF subtype that expresses CXC motif chemokine ligand 12 (CXCL12). Ablation of FAP-positive CAFs or inhibition of CXCL12 uncovers the antitumor activity of CTLA-4 and PD-L1-based immunotherapy[133]. A phase I/II clinical trial (NCT03168139) (https://clinicaltrials.gov/ct2/show/NCT03168139) was conducted to evaluate the treatment effect of pembrolizumab in patients receiving docetaxel (NOX-A12), an agent targeting CXCL12 and TME in metastatic PDAC. No results have been reported yet.

Cellular components in the TME, including MDSCs and TAMs, are also promising targets in the combinatory strategy for immunotherapy. MDSCs and TAMs induce an immunosuppressive TME, partially through colony-stimulating factor 1 receptor (CSF1R) and focal adhesion kinase (FAK)[134]. Small molecular inhibitors of CSF1R or FAK can reprogram the TME and improve T lymphocyte-mediated pancreatic cancer destruction[135,136]. Multiple clinical trials with CSF1R or FAK inhibitors combined with immunotherapy are currently ongoing (Table 4).

CONCLUSION

Despite advances in translational research, PDAC remains a highly lethal malignancy. Recent breakthroughs in immunotherapy have revolutionized cancer therapy and have shown great potential to transform future PDAC treatment. However, PDAC has shown inferior treatment outcomes toward

Table 4 Ongoing clinical trials with immunotherapy plus agents targeting the tumor microenvironment in pancreatic ductal adenocarcinoma

Strategy	Treatment	Phase	Number	Cancer stage
Immune checkpoint inhibitor (target) + CAFs/CXCL12 targeted agents	Pembrolizumab(PD-1) + Olaptesed pegol	I/II	NCT03168139	Metastatic PDAC
Immune checkpoint inhibitor (target)+ CSF1R targeted agent	Durvalumab (PD-L1) + Pexidartinib	I	NCT02777710	Metastatic/Advanced PDAC
	Nivolumab (PD-1) + Cabiralizumab	I	NCT02526017	Advanced PDAC
	Nivolumab (PD-1) + Cabiralizumab + Gemcitabine	II	NCT03697564	Advanced PDAC (Stage IV)
Immune checkpoint inhibitor (target) + FAK targeted agent	Pembrolizumab(PD-1) + Defactinib	I/IIa	NCT02758587	Advanced PDAC
	Pembrolizumab(PD-1) + Defactinib + Gemcitabine	I	NCT02546531	Advanced PDAC
	Pembrolizumab (PD-1) + Defactinib	II	NCT03727880	Resectable PDAC

https://clinicaltrials.gov/. PDAC: Pancreatic ductal adenocarcinoma; CTLA-4: Cytotoxic T lymphocyte-associated antigen-4; PD-1: Programmed cell death protein 1; PD-L1: Programmed cell death ligand 1; CAFs: Cancer-associated fibroblasts; CXCL12: CXC motif chemokine ligand 12; CSF1R: Colony-stimulating factor 1 receptor; FAK: Focal adhesion kinase.

various immunotherapy regimens compared to other cancer types. The TME has been considered as the fundamental underlying barrier to therapy resistance. To overcome this therapeutic resistance, further investigations with innovative treatment strategies will be needed.

FOOTNOTES

Author contributions: Smith C and Yin F collected and analyzed the data, made the tables and figure, wrote and finalized the manuscript; Zheng W, Dong J, Wang Y, Lai J and Liu X critically reviewed the manuscript; and All authors have approved the final manuscript.

Conflict-of-interest statement: The authors declare no competing interests in this study.

Open-Access: This article is an open-access article that was selected by an in-house editor and fully peer-reviewed by external reviewers. It is distributed in accordance with the Creative Commons Attribution NonCommercial (CC BY-NC 4.0) license, which permits others to distribute, remix, adapt, build upon this work non-commercially, and license their derivative works on different terms, provided the original work is properly cited and the use is non-commercial. See: https://creativecommons.org/Licenses/by-nc/4.0/

Country/Territory of origin: United States

ORCID number: Caitlyn Smith 0000-0001-8944-0480; Wei Zheng 0000-0003-3193-2655; Jixin Dong 0000-0002-2757-4464; Yaohong Wang 0000-0001-5964-0465; Jinping Lai 0000-0001-5365-2481; Xiuli Liu 0000-0001-5791-2017; Feng Yin 0000-0002-8444-1123.

S-Editor: Ma YJ
L-Editor: A
P-Editor: Ma YJ

REFERENCES

1 **Siegel RL**, Miller KD, Fuchs HE, Jemal A. Cancer Statistics, 2021. *CA Cancer J Clin* 2021; **71**: 7-33 [PMID: 33433946 DOI: 10.3322/caac.21654]
2 **Miller KD**, Siegel RL, Lin CC, Mariotto AB, Kramer JL, Rowland JH, Stein KD, Alteri R, Jemal A. Cancer treatment and survivorship statistics, 2016. *CA Cancer J Clin* 2016; **66**: 271-289 [PMID: 27253694 DOI: 10.3322/caac.21349]
3 **Porta M**, Fabregat X, Malats N, Guarner L, Carrato A, de Miguel A, Ruiz L, Jariod M, Costafreda S, Coll S, Alguacil J, Corominas JM, Solà R, Salas A, Real FX. Exocrine pancreatic cancer: symptoms at presentation and their relation to tumour site and stage. *Clin Transl Oncol* 2005; **7**: 189-197 [PMID: 15960930 DOI: 10.1007/BF02712816]
4 **De Souza A**, Khawaja KI, Masud F, Saif MW. Metformin and pancreatic cancer: Is there a role? *Cancer Chemother Pharmacol* 2016; **77**: 235-242 [PMID: 26740120 DOI: 10.1007/s00280-015-2948-8]
5 **Corbo V**, Tortora G, Scarpa A. Molecular pathology of pancreatic cancer: from bench-to-bedside translation. *Curr Drug*

Targets 2012; **13**: 744-752 [PMID: 22458520 DOI: 10.2174/138945012800564103]
6 **Sperti C**, Pasquali C, Pedrazzoli S. Ductal adenocarcinoma of the body and tail of the pancreas. *J Am Coll Surg* 1997; **185**: 255-259 [PMID: 9291403 DOI: 10.1016/s1072-7515(97)00056-2]
7 **Griffin JF**, Smalley SR, Jewell W, Paradelo JC, Reymond RD, Hassanein RE, Evans RG. Patterns of failure after curative resection of pancreatic carcinoma. *Cancer* 1990; **66**: 56-61 [PMID: 2354408 DOI: 10.1002/1097-0142(19900701)66:1<56::aid-cncr2820660112>3.0.co;2-6]
8 **Mizrahi JD**, Surana R, Valle JW, Shroff RT. Pancreatic cancer. *Lancet* 2020; **395**: 2008-2020 [PMID: 32593337 DOI: 10.1016/S0140-6736(20)30974-0]
9 **Ettrich TJ**, Seufferlein T. Systemic Therapy for Metastatic Pancreatic Cancer. *Curr Treat Options Oncol* 2021; **22**: 106 [PMID: 34665339 DOI: 10.1007/s11864-021-00895-4]
10 **Oberstein PE**, Olive KP. Pancreatic cancer: why is it so hard to treat? *Therap Adv Gastroenterol* 2013; **6**: 321-337 [PMID: 23814611 DOI: 10.1177/1756283X13478680]
11 **Conroy T**, Desseigne F, Ychou M, Bouché O, Guimbaud R, Bécouarn Y, Adenis A, Raoul JL, Gourgou-Bourgade S, de la Fouchardière C, Bennouna J, Bachet JB, Khemissa-Akouz F, Péré-Vergé D, Delbaldo C, Assenat E, Chauffert B, Michel P, Montoto-Grillot C, Ducreux M; Groupe Tumeurs Digestives of Unicancer; PRODIGE Intergroup. FOLFIRINOX versus gemcitabine for metastatic pancreatic cancer. *N Engl J Med* 2011; **364**: 1817-1825 [PMID: 21561347 DOI: 10.1056/NEJMoa1011923]
12 **Sarantis P**, Koustas E, Papadimitropoulou A, Papavassiliou AG, Karamouzis MV. Pancreatic ductal adenocarcinoma: Treatment hurdles, tumor microenvironment and immunotherapy. *World J Gastrointest Oncol* 2020; **12**: 173-181 [PMID: 32104548 DOI: 10.4251/wjgo.v12.i2.173]
13 **Storz P**, Crawford HC. Carcinogenesis of Pancreatic Ductal Adenocarcinoma. *Gastroenterology* 2020; **158**: 2072-2081 [PMID: 32199881 DOI: 10.1053/j.gastro.2020.02.059]
14 **Grant TJ**, Hua K, Singh A. Molecular Pathogenesis of Pancreatic Cancer. *Prog Mol Biol Transl Sci* 2016; **144**: 241-275 [PMID: 27865459 DOI: 10.1016/bs.pmbts.2016.09.008]
15 **Samuel N**, Hudson TJ. The molecular and cellular heterogeneity of pancreatic ductal adenocarcinoma. *Nat Rev Gastroenterol Hepatol* 2011; **9**: 77-87 [PMID: 22183185 DOI: 10.1038/nrgastro.2011.215]
16 **Lee CJ**, Li C, Simeone DM. Human pancreatic cancer stem cells: implications for how we treat pancreatic cancer. *Transl Oncol* 2008; **1**: 14-18 [PMID: 18607507 DOI: 10.1593/tlo.08013]
17 **Pham T**, Roth S, Kong J, Guerra G, Narasimhan V, Pereira L, Desai J, Heriot A, Ramsay R. An Update on Immunotherapy for Solid Tumors: A Review. *Ann Surg Oncol* 2018; **25**: 3404-3412 [PMID: 30039324 DOI: 10.1245/s10434-018-6658-4]
18 **Katayama ES**, Hue JJ, Bajor DL, Ocuin LM, Ammori JB, Hardacre JM, Winter JM. A comprehensive analysis of clinical trials in pancreatic cancer: what is coming down the pike? *Oncotarget* 2020; **11**: 3489-3501 [PMID: 33014285 DOI: 10.18632/oncotarget.27727]
19 **Goggins M**, Offerhaus GJ, Hilgers W, Griffin CA, Shekher M, Tang D, Sohn TA, Yeo CJ, Kern SE, Hruban RH. Pancreatic adenocarcinomas with DNA replication errors (RER+) are associated with wild-type K-ras and characteristic histopathology. Poor differentiation, a syncytial growth pattern, and pushing borders suggest RER+. *Am J Pathol* 1998; **152**: 1501-1507 [PMID: 9626054]
20 **Wilentz RE**, Goggins M, Redston M, Marcus VA, Adsay NV, Sohn TA, Kadkol SS, Yeo CJ, Choti M, Zahurak M, Johnson K, Tascilar M, Offerhaus GJ, Hruban RH, Kern SE. Genetic, immunohistochemical, and clinical features of medullary carcinoma of the pancreas: A newly described and characterized entity. *Am J Pathol* 2000; **156**: 1641-1651 [PMID: 10793075 DOI: 10.1016/S0002-9440(10)65035-3]
21 **Foucher ED**, Ghigo C, Chouaib S, Galon J, Iovanna J, Olive D. Pancreatic Ductal Adenocarcinoma: A Strong Imbalance of Good and Bad Immunological Cops in the Tumor Microenvironment. *Front Immunol* 2018; **9**: 1044 [PMID: 29868007 DOI: 10.3389/fimmu.2018.01044]
22 **Ren B**, Cui M, Yang G, Wang H, Feng M, You L, Zhao Y. Tumor microenvironment participates in metastasis of pancreatic cancer. *Mol Cancer* 2018; **17**: 108 [PMID: 30060755 DOI: 10.1186/s12943-018-0858-1]
23 **Waghray M**, Yalamanchili M, di Magliano MP, Simeone DM. Deciphering the role of stroma in pancreatic cancer. *Curr Opin Gastroenterol* 2013; **29**: 537-543 [PMID: 23892539 DOI: 10.1097/MOG.0b013e328363affe]
24 **Ho WJ**, Jaffee EM, Zheng L. The tumour microenvironment in pancreatic cancer - clinical challenges and opportunities. *Nat Rev Clin Oncol* 2020; **17**: 527-540 [PMID: 32398706 DOI: 10.1038/s41571-020-0363-5]
25 **Hessmann E**, Buchholz SM, Demir IE, Singh SK, Gress TM, Ellenrieder V, Neesse A. Microenvironmental Determinants of Pancreatic Cancer. *Physiol Rev* 2020; **100**: 1707-1751 [PMID: 32297835 DOI: 10.1152/physrev.00042.2019]
26 **Erkan M**, Hausmann S, Michalski CW, Fingerle AA, Dobritz M, Kleeff J, Friess H. The role of stroma in pancreatic cancer: diagnostic and therapeutic implications. *Nat Rev Gastroenterol Hepatol* 2012; **9**: 454-467 [PMID: 22710569 DOI: 10.1038/nrgastro.2012.115]
27 **Whatcott CJ**, Diep CH, Jiang P, Watanabe A, LoBello J, Sima C, Hostetter G, Shepard HM, Von Hoff DD, Han H. Desmoplasia in Primary Tumors and Metastatic Lesions of Pancreatic Cancer. *Clin Cancer Res* 2015; **21**: 3561-3568 [PMID: 25695692 DOI: 10.1158/1078-0432.CCR-14-1051]
28 **Karagiannis GS**, Poutahidis T, Erdman SE, Kirsch R, Riddell RH, Diamandis EP. Cancer-associated fibroblasts drive the progression of metastasis through both paracrine and mechanical pressure on cancer tissue. *Mol Cancer Res* 2012; **10**: 1403-1418 [PMID: 23024188 DOI: 10.1158/1541-7786.MCR-12-0307]
29 **Ferrara B**, Pignatelli C, Cossutta M, Citro A, Courty J, Piemonti L. The Extracellular Matrix in Pancreatic Cancer: Description of a Complex Network and Promising Therapeutic Options. *Cancers (Basel)* 2021; **13** [PMID: 34503252 DOI: 10.3390/cancers13174442]
30 **Binenbaum Y**, Na'ara S, Gil Z. Gemcitabine resistance in pancreatic ductal adenocarcinoma. *Drug Resist Updat* 2015; **23**: 55-68 [PMID: 26690340 DOI: 10.1016/j.drup.2015.10.002]
31 **Kultti A**, Zhao C, Singha NC, Zimmerman S, Osgood RJ, Symons R, Jiang P, Li X, Thompson CB, Infante JR, Jacobetz MA, Tuveson DA, Frost GI, Shepard HM, Huang Z. Accumulation of extracellular hyaluronan by hyaluronan synthase 3

promotes tumor growth and modulates the pancreatic cancer microenvironment. *Biomed Res Int* 2014; **2014**: 817613 [PMID: 25147816 DOI: 10.1155/2014/817613]

32 **Provenzano PP**, Cuevas C, Chang AE, Goel VK, Von Hoff DD, Hingorani SR. Enzymatic targeting of the stroma ablates physical barriers to treatment of pancreatic ductal adenocarcinoma. *Cancer Cell* 2012; **21**: 418-429 [PMID: 22439937 DOI: 10.1016/j.ccr.2012.01.007]

33 **Gulley JL**, Borre M, Vogelzang NJ, Ng S, Agarwal N, Parker CC, Pook DW, Rathenborg P, Flaig TW, Carles J, Saad F, Shore ND, Chen L, Heery CR, Gerritsen WR, Priou F, Langkilde NC, Novikov A, Kantoff PW. Phase III Trial of PROSTVAC in Asymptomatic or Minimally Symptomatic Metastatic Castration-Resistant Prostate Cancer. *J Clin Oncol* 2019; **37**: 1051-1061 [PMID: 30817251 DOI: 10.1200/JCO.18.02031]

34 **Van Cutsem E**, Tempero MA, Sigal D, Oh DY, Fazio N, Macarulla T, Hitre E, Hammel P, Hendifar AE, Bates SE, Li CP, Hingorani SR, de la Fouchardiere C, Kasi A, Heinemann V, Maraveyas A, Bahary N, Layos L, Sahai V, Zheng L, Lacy J, Park JO, Portales F, Oberstein P, Wu W, Chondros D, Bullock AJ; HALO 109-301 Investigators. Randomized Phase III Trial of Pegvorhyaluronidase Alfa With Nab-Paclitaxel Plus Gemcitabine for Patients With Hyaluronan-High Metastatic Pancreatic Adenocarcinoma. *J Clin Oncol* 2020; **38**: 3185-3194 [PMID: 32706635 DOI: 10.1200/JCO.20.00590]

35 **Coussens LM**, Fingleton B, Matrisian LM. Matrix metalloproteinase inhibitors and cancer: trials and tribulations. *Science* 2002; **295**: 2387-2392 [PMID: 11923519 DOI: 10.1126/science.1067100]

36 **Bramhall SR**, Neoptolemos JP, Stamp GW, Lemoine NR. Imbalance of expression of matrix metalloproteinases (MMPs) and tissue inhibitors of the matrix metalloproteinases (TIMPs) in human pancreatic carcinoma. *J Pathol* 1997; **182**: 347-355 [PMID: 9349239 DOI: 10.1002/(SICI)1096-9896(199707)182:3<347::AID-PATH848>3.0.CO;2-J]

37 **Xu Y**, Li Z, Jiang P, Wu G, Chen K, Zhang X, Li X. The co-expression of MMP-9 and Tenascin-C is significantly associated with the progression and prognosis of pancreatic cancer. *Diagn Pathol* 2015; **10**: 211 [PMID: 26652622 DOI: 10.1186/s13000-015-0445-3]

38 **Okada Y**, Eibl G, Guha S, Duffy JP, Reber HA, Hines OJ. Nerve growth factor stimulates MMP-2 expression and activity and increases invasion by human pancreatic cancer cells. *Clin Exp Metastasis* 2004; **21**: 285-292 [PMID: 15554384 DOI: 10.1023/b:clin.0000046131.24625.54]

39 **Schneiderhan W**, Diaz F, Fundel M, Zhou S, Siech M, Hasel C, Möller P, Gschwend JE, Seufferlein T, Gress T, Adler G, Bachem MG. Pancreatic stellate cells are an important source of MMP-2 in human pancreatic cancer and accelerate tumor progression in a murine xenograft model and CAM assay. *J Cell Sci* 2007; **120**: 512-519 [PMID: 17227797 DOI: 10.1242/jcs.03347]

40 **Ellenrieder V**, Alber B, Lacher U, Hendler SF, Menke A, Boeck W, Wagner M, Wilda M, Friess H, Büchler M, Adler G, Gress TM. Role of MT-MMPs and MMP-2 in pancreatic cancer progression. *Int J Cancer* 2000; **85**: 14-20 [PMID: 10585576 DOI: 10.1002/(sici)1097-0215(20000101)85:1<14::aid-ijc3>3.0.co;2-o]

41 **Crawford HC**, Scoggins CR, Washington MK, Matrisian LM, Leach SD. Matrix metalloproteinase-7 is expressed by pancreatic cancer precursors and regulates acinar-to-ductal metaplasia in exocrine pancreas. *J Clin Invest* 2002; **109**: 1437-1444 [PMID: 12045257 DOI: 10.1172/JCI15051]

42 **Marshall DC**, Lyman SK, McCauley S, Kovalenko M, Spangler R, Liu C, Lee M, O'Sullivan C, Barry-Hamilton V, Ghermazien H, Mikels-Vigdal A, Garcia CA, Jorgensen B, Velayo AC, Wang R, Adamkewicz JI, Smith V. Selective Allosteric Inhibition of MMP9 Is Efficacious in Preclinical Models of Ulcerative Colitis and Colorectal Cancer. *PLoS One* 2015; **10**: e0127063 [PMID: 25961845 DOI: 10.1371/journal.pone.0127063]

43 **Grünwald B**, Vandooren J, Gerg M, Ahomaa K, Hunger A, Berchtold S, Akbareian S, Schaten S, Knolle P, Edwards DR, Opdenakker G, Krüger A. Systemic Ablation of MMP-9 Triggers Invasive Growth and Metastasis of Pancreatic Cancer *via* Deregulation of IL6 Expression in the Bone Marrow. *Mol Cancer Res* 2016; **14**: 1147-1158 [PMID: 27489361 DOI: 10.1158/1541-7786.MCR-16-0180]

44 **Olive KP**, Jacobetz MA, Davidson CJ, Gopinathan A, McIntyre D, Honess D, Madhu B, Goldgraben MA, Caldwell ME, Allard D, Frese KK, Denicola G, Feig C, Combs C, Winter SP, Ireland-Zecchini H, Reichelt S, Howat WJ, Chang A, Dhara M, Wang L, Rückert F, Grützmann R, Pilarsky C, Izeradjene K, Hingorani SR, Huang P, Davies SE, Plunkett W, Egorin M, Hruban RH, Whitebread N, McGovern K, Adams J, Iacobuzio-Donahue C, Griffiths J, Tuveson DA. Inhibition of Hedgehog signaling enhances delivery of chemotherapy in a mouse model of pancreatic cancer. *Science* 2009; **324**: 1457-1461 [PMID: 19460966 DOI: 10.1126/science.1171362]

45 **Cheng X**, Kim JY, Ghafoory S, Duvaci T, Rafiee R, Theobald J, Alborzinia H, Holenya P, Fredebohm J, Merz KH, Mehrabi A, Hafezi M, Saffari A, Eisenbrand G, Hoheisel JD, Wölfl S. Methylisoindigo preferentially kills cancer stem cells by interfering cell metabolism *via* inhibition of LKB1 and activation of AMPK in PDACs. *Mol Oncol* 2016; **10**: 806-824 [PMID: 26887594 DOI: 10.1016/j.molonc.2016.01.008]

46 **Truong LH**, Pauklin S. Pancreatic Cancer Microenvironment and Cellular Composition: Current Understandings and Therapeutic Approaches. *Cancers (Basel)* 2021; **13** [PMID: 34638513 DOI: 10.3390/cancers13195028]

47 **Richards KE**, Zeleniak AE, Fishel ML, Wu J, Littlepage LE, Hill R. Cancer-associated fibroblast exosomes regulate survival and proliferation of pancreatic cancer cells. *Oncogene* 2017; **36**: 1770-1778 [PMID: 27669441 DOI: 10.1038/onc.2016.353]

48 **Olivares O**, Mayers JR, Gouirand V, Torrence ME, Gicquel T, Borge L, Lac S, Roques J, Lavaut MN, Berthezène P, Rubis M, Secq V, Garcia S, Moutardier V, Lombardo D, Iovanna JL, Tomasini R, Guillaumond F, Vander Heiden MG, Vasseur S. Collagen-derived proline promotes pancreatic ductal adenocarcinoma cell survival under nutrient limited conditions. *Nat Commun* 2017; **8**: 16031 [PMID: 28685754 DOI: 10.1038/ncomms16031]

49 **Sousa CM**, Biancur DE, Wang X, Halbrook CJ, Sherman MH, Zhang L, Kremer D, Hwang RF, Witkiewicz AK, Ying H, Asara JM, Evans RM, Cantley LC, Lyssiotis CA, Kimmelman AC. Pancreatic stellate cells support tumour metabolism through autophagic alanine secretion. *Nature* 2016; **536**: 479-483 [PMID: 27509858 DOI: 10.1038/nature19084]

50 **Özdemir BC**, Pentcheva-Hoang T, Carstens JL, Zheng X, Wu CC, Simpson TR, Laklai H, Sugimoto H, Kahlert C, Novitskiy SV, De Jesus-Acosta A, Sharma P, Heidari P, Mahmood U, Chin L, Moses HL, Weaver VM, Maitra A, Allison JP, LeBleu VS, Kalluri R. Depletion of carcinoma-associated fibroblasts and fibrosis induces immunosuppression and

accelerates pancreas cancer with reduced survival. *Cancer Cell* 2014; **25**: 719-734 [PMID: 24856586 DOI: 10.1016/j.ccr.2014.04.005]

51 **Lee JJ**, Perera RM, Wang H, Wu DC, Liu XS, Han S, Fitamant J, Jones PD, Ghanta KS, Kawano S, Nagle JM, Deshpande V, Boucher Y, Kato T, Chen JK, Willmann JK, Bardeesy N, Beachy PA. Stromal response to Hedgehog signaling restrains pancreatic cancer progression. *Proc Natl Acad Sci U S A* 2014; **111**: E3091-E3100 [PMID: 25024225 DOI: 10.1073/pnas.1411679111]

52 **Biffi G**, Tuveson DA. Diversity and Biology of Cancer-Associated Fibroblasts. *Physiol Rev* 2021; **101**: 147-176 [PMID: 32466724 DOI: 10.1152/physrev.00048.2019]

53 **Helms E**, Onate MK, Sherman MH. Fibroblast Heterogeneity in the Pancreatic Tumor Microenvironment. *Cancer Discov* 2020; **10**: 648-656 [PMID: 32014869 DOI: 10.1158/2159-8290.CD-19-1353]

54 **Öhlund D**, Handly-Santana A, Biffi G, Elyada E, Almeida AS, Ponz-Sarvise M, Corbo V, Oni TE, Hearn SA, Lee EJ, Chio II, Hwang CI, Tiriac H, Baker LA, Engle DD, Feig C, Kultti A, Egeblad M, Fearon DT, Crawford JM, Clevers H, Park Y, Tuveson DA. Distinct populations of inflammatory fibroblasts and myofibroblasts in pancreatic cancer. *J Exp Med* 2017; **214**: 579-596 [PMID: 28232471 DOI: 10.1084/jem.20162024]

55 **Sahai E**, Astsaturov I, Cukierman E, DeNardo DG, Egeblad M, Evans RM, Fearon D, Greten FR, Hingorani SR, Hunter T, Hynes RO, Jain RK, Janowitz T, Jorgensen C, Kimmelman AC, Kolonin MG, Maki RG, Powers RS, Puré E, Ramirez DC, Scherz-Shouval R, Sherman MH, Stewart S, Tlsty TD, Tuveson DA, Watt FM, Weaver V, Weeraratna AT, Werb Z. A framework for advancing our understanding of cancer-associated fibroblasts. *Nat Rev Cancer* 2020; **20**: 174-186 [PMID: 31980749 DOI: 10.1038/s41568-019-0238-1]

56 **Kalluri R**. The biology and function of fibroblasts in cancer. *Nat Rev Cancer* 2016; **16**: 582-598 [PMID: 27550820 DOI: 10.1038/nrc.2016.73]

57 **Yang X**, Lin Y, Shi Y, Li B, Liu W, Yin W, Dang Y, Chu Y, Fan J, He R. FAP Promotes Immunosuppression by Cancer-Associated Fibroblasts in the Tumor Microenvironment *via* STAT3-CCL2 Signaling. *Cancer Res* 2016; **76**: 4124-4135 [PMID: 27216177 DOI: 10.1158/0008-5472.CAN-15-2973]

58 **Shi M**, Yu DH, Chen Y, Zhao CY, Zhang J, Liu QH, Ni CR, Zhu MH. Expression of fibroblast activation protein in human pancreatic adenocarcinoma and its clinicopathological significance. *World J Gastroenterol* 2012; **18**: 840-846 [PMID: 22371645 DOI: 10.3748/wjg.v18.i8.840]

59 **Ziani L**, Chouaib S, Thiery J. Alteration of the Antitumor Immune Response by Cancer-Associated Fibroblasts. *Front Immunol* 2018; **9**: 414 [PMID: 29545811 DOI: 10.3389/fimmu.2018.00414]

60 **Kobayashi H**, Enomoto A, Woods SL, Burt AD, Takahashi M, Worthley DL. Cancer-associated fibroblasts in gastrointestinal cancer. *Nat Rev Gastroenterol Hepatol* 2019; **16**: 282-295 [PMID: 30778141 DOI: 10.1038/s41575-019-0115-0]

61 **Li T**, Yi S, Liu W, Jia C, Wang G, Hua X, Tai Y, Zhang Q, Chen G. Colorectal carcinoma-derived fibroblasts modulate natural killer cell phenotype and antitumor cytotoxicity. *Med Oncol* 2013; **30**: 663 [PMID: 23873014 DOI: 10.1007/s12032-013-0663-z]

62 **Fitzgerald AA**, Weiner LM. The role of fibroblast activation protein in health and malignancy. *Cancer Metastasis Rev* 2020; **39**: 783-803 [PMID: 32601975 DOI: 10.1007/s10555-020-09909-3]

63 **Aliru ML**, Schoenhals JE, Venkatesulu BP, Anderson CC, Barsoumian HB, Younes AI, K Mahadevan LS, Soeung M, Aziz KE, Welsh JW, Krishnan S. Radiation therapy and immunotherapy: what is the optimal timing or sequencing? *Immunotherapy* 2018; **10**: 299-316 [PMID: 29421979 DOI: 10.2217/imt-2017-0082]

64 **Ren X**, Ye F, Jiang Z, Chu Y, Xiong S, Wang Y. Involvement of cellular death in TRAIL/DR5-dependent suppression induced by CD4(+)CD25(+) regulatory T cells. *Cell Death Differ* 2007; **14**: 2076-2084 [PMID: 17762882 DOI: 10.1038/sj.cdd.4402220]

65 **Gondek DC**, Lu LF, Quezada SA, Sakaguchi S, Noelle RJ. Cutting edge: contact-mediated suppression by CD4+CD25+ regulatory cells involves a granzyme B-dependent, perforin-independent mechanism. *J Immunol* 2005; **174**: 1783-1786 [PMID: 15699103 DOI: 10.4049/jimmunol.174.4.1783]

66 **Tsuchikawa T**, Hirano S, Tanaka E, Matsumoto J, Kato K, Nakamura T, Ebihara Y, Shichinohe T. Novel aspects of preoperative chemoradiation therapy improving anti-tumor immunity in pancreatic cancer. *Cancer Sci* 2013; **104**: 531-535 [PMID: 23363422 DOI: 10.1111/cas.12119]

67 **Zhang Y**, Lazarus J, Steele NG, Yan W, Lee HJ, Nwosu ZC, Halbrook CJ, Menjivar RE, Kemp SB, Sirihorachai VR, Velez-Delgado A, Donahue K, Carpenter ES, Brown KL, Irizarry-Negron V, Nevison AC, Vinta A, Anderson MA, Crawford HC, Lyssiotis CA, Frankel TL, Bednar F, Pasca di Magliano M. Regulatory T-cell Depletion Alters the Tumor Microenvironment and Accelerates Pancreatic Carcinogenesis. *Cancer Discov* 2020; **10**: 422-439 [PMID: 31911451 DOI: 10.1158/2159-8290.CD-19-0958]

68 **Ugel S**, De Sanctis F, Mandruzzato S, Bronte V. Tumor-induced myeloid deviation: when myeloid-derived suppressor cells meet tumor-associated macrophages. *J Clin Invest* 2015; **125**: 3365-3376 [PMID: 26325033 DOI: 10.1172/JCI80006]

69 **De Cicco P**, Ercolano G, Ianaro A. The New Era of Cancer Immunotherapy: Targeting Myeloid-Derived Suppressor Cells to Overcome Immune Evasion. *Front Immunol* 2020; **11**: 1680 [PMID: 32849585 DOI: 10.3389/fimmu.2020.01680]

70 **Markowitz J**, Brooks TR, Duggan MC, Paul BK, Pan X, Wei L, Abrams Z, Luedke E, Lesinski GB, Mundy-Bosse B, Bekaii-Saab T, Carson WE 3rd. Patients with pancreatic adenocarcinoma exhibit elevated levels of myeloid-derived suppressor cells upon progression of disease. *Cancer Immunol Immunother* 2015; **64**: 149-159 [PMID: 25305035 DOI: 10.1007/s00262-014-1618-8]

71 **Di Caro G**, Cortese N, Castino GF, Grizzi F, Gavazzi F, Ridolfi C, Capretti G, Mineri R, Todoric J, Zerbi A, Allavena P, Mantovani A, Marchesi F. Dual prognostic significance of tumour-associated macrophages in human pancreatic adenocarcinoma treated or untreated with chemotherapy. *Gut* 2016; **65**: 1710-1720 [PMID: 26156960 DOI: 10.1136/gutjnl-2015-309193]

72 **Lankadasari MB**, Mukhopadhyay P, Mohammed S, Harikumar KB. TAMing pancreatic cancer: combat with a double edged sword. *Mol Cancer* 2019; **18**: 48 [PMID: 30925924 DOI: 10.1186/s12943-019-0966-6]

73 **Hu H**, Hang JJ, Han T, Zhuo M, Jiao F, Wang LW. The M2 phenotype of tumor-associated macrophages in the stroma confers a poor prognosis in pancreatic cancer. *Tumour Biol* 2016; **37**: 8657-8664 [PMID: 26738860 DOI: 10.1007/s13277-015-4741-z]

74 **Liu Q**, Li Y, Niu Z, Zong Y, Wang M, Yao L, Lu Z, Liao Q, Zhao Y. Atorvastatin (Lipitor) attenuates the effects of aspirin on pancreatic cancerogenesis and the chemotherapeutic efficacy of gemcitabine on pancreatic cancer by promoting M2 polarized tumor associated macrophages. *J Exp Clin Cancer Res* 2016; **35**: 33 [PMID: 26879926 DOI: 10.1186/s13046-016-0304-4]

75 **Dijkgraaf EM**, Heusinkveld M, Tummers B, Vogelpoel LT, Goedemans R, Jha V, Nortier JW, Welters MJ, Kroep JR, van der Burg SH. Chemotherapy alters monocyte differentiation to favor generation of cancer-supporting M2 macrophages in the tumor microenvironment. *Cancer Res* 2013; **73**: 2480-2492 [PMID: 23436796 DOI: 10.1158/0008-5472.CAN-12-3542]

76 **Young K**, Hughes DJ, Cunningham D, Starling N. Immunotherapy and pancreatic cancer: unique challenges and potential opportunities. *Ther Adv Med Oncol* 2018; **10**: 1758835918816281 [PMID: 30574212 DOI: 10.1177/1758835918816281]

77 **Zhang J**, Wolfgang CL, Zheng L. Precision Immuno-Oncology: Prospects of Individualized Immunotherapy for Pancreatic Cancer. *Cancers (Basel)* 2018; **10** [PMID: 29385739 DOI: 10.3390/cancers10020039]

78 **Iwai Y**, Ishida M, Tanaka Y, Okazaki T, Honjo T, Minato N. Involvement of PD-L1 on tumor cells in the escape from host immune system and tumor immunotherapy by PD-L1 blockade. *Proc Natl Acad Sci U S A* 2002; **99**: 12293-12297 [PMID: 12218188 DOI: 10.1073/pnas.192461099]

79 **Twomey JD**, Zhang B. Cancer Immunotherapy Update: FDA-Approved Checkpoint Inhibitors and Companion Diagnostics. *AAPS J* 2021; **23**: 39 [PMID: 33677681 DOI: 10.1208/s12248-021-00574-0]

80 **Royal RE**, Levy C, Turner K, Mathur A, Hughes M, Kammula US, Sherry RM, Topalian SL, Yang JC, Lowy I, Rosenberg SA. Phase 2 trial of single agent Ipilimumab (anti-CTLA-4) for locally advanced or metastatic pancreatic adenocarcinoma. *J Immunother* 2010; **33**: 828-833 [PMID: 20842054 DOI: 10.1097/CJI.0b013e3181eec14c]

81 **Torphy RJ**, Zhu Y, Schulick RD. Immunotherapy for pancreatic cancer: Barriers and breakthroughs. *Ann Gastroenterol Surg* 2018; **2**: 274-281 [PMID: 30003190 DOI: 10.1002/ags3.12176]

82 **Plate JM**, Plate AE, Shott S, Bograd S, Harris JE. Effect of gemcitabine on immune cells in subjects with adenocarcinoma of the pancreas. *Cancer Immunol Immunother* 2005; **54**: 915-925 [PMID: 15782312 DOI: 10.1007/s00262-004-0638-1]

83 **Aglietta M**, Barone C, Sawyer MB, Moore MJ, Miller WH Jr, Bagalà C, Colombi F, Cagnazzo C, Gioeni L, Wang E, Huang B, Fly KD, Leone F. A phase I dose escalation trial of tremelimumab (CP-675,206) in combination with gemcitabine in chemotherapy-naive patients with metastatic pancreatic cancer. *Ann Oncol* 2014; **25**: 1750-1755 [PMID: 24907635 DOI: 10.1093/annonc/mdu205]

84 **Weiss GJ**, Blaydorn L, Beck J, Bornemann-Kolatzki K, Urnovitz H, Schütz E, Khemka V. Phase Ib/II study of gemcitabine, nab-paclitaxel, and pembrolizumab in metastatic pancreatic adenocarcinoma. *Invest New Drugs* 2018; **36**: 96-102 [PMID: 29119276 DOI: 10.1007/s10637-017-0525-1]

85 **Mizugaki H**, Yamamoto N, Murakami H, Kenmotsu H, Fujiwara Y, Ishida Y, Kawakami T, Takahashi T. Phase I dose-finding study of monotherapy with atezolizumab, an engineered immunoglobulin monoclonal antibody targeting PD-L1, in Japanese patients with advanced solid tumors. *Invest New Drugs* 2016; **34**: 596-603 [PMID: 27363843 DOI: 10.1007/s10637-016-0371-6]

86 **O'Reilly EM**, Oh DY, Dhani N, Renouf DJ, Lee MA, Sun W, Fisher G, Hezel A, Chang SC, Vlahovic G, Takahashi O, Yang Y, Fitts D, Philip PA. Durvalumab With or Without Tremelimumab for Patients With Metastatic Pancreatic Ductal Adenocarcinoma: A Phase 2 Randomized Clinical Trial. *JAMA Oncol* 2019; **5**: 1431-1438 [PMID: 31318392 DOI: 10.1001/jamaoncol.2019.1588]

87 **Jardim DL**, Goodman A, de Melo Gagliato D, Kurzrock R. The Challenges of Tumor Mutational Burden as an Immunotherapy Biomarker. *Cancer Cell* 2021; **39**: 154-173 [PMID: 33125859 DOI: 10.1016/j.ccell.2020.10.001]

88 **Salman B**, Zhou D, Jaffee EM, Edil BH, Zheng L. Vaccine therapy for pancreatic cancer. *Oncoimmunology* 2013; **2**: e26662 [PMID: 24498551 DOI: 10.4161/onci.26662]

89 **Rosenberg A**, Mahalingam D. Immunotherapy in pancreatic adenocarcinoma-overcoming barriers to response. *J Gastrointest Oncol* 2018; **9**: 143-159 [PMID: 29564181 DOI: 10.21037/jgo.2018.01.13]

90 **Laheru D**, Biedrzycki B, Jaffee EM. Development of a cytokine-modified allogeneic whole cell pancreatic cancer vaccine. *Methods Mol Biol* 2013; **980**: 175-203 [PMID: 23359154 DOI: 10.1007/978-1-62703-287-2_9]

91 **Jaffee EM**, Hruban RH, Biedrzycki B, Laheru D, Schepers K, Sauter PR, Goemann M, Coleman J, Grochow L, Donehower RC, Lillemoe KD, O'Reilly S, Abrams RA, Pardoll DM, Cameron JL, Yeo CJ. Novel allogeneic granulocyte-macrophage colony-stimulating factor-secreting tumor vaccine for pancreatic cancer: a phase I trial of safety and immune activation. *J Clin Oncol* 2001; **19**: 145-156 [PMID: 11134207 DOI: 10.1200/JCO.2001.19.1.145]

92 **Lutz E**, Yeo CJ, Lillemoe KD, Biedrzycki B, Kobrin B, Herman J, Sugar E, Piantadosi S, Cameron JL, Solt S, Onners B, Tartakovsky I, Choi M, Sharma R, Illei PB, Hruban RH, Abrams RA, Le D, Jaffee E, Laheru D. A lethally irradiated allogeneic granulocyte-macrophage colony stimulating factor-secreting tumor vaccine for pancreatic adenocarcinoma. A Phase II trial of safety, efficacy, and immune activation. *Ann Surg* 2011; **253**: 328-335 [PMID: 21217520 DOI: 10.1097/SLA.0b013e3181fd271c]

93 **Chung V**, Kos FJ, Hardwick N, Yuan Y, Chao J, Li D, Waisman J, Li M, Zurcher K, Frankel P, Diamond DJ. Evaluation of safety and efficacy of p53MVA vaccine combined with pembrolizumab in patients with advanced solid cancers. *Clin Transl Oncol* 2019; **21**: 363-372 [PMID: 30094792 DOI: 10.1007/s12094-018-1932-2]

94 **Le DT**, Lutz E, Uram JN, Sugar EA, Onners B, Solt S, Zheng L, Diaz LA Jr, Donehower RC, Jaffee EM, Laheru DA. Evaluation of ipilimumab in combination with allogeneic pancreatic tumor cells transfected with a GM-CSF gene in previously treated pancreatic cancer. *J Immunother* 2013; **36**: 382-389 [PMID: 23924790 DOI: 10.1097/CJI.0b013e31829fb7a2]

95 **Osawa R**, Tsunoda T, Yoshimura S, Watanabe T, Miyazawa M, Tani M, Takeda K, Nakagawa H, Nakamura Y, Yamaue H. Identification of HLA-A24-restricted novel T Cell epitope peptides derived from P-cadherin and kinesin family member 20A. *J Biomed Biotechnol* 2012; **2012**: 848042 [PMID: 22778556 DOI: 10.1155/2012/848042]

96 **Asahara S**, Takeda K, Yamao K, Maguchi H, Yamaue H. Phase I/II clinical trial using HLA-A24-restricted peptide vaccine derived from KIF20A for patients with advanced pancreatic cancer. *J Transl Med* 2013; **11**: 291 [PMID: 24237633 DOI: 10.1186/1479-5876-11-291]

97 **Suzuki N**, Hazama S, Iguchi H, Uesugi K, Tanaka H, Hirakawa K, Aruga A, Hatori T, Ishizaki H, Umeda Y, Fujiwara T, Ikemoto T, Shimada M, Yoshimatsu K, Shimizu R, Hayashi H, Sakata K, Takenouchi H, Matsui H, Shindo Y, Iida M, Koki Y, Arima H, Furukawa H, Ueno T, Yoshino S, Nakamura Y, Oka M, Nagano H. Phase II clinical trial of peptide cocktail therapy for patients with advanced pancreatic cancer: VENUS-PC study. *Cancer Sci* 2017; **108**: 73-80 [PMID: 27783849 DOI: 10.1111/cas.13113]

98 **Miyazawa M**, Katsuda M, Maguchi H, Katanuma A, Ishii H, Ozaka M, Yamao K, Imaoka H, Kawai M, Hirono S, Okada KI, Yamaue H. Phase II clinical trial using novel peptide cocktail vaccine as a postoperative adjuvant treatment for surgically resected pancreatic cancer patients. *Int J Cancer* 2017; **140**: 973-982 [PMID: 27861852 DOI: 10.1002/ijc.30510]

99 **Kameshima H**, Tsuruma T, Kutomi G, Shima H, Iwayama Y, Kimura Y, Imamura M, Torigoe T, Takahashi A, Hirohashi Y, Tamura Y, Tsukahara T, Kanaseki T, Sato N, Hirata K. Immunotherapeutic benefit of α-interferon (IFNα) in survivin2B-derived peptide vaccination for advanced pancreatic cancer patients. *Cancer Sci* 2013; **104**: 124-129 [PMID: 23078230 DOI: 10.1111/cas.12046]

100 **Coveler AL**, Rossi GR, Vahanian NN, Link C, Chiorean EG. Algenpantucel-L immunotherapy in pancreatic adenocarcinoma. *Immunotherapy* 2016; **8**: 117-125 [PMID: 26787078 DOI: 10.2217/imt.15.113]

101 **Hardacre JM**, Mulcahy M, Small W, Talamonti M, Obel J, Krishnamurthi S, Rocha-Lima CS, Safran H, Lenz HJ, Chiorean EG. Addition of algenpantucel-L immunotherapy to standard adjuvant therapy for pancreatic cancer: a phase 2 study. *J Gastrointest Surg* 2013; **17**: 94-100; discussion p. 100 [PMID: 23229886 DOI: 10.1007/s11605-012-2064-6]

102 **McCormick KA**, Coveler AL, Rossi GR, Vahanian NN, Link C, Chiorean EG. Pancreatic cancer: Update on immunotherapies and algenpantucel-L. *Hum Vaccin Immunother* 2016; **12**: 563-575 [PMID: 26619245 DOI: 10.1080/21645515.2015.1093264]

103 **Hewitt DB**, Nissen N, Hatoum H, Musher B, Seng J, Coveler AL, Al-Rajabi R, Yeo CJ, Leiby B, Banks J, Balducci L, Vaccaro G, LoConte N, George TJ, Brenner W, Elquza E, Vahanian N, Rossi G, Kennedy E, Link C, Lavu H. A Phase 3 Randomized Clinical Trial of Chemotherapy With or Without Algenpantucel-L (HyperAcute-Pancreas) Immunotherapy in Subjects With Borderline Resectable or Locally Advanced Unresectable Pancreatic Cancer. *Ann Surg* 2022; **275**: 45-53 [PMID: 33630475 DOI: 10.1097/SLA.0000000000004669]

104 **Nath S**, Mukherjee P. MUC1: a multifaceted oncoprotein with a key role in cancer progression. *Trends Mol Med* 2014; **20**: 332-342 [PMID: 24667139 DOI: 10.1016/j.molmed.2014.02.007]

105 **Behrens ME**, Grandgenett PM, Bailey JM, Singh PK, Yi CH, Yu F, Hollingsworth MA. The reactive tumor microenvironment: MUC1 signaling directly reprograms transcription of CTGF. *Oncogene* 2010; **29**: 5667-5677 [PMID: 20697347 DOI: 10.1038/onc.2010.327]

106 **Lepisto AJ**, Moser AJ, Zeh H, Lee K, Bartlett D, McKolanis JR, Geller BA, Schmotzer A, Potter DP, Whiteside T, Finn OJ, Ramanathan RK. A phase I/II study of a MUC1 peptide pulsed autologous dendritic cell vaccine as adjuvant therapy in patients with resected pancreatic and biliary tumors. *Cancer Ther* 2008; **6**: 955-964 [PMID: 19129927]

107 **Gong YF**, Zhou QB, Liao YD, Mai C, Chen TJ, Tang YQ, Chen RF. Optimized construction of MUC1-VNTR$_n$ DNA vaccine and its anti-pancreatic cancer efficacy. *Oncol Lett* 2017; **13**: 2198-2206 [PMID: 28454381 DOI: 10.3892/ol.2017.5717]

108 **Palucka K**, Ueno H, Fay J, Banchereau J. Dendritic cells and immunity against cancer. *J Intern Med* 2011; **269**: 64-73 [PMID: 21158979 DOI: 10.1111/j.1365-2796.2010.02317.x]

109 **Mehrotra S**, Britten CD, Chin S, Garrett-Mayer E, Cloud CA, Li M, Scurti G, Salem ML, Nelson MH, Thomas MB, Paulos CM, Salazar AM, Nishimura MI, Rubinstein MP, Li Z, Cole DJ. Vaccination with poly(IC:LC) and peptide-pulsed autologous dendritic cells in patients with pancreatic cancer. *J Hematol Oncol* 2017; **10**: 82 [PMID: 28388966 DOI: 10.1186/s13045-017-0459-2]

110 **Yanagisawa R**, Koizumi T, Koya T, Sano K, Koido S, Nagai K, Kobayashi M, Okamoto M, Sugiyama H, Shimodaira S. WT1-pulsed Dendritic Cell Vaccine Combined with Chemotherapy for Resected Pancreatic Cancer in a Phase I Study. *Anticancer Res* 2018; **38**: 2217-2225 [PMID: 29599342 DOI: 10.21873/anticanres.12464]

111 **Kimura Y**, Tsukada J, Tomoda T, Takahashi H, Imai K, Shimamura K, Sunamura M, Yonemitsu Y, Shimodaira S, Koido S, Homma S, Okamoto M. Clinical and immunologic evaluation of dendritic cell-based immunotherapy in combination with gemcitabine and/or S-1 in patients with advanced pancreatic carcinoma. *Pancreas* 2012; **41**: 195-205 [PMID: 21792083 DOI: 10.1097/MPA.0b013e31822398c6]

112 **Kobayashi M**, Shimodaira S, Nagai K, Ogasawara M, Takahashi H, Abe H, Tanii M, Okamoto M, Tsujitani S, Yusa S, Ishidao T, Kishimoto J, Shibamoto Y, Nagaya M, Yonemitsu Y; DC Vaccine Study Group at the Japan Society of Innovative Cell Therapy (J-SICT). Prognostic factors related to add-on dendritic cell vaccines on patients with inoperable pancreatic cancer receiving chemotherapy: a multicenter analysis. *Cancer Immunol Immunother* 2014; **63**: 797-806 [PMID: 24777613 DOI: 10.1007/s00262-014-1554-7]

113 **Takakura K**, Koido S, Kan S, Yoshida K, Mori M, Hirano Y, Ito Z, Kobayashi H, Takami S, Matsumoto Y, Kajihara M, Misawa T, Okamoto M, Sugiyama H, Homma S, Ohkusa T, Tajiri H. Prognostic markers for patient outcome following vaccination with multiple MHC Class I/II-restricted WT1 peptide-pulsed dendritic cells plus chemotherapy for pancreatic cancer. *Anticancer Res* 2015; **35**: 555-562 [PMID: 25550602]

114 **Abou-Alfa GK**, Chapman PB, Feilchenfeldt J, Brennan MF, Capanu M, Gansukh B, Jacobs G, Levin A, Neville D, Kelsen DP, O'Reilly EM. Targeting mutated K-ras in pancreatic adenocarcinoma using an adjuvant vaccine. *Am J Clin Oncol* 2011; **34**: 321-325 [PMID: 20686403 DOI: 10.1097/COC.0b013e3181e84b1f]

115 **Palmer DH**, Valle JW, Ma YT, Faluyi O, Neoptolemos JP, Jensen Gjertsen T, Iversen B, Amund Eriksen J, Møller AS, Aksnes AK, Miller R, Dueland S. TG01/GM-CSF and adjuvant gemcitabine in patients with resected RAS-mutant adenocarcinoma of the pancreas (CT TG01-01): a single-arm, phase 1/2 trial. *Br J Cancer* 2020; **122**: 971-977 [PMID: 32063605 DOI: 10.1038/s41416-020-0752-7]

116 **Wedén S**, Klemp M, Gladhaug IP, Møller M, Eriksen JA, Gaudernack G, Buanes T. Long-term follow-up of patients with resected pancreatic cancer following vaccination against mutant K-ras. *Int J Cancer* 2011; **128**: 1120-1128 [PMID: 20473937 DOI: 10.1002/ijc.25449]

117 **Cohn A**, Morse MA, O'Neil B, Whiting S, Coeshott C, Ferraro J, Bellgrau D, Apelian D, Rodell TC. Whole Recombinant Saccharomyces cerevisiae Yeast Expressing Ras Mutations as Treatment for Patients With Solid Tumors Bearing Ras Mutations: Results From a Phase 1 Trial. *J Immunother* 2018; **41**: 141-150 [PMID: 29528991 DOI: 10.1097/CJI.0000000000000219]

118 **Muscarella P**, Bekaii-Saab T, McIntyre K, Rosemurgy A, Ross SB, Richards DA, Fisher WE, Flynn PJ, Mattson A, Coeshott C, Roder H, Roder J, Harrell FE, Cohn A, Rodell TC, Apelian D. A Phase 2 Randomized Placebo-Controlled Adjuvant Trial of GI-4000, a Recombinant Yeast Expressing Mutated RAS Proteins in Patients with Resected Pancreas Cancer. *J Pancreat Cancer* 2021; **7**: 8-19 [PMID: 33786412 DOI: 10.1089/pancan.2020.0021]

119 **Suehara N**, Mizumoto K, Muta T, Tominaga Y, Shimura H, Kitajima S, Hamasaki N, Tsuneyoshi M, Tanaka M. Telomerase elevation in pancreatic ductal carcinoma compared to nonmalignant pathological states. *Clin Cancer Res* 1997; **3**: 993-998 [PMID: 9815776]

120 **Bernhardt SL**, Gjertsen MK, Trachsel S, Møller M, Eriksen JA, Meo M, Buanes T, Gaudernack G. Telomerase peptide vaccination of patients with non-resectable pancreatic cancer: A dose escalating phase I/II study. *Br J Cancer* 2006; **95**: 1474-1482 [PMID: 17060934 DOI: 10.1038/sj.bjc.6603437]

121 **Middleton G**, Silcocks P, Cox T, Valle J, Wadsley J, Propper D, Coxon F, Ross P, Madhusudan S, Roques T, Cunningham D, Falk S, Wadd N, Harrison M, Corrie P, Iveson T, Robinson A, McAdam K, Eatock M, Evans J, Archer C, Hickish T, Garcia-Alonso A, Nicolson M, Steward W, Anthoney A, Greenhalf W, Shaw V, Costello E, Naisbitt D, Rawcliffe C, Nanson G, Neoptolemos J. Gemcitabine and capecitabine with or without telomerase peptide vaccine GV1001 in patients with locally advanced or metastatic pancreatic cancer (TeloVac): an open-label, randomised, phase 3 trial. *Lancet Oncol* 2014; **15**: 829-840 [PMID: 24954781 DOI: 10.1016/S1470-2045(14)70236-0]

122 **Morotti M**, Albukhari A, Alsaadi A, Artibani M, Brenton JD, Curbishley SM, Dong T, Dustin ML, Hu Z, McGranahan N, Miller ML, Santana-Gonzalez L, Seymour LW, Shi T, Van Loo P, Yau C, White H, Wietek N, Church DN, Wedge DC, Ahmed AA. Promises and challenges of adoptive T-cell therapies for solid tumours. *Br J Cancer* 2021; **124**: 1759-1776 [PMID: 33782566 DOI: 10.1038/s41416-021-01353-6]

123 **Rohaan MW**, Wilgenhof S, Haanen JBAG. Adoptive cellular therapies: the current landscape. *Virchows Arch* 2019; **474**: 449-461 [PMID: 30470934 DOI: 10.1007/s00428-018-2484-0]

124 **Matsui H**, Hazama S, Sakamoto K, Shindo Y, Kanekiyo S, Nakashima M, Matsukuma S, Tokuhisa Y, Iida M, Suzuki N, Yoshimura K, Takeda S, Ueno T, Yoshino S, Oka M, Nagano H. Postoperative Adjuvant Therapy for Resectable Pancreatic Cancer With Gemcitabine and Adoptive Immunotherapy. *Pancreas* 2017; **46**: 994-1002 [PMID: 28697053 DOI: 10.1097/MPA.0000000000000880]

125 **Chen Y**, Ayaru L, Mathew S, Morris E, Pereira SP, Behboudi S. Expansion of anti-mesothelin specific CD4+ and CD8+ T cell responses in patients with pancreatic carcinoma. *PLoS One* 2014; **9**: e88133 [PMID: 24520352 DOI: 10.1371/journal.pone.0088133]

126 **Watanabe K**, Luo Y, Da T, Guedan S, Ruella M, Scholler J, Keith B, Young RM, Engels B, Sorsa S, Siurala M, Havunen R, Tähtinen S, Hemminki A, June CH. Pancreatic cancer therapy with combined mesothelin-redirected chimeric antigen receptor T cells and cytokine-armed oncolytic adenoviruses. *JCI Insight* 2018; **3** [PMID: 29618658 DOI: 10.1172/jci.insight.99573]

127 **Hassan R**, Ebel W, Routhier EL, Patel R, Kline JB, Zhang J, Chao Q, Jacob S, Turchin H, Gibbs L, Phillips MD, Mudali S, Iacobuzio-Donahue C, Jaffee EM, Moreno M, Pastan I, Sass PM, Nicolaides NC, Grasso L. Preclinical evaluation of MORAb-009, a chimeric antibody targeting tumor-associated mesothelin. *Cancer Immun* 2007; **7**: 20 [PMID: 18088084]

128 **Hassan R**, Cohen SJ, Phillips M, Pastan I, Sharon E, Kelly RJ, Schweizer C, Weil S, Laheru D. Phase I clinical trial of the chimeric anti-mesothelin monoclonal antibody MORAb-009 in patients with mesothelin-expressing cancers. *Clin Cancer Res* 2010; **16**: 6132-6138 [PMID: 21037025 DOI: 10.1158/1078-0432.CCR-10-2275]

129 **Collins MA**, Bednar F, Zhang Y, Brisset JC, Galbán S, Galbán CJ, Rakshit S, Flannagan KS, Adsay NV, Pasca di Magliano M. Oncogenic Kras is required for both the initiation and maintenance of pancreatic cancer in mice. *J Clin Invest* 2012; **122**: 639-653 [PMID: 22232209 DOI: 10.1172/JCI59227]

130 **Qin C**, Yang G, Yang J, Ren B, Wang H, Chen G, Zhao F, You L, Wang W, Zhao Y. Metabolism of pancreatic cancer: paving the way to better anticancer strategies. *Mol Cancer* 2020; **19**: 50 [PMID: 32122374 DOI: 10.1186/s12943-020-01169-7]

131 **Kraman M**, Bambrough PJ, Arnold JN, Roberts EW, Magiera L, Jones JO, Gopinathan A, Tuveson DA, Fearon DT. Suppression of antitumor immunity by stromal cells expressing fibroblast activation protein-alpha. *Science* 2010; **330**: 827-830 [PMID: 21051638 DOI: 10.1126/science.1195300]

132 **Dominguez CX**, Müller S, Keerthivasan S, Koeppen H, Hung J, Gierke S, Breart B, Foreman O, Bainbridge TW, Castiglioni A, Senbabaoglu Y, Modrusan Z, Liang Y, Junttila MR, Klijn C, Bourgon R, Turley SJ. Single-Cell RNA Sequencing Reveals Stromal Evolution into LRRC15^{+} Myofibroblasts as a Determinant of Patient Response to Cancer Immunotherapy. *Cancer Discov* 2020; **10**: 232-253 [PMID: 31699795 DOI: 10.1158/2159-8290.CD-19-0644]

133 **Feig C**, Jones JO, Kraman M, Wells RJ, Deonarine A, Chan DS, Connell CM, Roberts EW, Zhao Q, Caballero OL, Teichmann SA, Janowitz T, Jodrell DI, Tuveson DA, Fearon DT. Targeting CXCL12 from FAP-expressing carcinoma-associated fibroblasts synergizes with anti-PD-L1 immunotherapy in pancreatic cancer. *Proc Natl Acad Sci U S A* 2013; **110**: 20212-20217 [PMID: 24277834 DOI: 10.1073/pnas.1320318110]

134 **Osipov A**, Saung MT, Zheng L, Murphy AG. Small molecule immunomodulation: the tumor microenvironment and overcoming immune escape. *J Immunother Cancer* 2019; **7**: 224 [PMID: 31439034 DOI: 10.1186/s40425-019-0667-0]

135 **Li M**, Li M, Yang Y, Liu Y, Xie H, Yu Q, Tian L, Tang X, Ren K, Li J, Zhang Z, He Q. Remodeling tumor immune microenvironment *via* targeted blockade of PI3K-γ and CSF-1/CSF-1R pathways in tumor associated macrophages for pancreatic cancer therapy. *J Control Release* 2020; **321**: 23-35 [PMID: 32035193 DOI: 10.1016/j.jconrel.2020.02.011]

136 **Jiang H**, Hegde S, Knolhoff BL, Zhu Y, Herndon JM, Meyer MA, Nywening TM, Hawkins WG, Shapiro IM, Weaver

DT, Pachter JA, Wang-Gillam A, DeNardo DG. Targeting focal adhesion kinase renders pancreatic cancers responsive to checkpoint immunotherapy. *Nat Med* 2016; **22**: 851-860 [PMID: 27376576 DOI: 10.1038/nm.4123]

World Journal of Gastroenterology

Submit a Manuscript: https://www.f6publishing.com

World J Gastroenterol 2022 July 21; 28(27): 3314-3333

DOI: 10.3748/wjg.v28.i27.3314

ISSN 1007-9327 (print) ISSN 2219-2840 (online)

REVIEW

Crosstalk between dietary patterns, obesity and nonalcoholic fatty liver disease

Danijela Ristic-Medic, Joanna Bajerska, Vesna Vucic

Specialty type: Gastroenterology and hepatology

Provenance and peer review: Invited article; Externally peer reviewed.

Peer-review model: Single blind

Peer-review report's scientific quality classification

Grade A (Excellent): A
Grade B (Very good): 0
Grade C (Good): C
Grade D (Fair): 0
Grade E (Poor): 0

P-Reviewer: Tziomalos K, Greece; Xing HC, China

Received: January 17, 2022
Peer-review started: January 17, 2022
First decision: April 11, 2022
Revised: May 3, 2022
Accepted: June 18, 2022
Article in press: June 18, 2022
Published online: July 21, 2022

Danijela Ristic-Medic, Vesna Vucic, Group for Nutritional Biochemistry and Dietology, Centre of Research Excellence in Nutrition and Metabolism, Institute for Medical Research, National Institute of Republic Serbia, Belgrade PO Box 102, Serbia

Joanna Bajerska, Department of Human Nutrition and Dietetics, Poznań University of Life Sciences, Poznań 60-624, Poland

Corresponding author: Danijela Ristic-Medic, Doctor, MD, PhD, Professor, Senior Researcher, Group for Nutritional Biochemistry and Dietology, Centre of Research Excellence in Nutrition and Metabolism, Institute for Medical Research, National Institute of Republic Serbia, Tadeusa Koscuska 1, Belgrade PO Box 102, Serbia. dristicmedic@gmail.com

Abstract

The prevalence of nonalcoholic fatty liver disease (NAFLD) is rising worldwide, paralleling the epidemic of obesity. The liver is a key organ for the metabolism of proteins, fats and carbohydrates. Various types of fats and carbohydrates in isocaloric diets differently influence fat accumulation in the liver parenchyma. Therefore, nutrition can manage hepatic and cardiometabolic complications of NAFLD. Even moderately reduced caloric intake, which leads to a weight loss of 5%-10% of initial body weight, is effective in improving liver steatosis and surrogate markers of liver disease status. Among dietary patterns, the Mediterranean diet mostly prevents the onset of NAFLD. Furthermore, this diet is also the most recommended for the treatment of NAFLD patients. However, clinical trials based on the dietary interventions in NAFLD patients are sparse. Since there are only a few studies examining dietary interventions in clinically advanced stages of NAFLD, such as active and fibrotic steatohepatitis, the optimal diet for patients in these stages of the disease must still be determined. In this narrative review, we aimed to critically summarize the associations between different dietary patterns, obesity and prevention/risk for NAFLD, to describe specific dietary interventions' impacts on liver steatosis in adults with NAFLD and to provide an updated overview of dietary recommendations that clinicians potentially need to apply in their daily practice.

Key Words: Nonalcoholic fatty liver disease; Dietary patterns; Obesity; Diet; Mediterranean diet; Nutrition; Treatment; Clinical guidance

©The Author(s) 2022. Published by Baishideng Publishing Group Inc. All rights reserved.

Core Tip: In this review, we emphasize that based on the current evidence, there is no consensus on the ideal macronutrient composition of the diet for nonalcoholic fatty liver disease (NAFLD) patients. We have shown that dietary habits are the most important factor in NAFLD prevention. The Mediterranean and healthy dietary pattern, characterized by high consumption of vegetables, fruits, nuts, olive oil, low-fat dairy products and fish, were linked with a reduced NAFLD risk. The Dietary Approach to Stop Hypertension diet, intermittent fasting and ketogenic diet are other dietary regimes that have growing interest among specialists who advise patients with NAFLD. Nevertheless, new studies designed to assess the effects of these diets on liver-related outcomes and liver histology are needed. We also noted that dietary advice should be personalized in NAFLD patients.

Citation: Ristic-Medic D, Bajerska J, Vucic V. Crosstalk between dietary patterns, obesity and nonalcoholic fatty liver disease. *World J Gastroenterol* 2022; 28(27): 3314-3333
URL: https://www.wjgnet.com/1007-9327/full/v28/i27/3314.htm
DOI: https://dx.doi.org/10.3748/wjg.v28.i27.3314

INTRODUCTION

Nonalcoholic fatty liver disease (NAFLD) is the accumulation of excess fat (more than 5%) in the liver parenchyma in people with no significant alcohol consumption or secondary causes of hepatic steatosis [1]. The prevalence of NAFLD is rising in many countries, paralleling the epidemic of obesity worldwide. The highest rates of NAFLD have been observed in North Africa (31%), the Middle East (32%) and Asia (27%)[2].

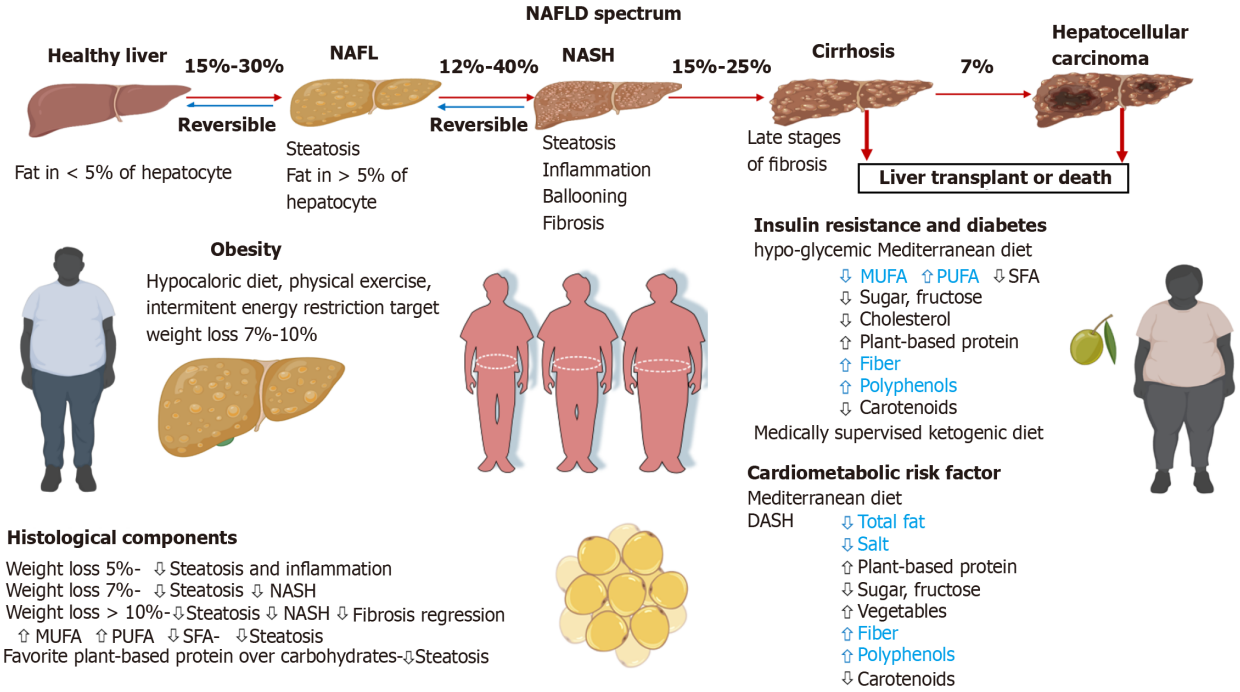
NAFLD represents a clinicopathological spectrum, ranging from benign hepatic steatosis to nonalcoholic steatohepatitis (NASH) and characterized by hepatocellular injury and inflammation, which leads to hepatic fibrosis[3,4]. Up to 20% of patients with fibrotic NASH progress to cirrhosis and associated complications[5,6]. Fibrotic NASH can lead to hepatocellular carcinoma, even at the pre-cirrhotic stage (Figure 1). Approximately 90% of the obese population, 60% of patients with diabetes type 2 and 50% of patients with dyslipidemia have NAFLD[6-8]. Moreover, NAFLD is a risk factor for severe coronavirus disease 2019, and thus nutritional prevention of coronavirus disease 2019 complications has been highlighted in a recent review[8].

Nevertheless, obesity, overnutrition, dietary components and a sedentary lifestyle are modifiable risk factors for NAFLD. Central obesity is probably the most significant modifiable risk factor for this disorder, which arises from energy imbalance[9]. The relationship between excessive caloric intake and the NAFLD development has been shown in interventional studies. Weight loss as a primary therapeutic approach produced clinically meaningful outcomes in patients with NAFLD[10,11]. However, the success of such weight loss interventions depends on the intensity of diet counseling and the frequency of visits to dietitians. Two dietary patterns that seem to promote the improvement of NAFLD with incorporated recommendations are the Mediterranean and the Dietary Approach to Stop Hypertension (DASH) diets[12].

This review critically summarizes the associations between dietary patterns, obesity and prevention/risk for NAFLD as well as the impact of specific dietary interventions on hepatic steatosis in adults with NAFLD. It also provides an updated overview of dietary recommendations that clinicians potentially need to apply in their daily practice.

LITERATURE SEARCH

This narrative review was based on PubMed electronic database search for relevant publications using the following terms ("fatty liver" OR "NAFLD" OR "non-alcoholic fatty liver disease" OR "steatosis of liver" OR "steatohepatitis" OR "steatosis") AND "obesity" AND ("diet" OR "dietary pattern" OR "dietary interventions" OR "nutrition") to identify the studies on the association between dietary patterns and NAFLD and specific clinical dietary intervention studies in adult patients with NAFLD. Also, we focused on systematic reviews with meta-analyses. Studies relevant to the topic, conducted in humans, published in English and preferably published in the last 10 years were included. All studies are checked in Reference Citation Analysis database (https://www.referencecitationanalysis.com/). The list of references was reduced because priority had been given to studies that are relevant to clinical practice. The final list of references was approved with the consent of the authors.



DOI: 10.3748/wjg.v28.i27.3314 Copyright ©The Author(s) 2022.

Figure 1 Progression of nonalcoholic fatty liver to cirrhosis and/or liver cancer and suggested dietary intervention in nonalcoholic fatty liver disease patients according to risk factors. DASH: Dietary Approach to Stop Hypertension; MUFA: Monounsaturated fatty acid; NAFL: Nonalcoholic fatty liver; NAFLD: Nonalcoholic fatty liver disease; NASH: Nonalcoholic steatohepatitis; PUFA: Polyunsaturated fatty acid; SFA: Saturated fatty acid. Blue fonts indicate evidence-based proven effect of the dietary component. Created in Biorender.com.

MECHANISMS OF LIVER INJURY IN PATIENTS WITH OBESITY

The pathophysiology of NAFLD involves multiple genetic and environmental factors. Genetic factors include specific polymorphisms and epigenetic modifications. As the most common genetic determinant of NAFLD, the I148M variant of patatin-like phospholipase domain-containing protein 3 gene has been recognized[13]. Environmental factors are related to diet and lifestyle, hormonal disturbances, insulin resistance (IR), obesity, oxidative stress, lipotoxicity, unfavorable gut microbiota and many others[9]. Despite well-established risk factors for NAFLD, the pathways leading to the disease are not elucidated, but the role of the diet is undeniable.

It is known that the liver utilizes fatty acids and sugars as primary metabolic substrates, but the overload of these substances results in the accumulation of toxic lipid products[14]. These products increase oxidative stress by overproduction of reactive oxygen species and inflammation in hepatocytes that leads to liver injury. Moreover, a higher intake of saturated fatty acids (SFAs) promotes hepatic liver accumulation and the development and progression of NAFLD[15]. On the contrary, intake of unsaturated fats has a protective role[16].

Recent studies revealed the underlying mechanism of this process, highlighting mitochondrial dysfunction as a key player (reviewed by Meex and Blank[17]). Hepatocytes are very rich in mitochondria, and intake of SFAs induces changes in their structure and function. The process starts with liver steatosis due to reduced oxidation and enhanced lipolysis of adipose tissues. Steatosis affects the efficacy of the respiratory transport chain[18]. Consequently, overproduction of reactive oxygen species and lipid peroxidation arise, eventually resulting in inflammation, apoptosis and damage of the liver. In addition, SFAs from food enter the mitochondrial membrane and alter its permeability and fluidity, contributing further to NAFLD progression[19].

Besides the diet itself, obesity is also associated with NAFLD pathophysiology. In obesity, the capacity of an expanded adipose tissue to store lipids is limited, and the excess of lipids is stored in hepatocytes. The main form of lipids stored in the liver are triglycerides (TGs). Namely, high levels of free fatty acids in circulation, derived from enhanced lipolysis or diminished absorption by subcutaneous adipose tissue, bring ectopic fat accumulation, mostly in the liver. The sources of free fatty acids that form in the liver TG are not only from the diet (around 15%) but from increased lipolysis of TGs in adipose tissue (approximately 60%) and *de novo* lipogenesis (DNL) in the liver (25%) from dietary sugars, glucose and fructose[20]. This is supported by a study using stable isotopes, which has shown that accumulated lipids in the liver of NAFLD patients are mainly attributable to DNL. This stage of fat accumulation in the liver is the beginning of NAFLD, and managing obesity at this stage is of crucial importance. The lack of successful obesity treatment leads to intrahepatic inflammation and infiltration

of immune cells, such as lymphocytes, monocytes and neutrophils, which release cytokines in the liver [21]. This process not only intensifies inflammation but also promotes intrahepatic fibrogenesis, leading to progression of NAFLD to NASH.

Another relationship between obesity and NAFLD has been established through adipokines[22]. Adipokines are hormones derived from adipose tissue, and they are commonly represented by leptin and adiponectin. While their synthesis is balanced in people with normal weight, in obesity the dysregulation of pro- and anti-inflammatory adipokines is present. The enlarged, hypertrophic adipocytes produce proinflammatory adipokines and cytokines and promote IR. Adiponectin suppresses the secretion of proinflammatory cytokines (interleukin 6, tumor necrosis factor α), promotes the release of anti-inflammatory interleukin 10 and negatively correlates with visceral adipose tissue mass[23]. On the contrary, leptin is a product of white adipose tissue, and its level in circulation depends on the fat tissue mass and adipocyte size[24]. This is a satiety hormone with pleiotropic effects, and its concentration is a marker of obesity-related complications: Neuropathy and atherosclerosis[25,26]. Hyperleptinemia is considered crucial for NAFLD progression, although the exact mechanisms are still unclear. However, new findings pinpointed that leptin mediates pyroptotic-like cell death of macrophages and hepatocytes through infiltrated CD8+ T lymphocytes[27]. These results can provide a new strategy for future treatment of NAFLD.

Among the other risk factors, metabolic syndrome (MetS) has demonstrated the strongest association with NAFLD and its advanced stage, NASH. Since MetS is characterized by several features, including waist circumference, hypertension, hyperglycemia and dyslipidemia (low high-density lipoprotein cholesterol and/or high TG level), the clearest biological link with NAFLD development and progression was found for glucose level[28]. In line with this, 75% of patients with diabetes mellitus have NAFLD as well. This relation is bidirectional: Patients with NAFLD have a higher risk of developing diabetes[29]. Although IR is involved in NAFLD pathogenesis, improving IR is often insufficient to prevent further progression of NAFLD[30].

Furthermore, increased central adiposity, an important component of MetS, is considered a more significant marker of NAFLD than total body fat. This is expected, considering the role of visceral fats in the biosynthesis of adipokines. According to a recent study, there is a cross-talk between IR, adipose tissue inflammation and NAFLD, with dipeptidyl peptidase 4 as the key factor. This enzyme, secreted by the hepatocytes, has been shown to promote IR and inflammation of visceral adipose tissue[31]. In support of that, Barchetta *et al*[32] reported that levels and activity of dipeptidyl peptidase 4 in circulation are independently associated with NAFLD presence and severity in patients with or without other metabolic diseases and with various grades of obesity. The authors proposed dipeptidyl peptidase 4 as a novel marker for NAFLD/NASH risk stratification and follow-up of NAFLD patients.

ASSOCIATIONS BETWEEN DIETARY PATTERNS AND RISK OF NAFLD

Since people do not consume nutrients in isolation, the best option to describe the relationship between nutrition and health outcomes is the analysis of dietary patterns. Dietary patterns are a combination of a variety of foods habitually consumed by an individual, which together create synergistic effects on our health[33]. Two main dietary patterns, such as a "Western dietary pattern" and "Mediterranean dietary pattern" have been significantly associated (although in the opposite direction) with NAFLD, independently of potential confounders[34]. However, there are more dietary patterns (*e.g.*, healthy, traditional) identified for these associations.

Mediterranean dietary pattern and NAFLD

Mediterranean diet (MD) is a plant-based diet containing significant amounts of fiber, antioxidants, vegetable proteins, monounsaturated fat and polyunsaturated fatty acids (PUFAs), and with an appropriate n-6/n-3 PUFA ratio. This diet is known as a high-fat diet, with a fat intake of up to 45% of total daily calories[35]. The basic source of dietary fat in this diet is olive oil[33,36], where oleic acid, a monounsaturated fatty acid (MUFA), is a major component[37]. The MD is also characterized by high amounts of PUFAs. Dietary sources of the PUFAs, especially long-chain n-3 fatty acids, which include eicosapentaenoic acid and docosahexaenoic acid, in the MD are fish and nuts[38]. The MD is therefore rich in macronutrients that have been shown to have a beneficial effect on glucose and lipidic metabolism, and consequently on NAFLD[39]. The observational studies on the association between MD and NAFLD are summarized in Table 1. A reverse association between high adherence to MD and NAFLD odds, even after adjusting for some confounders such as age, sex, diabetes, physical activity, energy intake, smoking status and supplements use was seen in two case-control studies[40,41] and one cross-sectional study[42]. It should be highlighted that higher consumption of nuts, fruits and vegetables, legumes and fish as well as lower intake of meat were reported to be protective against NAFLD[43].

However, Entezari *et al*[40] observed that the reverse relationship between adherence to MD and odds of NAFLD disappeared after controlling for the anthropometric variables (body mass index and waist-to-hip ratio), which means that the MD may improve fatty liver by body weight modification,

Table 1 Association between the Mediterranean dietary patterns and nonalcoholic fatty liver disease

Ref.	Country/Region	Assess adherence to the MD	Food groups associated with lower risk NAFLD	Study design	Number of patients and age range	Main results	Associations
Entezari *et al* [40]	Iran	MDS	↑ Intake nuts and fruits, vegetables, legumes, high MUFA/PUFA ratio, cereals and fish. ↓ EI, low-fat dairy and meats	C-C	247 (43.7% male); 18–55 yr	↑ Adherence to MD was associated with ↓ risk of NAFLD after controlling for age (OR: 0.40, 95%CI: 0.17–0.95) and sex, diabetes, PA and supplement intake (OR: 0.36, 95%CI: 0.15–0.89). This association disappeared after adjusting for BMI, WHR (OR: 0.70, 95%CI: 0.25–1.97)	↓, After controlling for anthropometrical variables ↔
Giraldi *et al* [41]	Italy	MDS	↑ Legumes consumption ↓ risk of NAFLD (OR: 0.62; 95%CI: 0.38-0.99) and ↑ fish intake ↓ risk of NAFLD (OR: 0.38; 95%CI: 0.17-0.85)	C-C	815 (371 with NAFLD); 59 ± 16 yr; 444 controls; 45 ± 14 yr	↑ Adherence to the MD was associated with ↓ risk of NAFLD (OR: 0.83; 95%CI: 0.71-0.98) after controlling for age, sex, EI, diabetes status, smoking status, BMI and PA	↓
Baratta *et al* [42]	Italy	MD questionnaire	↓ Meat intake	C-S	584 patients (61.8% males) with cardiometabolic risk factors screened for the presence of liver steatosis; 56.2 ± 12.4 yr	↑ Adherence to MD was associated with ↓ risk of NAFLD (intermediate *vs* low tertile OR: 0.12; $P < 0.05$; high *vs* low tertile OR: 0.09; $P < 0.05$)	↓
Aller[45]	Spain	14-item MD assessment tool	-	C-S	82 NAFLD patients (42.7% low and 57.3% high steatosis grade, 68.3% steatohepatitis and 51.2% liver fibrosis mean age 44 + 11 yr	↑ Adherence to MD was associated with ↓ likelihood of having steatohepatitis OR: 0.43; 95%CI: 0.29-0.64 and steatosis OR: 0.42; 95%CI: 0.26- 0.70	↓
Park *et al*[46]	United States; 5 targeted racial/ethnic groups: African American, Native Hawaiian, Japanese American, Latino and White	Alternate MDS	-	Nested C-C	2959 with NAFLD (509 with cirrhosis; 2450 without cirrhosis) and 29292 controls; mean age 44.2 + 11.3 yr	↑ Adherence to MD was not associated with lower NAFLD risk	↔
Chan *et al* [47]	Hong Kong of China	MDS	↑ Vegetables and legumes, fruits and dried fruits, vitamin C	C-S	797 (41.7% males) 27.6% had a fatty liver aged ≥ 18 yr	MDS was not associated with the prevalence of NAFLD	↔
Kontogianni *et al*[44]	Greece	MDS	-	C-S	73 overweight/obese patients with NAFLD (69% males) *vs* 58 age-sex- and BMI matched controls; mean age 45 yr	No difference in the MDS was observed between patients and controls. One unit increase in the MDS was associated with ↓ likelihood of having NASH (OR: 0.64; 95%CI: 0.45-0.92), after controlling for sex and abdominal fat	↓

BMI: Body mass index; C-C: Case-control; C-S: Cross-sectional; CI: Confidence interval; EI: Energy intake; MD: Mediterranean diet; MDS: Mediterranean Diet Score; MUFA/PUFA: Monounsaturated fatty acids/Polyunsaturated fatty acids; NAFLD: Non-alcoholic fatty liver disease; OR: Odds ratio; WHR: Waist to hip ratio; PA: Physical activity.

modulation of lipid profile and inflammatory markers. Although Kontogianni *et al*[44] did not find a significant difference between NAFLD patients and controls in terms of adherence to the MD, higher adherence to this diet was inversely associated with alcoholic steatohepatitis. Similar results were seen

in the study by Aller *et al*[45].

On the other hand, in a nested and matched case-control study[46] as well as a cross-sectional study [47] it was found that adherence to the MD in any models (crude or adjusted to some confounders) was not associated with the risk of NAFLD. It should be highlighted that the dietary indices that measure adherence to the MD vary among the included studies. Hence, the specific dietary components and/or food items included within each of these indices and the methods used to evaluate compliance should be taken into consideration when interpreting obtained results. Nevertheless, a recent meta-analysis has proven that MD reduced the risk of NAFLD by 23%[43]. Also, the European Association for the Study of the Liver, and the European Association for the Study of Diabetes-European Association for the Study of Obesity Clinical Practice Guidelines have encouraged the MD as a lifestyle choice for treating the disease[48].

Various mechanisms may be associated with the beneficial effects of the MD on metabolic health and NAFLD, but the most important for this association is an appropriate fatty acid composition due to high MUFA content and an appropriate n-6/n-3 PUFA ratio[49]. It has been proven that MUFA may prevent the development of NAFLD by improving blood lipid concentrations, lowering body fat contents and decreasing postprandial adiponectin expression[50]. MUFAs (oleic acid) from olive oil have numerous beneficial effects on NAFLD, including decreased oxidized low-density lipoprotein, low-density lipoprotein cholesterol (LDL-C) and TG concentration, without the concomitant decrease in high-density lipoprotein cholesterol (HDL-C)[51], as well as lowering blood pressure and improving insulin sensitivity[37]. Additional effects of the MD relate to its polyphenol content. For example, polyphenols present in olive oil, such as oleuropein, hydroxytyrosol and tyrosol, have important antioxidant and anti-inflammatory effects[51]. The high content of dietary fiber both in soluble and insoluble forms in the MD is associated with a decrease in serum TGs and blood glucose[40]. The beneficial effect of the MD on NAFLD progression is also linked with an absence of added sugars and fructose in this diet.

Healthy dietary patterns and risk/prevalence of NAFLD

A healthy dietary pattern is defined as an appropriate intake of fruits & vegetables, nuts, olive oil, low-fat dairy products and fish. MD is one example of a healthy dietary pattern, but there are also other specific healthy diets. In Table 2, associations between healthy dietary patterns and the risk/prevalence of NAFLD are summarized.

In nine out of ten collected studies–in two prospective studies[52,53], four case-control studies[33,54-56], and three cross-sectional studies[57-59], a healthy dietary pattern was associated with a decreased risk of NAFLD independent of several confounders added to the models. Moreover, in a study by Chung *et al*[60] "simple meal pattern" characterized by a high intake of root and yellow vegetables, fruits, dairy products, eggs and nuts also exhibited an inverse correlation with NAFLD. Kalafati *et al*[55] found that individuals in the second quartile of the unsaturated fatty acids pattern, a dietary pattern with strong antioxidant properties, had 55.7% reduced odds of developing NAFLD than those in the first quartile, after adjusting for several confounders. However, higher consumption of unsaturated fatty acids was not associated with further protection from NAFLD, which may be explained by the fact that a greater intake of this diet leads to higher energy intake. Moreover, the mentioned authors found that the score for the prudent pattern (recognized also as a healthy dietary pattern) based on oil-based cooked vegetables, legumes, potatoes, fruits, vegetables and fatty fish was negatively associated with TG and uric acid levels, mediators of the associations between obesity and the incidence of NAFLD[61]. Only one study, presented by Alferink *et al*[62], found that adherence to vegetable and fish patterns (a kind of healthy pattern) was not associated with the risk of NAFLD.

The protective effect of healthy diets on the risk of the NAFLD could be a consequence of high consumption of vegetables and moderate intake of fruits, which are sources of antioxidant vitamins, such as vitamins A, E and C (protective against oxidative stress)[43]. Moreover, fruits and vegetables are good sources of dietary fiber, which has an inverse association with IR and the risk of NAFLD progression. Fish are sources of long-chain n-3 PUFAs, which are capable of reducing TGs and have a protective role against NAFLD[38].

Western and traditional dietary patterns and risk/prevalence of NAFLD

Although definitions of Western dietary patterns vary, this diet is often characterized by high consumption of soft drinks, red and processed meat and refined cereals, with concurrently low intake of fish, fruit and vegetables as well as whole grains[63]. Therefore, this diet is characterized by a high intake of animal and trans fats, sugar and fructose and a low intake of fiber and phytochemicals[52]. It was observed that when a western diet is provided in excess, even for a short period of 1 wk, it leads to increased hepatic steatosis[33]. In Table 2, associations between Western and traditional and healthy dietary patterns and the risk/prevalence of NAFLD are summarized.

Oddy *et al*[52], in their prospective cohort study, found that a higher score of the Western dietary pattern at 14 years of age was associated with a greater risk of NAFLD at 17 years. Similar results were obtained in other observational studies[34,56]. On the other hand, some studies report significant associations of this diet with the risk of NAFLD[58,60]. In the literature, the following dietary patterns familiar to the western patterns are also present: Fast food[54,55]; animal food/high protein[53,54]; red meat and alcohol[62]; high-salt[57]; high-fat dairy and refined grains[62]; high-carbohydrate/sweet/sugar/high

Table 2 Characteristics of the observational studies on the association between different dietary patterns and nonalcoholic fatty liver disease

Ref.	Country/Region	Dietary pattern	Food items in dietary patterns	Type of study	N, age	Main results	Associations
Oddy *et al*[52]	Australia	Western	Takeaway foods, confectionery, red meat, refined grains, processed meats, chips, sauces, full-fat dairy products and soft drinks	P	995. FFQ completed at 14 yr and liver ultrasound at 17 yr	Higher western pattern score at 14 yr was associated with ↑ risk of NAFLD at 17 yr (OR: 1.59; 95%CI: 1.17–2.14; $P < 0.05$) before adjustment to BMI	↑
		Healthy	Whole grains, fruit, vegetables, legumes, fish			A healthy diet at 14 yr appeared protective against NAFLD at 17 yr in centrally obese adolescents (OR: 0.63; 95%CI 0.41-0.96; $P < 0.05$)	↓
Salehi-Sahlabadi *et al* [34]	Iran	Western	Fast foods, soft drinks, processed meat, high-fat dairy products, hydrogenated fats, mayonnaise, salty snacks, sugar sweetened desserts, organ meats and refined grains	C-C	675 (450 with NAFLD) NAFLD: 38.6 ± 8.7 yr; Controls: 37.9 ± 8.9 yr	The western pattern was associated with ↑ risk for NAFLD after adjustment for age, sex, BMI, PA, SES and EI	↑
		Healthy	Fish, skinless poultry, low-fat dairy, fresh fruits, natural juices, canned fruits, dried fruits, vegetables, nuts, olive and garlic			A healthy pattern was associated with ↓ risk for NAFLD, after controlling for mentioned variables	↓
		Traditional	Red meat, organ meats, skinless poultry, eggs, yogurt drink, tea, legumes, tomato sauce, sugar sweetened-desserts, potato, condiments, salt, pickles and broth			Lack of association between traditional pattern and risk of NAFLD adjusted for mentioned variables	↔
Chung *et al*[60]	Korea	Western and high-carbohydrate	Processed meats, bread, soft drinks, pork, noodles, beef, cakes, snacks, beef soup, sugar, coffee, chicken, processed fish and refined grains	C-S	1190 (331 with NAFLD) NAFLD: 53 ± 9 yr; Controls: 51 ± 10 yr	Lack of association between Western/high-carbohydrate pattern and risk of NAFLD after adjustment for age, sex, WC, smoking status, EI, diabetes and hypertension	↔
		Traditional	Vegetables; fermented vegetables such as kimchi and jjangajji; fish and seafood; mush-rooms; fermented, processed, natural soybeans			↑ Adherence to the traditional pattern was associated with ↑ risk of NAFLD (OR: 1.85; 95%CI: 1.11-3.08; $P < 0.05$) after controlling for mentioned variables	↑
		Simple meal	Fruits, root and yellow vegetables, eggs, dairy products and nuts			↑ Adherence to the simple meal pattern was associated with ↓ risk of NAFLD (OR: 0.59; 95%CI: 0.34-1.00; $P < 0.05$), after controlling for mentioned variables	↓
Dehghanseresht *et al*[54]	Iran	Ordinary	Sweets, oils, fruits, white meats, refined grains, tea and coffee, salt, biscuits, snacks as well as red and organ meats	C-C	244 (122 with NAFLD) aged 19–70 yr	↑ Adherence to the ordinary pattern was associated with ↑ risk of NAFLD; $P < 0.001$	↑
		Traditional	Red and organ meats, dairy products, condiments, salt, tea and coffee and low			↑ Adherence to the traditional pattern was associated with ↑ risk of	↑

			intake of fruits			NAFLD $P < 0.001$	
		Vegetables and dairy (healthy pattern)	Vegetables, whole grains, legumes and nuts and dairy products			↑ Adherence to the vegetables and dairy pattern was ↓ association with NAFLD risk (OR: 0.23; 95%CI: 0.09–0.58; $P < 0.05$)	↓
		Fast food	Sauces, pickles, fast foods, soft drinks, snacks and biscuits			No association between Fast food patterns and the risk of NAFLD	↔
Yang *et al*[57]	China	Traditional Chinese	Staple food, coarse grains, fruits, eggs, fish and shrimp, milk and tea	C-S	999 (345 with NAFLD) aged 45–60 yr	No association between traditional pattern and the risk of NAFLD	↔
		Animal food	Kelp/seaweed and mushroom, pork, beef, mutton, poultry, cooked meat, eggs, fish and shrimp, beans and grease			After controlling for potential confounders, animal food patterns had ↑ prevalence rate for NAFLD (PR: 1.35; 95%CI: 1.06–1.72; $P < 0.05$	↑
		Grains-vegetables (healthy pattern)	Coarse grains, tubers, vegetables, mushroom and kelp/seaweed, cooked meat and beans			After adjustment for BMI, a vegetable pattern had ↓ prevalence rate for NAFLD (PR: 0.78; 95%CI: 0.62–0.98, $P < 0.05$).	↓
		High-salt	Rice, pickled vegetables, processed meat, bacon, salted duck egg, salted fish and tea			No association between high salt and the risk of NAFLD	↔
Jia *et al*[65]	China	High-carbohydrate/sweet	Fruits, cakes and candied fruits	C-S	4365 (1339 with NAFLD: adults	↑ Adherence to a high-carbohydrate/sweet pattern was associated with ↑ the prevalence of NAFLD in females but not in males	↑ only in females not in males
Kalafati *et al*[55]	Greece	Fast food	Energy-dense foods rich in saturated fat and sugar and included fast foods, sweetened soft drinks, fried potatoes and savory and puff pastry snacks	C-C	351 (134 with NAFLD) Case: 50.0 ± 10.5 yr; Control 44.0 ± 11.0 yr	↑ Adherence to a fast-food pattern was associated with ↑ odds for NAFLD after adjustment for age, sex, EI, PA, pack-yr smoked, education, MS ($P < 0.01$)	↑
		Prudent (healthy pattern)	Oil-based cooked vegetables, legumes, potatoes, fruits, vegetables and fatty fish			↑ Adherence to the prudent pattern was associated with ↓ TG and uric acid levels (β: -5.96; $P < 0.05$; β: -0.15; $P < 0.05$, respectively)	↓
		High-protein	Red meat, poultry, eggs			The high protein pattern was not associated with any NAFLD-related biomarker	↔
		The unsaturated FA	Nuts, chocolate and other foods rich in unsaturated FA			Individuals in the second quartile of the unsaturated FA pattern had ↓ odds of developing NAFLD *vs* the first quartile after being adjusted for mentioned confounders ($P < 0.05$)	↓
Tutunchi *et al*[56]	Iran	Healthy	Vegetables, legumes, fruits and low-fat dairy products	C-C	210 (105 with NAFLD) Cases 46 ± 9 yr; Controls 45 ± 9 yr	A healthy pattern was associated with ↓ odds of NAFLD (OR: 0.34; 95%CI: 0.16–0.81) after controlling for sex, education, PA, BMI,	↓

						WC	
		Western	Sweet, hydrogenated fat, red and processed meat and soft drink dietary patterns			↑ Adherence to the western pattern was related to ↑ risk of NAFLD (OR: 2.68; 95%CI: 1.31–4.16), after controlling to mentioned confounders	↑
Zhang *et al*[61]	China	Sugar-rich	Strawberry, kiwi fruit, persimmon, sweets, candied fruits, Chinese cakes	P	17360 free from NAFLD at baseline; During a median follow-up of 4.2 yr, 4034 with NAFLD, aged > 18 yr	After adjusting for age, sex, BMI, smoking, alcohol, education, occupation, income, PA, EI, personal and family history of the disease, depressive symptoms, dietary supplement use, inflammation markers, WHR and each other dietary pattern score, the sugar-rich pattern was associated with ↑ risk of NAFLD (HR: 1.11; 95%CI 1.01, 1.23)	↑
		Vegetable (healthy pattern)	Cucumber, green leafy vegetables, Chinese cabbage, celery, pumpkin			After adjusting for mentioned confounders, vegetable diet was associated with ↓ risk of NAFLD (HR 0.96; 95%CI: 0.86, 1.07)	↓
		Animal food	Animal organs, animal blood, preserved eggs, instant noodles, pork skin, sausage			After adjusting for mentioned confounders, animal food diet was associated with ↑ risk of NAFLD (HR: 1.22; 95%CI: 1.10, 1.36)	↑
Alferink *et al* [62]	The Netherlands	Vegetable and fish (healthy pattern)	Vegetables, poultry, fish and fruit	P	963 (343 with NAFLD) Baseline: 71.0 yr; Follow-up: 75 yr	No associations between vegetable and fish diet and NAFLD	↔
		Red meat and alcohol	Red, refined or organ meat, salty snacks and beer or spirits and low intake of fruit and tea			No associations between red meat and alcohol pattern and NAFLD	↔
		Traditional	Vegetable oils and stanols and margarine or butter, potatoes, whole grains and sweet snacks or desserts			↑ Adherence to the Traditional pattern was associated with ↓ risk of NAFLD (OR: 0.40; 95%CI 0.15–1.00) adjustment for sex, age, baseline education level, PA, EI, alcohol intake and follow-up time, BMI, baseline type 2 diabetes mellitus and baseline hypertension	↓
		Salty snacks and sauces	Savory food groups such as nuts, legumes, salty snacks and sauces			No associations between salty snacks and sauces pattern and NAFLD	↔
		High-fat dairy and refined grain	Fruit juice, refined grains, high-fat dairy products and sweet snacks or desserts			No associations between high-fat dairy and refined grain pattern and NAFLD	↔
Fakhoury-Sayegh *et al*[64]	Lebanon	Traditional	Vegetables, chickpeas, red beans, lentils, peas, vegetable oil/olives	C-C	222 (112 with NAFLD) Cases: 40 ± 6 yr; Controls: 39 ± 13 yr	↑ Adherence to traditional pattern ↓ the odds of NAFLD (OR: 0.30; CI 95%: 0.11–0.86; $P < 0.05$) adjusted for MS, EI, education, PA, family history, smoking, place of residence and profession	↓

		High fruits	Fruits and fruit juices			↑ Adherence to high fruits pattern ↑ the odds of NAFLD (OR: 4.061; 95%CI: 1.320–12.100, $P < 0.05$, adjusted for mentioned confounders	↑
		The high meat and fast food diet: (Western-like dietary pattern)	Meat such as pork, chicken, beef meat and hotdog			↑ Adherence to Western pattern ↑ the odds of NAFLD (OR: 4.081; 95%CI: 1.36–12.28, $P < 0.05$) adjusted for mentioned confounders	↑
Nakashita *et al* [58]	Japan	Healthy	Seaweeds, vegetables, mushrooms, pulses, potatoes and starches	C-S	281 men (89 with NAFLD) NAFLD: 62 (57–67) yr; Controls: 61 (56–67) yr	A healthy pattern was correlated with the ↓ risk of NAFLD	↓
		Western	Fats and oils, meat, seasonings, spices			No correlation between western pattern and NAFLD	↔
		Snacks	Sugars and starches, beverages (tea, coffee, fruit juice, soft drinks), fruits			No correlation between snacks pattern and NAFLD	↔
Adriano *et al* [59]	Brazil	Healthy	Fruits, vegetables/legumes, white meat, olive oil, margarine, bread/toast (with significant negative loading for beef)	C-S	229 older adults (74.7% women) NAFLD: 67.0 ± 5.0 yr; Controls: 70.1 ± 7.0 yr	↑ Adherence to the healthy pattern was associated with ↓ prevalence of NAFLD (PR: 0.70; 95%CI: 0.50, 0.98, $P < 0.05$) after adjustment for sex, age, EI, BMI, smoking status, PA, family income and use of hypoglycemic drugs	↓
		Regional snacks (Northeast of Brazil)	Tea/coffee, dairy products, cassava flour/tapioca/cuscus, butter and olive oil			↑ Adherence to the regional snacks pattern was associated with the ↑ prevalence of NAFLD (PR: 1.42; 95%CI: 1.02, 1.92, $P < 0.05$) after adjustment for mentioned confounders	↑
		Energy-dense	Processed cold meats, beef, viscera, sweet products/desserts/sugar, soft drinks, tubers/spaghetti/pastries			No association between energy density pattern and NAFLD	↔
		Traditional	Rice, beans, bread/toast, tea/coffee, sweet products/desserts/sugar			No association between traditional pattern and NAFLD	↔

BMI: Body mass index; C-C: Case-control; C-S: Cross-sectional; CI: Confidence interval; EI: Energy intake; FA: Fatty acid; FFQ: Food frequency questionnaire; HR: Hazard ratio; NAFLD: Nonalcoholic fatty liver disease; MS: Metabolic syndrome; OR: Odds ratio; P: Prospective; PA: Physical activity; PR: Prevalence ratio; SES: Socioeconomic status; TG: Triglyceride; WC: Waist circumference; WHR: Waist-to-hip ratio.

fruits[53,64,65]; as well as, snacks and energy-dense dietary pattern[58,59,62]. The majority of these dietary patterns increased the risk of NAFLD. Although high-carbohydrate/sweet/sugar/high fruits dietary pattern was associated with a significantly higher risk of NAFLD, Jia *et al*[65] found that this diet was positively associated with the prevalence of NAFLD only in females but not in males. Overall, Hassani Zadeh *et al*[43], in their meta-analysis, found that Western dietary patterns increased the risk of NAFLD by 56%.

The Western dietary pattern rich in saturated and trans-fatty acids may affect the hepatic cell steatosis *via* chylomicron uptake[34]. This dietary pattern, due to high amounts of refined grains, white bread and sugar-sweetened beverages has been also strongly associated with IR, diabetes and obesity. Soft drinks, the main constituents of the Western diet, contain substantial amounts of added sugars and fructose[66]. It was indicated that a higher intake of fructose induces hepatic IR and inflammation, thereby fueling the development of NAFLD. In addition, fructose metabolism could promote hepatic lipogenesis by inhibiting the DNL pathway and regulating lipogenic gene expression in the liver[67]. It should be noted that moderate consumption of fruits due to the presence of other dietary components such as dietary fiber and antioxidant vitamins can have a protective effect against NAFLD. On the other hand, excessive fruit consumption, as was seen in a study by Fakhoury-Sayegh *et al*[64], may increase

the risk for NAFLD, due to the high content of simple sugars (especially fructose).

The traditional diet may differ depending on the region or country and encompasses the common foods eaten there. Since this pattern comprises both healthy and unhealthy food items in different proportions, in collected studies we can observe the different influences of this pattern on the risk of NAFLD. For example, in a Korean study[60] the traditional diet was characterized by high intake of vegetables, fermented vegetables, such as kimchi, fish and seafood, mushrooms and fermented, processed and natural soybeans and was associated with a higher risk of NAFLD independent of several confounders added to this model. A traditional Iranian dietary pattern characterized by intake of red and organ meats, dairy products, condiments, salt, tea and coffee and low fruits consumption was related to an increased risk of NAFLD[54]. However, in another Iranian study[34], a traditional diet, represented by a high intake of red meat organ meats, skinless poultry, eggs, yogurt drink, tea, legumes, tomato sauce, sugars sweets-desserts, potato, condiments, salt, pickles and broth, was not associated with risk of NAFLD. Similar observations were reported by Yang *et al*[57] and Adriano *et al*[59] where traditional Chinese food items (staple food, coarse grains, fruits, eggs, fish and shrimp, milk and tea) and traditional Brazilian foods (rice, beans, bread/toast, tea/coffee, and sweet products/desserts/sugar) were not associated with a risk of NAFLD. In turn, Alferink *et al*[62] found that traditional Dutch dietary patterns consisting of vegetable oils, stanols and margarine or butter, potatoes, whole grains, and sweet snacks or desserts were associated with regression of NAFLD. Similar observations revealed that the traditional Lebanon diet (characterized by high intake of vegetables, chickpeas, red beans, lentils, peas, and vegetable oil/olives) was also related to a lower risk of NAFLD [64].

DIETARY INTERVENTION STUDIES IN NAFLD PATIENTS

Lifestyle modification, including a change in diet, weight loss target and structured exercise/physical intervention is the first-line and a cornerstone therapy for the NAFLD condition. It is implemented to reduce the cardiometabolic risk factors and cardiovascular disease events and to resolve NAFLD. Table 3 displays the NAFLD diet treatment recommendations/guidelines of The European Association for the Study of the Liver[48] and the European Society for Clinical Nutrition and Metabolism[68], in addition to the American Association for the Study of Liver Diseases[69,70], the Asian Pacific Association for the Study of the Liver[71], the American Gastroenterological Association[7] and the World Gastroenterology Organization[72].

The primary dietary goal for patients with NAFLD is to implement a hypocaloric diet due to a caloric deficit. Most often, low-calorie diets lead to an energy deficit of 500-1000 calories. Ordinarily, overweight NAFLD patients are advised to have a deficit of at least 500 calories/d for weight loss[10,48,73,74]. A weight loss of 3%-5% of body weight is necessary to improve liver steatosis[10]. To improve most of the histopathological characteristics in NAFLD, hepatocyte ballooning, lobular inflammation and fibrosis, a greater loss of body weight of 7%-10% is required[75]. Meta-analysis of 8 randomized controlled trials confirm that a 7% reduction in body weight was associated with improvement of the NAFLD Activity Score[76]. But, it should be noted that 94% of patients who lost 5% of initial body weight stabilized/or improved liver fibrosis[77]. Meta-analyses of 22 randomized controlled trials with 2588 participants reported that weight-loss interventions were significantly associated with improvements in alanine aminotransferase (ALT), ultrasonography pronounced liver steatosis, NAFLD Activity Score and presence of steatohepatitis[11]. Caloric restriction alone or in combination with physical activity encourages the loss of body weight and reduces hepatic steatosis and subsequently promotes fat mobilization from the liver[70]. In adults with NAFLD, exercise alone may prevent, reduce and cured liver steatosis. However, the ability of physical activity to improve other NAFLD spectrum histological parameters remains unknown.

Based on the current evidence, there is no consensus on the ideal macronutrient composition of the diet for NAFLD patients. The best nutrition recommendation is a traceable diet, based on individual preferences, eating habits and behaviors[74]. Also, there is no solid evidence to support a particular macronutrient composition of a hypocaloric diet unique for use in NAFLD patients. Independent of weight loss, a diet low in carbohydrates and higher in protein intake is associated with improvements of metabolic parameters in NAFLD patients[73,78]. A recent meta-analysis 32 controlled isocaloric feeding studies with a constant proportion of protein in the diet and varying ratios of carbohydrate and fat indicates that diet differences are too small, which implies the importance of caloric intake in NAFLD patients[79]. Overall, more future studies on macronutrient composition in diet are needed.

As previously stated, Mediterranean dietary patterns prevent the onset of NAFLD. The MD is also the most recommended diet for the treatment of NAFLD patients[12]. It improves liver steatosis, as indicated by the results of several studies, regardless of whether there is a calorie restriction in the diet. Independent of weight loss, patients have greater reductions in intrahepatic lipid content and insulin sensitivity after following the MD compared to a low-fat/high-carbohydrate diet. Consumption of a MD with calories less than the required daily energy allowed male NAFLD patients to reduce body weight, lipid accumulation, visceral adiposity index, fatty liver index, hepatic steatosis index and IR, as well as a

Table 3 Summary of international guidelines on diet for nonalcoholic fatty liver disease patients

	EASL/EASD/EASO clinical practice guidelines for the management of NAFLD [48]	ESPEN guideline on clinical nutrition in liver disease[68]	AASLD practice guidance: The diagnosis and management of NAFLD[69,70]	APASL clinical practice guidelines for the management of MAFLD[71]	AGA clinical practice guidelines for diagnosis and management of NAFLD[7]	WGO guidance for NAFLD/NASH [72]
Target for weight loss	7%-10%	7%-10% (in obese patient); > 10% to improve fibrosis	3%-5% (to improve steatosis); 7%-10% for histological improvement	7%-10%	≥ 5% if steatosis; ≥ 7% if NASH; ≥ 10% if fibrosis	5%-10%
Macronutrient composition	Low to moderate fat and moderate to higher carbohydrate; low carbohydrate, ketogenic diets or high protein	Irrespective of macronutrient composition, MD to improve steatosis and IR	Less relevant	Low-carbohydrate, low-fat and Mediterranean-type diets	Minimize SFA, ↓ red and processed meat	Avoid trans-fats; ↑ omega 3/omega 6 PUFA
Energy restriction	Hypocaloric: Reduction of 500-1000 kcal/d target weight loss of 0.5-1.0 kg/wk	Hypocaloric diet according to obesity guidance	Hypocaloric diet reduction of 500-1000 kcal/d	Hypocaloric diet reduction of 500-1000 kcal/d	Hypocaloric: 1200-1500 kcal/d or ↓ from baseline 500-1000 kcal/d	Hypocaloric: ↓ calories intake 25%
Fructose intake	Avoid fructose-containing beverages and foods				Avoid fructose commercially produced	Avoid fructose and soft drinks
Coffee intake	No liver-related limitations	"More likely to benefit health than harm"		"More likely to benefit health than harm"		
Alcohol intake	Risk below (< 30 g men, < 20 g women)	Abstain	Not consume heavy amounts		Restrict	

AGA: American Gastroenterological Association; AASLD: American Association for the Study of the Liver; APASL: Asian Pacific Association for the Study of the Liver; EASL: European Association for the Study of the Liver; EASD: European Association for the Study of Diabetes; EASO: European Association for the Study of Obesity; ESPEN: European Society for Clinical Nutrition and Metabolism; IR: Insulin resistance; MAFLD: Metabolic associated fatty liver disease; MD: Mediterranean diet; NAFLD: Nonalcoholic fatty liver disease; NASH: Nonalcoholic steatohepatitis; PUFA: Polyunsaturated fatty acid; SFA: Saturated fatty acid; WGO: World Gastroenterology Organization.

reduced share of SFA in the serum fatty acid profile decreased serum levels of SFAs and increased serum levels of MUFAs and n-3 PUFA[80]. The MD has well-documented metabolic benefits to reduce cardiovascular risk and thus is well valued in the medical community[81]. This observation is important because NAFLD patients have an increased risk of cardiovascular disease.

A systematic review and meta-analysis of randomized controlled trials presented that Mediterranean and hypocaloric dietary interventions favoring unsaturated fatty acids led to improved intrahepatic lipid content and transaminases levels (ALT, aspartate aminotransferase) in NAFLD patients[82]. The gamma-glutamyl transferase level does not change significantly during the Mediterranean dietary interventions[82]. Diet compositions in randomized controlled trials used in these meta-analyses can be considered comparable. Based on the calculated NAFLD fibrosis score, the composite score of age, glucose levels, platelet count, albumin and aspartate aminotransferase/ALT ratio, indicated that risk for advanced hepatic fibrosis was 11% among NAFLD patients with incidentally discovered hepatic steatosis[76]. In patients with NAFLD, gamma-glutamyl transferase levels decreased only after low glycemic index-MD intervention[83]. Hence, it is confirmed that MD without caloric restriction reduced the liver fat. Since there are only a few studies examining dietary interventions in clinically advanced stages of NAFLD (active and fibrotic NASH), the optimal dietary recommendation for nutrition intervention in NAFLD remains to be defined.

Well-discussed risk factors for hepatic steatosis are high SFA intake and overconsumption of carbohydrates, such as fructose. This type of diet leads to obesity. Intervention studies provide clear and strong evidence of a link between excessive calorie intake and NAFLD development as well as being linked to excess energy intake with increased lipolysis, induced IR and increased harmful ceramides in plasma[15,16]. Excessive intake of SFA (1000 extra kcal/d) conducted in obese patients for 3 wk increased intrahepatic TG content more than the intake of unsaturated fats (+ 55% *vs* + 15%, respectively)[16]. Also, overconsumption of simple sugars increased the intrahepatic TG content (+ 33%) by stimulating DNL (+ 98%). In a review by Stokes *et al*[84], short-term hypocaloric diets (up to 16 wk) have shown beneficial effects in reducing intrahepatic lipid content. Also, research supports that carbohydrate restriction and consumption of unsaturated fatty acids have efficacious metabolic effects in NAFLD[12,81,84]. Obesity is closely related to low levels of n-3 PUFA in plasma phospholipids[85].

Dietary modifications including n-3 PUFA supplementation are considered to be suitable therapeutic strategies for obese NAFLD patients, though further clinical trials are required.

However, among NAFLD patients, weight loss is largely unsuccessful in the real world in the ambulatory and clinical settings[86]. However, more frequent clinical encounters and controls are associated with an increased likelihood of weight loss (enhanced probability of weight reduction). Therefore, national strategies are needed for targeted success in weight loss success in high-risk populations.

Time-restricted feeding and intermittent fasting

The newest popular dietary intervention in the past few years is time-restricted feeding as a form of daily intermittent fasting (IF). This dietary approach restricts the time between the first and last food intake, without emphasizing calorie restriction. IF implies a > 60% energy restriction on > 2 d/wk. In time-restricted eating, daily food intake is limited to 8-10 h. These diets with a limited eating window appear to be safe in the NAFLD population. Patients tolerate this diet well. The key feature of this dietetic approach is the so-called "metabolic switch" that occurs 12 h after the cessation of food intake, where glycogen stores in the liver are depleted, and adipose tissue lipolysis increases[87]. This type of diet seems to be effective for weight loss, whereas many authors denied that the effect is still the result of a real calorie restriction. Patients with NAFLD follow the IF diet based on metabolic changes that are presented among overweight/obese individuals. A recent meta-analysis, involving patients with NAFLD, has shown that IF is beneficial in weight loss and liver enzyme levels[88]. However, no additional metabolic benefit has been shown compared to calorie-restricted diets[89]. In patients with NAFLD improvement in fatty liver index correlates with the number of fasting days and with the degree reduction in body mass index[90].

In a study performed by Cai *et al*[91], 271 NAFLD patients were randomized to time-restricted feeding, alternate-day fasting and control groups and were followed for 12 wk[91]. Findings from this study indicated that alternate-day fasting could be an effective diet method for weight loss and amelioration of lipid metabolism, with no direct effect in steatosis regression. In one Malaysian randomized controlled trial, 8 wk of IF with alternate-day calorie restriction resulted in the reduction of body weight and liver enzymes as well as hepatic steatosis compared to a habitual diet[92]. 8 wk of IF with limited caloric intake on alternating days led to a decrease in body weight and liver enzymes, as well as hepatic steatosis compared to the usual diet. Additional evidence for the benefit of IF to diminish hepatic steatosis and body weight compared to common lifestyle modification has been reported by 5:2 diet (intermittent calorie restriction: 600 kcal/d for men and 500 kcal/d for women for 2 non-consecutive days per week). But, the same effect was obtained in another group of participants on a low-carbohydrate high-fat diet (daily caloric intake: 1900 kcal/d for men and 1600 kcal/d for women) [89]. Data regarding IF efficacy in the steatosis/fibrosis regression are lacking. For now, it is important for medical practitioners not to advise this diet to patients with cirrhosis caused by NAFLD due to the well-known effect of starvation on the development of sarcopenia.

DASH diet

Evidence from two observational studies revealed that high adherence to the DASH-style diet is inversely associated with the risk of developing NAFLD[93,94]. It is indicated that subjects who fully adhered to the DASH diet were 30% less likely to have NAFLD. DASH is a low-glycemic index and low energy-dense diet, emphasizing low sodium intake and minimal consumption of processed foods. It is well known that the DASH diet is associated with a reduction in cardiovascular risk, as originally intended for hypertension patients. A randomized controlled trial including 60 overweight/obese adults, with ultrasonography proven NAFLD showed that the DASH diet over 8 wk led to more effective weight loss, improvement of aminotransferases and markers of IR, TG and total-C/HDL-C ratio compared to a contemporary control diet[95]. The DASH diet may be a promising dietary option for NAFLD patients, as weight loss, improved cardiometabolic factors and regression of steatosis are surrogate markers of liver disease status and the main goals of NAFLD treatment. This diet has aroused interest among specialists who care for patients with NAFLD. Further studies are essential to assess the effects of the DASH diet on liver histology and the clinical outcome of patients with NAFLD.

Ketogenic diet

Ketogenic diet (KD) is the most popular low-carbohydrate eating plan based on a strict restriction in carbohydrates (less than 20-50 g/d) consumption. The KD became a popular weight loss intervention among obese patients due to its effectiveness despite safety concerns of this diet plan if dyslipidemia is present[96]. Therefore, KD could have a positive impact on NAFLD, due to very low content of carbohydrates in the diet. However, it is not known if ketosis plays an additional role. Several mechanisms may be proposed links between ketosis and improvement of NAFLD. First, a ketogenic diet decreases insulin levels that lead to increased rate of fatty acid oxidation and decreased lipogenesis [97]. Then, restriction of carbohydrates encourages the formation of ketone bodies, which cause satiety by a still-unknown mechanism[98]. In turn, reduced calorie intake leads to weight loss.

Few studies have tested KD as a treatment strategy for NAFLD patients. Based on fat content, KD can be a normocaloric, hypocaloric or non-restricted caloric diet. Pérez-Guisado *et al*[99] conducted a pilot study on 14 overweight male patients with MetS and with ultrasonography-proven NAFLD. Patients fed unrestricted Mediterranean high-fat KD, high in unsaturated fats (*i.e.* olive oil and fish oil rich with omega-3 fatty acids). Adherence to Mediterranean high-fat KD showed a significant improvement in body weight, aminotransferases and LDL-C levels, and steatosis degree (21% of the patients had complete fatty liver regression)[99].

Mardinoglu *et al*[100] reported a 2-wk KD intervention (carbohydrate 20–30 g/d, fat 241 g/d, 3115 kcal/d) in 17 obese patients with NAFLD. Despite a slight weight loss, liver fat content (assessed by magnetic resonance spectroscopy) was reduced by 43.8% in obese patients in this study. At the same time, a concomitant decrease in *de novo* gene for liver lipogenesis was obtained[100]. Moreover, literature data indicated that normocaloric high-fat KD inhibits DNL and induces fatty acid oxidation, caused sustained weight loss and reduced hepatic fat accumulation[16,101]. Based on the above findings KD could be a potential therapeutic dietary intervention for addressing steatosis regression and weight loss. Future studies are needed on the KD effect on fibrosis regression and resolution of inflammation. Because ketosis may have beneficial effects independently of the diet composition, studies aiming to identify the specific role that ketone bodies play in the pathophysiology of NAFLD are warranted.

Added sugars

Study evidence from cross-sectional trials pronounced a directly proportional association between the intake of refined sugar (especially high fructose corn syrup) due to the consumption of sweet sugar beverages with the risk of developing NAFLD[81,102]. Patients with NAFLD consume 2-3 times more fructose. Higher fructose consumption is also related to an increased risk of having steatohepatitis and advanced fibrosis in NAFLD patients. Based on current evidence, fructose supplementation was linked with higher adiposity and enhanced visceral fat, hypertriglyceridemia and IR, occurs due to increase DNL in liver, in spite of similar weight gain when compared to glucose[103]. Increasing the frequency of the snacks with added sugar consumption led to a prominent increase in the hepatic fat content. The augmented hepatic steatosis was proportional to visceral fat accumulation and to the rise in DNL.

Fructose-rich diets, based on sugar-sweetened beverages increase hepatic synthesis of TG and are recognized as a major mediator of NAFLD[73]. It was observed that carbohydrate overfeeding in overweight persons consumed 1000 kcal/d from simple carbohydrates (sugar-sweetened soft drinks, candy, pineapple juice) for 3 wk caused a 10-times greater relative increase in fat content in the liver than in body weight (27% *vs* 2%, respectively)[104]. The recommendation to avoid sweet sugar beverages reduced the intake of extra empty calories and supported a caloric deficit for weight loss. Notably, high fructose consumption in NAFLD patients was compiled, with an increase in hepatic fructokinase and fatty acid synthase mRNA when compared to healthy persons[105]. Fructose can advance hepatic steatosis both directly *via* DNL and indirectly *via* DNL feedback inhibition of fatty acids. Overconsumption of fructose may increase the risk of developing NASH and advanced fibrosis, although the relationship may be confounded by excess energy intake or by unhealthy dietary patterns and sedentary lifestyle, which are common in NAFLD patients[106].

Current literature evidence suggests that higher fructose intake (> 20E% or 100–220 g/d) may adversely affect disease onset and progression[81]. Meta-analyses reported that moderate fructose consumption lower than 10% of energy (< 50 g/d for a 2000 kcal diet) does not induce weight gain or dyslipidemia. Sugar-sweetened beverage intake of ≥ 1 serving/d rises the risk of having NAFLD by 50% [33] and liver fibrosis by 250%[107]. It seems that artificially sweetened beverages and defined 100% fruit juices have similar effects as sugar-sweetened beverages. The results of a systematic review indicated that fructose in the diet isocalorically replaced with other carbohydrate sources for 1-10 wk did not affect NAFLD biomarkers[108]. Fructose overconsumption increases intrahepatic lipids and ALT levels. This effect results from excess energy intake rather than fructose consumption[108]. In the future, long-term prospective clinical trials are essential to understand and confirm a link between NAFLD progression and fructose consumption.

Coffee consumption

NAFLD patients who drink three to four cups of coffee per day will have more health benefits than harm, with the reduction in risk for various health outcome[109]. Nevertheless, a recent meta-analysis of 11 epidemiological studies confirmed association with regular coffee consumption and decreased risk of NAFLD[110]. Moreover in patients already diagnosed with NAFLD, coffee consumption reduced risk for the development of liver fibrosis[97,110]. A case-control study showed involvement of coffee in the fatty liver score, pronounced by ultrasound in all coffee consumers[111]. A systematic review determined that coffee consumption was inversely related to the severity of steatohepatitis in NAFLD patients[112]. Prohibitive effects on fibrosis progression were determined by the FibroTest based on fasting biochemical markers presented in a prospective study in the general population[113]. It was noted that decaffeinated coffee has the same helpful effect on NAFLD[114]. It was considered that two cups of coffee/day helped in the prevention of hepatocellular carcinoma[115], while three cups of coffee/day prevented steatohepatitis and fibrosis[109]. As observations have so far been based on epidemiological studies, future clinical studies need to confirm whether coffee consumption can be

considered a preventative factor for NAFLD. Until then, routine prescription of coffee for NAFLD prevention/treatment is not recommended.

CONCLUSION

In conclusion, the Western dietary pattern characterized by high intake of soft drinks, red and processed meat and refined cereals with coincidentally low intake of fish, fruit and vegetables as well as whole grains tended to increase the risk of NAFLD. The healthy and Mediterranean dietary patterns characterized by high consumption of vegetables, fruits, nuts, olive oil, low-fat dairy products and fish were linked with a reduced NAFLD risk. More prospective cohort studies are needed to confirm the association between dietary patterns and NAFLD risk. Macronutrient composition and excessive caloric intake are critical determinates of obesity and liver health. DASH, IF and KD have aroused interest among specialists who care for patients with NAFLD. Further well-designed studies are needed to assess the effects of these diets on liver-related outcomes and liver histology. Dietary advice should be provided by a multidisciplinary team with a specialized dietitian as an individual approach, as we already know that our genetics and gut microbiota cause differences in the effects of the diet to our metabolism. Future research in field interaction overfeeding and genomics are warranted, as are of the inter-individual difference of liver steatoses.

FOOTNOTES

Author contributions: Ristic-Medic D designed the review; Ristic-Medic D and Bajerska J analyzed and interpreted the data and drafted the manuscript; Vucic V critically revised the paper.

Supported by Ministry of Education, Science and Technological Development of the Republic of Serbia, No. 451-03-68/2022-14/200042.

Conflict-of-interest statement: All the authors report no relevant conflicts of interest for this article.

Open-Access: This article is an open-access article that was selected by an in-house editor and fully peer-reviewed by external reviewers. It is distributed in accordance with the Creative Commons Attribution NonCommercial (CC BY-NC 4.0) license, which permits others to distribute, remix, adapt, build upon this work non-commercially, and license their derivative works on different terms, provided the original work is properly cited and the use is non-commercial. See: https://creativecommons.org/Licenses/by-nc/4.0/

Country/Territory of origin: Serbia

ORCID number: Danijela Ristic-Medic 0000-0002-7041-4220; Joanna Bajerska 0000-0002-2268-9326; Vesna Vucic 0000-0002-8563-594X.

S-Editor: Fan JR
L-Editor: A
P-Editor: Fan JR

REFERENCES

1 **Benedict M**, Zhang X. Non-alcoholic fatty liver disease: An expanded review. *World J Hepatol* 2017; **9**: 715-732 [PMID: 28652891 DOI: 10.4254/wjh.v9.i16.715]
2 **Wong MCS**, Huang JLW, George J, Huang J, Leung C, Eslam M, Chan HLY, Ng SC. The changing epidemiology of liver diseases in the Asia-Pacific region. *Nat Rev Gastroenterol Hepatol* 2019; **16**: 57-73 [PMID: 30158570 DOI: 10.1038/s41575-018-0055-0]
3 **Cotter TG**, Rinella M. Nonalcoholic Fatty Liver Disease 2020: The State of the Disease. *Gastroenterology* 2020; **158**: 1851-1864 [PMID: 32061595 DOI: 10.1053/j.gastro.2020.01.052]
4 **Adibi A**, Maleki S, Adibi P, Etminani R, Hovsepian S. Prevalence of Nonalcoholic Fatty Liver Disease and its Related Metabolic Risk Factors in Isfahan, Iran. *Adv Biomed Res* 2017; **6**: 47 [PMID: 28503502 DOI: 10.4103/2277-9175.204590]
5 **Wong MCS**, Huang J. The growing burden of liver cirrhosis: implications for preventive measures. *Hepatol Int* 2018; **12**: 201-203 [PMID: 29679258 DOI: 10.1007/s12072-018-9865-y]
6 **Godoy-Matos AF**, Silva Júnior WS, Valerio CM. NAFLD as a continuum: from obesity to metabolic syndrome and diabetes. *Diabetol Metab Syndr* 2020; **12**: 60 [PMID: 32684985 DOI: 10.1186/s13098-020-00570-y]
7 **Younossi ZM**, Corey KE, Lim JK. AGA Clinical Practice Update on Lifestyle Modification Using Diet and Exercise to Achieve Weight Loss in the Management of Nonalcoholic Fatty Liver Disease: Expert Review. *Gastroenterology* 2021; **160**: 912-918 [PMID: 33307021 DOI: 10.1053/j.gastro.2020.11.051]

8 **Ristic-Medic D**, Petrovic S, Arsic A, Vucic V. Liver disease and COVID-19: The link with oxidative stress, antioxidants and nutrition. *World J Gastroenterol* 2021; **27**: 5682-5699 [PMID: 34629794 DOI: 10.3748/wjg.v27.i34.5682]

9 **Polyzos SA**, Kountouras J, Mantzoros CS. Obesity and nonalcoholic fatty liver disease: From pathophysiology to therapeutics. *Metabolism* 2019; **92**: 82-97 [PMID: 30502373 DOI: 10.1016/j.metabol.2018.11.014]

10 **Sanyal AJ**. Putting non-alcoholic fatty liver disease on the radar for primary care physicians: how well are we doing? *BMC Med* 2018; **16**: 148 [PMID: 30139362 DOI: 10.1186/s12916-018-1149-9]

11 **Koutoukidis DA**, Astbury NM, Tudor KE, Morris E, Henry JA, Noreik M, Jebb SA, Aveyard P. Association of Weight Loss Interventions With Changes in Biomarkers of Nonalcoholic Fatty Liver Disease: A Systematic Review and Meta-analysis. *JAMA Intern Med* 2019; **179**: 1262-1271 [PMID: 31260026 DOI: 10.1001/jamainternmed.2019.2248]

12 **Pugliese N**, Plaz Torres MC, Petta S, Valenti L, Giannini EG, Aghemo A. Is there an 'ideal' diet for patients with NAFLD? *Eur J Clin Invest* 2022; **52**: e13659 [PMID: 34309833 DOI: 10.1111/eci.13659]

13 **Eslam M**, Valenti L, Romeo S. Genetics and epigenetics of NAFLD and NASH: Clinical impact. *J Hepatol* 2018; **68**: 268-279 [PMID: 29122391 DOI: 10.1016/j.jhep.2017.09.003]

14 **Mota M**, Banini BA, Cazanave SC, Sanyal AJ. Molecular mechanisms of lipotoxicity and glucotoxicity in nonalcoholic fatty liver disease. *Metabolism* 2016; **65**: 1049-1061 [PMID: 26997538 DOI: 10.1016/j.metabol.2016.02.014]

15 **Rosqvist F**, Kullberg J, Ståhlman M, Cedernaes J, Heurling K, Johansson HE, Iggman D, Wilking H, Larsson A, Eriksson O, Johansson L, Straniero S, Rudling M, Antoni G, Lubberink M, Orho-Melander M, Borén J, Ahlström H, Risérus U. Overeating Saturated Fat Promotes Fatty Liver and Ceramides Compared With Polyunsaturated Fat: A Randomized Trial. *J Clin Endocrinol Metab* 2019; **104**: 6207-6219 [PMID: 31369090 DOI: 10.1210/jc.2019-00160]

16 **Luukkonen PK**, Sädevirta S, Zhou Y, Kayser B, Ali A, Ahonen L, Lallukka S, Pelloux V, Gaggini M, Jian C, Hakkarainen A, Lundbom N, Gylling H, Salonen A, Orešič M, Hyötyläinen T, Orho-Melander M, Rissanen A, Gastaldelli A, Clément K, Hodson L, Yki-Järvinen H. Saturated Fat Is More Metabolically Harmful for the Human Liver Than Unsaturated Fat or Simple Sugars. *Diabetes Care* 2018; **41**: 1732-1739 [PMID: 29844096 DOI: 10.2337/dc18-0071]

17 **Meex RCR**, Blaak EE. Mitochondrial Dysfunction is a Key Pathway that Links Saturated Fat Intake to the Development and Progression of NAFLD. *Mol Nutr Food Res* 2021; **65**: e1900942 [PMID: 32574416 DOI: 10.1002/mnfr.201900942]

18 **Satapati S**, Kucejova B, Duarte JA, Fletcher JA, Reynolds L, Sunny NE, He T, Nair LA, Livingston KA, Fu X, Merritt ME, Sherry AD, Malloy CR, Shelton JM, Lambert J, Parks EJ, Corbin I, Magnuson MA, Browning JD, Burgess SC. Mitochondrial metabolism mediates oxidative stress and inflammation in fatty liver. *J Clin Invest* 2016; **126**: 1605 [PMID: 27035816 DOI: 10.1172/JCI86695]

19 **Sullivan EM**, Fix A, Crouch MJ, Sparagna GC, Zeczycki TN, Brown DA, Shaikh SR. Murine diet-induced obesity remodels cardiac and liver mitochondrial phospholipid acyl chains with differential effects on respiratory enzyme activity. *J Nutr Biochem* 2017; **45**: 94-103 [PMID: 28437736 DOI: 10.1016/j.jnutbio.2017.04.004]

20 **Donnelly KL**, Smith CI, Schwarzenberg SJ, Jessurun J, Boldt MD, Parks EJ. Sources of fatty acids stored in liver and secreted *via* lipoproteins in patients with nonalcoholic fatty liver disease. *J Clin Invest* 2005; **115**: 1343-1351 [PMID: 15864352 DOI: 10.1172/JCI23621]

21 **Nati M**, Haddad D, Birkenfeld AL, Koch CA, Chavakis T, Chatzigeorgiou A. The role of immune cells in metabolism-related liver inflammation and development of non-alcoholic steatohepatitis (NASH). *Rev Endocr Metab Disord* 2016; **17**: 29-39 [PMID: 26847547 DOI: 10.1007/s11154-016-9339-2]

22 **Zorena K**, Jachimowicz-Duda O, Ślęzak D, Robakowska M, Mrugacz M. Adipokines and Obesity. Potential Link to Metabolic Disorders and Chronic Complications. *Int J Mol Sci* 2020; **21** [PMID: 32443588 DOI: 10.3390/ijms21103570]

23 **Monda V**, Polito R, Lovino A, Finaldi A, Valenzano A, Nigro E, Corso G, Sessa F, Asmundo A, Nunno ND, Cibelli G, Messina G. Short-Term Physiological Effects of a Very Low-Calorie Ketogenic Diet: Effects on Adiponectin Levels and Inflammatory States. *Int J Mol Sci* 2020; **21** [PMID: 32370212 DOI: 10.3390/ijms21093228]

24 **Flehmig G**, Scholz M, Klöting N, Fasshauer M, Tönjes A, Stumvoll M, Youn BS, Blüher M. Identification of adipokine clusters related to parameters of fat mass, insulin sensitivity and inflammation. *PLoS One* 2014; **9**: e99785 [PMID: 24968098 DOI: 10.1371/journal.pone.0099785]

25 **Morioka T**, Emoto M, Yamazaki Y, Kawano N, Imamura S, Numaguchi R, Urata H, Motoyama K, Mori K, Fukumoto S, Koyama H, Shoji T, Inaba M. Leptin is associated with vascular endothelial function in overweight patients with type 2 diabetes. *Cardiovasc Diabetol* 2014; **13**: 10 [PMID: 24410779 DOI: 10.1186/1475-2840-13-10]

26 **Jung CH**, Kim BY, Mok JO, Kang SK, Kim CH. Association between serum adipocytokine levels and microangiopathies in patients with type 2 diabetes mellitus. *J Diabetes Investig* 2014; **5**: 333-339 [PMID: 24843783 DOI: 10.1111/jdi.12144]

27 **Zhang Q**, Wang J, Huang F, Yao Y, Xu L. Leptin induces NAFLD progression through infiltrated CD8+ T lymphocytes mediating pyroptotic-like cell death of hepatocytes and macrophages. *Dig Liver Dis* 2021; **53**: 598-605 [PMID: 33172809 DOI: 10.1016/j.dld.2020.10.025]

28 **Käräjämäki AJ**, Bloigu R, Kauma H, Kesäniemi YA, Koivurova OP, Perkiömäki J, Huikuri H, Ukkola O. Non-alcoholic fatty liver disease with and without metabolic syndrome: Different long-term outcomes. *Metabolism* 2017; **66**: 55-63 [PMID: 27423871 DOI: 10.1016/j.metabol.2016.06.009]

29 **Ballestri S**, Zona S, Targher G, Romagnoli D, Baldelli E, Nascimbeni F, Roverato A, Guaraldi G, Lonardo A. Nonalcoholic fatty liver disease is associated with an almost twofold increased risk of incident type 2 diabetes and metabolic syndrome. Evidence from a systematic review and meta-analysis. *J Gastroenterol Hepatol* 2016; **31**: 936-944 [PMID: 26667191 DOI: 10.1111/jgh.13264]

30 **Loomba R**, Abraham M, Unalp A, Wilson L, Lavine J, Doo E, Bass NM; Nonalcoholic Steatohepatitis Clinical Research Network. Association between diabetes, family history of diabetes, and risk of nonalcoholic steatohepatitis and fibrosis. *Hepatology* 2012; **56**: 943-951 [PMID: 22505194 DOI: 10.1002/hep.25772]

31 **Ghorpade DS**, Ozcan L, Zheng Z, Nicoloro SM, Shen Y, Chen E, Blüher M, Czech MP, Tabas I. Hepatocyte-secreted DPP4 in obesity promotes adipose inflammation and insulin resistance. *Nature* 2018; **555**: 673-677 [PMID: 29562231 DOI: 10.1038/nature26138]

32 **Barchetta I**, Ceccarelli V, Cimini FA, Barone E, Sentinelli F, Coluzzi M, Chiappetta C, Bertoccini L, Tramutola A,

Labbadia G, Di Cristofano C, Silecchia G, Leonetti F, Cavallo MG. Circulating dipeptidyl peptidase-4 is independently associated with the presence and severity of NAFLD/NASH in individuals with and without obesity and metabolic disease. *J Endocrinol Invest* 2021; **44**: 979-988 [PMID: 32852705 DOI: 10.1007/s40618-020-01392-5]

33 **Zelber-Sagi S**, Salomone F, Mlynarsky L. The Mediterranean dietary pattern as the diet of choice for non-alcoholic fatty liver disease: Evidence and plausible mechanisms. *Liver Int* 2017; **37**: 936-949 [PMID: 28371239 DOI: 10.1111/liv.13435]

34 **Salehi-Sahlabadi A**, Sadat S, Beigrezaei S, Pourmasomi M, Feizi A, Ghiasvand R, Hadi A, Clark CCT, Miraghajani M. Dietary patterns and risk of non-alcoholic fatty liver disease. *BMC Gastroenterol* 2021; **21**: 41 [PMID: 33509112 DOI: 10.1186/s12876-021-01612-z]

35 **Pérez-Martínez P**, Mikhailidis DP, Athyros VG, Bullo M, Couture P, Covas MI, de Koning L, Delgado-Lista J, Díaz-López A, Drevon CA, Estruch R, Esposito K, Fitó M, Garaulet M, Giugliano D, García-Ríos A, Katsiki N, Kolovou G, Lamarche B, Maiorino MI, Mena-Sánchez G, Muñoz-Garach A, Nikolic D, Ordovás JM, Pérez-Jiménez F, Rizzo M, Salas-Salvadó J, Schröder H, Tinahones FJ, de la Torre R, van Ommen B, Wopereis S, Ros E, López-Miranda J. Lifestyle recommendations for the prevention and management of metabolic syndrome: an international panel recommendation. *Nutr Rev* 2017; **75**: 307-326 [PMID: 28521334 DOI: 10.1093/nutrit/nux014]

36 **Bajerska J**, Chmurzynska A, Muzsik A, Krzyżanowska P, Mądry E, Malinowska AM, Walkowiak J. Weight loss and metabolic health effects from energy-restricted Mediterranean and Central-European diets in postmenopausal women: A randomized controlled trial. *Sci Rep* 2018; **8**: 11170 [PMID: 30042488 DOI: 10.1038/s41598-018-29495-3]

37 **Gosal H**, Kaur H, Chakwop Ngassa H, Elmenawi KA, Anil V, Mohammed L. The Significance of the Mediterranean Diet in the Management of Non-Alcoholic Fatty Liver Disease: A Systematic Review. *Cureus* 2021; **13**: e15618 [PMID: 34277236 DOI: 10.7759/cureus.15618]

38 **Gil A**, Gil F. Fish, a Mediterranean source of n-3 PUFA: benefits do not justify limiting consumption. *Br J Nutr* 2015; **113** Suppl 2: S58-S67 [PMID: 26148923 DOI: 10.1017/S0007114514003742]

39 **Kastorini CM**, Milionis HJ, Esposito K, Giugliano D, Goudevenos JA, Panagiotakos DB. The effect of Mediterranean diet on metabolic syndrome and its components: a meta-analysis of 50 studies and 534,906 individuals. *J Am Coll Cardiol* 2011; **57**: 1299-1313 [PMID: 21392646 DOI: 10.1016/j.jacc.2010.09.073]

40 **Entezari MR**, Talenezhad N, Mirzavandi F, Rahimpour S, Mozaffari-Khosravi H, Fallahzadeh H, Hosseinzadeh M. Mediterranean dietary pattern and non-alcoholic fatty liver diseases: a case-control study. *J Nutr Sci* 2021; **10**: e55 [PMID: 34367629 DOI: 10.1017/jns.2021.43]

41 **Giraldi L**, Miele L, Aleksovska K, Manca F, Leoncini E, Biolato M, Arzani D, Pirro MA, Marrone G, Cefalo C, Racco S, Liguori A, Rapaccini G, Miggiano GA, Gasbarrini A, Boccia S, Grieco A. Mediterranean diet and the prevention of non-alcoholic fatty liver disease: results from a case-control study. *Eur Rev Med Pharmacol Sci* 2020; **24**: 7391-7398 [PMID: 32706078 DOI: 10.26355/eurrev_202007_21907]

42 **Baratta F**, Pastori D, Polimeni L, Bucci T, Ceci F, Calabrese C, Ernesti I, Pannitteri G, Violi F, Angelico F, Del Ben M. Adherence to Mediterranean Diet and Non-Alcoholic Fatty Liver Disease: Effect on Insulin Resistance. *Am J Gastroenterol* 2017; **112**: 1832-1839 [PMID: 29063908 DOI: 10.1038/ajg.2017.371]

43 **Hassani Zadeh S**, Mansoori A, Hosseinzadeh M. Relationship between dietary patterns and non-alcoholic fatty liver disease: A systematic review and meta-analysis. *J Gastroenterol Hepatol* 2021; **36**: 1470-1478 [PMID: 33269500 DOI: 10.1111/jgh.15363]

44 **Kontogianni MD**, Tileli N, Margariti A, Georgoulis M, Deutsch M, Tiniakos D, Fragopoulou E, Zafiropoulou R, Manios Y, Papatheodoridis G. Adherence to the Mediterranean diet is associated with the severity of non-alcoholic fatty liver disease. *Clin Nutr* 2014; **33**: 678-683 [PMID: 24064253 DOI: 10.1016/j.clnu.2013.08.014]

45 **Aller R**, Izaola O, de la Fuente B, De Luis Román DA. Mediterranean diet is associated with liver histology in patients with non alcoholic fatty liver disease. *Nutr Hosp* 2015; **32**: 2518-2524 [PMID: 26667698 DOI: 10.3305/nh.2015.32.6.10074]

46 **Park SY**, Noureddin M, Boushey C, Wilkens LR, Setiawan VW. Diet Quality Association with Nonalcoholic Fatty Liver Disease by Cirrhosis Status: The Multiethnic Cohort. *Curr Dev Nutr* 2020; **4**: nzaa024 [PMID: 32190810 DOI: 10.1093/cdn/nzaa024]

47 **Chan R**, Wong VW, Chu WC, Wong GL, Li LS, Leung J, Chim AM, Yeung DK, Sea MM, Woo J, Chan FK, Chan HL. Diet-Quality Scores and Prevalence of Nonalcoholic Fatty Liver Disease: A Population Study Using Proton-Magnetic Resonance Spectroscopy. *PLoS One* 2015; **10**: e0139310 [PMID: 26418083 DOI: 10.1371/journal.pone.0139310]

48 **European Association for the Study of the Liver (EASL)**; European Association for the Study of Diabetes (EASD); European Association for the Study of Obesity (EASO). EASL-EASD-EASO Clinical Practice Guidelines for the management of non-alcoholic fatty liver disease. *J Hepatol* 2016; **64**: 1388-1402 [PMID: 27062661 DOI: 10.1016/j.jhep.2015.11.004]

49 **Anania C**, Perla FM, Olivero F, Pacifico L, Chiesa C. Mediterranean diet and nonalcoholic fatty liver disease. *World J Gastroenterol* 2018; **24**: 2083-2094 [PMID: 29785077 DOI: 10.3748/wjg.v24.i19.2083]

50 **Paniagua JA**, Gallego de la Sacristana A, Romero I, Vidal-Puig A, Latre JM, Sanchez E, Perez-Martinez P, Lopez-Miranda J, Perez-Jimenez F. Monounsaturated fat-rich diet prevents central body fat distribution and decreases postprandial adiponectin expression induced by a carbohydrate-rich diet in insulin-resistant subjects. *Diabetes Care* 2007; **30**: 1717-1723 [PMID: 17384344 DOI: 10.2337/dc06-2220]

51 **Assy N**, Nassar F, Nasser G, Grosovski M. Olive oil consumption and non-alcoholic fatty liver disease. *World J Gastroenterol* 2009; **15**: 1809-1815 [PMID: 19370776 DOI: 10.3748/wjg.15.1809]

52 **Oddy WH**, Herbison CE, Jacoby P, Ambrosini GL, O'Sullivan TA, Ayonrinde OT, Olynyk JK, Black LJ, Beilin LJ, Mori TA, Hands BP, Adams LA. The Western dietary pattern is prospectively associated with nonalcoholic fatty liver disease in adolescence. *Am J Gastroenterol* 2013; **108**: 778-785 [PMID: 23545714 DOI: 10.1038/ajg.2013.95]

53 **Zhang S**, Gu Y, Bian S, Górska MJ, Zhang Q, Liu L, Meng G, Yao Z, Wu H, Wang Y, Zhang T, Wang X, Sun S, Zhou M, Jia Q, Song K, Qi L, Niu K. Dietary patterns and risk of non-alcoholic fatty liver disease in adults: A prospective cohort study. *Clin Nutr* 2021; **40**: 5373-5382 [PMID: 34560608 DOI: 10.1016/j.clnu.2021.08.021]

54 **Dehghanseresht N**, Jafarirad S, Alavinejad SP, Mansoori A. Association of the dietary patterns with the risk of non-alcoholic fatty liver disease among Iranian population: a case-control study. *Nutr J* 2020; **19**: 63 [PMID: 32605646 DOI: 10.1186/s12937-020-00580-6]

55 **Kalafati IP**, Borsa D, Dimitriou M, Revenas K, Kokkinos A, Dedoussis GV. Dietary patterns and non-alcoholic fatty liver disease in a Greek case-control study. *Nutrition* 2019; **61**: 105-110 [PMID: 30708259 DOI: 10.1016/j.nut.2018.10.032]

56 **Tutunchi H**, Saghafi-Asl M, Asghari-Jafarabadi M, Ostadrahimi A. Association between Dietary Patterns and Non-alcoholic Fatty Liver Disease: Results from a Case-Control Study. *Arch Iran Med* 2021; **24**: 35-42 [PMID: 33588566 DOI: 10.34172/aim.2021.06]

57 **Yang CQ**, Shu L, Wang S, Wang JJ, Zhou Y, Xuan YJ, Wang SF. Dietary Patterns Modulate the Risk of Non-Alcoholic Fatty Liver Disease in Chinese Adults. *Nutrients* 2015; **7**: 4778-4791 [PMID: 26083112 DOI: 10.3390/nu7064778]

58 **Nakashita C**, Xi L, Inoue Y, Kabura R, Masuda S, Yamano Y, Katoh T. Impact of dietary compositions and patterns on the prevalence of nonalcoholic fatty liver disease in Japanese men: a cross-sectional study. *BMC Gastroenterol* 2021; **21**: 342 [PMID: 34481454 DOI: 10.1186/s12876-021-01919-x]

59 **Adriano LS**, Sampaio HA, Arruda SP, Portela CL, de Melo MLP, Carioca AA, Soares NT. Healthy dietary pattern is inversely associated with non-alcoholic fatty liver disease in elderly. *Br J Nutr* 2016; **115**: 2189-2195 [PMID: 27102566 DOI: 10.1017/S0007114516001410]

60 **Chung GE**, Youn J, Kim YS, Lee JE, Yang SY, Lim JH, Song JH, Doo EY, Kim JS. Dietary patterns are associated with the prevalence of nonalcoholic fatty liver disease in Korean adults. *Nutrition* 2019; **62**: 32-38 [PMID: 30826597 DOI: 10.1016/j.nut.2018.11.021]

61 **Zhang Q**, Ma X, Xing J, Shi H, Yang R, Jiao Y, Chen S, Wu S, Zhang S, Sun X. Serum Uric Acid Is a Mediator of the Association Between Obesity and Incident Nonalcoholic Fatty Liver Disease: A Prospective Cohort Study. *Front Endocrinol (Lausanne)* 2021; **12**: 657856 [PMID: 34054728 DOI: 10.3389/fendo.2021.657856]

62 **Alferink LJM**, Erler NS, de Knegt RJ, Janssen HLA, Metselaar HJ, Darwish Murad S, Kiefte-de Jong JC. Adherence to a plant-based, high-fibre dietary pattern is related to regression of non-alcoholic fatty liver disease in an elderly population. *Eur J Epidemiol* 2020; **35**: 1069-1085 [PMID: 32323115 DOI: 10.1007/s10654-020-00627-2]

63 **Drake I**, Sonestedt E, Ericson U, Wallström P, Orho-Melander M. A Western dietary pattern is prospectively associated with cardio-metabolic traits and incidence of the metabolic syndrome. *Br J Nutr* 2018; **119**: 1168-1176 [PMID: 29759108 DOI: 10.1017/S000711451800079X]

64 **Fakhoury-Sayegh N**, Younes H, Heraoui GNHA, Sayegh R. Nutritional Profile and Dietary Patterns of Lebanese Non-Alcoholic Fatty Liver Disease Patients: A Case-Control Study. *Nutrients* 2017; **9** [PMID: 29135945 DOI: 10.3390/nu9111245]

65 **Jia Q**, Xia Y, Zhang Q, Wu H, Du H, Liu L, Wang C, Shi H, Guo X, Liu X, Li C, Sun S, Wang X, Zhao H, Song K, Huang G, Wu Y, Cui N, Niu K. Dietary patterns are associated with prevalence of fatty liver disease in adults. *Eur J Clin Nutr* 2015; **69**: 914-921 [PMID: 25649235 DOI: 10.1038/ejcn.2014.297]

66 **Zhang S**, Gu Y, Bian S, Lu Z, Zhang Q, Liu L, Meng G, Yao Z, Wu H, Wang Y, Zhang T, Wang X, Sun S, Zhou M, Jia Q, Song K, Qi L, Niu K. Soft drink consumption and risk of nonalcoholic fatty liver disease: results from the Tianjin Chronic Low-Grade Systemic Inflammation and Health (TCLSIH) cohort study. *Am J Clin Nutr* 2021; **113**: 1265-1274 [PMID: 33564868 DOI: 10.1093/ajcn/nqaa380]

67 **Softic S**, Cohen DE, Kahn CR. Role of Dietary Fructose and Hepatic De Novo Lipogenesis in Fatty Liver Disease. *Dig Dis Sci* 2016; **61**: 1282-1293 [PMID: 26856717 DOI: 10.1007/s10620-016-4054-0]

68 **Bischoff SC**, Austin P, Boeykens K, Chourdakis M, Cuerda C, Jonkers-Schuitema C, Lichota M, Nyulasi I, Schneider SM, Stanga Z, Pironi L. ESPEN guideline on home enteral nutrition. *Clin Nutr* 2020; **39**: 5-22 [PMID: 31255350 DOI: 10.1016/j.clnu.2019.04.022]

69 The diagnosis and management of nonalcoholic fatty liver disease: Practice guidance from the American Association for the Study of Liver Diseases. *Clin Liver Dis (Hoboken)* 2018; **11**: 81 [PMID: 30992795 DOI: 10.1002/cld.722]

70 **Chalasani N**, Younossi Z, Lavine JE, Charlton M, Cusi K, Rinella M, Harrison SA, Brunt EM, Sanyal AJ. The diagnosis and management of nonalcoholic fatty liver disease: Practice guidance from the American Association for the Study of Liver Diseases. *Hepatology* 2018; **67**: 328-357 [PMID: 28714183 DOI: 10.1002/hep.29367]

71 **Eslam M**, Sarin SK, Wong VW, Fan JG, Kawaguchi T, Ahn SH, Zheng MH, Shiha G, Yilmaz Y, Gani R, Alam S, Dan YY, Kao JH, Hamid S, Cua IH, Chan WK, Payawal D, Tan SS, Tanwandee T, Adams LA, Kumar M, Omata M, George J. The Asian Pacific Association for the Study of the Liver clinical practice guidelines for the diagnosis and management of metabolic associated fatty liver disease. *Hepatol Int* 2020; **14**: 889-919 [PMID: 33006093 DOI: 10.1007/s12072-020-10094-2]

72 **Review Team**. , LaBrecque DR, Abbas Z, Anania F, Ferenci P, Khan AG, Goh KL, Hamid SS, Isakov V, Lizarzabal M, Peñaranda MM, Ramos JF, Sarin S, Stimac D, Thomson AB, Umar M, Krabshuis J, LeMair A; World Gastroenterology Organisation. World Gastroenterology Organisation global guidelines: Nonalcoholic fatty liver disease and nonalcoholic steatohepatitis. *J Clin Gastroenterol* 2014; **48**: 467-473 [PMID: 24921212 DOI: 10.1097/MCG.0000000000000116]

73 **Barrera F**, George J. The role of diet and nutritional intervention for the management of patients with NAFLD. *Clin Liver Dis* 2014; **18**: 91-112 [PMID: 24274867 DOI: 10.1016/j.cld.2013.09.009]

74 **Raynor HA**, Champagne CM. Position of the Academy of Nutrition and Dietetics: Interventions for the Treatment of Overweight and Obesity in Adults. *J Acad Nutr Diet* 2016; **116**: 129-147 [PMID: 26718656 DOI: 10.1016/j.jand.2015.10.031]

75 **Hohenester S**, Christiansen S, Nagel J, Wimmer R, Artmann R, Denk G, Bischoff M, Bischoff G, Rust C. Lifestyle intervention for morbid obesity: effects on liver steatosis, inflammation, and fibrosis. *Am J Physiol Gastrointest Liver Physiol* 2018; **315**: G329-G338 [PMID: 29878845 DOI: 10.1152/ajpgi.00044.2018]

76 **Musso G**, Cassader M, Rosina F, Gambino R. Impact of current treatments on liver disease, glucose metabolism and cardiovascular risk in non-alcoholic fatty liver disease (NAFLD): a systematic review and meta-analysis of randomised trials. *Diabetologia* 2012; **55**: 885-904 [PMID: 22278337 DOI: 10.1007/s00125-011-2446-4]

77 **Hsu CC**, Ness E, Kowdley KV. Nutritional Approaches to Achieve Weight Loss in Nonalcoholic Fatty Liver Disease.

Adv Nutr 2017; **8**: 253-265 [PMID: 28298270 DOI: 10.3945/an.116.013730]
78 **Miller EF**. Nutrition Management Strategies for Nonalcoholic Fatty Liver Disease: Treatment and Prevention. *Clin Liver Dis (Hoboken)* 2020; **15**: 144-148 [PMID: 32395240 DOI: 10.1002/cld.918]
79 **Hall KD**, Guo J. Obesity Energetics: Body Weight Regulation and the Effects of Diet Composition. *Gastroenterology* 2017; **152**: 1718-1727.e3 [PMID: 28193517 DOI: 10.1053/j.gastro.2017.01.052]
80 **Ristic-Medic D**, Kovacic M, Takic M, Arsic A, Petrovic S, Paunovic M, Jovicic M, Vucic V. Calorie-Restricted Mediterranean and Low-Fat Diets Affect Fatty Acid Status in Individuals with Nonalcoholic Fatty Liver Disease. *Nutrients* 2020; **13** [PMID: 33374554 DOI: 10.3390/nu13010015]
81 **George ES**, Forsyth A, Itsiopoulos C, Nicoll AJ, Ryan M, Sood S, Roberts SK, Tierney AC. Practical Dietary Recommendations for the Prevention and Management of Nonalcoholic Fatty Liver Disease in Adults. *Adv Nutr* 2018; **9**: 30-40 [PMID: 29438460 DOI: 10.1093/advances/nmx007]
82 **Houttu V**, Csader S, Nieuwdorp M, Holleboom AG, Schwab U. Dietary Interventions in Patients With Non-alcoholic Fatty Liver Disease: A Systematic Review and Meta-Analysis. *Front Nutr* 2021; **8**: 716783 [PMID: 34368214 DOI: 10.3389/fnut.2021.716783]
83 **Misciagna G**, Del Pilar Díaz M, Caramia DV, Bonfiglio C, Franco I, Noviello MR, Chiloiro M, Abbrescia DI, Mirizzi A, Tanzi M, Caruso MG, Correale M, Reddavide R, Inguaggiato R, Cisternino AM, Osella AR. Effect of a Low Glycemic Index Mediterranean Diet on Non-Alcoholic Fatty Liver Disease. A Randomized Controlled Clinici Trial. *J Nutr Health Aging* 2017; **21**: 404-412 [PMID: 28346567 DOI: 10.1007/s12603-016-0809-8]
84 **Stokes CS**, Lammert F, Krawczyk M. Short-term Dietary Interventions for the Management of Nonalcoholic Fatty Liver. *Curr Med Chem* 2019; **26**: 3483-3496 [PMID: 28482789 DOI: 10.2174/0929867324666170508144409]
85 **Arsic A**, Takic M, Kojadinovic M, Petrovic S, Paunovic M, Vucic V, Ristic Medic D. Metabolically healthy obesity: is there a link with polyunsaturated fatty acid intake and status? *Can J Physiol Pharmacol* 2021; **99**: 64-71 [PMID: 32822561 DOI: 10.1139/cjpp-2020-0317]
86 **Dudekula A**, Rachakonda V, Shaik B, Behari J. Weight loss in nonalcoholic Fatty liver disease patients in an ambulatory care setting is largely unsuccessful but correlates with frequency of clinic visits. *PLoS One* 2014; **9**: e111808 [PMID: 25375228 DOI: 10.1371/journal.pone.0111808]
87 **Kang J**, Ratamess NA, Faigenbaum AD, Bush JA, Beller N, Vargas A, Fardman B, Andriopoulos T. Effect of Time-Restricted Feeding on Anthropometric, Metabolic, and Fitness Parameters: A Systematic Review. *J Am Coll Nutr* 2021; 1-16 [PMID: 34491139 DOI: 10.1080/07315724.2021.1958719]
88 **Yin C**, Li Z, Xiang Y, Peng H, Yang P, Yuan S, Zhang X, Wu Y, Huang M, Li J. Effect of Intermittent Fasting on Non-Alcoholic Fatty Liver Disease: Systematic Review and Meta-Analysis. *Front Nutr* 2021; **8**: 709683 [PMID: 34322514 DOI: 10.3389/fnut.2021.709683]
89 **Holmer M**, Lindqvist C, Petersson S, Moshtaghi-Svensson J, Tillander V, Brismar TB, Hagström H, Stål P. Treatment of NAFLD with intermittent calorie restriction or low-carb high-fat diet - a randomised controlled trial. *JHEP Rep* 2021; **3**: 100256 [PMID: 33898960 DOI: 10.1016/j.jhepr.2021.100256]
90 **Wilhelmi de Toledo F**, Grundler F, Sirtori CR, Ruscica M. Unravelling the health effects of fasting: a long road from obesity treatment to healthy life span increase and improved cognition. *Ann Med* 2020; **52**: 147-161 [PMID: 32519900 DOI: 10.1080/07853890.2020.1770849]
91 **Cai H**, Qin YL, Shi ZY, Chen JH, Zeng MJ, Zhou W, Chen RQ, Chen ZY. Effects of alternate-day fasting on body weight and dyslipidaemia in patients with non-alcoholic fatty liver disease: a randomised controlled trial. *BMC Gastroenterol* 2019; **19**: 219 [PMID: 31852444 DOI: 10.1186/s12876-019-1132-8]
92 **Johari MI**, Yusoff K, Haron J, Nadarajan C, Ibrahim KN, Wong MS, Hafidz MIA, Chua BE, Hamid N, Arifin WN, Ma ZF, Lee YY. A Randomised Controlled Trial on the Effectiveness and Adherence of Modified Alternate-day Calorie Restriction in Improving Activity of Non-Alcoholic Fatty Liver Disease. *Sci Rep* 2019; **9**: 11232 [PMID: 31375753 DOI: 10.1038/s41598-019-47763-8]
93 **Hekmatdoost A**, Shamsipour A, Meibodi M, Gheibizadeh N, Eslamparast T, Poustchi H. Adherence to the Dietary Approaches to Stop Hypertension (DASH) and risk of Nonalcoholic Fatty Liver Disease. *Int J Food Sci Nutr* 2016; **67**: 1024-1029 [PMID: 27436528 DOI: 10.1080/09637486.2016.1210101]
94 **Xiao ML**, Lin JS, Li YH, Liu M, Deng YY, Wang CY, Chen YM. Adherence to the Dietary Approaches to Stop Hypertension (DASH) diet is associated with lower presence of non-alcoholic fatty liver disease in middle-aged and elderly adults. *Public Health Nutr* 2020; **23**: 674-682 [PMID: 31566148 DOI: 10.1017/S1368980019002568]
95 **Razavi Zade M**, Telkabadi MH, Bahmani F, Salehi B, Farshbaf S, Asemi Z. The effects of DASH diet on weight loss and metabolic status in adults with non-alcoholic fatty liver disease: a randomized clinical trial. *Liver Int* 2016; **36**: 563-571 [PMID: 26503843 DOI: 10.1111/liv.12990]
96 **Moreno B**, Bellido D, Sajoux I, Goday A, Saavedra D, Crujeiras AB, Casanueva FF. Comparison of a very low-calorie-ketogenic diet with a standard low-calorie diet in the treatment of obesity. *Endocrine* 2014; **47**: 793-805 [PMID: 24584583 DOI: 10.1007/s12020-014-0192-3]
97 **Watanabe M**, Tozzi R, Risi R, Tuccinardi D, Mariani S, Basciani S, Spera G, Lubrano C, Gnessi L. Beneficial effects of the ketogenic diet on nonalcoholic fatty liver disease: A comprehensive review of the literature. *Obes Rev* 2020; **21**: e13024 [PMID: 32207237 DOI: 10.1111/obr.13024]
98 **Westerbacka J**, Lammi K, Häkkinen AM, Rissanen A, Salminen I, Aro A, Yki-Järvinen H. Dietary fat content modifies liver fat in overweight nondiabetic subjects. *J Clin Endocrinol Metab* 2005; **90**: 2804-2809 [PMID: 15741262 DOI: 10.1210/jc.2004-1983]
99 **Pérez-Guisado J**, Muñoz-Serrano A. A pilot study of the Spanish Ketogenic Mediterranean Diet: an effective therapy for the metabolic syndrome. *J Med Food* 2011; **14**: 681-687 [PMID: 21612461 DOI: 10.1089/jmf.2010.0137]
100 **Mardinoglu A**, Wu H, Bjornson E, Zhang C, Hakkarainen A, Räsänen SM, Lee S, Mancina RM, Bergentall M, Pietiläinen KH, Söderlund S, Matikainen N, Ståhlman M, Bergh PO, Adiels M, Piening BD, Granér M, Lundbom N, Williams KJ, Romeo S, Nielsen J, Snyder M, Uhlén M, Bergström G, Perkins R, Marschall HU, Bäckhed F, Taskinen MR, Borén J. An Integrated Understanding of the Rapid Metabolic Benefits of a Carbohydrate-Restricted Diet on Hepatic

Steatosis in Humans. *Cell Metab* 2018; **27**: 559-571.e5 [PMID: 29456073 DOI: 10.1016/j.cmet.2018.01.005]

101 **Lundsgaard AM**, Holm JB, Sjøberg KA, Bojsen-Møller KN, Myrmel LS, Fjære E, Jensen BAH, Nicolaisen TS, Hingst JR, Hansen SL, Doll S, Geyer PE, Deshmukh AS, Holst JJ, Madsen L, Kristiansen K, Wojtaszewski JFP, Richter EA, Kiens B. Mechanisms Preserving Insulin Action during High Dietary Fat Intake. *Cell Metab* 2019; **29**: 50-63.e4 [PMID: 30269983 DOI: 10.1016/j.cmet.2018.08.022]

102 **Ouyang X**, Cirillo P, Sautin Y, McCall S, Bruchette JL, Diehl AM, Johnson RJ, Abdelmalek MF. Fructose consumption as a risk factor for non-alcoholic fatty liver disease. *J Hepatol* 2008; **48**: 993-999 [PMID: 18395287 DOI: 10.1016/j.jhep.2008.02.011]

103 **Stanhope KL**, Schwarz JM, Keim NL, Griffen SC, Bremer AA, Graham JL, Hatcher B, Cox CL, Dyachenko A, Zhang W, McGahan JP, Seibert A, Krauss RM, Chiu S, Schaefer EJ, Ai M, Otokozawa S, Nakajima K, Nakano T, Beysen C, Hellerstein MK, Berglund L, Havel PJ. Consuming fructose-sweetened, not glucose-sweetened, beverages increases visceral adiposity and lipids and decreases insulin sensitivity in overweight/obese humans. *J Clin Invest* 2009; **119**: 1322-1334 [PMID: 19381015 DOI: 10.1172/JCI37385]

104 **Sevastianova K**, Santos A, Kotronen A, Hakkarainen A, Makkonen J, Silander K, Peltonen M, Romeo S, Lundbom J, Lundbom N, Olkkonen VM, Gylling H, Fielding BA, Rissanen A, Yki-Järvinen H. Effect of short-term carbohydrate overfeeding and long-term weight loss on liver fat in overweight humans. *Am J Clin Nutr* 2012; **96**: 727-734 [PMID: 22952180 DOI: 10.3945/ajcn.112.038695]

105 **Roeb E**, Weiskirchen R. Fructose and Non-Alcoholic Steatohepatitis. *Front Pharmacol* 2021; **12**: 634344 [PMID: 33628193 DOI: 10.3389/fphar.2021.634344]

106 **Meng G**, Zhang B, Yu F, Li C, Zhang Q, Liu L, Wu H, Xia Y, Bao X, Shi H, Su Q, Gu Y, Fang L, Yang H, Yu B, Sun S, Wang X, Zhou M, Jia Q, Jiao H, Wang B, Guo Q, Carvalhoa LA, Sun Z, Song K, Yu M, Niu K. Soft drinks consumption is associated with nonalcoholic fatty liver disease independent of metabolic syndrome in Chinese population. *Eur J Nutr* 2018; **57**: 2113-2121 [PMID: 28702720 DOI: 10.1007/s00394-017-1485-0]

107 **Abdelmalek MF**, Suzuki A, Guy C, Unalp-Arida A, Colvin R, Johnson RJ, Diehl AM; Nonalcoholic Steatohepatitis Clinical Research Network. Increased fructose consumption is associated with fibrosis severity in patients with nonalcoholic fatty liver disease. *Hepatology* 2010; **51**: 1961-1971 [PMID: 20301112 DOI: 10.1002/hep.23535]

108 **Chiu S**, Sievenpiper JL, de Souza RJ, Cozma AI, Mirrahimi A, Carleton AJ, Ha V, Di Buono M, Jenkins AL, Leiter LA, Wolever TM, Don-Wauchope AC, Beyene J, Kendall CW, Jenkins DJ. Effect of fructose on markers of non-alcoholic fatty liver disease (NAFLD): a systematic review and meta-analysis of controlled feeding trials. *Eur J Clin Nutr* 2014; **68**: 416-423 [PMID: 24569542 DOI: 10.1038/ejcn.2014.8]

109 **Kositamongkol C**, Kanchanasurakit S, Auttamalang C, Inchai N, Kabkaew T, Kitpark S, Chaiyakunapruk N, Duangjai A, Saokaew S, Phisalprapa P. Coffee Consumption and Non-alcoholic Fatty Liver Disease: An Umbrella Review and a Systematic Review and Meta-analysis. *Front Pharmacol* 2021; **12**: 786596 [PMID: 34966282 DOI: 10.3389/fphar.2021.786596]

110 **Hayat U**, Siddiqui AA, Okut H, Afroz S, Tasleem S, Haris A. The effect of coffee consumption on the non-alcoholic fatty liver disease and liver fibrosis: A meta-analysis of 11 epidemiological studies. *Ann Hepatol* 2021; **20**: 100254 [PMID: 32920163 DOI: 10.1016/j.aohep.2020.08.071]

111 **Catalano D**, Martines GF, Tonzuso A, Pirri C, Trovato FM, Trovato GM. Protective role of coffee in non-alcoholic fatty liver disease (NAFLD). *Dig Dis Sci* 2010; **55**: 3200-3206 [PMID: 20165979 DOI: 10.1007/s10620-010-1143-3]

112 **Saab S**, Mallam D, Cox GA 2nd, Tong MJ. Impact of coffee on liver diseases: a systematic review. *Liver Int* 2014; **34**: 495-504 [PMID: 24102757 DOI: 10.1111/liv.12304]

113 **Zelber-Sagi S**, Salomone F, Webb M, Lotan R, Yeshua H, Halpern Z, Santo E, Oren R, Shibolet O. Coffee consumption and nonalcoholic fatty liver onset: a prospective study in the general population. *Transl Res* 2015; **165**: 428-436 [PMID: 25468486 DOI: 10.1016/j.trsl.2014.10.008]

114 **Kennedy OJ**, Fallowfield JA, Poole R, Hayes PC, Parkes J, Roderick PJ. All coffee types decrease the risk of adverse clinical outcomes in chronic liver disease: a UK Biobank study. *BMC Public Health* 2021; **21**: 970 [PMID: 34154561 DOI: 10.1186/s12889-021-10991-7]

115 **Bravi F**, Tavani A, Bosetti C, Boffetta P, La Vecchia C. Coffee and the risk of hepatocellular carcinoma and chronic liver disease: a systematic review and meta-analysis of prospective studies. *Eur J Cancer Prev* 2017; **26**: 368-377 [PMID: 27111112 DOI: 10.1097/CEJ.0000000000000252]

World Journal of Gastroenterology

Submit a Manuscript: https://www.f6publishing.com

World J Gastroenterol 2022 July 21; 28(27): 3334-3345

DOI: 10.3748/wjg.v28.i27.3334

ISSN 1007-9327 (print) ISSN 2219-2840 (online)

MINIREVIEWS

Application of intravoxel incoherent motion diffusion-weighted imaging in hepatocellular carcinoma

Yi Zhou, Jing Zheng, Cui Yang, Juan Peng, Ning Liu, Lin Yang, Xiao-Ming Zhang

Specialty type: Radiology, nuclear medicine and medical imaging

Provenance and peer review: Invited article; Externally peer reviewed.

Peer-review model: Single blind

Peer-review report's scientific quality classification

Grade A (Excellent): 0
Grade B (Very good): B, B, B
Grade C (Good): C, C
Grade D (Fair): 0
Grade E (Poor): 0

P-Reviewer: Marusic M, Croatia; Nath L, India; Sato T, Japan

Received: December 30, 2021
Peer-review started: December 30, 2021
First decision: April 16, 2022
Revised: April 26, 2022
Accepted: June 23, 2022
Article in press: June 23, 2022
Published online: July 21, 2022

Yi Zhou, Jing Zheng, Cui Yang, Juan Peng, Ning Liu, Lin Yang, Xiao-Ming Zhang, Medical Imaging Key Laboratory of Sichuan Province, Department of Radiology, Medical Research Center, The Affiliated Hospital of North Sichuan Medical College, Nanchong 637000, Sichuan Province, China

Yi Zhou, Department of Radiology, People's Hospital of Deyang City, Deyang 618000, Sichuan Province, China

Cui Yang, Department of Radiology, Panzhihua Central Hospital, Panzhihua 617000, Sichuan Province, China

Juan Peng, Department of Radiology, Sichuan Provincial People's Hospital Jinniu Hospital, Chengdu Jinniu District People's Hospital, Chengdu 610007, Sichuan Province, China

Corresponding author: Lin Yang, MD, Professor, Medical Imaging Key Laboratory of Sichuan Province, Department of Radiology, Medical Research Center, The Affiliated Hospital of North Sichuan Medical College, No. 63 Wenhua Road, Nanchong 637000, Sichuan Province, China. linyangmd@163.com

Abstract

The morbidity and mortality of hepatocellular carcinoma (HCC) rank 6th and 4th, respectively, among malignant tumors worldwide. Traditional diffusion-weighted imaging (DWI) uses the apparent diffusion coefficient (ADC) obtained by applying the monoexponential model to reflect water molecule diffusion in active tissue; however, the value of ADC is affected by microcirculation perfusion. Using a biexponential model, intravoxel incoherent motion (IVIM)-DWI quantitatively measures information related to pure water molecule diffusion and microcirculation perfusion, thus compensating for the shortcomings of DWI. The number of studies examining the application of IVIM-DWI in patients with HCC has gradually increased over the last few years, and many results show that IVIM-DWI has vital value for HCC differentiation, pathological grading, and predicting and evaluating the treatment response. The present study principally reviews the principle of IVIM-DWI and its research progress in HCC differentiation, pathological grading, predicting and evaluating the treatment response, predicting postoperative recurrence and predicting gene expression prediction.

Key Words: Hepatocellular carcinoma; Intravoxel incoherent motion; Differentiation; Pathological grading; Treatment response; Gene expression

©The Author(s) 2022. Published by Baishideng Publishing Group Inc. All rights reserved.

Core Tip: Intravoxel incoherent motion (IVIM) diffusion-weighted imaging (DWI) quantitatively measures information related to pure water molecule diffusion and microcirculation perfusion using a biexponential model, thus compensating for the shortcomings of traditional DWI. The number of studies assessing IVIM-DWI in patients with hepatocellular carcinoma (HCC) has gradually increased over the last few years. This review, which is based on the literature, identified an imaging biomarker for HCC differentiation, pathological grading, predicting and evaluating the treatment response, predicting postoperative recurrence and predicting gene expression prediction. The results of this analysis show that IVIM-DWI has important value in the treatment and diagnosis of HCC.

Citation: Zhou Y, Zheng J, Yang C, Peng J, Liu N, Yang L, Zhang XM. Application of intravoxel incoherent motion diffusion-weighted imaging in hepatocellular carcinoma. *World J Gastroenterol* 2022; 28(27): 3334-3345
URL: https://www.wjgnet.com/1007-9327/full/v28/i27/3334.htm
DOI: https://dx.doi.org/10.3748/wjg.v28.i27.3334

INTRODUCTION

The morbidity and mortality of hepatocellular carcinoma (HCC) rank 6th and 4th, respectively, among malignant tumors worldwide[1,2]. The apparent diffusion coefficient (ADC) obtained using traditional diffusion-weighted imaging (DWI) reflects water molecule diffusion in tissue[3]. However, many studies have shown that a voxel contains other diffusion information in addition to the diffusion movement of pure water molecules, namely, the microcirculation perfusion of the capillary network in tissue[3-6]. One limitation of traditional DWI is that it is unable to distinguish water molecule diffusion and microcirculation perfusion information. Le Bihan *et al*[6,7] proposed that intravoxel incoherent motion (IVIM) quantitatively obtains information on both pure water molecule diffusion and diffusion related to microcirculation perfusion, thus compensating for the shortcoming of traditional DWI. Therefore, IVIM has become a research hotspot in recent years. The liver is suitable for IVIM research because of its relatively large blood supply. Since the first application of IVIM-DWI for the study of liver disease by Yamada *et al*[8], the number of studies assessing IVIM-DWI in patients with HCC has progressively increased, and significant progress has been achieved. This study mainly reviews IVIM-DWI research progress in the diagnosis and treatment of HCC.

THE BASIC PRINCIPLES OF IVIM-DWI

DWI is currently the only functional magnetic resonance imaging (MRI) technology that noninvasively measures water molecule diffusion in living tissue[3]. According to the theory of traditional DWI, the movement of free water molecules is considered to conform to a Gaussian distribution. However, due to the presence of complex cell structures and multiple diffusion barriers, such as cell membranes, in biological tissues, the diffusion behavior of water in biological tissues is more complicated. Therefore, the displacement of water in tissue may substantially deviate from a Gaussian distribution, challenging the validity of the monoexponential model to varying degrees. Additionally, the ADC, which reflects the water molecule diffusion, is affected simultaneously by microcirculation perfusion[3,5,7]. IVIM-DWI uses sufficient b values and biexponential models for the acquisition and analysis of images and distinguishes information regarding the pure tissue diffusion of water molecules and diffusion related to microcirculation perfusion. Among IVIM-DWI parameters, the simple diffusion coefficient, which is also referred to as the slow apparent diffusion coefficient (D), reflects the diffusion movement of pure water molecules in the tissue in a region of interest (ROI). The false diffusion coefficient, which is also called the fast apparent diffusion coefficient (D*), reflects diffusion movement related to microcirculation perfusion in the capillary network in an ROI. The fraction of the fast apparent diffusion coefficient (f) represents the volume ratio of the local microcirculation perfusion-related effect to the total diffusion effect, which may reflect the blood volume in an ROI. The formula for determining the relationship between IVIM-DWI signal attenuation and b values in tissue is as follows:

$S_b/S_0 = (1 - f) \times \exp(-bD) + f \times \exp[-b(D + D^*)]$

Where b is the diffusion sensitivity coefficient with units of s/mm^2, while the unit for both D and D* is mm^2/s, and S represents intravoxel signal intensity, with S_0 and S_b representing the signal intensities when b = 0 and b has other values, respectively. The b value determines the effect of microcirculation perfusion on DWI signal attenuation[6]. When the b value is low (b < 200 s/mm^2), the effect of microcir-

culation perfusion accounts for a large proportion of the total diffusion effect, whereas when the b value is high (b ≥ 200 s/mm^2), signal attenuation basically reflects only the pure water molecule diffusion in a voxel.

HCC DIFFERENTIATION

To date, many studies have shown that IVIM-DWI has important value in differentiating HCC from other liver lesions[8-22]. In theory, malignant tumors restrict the movement of water molecules to a significantly greater extent than benign tumors; thus, the ADC and D values of malignant tumors are lower than those of benign tumors[23]. Studies have confirmed that the ADC and D values of malignant liver lesions are remarkably lower than those of benign liver lesions and are useful to distinguish benign from malignant liver lesions, with the D value showing higher differentiation efficiency[8,10-15,17]. Yoon *et al*[14] conducted an IVIM study on 169 lesions in 142 patients. The values of ADC and D in malignant liver lesions [1.14 ± 0.24, 0.95 ± 0.21, (× 10^{-3} mm^2/s), respectively] were significantly lower than those in benign liver lesions (1.72 ± 0.37, 1.61 ± 0.34, (× 10^{-3} mm^2/s), respectively). The area under the receiver operating characteristic (ROC) curve (AUC) values for the ADC value and D value in differentiating liver malignancies and hypervascular malignancies were 0.933 and 0.971, respectively, and 0.919 and 0.961, respectively (all $P < 0.0005$).

However, research results for D* values and f values in differentiating benign and malignant liver nodules are inconsistent. A study by Ichikawa *et al*[16] showed that the D* value of malignant liver lesions was significantly lower than that of benign lesions, but no difference in f values was observed between benign and malignant lesions. A study by Luo *et al*[10] also revealed that the D* values of HCC were obviously lower than those of focal nodular hyperplasia, with no significant difference in the f value between the two groups. However, another study[11] by the same group showed that the f value in the malignant group was significantly lower than that in the benign group, and the D* value did not differ significantly between the two groups. The studies by Klauss *et al*[12] and Doblas *et al*[18] both showed no significant differences in the D* and f values between benign and malignant liver lesions and no significance in the values of D* and f in differentiating those two types of liver lesions. Recently, Podgórska *et al*[24] reported that the perfusion-diffusion ratio was more effective than IVIM-DWI parameters in differentiating solid benign and malignant primary liver lesions.

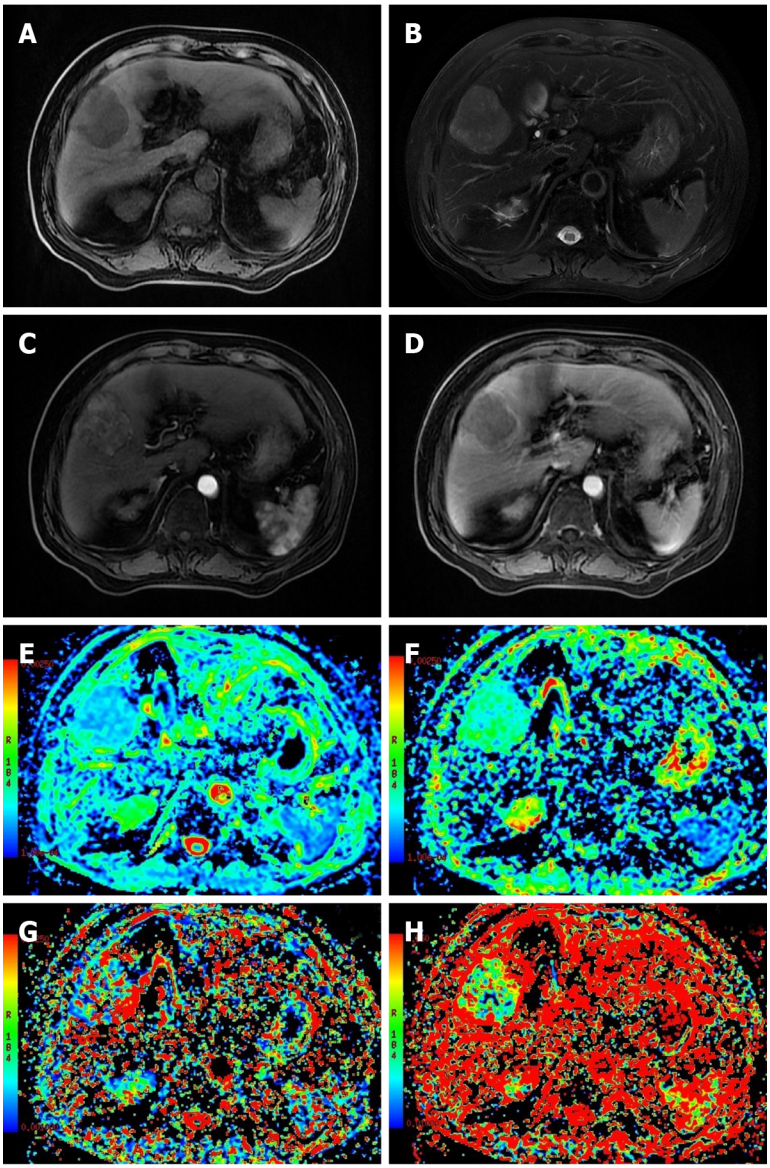
The inconsistencies in the results described above may be related to the following factors: (1) D* and f values not only reflect blood perfusion information but may also reflect other information, such as particle or gland excretion[10,15,25]; (2) the D* values of hepatic hemangioma with different blood supply types exhibit a range of fluctuation range[13]; and (3) interference from other factors, such as the b value distribution, ROI settings, and differences in tumor composition, may occur[16,23,26] (Figures 1 and 2).

Relatively few studies assessing the differentiation of malignant nodules with different pathological characteristics in the liver have been published. The few available studies have involved differentiating HCC from intrahepatic cholangiocarcinoma (ICC) and/or metastasis[9,27-29]. Our previous study[27] showed significantly lower ADC and D values for HCC than for ICC, a significantly higher D* value for HCC than for ICC, higher diagnostic efficiency for D* [AUC = 0.896], and no significant difference in f values between the two groups. According to other studies, ADC and D for HCC are obviously lower than those for ICC. However, the results for the IVIM-DWI parameters D* and f are not consistent. Choi *et al*[9] and Shao *et al*[28] reported that the f values of HCC were higher than those of ICC, while the D* values did not differ significantly between the two studied groups. Wei *et al*[29] did not document significant differences in either D* or f values between HCC and ICC groups.

The results of studies analyzing the differentiation between HCC and liver metastases differ substantially. Choi *et al*[9] found that the f value of HCC was significantly higher than that of liver metastases, but no significant differences were detected in other IVIM-DWI parameters. The study by Wu *et al*[30] indicated no obvious differences in the values of ADC, D, D*, and f for HCC from those for hepatic metastases, which may be due to changes in microcirculation and cell density caused by metastatic tumors of different origins. Dividing liver metastases into different subgroups according to different origins may be a more reasonable approach.

PREDICTION OF PATHOLOGICAL GRADING

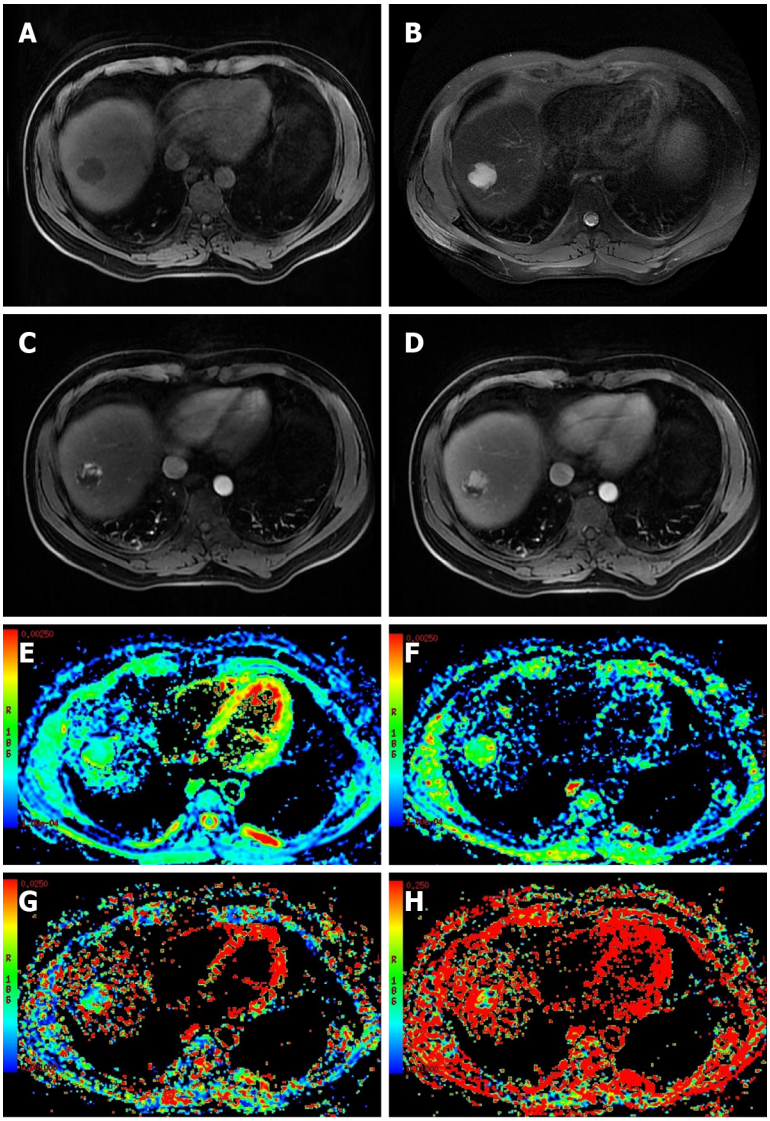
Preoperative prediction of the pathological grade of HCC has important value in formulating guidelines for individualized treatments. Studies have shown that IVIM helps predict the pathological grade of HCC before surgery[23,26,31-44]. A meta-analysis by Yang *et al*[32] included 16 studies (1428 cases of HCC) using IVIM-DWI for pathological grading and found that ADC and D values showed high accuracy for the pathological grading of noninvasive HCC and better differentiation efficiency for D values than for ADC values. The explanation for this result may be that a higher tumor pathological



DOI: 10.3748/wjg.v28.i27.3334 **Copyright** ©The Author(s) 2022.

Figure 1 Moderately differentiated hepatocellular carcinoma in an 85-year-old male. A 6.1-cm-sized mass in the right hepatic section shows hypointensity on unenhanced T1-weighted image, hyperintensity on unenhanced T2-weighted image, hyperenhancement in the image of the arterial phase, and wash-out in the image of the portal venous phase. A: Unenhanced T1-weighted image; B: Unenhanced T2-weighted image; C: Image of the arterial phase; D: Image of the portal venous phase; E: Image showing the apparent diffusion coefficient; F: Image showing D; G: Image showing D*; H: Image showing f.

grade indicates greater cellularity, a higher nuclear-to-cytoplasmic ratio, and a smaller extracellular space, resulting in more restricted water diffusion, which ultimately leads to lower ADC and D values [23,33,35]. A potential explanation for the superiority of D values compared to ADC values may be that D values theoretically avoid the effect of microcirculation perfusion information. The results for the correlation between D* and f values and pathological grading are inconsistent. In addition to reporting results for ADC and D values and tumor tissue grading consistent with those of previous studies, Li *et al* [36] used rat models and showed that the D* and f values of higher-grade lesions were higher than those of lower-grade lesions and that D* and f values were positively correlated with the tumor tissue grade. Sokmen *et al*[26] and Granata *et al*[38] found that f values were significantly correlated with the HCC pathological grade, while a significant correlation was not identified between D* values and the pathological grade. On the other hand, multiple studies by Zhu *et al*[23,33,35] showed that neither D* values nor f values were significantly correlated with the HCC pathological grade.



DOI: 10.3748/wjg.v28.i27.3334 **Copyright** ©The Author(s) 2022.

Figure 2 Hepatic hemangiomas in a 35-year-old male. A 3.0-cm-sized mass in the right hepatic section shows hypointensity on the unenhanced T1-weighted image, hyperintensity on the unenhanced T2-weighted image, peripheral globular enhancement in the image of the arterial phase and centripetal fill-in in the image of the portal venous phase. A: Unenhanced T1-weighted image; B: Unenhanced T2-weighted image; C: Image of the arterial phase; D: Image of the portal venous phase; E: Image showing the apparent diffusion coefficient; F: Image showing the D; G: Image showing the D*; H: Image showing the f.

PREDICTION AND EVALUATION OF TREATMENT RESPONSES

Locoregional therapy

IVIM-DWI accurately reflects microstructures and blood perfusion changes before and after tumor treatment and is particularly suitable for the prediction and evaluation of the responses to and efficacy of tumor locoregional therapy (LRT)[45]. Many researchers have investigated the value of IVIM-DWI in the prediction and evaluation of transarterial chemoembolization (TACE) efficacy in patients with HCC [46-52]. Park *et al*[50] reported that the preoperative D* value of HCC with better lipiodol deposition was markedly higher than that of HCC with poor lipiodol deposition, suggesting that the D* value may predict lipiodol deposition after TACE for patients with HCC. As shown in our previous study[46], the ADC and D values of HCC were obviously elevated four weeks after TACE treatment, the D* value was significantly reduced, and the f value did not change significantly.

Hectors *et al*[53] investigated the effect of yttrium 90 radioembolization on diffusion and perfusion in HCC. The authors performed multiparametric MRI including IVIM-DWI on 24 patients with HCC before (n = 24) and six weeks (n = 21) after radioembolization. The ADC and D values of HCC were significantly increased at six weeks after radioembolization (P < 0.0004), while the D* values were significantly reduced (P = 0.014), and no significant change was detected in f values (P = 0.765).

Server *et al*[54] administered LRT to 15 patients with HCC (11 patients underwent transarterial radioembolization, and four patients underwent TACE, and IVIM-DWI was performed before and eight

weeks after LRT). Their results indicated that the ADC and D values obtained after LRT were significantly higher than those recorded before treatment, but the f values were significantly lower than those recorded before LRT. In the responder group, the ADC and D values were significantly increased, and the f values were significantly reduced after LRT. No significant differences were detected in the nonresponder group. Based on these findings, IVIM effectively predicts and evaluates the response to and efficacy of LRT. In these studies, the potential explanation for the inconsistency in the blood perfusion parameters D* and f may be that they represent different types of perfusion in various aspects, with the former usually reflecting the blood flow rate in capillaries and the latter mainly reflecting blood volume (Table 1).

Systemic therapy

Changes in volume are often not obvious in the early stage of targeted therapy for HCC. Compared to traditional imaging methods, IVIM-DWI has more advantages in the early evaluation of the HCC response to targeted therapy[55-59]. Wagner *et al*[56] revealed that the D value of viable tumor regions in malignant liver tumors was significantly lower than that of necrotic tumor tissue but higher than that of fibrotic tumor regions. Joo *et al*[55] used IVIM-DWI to evaluate the efficacy of the vascular blocker CKD-516 against rabbit VX2 liver tumors and found that the D* and f values of the treatment group were noticeably reduced at four hours. Based on these studies, IVIM-DWI is useful to assess early responses to tumor vascular blockers[56]. Yang *et al*[57] investigated the values of IVIM-DWI in evaluating the response of 35 nude mice with HCC to sorafenib. Compared to the values recorded at baseline and in the control group, the ADC and D values of the treatment group at each time point were significantly higher, while the f value was significantly decreased at 7 d and increased at 21 d. The values of ADC, D, and f were significantly correlated with the necrotic fraction. Lewin *et al*[58] used IVIM parameters to evaluate the efficacy of sorafenib treatment in patients with advanced HCC. The f values of responder patients were obviously increased at two weeks and two months after treatment, while these values decreased in nonresponder patients. Therefore, the authors propose that the f value is useful as a reliable marker to evaluate sorafenib treatment efficacy in patients with advanced HCC. Shirota *et al*[59] used IVIM-DWI to evaluate the responses of patients with HCC undergoing sorafenib treatment and found that the D value at baseline was significantly higher in the responder group than in the nonresponder group. The sensitivity and specificity of the D value for evaluating the treatment response were 100% and 67%, respectively (Table 2).

Immunotherapy for HCC is an emerging method with promising results; it exerts an antitumor effect without affecting tumor size. Functional imaging methods will play an important role in evaluating the response to immunotherapy. Andersson *et al*[60] evaluated the response of patients with HCC to intratumoral injections of the immune primer ilixadencel using IVIM-DWI and a histogram analysis. Seventeen patients with HCC were enrolled in this study. Their results showed that the 10th percentile of D* decreased significantly after treatment to baseline, and significant correlations were identified between the 10th percentile and median D value. Chen *et al*[61] reported that both pretreatment IVIM-DWI and DCE-MRI parameters, especially ADC and slope, may predict progression-free survival and overall survival in patients with HCC receiving lenalidomide (a dual antiangiogenic and immunomodulatory agent) as second-line therapy. Recently, the application of immune checkpoint inhibitors in tumors has become a new research hotspot. Subsequently, IVIM-DWI will inevitably play a valuable role in predicting the response to and evaluating the efficacy of tumor immunotherapy.

PREDICTION OF POSTOPERATIVE RECURRENCE

Some researchers have reported the value of IVIM-DWI in predicting recurrence and prognosis after the surgical resection of HCC. Microvascular invasion (MVI) is one of the main factors affecting postoperative recurrence or survival among patients with HCC. IVIM-DWI predicts HCC MVI prior to surgery[62]. Wei *et al*[63] prospectively studied the predictive value of preoperative IVIM-DWI and conventional imaging characteristics for MVI. The results of the univariate analysis showed that the characteristics that were significantly correlated with HCC MVI were decreased ADC values, decreased D values, and irregular circumferential enhancement. In the multivariate analysis, only the D value was an independent risk factor for HCC MVI (the AUC was 0.815). Zhao *et al*[64] and Li *et al*[65] reported similar results. Zhang *et al*[66] studied 157 patients undergoing HCC resection and found that D values might serve as a marker for predicting HCC recurrence after hepatectomy and that the predictive capability would be improved if it was combined with age and the alpha-fetoprotein level.

PREDICTING GENE EXPRESSION

Recently, some studies have indicated that IVIM-DWI predicts gene expression in patients with HCC [67-69]. We recently investigated the correlations of HCC IVIM-DWI parameters with angiopoietin-2

Table 1 Summary of locoregional therapy studies

Ref.	Country	Subject number	Key findings
Juan *et al* [46], 2019	China	20	After TACE, the ADC and Dslow values of HCC increased significantly, and the value of Dfast decreased significantly; the f value did not change markedly.
Wu *et al* [47], 2019	China	55	Compared with nonresponders, the mean, median, and 25th percentile of the PF, ADC, and ADCtotal were higher in responders, while the skewness and kurtosis of PF, kurtosis of ADC and ADCtotal were lower
Lin *et al* [48], 2016	China	118	Before TACE, significant differences in ADC, Dslow and Dfast were observed between the effective and ineffective groups. After TACE, the effective group exhibited lower Dfast and higher ADC and Dslow values than the ineffective group. The tumor regression rate was negatively correlated with Dfast but positively correlated with ADC and Dslow
Park *et al* [50], 2014	Korea	44	The preoperative D* value was significantly increased in the good lipiodol uptake group compared with the poor uptake group after TACE, while the ADC, D, and f values were not significantly different between these two groups
Jia F *et al* [51], 2020	China	56	ROC curve analyses revealed that the combined model including APT SIs and D values was better able to predict the tumor response to TACE than the individual parameters
Wu L *et al* [52], 2017	China	30	The ADCtotal ratio and D ratio measured 24-48 h after TACE were independent predictors of the response to TACE of patients with HCC and showed stronger associations with PFS than mRECIST criteria
Hectors *et al*[53], 2020	United States	24	The ADC and D values of HCC were significantly increased at six weeks after radioembolization, while the D* values were significantly reduced, with no significant change in f values
Server *et al* [54], 2019	Turkey	15	The ADC and D values after LRT were significantly higher than those measured before treatment, while the f values were significantly lower than those recorded before LRT. In the responder group, the ADC and D values were significantly increased after LRT, whereas the f values were significantly reduced

TACE: Transarterial chemoembolization; ADC: Apparent diffusion coefficient; HCC: Hepatocellular carcinoma; PF: Perfusion fraction; ROC: Receiver operating characteristic; APT: Amide proton transfer; SIs: Signal intensities; PFS: Progression-free survival; LRT: Locoregional therapy.

Table 2 Summary of systemic therapy studies

Ref.	Country	Subject number	Key findings
Joo *et al*[55], 2014	Korea	21	The D* and f values of the treatment group were significantly decreased at four hours. The sizes of the decreases in f and fD* at four hours were negatively correlated with the tumor size at 7 d of follow-up
Wagner *et al* [56], 2012	France	48	The D values of viable tumor regions in malignant liver tumors were significantly lower than those of necrotic tumor tissue but higher than those of fibrotic tumor regions
Yang *et al* [57], 2017	China	35	Compared with the values at baseline and those recorded in the control group, the ADC and D values in the treatment group were significantly higher at each time point, whereas the f values decreased significantly at 7 d and increased at 21 d
Lewin *et al* [58], 2011	France	12	The f values increased significantly in responder patients at two weeks and two months after treatment but decreased in nonresponder patients. The f value was useful as a reliable marker to evaluate sorafenib treatment efficacy in patients with advanced HCC
Shirota *et al* [59], 2016	Japan	9	The D values at baseline were significantly higher in the responder group than in the nonresponder group. The sensitivity and specificity of the D values for evaluating treatment response were 100% and 67%, respectively

ADC: Apparent diffusion coefficient; HCC: Hepatocellular carcinoma.

(Ang-2) and transketolase (TKT) expression[67]. We observed significantly higher D* and f values in the high Ang-2 expression group than in the low Ang-2 expression group, and the values of D* and f were positively correlated with the Ang-2 expression levels . On the other hand, the ADC and D values of the TKT high expression group were significantly lower than those of the TKT low expression group, and the ADC and D values were negatively correlated with TKT expression. Based on this result, IVIM-DWI noninvasively predicts Ang-2 and TKT expression in HCC before surgery. Shi *et al*[68] performed IVIM-DWI of 52 patients with HCC and identified four IVIM-derived histogram metrics with the capability for differentiating Ki67 expression, with *P* values less than 0.05. By establishing a diagnostic model based on a logistic regression model, the AUC value for diagnosing high Ki67 expression was 0.861. The results of this study suggest that the histogram indicators obtained from IVIM-DWI scanning can accurately predict the Ki67 expression status.

CONCLUSION

IVIM-DWI accurately and precisely reflects tissue structures and pathophysiological changes and has important application value for HCC differentiation, pathological grading, and predicting and evaluating the treatment response. However, the factors affecting IVIM-DWI measurement results are complicated and diverse[8,20,25,70-76]. Factors including the number, distribution, and fitting methods of b values, other physiological activities (such as gland secretion and flow), ROI settings, scanning devices and field strength, imaging acquisition methods, and motion artifacts all affect data quality[23,25,34,41]. Increased standardization of data acquisition and analysis is imperative to facilitate the generation of reliable IVIM-DWI biomarker measures that are broadly applicable[74,77,78]. In addition, recent studies have shown that IVIM-DWI modeling of the perfusion component is constrained by the diffusion component, and a reduced D slow measure leads to artificially higher PF and D fast measures [75,76]. These results should also be considered in the design of future IVIM-DWI studies. We postulate that with advances in imaging technology and further in-depth research, IVIM-DWI will certainly play a more prominent role in the diagnosis and treatment of HCC.

FOOTNOTES

Author contributions: Zhou Y wrote the paper; Zheng J, Yang C, Peng J and Liu N collected the data; Yang L revised the paper; Zhang XM designed the research project.

Supported by the Project of Department of Science and Technology of Sichuan Province, No. 2016JY0105; Project of Medical Association of Sichuan Province, No. S20070; and the Project of City-University Science and Technology Strategic Cooperation of Nanchong City (North Sichuan Medical College), No. 20SXQT0324.

Conflict-of-interest statement: The authors have no conflicts of interest related to this article to declare.

Open-Access: This article is an open-access article that was selected by an in-house editor and fully peer-reviewed by external reviewers. It is distributed in accordance with the Creative Commons Attribution NonCommercial (CC BY-NC 4.0) license, which permits others to distribute, remix, adapt, build upon this work non-commercially, and license their derivative works on different terms, provided the original work is properly cited and the use is non-commercial. See: https://creativecommons.org/Licenses/by-nc/4.0/

Country/Territory of origin: China

ORCID number: Yi Zhou 0000-0002-1911-5380; Jing Zheng 0000-0002-2031-0845; Cui Yang 0000-0001-6751-9075; Juan Peng 0000-0002-7961-3533; Ning Liu 0000-0003-3587-5440; Lin Yang 0000-0001-8746-9255; Xiao-Ming Zhang 0000-0001-5327-8506.

S-Editor: Zhang H
L-Editor: A
P-Editor: Zhang H

REFERENCES

1 **Yang JD**, Hainaut P, Gores GJ, Amadou A, Plymoth A, Roberts LR. A global view of hepatocellular carcinoma: trends, risk, prevention and management. *Nat Rev Gastroenterol Hepatol* 2019; **16**: 589-604 [PMID: 31439937 DOI: 10.1038/s41575-019-0186-y]

2 **Global Burden of Disease Cancer Collaboration**, Fitzmaurice C, Allen C, Barber RM, Barregard L, Bhutta ZA, Brenner H, Dicker DJ, Chimed-Orchir O, Dandona R, Dandona L, Fleming T, Forouzanfar MH, Hancock J, Hay RJ, Hunter-Merrill R, Huynh C, Hosgood HD, Johnson CO, Jonas JB, Khubchandani J, Kumar GA, Kutz M, Lan Q, Larson HJ, Liang X, Lim SS, Lopez AD, MacIntyre MF, Marczak L, Marquez N, Mokdad AH, Pinho C, Pourmalek F, Salomon JA, Sanabria JR, Sandar L, Sartorius B, Schwartz SM, Shackelford KA, Shibuya K, Stanaway J, Steiner C, Sun J, Takahashi K, Vollset SE, Vos T, Wagner JA, Wang H, Westerman R, Zeeb H, Zoeckler L, Abd-Allah F, Ahmed MB, Alabed S, Alam NK, Aldhahri SF, Alem G, Alemayohu MA, Ali R, Al-Raddadi R, Amare A, Amoako Y, Artaman A, Asayesh H, Atnafu N, Awasthi A, Saleem HB, Barac A, Bedi N, Bensenor I, Berhane A, Bernabé E, Betsu B, Binagwaho A, Boneya D, Campos-Nonato I, Castañeda-Orjuela C, Catalá-López F, Chiang P, Chibueze C, Chitheer A, Choi JY, Cowie B, Damtew S, das Neves J, Dey S, Dharmaratne S, Dhillon P, Ding E, Driscoll T, Ekwueme D, Endries AY, Farvid M, Farzadfar F, Fernandes J, Fischer F, G/Hiwot TT, Gebru A, Gopalani S, Hailu A, Horino M, Horita N, Husseini A, Huybrechts I, Inoue M, Islami F, Jakovljevic M, James S, Javanbakht M, Jee SH, Kasaeian A, Kedir MS, Khader YS, Khang YH, Kim D, Leigh J, Linn S, Lunevicius R, El Razek HMA, Malekzadeh R, Malta DC, Marcenes W, Markos D, Melaku YA, Meles KG, Mendoza W, Mengiste DT, Meretoja TJ, Miller TR, Mohammad KA, Mohammadi A, Mohammed S, Moradi-Lakeh M, Nagel G, Nand D, Le Nguyen Q, Nolte S, Ogbo FA, Oladimeji KE, Oren E, Pa M, Park EK, Pereira DM, Plass D, Qorbani M, Radfar A, Rafay A, Rahman M, Rana SM, Søreide K, Satpathy M, Sawhney M, Sepanlou SG, Shaikh MA, She J, Shiue I, Shore HR, Shrime

MG, So S, Soneji S, Stathopoulou V, Stroumpoulis K, Sufiyan MB, Sykes BL, Tabarés-Seisdedos R, Tadese F, Tedla BA, Tessema GA, Thakur JS, Tran BX, Ukwaja KN, Uzochukwu BSC, Vlassov VV, Weiderpass E, Wubshet Terefe M, Yebyo HG, Yimam HH, Yonemoto N, Younis MZ, Yu C, Zaidi Z, Zaki MES, Zenebe ZM, Murray CJL, Naghavi M. Global, Regional, and National Cancer Incidence, Mortality, Years of Life Lost, Years Lived With Disability, and Disability-Adjusted Life-years for 32 Cancer Groups, 1990 to 2015: A Systematic Analysis for the Global Burden of Disease Study. *JAMA Oncol* 2017; **3**: 524-548 [PMID: 27918777 DOI: 10.1001/jamaoncol.2016.5688]

3 **Taouli B**, Koh DM. Diffusion-weighted MR imaging of the liver. *Radiology* 2010; **254**: 47-66 [PMID: 20032142 DOI: 10.1148/radiol.09090021]

4 **Lewis S**, Dyvorne H, Cui Y, Taouli B. Diffusion-weighted imaging of the liver: techniques and applications. *Magn Reson Imaging Clin N Am* 2014; **22**: 373-395 [PMID: 25086935 DOI: 10.1016/j.mric.2014.04.009]

5 **Bammer R**. Basic principles of diffusion-weighted imaging. *Eur J Radiol* 2003; **45**: 169-184 [PMID: 12595101 DOI: 10.1016/s0720-048x(02)00303-0]

6 **Le Bihan D**, Breton E, Lallemand D, Aubin ML, Vignaud J, Laval-Jeantet M. Separation of diffusion and perfusion in intravoxel incoherent motion MR imaging. *Radiology* 1988; **168**: 497-505 [PMID: 3393671 DOI: 10.1148/radiology.168.2.3393671]

7 **Le Bihan D**, Breton E, Lallemand D, Grenier P, Cabanis E, Laval-Jeantet M. MR imaging of intravoxel incoherent motions: application to diffusion and perfusion in neurologic disorders. *Radiology* 1986; **161**: 401-407 [PMID: 3763909 DOI: 10.1148/radiology.161.2.3763909]

8 **Yamada I**, Aung W, Himeno Y, Nakagawa T, Shibuya H. Diffusion coefficients in abdominal organs and hepatic lesions: evaluation with intravoxel incoherent motion echo-planar MR imaging. *Radiology* 1999; **210**: 617-623 [PMID: 10207458 DOI: 10.1148/radiology.210.3.r99fe17617]

9 **Choi IY**, Lee SS, Sung YS, Cheong H, Lee H, Byun JH, Kim SY, Lee SJ, Shin YM, Lee MG. Intravoxel incoherent motion diffusion-weighted imaging for characterizing focal hepatic lesions: Correlation with lesion enhancement. *J Magn Reson Imaging* 2017; **45**: 1589-1598 [PMID: 27664970 DOI: 10.1002/jmri.25492]

10 **Luo M**, Zhang L, Jiang XH, Zhang WD. Intravoxel incoherent motion: application in differentiation of hepatocellular carcinoma and focal nodular hyperplasia. *Diagn Interv Radiol* 2017; **23**: 263-271 [PMID: 28703102 DOI: 10.5152/dir.2017.16595]

11 **Luo M**, Zhang L, Jiang XH, Zhang WD. Intravoxel Incoherent Motion Diffusion-weighted Imaging: Evaluation of the Differentiation of Solid Hepatic Lesions. *Transl Oncol* 2017; **10**: 831-838 [PMID: 28866259 DOI: 10.1016/j.tranon.2017.08.003]

12 **Klauss M**, Mayer P, Maier-Hein K, Laun FB, Mehrabi A, Kauczor HU, Stieltjes B. IVIM-diffusion-MRI for the differentiation of solid benign and malign hypervascular liver lesions-Evaluation with two different MR scanners. *Eur J Radiol* 2016; **85**: 1289-1294 [PMID: 27235876 DOI: 10.1016/j.ejrad.2016.04.011]

13 **Zhu L**, Cheng Q, Luo W, Bao L, Guo G. A comparative study of apparent diffusion coefficient and intravoxel incoherent motion-derived parameters for the characterization of common solid hepatic tumors. *Acta Radiol* 2015; **56**: 1411-1418 [PMID: 25422515 DOI: 10.1177/0284185114559426]

14 **Yoon JH**, Lee JM, Yu MH, Kiefer B, Han JK, Choi BI. Evaluation of hepatic focal lesions using diffusion-weighted MR imaging: comparison of apparent diffusion coefficient and intravoxel incoherent motion-derived parameters. *J Magn Reson Imaging* 2014; **39**: 276-285 [PMID: 23633178 DOI: 10.1002/jmri.24158]

15 **Watanabe H**, Kanematsu M, Goshima S, Kajita K, Kawada H, Noda Y, Tatahashi Y, Kawai N, Kondo H, Moriyama N. Characterizing focal hepatic lesions by free-breathing intravoxel incoherent motion MRI at 3.0 T. *Acta Radiol* 2014; **55**: 1166-1173 [PMID: 24316660 DOI: 10.1177/0284185113514966]

16 **Ichikawa S**, Motosugi U, Ichikawa T, Sano K, Morisaka H, Araki T. Intravoxel incoherent motion imaging of focal hepatic lesions. *J Magn Reson Imaging* 2013; **37**: 1371-1376 [PMID: 23172819 DOI: 10.1002/jmri.23930]

17 **Penner AH**, Sprinkart AM, Kukuk GM, Gütgemann I, Gieseke J, Schild HH, Willinek WA, Mürtz P. Intravoxel incoherent motion model-based liver lesion characterisation from three b-value diffusion-weighted MRI. *Eur Radiol* 2013; **23**: 2773-2783 [PMID: 23666233 DOI: 10.1007/s00330-013-2869-z]

18 **Doblas S**, Wagner M, Leitao HS, Daire JL, Sinkus R, Vilgrain V, Van Beers BE. Determination of malignancy and characterization of hepatic tumor type with diffusion-weighted magnetic resonance imaging: comparison of apparent diffusion coefficient and intravoxel incoherent motion-derived measurements. *Invest Radiol* 2013; **48**: 722-728 [PMID: 23669588 DOI: 10.1097/RLI.0b013e3182915912]

19 **Regini F**, Colagrande S, Mazzoni LN, Busoni S, Matteuzzi B, Santini P, Wyttenbach R. Assessment of Liver Perfusion by IntraVoxel Incoherent Motion (IVIM) Magnetic Resonance-Diffusion-Weighted Imaging: Correlation With Phase-Contrast Portal Venous Flow Measurements. *J Comput Assist Tomogr* 2015; **39**: 365-372 [PMID: 25700227 DOI: 10.1097/RCT.0000000000000220]

20 **Dyvorne H**, Jajamovich G, Kakite S, Kuehn B, Taouli B. Intravoxel incoherent motion diffusion imaging of the liver: optimal b-value subsampling and impact on parameter precision and reproducibility. *Eur J Radiol* 2014; **83**: 2109-2113 [PMID: 25277521 DOI: 10.1016/j.ejrad.2014.09.003]

21 **Ai Z**, Han Q, Huang Z, Wu J, Xiang Z. The value of multiparametric histogram features based on intravoxel incoherent motion diffusion-weighted imaging (IVIM-DWI) for the differential diagnosis of liver lesions. *Ann Transl Med* 2020; **8**: 1128 [PMID: 33240977 DOI: 10.21037/atm-20-5109]

22 **Granata V**, Fusco R, Amato DM, Albino V, Patrone R, Izzo F, Petrillo A. Beyond the vascular profile: conventional DWI, IVIM and kurtosis in the assessment of hepatocellular carcinoma. *Eur Rev Med Pharmacol Sci* 2020; **24**: 7284-7293 [PMID: 32706066 DOI: 10.26355/eurrev_202007_21883]

23 **Woo S**, Lee JM, Yoon JH, Joo I, Han JK, Choi BI. Intravoxel incoherent motion diffusion-weighted MR imaging of hepatocellular carcinoma: correlation with enhancement degree and histologic grade. *Radiology* 2014; **270**: 758-767 [PMID: 24475811 DOI: 10.1148/radiol.13130444]

24 **Podgórska J**, Pasicz K, Skrzyński W, Gołębiewski B, Kuś P, Jasieniak J, Kiliszczyk A, Rogowska A, Benkert T, Pałucki J, Grabska I, Fabiszewska E, Jagielska B, Kukołowicz P, Cieszanowski A. Perfusion-Diffusion Ratio: A New IVIM Approach

in Differentiating Solid Benign and Malignant Primary Lesions of the Liver. *Biomed Res Int* 2022; **2022**: 2957759 [PMID: 35075424 DOI: 10.1155/2022/2957759]

25 **Kakite S**, Dyvorne H, Besa C, Cooper N, Facciuto M, Donnerhack C, Taouli B. Hepatocellular carcinoma: short-term reproducibility of apparent diffusion coefficient and intravoxel incoherent motion parameters at 3.0T. *J Magn Reson Imaging* 2015; **41**: 149-156 [PMID: 24415565 DOI: 10.1002/jmri.24538]

26 **Sokmen BK**, Sabet S, Oz A, Server S, Namal E, Dayangac M, Dogusoy GB, Tokat Y, Inan N. Value of Intravoxel Incoherent Motion for Hepatocellular Carcinoma Grading. *Transplant Proc* 2019; **51**: 1861-1866 [PMID: 31399170 DOI: 10.1016/j.transproceed.2019.02.027]

27 **Peng J**, Zheng J, Yang C, Wang R, Zhou Y, Tao YY, Gong XQ, Wang WC, Zhang XM, Yang L. Intravoxel incoherent motion diffusion-weighted imaging to differentiate hepatocellular carcinoma from intrahepatic cholangiocarcinoma. *Sci Rep* 2020; **10**: 7717 [PMID: 32382050 DOI: 10.1038/s41598-020-64804-9]

28 **Shao S**, Shan Q, Zheng N, Wang B, Wang J. Role of Intravoxel Incoherent Motion in Discriminating Hepatitis B Virus-Related Intrahepatic Mass-Forming Cholangiocarcinoma from Hepatocellular Carcinoma Based on Liver Imaging Reporting and Data System v2018. *Cancer Biother Radiopharm* 2019; **34**: 511-518 [PMID: 31314589 DOI: 10.1089/cbr.2019.2799]

29 **Wei Y**, Gao F, Zheng D, Huang Z, Wang M, Hu F, Chen C, Duan T, Chen J, Cao L, Song B. Intrahepatic cholangiocarcinoma in the setting of HBV-related cirrhosis: Differentiation with hepatocellular carcinoma by using Intravoxel incoherent motion diffusion-weighted MR imaging. *Oncotarget* 2018; **9**: 7975-7983 [PMID: 29487707 DOI: 10.18632/oncotarget.23807]

30 **Wu H**, Liang Y, Jiang X, Wei X, Liu Y, Liu W, Guo Y, Tang W. Meta-analysis of intravoxel incoherent motion magnetic resonance imaging in differentiating focal lesions of the liver. *Medicine (Baltimore)* 2018; **97**: e12071 [PMID: 30142864 DOI: 10.1097/MD.0000000000012071]

31 **Shan Q**, Kuang S, Zhang Y, He B, Wu J, Zhang T, Wang J. A comparative study of monoexponential versus biexponential models of diffusion-weighted imaging in differentiating histologic grades of hepatitis B virus-related hepatocellular carcinoma. *Abdom Radiol (NY)* 2020; **45**: 90-100 [PMID: 31595327 DOI: 10.1007/s00261-019-02253-3]

32 **Yang D**, She H, Wang X, Yang Z, Wang Z. Diagnostic accuracy of quantitative diffusion parameters in the pathological grading of hepatocellular carcinoma: A meta-analysis. *J Magn Reson Imaging* 2020; **51**: 1581-1593 [PMID: 31654537 DOI: 10.1002/jmri.26963]

33 **Wei Y**, Gao F, Wang M, Huang Z, Tang H, Li J, Wang Y, Zhang T, Wei X, Zheng D, Song B. Intravoxel incoherent motion diffusion-weighted imaging for assessment of histologic grade of hepatocellular carcinoma: comparison of three methods for positioning region of interest. *Eur Radiol* 2019; **29**: 535-544 [PMID: 30027411 DOI: 10.1007/s00330-018-5638-1]

34 **Ichikawa S**, Motosugi U, Hernando D, Morisaka H, Enomoto N, Matsuda M, Onishi H. Histological Grading of Hepatocellular Carcinomas with Intravoxel Incoherent Motion Diffusion-weighted Imaging: Inconsistent Results Depending on the Fitting Method. *Magn Reson Med Sci* 2018; **17**: 168-173 [PMID: 28819085 DOI: 10.2463/mrms.mp.2017-0047]

35 **Zhu SC**, Liu YH, Wei Y, Li LL, Dou SW, Sun TY, Shi DP. Intravoxel incoherent motion diffusion-weighted magnetic resonance imaging for predicting histological grade of hepatocellular carcinoma: Comparison with conventional diffusion-weighted imaging. *World J Gastroenterol* 2018; **24**: 929-940 [PMID: 29491686 DOI: 10.3748/wjg.v24.i8.929]

36 **Li M**, Zheng XJ, Huang ZX, Song B. [Predicting Histological Grade of HCC in Rats using Intravoxel Incoherent Motion Imaging]. *Sichuan Da Xue Xue Bao Yi Xue Ban* 2018; **49**: 243-247 [PMID: 29737069]

37 **Shan Q**, Chen J, Zhang T, Yan R, Wu J, Shu Y, Kang Z, He B, Zhang Z, Wang J. Evaluating histologic differentiation of hepatitis B virus-related hepatocellular carcinoma using intravoxel incoherent motion and AFP levels alone and in combination. *Abdom Radiol (NY)* 2017; **42**: 2079-2088 [PMID: 28337521 DOI: 10.1007/s00261-017-1107-6]

38 **Granata V**, Fusco R, Catalano O, Guarino B, Granata F, Tatangelo F, Avallone A, Piccirillo M, Palaia R, Izzo F, Petrillo A. Intravoxel incoherent motion (IVIM) in diffusion-weighted imaging (DWI) for Hepatocellular carcinoma: correlation with histologic grade. *Oncotarget* 2016; **7**: 79357-79364 [PMID: 27764817 DOI: 10.18632/oncotarget.12689]

39 **Nakanishi M**, Chuma M, Hige S, Omatsu T, Yokoo H, Nakanishi K, Kamiyama T, Kubota K, Haga H, Matsuno Y, Onodera Y, Kato M, Asaka M. Relationship between diffusion-weighted magnetic resonance imaging and histological tumor grading of hepatocellular carcinoma. *Ann Surg Oncol* 2012; **19**: 1302-1309 [PMID: 21927976 DOI: 10.1245/s10434-011-2066-8]

40 **Koh DM**, Collins DJ, Orton MR. Intravoxel incoherent motion in body diffusion-weighted MRI: reality and challenges. *AJR Am J Roentgenol* 2011; **196**: 1351-1361 [PMID: 21606299 DOI: 10.2214/AJR.10.5515]

41 **Granata V**, Fusco R, Filice S, Catalano O, Piccirillo M, Palaia R, Izzo F, Petrillo A. The current role and future prospectives of functional parameters by diffusion weighted imaging in the assessment of histologic grade of HCC. *Infect Agent Cancer* 2018; **13**: 23 [PMID: 29988667 DOI: 10.1186/s13027-018-0194-5]

42 **Wu B**, Jia F, Li X, Li L, Wang K, Han D. Comparative Study of Amide Proton Transfer Imaging and Intravoxel Incoherent Motion Imaging for Predicting Histologic Grade of Hepatocellular Carcinoma. *Front Oncol* 2020; **10**: 562049 [PMID: 33194630 DOI: 10.3389/fonc.2020.562049]

43 **Zhou Y**, Yang G, Gong XQ, Tao YY, Wang R, Zheng J, Yang C, Peng J, Yang L, Li JD, Zhang XM. A study of the correlations between IVIM-DWI parameters and the histologic differentiation of hepatocellular carcinoma. *Sci Rep* 2021; **11**: 10392 [PMID: 34001962 DOI: 10.1038/s41598-021-89784-2]

44 **Song Q**, Guo Y, Yao X, Rao S, Qian C, Ye D, Zeng M. Comparative study of evaluating the microcirculatory function status of primary small HCC between the CE (DCE-MRI) and Non-CE (IVIM-DWI) MR Perfusion Imaging. *Abdom Radiol (NY)* 2021; **46**: 2575-2583 [PMID: 33483778 DOI: 10.1007/s00261-020-02945-1]

45 **Hussein RS**, Tantawy W, Abbas YA. MRI assessment of hepatocellular carcinoma after locoregional therapy. *Insights Imaging* 2019; **10**: 8 [PMID: 30694398 DOI: 10.1186/s13244-019-0690-1]

46 **Peng J**, Yang C, Zheng J, Wang R, Zhou Y, Wang WC, Yang L, Zhang XM, Miao ND, Ren YJ, Xu H and Min XL. Intravoxel Incoherent Motion Diffusion Weighted Imaging for the Therapeutic Response of Transarterial

Chemoembolization for Hepatocellular Carcinoma. *J Cancer Ther* 2019; **10**: 591-601 [DOI: 10.4236/jct.2019.107048]

47 **Wu LF**, Rao SX, Xu PJ, Yang L, Chen CZ, Liu H, Huang JF, Fu CX, Halim A, Zeng MS. Pre-TACE kurtosis of ADC_{total} derived from histogram analysis for diffusion-weighted imaging is the best independent predictor of prognosis in hepatocellular carcinoma. *Eur Radiol* 2019; **29**: 213-223 [PMID: 29922932 DOI: 10.1007/s00330-018-5482-3]

48 **Lin M**, Tian MM, Zhang WP, Xu L, Jin P. Predictive values of diffusion-weighted imaging and perfusion-weighted imaging in evaluating the efficacy of transcatheter arterial chemoembolization for hepatocellular carcinoma. *Onco Targets Ther* 2016; **9**: 7029-7037 [PMID: 27895495 DOI: 10.2147/OTT.S112555]

49 **Yang K**, Zhang XM, Yang L, Xu H, Peng J. Advanced imaging techniques in the therapeutic response of transarterial chemoembolization for hepatocellular carcinoma. *World J Gastroenterol* 2016; **22**: 4835-4847 [PMID: 27239110 DOI: 10.3748/wjg.v22.i20.4835]

50 **Park YS**, Lee CH, Kim JH, Kim IS, Kiefer B, Seo TS, Kim KA, Park CM. Using intravoxel incoherent motion (IVIM) MR imaging to predict lipiodol uptake in patients with hepatocellular carcinoma following transcatheter arterial chemoembolization: a preliminary result. *Magn Reson Imaging* 2014; **32**: 638-646 [PMID: 24703575 DOI: 10.1016/j.mri.2014.03.003]

51 **Jia F**, Wu B, Yan R, Li L, Wang K, Han D. Prediction Model for Intermediate-Stage Hepatocellular Carcinoma Response to Transarterial Chemoembolization. *J Magn Reson Imaging* 2020; **52**: 1657-1667 [PMID: 32424881 DOI: 10.1002/jmri.27189]

52 **Wu L**, Xu P, Rao S, Yang L, Chen C, Liu H, Fu C, Zeng M. ADC_{total} ratio and D ratio derived from intravoxel incoherent motion early after TACE are independent predictors for survival in hepatocellular carcinoma. *J Magn Reson Imaging* 2017; **46**: 820-830 [PMID: 28276105 DOI: 10.1002/jmri.25617]

53 **Hectors SJ**, Lewis S, Kennedy P, Bane O, Said D, Segall M, Schwartz M, Kim E, Taouli B. Assessment of Hepatocellular Carcinoma Response to ^{90}Y Radioembolization Using Dynamic Contrast Material-enhanced MRI and Intravoxel Incoherent Motion Diffusion-weighted Imaging. *Radiol Imaging Cancer* 2020; **2**: e190094 [PMID: 32803165 DOI: 10.1148/rycan.2020190094]

54 **Server S**, Sabet S, Bilgin R, Inan N, Yuzer Y, Tokat Y. Intravoxel Incoherent Motion Parameters for Assessing the Efficiency of Locoregional Bridging Treatments before Liver Transplantation. *Transplant Proc* 2019; **51**: 2391-2396 [PMID: 31474296 DOI: 10.1016/j.transproceed.2019.01.161]

55 **Joo I**, Lee JM, Han JK, Choi BI. Intravoxel incoherent motion diffusion-weighted MR imaging for monitoring the therapeutic efficacy of the vascular disrupting agent CKD-516 in rabbit VX2 liver tumors. *Radiology* 2014; **272**: 417-426 [PMID: 24697148 DOI: 10.1148/radiol.14131165]

56 **Wagner M**, Doblas S, Daire JL, Paradis V, Haddad N, Leitão H, Garteiser P, Vilgrain V, Sinkus R, Van Beers BE. Diffusion-weighted MR imaging for the regional characterization of liver tumors. *Radiology* 2012; **264**: 464-472 [PMID: 22692032 DOI: 10.1148/radiol.12111530]

57 **Yang SH**, Lin J, Lu F, Han ZH, Fu CX, Lv P, Liu H, Gao DM. Evaluation of antiangiogenic and antiproliferative effects of sorafenib by sequential histology and intravoxel incoherent motion diffusion-weighted imaging in an orthotopic hepatocellular carcinoma xenograft model. *J Magn Reson Imaging* 2017; **45**: 270-280 [PMID: 27299302 DOI: 10.1002/jmri.25344]

58 **Lewin M**, Fartoux L, Vignaud A, Arrivé L, Menu Y, Rosmorduc O. The diffusion-weighted imaging perfusion fraction f is a potential marker of sorafenib treatment in advanced hepatocellular carcinoma: a pilot study. *Eur Radiol* 2011; **21**: 281-290 [PMID: 20683597 DOI: 10.1007/s00330-010-1914-4]

59 **Shirota N**, Saito K, Sugimoto K, Takara K, Moriyasu F, Tokuuye K. Intravoxel incoherent motion MRI as a biomarker of sorafenib treatment for advanced hepatocellular carcinoma: a pilot study. *Cancer Imaging* 2016; **16**: 1 [PMID: 26822946 DOI: 10.1186/s40644-016-0059-3]

60 **Andersson M**, Jalnefjord O, Montelius M, Rizell M, Sternby Eilard M, Ljungberg M. Evaluation of response in patients with hepatocellular carcinoma treated with intratumoral dendritic cell vaccination using intravoxel incoherent motion (IVIM) MRI and histogram analysis. *Acta Radiol* 2021; 2841851211065935 [PMID: 34904868 DOI: 10.1177/02841851211065935]

61 **Chen BB**, Shao YY, Lin ZZ, Hsu CH, Cheng AL, Hsu C, Liang PC, Shih TT. Dynamic Contrast-Enhanced and Intravoxel Incoherent Motion MRI Biomarkers Are Correlated to Survival Outcome in Advanced Hepatocellular Carcinoma. *Diagnostics (Basel)* 2021; **11** [PMID: 34441274 DOI: 10.3390/diagnostics11081340]

62 **Zeng Q**, Liu B, Xu Y, Zhou W. An attention-based deep learning model for predicting microvascular invasion of hepatocellular carcinoma using an intra-voxel incoherent motion model of diffusion-weighted magnetic resonance imaging. *Phys Med Biol* 2021; **66** [PMID: 34469880 DOI: 10.1088/1361-6560/ac22db]

63 **Wei Y**, Huang Z, Tang H, Deng L, Yuan Y, Li J, Wu D, Wei X, Song B. IVIM improves preoperative assessment of microvascular invasion in HCC. *Eur Radiol* 2019; **29**: 5403-5414 [PMID: 30877465 DOI: 10.1007/s00330-019-06088-w]

64 **Zhao W**, Liu W, Liu H, Yi X, Hou J, Pei Y, Feng D, Liu L, Li W. Preoperative prediction of microvascular invasion of hepatocellular carcinoma with IVIM diffusion-weighted MR imaging and Gd-EOB-DTPA-enhanced MR imaging. *PLoS One* 2018; **13**: e0197488 [PMID: 29771954 DOI: 10.1371/journal.pone.0197488]

65 **Li H**, Zhang J, Zheng Z, Guo Y, Chen M, Xie C, Zhang Z, Mei Y, Feng Y, Xu Y. Preoperative histogram analysis of intravoxel incoherent motion (IVIM) for predicting microvascular invasion in patients with single hepatocellular carcinoma. *Eur J Radiol* 2018; **105**: 65-71 [PMID: 30017300 DOI: 10.1016/j.ejrad.2018.05.032]

66 **Zhang Y**, Kuang S, Shan Q, Rong D, Zhang Z, Yang H, Wu J, Chen J, He B, Deng Y, Roberts N, Shen J, Venkatesh SK, Wang J. Can IVIM help predict HCC recurrence after hepatectomy? *Eur Radiol* 2019; **29**: 5791-5803 [PMID: 30972544 DOI: 10.1007/s00330-019-06180-1]

67 **Zheng J**, Gong XQ, Tao YY, Wang R, Yang G, Li JD, Ren T, Li ZM, Yang C, Wang WC, Yang L, Zhang XM. A Correlative Study Between IVIM-DWI Parameters and the Expression Levels of Ang-2 and TKT in Hepatocellular Carcinoma. *Front Oncol* 2020; **10**: 594366 [PMID: 33520706 DOI: 10.3389/fonc.2020.594366]

68 **Shi G**, Han X, Wang Q, Ding Y, Liu H, Zhang Y, Dai Y. Evaluation of Multiple Prognostic Factors of Hepatocellular Carcinoma with Intra-Voxel Incoherent Motions Imaging by Extracting the Histogram Metrics. *Cancer Manag Res* 2020;

12: 6019-6031 [PMID: 32765101 DOI: 10.2147/CMAR.S262973]

69 **Guo Y**, Chen J, Zhang Y, Guo Y, Jiang M, Dai Y, Yao X. Differentiating Cytokeratin 19 expression of hepatocellular carcinoma by using multi-b-value diffusion-weighted MR imaging with mono-exponential, stretched exponential, intravoxel incoherent motion, diffusion kurtosis imaging and fractional order calculus models. *Eur J Radiol* 2022; **150**: 110237 [PMID: 35278979 DOI: 10.1016/j.ejrad.2022.110237]

70 **Andreou A**, Koh DM, Collins DJ, Blackledge M, Wallace T, Leach MO, Orton MR. Measurement reproducibility of perfusion fraction and pseudodiffusion coefficient derived by intravoxel incoherent motion diffusion-weighted MR imaging in normal liver and metastases. *Eur Radiol* 2013; **23**: 428-434 [PMID: 23052642 DOI: 10.1007/s00330-012-2604-1]

71 **Dyvorne HA**, Galea N, Nevers T, Fiel MI, Carpenter D, Wong E, Orton M, de Oliveira A, Feiweier T, Vachon ML, Babb JS, Taouli B. Diffusion-weighted imaging of the liver with multiple b values: effect of diffusion gradient polarity and breathing acquisition on image quality and intravoxel incoherent motion parameters--a pilot study. *Radiology* 2013; **266**: 920-929 [PMID: 23220895 DOI: 10.1148/radiol.12120686]

72 **Patel J**, Sigmund EE, Rusinek H, Oei M, Babb JS, Taouli B. Diagnosis of cirrhosis with intravoxel incoherent motion diffusion MRI and dynamic contrast-enhanced MRI alone and in combination: preliminary experience. *J Magn Reson Imaging* 2010; **31**: 589-600 [PMID: 20187201 DOI: 10.1002/jmri.22081]

73 **Luciani A**, Vignaud A, Cavet M, Nhieu JT, Mallat A, Ruel L, Laurent A, Deux JF, Brugieres P, Rahmouni A. Liver cirrhosis: intravoxel incoherent motion MR imaging--pilot study. *Radiology* 2008; **249**: 891-899 [PMID: 19011186 DOI: 10.1148/radiol.2493080080]

74 **Wang YXJ**, Huang H, Zheng CJ, Xiao BH, Chevallier O, Wang W. Diffusion-weighted MRI of the liver: challenges and some solutions for the quantification of apparent diffusion coefficient and intravoxel incoherent motion. *Am J Nucl Med Mol Imaging* 2021; **11**: 107-142 [PMID: 34079640]

75 **Wáng YXJ**. Mutual constraining of slow component and fast component measures: some observations in liver IVIM imaging. *Quant Imaging Med Surg* 2021; **11**: 2879-2887 [PMID: 34079748 DOI: 10.21037/qims-21-187]

76 **Wáng YXJ**. Observed paradoxical perfusion fraction elevation in steatotic liver: An example of intravoxel incoherent motion modeling of the perfusion component constrained by the diffusion component. *NMR Biomed* 2021; **34**: e4488 [PMID: 33559161 DOI: 10.1002/nbm.4488]

77 **Tao YY**, Zhou Y, Wang R, Gong XQ, Zheng J, Yang C, Yang L, Zhang XM. Progress of intravoxel incoherent motion diffusion-weighted imaging in liver diseases. *World J Clin Cases* 2020; **8**: 3164-3176 [PMID: 32874971 DOI: 10.12998/wjcc.v8.i15.3164]

78 **Tramontano L**, Cavaliere C, Salvatore M, Brancato V. The Role of Non-Gaussian Models of Diffusion Weighted MRI in Hepatocellular Carcinoma: A Systematic Review. *J Clin Med* 2021; **10** [PMID: 34203995 DOI: 10.3390/jcm10122641]

World Journal of Gastroenterology

Submit a Manuscript: https://www.f6publishing.com

World J Gastroenterol 2022 July 21; 28(27): 3346-3358

DOI: 10.3748/wjg.v28.i27.3346

ISSN 1007-9327 (print) ISSN 2219-2840 (online)

MINIREVIEWS

Regulatory T cells and their associated factors in hepatocellular carcinoma development and therapy

Chun-Ye Zhang, Shuai Liu, Ming Yang

Specialty type: Gastroenterology and hepatology

Provenance and peer review: Invited article; Externally peer reviewed.

Peer-review model: Single blind

Peer-review report's scientific quality classification
Grade A (Excellent): 0
Grade B (Very good): B
Grade C (Good): C
Grade D (Fair): 0
Grade E (Poor): 0

P-Reviewer: Grassi G, Italy; Lu G, China

Received: January 3, 2022
Peer-review started: January 3, 2022
First decision: January 23, 2022
Revised: January 27, 2022
Accepted: June 23, 2022
Article in press: June 23, 2022
Published online: July 21, 2022

Chun-Ye Zhang, Department of Veterinary Pathobiology, University of Missouri, Columbia, MO 65211, United States

Shuai Liu, The First Affiliated Hospital, Zhejiang University, Hangzhou 310006, Zhejiang Province, China

Ming Yang, Department of Surgery, University of Missouri, Columbia, MO 65211, United States

Corresponding author: Ming Yang, DVM, PhD, Postdoctoral Fellow, Department of Surgery, University of Missouri, Room 2203, NexGen Precision Building, 1030 Hitt Street, Columbia, MO 65211, United States. yangmin@health.missouri.edu

Abstract

Liver cancer is the third leading cause of cancer-related death worldwide with primary type hepatocellular carcinoma (HCC). Factors, including carcinogens, infection of hepatitis viruses, alcohol abuse, and non-alcoholic fatty liver disease (NAFLD), can induce HCC initiation and promote HCC progression. The prevalence of NAFLD accompanying the increased incidence of obesity and type 2 diabetes becomes the most increasing factor causing HCC worldwide. However, the benefit of current therapeutic options is still limited. Intrahepatic immunity plays critically important roles in HCC initiation, development, and progression. Regulatory T cells (Tregs) and their associated factors such as metabolites and secreting cytokines mediate the immune tolerance of the tumor microenvironment in HCC. Therefore, targeting Tregs and blocking their mediated factors may prevent HCC progression. This review summarizes the functions of Tregs in HCC-inducing factors including alcoholic and NAFLD, liver fibrosis, cirrhosis, and viral infections. Overall, a better understanding of the role of Tregs in the development and progression of HCC provides treatment strategies for liver cancer treatment.

Key Words: Hepatocellular carcinoma; Regulatory T cells; Alcoholic fatty liver disease; Non-alcoholic fatty liver disease; Treatment; Clinical trials

©The Author(s) 2022. Published by Baishideng Publishing Group Inc. All rights reserved.

Core Tip: Liver cancer is the third leading cause of cancer-related death worldwide. Hepatocellular carcinoma (HCC) is the primary type of liver cancer. Factors, including carcinogenic infection of hepatitis viruses, alcohol abuse, and non-alcoholic fatty liver disease (NAFLD), can induce HCC initiation and promote HCC progression. The prevalence of NAFLD accompanying the increased incidence of obesity and type 2 diabetes becomes the most increasing factor causing HCC worldwide. However, the benefit of current therapeutic options is still limited. Intrahepatic immunity plays critically important roles in HCC initiation, development, and progression. Regulatory T cells (Tregs) and their associated factors such as metabolites and secreting cytokines mediate the immune tolerance of the tumor microenvironment in HCC. Therefore, targeting Tregs and blocking their mediated factors may prevent HCC progression. A better understanding of the role of Tregs in intrahepatic immunity is helpful to develop novel HCC treatment options.

Citation: Zhang CY, Liu S, Yang M. Regulatory T cells and their associated factors in hepatocellular carcinoma development and therapy. *World J Gastroenterol* 2022; 28(27): 3346-3358
URL: https://www.wjgnet.com/1007-9327/full/v28/i27/3346.htm
DOI: https://dx.doi.org/10.3748/wjg.v28.i27.3346

INTRODUCTION

Liver cancer is the third leading cause of cancer-related death worldwide with 8.3% of death ratio, following lung and colorectal cancers[1]. The most common type of primary liver cancer is hepatocellular carcinoma (HCC) and the second type is cholangiocarcinoma[2]. Factors, including carcinogens (*e.g.*, aflatoxin B1), infection of hepatitis viruses, alcohol abuse, and non-alcoholic fatty liver disease (NAFLD), can induce HCC and promote HCC progression[3-5]. In addition, accompanying the increasing incidence of obesity and type 2 diabetes (T2D), NAFLD becomes an increasing factor that causes HCC worldwide[6,7].

Surgical resection is a curative treatment option for the early stage of HCC. However, most cases in HCC were found in the late stage. In addition, other minimally invasive local therapies, such as radiofrequency ablation and microwave ablation, and systemic therapy, such as tyrosine kinase inhibitors, are treatment options for patients who are not suitable for surgery[8]. Furthermore, immunotherapy by targeting checkpoint inhibitors [*e.g.*, anti-programmed cell death protein 1 (PD-1)/programmed death-ligand 1 (PD-L1) antibodies] shows benefits against advanced HCC in the clinic. A combination treatment by blocking both PD-L1 (*e.g.*, atezolizumab) and vascular endothelial growth factor (VEGF) (*e.g.*, bevacizumab) is one of the best first-line treatments for advanced HCC[9]. Other potential immunotherapy options including T cell-mediated therapy such as chimeric antigen receptor-engineered T cells[10-12], peptide-based vaccines[13-15], and micro ribonucleic acids (miRNAs)-mediated therapies[16], are undergoing investigations for HCC treatment.

Intrahepatic immunity including both innate and adaptive immune responses plays pivotal roles in the development and progression of HCC, especially for T cells[17]. Among them, the imbalance between effector CD4 and/or CD8 T cells and regulatory T cells (Tregs) induces immunotolerance and promotes HCC progression[18,19]. Factors impacting the balance of effector T cells and Tregs include gut microbiota, transforming growth factor-beta (TGF-β), and treatments such as trans-arterial chemoembolization[18-20], *etc.* The expression of cytokines such as interleukin (IL)-2, IL-5, interferon (IFN)-γ was increased with an increased ratio of cytotoxic T lymphocytes (CTLs)/Tregs with the treatment of Lenvatinib, a multiple kinase inhibitor, while the expression of T-cell immunoglobulin mucin-3 (Tim-3) and CTL-associated antigen-4 (CTLA-4) was decreased on Treg cells[21]. Therefore, modulating the Treg frequency and the expression of related cytokines are critically important for anti-tumor immunotherapy.

In this review, functions of Tregs on HCC causing factors such as alcoholic liver disease (ALD), NAFLD, liver fibrosis, and cirrhosis are discussed. In addition, molecules mediated Treg functions and therapeutic options by targeting Tregs are summarized. Moreover, clinical trials by targeting Tregs to modulate immune response were analyzed.

TREGS IN CHRONIC LIVER DISEASE

Tregs in ALD

As immunosuppressive cells, Tregs play a pivotal role in chronic liver diseases, including ALD. For example, chronic-binge alcohol exposure in C57BL/6 mice induced the reduction of Treg cells, but increased T helper 17 cells (Th17) cells and the production of IL-17[22]. Treatment with ginsenoside F2

can ameliorate ALD by increasing the frequency of Foxp3$^+$Tregs and decreasing IL-17-producing Th17 cells compared to control groups[23]. However, the molecular mechanism of how Tregs impact the progression of ALD except for modulation of liver inflammation remains unclear.

Tregs in NAFLD and nonalcoholic steatohepatitis

The balance Th17 cells/Tregs plays an essential role in metabolic diseases by regulating immune response and glucose and lipid metabolism[8]. The lower Treg (forkhead box P3$^+$/FOXP3$^+$) and higher Th17 cell (IL-17-producing cells) numbers were found in portal or periportal tract in livers of adult NAFLD patients, whereas more Tregs were shown in pediatric NAFLD patients[24]. In addition, severe liver inflammation was positively associated with intralobular expression of FOXP3 in pediatric patients but was positively associated with higher expression of IL-17 and lower expression of FOXP3 in adult patients, indicating the role of Tregs in NAFLD is age-dependent. Intrahepatic imbalance of Th17/Treg cells promotes the progression of NAFLD, accompanying higher expression of inflammatory cytokines such as IL-6, IL-17, and IL-23 in both serum and liver[25]. Feeding a high-fat diet (HFD) can impact the balance of Th17/Treg cells and Th1/Th2 cells of CD4 T cells in mesenteric lymph nodes (MLN). In addition, those CD4 T cells can potentially migrate into the liver to promote liver inflammation to result in NAFLD progression[26]. The effects of CD4 T cells in MLN on liver inflammation and fat accumulation can be ameliorated by administration of antibiotics and probiotics, indicating an important role of gut microbiota in NAFLD pathogenesis[26].

Dywicki *et al*[27] showed intrahepatic Tregs were increased in high-fat high-carbohydrate (HF-HC) diet-induced nonalcoholic steatohepatitis (NASH) in BALB/c mice. In addition, depletion of adaptive immunity aggregated HF-HC diet-induced NASH in recombination activating 1-knockout BALB/c mice. Although Tregs showed an anti-inflammation effect in ALD[23], adoptive transfer of Tregs increased steatosis and serum level of alanine aminotransferase (ALT), indicating that Tregs enhance the progression of NAFLD[27]. Another study also showed that increasing Tregs in subcutaneous adipose tissue induced by adoptive transfer of Tregs from healthy C57BL/6J mice to high-fat HFD (HFHFD)-fed mice increased hepatic steatosis during NAFLD development[28].

Mechanistically, the formation of neutrophil extracellular traps during NASH progression can induce Treg differentiation from naïve CD4 T cells, which is dependent on Toll-like receptor 4 (TLR-4) and involved in NASH-HCC progression[29].

Tregs in liver fibrosis and cirrhosis

Progression of chronic liver disease, including ALD and NAFLD, can promote the development of liver fibrosis and its advanced stage liver cirrhosis. However, there are no currently available therapies that can treat or reverse liver cirrhosis. Deng *et al*[30] reported that co-infusion with human amniotic mesenchymal stromal cells (hAMSCs) and Tregs can prevent mild liver fibrosis. Tregs play a critical role in the secretion of hepatocyte growth factor (HGF) and cell differentiation of hAMSCs.

Furthermore, an imbalance of Th17 cells/Tregs was also shown in cirrhotic patients with hepatitis B virus (HBV) infection. The frequency of Tregs was reduced in peripheral blood, while the frequency of Th17 cells was increased, resulting in a decreased Treg/Th17 ratio as a potential diagnostic marker for decompensated liver cirrhosis[31]. Another study also showed that the frequencies of both Tregs and Th17 cells were increased in the blood of patients with HBV infection and cirrhotic livers but with a higher extent in Th17 cells, resulting in an increased ratio of Th17/Treg, compared to the control group [32]. In addition, the mRNA levels of proinflammatory cytokines IL-1β, IL-6, and tumor necrosis factor (TNF)-α, as well as the protein expression of nuclear factor κB in the liver were significantly increased in HBV-infected liver and cirrhotic liver compared to healthy controls. Another study also showed that HBV infection can induce IL-8/C-X-C motif chemokine receptor 1/TGF-β signaling to provoke Treg polarization, resulting in suppression of anti-tumor immunity and enhance of HCC metastasis[33]. Moreover, the frequency of Tregs in blood and plasma levels of IL-35 were increased and positively related to viral load in HCV infected patients with cirrhosis and HCC[34].

Tregs in HCC

A meta-analysis showed that a higher infiltration of CD3 T cells, CD8 T cells, and natural killer cells was associated with better overall survival (OS), disease-free survival (DFS), and recurrence-free survival (RFS). In contrast, a higher infiltration of Tregs and neutrophils indicated lower OS and DFS[35]. Another report also showed that an increase of Tregs or a decrease of M1 macrophages (proinflammatory phenotype) were associated with a poor prognosis of HCC patients[36]. C-C chemokine receptor type 4 (CCR4)$^+$Tregs are predominant Tregs that are recruited in tumor tissue of HCC associated infection of hepatitis viruses, which is associated with HCC resistance to sorafenib treatment[37]. The frequency of CD127^{low}, CD25$^+$, CD4$^+$, Tregs was increased significantly in the peripheral venous blood of HCC patients compared to healthy controls[38]. In addition, the serum levels of TGF-β1 and IL-10 in HCC patients were positively associated with the Treg population in the blood, which were decreased post-operation and chemotherapy treatments. C-C motif chemokine ligand (CCL) 5 expression on circulating tumor cells in HCC patients can attract Tregs to induce an immunosuppressive environment, one of the mechanisms for CTC escaping immune surveillance[39].

The expression of immune checkpoint proteins in the HCC microenvironment impacts Tregs and antitumor immunity. PD-L1^{+}neutrophils, Tregs, and neutrophil to lymphocyte ratio were significantly increased in peripheral blood of patients with poorly differentiated HCC with a worse prognosis compared to that in patients with highly-moderately differentiated HCC[40]. Zhou *et al*[41] reported that tumor-associated neutrophils can induce the infiltration of the macrophages and Tregs from HCC mice or patients *via* producing CCL2 and CCL17, resulting in HCC progression and resistance to sorafenib. CTLA-4 on Tregs in HCC impacts dendritic cell function by downregulating CD80/CD86 on dendritic cells (DCs)[42]. Therefore, blockade of CTLA-4 in HCC can improve DC-mediated anti-tumor immunity.

Treatment with tivozanib, a tyrosine kinase inhibitor, can suppress Tregs by inhibiting receptor tyrosine kinase c-Kit (CD117)/stem cell factor (SCF) axis and increased CD4^{+}PD-1^{+}T cells, resulting in a significant improvement in OS of HCC patients[43]. Treatment with Lenvatinib also can inhibit IL-2 mediated Treg differentiation except for decreasing PD-L1 expression in HCC cells[44]. Overall, the balance between Tregs with other T cells plays a vital in liver diseases, including the initiation and progression of HCC (Figure 1).

Furthermore, alteration of intrahepatic immunity is associated with HCC prognosis and treatment (Figure 2). An increase of Tregs, Th2, and Th17 T cells, as well as M2 macrophages, is usually and positively associated with HCC progression in patients, whereas an abundance of CD8 T cells, Th1 T cells, and M1 macrophages is associated with HCC therapy and good prognosis for HCC patients[45]. Single-cell RNA sequencing technologies have been applied to investigate the immune landscape of HCC samples to illustrate the subtypes of immune cells in HCC and their gene expressing profiles, as well as immune cell interactions, such as DCs with Tregs or CD8 T cells[46].

IMPORTANT MOLECULES MEDIATED TREG FUNCTION AND METABOLISM

HIF-1α

Hypoxia-inducible transcription factors (HIFs) regulate cell metabolism, proliferation, and migration in low oxygen or hypoxic environment, as well as angiogenesis[47]. It has been reported that the expression of HIF-1 alpha (HIF-1α) was higher in HCC tissues compared to that in corresponding adjacent tissues. In addition, overexpression of HIF-1α was associated with poor outcomes of HCC in human patients[48]. Chronic intermittent hypoxia can promote NASH progression *via* regulating the balance of Th17/Treg by inducing the expression of HIF-1α[49].

Gal-9

Tregs can be subclassified into inflamed-tissue related memory Tregs (mTregs) and non-related resting Treg (rTregs). During HBV infection, mTregs were increased accompanying liver inflammation and liver injury evidenced by an increase of serum ALT level, but not rTregs[50]. The S-type lectin galectin-9 (Gal-9) was increased in the HBV-infected liver, contributing to T cell depletion and exhaustion by binding Tim-3[51]. For example, activation of Gal-9/Tim-3 signaling in concanavalin A-induced mouse hepatitis suppressed the induction of effector T (Teff) cells and the production of IFN-γ[52]. In addition, the Gal-9/Tim-3 signaling pathway plays an important role in the expansion of mTregs[50].

GDF15

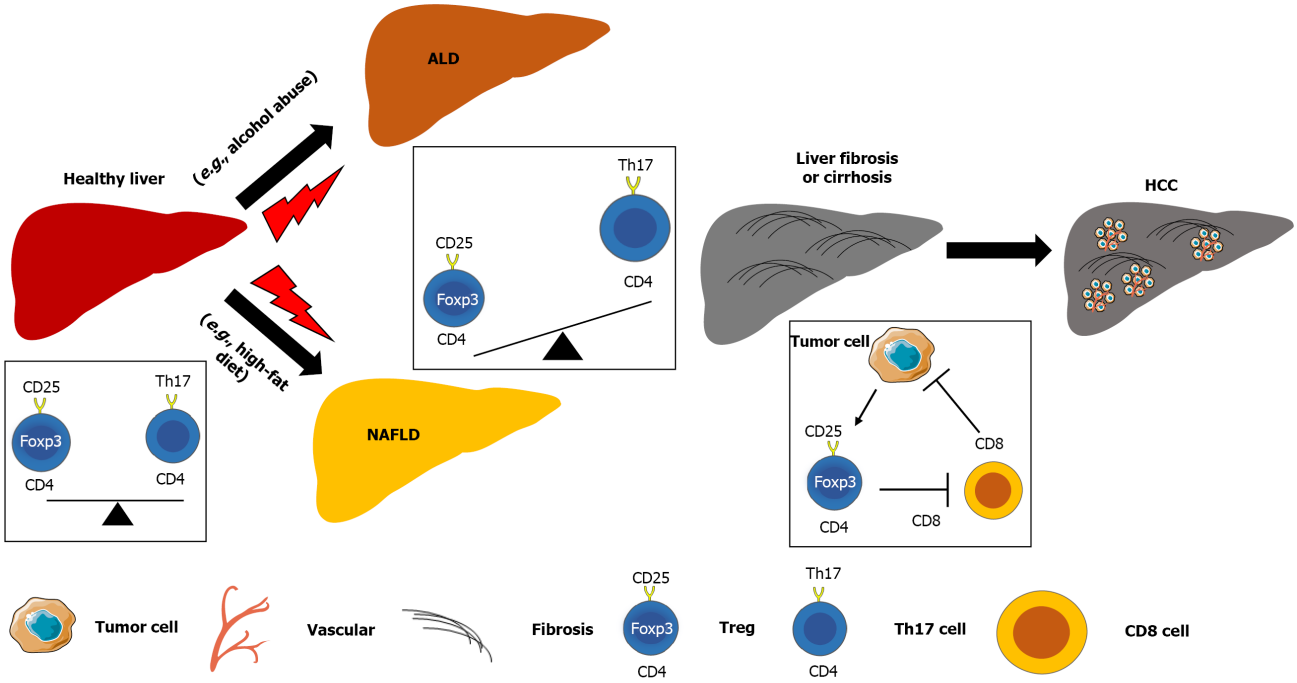
The expression of growth differentiation factor 15 (GDF15) was positively related to the frequency of Tregs in HCC. GDF15 can promote the suppressive effect of natural Tregs *via* binding with its unrecognized receptor CD48 on T cells to inhibit the function of homology and U-box containing protein 1, which can degrade FOXP3[53]. Thus, neutralizing GDF15 by an antibody can eradicate HCC and enhance anti-tumor immunity.

microRNAs

Hepatic expression of microRNA-195 (miR-195) was reduced in NAFLD development, accompanying an increased ratio of Th17/Treg ratio in the blood, as well as the expression IL-17, CD40, and TNF-α in rat liver[54]. Overexpression of miR-195 can maintain the balance of Th17/Treg to ameliorate NAFLD and liver inflammation. Many miRNAs can regulate Th17/Treg cell balance in NAFLD such as miR-29c *via* interacting with insulin-like growth factor binding protein 1/IGFBP1)[55]. In addition, other microRNAs such as miR-155[56,57], miR-423-5p[58], and miR-1246[59] play important roles in modulating the balance of Tregs with Th17 cells and their functions in liver disease.

TLRs

Activation of TLR signaling pathway can suppress the effect of Tregs on adaptive immune response, which is in part dependent on microbial production-induced expression of IL-6[60]. TLR9-deficiency increased the frequency of Treg cells in the intestine, resulting in a decrease of IL-17 and IFN-γ producing Teff cells[61]. The imbalance of Treg/Teff cells compromised immune response to oral



DOI: 10.3748/wjg.v28.i27.3346 **Copyright** ©The Author(s) 2022.

Figure 1 The imbalance of regulatory T cells and effector T cells promotes the progression of chronic liver diseases and hepatocellular carcinoma. Chronic liver diseases such as alcoholic liver disease and non-alcoholic fatty liver disease induced by factors such as alcohol abuse and high-fat diet, respectively, can induce liver fibrosis, cirrhosis, and even hepatocellular carcinoma. The imbalance of regulatory T cells with T helper 17 cells or CD8 T cells is involved in the pathogenesis of liver inflammation, fibrosis, and cancer progression. ALD: Alcoholic liver disease; HCC: Hepatocellular carcinoma; NAFLD: Non-alcoholic fatty liver disease; Treg: Regulatory T cells; Th: T helper.

infection, which can be reversed by reconstitution of gut flora deoxyribonucleic acid (DNA)[61]. In addition, the antibiotic treatment caused gut microbiota dysbiosis and recapitulated TLR9 deficiency-induced impaired immune response.

Yes-associated protein (YAP)

Yes-associated protein (YAP), a coactivator and a corepressor of the Hippo signaling pathway, plays a vital role in Tregs *in vivo* and *in vitro*[62]. Blocking YAP-mediated activation of activin can improve anti-tumor immunity *via* regulating TGF-β/mothers against decapentaplegic homolog (SMAD)[62]. Similarly, blockage of TGF-β signaling can compromise Treg function to improve anti-tumor immune response[63], which may expand the population of quiescent Tregs, $CD4^+CD25^-Foxp3^+$.

The above-mentioned molecules can modulate Treg metabolism and function as potential molecular targets for HCC treatment. In addition, modulation of these molecules can potentially recover the balance of Tregs with other tumor-infiltrating immune cells to activate anti-tumor immunity (Figure 3).

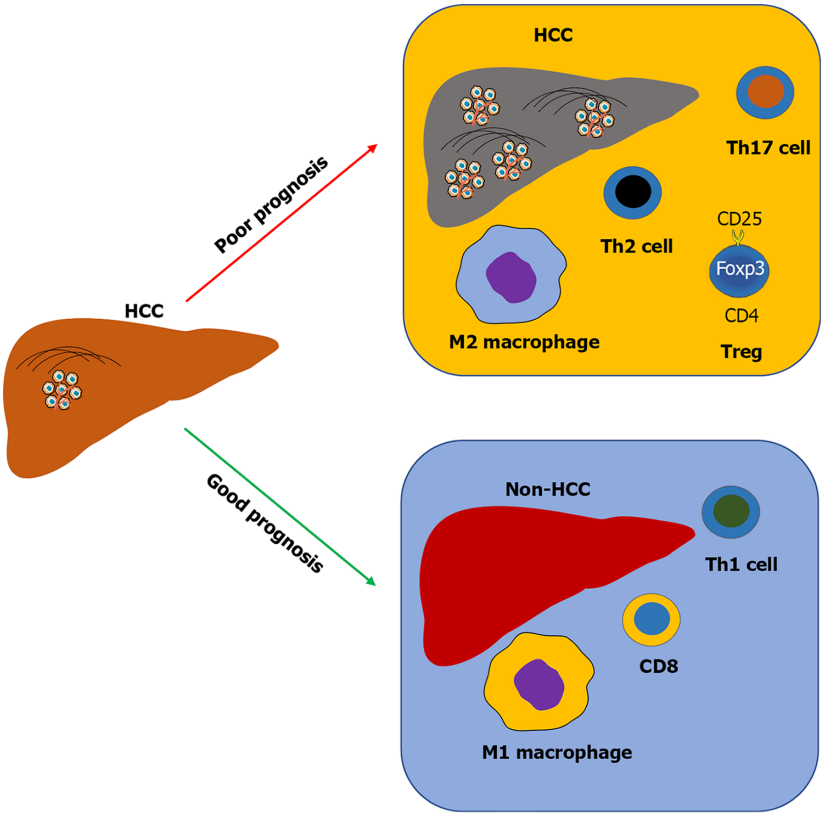
TREATMENT OPTIONS

Modulation of microRNAs

Administration of miR-26a can reduce the frequency of Tregs and the concentrations of alpha-fetoprotein, des-gamma carboxyprothrombin, and VEGF in Balb/c mice with diethylnitrosamine-induced HCC[64]. The suppressive effects of miR-26a on HCC growth and angiogenesis are mediated by targeting IL-6/signal transducer and activator of transcription 3 (Stat3) signaling[65] and HGF/HGF receptor (HGFR/c-Met) signaling[66], respectively. In addition, miR-26a inversely regulated the expression of F-box protein 11 (FBXO11), which was upregulated and played an oncogenic role in HCC [67].

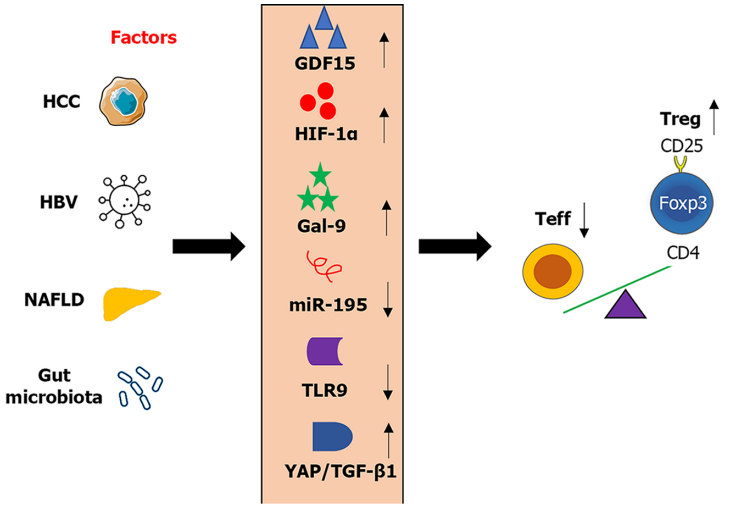
Adoptive transfer of cells

Adoptive transfer of Tregs attenuated triptolide-induced liver injury, while depletion of Tregs showed the opposite effect, indicating that Tregs contribute to the progression of liver injury[68]. Another study showed that adoptive transfer of hepatic stellate cell (HSC)-stimulated Tregs can significantly decrease liver injury in mice with autoimmune hepatitis by inducing the balance of Treg/Th17 ratio[69]. In addition, the adoptive transfer of HSCs promoted the differentiation of Tregs and decreased Th17 cells,



DOI: 10.3748/wjg.v28.i27.3346 **Copyright** ©The Author(s) 2022.

Figure 2 The alteration of intrahepatic immunity predicts the prognosis of hepatocellular carcinoma patients. Usually, an increase of regulatory T cells, T helper (Th) 2 cells, and Th17 cells, as well as M2 macrophages is positively associated with hepatocellular carcinoma (HCC) progression in patients, whereas an abundance of CD8 T cells, Th1 T cells, and M1 macrophages is associated with HCC therapy and good prognosis for HCC patients. HCC: Hepatocellular carcinoma; Treg: Regulatory T cells; Th: T helper.



DOI: 10.3748/wjg.v28.i27.3346 **Copyright** ©The Author(s) 2022

Figure 3 Factors mediated the imbalance of regulatory T cells/effector T cells. Factor such as Hepatitis B virus, gut microbiota, and non-alcoholic fatty liver disease, as well as hepatocellular carcinoma tumor cells, can modulate several important molecules produced in the liver. Alteration of these molecules has been associated with the change of frequency and/or function of regulatory T cells in chronic liver disease, resulting in an imbalance of regulatory T cells/effector T cells. HCC: Hepatocellular carcinoma; HBV: Hepatitis B virus; NAFLD: Non-alcoholic fatty liver disease; Teff: Effector T cells; Treg: Regulatory T cells; GDF: Growth differentiation factor; HIF: Hypoxia-inducible transcription factors; Gal: Galectin; miR: micro ribonucleic acid; TLR: Toll-like receptor; YAP: Yes-associated protein; TGF-β: Transforming growth factor-beta.

resulting in amelioration of liver injury[70]. Deng *et al*[30] reported that co-infusion with hAMSCs and Tregs can prevent mild liver fibrosis. Tregs play a critical role in the secretion of HGF and cell differentiation of hAMSCs.

Table 1 Treatment options for hepatocellular carcinoma by targeting regulatory T cells and relative signaling pathways

Treatment	Targets	Functions	Ref.
CCR4 antagonist	CCR4	Administration of a CCR4 antagonist or N-CCR4-Fc, a neutralizing pseudo-receptor that can block Tregs accumulation in HCC, can enhance therapeutic efficacy to PD-1 blockade and sorafenib	Gao *et al*[37], 2022
miR-26a	IL6/Stat3 and HGF/c-Met	The suppressive effects of miR-26a on HCC growth and angiogenesis are mediated by targeting IL-6/signal transducer and activator of transcription 3 signaling and HGF/HGFR/c-Met signaling, respectively	Yang *et al*[65], 2013; Yang *et al*[66], 2014
GDF15 neutralizing antibody	GDF15/CD48	Inhibiting GDF15 function by a neutralizing antibody can effectively eradicate HCC and promote a tumoricidal immune response in mice	Wang *et al*[53], 2021
Supplementation of *Lactobacillus rhamnosus* GG or its culture supernatant	The ratio of Treg and Th17 cells	Supplementation of *Lactobacillus rhamnosus* GG or its culture supernatant can ameliorate chronic alcohol-induced liver injury by reducing hepatic inflammation, enhancing intestinal barrier integrity, and inducing balance in the ratio of Treg and Th17 cells to reduce alcoholic-induced liver injury	Chen *et al*[22], 2016; Wang *et al*[72], 2013; Wang *et al*[73], 2012
Prohep, a novel probiotic mixture	Gut microbiota and Treg differentiation	Probiotic treatment regulated T-cell differentiation in the gut by reducing Th17 polarization and increasing the differentiation of anti-inflammatory Treg cells, by increasing the abundance of beneficial bacteria, such as *Prevotella* and *Oscillibacter*	Li *et al*[74], 2016
Anti-PD-1 and anti-PD-L1 antibodies	PD-1 and PD-L1	Another study also showed that Treg-mediated inhibition of IFN-γ production and cytotoxicity of CD8 T cells can be partially reduced by anti-PD-1 and anti-PD-L1 antibodies in HCC	Langhans *et al*[76], 2019
Dual anti-PD-1/VEGFR-2 therapy	VEGFR-2 and PD-1	Dual therapies increased CD8 T cell infiltration and activation, reduced Tregs and infiltration of $CCR2^{+}$monocytes, as well as the phenotype of tumor-associated macrophages (the M1/M2 ratio) in HCC tissue	Shigeta *et al*[75], 2020
Anti-CTLA-4 monoclonal antibody	Tregs	Treg depletion-mediated by anti-CTLA-4 monoclonal antibody (clone 9H10) restored the function of tumor antigen-specific CD8 T cells, with a synergistic effect with anti-PD-1 treatment	Lee *et al*[77], 2020
Resveratrol	Tregs and immunosuppressive cytokines including TGF-β1 and IL-10	Treatment with resveratrol, a natural phenol, can inhibit H22 (a mouse HCC cell line)-induced orthotopic HCC tumor growth *via* decreasing the frequency of $CD8^{+}CD122^{+}$Tregs and M2-like macrophages in mice	Zhang *et al*[79], 2020

CCR: C-C chemokine receptor; HGF: Hepatocyte growth factor; HGFR: Hepatocyte growth factor receptor; HCC: Hepatocellular carcinoma; PD-1: Programmed cell death protein 1; miR: micro ribonucleic acid; IL: Interleukin; GDF: Growth differentiation factor; Treg: Regulatory T cells; Th: T helper; IFN: Interferon; VEGFR: Vascular endothelial growth factor receptor; CTLA: Cytotoxic T lymphocyte-associated antigen; TGF-β: Transforming growth factor-beta.

Modulation of gut microbiota

Depletion of Tregs in the intestine caused an increase in the abundance of *Firmicutes* and intestinal inflammation[71]. Supplementation of *Lactobacillus rhamnosus* GG or its culture supernatant can ameliorate chronic alcohol-induced liver injury by reducing TNF-α expression *via* inhibition of TLR4- and TLR5-mediated hepatic inflammation[72], as well as amelioration of intestinal barrier integrity and suppression of alcohol-induced endotoxemia[73]. In addition, the culture supernatant can balance the ratio of Treg and Th17 cells to reduce alcoholic-induced liver injury[22].

Treatment with Prohep, a novel probiotic mixture, significantly inhibited the HCC growth compared to the control group, resulting in an abundance of beneficial bacteria, such as *Prevotella* and *Oscillibacter* [74]. This study also showed that probiotic treatment regulated T-cell differentiation in the gut by reducing Th17 polarization and increasing the differentiation of anti-inflammatory Treg cells.

Blockade of immune checkpoints

Dual anti-PD-1/VEGF receptor-2 therapy increased CD8 T cell infiltration and activation, reduced Tregs and infiltration of $CCR2^{+}$monocytes, as well as the phenotype of tumor-associated macrophages (the M1/M2 ratio) in HCC tissue[75]. Another study also showed that Treg-mediated inhibition of IFN-γ production and cytotoxicity of CD8 T cells can be partially reduced by anti-PD-1 and anti-PD-L1 antibodies in HCC[76].

Treg depletion-mediated by anti-CTLA-4 monoclonal antibody (clone 9H10) restored the function of tumor antigen-specific CD8 T cells, with a synergetic effect with anti-PD-1 treatment[77].

Other treatments

CCR4 expression in Tregs accompanied with an increased expression IL-10 and IL-35, resulting in suppression of CD8 T cells and HCC progression. Administration of a CCR4 antagonist or N-CCR4-Fc, a

Table 2 Clinical trials by targeting regulatory T cells to modulate the immune response

Trial	Phase	Treatment	Results	Ref.
NCT02476123	I	Anti-CCR4 antibody mogamulizumab	Treg depletion induced by anti-CCR4 antibody (mogamulizumab), in combination with anti-PD-1 antibody (nivolumab) showed antitumor activity and increased $CD8^+$ T cell infiltration	Doi *et al*[78], 2019; Sánchez-Fueyo *et al*[83], 2020
NCT02166177	I	Intravenous infusion of ex vivo expanded Tregs	Treg transfer can transiently increase circulating Tregs and inhibit anti-donor T cell responses in patients with liver transplants	Fueyo *et al*[83], 2020
NCT02166177	I	Autologous Treg therapy	To defect safety and efficacy study of regulatory T cell therapy in liver transplant patients	Whitehouse *et al* [84], 2017
NCT01624077	I	Injection of Tregs	To defect safety and efficacy study of regulatory T cell therapy in liver transplant patients	Whitehouse *et al* [84], 2017
NCT03654040	I	A single dose of alloantigen-reactive Tregs (arTreg) (≥ 90 × 10^6 total cells)	It is a single-center, prospective, open-label, non-randomized clinical trial exploring cellular therapy to facilitate immunosuppression withdrawal in liver transplant recipients	Cvetkovski *et al* [85], 2021
NCT03577431		arTreg-CSB (2.5 × 10^6 cells)		
NCT02260375	I	Infusion of mesenchymal stromal cells	MSC infusion in liver transplant recipients slightly increased circulating Treg/memory Treg over baseline, without a statistically significant, but not in the control group	Casiraghi *et al* [86], 2021
NCT02027116	I	DNA vaccine GLS-6150	GLS-6150 decreases Treg cell frequency and enhances HCV-specific T cell responses without significant side effects	Han *et al*[87], 2020
NCT02174276	II	GS-4774, a yeast-based therapeutic vaccine	Treatment with GS-4774 increased T-cell functions by increasing the production of IFN-γ and TNF and reducing the cell number of Tregs	Boni *et al*[88], 2019
NCT02360592	IV	Combined therapy with interferon plus IL-1 and hepatitis B Vaccine	Combination therapy increased the level of hepatitis B surface antigen with partial restoration of Tregs and NK cells	Wu *et al*[89], 2019
NCT02072486	None	Sorafenib, a multiple kinase inhibitor	Treatment with sorafenib can significantly suppress extracellular signal-regulated $kinases^+$ FMS-like tyrosine $kinase\ 3^+$ Tregs and myeloid-derived suppressor cells to benefit the survival of HCC patients	Kalathil *et al* [90], 2019

CCR: C-C chemokine receptor; CSB: Co-stimulatory blockade; PD-1: Programmed cell death protein 1; Treg: Regulatory T cells; MSC: Mesenchymal stromal cells; DNA: Deoxyribonucleic acid; GLS: Glutaminase; IFN: Interferon; TNF: Tumor necrosis factor; IL: Interleukin; NK: Natural killer; FMS: Feline McDonough sarcoma.

neutralizing pseudo-receptor that can block Tregs accumulation in HCC, can enhance therapeutic efficacy to PD-1 blockade and sorafenib[37]. Treg depletion induced by anti-CCR4 antibody (mogamulizumab), in combination with anti-PD-1 antibody (nivolumab) showed antitumor activity and increased CD8+ T cell infiltration[78].

Treatment with resveratrol, a natural phenol, can inhibit H22 (a mouse HCC cell line)-induced orthotopic HCC tumor growth *via* decreasing the frequency of $CD8^+CD122^+$Tregs and M2-like macrophages in mice[79].

Ren *et al*[80] reported that Tregs were further increased in HCC patients compared to healthy and cirrhosis controls, as well as in HCC patients with Barcelona clinic liver cancer (BCLC) stage C compared to that in HCC patients with BCLC stage B. The authors also showed that treatment with microparticles-transarterial chemoembolization dramatically decreased Treg cell proportion at 1-2 wk post-treatment. Overall, the treatment options for HCC associated with Treg regulation were summarized in Table 1.

CLINICAL TRIALS

Tregs display multiple roles in the development and progression of HCC. The ratio of Treg/Th17 cells in peripheral blood can be applied to monitor immune tolerance as immune markers in liver transplantation[81]. The balance of Treg/Th17 cells or other effector T cells is essential for suppressing autoimmune diseases and cancers[82]. Therefore, treatments including diverse immunomodulatory therapies can regulate Tregs to enhance the antitumor immune response. In Table 2, potential therapies in clinical trials were summarized. Treatments including infusion of Tregs[83-85] and mesenchymal stromal cells (MSCs)[86], vaccines[87-89], and kinase inhibitors[90].

CONCLUSION

Tregs modulate the intestinal and intrahepatic immune response, contributing critically important roles in the gut-liver axis. Functional changes of Tregs are involved in the pathogenesis of chronic liver diseases, such as ALD and NAFLD, causing factors for HCC. Several important molecules investigated in recent studies are summarized and targeting them may potentially treat HCC by modulating Treg function and/or frequency. Clinical trials are undergoing to further explore the new treatments for HCC, which modulate the function of the frequency of Tregs. In the future, multi-omic analysis including metabolic and proteomic data for Treg metabolism and function during the progression of HCC is critical to illustrate the underlying mechanisms of Tregs in HCC pathogenesis and find out new therapeutic targets.

FOOTNOTES

Author contributions: Zhang CY, Liu S, and Yang M designed and collected data, wrote, revised, and finalized the manuscript; all authors contributed equally, and shared the first authorship.

Conflict-of-interest statement: There are no conflicts of interest to report.

Open-Access: This article is an open-access article that was selected by an in-house editor and fully peer-reviewed by external reviewers. It is distributed in accordance with the Creative Commons Attribution NonCommercial (CC BY-NC 4.0) license, which permits others to distribute, remix, adapt, build upon this work non-commercially, and license their derivative works on different terms, provided the original work is properly cited and the use is non-commercial. See: https://creativecommons.org/Licenses/by-nc/4.0/

Country/Territory of origin: United States

ORCID number: Chun-Ye Zhang 0000-0003-2567-029X; Shuai Liu 0000-0001-9695-2492; Ming Yang 0000-0002-4895-5864.

S-Editor: Chen YL
L-Editor: A
P-Editor: Chen YL

REFERENCES

1 **Sung H**, Ferlay J, Siegel RL, Laversanne M, Soerjomataram I, Jemal A, Bray F. Global Cancer Statistics 2020: GLOBOCAN Estimates of Incidence and Mortality Worldwide for 36 Cancers in 185 Countries. *CA Cancer J Clin* 2021; **71**: 209-249 [PMID: 33538338 DOI: 10.3322/caac.21660]
2 **Zhang C**, Yang M. The Emerging Factors and Treatment Options for NAFLD-Related Hepatocellular Carcinoma. *Cancers (Basel)* 2021; **13** [PMID: 34359642 DOI: 10.3390/cancers13153740]
3 **Qi X**, Yang M, Stenberg J, Dey R, Fogwe L, Alam MS, Kimchi ET, Staveley-O'Carroll KF, Li G. Gut microbiota mediated molecular events and therapy in liver diseases. *World J Gastroenterol* 2020; **26**: 7603-7618 [PMID: 33505139 DOI: 10.3748/wjg.v26.i48.7603]
4 **De Battista D**, Zamboni F, Gerstein H, Sato S, Markowitz TE, Lack J, Engle RE, Farci P. Molecular Signature and Immune Landscape of HCV-Associated Hepatocellular Carcinoma (HCC): Differences and Similarities with HBV-HCC. *J Hepatocell Carcinoma* 2021; **8**: 1399-1413 [PMID: 34849372 DOI: 10.2147/JHC.S325959]
5 **Zhu Q**, Ma Y, Liang J, Wei Z, Li M, Zhang Y, Liu M, He H, Qu C, Cai J, Wang X, Zeng Y, Jiao Y. AHR mediates the aflatoxin B1 toxicity associated with hepatocellular carcinoma. *Signal Transduct Target Ther* 2021; **6**: 299 [PMID: 34373448 DOI: 10.1038/s41392-021-00713-1]
6 **Bertot LC**, Adams LA. Trends in hepatocellular carcinoma due to non-alcoholic fatty liver disease. *Expert Rev Gastroenterol Hepatol* 2019; **13**: 179-187 [PMID: 30791782 DOI: 10.1080/17474124.2019.1549989]
7 **Zhang C**, Liu S, Yang M. Hepatocellular Carcinoma and Obesity, Type 2 Diabetes Mellitus, Cardiovascular Disease: Causing Factors, Molecular Links, and Treatment Options. *Front Endocrinol (Lausanne)* 2021; **12**: 808526 [PMID: 35002979 DOI: 10.3389/fendo.2021.808526]
8 **Zhang C**, Yang M, Ericsson AC. The Potential Gut Microbiota-Mediated Treatment Options for Liver Cancer. *Front Oncol* 2020; **10**: 524205 [PMID: 33163393 DOI: 10.3389/fonc.2020.524205]
9 **Sangro B**, Sarobe P, Hervás-Stubbs S, Melero I. Advances in immunotherapy for hepatocellular carcinoma. *Nat Rev Gastroenterol Hepatol* 2021; **18**: 525-543 [PMID: 33850328 DOI: 10.1038/s41575-021-00438-0]
10 **Pang N**, Shi J, Qin L, Chen A, Tang Y, Yang H, Huang Y, Wu Q, Li X, He B, Li T, Liang B, Zhang J, Cao B, Liu M, Feng Y, Ye X, Chen X, Wang L, Tian Y, Li H, Li J, Hu H, He J, Hu Y, Zhi C, Tang Z, Gong Y, Xu F, Xu L, Fan W, Zhao M, Chen D, Lian H, Yang L, Li P, Zhang Z. IL-7 and CCL19-secreting CAR-T cell therapy for tumors with positive glypican-3 or mesothelin. *J Hematol Oncol* 2021; **14**: 118 [PMID: 34325726 DOI: 10.1186/s13045-021-01128-9]
11 **Li D**, Li N, Zhang YF, Fu H, Feng M, Schneider D, Su L, Wu X, Zhou J, Mackay S, Kramer J, Duan Z, Yang H, Kolluri A, Hummer AM, Torres MB, Zhu H, Hall MD, Luo X, Chen J, Wang Q, Abate-Daga D, Dropulic B, Hewitt SM, Orentas RJ,

Greten TF, Ho M. Persistent Polyfunctional Chimeric Antigen Receptor T Cells That Target Glypican 3 Eliminate Orthotopic Hepatocellular Carcinomas in Mice. *Gastroenterology* 2020; **158**: 2250-2265.e20 [PMID: 32060001 DOI: 10.1053/j.gastro.2020.02.011]

12 **Batra SA**, Rathi P, Guo L, Courtney AN, Fleurence J, Balzeau J, Shaik RS, Nguyen TP, Wu MF, Bulsara S, Mamonkin M, Metelitsa LS, Heczey A. Glypican-3-Specific CAR T Cells Coexpressing IL15 and IL21 Have Superior Expansion and Antitumor Activity against Hepatocellular Carcinoma. *Cancer Immunol Res* 2020; **8**: 309-320 [PMID: 31953246 DOI: 10.1158/2326-6066.CIR-19-0293]

13 **Tsuchiya N**, Yoshikawa T, Fujinami N, Saito K, Mizuno S, Sawada Y, Endo I, Nakatsura T. Immunological efficacy of glypican-3 peptide vaccine in patients with advanced hepatocellular carcinoma. *Oncoimmunology* 2017; **6**: e1346764 [PMID: 29123959 DOI: 10.1080/2162402X.2017.1346764]

14 **Charneau J**, Suzuki T, Shimomura M, Fujinami N, Nakatsura T. Peptide-Based Vaccines for Hepatocellular Carcinoma: A Review of Recent Advances. *J Hepatocell Carcinoma* 2021; **8**: 1035-1054 [PMID: 34513746 DOI: 10.2147/JHC.S291558]

15 **Zhang C**, Yang M, Ericsson AC. Antimicrobial Peptides: Potential Application in Liver Cancer. *Front Microbiol* 2019; **10**: 1257 [PMID: 31231341 DOI: 10.3389/fmicb.2019.01257]

16 **Roy B**, Ghose S, Biswas S. Therapeutic strategies for miRNA delivery to reduce hepatocellular carcinoma. *Semin Cell Dev Biol* 2022; **124**: 134-144 [PMID: 33926792 DOI: 10.1016/j.semcdb.2021.04.006]

17 **Zhang C**, Yang M. Targeting T Cell Subtypes for NAFLD and NAFLD-Related HCC Treatment: An Opinion. *Front Med (Lausanne)* 2021; **8**: 789859 [PMID: 34869507 DOI: 10.3389/fmed.2021.789859]

18 **Behary J**, Amorim N, Jiang XT, Raposo A, Gong L, McGovern E, Ibrahim R, Chu F, Stephens C, Jebeili H, Fragomeli V, Koay YC, Jackson M, O'Sullivan J, Weltman M, McCaughan G, El-Omar E, Zekry A. Gut microbiota impact on the peripheral immune response in non-alcoholic fatty liver disease related hepatocellular carcinoma. *Nat Commun* 2021; **12**: 187 [PMID: 33420074 DOI: 10.1038/s41467-020-20422-7]

19 **Dituri F**, Mancarella S, Serino G, Chaoul N, Lupo LG, Villa E, Fabregat I, Giannelli G. Direct and Indirect Effect of TGFβ on Treg Transendothelial Recruitment in HCC Tissue Microenvironment. *Int J Mol Sci* 2021; **22** [PMID: 34769191 DOI: 10.3390/ijms222111765]

20 **Pinato DJ**, Murray SM, Forner A, Kaneko T, Fessas P, Toniutto P, Mínguez B, Cacciato V, Avellini C, Diaz A, Boyton RJ, Altmann DM, Goldin RD, Akarca AU, Marafioti T, Mauri FA, Casagrande E, Grillo F, Giannini E, Bhoori S, Mazzaferro V. Trans-arterial chemoembolization as a loco-regional inducer of immunogenic cell death in hepatocellular carcinoma: implications for immunotherapy. *J Immunother Cancer* 2021; **9** [PMID: 34593621 DOI: 10.1136/jitc-2021-003311]

21 **Zhu J**, Fang P, Wang C, Gu M, Pan B, Guo W, Yang X, Wang B. The immunomodulatory activity of lenvatinib prompts the survival of patients with advanced hepatocellular carcinoma. *Cancer Med* 2021; **10**: 7977-7987 [PMID: 34605616 DOI: 10.1002/cam4.4312]

22 **Chen RC**, Xu LM, Du SJ, Huang SS, Wu H, Dong JJ, Huang JR, Wang XD, Feng WK, Chen YP. Lactobacillus rhamnosus GG supernatant promotes intestinal barrier function, balances Treg and TH17 cells and ameliorates hepatic injury in a mouse model of chronic-binge alcohol feeding. *Toxicol Lett* 2016; **241**: 103-110 [PMID: 26617183 DOI: 10.1016/j.toxlet.2015.11.019]

23 **Kim MH**, Kim HH, Jeong JM, Shim YR, Lee JH, Kim YE, Ryu T, Yang K, Kim KR, Jeon BM, Kim SC, Jung JK, Choi JK, Lee YS, Byun JS, Jeong WI. Ginsenoside F2 attenuates chronic-binge ethanol-induced liver injury by increasing regulatory T cells and decreasing Th17 cells. *J Ginseng Res* 2020; **44**: 815-822 [PMID: 33192125 DOI: 10.1016/j.jgr.2020.03.002]

24 **Cairoli V**, De Matteo E, Rios D, Lezama C, Galoppo M, Casciato P, Mullen E, Giadans C, Bertot G, Preciado MV, Valva P. Hepatic lymphocytes involved in the pathogenesis of pediatric and adult non-alcoholic fatty liver disease. *Sci Rep* 2021; **11**: 5129 [PMID: 33664397 DOI: 10.1038/s41598-021-84674-z]

25 **He B**, Wu L, Xie W, Shao Y, Jiang J, Zhao Z, Yan M, Chen Z, Cui D. The imbalance of Th17/Treg cells is involved in the progression of nonalcoholic fatty liver disease in mice. *BMC Immunol* 2017; **18**: 33 [PMID: 28646856 DOI: 10.1186/s12865-017-0215-y]

26 **Su L**, Wu Z, Chi Y, Song Y, Xu J, Tan J, Cong X, Liu Y. Mesenteric lymph node $CD4^+$ T lymphocytes migrate to liver and contribute to non-alcoholic fatty liver disease. *Cell Immunol* 2019; **337**: 33-41 [PMID: 30770094 DOI: 10.1016/j.cellimm.2019.01.005]

27 **Dywicki J**, Buitrago-Molina LE, Noyan F, Davalos-Misslitz AC, Hupa-Breier KL, Lieber M, Hapke M, Schlue J, Falk CS, Raha S, Prinz I, Koenecke C, Manns MP, Wedemeyer H, Hardtke-Wolenski M, Jaeckel E. The Detrimental Role of Regulatory T Cells in Nonalcoholic Steatohepatitis. *Hepatol Commun* 2022; **6**: 320-333 [PMID: 34532981 DOI: 10.1002/hep4.1807]

28 **Van Herck MA**, Vonghia L, Kwanten WJ, Vanwolleghem T, Ebo DG, Michielsen PP, De Man JG, Gama L, De Winter BY, Francque SM. Adoptive Cell Transfer of Regulatory T Cells Exacerbates Hepatic Steatosis in High-Fat High-Fructose Diet-Fed Mice. *Front Immunol* 2020; **11**: 1711 [PMID: 32849604 DOI: 10.3389/fimmu.2020.01711]

29 **Wang H**, Zhang H, Wang Y, Brown ZJ, Xia Y, Huang Z, Shen C, Hu Z, Beane J, Ansa-Addo EA, Huang H, Tian D, Tsung A. Regulatory T-cell and neutrophil extracellular trap interaction contributes to carcinogenesis in non-alcoholic steatohepatitis. *J Hepatol* 2021; **75**: 1271-1283 [PMID: 34363921 DOI: 10.1016/j.jhep.2021.07.032]

30 **Deng Z**, Zhou J, Mu X, Gu J, Li X, Shao Q, Li J, Yang C, Han G, Zhao J, Xia Y. Regulatory T Cells Improved the Anti-cirrhosis Activity of Human Amniotic Mesenchymal Stem Cell in the Liver by Regulating the TGF-β-Indoleamine 2,3-Dioxygenase Signaling. *Front Cell Dev Biol* 2021; **9**: 737825 [PMID: 34712665 DOI: 10.3389/fcell.2021.737825]

31 **Lan YT**, Wang ZL, Tian P, Gong XN, Fan YC, Wang K. Treg/Th17 imbalance and its clinical significance in patients with hepatitis B-associated liver cirrhosis. *Diagn Pathol* 2019; **14**: 114 [PMID: 31639000 DOI: 10.1186/s13000-019-0891-4]

32 **Mou H**, Wu S, Zhao G, Wang J. Changes of Th17/Treg ratio in the transition of chronic hepatitis B to liver cirrhosis and correlations with liver function and inflammation. *Exp Ther Med* 2019; **17**: 2963-2968 [PMID: 30936966 DOI: 10.3892/etm.2019.7299]

33 **Zhang C**, Gao Y, Du C, Markowitz GJ, Fu J, Zhang Z, Liu C, Qin W, Wang H, Wang F, Yang P. Hepatitis B-Induced IL8 Promotes Hepatocellular Carcinoma Venous Metastasis and Intrahepatic Treg Accumulation. *Cancer Res* 2021; **81**: 2386-

2398 [PMID: 33653774 DOI: 10.1158/0008-5472.CAN-20-3453]
34 **Abd El-Ghani EH**, Afifi NA, Ibrahim MA, Zahran AM, El-Mokhtar MA, Mekky MA, Hetta HF. Regulatory T Cells and IL35 in Chronic Hepatitis C Related Cirrhosis and Hepatocellular Carcinoma. *Egypt J Immunol* 2021; **28**: 46-52 [PMID: 34147053]
35 **Schoenberg MB**, Li X, Han Y, Hao J, Miksch RC, Koch D, Börner N, Beger NT, Bucher JN, Schiergens TS, Guba MO, Werner J, Bazhin AV. The predictive value of tumor infiltrating leukocytes in Hepatocellular Carcinoma: A systematic review and meta-analysis. *Eur J Surg Oncol* 2021; **47**: 2561-2570 [PMID: 33966947 DOI: 10.1016/j.ejso.2021.04.042]
36 **Yu S**, Wang Y, Hou J, Li W, Wang X, Xiang L, Tan D, Wang W, Jiang L, Claret FX, Jiao M, Guo H. Tumor-infiltrating immune cells in hepatocellular carcinoma: Tregs is correlated with poor overall survival. *PLoS One* 2020; **15**: e0231003 [PMID: 32240238 DOI: 10.1371/journal.pone.0231003]
37 **Gao Y**, You M, Fu J, Tian M, Zhong X, Du C, Hong Z, Zhu Z, Liu J, Markowitz GJ, Wang FS, Yang P. Intratumoral stem-like CCR4+ regulatory T cells orchestrate the immunosuppressive microenvironment in HCC associated with hepatitis B. *J Hepatol* 2022; **76**: 148-159 [PMID: 34689996 DOI: 10.1016/j.jhep.2021.08.029]
38 **Zhou W**, Deng J, Chen Q, Li R, Xu X, Guan Y, Li W, Xiong X, Li H, Li J, Cai X. Expression of CD4+CD25+CD127^{Low} regulatory T cells and cytokines in peripheral blood of patients with primary liver carcinoma. *Int J Med Sci* 2020; **17**: 712-719 [PMID: 32218692 DOI: 10.7150/ijms.44088]
39 **Sun YF**, Wu L, Liu SP, Jiang MM, Hu B, Zhou KQ, Guo W, Xu Y, Zhong Y, Zhou XR, Zhang ZF, Liu G, Liu S, Shi YH, Ji Y, Du M, Li NN, Li GB, Zhao ZK, Huang XY, Xu LQ, Yu QC, Peng DH, Qiu SJ, Sun HC, Dean M, Wang XD, Chung WY, Dennison AR, Zhou J, Hou Y, Fan J, Yang XR. Dissecting spatial heterogeneity and the immune-evasion mechanism of CTCs by single-cell RNA-seq in hepatocellular carcinoma. *Nat Commun* 2021; **12**: 4091 [PMID: 34215748 DOI: 10.1038/s41467-021-24386-0]
40 **Zhou L**, Wang J, Lyu SC, Pan LC, Shi XJ, Du GS, He Q. PD-L1^{+}NEUT, Foxp3^{+}Treg, and NLR as New Prognostic Marker with Low Survival Benefits Value in Hepatocellular Carcinoma. *Technol Cancer Res Treat* 2021; **20**: 15330338211045820 [PMID: 34605709 DOI: 10.1177/15330338211045820]
41 **Zhou SL**, Zhou ZJ, Hu ZQ, Huang XW, Wang Z, Chen EB, Fan J, Cao Y, Dai Z, Zhou J. Tumor-Associated Neutrophils Recruit Macrophages and T-Regulatory Cells to Promote Progression of Hepatocellular Carcinoma and Resistance to Sorafenib. *Gastroenterology* 2016; **150**: 1646-1658.e17 [PMID: 26924089 DOI: 10.1053/j.gastro.2016.02.040]
42 **Chen X**, Du Y, Hu Q, Huang Z. Tumor-derived CD4+CD25+regulatory T cells inhibit dendritic cells function by CTLA-4. *Pathol Res Pract* 2017; **213**: 245-249 [PMID: 28214198 DOI: 10.1016/j.prp.2016.12.008]
43 **Kalathil SG**, Wang K, Hutson A, Iyer R, Thanavala Y. Tivozanib mediated inhibition of c-Kit/SCF signaling on Tregs and MDSCs and reversal of tumor induced immune suppression correlates with survival of HCC patients. *Oncoimmunology* 2020; **9**: 1824863 [PMID: 33101775 DOI: 10.1080/2162402X.2020.1824863]
44 **Yi C**, Chen L, Lin Z, Liu L, Shao W, Zhang R, Lin J, Zhang J, Zhu W, Jia H, Qin L, Lu L, Chen J. Lenvatinib Targets FGF Receptor 4 to Enhance Antitumor Immune Response of Anti-Programmed Cell Death-1 in HCC. *Hepatology* 2021; **74**: 2544-2560 [PMID: 34036623 DOI: 10.1002/hep.31921]
45 **Lee YH**, Tai D, Yip C, Choo SP, Chew V. Combinational Immunotherapy for Hepatocellular Carcinoma: Radiotherapy, Immune Checkpoint Blockade and Beyond. *Front Immunol* 2020; **11**: 568759 [PMID: 33117354 DOI: 10.3389/fimmu.2020.568759]
46 **Zhang Q**, He Y, Luo N, Patel SJ, Han Y, Gao R, Modak M, Carotta S, Haslinger C, Kind D, Peet GW, Zhong G, Lu S, Zhu W, Mao Y, Xiao M, Bergmann M, Hu X, Kerkar SP, Vogt AB, Pflanz S, Liu K, Peng J, Ren X, Zhang Z. Landscape and Dynamics of Single Immune Cells in Hepatocellular Carcinoma. *Cell* 2019; **179**: 829-845.e20 [PMID: 31675496 DOI: 10.1016/j.cell.2019.10.003]
47 **Wilson GK**, Tennant DA, McKeating JA. Hypoxia inducible factors in liver disease and hepatocellular carcinoma: current understanding and future directions. *J Hepatol* 2014; **61**: 1397-1406 [PMID: 25157983 DOI: 10.1016/j.jhep.2014.08.025]
48 **Guo Y**, Xiao Z, Yang L, Gao Y, Zhu Q, Hu L, Huang D, Xu Q. Hypoxiainducible factors in hepatocellular carcinoma (Review). *Oncol Rep* 2020; **43**: 3-15 [PMID: 31746396 DOI: 10.3892/or.2019.7397]
49 **Liu J**, Li W, Zhu W, He W, Zhao H, Xiang Y, Liu C, Wu W. Chronic intermittent hypoxia promotes the development of experimental non-alcoholic steatohepatitis by modulating Treg/Th17 differentiation. *Acta Biochim Biophys Sin (Shanghai)* 2018; **50**: 1200-1210 [PMID: 30379980 DOI: 10.1093/abbs/gmy131]
50 **Hu CC**, Jeng WJ, Chen YC, Fang JH, Huang CH, Teng W, Hsieh YC, Lin YC, Chien RN, Sheen IS, Lin CY. Memory Regulatory T cells Increase Only In Inflammatory Phase of Chronic Hepatitis B Infection and Related to Galectin-9/Tim-3 interaction. *Sci Rep* 2017; **7**: 15280 [PMID: 29127350 DOI: 10.1038/s41598-017-15527-x]
51 **Nebbia G**, Peppa D, Schurich A, Khanna P, Singh HD, Cheng Y, Rosenberg W, Dusheiko G, Gilson R, ChinAleong J, Kennedy P, Maini MK. Upregulation of the Tim-3/galectin-9 pathway of T cell exhaustion in chronic hepatitis B virus infection. *PLoS One* 2012; **7**: e47648 [PMID: 23112829 DOI: 10.1371/journal.pone.0047648]
52 **Ju Y**, Shang X, Liu Z, Zhang J, Li Y, Shen Y, Liu Y, Liu C, Liu B, Xu L, Wang Y, Zhang B, Zou J. The Tim-3/galectin-9 pathway involves in the homeostasis of hepatic Tregs in a mouse model of concanavalin A-induced hepatitis. *Mol Immunol* 2014; **58**: 85-91 [PMID: 24333756 DOI: 10.1016/j.molimm.2013.11.001]
53 **Wang Z**, He L, Li W, Xu C, Zhang J, Wang D, Dou K, Zhuang R, Jin B, Zhang W, Hao Q, Zhang K, Wang S, Gao Y, Gu J, Shang L, Tan Z, Su H, Zhang Y, Zhang C, Li M. GDF15 induces immunosuppression *via* CD48 on regulatory T cells in hepatocellular carcinoma. *J Immunother Cancer* 2021; **9** [PMID: 34489334 DOI: 10.1136/jitc-2021-002787]
54 **Li Y**, Jiang HT, Han LB, Xiao L, Gan JH. MiR-195 regulates CD40 to maintain Th17/Treg balance in rats with non-alcoholic fatty liver disease. *Biomed Pharmacother* 2020; **124**: 109930 [PMID: 31991386 DOI: 10.1016/j.biopha.2020.109930]
55 **Cai C**, Chen DZ, Tu HX, Chen WK, Ge LC, Fu TT, Tao Y, Ye SS, Li J, Lin Z, Wang XD, Xu LM, Chen YP. MicroRNA-29c Acting on FOS Plays a Significant Role in Nonalcoholic Steatohepatitis Through the Interleukin-17 Signaling Pathway. *Front Physiol* 2021; **12**: 597449 [PMID: 33927635 DOI: 10.3389/fphys.2021.597449]
56 **Xia G**, Wu S, Wang X, Fu M. Inhibition of microRNA-155 attenuates concanavalin-A-induced autoimmune hepatitis by regulating Treg/Th17 cell differentiation. *Can J Physiol Pharmacol* 2018; **96**: 1293-1300 [PMID: 30290123 DOI:

10.1139/cjpp-2018-0467]
57 **Liu N**, Chang CW, Steer CJ, Wang XW, Song G. MicroRNA-15a/16-1 Prevents Hepatocellular Carcinoma by Disrupting the Communication Between Kupffer Cells and Regulatory T Cells. *Gastroenterology* 2022; **162**: 575-589 [PMID: 34678217 DOI: 10.1053/j.gastro.2021.10.015]
58 **Yu Z**, Zhao H, Feng X, Li H, Qiu C, Yi X, Tang H, Zhang J. Long Non-coding RNA FENDRR Acts as a miR-423-5p Sponge to Suppress the Treg-Mediated Immune Escape of Hepatocellular Carcinoma Cells. *Mol Ther Nucleic Acids* 2019; **17**: 516-529 [PMID: 31351327 DOI: 10.1016/j.omtn.2019.05.027]
59 **Xie K**, Liu L, Chen J, Liu F. Exosomal miR-1246 derived from human umbilical cord blood mesenchymal stem cells attenuates hepatic ischemia reperfusion injury by modulating T helper 17/regulatory T balance. *IUBMB Life* 2019; **71**: 2020-2030 [PMID: 31433911 DOI: 10.1002/iub.2147]
60 **Pasare C**, Medzhitov R. Toll pathway-dependent blockade of CD4+CD25+ T cell-mediated suppression by dendritic cells. *Science* 2003; **299**: 1033-1036 [PMID: 12532024 DOI: 10.1126/science.1078231]
61 **Hall JA**, Bouladoux N, Sun CM, Wohlfert EA, Blank RB, Zhu Q, Grigg ME, Berzofsky JA, Belkaid Y. Commensal DNA limits regulatory T cell conversion and is a natural adjuvant of intestinal immune responses. *Immunity* 2008; **29**: 637-649 [PMID: 18835196 DOI: 10.1016/j.immuni.2008.08.009]
62 **Ni X**, Tao J, Barbi J, Chen Q, Park BV, Li Z, Zhang N, Lebid A, Ramaswamy A, Wei P, Zheng Y, Zhang X, Wu X, Vignali P, Yang CP, Li H, Pardoll D, Lu L, Pan D, Pan F. YAP Is Essential for Treg-Mediated Suppression of Antitumor Immunity. *Cancer Discov* 2018; **8**: 1026-1043 [PMID: 29907586 DOI: 10.1158/2159-8290.CD-17-1124]
63 **Polanczyk MJ**, Walker E, Haley D, Guerrouahen BS, Akporiaye ET. Blockade of TGF-β signaling to enhance the antitumor response is accompanied by dysregulation of the functional activity of $CD4^+CD25^+Foxp3^+$ and $CD4^+CD25^-Foxp3^+$ T cells. *J Transl Med* 2019; **17**: 219 [PMID: 31288845 DOI: 10.1186/s12967-019-1967-3]
64 **Badr AM**, El-Ahwany E, Goda L, Nagy F, Helal N, El Deeb S. MicroRNA-26a systemic administration attenuates tumor formation in hepatocellular carcinoma mouse model. *Pak J Pharm Sci* 2021; **34**: 925-932 [PMID: 34602415]
65 **Yang X**, Liang L, Zhang XF, Jia HL, Qin Y, Zhu XC, Gao XM, Qiao P, Zheng Y, Sheng YY, Wei JW, Zhou HJ, Ren N, Ye QH, Dong QZ, Qin LX. MicroRNA-26a suppresses tumor growth and metastasis of human hepatocellular carcinoma by targeting interleukin-6-Stat3 pathway. *Hepatology* 2013; **58**: 158-170 [PMID: 23389848 DOI: 10.1002/hep.26305]
66 **Yang X**, Zhang XF, Lu X, Jia HL, Liang L, Dong QZ, Ye QH, Qin LX. MicroRNA-26a suppresses angiogenesis in human hepatocellular carcinoma by targeting hepatocyte growth factor-cMet pathway. *Hepatology* 2014; **59**: 1874-1885 [PMID: 24259426 DOI: 10.1002/hep.26941]
67 **Ma Y**, Deng F, Li P, Chen G, Tao Y, Wang H. The tumor suppressive miR-26a regulation of FBXO11 inhibits proliferation, migration and invasion of hepatocellular carcinoma cells. *Biomed Pharmacother* 2018; **101**: 648-655 [PMID: 29518611 DOI: 10.1016/j.biopha.2018.02.118]
68 **Wang X**, Sun L, Zhang L, Jiang Z. Effect of Adoptive Transfer or Depletion of Regulatory T Cells on Triptolide-induced Liver Injury. *Front Pharmacol* 2016; **7**: 99 [PMID: 27148057 DOI: 10.3389/fphar.2016.00099]
69 **Huang H**, Deng Z. Adoptive transfer of regulatory T cells stimulated by Allogeneic Hepatic Stellate Cells mitigates liver injury in mice with concanavalin A-induced autoimmune hepatitis. *Biochem Biophys Res Commun* 2019; **512**: 14-21 [PMID: 30853178 DOI: 10.1016/j.bbrc.2019.02.147]
70 **Feng M**, Wang Q, Jiang Z, Ding J, Wang H, Wang M, Lu L, Guan W. Adoptive transferred hepatic stellate cells attenuated drug-induced liver injury by modulating the rate of regulatory T cells/T helper 17 cells. *Clin Immunol* 2016; **165**: 12-18 [PMID: 26911201 DOI: 10.1016/j.clim.2016.02.006]
71 **Kehrmann J**, Effenberg L, Wilk C, Schoemer D, Ngo Thi Phuong N, Adamczyk A, Pastille E, Scholtysik R, Klein-Hitpass L, Klopfleisch R, Westendorf AM, Buer J. Depletion of $Foxp3^+$ regulatory T cells is accompanied by an increase in the relative abundance of Firmicutes in the murine gut microbiome. *Immunology* 2020; **159**: 344-353 [PMID: 31755554 DOI: 10.1111/imm.13158]
72 **Wang Y**, Liu Y, Kirpich I, Ma Z, Wang C, Zhang M, Suttles J, McClain C, Feng W. Lactobacillus rhamnosus GG reduces hepatic TNFα production and inflammation in chronic alcohol-induced liver injury. *J Nutr Biochem* 2013; **24**: 1609-1615 [PMID: 23618528 DOI: 10.1016/j.jnutbio.2013.02.001]
73 **Wang Y**, Liu Y, Sidhu A, Ma Z, McClain C, Feng W. Lactobacillus rhamnosus GG culture supernatant ameliorates acute alcohol-induced intestinal permeability and liver injury. *Am J Physiol Gastrointest Liver Physiol* 2012; **303**: G32-G41 [PMID: 22538402 DOI: 10.1152/ajpgi.00024.2012]
74 **Li J**, Sung CY, Lee N, Ni Y, Pihlajamäki J, Panagiotou G, El-Nezami H. Probiotics modulated gut microbiota suppresses hepatocellular carcinoma growth in mice. *Proc Natl Acad Sci U S A* 2016; **113**: E1306-E1315 [PMID: 26884164 DOI: 10.1073/pnas.1518189113]
75 **Shigeta K**, Datta M, Hato T, Kitahara S, Chen IX, Matsui A, Kikuchi H, Mamessier E, Aoki S, Ramjiawan RR, Ochiai H, Bardeesy N, Huang P, Cobbold M, Zhu AX, Jain RK, Duda DG. Dual Programmed Death Receptor-1 and Vascular Endothelial Growth Factor Receptor-2 Blockade Promotes Vascular Normalization and Enhances Antitumor Immune Responses in Hepatocellular Carcinoma. *Hepatology* 2020; **71**: 1247-1261 [PMID: 31378984 DOI: 10.1002/hep.30889]
76 **Langhans B**, Nischalke HD, Krämer B, Dold L, Lutz P, Mohr R, Vogt A, Toma M, Eis-Hübinger AM, Nattermann J, Strassburg CP, Gonzalez-Carmona MA, Spengler U. Role of regulatory T cells and checkpoint inhibition in hepatocellular carcinoma. *Cancer Immunol Immunother* 2019; **68**: 2055-2066 [PMID: 31724091 DOI: 10.1007/s00262-019-02427-4]
77 **Lee JC**, Mehdizadeh S, Smith J, Young A, Mufazalov IA, Mowery CT, Daud A, Bluestone JA. Regulatory T cell control of systemic immunity and immunotherapy response in liver metastasis. *Sci Immunol* 2020; **5** [PMID: 33008914 DOI: 10.1126/sciimmunol.aba0759]
78 **Doi T**, Muro K, Ishii H, Kato T, Tsushima T, Takenoyama M, Oizumi S, Gemmoto K, Suna H, Enokitani K, Kawakami T, Nishikawa H, Yamamoto N. A Phase I Study of the Anti-CC Chemokine Receptor 4 Antibody, Mogamulizumab, in Combination with Nivolumab in Patients with Advanced or Metastatic Solid Tumors. *Clin Cancer Res* 2019; **25**: 6614-6622 [PMID: 31455681 DOI: 10.1158/1078-0432.CCR-19-1090]
79 **Zhang Q**, Huang H, Zheng F, Liu H, Qiu F, Chen Y, Liang CL, Dai Z. Resveratrol exerts antitumor effects by downregulating $CD8^+CD122^+$ Tregs in murine hepatocellular carcinoma. *Oncoimmunology* 2020; **9**: 1829346 [PMID:

33150044 DOI: 10.1080/2162402X.2020.1829346]

80 **Ren Z**, Yue Y, Zhang Y, Dong J, Liu Y, Yang X, Lin X, Zhao X, Wei Z, Zheng Y, Wang T. Changes in the Peripheral Blood Treg Cell Proportion in Hepatocellular Carcinoma Patients After Transarterial Chemoembolization With Microparticles. *Front Immunol* 2021; **12**: 624789 [PMID: 33717135 DOI: 10.3389/fimmu.2021.624789]

81 **Jhun J**, Lee SH, Lee SK, Kim HY, Jung ES, Kim DG, Choi J, Bae SH, Yoon SK, Chung BH, Yang CW, Cho ML, Choi JY. Serial Monitoring of Immune Markers Being Represented Regulatory T Cell/T Helper 17 Cell Ratio: Indicating Tolerance for Tapering Immunosuppression after Liver Transplantation. *Front Immunol* 2018; **9**: 352 [PMID: 29545795 DOI: 10.3389/fimmu.2018.00352]

82 **Knochelmann HM**, Dwyer CJ, Bailey SR, Amaya SM, Elston DM, Mazza-McCrann JM, Paulos CM. When worlds collide: Th17 and Treg cells in cancer and autoimmunity. *Cell Mol Immunol* 2018; **15**: 458-469 [PMID: 29563615 DOI: 10.1038/s41423-018-0004-4]

83 **Sánchez-Fueyo A**, Whitehouse G, Grageda N, Cramp ME, Lim TY, Romano M, Thirkell S, Lowe K, Fry L, Heward J, Kerr A, Ali J, Fisher C, Lewis G, Hope A, Kodela E, Lyne M, Farzaneh F, Kordasti S, Rebollo-Mesa I, Jose Lozano J, Safinia N, Heaton N, Lechler R, Martínez-Llordella M, Lombardi G. Applicability, safety, and biological activity of regulatory T cell therapy in liver transplantation. *Am J Transplant* 2020; **20**: 1125-1136 [PMID: 31715056 DOI: 10.1111/ajt.15700]

84 **Whitehouse GP**, Hope A, Sanchez-Fueyo A. Regulatory T-cell therapy in liver transplantation. *Transpl Int* 2017; **30**: 776-784 [PMID: 28608637 DOI: 10.1111/tri.12998]

85 **Cvetkovski F**, Hexham JM, Berglund E. Strategies for Liver Transplantation Tolerance. *Int J Mol Sci* 2021; **22** [PMID: 33668238 DOI: 10.3390/ijms22052253]

86 **Casiraghi F**, Perico N, Podestà MA, Todeschini M, Zambelli M, Colledan M, Camagni S, Fagiuoli S, Pinna AD, Cescon M, Bertuzzo V, Maroni L, Introna M, Capelli C, Golay JT, Buzzi M, Mister M, Ordonez PYR, Breno M, Mele C, Villa A, Remuzzi G; MSC-LIVER Study Group. Third-party bone marrow-derived mesenchymal stromal cell infusion before liver transplantation: A randomized controlled trial. *Am J Transplant* 2021; **21**: 2795-2809 [PMID: 33370477 DOI: 10.1111/ajt.16468]

87 **Han JW**, Sung PS, Hong SH, Lee H, Koh JY, White S, Maslow JN, Weiner DB, Park SH, Jeong M, Heo J, Ahn SH, Shin EC. IFNL3-adjuvanted HCV DNA vaccine reduces regulatory T cell frequency and increases virus-specific T cell responses. *J Hepatol* 2020; **73**: 72-83 [PMID: 32088322 DOI: 10.1016/j.jhep.2020.02.009]

88 **Boni C**, Janssen HLA, Rossi M, Yoon SK, Vecchi A, Barili V, Yoshida EM, Trinh H, Rodell TC, Laccabue D, Alfieri A, Brillo F, Fisicaro P, Acerbi G, Pedrazzi G, Andreone P, Cursaro C, Margotti M, Santoro R, Piazzolla V, Brunetto MR, Coco B, Cavallone D, Zhao Y, Joshi A, Woo J, Lau AH, Gaggar A, Subramanian GM, Massetto B, Fung S, Ahn SH, Ma X, Mangia A, Ferrari C. Combined GS-4774 and Tenofovir Therapy Can Improve HBV-Specific T-Cell Responses in Patients With Chronic Hepatitis. *Gastroenterology* 2019; **157**: 227-241.e7 [PMID: 30930022 DOI: 10.1053/j.gastro.2019.03.044]

89 **Wu D**, Wang P, Han M, Chen Y, Chen X, Xia Q, Yan W, Wan X, Zhu C, Xie Q, Jiang J, Wei L, Tan D, Dou X, Yu Y, Hou J, Luo X, Ning Q. Sequential combination therapy with interferon, interleukin-2 and therapeutic vaccine in entecavir-suppressed chronic hepatitis B patients: the Endeavor study. *Hepatol Int* 2019; **13**: 573-586 [PMID: 31172415 DOI: 10.1007/s12072-019-09956-1]

90 **Kalathil SG**, Hutson A, Barbi J, Iyer R, Thanavala Y. Augmentation of IFN-γ+ CD8+ T cell responses correlates with survival of HCC patients on sorafenib therapy. *JCI Insight* 2019; **4** [PMID: 31391334 DOI: 10.1172/jci.insight.130116]

World Journal of Gastroenterology

Submit a Manuscript: https://www.f6publishing.com

World J Gastroenterol 2022 July 21; 28(27): 3359-3369

DOI: 10.3748/wjg.v28.i27.3359

ISSN 1007-9327 (print) ISSN 2219-2840 (online)

MINIREVIEWS

Single-incision laparoscopic surgery to treat hepatopancreatobiliary cancer: A technical review

Shu-Hung Chuang, Shih-Chang Chuang

Specialty type: Surgery

Provenance and peer review: Invited article; Externally peer reviewed.

Peer-review model: Single blind

Peer-review report's scientific quality classification

Grade A (Excellent): 0
Grade B (Very good): B, B
Grade C (Good): 0
Grade D (Fair): 0
Grade E (Poor): 0

P-Reviewer: A JD, China; Hiep LT, Viet Nam

Received: January 17, 2022
Peer-review started: January 17, 2022
First decision: March 9, 2022
Revised: March 20, 2022
Accepted: June 16, 2022
Article in press: June 16, 2022
Published online: July 21, 2022

Shu-Hung Chuang, Shih-Chang Chuang, Division of General and Digestive Surgery, Department of Surgery, Kaohsiung Medical University Hospital, Kaohsiung Medical University, Kaohsiung 80708, Taiwan

Shu-Hung Chuang, Shih-Chang Chuang, School of Medicine, College of Medicine, Kaohsiung Medical University, Kaohsiung 80708, Taiwan

Corresponding author: Shih-Chang Chuang, MD, PhD, Associate Professor, Director, Surgeon, Surgical Oncologist, Division of General and Digestive Surgery, Department of Surgery, Kaohsiung Medical University Hospital, Kaohsiung Medical University, No. 100 Shih-Chuan 1st Road, Sanmin District, Kaohsiung 80708, Taiwan. chuangsc@cc.kmu.edu.tw

Abstract

Single-incision laparoscopic surgery (SILS), or laparoendoscopic single-site surgery, was launched to minimize incisional traumatic effects in the 1990s. Minor SILS, such as cholecystectomies, have been gaining in popularity over the past few decades. Its application in complicated hepatopancreatobiliary (HPB) surgeries, however, has made slow progress due to instrumental and technical limitations, costs, and safety concerns. While minimally invasive abdominal surgery is pushing the boundaries, advanced laparoscopic HPB surgeries have been shown to be comparable to open operations in terms of patient and oncologic safety, including hepatectomies, distal pancreatectomies (DP), and pancreaticoduodenectomies (PD). In contrast, advanced SILS for HPB malignancy has only been reported in a few small case series. Most of the procedures involved minor liver resections and DP; major hepatectomies were rarely described. Single-incision laparoscopic PD has not yet been reported. We herein review the published SILS for HPB cancer in the literature and our three-year experience focusing on the technical aspects.

Key Words: Hepatectomy; Hepatopancreatobiliary cancer; Laparoendoscopic single-site surgery; Pancreatectomy; Pancreaticoduodenectomy; Single-incision laparoscopic surgery

©The Author(s) 2022. Published by Baishideng Publishing Group Inc. All rights reserved.

Core Tip: Single-incision laparoscopic surgery (SILS), or laparoendoscopic single-site surgery, has been introduced to minimize incisional traumatic effects over the past few decades. As minor SILS, such as cholecystectomies, have been gaining in popularity, major SILS for complicated hepatopancreatobiliary (HPB) surgeries have made slow progress due to instrumental and technical limitations, costs, and safety concerns. We herein review the published SILS for HPB cancer in the literature and our three-year experience focusing on the technical aspects.

Citation: Chuang SH, Chuang SC. Single-incision laparoscopic surgery to treat hepatopancreatobiliary cancer: A technical review. *World J Gastroenterol* 2022; 28(27): 3359-3369
URL: https://www.wjgnet.com/1007-9327/full/v28/i27/3359.htm
DOI: https://dx.doi.org/10.3748/wjg.v28.i27.3359

INTRODUCTION

Single-incision laparoscopic surgery (SILS), also known as laparoendoscopic single-site surgery, is an advanced minimally invasive procedure that leaves a single small incision after surgery. Since it was introduced in the 1990s, numerous studies regarding SILS for minor procedures have been published, such as for cholecystectomy[1]. In contrast, its application in advanced hepatopancreatobiliary (HPB) surgeries is rarely reported[2-8].

By minimizing the incision number, SILS has the potential advantages of less pain, fewer wound complications, faster recovery, and favorable cosmesis. Nevertheless, the existing literature regarding minor SILS fails to reach a conclusion. For example, single-incision laparoscopic cholecystectomies (SILC), the most published SILS to date, have been shown to be superior in marginal benefits such as less pain and shorter hospital stays, while incisional hernia and bile duct injury are considerable drawbacks[9-11]. Nevertheless, it is always necessary to remove a sizable specimen during advanced HPB surgeries. One of the small incisions in standard multi-incision laparoscopic surgeries (MILS) has to be enlarged to fit the specimen size as well as the only incision in SILS. Since incisional hernia has become a minor issue, patient and oncologic safety has attracted more concern in advanced single-incision laparoscopic HPB surgeries. MILS has been shown to be comparable to open operations for HPB malignancy, including hepatectomies, distal pancreatectomies (DP), and pancreaticoduodenectomies (PD), in recent years[12-24]. The fact that only a few case series of SILS for HPB cancer have been reported reflects the limitations of surgical techniques, instrumental technology, and adequate training. Although our previous study showed that practicing minor SILS helps to achieve competence in this technique for complicated diseases[25], there is still a long way to go. In this review, we conducted an updated literature search for SILS to treat malignant HPB diseases that were reported in English. Studies involving robotic technology were excluded. Meanwhile, a summary of our three-year experience focusing on the technical aspects was described.

SINGLE-INCISION LAPAROSCOPIC HEPATECTOMY (SILH) FOR MALIGNANCY

Literature review

Eight original studies[26-33] and 20 case reports[34-47] were identified with a cutoff value of 10 malignant cases. The outdated reports of sequential studies from the same groups were excluded. Nearly all the case reports involved minor liver resections [partial hepatectomies, monosegmentectomies, and left lateral sectionectomies (LLS)]. Three of the eight original articles described major hepatectomies (resection of over two segments), including nine right hemihepatectomies (RHs), 34 left hemihepatectomies, and seven right posterior sectionectomies (RPSs)[27,29,32] (Table 1). Most procedures were performed for malignant diseases. Five nonrandomized comparative studies between SILH and multi-incision laparoscopic hepatectomies (MILHs) were conducted[26-28,30,32]. Hyun *et al*[26] reported a shorter postoperative hospital stay and comparable pathologic features for minor SILH compared with minor MILH; long-term survival outcomes were absent. Mittermair *et al*[27] showed less blood loss, a lower number of patients with blood loss > 25 mL, and more blood transfusions in the major SILH group; no local tumor recurrence occurred during a median follow-up of 61 mo. Tsai *et al*[28] reported a shorter operative time and shorter postoperative hospital stays in the SILH group for LLS but not partial hepatectomies of segment 5-6; the 1-, 3-, and 5-year overall and recurrence-free survival rates for hepatocellular carcinoma were similar in both the SILH and MILH groups. Wang *et al*[30] showed shorter postoperative hospital stays for patients without cirrhosis undergoing LLS in the SILH group; the 1-year recurrence-free survival rates for hepatocellular carcinoma were similar in both the SILH and MILH groups. Han *et al*[32] reported a shorter operative time, less blood loss, and earlier

Table 1 English original researches of single-incision laparoscopic hepatectomies for malignancy retrieved online till December 2021

Ref.	Journal (year of publication)	SILH	Control group	RH	LH	RAS	RPS	LLS + MR
Hyun *et al*[26]	*J Gastrointest Surg* (2021)	15	MILH	0	0	0	0	15
Mittermair *et al*[27]	*J Clin Med* (2021)	34	MILH	4	6	0	7	17
Tsai *et al*[28]	*Surg Endosc* (2020)	54	MILH	0	0	0	0	54
Saad *et al*[29]	*ANZ J Surg* (2020)	54	No	0	11	0	0	43
Wang *et al*[30]	*Int J Surg* (2020)	33	MILH	0	0	0	0	33
Pan *et al*[31]	*Surg Laparosc Endosc Percutan Tech* (2019)	37	No	0	0	0	0	37
Han *et al*[32]	*World J Gastroenterol* (2018)	155	MILH	5	17	0	0	133
Weiss *et al*[33]	*J Hepatobiliary Pancreat Sci* (2015)	21	No	0	0	0	0	21
Our study	Under submission	31	No	3	2	3	3	20

SILH: Single-incision laparoscopic hepatectomies; MILH: Multi-incision laparoscopic hepatectomies; RH: Right hemihepatectomies; LH: Left hemihepatectomies; RAS: Right anterior sectionectomies; RPS: Right posterior sectionectomies; LLS: Left lateral sectionectomies; MR: Minor resections including monosegmentectomies and partial hepatectomies.

enteral feeding in the SILH group; the safety resection margins were similar in both the SILH and MILH groups. However, long-term survival outcomes were not presented.

In summary, SILH was superior to MILH in terms of shorter postoperative hospital stays in three comparative studies of minor liver resections[26,28,30]. For major hepatectomies, the two related studies came to a different conclusion. While Mittermair C *et al*[27] declared more substantial blood loss requiring transfusion in SILH, Han *et al*[32] reported a shorter operative time, less blood loss, and earlier enteral feeding for the single port technique.

Our experience and technical review

While SILC[25] and single-incision laparoscopic common bile duct exploration (SILCBD)[48] have become our standard of care for cholelithiasis over the past decade, we have developed more advanced SILS for malignant HPB diseases since 2016. The principles of standard MILS and surgical oncology were strictly followed to maintain a high standard of patient safety and prognosis. From July 2018 to July 2021, 31 SILH procedures were performed by the first author to treat malignant diseases (Table 1). Eleven (35.5%) major liver resections involved three RHs, two left hemohepatectomies (LHs), three right anterior sectionectomies (RASs), and three RPSs. The others were 20 (64.5%) minor resections. An additional port was needed in five (16.1%) procedures, and no open conversion occurred. There was one case of surgery-related 90-d mortality due to pulmonary infection.

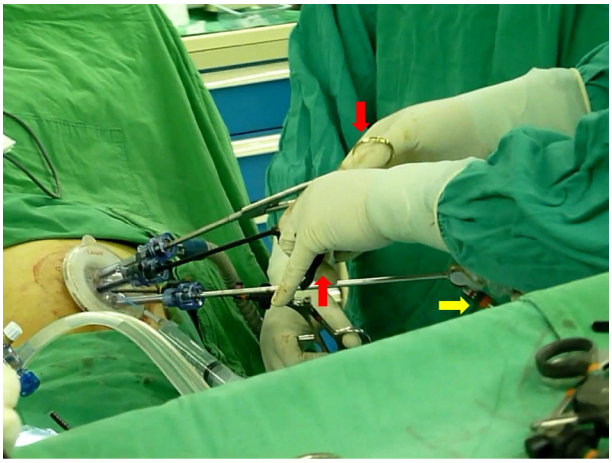
Patient position

During formal hepatic surgery, the patient was placed in a reverse Trendelenburg position with arms abducted and legs split. The surgeon stood between the patient's legs to facilitate hepatic hilar management. The assistant held the laparoscope at the patient's left/right side (between the left/right limbs) during right/Left hepatic resections. For LLS, the operative table could be tilted toward the patient's right side. In contrast, it should be tilted toward the patient's left side during RPS. Lateral decubitus positions were not favored because of impaired access to the hepatic hilum.

Port and instrument

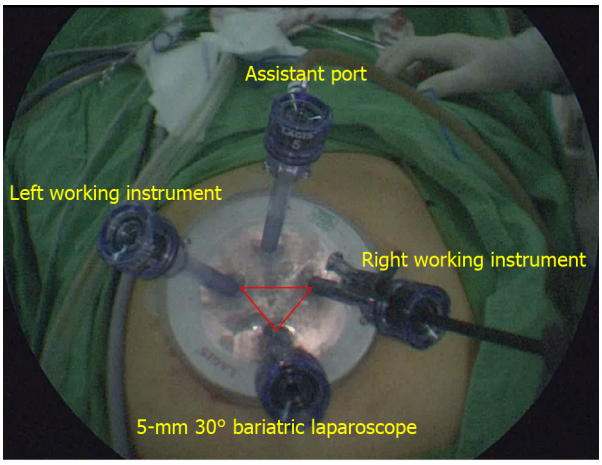
By using conventional laparoscopic ports and straight instruments through a 1.5-2.5 cm skin incision and multiple nearby punctures on the deep fascia, the costs can be reduced to a minimum. This single-incision multipuncture approach is only suitable for short-duration procedures such as SILC[25], SILCBDE[48], and minor SILH because of its inherent problem of air leakage. Otherwise, a 3-6 cm single skin and deep fascia incision with a homemade (surgical glove) or commercial multichannel port is recommended for major liver resections to remove a sizable specimen at the end of surgery.

We recommended 30° rigid laparoscopes and conventional straight instruments, as the latter could be manipulated more intuitively than curved or articulated instruments. A 5-mm 30° bariatric laparoscope can effectively prevent "sword fighting" between the light cable of the laparoscope and the instrument handles (Figure 1). The port configuration was arranged in a reverse triangular pattern (Figure 2). The 30° laparoscope passed through the lower port and the fulcrum to the upper part of the operative field to provide an overlooking view, and the two working instruments reached the lower part of the



DOI: 10.3748/wjg.v28.i27.3359 **Copyright** ©The Author(s) 2022.

Figure 1 The 5-mm 30° bariatric laparoscope effectively prevented "sword fighting" between the light cable (yellow arrow) of the laparoscope and the instrument handles (red arrows) in single-incision laparoscopic surgery.



DOI: 10.3748/wjg.v28.i27.3359 **Copyright** ©The Author(s) 2022.

Figure 2 The port configuration was arranged in a reverse triangular pattern on a commercial multichannel port in a single-incision laparoscopic surgery. The upper port served as an assistant port for additional traction or suction/irrigation.

operative field to perform the procedure. This configuration decreased collisions between the laparoscope and the working instruments. Finally, a fourth port could be used to perform traction or suction.

Abdominal incision

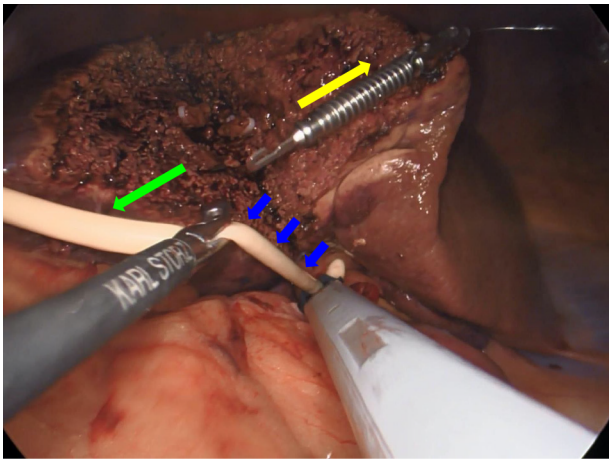
Considering that upper abdominal incisions induce more pain, we avoided making incisions above the umbilical level. A praumbilical incision with downward extension is good for performing single-incision laparoscopic LH or RH. Otherwise, a transverse incision at the same level of the umbilicus is suitable to perform single-incision laparoscopic RAS or RPS. The incision should be tailored to the specimen size for its removal.

Hepatic inflow control

For temporary hepatic inflow control (Pringle maneuver), we favored the use of a 14-French Foley catheter (Figure 3), which was introduced by Huang *et al*[49] in 2018. During selective inflow control for major SILH, such as the extra Glissonian approach or individual dissection, a laparoscopic right angle dissector or a goldfinger retractor is useful. As the working instruments were kept aligned with the laparoscope in SILH, it was difficult to see the distal ends of the instruments. Laparoscopic working instruments with curved or flexible ends were easier to manipulate under limited vision.

Parenchymal transection

To avoid interinstrumental collisions, auxiliary traction devices substituted for assistant tractions. We preferred EndoGrab™ (Virtual Ports Ltd., Hod Hasharon, Israel), while gravity would provide counter-



DOI: 10.3748/wjg.v28.i27.3359 **Copyright** ©The Author(s) 2022.

Figure 3 The hepatoduodenal ligament was encircled by a 14-French Foley catheter (blue arrows) for temporary hepatic inflow control (Pringle maneuver) in a single-incision laparoscopic right posterior sectionectomy. An EndoGrab™ (Virtual Ports Ltd., Hod Hasharon, Israel) provided traction in the direction of the yellow arrow, while gravity created countertraction (green arrow).

traction in some instances (Figure 3). The transection line should be kept aligned with the laparoscopic view at all times.

Single-incision laparoscopic suturing technique

Suturing is the last line of defense in patient safety for not only open but also laparoscopic surgeries. It can be applied in various difficult situations to stop bleeding or biliary leakage. While performing single-incision laparoscopic suturing technique (SILST), forward-backward, vertical, and rotational movements are frequently used rather than transverse movements. The curved tip of a Maryland dissector helps to form a loop made by two instruments nearly parallel to each other (Figure 4). In addition, monofilament threads make loops more easily in SILST due to their high elasticity.

SINGLE-INCISION LAPAROSCOPIC PANCREATECTOMY FOR MALIGNANCY

Literature review

While most reported single-incision laparoscopic DP (SILDP) was used to treat benign lesions, only three original studies[50-52] (Table 2) and three case reports[53-55] of SILDP for cancer were identified with a cutoff value of 10 cases. Series containing neoplasms with uncertain behavior were excluded, as well as outdated reports of sequential studies from the same groups. All three original studies were nonrandomized comparative studies. SILDP was compared with multi-incision laparoscopic DP (MILDP) in two studies and the robotic approach in the remaining study. SILDP was associated with a longer operative time, reduced postoperative pain, and lower spleen/splenic vessel preservation rates than MILDP[50,51]. Robotic DP and splenectomies required a longer operating room time than SILDP and splenectomies, but the operative durations were similar[52]. All the patients except one undergoing DP for neoplasms had R0 resections, and six (7 ± 6.6) lymph nodes were noted according to the pathologic reports. However, long-term survival outcomes were not provided.

For PD, one of the most complicated abdominal surgeries, we could not find any report of applying a single-incision laparoscopic technique.

Our experience and technical review

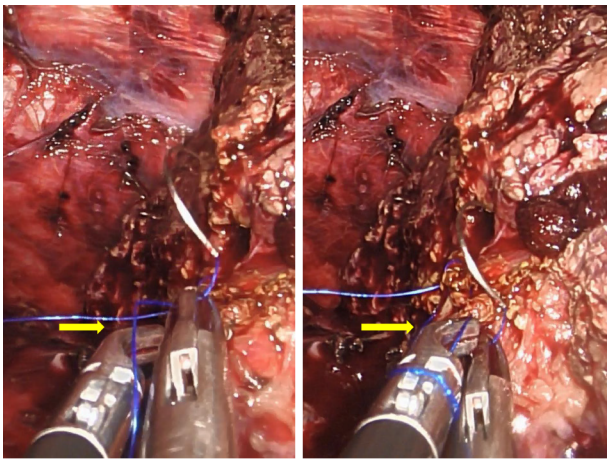
We have no experience in performing SILDP for malignancy. Two patients with benign lesions (serous cystadenoma) underwent this procedure in the last two years. However, we have performed single-incision laparoscopic PD (SILPD) on three patients since May 2020. All procedures were accomplished successfully without conversion to MILS or open operations. No major complications, such as postoperative pancreatic fistula, occurred, and there was no 90-day mortality. The pathology report was distal cholangiocarcinoma in the first patient and pancreatic ductal adenocarcinoma in the other two. Routine D2 Lymph node dissections and intraoperative frozen sections for checking resection margins were carried out for oncologic safety. To the best of our knowledge, this report is the first experience of SILPD in the world and is now under submission.

Table 2 English original researches of single-incision laparoscopic pancreatectomies for malignancy retrieved online till December 2021

Ref.	Journal (year of publication)	Procedure	Case number	Control group	Spleen preservation
Park *et al*[50]	*Hepatobiliary Pancreat Sci* (2019)	SILDP	26	MILDP	0[1]
Ağcaoğlu *et al*[51]	*Sisli Etfal Hastan Tip Bul* (2019)	SILDP	10	MILDP	1
Ryan *et al*[52]	*JSLS* (2015)	SILDPS	16	RDPS	N/A

[1]Splenic vessel preservation.

SILDP: Single-incision laparoscopic distal pancreatectomies; MILDP: Multi-incision laparoscopic distal pancreatectomies; SILDPS: Single-incision laparoscopic distal pancreatectomies and splenectomies; RDPS: Robotic distal pancreatectomies and splenectomies; N/A: Not applicable.



DOI: 10.3748/wjg.v28.i27.3359 **Copyright** ©The Author(s) 2022.

Figure 4 The curved tip of a Maryland dissector (yellow arrow) helped to form a loop made by two instruments nearly parallel to each other in a single-incision laparoscopic surgery. A monofilament thread was used in this case.

Patient position

During a single-incision laparoscopic pancreatectomy, the patient was placed in a reverse Trendelenburg position with the surgeon standing between their legs. The operative table could be tilted toward the patient's right side for SILDP. The assistant held the laparoscope at the patient's left side (between the left limbs) during the resection phase and hepaticojejunostomy during SILPD. In contrast, the assistant held the laparoscope at the patient's right side (between the right limbs) during SILDP and pancreaticojejunostomy/gastrojejunostomy in SILPD.

Port and instrument

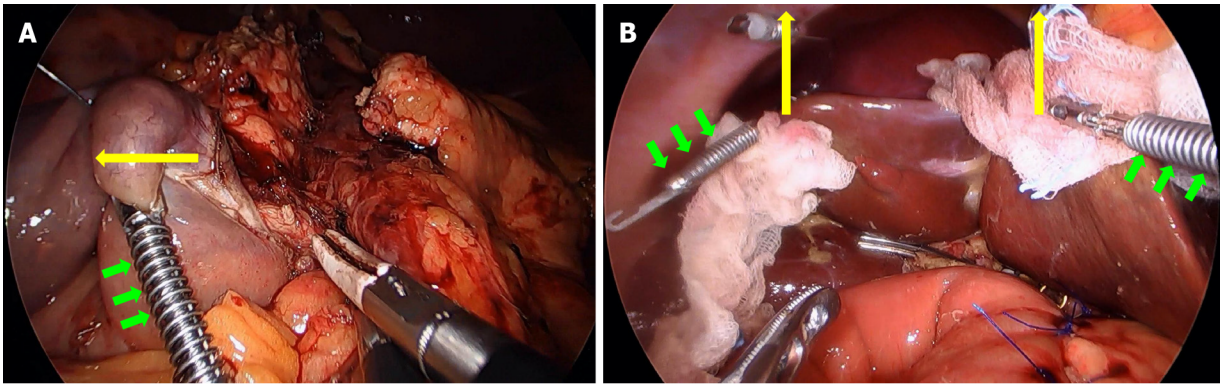
Major pancreatic and hepatic resections shared the same port configuration and instrument selection. Sometimes the surgeon had to cross the instruments to achieve an adequate approaching angle (the angle between the two working instruments) or solve a handedness problem, such as suturing a left target with a right-handed instrument.

Abdominal incision

In order to achieve less pain and better cosmesis, a several centimeter praumbilical incision with downward extension is good for performing a SILDP or a SILPD. The incision should be enlarged to facilitate specimen removal in a retrieval bag at the end of surgery if necessary.

Auxiliary traction

EndoGrab™ (Virtual Ports Ltd., Hod Hasharon, Israel) could be applied on the duodenum to be resected during the uncinate process dissection in a SILPD (Figure 5A). It was very useful for liver retraction during SILDP or SILPD (Figure 5B).



DOI: 10.3748/wjg.v28.i27.3359 **Copyright** ©The Author(s) 2022.

Figure 5 EndoGrab™ (Virtual Ports Ltd., Hod Hasharon, Israel) provided auxiliary traction during single-incision laparoscopic pancreatectomies. A: EndoGrab™ (green arrows) was applied on the duodenal 3rd portion to provide lateral traction (yellow arrow) during the uncinate process dissection in a single-incision laparoscopic pancreaticoduodenectomy (SILPD); B: Two EndoGrabs™ (green arrows) facilitated upward traction (yellow arrows) of the liver edges during the reconstruction phase in a SILPD. Two pieces of gauze served as cushions to minimize the traumatic effect of EndoGrabs™ (green arrows) on the liver.

SILST

Unlike hepatectomies, suturing constituted a major component in pancreatic resections, such as hemostasis (Video 1), closure of the pancreatic stump in a DP and creation of the three anastomoses (pancreaticojejunostomy, hepaticojejunostomy, and gastrojejunostomy) in a PD. During critical duct-to-mucosa pancreaticojejunostomy, we recommend interrupted suturing for the inner layer to prevent anastomotic stricture caused by a "purse-string effect". Holding the interrupted stitches with metallic clips before tying them helped to gain adequate space for the anastomosis. In our experience, up to three metallic clips could be used simultaneously during anastomosis without confusing the surgeon (Figure 6). While performing SILST, all the principles of suturing in open surgery and MILS should be followed on the basis of high quality. Otherwise, additional port(s) should be utilized to minimize anastomotic leakage.

Step-by-step procedures in SILPD

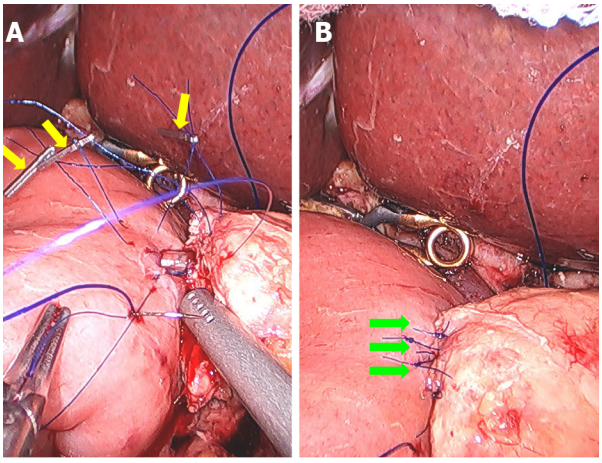
While the laparoscopic view was unchanged during SILPD, the procedural steps were standardized to shorten the operative time as well as the learning curve. These steps include division of the gastrocolic ligament, release of the hepatic flexure of the transverse colon, Kocher maneuver (Station 13 Lymph nodes harvest), division of Treitz's ligament, pulling of the proximal jejunum to the patient's right side, creation of the tunnel under the pancreatic neck, division of the proximal jejunum and its mesentery, division of the lesser omentum and distal stomach (Station 5 and 6 Lymph node harvest), division of the pancreatic neck, dissection of the uncinate process (Station 14 Lymph nodes harvest), Station 8 and 12 Lymph node harvest, division of the common hepatic duct, removal of the gallbladder from the liver bed, specimen extraction, pancreaticojejunostomy, hepaticojejunostomy, gastrojejunostomy, and peritoneal irrigation with drainage.

SINGLE-INCISION LAPAROSCOPIC BILE DUCT RESECTION (SILBDR) FOR MALIGNANCY

Literature review

We only found one case report of SILBDR in the literature[56]. Two patients with Bismuth–Corlette type I perihilar cholangiocarcinoma underwent the procedure, including hepatoduodenal ligament lymphadenectomy, successfully with good recovery. The resection margins of the proximal and distal bile ducts were free from tumor invasion, but long-term follow-up was pending. The authors concluded that SILBDR can be optional in strictly selected patients with Bismuth–Corlette type I perihilar cholangiocarcinoma.

As perihilar cholangiocarcinoma is relatively rare to diagnose in an early stage, more advanced procedures, such as hemihepatectomies, caudate lobectomies, or PD, are usually performed in addition to bile duct resections for a better prognosis. The feasibility of SILS for resecting advanced-stage perihilar cholangiocarcinoma, an extremely complicated, demanding, and time-consuming procedure, should be considered with caution.



DOI: 10.3748/wjg.v28.i27.3359 **Copyright** ©The Author(s) 2022.

Figure 6 Single-incision laparoscopic suturing technique was applied to a pancreatiojejunostomy. A: Three metallic clips (yellow arrows) were used at the same time during the inner duct-to-mucosa anastomosis of the pancreatiojejunostomy (PJ) in a single-incision laparoscopic pancreaticoduodenectomy; B: Completed inner duct-to-mucosa anastomosis (green arrows) of the PJ.

CONCLUSION

Minor SILH, such as LLS, monosegmentectomies, and partial liver resections, are feasible and safe to treat selected patients with cancer by experienced laparoscopic surgeons. Although the evidence level is low, minor SILH seems to be superior to minor MILH in terms of shorter postoperative hospital stay. The oncologic outcome is comparable for both procedures. Large-scale randomized controlled clinical trials are necessary to address this issue.

Major SILH might be feasible for highly selected patients by experienced laparoscopic surgeons in high-volume centers. The current evidence is limited and fails to determine its position compared with major MILH. Surgical skill refinement and technology advancement are anticipated to overcome this demanding procedure.

Although technically feasible, SILDP has been shown to be associated with longer operative time and lower spleen/splenic vessel preservation rates. Strict patient selection is mandatory for the possible accompanying splenectomy. Well-designed randomized controlled studies are needed to compare this procedure with MILDP. Robotic technology may have a positive effect on minimally invasive DP.

SILPD is just in its infancy, and this is also true for SILBDR. While developing these techniques, patient and oncologic safety should be prioritized. A low threshold to convert the procedures should always be kept in mind.

ACKNOWLEDGEMENTS

We gratefully acknowledge the work of Dr. Hsu JW in assisting with the surgical procedures and the data collection.

FOOTNOTES

Author contributions: Chuang SH drafted the manuscript; Chuang SC revised the manuscript; Both authors have read and approve the final manuscript.

Conflict-of-interest statement: The authors report no conflict of interest.

Open-Access: This article is an open-access article that was selected by an in-house editor and fully peer-reviewed by external reviewers. It is distributed in accordance with the Creative Commons Attribution NonCommercial (CC BY-NC 4.0) license, which permits others to distribute, remix, adapt, build upon this work non-commercially, and license their derivative works on different terms, provided the original work is properly cited and the use is non-commercial. See: https://creativecommons.org/Licenses/by-nc/4.0/

Country/Territory of origin: Taiwan

ORCID number: Shu-Hung Chuang 0000-0002-2007-0415; Shih-Chang Chuang 0000-0003-1481-1632.

S-Editor: Yan JP
L-Editor: A
P-Editor: Yan JP

REFERENCES

1 **Morales-Conde S**, Peeters A, Meyer YM, Antoniou SA, Del Agua IA, Arezzo A, Arolfo S, Yehuda AB, Boni L, Cassinotti E, Dapri G, Yang T, Fransen S, Forgione A, Hajibandeh S, Mazzola M, Migliore M, Mittermair C, Mittermair D, Morandeira-Rivas A, Moreno-Sanz C, Morlacchi A, Nizri E, Nuijts M, Raakow J, Sánchez-Margallo FM, Sánchez-Margallo JA, Szold A, Weiss H, Weiss M, Zorron R, Bouvy ND. European association for endoscopic surgery (EAES) consensus statement on single-incision endoscopic surgery. *Surg Endosc* 2019; **33**: 996-1019 [PMID: 30771069 DOI: 10.1007/s00464-019-06693-2]

2 **Machairas N**, Papaconstantinou D, Gaitanidis A, Hasemaki N, Paspala A, Stamopoulos P, Kykalos S, Sotiropoulos GC. Is Single-Incision Laparoscopic Liver Surgery Safe and Efficient for the Treatment of Malignant Hepatic Tumors? *J Gastrointest Cancer* 2020; **51**: 425-432 [PMID: 31388921 DOI: 10.1007/s12029-019-00285-y]

3 **Wang YB**, Xia J, Zhang JY, Gong JP, Wang XM. Effectiveness and safety of single-port versus multi-port laparoscopic surgery for treating liver diseases: a meta-analysis. *Surg Endosc* 2017; **31**: 1524-1537 [PMID: 27553801 DOI: 10.1007/s00464-016-5199-9]

4 **Karabicak I**, Karabulut K. Single port laparoscopic liver surgery: A minireview. *World J Gastrointest Endosc* 2016; **8**: 444-450 [PMID: 27358670 DOI: 10.4253/wjge.v8.i12.444]

5 **Benzing C**, Krenzien F, Atanasov G, Seehofer D, Sucher R, Zorron R, Pratschke J, Schmelzle M. Single incision laparoscopic liver resection (SILL) - a systematic review. *GMS Interdiscip Plast Reconstr Surg DGPW* 2015; **4**: Doc17 [PMID: 26734538 DOI: 10.3205/iprs000076]

6 **Ban D**, Kudo A, Irie T, Ochiai T, Aihara A, Matsumura S, Tanaka S, Tanabe M. Advances in reduced port laparoscopic liver resection. *Asian J Endosc Surg* 2015; **8**: 11-15 [PMID: 25510567 DOI: 10.1111/ases.12164]

7 **Chang SK**, Lee KY. Therapeutic advances: single incision laparoscopic hepatopancreatobiliary surgery. *World J Gastroenterol* 2014; **20**: 14329-14337 [PMID: 25339820 DOI: 10.3748/wjg.v20.i39.14329]

8 **Gkegkes ID**, Iavazzo C. Single incision laparoscopic hepatectomy: A systematic review. *J Minim Access Surg* 2014; **10**: 107-112 [PMID: 25013325 DOI: 10.4103/0972-9941.134872]

9 **Yao D**, Wu S, Tian Y, Fan Y, Kong J, Li Y. Transumbilical single-incision laparoscopic distal pancreatectomy: primary experience and review of the English literature. *World J Surg* 2014; **38**: 1196-1204 [PMID: 24357245 DOI: 10.1007/s00268-013-2404-z]

10 **Chatzizacharias NA**, Dajani K, Koong JK, Jah A. The Role of the Single Incision Laparoscopic Approach in Liver and Pancreatic Resectional Surgery. *Minim Invasive Surg* 2016; **2016**: 1454026 [PMID: 27891251 DOI: 10.1155/2016/1454026]

11 **Chuang SH**, Lin CS. Single-incision laparoscopic surgery for biliary tract disease. *World J Gastroenterol* 2016; **22**: 736-747 [PMID: 26811621 DOI: 10.3748/wjg.v22.i2.736]

12 **Hildebrand N**, Verkoulen K, Dewulf M, Heise D, Ulmer F, Coolsen M. Short-term outcomes of laparoscopic versus open hepatectomy in the elderly patient: systematic review and meta-analysis. *HPB (Oxford)* 2021; **23**: 984-993 [PMID: 33632653 DOI: 10.1016/j.hpb.2021.01.016]

13 **Machairas N**, Kostakis ID, Schizas D, Kykalos S, Nikiteas N, Sotiropoulos GC. Meta-analysis of laparoscopic versus open liver resection for intrahepatic cholangiocarcinoma. *Updates Surg* 2021; **73**: 59-68 [PMID: 33219937 DOI: 10.1007/s13304-020-00930-3]

14 **Cipriani F**, Ratti F, Fiorentini G, Reineke R, Aldrighetti L. Systematic review of perioperative and oncologic outcomes of minimally-invasive surgery for hilar cholangiocarcinoma. *Updates Surg* 2021; **73**: 359-377 [PMID: 33615423 DOI: 10.1007/s13304-021-01006-6]

15 **Lyu Y**, Cheng Y, Wang B, Zhao S, Chen L. Assessment of laparoscopic versus open distal pancreatectomy: a systematic review and meta-analysis. *Minim Invasive Ther Allied Technol* 2022; **31**: 350-358 [PMID: 32903097 DOI: 10.1080/13645706.2020.1812664]

16 **Gavriilidis P**, Roberts KJ, Sutcliffe RP. Laparoscopic versus open distal pancreatectomy for pancreatic adenocarcinoma: a systematic review and meta-analysis. *Acta Chir Belg* 2018; **118**: 278-286 [PMID: 29996721 DOI: 10.1080/00015458.2018.1492212]

17 **van Hilst J**, Korrel M, de Rooij T, Lof S, Busch OR, Groot Koerkamp B, Kooby DA, van Dieren S, Abu Hilal M, Besselink MG; DIPLOMA study group. Oncologic outcomes of minimally invasive versus open distal pancreatectomy for pancreatic ductal adenocarcinoma: A systematic review and meta-analysis. *Eur J Surg Oncol* 2019; **45**: 719-727 [PMID: 30579652 DOI: 10.1016/j.ejso.2018.12.003]

18 **Yang DJ**, Xiong JJ, Lu HM, Wei Y, Zhang L, Lu S, Hu WM. The oncological safety in minimally invasive versus open distal pancreatectomy for pancreatic ductal adenocarcinoma: a systematic review and meta-analysis. *Sci Rep* 2019; **9**: 1159 [PMID: 30718559 DOI: 10.1038/s41598-018-37617-0]

19 **Nickel F**, Haney CM, Kowalewski KF, Probst P, Limen EF, Kalkum E, Diener MK, Strobel O, Müller-Stich BP, Hackert T. Laparoscopic Versus Open Pancreaticoduodenectomy: A Systematic Review and Meta-analysis of Randomized Controlled Trials. *Ann Surg* 2020; **271**: 54-66 [PMID: 30973388 DOI: 10.1097/SLA.0000000000003309]

20 **Wang M**, Li D, Chen R, Huang X, Li J, Liu Y, Liu J, Cheng W, Chen X, Zhao W, Tan Z, Huang H, Zhu F, Qin T, Ma J, Yu G, Zhou B, Zheng S, Tang Y, Han W, Meng L, Ke J, Feng F, Chen B, Yin X, Chen W, Ma H, Xu J, Lin R, Dong Y, Yu Y, Zhang H, Qin R; Minimally Invasive Treatment Group in the Pancreatic Disease Branch of China's International Exchange and Promotion Association for Medicine and Healthcare (MITG-P-CPAM). Laparoscopic versus open

pancreatoduodenectomy for pancreatic or periampullary tumours: a multicentre, open-label, randomised controlled trial. *Lancet Gastroenterol Hepatol* 2021; **6**: 438-447 [PMID: 33915091 DOI: 10.1016/S2468-1253(21)00054-6]

21 **Katsuki R**, Jo T, Yasunaga H, Kumazawa R, Uda K. Outcomes of laparoscopic versus open pancreatoduodenectomy: A nationwide retrospective cohort study. *Surgery* 2021; **169**: 1427-1433 [PMID: 33487433 DOI: 10.1016/j.surg.2020.12.018]

22 **Yin Z**, Jian Z, Hou B, Jin H. Surgical and Oncological Outcomes of Laparoscopic Versus Open Pancreaticoduodenectomy in Patients With Pancreatic Duct Adenocarcinoma. *Pancreas* 2019; **48**: 861-867 [PMID: 31306305 DOI: 10.1097/MPA.0000000000001363]

23 **Jiang YL**, Zhang RC, Zhou YC. Comparison of overall survival and perioperative outcomes of laparoscopic pancreaticoduodenectomy and open pancreaticoduodenectomy for pancreatic ductal adenocarcinoma: a systematic review and meta-analysis. *BMC Cancer* 2019; **19**: 781 [PMID: 31391085 DOI: 10.1186/s12885-019-6001-x]

24 **Peng L**, Zhou Z, Cao Z, Wu W, Xiao W, Cao J. Long-Term Oncological Outcomes in Laparoscopic Versus Open Pancreaticoduodenectomy for Pancreatic Cancer: A Systematic Review and Meta-Analysis. *J Laparoendosc Adv Surg Tech A* 2019; **29**: 759-769 [PMID: 30835156 DOI: 10.1089/lap.2018.0683]

25 **Chuang SH**, Yang WJ, Chang CM, Lin CS, Yeh MC. Is routine single-incision laparoscopic cholecystectomy feasible? *Am J Surg* 2015; **210**: 315-321 [PMID: 25916613 DOI: 10.1016/j.amjsurg.2014.12.032]

26 **Hyun IG**, Choi Y, Han HS, Yoon YS, Cho JY, Kim KH, Han S. Feasibility of Solo Single-Incision Laparoscopic Surgery in Non-anatomical Minor Liver Resection: a Propensity Score-Matched Analysis. *J Gastrointest Surg* 2021; **25**: 681-687 [PMID: 32157607 DOI: 10.1007/s11605-020-04527-4]

27 **Mittermair C**, Weiss M, Schirnhofer J, Brunner E, Fischer K, Obrist C, de Cillia M, Kemmetinger V, Gollegger E, Hell T, Weiss H. The Shift from Multiport to Single Port Increases the Amount of Bleeding in Laparoscopic Major Hepatectomy. *J Clin Med* 2021; **10** [PMID: 33498169 DOI: 10.3390/jcm10030374]

28 **Tsai KY**, Chen HA, Wang WY, Huang MT. Long-term and short-term surgical outcomes of single-incision laparoscopic hepatectomy on anterolateral liver segments. *Surg Endosc* 2020; **34**: 2969-2979 [PMID: 31482356 DOI: 10.1007/s00464-019-07080-7]

29 **Saad MR**, Choi Y, Han HS, Yoon YS, Cho JY, Lee JS, Lee BR. Solo single-incision laparoscopic liver resection: a cohort series. *ANZ J Surg* 2020; **90**: 1108-1111 [PMID: 32378778 DOI: 10.1111/ans.15941]

30 **Wang JC**, Pan Y, Chen J, Hu D, Tuoheti Y, Zhou Z, Xu L, Chen M, Zhang Y. Single versus multiple port laparoscopic left lateral sectionectomy for hepatocellular carcinoma: A retrospective comparative study. *Int J Surg* 2020; **77**: 15-21 [PMID: 32179178 DOI: 10.1016/j.ijsu.2020.03.003]

31 **Pan Y**, Chen J, Xu L, Zhou Z, Chen M, Zhang Y. Single-Port Laparoscopic Hepatectomy for Liver Tumor: Operative Steps (With Video). *Surg Laparosc Endosc Percutan Tech* 2019; **29**: e98-e101 [PMID: 31567784 DOI: 10.1097/SLE.0000000000000724]

32 **Han JH**, You YK, Choi HJ, Hong TH, Kim DG. Clinical advantages of single port laparoscopic hepatectomy. *World J Gastroenterol* 2018; **24**: 379-386 [PMID: 29391760 DOI: 10.3748/wjg.v24.i3.379]

33 **Weiss M**, Mittermair C, Brunner E, Schirnhofer J, Obrist C, Pimpl K, Hell T, Weiss H. Inline radiofrequency pre-coagulation simplifies single-incision laparoscopic minor liver resection. *J Hepatobiliary Pancreat Sci* 2015; **22**: 831-836 [PMID: 26510122 DOI: 10.1002/jhbp.295]

34 **Tayar C**, Subar D, Salloum C, Malek A, Laurent A, Azoulay D. Single incision laparoscopic hepatectomy: Advances in laparoscopic liver surgery. *J Minim Access Surg* 2014; **10**: 14-17 [PMID: 24501503 DOI: 10.4103/0972-9941.124454]

35 **Pan M**, Jiang Z, Cheng Y, Xu X, Zhang Z, Zhou C, He G, Xu T, Liu H, Gao Y. Single-incision laparoscopic hepatectomy for benign and malignant hepatopathy: initial experience in 8 Chinese patients. *Surg Innov* 2012; **19**: 446-451 [PMID: 22474017 DOI: 10.1177/1553350612438412]

36 **Toyama Y**, Yoshida S, Okui N, Kitamura H, Yanagisawa S, Yanaga K. Transumbilical single-incision laparoscopic hepatectomy using precoagulation and clipless technique in a patient with combined hepatocellular-cholangiocarcinoma: a case report. *Surg Laparosc Endosc Percutan Tech* 2013; **23**: e194-e199 [PMID: 24105295 DOI: 10.1097/SLE.0b013e31828b8602]

37 **Camps Lasa J**, Cugat Andorrà E, Herrero Fonollosa E, García Domingo MI, Sánchez Martínez R, Vargas Pierola H, Rodríguez Campos A. Single-port laparoscopic approach of the left liver: initial experience. *Cir Esp* 2014; **92**: 589-594 [PMID: 24999088 DOI: 10.1016/j.ciresp.2014.05.009]

38 **Kim G**, Lau AC, Chang SK. Single-incision laparoscopic hepatic resection in patients with previous hepatic resections: a mini case series. *Asian J Endosc Surg* 2014; **7**: 63-66 [PMID: 24450347 DOI: 10.1111/ases.12072]

39 **Karabicak I**, Karabulut K, Yuruker S, Kesicioglu T, Ozen N. Single-Port Laparoscopic Liver Resection: Largest Turkish Experience. *Indian J Surg* 2017; **79**: 111-115 [PMID: 28442836 DOI: 10.1007/s12262-015-1435-0]

40 **Inoue Y**, Asakuma M, Hirokawa F, Hayashi M, Shimizu T, Uchiyama K. Single port access for laparoscopic lateral segmentectomy. *Wideochir Inne Tech Maloinwazyjne* 2017; **12**: 357-365 [PMID: 29362650 DOI: 10.5114/wiitm.2017.70260]

41 **Tzanis D**, Lainas P, Tranchart H, Pourcher G, Devaquet N, Perlemuter G, Naveau S, Dagher I. Atypical as well as anatomical liver resections are feasible by laparoendoscopic single-site surgery. *Int J Surg Case Rep* 2014; **5**: 580-583 [PMID: 25108073 DOI: 10.1016/j.ijscr.2013.11.009]

42 **Struecker B**, Haber P, Öllinger R, Bahra M, Pascher A, Pratschke J, Schmelzle M. Comparison of Single-Port Versus Standard Multiport Left Lateral Liver Sectionectomy. *Surg Innov* 2018; **25**: 136-141 [PMID: 29303066 DOI: 10.1177/1553350617752010]

43 **Belli G**, Fantini C, D'Agostino A, Cioffi L, Russo G, Belli A, Limongelli P. Laparoendoscopic single site liver resection for recurrent hepatocellular carcinoma in cirrhosis: first technical note. *Surg Laparosc Endosc Percutan Tech* 2011; **21**: e166-e168 [PMID: 21857451 DOI: 10.1097/SLE.0b013e3182207d3a]

44 **Wu S**, Yu XP, Tian Y, Siwo EA, Li Y, Yu H, Yao D, Lv C. Transumbilical single-incision laparoscopic resection of focal hepatic lesions. *JSLS* 2014; **18** [PMID: 25392646 DOI: 10.4293/JSLS.2014.00397]

45 **Dapri G**, Dimarco L, Cadière GB, Donckier V. Initial experience in single-incision transumbilical laparoscopic liver resection: indications, potential benefits, and limitations. *HPB Surg* 2012; **2012**: 921973 [PMID: 23082044 DOI:

10.1155/2012/921973]
46 **Røsok BI**, Edwin B. Single-Incision Laparoscopic Liver Resection for Colorectal Metastasis through Stoma Site at Time of Reversal of Diversion Ileostomy: A Case Report. *Minim Invasive Surg* 2011; **2011**: 502176 [PMID: 22091359 DOI: 10.1155/2011/502176]
47 **Cantos-Pallares M**, Mir-Labrador J, Rafael Redondo-Cano C, Nuñez-Ronda R, Artigues-Sanchez de Rojas E, Fabra-Ramis R. Single-port Laparoscopic Liver Resection in Patients with Previous Abdominal Surgeries: Is it a Feasible Approach? *J Coll Physicians Surg Pak* 2022; **32**: 96-98 [PMID: 34983156 DOI: 10.29271/jcpsp.2022.01.96]
48 **Chuang SH**, Chen PH, Chang CM, Tsai YF, Lin CS. Single-incision laparoscopic common bile duct exploration with conventional instruments: an innovative technique and a comparative study. *J Gastrointest Surg* 2014; **18**: 737-743 [PMID: 24347312 DOI: 10.1007/s11605-013-2420-1]
49 **Huang JW**, Su WL, Wang SN. Alternative Laparoscopic Intracorporeal Pringle Maneuver by Huang's Loop. *World J Surg* 2018; **42**: 3312-3315 [PMID: 29589115 DOI: 10.1007/s00268-018-4584-z]
50 **Park P**, Han HJ, Song TJ, Choi SB, Kim WB, Yoo YD, Kim DS, Cha JH. Single-port versus conventional laparoscopic distal pancreatectomy: a propensity score matched analysis and a learning curve of single-port approach. *J Hepatobiliary Pancreat Sci* 2019; **26**: 401-409 [PMID: 31211913 DOI: 10.1002/jhbp.646]
51 **Ağcaoğlu O**, Aksakal N, Azamat İF, Doğan S, Mercan S, Barbaros U. Comparison of Clinical Outcomes of Single-Incision Versus Conventional Multiport Laparoscopic Distal Pancreatectomy: A Single Institution Experience. *Sisli Etfal Hastan Tip Bul* 2019; **53**: 114-119 [PMID: 32377068 DOI: 10.14744/SEMB.2019.37880]
52 **Ryan CE**, Ross SB, Sukharamwala PB, Sadowitz BD, Wood TW, Rosemurgy AS. Distal pancreatectomy and splenectomy: a robotic or LESS approach. *JSLS* 2015; **19**: e2014.00246 [PMID: 25848192 DOI: 10.4293/JSLS.2014.00246]
53 **Kuroki T**, Kitasato A, Adachi T, Soyama A, Takatsuki M, Eguchi S. Single-incision laparoscopic distal pancreatectomy: our initial experience. *Hepatogastroenterology* 2014; **61**: 212-214 [PMID: 24895823 DOI: 10.1002/hep.24089]
54 **Misawa T**, Ito R, Futagawa Y, Fujiwara Y, Kitamura H, Tsutsui N, Shiba H, Wakiyama S, Ishida Y, Yanaga K. Single-incision laparoscopic distal pancreatectomy with or without splenic preservation: how we do it. *Asian J Endosc Surg* 2012; **5**: 195-199 [PMID: 23095300 DOI: 10.1111/j.1758-5910.2012.00155.x]
55 **Haugvik SP**, Røsok BI, Waage A, Mathisen O, Edwin B. Single-incision versus conventional laparoscopic distal pancreatectomy: a single-institution case-control study. *Langenbecks Arch Surg* 2013; **398**: 1091-1096 [PMID: 24177746 DOI: 10.1007/s00423-013-1133-y]
56 **Yu H**, Wu SD, Tian Y, Su Y, Li YN. Single-incision laparoscopic resection of Bismuth I hilar cholangiocarcinoma. *Surg Innov* 2013; **20**: 209-213 [PMID: 22393076 DOI: 10.1177/1553350612438414]

World Journal of Gastroenterology

Submit a Manuscript: https://www.f6publishing.com

World J Gastroenterol 2022 July 21; 28(27): 3370-3382

DOI: 10.3748/wjg.v28.i27.3370

ISSN 1007-9327 (print) ISSN 2219-2840 (online)

MINIREVIEWS

Probiotics and postbiotics in colorectal cancer: Prevention and complementary therapy

Monika Kvakova, Anna Kamlarova, Jana Stofilova, Veronika Benetinova, Izabela Bertkova

Specialty type: Gastroenterology and hepatology

Provenance and peer review: Invited article; Externally peer reviewed.

Peer-review model: Single blind

Peer-review report's scientific quality classification

Grade A (Excellent): 0
Grade B (Very good): B, B
Grade C (Good): 0
Grade D (Fair): 0
Grade E (Poor): 0

P-Reviewer: Ros J, Spain; Wen XL, China

Received: January 18, 2022
Peer-review started: January 18, 2022
First decision: March 8, 2022
Revised: March 22, 2022
Accepted: June 16, 2022
Article in press: June 16, 2022
Published online: July 21, 2022

Monika Kvakova, Anna Kamlarova, Jana Stofilova, Veronika Benetinova, Izabela Bertkova, Center of Clinical and Preclinical Research MEDIPARK, Faculty of Medicine, P.J. Safarik University in Kosice, Kosice 04011, Slovakia

Corresponding author: Monika Kvakova, PhD, Research Fellow, Research Scientist, Center of Clinical and Preclinical Research MEDIPARK, Faculty of Medicine, P.J. Safarik University in Kosice, Trieda SNP 1, Kosice 04011, Slovakia. monika.kvakova@upjs.sk

Abstract

Colorectal cancer (CRC) is a leading cause of human mortality worldwide. As conventional anticancer therapy not always being effective, there is growing interest in innovative "drug-free" cancer treatments or interventions that improve the efficacy of established therapy. CRC is associated with microbiome alterations, a process known as dysbiosis that involves depletion and/or enrichment of particular gut bacterial species and their metabolic functions. Supplementing patient treatment with traditional probiotics (with or without prebiotics), next-generation probiotics (NGP), or postbiotics represents a potentially effective and accessible complementary anticancer strategy by restoring gut microbiota composition and/or by signaling to the host. In this capacity, restoration of the gut microbiota in cancer patients can stabilize and enhance intestinal barrier function, as well as promote anticarcinogenic, anti-inflammatory, antimutagenic or other biologically important biochemical pathways that show high specificity towards tumor cells. Potential benefits of traditional probiotics, NGP, and postbiotics include modulating gut microbiota composition and function, as well as the host inflammatory response. Their application in CRC prevention is highlighted in this review, where we consider supportive *in vitro*, animal, and clinical studies. Based on emerging research, NGP and postbiotics hold promise in establishing innovative treatments for CRC by conferring physiological functions *via* the production of dominant natural products and metabolites that provide new host-microbiota signals to combat CRC. Although favorable results have been reported, further investigations focusing on strain and dose specificity are required to ensure the efficacy and safety of traditional probiotics, NGP, and postbiotics in CRC prevention and treatment.

Key Words: Colorectal cancer; Traditional probiotics; Next-generation probiotics; Postbiotics; Gut microbiota

©The Author(s) 2022. Published by Baishideng Publishing Group Inc. All rights reserved.

Core Tip: The effects of traditional probiotics, next-generation probiotics (NGP), or postbiotics in colorectal cancer (CRC) prevention and complementary therapy can be associated independently or in mutual cooperation with several mechanisms, including suppression of inflammation, enhancing apoptosis of tumor cells, restoring intestinal barrier function, competition with pathogens and by promoting healthy gut microbiota composition and function. Traditional probiotics, NGP, or postbiotics supplementation is also a potential strategy to boost the effectiveness of chemotherapy and immunotherapy, reduce the rate of postoperative complications, and improve the quality of lives of CRC patients.

Citation: Kvakova M, Kamlarova A, Stofilova J, Benetinova V, Bertkova I. Probiotics and postbiotics in colorectal cancer: Prevention and complementary therapy. *World J Gastroenterol* 2022; 28(27): 3370-3382
URL: https://www.wjgnet.com/1007-9327/full/v28/i27/3370.htm
DOI: https://dx.doi.org/10.3748/wjg.v28.i27.3370

INTRODUCTION

Colorectal cancer (CRC) is the third most commonly diagnosed cancer in males and the second in females worldwide; thus a significant change in lifestyle is required to facilitate effective CRC prevention[1]. CRC is a heterogeneous disease of the intestinal epithelium, comprising the colon, rectum, and anus. It is characterized by a dysregulated immune response, accumulation of stem cell mutations, intestinal barrier disruption, and dysbiosis, which is often regarded as an unfavorable alteration in gut microbiota composition and function. Up to 90% of CRC risk is thought to be lifestyle-dependent, primarily due to dietary or environmental factors including feeding patterns that modulate consumption of fiber, red and processed meat or alcohol consumption, and low omega-3 fatty acids and vitamin D intake. Obesity, lack of physical activity, and smoking are also significant risk factors that promote CRC-associated microbiota changes[2]. CRC is linked with microbiome alterations, which include depletion and/or enrichment in particular bacterial species that are present in CRC patients (extensively reviewed by Torres-Maravilla *et al*[3], Ternes *et al*[4], Janney *et al*[2], Fong *et al*[5], and Wirbel *et al*[6]).

The human microbiota is a complex ecosystem of bacteria, viruses, eukaryotes, and archea, which can regulate a variety of host physiological functions including digestion, immune response, metabolism, disease pathogenesis, elimination of toxins, and biosynthesis of key compounds such as essential vitamins and cofactors. Microbiota can even modulate gut-brain axis function to alter, for example, anxiety and mood. Symbiotic bacteria that colonize the human gut can be classified into several phyla comprising Bacteroidetes and Firmicutes, followed by Proteobacteria, Fusobacteria, Actinobacteria, Verrucomicrobia, and Spirochaetes. Microbiome composition varies between healthy individuals, as well as in CRC patients[7]. CRC-associated bacteria that have been identified to date include enrichment of *Fusobacterium nucleatum*, *Enterococcus faecalis*, *Streptococcus gallolyticus*, entero-toxigenic *Bacteroides fragilis*, *Escherichia coli*, *Peptostreptococcus* spp., and *Ruminococcus* spp. By contrast, *Lactobacillus* spp., *Bifidobacterium* spp., *Faecalibacterium* spp., *Roseburia* spp., *Clostridium* spp., *Granulicatella* spp., *Streptococcus thermophilus*, and other species of *Lachnospiraceae* family are depleted in CRC (Table 1)[2-5]. These altered microbiota signatures can potentially be used to provide future diagnostics, and their presence/absence may contribute to the pathogenesis or prevention/treatment of CRC. However, the pathophysiological role of dysbiosis in CRC still remains unclear, since microbiota changes may reflect changes in host health status and some bacteria may even confer protection as a compensatory response to disease progression. This complexity is clearly evident by the report of specific bacteria associated with tumor initiation phase (driver bacteria) whereas other bacteria are associated with tumor development during progressive stages of CRC (passenger bacteria). Driver bacteria reportedly contribute to the formation of a tumor microenvironment that is comprised of normal epithelial cells and cancer cells. In this milieu, secreted microbial metabolites trigger damage to normal host cells, thus reprograming their metabolism to change the intestinal microenvironment and microbiome profile towards a more "CRC supportive" composition[8-10]. Potential driver bacteria include *Bacteroides fragilis*, *Escherichia coli*, *Enterococcus Faecalis*, *Bacillus*, *Bradyrhizobium*, *Methylobacterium*, *Streptomyces*, *Shigella*, *Citrobacter*, *Salmonella*, *Intrasporangiaceae*, and *Sinobacteraceae*. On the other hand, passenger bacteria occupy an existing tumor microenvironment where they are thought to either promote or inhibit CRC progression. Reported passenger bacteria include species *Fusobacterium*, *Parvimonas*, *Peptostreptococcus*, *Campylobacter*, *Streptococcus*, *Schwartzia*, *Burkholderiales*, *Caulobacteraceae*, *Delftia*, *Oxalobacteraceae*, *Faecalibacterium*, and *Sutterella*[8-11]. The host gut microbiota and immune system play important roles in CRC prevention and development. Therefore, probiotics, next-generation probiotics

Table 1 Overview of the most relevant bacteria related to colorectal cancer

Enriched bacteria	Depleted bacteria	Ref.
Fusobacterium nucleatum, Peptostreptococcus spp., *Porphyromonas asaccharolytica, Prevotella* spp., *Parvimonas micra, Bacteroides fragilis, Streptococcus gallolyticus, Escherichia coli, Campylobacter* spp., *Shigella* spp., *Enterococcus faecalis*	*Blautia* spp., *Faecalibacterium prausnitzii, Clostridium butyricum, Streptococcus thermophilus, Roseburia* spp.	[4,55-57]

(NGP), or postbiotics could be used as weapons to prevent CRC, to support the treatment and to improve the clinical outcomes in CRC patients.

This minireview summarizes recent CRC findings from clinical, animal and *in vitro* studies, and discusses the efficiency of probiotics, NGP, and postbiotics in CRC prevention and therapy.

TRADITIONAL PROBIOTICS

Probiotics are defined as "live, non-pathogenic microorganisms that, when administered in adequate amounts, may confer a health benefit on the host"[12]. Probiotics have a centuries-long history of safe use as prevention and adjuvant therapy in combating human diseases. They are also promising candidates in modulating human gut microbiota composition and function in CRC patients. Traditional widely used probiotics mainly belong to *Bifidobacterium* spp., *Lactobacillus* spp. and other lactic-acid-producing bacteria, including species belonging to *Streptococcus, Enterococcus*, and *Lactococcus*, complemented by yeasts of the genus *Saccharomyces*. The beneficial effects of probiotics, functioning in a species and/or strain-specific manner, include sustaining a healthy microbiome, reversing dysbiosis, preventing pathogenic infections and mucosal adhesion of pathogens, stabilizing and enhancing intestinal barrier function. Probiotic bacteria may achieve these beneficial functions in part by producing anti-carcinogenic, anti-inflammatory, anti-mutagenic and other biologically important compounds such as short-chain fatty acids (SCFAs), vitamin K, or B-group vitamins[5,7,13,14].

Current research builds on a foundation of work demonstrating that gut microbiota modulation through administration of probiotics and/or prebiotics plays an important role in CRC prevention and therapy. In a randomized, double-blinded, placebo-controlled trial, 60 patients underwent surgical CRC resection, of whom 29 received the probiotic powder (*Bifidobacterium animalis* subsp. *lactis* HY8002 [1 × 10^8 CFU], *Lactobacillus casei* HY2782 [5 × 10^7 CFU], and *Lactobacillus plantarum* HY7712 [5 × 10^7 CFU]) and 31 placebo, for 4 wk, starting at 1 wk preoperatively. The treatment group receiving probiotic powder showed an increase in abundance of *Bifidobacterium*, *Akkermansia*, *Parabacteroides*, *Veillonella*, *Lactobacillus*, *Erysipelatoclostridium* and a reduction in bacteria associated with CRC, such as *Prevotella*, *Alloprevotella*, *Fusobacterium*, and *Porphyromonas*. Lower serum zonulin, improved postoperative bowel function, and postoperative recovery were evident in the probiotic group compared with placebo[15]. In another randomized clinical trial, a group of 31 CRC patients received probiotic supplement *Bifidobacterium longum* BB536 (5 × 10^{10} CFU/2 g/daily) preoperatively for 7–14 d and postoperatively for 2 wk. Attenuated postoperative inflammatory responses (high-sensitivity C-Reactive protein), reduced risk of postoperative infectious complications, and accelerated health recovery after colorectal resection were evident in the treatment group. Hospital stay was significantly shortened and correlated significantly with increased Actinobacteria and decreased Firmicutes after probiotic intervention[16]. Aisu *et al*[17] administered BIO THREE® 2 mg *Enterococcus faecalis* T110, 10 mg *Clostridium butyricum* TO-A, and 10 mg *Bacillus mesentericus* TO-A to 75 CRC patients 15 d prior to the surgery. Incidence of postoperative complications and superficial incisional infections were lower, and these health effects were as shown to associate with an increased mean proportion of beneficial *Bifidobacterium*, postoperatively, even though this organism was not administered as part of the probiotic regime. The change in microbial diversity and improved integrity of the mucosal barrier were also observed by Liu *et al*[18] after *Lactobacillus plantarum* CGMCC 1258, *Lactobacillus acidophilus* LA-11, *Bifidobacterium longum* BL-88 (2.6 × 10^{14} CFU/2 g/daily) administration 6 d preoperatively and 10 d postoperatively to CRC patients. The numbers of beneficial bacteria, including *Bifidobacteria* and *Lactobacilli*, increased in the probiotic group after surgery, whereas they decreased in the placebo group. By contrast, Enterobacteriales and *Pseudomonas*, were decreased in the probiotic group whereas they increased in the placebo group. Based on a number of clinical trials, the preoperative oral intake of probiotics combined with the postoperative treatment in patients who need gastrointestinal surgery is potentially recommended. Larger rigorously controlled clinical trials are required to endorse these preliminary positive outcome studies since avoidance of probiotic use has also been recommended in patients with immunodeficiency and dysbiosis. More studies and the key outcomes are listed in Table 2.

Table 2 Efficiency of probiotics in colorectal cancer prevention and therapy-clinical trials

Probiotic strain/synbiotics	Dose/length of the study	Trial type/sample size	Microbial changes/key outcomes	Ref.
Lactobacillus rhamnosus GG, *Bifidobacterium lactis* Bb12 + inulin enriched with oligofructose	10^{10} CFU and 10 g of prebiotic, 12 wk	Human prevention study-CRC patients (*n* = 15 placebo, *n* = 19 synbiotics), polypectomized patients (*n* =19 placebo, *n* = 21 synbiotics)	↑*Bifidobacterium*, ↑*Lactobacillus*, ↓*Clostridium perfringens*; ↓proliferation rate of colorectal cells and stimulation of peripheral blood mononuclear cells (↑IFNg, ↓IL-2)	Rafter *et al*[58]
Bifidobacterium longum BB536, *Lactobacillus johnsonii* La1	2×10^7 CFU or 2×10^9 CFU, 3 d preoperatively and 3 d postoperatively	CRC patients undergoing elective colorectal resection- Randomized double blind, placebo-controlled study (*n* = 10 placebo, *n* = 21 probiotics)	*B. longum* BB536 did not adhere to colonic mucosa only La1, ↓*Enterobacteriaceae* ↓*Enterococcus*, modulation of local immunity (↑CD3+, CD4+, CD8+, activity of dendritic cells); no clinical effect	Gianotti *et al*[59]
Bifidobacterium longum, *Lactobacillus acidophilus*, *Enterococcus faecalis*	3×10^8 CFU, 3 d (from -5 to -3 d) preoperatively	Single-center prospective randomized control study (*n* = 30 placebo, *n* = 30 probiotics)	↑*Bifidobacterium* and ↓*Escherichia*; ↓endotoxins, D-lactic acid, serum IL-6 and C-reactive protein; ↑serum IgG and IgA; ↓postoperative occurrence of infectious complications of CRC	Zhang *et al*[60]
Bifidobacterium longum, *Lactobacillus acidophilus* and *Enterococcus faecalis*	1:1:1 daily 6×10^7 CFU, 5 d	Perioperative intake of probiotics in CRC patients (*n* = 11 placebo, *n* = 11 probiotics)	↑richness and diversity of mucosal microbes, ↓*Peptostreptococcus*, ↓*Comamonas*, ↓*Fusobacterium*, ↑*Enterococcus*, ↑Proteobacteria; no clinical effect	Gao *et al*[61]
LactoLevure (*Lactobacillus acidophilus* LA-5, *Lacobacillus plantarum*, *Bifidobacterium lactis* BB-12, *Saccharomyces boulardii*)	1.75×10^9 CFU, 0.5×10^9 CFU, 1.75×10^9 CFU, 1.5×10^9 CFU, respectively, 1 d preoperatively and 15 d postoperatively	CRC patients undergoing surgery- Randomized, double-blind, placebo-controlled study (*n* = 80 placebo, *n* = 84 probiotics)	Reduction of the postoperative pneumonia rate, anastomotic leakage and surgical site infections; ↑gene expression of SOCS3; ↑circulating IL-6, TNF-α	Kotzampassi *et al*[62] (NCT02313519)
Colon Dophilus™ [*Bifidobacterium breve* HA-129 (25%), *Bifidobacterium bifidum* HA-132 HA (20%), *Bifidobacterium longum* HA-135 (14.5%), *Lactobacillus rhamnosus* HA-111 (8%), *Lactobacillus acidophilus* HA-122 (8%), *Lactobacillus casei* HA-108 (8%), *Lactobacillus plantarum* HA-119 (8%), *Streptococcus thermopilus* HA-110 (6%), *Lactobacillus brevis* HA-112 (2%), *Bifidobacterium infantis* HA-116 (0.5%)]	10×10^9CFU/ daily, 12 wk	Patients with CRC, concomitantly with irinotecan chemotherapy- Randomized, placebo-controlled study (*n* = 23 placebo, *n* = 23 probiotics)	Reduction in the incidence and severity of chemotherapy induced diarrhea and incidence of enterocolitis.	Mego *et al*[63] (NCT01410955)
Saccharomyces boulardii	7 d preoperatively	Randomized study (*n* = 18 conventional treatment, *n* = 15 probiotics)	↓mucosal IL-1β, IL-10, and IL-23A mRNA levels; no statistical impact on postoperative infection rates	Consoli *et al*[64]
ProBion Clinica (*Bifidobacterium lactis* Bl-04 and *Lactobacillus acidophilus* NCFM + inulin)	1.4×10^{10} CFU, 7×10^9 CFU and 0.63 g of prebiotic, 8-78 d	Prospective randomized intervention (*n* = 7 placebo, *n* = 8 probiotics)	Increased abundance of butyrate producing bacteria ↑Firmicutes, ↑*Faecalibacterium*, ↑*Eubacterium*, ↑*Roseburia* ↑*Lachnospira*; ↓CRC associated bacteria- *Fusobacterium* and *Peptostreptococcus*	Hibberd *et al*[65] (NCT03072641)
Simbio-flora (*Lactobacillus acidophilus* NCFM, *Lactobacillus rhamnosus* HN001, *Lactobacillus casei* LPC-37, *Bifidobacterium lactis* HN019 and fructooligosaccharide)	10^9 CFU and 6 g of prebiotic, 7 d preoperatively	Patients with CRC subjected to colorectal resection- Prospective, randomized, double-blind, placebo-controlled study (*n* = 37 placebo, *n* = 36 synbiotic)	Reduced inflammatory state (C-reactive protein, IL-6), reductions in morbidity, hospital length of stay, and use of antibiotics. Stimulated bowel function, decreased complications and reduced cumulative duration of antibiotic usage	Polakowski *et al*[66]
Lactobacillus acidophilus BCMC® 12,130, *Lactobacillus lactis* BCMC® 12,451, *Lactobacillus casei* subsp BCMC® 12,313, *Bifidobacterium longum* BCMC® 02120, *Bifidobacterium bifidum* BCMC® 02290 and *Bifidobacterium infantis* BCMC® 02129	30 billion CFU, twice daily for 6 mo	Randomized double-blind placebo-controlled trial (*n* = 25 placebo, *n* = 27 probiotics)	Reduction in the levels of pro-inflammatory cytokines, TNF-α, IL-6, IL-10, IL-12, IL-17A, IL-17C and IL-22.	Zaharuddin *et al*[32] (NCT03782428)

CRC: Colorectal cancer; IFNg: Interferon-gamma; Ig: Immunoglobulin; IL: Interleukin; TNF-α: Tumor necrosis factor-alpha.

NGP

One potential approach to achieve CRC prevention and treatment is through NGP administration. As described above, the most frequently used probiotics belong to *Bifidobacterium* spp. and *Lactobacillus* spp. However, recent studies using metagenomic approaches have revealed the importance of further identification and characterization of commensal species, mainly anaerobic ones, residing in the gastrointestinal tract that play an important role in regulating the immune system and maintaining overall gut health. Growing evidence suggests that dysbiosis may contribute to CRC progression as well as several other diseases[19-22]. Although there is no official definition of NGP, it is generally defined as live microorganisms identified on the basis of comparative microbiota analyses between healthy and sick individuals/animals that, when administered with strain-specificity and in dose dependent manner, confer health benefits on the host[23,24]. Compared with healthy individuals, patients with CRC possess a different compositional structure and physiological activity of the gut microbiota with SCFAs-producing bacteria being depleted. This suggests that SCFAs-producing bacteria might potentially exhibit anti-inflammatory and anticarcinogenic properties, as well as being NGP candidates in CRC prevention and therapy. SCFAs, primarily acetate, propionate, and butyrate, are key physiological metabolites of the microbial fermentation of dietary fiber in the colon. Butyrate is the major energy source for colonocyte homeostasis, promoting growth stimulation and production of protective cytokines that maintain gut barrier integrity and function[14,25-27]. Furthermore, increasing levels of SCFAs in the gut helps to create a favorable microenvironment for beneficial bacteria by inhibiting the growth and adhesion of pathogens, and by enhancing vitamin bioavailability, mineral absorption and promoting mucosal integrity. Most butyrate-producing bacteria in the human colon belong to the Firmicutes phylum, clostridial clusters IV and XIVa, the most dominant species being *Faecalibacterium prausnitzii* and *Eubacterium rectale,* followed by *Eubacterium* spp. as well as *Anaerostipes* spp. and *Roseburia* spp. In addition to butyrate-producing bacteria, other NGP candidates with important regulatory effects on gut homeostasis include *Akkermansia muciniphila*, non-toxigenic *Bacteroides fragilis*, *Propionibacterium freudenreichii,* and some strains of *Bacillus* spp. and *Clostridium* spp., which belong to Generally Recognized As Safe microorganisms[7,28,29].

Chronic oral administration of *Butyricicoccus pullicaecorum* BCRC 81109 (butyrate producing bacteria) to BALB/cByJNarl male mice decreased colon tumor progression over 9 wk. This protection against CRC clinical outcomes was linked to activation of the SCFAs transporter solute carrier family 5 member 8 and/or G-protein-coupled receptor (GPR) 43[30]. Chen *et al*[25] also observed in an *in vivo* animal study that application of butyrate producing bacteria *Clostridium butyricum* ATCC 19398 (2×10^9 CFU/0.2 mL 3 times a week for 12 wk) inhibited intestinal tumor development by an increasing apoptosis of CRC cells, by modulating the Wnt/β-catenin signaling pathway. There was also a reduction in pathogenic bacteria and bile acid-biotransforming bacteria, whereas an increase in beneficial *Lactobacillus* spp. and SCFAs-producing *Rumincoccaceae* and *Eubacterium* spp. was evident. Thus, reduction in colonic secondary bile acids increased cecal SCFAs levels and activated G-protein coupled receptors, GPR43 and GPR109A, which were mechanistically implicated. Growth of CRC cell lines (HCT-116 and SW1116) was significantly inhibited by strains *Bacillus subtilis* ATCC 23857 and *Clostridium butyricum* ATCC 19398, and by their main metabolites bacitracin and butyrate. mRNA levels of important receptors and transcriptional factors related to inflammation for example, TLR4, MYD88, nuclear factor-kappa B (NF-κB), interleukin 22 (IL-22), and survivin were decreased and expression of $p21^{WAF1}$ was increased after treatment of SW1116 cells with *Bacillus subtilis* and *Clostridium butyricum* NGP[31]. Purified components produced by NGP cells were also studied and inhibition of human cancer cell proliferation by controlling the cell cycle was detected. Polysaccharide A purified from *Bacteroides fragilis* NCTC9343 (non-toxigenic) induced the production of the pro-inflammatory cytokine IL-8[32] and aspartic protease Amuc_1434 (recombinant enzyme) from *Akkermansia muciniphila* upregulated the expression of tumor protein 53, increased mitochondrial reactive oxygen species (ROS) levels and promoted apoptosis of LS174T cells[33]. Pahle *et al*[34] employed *Clostridium perfringens* enterotoxin (CPE) in CPE gene therapy to selectively target claudin-3 and claudin-4 expressing colon carcinomas *in vitro* and *in vivo* by using a translation optimized CPE expressing vector. Elevated toxicity of the optimized CPE expressing vector was evident in claudin-positive cells 48 h after the transfection, with toxicity rates of 76%–92% and rapid cytotoxic effects such as membrane disruption and necrosis. Further *in vivo* studies focused on the efficiency of NGP application in CRC are listed in Table 3 and postbiotics derived from NGP are considered below.

POSTBIOTICS

Postbiotics is an extensively researched subject that remains a largely understudied topic in CRC. Due to the phenomenal number and variety of metabolites produced by bacteria, it has been an enormous challenge to isolate and characterize the specific compound/s responsible for the therapeutic efficacy. Moreover, defining safety profiles and appropriate application doses of particular postbiotics in the preclinical and clinical settings may require regulatory guidelines and approvals[5]. The International

Table 3 Efficiency of next-generation probiotics in colorectal cancer *in vivo*

NGP strain	Application	Study/ cohort	Mechanism/effect(s)	Ref.
Akkermansia muciniphila MucT ATCC BAA-835	pasteurized culture 1.5 × 10^8 CFU/100 μL or recombinant Amuc_1100 3 μg (specific outer membrane protein)/2 wk before AOM injection until sacrifice	23-wk *in vivo* animal study, acute colitis was induced by AOM (10 mg/kg) (intraperitoneally) + 2% DSS (in water)-male C57BL/6J mice	Prevention of AOM/DSS-induced tumorigenesis by DNA damage attenuation, cell apoptosis and abnormal proliferation. Significant amelioration of acute colitis, relieved colon shortening and splenomegaly, delayed tumor formation and reduced expression of γH2AX, cleaved caspase 3 and Ki67. Blunted CAC through the expansion and activation of cytotoxic T lymphocytes, indicated by TNF-α induction and PD-1 downregulation	Wang *et al* [67]
Akkermansia muciniphila ATCC BAA-835	1 × 10^8 CFU/mouse every other day (day 7-12), gavage administration	4-wk *in vivo* animal study, CRC induced by mice colon cancer cells CT-26 (1 × 10^6) (subcutaneously)-*n* = 70, male BALB/c mice	*A. muciniphila* colonization significantly increased inhibition rate/anti-cancer effect of FOLFOX (from 48% to 76%) and significantly decreased marker of proliferation-Ki67 (% of positively stained cells)	Hou *et al*[68]
Clostridium butyricum (powder by Kexing Biopharm CO., LTD)	2 × 10^8 CFU/0.2 mL/3 times *per* week, gavage administration	78 d *in vivo* animal study, CAC induced by intraperitoneal AOM (12.5 mg/kg) + 2.5% DSS (in water)-*n* = 30, C57BL/6 mice	Inhibition of NF-κB pathway and apoptosis promotion. Change in the microbiome composition-reduction of Firmicutes to Bacteroidetes ratio. Reduction of incidence and size of CRC and increase of tumor cells apoptosis. Reduction in cytokines including TNF-α, IL-6 and level of COX-2. Decrease in phosphorylation of NF-κB and level of Bcl-2. Increase in Bax expression	Liu *et al*[69]
Clostridium butyricum ATCC 19398 or *Bacillus subtilis* ATCC 23857	2.5 × 10^8 CFU/0.3 mL/3 times *per* week for 28 wk, oral administration	28 wk *in vivo* animal study. CRC induced with DMH (20 mg/kg body weight)/weekly (intraperitoneally)-*n* = 72, male C57BL/6 mice	Inhibition of intestinal tumorigenesis and modulation of immunity and inflammation. Reduction in tumor size and incidence. After supplementation with probiotics, mice showed decreased Th2 and Th17 expression and increased CD4/CD8 expression compared to DMH-treated mice. Reduced gene expression of TLR4–MYD88–NF-κB, IL-22 and increase of $P21^{waf1}$ and Tlr3 mRNA levels in intestinal mucosa	Chen *et al* [31]

AOM: Azoxymethane; CAC: Colitis-associated cancer; CRC: Colorectal cancer; DMH: 1,2-dimethylhydrazine; DSS: Dextran sulfate sodium; FOLFOX: Oxaliplatin, fluorouracil and calcium folinate; IL: Interleukin; NF-κB: Nuclear factor-kappa B; TNF-α: Tumor necrosis factor-alpha.

Scientific Association for Probiotics and Prebiotics (ISAPP) offers expertise in microbiology, microbial physiology, gastroenterology, nutrition, food science and pediatrics. ISAPP recently provided the clear definition and scope of postbiotics to include "preparation of inanimate microorganisms and/or their components that confer a health benefit on the host"[35]. Postbiotics, which exert desired physiological effects to the host, include inactivated microbial cells or cell components (cell surface proteins, endo- or exo-polysaccharides, peptidoglycan-derived muropeptides and teichoic acids) or important metabolites secreted by gut microbiota through a fermentation process or released under certain conditions such as a change in intestinal environment or after lysis (SCFAs including acetate, propionate and butyrate; enzymes; bacteriocins; reuterin; acetoin; organic acids, *etc*)[5,35,36]. Therefore, the isolation and characterization of new postbiotics is a growing field and requires careful biochemical characterization of beneficial mechanisms. Supplementation with postbiotics, can in some cases be an effective and safer strategy to prevent and/or treat diseases, compared with ingestion of viable probiotic bacteria[5].

Microbial metabolites undoubtedly play an important role in CRC pathogenesis. Certain postbiotics exert antitumor activity, including selective cytotoxicity against tumor cells suggesting their therapeutic potential (Figure 1)[5]. For example, SCFAs are well-known inhibitors of epigenetic enzymes histone deacetylases, which play a central role in gene regulation; thus, SCFAs have the ability to induce cell cycle arrest, and/or apoptosis in many cancer cell lines[37]. Cell-free supernatants (CFS) of different *Lactobacillus* and *Bifidobacterium* strains have been shown to induce apoptosis or inhibit proliferation of CRC cell lines[38-40]. Chen *et al*[41] demonstrated that supernatants of *Lactobacillus johnsonii* BCRC17010 and *Lactobacillus reuteri* BCRC14625 strains in high concentrations were able to damage HT-29 cell membranes causing elevated lactate dehydrogenase release. A recent study has reported a potent selective cytotoxicity effect of postbiotic metabolites from *Lactobacillus plantarum* strains *via* anti-proliferative effects and induction of apoptosis in HT-29 cells whilst sparing the normal cells[42]. Cousin *et al* [43] showed that metabolites from *Propionibacterium freudenreichii* ITG-P9, namely propionate and acetate, had induced intrinsic apoptosis of CRC cells, *via* the production and release of SCFAs acting on mitochondria. Moreover, CFS or SCFAs in combination with Tumor Necrosis Factor-Related Apoptosis-Inducing Ligand (TRAIL), increased the pro-apoptotic gene expression (TRAIL-R2/DR5), decreased the anti-apoptotic gene expression of FLIP and XIAP in HT-29 cancer cells and enhanced the cytotoxicity in CRC cells compared to human healthy intestinal epithelial cells. Further control studies are required to delineate specific molecular targets in these models since enhanced toxicity to fermentation induced acidic pH shifts remains a potential protective mechanism.

As inflammation is undeniably linked to carcinogenesis, any postbiotic that inhibits inflammation is also an important candidate acting as anti-tumor agent. It was shown that *Lactobacillus rhamnosus* GG-

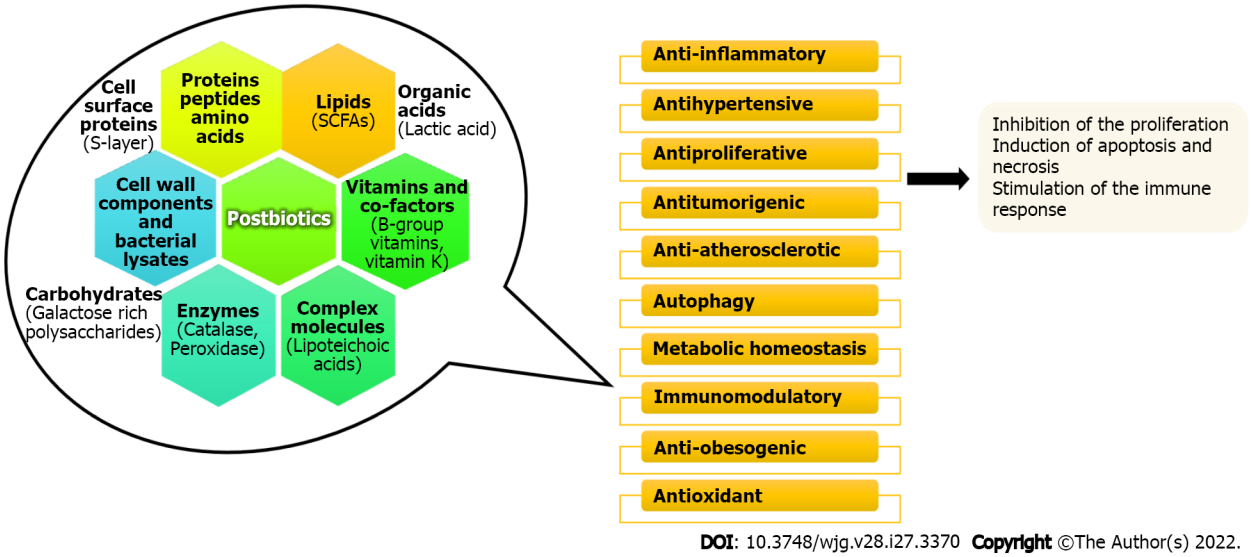


Figure 1 Examples of postbiotics and their proposed activity in patients with colorectal cancer. SCFAs: Short-chain fatty acids.

derived protein p40 can play a role in the prevention of CRC by suppressing intestinal epithelial inflammation, inhibiting epithelial cells apoptosis and by promoting IgA production[44-46]. CFS derived from several other probiotic strains, such as, *Lactobacillus acidophilus*, *Lactobacillus casei*, *Lactobacillus rhamnosus* GG and *Bifidobacterium breve*, were able to downregulate inflammation, exhibit antioxidant activity or maintained intestinal barrier integrity[47-49].

To date, only a few animal studies have been performed to evaluate the effectiveness of postbiotics in CRC prevention and therapy *in vivo*. The stage is now set to expand this work with the use of translational *in vivo* models and clinical trials, which are essential to demonstrate efficacy. Sharma and Shukla [50] observed that CFS from *Lactobacillus rhamnosus* MD 14 MH656799 containing acetamide, acetate, propionate, butyrate, thiocyanic acid and oxalic acid attenuated early colon carcinogenesis in Sprague–Dawley rats (n = 36). The protective mechanism was linked to reduced fecal procarcinogenic enzymes, oxidants, aberrant crypt foci, vis-à-vis downregulating oncogenes (β-catenin, K-ras, Cox-2, NF-κB) and upregulating tumor suppressor p53 gene leading to an almost healthy colon histology. De Moreno de LeBlanc *et al*[51] evaluated the effect of the enzyme catalase as a postbiotic from catalase-producing *Lactococcus lactis* htrA-NZ9000 on the prevention/regression of 1,2-dimethylhydrazine (DMH) induced CRC in BALB/c mice (n = 180-210). Catalase-producing *Lactococcus lactis* increased catalase activity in DMH-treated mice and reduced H_2O_2 levels compared with the control group. Using the histopathological grading scale of chemically induced CRC, mice that received catalase-producing *Lactococcus lactis* had significantly less colonic damage and inflammation (2.0 ± 0.4) compared to control animals that received non-catalase-producing *Lactococcus lactis* (4.0 ± 0.3) or placebo-treated animals (4.7 ± 0.5). Increased antioxidant activity reduced levels of H_2O_2 and ROS involved in CRC onset and progression.

There are also promising results from studies of postbiotics derived from NGP. Recently, numerous *in vitro* studies showed that supernatant from SCFAs-producing bacteria, such as *Butyricicoccus pullicaecorum* BCRC 81109[30], *Clostridium butyricum* ATCC 19398[25], *Propionibacterium freudenreichii* TL142[52], *Propionibacterium acidipropionici* CNRZ80, *Propionibacterium freudenreichii* subsp. *freudenreichii* ITG18, *Propionibacterium freudenreichii* subsp. *shermanii* SI41[53] suppressed CRC cells proliferation and induced apoptosis. The same results were documented by Zhao *et al*[54], where single strain CFS from human *Bacillus* strains BY38, BY40, BY43, BY45 exhibited inhibitory effects on the proliferation of CRC cells in a dose-dependent manner through the induction of cell apoptosis. These results suggest that NGP could represent novel and promising anti-tumor agents against CRC. Further *in vitro* studies focused on the activity of postbiotics derived from different probiotic strains in CRC cell lines are listed in Table 4.

CONCLUSION

Traditional probiotics have utility in the management of CRC as adjuvant treatment, mainly to reduce postoperative complications and to alleviate the side effects of chemotherapy. Antitumorigenic mechanisms of probiotics include the modification of intestinal microbiome, improvement of intestinal barrier integrity, immune potentiation and maintaining gut homeostasis. However, it is well known that the efficiency of probiotics is strain specific. The available clinical data indicate that CRC patients most

Table 4 Efficiency of postbiotics on cancer cells *in vitro*

Probiotic strain	Derived postbiotic	Cell line	Mechanism/effect(s)	Ref.
Lactobacilus casei ATCC334	CFS (ferrichrome)	Caco-2/bbe, SKCO-1, SW620	In CFS, ferrichrome subsequently identified as the responsible molecule that induced apoptosis *via* JNK-DDTI3 signaling axis, thus having tumor-suppressive effect and exerted minimal effect on normal intestinal epithelial cells	Konishi *et al*[70]
Lactobacillus rhamnosus MD 14 MH 656799	CFS (acetate, butyrate, propionate, acetamide, thiocyanic acid, and oxalic acid)	Caco-2, HT-29	CFS with metabolites exhibited both anti-genotoxic and cytotoxic potential against CRC cells	Sharma *et al*[71]
Bifidobacterium adolescentis SPM0212	CFS	Caco-2, HT-29, SW480	CFS significantly inhibited the proliferation of cancer cells	Kim *et al*[39]
Lactobacillus fermentum KCTC 3112	CFS	CCD18-Co, HCT-116, HT-29	Induction of cancer cells apoptosis by CFS up-regulating Caspase-3, Bax, Bak, Noxa, and Bid mRNA expressions	Lee *et al*[38]
Lactobacillus casei (ATCC 334), *Lactobacillus rhamnosus* (GG ATCC 53103)	CFS	HCT-116	Anti-metastatic effects of high molecular weight fractions	Escamilla *et al*[40]
Lactobacillus acidophilus ATCC 4356, *Lactococcus lactis* ATCC 11454, *Lactobacillus casei* ATCC 334, *Lactobacillus reuteri* ATCC 55148, *Saccharomyces boulardii* ATCC MYA-796	CFS	HT-29	Downregulation of the expression of PGE-2 and IL-8 in cancer cells by metabolites of probiotics. CFS differently modulated IL-1β, IL-6, TNF-α, and IL-10 production by human macrophages, suggesting a peculiar anti-inflammatory activity	De Marco *et al*[48]
Lactobacillus casei ATCC 393	Sonicated-cell suspension	CT26, HT-29	Inhibition of cancer cells proliferation and induction of apoptosis	Tiptiri-Kourpeti *et al* [72]
Lactobacillus reuteri PTCC 1655	Sonicated-cell suspension	HT-29-ShE	Anti-metastatic and anti-proliferative effects	Maghsood *et al*[73]
Lactococcus lactis PTCC 1336	Nisin, cell wall, cytoplasmic extract of nisin	SW480	Anti-proliferative effects, associated with the decreased expression of cyclin D1 in SW480 cell line	Hosseini *et al*[74]
Pediococcus pentosaceus FP3, *Lactobacillus salivarius* FP25/FP35, *Enterococcus faecium* FP51	SCFAs (butyrate and propionate)	Caco-2	Significant proliferation inhibition of Caco-2 cells and activation of apoptosis	Thirabunyanon and Hongwittayakorn [75]
Streptomyces levis ABRIINW111	Extracted metabolites	SW480	SW480 growth inhibition, increased Caspase-3 and reduced Ki67 expression in a concentration/time-dependent manner; subG$_1$ phase (apoptosis) increased by metabolites and cell cycle arrest in G$_1$, G$_2$/M and S phase; *p53* gene expression followed SW480 cells treatment significantly	Faramarzian Azimi Maragheh *et al*[76]
Streptomyces sp. MUM256	MUM256 extract	HT-29, Caco-2	Antioxidant properties, cytotoxicity against CRC cells by reduction in viability and induction of apoptosis (depolarization of mitochondrial membrane potential and arrest in subG$_1$ phase)	Tan *et al*[77]
Clostridium butyricum ATCC 19398	SCFAs	HCT-116, HCT-8, Caco-2	Suppression of the Wnt/b-catenin signaling pathway and modulation of the gut microbiota composition.	Chen *et al*[25]

CFS: Cell-free supernatant; CRC: Colorectal cancer; IL: Interleukin; SCFAs: Short-chain fatty acids; TNF-α: Tumor necrosis factor-alpha.

often benefit from combined administration of strains *Lactobacillus acidophilus*, *Lactobacillus casei*, *Bifidobacterium lactis*, and *Bifidobacterium longum*. Use of their combination or in combination with other species is more effective than individual supplementation. Nevertheless, consideration of each CRC patient's health status is still strictly recommended before administering viable probiotics. The gut microbiota is emerging as a contributing factor in the etiopathology of CRC. It is necessary to consider gut microbiota-drug interactions, including composition and metabolic activity of gut microbiota, which can both positively and negatively affect the outcome of CRC therapy. And even though research in this area is still in its infancy, it can be assumed that future clinical treatment and prevention of CRC will focus on supplementing the microbiome with commensal species (NGP candidates) that are predominantly anaerobic. Recent studies indicate that SCFAs-producing bacteria, especially butyrate producers, such as *Akkermansia muciniphila*, *Propionibacterium freudenreichi*, and *Butyricicoccus pullicaecorum* belong to

beneficial NGP that may have applicability in CRC therapy. Furthermore, it was discovered that strains previously defined as potential pathogens appear to possess probiotic properties when these lack key virulence factors, for example non-toxigenic *Bacteroides fragilis* NCTC9343 has positive effects on patient's health. A significant disadvantage of NGP is, above all, their safety as this has not yet been sufficiently confirmed in animal and clinical studies. Safety validation is of particular importance before administering NGP to oncology patients. Although NGP research is experimentally demanding, emerging data shows great potential. Therefore, it is necessary to continue and explore new possibilities of NGP use in the therapy or prevention of diseases, including CRC, especially through clinical trials. Supplementation with postbiotics should be favorable in CRC therapy, because postbiotics have the ability to stimulate immune responses, inhibit cancer cell proliferation, induce apoptosis and necrosis, and they can shape microbiome composition in CRC patients. The advantage of postbiotics is that they do not pose a risk of unwanted infection to the patient, although screening for product contamination will be important. Moreover, it is possible to accurately determine and verify administered doses of a particular postbiotic. However, this emerging research area currently lack *in vivo* or clinical data to assess feasibility. In conclusion, the administration of traditional probiotics, NGP or postbiotics, supported by various experimental studies, is an efficient complementary therapeutic approach to combat CRC. A protective effect of probiotics and postbiotics against CRC onset is also indicated, however, lifestyle changes are recommended as a first line of defense in CRC prevention.

ACKNOWLEDGEMENTS

We are thankful to Tor C Savidge, PhD for the editorial assistance.

FOOTNOTES

Author contributions: All authors contributed equally to the conceptualization and design of the manuscript; Kvakova M prepared and finalized the manuscript; Kamlarova A, Stofilova J, and Benetinova V reviewed the literature, and prepared the tables and figure; Bertkova I as senior author revised the manuscript; all authors approved the final manuscript.

Supported by Scientific Grant Agency of the Ministry of Education of Slovak Republic and Academy of Sciences VEGA, No. 1/0393/20; and the Operational Program Integrated Infrastructure Within the Project: Demand-Driven Research for the Sustainable and Innovative Food, Co-financed by the European Regional Development Fund, No. Drive4SIFood 313011V336.

Conflict-of-interest statement: All the authors report no relevant conflicts of interest for this article.

Open-Access: This article is an open-access article that was selected by an in-house editor and fully peer-reviewed by external reviewers. It is distributed in accordance with the Creative Commons Attribution NonCommercial (CC BY-NC 4.0) license, which permits others to distribute, remix, adapt, build upon this work non-commercially, and license their derivative works on different terms, provided the original work is properly cited and the use is non-commercial. See: https://creativecommons.org/Licenses/by-nc/4.0/

Country/Territory of origin: Slovakia

ORCID number: Monika Kvakova 0000-0002-9659-5584; Anna Kamlarova 0000-0001-7871-5338; Jana Stofilova 0000-0002-9409-4153; Veronika Benetinova 0000-0001-9523-8203; Izabela Bertkova 0000-0003-3076-2711.

S-Editor: Fan JR
L-Editor: Filipodia
P-Editor: Fan JR

REFERENCES

1 **Sung H**, Ferlay J, Siegel RL, Laversanne M, Soerjomataram I, Jemal A, Bray F. Global Cancer Statistics 2020: GLOBOCAN Estimates of Incidence and Mortality Worldwide for 36 Cancers in 185 Countries. *CA Cancer J Clin* 2021; **71**: 209-249 [PMID: 33538338 DOI: 10.3322/caac.21660]

2 **Janney A**, Powrie F, Mann EH. Host-microbiota maladaptation in colorectal cancer. *Nature* 2020; **585**: 509-517 [PMID: 32968260 DOI: 10.1038/s41586-020-2729-3]

3 **Torres-Maravilla E**, Boucard AS, Mohseni AH, Taghinezhad-S S, Cortes-Perez NG, Bermúdez-Humarán LG. Role of Gut Microbiota and Probiotics in Colorectal Cancer: Onset and Progression. *Microorganisms* 2021; **9** [PMID: 34068653 DOI: 10.3390/microorganisms9051021]

4 **Ternes D**, Karta J, Tsenkova M, Wilmes P, Haan S, Letellier E. Microbiome in Colorectal Cancer: How to Get from Meta-omics to Mechanism? *Trends Microbiol* 2020; **28**: 401-423 [PMID: 32298617 DOI: 10.1016/j.tim.2020.01.001]

5 **Fong W**, Li Q, Yu J. Gut microbiota modulation: a novel strategy for prevention and treatment of colorectal cancer. *Oncogene* 2020; **39**: 4925-4943 [PMID: 32514151 DOI: 10.1038/s41388-020-1341-1]

6 **Wirbel J**, Pyl PT, Kartal E, Zych K, Kashani A, Milanese A, Fleck JS, Voigt AY, Palleja A, Ponnudurai R, Sunagawa S, Coelho LP, Schrotz-King P, Vogtmann E, Habermann N, Niméus E, Thomas AM, Manghi P, Gandini S, Serrano D, Mizutani S, Shiroma H, Shiba S, Shibata T, Yachida S, Yamada T, Waldron L, Naccarati A, Segata N, Sinha R, Ulrich CM, Brenner H, Arumugam M, Bork P, Zeller G. Meta-analysis of fecal metagenomes reveals global microbial signatures that are specific for colorectal cancer. *Nat Med* 2019; **25**: 679-689 [PMID: 30936547 DOI: 10.1038/s41591-019-0406-6]

7 **Kvakova M**, Bertkova I, Stofilova J, Savidge TC. Co-Encapsulated Synbiotics and Immobilized Probiotics in Human Health and Gut Microbiota Modulation. *Foods* 2021; **10** [PMID: 34200108 DOI: 10.3390/foods10061297]

8 **Zhang M**, Lv Y, Hou S, Liu Y, Wang Y, Wan X. Differential Mucosal Microbiome Profiles across Stages of Human Colorectal Cancer. *Life (Basel)* 2021; **11** [PMID: 34440574 DOI: 10.3390/Life11080831]

9 **Wang Y**, Zhang C, Hou S, Wu X, Liu J, Wan X. Analyses of Potential Driver and Passenger Bacteria in Human Colorectal Cancer. *Cancer Manag Res* 2020; **12**: 11553-11561 [PMID: 33209059 DOI: 10.2147/CMAR.S275316]

10 **Xu S**, Yin W, Zhang Y, Lv Q, Yang Y, He J. Foes or Friends? *Cancers (Basel)* 2020; **12** [PMID: 32041122 DOI: 10.3390/cancers12020372]

11 **Tjalsma H**, Boleij A, Marchesi JR, Dutilh BE. A bacterial driver-passenger model for colorectal cancer: beyond the usual suspects. *Nat Rev Microbiol* 2012; **10**: 575-582 [PMID: 22728587 DOI: 10.1038/nrmicro2819]

12 **FAO/WHO**. Health and Nutritional Properties of Probiotics in Food Including Powder Milk with Live Lactic Acid Bacteria. 2006. [cited 20 December 2021]. Available from: www.fao.org

13 **Tripathy A**, Dash J, Kancharla S, Kolli P, Mahajan D, Senapati S, Jena MK. Probiotics: A Promising Candidate for Management of Colorectal Cancer. *Cancers (Basel)* 2021; **13** [PMID: 34202265 DOI: 10.3390/cancers13133178]

14 **Zhao Y**, Wang C, Goel A. Role of gut microbiota in epigenetic regulation of colorectal Cancer. *Biochim Biophys Acta Rev Cancer* 2021; **1875**: 188490 [PMID: 33321173 DOI: 10.1016/j.bbcan.2020.188490]

15 **Park IJ**, Lee JH, Kye BH, Oh HK, Cho YB, Kim YT, Kim JY, Sung NY, Kang SB, Seo JM, Sim JH, Lee JL, Lee IK. Effects of PrObiotics on the Symptoms and Surgical ouTComes after Anterior REsection of Colon Cancer (POSTCARE): A Randomized, Double-Blind, Placebo-Controlled Trial. *J Clin Med* 2020; **9** [PMID: 32664289 DOI: 10.3390/jcm9072181]

16 **Mizuta M**, Endo I, Yamamoto S, Inokawa H, Kubo M, Udaka T, Sogabe O, Maeda H, Shirakawa K, Okazaki E, Odamaki T, Abe F, Xiao JZ. Perioperative supplementation with bifidobacteria improves postoperative nutritional recovery, inflammatory response, and fecal microbiota in patients undergoing colorectal surgery: a prospective, randomized clinical trial. *Biosci Microbiota Food Health* 2016; **35**: 77-87 [PMID: 27200261 DOI: 10.12938/bmfh.2015-017]

17 **Aisu N**, Tanimura S, Yamashita Y, Yamashita K, Maki K, Yoshida Y, Sasaki T, Takeno S, Hoshino S. Impact of perioperative probiotic treatment for surgical site infections in patients with colorectal cancer. *Exp Ther Med* 2015; **10**: 966-972 [PMID: 26622423 DOI: 10.3892/etm.2015.2640]

18 **Liu Z**, Qin H, Yang Z, Xia Y, Liu W, Yang J, Jiang Y, Zhang H, Wang Y, Zheng Q. Randomised clinical trial: the effects of perioperative probiotic treatment on barrier function and post-operative infectious complications in colorectal cancer surgery - a double-blind study. *Aliment Pharmacol Ther* 2011; **33**: 50-63 [PMID: 21083585 DOI: 10.1111/j.1365-2036.2010.04492.x]

19 **Gautier T**, David-Le Gall S, Sweidan A, Tamanai-Shacoori Z, Jolivet-Gougeon A, Loréal O, Bousarghin L. Next-Generation Probiotics and Their Metabolites in COVID-19. *Microorganisms* 2021; **9** [PMID: 33925715 DOI: 10.3390/microorganisms9050941]

20 **Osman MA**, Neoh HM, Ab Mutalib NS, Chin SF, Mazlan L, Raja Ali RA, Zakaria AD, Ngiu CS, Ang MY, Jamal R. Parvimonas micra, Peptostreptococcus stomatis, Fusobacterium nucleatum and Akkermansia muciniphila as a four-bacteria biomarker panel of colorectal cancer. *Sci Rep* 2021; **11**: 2925 [PMID: 33536501 DOI: 10.1038/s41598-021-82465-0]

21 **Lv Y**, Ye T, Wang HP, Zhao JY, Chen WJ, Wang X, Shen CX, Wu YB, Cai YK. Suppression of colorectal tumorigenesis by recombinant *Bacteroides fragilis* enterotoxin-2 *in vivo*. *World J Gastroenterol* 2017; **23**: 603-613 [PMID: 28216966 DOI: 10.3748/wjg.v23.i4.603]

22 **Dai Z**, Coker OO, Nakatsu G, Wu WKK, Zhao L, Chen Z, Chan FKL, Kristiansen K, Sung JJY, Wong SH, Yu J. Multi-cohort analysis of colorectal cancer metagenome identified altered bacteria across populations and universal bacterial markers. *Microbiome* 2018; **6**: 70 [PMID: 29642940 DOI: 10.1186/s40168-018-0451-2]

23 **Martín R**, Langella P. Emerging Health Concepts in the Probiotics Field: Streamlining the Definitions. *Front Microbiol* 2019; **10**: 1047 [PMID: 31164874 DOI: 10.3389/fmicb.2019.01047]

24 **Lin TL**, Shu CC, Lai WF, Tzeng CM, Lai HC, Lu CC. Investiture of next generation probiotics on amelioration of diseases – Strains do matter. *Med Microecol* 2019; **1-2**: 100002 [DOI: 10.1016/j.medmic.2019.100002]

25 **Chen D**, Jin D, Huang S, Wu J, Xu M, Liu T, Dong W, Liu X, Wang S, Zhong W, Liu Y, Jiang R, Piao M, Wang B, Cao H. Clostridium butyricum, a butyrate-producing probiotic, inhibits intestinal tumor development through modulating Wnt signaling and gut microbiota. *Cancer Lett* 2020; **469**: 456-467 [PMID: 31734354 DOI: 10.1016/j.canlet.2019.11.019]

26 **Hu S**, Liu L, Chang EB, Wang JY, Raufman JP. Butyrate inhibits pro-proliferative miR-92a by diminishing c-Myc-induced miR-17-92a cluster transcription in human colon cancer cells. *Mol Cancer* 2015; **14**: 180 [PMID: 26463716 DOI: 10.1186/s12943-015-0450-x]

27 **Chen HM**, Yu YN, Wang JL, Lin YW, Kong X, Yang CQ, Yang L, Liu ZJ, Yuan YZ, Liu F, Wu JX, Zhong L, Fang DC, Zou W, Fang JY. Decreased dietary fiber intake and structural alteration of gut microbiota in patients with advanced colorectal adenoma. *Am J Clin Nutr* 2013; **97**: 1044-1052 [PMID: 23553152 DOI: 10.3945/ajcn.112.046607]

28 **Gu ZY**, Pei WL, Zhang Y, Zhu J, Li L, Zhang Z. Akkermansia muciniphila in inflammatory bowel disease and colorectal cancer. *Chin Med J (Engl)* 2021; **134**: 2841-2843 [PMID: 34711719 DOI: 10.1097/CM9.0000000000001829]

29 **Rivière A**, Selak M, Lantin D, Leroy F, De Vuyst L. Bifidobacteria and Butyrate-Producing Colon Bacteria: Importance and Strategies for Their Stimulation in the Human Gut. *Front Microbiol* 2016; **7**: 979 [PMID: 27446020 DOI:

10.3389/fmicb.2016.00979]
30 **Chang SC**, Shen MH, Liu CY, Pu CM, Hu JM, Huang CJ. A gut butyrate-producing bacterium *Butyricicoccus pullicaecorum* regulates short-chain fatty acid transporter and receptor to reduce the progression of 1,2-dimethylhydrazine-associated colorectal cancer. *Oncol Lett* 2020; **20**: 327 [PMID: 33101496 DOI: 10.3892/ol.2020.12190]
31 **Chen ZF**, Ai LY, Wang JL, Ren LL, Yu YN, Xu J, Chen HY, Yu J, Li M, Qin WX, Ma X, Shen N, Chen YX, Hong J, Fang JY. Probiotics Clostridium butyricum and Bacillus subtilis ameliorate intestinal tumorigenesis. *Future Microbiol* 2015; **10**: 1433-1445 [PMID: 26346930 DOI: 10.2217/fmb.15.66]
32 **Zaharuddin L**, Mokhtar NM, Muhammad Nawawi KN, Raja Ali RA. A randomized double-blind placebo-controlled trial of probiotics in post-surgical colorectal cancer. *BMC Gastroenterol* 2019; **19**: 131 [PMID: 31340751 DOI: 10.1186/s12876-019-1047-4]
33 **Meng X**, Zhang J, Wu H, Yu D, Fang X. *Akkermansia muciniphila* Aspartic Protease Amuc_1434* Inhibits Human Colorectal Cancer LS174T Cell Viability *via* TRAIL-Mediated Apoptosis Pathway. *Int J Mol Sci* 2020; **21** [PMID: 32403433 DOI: 10.3390/ijms21093385]
34 **Pahle J**, Menzel L, Niesler N, Kobelt D, Aumann J, Rivera M, Walther W. Rapid eradication of colon carcinoma by Clostridium perfringens Enterotoxin suicidal gene therapy. *BMC Cancer* 2017; **17**: 129 [PMID: 28193196 DOI: 10.1186/s12885-017-3123-x]
35 **Salminen S**, Collado MC, Endo A, Hill C, Lebeer S, Quigley EMM, Sanders ME, Shamir R, Swann JR, Szajewska H, Vinderola G. The International Scientific Association of Probiotics and Prebiotics (ISAPP) consensus statement on the definition and scope of postbiotics. *Nat Rev Gastroenterol Hepatol* 2021; **18**: 649-667 [PMID: 33948025 DOI: 10.1038/s41575-021-00440-6]
36 **Wegh CAM**, Geerlings SY, Knol J, Roeselers G, Belzer C. Postbiotics and Their Potential Applications in Early Life Nutrition and Beyond. *Int J Mol Sci* 2019; **20** [PMID: 31547172 DOI: 10.3390/ijms20194673]
37 **King J**, Patel M, Chandrasekaran S. Metabolism, HDACs, and HDAC Inhibitors: A Systems Biology Perspective. *Metabolites* 2021; **11** [PMID: 34822450 DOI: 10.3390/metabo11110792]
38 **Lee YP**, Chiu CC, Lin TJ, Hung SW, Huang WC, Chiu CF, Huang YT, Chen YH, Chen TH, Chuang HL. The germ-free mice monocolonization with *Bacteroides fragilis* improves azoxymethane/dextran sulfate sodium induced colitis-associated colorectal cancer. *Immunopharmacol Immunotoxicol* 2019; **41**: 207-213 [PMID: 30706742 DOI: 10.1080/08923973.2019.1569047]
39 **Kim Y**, Lee D, Kim D, Cho J, Yang J, Chung M, Kim K, Ha N. Inhibition of proliferation in colon cancer cell lines and harmful enzyme activity of colon bacteria by Bifidobacterium adolescentis SPM0212. *Arch Pharm Res* 2008; **31**: 468-473 [PMID: 18449504 DOI: 10.1007/s12272-001-1180-y]
40 **Escamilla J**, Lane MA, Maitin V. Cell-free supernatants from probiotic Lactobacillus casei and Lactobacillus rhamnosus GG decrease colon cancer cell invasion in vitro. *Nutr Cancer* 2012; **64**: 871-878 [PMID: 22830611 DOI: 10.1080/01635581.2012.700758]
41 **Chen ZY**, Hsieh YM, Huang CC, Tsai CC. Inhibitory Effects of Probiotic Lactobacillus on the Growth of Human Colonic Carcinoma Cell Line HT-29. *Molecules* 2017; **22** [PMID: 28075415 DOI: 10.3390/molecules22010107]
42 **Chuah LO**, Foo HL, Loh TC, Mohammed Alitheen NB, Yeap SK, Abdul Mutalib NE, Abdul Rahim R, Yusoff K. Postbiotic metabolites produced by Lactobacillus plantarum strains exert selective cytotoxicity effects on cancer cells. *BMC Complement Altern Med* 2019; **19**: 114 [PMID: 31159791 DOI: 10.1186/s12906-019-2528-2]
43 **Cousin FJ**, Jouan-Lanhouet S, Théret N, Brenner C, Jouan E, Le Moigne-Muller G, Dimanche-Boitrel MT, Jan G. The probiotic Propionibacterium freudenreichii as a new adjuvant for TRAIL-based therapy in colorectal cancer. *Oncotarget* 2016; **7**: 7161-7178 [PMID: 26771233 DOI: 10.18632/oncotarget.6881]
44 **Wang Y**, Liu L, Moore DJ, Shen X, Peek RM, Acra SA, Li H, Ren X, Polk DB, Yan F. An LGG-derived protein promotes IgA production through upregulation of APRIL expression in intestinal epithelial cells. *Mucosal Immunol* 2017; **10**: 373-384 [PMID: 27353252 DOI: 10.1038/mi.2016.57]
45 **Wang L**, Cao H, Liu L, Wang B, Walker WA, Acra SA, Yan F. Activation of epidermal growth factor receptor mediates mucin production stimulated by p40, a Lactobacillus rhamnosus GG-derived protein. *J Biol Chem* 2014; **289**: 20234-20244 [PMID: 24895124 DOI: 10.1074/jbc.M114.553800]
46 **Yan F**, Polk DB. Characterization of a probiotic-derived soluble protein which reveals a mechanism of preventive and treatment effects of probiotics on intestinal inflammatory diseases. *Gut Microbes* 2012; **3**: 25-28 [PMID: 22356855 DOI: 10.4161/gmic.19245]
47 **Gao J**, Li Y, Wan Y, Hu T, Liu L, Yang S, Gong Z, Zeng Q, Wei Y, Yang W, Zeng Z, He X, Huang SH, Cao H. A Novel Postbiotic From *Lactobacillus rhamnosus* GG With a Beneficial Effect on Intestinal Barrier Function. *Front Microbiol* 2019; **10**: 477 [PMID: 30923519 DOI: 10.3389/fmicb.2019.00477]
48 **De Marco S**, Sichetti M, Muradyan D, Piccioni M, Traina G, Pagiotti R, Pietrella D. Probiotic Cell-Free Supernatants Exhibited Anti-Inflammatory and Antioxidant Activity on Human Gut Epithelial Cells and Macrophages Stimulated with LPS. *Evid Based Complement Alternat Med* 2018; **2018**: 1756308 [PMID: 30069221 DOI: 10.1155/2018/1756308]
49 **Bermudez-Brito M**, Muñoz-Quezada S, Gomez-Llorente C, Matencio E, Bernal MJ, Romero F, Gil A. Cell-free culture supernatant of Bifidobacterium breve CNCM I-4035 decreases pro-inflammatory cytokines in human dendritic cells challenged with Salmonella typhi through TLR activation. *PLoS One* 2013; **8**: e59370 [PMID: 23555025 DOI: 10.1371/journal.pone.0059370]
50 **Sharma M**, Shukla G. Administration of Metabiotics Extracted From Probiotic *Lactobacillus rhamnosus* MD 14 Inhibit Experimental Colorectal Carcinogenesis by Targeting Wnt/β-Catenin Pathway. *Front Oncol* 2020; **10**: 746 [PMID: 32670864 DOI: 10.3389/fonc.2020.00746]
51 **de Moreno de LeBlanc A**, LeBlanc JG, Perdigón G, Miyoshi A, Langella P, Azevedo V, Sesma F. Oral administration of a catalase-producing Lactococcus lactis can prevent a chemically induced colon cancer in mice. *J Med Microbiol* 2008; **57**: 100-105 [PMID: 18065674 DOI: 10.1099/jmm.0.47403-0]
52 **Lan A**, Lagadic-Gossmann D, Lemaire C, Brenner C, Jan G. Acidic extracellular pH shifts colorectal cancer cell death from apoptosis to necrosis upon exposure to propionate and acetate, major end-products of the human probiotic

propionibacteria. *Apoptosis* 2007; **12**: 573-591 [PMID: 17195096 DOI: 10.1007/s10495-006-0010-3]
53 **Jan G**, Belzacq AS, Haouzi D, Rouault A, Métivier D, Kroemer G, Brenner C. Propionibacteria induce apoptosis of colorectal carcinoma cells *via* short-chain fatty acids acting on mitochondria. *Cell Death Differ* 2002; **9**: 179-188 [PMID: 11840168 DOI: 10.1038/sj.cdd.4400935]
54 **Zhao MF**, Liang GD, Zhou YJ, Chi ZP, Zhuang H, Zhu SL, Wang Y, Liu GR, Zhao JB, Liu SL. Novel Bacillus strains from the human gut exert anticancer effects on a broad range of malignancy types. *Invest New Drugs* 2020; **38**: 1373-1382 [PMID: 32734371 DOI: 10.1007/s10637-020-00906-5]
55 **Cheng Y**, Ling Z, Li L. The Intestinal Microbiota and Colorectal Cancer. *Front Immunol* 2020; **11**: 615056 [PMID: 33329610 DOI: 10.3389/fimmu.2020.615056]
56 **Zhao L**, Cho WC, Nicolls MR. Colorectal Cancer-Associated Microbiome Patterns and Signatures. *Front Genet* 2021; **12**: 787176 [PMID: 35003221 DOI: 10.3389/fgene.2021.787176]
57 **Rebersek M**. Gut microbiome and its role in colorectal cancer. *BMC Cancer* 2021; **21**: 1325 [PMID: 34895176 DOI: 10.1186/s12885-021-09054-2]
58 **Rafter J**, Bennett M, Caderni G, Clune Y, Hughes R, Karlsson PC, Klinder A, O'Riordan M, O'Sullivan GC, Pool-Zobel B, Rechkemmer G, Roller M, Rowland I, Salvadori M, Thijs H, Van Loo J, Watzl B, Collins JK. Dietary synbiotics reduce cancer risk factors in polypectomized and colon cancer patients. *Am J Clin Nutr* 2007; **85**: 488-496 [PMID: 17284748 DOI: 10.1093/ajcn/85.2.488]
59 **Gianotti L**, Morelli L, Galbiati F, Rocchetti S, Coppola S, Beneduce A, Gilardini C, Zonenschain D, Nespoli A, Braga M. A randomized double-blind trial on perioperative administration of probiotics in colorectal cancer patients. *World J Gastroenterol* 2010; **16**: 167-175 [PMID: 20066735 DOI: 10.3748/wjg.v16.i2.167]
60 **Zhang JW**, Du P, Gao J, Yang BR, Fang WJ, Ying CM. Preoperative probiotics decrease postoperative infectious complications of colorectal cancer. *Am J Med Sci* 2012; **343**: 199-205 [PMID: 22197980 DOI: 10.1097/MAJ.0b013e31823aace6]
61 **Gao Z**, Guo B, Gao R, Zhu Q, Wu W, Qin H. Probiotics modify human intestinal mucosa-associated microbiota in patients with colorectal cancer. *Mol Med Rep* 2015; **12**: 6119-6127 [PMID: 26238090 DOI: 10.3892/mmr.2015.4124]
62 **Kotzampassi K**, Stavrou G, Damoraki G, Georgitsi M, Basdanis G, Tsaousi G, Giamarellos-Bourboulis EJ. A Four-Probiotics Regimen Reduces Postoperative Complications After Colorectal Surgery: A Randomized, Double-Blind, Placebo-Controlled Study. *World J Surg* 2015; **39**: 2776-2783 [PMID: 25894405 DOI: 10.1007/s00268-015-3071-z]
63 **Mego M**, Chovanec J, Vochyanova-Andrezalova I, Konkolovsky P, Mikulova M, Reckova M, Miskovska V, Bystricky B, Beniak J, Medvecova L, Lagin A, Svetlovska D, Spanik S, Zajac V, Mardiak J, Drgona L. Prevention of irinotecan induced diarrhea by probiotics: A randomized double blind, placebo controlled pilot study. *Complement Ther Med* 2015; **23**: 356-362 [PMID: 26051570 DOI: 10.1016/j.ctim.2015.03.008]
64 **Consoli ML**, da Silva RS, Nicoli JR, Bruña-Romero O, da Silva RG, de Vasconcelos Generoso S, Correia MI. Randomized Clinical Trial: Impact of Oral Administration of Saccharomyces boulardii on Gene Expression of Intestinal Cytokines in Patients Undergoing Colon Resection. *JPEN J Parenter Enteral Nutr* 2016; **40**: 1114-1121 [PMID: 25917895 DOI: 10.1177/0148607115584387]
65 **Hibberd AA**, Lyra A, Ouwehand AC, Rolny P, Lindegren H, Cedgård L, Wettergren Y. Intestinal microbiota is altered in patients with colon cancer and modified by probiotic intervention. *BMJ Open Gastroenterol* 2017; **4**: e000145 [PMID: 28944067 DOI: 10.1136/bmjgast-2017-000145]
66 **Polakowski CB**, Kato M, Preti VB, Schieferdecker MEM, Ligocki Campos AC. Impact of the preoperative use of synbiotics in colorectal cancer patients: A prospective, randomized, double-blind, placebo-controlled study. *Nutrition* 2019; **58**: 40-46 [PMID: 30278428 DOI: 10.1016/j.nut.2018.06.004]
67 **Wang L**, Tang L, Feng Y, Zhao S, Han M, Zhang C, Yuan G, Zhu J, Cao S, Wu Q, Li L, Zhang Z. A purified membrane protein from *Akkermansia muciniphila* or the pasteurised bacterium blunts colitis associated tumourigenesis by modulation of $CD8^+$ T cells in mice. *Gut* 2020; **69**: 1988-1997 [PMID: 32169907 DOI: 10.1136/gutjnl-2019-320105]
68 **Hou X**, Zhang P, Du H, Chu W, Sun R, Qin S, Tian Y, Zhang Z, Xu F. *Akkermansia Muciniphila* Potentiates the Antitumor Efficacy of FOLFOX in Colon Cancer. *Front Pharmacol* 2021; **12**: 725583 [PMID: 34603035 DOI: 10.3389/fphar.2021.725583]
69 **Liu M**, Xie W, Wan X, Deng T. Clostridium butyricum modulates gut microbiota and reduces colitis associated colon cancer in mice. *Int Immunopharmacol* 2020; **88**: 106862 [PMID: 32771947 DOI: 10.1016/j.intimp.2020.106862]
70 **Konishi H**, Fujiya M, Tanaka H, Ueno N, Moriichi K, Sasajima J, Ikuta K, Akutsu H, Tanabe H, Kohgo Y. Probiotic-derived ferrichrome inhibits colon cancer progression *via* JNK-mediated apoptosis. *Nat Commun* 2016; **7**: 12365 [PMID: 27507542 DOI: 10.1038/ncomms12365]
71 **Sharma M**, Chandel D, Shukla G. Antigenotoxicity and Cytotoxic Potentials of Metabiotics Extracted from Isolated Probiotic, *Lactobacillus rhamnosus* MD 14 on Caco-2 and HT-29 Human Colon Cancer Cells. *Nutr Cancer* 2020; **72**: 110-119 [PMID: 31266374 DOI: 10.1080/01635581.2019.1615514]
72 **Tiptiri-Kourpeti A**, Spyridopoulou K, Santarmaki V, Aindelis G, Tompoulidou E, Lamprianidou EE, Saxami G, Ypsilantis P, Lampri ES, Simopoulos C, Kotsianidis I, Galanis A, Kourkoutas Y, Dimitrellou D, Chlichlia K. Lactobacillus casei Exerts Anti-Proliferative Effects Accompanied by Apoptotic Cell Death and Up-Regulation of TRAIL in Colon Carcinoma Cells. *PLoS One* 2016; **11**: e0147960 [PMID: 26849051 DOI: 10.1371/journal.pone.0147960]
73 **Maghsood F**, Johari B, Rohani M, Madanchi H, Saltanatpour Z, Kadivar M. Anti-proliferative and Anti-metastatic Potential of High Molecular Weight Secretory Molecules from Probiotic Lactobacillus Reuteri Cell-Free Supernatant Against Human Colon Cancer Stem-Like Cells (HT29-ShE). *Int J Pept Res Ther* 2020; **26**: 2619-2631 [DOI: 10.1007/s10989-020-10049-z]
74 **Hosseini SS**, Goudarzi H, Ghalavand Z, Hajikhani B, Rafeieiatani Z, Hakemi-Vala M. Anti-proliferative effects of cell wall, cytoplasmic extract of *Lactococcus lactis* and nisin through down-regulation of *cyclin D1* on SW480 colorectal cancer cell line. *Iran J Microbiol* 2020; **12**: 424-430 [PMID: 33603997 DOI: 10.18502/ijm.v12i5.4603]
75 **Thirabunyanon M**, Hongwittayakorn P. Potential probiotic lactic acid bacteria of human origin induce antiproliferation of colon cancer cells *via* synergic actions in adhesion to cancer cells and short-chain fatty acid bioproduction. *Appl Biochem*

Biotechnol 2013; **169**: 511-525 [PMID: 23239414 DOI: 10.1007/s12010-012-9995-y]

76 **Faramarzian Azimi Maragheh B**, Fatourachi P, Mohammadi SM, Valipour B, Behtari M, Dehnad A, Nozad Charoudeh H. *Streptomyces Levis ABRIINW111* Inhibits SW480 Cells Growth by Apoptosis Induction. *Adv Pharm Bull* 2018; **8**: 675-682 [PMID: 30607340 DOI: 10.15171/apb.2018.076]

77 **Tan LT**, Chan KG, Pusparajah P, Yin WF, Khan TM, Lee LH, Goh BH. Mangrove derived Streptomyces sp. MUM265 as a potential source of antioxidant and anticolon-cancer agents. *BMC Microbiol* 2019; **19**: 38 [PMID: 30760201 DOI: 10.1186/s12866-019-1409-7]

World Journal of Gastroenterology

Submit a Manuscript: https://www.f6publishing.com

World J Gastroenterol 2022 July 21; 28(27): 3383-3397

DOI: 10.3748/wjg.v28.i27.3383

ISSN 1007-9327 (print) ISSN 2219-2840 (online)

MINIREVIEWS

Interventional strategies in infected necrotizing pancreatitis: Indications, timing, and outcomes

Birte Purschke, Louisa Bolm, Max Nikolaus Meyer, Hiroki Sato

Specialty type: Gastroenterology and hepatology

Provenance and peer review: Invited article; Externally peer reviewed.

Peer-review model: Single blind

Peer-review report's scientific quality classification

Grade A (Excellent): 0
Grade B (Very good): B
Grade C (Good): C
Grade D (Fair): 0
Grade E (Poor): 0

P-Reviewer: Jiang M, China; Shalli K, United Kingdom

Received: January 20, 2022
Peer-review started: January 20, 2022
First decision: February 24, 2022
Revised: March 7, 2022
Accepted: June 15, 2022
Article in press: June 15, 2022
Published online: July 21, 2022

Birte Purschke, Louisa Bolm, Department of Gastrointestinal Surgery, Massachusetts General Hospital, Boston, MA 02114, United States

Max Nikolaus Meyer, Department of Radiation Oncology, Massachusetts General Hospital, Boston, MA 02114, United States

Hiroki Sato, Department of Medicine, Asahikawa Medical University, Asahikawa 0788510, Hokkaido, Japan

Hiroki Sato, Department of Gastroenterology, Asahikawa Kosei Hospital, Asahikawa 0788211, Hokkaido, Japan

Corresponding author: Hiroki Sato, MD, PhD, Academic Fellow, Chief Doctor, Research Fellow, Department of Medicine, Asahikawa Medical University, 1-1, Midorigaoka Higashi 2 Jyo 1 Chome, Asahikawa 0788510, Hokkaido, Japan. hirokisato@asahikawa-med.ac.jp

Abstract

Acute pancreatitis (AP) is one of the most common gastrointestinal diseases and remains a life-threatening condition. Although AP resolves to restitutio ad integrum in approximately 80% of patients, it can progress to necrotizing pancreatitis (NP). NP is associated with superinfection in a third of patients, leading to an increase in mortality rate of up to 40%. Accurate and early diagnosis of NP and associated complications, as well as state-of-the-art therapy are essential to improve patient prognoses. The emerging role of endoscopy and recent trials on multidisciplinary management of NP established the "step-up approach". This approach starts with endoscopic interventions and can be escalated to other interventional and ultimately surgical procedures if required. Studies showed that this approach decreases the incidence of new multiple-organ failure as well as the risk of interventional complications. However, the optimal interventional sequence and timing of interventional procedures remain controversial. This review aims to summarize the indications, timing, and treatment outcomes for infected NP and to provide guidance on multidisciplinary decision-making.

Key Words: Pancreatitis; Acute necrotizing pancreatitis; Necrosis; Superinfection; Endoscopy; Surgery

©The Author(s) 2022. Published by Baishideng Publishing Group Inc. All rights reserved.

Core Tip: Acute pancreatitis remains a potentially life-threatening disease. Necrotizing pancreatitis (NP) is associated with superinfection and increases the mortality rate. We summarized the current evidence and clinical recommendations of multidisciplinary approaches focusing on conservative, interventional, and surgical treatment. The interventional approach is often required as a first step in treating infected NP, while further options include minimal invasive or an escalation to open surgical treatment. Although this "step-up approach" is well-established, the exact timing, sequence, and procedure choice remain controversial; this review aims to summarize current evidence and to provide guidance for decision making in clinical practice.

Citation: Purschke B, Bolm L, Meyer MN, Sato H. Interventional strategies in infected necrotizing pancreatitis: Indications, timing, and outcomes. *World J Gastroenterol* 2022; 28(27): 3383-3397
URL: https://www.wjgnet.com/1007-9327/full/v28/i27/3383.htm
DOI: https://dx.doi.org/10.3748/wjg.v28.i27.3383

INTRODUCTION

Acute pancreatitis (AP) is one of the most common and severe gastrointestinal diseases[1]. The rate of AP-related hospitalization in the United States increased from 65.38 to 81.88 per 100000 United States adults per year from 2001 to 2014[2].

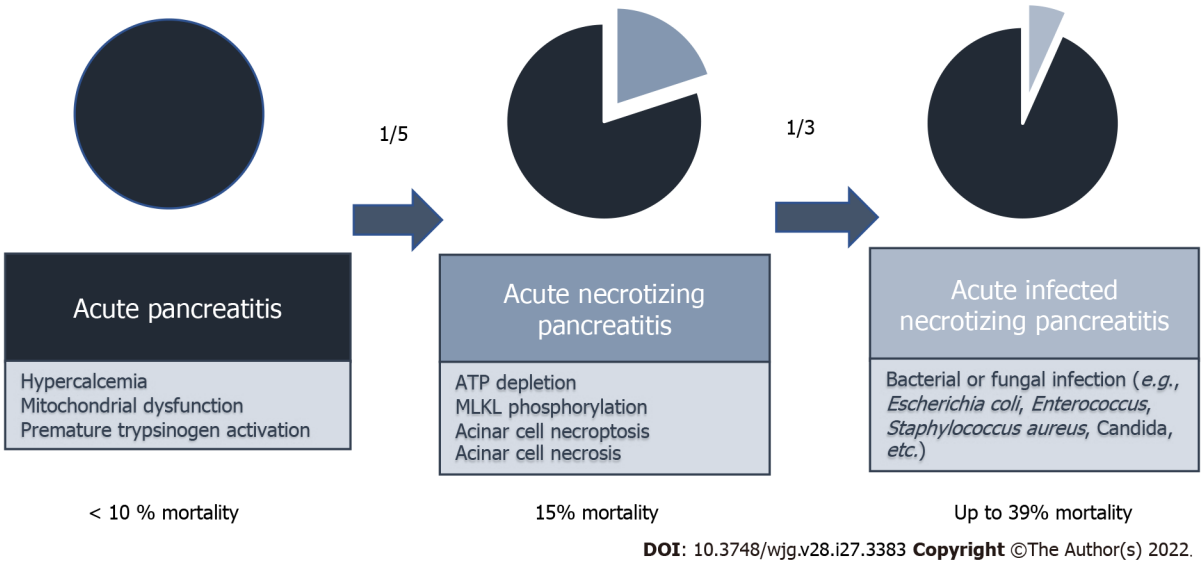
The pathophysiology of AP is characterized by acinar cell injury leading to premature intrapancreatic activation of digestive proteases. ATP depletion and mixed lineage kinase domain-like protein phosphorylation lead to acinar cell necroptosis and necrosis[3]. This results in a cascade effect leading to autodigestion of the pancreatic parenchyma. The acinar cell injury and autodigestion can be induced by different mechanisms; recent publications discuss, for example, the role of hypercalcemia and organelle dysfunction. Cholecystokinin, biliary acids, and alcohol consumption can lead to increased Ca^{2+} efflux by the endoplasmic reticulum (ER). In turn, hypercalcemia can damage the mitochondrial membrane, reducing ATP production and hence the function of the Ca^{2+} efflux mechanisms of the cell itself, which increases the intracellular Ca^{2+} levels even further. This intracellular Ca^{2+} overload ultimately leads to the release and activation of digestive enzymes, which results in premature activation of trypsin. In addition, bile acids, alcohol, and other pancreatic toxic substances can trigger the acinar cells themselves, leading to higher secretion of trypsin[4-6].

AP can be classified as either interstitial edematous or necrotizing pancreatitis (NP). While inflammation and edema of the pancreatic parenchyma and peripancreatic tissues characterize intestinal edematous pancreatitis, further pancreatic or peripancreatic necrosis is known as NP[6], which is a potentially life-threatening disease associated with a 15% mortality rate. In approximately a third of patients with NP, superinfection (fungal or bacterial infection) of necrosis occurs during the clinical course, mostly within 2 to 4 wk after disease onset. Infected NP (INP) results in an even higher mortality rate of up to 30% to 39% (Figure 1)[7-9]. The major causes of INP are obstructing gallstones (up to 50%) and alcohol abuse (20%)[10].

Several scores were introduced in order to predict the severity of AP and its mortality. A retrospective study from 2013 comparing some of these scores revealed that especially the Bedside Index for Severity in Acute Pancreatitis (BISAP) and Acute Physiology and Chronic Health Evaluation (APACHE-II) score stand out compared to scores like the computed tomography (CT) severity index, Ranson Score, body mass index, or hematocrit in terms of predicting severity, organ failure, and death. The BISAP score is a combination of the following five parameters, each worth one point: Altered mental state, blood urea nitrogen > 25.2 mg/dL or more, positive systemic inflammatory response syndrome criteria, age over 60 years, and pleural effusion on CT scan. In comparison, the APACHE-II score uses 14 different parameters, ranging from age to the Glasgow Coma Scale[11].

Another applicable score in INP is the Marshall Score, which determines the presence of organ failure, which, according to the 2012 revised Atlanta Classification of AP, is a criterion that differentiates between mild (no organ failure), moderate (organ failure after less than 48 h), and severe (organ failure after more than 48 h) pancreatitis. The Marshall Score assesses the respiratory system on a scale from 0 to 4 using PaO_2/FIO_2, the renal system using serum creatinine in mg/dL, and the cardiovascular system using the systolic blood pressure in mmHg. A score of 2 or higher for any of the systems indicates organ failure[12].

The clinical management of INP is complex and involves a multidisciplinary team of intensive care specialists, gastroenterologists, and surgeons. Recent trials have provided important insight into the disease mechanisms and have optimized the treatment strategies. However, the indications, timing, and outcomes of different interventional strategies remain controversial.



DOI: 10.3748/wjg.v28.i27.3383 **Copyright** ©The Author(s) 2022.

Figure 1 Mortality rates of acute pancreatitis and pathomechanisms. The mortality rate of all patients with acute pancreatitis (AP) is less than 10%. One-fifth of the patients developed necrotizing AP by ATP depletion, MLKL phosphorylation, acinar cell necroptosis, and/or acinar cell necrosis. One-third of the patients with necrotizing AP developed bacterial or fungal infection. The mortality rate of the infected necrotizing pancreatitis is up to 39%.

PHASES OF AP

According to the 2012 revised Atlanta classification of pancreatitis, two AP phases can be differentiated: the early (< 1 wk after onset) and late (> 1 wk after onset) phases. The early phase is characterized by the first clinical signs of pancreatitis: Abdominal pain, biochemical findings, and imaging findings consistent with pancreatitis. During this time, a pro-inflammatory sterile response occurs, which can lead to systemic inflammatory response syndrome (SIRS)[13]. Nevertheless, AP is self-limited in more than 80% of patients, and treatment in the early phase consists of supportive care instead of a curative intervention[14]. However, necrosis and acute necrotic collection (ANC) can occur in the late phase. ANC is considered a local complication of AP and is characterized by a collection of both fluid and necrosis without a defined wall[8]. ANC can resolve spontaneously or eventually become encapsulating, which allows the collection to become more organized within a well-defined inflammatory wall [15,16]. This process takes approximately 4-6 wk and the end-product is called a walled-off necrosis (WON)[17]. Once WON is diagnosed, whether the pancreatic or peripancreatic necrotic tissue and ANCs are sterile or infected must be determined to plan the subsequent treatment course. Superinfection of acute NP increases the mortality rate (24% *vs* 3.5%)[18,19]. In order to prevent SIRS, sepsis, and multiple (respiratory, cardiovascular, hepatic, and renal) organ failure, the treatment goal is to remove the infected non-vital tissue[13,18,20].

DIAGNOSIS OF ACUTE INP

The diagnosis of AP is mostly based on clinical symptoms; the major ones being abdominal pain, fever, nausea, and vomiting. The diagnosis is further narrowed by measuring the levels of serum amylase and/or lipase. As a diagnostic criterion for pancreatitis, these markers exceed the physiological range by approximately three times. Characteristic imaging findings, such as enlargement of the pancreas and hypodense areas within the parenchyma and/or the peripancreatic tissue, are radiological imaging criteria[8,17,21].

The primary imaging modality within the first 48 h is a transabdominal ultrasound, primarily to determine the need for cholecystectomy for biliary pancreatitis. If the diagnosis of AP remains uncertain, a CT scan can be performed. However, changes on CT are most evident approximately 72 h after AP onset[21].

To diagnose NP, contrast-enhanced CT (CECT) is the preferred imaging modality, as it can identify the presence of gas in the necrotic collection. Magnetic resonance imaging can also be used but is less sensitive than CECT[22]. The diagnosis of infected necrosis is based on clinical criteria including fever and rising serum inflammatory markers[23].

INP REQUIRES A MULTIDISCIPLINARY APPROACH

INP requires both closely monitored intensive care and interventional approaches to remove infected necrotic areas. Endoscopic interventional options involve endoscopic drainage and/or endoscopic necrosectomy. Further interventions are percutaneous transgastric drainage, minimally invasive or open necrosectomy. Using the acronym "PANCREAS", Gomes *et al*[24] summarized eight important steps in the management of severe AP: Perfusion, analgesia, nutrition, clinical and radiological assessment, endoscopy, antibiotics, and surgery.

Historically, INP patients have undergone early open debridement of necrotic tissue (median timing of the operation 21[25] to 28[26] d), mostly followed by local continuous lavage[26]. Recently, interventional strategies have shifted towards a so-called "step-up approach," which involves endoscopic or surgical interventions that comprise open and minimally invasive procedures. The approach starts with simple, less invasive interventions like endoscopic drainage, and escalates to more invasive and finally surgical procedures if these approaches fail.

CONSERVATIVE TREATMENT

INP patients require close monitoring and may need to be admitted to intensive care treatment due to the risk of sepsis and consequent organ failure[27]. The major components of conservative therapy are fluid administration, nutrition, and antibiotics.

FLUID ADMINISTRATION

Hypovolemia is a constant risk in AP patients; moreover, installing fluid infusions and closely monitoring patient circulation parameters is therefore essential. The duration of intravenous infusions as well as the total volume of fluids per day, are subject to ongoing debate[24].

A recent meta-analysis analyzed the impact of early aggressive fluid therapy (infusion rate of 3-5 mL/kg/h in the first 24 h) as compared to non-aggressive hydration. Eleven trials were included, and the authors could not detect a difference in mortality rate; however, aggressive fluid therapy increased the risk of acute kidney injury and pulmonary edema. Furthermore, there was no difference in overall outcomes such as incidence of SIRS, organ failure, or pancreatic necrosis for both therapeutic strategies [28]. Another study demonstrated that early rapid fluid therapy is associated with persistent organ failure, primarily of the respiratory system[29].

Recent studies have favored Ringer's lactate solution as the fluid of choice as opposed to saline solution, as the former reduced systemic inflammation[30]. Recent studies have concluded that the optimal AP regimen involves 3-4 L of Ringer's lactate solution every 24 h and predefined checkpoints at 6-8 h in order to tailor the fluid management to the condition of the patient. Furthermore, measuring urine output, intraabdominal pressure, and vital signs can help adjust the regimen of fluid therapy[31].

NUTRITION

While fasting was considered helpful in AP in the past, current evidence supports early oral or enteral nutrition even if patients experience AP-related complications. As patients with acute NP have increased energy requirements and sustained protein catabolism, an early start of enteral nutrition within the first 48 h of symptom onset is the current standard of care[32]. Regarding nutrition protocol, 25 kcal/kg/d up to a maximum of 30 kcal/kg/d with 1.2-1.5 g/kg of protein per day is recommended [24]. As compared to parenteral nutrition, enteral nutrition is associated with a lower rate of infectious complications and organ failure, shorter hospital stay, and reduced mortality rate[33,34].

ANTIBIOTICS AND PANCREATIC FUNGAL INFECTION

In contrast to patients with general AP, INP patients require immediate antibiotic therapy starting as soon as the diagnosis of INP is confirmed. INP should be initially treated with empirical antibiotics covering both aerobic and anaerobic Gram-negative and Gram-positive microorganisms, such as Imipenem or Ciprofloxacin[35]. A CT-guided fine-needle aspiration (FNA) can help design a more targeted treatment plan. The bacteria most frequently identified in IPN are *Escherichia coli*, *Enterococcus*, *Staphylococcus aureus*, *Staphylococcus epidermidis, Klebsiella pneumoniae, Pseudomonas spp*., and *Streptococcus spp*.[36].

Although antibiotic therapy is an essential tool in the treatment of INP patients, there is insufficient evidence to support the role of antibiotic prophylaxis after the diagnosis of sterile pancreatitis in order to prevent superinfection[36-38].

The use of prophylactic antibacterial therapy and duration of antibacterial therapy have been observed to increase the incidence of pancreatic fungal infection, which is a condition in patients with NP that is associated with increased mortality, intensive care unit admission rate, and length of stay. Its incidence was 26.6% in a study including 2151 patients with NP[39].

INVASIVE TREATMENT

Treatment planning and determining therapy concepts in INP patients should be performed within a multidisciplinary team of surgeons, interventional radiologists, and gastrointestinal endoscopists at experienced centers. Specialists should assess the feasibility of different access routes (transgastric, transduodenal, percutaneous, retroperitoneal, laparoscopic, or laparotomic) and weigh the treatment options, while considering the individual clinical condition of each patient (Table 1).

ENDOSCOPY

Endoscopy plays an emerging role in the treatment of INP[40]. Interventional approaches such as the placement of plastic or metal stents for endoscopic transluminal drainage (ETD) or direct necrosectomy are endoscopically feasible[41].

ETD AND STENT CHOICE

ETD is performed as the standard first step of endoscopic INP treatment. The aim of this procedure is to establish a temporary connection between the gastric cavity and necrotic cavity in the adjacent pancreas in order to drain necrotic collections.

ETD is performed with the assistance of endoscopic ultrasound, which helps avoid puncturing of vessels (*via* color doppler) or targets other than the necrotic collections[42]. The endoscopist then places either a plastic, double pigtail stent; a self-expandable metal stent (SEMS); or a lumen-apposing metal stent (LAMS). The metal stents are larger in diameter (15-20 mm) than the plastic stents (2.33–3.33 mm) and provide access for potential subsequent debridement (Figure 2). SEMS are not commonly used, as they have been reported to migrate into the collapsed fluid collection, posing a risk of major bleeding [43]. LAMS are designed to prevent migration and minimize the risk of leakage with their apposing features[44,45]. Another advantage of LAMS over plastic stents is the delivery system *via* a single-step platform, resulting in a shorter intervention time[46]. Retrospective studies comparing drainage with either LAMS or plastic stents found that the procedure time is significantly shorter for LAMS drainage [47,48]. One of these studies also shows that LAMS drainage results in increased clinical success, reduced need for surgery, and a lower recurrence rate[47].

A more recent randomized clinical trial, however, compared both stent types in a total of 60 patients (31 undergoing LAMS placement and 29 undergoing plastic stent placement) and found that LAMS was not superior to plastic stents. The authors detected no difference in treatment success, the number of procedures required, length of stay, adverse events (within < 3 wk of LAMS removal), readmissions, or overall treatment costs[49,50]. Moreover, the study showed significant stent-related adverse events if LAMS were left in place for more than 3 wk. Given these heterogeneous results, future studies are needed to further evaluate the outcomes of different ETD strategies. Nevertheless, the treating medical team should consider the different procedure duration, since the average time to place the LAMS is shorter compared to plastic stents (15 *vs* 40 min, $P < 0.001$)[51].

ENDOSCOPIC NECROSECTOMY

If the clinical condition of INP patients fails to improve 72 h after ETD, necrosectomy should be considered. Endoscopic transluminal necrosectomy (ETN) can be performed, using a LAMS as access route to the necrotic cavity. With help of forceps, nets, and lavage techniques with saline or hydrogen peroxide, the necrotic tissues are removed endoscopically. ETN can be performed several times if necroses cannot be removed in one procedure[52,53]. It is important to consider that multiple ETN attempts also cause an increased risk of procedure-related complications such as bleeding or perforation [42].

Table 1 Overview of possible interventions in infected necrotizing pancreatitis

		Indications	Contraindications	Most common complications	Ref.
Interventions	Endoscopic transluminal drainage	Standard first step for INP, standard for PFC treatment	Unencapsulated collections, distance from gastroduodenal duct (> 1 cm), vascular pseudoaneuryms	Major bleedings, perforation, post-procedure infection, recurrence, migration of the stent	[37, 38, 40]
	Endoscopic necrosectomy	No improvement in clinical condition within < 72 h after ETD, follow-up treatment	Large necrotic areas, dense necrosis, disconnected duct	Bleeding, perforation, pancreatic fistula, infections	[37, 48, 50]
	Percutaneous catheter drainage	Hardly accessible ANC, ETD not feasible, as combination with ETD	Intracystic haemorrhagia, pancreatic ascites	Intestinal fistula, infection	[36, 51]
	Open surgery	Infected necrosis, suspected perforation, abdominal compartment syndrome, ischemia, intrabadominal haemorrhagia, poorly walled off necrosis, final treatment option if other interventions fail	No clear contraindications reported	Bleeding, infection, perforation, multi-organ failure	[52, 53]
	Minimally invasive surgery	Infected necrosis	Extensive or hardly accessible collections	Bleeding, infection, perforation	[44, 57, 58]

INP: Infected necrotizing pancreatitis; ANC: Acute necrotic collection; ETD: Endoscopic transluminal drainage.

If a transgastric access is not possible or WONs are located in an inaccessible lateral position, a sinus tract endoscopy (STE) may be an option. In order to perform STE, a CT-guided percutaneous drainage catheter is placed 10 d prior to the procedure. The catheter causes the tract wall to mature, so the insertion of an adult gastroscope under fluoroscopic control can be performed safely. The necrotic cavity is lavaged and necrotic tissue is removed, as is done in the ETN procedure (Figure 3)[54].

Endoscopic necrosectomy reduces the rate of surgical interventions[55]. However, these interventions are limited to small necrotic areas and can be very time consuming (60-120 min)[56].

PERCUTANEOUS CATHETER DRAINAGE

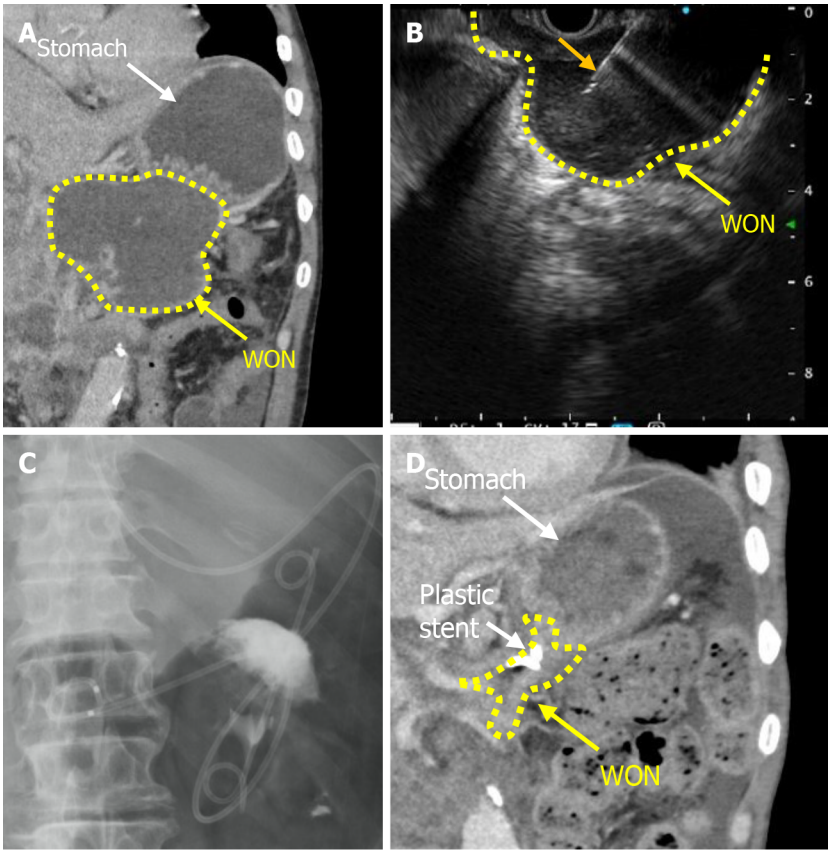
Percutaneous catheter drainage (PCD) is often used prior to endoscopic necrosectomy if the ANC is located in the flank or pelvic region and access *via* ETD is not possible. An interventional radiologist places a general-purpose pigtail drainage catheter into the necrotic collection using the Seldinger technique *via* the most direct transperitoneal route. The preferred route for PCD is through the retroperitoneum. In this case, the drain can be used to guide potential further minimally invasive retroperitoneal necrosectomy (*i.e.*, video-assisted retroperitoneal debridement or STE). A combination of endoscopic transluminal and PCD (also known as dual-modality drainage) is a further option in patients with large collections extending into the paracolic gutters or pelvic region[57]. PCD is the least invasive intervention and was the only intervention needed for patients with INP in 35% (15 out of 43) patients in the randomized PANTER trial[40].

SURGERY

Larger, more complex, and endoscopically not accessible necrotic areas may require minimally invasive or open surgical approaches[16].

OPEN SURGERY

AP can lead to severe complications, such as hemorrhage, perforation, or ischemia. These complications may require immediate open surgical treatment. Abdominal compartment syndrome is a further severe potential complication of AP that must be managed *via* laparotomy. The drainage or debridement of ANCs and contacting the omental bursa should be avoided during these surgical emergency procedures [58]. Beside emergency indications, INP itself is a well-accepted indication for surgical treatment[59].



DOI: 10.3748/wjg.v28.i27.3383 **Copyright** ©The Author(s) 2022.

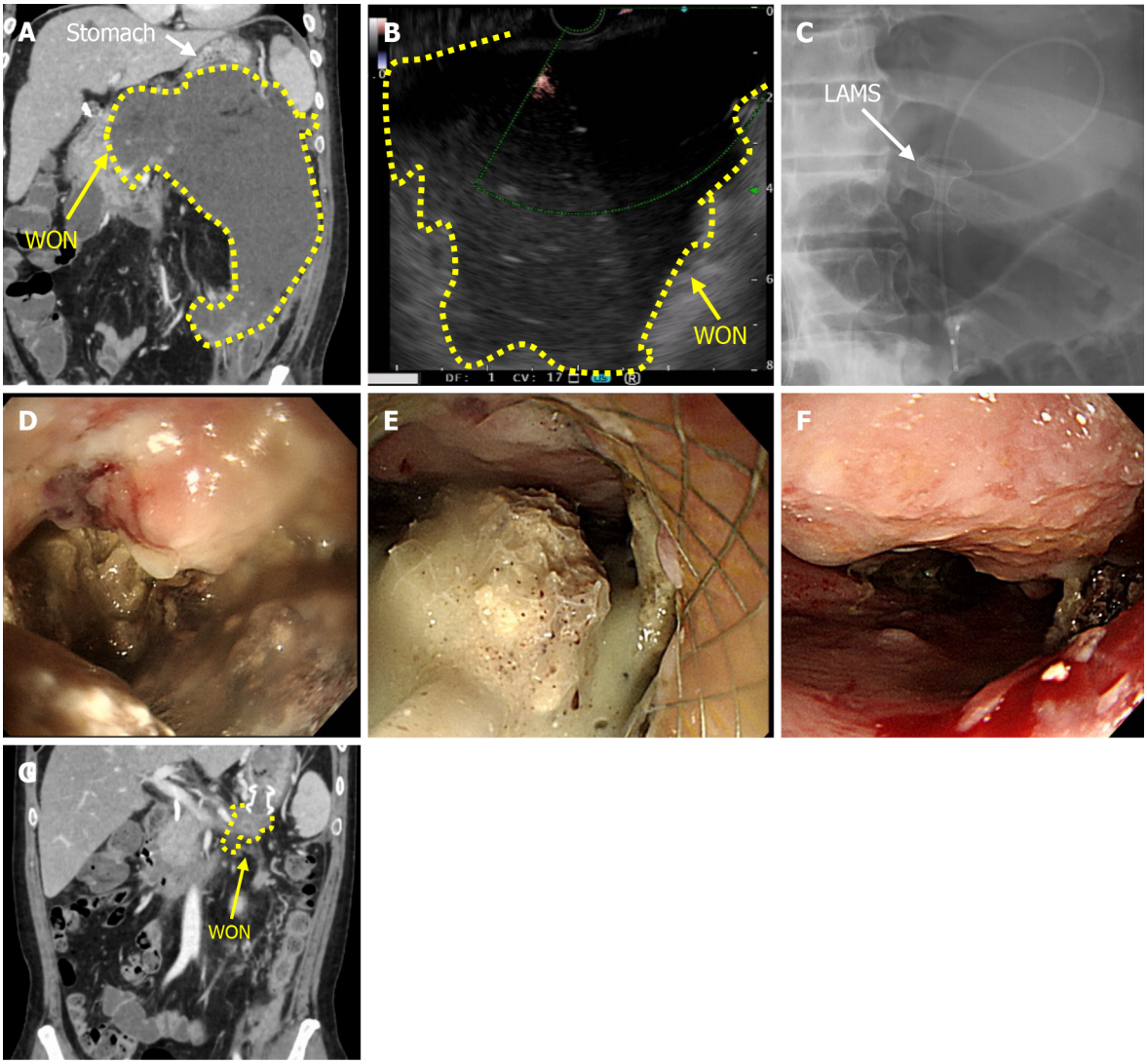
Figure 2 Endoscopic transluminal drainage with plastic stenting. A: A typical computed tomography (CT) scan with walled-off necrosis (WON) formed by necrotizing pancreatitis (white arrow shows stomach and yellow dotted line is the demarcation line of the WON); B: Endoscopic ultrasonography (EUS)-guided drainage for WON was performed (orange arrow shows the needle of 22-gauge EUS needle); C: Two plastic stents and nasobiliary drainage tube was placed into the WON; D: The size of the WON was reduced in the CT scan one month after the procedure. WON: Walled-off necrosis.

Open surgical necrosectomy follows the main principle of exposing the necrotic area and bluntly debriding necrotic tissue: Necrosectomy can be performed with: (1) Open packing; (2) Closed packing; (3) Closed continuous lavage; and (4) Planned re-laparotomies. Open packing involves packing the necrotic cavity with non-adherent dressing after surgical necrosectomy. Readmissions follow every 48 h until the abdomen can be closed after inserting drains. Closed packing is performed when multiple, large, gauze-filled Penrose drains are placed in the residual cavity after necrosectomy and the abdomen is subsequently closed. Closed continuous lavage is performed with the help of two or more double-lumen Salem sump tubes and single-lumen silicone rubber tubes, which are inserted from each flank side and have an in- and outflow of the lavage. Up to 40 L of lavage fluids are used. Planned re-laparotomies provide continuous removal of necrotic tissue over several following days. Surgeons often incorporate zippers into the abdominal wall facilitating repetitive surgical intervention[59].

The standard surgical access is performed either as a transperitoneal or retroperitoneal access. Transgastric access has been added more recently and is considered a fast single-stage option for the treatment of symptomatic WON in severely ill patients[60]. A recent study suggested choosing surgical transgastric necrosectomy whenever feasible in the case of a disconnected pancreatic duct, for dense and large necrosis, and if cholecystectomy must be performed. If the transgastric access is not possible, the authors suggested video-assisted retroperitoneal debridement (VARD) as an alternative procedure[61].

MINIMALLY INVASIVE SURGERY

The main procedures of minimal invasive management of INP are minimal access retroperitoneal pancreatic necrosectomy (MARPN) and VARD. MARPN involves the placement of a 12-French catheter under CT guidance by an interventional radiologist prior to surgery. The preformed access tract is then dilated up to 30-French during the minimal invasive procedure, so that a rigid nephroscope can be entered. The nephroscope serves as visualization instrument and working channel for necrosectomy at the same time. An irrigation drainage system for continuous lavage is installed at the end of the procedure. MARPN can be done multiple times until the patient's condition improves.



DOI: 10.3748/wjg.v28.i27.3383 **Copyright** ©The Author(s) 2022.

Figure 3 A case with endoscopic transluminal drainage with lumen-apposing metal stent. A: Computed tomography (CT) scan before performing the endoscopic ultrasonography (EUS)-guided drainage (White arrow shows the stomach and the yellow arrow shows the walled-off necrosis (WON); the yellow dotted line is the demarcation line of the WON); B: EUS (with color doppler) picture shows marked echoic lesion without vessels; C: Lumen-apposing metal stent (LAMS) and nasobiliary drainage tube were placed (white arrow shows LAMS: Hot AXIOS™ 15 mm × 10 mm, Boston Scientific, Marlborough, MA, United States; Boston Scientific Japan, Tokyo, Japan); D: Esophagogastroduodenoscopy was inserted into necrotic cavity through LAMS; E: Necrosectomy was performed using endoscopic retrieval net; F: Endoscopic findings of the WON one month after the multiple necrosectomy sessions (2-3 times/wk); G: CT scan shows marked reduction of WON cavity one month after multiple necrosectomy sessions. WON: Walled-off necrosis; LAMS: Lumen-apposing metal stent.

VARD consists of combined manual and laparoscopical necrosectomy. It was first reported in 2007 by van Santvoort *et al*[62], who described it as "a hybrid between pure endoscopic retroperitoneal necrosectomy and the open translumbar approach." The procedure starts with a left flank subcostal incision facilitating direct manual debridement followed by a laparoscopic deeper inspection and debridement by laparoscopic instruments. The intervention ends with a continuous lavage.

COMPARISON BETWEEN OPEN AND MINIMALLY INVASIVE SURGERY

Open surgical necrosectomy in AP was historically associated with a mortality rate of 50% or higher[63, 64]. Improved intensive care management, as well as advances in surgical techniques, including minimally invasive options, and the availability of first line endoscopic and minimally invasive procedures have improved patient outcomes over the past decades[65].

A retrospective study compared outcomes of INP patients between 1997-2008 and 2009-2013 and revealed decreased mortality (23.8% *vs* 11.2%, $P = 0.001$) and overall complication rates (73.3% *vs* 64.4%, $P = 0.80$) in the more recent cohort. Minimal invasive approaches contribute to better treatment success rates and improved outcomes in INP as compared to open surgery. MARPN also reportedly results in decreased postoperative multiorgan failure compared to open pancreatic necrosectomy (35% *vs* 20.4%, *P*

= 0.001)[66].

A recent retrospective cohort study comparing 88 patients with open surgical necrosectomy to 91 patients who were treated with minimal invasive surgery (MIS) showed that MIS results in a fivefold decrease in mortality[49]. A meta-analysis published in 2018 reported lower risk of death rates in the very high-risk group when comparing minimally invasive necrosectomy to open surgery[67].

STEP-UP APPROACH

The therapeutic approach in INP patients has shifted from open surgical treatment to a less invasive management that can be summarized by "three Ds": Delay – drain – debride. This approach leads to the introduction of the so-called "step-up approach", which was first described in 2006 by the Dutch Pancreatitis Study group in their PANTER trial[40].

Delay refers to the solidification and complete encapsulation of the pancreatic collection when WON occurs. This is presumed to optimize conditions for intervention, with a lower risk of bleeding and less reinterventions. Drain alludes to using a percutaneous or endoscopic transgastric catheter drainage to mitigate sepsis. Finally, when patients fail to show clinical improvement, debridement is required; in such cases, performing endoscopic or surgical necrosectomy is the next step[40]. A multidisciplinary team of INP experts can choose from different treatment options for each step and decides on the most suitable approach for each individual patient. Re-evaluation periods of 72 h between steps should be maintained[49]. This therapeutic management is also referred to as the "step-up approach", which comprises both an endoscopic and a surgical approach. The overall paradigm is to start with the least invasive and harmful intervention with an option to escalate to more radical approaches with continuous evaluation. The step-up approach decreased the incidence of new multiple-organ failure from 40% to 12% when compared to primary laparotomy[40]. It is the current state-of-the-art approach and has been implemented in all major guidelines (Figure 4)[23,68].

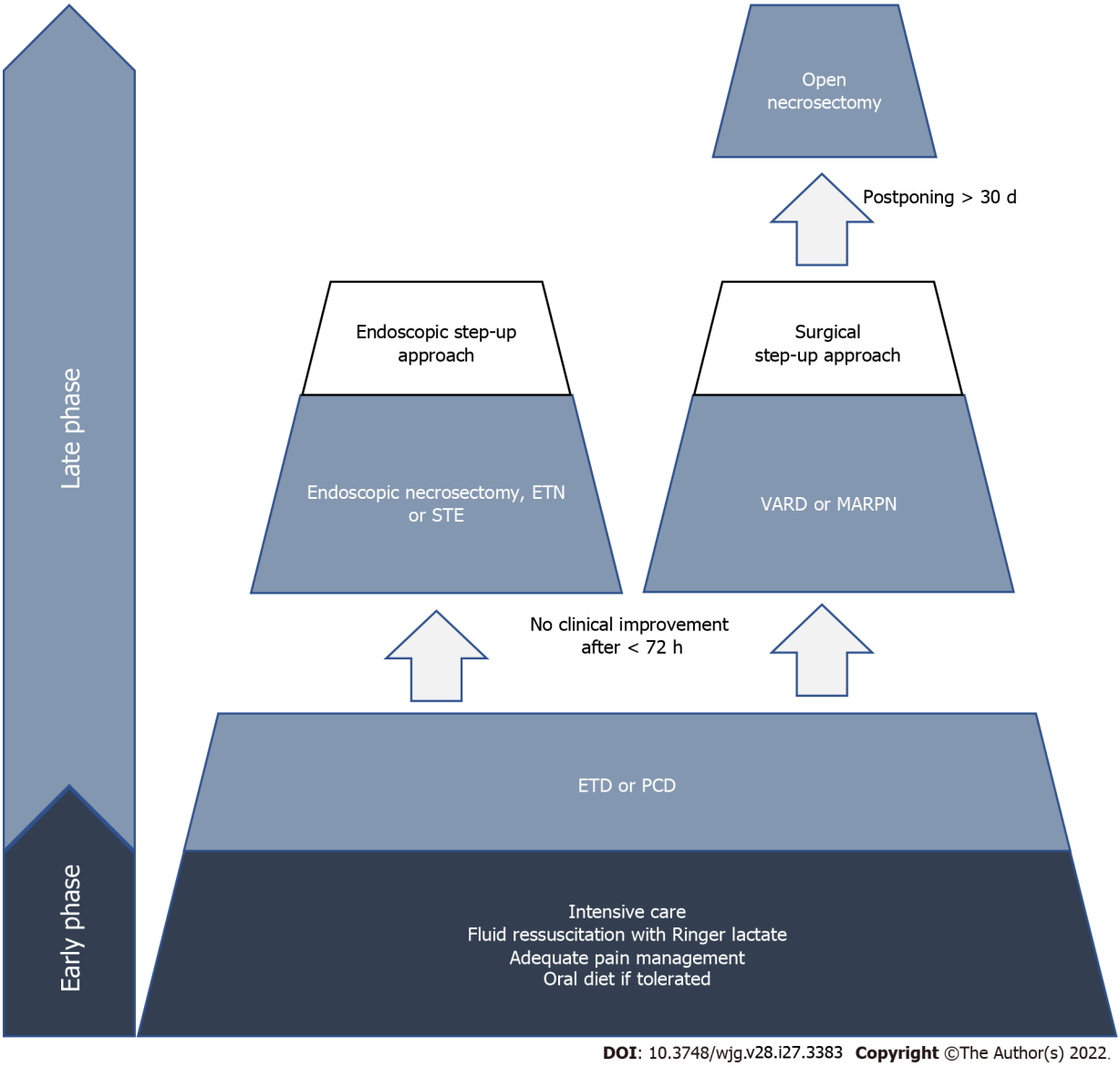
ENDOSCOPIC OR SURGICAL STEP-UP APPROACH

The step-up approach can be performed using endoscopic or surgical necrosectomy. Comparing both approaches has been subject of several randomized trials. From 2008 to 2010, the first prospective, multicentric randomized controlled trial comparing the surgical and endoscopic step-up approaches was performed in the Netherlands. The so-called PENGUIN trial compared endoscopic transgastric necrosectomy with prior retroperitoneal drainage and different techniques of surgical necrosectomy (VARD or, if not feasible, laparotomy) in 10 INP patients per group. The results demonstrated reduced inflammatory response as measured by serum interleukin 6 Levels, reduced rates of pancreatic fistulas (10% *vs* 70%, P = 0.020), and no occurrence of new-onset multiorgan failure (0% *vs* 50%, P = 0.030) in patients in the endoscopic arm[69]. The authors concluded that the endoscopic approach was associated with reduced physiological stress, while surgical access was more invasive.

The multicentric TENSION trial was conducted during 2011-2015 in the Netherlands and compared the outcomes of 51 patients following the endoscopic step-up approach to 47 following the surgical step-up approach. The findings showed no significant difference in mortality and major morbidity between both groups (43% in the endoscopic step-up approach *vs*. 45% in the surgical step-up approach, P = 0.880). However, the mean hospital stay was shorter (53 *vs* 69 d, P = 0.014), fewer pancreatic fistulas occurred (5% *vs* 32%, P = 0.001), and there was a lower overall mean cost (60228 € *vs* 73883 € in the endoscopic step-up approach group[70]).

From 2014 to 2017, the monocentric MISER trial was performed in the United States, comparing minimally invasive surgery (laparoscopic debridement or VARD) to the endoscopic step-up approach in a total of 66 patients. They included severely ill patient cohorts and excluded patients who had improved clinically with only percutaneous drainage as treatment. Consistent with the findings of the TENSION trial, MISER showed no difference in mortality rates (8.8% with the endoscopic step-up approach *vs*. 6.3% with minimally invasive surgery, P = 0.999). However, patients assigned to the endoscopic approach were less likely to develop enteral and pancreatic-cutaneous fistulas (0% *vs* 28.1%, P = 0.001), experienced a lower rate of major complications (12% *vs*. 41%, P = 0.007), and had lower rates of SIRS (20.6% *vs* 65.6 %, P < 0.001). Six months after treatment, patients in the surgical group had significantly more disease-related adverse events than did those in the endoscopic group (43.8 % *vs* 5.9 %, P < 0.001). Finally, the physical health scores for quality of life at 3 mo were better with the endoscopic approach (P = 0.039) and the mean total cost were lower ($75830) compared with the surgical approach ($117492)[49].

The currently available randomized controlled trials point to the endoscopic step-up approach as the preferred treatment for INP patients. However, if the endoscopic treatment is unfeasible, or the necrotic collection extends to the flank or pelvic region (which is difficult to access endoscopically), surgical interventions constitute the alternative when performed as a step-up approach. Each INP patient should be assessed and treated by a multidisciplinary team with sufficient experience in both approaches.



DOI: 10.3748/wjg.v28.i27.3383 **Copyright** ©The Author(s) 2022.

Figure 4 Overview of the step-up approaches of infected necrotizing pancreatitis patients. In the acute phase, multidisciplinary treatment for acute pancreatitis is recommended. Endoscopic necrosectomy or surgical step-up should be considered if there no clinical improvement is observed within 72 h. Open necrosectomy should be considered after video-assisted retroperitoneal debridement or minimal access retroperitoneal pancreatic necrosectomy. ETN: Endoscopic transluminal necrosectomy; STE: Sinus tract endoscopy; ETD: Endoscopic transluminal drainage; PCD: Percutaneous catheter drainage; VARD: Video-assisted retroperitoneal debridement; MARPN: Minimal access retroperitoneal pancreatic necrosectomy.

TIMING OF INTERVENTIONS

The optimal timing of interventions remains a controversial topic and is subject to ongoing debate. An international survey performed in 2016 among 87 pancreatologists revealed that 55% of experts routinely postponed invasive interventions after diagnosing infected necrosis in AP and awaited the effect of antibiotics. However, 33% of pancreatologists preferred surgical necrosectomy as early as possible in infected necrosis, while the remaining 67% would select that route only in the case of WON [71].

A 2014 prospective study including 223 patients revealed that a postponed surgical intervention after 30 d was associated with a lower mortality rate compared to that associated with surgical intervention before day 30 [10% (9/87) *vs* 21% (28/136), $P = 0.040$][72]. This study followed up on a retrospective study from 2007 that also revealed that patients receiving a postponed surgical necrosectomy exhibited lower mortality rates as compared to those receiving surgical treatment after 15-29 d and 1-14 d (8% *vs* 45% *vs* 75%, $P < 0.001$)[26].

A recent study of the Dutch Pancreatic Study Group, the POINTER trial, determined whether the outcomes in INP patients could be improved by early catheter drainage. In the study, catheter drainage was performed immediately in 55 patients, while 49 received the treatment after waiting until WON occurred. Patients were included when there was gas reported on CECT, positive gram/culture FNA,

and clinical suspicion for INP. The rate of organ failure was comparable in both groups and there was no difference in mortality rates. The total number of interventions was 4:1 in the early intervention group compared to the group with delayed intervention, and the total number of necrosectomies in the whole number of patients was 28 (51%) in the immediate as compared to 11 (22%) in the postponed drainage group. Postponing the intervention led to conservative treatment in nearly 40% of patients. This trial could not detect a benefit of immediate drainage over postponed drainage. Conversely, postponing intervention may ultimately avoid necrosectomy and its potential complications[73].

CONCLUSION

Recent advances in endoscopic and minimally invasive therapy have led to a shift in the interventional strategy for INP. Although no standardized approach suits every patient, the "step-up approach" has emerged as a paradigm to treat this severe disease. The key is to start with the least invasive procedure and potentially escalate to more invasive interventions after continuous evaluation, if necessary. This approach highlights the importance of a multidisciplinary team to guide therapeutic approaches in INP patients. The strategy should be based on the individual patient and should allow for dynamic changes in regard to the patient's clinical condition. This claim is also backed by the studies presented in this review that demonstrate lower rates of new multiorgan failure and reduction of hospitalization days, among other preferred outcomes. Even with these recent advances, INP continues to elicit a high mortality rate and further research is required to optimize strategic approaches.

ACKNOWLEDGEMENTS

We thank Hiramatsu K at Asahikawa Kosei Hospital for providing percutaneous radiological drainage pictures; We also thank Okada T, Kawamoto T, Fujinaga A, and Goto M at Asahikawa Kosei Hospital, as well as Hayashi A, the member of Division of Metabolism and Biosystemic Science, Gastroenterology and Hematology/Oncology Department of Medicine, Asahikawa Medical University for providing endoscopic drainage pictures.

FOOTNOTES

Author contributions: Purschke B wrote and edited the manuscript, and collected the clinical data and evidence; Bolm L edited the manuscript and reviewed the discussion about interventional surgical strategies; Meyer MN reviewed the manuscript and provided recommendations on treatment strategies; Sato H reviewed the manuscript and provided strategies and recommendations on the endoscopic intervention part; all authors have read and approved the final manuscript.

Supported by Japan Society for the Promotion of Science KAKENHI, No. 19K17480 and No. 21KK0283 (to Sato H).

Conflict-of-interest statement: Authors declare no conflicts of interests for this article.

Open-Access: This article is an open-access article that was selected by an in-house editor and fully peer-reviewed by external reviewers. It is distributed in accordance with the Creative Commons Attribution NonCommercial (CC BY-NC 4.0) license, which permits others to distribute, remix, adapt, build upon this work non-commercially, and license their derivative works on different terms, provided the original work is properly cited and the use is non-commercial. See: https://creativecommons.org/Licenses/by-nc/4.0/

Country/Territory of origin: Japan

ORCID number: Birte Purschke 0000-0002-6885-6345; Louisa Bolm 0000-0002-1612-1857; Max Nikolaus Meyer 0000-0003-2970-5752; Hiroki Sato 0000-0002-6994-1840.

Corresponding Author's Membership in Professional Societies: Japan Gastroenterological Endoscopy Society, No. 20190318; Japanese Society of Gastroenterology, No. 39625; American Gastroenterological Association, No. 1156949; Japan Society of Human Genetics, No. 1517082360; Japanese Society of Internal Medicine, No. 99021; Japanese Association for Medical Artificial Intelligence, No. 388; Japanese Board of Cancer Therapy, No. 1810053; Japan Society of Medical Oncology, No. 20-0076; Japanese Society for Helicobacter Research; Japan Society of Hepatology, No. 8987; Royal Society of Medicine, No. 00723754.

S-Editor: Yan JP
L-Editor: A
P-Editor: Yan JP

REFERENCES

1 **Peery AF**, Crockett SD, Murphy CC, Lund JL, Dellon ES, Williams JL, Jensen ET, Shaheen NJ, Barritt AS, Lieber SR, Kochar B, Barnes EL, Fan YC, Pate V, Galanko J, Baron TH, Sandler RS. Burden and Cost of Gastrointestinal, Liver, and Pancreatic Diseases in the United States: Update 2018. *Gastroenterology* 2019; **156**: 254-272.e11 [PMID: 30315778 DOI: 10.1053/j.gastro.2018.08.063]

2 **Gapp J**, Hall AG, Walters RW, Jahann D, Kassim T, Reddymasu S. Trends and Outcomes of Hospitalizations Related to Acute Pancreatitis: Epidemiology From 2001 to 2014 in the United States. *Pancreas* 2019; **48**: 548-554 [PMID: 30946239 DOI: 10.1097/MPA.0000000000001275]

3 **Zheng Z**, Ding YX, Qu YX, Cao F, Li F. A narrative review of acute pancreatitis and its diagnosis, pathogenetic mechanism, and management. *Ann Transl Med* 2021; **9**: 69 [PMID: 33553362 DOI: 10.21037/atm-20-4802]

4 **Mayerle J**, Sendler M, Hegyi E, Beyer G, Lerch MM, Sahin-Tóth M. Genetics, Cell Biology, and Pathophysiology of Pancreatitis. *Gastroenterology* 2019; **156**: 1951-1968.e1 [PMID: 30660731 DOI: 10.1053/j.gastro.2018.11.081]

5 **Habtezion A**, Gukovskaya AS, Pandol SJ. Acute Pancreatitis: A Multifaceted Set of Organelle and Cellular Interactions. *Gastroenterology* 2019; **156**: 1941-1950 [PMID: 30660726 DOI: 10.1053/j.gastro.2018.11.082]

6 **Mederos MA**, Reber HA, Girgis MD. Acute Pancreatitis: A Review. *JAMA* 2021; **325**: 382-390 [PMID: 33496779 DOI: 10.1001/jama.2020.20317]

7 **Werge M**, Novovic S, Schmidt PN, Gluud LL. Infection increases mortality in necrotizing pancreatitis: A systematic review and meta-analysis. *Pancreatology* 2016; **16**: 698-707 [PMID: 27449605 DOI: 10.1016/j.pan.2016.07.004]

8 **Colvin SD**, Smith EN, Morgan DE, Porter KK. Acute pancreatitis: an update on the revised Atlanta classification. *Abdom Radiol (NY)* 2020; **45**: 1222-1231 [PMID: 31494708 DOI: 10.1007/s00261-019-02214-w]

9 **van Santvoort HC**, Bakker OJ, Bollen TL, Besselink MG, Ahmed Ali U, Schrijver AM, Boermeester MA, van Goor H, Dejong CH, van Eijck CH, van Ramshorst B, Schaapherder AF, van der Harst E, Hofker S, Nieuwenhuijs VB, Brink MA, Kruyt PM, Manusama ER, van der Schelling GP, Karsten T, Hesselink EJ, van Laarhoven CJ, Rosman C, Bosscha K, de Wit RJ, Houdijk AP, Cuesta MA, Wahab PJ, Gooszen HG; Dutch Pancreatitis Study Group. A conservative and minimally invasive approach to necrotizing pancreatitis improves outcome. *Gastroenterology* 2011; **141**: 1254-1263 [PMID: 21741922 DOI: 10.1053/j.gastro.2011.06.073]

10 **Nesvaderani M**, Eslick GD, Vagg D, Faraj S, Cox MR. Epidemiology, aetiology and outcomes of acute pancreatitis: A retrospective cohort study. *Int J Surg* 2015; **23**: 68-74 [PMID: 26384834 DOI: 10.1016/j.ijsu.2015.07.701]

11 **Park JY**, Jeon TJ, Ha TH, Hwang JT, Sinn DH, Oh TH, Shin WC, Choi WC. Bedside index for severity in acute pancreatitis: comparison with other scoring systems in predicting severity and organ failure. *Hepatobiliary Pancreat Dis Int* 2013; **12**: 645-650 [PMID: 24322751 DOI: 10.1016/s1499-3872(13)60101-0]

12 **Foster BR**, Jensen KK, Bakis G, Shaaban AM, Coakley FV. Revised Atlanta Classification for Acute Pancreatitis: A Pictorial Essay. *Radiographics* 2016; **36**: 675-687 [PMID: 27163588 DOI: 10.1148/rg.2016150097]

13 **Zerem E**. Treatment of severe acute pancreatitis and its complications. *World J Gastroenterol* 2014; **20**: 13879-13892 [PMID: 25320523 DOI: 10.3748/wjg.v20.i38.13879]

14 **Kayar Y**, Senturk H, Tozlu M, Baysal B, Atay M, Ince AT. Prediction of Self-Limited Acute Pancreatitis Cases at Admission to Emergency Unit. *GE Port J Gastroenterol* 2019; **26**: 251-259 [PMID: 31328139 DOI: 10.1159/000493762]

15 **Yasuda I**, Takahashi K. Endoscopic management of walled-off pancreatic necrosis. *Dig Endosc* 2021; **33**: 335-341 [PMID: 32306430 DOI: 10.1111/den.13699]

16 **Heckler M**, Hackert T, Hu K, Halloran CM, Büchler MW, Neoptolemos JP. Severe acute pancreatitis: surgical indications and treatment. *Langenbecks Arch Surg* 2021; **406**: 521-535 [PMID: 32910276 DOI: 10.1007/s00423-020-01944-6]

17 **van Dijk SM**, Hallensleben NDL, van Santvoort HC, Fockens P, van Goor H, Bruno MJ, Besselink MG; Dutch Pancreatitis Study Group. Acute pancreatitis: recent advances through randomised trials. *Gut* 2017; **66**: 2024-2032 [PMID: 28838972 DOI: 10.1136/gutjnl-2016-313595]

18 **Büchler MW**, Gloor B, Müller CA, Friess H, Seiler CA, Uhl W. Acute necrotizing pancreatitis: treatment strategy according to the status of infection. *Ann Surg* 2000; **232**: 619-626 [PMID: 11066131 DOI: 10.1097/00000658-200011000-00001]

19 **da Costa DW**, Boerma D, van Santvoort HC, Horvath KD, Werner J, Carter CR, Bollen TL, Gooszen HG, Besselink MG, Bakker OJ. Staged multidisciplinary step-up management for necrotizing pancreatitis. *Br J Surg* 2014; **101**: e65-e79 [PMID: 24272964 DOI: 10.1002/bjs.9346]

20 **Werner J**, Feuerbach S, Uhl W, Büchler MW. Management of acute pancreatitis: from surgery to interventional intensive care. *Gut* 2005; **54**: 426-436 [PMID: 15710995 DOI: 10.1136/gut.2003.035907]

21 **Leppäniemi A**, Tolonen M, Tarasconi A, Segovia-Lohse H, Gamberini E, Kirkpatrick AW, Ball CG, Parry N, Sartelli M, Wolbrink D, van Goor H, Baiocchi G, Ansaloni L, Biffl W, Coccolini F, Di Saverio S, Kluger Y, Moore E, Catena F. 2019 WSES guidelines for the management of severe acute pancreatitis. *World J Emerg Surg* 2019; **14**: 27 [PMID: 31210778 DOI: 10.1186/s13017-019-0247-0]

22 **McPherson SJ**, O'Reilly DA, Sinclair MT, Smith N. The use of imaging in acute pancreatitis in United Kingdom hospitals: findings from a national quality of care study. *Br J Radiol* 2017; **90**: 20170224 [PMID: 28869389 DOI: 10.1259/bjr.20170224]

23 **Working Group IAP/APA Acute Pancreatitis Guidelines**. IAP/APA evidence-based guidelines for the management of acute pancreatitis. *Pancreatology* 2013; **13**: e1-15 [PMID: 24054878 DOI: 10.1016/j.pan.2013.07.063]

24 **Gomes CA**, Di Saverio S, Sartelli M, Segallini E, Cilloni N, Pezzilli R, Pagano N, Gomes FC, Catena F. Severe acute pancreatitis: eight fundamental steps revised according to the 'PANCREAS' acronym. *Ann R Coll Surg Engl* 2020; **102**: 555-559 [PMID: 32159357 DOI: 10.1308/rcsann.2020.0029]

25 **Fernández-del Castillo C**, Rattner DW, Makary MA, Mostafavi A, McGrath D, Warshaw AL. Débridement and closed packing for the treatment of necrotizing pancreatitis. *Ann Surg* 1998; **228**: 676-684 [PMID: 9833806 DOI: 10.1097/00000658-199811000-00007]

26 **Besselink MG**, Verwer TJ, Schoenmaeckers EJ, Buskens E, Ridwan BU, Visser MR, Nieuwenhuijs VB, Gooszen HG.

Timing of surgical intervention in necrotizing pancreatitis. *Arch Surg* 2007; **142**: 1194-1201 [PMID: 18086987 DOI: 10.1001/archsurg.142.12.1194]

27 **Schepers NJ**, Bakker OJ, Besselink MG, Ahmed Ali U, Bollen TL, Gooszen HG, van Santvoort HC, Bruno MJ; Dutch Pancreatitis Study Group. Impact of characteristics of organ failure and infected necrosis on mortality in necrotising pancreatitis. *Gut* 2019; **68**: 1044-1051 [PMID: 29950344 DOI: 10.1136/gutjnl-2017-314657]

28 **Gad MM**, Simons-Linares CR. Is aggressive intravenous fluid resuscitation beneficial in acute pancreatitis? *World J Gastroenterol* 2020; **26**: 1098-1106 [PMID: 32206000 DOI: 10.3748/wjg.v26.i10.1098]

29 **Li L**, Jin T, Wen S, Shi N, Zhang R, Zhu P, Lin Z, Jiang K, Guo J, Liu T, Philips A, Deng L, Yang X, Singh VK, Sutton R, Windsor JA, Huang W, Xia Q. Early Rapid Fluid Therapy Is Associated with Increased Rate of Noninvasive Positive-Pressure Ventilation in Hemoconcentrated Patients with Severe Acute Pancreatitis. *Dig Dis Sci* 2020; **65**: 2700-2711 [PMID: 31912265 DOI: 10.1007/s10620-019-05985-w]

30 **Wu BU**, Hwang JQ, Gardner TH, Repas K, Delee R, Yu S, Smith B, Banks PA, Conwell DL. Lactated Ringer's solution reduces systemic inflammation compared with saline in patients with acute pancreatitis. *Clin Gastroenterol Hepatol* 2011; **9**: 710-717.e1 [PMID: 21645639 DOI: 10.1016/j.cgh.2011.04.026]

31 **Garg PK**, Mahapatra SJ. Optimum Fluid Therapy in Acute Pancreatitis Needs an Alchemist. *Gastroenterology* 2021; **160**: 655-659 [PMID: 33412126 DOI: 10.1053/j.gastro.2020.12.017]

32 **Bakker OJ**, van Brunschot S, Farre A, Johnson CD, Kalfarentzos F, Louie BE, Oláh A, O'Keefe SJ, Petrov MS, Powell JJ, Besselink MG, van Santvoort HC, Rovers MM, Gooszen HG. Timing of enteral nutrition in acute pancreatitis: meta-analysis of individuals using a single-arm of randomised trials. *Pancreatology* 2014; **14**: 340-346 [PMID: 25128270 DOI: 10.1016/j.pan.2014.07.008]

33 **Li W**, Liu J, Zhao S, Li J. Safety and efficacy of total parenteral nutrition versus total enteral nutrition for patients with severe acute pancreatitis: a meta-analysis. *J Int Med Res* 2018; **46**: 3948-3958 [PMID: 29962261 DOI: 10.1177/0300060518782070]

34 **Oláh A**, Romics L Jr. Enteral nutrition in acute pancreatitis: a review of the current evidence. *World J Gastroenterol* 2014; **20**: 16123-16131 [PMID: 25473164 DOI: 10.3748/wjg.v20.i43.16123]

35 **Isenmann R**, Büchler MW, Friess H, Uhl W, Beger HG. Antibiotics in acute pancreatitis. *Dig Surg* 1996; **13**: 365-369 [DOI: 10.1159/000172465]

36 **Barie PS**. A critical review of antibiotic prophylaxis in severe acute pancreatitis. *Am J Surg* 1996; **172**: 38S-43S [PMID: 9003689 DOI: 10.1016/S0002-9610(96)00349-2]

37 **Villatoro E**, Mulla M, Larvin M. Antibiotic therapy for prophylaxis against infection of pancreatic necrosis in acute pancreatitis. *Cochrane Database Syst Rev* 2010; CD002941 [PMID: 20464721 DOI: 10.1002/14651858.CD002941.pub3]

38 **Jafri NS**, Mahid SS, Minor KS, Idstein SR, Hornung CA, Galandiuk S. Meta-analysis: antibiotic prophylaxis to prevent peristomal infection following percutaneous endoscopic gastrostomy. *Aliment Pharmacol Ther* 2007; **25**: 647-656 [PMID: 17311597 DOI: 10.1111/j.1365-2036.2007.03247.x]

39 **Singh RR**, Mitchell W, David Y, Cheesman A, Dixon RE, Nagula S, DiMaio CJ, Greenwald DA, Kumta NA. Pancreatic Fungal Infection in Patients With Necrotizing Pancreatitis: A Systematic Review and Meta-analysis. *J Clin Gastroenterol* 2021; **55**: 218-226 [PMID: 33252558 DOI: 10.1097/MCG.0000000000001467]

40 **Besselink MG**, van Santvoort HC, Nieuwenhuijs VB, Boermeester MA, Bollen TL, Buskens E, Dejong CH, van Eijck CH, van Goor H, Hofker SS, Lameris JS, van Leeuwen MS, Ploeg RJ, van Ramshorst B, Schaapherder AF, Cuesta MA, Consten EC, Gouma DJ, van der Harst E, Hesselink EJ, Houdijk LP, Karsten TM, van Laarhoven CJ, Pierie JP, Rosman C, Bilgen EJ, Timmer R, van der Tweel I, de Wit RJ, Witteman BJ, Gooszen HG; Dutch Acute Pancreatitis Study Group. Minimally invasive 'step-up approach' versus maximal necrosectomy in patients with acute necrotising pancreatitis (PANTER trial): design and rationale of a randomised controlled multicenter trial [ISRCTN13975868]. *BMC Surg* 2006; **6**: 6 [PMID: 16606471 DOI: 10.1186/1471-2482-6-6]

41 **Ruiz-Clavijo D**, de la Higuera BG, Vila JJ. Advances in the endoscopic management of pancreatic collections. *World J Gastrointest Endosc* 2015; **7**: 381-388 [PMID: 25901217 DOI: 10.4253/wjge.v7.i4.381]

42 **Trikudanathan G**, Attam R, Arain MA, Mallery S, Freeman ML. Endoscopic interventions for necrotizing pancreatitis. *Am J Gastroenterol* 2014; **109**: 969-81; quiz 982 [PMID: 24957157 DOI: 10.1038/ajg.2014.130]

43 **Talreja JP**, Shami VM, Ku J, Morris TD, Ellen K, Kahaleh M. Transenteric drainage of pancreatic-fluid collections with fully covered self-expanding metallic stents (with video). *Gastrointest Endosc* 2008; **68**: 1199-1203 [PMID: 19028232 DOI: 10.1016/j.gie.2008.06.015]

44 **Mussetto A**, Fugazza A, Fuccio L, Triossi O, Repici A, Anderloni A. Current uses and outcomes of lumen-apposing metal stents. *Ann Gastroenterol* 2018; **31**: 535-540 [PMID: 30174389 DOI: 10.20524/aog.2018.0287]

45 **Dalsania R**, Willingham FF. Treatment of walled-off pancreatic necrosis. *Curr Opin Gastroenterol* 2019; **35**: 478-482 [PMID: 31313686 DOI: 10.1097/MOG.0000000000000564]

46 **Bang JY**, Varadarajulu S. Lumen-apposing metal stents for endoscopic ultrasonography-guided interventions. *Dig Endosc* 2019; **31**: 619-626 [PMID: 31050068 DOI: 10.1111/den.13428]

47 **Chen YI**, Yang J, Friedland S, Holmes I, Law R, Hosmer A, Stevens T, Franco MC, Jang S, Pawa R, Mathur N, Sejpal DV, Inamdar S, Trindade AJ, Nieto J, Berzin TM, Sawhney M, DeSimone ML, DiMaio C, Kumta NA, Gupta S, Yachimski P, Anderloni A, Baron TH, James TW, Jamil LH, Ona MA, Lo SK, Gaddam S, Dollhopf M, Bukhari MA, Moran R, Gutierrez OB, Sanaei O, Fayad L, Ngamruengphong S, Kumbhari V, Singh V, Repici A, Khashab MA. Lumen apposing metal stents are superior to plastic stents in pancreatic walled-off necrosis: a large international multicenter study. *Endosc Int Open* 2019; **7**: E347-E354 [PMID: 30834293 DOI: 10.1055/a-0828-7630]

48 **Rana SS**, Sharma R, Dhalaria L, Gupta R. Efficacy and safety of plastic versus lumen-apposing metal stents for transmural drainage of walled-off necrosis: a retrospective single-center study. *Ann Gastroenterol* 2020; **33**: 426-432 [PMID: 32624665 DOI: 10.20524/aog.2020.0499]

49 **Bang JY**, Arnoletti JP, Holt BA, Sutton B, Hasan MK, Navaneethan U, Feranec N, Wilcox CM, Tharian B, Hawes RH, Varadarajulu S. An Endoscopic Transluminal Approach, Compared With Minimally Invasive Surgery, Reduces Complications and Costs for Patients With Necrotizing Pancreatitis. *Gastroenterology* 2019; **156**: 1027-1040.e3 [PMID:

30452918 DOI: 10.1053/j.gastro.2018.11.031]
50 **Bang JY**, Hasan MK, Navaneethan U, Sutton B, Frandah W, Siddique S, Hawes RH, Varadarajulu S. Lumen-apposing metal stents for drainage of pancreatic fluid collections: When and for whom? *Dig Endosc* 2017; **29**: 83-90 [PMID: 27199157 DOI: 10.1111/den.12681]
51 **Bang JY**, Navaneethan U, Hasan MK, Sutton B, Hawes R, Varadarajulu S. Non-superiority of lumen-apposing metal stents over plastic stents for drainage of walled-off necrosis in a randomised trial. *Gut* 2019; **68**: 1200-1209 [PMID: 29858393 DOI: 10.1136/gutjnl-2017-315335]
52 **Arvanitakis M**, Dumonceau JM, Albert J, Badaoui A, Bali MA, Barthet M, Besselink M, Deviere J, Oliveira Ferreira A, Gyökeres T, Hritz I, Hucl T, Milashka M, Papanikolaou IS, Poley JW, Seewald S, Vanbiervliet G, van Lienden K, van Santvoort H, Voermans R, Delhaye M, van Hooft J. Endoscopic management of acute necrotizing pancreatitis: European Society of Gastrointestinal Endoscopy (ESGE) evidence-based multidisciplinary guidelines. *Endoscopy* 2018; **50**: 524-546 [PMID: 29631305 DOI: 10.1055/a-0588-5365]
53 **Baron TH**. Endoscopic pancreatic necrosectomy. *Gastroenterol Hepatol (N Y)* 2008; **4**: 617-620 [PMID: 22798744 DOI: 10.1016/s0016-5085(08)60559-4]
54 **Goenka MK**, Goenka U, Mujoo MY, Tiwary IK, Mahawar S, Rai VK. Pancreatic Necrosectomy through Sinus Tract Endoscopy. *Clin Endosc* 2018; **51**: 279-284 [PMID: 29301065 DOI: 10.5946/ce.2017.066]
55 **Gardner TB**, Coelho-Prabhu N, Gordon SR, Gelrud A, Maple JT, Papachristou GI, Freeman ML, Topazian MD, Attam R, Mackenzie TA, Baron TH. Direct endoscopic necrosectomy for the treatment of walled-off pancreatic necrosis: results from a multicenter U.S. series. *Gastrointest Endosc* 2011; **73**: 718-726 [PMID: 21237454 DOI: 10.1016/j.gie.2010.10.053]
56 **Voermans RP**, Besselink MG, Fockens P. Endoscopic management of walled-off pancreatic necrosis. *J Hepatobiliary Pancreat Sci* 2015; **22**: 20-26 [PMID: 25345777 DOI: 10.1002/jhbp.180]
57 **Boxhoorn L**, Voermans RP, Bouwense SA, Bruno MJ, Verdonk RC, Boermeester MA, van Santvoort HC, Besselink MG. Acute pancreatitis. *Lancet* 2020; **396**: 726-734 [PMID: 32891214 DOI: 10.1016/S0140-6736(20)31310-6]
58 **Trikudanathan G**, Wolbrink DRJ, van Santvoort HC, Mallery S, Freeman M, Besselink MG. Current Concepts in Severe Acute and Necrotizing Pancreatitis: An Evidence-Based Approach. *Gastroenterology* 2019; **156**: 1994-2007.e3 [PMID: 30776347 DOI: 10.1053/j.gastro.2019.01.269]
59 **Werner J**, Hartwig W, Hackert T, Büchler MW. Surgery in the treatment of acute pancreatitis--open pancreatic necrosectomy. *Scand J Surg* 2005; **94**: 130-134 [PMID: 16111095 DOI: 10.1177/145749690509400209]
60 **Driedger M**, Zyromski NJ, Visser BC, Jester A, Sutherland FR, Nakeeb A, Dixon E, Dua MM, House MG, Worhunsky DJ, Munene G, Ball CG. Surgical Transgastric Necrosectomy for Necrotizing Pancreatitis: A Single-stage Procedure for Walled-off Pancreatic Necrosis. *Ann Surg* 2020; **271**: 163-168 [PMID: 30216220 DOI: 10.1097/SLA.0000000000003048]
61 **Luckhurst CM**, El Hechi M, Elsharkawy AE, Eid AI, Maurer LR, Kaafarani HM, Thabet A, Forcione DG, Fernández-Del Castillo C, Lillemoe KD, Fagenholz PJ. Improved Mortality in Necrotizing Pancreatitis with a Multidisciplinary Minimally Invasive Step-Up Approach: Comparison with a Modern Open Necrosectomy Cohort. *J Am Coll Surg* 2020; **230**: 873-883 [PMID: 32251846 DOI: 10.1016/j.jamcollsurg.2020.01.038]
62 **van Santvoort HC**, Besselink MG, Horvath KD, Sinanan MN, Bollen TL, van Ramshorst B, Gooszen HG; Dutch Acute Pancreatis Study Group. Videoscopic assisted retroperitoneal debridement in infected necrotizing pancreatitis. *HPB (Oxford)* 2007; **9**: 156-159 [PMID: 18333133 DOI: 10.1080/13651820701225688]
63 **Mier J**, León EL, Castillo A, Robledo F, Blanco R. Early versus late necrosectomy in severe necrotizing pancreatitis. *Am J Surg* 1997; **173**: 71-75 [PMID: 9074366 DOI: 10.1016/S0002-9610(96)00425-4]
64 **Götzinger P**, Sautner T, Kriwanek S, Beckerhinn P, Barlan M, Armbruster C, Wamser P, Függer R. Surgical treatment for severe acute pancreatitis: extent and surgical control of necrosis determine outcome. *World J Surg* 2002; **26**: 474-478 [PMID: 11910483 DOI: 10.1007/s00268-001-0252-8]
65 **Szeliga J**, Jackowski M. Minimally invasive procedures in severe acute pancreatitis treatment - assessment of benefits and possibilities of use. *Wideochir Inne Tech Maloinwazyjne* 2014; **9**: 170-178 [PMID: 25097683 DOI: 10.5114/wiitm.2014.41628]
66 **Gomatos IP**, Halloran CM, Ghaneh P, Raraty MG, Polydoros F, Evans JC, Smart HL, Yagati-Satchidanand R, Garry JM, Whelan PA, Hughes FE, Sutton R, Neoptolemos JP. Outcomes From Minimal Access Retroperitoneal and Open Pancreatic Necrosectomy in 394 Patients With Necrotizing Pancreatitis. *Ann Surg* 2016; **263**: 992-1001 [PMID: 26501713 DOI: 10.1097/SLA.0000000000001407]
67 **van Brunschot S**, Hollemans RA, Bakker OJ, Besselink MG, Baron TH, Beger HG, Boermeester MA, Bollen TL, Bruno MJ, Carter R, French JJ, Coelho D, Dahl B, Dijkgraaf MG, Doctor N, Fagenholz PJ, Farkas G, Castillo CFD, Fockens P, Freeman ML, Gardner TB, Goor HV, Gooszen HG, Hannink G, Lochan R, McKay CJ, Neoptolemos JP, Oláh A, Parks RW, Peev MP, Raraty M, Rau B, Rösch T, Rovers M, Seifert H, Siriwardena AK, Horvath KD, van Santvoort HC. Minimally invasive and endoscopic versus open necrosectomy for necrotising pancreatitis: a pooled analysis of individual data for 1980 patients. *Gut* 2018; **67**: 697-706 [PMID: 28774886 DOI: 10.1136/gutjnl-2016-313341]
68 **Tenner S**, Baillie J, DeWitt J, Vege SS; American College of Gastroenterology. American College of Gastroenterology guideline: management of acute pancreatitis. *Am J Gastroenterol* 2013; **108**: 1400-15; 1416 [PMID: 23896955 DOI: 10.1038/ajg.2013.218]
69 **Bakker OJ**, van Santvoort HC, van Brunschot S, Geskus RB, Besselink MG, Bollen TL, van Eijck CH, Fockens P, Hazebroek EJ, Nijmeijer RM, Poley JW, van Ramshorst B, Vleggaar FP, Boermeester MA, Gooszen HG, Weusten BL, Timmer R; Dutch Pancreatitis Study Group. Endoscopic transgastric vs surgical necrosectomy for infected necrotizing pancreatitis: a randomized trial. *JAMA* 2012; **307**: 1053-1061 [PMID: 22416101 DOI: 10.1001/jama.2012.276]
70 **van Brunschot S**, van Grinsven J, Voermans RP, Bakker OJ, Besselink MG, Boermeester MA, Bollen TL, Bosscha K, Bouwense SA, Bruno MJ, Cappendijk VC, Consten EC, Dejong CH, Dijkgraaf MG, van Eijck CH, Erkelens GW, van Goor H, Hadithi M, Haveman JW, Hofker SH, Jansen JJ, Laméris JS, van Lienden KP, Manusama ER, Meijssen MA, Mulder CJ, Nieuwenhuis VB, Poley JW, de Ridder RJ, Rosman C, Schaapherder AF, Scheepers JJ, Schoon EJ, Seerden T, Spanier BW, Straathof JW, Timmer R, Venneman NG, Vleggaar FP, Witteman BJ, Gooszen HG, van Santvoort HC, Fockens P; Dutch Pancreatitis Study Group. Transluminal endoscopic step-up approach versus minimally invasive surgical step-up

approach in patients with infected necrotising pancreatitis (TENSION trial): design and rationale of a randomised controlled multicenter trial [ISRCTN09186711]. *BMC Gastroenterol* 2013; **13**: 161 [PMID: 24274589 DOI: 10.1186/1471-230X-13-161]

71 **van Grinsven J**, van Brunschot S, Bakker OJ, Bollen TL, Boermeester MA, Bruno MJ, Dejong CH, Dijkgraaf MG, van Eijck CH, Fockens P, van Goor H, Gooszen HG, Horvath KD, van Lienden KP, van Santvoort HC, Besselink MG; Dutch Pancreatitis Study Group. Diagnostic strategy and timing of intervention in infected necrotizing pancreatitis: an international expert survey and case vignette study. *HPB (Oxford)* 2016; **18**: 49-56 [PMID: 26776851 DOI: 10.1016/j.hpb.2015.07.003]

72 **Guo Q**, Li A, Xia Q, Lu H, Ke N, Du X, Zhang Z, Hu W. Timing of intervention in necrotizing pancreatitis. *J Gastrointest Surg* 2014; **18**: 1770-1776 [PMID: 25091844 DOI: 10.1007/s11605-014-2606-1]

73 **Boxhoorn L**, van Dijk SM, van Grinsven J, Verdonk RC, Boermeester MA, Bollen TL, Bouwense SAW, Bruno MJ, Cappendijk VC, Dejong CHC, van Duijvendijk P, van Eijck CHJ, Fockens P, Francken MFG, van Goor H, Hadithi M, Hallensleben NDL, Haveman JW, Jacobs MAJM, Jansen JM, Kop MPM, van Lienden KP, Manusama ER, Mieog JSD, Molenaar IQ, Nieuwenhuijs VB, Poen AC, Poley JW, van de Poll M, Quispel R, Römkens TEH, Schwartz MP, Seerden TC, Stommel MWJ, Straathof JWA, Timmerhuis HC, Venneman NG, Voermans RP, van de Vrie W, Witteman BJ, Dijkgraaf MGW, van Santvoort HC, Besselink MG; Dutch Pancreatitis Study Group. Immediate versus Postponed Intervention for Infected Necrotizing Pancreatitis. *N Engl J Med* 2021; **385**: 1372-1381 [PMID: 34614330 DOI: 10.1056/NEJMoa2100826]

World Journal of Gastroenterology

Submit a Manuscript: https://www.f6publishing.com

World J Gastroenterol 2022 July 21; 28(27): 3398-3409

DOI: 10.3748/wjg.v28.i27.3398

ISSN 1007-9327 (print) ISSN 2219-2840 (online)

MINIREVIEWS

Artificial intelligence in liver ultrasound

Liu-Liu Cao, Mei Peng, Xiang Xie, Gong-Quan Chen, Shu-Yan Huang, Jia-Yu Wang, Fan Jiang, Xin-Wu Cui, Christoph F Dietrich

Specialty type: Gastroenterology and hepatology

Provenance and peer review: Invited article; Externally peer reviewed.

Peer-review model: Single blind

Peer-review report's scientific quality classification

Grade A (Excellent): 0
Grade B (Very good): 0
Grade C (Good): C, C
Grade D (Fair): 0
Grade E (Poor): 0

P-Reviewer: Hussain J, Oman; Li L, China

Received: February 7, 2022
Peer-review started: February 7, 2022
First decision: April 10, 2022
Revised: April 18, 2022
Accepted: June 19, 2022
Article in press: June 19, 2022
Published online: July 21, 2022

Liu-Liu Cao, Mei Peng, Xiang Xie, Fan Jiang, Department of Medical Ultrasound, The Second Hospital of Anhui Medical University, Hefei 230601, Anhui Province, China

Gong-Quan Chen, Department of Medical Ultrasound, Minda Hospital of Hubei Minzu University, Enshi 445000, Hubei Province, China

Shu-Yan Huang, Department of Medical Ultrasound, The First People's Hospital of Huaihua, Huaihua 418000, Hunan Province, China

Jia-Yu Wang, Xin-Wu Cui, Department of Medical Ultrasound, Tongji Hospital of Tongji Medical College, Huazhong University of Science and Technology, Wuhan 430030, Hubei Province, China

Christoph F Dietrich, Department Allgemeine Innere Medizin, Kliniken Hirslanden Beau Site, Salem und Permanence, Bern 3626, Switzerland

Corresponding author: Fan Jiang, MD, Associate Professor, Department of Medical Ultrasound, The Second Hospital of Anhui Medical University, No. 678 Furong Road, Economic and Technological Development Zone, Hefei 230601, Anhui Province, China.
ahultrasound2005@126.com

Abstract

Artificial intelligence (AI) is playing an increasingly important role in medicine, especially in the field of medical imaging. It can be used to diagnose diseases and predict certain statuses and possible events that may happen. Recently, more and more studies have confirmed the value of AI based on ultrasound in the evaluation of diffuse liver diseases and focal liver lesions. It can assess the severity of liver fibrosis and nonalcoholic fatty liver, differentially diagnose benign and malignant liver lesions, distinguish primary from secondary liver cancers, predict the curative effect of liver cancer treatment and recurrence after treatment, and predict microvascular invasion in hepatocellular carcinoma. The findings from these studies have great clinical application potential in the near future. The purpose of this review is to comprehensively introduce the current status and future perspectives of AI in liver ultrasound.

Key Words: Machine learning; Deep learning; Radiomics; Diffuse liver diseases; Focal liver diseases; Ultrasound

©The Author(s) 2022. Published by Baishideng Publishing Group Inc. All rights reserved.

Core Tip: Artificial intelligence (AI) is playing an increasingly important role in medicine, especially in the field of medical imaging. Currently, there is a need of a comprehensive review to introduce the application of AI based on ultrasound in diffuse and focal liver lesions. In this article, we introduce the application of AI in the assessment of liver fibrosis and nonalcoholic fatty liver and the differentiation of focal liver lesions. In addition, we discuss the performance of AI based on ultrasound in predicting curative effect, prognosis and microvascular invasion in hepatocellular carcinoma. Lastly, we illustrate the future prospect of AI in liver ultrasound.

Citation: Cao LL, Peng M, Xie X, Chen GQ, Huang SY, Wang JY, Jiang F, Cui XW, Dietrich CF. Artificial intelligence in liver ultrasound. *World J Gastroenterol* 2022; 28(27): 3398-3409
URL: https://www.wjgnet.com/1007-9327/full/v28/i27/3398.htm
DOI: https://dx.doi.org/10.3748/wjg.v28.i27.3398

INTRODUCTION

In the past several years, liver diseases have affected millions of lives and became one of the main causes of illness and death in the world[1]. It is reported that more than one-fifth of the Chinese population are affected by liver diseases, such as liver fibrosis, liver cancer and nonalcoholic fatty liver disease (NAFLD), contributing unambiguously to health loss. Therefore, paying more attention to liver diseases is of great significance.

Artificial intelligence (AI) is defined as the research of algorithms that enable machines to have the ability of reasoning and performing functions such as solving problems, recognizing object and word, inferring world states, and making decisions[2]. AI is a precise prediction technique that automates learning and recognizes patterns in data. Apart from this, AI has been extensively applied to medical diagnosis, especially in medical image analysis. This application mainly relies on deep learning, a subfield of machine learning. Deep learning is on the frontier of AI, which is based on deep neural networks (DNNs) with more than one hidden layer. Convolutional neural networks (CNNs) are a branch of DNNs that are particularly useful for recognizing images and have stimulated a large amount of interest from industry, academia and clinicians[3].

Compared to other medical imaging techniques, ultrasound is noninvasive, portable and can provide real-time imaging. In recent years, AI-powered ultrasound has become more developed and been implemented in clinical applications in order to reduce the subjectivity and improve the efficiency of ultrasound diagnosis[4]. Many studies have confirmed the value of AI in the evaluation of thyroid nodule, breast lesion and liver lesion classification by ultrasound. In addition to these applications, other AI applications in ultrasound have also been explored and achieved great progress.

In liver medical imaging, AI can make a quantitative assessment by recognizing imaging information automatically to aid physicians in making more precise and comprehensive imaging diagnoses[5]. This technique has been extensively applied to computed tomography (CT), positron emission tomography-CT, magnetic resonance imaging and ultrasound to diagnose liver lesions. For instance, deep learning based on CT and positron emission tomography-CT can be used to detect new liver tumors and metastatic liver malignancy, and to predict the primary origin of liver metastasis[6-8].

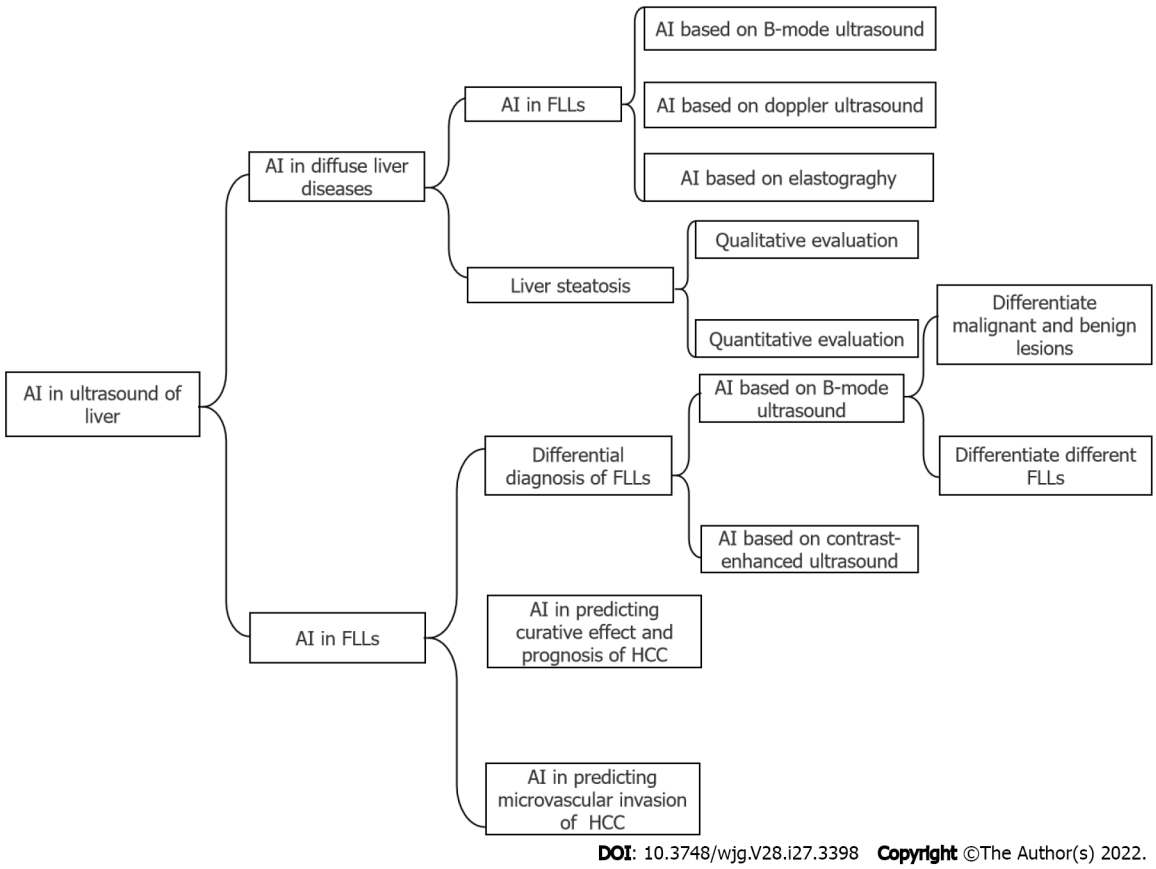
There are also many studies that have illustrated the application of AI in liver ultrasound, while a comprehensive review of AI in this field is lacking. In this review, we will introduce the application of AI based on ultrasound in diffuse liver diseases, including liver fibrosis and steatosis, and focal liver lesions (FLLs), including their differential diagnosis, prediction of a curative effect and prognosis and microvascular invasion (MVI) of hepatocellular carcinoma (HCC). The main structure of this review was illustrated in Figure 1.

APPLICATION OF AI IN DIFFUSE LIVER DISEASE

There are a variety of diffuse liver diseases that can be asymptomatic or cause severe liver dysfunction, and many of them may lead to cirrhosis, hepatic carcinoma, and death. We will introduce the applications of AI based on ultrasound in two common diffuse liver diseases, *i.e.* liver fibrosis and steatosis.

Liver fibrosis

Liver fibrosis is the early step of cirrhosis and an important pathological basis of HCC[9]. Therefore, the early detection and prevention of liver fibrosis is essential in the clinical setting. However, although liver biopsy is the gold standard for classifying liver fibrosis using the Metavir score[10] or New Inuyama classification[11] to distribute the score ranging from F0 (no fibrosis) to F4 (cirrhosis). The use



DOI: 10.3748/wjg.V28.i27.3398 Copyright ©The Author(s) 2022.

Figure 1 Main structure of this review. AI: Artificial intelligence; FLLs: Focal liver lesions; HCC: Hepatocellular carcinoma.

of tissue examination for the assessment of liver fibrosis is controversial because liver biopsy is invasive and liver fibrosis is not equably distributed throughout the liver. There are an increasing number of credible, noninvasive and available approaches being widely applied in clinical practice. Recently, a large number of noninvasive techniques have been used to prevent adverse outcomes through the application of AI based on ultrasound.

AI based on B-mode ultrasound: As early as 20 years ago, AI was used to assist the diagnosis of liver fibrosis. Badawi *et al*[12] creatively proposed an approach that employed fuzzy reasoning techniques to identify diffuse liver diseases automatically by using digital quantitative features measured from the ultrasound images. They extracted parameters only from B-mode images, and the results revealed that this approach had higher specificity and sensitivity for the diagnosis of liver fibrosis than the statistical classification techniques, which had a certain effect but could not help much.

Apart from this, a novel deep multi-scale texture network based entirely on B-mode ultrasound images that was proposed recently seems to be more convenient[13]. The area under the receiver operating characteristic curve of this approach was 0.92 for significant fibrosis (≥ F2) and 0.89 for cirrhosis (F4) in the validation group, which outperformed the ultrasonographers and three serum biomarkers during diagnosis. Although it cannot be used for liver fibrosis staging now, it has excellent potential in the future workflow.

AI based on Doppler ultrasound: On the basis of grey-scale parameters from B-mode images, Doppler parameters of intrahepatic blood vasculature were added as essential parameters. Eventually, five ultrasonographic variables, including the liver parenchyma, thickness of the spleen, the hepatic vein waveform, hepatic artery pulsatile index and damping index, were selected as the input neurons. A data optimization procedure was used in an artificial neural network for the diagnosis of liver fibrosis, which achieved an area under the curve of 0.92[14]. Although this model proved to predict liver cirrhosis accurately, it still could not provide a specific grading.

AI based on elastography: In recent years, with the development of ultrasound, studies have proposed computer-aided techniques based on elastography that is of great importance in ultrasound images to identify and stage liver fibrosis. Real-time tissue elastography (RTE) is one of the recently developed elastography techniques. In a study, 11 image features were extracted directly from the RTE software that was installed in the ultrasound system to quantify the patterns of the RTE images[15]. Then, the data were processed and divided among four classical classifiers. The results showed that the

performance of the adopted classifiers was much better than the previous liver fibrosis index method, which predicted the stage of fibrosis using RTE images and multiple regression analyses. The good performance in this study demonstrated that machine learning had the potential to perform as powerful tools for staging liver fibrosis.

Nowadays, most applications of AI in evaluating the stage of liver fibrosis are based on shear wave elastography. An automated approach including the image quality check, region of interest (ROI) selection and CNN classification based on shear wave elastography showed a more accurate detection of ≥ F2 fibrosis levels than a previously published baseline approach, with an area under curve of 0.89 *vs* 0.74[16]. The deep learning radiomics also presented the potential diagnostic performance in chronic hepatitis B patients compared with two-dimensional shear wave elastography[17]. AI could help stage liver fibrosis more accurately with the assistance of elastography.

Liver steatosis

Hepatic steatosis, characterized by the accumulation of fat droplets in hepatocytes, can develop into nonalcoholic fibrosis, steatohepatitis, cirrhosis, and even HCC[18,19]. Early detection and treatment may halt or reverse NAFLD progression[19]. As a consequence, there is a critical need to develop noninvasive imaging methods to assess hepatic steatosis. Noninvasive liver imaging methods including CT, magnetic resonance imaging and ultrasound have been extensively investigated[20].

Ultrasound is the first-line examination for identifying liver steatosis. It shows an enlarged liver with a greater number of echoes caused by fat droplets, and the liver is brighter and more hyperechoic compared with the right kidney. The image is qualitative and relies on the subjective judgement of the operator, which definitely leads to variable results and low reproducibility[21]. To overcome the observer bias, a series of quantitative and semi-quantitative parameters, including attenuation and backscatter coefficients, the hepato-renal index (HRI) and ultrasound envelope statistic parametric imaging (known as speckle statistics), have been implemented, some of which represent excellent reproducibility and reliability[21-24]. At present, almost all the studies published have concentrated on NAFLD.

It was reported that the detection of moderate and severe steatosis based on ultrasound has an 84.8% sensitivity and a 93.6% specificity, while mild steatosis has an even lower sensitivity[25]. Recently, some researchers applied AI to improve the ultrasound detection rate of NAFLD, and the results were promising. Table 1 shows the studies using AI based on ultrasound to identify steatosis. The studies showed that AI had tremendous potential in helping diagnose liver steatosis. Some studies attempted to optimize CNN models. In the future, classifying the degree of liver steatosis with the assistance of the AI could be a trend.

Qualitative evaluation: Deep learning has been applied to qualitatively evaluate NAFLD. An approach of assessing fatty liver disease by utilizing deep learning based on CNNs with B-mode images was proposed[26]. The study recruited 135 participants with known or suspected NAFLD to investigate the function of four liver views (three views in the transverse plane, including hepatic veins at the confluence with the inferior vena cava, right portal vein and right posterior portal vein, and one view in the sagittal plane, *i.e.* the liver and kidney view) in the assessment[27]. The study assessed attention maps for liver assessment based on CNNs, which illustrated that the available image features provided by each view could assess liver fat. Unlike the previous study, magnetic resonance imaging proton density fat fraction was used as a reference standard, which was not precise enough compared with liver biopsy.

A novel framework combining transfer learning with fine-tuning was proposed[28]. Although this study revealed that the new framework outperformed CNN, this conclusion was not entirely convincing because the radiologists' qualitative scores were the reference standard. This framework was also utilized in other studies and achieved a good performance.

With the development of deep learning, Chou *et al*[29] established two-class, three-class and four-class prediction models to classify the severity of steatosis by using B-mode ultrasound images from 2070 patients. Although liver biopsy is the gold standard, the deep learning model could select eligible patients for a liver biopsy by evaluating the severity of fatty liver preliminarily, which would reduce unnecessary tests.

Different deep learning algorithms tend to have different performances. The combined deep learning algorithm based on B-mode images had an area under the receiver operating characteristic curve of 0.9999 and accuracy of 0.9864 compared with other algorithms[30]. Therefore, in future studies selecting an optimal algorithm is important.

Quantitative evaluation: AI has also been applied to quantitatively evaluate NAFLD. Radiofrequency signals may negate the loss or change of data during translation to B-mode ultrasound images. A study acquired the diagnosis and fat fraction of NAFLD by inputting the original data based on one-dimensional algorithms[31]. The investigators obtained a 97% sensitivity and 94% specificity, and the positive predictive value was up to 97%, which demonstrated that the utilization of original ultrasound radiofrequency could be applied in diagnosing NAFLD and to quantifying liver fat fraction. Similarly, in an animal experiment, a CNN model based on radiofrequency signals was shown to have a better

Table 1 Studies using artificial intelligence based on ultrasound for fatty liver disease diagnosis

Task	Reference standard	Sample size	Method	Results	Ref.
Fatty liver disease diagnosis	Liver biopsy	55 patients with severe obesity, 38 of whom had fatty liver disease	Deep learning with B-mode image ultrasound	Sensitivity: 100%; specificity: 88%; accuracy: 96%; AUC: 0.98	[26]
Fatty liver disease diagnosis	Radiologist qualitative score	157 ultrasound liver images from unknown number of participants	Deep learning with B-mode image ultrasound	Sensitivity: 95%; specificity: 85%; accuracy: 90.6%; AUC: 0.96	[28]
NAFLD assessment	MRI proton density fat fraction	204 participants, 140 of whom had NAFLD, 64 control participants	One-dimensional CNNs	Sensitivity: 97%; specificity: 94%; accuracy: 96%; AUC: 0.98	[31]
NAFLD assessment	MRI proton density fat fraction	135 adult participants with known or suspected NAFLD	Transfer learning with a pretrained CNN by four ultrasound views of liver routinely obtained	SCC: 0.81; AUC: 0.91 (PDFF ≥ 5%)	[27]
NAFLD assessment	Liver biopsy	295 subjects, 198 mild fatty liver, one moderate degree of fatty liver	DCNN-based organ segmentation with Gaussian mixture modeling for automated quantification of the HRI	ICC of two radiologists and DCNN were 0.919, 0.916, 0.734	[33]
The severity of fatty liver	Abdominal ultrasound	21855 B-mode ultrasound images, 2070 patients with different severities from none to severe fatty liver	Pretrained CNN models with B-mode ultrasound images	The areas under the receiver operating characteristic curves were 0.974 (mild steatosis *vs* others), 0.971 (moderate steatosis *vs* others), 0.981 (severe steatosis *vs* others), 0.985 (any severity *vs* normal) and 0.996 (moderate-to-severe steatosis clinically abnormal *vs* normal-to-mild steatosis clinically normal)	[29]

AUC: Area under curve; CNN: Convolutional neural network; DCNN: Deep convolutional neural network; HRI: Hepato-renal index; ICC: Intraclass correlation; MRI: Magnetic resonance image; NAFLD: Nonalcoholic fatty liver disease; PDFF: Proton density fat fraction; SCC: Spearman correlation coefficient.

performance than the traditional quantitative ultrasound when classifying steatosis[32].

An HRI model based on CNNs was also tested for NAFLD evaluation. Cha *et al*[33] reported that an automated approach had no significant difference in hepatic measurements and HRI calculations compared with experienced radiologists, which indicated that the aid of deep learning could reduce a radiologist's workload and improve the residents' diagnostic accuracy. In this study, an automated HRI calculation algorithm was used, including liver and kidney segmentation, kidney ROI extraction, liver ROI extraction, and calculation of the HRI.

APPLICATION OF AI IN FLLS

HCC is the most conventional original malignant FLL, which is the sixth most common cancer in human beings as well as the fourth cause of cancer-related deaths in the world[1]. Hence, early accurate differential diagnosis of malignant and benign FLL is important for the management and prognosis of patients[34].

Ultrasound is the first-line imaging modality to identify FLLs in the clinical workflow. The development of AI provides a new method to improve the accuracy of ultrasound in diagnosing FLLs. Compared with radiologists viewing anatomical images, AI can better reflect monolithic tumor morphology as well as capture both granular and radiological patterns in a specific task, which is difficult by normal human vision[35]. Figure 2 illustrates the flowchart of the application of deep learning and radiomics in FLLs. Studies have confirmed that the application of AI can improve the diagnostic performance of ultrasound for FLLs (Table 2).

Differential diagnosis of FLLs

AI based on B-mode ultrasound: AI has been widely used in differentiating malignant and benign FLLs based on B-mode ultrasound. Gray level co-occurrence matrix could be used in extracting features from B-mode images, which has been used in differentiating malignant and benign FLLs combined with a fuzzy support vector machine[36]. This study achieved an area under the curve of 0.984 and 0.971 in database 1 and database 2, respectively, which confirmed the feasibility of AI in this field.

Table 2 Studies using artificial intelligence based on ultrasound for focal liver lesion diagnosis

Modality and task	Approach	Target disease: number of the case	Performance	Ref.
Classifying different FLLs based on B-mode	ANN	Cyst: 29; hemangioma: 37; malignant tumor: 33	Cyst *vs* hemangioma accuracy: 99.7%; cyst *vs* malignant tumor accuracy: 98.7%; hemangioma *vs* malignant tumor accuracy: 96.1%	[40]
Differentiating benign and malignant lesions based on B-mode	CNN	Benign lesions: 300; malignant lesions: 296	All lesion accuracy: 84%; uncertain set of lesion accuracy: 79%	[37]
Classifying different FLLs based on B-mode	ANN (sparse autoencoder)	Normal liver: 16; cyst: 44; hemangioma: 18; HCC: 30	overall accuracy: 97.2%; overall sensitivity: 98%; overall specificity: 95.7%	[41]
Differentiating benign and malignant lesions based on B-mode	FSVM	training set; DS1: benign lesions: 132, malignant lesions: 68; DS2: malignant liver cancer: 50, hepatocellular adenoma: 150, hemangioma: 35, focal nodular hyperplasia: 145, lipoma: 70	DS1: accuracy: 97%, sensitivity: 100%, specificity: 95.5%, AUC: 0.984; DS2: accuracy: 95.1%, sensitivity: 92.0%, specificity: 95.5%, AUC: 0.971	[36]
Classifying different FLLs based on B-mode	CNN	Non-tumorous liver: 258, hemangioma: 17, HCC: 6, cyst: 30, focal nodular hyperplasia: 8	AUC for tumor detection: 0.935; AUC for tumor discrimination (mean): 0.916	[42]
Diagnosing HCC based on B-mode	CNN	Malignant tumor: 1786; benign tumor: 427	AUC for EV: 0.924	[38]
Differentiating benign and malignant lesions based on B-mode	CNN	HCC: 6; cyst: 6600; hemangioma: 5374; focal fatty sparing: 5110; focal fatty infiltration: 934	IV: overall sensitivity: 83.9%; overall specificity: 97.1%; HCC detection rate: 85.3%; EV: overall sensitivity: 84.9%; overall specificity: 97.1%; HCC detection rate: 78.3%	[39]
Classifying different FLLs based on CEUS	ANN	hemangioma: 16; focal fatty liver: 23; HCC: 41; metastatic tumor: 32 (hypervascular: 20 hypovascular: 12)	Accuracy: 94.5%; sensitivity: 93.2%; specificity: 89.7%	[47]
Differentiating benign and malignant lesions based on CEUS	Deep belief networks	HCC: 6; hemangioma: 10; liver abscess: 4; metastases: 3; focal fatty sparing: 3	Accuracy: 83.4%; sensitivity: 83.3%; specificity: 87.5%	[59]
Differentiating benign and malignant lesions based on CEUS	SVM	Benign tumor: 30; malignant tumor: 22	Accuracy: 90.3%; sensitivity: 93.1%; specificity: 86.9%	[45]
Differentiating benign and malignant lesions based on CEUS	SVM	Benign tumor, HCC or metastatic tumor: 98	Benign *vs* malignant accuracy: 91.8%, sensitivity: 93.1%, specificity: 86.9%; benign *vs* HCC *vs* metastatic carcinoma: accuracy: 85.7%; sensitivity: 84.4%; specificity: 87.7%	[46]
Differentiating benign and malignant lesions based on CEUS	Deep canonical correlation analysis + multiple kernel learning	Benign tumor: 46; malignant tumor: 47	Accuracy: 90.4%; sensitivity: 93.6%; specificity: 86.9%	[43]
Differentiating benign and malignant lesions based on CEUS	3D-CNN	HCC: 2110; focal nodular hyperplasia: 2310	Accuracy: 93.1%; sensitivity: 94.5%; specificity: 93.6%	[44]
Differentiating benign and malignant lesions based on CEUS	Deep neural network	Focal nodular hyperplasia: 16; HCC: 30; hemangioma: 23; hypervascular metastasis: 11; hypovascular metastasis: 11	Top accuracy: 88%	[48]
Differentiating benign and malignant lesions based on CEUS	CNN	Development set: malignant tumor: 281, benign tumor: 82; testing set: malignant tumor: 164, benign tumor: 47	Accuracy: 91.0%; sensitivity: 92.7%; specificity: 85.1%; AUC: 0.934	[49]

ANN: Artificial neural network; AUC: Area under curve; CEUS: Contrast-enhanced ultrasound; CNN: Convolutional neural network; DS1: Database 1; DS2: Database 2; EV: External validation; FLL: Focal liver lesion; FSVM: Fuzzy support vector machine; HCC: Hepatocellular carcinoma; IV: Internal validation; SVM: Support vector machine; 3D: Three-dimensional.

With the development of AI, deep learning plays a more vital role in the differential diagnosis of FLLs. A CNN with ResNet50 was utilized to recognize benign from malignant solid liver lesions through ultrasonography. The performance was comparable to that of expert radiologists[37]. However, this study did not involve other information such as clinical factors. In another (multicenter) study, after adding seven clinical factors, a higher accuracy, sensitivity and specificity was obtained, compared with those from radiologists with 15 years of experience. The area under the curve for recognizing malignant from benign lesions reached up to 0.924 in the external validation cohort[38].

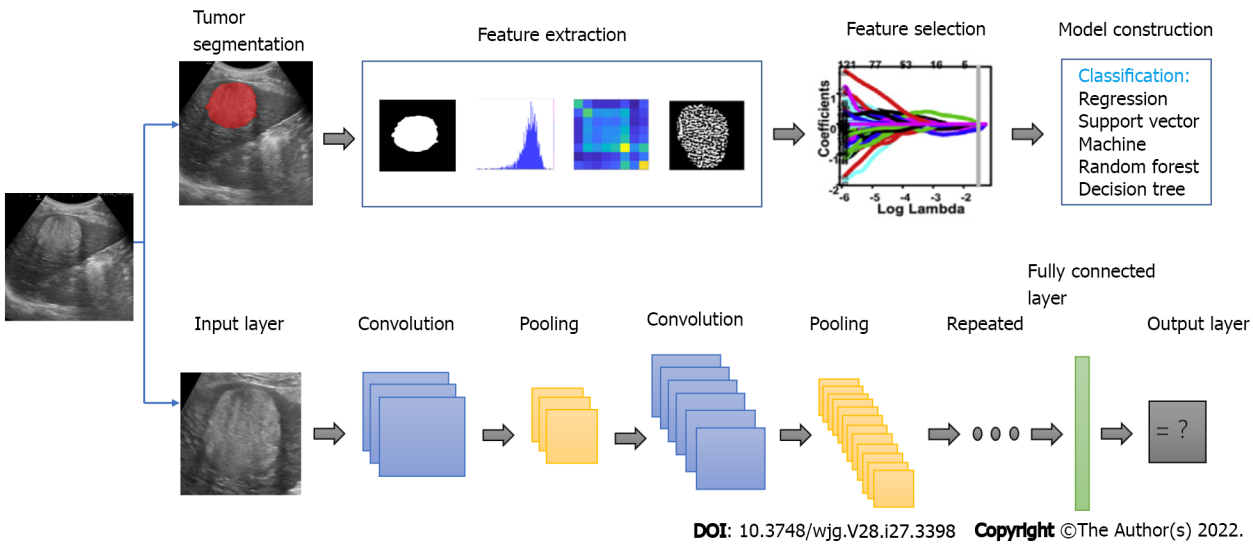


Figure 2 Illustration of the flowchart of the application of deep learning and radiomics in focal liver lesions. These two methods were based on big data, which contained image preprocessing, feature extraction and model construction.

However, the aforementioned studies only included common FLLs. Increasing the types of FLLs may confuse the diagnosis and reduce the accuracy. Similar to the previous study, a multicenter study estimating internal validation and external validation cohorts had a larger volume of training data and involved more varieties of FLLs, including cysts, HCC, hemangiomas, focal fatty infiltration and focal fatty sparing[39]. Although they obtained a lower sensitivity due to more types of diseases, the performance in the external validation cohorts was still satisfactory. In addition, they utilized videos as training materials to achieve real-time analysis in the future workflow. This novel approach would offer great convenience to radiologists in helping differentiate FLLs.

AI could also be used in the classification of FLLs. In order to optimize feature sets, a hybrid textural feature extraction system was proposed by Hwang *et al*[40]. In their preliminary study, a high accuracy was observed in classifying cysts *vs* hemangiomas and cysts *vs* malignant lesions. However, when classifying hemangiomas *vs* malignant lesions by extracting multiple ROI, the accuracy was only 80%. The proposed approach exhibited a better accuracy in all classification groups by quantifying the key features in ultrasound images, especially in classifying hemangioma *vs* malignant, with an accuracy of 96.13%.

Later, a sparse autoencoder system based on deep learning was proposed in diagnosing cysts, hemangiomas and malignant lesions, and it outperformed the three progressive techniques, including K-enarest neighbor, multi-support vector machine and naive Bayes, with an overall accuracy of 97.2% [41].

These two studies[40,41] focused on three kinds of FLLs. An algorithm that could simultaneously detect and characterize FLLs based on deep learning was proposed in diagnosing HCC, focal nodular hyperplasia, cysts, hemangiomas and metastasis, and it achieved an average area under the curve of 0.916[42]. That study yielded promising results by using a small amount of data. Larger databases would increase the accuracy of this model.

AI based on contrast-enhanced ultrasound: It is reported that contrast-enhanced ultrasound (CEUS) images had better sensitivity and specificity for differentiating between malignant and benign tumors compared with B-mode images, which indicated CEUS had a superior diagnostic performance. Combining AI with CEUS could differentiate benign and malignant FLLs and classify different kinds of malignant lesions.

AI could be used to differentiate malignant and benign FLLs based on three-phase CEUS images. A two-stage multiple view learning that represented the integration of deep canonical correlation analysis and multiple kernel learning was used to fuse the characteristics of three-phase patterns in CEUS, presenting an accuracy of 90.41%[43]. The proposed algorithm had both a low computational complex and a high predictive accuracy. For multiview CEUS images, utilizing a multimodal feature fusion algorithm is necessary.

Compared with deep canonical correlation analysis-multiple kernel learning, the use of a three-dimensioned CNN, which integrated the relationship between two temporally adjacent frames to extract features spatially and temporally, achieved a higher accuracy of 93.1%, sensitivity of 94.5% and specificity of 93.6%[44]. However, this algorithm still needs to be validated.

These two studies above[43,44] exploited heterogeneous visual morphology to describe the difference between liver masses. Apart from this method, time-intensity curve (TIC), which represents the contrast

intensity constantly and generates the fitted curve of enhanced intensity during the process, was used in many studies.

Support vector machine[45,46] and deep learning[47,48] based on TICs have presented good performances in differentiating FLLs. A support vector machine-based image analysis system was used for FLL classification and presented an area under the curve of 0.89[45]. An artificial neural network diagnostic system based on TICs was shown to have a similar accuracy and specificity in classifying five different liver tumors 10 years ago[47]. Later, deep learning became more mature, and TICs of the arterial and the portal vein phases of CEUS videos were extracted on the basis of the deep belief networks, a kind of neural network that was composed of layers of Boltzmann machines, to analyze the extracted TICs[48]. The accuracy of this deep learning method for classifying benign from malignant lesions was 83.36%. A novel evaluation procedure named 'leave-one-patient-out' and custom DNNs were creatively presented. That study involved various types of liver lesions and compared the custom DNN designs with the state-of-the-art architectures and obtained a maximal accuracy of 88% by utilizing the proposed evaluation procedure in both pretrained and trained-from-scratch models. This novel approach has a magnificent prospect for development, and it is worth further investigation.

AI based on CEUS was shown to assist in clinical settings as the reference and improve the performance of residents in the differentiation of benign and malignant FLLs[49]. In the future, it will likely play a supporting role in clinical work. However, AI based on TICs tends to complicate the calculation because generating TICs is a time-consuming process. Therefore, developing new approaches to extract features from CEUS images is important.

Application of AI in predicting curative effect and prognosis of HCC

It was reported that the Edmondson-Steiner grade is a vital preoperation predictor of tumor survival and recurrence after undergoing surgical resection[50,51]. Because preoperative pathological differentiation grade can only be obtained by an invasive biopsy[52], it is necessary to explore a noninvasive method to predict therapeutic effect, recurrence and metastasis to achieve personalized treatment.

Some studies[53-55] demonstrated the superiority of AI based on CEUS in predicting a curative effect and prognosis in HCC. Although the results revealed a better performance of AI models compared with a single clinical or ultrasound model, a better performance may be obtained by adding clinical factors in the future studies.

Predicting curative effect of HCC: Transarterial chemoembolization (TACE) is the first-line therapy in patients who are diagnosed with mid-stage HCC, and the response to the first TACE treatment is related to the subsequent curative effect and survival. Therefore, it is necessary to predict the personalized responses to the first TACE treatment. A deep learning radiomics-based CEUS model, machine learning radiomics-based B-mode image model and machine learning radiomics-based TIC of the CEUS model were established to achieve this function[53]. These models presented a better performance compared with the hepatoma arterial embolization prognostic score based on three indexes concerning liver function and tumor load, which will be of great benefit in selecting both first treatment and subsequent therapies after the first TACE treatment.

Predicting prognosis of patients with HCC: Radiofrequency ablation and surgical resection are recommended for early-stage HCC. Deep learning could also be used to predict the progression-free survival of these two therapies in HCC patients[54]. Two models based on these two kinds of therapies provided a satisfactory prediction accuracy and calibration of 2-year progression-free survival. In another study[55], a three dimensional-CNN model, which avoided missing information from CEUS images compared with extracting features from four-phase images, was used. It was observed that predicting prognosis of different treatments in advance and timely swapping of treatment would increase the 2-year progression-free survival, which could contribute to a better prognosis.

Application of AI in predicting MVI of HCC

MVI has shown to be the independent predictor of recurrence and poor outcomes of HCC. Therefore, making a noninvasive and accurate preoperative identification of MVI would be of great significance for HCC patients. The application of AI in predicting MVI achieved good performance based on gray-scale ultrasound images and CEUS.

The radiomics score based on ultrasound of HCC was established and shown to be an independent predictor of MVI[56]. The performance of the clinical nomogram improved significantly with the aid of a radiomics score, which demonstrated the important role of this technique.

Features of the peritumoral area have been shown to be more accurate recently[56]. The radiomic signatures from the gross and peritumoral region showed the best performance compared with the gross-tumoral region and the peritumoral region[57]. The area under the curves were 0.726 based on features of the gross and peritumoral region and 0.744 after the incorporation of essential clinical information.

These studies[56,57] mentioned above have confirmed the application of AI based on gray-scale ultrasound, and AI could be applied to CEUS in predicting MVI as well. Zhang *et al*[58] extracted radiomics features from the B-mode, artery phase, portal venous phase and delay phase images of

preoperative CEUS to construct four radiomics scores based on the primary dataset. Then, they used four radiomic scores and clinical factors for multivariate logistic regression analysis, which demonstrated that the portal venous phase and delay phase radiomics score, tumor size and alpha-fetoprotein level were independent risk factors in predicting MVI. The radiomics nomogram based on these four predictors indicated a better discrimination and a good calibration compared with the clinical model (based on tumor size and alpha-fetoprotein level) in both the primary dataset (area under the curve: 0.849 *vs* 0.690) and the validation dataset (area under the curve: 0.788 *vs* 0.661). This study developed a new noninvasive predictive nomogram based on CEUS that could provide useful information in predicting MVI preoperatively, thus facilitating the choice of a more appropriate surgical option.

CONCLUSION

In conclusion, AI can provide great assistance in the evaluation of diffuse liver diseases (including liver fibrosis and liver steatosis) and FLLs. First, it could be applied to identify and stage liver fibrosis on the basis of B-mode ultrasound, Doppler ultrasound, and elastography. Second, the application of deep learning could be used to make qualitative evaluation based entirely on B-mode images and quantitative evaluation based on radiofrequency signals and HRI, which would improve the ultrasound detection rate of NAFLD. Third, AI has the ability to differentiate malignant FLLs from benign FLLs as well as classify different kinds of FLLs with a better performance compared with clinical indexes. Fourth, the curative effect and prognosis of HCC treatment can be predicted, and an optimal personalized treatment can be chosen. Last, AI based on B-mode ultrasound and CEUS could predict MVI of HCC preoperatively, which could be helpful for more appropriate surgical planning. These applications had good specificity, accuracy and a comparable or even better performance compared with experts in the diagnosis and differentiation of diffuse and focal liver lesions.

There are also some limitations in the applications of AI using ultrasound. First, it is difficult to prepare a large-scale dataset, especially for medical images. Second, although deep learning is the widest used algorithm and has good performance in various studies, its interpretability and generalization is low. Third, the input data may vary from different equipment and operators, which would influence the performance of AI. Last, because a large amount of data is needed to train and validate the established algorithms, the conclusions of many single-center studies are not convincing. Therefore, researchers are expected to conduct more multicenter studies and incorporate more samples, as much as possible. At the same time, optimizing algorithms and creating standards for medical images are also necessary. Despite medical images, researchers could also build the database containing important clinical factors to establish a more comprehensive AI model for future work.

FOOTNOTES

Author contributions: Jiang F, Cui XW and Dietrich CF conceived and established the design of the paper; Cao LL, Peng M, Xie X, Chen GQ, Huang SY, Wang JY, Dietrich CF, Jiang F and Cui XW explored the literature data; Cao LL provided the first draft of the manuscript, which was discussed and revised critically for intellectual content by Peng M, Xie X, Dietrich CF, Jiang F and Cui XW; all authors discussed the statements and conclusions, and approved the final version to be published.

Supported by National Natural Science Foundation of China, No. 82071953; and 2020 Hunan Province Clinical Medical Technology Innovation Guidance Project.

Conflict-of-interest statement: All the authors report no relevant conflicts of interest for this article.

Open-Access: This article is an open-access article that was selected by an in-house editor and fully peer-reviewed by external reviewers. It is distributed in accordance with the Creative Commons Attribution NonCommercial (CC BY-NC 4.0) license, which permits others to distribute, remix, adapt, build upon this work non-commercially, and license their derivative works on different terms, provided the original work is properly cited and the use is non-commercial. See: https://creativecommons.org/Licenses/by-nc/4.0/

Country/Territory of origin: China

ORCID number: Liu-Liu Cao 0000-0001-8078-5634; Mei Peng 0000-0001-7809-9440; Xiang Xie 0000-0001-5514-2362; Gong-Quan Chen 0000-0002-4204-6133; Shu-Yan Huang 0000-0002-7050-9553; Jia-Yu Wang 0000-0001-9902-0666; Fan Jiang 0000-0001-8896-2009; Xin-Wu Cui 0000-0003-3890-6660; Christoph F Dietrich 0000-0001-6015-6347.

S-Editor: Fan JR
L-Editor: A
P-Editor: Fan JR

REFERENCES

1 **Xiao J**, Wang F, Wong NK, He J, Zhang R, Sun R, Xu Y, Liu Y, Li W, Koike K, He W, You H, Miao Y, Liu X, Meng M, Gao B, Wang H, Li C. Global liver disease burdens and research trends: Analysis from a Chinese perspective. *J Hepatol* 2019; **71**: 212-221 [PMID: 30871980 DOI: 10.1016/j.jhep.2019.03.004]

2 **Bellman RE**. An Introduction to Artificial Intelligence: Can Computers Think? Spring: 1978

3 **Chan HP**, Samala RK, Hadjiiski LM, Zhou C. Deep Learning in Medical Image Analysis. *Adv Exp Med Biol* 2020; **1213**: 3-21 [PMID: 32030660 DOI: 10.1007/978-3-030-33128-3_1]

4 **Akkus Z**, Cai J, Boonrod A, Zeinoddini A, Weston AD, Philbrick KA, Erickson BJ. A Survey of Deep-Learning Applications in Ultrasound: Artificial Intelligence-Powered Ultrasound for Improving Clinical Workflow. *J Am Coll Radiol* 2019; **16**: 1318-1328 [PMID: 31492410 DOI: 10.1016/j.jacr.2019.06.004]

5 **Ambinder EP**. A history of the shift toward full computerization of medicine. *J Oncol Pract* 2005; **1**: 54-56 [PMID: 20871680 DOI: 10.1200/jop.2005.1.2.54]

6 **Vivanti R**, Szeskin A, Lev-Cohain N, Sosna J, Joskowicz L. Automatic detection of new tumors and tumor burden evaluation in longitudinal liver CT scan studies. *Int J Comput Assist Radiol Surg* 2017; **12**: 1945-1957 [PMID: 28856515 DOI: 10.1007/s11548-017-1660-z]

7 **Preis O**, Blake MA, Scott JA. Neural network evaluation of PET scans of the liver: a potentially useful adjunct in clinical interpretation. *Radiology* 2011; **258**: 714-721 [PMID: 21339347 DOI: 10.1148/radiol.10100547]

8 **Ben-Cohen A**, Klang E, Diamant I, Rozendorn N, Raskin SP, Konen E, Amitai MM, Greenspan H. CT Image-based Decision Support System for Categorization of Liver Metastases Into Primary Cancer Sites: Initial Results. *Acad Radiol* 2017; **24**: 1501-1509 [PMID: 28778512 DOI: 10.1016/j.acra.2017.06.008]

9 **Yoo S**, Wang W, Wang Q, Fiel MI, Lee E, Hiotis SP, Zhu J. A pilot systematic genomic comparison of recurrence risks of hepatitis B virus-associated hepatocellular carcinoma with low- and high-degree liver fibrosis. *BMC Med* 2017; **15**: 214 [PMID: 29212479 DOI: 10.1186/s12916-017-0973-7]

10 **Bedossa P**, Poynard T. An algorithm for the grading of activity in chronic hepatitis C. The METAVIR Cooperative Study Group. *Hepatology* 1996; **24**: 289-293 [PMID: 8690394 DOI: 10.1002/hep.510240201]

11 **Yamada G**. [Histopathological characteristics and clinical significance of New Inuyama Classification in chronic hepatitis B]. *Nihon Rinsho* 2004; **62** Suppl 8: 290-292 [PMID: 15453332]

12 **Badawi AM**, Derbala AS, Youssef AM. Fuzzy logic algorithm for quantitative tissue characterization of diffuse liver diseases from ultrasound images. *Int J Med Inform* 1999; **55**: 135-147 [PMID: 10530829 DOI: 10.1016/s1386-5056(99)00010-6]

13 **Ruan D**, Shi Y, Jin L, Yang Q, Yu W, Ren H, Zheng W, Chen Y, Zheng N, Zheng M. An ultrasound image-based deep multi-scale texture network for liver fibrosis grading in patients with chronic HBV infection. *Liver Int* 2021; **41**: 2440-2454 [PMID: 34219353 DOI: 10.1111/liv.14999]

14 **Zhang L**, Li QY, Duan YY, Yan GZ, Yang YL, Yang RJ. Artificial neural network aided non-invasive grading evaluation of hepatic fibrosis by duplex ultrasonography. *BMC Med Inform Decis Mak* 2012; **12**: 55 [PMID: 22716936 DOI: 10.1186/1472-6947-12-55]

15 **Chen Y**, Luo Y, Huang W, Hu D, Zheng RQ, Cong SZ, Meng FK, Yang H, Lin HJ, Sun Y, Wang XY, Wu T, Ren J, Pei SF, Zheng Y, He Y, Hu Y, Yang N, Yan H. Machine-learning-based classification of real-time tissue elastography for hepatic fibrosis in patients with chronic hepatitis B. *Comput Biol Med* 2017; **89**: 18-23 [PMID: 28779596 DOI: 10.1016/j.compbiomed.2017.07.012]

16 **Brattain LJ**, Telfer BA, Dhyani M, Grajo JR, Samir AE. Objective Liver Fibrosis Estimation from Shear Wave Elastography. *Annu Int Conf IEEE Eng Med Biol Soc* 2018; **2018**: 1-5 [PMID: 30440285 DOI: 10.1109/EMBC.2018.8513011]

17 **Wang K**, Lu X, Zhou H, Gao Y, Zheng J, Tong M, Wu C, Liu C, Huang L, Jiang T, Meng F, Lu Y, Ai H, Xie XY, Yin LP, Liang P, Tian J, Zheng R. Deep learning Radiomics of shear wave elastography significantly improved diagnostic performance for assessing liver fibrosis in chronic hepatitis B: a prospective multicentre study. *Gut* 2019; **68**: 729-741 [PMID: 29730602 DOI: 10.1136/gutjnl-2018-316204]

18 **Loomba R**, Sanyal AJ. The global NAFLD epidemic. *Nat Rev Gastroenterol Hepatol* 2013; **10**: 686-690 [PMID: 24042449 DOI: 10.1038/nrgastro.2013.171]

19 **Friedman SL**, Neuschwander-Tetri BA, Rinella M, Sanyal AJ. Mechanisms of NAFLD development and therapeutic strategies. *Nat Med* 2018; **24**: 908-922 [PMID: 29967350 DOI: 10.1038/s41591-018-0104-9]

20 **Lăpădat AM**, Jianu IR, Ungureanu BS, Florescu LM, Gheonea DI, Sovaila S, Gheonea IA. Non-invasive imaging techniques in assessing non-alcoholic fatty liver disease: a current status of available methods. *J Med Life* 2017; **10**: 19-26 [PMID: 28255371]

21 **Lee DH**. Imaging evaluation of non-alcoholic fatty liver disease: focused on quantification. *Clin Mol Hepatol* 2017; **23**: 290-301 [PMID: 28994271 DOI: 10.3350/cmh.2017.0042]

22 **Ballestri S**, Nascimbeni F, Lugari S, Lonardo A, Francica G. A critical appraisal of the use of ultrasound in hepatic steatosis. *Expert Rev Gastroenterol Hepatol* 2019; **13**: 667-681 [PMID: 31104523 DOI: 10.1080/17474124.2019.1621164]

23 **Pirmoazen AM**, Khurana A, El Kaffas A, Kamaya A. Quantitative ultrasound approaches for diagnosis and monitoring hepatic steatosis in nonalcoholic fatty liver disease. *Theranostics* 2020; **10**: 4277-4289 [PMID: 32226553 DOI: 10.7150/thno.40249]

24 **Xia MF**, Yan HM, He WY, Li XM, Li CL, Yao XZ, Li RK, Zeng MS, Gao X. Standardized ultrasound hepatic/renal ratio and hepatic attenuation rate to quantify liver fat content: an improvement method. *Obesity (Silver Spring)* 2012; **20**: 444-452 [PMID: 22016092 DOI: 10.1038/oby.2011.302]

25 **Kotronen A**, Peltonen M, Hakkarainen A, Sevastianova K, Bergholm R, Johansson LM, Lundbom N, Rissanen A, Ridderstråle M, Groop L, Orho-Melander M, Yki-Järvinen H. Prediction of non-alcoholic fatty liver disease and liver fat using metabolic and genetic factors. *Gastroenterology* 2009; **137**: 865-872 [PMID: 19524579 DOI: 10.1053/j.gastro.2009.06.005]

26 **Byra M**, Styczynski G, Szmigielski C, Kalinowski P, Michałowski Ł, Paluszkiewicz R, Ziarkiewicz-Wróblewska B, Zieniewicz K, Sobieraj P, Nowicki A. Transfer learning with deep convolutional neural network for liver steatosis assessment in ultrasound images. *Int J Comput Assist Radiol Surg* 2018; **13**: 1895-1903 [PMID: 30094778 DOI: 10.1007/s11548-018-1843-2]

27 **Byra M**, Han A, Boehringer AS, Zhang YN, O'Brien WD Jr, Erdman JW Jr, Loomba R, Sirlin CB, Andre M. Liver Fat Assessment in Multiview Sonography Using Transfer Learning With Convolutional Neural Networks. *J Ultrasound Med* 2022; **41**: 175-184 [PMID: 33749862 DOI: 10.1002/jum.15693]

28 **Reddy DS**, Bharath R, Rajalakshmi P. A Novel Computer-Aided Diagnosis Framework Using Deep Learning for Classification of Fatty Liver Disease in Ultrasound Imaging. *Int Confer e-Health Network App Ser* 2018; 1-5

29 **Chou TH**, Yeh HJ, Chang CC, Tang JH, Kao WY, Su IC, Li CH, Chang WH, Huang CK, Sufriyana H, Su EC. Deep learning for abdominal ultrasound: A computer-aided diagnostic system for the severity of fatty liver. *J Chin Med Assoc* 2021; **84**: 842-850 [PMID: 34282076 DOI: 10.1097/JCMA.0000000000000585]

30 **Zamanian H**, Mostaar A, Azadeh P, Ahmadi M. Implementation of Combinational Deep Learning Algorithm for Non-alcoholic Fatty Liver Classification in Ultrasound Images. *J Biomed Phys Eng* 2021; **11**: 73-84 [PMID: 33564642 DOI: 10.31661/jbpe.v0i0.2009-1180]

31 **Han A**, Byra M, Heba E, Andre MP, Erdman JW Jr, Loomba R, Sirlin CB, O'Brien WD Jr. Noninvasive Diagnosis of Nonalcoholic Fatty Liver Disease and Quantification of Liver Fat with Radiofrequency Ultrasound Data Using One-dimensional Convolutional Neural Networks. *Radiology* 2020; **295**: 342-350 [PMID: 32096706 DOI: 10.1148/radiol.2020191160]

32 **Nguyen TN**, Podkowa AS, Park TH, Miller RJ, Do MN, Oelze ML. Use of a convolutional neural network and quantitative ultrasound for diagnosis of fatty liver. *Ultrasound Med Biol* 2021; **47**: 556-568 [PMID: 33358553 DOI: 10.1016/j.ultrasmedbio.2020.10.025]

33 **Cha DI**, Kang TW, Min JH, Joo I, Sinn DH, Ha SY, Kim K, Lee G, Yi J. Deep learning-based automated quantification of the hepatorenal index for evaluation of fatty liver by ultrasonography. *Ultrasonography* 2021; **40**: 565-574 [PMID: 33966363 DOI: 10.14366/usg.20179]

34 **Amarapurkar D**, Han KH, Chan HL, Ueno Y; Asia-Pacific Working Party on Prevention of Hepatocellular Carcinoma. Application of surveillance programs for hepatocellular carcinoma in the Asia-Pacific Region. *J Gastroenterol Hepatol* 2009; **24**: 955-961 [PMID: 19383082 DOI: 10.1111/j.1440-1746.2009.05805.x]

35 **Kumar V**, Gu Y, Basu S, Berglund A, Eschrich SA, Schabath MB, Forster K, Aerts HJ, Dekker A, Fenstermacher D, Goldgof DB, Hall LO, Lambin P, Balagurunathan Y, Gatenby RA, Gillies RJ. Radiomics: the process and the challenges. *Magn Reson Imaging* 2012; **30**: 1234-1248 [PMID: 22898692 DOI: 10.1016/j.mri.2012.06.010]

36 **Xian GM**. An identification method of malignant and benign liver tumors from ultrasonography based on GLCM texture features and fuzzy SVM. *Expert System App* 2010; **37**: 6737-6741 [DOI: 10.1016/J.ESWA.2010.02.067]

37 **Xi IL**, Wu J, Guan J, Zhang PJ, Horii SC, Soulen MC, Zhang Z, Bai HX. Deep learning for differentiation of benign and malignant solid liver lesions on ultrasonography. *Abdom Radiol (NY)* 2021; **46**: 534-543 [PMID: 32681268 DOI: 10.1007/s00261-020-02564-w]

38 **Yang Q**, Wei J, Hao X, Kong D, Yu X, Jiang T, Xi J, Cai W, Luo Y, Jing X, Yang Y, Cheng Z, Wu J, Zhang H, Liao J, Zhou P, Song Y, Zhang Y, Han Z, Cheng W, Tang L, Liu F, Dou J, Zheng R, Yu J, Tian J, Liang P. Improving B-mode ultrasound diagnostic performance for focal liver lesions using deep learning: A multicentre study. *EBioMedicine* 2020; **56**: 102777 [PMID: 32485640 DOI: 10.1016/j.ebiom.2020.102777]

39 **Tiyarattanachai T**, Apiparakoon T, Marukatat S, Sukcharoen S, Geratikornsupuk N, Anukulkarnkusol N, Mekaroonkamol P, Tanpowpong N, Sarakul P, Rerknimitr R, Chaiteerakij R. Development and validation of artificial intelligence to detect and diagnose liver lesions from ultrasound images. *PLoS One* 2021; **16**: e0252882 [PMID: 34101764 DOI: 10.1371/journal.pone.0252882]

40 **Hwang YN**, Lee JH, Kim GY, Jiang YY, Kim SM. Classification of focal liver lesions on ultrasound images by extracting hybrid textural features and using an artificial neural network. *Biomed Mater Eng* 2015; **26** Suppl 1: S1599-S1611 [PMID: 26405925 DOI: 10.3233/BME-151459]

41 **Hassan TM**, Elmogy M, Sallam ES. Diagnosis of Focal Liver Diseases Based on Deep Learning Technique for Ultrasound Images. *J Sci Engi* 2017; **42**: 3127-3140 [DOI: 10.1007/S13369-016-2387-9]

42 **Schmauch B**, Herent P, Jehanno P, Dehaene O, Saillard C, Aubé C, Luciani A, Lassau N, Jégou S. Diagnosis of focal liver lesions from ultrasound using deep learning. *Diagn Interv Imaging* 2019; **100**: 227-233 [PMID: 30926443 DOI: 10.1016/j.diii.2019.02.009]

43 **Guo LH**, Wang D, Qian YY, Zheng X, Zhao CK, Li XL, Bo XW, Yue WW, Zhang Q, Shi J, Xu HX. A two-stage multi-view learning framework based computer-aided diagnosis of liver tumors with contrast enhanced ultrasound images. *Clin Hemorheol Microcirc* 2018; **69**: 343-354 [PMID: 29630528 DOI: 10.3233/CH-170275]

44 **Pan F**, Huang Q, Li X. Classification of liver tumors with CEUS based on 3D-CNN. *Int Confer Adv Rob Mechat* 2019; 845-849

45 **Gatos I**, Tsantis S, Spiliopoulos S, Skouroliakou A, Theotokas I, Zoumpoulis P, Hazle JD, Kagadis GC. A new automated quantification algorithm for the detection and evaluation of focal liver lesions with contrast-enhanced ultrasound. *Med Phys* 2015; **42**: 3948-3959 [PMID: 26133595 DOI: 10.1118/1.4921753]

46 **Kondo S**, Takagi K, Nishida M, Iwai T, Kudo Y, Ogawa K, Kamiyama T, Shibuya H, Kahata K, Shimizu C. Computer-Aided Diagnosis of Focal Liver Lesions Using Contrast-Enhanced Ultrasonography With Perflubutane Microbubbles. *IEEE Trans Med Imaging* 2017; **36**: 1427-1437 [PMID: 28141517 DOI: 10.1109/TMI.2017.2659734]

47 **Streba CT**, Ionescu M, Gheonea DI, Sandulescu L, Ciurea T, Saftoiu A, Vere CC, Rogoveanu I. Contrast-enhanced ultrasonography parameters in neural network diagnosis of liver tumors. *World J Gastroenterol* 2012; **18**: 4427-4434 [PMID: 22969209 DOI: 10.3748/wjg.v18.i32.4427]

48 **Căleanu CD**, Sîrbu CL, Simion G. Deep Neural Architectures for Contrast Enhanced Ultrasound (CEUS) Focal Liver Lesions Automated Diagnosis. *Sensors (Basel)* 2021; **21** [PMID: 34208548 DOI: 10.3390/s21124126]

49 **Hu HT**, Wang W, Chen LD, Ruan SM, Chen SL, Li X, Lu MD, Xie XY, Kuang M. Artificial intelligence assists

identifying malignant *vs* benign liver lesions using contrast-enhanced ultrasound. *J Gastroenterol Hepatol* 2021; **36**: 2875-2883 [PMID: 33880797 DOI: 10.1111/jgh.15522]

50 **Zhou L**, Rui JA, Zhou WX, Wang SB, Chen SG, Qu Q. Edmondson-Steiner grade: A crucial predictor of recurrence and survival in hepatocellular carcinoma without microvascular invasio. *Pathol Res Pract* 2017; **213**: 824-830 [PMID: 28554743 DOI: 10.1016/j.prp.2017.03.002]

51 **Zhou L**, Rui JA, Wang SB, Chen SG, Qu Q, Chi TY, Wei X, Han K, Zhang N, Zhao HT. Factors predictive for long-term survival of male patients with hepatocellular carcinoma after curative resection. *J Surg Oncol* 2007; **95**: 298-303 [PMID: 17326130 DOI: 10.1002/jso.20678]

52 **Court CM**, Harlander-Locke MP, Markovic D, French SW, Naini BV, Lu DS, Raman SS, Kaldas FM, Zarrinpar A, Farmer DG, Finn RS, Sadeghi S, Tomlinson JS, Busuttil RW, Agopian VG. Determination of hepatocellular carcinoma grade by needle biopsy is unreliable for liver transplant candidate selection. *Liver Transpl* 2017; **23**: 1123-1132 [PMID: 28688158 DOI: 10.1002/lt.24811]

53 **Liu D**, Liu F, Xie X, Su L, Liu M, Kuang M, Huang G, Wang Y, Zhou H, Wang K, Lin M, Tian J. Accurate prediction of responses to transarterial chemoembolization for patients with hepatocellular carcinoma by using artificial intelligence in contrast-enhanced ultrasound. *Eur Radiol* 2020; **30**: 2365-2376 [PMID: 31900703 DOI: 10.1007/s00330-019-06553-6]

54 **Liu F**, Liu D, Wang K, Xie X, Su L, Kuang M, Huang G, Peng B, Wang Y, Lin M, Tian J. Deep Learning Radiomics Based on Contrast-Enhanced Ultrasound Might Optimize Curative Treatments for Very-Early or Early-Stage Hepatocellular Carcinoma Patients. *Liver Cancer* 2020; **9**: 397-413 [PMID: 32999867 DOI: 10.1159/000505694]

55 **Wang W**, Wu SS, Zhang JC, Xian MF, Huang H, Li W, Zhou ZM, Zhang CQ, Wu TF, Li X, Xu M, Xie XY, Kuang M, Lu MD, Hu HT. Preoperative Pathological Grading of Hepatocellular Carcinoma Using Ultrasomics of Contrast-Enhanced Ultrasound. *Acad Radiol* 2021; **28**: 1094-1101 [PMID: 32622746 DOI: 10.1016/j.acra.2020.05.033]

56 **Hu HT**, Wang Z, Huang XW, Chen SL, Zheng X, Ruan SM, Xie XY, Lu MD, Yu J, Tian J, Liang P, Wang W, Kuang M. Ultrasound-based radiomics score: a potential biomarker for the prediction of microvascular invasion in hepatocellular carcinoma. *Eur Radiol* 2019; **29**: 2890-2901 [PMID: 30421015 DOI: 10.1007/s00330-018-5797-0]

57 **Dong Y**, Zhou L, Xia W, Zhao XY, Zhang Q, Jian JM, Gao X, Wang WP. Preoperative Prediction of Microvascular Invasion in Hepatocellular Carcinoma: Initial Application of a Radiomic Algorithm Based on Grayscale Ultrasound Images. *Front Oncol* 2020; **10**: 353 [PMID: 32266138 DOI: 10.3389/fonc.2020.00353]

58 **Zhang D**, Wei Q, Wu GG, Zhang XY, Lu WW, Lv WZ, Liao JT, Cui XW, Ni XJ, Dietrich CF. Preoperative Prediction of Microvascular Invasion in Patients With Hepatocellular Carcinoma Based on Radiomics Nomogram Using Contrast-Enhanced Ultrasound. *Front Oncol* 2021; **11**: 709339 [PMID: 34557410 DOI: 10.3389/fonc.2021.709339]

59 **Wu K**, Chen X, Ding M. Deep learning based classification of focal liver lesions with contrast-enhanced ultrasound. *Optik* 2014; **125**: 4057-4063 [DOI: 10.1016/J.IJLEO.2014.01.114]

World Journal of Gastroenterology

Submit a Manuscript: https://www.f6publishing.com

World J Gastroenterol 2022 July 21; 28(27): 3410-3421

DOI: 10.3748/wjg.v28.i27.3410

ISSN 1007-9327 (print) ISSN 2219-2840 (online)

MINIREVIEWS

Risk factors and diagnostic biomarkers for nonalcoholic fatty liver disease-associated hepatocellular carcinoma: Current evidence and future perspectives

Masayuki Ueno, Haruhiko Takeda, Atsushi Takai, Hiroshi Seno

Specialty type: Gastroenterology and hepatology

Provenance and peer review: Invited article; Externally peer reviewed.

Peer-review model: Single blind

Peer-review report's scientific quality classification

Grade A (Excellent): 0
Grade B (Very good): B
Grade C (Good): C
Grade D (Fair): 0
Grade E (Poor): 0

P-Reviewer: Ulasoglu C, Turkey; Wang YL, China

Received: February 2, 2022
Peer-review started: February 2, 2022
First decision: April 10, 2022
Revised: April 24, 2022
Accepted: June 15, 2022
Article in press: June 15, 2022
Published online: July 21, 2022

Masayuki Ueno, Haruhiko Takeda, Atsushi Takai, Hiroshi Seno, Department of Gastroenterology and Hepatology, Kyoto University Graduate School of Medicine, Kyoto 6068507, Japan

Corresponding author: Atsushi Takai, MD, PhD, Assistant Professor, Department of Gastroenterology and Hepatology, Kyoto University Graduate School of Medicine, 54 Shogoin-Kawahara-cho, Sakyo-ku, Kyoto 6068507, Japan. atsushit@kuhp.kyoto-u.ac.jp

Abstract

High rates of excessive calorie intake diets and sedentary lifestyles have led to a global increase in nonalcoholic fatty liver disease (NAFLD). As a result, this condition has recently become one of the leading causes of hepatocellular carcinoma (HCC). Furthermore, the incidence of NAFLD-associated HCC (NAFLD-HCC) is expected to increase in the near future. Advanced liver fibrosis is the most common risk factor for NAFLD-HCC. However, up to 50% of NAFLD-HCC cases develop without underlying liver cirrhosis. Epidemiological studies have revealed many other risk factors for this condition; including diabetes, other metabolic traits, obesity, old age, male sex, Hispanic ethnicity, mild alcohol intake, and elevated liver enzymes. Specific gene variants, such as single-nucleotide polymorphisms of patatin-like phospholipase domain 3, transmembrane 6 superfamily member 2, and membrane-bound O-acyl-transferase domain-containing 7, are also associated with an increased risk of HCC in patients with NAFLD. This clinical and genetic information should be interpreted together for accurate risk prediction. Alpha-fetoprotein (AFP) is the only biomarker currently recommended for HCC screening. However, it is not sufficiently sensitive in addressing this diagnostic challenge. The GALAD score can be calculated based on sex, age, lectin-bound AFP, AFP, and des-carboxyprothrombin and is reported to show better diagnostic performance for HCC. In addition, emerging studies on genetic and epigenetic biomarkers have also yielded promising diagnostic potential. However, further research is needed to establish an effective surveillance program for the early diagnosis of NAFLD-HCC.

Key Words: Nonalcoholic fatty liver disease; Hepatocellular carcinoma; Risk factors; Biomarkers; Tumor markers; Genetics

©The Author(s) 2022. Published by Baishideng Publishing Group Inc. All rights reserved.

Core Tip: This review summarizes the risk factors and diagnostic biomarkers for nonalcoholic fatty liver disease (NAFLD)-associated hepatocellular carcinoma (HCC). The highlighted risk factors include liver fibrosis, diabetes, age, sex, race, alcohol intake, elevated liver enzymes, and specific genetic variants. Currently available diagnostic biomarkers include alpha-fetoprotein (AFP), des-carboxyprothrombin, and the AFP isoform L3. The combined use of these biomarkers may increase the diagnostic sensitivity of NAFLD-HCC detection. However, more discussion will be necessary on the cost-effectiveness of these approaches. This review also summarizes emerging means of discovering novel biomarkers using omics techniques. A better understanding of these risk factors and diagnostic biomarkers will facilitate the effective surveillance of NAFLD-HCC.

Citation: Ueno M, Takeda H, Takai A, Seno H. Risk factors and diagnostic biomarkers for nonalcoholic fatty liver disease-associated hepatocellular carcinoma: Current evidence and future perspectives. *World J Gastroenterol* 2022; 28(27): 3410-3421
URL: https://www.wjgnet.com/1007-9327/full/v28/i27/3410.htm
DOI: https://dx.doi.org/10.3748/wjg.v28.i27.3410

INTRODUCTION

Hepatocellular carcinoma (HCC) accounts for the majority of primary liver cancers[1]. It is the sixth most common form of cancer and the fourth leading cause of worldwide cancer-related deaths[2]. By contrast to the declining trends for other major cancers, mortality rates from liver cancer have increased by almost 3% *per* year[3]. Chronic liver infection from hepatitis B or C virus (HBV or HCV, respectively) and alcohol abuse are the most common causes of HCC[1,4]. However, there is a growing concern about the rapid increase in nonalcoholic fatty liver disease (NAFLD) as another cause of HCC.

NAFLD is a spectrum of chronic liver diseases characterized by excess fat accumulation in hepatocytes[5]. The prevalence of NAFLD is rapidly increasing worldwide, with recent studies reporting a global percentage of approximately 25%[6]. Unsurprisingly, the incidence of NAFLD-associated HCC (NAFLD-HCC) is also increasing in many areas of the world. In the United States, the proportion of NAFLD-HCC among all HCC patients has significantly increased from 9.3% to 13.6% over the past decade[7]. In a French cohort of patients who underwent liver resection, the prevalence of NAFLD-HCC increased from 2.6% (1995-1999) to 19.5% (2010-2014)[8]. Similar trends are also seen in Asian countries. According to a nationwide survey conducted in Japan, the proportion of nonalcoholic steatohepatitis (NASH)-related HCC has increased from 1.5% (2007 or before) to 7.2% (2014–2016)[9]. Universal HBV vaccination and widespread use of direct-acting antiviral agents for HCV are expected to decrease the number of virus-related HCC cases. Nonetheless, NAFLD-HCC is expected to continue to rise in the future[10,11].

NAFLD-HCC is often diagnosed at an advanced stage due to a lack of efficient surveillance policies [11]. In the Veteran Affairs population, only 40% of NAFLD-HCC patients underwent HCC surveillance compared to more than 80% of patients with HCV-related HCC[12]. From the perspective of cost-effectiveness, HCC screening should be considered when the annual risk of HCC exceeds 0.4–2.0%[13,14]. However, in a large-scale retrospective cohort study, out of 2382289 person-years of follow-up, only 490 patients with NAFLD were diagnosed with HCC (0.21/1000 person-years)[15]. Thus, it is necessary to more effectively identify high-risk patients who will benefit from HCC surveillance. Additionally, the diagnostic performance of the implemented examination is important for effective surveillance. Although ultrasonography with or without alpha-fetoprotein (AFP) is recommended for HCC screening [16], the sensitivity and specificity of these examinations are insufficient in patients with NAFLD. The high prevalence of obesity in patients with NAFLD impairs ultrasonography performance[17]. Therefore, many researchers have been searching for alternative NAFLD-HCC surveillance tools to increase the chances of early diagnosis. Recent advances in omics technology have enabled easier genetic and epigenetic benchmark analysis. Thus, many potential biomarkers are currently under investigation.

In this review, we discuss the current evidence for clinical and genetic HCC risk factors. We also summarize previous reports on the diagnostic biomarkers of NAFLD-HCC, including those under development. Finally, we briefly address future perspectives on HCC surveillance for NAFLD patients.

CLINICAL RISK FACTORS

Liver fibrosis

Liver fibrosis is the most important risk factor for the development of HCC in patients with NAFLD[18,

19]. In a large retrospective cohort study, the annual HCC incidence rates amongst NAFLD patients with and without cirrhosis were 10.6 and 0.08 *per* 1000 person-years, respectively[15]. This indicates that the presence of liver cirrhosis increases the risk of NAFLD-HCC by more than 10-fold (Table 1).

Liver biopsy is the gold standard for evaluating the fibrotic stage of the liver[20]. However, noninvasive examinations are more widely used in clinical practice. Available serum biomarkers for assessing fibrosis include the aspartate transaminase (AST)-to-platelet ratio index, Fibrosis-4 (FIB-4) index, and enhanced liver fibrosis score[21]. The FIB-4 index is calculated using various factors; including age, AST, alanine aminotransferase (ALT), and platelet count. Furthermore, a significant association between the FIB-4 index and HCC risk in NAFLD patients has been reported[15,22]. The Mac-2-binding protein glycosylation isomer is a novel serum biomarker that shows relatively high efficacy at assessing liver fibrosis[23]. It may also be useful in predicting the risk of hepatocarcinogenesis among NAFLD patients[24].

Additionally, elastography techniques using ultrasound or magnetic resonance imaging are useful tools for noninvasive evaluation of degree of fibrosis[21]. A retrospective study from Japan suggested that shear wave velocity measurements can be used for HCC risk assessment in NAFLD patients[25].

Diabetes mellitus and other metabolic traits

Several studies have demonstrated that (mostly type 2) diabetes mellitus is associated with an increased risk of HCC development in NAFLD patients. The hazard ratio for HCC in diabetic patients has been reported to be around 2.2–4.2[22,26,27] (Table 1). In a nationwide Japanese study, the annual incidence of HCC was only 0.11% in diabetes patients overall. However, it increased to 1.0% when they had an FIB-4 index of 3.5 or more[14]. Therefore, the degree of liver fibrosis, together with presence or absence of diabetes, should be assessed to predict the risk of NAFLD-HCC.

There have been conflicting reports regarding the association between other metabolic traits such as hypertension, dyslipidemia, with NAFLD-HCC[28]. However, a recent study showed that these conditions were also risk factors for NAFLD-HCC (Table 1). Furthermore, the hazard ratio for HCC was 5.6 in patients with diabetes, hypertension, and dyslipidemia[27,29].

Obesity

Regardless of underlying liver diseases, obesity is associated with an increased risk of HCC[30]. This relationship has also been confirmed in patients with NAFLD[29,31]. In a cohort of NAFLD-HCC patients treated with curative radiofrequency ablation, the degree of visceral fat accumulation, but not body mass index (BMI), was independently associated with an increased risk of HCC recurrence[32]. A propensity score-matched study showed that the incidence of both NASH and HCC were significantly lower in patients who underwent bariatric surgery, indicating a protective role of sustained weight loss by bariatric surgery[33].

Age, sex, and race

Old age, male sex, and Hispanic ethnicity are also known risk factors for NAFLD-HCC (Table 1); the details are described in another review article[31]. In the United States, a multicenter case-control study showed that old age (*per* year) and male sex were independently associated with a higher NAFLD-HCC risk [odds ratios (OR), 1.08 and 4.34, respectively][34]. In another study, age ≥ 65 years was associated with a 1.83 times higher NAFLD-HCC risk compared to age < 65 years[15]. Regarding ethnicity, a previous study showed that Hispanic patients had a lower NAFLD-HCC risk (OR, 0.3). By contrast, another study showed the opposite result (hazard ratio, 1.59)[15,34]. Several other studies have shown that Hispanic ethnicity is, in itself, a risk factor for NAFLD, partly because of the high prevalence of patatin-like phospholipase domain 3 (*PNPLA3*) variants among Hispanic people[35,36].

Alcohol intake and smoking

NAFLD is defined as hepatic steatosis without harmful alcohol intake (more than 30 g/day for men and 20 g/day for women). However, mild alcohol intake can also be a risk factor for NAFLD-HCC[37]. Previous studies have shown that mild drinking habits were associated with 3.6–4.8 times higher risk of HCC in NAFLD patients compared to no habits of drinking[38,39] (Table 1). No study has specifically investigated the association between smoking and NAFLD-HCC. However, smoking is associated with an increased risk of HCC. Additionally, it has been reported to be associated with advanced liver fibrosis in NAFLD patients[31,40]. Because these factors are modifiable, NAFLD patients should be informed that cessation of alcohol intake and smoking may reduce the risk of future HCC development.

Elevated liver enzymes

Patients with NASH are thought to have a higher risk of HCC than those with NAFLD[18]. However, liver biopsy is required to accurately distinguish these conditions. Therefore, elevated liver enzyme levels are often used as surrogate markers for NASH in clinical practice. Several studies have shown that elevated liver enzymes in NAFLD patients are significantly associated with an increased risk of HCC (hazard ratio, 2.07–8.20)[41-43] (Table 1). At the same time, however, normal transaminase levels do not exclude the possibility of advanced liver fibrosis[44].

Table 1 Clinical risk factors for nonalcoholic fatty liver disease-associated hepatocellular carcinoma

Risk factors	Reported evidence	Ref.
Liver fibrosis	The annual incidence rate of HCC in NAFLD patients with cirrhosis was more than 10 times higher than in those without	[15,22,24,25]
	Non-invasive fibrosis markers (*e.g.*, FIB-4 index, M2BPGi, and shear wave velocity in VTQ) also had significant associations with the risk of NAFLD-HCC	
Diabetes	Associated with increased risk of HCC in NAFLD patients (hazard ratio: 2.2–4.2)	[22,26,27]
Hypertension	May be an independent risk factor for NAFLD-HCC	[29]
Dyslipidemia	May be an independent risk factor for NAFLD-HCC	[29]
Age	Increased age was an independent risk factor for HCC in patients with NASH-related cirrhosis	[15,34]
	NAFLD patients aged ≥ 65 had 1.83 times higher risk of HCC than those aged < 65	
Male sex	Male patients with NASH-related cirrhosis had 4.34 times higher risk of HCC than female patients	[34]
Ethnicity	Hispanic ethnicity was associated with 1.59 times higher risk of HCC in NAFLD patients compared to white ethnicity (however, there have been conflicting results)	[15]
Mild alcohol intake	Associated with increased risk of HCC in NAFLD patients (hazard ratio: 3.6–4.8)	[38,39]
Elevated liver enzymes	Associated with increased risk of HCC in NAFLD patients (hazard ratio: 2.1–8.2)	[41-43]

HCC: Hepatocellular carcinoma; NAFLD: Nonalcoholic fatty liver disease; FIB-4: Fibrosis-4; M2BPGi: Mac-2-binding protein glycosylation isomer; VTQ: Virtual touch quantification; NASH: Nonalcoholic steatohepatitis.

Combined risk assessment

As we described above, many factors influence the risk of HCC in NAFLD patients. Therefore, integrating multiple factors will improve the accuracy of risk assessment. Lee *et al*[45] proposed a risk prediction model consisting of age, platelet count, and liver stiffness. This showed relatively good prediction performance in the validation cohort (*i.e.*, area under the receiver operating characteristic curve (AUROC), 0.78)[45]. Ioannou *et al*[46] reported another prediction model with a similar predictive value (AUROC, 0.75), consisting of age, sex, diabetes, BMI, platelet count, serum albumin, and AST/√ALT ratio[46].

GENETIC RISK FACTORS

Although NAFLD development and progression is largely determined by environmental factors, several genetic factors are involved in NAFLD pathogenesis. These genes included *PNPLA3*, transmembrane 6 superfamily member 2 (*TM6SF2*), glucokinase regulator (*GCKR*), membrane-bound O-acyl-transferase domain-containing 7 (*MBOAT7*), and 17-beta-hydroxysteroid dehydrogenase 13 (*HSD17B13*)[5,47]. Epigenetic factors, such as DNA methylation, histone modification, and non-coding RNAs, also play roles in the progression of NAFLD and hepatocarcinogenesis[48]. The risk of severe liver fibrosis has been reported to be 12.5-fold higher in patients with first-degree relatives with NAFLD-related cirrhosis than those without[49].

Single-nucleotide polymorphisms (SNPs) of *PNPLA3* have been the most studied for its association with HCC[50]. In a cohort of European Caucasian patients with NAFLD, the *PNPLA3* rs738409 polymorphism was significantly associated with HCC risk. GG carriers were found to evince a 5-fold increased risk compared to CC carriers[51]. This association was confirmed by subsequent studies[52,53]. The *TM6SF2* rs58542926 polymorphism has been reported to be another risk factor for HCC and advanced fibrosis/cirrhosis[54,55]. In addition, the *MBOAT7* rs641738 variant has also been reported as a risk factor for NAFLD-HCC. Furthermore, in an Italian cohort, the rs6417338 C-to-T variant was associated with a 1.65-fold increased risk of HCC[56]. Other reported SNPs associated with NAFLD-HCC risk include Toll-like receptor 5 rs5744174[57], signal transducer transcription 6 rs167769[58] activator, yes-associated protein 1 rs11225163[58], *HSD17B13* rs72613567[55], and dystrophy-associated fer-1-like protein rs17007417[59] (Table 2).

Zhang *et al*[55] reported a combined risk assessment model consisting of *PNPLA3*, *TM6SF2*, and *HSD17B13* variants[55]. In this study, patients with the highest score had a 29-fold higher risk of developing HCC. Bianco *et al*[60] reported another polygenic risk assessment model consisting of *PNPLA3*, *TM6SF2*, *GCKR*, *MBOAT7*, and *HSD17B13*[60]. The sensitivity and specificity for diagnosing HCC were 0.43 and 0.79%, respectively (AUROC, 0.65).

Table 2 Genetic risk factors for nonalcoholic fatty liver disease-associated hepatocellular carcinoma

Risk factors	Reported evidence	Ref.
PNPLA3	Carriage of rs738409 GG polymorphism is associated with 5.1–6.4-fold increased risk of HCC in NAFLD patients	[51-53,60]
	PNPLA3 G variant (GG *vs* CG *vs* CC) was not significantly associated with the risk of cardiovascular events extrahepatic cancers or overall death, but was associated with HCC (HR: 2.66) and liver-related death (HR: 2.42)	
	Used for developing polygenic risk scores	
TM6SF2	*TM6SF2* minor allele carriage (rs58542926 C>T) was associated with advanced fibrosis/cirrhosis and HCC (OR, 2.8) in NAFLD patients	[54,55,60]
	Combined assessment with *PNPLA3* and *HSD17B13* variants were useful for risk stratification of NAFLD-HCC	
	Used for developing polygenic risk scores	
MBOAT7	*MBOAT7* rs641738 C>T variants were associated with higher risk of HCC in NAFLD patients (OR, 1.65–2.10)	[56,60]
	Used for developing polygenic risk scores	
TLR5	*TLR5* rs5744174 TT genotype was a risk factor of HCC in patients with steatohepatitis-related cirrhosis (OR, 1.9)	[57]
STAT6	*STAT6* rs167769 CC genotype was inversely associated with the risk of HCC in NASH patients (OR, 0.015)	[58]
YAP1	Carriage of *YAP1* rs11225163 C allele was inversely associated with the risk of HCC in NASH patients (OR, 0.047)	[58]
HSD17B13	Combined assessment with *PNPLA3* and *TM6SF2* variants were useful for risk stratification of NAFLD-HCC	[55]
DYSF	*DYSF* rs17007417 T allele carriage was associated with increased risk of HCC in NAFLD patients (OR, 2.74)	[59]
GCKR	*GCKR* rs1260326 T allele carriage was associated with increased risk of HCC in NAFLD patients (OR, 1.38)	[59,60]
	Used for developing polygenic risk scores	

PNPLA3: Patatin-like phospholipase domain 3; HCC: Hepatocellular carcinoma; NAFLD: Nonalcoholic fatty liver disease; HR: Hazard ratio; TM6SF2: Transmembrane 6 superfamily member 2; HSD17B13: 7-beta-Hydroxysteroid dehydrogenase 13; OR: Odds ratio; MBOAT7: Membrane-bound O-acyltransferase domain-containing 7; TLR5: Toll-like receptor 5; STAT6: Signal transducer activator of transcription 6; NASH: Nonalcoholic steatohepatitis; YAP1: Yes-associated protein 1; DYSF: Dystrophy-associated fer-1-like protein; GCKR: Glucokinase regulator.

DIAGNOSTIC BIOMARKERS

Currently available biomarkers

The currently available serum biomarkers for diagnosing HCC include AFP, des-carboxyprothrombin (DCP), and AFP isoform L3 (AFP-L3) (Table 3). Only AFP is recommended for HCC surveillance as *per* the major guidelines[31]. However, patients with NAFLD-HCC tend to have lower AFP levels than those with viral HCC[12,61]. Thus, the combined use of multiple tumor markers may be considered to increase the detection rate of HCC[62]. The GALAD score is a scoring system for the diagnosis of HCC. This score can be calculated by sex, age, lectin-bound AFP, AFP, and DCP. In a German cohort of NASH patients with and without HCC, the GALAD score exhibited excellent diagnostic performance (AUROC, 0.96). This was significantly better than AFP (AUROC, 0.88), DCP (AUROC, 0.87), and AFP-L3 (AUROC, 0.86) alone[63]. However, it must be noted that that only 20% of the HCC patients included in this study were within the Milan criteria. In addition, further research is needed from the perspective of cost effectiveness to determine whether this scoring system should be recommended for routine HCC screening in patients with NAFLD.

Potential biomarkers under investigation

Many serum biomarkers are under investigation for more accurate diagnosis of NAFLD-HCC without imaging. These biomarkers include iron and transferrin saturation[64], glypican-3 and adiponectin[65], midkine[66], apoptosis inhibitor of macrophages[67,68], glycosylation patterns of glycoproteins[69], and specific types of glycopeptides[70,71] (Table 3). Recently, Kozumi *et al*[72] showed that intrahepatic and serum thrombospondin 2 (*THBS2*) expression levels are strongly associated with advanced fibrosis in patients with NASH[72]. In their study, HCC was observed only in patients with high serum levels of

Table 3 Currently available and potential diagnostic biomarkers for nonalcoholic fatty liver disease-associated hepatocellular carcinoma

Biomarkers	Reported evidence	Ref.
Currently available		
AFP	Modest diagnostic ability for HCC in NAFLD patients (AUROC, 0.71–0.88)	[63,84]
DCP	The diagnostic ability for NAFLD-HCC was similar to that of AFP	[63,84]
	Combined use with AFP improved the diagnostic performance	
	Used for calculation of GALAD score	
AFP-L3	The diagnostic ability for NAFLD-HCC was similar to that of AFP	[63]
	Used for calculation of GALAD score	
Under development		
Iron status	Elevations of serum iron levels and transferrin saturation were associated with increased risk of HCC in NAFLD patients (HR, 2.91 and 2.02, respectively)	[64]
Proteins	Midkine increased the diagnostic yield in AFP-negative HCC in NAFLD patients; 59.2% of AFP-negative NAFLD-HCC patients had elevation of serum midkine levels	[65-67,72]
	IgM-free AIM had better diagnostic performance for NASH-HCC than AFP or DCP (AUROC, 0.905–0.929)	
	Serum TSP-2 levels were significantly associated with advanced fibrosis in NASH patients. Among 164 patients with NAFLD, HCC occurred only in patients with high serum levels of TSP-2	
Glycoprotein	Glycosylation patterns of alpha-1 acid glycoprotein may serve as a diagnostic biomarker for AFP-negative HCC in NAFLD patients	[69]
Proteoglycan	Glypican-3 had modest diagnostic ability (AUROC, 0.759), similar to AFP (AUROC, 0.763). When combined with age, sex, DCP and adiponectin, the AUROC increased to 0.948	[65]
Glycopeptide	Site-specific N-glycopeptides from vitronectin may serve as diagnostic biomarkers for NASH-HCC. When used together with AFP, the AUROC were 0.834 and 0.847, compared to 0.791 of AFP alone	[70,71]
	Site-specific N-glycopeptides from serum haptoglobin showed better diagnostic accuracy for NASH-HCC than AFP	
Cytokine (adipokine)	Adiponectin had slightly better diagnostic ability (AUROC, 0.770) than AFP (AUROC, 0.763). When combined with age, sex, DCP and glypican-3, the AUROC increased to 0.948	[65]
Cell-free DNA	*TERT* promoter mutation (C228T) in serum cfDNA showed better diagnostic ability for early NAFLD-HCC than AFP and DCP	[76,78]
	Methylation biomarkers in cfDNA improved the diagnostic performance when combined with AFP	
microRNA	The expression levels of exosomal miR-182, miR-301a and miR-373 in both serum and ascetic fluid were higher in NASH-cirrhosis patients with HCC than in those without HCC	[77]

AFP: Alpha-fetoprotein; HCC: Hepatocellular carcinoma; NAFLD: Nonalcoholic fatty liver disease; AUROC: Area under receiver operating characteristic curve; DCP: Des-carboxyprothrombin; AFP-L3: AFP isoform L3; HR: Hazard ratio; IgM: Immunoglobulin M; AIM: Apoptosis inhibitor of macrophages; TSP-2: Thrombospondin-2; NASH: Nonalcoholic steatohepatitis; TERT: Telomerase reverse transcriptase; cfDNA: Cell-free DNA; miR: microRNA.

thrombospondin-2 (TSP-2). Thus, serum TSP-2 testing may also be useful for NAFLD-HCC surveillance.

Genetic and epigenetic biomarkers have attracted increasing attention in recent years (Table 3). For example, telomerase reverse transcriptase (*TERT*) promoter mutations, the most common form of HCC genetic alteration[73-75], can be analyzed using cell-free DNA (cfDNA). Akuta *et al*[76] reported that *TERT* C228T mutation could be detected in 63.9% of NAFLD-HCC patients by analyzing cfDNA[76]. Notably, it can be positive, even in patients with normal AFP and DCP levels. Another example of circulating biomarkers is non-coding RNAs, especially microRNAs. In a preliminary study, the serum expression levels of miR-182, miR-301a, and miR-373 were significantly higher in NASH-HCC patients than in NASH patients without HCC[77]. DNA methylation can also be analyzed using peripheral blood. In a recent study, methylation cfDNA biomarkers provided a modest diagnostic value for NAFLD-HCC with a sensitivity of 87.5% and specificity of 39.4%[78]. The combination of this DNA methylation panel and AFP led to a better cohort wide diagnostic performance than either of them used

alone. Although the utility of these biomarkers is yet to be validated, in the near future, advances in omics technology will surely provide better diagnostic tools for NAFLD-HCC than conventional tumor markers.

FUTURE PERSPECTIVES

A more effective surveillance approach is strongly desired to reduce the number of deaths due to NAFLD-HCC. As advanced liver fibrosis is the most common risk factor for NAFLD-HCC, current screening recommendations primarily focus on patients with cirrhosis. However, in a French study, only 37% of patients undergoing liver resection for NAFLD-HCC had bridging fibrosis or cirrhosis; with a frequency significantly lower than that of other etiologies[8]. Similar results were observed in a Japanese multicenter study; in which only 49% of patients with NAFLD-HCC had underlying cirrhosis [79]. Therefore, more than half of patients with NAFLD-HCC will lose the chance of early detection if no other risk factors are considered. As discussed above, other clinical factors and specific genetic variants have robust associations with NAFLD-HCC risk. We should make the best use of this evidence to enhance effective HCC surveillance. In addition, more accurate diagnostic biomarkers for NAFLD-HCC are needed. Among the currently available biomarkers, the GALAD score seems to be the most reliable. However, advances in omics technology will certainly provide more powerful diagnostic tools in the future. For instance, a recent study showed that fragmentomic cfDNA analysis offered excellent accuracy in detecting primary liver tumors (AUROC, 0.995), regardless of the underlying liver disease [80]. Moreover, it showed a sensitivity of over 95%, even for stage I tumors. Thus, further research on genetic and epigenetic biomarkers is very much needed.

Novel conceptional criteria for metabolic dysfunction-associated fatty liver disease (MAFLD) were proposed in 2020[81]. Although MAFLD has been reported as a more practical definition for identifying patients with fatty liver disease with high risk of disease progression[82], it remains unclear whether the evidence of risk factors and diagnostic markers for NAFLD-HCC can be extended to MAFLD-HCC. A nationwide cohort study conducted in Taiwan revealed that patients with NAFLD/MAFLD overlap had similar risk of HCC compared to those with NAFLD alone[83]. Nonetheless, further studies are warranted on this topic.

CONCLUSION

The incidence of NAFLD-HCC is increasing rapidly worldwide. Thus, an effective surveillance approach is required to reduce the number of deaths due to this condition. Although advanced fibrosis is the most important risk factor for NAFLD-HCC, other clinical risk factors such as diabetes, old age, male sex, and elevated liver enzymes should also be considered. Recent advances in omics technology have revealed that genetic factors such as the SNP of *PNPLA3* also affect the risk of hepatocarcinogenesis in patients with NAFLD. With regards to the diagnostic biomarkers for NAFLD-HCC, only AFP is recommended for surveillance as *per* major guidelines. A recent study showed that the GALAD score evinced a more effective diagnostic performance than when AFP was used alone. However, clinical implementation should be discussed from the perspective of cost-effectiveness. Specific gene mutations and DNA methylation can be detected in cfDNA and are expected to be novel biomarkers for the early NAFLD-HCC diagnosis, as well as specific proteins, glycopeptides, and adipokines.

ACKNOWLEDGEMENTS

We would like to thank Drs. Ken Takahashi, Takahiro Shimizu, Yuji Eso, Eriko Iguchi, Ken Kumagai, Masako Mishima, Mari Teramura, Shigeharu Nakano, Takahiko Ito, Haruka Amino, and Takahiro Inoue for their helpful discussions and comments on the manuscript.

FOOTNOTES

Author contributions: Ueno M drafted the manuscript and prepared the tables; Takeda H and Takai A designed the outline and coordinated the writing of the manuscript; Seno H supervised data interpretation and revised the manuscript.

Conflict-of-interest statement: All the authors report no relevant conflicts of interest for this article.

Open-Access: This article is an open-access article that was selected by an in-house editor and fully peer-reviewed by external reviewers. It is distributed in accordance with the Creative Commons Attribution NonCommercial (CC BY-

NC 4.0) license, which permits others to distribute, remix, adapt, build upon this work non-commercially, and license their derivative works on different terms, provided the original work is properly cited and the use is non-commercial. See: https://creativecommons.org/Licenses/by-nc/4.0/

Country/Territory of origin: Japan

ORCID number: Masayuki Ueno 0000-0002-2497-9327; Haruhiko Takeda 0000-0002-8954-9133; Atsushi Takai 0000-0002-5233-4120; Hiroshi Seno 0000-0002-8509-8128.

S-Editor: Fan JR
L-Editor: A
P-Editor: Fan JR

REFERENCES

1 **Villanueva A**. Hepatocellular Carcinoma. *N Engl J Med* 2019; **380**: 1450-1462 [PMID: 30970190 DOI: 10.1056/NEJMra1713263]
2 **Bray F**, Ferlay J, Soerjomataram I, Siegel RL, Torre LA, Jemal A. Global cancer statistics 2018: GLOBOCAN estimates of incidence and mortality worldwide for 36 cancers in 185 countries. *CA Cancer J Clin* 2018; **68**: 394-424 [PMID: 30207593 DOI: 10.3322/caac.21492]
3 **Miller KD**, Fidler-Benaoudia M, Keegan TH, Hipp HS, Jemal A, Siegel RL. Cancer statistics for adolescents and young adults, 2020. *CA Cancer J Clin* 2020; **70**: 443-459 [PMID: 32940362 DOI: 10.3322/caac.21637]
4 **Takeda H**, Takai A, Inuzuka T, Marusawa H. Genetic basis of hepatitis virus-associated hepatocellular carcinoma: linkage between infection, inflammation, and tumorigenesis. *J Gastroenterol* 2017; **52**: 26-38 [PMID: 27714455 DOI: 10.1007/s00535-016-1273-2]
5 **Brunt EM**, Wong VW, Nobili V, Day CP, Sookoian S, Maher JJ, Bugianesi E, Sirlin CB, Neuschwander-Tetri BA, Rinella ME. Nonalcoholic fatty liver disease. *Nat Rev Dis Primers* 2015; **1**: 15080 [PMID: 27188459 DOI: 10.1038/nrdp.2015.80]
6 **Younossi Z**, Anstee QM, Marietti M, Hardy T, Henry L, Eslam M, George J, Bugianesi E. Global burden of NAFLD and NASH: trends, predictions, risk factors and prevention. *Nat Rev Gastroenterol Hepatol* 2018; **15**: 11-20 [PMID: 28930295 DOI: 10.1038/nrgastro.2017.109]
7 **Hester D**, Golabi P, Paik J, Younossi I, Mishra A, Younossi ZM. Among Medicare Patients With Hepatocellular Carcinoma, Non-alcoholic Fatty Liver Disease is the Most Common Etiology and Cause of Mortality. *J Clin Gastroenterol* 2020; **54**: 459-467 [PMID: 30672817 DOI: 10.1097/MCG.0000000000001172]
8 **Pais R**, Fartoux L, Goumard C, Scatton O, Wendum D, Rosmorduc O, Ratziu V. Temporal trends, clinical patterns and outcomes of NAFLD-related HCC in patients undergoing liver resection over a 20-year period. *Aliment Pharmacol Ther* 2017; **46**: 856-863 [PMID: 28857208 DOI: 10.1111/apt.14261]
9 **Enomoto H**, Ueno Y, Hiasa Y, Nishikawa H, Hige S, Takikawa Y, Taniai M, Ishikawa T, Yasui K, Takaki A, Takaguchi K, Ido A, Kurosaki M, Kanto T, Nishiguchi S; Japan Etiology of Liver Cirrhosis Study Group in the 54th Annual Meeting of JSH. The transition in the etiologies of hepatocellular carcinoma-complicated liver cirrhosis in a nationwide survey of Japan. *J Gastroenterol* 2021; **56**: 158-167 [PMID: 33219410 DOI: 10.1007/s00535-020-01748-x]
10 **Estes C**, Anstee QM, Arias-Loste MT, Bantel H, Bellentani S, Caballeria J, Colombo M, Craxi A, Crespo J, Day CP, Eguchi Y, Geier A, Kondili LA, Kroy DC, Lazarus JV, Loomba R, Manns MP, Marchesini G, Nakajima A, Negro F, Petta S, Ratziu V, Romero-Gomez M, Sanyal A, Schattenberg JM, Tacke F, Tanaka J, Trautwein C, Wei L, Zeuzem S, Razavi H. Modeling NAFLD disease burden in China, France, Germany, Italy, Japan, Spain, United Kingdom, and United States for the period 2016-2030. *J Hepatol* 2018; **69**: 896-904 [PMID: 29886156 DOI: 10.1016/j.jhep.2018.05.036]
11 **Degasperi E**, Colombo M. Distinctive features of hepatocellular carcinoma in non-alcoholic fatty liver disease. *Lancet Gastroenterol Hepatol* 2016; **1**: 156-164 [PMID: 28404072 DOI: 10.1016/S2468-1253(16)30018-8]
12 **Mittal S**, Sada YH, El-Serag HB, Kanwal F, Duan Z, Temple S, May SB, Kramer JR, Richardson PA, Davila JA. Temporal trends of nonalcoholic fatty liver disease-related hepatocellular carcinoma in the veteran affairs population. *Clin Gastroenterol Hepatol* 2015; **13**: 594-601.e1 [PMID: 25148760 DOI: 10.1016/j.cgh.2014.08.013]
13 **Parikh ND**, Singal AG, Hutton DW, Tapper EB. Cost-Effectiveness of Hepatocellular Carcinoma Surveillance: An Assessment of Benefits and Harms. *Am J Gastroenterol* 2020; **115**: 1642-1649 [PMID: 32530829 DOI: 10.14309/ajg.0000000000000715]
14 **Tateishi R**, Matsumura T, Okanoue T, Shima T, Uchino K, Fujiwara N, Senokuchi T, Kon K, Sasako T, Taniai M, Kawaguchi T, Inoue H, Watada H, Kubota N, Shimano H, Kaneko S, Hashimoto E, Watanabe S, Shiota G, Ueki K, Kashiwabara K, Matsuyama Y, Tanaka H, Kasuga M, Araki E, Koike K; LUCID study investigators. Hepatocellular carcinoma development in diabetic patients: a nationwide survey in Japan. *J Gastroenterol* 2021; **56**: 261-273 [PMID: 33427937 DOI: 10.1007/s00535-020-01754-z]
15 **Kanwal F**, Kramer JR, Mapakshi S, Natarajan Y, Chayanupatkul M, Richardson PA, Li L, Desiderio R, Thrift AP, Asch SM, Chu J, El-Serag HB. Risk of Hepatocellular Cancer in Patients With Non-Alcoholic Fatty Liver Disease. *Gastroenterology* 2018; **155**: 1828-1837.e2 [PMID: 30144434 DOI: 10.1053/j.gastro.2018.08.024]
16 **Kim TH**, Kim SY, Tang A, Lee JM. Comparison of international guidelines for noninvasive diagnosis of hepatocellular carcinoma: 2018 update. *Clin Mol Hepatol* 2019; **25**: 245-263 [PMID: 30759967 DOI: 10.3350/cmh.2018.0090]
17 **Harris PS**, Hansen RM, Gray ME, Massoud OI, McGuire BM, Shoreibah MG. Hepatocellular carcinoma surveillance: An evidence-based approach. *World J Gastroenterol* 2019; **25**: 1550-1559 [PMID: 30983815 DOI: 10.3748/wjg.v25.i13.1550]
18 **Younossi ZM**, Henry L. Epidemiology of non-alcoholic fatty liver disease and hepatocellular carcinoma. *JHEP Rep* 2021;

3: 100305 [PMID: 34189448 DOI: 10.1016/j.jhepr.2021.100305]
19 **Ito T**, Ishigami M, Ishizu Y, Kuzuya T, Honda T, Hayashi K, Nishimura D, Toyoda H, Kumada T, Goto H, Hirooka Y. Utility and limitations of noninvasive fibrosis markers for predicting prognosis in biopsy-proven Japanese non-alcoholic fatty liver disease patients. *J Gastroenterol Hepatol* 2019; **34**: 207-214 [PMID: 30144360 DOI: 10.1111/jgh.14448]
20 **Berger D**, Desai V, Janardhan S. Con: Liver Biopsy Remains the Gold Standard to Evaluate Fibrosis in Patients With Nonalcoholic Fatty Liver Disease. *Clin Liver Dis (Hoboken)* 2019; **13**: 114-116 [PMID: 31061705 DOI: 10.1002/cld.740]
21 **Castera L**, Friedrich-Rust M, Loomba R. Noninvasive Assessment of Liver Disease in Patients With Nonalcoholic Fatty Liver Disease. *Gastroenterology* 2019; **156**: 1264-1281.e4 [PMID: 30660725 DOI: 10.1053/j.gastro.2018.12.036]
22 **Alexander M**, Loomis AK, van der Lei J, Duarte-Salles T, Prieto-Alhambra D, Ansell D, Pasqua A, Lapi F, Rijnbeek P, Mosseveld M, Waterworth DM, Kendrick S, Sattar N, Alazawi W. Risks and clinical predictors of cirrhosis and hepatocellular carcinoma diagnoses in adults with diagnosed NAFLD: real-world study of 18 million patients in four European cohorts. *BMC Med* 2019; **17**: 95 [PMID: 31104631 DOI: 10.1186/s12916-019-1321-x]
23 **Kamada Y**, Ono M, Hyogo H, Fujii H, Sumida Y, Yamada M, Mori K, Tanaka S, Maekawa T, Ebisutani Y, Yamamoto A, Takamatsu S, Yoneda M, Kawada N, Chayama K, Saibara T, Takehara T, Miyoshi E; Japan Study Group of Nonalcoholic Fatty Liver Disease (JSG-NAFLD). Use of Mac-2 binding protein as a biomarker for nonalcoholic fatty liver disease diagnosis. *Hepatol Commun* 2017; **1**: 780-791 [PMID: 29404494 DOI: 10.1002/hep4.1080]
24 **Kawanaka M**, Tomiyama Y, Hyogo H, Koda M, Shima T, Tobita H, Hiramatsu A, Nishino K, Okamoto T, Sato S, Hara Y, Nishina S, Kawamoto H, Chayama K, Okanoue T, Hino K. Wisteria floribunda agglutinin-positive Mac-2 binding protein predicts the development of hepatocellular carcinoma in patients with non-alcoholic fatty liver disease. *Hepatol Res* 2018; **48**: 521-528 [PMID: 29316028 DOI: 10.1111/hepr.13054]
25 **Takamura M**, Kanefuji T, Suda T, Yokoo T, Kamimura H, Tsuchiya A, Kamimura K, Tamura Y, Igarashi M, Kawai H, Yamagiwa S, Nomoto M, Aoyagi Y. Value of shear wave velocity measurements for the risk assessment of hepatocellular carcinoma development in patients with nonalcoholic fatty liver disease : HCC risk assessment by VTTQ. *Hepatol Int* 2014; **8**: 240-249 [PMID: 26202505 DOI: 10.1007/s12072-014-9517-9]
26 **Grgurevic I**, Bozin T, Mikus M, Kukla M, O'Beirne J. Hepatocellular Carcinoma in Non-Alcoholic Fatty Liver Disease: From Epidemiology to Diagnostic Approach. *Cancers (Basel)* 2021; **13** [PMID: 34830997 DOI: 10.3390/cancers13225844]
27 **Fassio E**, Barreyro FJ, Pérez MS, Dávila D, Landeira G, Gualano G, Ruffillo G. Hepatocellular carcinoma in patients with metabolic dysfunction-associated fatty liver disease: Can we stratify at-risk populations? *World J Hepatol* 2022; **14**: 354-371 [PMID: 35317172 DOI: 10.4254/wjh.v14.i2.354]
28 **Benhammou JN**, Lin J, Hussain SK, El-Kabany M. Emerging risk factors for nonalcoholic fatty liver disease associated hepatocellular carcinoma. *Hepatoma Res* 2020; **6** [PMID: 32685690 DOI: 10.20517/2394-5079.2020.16]
29 **Jarvis H**, Craig D, Barker R, Spiers G, Stow D, Anstee QM, Hanratty B. Metabolic risk factors and incident advanced liver disease in non-alcoholic fatty liver disease (NAFLD): A systematic review and meta-analysis of population-based observational studies. *PLoS Med* 2020; **17**: e1003100 [PMID: 32353039 DOI: 10.1371/journal.pmed.1003100]
30 **Chen Y**, Wang X, Wang J, Yan Z, Luo J. Excess body weight and the risk of primary liver cancer: an updated meta-analysis of prospective studies. *Eur J Cancer* 2012; **48**: 2137-2145 [PMID: 22446023 DOI: 10.1016/j.ejca.2012.02.063]
31 **Huang DQ**, El-Serag HB, Loomba R. Global epidemiology of NAFLD-related HCC: trends, predictions, risk factors and prevention. *Nat Rev Gastroenterol Hepatol* 2021; **18**: 223-238 [PMID: 33349658 DOI: 10.1038/s41575-020-00381-6]
32 **Ohki T**, Tateishi R, Shiina S, Goto E, Sato T, Nakagawa H, Masuzaki R, Goto T, Hamamura K, Kanai F, Yoshida H, Kawabe T, Omata M. Visceral fat accumulation is an independent risk factor for hepatocellular carcinoma recurrence after curative treatment in patients with suspected NASH. *Gut* 2009; **58**: 839-844 [PMID: 19174415 DOI: 10.1136/gut.2008.164053]
33 **Kwak M**, Mehaffey JH, Hawkins RB, Hsu A, Schirmer B, Hallowell PT. Bariatric surgery is associated with reduction in non-alcoholic steatohepatitis and hepatocellular carcinoma: A propensity matched analysis. *Am J Surg* 2020; **219**: 504-507 [PMID: 31575419 DOI: 10.1016/j.amjsurg.2019.09.006]
34 **Corey KE**, Gawrieh S, deLemos AS, Zheng H, Scanga AE, Haglund JW, Sanchez J, Danford CJ, Comerford M, Bossi K, Munir S, Chalasani N, Wattacheril J. Risk factors for hepatocellular carcinoma in cirrhosis due to nonalcoholic fatty liver disease: A multicenter, case-control study. *World J Hepatol* 2017; **9**: 385-390 [PMID: 28321274 DOI: 10.4254/wjh.v9.i7.385]
35 **Romeo S**, Kozlitina J, Xing C, Pertsemlidis A, Cox D, Pennacchio LA, Boerwinkle E, Cohen JC, Hobbs HH. Genetic variation in PNPLA3 confers susceptibility to nonalcoholic fatty liver disease. *Nat Genet* 2008; **40**: 1461-1465 [PMID: 18820647 DOI: 10.1038/ng.257]
36 **Thandra KC**, Barsouk A, Saginala K, Aluru JS, Rawla P. Epidemiology of non-alcoholic fatty liver disease and risk of hepatocellular carcinoma progression. *Clin Exp Hepatol* 2020; **6**: 289-294 [PMID: 33511275 DOI: 10.5114/ceh.2020.102153]
37 **Petroni ML**, Brodosi L, Marchignoli F, Musio A, Marchesini G. Moderate Alcohol Intake in Non-Alcoholic Fatty Liver Disease: To Drink or Not to Drink? *Nutrients* 2019; **11** [PMID: 31847199 DOI: 10.3390/nu11123048]
38 **Kimura T**, Tanaka N, Fujimori N, Sugiura A, Yamazaki T, Joshita S, Komatsu M, Umemura T, Matsumoto A, Tanaka E. Mild drinking habit is a risk factor for hepatocarcinogenesis in non-alcoholic fatty liver disease with advanced fibrosis. *World J Gastroenterol* 2018; **24**: 1440-1450 [PMID: 29632425 DOI: 10.3748/wjg.v24.i13.1440]
39 **Protopapas AA**, Cholongitas E, Chrysavgis L, Tziomalos K. Alcohol consumption in patients with nonalcoholic fatty liver disease: yes, or no? *Ann Gastroenterol* 2021; **34**: 476-486 [PMID: 34276185 DOI: 10.20524/aog.2021.0641]
40 **Ou H**, Fu Y, Liao W, Zheng C, Wu X. Association between Smoking and Liver Fibrosis among Patients with Nonalcoholic Fatty Liver Disease. *Can J Gastroenterol Hepatol* 2019; **2019**: 6028952 [PMID: 31737583 DOI: 10.1155/2019/6028952]
41 **Kawamura Y**, Arase Y, Ikeda K, Seko Y, Imai N, Hosaka T, Kobayashi M, Saitoh S, Sezaki H, Akuta N, Suzuki F, Suzuki Y, Ohmoto Y, Amakawa K, Tsuji H, Kumada H. Large-scale long-term follow-up study of Japanese patients with non-alcoholic Fatty liver disease for the onset of hepatocellular carcinoma. *Am J Gastroenterol* 2012; **107**: 253-261 [PMID: 22008893 DOI: 10.1038/ajg.2011.327]
42 **Natarajan Y**, Kramer JR, Yu X, Li L, Thrift AP, El-Serag HB, Kanwal F. Risk of Cirrhosis and Hepatocellular Cancer in

Patients With NAFLD and Normal Liver Enzymes. *Hepatology* 2020; **72**: 1242-1252 [PMID: 32022277 DOI: 10.1002/hep.31157]

43 **Lee TY**, Wu JC, Yu SH, Lin JT, Wu MS, Wu CY. The occurrence of hepatocellular carcinoma in different risk stratifications of clinically noncirrhotic nonalcoholic fatty liver disease. *Int J Cancer* 2017; **141**: 1307-1314 [PMID: 28509327 DOI: 10.1002/ijc.30784]

44 **Makker J**, Tariq H, Kumar K, Ravi M, Shaikh DH, Leung V, Hayat U, Hassan MT, Patel H, Nayudu S, Chilimuri S. Prevalence of advanced liver fibrosis and steatosis in type-2 diabetics with normal transaminases: A prospective cohort study. *World J Gastroenterol* 2021; **27**: 523-533 [PMID: 33642826 DOI: 10.3748/wjg.v27.i6.523]

45 **Lee JS**, Sinn DH, Park SY, Shin HJ, Lee HW, Kim BK, Park JY, Kim DY, Ahn SH, Oh JH, Lee JI, Kim SU. Liver Stiffness-Based Risk Prediction Model for Hepatocellular Carcinoma in Patients with Nonalcoholic Fatty Liver Disease. *Cancers (Basel)* 2021; **13** [PMID: 34572795 DOI: 10.3390/cancers13184567]

46 **Ioannou GN**, Green P, Kerr KF, Berry K. Models estimating risk of hepatocellular carcinoma in patients with alcohol or NAFLD-related cirrhosis for risk stratification. *J Hepatol* 2019; **71**: 523-533 [PMID: 31145929 DOI: 10.1016/j.jhep.2019.05.008]

47 **Carlsson B**, Lindén D, Brolén G, Liljeblad M, Bjursell M, Romeo S, Loomba R. Review article: the emerging role of genetics in precision medicine for patients with non-alcoholic steatohepatitis. *Aliment Pharmacol Ther* 2020; **51**: 1305-1320 [PMID: 32383295 DOI: 10.1111/apt.15738]

48 **Tian Y**, Wong VW, Chan HL, Cheng AS. Epigenetic regulation of hepatocellular carcinoma in non-alcoholic fatty liver disease. *Semin Cancer Biol* 2013; **23**: 471-482 [PMID: 24018165 DOI: 10.1016/j.semcancer.2013.08.010]

49 **Caussy C**, Soni M, Cui J, Bettencourt R, Schork N, Chen CH, Ikhwan MA, Bassirian S, Cepin S, Gonzalez MP, Mendler M, Kono Y, Vodkin I, Mekeel K, Haldorson J, Hemming A, Andrews B, Salotti J, Richards L, Brenner DA, Sirlin CB, Loomba R; Familial NAFLD Cirrhosis Research Consortium. Nonalcoholic fatty liver disease with cirrhosis increases familial risk for advanced fibrosis. *J Clin Invest* 2017; **127**: 2697-2704 [PMID: 28628033 DOI: 10.1172/JCI93465]

50 **Anstee QM**, Day CP. The Genetics of Nonalcoholic Fatty Liver Disease: Spotlight on PNPLA3 and TM6SF2. *Semin Liver Dis* 2015; **35**: 270-290 [PMID: 26378644 DOI: 10.1055/s-0035-1562947]

51 **Oda K**, Uto H, Mawatari S, Ido A. Clinical features of hepatocellular carcinoma associated with nonalcoholic fatty liver disease: a review of human studies. *Clin J Gastroenterol* 2015; **8**: 1-9 [PMID: 25575848 DOI: 10.1007/s12328-014-0548-5]

52 **Seko Y**, Sumida Y, Tanaka S, Mori K, Taketani H, Ishiba H, Hara T, Okajima A, Umemura A, Nishikawa T, Yamaguchi K, Moriguchi M, Kanemasa K, Yasui K, Imai S, Shimada K, Itoh Y. Development of hepatocellular carcinoma in Japanese patients with biopsy-proven non-alcoholic fatty liver disease: Association between PNPLA3 genotype and hepatocarcinogenesis/fibrosis progression. *Hepatol Res* 2017; **47**: 1083-1092 [PMID: 27862719 DOI: 10.1111/hepr.12840]

53 **Wang Z**, Budhu AS, Shen Y, Wong LL, Hernandez BY, Tiirikainen M, Ma X, Irwin ML, Lu L, Zhao H, Lim JK, Taddei T, Mishra L, Pawlish K, Stroup A, Brown R, Nguyen MH, Koshiol J, Hernandez MO, Forgues M, Yang HI, Lee MH, Huang YH, Iwasaki M, Goto A, Suzuki S, Matsuda K, Tanikawa C, Kamatani Y, Mann D, Guarnera M, Shetty K, Thomas CE, Yuan JM, Khor CC, Koh WP, Risch H, Wang XW, Yu H. Genetic susceptibility to hepatocellular carcinoma in chromosome 22q13.31, findings of a genome-wide association study. *JGH Open* 2021; **5**: 1363-1372 [PMID: 34950780 DOI: 10.1002/jgh3.12682]

54 **Liu YL**, Reeves HL, Burt AD, Tiniakos D, McPherson S, Leathart JB, Allison ME, Alexander GJ, Piguet AC, Anty R, Donaldson P, Aithal GP, Francque S, Van Gaal L, Clement K, Ratziu V, Dufour JF, Day CP, Daly AK, Anstee QM. TM6SF2 rs58542926 influences hepatic fibrosis progression in patients with non-alcoholic fatty liver disease. *Nat Commun* 2014; **5**: 4309 [PMID: 24978903 DOI: 10.1038/ncomms5309]

55 **Zhang HB**, Su W, Xu H, Zhang XY, Guan YF. HSD17B13: A Potential Therapeutic Target for NAFLD. *Front Mol Biosci* 2021; **8**: 824776 [PMID: 35071330 DOI: 10.3389/fmolb.2021.824776]

56 **Donati B**, Dongiovanni P, Romeo S, Meroni M, McCain M, Miele L, Petta S, Maier S, Rosso C, De Luca L, Vanni E, Grimaudo S, Romagnoli R, Colli F, Ferri F, Mancina RM, Iruzubieta P, Craxi A, Fracanzani AL, Grieco A, Corradini SG, Aghemo A, Colombo M, Soardo G, Bugianesi E, Reeves H, Anstee QM, Fargion S, Valenti L. MBOAT7 rs641738 variant and hepatocellular carcinoma in non-cirrhotic individuals. *Sci Rep* 2017; **7**: 4492 [PMID: 28674415 DOI: 10.1038/s41598-017-04991-0]

57 **Nischalke HD**, Fischer J, Klüners A, Matz-Soja M, Krämer B, Langhans B, Goeser F, Soyka M, Stickel F, Spengler U, Nattermann J, Strassburg CP, Berg T, Lutz P. A genetic variant in toll-like receptor 5 is linked to chemokine levels and hepatocellular carcinoma in steatohepatitis. *Liver Int* 2021; **41**: 2139-2148 [PMID: 34051061 DOI: 10.1111/liv.14980]

58 **El-Derany MO**. Polymorphisms in Interleukin 13 Signaling and Interacting Genes Predict Advanced Fibrosis and Hepatocellular Carcinoma Development in Non-Alcoholic Steatohepatitis. *Biology (Basel)* 2020; **9** [PMID: 32283835 DOI: 10.3390/biology9040075]

59 **Kawaguchi T**, Shima T, Mizuno M, Mitsumoto Y, Umemura A, Kanbara Y, Tanaka S, Sumida Y, Yasui K, Takahashi M, Matsuo K, Itoh Y, Tokushige K, Hashimoto E, Kiyosawa K, Kawaguchi M, Itoh H, Uto H, Komorizono Y, Shirabe K, Takami S, Takamura T, Kawanaka M, Yamada R, Matsuda F, Okanoue T. Risk estimation model for nonalcoholic fatty liver disease in the Japanese using multiple genetic markers. *PLoS One* 2018; **13**: e0185490 [PMID: 29385134 DOI: 10.1371/journal.pone.0185490]

60 **Bianco C**, Jamialahmadi O, Pelusi S, Baselli G, Dongiovanni P, Zanoni I, Santoro L, Maier S, Liguori A, Meroni M, Borroni V, D'Ambrosio R, Spagnuolo R, Alisi A, Federico A, Bugianesi E, Petta S, Miele L, Vespasiani-Gentilucci U, Anstee QM, Stickel F, Hampe J, Fischer J, Berg T, Fracanzani AL, Soardo G, Reeves H, Prati D, Romeo S, Valenti L. Non-invasive stratification of hepatocellular carcinoma risk in non-alcoholic fatty liver using polygenic risk scores. *J Hepatol* 2021; **74**: 775-782 [PMID: 33248170 DOI: 10.1016/j.jhep.2020.11.024]

61 **Than NN**, Ghazanfar A, Hodson J, Tehami N, Coldham C, Mergental H, Manas D, Shah T, Newsome PN, Reeves H, Shetty S. Comparing clinical presentations, treatments and outcomes of hepatocellular carcinoma due to hepatitis C and non-alcoholic fatty liver disease. *QJM* 2017; **110**: 73-81 [PMID: 27634970 DOI: 10.1093/qjmed/hcw151]

62 **Ertle JM**, Heider D, Wichert M, Keller B, Kueper R, Hilgard P, Gerken G, Schlaak JF. A combination of α-fetoprotein and

des-γ-carboxy prothrombin is superior in detection of hepatocellular carcinoma. *Digestion* 2013; **87**: 121-131 [PMID: 23406785 DOI: 10.1159/000346080]

63 **Best J**, Bechmann LP, Sowa JP, Sydor S, Dechêne A, Pflanz K, Bedreli S, Schotten C, Geier A, Berg T, Fischer J, Vogel A, Bantel H, Weinmann A, Schattenberg JM, Huber Y, Wege H, von Felden J, Schulze K, Bettinger D, Thimme R, Sinner F, Schütte K, Weiss KH, Toyoda H, Yasuda S, Kumada T, Berhane S, Wichert M, Heider D, Gerken G, Johnson P, Canbay A. GALAD Score Detects Early Hepatocellular Carcinoma in an International Cohort of Patients With Nonalcoholic Steatohepatitis. *Clin Gastroenterol Hepatol* 2020; **18**: 728-735.e4 [PMID: 31712073 DOI: 10.1016/j.cgh.2019.11.012]

64 **Yu YC**, Luu HN, Wang R, Thomas CE, Glynn NW, Youk AO, Behari J, Yuan JM. Serum Biomarkers of Iron Status and Risk of Hepatocellular Carcinoma Development in Patients with Nonalcoholic Fatty Liver Disease. *Cancer Epidemiol Biomarkers Prev* 2022; **31**: 230-235 [PMID: 34649958 DOI: 10.1158/1055-9965.EPI-21-0754]

65 **Caviglia GP**, Armandi A, Rosso C, Gaia S, Aneli S, Rolle E, Abate ML, Olivero A, Nicolosi A, Guariglia M, Ribaldone DG, Carucci P, Saracco GM, Bugianesi E. Biomarkers of Oncogenesis, Adipose Tissue Dysfunction and Systemic Inflammation for the Detection of Hepatocellular Carcinoma in Patients with Nonalcoholic Fatty Liver Disease. *Cancers (Basel)* 2021; **13** [PMID: 34064999 DOI: 10.3390/cancers13102305]

66 **Vongsuvanh R**, van der Poorten D, Iseli T, Strasser SI, McCaughan GW, George J. Midkine Increases Diagnostic Yield in AFP Negative and NASH-Related Hepatocellular Carcinoma. *PLoS One* 2016; **11**: e0155800 [PMID: 27219517 DOI: 10.1371/journal.pone.0155800]

67 **Sumida Y**, Yoneda M, Seko Y, Ishiba H, Hara T, Toyoda H, Yasuda S, Kumada T, Hayashi H, Kobayashi T, Imajo K, Tada T, Kawaguchi T, Eguchi Y, Oeda S, Takahashi H, Tomita E, Okanoue T, Nakajima A; Japan Study Group Of Nafld Jsg-Nafld. Surveillance of Hepatocellular Carcinoma in Nonalcoholic Fatty Liver Disease. *Diagnostics (Basel)* 2020; **10** [PMID: 32785100 DOI: 10.3390/diagnostics10080579]

68 **Shimizu T**, Sawada T, Asai T, Kanetsuki Y, Hirota J, Moriguchi M, Nakajima T, Miyazaki T, Okanoue T. Hepatocellular carcinoma diagnosis using a novel electrochemiluminescence immunoassay targeting serum IgM-free AIM. *Clin J Gastroenterol* 2022; **15**: 41-51 [PMID: 34981443 DOI: 10.1007/s12328-021-01567-4]

69 **Liang J**, Zhu J, Wang M, Singal AG, Odewole M, Kagan S, Renteria V, Liu S, Parikh ND, Lubman DM. Evaluation of AGP Fucosylation as a Marker for Hepatocellular Carcinoma of Three Different Etiologies. *Sci Rep* 2019; **9**: 11580 [PMID: 31399619 DOI: 10.1038/s41598-019-48043-1]

70 **Zhu J**, Huang J, Zhang J, Chen Z, Lin Y, Grigorean G, Li L, Liu S, Singal AG, Parikh ND, Lubman DM. Glycopeptide Biomarkers in Serum Haptoglobin for Hepatocellular Carcinoma Detection in Patients with Nonalcoholic Steatohepatitis. *J Proteome Res* 2020; **19**: 3452-3466 [PMID: 32412768 DOI: 10.1021/acs.jproteome.0c00270]

71 **Lin Y**, Zhu J, Pan L, Zhang J, Tan Z, Olivares J, Singal AG, Parikh ND, Lubman DM. A Panel of Glycopeptides as Candidate Biomarkers for Early Diagnosis of NASH Hepatocellular Carcinoma Using a Stepped HCD Method and PRM Evaluation. *J Proteome Res* 2021; **20**: 3278-3289 [PMID: 33929864 DOI: 10.1021/acs.jproteome.1c00175]

72 **Kozumi K**, Kodama T, Murai H, Sakane S, Govaere O, Cockell S, Motooka D, Kakita N, Yamada Y, Kondo Y, Tahata Y, Yamada R, Hikita H, Sakamori R, Kamada Y, Daly AK, Anstee QM, Tatsumi T, Morii E, Takehara T. Transcriptomics Identify Thrombospondin-2 as a Biomarker for NASH and Advanced Liver Fibrosis. *Hepatology* 2021; **74**: 2452-2466 [PMID: 34105780 DOI: 10.1002/hep.31995]

73 **Totoki Y**, Tatsuno K, Covington KR, Ueda H, Creighton CJ, Kato M, Tsuji S, Donehower LA, Slagle BL, Nakamura H, Yamamoto S, Shinbrot E, Hama N, Lehmkuhl M, Hosoda F, Arai Y, Walker K, Dahdouli M, Gotoh K, Nagae G, Gingras MC, Muzny DM, Ojima H, Shimada K, Midorikawa Y, Goss JA, Cotton R, Hayashi A, Shibahara J, Ishikawa S, Guiteau J, Tanaka M, Urushidate T, Ohashi S, Okada N, Doddapaneni H, Wang M, Zhu Y, Dinh H, Okusaka T, Kokudo N, Kosuge T, Takayama T, Fukayama M, Gibbs RA, Wheeler DA, Aburatani H, Shibata T. Trans-ancestry mutational landscape of hepatocellular carcinoma genomes. *Nat Genet* 2014; **46**: 1267-1273 [PMID: 25362482 DOI: 10.1038/ng.3126]

74 **Takeda H**, Takai A, Kumagai K, Iguchi E, Arasawa S, Eso Y, Shimizu T, Ueda Y, Taura K, Uemoto S, Kita R, Haga H, Marusawa H, Fujimoto A, Seno H. Multiregional whole-genome sequencing of hepatocellular carcinoma with nodule-in-nodule appearance reveals stepwise cancer evolution. *J Pathol* 2020; **252**: 398-410 [PMID: 32815153 DOI: 10.1002/path.5533]

75 **Ki Kim S**, Ueda Y, Hatano E, Kakiuchi N, Takeda H, Goto T, Shimizu T, Yoshida K, Ikura Y, Shiraishi Y, Chiba K, Tanaka H, Miyano S, Uemoto S, Chiba T, Ogawa S, Marusawa H. TERT promoter mutations and chromosome 8p loss are characteristic of nonalcoholic fatty liver disease-related hepatocellular carcinoma. *Int J Cancer* 2016; **139**: 2512-2518 [PMID: 27511114 DOI: 10.1002/ijc.30379]

76 **Akuta N**, Kawamura Y, Kobayashi M, Arase Y, Saitoh S, Fujiyama S, Sezaki H, Hosaka T, Suzuki Y, Suzuki F, Ikeda K, Kumada H. TERT Promoter Mutation in Serum Cell-Free DNA Is a Diagnostic Marker of Primary Hepatocellular Carcinoma in Patients with Nonalcoholic Fatty Liver Disease. *Oncology* 2021; **99**: 114-123 [PMID: 32998139 DOI: 10.1159/000510366]

77 **Muhammad Yusuf AN**, Raja Ali RA, Muhammad Nawawi KN, Mokhtar NM. Potential biomarkers in NASH-induced liver cirrhosis with hepatocellular carcinoma: A preliminary work on roles of exosomal miR-182, miR-301a, and miR-373. *Malays J Pathol* 2020; **42**: 377-384 [PMID: 33361718]

78 **Lewin J**, Kottwitz D, Aoyama J, deVos T, Garces J, Hasinger O, Kasielke S, Knaust F, Rathi P, Rausch S, Weiss G, Zipprich A, Mena E, Fong TL. Plasma cell free DNA methylation markers for hepatocellular carcinoma surveillance in patients with cirrhosis: a case control study. *BMC Gastroenterol* 2021; **21**: 136 [PMID: 33765926 DOI: 10.1186/s12876-021-01714-8]

79 **Yasui K**, Hashimoto E, Komorizono Y, Koike K, Arii S, Imai Y, Shima T, Kanbara Y, Saibara T, Mori T, Kawata S, Uto H, Takami S, Sumida Y, Takamura T, Kawanaka M, Okanoue T; Japan NASH Study Group, Ministry of Health, Labour, and Welfare of Japan. Characteristics of patients with nonalcoholic steatohepatitis who develop hepatocellular carcinoma. *Clin Gastroenterol Hepatol* 2011; **9**: 428-33; quiz e50 [PMID: 21320639 DOI: 10.1016/j.cgh.2011.01.023]

80 **Zhang X**, Wang Z, Tang W, Wang X, Liu R, Bao H, Chen X, Wei Y, Wu S, Wu X, Shao Y, Fan J, Zhou J. Ultra-Sensitive and Affordable Assay for Early Detection of Primary Liver Cancer Using Plasma cfDNA Fragmentomics. *Hepatology* 2021 [DOI: 10.1002/hep.32308]

81 **Eslam M**, Sanyal AJ, George J; International Consensus Panel. MAFLD: A Consensus-Driven Proposed Nomenclature for Metabolic Associated Fatty Liver Disease. *Gastroenterology* 2020; **158**: 1999-2014.e1 [PMID: 32044314 DOI: 10.1053/j.gastro.2019.11.312]

82 **Lin S**, Huang J, Wang M, Kumar R, Liu Y, Liu S, Wu Y, Wang X, Zhu Y. Comparison of MAFLD and NAFLD diagnostic criteria in real world. *Liver Int* 2020; **40**: 2082-2089 [PMID: 32478487 DOI: 10.1111/liv.14548]

83 **Chen YG**, Yang CW, Chung CH, Ho CL, Chen WL, Chien WC. The association between metabolic risk factors, nonalcoholic fatty liver disease, and the incidence of liver cancer: a nationwide population-based cohort study. *Hepatol Int* 2022 [PMID: 35064545 DOI: 10.1007/s12072-021-10281-9]

84 **Beale G**, Chattopadhyay D, Gray J, Stewart S, Hudson M, Day C, Trerotoli P, Giannelli G, Manas D, Reeves H. AFP, PIVKAII, GP3, SCCA-1 and follisatin as surveillance biomarkers for hepatocellular cancer in non-alcoholic and alcoholic fatty liver disease. *BMC Cancer* 2008; **8**: 200 [PMID: 18638391 DOI: 10.1186/1471-2407-8-200]

World Journal of Gastroenterology

Submit a Manuscript: https://www.f6publishing.com

World J Gastroenterol 2022 July 21; 28(27): 3422-3434

DOI: 10.3748/wjg.v28.i27.3422

ISSN 1007-9327 (print) ISSN 2219-2840 (online)

ORIGINAL ARTICLE

Basic Study

Accumulation of poly (adenosine diphosphate-ribose) by sustained supply of calcium inducing mitochondrial stress in pancreatic cancer cells

Keun-Yeong Jeong, Jae Jun Sim, Minhee Park, Hwan Mook Kim

Specialty type: Gastroenterology and hepatology

Provenance and peer review: Invited article; Externally peer reviewed.

Peer-review model: Single blind

Peer-review report's scientific quality classification

Grade A (Excellent): 0
Grade B (Very good): B
Grade C (Good): C, C
Grade D (Fair): 0
Grade E (Poor): 0

P-Reviewer: Prasetyo EP, Indonesia; Tang D, China; Zuo CJ, China

Received: January 11, 2022
Peer-review started: January 11, 2022
First decision: March 8, 2022
Revised: March 15, 2022
Accepted: June 26, 2022
Article in press: June 26, 2022
Published online: July 21, 2022

Keun-Yeong Jeong, Jae Jun Sim, Minhee Park, Hwan Mook Kim, Research and Development, Metimedi Pharmaceuticals, Incheon 22006, South Korea

Corresponding author: Keun-Yeong Jeong, PhD, Executive Vice President, Research Assistant Professor, Research and Development, Metimedi Pharmaceuticals, 263 Central-ro, Incheon 22006, South Korea. alvirus@naver.com

Abstract

BACKGROUND

The biochemical phenomenon defined as poly adenosine diphosphate (ADP)-ribosylation (PARylation) is essential for the progression of pancreatic cancer. However, the excessive accumulation of poly ADP-ribose (PAR) induces apoptosis-inducing factor (AIF) release from mitochondria and energy deprivation resulting in the caspase-independent death of cancer cells.

AIM

To investigate whether sustained calcium supply could induce an anticancer effect on pancreatic cancer by PAR accumulation.

METHODS

Two pancreatic cancer cell lines, AsPC-1 and CFPAC-1 were used for the study. Calcium influx and mitochondrial reactive oxygen species (ROS) were observed by fluorescence staining. Changes in enzyme levels, as well as PAR accumulation and energy metabolism, were measured using assay kits. AIF-dependent cell death was investigated followed by confirming *in vivo* anticancer effects by sustained calcium administration.

RESULTS

Mitochondrial ROS levels were elevated with increasing calcium influx into pancreatic cancer cells. Then, excess PAR accumulation, decreased PAR glycohydrolase and ADP-ribosyl hydrolase 3 levels, and energy deprivation were observed. *In vitro* and *in vivo* antitumor effects were confirmed to accompany elevated AIF levels.

CONCLUSION

This study visualized the potential anticancer effects of excessive PAR accumu-

lation by sustained calcium supply on pancreatic cancer, however elucidating a clear mode of action remains a challenge, and it should be accompanied by further studies to assess its potential for clinical application.

Key Words: Pancreatic cancer; Calcium; Reactive oxygen species; Poly adenosine diphosphate-ribose; Poly adenosine diphosphate-ribosylation; Poly adenosine diphosphate-ribose polymerase; Apoptosis-inducing factor; Nicotinamide adenine dinucleotide; Anticancer effect

©The Author(s) 2022. Published by Baishideng Publishing Group Inc. All rights reserved.

Core Tip: Accumulation of poly adenosine diphosphate-ribose (PAR) was induced by an increase in reactive oxygen species following sustained calcium supply, which in turn led to the death of pancreatic cancer cells by energy deprivation and apoptosis-inducing factor expression. Although calcium-mediated accumulation of PAR would be a potential strategy for the treatment of pancreatic cancer, the association with the mechanical role of calcium in enabling the inactivation of PAR-degrading enzymes needs to be elucidated.

Citation: Jeong KY, Sim JJ, Park M, Kim HM. Accumulation of poly (adenosine diphosphate-ribose) by sustained supply of calcium inducing mitochondrial stress in pancreatic cancer cells. *World J Gastroenterol* 2022; 28(27): 3422-3434
URL: https://www.wjgnet.com/1007-9327/full/v28/i27/3422.htm
DOI: https://dx.doi.org/10.3748/wjg.v28.i27.3422

INTRODUCTION

Recent literature emphasizes that the biochemical phenomenon defined as poly adenosine diphosphate (ADP)-ribosylation (PARylation) is essential for the progression of cancer[1]. Poly ADP-ribose (PAR) is synthesized by the biochemical reaction of PAR polymerase-1 (PARP-1), which catalyzes the polymerization of ADP-ribose from the donor nicotinamide adenine dinucleotide (NAD+) to form a linear or branched PAR polymer[2]. Because PARylation is implicated in the multistep process involving various physiological maintenance factors and overcoming stress conditions for cancer cell survival, there might be connections between PARP-1 function and pancreatic cancer progression as a bridgehead linked by PARylation[1,2].

Although PARylation is essential for cancer survival, the excessive accumulation of PAR can mediate apoptosis-inducing factor (AIF) release from mitochondria and its nuclear translocation, resulting in the caspase-independent death of cancer cells[3]. The mode of action of the relationship between AIF and PAR involved in cell death has not been elucidated, but AIF translocation to the nucleus leading to chromatin condensation and large-scale DNA fragmentation is a well-established theory[3,4]. Cell death following PAR accumulation was recently defined as parthanatos, which is considered another death mechanism in a large category of apoptosis-type reactions[4]. Therefore, targeting ADP-ribosyl hydrolase 3 (ARH3), a type of PAR-degrading protein, and PAR glycohydrolase (PARG), a reversible covalent-modifier targeting PAR, might be potential methods to induce anticancer effects *via* PAR accumulation[5-7]. Although approaches to inhibit such enzymes through RNA interference or genetic manipulation have been tried, there have been few studies of the relevant mechanisms targeting pancreatic cancer[6,7].

Calcium is a key element in physiological signal transduction that enables the adjustment of energy production to cellular demand[8]; however, some reports indicated that cancer cells were affected during the influx of a high concentration of calcium resulting in excessive reactive oxygen species (ROS) produced from mitochondria[9]. Furthermore, there was an association between PARP-1 and an increase in ROS[1,10,11]. It was reported that the hyperactivation of PARP-1 was induced by an increase in ROS caused by intracellular calcium influx, the activation of PARP-1 as a response to DNA damage, or to drive an antioxidant program to protect cells from ROS[1,10,11]. This implies that excessive PAR accumulation can be induced as a result of PARP-1 hyperactivation followed by PARylation, suggesting the prospect of influencing pancreatic cancer cell survival by supplying high concentrations of calcium. The study aimed to investigate whether a sustained calcium supply induced intracellular PAR accumulation with an increase in ROS and to demonstrate the potential of this phenomenon to promote anticancer effects on pancreatic cancer.

MATERIALS AND METHODS

Cell lines and culture conditions

AsPC-1 and CFPAC-1 were obtained from the American Type Culture Collection (Manassas, VA, United States). The cells were grown in Roswell Park Memorial Institute 1640 and Iscove's Modified Dubecco's Medium supplemented with 10% fetal bovine serum (Welgene, Gyeongsan, Korea) and 1% penicillin/streptomycin (Welgene, Gyeongsan, Korea). All cells were cultured under a humidified atmosphere at 37 °C containing 5% CO_2.

Reagents

Lactate calcium salt (CaLac) and calpeptin were purchased from Sigma-Aldrich (St. Louis, MO, United States) and dissolved in distilled water. The solutions were stored at 4 °C until use.

Measurement of intracellular calcium

Calcium concentrations were measured using a confocal laser scanning microscope (Leica, Heidelberg, Germany). Cultured pancreatic cancer cells were loaded with 10 μM Fluo-3/AM (Invitrogen, Frederick, MD, United States) dissolved in dimethyl sulfoxide (Sigma-Aldrich). Then the cells were incubated for 30 min at 37 °C. Fluo-3/AM was excited at 488 nm and emitted fluorescence was measured at 515 nm.

Immunocytochemistry

Pancreatic cancer cells were fixed on bio-coated coverslips (BD bioscience, NJ, United States) using 4% paraformaldehyde, and incubated for 15 h with the primary antibody against AIF (1:200, Santa Cruz Biotechnology, Santa Cruz, CA, United States). Subsequently, the cells were incubated with an anti-rabbit secondary biotinylated anti-body (1:5000, Abcam) and visualized with streptavidin conjugated to fluorescein (Vector Laboratories, Burlingame, CA, United States). MitoSOX Red (Thermo Fisher Scientific, Waltham, MA, United States) was used to detect mitochondrial superoxide production. Fluorescence was measured using a confocal laser scanning microscope (Leica). Signal intensities were quantified and analyzed using the Xenogen Imaging System (IVIS® 100 series, Caliper Life Science, MA, United States).

Enzyme-linked immunosorbent assay

PARG, RNF-146, PAR, and AIF levels were quantified from 1×10^6 number of pancreatic cancer cells or 2 mm^3 volume of tumor tissues using each assay kit (PARG assay kit: Trevigen, Gaithersburg, MD, United States; RNF-146 ELISA kit: Abbexa, Houston, TX, United States; PAR ELISA kit: Cell Biolabs, San Diego, CA, United States; AIF ELISA kit: Abcam, Cambridge, England), according to the manufacturer's instructions.

Adenosine triphosphate assay

The cell culture medium was supplemented with CaLac, and cultures were incubated for 24 h. 1×10^6 cells were then sonicated. The cells were centrifuged at 1500 g for 20 min to remove insoluble material, and the supernatant was collected. Adenosine triphosphate (ATP) was measured by ATP colorimetric assay kit (Abcam) according to manufacturer's instructions.

NAD+ and NADH assay

The cell culture medium was supplemented with CaLac, and the cultures were incubated for 24 h. 1×10^6 cells were then sonicated. The cells were washed twice with phosphate buffer solution (PBS), and NAD+ and NADH levels were measured using the NAD/NADH quantitation kit (Sigma) according to the manufacturer's protocol.

Transferase-mediated dUTP nick end labeling assay

Pancreatic cancer cells were treated with CaLac for 24 h and then washed with cold PBS. The cells were fixed with 4% paraformaldehyde for 30 min and washed twice with PBS for 2 min. Fixed cells in permeabilization solution (0.1% Triton X-100 and 0.1% Sodium citrate) were washed. The tumors were fixed in 10% neutral buffered formalin and embedded in paraffin. Tissue sections (4 μm) were made from paraffin-embedded blocks on a microtome, and then the sections were deparaffinized and rehydrated. To detect cell death, the DeadEnd™ Fluorometric transferase-mediated dUTP nick end labeling (TUNEL) system kit (Promega, Madison, WI, United States) was used according to the manufacturer's instructions.

FACS analysis

Annexin V and propidium iodide (PI) staining was performed using an Annexin V-FITC Apoptosis Detection Kit (BD Biosciences). 2.5×10^6 of AsPC-1 and CFPAC-1 cells were exposed to CaLac for 24 h. The cells were resuspended in 100 μL of Annexin V-FITC binding buffer, and then 5 μL of Annexin V-FITC conjugate and 10 μL of PI buffer were added. Annexin V and PI were analyzed using a FACS

CaliburTM instrument (BD Biosciences).

Cell viability assay

Pancreatic cancer cells were cultured in a 96-well plate (3×10^3 cells/well) for 24 h, and then treated with CaLac for 24 h at 37 °C. Then, 10 μL of 3-(4,5-dimethylthiazol-2-yl)-2,5-diphenyltetrazolium bromide was added to each well, and the cells were incubated at 37 °C for 1 h in a humidified environment containing 5% CO_2. After the media was discarded, 200 μL of dimethyl sulfoxide (Cell Signaling Technology, Danvers, MA, United States) was added to each well. The absorbance was read at 570 nm using a microplate reader (iMark Microplate Absorbance Reader, Bio-Rad, CA, United States).

Xenograft animal model

Twenty-eight male Balb/c nude mice (5 wk of age) were purchased from the Charles River Breeding Laboratories (Wilmington, MA, United States). All animals were maintained on a 12 h light/dark cycle (light on, 08:00) at 22-25 °C, with free access to food and water. To investigate the antitumor activity of CaLac *in vivo*, a therapeutic strategy was devised to investigate its effect on the heterotopic xenograft animal model. Fourteen mice were used for establishing a heterotopic xenograft model using AsPC-1 cells (5×10^6) resuspended in 100 μL of phosphate-buffered saline. The cells were injected subcutaneously into the left flank of mice. Once the tumors reached a diameter of 8 mm, 7 mice were randomly divided into the untreated group, and 7 mice were divided into the CaLac-treated group. 20 mg/kg of CaLac was subcutaneously injected daily for 21 d. Tumor growth was monitored three times per week. To harvest tumors for histological and molecular biology analysis, carbon dioxide inhalation was used for euthanasia at the end of the experiments.

Immunohistochemistry

The tumors were fixed in 10% neutral buffered formalin and embedded in paraffin. Tissue sections (4 μm) were made from paraffin-embedded blocks on a microtome, and then the sections were deparaffinized and rehydrated. Endogenous peroxidase activity was blocked by 3% H_2O_2 in distilled water for 30 min. Antigen retrieval was induced by slide heating with 10 mmol/L citrate buffer (pH 6.0) using a microwave oven. The sections were blocked using a blocking agent (Invitrogen, Frederick, MD, United States) and incubated overnight with the primary antibodies at 4 °C. The primary antibodies were as follows: Ki-67 (1:200, Santa Cruz Biotechnology) and proliferating cell nuclear antigen (PCNA, 1:200, Santa Cruz Biotechnology). The sections were then incubated with biotinylated anti-mouse antibody (1:500, Vector Laboratories, Burlingame, CA, United States) for 1 h. After a PBST wash, the sections were treated with 3,3'-diaminobenzidine substrate (Dako, Carpentaria, CA, United States) and counterstained with hematoxylin (Thermo Fisher Scientific). A Leica DM 1000 LED microscope (Leica Microsystems, Wetzlar, Germany) was used for image analysis.

Statistical analysis

Data are presented as the means ± SD. Statistical significance was analyzed using the Student's *t*-test or one-way analysis of variance, depending on the normality of the data distribution. $P < 0.05$ was considered as statistically significant. All statistical analyses were performed by Sigma Stat v3.5 (Systat Software Inc., Chicago, IL, United States).

RESULTS

Calcium influx increases mitochondrial ROS in pancreatic cancer cells

The fluorescence intensity of fluo-3 by calcium reaction was increased in cells of both types of pancreatic cancer, AsPC-1 and CFPAC-1, following CaLac treatment (Figure 1A). In a quantitative analysis of fluorescence intensity, intracellular calcium levels were significantly increased by sustained calcium supply to about 2.1- and 1.9-fold in AsPC-1 and CFPAC-1, respectively, compared with the untreated group (Figure 1B). The increase in red fluorescence level in pancreatic cancer cells indicated increased ROS generation in pancreatic cancer cells by sustained calcium supply, indicating that ROS originated from mitochondria by the simultaneous use of a mitochondrial tracer showing green fluorescence (Figure 1C). In an analysis of the mean fluorescence intensity (MFI), mitochondrial ROS levels detected by MitoSOX™ were significantly increased by sustained calcium supply to about 2.33- and 2.63-fold in ASPC-1 and CFPAC-1, respectively, compared with the untreated group (Figures 1D and E).

An increase in ROS causes the excessive accumulation of PAR and energy deprivation

In addition to the immediate association of PAR accumulation by increased ROS levels, PARG and RNF-146 were supplementally investigated to confirm a change in the enzyme levels involved in PAR accumulation. A decrease in the enzymatic activity of PARG and ARH3 following calcium supply was observed (Figures 2A and B), accompanied by the accumulation of PAR in pancreatic cancer cells (Figure 2C). Changes in coenzyme factors involved in energy metabolism following the accumulation of

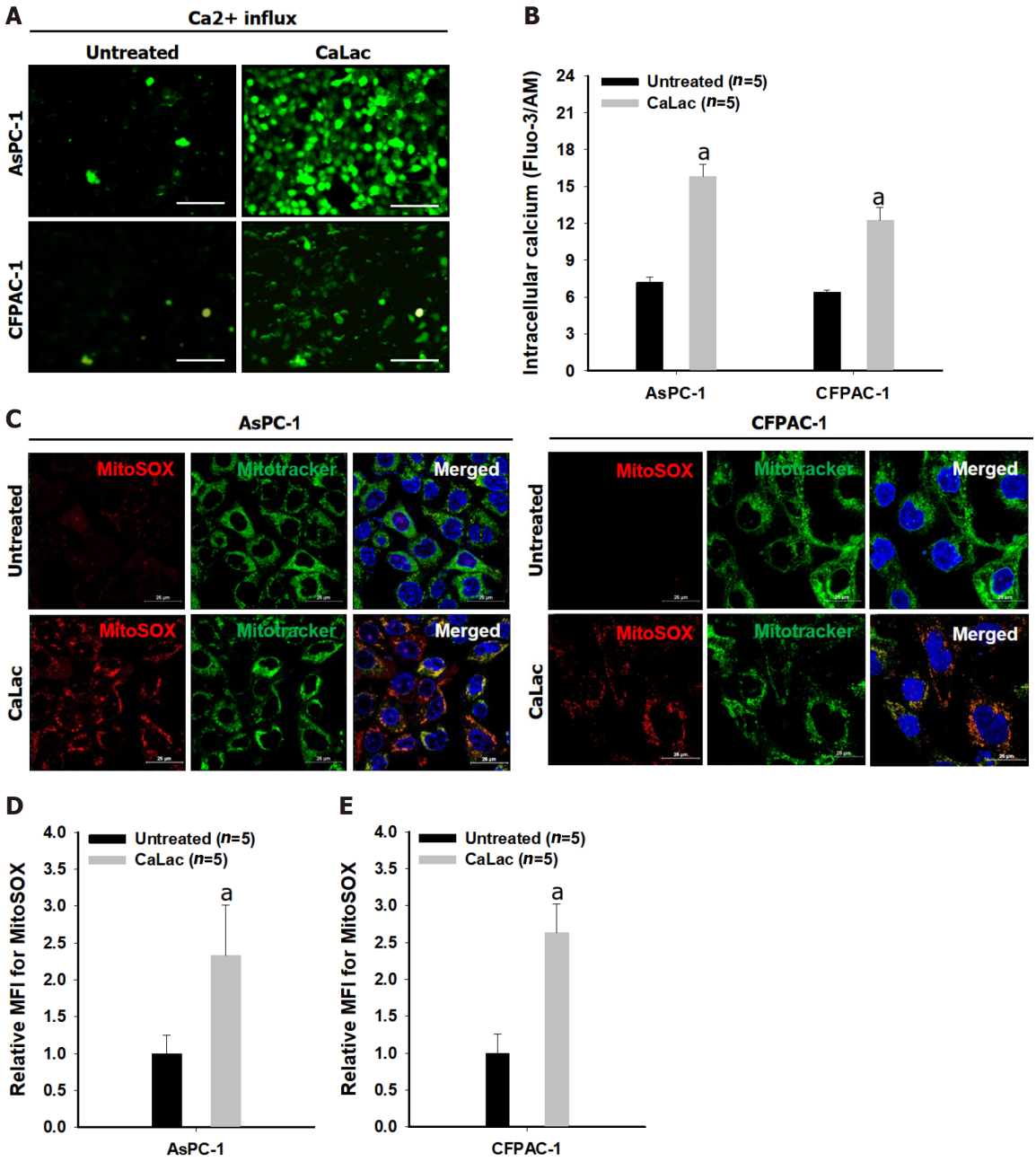


Figure 1 Confirmation of mitochondrial reactive oxygen species generation by sustained calcium supply. A: Fluorescent calcium imaging following lactate calcium salt (CaLac) treatment of pancreatic cancer cells (AsPC-1 and CFPAC-1). Scale bars: 100 μm; B: Quantitative analysis of the fluorescence intensity of calcium; C: Confocal imaging of mitochondrial reactive oxygen species (ROS) in pancreatic cancer cells. Red dye: Mitochondrial superoxide indicator; Green dye: Mitochondrial indicator. Scale bars: 25 μm; D: Quantitative analysis of the fluorescence intensity of mitochondrial ROS in AsPC-1; E: Quantitative analysis of the fluorescence intensity of mitochondrial ROS in CFPAC-1. The fluorescence intensity was calculated by the mean fluorescence intensity. The cells were treated with 2.5 mM CaLac for 72 h. Results represent the mean ± SD. $^{a}P < 0.001$ *vs* untreated. CaLac: Lactate calcium salt; MitoSOX: Mitochondrial superoxide indicator.

PAR were also identified (Figures 2D and E). These results indicated that the excessive synthesis of PAR resulted in reduced NAD+ levels (Figure 2D) and the increase of NADH levels (Figure 2E), which led to a depletion of ATP (Figure 2F).

An increase in AIF expression induces the death of pancreatic cancer cells

The results of immunocytochemical staining for the co-expression of AIF with the mitochondrial tracker in two types of pancreatic cancer cells indicated the calcium supply induced the translocation of AIF from the cytoplasm into the nucleus, whereas only cytoplasmic co-expression was observed in the untreated group (Figure 3A). Furthermore, it was quantitatively increased by calcium supply when the expression of AIF only was confirmed as a separate result through MFI analysis (Figures 3B and C). Then, the reaction ratio by TUNEL staining per total cells was significantly increased (Figures 3D and E), and Annexin V labeled cells increased from 6.61% to 37.61% and from 4.8% to 26.91% in AsPC-1 and CFPAC-1, respectively (Figure 3F). A decrease in cell viability by calcium supply was macroscopically

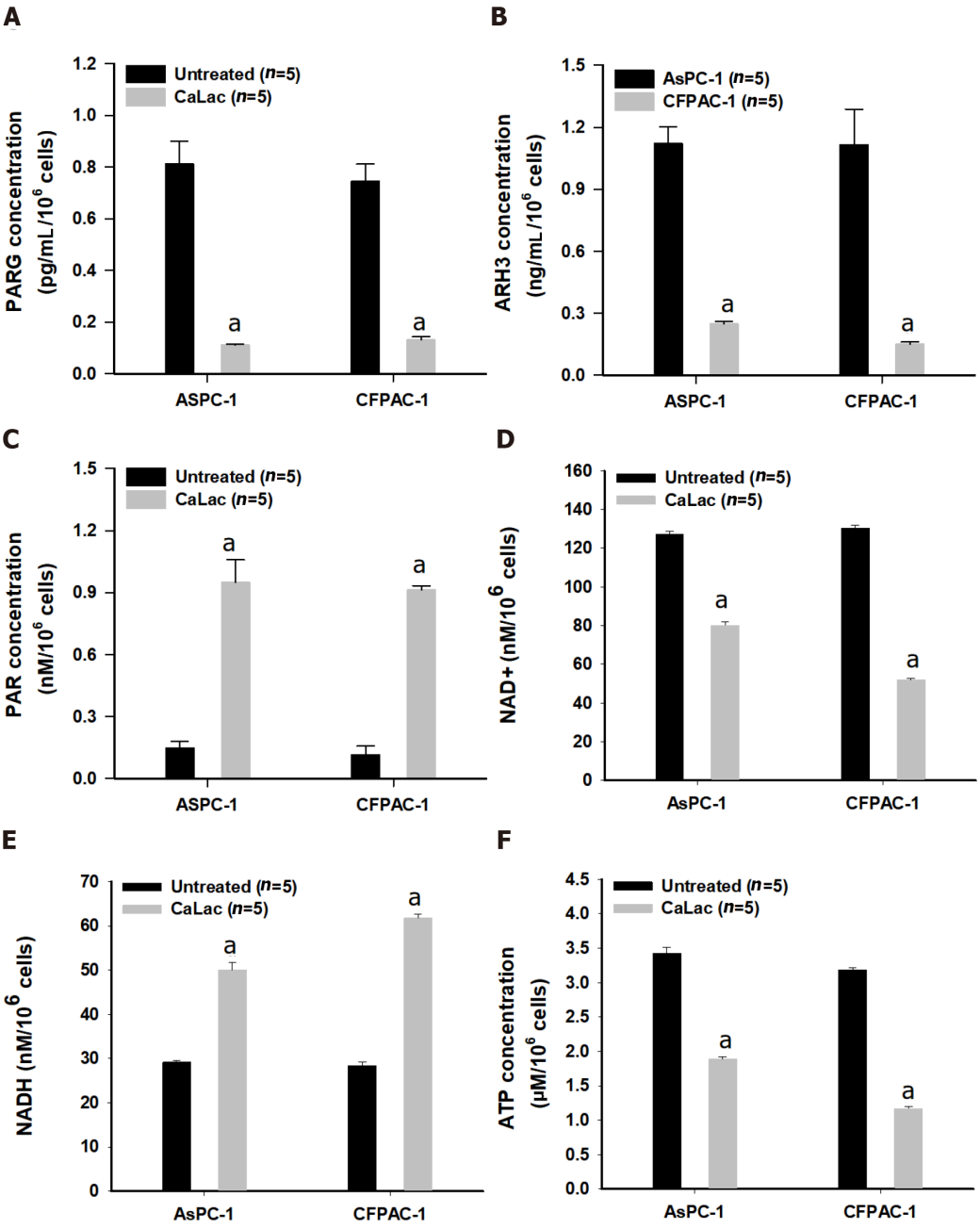


Figure 2 Confirmation of enzyme change and poly adenosine diphosphate-ribose accumulation by calcium supply resulting in energy crisis. A: Quantitative analysis of the enzyme levels of poly adenosine diphosphate (ADP)-ribose (PAR) glycohydrolase in pancreatic cancer cells (AsPC-1 and CFPAC-1); B: Quantitative analysis of the enzyme levels of ADP-ribosyl hydrolase 3 in AsPC-1 and CFPAC-1; C: Quantitative analysis of PAR levels; D: Quantitative analysis of nicotinamide adenine dinucleotide levels; E: Quantitative analysis of NADH levels; F: Quantitative analysis of adenosine triphosphate (ATP) levels. The cells were treated with 2.5 mM lactate calcium salt for 72 h. Results represent the mean ± SD. $^{a}P < 0.001$ *vs* untreated. CaLac: Lactate calcium salt; PARG: Poly adenosine diphosphate-ribose glycohydrolase; ARH3: Adenosine diphosphate-ribosyl hydrolase 3; NAD+: Nicotinamide adenine dinucleotide; ATP: Adenosine triphosphate.

observed by microphotographs (Figure 3G), and the CaLac group (calcium supply) showed low cell viability (mean 35.5%) when defining the total cell viability of the untreated group as 100% (Figure 3H).

An increase in PAR accumulation relates to calcium-dependent proteolytic enzyme activity in pancreatic cancer cells

To elucidate an increase in PAR accumulation by sustained calcium supply, the calpain inhibitor, calpeptin, was introduced. Changes in PARG, ARH3, PAR, and AIF were sequentially observed in pancreatic cancer cells (Figure 4). Although PARG levels were significantly decreased by sustained calcium supply, there was only a slight decrease (no significant difference) when combining calpeptin with calcium supply (Figures 4A and B). Calpeptin itself did not directly change the levels of PARG (Figures 4A and B) similar to that of ARH3 (Figures 4C and D). Furthermore, the levels of PAR and AIF

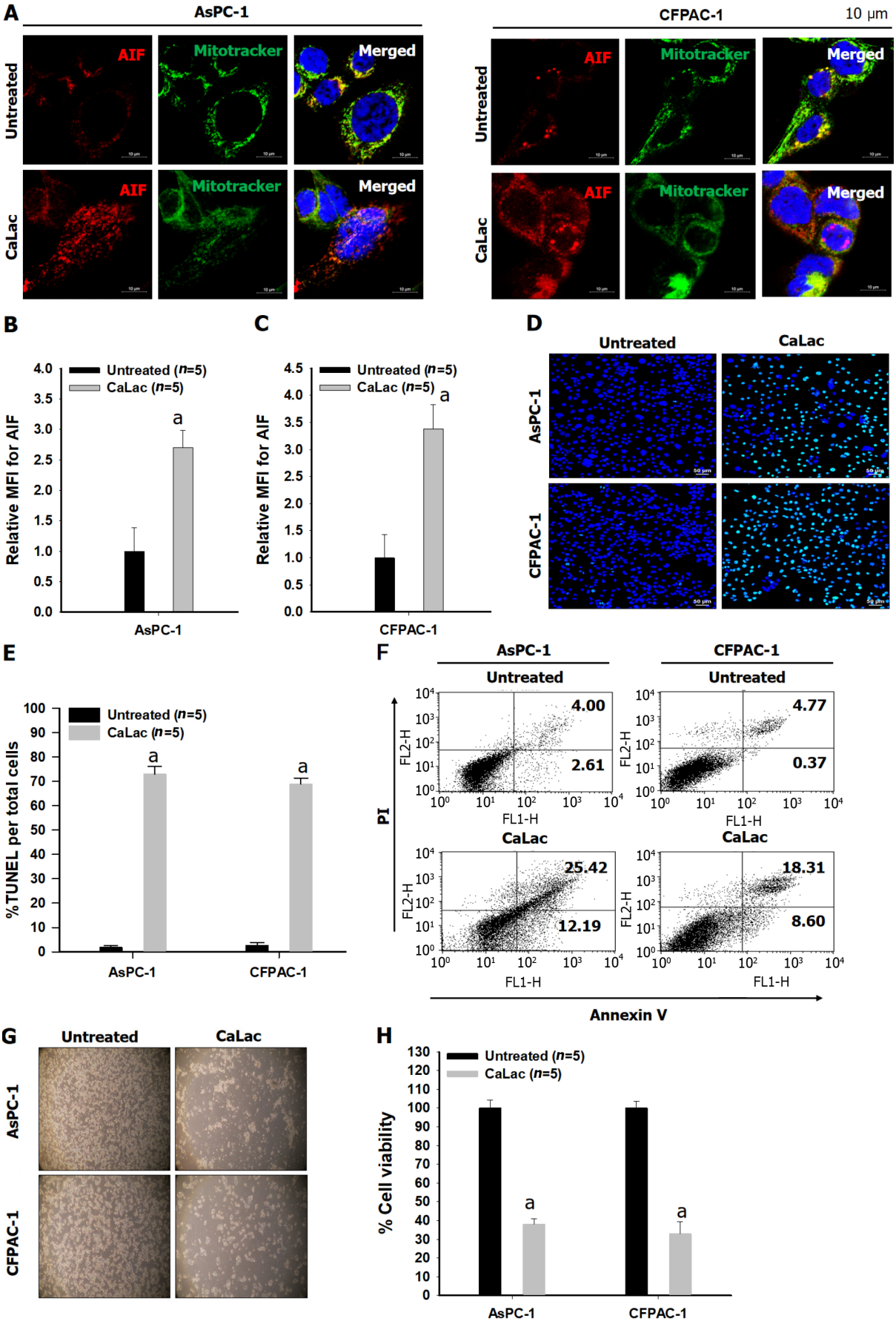


Figure 3 Confirmation of the expression of apoptosis-inducing factor followed by an increase in apoptosis in pancreatic cancer cells (AsPC-1 and CFPAC-1). A: Immunocytochemical staining for apoptosis-inducing factor (AIF) release from mitochondria and translocation into the nucleus. Red dye: AIF; Green dye: Mitochondrial indicator. Scale bars: 10 μm; B: Quantitative analysis of the mean fluorescence intensity (MFI) of AIF in CFPAC-1; C: Quantitative

analysis of the MFI of AIF in AsPC-1; D: Fluorescent microphotographs for colorimetric terminal deoxynucleotidyl transferase -mediated dUTP nick end labeling (TUNEL) detection. Green dye: TUNEL staining. Scale bars: 50 μm; E: Quantitative analysis of the % ratio of TUNEL detected cells per total pancreatic cancer cells; F: Representative flow cytometry plots using Annexin V-fluorescein-5-isothiocyanate/propidium iodide staining for apoptosis; G: Representative microphotographs to compare cell condition after calcium supply; H: Quantitative analysis of the percent cell viability following calcium supply. The cells were treated with 2.5 mM lactate calcium salt for 72 h. Results represent the mean ± SD. $^{a}P < 0.001$ *vs* untreated. CaLac: Lactate calcium salt; AIF: Apoptosis-inducing factor; MFI: Mean fluorescence intensity; TUNEL: Transferase-mediated dUTP nick end labeling.

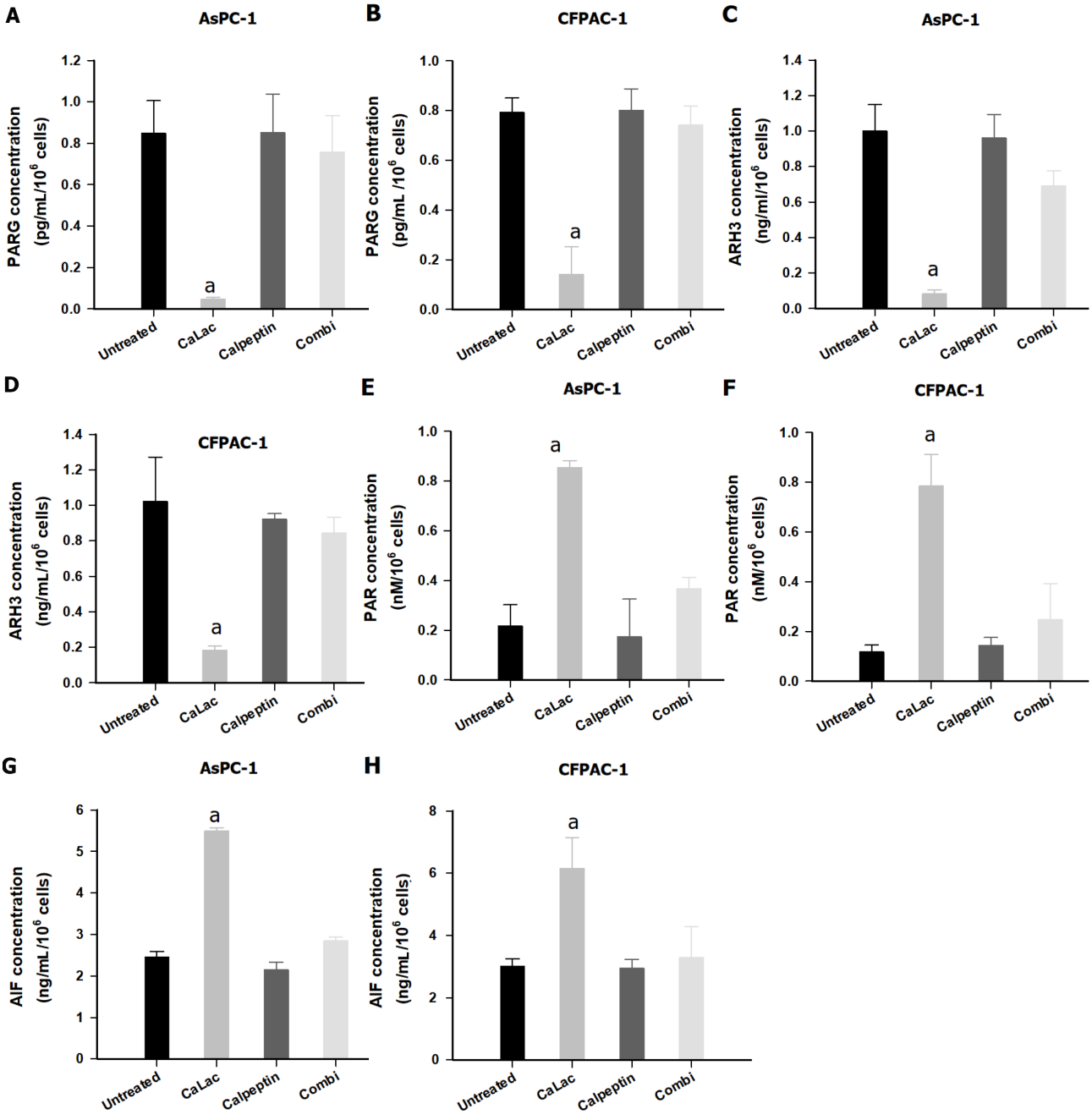


Figure 4 Confirmation of poly-adenosine diphosphate ribose accumulation in pancreatic cancer cells (AsPC-1 and CFPAC-1) by calcium-mediated proteasomal activity. A: Quantitative analysis of poly adenosine diphosphate-ribose glycohydrolase (PARG) levels in AsPC-1; B: Quantitative analysis of PARG levels in CFPAC-1; C: Quantitative analysis of ADP-ribosyl hydrolase 3 (ARH3) levels in AsPC-1; D: Quantitative analysis of ARH3 levels in CFPAC-1; E: Quantitative analysis of PAR levels in AsPC-1; F: Quantitative analysis of PAR levels in CFPAC-1; G: Quantitative analysis of apoptosis-inducing factor (AIF) levels in AsPC-1; H: Quantitative analysis of AIF levels in CFPAC-1. Calpeptin was used for proteasome inhibition. The cells were treated with 2.5 mM lactate calcium salt for 72 h. Results represent the mean ± SD. $^{a}P < 0.001$ *vs* untreated. CaLac: Lactate calcium salt; PARG: Poly adenosine diphosphate-ribose glycohydrolase; ARH3: Adenosine diphosphate-ribosyl hydrolase 3; AIF: Apoptosis-inducing factor.

were increased by calcium supply, which was restored to a level similar to that of the untreated group under culture conditions in which calpeptin was added (Figures 4E-H).

Sustained calcium administration induces anticancer effects on pancreatic cancer

Comparative results of tumor growth in heterotopic xenograft models demonstrated the inhibition of pancreatic cancer growth by calcium administration (Figures 5Aand B, Figure 6). The tumor volume on the last day of measurement was 830.37 ± 138.36 and 431.41 ± 91.98 in the untreated and the CaLac groups, respectively. Tumor volume was reduced by about 48.1% in the CaLac group compared with the untreated group (Figure 5B). There were few viable cells capable of discriminating the staining of nuclei in tumor tissues of the CaLac group (Figure 5C), indicating an increase in PAR-dependent AIF expression following sustained calcium-induced apoptosis (Figures 5D and E). The apoptotic signal in tumor tissues was increased 5.13-fold in the CaLac group compared with the untreated group (Figures 5F and G). As a result of apoptosis, the malignancy indicators of tumors were significantly reduced (Figure 5H) and the expressions of Ki-67 and PCNA were significantly reduced by about 64% and 68%, respectively in the CaLac group (Figures 5I and J).

DISCUSSION

This study demonstrated that the accumulation of PAR was induced by an increase in ROS following sustained calcium supply, which in turn led to the death of pancreatic cancer cells by energy deprivation and AIF expression. CaLac is a small molecule generated by the reaction of lactic acid with calcium carbonate and is characterized as a weak electrolyte with a neutralized charge[12]. Such a characteristic of CaLac suggests it might readily cross cell membranes as a bound form. Therefore, the accumulation of calcium was greatly increased in pancreatic cancer cells by the sustained treatment of CaLac, which was in line with our direction of research targeting intracellular calcium accumulation. It is well known that intracellular calcium uptake can promote ROS formation in mitochondria by stimulating tricarboxylic acid cycle enzymes and electron transport chain activity[9]. The results indicated that calcium accumulation by CaLac led to an increase in the mitochondrial ROS of pancreatic cancer cells. An active calcium signal must operate within physiological levels, but when intracellular calcium levels exceed this threshold, excessive ROS production can have a detrimental effect on cell survival by disrupting mitochondrial bioenergetic regulation and cellular functions[13]. The main reason for investigating an increase in PAR synthesis among the various biological phenomena mediated by calcium-dependent excessive ROS is its key function as a protective mechanism for cancer cell survival under hostile conditions[1,10,11,14]. ROS can be spontaneously generated during the ceaseless process of the rapid growth of cancer cells, but excessive ROS can cause DNA damage by irreversible oxidative stress[15]. PAR synthesis is defined as PARylation by PARP-1 recruits or modifies several nuclear proteins during the DNA damage response against harmful oxidative stress; however, the excessive synthesis of PAR can lead to cell death[1,14]. A sustained calcium supply causes the accumulation of PAR to cope with long-lasting DNA damage along with an increase of ROS in pancreatic cancer cells. Well-established phenomena induced by PAR accumulation include energy deprivation and AIF release from mitochondria[3,4,16]. Because PAR is catalyzed for synthesis from donor NAD+, excessive PAR accumulation causes a decrease in the intracellular level of NAD+, leading to energy deprivation[8,17]. Furthermore, an increase in AIF release induces cell death by large-scale DNA fragmentation defined as parthanatos, although a clear mechanism has not been elucidated[4,16]. The results indicated that AIF migrates from the mitochondria to the cytoplasm and nucleus in response to the accumulation of PAR followed by inducing the death of pancreatic cancer cells. Therefore, excessive PAR accumulation caused by an increase in ROS by sustained calcium supply can be considered to mediate anticancer activity as the main mechanism with energy deprivation and AIF release in pancreatic cancer cells. Cancer cells activate PAR erasing enzymes PARG and ARH3 to hydrolyze ribose-ribose bonds, PAR itself, or O-acetyl-ADP-ribose resulting in the prevention of excessive PAR accumulation[6,18]. These hydrolytic reactions form a biochemical mechanism to counter the PAR-mediated death of cancer cells[4,19,20]. In this study, it was confirmed that the enzymatic activities of PARG and ARH3 were significantly decreased after sustained calcium supply; however, the activity was restored by treatment with calpeptin, a potent, cell-permeable calpain inhibitor. Calpain is a break-down molecule and a calcium-dependent cysteine protease that can also induce ROS production depending on its activation, and it may also damage ion channels, cell adhesion molecules, and cell surface receptors as well as various enzymes[21,22]. On this basis, it is anticipated that calcium-dependent calpain activation would directly induce the enzymatic inactivity of PARG and ARH according to the results of calpeptin application on pancreatic cancer cells. However, the current research outcome was unable to provide a clear mechanistic basis for the enzymatic inactivation of PARG and ARH by calpain. Because PARG and ARH3 are directly related to the accumulation of PAR in pancreatic cancer cells, we wish to investigate this further in more detail.

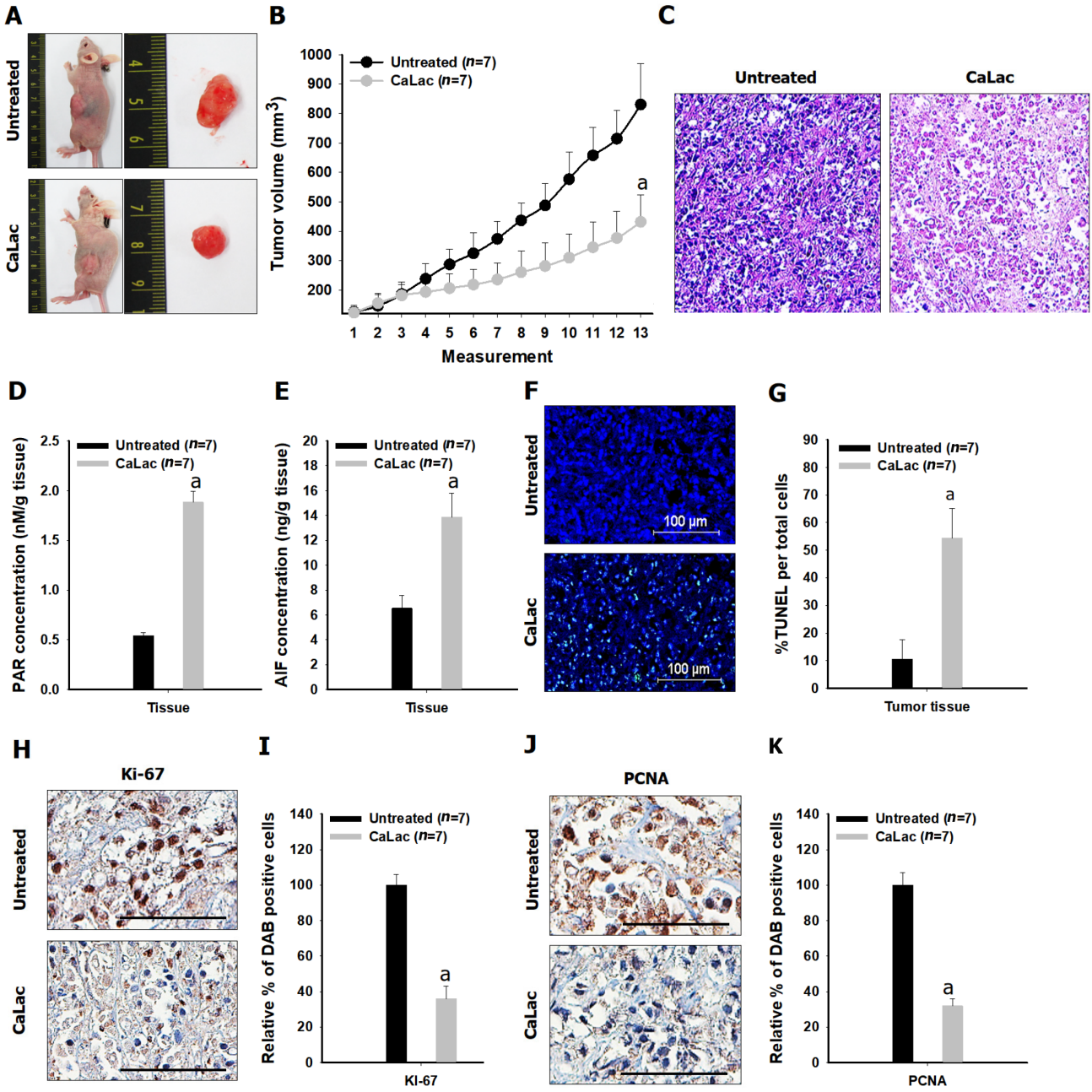


Figure 5 Confirmation of the *in vivo* antitumor effect on pancreatic cancer following sustained calcium administration. A: Macroscopic observation of the tumor mass; B: Comparison of tumor volume between the untreated and calcium-administered groups. Lactate calcium salt (CaLac): 20 mg/kg/mouse, subcutaneous injection, daily for 21 d; C: Hematoxylin and eosin staining. Scale bars: 100 μm; D: Comparison of poly adenosine diphosphate ribose expression in tumor tissues; E: Comparison of apoptosis-inducing factor expression in tumor tissues; F and G: % terminal deoxynucleotidyl transferase-mediated dUTP nick end labeling expression to compare increased apoptosis in tumor tissues. Scale bars: 100 μm; H and I: Comparison of Ki-67 expression in tumor tissues. Scale bars: 50 μm; J and K: Comparison of proliferating cell nuclear antigen in tumor tissues. Scale bars: 50 μm. $^{a}P < 0.001$ *vs* untreated. Results are the mean ± SD. PAR: Poly adenosine diphosphate ribose; AIF: Apoptosis-inducing factor; TUNEL: Transferase-mediated dUTP nick end labeling; PCNA: Proliferating cell nuclear antigen; CaLac: Lactate calcium salt.

CONCLUSION

This study focused on the accumulation of PAR to induce energy deprivation and AIF release by sustained calcium supply to investigate its potential anticancer effect on pancreatic cancer. We demonstrated that an increase in ROS and inhibition of PAR-erasing enzymes might be the main contributors to these effects. However, the connection to the mechanistic role of calcium in enabling the inactivation of PAR-degrading enzyme needs to be elucidated, and additional studies to explore the potential of clinical application are required.

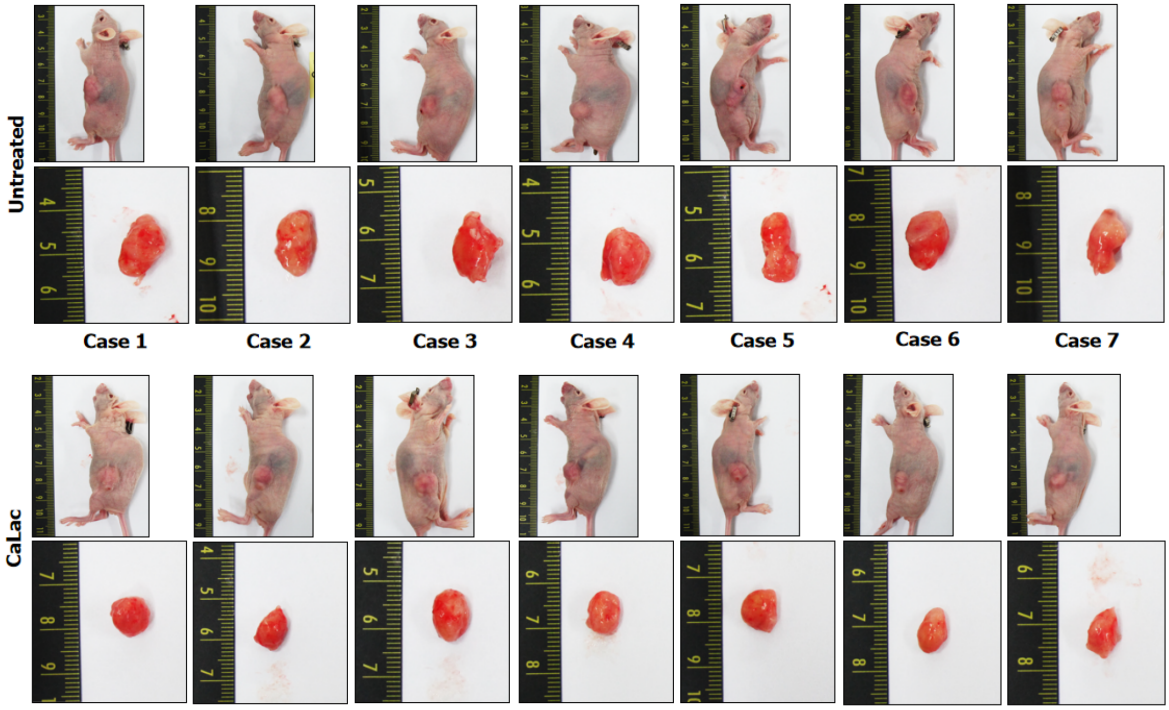


Figure 6 Tumor pictures of all xenograft mice following the end of 20 mg/kg lactate calcium salt administration for 21 d. CaLac: Lactate calcium salt.

ARTICLE HIGHLIGHTS

Research background

The excessive accumulation of poly adenosine diphosphate(ADP)-ribose (PAR) induces energy deprivation and apoptosis-inducing factor (AIF) release from mitochondria resulting in the caspase-independent death of cancer cells, and an increase in PAR is closely related to an increase in reactive oxygen species (ROS).

Research motivation

Increasing ROS can be induced in cancer cells by calcium influx. Therefore, it would be possible to expect the anticancer effect targeting pancreatic cancer through calcium-dependent PAR accumulation.

Research objectives

This study focused on the accumulation of PAR to induce energy deprivation and AIF release by sustained calcium supply to investigate its potential anticancer effect on pancreatic cancer.

Research methods

Two pancreatic cancer cell lines, AsPC-1 and CFPAC-1 were used for the study. Calcium influx and mitochondrial ROS were observed by fluorescence staining. Changes in enzyme levels, as well as PAR accumulation and energy metabolism, were measured using assay kits. AIF-dependent cell death was investigated followed by confirming *in vivo* anticancer effects by sustained calcium administration.

Research results

Mitochondrial ROS levels were elevated with increasing calcium influx into pancreatic cancer cells. Then, excess PAR accumulation, decreased PAR glycohydrolase and ADP-ribosyl hydrolase 3 levels, and energy crisis were observed. *In vitro* and *in vivo* antitumor effects were confirmed to accompany elevated AIF levels.

Research conclusions

Accumulation of PAR was induced by an increase in ROS following sustained calcium supply, which in turn led to the death of pancreatic cancer cells by energy deprivation and AIF expression. Calcium-mediated accumulation of PAR would be a potential strategy for the treatment of pancreatic cancer.

Research perspectives

Although this study visualized the potential anticancer effects of excessive PAR accumulation by sustained calcium supply on pancreatic cancer, elucidating a clear mode of action remains a challenge, and it should be accompanied by further studies to assess its potential for clinical application.

FOOTNOTES

Author contributions: Jeong KY conceived the project and wrote the paper; Jeong KY and Sim JJ designed the experiments; Jeong KY, Sim JJ, and Park MH performed the experiments; Jeong KY, Sim JJ, and Kim HM analyzed the data; and all authors discussed the results and revised the manuscript.

Institutional animal care and use committee statement: Animal care and experimental procedures were authorized by the Institutional Animal Care and Use Committee at Gachon University (IACUC-LCDI-2019-0102, 16 July 2019).

Conflict-of-interest statement: All the authors report no relevant conflicts of interest for this article.

Data sharing statement: No additional data are available.

ARRIVE guidelines statement: The authors have read the ARRIVE guidelines, and the manuscript was prepared and revised according to the ARRIVE guidelines.

Open-Access: This article is an open-access article that was selected by an in-house editor and fully peer-reviewed by external reviewers. It is distributed in accordance with the Creative Commons Attribution NonCommercial (CC BY-NC 4.0) license, which permits others to distribute, remix, adapt, build upon this work non-commercially, and license their derivative works on different terms, provided the original work is properly cited and the use is non-commercial. See: https://creativecommons.org/Licenses/by-nc/4.0/

Country/Territory of origin: South Korea

ORCID number: Keun-Yeong Jeong 0000-0002-4933-3493; Jae Jun Sim 0000-0002-3851-5689; Minhee Park 0000-0002-2513-2080; Hwan Mook Kim 0000-0001-7649-9790.

S-Editor: Wang JJ
L-Editor: A
P-Editor: Qi WW

REFERENCES

1 **Jeong KY**, Park MH. The Significance of Targeting Poly (ADP-Ribose) Polymerase-1 in Pancreatic Cancer for Providing a New Therapeutic Paradigm. *Int J Mol Sci* 2021; **22** [PMID: 33805293 DOI: 10.3390/ijms22073509]
2 **Alemasova EE**, Lavrik OI. Poly(ADP-ribosyl)ation by PARP1: reaction mechanism and regulatory proteins. *Nucleic Acids Res* 2019; **47**: 3811-3827 [PMID: 30799503 DOI: 10.1093/nar/gkz120]
3 **Kamaletdinova T**, Fanaei-Kahrani Z, Wang ZQ. The Enigmatic Function of PARP1: From PARylation Activity to PAR Readers. *Cells* 2019; **8** [PMID: 31842403 DOI: 10.3390/cells8121625]
4 **Wang Y**, Dawson VL, Dawson TM. Poly(ADP-ribose) signals to mitochondrial AIF: a key event in parthanatos. *Exp Neurol* 2009; **218**: 193-202 [PMID: 19332058 DOI: 10.1016/j.expneurol.2009.03.020]
5 **O'Sullivan J**, Tedim Ferreira M, Gagné JP, Sharma AK, Hendzel MJ, Masson JY, Poirier GG. Emerging roles of eraser enzymes in the dynamic control of protein ADP-ribosylation. *Nat Commun* 2019; **10**: 1182 [PMID: 30862789 DOI: 10.1038/s41467-019-08859-x]
6 **Harrision D**, Gravells P, Thompson R, Bryant HE. Poly(ADP-Ribose) Glycohydrolase (PARG) vs. Poly(ADP-Ribose) Polymerase (PARP) - Function in Genome Maintenance and Relevance of Inhibitors for Anti-cancer Therapy. *Front Mol Biosci* 2020; **7**: 191 [PMID: 33005627 DOI: 10.3389/fmolb.2020.00191]
7 **Jain A**, Agostini LC, McCarthy GA, Chand SN, Ramirez A, Nevler A, Cozzitorto J, Schultz CW, Lowder CY, Smith KM, Waddell ID, Raitses-Gurevich M, Stossel C, Gorman YG, Atias D, Yeo CJ, Winter JM, Olive KP, Golan T, Pishvaian MJ, Ogilvie D, James DI, Jordan AM, Brody JR. Poly (ADP) Ribose Glycohydrolase Can Be Effectively Targeted in Pancreatic Cancer. *Cancer Res* 2019; **79**: 4491-4502 [PMID: 31273064 DOI: 10.1158/0008-5472.CAN-18-3645]
8 **Rossi A**, Pizzo P, Filadi R. Calcium, mitochondria and cell metabolism: A functional triangle in bioenergetics. *Biochim Biophys Acta Mol Cell Res* 2019; **1866**: 1068-1078 [PMID: 30982525 DOI: 10.1016/j.bbamcr.2018.10.016]
9 **Bertero E**, Maack C. Calcium Signaling and Reactive Oxygen Species in Mitochondria. *Circ Res* 2018; **122**: 1460-1478 [PMID: 29748369 DOI: 10.1161/CIRCRESAHA.118.310082]
10 **Pazzaglia S**, Pioli C. Multifaceted Role of PARP-1 in DNA Repair and Inflammation: Pathological and Therapeutic Implications in Cancer and Non-Cancer Diseases. *Cells* 2019; **9** [PMID: 31877876 DOI: 10.3390/cells9010041]
11 **Martí JM**, Fernández-Cortés M, Serrano-Sáenz S, Zamudio-Martinez E, Delgado-Bellido D, Garcia-Diaz A, Oliver FJ. The Multifactorial Role of PARP-1 in Tumor Microenvironment. *Cancers (Basel)* 2020; **12** [PMID: 32245040 DOI:

10.3390/cancers12030739]
12 **Jeong KY**, Sim JJ, Park MH, Kim HM. Remodeling of Cancer-Specific Metabolism under Hypoxia with Lactate Calcium Salt in Human Colorectal Cancer Cells. *Cancers (Basel)* 2021; **13** [PMID: 33806179 DOI: 10.3390/cancers13071518]
13 **Hempel N**, Trebak M. Crosstalk between calcium and reactive oxygen species signaling in cancer. *Cell Calcium* 2017; **63**: 70-96 [PMID: 28143649 DOI: 10.1016/j.ceca.2017.01.007]
14 **Gupte R**, Liu Z, Kraus WL. PARPs and ADP-ribosylation: recent advances linking molecular functions to biological outcomes. *Genes Dev* 2017; **31**: 101-126 [PMID: 28202539 DOI: 10.1101/gad.291518.116]
15 **Perillo B**, Di Donato M, Pezone A, Di Zazzo E, Giovannelli P, Galasso G, Castoria G, Migliaccio A. ROS in cancer therapy: the bright side of the moon. *Exp Mol Med* 2020; **52**: 192-203 [PMID: 32060354 DOI: 10.1038/s12276-020-0384-2]
16 **Mashimo M**, Onishi M, Uno A, Tanimichi A, Nobeyama A, Mori M, Yamada S, Negi S, Bu X, Kato J, Moss J, Sanada N, Kizu R, Fujii T. The 89-kDa PARP1 cleavage fragment serves as a cytoplasmic PAR carrier to induce AIF-mediated apoptosis. *J Biol Chem* 2021; **296**: 100046 [PMID: 33168626 DOI: 10.1074/jbc.RA120.014479]
17 **Murata MM**, Kong X, Moncada E, Chen Y, Imamura H, Wang P, Berns MW, Yokomori K, Digman MA. NAD+ consumption by PARP1 in response to DNA damage triggers metabolic shift critical for damaged cell survival. *Mol Biol Cell* 2019; **30**: 2584-2597 [PMID: 31390283 DOI: 10.1091/mbc.E18-10-0650]
18 **Kassab MA**, Yu LL, Yu X. Targeting dePARylation for cancer therapy. *Cell Biosci* 2020; **10**: 7 [PMID: 32010441 DOI: 10.1186/s13578-020-0375-y]
19 **Liu L**, Li J, Ke Y, Zeng X, Gao J, Ba X, Wang R. The key players of parthanatos: opportunities for targeting multiple levels in the therapy of parthanatos-based pathogenesis. *Cell Mol Life Sci* 2022; **79**: 60 [PMID: 35000037 DOI: 10.1007/s00018-021-04109-w]
20 **Fatokun AA**, Dawson VL, Dawson TM. Parthanatos: mitochondrial-linked mechanisms and therapeutic opportunities. *Br J Pharmacol* 2014; **171**: 2000-2016 [PMID: 24684389 DOI: 10.1111/bph.12416]
21 **Randriamboavonjy V**, Kyselova A, Fleming I. Redox Regulation of Calpains: Consequences on Vascular Function. *Antioxid Redox Signal* 2019; **30**: 1011-1026 [PMID: 30266074 DOI: 10.1089/ars.2018.7607]
22 **Johnson DE**. Noncaspase proteases in apoptosis. *Leukemia* 2000; **14**: 1695-1703 [PMID: 10995018 DOI: 10.1038/sj.leu.2401879]

World Journal of Gastroenterology

Submit a Manuscript: https://www.f6publishing.com

World J Gastroenterol 2022 July 21; 28(27): 3435-3454

DOI: 10.3748/wjg.v28.i27.3435

ISSN 1007-9327 (print) ISSN 2219-2840 (online)

ORIGINAL ARTICLE

Basic Study

RING finger and WD repeat domain 3 regulates proliferation and metastasis through the Wnt/β-catenin signalling pathways in hepatocellular carcinoma

Ruo-Peng Liang, Xiao-Xue Zhang, Jie Zhao, Qin-Wei Lu, Rong-Tao Zhu, Wei-Jie Wang, Jian Li, Kai Bo, Chi-Xian Zhang, Yu-Ling Sun

Specialty type: Gastroenterology and hepatology

Provenance and peer review: Unsolicited article; Externally peer reviewed.

Peer-review model: Single blind

Peer-review report's scientific quality classification

Grade A (Excellent): 0
Grade B (Very good): B
Grade C (Good): C
Grade D (Fair): 0
Grade E (Poor): 0

P-Reviewer: Gupta T, India; Limaiem F, Tunisia
A-Editor: Morozov S, Russia

Received: February 7, 2022
Peer-review started: February 7, 2022
First decision: April 5, 2022
Revised: April 16, 2022
Accepted: June 3, 2022
Article in press: June 3, 2022
Published online: July 21, 2022

Ruo-Peng Liang, Jie Zhao, Qin-Wei Lu, Rong-Tao Zhu, Wei-Jie Wang, Jian Li, Kai Bo, Chi-Xian Zhang, Yu-Ling Sun, Department of Hepatobiliary and Pancreatic Surgery, The First Affiliated Hospital of Zhengzhou University, Zhengzhou 450052, Henan Province, China

Xiao-Xue Zhang, Department of Physical Examination, The First Affiliated Hospital of Zhengzhou University, Zhengzhou 450052, Henan Province, China

Corresponding author: Yu-Ling Sun, MD, PhD, Chief Doctor, Department of Hepatobiliary and Pancreatic Surgery, The First Affiliated Hospital of Zhengzhou University, No. 50 West Jianshe Road, Zhengzhou 450052, Henan Province, China. ylsun@zzu.edu.cn

Abstract

BACKGROUND

Hepatocellular carcinoma (HCC) exhibits high invasiveness and mortality rates, and the molecular mechanisms of HCC have gained increasing research interest. The abnormal DNA damage response has long been recognized as one of the important factors for tumor occurrence and development. Recent studies have shown the potential of the protein RING finger and WD repeat domain 3 (RFWD3) that positively regulates p53 stability in response to DNA damage as a therapeutic target in cancers.

AIM

To investigate the relationship between HCC and RFWD3 *in vitro* and *in vivo* and explored the underlying molecular signalling transduction pathways.

METHODS

RFWD3 gene expression was analyzed in HCC tissues and adjacent normal tissues. Lentivirus was used to stably knockdown RFWD3 expression in HCC cell lines. After verifying the silencing efficiency, Celigo/cell cycle/apoptosis and MTT assays were used to evaluate cell proliferation and apoptosis. Subsequently, cell migration and invasion were assessed by wound healing and transwell assays. In addition, transduced cells were implanted subcutaneously and injected into the tail vein of nude mice to observe tumor growth and metastasis. Next, we used lentiviral-mediated rescue of RFWD3 shRNA to verify the phenotype.

Finally, the microarray, ingenuity pathway analysis, and western blot analysis were used to analyze the regulatory network underlying HCC.

RESULTS

Compared with adjacent tissues, RFWD3 expression levels were significantly higher in clinical HCC tissues and correlated with tumor size and TNM stage ($P < 0.05$), which indicated a poor prognosis state. RFWD3 silencing in BEL-7404 and HCC-LM3 cells increased apoptosis, decreased growth, and inhibited the migration in shRNAi cells compared with those in shCtrl cells ($P < 0.05$). Furthermore, the *in vitro* results were supported by the findings of the *in vivo* experiments with the reduction of tumor cell invasion and migration. Moreover, the rescue of RFWD3 shRNAi resulted in the resumption of invasion and metastasis in HCC cell lines. Finally, gene expression profiling and subsequent experimental verification revealed that RFWD3 might influence the proliferation and metastasis of HCC *via* the Wnt/β-catenin signalling pathway.

CONCLUSION

We provide evidence for the expression and function of RFWD3 in HCC. RFWD3 affects the prognosis, proliferation, invasion, and metastasis of HCC by regulating the Wnt/β-catenin signalling pathway.

Key Words: RING finger and WD repeat domain 3; Hepatocellular carcinoma; Invasion; Proliferation; Metastasis; Wnt/β-catenin signaling pathways

©The Author(s) 2022. Published by Baishideng Publishing Group Inc. All rights reserved.

Core Tip: The relationship between RING finger and WD repeat domain 3 (RFWD3) and tumorigenesis process has been reported occasionally, but the relationship between RFWD3 and hepatocellular carcinoma (HCC) is still unclear. This research reports the significant role of RFWD3 in HCC development by using bioinformatics databases, clinical samples, cell phenotypes, *in vivo* experiments, and microarray analyses. It provides evidence that RFWD3 expression might affect the tumorigenesis process of HCC by regulating the Wnt/β-catenin signalling pathways, laying a basic foundation for future relevant studies.

Citation: Liang RP, Zhang XX, Zhao J, Lu QW, Zhu RT, Wang WJ, Li J, Bo K, Zhang CX, Sun YL. RING finger and WD repeat domain 3 regulates proliferation and metastasis through the Wnt/β-catenin signalling pathways in hepatocellular carcinoma. *World J Gastroenterol* 2022; 28(27): 3435-3454
URL: https://www.wjgnet.com/1007-9327/full/v28/i27/3435.htm
DOI: https://dx.doi.org/10.3748/wjg.v28.i27.3435

INTRODUCTION

Hepatocellular carcinoma (HCC) is one of the most common malignant tumors and is highly invasive with a high mortality rate[1]. Reportedly, the incidence of HCC has increased rapidly by approximately 3%–4% *per* year in the United States[2]. Despite advances in medical research, early diagnosis of HCC remains difficult, and most patients are diagnosed with middle-or late-stage disease[3-5]. Moreover, even though some progress has been made in the clinical diagnosis and treatment of HCC, the long-term survival after treatment for patients diagnosed with early-stage HCC is low[6]. With the development of biomedicine, more basic studies have been carried out on HCC, but the underlying mechanism remains unclear, warranting promising interventions[7,8].

Multiple signal transduction pathways have been demonstrated to be involved in cellular responses to stress. For example, the ubiquitin-proteasome system (UPS) plays an important role in DNA damage repair, transcription regulation, cell cycle arrest, and apoptosis[9-11]. Several studies have focused on the role of the protein RING finger and WD repeat domain 3 (RFWD3) in the ataxia telangiectasia-mutated (ATM)/ATM-Rad3-related pathways of DNA damage response[12-16]. RFWD3 contains a RING finger domain and displays *in vitro* E3 ubiquitin ligase activity. It comprises an SQ-rich region in the N-terminus, a coiled-coil domain, and a WD40 domain in the C-terminus. In addition, sequence comparison revealed that the residues flanking serine 46 and serine 63 of RFWD3 are conserved[17]. According to the current literature, RFWD3 accumulates at stalled replication forks as part of the DNA damage response[18,19]. At these sites, RFWD3 co-localizes with replication protein A (RPA) and binds *via* its WD40 domain at the C-terminus to RPA2[20,21]. It functions in replication checkpoint signalling

upon replication stress and promotes replication fork restart after homologous recombination (HR)[22, 23]. RFWD3 is regarded as a tumor suppressor gene, and recent functional and mechanistic studies have indicated that it maintains the stability of p53[24]. Feeney *et al*[25] reported that it facilitates RPA-mediated DNA damage response[25]. Furthermore, RFWD3 is required for the proliferation of non-small-cell lung cancer, gastric carcinoma, and colorectal cancer cells and may have an important role[26-28]. However, the relationship between HCC and RFWD3 has not been explored.

In a preliminary experiment using a small number of HCC samples, our team found that RFWD3 expression was higher in HCC tissues than in adjacent non-cancerous tissues[29]. To rule out the effects of small sample numbers, the results were then verified using the open-source database. For this purpose, we chose RNA SEQ data (FPKM normalized) of liver cancer from The Cancer Genome Atlas (TCGA) database directly downloaded from the UCSC Xena database and further transformed it into log2 (TPM + 1) format. The results were concordant with our preliminary findings. Furthermore, the immunohistochemical analysis demonstrated that RFWD3 expression was associated with the clinical TNM stage (and with survival, according to the database). Therefore, in this study, we tested the hypothesis that RFWD3 plays a significant role in HCC development.

To test this hypothesis, in this study, we investigate the relationship between HCC and RFWD3 *in vitro* using human HCC cell lines and *in vivo* using HCC xenograft models in nude mice. Further, we unravel the underlying molecular signalling transduction pathways in HCC. The findings of this study provide evidence for the first time that RFWD3 plays a significant role in HCC cell proliferation and may serve as a potential therapeutic target for HCC.

MATERIALS AND METHODS

Tissue samples

Sixty tissue sample pairs (HCC and adjacent normal liver tissues) were obtained from clinical patients who underwent surgical HCC resection at the First Affiliated Hospital of Zhengzhou University (Zhengzhou, China). Before the operation, all patients were informed that the resected tissues could be used for research, and consent was obtained from each patient. After resection, the tissues were snap-frozen immediately and stored at −80 °C. All the experimental procedures were approved by the Ethics Committee of the First Affiliated Hospital of Zhengzhou University (Approval No. 10[2017]).

TCGA liver HCC cohort assessment

TCGA liver HCC cohort included 374 cancer tissues and 50 adjacent normal tissues. According to the expression level of *RFWD3* gene, we used the best cut-off value to divide the HCC patients into high and low expression groups by the Surv function of the survminer package. Then, the Kaplan-Meier method and log-rank test were used to evaluate the differences in overall survival and recurrence-free survival between the two groups. All data processing, statistical analyses, and graphical presentations (of this section) were carried out using R 4.0.5 software.

Immunohistochemical analysis of human HCC tissues

HCC tissue microarray data of 60 HCC and adjacent tissues, including some basic clinical data shown in Table 1, were obtained from BiochipTech (Zhengzhou, China). Immunohistochemistry (IHC) was performed using a 1:100 dilution of a primary antibody against *RFWD3* (Multi Sciences, Hangzhou, China), and all immunohistochemical procedures were performed according to a common standard protocol. First, the expression levels of RFWD3 between HCC and adjacent tissues were compared with a histochemical score (H-score). Then, a scoring system that combined the staining intensity (SI: 0, negative; 1, weak; 2, moderate; 3, strong) and the percentage of positive cells (PP: 0, < 5%; 1, 6%–25%; 2, 26%–50%; 3, 51%–75%; 4, > 75%) was used to compare the correlation of clinical data in patients with RFWD3 expression (SI × PP > 4 was considered high expression; SI × PP ≤ 4 was considered low expression).

Cell lines and culturing, lentivirus vector construction, and transduction

The human HCC cell lines BEL-7404 and HCC-LM3, maintained in our laboratory, were cultured (BEL-7404: 10% FBS, 90% RPMI-1640; HCC-LM3: 10% FBS, 90% DMEM; all purchased from Gibco, United States) according to the American type culture collection protocol. All cells were cultured in 50 ml/L CO_2 at 37°C in a moderately humid environment. The RFWD3 siRNA sequence (5-CAGAGAATGATG-GCAACAT-3) was synthesized and cloned into the AgeI/EcoRI sites of the lentivirus-based GV493-puromycin vector (shRNAi). The negative control lentiviral vector (5-TTCTCCGAACGTGTCACGT-3) was used as a control (shCtrl). The cells were divided into two groups (shCtrl and shRNAi), seeded in six-well plates, and allowed to grow until the logarithmic phase and less than 70% confluency. After verifying the transfection efficiency, the cells were harvested for subsequent *in vivo* and *in vitro* experiments. Additionally, the *RFWD3*-reverse mutation sequence (5-CTGAGAACGACGGAAATAT-3) was synthesized and cloned into the *BamHI*/*AgeI* sites of the lentivirus-based GV557-neomycin vector

Table 1 Clinicopathological features in hepatocellular carcinoma tissue microarrays

Clinicopathological parameters	Number	Expression of RFWD3		*P* value
		Low[1]	High[1]	
Total	60	25	35	
Gender				
Male	24	9	15	
Female	36	16	20	0.592
HBsAg				
Positive	39	17	22	
Negative	21	8	13	0.68
Age (yr)				
< 60	34	17	17	
≥ 60	26	8	18	0.134
Tumor size				
< 5 cm	27	15	12	
≥ 5 cm	33	10	23	0.048[a]
TNM stage[2]				
I–II	31	17	14	
III–IV	29	8	21	0.032[a]

[1]Staining intensity (SI) × percentage of positive (PP) > 4 was considered high expression; SI × PP < 4 was considered low expression.
[2]TNM stage was determined according to the guidelines of the American Joint Committee on Cancer (2010).
[a]$P < 0.05$.
RFWD3: RING finger and WD repeat domain 3.

(KD-OE). The virus without anti-Smad served as negative controls (KD-OE-NC) for subsequent phenotypic validation. The GV493-puromycin and GV557-neomycin vectors were obtained from GeneChem (Shanghai, China).

Quantitative reverse transcription-polymerase chain reaction

Quantitative reverse transcription-polymerase chain reaction (qRT-PCR) was used to detect the mRNA expression level of RFWD3 using the following primers: Forward: 5′-AGAGTATGGAGGGGT-TGTTGAC-3′ and reverse: 5′-TAGAAGCAGAAGGTAGCAGAGG-3′. Total RNA was extracted from tissues and cells using TRIzol reagent (Thermo Fisher Scientific, United States) and reverse transcribed into cDNA using a Prime-Script RT Reagent Kit with gDNA Eraser (Takara Bio, Japan). Following a common standard protocol, qRT-PCR was performed in a total volume of 10 μL on a 7900-HT Fast Real-time PCR System (Applied Biosystems Inc., United States) to evaluate RFWD3 expression in 60 pairs of HCC tissues and determine the RFWD3 knockdown efficiency in cells transduced with shCtrl and shRNAi.

Western blot analysis

To determine the RFWD3 virus transfection efficiency in cells transduced with shCtrl, shRNAi, KD-OE, and KD-OE-NC, the levels of RFWD3 protein expression were assessed by western blot (WB). Briefly, the total protein was extracted by incubating the cells in RIPA lysis buffer (Thermo Fisher Scientific, United States) supplemented with a protease inhibitor cocktail (Thermo Fisher Scientific, United States) for 1 h on ice, followed by sonication (Shanghai Experimental Instruments, China) for three 5 s cycles on ice. After centrifugation (14000 ×*g*, 4 °C, 15 min), the supernatant was collected for protein concentration measurement using a bicinchoninic acid protein assay kit (Pierce Biotechnology, United States). Denatured protein samples (30 μg/10 μL) were separated by SDS-PAGE (Invitrogen, United States) and transferred to polyvinylidene fluoride membranes (Bio-Rad, United States). Afterward, the membranes were blocked with 5% non-fat milk (BD Biosciences, United States) dissolved in 30 mL Tris-buffered saline with Tween-20 (TBST) for 2 h at common room temperature. The membranes were then incubated overnight at 4 °C with primary antibodies against GAPDH (1:1000; Abcam, United States) and RFWD3 (1:1000; Multi Sciences, Hangzhou, China). After three 5 min washes in TBST with agitation, the membranes were incubated for 1 h at room temperature with the appropriate secondary

horseradish peroxidase-linked antibodies, including goat anti-rabbit IgG for GAPDH (1:2000; Abcam, United States) and goat anti-rabbit IgG for RFWD3 (*1:2000*; Multi Sciences, Hangzhou, China). An ECL kit (Pierce Biotechnology, United States) was used to visualize the protein bands.

Cell growth and proliferation assays

A Celigo imaging cytometer (Celigo; Nexcelom Bioscience, United States) and MTT assays were used to detect the number of cells at each time point, and the growth status of the cells was analyzed. For the Celigo assay, cells in the logarithmic phase were digested with trypsin (Sangon Biotech, Shanghai, China), seeded in 96-well plates (2000 cells/well in 100 μL medium) with three wells *per* condition, and cultured in a 37 °C incubator with 50 mL/L CO_2. From the first day to the fifth day after seeding, the plate was subjected to high-throughput screening every day. GFP fluorescence was measured in each scan to generate a five days cell proliferation curve. For the MTT assay, two groups of cells were seeded in 96-well plates (2000 cells/well) with three wells *per* condition and incubated at 37 °C for six consecutive days. Cell viability was analyzed every 24 h by washing the cells twice with PBS and adding MTT solution (5 mg/mL) to each well. After 4 h of incubation, the supernatant in each well was removed, and 100 μL DMSO was added to solubilize the formazan crystals. After 10 min, the optical density (OD) was measured at an excitation wavelength of 490 nm and an emission wavelength of 570 nm using a microplate reader (VarioskanFlash; Thermo Fisher Scientific, United States).

Cell cycle assays

Cell cycle progression was examined using propidium iodide (PI; Sigma, United States) and RNase A (Thermo Fisher, United States). Cells in the logarithmic growth phase in six-well culture plates were digested with trypsin (Sangon Biotech, Shanghai, China) and diluted with the culture medium. Three replicate tubes were analyzed for both the shCtrl and shRNAi groups (1×10^6 cells/tube). The cells were centrifuged at 1300 rpm for 5 min, and the supernatant was discarded. The cell pellet was washed with pre-cooled D-Hanks equilibrium solution (4 °C with pH = 7.2–7.4), and the harvested cells were fixed with 70% cold ethanol at 4 °C overnight. Afterward, the cells were washed twice with 4 °C D-Hanks solution and incubated with 10 mg/mL RNase at 37 °C. Cell cycle progression was monitored by staining the nuclei with PI. The fluorescence of DNA-bound PI in cells was measured using flow cytometry (FCM; FC500 flow cytometer; Cytomics, United States). Finally, ModFit LT software (Windows version 4.0; Verity Software House, United States) was used to analyze the cell populations in different phases of the cell cycle.

Cell apoptosis assays

Cell apoptosis was assayed using an Annexin V-APC/PI apoptosis detection kit (Biosciences, Thermo Fisher, United States). Cells in the logarithmic phase were digested with trypsin (Sangon Biotech, Shanghai, China) and diluted with the culture medium. Three replicate tubes each were analyzed for the shCtrl, shRNAi, KD-OE, and KD-OE-NC groups of each cell line (1×10^4 cells/tube). The cells were centrifuged at 1300 rpm for 5 min, and the supernatant was discarded. The cell pellet was washed with a pre-cooled D-Hanks equilibrium solution (4 °C with pH = 7.2–7.4). The cells were then washed with 1 × binding buffer, centrifuged at 1300 rpm for 3 min, and resuspended in 200 μL 1 × binding buffer. Next, 10 μL Annexin V-APC staining solution was added, and the samples were incubated for 10–15 min at room temperature in the dark. Finally, apoptosis was detected in the samples.

Cell invasion and migration assays

Cell migration was assayed using wound healing and transwell assays. For the wound-healing assay, cells were plated in 6-well plates and scratched with a sterile pipette tip. The cells were then imaged using a microscope (Olympus, Japan) to observe migration after 12 and 24 h. For the invasion and migration assays, the upper surfaces of transwell chambers (Costar, Cambridge, MA, United States) were uncoated (for the migration experiments) or coated with Matrigel (1:4, BD, United States) (for the invasion experiments). Cells were then added to the upper chambers containing 200 μL serum-free medium (BEL-7404: RPMI-1640; HCC-LM3: DMEM) *per* well, and 500 μL medium (with 10% FBS) was added to the lower chambers. After 48 h, the chambers were cleaned, stained with hematoxylin, transferred to glass slides after the operation, and then observed under a microscope (Olympus, Japan). Six fields *per* chamber were used to quantify the invaded cell numbers with 100 × and 200 × magnifications.

Establishment of HCC xenograft models in nude mice

All animal experimental protocols were conducted following the ARRIVE (Animal Research: Reporting In Vivo Experiments) guidelines (https://www.nc3rs.org.uk/arrive-guidelines) and performed following protocols approved by the Research Ethics Committee of the First Affiliated Hospital of Zhengzhou University (Approval No. 10[2017]). Nude mice were purchased from Shanghai B&K Universal Group Limited (certificate number: SCXK 2013-0016; Shanghai, China). For the proliferation assay, 5×10^6 HCC-LM3 cells stably transduced with the lentiviral pSC-1-GFP vector carrying shCtrl or shRNAi were suspended in PBS and injected subcutaneously into the flank region of 6-week-old male

athymic nude mice (six mice in each group). For the metastasis assay, 2×10^6 HCC-LM3 cells transduced as described above were injected into the tail vein of nude mice. The animals were acclimatized to laboratory conditions (23 °C, 12 h/12 h light/dark, 50% humidity, ad libitum access to food and water). After four weeks, the mice were euthanized by barbiturate overdose (intravenous injection, 150 mg/kg pentobarbital sodium) for tissue collection and photographed.

Microarray-based gene expression analysis

To elucidate the molecular mechanisms involved in the association between RFWD3 and HCC, we performed microarray-based gene expression analysis to compare gene expression between the shCtrl and shRNAi groups. We then used ingenuity pathway analysis (IPA) to explore the molecular signal transduction pathways involved in HCC. All procedures were performed according to a common protocol, and assistance was provided by the Shanghai Biotechnology Corporation (SBC, Shanghai, China).

Statistical Analysis

Statistical analyses and related statistical illustrations were performed using SPSS (version 21.0; IBM, Armonk, NY, United States) and GraphPad Prism software (ver. *5.0* for Windows; GraphPad Software Inc., United States). The Pearson chi-square test was used to determine the correlation between clinical characteristics and immunohistochemical staining. Other results are expressed as mean ± SD. A t-test was used to compare the two groups, and a P value of < 0.05 was considered statistically significant.

RESULTS

RFWD3 is ppregulated in HCC and correlated with worse prognosis

RFWD3 expression was examined in HCC tissues and matched adjacent normal tissues. IHC analysis of 60 tissue pairs revealed that HCC tissues exhibited a higher H-score than non-tumor tissues (Figure 1A) [30]. This result was supported by the qRT-PCR analysis of 54 tissue sample pairs (some outlier value pairs were excluded) (Figure 1B). These results were concordant with the RFWD3 expression data obtained by analyzing the bioinformatics database (Figure 1C). In addition, the bioinformatics database showed that higher RFWD3 expression represents a worse prognosis in HCC (Figure 1D and E). These data indicate that high RFWD3 expression might predict poor HCC development and prognosis (Table 1).

Validation of lentiviral-mediated knockdown efficiency in cell lines

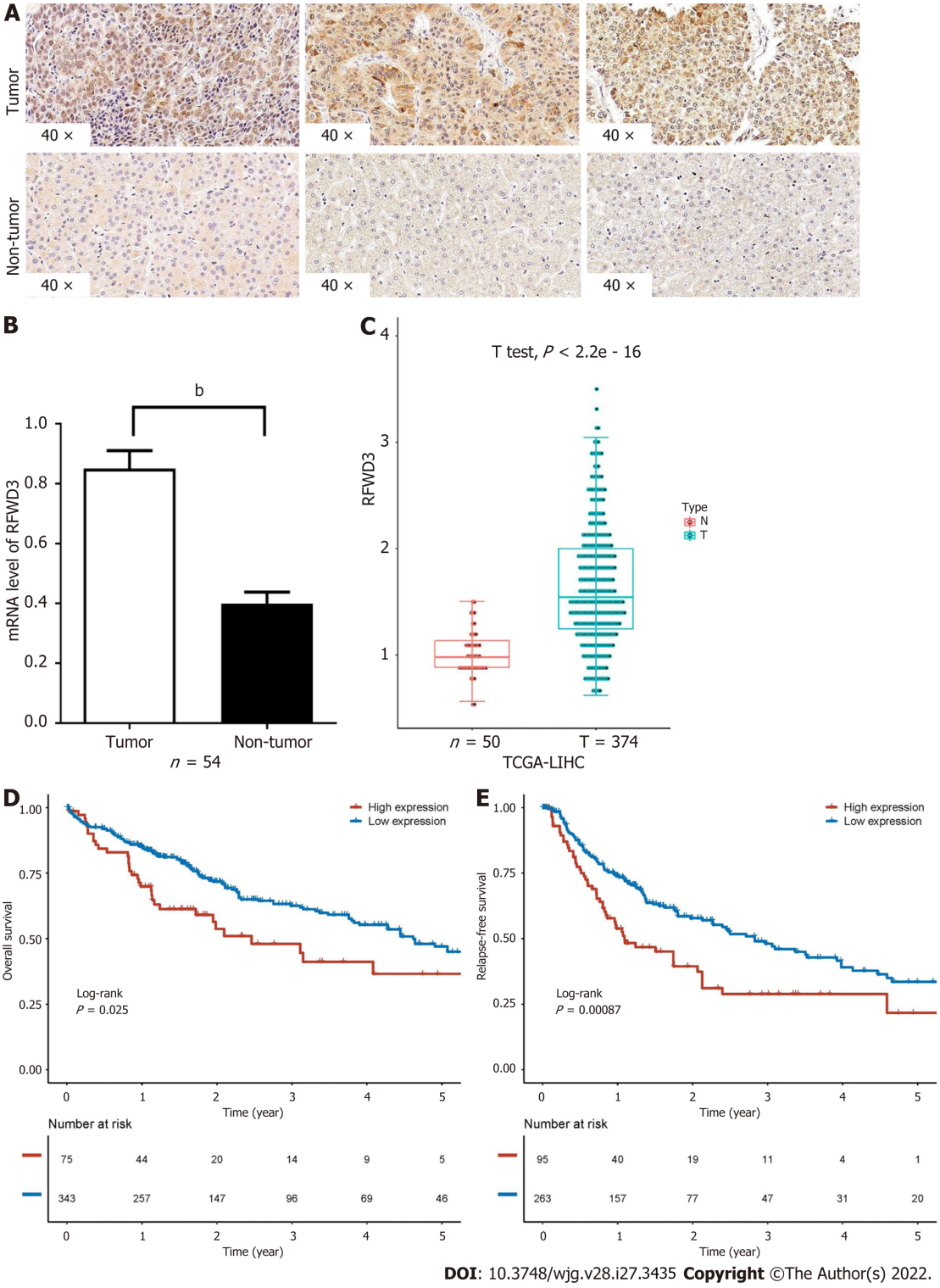
After verifying the high expression of RFWD3 in HCC tissues, we selected HCC cell lines for further *in vitro* experiments. BEL-7404, HCC-LM3, SMMC-7721, and BEL-7402 cells were evaluated for the stable expression of RFWD3. Based on qRT-PCR and cell growth analyses, we chose BEL-7404 and HCC-LM3 cells for lentiviral-mediated knockdown of RFWD3 expression (Figure 2A). After lentiviral transduction, compared with the shCtrl group, the shRNAi group showed obvious knockdown of RFWD3 (qRT-PCR: BEL-7404: $P < 0.01$; HCC-LM3: $P < 0.01$) (Figure 2B). These results were subsequently confirmed with WB analysis and GFP fluorescence imaging (Figure 2C and D).

RFWD3 knockdown inhibits HCC growth and proliferation in vitro

A high-content screening assay (Celigo) was performed to monitor cell growth for five days. The total cell count and growth rate were lower in the shRNAi group than in the shCtrl group (Figure 3A). To further verify these results, we used an MTT assay. After five days of incubation in the same environment, consistent with the Celigo results, the OD value was significantly lower in the shRNAi group than that in the shCtrl group (Figure 3B). Taken together, these results indicate that RFWD3 knockdown significantly reduced the proliferation of HCC cells.

RFWD3 knockdown induces cell cycle arrest

To determine whether RFWD3 affects cell proliferation by regulating the cell cycle, we used PI staining to evaluate cell cycle progression. In the shCtrl and shRNAi groups, the cell cycle distributions were as follows (presented as the mean value of three replicates). For BEL-7404 shCtrl cells, 40.09% were in G0/G1 phase, 35.01% were in the S phase, and 24.9% were in the G2/M phase, while for BEL-7404 shRNAi cells, 37.82% were in G0/G1 phase, 30.03% were in S phase, and 32.15% were in G2/M phase. For HCC-LM3 shCtrl cells, 55.07% were in G0/G1 phase, 36.98% were in the S phase, and 7.95% were in the G2/M phase, while for HCC-LM3 shRNAi cells, 54.98% were in G0/G1 phase, 29.84% were in S phase, and 15.18% were in G2/M phase. Compared with shCtrl cells, shRNAi cells showed a reduced percentage of cells in G0/G1 (BEL-7404: $P < 0.01$) and S phase (BEL-7404: $P < 0.01$; HCC-LM3: $P < 0.01$), and the fraction of cells in the G2/M phase was significantly increased (BEL-7404: $P < 0.01$; HCC-LM3: $P < 0.01$). These results indicated that RFWD3 knockdown blocked cell cycle progression through the G2/M phase (Figure 3C and D).

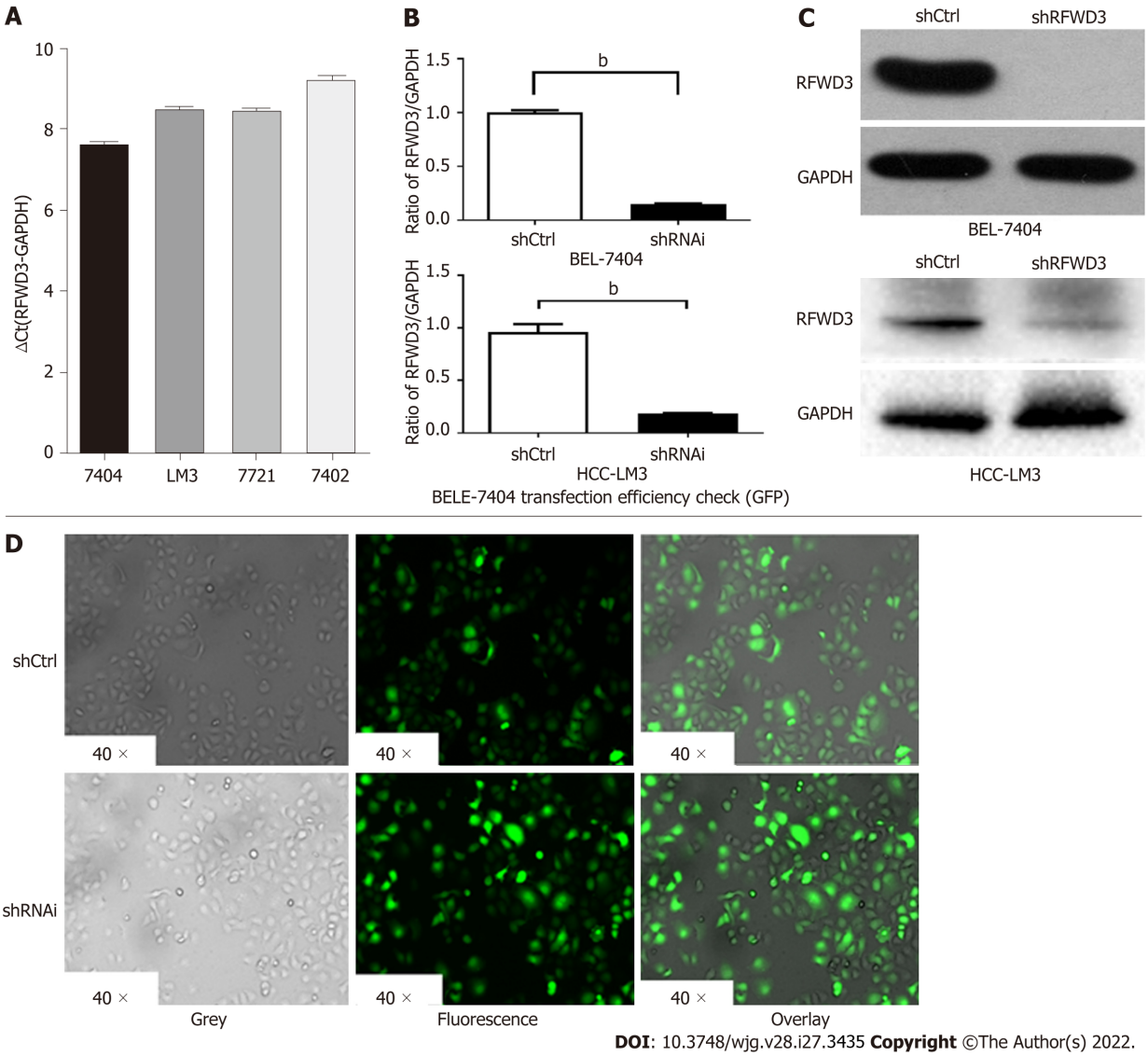


DOI: 10.3748/wjg.v28.i27.3435 **Copyright** ©The Author(s) 2022.

Figure 1 Expression of RING finger and WD repeat domain 3 in hepatocellular carcinoma and its correlation with a worse prognosis. A: RING finger and WD repeat domain 3 (RFWD3) expression in hepatocellular carcinoma (HCC) tumor and non-tumor tissues detected using immunohistochemical staining; B: Expression analysis of RFWD3 in 54 tissue sample pairs (some invalid samples were removed) using quantitative reverse transcription-polymerase chain reaction ($^bP < 0.01$); C: Comparison of RFWD3 expression between tumor and non-tumor tissues in HCC patients (T = 374, *n* = 50, the data source is the Cancer Genome Atlas (TCGA) (TCGA) database); D and E: Kaplan-Meier survival curves of HCC patients with high and low expression of RFWD3 (*n* = 91, the data source is the TCGA database).

RFWD3 knockdown increased cell apoptosis

To determine whether RFWD3 affects cell proliferation by inducing apoptosis, an Annexin V-APC/PI apoptosis detection kit (AV/PI) was used to detect apoptosis in the two groups of cells by FCM. The apoptosis ratios were (presented as the mean value of three replicates) 4.47 ± 0.3748 for BEL-7404 shCtrl cells, 9.77 ± 0.1142 for BEL-7404 shRNAi cells, 2.14 ± 0.2234 for HCC-LM3 shCtrl cells, and 9.01 ± 0.2230



DOI: 10.3748/wjg.v28.i27.3435 **Copyright** ©The Author(s) 2022.

Figure 2 Validation of lentivirus knockdown efficiency in cell lines. A: RING finger and WD repeat domain 3 (RFWD3) expression in BEL-7404 and Hepatocellular carcinoma (HCC)-LM3 cells obtained using quantitative reverse transcription-polymerase chain reaction (qRT-PCR) analysis; B and C: The shRNAi group shows obvious knockdown of RFWD3 [BEL-7404: qRT-PCR: $^{b}P < 0.01$, western blot (WB): $^{b}P < 0.01$; HCC-LM3: qRT-PCR: $^{b}P < 0.01$, WB: $^{b}P < 0.01$]; D: Confirmation of the lentivirus transduction efficiency using GFP fluorescence imaging.

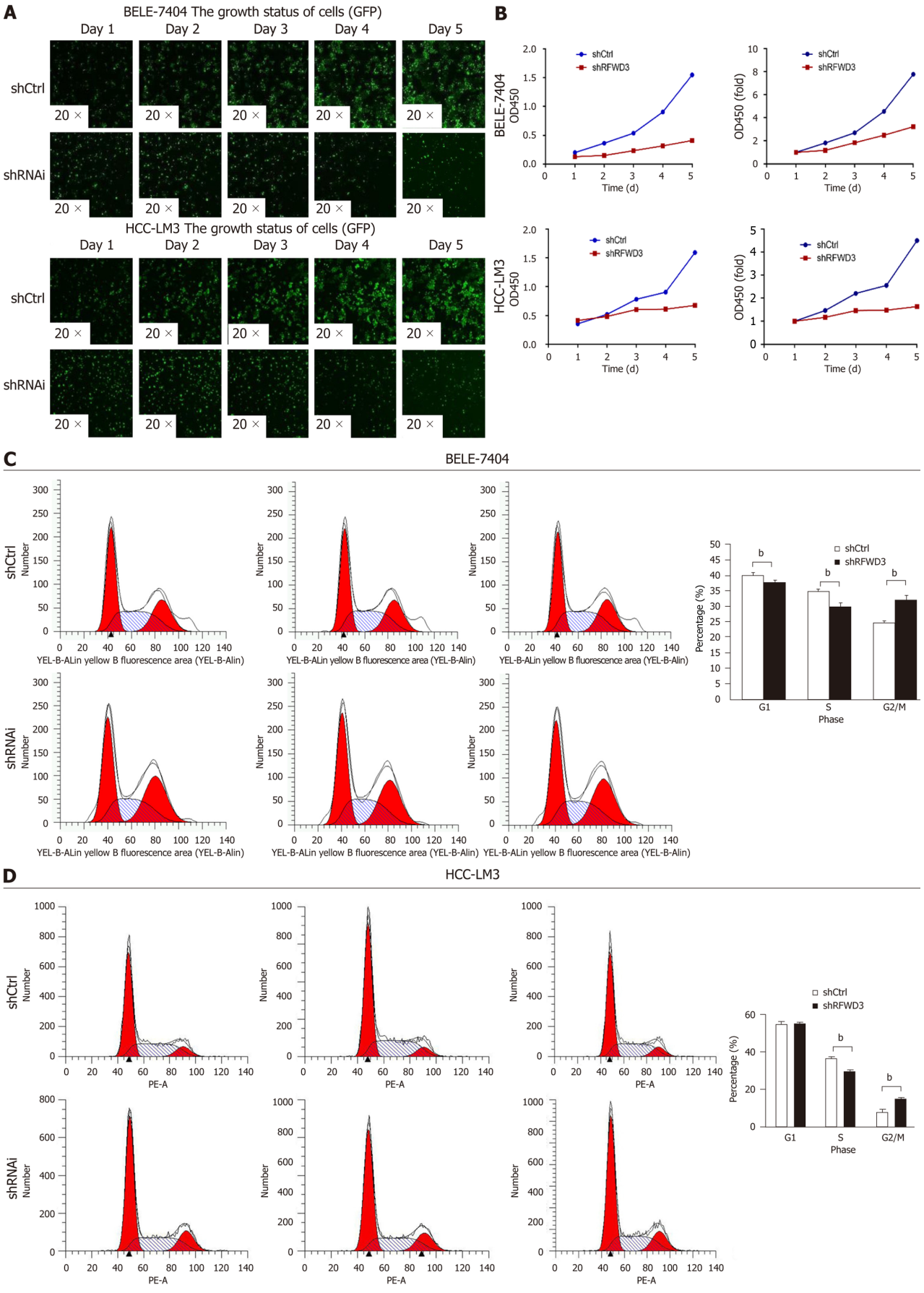
for HCC-LM3 shRNAi cells. Compared with shCtrl cells, shRNAi cells had a higher apoptosis rate (BEL-7404: $P < 0.01$; HCC-LM3: $P < 0.01$). This result demonstrated that RFWD3 knockdown increased the apoptosis ratio, thus affecting the proliferation of HCC cells (Figure 3E and F).

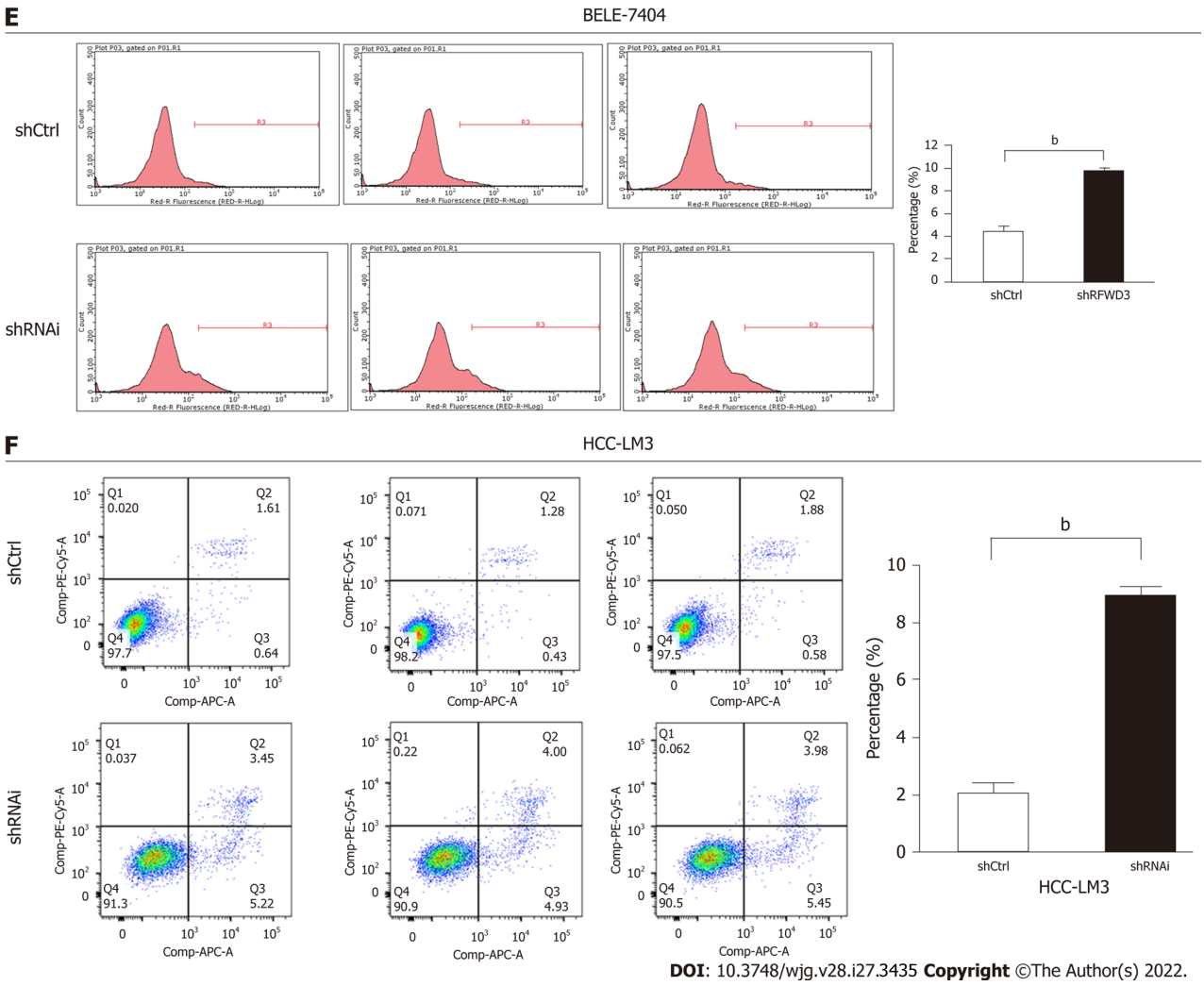
RFWD3 knockdown reduced HCC cell invasion and migration

Wound healing and transwell assays were used to evaluate HCC cell invasion and migration. In the wound healing assay, the shCtrl groups exhibited better healing ability ($P < 0.05$). After 12 h, the wound area was 103.40 ± 1.32 in BEL-7404 shCtrl cells, 125.90 ± 4.46 in BEL-7404 shRNAi cells, 145.40 ± 0.84 in HCC-LM3 shCtrl cells and 159.50 ± 2.21 in HCC-LM3 shRNAi cells. Over time, the difference in the size of the wound area between the two groups increased. After 24 h, the wound area was 22.97 ± 0.22 in BEL-7404 shCtrl cells, 60.94 ± 2.41 in BEL shRNAi cells, 60.22 ± 12.68 in HCC-LM3 shCtrl cells and 134.40 ± 0.84 in HCC-LM3 shRNAi cells (Figure 4A). We next examined cell migration and invasion with transwell assays. The migration of both BEL-7404 and HCC-LM3 shRNAi cells was attenuated compared with shCtrl cells ($P < 0.05$). Similar results were observed in the invasion assay (Figure 4B). These data revealed that RFWD3 knockdown reduced HCC cell invasion and migration.

RFWD3 knockdown decreased HCC cell proliferation, invasion, and metastasis in vivo

We established an HCC xenograft model in nude mice to verify the results *in vivo*. HCC-LM3 shCtrl and shRNAi cells were injected subcutaneously (Figure 5A) and into the tail vein (Figure 5B) of nude mice (six mice in each group). After four weeks, the mice were euthanized by cervical dislocation. The tumors


A
BELE-7404 The growth status of cells (GFP)
Day 1
Day 2
Day 3
Day 4
Day 5
shCtrl
shRNAi
20 ×
HCC-LM3 The growth status of cells (GFP)
B
BELE-7404 OD450
HCC-LM3 OD450
OD450 (fold)
shCtrl
shRFWD3
Time (d)
C
BELE-7404
shCtrl
shRNAi
Number
YEL-B-ALin yellow B fluorescence area (YEL-B-Alin)
Percentage (%)
G1
S
G2/M
Phase
D
HCC-LM3
PE-A



DOI: 10.3748/wjg.v28.i27.3435 **Copyright** ©The Author(s) 2022.

Figure 3 RING finger and WD repeat domain 3 knockdown inhibits cell growth and proliferation and induces cell cycle arrest and apoptosis. A: Cell growth and proliferation of BEL-7404, Hepatocellular carcinoma (HCC)-LM3 shRNAi, and shCtrl cells continuously monitored using a Celigo instrument for five days; B: MTT assay demonstrating that RING finger and WD repeat domain 3 siRNA significantly reduced the proliferation of HCC cells; C and D: The cell cycle progression evaluated by flow cytometry (FCM) with propidium iodide (PI) and RNase A ($^bP < 0.01$); E and F: FCM to assess the apoptosis in shRNAi and shCtrl groups of cells using Annexin V-APC/PI Apoptosis Detection Kit ($^bP < 0.01$).

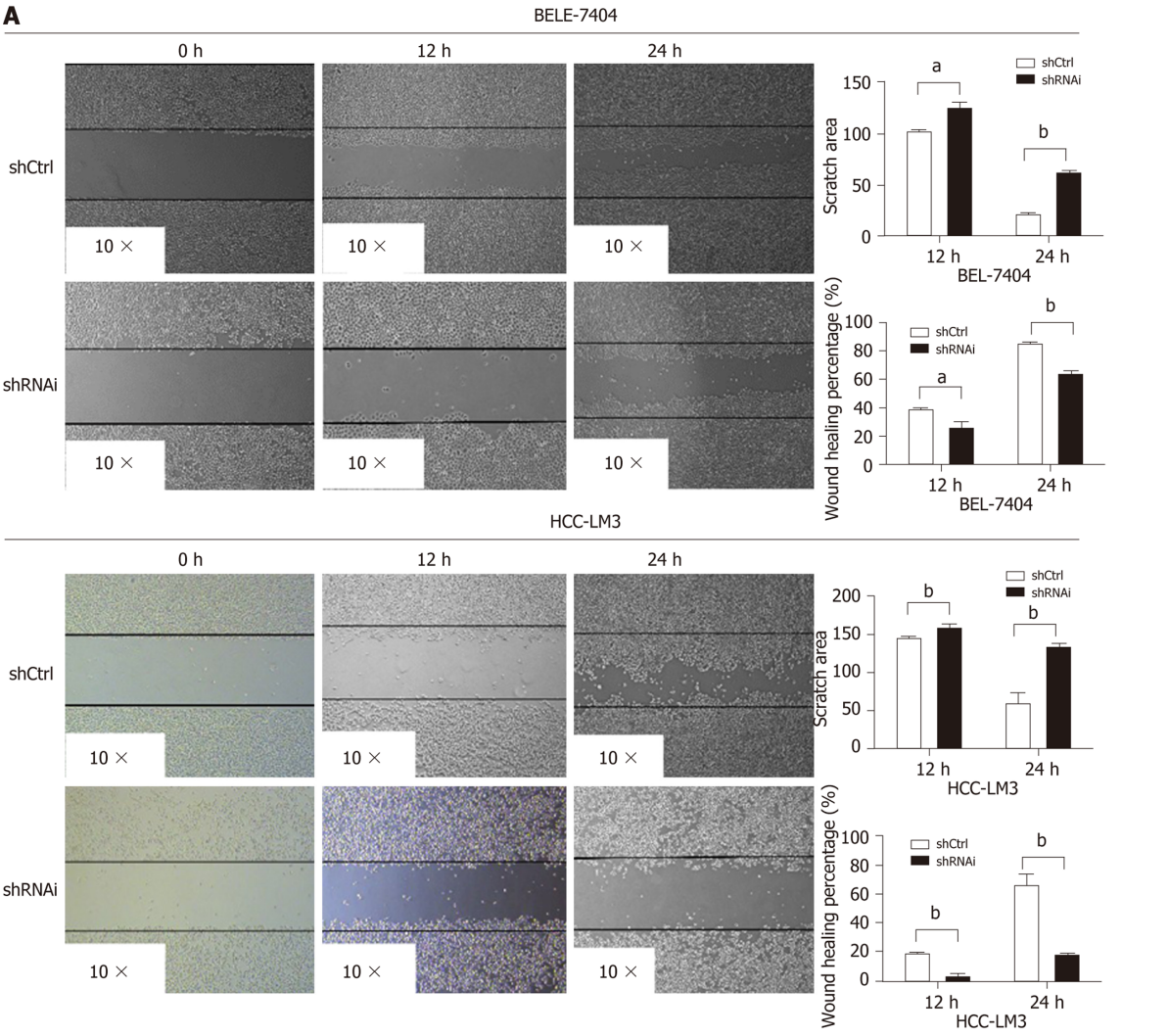
(subcutaneous injection groups) and lung tissues (tail vein injection groups) were removed for imaging analysis. The growth and invasion ability of tumors was significantly lower in mice injected with shRNAi cells than in mice injected with shCtrl cells. These results show that silencing RFWD3 effectively reduced HCC tumor proliferation, invasion, and metastasis in vivo.

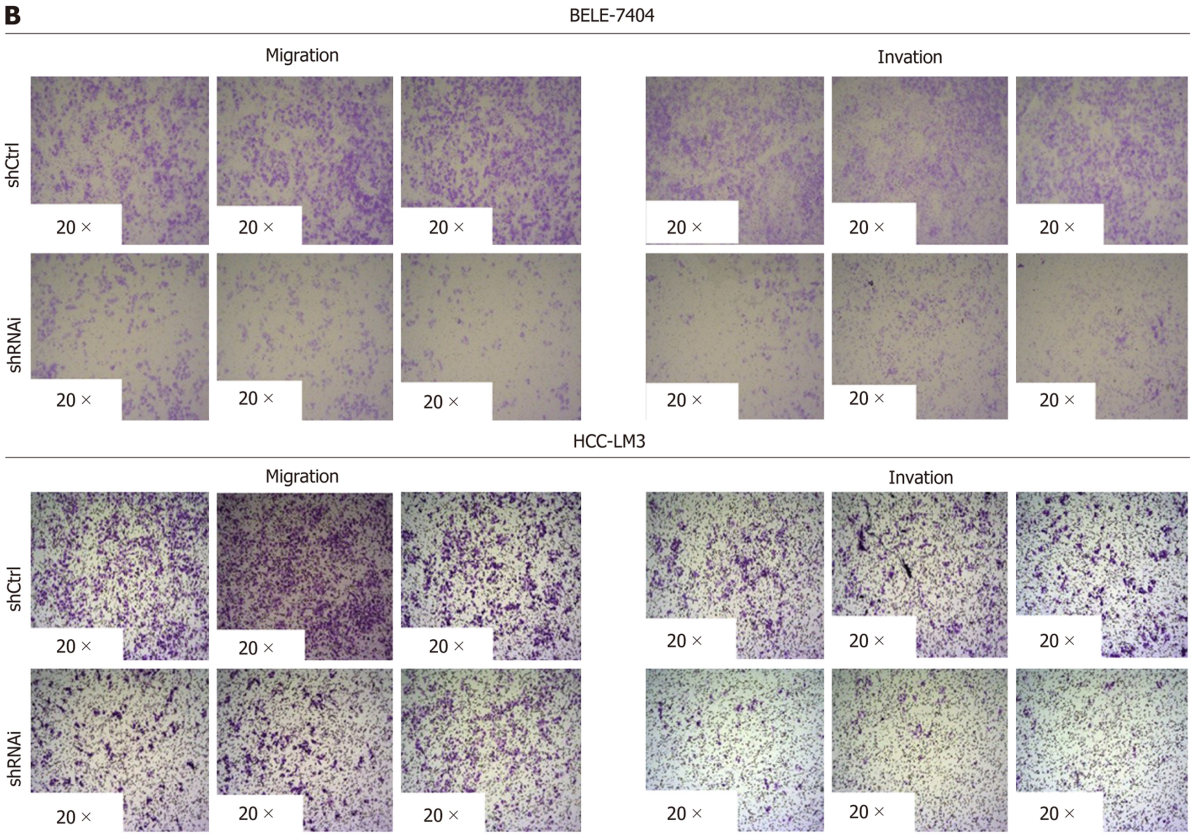
Validation of the efficiency of lentiviral-mediated rescue of RFWD3 shRNAi in cell lines

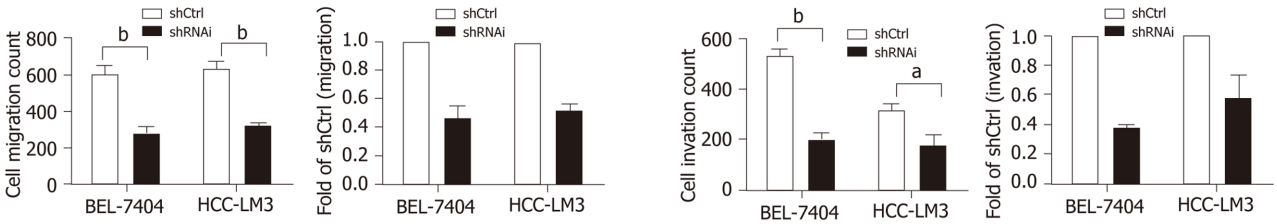
To rule out off-target effects and confirm the biological function of RFWD3 shRNAi, a rescue experiment was performed with RFWD3-KD-OE in HCC cells. After transfection with an LV-RFWD3 lentiviral vector, we used GFP fluorescence imaging to confirm transduction efficiency (Figure 6A). Compared with the RFWD3-KD-OE-NC group, the RFWD3-KD-OE group showed upregulation of RFWD3 in qRT-PCR (Figure 6B). WB analysis also confirmed the lentivirus transduction efficiency (Figure 6C).

RFWD3-KD-OE resume shRNAi HCC cells proliferation, invasion, and migration

In the MTT assay, the OD value of the RFWD3-KD-OE group was higher than that of the RFWD3-KD-OE-NC group. These results indicate that RFWD3-KD-OE rescued the proliferation of shRNAi BEL-7404 cells (Figure 7A). Furthermore, no difference was observed between the G1 and S phases in the two groups of cell cycle progression assays. However, in the G2/M phase, the fraction of RFWD3-KD-OE-NC cells was increased (the average value was 30.51% in RFWD3-KD-OE-NC cells, 29.74% in RFWD3-KD-OE cells, $P < 0.05$); however, the gap in data was diminished compared with previous BEL-7404 RNAi groups (24.9% in shCtrl cells, 32.15% in shRNAi cells, $P < 0.05$) (Figure 7B). In the subsequent apoptosis experiments, BEL-7404 RFWD3-KD-OE-NC cells had a higher apoptosis rate (the average

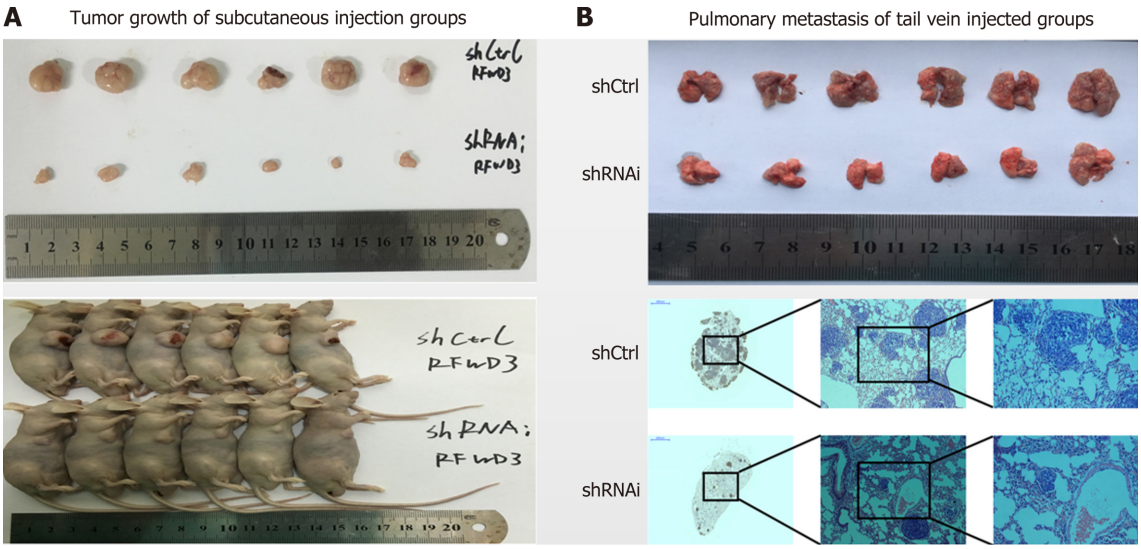

A
BELE-7404
0 h
12 h
24 h
shCtrl
shRNAi
10 ×
Scratch area
shCtrl
shRNAi
a
b
12 h
24 h
BEL-7404
Wound healing percentage (%)
HCC-LM3


B
BELE-7404
Migration
Invation
shCtrl
shRNAi
20 ×
HCC-LM3



DOI: 10.3748/wjg.v28.i27.3435 **Copyright** ©The Author(s) 2022.

Figure 4 RING finger and WD repeat domain 3 knockdown reduces hepatocellular carcinoma cell invasion and migration. A: Wound-healing assay in the shCtrl and shRNAi groups ($^{a}P < 0.05$, $^{b}P < 0.01$); B: The migration ability of both BEL-7404 and hepatocellular carcinoma-LM3 shRNAi cells. Invasion assays demonstrating similar results ($^{a}P < 0.05$, $^{b}P < 0.01$).



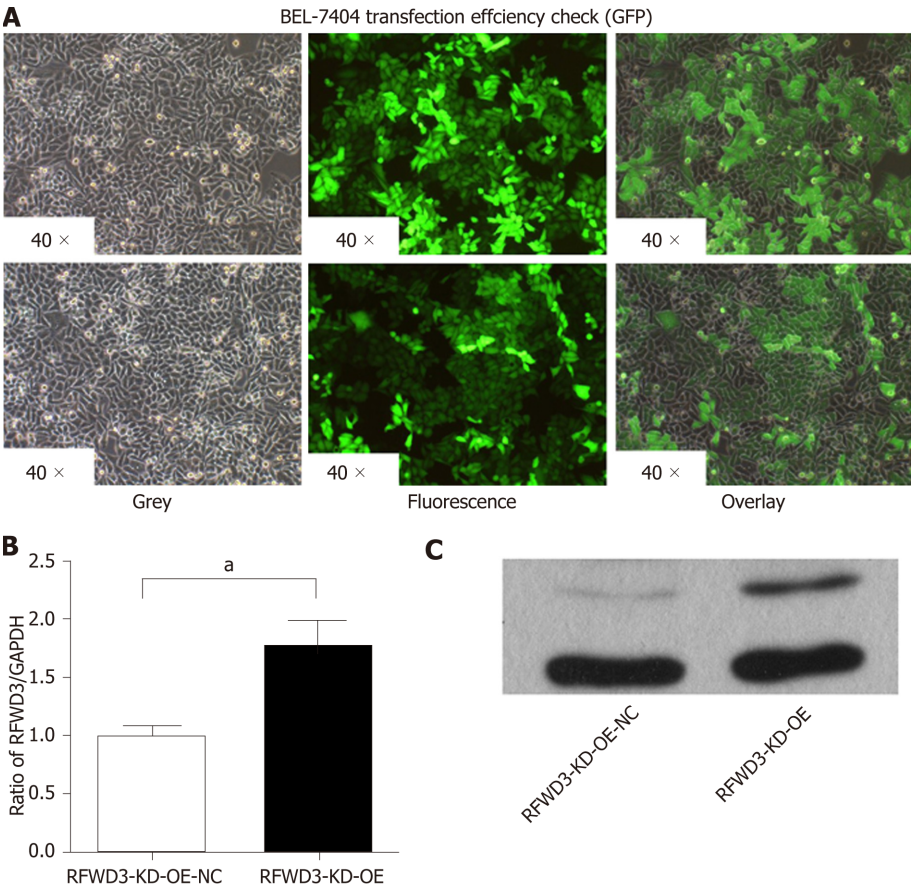
DOI: 10.3748/wjg.v28.i27.3435 **Copyright** ©The Author(s) 2022.

Figure 5 RING finger and WD repeat domain 3 knockdown reduces hepatocellular carcinoma cell growth *in vivo*. A: Imaging analysis of the tumor and lung tissues of mice injected with shRNAi and shCtrl cells; B: Imaging analysis of pulmonary metastasis of hepatocellular carcinoma cells in mice injected with shRNAi and shCtrl cells.

value was 20.47% in RFWD3-KD-OE-NC cells, 18.03% in RFWD3-KD-OE cells, $P < 0.01$) (Figure 7C). This result demonstrated that RFWD3-KD-OE reduced the apoptosis ratio, thus affecting the proliferation of shRNAi BEL-7404 cells. In transwell assays, the migration of BEL-7404 RFWD3-KD-OE cells was higher than that of RFWD3-KD-OE-NC cells ($P < 0.01$) (Figure 7D). Similar results were observed in the invasion assay ($P < 0.01$; Figure 7E). These data revealed that RFWD3-KD-OE rescued BEL-7404 shRNAi cell invasion and migration.

RFWD3 influence the progress of HCC via the Wnt/β-catenin signalling pathway

To further validate the results of the *in vitro* and *in vivo* experiments, we performed microarray analysis to explore the molecular mechanism underlying the differential RFWD3 expression between shCtrl and shRNAi HCC cells. A total of 454 genes (Figure 8A) exhibited differential mRNA expression between the two groups (> 2-fold, $P < 0.05$). We then analyzed the disease and function to determine the enriched gene sets. Genes involved in cell death, viability and survival, cell movement and invasion, cellular assembly and organization, DNA replication, recombination and repair, and cellular function and maintenance were significantly enriched ($P < 0.05$, Figure 8B). Classical pathway analysis revealed that, in addition to the previously reported p53 and cell cycle checkpoint control pathways, the Wnt/β-catenin signalling pathway was altered following RFWD3 silencing ($P < 0.05$, Figure 8C and D). Next, we used IPA to analyze the knowledge-based interactome associated with the regulation of these pathways (Figure 8E). Some genes involved in tumorigenesis were shown to be regulated by RFWD3, including *CREBBP*, *KREMEN-1*, *LRP6*, *JUN*, *WNT5A*, and *WNT7B*. Finally, we tested the protein expression between shCtrl and shRNAi and RFWD3-KD-OE *vs* RFWD3-KD-OE-NC groups and found that the expression of *CREBBP*, *WNT5A*, *JUN*, *WNT7B*, and *LRP6* were decreased, and the expression of *KREMEN-1* was increased in the shRNAi and RFWD3-KD-OE-NC groups than that in shCtrl and RFWD3-KD-OE groups (Figure 8F-I). These results indicate that the Wnt/β-catenin signalling pathway is involved in the RFWD3-mediated promotion of HCC tumorigenesis.



DOI: 10.3748/wjg.v28.i27.3435 **Copyright** ©The Author(s) 2022.

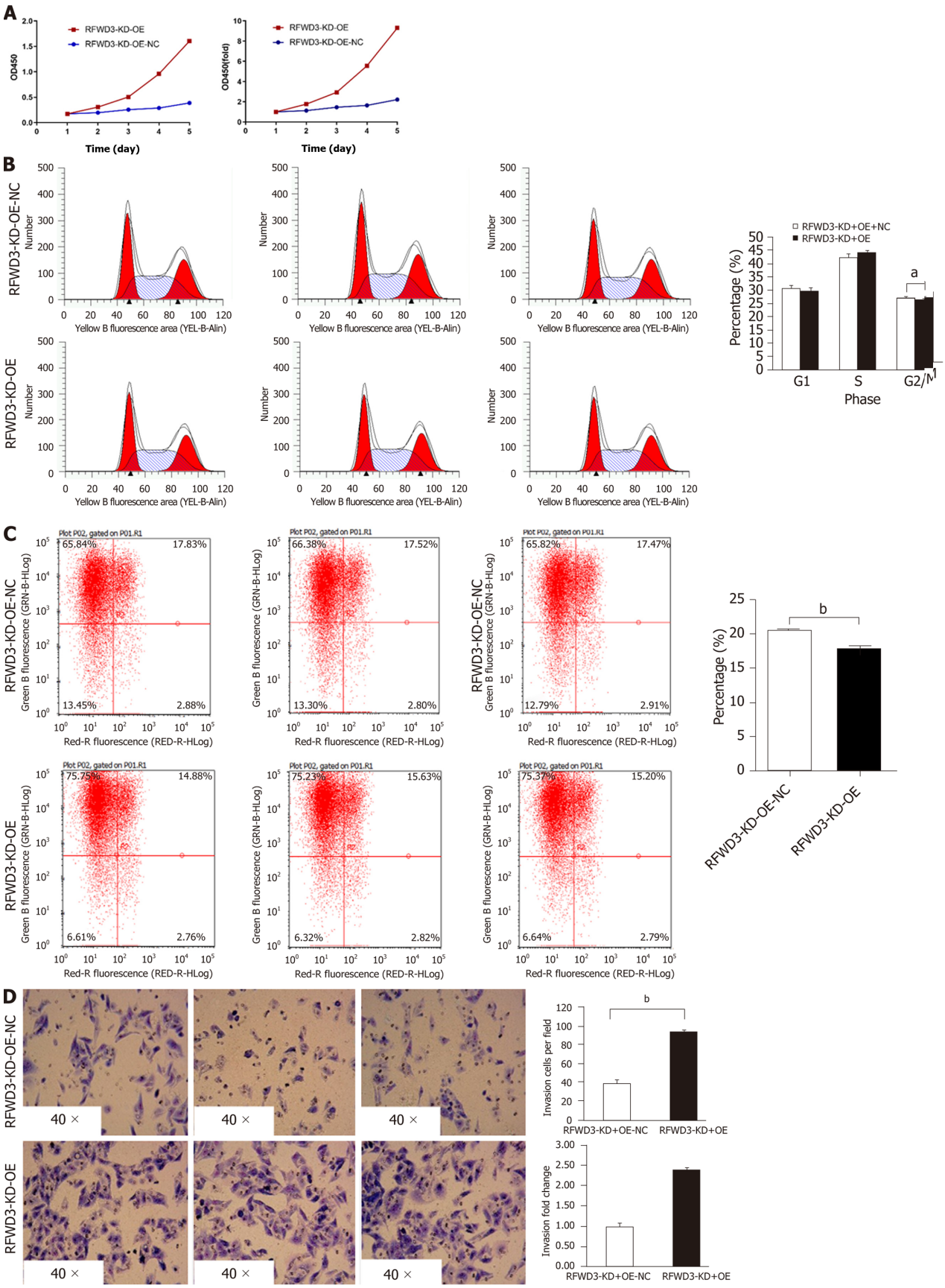
Figure 6 Validation of lentiviral-mediated rescue RING finger and WD repeat domain 3 shRNAi efficiency in cell lines. A: GFP fluorescence imaging confirms the lentivirus transduction efficiency; B: Compared with the RING finger and WD repeat domain 3 (RFWD3)-KD-OE-NC group, the RFWD3-KD-OE group shows upregulated RFWD3 in the quantitative reverse transcription-polymerase chain reaction analysis ($^aP < 0.05$); C: Western blot analysis confirms the same upshot.

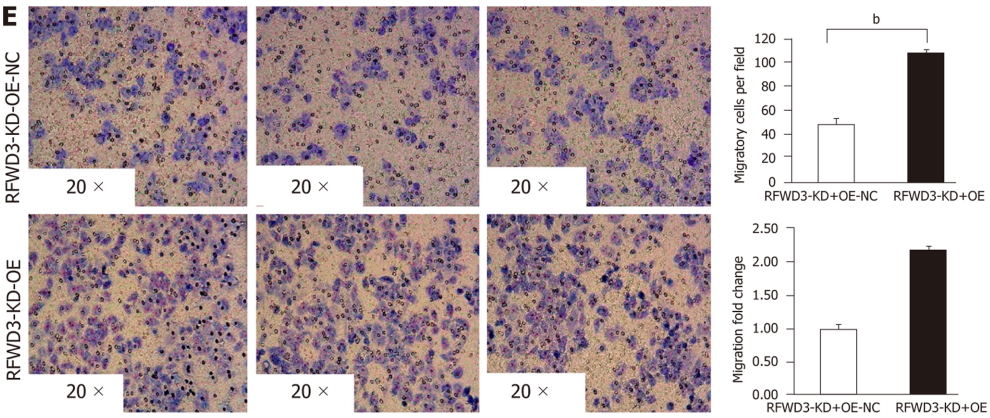
DISCUSSION

In this study, we demonstrated reduced growth and proliferation of HCC cells in the shRNAi group. Subsequent evaluation of cell cycle progression revealed disrupted cell cycle progression at the G2/M phase, whereas the FCM analysis showed a higher rate of apoptosis in the shRNAi group than in the ShCtrl group. These results confirmed that RFWD3 silencing caused both cell cycle arrest at the G2/M phase and apoptosis. Furthermore, the *in vitro* experiments revealed that shCtrl cells had better healing abilities than shRNAi cells. In the subsequent transwell experiments, we also found that the shRNAi cells had about half the metastatic capacity of the shCtrl cells. These results were validated *in vivo* using mice models, which showed that the tumor volumes in mice injected subcutaneously with shRNAi cells were significantly smaller than those in mice injected with shCtrl cells. Furthermore, the pulmonary metastasis group revealed that lung metastasis was significantly reduced in mice injected with shRNAi cells than in those injected with shCtrl cells.

To rule out off-target effects with RFWD3-shRNAi, we performed a rescue experiment. After verifying the transfection efficiency and screening of stable cell lines, we carried out phenotype verification. Compared with the control group, the cell growth state was restored in the RFWD3-KD-OE group. It also showed a higher OD value in the MTT assay, decreased fraction of G2/M phase, and diminution gap of data compared with RFWD3-KD-OE-NC group. Furthermore, in the apoptosis experiments, the RFWD3-KD-OE group had a lower apoptosis rate than the RFWD3-KD-OE-NC group. The same results were observed in the transwell assays, and the migration and invasion abilities of the RFWD3-KD-OE group were recovered. These data revealed that RFWD3-KD-OE resumed BEL-7404 shRNAi cell invasion and metastasis and proved that the previous RFWD3-shRNAi experimental results were not due to off-target effects.

Subsequently, we proved that RFWD3 silencing plays a positive role in inhibiting the proliferation, invasion, and metastasis of HCC. Previous studies have reported that the essential role of RFWD3 in HR makes it important for cell survival, as it promotes the repair of DNA damage. Therefore, the increased apoptosis could be attributed to the unrepaired DNA damage upon RFWD3 loss. On the contrary, the migration and metastasis phenotypes could be explained by decreased viability due to increased


A
RFWD3-KD-OE
RFWD3-KD-OE-NC
OD450
OD450(fold)
Time (day)
B
RFWD3-KD-OE-NC
RFWD3-KD-OE
Number
Yellow B fluorescence area (YEL-B-Alin)
RFWD3-KD+OE+NC
RFWD3-KD+OE
Percentage (%)
G1
S
G2/M
Phase
a
C
Plot P02, gated on P01.R1
Green B fluorescence (GRN-B-HLog)
Red-R fluorescence (RED-R-HLog)
65.84%
17.83%
13.45%
2.88%
66.38%
17.52%
13.30%
2.80%
65.82%
17.47%
12.79%
2.91%
75.75%
14.88%
6.61%
2.76%
75.23%
15.63%
6.32%
2.82%
75.37%
15.20%
6.64%
2.79%
b
D
40 ×
Invasion cells per field
Invasion fold change



DOI: 10.3748/wjg.v28.i27.3435 **Copyright** ©The Author(s) 2022.

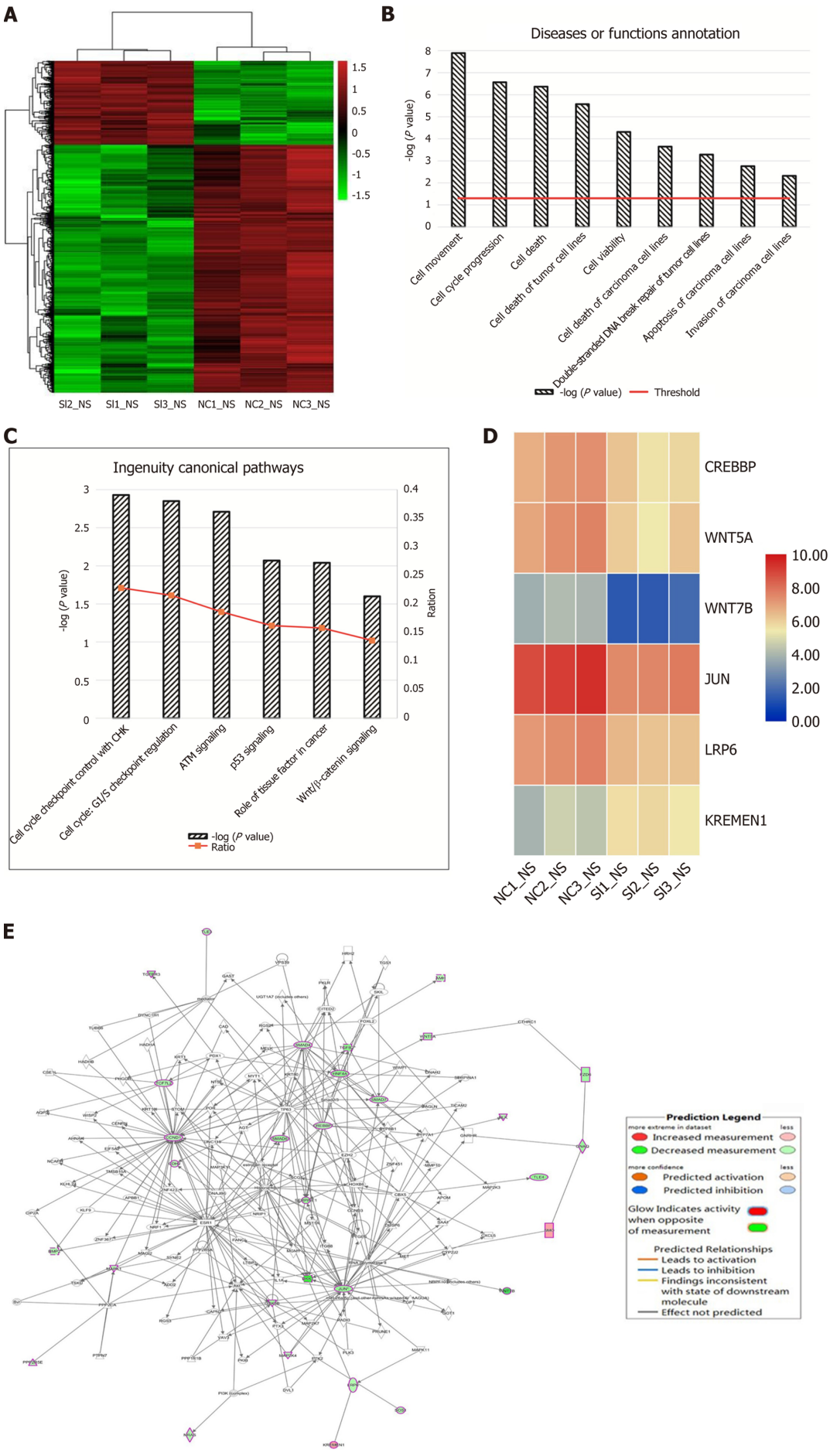
Figure 7 RING finger and WD repeat domain 3-KD-OE reverses the cell phenotype of shRNAi BEL-7404 cells. A: MTT assay; B: The cell cycle distribution in RING finger and WD repeat domain 3 (RFWD3)-KD-OE-NC and RFWD3-KD-OE cells ($^aP < 0.05$); C: Rate of apoptosis in RFWD3-KD-OE-NC and RFWD3-KD-OE groups ($^bP < 0.01$); D and E: RFWD3-KD-OE resumes BEL-7404 shRNAi cell invasion and migration ability in transwell ($^bP < 0.01$) and invasion assays ($^bP < 0.01$).

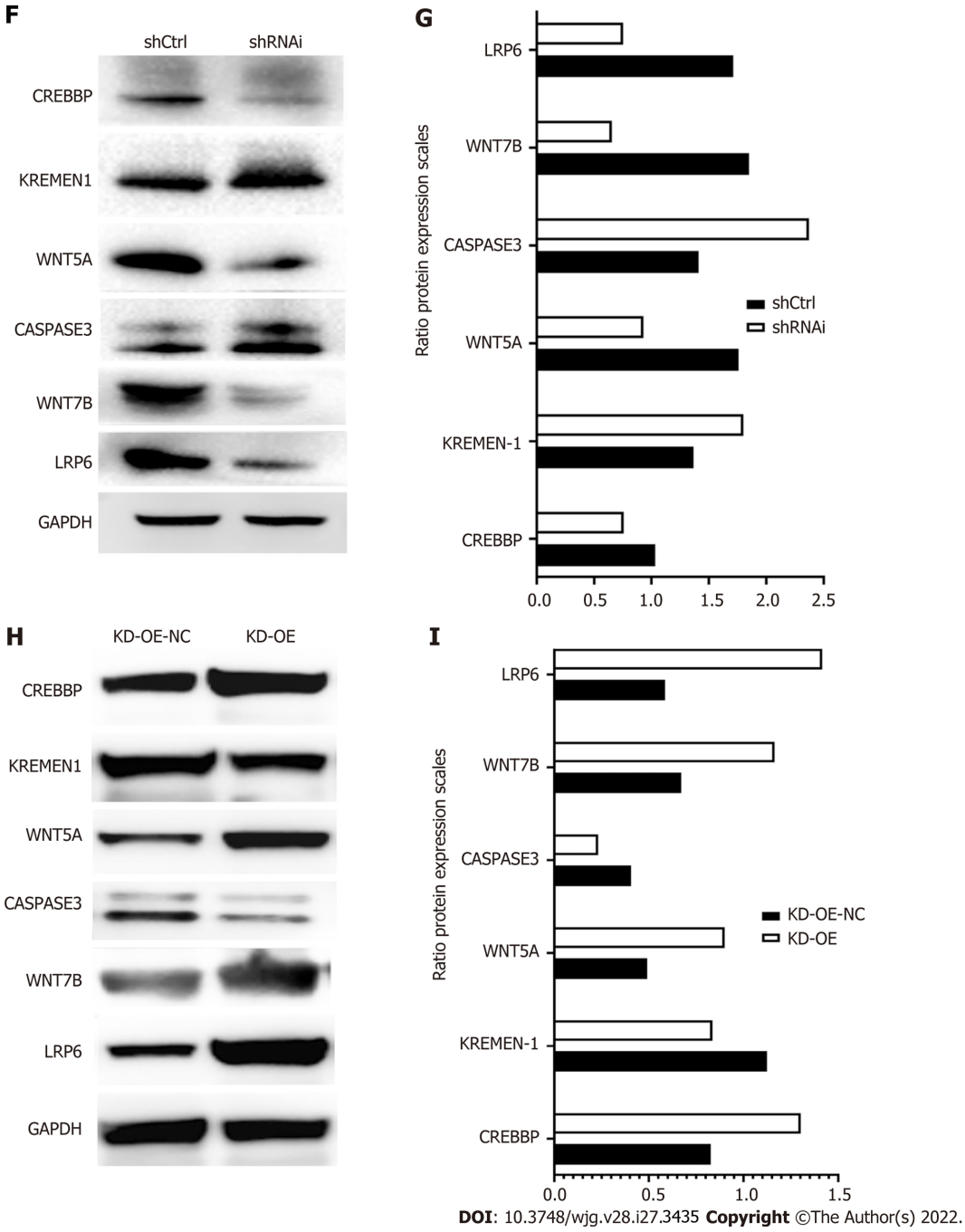
RFWD3 function during DNA repair. In other words, this condition may be explained by a common theory: "There are more firefighters on the fire scene than ordinary people." However, the questions like whether the increased expression of RFWD3 in HCC is a compensatory mechanism to deal with increased genomic instability or whether RFWD3 is regulated by a Janus-faced regulator that plays other roles in HCC, consequently promoting the progression of HCC remained unanswered.

To answer these questions, we explored the mechanism underlying HCC and identified the molecular signalling transduction pathways using microarray-based gene expression analyses and IPA. The raw data (Supplementary materials 1) were verified with the uniformity, integrity and reliability (Supplementary materials 2). Gene expression profiling revealed that RFWD3 silencing enriched the expression of genes involved in cellular function and maintenance, cell death, viability, movement, invasion and survival, and DNA replication, recombination, and repair (Supplementary materials 3). In terms of the gene pathways involved, in addition to the p53 and cell replication cycle pathways that were previously reported in the literature, we found that the Wnt/β-catenin signalling pathway also had a significant impact. Further examination of the knowledge-based interactome associated with the regulation of Wnt/β-catenin *via* IPA analysis demonstrated that *CREMEN1, JUN, CREBBP, WNT5A, WNT7B,* and *LRP6*, which have been implicated in the proliferation and metastasis of various cancers, were differentially regulated by RFWD3 (> 2-fold, $P < 0.05$).

Reportedly, Wnt/β-catenin signalling plays an important role in embryonic liver development and regeneration and preserves liver health. An aberrant Wnt signalling activity has been implicated in several human cancers[31,32]. In normal tissues, only a small amount of β-catenin is found in the cytoplasm and is quickly degraded by the UPS. It is bound by a destruction complex containing *GSK3B, AXIN,* and *APC* and then ubiquitinated by β-transducin repeat-containing protein and subsequently degraded by the proteasome[33]. In the traditional Wnt/β-catenin pathway in tumors, the destruction complex is disassembled by the phosphorylation of *LRP6* and *GSK3β*, thereby preventing β-catenin degradation[34]. The accumulated β-catenin is transferred from the cytoplasm to the nucleus, where it competes with Groucho to form the *β-catenin-TCF/LEF* transcriptional complex. Finally, the Wnt signalling pathway is activated to regulate the transcription of target genes such as *cyclin D1*, *c-myc*, and *MMP9* under the synergistic effect of auxiliary factors, thus regulating tumor progression[35]. *KREMEN-1* is a transmembrane protein that contains a kringle domain. Studies have shown that it is a high-affinity receptor for *DKK*. *KREMEN-1, DKK*, and *LRP5/6* form a ternary complex that inhibits Wnt/β-catenin signalling, thus inducing head defects in Xenopus embryos[36,37]. Furthermore, *KREMEN-1* expression is prevalent in adult mammals but is often lacking in tumors. It has been shown that Wnt/β-catenin signalling maintains the low differentiation state of stem cells and undifferentiated cells, but *Dickkopf-KREMEN* blocks Wnt/β-catenin signalling causing cells to differentiate[38].

Collectively, the findings demonstrated that factors involved in Wnt/β-catenin signallings, such as *CREBBP, WNT5A, JUN, WNT7B,* and *LRP6*, were downregulated by RFWD3 silencing, and the expression of *KREMEN-1* was increased, indicating that RFWD3 might influence the progression of HCC *via* the Wnt/β-catenin signalling pathway. Based on these findings, it can be inferred that RFWD3 affects the Wnt/β-catenin signalling pathway and therefore affects HCC tumorigenesis. However, the detailed regulatory mechanism is still unclear and should be explored in future studies.


A
1.5
1
0.5
0
-0.5
-1
-1.5
SI2_NS
SI1_NS
SI3_NS
NC1_NS
NC2_NS
NC3_NS
B
Diseases or functions annotation
-log (P value)
Cell movement
Cell cycle progression
Cell death
Cell death of tumor cell lines
Cell viability
Cell death of carcinoma cell lines
Double-stranded DNA break repair of tumor cell lines
Apoptosis of carcinoma cell lines
Invasion of carcinoma cell lines
-log (P value)
Threshold
C
Ingenuity canonical pathways
-log (P value)
Ration
Cell cycle checkpoint control with CHK
Cell cycle: G1/S checkpoint regulation
ATM signaling
p53 signaling
Role of tissue factor in cancer
Wnt/β-catenin signaling
-log (P value)
Ratio
D
CREBBP
WNT5A
WNT7B
JUN
LRP6
KREMEN1
10.00
8.00
6.00
4.00
2.00
0.00
NC1_NS
NC2_NS
NC3_NS
SI1_NS
SI2_NS
SI3_NS
E
Prediction Legend
more extreme in dataset
less
Increased measurement
Decreased measurement
more confidence
less
Predicted activation
Predicted inhibition
Glow Indicates activity when opposite of measurement
Predicted Relationships
Leads to activation
Leads to inhibition
Findings inconsistent with state of downstream molecule
Effect not predicted



DOI: 10.3748/wjg.v28.i27.3435 **Copyright** ©The Author(s) 2022.

Figure 8 shRFWD3i influences the progress of hepatocellular carcinoma through the Wnt/β-catenin signalling pathway. A: Heatmap analysis showing the gene expression changes after RING finger and WD repeat domain 3 (RFWD3) silencing (454 genes, above 2-fold); B: Disease and functional analysis to classify genes enriched after RFWD3 silencing; C: Classical pathway analysis indicates genes enriched after RFWD3 silencing; D: The microarray analysis reveals alteration in the Wnt/β-catenin signalling pathway following RFWD3 silencing; E: Knowledge-based interaction network of Wnt/β-catenin signalling targets (> 2-fold change, $P < 0.05$). The intensity of the node color indicates the degree of upregulation (red) or downregulation (green) following RFWD3 silencing in hepatocellular carcinoma cells; F-I: The expression of *CREBBP, Wnt5A, JUN, Wnt7B* and *LRP6* were decreased, and the expression of *KREMEN-1* was increased in the shRNAi group using western blot analysis, in rescue experiment, the results are reversed.

CONCLUSION

In this study, we validated the expression and function of RFWD3 in HCC and demonstrated that RFWD3 expression might affect the proliferation and metastasis of HCC by regulating the Wnt/β-catenin signalling pathway. The findings suggest that RFWD3 could be a potential therapeutic target for HCC; however, it warrants further investigations to ascertain these possibilities.

ARTICLE HIGHLIGHTS

Research background

Hepatocellular carcinoma (HCC) is one of the most common malignant tumors with a high mortality rate. The molecular biology research of HCC can reveal the potential mechanism and provide direction for its comprehensive treatment.

Research motivation

The relationship between RING finger and WD repeat domain 3 (RFWD3) and the tumorigenesis process has been reported occasionally; however, the relationship between RFWD3 and HCC is still unclear.

Research objectives

We aimed to investigate the relationship between HCC and RFWD3 and explore the underlying molecular signalling transduction pathways.

Research methods

We analyzed RFWD3 expression in HCC tissues and evaluated cell phenotypes such as proliferation, apoptosis, migration, and invasion using Lentivirus mediated RFWD3 knockdown. In addition, *in vivo* experiments were performed to observe tumor growth and metastasis. Next, the phenotype was verified using the lentiviral-mediated rescue of RFWD3 shRNA. Finally, we unraveled the regulatory network underlying HCC using microarray, bioinformatics, and western blot analyses.

Research results

RFWD3 expression levels were correlated with tumor size and TNM stage in clinical samples. RFWD3 silencing increased apoptosis, decreased growth, and inhibited migration in HCC cell lines and nude mice, which were resumed with RFWD3 shRNAi rescue. Subsequent experiments revealed that RFWD3 might influence the proliferation and metastasis of HCC *via* the Wnt/β-catenin signalling pathway.

Research conclusions

This study shows that RFWD3 affects the Wnt/β-catenin signalling pathway and therefore affects HCC tumorigenesis.

Research perspectives

The findings suggest that RFWD3 could be a potential therapeutic target for HCC. However, it warrants further investigations to ascertain these inferences.

ACKNOWLEDGEMENTS

We would like to thank Wen-Feng Song, Hao Chen, Liang-Jie Hong, Dan-Jing Guo, Rong Su, Hao-Hao Chen and Han-Wen Zhang for their technical assistance.

FOOTNOTES

Author contributions: Sun YL conceived the experiments; Liang RP, Zhang XX, Zhao J, Lu QW, Zhu RT, Wang WJ, Li J, Bo K and Zhang CX contributed sample collection/reagents/materials/analysis tools, performed all experiments, and analyzed the data; Liang RP, Zhang XX and Zhao J analyzed the results and wrote the paper; all authors have read and approve the final manuscript.

Supported by National Natural Science Foundation of China, No. 82172944 and No. 81900558; Co-operation Research Plan of Medical Science and Technology of Henan Province, No. LHGJ20190149; and The Key Scientific Research Projects of Universities of Henan Province, No. 21A320052.

Institutional review board statement: This study was reviewed and approved by the First Affiliated Hospital of Zhengzhou University, Zhengzhou, China, No. 10[2017].

Institutional animal care and use committee statement: All animal experimental protocols were conducted following the ARRIVE guidelines (Animal Research: Reporting In Vivo Experiments, https://www.nc3rs.org.uk/arrive-guidelines) and approved by Laboratory Animals and the Institutional Animal Care and Use Committee of the First Affiliated Hospital of Zhengzhou University (Approval Number: 10[2017]).

Conflict-of-interest statement: All the authors report no relevant conflicts of interest for this article.

Data sharing statement: The data are available from the corresponding author on reasonable request.

ARRIVE guidelines statement: The authors have read the ARRIVE guidelines, and the manuscript was prepared and revised according to the ARRIVE guidelines.

Open-Access: This article is an open-access article that was selected by an in-house editor and fully peer-reviewed by external reviewers. It is distributed in accordance with the Creative Commons Attribution NonCommercial (CC BY-NC 4.0) license, which permits others to distribute, remix, adapt, build upon this work non-commercially, and license their derivative works on different terms, provided the original work is properly cited and the use is non-commercial. See: https://creativecommons.org/Licenses/by-nc/4.0/

Country/Territory of origin: China

ORCID number: Ruo-Peng Liang 0000-0002-3789-1666; Xiao-Xue Zhang 0000-0003-2272-3405; Jie Zhao 0000-0001-7701-1654; Qin-Wei Lu 0000-0003-3801-8217; Rong-Tao Zhu 0000-0003-3655-9458; Wei-Jie Wang 0000-0003-3136-8628; Jian Li 0000-0001-7756-2312; Kai Bo 0000-0002-0039-0585; Chi-Xian Zhang 0000-0002-4387-7182; Yu-Ling Sun 0000-0001-5289-4673.

S-Editor: Fan JR
L-Editor: A
P-Editor: Zhang YL

REFERENCES

1 **Chen W**, Zheng R, Baade PD, Zhang S, Zeng H, Bray F, Jemal A, Yu XQ, He J. Cancer statistics in China, 2015. *CA Cancer J Clin* 2016; **66**: 115-132 [PMID: 26808342 DOI: 10.3322/caac.21338]
2 **Siegel RL**, Miller KD, Jemal A. Cancer statistics, 2020. *CA Cancer J Clin* 2020; **70**: 7-30 [PMID: 31912902 DOI: 10.3322/caac.21590]
3 **Li J**, Qiu X, Guo W, Yan B, Zhang S. Prospective analysis of tiopronin in prevention of sorafenib and antiviral therapy inducing liver toxicity in advanced hepatitis B virus-related hepatocellular carcinoma. *Med Oncol* 2015; **32**: 238 [PMID: 26330362 DOI: 10.1007/s12032-015-0684-x]
4 **Tsai CL**, Hsu FM, Cheng JC. How to Improve Therapeutic Ratio in Radiotherapy of HCC. *Liver Cancer* 2016; **5**: 210-220 [PMID: 27493896 DOI: 10.1159/000367767]
5 **Kim KI**, Chung HK, Park JH, Lee YJ, Kang JH. Alpha-fetoprotein-targeted reporter gene expression imaging in hepatocellular carcinoma. *World J Gastroenterol* 2016; **22**: 6127-6134 [PMID: 27468205 DOI: 10.3748/wjg.v22.i27.6127]
6 **Trojan J**, Zangos S, Schnitzbauer AA. Diagnostics and Treatment of Hepatocellular Carcinoma in 2016: Standards and Developments. *Visc Med* 2016; **32**: 116-120 [PMID: 27413729 DOI: 10.1159/000445730]
7 **Tang ZY**. Hepatocellular carcinoma--cause, treatment and metastasis. *World J Gastroenterol* 2001; **7**: 445-454 [PMID: 11819809 DOI: 10.3748/wjg.v7.i4.445]
8 **Hu L**, Lau SH, Tzang CH, Wen JM, Wang W, Xie D, Huang M, Wang Y, Wu MC, Huang JF, Zeng WF, Sham JS, Yang M, Guan XY. Association of Vimentin overexpression and hepatocellular carcinoma metastasis. *Oncogene* 2004; **23**: 298-302 [PMID: 14647434 DOI: 10.1038/sj.onc.1206483]
9 **Harper JW**, Elledge SJ. The DNA damage response: ten years after. *Mol Cell* 2007; **28**: 739-745 [PMID: 18082599 DOI: 10.1016/j.molcel.2007.11.015]
10 **Turnbull AP**, Ioannidis S, Krajewski WW, Pinto-Fernandez A, Heride C, Martin ACL, Tonkin LM, Townsend EC, Buker SM, Lancia DR, Caravella JA, Toms AV, Charlton TM, Lahdenranta J, Wilker E, Follows BC, Evans NJ, Stead L, Alli C, Zarayskiy VV, Talbot AC, Buckmelter AJ, Wang M, McKinnon CL, Saab F, McGouran JF, Century H, Gersch M, Pittman MS, Marshall CG, Raynham TM, Simcox M, Stewart LMD, McLoughlin SB, Escobedo JA, Bair KW, Dinsmore CJ, Hammonds TR, Kim S, Urbé S, Clague MJ, Kessler BM, Komander D. Molecular basis of USP7 inhibition by selective small-molecule inhibitors. *Nature* 2017; **550**: 481-486 [PMID: 29045389 DOI: 10.1038/nature24451]
11 **Hou CC**, Yang WX. New insights to the ubiquitin-proteasome pathway (UPP) mechanism during spermatogenesis. *Mol Biol Rep* 2013; **40**: 3213-3230 [PMID: 23268313 DOI: 10.1007/s11033-012-2397-y]
12 **Shiloh Y**. ATM and related protein kinases: safeguarding genome integrity. *Nat Rev Cancer* 2003; **3**: 155-168 [PMID: 12612651 DOI: 10.1038/nrc1011]
13 **Cimprich KA**, Cortez D. ATR: an essential regulator of genome integrity. *Nat Rev Mol Cell Biol* 2008; **9**: 616-627 [PMID: 18594563 DOI: 10.1038/nrm2450]
14 **Mu JJ**, Wang Y, Luo H, Leng M, Zhang J, Yang T, Besusso D, Jung SY, Qin J. A proteomic analysis of ataxia telangiectasia-mutated (ATM)/ATM-Rad3-related (ATR) substrates identifies the ubiquitin-proteasome system as a regulator for DNA damage checkpoints. *J Biol Chem* 2007; **282**: 17330-17334 [PMID: 17478428 DOI: 10.1074/jbc.C700079200]
15 **Matsuoka S**, Ballif BA, Smogorzewska A, McDonald ER 3rd, Hurov KE, Luo J, Bakalarski CE, Zhao Z, Solimini N, Lerenthal Y, Shiloh Y, Gygi SP, Elledge SJ. ATM and ATR substrate analysis reveals extensive protein networks responsive to DNA damage. *Science* 2007; **316**: 1160-1166 [PMID: 17525332 DOI: 10.1126/science.1140321]
16 **Smolka MB**, Albuquerque CP, Chen SH, Zhou H. Proteome-wide identification of *in vivo* targets of DNA damage

checkpoint kinases. *Proc Natl Acad Sci U S A* 2007; **104**: 10364-10369 [PMID: 17563356 DOI: 10.1073/pnas.0701622104]
17 **Fu X**, Yucer N, Liu S, Li M, Yi P, Mu JJ, Yang T, Chu J, Jung SY, O'Malley BW, Gu W, Qin J, Wang Y. RFWD3-Mdm2 ubiquitin ligase complex positively regulates p53 stability in response to DNA damage. *Proc Natl Acad Sci U S A* 2010; **107**: 4579-4584 [PMID: 20173098 DOI: 10.1073/pnas.0912094107]
18 **Elia AE**, Wang DC, Willis NA, Boardman AP, Hajdu I, Adeyemi RO, Lowry E, Gygi SP, Scully R, Elledge SJ. RFWD3-Dependent Ubiquitination of RPA Regulates Repair at Stalled Replication Forks. *Mol Cell* 2015; **60**: 280-293 [PMID: 26474068 DOI: 10.1016/j.molcel.2015.09.011]
19 **Zhang W**, Sidhu SS. Development of inhibitors in the ubiquitination cascade. *FEBS Lett* 2014; **588**: 356-367 [PMID: 24239534 DOI: 10.1016/j.febslet.2013.11.003]
20 **Knies K**, Inano S, Ramírez MJ, Ishiai M, Surrallés J, Takata M, Schindler D. Biallelic mutations in the ubiquitin ligase RFWD3 cause Fanconi anemia. *J Clin Invest* 2017; **127**: 3013-3027 [PMID: 28691929 DOI: 10.1172/JCI92069]
21 **Wolberger C**. Mechanisms for regulating deubiquitinating enzymes. *Protein Sci* 2014; **23**: 344-353 [PMID: 24403057 DOI: 10.1002/pro.2415]
22 **Gong Z**, Chen J. E3 Ligase RFWD3 participates in replication checkpoint control. *J Biol Chem* 2011; **286**: 22308-22313 [PMID: 21504906 DOI: 10.1074/jbc.M111.222869]
23 **Sokratous K**, Hadjisavvas A, Diamandis EP, Kyriacou K. The role of ubiquitin-binding domains in human pathophysiology. *Crit Rev Clin Lab Sci* 2014; **51**: 280-290 [PMID: 24901807 DOI: 10.3109/10408363.2014.915287]
24 **Liu S**, Chu J, Yucer N, Leng M, Wang SY, Chen BP, Hittelman WN, Wang Y. RING finger and WD repeat domain 3 (RFWD3) associates with replication protein A (RPA) and facilitates RPA-mediated DNA damage response. *J Biol Chem* 2011; **286**: 22314-22322 [PMID: 21558276 DOI: 10.1074/jbc.M111.222802]
25 **Feeney L**, Muñoz IM, Lachaud C, Toth R, Appleton PL, Schindler D, Rouse J. RPA-Mediated Recruitment of the E3 Ligase RFWD3 Is Vital for Interstrand Crosslink Repair and Human Health. *Mol Cell* 2017; **66**: 610-621.e4 [PMID: 28575657 DOI: 10.1016/j.molcel.2017.04.021]
26 **Zhang Y**, Zhao X, Zhou Y, Wang M, Zhou G. Identification of an E3 Ligase-encoding gene RFWD3 in non-small cell lung cancer. *Front Med* 2020; **14**: 318-326 [PMID: 31571161 DOI: 10.1007/s11684-019-0708-6]
27 **Jia J**, Yang Y, Yan T, Chen T, Lu G. Down-regulation of RFWD3 inhibits cancer cells proliferation and migration in gastric carcinoma. *Gen Physiol Biophys* 2020; **39**: 363-371 [PMID: 32902405 DOI: 10.4149/gpb_2020009]
28 **Xu F**, Xiao Z, Fan L, Ruan G, Cheng Y, Tian Y, Chen M, Chen D, Wei Y. RFWD3 Participates in the Occurrence and Development of Colorectal Cancer *via* E2F1 Transcriptional Regulation of BIRC5. *Front Cell Dev Biol* 2021; **9**: 675356 [PMID: 34712656 DOI: 10.3389/fcell.2021.675356]
29 **Wang WJ**, Jin WW, Pan J, Wang LB, Zhu RT, Li J, Zhang CX, Liang RP. The expression of ring finger and WD repeat domain 3 in hepatocellular carcinoma and its clinical relevance. *J Hepatopancreat Sur* 2019; **31**: 741-745 [DOI: 10.11952/j.issn.1007-1954.2019.12.009]
30 **Rutgers M**, van Pelt MJ, Dhert WJ, Creemers LB, Saris DB. Evaluation of histological scoring systems for tissue-engineered, repaired and osteoarthritic cartilage. *Osteoarthritis Cartilage* 2010; **18**: 12-23 [PMID: 19747584 DOI: 10.1016/j.joca.2009.08.009]
31 **McLin VA**, Rankin SA, Zorn AM. Repression of Wnt/beta-catenin signaling in the anterior endoderm is essential for liver and pancreas development. *Development* 2007; **134**: 2207-2217 [PMID: 17507400 DOI: 10.1242/dev.001230]
32 **Brafman D**, Willert K. Wnt/β-catenin signaling during early vertebrate neural development. *Dev Neurobiol* 2017; **77**: 1239-1259 [PMID: 28799266 DOI: 10.1002/dneu.22517]
33 **Fatima S**, Luk JM, Poon RT, Lee NP. Dysregulated expression of dickkopfs for potential detection of hepatocellular carcinoma. *Expert Rev Mol Diagn* 2014; **14**: 535-548 [PMID: 24809435 DOI: 10.1586/14737159.2014.915747]
34 **Murillo-Garzón V**, Kypta R. WNT signalling in prostate cancer. *Nat Rev Urol* 2017; **14**: 683-696 [PMID: 28895566 DOI: 10.1038/nrurol.2017.144]
35 **Lee HC**, Kim M, Wands JR. Wnt/Frizzled signaling in hepatocellular carcinoma. *Front Biosci* 2006; **11**: 1901-1915 [PMID: 16368566 DOI: 10.2741/1933]
36 **Nakamura T**, Aoki S, Kitajima K, Takahashi T, Matsumoto K, Nakamura T. Molecular cloning and characterization of Kremen, a novel kringle-containing transmembrane protein. *Biochim Biophys Acta* 2001; **1518**: 63-72 [PMID: 11267660 DOI: 10.1016/s0167-4781(01)00168-3]
37 **Mishra SK**, Funair L, Cressley A, Gittes GK, Burns RC. High-affinity Dkk1 receptor Kremen1 is internalized by clathrin-mediated endocytosis. *PLoS One* 2012; **7**: e52190 [PMID: 23251700 DOI: 10.1371/journal.pone.0052190]
38 **Nakamura T**, Nakamura T, Matsumoto K. The functions and possible significance of Kremen as the gatekeeper of Wnt signalling in development and pathology. *J Cell Mol Med* 2008; **12**: 391-408 [PMID: 18088386 DOI: 10.1111/j.1582-4934.2007.00201.x]

World Journal of Gastroenterology

Submit a Manuscript: https://www.f6publishing.com

World J Gastroenterol 2022 July 21; 28(27): 3455-3475

DOI: 10.3748/wjg.v28.i27.3455

ISSN 1007-9327 (print) ISSN 2219-2840 (online)

ORIGINAL ARTICLE

Basic Study

Associations of gut microbiota with dyslipidemia based on sex differences in subjects from Northwestern China

Lei Guo, Yang-Yang Wang, Ji-Han Wang, He-Ping Zhao, Yan Yu, Guo-Dong Wang, Kun Dai, Yu-Zhu Yan, Yan-Jie Yang, Jing Lv

Specialty type: Gastroenterology and hepatology

Provenance and peer review: Invited article; Externally peer reviewed.

Peer-review model: Single blind

Peer-review report's scientific quality classification

Grade A (Excellent): 0
Grade B (Very good): B, B
Grade C (Good): 0
Grade D (Fair): D
Grade E (Poor): 0

P-Reviewer: Amedei A, Italy; Panduro A, Mexico; Papazafiropoulou A, Greece

Received: February 18, 2022
Peer-review started: February 18, 2022
First decision: May 9, 2022
Revised: May 17, 2022
Accepted: June 20, 2022
Article in press: June, 20, 2022
Published online: July 21, 2022

Lei Guo, Department of Spine Surgery, Honghui Hospital, Xi'an Jiaotong University, Xi'an 710054, Shaanxi Province, China

Yang-Yang Wang, School of Electronics and Information, Northwestern Polytechnical University, Xi'an 710129, Shaanxi Province, China

Ji-Han Wang, Institute of Medical Research, Northwestern Polytechnical University, Xi'an 710072, Shaanxi Province, China

He-Ping Zhao, Yan Yu, Yu-Zhu Yan, Jing Lv, Department of Clinical Laboratory, Honghui Hospital, Xi'an Jiaotong University, Xi'an 710054, Shaanxi Province, China

Guo-Dong Wang, Department of Quality Control, Xi'an Mental Health Center, Xi'an 710100, Shaanxi Province, China

Kun Dai, Department of Clinical Laboratory, Yanliang Railway Hospital of Xi'an, Xi'an 710089, Shaanxi Province, China

Yan-Jie Yang, Department of Cardiology, The First Affiliated Hospital of Xi'an Jiaotong University, Xi'an 710061, Shaanxi Province, China

Corresponding author: Jing Lv, MD, Doctor, Department of Clinical Laboratory, Honghui Hospital, Xi'an Jiaotong University, No. 555 You Yi Dong Road, Xi'an 710054, Shaanxi Province, China. lvjing-1219@163.com

Abstract

BACKGROUND

The gut microbiota (GM) has been proven to play a role in the regulation of host lipid metabolism, which provides a new theory about the pathogenesis of dyslipidemia. However, the associations of GM with dyslipidemia based on sex differences remain unclear and warrant elucidation.

AIM

To investigate the associations of GM features with serum lipid profiles based on sex differences in a Chinese population.

METHODS

This study ultimately recruited 142 participants (73 females and 69 males) at

Honghui Hospital, Xi'an Jiaotong University. The anthropometric and blood metabolic parameters of all participants were measured. According to their serum lipid levels, female and male participants were classified into a high triglyceride (H_TG) group, a high total cholesterol (H_CHO) group, a low high-density lipoprotein cholesterol (L_HDL-C) group, and a control (CON) group with normal serum lipid levels. Fresh fecal samples were collected for 16S rRNA gene sequencing. UPARSE software, QIIME software, the RDP classifier and the FAPROTAX database were used for sequencing analyses.

RESULTS

The GM composition at the phylum level included Firmicutes and Bacteroidetes as the core GM. Different GM features were identified between females and males, and the associations between GM and serum lipid profiles were different in females and males. The GM features in different dyslipidemia subgroups changed in both female patients and male patients. Proteobacteria, Lactobacillaceae, *Lactobacillus* and *Lactobacillus_salivarius* were enriched in H_CHO females compared with CON females, while Coriobacteriia were enriched in L_HDL-C females. In the comparison among the three dyslipidemia subgroups in females, *Lactobacillus_salivarius* were enriched in H_CHO females, and Prevotellaceae were enriched in L_HDL-C females. Compared with CON or H_TG males, Prevotellaceae, *unidentified_Ruminococcaceae*, *Roseburia* and *Roseburia_inulinivorans* were decreased in L_HDL-C males (P value < 0.05), and linear discriminant analysis effect size analysis indicated an enrichment of the above GM taxa in H_TG males compared with other male subgroups. Additionally, *Roseburia_inulinivorans* abundance was positively correlated with serum TG and total cholesterol levels, and *Roseburia* were positively correlated with serum TG level. Furthermore, Proteobacteria (0.724, 95%CI: 0.567-0.849), Lactobacillaceae (0.703, 95%CI: 0.544-0.832), *Lactobacillus* (0.705, 95%CI: 0.547-0.834) and *Lactobacillus_salivarius* (0.706, 95%CI: 0.548-0.835) could distinguish H_CHO females from CON females, while Coriobacteriia (0.710, 95%CI: 0.547-0.841), Coriobacteriales (0.710, 95%CI: 0.547-0.841), Prevotellaceae (0.697, 95%CI: 0.534-0.830), *Roseburia* (0.697, 95%CI: 0.534-0.830) and *Roseburia_inulinivorans* (0.684, 95%CI: 0.520-0.820) could discriminate H_TG males from CON males. Based on the predictions of GM metabolic capabilities with the FAPROTAX database, a total of 51 functional assignments were obtained in females, while 38 were obtained in males. This functional prediction suggested that cellulolysis increased in L_HDL-C females compared with CON females, but decreased in L_HDL-C males compared with CON males.

CONCLUSION

This study indicates associations of GM with serum lipid profiles, supporting the notion that GM dysbiosis may participate in the pathogenesis of dyslipidemia, and sex differences should be considered.

Key Words: Dyslipidemia; Gut microbiota; 16S rRNA; Sequencing; Sex differences; Northwestern China

©The Author(s) 2022. Published by Baishideng Publishing Group Inc. All rights reserved.

Core Tip: Dyslipidemia is the circulating lipid expression of metabolic syndrome, and alterations of gut microbiota (GM) are indicated to participate in the pathogenesis of dyslipidemia; however, little evidence was found in the literature on sex differences for these associations. Our results demonstrated the GM features in different dyslipidemia subgroups in females and males, suggesting a complex interaction between GM and lipid metabolism. Our observations may provide new evidence that different GM taxa may be associated with distinct lipids, and that GM may affect specific aspects of lipid metabolism. More studies are required to propose specific taxa that have the potential to ameliorate dyslipidemia.

Citation: Guo L, Wang YY, Wang JH, Zhao HP, Yu Y, Wang GD, Dai K, Yan YZ, Yang YJ, Lv J. Associations of gut microbiota with dyslipidemia based on sex differences in subjects from Northwestern China. *World J Gastroenterol* 2022; 28(27): 3455-3475

URL: https://www.wjgnet.com/1007-9327/full/v28/i27/3455.htm

DOI: https://dx.doi.org/10.3748/wjg.v28.i27.3455

INTRODUCTION

Obesity has become a worldwide public health challenge, with its prevalence nearly tripled since 1975 [1]. Obesity is defined as a chronic accumulation of excessive lipids in tissues[2], which is related to the disruption of lipid metabolism[3]. As a defect in lipid metabolism, dyslipidemia is defined as any abnormality in blood lipid levels, and is characterized by an elevation of circulating triglyceride (TG), total cholesterol (TC), and low-density lipoprotein cholesterol (LDL-C), or a decrease in high-density lipoprotein cholesterol (HDL-C). Since observational studies have shown that 60%-70% of adults have lipid levels outside the recommended range[4,5], it is essential to reveal the underlying mechanism of dyslipidemia. Circulating lipid levels are known to have an important genetic contribution from over 500 single-nucleotide polymorphisms in more than 150 Loci, explaining approximately 40% of the total individual variation[6]. However, the unexplained 60% variation has been attributed to undiscovered elements and unquantified environmental factors, such as dietary intake and physical activity[7,8]. In recent years, considerable progress has been made in elucidating the mechanism responsible for dyslipidemia, and accumulated evidence has shown that the gut microbiota (GM) may play a potential role in obesity and related metabolic diseases, such as dyslipidemia[9-12].

The human gastrointestinal tract harbors over 100 trillion microorganisms[13], and the gut bacteria having effects on human health are the most prevalent and well-studied. In humans, GM profiles vary among different ethnicities (host genetics) and between different sexes[14,15], and are mainly shaped by early life events and stabilize in adolescence[16]. However, its composition and activity can be dynamic, and may be altered dramatically by multiple factors, such as medications, chronic dietary patterns and other environmental exposures[15,17,18]. This "microbial organ" has been recognized to perform various physiological functions[19-21], and is often called "a new virtual metabolic organ"[22,23]. The first indication of associations between GM and disorder statuses were for inflammation[24], and altered GM community (dysbiosis) has now been established in the development of cardiometabolic phenotypes[25]. These lines of evidence have raised an interest in GM as an important candidate in accounting for the unexplained variation in serum lipid levels in humans, and as a target for the therapeutic benefit of dyslipidemia[26]. Recent studies have convincingly linked GM to dyslipidemia, and GM was reported to explain substantial variation in TG and HDL-C levels independent of genetic factors in a Dutch study[26]. In addition, accumulating data from animal studies demonstrate that GM can affect host lipid metabolism through multiple direct and indirect biological mechanisms[27,28]. Nevertheless, determining associations between GM and host lipid metabolism remains a challenge in humans. Furthermore, sex is an important factor that may influence GM profiles, and sex differences can be observed in serum lipid profiles[29-31]. However, the relationship between GM and dyslipidemia based on sex differences remains unclear.

Collectively, ethnicity, geography and sex are potent factors that could influence the GM community [14,15,32]. Thus, this study focused on the associations of GM features with dyslipidemia based on sex differences in a northwestern Chinese population. We first reveal sex differences regarding GM features and then introduce dyslipidemia, highlighting its intricate relationships with GM, and discuss possible altered GM functions.

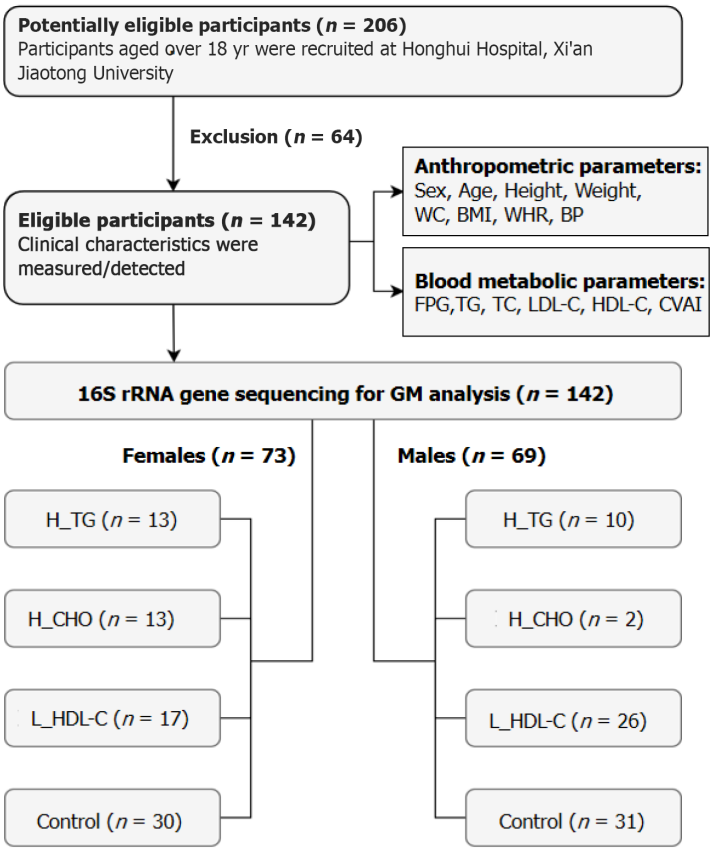
MATERIALS AND METHODS

Study design

From July 2018 to January 2020, this study recruited 206 adult individuals (107 females and 99 males) from the outpatient clinics at Honghui Hospital, Xi'an Jiaotong University, China. Individuals were excluded if one of the following conditions existed: (1) With any gastrointestinal diseases, infectious or chronic diseases, serious systematic dysfunctions, or surgery histories of the gastrointestinal tract; (2) Taking any medications that could disrupt the original GM community, such as probiotics or prebiotics, antimicrobial therapies, anti-inflammatory drugs, acid-suppressing drugs, immunosuppressants, or anti-dyslipidemia/anti-dysglycemia/anti-hypertension drugs within the past month prior to sampling [33]; and (3) Females who were pregnant or lactating. The individuals who met the above conditions were included as participants in this study, and informed consent was obtained. Finally, 142 participants (73 females and 69 males) were recruited, including 81 dyslipidemia patients and 61 controls (CON) with normal serum lipid levels. Data privacy was ensured by using anonymized identifiers, and the study flow is shown in Figure 1. This study was approved by the Ethical Committee of Honghui Hospital, Xi'an Jiaotong University (Protocol Number: 201801022, approved January 8, 2018).

Measurement of anthropometric parameters

On their first visit, related medical information was documented for all participants. Body weight (W) and height (H) were measured without shoes and heavy clothing to the nearest 0.1 cm and 0.1 kg, respectively. Waist circumference (WC) was measured in the middle of the lower rib margin and the iliac crest with a nonexpandable tape to the nearest 0.1 cm in the standing position. Body mass index



DOI: 10.3748/wjg.v28.i27.3455 **Copyright** ©The Author(s) 2022.

Figure 1 Flow chart of this study. WC: Waist circumference; BMI: Body mass index; WHR: Waist circumference/height ratio; BP: Blood pressure; FPG: Fasting plasma glucose; TG: Triglyceride; TC: Total cholesterol; LDL-C: Low-density lipoprotein cholesterol; HDL-C: High-density lipoprotein cholesterol; CVAI: Chinese visceral adiposity index; GM: Gut microbiota; H_TG: High triglyceride group; H_CHO: High cholesterol group; L_HDL-C: Low high-density lipoprotein cholesterol group.

(BMI) and WC/height ratio (WHR) were calculated accordingly. Blood pressure (BP) was assessed using a medical electronic sphygmomanometer (HEM-7130 professional, OMRON, Dalian, China) on the left arm positioned at the heart level with palm face up in a sitting position. The participants were required to rest in a seated position for at least 5 min before BP assessment, with triplicate measurements at 1-min intervals. All equipment was calibrated at the beginning of the study.

Detection and computation of metabolic indicators

Venous blood samples were drawn from an antecubital vein in the morning following an overnight (at least 8 h) fast. Levels of fasting plasma glucose, TG, TC, LDL-C and HDL-C were detected by an automatic biochemical analyzer (Cobas c701, Roche, Mannheim, Germany). This instrument system was calibrated regularly. Moreover, the Chinese visceral adiposity index (CVAI) was calculated using the formula[34]: CVAI for females = -187.32 + 1.71 × age + 4.23 × BMI + 1.12 × WC (cm) + 39.76 × Log_{10}TG (mmol/L) - 11.66 × HDL-C (mmol/L), and CVAI for males = -267.93 + 0.68 × age + 0.03 × BMI + 4.00 × WC + 22.00 × Log_{10}TG - 16.32 × HDL-C.

Diagnostic criteria and grouping

In accordance with the "Guidelines for prevention and treatment of dyslipidemia in Chinese adults" (revised in 2016)[35] and the stratification standard of dyslipidemia in the primary prevention population of arteriosclerotic cardiovascular disease in China[36], dyslipidemia was defined as the presence of one or more abnormal serum lipid levels without any lipid-lowering medication: TG ≥ 1.7 mmol/L, TC ≥ 5.2 mmol/L, LDL-C ≥ 3.4 mmol/L, and/or HDL-C < 1.0 mmol/L. Subsequently, participants were divided into subgroups according to their serum lipid profiles. Specifically, patients were classified into the high TG (H_TG) group if only high TG level existed. Patients with increased serum TC and/or LDL-C levels and without HDL-C or TG abnormalities were classified into the high cholesterol (H_CHO) group. Patients were classified into the low HDL-C (L_HDL-C) group if only low serum HDL-C level existed. Participants with normal serum lipid profiles served as CON.

Fecal sample collection, DNA extraction, and 16S rRNA gene sequencing

Fresh fecal samples were collected from each participant at home, and stored in foam boxes with frozen cold packs[37]. Within 6 h after defecation, all fecal samples were transported to the Clinical Laboratory of Honghui Hospital, Xi'an Jiaotong University, and immediately stored at -80 °C until further processing. Genomic DNA was extracted from all samples using the QIAamp Fast DNA Stool Mini Kit (Qiagen, Hilden, Germany) following the manufacturer's instructions. After quality evaluation and concentration determination, DNA samples, greater than 1 μg and with an OD value between 1.8-2.0, were considered to be qualified for subsequent sequencing. Then, the V3-V4 regions of the 16S rRNA gene were amplified by universal primers (338F: 5'-ACT CCT ACG GGA GGC AGC AG-3'; 806R: 5'-GGA CTA CHV GGG TWT CTA AT-3') with barcodes, and all PCRs were performed using Phusion® High Fidelity PCR Master Mix (New England Biolabs, Ipswich, MA, United States). Next, the PCR products were mixed and purified using a GeneJET™ Gel Extraction Kit (Thermo Scientific, Waltham, MA, United States). The sequencing library for each sample was constructed with the NEB Next® Ultra ™ DNA Library Prep Kit for Illumina (New England Biolabs, Ipswich, MA, United States), and library quality was assessed on a Qubit® 2.0 Fluorometer (Thermo Scientific, Waltham, MA, United States). Finally, the generated libraries were pair-end (2 × 250 bp) sequenced on the Illumina NovaSeq 6000 platform (Illumina, San Diego, CA, United States).

16S rRNA gene sequencing analyses

UPARSE (v7.0.1001) and QIIME software (v1.7.0) were introduced for sequencing analyses. According to a similarity threshold of 97%, acquired clean reads with high quality were de novo clustered into the same operational taxonomic unit (OTU), and the representative sequence of each OTU was screened and used to annotate taxonomic information based on the RDP classifier (v2.2). The GM diversity and composition were assessed based on the annotated OTUs. The alpha diversity (α-diversity) of GM was estimated by four indices, including Chao1, abundance coverage-based estimator (Ace), Shannon and Simpson. The comparisons of these indices between groups were conducted by the Wilcoxon rank-sum test, using function *wilcox.test* from the R package stats. To investigate the significance of differences in the GM community, beta diversity (β-diversity) was estimated using the unweighted UniFrac method to calculate the distances between samples, and visualized by the principal coordinates analysis (PCoA) model. The "*WGCNA*", "*stats*" and "*ggplot2*" packages in R were utilized. The top ten GM taxa sorted by higher relative abundances at the six taxonomic levels, including phylum, class, order, family, genus and species, were identified and visualized in each group. The linear discriminant analysis (LDA) effect size (LEfSe) algorithm was applied to identify the enriched significant taxa in each group. The LDA score threshold was set to 2 on a log10 scale. The FAPROTAX (v1.2.2) database, containing 90 different types of metabolic assignments, was introduced to obtain the functional information of the GM community[38], and the differences between groups were assessed by the Wilcoxon rank-sum test, with a P value < 0.05 considered significant.

Statistical analysis

SPSS (v23.0.0.0, IBM SPSS Inc., Chicago, IL), R platform (v4.0.2, R Foundation, Vienna, Austria), GraphPad Prism (v8.4.3, GraphPad Software Inc., San Diego, CA, United States) and MedCalc (v19.0.4, MedCalc Software Bvba, Ostend, Belgium) were employed for statistical analysis and figure construction. The normal distribution of quantitative variables was assessed by the Shapiro-Wilk test. Clinical parameters are presented as the mean ± SD, and were analyzed among groups by the variance analysis (ANOVA) or Welch's ANOVA depending on the homogeneity of variance. In addition, the Games-Howell test was used for multiple comparisons if a P value < 0.05 existed. The "*ggcorrplot*" package in R was utilized for Spearman correlation analysis between clinical parameters. Moreover, Spearman correlation analysis was also applied to evaluate the potential associations between GM features and clinical parameters, using the function *cor.test (method = spearman)* in R. Receiver operating characteristic (ROC) curve analysis, with areas under the curve, was applied to evaluate the diagnostic performance of specific GM taxa. All statistical tests with a P value < 0.05 were considered significant.

The bioinformatics analyses and statistical methods/techniques mentioned in this study were conducted, verified and reviewed by our expert Ji-Han Wang, PhD, from Institute of Medical Research, Northwestern Polytechnical University, and Guo-Dong Wang, Master Degree, from Department of Quality Control, Xi'an Mental Health Center.

RESULTS

Basic information of the study population

The present study finally included 142 participants (73 females and 69 males), as shown in Figure 1. Table 1 shows the clinical characteristics of all the participants grouped by sex and serum lipid profiles. Serum lipid levels and CVAI showed differences among female subgroups as did height, WC and WHR (P value < 0.05). Serum lipid levels and CVAI showed differences among male subgroups as well (P

Table 1 Clinical characteristics of the study population

	Females					Males				
	High TG	High CHO	Low HDL-C	Control	*P* value	High TG	High CHO	Low HDL-C	Control	*P* value
Number	13	13	17	30		10	2	26	31	
Age (yr)	55 ± 8	56 ± 5	54 ± 16	52 ± 12	0.420	54 ± 12	58 ± 11	52 ± 12	56 ± 13	0.770
Height (cm)	155.0 ± 7.2	147.0 ± 5.8	153.6 ± 5.4	154.3 ± 4.8	0.001[a]	164.7 ± 6.2	160.0 ± 1.2	166.8 ± 5.4	164.8 ± 6.1	0.300
Weight (kg)	61.6 ± 9.3	53.6 ± 8.6	55.0 ± 9.2	55.3 ± 8.8	0.102	65.8 ± 9.0	56.2 ± 4.9	65.0 ± 8.3	61.0 ± 10.5	0.231
WC (cm)	90.2 ± 9.6	85.4 ± 7.2	82.3 ± 7.8	82.4 ± 8.6	0.035[a]	88.3 ± 6.1	75.2 ± 9.5	87.0 ± 8.2	83.1 ± 8.8	0.066
BMI (kg/m^2)	25.7 ± 3.7	24.7 ± 3.3	23.3 ± 3.2	23.2 ± 3.2	0.103	24.2 ± 3.0	22.0 ± 2.2	23.3 ± 2.8	22.4 ± 3.6	0.403
WHR	0.58 ± 0.07	0.58 ± 0.05	0.54 ± 0.06	0.53 ± 0.06	0.017[a]	0.54 ± 0.03	0.47 ± 0.06	0.52 ± 0.05	0.50 ± 0.50	0.153
SBP (mmHg)	141 ± 17	139 ± 17	125 ± 19	129 ± 25	0.127	137 ± 23	136 ± 12	128 ± 21	134 ± 18	0.569
DBP (mmHg)	82 ± 10	78 ± 8	73 ± 9	76 ± 11	0.110	84 ± 12	80 ± 5	78 ± 11	81 ± 10	0.509
FPG (mmol/L)	5.00 ± 1.33	4.96 ± 0.57	5.48 ± 1.17	4.90 ± 0.59	0.346	5.05 ± 0.73	4.85 ± 2.23	4.81 ± 0.80	4.97 ± 1.10	0.895
TG (mmol/L)	2.15 ± 0.48	1.40 ± 0.22	1.01 ± 0.31	1.21 ± 0.33	< 0.001[a]	4.04 ± 0.86	5.75 ± 0.65	3.07 ± 0.76	3.97 ± 0.55	0.012[a]
TC (mmol/L)	4.31 ± 0.50	5.58 ± 0.43	2.57 ± 0.63	0.41 ± 0.67	< 0.001[a]	2.01 ± 0.68	4.26 ± 0.95	1.77 ± 0.54	2.19 ± 0.45	< 0.001[a]
LDL-C (mmol/L)	2.16 ± 0.43	3.44±0.49	1.51 ± 0.56	2.25 ± 0.56	< 0.001[a]	1.13 ± 0.09	1.20 ± 0.27	0.79 ± 0.14	1.48 ± 0.32	0.001[a]
HDL-C (mmol/L)	1.29 ± 0.23	1.75±0.31	0.77 ± 0.15	1.50 ± 0.36	< 0.001[a]	2.98 ± 0.78	4.55 ± 0.92	2.28 ± 0.69	2.49 ± 0.54	< 0.001[a]
CVAI	113.63 ± 25.96	94.16 ± 19.92	86.84 ± 32.86	76.30 ± 37.05	0.008[a]	112.13 ± 26.62	54.08 ± 53.32	103.91 ± 36.87	78.76 ± 38.08	0.011[a]

[a]$P < 0.05$.

Data are presented as mean ± SD. *P* values are from the variance analysis (ANOVA) or Welch's ANOVA depending on the homogeneity of variance. CHO: Cholesterol; WC: Waist circumference; BMI: Body mass index; WHR: Waist circumference/height ratio; SBP: Systolic blood pressure; DBP: Diastolic blood pressure; FPG: Fasting plasma glucose; TG: Triglyceride; TC: Total cholesterol; LDL-C: Low-density lipoprotein cholesterol; HDL-C: High-density lipoprotein cholesterol; CVAI: Chinese visceral adiposity index.

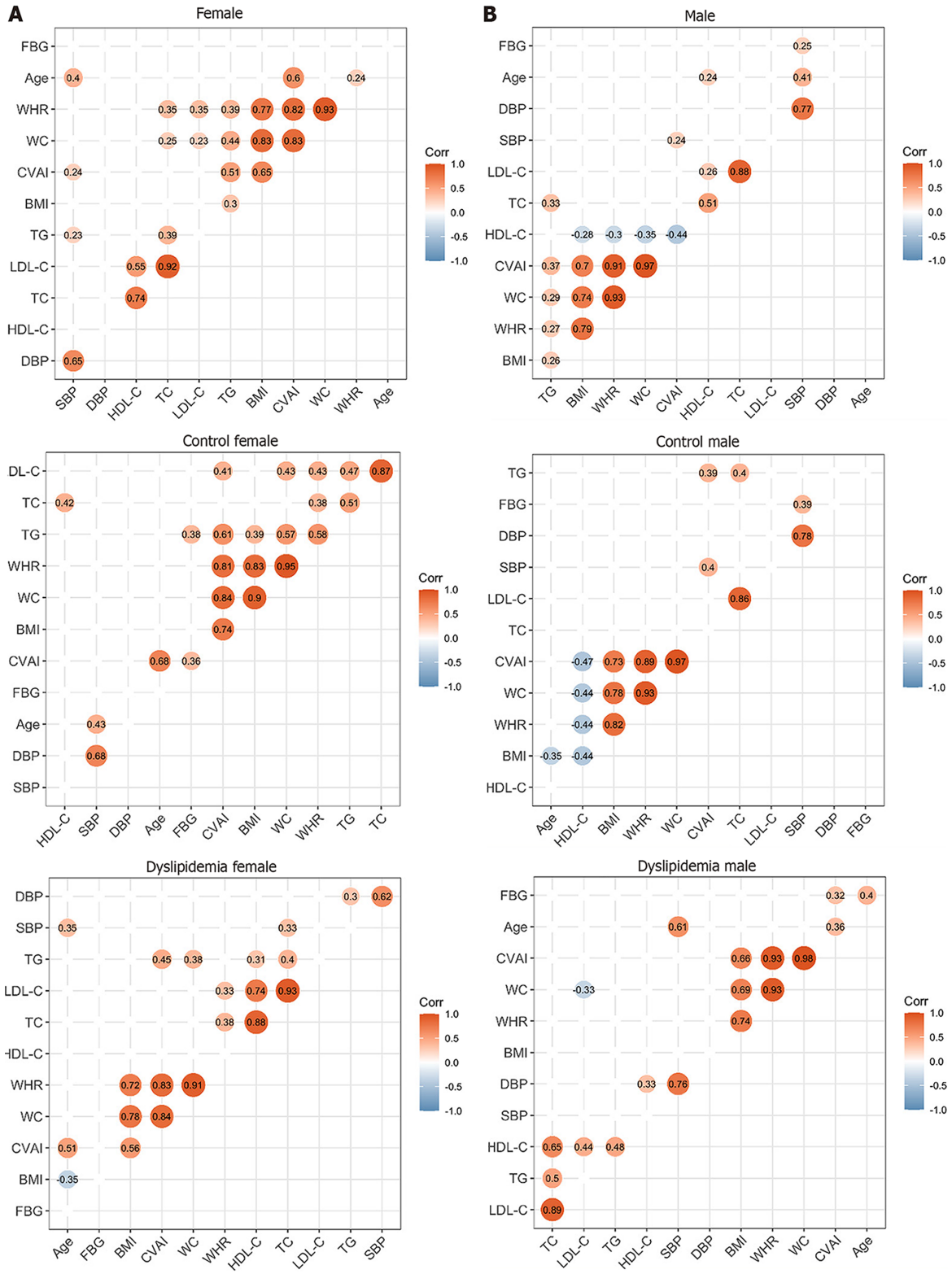
value < 0.05). Please refer to Supplementary Table 1 for detailed information and differences between females and males. The correlation analysis between the clinical characteristics of females and males is shown in Figure 2, and indicates positive correlations between the serum lipid indicators.

Diversity analysis of GM in the study population

To identify the associations of GM features with serum lipid profiles, we performed 16S rRNA gene sequencing analyses of GM from fecal samples. After quality CON, sequencing reads from 142 fecal samples were processed to determine the OTUs. Our data indicated that females had more unique OTUs, and the number of common OTUs shared by the female subgroups was larger than that shared by the male subgroups (data not shown).

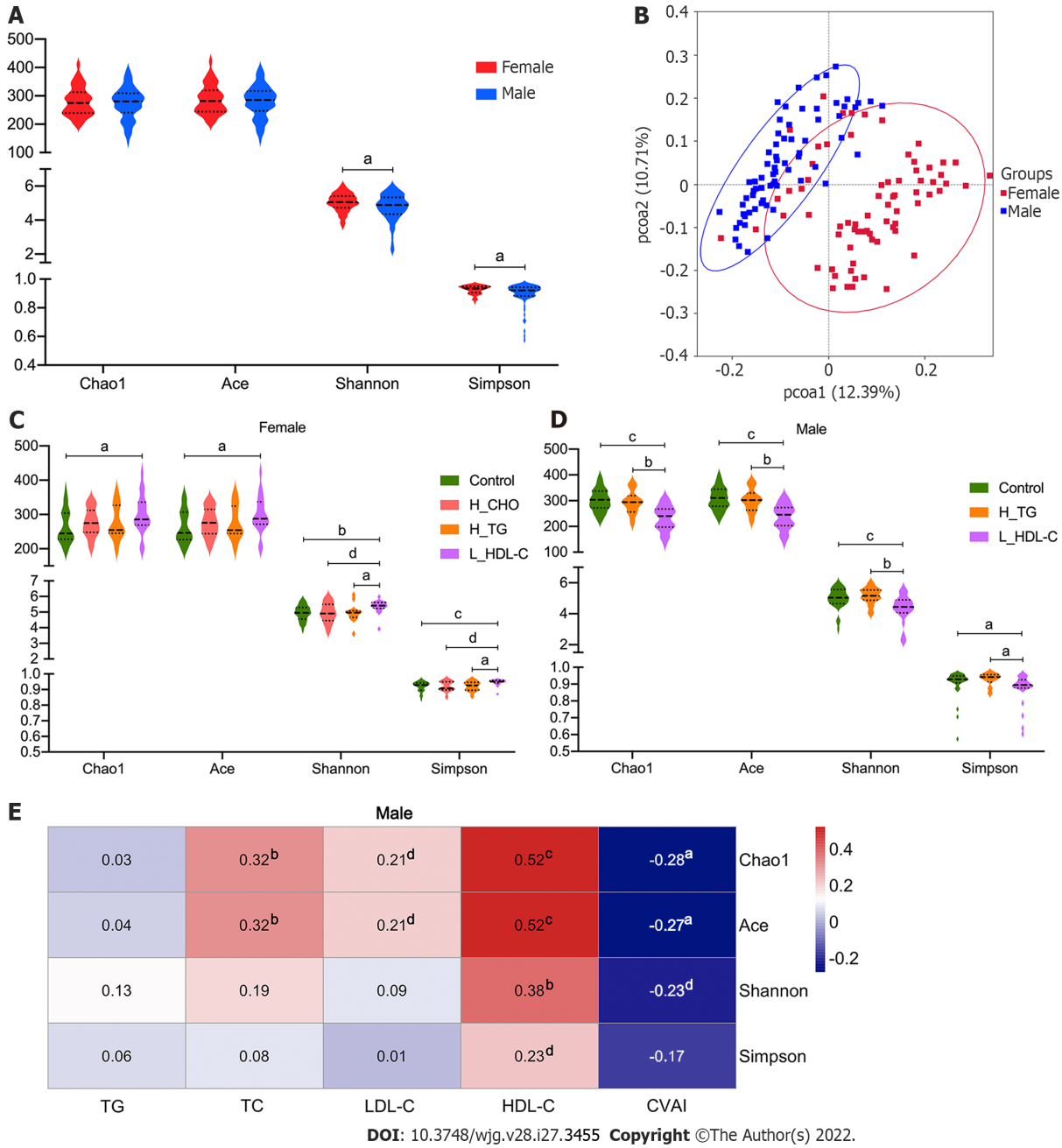
We evaluated the diversity of the GM community to assess the richness and evenness for females and males, and Shannon and Simpson indices suggested a higher α-diversity in females (*P* value < 0.05, Figure 3A). In addition, a dissimilarity between females and males was observed according to the visualized PCoA model for β-diversity analysis (Figure 3B). Since sex is an important determinant of GM and serum lipids[30,32,39], the study population was divided into a female group and a male group for the subsequent analyses.

To reveal the associations of GM diversity with serum lipid profiles based on sex differences, we conducted analogous analyses in the enrolled females and males. Our results showed that the α-diversity of GM was different in different dyslipidemia subgroups in females and males (Figure 3C and D). Of note, the α-diversity in L_HDL-C females was higher than that in CON females (*P* value < 0.05), while it was lower in L_HDL-C males than that in CON males (*P* value < 0.05). Additionally, the α-diversity of GM in H_TG males was higher than that in L_HDL-C males (*P* value < 0.05). The PCoA results suggested that the GM community in different dyslipidemia subgroups varied from that in the CON group in females and males, respectively, but could not be separated accurately and clearly (data not shown). Furthermore, the α-diversity of GM was found to be correlated with the serum lipid profiles and CVAI in males (Figure 3E). Specifically, the Chao1, Ace and Shannon indices were positively correlated with the serum HDL-C levels, while the Chao1 and Ace indices were negatively correlated



DOI: 10.3748/wjg.v28.i27.3455 **Copyright** ©The Author(s) 2022.

Figure 2 Correlations between the clinical characteristics in the study population. A: Correlations between the clinical characteristics of the enrolled females; B: Correlations between the clinical characteristics of the enrolled males. The circle represents the correlation coefficient of each two parameters (*P* value < 0.05). The number presented in the circle is the correlation coefficient. The larger the absolute value is, the stronger the correlation is. Blue indicates a negative correlation and orange indicates a positive correlation. The depth of the color represents the strength of the correlation. The deeper the color is, the stronger the correlation is. The "*ggcorrplot*" package in R was utilized for Spearman's correlation analysis. WC: Waist circumference; BMI: Body mass index; WHR: Waist circumference/height ratio; SBP: Systolic blood pressure; DBP: Diastolic blood pressure; TG: Triglyceride; TC: Total cholesterol; LDL-C: Low-density lipoprotein cholesterol; HDL-C: High-density lipoprotein cholesterol; CVAI: Chinese visceral adiposity index.



DOI: 10.3748/wjg.v28.i27.3455 **Copyright** ©The Author(s) 2022.

Figure 3 Diversity analysis of gut microbiota in the study population. A: Violin plots of α-diversity analysis of gut microbiota (GM) in females and males of the study population. Each plot represents one index of the α-diversity distribution of GM, including Chao1, Ace, Shannon and Simpson indices, for each group. The Wilcoxon rank-sum test was used to evaluate the differences between groups; B: Plots of principal coordinate analysis (PCoA) based on the operational taxonomic unit level in females and males of the study population. Each square represents the GM community in one sample, and the axis title represents the percentage change of interpretation. The distance between squares represents the similarity or dissimilarity of the GM community in the study population, and PCoA analysis was conducted by unweighted UniFrac method; C: Violin plots of α-diversity analysis of GM in females of the study population; D: Violin plots of α-diversity analysis of GM in males of the study population; E: Correlations between GM diversity and serum lipid profiles in males of the study population. Spearman's correlation analysis was conducted. The number presented in each cell is the correlation coefficient. The larger the absolute value is, the stronger the correlation is. Blue indicates a negative correlation and red indicates a positive correlation. The depth of the color represents the strength of the correlation. The deeper the color is, the stronger the correlation is. $^{a}P < 0.05$, $^{b}P < 0.01$, $^{c}P < 0.001$, $^{d}P < 0.1$. TG: Triglyceride; TC: Total cholesterol; LDL-C: Low-density lipoprotein cholesterol; HDL-C: High-density lipoprotein cholesterol; CVAI: Chinese visceral adiposity index; H_CHO: High total cholesterol; H_TG: high triglyceride; L_HDL-C: Low high-density lipoprotein cholesterol.

with CVAI. However, similar results could not be observed in females. The bioinformatics analyses above revealed the associations between the general state of GM and the human serum lipid profiles.

Taxonomic composition of GM in the study population

After diversity analysis, we focused on the relative abundances of GM taxa at six different taxonomic levels in different groups, and the top ten taxa with higher relative abundances at each level are shown in Supplementary Figure 1 for females and males. Similarly, the top ten taxa at each level were

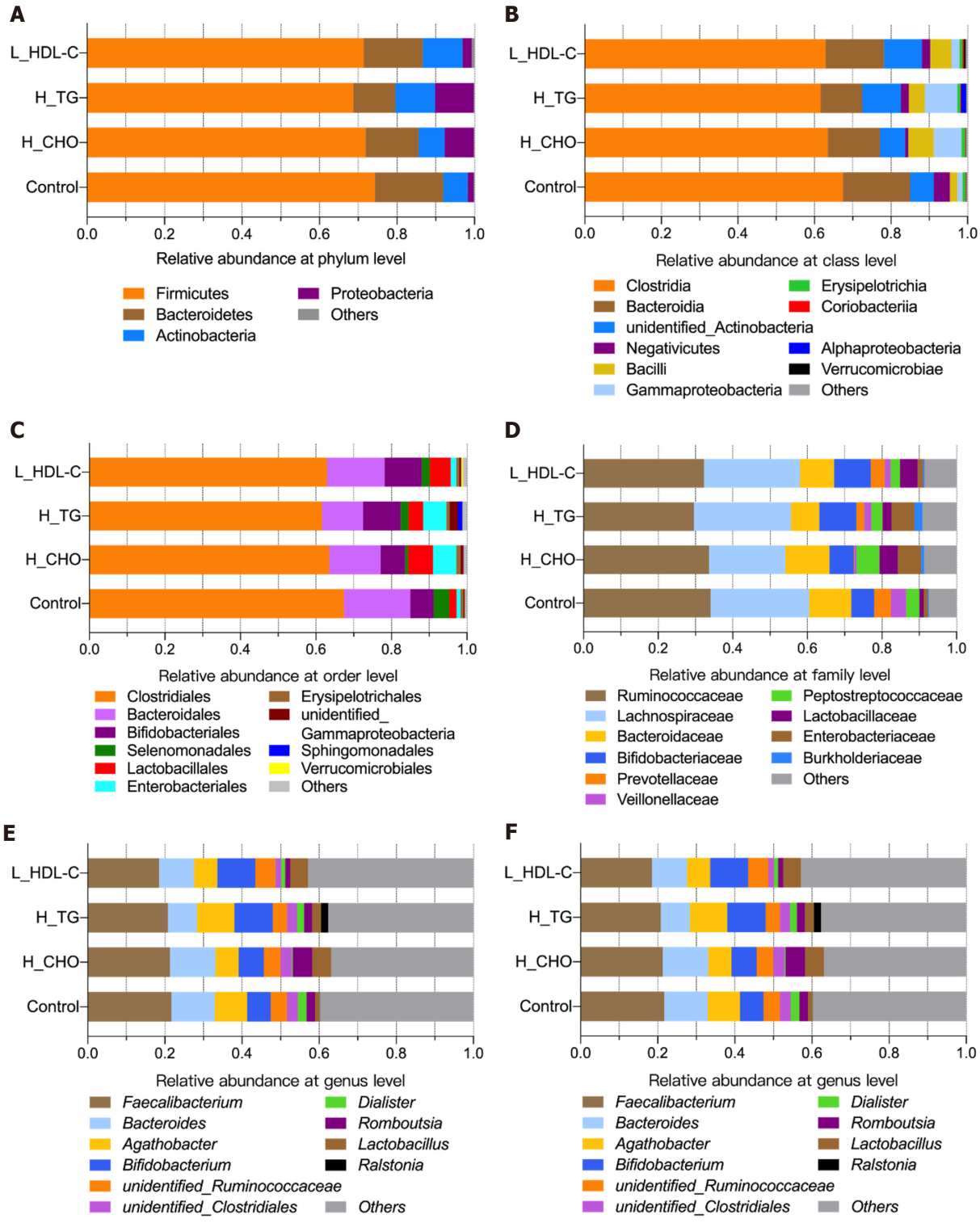
identified in the female subgroups (Figure 4). Consistent with previous data, the GM composition at the phylum level included Firmicutes and Bacteroidetes as the core GM, with lower relative abundances of Actinobacteria, Proteobacteria and others. The most abundant GM taxa were Clostridia, Bacteroidia, Clostridiales, Bacteroides, Ruminococcaceae, Lachnospiraceae, Bacteroidaceae, *Faecalibacterium* and *Bacteroides*. GM taxa with relative abundances of no less than 0.0001 at each level were included in the following analyses. The relative abundances of Proteobacteria, Lactobacillaceae and *Lactobacillus* were no less than 0.010 in H_CHO females, and were greater than those in CON females (P value < 0.05); while the relative abundance of Coriobacteriia was higher in L_HDL-C females than that in CON females (P value < 0.05). In the comparison of H_CHO and L_HDL-C females, Prevotellaceae abundance was greater in L_HDL-C females (P value < 0.05), and *Lactobacillus_salivarius* abundance was greater in H_CHO females (P value < 0.05). In the comparison of H_CHO and H_TG females, *Agathobacter* abundance was higher in H_TG females (P value < 0.05), while the relative abundances of *Ruminococcus_bromii* and *Lactobacillus_salivarius* were higher in H_CHO females (P value < 0.05). Additionally, Prevotellaceae abundance was greater in L_HDL-C females than that in H_TG females (P value < 0.05). Subsequently, analogous comparison analysis was conducted in the male subgroups (Figure 5). The most abundant taxa were Clostridia, Bacteroidia, Clostridiales, Bacteroidales, Ruminococcaceae, Lachnospiraceae, *Faecalibacterium*, *Bifidobacterium*, *Bifidobacterium_pseudocatenulatum* and *Clostridium_disporicum*. In the comparison of L_HDL-C and CON males, the relative abundances of Bacteroidetes, Bacteroidia, Bacteroidales, Prevotellaceae, *unidentified_Ruminococcaceae*, *Roseburia* and *Roseburia_inulinivorans* were lower in L_HDL-C males (P value < 0.05). Meanwhile, Coriobacteriia, Coriobacteriales, Prevotellaceae, *unidentified_Ruminococcaceae*, *Roseburia* and *Roseburia_inulinivorans* were lower in L_HDL-C males than those in H_TG males (P value < 0.05). Interestingly, no differences were observed in the comparison between the H_TG group and CON group (P value > 0.05) in females or males.

LEfSe analysis was conducted in different dyslipidemia subgroups and the CON group in females and males. Compared with CON females (Figure 6), LEfSe analysis revealed the enrichment of Proteobacteria, Lactobacillaceae, *Lactobacillus* and *Lactobacillus_salivarius* in H_CHO females, and the enrichment of Coriobacteriia in L_HDL-C females. In the comparison among the three dyslipidemia subgroups in females, *Lactobacillus_salivarius* were enriched in H_CHO females, and Prevotellaceae were enriched in L_HDL-C females. Simultaneously, LEfSe analysis revealed that Prevotellaceae, *unidentified_Ruminococcaceae*, *Roseburia*, *Roseburia_inulinivorans*, Coriobacteriia, Coriobacteriales and Verrucomicrobiae were enriched in H_TG males compared with other males (Figure 7).

Associations of GM taxa with serum lipid profiles in the study population

To further explore the clinical implications of GM in dyslipidemia, Spearman correlation analysis was introduced to assess the associations between differential GM taxa and the serum lipid profiles/CVAI, and a number of reliable correlations were revealed. In females, a positive correlation of *Bacteroides_coprocola* with serum TG level was observed, while negative correlations of Bacteroidetes, Bacteroidia and Bacteroidales with CVAI were noted (P value < 0.05, Figure 8A). Moreover, more correlations were identified in males (P value < 0.05, Figure 8B). Specifically, the relative abundances of Actinobacteria, unidentified_Actinobacteria, Bifidobacteriales, Bifidobacteriaceae and *Bifidobacterium* were negatively correlated with the serum TG and TC levels, the relative abundance of *Roseburia_inulinivorans* was positively correlated with the serum TG and TC levels, and the relative abundance of *Roseburia* was positively correlated with the serum TG level. In addition, the relative abundances of Leuconostocaceae, *Weissella* and *Weissella_cibaria* were correlated with increased serum TC and LDL-C levels, and the relative abundance of *Bacteroides_vulgatus* was correlated with decreased serum LDL-C level. Furthermore, we found that the relative abundances of Bacteroidetes, Bacteroidia, Bacteroidales, Coriobacteriales, Prevotellaceae, *unidentified_Ruminococcaceae* and *Roseburia_inulinivorans* were positively correlated with serum HDL-C level, and the relative abundances of Bacteroidetes, Bacteroidia, Bacteroidales and *Bacteroides_vulgatus* were negatively correlated with CVAI in males.

To search for the specific GM taxa that may facilitate the differentiation of lipid profiles in dyslipidemia patients from CON, ROC curve analysis was conducted in the female and male subgroups (P value < 0.05, Figure 9). The GM taxa, that effectively distinguished H_CHO females from CON females, were Proteobacteria (0.724, 95%CI: 0.567-0.849), Lactobacillaceae (0.703, 95%CI: 0.544-0.832), *Lactobacillus* (0.705, 95%CI: 0.547-0.834) and *Lactobacillus_salivarius* (0.706, 95%CI: 0.548-0.835). In addition, Coriobacteriia (0.697, 95%CI: 0.546-0.822) may help discriminate L_HDL-C females from CON females. Moreover, the GM taxa in favor of the differentiation of H_TG males from CON males were Coriobacteriia (0.710, 95%CI: 0.547-0.841), Coriobacteriales (0.710, 95%CI: 0.547-0.841), Prevotellaceae (0.697, 95%CI: 0.534-0.830), *Roseburia* (0.697, 95%CI: 0.534-0.830) and *Roseburia_inulinivorans* (0.684, 95%CI: 0.520-0.820). Additionally, seven GM taxa may play a role in distinguishing L_HDL-C males from CON males: Bacteroidetes (0.676, 95%CI: 0.539-0.794), Bacteroidia (0.676, 95%CI: 0.539-0.794), Bacteroidales (0.676, 95%CI: 0.538-0.793), Prevotellaceae (0.685, 95%CI: 0.548-0.802), *unidentified_Ruminococcaceae* (0.687, 95%CI: 0.551-0.804), *Roseburia* (0.662, 95%CI: 0.524-0.782) and *Roseburia_inulinivorans* (0.682, 95%CI: 0.545-0.799).

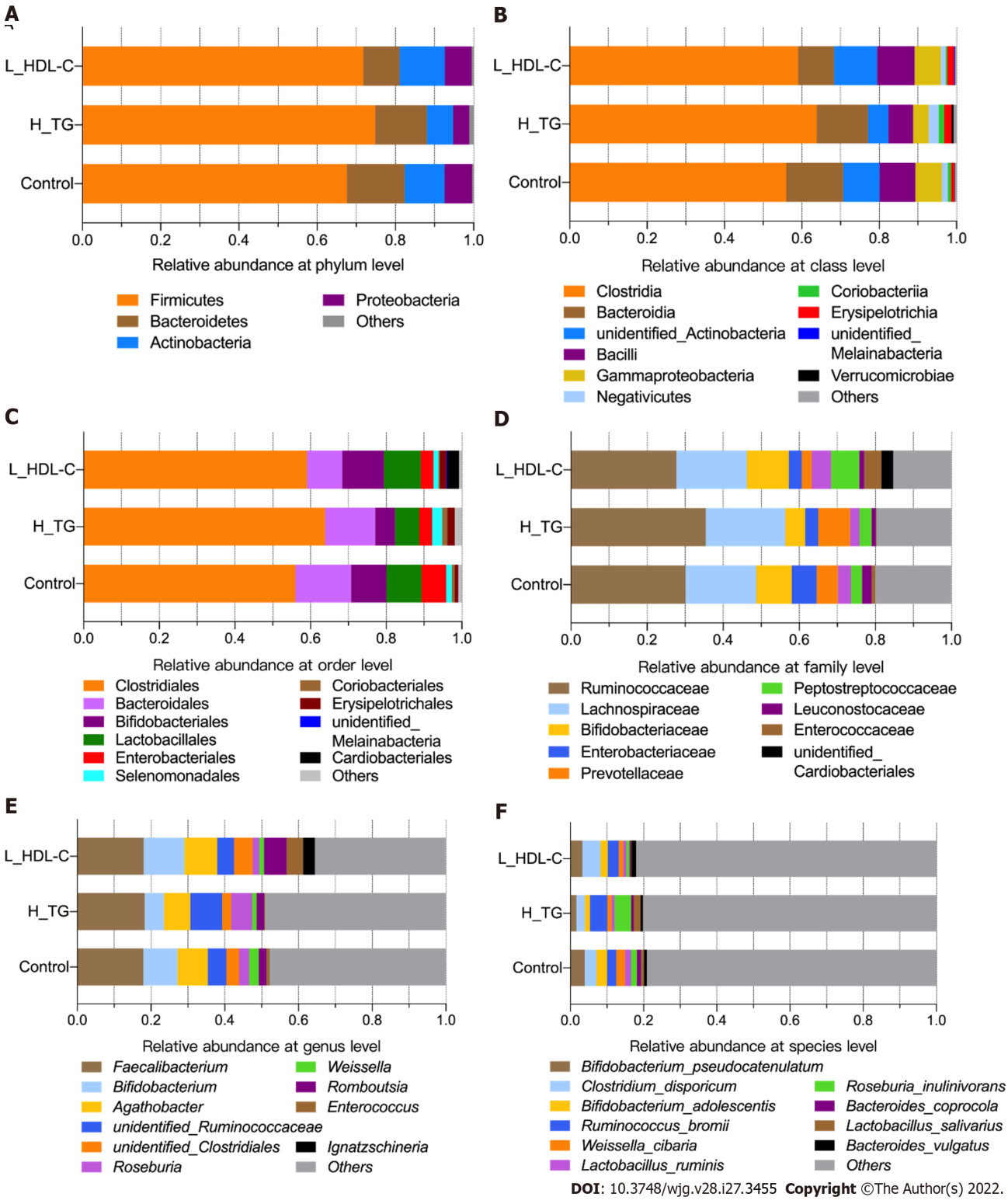


DOI: 10.3748/wjg.v28.i27.3455 **Copyright** ©The Author(s) 2022.

Figure 4 The taxonomic composition of gut microbiota in females of the study population. Bar plots show the relative abundances of the top ten taxa at the six taxonomic levels, including phyla, class, orders, family, genus and species, in females. Each component of the cumulative bar chart indicates a phylum, a class, an order, a family, a genus or a species. A: Relative abundance at phylum level; B: Relative abundance at class level; C: Relative abundance at order level; D: Relative abundance at family level; E: Relative abundance at genus level; F: Relative abundance at species level. H_CHO: High total cholesterol; H_TG: high triglyceride; L_HDL-C: Low high-density lipoprotein cholesterol.

Functional analysis of GM in the study population

Finally, we evaluated the functions of the GM community using the FAPROTAX database, and obtained the main metabolic processes of microorganisms associated with different biogeochemical cycles. A total of 51 functional assignments, with relative abundances larger than 0.0001 of the average level, were obtained in females, and 38 assignments were obtained in males. Apparently, GM functions showed



DOI: 10.3748/wjg.v28.i27.3455 **Copyright** ©The Author(s) 2022.

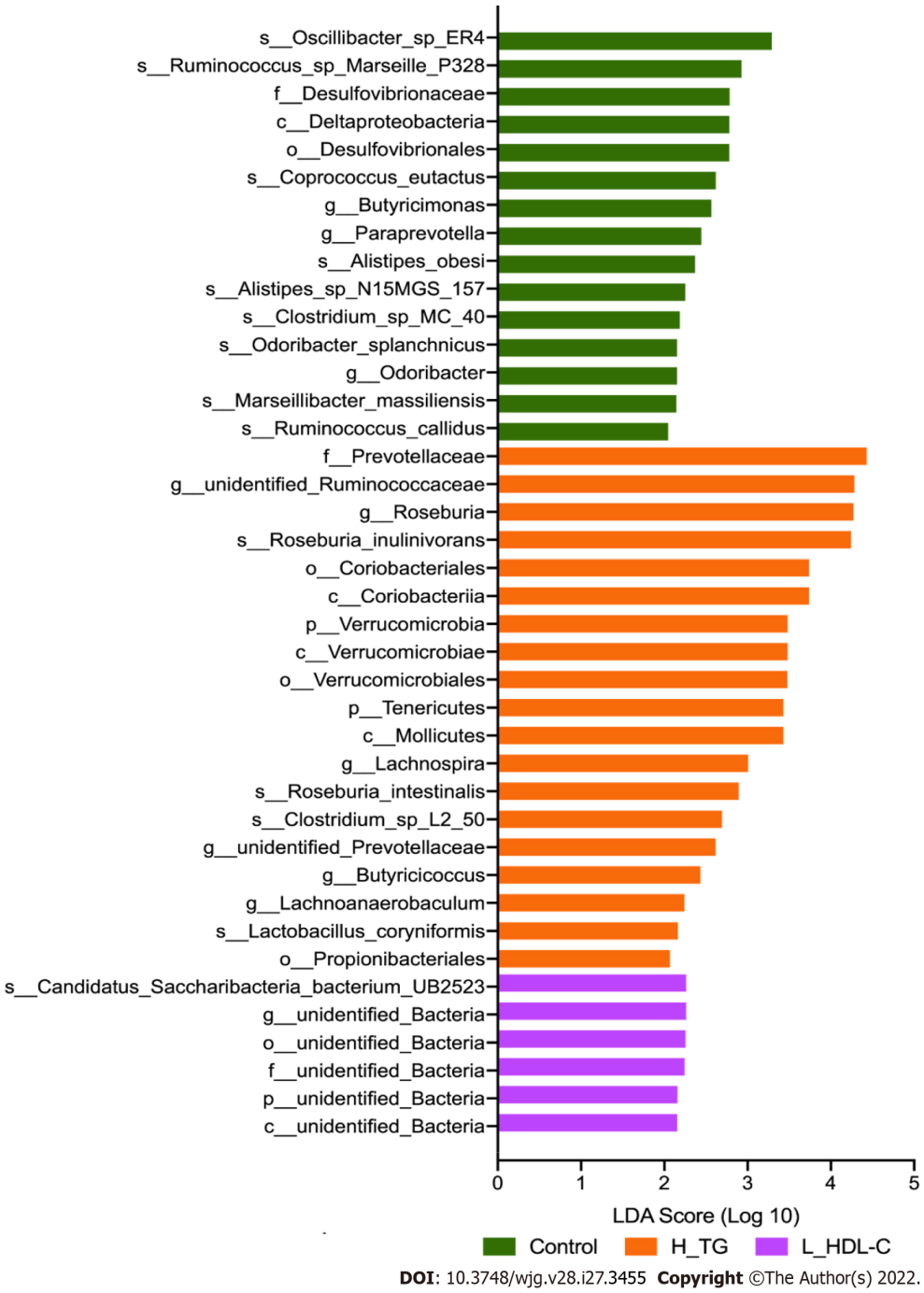
Figure 5 The taxonomic composition of gut microbiota in males of the study population. Bar plots show the relative abundances of the top ten taxa at the six taxonomic levels, including phyla, class, orders, family, genus and species, in males. Each component of the cumulative bar chart indicates a phylum, a class, an order, a family, a genus or a species. A: Relative abundance at phylum level; B: Relative abundance at class level; C: Relative abundance at order level; D: Relative abundance at family level; E: Relative abundance at genus level; F: Relative abundance at species level. H_TG: high triglyceride; L_HDL-C: Low high-density lipoprotein cholesterol.

different patterns between females and males, further supporting our strategy of separation and independent analysis in females and males. The top twenty annotated functions with higher relative abundances in females and males are shown in Figure 10. Furthermore, comparison analysis between the different subgroups was conducted. Compared with CON females, the relative abundance of aerobic chemoheterotrophy was increased in H_CHO females (P value < 0.05), while cellulolysis



DOI: 10.3748/wjg.v28.i27.3455 **Copyright** ©The Author(s) 2022.

Figure 6 Linear discriminant analysis effect size analysis in females of the study population. Linear discriminant analysis (LDA) scores indicate differentially represented gut microbiota taxa (biomarkers) in each female subgroups. The length of each bar represents the LDA score format with log 10, and the logarithmic threshold for discriminative features was set to 2.0. H_CHO: High total cholesterol; H_TG: high triglyceride; L_HDL-C: Low high-density lipoprotein cholesterol.



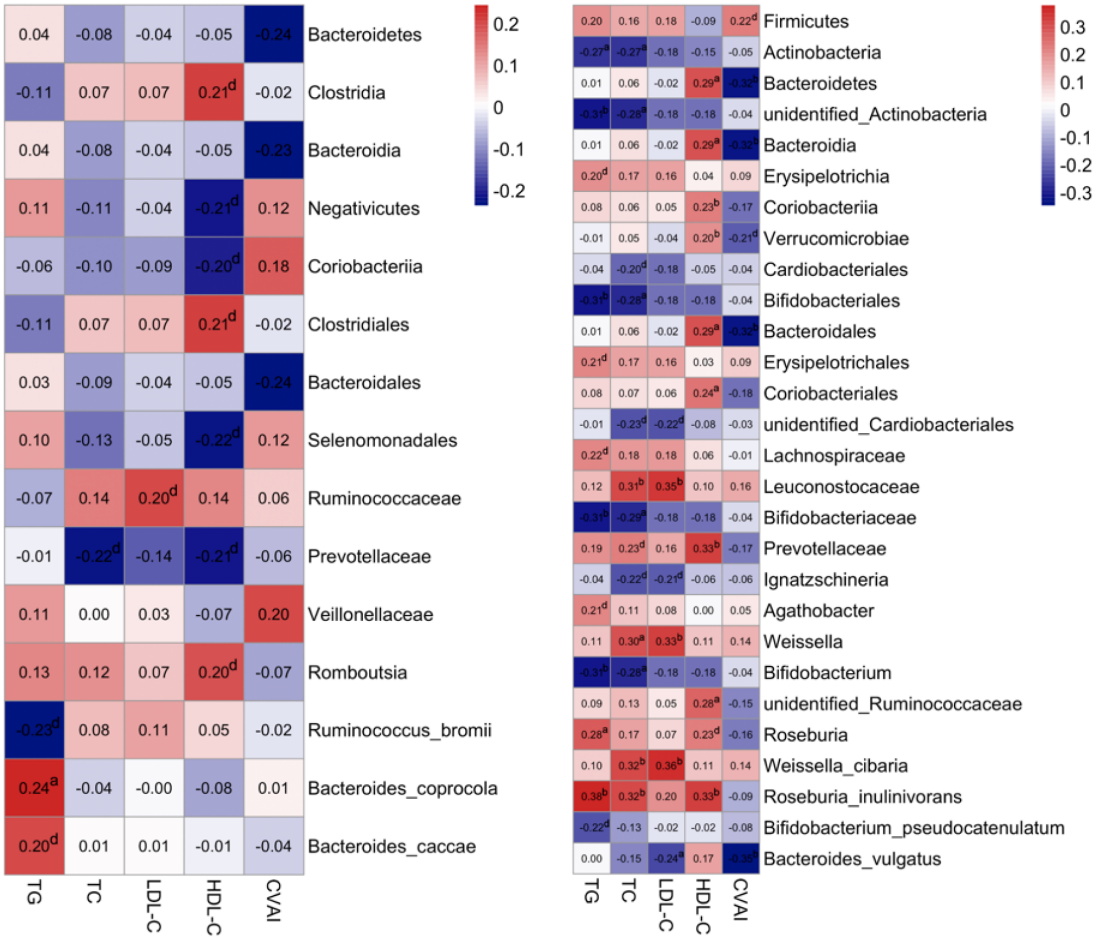
DOI: 10.3748/wjg.v28.i27.3455 **Copyright** ©The Author(s) 2022.

Figure 7 Linear discriminant analysis effect size analysis in males of the study population. Linear discriminant analysis (LDA) scores indicate differentially represented gut microbiota taxa (biomarkers) in each male subgroups. The length of each bar represents the LDA score format with log 10, and the logarithmic threshold for discriminative features was set to 2.0. H_TG: high triglyceride; L_HDL-C: Low high-density lipoprotein cholesterol.

abundance was increased in L_HDL-C females (P value < 0.05). Additionally, cellulolysis abundance was increased in L_HDL-C females when compared with that in H_CHO females (P value < 0.05). Compared with CON males, the relative abundances of sulfate respiration, respiration of sulfur compounds and cellulolysis were decreased in L_HDL-C males (P value < 0.05), while the relative abundance of nitrate respiration was increased in L_HDL-C males (P value < 0.05).

DISCUSSION

Dyslipidemia is considered a defect of lipid metabolism in circulation, characterized by increased or decreased levels of serum lipids. Notably, alterations in the GM community may participate in the pathogenesis of dyslipidemia, and the GM composition could be influenced by sex, host genotype and



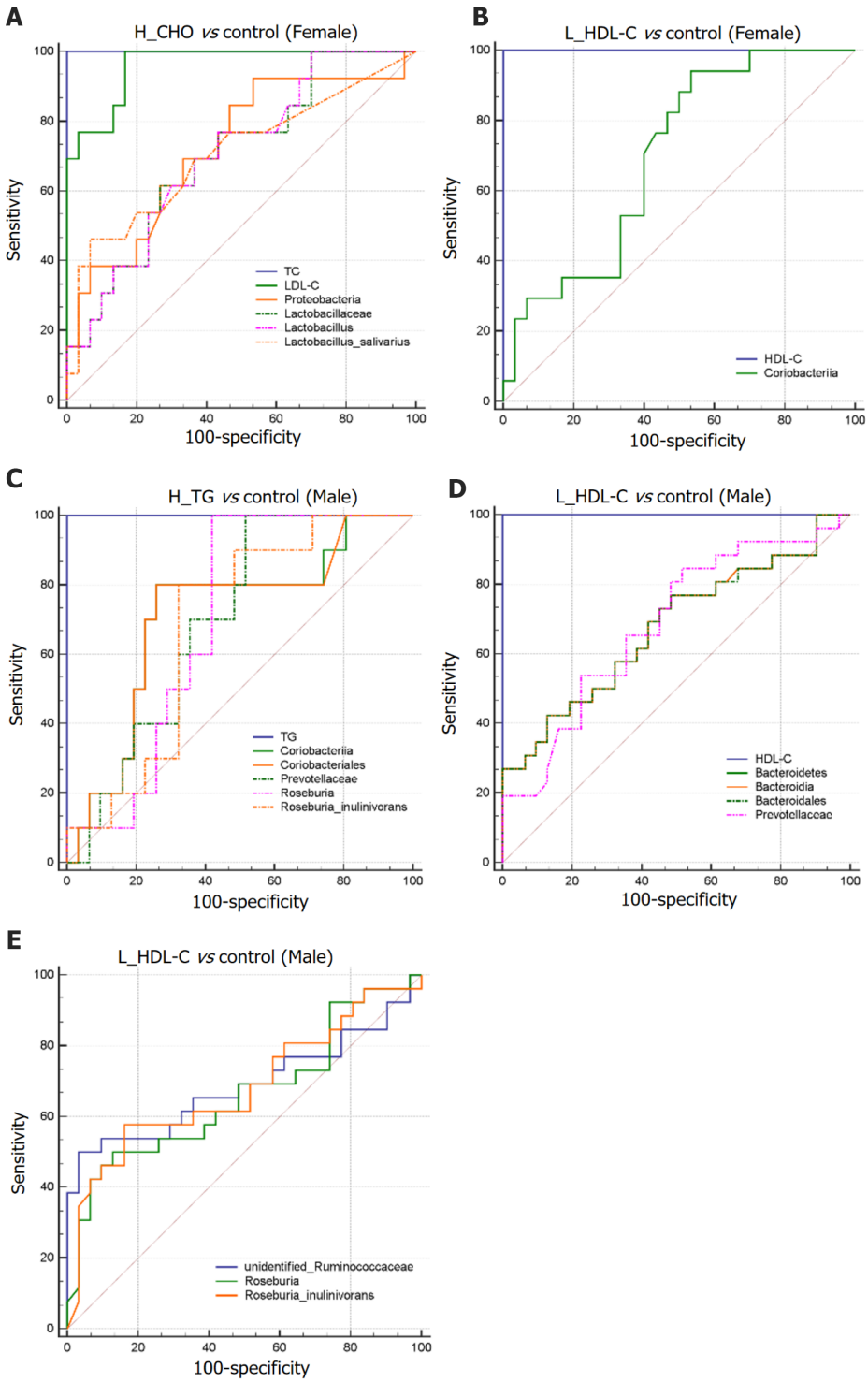
DOI: 10.3748/wjg.v28.i27.3455 **Copyright** ©The Author(s) 2022.

Figure 8 Associations of gut microbiota taxa with serum lipid indicators in the study population. A: Correlations of gut microbiota (GM) taxa with serum lipid indicators in females. Spearman's correlation analysis was conducted. The number presented in each cell is the correlation coefficient. The larger the absolute value is, the stronger the correlation is. Blue indicates a negative correlation and red indicates a positive correlation. The depth of the color represents the strength of the correlation. The deeper the color is, the stronger the correlation is; B: Correlations of GM taxa with serum lipid indicators in males. $^{a}P < 0.05$, $^{b}P < 0.01$, $^{d}P < 0.1$. TG: Triglyceride; TC: Total cholesterol; LDL-C: Low-density lipoprotein cholesterol; HDL-C: High-density lipoprotein cholesterol; CVAI: Chinese visceral adiposity index.

geographic location. To our knowledge, little evidence is present in the literature on the correlations between GM and serum lipids based on sex differences[39]; hence, the initial objective of this study was to identify the associations of GM features with serum lipid profiles based on sex differences in a Chinese population.

Considered as a whole, there were significant differences in serum lipid profiles and GM features between females and males. Specifically, females have higher GM diversities, and the GM composition was quite different from that in males, which is consistent with previous data[40]. In addition, the functional analysis of GM also showed an obvious dissimilarity between females and males, further supporting our strategy of respective GM analysis in females and males[14]. Of note, the associations between GM and dyslipidemia in humans have been investigated and demonstrated by various studies, suggesting the alteration of GM in patients with impaired lipid metabolism[28,41]. For instance, Cotillard *et al*[42] noted that reduced GM richness, commonly observed in obese patients, was linked to increased serum TG and TC levels. Following that study, more studies have demonstrated negative correlations of circulating TG and LDL-C levels with GM diversity, and a positive correlation of HDL-C with GM richness[9,26,43,44]. Moreover, certain GM taxa were found to be correlated with specific lipid profiles, suggesting that different GM taxa may affect distinct classes of lipids[26,42,43]. Although the present data have not clearly defined the GM pattern of patients with dyslipidemia, these observations provide new avenues for validation and follow-up studies. Therefore, dyslipidemia female and male patients in this study were divided into a H_TG group, a H_CHO group and a L_HDL-C group, for a more targeted investigation and interpretation.

As an important indicator of the GM community and a general measure of gut health, higher GM diversities have been proposed to be associated with healthy lipid levels, such as increased HDL-C and decreased TG levels[26]. Our results showed a positive correlation between GM diversities and the serum HDL-C level in males, consistent with previous data[26]. Additionally, GM diversities were

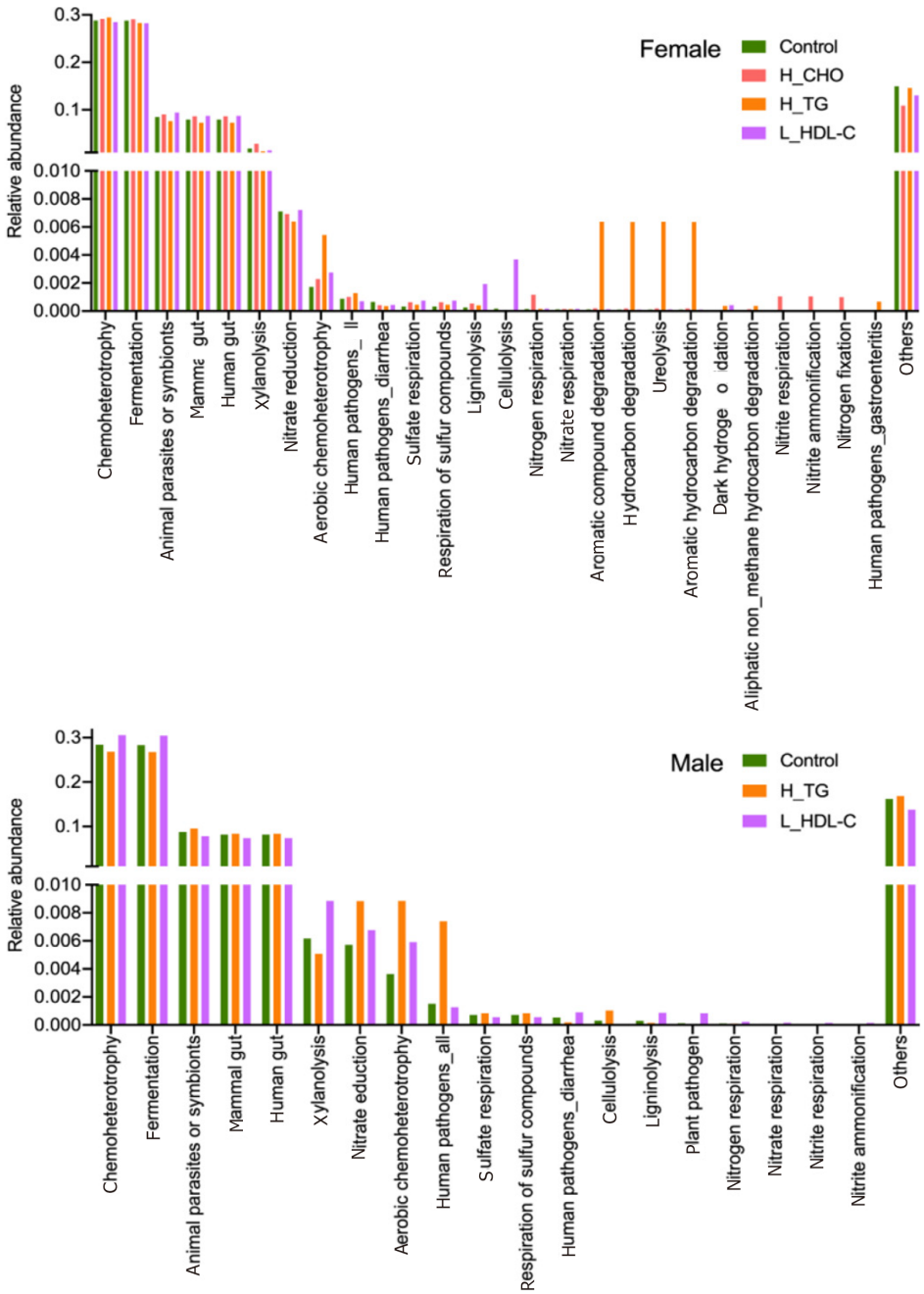


DOI: 10.3748/wjg.v28.i27.3455 **Copyright** ©The Author(s) 2022.

Figure 9 Differential gut microbiota taxa-based classification of dyslipidemia in the study population. Receiver operating characteristic curve analysis for identifying dyslipidemia subgroup from controls by gut microbiota taxa in females and males. A: High total cholesterol *vs* control (Female); B: Low high-density lipoprotein cholesterol (L_HDL-C) *vs* control (Female); C: High triglyceride *vs* control (Male); D and E: L_HDL-C *vs* control (Male). H_CHO: High total cholesterol; H_TG: high triglyceride; L_HDL-C: Low high-density lipoprotein cholesterol.

negatively correlated with CVAI in males. As a valuable indicator of "adipose distribution and function", CVAI has been suggested to be a reliable and applicable indicator for the evaluation of visceral fat dysfunction in Chinese individuals, which is based on simple and obtainable clinical parameters and the serum lipid levels[34,45]. The CVAI is essentially correlated with lipid metabolism, and its negative correlation with GM diversities could further support the reliability of our data.

Butyrate has been suggested to facilitate the prevention and treatment of diet-induced obesity by reducing fat accumulation and insulin resistance[46,47], and the ability to produce butyrate is widely distributed among gram-positive anaerobic bacteria[48]. As members of the butyrate-producing bacteria



DOI: 10.3748/wjg.v28.i27.3455 **Copyright** ©The Author(s) 2022.

Figure 10 The main functional annotations of gut microbiota in the study population. Bar plots show the relative abundances of top twenty annotated functions with higher relative abundances in female subgroups and male subgroups, respectively, using the FAPROTAX database. H_CHO: High total cholesterol; H_TG: high triglyceride; L_HDL-C: Low high-density lipoprotein cholesterol.

[48], *Roseburia* and *Roseburia_inulinivorans* have been investigated in certain diseases. By analyzing the GM composition of patients with symptomatic atherosclerosis, Karlsson *et al*[49] noted an enrichment of *Roseburia* in CVD patients, while a lower abundance of *Roseburia* was be observed in patients with diabetes[44]. In this study, we found that *Roseburia_inulinivorans* were positively correlated with the serum TG, TC and HDL-C levels, and *Roseburia* were positively correlated with the serum TG level in males. In addition, decreased *Roseburia* and *Roseburia_inulinivorans* abundances distinguished L_HDL-C males from CON males, while increased *Roseburia* and *Roseburia_inulinivorans* abundances distinguished H_TG males from CON males. Furthermore, strains of *Bifidobacterium* and *Lactobacillus* have potential therapeutic purposes[50]. An *et al*[51] once described a comparable, positive anti-obesity and lipid-lowering effect of *Bifidobacterium* spp. in obese rats fed a high-fat diet. Consistent with the evidence, our results demonstrated that the relative abundances of Bifidobacteriales, Bifidobacteriaceae and *Bifidobacterium* were negatively correlated with the serum TG and TC levels in males. However, certain favorable GM taxa, such as Lactobacillaceae, *Lactobacillus* and *Lactobacillus_salivarius*, were enriched in H_CHO females. As a probiotic supplement, *Lactobacillus* were noted to have a negative correlation with serum

lipid profiles[52]. An animal study, focused on mice fed a high-fat high-cholesterol diet and supplemented with *Lactobacillus curvatus* and/or *Lactobacillus plantarum*, revealed that these probiotic bacteria play important roles in normalizing lipid metabolism, such as decreasing TC levels in plasma and liver, and reducing the accumulation of hepatic TG[53]. Obviously, certain conflicting findings exist, which should be further investigated. Nevertheless, these observations indicate that different GM taxa associate with certain lipids, and may affect specific aspects of lipid metabolism[26,42,43].

A recent study on rats[54] demonstrated that a high-fat diet decreased the proportions of Bacteroidetes and its genera *Bacteroides* and *Prevotella*, and a study on swine indicated that decreased Bacteroidetes proportions were accompanied by decreases in the circulating TG level[55]; however, whether Bacteroidetes can alter cholesterol or TG levels in humans remains disputed. In humans, decreased Bacteroidetes proportions, including *Bacteroides_vulgatus* and *Bacteroides_dorei*, were observed in patients with coronary artery disease[56,57]. In addition, some species of *Bacteroides* were shown to be decreased in patients with CVDs[49], and may be used as biomarkers for evaluating the alleviation of obesity[54]. Our results showed that *Bacteroides_vulgatus* were negatively correlated with the serum LDL-C level but positively correlated with the serum TG level in females, while Bacteroidetes, Bacteroidia and Bacteroidales were negatively correlated with CVAI in females. Moreover, Bacteroidetes, Bacteroidia and Bacteroidales were positively correlated with the serum HDL-C level, differentiated L_HDL-C males from CON males, and were negatively correlated with CVAI in males. These observed associations may further support their roles in the favorable regulation of lipid metabolism. Interestingly, Prevotellaceae were enriched in L_HDL-C group in the comparison among the three dyslipidemia subgroups in females. However, the relative abundance of Prevotellaceae was decreased significantly in L_HDL-C males, and could distinguish L_HDL-C males from CON males. Additionally, increased Prevotellaceae also helped discriminate H_TG males from CON males in our study. Of note, Kelly *et al*[58] reported that genera within the family Prevotellaceae had different effects; some were associated with an increased and others with a decreased CVD risk profile. Meanwhile, Coriobacteriia were indicated to be enriched in L_HDL-C females, and could differentiate L_HDL-C females from CON females. Moreover, we identified that Coriobacteriales were correlated with the increased serum HDL-C level in males, and increased Coriobacteriia and Coriobacteriales could distinguish H_TG males from CON males. However, these taxa have not been studied thoroughly, and it is difficult to assess their metabolic functions in human lipid metabolism.

Different GM taxa may have distinct activities and modes of action[50,59], and certain taxa may exert synergistic and cooperative interactions[60], indicating the importance of balance in the GM community. Our results may suggest a complex interaction between GM and distinct lipid metabolisms based on sex differences, and provide new evidence of the involvement of GM in dyslipidemia. Nevertheless, more studies are required to determine which specific taxa have the potential to ameliorate dyslipidemia.

There were several limitations in this study, the most marked of which was the small sample size in each subgroup. This was a single-center study, recruiting Chinese participants near Xi'an, a central city in northwestern China. In addition, certain confounders, such as dietary habit, that could have influenced the GM composition[61], must be taken into consideration. However, elucidation of certain associations of GM taxa with host lipid metabolism in this study is still valuable. We hope that our observations will facilitate prospective studies investigating diverse aspects of GM influences on human dyslipidemia based on sex differences. In future studies, it is recommended that the sample size be increased, more confounders be considered, and various research methods be integrated to ascertain potential associations.

CONCLUSION

Based on the thorough analyses of GM features with dyslipidemia in females and males, potent associations of GM-host relations based on sex differences were revealed, and the potential of GM for dyslipidemia diagnosis was demonstrated. Although this study could not provide a conclusive association between GM and dyslipidemia, it may provide new insights into the pathogenesis of dyslipidemia.

ARTICLE HIGHLIGHTS

Research background

Dyslipidemia is a common chronic disorder, and is defined as any abnormality in blood lipid levels. In recent years, considerable progress has been made in elucidating the mechanisms of dyslipidemia, and the gut microbiota (GM) has been indicated to play a pivotal role in its pathophysiology. However, the associations between GM and dyslipidemia remain to be elucidated.

Research motivation

Although recent studies have convincingly linked GM to dyslipidemia, proving the associations between GM and host lipid metabolism remains a challenge in humans. In addition, ethnicity, geography and sex are potent factors that could influence the GM community. Therefore, it is important to clarify the relationship between GM and dyslipidemia, and to explore the importance of sex differences. In this study, we first revealed sex differences regarding the GM features, and then introduced dyslipidemia, highlighting its intricate relationships with GM and possible altered GM functions.

Research objectives

This study focused on the associations of GM features with dyslipidemia based on sex differences in a northwestern Chinese population.

Research methods

This study finally recruited 142 participants (73 females and 69 males) at Honghui Hospital, Xi'an Jiaotong University, who fulfilled the criteria for the diagnosis of dyslipidemia according to the "Guidelines for prevention and treatment of dyslipidemia in Chinese adults". The anthropometric and blood metabolic parameters of all participants were measured. According to their detected serum lipid levels, female and male participants were classified into a high triglyceride (H_TG) group, a high total cholesterol (H_CHO) group, a low high-density lipoprotein cholesterol (L_HDL-C) group, and a control (CON) group with normal serum lipid levels. Fresh fecal samples were collected for 16S rRNA gene sequencing, and UPARSE software, QIIME software, the RDP classifier tool and the FAPROTAX database were used for sequencing analyses.

Research results

Different GM features were identified between females and males, and the associations between GM and serum lipid profiles were different between females and males. In the comparison of the three dyslipidemia subgroups in females, *Lactobacillus_salivarius* were enriched in H_CHO females, and Prevotellaceae were enriched in L_HDL-C females. Compared with CON or H_TG males, Prevotellaceae, *unidentified_Ruminococcaceae*, *Roseburia* and *Roseburia_inulinivorans* were decreased in L_HDL-C males; while linear discriminant analysis effect size analysis indicated an enrichment of these above GM taxa in H_TG males in comparison to other male subgroups. Additionally, *Roseburia_inulinivorans* abundance was positively correlated with the serum TG and total cholesterol levels, and *Roseburia* were positively correlated with the serum TG level. Furthermore, Proteobacteria, Lactobacillaceae, *Lactobacillus* and *Lactobacillus_salivarius* distinguished H_CHO females from CON females, while Coriobacteriia, Coriobacteriales, Prevotellaceae, *Roseburia* and *Roseburia_inulinivorans* distinguished H_TG males from CON males. Based on the predictions of GM metabolic capabilities from the FAPROTAX database, cellulolysis was increased in L_HDL-C females compared with CON females, but was decreased in L_HDL-C males compared with CON males.

Research conclusions

This study provides evidence of the associations between GM and serum lipid profiles based on sex differences, suggesting a complex interaction between GM and distinct lipid metabolisms, and providing new insights into the pathogenesis of dyslipidemia.

Research perspectives

Future studies are needed to determine which specific taxa have the potential to ameliorate dyslipidemia, to investigate the underlying biological functions of the key GM in dyslipidemia, and to explore the differences in diet and other factors between females and males as possible causes for the observed differences in GM and the lipid profiles.

FOOTNOTES

Author contributions: All the authors solely contributed to this article; Guo L and Lv J searched and reviewed published articles, interpreted data, constructed tables, drafted the article, and made substantial contributions to the conception and design of this study; Wang YY, Wang JH and Yan YZ conducted the experiments, performed sequencing analysis and constructed the figures; Wang YY, Wang JH and Wang GD performed statistical analysis; Zhao HP, Yu Y and Dai K constructed the figures and tables; Yang YJ contributed to the conception of the study; and all authors critically reviewed the manuscript, and approved the final version to be published.

Supported by Youth Program of Xi'an Municipal Health Commission of China, No. 2022qn07; General Program of Xi'an Municipal Health Commission of China, No. 2020ms14; and National Natural Science Foundation of China, No. 81702067.

Institutional review board statement: This study was reviewed and approved by the Ethics Committee of Honghui Hospital, Xi'an Jiaotong University, No. 201801022.

Informed consent statement: All study participants provided informed consent prior to study enrollment.

Conflict-of-interest statement: All the authors report no relevant conflicts of interest for this article.

Data sharing statement: The raw data supporting the conclusions of this article available from the corresponding author at lvjing-1219@163.com.

Open-Access: This article is an open-access article that was selected by an in-house editor and fully peer-reviewed by external reviewers. It is distributed in accordance with the Creative Commons Attribution NonCommercial (CC BY-NC 4.0) license, which permits others to distribute, remix, adapt, build upon this work non-commercially, and license their derivative works on different terms, provided the original work is properly cited and the use is non-commercial. See: https://creativecommons.org/Licenses/by-nc/4.0/

Country/Territory of origin: China

ORCID number: Lei Guo 0000-0002-5166-5374; Yang-Yang Wang 0000-0002-4259-2804; Ji-Han Wang 0000-0003-1925-330X; He-Ping Zhao 0000-0002-7896-6636; Yan Yu 0000-0003-1587-7748; Guo-Dong Wang 0000-0002-1346-8396; Kun Dai 0000-0001-5091-7800; Yu-Zhu Yan 0000-0003-1355-0266; Yan-Jie Yang 0000-0002-7259-2995; Jing Lv 0000-0003-2801-743X.

S-Editor: Fan JR
L-Editor: A
P-Editor: Qi WW

REFERENCES

1 **World Health Organization**. Obesity and overweight Fact Sheet. 2021. [cited 10 January 2022]. Available from: https://www.who.int/news-room/fact-sheets/detail/obesity-and-overweight
2 **Sun B**, Karin M. Obesity, inflammation, and liver cancer. *J Hepatol* 2012; **56**: 704-713 [PMID: 22120206 DOI: 10.1016/j.jhep.2011.09.020]
3 **Bloor ID**, Symonds ME. Sexual dimorphism in white and brown adipose tissue with obesity and inflammation. *Horm Behav* 2014; **66**: 95-103 [PMID: 24589990 DOI: 10.1016/j.yhbeh.2014.02.007]
4 **Gao N**, Yu Y, Zhang B, Yuan Z, Zhang H, Song Y, Zhao M, Ji J, Liu L, Xu C, Zhao J. Dyslipidemia in rural areas of North China: prevalence, characteristics, and predictive value. *Lipids Health Dis* 2016; **15**: 154 [PMID: 27619340 DOI: 10.1186/s12944-016-0328-y]
5 **Tóth PP**, Potter D, Ming EE. Prevalence of lipid abnormalities in the United States: the National Health and Nutrition Examination Survey 2003-2006. *J Clin Lipidol* 2012; **6**: 325-330 [PMID: 22836069 DOI: 10.1016/j.jacl.2012.05.002]
6 **García-Giustiniani D**, Stein R. Genetics of Dyslipidemia. *Arq Bras Cardiol* 2016; **106**: 434-438 [PMID: 27305287 DOI: 10.5935/abc.20160074]
7 **Kokkinos PF**, Fernhall B. Physical activity and high density lipoprotein cholesterol levels: what is the relationship? *Sports Med* 1999; **28**: 307-314 [PMID: 10593643 DOI: 10.2165/00007256-199928050-00002]
8 **O'Doherty AF**, Jones HS, Sathyapalan T, Ingle L, Carroll S. The Effects of Acute Interval Exercise and Strawberry Intake on Postprandial Lipemia. *Med Sci Sports Exerc* 2017; **49**: 2315-2323 [PMID: 29045326 DOI: 10.1249/MSS.0000000000001341]
9 **Matey-Hernandez ML**, Williams FMK, Potter T, Valdes AM, Spector TD, Menni C. Genetic and microbiome influence on lipid metabolism and dyslipidemia. *Physiol Genomics* 2018; **50**: 117-126 [PMID: 29341867 DOI: 10.1152/physiolgenomics.00053.2017]
10 **Tremaroli V**, Bäckhed F. Functional interactions between the gut microbiota and host metabolism. *Nature* 2012; **489**: 242-249 [PMID: 22972297 DOI: 10.1038/nature11552]
11 **Cani PD**. Metabolism in 2013: The gut microbiota manages host metabolism. *Nat Rev Endocrinol* 2014; **10**: 74-76 [PMID: 24322652 DOI: 10.1038/nrendo.2013.240]
12 **Plaza-Diaz J**. Nutrition, Microbiota and Noncommunicable Diseases. *Nutrients* 2020; **12** [PMID: 32630712 DOI: 10.3390/nu12071971]
13 **Turnbaugh PJ**, Ley RE, Hamady M, Fraser-Liggett CM, Knight R, Gordon JI. The human microbiome project. *Nature* 2007; **449**: 804-810 [PMID: 17943116 DOI: 10.1038/nature06244]
14 **Yatsunenko T**, Rey FE, Manary MJ, Trehan I, Dominguez-Bello MG, Contreras M, Magris M, Hidalgo G, Baldassano RN, Anokhin AP, Heath AC, Warner B, Reeder J, Kuczynski J, Caporaso JG, Lozupone CA, Lauber C, Clemente JC, Knights D, Knight R, Gordon JI. Human gut microbiome viewed across age and geography. *Nature* 2012; **486**: 222-227 [PMID: 22699611 DOI: 10.1038/nature11053]
15 **Schloissnig S**, Arumugam M, Sunagawa S, Mitreva M, Tap J, Zhu A, Waller A, Mende DR, Kultima JR, Martin J, Kota K, Sunyaev SR, Weinstock GM, Bork P. Genomic variation landscape of the human gut microbiome. *Nature* 2013; **493**: 45-50 [PMID: 23222524 DOI: 10.1038/nature11711]
16 **Dominguez-Bello MG**, Blaser MJ, Ley RE, Knight R. Development of the human gastrointestinal microbiota and insights

from high-throughput sequencing. *Gastroenterology* 2011; **140**: 1713-1719 [PMID: 21530737 DOI: 10.1053/j.gastro.2011.02.011]

17 **Jernberg C**, Löfmark S, Edlund C, Jansson JK. Long-term impacts of antibiotic exposure on the human intestinal microbiota. *Microbiology (Reading)* 2010; **156**: 3216-3223 [PMID: 20705661 DOI: 10.1099/mic.0.040618-0]

18 **Wu GD**, Chen J, Hoffmann C, Bittinger K, Chen YY, Keilbaugh SA, Bewtra M, Knights D, Walters WA, Knight R, Sinha R, Gilroy E, Gupta K, Baldassano R, Nessel L, Li H, Bushman FD, Lewis JD. Linking long-term dietary patterns with gut microbial enterotypes. *Science* 2011; **334**: 105-108 [PMID: 21885731 DOI: 10.1126/science.1208344]

19 **Sommer F**, Bäckhed F. The gut microbiota--masters of host development and physiology. *Nat Rev Microbiol* 2013; **11**: 227-238 [PMID: 23435359 DOI: 10.1038/nrmicro2974]

20 **Rinninella E**, Raoul P, Cintoni M, Franceschi F, Miggiano GAD, Gasbarrini A, Mele MC. What is the Healthy Gut Microbiota Composition? *Microorganisms* 2019; **7** [PMID: 30634578 DOI: 10.3390/microorganisms7010014]

21 **Oliphant K**, Allen-Vercoe E. Macronutrient metabolism by the human gut microbiome: major fermentation by-products and their impact on host health. *Microbiome* 2019; **7**: 91 [PMID: 31196177 DOI: 10.1186/s40168-019-0704-8]

22 **Evans JM**, Morris LS, Marchesi JR. The gut microbiome: the role of a virtual organ in the endocrinology of the host. *J Endocrinol* 2013; **218**: R37-R47 [PMID: 23833275 DOI: 10.1530/JOE-13-0131]

23 **Dieterich W**, Schink M, Zopf Y. Microbiota in the Gastrointestinal Tract. *Med Sci (Basel)* 2018; **6** [PMID: 30558253 DOI: 10.3390/medsci6040116]

24 **Blander JM**, Longman RS, Iliev ID, Sonnenberg GF, Artis D. Regulation of inflammation by microbiota interactions with the host. *Nat Immunol* 2017; **18**: 851-860 [PMID: 28722709 DOI: 10.1038/ni.3780]

25 **Nicholson JK**, Holmes E, Kinross J, Burcelin R, Gibson G, Jia W, Pettersson S. Host-gut microbiota metabolic interactions. *Science* 2012; **336**: 1262-1267 [PMID: 22674330 DOI: 10.1126/science.1223813]

26 **Fu J**, Bonder MJ, Cenit MC, Tigchelaar EF, Maatman A, Dekens JA, Brandsma E, Marczynska J, Imhann F, Weersma RK, Franke L, Poon TW, Xavier RJ, Gevers D, Hofker MH, Wijmenga C, Zhernakova A. The Gut Microbiome Contributes to a Substantial Proportion of the Variation in Blood Lipids. *Circ Res* 2015; **117**: 817-824 [PMID: 26358192 DOI: 10.1161/CIRCRESAHA.115.306807]

27 **Ghazalpour A**, Cespedes I, Bennett BJ, Allayee H. Expanding role of gut microbiota in lipid metabolism. *Curr Opin Lipidol* 2016; **27**: 141-147 [PMID: 26855231 DOI: 10.1097/MOL.0000000000000278]

28 **Schoeler M**, Caesar R. Dietary lipids, gut microbiota and lipid metabolism. *Rev Endocr Metab Disord* 2019; **20**: 461-472 [PMID: 31707624 DOI: 10.1007/s11154-019-09512-0]

29 **Magkos F**, Mittendorfer B. Gender differences in lipid metabolism and the effect of obesity. *Obstet Gynecol Clin North Am* 2009; **36**: 245-265, vii [PMID: 19501312 DOI: 10.1016/j.ogc.2009.03.001]

30 **Palmisano BT**, Zhu L, Eckel RH, Stafford JM. Sex differences in lipid and lipoprotein metabolism. *Mol Metab* 2018; **15**: 45-55 [PMID: 29858147 DOI: 10.1016/j.molmet.2018.05.008]

31 **Imamura F**, Micha R, Khatibzadeh S, Fahimi S, Shi P, Powles J, Mozaffarian D; Global Burden of Diseases Nutrition and Chronic Diseases Expert Group (NutriCoDE). Dietary quality among men and women in 187 countries in 1990 and 2010: a systematic assessment. *Lancet Glob Health* 2015; **3**: e132-e142 [PMID: 25701991 DOI: 10.1016/S2214-109X(14)70381-X]

32 **Kim YS**, Unno T, Kim BY, Park MS. Sex Differences in Gut Microbiota. *World J Mens Health* 2020; **38**: 48-60 [PMID: 30929328 DOI: 10.5534/wjmh.190009]

33 **Zheng W**, Ma Y, Zhao A, He T, Lyu N, Pan Z, Mao G, Liu Y, Li J, Wang P, Wang J, Zhu B, Zhang Y. Compositional and functional differences in human gut microbiome with respect to equol production and its association with blood lipid level: a cross-sectional study. *Gut Pathog* 2019; **11**: 20 [PMID: 31168326 DOI: 10.1186/s13099-019-0297-6]

34 **Xia MF**, Chen Y, Lin HD, Ma H, Li XM, Aleteng Q, Li Q, Wang D, Hu Y, Pan BS, Li XJ, Li XY, Gao X. A indicator of visceral adipose dysfunction to evaluate metabolic health in adult Chinese. *Sci Rep* 2016; **6**: 38214 [PMID: 27905531 DOI: 10.1038/srep38214]

35 **Joint Committee on Revision of guidelines for prevention and treatment of dyslipidemia in Chinese adults**. Guidelines for Prevention and Treatment of Dyslipidemia in Chinese Adults (Revised Edition 2016). *Zhongguo Xunhuan Zazhi* 2016; **31**: 937-953 [DOI: 10.3969/j.issn.1000-3614.2016.10.001]

36 **Zhu X**, Li Y, Jiang Y, Zhang J, Duan R, Liu L, Liu C, Xu X, Yu L, Wang Q, Xiong F, Ni C, Xu L, He Q. Prediction of Gut Microbial Community Structure and Function in Polycystic Ovary Syndrome With High Low-Density Lipoprotein Cholesterol. *Front Cell Infect Microbiol* 2021; **11**: 665406 [PMID: 34350129 DOI: 10.3389/fcimb.2021.665406]

37 **Franzosa EA**, Morgan XC, Segata N, Waldron L, Reyes J, Earl AM, Giannoukos G, Boylan MR, Ciulla D, Gevers D, Izard J, Garrett WS, Chan AT, Huttenhower C. Relating the metatranscriptome and metagenome of the human gut. *Proc Natl Acad Sci U S A* 2014; **111**: E2329-E2338 [PMID: 24843156 DOI: 10.1073/pnas.1319284111]

38 **Louca S**, Parfrey LW, Doebeli M. Decoupling function and taxonomy in the global ocean microbiome. *Science* 2016; **353**: 1272-1277 [PMID: 27634532 DOI: 10.1126/science.aaf4507]

39 **Razavi AC**, Potts KS, Kelly TN, Bazzano LA. Sex, gut microbiome, and cardiovascular disease risk. *Biol Sex Differ* 2019; **10**: 29 [PMID: 31182162 DOI: 10.1186/s13293-019-0240-z]

40 **Markle JG**, Frank DN, Mortin-Toth S, Robertson CE, Feazel LM, Rolle-Kampczyk U, von Bergen M, McCoy KD, Macpherson AJ, Danska JS. Sex differences in the gut microbiome drive hormone-dependent regulation of autoimmunity. *Science* 2013; **339**: 1084-1088 [PMID: 23328391 DOI: 10.1126/science.1233521]

41 **Castaner O**, Goday A, Park YM, Lee SH, Magkos F, Shiow STE, Schröder H. The Gut Microbiome Profile in Obesity: A Systematic Review. *Int J Endocrinol* 2018; **2018**: 4095789 [PMID: 29849617 DOI: 10.1155/2018/4095789]

42 **Cotillard A**, Kennedy SP, Kong LC, Prifti E, Pons N, Le Chatelier E, Almeida M, Quinquis B, Levenez F, Galleron N, Gougis S, Rizkalla S, Batto JM, Renault P; ANR MicroObes consortium, Doré J, Zucker JD, Clément K, Ehrlich SD. Dietary intervention impact on gut microbial gene richness. *Nature* 2013; **500**: 585-588 [PMID: 23985875 DOI: 10.1038/nature12480]

43 **Le Chatelier E**, Nielsen T, Qin J, Prifti E, Hildebrand F, Falony G, Almeida M, Arumugam M, Batto JM, Kennedy S, Leonard P, Li J, Burgdorf K, Grarup N, Jørgensen T, Brandslund I, Nielsen HB, Juncker AS, Bertalan M, Levenez F, Pons

N, Rasmussen S, Sunagawa S, Tap J, Tims S, Zoetendal EG, Brunak S, Clément K, Doré J, Kleerebezem M, Kristiansen K, Renault P, Sicheritz-Ponten T, de Vos WM, Zucker JD, Raes J, Hansen T; MetaHIT consortium, Bork P, Wang J, Ehrlich SD, Pedersen O. Richness of human gut microbiome correlates with metabolic markers. *Nature* 2013; **500**: 541-546 [PMID: 23985870 DOI: 10.1038/nature12506]

44 **Karlsson FH**, Tremaroli V, Nookaew I, Bergström G, Behre CJ, Fagerberg B, Nielsen J, Bäckhed F. Gut metagenome in European women with normal, impaired and diabetic glucose control. *Nature* 2013; **498**: 99-103 [PMID: 23719380 DOI: 10.1038/nature12198]

45 **Amato MC**, Giordano C, Galia M, Criscimanna A, Vitabile S, Midiri M, Galluzzo A; AlkaMeSy Study Group. Visceral Adiposity Index: a reliable indicator of visceral fat function associated with cardiometabolic risk. *Diabetes Care* 2010; **33**: 920-922 [PMID: 20067971 DOI: 10.2337/dc09-1825]

46 **Gao Z**, Yin J, Zhang J, Ward RE, Martin RJ, Lefevre M, Cefalu WT, Ye J. Butyrate improves insulin sensitivity and increases energy expenditure in mice. *Diabetes* 2009; **58**: 1509-1517 [PMID: 19366864 DOI: 10.2337/db08-1637]

47 **Hatayama H**, Iwashita J, Kuwajima A, Abe T. The short chain fatty acid, butyrate, stimulates MUC2 mucin production in the human colon cancer cell line, LS174T. *Biochem Biophys Res Commun* 2007; **356**: 599-603 [PMID: 17374366 DOI: 10.1016/j.bbrc.2007.03.025]

48 **Louis P**, Flint HJ. Diversity, metabolism and microbial ecology of butyrate-producing bacteria from the human large intestine. *FEMS Microbiol Lett* 2009; **294**: 1-8 [PMID: 19222573 DOI: 10.1111/j.1574-6968.2009.01514.x]

49 **Karlsson FH**, Fåk F, Nookaew I, Tremaroli V, Fagerberg B, Petranovic D, Bäckhed F, Nielsen J. Symptomatic atherosclerosis is associated with an altered gut metagenome. *Nat Commun* 2012; **3**: 1245 [PMID: 23212374 DOI: 10.1038/ncomms2266]

50 **Suharja AAS**, Henriksson A, Liu SQ. Impact of Saccharomyces cerevisiae on viability of probiotic Lactobacillus rhamnosus in fermented milk under ambient conditions. *J Food Process Preserv* 2014; **38**: 326-337 [DOI: 10.1111/j.1745-4549.2012.00780.x]

51 **An HM**, Park SY, Lee DK, Kim JR, Cha MK, Lee SW, Lim HT, Kim KJ, Ha NJ. Antiobesity and lipid-lowering effects of Bifidobacterium spp. in high fat diet-induced obese rats. *Lipids Health Dis* 2011; **10**: 116 [PMID: 21745411 DOI: 10.1186/1476-511X-10-116]

52 **Huang ZR**, Chen M, Guo WL, Li TT, Liu B, Bai WD, Ai LZ, Rao PF, Ni L, Lv XC. Monascus purpureus-fermented common buckwheat protects against dyslipidemia and non-alcoholic fatty liver disease through the regulation of liver metabolome and intestinal microbiome. *Food Res Int* 2020; **136**: 109511 [PMID: 32846589 DOI: 10.1016/j.foodres.2020.109511]

53 **Yoo SR**, Kim YJ, Park DY, Jung UJ, Jeon SM, Ahn YT, Huh CS, McGregor R, Choi MS. Probiotics L. plantarum and L. curvatus in combination alter hepatic lipid metabolism and suppress diet-induced obesity. *Obesity (Silver Spring)* 2013; **21**: 2571-2578 [PMID: 23512789 DOI: 10.1002/oby.20428]

54 **Zhu Y**, Zhang JY, Wei YL, Hao JY, Lei YQ, Zhao WB, Xiao YH, Sun AD. The polyphenol-rich extract from chokeberry (*Aronia melanocarpa* L.) modulates gut microbiota and improves lipid metabolism in diet-induced obese rats. *Nutr Metab (Lond)* 2020; **17**: 54 [PMID: 32655675 DOI: 10.1186/s12986-020-00473-9]

55 **Cui C**, Shen CJ, Jia G, Wang KN. Effect of dietary Bacillus subtilis on proportion of Bacteroidetes and Firmicutes in swine intestine and lipid metabolism. *Genet Mol Res* 2013; **12**: 1766-1776 [PMID: 23765983 DOI: 10.4238/2013.May.23.1]

56 **Emoto T**, Yamashita T, Sasaki N, Hirota Y, Hayashi T, So A, Kasahara K, Yodoi K, Matsumoto T, Mizoguchi T, Ogawa W, Hirata K. Analysis of Gut Microbiota in Coronary Artery Disease Patients: a Possible Link between Gut Microbiota and Coronary Artery Disease. *J Atheroscler Thromb* 2016; **23**: 908-921 [PMID: 26947598 DOI: 10.5551/jat.32672]

57 **Yoshida N**, Emoto T, Yamashita T, Watanabe H, Hayashi T, Tabata T, Hoshi N, Hatano N, Ozawa G, Sasaki N, Mizoguchi T, Amin HZ, Hirota Y, Ogawa W, Yamada T, Hirata KI. Bacteroides vulgatus and Bacteroides dorei Reduce Gut Microbial Lipopolysaccharide Production and Inhibit Atherosclerosis. *Circulation* 2018; **138**: 2486-2498 [PMID: 30571343 DOI: 10.1161/CIRCULATIONAHA.118.033714]

58 **Kelly TN**, Bazzano LA, Ajami NJ, He H, Zhao J, Petrosino JF, Correa A, He J. Gut Microbiome Associates With Lifetime Cardiovascular Disease Risk Profile Among Bogalusa Heart Study Participants. *Circ Res* 2016; **119**: 956-964 [PMID: 27507222 DOI: 10.1161/CIRCRESAHA.116.309219]

59 **Hendijani F**, Akbari V. Probiotic supplementation for management of cardiovascular risk factors in adults with type II diabetes: A systematic review and meta-analysis. *Clin Nutr* 2018; **37**: 532-541 [PMID: 28318686 DOI: 10.1016/j.clnu.2017.02.015]

60 **Chapman CM**, Gibson GR, Rowland I. Health benefits of probiotics: are mixtures more effective than single strains? *Eur J Nutr* 2011; **50**: 1-17 [PMID: 21229254 DOI: 10.1007/s00394-010-0166-z]

61 **Makki K**, Deehan EC, Walter J, Bäckhed F. The Impact of Dietary Fiber on Gut Microbiota in Host Health and Disease. *Cell Host Microbe* 2018; **23**: 705-715 [PMID: 29902436 DOI: 10.1016/j.chom.2018.05.012]

World Journal of Gastroenterology

Submit a Manuscript: https://www.f6publishing.com

World J Gastroenterol 2022 July 21; 28(27): 3476-3487

DOI: 10.3748/wjg.v28.i27.3476

ISSN 1007-9327 (print) ISSN 2219-2840 (online)

ORIGINAL ARTICLE

Retrospective Cohort Study

Prognostic significance of hemoglobin, albumin, lymphocyte, platelet in gastrointestinal stromal tumors: A propensity matched retrospective cohort study

Zhou Zhao, Xiao-Nan Yin, Jian Wang, Xin Chen, Zhao-Lun Cai, Bo Zhang

Specialty type: Gastroenterology and hepatology

Provenance and peer review: Unsolicited article; Externally peer reviewed.

Peer-review model: Single blind

Peer-review report's scientific quality classification

Grade A (Excellent): A
Grade B (Very good): B
Grade C (Good): 0
Grade D (Fair): 0
Grade E (Poor): 0

P-Reviewer: Elpek GO, Turkey; Fusaroli P, Italy

Received: February 11, 2022
Peer-review started: February 11, 2022
First decision: April 10, 2022
Revised: April 19, 2022
Accepted: June 19, 2022
Article in press: June 19, 2022
Published online: July 21, 2022

Zhou Zhao, Xiao-Nan Yin, Jian Wang, Xin Chen, Zhao-Lun Cai, Bo Zhang, Department of Gastrointestinal Surgery, Sichuan University West China Hospital, Chengdu 610041, Sichuan Province, China

Corresponding author: Bo Zhang, MD, PhD, Professor, Department of Gastrointestinal Surgery, Sichuan University West China Hospital, No. 37 Guoxue Alley, Wuhou District, Chengdu 610041, Sichuan Province, China. hxwcwk@126.com

Abstract

BACKGROUND

The combined index of hemoglobin, albumin, lymphocyte, and platelet (HALP) can reflect systemic inflammation and nutritional status simultaneously, with some evidence revealing its prognostic value for some tumors. However, the effect of HALP on recurrence-free survival (RFS) in patients with gastrointestinal stromal tumors (GISTs) has not been reported.

AIM

To investigate the prognostic value of HALP in GIST patients.

METHODS

Data from 591 untreated patients who underwent R0 resection for primary and localized GISTs at West China Hospital between December 2008 and December 2016 were included. Clinicopathological data, preoperative albumin, blood routine information, postoperative treatment, and recurrence status were recorded. To eliminate baseline inequivalence, the propensity scores matching (PSM) method was introduced. Ultimately, the relationship between RFS and preoperative HALP was investigated.

RESULTS

The optimal cutoff value for HALP was determined to be 31.5 by X-tile analysis. HALP was significantly associated with tumor site, tumor size, mitosis, Ki67, National Institutes of Health (NIH) risk category, and adjuvant therapy (all $P < 0.001$). Before PSM, GIST patients with an increased HALP had a significantly poor RFS ($P < 0.001$), and low HALP was an independent risk factor for poor RFS [hazard ratio (HR): 0.506, 95% confidence interval (95%CI): 0.291-0.879, $P = 0.016$]. In NIH high-risk GIST patients, GIST patients with low HALP had a worse RFS

than patients with high HALP ($P < 0.05$). After PSM, 458 GIST patients were identified; those with an increased HALP still had significantly poor RFS after PSM ($P < 0.001$) and low HALP was still an independent risk factor for poor RFS (HR: 0.558, 95%CI: 0.319-0.976, $P = 0.041$).

CONCLUSION

HALP was significantly correlated with postoperative pathology and postoperative treatment. Furthermore, HALP showed a strong ability to predict RFS in GIST patients who underwent radical resection.

Key Words: Gastrointestinal stromal tumors; Nutrition assessment; Immuno-inflammatory-based prognostic scores; Prognosis; Propensity score

©The Author(s) 2022. Published by Baishideng Publishing Group Inc. All rights reserved.

Core Tip: The combined index of hemoglobin, albumin, lymphocyte, and platelet (HALP) can reflect systemic inflammation and nutritional status simultaneously. We demonstrated that HALP has a statistically significant correlation with postoperative pathology and postoperative treatment in patients with gastrointestinal stromal tumors (GISTs). Furthermore, we revealed that a low level of HALP was an independent risk factor for poor recurrence-free survival in GIST patients following radical resection before and after propensity scores matching.

Citation: Zhao Z, Yin XN, Wang J, Chen X, Cai ZL, Zhang B. Prognostic significance of hemoglobin, albumin, lymphocyte, platelet in gastrointestinal stromal tumors: A propensity matched retrospective cohort study. *World J Gastroenterol* 2022; 28(27): 3476-3487

URL: https://www.wjgnet.com/1007-9327/full/v28/i27/3476.htm

DOI: https://dx.doi.org/10.3748/wjg.v28.i27.3476

INTRODUCTION

Gastrointestinal stromal tumors (GISTs), a rare type of tumor, are the most frequent mesenchymal tumors arising from the gastrointestinal tract[1]. GISTs may occur anywhere in the digestive tract and even occasionally outside the gastrointestinal tract, with the stomach accounting for 60% and the small intestine 30% of all GISTs[2]. The morphology, immunohistochemistry, and molecular markers are helpful to the diagnosis of GISTs. Surgical resection is the standard treatment for resectable GISTs[3]. Nowadays, novel small molecular tyrosine kinase inhibitors, such as imatinib and sunitinib, have revolutionized the integrated treatment of GISTs and greatly improved the long-term prognosis of patients[4].

Some GIST-specific parameters based on postoperative pathologies, such as tumor size, primary tumor location, mitotic index, and tumor rupture, have been used to stratify the risk of recurrence for GISTs[2,5-7]. Meanwhile, a recent effort has shed light on the role of preoperative cancer-related inflammation and nutrition status in progression of various cancers, such as those of gastric[8], colorectal[9], non-small lung[10], and GIST[11-15]. Several preoperative immuno-inflammatory-based prognostic scores, such as the preoperative neutrophil-to-lymphocyte ratio (NLR), the lymphocyte-to-monocyte ratio (LMR), and the platelet-to-lymphocyte ratio (PLR), reflect the systematic inflammatory response, with some evidence supporting their prognostic ability for GISTs[13-17]. Furthermore, nutritional status, such as measured by the prognostic nutritional index (PNI), has also been shown to play an important role in GIST progression[10,11].

Recent studies have proposed a new combined index of hemoglobin, albumin, lymphocyte, and platelet (HALP) which can reflect systemic inflammation and nutritional status simultaneously[18]. It has already been reported as related to the prognosis of patients with pancreatic cancer[19], renal cancer [20], gastric cancer[18], prostate cancer[21], bladder cancer[22], esophageal cancer[23], and small cell lung cancer[24]. However, there are no studies on the relationship between HALP and recurrence in GIST patients who undergo radical resection. Therefore, this study aimed to investigate the prognostic value of preoperative HALP in resected GIST patients.

MATERIALS AND METHODS

Patient population

A flow diagram of the patient selection process is shown in Figure 1. Data from consecutive, previously untreated patients who underwent R0 resection for primary, localized GISTs at West China Hospital between December 2008 and December 2016 were included in this study. Patients who were younger than 18 years in age, without complete preoperative blood routine information or medical history, or with infectious diseases, blood counts with white blood cells (WBCs) > 10×10^9/L, neutrophils > 8×10^9/L, or lymphocytes > 5×10^9/L, other tumors, severe liver, kidney or heart diseases, emergency surgery, or follow-up less than 6 mo were excluded. In total, 591 GIST patients were enrolled for the current analysis.

This study was reviewed and approved by the Ethics Committee of the West China Hospital of Sichuan University, No. 1135(2019) and adhered to the tenets of the Declaration of Helsinki. All patients provided written informed consent.

Definition

Recurrence-free survival (RFS) was defined as the time interval between the time of surgery and the time of the first documented appearance of tumor after complete resection. The HALP, PNI, NLR, PLR, and LMR were calculated using the following formulas: HALP = hemoglobin level (g/L) × albumin level (g/L) × lymphocyte count (/L)/platelet count (/L)[19]; PNI = albumin level (g/L) + 5 × lymphocyte count (n/mm^3)[25]; NLR = neutrophil count (n/mm^3)/lymphocyte count (n/mm^3)[15,16]; PLR = platelet count (n/mm^3)/lymphocyte count (n/mm^3)[14]; LMR = lymphocyte count (n/mm^3)/monocyte count (n/mm^3)[26].

Data collection

Clinicopathological data, postoperative treatment, and recurrence status were recorded. The following data of each patient were retrieved from the self-built GISTs database: Demographic characteristics, tumor sites, tumor size, mitotic index [mitosis/50 high-power field (HPF) or mitosis/50 mm^2], morphology, immunohistochemistry, molecular markers, preoperative hemoglobin, albumin, WBC count, absolute neutrophil count, monocyte count, platelet count, and lymphocyte count. Tumor risk stratification was determined based on the modified National Institutes of Health (NIH) classification [27].

Perioperative evaluation and postoperative histopathological diagnosis

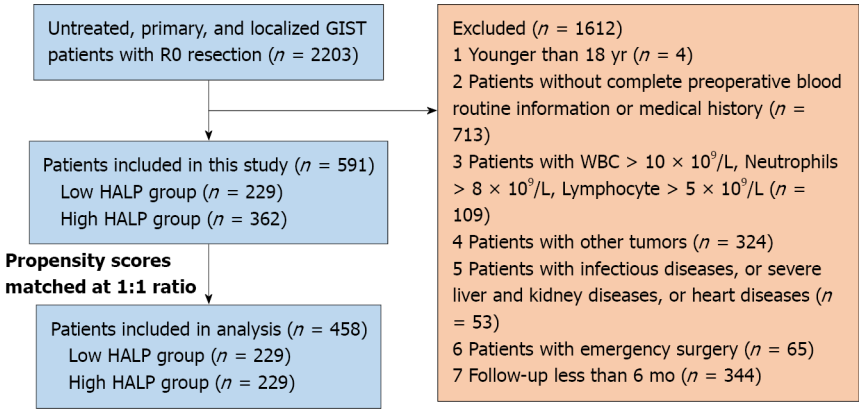
For all patients, the laboratory tests were evaluated within 1 wk before operation. Preoperative blood routine and blood biochemical examination were performed by the Laboratory Department of Sichuan University West China Hospital. The parameters included complete blood cell count and serum albumin. Histopathological diagnosis was performed by the Department of Pathology of Sichuan University West China Hospital; the postoperative pathological findings included data on gross appearance, tumor size, tumor site, resection margin status, tumor cell morphology, lymph node metastasis status, and immunohistochemical staining, *etc*.

Follow-up

Abdominal/pelvic computed tomography was performed every 3-6 mo in the first 3 years after operation, and then every 6-12 mo, until 5 years after the operation, and then once a year until recurrence. Recurrence status was ascertained up to December 2020.

Statistical analysis

The optimal cutoff values for the HALP, PNI, NLR, PLR, and LMR were determined to be 31.5, 48.6, 2.60, 134.8, and 4.0, respectively, by X-tile analysis[28]. Propensity scores matching (PSM) was performed as 1:1 matching and a 0.02 caliper based on the patient's age, tumor size, tumor site, mitosis, and adjuvant targeted therapy using nearest neighbor matching with the MatchIt R package (https://cran.r-project.org/web/packages/MatchIt/MatchIt.pdf). The categorical variables are reported as n (%) and quantitative variables are reported as mean ± SD or median (range). Statistical significance of group comparisons was analyzed *via* parametric and nonparametric tests for continuous variables and *via* chi-square analysis or Fisher's test for categorical variables. Survival curves of the RFS were calculated by the Kaplan-Meier methods and compared by log-rank tests. Hazard ratio (HR) for recurrence was calculated by Cox regression analysis. Sensitivity and specificity of HALP, PNI, NLR, LMR, and PLR were defined using time-dependent receiver operating characteristic (ROC) curves, and areas under the curve (AUCs) were detected utilizing survival ROC R package[29]. All statistical analyses were performed using SPSS Statistics version 21 (SPSS 21.0; IBM Corp., Armonk, NY, United States) and GraphPad Prism version 7.0 (GraphPad Software, La Jolla, CA, United States). Statistical significance was set at $P < 0.05$ as two-sided.



DOI: 10.3748/wjg.v28.i27.3476 **Copyright** ©The Author(s) 2022.

Figure 1 Flow diagram of the patient selection process. GIST: Gastrointestinal stromal tumor; HALP: Combination index of hemoglobin, albumin, lymphocyte, and platelet; WBC: White blood cell.

RESULTS

Baseline characteristics

The demographic and clinicopathological characteristics of the 591 GIST patients are listed in Table 1 and Supplementary Table 1. The study population consisted of 280 (46.8%) male and 311 (53.2%) female patients. The median age was 57 (range: 21-86) years. The median follow-up time was 56 (range: 4-138) mo. The mean ± SD findings for the HALP, PNI, NLR, PLR, and LMR values were 45.81 ± 33.73, 49.04 ± 5.43, 2.64 ± 1.74, 152.8 ± 84.6 and 5.13 ± 3.00, respectively. The mean ± SD of tumor size was 6.16 ± 4.87 cm. One hundred ninety-one tumors (32.3%) had a mitotic index of > 5/50 HPF. A total of 34.0% (201/691) of the GIST patients received adjuvant therapy with imatinib or sunitinib. According to NIH risk classification, 72 (12.2%) patients were classified as very low risk, 178 (30.1%) patients as low risk, 114 (19.3%) patients as intermediate risk, and 227 (38.4%) patients as high risk. Recurrence occurred in 62 GIST patients.

Association of HALP and clinicopathological factors

The clinicopathological characteristics between the high and low groups of HALP were categorized and analyzed as shown in Table 1 and Supplementary Table 1. Together, 229 patients were assigned to the low HALP group and 362 patients to the high HALP group. The results demonstrated that tumor site, tumor size, mitotic index, Ki67, NIH risk category, and adjuvant therapy were significantly associated with HALP (all $P < 0.05$).

PSM analysis was further carried out to avoid confounding variables that might interfere with the association between RFS and HALP level. After 1:1 matching, PSM analysis identified 229 pairs of GIST patients. After PSM, HALP was still associated with sex, Ki67, and recurrence but not with any other clinicopathological characteristics (Table 1 and Supplementary Table 1).

Association of clinicopathological factors and RFS

Before PSM, tumor site, tumor size, mitotic index, Ki67, NIH risk category, NLR, PLR, PNI, and HALP were associated with RFS (all $P < 0.05$) (Table 2). RFS in GIST patients with low HALP was significantly worse than in those with high HALP (Figure 2). Cox multiple regression analysis showed that HALP was an independent prognostic factor for RFS in GIST patients before PSM [HR: 0.506, 95% confidence interval (CI): 0.291-0.879, $P = 0.016$].

After PSM, tumor site, tumor size, mitotic index, Ki67, NIH risk category, PNI, NLR, PLR, and HALP were still related to RFS (all $P < 0.05$) (Table 2). RFS was also significantly worse in GIST patients with low HALP than in those with high HALP (Figure 2). Furthermore, Cox multiple regression analysis showed that HALP was an independent prognostic factor for RFS in GIST patients (HR: 0.558, 95%CI: 0.319-0.976, $P = 0.041$).

Subgroup analysis

The clinicopathological characteristics of high-risk GIST patients between the high and low groups of HALP were categorized in Supplementary Table 1. Together, 125 patients were assigned to the low HALP group and 102 patients to the high HALP group. The results demonstrated that sex and Ki67 were associated with HALP (both $P < 0.05$). Not surprisingly, patients in the low HALP group had significantly worse survival than patients in the high HALP group (Figure 2). Furthermore, Cox multiple regression analysis indicated that HALP was an independent prognostic factor for RFS in GIST patients (HR: 0.469, 95%CI: 0.245-0.896, $P = 0.022$) (Supplementary Table 2).

Table 1 Baseline characteristics in patients with high or low combination index of hemoglobin, albumin, lymphocyte, and platelet before and after propensity scores matching (mean ± SD)

Characteristics	Before PSM[1]				After PSM			
	All	Low HALP, < 31.5	High HALP, ≥ 31.5	*P* value	All	Low HALP, < 31.5	High HALP, ≥ 31.5	*P* value
n (%)	591	229 (38.7)	362 (61.3)	-	458	229 (50)	229 (50)	-
Age in yr	56.3 ± 12.0	56.7 ± 12.2	56.1 ± 11.8		56.8 ± 12.1	56.7 ± 12.2	57.0 ± 12.1	
< 60	337 (57.0)	129	208		256 (55.9)	129	127	
≥ 60	254 (43.0)	100	154	0.788	202 (44.1)	100	102	0.851
Sex								
Male	280 (47.4)	98	182		233 (50.9)	131	102	
Female	311 (52.6)	131	180	0.076	225 (49.1)	98	127	0.007[a]
Tumor site								
Stomach	424 (71.7)	143	281		299 (65.3)	143	156	
Non-stomach	167 (28.3)	86	81	< 0.001[a]	159 (34.7)	86	73	0.202
Tumor size in cm	6.16 ± 4.87	7.69 ± 5.65	5.18 ± 4.02		7.13 ± 5.08	7.69 ± 5.65	6.57 ± 4.38	
≤ 2	86 (14.6)	10	76		27 (5.9)	10	17	
2.1-5.0	251 (42.5)	87	164		177 (38.6)	87	90	
5.1-10.0	184 (31.1)	95	89		184 (40.2)	95	89	
> 10.0	70 (11.8)	37	33	< 0.001[a]	70 (15.3)	37	33	0.514
Mitotic index/50 HPF								
≤ 5	332 (56.2)	107	225		220 (48.0)	107	113	
6-10	100 (16.9)	45	55		91 (19.9)	45	46	
> 10	91 (15.4)	49	42		89 (19.4)	49	40	
Unknown	68 (11.5)	28	40	0.001[a]	58 (12.7)	28	30	0.764
Ki67								
≤ 10	417 (70.6)	140	277		308 (67.3)	140	168	
> 10	98 (16.6)	61	37		94 (20.5)	61	33	
Unknown	76 (12.9)	28	48	< 0.001[a]	26 (12.2)	28	28	0.004[a]
NIH risk category								
Very low risk	72 (12.2)	9	63		21 (4.6)	9	12	
Low risk	178 (30.1)	52	126		113 (24.7)	52	61	
Intermediate risk	114 (19.3)	43	71		100 (21.8)	43	57	
High risk	227 (38.4)	125	102	< 0.001[a]	224 (48.9)	125	99	0.106
Adjuvant therapy								
Yes	201 (34.0)	99	102		193 (42.1)	99	94	
No	390 (66.0)	130	260	< 0.001[a]	265 (57.9)	130	135	0.636
Recurrence								
Yes	62 (10.5)	42	20		61 (13.3)	42	19	
No	529 (89.5)	187	342	< 0.001[a]	397 (86.7)	187	210	0.002[a]

[1]Method = nearest; Cliper value = 0.02.

[a]$P < 0.05$ was considered statistically significant.

HALP: Combination index of hemoglobin, albumin, lymphocyte, and platelet; HPF: High-power field; NIH: National Institutes of Health; PSM: Propensity scores matching; SD: Standard deviation.

Sensitivity analysis

Time-dependent ROCs were generated for HALP, PNI, NLR, LMR, and PLR to predict 5-year RFS. According to the results, the 5-year AUC reached 0.661 in the HALP group, while PNI, NLR, LMR, and PLR reached 0.622, 0.591, 0.505, and 0.627, respectively (Figure 3).

DISCUSSION

There is growing evidence that preoperative nutritional status and inflammatory response may be a potentially powerful predictor of the prognosis of cancer patients. Consistent with previous research, the present study found that preoperative inflammation scores, such as NLR and PLR, were associated with the prognosis of GIST patients, both before and after PSM[14,16,30,31] (Supplementary Figure 1). However, LMR seemed to have no effect on the RFS of GIST patients (Supplementary Figure 1), which differs from findings of previous studies[14]. In addition, the PNI, a nutritional score based on albumin levels and lymphocytes, was also related to RFS of GIST patients, both before and after PSM in the present study[11,12] (Supplementary Figure 1).

In this study, we also found that preoperative HALP was significantly correlated with tumor site, tumor size, mitosis, Ki67, NIH risk category, and adjuvant therapy (Table 1). To balance the patient characteristics and standard prognostic factors between groups, we utilized the PSM method to balance patient's age, tumor size, tumor site, mitosis, and adjuvant targeted therapy. After PSM, sex, Ki67, PNI, NLR, LMR, and PLR were still associated with HALP (Supplementary Table 1). Notably, there was no difference in standard prognostic factors (*i.e.* tumor site, tumor size, mitosis, NIH risk category, and adjuvant therapy) between the low and high HALP groups (Table 1). Given that HALP shared several parameters with PNI, NLR, LMR, and PLR, their statistically significant correlation is unsurprising. The correlation between HALP and sex may be due to the fact that the male and female patients had significantly different hemoglobin levels (123.22 ± 2.08 g/L for males and 105.46 ± 1.84 g/L for females, $P < 0.001$). Remarkably, recurrence was not associated with either sex or histologic subtype (Supplementary Table 1). Subgroup analysis by sex revealed that a low level of HALP was associated with recurrence in both male and female patients ($P = 0.048$ and $P = 0.018$, respectively) (Supplementary Figure 2).

Finally, consistent with previous research on HALP in other tumors[18,19], our findings revealed prognostic value of HALP in GIST[20-24]. HALP was an independent risk factor for GIST patients before PSM, after PSM, and in high-risk subgroups (Table 2 and Supplementary Table 3). Thus, HALP can be used to not only evaluate GIST patients' postoperative risk prior to surgery but also to assess their prognosis. Notably, the HALP index can be utilized to predict the prognosis of patients in a convenient and cost-effective manner.

Although the underlying mechanism of systemic inflammation in tumorigenesis, progression and metastasis remains obscure, some theories suggest that it stimulates angiogenesis, immunosuppression, and formation of the supporting microenvironment. Lymphocytes are well known to play a critical role in tumor growth inhibition[32-34]. A higher lymphocyte signature is associated with improved prognosis in a variety of tumors[34], whereas platelets can infiltrate the tumor microenvironment and interact directly with cancer cells[35,36], assisting circulating tumor cells in adhering to endothelial cells and establishing a niche environment prior to metastasis[37-41].

Anemia is one of the most common symptoms of GIST, which can be caused by both gastrointestinal bleeding and intratumoral bleeding[42]. Yang *et al*[43] identified GIST with gastrointestinal bleeding as an independent prognostic predictor of poor RFS. Several studies have demonstrated that low hemoglobin levels can result in tumor hypoxia, which is associated with an increased risk of local failure and distant metastasis[31,44]. Furthermore, a hypoxic tumor environment may result in limited drug accumulation and hinder drug efficacy[45]. Most importantly, anemia is a common adverse effect of imatinib[46], which may require the prescribing physician to stop the drug or reduce the dose. High levels of preoperative hemoglobin may help to prevent this adverse effect.

Low levels of serum albumin are also associated with poor long-term survival in GIST patients[44,45], which is consistent with our findings. Serum albumin is generally considered as associated with nutritional status and liver or renal function, both of which may affect the prescribing physician's decision-making, similar to hemoglobin. Additionally, tumor tissues have abnormal vascular endothelial gaps and lack effective lymphatic drainage, allowing macromolecules, such as albumin, to accumulate more readily in tumor tissue than in normal tissue[47,48]. Consequently, serum albumin is suspected of being a possible nutritional source for tumor growth, due to its elevated accumulation in tumors[49-51]. This effect is referred to as the 'enhanced permeability and retention effect'. Moreover, about 95% of imatinib is bound to serum proteins, mainly albumin and 1-acid glycoprotein, which may facilitate drug accumulation in tumors and improve therapeutic effect[52,53]. Subsequently, serum albumin levels have been shown to be an independent prognostic factor of survival in a variety of cancers, including those of colorectal[54], gastric[55], pancreatic[56], and breast[57]. As a result, it is unsurprising that HALP, which reflects systemic inflammation and nutritional status simultaneously, is associated with the risk and prognosis of GIST.

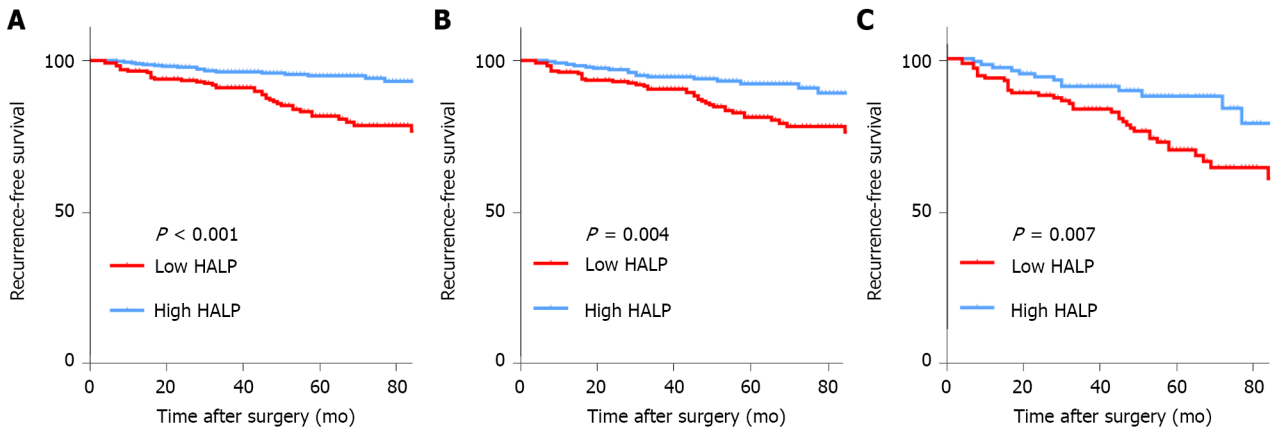
Table 2 Univariate and multivariate regression analysis of prognostic factors in patients before and after propensity scores matching

Risk factors	Before PSM				After PSM			
	Univariate analysis, HR (95%CI)	Univariate analysis, *P* value	Multivariate analysis, HR (95%CI)	Multivariate analysis, *P* value	Univariate analysis, HR (95%CI)	Univariate analysis, *P* value	Multivariate analysis, HR (95%CI)	Multivariate analysis, *P* value
Age	1.009 (0.987-1.030)	0.431		NS	1.006 (0.984-1.027)	0.607		NS
Sex: Male *vs* female	0.639 (0.386-1.056)	0.081		NS	0.711 (0.429-1.179)	0.186		NS
Tumor site: Stomach *vs* non-stomach	2.273 (1.377-3.752)	0.001[a]	2.979 (1.716-5.171)	< 0.001[a]	1.702 (1.028-2.818)	0.039[a]	2.865 (1.631-5.032)	< 0.001[a]
Tumor size in cm: ≤ 2/2.1-5.0/5.1-10.0/> 10.0	2.629 (1.948-3.548)	< 0.001[a]	1.070 (1.032-1.109)	0.001[a]	1.086 (1.056-1.116)	< 0.001[a]	1.068 (1.029-1.107)	< 0.001[a]
Mitotic index as/50 HPF: ≤ 5/6-10/> 10/unknown	2.071 (1.686-2.545)	< 0.001[a]		< 0.001[a]		< 0.001[a]		0.001[a]
≤ 5 *vs* 6-10			5.659 (2.151-14.887)	0.002[a]	5.442 (2.067-14.323)	0.001[a]	5.444 (1.955-15.162)	0.001[a]
≤ 5 *vs* > 10			8.259 (3.140-21.720)	< 0.001[a]	14.722 (6.037-35.904)	< 0.001[a]	7.675 (2.759-21.348)	< 0.001[a]
≤ 5 *vs* unknown			5.299 (2.041-13.757)	< 0.001[a]	9.851 (3.843-25.251)	< 0.001[a]	5.107 (1.873-13.923)	0.001[a]
CD117: +/-	1.231 (0.300-5.059)	0.773		NA	1.291 (0.314-5.313)	0.723	-	NA
DOG1: +/-/unknown	1.464 (0.773-2.774)	0.242		NA	1.626 (0.853-3.102)	0.140	-	NA
Ki67: ≤ 10/> 10/unknown	1.919 (1.453-2.533)	< 0.001[a]		0.001[a]		< 0.001[a]		0.001[a]
< 10 *vs* ≤ 10			3.579 (1.771-7.233)	< 0.001[a]	8.625 (4.750-15.660)	< 0.001[a]	3.710 (1.811-7.599)	< 0.001[a]
Unknown *vs* ≤ 10			2.844 (1.290-6.270)	0.024[a]	3.310 (1.528-7.169)	0.002[a]	3.050 (1.365-6.816)	0.007
Histologic subtypes: Spindle/epithelioid/mixed	1.361 (0.981-1.889)	0.065		NS	1.236 (0.891-1.715)	0.204	-	NA
NIH risk category: Very low/low/intermediate/high	3.218 (2.180-4.751)	< 0.001[a]		NS	2.892 (1.865-4.484)	< 0.001[a]	-	NS
Adjuvant therapy: Yes/no	1.289 (0.768-2.162)	0.336	0.445 (0.257-0.769)	0.004[a]	0.923 (0.549-1.551)	0.761		0.003[a]
NLR: < 2.60/≥ 2.60	2.025 (1.229-3.337)	0.006[a]		NS	1.746 (1.055-2.890)	0.030[a]		NS
PLR: < 134.8/≥ 134.8	2.925 (1.673-5.112)	< 0.001[a]		NS	1.991 (1.137-3.486)	0.016[a]		NS
LMR: < 4.0/≥ 4.0	1.296 (0.777-2.163)	0.321		NA	1.088 (0.650-1.821)	0.749	-	NA
PNI: < 48.6/≥ 48.6	0.291 (0.171-0.496)	< 0.001[a]		NS	1.991 (1.137-3.486)	0.016[a]		NS
HALP: < 31.5/≥ 31.5	0.341 (0.197-0.590)	< 0.001[a]	0.506 (0.291-0.879)	0.016[a]	0.457 (0.265-0.785)	0.005[a]	0.558 (0.319-0.976)	0.041[a]

[a]*P* < 0.05 was considered statistically significant.

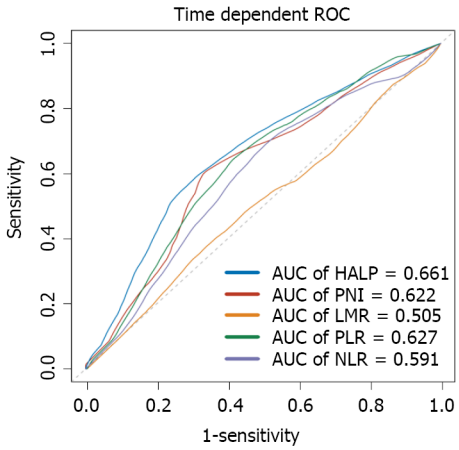
CI: Confidence interval; HALP: Combination index of hemoglobin, albumin, lymphocyte, and platelet; HPF: High-power field; HR: Hazard ratio; NA: Not adopted; LMR: Lymphocyte-to-monocyte ratio; NIH: National Institutes of Health; NLR: Neutrophil-to-lymphocyte ratio; NS: Not significant; PLR: Platelet-to-lymphocyte ratio; PNI: Prognostic nutritional index; PSM: Propensity scores matching.

There are some limitations to this study. First, because this is a retrospective study, biases in the data collection process are possible. Second, our cases were collected between 2008 and 2016, the period during which imatinib was used for adjuvant treatment of GIST in China. Despite the adverse reaction



DOI: 10.3748/wjg.v28.i27.3476 Copyright ©The Author(s) 2022.

Figure 2 Kaplan-Meier curves of recurrence-free survival. A: Stratified by low/high levels of the combination index of hemoglobin, albumin, lymphocyte, and platelet (HALP) in gastrointestinal stromal tumors (GISTs) patients before propensity scores matching (PSM); B: Stratified by low/high levels of HALP in GIST patients after PSM; C: Stratified by low/high levels of HALP in high-risk GIST patients. GIST: Gastrointestinal stromal tumors; PSM: Propensity scores matching; HALP: Hemoglobin, albumin, lymphocyte, and platelet.



DOI: 10.3748/wjg.v28.i27.3476 Copyright ©The Author(s) 2022.

Figure 3 Comparison of hemoglobin, albumin, lymphocyte, and platelet and other parameters in prediction ability of 5-year recurrence-free survival by receiver operating characteristic curve analysis before propensity scores matching. AUC: Area under the curve; HALP: Hemoglobin, albumin, lymphocyte, and platelet; LMR: Lymphocyte-to-monocyte ratio; NLR: Neutrophil-to-lymphocyte ratio; PLR: Platelet-to-lymphocyte ratio; PNI: Prognostic nutritional index; PSM: Propensity scores matching; ROC: Receiver operating characteristic.

and high costs, 201/591 (34.0%) of GIST patients still received adjuvant imatinib therapy. As an important treatment after GIST, adjuvant imatinib therapy can significantly improve the prognosis of GIST patients[58], and its benefits are also shown in the present study (Supplementary Figure 3). However, there was no adequate collection and analysis of the time, dose, and adverse reactions of patients with imatinib or sunitinib therapy, which may also be related to HALP. Moreover, this study did not evaluate other clinicopathological factors related to prognosis, especially gene mutation status. Furthermore, the effect of preoperative or postoperative improvement of nutritional status or inflammation response on the prognosis of GIST remains obscure, and will require further confirmation in clinical studies.

CONCLUSION

HALP was associated with postoperative pathological data (*i.e.* tumor site, tumor size, mitosis, Ki67, NIH risk category) and adjuvant therapy. Furthermore, HALP was an independent risk factor for RFS in GIST patients who underwent radical resection.

ARTICLE HIGHLIGHTS

Research background

The combination index of hemoglobin, albumin, lymphocyte, and platelet (HALP) has been reported as associated with prognosis in many cancers but not yet in gastrointestinal stromal tumors (GISTs). Therefore, this study aimed to investigate the prognostic value of preoperative HALP in resected GIST patients.

Research motivation

At present, the risk of GIST is mainly based on postoperative pathological indicators. The motivation for this article involved the need to find a convenient, non-invasive, preoperative indicator that will assist in prognostic prediction of GIST.

Research objectives

To investigate the prognostic value of HALP in GIST patients.

Research methods

This retrospective cohort study enrolled patients with GIST using propensity scores matching to explore the relationship between HALP, postoperative clinicopathological data, and the prognostic significance of HALP.

Research results

HALP can be conveniently used preoperatively to assess risk and prognosis of GIST patients. However, the effect of improving nutritional status or immune-inflammatory status on the prognosis of GIST is still unclear and requires further confirmation through clinical studies.

Research conclusions

HALP was associated with postoperative pathological data (*i.e.* tumor site, tumor size, mitosis, Ki67, National Institutes of Health risk category) and adjuvant therapy. Furthermore, HALP was an independent risk factor for recurrence-free survival in GIST patients who underwent radical resection. This study is the first to report the prognostic significance of HALP in GIST. In this study, HALP was found to be an independent risk factor for GIST patients with R0 resection. Consistent with reports of HALP in other tumors, HALP is also associated with prognosis in GIST. HALP was also found to be an independent risk factor for GIST patients with R0 resection. In clinical practice, convenient and non-invasive preoperative HALP may be used to assist in the prediction of risk and prognosis for GIST patients.

Research perspectives

Through this retrospective cohort study, we found the prognostic significance of HALP in GIST. This study did not evaluate other clinicopathological factors related to prognosis, especially gene mutation status. Subsequent studies should employ a prospective cohort method and incorporate additional factors to further explore the prognostic significance of HALP in GIST patients.

FOOTNOTES

Author contributions: All authors made a significant contribution to the work reported, whether that is in the conception, study design, execution, acquisition of data, analysis and interpretation, or in all these areas; and all authors took part in drafting, revising or critically reviewing the article, gave final approval of the version to be published, agreed on the journal to which the article has been submitted and agreed to be accountable for all aspects of the work.

Supported by National Natural Science Foundation of China, No. 81572931; and The 1.3.5 Project for Disciplines of Excellence, West China Hospital, Sichuan University, No. ZYJC18034.

Institutional review board statement: The Institutional Review Board of the West China Hospital of Sichuan University provided approval for this study, No. 1135(2019).

Informed consent statement: This study examined only patients' electronic health records. Each patient had been asked to sign an informed consent form authorizing the use of their electronic health record for scientific research. If the patient had not consented, we were unable to access his/her information in the hospital's information system.

Conflict-of-interest statement: All the authors report no relevant conflicts of interest for this article.

Data sharing statement: The data that supporting the findings of this study are available from the corresponding author (e-mail: hxwcwk@126.com) upon reasonable request.

STROBE statement: The authors have read the STROBE Statement – checklist of items, and the manuscript was prepared and revised according to the STROBE Statement – checklist of items.

Open-Access: This article is an open-access article that was selected by an in-house editor and fully peer-reviewed by external reviewers. It is distributed in accordance with the Creative Commons Attribution NonCommercial (CC BY-NC 4.0) license, which permits others to distribute, remix, adapt, build upon this work non-commercially, and license their derivative works on different terms, provided the original work is properly cited and the use is non-commercial. See: https://creativecommons.org/Licenses/by-nc/4.0/

Country/Territory of origin: China

ORCID number: Zhou Zhao 0000-0001-7349-7159; Xiao-Nan Yin 0000-0003-4525-1877; Jian Wang 0000-0002-7407-2504; Xin Chen 0000-0001-7025-0337; Zhao-Lun Cai 0000-0002-3706-6703; Bo Zhang 0000-0002-0254-5843.

S-Editor: Fan JR
L-Editor: A
P-Editor: Fan JR

REFERENCES

1 **Ma GL**, Murphy JD, Martinez ME, Sicklick JK. Epidemiology of gastrointestinal stromal tumors in the era of histology codes: results of a population-based study. *Cancer Epidemiol Biomarkers Prev* 2015; **24**: 298-302 [PMID: 25277795 DOI: 10.1158/1055-9965.EPI-14-1002]
2 **Nishida T**, Blay JY, Hirota S, Kitagawa Y, Kang YK. The standard diagnosis, treatment, and follow-up of gastrointestinal stromal tumors based on guidelines. *Gastric Cancer* 2016; **19**: 3-14 [PMID: 26276366 DOI: 10.1007/s10120-015-0526-8]
3 **Barrios CH**, Blackstein ME, Blay JY, Casali PG, Chacon M, Gu J, Kang YK, Nishida T, Purkayastha D, Woodman RC, Reichardt P. The GOLD ReGISTry: a Global, Prospective, Observational Registry Collecting Longitudinal Data on Patients with Advanced and Localised Gastrointestinal Stromal Tumours. *Eur J Cancer* 2015; **51**: 2423-2433 [PMID: 26248685 DOI: 10.1016/j.ejca.2015.07.010]
4 **DeMatteo RP**, Ballman KV, Antonescu CR, Corless C, Kolesnikova V, von Mehren M, McCarter MD, Norton J, Maki RG, Pisters PW, Demetri GD, Brennan MF, Owzar K; American College of Surgeons Oncology Group (ACOSOG) Intergroup Adjuvant GIST Study Team for the Alliance for Clinical Trials in Oncology. Long-term results of adjuvant imatinib mesylate in localized, high-risk, primary gastrointestinal stromal tumor: ACOSOG Z9000 (Alliance) intergroup phase 2 trial. *Ann Surg* 2013; **258**: 422-429 [PMID: 23860199 DOI: 10.1097/SLA.0b013e3182a15eb7]
5 **Demetri GD**, von Mehren M, Antonescu CR, DeMatteo RP, Ganjoo KN, Maki RG, Pisters PW, Raut CP, Riedel RF, Schuetze S, Sundar HM, Trent JC, Wayne JD. NCCN Task Force report: update on the management of patients with gastrointestinal stromal tumors. *J Natl Compr Canc Netw* 2010; **8** Suppl 2: S1-41; quiz S42 [PMID: 20457867 DOI: 10.6004/jnccn.2010.0116]
6 **Casali PG**, Abecassis N, Aro HT, Bauer S, Biagini R, Bielack S, Bonvalot S, Boukovinas I, Bovee JVMG, Brodowicz T, Broto JM, Buonadonna A, De Álava E, Dei Tos AP, Del Muro XG, Dileo P, Eriksson M, Fedenko A, Ferraresi V, Ferrari A, Ferrari S, Frezza AM, Gasperoni S, Gelderblom H, Gil T, Grignani G, Gronchi A, Haas RL, Hassan B, Hohenberger P, Issels R, Joensuu H, Jones RL, Judson I, Jutte P, Kaal S, Kasper B, Kopeckova K, Krákorová DA, Le Cesne A, Lugowska I, Merimsky O, Montemurro M, Pantaleo MA, Piana R, Picci P, Piperno-Neumann S, Pousa AL, Reichardt P, Robinson MH, Rutkowski P, Safwat AA, Schöffski P, Sleijfer S, Stacchiotti S, Sundby Hall K, Unk M, Van Coevorden F, van der Graaf WTA, Whelan J, Wardelmann E, Zaikova O, Blay JY; ESMO Guidelines Committee and EURACAN. Gastrointestinal stromal tumours: ESMO-EURACAN Clinical Practice Guidelines for diagnosis, treatment and follow-up. *Ann Oncol* 2018; **29**: iv68-iv78 [PMID: 29846513 DOI: 10.1093/annonc/mdy095]
7 **Koo DH**, Ryu MH, Kim KM, Yang HK, Sawaki A, Hirota S, Zheng J, Zhang B, Tzen CY, Yeh CN, Nishida T, Shen L, Chen LT, Kang YK. Asian Consensus Guidelines for the Diagnosis and Management of Gastrointestinal Stromal Tumor. *Cancer Res Treat* 2016; **48**: 1155-1166 [PMID: 27384163 DOI: 10.4143/crt.2016.187]
8 **Ubukata H**, Motohashi G, Tabuchi T, Nagata H, Konishi S. Evaluations of interferon-γ/interleukin-4 ratio and neutrophil/lymphocyte ratio as prognostic indicators in gastric cancer patients. *J Surg Oncol* 2010; **102**: 742-747 [PMID: 20872813 DOI: 10.1002/jso.21725]
9 **Malietzis G**, Giacometti M, Askari A, Nachiappan S, Kennedy RH, Faiz OD, Aziz O, Jenkins JT. A preoperative neutrophil to lymphocyte ratio of 3 predicts disease-free survival after curative elective colorectal cancer surgery. *Ann Surg* 2014; **260**: 287-292 [PMID: 24096764 DOI: 10.1097/SLA.0000000000000216]
10 **Pinato DJ**, Shiner RJ, Seckl MJ, Stebbing J, Sharma R, Mauri FA. Prognostic performance of inflammation-based prognostic indices in primary operable non-small cell lung cancer. *Br J Cancer* 2014; **110**: 1930-1935 [PMID: 24667648 DOI: 10.1038/bjc.2014.145]
11 **Sun J**, Mei Y, Zhu Q, Shou C, Tjhoi WEH, Yang W, Yu H, Zhang Q, Liu X, Yu J. Relationship of prognostic nutritional index with prognosis of gastrointestinal stromal tumors. *J Cancer* 2019; **10**: 2679-2686 [PMID: 31258776 DOI: 10.7150/jca.32299]

12 **Shi WK**, Zhang XH, Zhang J, Yu M, Yuan YJ, Xiong W, Zhang CH, He YL, Wei ZW. Predictive ability of prognostic nutritional index in surgically resected gastrointestinal stromal tumors: a propensity score matching analysis. *Jpn J Clin Oncol* 2019; **49**: 823-831 [PMID: 31162583 DOI: 10.1093/jjco/hyz078]

13 **Yin XN**, Tang SM, Yin Y, Shen CY, Zhang B, Chen ZX. [Associations of Preoperative Platelet-to-lymphocyte Ratio and Derived Neutrophil-to-lymphocyte Ratio with thePrognosis of Gastrointestinal Stromal Tumor]. *Sichuan Da Xue Xue Bao Yi Xue Ban* 2017; **48**: 239-243 [PMID: 28612534]

14 **Feng F**, Tian Y, Liu S, Zheng G, Liu Z, Xu G, Guo M, Lian X, Fan D, Zhang H. Combination of PLR, MLR, MWR, and Tumor Size Could Significantly Increase the Prognostic Value for Gastrointestinal Stromal Tumors. *Medicine (Baltimore)* 2016; **95**: e3248 [PMID: 27057867 DOI: 10.1097/MD.0000000000003248]

15 **Yin Z**, Gao J, Liu W, Huang C, Shuai X, Wang G, Tao K, Zhang P. Clinicopathological and Prognostic Analysis of Primary Gastrointestinal Stromal Tumor Presenting with Gastrointestinal Bleeding: a 10-Year Retrospective Study. *J Gastrointest Surg* 2017; **21**: 792-800 [PMID: 28275959 DOI: 10.1007/s11605-017-3385-2]

16 **Racz JM**, Cleghorn MC, Jimenez MC, Atenafu EG, Jackson TD, Okrainec A, Venkat Raghavan L, Quereshy FA. Predictive Ability of Blood Neutrophil-to-Lymphocyte and Platelet-to-Lymphocyte Ratios in Gastrointestinal Stromal Tumors. *Ann Surg Oncol* 2015; **22**: 2343-2350 [PMID: 25472648 DOI: 10.1245/s10434-014-4265-6]

17 **Luo XF**, Zhou LH. Prognostic significance of neutrophil to lymphocyte ratio in patients with gastrointestinal stromal tumors: A meta-analysis. *Clin Chim Acta* 2018; **477**: 7-12 [PMID: 29175648 DOI: 10.1016/j.cca.2017.11.029]

18 **Chen XL**, Xue L, Wang W, Chen HN, Zhang WH, Liu K, Chen XZ, Yang K, Zhang B, Chen ZX, Chen JP, Zhou ZG, Hu JK. Prognostic significance of the combination of preoperative hemoglobin, albumin, lymphocyte and platelet in patients with gastric carcinoma: a retrospective cohort study. *Oncotarget* 2015; **6**: 41370-41382 [PMID: 26497995 DOI: 10.18632/oncotarget.5629]

19 **Xu SS**, Li S, Xu HX, Li H, Wu CT, Wang WQ, Gao HL, Jiang W, Zhang WH, Li TJ, Ni QX, Liu L, Yu XJ. Haemoglobin, albumin, lymphocyte and platelet predicts postoperative survival in pancreatic cancer. *World J Gastroenterol* 2020; **26**: 828-838 [PMID: 32148380 DOI: 10.3748/wjg.v26.i8.828]

20 **Peng D**, Zhang CJ, Tang Q, Zhang L, Yang KW, Yu XT, Gong Y, Li XS, He ZS, Zhou LQ. Prognostic significance of the combination of preoperative hemoglobin and albumin levels and lymphocyte and platelet counts (HALP) in patients with renal cell carcinoma after nephrectomy. *BMC Urol* 2018; **18**: 20 [PMID: 29544476 DOI: 10.1186/s12894-018-0333-8]

21 **Guo Y**, Shi D, Zhang J, Mao S, Wang L, Zhang W, Zhang Z, Jin L, Yang B, Ye L, Yao X. The Hemoglobin, Albumin, Lymphocyte, and Platelet (HALP) Score is a Novel Significant Prognostic Factor for Patients with Metastatic Prostate Cancer Undergoing Cytoreductive Radical Prostatectomy. *J Cancer* 2019; **10**: 81-91 [PMID: 30662528 DOI: 10.7150/jca.27210]

22 **Peng D**, Zhang CJ, Gong YQ, Hao H, Guan B, Li XS, Zhou LQ. Prognostic significance of HALP (hemoglobin, albumin, lymphocyte and platelet) in patients with bladder cancer after radical cystectomy. *Sci Rep* 2018; **8**: 794 [PMID: 29335609 DOI: 10.1038/s41598-018-19146-y]

23 **Cong L**, Hu L. The value of the combination of hemoglobin, albumin, lymphocyte and platelet in predicting platinum-based chemoradiotherapy response in male patients with esophageal squamous cell carcinoma. *Int Immunopharmacol* 2017; **46**: 75-79 [PMID: 28268208 DOI: 10.1016/j.intimp.2017.02.027]

24 **Shen XB**, Zhang YX, Wang W, Pan YY. The Hemoglobin, Albumin, Lymphocyte, and Platelet (HALP) Score in Patients with Small Cell Lung Cancer Before First-Line Treatment with Etoposide and Progression-Free Survival. *Med Sci Monit* 2019; **25**: 5630-5639 [PMID: 31356586 DOI: 10.12659/MSM.917968]

25 **Ichikawa K**, Mizuno S, Hayasaki A, Kishiwada M, Fujii T, Iizawa Y, Kato H, Tanemura A, Murata Y, Azumi Y, Kuriyama N, Usui M, Sakurai H, Isaji S. Prognostic Nutritional Index After Chemoradiotherapy Was the Strongest Prognostic Predictor Among Biological and Conditional Factors in Localized Pancreatic Ductal Adenocarcinoma Patients. *Cancers (Basel)* 2019; **11** [PMID: 30974894 DOI: 10.3390/cancers11040514]

26 **Hsu JT**, Wang CC, Le PH, Chen TH, Kuo CJ, Lin CJ, Chou WC, Yeh TS. Lymphocyte-to-monocyte ratios predict gastric cancer surgical outcomes. *J Surg Res* 2016; **202**: 284-290 [PMID: 27229102 DOI: 10.1016/j.jss.2016.01.005]

27 **Joensuu H**. Risk stratification of patients diagnosed with gastrointestinal stromal tumor. *Hum Pathol* 2008; **39**: 1411-1419 [PMID: 18774375 DOI: 10.1016/j.humpath.2008.06.025]

28 **Camp RL**, Dolled-Filhart M, Rimm DL. X-tile: a new bio-informatics tool for biomarker assessment and outcome-based cut-point optimization. *Clin Cancer Res* 2004; **10**: 7252-7259 [PMID: 15534099 DOI: 10.1158/1078-0432.Ccr-04-0713]

29 **Heagerty PJ**, Lumley T, Pepe MS. Time-dependent ROC curves for censored survival data and a diagnostic marker. *Biometrics* 2000; **56**: 337-344 [PMID: 10877287 DOI: 10.1111/j.0006-341x.2000.00337.x]

30 **Goh BK**, Chok AY, Allen JC Jr, Quek R, Teo MC, Chow PK, Chung AY, Ong HS, Wong WK. Blood neutrophil-to-lymphocyte and platelet-to-lymphocyte ratios are independent prognostic factors for surgically resected gastrointestinal stromal tumors. *Surgery* 2016; **159**: 1146-1156 [PMID: 26688506 DOI: 10.1016/j.surg.2015.10.021]

31 **Rutkowski P**, Teterycz P, Klimczak A, Bylina E, Szamotulska K, Lugowska I. Blood neutrophil-to-lymphocyte ratio is associated with prognosis in advanced gastrointestinal stromal tumors treated with imatinib. *Tumori* 2018; **104**: 415-422 [PMID: 29714669 DOI: 10.1177/0300891618765543]

32 **Ostroumov D**, Fekete-Drimusz N, Saborowski M, Kühnel F, Woller N. CD4 and CD8 T lymphocyte interplay in controlling tumor growth. *Cell Mol Life Sci* 2018; **75**: 689-713 [PMID: 29032503 DOI: 10.1007/s00018-017-2686-7]

33 **Shankaran V**, Ikeda H, Bruce AT, White JM, Swanson PE, Old LJ, Schreiber RD. IFNgamma and lymphocytes prevent primary tumour development and shape tumour immunogenicity. *Nature* 2001; **410**: 1107-1111 [PMID: 11323675 DOI: 10.1038/35074122]

34 **Thorsson V**, Gibbs DL, Brown SD, Wolf D, Bortone DS, Ou Yang TH, Porta-Pardo E, Gao GF, Plaisier CL, Eddy JA, Ziv E, Culhane AC, Paull EO, Sivakumar IKA, Gentles AJ, Malhotra R, Farshidfar F, Colaprico A, Parker JS, Mose LE, Vo NS, Liu J, Liu Y, Rader J, Dhankani V, Reynolds SM, Bowlby R, Califano A, Cherniack AD, Anastassiou D, Bedognetti D, Mokrab Y, Newman AM, Rao A, Chen K, Krasnitz A, Hu H, Malta TM, Noushmehr H, Pedamallu CS, Bullman S, Ojesina AI, Lamb A, Zhou W, Shen H, Choueiri TK, Weinstein JN, Guinney J, Saltz J, Holt RA, Rabkin CS; Cancer Genome Atlas Research Network, Lazar AJ, Serody JS, Demicco EG, Disis ML, Vincent BG, Shmulevich I. The Immune

Landscape of Cancer. *Immunity* 2018; **48**: 812-830.e14 [PMID: 29628290 DOI: 10.1016/j.immuni.2018.03.023]
35 **Nash GF**, Turner LF, Scully MF, Kakkar AK. Platelets and cancer. *Lancet Oncol* 2002; **3**: 425-430 [PMID: 12142172 DOI: 10.1016/s1470-2045(02)00789-1]
36 **Haemmerle M**, Stone RL, Menter DG, Afshar-Kharghan V, Sood AK. The Platelet Lifeline to Cancer: Challenges and Opportunities. *Cancer Cell* 2018; **33**: 965-983 [PMID: 29657130 DOI: 10.1016/j.ccell.2018.03.002]
37 **Davì G**, Patrono C. Platelet activation and atherothrombosis. *N Engl J Med* 2007; **357**: 2482-2494 [PMID: 18077812 DOI: 10.1056/NEJMra071014]
38 **Abdol Razak NB**, Jones G, Bhandari M, Berndt MC, Metharom P. Cancer-Associated Thrombosis: An Overview of Mechanisms, Risk Factors, and Treatment. *Cancers (Basel)* 2018; **10** [PMID: 30314362 DOI: 10.3390/cancers10100380]
39 **Olsson AK**, Cedervall J. The pro-inflammatory role of platelets in cancer. *Platelets* 2018; **29**: 569-573 [PMID: 29584534 DOI: 10.1080/09537104.2018.1453059]
40 **Schlesinger M**. Role of platelets and platelet receptors in cancer metastasis. *J Hematol Oncol* 2018; **11**: 125 [PMID: 30305116 DOI: 10.1186/s13045-018-0669-2]
41 **Wojtukiewicz MZ**, Sierko E, Hempel D, Tucker SC, Honn KV. Platelets and cancer angiogenesis nexus. *Cancer Metastasis Rev* 2017; **36**: 249-262 [PMID: 28681240 DOI: 10.1007/s10555-017-9673-1]
42 **Sorour MA**, Kassem MI, Ghazal Ael-H, El-Riwini MT, Abu Nasr A. Gastrointestinal stromal tumors (GIST) related emergencies. *Int J Surg* 2014; **12**: 269-280 [PMID: 24530605 DOI: 10.1016/j.ijsu.2014.02.004]
43 **Yang Z**, Wang F, Liu S, Guan W. Comparative clinical features and short-term outcomes of gastric and small intestinal gastrointestinal stromal tumours: a retrospective study. *Sci Rep* 2019; **9**: 10033 [PMID: 31296939 DOI: 10.1038/s41598-019-46520-1]
44 **Italiano A**, Cioffi A, Coco P, Maki RG, Schöffski P, Rutkowski P, Le Cesne A, Duffaud F, Adenis A, Isambert N, Bompas E, Blay JY, Casali P, Keohan ML, Toulmonde M, Antonescu CR, Debiec-Rychter M, Coindre JM, Bui B. Patterns of care, prognosis, and survival in patients with metastatic gastrointestinal stromal tumors (GIST) refractory to first-line imatinib and second-line sunitinib. *Ann Surg Oncol* 2012; **19**: 1551-1559 [PMID: 22065192 DOI: 10.1245/s10434-011-2120-6]
45 **Hompland I**, Bruland ØS, Hølmebakk T, Poulsen JP, Stoldt S, Hall KS, Boye K. Prediction of long-term survival in patients with metastatic gastrointestinal stromal tumor: analysis of a large, single-institution cohort. *Acta Oncol* 2017; **56**: 1317-1323 [PMID: 28557540 DOI: 10.1080/0284186X.2017.1330555]
46 **Xia Y**, Chen S, Luo M, Wu J, Cai S, He Y, Chen X, Zhang X. Correlations between imatinib plasma trough concentration and adverse reactions in Chinese patients with gastrointestinal stromal tumors. *Cancer* 2020; **126** Suppl 9: 2054-2061 [PMID: 32293723 DOI: 10.1002/cncr.32751]
47 **Allen TM**, Cullis PR. Drug delivery systems: entering the mainstream. *Science* 2004; **303**: 1818-1822 [PMID: 15031496 DOI: 10.1126/science.1095833]
48 **Kalyane D**, Raval N, Maheshwari R, Tambe V, Kalia K, Tekade RK. Employment of enhanced permeability and retention effect (EPR): Nanoparticle-based precision tools for targeting of therapeutic and diagnostic agent in cancer. *Mater Sci Eng C Mater Biol Appl* 2019; **98**: 1252-1276 [PMID: 30813007 DOI: 10.1016/j.msec.2019.01.066]
49 **Babson AL**, Winnick T. Protein transfer in tumor-bearing rats. *Cancer Res* 1954; **14**: 606-611 [PMID: 13199806]
50 **Kratz F**. Albumin as a drug carrier: design of prodrugs, drug conjugates and nanoparticles. *J Control Release* 2008; **132**: 171-183 [PMID: 18582981 DOI: 10.1016/j.jconrel.2008.05.010]
51 **Kratz F**, Beyer U. Serum proteins as drug carriers of anticancer agents: a review. *Drug Deliv* 1998; **5**: 281-299 [PMID: 19569996 DOI: 10.3109/10717549809065759]
52 **Peng B**, Lloyd P, Schran H. Clinical pharmacokinetics of imatinib. *Clin Pharmacokinet* 2005; **44**: 879-894 [PMID: 16122278 DOI: 10.2165/00003088-200544090-00001]
53 **Kim B**, Seo B, Park S, Lee C, Kim JO, Oh KT, Lee ES, Choi HG, Youn YS. Albumin nanoparticles with synergistic antitumor efficacy against metastatic lung cancers. *Colloids Surf B Biointerfaces* 2017; **158**: 157-166 [PMID: 28688365 DOI: 10.1016/j.colsurfb.2017.06.039]
54 **Boonpipattanapong T**, Chewatanakornkul S. Preoperative carcinoembryonic antigen and albumin in predicting survival in patients with colon and rectal carcinomas. *J Clin Gastroenterol* 2006; **40**: 592-595 [PMID: 16917399 DOI: 10.1097/00004836-200608000-00006]
55 **Oñate-Ocaña LF**, Aiello-Crocifoglio V, Gallardo-Rincón D, Herrera-Goepfert R, Brom-Valladares R, Carrillo JF, Cervera E, Mohar-Betancourt A. Serum albumin as a significant prognostic factor for patients with gastric carcinoma. *Ann Surg Oncol* 2007; **14**: 381-389 [PMID: 17160496 DOI: 10.1245/s10434-006-9093-x]
56 **Siddiqui A**, Heinzerling J, Livingston EH, Huerta S. Predictors of early mortality in veteran patients with pancreatic cancer. *Am J Surg* 2007; **194**: 362-366 [PMID: 17693283 DOI: 10.1016/j.amjsurg.2007.02.007]
57 **Lis CG**, Grutsch JF, Vashi PG, Lammersfeld CA. Is serum albumin an independent predictor of survival in patients with breast cancer? *JPEN J Parenter Enteral Nutr* 2003; **27**: 10-15 [PMID: 12549592 DOI: 10.1177/014860710302700110]
58 **Cohen MH**, Cortazar P, Justice R, Pazdur R. Approval summary: imatinib mesylate in the adjuvant treatment of malignant gastrointestinal stromal tumors. *Oncologist* 2010; **15**: 300-307 [PMID: 20200041 DOI: 10.1634/theoncologist.2009-0120]

World Journal of Gastroenterology

Submit a Manuscript: https://www.f6publishing.com

World J Gastroenterol 2022 July 21; 28(27): 3488-3502

DOI: 10.3748/wjg.v28.i27.3488

ISSN 1007-9327 (print) ISSN 2219-2840 (online)

ORIGINAL ARTICLE

Retrospective Study

Contrast-enhanced ultrasound Liver Imaging Reporting and Data System: Lights and shadows in hepatocellular carcinoma and cholangiocellular carcinoma diagnosis

Gianpaolo Vidili, Marco Arru, Giuliana Solinas, Diego Francesco Calvisi, Pierluigi Meloni, Assunta Sauchella, Davide Turilli, Claudio Fabio, Antonio Cossu, Giordano Madeddu, Sergio Babudieri, Maria Assunta Zocco, Giovanni Iannetti, Enza Di Lembo, Alessandro Palmerio Delitala, Roberto Manetti

Specialty type: Medicine, research and experimental

Provenance and peer review: Invited article; Externally peer reviewed.

Peer-review model: Single blind

Peer-review report's scientific quality classification

Grade A (Excellent): 0
Grade B (Very good): B
Grade C (Good): C
Grade D (Fair): D, D
Grade E (Poor): 0

P-Reviewer: Cao X, China; Kamimura H, Japan; Lu Q, China; Zhou JH, China

A-Editor: Chen Z, China

Received: December 17, 2021
Peer-review started: December 17, 2021
First decision: January 27, 2022
Revised: February 10, 2022
Accepted: June 16, 2022
Article in press: June 16, 2022
Published online: July 21, 2022

Gianpaolo Vidili, Marco Arru, Diego Francesco Calvisi, Pierluigi Meloni, Assunta Sauchella, Davide Turilli, Claudio Fabio, Antonio Cossu, Giordano Madeddu, Sergio Babudieri, Alessandro Palmerio Delitala, Roberto Manetti, Department of Medical, Surgical and Experimental Sciences, University of Sassari, Sassari 07100, Italy

Giuliana Solinas, Department of Biomedical Sciences, Public Health-Laboratory of Biostatistics, University of Sassari, Sassari 07100, Italy

Maria Assunta Zocco, Department of Internal Medicine and Gastroenterology, Fondazione Policlinico Universitario A. Gemelli IRCCS, Catholic University, Rome 00168, Italy

Giovanni Iannetti, Enza Di Lembo, Ultrasound Unit, Ospedale S. Spirito, Pescara 65123, Italy

Corresponding author: Gianpaolo Vidili, MD, Assistant Professor, Department of Medical, Surgical and Experimental Sciences, University of Sassari, 8 Viale San Pietro, Sassari 07100, Italy. gianpaolovidili@uniss.it

Abstract

BACKGROUND

Contrast-enhanced ultrasound (CEUS) is considered a secondary examination compared to computed tomography (CT) and magnetic resonance imaging (MRI) in the diagnosis of hepatocellular carcinoma (HCC), due to the risk of misdiagnosing intrahepatic cholangiocarcinoma (ICC). The introduction of CEUS Liver Imaging Reporting and Data System (CEUS LI-RADS) might overcome this limitation. Even though data from the literature seems promising, its reliability in real-life context has not been well-established yet.

AIM

To test the accuracy of CEUS LI-RADS for correctly diagnosing HCC and ICC in cirrhosis.

METHODS

CEUS LI-RADS class was retrospectively assigned to 511 nodules identified in 269 patients suffering from liver cirrhosis. The diagnostic standard for all nodules was

either biopsy (102 nodules) or CT/MRI (409 nodules). Common diagnostic accuracy indexes such as sensitivity, specificity, positive predictive value (PPV), and negative predictive value (NPV) were assessed for the following associations: CEUS LR-5 and HCC; CEUS LR-4 and 5 merged class and HCC; CEUS LR-M and ICC; and CEUS LR-3 and malignancy. The frequency of malignant lesions in CEUS LR-3 subgroups with different CEUS patterns was also determined. Inter-rater agreement for CEUS LI-RADS class assignment and for major CEUS pattern identification was evaluated.

RESULTS

CEUS LR-5 predicted HCC with a 67.6% sensitivity, 97.7% specificity, and 99.3% PPV ($P < 0.001$). The merging of LR-4 and 5 offered an improved 93.9% sensitivity in HCC diagnosis with a 94.3% specificity and 98.8% PPV ($P < 0.001$). CEUS LR-M predicted ICC with a 91.3% sensitivity, 96.7% specificity, and 99.6% NPV ($P < 0.001$). CEUS LR-3 predominantly included benign lesions (only 28.8% of malignancies). In this class, the hypo-hypo pattern showed a much higher rate of malignant lesions (73.3%) than the iso-iso pattern (2.6%). Inter-rater agreement between internal raters for CEUS-LR class assignment was almost perfect ($n = 511$, $k = 0.94$, $P < 0.001$), while the agreement among raters from separate centres was substantial ($n = 50$, $k = 0.67$, $P < 0.001$). Agreement was stronger for arterial phase hyperenhancement (internal $k = 0.86$, $P < 2.7 \times 10^{-214}$; external $k = 0.8$, $P < 0.001$) than washout (internal $k = 0.79$, $P < 1.6 \times 10^{-202}$; external $k = 0.71$, $P < 0.001$).

CONCLUSION

CEUS LI-RADS is effective but can be improved by merging LR-4 and 5 to diagnose HCC and by splitting LR-3 into two subgroups to differentiate iso-iso nodules from other patterns.

Key Words: Contrast-enhanced ultrasound Liver Imaging Reporting and Data System; Hepatocellular carcinoma; Intrahepatic cholangiocarcinoma; Cirrhosis; Contrast-enhanced ultrasound; Liver

©The Author(s) 2022. Published by Baishideng Publishing Group Inc. All rights reserved.

Core Tip: This is a retrospective study to evaluate the accuracy of contrast-enhanced ultrasound Liver Imaging Reporting and Data System (CEUS LI-RADS) in correctly diagnosing hepatocellular carcinoma (HCC) and intrahepatic cholangiocarcinoma (ICC) in patients with cirrhosis. CEUS LR-5 showed a 97.7% specificity for HCC with a low sensitivity (67.6%), while the CEUS LR-4 and 5 merged class showed a 93.9% sensitivity and 94.3% specificity for HCC. CEUS LR-M predicted ICC with a 91.3% sensitivity and 96.7% specificity. CEUS LR-3 predominantly included benign lesions (28.8% of malignancies) but was heterogeneous as the hypo-hypo pattern showed a higher rate of malignant lesions (73.3%) than the iso-iso pattern (2.6%).

Citation: Vidili G, Arru M, Solinas G, Calvisi DF, Meloni P, Sauchella A, Turilli D, Fabio C, Cossu A, Madeddu G, Babudieri S, Zocco MA, Iannetti G, Di Lembo E, Delitala AP, Manetti R. Contrast-enhanced ultrasound Liver Imaging Reporting and Data System: Lights and shadows in hepatocellular carcinoma and cholangiocellular carcinoma diagnosis. *World J Gastroenterol* 2022; 28(27): 3488-3502
URL: https://www.wjgnet.com/1007-9327/full/v28/i27/3488.htm
DOI: https://dx.doi.org/10.3748/wjg.v28.i27.3488

INTRODUCTION

Liver cirrhosis is a strong risk factor for primitive liver cancer, the seventh most commonly diagnosed malignancy worldwide and the third most common cause of cancer-related death[1]. In this scenario, the most prevalent malignant lesion is hepatocellular carcinoma (HCC), followed by intrahepatic cholangiocarcinoma (ICC); however, other types of cancer are rare. The development of a malignant lesion represents a critical point in the clinical history of chronic liver diseases since it significantly reduces life expectancy, especially in case of late diagnosis. Therefore, regular follow-up is essential for these patients with mandatory ultrasonography every 6 mo for detecting solid focal liver lesions[2-5].

Contrast-enhanced ultrasound (CEUS) is an effective, well-recognized, and safe imaging technique for visualising the onset of new nodules in liver cirrhosis, that adheres to national and international guidelines[2,6,7]. One of the initial limitations of CEUS, reported in 2010, was the possibility of missing ICC cases, since a significant proportion of the ICC nodules that develop in a cirrhotic liver show the

same enhancement pattern as HCC[8]. Since then, subsequent studies have demonstrated that the timing and intensity of washout are different in HCC and ICC. In particular, for the vast majority of ICC nodules (50%-85%), washout starts earlier than 60 *s*, while this is rarely observed in HCC. Furthermore, washout intensity during late phase is clearer in ICC than in HCC[9-14]. These findings led the American College of Radiology to release the CEUS Liver Imaging Reporting and Data System (CEUS LI-RADS), similar to previous releases for computed tomography (CT) and magnetic resonance imaging (MRI). The algorithm was officially approved in June 2016, and the latest update was published in 2017 [15].

CEUS LI-RADS is a standardized system for technique, interpretation, reporting, and data collection on focal liver lesions in patients at high risk for HCC. It encompasses features such as size, conventional ultrasound morphology, contrast enhancement behaviours, and dimensional variations in order to stratify the risk of HCC and to avoid ICC misdiagnosis[16-20]. In particular, CEUS LR-5 is a class specifically designed to include HCC. It encompasses nodules > 1 cm that show arterial phase hyperenhancement (APHE) that is neither rim nor globular, followed by a late (> 60 *s*) mild-degree washout. Other CEUS LI-RADS categories (*e.g.*, CEUS LR-4 and 3) express a very probable and intermediate risk of HCC, while CEUS LR-M has an intermediate/high risk of malignancy without a typical HCC pattern. CEUS LR-M includes lesions of any size that show arterial phase rim enhancement pattern and/or early (before 60 *s*) washout and/or marked washout.

So far, only a few studies have presented actual data from the application of CEUS LI-RADS diagnostic algorithm in cirrhotic patients with suspicious nodules[21-27]. The aim of this study was to test the capability of CEUS LI-RADS in accurately diagnosing focal liver lesions in patients affected by cirrhosis. In particular, we tested the accuracy of CEUS LR-5 and LR-M in correctly diagnosing HCC and ICC, respectively. In addition, we merged classes LR-4 and LR-5 and tested their accuracy in correctly diagnosing HCC as a joint class. Finally, we assessed the rate of malignancy for specific LR-3 class patterns.

MATERIALS AND METHODS

Study design and data collection

The present retrospective study involved patients with cirrhosis associated nodules that were visible using conventional ultrasound, for which it was possible to review the basal appearance and dynamic pattern of the ultrasound contrast agent. Cirrhosis was diagnosed on the basis of clinical data, biochemical parameters, imaging criteria, and elastosonography.

We reviewed all the liver CEUS performed at our centre (Medical Ultrasound Unit, University Hospital, Sassari, Italy) between December 2008 and January 2020. All examinations aimed to characterize a new nodule developed in the context of surveillance programmes for liver cirrhosis. Nodules located in different liver segments were analysed separately with individual boluses of contrast. Within the same segment, only one target nodule was included for analysis based on best visualization criteria.

CT and/or MRI, when typical for HCC or definitely benign (haemangioma, hepatic fat deposition/sparing, and hypertrophic pseudomass), were used as the gold standard imaging modalities. For all other cases, histology obtained by a percutaneous biopsy or surgical resection was considered the reference standard (Supplementary Figures 1 and 2).

Specifically, nodules showing a CT/MRI dynamic pattern with hyperenhancement during the arterial phase followed by washout in the portal or late phase (Supplementary Figures 3 and 4), were diagnosed as HCC in accordance with both the American Association for the Study of Liver Diseases (AASLD) and the Italian Association for the Study of the Liver (AISF) guidelines[2,28]. Benign lesions received a further 2-year follow-up; in case of any increase in size and/or CEUS enhancement variations, a biopsy was performed.

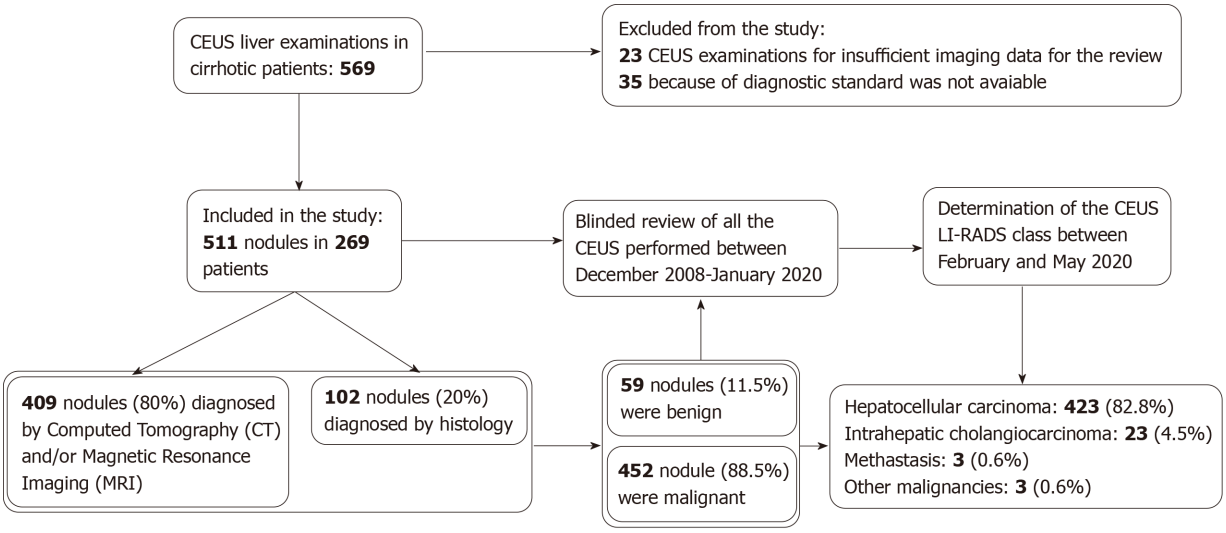
All cases where it was not possible to review the timing and the degree of washout on CEUS (23 cases), or a validated diagnostic reference standard, either CT/MRI scan or histology, was not available (35 cases), were excluded. The algorithm of the study is shown in Figure 1.

CEUS examination and CEUS LI-RADS classification

All CEUS examinations were performed by a physician with 15 years of experience (G.V.) using a second-generation ultrasound contrast agent (SonoVue, Bracco, Milan, Italy).

The signal coming from the bubbles was detected through the following ultrasound scanners: (1) Acuson Sequoia 512 with a 4C1 convex probe and cadence contrast pulse sequencing (CPS, Acuson Siemens, Mountain View, CA, United States) until 2014; and (2) Aixplorer (SuperSonic Imaging, S.A., Aix en Provence, France) with a convex broadband probe (SC6-1) and dedicated software also known as Power Modulated Pulse Inversion (PMPI) from January 2015 until the end of the study.

The CEUS examination was performed continuously for 120 s starting from the injection of contrast. Subsequently, short clips lasting 15-30 *s* were recorded until 5 min after injection.



DOI: 10.3748/wjg.v28.i27.3488 **Copyright** © The Author(s) 2022.

Figure 1 Flow chart of the study.

The CEUS LI-RADS patterns were established after evaluation of all clips and images, with particular attention to the behaviour of intranodular contrast enhancement in dynamic phases.

The review process was independently performed by two operators (G.V. and M.A.) with 15 and 2 years of experience, respectively. In case of disagreement, the class indicated by the more experienced operator was assigned.

The reviewers were blinded to patient identity and final diagnosis. The specific targets of the review process were: (1) Nodule size; (2) the presence of APHE and the type of filling (global, rim, or peripheral discontinuous globular enhancement); and (3) the presence of washout during portal and parenchymal phases, focusing on its timing (before or after 60 *s*) and intensity (mild or marked); washout before 60 *s* was considered early, while washout happening after 60 *s* was considered late.

Inter-rater reliability of CEUS LI-RADS class assignment and of CEUS major features between the two raters (internal agreement) was evaluated for all the nodules (n = 511). Inter-rater reliability among our centre and two other operators from external centres (M.A.Z and G.I., both with more than 20 years of experience in CEUS) was also evaluated for a subgroup of 50 nodules (external agreement). To avoid an excess of typical HCCs, a total of 26 HCCs, 11 ICCs, 11 benign lesions, and 2 other malignancies were randomly selected for the external agreement analysis.

The entire process, including folder preparation, CEUS LI-RADS class assignment, and dataset preparation for analysis, was completed over a period of 5 mo. A systematic review of all CT and MRI scans was not performed.

Statistical analysis

Descriptive statistics (median, interquartile range, range, and percentage) were calculated for patients' demographic and clinical characteristics (age, sex, aetiology of cirrhosis, number, and size of nodules). The normal distribution of continuous variables was evaluated through Shapiro-Wilk test. Discrete and qualitative variables are expressed as frequencies and percentages.

Sensitivity, specificity, positive predictive value (PPV), negative predictive value (NPV), diagnostic accuracy, Youden's index, relative risk, odds ratio, positive likelihood ratio, and negative likelihood ratio were calculated to assess the accuracy of different CEUS-LR classes and subclasses in diagnosing HCC (LR-5, LR-4, and LR-4 and 5 merging class), ICC (LR-M), and malignancies (LR-3). The associations between different CEUS LI-RADS classes and definite diagnosis were evaluated by Pearson's chi-square test or Fisher's exact test. To determine the uncertainty of the estimates on sensitivity, specificity, PPV, NPV, and diagnostic accuracy, 95% confidence intervals (CIs) were calculated.

Cohen's k and Fleiss' k statistics were used to evaluate the interobserver agreement among different examiners in the assignment of the CEUS LI-RADS classes and identification of APHE (absent, homogeneous, or rim-like), and washout (absent, late and mild, or early and/or marked). Additionally, a visual graphical representation of the agreement was created, based on the agreement chart proposed by Bangdiwala[29]. All statistical tests were considered significant for a P value < 0.05. Data were analysed using Stata/MP version 17.0 (Statacorp LP, TX, United States) and R version 4.1.1 (The R Foundation for Statistical Computing, Vienna, Austria).

RESULTS

A total of 511 nodules identified in 269 patients were considered in this study. The complete dataset concerning patients and nodule characteristics is shown in Table 1.

Four-hundred and fifty-two out of 511 nodules (88.5%) turned out to be malignant, consisting of 423 HCCs (82.8%), 23 ICCs (4.5%), 3 metastases (0.6%), and 3 other malignancies (0.6%). Non-invasive diagnosis was obtained for 409 nodules (80%), while histology was followed for 102 nodules (20%). Complete data concerning each definite diagnosis rate for every CEUS LI-RADS class are reported in Table 2. Table 3 shows the rates of HCC and ICC in different CEUS LI-RADS classes. The pathological findings for hepatic nodules are shown in Supplementary Table 1.

The most prevalent pattern in the arterial phase was homogeneous APHE (79.1% of all nodules), followed by isoenhancement (12.7%). In the portal and late phases, the majority of nodules showed a late and mild washout (60.7%) while the second most frequent pattern was isoenhancement (30.7%). See Table 4 and Table 5 for complete data on CEUS pattern in the arterial and venous phases, respectively.

LR-M nodules

Thirty-seven lesions (7.2%) were assigned to the CEUS LR-M class (Figure 2A). Twenty-one of these nodules turned out to be ICCs, eleven were HCCs, three were metastases, one was a lymphoepithelioma, and one was benign. CEUS LR-M predicted ICC with a 91.3% sensitivity, 96.7% specificity, 56.8% PPV, 99.6% NPV, and 96.5% diagnostic accuracy ($P < 0.001$) (Table 6). Examining the CEUS behaviour of ICC, it was observed that 16 out of 21 nodules (76%) showed a rim APHE, while 11 out of 21 nodules (52%) showed an early washout (Supplementary Table 2). HCC nodules reported as LR-M showed a rim APHE in 6 out of 11 cases (54.5%) and an early washout in 7 out of 11 cases (63.6%; Supplementary Table 3).

LR-5 nodules

A total of 288 nodules (56.4%) were categorized as CEUS LR-5 (Figure 2B), of which 286 turned out to be HCC, and 2 were benign lesions. The median diameter of these nodules was 25 mm. The conclusive diagnosis was achieved by CT/MRI for 248 nodules and by histology for 40. CEUS LR-5 class predicted HCC with a 67.6% sensitivity, 97.7% specificity, 99.3% PPV, 38.6% NPV, and 72.8% diagnostic accuracy ($P < 0.001$) (Table 6).

LR-4 nodules

One-hundred and fourteen nodules (22.3%) were reported as CEUS LR-4 (Figure 2C), of which 111 were HCC and 3 were regenerative nodules, as confirmed by histology. The median diameter of these nodules was 21.5 mm. In 95 cases, the diagnosis was given by CT/MRI and in 19 cases by biopsy. CEUS LR-4 predicted HCC with a 26.2% sensitivity, 96.6% specificity, 97.4% PPV, 21.4% NPV, and 38.4% diagnostic accuracy ($P < 0.001$) (Table 6). Table 7 show data relative to different LR-4 patterns.

LR 4-5 merged class

The merging of CEUS LR-4 and CEUS LR-5 classes predicted HCC with a 93.9% sensitivity, 94.3% specificity, 98.8% PPV, 76.1% NPV, and 93.9% diagnostic accuracy ($P < 0.001$) (Table 6).

LR-3 nodules

Sixty-six lesions (12.9%) were assigned to the CEUS LR-3 class (Figure 2D and E). Specifically, 15 of these nodules were HCCs, 2 were ICCs, 2 were other malignancies, and 47 were benign lesions. The median diameter of these nodules was 16 mm. Fifty-three lesions were diagnosed non-invasively by CT/MRI, while 13 by biopsy. CEUS LR-3 predicted benign lesions with a 79.7% sensitivity, 95.8% specificity, 71.2% PPV, 97.3% NPV, and 93.9% diagnostic accuracy ($P < 0.001$) (Table 6). Lesions belonging to the CEUS LR-3 class showed great heterogeneity. In fact, iso-iso nodules (Figure 2D) were most likely benign (only 1 malignancy out of 39 nodules), while other patterns showed a higher risk of cancer (18 malignancies out of 27). The second most frequent CEUS LR-3 pattern was the hypo-hypo pattern assigned to 15 nodules (Figure 2E), of which 11 were malignant (7 HCCs, 2 ICCs, 1 lymphoma, and 1 carcinosarcoma). The rate of malignancy for the CEUS LR-3 class and its subclasses are shown in Figure 3. We also calculated the correlation between specific CEUS LR-3 subgroups and malignancy, with analysis limited to CEUS LR-3 nodules ($n = 66$). It was observed that CEUS LR-3 iso-iso pattern predicted malignancy with a 5.3% sensitivity, 19.1% specificity, 2.6% PPV, 33.3% NPV, and 15.2% diagnostic accuracy ($P < 0.001$). Conversely, CEUS LR-3 hypo-hypo pattern predicted malignancy with a 57.9% sensitivity, 91.5% specificity, 73.3% PPV, 84.3% NPV, and 81.8% diagnostic accuracy ($P < 0.001$) (Table 6). Data concerning different LR-3 patterns are reported in Table 7.

LR 1-2 nodules

Only one nodule (0.2%) was categorized as CEUS LR-1, and five nodules (1%) as CEUS LR-2. All these nodules were found to be benign.

Table 1 Characteristics of patients and hepatic nodules

Item	Number or range
Nodules, *n*	511
Patients, *n*	269
Males, *n* (%)	219 (81.4)
Females, *n* (%)	50 (18.6)
Median age at first nodule (IQR; range)	69 years (61-75; 43-88)
Males (IQR; range)	67 years (59-74; 43-88)
Females (IQR; range)	74.5 years (71-78; 59-85)
Hepatic cirrhosis aetiology (n)	
Chronic HCV infection, *n* (%)	129 (48)
Alcohol abuse, *n* (%)	45 (16.7)
Chronic HBV infection, *n* (%)	24 (8.9)
Chronic HCV infection + alcohol abuse, *n* (%)	21 (7.8)
Chronic HBV + HCV infection, *n* (%)	8 (3)
NASH, *n* (%)	6 (2.2)
ChronicHBV infection + alcohol abuse, *n* (%)	5 (1.9)
Other aetiologies, *n* (%)	6 (2.2)
Unknown aetiology, *n* (%)	25 (9.3)
Median diameter of nodules (IQR; range)	24 mm (16-36; 5-200)

IQR: Inter quartile range; HCV: Hepatitis C virus; HBV: Hepatitis B virus; NASH: Non-alcoholic steatohepatitis.

Table 2 Rates of different conclusive diagnoses for each Contrast-enhanced ultrasound Liver Imaging Reporting and Data System class

		Conclusive diagnosis						%
		HCC	ICC	Metastasis	Other malignancy	Benign lesion	Total	
CEUS LI-RADS class	CEUS LR-M	11	21	3	1	1	37	7.2
	CEUS LR-5	286	0	0	0	2	288	56.4
	CEUS LR-4	111	0	0	0	3	114	22.3
	CEUS LR-3	15	2	0	2	47	66	12.9
	CEUS LR-2	0	0	0	0	5	5	1.0
	CEUS LR-1	0	0	0	0	1	1	0.2
	Total	423	23	3	3	59	511	100.0
%		82.8	4.5	0.6	0.6	11.5	100.0	

CEUS LI-RADS: Contrast-enhanced ultrasound Liver Imaging Reporting and Data System; HCC: Hepatocellular carcinoma; ICC: Intrahepatic cholangiocarcinoma.

Interobserver agreement

The observed agreement between the two internal raters (1 and 2) for the assignment of CEUS LI-RADS class was 95.7%, with Cohen's $k = 0.94$ (95%CI: 0.92-0.97, $P < 0.0001$), which represents an almost perfect agreement, according to Landis and Koch[30] classification. The agreement is clearly visualized in Figure 4A. Supplementary Table 4 shows the assignments of the two raters.

The observed agreement among the three raters from different centres (2, 3, and 4) for the assignment of CEUS LI-RADS class was 68% and Fleiss's k coefficient showed a value of 0.67 ($P < 0.0001$), which represents a substantial agreement. In particular, the agreement was almost perfect between raters 2 and

Table 3 Rates of hepatocellular carcinoma and intrahepatic cholangiocarcinoma in different Contrast-enhanced ultrasound Liver Imaging Reporting and Data System classes

CEUS LI-RADS class	HCC	ICC
LR-3	15/66 (22.7%)	2/66 (3%)
LR-4	111/114 (97.4%)	0/114 (0%)
LR-5	286/288 (99.3%)	0/288 (0%)
LR-M	11/37 (29.7%)	21/37 (56.8%)

CEUS LI-RADS: Contrast-enhanced ultrasound Liver Imaging Reporting and Data System; HCC: Hepatocellular carcinoma; ICC: Intrahepatic cholangiocarcinoma.

Table 4 Rates of different contrast-enhanced ultrasound patterns in arterial phase

Arterial phase CEUS pattern	Nodules, *n* (%)
Homogeneous hyperenhancement	404 (79.1)
Rim hyperenhancement	23 (4.5)
Globular hyperenhancement	1 (0.2)
Isoenhancement	65 (12.7)
Hypoenhancement	18 (3.5)

CEUS: Contrast-enhanced ultrasound.

Table 5 Rate of different portal and late phase contrast-enhanced ultrasound patterns

Portal and late phase CEUS pattern	Nodules, *n* (%)
Late and mild washout	310 (60.7%)
Early/marked washout	27 (5.3%)
Isoenhancement	157 (30.7%)
Hypoenhancement	15 (2.9%)
Hyperenhancement	2 (0.4%)

CEUS: Contrast-enhanced ultrasound.

3 (k = 0.88, $P < 1.7 \times 10^{-68}$), substantial between raters 2 and 4 (k = 0.66, $P < 1.5 \times 10^{-14}$), and substantial between raters 3 and 4 (k = 0.61, $P < 8.5 \times 10^{-10}$). The agreement is visualized in Figure 4B-D.

With regards to specific CEUS patterns, we found a higher degree of agreement for APHE (internal k = 0.86, $P < 2.7 \times 10^{-214}$; external k = 0.8, $P < 0.001$) than for washout (internal k = 0.79, $P < 1.6 \times 10^{-202}$; external k = 0.71, $P < 0.001$).

DISCUSSION

CEUS LI-RADS is a valuable diagnostic tool for non-invasive differential diagnosis of focal liver lesions in patients with cirrhosis. Based on our experience, employing this approach improves the performance of CEUS in the characterization of nodules, especially to discriminate between HCC and ICC.

In the current study, CEUS LR-5 was extremely specific for HCC with a very high PPV (99.3%). Only two false-positive results were observed, which were not ICC. We can therefore maintain that CEUS LR-5 is an appropriate tool for non-invasive diagnosis of HCC with virtually no risk of ICC misdiagnosis. Our data agree with recent publications on the subject[22]. However, CEUS LR-5 lacked sensitivity (67.6%) due to the large number of CEUS LR-4 nodules with a final diagnosis of HCC (97.4%). The high specificity of CEUS LR-5 for HCC combined with a low sensitivity was confirmed by a recent prospective multicentric study that compared the accuracy of different CEUS algorithms for the non-

Table 6 Diagnostic statistics of different contrast-enhanced ultrasound Liver Imaging Reporting and Data System classes for different diagnosis

Tested association	Sensitivity (%)	Specificity (%)	PPV (%)	NPV (%)	Diagnostic accuracy (%)	Youden's index	Odds Ratio	*P* value
CEUS LR M-ICC	91.3 (72.0-98.9)	96.7 (94.7-98.1)	56.8 (39.5-72.9)	99.6 (98.5-99.9)	96.5 (94.5-97.9)	0.880	309.75	< 0.001
CEUS LR 5-HCC	67.6 (62.9-72.1)	97.7 (92.0-99.7)	99.3 (97.5-99.9)	38.6 (32.1-45.3)	72.8 (68.7-76.6)	0.653	89.80	< 0.001
CEUS LR 4-HCC	26.2 (22.1-30.7)	96.6 (90.4-99.3)	97.4 (92.5-99.5)	21.4 (17.5-25.8)	38.4 (34.1-42.7)	0.228	10.10	< 0.001
CEUS LR 4/5-HCC	93.9 (91.1-95.9)	94.3 (87.2-98.1)	98.8 (97.1-99.6)	76.1 (67.0-83.8)	93.9 (91.5-95.8)	0.882	253.50	< 0.001
CEUS LR 3-benign lesion	79.7 (67.2-89.0)	95.8 (93.5-97.5)	71.2 (58.7-81.7)	97.3 (95.3-98.6)	93.9 (91.5-95.8)	0.755	89.26	< 0.001
CEUS LR-3-malignancy	4.2 (2.5-6.5)	20.3 (11.0-32.8)	28.8 (18.3-41.3)	2.7 (1.4-4.7)	6.0 (4.2-8.5)	-0.755	0.01	< 0.001
CEUS LR-3-iso-iso-malignancy	5.3 (0.1-26.0)	19.1 (9.1-33.3)	2.6 (0.1-13.5)	33.3 (16.5-54.0)	15.2 (7.5-26.1)	-0.756	0.01	< 0.001
CEUS LR-3-hypo-hypo-malignancy	57.9 (33.5-79.7)	91.5 (79.6-97.6)	73.3 (44.9-92.2)	84.3 (71.4-93.0)	81.8 (70.4-90.2)	0.494	14.78	< 0.001

CEUS: Contrast-enhanced ultrasound; HCC: Hepatocellular carcinoma; ICC: Intrahepatic cholangiocarcinoma; PPV: Positive predictive value; NPV: Negative predictive value.

Table 7 Classification of nodules for LR-3, LR-4, and LR-5 classes, reported in yellow, orange, and red, respectively

Nodule size	No APHE[1]		APHE[1]		Total
	< 20 mm	≥ 20 mm	< 10 mm	≥ 10 mm	
No washout of any type	37 (4)	21 (5)	1 (1)	106 (104)	165
Late and mild washout	7 (5)	8 (7)	0	288 (286)	303
Total	44	29	1	394	468

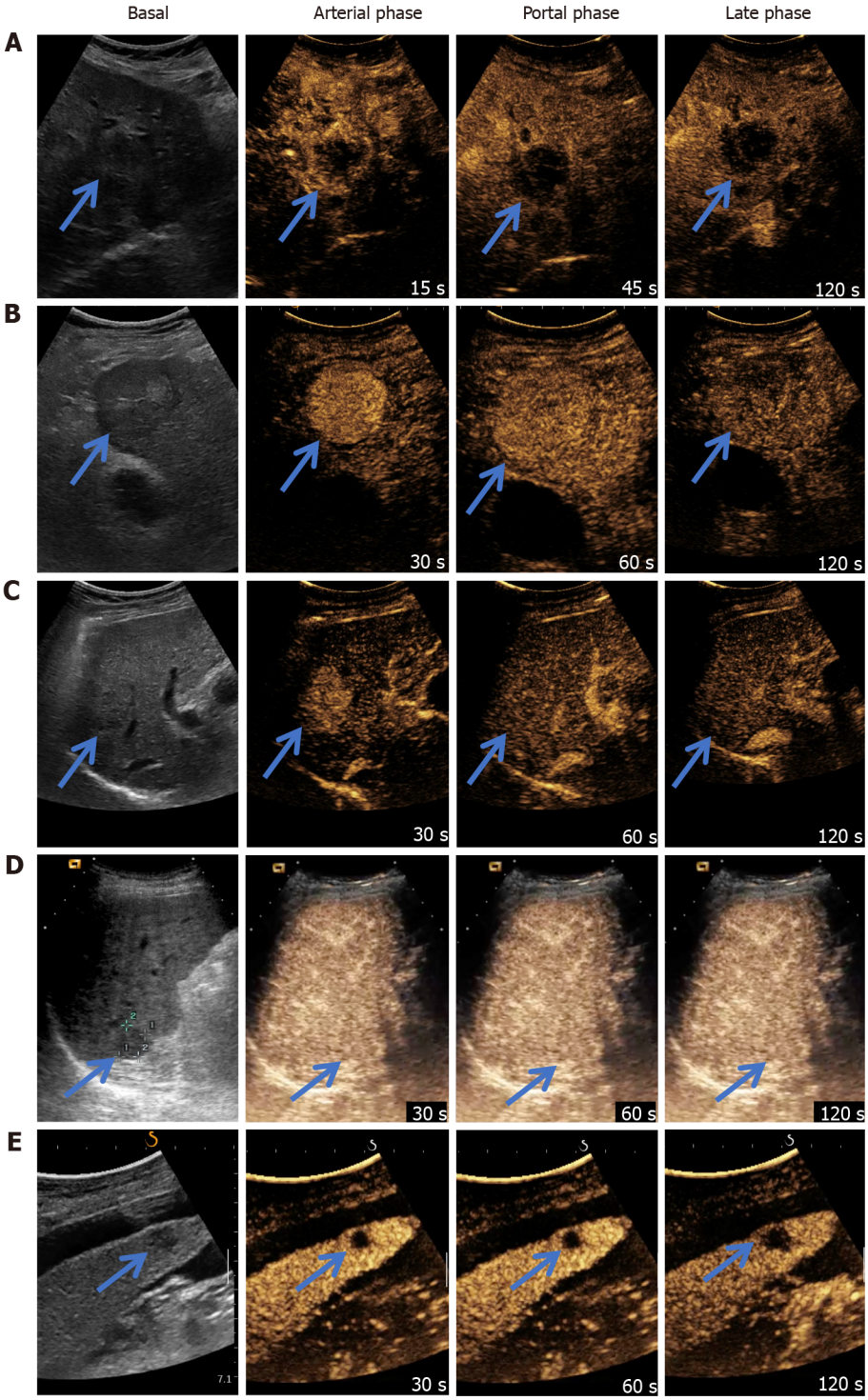
[1]With the exclusion of nodules with rim and peripheral discontinuous globular arterial phase hyper-enhancement belonging to contrast-enhanced ultrasound LR-M and contrast-enhanced ultrasound LR-1 classes, respectively.
Number of hepatocellular carcinomas in brackets. APHE: Arterial phase hyperenhancement.

invasive diagnosis of HCC[31] and a recent meta-analysis[32].

Considering the high risk of HCC for the LR-4 class (97.4% PPV), the possibility of merging LR-4 and 5 classes was tested. By doing so, sensitivity in identifying HCC rose from 67.6% to 93.9%. The loss in specificity was low (from 97.7% to 94.3%), and was entirely attributed to two nodules > 10 mm classified as CEUS LR-4, which turned out to be benign. Data from the literature supports such an approach, showing that around 50% of HCCs do not display any washout in the portal and late venous phases on CEUS. In particular, Giorgio *et al*[33] demonstrated in their series that 55.4% of the biopsied HCC nodules < 20 mm showed this pattern after APHE. These findings were further corroborated by Leoni *et al*[34], who found that the hyper-iso pattern shows a high PPV (94%) for HCC and identifies nodules that are HCC or with a strong tendency to malignant progression. This pattern was detected in 36.2% (46 out 127) of HCCs[34].

Therefore, it should be considered that the introduction of the washout criteria in CEUS is based on findings from studies exploring the role of contrast-enhanced CT in the non-invasive diagnosis of HCC [35-37]. These findings were then extended to CEUS and MRI with little consideration for the differences in the pharmacokinetics of contrast agents among these techniques and the importance of the nodule visibility at baseline. Indeed, the requirement for washout as a diagnostic criterion is less stringent for CEUS and MRI, since these techniques have an improved capability to evaluate and determine whether APHE reflects the presence of a distinct nodule or merely abnormalities of intrahepatic vessels. CEUS, in particular, is performed for improved characterization of a nodule that has already been detected through conventional ultrasound.

Unfortunately, the introduction of washout in CEUS has significantly lowered the sensitivity of non-invasive diagnostic criteria for HCC. The inclusion of hyper-iso pattern among criteria for non-invasive HCC diagnosis might be a solution to increase CEUS sensitivity. Using this strategy, it can be concluded that there is no significant risk of overestimating the diagnosis of HCC, as in our series 98% of the

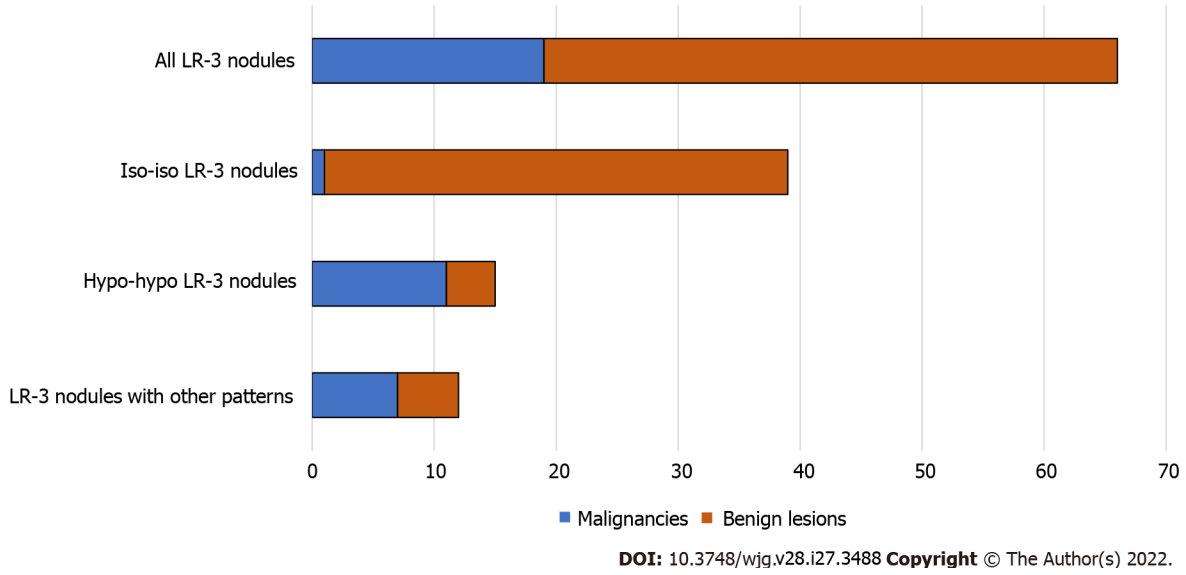


DOI: 10.3748/wjg.v28.i27.3488 **Copyright** © The Author(s) 2022.

Figure 2 Examples of different contrast-enhanced ultrasound Liver Imaging Reporting and Data System classes. A: Contrast-enhanced ultrasound (CEUS) LR-M. Notice rim arterial phase hyperenhancement and early washout, before 60 *s*; B: CEUS LR-5. Notice homogeneous arterial phase hyperenhancement, isoenhancement in portal phase, and mild washout in the late phase; C: CEUS LR-4. Notice homogeneous arterial phase hyperenhancement and isoenhancement in both portal and late phases; D: CEUS LR-3 iso-iso. Notice isoenhancement in all phases; E: CEUS LR-3 hypo-hypo. Notice hypoenhancement in all phases. The arrows show the target lesion.

nodules with the hyper-iso pattern were HCCs and only 2% were benign nodules. These considerations and results agree with another study on the combination of CEUS LR-4 and LR-5 criteria[38]. Furthermore, different studies demonstrated that the identification of washout has higher inter-rater variability than APHE identification[39,40]. These findings are also confirmed by the present study.

Regarding ICC, we observed that the majority of the nodules (21/23, 91.3%) were correctly diagnosed using the LR-M class of risk. Only two ICC cases were not assigned to this class due to a hypovascular aspect in all phases. The high sensitivity and specificity of the CEUS LR-M class for ICC (91.3% and

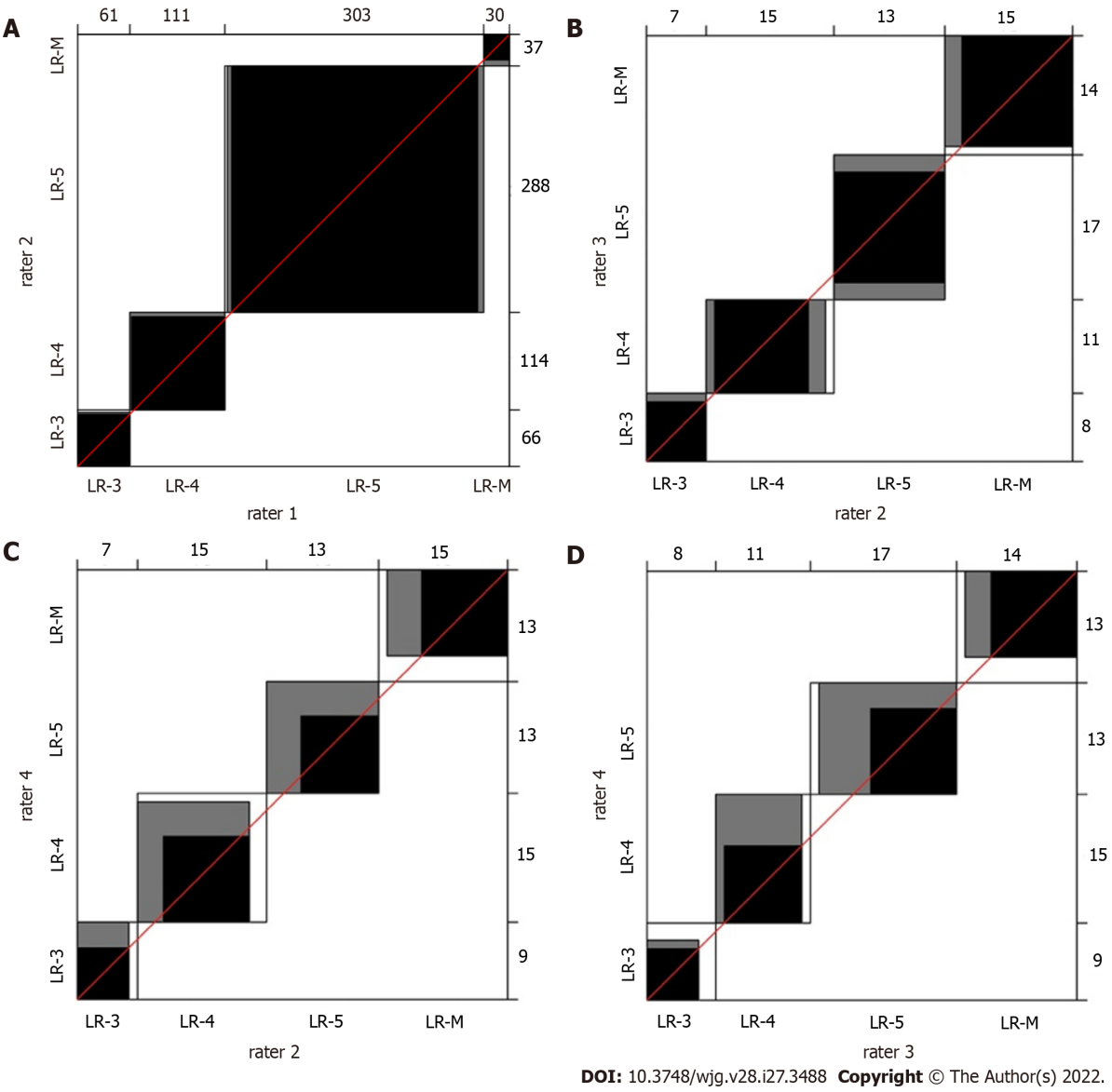


DOI: 10.3748/wjg.v28.i27.3488 **Copyright** © The Author(s) 2022.

Figure 3 Absolute frequency (*n*) of malignancies and benign lesions in LR-3 nodules and LR-3 subgroups with different contrast-enhanced ultrasound patterns.

96.7%, respectively) in our series of patients demonstrate that this class is a valuable diagnostic tool for this type of cancer. Still, this class is not entirely specific for ICC as other types of malignancy can be found, such as HCC, metastatic lesions, and rarer malignancies[41]. We found that 11 out of 37 nodules (30%) classified as LR–M turned out to be HCC. This was due to the presence of an early washout (63.6% of nodules) and/or a rim enhancement pattern (54.5% of nodules). These observations are in agreement with the previously published literature. In particular, a multicentre retrospective study published by Terzi *et al*[22] reported that about 40% of LR-M lesions were HCCs. Another study by Wilson *et al*[16] identified that 35% of HCCs were reported to be LR-M. Several other authors have attempted to decrease the risk of HCC misdiagnosis by proposing a modified LR-M class of risk with the introduction of new criteria, such as the shortening of washout timing to < 45 *s* or the possibility to detect a significant washout to < 3 min[42-44]. Interestingly, Chen *et al*[45] were able to reduce the ICC misdiagnosis rate with CEUS LR-M from 38 to 12 cases by considering other criteria such as the presence of an intratumoral vein or an unclear boundary of the intratumoral non-enhanced area. However, we did not test these new criteria that require validation in multicentric and prospective studies. Another recent study by Huang *et al*[46] suggested that the integration of CEUS with the dosage of serum tumour markers (AFP and CA 19.9) improves the differentiation of LR-M nodules. Even though there are some limitations related to LR-M in this scenario, the adoption of this class of risk allows the improvement of diagnostic performance of CEUS for ICC, overcoming the drawbacks that resulted in the elimination of CEUS from the diagnostic flow charts of the most important hepatological international guidelines[3,8].

At present, CEUS LR-3 lesions are considered to hold an intermediate risk of malignancy, which is around 50% according to a recent study published by Terzi *et al*[22]. This rate was much lower in our case series (28.8%), which might be attributable to the lower figures of our study. Still, looking at the data from single centres in the multicentric study by Terzi *et al*[22], the rate of HCC in the CEUS LR-3 class ranged between 28.3% and 74.3%. One possible explanation for these results could be the high intrinsic heterogeneity of this class. Indeed, the algorithm only considers either the presence or absence of APHE, without any distinction between isoenhancement and hypoenhancement in all phases. However, in our clinical experience, hypo-hypo lesions are more likely to be malignant than iso-iso lesions. The present study confirmed this observation: Within the CEUS LR-3 class, the PPV for malignancy moved from 28.8% for CEUS LR-3 overall class to 2.6% for CEUS LR-3 iso-iso nodules, and 73.3% for CEUS LR-3 hypo-hypo nodules (Table 5). These considerations are in concordance with studies published before the advent of CEUS LI-RADS, when the problem of hypovascular nodules, which represent around 10% of HCC, was highlighted[47-49]. Likewise, we should be aware of the possibility of detecting ICC nodules in this class when a nodule shows hypoenhancement in all the phases; as observed in two out of 15 (13%) hypo-hypo nodules in our study. In light of these observations, we believe that it might be advantageous to split the CEUS LR-3 class into two subgroups (*e.g.*, CEUS LR-3a and CEUS LR-3b) in order to separate iso-iso lesions from other patterns. To the best of our knowledge, this is the first study suggesting a CEUS LR-3 refinement based on real-life results. We believe that more attention should be directed towards the behaviour of nodule enhancement, rather than focusing on the size of the lesion alone.



DOI: 10.3748/wjg.v28.i27.3488 **Copyright** © The Author(s) 2022.

Figure 4 Bangdiwala's agreement charts of the Contrast-enhanced ultrasound Liver Imaging Reporting and Data System class assignments between different raters. In the case of perfect agreement, the *k* rectangles are represented by perfect squares and the shaded squares determined by the diagonal cell entries are exactly equal to the rectangles; lesser agreement is visualized by comparing the area of the blackened squares to the area of the rectangles. A: Agreement chart between the two internal raters (1 and 2), with the exclusion of LR-1 and LR-2 classes due to their rarity (n = 505); B-D: Agreement charts among the three raters from different centres (2, 3, and 4) for the subgroup of 50 nodules. We list the agreement charts between raters 2 and 3 (B), between raters 2 and 4 (C), and between raters 3 and 4 (D).

Finally, this study demonstrated excellent inter-rater reliability of this classification system. Therefore, the use of CEUS LI-RADS in clinical practice could improve the reproducibility of CEUS and partially reduce the gap due to the difference in experience, as suggested by a recent study[50].

Our study also has some critical shortcomings, namely, its retrospective nature and the limited number of nodules analysed. These drawbacks are primarily due to the fact that data were collected from a single centre. Another debatable aspect of our investigation is the limited number of biopsies. However, we would like to highlight that current guidelines do not routinely recommend biopsy for nodules with typical HCC pattern on CT or MRI, allowing a non-invasive diagnosis[4,28].

Further prospective multicentric studies are warranted to confirm our findings and to investigate whether our considerations could be applied to the general population of patients with cirrhosis.

CONCLUSION

The present study supports the use of CEUS LI-RADS for the characterization of focal liver lesions in liver cirrhosis and the usefulness of LR-5 and LR-M classes to diagnose HCC and ICC, respectively. Additionally, our findings suggest that the merging of LR-4 and LR-5 classes provides innovative

benefits in terms of diagnostic accuracy for HCC. Furthermore, it seems reasonable to split the CEUS LR-3 class into two subgroups to differentiate the risk of malignancy between iso-iso nodules, which are more likely to be benign, and other patterns, namely, hypo-hypo nodules, which are more likely to be malignant and not specific for HCC.

ARTICLE HIGHLIGHTS

Research background

Patients affected by liver cirrhosis are at high risk of developing hepatocellular carcinoma (HCC) and other malignancies such us intrahepatic cholangiocellular carcinoma (ICC). Diagnostic tools to characterize new-onset nodules in cirrhosis include contrast-enhanced ultrasound (CEUS), but this technique has been challenged for the possibility of misdiagnosing HCC and ICC.

Research motivation

The CEUS Liver Imaging Reporting and Data System (CEUS LI-RADS) aims to refine CEUS interpretation in order to improve the differentiation of HCC from other malignancies. Nevertheless, its effectiveness in real-life context has not yet been well established.

Research objectives

To test the accuracy of CEUS LI-RADS in correctly diagnosing HCC and ICC in cirrhosis with LR-5 and LR-M class, respectively, to evaluate the performance of LR-4 and 5 merging class in the diagnosis of HCC, and to investigate the rate of malignancies in different LR-3 patterns.

Research methods

This study consecutively collected 511 nodules in 269 cirrhotic patients from December 2008 to January 2020. A CEUS LI-RADS class was retrospectively attributed to each nodule based on review of CEUS examination. Common diagnostic accuracy indexes were assessed for the following associations: CEUS LR-5 and HCC; CEUS LR-4 and 5 merged class and HCC; CEUS LR-M and ICC; CEUS LR-3 and malignancy. The diagnostic standard was either biopsy or computed tomography/magnetic resonance imaging. The frequency of malignant lesions in CEUS LR-3 subgroups with different CEUS patterns was also determined.

Research results

CEUS LR-5 showed a 97.7% specificity for HCC with a low sensitivity (67.6%), while the CEUS LR-4 and 5 merged class showed a 93.9% sensitivity and 94.3% specificity for HCC. CEUS LR-M predicted ICC with a 91.3% sensitivity and 96.7% specificity. CEUS LR-3 predominantly included benign lesions (28.8% of malignancies) but was heterogeneous as the hypo-hypo pattern showed a higher rate of malignant lesions (73.3%) than the iso-iso pattern (2.6%).

Research conclusions

HCC diagnosis could benefit from the merging of CEUS LI-RADS classes 4 and 5. In addition, splitting LR-3 class could be advantageous to differentiate iso-iso nodules from other patterns with a higher risk of malignancy.

Research perspectives

Further prospective multicentric studies are necessary to confirm and extend our findings to the general population.

ACKNOWLEDGEMENTS

The authors thank Cabigiosu F for his help in data entry, and Fois SS for contributing to English language revision of the manuscript.

FOOTNOTES

Author contributions: Vidili G designed the study, performed contrast-enhanced ultrasound examinations, biopsies, and the blinded review of cases, and wrote and revised the manuscript; Arru M performed the blinded review of the cases, collected and analysed the data, and participated in paper writing and review; Solinas G performed the statistical analysis and participated in the final draft; Calvisi DF collected and analysed the data, and participated in writing, review, and editing of the manuscript; Meloni P, Sauchella A, and Di Lembo E participated in collecting and

preparing the data for the analysis; Turilli D and Fabio C performed computed tomography and magnetic resonance imaging scans and participated in data collection; Cossu A reviewed the pathology material; Madeddu G participated in data collection and writing the paper; Zocco MA and Iannetti G performed the external blinded review of the cases; Delitala AP and Babudieri S participated in data analysis and writing of the manuscript; Manetti R participated in writing and reviewing the final draft; all authors have read and agreed to the final version of the manuscript.

Supported by the Fondazione di Sardegna, No. FDS2019VIDILI; and the University of Sassari, No. FAR2019.

Institutional review board statement: This study was reviewed and approved by the Ethics Committee of Azienda Ospedaliero Universitaria di Sassari and the Ethics Committee of Azienda Ospedaliero Universitaria di Cagliari (No. PG/2020/16814).

Informed consent statement: All study participants, or their legal guardian, provided informed written consent prior to study enrollment.

Conflict-of-interest statement: There are no conflicts of interest to report.

Data sharing statement: Data presented in this study is available on request from the corresponding author.

Open-Access: This article is an open-access article that was selected by an in-house editor and fully peer-reviewed by external reviewers. It is distributed in accordance with the Creative Commons Attribution NonCommercial (CC BY-NC 4.0) license, which permits others to distribute, remix, adapt, build upon this work non-commercially, and license their derivative works on different terms, provided the original work is properly cited and the use is non-commercial. See: https://creativecommons.org/Licenses/by-nc/4.0/

Country/Territory of origin: Italy

ORCID number: Gianpaolo Vidili 0000-0003-0003-1272; Marco Arru 0000-0002-7112-5025; Giuliana Solinas 0000-0003-2174-0983; Diego Francesco Calvisi 0000-0002-6038-8567; Pierluigi Meloni 0000-0003-3313-0445; Assunta Sauchella 0000-0003-1116-7458; Davide Turilli 0000-0002-2063-994X; Claudio Fabio 0000-0002-5372-1552; Antonio Cossu 0000-0002-2390-2205; Giordano Madeddu 0000-0001-6099-2273; Sergio Babudieri 0000-0001-7291-8687; Maria Assunta Zocco 0000-0002-0814-9542; Giovanni Iannetti 0000-0002-1880-0829; Enza Di Lembo 0000-0003-1652-600X; Alessandro Palmerio Delitala 0000-0003-1729-8969; Roberto Manetti 0000-0001-7376-2303.

S-Editor: Chen YL
L-Editor: Wang TQ
P-Editor: Wu RR

REFERENCES

1 **Sung H**, Ferlay J, Siegel RL, Laversanne M, Soerjomataram I, Jemal A, Bray F. Global Cancer Statistics 2020: GLOBOCAN Estimates of Incidence and Mortality Worldwide for 36 Cancers in 185 Countries. *CA Cancer J Clin* 2021; **71**: 209-249 [PMID: 33538338 DOI: 10.3322/caac.21660]

2 **Italian Association for the Study of the Liver (AISF)**, AISF Expert Panel; AISF Coordinating Committee, Bolondi L, Cillo U, Colombo M, Craxì A, Farinati F, Giannini EG, Golfieri R, Levrero M, Pinna AD, Piscaglia F, Raimondo G, Trevisani F, Bruno R, Caraceni P, Ciancio A, Coco B, Fraquelli M, Rendina M, Squadrito G, Toniutto P. Position paper of the Italian Association for the Study of the Liver (AISF): the multidisciplinary clinical approach to hepatocellular carcinoma. *Dig Liver Dis* 2013; **45**: 712-723 [PMID: 23769756 DOI: 10.1016/j.dld.2013.01.012]

3 **European Association For The Study Of The Liver**. EASL-EORTC clinical practice guidelines: management of hepatocellular carcinoma. *J Hepatol* 2012; **56**: 908-943 [DOI: 10.1016/j.jhep.2012.03.006]

4 **European Association for the Study of the Liver**. EASL Clinical Practice Guidelines: Management of hepatocellular carcinoma. *J Hepatol* 2018; **69**: 182-236 [DOI: 10.1016/j.jhep.2018.03.019]

5 **Bolondi L**, Sofia S, Siringo S, Gaiani S, Casali A, Zironi G, Piscaglia F, Gramantieri L, Zanetti M, Sherman M. Surveillance programme of cirrhotic patients for early diagnosis and treatment of hepatocellular carcinoma: a cost effectiveness analysis. *Gut* 2001; **48**: 251-259 [PMID: 11156649 DOI: 10.1136/gut.48.2.251]

6 **Vidili G**, De Sio I, D'Onofrio M, Mirk P, Bertolotto M, Schiavone C; SIUMB experts committee. SIUMB guidelines and recommendations for the correct use of ultrasound in the management of patients with focal liver disease. *J Ultrasound* 2019; **22**: 41-51 [PMID: 30580390 DOI: 10.1007/s40477-018-0343-0]

7 **Claudon M**, Dietrich CF, Choi BI, Cosgrove DO, Kudo M, Nolsøe CP, Piscaglia F, Wilson SR, Barr RG, Chammas MC, Chaubal NG, Chen MH, Clevert DA, Correas JM, Ding H, Forsberg F, Fowlkes JB, Gibson RN, Goldberg BB, Lassau N, Leen EL, Mattrey RF, Moriyasu F, Solbiati L, Weskott HP, Xu HX; World Federation for Ultrasound in Medicine; European Federation of Societies for Ultrasound. Guidelines and good clinical practice recommendations for Contrast Enhanced Ultrasound (CEUS) in the liver - update 2012: A WFUMB-EFSUMB initiative in cooperation with representatives of AFSUMB, AIUM, ASUM, FLAUS and ICUS. *Ultrasound Med Biol* 2013; **39**: 187-210 [PMID: 23137926 DOI: 10.1016/j.ultrasmedbio.2012.09.002]

8 **Vilana R**, Forner A, Bianchi L, García-Criado A, Rimola J, de Lope CR, Reig M, Ayuso C, Brú C, Bruix J. Intrahepatic

peripheral cholangiocarcinoma in cirrhosis patients may display a vascular pattern similar to hepatocellular carcinoma on contrast-enhanced ultrasound. *Hepatology* 2010; **51**: 2020-2029 [PMID: 20512990 DOI: 10.1002/hep.23600]

9 **de Sio I**, Iadevaia MD, Vitale LM, Niosi M, Del Prete A, de Sio C, Romano L, Funaro A, Meucci R, Federico A, Loguercio C, Romano M. Optimized contrast-enhanced ultrasonography for characterization of focal liver lesions in cirrhosis: A single-center retrospective study. *United European Gastroenterol J* 2014; **2**: 279-287 [PMID: 25083285 DOI: 10.1177/2050640614538964]

10 **Forner A**, Vidili G, Rengo M, Bujanda L, Ponz-Sarvisé M, Lamarca A. Clinical presentation, diagnosis and staging of cholangiocarcinoma. *Liver Int* 2019; **39** Suppl 1: 98-107 [PMID: 30831002 DOI: 10.1111/liv.14086]

11 **Wildner D**, Schellhaas B, Strack D, Goertz RS, Pfeifer L, Fiessler C, Neurath MF, Strobel D. Differentiation of malignant liver tumors by software-based perfusion quantification with dynamic contrast-enhanced ultrasound (DCEUS). *Clin Hemorheol Microcirc* 2019; **71**: 39-51 [PMID: 29865043 DOI: 10.3233/CH-180378]

12 **Liu GJ**, Wang W, Lu MD, Xie XY, Xu HX, Xu ZF, Chen LD, Wang Z, Liang JY, Huang Y, Li W, Liu JY. Contrast-Enhanced Ultrasound for the Characterization of Hepatocellular Carcinoma and Intrahepatic Cholangiocarcinoma. *Liver Cancer* 2015; **4**: 241-252 [PMID: 26779444 DOI: 10.1159/000367738]

13 **Galassi M**, Iavarone M, Rossi S, Bota S, Vavassori S, Rosa L, Leoni S, Venerandi L, Marinelli S, Sangiovanni A, Veronese L, Fraquelli M, Granito A, Golfieri R, Colombo M, Bolondi L, Piscaglia F. Patterns of appearance and risk of misdiagnosis of intrahepatic cholangiocarcinoma in cirrhosis at contrast enhanced ultrasound. *Liver Int* 2013; **33**: 771-779 [PMID: 23445369 DOI: 10.1111/liv.12124]

14 **Chen LD**, Ruan SM, Liang JY, Yang Z, Shen SL, Huang Y, Li W, Wang Z, Xie XY, Lu MD, Kuang M, Wang W. Differentiation of intrahepatic cholangiocarcinoma from hepatocellular carcinoma in high-risk patients: A predictive model using contrast-enhanced ultrasound. *World J Gastroenterol* 2018; **24**: 3786-3798 [PMID: 30197484 DOI: 10.3748/wjg.v24.i33.3786]

15 **American College of Radiology**. CEUS LI RADS v2017 CORE. 2017. Avaiable from: https://www.acr.org/Quality-Safety/Resources/LIRADS

16 **Wilson SR**, Lyshchik A, Piscaglia F, Cosgrove D, Jang HJ, Sirlin C, Dietrich CF, Kim TK, Willmann JK, Kono Y. CEUS LI-RADS: algorithm, implementation, and key differences from CT/MRI. *Abdom Radiol (NY)* 2018; **43**: 127-142 [PMID: 28819825 DOI: 10.1007/s00261-017-1250-0]

17 **Lyshchik A**, Kono Y, Dietrich CF, Jang HJ, Kim TK, Piscaglia F, Vezeridis A, Willmann JK, Wilson SR. Contrast-enhanced ultrasound of the liver: technical and lexicon recommendations from the ACR CEUS LI-RADS working group. *Abdom Radiol (NY)* 2018; **43**: 861-879 [PMID: 29151131 DOI: 10.1007/s00261-017-1392-0]

18 **Kim TK**, Noh SY, Wilson SR, Kono Y, Piscaglia F, Jang HJ, Lyshchik A, Dietrich CF, Willmann JK, Vezeridis A, Sirlin CB. Contrast-enhanced ultrasound (CEUS) liver imaging reporting and data system (LI-RADS) 2017 - a review of important differences compared to the CT/MRI system. *Clin Mol Hepatol* 2017; **23**: 280-289 [PMID: 28911220 DOI: 10.3350/cmh.2017.0037]

19 **Rimola J**, Forner A, Tremosini S, Reig M, Vilana R, Bianchi L, Rodríguez-Lope C, Solé M, Ayuso C, Bruix J. Non-invasive diagnosis of hepatocellular carcinoma ≤ 2 cm in cirrhosis. Diagnostic accuracy assessing fat, capsule and signal intensity at dynamic MRI. *J Hepatol* 2012; **56**: 1317-1323 [PMID: 22314420 DOI: 10.1016/j.jhep.2012.01.004]

20 **Barreiros AP**, Piscaglia F, Dietrich CF. Contrast enhanced ultrasound for the diagnosis of hepatocellular carcinoma (HCC): comments on AASLD guidelines. *J Hepatol* 2012; **57**: 930-932 [PMID: 22739095 DOI: 10.1016/j.jhep.2012.04.018]

21 **Huang JY**, Li JW, Lu Q, Luo Y, Lin L, Shi YJ, Li T, Liu JB, Lyshchik A. Diagnostic Accuracy of CEUS LI-RADS for the Characterization of Liver Nodules 20 mm or Smaller in Patients at Risk for Hepatocellular Carcinoma. *Radiology* 2020; **294**: 329-339 [PMID: 31793849 DOI: 10.1148/radiol.2019191086]

22 **Terzi E**, Iavarone M, Pompili M, Veronese L, Cabibbo G, Fraquelli M, Riccardi L, De Bonis L, Sangiovanni A, Leoni S, Zocco MA, Rossi S, Alessi N, Wilson SR, Piscaglia F; CEUS LI-RADS Italy study group collaborators:. Contrast ultrasound LI-RADS LR-5 identifies hepatocellular carcinoma in cirrhosis in a multicenter restropective study of 1,006 nodules. *J Hepatol* 2018; **68**: 485-492 [PMID: 29133247 DOI: 10.1016/j.jhep.2017.11.007]

23 **Huang Z**, Zhou P, Li S, Li K. MR versus CEUS LI-RADS for Distinguishing Hepatocellular Carcinoma from other Hepatic Malignancies in High-Risk Patients. Ultrasound Med Biol 2021; 47: 1244-1252 [PMID: 33610338 DOI: 10.1016/j.ultrasmedbio.2021.01.020]

24 **Li S**, Zhou L, Chen R, Chen Y, Niu Z, Qian L, Fang Y, Xu L, Xu H, Zhang L. Diagnostic efficacy of contrast-enhanced ultrasound versus MRI Liver Imaging Reporting and Data System (LI-RADS) for categorising hepatic observations in patients at risk of hepatocellular carcinoma. Clin Radiol 2021; 76: 161.e1-161.e10 [PMID: 33198943 DOI: 10.1016/j.crad.2020.10.009]

25 **Makoyeva A**, Kim TK, Jang HJ, Medellin A, Wilson SR. Use of CEUS LI-RADS for the Accurate Diagnosis of Nodules in Patients at Risk for Hepatocellular Carcinoma: A Validation Study. *Radiol Imaging Cancer* 2020; **2**: e190014 [PMID: 33778701 DOI: 10.1148/rycan.2020190014]

26 **Pan JM**, Chen W, Zheng YL, Cheng MQ, Zeng D, Huang H, Huang Y, Xie XY, Lu MD, Kuang M, Hu HT, Chen LD, Wang W. Tumor size-based validation of contrast-enhanced ultrasound liver imaging reporting and data system (CEUS LI-RADS) 2017 for hepatocellular carcinoma characterizing. *Br J Radiol* 2021; **94**: 20201359 [PMID: 34545763 DOI: 10.1259/bjr.20201359]

27 **Lv K**, Cao X, Dong Y, Geng D, Zhang J. CT/MRI LI-RADS version 2018 versus CEUS LI-RADS version 2017 in the diagnosis of primary hepatic nodules in patients with high-risk hepatocellular carcinoma. Ann Transl Med 2021; 9: 1076 [PMID: 34422988 DOI: 10.21037/atm-21-1035]

28 **Bruix J**, Sherman M; American Association for the Study of Liver Diseases. Management of hepatocellular carcinoma: an update. *Hepatology* 2011; **53**: 1020-1022 [PMID: 21374666 DOI: 10.1002/hep.24199]

29 **Bangdiwala SI**, Shankar V. The agreement chart. *BMC Med Res Methodol* 2013; **13**: 97 [PMID: 23890315 DOI: 10.1186/1471-2288-13-97]

30 **Landis JR**, Koch GG. The measurement of observer agreement for categorical data. *Biometrics* 1977; **33**: 159-174 [PMID:

843571]
31 **Schellhaas B**, Bernatik T, Bohle W, Borowitzka F, Chang J, Dietrich CF, Dirks K, Donoval R, Drube K, Friedrich-Rust M, Gall C, Gittinger F, Gutermann M, Haenle MM, von Herbay A, Ho CH, Hochdoerffer R, Hoffmann T, Hüttig M, Janson C, Jung EM, Jung N, Karlas T, Klinger C, Kornmehl A, Kratzer W, Krug S, Kunze G, Leitlein J, Link A, Lottspeich C, Marano A, Mauch M, Moleda L, Neesse A, Petzold G, Potthoff A, Praktiknjo M, Rösner KD, Schanz S, Schultheiß M, Sivanathan V, Stock J, Thomsen T, Vogelpohl J, Vogt C, Wagner S, Wiegard C, Wiesinger I, Will U, Ziesch M, Zimmermann P, Strobel D. Contrast-Enhanced Ultrasound Algorithms (CEUS-LIRADS/ESCULAP) for the Noninvasive Diagnosis of Hepatocellular Carcinoma - A Prospective Multicenter DEGUM Study. *Ultraschall Med* 2021; **42**: e20 [PMID: 32717752 DOI: 10.1055/a-1220-8561]
32 **Peng J**, Zhang T, Wang H, Ma X. The Value of Contrast-Enhanced Ultrasound Liver Imaging Reporting and Data System in the Diagnosis of Hepatocellular Carcinoma: A Meta-Analysis. *J Ultrasound Med* 2022; **41**: 1537-1547 [PMID: 34617296 DOI: 10.1002/jum.15837]
33 **Giorgio A**, Montesarchio L, Gatti P, Amendola F, Matteucci P, Santoro B, Merola MG, Merola F, Coppola C, Giorgio V. Contrast-Enhanced Ultrasound: a Simple and Effective Tool in Defining a Rapid Diagnostic Work-up for Small Nodules Detected in Cirrhotic Patients during Surveillance. *J Gastrointestin Liver Dis* 2016; **25**: 205-211 [PMID: 27308652 DOI: 10.15403/jgld.2014.1121.252.chu]
34 **Leoni S**, Piscaglia F, Granito A, Borghi A, Galassi M, Marinelli S, Terzi E, Bolondi L. Characterization of primary and recurrent nodules in liver cirrhosis using contrast-enhanced ultrasound: which vascular criteria should be adopted? *Ultraschall Med* 2013; **34**: 280-287 [PMID: 23616066 DOI: 10.1055/s-0033-1335024]
35 **Baron RL**, Oliver JH 3rd, Dodd GD 3rd, Nalesnik M, Holbert BL, Carr B. Hepatocellular carcinoma: evaluation with biphasic, contrast-enhanced, helical CT. *Radiology* 1996; **199**: 505-511 [PMID: 8668803 DOI: 10.1148/radiology.199.2.8668803]
36 **Oliver JH 3rd**, Baron RL, Federle MP, Rockette HE Jr. Detecting hepatocellular carcinoma: value of unenhanced or arterial phase CT imaging or both used in conjunction with conventional portal venous phase contrast-enhanced CT imaging. *AJR Am J Roentgenol* 1996; **167**: 71-77 [PMID: 8659425 DOI: 10.2214/ajr.167.1.8659425]
37 **Hwang GJ**, Kim MJ, Yoo HS, Lee JT. Nodular hepatocellular carcinomas: detection with arterial-, portal-, and delayed-phase images at spiral CT. *Radiology* 1997; **202**: 383-388 [PMID: 9015062 DOI: 10.1148/radiology.202.2.9015062]
38 **Schellhaas B**, Görtz RS, Pfeifer L, Kielisch C, Neurath MF, Strobel D. Diagnostic accuracy of contrast-enhanced ultrasound for the differential diagnosis of hepatocellular carcinoma: ESCULAP versus CEUS-LI-RADS. *Eur J Gastroenterol Hepatol* 2017; **29**: 1036-1044 [PMID: 28562394 DOI: 10.1097/MEG.0000000000000916]
39 **Li J**, Ling W, Chen S, Ma L, Yang L, Lu Q, Luo Y. The interreader agreement and validation of contrast-enhanced ultrasound liver imaging reporting and data system. *Eur J Radiol* 2019; **120**: 108685 [PMID: 31606712 DOI: 10.1016/j.ejrad.2019.108685]
40 **Schellhaas B**, Pfeifer L, Kielisch C, Goertz RS, Neurath MF, Strobel D. Interobserver Agreement for Contrast-Enhanced Ultrasound (CEUS)-Based Standardized Algorithms for the Diagnosis of Hepatocellular Carcinoma in High-Risk Patients. *Ultraschall Med* 2018; **39**: 667-674 [PMID: 29879746 DOI: 10.1055/a-0612-7887]
41 **Yang J**, Zhang YH, Li JW, Shi YY, Huang JY, Luo Y, Liu JB, Lu Q. Contrast-enhanced ultrasound in association with serum biomarkers for differentiating combined hepatocellular-cholangiocarcinoma from hepatocellular carcinoma and intrahepatic cholangiocarcinoma. *World J Gastroenterol* 2020; **26**: 7325-7337 [PMID: 33362387 DOI: 10.3748/wjg.v26.i46.7325]
42 **Li F**, Li Q, Liu Y, Han J, Zheng W, Huang Y, Zheng X, Cao L, Zhou JH. Distinguishing intrahepatic cholangiocarcinoma from hepatocellular carcinoma in patients with and without risks: the evaluation of the LR-M criteria of contrast-enhanced ultrasound liver imaging reporting and data system version 2017. *Eur Radiol* 2020; **30**: 461-470 [PMID: 31297632 DOI: 10.1007/s00330-019-06317-2]
43 **Ding J**, Qin Z, Zhou Y, Zhou H, Zhang Q, Wang Y, Jing X, Wang F. Impact of Revision of the LR-M Criteria on the Diagnostic Performance of Contrast-Enhanced Ultrasound LI-RADS. *Ultrasound Med Biol* 2021; **47**: 3403-3410 [PMID: 34598799 DOI: 10.1016/j.ultrasmedbio.2021.08.007]
44 **Zeng D**, Xu M, Liang JY, Cheng MQ, Huang H, Pan JM, Huang Y, Tong WJ, Xie XY, Lu MD, Kuang M, Chen LD, Hu HT, Wang W. Using new criteria to improve the differentiation between HCC and non-HCC malignancies: clinical practice and discussion in CEUS LI-RADS 2017. *Radiol Med* 2022; **127**: 1-10 [PMID: 34665430 DOI: 10.1007/s11547-021-01417-w]
45 **Chen LD**, Ruan SM, Lin Y, Liang JY, Shen SL, Hu HT, Huang Y, Li W, Wang Z, Xie XY, Lu MD, Kuang M, Wang W. Comparison between M-score and LR-M in the reporting system of contrast-enhanced ultrasound LI-RADS. *Eur Radiol* 2019; **29**: 4249-4257 [PMID: 30569182 DOI: 10.1007/s00330-018-5927-8]
46 **Huang JY**, Li JW, Ling WW, Li T, Luo Y, Liu JB, Lu Q. Can contrast enhanced ultrasound differentiate intrahepatic cholangiocarcinoma from hepatocellular carcinoma? *World J Gastroenterol* 2020; **26**: 3938-3951 [PMID: 32774068 DOI: 10.3748/wjg.v26.i27.3938]
47 **Boozari B**, Soudah B, Rifai K, Schneidewind S, Vogel A, Hecker H, Hahn A, Schlue J, Dietrich CF, Bahr MJ, Kubicka S, Manns MP, Gebel M. Grading of hypervascular hepatocellular carcinoma using late phase of contrast enhanced sonography - a prospective study. *Dig Liver Dis* 2011; **43**: 484-490 [PMID: 21377941 DOI: 10.1016/j.dld.2011.01.001]
48 **Choi BI**, Lee JM, Kim TK, Dioguardi Burgio M, Vilgrain V. Diagnosing Borderline Hepatic Nodules in Hepatocarcinogenesis: Imaging Performance. *AJR Am J Roentgenol* 2015; **205**: 10-21 [PMID: 26102378 DOI: 10.2214/AJR.14.12655]
49 **Bolondi L**, Gaiani S, Celli N, Golfieri R, Grigioni WF, Leoni S, Venturi AM, Piscaglia F. Characterization of small nodules in cirrhosis by assessment of vascularity: the problem of hypovascular hepatocellular carcinoma. *Hepatology* 2005; **42**: 27-34 [PMID: 15954118 DOI: 10.1002/hep.20728]
50 **Li W**, Li L, Zhuang BW, Ruan SM, Hu HT, Huang Y, Lin MX, Xie XY, Kuang M, Lu MD, Chen LD, Wang W. Inter-reader agreement of CEUS LI-RADS among radiologists with different levels of experience. *Eur Radiol* 2021; **31**: 6758-6767 [PMID: 33675388 DOI: 10.1007/s00330-021-07777-1]

World Journal of Gastroenterology

Submit a Manuscript: https://www.f6publishing.com

World J Gastroenterol 2022 July 21; 28(27): 3503-3513

DOI: 10.3748/wjg.v28.i27.3503

ISSN 1007-9327 (print) ISSN 2219-2840 (online)

ORIGINAL ARTICLE

Retrospective Study

Novel index for the prediction of significant liver fibrosis and cirrhosis in chronic hepatitis B patients in China

Min-Jun Liao, Jun Li, Wei Dang, Dong-Bo Chen, Wan-Ying Qin, Pu Chen, Bi-Geng Zhao, Li-Ying Ren, Ting-Feng Xu, Hong-Song Chen, Wei-Jia Liao

Specialty type: Gastroenterology and hepatology

Provenance and peer review: Unsolicited article; Externally peer reviewed.

Peer-review model: Single blind

Peer-review report's scientific quality classification
Grade A (Excellent): 0
Grade B (Very good): B
Grade C (Good): C
Grade D (Fair): 0
Grade E (Poor): 0

P-Reviewer: Jiang KP, China; Leowattana W, Thailand

Received: February 14, 2022
Peer-review started: February 14, 2022
First decision: March 9, 2022
Revised: March 23, 2022
Accepted: June 18, 2022
Article in press: June 18, 2022
Published online: July 21, 2022

Min-Jun Liao, Jun Li, Wei Dang, Wan-Ying Qin, Bi-Geng Zhao, Li-Ying Ren, Ting-Feng Xu, Wei-Jia Liao, Laboratory of Hepatobiliary and Pancreatic Surgery, The Affiliated Hospital of Guilin Medical University, Guilin 541001, Guangxi Zhuang Autonomous Region, China

Min-Jun Liao, Guangdong Provincial Key Laboratory of Gastroenterology, Department of Gastroenterology and Hepatology Unit, Nanfang Hospital, Southern Medical University, Guangzhou 510515, Guangdong Province, China

Jun Li, Genetics and Precision Medicine Laboratory, The Affiliated Hospital of Guilin Medical University, Guilin 541001, Guangxi Zhuang Autonomous Region, China

Dong-Bo Chen, Pu Chen, Hong-Song Chen, Beijing Key Laboratory of Hepatitis C and Immunotherapy for Liver Disease, Peking University People's Hospital, Beijing 100044, China

Corresponding author: Wei-Jia Liao, MD, Chief Doctor, Professor, Laboratory of Hepatobiliary and Pancreatic Surgery, The Affiliated Hospital of Guilin Medical University, No. 15 Lequn Road, Xiufeng District, Guilin 541001, Guangxi Zhuang Autonomous Region, China. liaoweijia288@163.com

Abstract

BACKGROUND

Noninvasive, practical, and convenient means of detection for the prediction of liver fibrosis and cirrhosis in China are greatly needed.

AIM

To develop a precise noninvasive test to stage liver fibrosis and cirrhosis.

METHODS

With liver biopsy as the gold standard, we established a new index, [alkaline phosphatase (U/L) + gamma-glutamyl transpeptidase (U/L)/platelet (10^9/L) (AGPR)], to predict liver fibrosis and cirrhosis. In addition, we compared the area under the receiver operating characteristic curve (AUROC) of AGPR, gamma-glutamyl transpeptidase to platelet ratio, aspartate transaminase to platelet ratio index, and FIB-4 and evaluated the accuracy of these routine laboratory indices in predicting liver fibrosis and cirrhosis.

RESULTS

Correlation analysis revealed a significant positive correlation between AGPR and liver fibrosis stage ($P < 0.001$). In the training cohort, the AUROC of AGPR was 0.83 (95%CI: 0.78-0.87) for predicting fibrosis (≥ F2), 0.84 (95%CI: 0.79-0.88) for predicting extensive fibrosis (≥ F3), and 0.87 (95%CI: 0.83-0.91) for predicting cirrhosis (F4). In the validation cohort, the AUROCs of AGPR to predict ≥ F2, ≥ F3 and F4 were 0.83 (95%CI: 0.77-0.88), 0.83 (95%CI: 0.77-0.89), and 0.84 (95%CI: 0.78-0.89), respectively.

CONCLUSION

The AGPR index should become a new, simple, accurate, and noninvasive marker to predict liver fibrosis and cirrhosis in chronic hepatitis B patients.

Key Words: Liver; Fibrosis; Cirrhosis; Prediction; Novel noninvasive marker; Chronic hepatitis B

©The Author(s) 2022. Published by Baishideng Publishing Group Inc. All rights reserved.

Core Tip: Chronic hepatitis B virus (HBV) infection is highly endemic in China, and routine assessment of chronic hepatitis B patients is greatly needed to guide management and indicate the need for treatment. In this study, we established a new index to stage liver fibrosis and cirrhosis in patients with chronic HBV infection in China. In addition, the study compared the predictive performance between the new index and other noninvasive indices. The new index is suitable for regular monitoring and is crucial for the management of patients with liver fibrosis/cirrhosis.

Citation: Liao MJ, Li J, Dang W, Chen DB, Qin WY, Chen P, Zhao BG, Ren LY, Xu TF, Chen HS, Liao WJ. Novel index for the prediction of significant liver fibrosis and cirrhosis in chronic hepatitis B patients in China. *World J Gastroenterol* 2022; 28(27): 3503-3513
URL: https://www.wjgnet.com/1007-9327/full/v28/i27/3503.htm
DOI: https://dx.doi.org/10.3748/wjg.v28.i27.3503

INTRODUCTION

Chronic hepatitis B virus (HBV) infection is a public issue that affects human health. Patients who are chronically infected with HBV have a tendency to develop liver fibrosis, liver cirrhosis and even more serious conditions, such as hepatocellular carcinoma (HCC). It has been reported that liver fibrosis can be reversed in patients with varying degrees of fibrosis by removing pathogenic factors, including HBV infection and alcohol[1,2]. It would benefit patients to obtain early diagnosis and effective treatment of liver fibrosis before the disease worsens. Hence, measures should be taken to achieve early diagnosis of liver fibrosis to avoid disease progression caused by HBV infection.

Liver biopsy has always been regarded as the gold standard to evaluate liver histology and assess the degree of fibrosis[3]. However, liver biopsy has shortcomings. Like any surgery, liver biopsy carries some risks, such as puncture of the lung or gallbladder, infection, bleeding, and pain, although these complications are rare[4]. In addition, a major problem is the sampling error and significant variability of fibrosis assessment by liver biopsy[5]. Transient elastography performed with FibroScan is a new technique to measure liver stiffness, and it has the advantages of noninvasiveness, good reproducibility and higher objectivity[6-8]. However, the FibroScan device and its maintenance are expensive, limiting the use of transient elastography in low- and middle-income countries and making it unsuitable for routine monitoring of liver fibrosis/cirrhosis in patients with chronic liver disease in economically poor areas. In recent years, researchers have been interested in finding a potential marker of liver fibrosis/cirrhosis or developing a multifactorial model from peripheral blood[9]. Noninvasive fibrosis tests based on routine laboratory indices have become available and are increasingly used to both assess and stage liver fibrosis; these include the aspartate transaminase (AST)-to-platelet (PLT) ratio index (APRI)[10], FIB-4[11] and the gamma-glutamyl transpeptidase (γ-GT) to PLT ratio (GPR)[12]. These indices are inexpensive, available and noninvasive for assessment of the stages of fibrosis/cirrhosis and can be easily performed in outpatient settings with limited conditions. Among these, the APRI was recommended by the World Health Organization as the most useful noninvasive tool to assess cirrhosis in resource-limited settings; however, FIB-4 was not recommended because it is not used for the detection of cirrhosis[13]. However, the levels of sensitivity and positive predictive value were low for APRI[14]. Therefore, there is an urgent need to find a more reliable method that is noninvasive, inexpensive, convenient and feasible for assessing liver disease stage and identifying patients who need treatment.

Table 1 Clinical and biochemical data of examined patients

Parameter	Training cohort (*n* = 296)[1]	Validation cohort (*n* = 211)[1]	*P* value
Age (yr)	42.47 ± 11.98	41.21 ± 11.36	0.167
Gender: Female/male (*n*)	75/221	40/171	0.091
Drinking: Yes/no (*n*)	127/169	101/110	0.268
Smoking: Yes/no (*n*)	92/204	68/143	0.784
HbeAg: Negative/positive	16/280	15/196	0.430
Fibrosis stage: F0/F1/F2/F3/F4	55/58/75/64/44	47/47/37/54/26	0.194
Activity grade: A0/A1/A2/A3/A4	16/92/113/69/6	15/72/69/52/3	0.446
WBC (× 10^9/L)	5.89 ± 2.55	6.34 ± 4.32	0.150
NEUT × 10^9/L)	3.55 ± 2.44	3.66 ± 2.61	0.611
LYMPH (× 10^9/L)	1.72 ± 0.62	1.80 ± 0.63	0.063
PLT (× 10^9/L)	171.61 ± 66.87	174.48 ± 61.62	0.636
Albumin (g/L)	41.12 ± 19.09	39.94 ± 6.07	0.380
Globulin (g/L)	29.67 ± 5.45	29.14 ± 5.80	0.298
TBIL (μmol/L)	16.51 ± 8.44	16.73 ± 7.63	0.768
DBIL (μmol/L)	6.91 ± 5.03	7.07 ± 4.33	0.699
ALT (U/L)	73.31 ± 65.41	96.85 ± 83.62	0.002
AST (U/L)	72.59 ± 63.29	77.44 ± 67.34	0.411
ALP (U/L)	97.70 ± 41.98	104.32 ± 49.25	0.104
γ-GT (U/L)	85.64 ± 69.68	97.98 ± 75.36	0.058
AGPR	1.26 ± 0.84	1.32 ± 0.89	0.431

[1]Data presented as the mean ± SD or proportions.

HbeAg: Hepatitis B e-antigen; WBC: White blood cell; NEUT: Neutrophil count; LYMPH: Lymphocyte count; PLT: Platelet; TBIL: Total bilirubin; DBIL: Direct bilirubin; ALT: Alanine aminotransferase; AST: Aspartate aminotransferase; ALP: Alkaline phosphatase; γ-GT: Gamma-glutamyl transpeptidase; AGPR: [Alkaline phosphatase (U/L) + gamma-glutamyl transpeptidase (U/L)]/platelet (10^9/L).

In this study, we tested a novel noninvasive index, the alkaline phosphatase (ALP) and γ-GT to PLT ratio (AGPR), for the assessment of liver fibrosis and cirrhosis through statistical analysis of clinical data. Moreover, we compared the diagnostic values of the AGPR, GPR, APRI and FIB-4 indices.

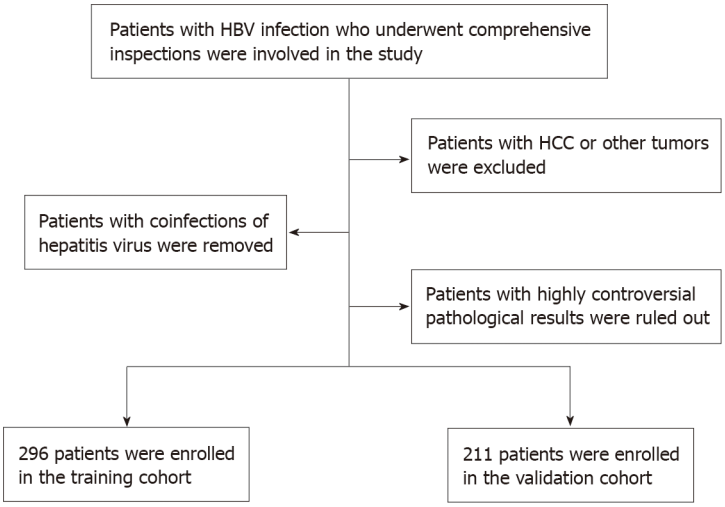
MATERIALS AND METHODS

Patients

The patients who participated in this study were divided into a training set and a validation set. Patients in the training set received treatment at the Affiliated Hospital of Guilin Medical University (Guilin, People's Republic of China). Patients in the validation set received treatments at the Peking University People's Hospital (Beijing, Guangxi Zhuang Autonomous Region, China). All patients were under treatment from May 2005 to October 2016, and all underwent systematic examinations, including abdominal ultrasound, routine laboratory tests and liver histological examination tests. The clinicopathologic characteristics of all patients, including age, gender, alcohol consumption, smoking status, hepatitis B e-antigen (HbeAg) status, fibrosis and cirrhosis stage, activity grade, white blood cell (WBC) count, neutrophil count (NEUT), lymphocyte count (LYMPH), PLT count, albumin, globulin, total bilirubin (TBIL), direct bilirubin (DBIL), alanine aminotransferase (ALT), AST, ALP, γ-GT and AGPR were collected and are detailed in Table 1. All patients in the study were chronically infected with HBV and were positive for hepatitis B surface antigen.

Liver histological examination

Some basic clinical examinations that ensure that patients are relatively safe when performing liver puncture surgery should be performed. In addition, physicians should obtain informed consent from



DOI: 10.3748/wjg.v28.i27.3503 **Copyright** ©The Author(s) 2022.

Figure 1 Selection principles of study population. HBV: Hepatitis B virus; HCC: Hepatocellular carcinoma.

the patients prior to surgery. Ultrasound localization was performed on consenting and suitable patients for liver biopsy procedures. Qualified liver tissue samples were formalin-fixed and paraffin-embedded for pathological analysis. Liver fibrosis and cirrhosis were graded as follows according to the METAVIR system: F0, no fibrosis; F1, fibrosis in the portal vein zone but no fibrous septa; F2, a small amount of fibrous septa; F3, many fibrous septa but no cirrhosis; F4, cirrhosis[15]. All biopsy samples were assessed separately by two liver pathologists who were blinded to the clinical information. If the results of their evaluation were discordant, a third highly experienced hepatopathologist blinded to patient information reviewed the contested samples. Samples were excluded from the study population if the pathologists failed to reach consensus.

Computational formula

AGPR was calculated as [ALP (U/L) + γ-GT (U/L)]/PLT count (10^9/L). APRI was calculated as (AST/ULN)/PLT count (10^9/L) × 100[10]. FIB-4 was calculated by the formula: Age (years) × AST (U/L)/[PLT (10^9/L) × ALT (U/L)$^{1/2}$][11]. The formula for GPR was γ-GT/ULN of γ-GT/PLT count (10^9/L) × 100[12].

Statistical analysis

Student's *t* test was used for continuous variables, and Pearson's χ^2 test or Fisher's exact test was used for categorical variables to compare baseline characteristics. Data are presented as the mean ± SD or proportions. Univariable logistic regression was used for the variables of age, gender, WBC, NEUT, LYMPH, PLT, albumin, globulin, TBIL, DBIL, ALT, AST, ALP, γ-GT and AGPR. The receiver operating characteristic (ROC) curves were drawn to evaluate the accuracy rate of diagnosis for the AGPR, GPR, APRI, and FIB-4. The sensitivity, specificity, positive and negative predictive values, positive and negative likelihood ratio, hazard ratio and the area under the ROC curve (AUROC) of the four non-invasive markers for fibrosis and cirrhosis staging were obtained through comparison and analysis of F0-1 *vs* F2-4, F0-2 *vs* F3-4, and F0-3 *vs* F4, respectively. Data analysis was performed using SPSS software (version 24.0). A P value < 0.05 was regarded as statistically significant.

RESULTS

Study populations of the training and validation cohorts

Patients involved in this study needed to meet certain criteria. Those criteria were as follows: (1) Study patients were infected with HBV and underwent systematic examinations, including abdominal ultrasound, routine laboratory tests and liver biopsies; (2) Patients with HCC or other tumors were excluded; (3) Patients with coinfection of HCV, HIV or HDV were excluded; and (4) Patients with highly controversial results on liver fibrosis pathological grading were excluded. Figure 1 displays the selection principles.

Clinical data related to this study are summarized in Table 1. There were no statistically significant differences between the training and validation cohorts in terms of age, gender, drinking status, smoking status, HbeAg, fibrosis stage, activity grade, WBC, NEUT, LYMPH, PLT, albumin, globulin, TBIL, DBIL, ALT, AST, ALP, γ-GT or AGPR (P > 0.05). Nonsignificant differences between the two

Table 2 Univariate analysis in the training cohort

Parameter	Fibrosis (F0-1) (*n* = 113)[1]	Fibrosis (F2-4) (*n* = 183)[1]	*P* value
Age (yr)	45.15 ± 14.97	43.63 ± 13.32	0.363
Gender: Female/male (*n*)	37/76	38/145	0.021
WBC (× 10^9/L)	6.45 ± 3.02	5.55 ± 2.14	0.003
NEUT (× 10^9/L)	4.14 ± 3.0	3.18 ± 1.95	0.001
LYMPH (× 10^9/L)	1.67 ± 0.60	1.68 ± 0.63	0.828
PLT (× 10^9/L)	206.0 ± 68.39	150.55 ± 56.49	< 0.001
Albumin (g/L)	41.26 ± 5.93	39.29 ± 5.66	0.005
Globulin (g/L)	27.46 ± 4.46	31.04 ± 5.56	< 0.001
TBIL (μmol/L)	13.82 ± 7.06	17.12 ± 8.8	< 0.001
DBIL (μmol/L)	6.43 ± 3.72	7.81 ± 4.49	< 0.001
ALT (U/L)	65.01 ± 70.72	78.42 ± 66.62	0.101
AST (U/L)	56.61 ± 55.11	82.45 ± 66.09	0.001
ALP (U/L)	79.06 ± 34.16	109.2 ± 42.31	< 0.001
γ-GT (U/L)	51.84 ± 47.06	106.5 ± 73.21	< 0.001
AGPR	0.72 ± 0.49	1.61 ± 0.83	< 0.001

[1]Data presented as the mean ± SD or proportions.
WBC: White blood cell; NEUT: Neutrophil count; LYMPH: Lymphocyte count; PLT: Platelet; TBIL: Total bilirubin; DBIL: Direct bilirubin; ALT: Alanine aminotransferase; AST: Aspartate aminotransferase; ALP: Alkaline phosphatase; γ-GT: Gamma-glutamyl transpeptidase; AGPR: [Alkaline phosphatase (U/L) + gamma-glutamyl transpeptidase (U/L)]/platelet (10^9/L).

study groups revealed that the selection of training and validation cohorts was reasonable.

AGPR predicts significant hepatic fibrosis and cirrhosis

Univariable analyses showed that the presence of significant liver fibrosis (≥ F2) was related to gender, WBC, NEUT, PLT, albumin, globulin, TBIL, DBIL, AST, ALP, γ-GT and AGPR (Table 2). In the training cohort, correlation analysis revealed a significant positive correlation between AGPR and liver fibrosis stage (r = 0.567, P < 0.001) (Figure 2A). In the validation cohort, there was also a positive correlation between AGPR and liver fibrosis stage (r = 0.524, P < 0.001), as shown in Supplementary Table 1 and Supplementary Figure 1A. Box plots showed that liver fibrosis stage positively correlated with ALP + γ-GT (r = 0.352, P < 0.001), GPR (r = 0.509, P < 0.001), APRI (r = 0.428, P < 0.001) and FIB-4 (r = 0.416, P < 0.001) in the training cohort (Figure 2B and D-F). The severity of liver fibrosis stage correlated significantly with a gradual increase in the levels of these indicators. There was a negative correlation between PLT count and liver fibrosis stage (r = -0.362, P < 0.001) in the training cohort (Figure 2C). The severity of liver fibrosis decreased with increasing PLT count. Similar results were obtained in the validation cohort, and the specific data related to these results are shown in Supplementary Figure 1B-F and Supplementary Table 2.

Comparisons of AUROC between AGPR and other noninvasive indices

The summary AUROC, sensitivity, specificity, positive and negative predictive values, positive and negative likelihood ratios, and hazard ratios for the detection of fibrosis and cirrhosis for AGPR, GPR, APRI and FIB-4 are displayed in Table 3. In the training cohort, the AUROC of AGPR (0.83, 95%CI: 0.78-0.87) was higher than that of GPR (0.77, 95%CI: 0.72-0.82; P = 0.008), APRI (0.72, 95%CI: 0.67-0.77; P < 0.0001) and FIB-4 (0.74, 95%CI: 0.69-0.79; P = 0.0004) for the prediction of significant fibrosis (≥ F2). For the assessment of extensive fibrosis (≥ F3), the AUROC of AGPR (0.84, 95%CI: 0.79-0.88) was also higher than that of GPR (0.81, 95%CI: 0.76-0.85; P < 0.0001), APRI (0.70, 95%CI: 0.64-0.75; P < 0.0001) and FIB-4 (0.75, 95%CI: 0.69-0.80; P = 0.0005). For the diagnosis of cirrhosis (F4), the AUROC of AGPR was 0.87 (95%CI: 0.83-0.91), which was higher than that of GPR (0.80, 95%CI: 0.75-0.84; P = 0.0001), APRI (0.76, 95%CI: 0.70-0.8; P = 0.0002) and FIB-4 (0.80, 95%CI: 0.75-0.84; P = 0.022) (Figure 3A and Table 3). For identifying patients with significant fibrosis and cirrhosis, the summary sensitivities of AGPR were 83.1% and 88.6%, respectively, while the summary specificities of AGPR were 73.4% and 75.4%, respectively. The sensitivity, specificity, positive and negative predictive values, positive and negative likelihood ratios, and hazard ratios of the other noninvasive indices are detailed in Table 3. Our results

Table 3 Comparisons of the receiver operating characteristic curve between different non-invasive indices

	Training cohort (*n* = 296)			Validation cohort (*n* = 211)		
	F0-1 *vs* F2-4	F0-2 *vs* F3-4	F0-3 *vs* F4	F0-1 *vs* F2-4	F0-2 *vs* F3-4	F0-3 *vs* F4
AGPR						
AUROC (95%CI)	0.83 (0.78-0.87)	0.84 (0.79-0.88)	0.87 (0.83-0.91)	0.83 (0.77-0.88)	0.83 (0.77-0.89)	0.84 (0.78-0.89)
Cut-off values	0.87	1.20	1.40	0.87	1.20	1.40
Se/Sp (%)	83.1/73.4	72.22/80.3	88.6/75.4	85.5/68.1	78.7/70.2	92.3/67.0
PPV/NPV (%)	83.5/72.8	67.8/83.4	38.6/97.4	76.9/79.0	61.8/84.4	28.2/98.4
Positive/negative LR	3.13/0.23	3.67/0.35	3.60/0.15	2.68/0.21	2.65/0.30	2.80/0.11
HR (95%CI)	8.48 (5.22-14.33)	7.56 (4.76-9.83)	8.10 (5.11-11.63)	8.02 (4.95-15.62)	7.06 (4.51-12.35)	5.06 (3.89-7.72)
GPR						
AUROC (95%CI)	0.77 (0.72-0.82)	0.81 (0.76-0.85)	0.80 (0.75-0.84)	0.80 (0.74-0.85)	0.81 (0.74-0.87)	0.78 (0.71-0.83)
Cut-off values	0.32	0.32	0.56	0.32	0.32	0.56
Se/Sp (%)	73.7/70.8	76.8/54.8	79.5/65.9	86.3/67.0	91.2/56.5	75.0/62.3
PPV/NPV (%)	80.4/62.5	49.4/80.5	28.9/94.9	76.5/79.7	56.2/91.4	26.5/86.9
Positive/negative LR	2.53/0.37	1.70/0.42	2.33/0.31	2.62/0.20	2.10/0.15	1.95/0.41
HR (95%CI)	6.53 (4.81-9.62)	6.72 (3.96-9.63)	6.47 (4.08-9.83)	6.45 (3.58-11.61)	7.30 (3.87-14.62)	4.84 (3.28-7.95)
APRI						
AUROC (95%CI)	0.72 (0.67-0.77)	0.70 (0.64-0.75)	0.76 (0.70-0.81)	0.76 (0.70-0.82)	0.74 (0.67-0.82)	0.77 (0.70-0.83)
Cut-off values	0.5 1.5	-	1.0 2.0	0.5 1.5	- 1.0	2.0
Se/Sp (%)	80.9/58.4 36.1/79.7	-	77.3/64.7 43.2/83.3	83.8/54.3 34.1/76.6	- 70.1/68.6	50.1/78.3
PPV/NPV (%)	75.9/65.3 74.2/43.5	-	27.6/94.2 31.1/89.4	69.5/72.9 64.5/48.3	- 26.3/92.7	30.8/91.9
Positive/negative LR	1.94/0.33 1.77/0.80	-	2.19/0.35 2.59/0.68	1.83/0.30 1.46/0.86	- 2.12/0.44	3.16/0.63
HR (95%CI)	2.61 (1.85-3.67)	1.85 (1.41-2.42)	2.09 (1.63-2.55)	1.59 (1.23-2.07)	2.64 (1.76-4.32)	2.13 (1.71-2.58)
FIB-4						
AUROC (95%CI)	0.74 (0.69-0.79)	0.75 (0.69-0.80)	0.80 (0.75-0.84)	0.74 (0.67-0.80)	0.79 (0.73-0.84)	0.77 (0.71-0.83)
Cut-off values	-	1.45 3.25	-	-	1.45 3.25	-
Se/Sp (%)	-	87.9/47.3 42.6/87.2	-	-	77.5/58.1 37.5/93.1	-
PPV/NPV (%)	-	49.0/87.3 65.7/72.6	-	-	53.0/80.9 76.9/70.9	-
Positive/negative LR	-	1.67/0.25 3.34/0.66	-	-	1.85/0.39 5.46/0.67	-
HR (95%CI)	1.86 (1.52-2.53)	1.94 (1.55-2.42)	2.17 (1.77-2.56)	1.98 (1.50-2.62)	2.11 (1.63-2.74)	1.87 (1.68-2.36)
Comparison of AUROC						
AGPR and GPR	$P = 0.008$	$P < 0.0001$	$P = 0.0001$	$P = 0.028$	$P = 0.005$	$P = 0.0008$
AGPR and APRI	$P < 0.0001$	$P < 0.0001$	$P = 0.0002$	$P = 0.0001$	$P = 0.0001$	$P = 0.134$
AGPR and FIB-4	$P = 0.0004$	$P = 0.0005$	$P = 0.022$	$P = 0.007$	$P = 0.174$	$P = 0.100$
GPR and APRI	$P = 0.0007$	$P = 0.0028$	$P = 0.284$	$P = 0.003$	$P = 0.016$	$P = 0.831$

GPR and FIB-4	$P = 0.026$	$P = 0.331$	$P = 0.922$	$P = 0.093$	$P = 0.929$	$P = 0.591$
APRI and FIB-4	$P = 0.455$	$P = 0.028$	$P = 0.061$	$P = 0.248$	$P = 0.008$	$P = 0.795$

AGPR: [Alkaline phosphatase (U/L) + gamma-glutamyl transpeptidase (U/L)]/platelet count (10^9/L); AUROC: Area under the receiver operating characteristic curve; Se: Sensitivity; Sp: Specificity; PPV: Positive predictive value; NPV: Negative predictive value; LR: Likelihood ratio; HR: Hazard ratio; CI: Confidence interval; GPR: Gamma-glutamyl transpeptidase to platelet ratio; APRI: Aspartate aminotransferase-to-platelet ratio index; FIB-4: Age (years) × aspartate aminotransferase (U/L)/[platelet (10^9/L) × alanine aminotransferase (U/L)$^{1/2}$].

revealed that AGPR had the best overall performance among these noninvasive indices.

We further evaluated the diagnostic accuracy and performance of these noninvasive indices in the validation cohort. Similar to the results from the training cohort, the AUROC of AGPR was better than that of GPR (0.78, 95%CI: 0.71-0.83), APRI (0.77, 95%CI: 0.70-0.83), and FIB-4 (0.77, 95%CI: 0.71-0.83) (Figure 3B and Table 3).

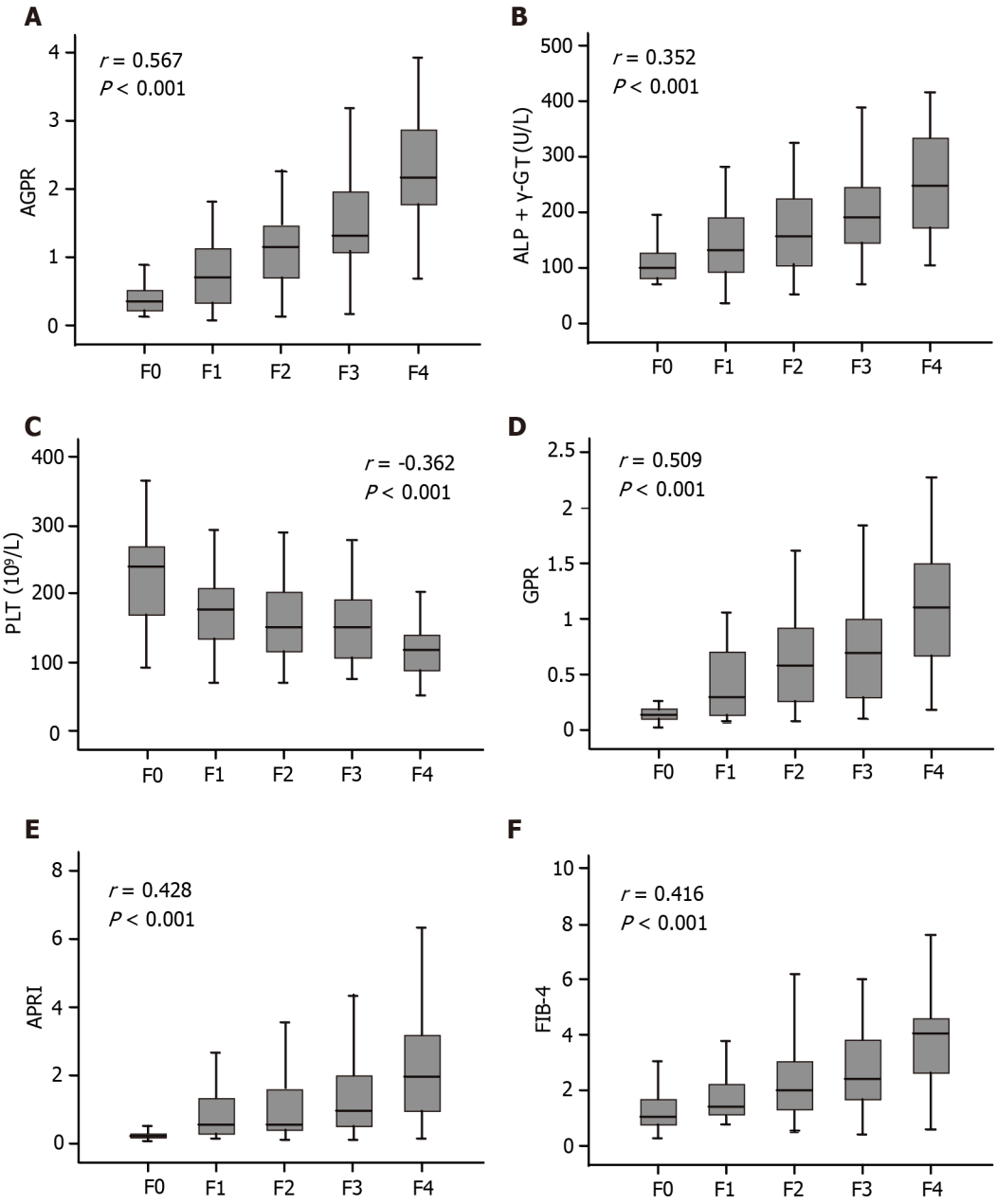
DISCUSSION

Cirrhosis is one of the top 20 causes of disability-adjusted life years and life lost years, accounting for 1.6% and 2.1% of the global burden, respectively[16]. Cirrhosis is also the 11th most common cause of death worldwide[16]. Recently, Xu *et al*[17] provided updated guidelines for the management of liver cirrhosis in China. However, better screening for early fibrosis or cirrhosis remains a challenge. Finding an inexpensive, noninvasive, convenient, feasible and precise parameter to stage liver fibrosis is the expectation of all medical staff in China. Although liver biopsy is a good measure for the assessment of liver fibrosis grade, many patients do not accept it, or they are not suitable for the test[18,19]. FibroScan is a noninvasive diagnostic technique and its diagnostic accuracy is high. However, its application is limited because of its high cost[20]. Consequently, the development of noninvasive assessment methods for liver fibrosis in patients with chronic HBV infection appears especially important in clinical practice.

In the present study, we developed a new simple, convenient and noninvasive index (AGPR) to predict significant liver fibrosis in chronic HBV-infected patients in China. The correlation coefficients between liver fibrosis stage and AGPR suggest that AGPR is a good test for the assessment of significant liver fibrosis and cirrhosis.

The AGPR index was established on the basis of ALP, γ-GT and PLT. These three indicators are clinical evaluations of features of fibrosis/cirrhosis and evidence of decompensation. Hepatitis is related to ALP[21,22] and γ-GT[23,24]. ALP is useful in the diagnosis of chronic liver diseases[25]. A study showed that serum ALP level was significantly different in patients with or without liver cirrhosis[26]. In a report, γ-GT was demonstrated to be an independent predictor of hepatic fibrosis[27]. The circulating PLT count has been recommended as a biomarker of hepatic fibrosis and cirrhosis[28]. Based on these findings, each of the three variables is related to the degree of liver fibrosis. The antiviral treatment, anti-inflammatory and hepatoprotective treatment have a greater impact on serum levels of aminotransferases, such as AST and ALT. However, according to clinical observation, ALP and γ-GT are regarded as less specific for liver injury than AST and ALT. The effects of antiviral therapy, anti-inflammatory therapy and hepatoprotective therapy on ALP and γ-GT are not as obvious as on AST and ALT. As a matter of fact, elevated serum γ-GT levels are strongly associated with alcohol consumption. However, the researchers have reported that the high-risk liver disease mortality due to elevated γ-GT was not affected by alcohol consumption[29].

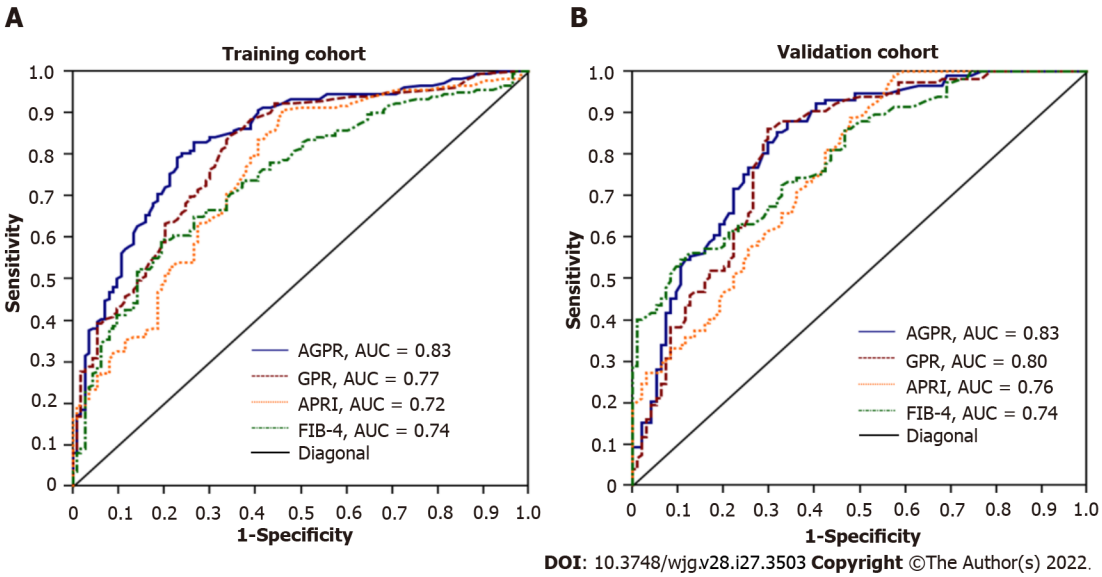
A routine assessment of liver fibrosis stage for patients with chronic HBV infection is needed to guide management and to indicate the need for treatment. However, the diagnosis of liver fibrosis and compensated cirrhosis cannot be based on clinically obvious features. Noninvasive fibrosis tests are now increasingly used for evaluating liver fibrosis, reducing the need for liver biopsy. AGPR may be a new promising noninvasive fibrosis test to assist in the selection of optimal candidates for antiviral therapy. The AGPR test is inexpensive, routinely available at health-care facilities, and can be performed by untrained staff. It is suitable for conventional monitoring of hepatic fibrosis and cirrhosis. The Guidelines Development Group prioritized urgent initiation of antiviral therapy for patients with cirrhosis based on APRI score > 2 in adults, regardless of ALT or HBV DNA levels[13]. However, when applying an APRI score > 2 in this study, the sensitivity for the diagnosis of cirrhosis was only 43.2% and 50.1% in the training and validation cohorts, respectively. This suggested that more than 50% of patients with cirrhosis would be incorrectly classified as not having cirrhosis, which may lead to delayed initiation of treatment. In contrast, the sensitivity of AGPR for the diagnosis of cirrhosis was high at 88.6% and 92.3% in the training and validation cohorts, respectively. Therefore, our data suggested that AGPR may be a preferred noninvasive test to detect the presence of significant fibrosis and cirrhosis. It may serve as a simple index to make treatment decisions in patients without evidence of cirrhosis in China and other resource-limited settings where HBV infection is endemic.



DOI: 10.3748/wjg.v28.i27.3503 **Copyright** ©The Author(s) 2022.

Figure 2 Box plots of [alkaline phosphatase (U/L) + gamma-glutamyl transpeptidase (U/L)]/platelet (10^9/L) (A), alkaline phosphatase + gamma-glutamyl transpeptidase (B), platelet (C), gamma-glutamyl transpeptidase to platelet ratio (D), aspartate aminotransferase-to-platelet ratio index (E), and age × aspartate transaminase/platelet × alanine aminotransferase (F) according to the METAVIR fibrosis stage in the training cohort. AGPR: [Alkaline phosphatase (U/L) + gamma-glutamyl transpeptidase (U/L)]/platelet (10^9/L); ALP + γ-GT: Alkaline phosphatase + gamma-glutamyl transpeptidase; PLT: Platelet; GPR: Gamma-glutamyl transpeptidase to platelet ratio; APRI: Aspartate aminotransferase-to-platelet ratio index; FIB-4: Age × aspartate transaminase/platelet × alanine aminotransferase.

Our study has some limitations. First, the selection of samples was limited to a population with chronic HBV infection in China. Whether AGPR can be generalized to different geographical areas (the infection of hepatitis C virus is endemic) remains to be determined. Second, the time span of over 10 years for our selected samples was too long (from May 2005 to October 2016). Over this time period, substantial changes have taken place in terms of medical equipment and physical examination technologies, which may reduce the accuracy of our study results. Finally, there are many factors involved in liver fibrosis. The impact of various interference factors on the diagnostic accuracy of the AGPR index has not been fully evaluated. Some interference may affect the precision of our index.



DOI: 10.3748/wjg.v28.i27.3503 **Copyright** ©The Author(s) 2022.

Figure 3 The receiver operating characteristic analysis of [alkaline phosphatase (U/L) + gamma-glutamyl transpeptidase (U/L)]/platelet (10^9/L), amma-glutamyl transpeptidase to platelet ratio, aspartate aminotransferase-to-platelet ratio index and age × aspartate transaminase/platelet × alanine aminotransferase in the training (A) and validation cohorts (B). AGPR: [Alkaline phosphatase (U/L) + gamma-glutamyl transpeptidase (U/L)]/platelet (10^9/L); GPR: Gamma-glutamyl transpeptidase to platelet ratio; APRI: Aspartate aminotransferase-to-platelet ratio index; FIB-4: Age × aspartate transaminase/platelet × alanine aminotransferase; AUC: Area under the curve.

CONCLUSION

In summary, the AGPR index may be an accurate noninvasive test for predicting significant liver fibrosis and cirrhosis in patients with chronic HBV infection in China. In addition, it is suitable for conventional monitoring. Therefore, for the prediction of liver fibrosis and cirrhosis, the AGPR index is a promising noninvasive marker that is worthy of further attention and research.

ARTICLE HIGHLIGHTS

Research background

Patients infected with hepatitis B virus (HBV) tend to develop liver fibrosis and liver cirrhosis. Those with cirrhosis have a high risk of hepatic decompensation and hepatitis B- related hepatocellular carcinoma.

Research motivation

Liver biopsy was used to ascertain the degree of fibrosis/cirrhosis. However, as an invasive procedure, liver biopsy has many disadvantages. The Guidelines Development Group recommended the use of noninvasive tests to assist in the assessment of liver disease stage and the diagnosis of fibrosis/cirrhosis. The use of a noninvasive test can reduce the need for liver biopsy.

Research objectives

The present study aimed to develop a precise noninvasive test to stage liver fibrosis/cirrhosis and compare the diagnostic values between different noninvasive methods.

Research methods

Univariable logistic regression was used to identify significant predictive factors. Correlation analysis was performed to reveal the correlation between clinical parameters and liver stage. Receiver operating characteristic (ROC) curves were drawn to evaluate the diagnostic accuracy of different noninvasive methods.

Research results

The presence of liver fibrosis was significantly related to alkaline phosphatase and the gamma-glutamyl transpeptidase to platelet ratio (AGPR). There was a significant positive correlation between AGPR and liver fibrosis stage. The area under the ROC curve values of AGPR were 0.83, 0.84, and 0.87 for the prediction of significant fibrosis, extensive fibrosis, and cirrhosis, respectively. The AGPR index had a

better overall performance than other noninvasive indices.

Research conclusions

AGPR can be used to detect the presence of significant fibrosis, extensive fibrosis, and cirrhosis with high diagnostic accuracy, sensitivity, and specificity in patients with chronic HBV infection.

Research perspectives

The AGPR index is a promising noninvasive marker for assessing liver disease stage. The use of AGPR can help with the routine monitoring of hepatic fibrosis and cirrhosis.

FOOTNOTES

Author contributions: Liao MJ, Li J, and Dang W contributed equally to this work; Liao WJ was the guarantor and designed the study; Liao MJ, Li J, Chen DB, Qin WY, Chen P, Zhao BG, Ren LY, Xu TF, and Liao WJ participated in the acquisition, analysis, and interpretation of the data; Li J and Dang W drafted the initial manuscript; Chen HS and Liao WJ revised the article critically for important intellectual content.

Supported by the National Natural Science Foundation of China, No. 81372163; the Natural Science Foundation of Guangxi, No. 2018GXNSFDA138001; the Science and Technology Planning Project of Guilin, No. 20190218-1; the Opening Project of Key laboratory of High-Incidence-Tumor Prevention & Treatment (Guangxi Medical University), Ministry of Education, No. GKE-KF202101; and the Program of Guangxi Zhuang Autonomous Region Health and Family Planning Commission, No. Z20210706 and No. Z20190665.

Institutional review board statement: The study was reviewed and approved by the research ethics committee of Affiliated Hospital of Guilin Medical University.

Informed consent statement: Informed consent was obtained from all patients.

Conflict-of-interest statement: There are no conflicts of interest to report.

Data sharing statement: No additional data are available.

Open-Access: This article is an open-access article that was selected by an in-house editor and fully peer-reviewed by external reviewers. It is distributed in accordance with the Creative Commons Attribution NonCommercial (CC BY-NC 4.0) license, which permits others to distribute, remix, adapt, build upon this work non-commercially, and license their derivative works on different terms, provided the original work is properly cited and the use is non-commercial. See: https://creativecommons.org/Licenses/by-nc/4.0/

Country/Territory of origin: China

ORCID number: Min-Jun Liao 0000-0002-2328-8209; Jun Li 0000-0002-6210-4062; Wei Dang 0000-0002-9263-5841; Dong-Bo Chen 0000-0001-5173-6999; Wan-Ying Qin 0000-0001-6040-9340; Pu Chen 0000-0003-1437-2617; Bi-Geng Zhao 0000-0001-6203-4159; Li-Ying Ren 0000-0003-3624-5483; Ting-Feng Xu 0000-0003-0303-5471; Hong-Song Chen 0000-0001-6858-8398; Wei-Jia Liao 0000-0002-8906-8612.

S-Editor: Yan JP
L-Editor: A
P-Editor: Yan JP

REFERENCES

1 **Sun M**, Kisseleva T. Reversibility of liver fibrosis. *Clin Res Hepatol Gastroenterol* 2015; **39** Suppl 1: S60-S63 [PMID: 26206574 DOI: 10.1016/j.clinre.2015.06.015]
2 **Rockey DC**. Liver Fibrosis Reversion After Suppression of Hepatitis B Virus. *Clin Liver Dis* 2016; **20**: 667-679 [PMID: 27742006 DOI: 10.1016/j.cld.2016.06.003]
3 **Park YE**, Kim BK, Park JY, Kim DY, Ahn SH, Han KH, Han S, Jeon MY, Heo JY, Song K, Kim SU. Gamma-glutamyl transpeptidase-to-platelet ratio is an independent predictor of hepatitis B virus-related liver cancer. *J Gastroenterol Hepatol* 2017; **32**: 1221-1229 [PMID: 27859587 DOI: 10.1111/jgh.13653]
4 **Li Y**, Chen Y, Zhao Y. The diagnostic value of the FIB-4 index for staging hepatitis B-related fibrosis: a meta-analysis. *PLoS One* 2014; **9**: e105728 [PMID: 25165830 DOI: 10.1371/journal.pone.0105728]
5 **Friedman LS**. Controversies in liver biopsy: who, where, when, how, why? *Curr Gastroenterol Rep* 2004; **6**: 30-36 [PMID: 14720451 DOI: 10.1007/s11894-004-0023-4]
6 **Meng F**, Zheng Y, Zhang Q, Mu X, Xu X, Zhang H, Ding L. Noninvasive evaluation of liver fibrosis using real-time tissue elastography and transient elastography (FibroScan). *J Ultrasound Med* 2015; **34**: 403-410 [PMID: 25715361 DOI:

10.7863/ultra.34.3.403]
7 **Dong DR**, Hao MN, Li C, Peng Z, Liu X, Wang GP, Ma AL. Acoustic radiation force impulse elastography, FibroScan®, Forns' index and their combination in the assessment of liver fibrosis in patients with chronic hepatitis B, and the impact of inflammatory activity and steatosis on these diagnostic methods. *Mol Med Rep* 2015; **11**: 4174-4182 [PMID: 25651500 DOI: 10.3892/mmr.2015.3299]
8 **Jia J**, Hou J, Ding H, Chen G, Xie Q, Wang Y, Zeng M, Zhao J, Wang T, Hu X, Schuppan D. Transient elastography compared to serum markers to predict liver fibrosis in a cohort of Chinese patients with chronic hepatitis B. *J Gastroenterol Hepatol* 2015; **30**: 756-762 [PMID: 25353058 DOI: 10.1111/jgh.12840]
9 **Liao Y**, Wei R, Yao R, Qin L, Li J, Yu J, Liao W. AGLR is a novel index for the prognosis of hepatocellular carcinoma patients: a retrospective study. *BMC Surg* 2021; **21**: 72 [PMID: 33536005 DOI: 10.1186/s12893-020-01037-7]
10 **Wai CT**, Greenson JK, Fontana RJ, Kalbfleisch JD, Marrero JA, Conjeevaram HS, Lok AS. A simple noninvasive index can predict both significant fibrosis and cirrhosis in patients with chronic hepatitis C. *Hepatology* 2003; **38**: 518-526 [PMID: 12883497 DOI: 10.1053/jhep.2003.50346]
11 **Sterling RK**, Lissen E, Clumeck N, Sola R, Correa MC, Montaner J, S Sulkowski M, Torriani FJ, Dieterich DT, Thomas DL, Messinger D, Nelson M; APRICOT Clinical Investigators. Development of a simple noninvasive index to predict significant fibrosis in patients with HIV/HCV coinfection. *Hepatology* 2006; **43**: 1317-1325 [PMID: 16729309 DOI: 10.1002/hep.21178]
12 **Lemoine M**, Shimakawa Y, Nayagam S, Khalil M, Suso P, Lloyd J, Goldin R, Njai HF, Ndow G, Taal M, Cooke G, D'Alessandro U, Vray M, Mbaye PS, Njie R, Mallet V, Thursz M. The gamma-glutamyl transpeptidase to platelet ratio (GPR) predicts significant liver fibrosis and cirrhosis in patients with chronic HBV infection in West Africa. *Gut* 2016; **65**: 1369-1376 [PMID: 26109530 DOI: 10.1136/gutjnl-2015-309260]
13 **World Health Organization**. Guidelines for the Prevention, Care and Treatment of Persons with chronic Hepatitis B infection. 2015. [Cited 13 Mar 2018]. Available from: http://whoint/hiv/pub/hepatitis/hepatitis-b-guidelines/en/
14 **Li Q**, Song J, Huang Y, Li X, Zhuo Q, Li W, Chen C, Lu C, Qi X, Chen L. The Gamma-Glutamyl-Transpeptidase to Platelet Ratio Does not Show Advantages than APRI and Fib-4 in Diagnosing Significant Fibrosis and Cirrhosis in Patients With Chronic Hepatitis B: A Retrospective Cohort Study in China. *Medicine (Baltimore)* 2016; **95**: e3372 [PMID: 27100421 DOI: 10.1097/MD.0000000000003372]
15 **Bedossa P**, Poynard T. An algorithm for the grading of activity in chronic hepatitis C. The METAVIR Cooperative Study Group. *Hepatology* 1996; **24**: 289-293 [PMID: 8690394 DOI: 10.1002/hep.510240201]
16 **Asrani SK**, Devarbhavi H, Eaton J, Kamath PS. Burden of liver diseases in the world. *J Hepatol* 2019; **70**: 151-171 [PMID: 30266282 DOI: 10.1016/j.jhep.2018.09.014]
17 **Xu XY**, Ding HG, Li WG, Xu JH, Han Y, Jia JD, Wei L, Duan ZP, Ling-Hu EQ, Zhuang H. Chinese guidelines on the management of liver cirrhosis (abbreviated version). *World J Gastroenterol* 2020; **26**: 7088-7103 [PMID: 33362370 DOI: 10.3748/wjg.v26.i45.7088]
18 **McGill DB**, Rakela J, Zinsmeister AR, Ott BJ. A 21-year experience with major hemorrhage after percutaneous liver biopsy. *Gastroenterology* 1990; **99**: 1396-1400 [PMID: 2101588 DOI: 10.1016/0016-5085(90)91167-5]
19 **Nalbantoglu IL**, Brunt EM. Role of liver biopsy in nonalcoholic fatty liver disease. *World J Gastroenterol* 2014; **20**: 9026-9037 [PMID: 25083076 DOI: 10.3748/wjg.v20.i27.9026]
20 **Sun W**, Cui H, Li N, Wei Y, Lai S, Yang Y, Yin X, Chen DF. Comparison of FIB-4 index, NAFLD fibrosis score and BARD score for prediction of advanced fibrosis in adult patients with non-alcoholic fatty liver disease: A meta-analysis study. *Hepatol Res* 2016; **46**: 862-870 [PMID: 26763834 DOI: 10.1111/hepr.12647]
21 **Aggarwal SK**, Radhakrishnan S. Syphilitic hepatitis: Look for raised alkaline phosphatase level. *Med J Armed Forces India* 2016; **72**: 192-193 [PMID: 27257335 DOI: 10.1016/j.mjafi.2015.11.011]
22 **Kasztelan-Szczerbinska B**, Slomka M, Celinski K, Szczerbinski M. Alkaline phosphatase: the next independent predictor of the poor 90-day outcome in alcoholic hepatitis. *Biomed Res Int* 2013; **2013**: 614081 [PMID: 24151614 DOI: 10.1155/2013/614081]
23 **Huang CF**, Chuang WL, Yu ML. Interference of diabetes on the association of γ-glutamyl transpeptidase to platelet ratio with liver fibrosis in chronic hepatitis C. *Kaohsiung J Med Sci* 2016; **32**: 334-335 [PMID: 27377848 DOI: 10.1016/j.kjms.2016.04.004]
24 **Benini F**, Pigozzi MG, Baisini O, Romanini L, Ahmed H, Pozzi A, Ricci C, Lanzini A. Increased serum gamma-glutamyl-transpeptidase concentration is associated with nonalcoholic steatosis and not with cholestasis in patients with chronic hepatitis C. *J Gastroenterol Hepatol* 2007; **22**: 1621-1626 [PMID: 17845689 DOI: 10.1111/j.1440-1746.2006.04733.x]
25 **Barreto AV**, Alecrim VM, Medeiros TB, Domingues AL, Lopes EP, Martins JR, Nader HB, Diniz GT, Montenegro SM, Morais CN. New index for the diagnosis of liver fibrosis in Schistosomiasis mansoni. *Arq Gastroenterol* 2017; **54**: 51-56 [PMID: 28079240 DOI: 10.1590/S0004-2803.2017v54n1-10]
26 **Cho HJ**, Kim SS, Ahn SJ, Park JH, Kim DJ, Kim YB, Cho SW, Cheong JY. Serum transferrin as a liver fibrosis biomarker in patients with chronic hepatitis B. *Clin Mol Hepatol* 2014; **20**: 347-354 [PMID: 25548740 DOI: 10.3350/cmh.2014.20.4.347]
27 **Nishikawa H**, Hasegawa K, Ishii A, Takata R, Enomoto H, Yoh K, Kishino K, Shimono Y, Iwata Y, Nakano C, Nishimura T, Aizawa N, Sakai Y, Ikeda N, Takashima T, Iijima H, Nishiguchi S. A proposed predictive model for advanced fibrosis in patients with chronic hepatitis B and its validation. *Medicine (Baltimore)* 2016; **95**: e4679 [PMID: 27583895 DOI: 10.1097/MD.0000000000004679]
28 **Pradella P**, Bonetto S, Turchetto S, Uxa L, Comar C, Zorat F, De Angelis V, Pozzato G. Platelet production and destruction in liver cirrhosis. *J Hepatol* 2011; **54**: 894-900 [PMID: 21145808 DOI: 10.1016/j.jhep.2010.08.018]
29 **Ruhl CE**, Everhart JE. Elevated serum alanine aminotransferase and gamma-glutamyltransferase and mortality in the United States population. *Gastroenterology* 2009; **136**: 477-85.e11 [PMID: 19100265 DOI: 10.1053/j.gastro.2008.10.052]

World Journal of Gastroenterology

Submit a Manuscript: https://www.f6publishing.com

World J Gastroenterol 2022 July 21; 28(27): 3514-3523

DOI: 10.3748/wjg.v28.i27.3514

ISSN 1007-9327 (print) ISSN 2219-2840 (online)

SYSTEMATIC REVIEWS

Percutaneous transhepatic cholangiography *vs* endoscopic ultrasound-guided biliary drainage: A systematic review

Zeinab Hassan, Eyad Gadour

Specialty type: Gastroenterology and hepatology

Provenance and peer review: Unsolicited article; Externally peer reviewed

Peer-review model: Single blind

Peer-review report's scientific quality classification

Grade A (Excellent): A
Grade B (Very good): 0
Grade C (Good): C
Grade D (Fair): 0
Grade E (Poor): 0

P-Reviewer: Jin G, China; Villa E, United States

Received: November 22, 2021
Peer-review started: November 23, 2021
First decision: January 9, 2022
Revised: January 21, 2022
Accepted: June 23, 2022
Article in press: June 23, 2022
Published online: July 21, 2022

Zeinab Hassan, Internal Medicine, Stockport Hospitals NHS Foundation Trust, Manchester SK2 7JE, United Kingdom

Eyad Gadour, Department of Gastroenterology, University Hospitals of Morecambe Bay NHS Foundation Trust, Lancaster LA1 4RP, United Kingdom

Corresponding author: Eyad Gadour, CCST, FRCP, MBBS, MRCP, Consultant Physician-Scientist, Department of Gastroenterology, University Hospitals of Morecambe Bay NHS Foundation Trust, Royal Lancaster Infirmary, Lancaster LA1 4RP, United Kingdom.
eyadgadour@doctors.org.uk

Abstract

BACKGROUND

Percutaneous transhepatic cholangiography is a diagnostic and therapeutic procedure that involves inserting a needle into the biliary tree, followed by the immediate insertion of a catheter. Endoscopic ultrasound-guided biliary drainage (EUS-BD) is a novel technique that allows BD by echoendoscopy and fluoroscopy using a stent from the biliary tree to the gastrointestinal tract.

AIM

To compare the technical aspects and outcomes of percutaneous transhepatic BD (PTBD) and EUS-BD.

METHODS

Different databases, including PubMed, Embase, clinicaltrials.gov, the Cochrane library, Scopus, and Google Scholar, were searched according to the guidelines for Preferred Reporting Items for Systematic reviews and Meta-Analyses to obtain studies comparing PTBD and EUS-BD.

RESULTS

Among the six studies that fulfilled the inclusion criteria, PTBD patients underwent significantly more reinterventions (4.9 *vs* 1.3), experienced more postprocedural pain (4.1 *vs* 1.9), and experienced more late adverse events (53.8% *vs* 6.6%) than EUS-BD patients. There was a significant reduction in the total bilirubin levels in both the groups (16.4-3.3 μmol/L and 17.2-3.8 μmol/L for EUS-BD and PTBD, respectively; P = 0.002) at the 7-d follow-up. There were no significant differences observed in the complication rates between PTBD and EUS-BD (3.3 *vs* 3.8). PTBD was associated with a higher adverse event rate than EUS-BD in all the procedures, including reinterventions (80.4% *vs* 15.7%, respectively)

and a higher index procedure (39.2% *vs* 18.2%, respectively).

CONCLUSION
The findings of this systematic review revealed that EUS-BD is linked with a higher rate of effective BD and a more manageable procedure-related adverse event profile than PTBD. These findings highlight the evidence for successful EUS-BD implementation.

Key Words: Percutaneous transhepatic cholangiography; Endoscopic ultrasound; Biliary drainage; Obstructive cholangiopathy

©The Author(s) 2022. Published by Baishideng Publishing Group Inc. All rights reserved.

Core Tip: Endoscopic transpapillary biliary drainage (BD) is the preferred approach for biliary decompression in patients with unresectable pancreatic cancer and obstructive jaundice. We conducted a systematic review of studies comparing the technical aspects and outcomes of two distinct approaches for BD: Endoscopic ultrasound-guided BD (EUS-BD) and percutaneous transhepatic BD (PTBD). The evaluation of six studies that fulfilled the inclusion criteria revealed that PTBD was associated with more reinterventions, postprocedural pain, and late adverse events compared with EUS-BD. Both procedures were associated with a significant reduction in the total bilirubin levels at the 7-d follow-up, and there were no significant differences in the complication rates between the two procedures. In summary, EUS-BD was associated with a higher rate of effective BD and manageable procedure-related adverse events compared with PTBD, highlighting its utility in successful BD.

Citation: Hassan Z, Gadour E. Percutaneous transhepatic cholangiography *vs* endoscopic ultrasound-guided biliary drainage: A systematic review. *World J Gastroenterol* 2022; 28(27): 3514-3523
URL: https://www.wjgnet.com/1007-9327/full/v28/i27/3514.htm
DOI: https://dx.doi.org/10.3748/wjg.v28.i27.3514

INTRODUCTION

Endoscopic transpapillary biliary drainage (BD) is the preferred approach for biliary decompression in patients with unresectable pancreatic cancer and obstructive jaundice[1]. Percutaneous transhepatic cholangiography (PTC) is a diagnostic and therapeutic procedure that involves inserting a needle into the biliary tree, followed by immediately inserting a catheter to achieve percutaneous BD. During the procedure, contrast is injected into one or more bile ducts (cholangiography) and sometimes into the duodenum. PTC can be performed using fluoroscopic guidance alone or using both fluoroscopic and ultrasound guidance[2,3].

In cases of suspected malignant biliary stricture, imaging alone may not be sufficient to provide a precise diagnosis. PTC was first introduced several decades ago to visualize biliary obstructions, treat malignant obstructive jaundice palliatively, and access BD[4]. Fine needle aspiration (FNA), brush cytology, and forceps biopsy have been performed using percutaneous biliary catheterization during PTC since the 1980s[5]. For biliary stenosis, endoscopic retrograde cholangiopancreatography (ERCP) has recently been recognized as a reliable diagnostic and therapeutic procedure.

Endoscopic retrograde BD (ERBD) is the most commonly used method of biliary decompression in patients with blockage of the distal central bile duct. This technique has a success rate of 90%-95% in the United States[6]. Altered anatomy, presenting pathology (tumor infiltration, impacted stone, and duodenal compression by a pancreatic pseudocyst), previous surgery, or variations in normal anatomy (periampullary diverticula and tortuous ducts) can contribute to the failure of ERBD. The failure rate of ERBD is 6%-7% in cases with obstructive jaundice caused by a blockage or altered anatomy[7]. Percutaneous transhepatic BD (PTBD) has a lower risk of complications than surgical decompression, but it is associated with complications such as fistula formation, repeat intervention, recurrent infection, and the requirement for long-term external catheter drainage, which contribute to a low quality of life [8]. Although PTBD is associated with severe morbidity and mortality, the only relative contraindication of PTBD is perihepatic ascites[6-9]. Furthermore, PTBD usually requires separate surgery after the failure of ERCP BD, thereby increasing the morbidity associated with biliary stasis.

Endoscopic ultrasound-guided BD (EUS-BD) has become more widely used as an alternative to PTBD in patients with anatomical abnormalities, which make endoscopic transpapillary insertion of a biliary stent difficult[10]. It offers advantages of being compatible with anatomic internal drainage, being more comfortable, and resulting in a recovery associated with fewer complications and reduced expenditure [11].

EUS is an extremely useful imaging method for examining the gastrointestinal luminal wall and surrounding tissues. The proximity of the EUS probe to the area of interest enables high-resolution imaging and EUS-guided FNA tissue collection in real time. EUS has become a crucial diagnostic technique due to its high-quality imaging and FNA capacity and is also used as a treatment tool. However, until recently, its use was limited to the introduction of various drugs[12,13]. The therapeutic uses of EUS have been expanded due to larger channel echoendoscopes, which combine the benefits of real-time ultrasound and fluoroscopy imaging with the use of ERCP-based devices and procedures, such as EUS-BD. In 1996, Wiersema *et al*[14] first reported EUS-guided diagnostic cholangiography and in 2001, Giovannini *et al*[10] first reported EUS-BD in a patient with pancreatic cancer, establishing a choledochoduodenal fistula with a needle knife followed by transduodenal stenting.

These early reports were followed by modified techniques and expanded indications, such as EUS-guided hepatic gastrostomy with stent placement[15], transduodenal EUS-rendezvous (EUS-RV) biliary access[16], and EUS-guided choledocholithiasis therapy with the creation of a neo papilla[17]. Since then, several studies have reported modifications to these techniques, including the use of a covered metal stent as a conduit for interventional endoscopic procedures in the bile duct[18,19]. Few studies have compared EUS-BD and PTBD in failed ERCP cases in terms of success rate and adverse event profile[20]; therefore, we performed a systematic review of the relevant literature to investigate the combined efficacy and adverse effects of EUS-BD and PTBD.

MATERIALS AND METHODS

Literature search

This systematic review was conducted using an electronic search of different databases, including PubMed, Embase, clinicaltrials.gov, the Cochrane library, Scopus, and Google Scholar using the guidelines for Preferred Reporting Items for Systematic reviews and Meta-Analyses[21]. Two investigators independently searched for the following key terms: all field "failed EUS", all field "Percutaneous biliary drainage", and all field "EUS-guided biliary drainage". All the three search headings were connected using the Boolean operator "AND". Studies published in English comparing PTBD with EUS-BD were chronologically limited to those published from their inception to October 2021. After completing the literature search, the references were imported to Endnote citation manager (Endnote X9) for removing any duplicates, following which the abstracts were screened for potential relevance by two independent investigators. This study included intervention studies, retrospective or prospective observational studies, case reports, randomized controlled trials, and published abstracts that reported at least some adverse events. And this study also cited high-quality articles in Reference Citation Analysis (https://www.referencecitationanalysis.com).

Letters, comments, seminar proceedings, and animal studies were excluded from our analysis. Moreover, only human studies were included and limited to the English language. Publications judged to be potentially relevant underwent a full text assessment by two independent investigators to determine their inclusion. Disagreements regarding study eligibility were resolved by consensus or adjudication between the investigators.

Data extraction

The baseline study details, including study identifiers, such as first author, publication year, title, and country, and study-specific methodological data, such as sample size, study design, single-center *vs* multicenter study types, and healthcare setting, are presented in Table 1. Technical and clinical success rates, including the total number of patients enrolled, number of patients in each arm, mean age, sex ratio, comorbidity index, mean preprocedural bilirubin, mean diameter of the bile duct, etiology of biliary obstruction, and reasons for EUS failure are shown in Table 2.

Risk of bias evaluation

The GRADE checklist was used to evaluate the risk of bias in the included studies[22]. Table 3 shows a summary of the methodological qualities of studies reporting the prevalence data. Questions were answered as "yes", "no", "unclear", or "not applicable".

RESULTS

Our literature search yielded 315 manuscripts, of which 132 studies remained after excluding duplicate studies. After reviewing the title and abstract, only nine articles were left for the thorough screening of data by reviewing the full text. Further, two studies were eliminated after reading the manuscripts because they included primary EUS-BD cases wherein EUS was not attempted as the primary procedure. The third study was excluded, as it did not contain full text. A total of six studies met the abovementioned inclusion criteria of the study[23-28] (Figure 1).

Table 1 Baseline characteristics of the studies

Ref.	Artifon *et al*[23]	Bapaye *et al*[24]	Khashab *et al*[25]	Giovannini[26]	Jung *et al*[27]	Sharaiha *et al*[28]
Type of study (country)	Single-center, prospective, randomized, controlled trial(Brazil)	Single-center, retrospective, comparative study (India)	Single-center, retrospective, comparative, cohort study (United States)	Multicenter, randomized, phase II trial (France)	Multicenter, prospective, randomized, controlled trial (South Korea)	Single-center, retrospective, cohort review (United States)
Age [mean (SD)/median ± SD], yr	63.4 (11.1) *vs* 71.0 (11.9)	59.9 ± 13.3 *vs* 62.4 ± 10.2	64.9 ± 12.5 *vs* 66.9 ± 12.5	N/A	66.5 *vs* 68.4	68.7 ± 13.9 *vs* 58.8 ± 13.6
Males/females	2.25 *vs* 2.0	1.08 *vs* 1.6	1.2 *vs* 1.31	0.91 *vs* 9	3.25 *vs* 3	12 *vs* 1.47
Comorbidity/quality index (mean)	58.3 *vs* 57.8 (QoL sF 36)	N/A	N/A	N/A	40.7 *vs* 40.5 (global health status/QoL)	5.9 *vs* 6.4 (Charleston comorbidity index)
Total bilirubin (mean), mg/dL	16.4 *vs* 17.2	7.11 ± 7.6 *vs* 9.41 ± 12.4	15.8 ± 11.3 *vs* 14.5 ± 8.8	N/A	10.4 *vs* 11.8	N/A
Mean diameter of bile duct	13.7 *vs* 11.9	N/A	N/A	N/A	11.22 *vs* 12.6	N/A
Etiology of obstruction						
Adenocarcinoma of the pancreatic	10 *vs* 6	15 *vs* 18	43	N/A	12 *vs* 12	22
Advanced lymphoma/liposarcoma	0 *vs* 1	0	1	N/A	0	0
Cholangiocarcinoma	1 *vs* 1	2 *vs* 2	12	N/A	7 *vs* 14	9
Duodenal carcinoma	0	0	1	N/A	3 *vs* 0	5
Gall bladder cancer	0	0	0	N/A	5 *vs* 5	0
Gastric carcinoma	0 *vs* 1	0	1	N/A	3 *vs* 2	4
Metastasis	0 *vs* 3	0	12	N/A	3 *vs* 1	7
Plasmacytoma	1 *vs* 0	0	0	N/A	0	0
Total malignancy		0	37	N/A		
Reason for ERCP failure						
Altered anatomy	1	9	0	N/A	12 *vs* 10	N/A
Duodenal/stomach invasion	8	32	0	N/A	22 *vs* 22	N/A
Indwelling duodenal stent	0	16	0	N/A	0	N/A
Unable to cannulate	16	42	0	N/A	0	N/A

N/A: Not applicable; QoL sF: Quality of life Short Form Survey (SF-36); ERCP: Endoscopic retrograde cholangiopancreatography.

DISCUSSION

The most common method for gaining access to the biliary tree is ERCP. In patients with unmodified upper gastrointestinal anatomy, the success rate of bile duct cannulation using ERCP is > 90%[25]. Affected or variant anatomy, ampullary pathology (stones, stenosis, and tumor infiltration), periampullary diverticulum, gastric outlet obstruction, indwelling duodenal stent, and previous gastric bypass surgery are the prevalent causes of failed cannulation[29]. The rate of adverse outcomes associated with PTBD and surgery is extremely high, although these approaches are traditionally used to treat these clinical conditions[30]. The most prevalent issues related to long-term PTBD therapy are drain blockage, dislocation, and cholangitis, which require multiple interventions and longer hospital stays[31]. Moreover, patients are left with a permanent external drain, resulting in poor quality of life[32]. EUS-BD has emerged as a viable, extremely safe, effective, and minimally invasive approach[33]. Using echoendoscopy and fluoroscopy, the biliary tree is accessed from the gastrointestinal lumen, a fistulous tract is created, and a stent is deployed in a single step, eliminating the need for an external drain[34]. However, the rates of success and adverse events associated with EUS-BD remain unclear. The use of EUS-BD was first reported by Giovannini *et al*[10] in 2001. Subsequently, several studies reported the

Table 2 Rates of clinical and technical success in the included studies

Ref.	Technical success		Clinical success	
	EUS-guided Choledochoduodenostomy	Percutaneous transhepatic biliarydrainage	EUS-guided Choledochoduodenostomy	Percutaneous transhepatic biliarydrainage
Artifon *et al* [23]	13/13	12/12	13/13	12/12
Bapaye *et al* [24]	23/25	26/26	23/25	26/26
Khashab *et al* [25]	19/22	51/51	19/19	47/51
Giovannini [26]	19/20	17/17	18/19	17/17
Jung *et al*[27]	32/34	31/32	28/32	27/31
Sharaiha *et al* [28]	43/47	12/13	27/43	3/12

Table 3 Quality of identified studies

Ref.	Criteria									Overall appraisal
	C1	C2	C3	C4	C5	C6	C7	C8	C9	
Artifon *et al*[23]	Yes	Yes	Yes	Yes	Yes	Yes	Yes	Unclear	Yes	Included
Bapaye *et al*[24]	Yes	Yes	Yes	Yes	Yes	Yes	Yes	Yes	Yes	Included
Khashab *et al*[25]	Yes	Yes	Yes	Yes	Yes	Yes	Yes	Yes	Yes	Included
Giovannini[26]	Unclear	Yes	Yes	Yes	Yes	Yes	Yes	Yes	Yes	Included
Jung *et al*[27]	Yes	Yes	Yes	Yes	Yes	Yes	Yes	Unclear	Yes	Included
Sharaiha *et al*[28]	Yes	Yes	Yes	Yes	Yes	Unclear	Yes	Yes	Yes	Included

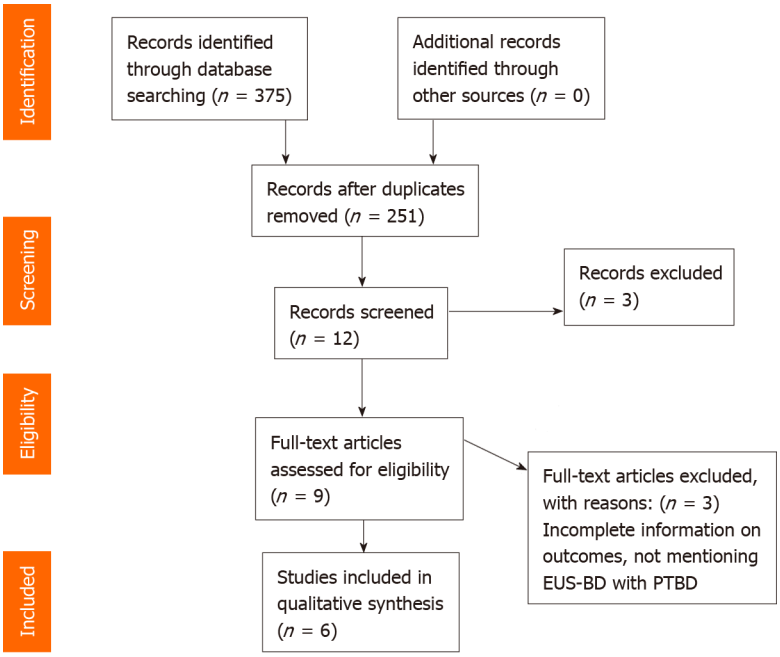
C1: Did the study sample represent the target population? C2: Were participants in the study appropriately recruited? C3: Was the sample size adequate? C4: Were the study subjects and study setting described in detail? C5: Did the data analysis cover a sufficient portion of the identified population? C6: Were objective and standard criteria used to measure the condition of interest? C7: Was the condition reliably measured? C8: Was the statistical analysis appropriate? C9: Were all important confounding factors/subgroups/differences identified and taken into account?

efficacy of EUS-BD as an alternative BD method after a failed ERCP. The EUS-BD procedures are divided into three techniques: (1) EUS-RV; (2) EUS-guided antegrade (EUS-AG); and (3) EUS-guided transluminal BD, including EUS-guided choledochoduodenostomy (EUS-CDS) and EUS-guided hepaticogastrostomy (EUS-HGS)[6]. In EUS-RV, the biliary duct is accessed using fluoroscopy and EUS, forming a temporary fistula, followed by guidewire placement into the duodenum *via* the biliary duct and ampulla. After guidewire placement, ERCP is performed using the EUS-placed guidewire, which is removed once biliary cannulation is obtained. Thus, EUS-RV should be performed in patients with an endoscopically accessible ampulla after unsuccessful biliary cannulation using conventional ERCP.

In EUS-AG, the intrahepatic biliary duct is accessed by creating a temporary fistula between the intestine and intrahepatic biliary duct from the upper intestine. Stent placement or balloon dilation is performed after the dilation of the fistula to achieve biliary obstruction through the fistula without reaching the ampulla using the endoscope. This technique is appropriate when reaching the biliary orifice using endoscopy is impossible or unmanageable, such as in biliary obstruction in patients with surgically altered anatomy or upper intestinal obstruction.

In EUS-guided transluminal BD, including EUS-CDS and EUS-HGS, the biliary duct is accessed followed by guidewire placement and fistula dilation under EUS guidance. For BD, a permanent fistula is created by inserting the stent between the biliary duct and the intestine. This procedure can be performed in cases where reaching the biliary orifice using endoscopy is possible or accessible; however, in patients with unresectable malignant biliary obstruction, its indication should be limited given the features of permanent fistula creation.

Recent studies have demonstrated that EUS-BD could be an alternative to PTBD in patients with inoperable malignant biliary blockage and failed ERCP. However, individual study outcomes show inconsistent results. We performed a systemic analysis to aggregate information from individual trials



DOI: 10.3748/wjg.v28.i27.3514 **Copyright** ©The Author(s) 2022.

Figure 1 PRISMA Flow Diagram. EUS-BD: Endoscopic ultrasound-guided biliary drainage; PTBD: Percutaneous transhepatic biliary drainage.

and examine the overall outcomes of EUS-BD compared with PTBD. EUS-BD was associated with a lower rate of adverse events compared with PTBD. The healthcare cost of PTBD was twice that of EUS-BD due to the high reintervention rate in the PTBD group. A retrospective study by Sharaiha *et al*[28] reported that the technical success rate was comparable between PTBD and EUS-BD in patients with inoperable malignant biliary obstruction and inaccessible papilla. In a retrospective study examining patients with incurable malignant biliary obstruction with failed ERCP due to an inaccessible papilla, Bapaye *et al*[24] found that the EUS-BD group had a higher success rate of BD (92% *vs* 46%, respectively, $P > 0.05$) and a lower rate of adverse events than the PTBD group (20% *vs* 46%, respectively, $P = 0.05$) [24]. These results were partially due to the use of EUS-BD in high-volume centers by experienced endoscopists. The rates of success and the complications of EUS-BD are expected to improve with technical advances.

In the present systematic review, the only randomized controlled study comparing EUS-BD and PTBD in patients with inoperable malignant biliary blockage was conducted by Artifon *et al*[8]. The study, which included 13 patients in the EUS-BD group and 12 patients in the PTBD group, reported that EUS-BD and PTBD were comparable in terms of cost, adverse events, and clinically meaningful improvements in bilirubin levels. The bilirubin levels in the EUS-BD group declined from 16.4 μmol/L to 3.3 μmol/L, whereas the bilirubin levels in the PTBD group declined from 17.2 μmol/L to 3.3 μmol/L [8]. The postprocedural follow-up period was 7 d in both the groups. Choi *et al*[32] reported a higher technical success rate in the PTBD group than in the EUS-BD group, although the functional success rate was comparable between the two groups[35].

In most facilities, PTBD is used as an alternative technique in cases of failed ERCP. In high-volume clinics, endoscopic ultrasound-guided gallbladder drainage has begun replacing PTBD, which was developed only a decade ago as the fourth approach for biliary decompression after surgical drainage, percutaneous transhepatic drainage, and endoscopic transpapillary drainage[36]. Although the type of BD approach used in cases of failed ERCP is currently determined by local competence, EUS-BD is a less intrusive and more physiologic technique. This approach improves nutrition absorption, prevents electrolyte loss, reduces reinterventions, and eliminates the stress of external drainage[37]. EUS-BD can also be performed in a single setting before ERCP if the patient agrees.

However, EUS-BD is associated with several specific issues. Only a small number of centers have the operational skills to perform EUS-BD, whereas most centers have extensive experience and skills to perform PTBD, and interventional radiologists are well-trained and equipped to perform PTBD[25]. The inherent risk of advanced endoscopy necessitates specialized training. Therefore, EUS-BD can only be performed in high-volume treatment institutions with adequate interventional radiology and surgical backup to prevent complications such as bile leak, pneumoperitoneum, hemorrhage, and stent migration[38,39].

The invasion of the sterile biliary tree by transmural puncture from the luminal side of the gastrointestinal tract poses a modest theoretical risk of infection in EUS-BD[40]. However, such negative events should improve with the further evolution of this technique. Despite its classification as a rescue

treatment for failed ERCP, primary EUS-BD is currently compared with ERCP, and a recent study indicated similar short-term outcomes between EUS-BD and ERCP[41]. In addition, unlike ERCP, there is no risk of pancreatitis following EUS-BD. Furthermore, the clinical success rates and complications do not differ between EUS-BD and ERCP if performed by skilled endoscopists. The current systematic review revealed that EUS-BD was safe and effective when performed by skilled individuals, with a lower risk of adverse events and similar technical and clinical success rates.

Our analyses also indicated that: In patients with inoperable biliary blockage after a failed ERCP, EUS-BD was associated with a higher chance of successful BD and a lower risk of procedure-related adverse effects and infectious complications compared with PTBD. Furthermore, the number of patients with bile leaks was lower in the EUS-BD group than in the PTBD group.

CONCLUSION

Several case reports, series, and retrospective investigations regarding EUS-BD have been published to date. However, no prospective studies or comparisons of the various BD systems have been published; therefore, the technical success, functional success, adverse events, and stent patency of EUS-BD with long-term follow-up remain unknown. Prospective, randomized controlled studies are required to clarify these issues. However, it is clear that EUS-BD is clinically useful as a BD option. EUS-BD could become a first-line BD treatment instead of ERCP if the outcomes of clinical studies are positive and technologies are simplified.

ARTICLE HIGHLIGHTS

Research background

Percutaneous transhepatic cholangiography is a diagnostic and therapeutic procedure. Endoscopic ultrasound-guided biliary drainage (EUS-BD) is a novel technique that allows BD whose technicality, success rate, and outcomes are not negligible.

Research motivation

We aimed to compare the technical details and outcomes of 132 studies concerning interventional BD procedures in patients with obstructive cholangiopathy. We conducted a systematic review of six studies that met the inclusion criteria.

Research objectives

To assess the suitability and appropriability of different clinical biliary interventions in achieving optimal BD for obstructive cholangiopathy.

Research methods

An extensive systematic review was independently conducted by two investigators using an electronic search of different databases, including PubMed, Embase, clinicaltrials.gov, the Cochrane library, Scopus, and Google Scholar, using the guidelines for Preferred Reporting Items for Systematic reviews and Meta-Analyses to identify studies comparing percutaneous transhepatic BD (PTBD) and EUS-BD.

Research results

PTBD patients underwent significantly more reinterventions (4.9 *vs* 1.3), experienced more postprocedural pain (4.1 *vs* 1.9), and experienced more late adverse events (53.8% *vs* 6.6%) than EUS-BD patients. There was a significant reduction in the total bilirubin levels in both the groups (16.4-3.3 μmol/L and 17.2-3.8 μmol/L in the EUS-BD and PTBD groups, respectively; $P = 0.002$) at the postprocedural 7-d follow-up. There were no significant differences in the complication rates between the PTBD and EUS-BD groups (3.3 *vs* 3.8). PTBD was associated with a higher adverse event rate than EUS-BD in all the procedures, including reinterventions (80.4% *vs* 15.7%, respectively) and a higher rate of index procedure (39.2% *vs* 18.2%, respectively).

Research conclusions

EUS-BD might be considered as a first-line BD treatment instead of PTBD if the outcomes of clinical studies are favorable and the technical approach is simplified.

Research perspectives

EUS-BD following failed ERCP was superior to PTBD in patients with obstructive cholangiopathy.

FOOTNOTES

Author contributions: Hassan Z contributed in study selection, data analysis, and writing of the manuscript; Gadour E contributed in study conception, analysis and interpretation of the data, and drafting of the manuscript; and all authors have approved the final manuscript.

Conflict-of-interest statement: All the authors report no relevant conflicts of interest for this article.

PRISMA 2009 Checklist statement: The authors have read the PRISMA 2009 Checklist, and the manuscript was prepared and revised according to the PRISMA 2009 Checklist.

Open-Access: This article is an open-access article that was selected by an in-house editor and fully peer-reviewed by external reviewers. It is distributed in accordance with the Creative Commons Attribution NonCommercial (CC BY-NC 4.0) license, which permits others to distribute, remix, adapt, build upon this work non-commercially, and license their derivative works on different terms, provided the original work is properly cited and the use is non-commercial. See: https://creativecommons.org/Licenses/by-nc/4.0/

Country/Territory of origin: United Kingdom

ORCID number: Zeinab Hassan 0000-0003-0703-6500; Eyad Gadour 0000-0001-5087-1611.

Corresponding Author's Membership in Professional Societies: British Society of Gastroenterology, BSG64346.

S-Editor: Wang JJ
L-Editor: A
P-Editor: Wang JJ

REFERENCES

1 **Ang TL**, Teo EK, Fock KM. EUS-guided transduodenal biliary drainage in unresectable pancreatic cancer with obstructive jaundice. *JOP* 2007; **8**: 438-443 [PMID: 17625296]
2 **Mastier C**, Valette PJ, Adham M, Mabrut JY, Glehen O, Ponchon T, Rousset P, Rode A. Complex Biliary Leaks: Effectiveness of Percutaneous Radiological Treatment Compared to Simple Leaks in 101 Patients. *Cardiovasc Intervent Radiol* 2018; **41**: 1566-1572 [PMID: 29872897 DOI: 10.1007/s00270-018-2005-1]
3 **Azeemuddin M**, Turab N Al Qamari, Chaudhry MBH, Hamid S, Hasan M, Sayani R. Percutaneous Management of Biliary Enteric Anastomotic Strictures: An Institutional Review. *Cureus* 2018; **10**: e2228 [PMID: 29713573 DOI: 10.7759/cureus.2228]
4 **DeMasi CJ**, Akdamar K, Hunter FM, Sparks RD. Percutaneous transhepatic cholangiography in the diagnosis of jaundice. *Am J Med Sci* 1967; **254**: 316-321 [PMID: 6054533 DOI: 10.1097/00000441-196709000-00006]
5 **Voegeli DR**, Crummy AB, Weese JL. Percutaneous transhepatic cholangiography, drainage, and biopsy in patients with malignant biliary obstruction. An alternative to surgery. *Am J Surg* 1985; **150**: 243-247 [DOI: 10.1016/0002-9610(85)90129-1]
6 **Komaki T**, Kitano M, Sakamoto H, Kudo M. Endoscopic ultrasonography-guided biliary drainage: evaluation of a choledochoduodenostomy technique. *Pancreatology* 2011; **11** Suppl 2: 47-51 [PMID: 21464587 DOI: 10.1159/000323508]
7 **Enochsson L**, Swahn F, Arnelo U, Nilsson M, Löhr M, Persson G. Nationwide, population-based data from 11,074 ERCP procedures from the Swedish Registry for Gallstone Surgery and ERCP. *Gastrointest Endosc* 2010; **72**: 1175-1184, 1184.e1 [PMID: 20970787 DOI: 10.1016/j.gie.2010.07.047]
8 **Artifon EL**, Sakai P, Cunha JE, Dupont A, Filho FM, Hondo FY, Ishioka S, Raju GS. Surgery or endoscopy for palliation of biliary obstruction due to metastatic pancreatic cancer. *Am J Gastroenterol* 2006; **101**: 2031-2037 [PMID: 16968509 DOI: 10.1111/j.1572-0241.2006.00764.x]
9 **Weber A**, Gaa J, Rosca B, Born P, Neu B, Schmid RM, Prinz C. Complications of percutaneous transhepatic biliary drainage in patients with dilated and nondilated intrahepatic bile ducts. *Eur J Radiol* 2009; **72**: 412-417 [PMID: 18926655 DOI: 10.1016/j.ejrad.2008.08.012]
10 **Giovannini M**, Moutardier V, Pesenti C, Bories E, Lelong B, Delpero JR. Endoscopic ultrasound-guided bilioduodenal anastomosis: a new technique for biliary drainage. *Endoscopy* 2001; **33**: 898-900 [PMID: 11571690 DOI: 10.1055/s-2001-17324]
11 **Lesmana CRA**, Gani RA, Hasan I, Sulaiman AS, Ho KY, Dhir V, Lesmana LA. Palliative Endoscopic Ultrasound Biliary Drainage for Advanced Malignant Biliary Obstruction: Should It Replace the Percutaneous Approach? *Case Rep Gastroenterol* 2019; **13**: 385-397 [PMID: 31616233 DOI: 10.1159/000502835]
12 **Kozarek RA**. Malignant jaundice. *Eur J Cancer Suppl* 2005; **3**: 183-190 [DOI: 10.1016/S1359-6349(05)80275-7]
13 **Collins D**, Penman I, Mishra G, Draganov P. EUS-guided celiac block and neurolysis. *Endoscopy* 2006; **38**: 935-939 [PMID: 16981114 DOI: 10.1055/s-2006-944734]
14 **Wiersema MJ**, Sandusky D, Carr R, Wiersema LM, Erdel WC, Frederick PK. Endosonography-guided cholangiopancreatography. *Gastrointest Endosc* 1996; **43**: 102-106 [PMID: 8635700 DOI: 10.1016/s0016-5107(06)80108-2]
15 **Giovannini M**, Dotti M, Bories E, Moutardier V, Pesenti C, Danisi C, Delpero JR. Hepaticogastrostomy by echo-endoscopy as a palliative treatment in a patient with metastatic biliary obstruction. *Endoscopy* 2003; **35**: 1076-1078 [PMID:

14648424 DOI: 10.1055/s-2003-44596]
16 **Mallery S**, Matlock J, Freeman ML. EUS-guided rendezvous drainage of obstructed biliary and pancreatic ducts: Report of 6 cases. *Gastrointest Endosc* 2004; **59**: 100-107 [PMID: 14722561 DOI: 10.1016/s0016-5107(03)02300-9]
17 **Itoi T**, Itokawa F, Sofuni A, Kurihara T, Tsuchiya T, Ishii K, Tsuji S, Ikeuchi N, Moriyasu F. Endoscopic ultrasound-guided choledochoduodenostomy in patients with failed endoscopic retrograde cholangiopancreatography. *World J Gastroenterol* 2008; **14**: 6078-6082 [PMID: 18932289 DOI: 10.3748/wjg.14.6078]
18 **Kahaleh M**, Yoshida C, Kane L, Yeaton P. Interventional EUS cholangiography: A report of five cases. *Gastrointest Endosc* 2004; **60**: 138-142 [PMID: 15229448 DOI: 10.1016/s0016-5107(04)01528-7]
19 **Chavalitdhamrong D**, Draganov PV. Endoscopic ultrasound-guided biliary drainage. *World J Gastroenterol* 2012; **18**: 491-497 [PMID: 22363114 DOI: 10.3748/wjg.v18.i6.491]
20 **Lee TH**, Choi JH, Park do H, Song TJ, Kim DU, Paik WH, Hwangbo Y, Lee SS, Seo DW, Lee SK, Kim MH. Similar Efficacies of Endoscopic Ultrasound-guided Transmural and Percutaneous Drainage for Malignant Distal Biliary Obstruction. *Clin Gastroenterol Hepatol* 2016; **14**: 1011-1019.e3 [PMID: 26748220 DOI: 10.1016/j.cgh.2015.12.032]
21 **Beller EM**, Glasziou PP, Altman DG, Hopewell S, Bastian H, Chalmers I, Gøtzsche PC, Lasserson T, Tovey D; PRISMA for Abstracts Group. PRISMA for Abstracts: reporting systematic reviews in journal and conference abstracts. *PLoS Med* 2013; **10**: e1001419 [PMID: 23585737 DOI: 10.1371/journal.pmed.1001419]
22 **Guyatt GH**, Oxman AD, Schünemann HJ, Tugwell P, Knottnerus A. GRADE guidelines: a new series of articles in the Journal of Clinical Epidemiology. *J Clin Epidemiol* 2011; **64**: 380-382 [PMID: 21185693 DOI: 10.1016/j.jclinepi.2010.09.011]
23 **Artifon EL**, Aparicio D, Paione JB, Lo SK, Bordini A, Rabello C, Otoch JP, Gupta K. Biliary drainage in patients with unresectable, malignant obstruction where ERCP fails: endoscopic ultrasonography-guided choledochoduodenostomy versus percutaneous drainage. *J Clin Gastroenterol* 2012; **46**: 768-774 [PMID: 22810111 DOI: 10.1097/MCG.0b013e31825f264c]
24 **Bapaye A**, Dubale N, Aher A. Comparison of endosonography-guided vs. percutaneous biliary stenting when papilla is inaccessible for ERCP. *United European Gastroenterol J* 2013; **1**: 285-293 [PMID: 24917973 DOI: 10.1177/2050640613490928]
25 **Khashab MA**, Valeshabad AK, Afghani E, Singh VK, Kumbhari V, Messallam A, Saxena P, El Zein M, Lennon AM, Canto MI, Kalloo AN. A comparative evaluation of EUS-guided biliary drainage and percutaneous drainage in patients with distal malignant biliary obstruction and failed ERCP. *Dig Dis Sci* 2015; **60**: 557-565 [PMID: 25081224 DOI: 10.1007/s10620-014-3300-6]
26 **Giovannini M**. Learning in therapeutic EUS. *Endosc Ultrasound* 2021; **10**: 317-318 [PMID: 34677158 DOI: 10.4103/EUS-D-21-00205]
27 **Jung Y**, Lee J, Cho JY, Kim YD, Park CG, Kim MW, Kim KJ, Kim SW. Comparison of efficacy and safety between endoscopic submucosal dissection and transanal endoscopic microsurgery for the treatment of rectal tumor. *Saudi J Gastroenterol* 2018; **24**: 115-121 [PMID: 29637919 DOI: 10.4103/sjg.SJG_440_17]
28 **Sharaiha RZ**, Kumta NA, Desai AP, DeFilippis EM, Gabr M, Sarkisian AM, Salgado S, Millman J, Benvenuto A, Cohen M, Tyberg A, Gaidhane M, Kahaleh M. Endoscopic ultrasound-guided biliary drainage versus percutaneous transhepatic biliary drainage: predictors of successful outcome in patients who fail endoscopic retrograde cholangiopancreatography. *Surg Endosc* 2016; **30**: 5500-5505 [PMID: 27129552 DOI: 10.1007/s00464-016-4913-y]
29 **Laméris JS**, Stoker J, Nijs HG, Zonderland HM, Terpstra OT, van Blankenstein M, Schütte HE. Malignant biliary obstruction: percutaneous use of self-expandable stents. *Radiology* 1991; **179**: 703-707 [PMID: 2027978 DOI: 10.1148/radiology.179.3.2027978]
30 **Smith AC**, Dowsett JF, Russell RC, Hatfield AR, Cotton PB. Randomised trial of endoscopic stenting versus surgical bypass in malignant low bileduct obstruction. *Lancet* 1994; **344**: 1655-1660 [PMID: 7996958 DOI: 10.1016/S0140-6736(94)90455-3]
31 **Nennstiel S**, Weber A, Frick G, Haller B, Meining A, Schmid RM, Neu B. Drainage-related Complications in Percutaneous Transhepatic Biliary Drainage: An Analysis Over 10 Years. *J Clin Gastroenterol* 2015; **49**: 764-770 [PMID: 25518004 DOI: 10.1097/MCG.0000000000000275]
32 **Choi JH**, Kim HW, Lee JC, Paik KH, Seong NJ, Yoon CJ, Hwang JH, Kim J. Percutaneous transhepatic versus EUS-guided gallbladder drainage for malignant cystic duct obstruction. *Gastrointest Endosc* 2017; **85**: 357-364 [PMID: 27566055 DOI: 10.1016/j.gie.2016.07.067]
33 **Irani S**, Baron TH, Grimm IS, Khashab MA. EUS-guided gallbladder drainage with a lumen-apposing metal stent (with video). *Gastrointest Endosc* 2015; **82**: 1110-1115 [PMID: 26142558 DOI: 10.1016/j.gie.2015.05.045]
34 **Teoh AY**, Binmoeller KF, Lau JY. Single-step EUS-guided puncture and delivery of a lumen-apposing stent for gallbladder drainage using a novel cautery-tipped stent delivery system. *Gastrointest Endosc* 2014; **80**: 1171 [PMID: 24830582 DOI: 10.1016/j.gie.2014.03.038]
35 **Caglar E**, Atasoy D, Tozlu M, Altınkaya E, Dogan S, Senturk H. Experience of the Endoscopists Matters in Endoscopic Retrograde Cholangiopancreatography in Billroth II Gastrectomy Patients. *Clin Endosc* 2020; **53**: 82-89 [PMID: 31476843 DOI: 10.5946/ce.2019.073]
36 **Baniya R**, Upadhaya S, Madala S, Subedi SC, Shaik Mohammed T, Bachuwa G. Endoscopic ultrasound-guided biliary drainage versus percutaneous transhepatic biliary drainage after failed endoscopic retrograde cholangiopancreatography: a meta-analysis. *Clin Exp Gastroenterol* 2017; **10**: 67-74 [PMID: 28408850 DOI: 10.2147/CEG.S132004]
37 **Holt BA**, Hawes R, Hasan M, Canipe A, Tharian B, Navaneethan U, Varadarajulu S. Biliary drainage: role of EUS guidance. *Gastrointest Endosc* 2016; **83**: 160-165 [PMID: 26215648 DOI: 10.1016/j.gie.2015.06.019]
38 **Kahaleh M**, Artifon EL, Perez-Miranda M, Gupta K, Itoi T, Binmoeller KF, Giovannini M. Endoscopic ultrasonography guided biliary drainage: summary of consortium meeting, May 7th, 2011, Chicago. *World J Gastroenterol* 2013; **19**: 1372-1379 [PMID: 23538784 DOI: 10.3748/wjg.v19.i9.1372]
39 **Kawakubo K**, Isayama H, Kato H, Itoi T, Kawakami H, Hanada K, Ishiwatari H, Yasuda I, Kawamoto H, Itokawa F, Kuwatani M, Iiboshi T, Hayashi T, Doi S, Nakai Y. Multicenter retrospective study of endoscopic ultrasound-guided biliary

drainage for malignant biliary obstruction in Japan. *J Hepatobiliary Pancreat Sci* 2014; **21**: 328-334 [PMID: 24026963 DOI: 10.1002/jhbp.27]

40 **Lakhtakia S**. Complications of diagnostic and therapeutic Endoscopic Ultrasound. *Best Pract Res Clin Gastroenterol* 2016; **30**: 807-823 [PMID: 27931638 DOI: 10.1016/j.bpg.2016.10.008]

41 **Dhir V**, Itoi T, Khashab MA, Park DH, Yuen Bun Teoh A, Attam R, Messallam A, Varadarajulu S, Maydeo A. Multicenter comparative evaluation of endoscopic placement of expandable metal stents for malignant distal common bile duct obstruction by ERCP or EUS-guided approach. *Gastrointest Endosc* 2015; **81**: 913-923 [PMID: 25484326 DOI: 10.1016/j.gie.2014.09.054]

World Journal of Gastroenterology

Submit a Manuscript: https://www.f6publishing.com

World J Gastroenterol 2022 July 21; 28(27): 3524-3531

DOI: 10.3748/wjg.v28.i27.3524

ISSN 1007-9327 (print) ISSN 2219-2840 (online)

CASE REPORT

Isolated gastric variceal bleeding related to non-cirrhotic portal hypertension following oxaliplatin-based chemotherapy: A case report

Xu Zhang, Yan-Ying Gao, De-Zhao Song, Bao-Xin Qian

Specialty type: Medicine, general and internal

Provenance and peer review: Unsolicited article; Externally peer reviewed.

Peer-review model: Single blind

Peer-review report's scientific quality classification

Grade A (Excellent): 0
Grade B (Very good): B, B
Grade C (Good): C
Grade D (Fair): D
Grade E (Poor): 0

P-Reviewer: Dambrauskas Z, Lithuania; Fiorentini G, Italy; Yeoh SW, Australia; Yoshida H, Japan

Received: December 26, 2021
Peer-review started: December 26, 2021
First decision: April 16, 2022
Revised: April 27, 2022
Accepted: June 26, 2022
Article in press: June 26, 2022
Published online: July 21, 2022

Xu Zhang, Yan-Ying Gao, Department of Gastroenterology and Hepatology, The Third Central Hospital of Tianjin; Tianjin Key Laboratory of Extra-corporeal Life Support for Critical Diseases; Artificial Cell Engineering Technology Research Center; Tianjin Institute of Hepatobiliary Disease, Tianjin 300000, China

De-Zhao Song, Department of Interventional Radiology, The Third Central Hospital of Tianjin; Tianjin Key Laboratory of Extracorporeal Life Support for Critical Diseases; Artificial Cell Engineering Technology Research Center; Tianjin Institute of Hepatobiliary Disease, Tianjin 300000, China

Bao-Xin Qian, Department of Gastroenterology and Hepatology, The Third Central Hospital of Tianjin; Tianjin Key Laboratory of Extracorporeal Life Support for Critical Diseases; Artificial Cell Engineering Technology Research Center; Tianjin Institute of Hepatobiliary Disease, Tianjin 300000, China

Corresponding author: Bao-Xin Qian, MD, Attending Doctor, Department of Gastroenterology and Hepatology, The Third Central Hospital of Tianjin; Tianjin Key Laboratory of Extracorporeal Life Support for Critical Diseases; Artificial Cell Engineering Technology Research Center; Tianjin Institute of Hepatobiliary Disease, No. 83 Jintang Road, Hedong District, Tianjin 300000, China. baoxinqian@126.com

Abstract

BACKGROUND

Sinusoidal obstruction syndrome has been reported after oxaliplatin-based chemotherapy, but liver fibrosis and non-cirrhotic portal hypertension (NCPH) are rarely reported.

CASE SUMMARY

Here, we describe the case of a 64-year-old woman who developed isolated gastric variceal bleeding 16 mo after completing eight cycles of oxaliplatin combined with capecitabine chemotherapy after colon cancer resection. Surprisingly, splenomegaly and thrombocytopenia were not accompanied by variceal bleeding, which has been reported to have predictive value for gastric variceal formation. However, a liver biopsy showed fibrosis in the portal area, suggesting NCPH. The patient underwent endoscopic treatment and experienced no further symptoms.

CONCLUSION
It is necessary to guard against long-term complications after oxaliplatin-based chemotherapy. Sometimes splenic size and platelet level may not always accurately predict the occurrence of portal hypertension.

Key Words: Non-cirrhotic portal hypertension; Sinusoidal obstruction syndrome; Isolated gastric varices; Oxaliplatin chemotherapy; Colon cancer; Case report

©The Author(s) 2022. Published by Baishideng Publishing Group Inc. All rights reserved.

Core Tip: The occurrence of portal hypertension after oxaliplatin chemotherapy is mostly considered to be related to sinusoidal obstruction syndrome, and few studies clearly support non-cirrhotic portal hypertension (NCPH). We present a case of isolated gastric variceal bleeding after oxaliplatin chemotherapy. The pathological results support NCPH.

Citation: Zhang X, Gao YY, Song DZ, Qian BX. Isolated gastric variceal bleeding related to non-cirrhotic portal hypertension following oxaliplatin-based chemotherapy: A case report. *World J Gastroenterol* 2022; 28(27): 3524-3531
URL: https://www.wjgnet.com/1007-9327/full/v28/i27/3524.htm
DOI: https://dx.doi.org/10.3748/wjg.v28.i27.3524

INTRODUCTION

The third-generation platinum anticancer drug, oxaliplatin, is often used in combination with 5-fluorouracil or capecitabine as one of the main chemotherapy strategies for neoadjuvant/adjuvant treatment of stage III and metastatic colon cancer[1]. Oxaliplatin can induce different degrees of liver injury, from mild to acute liver failure, and sinusoidal obstruction syndrome (SOS) is a characteristic manifestation. In addition, chronic injury from endothelial cell damage and architectural distortion may develop nodular regenerative hyperplasia (NRH) and non-cirrhotic portal hypertension (NCPH) years after chemotherapy[2]. As a result, there are manifestations of portal hypertension, such as splenomegaly, thrombocytopenia, ascites, and esophagogastric varices. Since these complications occur long after chemotherapy completion, clinicians may not attribute these findings to oxaliplatin. Here, we report the case of a 64-year-old woman who was treated with eight cycles of oxaliplatin combined with capecitabine after radical resection of the right colon for ascending colon cancer. Isolated gastric variceal bleeding was diagnosed and treated endoscopically, but there was no obvious accompanying splenomegaly, thrombocytopenia, or broadened portal vein. The liver biopsy was indicative of NCPH.

CASE PRESENTATION

Chief complaints

A 64-year-old woman was transferred to our hospital on account of hematemesis and melena.

History of present illness

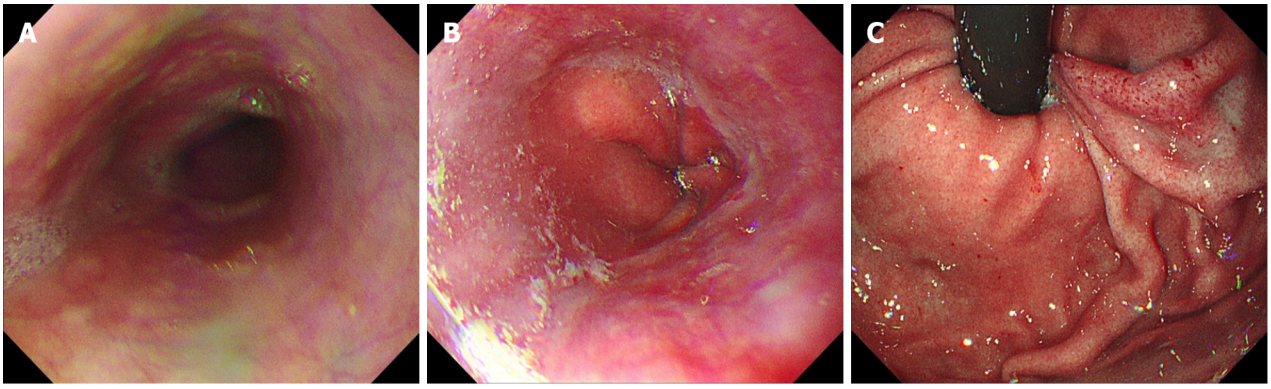
The patient complained of hematemesis and melena 2 d prior to presentation. She underwent hemostasis and rehydration at the previous hospital. Colonoscopy and gastroscopy were successively performed, and severe gastric varices were found before administration.

History of past illness

Laparoscopic radical resection of right colon cancer had been performed 16 mo earlier due to ascending colon cancer (pT4N2Mx). Preoperative gastroscopy did not show any abnormalities (Figure 1). She received eight cycles of oxaliplatin combined with capecitabine for 6 mo postoperatively. No tumor recurrence was found after intermittent re-examination.

Personal and family history

The patient had no known history of liver disease. She had no history of habitual use of alcohol and no significant history of exposure to liver injury-inducing drugs other than chemotherapy.



DOI: 10.3748/wjg.v28.i27.3524 **Copyright** ©The Author(s) 2022.

Figure 1 Gastroscopic images taken before colon cancer surgery. A: Upper esophageal segment; B: Lower esophageal segment; C: The gastric fundus. No varices were found.

Physical examination

The patient's temperature was 36.6°C, heart rate was 93 bpm, respiratory rate was 16 breaths per minute, blood pressure was 125/65 mmHg, and oxygen saturation in room air was 98%. The patient had an anemic appearance and pale palpebral conjunctiva. No signs of chronic liver disease, such as palmar erythema and spider nevus, were found. No significant enlargement of the liver or spleen was detected on palpation.

Laboratory examinations

Blood examination indicated severe anemia with normal levels of leukocytes and platelets. Prothrombin time was normal with a slight increase in plasma D-dimer level. Liver function test indicated mild hypoproteinemia with normal transaminase and bilirubin levels; renal function was normal. Liver tests were negative for hepatitis viruses; autoimmune liver diseases; and metabolic liver diseases, such as hepatolenticular degeneration and hemochromatosis (Table 1).

Imaging examinations

An enhanced computed tomography (CT) scan of the abdomen and pelvis showed postoperative changes of the colon, an irregular liver contour, slightly enlarged spleen, low-grade fatty liver, and varices in the gastric fundus with gastro-renal shunting (Figure 2). Contrast-enhanced ultrasonography showed that the size of the spleen was 4.2 cm × 11.2 cm. The diameter of the retropancreatic splenic vein was 0.67 cm with a mean blood flow velocity of 33.0 cm/s and volume flow of 528.7 mL/min.

Pathological examination

A transjugular liver biopsy was performed, and the hepatic venous pressure gradient (HVPG, wedged hepatic venous pressure – free hepatic venous pressure) was measured as 15 mmHg. Liver biopsy showed that the hepatic lobule was essentially complete with sinusoidal dilatation, and no pseudolobular formation was observed. Hepatocyte nuclear size slightly varied. Focal perisinusoidal fibrosis could be observed in the hepatic central vein area, which showed a diffuse distribution of necrotic hepatocytes engulfed by phagocytes. There were slight inflammatory reactions in hepatic portal areas, with slight fibrosis in the interstitium and around the bile duct. The vascular wall of the portal vein was thickened, indicating portal hypertension, and the final pathological diagnosis considered NCPH (Figure 3).

FINAL DIAGNOSIS

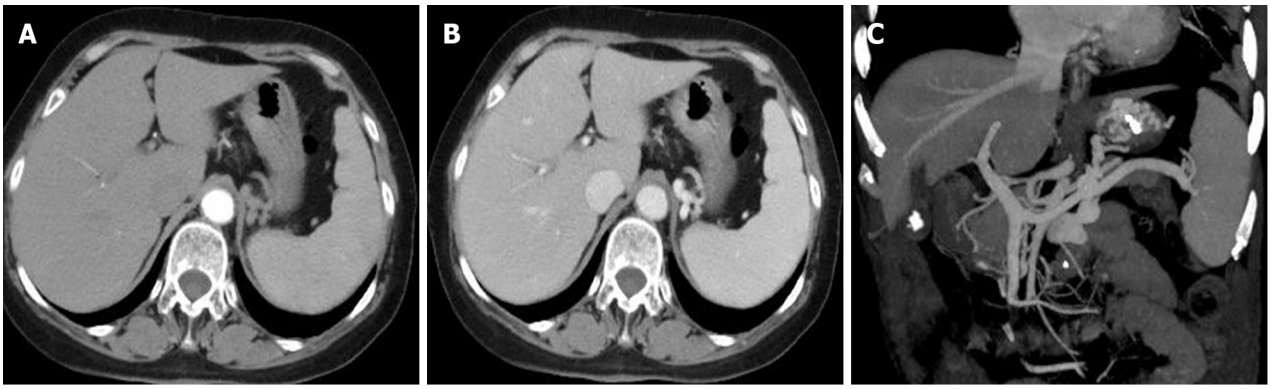
The final diagnosis of the presented case was NCPH due to oxaliplatin.

TREATMENT

After admission, the patient was immediately administered with octreotide (50 μg/h, iv, for 72 h), proton pump inhibitor, omeprazole (8 mg/h, iv, for 72 h), and hemocoagulase. An erythrocyte suspension of volume, 400 mL, was transfused. Gastroscopy after cessation of active gastrointestinal bleeding revealed severe isolated gastric varices in the fundus of the stomach, Lg-f, F3, Cb, and RC2

Table 1 Clinical indicators

Routine examination		Biochemical examination		Immune examination	
White blood count	11.95 x 10^9/L	Alaninetransaminase	1831 U/L	Hepatitis B surface antigen	(-)
Red blood count	1.9 x 10^{12}/L	Aspartate transaminase	31 U/L	Hepatitis C antibody	(-)
Hemoglobin	60 g/L	Alkaline phosphatase	103 U/L	Antinuclear antibody	(-)
Platelet	171 x 10^9/L	Gamma glutamyl transpeptidase	29 U/L	Antimitochondrial antibody	(-)
Prothrombin time	14.3 s	Total bilirubin	12.0 mmol/L	Immunoglobulin G	(-)
International standard ratio	1.12	Direct bilirubin	1.2 mmol/L	Immunoglobulin M	(-)
D-dimer	4.38 mg/L	Albumin	33.7 g/L	Immunoglobulin G4	(-)
		Globulose	29.3 g/L		
		Serum creatinine	82 mmol/L		
		Potassium	3.58 mmol/L		
		Ferritin	(-)		
		Ceruloplasmin	(-)		



DOI: 10.3748/wjg.v28.i27.3524 **Copyright** ©The Author(s) 2022.

Figure 2 Abdominal enhanced computed tomography images. A: Arterial phase; B: Portal vein phase. There was no atrophy or cirrhotic features, and the liver parenchyma density was uniform; C: 3D vascular reconstruction of portal vein system. The blood flows of the portal and retropancreatic splenic veins were unobstructed without obvious widening of the inner diameters. Severe gastric fundal varices were clearly visible.

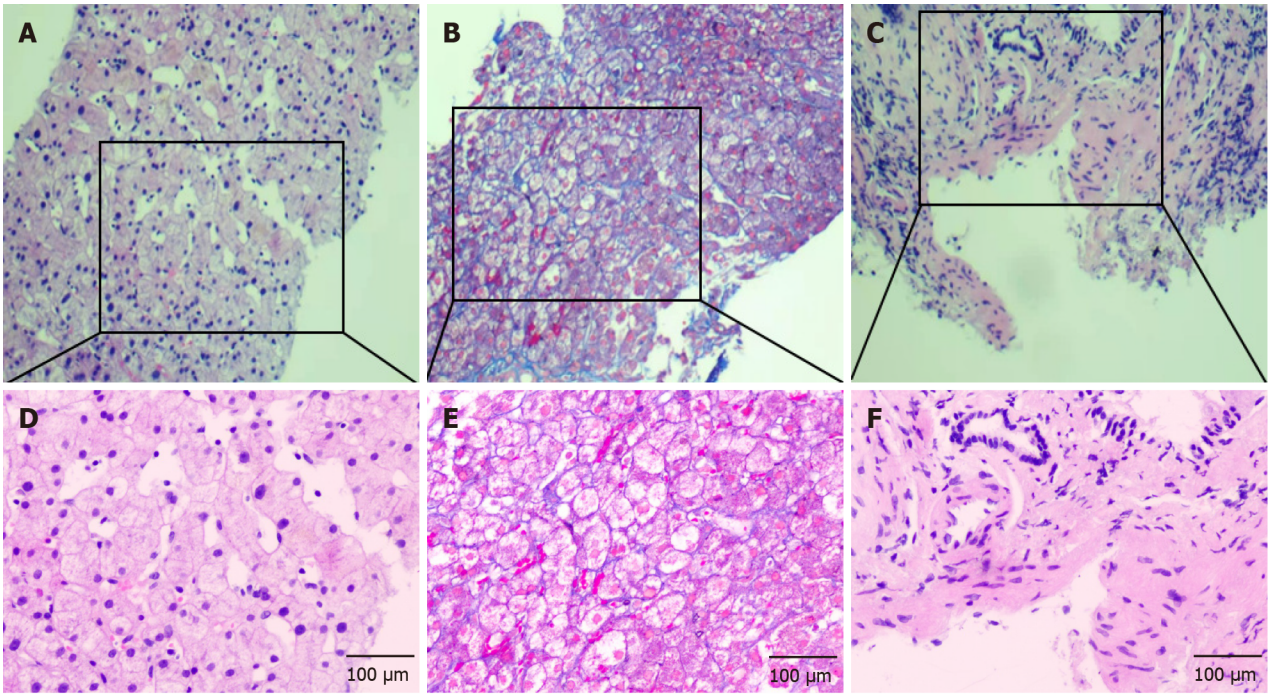
(Figure 4). Cyanoacrylate glue was injected.

OUTCOME AND FOLLOW-UP

The patient had an uneventful postoperative clinical course. Therefore, she was discharged 7 d after operation. Beta blockers were not administered because the patient' s mean heart rate was 58 ± 6 bpm. During a follow-up visit 2 mo after the operation, signs of anemia was absent and a new gastroscopy showed varices in fundus of stomach relieved obviously.

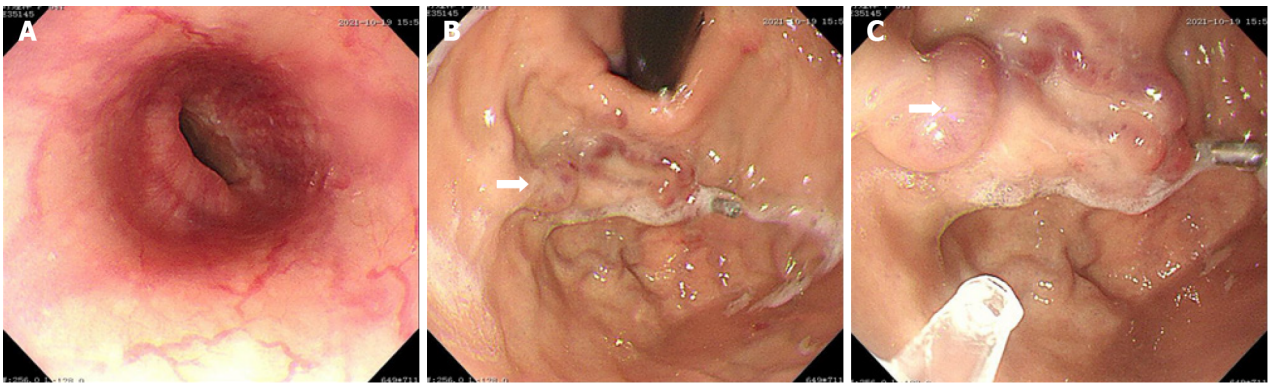
DISCUSSION

As one of the main chemotherapeutic agents for stage III and metastatic colon cancer, oxaliplatin is widely used in chemotherapy. Common side effects of oxaliplatin are neurotoxicity, gastrointestinal reactions, and hematological toxicity. In recent years, SOS has received more attention as a long-term complication of oxaliplatin use, and its reported incidence rate ranges from 19% to 52%[3,4]. SOS is an obliterative venulitis of the terminal hepatic venules, which is characterized by jaundice, right upper quadrant pain, tender hepatomegaly, ascites, and unexplained weight gain. SOS usually occurs as a result of cytoreductive therapy prior to hematopoietic stem cell transplantation. In China, it is often associated with the oral intake of plants that contain pyrrolidine alkaloids. This patient did not have any



DOI: 10.3748/wjg.v28.i27.3524 **Copyright** ©The Author(s) 2022.

Figure 3 Pathological examination images. A, D: Hematoxylin and eosin (HE) staining showed obvious sinusoidal dilatation (A: 100 ×; D: 200 ×); B, E: Masson staining showed mild peri-sinusoidal fibrosis (B: 100 ×; E: 200 ×); C, F: HE staining showed obvious portal vein wall thickening and mild fibrosis in the portal area (C: 100 ×; F: 200 ×).



DOI: 10.3748/wjg.v28.i27.3524 **Copyright** ©The Author(s) 2022.

Figure 4 Gastroscopic examination and treatment images in our hospital. A: Image showing smooth esophageal mucosa without varices; B: Isolated gastric fundus varices (white arrow); C: Cyanoacrylate glue injection (white arrow) was administered for varices after blocking blood flow with a titanium clip to prevent ectopic embolism.

significant history of exposure to liver injury-inducing drugs other than chemotherapy. Therefore, the liver damage was considered to be directly related to oxaliplatin-containing chemotherapy.

The mechanism by which oxaliplatin causes hepatic sinusoidal injury is relatively clear. The inflammation caused by oxaliplatin can increase the expression of many cytokines and chemokines[5], leading to atrophy and apoptosis of hepatocytes around the hepatic sinusoids, which decreases the supporting capacity. Oxidative stress[6] and glutathione depletion[7] caused by oxaliplatin metabolism could destroy the integrity and permeability of liver sinusoidal endothelial cells (LSECs). Necrotic LSECs and red blood cells can then form emboli with platelets, which causes obstruction and expansion of the hepatic sinusoids, leading to SOS. LSECs produce cytokines and inflammatory factors, such as interleukin-6, platelet-derived growth factor, tissue inhibitor of metalloproteinase, matrix metalloproteinases, and vascular endothelial growth factor. These activate hepatic stellate cells to increase collagen levels in the extracellular matrix, ultimately leading to hepatic fibrosis[8] that can progress to NRH, NCPH, and portal sclerosis in subsequent years.

In the pathological examination of our patient, there was an obvious expansion of the hepatic sinusoids with fibrosis in the hepatic sinusoids and portal areas. The lack of typical SOS manifestations, such as intrasinusoidal hemorrhage, thrombosis, and obstruction, suggested NCPH. This pathological manifestation was similar to that described by Ryuta *et al*[9]. In that case, esophageal and gastric varices were found 3.5 years after the termination of oxaliplatin-based chemotherapy, compared to 16 mo in this report. Both patients developed long-term portal complications after chemotherapy completion. Vigano *et al*[10] analyzed liver injury reversibility after the interruption of chemotherapy and reported that SOS may resolve within 9 mo. Therefore, we suspected that the sinusoidal injury in this patient was not enough to cause typical clinical presentations of SOS, which had gradually recovered after chemotherapy termination. However, fibrosis persisted in the hepatic sinusoids and portal areas, resulting in portal hypertension and severe gastric variceal bleeding.

NCPH etiology can be divided into five groups: infection, immune disorders, thrombophilia, genetic defect, and exposure history of drugs or poisons[11]. Currently, drugs that can reportedly induce NCPH include difenoxin, azathioprine, mercaptopurine, and allopurinol[12,13]. A recent study proposed that oxaliplatin is related to NCPH[2]. The main clinical manifestations of NCPH are esophagogastric varices, splenomegaly, thrombocytopenia, and ascites, with the first being the most common[14]. Park *et al*[15] investigated the predictors of portal hypertension formation related to oxaliplatin use and found that noninvasive fibrosis prediction models including, the age-platelet index, aspartate aminotransferase-to-platelet ratio index, platelet-to-spleen ratio, and fibrosis-4 score, have good predictive values. Satta *et al*[16] reported that platelet count and spleen index under CT correlated with esophagogastric variceal formation. These indicators are often used to screen whether patients need gastroscopy because they are easily obtained. However, in this case, the patient had severe isolated gastric varices accompanied by gastro-renal shunting. No obvious increase in splenic volume or thrombocytopenia during or after chemotherapy was observed, and no widening of the portal vein was observed on enhanced CT, which was different from common esophagogastric varices related to oxaliplatin. These findings exemplify why diagnoses may be missed. Apparently, gastroscopy was not performed during follow-up after surgery and chemotherapy, which is why the varices were not discovered until bleeding occurred.

Notably, NCPH is considered as pre-sinusoidal portal hypertension. Therefore, HVPG in patients with NCPH may not exactly reflect portal hypertension with measurements lower than those in patients with liver cirrhosis. A retrospective study reported that the average HVPG of patients with NCPH was 8.3 ± 4.5 mmHg, 60% of patients had normal or slightly elevated HVPG (≤ 10 mmHg), and 40% of patients had HVPG > 11 mmHg[14]. The HVPG level in our patient was 15 mmHg, which was significantly higher than normal, possibly due to hepatic sinusoidal injury and peri-sinusoidal fibrosis.

Ligation and cyanoacrylate glue injection under gastroscopy are the first-line treatment options for esophageal and gastric variceal bleeding in liver cirrhosis[17], but whether they are appropriate for esophageal and gastric variceal bleeding related to NCPH remains controversial. A previous study reported that the effect of endoscopic therapy in preventing variceal rebleeding in patients with NCPH is not ideal, compared to its effect in preventing hepatitis B cirrhosis-related portal hypertension[18]. Due to good functional liver reserve in patients with NCPH, transjugular intrahepatic portosystemic shunt (TIPS) treatment has a lower rebleeding rate, and the incidence and mortality of postoperative hepatic encephalopathy are lower[19]. For these reasons, TIPS may be used as the first-line treatment for esophageal and gastric variceal bleeding due to NCPH.

However, this report describes a patient with NCPH who underwent colon cancer resection. Therefore, it is necessary to guard against the possibility of malignant tumor recurrence and maintain good liver function, in case reoperation and additional chemotherapy rounds are required. Liver compensation ability may decrease after TIPS treatment. Instead, gastroscopic therapy was performed with successful cyanoacrylate glue injection, and the patient was discharged.

CONCLUSION

Oxaliplatin can cause hepatic sinusoidal injury and SOS, which could lead to portal hypertension years later. Splenomegaly and thrombocytopenia have a certain predictive value for SOS occurrence in patients who previously received chemotherapy, but few unique cases remain in the clinic. The formation of esophageal and gastric varices is the only manifestation of portal hypertension; therefore, these patients are likely to be misdiagnosed. Therefore, gastroscopy should be considered as part of follow-up after oxaliplatin-based chemotherapy.

FOOTNOTES

Author contributions: Zhang X and Gao YY contributed equally to this article; Zhang X and Gao YY contributed to writing-original draft preparation; Song DZ contributed to performing transjugular liver biopsy; and Qian BX contributed to writing-reviewing and editing.

Supported by Tianjin Science and Technology Plan Project, No. 19ZXDBSY00030.

Informed consent statement: The legal guardian of the study participant provided informed written consent prior to study enrollment.

Conflict-of-interest statement: All authors report no relevant conflicts of interest for this article.

CARE Checklist (2016) statement: The authors have read the CARE Checklist (2016), and the manuscript was prepared and revised according to the CARE Checklist (2016).

Open-Access: This article is an open-access article that was selected by an in-house editor and fully peer-reviewed by external reviewers. It is distributed in accordance with the Creative Commons Attribution NonCommercial (CC BY-NC 4.0) license, which permits others to distribute, remix, adapt, build upon this work non-commercially, and license their derivative works on different terms, provided the original work is properly cited and the use is non-commercial. See: https://creativecommons.org/Licenses/by-nc/4.0/

Country/Territory of origin: China

ORCID number: Xu Zhang 0000-0001-7399-0509; Yan-Ying Gao 0000-0001-6102-9681; De-Zhao Song 0000-0003-3405-531X; Bao-Xin Qian 0000-0001-7462-8034.

S-Editor: Ma YJ
L-Editor: A
P-Editor: Ma YJ

REFERENCES

1 **André T**, Boni C, Mounedji-Boudiaf L, Navarro M, Tabernero J, Hickish T, Topham C, Zaninelli M, Clingan P, Bridgewater J, Tabah-Fisch I, de Gramont A; Multicenter International Study of Oxaliplatin/5-Fluorouracil/Leucovorin in the Adjuvant Treatment of Colon Cancer (MOSAIC) Investigators. Oxaliplatin, fluorouracil, and leucovorin as adjuvant treatment for colon cancer. *N Engl J Med* 2004; **350**: 2343-2351 [PMID: 15175436 DOI: 10.1056/NEJMoa032709]

2 **Tavernier E**, Chalayer E, Cornillon J, Pouvaret A, Martignoles JA, Casteillo F, Terreaux J, Daguenet E, Guyotat D. Fulminant hepatitis due to very severe sinusoidal obstruction syndrome (SOS/VOD) after autologous peripheral stem cell transplantation: a case report. *BMC Res Notes* 2018; **11**: 436 [PMID: 29970140 DOI: 10.1186/s13104-018-3533-0]

3 **Rubbia-Brandt L**, Audard V, Sartoretti P, Roth AD, Brezault C, Le Charpentier M, Dousset B, Morel P, Soubrane O, Chaussade S, Mentha G, Terris B. Severe hepatic sinusoidal obstruction associated with oxaliplatin-based chemotherapy in patients with metastatic colorectal cancer. *Ann Oncol* 2004; **15**: 460-466 [PMID: 14998849 DOI: 10.1093/annonc/mdh095]

4 **Rubbia-Brandt L**, Lauwers GY, Wang H, Majno PE, Tanabe K, Zhu AX, Brezault C, Soubrane O, Abdalla EK, Vauthey JN, Mentha G, Terris B. Sinusoidal obstruction syndrome and nodular regenerative hyperplasia are frequent oxaliplatin-associated liver lesions and partially prevented by bevacizumab in patients with hepatic colorectal metastasis. *Histopathology* 2010; **56**: 430-439 [PMID: 20459550 DOI: 10.1111/j.1365-2559.2010.03511.x]

5 **Robinson SM**, Mann J, Vasilaki A, Mathers J, Burt AD, Oakley F, White SA, Mann DA. Pathogenesis of FOLFOX induced sinusoidal obstruction syndrome in a murine chemotherapy model. *J Hepatol* 2013; **59**: 318-326 [PMID: 23624001 DOI: 10.1016/j.jhep.2013.04.014]

6 **Takada S**, Miyashita T, Yamamoto Y, Kanou S, Munesue S, Ohbatake Y, Nakanuma S, Okamoto K, Sakai S, Kinoshita J, Makino I, Nakamura K, Tajima H, Takamura H, Ninomiya I, Fushida S, Ohta T. Soluble Thrombomodulin Attenuates Endothelial Cell Damage in Hepatic Sinusoidal Obstruction Syndrome. *In Vivo* 2018; **32**: 1409-1417 [PMID: 30348695 DOI: 10.21873/invivo.11393]

7 **Vreuls CP**, Olde Damink SW, Koek GH, Winstanley A, Wisse E, Cloots RH, van den Broek MA, Dejong CH, Bosman FT, Driessen A. Glutathione S-transferase M1-null genotype as risk factor for SOS in oxaliplatin-treated patients with metastatic colorectal cancer. *Br J Cancer* 2013; **108**: 676-680 [PMID: 23287989 DOI: 10.1038/bjc.2012.590]

8 **Rubbia-Brandt L**, Tauzin S, Brezault C, Delucinge-Vivier C, Descombes P, Dousset B, Majno PE, Mentha G, Terris B. Gene expression profiling provides insights into pathways of oxaliplatin-related sinusoidal obstruction syndrome in humans. *Mol Cancer Ther* 2011; **10**: 687-696 [PMID: 21330458 DOI: 10.1158/1535-7163.MCT-10-1072]

9 **Shigefuku R**, Watanabe T, Mizukami T, Matsunaga K, Hattori N, Ehira T, Suzuki T, Nakano H, Sato Y, Matsuo Y, Nakahara K, Ikeda H, Matsumoto N, Tsuda T, Katayama M, Koizumi S, Okuse C, Suzuki M, Otsubo T, Nakajima TE, Yasuda H, Itoh F. Esophagogastric varices were diagnosed in a non-cirrhotic liver case during long-term follow-up after oxaliplatin-based chemotherapy. *Clin J Gastroenterol* 2018; **11**: 487-492 [PMID: 29948819 DOI: 10.1007/s12328-018-0873-1]

10 **Vigano L**, De Rosa G, Toso C, Andres A, Ferrero A, Roth A, Sperti E, Majno P, Rubbia-Brandt L. Reversibility of chemotherapy-related liver injury. *J Hepatol* 2017; **67**: 84-91 [PMID: 28284915 DOI: 10.1016/j.jhep.2017.02.031]

11 **Schouten JN**, Garcia-Pagan JC, Valla DC, Janssen HL. Idiopathic noncirrhotic portal hypertension. *Hepatology* 2011; **54**: 1071-1081 [PMID: 21574171 DOI: 10.1002/hep.24422]

12 **Cachay ER**, Peterson MR, Goicoechea M, Mathews WC. Didanosine Exposure and Noncirrhotic Portal Hypertension in a HIV Clinic in North America: a Follow-up Study. *Br J Med Med Res* 2011; **1**: 346-355 [PMID: 22268001 DOI: 10.9734/bjmmr/2011/554]

13 **Seinen ML**, van Asseldonk DP, de Boer NK, Bouma G, van Nieuwkerk CM, Mulder CJ, Bloemena E, van Bodegraven AA. Nodular Regenerative Hyperplasia of the Liver in Patients with IBD Treated with Allopurinol-Thiopurine Combination Therapy. *Inflamm Bowel Dis* 2017; **23**: 448-452 [PMID: 28151736 DOI: 10.1097/MIB.0000000000001036]

14 **Siramolpiwat S**, Seijo S, Miquel R, Berzigotti A, Garcia-Criado A, Darnell A, Turon F, Hernandez-Gea V, Bosch J, Garcia-Pagán JC. Idiopathic portal hypertension: natural history and long-term outcome. *Hepatology* 2014; **59**: 2276-2285 [PMID: 24155091 DOI: 10.1002/hep.26904]

15 **Park S**, Kim HY, Kim H, Park JH, Kim JH, Kim KH, Kim W, Choi IS, Jung YJ, Kim JS. Changes in Noninvasive Liver Fibrosis Indices and Spleen Size During Chemotherapy: Potential Markers for Oxaliplatin-Induced Sinusoidal Obstruction Syndrome. *Medicine (Baltimore)* 2016; **95**: e2454 [PMID: 26765438 DOI: 10.1097/MD.0000000000002454]

16 **Satta Y**, Shigefuku R, Watanabe T, Mizukami T, Tsuda T, Suzuki T, Ehira T, Hattori N, Kiyokawa H, Nakahara K, Ikeda H, Matsunaga K, Takahashi H, Matsumoto N, Okuse C, Suzuki M, Sunakawa Y, Yasuda H, Itoh F. Prediction of esophagogastric varices associated with oxaliplatin administration. *JGH Open* 2021; **5**: 1289-1297 [PMID: 34816015 DOI: 10.1002/jgh3.12668]

17 **He FL**, Qi RZ, Zhang YN, Zhang K, Zhu-Ge YZ, Wang M, Wang Y, Jia JD, Liu FQ. Transjugular intrahepatic portosystemic shunt and splenectomy are more effective than endoscopic therapy for recurrent variceal bleeding in patients with idiopathic noncirrhotic portal hypertension. *World J Clin Cases* 2020; **8**: 1871-1877 [PMID: 32518776 DOI: 10.12998/wjcc.v8.i10.1871]

18 **Huang X**, Li F, Wang L, Xiao M, Ni L, Jiang S, Ji Y, Zhang C, Zhang W, Wang J, Chen S. Endoscopic treatment of gastroesophageal variceal bleeding after oxaliplatin-based chemotherapy in patients with colorectal cancer. *Endoscopy* 2020; **52**: 727-735 [PMID: 32380558 DOI: 10.1055/a-1157-8611]

19 **Lv Y**, Li K, He C, Luo B, Zhang B, Liu H, Wang Z, Guo W, Wang Q, Chen H, Bai W, Yuan X, Yu T, Li X, Yuan J, Han N, Zhu Y, Niu J, Xie H, Wang J, Chen L, Yin Z, Fan D, Li Z, Han G. TIPSS for variceal bleeding in patients with idiopathic non-cirrhotic portal hypertension: comparison with patients who have cirrhosis. *Aliment Pharmacol Ther* 2019; **49**: 926-939 [PMID: 30820990 DOI: 10.1111/apt.15186]

World Journal of Gastroenterology

Submit a Manuscript: https://www.f6publishing.com

World J Gastroenterol 2022 July 21; 28(27): 3532-3534

DOI: 10.3748/wjg.v28.i27.3532

ISSN 1007-9327 (print) ISSN 2219-2840 (online)

LETTER TO THE EDITOR

Hepatitis B core-related antigen: Are we near a treatment endpoint?

Tarana Gupta

Specialty type: Gastroenterology and hepatology

Provenance and peer review: Unsolicited article; Externally peer reviewed

Peer-review model: Single blind

Peer-review report's scientific quality classification

Grade A (Excellent): 0
Grade B (Very good): B
Grade C (Good): C, C, C, C
Grade D (Fair): D
Grade E (Poor): 0

P-Reviewer: Caviglia GP, Italy; Feng B, China; Tong GD, China; Yin GQ, China

Received: November 7, 2021
Peer-review started: November 7, 2021
First decision: December 12, 2021
Revised: December 25, 2021
Accepted: June 24, 2022
Article in press: June 24, 2022
Published online: July 21, 2022

Tarana Gupta, Medicine, Pandit Bhagwat Dayal Sharma Post Graduate Institute of Medical Sciences, Rohtak 124001, Haryana, India

Corresponding author: Tarana Gupta, Doctor, MBBS, MD, Professor, Medicine, Pandit Bhagwat Dayal Sharma Post Graduate Institute of Medical Sciences, House No. 1065 A Sector 1, Rohtak 124001, Haryana, India. taranagupta@gmail.com

Abstract

Different serological and virological markers in chronic hepatitis B patients guide staging of viral infection, and initiation and response to therapy. Due to the persistence of intrahepatic covalently closed circular DNA (cccDNA) in the hepatocyte nucleus, hepatitis B is not curable. Even after undetectable hepatitis B virus DNA levels, the persistence of hepatitis B surface antigen and novel markers such as hepatitis B core-related antigen (HBcrAg) indicate the persistence of intrahepatic cccDNA. In this study, HBcrAg levels at baseline and after 24 and 48 wk of antiviral therapy predicted hepatitis B e antigen seroconversion. Due to the poor sensitivity of assays and detectable levels in HBsAg-negative patients, the long-term utility of HBcrAg needs future research.

Key Words: Hepatitis B core-related antigen; Chronic hepatitis B; Covalently closed circular DNA; Hepatitis B e antigen seroconversion; Hepatitis B virus DNA; Pregenomic RNA

©The Author(s) 2022. Published by Baishideng Publishing Group Inc. All rights reserved.

Core Tip: This study highlights the predictive role of hepatitis B core-related antigen (HBcrAg) levels at baseline, and after 24 and 48 wk of antiviral therapy for hepatitis B e antigen seroconversion in chronic hepatitis B patients. The issues related to poor sensitivity of assays and detectable levels in hepatitis B surface antigen-negative patients are major concerns. Future research on the utility of HBcrAg in hepatitis B virus (HBV) flare after nucleotide cessation, occult HBV reactivation, and risk of developing hepatocellular carcinoma is also needed.

Citation: Gupta T. Hepatitis B core-related antigen: Are we near a treatment endpoint? *World J Gastroenterol* 2022; 28(27): 3532-3534
URL: https://www.wjgnet.com/1007-9327/full/v28/i27/3532.htm
DOI: https://dx.doi.org/10.3748/wjg.v28.i27.3532

TO THE EDITOR

We read with interest the study titled, "Serum hepatitis B core-related antigen as a surrogate marker of hepatitis B e antigen seroconversion in chronic hepatitis B" by Chi *et al*[1] in the World Journal of Gastroenterology. Hepatitis B core-related antigen (HBcrAg) and hepatitis B virus (HBV) RNA are potential serological markers of chronic hepatitis B infection and activity. In the HBV life cycle, intrahepatic covalently closed circular DNA (cccDNA) is transcribed into five RNAs of which pregenomic RNA is a precursor to synthesis of the viral genome by reverse transcription and precore mRNA is precursor to proteins hepatitis B core antigen. Hepatitis B e antigen (HBeAg) and p22cr are collectively called HBcrAg due to their identical 149 amino acid sequences. In addition, viral sequences also integrate in the host genome and can express hepatitis B surface antigen (HBsAg). Therefore, HBsAg quantification may not be exactly reflective of intrahepatic cccDNA levels. On the other hand, only cccDNA can express the viral genome. In real world settings, liver biopsy is not feasible for cccDNA quantification and a surrogate marker is needed in serum for intrahepatic cccDNA quantification. HBcrAg-related proteins can be detected in Dane particles, HBV DNA-negative Dane particles, and possibly in HBV RNA-containing virions[2]. Interestingly, nucleotide analogues (NAs) inhibit DNA polymerase and viral replication; they do not affect production of viral intermediate proteins such as HBcrAg. Therefore, even on antiviral treatment, HBcrAg can reflect cccDNA quantity and activity in hepatocytes.

This study determined the predictive role of HBcrAg for HBeAg seroconversion in chronic hepatitis B (CHB) patients. All patients were analyzed for HBcrAg, HBV RNA, and HBV DNA levels in blood and cccDNA quantification in liver biopsy specimen. Although there is treatment heterogeneity with two different cohorts of entecavir (n = 109) and pegylated-interferon (PEG-IFN) (n = 30) therapy, the authors found baseline HBcrAg levels correlating with cccDNA levels in patients with and without HBeAg seroconversion. However, the PEG-IFN group only had 30 patients, and as IFNs are immunomodulators that increase innate immune response in controlling HBV infection with higher HBeAg seroconversion rates compared to NA therapy, it may be premature to conclude that it only affects viral replication and not the production of other viral proteins. Therefore, some bias may be related to treatment heterogeneity.

This study also highlights that serum qHBcrAg levels at 24 and 48 wk of treatment better predict HBeAg seroconversion than qHBcrAg levels at baseline. Song *et al*[3] showed baseline HBcrAg levels < 4.9 log U/mL, > 2 log reduction of HBcrAg at week 28 having a positive predictive value 74% and 76%, and negative predictive value of 96% and 94%, respectively, for the prediction of spontaneous HBeAg seroconversion. In HBeAg-positive CHB patients, HBcrAg is high in the immune tolerant phase compared to the immune clearance phase. And in HBeAg-negative patients, lower HBcrAg levels are present in the inactive carrier state than in HBeAg-negative CHB. Recently Ghany *et al*[4] demonstrated a correlation of HBV RNA and HBcrAg levels with HBV DNA in different phases of CHB infection.

Wong *et al*[5] demonstrated that correlation coefficients of serum HBV DNA and HBcrAg with intrahepatic cccDNA are 0.7 and 0.64-0.7, respectively, which are similar; however, in patients on antiviral therapy with undetectable serum HBV DNA, HBcrAg is the preferred marker for estimating intrahepatic cccDNA levels. Tseng *et al*[6] recently showed risk stratification of development of cirrhosis, and its complications and liver-related mortality in CHB patients over a period of 15.9 years by baseline HBcrAg levels. Carey *et al*[7] showed that HBcrAg and HBV RNA predict clinical flares in HBeAg-negative CHB patients with suppressed HBV DNA levels on nucleotide analogue therapy. Together, HBcrAg is a promising novel serum marker but with many limitations. First, with current available assays, the lower limit of detection is 2 log U/mL, so more sensitive assays are needed. Second, one study found detectable serum HBcrAg in 40% patients with HBsAg seroclearance[8]. Finally, large-scale studies in different ethnic groups are needed to determine the predictive value of HBcrAg with certain cut-off values in clinical practice especially occult HBV reactivation, HBV flare after nucleotide analogue cessation, and risk of hepatocellular carcinoma development.

FOOTNOTES

Author contributions: Gupta T wrote and critically revised the manuscript.

Conflict-of-interest statement: The author has no conflicts of interest to declare.

Open-Access: This article is an open-access article that was selected by an in-house editor and fully peer-reviewed by external reviewers. It is distributed in accordance with the Creative Commons Attribution NonCommercial (CC BY-NC 4.0) license, which permits others to distribute, remix, adapt, build upon this work non-commercially, and license their derivative works on different terms, provided the original work is properly cited and the use is non-commercial. See: https://creativecommons.org/Licenses/by-nc/4.0/

Country/Territory of origin: India

ORCID number: Tarana Gupta 0000-0003-3453-2040.

S-Editor: Wang JJ
L-Editor: Filipodia
P-Editor: Wang JJ

REFERENCES

1 **Chi XM**, Wang XM, Wang ZF, Wu RH, Gao XZ, Xu HQ, Ding YH, Niu JQ. Serum hepatitis B core-related antigen as a surrogate marker of hepatitis B e antigen seroconversion in chronic hepatitis B. *World J Gastroenterol* 2021; **27**: 6927-6938 [PMID: 34790015 DOI: 10.3748/wjg.v27.i40.6927]
2 **Park Y**, Hong DJ, Shin S, Cho Y, Kim HS. Performance evaluation of new automated hepatitis B viral markers in the clinical laboratory: two quantitative hepatitis B surface antigen assays and an HBV core-related antigen assay. *Am J Clin Pathol* 2012; **137**: 770-777 [PMID: 22523216 DOI: 10.1309/AJCP8QDN7NAUXJFJ]
3 **Song G**, Yang R, Rao H, Feng B, Ma H, Jin Q, Wei L. Serum HBV core-related antigen is a good predictor for spontaneous HBeAg seroconversion in chronic hepatitis B patients. *J Med Virol* 2017; **89**: 463-468 [PMID: 27505145 DOI: 10.1002/jmv.24657]
4 **Ghany MG**, King WC, Lisker-Melman M, Lok ASF, Terrault N, Janssen HLA, Khalili M, Chung RT, Lee WM, Lau DTY, Cloherty GA, Sterling RK. Comparison of HBV RNA and Hepatitis B Core Related Antigen With Conventional HBV Markers Among Untreated Adults With Chronic Hepatitis B in North America. *Hepatology* 2021; **74**: 2395-2409 [PMID: 34133774 DOI: 10.1002/hep.32018]
5 **Wong DK**, Seto WK, Cheung KS, Chong CK, Huang FY, Fung J, Lai CL, Yuen MF. Hepatitis B virus core-related antigen as a surrogate marker for covalently closed circular DNA. *Liver Int* 2017; **37**: 995-1001 [PMID: 27992681 DOI: 10.1111/liv.13346]
6 **Tseng TC**, Liu CJ, Yang WT, Hsu CY, Hong CM, Su TH, Tsai CH, Chen CL, Yang HC, Liu CH, Chen HH, Chen PJ, Kao JH. Serum hepatitis B core-related antigen level stratifies risk of disease progression in chronic hepatitis B patients with intermediate viral load. *Aliment Pharmacol Ther* 2021; **53**: 908-918 [PMID: 33465271 DOI: 10.1111/apt.16266]
7 **Carey I**, Gersch J, Wang B, Moigboi C, Kuhns M, Cloherty G, Dusheiko G, Agarwal K. Pregenomic HBV RNA and Hepatitis B Core-Related Antigen Predict Outcomes in Hepatitis B e Antigen-Negative Chronic Hepatitis B Patients Suppressed on Nucleos(T)ide Analogue Therapy. *Hepatology* 2020; **72**: 42-57 [PMID: 31701544 DOI: 10.1002/hep.31026]
8 **Seto WK**, Wong DK, Fung J, Huang FY, Liu KS, Lai CL, Yuen MF. Linearized hepatitis B surface antigen and hepatitis B core-related antigen in the natural history of chronic hepatitis B. *Clin Microbiol Infect* 2014; **20**: 1173-1180 [PMID: 24975365 DOI: 10.1111/1469-0691.12739]



Published by **Baishideng Publishing Group Inc**
7041 Koll Center Parkway, Suite 160, Pleasanton, CA 94566, USA
Telephone: +1-925-3991568
E-mail: bpgoffice@wjgnet.com
Help Desk: https://www.f6publishing.com/helpdesk
https://www.wjgnet.com



© 2022 Baishideng Publishing Group Inc. All rights reserved.

ISSN 1007-9327 (print)
ISSN 2219-2840 (online)

World Journal of *Gastroenterology*

World J Gastroenterol 2022 July 28; 28(28): 3535-3752



Published by Baishideng Publishing Group Inc

World Journal of Gastroenterology

Contents

Weekly Volume 28 Number 28 July 28, 2022

REVIEW

3535 Peroxisome proliferator-activated receptor gamma as a therapeutic target for hepatocellular carcinoma: Experimental and clinical scenarios

Katoch S, Sharma V, Patial V

3555 Gut microbiota alteration and modulation in hepatitis B virus-related fibrosis and complications: Molecular mechanisms and therapeutic inventions

Li YG, Yu ZJ, Li A, Ren ZG

MINIREVIEWS

3573 Combination approaches in hepatocellular carcinoma: How systemic treatment can benefit candidates to locoregional modalities

da Fonseca LG, Araujo RLC

3586 Update on endoscopic ultrasound-guided liver biopsy

Rangwani S, Ardeshna DR, Mumtaz K, Kelly SG, Han SY, Krishna SG

3595 Non-alcoholic fatty liver disease-related hepatocellular carcinoma: Is there a role for immunotherapy?

Mattos ÂZ, Debes JD, Vogel A, Arrese M, Revelo X, Pase THS, Manica M, Mattos AA

3608 Potassium-competitive acid blockers and gastroesophageal reflux disease

Leowattana W, Leowattana T

3620 Making the case for multidisciplinary pediatric aerodigestive programs

Kanotra SP, Weiner R, Rahhal R

3627 Therapeutic potential of mesenchymal stem cells in the treatment of acute liver failure

Harrell CR, Pavlovic D, Djonov V, Volarevic V

3637 Effective combinations of anti-cancer and targeted drugs for pancreatic cancer treatment

Nishimoto A

ORIGINAL ARTICLE

Basic Study

3644 Mechanism of electroacupuncture and herb-partitioned moxibustion on ulcerative colitis animal model: A study based on proteomics

Qi Q, Zhong R, Liu YN, Zhao C, Huang Y, Lu Y, Ma Z, Zheng HD, Wu LY

World Journal of Gastroenterology

Weekly Volume 28 Number 28 July 28, 2022

Contents

Retrospective Study

3666 How has the disease course of pediatric ulcerative colitis changed throughout the biologics era? A comparison with the IBSEN study

Kwon Y, Kim ES, Choe YH, Kim MJ

3682 Gastric mucosal precancerous lesions in *Helicobacter pylori*-infected pediatric patients in central China: A single-center, retrospective investigation

Yu M, Ma J, Song XX, Shao QQ, Yu XC, Khan MN, Qi YB, Hu RB, Wei PR, Xiao W, Jia BL, Cheng YB, Kong LF, Chen CL, Ding SZ

Observational Study

3695 Secular trends of intrahepatic cholangiocarcinoma in a high endemic area: A population-based study

Lin CR, Lee YK, Chiang CJ, Yang YW, Chang HC, You SL

3706 Family-based *Helicobacter pylori* infection status and transmission pattern in central China, and its clinical implications for related disease prevention

Yu XC, Shao QQ, Ma J, Yu M, Zhang C, Lei L, Zhou Y, Chen WC, Zhang W, Fang XH, Zhu YZ, Wu G, Wang XM, Han SY, Sun PC, Ding SZ

SCIENTOMETRICS

3720 Global research on *Clostridium difficile*-associated diarrhoea: A visualized study

Zyoud SH

CASE REPORT

3732 Delayed immune-related sclerosing cholangitis after discontinuation of pembrolizumab: A case report

Tanaka T, Sakai A, Tsujimae M, Yamada Y, Kobayashi T, Masuda A, Kodama Y

LETTER TO THE EDITOR

3739 Prednisolone induced pneumatosis coli and pneumoperitoneum

Goh SSN, Shelat V

3743 Is patient satisfaction sufficient to validate endoscopic anti-reflux treatments?

Bortolotti M

3747 Endoluminal vacuum-assisted therapy as a treatment for anastomotic leakage in colorectal surgery

Chiarello MM, Bianchi V, Fransvea P, Brisinda G

Contents

ABOUT COVER

Editorial Board Member of *World Journal of Gastroenterology*, Giovanna Ferraioli, MD, FAIUM, Researcher, Department of Clinical Surgical, Diagnostic and Pediatric Sciences, Medical School University of Pavia, Viale Brambilla 74, Pavia 27100, Italy. giovanna.ferraioli@unipv.it

AIMS AND SCOPE

The primary aim of *World Journal of Gastroenterology* (*WJG*, *World J Gastroenterol*) is to provide scholars and readers from various fields of gastroenterology and hepatology with a platform to publish high-quality basic and clinical research articles and communicate their research findings online. *WJG* mainly publishes articles reporting research results and findings obtained in the field of gastroenterology and hepatology and covering a wide range of topics including gastroenterology, hepatology, gastrointestinal endoscopy, gastrointestinal surgery, gastrointestinal oncology, and pediatric gastroenterology.

INDEXING/ABSTRACTING

The *WJG* is now abstracted and indexed in Science Citation Index Expanded (SCIE, also known as SciSearch®), Current Contents/Clinical Medicine, Journal Citation Reports, Index Medicus, MEDLINE, PubMed, PubMed Central, Scopus, Reference Citation Analysis, China National Knowledge Infrastructure, China Science and Technology Journal Database, and Superstar Journals Database. The 2022 edition of Journal Citation Reports® cites the 2021 impact factor (IF) for *WJG* as 5.374; IF without journal self cites: 5.187; 5-year IF: 5.715; Journal Citation Indicator: 0.84; Ranking: 31 among 93 journals in gastroenterology and hepatology; and Quartile category: Q2. The *WJG*'s CiteScore for 2021 is 8.1 and Scopus CiteScore rank 2021: Gastroenterology is 18/149.

RESPONSIBLE EDITORS FOR THIS ISSUE

Production Editor: *Yu-Xi Chen*; **Production Department Director:** *Xu Guo*; **Editorial Office Director:** *Jia-Ru Fan*.

NAME OF JOURNAL
World Journal of Gastroenterology

ISSN
ISSN 1007-9327 (print) ISSN 2219-2840 (online)

LAUNCH DATE
October 1, 1995

FREQUENCY
Weekly

EDITORS-IN-CHIEF
Andrzej S Tarnawski

EDITORIAL BOARD MEMBERS
http://www.wjgnet.com/1007-9327/editorialboard.htm

PUBLICATION DATE
July 28, 2022

COPYRIGHT
© 2022 Baishideng Publishing Group Inc

INSTRUCTIONS TO AUTHORS
https://www.wjgnet.com/bpg/gerinfo/204

GUIDELINES FOR ETHICS DOCUMENTS
https://www.wjgnet.com/bpg/GerInfo/287

GUIDELINES FOR NON-NATIVE SPEAKERS OF ENGLISH
https://www.wjgnet.com/bpg/gerinfo/240

PUBLICATION ETHICS
https://www.wjgnet.com/bpg/GerInfo/288

PUBLICATION MISCONDUCT
https://www.wjgnet.com/bpg/gerinfo/208

ARTICLE PROCESSING CHARGE
https://www.wjgnet.com/bpg/gerinfo/242

STEPS FOR SUBMITTING MANUSCRIPTS
https://www.wjgnet.com/bpg/GerInfo/239

ONLINE SUBMISSION
https://www.f6publishing.com

© 2022 Baishideng Publishing Group Inc. All rights reserved. 7041 Koll Center Parkway, Suite 160, Pleasanton, CA 94566, USA

E-mail: bpgoffice@wjgnet.com https://www.wjgnet.com

World Journal of Gastroenterology

Submit a Manuscript: https://www.f6publishing.com

World J Gastroenterol 2022 July 28; 28(28): 3535-3554

DOI: 10.3748/wjg.v28.i28.3535

ISSN 1007-9327 (print) ISSN 2219-2840 (online)

REVIEW

Peroxisome proliferator-activated receptor gamma as a therapeutic target for hepatocellular carcinoma: Experimental and clinical scenarios

Swati Katoch, Vinesh Sharma, Vikram Patial

Specialty type: Gastroenterology and hepatology

Provenance and peer review: Invited article; Externally peer reviewed.

Peer-review model: Single blind

Peer-review report's scientific quality classification

Grade A (Excellent): 0
Grade B (Very good): B
Grade C (Good): C, C
Grade D (Fair): 0
Grade E (Poor): 0

P-Reviewer: Cao X, China; Cao ZF, China; Jeong KY, South Korea

Received: January 17, 2022
Peer-review started: January 17, 2022
First decision: April 11, 2022
Revised: April 25, 2022
Accepted: June 24, 2022
Article in press: June 24, 2022
Published online: July 28, 2022

Swati Katoch, Vinesh Sharma, Vikram Patial, Division of Dietetics and Nutrition Technology, Institute of Himalayan Bioresource Technology, Palampur 176061, Himachal Pradesh, India

Swati Katoch, Vinesh Sharma, Vikram Patial, Academy of Scientific and Innovative Research, Ghaziabad 201002, UP, India

Corresponding author: Vikram Patial, PhD, Senior Scientist, Division of Dietetics and Nutrition Technology, Institute of Himalayan Bioresource Technology, Palampur 176061, Himachal Pradesh, India. vikrampatial@ihbt.res.in

Abstract

Hepatocellular carcinoma (HCC) is the most common type of liver cancer worldwide. Viral hepatitis is a significant risk factor for HCC, although metabolic syndrome and diabetes are more frequently associated with the HCC. With increasing prevalence, there is expected to be > 1 million cases annually by 2025. Therefore, there is an urgent need to establish potential therapeutic targets to cure this disease. Peroxisome-proliferator-activated receptor gamma (PPARγ) is a ligand-activated transcription factor that plays a crucial role in the patho-physiology of HCC. Many synthetic agonists of PPARγ suppress HCC in experimental studies and clinical trials. These synthetic agonists have shown promising results by inducing cell cycle arrest and apoptosis in HCC cells and preventing the invasion and metastasis of HCC. However, some synthetic agonists also pose severe side effects in addition to their therapeutic efficacy. Thus natural PPARγ agonists can be an alternative to exploit this potential target for HCC treatment. In this review, the regulatory role of PPARγ in the pathogenesis of HCC is elucidated. Furthermore, the experimental and clinical scenario of both synthetic and natural PPARγ agonists against HCC is discussed. Most of the available literature advocates PPARγ as a potential therapeutic target for the treatment of HCC.

Key Words: Anticancer; Hepatocellular carcinoma; Natural agonists; Peroxisome proliferator-activated receptor-γ; Thiazolidinediones

©The Author(s) 2022. Published by Baishideng Publishing Group Inc. All rights reserved.

Core Tip: Hepatocellular carcinoma (HCC) is the most common type of liver cancer worldwide. Viral infections and metabolic syndrome are the major risk factors for HCC, and its incidence is expected to increase to > 1 million cases annually by 2025. The crucial role of peroxisome-proliferator-activated receptor gamma (PPARγ) in HCC pathophysiology makes it a potential therapeutic target. Along with synthetic agonists, natural PPARγ agonists provide alternative and safer options for HCC treatment; however, they need to be validated clinically. This review discusses the regulatory role of PPARγ in HCC pathogenesis and experimental and clinical scenarios of PPARγ agonists in HCC treatment.

Citation: Katoch S, Sharma V, Patial V. Peroxisome proliferator-activated receptor gamma as a therapeutic target for hepatocellular carcinoma: Experimental and clinical scenarios. *World J Gastroenterol* 2022; 28(28): 3535-3554
URL: https://www.wjgnet.com/1007-9327/full/v28/i28/3535.htm
DOI: https://dx.doi.org/10.3748/wjg.v28.i28.3535

INTRODUCTION

Liver cancer is the sixth most common cause of cancer-related death worldwide, with a higher prevalence in men than women. Hepatocellular carcinoma (HCC) incidence was expected to increase to > 1 million individuals annually by 2025[1]. HCC, a primary subtype of liver cancer, primarily occurs in Asia and Africa due to the high prevalence of hepatitis B virus (HBV), hepatitis C virus, and diabetes [2]. These conditions are linked to the inflammatory response in the liver, leading to the development of HCC. Furthermore, other conditions such as obesity, dietary mycotoxin exposure, and excessive alcohol consumption are also among the risk factors for the development of HCC. These factors lead to the development of cirrhosis in 70%-80% of HCC patients. Liver transplantation is currently the best option for curing HCC, but there is a limitation to the availability of donors[3]. During the last two decades, the understanding and management of HCC have changed dramatically due to the extensive basic and clinical research, which may further help to reveal potential targets for the treatment of HCC. Sorafenib is the first-line defense therapy approved by the United States food and Drug Administration (FDA) for the advanced stages of HCC. It is a type of multikinase inhibitor that shows tumor-suppressing activity *via* targeting vascular endothelial growth factor receptor, adenosine monophosphate-activated protein kinase (AMPK), and platelet-derived growth factor receptor[4]. Apart from their therapeutic potential, sorafenib shows acquired resistance in HCC cells. The low response rate indicates that patients sensitive to sorafenib during the treatment will develop resistance within 6 mo. These negative impacts of approved drugs prompted many researchers to find novel drugs or targets to cure HCC[5].

Peroxisome proliferator-activated receptor gamma (PPARγ) is a ligand-activated nuclear receptor activated by synthetic and natural agonists[6]. It is highly expressed in adipose tissue, where it plays a central role in regulating adipose tissue function. Many studies have established the role of PPARγ in the pathophysiology of HCC. *In vitro* and *in vivo* data have shown the inhibitory role of PPARγ activation in tumor cell growth, migration, and invasion suggesting its therapeutic role in the growth regulation of HCC[7,8]. The antitumor effects of PPARγ are fulfilled by various mechanisms, including the induction of cell cycle arrest and activation of genes/proteins involved in immune and inflammatory responses[9]. Previous reports have revealed the mechanism underlying the development of HCC and suggested the presence of PPARγ in human HCC tissues, which shows a dose-dependent decrease in the growth of HCC cell lines[10]. Thus, molecules modulating PPARγ signaling pathways will provide a novel solution for the effective treatment of HCC. This review focuses on the role of PPARγ in the HCC pathophysiology and the experimental and clinical status of PPARγ agonists in the treatment of HCC.

MOLECULAR ARRANGEMENT OF PPARγ

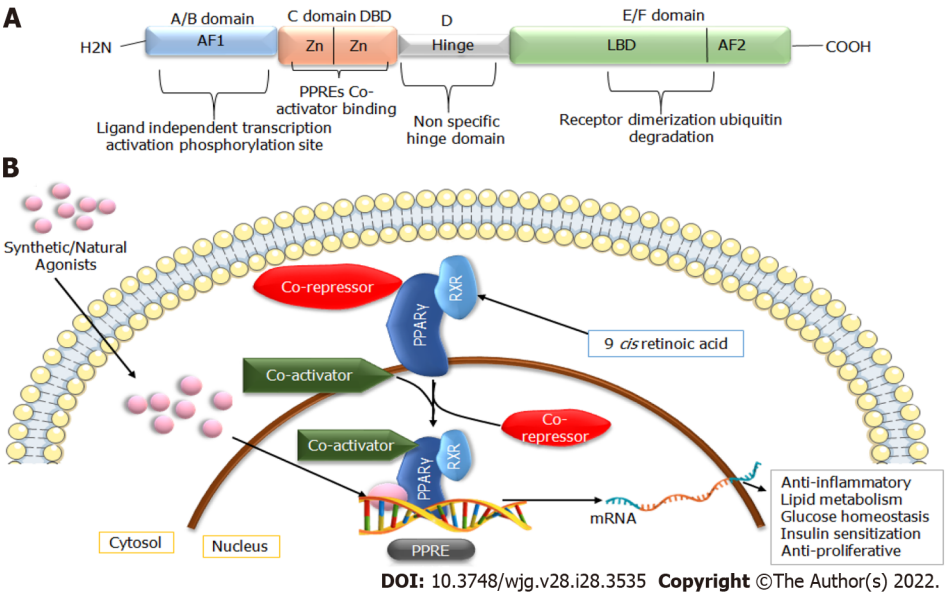
The PPARs protein belong to the superfamily of nuclear hormone factors containing 48 members. PPARs were mainly recognized for their proficiency in promoting peroxisome proliferation in the liver, and their expression is mainly regulated in response to ligand binding[11]. Three isoforms of PPARs, namely PPARα, PPARγ, and PPARδ, have been studied to a large extent. Of these isoforms, PPARγ is highly expressed in adipose tissue, where it plays a vital role in regulating lipid homeostasis, energy balance, adipogenesis, and inflammation. Due to the presence of different promotor regions and 5′ exons, PPARγ has three distinct mRNAs (PPARγ1, PPARγ2, and PPARγ3). The translation products of PPARγ1 and PPARγ3 yield identical proteins; however, PPARγ2 results in a product with an additional N-terminal region[12]. PPARγ1 and PPARγ3 are biologically expressed in different tissues (hepatocytes, muscles, and endothelial cells), whereas PPARγ2 is only widely expressed in adipose tissue[9,13]. PPARγ plays a significant role in maintaining metabolic alterations, inflammation, glucose homeostasis,

cell cycle regulation, differentiation, and migration, making it a potential therapeutic target for treating metabolic disorders and cancers[14]. The structural arrangement of PPARs is similar to steroid and thyroid hormone receptors. Its ligand-binding cavity is 3- to 4 -times higher than that of the other nuclear receptors. They can be activated by various natural and synthetic agonists, such as essential fatty acids[15,16]. The three-dimensional structure of PPARγ consists of a canonical domain shared with other nuclear receptors, named A-E from N to C terminus (Figure 1). These domains include the amino-terminal AF-1 domain, a DNA-binding domain with two zinc finger motifs, and a ligand-binding domain (LBD or E/F domain) at the C-terminus responsible for specific ligand binding at the peroxisome proliferator response element (PPRE)[16,17]. After interaction with specific ligands, the LBD facilitates the heterodimerization of PPARs with retinoid X receptor (RXR), which subsequently binds to the PPRE of the target gene. RXR is activated by the natural ligand 9-cis-retinoic acid receptor and synthetic retinoids receptors. However, in the absence of specific ligands, heterodimers bind with co-repressors, ultimately inhibiting the gene[12]. This complex subsequently recruits coactivation or co-repressors to regulate the expression of targets genes related to lipid glucose metabolisms and inflammation (Figure 1)[6].

ROLE OF PPARγ IN HCC

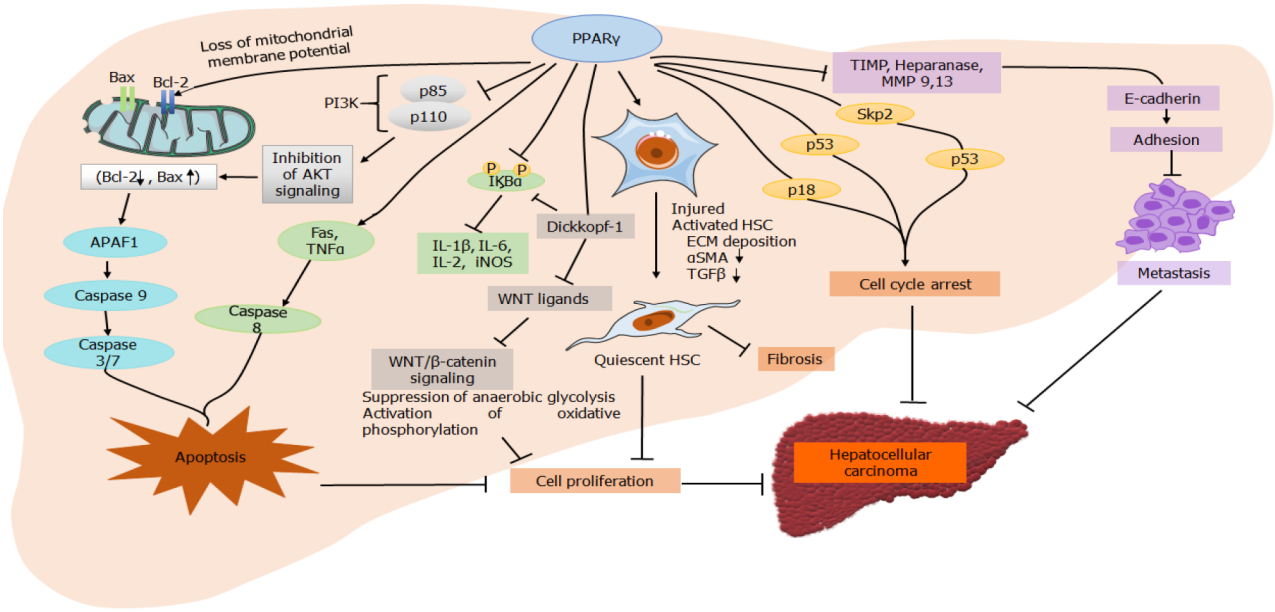
PPARγ plays a multifunctional role in many tissues and cell types such as adipocytes, pancreas, macrophages, liver, kidney, and skeletal muscle. It plays a regulatory role in adipocyte differentiation, lipid metabolism, and insulin sensitivity *via* downregulating leptin concentration[7]. Despite the low expression in the healthy liver, PPARγ plays a significant role in several hepatic conditions such as fatty liver, fibrosis, and HCC. Many *in vitro* and *in vivo* studies have reported that natural and synthetic PPARγ agonists inhibit tumor growth and cell migration in HCC[18]. The activation of PPARγ inhibits cell growth by inducing G0/G1 cell cycle arrest in HCC cells, which is suggested to be associated with p21, p27, and p18 upregulation (Figure 2). Furthermore, p27 upregulation downregulates S-phase kinase-associated protein-2 (Skp2) in HCC, an F-box protein component of the Skp, Cullin, F-box ubiquitin-ligase complex. p27 plays a vital role in G0/G1 arrest instead of p21[10,19]. The direct overexpression of PPARγ in hepatic cancerous cells also inhibits cell growth; however, the cells are arrested in the G2/M phase instead of the G0/G1 phase after PPARγ agonist treatment. G2/M phase arrest in PPARγ overexpression is attributed to activating cell division cycle 25C phosphatase by Ser216 phosphorylation and preventing premature mitosis[20]. Compared to wild-type mice, another study on PPARγ-deficient mice showed increased hepatocarcinogenesis after treatment of diethylnitrosamine (DENA). Growth differentiation factor 15 (GDF 15) is a target gene of PPARγ and is induced by its activation. GDF 15 overexpression in many cancers is associated with an antitumorigenic response, as it was suggested to reduce cancer cell viability and induce cell apoptosis. PPARγ activation by agonist or direct overexpression induces apoptosis by intrinsic and extrinsic pathways[21]. Activation of the extrinsic apoptosis pathway by PPARγ overexpression is attributed to the induction of tumor necrosis factor α (TNFα) and Fas, leading to the activation of downstream caspases (Figure 2). In the intrinsic pathway, PPARγ overexpression stimulates B-cell lymphoma 2 (Bcl-2)-associated X protein transcription and release into the cytosol, activating apoptotic protease activating factor 1 and caspase-9 complex, which further triggers caspase 3 and 7 to induce apoptosis[6,21]. The antitumorigenic effect of PPARγ in HCC is also suggested *via* modulation of the phosphoinositide 3-kinase (PI3K)/Akt pathway [22]. PPARγ activation attenuates p85 activation, which is essential for Akt induction, thus inhibiting PI3K/Akt signaling and inducing apoptosis[23].

Hepatic inflammation is crucial in the progression of HCC, and PPARγ plays a central role in regulating inflammation. PPARγ inhibits inflammation by interfering with nuclear factor-kappa B (NF-κB) and suppressing the production of proinflammatory cytokines (TNFα and interleukin 1 beta [IL-1β]). Activation of PPARγ by specific ligands in T-cell differentiation promotes an inflammatory response, thereby playing a significant role in the adaptive immune response. Thus, PPARγ act as an important therapeutic target for regulating inflammatory markers (TNFα, IL-2, IL-1β, and IL-6) against the progression of several diseases[7,16]. Hepatic stellate cell (HSC) activation and fibrogenic factor significantly contribute to the development of HCC (Figure 2). PPARγ is highly expressed in quiescent HSCs and has a role in their transdifferentiation. HSC activation and PPARγ are inversely related as increased expression of PPARγ inhibits HSC proliferation and induces apoptosis in activated HSCs[24]. It also reduces the expression of alpha-smooth muscle actin (αSMA) and hydroxyproline to inhibit hepatic fibrosis. Hepatic injury induces microvascular complications in the liver, stimulating various sinusoidal cells such as HSCs, liver sinusoidal endothelial cells, and Kupffer cells. PPARγ regulates the role of these cells in liver inflammation and fibrosis. The deactivation of HSCs by PPARγ agonists further reduces extracellular matrix deposition and expression patterns of matrix metalloproteinase (MMP)/tissue inhibitors of MMPs (TIMP). The expression of MMP9 and MMP13, TIMP, heparinase, and E-cadherin is associated with cancer cell migration and metastasis[25]. The expression patterns of these markers are directly linked to PPARγ activation. Reports also link PPARγ activation with autophagy in HCC. Autophagy is thought to be inhibited after autophagosome formation in the absence



DOI: 10.3748/wjg.v28.i28.3535 **Copyright** ©The Author(s) 2022.

Figure 1 General structure and ligand-activated transcription of peroxisome proliferator-activated receptor-gamma. A: Peroxisome proliferator-activated receptor (PPAR) structure includes four distinct structural domains A/B, C, D, and E/F; B: Ligand-activated transcription of PPARγ, which includes heterodimerization with nuclear receptor retinoid X receptor (RXR) and binding with peroxisome proliferator response elements located in the target genes through the DNA-binding domain (DBD). In the absence of ligand, PPAR is linked with the corepressor complex, whereas, in the presence of ligand, it is associated with the coactivator complex. LBD: Ligand-binding domain; PPRE: Peroxisome proliferator response element.



DOI: 10.3748/wjg.v28.i28.3535 **Copyright** ©The Author(s) 2022.

Figure 2 Schematic diagram showing the protective effect of peroxisome proliferator-activated receptor γ against the progression of hepatocellular carcinoma. Activated peroxisome proliferator-activated receptor γ (PPARγ) interacts with multiple pathways, leading to cell cycle arrest, apoptosis, inhibition of cell proliferation, and cell metastasis in hepatocellular carcinoma. BAX: B-cell lymphoma 2 (Bcl-2)-associated X protein; IκBα: Nuclear factor of kappa light polypeptide gene enhancer in B-cells inhibition alpha; IL: Interleukin; TIMP: Tissue inhibitor of metalloproteinases; MMP: Matrix metalloproteinase; ECM: Extracellular matrix; αSMA: Alpha-smooth muscle actin; TGFβ: Transforming growth factor beta; iNOS: Inducible nitric oxide synthase; TNFα: Tumor necrosis factor alpha; APF1: Apoptotic protease activating factor 1.

of PPARγ, resulting in increased light chain 3 protein expression and accumulation of p62 in the autophagosome[26,27]. Therefore, induction of autophagy in HCC is linked to the activation of PPARγ in HCC. A recent study elucidated the role of PPARγ coactivator-1α (PGC1α) in suppressing HCC metastasis. The levels of PGC1α were downregulated in human HCC and associated with a poor prognosis, large tumor size, and vascular invasion[28]. However, PGC1α overexpression in the HCC cells inhibited tumor cell migration and invasion. The suppression of metastasis by PGC1α overex-

pression was suggested due to PPARγ-dependent downregulation of pyruvate dehydrogenase kinase isozyme 1 and inhibition of aerobic glycolysis through Wnt/β-catenin/pyruvate dehydrogenase kinase-1 (PDK1) axis regulation[29].

Zinc finger protein 746 (ZNF746) is a Parkin-interacting substrate (PARIS), acting as a transcriptional regulator of PPARγ co-activator 1 alpha (PGC1α) which further regulates the activity of PPARγ and is involved in the onset of HCC. The elevated levels of insoluble parkin with PARIS accretion in the hepatic cells of diethylnitrosamine (DEN)-injected mice were observed with the downregulation of PGC1α and NRF1. Moreover, Chang liver cells treated with hydrogen peroxide showed PARIS accretion and alleviation of PGC1α. As the co-activator, PGC1α is directly linked to PPARγ regulation, further monitoring the oncogenic stress promoting cancer development. Thus, the modulation of PPARγ and its co-activators can be a promising therapeutic target for HCC[30]. In a clinical study, it was subsequently observed that the expression of PGC1α is negatively associated with tumor size and vascular influx. The increased expression of PGC1α could elevate the degree of oxidative phosphorylation, further slowing down the rate of metastasis and the Warburg effect of HCC cells[31]. Rapid proliferation is the prime feature of cancerous cells for which cells need to meet the high energy demand through the aerobic glycolysis pathway rather than the pyruvate oxidation pathway. The canonical Wnt/β-catenin signaling was also targeted to observe the expression of PDK1 in the PGC1α knockdown model by employing two popular inhibitors of this signaling pathway (XAV-939 and ICG-001). Gene Set Enrichment Analysis indicated that these inhibitors alleviate the overexpression of extracellular lactate, suggesting the possible role of PGC1α in the inhibition of aerobic glycolysis *via* Wnt/β-catenin signaling. Dual-luciferase reporter assays showed that the transcriptional actions of PPARγ are significantly increased in HCCLM3 and MHCC97H cells with PGC1α augmentation. These results show that the tumor-suppressive activity of PGC1α depends on PPARγ, which makes PPARγ a key regulator of HCC[29,32]. An earlier report revealed the role of PPARγ in HCC by analyzing the mRNA and protein expression in 20 patients with cirrhosis and chronic hepatitis. The results indicated a statistically pronounced drop in levels of PPARγ in HCC compared to the non-tumorous liver tissue[33]. A report confirmed that miR-130b aids cell aggressiveness by suppressing PPARγ in human HCC[34]. Similarly, evidence on the oncogenic role of miR-1468 in HCC *via* activating the PPARγ/Akt pathway was also recently confirmed. The increased levels of miR-1468 elevated the malignant prognostic features and improved survival. Carboxy-terminal domain 2 and UPF1 RNA Helicase And ATPase were identified as the downstream targets for miR-1468, which regulate PPARγ/Akt pathway activation. Restoration of the expression of these targets partially abolished the effects of miR-1468, explaining the regulation *via* PPARγ/Akt signaling[35].

EXPERIMENTAL AND CLINICAL SCENARIOS

Many studies have explored the therapeutic effects of synthetic and natural PPARγ agonists against HCC in preclinical and clinical trials. The activation of PPARγ significantly suppresses HCC progression and invasion. Several findings have identified PPARγ as a target for tumor suppression, a mediator of apoptosis, and a suppressor of carcinogenesis and metastasis by triggering intrinsic pathways and mainly inhibiting the PI3K/Akt survival pathway[8,21,36]. The various synthetic and natural PPARγ agonists used for HCC are listed in Table 1.

SYNTHETIC PPARγ AGONISTS IN HCC

PPARγ itself and its agonists have anticancer activities, such as growth inhibition, induction of apoptosis, and cell differentiation. Thiazolidinediones (TZDs) are a class of synthetic PPARγ agonists, and many compounds of this class have been studied for their efficacy in experimental models and clinical trials. These compounds were used as a bioregulatory remedial approach to target the communicative framework of HCC in patients with non-curative HCC[37]. TZDs are also effective for glycemic control and the likelihood of HCC and hepatic manifestation in diabetic patients with chronic hepatitis B (CHB). Of the 28999 patients with CHB, 3963 patients developed HCC at a median follow-up of 7.1 years, whereas 1153 patients were administered TZD during the follow-ups. The findings showed the co-relation of TZD use with lowering the risk of poor hepatic manifestations in diabetic patients with CHB[38]. A population-based case-control study performed in 23580 diabetic patients demonstrated the negative relationship between the risk of HCC and use of TZDs. There is a time-dependent effect of TZD use on the risk of HCC. The longer the duration of TZD use, the lower the risk of HCC[39-41]. Many other reports have also suggested that the administration of PPARγ agonists ameliorates several types of cancers, *i.e.* colorectal, bladder, lung, and liver cancers. The effects are more substantial at higher cumulative dosages with longer durations[42].

Table 1 Various synthetic and natural peroxisome-proliferator-activated receptor gamma agonist used in experimental and clinical trials for hepatocellular carcinoma

Agonist name	Drug bank/ PubChem ID	Model	Concentration/dose of agonist	Effects	Ref.
Synthetic agonists					
Pioglitazone	DB01132	*In vivo* (Rats, and Mice)	3 mg/kg; 10 mg/kg	Reduced HCC progression and decreased tumor size and volume	[44]
Rosiglitazone	DB00412	*In vivo* (Orthotopic Mice) *In vitro* (MHCC97L, and BEL-7404)	50 μmol/L	Decreased HCC migration, and invasiveness	[25]
		In vitro (HepG2 and PC3)	0.1, 1, 10, 100 μmol/L	Reduced cancer growth, Increased apoptosis	[49]
		In vitro (HepG2 and Hep3B)	80 μmol/L	Restricted the oncogenic activity of SEPT2	[50]
Telmisartan	DB00966	*In vitro* (HLF, HLE, HuH-7, PLC/PRF/5, and HepG2)	10, 50 or 100 μmol/L	Inhibit proliferation, induce cell cycle arrest	[53]
		In vivo (Mice)	15 mg/kg	Reversed malignant anomalies, antioxidant, anti-inflammatory	[54]
Troglitazone	DB00197	*In vitro* (Hep G2, HuH-7, KYN-1, and KYN-2)	5, 10, 25 μmol/L	Reduced cell proliferation and increased apoptosis	[56]
		In vitro (HepG2)	5, 10, 20, 40, 80, and 100 μmol/L	Apoptosis and growth inhibition	[57]
		In vitro (Hep G2, HuH-7, KYN-1, and KYN-2)	5, 10, and 25 μmol/L	Inhibited DNA synthesis, cell cycle growth, and α-fetoprotein levels	[58]
		In vitro (PLC/PRF/5, and HuH-7)	5, 10, 20, 40, 60, 80, and 100 μmol/L	Reduced cell proliferation and increased apoptosis	[59]
		In vitro (HLF, HAK-1A, HAK-1B, and HAK-5)	10, 20, 30, 40, and 50 μmol/L	Reduced cell proliferation and increased apoptosis	[19]
Saroglitazar	DB13115	*In vivo* (Mice)	4 mg/kg	Reduced inflammation in hepatic lobules, hepatocellular ballooning, and steatosis	[61]
		In vivo (Rats)	4 mg/kg	Improved lipid profile, and histopathological changes	[62]
Natural agonists					
Cannabinol, Cannabinoids	DB14737	*In vitro* (HepG2 and HUH-7); *In vivo* (Mice)	8 μmol/L; 15 mg/kg	Increased apoptosis, autophagy, anti-proliferative	[66]
		In vitro (HEK-293T and Neuro-2a); *In vivo* (Mice)	1, 5, 10, 25 μmol/L; 20 mg/kg	Antitumor, antioxidant, anti-inflammatory	[68]
Capsaicin	DB06774	*In vivo* (Rats)	0.5 and 1 mg/kg	Inhibit hepatic injury, and collagen deposition, anti-inflammatory	[71]
Curcumin	DB11672	*In vivo* (Rats)	20 mg/kg	Attenuated histopathological, serological, proliferative, and apoptotic parameters	[77]
		In vitro (H22); *In vivo* (Mice)	5, 10, 20, 40, and 80 μmol/L; 50, 100 mg/kg	Antiproliferative, decrease tumor growth, induce apoptosis	[78]
		In vivo (Mice)	150 mg/kg	Reduced inflammation, and tumor size	[79]
		In vivo (Rats)	0.5, 1, 2, 5, 10, 15, and 20 ng/mL	Interrupted TGFβ signaling, activated hepatic stellate cells	[80]
		In vitro (SMMC7721 and Huh-7)	10, 20, 40, 80, and 160 μmol/L	Suppressed cellular proliferation	[82]
Hesperidin	DB04703	*In vivo* (Rats)	50 and 100 mg/kg	Suppressed TGFβ signaling and hepatocarcinogenesis	[85]
		In vivo (Rats)	200 mg/kg	Inhibited PI3K/Akt pathway, Antioxidant	[86]

		In vitro (HepG2); *In vivo* (Rats)	100 μmol/L; 150 mg/kg	Inhibited Wnt3a/5a signaling pathway, anti-inflammatory	[87]
Hispidulin	DB14008	*In vitro* (SMMC7721 and Bel7402); *In vivo* (mouse tumor xenograft)	10 and 20 μmol/L; 20 and 40 mg /kg	Anticancerous, inhibited cell migration	[89]
		In vitro (NCI-H460 and A549)	4, 8, 15, 30, and 60 μmol/L	Induced ROS-mediated apoptosis, anti-cancerous	[90]
Isoflavone	DB12007	*In vivo* (Bel-7402 and SK-Hep-1)*In vivo* (Mice)	75 and 12 μmol/L resp.; 25 and 7.5 mg/kg resp.	Anti-inflammatory, anti-tumorigenic, reduced the size and volume of tumor	[94]
		In vitro (Hepa 1-6 cells)	1, 5, 10, 15, 20, 25, 50, 75, and 100 μmol/L	Antitumorigenic and antiproliferative	[95]
		In vitro (HCC-LM3, SMMC-7721, Hep3B, Bel-7402, and Huh-7)*In vivo* (Mice)	40, 60, and 80 μmol/L; 20, 40, and 80 mg/kg	Suppressed aerobic glycolysis and increased apoptotic rate	[96]
Oroxyloside	14655551	*In vitro* (HepG2) and SMMC-7721); *In vivo* (Mice)	100, 200, and 300 μmol/L; 90 mg/kg	Cell cycle arrest and growth repression	[100]
Resveratrol	DB02709	*In vivo* (Rats)	100 mg/kg	Antioxidant, anti-inflammatory, anticancer	[101]
		In vitro (HepG2); *In vivo* (Rats)	7.81, 15.63, 31.25, 62.5, 125, and 250 μg/mL; 20 mg/kg	Attenuated histopathological, serological, proliferative, and apoptotic parameters	[102]
Miscellaneous					
Avicularin	5490064	*In vitro* (HuH-7)	25, 50, and 100 μg/mL	Decreased the cell migration and invasiveness	[107]
Honokiol	72303	*In vitro* (HEK-293 and 3T3-L1); *In vivo* (Mice)	1, 3, and 10 μmol/L; 100 mg/kg	Activated PPARγ/RXR heterodimers; Reduced hyperglycemia	[108]
Chrysin	DB15581	*In vitro* (MDA-MB-231 and HepG2)*In vivo* (Mice)	10 μmol/L; 10 mg/kg	Increased apoptosis	[112]
Quercetin	DB04216	*In vitro* (HepG2 and SMCC-7721); *In vivo* (Mice)	0.05, 0.1, and 0.15 mmol/L; 40 mg/kg	Promoted the autophagy	[114]
		In vitro (PATU-8988 and PANC-1)	20, 40, 80, and 160 μmol/L	Suppressed HCC *via* STAT3 pathway	[117]
		In vitro (LM3); *In vivo* (Mice)	40, 80, and 120 μmol/L; 100 mg/kg	Reduced invasiveness, Cell cycle regulation	[118]
Clinical trials					
		Population type	No. of patients		
Thiazolidinediones	NA	Hongkong	1153	Reduce the synergistic effect of diabetes with liver disorders; Reduced risk of HCC	[38],[39], [40],[41]
		Taiwanese	77396		
			32891		
			76349		
Pioglitazone	DB01132	Chinese	75	Blocked RAGE signaling; Reduced HCC	[45]
		Japanese	85	Reduced growth and invasion of HCC cells	[46]
		Thai	10000	Reduced risk of HCC	[47]
Rosiglitazone	DB00412	French	44	Reduced NASH activity and ballooning score, Ameliorated histopathological aberrations	[51]
Saroglitazar	DB13115	Indian	30	Improved glycemic index and liver stiffness	[63]
			90	Improved fibrosis score	[64]

Isoflavone	DB12007	Japanese	302	Antioxidant, reduced risk of HCC	[97]
			191	Antioxidant, reduced risk of HCC	[98]

Akt/PKB: Protein kinase B; HCC: Hepatocellular carcinoma; NASH: Non-alcoholic steatohepatitis; PI3K: Phosphoinositide 3-kinase; PPARγ: Peroxisome proliferator-activated receptor gamma; RAGE: Receptor for advanced glycation end products; ROS: Reactive oxygen species; RXR: Retinoid X receptor; SEPT2: Septin 2; STAT3: Signal transducer and activator of transcription 3; TGFβ: Transforming growth factor beta; Wnt: Wingless-related integration site.

Pioglitazone

Pioglitazone (PGZ), a PPARγ ligand, works by improving the insulin sensitivity of tissues and exhibits anticancer activity. It selectively stimulates PPARγ *via* modulating the transcriptional alterations of genes involved in glucose metabolism and insulin resistance and further decreasing the gluconeogenesis and levels of glycated hemoglobin in the bloodstream[43]. PGZ treatment inhibits fibrosis progression and HCC development and reduces tumor size in DENA-induced rats at 3 mg/kg and mice at 10 mg/kg. PGZ is suggested to exhibit protective effects by reducing mitogen-activated protein kinase (MAPK) and upregulating adiponectin levels, resulting in activation of the hepatoprotective AMPK pathway[44].

The anticancer activity of PGZ is attributed to the pathological receptors for advanced glycation end products (RAGE). HCC tissues from 75 patients showed high expression of RAGE in HCC tissues, which was closely linked to pathological staging and lymph-vascular space influx. However, PGZ treatment suppressed cellular proliferation, ameliorated apoptosis, and cell cycle arrest, which further elevated PPARγ expression and decreased the expression of RAGE, NF-κB, high mobility group box 1, p38MAPK Ki-67, MMP2, and cyclin D1. The results demonstrated that PGZ as a PPARγ agonist possibly slows down the growth and invasion of HCC cells by blocking RAGE signaling[45]. Another prospective study confirmed the effect of PGZ on HCC by investigating 85 patients with HCC and hepatitis C virus infection to investigate recurrence-free survival. The spline-model analysis showed that the lessened risk of HCC recurrence is associated with increased body weight and body mass index ≥ 23. PGZ was also observed to alleviate insulin resistance and serum adiponectin levels[46]. A lifetime Markov model was employed among the population of Thailand to study the life expectancy, quality-adjusted life years, lifetime costs, and the incremental cost-effectiveness ratios in HCC patients. The weight reduction program with the administration of PGZ demonstrated that PGZ can reduce the number of HCC cases[47]. These therapeutic potentials also have limitations. PGZ has adverse effects such as body weight gain, peripheral edema, bone loss, and heart failure. Additionally, the risk of bladder cancer significantly limits the use of this agonist in the medical field[48].

Rosiglitazone

Rosiglitazone is a member of the TZD class of insulin-sensitizing PPARγ agonists. An inhibitory effect of PPARγ was reported on the invasive and metastatic potential of HCC *in vitro* (MHCC97L and BEL-7404 cell lines) and *in vivo* (orthotopic HCC mouse model). A pronounced expression of PPARγ was demonstrated in HCC cell lines treated with adenovirus-expressing mouse PPARγ1 (Ad-PPARγ), rosiglitazone (50 μmol/L), or Ad-PPARγ plus rosiglitazone. The induction of PPARγ markedly repressed HCC cell migration, invasiveness, levels of pro-metastatic genes (MMP9, MMP13, heparanase [HPSE]), and hepatocyte growth factor. However, the levels of cell adhesion genes (E-cadherin and SYP), extracellular matrix regulator TIMP3, and tumor suppressor gene retinoblastoma 1 were elevated. Additionally, direct transcriptional regulation of the genes TIMP3, MMP9, MMP13, and HPSE regulating PPARγ levels was also validated by chromatin immunoprecipitation-PCR[25]. Bcl-2 is a well-known family of anti-apoptotic proteins regulating endogenous apoptotic pathways and are highly expressed in carcinomas. (-)-gossypol ((-)-G) is the (-) enantiomer of gossypol that acts as a small molecule to induce apoptosis in several types of cancers by inhibiting Bcl-2 proteins. In a study, rosiglitazone was employed to sensitize (-)-G to induce apoptosis at different concentrations (0.1, 1, 10, 100 μmol/L). The (-)-G induced Mcl-1 (myeloid cell leukemia-1) stability was the prime concern for its apoptotic activity. However, rosiglitazone attenuated this stability *via* Janus kinase phosphorylation, further repressing cancer growth. These results suggest that rosiglitazone can reduce cancer growth and sensitize the other apoptotic factors for performing a similar activity. The study also provides insights into the novel cancer therapeutic activity of BH3 mimetics in the case of carcinomas based on the combination of PPARγ agonists and BH3 mimetics[49]. Rosiglitazone (80 μmol/L) also inhibits HCC cell growth by restricting the oncogenic activity of septin 2[50].

A long-term clinical trial was conducted in which 53 patients underwent liver biopsies and were further treated with rosiglitazone (8 mg/d) for the next 2 years. Forty-four patients fulfilled the criteria of the extension period and underwent another biopsy. During the extension phase, serum insulin and alanine aminotransferase (ALT) levels were decreased by 26% and 24%, respectively. Non-alcoholic steatohepatitis activity, ballooning, and fibrotic stage were decreased but not on a significant scale. The treatment was continued for another 2 years, but no significant results were obtained, showing that rosiglitazone does attenuate insulin sensitivity and transaminase levels but might not significantly

improve other histopathological parameters. However, additional targets were suggested to be explored [51]. However, there is increasing evidence of bone fractures in females medicated with rosiglitazone after menopause, limiting its use. In September 2010, the FDA restricted the use of rosiglitazone based on meta-analyses of mostly short-term randomized controlled trials, which showed evidence of myocardial infection risk. However, these restrictions were removed in 2013 based on other large clinical trials by Duke Clinical Research Institute, which showed no complications regarding heart failure[52].

Telmisartan

Telmisartan (TEL) is an angiotensin II receptor blocker with a high affinity for the angiotensin II receptor type 1, whose impromptu link with HCC has been discovered; however, the underlying mechanism is not clear. TEL shows basal resemblance with a well-known PPARγ agonist, PGZ. TEL (at concentrations of 10, 50, or 100 μmol/L) inhibits the proliferation and G0 to G1 cell cycle transition leading to G0/G1 cell cycle arrest in hepatic cancer cells (HLF, HLE, HuH-7, PLC/PRF/5, and HepG2) in a dose-dependent manner. The cell cycle arrest was accompanied by reduced cell cycle-related proteins, including cyclin D1 and cyclin E. Further TEL was suggested to increase the activity of AMPK and inhibit the mammalian target of rapamycin (mTOR) pathway[53]. Another study used a DENA-induced HCC mouse model to evaluate the effects of TEL (15 mg/kg), sorafenib (SRF) (30 mg/kg), and a combination of these two agonists. The treatment downregulated the mRNA expression of NF-κBp65, AFP, TNFα, and transforming growth factor beta 1 (TGFβ1) resulting in the reversion of malignant anomalies and suppression of extracellular signalregulated protein kinase 1/2 (ERK1/2) activation. SRF and TEL showed antiproliferative, antimetastatic, and anti-angiogenic effects by improving the expression of hepatic cyclin D1, MMP2, and vascular endothelial growth factor (VEGF). However, only TEL has exhibited agonistic activity for PPARγ receptors, as indicated by the elevated PPARγ DNA-binding activity, mRNA expression of cluster of differentiation 36, heme oxygenase 1, and enhanced hepatic antioxidant capacity. Moreover, TEL and SRF both ameliorate phosphorylation-induced activation of TGFβ-activated kinase 1 (TAK1), suggesting that TAK1 might act as the core mediator for the interaction between ERK1/2 and NF-κB. TEL exerts its anticancer effects by modulating the ERK1/2, TAK1, and NF-κB signaling axis from the perspective of its PPARγ agonistic activity. Thus, TEL may be a useful PPARγ agonist for further clinical studies in the context of HCC treatment[54]. Despite its potential, it has adverse effects including headaches, dizziness, fatigue, upper respiratory tract or stomach-related infections, sinusitis, nonspecific pain, and diarrhea[55].

Troglitazone

Troglitazone (TGZ) is a member of the TZD class of drugs and acts as a PPARγ agonist. The antiproliferative and antitumorigenic effects of TGZ were studied in the BEL-7402 HCC cell line at 5, 10, and 25 μmol/L concentrations. TGZ induced cell death in a concentration-dependent manner resulting in the increased presence of fragmented DNA and terminal deoxynucleotidyl transferase dUTP nick end labeling (TUNEL)-positive cells. TGZ enhanced cell cycle arrest in the G0/G1 phase and increased caspase activities (caspase 3, 6, 7, and 9), indicating increased cell apoptosis[56]. In another study, the HepG2 cell line treated with TGZ showed significant growth inhibition in a dose-dependent manner. The TUNEL assay and immunohistochemistry showed apoptosis induction and elevated expression of apoptotic proteins such as caspase 3 and survivin[57]. PPARγ was functionally expressed in hepatic cancer cell lines (HepG2, HuH-7, KYN-1, and KYN-2) with TGZ treatment. This was followed by the profound inhibition of cellular proliferation, DNA synthesis, cell cycle growth, and α-fetoprotein levels [58]. Similar results have also been shown by other groups that used other HCC cell lines such as PLC/PRF/5, HuH-7[59], HLF, HAK-1A, HAK-1B, and HAK-5 with TGZ[10,19]. The reduction in cell proliferation and increased apoptosis in most of these studies demonstrated the usefulness of TGZ for chemoprevention in HCC. Some recent studies showed the hepatotoxic effect of TGZ on diabetic patients. There is a significant elevation in liver enzymes level (ALT and aspartate aminotransferase [AST]) in 1.9% of patients with diabetes treated with TGZ for 24 to 48 wk. Furthermore, the cost of TGZ is much higher than that of other oral antihyperglycemic agents or insulin, which also limits the use of TGZ[60].

Saroglitazar

Saroglitazar is a first-class drug that acts as a dual PPARα/γ agonist. It is indicated for enhanced diabetic dyslipidemia, inflammation, steatosis, ballooning, and fibrosis progression. The agonistic effects of this drug have a favorable impact on insulin resistance and lipid profile. Saroglitazar treatment is thought to ameliorate high-fat diet-induced aberrations. The improvements were observed in hepatic lobular inflammation, hepatocellular ballooning, steatosis, and fibrosis. The effects of saroglitazar were more pronounced compared to PGZ. Transcriptomic analyses revealed the elevated expression of PPARγ in hepatic tissue with the anti-inflammatory effects of saroglitazar treatment[61]. Similarly, saroglitazar improved liver function parameters, degenerative changes, glucose and insulin levels, and lipid profile in high-fat emulsion plus lipopolysaccharide (LPS)-treated rats. The positive effects on serum leptin, TNFα, and adiponectin levels were also observed. The multiple protective roles of PPARα

/γ agonists in liver disorders suggest the usefulness of saroglitazar in managing liver cancer[62].

In a prospective observational study, 30 diabetic patients with liver fibrosis were enrolled and treated with 4 mg saroglitazar daily for 6 mo. A profound improvement in glycemic index, liver stiffness, and serum triglyceride levels of the patients was observed with no significant adverse side effects[63]. Another study conducted in 90 NAFLD patients who underwent liver biopsies, fibrosis scores, and other non-invasive parameters showed that saroglitazar treatment significantly improved the serum biomarker levels and fibrosis score. The study concluded the reversal effect of saroglitazar on fibrosis and advocated its use in treating HCC[64]. The most common adverse events associated with saroglitazar included asthenia, gastritis, chest discomfort, peripheral edema, dizziness, and tremors[65].

NATURAL PPARγ AGONISTS IN HCC

Natural PPARγ agonists have many beneficial properties including antioxidant, anti-inflammatory, antifibrotic, and antitumor effects. In addition to therapeutic effects, synthetic drugs have many adverse effects due to full PPARγ activation. Therefore, researchers are exploring potential natural PPARγ modulators with high specificity in terms of their binding at the active site and improving drug safety. The PPARγ-activating effect of natural products is recognized as having great potential in developing anticancer therapy. There are many reports on the natural PPARγ agonist against HCC in various experimental models.

Cannabinoids

The hemp plant *Cannabis sativa L.* produces approximately 60 unique compounds known as cannabinoids, of which ∆9-tetrahydrocannabinol (THC) is the most important due to its high potency and abundance in cannabis. Various studies have reported the fair safety profile of cannabinoids, in accordance with its probable antiproliferative activity on cancerous cells, may set the basis for future trials to evaluate the potential antitumor activity of cannabinoids. Vara *et al*[66] reported that cannabinoids THC and JWH-015 increased the intracellular mRNA and protein levels of PPARγ in HCC cells, and inhibition of PPARγ decreased cannabinoid-induced cell death and apoptosis. Further, increased PPARγ levels were correlated with endoplasmic reticulum stress and autophagy in HCC cells, suggesting the antiproliferative effects of cannabinoids through PPARγ-dependent pathways. The antitumor activity of THC was evaluated in patients who had failed standard therapy norms. *In vitro* studies have shown the suppression of tumor cell proliferation, and Ki67 immunostaining exhibits a reduced number of tumor cells[67]. THC is suggested to induce transcriptional modulation of the PPARγ pathway, and the activation is much more potent by cannabinoid acids than its decarboxylated products, indicating that cannabinoids act as a PPARγ agonist[68]. *Cannabis* contains some psychoactive agents that increase sociability and exert euphoric effects. Repeated use of *cannabis* has been linked to short- and long-term side effects, including respiratory and cardiovascular disorders, cognitive alterations, psychosis, schizophrenia, and mood disorders[69]. A recent study highlighted the side effects of a common preparation from *C. sativa* named *marijuana*. This study gave the putative association of the use of *cannabis* with a higher risk of gingival and periodontal diseases, oral infection, and cancer of the oral cavity[70]. Given the growing popularity of cannabinoid-based drugs for recreational and medical purposes and their potentially harmful effects, there is a need for further investigation in this field.

Capsaicin

Capsaicin (8-methyl-N-vanillyl-6-nonenamide) is a vital constituent of chili peppers belonging to the family of Capsicum. These phytoconstituents possess anti-inflammatory and chemopreventive properties. They counter various compounds' mutagenic properties and exert anticancer effects on breast, colon, prostate, and hepatic cancers. The DENA-induced models of HCC in rats and hepatic stellate cell lines were used to study the effects of capsaicin. Capsaicin was observed to inhibit hepatic injury, NF-κB activation, and collagen deposition. It has also ameliorated the levels of α-SMA, collagen type I, MMP2, TGFβ1, and TNFα. Furthermore, TGFβ1 expression and the phosphorylation of Smad2/3 were also inhibited through induction of PPARγ expression. The findings showed that capsaicin attenuates hepatic fibrosis by upregulating PPARγ expression[71]. The limitations of this natural PPARγ agonist should be mentioned. Capsaicin is a well-known irritant responsible for producing a painful, burning sensation when applied to the skin. Exposure to the eyes is painful and causes tearing, conjunctivitis, and blepharospasm[72]. Capsaicin is also a tussive agent, and inhaled capsaicin can be used to induce cough under experimental conditions. In humans, inhaled capsaicin induces a cough response immediately upon administration[73,74]. Interestingly, there is evidence that topical capsaicin can exacerbate angiotensin-converting enzyme (ACE) inhibitor-induced cough. A patient taking an ACE inhibitor for several years with no complaint of coughing reported coughing associated with applying a 0.075% capsaicin cream[75]. Additionally, oral administration of the ACE inhibitor captopril was found to cause a shift in the dose-response curve of inhaled capsaicin-induced cough in a trial with healthy adults[76].

Curcumin

Curcumin is a polyphenol compound present in *Curcuma longa* and is well known for its multiple therapeutic effects. Our previous study reported the effect of curcumin and piperine on DENA-induced HCC in rats. Curcumin prevented HCC progression by improving hepatic pathology, apoptosis induction, and inhibiting cell proliferation. However, the synergistic effect on HCC suppression was observed with the combination of curcumin and piperine[77]. Similarly, another study also reported the inhibition of cell proliferation, tumor growth, and apoptosis induction by curcumin treatment in HCC. The effect was suggested to decrease VEGF expression and PI3K/Akt signaling[78]. A study in a transgenic mouse model (expressing double HBV oncoproteins, HBx and pre-S2 in the liver) of HBV-related HCC reported the protective effects of phytosomal curcumin *via* targeting PPARγ as a key regulator. Curcumin decreased HCC formation and reduced the tumor size. Moreover, considerably more potent effects were observed on activation of PPARγ and inhibition of NF-κB. The report suggested that curcumin is an agonist for PPARγ, upregulating the genes involved in lipid metabolism, antiproliferation, and anti-inflammation. Furthermore, PPARγ activation regulates the suppression of NF-κB and subsequent pro-inflammatory cytokines. In addition, curcumin also is suggested to repress mTOR[79]. Recently, the antitumor effect of curcumin on HCC was suggested due to the involvement of miR-21 targeting TIMP3 and inhibition of the TGFβ1/Smad3 signaling pathway. The inhibition of TGFβ 1/Smad3 signaling by curcumin is reportedly linked to activation of the PPARγ gene[80,81]. It was further suggested to suppress cell proliferation through long non-coding RNA downregulation and inhibition of Wnt/β-catenin signaling[82]. The major disadvantage of this medication is the usage of high doses, which ultimately leads to liver injury in humans and experimental animals. A study showed that curcumin supplementation with paracetamol at doses of 50 and 100 mg/kg per day in experimental rabbits showed elevation of liver injury markers (ALT, AST, ALP, total protein, and albumin level) in plasma. Furthermore, levels of red blood cells and platelets were raised[83]. Also, the poor bioavailability of curcumin leads to its combined usage with other drugs such as piperine, which reportedly causes adverse drug reactions[84].

Hesperidin

Hesperidin is a flavanone glycoside found in the rind of citrus fruits including oranges and lemon. It possesses several pharmacological activities including antioxidant, anti-inflammatory, and anticancer effects. The chemopreventive efficacy of hesperidin was evaluated in DENA-induced HCC in rats. The hesperidin significantly reduced hepatic serological and tumor biomarkers along with TNFα. Furthermore, it also reduced the hepatic degenerative changes, oxidative stress, collagen deposition, TGFβ1, and NF-κB expression. However, the upregulated expression of nuclear factor erythroid 2–related factor 2, HO-1, and PPARγ suggested the effect of hesperidin *via* suppressing TGFβ signaling and subsequently activating PPARγ[85]. Another study investigated the efficacy of hesperidin *via* the PI3K/Akt pathway as a probable mechanism for curing HCC. Treatment with hesperidin elevated the protein levels of PI3K, Akt, and cyclin-dependent kinase 2 and ameliorated HCC progression[86]. In addition, hesperidin reportedly alters Wnt3a/β-catenin signaling in preventing HCC[87]. There are few reports on the bioavailability and solubility of hesperidin. Ameer *et al*[88] reported that hesperidin is absorbed across the gastrointestinal tract on oral administration, but cumulative recovery indicates low bioavailability. The factors limiting the bioavailability of hesperidin are poor water solubility and its precipitation in an acidic environment.

Hispidulin

Hispidulin, a phenolic flavonoid, exhibits anticancer activity against several types of cancers. The effect of hispidulin on HCC was studied in tumor cell lines (SMMC7721 and Bel7402) and mouse tumor xenograft models. Hispidulin activates caspase 3, triggers apoptosis, and inhibits cell migration *via* PPARγ activation, which is further linked to escalated phosphorylation of AMPK, ERK, and JNK *in vitro*. Specifically, GW9662 (a PPARγ inhibitor), compound C (an AMPK inhibitor), and PD98059 (a MEK inhibitor) negated the protective effects of hispidulin on PPARγ signaling. However, no pronounced changes in PPARγ levels were noted with pre-treatment of SP6000125 (a JNK inhibitor) *in vitro,* whereas it attenuated the anticancer activity of hispidulin. The suppression of Bel7402 xenograft tumor growth was successfully achieved by hispidulin through PPARγ activation, indicating the cardinal role of PPARγ signaling in HCC cell growth[89]. Recently, Lv *et al*[90] suggested that induction of reactive oxygen speciesmediated apoptosis through activation of the endoplasmic reticulum stress pathway is also responsible for the anticancer effect of hispidulin. Some evidence links hispidulin to its limited large-scale preparation. Studies have shown the lack of a single-dose design of hispidulin, which further limits the bioavailability[91,92].

Isoflavones

Isoflavones are a group of phytochemicals, a type of naturally occurring isoflavonoids. Studies have shown the anticancer effects of different isoflavones in the case of HCC[93]. A combination of two well-known isoflavones, Biochanin A and SB590885, was evaluated for their anticancer activities in HCC. The combination showed synergistic inhibition of cell growth and induced cell cycle arrest and apoptosis *in*

vitro. The inhibition of cellular proliferation and tumor suppression were attributed to the aberration of ERK MAPK and PI3K/Akt pathways. *In vivo*, a profound reduction in the size and volume of HCC tumors was noted, indicating the combination therapy of isoflavones as a potential lead for the management and treatment of advanced HCC[94]. The antitumorigenic and antiproliferative role of genistein was also studied in HCC *in vitro*. The isoflavone suppressed the proliferation of Hepa 1-6 cells and caused apoptosis in time- and dose-dependent manners[95]. In another study, genistein treatment suppressed aerobic glycolysis and increased the apoptotic rate in HCC cell lines. Additionally, genistein exhibited inhibitory effects on tumor progression and aerobic glycolysis. This may be identified as an effective treatment for advanced HCC[96]. Studies have reported the PPARγ-modulating effect of isoflavones and inhibition of HCC through inhibition of the PI3K/Akt pathway, and aerobic glycolysis further validates the involvement of PPARγ signaling. Clinical studies have also suggested that the more the dietary intake of flavonoids, the lesser the risk of developing HCC. In the Japanese population, a correlation between the isoflavone-rich diet and risk of HCC was observed[97,98]. Despite the therapeutic potential, some contentious health issues are associated with their intake. Soy proteins rich in isoflavones showed unfavorable effects at a higher dose, including gastrointestinal upset, constipation, nausea, allergic reactions, and loss of appetite. In animals, the intake of isoflavone (genistein) reportedly impacts the fertility and morphogenesis of ovaries. In addition, long-term use of soy extract may result in abnormal tissue growth in the uterus[99].

Oroxyloside

Oroxyloside (OAG), a flavonoid, was explored as a new dual agonist of PPARγ/α, which acts as a potent cell proliferation inhibitor in HCC-based metabolic transition. It regulates the glycolipid metabolic enzymes (PPAR-dependent or PPAR-independent), inhibits the breakdown of glucose, and promotes fatty acid oxidation, which generates acetyl-CoA for the tricarboxylic acid cycle and oxidative phosphorylation. The metabolic transition produced by OAG exhibits a profound generation of reactive oxygen species, leading to G1 cell cycle arrest and growth repression of HCC cells. OAG requires pyruvate dehydrogenase kinase 4 and β-oxidation to inhibit cell proliferation, explaining its PPARγ agonistic behavior. OAG is a new PPARγ/α agonist drug candidate and an effective therapeutic approach for HCC based on metabolic reprogramming[100]. Although many bioactive flavones' sources are very well known, information on their bioavailability and their active forms *in vivo* is limited. In particular, most flavonoid agents' absorption, metabolism, and blood delivery are poorly understood. Due to limited literature, it is difficult to elucidate the whole molecular mechanism. Hence, further studies are required to uncover their therapeutic potential against liver diseases.

Resveratrol

Resveratrol (RS) is a popular natural polyphenolic PPARγ agonist, well known for its anticancer properties, and has been recognized as the alternate mode in cancer treatment. A study revealed the effect of RS against alcohol-aflatoxin B1-induced HCC. During the progression of HCC, a decline in the antioxidant markers was effectively restored by resveratrol treatment. RS modulated the activity of the sirtuin 1 (SIRT1) enzyme in HCC by negatively regulating the levels of NF-κB, and cross-talk between this PPARγ agonist and SIRT1 signaling was observed[101]. A nano-formulation of RS using liposomes was developed to establish a specific drug delivery system for managing HCC. *In vitro* studies have revealed the increased internalization and enhanced anticancer activity of liposomal formulation (RL5) compared to naïve RS. A profound reduction in liver injury markers, hepatocyte nodules, and degenerative changes in the liver was observed in an *in vivo* HCC model. The results indicated the promising action of nano-formulation of RS and its substantial activity in controlling the severity of HCC[102]. Earlier, similar approaches were briefly reviewed by Santos *et al*[103] to study the pharmacokinetics of RS-loaded nanoparticles (RS-NPs) and study their effects on cancer tissue. A comprehensive analysis was carried out in various *in vivo* models, which revealed the markedly enhanced anticancer activity of RS-NPs. However, the poor bioavailability and rapid metabolism restricted the successful translation of resveratrol to clinical form. The *in vivo* efficacy of RS is affected due to its low solubility and low bioavailability. Oral intake of 25 mg of RS showed extremely low bioavailability; only a trace amount of unmetabolized RS was detected in plasma. The gastrointestinal tract absorbs approximately 70% of RS, but it is further metabolized by three distinct metabolic pathways leading to low bioavailability[104].

Miscellaneous

Avicularin (quercetin-3-α L arabinofuranoside), a glycoside related to quercetin, reportedly reduces obesity, inflammation, and drug resistance[105,106]. It also induces cytotoxicity in cancer cells by promoting intrinsic apoptosis pathways. One study investigated the activity of avicularin in HCC by employing HuH-7 cell lines. Avicularin inhibited cell proliferation in a dose-dependent manner and markedly decreased the cell migration and invasiveness of the cancer cells. Gene and protein expression studies revealed reduced levels of NF-κB, cyclooxygenase 2, and PPARγ. Avicularin may have the potential to modulate PPARγ to induce antineoplastic activity in HCC[107].

Honokiol (C18H18O2) is a bioactive, biphenolic phytoconstituent derived from the bark and leaves of *Magnolia Officinalis*. Honokiol exhibits various protective activities such as anticarcinogenic, anti-inflammatory, anti-angiogenic, antioxidative, and repressive potency towards the malignant conversion of papillomas to carcinomas without any noticeable toxicity effects. A group of researchers employed a great blend of *in silico, in vitro*, and *in vivo* techniques to pinpoint and validate honokiol as a potent lead for being a PPARγ agonist. The binding of honokiol into the ligand-binding pocket of PPARγ was anticipated *via* various *in silico* techniques. The luciferase reporter assay confirmed this binding and advocated that honokiol could act as a partial PPARγ agonist. Further, using 3T3-L1 and mouse embryonic cell lines, it was observed that honokiol stimulated basal glucose uptake but did not induce adipogenesis. However, the oral administration of honokiol resulted in reduced hyperglycemia and weight gain[108]. Various studies have suggested that honokiol acts as an RXR agonist forming RXR dimers and activating PPARγ/RXR heterodimers. Additionally, it also potentiates the activation of PPARγ/RXR heterodimers induced by rosiglitazone[109-111]. Also, no peer-reviewed papers proving the abuse, misuse, or dependence on or addiction to avicularin and honokiol have been retrieved yet.

Chrysin is a dihydroxyflavone belonging to the family of flavonoids. A study revealed that chrysin reduced cell viability and promoted apoptosis in all cell lines *via* inhibiting the Skp2 and low-density lipoprotein receptor-related protein 6 expression. However, reduced MMP2, MMP9, and fibronectin levels were observed[112]. Despite these interesting bioactivities, the clinical applications of chrysin have been constrained by its hydrophobicity, poor bioavailability, and degradation at alkaline pH[113]. Similarly, quercetin (QE) is a classic flavonoid and a yellow crystalline pigment present in plants, used as a food supplement to reduce allergic responses or boost immunity. It has been known to inhibit the development of various types of cancer hepatic conditions[114,115]. QE was suggested to effectively suppress HCC due to its close interaction with the signal transducer and activator of transcription 3 (STAT3) pathway[116,117]. It inhibits cell proliferation, cell cycle regulation, and invasiveness of the cancer cells by promoting the autophagy of HCC[118]. However, the bioavailability of QE is very low due to its poor aqueous solubility and instability, challenging its therapeutic application in the pharma sector[119].

CONTRADICTORY ROLE OF PPARγ

Cancer tissues display metabolic and thermodynamic aberrations with dysregulated cellular growth. Although the role of PPARγ and its agonists in HCC and other cancers have been extensively studied, as discussed above, several conflicting reports exist concerning the PPARγ expression in cancers. It is unclear whether PPARγ induction promotes or suppresses tumor growth and viability. In the case of several cancers, PPARγ mainly exhibits the down-regulated expressions while activating several other pathways like the canonical Wnt/beta-catenin pathway, PI3K/Akt pathway, STAT3 pathway, *etc*[82,87,118]. The activation of Wnt/β-catenin signaling leads to the upregulated PDK1, which leads to aerobic glycolysis and mitochondrial stress[29]. A recent report by Galbraith *et al*[120] revealed that the activation of PPARγ, in turn, induced Akt serine/threonine kinase 3 (AKT3), which eventually led to the more aggressive form of cancer. AKT3 enhances PGC1α localization to the nuclear space by repressing chromosome maintenance region 1, while the latter served as the downstream target for PGC1α. All these led to mitochondrial biogenesis, which fueled the progression of the tumor. Previous studies have also reported such inconsistent findings for PPARγ in HCC. Koga *et al*[10] tested five patients with cirrhotic livers and found no significant change in the PPARγ expressions compared to the surrounding non-cancerous tissue. Another study reported the consistently overexpressed PPARγ in HCC tissue having null expression in the surrounding tissues, even though all the patients were infected with viral hepatitis (B or C)[121]. Although the well-known inhibitory effects of PPARγ agonists are reported, they are also suggested to have PPARγ-independent effects on cancers. Troglitazone, as discussed above, has a prominent antitumorigenic role in HCC. However, there are reports of it exhibiting PPARγ-independent activity. Palakurthi *et al*[122] studied troglitazone and ciglitazone on both PPARγ-/- and PPARγ+/+ mouse embryonic stem cells considering various concentrations. Both the agonists could inhibit cellular proliferation in a dose-dependent manner by suppressing the G1-S transition. This evidence demonstrated that the antiproliferative effect was induced by suppressing the translation initiation. More similar reports back up the PPARγ-independent antitumorigenic property of PPARγ agonists[123,124]. One of the studies focused on the HCC progression in HBV-transgenic mice demonstrated that the anticancerous, antiproliferative, and apoptotic effects of TZD were more significant in PPARγ-deficient mice in comparison with the control mice, exhibiting normal PPARγ levels[125]. It is well-understood that PPARγ could potentially affect various pathways, so it is vital to understand the underlying mechanisms critically. This understanding is an absolute requirement as PPARγ may be inconsistent. However, it highlights its crucial role in tumor development, suggesting that targeted biomedical research against PPARγ could provide a highly efficacious avenue for treating and managing of HCC and various other cancers.

CONCLUSION

The majority of current studies support the fact that PPARγ may be a potential target against the progression of HCC. They have extensively explored the various signaling cascades through which PPARγ exerted inhibitory against HCC using synthetic and natural agonists in preclinical and clinical trials. PPARγ was suggested as a potential target as it suppresses cell proliferation, migration, and invasion in HCC cells through different signaling pathways. TZD, a class of synthetic PPARγ agonists, were extensively studied for their efficacy against HCC. TZD showed significant results against the progression of HCC; however, due to their adverse effect on different organs, these drugs are not approved for any cancer treatment. Therefore, increased focus was employed to identify natural and endogenous PPARγ agonists having high bioavailability and specificity in terms of their binding at the active site. Several studies reported the safety profiles and therapeutic role of natural agonists against HCC in various experiment modals. Natural agonists are also effectively reported to mediate apoptosis and inhibit cell proliferation, tumor growth, and metastasis in HCC. Few reports also highlighted the contradictory role of PPARγ in HCC. These contradictions might be due to some unidentified link between PPARγ and cancer. With the well-established role of PPARγ in the progression of HCC, better efficacy of its agonists may be achieved by a complete understanding of underlying mechanisms through which PPARγ showed therapeutic effects. Future studies should be focused on developing novel PPARγ targeting therapy for the treatment of HCC.

ACKNOWLEDGEMENTS

The authors are thankful to the Director, CSIR-IHBT, Palampur, India, for his continuous support. The CSIR-IHBT communication number is 5016.

FOOTNOTES

Author contributions: Katoch S and Sharma V wrote the manuscript and contributed equally to the manuscript; Patial V contributed to the conception of the study, manuscript writing and editing; All authors have read and approved the final manuscript.

Supported by CSIR, India, No. MLP0204.

Conflict-of-interest statement: The authors have no conflict of interests to declare.

Open-Access: This article is an open-access article that was selected by an in-house editor and fully peer-reviewed by external reviewers. It is distributed in accordance with the Creative Commons Attribution NonCommercial (CC BY-NC 4.0) license, which permits others to distribute, remix, adapt, build upon this work non-commercially, and license their derivative works on different terms, provided the original work is properly cited and the use is non-commercial. See: https://creativecommons.org/Licenses/by-nc/4.0/

Country/Territory of origin: India

ORCID number: Swati Katoch 0000-0001-9120-6327; Vinesh Sharma 0000-0003-3767-4124; Vikram Patial 0000-0002-4912-9871.

S-Editor: Ma YJ
L-Editor: Filipodia
P-Editor: Ma YJ

REFERENCES

1 **El-Serag HB**. Epidemiology of viral hepatitis and hepatocellular carcinoma. *Gastroenterology* 2012; **142**: 1264-1273.e1 [PMID: 22537432 DOI: 10.1053/j.gastro.2011.12.061]
2 **Sayiner M**, Golabi P, Younossi ZM. Disease Burden of Hepatocellular Carcinoma: A Global Perspective. *Dig Dis Sci* 2019; **64**: 910-917 [PMID: 30835028 DOI: 10.1007/s10620-019-05537-2]
3 **Santopaolo F**, Lenci I, Milana M, Manzia TM, Baiocchi L. Liver transplantation for hepatocellular carcinoma: Where do we stand? *World J Gastroenterol* 2019; **25**: 2591-2602 [PMID: 31210712 DOI: 10.3748/wjg.v25.i21.2591]
4 **Llovet JM**, Ricci S, Mazzaferro V, Hilgard P, Gane E, Blanc JF, de Oliveira AC, Santoro A, Raoul JL, Forner A, Schwartz M, Porta C, Zeuzem S, Bolondi L, Greten TF, Galle PR, Seitz JF, Borbath I, Häussinger D, Giannaris T, Shan M, Moscovici M, Voliotis D, Bruix J; SHARP Investigators Study Group. Sorafenib in advanced hepatocellular carcinoma. *N Engl J Med* 2008; **359**: 378-390 [PMID: 18650514 DOI: 10.1056/NEJMoa0708857]

5 **Fan G**, Wei X, Xu X. Is the era of sorafenib over? *Ther Adv Med Oncol* 2020; **12**: 1758835920927602 [PMID: 32518599 DOI: 10.1177/1758835920927602]
6 **Hsu HT**, Chi CW. Emerging role of the peroxisome proliferator-activated receptor-gamma in hepatocellular carcinoma. *J Hepatocell Carcinoma* 2014; **1**: 127-135 [PMID: 27508182 DOI: 10.2147/JHC.S48512]
7 **Willson TM**, Lambert MH, Kliewer SA. Peroxisome proliferator-activated receptor gamma and metabolic disease. *Annu Rev Biochem* 2001; **70**: 341-367 [PMID: 11395411 DOI: 10.1146/annurev.biochem.70.1.341]
8 **Wu CW**, Farrell GC, Yu J. Functional role of peroxisome-proliferator-activated receptor γ in hepatocellular carcinoma. *J Gastroenterol Hepatol* 2012; **27**: 1665-1669 [PMID: 22742931 DOI: 10.1111/j.1440-1746.2012.]
9 **Tan Y**, Wang M, Yang K, Chi T, Liao Z, Wei P. PPAR-α Modulators as Current and Potential Cancer Treatments. *Front Oncol* 2021; **11**: 599995 [PMID: 33833983 DOI: 10.3389/fonc.2021.599995]
10 **Koga H**, Sakisaka S, Harada M, Takagi T, Hanada S, Taniguchi E, Kawaguchi T, Sasatomi K, Kimura R, Hashimoto O, Ueno T, Yano H, Kojiro M, Sata M. Involvement of p21(WAF1/Cip1), p27(Kip1), and p18(INK4c) in troglitazone-induced cell-cycle arrest in human hepatoma cell lines. *Hepatology* 2001; **33**: 1087-1097 [PMID: 11343236 DOI: 10.1053/jhep.2001.24024]
11 **Lee WS**, Kim J. Peroxisome Proliferator-Activated Receptors and the Heart: Lessons from the Past and Future Directions. *PPAR Res* 2015; **2015**: 271983 [PMID: 26587015 DOI: 10.1155/2015/271983]
12 **Mirza AZ**, Althagafi II, Shamshad H. Role of PPAR receptor in different diseases and their ligands: Physiological importance and clinical implications. *Eur J Med Chem* 2019; **166**: 502-513 [PMID: 30739829 DOI: 10.1016/j.ejmech.2019.01.067]
13 **Aouali N**, Broukou A, Bosseler M, Keunen O, Schlesser V, Janji B, Palissot V, Stordeur P, Berchem G. Epigenetic Activity of Peroxisome Proliferator-Activated Receptor Gamma Agonists Increases the Anticancer Effect of Histone Deacetylase Inhibitors on Multiple Myeloma Cells. *PLoS One* 2015; **10**: e0130339 [PMID: 26091518 DOI: 10.1371/journal.pone.0130339]
14 **Peters JM**, Shah YM, Gonzalez FJ. The role of peroxisome proliferator-activated receptors in carcinogenesis and chemoprevention. *Nat Rev Cancer* 2012; **12**: 181-195 [PMID: 22318237 DOI: 10.1038/nrc3214]
15 **Tyagi S**, Gupta P, Saini AS, Kaushal C, Sharma S. The peroxisome proliferator-activated receptor: A family of nuclear receptors role in various diseases. *J Adv Pharm Technol Res* 2011; **2**: 236-240 [PMID: 22247890 DOI: 10.4103/2231-4040.90879]
16 **Grygiel-Górniak B**. Peroxisome proliferator-activated receptors and their ligands: nutritional and clinical implications--a review. *Nutr J* 2014; **13**: 17 [PMID: 24524207 DOI: 10.1186/1475-2891-13-17]
17 **Guan Y**. Peroxisome proliferator-activated receptor family and its relationship to renal complications of the metabolic syndrome. *J Am Soc Nephrol* 2004; **15**: 2801-2815 [PMID: 15504933 DOI: 10.1097/01.ASN.0000139067.83419.46]
18 **Wu L**, Guo C, Wu J. Therapeutic potential of PPARγ natural agonists in liver diseases. *J Cell Mol Med* 2020; **24**: 2736-2748 [PMID: 32031298 DOI: 10.1111/jcmm.15028]
19 **Koga H**, Harada M, Ohtsubo M, Shishido S, Kumemura H, Hanada S, Taniguchi E, Yamashita K, Kumashiro R, Ueno T, Sata M. Troglitazone induces p27Kip1-associated cell-cycle arrest through down-regulating Skp2 in human hepatoma cells. *Hepatology* 2003; **37**: 1086-1096 [PMID: 12717389 DOI: 10.1053/jhep.2003.50186]
20 **Cheung KF**, Zhao J, Hao Y, Li X, Lowe AW, Cheng AS, Sung JJ, Yu J. CITED2 is a novel direct effector of peroxisome proliferator-activated receptor γ in suppressing hepatocellular carcinoma cell growth. *Cancer* 2013; **119**: 1217-1226 [PMID: 23212831 DOI: 10.1002/cncr.27865]
21 **Yu J**, Shen B, Chu ES, Teoh N, Cheung KF, Wu CW, Wang S, Lam CN, Feng H, Zhao J, Cheng AS, To KF, Chan HL, Sung JJ. Inhibitory role of peroxisome proliferator-activated receptor gamma in hepatocarcinogenesis in mice and in vitro. *Hepatology* 2010; **51**: 2008-2019 [PMID: 20512989 DOI: 10.1002/hep.23550]
22 **Yousefnia S**, Momenzadeh S, Seyed Forootan F, Ghaedi K, Nasr Esfahani MH. The influence of peroxisome proliferator-activated receptor γ (PPARγ) ligands on cancer cell tumorigenicity. *Gene* 2018; **649**: 14-22 [PMID: 29369787 DOI: 10.1016/j.gene.2018.01.018]
23 **Bo QF**, Sun XM, Liu J, Sui XM, Li GX. Antitumor action of the peroxisome proliferator-activated receptor-γ agonist rosiglitazone in hepatocellular carcinoma. *Oncol Lett* 2015; **10**: 1979-1984 [PMID: 26622783 DOI: 10.3892/ol.2015.3554]
24 **Zhang Q**, Xiang S, Liu Q, Gu T, Yao Y, Lu X. PPARγ Antagonizes Hypoxia-Induced Activation of Hepatic Stellate Cell through Cross Mediating PI3K/AKT and cGMP/PKG Signaling. *PPAR Res* 2018; **2018**: 6970407 [PMID: 29686697 DOI: 10.1155/2018/6970407]
25 **Shen B**, Chu ES, Zhao G, Man K, Wu CW, Cheng JT, Li G, Nie Y, Lo CM, Teoh N, Farrell GC, Sung JJ, Yu J. PPAR gamma inhibits hepatocellular carcinoma metastases *in vitro* and in mice. *Br J Cancer* 2012; **106**: 1486-1494 [PMID: 22472882 DOI: 10.1038/bjc.2012.130]
26 **Mahmood DFD**, Jguirim-Souissi I, Khadija EH, Blondeau N, Diderot V, Amrani S, Slimane MN, Syrovets T, Simmet T, Rouis M. Peroxisome proliferator-activated receptor gamma induces apoptosis and inhibits autophagy of human monocyte-derived macrophages *via* induction of cathepsin L: potential role in atherosclerosis. *J Biol Chem* 2011; **286**: 28858-28866 [PMID: 21700710 DOI: 10.1074/jbc.M111.273292]
27 **Sun M**, Tan L, Hu M. The role of autophagy in hepatic fibrosis. *Am J Transl Res* 2021; **13**: 5747-5757 [PMID: 34306323]
28 **Mastropasqua F**, Girolimetti G, Shoshan M. PGC1α: Friend or Foe in Cancer? *Genes (Basel)* 2018; **9** [PMID: 29361779 DOI: 10.3390/genes9010048]
29 **Zuo Q**, He J, Zhang S, Wang H, Jin G, Jin H, Cheng Z, Tao X, Yu C, Li B, Yang C, Wang S, Lv Y, Zhao F, Yao M, Cong W, Wang C, Qin W. PPARγ Coactivator-1α Suppresses Metastasis of Hepatocellular Carcinoma by Inhibiting Warburg Effect by PPARγ-Dependent WNT/β-Catenin/Pyruvate Dehydrogenase Kinase Isozyme 1 Axis. *Hepatology* 2021; **73**: 644-660 [PMID: 32298475 DOI: 10.1002/hep.31280]
30 **Kim H**, Lee JY, Park SJ, Kwag E, Koo O, Shin JH. ZNF746/PARIS promotes the occurrence of hepatocellular carcinoma. *Biochem Biophys Res Commun* 2021; **563**: 98-104 [PMID: 34062393 DOI: 10.1016/j.bbrc.2021.05.051]
31 **Bost F**, Kaminski L. The metabolic modulator PGC-1α in cancer. *Am J Cancer Res* 2019; **9**: 198-211 [PMID: 30906622]
32 **Gerhold DL**, Liu F, Jiang G, Li Z, Xu J, Lu M, Sachs JR, Bagchi A, Fridman A, Holder DJ, Doebber TW, Berger J,

Elbrecht A, Moller DE, Zhang BB. Gene expression profile of adipocyte differentiation and its regulation by peroxisome proliferator-activated receptor-gamma agonists. *Endocrinology* 2002; **143**: 2106-2118 [PMID: 12021175 DOI: 10.1210/endo.143.6.8842]

33 **Yu J**, Qiao L, Zimmermann L, Ebert MP, Zhang H, Lin W, Röcken C, Malfertheiner P, Farrell GC. Troglitazone inhibits tumor growth in hepatocellular carcinoma in vitro and in vivo. *Hepatology* 2006; **43**: 134-143 [PMID: 16374840 DOI: 10.1002/hep.20994]

34 **Tu K**, Zheng X, Dou C, Li C, Yang W, Yao Y, Liu Q. MicroRNA-130b promotes cell aggressiveness by inhibiting peroxisome proliferator-activated receptor gamma in human hepatocellular carcinoma. *Int J Mol Sci* 2014; **15**: 20486-20499 [PMID: 25387077 DOI: 10.3390/ijms151120486]

35 **Liu Z**, Wang Y, Dou C, Sun L, Li Q, Wang L, Xu Q, Yang W, Liu Q, Tu K. MicroRNA-1468 promotes tumor progression by activating PPAR-γ-mediated AKT signaling in human hepatocellular carcinoma. *J Exp Clin Cancer Res* 2018; **37**: 49 [PMID: 29510736 DOI: 10.1186/s13046-018-0717-3]

36 **Hyun S**, Kim MS, Song YS, Bak Y, Ham SY, Lee DH, Hong J, Yoon DY. Peroxisome proliferator-activated receptor-gamma agonist 4-O-methylhonokiol induces apoptosis by triggering the intrinsic apoptosis pathway and inhibiting the PI3K/Akt survival pathway in SiHa human cervical cancer cells. *J Microbiol Biotechnol* 2015; **25**: 334-342 [PMID: 25563418 DOI: 10.4014/jmb.1411.11073]

37 **Walter I**, Schulz U, Vogelhuber M, Wiedmann K, Endlicher E, Klebl F, Andreesen R, Herr W, Ghibelli L, Hackl C, Wiest R, Reichle A. Communicative reprogramming non-curative hepatocellular carcinoma with low-dose metronomic chemotherapy, COX-2 inhibitor and PPAR-gamma agonist: a phase II trial. *Med Oncol* 2017; **34**: 192 [PMID: 29098441 DOI: 10.1007/s12032-017-1040-0]

38 **Yip TC**, Wong VW, Chan HL, Tse YK, Hui VW, Liang LY, Lee HW, Lui GC, Kong AP, Wong GL. Thiazolidinediones reduce the risk of hepatocellular carcinoma and hepatic events in diabetic patients with chronic hepatitis B. *J Viral Hepat* 2020; **27**: 904-914 [PMID: 32340077 DOI: 10.1111/jvh.13307]

39 **Lai SW**, Chen PC, Liao KF, Muo CH, Lin CC, Sung FC. Risk of hepatocellular carcinoma in diabetic patients and risk reduction associated with anti-diabetic therapy: a population-based cohort study. *Am J Gastroenterol* 2012; **107**: 46-52 [PMID: 22085817 DOI: 10.1038/ajg.2011.384]

40 **Lin HC**, Hsu YT, Kachingwe BH, Hsu CY, Uang YS, Wang LH. Dose effect of thiazolidinedione on cancer risk in type 2 diabetes mellitus patients: a six-year population-based cohort study. *J Clin Pharm Ther* 2014; **39**: 354-360 [PMID: 24661226 DOI: 10.1111/jcpt.12151]

41 **Huang MY**, Chung CH, Chang WK, Lin CS, Chen KW, Hsieh TY, Chien WC, Lin HH. The role of thiazolidinediones in hepatocellular carcinoma risk reduction: a population-based cohort study in Taiwan. *Am J Cancer Res* 2017; **7**: 1606-1616 [PMID: 28744408]

42 **Chang CH**, Lin JW, Wu LC, Lai MS, Chuang LM, Chan KA. Association of thiazolidinediones with liver cancer and colorectal cancer in type 2 diabetes mellitus. *Hepatology* 2012; **55**: 1462-1472 [PMID: 22135104 DOI: 10.1002/hep.25509]

43 **Yan H**, Wu W, Chang X, Xia M, Ma S, Wang L, Gao J. Gender differences in the efficacy of pioglitazone treatment in nonalcoholic fatty liver disease patients with abnormal glucose metabolism. *Biol Sex Differ* 2021; **12**: 1 [PMID: 33397443 DOI: 10.1186/s13293-020-00344-1]

44 **Li S**, Ghoshal S, Sojoodi M, Arora G, Masia R, Erstad DJ, Lanuti M, Hoshida Y, Baumert TF, Tanabe KK, Fuchs BC. Pioglitazone Reduces Hepatocellular Carcinoma Development in Two Rodent Models of Cirrhosis. *J Gastrointest Surg* 2019; **23**: 101-111 [PMID: 30367397 DOI: 10.1007/s11605-018-4004-6]

45 **Yang Y**, Zhao LH, Huang B, Wang RY, Yuan SX, Tao QF, Xu Y, Sun HY, Lin C, Zhou WP. Pioglitazone, a PPARγ agonist, inhibits growth and invasion of human hepatocellular carcinoma *via* blockade of the rage signaling. *Mol Carcinog* 2015; **54**: 1584-1595 [PMID: 25307746 DOI: 10.1002/mc.22231]

46 **Sumie S**, Kawaguchi T, Kawaguchi A, Kuromatsu R, Nakano M, Satani M, Yamada S, Okamura S, Yonezawa Y, Kakuma T, Torimura T, Sata M. Effect of pioglitazone on outcome following curative treatment for hepatocellular carcinoma in patients with hepatitis C virus infection: A prospective study. *Mol Clin Oncol* 2015; **3**: 115-120 [PMID: 25469280 DOI: 10.3892/mco.2014.435]

47 **Chongmelaxme B**, Phisalprapa P, Sawangjit R, Dilokthornsakul P, Chaiyakunapruk N. Weight Reduction and Pioglitazone are Cost-Effective for the Treatment of Non-Alcoholic Fatty Liver Disease in Thailand. *Pharmacoeconomics* 2019; **37**: 267-278 [PMID: 30430467 DOI: 10.1007/s40273-018-0736-0]

48 **Shah P**, Mudaliar S. Pioglitazone: side effect and safety profile. *Expert Opin Drug Saf* 2010; **9**: 347-354 [PMID: 20175701 DOI: 10.1517/14740331003623218]

49 **Li X**, He J, Li B, Gao M, Zeng Y, Lian J, Shi C, Huang Y, He F. The PPARγ agonist rosiglitazone sensitizes the BH3 mimetic (-)-gossypol to induce apoptosis in cancer cells with high level of Bcl-2. *Mol Carcinog* 2018; **57**: 1213-1222 [PMID: 29856104 DOI: 10.1002/mc.22837]

50 **Cao LQ**, Shao ZL, Liang HH, Zhang DW, Yang XW, Jiang XF, Xue P. Activation of peroxisome proliferator-activated receptor-γ (PPARγ) inhibits hepatoma cell growth *via* downregulation of SEPT2 expression. *Cancer Lett* 2015; **359**: 127-135 [PMID: 25592041 DOI: 10.1016/j.canlet.2015.01.004]

51 **Ratziu V**, Charlotte F, Bernhardt C, Giral P, Halbron M, Lenaour G, Hartmann-Heurtier A, Bruckert E, Poynard T; LIDO Study Group. Long-term efficacy of rosiglitazone in nonalcoholic steatohepatitis: results of the fatty liver improvement by rosiglitazone therapy (FLIRT 2) extension trial. *Hepatology* 2010; **51**: 445-453 [PMID: 19877169 DOI: 10.1002/hep.23270]

52 **Mitka M**. Panel recommends easing restrictions on rosiglitazone despite concerns about cardiovascular safety. *JAMA* 2013; **310**: 246-247 [PMID: 23860970 DOI: 10.1001/jama.2013.8141]

53 **Oura K**, Tadokoro T, Fujihara S, Morishita A, Chiyo T, Samukawa E, Yamana Y, Fujita K, Sakamoto T, Nomura T, Yoneyama H, Kobara H, Mori H, Iwama H, Okano K, Suzuki Y, Masaki T. Telmisartan inhibits hepatocellular carcinoma cell proliferation in vitro by inducing cell cycle arrest. *Oncol Rep* 2017; **38**: 2825-2835 [PMID: 29048654 DOI: 10.3892/or.2017.5977]

54 **Saber S**, Khodir AE, Soliman WE, Salama MM, Abdo WS, Elsaeed B, Nader K, Abdelnasser A, Megahed N, Basuony M, Shawky A, Mahmoud M, Medhat R, Eldin AS. Telmisartan attenuates N-nitrosodiethylamine-induced hepatocellular carcinoma in mice by modulating the NF-κB-TAK1-ERK1/2 axis in the context of PPARγ agonistic activity. *Naunyn Schmiedebergs Arch Pharmacol* 2019; **392**: 1591-1604 [PMID: 31367864 DOI: 10.1007/s00210-019-01706-2]

55 **Unger T**, Schupp M. Telmisartan: from lowering blood pressure to end-organ protection. *Future Cardiol* 2005; **1**: 7-15 [PMID: 19804057 DOI: 10.1517/14796678.1.1.7]

56 **Li MY**, Deng H, Zhao JM, Dai D, Tan XY. Peroxisome proliferator-activated receptor gamma ligands inhibit cell growth and induce apoptosis in human liver cancer BEL-7402 cells. *World J Gastroenterol* 2003; **9**: 1683-1688 [PMID: 12918101 DOI: 10.3748/wjg.v9.i8.1683]

57 **Zhou YM**, Wen YH, Kang XY, Qian HH, Yang JM, Yin ZF. Troglitazone, a peroxisome proliferator-activated receptor gamma ligand, induces growth inhibition and apoptosis of HepG2 human liver cancer cells. *World J Gastroenterol* 2008; **14**: 2168-2173 [PMID: 18407589 DOI: 10.3748/wjg.14.2168]

58 **Rumi MA**, Sato H, Ishihara S, Kawashima K, Hamamoto S, Kazumori H, Okuyama T, Fukuda R, Nagasue N, Kinoshita Y. Peroxisome proliferator-activated receptor gamma ligand-induced growth inhibition of human hepatocellular carcinoma. *Br J Cancer* 2001; **84**: 1640-1647 [PMID: 11401318 DOI: 10.1054/bjoc.2001.1821]

59 **Toyoda M**, Takagi H, Horiguchi N, Kakizaki S, Sato K, Takayama H, Mori M. A ligand for peroxisome proliferator activated receptor gamma inhibits cell growth and induces apoptosis in human liver cancer cells. *Gut* 2002; **50**: 563-567 [PMID: 11889080 DOI: 10.1136/gut.50.4.563]

60 **Kores K**, Konc J, Bren U. Mechanistic Insights into Side Effects of Troglitazone and Rosiglitazone Using a Novel Inverse Molecular Docking Protocol. *Pharmaceutics* 2021; **13** [PMID: 33670968 DOI: 10.3390/pharmaceutics13030315]

61 **Kumar DP**, Caffrey R, Marioneaux J, Santhekadur PK, Bhat M, Alonso C, Koduru SV, Philip B, Jain MR, Giri SR, Bedossa P, Sanyal AJ. The PPAR α/γ Agonist Saroglitazar Improves Insulin Resistance and Steatohepatitis in a Diet Induced Animal Model of Nonalcoholic Fatty Liver Disease. *Sci Rep* 2020; **10**: 9330 [PMID: 32518275 DOI: 10.1038/s41598-020-66458-z]

62 **Hassan NF**, Nada SA, Hassan A, El-Ansary MR, Al-Shorbagy MY, Abdelsalam RM. Saroglitazar Deactivates the Hepatic LPS/TLR4 Signaling Pathway and Ameliorates Adipocyte Dysfunction in Rats with High-Fat Emulsion/LPS Model-Induced Non-alcoholic Steatohepatitis. *Inflammation* 2019; **42**: 1056-1070 [PMID: 30737662 DOI: 10.1007/s10753-019-00967-6]

63 **Mitra A**. An Observational Study of Reduction in Glycemic Parameters and Liver Stiffness by Saroglitazar 4 mg in Patients With Type 2 Diabetes Mellitus and Nonalcoholic Fatty Liver Disease. *Cureus* 2020; **12**: e9065 [PMID: 32782883 DOI: 10.7759/cureus.9065]

64 **Shafi SM**, Yattoo GN. Spectrum, Clinico-pathological Profile of Non-Alcoholic Fatty Liver Disease and its Treatment Response with 48 wk Therapy of Saroglitazar. *JMS SKIMS* 2021; 24

65 **Sosale A**, Saboo B, Sosale B. Saroglitazar for the treatment of hypertrig-lyceridemia in patients with type 2 diabetes: current evidence. *Diabetes Metab Syndr Obes* 2015; **8**: 189-196 [PMID: 25926748 DOI: 10.2147/DMSO.S49592]

66 **Vara D**, Morell C, Rodríguez-Henche N, Diaz-Laviada I. Involvement of PPARγ in the antitumoral action of cannabinoids on hepatocellular carcinoma. *Cell Death Dis* 2013; **4**: e618 [PMID: 23640460 DOI: 10.1038/cddis.2013.141]

67 **Guzmán M**, Duarte MJ, Blázquez C, Ravina J, Rosa MC, Galve-Roperh I, Sánchez C, Velasco G, González-Feria L. A pilot clinical study of Delta9-tetrahydrocannabinol in patients with recurrent glioblastoma multiforme. *Br J Cancer* 2006; **95**: 197-203 [PMID: 16804518 DOI: 10.1038/sj.bjc.6603236]

68 **Nadal X**, Del Río C, Casano S, Palomares B, Ferreiro-Vera C, Navarrete C, Sánchez-Carnerero C, Cantarero I, Bellido ML, Meyer S, Morello G, Appendino G, Muñoz E. Tetrahydrocannabinolic acid is a potent PPARγ agonist with neuroprotective activity. *Br J Pharmacol* 2017; **174**: 4263-4276 [PMID: 28853159 DOI: 10.1111/bph.14019]

69 **Cohen K**, Weizman A, Weinstein A. Positive and Negative Effects of Cannabis and Cannabinoids on Health. *Clin Pharmacol Ther* 2019; **105**: 1139-1147 [PMID: 30703255 DOI: 10.1002/cpt.1381]

70 **Bellocchio L**, Inchingolo AD, Inchingolo AM, Lorusso F, Malcangi G, Santacroce L, Scarano A, Bordea IR, Hazballa D, D'Oria MT, Isacco CG, Nucci L, Serpico R, Tartaglia GM, Giovanniello D, Contaldo M, Farronato M, Dipalma G, Inchingolo F. Cannabinoids Drugs and Oral Health-From Recreational Side-Effects to Medicinal Purposes: A Systematic Review. *Int J Mol Sci* 2021; **22** [PMID: 34361095 DOI: 10.3390/ijms22158329]

71 **Choi JH**, Jin SW, Choi CY, Kim HG, Lee GH, Kim YA, Chung YC, Jeong HG. Capsaicin Inhibits Dimethylnitrosamine-Induced Hepatic Fibrosis by Inhibiting the TGF-β1/Smad Pathway *via* Peroxisome Proliferator-Activated Receptor Gamma Activation. *J Agric Food Chem* 2017; **65**: 317-326 [PMID: 27991776 DOI: 10.1021/acs.jafc.6b04805]

72 **Clark R**, Lee SH. Anticancer Properties of Capsaicin Against Human Cancer. *Anticancer Res* 2016; **36**: 837-843 [PMID: 26976969]

73 **Collier JG**, Fuller RW. Capsaicin inhalation in man and the effects of sodium cromoglycate. *Br J Pharmacol* 1984; **81**: 113-117 [PMID: 6423016 DOI: 10.1111/j.1476-5381.1984.tb10750.x]

74 **Midgren B**, Hansson L, Karlsson JA, Simonsson BG, Persson CG. Capsaicin-induced cough in humans. *Am Rev Respir Dis* 1992; **146**: 347-351 [PMID: 1489123 DOI: 10.1164/ajrccm/146.2.347]

75 **Hakas JF Jr**. Topical capsaicin induces cough in patient receiving ACE inhibitor. *Ann Allergy* 1990; **65**: 322-323 [PMID: 2221491]

76 **Morice AH**, Brown MJ, Higenbottam T. Cough associated with angiotensin converting enzyme inhibition. *J Cardiovasc Pharmacol* 1989; **13** Suppl 3: S59-S62 [PMID: 2474106 DOI: 10.1097/00005344-198900133-00015]

77 **Patial V**, S M, Sharma S, Pratap K, Singh D, Padwad YS. Synergistic effect of curcumin and piperine in suppression of DENA-induced hepatocellular carcinoma in rats. *Environ Toxicol Pharmacol* 2015; **40**: 445-452 [PMID: 26278679 DOI: 10.1016/j.etap.2015.07.012]

78 **Pan Z**, Zhuang J, Ji C, Cai Z, Liao W, Huang Z. Curcumin inhibits hepatocellular carcinoma growth by targeting VEGF expression. *Oncol Lett* 2018; **15**: 4821-4826 [PMID: 29552121 DOI: 10.3892/ol.2018.7988]

79 **Teng CF**, Yu CH, Chang HY, Hsieh WC, Wu TH, Lin JH, Wu HC, Jeng LB, Su IJ. Chemopreventive Effect of

Phytosomal Curcumin on Hepatitis B Virus-Related Hepatocellular Carcinoma in A Transgenic Mouse Model. *Sci Rep* 2019; **9**: 10338 [PMID: 31316146 DOI: 10.1038/s41598-019-46891-5]

80 **Zheng S**, Chen A. Disruption of transforming growth factor-beta signaling by curcumin induces gene expression of peroxisome proliferator-activated receptor-gamma in rat hepatic stellate cells. *Am J Physiol Gastrointest Liver Physiol* 2007; **292**: G113-G123 [PMID: 16959952 DOI: 10.1152/ajpgi.00200.2006]

81 **Li J**, Wei H, Liu Y, Li Q, Guo H, Guo Y, Chang Z. Curcumin Inhibits Hepatocellular Carcinoma *via* Regulating miR-21/TIMP3 Axis. *Evid Based Complement Alternat Med* 2020; **2020**: 2892917 [PMID: 32724322 DOI: 10.1155/2020/2892917]

82 **Shao J**, Shi CJ, Li Y, Zhang FW, Pan FF, Fu WM, Zhang JF. LincROR Mediates the Suppressive Effects of Curcumin on Hepatocellular Carcinoma Through Inactivating Wnt/β-Catenin Signaling. *Front Pharmacol* 2020; **11**: 847 [PMID: 32714183 DOI: 10.3389/fphar.2020.00847]

83 **Sayed MM**, El-Kordy EA. The protective effect of curcumin on paracetamol-induced liver damage in adult male rabbits: biochemical and histological studies. *Egyptian J Histol* 2014; **37**: 629-39

84 **Anand P**, Kunnumakkara AB, Newman RA, Aggarwal BB. Bioavailability of curcumin: problems and promises. *Mol Pharm* 2007; **4**: 807-818 [PMID: 17999464 DOI: 10.1021/mp700113r]

85 **Mahmoud AM**, Mohammed HM, Khadrawy SM, Galaly SR. Hesperidin protects against chemically induced hepatocarcinogenesis *via* modulation of Nrf2/ARE/HO-1, PPARγ and TGF-β1/Smad3 signaling, and amelioration of oxidative stress and inflammation. *Chem Biol Interact* 2017; **277**: 146-158 [PMID: 28935427 DOI: 10.1016/j.cbi.2017.09.015]

86 **Mo'men YS**, Hussein RM, Kandeil MA. Involvement of PI3K/Akt pathway in the protective effect of hesperidin against a chemically induced liver cancer in rats. *J Biochem Mol Toxicol* 2019; **33**: e22305 [PMID: 30779474 DOI: 10.1002/jbt.22305]

87 **Zaghloul RA**, Elsherbiny NM, Kenawy HI, El-Karef A, Eissa LA, El-Shishtawy MM. Hepatoprotective effect of hesperidin in hepatocellular carcinoma: Involvement of Wnt signaling pathways. *Life Sci* 2017; **185**: 114-125 [PMID: 28754618 DOI: 10.1016/j.lfs.2017.07.026]

88 **Ameer B**, Weintraub RA, Johnson JV, Yost RA, Rouseff RL. Flavanone absorption after naringin, hesperidin, and citrus administration. *Clin Pharmacol Ther* 1996; **60**: 34-40 [PMID: 8689809 DOI: 10.1016/S0009-9236(96)90164-2]

89 **Han M**, Gao H, Ju P, Gao MQ, Yuan YP, Chen XH, Liu KL, Han YT, Han ZW. Hispidulin inhibits hepatocellular carcinoma growth and metastasis through AMPK and ERK signaling mediated activation of PPARγ. *Biomed Pharmacother* 2018; **103**: 272-283 [PMID: 29656183 DOI: 10.1016/j.biopha.2018.04.014]

90 **Lv L**, Zhang W, Li T, Jiang L, Lu X, Lin J. Hispidulin exhibits potent anticancer activity in vitro and in vivo through activating ER stress in nonsmallcell lung cancer cells. *Oncol Rep* 2020; **43**: 1995-2003 [PMID: 32236602 DOI: 10.3892/or.2020.7568]

91 **Kavvadias D**, Sand P, Youdim KA, Qaiser MZ, Rice-Evans C, Baur R, Sigel E, Rausch WD, Riederer P, Schreier P. The flavone hispidulin, a benzodiazepine receptor ligand with positive allosteric properties, traverses the blood-brain barrier and exhibits anticonvulsive effects. *Br J Pharmacol* 2004; **142**: 811-820 [PMID: 15231642 DOI: 10.1038/sj.bjp.0705828]

92 **Chen LC**, Hsu KC, Chiou LC, Tseng HJ, Huang WJ. Total Synthesis and Metabolic Stability of Hispidulin and Its d-Labelled Derivative. *Molecules* 2017; **22** [PMID: 29113055 DOI: 10.3390/molecules22111897]

93 **Moselhy J**, Srinivasan S, Ankem MK, Damodaran C. Natural Products That Target Cancer Stem Cells. *Anticancer Res* 2015; **35**: 5773-5788 [PMID: 26503998]

94 **Xiao Y**, Gong Q, Wang W, Liu F, Kong Q, Pan F, Zhang X, Yu C, Hu S, Fan F, Li S, Liu Y. The combination of Biochanin A and SB590885 potentiates the inhibition of tumour progression in hepatocellular carcinoma. *Cancer Cell Int* 2020; **20**: 371 [PMID: 32774165 DOI: 10.1186/s12935-020-01463-w]

95 **Sanaei M**, Kavoosi F, Valiani A, Ghobadifar MA. Effect of Genistein on Apoptosis and Proliferation of Hepatocellular Carcinoma Hepa1-6 Cell Line. *Int J Prev Med* 2018; **9**: 12 [PMID: 29541427 DOI: 10.4103/ijpvm.IJPVM_249_16]

96 **Li S**, Li J, Dai W, Zhang Q, Feng J, Wu L, Liu T, Yu Q, Xu S, Wang W, Lu X, Chen K, Xia Y, Lu J, Zhou Y, Fan X, Mo W, Xu L, Guo C. Genistein suppresses aerobic glycolysis and induces hepatocellular carcinoma cell death. *Br J Cancer* 2017; **117**: 1518-1528 [PMID: 28926527 DOI: 10.1038/bjc.2017.323]

97 **Sharp GB**, Lagarde F, Mizuno T, Sauvaget C, Fukuhara T, Allen N, Suzuki G, Tokuoka S. Relationship of hepatocellular carcinoma to soya food consumption: a cohort-based, case-control study in Japan. *Int J Cancer* 2005; **115**: 290-295 [PMID: 15688396 DOI: 10.1002/ijc.20897]

98 **Zamora-Ros R**, Fedirko V, Trichopoulou A, González CA, Bamia C, Trepo E, Nöthlings U, Duarte-Salles T, Serafini M, Bredsdorff L, Overvad K, Tjønneland A, Halkjaer J, Fagherazzi G, Perquier F, Boutron-Ruault MC, Katzke V, Lukanova A, Floegel A, Boeing H, Lagiou P, Trichopoulos D, Saieva C, Agnoli C, Mattiello A, Tumino R, Sacerdote C, Bueno-de-Mesquita HB, Peeters PH, Weiderpass E, Engeset D, Skeie G, Argüelles MV, Molina-Montes E, Dorronsoro M, Tormo MJ, Ardanaz E, Ericson U, Sonestedt E, Sund M, Landberg R, Khaw KT, Wareham NJ, Crowe FL, Riboli E, Jenab M. Dietary flavonoid, lignan and antioxidant capacity and risk of hepatocellular carcinoma in the European prospective investigation into cancer and nutrition study. *Int J Cancer* 2013; **133**: 2429-2443 [PMID: 23649669 DOI: 10.1002/ijc.28257]

99 **Yu J**, Bi X, Yu B, Chen D. Isoflavones: Anti-Inflammatory Benefit and Possible Caveats. *Nutrients* 2016; **8** [PMID: 27294954 DOI: 10.3390/nu8060361]

100 **Zhou Y**, Guo Y, Zhu Y, Sun Y, Li W, Li Z, Wei L. Dual PPARγ/α agonist oroxyloside suppresses cell cycle progression by glycolipid metabolism switch-mediated increase of reactive oxygen species levels. *Free Radic Biol Med* 2021; **167**: 205-217 [PMID: 33713839 DOI: 10.1016/j.freeradbiomed.2021.02.032]

101 **Rawat D**, Chhonker SK, Naik RA, Koiri RK. Modulation of antioxidant enzymes, SIRT1 and NF-κB by resveratrol and nicotinamide in alcohol-aflatoxin B1-induced hepatocellular carcinoma. *J Biochem Mol Toxicol* 2021; **35**: e22625 [PMID: 32894639 DOI: 10.1002/jbt.22625]

102 **Jagwani S**, Jalalpure S, Dhamecha D, Jadhav K, Bohara R. Pharmacokinetic and Pharmacodynamic Evaluation of Resveratrol Loaded Cationic Liposomes for Targeting Hepatocellular Carcinoma. *ACS Biomater Sci Eng* 2020; **6**: 4969-

4984 [PMID: 33455290 DOI: 10.1021/acsbiomaterials.0c00429]
103 **Santos AC**, Pereira I, Magalhães M, Pereira-Silva M, Caldas M, Ferreira L, Figueiras A, Ribeiro AJ, Veiga F. Targeting Cancer Via Resveratrol-Loaded Nanoparticles Administration: Focusing on In Vivo Evidence. *AAPS J* 2019; **21**: 57 [PMID: 31016543 DOI: 10.1208/s12248-019-0325-y]
104 **Shaito A**, Posadino AM, Younes N, Hasan H, Halabi S, Alhababi D, Al-Mohannadi A, Abdel-Rahman WM, Eid AH, Nasrallah GK, Pintus G. Potential Adverse Effects of Resveratrol: A Literature Review. *Int J Mol Sci* 2020; **21** [PMID: 32197410 DOI: 10.3390/ijms21062084]
105 **Fujimori K**, Shibano M. Avicularin, a plant flavonoid, suppresses lipid accumulation through repression of C/EBPα-activated GLUT4-mediated glucose uptake in 3T3-L1 cells. *J Agric Food Chem* 2013; **61**: 5139-5147 [PMID: 23647459 DOI: 10.1021/jf401154c]
106 **Guo XF**, Liu JP, Ma SQ, Zhang P, Sun WD. Avicularin reversed multidrug-resistance in human gastric cancer through enhancing Bax and BOK expressions. *Biomed Pharmacother* 2018; **103**: 67-74 [PMID: 29635130 DOI: 10.1016/j.biopha.2018.03.110]
107 **Wang Z**, Li F, Quan Y, Shen J. Avicularin ameliorates human hepatocellular carcinoma *via* the regulation of NFκB/COX2/PPARγ activities. *Mol Med Rep* 2019; **19**: 5417-5423 [PMID: 31059053 DOI: 10.3892/mmr.2019.10198]
108 **Atanasov AG**, Wang JN, Gu SP, Bu J, Kramer MP, Baumgartner L, Fakhrudin N, Ladurner A, Malainer C, Vuorinen A, Noha SM, Schwaiger S, Rollinger JM, Schuster D, Stuppner H, Dirsch VM, Heiss EH. Honokiol: a non-adipogenic PPARγ agonist from nature. *Biochim Biophys Acta* 2013; **1830**: 4813-4819 [PMID: 23811337 DOI: 10.1016/j.bbagen.2013.06.021]
109 **Kotani H**, Tanabe H, Mizukami H, Amagaya S, Inoue M. A naturally occurring rexinoid, honokiol, can serve as a regulator of various retinoid x receptor heterodimers. *Biol Pharm Bull* 2012; **35**: 1-9 [PMID: 22223330 DOI: 10.1248/bpb.35.1]
110 **Pérez E**, Bourguet W, Gronemeyer H, de Lera AR. Modulation of RXR function through ligand design. *Biochim Biophys Acta* 2012; **1821**: 57-69 [PMID: 21515403 DOI: 10.1016/j.bbalip.2011.04.003]
111 **Kotani H**, Tanabe H, Mizukami H, Makishima M, Inoue M. Identification of a naturally occurring rexinoid, honokiol, that activates the retinoid X receptor. *J Nat Prod* 2010; **73**: 1332-1336 [PMID: 20695472 DOI: 10.1021/np100120c]
112 **Huang C**, Wei YX, Shen MC, Tu YH, Wang CC, Huang HC. Chrysin, Abundant in Morinda citrifolia Fruit Water-EtOAc Extracts, Combined with Apigenin Synergistically Induced Apoptosis and Inhibited Migration in Human Breast and Liver Cancer Cells. *J Agric Food Chem* 2016; **64**: 4235-4245 [PMID: 27137679 DOI: 10.1021/acs.jafc.6b00766]
113 **Zhang Y**, Zhao J, Afzal O, Kazmi I, Al-Abbasi FA, Altamimi ASA, Yang Z. Neuroprotective role of chrysin-loaded poly(lactic-co-glycolic acid) nanoparticle against kindling-induced epilepsy through Nrf2/ARE/HO-1 pathway. *J Biochem Mol Toxicol* 2021; **35**: e22634 [PMID: 32991785 DOI: 10.1002/jbt.22634]
114 **Dai W**, Gao Q, Qiu J, Yuan J, Wu G, Shen G. Quercetin induces apoptosis and enhances 5-FU therapeutic efficacy in hepatocellular carcinoma. *Tumour Biol* 2016; **37**: 6307-6313 [PMID: 26628295 DOI: 10.1007/s13277-015-4501-0]
115 **Srisa-Nga K**, Mankhetkorn S, Okonogi S, Khonkarn R. Delivery of Superparamagnetic Polymeric Micelles Loaded With Quercetin to Hepatocellular Carcinoma Cells. *J Pharm Sci* 2019; **108**: 996-1006 [PMID: 30121312 DOI: 10.1016/j.xphs.2018.08.008]
116 **Casella ML**, Parody JP, Ceballos MP, Quiroga AD, Ronco MT, Francés DE, Monti JA, Pisani GB, Carnovale CE, Carrillo MC, de Luján Alvarez M. Quercetin prevents liver carcinogenesis by inducing cell cycle arrest, decreasing cell proliferation and enhancing apoptosis. *Mol Nutr Food Res* 2014; **58**: 289-300 [PMID: 24124108 DOI: 10.1002/mnfr.201300362]
117 **Yu D**, Ye T, Xiang Y, Shi Z, Zhang J, Lou B, Zhang F, Chen B, Zhou M. Quercetin inhibits epithelial-mesenchymal transition, decreases invasiveness and metastasis, and reverses IL-6 induced epithelial-mesenchymal transition, expression of MMP by inhibiting STAT3 signaling in pancreatic cancer cells. *Onco Targets Ther* 2017; **10**: 4719-4729 [PMID: 29026320 DOI: 10.2147/OTT.S136840]
118 **Wu L**, Li J, Liu T, Li S, Feng J, Yu Q, Zhang J, Chen J, Zhou Y, Ji J, Chen K, Mao Y, Wang F, Dai W, Fan X, Wu J, Guo C. Quercetin shows anti-tumor effect in hepatocellular carcinoma LM3 cells by abrogating JAK2/STAT3 signaling pathway. *Cancer Med* 2019; **8**: 4806-4820 [PMID: 31273958 DOI: 10.1002/cam4.2388]
119 **Cai X**, Fang Z, Dou J, Yu A, Zhai G. Bioavailability of quercetin: problems and promises. *Curr Med Chem* 2013; **20**: 2572-2582 [PMID: 23514412 DOI: 10.2174/09298673113209990120]
120 **Galbraith LCA**, Mui E, Nixon C, Hedley A, Strachan D, MacKay G, Sumpton D, Sansom OJ, Leung HY, Ahmad I. PPAR-gamma induced AKT3 expression increases levels of mitochondrial biogenesis driving prostate cancer. *Oncogene* 2021; **40**: 2355-2366 [PMID: 33654198 DOI: 10.1038/s41388-021-01707-7]
121 **Schaefer KL**, Wada K, Takahashi H, Matsuhashi N, Ohnishi S, Wolfe MM, Turner JR, Nakajima A, Borkan SC, Saubermann LJ. Peroxisome proliferator-activated receptor gamma inhibition prevents adhesion to the extracellular matrix and induces anoikis in hepatocellular carcinoma cells. *Cancer Res* 2005; **65**: 2251-2259 [PMID: 15781638 DOI: 10.1158/0008-5472.CAN-04-3037]
122 **Palakurthi SS**, Aktas H, Grubissich LM, Mortensen RM, Halperin JA. Anticancer effects of thiazolidinediones are independent of peroxisome proliferator-activated receptor gamma and mediated by inhibition of translation initiation. *Cancer Res* 2001; **61**: 6213-6218 [PMID: 11507074]
123 **Baek SJ**, Wilson LC, Hsi LC, Eling TE. Troglitazone, a peroxisome proliferator-activated receptor gamma (PPAR gamma) ligand, selectively induces the early growth response-1 gene independently of PPAR gamma. A novel mechanism for its anti-tumorigenic activity. *J Biol Chem* 2003; **278**: 5845-5853 [PMID: 12475986]
124 **Gardner OS**, Shiau CW, Chen CS, Graves LM. Peroxisome proliferator-activated receptor gamma-independent activation of p38 MAPK by thiazolidinediones involves calcium/calmodulin-dependent protein kinase II and protein kinase R: correlation with endoplasmic reticulum stress. *J Biol Chem* 2005; **280**: 10109-10118 [PMID: 15649892 DOI: 10.1074/jbc.M410445200]
125 **Galli A**, Ceni E, Mello T, Polvani S, Tarocchi M, Buccoliero F, Lisi F, Cioni L, Ottanelli B, Foresta V, Mastrobuoni G, Moneti G, Pieraccini G, Surrenti C, Milani S. Thiazolidinediones inhibit hepatocarcinogenesis in hepatitis B virus-

transgenic mice by peroxisome proliferator-activated receptor gamma-independent regulation of nucleophosmin. *Hepatology* 2010; **52**: 493-505 [PMID: 20683949 DOI: 10.1002/hep.23669]

World Journal of Gastroenterology

Submit a Manuscript: https://www.f6publishing.com

World J Gastroenterol 2022 July 28; 28(28): 3555-3572

DOI: 10.3748/wjg.v28.i28.3555

ISSN 1007-9327 (print) ISSN 2219-2840 (online)

REVIEW

Gut microbiota alteration and modulation in hepatitis B virus-related fibrosis and complications: Molecular mechanisms and therapeutic inventions

Yao-Guang Li, Zu-Jiang Yu, Ang Li, Zhi-Gang Ren

Specialty type: Gastroenterology and hepatology

Provenance and peer review: Unsolicited article; Externally peer reviewed.

Peer-review model: Single blind

Peer-review report's scientific quality classification

Grade A (Excellent): 0
Grade B (Very good): B
Grade C (Good): C
Grade D (Fair): 0
Grade E (Poor): 0

P-Reviewer: Gerlich W, Germany; Han G

Received: April 4, 2022
Peer-review started: April 4, 2022
First decision: May 9, 2022
Revised: June 6, 2022
Accepted: June 24, 2022
Article in press: June 24, 2022
Published online: July 28, 2022

Yao-Guang Li, Zu-Jiang Yu, Zhi-Gang Ren, Department of Infectious Diseases, The First Affiliated Hospital of Zhengzhou University, Zhengzhou 450052, Henan Province, China

Yao-Guang Li, Zu-Jiang Yu, Ang Li, Gene Hospital of Henan Province, Precision Medicine Center, The First Affiliated Hospital of Zhengzhou University, Zhengzhou 450052, Henan Province, China

Zhi-Gang Ren, Jinan Microecological Biomedicine Shandong Laboratory, Jinan 250000, Shandong Province, China

Corresponding author: Zhi-Gang Ren, MD, PhD, Assistant Professor, Doctor, Department of Infectious Diseases, The First Affiliated Hospital of Zhengzhou University, No. 1 Jianshe East Road, Zhengzhou 450052, Henan Province, China. fccrenzg@zzu.edu.cn

Abstract

Hepatitis B virus (HBV) has posed a threat to public health, mainly resulting in liver damage. With long-term accumulation of extracellular matrix, patients with chronic hepatitis B are at high risk of developing into liver fibrosis and cirrhosis and even life-threatening hepatic carcinoma. The occurrence of complications such as spontaneous bacterial peritonitis and hepatic encephalopathy greatly increases disability and mortality. With deeper understanding of the bidirectional interaction between the liver and the gut (gut-liver axis), there is a growing consensus that the human health closely relates to the gut microbiota. Supported by animal and human studies, the gut microbiota alters as the HBV-related liver fibrosis initials and progresses, characterized as the decrease of the ratio between "good" and "potentially pathogenic" microbes. When the primary disease is controlled *via* antiviral treatment, the gut microbiota dysfunction tends to be improved. Conversely, the recovery of gut microbiota can promote the regression of liver fibrosis. Therapeutic strategies targeted on gut microbiota (rifaximin, probiotics, engineered probiotics and fecal microbiota transplantation) have been applied to animal models and patients, obtaining satisfactory results.

Key Words: Hepatitis B virus; Gut microbiota; Liver fibrosis; Liver cirrhosis; Hepatic encephalopathy; Fecal microbiota transplantation

©The Author(s) 2022. Published by Baishideng Publishing Group Inc. All rights reserved.

Core Tip: Intimate connection between the gut microbiota alteration and hepatitis B virus (HBV)-related fibrosis and complications has been supported by animal and human studies. Researchers and clinicians are making effort to control and reverse fibrosis by rebuilding a healthy gut microbiota. We herein discuss the gut microbiota alteration in HBV-related fibrosis and therapies targeted on reconstruction of gut microbiota homeostasis.

Citation: Li YG, Yu ZJ, Li A, Ren ZG. Gut microbiota alteration and modulation in hepatitis B virus-related fibrosis and complications: Molecular mechanisms and therapeutic inventions. *World J Gastroenterol* 2022; 28(28): 3555-3572
URL: https://www.wjgnet.com/1007-9327/full/v28/i28/3555.htm
DOI: https://dx.doi.org/10.3748/wjg.v28.i28.3555

INTRODUCTION

Hepatitis B virus (HBV) has brought about substantial global health problems, giving rise to approximately 1.5 million new infections in 2019[1]. Balancing the pathogenic ability and immunity defense, some patients may experience chronic HBV infection, and even chronic hepatitis B (CHB). The different phrases are designed by the presence of hepatitis B e antigen (HBeAg), HBV DNA levels, alanine aminotransferase (ALT) values and liver inflammation, and CHB is mainly characterized by elevated ALT levels and moderate/severe liver diseases[2]. Chronic HBV infection tends to be asymptomatic initially, however, tissue repair against chronic inflammation may result in an immoderate accumulation of extracellular matrix (ECM), so CHB patients are at high risk of developing progressive fibrosis and life-threatening cirrhosis. Complications, such as portal hypertension, spontaneous bacterial peritonitis (SBP)[3] and hepatic encephalopathy (HE)[4], are difficult to prevent and address. With hepatocellular carcinoma (HCC) coming along stealthily[5], approximately 820000 deaths were caused by HBV infection–related causes in 2019[1].

The human intestine, as an organ directly connected with the outside world, is colonized by microbes progressively after birth[6]. The human gut microbiota is now considered to be composed of approximately 10^{14} bacteria[7], 200-300 fungal species[8] and abundant bacteriophages[9], and is increasingly seen as a significant superorganism[10]. Predominant strains in the adult intestine belong to *Bacteroidetes*, *Firmicutes*, *Actinobacteria* and *Proteobacteria*: *Bacteroidetes* and *Firmicutes* are the most dominant phyla and are mainly composed of gram-negative bacteria and gram-positive clostridia respectively[11]. The composition of the gut microbiota is influenced by age, race, nutrition, diet, immunity, disease and medication use, and has a strong interaction with the host[12-14]. The intimate association between gut microbiota homeostasis and multiple organ disease progression has been confirmed in the past decade, especially in some metabolic disorders[15], and intestinal and liver diseases[16].

The liver is closely connected with the gut *via* the gut-liver axis, defined as the bidirectional interaction between the liver and the gut *via* transport of bile acids, immunoreactive substances, nutrients, *etc.*[17]. When impairment of intestinal barriers and disturbances of the gut microbiota occur, gut-derived microbe/antigen translocation may lead to invasion of the liver. The association between gut microbiota alterations and chronic liver diseases (CLDs) has received great attention.

This review will concentrate on gut microbiota alterations in HBV-related liver fibrosis and summarize the cutting edge of new therapeutic strategies. We will summarize and discuss: (1) Gut microbiota alteration in HBV-related liver fibrosis; (2) Gut microbiota-related mechanisms of liver fibrosis; (3) Gut microbiota dysfunction in liver fibrosis complications; and (4) Gut microbiota-related treatment toward HBV-related fibrosis and complications.

GUT MICROBIOTA ALTERATION IN HBV-RELATED LIVER FIBROSIS

HBV-infected populations tend to obtain a gut microbiota that differs from that of healthy people (Table 1). Depending on host and viral factors, patients with HBV infection may experience different phrases[2]. In this part, gut microbiota alteration in the HBV persistence and different stages of HBV infection will be discussed.

HBV persistence

After the infection, HBV may be spontaneously cleared or cause chronic infection in different individuals: 95% of adult-acquired infections result in spontaneous clearance, while over 90% of newborn infections lead to chronic infections[18]. The same phenomenon has been observed in animal

Table 1 Gut microbiota alteration and additional findings in hepatitis B virus-related fibrosis

Ref.	Population (*n*)	Detection method	Gut microbiota alteration	Additional findings
Lu *et al* [30]	Healthy volunteers (*n* = 32); HBV carriers (*n* = 30); CHB (*n* = 31); Decompensated HBV-LC (*n* = 31)	qPCR	Phylum *Bacteroidetes* ↓ *Firmicutes* ↓ Family *Bifidobacteria*/*Enterobacteriaceae* ↓	Copies of operons that code for virulence factors markedly increased. Fecal sIgA and TNF-α in decompensated HBV-LC patients were higher than other groups
Xu *et al*[142]	Healthy volunteers (*n* = 15); CHB (*n* = 16); HBV-LC (*n* = 16)	qPCR	Species (*Bifidobacterium* specific) *B. catenulatum* ↓ *B. longum* ↓ *B. dentinum* ↑	*B. dentium*, which was considered to be an opportunistic pathogen, increased in HBV-LC patients. Species composition of *Bifidobacterium* shifted from beneficial to pathogenic
Wu *et al*[143]	Healthy volunteers (*n* = 38); Decompensated HBV-LC (*n* = 61); HBV-LT (after LC) (n =74)	qPCR	Species (*Lactobacilli* specific) *L. rhamnosus* ↓ *L. fermentus* ↓	Less complex fecal *lactobacilli* composition was found especially in decompensated HBV-LC patients
Wei *et al*[38]	Healthy volunteers (*n* = 120); HBV-LC (*n* = 120): CTP-A (*n* = 40); CTP-B (*n* = 40); CTP-C (*n* = 40)	Solexa sequencing	Phylum *Bacteroidetes* ↓ *Proteobacteria* ↑ Family *Enterobacteriaceae* ↑ Genera *Veillonella* ↑	A negative correlation was observed between the Child-Turcotte-Pugh scores and *Bacteroidetes* ($P < 0.01$)
Wang *et al* [23]	Healthy volunteers (*n* = 22); CHB (*n* = 85): CP-A (*n* = 76); CP-B (*n* = 9)	16S rRNA sequencing	Family *Lachnospiraceae* ↓ *Rikenellaceae*, ↓ *Porphyromonadaceae* ↓ *Ruminococcaceae* ↓ *Veillonellaceae* ↑	*Streptococcus*, *Veillonella*, *Streptococcus* and *Haemophilus* had strong correlations with liver function indices and serum metabolites. They were significantly higher in patients with higher Child-Pugh scores. The gut microbiota may be partially involved in the abnormal accumulation of serum metabolites
Deng *et al* [29]	Healthy volunteers (*n* = 20); HBV-LC (*n* = 80): CP-A (*n* = 30); CP-B (*n* = 31); CP-C (*n* = 19)	16S rRNA sequencing	Phylum *Firmicutes/Bacteroidetes* ↑ Genera *Megamonas* ↓ *Veillonella* ↓	Gut microbiota alteration mentioned on the left were all independent risk or protective factors for HBV-LC. Serum endotoxin increased in patients with higher CP classes ($P = 0.000$)
Zeng *et al* [140]	Healthy volunteers (*n* = 15); CHB (*n* = 21); HBV-LC (*n* = 25); HBV-HCC (*n* = 21)	16S rRNA sequencing	Phylum *Proteobacteria* ↑ *Bacteroidetes* ↑ *Firmicutes* ↓ Family *Bifidobacteria/Enterobacteriaceae* ↓	Higher *Bacteroidetes/firmicutes* ratio represented for higher LPS exposure
Wang *et al*	Healthy volunteers (*n* = 21); CHB (*n* = 69); F0-1 (*n* = 25);	16S rRNA sequencing	Genera *Prevotella* ↑	Genera responsible for bile acid metabolism decreased in CHB fibrosis patients

[59]	F2-4 (n = 44)		*Bacteroides* ↓ *Ruminococcus* ↓	
Chen *et al* [28]	Healthy volunteers (n = 21); HBV carriers (n = 23); CHB (n = 28); HBV-LC (n = 25)	16S rRNA sequencing	Phylum *Actinobacteria* ↑ *Bacteroidetes* ↓ *Firmicutes* ↓ *Proteobacteria* ↑	HBV-LC patients had higher bacterial network complexity with lower abundance of potential beneficial bacterial taxa
Yang *et al* [27]	Healthy volunteers (n = 31); HBV carriers (n = 24); CHB (n = 56); HBV-LC (n = 54); HBV-ACLF (n = 52)	16S rRNA sequencing	There are fluctuations in the changes	HBV carriers might be the most suitable donors for FMT for higher α diversity and abundance of potential beneficial bacteria
Wang *et al* [37]	Healthy volunteers (n = 877); CHB (n = 252); HBV-LC (n = 162); HBV-ACLF (n = 212)	16S rRNA sequencing; metagenomic sequencing	Species *Enterococcus faecium* ↑	High abundance of *Enterococcus* is associated with progression while that of *Faecalibacterium* is associated with regression of HBV-ACLF

HBV: Hepatitis B virus; CHB: Chronic hepatitis B; ACLF: Acute-on-chronic liver failure; CP: Child-Pugh scores; CTP, Child-Turcotte-Pugh scores; FMT: Faecal microbiota transplantation; LC: Liver cirrhosis; LT: Liver transplant; qPCR: Quantitative polymerase chain reaction.

experiments, in which hepatitis B surface antigen (HBsAg) of immature mice remained positive[19]. The age-related difference in immune clearance of HBV is consistent with the stabilization time of the gut microbiota, and maturation appears to facilitate HBV clearance by diminishing the tolerance phenotype and stimulating the immunoreactive pathway[19,20]. Similarly, if the gut microbiota was greatly imbalanced by antibiotics, the depletion can impair intestinal barrier function and weaken the ability of humoral and cellular immunity to clear HBV: adult mice with a mature gut microbiota managed to clear HBV after 6 wk of infection, while they failed to do so after antibiotic use[19,21].

Acute HBV infection

Due to the difficulty of studying acute HBV infection in humans, animal studies have been used: the ratio of *Firmicutes*/*Bacteroides* increased in the early stages of infection (Day 14) and decreased significantly over time (Day 49) in two mouse groups that were constructed with different plasmids[22].

Chronic HBV infection and non-end-stage CHB

Compositional changes have already occurred in the gut microbiota in early-stage CHB patients: in the Child-Pugh A and B groups, the abundance of 5 operational taxonomic units (OTUs) belonging to *Actinomyces*, *Clostridium sensu stricto*, unclassified *Lachnospiraceae* and *Megamonas* increased, while 27 OTUs decreased, which belong to *Alistipes*, *Asaccharobacter*, *Bacteroides*, *Butyricimonas*, *Clostridium IV*, *etc.* [23].

To further understand the gut microbiota dynamics in chronic HBV infection and CHB, there are also studies concentrating on the association with clinical indicators reflecting liver function and infection state. The gut microbiota of subjects from the chronic HBV infection group with normal ALT (NALT) levels was rather similar to those from the healthy volunteers, while significantly different from those from the high ALT level group[24]; however, in a recent study, the authors presented a slightly different perspective that the microbial diversity and abundance of *Lactobacillus*, *Clostridium*, and *Bifidobacterium* were lower in CHB-NALT patients than in healthy volunteers[25]. *Streptococcus*, *Veillonella*, *Streptococcus* and *Haemophilus* showed high correlations with some serum metabolites, including aromatic amino acids (phenylalanine and tyrosine), which are assumed to play pathogenic roles the progression of CHB [23]. The gut microbiota also varies according to viral load: HBV-infected individuals with a low viral load showed high diversity and carry a predominance of taxa associated with fatty acid and lipid metabolism[26].

As the disease progresses, the gut microbiota changes dynamically: the α diversity of asymptomatic HBV carriers slightly increased compared with that of healthy donators, while that of patients in the other three groups (CHB, liver cirrhosis, and acute-on-chronic liver failure (ACLF)) decreased with the severity of the disease[27]. The gut microbiota of patients with liver cirrhosis showed lower diversity and higher network complexity[28]. *Veillonellaceae* and *Lachnospiraceae* families were depleted in patients with liver cirrhosis compared with those in healthy volunteers, while *Megamonas* and *Veillonella* genera were depleted and enriched in patients, respectively[29]. Additionally, copy numbers of *Enterobacteriaceae* increased and lactic acid bacteria were depleted, with marked variation in the intestinal community of CHB patients[30]. The *Bifidobacteria*/*Enterobacteriaceae* ratio can be used for tracing the progression of liver disease[30]. With the magnitude of severity of liver disease (estimated as increasing liver Child-Pugh score), partial functional genes were correlated, such as those encoding aspartate-

ammonia ligase, transaldolase, adenylosuccinate synthetase and IMP dehydrogenase[31]. According to the combined results of multiple studies, there is a well-acknowledged decrease in *Firmicutes* abundance and increase in *Proteobacteria* during the progression of HBV-related fibrosis.

HCC and end-stage CHB

Liver cirrhosis is a dangerous premalignant condition with an increasing incidence of genetic aberrations and an elevated risk of HCC[32,33]. HCC patients tend to present a distempered gut microbiota and abnormal metabolites[34]. The butyrate-producing genera were depleted, while lipopolysaccharide (LPS)-producing genera were enriched in liver cirrhosis and HCC patients, and *Clostridioides* abundance was generally observed to be positively related to the tumor size of HCC[35]. In another study, *Bacteroides*, *Lachnospiracea incertae sedis*, and *Clostridium XIVa* were enriched in HCC patients, and there was a consistency of positive correlation with the tumor burden[36]. By integrating the clinical characteristics and database analysis, serum bile acids may be the communication mediators between these three genera and the host transcriptome[36]. HCC can be secondary to a number of causes, including HBV, *Hepatitis C virus* (HCV) and so on. Compared with non-HBV non-HCV HCC, the abundance of *Prevotella* was much greater in HBV-related HCC group[34]. HBV-related HCC group had higher abundance of pathways related to DNA formation and function (including chaperones and folding catalysts, DNA replication proteins and chromosome), which supported that HBV can impair the normal function of DNA[34].

Additionally, dynamic alteration of gut microbiota is a valuable indicator to predict the prognosis of end-stage liver disease. The richness of *Enterococcus* was significantly higher in the HBV-related ACLF progression group, while a high abundance of *Faecalibacterium* was associated with regression (groups were divided according to the model for end-stage liver disease at discharge)[37]; a higher abundance of *E. coli* is consistent with an increasing level of LPS ligand in the circulation of patients with end-stage liver disease[38-40].

GUT MICROBIOTA-RELATED MECHANISMS OF LIVER FIBROSIS

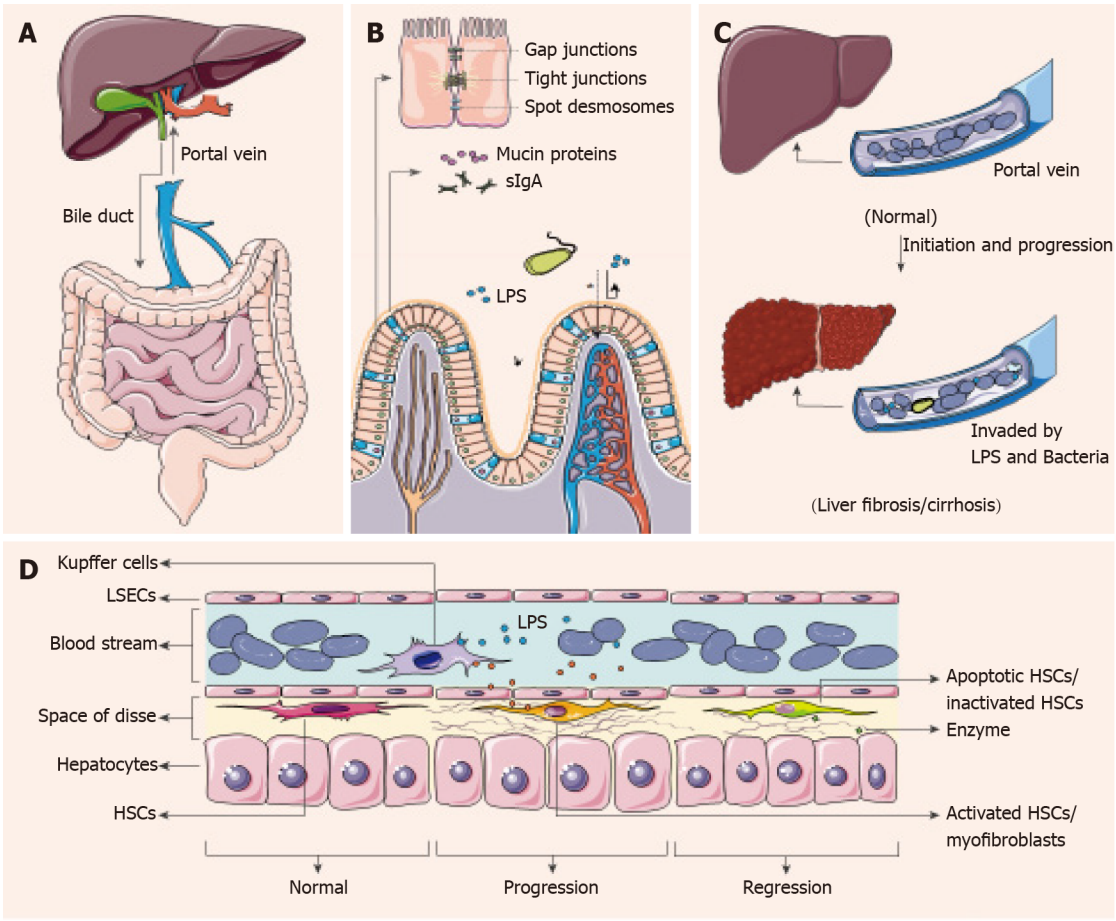
Liver fibrosis is fibrous scar caused by excess accumulation of ECM[41]. It is driven by the chronic and persistent occurrence of parenchymal injury and the activation of the inflammatory response, followed by a continuous repair reaction and liver fibrogenesis[42]. For HBV infection, liver infringement comes from not only HBV but also gut-derived microbe/antigen translocation and abnormal metabolites.

There is a close connection between the gut and liver through known organic pipelines (bile duct and portal vein)[43], and whether there are detours needs further study. The liver produces and sends primary bile acids (BAs) and immunologic active materials (some antimicrobial peptides) through the biliary tract to assist in intestinal digestion and immunity. Conversely, the portal vein carries secondary BAs, nutrients, gastrointestinal metabolites from the gut to the liver, to provide nutrients and get detoxification and biotransformation[17,44] (Figure 1A).

In a non-disease state, intestinal physical and chemical barriers effectively block pathogens or toxic substances and decrease bacterial colonization. The barriers mainly include mucin proteins secreted by goblet cells, secretory IgA (sIgA) secreted by plasma cells in lymphoid follicles of the lamina propria and tight junctions between intestinal epithelial cells (IECs)[45] (Figure 1B). Disorders of these barriers can lead to increased intestinal permeability and translocation of microbial components or metabolites (LPS, microbial DNA) in CLD patients, allowing microbes and antigens to translocate into the portal vein[45], and subsequently induce chronic or acute inflammatory responses of different tissues and organs[46] (Figure 1C).

Intestinal barrier impairment

The gastrointestinal mucus layer is the first line of defense against microbes, and the mobility enables the layer to carry pathogens distally and reduce microbial colonization[47]. The experimental mouse models with liver cirrhosis [induced by bile-duct ligation (BDL) or tetrachloromethane (CCl_4)] show a reduced thickness of the mucus layer, with loss of goblet cells[48]. These cirrhotic mice show pathological bacterial translocation, which has not been found in healthy or pre-hepatic portal-hypertensive mice[48]. sIgA is the predominant contributor to mucosal immunity, recognizing and eliminating bacterial protein antigens, and it also participates in barrier layer limitation of microbe/antigen translocation[49]. Patients with HBV-induced decompensated cirrhosis have increased sIgA content in blood and stool[30], consistent with the increased bacterial migration. Simultaneously, intestinal tight junctions are weakened in patients with liver cirrhosis, and the expression of tight junction proteins is decreased[50,51]. Zonulin, an effective physiological regulator of tight junctions, is one of the markers of intestinal permeability[52]. Serum zonulin content is significantly increased in HBV-related liver cirrhosis and HCC patients and the levels are correlated with the stages[53].



DOI: 10.3748/wjg.v28.i28.3555 **Copyright** ©The Author(s) 2022.

Figure 1 Mechanism of gut microbiota-related liver fibrosis/cirrhosis. A: Gut-liver axis. The close bidirectional connection between gut and liver is mainly through the portal vein and bile duct; B: Intestinal barriers. From the intestine lumen, intestinal barriers are mainly formed by mucin proteins, sIgA and intercellular junctions, especially tight junctions between intestinal epithelial cells. The asterisk means when the intestinal barriers are weakened or broken, microbe/antigen translocation ensues; C: Liver fibrosis/cirrhosis and gut microbe/antigen translocation. Compared with normal state, gut microbe/antigen translocation and liver fibrosis/cirrhosis may drive each other in chronic hepatitis B patients; D: Mechanisms of liver fibrosis/cirrhosis process and regression. Receiving the activation signal, hepatic stellate cells (HSCs) are activated into fibroblasts to form the fiber. As the activation signal ceases, the activated HSCs are inactivated or apoptotic. When fiber degradation predominated, fibrosis is reversed. HSCs: Hepatic stellate cells; LPS: Lipopolysaccharide; LSECs: Liver sinusoidal endothelial cells.

Gut-derived microbe/antigen translocation and metabolic dysbiosis

The impairment of the intestinal barrier greatly reduces the efficiency of blocking microbe/antigen translocation. Gut-derived microbes or fragments and metabolites enter the venous system, travel through the portal vein to invade the liver. Diversity of circulating bacteria in cirrhosis patients is consistent with the presence of dysbiosis[54]. Recent studies have also supported that the occurrence of intestinal bacterial overgrowth and bacterial translocation in cirrhosis using methods such as bacterial DNA sequencing[55] and fluorescence microscopy[21] and suggested that the mechanism is associated with antimicrobial host defense[56]. Simultaneously, LPS is one of the component of the outer membrane of Gram-negative bacteria, mainly from *Enterobacteriaceae*[57]. The dysbiosis of the gut microbiota in mice leads to endotoxemia, which may bring about Kupffer Cell (KC) IL-10 production and KC-mediated T cell suppression[57]. And endotoxemia is highly related to the severity in liver diseases and complications[58].

Additionally, abnormal composition of the gut microbiota results in metabolic disorders, among which the metabolism of BAs has aroused great concern[25]. The level of fecal total BAs decreased and the ratio of conjugated and primary BAs increased in CHB patients without liver cirrhosis, which may be the prelude of following changes[25]. And there is a trend that abundance of the bacteria genera responsible for BA metabolism is decreased in CHB patients with moderate/advanced fibrosis[59,60]. There is also a link between gut bacteria-controlled BA metabolism and liver antitumor immunosurveillance *via* natural killer T (NKT) cells[61].

Immune-mediated fibrosis and regression

Pattern recognition receptors (PRRs) are highly conserved host sensors that are able to recognize

exogenous and endogenous antigens, including pathogen-associated molecular patterns (PAMPs) and host-derived damage-associated molecular patterns (DAMPs)[62]. PRRs are expressed by a plethora of immune cells, especially macrophages[63]. Macrophages could be at the center of innate immune regulation, linking microbe/antigen translocation and liver inflammation or fibrosis[64]. Recognition of PRRs sends the initial signal to active downstream adaptor proteins to undergo maturation and assemble transcription factors, such as nuclear factor (NF)-κB[65,66]. The produced cytokines then recruit inflammatory cells, drive antimicrobial activities and promote myofibroblast formation[67].

Myofibroblasts, the collagen-producing cells, are not present in healthy livers[68]. In response to toxic liver injury, myofibroblasts are mainly transformed from activated hepatic stellate cells (HSCs)[69]. There are four different stages of HSCs, namely, quiescent, activated (equivalent to collagen type I-producing myofibroblasts), inactivated and senescent[41]. Under physiological conditions, quiescent HSCs stay in the space of Disse and function as the major vitamin A storage site[70]. Simulated by several cytokines (especially transforming growth factor (TGF)-β)[71], quiescent HSCs modulate phenotypes and transform into activated HSCs, and the activated HSCs migrate and secrete ECM to produce a fibrous scar[41]. After removing the initial driver, there is a decrease in the levels of pro-inflammatory cytokines (interleukin-6, interleukin-1β and tumor necrosis factor) and TGF-β, and a rapid decline of the counts of activated HSCs[41]. Activated HSCs can be transformed into inactivated or senescent cells, and stop producing type-I collagen fibers[72]. Later, when fiber degradation by matrix metalloproteinases overwhelms fiber formation, liver fibrosis can be controlled, regressed and even reversed[73].

In conclusion, increased microbe and endotoxin loads in the portal vein cause PRR activation on immune cells, especially on macrophages, which leads to the activation of quiescent HSCs into activated HSCs[44,66]. Later, activated HSCs proliferate in response to various cytokines, secrete type-I collagen fiber and make liver fibrotic[41]. Upon cessation of underlying injury, myofibroblasts undergo inactivation or apoptosis, and fibrosis can be discontinued or reversed[41] (Figure 1D). This is the mechanism of effective treatment to control and regress liver fibrosis.

GUT MICROBIOTA DYSFUNCTION IN LIVER FIBROSIS COMPLICATIONS

As mentioned above, gut microbiota alterations may drive immune-related inflammation and fibrosis in the liver. Due to the accumulation of collagen fiber, liver stiffness is increased, bloodstream transport is blocked, healthy liver parenchyma is replaced and liver biotransformation and detoxification abilities are weakened[74]. As the disease progresses into the decompensation stage, patients may experience deadly complications, such as portal hypertension, spontaneous bacterial peritonitis (SBP) and HE. The relationship among gut microbiota alteration, liver fibrosis and portal hypertension is similar to the question of the chicken and the egg, as they drive and affect each other[75]. Compared with compensated cirrhosis, gut microbiota composition is characterized by an increase in the abundance of potentially pathogenic bacteria in the decompensation stage, especially *Alcaligenaceae*, *Porphyromonadaceae*, *Veillonellaceae* and *Enterobacteriaceae*[76].

SBP

SBP refers to the infection of ascites without an apparent intra-abdominal focus[77]. It is a severe infection and is often fatal in patients with cirrhosis and ascites[78]. The pathogen of SBP in liver cirrhosis patients is mainly from the intestinal tract.

More than two decades ago, DNA fragments of 30 bacterial isolated from ascites, mesenteric lymph nodes, portal blood, and ileal flora were compared[79]. The same bacterial strain was simultaneously isolated in ascites and in mesenteric lymph nodes and/or the ileum in 7/8 (87%) instances[79]. Intraperitoneal LPS increased TLR4 (Toll-like receptor 4, the canonical PRR for LPS) expression and amplified portal hypertension in rat liver fibrosis[80].

HE

HE is a fatal central nervous system complication caused by acute and chronic hepatitis or decompensated cirrhosis[81], which is considered consciousness disturbance after ammonia-related cerebral edema[82]. HE patients tend to have a poor prognosis and high mortality and recurrence rates, with greatly increasing economic and nursing burdens[83].

Currently, there is an increasing consensus that the gut microbiota and gastrointestinal metabolites play an important role in the initiation and progress of HE. On the basis of the gut-liver axis mentioned above, researchers proposed the concept of the gut-brain-liver axis to describe the role of the gut microbiota[84]. Cognitive dysfunction in cirrhosis is related to a decrease in the abundance of autochthonous families and an increase in *Alcaligenaceae* and *Porphyromonadaceae*[85,86].

On the one hand, gut microbiota alteration in the decompensation stage is consistent with the accumulation of microbe-derived products, including ammonia, mercaptans, benzodiazepine-like substances, and indoles[76]. These products can pass the blood-brain barrier and alter astrocyte function, resulting in osmotic or oxidative stress, mitochondrial dysfunction, neurotransmission

disorder, *etc.*[81]. On the other hand, neurotransmitters produced by the microbiota, including serotonin, dopamine, and aminobutyric acid, can act on specific receptors of exogenous primary afferent neuron cells, or cross the blood-brain barrier to act as active neurotransmitters[87]. The complex network among the enteric nervous system, the autonomic nervous system and the neuroendocrine and neuroimmunity systems of the central nervous system has a mutual impact on the gut microbiota, and the up-down or down-up regulation mechanisms need further exploration[84].

GUT MICROBIOTA-RELATED TREATMENT TOWARD HBV-RELATED FIBROSIS AND COMPLICATIONS

Based on the fibrosis regression theory mentioned above, removing the cause is the key to controlling and reversing liver fibrosis (Tables 2 and 3). For more than a decade, antiviral therapy has been recognized as an effective method to prevent, control and even reverse fibrosis and cirrhosis[88]. Rifaximin reduces the virulence of the overgrown gut microbiota[89]. With further understanding of the connection between the gut microbiota and HBV-related fibrosis, scientists have suggested that host health depends on the balance of the composition of the entire microbial community rather than one or a few dominant organisms[90]. New therapeutic strategies for HBV-related fibrosis, cirrhosis and complications have been broadened to regulate the gut microbiota through probiotic supplementation and microbiota transplantation from healthy donors.

Gut microbiota stabilization with antiviral treatment

At present, the main endpoint of all current treatment strategies is to maintain long-term suppression of HBV replication[2]. Two main options are nucleoside analogs (NAs) and interferon alpha[91]. NAs with a high barrier to HBV resistance, including entecavir (ETV), tenofovir disoproxil fumarate (TDF) and tenofovir alafenamide (TAF), are believed to be favorably safe and long-acting[92]. Antiviral treatment (AVT) exerts a positive influence on survival rate and quality of life by preventing disease progression, reversing and degrading fibrosis and cirrhosis[93,94], and even reducing HCC incidence and mortality in CHB patients[95].

ETV therapy reverses gut microbiota dysbiosis induced by HBV infection in a mouse model[96]. And in a controlled cross-sectional and longitudinal real-world study, the species abundance of the gut microbiota increased markedly after ETV treatment[97]. After 8 wk of ETV treatment, the abundance of *Clostridium sensu stricto 1*, *Erysipelotrichaceae UCG-007* and *Intestinibacter* increased significantly, and that of *Streptococcus*, *Atopobium* and *Murdochiella* was markedly reduced[97]. Although the addition of *Clostridium butyricum* (CB) to ETV failed to improve the serum biochemical, immunologic and virologic variables, addition of CB affected the gut microbiota in CHB patients treated with ETV[98]. While there is a lack of dynamic and synergetic studies on liver fibrosis outcomes and gut microbiota alterations during AVT, collaborative microbes contributing the most to antiviral-intervened HBV-related fibrosis cannot be pinpointed definitively.

Rifaximin

Rifaximin is a rifamycin-based nonsystemic antibiotic with low gastrointestinal absorption and good antibacterial activity[89,99]. The gastrointestinal tract is the main therapeutic target of rifaximin, and it has been widely used in controlling HE with infrequent side effects and a favorable long-term safety profile[100,101].

Current ideas suggest that rifaximin may have positive implications for liver cirrhosis and complications by acting on the gut microbiota. However, according to a randomized trial, there seems to be a minor impact on the composition of the gut microbiota[102]. Enrolled patients with cirrhosis and ascites were divided into two groups to receive rifaximin or placebo for 4 wk. Rifaximin decreased gut bacterial abundance, while no effect on particular species was observed; blood bacterial richness was decreased and the difference in *Pseudomonadales* abundance was relatively obvious[102]. And there was no difference in circulating markers of inflammation between the two groups[102]. Two additional studies also supported that rifaximin has little influence on gut microbiota abundance[103], but the metabolite levels altered: after rifaximin application, endotoxemia was relieved, and serum saturated and unsaturated fatty acid levels were increased significantly[104]. The former conclusion agreed with a study on experimental mice[105]. Therefore, rather than having a bactericidal effect, rifaximin seems to have direct effects on bacterial function and virulence[89].

Probiotics and synthetic probiotics

Probiotics are living nonpathogenic microorganisms, and treatment doses (at least 10^6 viable CFU/g) may help temper the gut microbiota[106]. *Lactobacillus* and *Bifidobacterium* genera are widely reported as clinically available probiotics[107]. In recent studies, probiotics have been broadly used to regulate the gut microbiota for further positive influences on primary diseases, such as gastrointestinal dysfunctions [108,109], metabolic diseases[110,111] and psychoneurotic disorders[112,113].

Table 2 Gut microbiota-related treatment toward hepatitis B virus-related fibrosis and complications (studies in animal models)

Ref.	Study populations (*n*)	Treatment and grouping (*n*)	Conclusions
Antiviral therapy			
Li *et al*[96]	AAV-mediated persistent HBV infection (AAV-HBV) mice (*n* = 10)	35 d after HBV infection, 4 wk of daily ETV treatment. ETV (*n* = 5)	Gut microbiota dysbiosis of the AAV-HBV mice was reversed by ETV treatment with restored α diversity and changed proportion of *Akkermansia*, *Lacnospiracea* and *Marvinbryantia*
Rifaximin			
Kang *et al* [105]	Germ-free mice (*n* = 16)	15 d of rifaximin 100 mg/(kg·d), or humanized with stools from a HCV-induced cirrhotic patient with MHE. Rifaximin (*n* = 4); Humanized (*n* = 4); Rifaximin + humanized (*n* = 4)	Rifaximin beneficially altered intestinal ammonia generation by regulating intestinal glutaminase expression independent of gut microbiota. MHE-associated fecal colonization resulted in intestinal and systemic inflammation. It was ameliorated with rifaximin
Engineered probiotics			
Nicaise *et al*[120]	Ornithine transcarbamoylase-deficient Sparse-fur mice; Carbon tetrachloride rats; Thioacetamide-induced acute liver failure mice	NCIMB8826 (wild-type strain *Lactobacillus plantarum*), or EV101 (engineered *Lactobacillus plantarum*, $LDH^-/AlaD^+$) oral and intrarectal administration	EV101 administration was effective in controlling hyperammonemia in constitutive animal models with a significant effect on survival, which might be involved with direct ammonia consumption in the gut
Kurtz *et al* [121]	Ornithine transcarbamylase-deficient *spfash* mice; Thioacetamide-induced acute liver failure mice; Healthy volunteers (*n* = 52)	Non-modified *Escherichia coli* Nissle 1917 (EcN), SYNB1020 (engineered EcN, Δ argR, Δ thyA, malEK:PfnrS-$argA^{fbr}$) administration	SYNB1020 converted NH3 to l-arginine in vitro, and reduced systemic hyperammonemia, improved survival in mouse models. SYNB1020 was well tolerated in healthy volunteers
Ochoa-Sanchez *et al*[122]	Bile-duct ligated rats	Non-modified EcN, S-ARG, or S-ARG + BUT administration	S-ARG converted ammonia to arginine, it was further modified to additionally synthesize butyrate, which had the potential to prevent HE
FMT			
Liu *et al* [134]	Germ-free mice	Sterile supernatant or entire stool from pre-FMT and post-FMT cirrhotic patients with HE was transplanted to Germ-free mice	Transferred microbiota mediated neuroinflammation. Cirrhosis-associated dysregulation of gut microbiota was related with frontal cortical inflammation

AAV: Adeno-associated virus; HBV: Hepatitis B virus; ETV: Entecavir; HCV: Hepatitis C virus; MHE: Minimal hepatic encephalopathy; HE: Hepatic encephalopathy; FMT: Fecal microbiota transplantation.

The role of probiotics in complications of HBV-related fibrosis and cirrhosis has been validated, especially for HE. Probiotics can drive the gut microbiota, triggering emotional brain signatures[114]. For minimal HE, probiotic therapy (*Lactobacillus acidophilus*) can improve blood ammonia and psychometric tests and reduce the risk of overt encephalopathy deterioration[115]. Further studies confirmed that patients' cognition, venous ammonia level and intestinal mucosal barrier function were significantly improved after 3 mo of probiotic use (*Clostridium butyricum* combined with *Bifidobacterium infantis*), and the predominant bacteria (*Clostridium cluster I* and *Bifidobacterium*) were obviously enriched in the probiotic-treated group, while *Enterococcus* and *Enterobacteriaceae* were depleted[116]. The combination of probiotics and lactulose is effective for the secondary prophylaxis of HE patients with cirrhosis[117]. Simultaneously, probiotics may work by promoting the growth of beneficial microbes and preventing PAMP-mediated liver inflammation and the anti-proliferative, anti-angiogenic, and anti-metastatic effects of the antioxidant can block the progress of HCC[118].

Additionally, rapid progress in synthetic biology has brought more options, which makes engineered live biotherapeutics an available and promising strategy[119]. More than one decade ago, the genetically engineered ammonia-hyperconsuming strain NCIMB8826 was verified to exhibit a beneficial effect at a lower dose than its wild-type counterpart[120]. In recent years, more engineered bacteria have been constructed to accelerate ammonia metabolism, reduce blood ammonia concentration and reduce HE incidence[121,122]. One team from Synlogic Inc. engineered oral probiotic *Escherichia coli Nissle 1917* (Ecn) to create strain SYNB1020[121]. SYNB1020 is able to convert NH_3 to L-arginine *in vivo* and reduce hyperammonemia in two mouse models (ornithine transcarbamylase-deficient spfash mice and thioacetamide-induced liver injury mice). Satisfyingly, it showed metabolic activity and good tolerance in a phase 1 clinical study of 52 healthy adult volunteers. Later, another group modified Ecn to consume and convert ammonia to arginine, which was further modified to additionally synthesize butyrate[122]. Both of these studies showed that engineered probiotics have positive therapeutic significance for hyperammonemia and underlying potential for HE prevention. However, these strains have not progressed to clinical studies in hyperammonemia patients, and the clinical effects need further study.

Table 3 Gut microbiota-related treatment toward hepatitis B virus-related fibrosis and complications (studies in human)

Ref.	Study populations (*n*)	Treatment and grouping (*n*)	Conclusions
Antiviral therapy			
Lu *et al* [97]	Healthy volunteers (*n* = 30); CHB (*n* = 30)	8 wk of daily ETV treatment. ETV (*n* = 30)	After ETV treatment, gut microbiota abundance increased markedly, blood biochemical, immunological and virological responses improved significantly
Lu *et al* [98]	Healthy volunteers (*n* = 30); CHB patients (*n* = 60)	8 wk of daily ETV treatment, or with additional CB. ETV (*n* = 30); ETV + CB (*n* = 30)	Additional CB fail to improve blood biochemical, immunological and virological responses, but affects the gut microbiota in the CHB patients treated with ETV
Rifaximin			
Bajaj *et al* [104]	Decompensated LC patients with MHE (*n* = 20):CHB (NM)	8 wk of rifaximin 550-mg BD. Rifaximin (*n* = 20)	Rifaximin affected little on gut microbiota, there was just a modest decrease in *Veillonellaceae* and increase in *Eubacteriaceae*. Rifaximin significantly improved cognition and endotoxemia, it increased increase in serum saturated and unsaturated fatty acids post-rifaximin
Lutz *et al* [144]	Decompensated LC patients with ascites (*n* = 152): Viral hepatitis (*n* = 35)	Prophylactic antibiotic treatment before the time of paracentesis. Rifaximin (*n* = 27); Other systemic antibiotics (*n* = 17)	Prophylactic rifaximin did not reduce SBP occurrence. Prophylactic rifaximin was associated with the dominant bacteria in ascites: *Escherichia coli* and *enterococci* were dominant of patients without prophylaxis, klebsiella species were mostly recovered from the rifaximin group
Kimer *et al* [102]	Decompensated LC patients (*n* = 54): CHB (NM)	4 wk of rifaximin 550-mg BD or placebo BD. Rifaximin (*n* = 36); Placebo (*n* = 18)	Rifaximin had minor effects on bacteria translocation and gut microbiota. Rifaximin showed little impact on the inflammatory state (reflected as the level of TNF-α, IL-6, IL-10, IL-18, SDF-1α, TGF-1β, CRP)
Kaji *et al* [103]	Decompensated LC patients (*n* = 30): CHB (*n* = 4)	4 wk of rifaximin 1200 mg/d. Rifaximin (*n* = 30)	Rifaximin alleviated HE and endotoxemia with improved intestinal hyperpermeability, and it is involved in a gut microbial change. Rifaximin didn't affect serum proinflammatory cytokine levels (TNF-α, IL-6, IFN-γ, IL-10)
Probiotics			
Agrawal *et al*[117]	LC patients with recovered HE (*n* = 235): CHB (*n* = 49)	3 mo of lactulose 30–60 mL/d, or 3 capsules of probiotics per day, which contained 4 strains of *Lactobacillus*. Lactulose (*n* = 80); Probiotics (*n* = 77)	Lactulose and probiotics were effective for secondary prophylaxis of HE in cirrhotic patients
Ziada *et al* [115]	Decompensated LC patients with MHE (*n* = 90): CHB (NM)	4 wk of lactulose 30–60 mL/d, or 3 capsules of probiotics per day, which contained *Lactobacillus acidophilus*. Lactulose (*n* = 30); Probiotics (*n* = 30)	Probiotic was better tolerated than lactulose. Both of them can improve blood ammonia and psychometric tests and reduce the risk of developing overt HE. Magnetic resonance spectroscopy showed more improvement in the levels of brain neurometabolites in the probiotic group
Xia *et al* [116]	Decompensated HBV-LC patients with MHE (*n* = 67)	3 mo of probiotics 1500-mg TD, which contained *Clostridium butyricum* combined with *Bifidobacterium infantis*. Probiotics (*n* = 30)	After probiotics treatment, the therapeutic bacteria were significantly enriched, while *Enterococcus* and *Enterobacteriaceae* were decreased. Probiotics contributed to the improved cognition and the decreased ammonia levels
FMT			
Ren *et al* [132]	CHB with positive HBeAg, received over 3 yr of antiviral treatment (*n* = 18)	FMT was performed by gastroscope every 4 wk until HBeAg clearance. FMT (*n* = 5)	FMT was effective on HBeAg-positive CHB, especially in patients who could not cease the oral antiviral treatment even after long-term treatment
Bajaj *et al* [135]	Decompensated LC patients with recurrent HE (*n* = 20). CHB (NM)	After 5 d of antibiotics, FMT was performed by enema, or standard of care (SOC, rifaximin/lactulose) was applied. FMT (*n* = 10); SOC (*n* = 10)	FMT increased diversity and beneficial taxa of gut microbiota, improved cognition and showed good tolerance, other than SOC
Bajaj *et al* [136]	Decompensated LC patients with recurrent HE (*n* = 20). CHB (NM)	FMT was performed by enema, or standard of care (SOC, rifaximin/lactulose) was applied. FMT (*n* = 10); SOC (*n* = 10)	Oral FMT capsules are safe and well tolerated. Post-FMT, duodenal mucosal diversity increased with higher *Ruminococcaceae* and *Bifidobacteriaceae* and lower *Streptococcaceae* and *Veillonellaceae*. Reduction in *Veillonellaceae* were noted post-FMT in sigmoid and stool
Chauhan *et al*[133]	CHB with positive HBeAg, received over 1 years of antiviral treatment (*n* = 18)	6 FMTs were performed by gastroscope every 4 wk FMT (*n* = 12)	FMT appeared to be safe and effective on HBeAg-positive CHB in viral suppression and HBeAg clearance

CHB: Chronic hepatitis B; CB: *Clostridium butyricum*; CRP: C-reactive protein; EcN: *Escherichia coli* Nissle 1917; ETV: Entecavir; HBeAg: Hepatitis B e antigen; HE: Hepatic encephalopathy; IFN: Interferon; IL: Interleukin; LC: Liver cirrhosis; MHE: Minimal hepatic encephalopathy; NM: Not mentioned; SBP: Spontaneous bacterial peritonitis; SDF-1α: Stromal cell-derived factor 1-α; TDF: Tenofovir disoproxil fumarate; TGF-1β: Transforming growth factor β-1; TNF: Tumor necrosis factor; FMT: Faecal microbiota transplantation.

Fecal microbiota transplantation

Fecal microbiota transplantation (FMT) is an emerging treatment method that transfers the gut microbiota from a healthy donor to a patient[123]. Due to its ability to directly reshape or rebuild the recipient's gut microbial communities, FMT is one of the most promising therapies balancing and stabilizing the gut microbiota[76], and it has been applied to research-based treatment in animal models of a variety of diseases[124,125] and to study the mechanisms[126,127]. In recent years, FMT has been expanded to clinical treatment for human disease as a noninvasive strategy for conditions including recurrent *Clostridium difficile* infection[128], inflammatory bowel disease[129], severe obesity and metabolic syndrome[130]. Regarding the mechanism, the gut microbiota structure can be improved by FMT, and a clinical trial employing autologous FMT supported this point[131].

Clinical trials have also aimed to determine whether CHB patients can benefit from FMT therapy. In a pilot study carried out in China, FMT showed the potential to induce HBeAg clearance in HBeAg-positive CHB patients after long-term AVT: There was a significant HBeAg level decline in the FMT group (FMT combined with AVT), while no decline in the control group (AVT only) was found[132]. The results were consistent with a nonrandomized controlled clinical trial carried out in India: after 1 year of FMT therapy for 6 terms, the FMT group (FMT + AVT) seemed to show potential effectiveness and safety compared with those of the AVT group (AVT only)[133]. Some researchers have also hypothesized that FMT of some potential beneficial bacteria can change the occurrence of disease, and HBV carriers might be the most suitable donors for slightly higher microbiota abundance[27]. However, due to the limitations of a small number of participants and a lack of randomized clinical trials, further well-designed clinical trials are needed to confirm the initial assumptions and promote clinical practicability.

Studies on FMT for HE animal models or patients show satisfactory results. In animal experiments, neuroinflammation alleviation was found in cirrhosis model mice receiving FMT[134]. In a randomized clinical trial, FMT from rationally selected donors helped reduce and improve hospitalizations and improve cognition and dysbiosis for cirrhosis with recurrent HE[135]. Later, the same team verified the safety of FMT capsules through a phase 1, randomized and placebo-controlled clinical trial[136]. In addition to integral inoculation, selective inoculation of specific strains also plays an ameliorating role. Transplanting low-urease altered Schaedler flora to mice prepared with a depleted microbiota leaded to durable reduction in fecal urease activity and ammonia production[137]. The symbiotic pair of *Lactobacillus reuteri* JBD400 and *Streptococcus rubneri* JBD420 cooperatively improved transplantation efficiency 2.3×10^3 times more than that of sole transplantation and significantly lowered blood ammonia levels [138].

CONCLUSION

Consequently, gut microbiota alteration has been observed to be related to HBV-related fibrosis initiation and progression, and it is a promising therapeutic target. According to current studies, HBV persistence and clearance show consistency with the maturity and health of the gut microbiota[19,21]. With an increase of Child-Pugh scores and the model for end-stage liver disease, the gut microbiota is characterized by a decrease in the ratio of "good" to "potentially pathogenic" bacteria, and species diversity tends to decrease[139,140]. However, it is difficult to clarify which is the initiating factor between gut microbiota alteration and HBV-related fibrosis progression. Existing studies tend to be descriptive and lack HBV-specific exploration. Gut microbiota-related mechanisms are based on the gut-liver axis and immune-mediated response, briefly including intestinal barrier impairment, PRR activation, cytokine production, HSC activation and transformation, and fiber secretion and formation [41]. When the driver is removed, activated HSCs are inhibited or become apoptotic, and fiber scars are degraded, resulting in fibrosis regression[41].

Beyond theory, quite a few studies have begun examining therapeutic inventions. AVT can effectively control or even reverse HBV-related liver fibrosis, during which the gut microbiota gradually returns to homeostasis[96,97]. Rifaximin may decrease the virulence of the overgrown gut microbiota[89]. Probiotics and FMT are the most popular gut microbiota targeted therapies, and they are moving from the laboratory to the clinic. In addition, synthetic probiotics and selective microbiota transplantation may make these therapies more precise, and bring fewer side effects.

However, current studies do have limitations. There is a lack of in-depth research on the specific molecular mechanisms of the gut microbiota. Further clinical studies are needed to determine its effectiveness in patients with HBV-induced liver cirrhosis in the real world[141]. We must also admit that age, host location, dietary habits have a great impact on the gut microbiota, which leads to the lack of consistency and comparability of the alterations in gut microbiota in different studies. Therefore, diagnosis potential of microbial markers should be considered the factors mentioned above. We are looking forward to more powerful studies to strengthen the theoretical foundation and promote clinical application.

FOOTNOTES

Author contributions: Ren ZG and Li A designed the study; Li YG, Yu ZJ, Li A and Ren ZG collected data and summary viewpoints; Li YG wrote the manuscript; Ren ZG and Li A revised the manuscript; and All authors reviewed and approved the manuscript.

Supported by National Key Research and Development Program of China, No. 2018YFC2000500; Research Project of Jinan Microecological Biomedicine Shandong Laboratory, No. JNL-2022001A; and National Natural Science Foundation of China, No. U2004121, No. 82070643 and No. U1904164.

Conflict-of-interest statement: All authors report no relevant conflicts of interest for this article.

Open-Access: This article is an open-access article that was selected by an in-house editor and fully peer-reviewed by external reviewers. It is distributed in accordance with the Creative Commons Attribution NonCommercial (CC BY-NC 4.0) license, which permits others to distribute, remix, adapt, build upon this work non-commercially, and license their derivative works on different terms, provided the original work is properly cited and the use is non-commercial. See: https://creativecommons.org/Licenses/by-nc/4.0/

Country/Territory of origin: China

ORCID number: Yao-Guang Li 0000-0001-6963-0957; Zu-Jiang Yu 0000-0002-5224-8919; Ang Li 0000-0002-4972-4910; Zhi-Gang Ren 0000-0003-0798-3444.

S-Editor: Ma YJ
L-Editor: A
P-Editor: Ma YJ

REFERENCES

1 **World Health Organization**. Global progress report on HIV, viral hepatitis and sexually transmitted infections, 2021. 2021. Available from: https://www.who.int/publications/i/item/9789240027077
2 **European Association for the Study of the Liver**. EASL 2017 Clinical Practice Guidelines on the management of hepatitis B virus infection. *J Hepatol* 2017; **67**: 370-398 [PMID: 28427875 DOI: 10.1016/j.jhep.2017.03.021]
3 **Merli M**, Lucidi C, Giannelli V, Giusto M, Riggio O, Falcone M, Ridola L, Attili AF, Venditti M. Cirrhotic patients are at risk for health care-associated bacterial infections. *Clin Gastroenterol Hepatol* 2010; **8**: 979-985 [PMID: 20621200 DOI: 10.1016/j.cgh.2010.06.024]
4 **D'Amico G**, Morabito A, D'Amico M, Pasta L, Malizia G, Rebora P, Valsecchi MG. Clinical states of cirrhosis and competing risks. *J Hepatol* 2018; **68**: 563-576 [PMID: 29111320 DOI: 10.1016/j.jhep.2017.10.020]
5 **Yang R**, Xu Y, Dai Z, Lin X, Wang H. The Immunologic Role of Gut Microbiota in Patients with Chronic HBV Infection. *J Immunol Res* 2018; **2018**: 2361963 [PMID: 30148173 DOI: 10.1155/2018/2361963]
6 **Milani C**, Duranti S, Bottacini F, Casey E, Turroni F, Mahony J, Belzer C, Delgado Palacio S, Arboleya Montes S, Mancabelli L, Lugli GA, Rodriguez JM, Bode L, de Vos W, Gueimonde M, Margolles A, van Sinderen D, Ventura M. The First Microbial Colonizers of the Human Gut: Composition, Activities, and Health Implications of the Infant Gut Microbiota. *Microbiol Mol Biol Rev* 2017; **81** [PMID: 29118049 DOI: 10.1128/MMBR.00036-17]
7 **Doré J**, Simrén M, Buttle L, Guarner F. Hot topics in gut microbiota. *United European Gastroenterol J* 2013; **1**: 311-318 [PMID: 24917977 DOI: 10.1177/2050640613502477]
8 **Hillman ET**, Lu H, Yao T, Nakatsu CH. Microbial Ecology along the Gastrointestinal Tract. *Microbes Environ* 2017; **32**: 300-313 [PMID: 29129876 DOI: 10.1264/jsme2.ME17017]
9 **Reyes A**, Semenkovich NP, Whiteson K, Rohwer F, Gordon JI. Going viral: next-generation sequencing applied to phage populations in the human gut. *Nat Rev Microbiol* 2012; **10**: 607-617 [PMID: 22864264 DOI: 10.1038/nrmicro2853]
10 **Biedermann L**, Rogler G. The intestinal microbiota: its role in health and disease. *Eur J Pediatr* 2015; **174**: 151-167 [PMID: 25563215 DOI: 10.1007/s00431-014-2476-2]
11 **Marchesi JR**, Adams DH, Fava F, Hermes GD, Hirschfield GM, Hold G, Quraishi MN, Kinross J, Smidt H, Tuohy KM, Thomas LV, Zoetendal EG, Hart A. The gut microbiota and host health: a new clinical frontier. *Gut* 2016; **65**: 330-339 [PMID: 26338727 DOI: 10.1136/gutjnl-2015-309990]
12 **Odamaki T**, Kato K, Sugahara H, Hashikura N, Takahashi S, Xiao JZ, Abe F, Osawa R. Age-related changes in gut microbiota composition from newborn to centenarian: a cross-sectional study. *BMC Microbiol* 2016; **16**: 90 [PMID: 27220822 DOI: 10.1186/s12866-016-0708-5]
13 **Chen L**, Zhang YH, Huang T, Cai YD. Gene expression profiling gut microbiota in different races of humans. *Sci Rep* 2016; **6**: 23075 [PMID: 26975620 DOI: 10.1038/srep23075]
14 **Wu GD**, Compher C, Chen EZ, Smith SA, Shah RD, Bittinger K, Chehoud C, Albenberg LG, Nessel L, Gilroy E, Star J, Weljie AM, Flint HJ, Metz DC, Bennett MJ, Li H, Bushman FD, Lewis JD. Comparative metabolomics in vegans and omnivores reveal constraints on diet-dependent gut microbiota metabolite production. *Gut* 2016; **65**: 63-72 [PMID: 25431456 DOI: 10.1136/gutjnl-2014-308209]
15 **Agus A**, Clément K, Sokol H. Gut microbiota-derived metabolites as central regulators in metabolic disorders. *Gut* 2021; **70**: 1174-1182 [PMID: 33272977 DOI: 10.1136/gutjnl-2020-323071]

16 **Jones RM**, Neish AS. Gut Microbiota in Intestinal and Liver Disease. *Annu Rev Pathol* 2021; **16**: 251-275 [PMID: 33234022 DOI: 10.1146/annurev-pathol-030320-095722]

17 **Tripathi A**, Debelius J, Brenner DA, Karin M, Loomba R, Schnabl B, Knight R. The gut-liver axis and the intersection with the microbiome. *Nat Rev Gastroenterol Hepatol* 2018; **15**: 397-411 [PMID: 29748586 DOI: 10.1038/s41575-018-0011-z]

18 **Wu LL**, Huang TS, Shyu YC, Wang CL, Wang HY, Chen PJ. Gut microbiota in the innate immunity against hepatitis B virus - implication in age-dependent HBV clearance. *Curr Opin Virol* 2021; **49**: 194-202 [PMID: 34242953 DOI: 10.1016/j.coviro.2021.06.006]

19 **Chou HH**, Chien WH, Wu LL, Cheng CH, Chung CH, Horng JH, Ni YH, Tseng HT, Wu D, Lu X, Wang HY, Chen PJ, Chen DS. Age-related immune clearance of hepatitis B virus infection requires the establishment of gut microbiota. *Proc Natl Acad Sci U S A* 2015; **112**: 2175-2180 [PMID: 25646429 DOI: 10.1073/pnas.1424775112]

20 **Xu D**, Huang Y, Wang J. Gut microbiota modulate the immune effect against hepatitis B virus infection. *Eur J Clin Microbiol Infect Dis* 2015; **34**: 2139-2147 [PMID: 26272175 DOI: 10.1007/s10096-015-2464-0]

21 **Guo W**, Zhou X, Li X, Zhu Q, Peng J, Zhu B, Zheng X, Lu Y, Yang D, Wang B, Wang J. Depletion of Gut Microbiota Impairs Gut Barrier Function and Antiviral Immune Defense in the Liver. *Front Immunol* 2021; **12**: 636803 [PMID: 33841420 DOI: 10.3389/fimmu.2021.636803]

22 **Zhu Q**, Xia P, Zhou X, Li X, Guo W, Zhu B, Zheng X, Wang B, Yang D, Wang J. Hepatitis B Virus Infection Alters Gut Microbiota Composition in Mice. *Front Cell Infect Microbiol* 2019; **9**: 377 [PMID: 31750262 DOI: 10.3389/fcimb.2019.00377]

23 **Wang J**, Wang Y, Zhang X, Liu J, Zhang Q, Zhao Y, Peng J, Feng Q, Dai J, Sun S, Zhao L, Zhang Y, Hu Y, Zhang M. Gut Microbial Dysbiosis Is Associated with Altered Hepatic Functions and Serum Metabolites in Chronic Hepatitis B Patients. *Front Microbiol* 2017; **8**: 2222 [PMID: 29180991 DOI: 10.3389/fmicb.2017.02222]

24 **Yun Y**, Chang Y, Kim HN, Ryu S, Kwon MJ, Cho YK, Kim HL, Cheong HS, Joo EJ. Alterations of the Gut Microbiome in Chronic Hepatitis B Virus Infection Associated with Alanine Aminotransferase Level. *J Clin Med* 2019; **8** [PMID: 30717396 DOI: 10.3390/jcm8020173]

25 **Sun Z**, Huang C, Shi Y, Wang R, Fan J, Yu Y, Zhang Z, Zhu K, Li M, Ni Q, Chen Z, Zheng M, Yang Z. Distinct Bile Acid Profiles in Patients With Chronic Hepatitis B Virus Infection Reveal Metabolic Interplay Between Host, Virus and Gut Microbiome. *Front Med (Lausanne)* 2021; **8**: 708495 [PMID: 34671614 DOI: 10.3389/fmed.2021.708495]

26 **Joo EJ**, Cheong HS, Kwon MJ, Sohn W, Kim HN, Cho YK. Relationship between gut microbiome diversity and hepatitis B viral load in patients with chronic hepatitis B. *Gut Pathog* 2021; **13**: 65 [PMID: 34717727 DOI: 10.1186/s13099-021-00461-1]

27 **Yang XA**, Lv F, Wang R, Chang Y, Zhao Y, Cui X, Li H, Yang S, Li S, Zhao X, Mo Z, Yang F. Potential role of intestinal microflora in disease progression among patients with different stages of Hepatitis B. *Gut Pathog* 2020; **12**: 50 [PMID: 33117435 DOI: 10.1186/s13099-020-00391-4]

28 **Chen Z**, Xie Y, Zhou F, Zhang B, Wu J, Yang L, Xu S, Stedtfeld R, Chen Q, Liu J, Zhang X, Xu H, Ren J. Featured Gut Microbiomes Associated With the Progression of Chronic Hepatitis B Disease. *Front Microbiol* 2020; **11**: 383 [PMID: 32265857 DOI: 10.3389/fmicb.2020.00383]

29 **Deng YD**, Peng XB, Zhao RR, Ma CQ, Li JN, Yao LQ. The intestinal microbial community dissimilarity in hepatitis B virus-related liver cirrhosis patients with and without at alcohol consumption. *Gut Pathog* 2019; **11**: 58 [PMID: 31788031 DOI: 10.1186/s13099-019-0337-2]

30 **Lu H**, Wu Z, Xu W, Yang J, Chen Y, Li L. Intestinal microbiota was assessed in cirrhotic patients with hepatitis B virus infection. Intestinal microbiota of HBV cirrhotic patients. *Microb Ecol* 2011; **61**: 693-703 [PMID: 21286703 DOI: 10.1007/s00248-010-9801-8]

31 **Chen Y**, Qin N, Guo J, Qian G, Fang D, Shi D, Xu M, Yang F, He Z, Van Nostrand JD, Yuan T, Deng Y, Zhou J, Li L. Functional gene arrays-based analysis of fecal microbiomes in patients with liver cirrhosis. *BMC Genomics* 2014; **15**: 753 [PMID: 25179593 DOI: 10.1186/1471-2164-15-753]

32 **Ganesan M**, Eikenberry A, Poluektova LY, Kharbanda KK, Osna NA. Role of alcohol in pathogenesis of hepatitis B virus infection. *World J Gastroenterol* 2020; **26**: 883-903 [PMID: 32206001 DOI: 10.3748/wjg.v26.i9.883]

33 **Tang Y**, Zhou H, Xiang Y, Cui F. The diagnostic potential of gut microbiome for early hepatitis B virus-related hepatocellular carcinoma. *Eur J Gastroenterol Hepatol* 2021; **33**: e167-e175 [PMID: 33208683 DOI: 10.1097/MEG.0000000000001978]

34 **Liu Q**, Li F, Zhuang Y, Xu J, Wang J, Mao X, Zhang Y, Liu X. Alteration in gut microbiota associated with hepatitis B and non-hepatitis virus related hepatocellular carcinoma. *Gut Pathog* 2019; **11**: 1 [PMID: 30675188 DOI: 10.1186/s13099-018-0281-6]

35 **Zheng R**, Wang G, Pang Z, Ran N, Gu Y, Guan X, Yuan Y, Zuo X, Pan H, Zheng J, Wang F. Liver cirrhosis contributes to the disorder of gut microbiota in patients with hepatocellular carcinoma. *Cancer Med* 2020; **9**: 4232-4250 [PMID: 32281295 DOI: 10.1002/cam4.3045]

36 **Huang H**, Ren Z, Gao X, Hu X, Zhou Y, Jiang J, Lu H, Yin S, Ji J, Zhou L, Zheng S. Integrated analysis of microbiome and host transcriptome reveals correlations between gut microbiota and clinical outcomes in HBV-related hepatocellular carcinoma. *Genome Med* 2020; **12**: 102 [PMID: 33225985 DOI: 10.1186/s13073-020-00796-5]

37 **Wang K**, Zhang Z, Mo ZS, Yang XH, Lin BL, Peng L, Xu Y, Lei CY, Zhuang XD, Lu L, Yang RF, Chen T, Gao ZL. Gut microbiota as prognosis markers for patients with HBV-related acute-on-chronic liver failure. *Gut Microbes* 2021; **13**: 1-15 [PMID: 34006193 DOI: 10.1080/19490976.2021.1921925]

38 **Wei X**, Yan X, Zou D, Yang Z, Wang X, Liu W, Wang S, Li X, Han J, Huang L, Yuan J. Abnormal fecal microbiota community and functions in patients with hepatitis B liver cirrhosis as revealed by a metagenomic approach. *BMC Gastroenterol* 2013; **13**: 175 [PMID: 24369878 DOI: 10.1186/1471-230X-13-175]

39 **Roderburg C**, Luedde T. The role of the gut microbiome in the development and progression of liver cirrhosis and hepatocellular carcinoma. *Gut Microbes* 2014; **5**: 441-445 [PMID: 25006881 DOI: 10.4161/gmic.29599]

40 **Mohamadkhani A**. On the potential role of intestinal microbial community in hepatocarcinogenesis in chronic hepatitis

B. *Cancer Med* 2018 [PMID: 29761927 DOI: 10.1002/cam4.1550]
41 **Kisseleva T**, Brenner D. Molecular and cellular mechanisms of liver fibrosis and its regression. *Nat Rev Gastroenterol Hepatol* 2021; **18**: 151-166 [PMID: 33128017 DOI: 10.1038/s41575-020-00372-7]
42 **Parola M**, Pinzani M. Liver fibrosis: Pathophysiology, pathogenetic targets and clinical issues. *Mol Aspects Med* 2019; **65**: 37-55 [PMID: 30213667 DOI: 10.1016/j.mam.2018.09.002]
43 **Milosevic I**, Vujovic A, Barac A, Djelic M, Korac M, Radovanovic Spurnic A, Gmizic I, Stevanovic O, Djordjevic V, Lekic N, Russo E, Amedei A. Gut-Liver Axis, Gut Microbiota, and Its Modulation in the Management of Liver Diseases: A Review of the Literature. *Int J Mol Sci* 2019; **20** [PMID: 30658519 DOI: 10.3390/ijms20020395]
44 **Hrncir T**, Hrncirova L, Kverka M, Hromadka R, Machova V, Trckova E, Kostovcikova K, Kralickova P, Krejsek J, Tlaskalova-Hogenova H. Gut Microbiota and NAFLD: Pathogenetic Mechanisms, Microbiota Signatures, and Therapeutic Interventions. *Microorganisms* 2021; **9** [PMID: 33946843 DOI: 10.3390/microorganisms9050957]
45 **Chen D**, Le TH, Shahidipour H, Read SA, Ahlenstiel G. The Role of Gut-Derived Microbial Antigens on Liver Fibrosis Initiation and Progression. *Cells* 2019; **8** [PMID: 31717860 DOI: 10.3390/cells8111324]
46 **Nagpal R**, Yadav H. Bacterial Translocation from the Gut to the Distant Organs: An Overview. *Ann Nutr Metab* 2017; **71** Suppl 1: 11-16 [PMID: 28950279 DOI: 10.1159/000479918]
47 **Johansson ME**, Sjövall H, Hansson GC. The gastrointestinal mucus system in health and disease. *Nat Rev Gastroenterol Hepatol* 2013; **10**: 352-361 [PMID: 23478383 DOI: 10.1038/nrgastro.2013.35]
48 **Sorribas M**, Jakob MO, Yilmaz B, Li H, Stutz D, Noser Y, de Gottardi A, Moghadamrad S, Hassan M, Albillos A, Francés R, Juanola O, Spadoni I, Rescigno M, Wiest R. FXR modulates the gut-vascular barrier by regulating the entry sites for bacterial translocation in experimental cirrhosis. *J Hepatol* 2019; **71**: 1126-1140 [PMID: 31295531 DOI: 10.1016/j.jhep.2019.06.017]
49 **Macpherson AJ**, Uhr T. Induction of protective IgA by intestinal dendritic cells carrying commensal bacteria. *Science* 2004; **303**: 1662-1665 [PMID: 15016999 DOI: 10.1126/science.1091334]
50 **Assimakopoulos SF**, Tsamandas AC, Tsiaoussis GI, Karatza E, Triantos C, Vagianos CE, Spiliopoulou I, Kaltezioti V, Charonis A, Nikolopoulou VN, Scopa CD, Thomopoulos KC. Altered intestinal tight junctions' expression in patients with liver cirrhosis: a pathogenetic mechanism of intestinal hyperpermeability. *Eur J Clin Invest* 2012; **42**: 439-446 [PMID: 22023490 DOI: 10.1111/j.1365-2362.2011.02609.x]
51 **Pijls KE**, Koek GH, Elamin EE, de Vries H, Masclee AA, Jonkers DM. Large intestine permeability is increased in patients with compensated liver cirrhosis. *Am J Physiol Gastrointest Liver Physiol* 2014; **306**: G147-G153 [PMID: 24264047 DOI: 10.1152/ajpgi.00330.2013]
52 **Fasano A**, Not T, Wang W, Uzzau S, Berti I, Tommasini A, Goldblum SE. Zonulin, a newly discovered modulator of intestinal permeability, and its expression in coeliac disease. *Lancet* 2000; **355**: 1518-1519 [PMID: 10801176]
53 **Wang X**, Li MM, Niu Y, Zhang X, Yin JB, Zhao CJ, Wang RT. Serum Zonulin in HBV-Associated Chronic Hepatitis, Liver Cirrhosis, and Hepatocellular Carcinoma. *Dis Markers* 2019; **2019**: 5945721 [PMID: 31485278 DOI: 10.1155/2019/5945721]
54 **Kajihara M**, Koido S, Kanai T, Ito Z, Matsumoto Y, Takakura K, Saruta M, Kato K, Odamaki T, Xiao JZ, Sato N, Ohkusa T. Characterisation of blood microbiota in patients with liver cirrhosis. *Eur J Gastroenterol Hepatol* 2019; **31**: 1577-1583 [PMID: 31441799 DOI: 10.1097/MEG.0000000000001494]
55 **Guarner C**, Runyon BA, Young S, Heck M, Sheikh MY. Intestinal bacterial overgrowth and bacterial translocation in cirrhotic rats with ascites. *J Hepatol* 1997; **26**: 1372-1378 [PMID: 9210626 DOI: 10.1016/s0168-8278(97)80474-6]
56 **Teltschik Z**, Wiest R, Beisner J, Nuding S, Hofmann C, Schoelmerich J, Bevins CL, Stange EF, Wehkamp J. Intestinal bacterial translocation in rats with cirrhosis is related to compromised Paneth cell antimicrobial host defense. *Hepatology* 2012; **55**: 1154-1163 [PMID: 22095436 DOI: 10.1002/hep.24789]
57 **Zhou W**, Luo J, Xie X, Yang S, Zhu D, Huang H, Yang D, Liu J. Gut Microbiota Dysbiosis Strengthens Kupffer Cell-mediated Hepatitis B Virus Persistence through Inducing Endotoxemia in Mice. *J Clin Transl Hepatol* 2022; **10**: 17-25 [PMID: 35233369 DOI: 10.14218/JCTH.2020.00161]
58 **Lin RS**, Lee FY, Lee SD, Tsai YT, Lin HC, Lu RH, Hsu WC, Huang CC, Wang SS, Lo KJ. Endotoxemia in patients with chronic liver diseases: relationship to severity of liver diseases, presence of esophageal varices, and hyperdynamic circulation. *J Hepatol* 1995; **22**: 165-172 [PMID: 7790704 DOI: 10.1016/0168-8278(95)80424-2]
59 **Wang X**, Chen L, Wang H, Cai W, Xie Q. Modulation of bile acid profile by gut microbiota in chronic hepatitis B. *J Cell Mol Med* 2020; **24**: 2573-2581 [PMID: 31925905 DOI: 10.1111/jcmm.14951]
60 **Kakiyama G**, Pandak WM, Gillevet PM, Hylemon PB, Heuman DM, Daita K, Takei H, Muto A, Nittono H, Ridlon JM, White MB, Noble NA, Monteith P, Fuchs M, Thacker LR, Sikaroodi M, Bajaj JS. Modulation of the fecal bile acid profile by gut microbiota in cirrhosis. *J Hepatol* 2013; **58**: 949-955 [PMID: 23333527 DOI: 10.1016/j.jhep.2013.01.003]
61 **Ma C**, Han M, Heinrich B, Fu Q, Zhang Q, Sandhu M, Agdashian D, Terabe M, Berzofsky JA, Fako V, Ritz T, Longerich T, Theriot CM, McCulloch JA, Roy S, Yuan W, Thovarai V, Sen SK, Ruchirawat M, Korangy F, Wang XW, Trinchieri G, Greten TF. Gut microbiome-mediated bile acid metabolism regulates liver cancer *via* NKT cells. *Science* 2018; **360** [PMID: 29798856 DOI: 10.1126/science.aan5931]
62 **Paludan SR**, Pradeu T, Masters SL, Mogensen TH. Constitutive immune mechanisms: mediators of host defence and immune regulation. *Nat Rev Immunol* 2021; **21**: 137-150 [PMID: 32782357 DOI: 10.1038/s41577-020-0391-5]
63 **Tacke F**. Targeting hepatic macrophages to treat liver diseases. *J Hepatol* 2017; **66**: 1300-1312 [PMID: 28267621 DOI: 10.1016/j.jhep.2017.02.026]
64 **Tacke F**, Zimmermann HW. Macrophage heterogeneity in liver injury and fibrosis. *J Hepatol* 2014; **60**: 1090-1096 [PMID: 24412603 DOI: 10.1016/j.jhep.2013.12.025]
65 **Żeromski J**, Kierepa A, Brzezicha B, Kowala-Piaskowska A, Mozer-Lisewska I. Pattern Recognition Receptors: Significance of Expression in the Liver. *Arch Immunol Ther Exp (Warsz)* 2020; **68**: 29 [PMID: 32944845 DOI: 10.1007/s00005-020-00595-1]
66 **Kassa Y**, Million Y, Gedefie A, Moges F. Alteration of Gut Microbiota and Its Impact on Immune Response in Patients with Chronic HBV Infection: A Review. *Infect Drug Resist* 2021; **14**: 2571-2578 [PMID: 34262302 DOI:

10.2147/IDR.S305901]
67 **Fitzgerald KA**, Kagan JC. Toll-like Receptors and the Control of Immunity. *Cell* 2020; **180**: 1044-1066 [PMID: 32164908 DOI: 10.1016/j.cell.2020.02.041]
68 **Friedman SL**. Mechanisms of hepatic fibrogenesis. *Gastroenterology* 2008; **134**: 1655-1669 [PMID: 18471545 DOI: 10.1053/j.gastro.2008.03.003]
69 **Iwaisako K**, Jiang C, Zhang M, Cong M, Moore-Morris TJ, Park TJ, Liu X, Xu J, Wang P, Paik YH, Meng F, Asagiri M, Murray LA, Hofmann AF, Iida T, Glass CK, Brenner DA, Kisseleva T. Origin of myofibroblasts in the fibrotic liver in mice. *Proc Natl Acad Sci U S A* 2014; **111**: E3297-E3305 [PMID: 25074909 DOI: 10.1073/pnas.1400062111]
70 **Senoo H**, Kojima N, Sato M. Vitamin A-storing cells (stellate cells). *Vitam Horm* 2007; **75**: 131-159 [PMID: 17368315 DOI: 10.1016/S0083-6729(06)75006-3]
71 **Xu F**, Liu C, Zhou D, Zhang L. TGF-β/SMAD Pathway and Its Regulation in Hepatic Fibrosis. *J Histochem Cytochem* 2016; **64**: 157-167 [PMID: 26747705 DOI: 10.1369/0022155415627681]
72 **Kendall TJ**, Hennedige S, Aucott RL, Hartland SN, Vernon MA, Benyon RC, Iredale JP. p75 Neurotrophin receptor signaling regulates hepatic myofibroblast proliferation and apoptosis in recovery from rodent liver fibrosis. *Hepatology* 2009; **49**: 901-910 [PMID: 19072833 DOI: 10.1002/hep.22701]
73 **Issa R**, Zhou X, Constandinou CM, Fallowfield J, Millward-Sadler H, Gaca MD, Sands E, Suliman I, Trim N, Knorr A, Arthur MJ, Benyon RC, Iredale JP. Spontaneous recovery from micronodular cirrhosis: evidence for incomplete resolution associated with matrix cross-linking. *Gastroenterology* 2004; **126**: 1795-1808 [PMID: 15188175 DOI: 10.1053/j.gastro.2004.03.009]
74 **Ginès P**, Krag A, Abraldes JG, Solà E, Fabrellas N, Kamath PS. Liver cirrhosis. *Lancet* 2021; **398**: 1359-1376 [PMID: 34543610 DOI: 10.1016/S0140-6736(21)01374-X]
75 **Arab JP**, Martin-Mateos RM, Shah VH. Gut-liver axis, cirrhosis and portal hypertension: the chicken and the egg. *Hepatol Int* 2018; **12**: 24-33 [PMID: 28550391 DOI: 10.1007/s12072-017-9798-x]
76 **Paratore M**, Santopaolo F, Cammarota G, Pompili M, Gasbarrini A, Ponziani FR. Fecal Microbiota Transplantation in Patients with HBV Infection or Other Chronic Liver Diseases: Update on Current Knowledge and Future Perspectives. *J Clin Med* 2021; **10** [PMID: 34204748 DOI: 10.3390/jcm10122605]
77 **European Association for the Study of the Liver**. EASL Clinical Practice Guidelines for the management of patients with decompensated cirrhosis. *J Hepatol* 2018; **69**: 406-460 [PMID: 29653741 DOI: 10.1016/j.jhep.2018.03.024]
78 **Dever JB**, Sheikh MY. Review article: spontaneous bacterial peritonitis--bacteriology, diagnosis, treatment, risk factors and prevention. *Aliment Pharmacol Ther* 2015; **41**: 1116-1131 [PMID: 25819304 DOI: 10.1111/apt.13172]
79 **Llovet JM**, Bartolí R, March F, Planas R, Viñado B, Cabré E, Arnal J, Coll P, Ausina V, Gassull MA. Translocated intestinal bacteria cause spontaneous bacterial peritonitis in cirrhotic rats: molecular epidemiologic evidence. *J Hepatol* 1998; **28**: 307-313 [PMID: 9580278 DOI: 10.1016/0168-8278(88)80018-7]
80 **Steib CJ**, Hartmann AC, v Hesler C, Benesic A, Hennenberg M, Bilzer M, Gerbes AL. Intraperitoneal LPS amplifies portal hypertension in rat liver fibrosis. *Lab Invest* 2010; **90**: 1024-1032 [PMID: 20212458 DOI: 10.1038/labinvest.2010.60]
81 **Wijdicks EF**. Hepatic Encephalopathy. *N Engl J Med* 2016; **375**: 1660-1670 [PMID: 27783916 DOI: 10.1056/NEJMra1600561]
82 **Gu X**, Lu Q, Zhang C, Tang Z, Chu L. Clinical Application and Progress of Fecal Microbiota Transplantation in Liver Diseases: A Review. *Semin Liver Dis* 2021; **41**: 495-506 [PMID: 34261137 DOI: 10.1055/s-0041-1732319]
83 Retraction notice to: Clinical significance of the best response during repeated transarterial chemoembolization in the treatment of hepatocellular carcinoma [J. Hepatol. 2014; 60: 1212–1218]. *J Hepatol* 2015; **62**: 252 [PMID: 25538970 DOI: 10.1016/j.jhep.2014.10.038]
84 **Ding JH**, Jin Z, Yang XX, Lou J, Shan WX, Hu YX, Du Q, Liao QS, Xie R, Xu JY. Role of gut microbiota *via* the gut-liver-brain axis in digestive diseases. *World J Gastroenterol* 2020; **26**: 6141-6162 [PMID: 33177790 DOI: 10.3748/wjg.v26.i40.6141]
85 **Bajaj JS**, Ridlon JM, Hylemon PB, Thacker LR, Heuman DM, Smith S, Sikaroodi M, Gillevet PM. Linkage of gut microbiome with cognition in hepatic encephalopathy. *Am J Physiol Gastrointest Liver Physiol* 2012; **302**: G168-G175 [PMID: 21940902 DOI: 10.1152/ajpgi.00190.2011]
86 **Ahluwalia V**, Betrapally NS, Hylemon PB, White MB, Gillevet PM, Unser AB, Fagan A, Daita K, Heuman DM, Zhou H, Sikaroodi M, Bajaj JS. Impaired Gut-Liver-Brain Axis in Patients with Cirrhosis. *Sci Rep* 2016; **6**: 26800 [PMID: 27225869 DOI: 10.1038/srep26800]
87 **Johnson KV**, Foster KR. Why does the microbiome affect behaviour? *Nat Rev Microbiol* 2018; **16**: 647-655 [PMID: 29691482 DOI: 10.1038/s41579-018-0014-3]
88 **Peng CY**, Chien RN, Liaw YF. Hepatitis B virus-related decompensated liver cirrhosis: benefits of antiviral therapy. *J Hepatol* 2012; **57**: 442-450 [PMID: 22504333 DOI: 10.1016/j.jhep.2012.02.033]
89 **Caraceni P**, Vargas V, Solà E, Alessandria C, de Wit K, Trebicka J, Angeli P, Mookerjee RP, Durand F, Pose E, Krag A, Bajaj JS, Beuers U, Ginès P; Liverhope Consortium. The Use of Rifaximin in Patients With Cirrhosis. *Hepatology* 2021; **74**: 1660-1673 [PMID: 33421158 DOI: 10.1002/hep.31708]
90 **Woodhouse CA**, Patel VC, Singanayagam A, Shawcross DL. Review article: the gut microbiome as a therapeutic target in the pathogenesis and treatment of chronic liver disease. *Aliment Pharmacol Ther* 2018; **47**: 192-202 [PMID: 29083037 DOI: 10.1111/apt.14397]
91 **European Association For The Study Of The Liver**. EASL clinical practice guidelines: Management of chronic hepatitis B virus infection. *J Hepatol* 2012; **57**: 167-185 [PMID: 22436845 DOI: 10.1016/j.jhep.2012.02.010]
92 **Lok AS**, McMahon BJ, Brown RS Jr, Wong JB, Ahmed AT, Farah W, Almasri J, Alahdab F, Benkhadra K, Mouchli MA, Singh S, Mohamed EA, Abu Dabrh AM, Prokop LJ, Wang Z, Murad MH, Mohammed K. Antiviral therapy for chronic hepatitis B viral infection in adults: A systematic review and meta-analysis. *Hepatology* 2016; **63**: 284-306 [PMID: 26566246 DOI: 10.1002/hep.28280]
93 **Marcellin P**, Gane E, Buti M, Afdhal N, Sievert W, Jacobson IM, Washington MK, Germanidis G, Flaherty JF, Aguilar

Schall R, Bornstein JD, Kitrinos KM, Subramanian GM, McHutchison JG, Heathcote EJ. Regression of cirrhosis during treatment with tenofovir disoproxil fumarate for chronic hepatitis B: a 5-year open-label follow-up study. *Lancet* 2013; **381**: 468-475 [PMID: 23234725 DOI: 10.1016/S0140-6736(12)61425-1]

94 **Liaw YF**. Reversal of cirrhosis: an achievable goal of hepatitis B antiviral therapy. *J Hepatol* 2013; **59**: 880-881 [PMID: 23673137 DOI: 10.1016/j.jhep.2013.05.007]

95 **Su TH**, Hu TH, Chen CY, Huang YH, Chuang WL, Lin CC, Wang CC, Su WW, Chen MY, Peng CY, Chien RN, Huang YW, Wang HY, Lin CL, Yang SS, Chen TM, Mo LR, Hsu SJ, Tseng KC, Hsieh TY, Suk FM, Hu CT, Bair MJ, Liang CC, Lei YC, Tseng TC, Chen CL, Kao JH; C-TEAM study group and the Taiwan Liver Diseases Consortium. Four-year entecavir therapy reduces hepatocellular carcinoma, cirrhotic events and mortality in chronic hepatitis B patients. *Liver Int* 2016; **36**: 1755-1764 [PMID: 27634134 DOI: 10.1111/liv.13253]

96 **Li X**, Wu S, Du Y, Yang L, Li Y, Hong B. Entecavir therapy reverses gut microbiota dysbiosis induced by hepatitis B virus infection in a mouse model. *Int J Antimicrob Agents* 2020; **56**: 106000 [PMID: 32360229 DOI: 10.1016/j.ijantimicag.2020.106000]

97 **Lu YX**, He CZ, Wang YX, Ai ZS, Liang P, Yang CQ. Effect of Entecavir on the Intestinal Microflora in Patients with Chronic Hepatitis B: A Controlled Cross-Sectional and Longitudinal Real-World Study. *Infect Dis Ther* 2021; **10**: 241-252 [PMID: 33111216 DOI: 10.1007/s40121-020-00355-w]

98 **Lu YX**, Chang YZ, Liang P, Yang CQ. Effect of Additional Clostridium butyricum on the Intestinal Flora of Chronic Hepatitis B Patients Treated with Entecavir. *Infect Dis Ther* 2021; **10**: 1519-1530 [PMID: 34132991 DOI: 10.1007/s40121-021-00463-1]

99 **Alimirah M**, Sadiq O, Gordon SC. Novel Therapies in Hepatic Encephalopathy. *Clin Liver Dis* 2020; **24**: 303-315 [PMID: 32245535 DOI: 10.1016/j.cld.2020.01.009]

100 **Scarpignato C**, Pelosini I. Rifaximin, a poorly absorbed antibiotic: pharmacology and clinical potential. *Chemotherapy* 2005; **51** Suppl 1: 36-66 [PMID: 15855748]

101 **Bajaj JS**, Heuman DM, Wade JB, Gibson DP, Saeian K, Wegelin JA, Hafeezullah M, Bell DE, Sterling RK, Stravitz RT, Fuchs M, Luketic V, Sanyal AJ. Rifaximin improves driving simulator performance in a randomized trial of patients with minimal hepatic encephalopathy. *Gastroenterology* 2011; **140**: 478-487.e1 [PMID: 20849805 DOI: 10.1053/j.gastro.2010.08.061]

102 **Kimer N**, Pedersen JS, Tavenier J, Christensen JE, Busk TM, Hobolth L, Krag A, Al-Soud WA, Mortensen MS, Sørensen SJ, Møller S, Bendtsen F; members of the CoRif study group. Rifaximin has minor effects on bacterial composition, inflammation, and bacterial translocation in cirrhosis: A randomized trial. *J Gastroenterol Hepatol* 2018; **33**: 307-314 [PMID: 28671712 DOI: 10.1111/jgh.13852]

103 **Kaji K**, Saikawa S, Takaya H, Fujinaga Y, Furukawa M, Kitagawa K, Ozutsumi T, Kaya D, Tsuji Y, Sawada Y, Kawaratani H, Moriya K, Namisaki T, Akahane T, Mitoro A, Yoshiji H. Rifaximin Alleviates Endotoxemia with Decreased Serum Levels of Soluble CD163 and Mannose Receptor and Partial Modification of Gut Microbiota in Cirrhotic Patients. *Antibiotics (Basel)* 2020; **9** [PMID: 32235367 DOI: 10.3390/antibiotics9040145]

104 **Bajaj JS**, Heuman DM, Sanyal AJ, Hylemon PB, Sterling RK, Stravitz RT, Fuchs M, Ridlon JM, Daita K, Monteith P, Noble NA, White MB, Fisher A, Sikaroodi M, Rangwala H, Gillevet PM. Modulation of the metabiome by rifaximin in patients with cirrhosis and minimal hepatic encephalopathy. *PLoS One* 2013; **8**: e60042 [PMID: 23565181 DOI: 10.1371/journal.pone.0060042]

105 **Kang DJ**, Kakiyama G, Betrapally NS, Herzog J, Nittono H, Hylemon PB, Zhou H, Carroll I, Yang J, Gillevet PM, Jiao C, Takei H, Pandak WM, Iida T, Heuman DM, Fan S, Fiehn O, Kurosawa T, Sikaroodi M, Sartor RB, Bajaj JS. Rifaximin Exerts Beneficial Effects Independent of its Ability to Alter Microbiota Composition. *Clin Transl Gastroenterol* 2016; **7**: e187 [PMID: 27560928 DOI: 10.1038/ctg.2016.44]

106 **Bezirtzoglou E**, Stavropoulou E. Immunology and probiotic impact of the newborn and young children intestinal microflora. *Anaerobe* 2011; **17**: 369-374 [PMID: 21515397 DOI: 10.1016/j.anaerobe.2011.03.010]

107 **Stavropoulou E**, Bezirtzoglou E. Probiotics in Medicine: A Long Debate. *Front Immunol* 2020; **11**: 2192 [PMID: 33072084 DOI: 10.3389/fimmu.2020.02192]

108 **Lai HH**, Chiu CH, Kong MS, Chang CJ, Chen CC. Probiotic *Lactobacillus casei*: Effective for Managing Childhood Diarrhea by Altering Gut Microbiota and Attenuating Fecal Inflammatory Markers. *Nutrients* 2019; **11** [PMID: 31126062 DOI: 10.3390/nu11051150]

109 **Korpela K**, Salonen A, Vepsäläinen O, Suomalainen M, Kolmeder C, Varjosalo M, Miettinen S, Kukkonen K, Savilahti E, Kuitunen M, de Vos WM. Probiotic supplementation restores normal microbiota composition and function in antibiotic-treated and in caesarean-born infants. *Microbiome* 2018; **6**: 182 [PMID: 30326954 DOI: 10.1186/s40168-018-0567-4]

110 **Zhang Y**, Gu Y, Ren H, Wang S, Zhong H, Zhao X, Ma J, Gu X, Xue Y, Huang S, Yang J, Chen L, Chen G, Qu S, Liang J, Qin L, Huang Q, Peng Y, Li Q, Wang X, Kong P, Hou G, Gao M, Shi Z, Li X, Qiu Y, Zou Y, Yang H, Wang J, Xu G, Lai S, Li J, Ning G, Wang W. Gut microbiome-related effects of berberine and probiotics on type 2 diabetes (the PREMOTE study). *Nat Commun* 2020; **11**: 5015 [PMID: 33024120 DOI: 10.1038/s41467-020-18414-8]

111 **Sergeev IN**, Aljutaily T, Walton G, Huarte E. Effects of Synbiotic Supplement on Human Gut Microbiota, Body Composition and Weight Loss in Obesity. *Nutrients* 2020; **12** [PMID: 31952249 DOI: 10.3390/nu12010222]

112 **Kang DW**, Adams JB, Gregory AC, Borody T, Chittick L, Fasano A, Khoruts A, Geis E, Maldonado J, McDonough-Means S, Pollard EL, Roux S, Sadowsky MJ, Lipson KS, Sullivan MB, Caporaso JG, Krajmalnik-Brown R. Microbiota Transfer Therapy alters gut ecosystem and improves gastrointestinal and autism symptoms: an open-label study. *Microbiome* 2017; **5**: 10 [PMID: 28122648 DOI: 10.1186/s40168-016-0225-7]

113 **Chahwan B**, Kwan S, Isik A, van Hemert S, Burke C, Roberts L. Gut feelings: A randomised, triple-blind, placebo-controlled trial of probiotics for depressive symptoms. *J Affect Disord* 2019; **253**: 317-326 [PMID: 31078831 DOI: 10.1016/j.jad.2019.04.097]

114 **Bagga D**, Reichert JL, Koschutnig K, Aigner CS, Holzer P, Koskinen K, Moissl-Eichinger C, Schöpf V. Probiotics drive gut microbiome triggering emotional brain signatures. *Gut Microbes* 2018; **9**: 486-496 [PMID: 29723105 DOI:

10.1080/19490976.2018.1460015]
115 **Ziada DH**, Soliman HH, El Yamany SA, Hamisa MF, Hasan AM. Can Lactobacillus acidophilus improve minimal hepatic encephalopathy? *Arab J Gastroenterol* 2013; **14**: 116-122 [PMID: 24206740 DOI: 10.1016/j.ajg.2013.08.002]
116 **Xia X**, Chen J, Xia J, Wang B, Liu H, Yang L, Wang Y, Ling Z. Role of probiotics in the treatment of minimal hepatic encephalopathy in patients with HBV-induced liver cirrhosis. *J Int Med Res* 2018; **46**: 3596-3604 [PMID: 29806520 DOI: 10.1177/0300060518776064]
117 **Agrawal A**, Sharma BC, Sharma P, Sarin SK. Secondary prophylaxis of hepatic encephalopathy in cirrhosis: an open-label, randomized controlled trial of lactulose, probiotics, and no therapy. *Am J Gastroenterol* 2012; **107**: 1043-1050 [PMID: 22710579 DOI: 10.1038/ajg.2012.113]
118 **Thilakarathna WPDW**, Rupasinghe HPV, Ridgway ND. Mechanisms by Which Probiotic Bacteria Attenuate the Risk of Hepatocellular Carcinoma. *Int J Mol Sci* 2021; **22** [PMID: 33807605 DOI: 10.3390/ijms22052606]
119 **Ozdemir T**, Fedorec AJH, Danino T, Barnes CP. Synthetic Biology and Engineered Live Biotherapeutics: Toward Increasing System Complexity. *Cell Syst* 2018; **7**: 5-16 [PMID: 30048620 DOI: 10.1016/j.cels.2018.06.008]
120 **Nicaise C**, Prozzi D, Viaene E, Moreno C, Gustot T, Quertinmont E, Demetter P, Suain V, Goffin P, Devière J, Hols P. Control of acute, chronic, and constitutive hyperammonemia by wild-type and genetically engineered Lactobacillus plantarum in rodents. *Hepatology* 2008; **48**: 1184-1192 [PMID: 18697211 DOI: 10.1002/hep.22445]
121 **Kurtz CB**, Millet YA, Puurunen MK, Perreault M, Charbonneau MR, Isabella VM, Kotula JW, Antipov E, Dagon Y, Denney WS, Wagner DA, West KA, Degar AJ, Brennan AM, Miller PF. An engineered *E. coli* Nissle improves hyperammonemia and survival in mice and shows dose-dependent exposure in healthy humans. *Sci Transl Med* 2019; **11** [PMID: 30651324 DOI: 10.1126/scitranslmed.aau7975]
122 **Ochoa-Sanchez R**, Oliveira MM, Tremblay M, Petrazzo G, Pant A, Bosoi CR, Perreault M, Querbes W, Kurtz CB, Rose CF. Genetically engineered E. coli Nissle attenuates hyperammonemia and prevents memory impairment in bile-duct ligated rats. *Liver Int* 2021; **41**: 1020-1032 [PMID: 33548108 DOI: 10.1111/liv.14815]
123 **Khoruts A**, Sadowsky MJ. Understanding the mechanisms of faecal microbiota transplantation. *Nat Rev Gastroenterol Hepatol* 2016; **13**: 508-516 [PMID: 27329806 DOI: 10.1038/nrgastro.2016.98]
124 **Marotz CA**, Zarrinpar A. Treating Obesity and Metabolic Syndrome with Fecal Microbiota Transplantation. *Yale J Biol Med* 2016; **89**: 383-388 [PMID: 27698622]
125 **Niina A**, Kibe R, Suzuki R, Yuchi Y, Teshima T, Matsumoto H, Kataoka Y, Koyama H. Fecal microbiota transplantation as a new treatment for canine inflammatory bowel disease. *Biosci Microbiota Food Health* 2021; **40**: 98-104 [PMID: 33996366 DOI: 10.12938/bmfh.2020-049]
126 **Geng S**, Cheng S, Li Y, Wen Z, Ma X, Jiang X, Wang Y, Han X. Faecal Microbiota Transplantation Reduces Susceptibility to Epithelial Injury and Modulates Tryptophan Metabolism of the Microbial Community in a Piglet Model. *J Crohns Colitis* 2018; **12**: 1359-1374 [PMID: 30010734 DOI: 10.1093/ecco-jcc/jjy103]
127 **Sun MF**, Zhu YL, Zhou ZL, Jia XB, Xu YD, Yang Q, Cui C, Shen YQ. Neuroprotective effects of fecal microbiota transplantation on MPTP-induced Parkinson's disease mice: Gut microbiota, glial reaction and TLR4/TNF-α signaling pathway. *Brain Behav Immun* 2018; **70**: 48-60 [PMID: 29471030 DOI: 10.1016/j.bbi.2018.02.005]
128 **Kelly CR**, Khoruts A, Staley C, Sadowsky MJ, Abd M, Alani M, Bakow B, Curran P, McKenney J, Tisch A, Reinert SE, Machan JT, Brandt LJ. Effect of Fecal Microbiota Transplantation on Recurrence in Multiply Recurrent Clostridium difficile Infection: A Randomized Trial. *Ann Intern Med* 2016; **165**: 609-616 [PMID: 27547925 DOI: 10.7326/M16-0271]
129 **Khanna S**, Vazquez-Baeza Y, González A, Weiss S, Schmidt B, Muñiz-Pedrogo DA, Rainey JF 3rd, Kammer P, Nelson H, Sadowsky M, Khoruts A, Farrugia SL, Knight R, Pardi DS, Kashyap PC. Changes in microbial ecology after fecal microbiota transplantation for recurrent C. difficile infection affected by underlying inflammatory bowel disease. *Microbiome* 2017; **5**: 55 [PMID: 28506317 DOI: 10.1186/s40168-017-0269-3]
130 **Mocanu V**, Zhang Z, Deehan EC, Kao DH, Hotte N, Karmali S, Birch DW, Samarasinghe KK, Walter J, Madsen KL. Fecal microbial transplantation and fiber supplementation in patients with severe obesity and metabolic syndrome: a randomized double-blind, placebo-controlled phase 2 trial. *Nat Med* 2021; **27**: 1272-1279 [PMID: 34226737 DOI: 10.1038/s41591-021-01399-2]
131 **Suez J**, Zmora N, Zilberman-Schapira G, Mor U, Dori-Bachash M, Bashiardes S, Zur M, Regev-Lehavi D, Ben-Zeev Brik R, Federici S, Horn M, Cohen Y, Moor AE, Zeevi D, Korem T, Kotler E, Harmelin A, Itzkovitz S, Maharshak N, Shibolet O, Pevsner-Fischer M, Shapiro H, Sharon I, Halpern Z, Segal E, Elinav E. Post-Antibiotic Gut Mucosal Microbiome Reconstitution Is Impaired by Probiotics and Improved by Autologous FMT. *Cell* 2018; **174**: 1406-1423.e16 [PMID: 30193113 DOI: 10.1016/j.cell.2018.08.047]
132 **Ren YD**, Ye ZS, Yang LZ, Jin LX, Wei WJ, Deng YY, Chen XX, Xiao CX, Yu XF, Xu HZ, Xu LZ, Tang YN, Zhou F, Wang XL, Chen MY, Chen LG, Hong MZ, Ren JL, Pan JS. Fecal microbiota transplantation induces hepatitis B virus e-antigen (HBeAg) clearance in patients with positive HBeAg after long-term antiviral therapy. *Hepatology* 2017; **65**: 1765-1768 [PMID: 28027582 DOI: 10.1002/hep.29008]
133 **Chauhan A**, Kumar R, Sharma S, Mahanta M, Vayuuru SK, Nayak B, Kumar S, Shalimar. Fecal Microbiota Transplantation in Hepatitis B e Antigen-Positive Chronic Hepatitis B Patients: A Pilot Study. *Dig Dis Sci* 2021; **66**: 873-880 [PMID: 32279172 DOI: 10.1007/s10620-020-06246-x]
134 **Liu R**, Kang JD, Sartor RB, Sikaroodi M, Fagan A, Gavis EA, Zhou H, Hylemon PB, Herzog JW, Li X, Lippman RH, Gonzalez-Maeso J, Wade JB, Ghosh S, Gurley E, Gillevet PM, Bajaj JS. Neuroinflammation in Murine Cirrhosis Is Dependent on the Gut Microbiome and Is Attenuated by Fecal Transplant. *Hepatology* 2020; **71**: 611-626 [PMID: 31220352 DOI: 10.1002/hep.30827]
135 **Bajaj JS**, Kassam Z, Fagan A, Gavis EA, Liu E, Cox IJ, Kheradman R, Heuman D, Wang J, Gurry T, Williams R, Sikaroodi M, Fuchs M, Alm E, John B, Thacker LR, Riva A, Smith M, Taylor-Robinson SD, Gillevet PM. Fecal microbiota transplant from a rational stool donor improves hepatic encephalopathy: A randomized clinical trial. *Hepatology* 2017; **66**: 1727-1738 [PMID: 28586116 DOI: 10.1002/hep.29306]
136 **Bajaj JS**, Salzman NH, Acharya C, Sterling RK, White MB, Gavis EA, Fagan A, Hayward M, Holtz ML, Matherly S, Lee H, Osman M, Siddiqui MS, Fuchs M, Puri P, Sikaroodi M, Gillevet PM. Fecal Microbial Transplant Capsules Are Safe in

Hepatic Encephalopathy: A Phase 1, Randomized, Placebo-Controlled Trial. *Hepatology* 2019; **70**: 1690-1703 [PMID: 31038755 DOI: 10.1002/hep.30690]

137 **Shen TC**, Albenberg L, Bittinger K, Chehoud C, Chen YY, Judge CA, Chau L, Ni J, Sheng M, Lin A, Wilkins BJ, Buza EL, Lewis JD, Daikhin Y, Nissim I, Yudkoff M, Bushman FD, Wu GD. Engineering the gut microbiota to treat hyperammonemia. *J Clin Invest* 2015; **125**: 2841-2850 [PMID: 26098218 DOI: 10.1172/JCI79214]

138 **Liu J**, Zhai C, Rho JR, Lee S, Heo HJ, Kim S, Kim HJ, Hong ST. Treatment of Hyperammonemia by Transplanting a Symbiotic Pair of Intestinal Microbes. *Front Cell Infect Microbiol* 2021; **11**: 696044 [PMID: 35071025 DOI: 10.3389/fcimb.2021.696044]

139 **Ponziani FR**, Gerardi V, Pecere S, D'Aversa F, Lopetuso L, Zocco MA, Pompili M, Gasbarrini A. Effect of rifaximin on gut microbiota composition in advanced liver disease and its complications. *World J Gastroenterol* 2015; **21**: 12322-12333 [PMID: 26604640 DOI: 10.3748/wjg.v21.i43.12322]

140 **Zeng Y**, Chen S, Fu Y, Wu W, Chen T, Chen J, Yang B, Ou Q. Gut microbiota dysbiosis in patients with hepatitis B virus-induced chronic liver disease covering chronic hepatitis, liver cirrhosis and hepatocellular carcinoma. *J Viral Hepat* 2020; **27**: 143-155 [PMID: 31600845 DOI: 10.1111/jvh.13216]

141 **Kang Y**, Cai Y. Gut microbiota and hepatitis-B-virus-induced chronic liver disease: implications for faecal microbiota transplantation therapy. *J Hosp Infect* 2017; **96**: 342-348 [PMID: 28545829 DOI: 10.1016/j.jhin.2017.04.007]

142 **Xu M**, Wang B, Fu Y, Chen Y, Yang F, Lu H, Xu J, Li L. Changes of fecal Bifidobacterium species in adult patients with hepatitis B virus-induced chronic liver disease. *Microb Ecol* 2012; **63**: 304-313 [PMID: 21814872 DOI: 10.1007/s00248-011-9925-5]

143 **Wu ZW**, Lu HF, Wu J, Zuo J, Chen P, Sheng JF, Zheng SS, Li LJ. Assessment of the fecal lactobacilli population in patients with hepatitis B virus-related decompensated cirrhosis and hepatitis B cirrhosis treated with liver transplant. *Microb Ecol* 2012; **63**: 929-937 [PMID: 21965156 DOI: 10.1007/s00248-011-9945-1]

144 **Lutz P**, Parcina M, Bekeredjian-Ding I, Nischalke HD, Nattermann J, Sauerbruch T, Hoerauf A, Strassburg CP, Spengler U. Impact of rifaximin on the frequency and characteristics of spontaneous bacterial peritonitis in patients with liver cirrhosis and ascites. *PLoS One* 2014; **9**: e93909 [PMID: 24714550 DOI: 10.1371/journal.pone.0093909]

World Journal of Gastroenterology

Submit a Manuscript: https://www.f6publishing.com

World J Gastroenterol 2022 July 28; 28(28): 3573-3585

DOI: 10.3748/wjg.v28.i28.3573

ISSN 1007-9327 (print) ISSN 2219-2840 (online)

MINIREVIEWS

Combination approaches in hepatocellular carcinoma: How systemic treatment can benefit candidates to locoregional modalities

Leonardo Gomes da Fonseca, Raphael L C Araujo

Specialty type: Oncology

Provenance and peer review: Invited article; Externally peer reviewed.

Peer-review model: Single blind

Peer-review report's scientific quality classification

Grade A (Excellent): A
Grade B (Very good): 0
Grade C (Good): C, C
Grade D (Fair): 0
Grade E (Poor): 0

P-Reviewer: Abdalla AN, Saudi Arabia; Li S, China; Liu B, China

Received: January 17, 2022
Peer-review started: January 17, 2022
First decision: April 11, 2022
Revised: April 19, 2022
Accepted: June 26, 2022
Article in press: June 26, 2022
Published online: July 28, 2022

Leonardo Gomes da Fonseca, Department of Medical Oncology, Instituto do Cancer do Estado de Sao Paulo, University of Sao Paulo, São Paulo 01246-000, São Paulo, Brazil

Leonardo Gomes da Fonseca, Raphael L C Araujo, Hospital e Maternidade Brasil - Rede D'Or São Luiz, Santo André 09030-590, São Paulo, Brazil

Raphael L C Araujo, Department of Digestive Surgery, Escola Paulista de Medicina - UNIFESP, São Paulo 04023-062, São Paulo, Brazil

Corresponding author: Raphael L C Araujo, MD, PhD, Adjunct Professor, Surgical Oncologist, Department of Digestive Surgery, Escola Paulista de Medicina - UNIFESP, Rua Botucatu, 740, Vila Clementino, São Paulo 04023-062, São Paulo, Brazil. raphael.l.c.araujo@gmail.com

Abstract

The management of hepatocellular carcinoma (HCC) is challenging because most patients have underlying cirrhosis, and the treatment provides, historically, a limited impact on the natural history of patients with advanced-stage disease. Additionally, recurrence rates are high for those patients who receive local and locoregional modalities, such as surgical (resection and transplantation) or image-guided (ablation and intra-arterial) therapies. Translational research has led to new concepts that are reshaping the current clinical practice. Substantial advancements were achieved in the understanding of the hallmarks that drive hepatocarcinogenesis. This has primed a successful incorporation of novel agents with different targets, such as anti-angiogenic drugs, targeted-therapies, and immune-checkpoint inhibitors. Although clinical trials have proven efficacy of systemic agents in advanced stage disease, there is no conclusive evidence to support their use in combination with loco-regional therapy. While novel local modalities are being incorporated (*e.g.*, radioembolization, microwave ablation, and irreversible electroporation), emerging data indicate that locoregional treatments may induce tumor microenvironment changes, such as hyperexpression of growth factors, release of tumor antigens, infiltration of cytotoxic lymphocytes, and modulation of adaptative and innate immune response. Past trials that evaluated the use of antiangiogenic drugs in the adjuvant setting after ablation or chemoembolization fail to demonstrate a substantial improvement. Current efforts are directed to investigate the role of immunotherapy-based regimens in this context. The present review aims to describe the current landscape of systemic and locoregional treatments for HCC, present evidence to support combination approaches, and address future perspectives.

Key Words: Liver cancer; Hepatocellular carcinoma; Immunotherapy; Systemic therapy; Ablation; Embolization

©The Author(s) 2022. Published by Baishideng Publishing Group Inc. All rights reserved.

Core Tip: Management of hepatocellular carcinoma (HCC) is based on stages defined by tumor burden, liver function, and performance status. With the advent of more effective systemic treatments, such as immunotherapy and immunotherapy-based combinations, patients with advanced stage disease have better outcomes. The migration of systemic treatment to earlier stages, in combination with locoregional therapies, are expected to improve the outcomes and cure rates. Currently, the research field is moving towards an increasing interest in combining locoregional and systemic treatments for HCC.

Citation: da Fonseca LG, Araujo RLC. Combination approaches in hepatocellular carcinoma: How systemic treatment can benefit candidates to locoregional modalities. *World J Gastroenterol* 2022; 28(28): 3573-3585
URL: https://www.wjgnet.com/1007-9327/full/v28/i28/3573.htm
DOI: https://dx.doi.org/10.3748/wjg.v28.i28.3573

INTRODUCTION

Hepatocellular carcinoma (HCC) is a highly fatal disease, representing the fourth cause of cancer-related mortality worldwide[1]. This situation is attributed to the challenging management of patients with HCC *per se* in concomitance with an underlying liver disease and cirrhosis-related complications. Moreover, a significant proportion of patients are diagnosed with advanced stage disease, not amenable to curative options. Finally, even patients who are treated with local therapies, such as surgery and ablation, present high rates of recurrence, reaching up to 70% in 5 years[2].

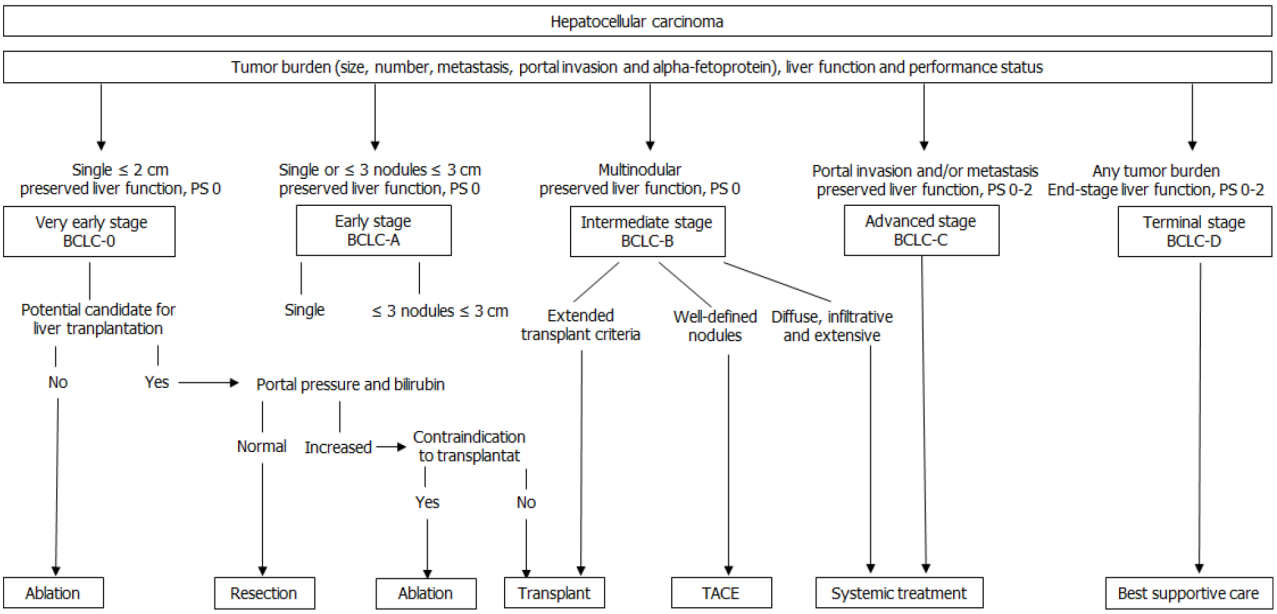
Treatment options for HCC are selected based on liver function, performance status, and tumor burden (size, number of lesions, metastatic spread, and vascular invasion). These patient- and tumor-centered characteristics define the stage of the cancer, each with a different prognosis[3]. Thus, clinical practice guidelines according to both tumor presentation and liver function integrate the available evidence based on well-delineated clinical trials and recommend treatment strategies for each stage[2,4] (Figure 1).

Liver resection, local ablation, and liver transplantation are recommended for very-early and early-stage disease and are considered curative-intent treatments for HCC. Intra-arterial therapies, such as transarterial chemoembolization (TACE), are indicated for cases classified as intermediate stage (multinodular liver disease beyond Milan-criteria with preserved liver function), and systemic treatments are used for patients with advanced stage disease[3]. Therapeutic management of HCC is evolving rapidly with the incorporation of novel locoregional techniques and the increasing number of systemic agents tested in clinical trials, including immunotherapy. Each treatment approach is directed to treat HCC at different stages, and there is a lack of evidence to support the use of combined systemic and locoregional treatments. Therefore, the biological rational behind combination strategies and the urgent need to improve outcomes for this lethal disease prime intense research activity in both basic and clinical fields. This review aims to address the current landscape of systemic and locoregional treatments and the future perspectives regarding combined approaches.

SYSTEMIC TREATMENT FOR HCC: CURRENT LANDSCAPE AND PERSPECTIVES

Systemic treatment is recommended for patients with advanced stage disease (preserved liver function, performance status 0-2, metastatic spread, and/or macrovascular invasion) and for patients in earlier stages who have contra-indications or progressed after locoregional modalities according to the concept of treatment stage migration[3].

The natural history of advanced HCC is poor, with a median overall survival of 4-8 mo without active treatments[5]. Since 2008, the use of agents that target hallmarks of hepatocarcinogenesis are gradually improving prognosis and achieving substantial clinical benefit for HCC patients. Sorafenib, a multikinase inhibitor, has been shown to improve overall survival over placebo in the SHARP and Asia-Pacific trials and became the first approved drug for advanced HCC[6,7]. After almost a decade, other drugs of the same class were tested with positive results in phase III trials, such as lenvatinib (non-inferior to sorafenib in first-line)[8], regorafenib (superior over placebo in second-line for patients who tolerated sorafenib)[9], and cabozantinib (superior over placebo after sorafenib failure)[10]. These drugs



DOI: 10.3748/wjg.v28.i28.3573 **Copyright** ©The Author(s) 2022.

Figure 1 Treatment algorithm for hepatocellular carcinoma based on level-1 evidence. The algorithm establishes five stages according to liver function, tumor burden, and performance status. Each stage is linked to first-line treatment recommendation, although individual decisions can be defined according to patient profile and available treatment options. Adapted from Ref. [3]. BCLC: Barcelona clinic liver cancer; TACE: Transarterial chemoembolization.

share common targets, such as vascular endothelial growth factor receptor (VEGFR) and platelet-derived growth factor receptor, while some of them present, individually, more direct actions against specific targets, such as the case of lenvatinib against fibroblast growth factor receptor, and cabozantinib against mesenchymal-epithelial transition (MET) receptor. Additionally, ramucirumab, a monoclonal antibody against VEGFR, was shown to improve overall survival over placebo in patients who present with alpha-fetoprotein (AFP) ≥ 400 ng/mL after sorafenib failure and is also approved for clinical use [11]. Generally, these drugs present antiangiogenic activity and promote clinical benefit by delaying tumor progression rather than inducing a substantial reduction in tumor burden. Trials with these drugs are consistent in showing a statically significant, but modest, increase in overall survival, with survivals around 11-13 mo in the first line, a response rate of less than 10% (except for lenvatinib, with a response rate of 18.8% in the REFLECT trial), and a range of class-related adverse events, such as fatigue, arterial hypertension, skin reaction, and diarrhea[12].

In the past years, the advent of immune-based treatments, such as immune checkpoint inhibitors, brought huge advances in HCC management. The biological background for the use of immunotherapy in HCC is based on the remarkable immunotolerance of the liver due to the high antigenic load derived from the enteral-portal circulation. Additionally, HCC develops in a microenvironment of chronic inflammation and underlying liver disease. Low infiltration of CD8 + T lymphocytes, responsible for the antitumor immune response, and a marked presence of exhausted lymphocytes and regulatory T lymphocytes are described in HCC, contributing to an immunosuppressive and procarcinogenic microenvironment[13,14].

The immune checkpoint inhibitors aimed at boosting anti-tumoral immunity in the priming phase by the recognition of antigens presented by dendritic cells to lymphocytes (anti-CTLA4 agents) and in the effector phase of T-CD8 cytotoxic cells against tumor cells (anti-PD1, anti-PDL1) were tested in phase I/II trials showing durable response rates of around 15%-20%. Therefore, pembrolizumab and nivolumab (anti-PD1 drugs) received approval for use in second-line treatments[15,16]. However, comparative trials showed that immune checkpoint inhibitors as monotherapy did not improve outcomes comparing to the available treatments. In a phase III trial, nivolumab was not proven to improve survival compared to sorafenib in the first line[17] and pembrolizumab did not achieve statistical superiority over placebo in the second-line[18].

The use of combinations of agents with different mechanisms of action can improve results of immunotherapy through additive effect and because VEGF can enhance the immunosuppression of the tumor microenvironment by inhibiting the function of effector T cells, increasing the recruitment of regulatory T cells and myeloid-derived suppressor cells[19]. This combination was explored in the IMBRAVE150 trial, which randomized patients to receive sorafenib *vs* a combination of bevacizumab (an anti-VEGF antibody) and atezolizumab (an anti-PD-L1 antibody). This trial demonstrated a significant improvement in overall survival (19.2 mo *vs* 13.4 mo), and also in progression-free survival and response rate[20,21]. IMBRAVE150 trial was a landmark in HCC management and marked the transition towards the use of combined systemic therapies (using dual-immunotherapy or antian-

giogenic plus immunotherapy combinations). Several combinations showed encouraging results in phases I and II trials, such as lenvatinib plus pembrolizumab[22], pembrolizumab plus regorafenib[23], nivolumab plus ipilimumab[24], and nivolumab, ipilimumab, and cabozantinib[25]. These preliminary results suggested that combinations may yield response rates of more than 20% according to RECIST criteria, which seems to compare favorably to the rates with multikinase inhibitors. However, it is important to point out some limitations of early phase trials. Firstly, non-comparative trials are not adequate to draw definitive conclusions. Besides, the response rate is not a surrogate marker for survival benefit in HCC, even more considering that RECIST may not capture the spectrum and patterns of progression and response in patients under immunotherapy.

Recently, durvalumab and tremelimumab as a combination treatment was announced to yield survival benefit over sorafenib in a phase III trial and is expected to be incorporated in the first-line setting as an alternative to atezolizumab plus bevacizumab[26,27]. Currently, other phase III trials are awaiting results in the context of combination therapies for advanced HCC (Table 1).

ROLE OF LOCOREGIONAL THERAPIES IN HCC: IS THERE ROOM FOR IMPROVING OUTCOMES?

Liver resection is indicated in early HCC, regardless of the presence of cirrhosis, since the liver function remains compensated, and is rarely is does the patient have a clinically significant portal hypertension. However, the risk of liver decompensation after resection in patients with restricted hepatic functional reserve is a concern, especially in cases requiring major hepatectomies (3 or more segments)[2,28,29]. On the other side, liver transplantation has the advantage of treating both cirrhosis and offer curative-intent treatment for HCC. Thus, liver transplantation decreases both the risk of recurrence, since the most recurrence is in the liver, and *de novo* lesions by removing the cirrhotic liver. But its application in clinical practice is hampered by organ shortage, complexity, heterogenous availability in different worldwide regions, and the risk of progression on waiting list[30].

In patients with liver-only disease not amenable to surgical modalities, locoregional interventional procedures play a key role. Locoregional treatment is defined as imaging-guided tumor directed procedures, and it is estimated that 50% of patients with HCC might receive any of these treatments during the course of the disease[31,32]. Basically, there are two groups of locoregional therapies: (1) Ablative therapies; or (2) Intra-arterial therapies. Although both modalities are consolidated with high level evidence, emerging approaches and techniques are being increasingly adopted and are expected to improve clinical outcomes. Besides, the risk of recurrence and progression in patients treated with locoregional therapies has led to intense research activity towards combination with systemic treatment [2,4].

ABLATIVE THERAPIES

Current evidence of ablative methods in HCC

Ablative therapies induce tumor destruction through different mechanisms according to the method: Chemical [percutaneous ethanol injection (PEI)], thermal [radiofrequency ablation (RFA), microwave (MWA), and cryoablation], and short pulses of high voltage (irreversible electroporation). In general, ablative techniques are considered a curative therapy for HCC < 2-3 cm and is associated with complete responses in 70%-90% of the cases, although recurrences occur in approximately 50% of the cases within 5 years[33-35].

The most used and recommended method is RFA, which has shown survival superiority over PEI in randomized trials[33]. Tumor size, number of nodules, and Child-Pugh class are associated with prognosis in patients treated with RFA[36-38]. Comparative studies *vs* resection demonstrated that RFA seems to be inferior to surgery in tumors > 3 cm[39]. Limitations to RFA include proximity to large vessels (due to heat effect), size, and location.

MWA is another technique that has been increasingly used and has the advantage of achieving a faster heating over a larger volume and being less susceptible to heat sink effect. Most studies that addressed comparisons between RFA and MWA showed similar efficacy, with a trend toward best results with MWA in tumors > 3 cm[40-42].

Alternative techniques, such as IRE and cryoablation, are under active research, with a small series of studies showing encouraging results[43,44]. IRE has the advantage of causing less thermal damage to adjacent tissues. However, more data are still required for IRE and cryoablation in order to fully incorporate these techniques into clinical practice guidelines.

Combination of ablative and systemic treatment: rationale and current evidence

The high risk of local and distant recurrence after ablation indicates the need for adjuvant strategies to improve cure rates. Features, such as large tumors, multinodularity, and vascular invasion (macroscopic

Table 1 Clinical trials in advanced hepatocellular carcinoma with combination of systemic treatment

Study name	Design	Experimental arm	Median overall survival, mo	Response rate-RECIST, %	Grade 3 - 4 treatment-related adverse events
IMBRAVE 150[21]	Phase III; First-line	Atezolizumab + Bevacizumab	19.2	30%	36%
KEYNOTE 524/Study 116[22]	Phase Ib; First-line	Pembrolizumab + Lenvatinib	22	36%	67%
REG-PEMBRO-HCC [23]	Phase Ib; First-line	Pembrolizumab + Regorafenib	26.5	32%	86%
CHECKMATE 040[24]	Phase II; Second-line	Nivolumab + Ipilimumab (arm A)	22.8	32%	53%
STUDY 22[27]	Phase II; Second-line	Durvalumab + Tremelimumab	18.7	24%	35.1%
CHECKMATE-040[25]	Phase II; First and second-line	Nivolumab + Ipilimumab + Cabozantinib	Not-reached	26%	71%

or microscopic), are significantly related to higher recurrence rates. Novel markers, such as genetic signatures, circulating microRNA, circulating non-coding RNA, circulating cell-free DNA, gut microbiota, and circulating tumor cells, have also been shown to predict the risk of recurrence[45-47].

To evaluate the impact of multikinase inhibitors with antiangiogenic activity combined with ablation, the STORM trial randomized patients treated with resection (n = 900) or ablation (n = 214) to sorafenib or placebo for a total of 4 years. Unfortunately, there was no difference in recurrence-free survival between groups, with a median to time to recurrence of 33.3 mo in the sorafenib group and 33.7 mo for the placebo group (HR = 0.94, P = 0.26)[48]. Thus, the positive results obtained with sorafenib in advanced disease have not been reproduced in the context of adjuvant post-resection or ablation. Other drugs used in the advanced stage, such as cabozantinib, regorafenib, ramucirumab, and lenvatinib have not been evaluated in patients after ablation. In sum, VEGFR-directed therapies as monotherapy do not seem to improve the results of ablation.

Recently, the immune features of localized HCC and the response to local treatment are being investigated[49-51]. The concentration of intratumor CD3 + and CD8 + T cells and the expression of programmed death ligand 1 (PD-L1) by immune and tumor cells appear to be associated with HCC aggressiveness and risk of recurrence after curative treatments, such as ablation and surgery[13]. The high expression of PD1 can lead a condition of exhausted CD8 + impairing cytotoxicity and decreasing of pro-inflammatory cytokines production and anti-tumor ability[13].

Ablation can induce stimulate inflammatory and cytokine production within the treated site. The tumor debris released upon ablation represent a tumor antigen repertoire that can boost antitumoral immunologic response. Indeed, tumor antigens can be found in dendritic cells in lymph nodes following ablation[52]. This background indicates a potential role for immune checkpoint inhibitors directed to PD1 and PD-L1 in combination with ablative therapies (Figure 2). A phase I trial including 32 patients treated with tremelimumab and ablation showed accumulation of CD8+ cells, suggesting immune system activation[53]. Preliminary results of the NIVOLVE trial were presented in 2021. In this phase II single arm trial, 55 patients after surgery (n = 33) or ablation (n = 22) received nivolumab for 12 mo. The median recurrence-free survival was 26 mo. In this trial, the authors suggested that patients with tumor-infiltrating lymphocytes, positive PD-L1, and negative staining for beta-catenin tend to develop fewer recurrences[54]; however, larger and comparative studies are needed to confirm these findings. Currently, several active trials (recruiting or waiting results) are addressing the role of immune-checkpoint inhibitors in combination with anti-VEGFR agents or alone after curative treatments, such as ablation (Table 2).

INTRA-ARTERIAL THERAPIES

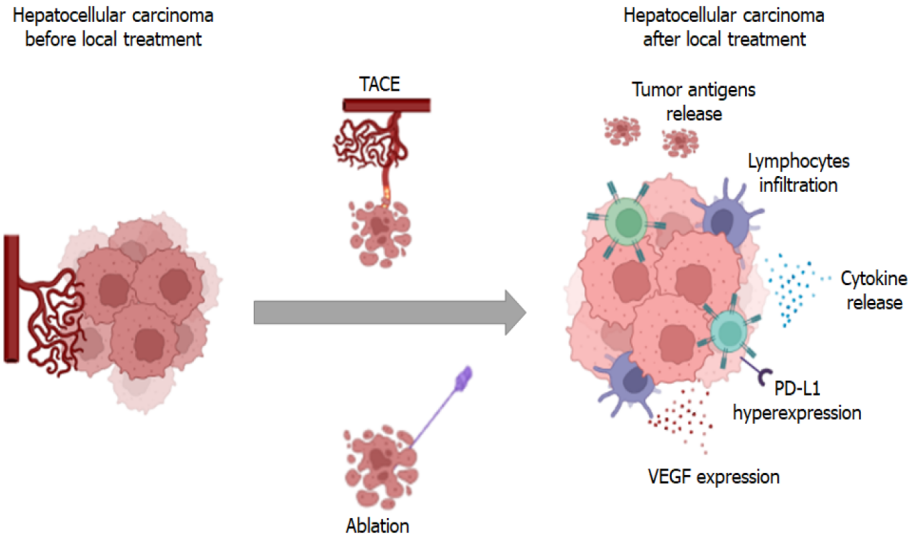
Current evidence of intra-arterial therapy in HCC

Intra-arterial therapies harness the arterial supply of HCC that differs from the liver parenchyma, which receives its blood supply predominantly from the portal vein. This group of therapies are composed of transarterial embolization (TAE), chemoembolization (TACE), and selective internal radiotherapy (SIRT) or radioembolization (TARE).

The mechanism of action of TAE is based on the obstruction of the blood supply causing ischemia, while TACE adds a cytotoxic agent (most commonly doxorubicin) and a carrier agent (commonly lipiodol). Drug-eluting bead (DEB)-TACE uses microspheres carrying cytotoxic agents which are associated with a sustained drug release and, theoretically, a lower systemic exposure to chemotherapy

Table 2 Clinical trials approaching combination of systemic treatment and ablation enrolling, recruiting, or waiting for final results

Trial	Trial registration	Drug	Control	*n*	Disease stage	Local treatment	Expected termination	Primary end-point
CHECKMATE 9DX	NCT03383458	Nivolumab	Placebo	530	Early/intermediate	Surgery/Ablation	2025	Recurrence-free survival
KEYNOTE 937	NCT03867084	Pembrolizumab	Placebo	950	Early/intermediate	Surgery/Ablation	2025	Recurrence-free survival and overall survival
IMBRAVE 050	NCT04102098	Atezolizumab + Bevacizumab	Surveillance	662	Early/intermediate /advanced	Surgery/Ablation	2027	Recurrence-free survival
EMERALD-2	NCT03847428	Durvalumab + Bevacizumab	Placebo	888	Early/intermediate	Surgery/Ablation	2024	Recurrence-free survival



DOI: 10.3748/wjg.v28.i28.3573 **Copyright** ©The Author(s) 2022.

Figure 2 Mechanisms of tumor microenvironment changes after locoregional therapies. After local interventions, tumor immune microenvironment may change with a pronounced release of tumor antigens, cytokines, lymphocyte infiltration, and hyperexpression of vascular endothelial growth factor. TACE: Transarterial chemoembolization; PD-L1: Programmed death ligand 1; VEGF: Vascular endothelial growth factor.

[55].

Based on randomized clinical trials of TACE *vs* no active treatment and also in a large meta-analysis, this is considered the standard of care for patients with intermediate-stage [Barcelona clinic liver cancer (BCLC)-B: Multinodular disease, preserved liver function, and performance status of 0][56,57]. In published cohorts with selected patients, the median overall survival with TACE reaches 48 mo[58]. There is no definitive evidence for the superiority of TACE over TAE, although data from meta-analysis suggests that the former is associated with better outcomes[57]. A prospective trial demonstrated that DEB-TACE presents lower treatment-related toxicities and a trend towards a better objective response rate compared to conventional TACE[59].

Guidelines recommend that patients who present progression with infiltrative tumors, vascular invasion, metastatic spread, or absence of a significant response after two TACEs should be considered for systemic treatment[2,4]. The risk of liver deterioration should be carefully monitored after TACE due to the prognostic impact of liver decompensation in patients with HCC[60]. The decision to declare TACE failure and switch to systemic treatment is heterogenous in different parts of the world, and many scores have been proposed to help in this decision, although some of them still require further validation in a population treated strictly according to the BCLC algorithm[61-65]. For example, the hepatoma-arterial embolization (HAP) score includes albumin, AFP, bilirubin and tumor diameter and was concepted to predict prognosis before the first TACE in a heterogeneous cohort with around 30% of BCLC-C patients[64]. The Assessment for Retreatment with TACE (ART) score was designed to evaluate benefit of a 2nd TACE and assess Child-Pugh score, AST levels, and tumor response after the first TACE. The ART score was originally developed in a cohort that included around 20% of patients with impaired liver function (Child-Pugh B8 or more)[66].

With the availability of more effective systemic agents, the migration from TACE to systemic treatment is a key decision in the management of HCC and should not be delayed at a point of

irreversible deterioration of liver function or performance status.

TARE has been increasingly studied in HCC and has become a common practice in many centers. Data comparing TACE to TARE demonstrated in patients with early or intermediate stage a longer time to progression favoring TARE, but no survival benefit[67]. Although encouraging, there is no solid evidence that TARE should became standard of care in patients eligible to intra-arterial therapies.

A recent single-arm retrospective study including patients with solitary HCC ≤ 8 cm reported objective response rates of 88.3% and a 3-years survival of 86.6%. In this study TARE served as a neoadjuvant therapy for transplantation or resection in 21% and 6.8% of patients, respectively[68].

In uncontrolled trials, TARE was suggested to be safe in patients with portal vein invasion[69]. However, randomized trials in the setting of advanced stage HCC did not prove superiority of TARE over sorafenib in overall survival[70,71]. Therefore, TARE is not recommended as a standard therapy in patients classified as BCLC-C. There is a need to better explore the role of TARE in HCC in prospective and randomized trials, especially for subgroups of patients requiring downstaging, segmental portal vein thrombosis, and using rigorous dosimetry.

Combination of intra-arterial and systemic treatment: rationale and current evidence

Although TACE is the standard treatment for intermediate stage, only around 50% of patients present objective response rate and most of them will eventually present distant and local progression[72]. This has led to studies focused on improving the outcomes for HCC patients treated with TACE by combining multikinase inhibitors.

The rational for testing these combinations comes from the demonstration of increased intratumorally micro vessel density and VEGF expression in residual tumors after TACE, suggesting that TACE may stimulate tumor angiogenesis[73]. However, antiangiogenic drugs, such as sorafenib[74,75], brivanib [76], and bevacizumab[77], failed to demonstrated survival benefit in combination with TACE in controlled trials.

Recently, TACTIS trials randomized patients to TACE alone or combined with sorafenib and showed that sorafenib improved progression-free survival (25.2 mo *vs* 13.5 mo; P = 0.006), but with no significant impact on overall survival (36.2 mo *vs* 30.8 mo; P = 0.40)[78,79]. Currently, available evidence fails to encourage the use of multikinase inhibitors in combination with TACE as a standard practice, but there is a growing enthusiasm with the use of immunotherapy in this setting.

Similar to ablative treatments, intra-arterial therapies may modulate innate and adaptative immunity by releasing cellular debris and inflammatory cytokines and inducing T-cell responses, what is suggested to be related to improved prognosis[80,81] (Figure 2). A recent study compared HCC tissue from patients who were previously submitted to TACE to patients not treated with TACE and found that the former had a lower density of immune-exhausted effector cytotoxic and T-regs with an upregulation of pro-inflammatory pathways[82]. Considering this background, strategies aimed at blocking negative regulators such as PD-1 and CTLA4 are promising and are being investigated in phase III clinical trials (Table 3).

TARE also seems to modulate immunological microenvironment in HCC. A study that compared findings before and after TARE showed that tumor-infiltrating lymphocytes after TARE exhibited signs of immune activation, such as higher expression of granzyme-B and infiltration of CD8+Tcells, NK cells, and antigen-presenting cells[83,84]. Initial data on the combination of nivolumab and SIRT showed favorable safety profile, but efficacy data are pending[85,86].

Besides the biological background, the use of systemic treatment in earlier stages (combined with locoregional treatment) may benefit those patients who would present clinical deterioration or liver function worsening during TACE-refractoriness and would not found fit to receive further systemic treatment in that situation.

CONCLUSION

The treatment landscape of HCC management evolved rapidly in the past years. The most relevant achievements took place in the management of advanced stage disease. The median overall survival in pivotal clinical trials shifted from 5-8 mo in placebo arms[6], to almost 20 mo with immunotherapy combinations[21]. Still, some questions remain to be answer regarding the identification of predictive biomarkers and the optimal sequence in first-, second-, and later lines[87-89].

On the other, the field evolved modestly in the setting of local and locoregional stages, comprising early and intermediate stages. Patients in the early stage are offered surgical resection, liver transplantation, or ablation. Due to organ shortage and strict criteria to transplant, surgery and ablation has been widely used. Unfortunately, their recurrence rates are high and determine results in long-term mortality[33-35]. Although attempts were made, no systemic treatment has improved outcomes in early stage. Robust evidence supports those immunological changes occur after tumor ablation and the use immunotherapy is encouraging.

Patients in the intermediate stage have historically been offered TACE with the aim to achieve tumor control. Similarly, most of them will eventually present local or distant progression and will be

Table 3 Clinical trials approaching combination of systemic treatment and intra-arterial actually enrolling, recruiting or waiting for final results

Trial	Trial registration	Drug	Control	*n*	Disease stage	Local treatment	Expected termination	Primary end-point
EMERALD-1	NCT03778957	Durvalumab + Bevacizumab plus TACE	TACE plusplacebo	600	Intermediate/advanced	TACE	2024	Progression-free survival
TACE-3	NCT04268888	Nivolumab plus DEB-TACE	DEB- TACE	522	Intermediate	DEB-TACE	2026	Overall survival
LEAP-012	NCT04246177	Lenvatinib plus Pembrol-izumab plus cTACE	cTACE	950	Intermediate	Surgery/Ablation	2029	Overall survival and progression-free survival
CheckMate 74 W	NCT04340193	Nivolumab plusIpilimumab/placebo plus cTACE	cTACE plusplacebo	765	Intermediate	Surgery/Ablation	Non-available	Time-to-progression and overall survival

c: Conventional; DEB: Drug-eluting beads; TACE: Transarterial chemoembolization.

considered for systemic treatment. The concomitant use of immunotherapy-based systemic agents and intra-arterial therapies may enhance anti-tumor immune response and impact positively on the outcomes. Several clinical trials are eagerly awaited.

The most promising ongoing trials approach the combination of TACE and immunotherapy, with the aim to significantly delay time-to-progression and, hopefully, increase cure rates for patients who achieve complete response with locoregional treatment. Similarly, trials that test adjuvant immunotherapy after ablation may increase cure rates by reducing the risk of recurrence and -*de novo* tumors. It is likely that biomarkers and subsets of clinical features will emerge from these trials and will support the selection of patients that will derive more benefit from combination approaches.

Finally, it is key to consider that if active trials succeed in showing a better anti-tumor efficacy with combination of locoregional and systemic treatment, a longer survival of patients with HCC will be expected. Furthermore, this will highlight the burden of cirrhosis-related complications as a competing risk of mortality and the importance of multidisciplinary teams as the standard approach for HCC.

FOOTNOTES

Author contributions: Both authors performed the writing and prepared the figures and tables; Both authors designed the outline and coordinated the writing of the paper.

Conflict-of-interest statement: All authors report no relevant conflicts of interest for this article.

Open-Access: This article is an open-access article that was selected by an in-house editor and fully peer-reviewed by external reviewers. It is distributed in accordance with the Creative Commons Attribution Noncommercial (CC BY-NC 4.0) license, which permits others to distribute, remix, adapt, build upon this work non-commercially, and license their derivative works on different terms, provided the original work is properly cited and the use is non-commercial. See: https://creativecommons.org/Licenses/by-nc/4.0/

Country/Territory of origin: Brazil

ORCID number: Leonardo Gomes da Fonseca 0000-0002-0216-3618; Raphael L C Araujo 0000-0002-7834-5944.

S-Editor: Ma YJ
L-Editor: Filipodia
P-Editor: Ma YJ

REFERENCES

1 **Llovet JM**, Zucman-Rossi J, Pikarsky E, Sangro B, Schwartz M, Sherman M, Gores G. Hepatocellular carcinoma. *Nat Rev Dis Primers* 2016; **2**: 16018 [PMID: 27158749 DOI: 10.1038/nrdp.2016.18]

2 **European Association for the Study of the Liver**. EASL Clinical Practice Guidelines: Management of hepatocellular carcinoma. *J Hepatol* 2018; **69**: 182-236 [PMID: 29628281 DOI: 10.1016/j.jhep.2018.03.019]

3 **Reig M**, Forner A, Rimola J, Ferrer-Fàbrega J, Burrel M, Garcia-Criado Á, Kelley RK, Galle PR, Mazzaferro V, Salem R, Sangro B, Singal AG, Vogel A, Fuster J, Ayuso C, Bruix J. BCLC strategy for prognosis prediction and treatment recommendation: The 2022 update. *J Hepatol* 2022; **76**: 681-693 [PMID: 34801630 DOI: 10.1016/j.jhep.2021.11.018]

4 **Heimbach JK**, Kulik LM, Finn RS, Sirlin CB, Abecassis MM, Roberts LR, Zhu AX, Murad MH, Marrero JA. AASLD guidelines for the treatment of hepatocellular carcinoma. *Hepatology* 2018; **67**: 358-380 [PMID: 28130846 DOI: 10.1002/hep.29086]

5 **Llovet JM**, Bustamante J, Castells A, Vilana R, Ayuso Mdel C, Sala M, Brú C, Rodés J, Bruix J. Natural history of untreated nonsurgical hepatocellular carcinoma: rationale for the design and evaluation of therapeutic trials. *Hepatology* 1999; **29**: 62-67 [PMID: 9862851 DOI: 10.1002/hep.510290145]

6 **Llovet JM**, Ricci S, Mazzaferro V, Hilgard P, Gane E, Blanc JF, de Oliveira AC, Santoro A, Raoul JL, Forner A, Schwartz M, Porta C, Zeuzem S, Bolondi L, Greten TF, Galle PR, Seitz JF, Borbath I, Häussinger D, Giannaris T, Shan M, Moscovici M, Voliotis D, Bruix J; SHARP Investigators Study Group. Sorafenib in advanced hepatocellular carcinoma. *N Engl J Med* 2008; **359**: 378-390 [PMID: 18650514 DOI: 10.1056/NEJMoa0708857]

7 **Cheng AL**, Kang YK, Chen Z, Tsao CJ, Qin S, Kim JS, Luo R, Feng J, Ye S, Yang TS, Xu J, Sun Y, Liang H, Liu J, Wang J, Tak WY, Pan H, Burock K, Zou J, Voliotis D, Guan Z. Efficacy and safety of sorafenib in patients in the Asia-Pacific region with advanced hepatocellular carcinoma: a phase III randomised, double-blind, placebo-controlled trial. *Lancet Oncol* 2009; **10**: 25-34 [PMID: 19095497 DOI: 10.1016/S1470-2045(08)70285-7]

8 **Kudo M**, Finn RS, Qin S, Han KH, Ikeda K, Piscaglia F, Baron A, Park JW, Han G, Jassem J, Blanc JF, Vogel A, Komov D, Evans TRJ, Lopez C, Dutcus C, Guo M, Saito K, Kraljevic S, Tamai T, Ren M, Cheng AL. Lenvatinib versus sorafenib in first-line treatment of patients with unresectable hepatocellular carcinoma: a randomised phase 3 non-inferiority trial. *Lancet* 2018; **391**: 1163-1173 [PMID: 29433850 DOI: 10.1016/S0140-6736(18)30207-1]

9 **Bruix J**, Qin S, Merle P, Granito A, Huang YH, Bodoky G, Pracht M, Yokosuka O, Rosmorduc O, Breder V, Gerolami R, Masi G, Ross PJ, Song T, Bronowicki JP, Ollivier-Hourmand I, Kudo M, Cheng AL, Llovet JM, Finn RS, LeBerre MA, Baumhauer A, Meinhardt G, Han G; RESORCE Investigators. Regorafenib for patients with hepatocellular carcinoma who progressed on sorafenib treatment (RESORCE): a randomised, double-blind, placebo-controlled, phase 3 trial. *Lancet* 2017; **389**: 56-66 [PMID: 27932229 DOI: 10.1016/S0140-6736(16)32453-9]

10 **Abou-Alfa GK**, Meyer T, Cheng AL, El-Khoueiry AB, Rimassa L, Ryoo BY, Cicin I, Merle P, Chen Y, Park JW, Blanc JF, Bolondi L, Klümpen HJ, Chan SL, Zagonel V, Pressiani T, Ryu MH, Venook AP, Hessel C, Borgman-Hagey AE, Schwab G, Kelley RK. Cabozantinib in Patients with Advanced and Progressing Hepatocellular Carcinoma. *N Engl J Med* 2018; **379**: 54-63 [PMID: 29972759 DOI: 10.1056/NEJMoa1717002]

11 **Zhu AX**, Park JO, Ryoo BY, Yen CJ, Poon R, Pastorelli D, Blanc JF, Chung HC, Baron AD, Pfiffer TE, Okusaka T, Kubackova K, Trojan J, Sastre J, Chau I, Chang SC, Abada PB, Yang L, Schwartz JD, Kudo M; REACH Trial Investigators. Ramucirumab versus placebo as second-line treatment in patients with advanced hepatocellular carcinoma following first-line therapy with sorafenib (REACH): a randomised, double-blind, multicentre, phase 3 trial. *Lancet Oncol* 2015; **16**: 859-870 [PMID: 26095784 DOI: 10.1016/S1470-2045(15)00050-9]

12 **da Fonseca LG**, Reig M, Bruix J. Tyrosine Kinase Inhibitors and Hepatocellular Carcinoma. *Clin Liver Dis* 2020; **24**: 719-737 [PMID: 33012455 DOI: 10.1016/j.cld.2020.07.012]

13 **Ma J**, Zheng B, Goswami S, Meng L, Zhang D, Cao C, Li T, Zhu F, Ma L, Zhang Z, Zhang S, Duan M, Chen Q, Gao Q, Zhang X. $PD1^{Hi}$ $CD8^{+}$ T cells correlate with exhausted signature and poor clinical outcome in hepatocellular carcinoma. *J Immunother Cancer* 2019; **7**: 331 [PMID: 31783783 DOI: 10.1186/s40425-019-0814-7]

14 **Makarova-Rusher OV**, Medina-Echeverz J, Duffy AG, Greten TF. The yin and yang of evasion and immune activation in HCC. *J Hepatol* 2015; **62**: 1420-1429 [PMID: 25733155 DOI: 10.1016/j.jhep.2015.02.038]

15 **Zhu AX**, Finn RS, Edeline J, Cattan S, Ogasawara S, Palmer D, Verslype C, Zagonel V, Fartoux L, Vogel A, Sarker D, Verset G, Chan SL, Knox J, Daniele B, Webber AL, Ebbinghaus SW, Ma J, Siegel AB, Cheng AL, Kudo M; KEYNOTE-224 investigators. Pembrolizumab in patients with advanced hepatocellular carcinoma previously treated with sorafenib (KEYNOTE-224): a non-randomised, open-label phase 2 trial. *Lancet Oncol* 2018; **19**: 940-952 [PMID: 29875066 DOI: 10.1016/S1470-2045(18)30351-6]

16 **El-Khoueiry AB**, Sangro B, Yau T, Crocenzi TS, Kudo M, Hsu C, Kim TY, Choo SP, Trojan J, Welling TH Rd, Meyer T, Kang YK, Yeo W, Chopra A, Anderson J, Dela Cruz C, Lang L, Neely J, Tang H, Dastani HB, Melero I. Nivolumab in patients with advanced hepatocellular carcinoma (CheckMate 040): an open-label, non-comparative, phase 1/2 dose escalation and expansion trial. *Lancet* 2017; **389**: 2492-2502 [PMID: 28434648 DOI: 10.1016/S0140-6736(17)31046-2]

17 **Yau T**, Park JW, Finn RS, Cheng AL, Mathurin P, Edeline J, Kudo M, Harding JJ, Merle P, Rosmorduc O, Wyrwicz L, Schott E, Choo SP, Kelley RK, Sieghart W, Assenat E, Zaucha R, Furuse J, Abou-Alfa GK, El-Khoueiry AB, Melero I, Begic D, Chen G, Neely J, Wisniewski T, Tschaika M, Sangro B. Nivolumab versus sorafenib in advanced hepatocellular carcinoma (CheckMate 459): a randomised, multicentre, open-label, phase 3 trial. *Lancet Oncol* 2022; **23**: 77-90 [PMID: 34914889 DOI: 10.1016/S1470-2045(21)00604-5]

18 **Finn RS**, Ryoo BY, Merle P, Kudo M, Bouattour M, Lim HY, Breder V, Edeline J, Chao Y, Ogasawara S, Yau T, Garrido M, Chan SL, Knox J, Daniele B, Ebbinghaus SW, Chen E, Siegel AB, Zhu AX, Cheng AL; KEYNOTE-240 investigators. Pembrolizumab As Second-Line Therapy in Patients With Advanced Hepatocellular Carcinoma in KEYNOTE-240: A Randomized, Double-Blind, Phase III Trial. *J Clin Oncol* 2020; **38**: 193-202 [PMID: 31790344 DOI: 10.1200/JCO.19.01307]

19 **Hegde PS**, Wallin JJ, Mancao C. Predictive markers of anti-VEGF and emerging role of angiogenesis inhibitors as immunotherapeutics. *Semin Cancer Biol* 2018; **52**: 117-124 [PMID: 29229461 DOI: 10.1016/j.semcancer.2017.12.002]

20 **Cheng AL**, Qin S, Ikeda M, Galle PR, Ducreux M, Kim TY, Lim HY, Kudo M, Breder V, Merle P, Kaseb AO, Li D, Verret W, Ma N, Nicholas A, Wang Y, Li L, Zhu AX, Finn RS. Updated efficacy and safety data from IMbrave150: Atezolizumab plus bevacizumab vs. sorafenib for unresectable hepatocellular carcinoma. *J Hepatol* 2022; **76**: 862-873 [PMID: 34902530 DOI: 10.1016/j.jhep.2021.11.030]

21 **Finn RS**, Qin S, Ikeda M, Galle PR, Ducreux M, Kim TY, Kudo M, Breder V, Merle P, Kaseb AO, Li D, Verret W, Xu DZ, Hernandez S, Liu J, Huang C, Mulla S, Wang Y, Lim HY, Zhu AX, Cheng AL; IMbrave150 Investigators.

Atezolizumab plus Bevacizumab in Unresectable Hepatocellular Carcinoma. *N Engl J Med* 2020; **382**: 1894-1905 [PMID: 32402160 DOI: 10.1056/NEJMoa1915745]

22 **Finn RS**, Ikeda M, Zhu AX, Sung MW, Baron AD, Kudo M, Okusaka T, Kobayashi M, Kumada H, Kaneko S, Pracht M, Mamontov K, Meyer T, Kubota T, Dutcus CE, Saito K, Siegel AB, Dubrovsky L, Mody K, Llovet JM. Phase Ib Study of Lenvatinib Plus Pembrolizumab in Patients With Unresectable Hepatocellular Carcinoma. *J Clin Oncol* 2020; **38**: 2960-2970 [PMID: 32716739 DOI: 10.1200/JCO.20.00808]

23 **El-Khoueiry AB**, Kim RD, Harris WP, Sung MW, Galle PR. Phase Ib study of regorafenib (REG) plus pembrolizumab (PEMBRO) for first-line treatment of advanced hepatocellular carcinoma (HCC). *J Clin Oncol* 2020; **38**: 564-564 [DOI: 10.1200/JCO.2020.38.4_suppl.564]

24 **Yau T**, Kang YK, Kim TY, El-Khoueiry AB, Santoro A, Sangro B, Melero I, Kudo M, Hou MM, Matilla A, Tovoli F, Knox JJ, Ruth He A, El-Rayes BF, Acosta-Rivera M, Lim HY, Neely J, Shen Y, Wisniewski T, Anderson J, Hsu C. Efficacy and Safety of Nivolumab Plus Ipilimumab in Patients With Advanced Hepatocellular Carcinoma Previously Treated With Sorafenib: The CheckMate 040 Randomized Clinical Trial. *JAMA Oncol* 2020; **6**: e204564 [PMID: 33001135 DOI: 10.1001/jamaoncol.2020.4564]

25 **Yau T**, Zagonel V, Santoro A, Acosta-Rivera M, Choo SP, Matilla A, He AR, Gracián AC, El-Khoueiry AB, Sangro B, Eldawy T, Bruix J, Frassineti G, Vaccaro GM, Tschaika M, Scheffold C, Shen Y, Neely J, Piscaglia F. Nivolumab (NIVO) + ipilimumab (IPI) + cabozantinib (CABO) combination therapy in patients (pts) with advanced hepatocellular carcinoma (aHCC): Results from CheckMate 040. *J Clin Oncol* 2020; **38**: 478-478 [DOI: 10.1200/jco.2020.38.4_suppl.478]

26 **AstraZeneca**. Imfinzi plus tremelimumab significantly improved overall survival in HIMALAYA Phase III trial in 1st-line unresectable liver cancer. [cited January 2, 2022] Available from: https://www.astrazeneca.com/media-centre/press-releases/2021/imfinzi-and-tremelimumab-improved-os-in-liver-cancer.html

27 **Kelley RK**, Sangro B, Harris W, Ikeda M, Okusaka T, Kang YK, Qin S, Tai DW, Lim HY, Yau T, Yong WP, Cheng AL, Gasbarrini A, Damian S, Bruix J, Borad M, Bendell J, Kim TY, Standifer N, He P, Makowsky M, Negro A, Kudo M, Abou-Alfa GK. Safety, Efficacy, and Pharmacodynamics of Tremelimumab Plus Durvalumab for Patients With Unresectable Hepatocellular Carcinoma: Randomized Expansion of a Phase I/II Study. *J Clin Oncol* 2021; **39**: 2991-3001 [PMID: 34292792 DOI: 10.1200/JCO.20.03555]

28 **Makary MS**, Ramsell S, Miller E, Beal EW, Dowell JD. Hepatocellular carcinoma locoregional therapies: Outcomes and future horizons. *World J Gastroenterol* 2021; **27**: 7462-7479 [PMID: 34887643 DOI: 10.3748/wjg.v27.i43.7462]

29 **Kong FH**, Miao XY, Zou H, Xiong L, Wen Y, Chen B, Liu X, Zhou JJ. End-stage liver disease score and future liver remnant volume predict post-hepatectomy liver failure in hepatocellular carcinoma. *World J Clin Cases* 2019; **7**: 3734-3741 [PMID: 31799298 DOI: 10.12998/wjcc.v7.i22.3734]

30 **Bhoori S**, Mazzaferro V. Current challenges in liver transplantation for hepatocellular carcinoma. *Best Pract Res Clin Gastroenterol* 2014; **28**: 867-879 [PMID: 25260314 DOI: 10.1016/j.bpg.2014.08.001]

31 **Park JW**, Chen M, Colombo M, Roberts LR, Schwartz M, Chen PJ, Kudo M, Johnson P, Wagner S, Orsini LS, Sherman M. Global patterns of hepatocellular carcinoma management from diagnosis to death: the BRIDGE Study. *Liver Int* 2015; **35**: 2155-2166 [PMID: 25752327 DOI: 10.1111/liv.12818]

32 **Llovet JM**, Kelley RK, Villanueva A, Singal AG, Pikarsky E, Roayaie S, Lencioni R, Koike K, Zucman-Rossi J, Finn RS. Hepatocellular carcinoma. *Nat Rev Dis Primers* 2021; **7**: 6 [PMID: 33479224 DOI: 10.1038/s41572-020-00240-3]

33 **Cho YK**, Kim JK, Kim MY, Rhim H, Han JK. Systematic review of randomized trials for hepatocellular carcinoma treated with percutaneous ablation therapies. *Hepatology* 2009; **49**: 453-459 [PMID: 19065676 DOI: 10.1002/hep.22648]

34 **Breen DJ**, Lencioni R. Image-guided ablation of primary liver and renal tumours. *Nat Rev Clin Oncol* 2015; **12**: 175-186 [PMID: 25601446 DOI: 10.1038/nrclinonc.2014.237]

35 **Kloeckner R**, Galle PR, Bruix J. Local and Regional Therapies for Hepatocellular Carcinoma. *Hepatology* 2021; **73** Suppl 1: 137-149 [PMID: 32557715 DOI: 10.1002/hep.31424]

36 **Yao XS**, Yan D, Jiang XX, Li X, Zeng HY, Li H. Short-term outcomes of radiofrequency ablation for hepatocellular carcinoma using cone-beam computed tomography for planning and image guidance. *World J Clin Cases* 2021; **9**: 1580-1591 [PMID: 33728301 DOI: 10.12998/wjcc.v9.i7.1580]

37 **Lee DH**, Lee JM, Lee JY, Kim SH, Yoon JH, Kim YJ, Han JK, Choi BI. Radiofrequency ablation of hepatocellular carcinoma as first-line treatment: long-term results and prognostic factors in 162 patients with cirrhosis. *Radiology* 2014; **270**: 900-909 [PMID: 24475823 DOI: 10.1148/radiol.13130940]

38 **N'Kontchou G**, Mahamoudi A, Aout M, Ganne-Carrié N, Grando V, Coderc E, Vicaut E, Trinchet JC, Sellier N, Beaugrand M, Seror O. Radiofrequency ablation of hepatocellular carcinoma: long-term results and prognostic factors in 235 Western patients with cirrhosis. *Hepatology* 2009; **50**: 1475-1483 [PMID: 19731239 DOI: 10.1002/hep.23181]

39 **Xia Y**, Li J, Liu G, Wang K, Qian G, Lu Z, Yang T, Yan Z, Lei Z, Si A, Wan X, Zhang H, Gao C, Cheng Z, Pawlik TM, Wang H, Lau WY, Wu M, Shen F. Long-term Effects of Repeat Hepatectomy vs Percutaneous Radiofrequency Ablation Among Patients With Recurrent Hepatocellular Carcinoma: A Randomized Clinical Trial. *JAMA Oncol* 2020; **6**: 255-263 [PMID: 31774468 DOI: 10.1001/jamaoncol.2019.4477]

40 **Glassberg MB**, Ghosh S, Clymer JW, Qadeer RA, Ferko NC, Sadeghirad B, Wright GW, Amaral JF. Microwave ablation compared with radiofrequency ablation for treatment of hepatocellular carcinoma and liver metastases: a systematic review and meta-analysis. *Onco Targets Ther* 2019; **12**: 6407-6438 [PMID: 31496742 DOI: 10.2147/OTT.S204340]

41 **Tan W**, Deng Q, Lin S, Wang Y, Xu G. Comparison of microwave ablation and radiofrequency ablation for hepatocellular carcinoma: a systematic review and meta-analysis. *Int J Hyperthermia* 2019; **36**: 264-272 [PMID: 30676100 DOI: 10.1080/02656736.2018.1562571]

42 **Harari CM**, Magagna M, Bedoya M, Lee FT Jr, Lubner MG, Hinshaw JL, Ziemlewicz T, Brace CL. Microwave Ablation: Comparison of Simultaneous and Sequential Activation of Multiple Antennas in Liver Model Systems. *Radiology* 2016; **278**: 95-103 [PMID: 26133361 DOI: 10.1148/radiol.2015142151]

43 **Sutter O**, Calvo J, N'Kontchou G, Nault JC, Ourabia R, Nahon P, Ganne-Carrié N, Bourcier V, Zentar N, Bouhafs F, Sellier N, Diallo A, Seror O. Safety and Efficacy of Irreversible Electroporation for the Treatment of Hepatocellular Carcinoma Not Amenable to Thermal Ablation Techniques: A Retrospective Single-Center Case Series. *Radiology* 2017;

284: 877-886 [PMID: 28453431 DOI: 10.1148/radiol.2017161413]
44 **Wang C**, Wang H, Yang W, Hu K, Xie H, Hu KQ, Bai W, Dong Z, Lu Y, Zeng Z, Lou M, Gao X, Chang X, An L, Qu J, Li J, Yang Y. Multicenter randomized controlled trial of percutaneous cryoablation versus radiofrequency ablation in hepatocellular carcinoma. *Hepatology* 2015; **61**: 1579-1590 [PMID: 25284802 DOI: 10.1002/hep.27548]
45 **Dapito DH**, Mencin A, Gwak GY, Pradere JP, Jang MK, Mederacke I, Caviglia JM, Khiabanian H, Adeyemi A, Bataller R, Lefkowitch JH, Bower M, Friedman R, Sartor RB, Rabadan R, Schwabe RF. Promotion of hepatocellular carcinoma by the intestinal microbiota and TLR4. *Cancer Cell* 2012; **21**: 504-516 [PMID: 22516259 DOI: 10.1016/j.ccr.2012.02.007]
46 **Portolani N**, Coniglio A, Ghidoni S, Giovanelli M, Benetti A, Tiberio GA, Giulini SM. Early and late recurrence after liver resection for hepatocellular carcinoma: prognostic and therapeutic implications. *Ann Surg* 2006; **243**: 229-235 [PMID: 16432356 DOI: 10.1097/01.sla.0000197706.21803.a1]
47 **Okajima W**, Komatsu S, Ichikawa D, Miyamae M, Ohashi T, Imamura T, Kiuchi J, Nishibeppu K, Arita T, Konishi H, Shiozaki A, Morimura R, Ikoma H, Okamoto K, Otsuji E. Liquid biopsy in patients with hepatocellular carcinoma: Circulating tumor cells and cell-free nucleic acids. *World J Gastroenterol* 2017; **23**: 5650-5668 [PMID: 28883691 DOI: 10.3748/wjg.v23.i31.5650]
48 **Bruix J**, Takayama T, Mazzaferro V, Chau GY, Yang J, Kudo M, Cai J, Poon RT, Han KH, Tak WY, Lee HC, Song T, Roayaie S, Bolondi L, Lee KS, Makuuchi M, Souza F, Berre MA, Meinhardt G, Llovet JM; STORM investigators. Adjuvant sorafenib for hepatocellular carcinoma after resection or ablation (STORM): a phase 3, randomised, double-blind, placebo-controlled trial. *Lancet Oncol* 2015; **16**: 1344-1354 [PMID: 26361969 DOI: 10.1016/S1470-2045(15)00198-9]
49 **Pu T**, Li ZH, Jiang D, Chen JM, Guo Q, Cai M, Chen ZX, Xie K, Zhao YJ, Liu FB. Nomogram based on inflammation-related markers for predicting survival of patients undergoing hepatectomy for hepatocellular carcinoma. *World J Clin Cases* 2021; **9**: 11193-11207 [PMID: 35071550 DOI: 10.12998/wjcc.v9.i36.11193]
50 **Liu P**, Tan XZ, Zhang T, Gu QB, Mao XH, Li YC, He YQ. Prediction of microvascular invasion in solitary hepatocellular carcinoma ≤ 5 cm based on computed tomography radiomics. *World J Gastroenterol* 2021; **27**: 2015-2024 [PMID: 34007136 DOI: 10.3748/wjg.v27.i17.2015]
51 **Tian YL**, Ji JJ, Chen LN, Cui XL, Liu ST, Mao L, Qiu YD, Li BB. Risk factors for long-term prognosis of hepatocellular carcinoma patients after anatomic hepatectomy. *World J Clin Cases* 2020; **8**: 713-722 [PMID: 32149055 DOI: 10.12998/wjcc.v8.i4.713]
52 **den Brok MH**, Sutmuller RP, Nierkens S, Bennink EJ, Toonen LW, Figdor CG, Ruers TJ, Adema GJ. Synergy between in situ cryoablation and TLR9 stimulation results in a highly effective in vivo dendritic cell vaccine. *Cancer Res* 2006; **66**: 7285-7292 [PMID: 16849578 DOI: 10.1158/0008-5472.CAN-06-0206]
53 **Duffy AG**, Ulahannan SV, Makorova-Rusher O, Rahma O, Wedemeyer H, Pratt D, Davis JL, Hughes MS, Heller T, ElGindi M, Uppala A, Korangy F, Kleiner DE, Figg WD, Venzon D, Steinberg SM, Venkatesan AM, Krishnasamy V, Abi-Jaoudeh N, Levy E, Wood BJ, Greten TF. Tremelimumab in combination with ablation in patients with advanced hepatocellular carcinoma. *J Hepatol* 2017; **66**: 545-551 [PMID: 27816492 DOI: 10.1016/j.jhep.2016.10.029]
54 **Kudo M**, Ueshima K, Nakahira S, Nishida N, Ida H, Minami Y, Nakai T, Wada H, Kubo S, Ohkawa K, Morishita A, Nomi T, Ishida K, Kobayashi S, Umeda M, Tsurusaki M, Chiba Y, Yoshimura K, Sakai K, Nishio K. Adjuvant nivolumab for hepatocellular carcinoma (HCC) after surgical resection (SR) or radiofrequency ablation (RFA) (NIVOLVE): A phase 2 prospective multicenter single-arm trial and exploratory biomarker analysis. *J Clin Oncol* 2021; **39**: 4070-4070 [DOI: 10.1200/JCO.2021.39.15_suppl.4070]
55 **Salem R**, Lewandowski RJ. Chemoembolization and radioembolization for hepatocellular carcinoma. *Clin Gastroenterol Hepatol* 2013; **11**: 604-11; quiz e43 [PMID: 23357493 DOI: 10.1016/j.cgh.2012.12.039]
56 **Llovet JM**, Real MI, Montaña X, Planas R, Coll S, Aponte J, Ayuso C, Sala M, Muchart J, Solà R, Rodés J, Bruix J; Barcelona Liver Cancer Group. Arterial embolisation or chemoembolisation versus symptomatic treatment in patients with unresectable hepatocellular carcinoma: a randomised controlled trial. *Lancet* 2002; **359**: 1734-1739 [PMID: 12049862 DOI: 10.1016/s0140-6736(02)08649-x]
57 **Llovet JM**, Bruix J. Systematic review of randomized trials for unresectable hepatocellular carcinoma: Chemoembolization improves survival. *Hepatology* 2003; **37**: 429-442 [PMID: 12540794 DOI: 10.1053/jhep.2003.50047]
58 **Burrel M**, Reig M, Forner A, Barrufet M, de Lope CR, Tremosini S, Ayuso C, Llovet JM, Real MI, Bruix J. Survival of patients with hepatocellular carcinoma treated by transarterial chemoembolisation (TACE) using Drug Eluting Beads. Implications for clinical practice and trial design. *J Hepatol* 2012; **56**: 1330-1335 [PMID: 22314428 DOI: 10.1016/j.jhep.2012.01.008]
59 **Lammer J**, Malagari K, Vogl T, Pilleul F, Denys A, Watkinson A, Pitton M, Sergent G, Pfammatter T, Terraz S, Benhamou Y, Avajon Y, Gruenberger T, Pomoni M, Langenberger H, Schuchmann M, Dumortier J, Mueller C, Chevallier P, Lencioni R; PRECISION V Investigators. Prospective randomized study of doxorubicin-eluting-bead embolization in the treatment of hepatocellular carcinoma: results of the PRECISION V study. *Cardiovasc Intervent Radiol* 2010; **33**: 41-52 [PMID: 19908093 DOI: 10.1007/s00270-009-9711-7]
60 **Pipa-Muñiz M**, Sanmartino S, Mesa A, Álvarez-Navascués C, González-Diéguez ML, Cadahía V, Rodríguez JE, Vega F, Rodríguez M, Costilla-García SM, Varela M. The development of early ascites is associated with shorter overall survival in patients with hepatocellular carcinoma treated with drug-eluting embolic chemoembolization. *BMC Gastroenterol* 2020; **20**: 166 [PMID: 32487071 DOI: 10.1186/s12876-020-01307-x]
61 **Teyateeti A**, Mahvash A, Long J, Abdelsalam M, Avritscher R, Kaseb A, Odisio B, Ravizzini G, Surasi D, Teyateeti A, Macapinlac H, Kappadath SC. Disease control and failure patterns of unresectable hepatocellular carcinoma following transarterial radioembolization with yttrium-90 microspheres and with/without sorafenib. *World J Gastroenterol* 2021; **27**: 8166-8181 [PMID: 35068861 DOI: 10.3748/wjg.v27.i47.8166]
62 **Romano F**, Chiarelli M, Garancini M, Scotti M, Zago M, Cioffi G, De Simone M, Cioffi U. Rethinking the Barcelona clinic liver cancer guidelines: Intermediate stage and Child-Pugh B patients are suitable for surgery? *World J Gastroenterol* 2021; **27**: 2784-2794 [PMID: 34135554 DOI: 10.3748/wjg.v27.i21.2784]
63 **Inchingolo R**, Acquafredda F, Tedeschi M, Laera L, Surico G, Surgo A, Fiorentino A, Spiliopoulos S, de'Angelis N, Memeo R. Worldwide management of hepatocellular carcinoma during the COVID-19 pandemic. *World J Gastroenterol*

2021; **27**: 3780-3789 [PMID: 34321843 DOI: 10.3748/wjg.v27.i25.3780]

64 **Kadalayil L**, Benini R, Pallan L, O'Beirne J, Marelli L, Yu D, Hackshaw A, Fox R, Johnson P, Burroughs AK, Palmer DH, Meyer T. A simple prognostic scoring system for patients receiving transarterial embolisation for hepatocellular cancer. *Ann Oncol* 2013; **24**: 2565-2570 [PMID: 23857958 DOI: 10.1093/annonc/mdt247]

65 **Raoul JL**, Forner A, Bolondi L, Cheung TT, Kloeckner R, de Baere T. Updated use of TACE for hepatocellular carcinoma treatment: How and when to use it based on clinical evidence. *Cancer Treat Rev* 2019; **72**: 28-36 [PMID: 30447470 DOI: 10.1016/j.ctrv.2018.11.002]

66 **Sieghart W**, Hucke F, Pinter M, Graziadei I, Vogel W, Müller C, Heinzl H, Trauner M, Peck-Radosavljevic M. The ART of decision making: retreatment with transarterial chemoembolization in patients with hepatocellular carcinoma. *Hepatology* 2013; **57**: 2261-2273 [PMID: 23316013 DOI: 10.1002/hep.26256]

67 **Salem R**, Gordon AC, Mouli S, Hickey R, Kallini J, Gabr A, Mulcahy MF, Baker T, Abecassis M, Miller FH, Yaghmai V, Sato K, Desai K, Thornburg B, Benson AB, Rademaker A, Ganger D, Kulik L, Lewandowski RJ. Y90 Radioembolization Significantly Prolongs Time to Progression Compared With Chemoembolization in Patients With Hepatocellular Carcinoma. *Gastroenterology* 2016; **151**: 1155-1163.e2 [PMID: 27575820 DOI: 10.1053/j.gastro.2016.08.029]

68 **Salem R**, Johnson GE, Kim E, Riaz A, Bishay V, Boucher E, Fowers K, Lewandowski R, Padia SA. Yttrium-90 Radioembolization for the Treatment of Solitary, Unresectable HCC: The LEGACY Study. *Hepatology* 2021; **74**: 2342-2352 [PMID: 33739462 DOI: 10.1002/hep.31819]

69 **Vilgrain V**, Pereira H, Assenat E, Guiu B, Ilonca AD, Pageaux GP, Sibert A, Bouattour M, Lebtahi R, Allaham W, Barraud H, Laurent V, Mathias E, Bronowicki JP, Tasu JP, Perdrisot R, Silvain C, Gerolami R, Mundler O, Seitz JF, Vidal V, Aubé C, Oberti F, Couturier O, Brenot-Rossi I, Raoul JL, Sarran A, Costentin C, Itti E, Luciani A, Adam R, Lewin M, Samuel D, Ronot M, Dinut A, Castera L, Chatellier G; SARAH Trial Group. Efficacy and safety of selective internal radiotherapy with yttrium-90 resin microspheres compared with sorafenib in locally advanced and inoperable hepatocellular carcinoma (SARAH): an open-label randomised controlled phase 3 trial. *Lancet Oncol* 2017; **18**: 1624-1636 [PMID: 29107679 DOI: 10.1016/S1470-2045(17)30683-6]

70 **Ricke J**, Klümpen HJ, Amthauer H, Bargellini I, Bartenstein P, de Toni EN, Gasbarrini A, Pech M, Peck-Radosavljevic M, Popovič P, Rosmorduc O, Schott E, Seidensticker M, Verslype C, Sangro B, Malfertheiner P. Impact of combined selective internal radiation therapy and sorafenib on survival in advanced hepatocellular carcinoma. *J Hepatol* 2019; **71**: 1164-1174 [PMID: 31421157 DOI: 10.1016/j.jhep.2019.08.006]

71 **Chow PKH**, Gandhi M, Tan SB, Khin MW, Khasbazar A, Ong J, Choo SP, Cheow PC, Chotipanich C, Lim K, Lesmana LA, Manuaba TW, Yoong BK, Raj A, Law CS, Cua IHY, Lobo RR, Teh CSC, Kim YH, Jong YW, Han HS, Bae SH, Yoon HK, Lee RC, Hung CF, Peng CY, Liang PC, Bartlett A, Kok KYY, Thng CH, Low AS, Goh ASW, Tay KH, Lo RHG, Goh BKP, Ng DCE, Lekurwale G, Liew WM, Gebski V, Mak KSW, Soo KC; Asia-Pacific Hepatocellular Carcinoma Trials Group. SIRveNIB: Selective Internal Radiation Therapy Versus Sorafenib in Asia-Pacific Patients With Hepatocellular Carcinoma. *J Clin Oncol* 2018; **36**: 1913-1921 [PMID: 29498924 DOI: 10.1200/JCO.2017.76.0892]

72 **Kwak MS**, Lee JH, Yoon JH, Yu SJ, Cho EJ, Jang ES, Kim YJ, Lee HS. Risk factors, clinical features, and prognosis of the hepatocellular carcinoma with peritoneal metastasis. *Dig Dis Sci* 2012; **57**: 813-819 [PMID: 22147252 DOI: 10.1007/s10620-011-1995-1]

73 **Wang B**, Xu H, Gao ZQ, Ning HF, Sun YQ, Cao GW. Increased expression of vascular endothelial growth factor in hepatocellular carcinoma after transcatheter arterial chemoembolization. *Acta Radiol* 2008; **49**: 523-529 [PMID: 18568538 DOI: 10.1080/02841850801958890]

74 **Meyer T**, Fox R, Ma YT, Ross PJ, James MW, Sturgess R, Stubbs C, Stocken DD, Wall L, Watkinson A, Hacking N, Evans TRJ, Collins P, Hubner RA, Cunningham D, Primrose JN, Johnson PJ, Palmer DH. Sorafenib in combination with transarterial chemoembolisation in patients with unresectable hepatocellular carcinoma (TACE 2): a randomised placebo-controlled, double-blind, phase 3 trial. *Lancet Gastroenterol Hepatol* 2017; **2**: 565-575 [PMID: 28648803 DOI: 10.1016/S2468-1253(17)30156-5]

75 **Lencioni R**, Llovet JM, Han G, Tak WY, Yang J, Guglielmi A, Paik SW, Reig M, Kim DY, Chau GY, Luca A, Del Arbol LR, Leberre MA, Niu W, Nicholson K, Meinhardt G, Bruix J. Sorafenib or placebo plus TACE with doxorubicin-eluting beads for intermediate stage HCC: The SPACE trial. *J Hepatol* 2016; **64**: 1090-1098 [PMID: 26809111 DOI: 10.1016/j.jhep.2016.01.012]

76 **Kudo M**, Han G, Finn RS, Poon RT, Blanc JF, Yan L, Yang J, Lu L, Tak WY, Yu X, Lee JH, Lin SM, Wu C, Tanwandee T, Shao G, Walters IB, Dela Cruz C, Poulart V, Wang JH. Brivanib as adjuvant therapy to transarterial chemoembolization in patients with hepatocellular carcinoma: A randomized phase III trial. *Hepatology* 2014; **60**: 1697-1707 [PMID: 24996197 DOI: 10.1002/hep.27290]

77 **Buijs M**, Reyes DK, Pawlik TM, Blackford AL, Salem R, Messersmith WA, Weekes CD, Mulcahy M, Kamel IR, Geschwind JF. Phase 2 trial of concurrent bevacizumab and transhepatic arterial chemoembolization in patients with unresectable hepatocellular carcinoma. *Cancer* 2013; **119**: 1042-1049 [PMID: 23132335 DOI: 10.1002/cncr.27859]

78 **Kudo M**, Ueshima K, Ikeda M, Torimura T, Aikata H, Izumi N, Yamasaki T, Hino K, Kuzuya T, Isoda N, Yasui K, Aino H, Ido A, Kawabe N, Nakao K, Wada Y, Yoshimura K, Okusaka T, Furuse J, Arai Y. TACTICS: Final overall survival (OS) data from a randomized, open label, multicenter, phase II trial of transcatheter arterial chemoembolization (TACE) therapy in combination with sorafenib as compared with TACE alone in patients (pts) with hepatocellular carcinoma (HCC). *J Clin Oncol* 2021; **39**: 270-270 [DOI: 10.1200/JCO.2021.39.3_suppl.270]

79 **Kudo M**, Ueshima K, Ikeda M, Torimura T, Tanabe N, Aikata H, Izumi N, Yamasaki T, Nojiri S, Hino K, Tsumura H, Kuzuya T, Isoda N, Yasui K, Aino H, Ido A, Kawabe N, Nakao K, Wada Y, Yokosuka O, Yoshimura K, Okusaka T, Furuse J, Kokudo N, Okita K, Johnson PJ, Arai Y; TACTICS study group. Randomised, multicentre prospective trial of transarterial chemoembolisation (TACE) plus sorafenib as compared with TACE alone in patients with hepatocellular carcinoma: TACTICS trial. *Gut* 2020; **69**: 1492-1501 [PMID: 31801872 DOI: 10.1136/gutjnl-2019-318934]

80 **Tampaki M**, Ionas E, Hadziyannis E, Deutsch M, Malagari K, Koskinas J. Association of TIM-3 with BCLC Stage, Serum PD-L1 Detection, and Response to Transarterial Chemoembolization in Patients with Hepatocellular Carcinoma. *Cancers (Basel)* 2020; **12** [PMID: 31952209 DOI: 10.3390/cancers12010212]

81 **Singh P**, Toom S, Avula A, Kumar V, Rahma OE. The Immune Modulation Effect of Locoregional Therapies and Its Potential Synergy with Immunotherapy in Hepatocellular Carcinoma. *J Hepatocell Carcinoma* 2020; **7**: 11-17 [PMID: 32104669 DOI: 10.2147/JHC.S187121]

82 **Pinato DJ**, Murray SM, Forner A, Kaneko T, Fessas P, Toniutto P, Mínguez B, Cacciato V, Avellini C, Diaz A, Boyton RJ, Altmann DM, Goldin RD, Akarca AU, Marafioti T, Mauri FA, Casagrande E, Grillo F, Giannini E, Bhoori S, Mazzaferro V. Trans-arterial chemoembolization as a loco-regional inducer of immunogenic cell death in hepatocellular carcinoma: implications for immunotherapy. *J Immunother Cancer* 2021; **9** [PMID: 34593621 DOI: 10.1136/jitc-2021-003311]

83 **Craciun L**, de Wind R, Demetter P, Lucidi V, Bohlok A, Michiels S, Bouazza F, Vouche M, Tancredi I, Verset G, Garaud S, Naveaux C, Galdon MG, Gallo KW, Hendlisz A, Derijckere ID, Flamen P, Larsimont D, Donckier V. Retrospective analysis of the immunogenic effects of intra-arterial locoregional therapies in hepatocellular carcinoma: a rationale for combining selective internal radiation therapy (SIRT) and immunotherapy. *BMC Cancer* 2020; **20**: 135 [PMID: 32075608 DOI: 10.1186/s12885-020-6613-1]

84 **Chew V**, Lee YH, Pan L, Nasir NJM, Lim CJ, Chua C, Lai L, Hazirah SN, Lim TKH, Goh BKP, Chung A, Lo RHG, Ng D, Filarca RLF, Albani S, Chow PKH. Immune activation underlies a sustained clinical response to Yttrium-90 radioembolisation in hepatocellular carcinoma. *Gut* 2019; **68**: 335-346 [PMID: 29440463 DOI: 10.1136/gutjnl-2017-315485]

85 **Tai D**, Loke K, Gogna A, Kaya NA, Tan SH, Hennedige T, Ng D, Irani F, Lee J, Lim JQ, Too CW, Ng MCH, Tham CK, Lam J, Koo SL, Chong HS, Goh GB, Huang HL, Venkatanarasimha N, Lo R, Chow PKH, Goh BKP, Chung A, Toh HC, Thng CH, Lim TKH, Yeong J, Zhai W, Chan CY, Choo SP. Radioembolisation with Y90-resin microspheres followed by nivolumab for advanced hepatocellular carcinoma (CA 209-678): a single arm, single centre, phase 2 trial. *Lancet Gastroenterol Hepatol* 2021; **6**: 1025-1035 [PMID: 34695377 DOI: 10.1016/S2468-1253(21)00305-8]

86 **Berberabe T**. SIRT Administered With Nivolumab Demonstrates Positive Safety, Tolerability Results in HCC. *Targeted Therapies Oncol* 2020; **9**: 24

87 **Han Y**, Zhi WH, Xu F, Zhang CB, Huang XQ, Luo JF. Selection of first-line systemic therapies for advanced hepatocellular carcinoma: A network meta-analysis of randomized controlled trials. *World J Gastroenterol* 2021; **27**: 2415-2433 [PMID: 34040331 DOI: 10.3748/wjg.v27.i19.2415]

88 **Long HY**, Huang TY, Xie XY, Long JT, Liu BX. Treatment strategies for hepatocellular carcinoma with extrahepatic metastasis. *World J Clin Cases* 2021; **9**: 5754-5768 [PMID: 34368295 DOI: 10.12998/wjcc.v9.i21.5754]

89 **Piñero F**, da Fonseca LG. Trial eligibility in advanced hepatocellular carcinoma: Does it support clinical practice in underrepresented subgroups? *World J Gastroenterol* 2021; **27**: 3429-3439 [PMID: 34239261 DOI: 10.3748/wjg.v27.i24.3429]

World Journal of Gastroenterology

Submit a Manuscript: https://www.f6publishing.com

World J Gastroenterol 2022 July 28; 28(28): 3586-3594

DOI: 10.3748/wjg.v28.i28.3586

ISSN 1007-9327 (print) ISSN 2219-2840 (online)

MINIREVIEWS

Update on endoscopic ultrasound-guided liver biopsy

Shiva Rangwani, Devarshi R Ardeshna, Khalid Mumtaz, Sean G Kelly, Samuel Y Han, Somashekar G Krishna

Specialty type: Gastroenterology and hepatology

Provenance and peer review: Invited article; Externally peer reviewed.

Peer-review model: Single blind

Peer-review report's scientific quality classification

Grade A (Excellent): A
Grade B (Very good): B
Grade C (Good): C
Grade D (Fair): D
Grade E (Poor): 0

P-Reviewer: Alali AA, Kuwait; El-Karaksy H, Egypt; Treeprasertsuk S, Thailand; Zhu YY, China

Received: January 16, 2022
Peer-review started: January 16, 2022
First decision: March 8, 2022
Revised: April 21, 2022
Accepted: June 23, 2022
Article in press: June 23, 2022
Published online: July 28, 2022

Shiva Rangwani, Devarshi R Ardeshna, Khalid Mumtaz, Sean G Kelly, Samuel Y Han, Somashekar G Krishna, Division of Gastroenterology, Hepatology, and Nutrition,Department of Internal Medicine, Ohio State University Wexner Medical Center, Columbus, OH 43210, United States

Corresponding author: Somashekar G Krishna, AGAF, FACG, FASGE, MD, Professor, Division of Gastroenterology, Hepatology, and Nutrition, Ohio State University Wexner Medical Center, 395 W 12th Avenue, Suite 262, Columbus, OH 43210, United States. somashekar.krishna@osumc.edu

Abstract

Endoscopic ultrasound guided liver biopsy (EUS-LB) has emerged as a minimally-invasive alternative to the traditional (percutaneous or transjugular) liver biopsy techniques for the diagnosis of liver parenchymal diseases. Potentially, EUS-LB combines the advantages of percutaneous and transjugular liver biopsy in addressing focused sampling in addition to measuring portal pressure. Additionally, EUS-LB facilitates access to both the lobes of the liver which is not considered with the traditional percutaneous liver biopsy. Multiple studies have compared EUS-LB with conventional liver biopsy and reported comparable diagnostic yield, increased acquisition of complete portal tracts, and longer specimen length as compared to the traditional approaches. EUS-LB is associated with lesser post-procedural pain and shorter recovery time, while providing lower risk of complications when compared to traditional liver biopsy. Innovations in needle types, needle sizes and suction techniques have aimed at further optimizing the EUS-LB technique. This review article updates current literature with focus on the variations in the technique and equipment used for EUS-LB, and compares EUS-LB with traditional methods of liver biopsy.

Key Words: Endoscopic ultrasound guided liver biopsy; Liver biopsy; Percutaneous liver biopsy; Transjugular liver biopsy; Liver parenchymal disease; Portal pressure gradient

©The Author(s) 2022. Published by Baishideng Publishing Group Inc. All rights reserved.

Core Tip: Endoscopic ultrasound guided liver biopsy (EUS-LB) has emerged as a minimally invasive alternative to the traditional (percutaneous or transjugular) liver biopsy techniques for the diagnosis of liver parenchymal diseases. EUS-LB facilitates access to both the lobes of the liver and allows measurement of portal pressure. EUS-LB has comparable diagnostic accuracy, increased yield of complete portal tracts, and longer specimen length compared to the traditional approaches. Innovations in needle technology and variations in suction have further optimized the EUS-LB technique. This review article updates current literature comparing EUS-LB to traditional liver biopsy and advances in this field.

Citation: Rangwani S, Ardeshna DR, Mumtaz K, Kelly SG, Han SY, Krishna SG. Update on endoscopic ultrasound-guided liver biopsy. *World J Gastroenterol* 2022; 28(28): 3586-3594
URL: https://www.wjgnet.com/1007-9327/full/v28/i28/3586.htm
DOI: https://dx.doi.org/10.3748/wjg.v28.i28.3586

INTRODUCTION

Liver biopsy is helpful in diagnosis of parenchymal pathologies such as alcoholic liver disease, autoimmune hepatitis, viral hepatitis, metabolic liver diseases (non-alcoholic fatty liver disease, alfa-1 anti-trypsin deficiency, Wilson disease, hemochromatosis, Gaucher's disease, *etc.*), drug-induced liver injury and infiltrative liver disease (*i.e.*, malignancy, abscess, sarcoidosis, *etc.*). Tissue examination also allows for diagnosis of rare overlapping liver diseases. The liver biopsy has traditionally been obtained *via* two routes: percutaneous liver biopsy (PC-LB) and transjugular liver biopsy (TJ-LB). In recent years, endoscopic technique and hardware advancement have led to the rise of endoscopic ultrasound-guided liver biopsy (EUS-LB). There is changing epidemiology of liver disease with increased global incidence of non-alcoholic fatty liver disease over the last two decades; it has reached to an estimated global prevalence of 25%[1]. This increased prevalence has led to advancements in lesser or non-invasive diagnostic tests such as ultrasound-elastography and MRI-proton density fat fraction[2]. Although these tests provide greater diagnostic accuracy compared to traditional peripheral blood laboratory tests, liver biopsy remains the gold standard for diagnosing focal lesions and parenchymal liver disease[3]. In this review, we will compare EUS-LB with traditional liver biopsy and highlight its, advantages and disadvantages in context of changing epidemiology of liver disease. Further, we will summarize the latest advancements on EUS-LB, focusing on technique, needle types/size, and suction type.

METHODS OF LIVER BIOPSY

The first mode of acquisition of liver tissue was PC-LB, as it provides the most direct route to access the liver. Percutaneous needle aspiration biopsies have been performed since the late 19th century and popularized in the 1930s[4]. Initial PC-LB techniques used percussion to guide needle placement; however, modern PC-LB is done under ultrasound- or fluoroscopic-image guidance[5]. If hepatomegaly is present, a subcostal route for PC-LB is preferred; however, a transthoracic approach is employed in the absence of hepatomegaly. In the early days of PC-LB, interventionists preferred 14 gauge (G) or 16 G needles to provide large, intact tissue samples. In recent years, spring-loaded 18 G and 20 G needles have been common[6]. PC-LB is usually done while the patient is awake with local anesthesia, but conscious sedation is often used. Common complications of PC-LB include pain (74%), minor bleeding (30%), and infection at the biopsy site[7,8]. As the liver capsule is punctured to obtain biopsy, intraperitoneal hemorrhage is a severe, albeit rare complication[7]. Other less-common complications include pneumothorax and hemothorax if the transthoracic approach is employed (0.1%-0.9%)[7-9]. Contraindications to PC-LB include significant ascites, large body-habitus, and severe coagulopathy[5]. As it has been a long-standing method of biopsy, PC-LB is widely available. Furthermore, given its short procedure time and the fact that general anesthesia is not required, PC-LB provides a cost-effective approach to diagnosing liver diseases. Drawbacks to PC-LB include access to only the right hepatic lobe and a limited view of surrounding anatomy. Further, if real-time imaging is not used for guidance, there is an increased risk of serious complications[10].

More recently, TJ-LB has been developed to obtain liver samples in patients with contraindications to PC-LB. In this technique, an interventional radiologist cannulates the internal jugular vein and accesses one of the hepatic vein under fluoroscopic guidance. Biopsy of the right hepatic lobe is preferred because of its size and the acute angulation of the veins with the inferior vena cava[11]. This procedure can be performed in patients with high body mass index, and significant ascites. Additionally, as the liver capsule is not punctured, it is the preferred method in those with profound coagulopathies[11]. This technique provides the added benefit of assessing the hepatic venous pressure gradient (HVPG), which is an indirect measure of the absence, presence and degree of portal hypertension. HVPG

measurement will be compared to EUS-guided measurement of portal pressure in the discussion of future research and practice below. Complications from TJ-LB include pain, hematoma, hemobilia, arterial aneurysm, and major hemorrhage[11]. In addition to subverting contraindications posed by the PC-LB, advantages of TJ-LB include lack of capsular puncture and the ability to obtain a portal pressure gradient measurement[7,10,11]. One of the limitation of TJ-LB is inability to obtain tissue from a focal lesion, due to limited view of surrounding structures[10].

Endoscopic ultrasound-guided fine-needle aspiration was first done in 1993 and EUS-LB was first described by Mathew in 2007[12,13]. EUS-LB poses several advantages over the traditional LB techniques. Firstly, EUS-LB allows access to both lobes of the liver (except in patients with Roux-en-Y or gastric bypass anatomy)[10]. Secondly, like TJ-LB, EUS-LB enables a practitioner to obtain liver tissue regardless of body habitus or ascites. The most advantageous aspects of EUS-LB, when compared to PC-LB and TJ-LB, lie in its real-time multi-dimensional evaluative abilities. Those undergoing workup for liver disease often require endoscopic evaluation – the advent of EUS-LB posed a solution to facilitate patients to undergo multiple endoscopic procedures in the same session. With EUS, a liver biopsy can be performed along with simultaneous evaluation for varices (esophageal and gastric) and portal pressure measurement. Further, the use of EUS in close proximity to the liver allows for better visualization of liver lesions for targeted liver biopsies[10]. In fact, multiple studies have shown a diagnostic accuracy between 85%-90% for solid liver masses using EUS-guided FNB[14-16]. Use of ultrasound-guided technique also allows practitioners to avoid critical structures during biopsy procurement. The drawbacks to EUS-LB mirror some of the drawbacks found in PC-LB and TJ-LB. Although the number of EUS-trained practitioners have grown rapidly over the past ten years in the United States, this procedure is less widely accessible when compared to PC-LB[10]. Further, unlike TJ-LB, EUS-LB does require capsular puncture and is not readily performed in patients with severe coagulopathy. Additionally, EUS-LB does require moderate or deep sedation, as with TJ-LB.

METHODS OF LIVER BIOPSY - COMPARISONS

Recovery times and complications

With the advent of multiple modalities for obtaining liver biopsies, recent studies have comparatively evaluated these approaches. The comparison between each of the three liver biopsy methods is summarized in Table 1. With regards to length of recovery, EUS-LB patients (n = 30) experienced a shorter post-procedural monitoring time (3 h) when compared to those (n = 60) undergoing PC-LB (4.2 h, P = 0.004)[17]. A recent study done in 2021 showed the mean recovery time for those undergoing EUS-LB was 90 min *vs* 141.3 min (P = 0.004) for TJ-LB[18]. The most common minor complication in each of the three modes of liver biopsy is pain. In a 2020 study, EUS-LB had significantly less pain scores when compared to PC-LB (0/10 for EUS-LB *vs* 3.5 for PC-LB, P = 0.0009)[17]. When comparing pain in EUS-LB and TJ-LB patients, one 2019 study found a significantly higher incidence of post-procedural pain in TJ-LB patients compared to EUS-LB patients, 8% *vs* 0% (P < 0.0001), respectively[19]. Adverse events with regard to liver biopsy include, but are not limited to, severe hemorrhage, hemobilia, abdominal wall injury, and intraperitoneal injury. Although no studies have directly compared adverse event rates between the three liver biopsy modalities, adverse event rates appear to be similar across each modality – EUS-LB: 1%-2.3%, PC-LB: 0.9%-3.1%, TJ-LB: 0.56%-6.5%[18-22].

Specimen adequacy

Regarding histological adequacy of liver biopsy samples, the American Association for the Study of Liver Diseases recommends a tissue length of between 2-3 cm with greater-than-or-equal-to 11 complete portal tracts (CPT)[23]. Systematic reviews have shown a total specimen length for PC-LB to be 17.7mm (± 5.5 mm), TJ-LB: 13.5 mm (± 4.5 mm), and EUS-LB 36.9 mm (± 6.2 mm)[20,24]. CPT numbers in these same studies revealed an aggregate CPT for PC-LB of 7.7 (± 3.4), TJ-LB: 6.8 (± 2.3), and EUS-LB: 9.0 (± 3.1)[20,24]. A recent 2021 study compared each liver biopsy technique head-to-head and found that EUS-LB (n = 53) had a significantly greater mean aggregate length (22.95 mm) compared to PC-LB (n = 20) (14.5 mm) (P = 0.03) and TJ-LB (n = 20) (14.6 mm) (P = 0.02)[18]. Further, both EUS-LB and TJ-LB provided a greater number of CPTs when compared to PC-LB: EUS-LB (19.36), TJ-LB (20.2), PC-LB (9.1) (EUS-LB *vs* PC-LB: P < 0.0001, EUS-LB *vs* TJ-LB P = 1)[18].

TECHNIQUE OF EUS-GUIDED LIVER BIOPSY

Since the inception of EUS-LB in 2007 with a Tru-Cut core biopsy needle (QuickCore, Cook Medical, Winston Salem, NC, United States), multiple studies have aimed at optimizing EUS-LB technique[13]. These changes coincided with procedural upgrades and improvements in needle technology. Incorporating these advancements into EUS-LB comes with technical (skills and training) and logical challenges (cost and availability). However, the essential technique of EUS-LB remains unchanged.

Table 1 Comparison of liver biopsy methods[1]

	Percutaneous liver biopsy	Transjugular liver biopsy	Endoscopic ultrasound-guided liver biopsy
Most common form of anesthesia	Local	Moderate sedation	Moderate sedation, deep sedation
Imaging	Fluoroscopy, ultrasound	Fluoroscopy	Ultrasound
Capsular puncture	Yes	No	Yes
Ability to evaluate focal hepatic lesions	No	No	Yes
Liver lobe access	Right	Right	Right, left
Contraindications	INR > 1.5, body habitus, significant ascites	Venous thrombosis, cholangitis	INR > 1.5
Post-procedural pain	+++	+	+
Post-procedural minor bleeding	+	+	+
Adverse event rate	+	+	+
Post-procedural recovery time	+++	++	+
Specimen length	+	+	+++
Total complete portal tracts	+	++	+++
Procedure cost	+	++	+++
Institutional availability	+++	++	+

[1]Information adapted using the Ref. [10,17,18,21].
+: Low/less; ++: Medium; +++: High/most; INR: International normalized ratio.

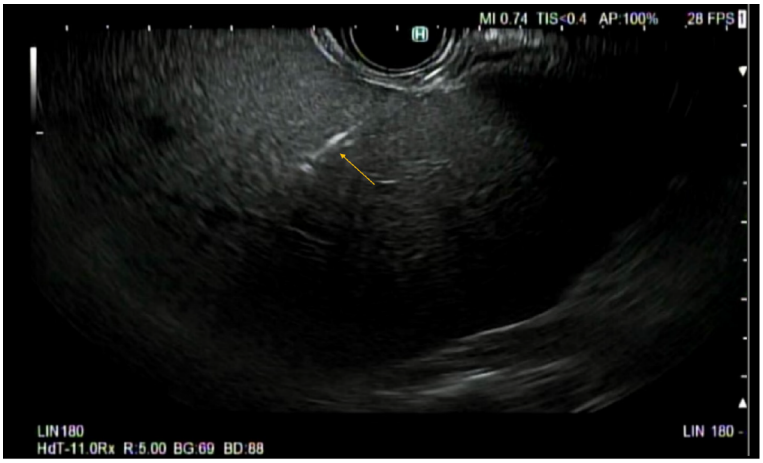
General technique

Patients undergoing EUS-LB are either moderately sedated with short-acting benzodiazepines and opiates or deeply sedated with propofol, per the availability of dedicated anesthetists. The patients are prone positioned and a linear array echo-endoscope is inserted for endo-sonography. Once the area of interest is identified, the stylet is removed, and a needle primed (with heparin or saline) or unprimed (air) is inserted[6,10]. Per endoscopist and center preference, the needle should be attached either to a wet suction (saline or heparin) or a dry suction (air). Before needle puncture, color Doppler should be used to ensure there are no vascular structures in the trajectory of the needle. Suction should be applied *via* a syringe once adequate liver parenchymal penetration is achieved (depending on the needle selection). Figure 1 shows the echoendoscopic image of a needle passing through into the left hepatic lobe. In 1 pass, actuations or fanning back-and-forth motions can be done with continued suction to allow for improved tissue acquisition[25]. Multiple such passes can be done overall to increase tissue acquisition. After each pass, the needle should be removed from the echo-endoscope and the tissue should be stored in formalin solution directly for preservation[6,10]. This gross tissue can be analyzed for adequacy and should guide the decision if more passes are required. Following the procedure, patients can be discharged after 1-2 h observation in the recovery unit.

Accessing liver parenchyma requires identification of endoscopic gastric landmarks. The left lobe of liver adjoins the gastroesophageal junction can be accessed through the gastroesophageal junction in the proximal stomach. The right lobe of the liver can be accessed through the duodenal bulb[26]. Among patients with altered anatomy, EUS-LB is limited. For Roux-en-Y gastric bypass patients, only left liver lobe biopsy is feasible through the transgastric approach[10].

Suction

Suction can be applied in a wet or dry fashion. In dry suction, an empty 10 cc or 20 cc syringe is applied to maintain suction after passing the needle into the liver parenchyma. In wet suction, the needle lumen is primed with fluid, causing negative pressure at the needle tip. As outlined above, wet suction utilizes either saline or heparin. A 2018 study compared wet heparin suction technique with dry suction technique. The study showed significantly increased aggregate specimen length (wet: 49.2 mm, dry: 23.9 mm, P = 0.003) and number of CPTs (7.0 *vs* 4.0, P = 0.01) for wet suction compared to dry suction techniques[27]. With wet suction, the sample is suspended in a column of fluid—leading to reduced shearing forces as it is not in contact with the needle wall. This likely leads to increased CPTs and intact specimen length for wet suction technique. To our knowledge, no studies directly comparing wet suction with saline *vs* heparin have been performed.



DOI: 10.3748/wjg.v28.i28.3586 **Copyright** ©The Author(s) 2022.

Figure 1 Needle for endoscopic ultrasound guided liver biopsy accessing left lobe of the liver. Orange arrow denotes needle. Image obtained by Krishna SG at the Ohio State University Wexner Medical Center Division of Gastroenterology, Hepatology, and Nutrition.

In contrast, specimens can be obtained without applying suction *via* stylet, in a "slow-pull" technique. A 2020 meta-analysis showed that FNB with a slow-pull technique provided similar total specimen length (44.3 mm *vs* 53.9 mm, $P = 0.40$) when compared to suction application; however, the slow-pull technique provided improved CPT than suction (30 *vs* 14.6, $P < 0.001$)[28]. Authors hypothesize that this stems from reduced fragmentation of the tissue specimen as it is subjected to an environment of less negative pressure with the slow-pull technique.

Needle pass/Actuation

Needle pass refers to the number of times a needle is introduced into the liver parenchyma through puncture of the liver capsule, while actuation refers to the number of back-and-forth motions are made in a specified needle pass. Through our literature review, it appears the 1-pass 1-actuation technique is the most common mode of EUS-LB acquisition[25,29]. There are few studies that have been done comparing needle pass and needle actuation with regards to pain, adverse events, and specimen quality. A 2021 study showed that EUS-LB using a 1-pass, 3-actuation technique ($n = 40$) provided longer liver cores with more CPTs than a 1-to-1 technique ($n = 40$), with an equivalent safety profile: CPT (24.5 *vs* 17.25, $P < 0.008$), aggregate specimen length (12.85 cm *vs* 6.89 cm $P < 0.001$)[25].

Needle selection: Size

When considering needle selection, a EUS-LB practitioner must take needle size and type into account. With regards to needle size, multiple studies have been done to determine the optimal needle size for EUS-LB. In the early days of EUS-LB, large 14G – 16 G spring-loaded cutting needles were used; however, these needles had varied diagnostic yields ranging from 29%-100%[30,31]. As time progressed, researchers found that smaller-gauge needles provided better results than their 14-16 G counterparts. In a 2017 study, 18 G percutaneous, 19 G FNA, 19G FNB, and 22 G FNB needles were compared on human cadaveric tissue to test for tissue adequacy. The study showed that a 19 G needle provided a significantly greater number of CPTs when compared to its 22 G and 18 G counterparts (6.2 *vs* 3.5 *vs* 3.2, respectively, $P < 0.001$ for both comparisons)[32]. In a similar study in 2019 on fresh bovine liver, 19 G and 20 G fork-tip needles yielded similar CPTs and total specimen length; however, both the 19 G and 20 G fork-tip needles significantly outperformed their 22 G fork-tip counterpart in terms of CPTs and specimen length[33].

More recent *in vivo* studies have confirmed the superiority of 19 G needles when compared to 22 G needles. A recent (2021) study showed that 19 G Franseen tip needle performed better than a 22 G Franseen tip needle in terms of specimen adequacy (19 G: 81.5%, 22 G: 66.7%, $P < 0.01$)[34]. The researchers posit that the 22 G samples had greater fragmentation, leading to reduced intact specimen length and CPT, reducing histological adequacy. The advantage of 19 G compared to 22 G needle was also shown in core needles, where 19 G core needles had a greater CPT (8.8 *vs* 3, $P < 0.0001$), longer core length (2.5 cm *vs* 1.1 cm, $P < 0.0001$), and a higher rate of pathological diagnostic samples (85% *vs* 10%, $P < 0.0001$) when compared to 22 G core needles[35].

Needle selection: Tip and design

As noted earlier, large spring-loaded cutting needles were initially used to perform EUS-LB. As EUS-LB grew, practitioners noted that fine-needle biopsy (FNB) needles may provide better samples in the endoscopic setting. In 2015, Dewitt *et al*[36] showed that a 19 G FNB histology needle performed better

than a 19 G spring-loaded cutting needle and provided longer specimens (19.4 mm *vs* 4.3 mm, P = 0.0001), greater CPTs (10.4 *vs* 1.3, P = 0.0004), and a higher percent of diagnostic histology (85% *vs* 57%, P = 0.006)[36].

Holding needle gauge constant, Franseen needle types have shown to be superior than their counterparts in recent studies. A 2019 study showed that a 19 G Franseen needle provided lengthier specimens when compared to a 19 G FNA needle for *in vivo* EUS-LB (2.09 cm *vs* 1.47 cm, P < 0.001), more CPTs (42.6 *vs* 18.1, P < 0.001), and similar pain scores[37]. In the late portion of the last decade, EUS-LB has been most commonly performed with either Franseen or Fork-Tip biopsy needles. Multiple studies have compared the effectiveness with regards to specimen quality and adverse events between these two needles. A 2020 study showed a similar adverse event and abdominal pain profile between the use of 19 G Franseen and fork-tip needles[29]. The Franseen needle, however, had a significantly greater total specimen length when compared to the fork-tip needle (3.1 cm *vs* 2.7 cm, P = 0.01) and greater total CPTs (24.0 *vs* 19.55, P < 0.01)[29]. The Franseen tip has also shown equal-to-superior diagnostic yield when compared to fork-tip, with one study showing nonsignificant-difference in histological adequacy rates but an increased number of CPTs (14.4 *vs* 9.5, P < 0.001) and another study showing a higher diagnostic yield of 97.2% for Franseen tip compared to 79.4% for fork-tip (P < 0.001)[38,39].

FUTURE RESEARCH AND PRACTICE

Portal pressure gradient

In trained hands it has become possible to obtain accurate measures of portal pressure gradients by various approaches[36]. The measure of the portal pressure gradient is primarily done through the transjugular approach. Although described as the gold standard, the hepatic venous pressure gradient (HVPG) is actually an indirect measure of portal pressure calculated by subtracting the free hepatic venous pressure from the wedge hepatic venous pressure[40]. In contrast, EUS-guided measurement of portal pressure is a direct measurement of sinusoidal pressure rather than an estimate, and may prove to be more accurate[40]. To obtain EUS-guided measurement of portal pressure, endoscopists first puncture the hepatic vein *via* a transgastric transhepatic approach, with the needle hooked up to a digital manometer *via* non-compressible tubing[41]. Once obtaining hepatic vein pressure averages, endoscopists then turn their attention to the portal vein, which is accessed in a transgastric transhepatic approach usually at the umbilical portion of the portal vein. Once the portal vein pressure is obtained, the portal pressure gradient is calculated by subtracting the mean portal vein pressure from the mean hepatic vein pressure[41]. These readings are usually obtained with a small-gauge (25 G) FNA needle [40,41].

Since the HVPG can be obtained without performing a liver biopsy, it is a very safe procedure when performed alone, mainly imparting the risk associated with right internal jugular access[9,11]. Therefore, it is essential to ensure that EUS-guided measurement of portal pressure is performed with specific indications to ensure safety. For example, patients with splenomegaly may benefit from EUS-LB and EUS-guided measurement of portal pressure to confirm whether cirrhosis and portal hypertension are the underlying causes of splenomegaly. However, if a patient has esophageal or gastric varices, it can be safely assumed that the portal pressure is 10 mmHg or higher and the patient has clinically significant portal hypertension[40]. That information should be used to determine whether EUS-guided measurement of portal pressure is warranted at the time of the procedure.

Concomitant EUS-LB with other endoscopic procedures

EUS-LB provides an exciting new method for liver tissue acquisition. A novel application is for special patient populations such as liver transplant recipients (LTRs). Laboratory abnormalities in liver transplant patients often requires an extensive workup including imaging, liver biopsy, and ERCP. Combining EUS-LB with ERCP can potentially provide a "one-stop-shop" for evaluation in this patient population. This will hopefully reduce the time, cost, and healthcare resources needed to accurately diagnose and treat post-transplant liver function abnormalities. Our group at Ohio State University, has recently submitted a case series of 12 consecutive LTRs with abnormal liver function tests (Han S, Jalil S, Groce JR, Krishna SG, Lara L, Lee P, Limkemann A, Papachristou GI, Mumtaz K. Feasibility of Single-Session EUS-guided Liver Biopsy and ERCP in Liver Transplant Recipients with Abnormal Liver Function Tests), who underwent concomitant EUS-LB and ERCP. In this case series, tissue adequacy was obtained in 100% of patients with the most common diagnoses including anastomotic stricture (75%) and T-cell mediated rejection (66.7%). Seven (58.3%) patients had dual diagnoses of T-cell mediated rejection and anastomotic stricture. There were no 30 d adverse events. Authors concluded that **s**ingle-session EUS-guided LB and ERCP for the evaluation of elevated liver function tests in LTRs appears to be safe and feasible, but larger studies are needed to verify these findings.

Similarly, a recent study published by Hajifathalian *et al*[42] on concomitant EUS-LB and portal pressure gradient measurement reported 24 (100%) and 23 (96%) patients had successful portosystemic gradient (PSG) measurement and EUS-liver biopsy, respectively. Analysis revealed a significant

association between both PSG and liver stiffness measured on transient elastography (P = 0.01) and FIB-4 score (P = 0.02). There was no significant correlation between the fibrosis stage on histology and measured PSG (P = 0.56)[42].

Lastly, EUS-LB has been discussed anecdotally as a more effective option in pediatric population, as it may reduce patient anxiety when compared to PC-LB or TJ-LB – although, to our knowledge, formal studies in pediatric populations are yet to be done.

CONCLUSION

Overall, EUS-LB provides unique advantages when compared to its counterparts: ability to evaluate the GI tract and pancreato-biliary system, while obtaining access to both lobes of the liver. It also has proven to produce more histologically/pathologically complete samples than PC-LB and TJ-LB. EUS-LB appears to be a safe, diagnostic modality for obtaining liver tissue. Concomitant EUS-LB, EUS portal pressure gradient measurement and other endoscopic procedure (simple endoscopy and ERCP) is another emerging area in the field of endo-hepatology.

FOOTNOTES

Author contributions: Rangwani S and Ardeshna DR performed the majority of the literature search, writing, and preparation of tables; Mumtaz K, Kelly SG, and Han SY reviewed the final manuscript; Krishna SG provided figures, input in the writing process, and review of the final manuscript.

Conflict-of-interest statement: All authors report no relevant conflicts of interest for this article.

Open-Access: This article is an open-access article that was selected by an in-house editor and fully peer-reviewed by external reviewers. It is distributed in accordance with the Creative Commons Attribution NonCommercial (CC BY-NC 4.0) license, which permits others to distribute, remix, adapt, build upon this work non-commercially, and license their derivative works on different terms, provided the original work is properly cited and the use is non-commercial. See: https://creativecommons.org/Licenses/by-nc/4.0/

Country/Territory of origin: United States

ORCID number: Shiva Rangwani 0000-0002-4292-5189; Devarshi R Ardeshna 0000-0002-1849-0867; Khalid Mumtaz 0000-0001-7868-6514; Sean G Kelly 0000-0002-9434-9924; Samuel Y Han 0000-0001-7373-7984; Somashekar G Krishna 0000-0001-5748-7890.

S-Editor: Ma YJ
L-Editor: A
P-Editor: Ma YJ

REFERENCES

1 **Younossi ZM**, Koenig AB, Abdelatif D, Fazel Y, Henry L, Wymer M. Global epidemiology of nonalcoholic fatty liver disease-Meta-analytic assessment of prevalence, incidence, and outcomes. *Hepatology* 2016; **64**: 73-84 [PMID: 26707365 DOI: 10.1002/hep.28431]
2 **Piazzolla VA**, Mangia A. Noninvasive Diagnosis of NAFLD and NASH. *Cells* 2020; **9** [PMID: 32316690 DOI: 10.3390/cells9041005]
3 **Castera L**, Friedrich-Rust M, Loomba R. Noninvasive Assessment of Liver Disease in Patients With Nonalcoholic Fatty Liver Disease. *Gastroenterology* 2019; **156**: 1264-1281.e4 [PMID: 30660725 DOI: 10.1053/j.gastro.2018.12.036]
4 **McLoughlin MJ**, Ho CS, Tao LC. Percutaneous needle aspiration biopsy. *Can Med Assoc J* 1978; **119**: 1324-1328 [PMID: 367550]
5 **Gilmore IT**, Burroughs A, Murray-Lyon IM, Williams R, Jenkins D, Hopkins A. Indications, methods, and outcomes of percutaneous liver biopsy in England and Wales: an audit by the British Society of Gastroenterology and the Royal College of Physicians of London. *Gut* 1995; **36**: 437-441 [PMID: 7698705 DOI: 10.1136/gut.36.3.437]
6 **Diehl DL**. Endoscopic Ultrasound-guided Liver Biopsy. *Gastrointest Endosc Clin N Am* 2019; **29**: 173-186 [PMID: 30846147 DOI: 10.1016/j.giec.2018.11.002]
7 **Shah AR**, Al-Hanayneh M, Chowdhry M, Bilal M, Singh S. Endoscopic ultrasound guided liver biopsy for parenchymal liver disease. *World J Hepatol* 2019; **11**: 335-343 [PMID: 31114638 DOI: 10.4254/wjh.v11.i4.335]
8 **Chi H**, Hansen BE, Tang WY, Schouten JN, Sprengers D, Taimr P, Janssen HL, de Knegt RJ. Multiple biopsy passes and the risk of complications of percutaneous liver biopsy. *Eur J Gastroenterol Hepatol* 2017; **29**: 36-41 [PMID: 27556687 DOI: 10.1097/MEG.0000000000000731]
9 **Lavian JD**, Thornton LM, Zybulewski A, Kim E, Nowakowski SF, Ranade M, Patel RS, Lookstein RA, Fischman A, Bishay V. Safety of percutaneous versus transjugular liver biopsy: A propensity score matched analysis. *Eur J Radiol* 2020;

133: 109399 [PMID: 33202374 DOI: 10.1016/j.ejrad.2020.109399]
10 **Madhok IK**, Parsa N, Nieto JM. Endoscopic Ultrasound-Guided Liver Biopsy. *Clin Liver Dis* 2022; **26**: 127-138 [PMID: 34802658 DOI: 10.1016/j.cld.2021.09.002]
11 **Kalambokis G**, Manousou P, Vibhakorn S, Marelli L, Cholongitas E, Senzolo M, Patch D, Burroughs AK. Transjugular liver biopsy--indications, adequacy, quality of specimens, and complications--a systematic review. *J Hepatol* 2007; **47**: 284-294 [PMID: 17561303 DOI: 10.1016/j.jhep.2007.05.001]
12 **Gress FG**. The Early History of Interventional Endoscopic Ultrasound. *Gastrointest Endosc Clin N Am* 2017; **27**: 547-550 [PMID: 28918797 DOI: 10.1016/j.giec.2017.06.015]
13 **Mathew A**. EUS-guided routine liver biopsy in selected patients. *Am J Gastroenterol* 2007; **102**: 2354-2355 [PMID: 17897349 DOI: 10.1111/j.1572-0241.2007.01353_7.x]
14 **Chon HK**, Yang HC, Choi KH, Kim TH. Endoscopic Ultrasound-Guided Liver Biopsy Using a Core Needle for Hepatic Solid Mass. *Clin Endosc* 2019; **52**: 340-346 [PMID: 31302987 DOI: 10.5946/ce.2018.175]
15 **Lee YN**, Moon JH, Kim HK, Choi HJ, Choi MH, Kim DC, Lee TH, Cha SW, Kim SG, Kim YS. Usefulness of endoscopic ultrasound-guided sampling using core biopsy needle as a percutaneous biopsy rescue for diagnosis of solid liver mass: Combined histological-cytological analysis. *J Gastroenterol Hepatol* 2015; **30**: 1161-1166 [PMID: 25684303 DOI: 10.1111/jgh.12922]
16 **Kongkam P**, Nalinthassanai N, Prueksapanich P, Sanpavat A, Cañones AR, Luangsukrerk T, Angsuwatcharakon P, Ridtitid W, Kullavanijaya P, Treeprasertsuk S, Rerknimitr R. A comparison of the antegrade core trap and reverse bevel needles for EUS-guided fine-needle biopsy sampling of liver mass: a prospective randomized cross over study. *HPB (Oxford)* 2022; **24**: 797-805 [PMID: 34794898 DOI: 10.1016/j.hpb.2021.10.009]
17 **Ali AH**, Panchal S, Rao DS, Gan Y, Al-Juboori A, Samiullah S, Ibdah JA, Hammoud GM. The efficacy and safety of endoscopic ultrasound-guided liver biopsy versus percutaneous liver biopsy in patients with chronic liver disease: a retrospective single-center study. *J Ultrasound* 2020; **23**: 157-167 [PMID: 32141043 DOI: 10.1007/s40477-020-00436-z]
18 **Patel HK**, Therapondos G, Galliano G, Romero R, Evans J, Cohen A, Mubarak MF, Shah JN, Chafic AHE. Endoscopic Ultrasound Guided Liver Biopsy Using Newer 19G FNB Needles Compared to Percutaneous and Trans-jugular Liver Biopsy: A Tertiary Center Experience. *Tech Innov Gastrointest Endosc* 2022; **24**: 127-135 [DOI: 10.1016/j.tige.2021.11.009]
19 **Shuja A**, Alkhasawneh A, Fialho A, Shukri A, Harris C, Smotherman C, Malespin M, de Melo SW Jr. Comparison of EUS-guided versus percutaneous and transjugular approaches for the performance of liver biopsies. *Dig Liver Dis* 2019; **51**: 826-830 [PMID: 30755347 DOI: 10.1016/j.dld.2019.01.006]
20 **Dhar J**, Samanta J. Role of endoscopic ultrasound in the field of hepatology: Recent advances and future trends. *World J Hepatol* 2021; **13**: 1459-1483 [PMID: 34904024 DOI: 10.4254/wjh.v13.i11.1459]
21 **Facciorusso A**, Crinò SF, Ramai D, Fabbri C, Mangiavillano B, Lisotti A, Muscatiello N, Cotsoglou C, Fusaroli P. Diagnostic yield of endoscopic ultrasound-guided liver biopsy in comparison to percutaneous liver biopsy: a systematic review and meta-analysis. *Expert Rev Gastroenterol Hepatol* 2022; **16**: 51-57 [PMID: 34918578 DOI: 10.1080/17474124.2022.2020645]
22 **Johnson KD**, Laoveeravat P, Yee EU, Perisetti A, Thandassery RB, Tharian B. Endoscopic ultrasound guided liver biopsy: Recent evidence. *World J Gastrointest Endosc* 2020; **12**: 83-97 [PMID: 32218888 DOI: 10.4253/wjge.v12.i3.83]
23 **Rockey DC**, Caldwell SH, Goodman ZD, Nelson RC, Smith AD; American Association for the Study of Liver Diseases. Liver biopsy. *Hepatology* 2009; **49**: 1017-1044 [PMID: 19243014 DOI: 10.1002/hep.22742]
24 **Cholongitas E**, Senzolo M, Standish R, Marelli L, Quaglia A, Patch D, Dhillon AP, Burroughs AK. A systematic review of the quality of liver biopsy specimens. *Am J Clin Pathol* 2006; **125**: 710-721 [PMID: 16707372 DOI: 10.1309/W3XC-NT4H-KFBN-2G0B]
25 **Ching-Companioni RA**, Johal AS, Confer BD, Forster E, Khara HS, Diehl DL. Single-pass 1-needle actuation versus single-pass 3-needle actuation technique for EUS-guided liver biopsy sampling: a randomized prospective trial (with video). *Gastrointest Endosc* 2021; **94**: 551-558 [PMID: 33771557 DOI: 10.1016/j.gie.2021.03.023]
26 **Bhatia V**, Hijioka S, Hara K, Mizuno N, Imaoka H, Yamao K. Endoscopic ultrasound description of liver segmentation and anatomy. *Dig Endosc* 2014; **26**: 482-490 [PMID: 24355092 DOI: 10.1111/den.12216]
27 **Mok SRS**, Diehl DL, Johal AS, Khara HS, Confer BD, Mudireddy PR, Kirchner HL, Chen ZE. A prospective pilot comparison of wet and dry heparinized suction for EUS-guided liver biopsy (with videos). *Gastrointest Endosc* 2018; **88**: 919-925 [PMID: 30120956 DOI: 10.1016/j.gie.2018.07.036]
28 **Baran B**, Kale S, Patil P, Kannadath B, Ramireddy S, Badillo R, DaVee RT, Thosani N. Endoscopic ultrasound-guided parenchymal liver biopsy: a systematic review and meta-analysis. *Surg Endosc* 2021; **35**: 5546-5557 [PMID: 33052529 DOI: 10.1007/s00464-020-08053-x]
29 **Nieto J**, Khaleel H, Challita Y, Jimenez M, Baron TH, Walters L, Hathaway K, Patel K, Lankarani A, Herman M, Holloman D, Saab S. EUS-guided fine-needle core liver biopsy sampling using a novel 19-gauge needle with modified 1-pass, 1 actuation wet suction technique. *Gastrointest Endosc* 2018; **87**: 469-475 [PMID: 28551024 DOI: 10.1016/j.gie.2017.05.013]
30 **Dewitt J**, McGreevy K, Cummings O, Sherman S, Leblanc JK, McHenry L, Al-Haddad M, Chalasani N. Initial experience with EUS-guided Tru-cut biopsy of benign liver disease. *Gastrointest Endosc* 2009; **69**: 535-542 [PMID: 19231495 DOI: 10.1016/j.gie.2008.09.056]
31 **Gleeson FC**, Clayton AC, Zhang L, Clain JE, Gores GJ, Rajan E, Smyrk TC, Topazian MD, Wang KK, Wiersema MJ, Levy MJ. Adequacy of endoscopic ultrasound core needle biopsy specimen of nonmalignant hepatic parenchymal disease. *Clin Gastroenterol Hepatol* 2008; **6**: 1437-1440 [PMID: 19081532 DOI: 10.1016/j.cgh.2008.07.015]
32 **Schulman AR**, Thompson CC, Odze R, Chan WW, Ryou M. Optimizing EUS-guided liver biopsy sampling: comprehensive assessment of needle types and tissue acquisition techniques. *Gastrointest Endosc* 2017; **85**: 419-426 [PMID: 27530070 DOI: 10.1016/j.gie.2016.07.065]
33 **Eskandari A**, Koo P, Bang H, Gui D, Urayama S. Comparison of Endoscopic Ultrasound Biopsy Needles for Endoscopic Ultrasound-Guided Liver Biopsy. *Clin Endosc* 2019; **52**: 347-352 [PMID: 31288504 DOI: 10.5946/ce.2019.005]

34 **Patel HK**, Saxena R, Rush N, Patel SK, Dasari CS, Mneimneh W, Quickery A, Rahal MA, Temnykh L, DeWitt J, Al-Haddad M. A Comparative Study of 22G versus 19G Needles for EUS-Guided Biopsies for Parenchymal Liver Disease: Are Thinner Needles Better? *Dig Dis Sci* 2021; **66**: 238-246 [PMID: 32128647 DOI: 10.1007/s10620-020-06165-x]

35 **Shah RM**, Schmidt J, John E, Rastegari S, Acharya P, Kedia P. Superior Specimen and Diagnostic Accuracy with Endoscopic Ultrasound-Guided Liver Biopsies Using 19-Gauge versus 22-Gauge Core Needles. *Clin Endosc* 2021; **54**: 739-744 [PMID: 33189102 DOI: 10.5946/ce.2020.212]

36 **DeWitt J**, Cho CM, Lin J, Al-Haddad M, Canto MI, Salamone A, Hruban RH, Messallam AA, Khashab MA. Comparison of EUS-guided tissue acquisition using two different 19-gauge core biopsy needles: a multicenter, prospective, randomized, and blinded study. *Endosc Int Open* 2015; **3**: E471-E478 [PMID: 26528504 DOI: 10.1055/s-0034-1392222]

37 **Ching-Companioni RA**, Diehl DL, Johal AS, Confer BD, Khara HS. 19 G aspiration needle versus 19 G core biopsy needle for endoscopic ultrasound-guided liver biopsy: a prospective randomized trial. *Endoscopy* 2019; **51**: 1059-1065 [PMID: 31342474 DOI: 10.1055/a-0956-6922]

38 **Aggarwal SN**, Magdaleno T, Klocksieben F, MacFarlan JE, Goonewardene S, Zator Z, Shah S, Shah HN. A prospective, head-to-head comparison of 2 EUS-guided liver biopsy needles in vivo. *Gastrointest Endosc* 2021; **93**: 1133-1138 [PMID: 33045222 DOI: 10.1016/j.gie.2020.09.050]

39 **Hashimoto R**, Lee DP, Samarasena JB, Chandan VS, Guo W, Lee JG, Chang KJ. Comparison of Two Specialized Histology Needles for Endoscopic Ultrasound (EUS)-Guided Liver Biopsy: A Pilot Study. *Dig Dis Sci* 2021; **66**: 1700-1706 [PMID: 32556821 DOI: 10.1007/s10620-020-06391-3]

40 **Rudnick SR**, Conway JD, Russo MW. Current state of endohepatology: Diagnosis and treatment of portal hypertension and its complications with endoscopic ultrasound. *World J Hepatol* 2021; **13**: 887-895 [PMID: 34552695 DOI: 10.4254/wjh.v13.i8.887]

41 **Samarasena JB**, Chang KJ. Endoscopic Ultrasound-Guided Interventions for the Measurement and Treatment of Portal Hypertension. *Gastrointest Endosc Clin N Am* 2019; **29**: 311-320 [PMID: 30846155 DOI: 10.1016/j.giec.2018.12.004]

42 **Hajifathalian K**, Westerveld D, Kaplan A, Dawod E, Herr A, Ianelli M, Saggese A, Kumar S, Fortune BE, Sharaiha RZ. Simultaneous EUS-guided portosystemic pressure measurement and liver biopsy sampling correlate with clinically meaningful outcomes. *Gastrointest Endosc* 2022; **95**: 703-710 [PMID: 34890694 DOI: 10.1016/j.gie.2021.11.037]

World Journal of Gastroenterology

Submit a Manuscript: https://www.f6publishing.com

World J Gastroenterol 2022 July 28; 28(28): 3595-3607

DOI: 10.3748/wjg.v28.i28.3595

ISSN 1007-9327 (print) ISSN 2219-2840 (online)

MINIREVIEWS

Non-alcoholic fatty liver disease-related hepatocellular carcinoma: Is there a role for immunotherapy?

Ângelo Z Mattos, Jose D Debes, Arndt Vogel, Marco Arrese, Xavier Revelo, Tales Henrique S Pase, Muriel Manica, Angelo A Mattos

Specialty type: Gastroenterology and hepatology

Provenance and peer review: Invited article; Externally peer reviewed.

Peer-review model: Single blind

Peer-review report's scientific quality classification

Grade A (Excellent): A
Grade B (Very good): B
Grade C (Good): 0
Grade D (Fair): 0
Grade E (Poor): 0

P-Reviewer: Ghoneim S, United States; Marchesini G, Italy

Received: February 14, 2022
Peer-review started: February 14, 2022
First decision: April 5, 2022
Revised: June 26, 2022
Accepted: June 26, 2022
Article in press: June 26, 2022
Published online: July 28, 2022

Ângelo Z Mattos, Angelo A Mattos, Graduate Program in Medicine: Hepatology, Federal University of Health Sciences of Porto Alegre, Porto Alegre 90050-170, Brazil

Ângelo Z Mattos, Angelo A Mattos, Gastroenterology and Hepatology Unit, Irmandade Santa Casa de Misericórdia de Porto Alegre, Porto Alegre 90050-170, Brazil

Jose D Debes, Department of Medicine, University of Minnesota, Minneapolis, MN 55455, United States

Jose D Debes, Department of Gastroenterology and Hepatology, Erasmus Medical Center, Rotterdam 999025, Netherlands

Arndt Vogel, Department of Gastroenterology, Hepatology and Endocrinology, Hannover Medical School, Hannover 30625, Germany

Marco Arrese, Department of Gastroenterology, School of Medicine and Center for Aging and Regeneration, Faculty of Biological Sciences, Pontificia Universidad Católica de Chile, Santiago 3580000, Chile

Xavier Revelo, Department of Integrative Biology and Physiology, University of Minnesota, Minneapolis, MN 55455, United States

Tales Henrique S Pase, Muriel Manica, Internal Medicine Unit, Irmandade Santa Casa de Misericórdia de Porto Alegre, Porto Alegre 90020-090, Brazil

Corresponding author: Ângelo Z Mattos, MD, MSc, PhD, Professor, Graduate Program in Medicine: Hepatology, Federal University of Health Sciences of Porto Alegre, 245 Sarmento Leite St., Porto Alegre 90050-170, Brazil. angmattos@hotmail.com

Abstract

Hepatocellular carcinoma (HCC) is among the most common cancers and it is a major cause of cancer-related deaths. Non-alcoholic fatty liver disease (NAFLD) affects approximately one fourth of individuals worldwide and it is becoming one of the most important causes of HCC. The pathogenic mechanisms leading to NAFLD-related HCC are complex and not completely understood. However, metabolic, fibrogenic, oncogenic, inflammatory and immunological pathways seem to be involved. First-line therapy of advanced HCC has recently undergone major changes, since the combination of atezolizumab and bevacizumab was

proven to increase survival when compared to sorafenib. Other immune-oncology drugs are also demonstrating promising results in patients with advanced HCC when compared to traditional systemic therapy. However, initial studies raised concerns that the advantages of immunotherapy might depend on the underlying liver disease, which seems to be particularly important in NAFLD-related HCC, as these tumors might not benefit from it. This article will review the mechanisms of NAFLD-related hepatocarcinogenesis, with an emphasis on its immune aspects, the efficacy of traditional systemic therapy for advanced NAFLD-related HCC, and the most recent data on the role of immunotherapy for this specific group of patients, showing that the management of this condition should be individualized and that a general recommendation cannot be made at this time.

Key Words: Non-alcoholic fatty liver disease; Hepatocellular carcinoma; Hepatocarcinogenesis; Immunology; Immunotherapy; Tyrosine kinase inhibitors

©The Author(s) 2022. Published by Baishideng Publishing Group Inc. All rights reserved.

Core Tip: Non-alcoholic fatty liver disease (NAFLD) is an important cause of hepatocellular carcinoma (HCC). While the treatment of advanced HCC has recently undergone a revolution led by immunotherapy, concerns have been raised that NAFLD-related HCC might not respond well to these new therapies. This review will approach the pathophysiology of NAFLD-related liver cancer, the evidence on traditional systemic treatments and the most recent data on immunotherapy for this particular group of patients, showing that the management of this condition should be individualized.

Citation: Mattos ÂZ, Debes JD, Vogel A, Arrese M, Revelo X, Pase THS, Manica M, Mattos AA. Non-alcoholic fatty liver disease-related hepatocellular carcinoma: Is there a role for immunotherapy? *World J Gastroenterol* 2022; 28(28): 3595-3607

URL: https://www.wjgnet.com/1007-9327/full/v28/i28/3595.htm

DOI: https://dx.doi.org/10.3748/wjg.v28.i28.3595

INTRODUCTION

The incidence of liver cancer worldwide was 11.6/100000 individuals in 2020 and its mortality rate reached 10.7/100000 in the same year, making it the sixth most common cancer and the second cause of cancer-related mortality[1]. Furthermore, it is estimated that its incidence rate will continue to increase until 2030[2]. Hepatocellular carcinoma (HCC) is by far the most common among primary liver cancers [3,4].

Non-alcoholic fatty liver disease (NAFLD) has a striking prevalence of 25% worldwide[5], which highlights its relevance as an underlying cause of HCC[6]. In the year of 2019, for instance, NAFLD was estimated to be associated with 36300 new cases of HCC, as well as with 34700 HCC-related deaths[7]. As it would be expected, the burden of NAFLD as a cause of HCC seems to be growing. It is estimated that the age-standardized incidence rate of NAFLD-related liver cancer will raise from 0.92 to 1.18/100000 individuals between 2018 and 2030[2]. Moreover, while a multinational cohort study demonstrated that NAFLD was responsible for 9% of HCC cases followed between 2005 and 2015 in South America (an area with high prevalence of NAFLD)[8], the same group verified that it was responsible for 34% of cases followed between 2019 and 2020[9].

Cirrhosis in general predisposes to HCC, and the annual incidence of HCC in patients with NAFLD-related cirrhosis ranges between 0.5% and 2.6%[10-13]. However, some specific mechanisms associated with NAFLD, which will be further discussed in this article, also allow for the development of HCC in the absence of cirrhosis, making NAFLD itself etiologically associated to hepatocarcinogenesis[6,14-16]. According to a meta-analysis, approximately 38% of NAFLD-related HCCs would develop in non-cirrhotic settings[17]. Still, it must be highlighted that the risk of developing HCC is much lower in patients with NAFLD who do not have cirrhosis than in those with NAFLD-related cirrhosis, as it has been recently shown in another meta-analysis (incidence of 0.03 *vs* 3.78/100 person-years)[18].

Significant progress has been recently made in the treatment of advanced HCC, when immunotherapy was proven superior to the systemic therapy used for over a decade[19,20]. Table 1 shows a summary of the most important randomized controlled trials on systemic therapy for advanced HCC.

Nevertheless, initial studies raised concerns that the advantages of immunotherapy might depend on the underlying liver disease, and that patients with NAFLD-related HCC might benefit less from it[21,22]. Considering the epidemiological importance of NAFLD-related HCC, this article aims to review the

Table 1 Summary of randomized controlled trials on systemic therapy for advanced hepatocellular carcinoma

Ref.	Interventions	Mechanisms of action	Main results
Llovet *et al* [57]	Sorafenib × placebo	TKI × placebo	Increased OS with sorafenib
Cheng *et al* [56]	Sorafenib × placebo	TKI × placebo	Increased OS with sorafenib
Bruix[1] et al [59]	Regorafenib × placebo	TKI × placebo	Increased OS with regorafenib
Kudo *et al* [61]	Lenvatinib × sorafenib	TKI × TKI	Non-inferior OS
Abou-Alfa[2] et al[58]	Cabozantinib × placebo	TKI × placebo	Increased OS with cabozantinib
Zhu[1,3] et al [60]	Ramucirumab × placebo	Anti-VEGF receptor 2 × placebo	Increased OS with ramucirumab
Yau *et al*[73]	Nivolumab × sorafenib	Anti-PD-1 × TKI	No increase in OS[4]
Finn[1] et al [74]	Pembrolizumab × placebo	Anti-PD-L1 × placebo	No increase in OS[4]
Finn *et al*[19]	Atezolizumab + bevacizumab × sorafenib	Anti-PD-L1 + anti-VEGF × TKI	Increased OS with atezolizumab + bevacizumab
Kelley *et al* [79]	Atezolizumab + cabozantinib × sorafenib × cabozantinib	Anti-PD-L1 + TKI × TKI × TKI	No increase in OS[4]
Abou-Alfa *et al*[82]	Tremelimumab + durvalumab × durvalumab × sorafenib	Anti-CTLA-4 + anti-PD-L1 × anti-PD-L1 × TKI	Increased OS with tremelimumab + durvalumab (× sorafenib). Non-inferior OS with durvalumab (× sorafenib)

[1]2nd line treatment.
[2]2nd or 3rd line treatment.
[3]Individuals with alpha-fetoprotein ≥ 400 ng/mL.
[4]Primary endpoint not reached.
TKI: Tyrosine kinase inhibitor; OS: Overall survival; VEGF: Vascular endothelial growth factor; PD-1: Programmed cell death protein 1; PD-L1: Programmed cell death ligand-1; CTLA-4: Cytotoxic T-lymphocyte-associated protein 4.

mechanisms behind NAFLD-related hepatocarcinogenesis, with an emphasis on its immune aspects, the knowledge gathered over the years on the efficacy of traditional systemic therapy for advanced NAFLD-related HCC, and the most up-to-date evidence on the role of immunotherapy for this specific group of patients.

PATHOPHYSIOLOGY OF NAFLD-RELATED HCC

The underlying pathogenic mechanisms leading to NAFLD-related HCC are complex and not completely understood[10,23,24]. Metabolic dysfunction as well as inflammatory, fibrogenic and oncogenic pathways are involved, which are in turn modulated by a myriad of factors. These include, among others, genetic and epigenetic changes, different degrees of dysregulation of multiorgan metabolic and endocrine signaling, altered immunologic responses and changes in gut microbiota[24,25].

A disturbed systemic metabolic milieu characterized mainly by insulin resistance and a low-grade inflammatory state seems to be a key in promoting carcinogenesis in a fat-laden liver. Both type 2 diabetes and obesity are known risk factors for NAFLD-related HCC, which may act additively with other metabolic syndrome traits (*i.e.*, dyslipidemia and hypertension) in increasing the risk of HCC development[25,26]. However, the precise molecular mechanisms underpinning the connection between metabolic dysfunction and HCC remain incompletely understood. Metabolic dysfunction-related changes in lipid metabolism (including uncontrolled lipolysis in adipose tissue leading to fatty acid overflow towards the liver and stimulation of hepatic de novo lipogenesis) lead to hepatocyte lipid overload that, in turn, triggers some compensatory adaptations such as downregulation of carnitine palmitoyltransferase 2, which may promote hepatocarcinogenesis. Accumulation of acylcarnitine has been suggested as a potential mechanism in this regard[27]. Also, changes in sterol regulatory element-binding proteins transcription factors, key regulators of sterol and fatty acid biosynthesis, may contribute through interaction with tumor suppressor genes such as p53[28].

Importantly, lipid overload also leads to the occurrence of oxidative stress, endoplasmic reticulum stress, mitochondrial dysfunction, cell injury and cell death, all triggering inflammatory responses and activating fibrogenic processes[29]. Moreover, numerous signaling pathways are also dysregulated, including activation of interleukin (IL)-6/Janus kinase/signal transducer and activator of transcription (STAT) pathway and insulin-like growth factor, among others[30].

Of note, in the setting of a chronic inflammatory microenvironment, death of hepatocytes by different mechanisms (necrosis, apoptosis, pyroptosis and other forms of the cell death) determines a compensatory hepatocyte proliferation. This proliferative response is associated with genetic and epigenetic changes that play a pivotal role in hepatocarcinogenesis. Among these genetic changes, different studies have identified mutations in the telomerase reverse transcriptase promoter, *p53* gene and wingless-related integration site (Wnt)/β-catenin signaling pathway genes as the most consistent genetic changes during HCC development[26]. Finally, epigenetic modifications have been shown to be involved in HCC progression in the context of NAFLD. A broad range of changes in chromatin remodeling, histone alterations, DNA methylation, and noncoding RNA expression has been described and reviewed recently[31]. Such processes have diagnostic, prognostic, and therapeutic implications[32].

Experimental evidence generated in mouse models and some human data strongly suggest that altered gut microbiota may be an important contributing factor to HCC development in the setting of NAFLD/nonalcoholic steatohepatitis (NASH)[33]. The occurrence of dysbiosis is common in NAFLD/NASH, as well as in its commonly associated comorbidities, such as obesity and type 2 diabetes. Nevertheless, although microbiome changes have been characterized in different studies involving subjects with NASH or NAFLD-related cirrhosis, there is considerable variability across different reports, and only few studies have focused specifically on NAFLD-related HCC. Ponziani *et al* [34] showed that cirrhotic NAFLD-related HCC patients had a microbiome profile enriched in Bacteroides and Ruminococcaceae compared to patients with NAFLD-related cirrhosis without HCC [34]. This microbiota profile was associated with increased levels of some circulating proinflammatory cytokines. However, it remains unclear if this is just an epiphenomenon or has pathogenetic relevance.

Mechanistically, dysbiosis leads to altered intestinal permeability, which in turn contributes to hepatic inflammation *via* toll-like receptor 4 (TLR4) stimulation by bacterial derived products. Sustained hepatic inflammation triggered by this pathway can then contribute to hepatocarcinogenesis through multiple mechanisms[23]. Consistent with this proposed mechanism, TLR4 ablation has been shown to prevent HCC development in NASH models[35]. Additionally, changes in gut microbiota critically influence bile acid metabolism. Thus, animals fed with a NASH-promoting diet exhibit a change in their bile acid pool composition, which become enriched in secondary bile acids, particularly deoxycholic acid[33]. Moreover, microbiome changes may induce the transition of hepatic stellate cells (HSCs) in the stroma into a senescence-associated secretory phenotype, which are cells associated with suppression of antitumor immunity[36].

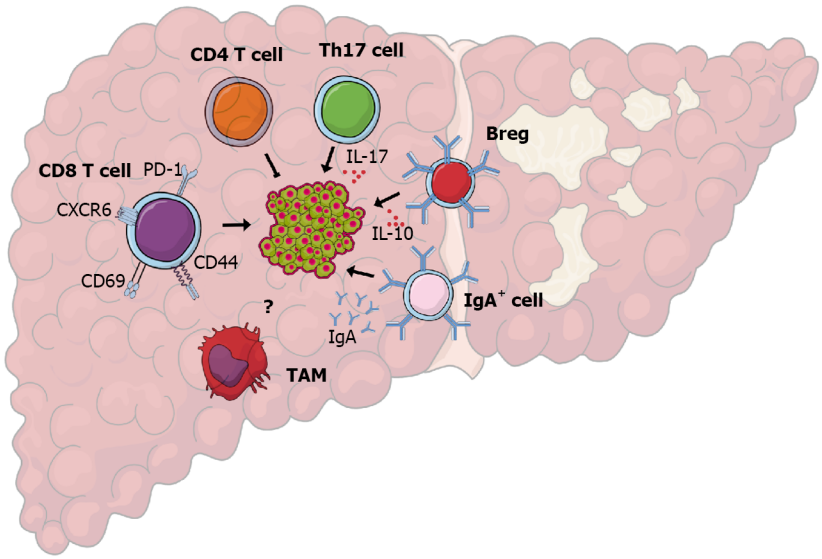
Specific genetic polymorphisms that influence NAFLD susceptibility and severity, such as patatin-like phospholipase domain containing protein 3 (PNPLA3), transmembrane 6 superfamily member 2 and membrane bound O-acetyltransferase domain containing 7, have been linked to a higher risk for NAFLD-related HCC[26]. Of these polymorphisms, the I148M variant of PNPLA3 is one of striking relevance in HCC development[37]. Carriage of this variant critically influences triacylglycerol remodeling in hepatocytes, and recent evidence shows that it also influences fibrogenesis and carcinogenesis by impairing retinol release from HSCs[38].

NAFLD-related HCC generally emerges in the setting of cirrhosis, but may arise also in a non-cirrhotic liver. Some pathways have been shown to play a role in this scenario. Increased STAT-3 signaling has been shown to be associated to the development of HCC independently of NASH and fibrosis. Also, disruption of circadian homeostasis has been shown to be related to HCC development independently of cirrhosis[39].

In summary, pathobiological mechanisms of hepatocarcinogenesis result from a complex interaction of the above-mentioned factors leading to uncontrolled proliferative responses, dysregulation of DNA-damage-response pathways, activation of survival signaling, angiogenesis, evasion of immune surveillance, genomic instability and ultimately to cancer development. It is likely that, in NAFLD patients, mechanisms leading to HCC vary from one subject to another given the heterogenous population grouped under the acronym[40]. Precision medicine approaches based on advanced biomarkers may help identify those at higher risk of developing HCC in order to include them in surveillance programs or, once diagnosed, may allow treatment with targeted therapies.

IMMUNE ASPECTS OF NAFLD-RELATED HCC

Emerging evidence suggests that the chronic inflammatory process of NAFLD and NASH sets the basis for the development of HCC[41]. In addition, there seems to be a role for innate and adaptive immune cells in the pathogenesis of NAFLD-related HCC (Figure 1). However, the immune mechanisms that are specific to NAFLD as the underlying cause of HCC are largely unclear. For example, numerous studies have demonstrated the critical involvement of hepatic macrophages, including resident Kupffer cells



DOI: 10.3748/wjg.v28.i28.3595 **Copyright** ©The Author(s) 2022.

Figure 1 Immune mechanisms in nonalcoholic fatty liver disease-related hepatocellular carcinoma pathogenesis. Studies using human specimens and mouse models have shown that activated non-alcoholic steatohepatitis-associated, programmed cell death protein 1 + CD8 T cells can cause non-specific cell death of hepatocytes and promote hepatocellular carcinoma development. T helper 17 cell-derived interleukin-17, immunoglobulin A-producing cells promote non-alcoholic steatohepatitis-derived hepatocellular carcinoma development, while an overall loss of CD4 T cells may increase tumor burden size. Bregs are abundant in hepatocellular carcinoma and promote disease progression, but are not specific to nonalcoholic fatty liver disease-related hepatocellular carcinoma. The role of tumor associated macrophages in the progression of nonalcoholic fatty liver disease-related hepatocellular carcinoma is unclear. Figure created in the Mind the Graph platform, available at www.mindthegraph.com. Th: T helper; PD-1: Programmed cell death protein 1; IL: Interleukin; Bregs: Regulatory B cells; IgA: Immunoglobulin A; CXCR6: C-X-C Motif Chemokine Receptor 6; TAM: Tumor associated macrophages.

and recruited monocyte-derived macrophages in the pathogenesis of NASH[42]. The activation of Kupffer cells is crucial for tumor development in the early stage of chemical-induced carcinogenesis[43] and tumor-associated macrophages play a prominent role in promoting HCC once a primary tumor is established[44]. Nevertheless, the role of hepatic macrophages in NAFLD-related HCC has not been investigated yet.

Regarding the role of adaptive immunity as a central player in the progression of NAFLD-related HCC, several reports have shown increased recruitment of adaptive immune cells such as T and B lymphocytes into the liver of these patients. For instance, whole-exome sequencing of livers from patients with NAFLD-related HCC shows enrichment of gene signatures associated with T lymphocytes suggesting increased hepatic T cell accumulation[45]. Notably, studies show that HCC cases from NAFLD-related cirrhosis display features of immune exhaustion, indicating a state of dysfunction likely due to stimulation by tumor antigens[45].

Experimental murine models of NAFLD-related HCC have shed light on the potential mechanisms by which T cells regulate HCC development. In a mouse model of NAFLD-related HCC that recapitulates metabolic disease, intrahepatic CD8 T cells become activated and express CD44 and CD69, suggesting that they can directly induce liver damage through interactions with hepatocytes[46]. Indeed, genetic ablation of CD8 T cells in this mouse model ameliorates liver damage, NASH, and HCC development, suggesting that CD8 T cells directly instigate disease progression[46]. The increased T cell infiltration in NAFLD-related HCC has been attributed to the inactivation of T cell protein tyrosine phosphatase in hepatocytes and increased expression of T cell chemoattractants[47]. Mechanistically, NASH programs CD8 T cells to acquire an activated exhausted phenotype and express increased levels of programmed cell death protein 1 (PD-1) in response to metabolic signals as well as to IL-15, instigating their non-specific killing of hepatocytes and disease progression[48]. In addition to exhaustion markers, NASH-derived PD-1 positive CD8 T cells express high levels of effector function molecules such as tumor necrosis factor α, interferon γ, and granzyme[21]. The increased activity of exhausted PD-1 positive CD8 T cells in the NASH liver is not limited to accelerating liver damage but can result in impaired immune surveillance and subsequent HCC[21].

In contrast to the accumulation of CD8 T cells, lipid dysregulation has been shown to cause a loss of CD4 T cells in tumor-free and tumor-bearing environments in the liver of mice with NASH induced by a methionine and choline-deficient L-amino acid-defined diet[49]. Importantly, depletion of total CD4 T cells promoted hepatic carcinogenesis in a MYC oncogene model of HCC, suggesting that the overall function of CD4 T cells is to provide antitumor immunity[49]. However, nutrient overload induces a subset of CD4 T cells known as T helper-17 cells that produce large amounts of IL-17A to promote tumorigenesis in NAFLD-related HCC[50]. Overall, these findings suggest that the exhaustion of hepatic CD8 T cells and the loss of CD4 T cells in NASH compromise the hepatic antitumor surveillance

and increase the susceptibility to HCC.

In addition to T cells, emerging evidence suggests that immunoglobulin A (IgA)-producing B cells play a critical role in the progression of NAFLD-related HCC. In humans, the number of tumor-infiltrating B cells correlates with tumor progression[51]. Likewise, patients with HCC that have fewer tumor-infiltrating plasma cells present a better prognosis[52]. Feeding a high fat diet to major urinary protein-urokinase-type plasminogen activator transgenic mice, a reliable model of NAFLD-related HCC, instigates IgA-producing cells to interfere with the protective role of anti-tumor cytotoxic CD8 T cells[53]. The IgA positive B cells inhibit the activity of CD8 T cells through the expression of programmed death-ligand 1 (PD-L1) and the production of the immunosuppressive cytokine IL-10[53]. Regulatory B cells, a subset of B cells, can also inhibit anti-tumor immunity through IL-10 production and promote HCC growth through direct interactions with the tumor cells[54]. As B cells promote NAFLD through the production of pro-inflammatory cytokines and regulation of intrahepatic T cells in NASH[55], future studies are needed to clarify the precise role of liver B cells in NAFLD-related HCC.

TRADITIONAL SYSTEMIC TREATMENT FOR ADVANCED NAFLD-RELATED HCC

Systemic therapy for HCC is relatively young in comparison to other cancers, becoming available only after 2007, with the arrival of sorafenib, a multikinase inhibitor that showed improved survival against placebo in both the SHARP and Asia-Pacific trials[56,57]. For 10 years, sorafenib was the only available systemic therapy for HCC, until the field expanded significantly over the last 5 years with trials showing benefit from regorafenib, lenvatinib, cabozantinib and ramucirumab[58-61]. All of these studies were performed on HCCs from multiple etiologies, but primarily viral hepatitis-related tumors. Recently, attention has shifted to the importance of HCC etiology as a predictor of response to systemic therapy. This issue has been most evident in HCC immunotherapy, but potentially applies to other systemic therapies as well.

NAFLD-related HCC represents a unique conundrum for systemic therapy, as metabolic issues beyond that of HCC may play a role[62]. Individuals with NAFLD-related HCC are more likely to be obese, and are more likely to be on hormone-related medications, both of which could affect the pharmacokinetics of systemic therapy. Indeed, a small study showed that patients on sorafenib who were receiving metformin for diabetes mellitus had worse survival than those on insulin, regardless of the cause of HCC[63].

Due to the temporal dynamics of HCC systemic therapy in the last 15 years, most of the available data is from sorafenib studies. Sorafenib is known to perform best when used in patients with viral hepatitis-related HCC, particularly hepatitis C infection. However, most studies addressed hepatitis C *vs* alcohol-related HCC, or viral hepatitis *vs* other causes of HCC, clouding the understanding of the role of sorafenib in NAFLD-related HCC specifically[64-66]. An international study, presented only in abstract form, found similar overall survival (OS) in patients treated with sorafenib with NAFLD-related HCC *vs* other causes [hazard ratio (HR): 0.94, 95% confidence interval (CI): 0.76-1.16, $P = 0.57$]. However, the NAFLD portion of the study included only 187 patients (3.5% of the total cohort), and further details are awaited with the full peer-reviewed version[67]. A recent retrospective subgroup analysis including 483 NAFLD-related HCC patients treated with sorafenib also found no significant difference in univariate analysis of survival between NAFLD and other etiologies (10.2 mo *vs* 12.3 mo; HR: 1.06; 95%CI: 0.83-1.34, $P = 0.63$)[68].

Information on NAFLD-related HCC for other non-immune forms of systemic therapy remains rather elusive, although very recent studies are shedding some light on the field. The initial trials for regorafenib (RESORCE), cabozantinib (CELESTIAL) and ramucirumab (REACH-2) included very limited numbers of patients with NAFLD-related HCC (6.6%, 9.3% and 7.9% respectively), and most subgroup analyses did not specifically evaluate NAFLD-related HCC[58-60]. The CELESTIAL trial for cabozantinib indicated benefit of the drug across all subgroups of etiologic factors and found no difference for OS between viral hepatitis-related HCC and other etiologies (HR: 0.76, 95%CI: 0.63-0.92 *vs* HR: 0.72, 95%CI: 0.54-0.96). However, the "other etiologies" group included all non-viral hepatitis-related tumors, with the NASH proportion conforming 43 patients. Also, this trial evaluated cabozantinib as second line therapy[58].

More recently, retrospective studies have evaluated lenvatinib in NAFLD-related HCC, suggesting an advantage for this multikinase inhibitor in this group of patients. A multicenter analysis of 236 NAFLD-related HCCs treated with lenvatinib (19% of the entire cohort) found a better OS for NAFLD-related HCC compared to other etiologies (22.2 mo *vs* 15.1 mo, HR: 0.69, 95%CI: 0.56-0.85, $P = 0.0006$)[68]. A Japanese study (also retrospective) of lenvatinib in unresectable tumors involving 103 NAFLD-related HCCs found no difference in OS compared to other etiologies, but the progression free survival (PFS) was better in the NAFLD group (median 9.3 mo *vs* 7.5 mo, $P = 0.01$)[69]. Furthermore, the retrospective multicenter ELEVATOR study, in which 200 patients were treated with lenvatinib, observed a similar survival in patients with viral and non-viral (NASH and alcoholic steatohepatitis) related HCC[70].

This early evidence suggests that sorafenib or cabozantinib are not particularly better (or worse) for NAFLD-related HCC, and that the use of lenvatinib might pose an advantage, with no specific data, so

far, for regorafenib. Nevertheless, it should be noted that better studies are needed in order to draw significant conclusions.

IMMUNOTHERAPY FOR ADVANCED NAFLD-RELATED HCC

In recent years, besides several tyrosine kinase inhibitors and a monoclonal antibody against vascular endothelial growth factor (VEGF) receptor-2 being added to the treatment armamentarium, immunotherapy with immune checkpoint blockers has been extensively investigated in patients with HCC[71]. Nivolumab, pembrolizumab, and the combination of nivolumab plus ipilimumab have been approved by the United States Food and Drug Administration (FDA) based on very promising phase II studies [72], but nivolumab and pembrolizumab failed to reach their primary endpoints in subsequent phase III trials in first- and second-line, respectively[73,74].

Atezolizumab plus bevacizumab

Overexpression of VEGF has been associated with liver cancer development and progression, and small phase II studies have shown modest anti-tumor efficacy of bevacizumab as monotherapy in advanced HCC[75]. In addition to the antiangiogenic effects, there is increasing evidence that anti-VEGF therapies may enhance the efficacy of anti-PD-1 and anti-PD-L1 by reversing VEGF-mediated immunosuppression and promoting T-cell infiltration in tumors[76]. Based on these observations, the PD-L1 inhibitor atezolizumab was evaluated together with the VEGF inhibitor bevacizumab in the phase III IMbrave150 study. The combination significantly improved all efficacy endpoints with a statistically significant and clinically meaningful survival benefit compared to sorafenib[19,77]. Side effect profiles of the drugs were in line with their respective mechanism of action and no new safety signals were observed. Additionally, patient-reported outcomes revealed that deteriorations in quality of life were significantly delayed in the combination arm compared to the sorafenib arm[78]. The combination has been approved by the FDA and by the European Medicines Agency (EMA), and it is currently regarded as the standard of care in first-line therapy of advanced HCC.

Atezolizumab plus cabozantinib

In the COSMIC-312 trial, in which 837 patients with HCC were randomized to be treated with atezolizumab plus cabozantinib, sorafenib in monotherapy or cabozantinib in monotherapy (2:1:1), PFS was 6.8 mo for the group receiving combination therapy, compared to 4.2 mo for the group under sorafenib (HR: 0.63, 95%CI: 0.44-0.91, P = 0.0012). Regarding OS, an interim analysis did not demonstrate a significant difference between combination treatment and monotherapy with sorafenib (HR: 0.90, 95%CI: 0.69-1.18, P = 0.438). Finally, the interim analysis on the comparison between cabozantinib and sorafenib showed a tendency favoring cabozantinib regarding PFS (HR: 0.71, 95%CI: 0.51-1.01)[79].

Dual checkpoint inhibition

Two antibodies against cytotoxic T-lymphocyte-associated protein 4 (CTLA-4) have been investigated in advanced HCC. The combination of nivolumab and ipilimumab has already shown improved OS in HCC patients in the phase I/II CheckMate040 study[80,81]. The pure immune-oncology (IO) combination achieved a high overall response rate with a promising OS of almost 23 mo. The most common immune related adverse events were rash, hepatitis, and adrenal insufficiency. Based on these results, the FDA approved nivolumab plus ipilimumab as second-line treatment for patients with advanced HCC previously treated with sorafenib. Currently, the checkmate 9DW study evaluates the efficacy of nivolumab plus ipilimumab compared to sorafenib or lenvatinib as first-line therapy.

Similar to ipilimumab, tremelimumab has also been studied as an anti-CTLA-4 antibody in HCC. Based on promising phase II data, the combination of durvalumab and tremelimumab was compared with durvalumab in monotherapy or sorafenib in monotherapy as first-line therapy for unresectable HCC in the HIMALAYA trial. Regarding the comparison between combination therapy and monotherapy with sorafenib, there was a significant improvement in OS favoring combination therapy (16.4 mo *vs* 13.8 mo, HR: 0.78, 95%CI: 0.65-0.92, P = 0.0035), and durvalumab plus tremelimumab may be approved by the FDA and EMA in the near future as an additional option for first-line treatment in HCC. Finally, monotherapy with durvalumab was noninferior to sorafenib regarding OS (HR: 0.86, 95%CI: 0.73-1.03)[82].

Etiology of liver disease and immunotherapy

A very recent study suggested that clinicians might need to consider the underlying liver disease for treatment selection in HCC. Pfister *et al*[21] provided provocative preclinical and limited clinical evidence that patients with NAFLD-related HCC may benefit less from immune checkpoint inhibition than patients with viral hepatitis-related HCC. Regarding preclinical data, authors evaluated immunotherapy in mice with NAFLD-related HCC. Despite the hepatic abundance of PD-1 positive CD8 T cells with features of exhaustion and effector functions in mice with NASH, which might be suggestive of a good response to immunotherapy, none of the pre-existing tumors regressed with treatment, and there

was evidence indicating that immunotherapy could even play a role in hepatocarcinogenesis in mice with NASH. In the same publication, a meta-analysis of three randomized controlled phase III trials failed to demonstrate evidence of survival improvement for patients with non-viral hepatitis-related HCC receiving immunotherapy. The authors also investigated a cohort of 130 HCC cases, in which 13 were NAFLD-related and had OS after immunotherapy of 5.4 mo, significantly lower than that of patients with HCCs related to other causes of liver disease (11.0 mo, P = 0.023). Finally, authors validated these findings in yet another cohort of 118 individuals with HCC, in which 11 were NAFLD-related and had OS of 8.8 mo, while patients with HCC related to other causes of liver disease had OS of 17.7 mo (P = 0.034)[21]. Nevertheless, important remarks on this study have been made in an editorial, which highlighted that patients with NASH were not separated from those with other non-viral hepatitis etiologies of liver disease in the meta-analysis presented in the paper, and that the small number of patients evaluated in the cohorts must be kept in mind when considering their results[83].

In the same line, both the Checkmate-459 and the IMBrave150 trials found that HR for OS was worse in patients with non-viral hepatitis-related HCC compared with patients with viral hepatitis-related cancer. However, neither study distinguished between patients with NASH and alcoholic steatohepatitis. In addition, it should be noted that the poor HRs in the non-viral hepatitis group were not solely due to the shorter survival in the IO arm, but also to a surprisingly long survival in the sorafenib arm of both trials[19,84]. Similarly, in the COSMIC-312 trial, when a subgroup analysis on etiology of the underlying liver disease was performed, the benefit of atezolizumab plus cabozantinib on PFS seemed to be driven by the hepatitis B-related HCC group, and there was no significant difference between combination therapy and sorafenib for patients with non-viral hepatitis related-HCC (HR: 0.92, 95%CI: 0.60-1.41)[79].

Another recent meta-analysis of randomized controlled trials helped fuel this debate, when it also demonstrated that immune checkpoint inhibitors were significantly more effective for viral hepatitis-related HCCs than for tumors associated with other kinds of liver disease. On the other hand, the etiology of liver disease did not seem to interfere with the efficacy of tyrosine-kinase inhibitors or anti-VEGF therapies[22].

In contrast to these observations, underlying liver disease (viral hepatitis *vs* alcohol *vs* NASH) did not significantly impact PFS and OS in a recent real-world cohort treated with atezolizumab and bevacizumab[85]. Moreover, in the HIMALAYA trial, the benefit of the combination of durvalumab and tremelimumab on OS persisted in the subgroup analysis in patients with non-viral hepatitis related-HCC (HR: 0.74, 95%CI: 0.57-0.95)[82].

Perhaps the decision to start immunotherapy might be guided by prognostic biomarkers, rather than solely by the etiology of liver disease. Several predictive biomarkers for immunotherapy response have been proposed, including PD-L1 expression[86] and evidence of activated Wnt/β-catenin signaling[87], but currently no validated biomarker exists to guide treatment decisions in HCC patients undergoing immunotherapy. The recently proposed CRAFITY score (C reactive protein and alpha-fetoprotein in ImmunoTherapY) may be an easy-to-use tool to predict outcomes of patients undergoing immunotherapy for HCC, regardless of Child-Pugh class and performance status[88].

CONCLUSION

As the field moves forward, and with early evidence suggesting a potential decreased response of NAFLD-related HCC to immunotherapy, studies of non-immune systemic therapy for this group of patients should become more frequent and more robust. Moreover, randomized controlled trials evaluating immunotherapy in this particular group of patients are of the utmost importance. Multiple issues should be taken into account in such studies, including the strict definition of NAFLD, metabolic associated fatty liver disease or NASH, the heterogeneity of this group which includes lean NAFLD, NAFLD related to metabolic syndrome and others, as well as the impact of other co-morbidities and medication profiles.

FOOTNOTES

Author contributions: All authors contributed to this paper with conception of the manuscript, literature review and analysis, drafting and critical revision of the manuscript, and approval of the final version of the paper.

Supported by European-Latin American ESCALON Consortium, Funded By The EU Horizon 2020 Program, No. 825510; Robert Wood Johnson Foundation, Harold Amos Medical Faculty Development Program to JDD; University of Minnesota Academic Investment Research Program–AIRP Grant to JDD; Fondo Nacional de Ciencia y Tecnología de Chilex to MA, No. FONDECYT-1191145; Agencia Nacional de Investigación y Desarrollo to MA, No. ANID-ACE 210009.

Conflict-of-interest statement: Dr. Mattos reports grants from EU Horizon 2020 program, grants from Robert Wood

Johnson Foundation, Harold Amos Medical Faculty Development Program, grants from Fondo Nacional de Ciencia y Tecnología de Chile and Comisión Nacional de Investigación, Ciencia y Tecnología , grants from University of Minnesota Academic Investment Research Program–AIRP grant, grants from Agencia Nacional de Investigación y Desarrollo (ANID ACE 210009), during the conduct of the study.

Open-Access: This article is an open-access article that was selected by an in-house editor and fully peer-reviewed by external reviewers. It is distributed in accordance with the Creative Commons Attribution NonCommercial (CC BY-NC 4.0) license, which permits others to distribute, remix, adapt, build upon this work non-commercially, and license their derivative works on different terms, provided the original work is properly cited and the use is non-commercial. See: https://creativecommons.org/Licenses/by-nc/4.0/

Country/Territory of origin: Brazil

ORCID number: Ângelo Z Mattos 0000-0002-3063-0199.

Corresponding Author's Membership in Professional Societies: Federação Brasileira De Gastroenterologia.

S-Editor: Fan JR
L-Editor: A
P-Editor: Fan JR

REFERENCES

1 **World Health Organization**. Global Cancer Observatory-GLOBOCAN 2020. [cited 14 February 2022]. Available from: https://gco.iarc.fr/
2 **Liu Z**, Xu K, Jiang Y, Cai N, Fan J, Mao X, Suo C, Jin L, Zhang T, Chen X. Global trend of aetiology-based primary liver cancer incidence from 1990 to 2030: a modelling study. *Int J Epidemiol* 2021; **50**: 128-142 [PMID: 33349860 DOI: 10.1093/ije/dyaa196]
3 **McGlynn KA**, Petrick JL, El-Serag HB. Epidemiology of Hepatocellular Carcinoma. *Hepatology* 2021; **73** Suppl 1: 4-13 [PMID: 32319693 DOI: 10.1002/hep.31288]
4 **Arnold M**, Abnet CC, Neale RE, Vignat J, Giovannucci EL, McGlynn KA, Bray F. Global Burden of 5 Major Types of Gastrointestinal Cancer. *Gastroenterology* 2020; **159**: 335-349.e15 [PMID: 32247694 DOI: 10.1053/j.gastro.2020.02.068]
5 **Younossi ZM**, Koenig AB, Abdelatif D, Fazel Y, Henry L, Wymer M. Global epidemiology of nonalcoholic fatty liver disease-Meta-analytic assessment of prevalence, incidence, and outcomes. *Hepatology* 2016; **64**: 73-84 [PMID: 26707365 DOI: 10.1002/hep.28431]
6 **Anstee QM**, Reeves HL, Kotsiliti E, Govaere O, Heikenwalder M. From NASH to HCC: current concepts and future challenges. *Nat Rev Gastroenterol Hepatol* 2019; **16**: 411-428 [PMID: 31028350 DOI: 10.1038/s41575-019-0145-7]
7 **GBD 2019 Diseases and Injuries Collaborators**. Global burden of 369 diseases and injuries in 204 countries and territories, 1990-2019: a systematic analysis for the Global Burden of Disease Study 2019. *Lancet* 2020; **396**: 1204-1222 [PMID: 33069326 DOI: 10.1016/S0140-6736(20)30925-9]
8 **Debes JD**, Chan AJ, Balderramo D, Kikuchi L, Gonzalez Ballerga E, Prieto JE, Tapias M, Idrovo V, Davalos MB, Cairo F, Barreyro FJ, Paredes S, Hernandez N, Avendaño K, Diaz Ferrer J, Yang JD, Carrera E, Garcia JA, Mattos AZ, Hirsch BS, Gonçalves PT, Carrilho FJ, Roberts LR. Hepatocellular carcinoma in South America: Evaluation of risk factors, demographics and therapy. *Liver Int* 2018; **38**: 136-143 [PMID: 28640517 DOI: 10.1111/liv.13502]
9 **Farah M**, Diaz Ferrer J, Baca EL, Mattos A, Arrese M, Prieto Ortiz JE, Balderramo D, Carrera E, Boonstra A, Debes JD. Changing epidemiology of hepatocellular carcinoma in South America: a report from the ESCALON Network. *Hepatology* 2021; **74** Suppl 1: 681A
10 **Banini BA**, Sanyal AJ. NAFLD-related HCC. *Adv Cancer Res* 2021; **149**: 143-169 [PMID: 33579423 DOI: 10.1016/bs.acr.2020.11.001]
11 **Ascha MS**, Hanouneh IA, Lopez R, Tamimi TA, Feldstein AF, Zein NN. The incidence and risk factors of hepatocellular carcinoma in patients with nonalcoholic steatohepatitis. *Hepatology* 2010; **51**: 1972-1978 [PMID: 20209604 DOI: 10.1002/hep.23527]
12 **Yatsuji S**, Hashimoto E, Tobari M, Taniai M, Tokushige K, Shiratori K. Clinical features and outcomes of cirrhosis due to non-alcoholic steatohepatitis compared with cirrhosis caused by chronic hepatitis C. *J Gastroenterol Hepatol* 2009; **24**: 248-254 [PMID: 19032450 DOI: 10.1111/j.1440-1746.2008.05640.x]
13 **Amarapurkar DN**, Dharod M, Gautam S, Patel N. Risk of development of hepatocellular carcinoma in patients with NASH-related cirrhosis. *Trop Gastroenterol* 2013; **34**: 159-163 [PMID: 24851525 DOI: 10.7869/tg.120]
14 **Levrero M**, Zucman-Rossi J. Mechanisms of HBV-induced hepatocellular carcinoma. *J Hepatol* 2016; **64**: S84-S101 [PMID: 27084040 DOI: 10.1016/j.jhep.2016.02.021]
15 **Geh D**, Manas DM, Reeves HL. Hepatocellular carcinoma in non-alcoholic fatty liver disease-a review of an emerging challenge facing clinicians. *Hepatobiliary Surg Nutr* 2021; **10**: 59-75 [PMID: 33575290 DOI: 10.21037/hbsn.2019.08.08]
16 **Villanueva A**. Hepatocellular Carcinoma. *N Engl J Med* 2019; **380**: 1450-1462 [PMID: 30970190 DOI: 10.1056/NEJMra1713263]
17 **Stine JG**, Wentworth BJ, Zimmet A, Rinella ME, Loomba R, Caldwell SH, Argo CK. Systematic review with meta-analysis: risk of hepatocellular carcinoma in non-alcoholic steatohepatitis without cirrhosis compared to other liver

diseases. *Aliment Pharmacol Ther* 2018; **48**: 696-703 [PMID: 30136293 DOI: 10.1111/apt.14937]

18 **Orci LA**, Sanduzzi-Zamparelli M, Caballol B, Sapena V, Colucci N, Torres F, Bruix J, Reig M, Toso C. Incidence of Hepatocellular Carcinoma in Patients With Nonalcoholic Fatty Liver Disease: A Systematic Review, Meta-analysis, and Meta-regression. *Clin Gastroenterol Hepatol* 2022; **20**: 283-292.e10 [PMID: 33965578 DOI: 10.1016/j.cgh.2021.05.002]

19 **Finn RS**, Qin S, Ikeda M, Galle PR, Ducreux M, Kim TY, Kudo M, Breder V, Merle P, Kaseb AO, Li D, Verret W, Xu DZ, Hernandez S, Liu J, Huang C, Mulla S, Wang Y, Lim HY, Zhu AX, Cheng AL; IMbrave150 Investigators. Atezolizumab plus Bevacizumab in Unresectable Hepatocellular Carcinoma. *N Engl J Med* 2020; **382**: 1894-1905 [PMID: 32402160 DOI: 10.1056/NEJMoa1915745]

20 **Reig M**, Forner A, Rimola J, Ferrer-Fàbrega J, Burrel M, Garcia-Criado Á, Kelley RK, Galle PR, Mazzaferro V, Salem R, Sangro B, Singal AG, Vogel A, Fuster J, Ayuso C, Bruix J. BCLC strategy for prognosis prediction and treatment recommendation: The 2022 update. *J Hepatol* 2022; **76**: 681-693 [PMID: 34801630 DOI: 10.1016/j.jhep.2021.11.018]

21 **Pfister D**, Núñez NG, Pinyol R, Govaere O, Pinter M, Szydlowska M, Gupta R, Qiu M, Deczkowska A, Weiner A, Müller F, Sinha A, Friebel E, Engleitner T, Lenggenhager D, Moncsek A, Heide D, Stirm K, Kosla J, Kotsiliti E, Leone V, Dudek M, Yousuf S, Inverso D, Singh I, Teijeiro A, Castet F, Montironi C, Haber PK, Tiniakos D, Bedossa P, Cockell S, Younes R, Vacca M, Marra F, Schattenberg JM, Allison M, Bugianesi E, Ratziu V, Pressiani T, D'Alessio A, Personeni N, Rimassa L, Daly AK, Scheiner B, Pomej K, Kirstein MM, Vogel A, Peck-Radosavljevic M, Hucke F, Finkelmeier F, Waidmann O, Trojan J, Schulze K, Wege H, Koch S, Weinmann A, Bueter M, Rössler F, Siebenhüner A, De Dosso S, Mallm JP, Umansky V, Jugold M, Luedde T, Schietinger A, Schirmacher P, Emu B, Augustin HG, Billeter A, Müller-Stich B, Kikuchi H, Duda DG, Kütting F, Waldschmidt DT, Ebert MP, Rahbari N, Mei HE, Schulz AR, Ringelhan M, Malek N, Spahn S, Bitzer M, Ruiz de Galarreta M, Lujambio A, Dufour JF, Marron TU, Kaseb A, Kudo M, Huang YH, Djouder N, Wolter K, Zender L, Marche PN, Decaens T, Pinato DJ, Rad R, Mertens JC, Weber A, Unger K, Meissner F, Roth S, Jilkova ZM, Claassen M, Anstee QM, Amit I, Knolle P, Becher B, Llovet JM, Heikenwalder M. NASH limits anti-tumour surveillance in immunotherapy-treated HCC. *Nature* 2021; **592**: 450-456 [PMID: 33762733 DOI: 10.1038/s41586-021-03362-0]

22 **Haber PK**, Puigvehí M, Castet F, Lourdusamy V, Montal R, Tabrizian P, Buckstein M, Kim E, Villanueva A, Schwartz M, Llovet JM. Evidence-Based Management of Hepatocellular Carcinoma: Systematic Review and Meta-analysis of Randomized Controlled Trials (2002-2020). *Gastroenterology* 2021; **161**: 879-898 [PMID: 34126063 DOI: 10.1053/j.gastro.2021.06.008]

23 **Shetty K**, Chen J, Shin JH, Jogunoori W, Mishra L. Pathogenesis of hepatocellular carcinoma development in non alcoholic fatty liver disease. *Curr Hepatol Rep* 2015; **14**: 119-127 [PMID: 26114083 DOI: 10.1007/s11901-015-0260-z]

24 **Kanda T**, Goto T, Hirotsu Y, Masuzaki R, Moriyama M, Omata M. Molecular Mechanisms: Connections between Nonalcoholic Fatty Liver Disease, Steatohepatitis and Hepatocellular Carcinoma. *Int J Mol Sci* 2020; **21** [PMID: 32102237 DOI: 10.3390/ijms21041525]

25 **Wegermann K**, Hyun J, Diehl AM. Molecular Mechanisms Linking Nonalcoholic Steatohepatitis to Cancer. *Clin Liver Dis (Hoboken)* 2021; **17**: 6-10 [PMID: 33552478 DOI: 10.1002/cld.1006]

26 **Valenti L**, Pedica F, Colombo M. Distinctive features of hepatocellular carcinoma in non-alcoholic fatty liver disease. *Dig Liver Dis* 2022; **54**: 154-163 [PMID: 34294580 DOI: 10.1016/j.dld.2021.06.023]

27 **Fujiwara N**, Nakagawa H, Enooku K, Kudo Y, Hayata Y, Nakatsuka T, Tanaka Y, Tateishi R, Hikiba Y, Misumi K, Tanaka M, Hayashi A, Shibahara J, Fukayama M, Arita J, Hasegawa K, Hirschfield H, Hoshida Y, Hirata Y, Otsuka M, Tateishi K, Koike K. CPT2 downregulation adapts HCC to lipid-rich environment and promotes carcinogenesis *via* acylcarnitine accumulation in obesity. *Gut* 2018; **67**: 1493-1504 [PMID: 29437870 DOI: 10.1136/gutjnl-2017-315193]

28 **Wu H**, Ng R, Chen X, Steer CJ, Song G. MicroRNA-21 is a potential link between non-alcoholic fatty liver disease and hepatocellular carcinoma *via* modulation of the HBP1-p53-Srebp1c pathway. *Gut* 2016; **65**: 1850-1860 [PMID: 26282675 DOI: 10.1136/gutjnl-2014-308430]

29 **Schuster S**, Cabrera D, Arrese M, Feldstein AE. Triggering and resolution of inflammation in NASH. *Nat Rev Gastroenterol Hepatol* 2018; **15**: 349-364 [PMID: 29740166 DOI: 10.1038/s41575-018-0009-6]

30 **Garcia-Lezana T**, Lopez-Canovas JL, Villanueva A. Signaling pathways in hepatocellular carcinoma. *Adv Cancer Res* 2021; **149**: 63-101 [PMID: 33579428 DOI: 10.1016/bs.acr.2020.10.002]

31 **Nagaraju GP**, Dariya B, Kasa P, Peela S, El-Rayes BF. Epigenetics in hepatocellular carcinoma. *Semin Cancer Biol* 2021 [PMID: 34324953 DOI: 10.1016/j.semcancer.2021.07.017]

32 **Geh D**, Anstee QM, Reeves HL. NAFLD-Associated HCC: Progress and Opportunities. *J Hepatocell Carcinoma* 2021; **8**: 223-239 [PMID: 33854987 DOI: 10.2147/JHC.S272213]

33 **Akkız H**. The Gut Microbiome and Hepatocellular Carcinoma. *J Gastrointest Cancer* 2021; **52**: 1314-1319 [PMID: 34870783 DOI: 10.1007/s12029-021-00748-1]

34 **Ponziani FR**, Bhoori S, Castelli C, Putignani L, Rivoltini L, Del Chierico F, Sanguinetti M, Morelli D, Paroni Sterbini F, Petito V, Reddel S, Calvani R, Camisaschi C, Picca A, Tuccitto A, Gasbarrini A, Pompili M, Mazzaferro V. Hepatocellular Carcinoma Is Associated With Gut Microbiota Profile and Inflammation in Nonalcoholic Fatty Liver Disease. *Hepatology* 2019; **69**: 107-120 [PMID: 29665135 DOI: 10.1002/hep.30036]

35 **Miura K**, Ishioka M, Minami S, Horie Y, Ohshima S, Goto T, Ohnishi H. Toll-like Receptor 4 on Macrophage Promotes the Development of Steatohepatitis-related Hepatocellular Carcinoma in Mice. *J Biol Chem* 2016; **291**: 11504-11517 [PMID: 27022031 DOI: 10.1074/jbc.M115.709048]

36 **Yoshimoto S**, Loo TM, Atarashi K, Kanda H, Sato S, Oyadomari S, Iwakura Y, Oshima K, Morita H, Hattori M, Honda K, Ishikawa Y, Hara E, Ohtani N. Obesity-induced gut microbial metabolite promotes liver cancer through senescence secretome. *Nature* 2013; **499**: 97-101 [PMID: 23803760 DOI: 10.1038/nature12347]

37 **Liu YL**, Patman GL, Leathart JB, Piguet AC, Burt AD, Dufour JF, Day CP, Daly AK, Reeves HL, Anstee QM. Carriage of the PNPLA3 rs738409 C >G polymorphism confers an increased risk of non-alcoholic fatty liver disease associated hepatocellular carcinoma. *J Hepatol* 2014; **61**: 75-81 [PMID: 24607626 DOI: 10.1016/j.jhep.2014.02.030]

38 **Bruschi FV**, Claudel T, Tardelli M, Caligiuri A, Stulnig TM, Marra F, Trauner M. The PNPLA3 I148M variant modulates the fibrogenic phenotype of human hepatic stellate cells. *Hepatology* 2017; **65**: 1875-1890 [PMID: 28073161 DOI:

10.1002/hep.29041]
39 **Kettner NM**, Voicu H, Finegold MJ, Coarfa C, Sreekumar A, Putluri N, Katchy CA, Lee C, Moore DD, Fu L. Circadian Homeostasis of Liver Metabolism Suppresses Hepatocarcinogenesis. *Cancer Cell* 2016; **30**: 909-924 [PMID: 27889186 DOI: 10.1016/j.ccell.2016.10.007]
40 **Arrese M**, Arab JP, Barrera F, Kaufmann B, Valenti L, Feldstein AE. Insights into Nonalcoholic Fatty-Liver Disease Heterogeneity. *Semin Liver Dis* 2021; **41**: 421-434 [PMID: 34233370 DOI: 10.1055/s-0041-1730927]
41 **Giraud J**, Chalopin D, Blanc JF, Saleh M. Hepatocellular Carcinoma Immune Landscape and the Potential of Immunotherapies. *Front Immunol* 2021; **12**: 655697 [PMID: 33815418 DOI: 10.3389/fimmu.2021.655697]
42 **Krenkel O**, Tacke F. Liver macrophages in tissue homeostasis and disease. *Nat Rev Immunol* 2017; **17**: 306-321 [PMID: 28317925 DOI: 10.1038/nri.2017.11]
43 **Wu J**, Li J, Salcedo R, Mivechi NF, Trinchieri G, Horuzsko A. The proinflammatory myeloid cell receptor TREM-1 controls Kupffer cell activation and development of hepatocellular carcinoma. *Cancer Res* 2012; **72**: 3977-3986 [PMID: 22719066 DOI: 10.1158/0008-5472.CAN-12-0938]
44 **Noy R**, Pollard JW. Tumor-associated macrophages: from mechanisms to therapy. *Immunity* 2014; **41**: 49-61 [PMID: 25035953 DOI: 10.1016/j.immuni.2014.06.010]
45 **Pinyol R**, Torrecilla S, Wang H, Montironi C, Piqué-Gili M, Torres-Martin M, Wei-Qiang L, Willoughby CE, Ramadori P, Andreu-Oller C, Taik P, Lee YA, Moeini A, Peix J, Faure-Dupuy S, Riedl T, Schuehle S, Oliveira CP, Alves VA, Boffetta P, Lachenmayer A, Roessler S, Minguez B, Schirmacher P, Dufour JF, Thung SN, Reeves HL, Carrilho FJ, Chang C, Uzilov AV, Heikenwalder M, Sanyal A, Friedman SL, Sia D, Llovet JM. Molecular characterisation of hepatocellular carcinoma in patients with non-alcoholic steatohepatitis. *J Hepatol* 2021; **75**: 865-878 [PMID: 33992698 DOI: 10.1016/j.jhep.2021.04.049]
46 **Wolf MJ**, Adili A, Piotrowitz K, Abdullah Z, Boege Y, Stemmer K, Ringelhan M, Simonavicius N, Egger M, Wohlleber D, Lorentzen A, Einer C, Schulz S, Clavel T, Protzer U, Thiele C, Zischka H, Moch H, Tschöp M, Tumanov AV, Haller D, Unger K, Karin M, Kopf M, Knolle P, Weber A, Heikenwalder M. Metabolic activation of intrahepatic CD8+ T cells and NKT cells causes nonalcoholic steatohepatitis and liver cancer *via* cross-talk with hepatocytes. *Cancer Cell* 2014; **26**: 549-564 [PMID: 25314080 DOI: 10.1016/j.ccell.2014.09.003]
47 **Grohmann M**, Wiede F, Dodd GT, Gurzov EN, Ooi GJ, Butt T, Rasmiena AA, Kaur S, Gulati T, Goh PK, Treloar AE, Archer S, Brown WA, Muller M, Watt MJ, Ohara O, McLean CA, Tiganis T. Obesity Drives STAT-1-Dependent NASH and STAT-3-Dependent HCC. *Cell* 2018; **175**: 1289-1306.e20 [PMID: 30454647 DOI: 10.1016/j.cell.2018.09.053]
48 **Dudek M**, Pfister D, Donakonda S, Filpe P, Schneider A, Laschinger M, Hartmann D, Hüser N, Meiser P, Bayerl F, Inverso D, Wigger J, Sebode M, Öllinger R, Rad R, Hegenbarth S, Anton M, Guillot A, Bowman A, Heide D, Müller F, Ramadori P, Leone V, Garcia-Caceres C, Gruber T, Seifert G, Kabat AM, Mallm JP, Reider S, Effenberger M, Roth S, Billeter AT, Müller-Stich B, Pearce EJ, Koch-Nolte F, Käser R, Tilg H, Thimme R, Boettler T, Tacke F, Dufour JF, Haller D, Murray PJ, Heeren R, Zehn D, Böttcher JP, Heikenwälder M, Knolle PA. Auto-aggressive CXCR6^{+} CD8 T cells cause liver immune pathology in NASH. *Nature* 2021; **592**: 444-449 [PMID: 33762736 DOI: 10.1038/s41586-021-03233-8]
49 **Ma C**, Kesarwala AH, Eggert T, Medina-Echeverz J, Kleiner DE, Jin P, Stroncek DF, Terabe M, Kapoor V, ElGindi M, Han M, Thornton AM, Zhang H, Egger M, Luo J, Felsher DW, McVicar DW, Weber A, Heikenwalder M, Greten TF. NAFLD causes selective CD4(+) T lymphocyte loss and promotes hepatocarcinogenesis. *Nature* 2016; **531**: 253-257 [PMID: 26934227 DOI: 10.1038/nature16969]
50 **Gomes AL**, Teijeiro A, Burén S, Tummala KS, Yilmaz M, Waisman A, Theurillat JP, Perna C, Djouder N. Metabolic Inflammation-Associated IL-17A Causes Non-alcoholic Steatohepatitis and Hepatocellular Carcinoma. *Cancer Cell* 2016; **30**: 161-175 [PMID: 27411590 DOI: 10.1016/j.ccell.2016.05.020]
51 **Faggioli F**, Palagano E, Di Tommaso L, Donadon M, Marrella V, Recordati C, Mantero S, Villa A, Vezzoni P, Cassani B. B lymphocytes limit senescence-driven fibrosis resolution and favor hepatocarcinogenesis in mouse liver injury. *Hepatology* 2018; **67**: 1970-1985 [PMID: 29105104 DOI: 10.1002/hep.29636]
52 **Zhang S**, Liu Z, Wu D, Chen L, Xie L. Single-Cell RNA-Seq Analysis Reveals Microenvironmental Infiltration of Plasma Cells and Hepatocytic Prognostic Markers in HCC With Cirrhosis. *Front Oncol* 2020; **10**: 596318 [PMID: 33224891 DOI: 10.3389/fonc.2020.596318]
53 **Shalapour S**, Lin XJ, Bastian IN, Brain J, Burt AD, Aksenov AA, Vrbanac AF, Li W, Perkins A, Matsutani T, Zhong Z, Dhar D, Navas-Molina JA, Xu J, Loomba R, Downes M, Yu RT, Evans RM, Dorrestein PC, Knight R, Benner C, Anstee QM, Karin M. Inflammation-induced IgA+ cells dismantle anti-liver cancer immunity. *Nature* 2017; **551**: 340-345 [PMID: 29144460 DOI: 10.1038/nature24302]
54 **Shao Y**, Lo CM, Ling CC, Liu XB, Ng KT, Chu AC, Ma YY, Li CX, Fan ST, Man K. Regulatory B cells accelerate hepatocellular carcinoma progression *via* CD40/CD154 signaling pathway. *Cancer Lett* 2014; **355**: 264-272 [PMID: 25301451 DOI: 10.1016/j.canlet.2014.09.026]
55 **Barrow F**, Khan S, Fredrickson G, Wang H, Dietsche K, Parthiban P, Robert S, Kaiser T, Winer S, Herman A, Adeyi O, Mouzaki M, Khoruts A, Hogquist KA, Staley C, Winer DA, Revelo XS. Microbiota-Driven Activation of Intrahepatic B Cells Aggravates NASH Through Innate and Adaptive Signaling. *Hepatology* 2021; **74**: 704-722 [PMID: 33609303 DOI: 10.1002/hep.31755]
56 **Cheng AL**, Kang YK, Chen Z, Tsao CJ, Qin S, Kim JS, Luo R, Feng J, Ye S, Yang TS, Xu J, Sun Y, Liang H, Liu J, Wang J, Tak WY, Pan H, Burock K, Zou J, Voliotis D, Guan Z. Efficacy and safety of sorafenib in patients in the Asia-Pacific region with advanced hepatocellular carcinoma: a phase III randomised, double-blind, placebo-controlled trial. *Lancet Oncol* 2009; **10**: 25-34 [PMID: 19095497 DOI: 10.1016/S1470-2045(08)70285-7]
57 **Llovet JM**, Ricci S, Mazzaferro V, Hilgard P, Gane E, Blanc JF, de Oliveira AC, Santoro A, Raoul JL, Forner A, Schwartz M, Porta C, Zeuzem S, Bolondi L, Greten TF, Galle PR, Seitz JF, Borbath I, Häussinger D, Giannaris T, Shan M, Moscovici M, Voliotis D, Bruix J; SHARP Investigators Study Group. Sorafenib in advanced hepatocellular carcinoma. *N Engl J Med* 2008; **359**: 378-390 [PMID: 18650514 DOI: 10.1056/NEJMoa0708857]
58 **Abou-Alfa GK**, Meyer T, Cheng AL, El-Khoueiry AB, Rimassa L, Ryoo BY, Cicin I, Merle P, Chen Y, Park JW, Blanc JF, Bolondi L, Klümpen HJ, Chan SL, Zagonel V, Pressiani T, Ryu MH, Venook AP, Hessel C, Borgman-Hagey AE,

Schwab G, Kelley RK. Cabozantinib in Patients with Advanced and Progressing Hepatocellular Carcinoma. *N Engl J Med* 2018; **379**: 54-63 [PMID: 29972759 DOI: 10.1056/NEJMoa1717002]

59 **Bruix J**, Qin S, Merle P, Granito A, Huang YH, Bodoky G, Pracht M, Yokosuka O, Rosmorduc O, Breder V, Gerolami R, Masi G, Ross PJ, Song T, Bronowicki JP, Ollivier-Hourmand I, Kudo M, Cheng AL, Llovet JM, Finn RS, LeBerre MA, Baumhauer A, Meinhardt G, Han G; RESORCE Investigators. Regorafenib for patients with hepatocellular carcinoma who progressed on sorafenib treatment (RESORCE): a randomised, double-blind, placebo-controlled, phase 3 trial. *Lancet* 2017; **389**: 56-66 [PMID: 27932229 DOI: 10.1016/S0140-6736(16)32453-9]

60 **Zhu AX**, Kang YK, Yen CJ, Finn RS, Galle PR, Llovet JM, Assenat E, Brandi G, Pracht M, Lim HY, Rau KM, Motomura K, Ohno I, Merle P, Daniele B, Shin DB, Gerken G, Borg C, Hiriart JB, Okusaka T, Morimoto M, Hsu Y, Abada PB, Kudo M; REACH-2 study investigators. Ramucirumab after sorafenib in patients with advanced hepatocellular carcinoma and increased α-fetoprotein concentrations (REACH-2): a randomised, double-blind, placebo-controlled, phase 3 trial. *Lancet Oncol* 2019; **20**: 282-296 [PMID: 30665869 DOI: 10.1016/S1470-2045(18)30937-9]

61 **Kudo M**, Finn RS, Qin S, Han KH, Ikeda K, Piscaglia F, Baron A, Park JW, Han G, Jassem J, Blanc JF, Vogel A, Komov D, Evans TRJ, Lopez C, Dutcus C, Guo M, Saito K, Kraljevic S, Tamai T, Ren M, Cheng AL. Lenvatinib *vs* sorafenib in first-line treatment of patients with unresectable hepatocellular carcinoma: a randomised phase 3 non-inferiority trial. *Lancet* 2018; **391**: 1163-1173 [PMID: 29433850 DOI: 10.1016/S0140-6736(18)30207-1]

62 **Foerster F**, Gairing SJ, Müller L, Galle PR. NAFLD-driven HCC: Safety and efficacy of current and emerging treatment options. *J Hepatol* 2022; **76**: 446-457 [PMID: 34555422 DOI: 10.1016/j.jhep.2021.09.007]

63 **Casadei Gardini A**, Faloppi L, De Matteis S, Foschi FG, Silvestris N, Tovoli F, Palmieri V, Marisi G, Brunetti O, Vespasiani-Gentilucci U, Perrone G, Valgiusti M, Granato AM, Ercolani G, Negrini G, Tamburini E, Aprile G, Passardi A, Santini D, Cascinu S, Frassineti GL, Scartozzi M. Metformin and insulin impact on clinical outcome in patients with advanced hepatocellular carcinoma receiving sorafenib: Validation study and biological rationale. *Eur J Cancer* 2017; **86**: 106-114 [PMID: 28985579 DOI: 10.1016/j.ejca.2017.09.003]

64 **Bruix J**, Cheng AL, Meinhardt G, Nakajima K, De Sanctis Y, Llovet J. Prognostic factors and predictors of sorafenib benefit in patients with hepatocellular carcinoma: Analysis of two phase III studies. *J Hepatol* 2017; **67**: 999-1008 [PMID: 28687477 DOI: 10.1016/j.jhep.2017.06.026]

65 **Bruix J**, Raoul JL, Sherman M, Mazzaferro V, Bolondi L, Craxi A, Galle PR, Santoro A, Beaugrand M, Sangiovanni A, Porta C, Gerken G, Marrero JA, Nadel A, Shan M, Moscovici M, Voliotis D, Llovet JM. Efficacy and safety of sorafenib in patients with advanced hepatocellular carcinoma: subanalyses of a phase III trial. *J Hepatol* 2012; **57**: 821-829 [PMID: 22727733 DOI: 10.1016/j.jhep.2012.06.014]

66 **Leathers JS**, Balderramo D, Prieto J, Diehl F, Gonzalez-Ballerga E, Ferreiro MR, Carrera E, Barreyro F, Diaz-Ferrer J, Singh D, Mattos AZ, Carrilho F, Debes JD. Sorafenib for Treatment of Hepatocellular Carcinoma: A Survival Analysis From the South American Liver Research Network. *J Clin Gastroenterol* 2019; **53**: 464-469 [PMID: 29952857 DOI: 10.1097/MCG.0000000000001085]

67 **Howell J**, Samani A, Mannan B, Hajiev S, Aval LM, Abdelmalak R, Tam VC, Bettinger D, Thimme R, Taddei TH, Kaplan DE, Seidensticker M, Sharma R. Impact of NAFLD on clinical outcomes in hepatocellular carcinoma treated with sorafenib: An international cohort study. *J Clin Oncol* 2021; **39** Suppl 3: 289 [DOI: 10.1200/JCO.2021.39.3_suppl.289]

68 **Rimini M**, Kudo M, Tada T, Shigeo S, Kang W, Suda G, Jefremow A, Burgio V, Iavarone M, Tortora R, Marra F, Lonardi S, Tamburini E, Piscaglia F, Masi G, Cabibbo G, Foschi FG, Silletta M, Kumada T, Iwamoto H, Aoki T, Goh MJ, Sakamoto N, Siebler J, Hiraoka A, Niizeki T, Ueshima K, Sho T, Atsukawa M, Hirooka M, Tsuji K, Ishikawa T, Takaguchi K, Kariyama K, Itobayashi E, Tajiri K, Shimada N, Shibata H, Ochi H, Yasuda S, Toyoda H, Fukunishi S, Ohama H, Kawata K, Tani J, Nakamura S, Nouso K, Tsutsui A, Nagano T, Takaaki T, Itokawa N, Okubo T, Arai T, Imai M, Joko K, Koizumi Y, Hiasa Y, Cucchetti A, Ratti F, Aldrighetti L, Cascinu S, Casadei-Gardini A. Nonalcoholic steatohepatitis in hepatocarcinoma: new insights about its prognostic role in patients treated with lenvatinib. *ESMO Open* 2021; **6**: 100330 [PMID: 34847382 DOI: 10.1016/j.esmoop.2021.100330]

69 **Hiraoka A**, Kumada T, Tada T, Tani J, Kariyama K, Fukunishi S, Atsukawa M, Hirooka M, Tsuji K, Ishikawa T, Takaguchi K, Itobayashi E, Tajiri K, Shimada N, Shibata H, Ochi H, Kawata K, Yasuda S, Toyoda H, Aoki T, Tanaka T, Ohama H, Nouso K, Tsutsui A, Nagano T, Itokawa N, Arai T, Okubo T, Imai M, Koizumi Y, Nakamura S, Joko K, Hiasa Y, Kudo M; Real-life Practice Experts for HCC (RELPEC) Study Group and HCC 48 Group (hepatocellular carcinoma experts from 48 clinics in Japan). Efficacy of lenvatinib for unresectable hepatocellular carcinoma based on background liver disease etiology: multi-center retrospective study. *Sci Rep* 2021; **11**: 16663 [PMID: 34404856 DOI: 10.1038/s41598-021-96089-x]

70 **Welland S**, Leyh C, Finkelmeier F, Jefremow A, Shmanko K, Gonzalez-Carmona MA, Kandulski A, Jeliazkova P, Best J, Fründt TW, Djanani A, Pangerl M, Maieron A, Greil R, Fricke C, Sookthai D, Günther R, Schmiderer A, Wege H, Venerito M, Ehmer U, Müller M, Strassburg CP, Weinmann A, Siebler J, Waidmann O, Lange CM, Saborowski A, Vogel A. Real-World Data for Lenvatinib in Hepatocellular Carcinoma (ELEVATOR): A retrospective multicenter study. *Liver Cancer* 2022 [DOI: 10.1159/000521746]

71 **Vogel A**, Martinelli E; ESMO Guidelines Committee. Electronic address: clinicalguidelines@esmo.org; ESMO Guidelines Committee. Updated treatment recommendations for hepatocellular carcinoma (HCC) from the ESMO Clinical Practice Guidelines. *Ann Oncol* 2021; **32**: 801-805 [PMID: 33716105 DOI: 10.1016/j.annonc.2021.02.014]

72 **Díaz-González Á**, Sanduzzi-Zamparelli M, da Fonseca LG, Di Costanzo GG, Alves R, Iavarone M, Leal C, Sacco R, Matilla AM, Hernández-Guerra M, Aballay Soteras G, Wörns MA, Pinter M, Varela M, Ladekarl M, Chagas AL, Mínguez B, Arenas JI, Granito A, Sánchez-Torrijos Y, Rojas Á, Rodríguez de Lope C, Alvares-da-Silva MR, Pascual S, Rimassa L, Lledó JL, Huertas C, Sangro B, Giannini EG, Delgado M, Vergara M, Perelló C, Lue A, Sala M, Gallego A, Coll S, Hernáez T, Piñero F, Pereira G, França A, Marín J, Anders M, Mello V, Lozano M, Nault JC, Menéndez J, García Juárez I, Bruix J, Reig M. International and multicenter real-world study of sorafenib-treated patients with hepatocellular carcinoma under dialysis. *Liver Int* 2020; **40**: 1467-1476 [PMID: 32170821 DOI: 10.1111/liv.14436]

73 **Yau T**, Park JW, Finn RS, Cheng AL, Mathurin P, Edeline J, Kudo M, Harding JJ, Merle P, Rosmorduc O, Wyrwicz L, Schott E, Choo SP, Kelley RK, Sieghart W, Assenat E, Zaucha R, Furuse J, Abou-Alfa GK, El-Khoueiry AB, Melero I,

Begic D, Chen G, Neely J, Wisniewski T, Tschaika M, Sangro B. Nivolumab *vs* sorafenib in advanced hepatocellular carcinoma (CheckMate 459): a randomised, multicentre, open-label, phase 3 trial. *Lancet Oncol* 2022; **23**: 77-90 [PMID: 34914889 DOI: 10.1016/S1470-2045(21)00604-5]

74 **Finn RS**, Ryoo BY, Merle P, Kudo M, Bouattour M, Lim HY, Breder V, Edeline J, Chao Y, Ogasawara S, Yau T, Garrido M, Chan SL, Knox J, Daniele B, Ebbinghaus SW, Chen E, Siegel AB, Zhu AX, Cheng AL; KEYNOTE-240 investigators. Pembrolizumab As Second-Line Therapy in Patients With Advanced Hepatocellular Carcinoma in KEYNOTE-240: A Randomized, Double-Blind, Phase III Trial. *J Clin Oncol* 2020; **38**: 193-202 [PMID: 31790344 DOI: 10.1200/JCO.19.01307]

75 **Siegel AB**, Cohen EI, Ocean A, Lehrer D, Goldenberg A, Knox JJ, Chen H, Clark-Garvey S, Weinberg A, Mandeli J, Christos P, Mazumdar M, Popa E, Brown RS Jr, Rafii S, Schwartz JD. Phase II trial evaluating the clinical and biologic effects of bevacizumab in unresectable hepatocellular carcinoma. *J Clin Oncol* 2008; **26**: 2992-2998 [PMID: 18565886 DOI: 10.1200/JCO.2007.15.9947]

76 **Hughes PE**, Caenepeel S, Wu LC. Targeted Therapy and Checkpoint Immunotherapy Combinations for the Treatment of Cancer. *Trends Immunol* 2016; **37**: 462-476 [PMID: 27216414 DOI: 10.1016/j.it.2016.04.010]

77 **Finn RS**, Qin S, Ikeda M, Galle PR, Ducreux M, Kim TY, Lim HY, Kudo M, Breder VV, Merle P, Kaseb AO, Li D, Verret W, Shao H, Liu J, Li L, Zhu AX, Cheng AL. IMbrave150: Updated overall survival (OS) data from a global, randomized, open-label phase III study of atezolizumab (atezo) + bevacizumab (bev) *vs* sorafenib (sor) in patients (pts) with unresectable hepatocellular carcinoma (HCC). *J Clin Oncol* 2021; **39** Suppl 3: 267 [DOI: 10.1200/JCO.2021.39.3_suppl.267]

78 **Galle PR**, Finn RS, Qin S, Ikeda M, Zhu AX, Kim TY, Kudo M, Breder V, Merle P, Kaseb A, Li D, Mulla S, Verret W, Xu DZ, Hernandez S, Ding B, Liu J, Huang C, Lim HY, Cheng AL, Ducreux M. Patient-reported outcomes with atezolizumab plus bevacizumab *vs* sorafenib in patients with unresectable hepatocellular carcinoma (IMbrave150): an open-label, randomised, phase 3 trial. *Lancet Oncol* 2021; **22**: 991-1001 [PMID: 34051880 DOI: 10.1016/S1470-2045(21)00151-0]

79 **Kelley R**, Yau T, Cheng A, Kaseb A, Qin A, Zhu AX, Chan S, Sukeepaisarnjaroen W, Breder V, Verset G, Gane E, Borbath I, Gomez Rangel JD, Merle P, Benzaghou FM, Banerjee K, Hazra S, Fawcett J, Rimassa L. Cabozantinib (C) plus atezolizumab (A) *vs* sorafenib (S) as first-line systemic treatment for advanced hepatocellular carcinoma (aHCC): Results from the randomized phase III COSMIC-312 trial. *Ann Oncol* 2022; **33**: 114-116 [DOI: 10.1016/j.annonc.2021.10.008]

80 **El-Khoueiry AB**, Sangro B, Yau T, Crocenzi TS, Kudo M, Hsu C, Kim TY, Choo SP, Trojan J, Welling TH Rd, Meyer T, Kang YK, Yeo W, Chopra A, Anderson J, Dela Cruz C, Lang L, Neely J, Tang H, Dastani HB, Melero I. Nivolumab in patients with advanced hepatocellular carcinoma (CheckMate 040): an open-label, non-comparative, phase 1/2 dose escalation and expansion trial. *Lancet* 2017; **389**: 2492-2502 [PMID: 28434648 DOI: 10.1016/S0140-6736(17)31046-2]

81 **Yau T**, Kang YK, Kim TY, El-Khoueiry AB, Santoro A, Sangro B, Melero I, Kudo M, Hou MM, Matilla A, Tovoli F, Knox JJ, Ruth He A, El-Rayes BF, Acosta-Rivera M, Lim HY, Neely J, Shen Y, Wisniewski T, Anderson J, Hsu C. Efficacy and Safety of Nivolumab Plus Ipilimumab in Patients With Advanced Hepatocellular Carcinoma Previously Treated With Sorafenib: The CheckMate 040 Randomized Clinical Trial. *JAMA Oncol* 2020; **6**: e204564 [PMID: 33001135 DOI: 10.1001/jamaoncol.2020.4564]

82 **Abou-Alfa G**, Chan S, Kudo M, Lau G, Kelley RK, Furuse J, Sukeepaisarnjaroen W, Kang YK, Dao TV, De Toni EN, Rimassa L, Breder VV, Vasilyev A, Heurgue A, Tam V, Mody K, Thungappa SC, He P, Negro A, Sangro B. Phase 3 randomized, open-label, multicenter study of tremelimumab (T) and durvalumab (D) as first-line therapy in patients (pts) with unresectable hepatocellular carcinoma (uHCC): HIMALAYA. *J Clin Oncol* 2022; **40** Suppl 4: 379

83 **Kelley RK**, Greten TF. Hepatocellular Carcinoma - Origins and Outcomes. *N Engl J Med* 2021; **385**: 280-282 [PMID: 34260842 DOI: 10.1056/NEJMcibr2106594]

84 **Yau T**, Park JW, Finn RS, Cheng AL, Mathurin P, Edeline J, Kudo M, Han KH, Harding JJ, Merle P, Rosmorduc O, Wyrwicz L, Schott E, Choo SP, Kelley RK, Begic D, Chen G, Neely J, Anderson J, Sangro B. CheckMate 459: A randomized, multi-center phase III study of nivolumab (NIVO) *vs* sorafenib (SOR) as first-line (1L) treatment in patients (pts) with advanced hepatocellular carcinoma (aHCC). *Ann Oncol* 2019; **30** Suppl 5 [DOI: 10.1093/annonc/mdz394.029]

85 **de Castro T**, Jochheim LS, Bathon M, Welland S, Scheiner B, Shmanko K, Roessler D, Ben Khaled N, Jeschke M, Ludwig JM, Marquardt JU, Weinmann A, Pinter M, Lange CM, Vogel A, Saborowski A. Atezolizumab and bevacizumab in patients with advanced hepatocellular carcinoma with impaired liver function and prior systemic therapy: a real-world experience. *Ther Adv Med Oncol* 2022; **14**: 17588359221080298 [PMID: 35251317 DOI: 10.1177/17588359221080298]

86 **Sangro B**, Melero I, Wadhawan S, Finn RS, Abou-Alfa GK, Cheng AL, Yau T, Furuse J, Park JW, Boyd Z, Tang HT, Shen Y, Tschaika M, Neely J, El-Khoueiry A. Association of inflammatory biomarkers with clinical outcomes in nivolumab-treated patients with advanced hepatocellular carcinoma. *J Hepatol* 2020; **73**: 1460-1469 [PMID: 32710922 DOI: 10.1016/j.jhep.2020.07.026]

87 **Sia D**, Jiao Y, Martinez-Quetglas I, Kuchuk O, Villacorta-Martin C, Castro de Moura M, Putra J, Camprecios G, Bassaganyas L, Akers N, Losic B, Waxman S, Thung SN, Mazzaferro V, Esteller M, Friedman SL, Schwartz M, Villanueva A, Llovet JM. Identification of an Immune-specific Class of Hepatocellular Carcinoma, Based on Molecular Features. *Gastroenterology* 2017; **153**: 812-826 [PMID: 28624577 DOI: 10.1053/j.gastro.2017.06.007]

88 **Scheiner B**, Pomej K, Kirstein MM, Hucke F, Finkelmeier F, Waidmann O, Himmelsbach V, Schulze K, von Felden J, Fründt TW, Stadler M, Heinzl H, Shmanko K, Spahn S, Radu P, Siebenhüner AR, Mertens JC, Rahbari NN, Kütting F, Waldschmidt DT, Ebert MP, Teufel A, De Dosso S, Pinato DJ, Pressiani T, Meischl T, Balcar L, Müller C, Mandorfer M, Reiberger T, Trauner M, Personeni N, Rimassa L, Bitzer M, Trojan J, Weinmann A, Wege H, Dufour JF, Peck-Radosavljevic M, Vogel A, Pinter M. Prognosis of patients with hepatocellular carcinoma treated with immunotherapy - development and validation of the CRAFITY score. *J Hepatol* 2022; **76**: 353-363 [PMID: 34648895 DOI: 10.1016/j.jhep.2021.09.035]

World Journal of Gastroenterology

Submit a Manuscript: https://www.f6publishing.com

World J Gastroenterol 2022 July 28; 28(28): 3608-3619

DOI: 10.3748/wjg.v28.i28.3608

ISSN 1007-9327 (print) ISSN 2219-2840 (online)

MINIREVIEWS

Potassium-competitive acid blockers and gastroesophageal reflux disease

Wattana Leowattana, Tawithep Leowattana

Specialty type: Gastroenterology and hepatology

Provenance and peer review: Invited article; Externally peer reviewed.

Peer-review model: Single blind

Peer-review report's scientific quality classification
Grade A (Excellent): 0
Grade B (Very good): 0
Grade C (Good): C, C
Grade D (Fair): 0
Grade E (Poor): 0

P-Reviewer: Lan C, China; Sintusek P, Thailand

Received: February 16, 2022
Peer-review started: February 16, 2022
First decision: April 12, 2022
Revised: April 24, 2022
Accepted: June 24, 2022
Article in press: June 24, 2022
Published online: July 28, 2022

Wattana Leowattana, Clinical Tropical Medicine, Faculty of Tropical Medicine, Mahidol University, Bangkok 10400, Thailand

Tawithep Leowattana, Department of Medicine, Faculty of Medicine, Srinakharinwirot University, Bangkok 10110, Thailand

Corresponding author: Wattana Leowattana, MD, MSc, PhD, Professor, Clinical Tropical Medicine, Faculty of Tropical Medicine, Mahidol University, 420/6 Rajavithi Road, Rachatawee, Bangkok 10400, Thailand. wattana.leo@mahidol.ac.th

Abstract

Proton pump inhibitors (PPIs), the most commonly used antisecretory medications in the management of reflux illness, virtually eliminate elective surgery for ulcer disease, and relegate anti-reflux surgery to patients with gastroesophageal reflux disease (GERD) who are inadequately managed by medical therapy. However, PPI medications still leave some therapeutic demands of GERD unmet. Furthermore, up to 40%-55% of daily PPI users have chronic symptoms, due to PPI refractoriness. Potassium-competitive acid blockers (P-CABs) transcend many of the problems and limits of PPIs, delivering quick, powerful, and extended acid suppression and allowing for treatment of numerous unmet needs. Recently, it has become clear that compromised mucosal integrity plays a role in the etiology of GERD. As a result, esophageal mucosal protection has emerged as a novel and potential treatment approach. An increasing body of research demonstrates that when P-CABs are used as primary drugs or add-on drugs (to regular treatment), they provide a considerable extra benefit, particularly in alleviating symptoms that do not respond to PPI therapy.

Key Words: Potassium-competitive acid blocker; Gastroesophageal reflux disease; Proton pump inhibitors; Treatment outcome; Proton pump inhibitor-refractory patients; Esophageal mucosal resistance

©The Author(s) 2022. Published by Baishideng Publishing Group Inc. All rights reserved.

Core Tip: The potassium-competitive acid blocker (P-CAB) has been discovered as a possible acid suppression therapeutic option. At the enzyme level, P-CABs compete with K^+ to suppress acid formation; the binding location of these compounds is separate from the probable pocket that K^+ occupies. When the P-CAB binds to the enzyme, it stops K^+ from attaching and activating it. According to clinical trials, P-CABs are extremely selective for gastric H^+, K^+-ATPase, restricting stomach acid production while acting quickly. Such medicines, which can have a rapid onset of action and a longer duration, may offer considerable advantages to individuals suffering from gastroesophageal reflux disease and other acid-related disorders.

Citation: Leowattana W, Leowattana T. Potassium-competitive acid blockers and gastroesophageal reflux disease. *World J Gastroenterol* 2022; 28(28): 3608-3619
URL: https://www.wjgnet.com/1007-9327/full/v28/i28/3608.htm
DOI: https://dx.doi.org/10.3748/wjg.v28.i28.3608

INTRODUCTION

Gastroesophageal reflux, the reflux of stomach contents into the esophagus, usually occurs after large and fatty meals. Nonetheless, under normal settings, efficient esophageal cleaning mechanisms return the bulk of the refluxed material to the stomach, and symptoms do not occur. However, when stomach reflux is severe or physically aggressive, it causes symptoms and difficulties, as well as a decrease in quality of life, thus creating gastroesophageal reflux disease (GERD)[1,2]. Since the 1990s, the prevalence of GERD has grown consistently, particularly in East Asia and North America (2.5%-7.8%, and 10%-20%, respectively)[3-5]. Heartburn and regurgitation are common esophageal symptoms, accompanied by consequent chest discomfort and dysphagia. Chronic cough, hoarseness of voice, and asthma are other extra-esophageal symptoms that have been linked to GERD in population-based research. The three GERD phenotypes are erosive esophagitis (EE), non-erosive reflux disease (NERD), and Barrett's esophagitis. Their responses to therapy vary greatly. Of note, the majority (70%) of GERD patients have an endoscopically normal mucosa and are regarded as having NERD.

Pharmacologic, endoscopic, and surgical options for GERD treatment are now available. The most often recommended drugs for GERD treatment in clinical practice are proton pump inhibitors (PPIs) and histamine-2 receptor antagonists. Other, less potent agents typically used to treat mild or intermittent symptoms or as adjunct therapies include antacids, sucralfate, baclofen, alginate, and prokinetics[6,7]. The goals of GERD management include symptom relief, esophageal inflammation healing, esophageal inflammation maintenance and prevention, and quality of life enhancement. PPIs have long been thought to be the basis of GERD treatment. Because of their significant and consistent antisecretory action, PPIs have proven particularly useful in treating EE, managing symptoms, and preventing GERD-related complications such as esophageal ulcers, esophageal bleeding, and peptic stricture. Overall, PPIs have been regarded as a relatively safe class of drugs, with many patients taking them for an extended time. Despite the success of PPIs in addressing many aspects of GERD, there are still many unmet needs[8-10]. Advanced EE, NERD, overnight heartburn, maintenance therapy, and refractory GERD are among them.

Furthermore, PPIs are ineffective for postprandial heartburn and are currently not recommended for atypical or extra-esophageal GERD presentations as well as GERD complications[11,12]. Importantly, prolonged PPI medications have been linked to side effects, generating worries among physicians and patients alike about their safety profile. This review looks at the development and quality of present and potential acid suppression medications, focusing on the potassium-competitive acid blocker (P-CAB) class and exploring their clinical studies.

ROLE OF POTASSIUM ION IN ACID SECRETION

Gastric acid is essential for food and water purification and digestion. Gastric juice has an extremely low pH (pH = 1) because parietal cells in the oxyntic mucosa of the stomach secrete H^+ and Cl^- ions to make hydrochloric acid. These cells secrete 1-2 L of hydrochloric acid every day. The action of gastric H^+/K^+-ATPase in the apical membrane of parietal cells promotes a very high concentration of H^+ in the lumen compared to plasma. The potassium ion plays an essential role in activating gastric H^+/K^+-ATPase and is required for the enzyme to function. At rest, H^+/K^+-ATPase is confined to tubulovesicular regions of a parietal cell with low K^+ concentrations and membranes that are impermeable to K^+. As a result, the enzyme is incapable of activating and transporting H^+ ions. When the parietal cell is stimulated, the tubulovesicular components merge with the cell's apical membrane. After being exposed to K^+-containing luminal fluid, the H^+/K^+-ATPase enzyme can begin to exchange H^+ for K^+[13-15]. Due to its

important involvement in the production of gastric juice, K^+ is a possible therapeutic target for acid blockers. One technique is to block the K^+ channels that allow ions to flow through the apical membrane of parietal cells, while another is to compete with K^+ at the level of the parietal cells' H^+/K^+-ATPase.

P-CABs

The surface of the stomach H^+/K^+-ATPase (the proton pump) is exposed to the extremely acidic parietal cell canaliculus, which has a high affinity for K^+ during acid secretion. Given the significance of the cation for enzyme activity, drugs that compete for K^+ binding have the potential to inhibit acid secretion. The mechanism of action of P-CAB is based on this premise. P-CABs were initially developed in the 1980s and have been studied by many pharmaceutical companies worldwide due to their ability to block the proton pump quickly, efficiently, and reversibly. Schering-Plough was one of those companies that developed a prototype P-CAB, SCH28080. Although the mechanism of action was not fully known at that time, this drug was discovered to lower stomach acid output in humans[16,17]. SCH28080 was later demonstrated to inhibit gastric H^+/K^+-ATPase by competing with K^+[18,19]. However, clinical development of SCH28080 was halted due to hepatotoxicity produced by repeated treatment. This condition sparked research into several kinds of SCH28080 derivatives, such as imidazopyridine derivatives (BY841), imidazo-naphthyridine derivatives (soraprazan), imidazo-thienopyridines (SPI-447), quinolone derivatives (SK&F96067)[20-23], pyrrolo-pyridazine derivatives (CS-526), pyrimidine derivatives (revaprazan), and pyrrole derivatives [vonoprazanm (VPZ)][24-26].

These novel antisecretory medicines vary from PPIs in that they compete with K^+ and cause a dose-dependent selective and reversible inhibition of the proton pump. Because they aren't prodrugs that need to be activated in parietal cells like PPIs, they start working right away, and control of acid secretion begins within the first day of treatment after starting the first dose. In addition, their dissociation from the proton pump is sluggish, and they can stay in the stomach mucosa for up to 24 h. As a result, unlike PPIs, which are less effective at night, their acid inhibitory action persists throughout the day and night[27,28]. Table 1 compares the key differences in the mechanisms of action of P-CABs and PPIs.

ACTION MECHANISM OF P-CABs

P-CABs are classified into many chemical classes (Figure 1). They are a varied class of medications while having a similar mechanism of action. P-CABs are lipophilic, weak bases with limited pH stability and high pKa values. They may concentrate in acidic environments because of the combination of these properties. In the parietal cell canaliculi (pH = 1), a P-CAB with pKa of 6.0 would be 100000-fold larger than in the plasma (pH = 7.4). *In vitro* and *in vivo* investigations using AZD0865 and revaprazan showed a concentrated P-CAB in the gastric mucosa[29-31]. By binding ionically to the enzyme, P-CAB inhibits gastric H^+/K^+-ATPase and prevents further activation by K^+. P-CABs are expected to bind at or near the K^+ binding site, preventing the K^+ from accessing the site (Figure 2). Although these novel drugs exhibit quick and potent antisecretory action, not all of their attractive pharmacodynamic features have translated into therapeutic advantages due to their hepatotoxicity and insufficient efficacy. In addition, linaprazan (AZD0865) failed to outperform standard-dose PPIs in the treatment of peptic ulcers and reflux esophagitis (RE)[32,33]. Soraprazan (BY359) and CS526 (R105366) have fulfilled their proof of effectiveness and safety goals in phase II tests, but data on these medicines have not been published[34].

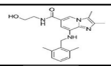
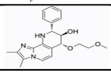
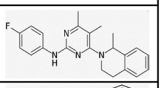
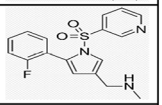
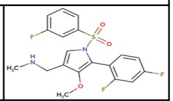
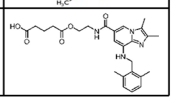
PHARMACOKINETICS AND PHARMACODYNAMICS OF P-CABs

P-CABs reach peak plasma concentrations quickly after oral administration, in part because they are acid-stable and may be administered as immediate-release formulations. In healthy men, a single dose of revaprazan (100 to 200 mg) resulted in peak plasma concentrations at 1.7 to 1.8 h, which declined to a mean elimination time (T1/2) of 2.2 h to 2.4 h with repeated administration. The pharmacokinetics and concentration-time profiles of revaprazan were comparable following repeated administration (on day 7) to those reported after the initial dosage on day 1[35]. In 2004, Yu *et al*[36] conducted a single-blind, dose-rising, parallel-group, randomized, placebo-controlled trial in 46 healthy subjects. In the single-dose research, plasma concentrations of revaprazan attained peak values 1.3 h to 2.5 h after administration and thereafter decreased mono-exponentially with a terminal T1/2 of 2.2 h to 2.4 h in dosage groups up to 200 mg. Revaprazan has linear pharmacokinetic properties, with negligible accumulation after numerous doses. The onset of pharmacological effects was quick, with the greatest benefits shown on the first day of treatment with repeated doses. They concluded that revaprazan was safe, well-tolerated, and efficiently suppressed acid secretion by increasing intragastric pH in a dose-dependent manner.

Table 1 Main differences in the mechanisms of action between proton pump inhibitors and potassium-competitive acid blockers[12]

Proton pump inhibitors	Potassium-competitive acid blockers
Prodrug requires transformation to the active form, sulphenamide	Direct action on the H^+/K^+ ATPase after protonation
Sulphenamide binds covalently to H^+/K^+-ATPase	P-CABs bind competitively to the K^+ binding site of H^+/K^+-ATPase
Irreversible binding to the proton pump	Reversible binding to the proton pump
The full effect after repeated doses	The full effect after the first dose
PK affected by genetic polymorphism	PK not affected by genetic polymorphism
PD effect more significant during the daytime	PD effect lasting for both the daytime and nocturnal hours
Meal-dependent antisecretory activity	Meal-independent antisecretory activity
Concentrate in parietal cell acid space (1000-fold higher than in plasma)	Super concentrates in parietal cell acid space (100000-fold higher than in plasma)
Duration of effect related to the half-life of the sulphenamide-enzyme complex	Duration of effect related to the half-life of the drug in plasma

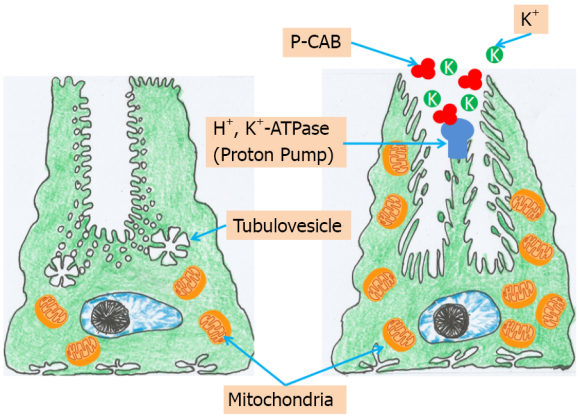
P-CAB: Potassium-competitive acid blocker; PD: Pharmacodynamic; PK: Pharmacokinetic.

P-CABs	Chemical class	Development phase	Company	Chemical structure
P-CABs whose development has been stopped				
Linaprazan (AZD0865)	Imidazopyridine	Stopped after phase III	AstraZeneca	
CS526 (R105266)	Pyrrolopyridazine	Stopped after phase I	Sankyo and Ube/ Novartis	
Soraprazan (BY359)	Imidazonaphthyridine	Stopped after phase II	Altana	
Available P-CABs in the market				
Revaprazan (YH1885)	Pyrimidine	Marketed in South Korea and India	Yuhan	
Vonoprazan (TAK-438)	Pyrrole	Marketed in Japan; Phase III in Europe /United States	Takeda and Phathom	
Tegoprazan (RQ-00000004)	Benzimidazole	Marketed in South Korea	Raqualia	
P-CABs under active study				
Fexuprazan (DWP14012)	Pyrrole	Phase III in South Korea	Daewoong	
X842 (Linaprazan pro-drug)	Imidazopyridine	Phase II in Europe	Cinclus Pharma	

DOI: 10.3748/wjg.v28.i28.3608 **Copyright** ©The Author(s) 2022.

Figure 1 Differences in chemical classes and chemical structures of potassium-competitive acid blockers[12]. P-CAB: Potassium-competitive acid blocker.

In 2015, Sakurai *et al*[37] conducted 2 phase I, single rising-dose, randomized, double-blind, placebo-controlled trials in 84 volunteers from Japan using 1-120 mg VPZ and 63 healthy males from the United Kingdom using 1-40 mg VPZ to evaluate the pharmacokinetics, pharmacodynamics, safety, and tolerability. They discovered that VPZ plasma concentration-time profiles exhibited fast absorption at all doses, with a median T_{max} of up to 2 h. $T_{1/2}$ was predicted to be up to 9 h. The acid suppression effect was dose-dependent, with a 24-h intragastric pH 4 holding time for 40 mg VPZ being 92% in Japanese males and 87% in British males. They determined that single oral doses of 20-120 mg VPZ suppressed gastric acid production in healthy male participants in a quick, deep, and 24-h manner. Furthermore, VPZ was well tolerated at all dosages tested, suggesting that it might be used as an alternate therapy for



DOI: 10.3748/wjg.v28.i28.3608 **Copyright** ©The Author(s) 2022.

Figure 2 Potassium-competitive acid blockers inhibit gastric H⁺/K⁺-ATPase by binding ionically to the enzyme and prevent further activation by the K⁺[7]. P-CAB: Potassium-competitive acid blocker.

acid-related diseases.

Recently, Han *et al*[38] performed a phase I, randomized, placebo-controlled study in 56 healthy volunteers without *Helicobacter pylori* infection to evaluate the safety, tolerability, pharmacokinetics, and pharmacodynamics of tegoprazan (TPZ). They found that TPZ was well tolerated. The majority of the adverse events were mild and resolved without any long-term consequences. On day 7, despite multiple dosages of TPZ, there was no accumulation in the plasma. The pharmacodynamics study found that TPZ suppressed gastric acid rapidly in a dose-dependent manner. They concluded that TPZ was well tolerated and demonstrated rapid and potent gastric acid suppression.

Sunwoo *et al*[39] conducted a randomized, double-blind, double-dummy, placebo-controlled study to evaluate a single ascending dose and multiple ascending doses of fexuprazan (FPZ) in 120 healthy male subjects without *Helicobacter pylori* (*H. pylori*) infection. They discovered that FPZ was well tolerated and suppressed gastric acid output for 24 h after delivery. In the multiple ascending doses trial, FPZ plasma concentrations grew in a dose-proportional way, but it did not appreciably accumulate in the plasma in the single ascending dosage study. They concluded that FPZ showed an immediate, long-lasting gastric acid suppression effect and was safe.

In 2020, Hwang *et al*[40] conducted a single- and multiple-dose, randomized, double-blind, placebo-controlled trial to elucidate the pharmacodynamics, pharmacokinetics, and safety of FPZ among healthy volunteers of Korean, Caucasian, and Japanese descent. FPZ (40, 60, or 80 mg for Koreans; 40 or 80 mg for Caucasians; 20, 40, or 80 mg for Japanese) or a placebo were given to ten participants in each group at random. Gastric acid suppression was shown to be consistent across ethnic groups. After successive doses of 40 mg, the mean percentages of time when the intragastric pH was over 4 in Korean, Caucasian, and Japanese participants were 64.3 percent, 62.8 percent, and 70.3 percent, respectively. Furthermore, the 80 mg dose that could effectively suppress gastric secretion was 94.8%, 90.6%, and 90.6% for the Korean, Caucasian, and Japanese subjects, respectively. They determined that FPZ suppressed stomach acid in the same way in Korean, Caucasian, and Japanese patients, and that the pharmacokinetic and pharmacodynamic correlations, as well as the safety, were the same in all three ethnic groups. The FPZ could be utilized regardless of ethnicity.

X842 is a linaprazan prodrug that is currently under development. X842 has a $T_{1/2}$ of 10 h and enables improved intragastric pH regulation over 24 h. Linaprazan was established in a phase I study that used a single dose or multiple escalating dosage design to assess the drug's safety and tolerability in healthy volunteers as the primary endpoint[41]. X842 was shown to be safe and well tolerated by the participants in the study. During the trial, no severe or significant adverse events were recorded. When both pharmacodynamics and pharmacokinetics were evaluated, precise dose linearity was identified. The mean median intragastric pH at each X842 dosage was never less than 4.

P-CABs EFFICACY IN GERD

VPZ efficacy in GERD

In 2015, Ashida *et al*[42] undertook a parallel-group, dose-ranging, multicenter, randomized, double-blind trial in 732 patients with EE to assess the effectiveness and safety of VPZ *vs* lansoprazole (LPZ). The eligible EE individuals were randomized 1:1:1:1:1 to undergo an 8-wk therapy with LPZ 30 mg, VPZ 5 mg, VPZ 10 mg, VPZ 20 mg, and VPZ 40 mg. They discovered that with VPZ 5, 10, 20, and 40 mg,

and LPZ 30 mg, the proportion of healed EE individuals at week 4 was 92.3%, 92.5%, 94.4%, 97.0% and 93.2%, respectively. When corrected for baseline Los Angeles (LA) grades A/B and C/D, all VPZ regimens were non-inferior to LPZ 30 mg therapy. With VPZ 5, 10, 20, 40 mg, and LPZ 30 mg, the proportions of healed EE individuals were 87.3%, 86.4%, 100%, 96.0%, and 87.0%, respectively, for LA grades C/D. The incidence of adverse events was the same in all groups. They indicated that VPZ was efficacious and comparable to LPZ in the treatment of EE. For severe EE (LA grades C/D), they advised VPZ doses of 20 mg or more.

Furthermore, Ashida *et al*[43] performed another parallel-group comparison, multicenter, randomized, double-blind trial to evaluate the non-inferiority, long-term efficacy, and safety as maintenance therapy of VPZ 20 mg compared with LPZ 30 mg in 409 endoscopically confirmed EE patients (LA grades A-D). They discovered that the proportion of patients with healed EE up to week 8 for VPZ (203/205) and 95.5% for LPZ (190/199) was 99.0% for VPZ (203/205) and 95.5% for LPZ (190/199), demonstrating the non-inferiority of VPZ 20 mg therapy. There were a few EE recurrences (< 10%) for long-term maintenance evaluation in patients treated with VPZ 10 mg or 20 mg. They stated that the comparative trial demonstrated the non-inferiority of VPZ 20 mg to LPZ 30 mg in EE, and that VPZ was well tolerated and efficacious among long-term maintenance EE patients (Table 2).

In 2017, Iwakiri *et al*[44] conducted a randomized, double-blind, multicenter trial of VPZ 20 mg or 40 mg in 19 patients with PPI-resistant (LPZ 30 mg) EE to measure stomach and esophageal pH over 24 h. Patients with endoscopically proven PPI-resistant EE received VPZ 20 mg (9 cases) or VPZ 40 mg (10 cases) for 8 wk after a 7- to 14-d run-in period with LPZ 30 mg therapy. The percentage of stomach pH 4 [pH 4 holding time ratio (HTR)] increased significantly in both groups from baseline: In the 20 mg group, it increased from 73.21% to 96.46%, and in the 40 mg group, it increased from 69.97% to 100.00%. There were no significant increases in esophageal pH 4 HTRs from baseline. After 8 wk of treatment, the healing rate in patients with baseline EE grades A-D was 60.0% in the 20 mg group and 71.4% in the 40 mg group. They concluded that VPZ 20 mg and 40 mg substantially suppressed gastric acid secretion over 24 h with considerably higher gastric pH at 4 HTR, resulting in an EE repair rate greater than 60%.

In the same year, Yamashita *et al*[45] conducted a study to evaluate the effects of VPZ and PPIs in 8 RE patients using multichannel intraluminal impedance-pH. They found that the mucosal lesions in 7/8 patients (87.5%) with persistent gastric mucosal injury after completing an 8-wk standard PPI therapy had entirely healed after VPZ therapy. From 26.5% to 78.0%, there was a considerable rise in stomach pH > 4 HTR. In addition, a decrease in esophageal pH of 4 HTR was seen, although it was not statistically significant. The overall number of reflux events, comprising acid and proximal reflux episodes, as well as the time it took for acid to clear, were both dramatically reduced. They concluded that VPZ should be used in patients with PPI-refractory RE.

In 2018, Ashida *et al*[46] conducted a study to compare VPZ 10 mg (n = 202) and 20 mg (n = 204) with LPZ 15 mg (n = 201) as maintenance treatment in 607 patients with healed EE. EE recurrence rates with LPZ 15 mg, VPZ 10 mg, and VPZ 20 mg were 16.8%, 5.1%, and 2.0%, respectively, throughout a 24-wk maintenance period. VPZ was shown to be non-inferior to 15 mg LPZ. The 10 mg and 20 mg VPZ were significantly lower than the LPZ at 15 mg. The EE recurrence rate, on the other hand, did not change substantially between the two VPZ dosages. They determined that VPZ 10 mg and 20 mg were non-inferior to LPZ 15 mg as maintenance treatment for individuals with healed EE.

A retrospective cohort study that recruited 55 patients with symptomatic GERD (NERD = 30, EE = 25) treated with VPZ 10 mg who had been followed for more than 1 year was conducted by Shinozaki *et al*[47]. They discovered that taking VPZ 10 mg for one month relieved GERD symptoms in 89% of patients and was maintained in 82% after one year without further treatment. In 47% of cases, 1-year maintenance treatment resulted in long-term relief of GERD symptoms. Nine of the forty-nine responders experienced a return of GERD symptoms, while VPZ dosage escalation relieved symptoms in 67% (6/9) of patients. Postprandial discomfort, postprandial distress, constipation, and diarrhea significantly decreased after 1 m and remained stable after a year. After 1 year of therapy, the endoscopic healing rate of EE was 95%. They concluded that 1 year of VPZ therapy reduces GERD symptoms significantly, and endoscopic healing of EE is good. VPZ is an efficient and beneficial long-term treatment for GERD.

In 2019, Oshima *et al*[48] conducted a randomized, placebo-controlled experiment in 32 patients with endoscopically proven EE who had heartburn at least once a week to see how quickly VPZ and LPZ relieve heartburn. For 14 d, the patients were given either VPZ 20 mg or LPZ 30 mg before breakfast. They found that heartburn was relieved earlier with VPZ than with LPZ. Furthermore, on day 1, VPZ and LPZ totally cured heartburn in 31.3% and 12.5% of patients, respectively. With VPZ medication, significantly more patients experienced full nighttime heartburn resolution compared with LPZ treatment. They concluded that during the first week of therapy, VPZ provided more prolonged heartburn relief than LPZ.

Recently, Akiyama *et al*[49] studied the efficacy of VPZ 20 mg in 13 patients with PPI-refractory GERD who exhibited continued pathological esophageal acid exposure (EAE). Among 13 patients who were observed by multichannel intraluminal impedance-pH at baseline (PPI treatment) and after VPZ 20 mg therapy, the median gastric acid exposure times of the VPZ group were lower than those of the PPI group, both during daytime and nocturnal observations. Furthermore, during the 24-h monitoring period, VPZ 20 mg treatment resulted in lower median EAE values (4.5%) than PPI therapy (10.6%).

Table 2 Clinical studies regarding the efficacy of potassium-competitive acid blocker in gastroesophageal reflux disease treatment

Ref.	Country/region	Study design	Patients, *n*	Diagnosis	Treatment groups	Duration of treatment, wk	Clinical outcomes
Ashida *et al*[42]	Japan	Multicenter, randomized, double-blind	732	EE	LPZ 30 mg; VPZ 5 mg; VPZ 10 mg; VPZ 20 mg; VPZ 40 mg	8	All VPZ regimens were non-inferior to LPZ 30 mg treatment. The proportions of healed EE subjects were 87.3%, 86.4%, 100%, 96.0%, and 87.0% with VPZ 5, 10, 20, 40 mg, and LPZ 30 mg, respectively
Ashida *et al*[43]	Japan	Multicenter, randomized, double-blind	607	EE	LPZ 15 mg; VPZ 10 mg; VPZ 20 mg	24	The EE recurrence rates were 16.8%, 5.1%, and 2.0% with LPZ 15 mg, VPZ 10 mg, and VPZ 20 mg, respectively, over the 24-wk maintenance period
Shinozaki *et al*[47]	Japan	Retrospective cohort	55	NERD = 30; EE = 25	VPZ 10 mg	4	The VPZ 10 mg for 1-mo alleviated GERD symptoms in 89% and were sustained in 82% after 1 yr without further therapy
Oshima *et al*[48]	Japan	Randomized placebo control	32	EE	LPZ 30 mg; VPZ 20 mg	2	The heartburn was relieved earlier with VPZ than with LPZ, and it was completely relieved in 31.3% and 12.5% of patients on day 1 with VPZ and LPZ, respectively
Akiyama *et al*[49]	Japan	Retrospective cohort with prospective study	13	PPI-refractory GERD	PPIs switch to VPZ 20 mg	8	The median gastric acid exposure times of the VPZ 20 mg were lower than the median gastric acid exposure times of the PPI treatment in both daytime and nocturnal observations. The VPZ 20 mg outperforms PPIs in stomach acid suppression, EAE control, symptom alleviation, and esophagitis healing in patients with PPI-refractory GERD
Mizuno *et al*[50]	Japan	Open-label, single-center, prospective study	50	PPI-refractory RE	PPIs switch to VPZ 20 mg for 4 wk and VPZ 10 mg	48	VPZ 10 mg prevented the recurrence of esophageal mucosal breaks in 43 of 50 (86.0%) patients. VPZ 10 mg is clinically efficacious for the long-term maintenance of healed RE
Xiao *et al* [51]	China, South Korea, Taiwan, Malaysia	Phase III, double-blind, multicenter study	481	EE	LPZ 30 mg; VPZ 20 mg	8	The 8-wk EE healing rates in the VPZ and LPZ groups were 92.4% and 91.3%, respectively. VPZ 20 mg was not inferior to LPZ 30 mg in EE healing at 8 wk
Okanobu *et al*[52]	Japan	Randomized control study	73	EE	VPZ 10 mg; VPZ 20 mg	Each dose for 4 wk and VPZ 10 mg for 8 wk	VPZ 10 mg had the same result as VPZ 20 mg in mucosal healing and symptom reduction at 4 wk and throughout the trial
Matsuda *et al*[53]	Japan	Multicenter, randomized, cross-over study	122	Erosive GERD	VPZ 10 mg; LPZ 15 mg	Every 2nd day for 4 wk and cross-over for more 4 wk	GERD symptoms were significantly reduced with VPZ 10 mg every other day, as measured by the FSSG and the gastrointestinal symptom rating scale
Lee *et al* [54]	South Korea	Randomized, double-blind, parallel-group comparison study	302	EE	TPZ 50 mg; TPZ 100 mg; EPZ 40 mg	4 and 8	At week 8, the cumulative healing rates for TPZ 50 mg, TPZ 100 mg, and EPZ 40 mg were 98.9%, 98.9%, and 98.9%, respectively
Kim *et al* [55]	South Korea	Phase III, double-blind, placebo-controlled, multicenter study	324	NERD	TPZ 50 mg; TPZ 100 mg; placebo	4	The proportions of heartburn-free days and full-resolution rates of heartburn were significantly higher in both TPZ groups than in the placebo group
Lee *et al* [56]	South Korea	Phase III, multicenter, randomized, double-blind trial	260	EE	FPZ 40 mg; EPZ 40 mg	8	FPZ 40 mg was non-inferior to EPZ 40 mg. FPZ 40 mg provided better symptom relief in patients with moderate to severe heartburn, with the effect lasting throughout the night

EAE: Esophageal acid exposure; EE: Erosive esophagitis; EPZ: Esomeprazole; FPZ: Fexuprazan; FSSG: Frequency scale for the symptoms of gastroesophageal reflux disease; GERD: Gastroesophageal reflux disease; LPZ: Lansoprazole; NERD: Non-erosive reflux disease; PPI: Proton pump

inhibitor; RE: Reflux esophagitis; TPZ: Tegoprazan; VPZ: Vonoprazan.

EAE normalization occurred in 46% of VPZ-treated people, and it was connected to complete stomach acid reduction (P = 0.005). Reflux symptoms (P = 0.01) and EE (P = 0.01) improved after switching to VPZ 20 mg. They concluded that VPZ 20 mg outperforms PPIs in stomach acid suppression, EAE control, symptom alleviation, and esophagitis healing in patients with PPI-refractory GERD.

Mizuno *et al*[50] carried out a study to assess the effectiveness of VPZ 10 mg as a maintenance treatment for healed RE in 50 patients who completed 48-wk maintenance therapy. Maintenance therapy with VPZ 10 mg at 48 wk avoided the recurrence of esophageal mucosal breaches in 43 of 50 patients (86.0%). Throughout the 48-wk maintenance therapy, the symptomatic non-relapse rate for acid reflux-related symptom score on the frequency scale for GERD symptoms and acid reflux score on the gastrointestinal symptom rating scale was 70.0% and 72.0%, respectively. They determined that VPZ 10 mg is clinically efficacious for the long-term maintenance of healed RE.

In 2020, Xiao *et al*[51] conducted a phase III, double-blind, multicenter study in 468 endoscopically confirmed EE patients and randomly assigned them to take either VPZ 20 mg (238) or LPZ 30 mg (230) once daily for 8 wk. They found that the 8-wk EE healing rates in the VPZ and LPZ groups were 92.4% and 91.3%, respectively. Moreover, in patients with a baseline LA classification of C/D, VPZ had higher 2-wk, 4-wk, and 8-wk EE healing rates than LPZ. Overall, the rates of EE healing appeared to be greater with VPZ than with LPZ. They concluded that VPZ is not inferior to LPZ in EE healing at 8 wk, and the two treatment groups had identical safety results.

Last year, Okanobu *et al*[52] performed a randomized control study to evaluate the efficacy of VPZ 10 mg (n = 36) compared with VPZ 20 mg (n = 37) in 73 patients with EE. The patients were given each dose for four weeks as an initial treatment, followed by eight weeks of maintenance therapy with VPZ 10 mg. The endoscopic healing rates of the 20 mg and 10 mg groups were 94.6% and 94.4%, respectively, after four wk. In both treatment groups, the frequency scale for GERD symptoms decreased significantly, from 13 to 4 and 14 to 3, respectively, in the 20 mg and 10 mg groups. The scores have plummeted to 2 after 12 wk. They determined that after 4 wk and throughout the experiment, VPZ 10 mg medication had a similar therapeutic response to VPZ 20 mg treatment in terms of mucosal repair and symptom reduction. These results were also the same in LA classification grade A/B patients but not in grade C/D patients.

A prospective, multicenter, open-label, randomized cross-over trial with two periods was conducted by Matsuda *et al*[53] to clarify the efficacy and superiority of VPZ 10 mg every other day over LPZ 15 mg in the maintenance management of 122 erosive GERD patients. They observed that 93.6% of the VPZ group and 82.1% of the LPZ group had well-controlled symptoms, with a significant difference (P = 0.003) using McNemar's test. The VPZ-LPZ and LPZ-VPZ groups, respectively, had 96.7% and 80.0% of patients well managed throughout the first four weeks (P = 0.007). For the second 4 wk, 94.4% of patients in the VPZ-LPZ and 76.7% of patients in the LPZ-VPZ groups were well controlled following 6 consecutive days a week (P = 0.009). They found that taking VPZ 10 mg every other day decreased GERD symptoms considerably, as indicated by the frequency scale for the gastrointestinal symptom rating scale and GERD symptoms.

TPZ efficacy in GERD

Lee *et al*[54] conducted a parallel-group, multicenter, randomized, double-blind comparative trial in 302 Korean patients with endoscopically confirmed EE in 2019. The patients were randomly assigned to receive TPZ 50 mg, TPZ 100 mg, or EPZ 40 mg for 4 wk or 8 wk. They confirmed that at week 8, the cumulative healing rates for TPZ 50 mg, TPZ 100 mg, and EPZ 40 mg were 98.9% (91/92), 98.9% (90/91), and 98.9% (87/88), respectively. Both TPZ dosages were non-inferior to EPZ 40 mg, and TPZ was well tolerated.

Kim *et al*[55] undertook a multicenter, double-blind, placebo-controlled, phase III trial in 324 Korean patients with NERD in 2021 to investigate the safety and effectiveness characteristics of TPZ relative to placebo. They were randomized into three groups with TPZ 50 mg, TPZ 100 mg, and placebo once daily for 4 wk. After 4 wk of therapy with TPZ 50 mg, TPZ 100 mg, or placebo, 42.5% (45/106), 48.5% (48/99), and 24.2% (24/99) of patients achieved full relief of significant symptoms. TPZ 50 mg and 100 mg performed better than the placebo by a substantial statistical difference. Both the TPZ and placebo groups had significantly greater percentages of heartburn-free days and full-resolution rates of heartburn. Furthermore, no apparent change in the occurrence of treatment-emergent adverse events was observed.

FPZ efficacy in GERD

In a phase III, multicenter, randomized, double-blind trial, FPZ, the antisecretory action of a pyrrole derivative with a quick and full onset was tested. A total of 260 adult patients with endoscopically proven EE (LA grades A to D) were given either FPZ 40 mg or EPZ 40 mg *per* day. The cumulative proportion of patients with healed mucosal breaks, as evaluated by endoscopy, was the main outcome

measure at week 8. The healing rate, symptoms, and quality of life were assessed at week 4, and it was discovered that FPZ was non-inferior to EPZ, with the groups having identical cumulative healing rates at 8 wk and equivalent rates at 4 wk. In individuals with moderate to severe heartburn, FPZ provided superior symptom alleviation that lasted throughout the night. The medication was well tolerated, with similar rates of side effects across treatment groups[56].

SAFETY OF P-CABs

Despite the fact that PPIs are one of the safest pharmacological classes available and have been used for almost 30 years, the number of papers on delayed-release PPI safety has skyrocketed, with many extensively discussed subjects appearing in high-profile journals[57,58]. Clinical studies and subsequent meta-analyses have revealed that VPZ has outstanding short and medium-term safety when compared to the performance of PPIs[42-53,59,60]. Because serum gastrin and pepsinogen I levels in healthy volunteers and GERD patients mirrored the antisecretory effect of VPZ, hypergastrinemia associated with long-term therapy may be a concern[61,62]. Clinical studies and subsequent meta-analyses have revealed that VPZ has outstanding short and medium-term safety when compared to the performance of PPIs[63]. Long-term PPI therapy has been associated with dysbiosis and changes in the gut microbiome, and similar changes have now been reported with VPZ[64-66]. Lipopolysaccharide biosynthesis proteins and lipopolysaccharide biosynthesis were the most dramatically elevated pathways in response to VPZ. They are most likely caused by an increase in intraluminal pH and are analogous to *H. pylori* responses to external pH changes. Because lipopolysaccharide is a potent immune response stimulator generated by Gram-negative bacteria, these data imply that VPZ may increase bacterial growth[67-69].

CONCLUSION

Many of the disadvantages and limitations of delayed-release PPIs are overcome by P-CABs. Mucosal healing in acid-related disorders is linked to the duration and degree of acid suppression, and also the length of treatment. Given the challenges in achieving good symptom management, particularly at night, with presently available delayed-release PPIs once daily, this novel family of medicines, P-CABs, delivers immediate, powerful, and extended acid suppression. They have the potential to address many of the unmet therapeutic needs in GERD, such as obtaining immediate heartburn relief and fast and specific healing of severe RE. The benefits of long-term acid suppression extend to *H. pylori* eradication, where intragastric pH control, especially at night, is crucial. Moreover, VPZ may be an optimum dual therapy as a straightforward, dependable, and successful first-line treatment for GERD. More thorough evaluations of VPZ, TPZ, and FPZ are needed, especially in Europe and North America. After extensive worldwide use of P-CABs, clinicians will justify whether it is effective, safe, and superior to currently available treatment with PPIs. In our opinion, VPZ or other P-CABs should be reserved for difficult-to-treat acid-related illnesses and unmet requirements, where the benefit-to-risk ratio is predicted to be the best.

FOOTNOTES

Author contributions: Leowattana W wrote the paper; Leowattana T collected the data.

Conflict-of-interest statement: All the authors report no relevant conflicts of interest for this article.

Open-Access: This article is an open-access article that was selected by an in-house editor and fully peer-reviewed by external reviewers. It is distributed in accordance with the Creative Commons Attribution NonCommercial (CC BY-NC 4.0) license, which permits others to distribute, remix, adapt, build upon this work non-commercially, and license their derivative works on different terms, provided the original work is properly cited and the use is non-commercial. See: https://creativecommons.org/Licenses/by-nc/4.0/

Country/Territory of origin: Togo

ORCID number: Wattana Leowattana 0000-0003-4257-2480; Tawithep Leowattana 0000-0003-2316-3585.

S-Editor: Fan JR
L-Editor: A
P-Editor: Fan JR

REFERENCES

1 **Tack J**, Pandolfino JE. Pathophysiology of Gastroesophageal Reflux Disease. *Gastroenterology* 2018; **154**: 277-288 [PMID: 29037470 DOI: 10.1053/j.gastro.2017.09.047]
2 **Chatila AT**, Nguyen MTT, Krill T, Roark R, Bilal M, Reep G. Natural history, pathophysiology and evaluation of gastroesophageal reflux disease. *Dis Mon* 2020; **66**: 100848 [PMID: 30803725 DOI: 10.1016/j.disamonth.2019.02.001]
3 **El-Serag HB**, Sweet S, Winchester CC, Dent J. Update on the epidemiology of gastro-oesophageal reflux disease: a systematic review. *Gut* 2014; **63**: 871-880 [PMID: 23853213 DOI: 10.1136/gutjnl-2012-304269]
4 **Richter JE**, Rubenstein JH. Presentation and Epidemiology of Gastroesophageal Reflux Disease. *Gastroenterology* 2018; **154**: 267-276 [PMID: 28780072 DOI: 10.1053/j.gastro.2017.07.045]
5 **Fock KM**, Talley N, Goh KL, Sugano K, Katelaris P, Holtmann G, Pandolfino JE, Sharma P, Ang TL, Hongo M, Wu J, Chen M, Choi MG, Law NM, Sheu BS, Zhang J, Ho KY, Sollano J, Rani AA, Kositchaiwat C, Bhatia S. Asia-Pacific consensus on the management of gastro-oesophageal reflux disease: an update focusing on refractory reflux disease and Barrett's oesophagus. *Gut* 2016; **65**: 1402-1415 [PMID: 27261337 DOI: 10.1136/gutjnl-2016-311715]
6 **Hershcovici T**, Fass R. Gastro-oesophageal reflux disease: beyond proton pump inhibitor therapy. *Drugs* 2011; **71**: 2381-2389 [PMID: 22117130 DOI: 10.2165/11597300-000000000-00000]
7 **Shibli F**, Kitayama Y, Fass R. Novel Therapies for Gastroesophageal Reflux Disease: Beyond Proton Pump Inhibitors. *Curr Gastroenterol Rep* 2020; **22**: 16 [PMID: 32185589 DOI: 10.1007/s11894-020-0753-y]
8 **Spechler SJ**. Evaluation and Treatment of Patients with Persistent Reflux Symptoms Despite Proton Pump Inhibitor Treatment. *Gastroenterol Clin North Am* 2020; **49**: 437-450 [PMID: 32718563 DOI: 10.1016/j.gtc.2020.04.003]
9 **Wijarnpreecha K**, Thongprayoon C, Chesdachai S, Panjawatanana P, Ungprasert P, Cheungpasitporn W. Associations of Proton-Pump Inhibitors and H2 Receptor Antagonists with Chronic Kidney Disease: A Meta-Analysis. *Dig Dis Sci* 2017; **62**: 2821-2827 [PMID: 28836158 DOI: 10.1007/s10620-017-4725-5]
10 **Yadlapati R**, DeLay K. Proton Pump Inhibitor-Refractory Gastroesophageal Reflux Disease. *Med Clin North Am* 2019; **103**: 15-27 [PMID: 30466671 DOI: 10.1016/j.mcna.2018.08.002]
11 **Moore JM**, Vaezi MF. Extraesophageal manifestations of gastroesophageal reflux disease: real or imagined? *Curr Opin Gastroenterol* 2010; **26**: 389-394 [PMID: 20473157 DOI: 10.1097/MOG.0b013e32833adc8d]
12 **Rettura F**, Bronzini F, Campigotto M, Lambiase C, Pancetti A, Berti G, Marchi S, de Bortoli N, Zerbib F, Savarino E, Bellini M. Refractory Gastroesophageal Reflux Disease: A Management Update. *Front Med (Lausanne)* 2021; **8**: 765061 [PMID: 34790683 DOI: 10.3389/fmed.2021.765061]
13 **Engevik AC**, Kaji I, Goldenring JR. The Physiology of the Gastric Parietal Cell. *Physiol Rev* 2020; **100**: 573-602 [PMID: 31670611 DOI: 10.1152/physrev.00016.2019]
14 **DuBose TD Jr**, Codina J. H,K-ATPase. *Curr Opin Nephrol Hypertens* 1996; **5**: 411-416 [PMID: 8937809 DOI: 10.1097/00041552-199609000-00006]
15 **Sakai H**, Fujii T, Takeguchi N. Proton-Potassium (H(+)/K(+)) ATPases: Properties and Roles in Health and Diseases. *Met Ions Life Sci* 2016; **16**: 459-483 [PMID: 26860309 DOI: 10.1007/978-3-319-21756-7_13]
16 **Ene MD**, Khan-Daneshmend T, Roberts CJ. A study of the inhibitory effects of SCH 28080 on gastric secretion in man. *Br J Pharmacol* 1982; **76**: 389-391 [PMID: 7104515 DOI: 10.1111/j.1476-5381.1982.tb09232.x]
17 **Long JF**, Chiu PJ, Derelanko MJ, Steinberg M. Gastric antisecretory and cytoprotective activities of SCH 28080. *J Pharmacol Exp Ther* 1983; **226**: 114-120 [PMID: 6864535]
18 **Beil W**, Hackbarth I, Sewing KF. Mechanism of gastric antisecretory effect of SCH 28080. *Br J Pharmacol* 1986; **88**: 19-23 [PMID: 3011171 DOI: 10.1111/j.1476-5381.1986.tb09466.x]
19 **Kaunitz JD**, Sachs G. Identification of a vanadate-sensitive potassium-dependent proton pump from rabbit colon. *J Biol Chem* 1986; **261**: 14005-14010 [PMID: 3021724]
20 **Keeling DJ**, Malcolm RC, Laing SM, Ife RJ, Leach CA. SK&F 96067 is a reversible, lumenally acting inhibitor of the gastric (H+ + K+)-ATPase. *Biochem Pharmacol* 1991; **42**: 123-130 [PMID: 1648919 DOI: 10.1016/0006-2952(91)90690-7]
21 **Tsukimi Y**, Ushiro T, Yamazaki T, Ishikawa H, Hirase J, Narita M, Nishigaito T, Banno K, Ichihara T, Tanaka H. Studies on the mechanism of action of the gastric H+,K(+)-ATPase inhibitor SPI-447. *Jpn J Pharmacol* 2000; **82**: 21-28 [PMID: 10874584 DOI: 10.1254/jjp.82.21]
22 **Wurst W**, Hartmann M. Current status of acid pump antagonists (reversible PPIs). *Yale J Biol Med* 1996; **69**: 233-243 [PMID: 9165692]
23 **Simon WA**, Herrmann M, Klein T, Shin JM, Huber R, Senn-Bilfinger J, Postius S. Soraprazan: setting new standards in inhibition of gastric acid secretion. *J Pharmacol Exp Ther* 2007; **321**: 866-874 [PMID: 17369284 DOI: 10.1124/jpet.107.120428]
24 **Ito K**, Kinoshita K, Tomizawa A, Morikawa-Inomata Y, Inaba F, Fujita Y, Tabata K, Shibakawa N. The effect of subchronic administration of 7-(4-fluorobenzyloxy)-2,3-dimethyl-1-{[(1S,2S)-2-methylcyclopropyl]methyl}-1H-pyrrolo[2,3-d]pyridazine (CS-526), a novel acid pump antagonist, on gastric acid secretion and gastrin levels in rats. *J Pharmacol Exp Ther* 2008; **326**: 163-170 [PMID: 18411413 DOI: 10.1124/jpet.108.137299]
25 **Mori H**, Tonai-Kachi H, Ochi Y, Taniguchi Y, Ohshiro H, Takahashi N, Aihara T, Hirao A, Kato T, Sakakibara M, Kurebayashi Y. N-(2-hydroxyethyl)-N,2-dimethyl-8-{[(4R)-5-methyl-3,4-dihydro-2H-chromen-4-yl]amino}imidazo[1,2-a]pyridine-6-carboxamide (PF-03716556), a novel, potent, and selective acid pump antagonist for the treatment of gastroesophageal reflux disease. *J Pharmacol Exp Ther* 2009; **328**: 671-679 [PMID: 18981288 DOI: 10.1124/jpet.108.146415]
26 **Arikawa Y**, Nishida H, Kurasawa O, Hasuoka A, Hirase K, Inatomi N, Hori Y, Matsukawa J, Imanishi A, Kondo M, Tarui N, Hamada T, Takagi T, Takeuchi T, Kajino M. Discovery of a novel pyrrole derivative 1-[5-(2-fluorophenyl)-1-(pyridin-3-ylsulfonyl)-1H-pyrrol-3-yl]-N-methylmethanamine fumarate (TAK-438) as a potassium-competitive acid blocker (P-CAB). *J Med Chem* 2012; **55**: 4446-4456 [PMID: 22512618 DOI: 10.1021/jm300318t]

27 **Scarpignato C**, Pelosini I, Di Mario F. Acid suppression therapy: where do we go from here? *Dig Dis* 2006; **24**: 11-46 [PMID: 16699262 DOI: 10.1159/000091298]

28 **Savarino V**, Marabotto E, Zentilin P, Demarzo MG, de Bortoli N, Savarino E. Pharmacological Management of Gastro-Esophageal Reflux Disease: An Update of the State-of-the-Art. *Drug Des Devel Ther* 2021; **15**: 1609-1621 [PMID: 33907381 DOI: 10.2147/DDDT.S306371]

29 **Gedda K**, Briving C, Svensson K, Maxvall I, Andersson K. Mechanism of action of AZD0865, a K+-competitive inhibitor of gastric H+,K+-ATPase. *Biochem Pharmacol* 2007; **73**: 198-205 [PMID: 17081503 DOI: 10.1016/j.bcp.2006.09.020]

30 **Kirchhoff P**, Andersson K, Socrates T, Sidani S, Kosiek O, Geibel JP. Characteristics of the K+-competitive H+,K+-ATPase inhibitor AZD0865 in isolated rat gastric glands. *Am J Physiol Gastrointest Liver Physiol* 2006; **291**: G838-G843 [PMID: 16798725 DOI: 10.1152/ajpgi.00120.2006]

31 **Sunwoo J**, Ji SC, Oh J, Ban MS, Nam JY, Kim B, Song GS, Yu KS, Jang IJ, Lee S. Pharmacodynamics of tegoprazan and revaprazan after single and multiple oral doses in healthy subjects. *Aliment Pharmacol Ther* 2020; **52**: 1640-1647 [PMID: 33131095 DOI: 10.1111/apt.16121]

32 **Kahrilas PJ**, Dent J, Lauritsen K, Malfertheiner P, Denison H, Franzén S, Hasselgren G. A randomized, comparative study of three doses of AZD0865 and esomeprazole for healing of reflux esophagitis. *Clin Gastroenterol Hepatol* 2007; **5**: 1385-1391 [PMID: 17950677 DOI: 10.1016/j.cgh.2007.08.014]

33 **Dent J**, Kahrilas PJ, Hatlebakk J, Vakil N, Denison H, Franzén S, Lundborg P. A randomized, comparative trial of a potassium-competitive acid blocker (AZD0865) and esomeprazole for the treatment of patients with nonerosive reflux disease. *Am J Gastroenterol* 2008; **103**: 20-26 [PMID: 18184117 DOI: 10.1111/j.1572-0241.2007.01544.x]

34 **Metz DC**, Vakil N, Keeffe EB, Lichtenstein GR. Advances in gastrointestinal pharmacotherapy. *Clin Gastroenterol Hepatol* 2005; **3**: 1167-1179 [PMID: 16361040 DOI: 10.1016/s1542-3565(05)00895-5]

35 **Kim HK**, Park SH, Cheung DY, Cho YS, Kim JI, Kim SS, Chae HS, Kim JK, Chung IS. Clinical trial: inhibitory effect of revaprazan on gastric acid secretion in healthy male subjects. *J Gastroenterol Hepatol* 2010; **25**: 1618-1625 [PMID: 20880169 DOI: 10.1111/j.1440-1746.2010.06408.x]

36 **Yu KS**, Bae KS, Shon JH, Cho JY, Yi SY, Chung JY, Lim HS, Jang IJ, Shin SG, Song KS, Moon BS. Pharmacokinetic and pharmacodynamic evaluation of a novel proton pump inhibitor, YH1885, in healthy volunteers. *J Clin Pharmacol* 2004; **44**: 73-82 [PMID: 14681344 DOI: 10.1177/0091270003261321]

37 **Sakurai Y**, Nishimura A, Kennedy G, Hibberd M, Jenkins R, Okamoto H, Yoneyama T, Jenkins H, Ashida K, Irie S, Täubel J. Safety, Tolerability, Pharmacokinetics, and Pharmacodynamics of Single Rising TAK-438 (Vonoprazan) Doses in Healthy Male Japanese/non-Japanese Subjects. *Clin Transl Gastroenterol* 2015; **6**: e94 [PMID: 26111126 DOI: 10.1038/ctg.2015.18]

38 **Han S**, Choi HY, Kim YH, Nam JY, Kim B, Song GS, Lim HS, Bae KS. Randomised clinical trial: safety, tolerability, pharmacokinetics, and pharmacodynamics of single and multiple oral doses of tegoprazan (CJ-12420), a novel potassium-competitive acid blocker, in healthy male subjects. *Aliment Pharmacol Ther* 2019; **50**: 751-759 [PMID: 31437865 DOI: 10.1111/apt.15438]

39 **Sunwoo J**, Oh J, Moon SJ, Ji SC, Lee SH, Yu KS, Kim HS, Lee A, Jang IJ. Safety, tolerability, pharmacodynamics and pharmacokinetics of DWP14012, a novel potassium-competitive acid blocker, in healthy male subjects. *Aliment Pharmacol Ther* 2018; **48**: 206-218 [PMID: 29863280 DOI: 10.1111/apt.14818]

40 **Hwang JG**, Jeon I, Park SA, Lee A, Yu KS, Jang IJ, Lee S. Pharmacodynamics and pharmacokinetics of DWP14012 (fexuprazan) in healthy subjects with different ethnicities. *Aliment Pharmacol Ther* 2020; **52**: 1648-1657 [PMID: 33111337 DOI: 10.1111/apt.16131]

41 **Unge P**, Andersson K. A first-in-human, open-label, healthy volunteer study of the new P-CAB X842 demonstrating 24h acid control for treatment of acid related diseases. *Gastroenterology* 2017; **154**: S238 [DOI: 10.1016/S0016-5085(18)31174-0]

42 **Ashida K**, Sakurai Y, Nishimura A, Kudou K, Hiramatsu N, Umegaki E, Iwakiri K, Chiba T. Randomised clinical trial: a dose-ranging study of vonoprazan, a novel potassium-competitive acid blocker, vs. lansoprazole for the treatment of erosive oesophagitis. *Aliment Pharmacol Ther* 2015; **42**: 685-695 [PMID: 26201312 DOI: 10.1111/apt.13331]

43 **Ashida K**, Sakurai Y, Hori T, Kudou K, Nishimura A, Hiramatsu N, Umegaki E, Iwakiri K. Randomised clinical trial: vonoprazan, a novel potassium-competitive acid blocker, vs. lansoprazole for the healing of erosive oesophagitis. *Aliment Pharmacol Ther* 2016; **43**: 240-251 [PMID: 26559637 DOI: 10.1111/apt.13461]

44 **Iwakiri K**, Sakurai Y, Shiino M, Okamoto H, Kudou K, Nishimura A, Hiramatsu N, Umegaki E, Ashida K. A randomized, double-blind study to evaluate the acid-inhibitory effect of vonoprazan (20 mg and 40 mg) in patients with proton-pump inhibitor-resistant erosive esophagitis. *Therap Adv Gastroenterol* 2017; **10**: 439-451 [PMID: 28567114 DOI: 10.1177/1756283X17705329]

45 **Yamashita H**, Kanamori A, Kano C, Hashimura H, Matsumoto K, Tsujimae M, Yoshizaki T, Momose K, Obata D, Eguchi T, Fujita M, Okada A. The Effects of Switching to Vonoprazan, a Novel Potassium-Competitive Acid Blocker, on Gastric Acidity and Reflux Patterns in Patients with Erosive Esophagitis Refractory to Proton Pump Inhibitors. *Digestion* 2017; **96**: 52-59 [PMID: 28662503 DOI: 10.1159/000478255]

46 **Ashida K**, Iwakiri K, Hiramatsu N, Sakurai Y, Hori T, Kudou K, Nishimura A, Umegaki E. Maintenance for healed erosive esophagitis: Phase III comparison of vonoprazan with lansoprazole. *World J Gastroenterol* 2018; **24**: 1550-1561 [PMID: 29662293 DOI: 10.3748/wjg.v24.i14.1550]

47 **Shinozaki S**, Osawa H, Kobayashi Y, Sakamoto H, Hayashi Y, Miura Y, Kawarai Lefor A, Yamamoto H. Long-term outcomes of patients with symptomatic gastroesophageal reflux disease treated with vonoprazan. *Scand J Gastroenterol* 2018; **53**: 897-904 [PMID: 30056768 DOI: 10.1080/00365521.2018.1486883]

48 **Oshima T**, Arai E, Taki M, Kondo T, Tomita T, Fukui H, Watari J, Miwa H. Randomised clinical trial: vonoprazan *vs* lansoprazole for the initial relief of heartburn in patients with erosive oesophagitis. *Aliment Pharmacol Ther* 2019; **49**: 140-146 [PMID: 30589965 DOI: 10.1111/apt.15062]

49 **Akiyama J**, Hosaka H, Kuribayashi S, Moriyasu S, Hisada Y, Okubo H, Watanabe K, Imbe K, Nagata N, Kojima Y, Yokoi C, Uemura N, Shimoyama Y, Kawamura O, Yamada M, Kusano M. Efficacy of Vonoprazan, a Novel Potassium-

Competitive Acid Blocker, in Patients with Proton Pump Inhibitor-Refractory Acid Reflux. *Digestion* 2020; **101**: 174-183 [PMID: 30897577 DOI: 10.1159/000497775]

50 **Mizuno H**, Nishino M, Yamada K, Kamiyamamoto S, Hinoue Y. Efficacy of Vonoprazan for 48-Week Maintenance Therapy of Patients with Healed Reflux Esophagitis. *Digestion* 2020; **101**: 411-421 [PMID: 31129668 DOI: 10.1159/000500399]

51 **Xiao Y**, Zhang S, Dai N, Fei G, Goh KL, Chun HJ, Sheu BS, Chong CF, Funao N, Zhou W, Chen M. Phase III, randomised, double-blind, multicentre study to evaluate the efficacy and safety of vonoprazan compared with lansoprazole in Asian patients with erosive oesophagitis. *Gut* 2020; **69**: 224-230 [PMID: 31409606 DOI: 10.1136/gutjnl-2019-318365]

52 **Okanobu H**, Kohno T, Mouri R, Hatsushika Y, Yamashita Y, Miyaki E, Fukuhara T, Okazaki A, Sakano A, Urabe A, Takaki S, Mori N, Tsuji K, Ochi H, Furukawa Y. Efficacy of vonoprazan 10 mg compared with 20 mg for the initial treatment in patients with erosive esophagitis: a randomized pilot study. *Esophagus* 2021; **18**: 669-675 [PMID: 33221955 DOI: 10.1007/s10388-020-00798-7]

53 **Matsuda S**, Kato M, Sakakibara Y, Hamada H, Sasaki Y, Mori H, Hirai Y, Inoue S, Toyokawa T, Kagaya T, Kuwai T, Esaka N, Yamashita H, Watanabe N, Matsumoto M, Fujii H, Demura M, Kubo K, Mabe K, Harada N. A study for every second day administration of vonoprazan for maintenance treatment of erosive GERD (ESD von GERD): a multicenter randomized cross-over study. *J Gastroenterol* 2022; **57**: 133-143 [PMID: 35092498 DOI: 10.1007/s00535-022-01850-2]

54 **Lee KJ**, Son BK, Kim GH, Jung HK, Jung HY, Chung IK, Sung IK, Kim JI, Kim JH, Lee JS, Kwon JG, Park JH, Huh KC, Park KS, Park MI, Kim N, Lee OY, Jee SR, Lee SK, Youn SJ, Kim SK, Lee ST, Hong SJ, Choi SC, Kim TN, Youn YH, Park HJ, Kang MJ, Park CH, Kim BT, Youn S, Song GS, Rhee PL. Randomised phase 3 trial: tegoprazan, a novel potassium-competitive acid blocker, vs. esomeprazole in patients with erosive oesophagitis. *Aliment Pharmacol Ther* 2019; **49**: 864-872 [PMID: 30843245 DOI: 10.1111/apt.15185]

55 **Kim SH**, Cho KB, Chun HJ, Lee SW, Kwon JG, Lee DH, Kim SG, Jung HY, Kim JW, Lee JS, Park H, Choi SC, Jee SR, Kim HS, Ko KH, Park SJ, Lee YC, Park SH, Kim AR, Kim EJ, Park HW, Kim BT, Song GS. Randomised clinical trial: comparison of tegoprazan and placebo in non-erosive reflux disease. *Aliment Pharmacol Ther* 2021; **54**: 402-411 [PMID: 34227708 DOI: 10.1111/apt.16477]

56 **Lee OY**, Chun HJ, Kim JJ, Kim JI, Kim SK, Lee SW, Park KS, Lee KL, Choi SC, Jang JY. A phase 3, non-inferiority randomized controlled trial with fexuprazan, a novel potassium competitive acid blocker vs. esomeprazole in patients with erosive esophagitis. *Gastroenterology* 2020; **158**: S1072

57 **Vaezi MF**, Yang YX, Howden CW. Complications of Proton Pump Inhibitor Therapy. *Gastroenterology* 2017; **153**: 35-48 [PMID: 28528705 DOI: 10.1053/j.gastro.2017.04.047]

58 **Malfertheiner P**, Kandulski A, Venerito M. Proton-pump inhibitors: understanding the complications and risks. *Nat Rev Gastroenterol Hepatol* 2017; **14**: 697-710 [PMID: 28930292 DOI: 10.1038/nrgastro.2017.117]

59 **Cheng Y**, Liu J, Tan X, Dai Y, Xie C, Li X, Lu Q, Kou F, Jiang H, Li J. Direct Comparison of the Efficacy and Safety of Vonoprazan Versus Proton-Pump Inhibitors for Gastroesophageal Reflux Disease: A Systematic Review and Meta-Analysis. *Dig Dis Sci* 2021; **66**: 19-28 [PMID: 32095968 DOI: 10.1007/s10620-020-06141-5]

60 **Miwa H**, Igarashi A, Teng L, Uda A, Deguchi H, Tango T. Systematic review with network meta-analysis: indirect comparison of the efficacy of vonoprazan and proton-pump inhibitors for maintenance treatment of gastroesophageal reflux disease. *J Gastroenterol* 2019; **54**: 718-729 [PMID: 30919071 DOI: 10.1007/s00535-019-01572-y]

61 **Kojima Y**, Takeuchi T, Sanomura M, Higashino K, Kojima K, Fukumoto K, Takata K, Sakamoto H, Sakaguchi M, Tominaga K, Higuchi K. Does the Novel Potassium-Competitive Acid Blocker Vonoprazan Cause More Hypergastrinemia than Conventional Proton Pump Inhibitors? *Digestion* 2018; **97**: 70-75 [PMID: 29393198 DOI: 10.1159/000484217]

62 **Uemura N**, Kinoshita Y, Haruma K, Yao T, Kushima R, Kanoo T. Rationale and design of the VISION study: a randomized, open-label study to evaluate the long-term safety of vonoprazan as maintenance treatment in patients with erosive esophagitis. *Clin Exp Gastroenterol* 2018; **11**: 51-56 [PMID: 29416369 DOI: 10.2147/CEG.S144149]

63 **Hafiz RA**, Wong C, Paynter S, David M, Peeters G. The Risk of Community-Acquired Enteric Infection in Proton Pump Inhibitor Therapy: Systematic Review and Meta-analysis. *Ann Pharmacother* 2018; **52**: 613-622 [PMID: 29457492 DOI: 10.1177/1060028018760569]

64 **Naito Y**, Kashiwagi K, Takagi T, Andoh A, Inoue R. Intestinal Dysbiosis Secondary to Proton-Pump Inhibitor Use. *Digestion* 2018; **97**: 195-204 [PMID: 29316555 DOI: 10.1159/000481813]

65 **Singh A**, Cresci GA, Kirby DF. Proton Pump Inhibitors: Risks and Rewards and Emerging Consequences to the Gut Microbiome. *Nutr Clin Pract* 2018; **33**: 614-624 [PMID: 30071147 DOI: 10.1002/ncp.10181]

66 **Kakiuchi T**, Yamamoto K, Imamura I, Hashiguchi K, Kawakubo H, Yamaguchi D, Fujioka Y, Okuda M. Gut microbiota changes related to Helicobacter pylori eradication with vonoprazan containing triple therapy among adolescents: a prospective multicenter study. *Sci Rep* 2021; **11**: 755 [PMID: 33436953 DOI: 10.1038/s41598-020-80802-3]

67 **Otsuka T**, Sugimoto M, Inoue R, Ohno M, Ban H, Nishida A, Inatomi O, Takahashi S, Naito Y, Andoh A. Influence of potassium-competitive acid blocker on the gut microbiome of *Helicobacter pylori*-negative healthy individuals. *Gut* 2017; **66**: 1723-1725 [PMID: 27965281 DOI: 10.1136/gutjnl-2016-313312]

68 **Marcus EA**, Inatomi N, Nagami GT, Sachs G, Scott DR. The effects of varying acidity on Helicobacter pylori growth and the bactericidal efficacy of ampicillin. *Aliment Pharmacol Ther* 2012; **36**: 972-979 [PMID: 23009227 DOI: 10.1111/apt.12059]

69 **Cochet F**, Peri F. The Role of Carbohydrates in the Lipopolysaccharide (LPS)/Toll-Like Receptor 4 (TLR4) Signalling. *Int J Mol Sci* 2017; **18** [PMID: 29099761 DOI: 10.3390/ijms18112318]

World Journal of Gastroenterology

Submit a Manuscript: https://www.f6publishing.com

World J Gastroenterol 2022 July 28; 28(28): 3620-3626

DOI: 10.3748/wjg.v28.i28.3620

ISSN 1007-9327 (print) ISSN 2219-2840 (online)

MINIREVIEWS

Making the case for multidisciplinary pediatric aerodigestive programs

Sohit P Kanotra, Rebecca Weiner, Riad Rahhal

Specialty type: Gastroenterology and hepatology

Provenance and peer review: Invited article; Externally peer reviewed.

Peer-review model: Single blind

Peer-review report's scientific quality classification
Grade A (Excellent): 0
Grade B (Very good): B
Grade C (Good): C
Grade D (Fair): 0
Grade E (Poor): 0

P-Reviewer: Aydin S, Turkey; Pandey A, India

Received: February 21, 2022
Peer-review started: February 21, 2022
First decision: May 9, 2022
Revised: May 23, 2022
Accepted: June 22, 2022
Article in press: June 22, 2022
Published online: July 28, 2022

Sohit P Kanotra, Department of Otolaryngology-Head and Neck Surgery, University of Iowa, Iowa City, IA 52242, United States

Rebecca Weiner, Department of Pediatrics, Division of Pediatric Pulmonology, University of Iowa, Iowa City, IA 52242, United States

Riad Rahhal, Department of Pediatrics, Division of Pediatric Gastroenterology, University of Iowa, Iowa City, IA 52242, United States

Corresponding author: Riad Rahhal, MD, MS, Professor, Department of Pediatrics, Division of Pediatric Gastroenterology, University of Iowa, 200 Hawkins Dr, Iowa City, IA 52242, United States. riad-rahhal@uiowa.edu

Abstract

Multidisciplinary pediatric aerodigestive centers have been proposed to address the needs of children with complex multi-system problems affecting the respiratory and upper gastrointestinal tracts. The setup of a multidisciplinary service allows for the complex coordination needed between different subspecialties. This allows for rapid communication and family-centered decision making and agreement on further diagnostic and/or therapeutic next steps such as offering triple endoscopy when indicated. Triple endoscopy entails performing rigid upper airway assessment, flexible bronchoscopy and upper gastrointestinal endoscopy and has been linked to reduced time to diagnosis/treatment, reduced costs and anesthesia exposure. This review summarizes the available literature on the structure and benefits of multidisciplinary pediatric aerodigestive services.

Key Words: Aerodigestive; Multidisciplinary; Pediatric; Triple endoscopy

©The Author(s) 2022. Published by Baishideng Publishing Group Inc. All rights reserved.

Core Tip: Multidisciplinary pediatric aerodigestive programs serve patients with multisystem problems affecting the respiratory and upper gastrointestinal tracts and require the participation and expertise of essential subspecialists including gastroenterologists. This setup allows for coordinated diagnostic and therapeutic interventions such as triple endoscopy. Benefits include reducing time to diagnosis and/or treatment, reducing healthcare costs and limiting exposure to radiation and anesthesia, providing a strong example of value-based healthcare delivery.

Citation: Kanotra SP, Weiner R, Rahhal R. Making the case for multidisciplinary pediatric aerodigestive programs. *World J Gastroenterol* 2022; 28(28): 3620-3626
URL: https://www.wjgnet.com/1007-9327/full/v28/i28/3620.htm
DOI: https://dx.doi.org/10.3748/wjg.v28.i28.3620

INTRODUCTION

Multidisciplinary programs for complex medical conditions such as cystic fibrosis and asthma have been shown to optimize the value of healthcare delivery by improving outcomes and reducing cost[1,2]. There is growing literature supporting this concept for aerodigestive programs[3,4]. Multidisciplinary pediatric aerodigestive programs have been proposed to address the specific needs of children with complex multi-system problems affecting the respiratory and upper gastrointestinal (GI) tracts. Conditions managed by aerodigestive programs are diverse and may include structural or physiological airway disease, chronic parenchymal lung disease, lung injury from aspiration or infection, dysphagia, and esophageal mucosal, motility and anatomic abnormalities[1,5]. One main aim of this coordinated interdisciplinary approach is to allow for expedited patient evaluation in a single clinical setting, including diagnostic and therapeutic interventions. Several benefits have been attributed to aerodigestive programs, as opposed to independent evaluations by different subspecialists at different times. Benefits include shorter time to diagnosis, reduced radiation and anesthesia exposure and lower healthcare related costs. The purpose of the review is to shed light on the structure, services and impacts of aerodigestive programs and to highlight the need for gastroenterology expertise and involvement within these programs.

Advances in the care of critically ill infants and children have created a growing population of patients with complex chronic multi-system diseases requiring a collaborative multispecialty approach to their management[6]. This includes multidisciplinary aerodigestive programs that focus on children with a combination of multiple and interrelated congenital and/or acquired conditions affecting airway, breathing, feeding, and concerns about growth/nutrition (Table 1). Key service components of an aerodigestive program include a pediatric otolaryngologist, pediatric pulmonologist and pediatric gastroenterologist along with a speech language pathologist, social worker and nutritionist. The first consensus statement on aerodigestive programs, published in 2018, provided a definition of an aerodigestive patient, specified needed participation of vital pediatric disciplines and their levels of expertise, and highlighted essential care components, assessments and therapies including endoscopic procedures [5].

Results of a survey published in 2019 noted the number of pediatric aerodigestive programs to be rapidly proliferating with diffuse geographic presence throughout the United States, with the largest subset operating in academic centers[7]. This was a recent phenomenon as a considerable percent of these programs had been operating for just a few years.

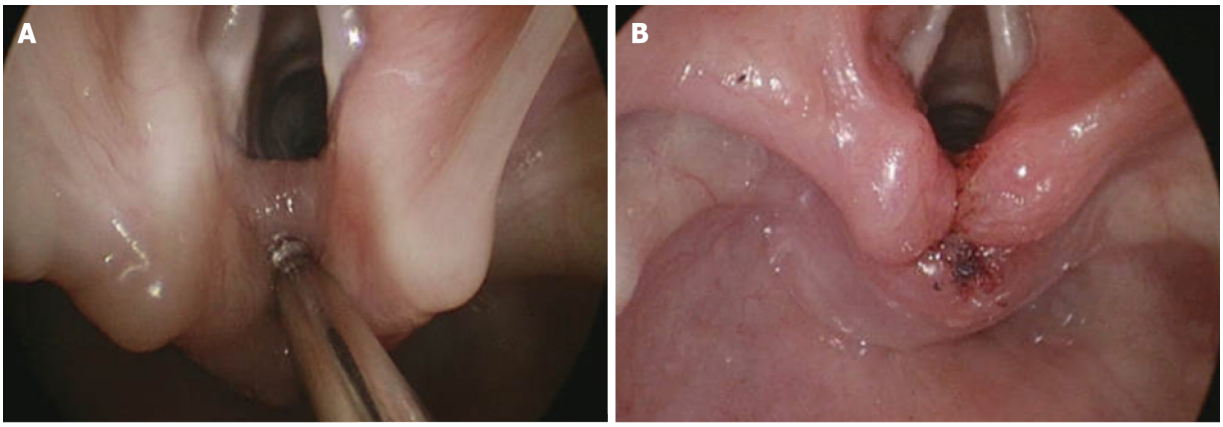
AERODIGESTIVE PROGRAM SERVICES

Aerodigestive programs not only offer expertise from different specialties in a single setting, but also enable the coordination of evaluation and intervention. Depending on patient presentation and the differential diagnoses, management includes education, discussion of potential treatment options and risks and benefits of treatment modalities and further testing. Evaluation can include a list of airway and GI interventions offered individually or in combination.

From the airway perspective, evaluation can include awake in-office flexible laryngoscopy and swallow assessment. Further workup may include drug induced sleep endoscopy, direct laryngoscopy and rigid bronchoscopy, while therapeutic interventions targeting specific pathology such as endoscopic repair of laryngeal cleft (Figure 1), laser excision of cysts, balloon dilation of subglottic stenosis and more advanced open airway interventions. These procedures have benefits and risks which should be taken in consideration and clearly discussed with caregivers. Some evaluation can take place without sedation while others require various levels of sedation, often performed in the operating room with the assistance of anesthesia services.

Table 1 Common aerodigestive problems (with overall among subspecialists)

Pulmonary	Otolaryngology	Gastroenterology
Chronic cough	Tracheostomy dependence	Dysphagia
Stridor	Stridor	Feeding intolerance
Wheezing	Noisy breathing	Gastroesophageal reflux disease
Recurrent pneumonia	Recurrent croup	Eosinophilic esophagitis
Tracheomalacia	Laryngeal cleft	Esophageal stricture
Bronchomalacia	Laryngeal stenosis	Congenital esophageal anomalies
Chronic lung disease	Laryngomalacia	Malnutrition
Need for ventilatory support	Vocal cord paralysis	Feeding tube dependence
	Subglottic stenosis	
	Tracheal stenosis	



DOI: 10.3748/wjg.v28.i28.3620 **Copyright** ©The Author(s) 2022.

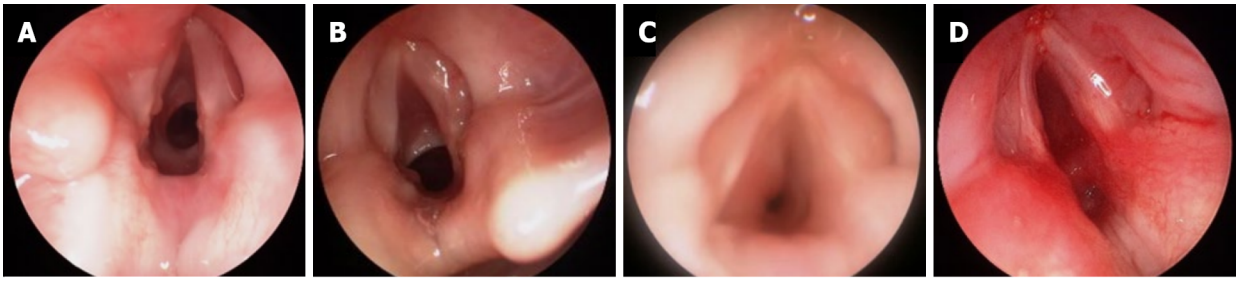
Figure 1 Endoscopic assessment and management for a laryngeal cleft which can contribute to aspiration. A: Probing of interaytenoid region to assess for cleft; B: Post laryngeal cleft repair using laser and suturing.

Awake in-office flexible laryngoscopy allows for a non-sedated evaluation of the upper airway. This allows for the assessment of upper airway dynamics and abnormalities such as vocal cord lesions and vocal cord movement, tongue base obstruction, hypopharyngeal collapse, adenoid or tonsillar hypertrophy and laryngomalacia. Assessment of dysphagia and aspiration can also be undertaken during in-office flexible laryngoscopy, *via* a procedure referred to as Fiberoptic Endoscopic Evaluation of Swallowing. Even though an invaluable tool for assessment of airway and swallowing abnormalities in the children, in-office flexible laryngoscopy has some disadvantages including limited assessment of structures below the vocal cords and dependence on patient compliance. In addition, therapeutic airway interventions are not possible in the office setting.

Drug induced sleep endoscopy (DISE) allows for upper airway evaluation using a flexible endoscope while a patient is in a pharmacologically induced sleep-like state. During DISE, an endoscope is passed through the nares to assess the nasopharynx, oropharynx, larynx, and in some cases the trachea. The procedure is often carried out either with propofol or dexmedetomidine sedation, which simulates natural sleep and can demonstrate lesions causing obstruction that may not be evident on an awake in-office flexible laryngoscopy[8].

Rigid endoscopy is considered the gold standard for diagnostic airway assessment of structures below the vocal cords, including trachea and bronchi. It offers better optics, ability to size areas of narrowing and provides an opportunity to perform a variety of interventions (Figure 2). This procedure requires patient sedation and thus is not hampered by patient tolerance or compliance. Spontaneous breathing can be maintained, which allows for examination of the dynamic status of the airway. The sedated status allows for surgical interventions such as biopsy, laryngeal cleft injection or suturing, epiglottopexy, balloon dilation, vocal cord injection, and laryngotracheal reconstruction[9,10].

Upper GI evaluation may include video fluoroscopic evaluation of swallowing, contrast imaging for esophageal strictures, impedance pH testing for gastroesophageal reflux disease (GERD), esophageal manometry for motility disorders and mucosal endoscopic assessment for esophagitis including eosino-



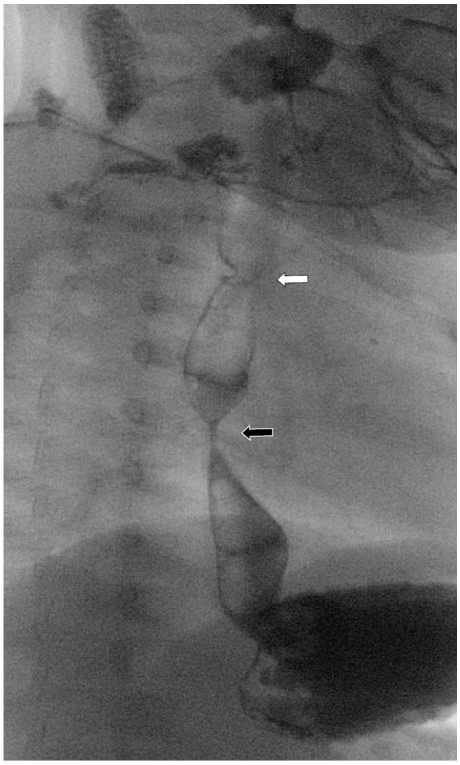
DOI: 10.3748/wjg.v28.i28.3620 **Copyright** ©The Author(s) 2022.

Figure 2 Endoscopic grading of subglottic stenosis. A: Grade I: 0%-50% obstruction; B: Grade II: 51%-70% obstruction; C: Grade III: 71%-99%; D: Grade IV: No detectable lumen.

philic esophagitis (EoE). Aerodigestive patients often have feeding problems and are at high risk for malnutrition, necessitating feeding tube placement and use[11]. Some patients can be managed with nasogastric and gastrostomy tubes while others require jejunal feeds due to persistent GERD and/or intolerance to intragastric feeds. The choice, placement and maintenance of feeding tubes can be managed by a pediatric gastroenterologist within an aerodigestive program[12].

Specific patient categories presenting to an aerodigestive clinic may have a particularly higher risk for upper GI abnormalities contributing the symptoms. These include patients previously treated for esophageal atresia and tracheoesophageal fistula (Figure 3). Common complications among these patients include esophagitis[13], recurrent respiratory tract infection, tracheomalacia and poor growth with increased healthcare utilization[14-16]. Pediatric gastroenterology input can be crucial to evaluate for anatomic and mucosal esophageal abnormalities and for persistent tracheoesophageal fistula, which can be difficult to diagnosis. Simultaneous tracheal and esophageal endoscopic assessment can help in challenging cases when imaging modalities are not definitive (Figure 4).

In some patients, flexible bronchoscopy, flexible upper GI endoscopy, direct laryngoscopy, and rigid bronchoscopy are indicated and can be offered in combination aptly named as "triple endoscopy". A triple endoscopy provides efficient, organized and thorough evaluation of the patient's disorders without requiring multiple, separate procedures under anesthesia. This allows for complementary modalities for evaluation of upper GI and airway structures and dynamics and facilitates real-time discovery, discussion, and planning amongst all the specialists involved, allowing for excellent, patient-centric care. A consensus on the core data elements to be gathered during triple endoscopy has been published[17]. From the gastroenterology standpoint, the importance of assessing for EoE is highlighted due to potential contribution to aerodigestive symptoms. An upper endoscopy should therefore be considered as part of a triple endoscopy in patients presenting with symptoms potentailly arising from esophageal mucosal disease (especially EoE) as well as anatomic GI disorders (such as esophageal strictures). Another common indication for triple endoscopy is in the preoperative evaluation of children undergoing open airway reconstructive surgery (like patients with tracheostomies moving towards decannulation). Triple endoscopy has also shown high yield in the evaluation of chronic cough, aspiration, apparent life-threatening episodes, recurrent croup and recurrent pneumonias. Triple endoscopy can assess factors that can predict outcomes of open airway reconstruction such as laryngo-tracheal reconstruction, cricotracheal resections and tracheal resections, allowing for risk modification to optimize patient outcomes. Triple endoscopy serves to provide a comprehensive assessment including evaluating grade of subglottic stenosis, ruling out secondary airway lesions (such as tracheobron-chomalacia). Active esophageal disorders, like EoE and GERD, have been linked to unfavorable effect outcomes of open airway reconstruction so it is important for identify these conditions and optimize their management[18,19]. In this patient population, flexible bronchoscopy with bronchoalveolar lavage provides evidence of bacterial colonization which can direct prophylactic antibiotics. Patients with tracheostomies, frequently evaluated by aerodigestive programs, commonly have airway colonization with *Pseudomonas aeruginosa*. Pseudomonal wound infection during open airway reconstruction surgeries leads to increased morbidity[20,21]. Implementation of culture directed antibiotics prior to or during open airway reconstruction surgery can therefore improve outcomes. Studies have demonstrated that specific subsets of aerodigestive patients are more likely to have abnormal mucosal histology on upper GI endoscopy and/or abnormal impedance pH testing[22,23]. This includes those with previously diagnosed asthma, feeding difficulty, and esophageal atresia with or without tracheoesophageal fistula, with 40%-50% yield on upper GI testing[22]. Findings noted included reflux esophagitis and EoE. It is important to note that in many studies a large percent of patients (> 50%) were on acid suppressive therapy which may have treated underlying proton pump inhibitor responsive eosinophilia (now considered a subset of EoE) which requires prolonged treatment and monitoring[24].



DOI: 10.3748/wjg.v28.i28.3620 **Copyright** ©The Author(s) 2022.

Figure 3 Fluoroscopic esophageal evaluation in high-risk patients. Esophagram in 10-month-old with repaired esophageal atresia presenting with feeding difficulty and poor growth, showing previously unrecognized distal esophageal congenital stricture (black arrow), far below the surgical repair site (white arrow).



DOI: 10.3748/wjg.v28.i28.3620 **Copyright** ©The Author(s) 2022.

Figure 4 Simultaneous tracheal and esophageal endoscopy in a patient with history of esophageal atresia to assess for persistent tracheoesophageal fistula.

AERODIGESTIVE PROGRAM OUTCOMES

As aerodigestive programs expand, there has been more emphasis on measuring program impact on patients, their families and the healthcare system. Clinical outcomes typically followed can include documented improvement in swallowing (control of aspiration), frequency of respiratory infections, rate of decannulation in patients with tracheostomies and overall patient mortality. Other important outcomes studied include time to reach a diagnosis and/or initiate treatment, impact of health-related quality of life, healthcare costs and utilization.

Studies have demonstrated numerous positive impacts of aerodigestive programs. These include lower technical direct cost (by as much as 70%) and fewer inpatient days after enrolling patients in an aerodigestive program[3]. Frequency of unnecessary evaluation (swallow studies and impedance pH testing) dropped when such programs were established[24,25]. Aerodigestive programs have been linked to improved patient quality of life and reduced caregiver burden[11]. Studies have also noted

shortened time to diagnosis (6 d *vs* 150 d, $P < 0.001$), fewer specialist consultations, lower hospital charges, less radiation exposure and reduced anesthesia exposure when aerodigestive programs were established[4,26]. The benefit of reducing anesthesia exposure is of particular interest in infants and young children in terms of diminishing neurocognitive risks associated with repeated exposure to anesthetics[27].

Further advantages of triple endoscopy include a significant reduction in mean anesthesia time (54 min *vs* 89 min, $P < 0.0001$) compared to having the 3 procedures done separately[28]. Charges and direct costs for triple endoscopy were also significantly lower as compared to performing these as separate procedures[28]. It is important to note that not all patients who present to an aerodigestive require a triple endoscopy. Patients with isolated surgical pathology such as cystic lesions (for example vallecular cyst) are likely to only require otolaryngologist intervention only.

CONCLUSION

Aerodigestive programs have specific requirements for essential subspecialist participation and expertise which includes gastroenterology services. These programs offer numerous advantages in the management of complex multi-system problems affecting the respiratory and upper GI tracts especially with the diverse and overlapping contributions of conditions leading to a range of patient signs and symptoms. The setup of an aerodigestive program allows for diagnostic and therapeutic interventions, offered individually or in combination. Benefits of aerodigestive programs have been demonstrated and include reducing time to diagnosis and/or initiating of treatment, reducing healthcare costs and limiting patient radiation and anesthesia exposure, providing a strong example of value-based healthcare.

FOOTNOTES

Author contributions: Rahhal R contributed to the study conception and design, drafted the initial article and approved the final article; Weiner R and Kanotra S contributed to the study conception and design, provided critical revision of the manuscript and approved the final article.

Conflict-of-interest statement: All the authors report no relevant conflicts of interest for this article.

Open-Access: This article is an open-access article that was selected by an in-house editor and fully peer-reviewed by external reviewers. It is distributed in accordance with the Creative Commons Attribution NonCommercial (CC BY-NC 4.0) license, which permits others to distribute, remix, adapt, build upon this work non-commercially, and license their derivative works on different terms, provided the original work is properly cited and the use is non-commercial. See: https://creativecommons.org/Licenses/by-nc/4.0/

Country/Territory of origin: United States

ORCID number: Sohit P Kanotra 0000-0001-9510-5689; Rebecca Weiner 0000-0002-5491-6896; Riad Rahhal 0000-0002-3326-1042.

S-Editor: Fan JR
L-Editor: A
P-Editor: Fan JR

REFERENCES

1 **Condren M**, Boger JA. Impact of a pediatric clinic-based multidisciplinary asthma education and management program. *J Pediatr Pharmacol Ther* 2005; **10**: 254-258 [PMID: 23118641 DOI: 10.5863/1551-6776-10.4.254]
2 **Sawicki GS**, Goss CH. Tackling the increasing complexity of CF care. *Pediatr Pulmonol* 2015; **50** Suppl 40: S74-S79 [PMID: 26335957 DOI: 10.1002/ppul.23244]
3 **Appachi S**, Banas A, Feinberg L, Henry D, Kenny D, Kraynack N, Rosneck A, Carl J, Krakovitz P. Association of Enrollment in an Aerodigestive Clinic With Reduced Hospital Stay for Children With Special Health Care Needs. *JAMA Otolaryngol Head Neck Surg* 2017; **143**: 1117-1121 [PMID: 28983551 DOI: 10.1001/jamaoto.2017.1743]
4 **Collaco JM**, Aherrera AD, Au Yeung KJ, Lefton-Greif MA, Hoch J, Skinner ML. Interdisciplinary pediatric aerodigestive care and reduction in health care costs and burden. *JAMA Otolaryngol Head Neck Surg* 2015; **141**: 101-105 [PMID: 25473812 DOI: 10.1001/jamaoto.2014.3057]
5 **Boesch RP**, Balakrishnan K, Acra S, Benscoter DT, Cofer SA, Collaco JM, Dahl JP, Daines CL, DeAlarcon A, DeBoer EM, Deterding RR, Friedlander JA, Gold BD, Grothe RM, Hart CK, Kazachkov M, Lefton-Greif MA, Miller CK, Moore PE, Pentiuk S, Peterson-Carmichael S, Piccione J, Prager JD, Putnam PE, Rosen R, Rutter MJ, Ryan MJ, Skinner ML,

Torres-Silva C, Wootten CT, Zur KB, Cotton RT, Wood RE. Structure and Functions of Pediatric Aerodigestive Programs: A Consensus Statement. *Pediatrics* 2018; **141** [PMID: 29437862 DOI: 10.1542/peds.2017-1701]

6 **Burns KH**, Casey PH, Lyle RE, Bird TM, Fussell JJ, Robbins JM. Increasing prevalence of medically complex children in US hospitals. *Pediatrics* 2010; **126**: 638-646 [PMID: 20855383 DOI: 10.1542/peds.2009-1658]

7 **Gumer L**, Rosen R, Gold BD, Chiou EH, Greifer M, Cohen S, Friedlander JA. Size and Prevalence of Pediatric Aerodigestive Programs in 2017. *J Pediatr Gastroenterol Nutr* 2019; **68**: e72-e76 [PMID: 31022094 DOI: 10.1097/MPG.0000000000002268]

8 **Arganbright JM**, Lee JC, Weatherly RA. Pediatric drug-induced sleep endoscopy: An updated review of the literature. *World J Otorhinolaryngol Head Neck Surg* 2021; **7**: 221-227 [PMID: 34430829 DOI: 10.1016/j.wjorl.2021.05.002]

9 **Wineski RE**, Panico E, Karas A, Rosen P, Van Diver B, Norwood TG, Grayson JW, Beltran-Ale G, Dimmitt R, Kassel R, Rogers A, Leonard M, Chapman A, Boehm L, Wiatrak B, Harris WT, Smith N. Optimal timing and technique for endoscopic management of dysphagia in pediatric aerodigestive patients. *Int J Pediatr Otorhinolaryngol* 2021; **150**: 110874 [PMID: 34392101 DOI: 10.1016/j.ijporl.2021.110874]

10 **Day KE**, Smith NJ, Kulbersh BD. Early surgical intervention in type I laryngeal cleft. *Int J Pediatr Otorhinolaryngol* 2016; **90**: 236-240 [PMID: 27729141 DOI: 10.1016/j.ijporl.2016.09.017]

11 **Kim S**, Park M, Kim E, Kim GE, Jung JH, Kim SY, Kim MJ, Kim DH, Park S, Koh H, Ho IG, Kim SK, Hwang S, Shin KH, Lee H, Lee B, Sohn MH, Rha DW, Kim KW. Development of a Multidisciplinary Aerodigestive Program: An Institutional Experience. *Children (Basel)* 2021; **8** [PMID: 34201876 DOI: 10.3390/children8070535]

12 **Al-Zubeidi D**, Demir H, Bishop WP, Rahhal RM. Gastrojejunal feeding tube use by gastroenterologists in a pediatric academic center. *J Pediatr Gastroenterol Nutr* 2013; **56**: 523-527 [PMID: 23254445 DOI: 10.1097/MPG.0b013e318282a8db]

13 **Tambucci R**, Rea F, Angelino G, Malamisura M, Mennini M, Riccardi C, Farello G, Valfré L, Dall'Oglio L, Markowitz JE, Fiocchi AG, De Angelis P. Eosinophilic esophagitis in esophageal atresia: Tertiary care experience of a "selective" approach for biopsy sampling. *World Allergy Organ J* 2020; **13**: 100116 [PMID: 32256942 DOI: 10.1016/j.waojou.2020.100116]

14 **Tuğba RG**, Tuğba ŞE, Ayşe TA, Zeynep RO, Pelin A, Cem K, Ramazan K. Review of Complications of Operated Esophageal Atresia and Tracheoesophageal Fistula Patients. *Turk Arch Pediatr* 2021; **56**: 380-385 [PMID: 35005734 DOI: 10.5152/TurkArchPediatr.2021.20125]

15 **Leibovitch L**, Zohar I, Maayan-Mazger A, Mazkereth R, Strauss T, Bilik R. Infants Born with Esophageal Atresia with or without Tracheo-Esophageal Fistula: Short- and Long-Term Outcomes. *Isr Med Assoc J* 2018; **20**: 161-166 [PMID: 29527854]

16 **Cartabuke RH**, Lopez R, Thota PN. Long-term esophageal and respiratory outcomes in children with esophageal atresia and tracheoesophageal fistula. *Gastroenterol Rep (Oxf)* 2016; **4**: 310-314 [PMID: 26475129 DOI: 10.1093/gastro/gov055]

17 **Boesch RP**, de Alarcon A, Piccione J, Prager J, Rosen R, Sidell DR, Wootten C, Balakrishnan K; Aerodigestive Research Collaborative. Consensus on Triple Endoscopy Data Elements Preparatory to Development of an Aerodigestive Registry. *Laryngoscope* 2022 [PMID: 35122443 DOI: 10.1002/lary.30038]

18 **Ludemann JP**, Hughes CA, Noah Z, Holinger LD. Complications of pediatric laryngotracheal reconstruction: prevention strategies. *Ann Otol Rhinol Laryngol* 1999; **108**: 1019-1026 [PMID: 10579227 DOI: 10.1177/000348949910801101]

19 **Halstead LA**. Gastroesophageal reflux: A critical factor in pediatric subglottic stenosis. *Otolaryngol Head Neck Surg* 1999; **120**: 683-688 [PMID: 10229593 DOI: 10.1053/hn.1999.v120.a91766]

20 **Sasaki CT**, Horiuchi M, Koss N. Tracheostomy-related subglottic stenosis: bacteriologic pathogenesis. *Laryngoscope* 1979; **89**: 857-865 [PMID: 449531 DOI: 10.1288/00005537-197906000-00001]

21 **Gray S**, Miller R, Myer CM 3rd, Cotton RT. Adjunctive measures for successful laryngotracheal reconstruction. *Ann Otol Rhinol Laryngol* 1987; **96**: 509-513 [PMID: 3674646 DOI: 10.1177/000348948709600506]

22 **DeBoer EM**, Kinder S, Duggar A, Prager JD, Soden J, Deterding RR, Ruiz AG, Jensen EL, Weinman J, Wine T, Fortunato JE, Friedlander JA. Evaluating the yield of gastrointestinal testing in pediatric patients in aerodigestive clinic. *Pediatr Pulmonol* 2018; **53**: 1517-1524 [PMID: 30288952 DOI: 10.1002/ppul.24170]

23 **Rosen R**, Amirault J, Johnston N, Haver K, Khatwa U, Rubinstein E, Nurko S. The utility of endoscopy and multichannel intraluminal impedance testing in children with cough and wheezing. *Pediatr Pulmonol* 2014; **49**: 1090-1096 [PMID: 24178927 DOI: 10.1002/ppul.22949]

24 **Hart CK**, de Alarcon A, Tabangin ME, Hamilton S, Rutter MJ, Pentiuk SP, Garza JM. Impedance probe testing prior to pediatric airway reconstruction. *Ann Otol Rhinol Laryngol* 2014; **123**: 641-646 [PMID: 24707014 DOI: 10.1177/0003489414528867]

25 **Wentland C**, Hersh C, Sally S, Fracchia MS, Hardy S, Liu B, Garcia JA, Hartnick CJ. Modified Best-Practice Algorithm to Reduce the Number of Postoperative Videofluoroscopic Swallow Studies in Patients With Type 1 Laryngeal Cleft Repair. *JAMA Otolaryngol Head Neck Surg* 2016; **142**: 851-856 [PMID: 27356238 DOI: 10.1001/jamaoto.2016.1252]

26 **Boesch RP**, Balakrishnan K, Grothe RM, Driscoll SW, Knoebel EE, Visscher SL, Cofer SA. Interdisciplinary aerodigestive care model improves risk, cost, and efficiency. *Int J Pediatr Otorhinolaryngol* 2018; **113**: 119-123 [PMID: 30173969 DOI: 10.1016/j.ijporl.2018.07.038]

27 **Gascon E**, Klauser P, Kiss JZ, Vutskits L. Potentially toxic effects of anaesthetics on the developing central nervous system. *Eur J Anaesthesiol* 2007; **24**: 213-224 [PMID: 17261215 DOI: 10.1017/s0265021506002365]

28 **Ruiz AG**, Bhatt JM, DeBoer EM, Friedlander J, Janosy N, Peterson MB, Wine T, Deterding R, Prager JD. Demonstrating the benefits of a multidisciplinary aerodigestive program. *Laryngoscope* 2020; **130**: 521-525 [PMID: 30919460 DOI: 10.1002/lary.27939]

World Journal of Gastroenterology

Submit a Manuscript: https://www.f6publishing.com

World J Gastroenterol 2022 July 28; 28(28): 3627-3636

DOI: 10.3748/wjg.v28.i28.3627

ISSN 1007-9327 (print) ISSN 2219-2840 (online)

MINIREVIEWS

Therapeutic potential of mesenchymal stem cells in the treatment of acute liver failure

Carl Randall Harrell, Dragica Pavlovic, Valentin Djonov, Vladislav Volarevic

Specialty type: Gastroenterology and hepatology

Provenance and peer review: Invited article; Externally peer reviewed.

Peer-review model: Single blind

Peer-review report's scientific quality classification

Grade A (Excellent): A
Grade B (Very good): B
Grade C (Good): 0
Grade D (Fair): 0
Grade E (Poor): 0

P-Reviewer: Salim A, Pakistan; Lu CX, China

Received: March 24, 2022
Peer-review started: March 24, 2022
First decision: April 25, 2022
Revised: May 8, 2022
Accepted: June 24, 2022
Article in press: June 24, 2022
Published online: July 28, 2022

Carl Randall Harrell, Regenerative Processing Plant LLC, Palm Harbor, FL 34176, United States

Dragica Pavlovic, Department of Genetics, Faculty of Medical Sciences, University of Kragujevac, Kragujevac 34000, Serbia

Valentin Djonov, Institute of Anatomy, University of Bern, Bern 3012, Switzerland

Vladislav Volarevic, Department of Medical Genetics and Microbiology and Immunology, Faculty of Medical Sciences, University of Kragujevac, Kragujevac 34000, Serbia

Corresponding author: Vladislav Volarevic, MD, Full Professor, Department of Medical Genetics and Microbiology and Immunology, Faculty of Medical Sciences, University of Kragujevac, 69 Svetozara Markovica Street, Kragujevac 34000, Serbia.
vladislav.volarevic@gmail.com

Abstract

Acute liver failure (ALF) is a severe and life-threatening condition in which rapid deterioration of liver function develops in a patient who has no preexisting liver disease. Mesenchymal stem cells (MSCs) are immunoregulatory stem cells which are able to modulate phenotype and function of all immune cells that play pathogenic role in the development and progression of ALF. MSCs in juxtacrine and paracrine manner attenuate antigen-presenting properties of dendritic cells and macrophages, reduce production of inflammatory cytokines in T lymphocytes, suppress hepatotoxicity of natural killer T (NKT) cells and promote generation and expansion of immunosuppressive T, B and NKT regulatory cells in acutely inflamed liver. Due to their nano-sized dimension and lipid envelope, intravenously injected MSC-derived exosomes (MSC-Exos) may by-pass all biological barriers to deliver MSC-sourced immunoregulatoy factors directly into the liver-infiltrated immune cells and injured hepatocytes. Results obtained by us and others revealed that intravenous administration of MSCs and MSC-Exos efficiently attenuated detrimental immune response and acute inflammation in the liver, suggesting that MSCs and MSC-Exos could be considered as potentially new remedies in the immunotherapy of ALF. In this review, we emphasize the current knowledge about molecular and cellular mechanisms which are responsible for MSC-based modulation of liver-infiltrated immune cells and we discuss different insights regarding the therapeutic potential of MSCs in liver regeneration.

Key Words: Mesenchymal stem cells; Acute liver failure; Therapy; Immunomodulation; Regeneration

©The Author(s) 2022. Published by Baishideng Publishing Group Inc. All rights reserved.

Core Tip: Due to their potent immunoregulatory, angiomodulatory and hepatoprotective properties, mesenchymal stem cells and their exosomes suppress detrimental immune response, prevent apoptosis and promote survival of injured hepatocytes which results in an enhanced repair and regeneration of acutely injured liver.

Citation: Harrell CR, Pavlovic D, Djonov V, Volarevic V. Therapeutic potential of mesenchymal stem cells in the treatment of acute liver failure. *World J Gastroenterol* 2022; 28(28): 3627-3636
URL: https://www.wjgnet.com/1007-9327/full/v28/i28/3627.htm
DOI: https://dx.doi.org/10.3748/wjg.v28.i28.3627

INTRODUCTION

The liver is the largest solid organ in the human body. It consists of large sections (lobes) which are divided in a thousand, hexagonally-shaped small units (lobules)[1]. The lobule is the main structural unit of the liver consisting of a portal triad, hepatocytes and a central vein[1]. The liver is essential organ which performs many functions including bile production, removal of waste products and toxins from the bloodstream, regulation of blood clotting, storage of fat-soluble vitamins, minerals (copper, iron) and glycogen[1]. The liver conjugates bilirubin, handles cholesterol homeostasis, regulates sex hormone metabolism and produces proteins which are important for optimal functioning of endocrine, gastrointestinal, reproductive and immune system. Since liver regulates many vital functions, severe and massive liver injury results in the development of life-threatening multi-organ dysfunction[1].

Acute liver failure (ALF) is a clinical syndrome characterized by rapid deterioration of liver function followed by ascites, coagulopathy, hepatic encephalopathy and multi-organ failure which occur in a patient who has no preexisting liver disease[2]. An annual incidence of ALF is 5.5-6.2 cases per million population per year[3]. ALF is a consequence of severe drug-induced liver injury, hepatic ischemia, invasion of hepatotropic viruses and develops due to the generation of detrimental immune response against foreign or self-antigens, released from injured hepatocytes[4].

Pathogen-associated molecular patterns expressed on invading pathogens or damage-associated molecular patterns and alarmins released from damaged-hepatocytes activate liver resident professional antigen presenting cells [dendritic cells (DCs) and Kupffer cells][2,5]. Activated DCs present lipid antigens to the liver natural killer T (NKT) cells in CD1-dependent manner, enabling their activation and polarization in inflammatory, interferon gamma (IFN-γ)-producing NKT1 and interleukin (IL)-17-producing NKT17 cells[6]. Additionally, activated liver DCs capture microbial proteins and self-proteins released from injured hepatocytes, and present them to the antigen-specific naïve CD4+ and CD8+ T cells[7]. DC-derived IL-12 induce activation and differentiation of naïve CD4+T cells in effector, IFN-γ-producing Th1 cells while DC-sourced IL-1, IL-6 and IL-23 induce generation of IL-17 and IL-22-producing effector Th17 cells[7].

Activated Kupffer cells produce tumor necrosis factor alpha (TNF-α) and IL-1β which induce enhanced expression of E and P selectins on liver endothelial cells, enabling massive influx of circulating neutrophils and monocytes in the injured livers[2,5]. Additionally, activated Kupffer cells release Th1 and Th17 cell-attracting chemokines (CXCL3 and CCL20) and recruit effector CXCR3-expressing CD4+Th1 cells and CCR6-expressing CD4+Th17 cells in the inflamed livers[6]. NKT1/Th1 cell-derived IFN-γ and NKT17/Th17 cell-sourced IL-17 induce enhanced synthesis of hepatotoxic TNF-α , nitric oxide (NO) and reactive oxygen species in Kupffer cells and liver-infiltrated neutrophils, resulting in massive necrosis of hepatocytes[6,7].

Transplantation of bio-artificial livers and hepatocytes could provide support of liver function temporarily and are therefore used as therapeutic approaches for the treatment of ALF[8]. Restored liver function and reduced incidence of extra hepatic complications were observed in ALF patients who underwent transplantation of hepatocytes[2]. However, short-term viability of engrafted hepatocytes and immune rejection against major histocompatibility complex (MHC) miss-matched transplanted hepatic cells significantly limited therapeutic efficacy of liver transplantation. Immunosuppressive therapy managed to temporarily improve survival of ALF patients who underwent liver transplantation [8,9]. Nevertheless, continuous and long-term use of immunosuppressive drugs may induce severe and life-threatening immunosuppression which may be fatal for ALF-treated patients[9]. Accordingly, there is an urgent need for the development and therapeutic use of new immunoregulatory and hepatoprotective agent which could create immunosuppressive microenvironment in injured liver, suppress

detrimental immune response, alleviate liver inflammation and, at the same time, promote hepatocyte proliferation without causing severe, systemic immunosuppression.

Mesenchymal stem cells (MSCs) are adult stem cells that reside in almost all postnatal organs, where participate in the elimination of microbial pathogens, suppress detrimental immune response, promote survival of injured parenchymal cells and enhance tissue repair and regeneration[10]. A large number of experimental and clinical studies demonstrated therapeutic efficacy of MSCs and their secretome in the treatment of ALF[11,12]. MSCs were either directly transplanted in the injured livers or were infused *via* peripheral, portal, splenic veins and hepatic artery. Sang *et al*[13] and Cao *et al*[14] demonstrated that MSCs administered *via* portal vein had better capability to attenuate liver inflammation, reduce necrosis and promote liver regeneration than MSCs which were transplanted *via* hepatic artery, peripheral vein or MSCs which were directly injected in the damaged livers. Teshima and colleagues observed that MSCs which were transplanted *via* splenic vein more efficiently suppressed liver inflammation and enhanced liver regeneration than MSCs which were injected *via* peripheral vein[15]. Opposite to these findings were results reported by Sun *et al*[16] who showed that there was no significant difference in the regeneration of acutely injured livers of animals that received MSCs *via* hepatic artery, portal or peripheral vein, suggesting that route of MSCs injection was not crucially important for their therapeutic effects in the treatment of ALF.

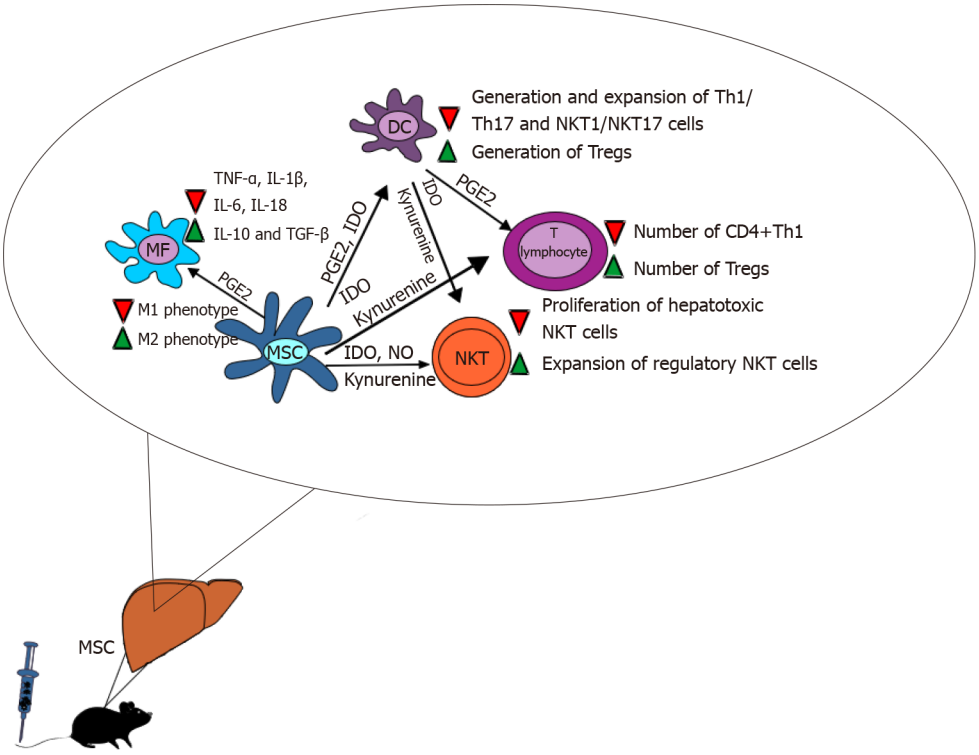
mmUpon engraftment, transplanted MSCs in juxtacrine (cell-to-cell contact-dependent signaling) and paracrine manner [through the activity of MSC-sourced soluble factors: Prostaglandin E2 (PGE2), IL-10, transforming growth factor beta (TGF-β), indoleamine 2, 3 dyoxigenase (IDO), NO, hepatic growth factor (HGF), IL-1 receptor antagonist] modulate phenotype and function of all immune cells that play pathogenic role in the development and progression of acute liver injury[11,12]. MSCs also produce various growth and angiomodulatory factors [HGF, IL-6, vascular endothelial growth factor, basic fibroblast growth factor (bFGF)] which support survival and proliferation of injured hepatocytes[10,13]. Herewith, in this review article, we summarized current knowledge about molecular and cellular pathways that were responsible for hepatoprotective, immunoregulatory and angiomodulatory effects of MSCs and their secretome in the therapy of ALF. An extensive literature review was carried out in March 2022 across several databases (MEDLINE, EMBASE, Google Scholar, ClinicalTrials.gov). Keywords used in the selection were: "mesenchymal stem cells", "secretome", "exosomes", "acute liver injury", "immunomodulation", "immunosuppression", "hepatocytes", "differentiation", "ischemia", "angiomodulation", "therapeutic potential", "liver repair and regeneration". All journals were considered, and an initial search retrieved 125 articles. The abstracts of all these articles were subsequently reviewed by two of the authors (CRH and VV) to check their relevance to the subject of this manuscript. Eligible studies had to delineate the effects of MSCs and their secretome on hepatocyte survival, phenotype and function of liver-infiltrated immune cells, and their findings were analyzed in this review.

MSC-DEPENDENT MODULATION OF LIVER-INFILTRATED IMMUNE CELLS

A large number of experimental studies demonstrated that hepatoprotective effects of MSCs were mainly relied on the immunoregulatory properties of MSCs[17-20]. MSCs attenuated acute liver inflammation and promoted liver regeneration by inducing immunosuppressive phenotype of liver macrophages, DCs, T lymphocytes and NKT cells[21-24].

MOLECULAR MECHANISMS RESPONSIBLE FOR MSC-BASED SUPPRESSION OF INFLAMMATORY MACROPHAGES IN INJURED LIVERS

Wang and colleagues showed that beneficial effects of MSCs in the attenuation of ALF were relied on the suppression of inflammatory M1 macrophages which hold central function in initiating acute liver inflammation[17]. Murine BM-MSCs alleviated murine D-galactosamine (D-Gal)-induced ALF by inducing generation of immunosuppressive M2 phenotype in liver macrophages in PGE2-dependent manner (Figure 1). MSC-derived PGE2 bound to the EP4 receptor and inhibited TGF-β-activated kinase 1-driven activation of nucleotide-binding and oligomerization domain-like receptor 3 (NLRP3) inflammasome in Kupffer cells[17]. PGE2-dependent suppression of NLRP3 inflammasome in liver macrophages resulted in down-regulated secretion of inflammatory cytokines (IL-1β, IL-6 and IL-18) which led to the alleviation of acute liver inflammation[17]. Additionally, MSC-sourced PGE2 induced phosphorylation and activation of transcriptional factor STAT6 which modulated mammalian target of rapamycin (mTOR) signaling that resulted in the generation of immunosuppressive M2 phenotype in liver macrophages. By producing anti-inflammatory cytokines (IL-10 and TGF-β), M2 macrophages attenuated on-going inflammation and promoted repair and regeneration of D-Gal-injured livers[17]. Similar findings were reported by Miao and colleagues who provided evidence that PGE2-dependent repression of NLRP3 inflammasome in Kupffer cells was mainly responsible for beneficial effects of BM-



DOI: 10.3748/wjg.v28.i28.3627 **Copyright** ©The Author(s) 2022.

Figure 1 Mesenchymal stem cells-based modulation of immune cells in acute liver injury. Mesenchymal stem cells (MSCs), in prostaglandin E2 (PGE2) dependent manner, prevent generation of inflammatory (M1) phenotype and induce generation of immunosuppressive (M2) phenotype in liver macrophages by down-regulating synthesis of inflammatory cytokines [tumor necrosis factor alpha, interleukin (IL)-1β, IL-6, IL-18] and by promoting production of anti-inflammatory cytokines (IL-10 and transforming growth factor beta). Increased indoleamine 2, 3 dyoxigenase (IDO) activity and enhanced secretion of PGE2 are mainly responsible for MSC-based generation of tolerogenic dendritic cells (DCs) which suppress expansion of Th1/Th17 lymphocytes and natural killer T (NKT) 1/NKT17 cells, but favor proliferation of immunosuppressive T regulatory cells (Tregs). MSC-generated tolerogenic DCs, in PGE2-dependent manner, suppress expansion of inflammatory CD4+ Th1 cells and induce expansion of Tregs, while in IDO/Kynurenine-dependent manner attenuate proliferation of hepatotoxic NKT cells and induce expansion of NKT regulatory cells (NKTregs). MSC-sourced nitric oxide, in autocrine manner, induces enhanced IDO activity in MSCs. MSC-derived IDO and Kynurenine suppress proliferation of inflammatory Th1 and NKT cells in the liver and were mainly responsible for MSC-dependent expansion of immunosuppressive Tregs and NKTregs in injured livers. MSCs: Mesenchymal stem cells; PGE2: Prostaglandin E2; TNF-α: Tumor necrosis factor alpha; IL: Interleukin; TGF-β: Transforming growth factor beta; IDO: Indoleamine 2, 3 dioxygenase; NKT: Natural killer T cells; Tregs: T regulatory cells; NKTregs: Natural killer T regulatory cells; NO: Nitric oxide.

MSCs in the attenuation of acute liver injury during lipopolysaccharide (LPS)-induced sepsis in mice [18]. BM-MSC-sourced PGE2 generated immunosuppressive phenotype and increased IL-10 production by modulating activity of extracellular signal-regulated kinase 1 (ERK1) in Kupffer cells[18].

Liu *et al*[19] who analyzed the frequency of F4/80-expressing macrophages in the livers of CCL4+MSC-treated mice confirmed that MSC-based therapy significantly altered phenotype and function of Kupffer cells in inflamed livers. During the initial phase of ALF (first 48 h after CCL4 injection), significantly higher number of inflammatory M1 macrophages was observed in injured livers while immunosuppressive M2 macrophages were dominant subpopulation of liver macrophages during the recovery phase (7 d after CCL4 injection)[19]. Intravenous injection of murine MSCs (5×10^5 cells/mice) which were obtained from compact bone attenuated liver inflammation and completely regenerate CCL4-injured livers. During the injured phase, the number of inflammatory monocyte-derived macrophages was significantly increased by MSC treatment while during the recovery phase of acute liver injury MSCs favored generation and expansion of immunosuppressive M2 macrophages, crucially contributed to the creation of immunosuppressive microenvironment in regenerated livers[19].

Hua *et al*[20] demonstrated that amnion-derived MSCs (A-MSCs) suppressed inducible nitric oxide synthase (iNOS) activity and NO production, attenuated synthesis of inflammatory cytokines (TNF-α, IL-6) and induced generation of anti-inflammatory phenotype in liver macrophages by promoting production of immunosuppressive IL-10. A-MSC-dependent modulation of liver macrophages was relied on modulation of autophagy, as evidenced by down-regulated expression of microtubule-associated protein 1 light chain 3 in A-MSC-treated Kupffer cells[20]. Single injection of A-MSCs (1×10^6 cells/mice) alleviated acetaminophen (APAP)-induced ALF in mice by inducing alternative activation of Kupffer cells. Liposome-induced macrophage depletion almost completely diminished beneficial effects of A-MSCs, indicating that macrophages were the main cellular targets of A-MSCs in the treatment of APAP-induced ALF[20].

THE CROSS-TALK BETWEEN MSCS, DCS, T LYMPHOCYTES AND NKT CELLS IN INJURED LIVERS

We and others demonstrated that MSCs and their secretome [MSC-derived conditioned medium (MSC-CM)] attenuated antigen-presenting properties of liver-infiltrated DCs, reducing their capacity for the generation and expansion of inflammatory Th1/Th17 and NKT1/NKT17 cells in injured livers[21-24]. MSC-sourced PGE2 and IDO were mainly responsible for the suppression of DC-dependent activation of liver T and NKT cells (Figure 1)[21-24].

Zhang *et al*[21] showed that intravenously injected BM-MSCs prevented progression of *Propionibacterium acnes* (*P. acnes*)-induced ALF in mice by inducing regulatory phenotype in liver DCs. MSCs-treated livers had normal morphology and structure without any signs of massive hepatocyte injury. MSCs down-regulated production of Th1 cell-attracting chemokines (CXCL9, CXCL10, CCL3, CCL21) which resulted in reduced influx of CXCR3 and CCR5-expressing effector CD4+ Th1 cells and CCR7-expressing memory CD4+ Th1 cells in the livers of *P. acnes*-treated mice[21]. Accordingly, only small number of liver-infiltrating lymphocytes was observed around the central veins of *P. acnes* + MSC-treated mice. Flow cytometry analysis of liver-infiltrated CD4+T cells revealed decreased expression of activating markers (CD44, CD69), indicating that MSCs suppressed activation of CD4+ T cells in *P. acnes* -treated animals[21]. MSCs attenuated ALF in mice by suppressing production of inflammatory and hepatotoxic cytokines (TNF-α and IFN-γ) in liver CD4+Th1 cells which was followed by the attenuation of systemic inflammation and by complete restoration of liver function[21]. Reduced number of CD4+ Th1 cells was accompanied with increased presence of FoxP3-expressing CD4+ CD25+ T regulatory cells (Tregs) in the livers of *P. acnes* + MSC-treated mice. Suppression of Th1 cell-driven liver inflammation was a consequence of MSC-dependent modulation of hepatic DCs[21]. DCs isolated from the livers of *P. acnes* + MSC-treated animals had regulatory phenotype, characterized by low expression of co-stimulatory molecules (CD80, CD86), decreased production of Th1 cell-related inflammatory cytokines (TNF-α, IL-1β, IL-12) and increased production of immunosuppressive cytokines (IL-10 and TGF-β) which induced generation and expansion of FoxP3-expressing CD4+ CD25+ Tregs in injured livers[21]. MSCs induced generation of regulatory phenotype in CD11c+ B220- precursor DCs through the activation of PI3K signaling pathway. By activating EP4 receptor, MSC-sourced PGE2 induced phosphorylation of PI3K and ERK1/2 kinases and elicited generation of tolerogenic, immunosuppressive phenotype in liver DCs[21]. Importantly, MSC-generated DCs possessed potent immunosuppressive and hepatoprotective properties. Passive transfer of MSC-generated regulatory DCs induced generation of hepatic Tregs, attenuated liver inflammation and prevented development of ALF in *P. acnes*-treated mice[21]. MSCs and DC-dependent expansion of Tregs was responsible for beneficial effects of MSCs since Treg depletion completely abrogated MSC-based attenuation of acute liver inflammation[21,22].

By using Concanavalin (Con A) and alpha-galactoceramide (α-GalCer)-induced hepatitis as murine models of ALF, we showed that MSC-dependent modulation of the cross-talk between DCs and NKT play important role in MSC-based attenuation of ALF[22-25]. Intravenously injected BM-MSCs significantly alleviated serum levels of AST and ALT, reduced apoptosis of hepatocytes and improved survival of Con A- and α-GalCer-treated mice[22-24]. Cellular make-up of the livers of MSC-treated animals revealed significantly reduced number of hepatotoxic, FasL, NKG2D and CD107-expressing NKT cells, indicating that MSCs suppressed cytotoxic properties of NKT cells[23]. The same phenomenon was observed in Con A- and α-GalCer-treated mice that received BM-MSC-CM, suggesting that MSCs suppressed NKT cell-driven liver inflammation in paracrine manner[22,23]. Among various MSC-derived immunosuppressive factors, NO and Kynurenine (IDO metabolite) were present in the highest concentration in BM-MSC-CM[23]. Additionally, inhibition of iNOS and IDO activity completely diminished hepatoprotective properties of MSCs, confirming the importance of NO and IDO/Kynurenine for MSC-dependent suppression of ALF[23,24]. MSC-sourced NO inhibited proliferation of hepatotoxic NKT cells while MSC-derived IDO induced generation of regulatory and immunosuppressive phenotype in NKT cells[23,25]. Additionally, MSC-sourced IDO prevented trans-differentiation of NKT regulatory cells (NKTregs) in inflammatory NKT17 cells by activating general control nonderepressible 2 (GCN2) kinase which suppressed protein kinase B/mTOR-dependent synthesis of inflammatory cytokines IL-17 and IL-22 in NKTregs[23,25].

In addition to their direct immunoregulatory effects on hepatotoic NKT cells, BM-MSCs and BM-MSC-CM suppressed effector functions of liver NKT cells indirectly, through the modulation of phenotype and function of hepatic DCs[25]. Liver DCs play important role in MSC-dependent suppression of liver NKT cells since their depletion abrogated hepatoprotective effects of MSCs and aggravated liver injury in MSC-treated mice[23,25]. MSCs attenuated antigen-presenting properties of hepatic DCs by down-regulating expression of MHC class II and co-stimulatory molecules on their membranes and by reducing synthesis of NKT1 and NKT17 cell- related inflammatory cytokines (TNF-α , IL-β, IL-12, IL-23, IFN-γ, IL-17)[22-25]. In similar manner as it was observed by Zhang *et al*[16], we also noticed that MSCs induced generation of regulatory and tolerogenic phenotype in hepatic DCs[22-25]. Increased IDO activity and enhanced production of anti-inflammatory cytokines (TGF-β and IL-10) were observed in the DCs which were isolated from the livers of Con A + MSCs and α-GalCer + MSCs-treated

mice[23]. MSC-generated regulatory DCs induced generation and expansion of IL-10 and TGF-β-producing NKTregs, contributing to the creation of immunosuppressive microenvironment in injured livers[24]. Additionally, BM-MSCs reduced presence of inflammatory, IFN-γ and TNF-α-producing NKT1 and IL-17-producing NKT17 cells in the livers of Con A + MSCs and α-GalCer + MSCs-treated mice which resulted in alleviated liver inflammation[24]. MSC-sourced IDO and its metabolite Kynurenine were mainly responsible for MSC-dependent generation of regulatory DCs[24,25]. Inhibition of IDO activity in MSCs attenuated their capacity for the generation of tolerogenic phenotype in hepatic DCs and diminished their hepatoprotective and immunosuppressive effects[24].

MSCS AS POTENTIALLY NEW THERAPEUTIC AGENTS IN REGENERATIVE HEPATOLOGY

MSCs represent heterogeneous population of immunoregulatory and angiomodulatory stem cells which possess enormous differentiation potential[25]. All subpopulations of MSCs spontaneously differentiate into the cells of mesodermal origin[25]. However, under appropriate conditions, MSCs may generate cells of ectodermal and endodermal origin, including hepatocyte-like cells (HLCs)[26-29].

Local tissue microenvironment, particularly oxygen supply and cytokines/growth factors released by parenchymal and tissue-resident immune cells modulate phenotype of MSCs[25,26]. MSCs are usually derived from bone marrow, adipose tissue, amniotic fluid, placenta, umbilical cord, dental pulp, compact bone and peripheral blood[10]. The development origin significantly affects potential for differentiation and other functional characteristics of tissue-specific MSCs[26]. BM-MSCs possess great genomic stability after long-term propagation[26]. An improved engraftment and increased life span are the main characteristics of adipose tissue-derived MSCs (AT-MSCs)[26]. Dental pulp-derived MSCs, amniotic fluid derived MSCs and placental derived MSCs have increased capacity for differentiation in neural cells, while BM-MSCs, AT-MSCs and umbilical cord derived MSCs (UC-MSCs) have great differentiation potential towards the cells of endodermal origin, including HLCs[26].

Accordingly, a large number of evidence demonstrated that human BM-MSC-, AT-MSC- and UC-MSC-derived HLCs represent valuable and promising cell source for the regeneration of injured livers [25-29].

Two step protocol is the most usually used for the generation of human MSC-derived HLCs[29]. After isolation from BM, AT and UC, MSCs are, under standard conditions (at 37 ℃ in a humidified atmosphere containing 5% CO_2), cultured in complete Dulbecco's modified Eagle's medium (DMEM) supplemented with fetal bovine serum (FBS) until they reach 75%-80% of confluence. Then, MSCs are cultured for 48 h in the FBS-free DMEM medium supplemented with endothelial growth factor (20 ng/mL) and basic fibroblast growth factor (bFGF, 10 ng/mL) to be committed towards endodermal lineage[29]. Afterwards, MSCs were seven days exposed to HLC step-1 differentiation medium, consisting of HGF (20 ng/mL), bFGF (10 ng/mL) and nicotin-amide (0.61 g/L). By binding to the c-met receptor on differentiated cells, HGF activates intracellular signaling molecules (Grb2-associated binder-1, son of sevenless), ERK kinase and mitogen-activated protein kinase which are important in the early stages of hepatogenesis[29]. Intracellular signaling elicited by HGF/c-met are enhanced by nicotin-amide which acts as selective kinase inhibitor that improves cell survival and proliferation during the initial stage of endodermal patterning. Finally, MSCs are cultured in HLC step-2 differentiation medium consisting of oncostatin (OSM, 20 ng/mL), dexamethasone (1 mmol/L) and insulin, transferrin and selenium (ITS, 50 mg/mL). OSM promotes maturation of hepatocytes, dexamethasone induces enhanced expression of liver-enriched transcription factors [CCAAT/enhancer-binding protein alpha (C/EBPα), hepatocyte nuclear factor (HNF)-4α], while ITS promotes the proliferation and survival of differentiated HLCs[29]. At the end of the differentiation process, HLCs generated from BM-, AT- and UC-MSCs, fully obtain hepatocyte-like polygonal morphology with cytoplasmic granulation and prominent centrally positioned nucleus[29]. Exposition to HLC differentiation mediums do not alter telomerase activity and do not induce genetic instability in human BM-, AT- and UC-MSC-derived HLCs[29].

MSC-derived HLCs had gene expression profile similar to fetal or adult hepatocytes[25-29]. During the early stage of differentiation, MSC-derived HLCs express several early hepatocyte differentiation markers [alfa-fetoprotein, cytokeratin (CK)7, GATA4, HNF1α, HNF3β, HNF4α, C/EBPα] while during the late stage of differentiation, MSC-derived HLCs express cell markers of mature hepatocytes (forkhead transcription factor which has a crucial role in hepatocyte differentiation), hepatocyte-specific gap junction protein connexin 32 and hepatocyte paraffin 1, localized in hepatocytes mitochondria). Finally, at the end of differentiation, MSC-derived HLCs are able to produce hepatocyte-specific proteins (albumin, fibrinogen, transferrin) and enzymes (cytochrome P450 subtypes 3A4 and 1A1, phosphoenolpyruvate carboxykinase 1 and carbamoylphosphate synthetase[26-29].

The analysis of functional characteristics of BM-, AT- and UC-MSCs-derived HLCs revealed that AT-MSC- and BM-MSC-derived HLCs had the higher capacity for glycogen storage than UC-MSCs-derived HLCs and their gene expressions were more consistent with the normal hepatocyte-differentiation profile[30]. Albumin gene expression increased progressively during the differentiation process of AT-

MSC- and BM-MSC-derived HLCs. In contrast, only transitory expression of albumin was observed in UC-MSC-derived HLCs (between day 7 and day 25). Additionally, HLCs which were generated from AT-MSCs and BM-MSCs displayed clusters arrangements and had increased proliferation rate compared to UC-MSC-derived HLCs which were not expanded as expected, hampering their potential for *in vivo* use[30]. Accordingly, only therapeutic potential of AT-MSC-derived HLCs and BM-MSC-derived HLCs was examined *in vivo*, in murine model of CCL4-induced acute liver injury[30]. Intravenously injected human AT-MSC-and BM-MSC-derived HLCs (1×10^6 cells), managed to completely regenerate CCL4-injured livers of immunodeficient mice. Hepatocytes isolated from the livers of CCL4-treated mice displayed normal morphology two weeks after the transplantation of human AT-MSC- and BM-MSC-derived HLCs. Importantly, hepatocytes in the regenerated livers of experimental mice express human albumin and CK19 confirming that they were generated from transplanted human AT-MSC- and BM-MSC-derived HLCs[30]. Accordingly, both AT-MSCs and BM-MSCs represent valuable cell source for the generation of functional HLCs which may repopulate and regenerate injured livers of ALF patients[30]. Nevertheless, it should be noted that progression of ALF is mainly a consequence of immune cell-dependent massive damage of hepatocytes[2,6]. Accordingly, detrimental immune response could induce injury of engrafted HLCs as well. Therefore, co-transplantation of MSC-derived HLCs and immunosuppressive MSCs should be explored as new therapeutic approach which could successfully regenerate injured livers of ALF patients.

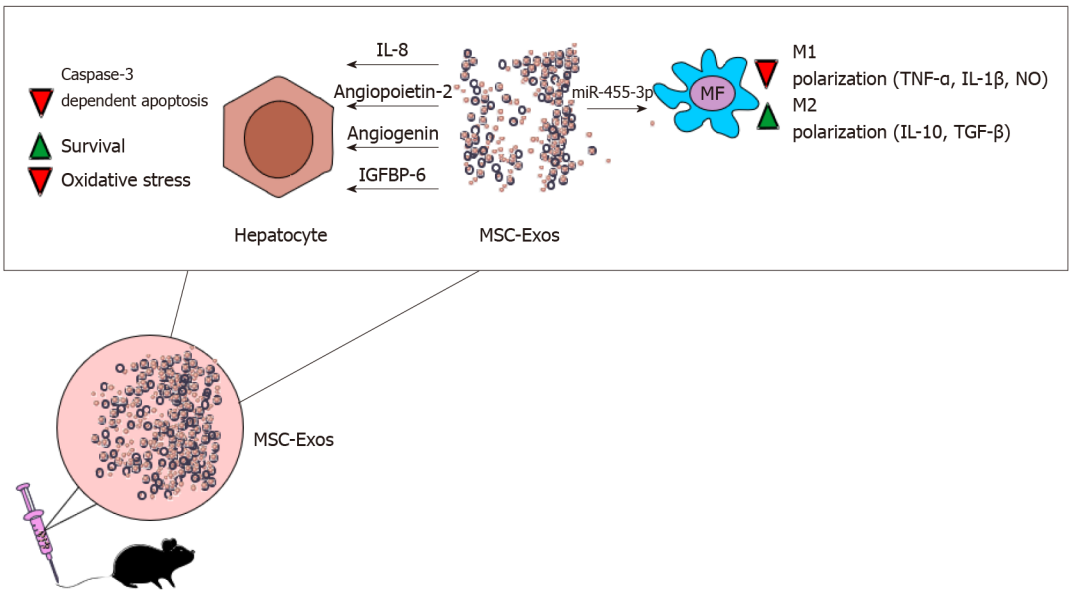
THERAPEUTIC POTENTIAL OF MSC-EXOS IN THE TREATMENT OF ACUTE LIVER INJURY

Although results obtained in animal studies strongly suggest that MSCs could be considered as new therapeutic agents in regenerative hepatology, there are several safety issues which limit clinical use of MSCs[31]. Firstly, MSCs are not constitutively immunosuppressive cells[32]. MSCs may adopt phenotype and function under the influence of biological factors to which they are exposed. When MSCs engraft in the tissue with low level of TNF-α and IFN-γ, they obtain pro-inflammatory MSC1 phenotype and secrete large number of bioactive factors which aggravate on-going inflammation. On the contrary, when MSCs are exposed to the high levels of TNF-α and IFN-γ, they acquire immunosuppressive MSC2 phenotype and produce immunoregulatory factors that suppress inflammatory immune cells[32]. Since local tissue concentration of TNF-α and IFN-γ differ in initial and recovery phases of acute liver inflammation, there is a concern that MSCs which will be engrafted in the injured livers with low level of TNF-α and IFN-γ may obtain pro-inflammatory MSC1 phenotype and may aggravate on-going inflammation[31,32]. Additionally, TGF-β and bone morphogenetic protein, released by macrophages in inflamed and regenerated tissues, may induce spontaneous and unwanted chondrogenic and osteogenic differentiation of MSCs[33]. Possible unwanted differentiation of transplanted MSCs represents an important safety concern which limits clinical use of MSCs in regenerative hepatology[33].

MSC-Exos are nano-sized extracellular vesicles which contain all of MSC-sourced immunoregulatory and angiomodulatory factors[34]. Due to their nano-sized dimension and lipid envelope, intravenously injected MSC-Exos by-pass all biological barriers and deliver their cargo (miRNAs) anti-inflammatory cytokines, growth factors) directly into the target liver-infiltrated immune cells and injured hepatocytes. Since the majority of MSC-dependent beneficial effects in attenuation of liver inflammation were relied on the activity of MSCs-sourced bioactive factors[25], administration of MSC-Exos is considered as an alternative therapeutic approach to MSC-based therapy since it addresses all safety concerns related to the transplantation of MSCs[34]. A detailed proteomic analysis revealed that MSC-Exos contained proteins that regulate hepatocyte survival, oxidative stress, tissue remodeling, activation and migration of immune cells[34]. Accordingly, several experimental studies demonstrated therapeutic potential of MSC-Exos in the treatment of ALF[35-37].

After intravenous injection, MSC-Exos obtained from MB-MSC-Exos migrated in the liver, attenuated D-Gal/LPS-induced acute liver inflammation and improved survival of in D-Gal/LPS-treated mice suffering from ALF[35]. By delivering immunosuppressive molecules and trophic factors in inflamed livers [IL-8, angiopoietin-2, angiogenin, insulin-like growth factor binding protein-6 (IGFBP-6)] MB-MSC-Exos attenuated caspase-3-dependent apoptosis of injured hepatocytes[35]. MB-MSCs-sourced IL-8 inhibited TNF-α-induced activation of caspase-3 and prevented apoptosis of hepatocytes while angiopoietin-2, angiogenin and IGFBP-6 promoted survival of hepatocytes by preventing the progression of ischemia-induced injury in inflamed livers[35].

The importance of anti-apoptotic effects of MSC-Exos in the treatment of ALF was confirmed in murine model of CCL4-induced acute liver injury[36]. Jiang and colleagues demonstrated that hepato-protective effects of Exos isolated from the secretome of human UC-MSCs (UC-MSC-Exos) were relied on their capacity to inhibit caspase 3 and Bcl-2-associated X protein-driven apoptosis of hepatocytes [36]. Additionally, significant decrease of oxidase metabolite 8-hydroxy-2-deoxyguanosine was observed in CCL4-injured livers 24 h after administration of UC-MSC-Exos, indicating that UC-MSC-Exos-dependent inhibition of oxidative stress in injured hepatocytes was, at least partially, responsible



DOI: 10.3748/wjg.v28.i28.3627 **Copyright** ©The Author(s) 2022.

Figure 2 Molecular mechanisms responsible for the beneficial effects of mesenchymal stem cell derived exosomes in attenuation of acute liver failure. By delivering interleukin (IL)-8, angiopoietin-2, angiogenin, insulin-like growth factor binding protein-6, mesenchymal stem cell derived exosomes (MSC-Exos) attenuate oxidative stress, suppress caspase-3-dependent apoptosis and promoted survival of hepatocytes in acutely injured livers. MSC-Exos, in miRNA-455-3p-dependent manner, alleviate on-going liver inflammation by inhibiting inflammatory, tumor necrosis factor alpha, IL-1β and nitric oxide-producing M1 macrophages and by promoting generation of immunosuppressive, transforming growth factor beta-β and IL-10-producing M2 macrophages. Abbreviations: MSC-Exos: Mesenchymal stem cell derived exosomes; IL: Interleukin; IGFBP6: Insulin like growth factor binding protein 6; TNF-α: Tumor necrosis factor alpha; NO: Nitric oxide.

for the alleviation of ALF in experimental mice[36].

As evidenced by Shao and colleagues, MSC-Exo-sourced miR-455-3p was crucially responsible for MSC-dependent immunosuppression in ALF[37]. MSC-derived miR-455-3p modulated activation of PI3K and attenuated synthesis of inflammatory cytokines IL-6, G-CSF, IL-17, IP-10, and MCP-1 in liver macrophages[37]. Significantly reduced necrosis of hepatocytes, down-regulated serum levels of aspartate aminotransferase, alanine transaminase and bilirubin were observed in CCL4 + miR-455-3p-treated mice. Additionally, miR-455-3p significantly reduced presence of CD68-expressing macrophages in the liver and decreased total number of circulating inflammatory CD14+ CD16+ and CCR2+ CD16+ monocytes in peripheral blood of CCL4-treated animals, indicating that beneficial effects of miR-455-3p was mainly relied on the suppression of inflammatory monocytes/macrophages[37] (Figure 2).

CONCLUSION

MSCs possess potent immunoregulatory, angiomodulatory and hepatoprotective properties[25,38]. Results obtained in experimental studies showed that MSCs and MSC-Exos were able to efficiently attenuate acute liver inflammation and to promote enhanced repair and regeneration of injured liver tissue, suggesting their potential clinical use in the therapy of ALF[25,38].

However, it should be noted that there are several issues that need to be addressed before MSCs and their exosomes could be offered as new remedy in regenerative hepatology. The optimal tissue source, dose, and frequency of MSCs/MSC-Exos should be defined. Up-coming studies should also precisely determine all MSC-sourced immunoregulatory and hepatoprotective factors which are responsible for their beneficial effects. Afterwards, bioengineering of MSCs which will massively produce these bioactive molecules should be performed. It is highly expected that these newly developed MSCs and their exosomes will have significantly enhanced efficacy in in the treatment of ALF.

FOOTNOTES

Author contributions: Harrell CR, Djonov V and Volarevic V analyzed the data and wrote the manuscript; Pavlovic D designed and created figures and wrote the manuscript; All authors have read and approve the final manuscript.

Conflict-of-interest statement: Authors declare no conflict of interests for this article.

Open-Access: This article is an open-access article that was selected by an in-house editor and fully peer-reviewed by external reviewers. It is distributed in accordance with the Creative Commons Attribution NonCommercial (CC BY-NC 4.0) license, which permits others to distribute, remix, adapt, build upon this work non-commercially, and license their derivative works on different terms, provided the original work is properly cited and the use is non-commercial. See: https://creativecommons.org/Licenses/by-nc/4.0/

Country/Territory of origin: Serbia

ORCID number: C Randall Harrell 0000-0002-5906-9198; Dragica Pavlovic 0000-0002-1948-5365; Valentin Djonov 0000-0003-0529-9665; Vladislav Volarevic 0000-0001-5948-9902.

S-Editor: Zhang H
L-Editor: A
P-Editor: Zhang H

REFERENCES

1 **Trefts E**, Gannon M, Wasserman DH. The liver. *Curr Biol* 2017; **27**: R1147-R1151 [PMID: 29112863 DOI: 10.1016/j.cub.2017.09.019]
2 **Stravitz RT**, Lee WM. Acute liver failure. *Lancet* 2019; **394**: 869-881 [PMID: 31498101 DOI: 10.1016/S0140-6736(19)31894-X]
3 **Bower WA**, Johns M, Margolis HS, Williams IT, Bell BP. Population-based surveillance for acute liver failure. *Am J Gastroenterol* 2007; **102**: 2459-2463 [PMID: 17608778 DOI: 10.1111/j.1572-0241.2007.01388.x]
4 **Lemmer P**, Pospiech JC, Canbay A. Liver failure-future challenges and remaining questions. *Ann Transl Med* 2021; **9**: 734 [PMID: 33987432 DOI: 10.21037/atm-20-4968]
5 **Dong V**, Nanchal R, Karvellas CJ. Pathophysiology of Acute Liver Failure. *Nutr Clin Pract* 2020; **35**: 24-29 [PMID: 31840297 DOI: 10.1002/ncp.10459]
6 **Zhang H**, Jiang Z, Zhang L. Dual effect of T helper cell 17 (Th17) and regulatory T cell (Treg) in liver pathological process: From occurrence to end stage of disease. *Int Immunopharmacol* 2019; **69**: 50-59 [PMID: 30669025 DOI: 10.1016/j.intimp.2019.01.005]
7 **Przybyl H**, Grindler J, Lauer D. Unfreezing What's Hot in Liver Transplantation: A Review of Current Trends. *AACN Adv Crit Care* 2022; **33**: 56-67 [PMID: 35259225 DOI: 10.4037/aacnacc2022728]
8 **Biolato M**, Bianco A, Lucchini M, Gasbarrini A, Mirabella M, Grieco A. The Disease-Modifying Therapies of Relapsing-Remitting Multiple Sclerosis and Liver Injury: A Narrative Review. *CNS Drugs* 2021; **35**: 861-880 [PMID: 34319570 DOI: 10.1007/s40263-021-00842-9]
9 **Hu C**, Li L. Improvement of mesenchymal stromal cells and their derivatives for treating acute liver failure. *J Mol Med (Berl)* 2019; **97**: 1065-1084 [PMID: 31197403 DOI: 10.1007/s00109-019-01804-x]
10 **Hu C**, Wu Z, Li L. Mesenchymal stromal cells promote liver regeneration through regulation of immune cells. *Int J Biol Sci* 2020; **16**: 893-903 [PMID: 32071558 DOI: 10.7150/ijbs.39725]
11 **Zhou JH**, Lu X, Yan CL, Sheng XY, Cao HC. Mesenchymal stromal cell-dependent immunoregulation in chemically-induced acute liver failure. *World J Stem Cells* 2021; **13**: 208-220 [PMID: 33815670 DOI: 10.4252/wjsc.v13.i3.208]
12 **Wu R**, Fan X, Wang Y, Shen M, Zheng Y, Zhao S, Yang L. Mesenchymal Stem Cell-Derived Extracellular Vesicles in Liver Immunity and Therapy. *Front Immunol* 2022; **13**: 833878 [PMID: 35309311 DOI: 10.3389/fimmu.2022.833878]
13 **Sang JF**, Shi XL, Han B, Huang T, Huang X, Ren HZ, Ding YT. Intraportal mesenchymal stem cell transplantation prevents acute liver failure through promoting cell proliferation and inhibiting apoptosis. *Hepatobiliary Pancreat Dis Int* 2016; **15**: 602-611 [PMID: 27919849 DOI: 10.1016/s1499-3872(16)60141-8]
14 **Cao H**, Yang J, Yu J, Pan Q, Li J, Zhou P, Li Y, Pan X, Wang Y, Li L. Therapeutic potential of transplanted placental mesenchymal stem cells in treating Chinese miniature pigs with acute liver failure. *BMC Med* 2012; **10**: 56 [PMID: 22673529 DOI: 10.1186/1741-7015-10-56]
15 **Teshima T**, Matsumoto H, Michishita M, Matsuoka A, Shiba M, Nagashima T, Koyama H. Allogenic Adipose Tissue-Derived Mesenchymal Stem Cells Ameliorate Acute Hepatic Injury in Dogs. *Stem Cells Int* 2017; **2017**: 3892514 [PMID: 29445402 DOI: 10.1155/2017/3892514]
16 **Sun L**, Fan X, Zhang L, Shi G, Aili M, Lu X, Jiang T, Zhang Y. Bone mesenchymal stem cell transplantation *via* four routes for the treatment of acute liver failure in rats. *Int J Mol Med* 2014; **34**: 987-996 [PMID: 25110277 DOI: 10.3892/ijmm.2014.1890]
17 **Wang J**, Liu Y, Ding H, Shi X, Ren H. Mesenchymal stem cell-secreted prostaglandin E_2 ameliorates acute liver failure *via* attenuation of cell death and regulation of macrophage polarization. *Stem Cell Res Ther* 2021; **12**: 15 [PMID: 33413632 DOI: 10.1186/s13287-020-02070-2]
18 **Miao CM**, Jiang XW, He K, Li PZ, Liu ZJ, Cao D, Ou ZB, Gong JP, Liu CA, Cheng Y. Bone marrow stromal cells attenuate LPS-induced mouse acute liver injury *via* the prostaglandin E 2-dependent repression of the NLRP3 inflammasome in Kupffer cells. *Immunol Lett* 2016; **179**: 102-113 [PMID: 27666012 DOI: 10.1016/j.imlet.2016.09.009]
19 **Liu J**, Feng B, Xu Y, Zhu J, Feng X, Chen W, Sheng X, Shi X, Pan Q, Yu J, Zeng X, Cao H, Li L. Immunomodulatory effect of mesenchymal stem cells in chemical-induced liver injury: a high-dimensional analysis. *Stem Cell Res Ther* 2019; **10**: 262 [PMID: 31443686 DOI: 10.1186/s13287-019-1379-6]
20 **Hua D**, Ju Z, Gan X, Wang Q, Luo C, Gu J, Yu Y. Human amniotic mesenchymal stromal cells alleviate acute liver injury

by inhibiting the pro-inflammatory response of liver resident macrophage through autophagy. *Ann Transl Med* 2019; **7**: 392 [PMID: 31555706 DOI: 10.21037/atm.2019.08.83]

21 **Zhang Y**, Cai W, Huang Q, Gu Y, Shi Y, Huang J, Zhao F, Liu Q, Wei X, Jin M, Wu C, Xie Q, Zhang Y, Wan B. Mesenchymal stem cells alleviate bacteria-induced liver injury in mice by inducing regulatory dendritic cells. *Hepatology* 2014; **59**: 671-682 [PMID: 23929707 DOI: 10.1002/hep.26670]

22 **Gazdic M**, Markovic BS, Arsenijevic A, Jovicic N, Acovic A, Harrell CR, Fellabaum C, Djonov V, Arsenijevic N, Lukic ML, Volarevic V. Crosstalk between mesenchymal stem cells and T regulatory cells is crucially important for the attenuation of acute liver injury. *Liver Transpl* 2018; **24**: 687-702 [PMID: 29500914 DOI: 10.1002/lt.25049]

23 **Gazdic M**, Simovic Markovic B, Vucicevic L, Nikolic T, Djonov V, Arsenijevic N, Trajkovic V, Lukic ML, Volarevic V. Mesenchymal stem cells protect from acute liver injury by attenuating hepatotoxicity of liver natural killer T cells in an inducible nitric oxide synthase- and indoleamine 2,3-dioxygenase-dependent manner. *J Tissue Eng Regen Med* 2018; **12**: e1173-e1185 [PMID: 28488390 DOI: 10.1002/term.2452]

24 **Milosavljevic N**, Gazdic M, Simovic Markovic B, Arsenijevic A, Nurkovic J, Dolicanin Z, Djonov V, Lukic ML, Volarevic V. Mesenchymal stem cells attenuate acute liver injury by altering ratio between interleukin 17 producing and regulatory natural killer T cells. *Liver Transpl* 2017; **23**: 1040-1050 [PMID: 28481005 DOI: 10.1002/lt.24784]

25 **Gazdic M**, Arsenijevic A, Markovic BS, Volarevic A, Dimova I, Djonov V, Arsenijevic N, Stojkovic M, Volarevic V. Mesenchymal Stem Cell-Dependent Modulation of Liver Diseases. *Int J Biol Sci* 2017; **13**: 1109-1117 [PMID: 29104502 DOI: 10.7150/ijbs.20240]

26 **Musina RA**, Bekchanova ES, Belyavskii AV, Sukhikh GT. Differentiation potential of mesenchymal stem cells of different origin. *Bull Exp Biol Med* 2006; **141**: 147-151 [PMID: 16929987 DOI: 10.1007/s10517-006-0115-2]

27 **Taléns-Visconti R**, Bonora A, Jover R, Mirabet V, Carbonell F, Castell JV, Gómez-Lechón MJ. Hepatogenic differentiation of human mesenchymal stem cells from adipose tissue in comparison with bone marrow mesenchymal stem cells. *World J Gastroenterol* 2006; **12**: 5834-5845 [PMID: 17007050 DOI: 10.3748/wjg.v12.i36.5834]

28 **Sawitza I**, Kordes C, Götze S, Herebian D, Häussinger D. Bile acids induce hepatic differentiation of mesenchymal stem cells. *Sci Rep* 2015; **5**: 13320 [PMID: 26304833 DOI: 10.1038/srep13320]

29 **Chivu M**, Dima SO, Stancu CI, Dobrea C, Uscatescu V, Necula LG, Bleotu C, Tanase C, Albulescu R, Ardeleanu C, Popescu I. In vitro hepatic differentiation of human bone marrow mesenchymal stem cells under differential exposure to liver-specific factors. *Transl Res* 2009; **154**: 122-132 [PMID: 19665688 DOI: 10.1016/j.trsl.2009.05.007]

30 **Manzini BM**, da Silva Santos Duarte A, Sankaramanivel S, Ramos AL, Latuf-Filho P, Escanhoela C, Kharmandayan P, Olalla Saad ST, Boin I, Malheiros Luzo ÂC. Useful properties of undifferentiated mesenchymal stromal cells and adipose tissue as the source in liver-regenerative therapy studied in an animal model of severe acute fulminant hepatitis. *Cytotherapy* 2015; **17**: 1052-1065 [PMID: 26139545 DOI: 10.1016/j.jcyt.2015.04.010]

31 **Volarevic V**, Markovic BS, Gazdic M, Volarevic A, Jovicic N, Arsenijevic N, Armstrong L, Djonov V, Lako M, Stojkovic M. Ethical and Safety Issues of Stem Cell-Based Therapy. *Int J Med Sci* 2018; **15**: 36-45 [PMID: 29333086 DOI: 10.7150/ijms.21666]

32 **Gazdic M**, Volarevic V, Arsenijevic N, Stojkovic M. Mesenchymal stem cells: a friend or foe in immune-mediated diseases. *Stem Cell Rev Rep* 2015; **11**: 280-287 [PMID: 25592610 DOI: 10.1007/s12015-014-9583-3]

33 **Rahman MS**, Akhtar N, Jamil HM, Banik RS, Asaduzzaman SM. TGF-β/BMP signaling and other molecular events: regulation of osteoblastogenesis and bone formation. *Bone Res* 2015; **3**: 15005 [PMID: 26273537 DOI: 10.1038/boneres.2015.5]

34 **Harrell CR**, Jovicic N, Djonov V, Arsenijevic N, Volarevic V. Mesenchymal Stem Cell-Derived Exosomes and Other Extracellular Vesicles as New Remedies in the Therapy of Inflammatory Diseases. *Cells* 2019; **8** [PMID: 31835680 DOI: 10.3390/cells8121605]

35 **Chen L**, Xiang B, Wang X, Xiang C. Exosomes derived from human menstrual blood-derived stem cells alleviate fulminant hepatic failure. *Stem Cell Res Ther* 2017; **8**: 9 [PMID: 28115012 DOI: 10.1186/s13287-016-0453-6]

36 **Jiang W**, Tan Y, Cai M, Zhao T, Mao F, Zhang X, Xu W, Yan Z, Qian H, Yan Y. Human Umbilical Cord MSC-Derived Exosomes Suppress the Development of CCl_4-Induced Liver Injury through Antioxidant Effect. *Stem Cells Int* 2018; **2018**: 6079642 [PMID: 29686713 DOI: 10.1155/2018/6079642]

37 **Shao M**, Xu Q, Wu Z, Chen Y, Shu Y, Cao X, Chen M, Zhang B, Zhou Y, Yao R, Shi Y, Bu H. Exosomes derived from human umbilical cord mesenchymal stem cells ameliorate IL-6-induced acute liver injury through miR-455-3p. *Stem Cell Res Ther* 2020; **11**: 37 [PMID: 31973730 DOI: 10.1186/s13287-020-1550-0]

38 **Harrell CR**, Djonov V, Volarevic V. The Cross-Talk between Mesenchymal Stem Cells and Immune Cells in Tissue Repair and Regeneration. *Int J Mol Sci* 2021; **22** [PMID: 33804369 DOI: 10.3390/ijms22052472]

World Journal of Gastroenterology

Submit a Manuscript: https://www.f6publishing.com

World J Gastroenterol 2022 July 28; 28(28): 3637-3643

DOI: 10.3748/wjg.v28.i28.3637

ISSN 1007-9327 (print) ISSN 2219-2840 (online)

MINIREVIEWS

Effective combinations of anti-cancer and targeted drugs for pancreatic cancer treatment

Arata Nishimoto

Specialty type: Oncology

Provenance and peer review: Invited article; Externally peer reviewed.

Peer-review model: Single blind

Peer-review report's scientific quality classification

Grade A (Excellent): 0
Grade B (Very good): B, B
Grade C (Good): 0
Grade D (Fair): 0
Grade E (Poor): 0

P-Reviewer: Chen H, China; lee Y, South Korea

Received: April 1, 2022
Peer-review started: April 1, 2022
First decision: May 9, 2022
Revised: June 6, 2022
Accepted: June 30, 2022
Article in press: June 30, 2022
Published online: July 28, 2022

Arata Nishimoto, Division of Basic Pharmaceutical Science, Department of Pharmacy, Faculty of Pharmaceutical Sciences, Sanyo-Onoda City University, Sanyo-Onoda City 756-0884, Yamaguchi, Japan

Corresponding author: Arata Nishimoto, PhD, Professor, Division of Basic Pharmaceutical Science, Department of Pharmacy, Faculty of Pharmaceutical Sciences, Sanyo-Onoda City University, 1-1-1 Daigaku-dori , Sanyo-Onoda City 756-0884, Yamaguchi, Japan.
anishimo@rs.socu.ac.jp

Abstract

Pancreatic cancer is highly aggressive and lethal. Due to the lack of effective methods for detecting the disease at an early stage, pancreatic cancer is frequently diagnosed late. Gemcitabine has been the standard chemotherapy drug for patients with pancreatic cancer for over 20 years, but its anti-tumor effect is limited. Therefore, FOLFIRINOX (leucovorin, fluorouracil, irinotecan, oxaliplatin) as well as combination therapies using gemcitabine and conventional agents, such as cisplatin and capecitabine, has also been administered; however, these have not resulted in complete remission. Therefore, there is a need to develop novel and effective therapies for pancreatic cancer. Recently, some studies have reported that combinations of gemcitabine and targeted drugs have had significant anti-tumor effects on pancreatic cancer cells. As gemcitabine induced DNA damage response, the proteins related to DNA damage response can be suitable additional targets for novel gemcitabine-based combination therapy. Furthermore, KRAS/RAF/MEK/ERK signaling triggered by oncogenic mutated *KRAS* and autophagy are frequently activated in pancreatic cancer. Therefore, these characteristics of pancreatic cancer are potential targets for developing effective novel therapies.

In this minireview, combinations of gemcitabine and targeted drugs to these characteristics, combinations of targeted drugs, combinations of natural products and anti-cancer agents, including gemcitabine, and combinations among natural products are discussed.

Key Words: Pancreatic cancer; Gemcitabine; Targeted drug; Combination therapy

©The Author(s) 2022. Published by Baishideng Publishing Group Inc. All rights reserved.

Core Tip: Gemcitabine has been the standard chemotherapy drug for patients with pancreatic cancer; however, its effectiveness is limited. Therefore, various combination therapies involving gemcitabine and targeted drugs are being explored. A review of combination therapies based mainly on clinical studies has been published recently; therefore, this minireview focuses on the findings of basic studies and discusses combinations of gemcitabine and targeted drugs, combinations of targeted drugs, combinations of natural products and anti-cancer agents, including gemcitabine, and combinations among natural products.

Citation: Nishimoto A. Effective combinations of anti-cancer and targeted drugs for pancreatic cancer treatment. *World J Gastroenterol* 2022; 28(28): 3637-3643
URL: https://www.wjgnet.com/1007-9327/full/v28/i28/3637.htm
DOI: https://dx.doi.org/10.3748/wjg.v28.i28.3637

INTRODUCTION

Pancreatic cancer is fatal and has a 5-year survival rate of approximate 10%[1]. It is estimated that pancreatic cancer will become the second most common cause of cancer-related deaths in the United States by 2030[2]. Pancreatic cancer is frequently diagnosed at a late stage owing to the lack of effective methods for detecting it at earlier stages and non-specific symptoms. Therefore, there is an urgent need to develop both novel effective therapies for pancreatic cancer that has progressed to a late stage and effective methods for detecting pancreatic cancer at an early stage.

Gemcitabine is the standard treatment for patients with pancreatic cancer. However, as the anti-tumor effect of gemcitabine is limited, FOLFIRINOX (leucovorin, fluorouracil, irinotecan, oxaliplatin) as well as combination therapies of gemcitabine and conventional agents, such as cisplatin and capecitabine, has also been administered[3-5]. Although these combination therapies improved overall survival compared to gemcitabine alone, they did not achieve complete remission. In addition, the incidence of toxicity associated with these combination therapies has increased[3-6].

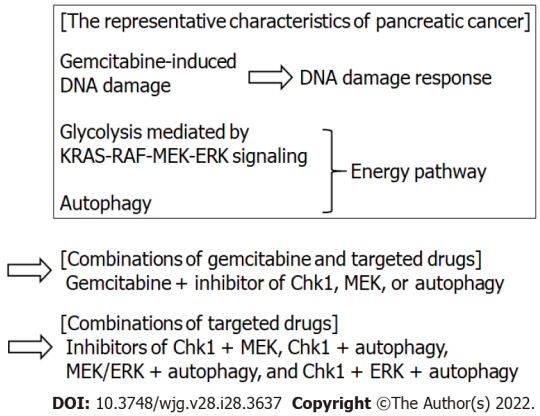
Recent studies have attempted to identify effective combinations of gemcitabine and targeted drugs for pancreatic cancer. As gemcitabine, a well-known DNA-damaging agent, induced DNA damage response, the proteins related to DNA damage response can be suitable additional targets for novel gemcitabine-based combination therapy. Furthermore, KRAS/RAF/MEK/ERK signaling triggered by oncogenic mutated *KRAS* and autophagy, which are described as the characteristics of pancreatic ductal adenocarcinoma (PDAC), are frequently activated. Therefore, these characteristics are promising targets for effective novel therapeutic strategies[7-12]. An excellent review on effective combination therapies for pancreatic cancer was published recently[13]. This review was based mainly on the findings of preclinical and clinical studies[13]; therefore, this minireview focuses on the findings of basic studies and discusses combinations of gemcitabine and targeted drugs, combinations of targeted drugs, combinations of natural products and anti-cancer agents, including gemcitabine, and combinations among natural products.

COMBINATIONS OF GEMCITABINE AND TARGETED DRUGS

Gemcitabine, a well-known DNA-damaging agent, has been the standard first-line drug for patients with pancreatic cancer. However, the efficacy of gemcitabine in pancreatic cancer is limited and a novel gemcitabine-based combination therapy is required. In this section and Figure 1, combinations of gemcitabine and targeted drugs to enhance the anti-tumor effect are summarized.

Gemcitabine and Chk1 inhibitor

Quinone-methide triterpenoid pristimerin induces lysosomal degradation of checkpoint kinase 1 (Chk1) and augments the expression of γ-H2AX, which is a biomarker of DNA damage following gemcitabine treatment[14]. Furthermore, the combination of gemcitabine and pristimerin was shown to increase apoptosis of pancreatic cancer cells[14]. The Chk1 inhibitor MK-8776 also enhances the sensitivity of multiple human cancer cell lines, including pancreatic cancer cells, to gemcitabine[15]. The DNA damage response mediated by Chk1 in pancreatic cancer stem cells was greater than that in non-pancreatic cancer stem cells, indicating that Chk1 inhibition selectively sensitizes pancreatic cancer stem cells to gemcitabine[16]. The combination of Chk1 inhibition and gemcitabine reduces the ability of tumor initiation in pancreatic cancer stem cells[16]. The anti-tumor effect of the combination of gemcitabine and doublecortin-like kinase 1 (Dclk1) inhibitor has also been reported[17]. The latter significantly decreased the expression of gemcitabine-induced phosphorylated Chk1 in pancreatic cancer cells. The combination of gemcitabine and Dclk1 inhibitor did not arrest the cell cycle at the S



DOI: 10.3748/wjg.v28.i28.3637 **Copyright** ©The Author(s) 2022.

Figure 1 The representative characteristics of pancreatic cancer as potential targets for effective combination therapy.

phase and allowed cell cycle progression[17]. In addition, the combination of gemcitabine and Dclk1 inhibitor increased the rate of γ-H2AX-positive cells compared to individual treatments. The combination of gemcitabine and Dclk1 inhibitor induced PARP1 cleavage as well as caspase-3 activation and significantly decreased the survival rate of pancreatic cancer cells compared to gemcitabine treatment alone[17].

Gemcitabine and KRAS antibody/MEK inhibitor

Oncogenic *KRAS* mutations are present in approximately 90% of pancreatic cancer cases. Consequently, KRAS and its downstream proteins, such as RAF, MEK, and ERK, are activated in pancreatic cancer cases and contribute to the progression of the disease. Therefore, inhibitors targeting these proteins may be effective in inhibiting this progression.

Antibodies that bind intracellularly to the activated GTP-bound form of oncogenic KRAS mutants have been developed and significantly sensitize pancreatic cancer cells to gemcitabine[18,19]. These antibodies synergistically increase the anti-tumor effect of gemcitabine by inhibiting the RAF/MEK/ERK signaling pathway downstream of KRAS[18,19]. The antibodies are internalized in the cytoplasm by endocytosis through the tumor-associated receptors of extracellular epithelial cell adhesion molecules[19]. These antibodies synergistically increase the anti-tumor effect of gemcitabine by inhibiting KRAS/RAF/MEK/ERK signaling in pancreatic cancer cells[18,19].

The MEK inhibitor, trametinib, both alone and in combination with gemcitabine, was shown to exhibit significantly enhanced anti-tumor effects compared to gemcitabine alone[20]. The combination of gemcitabine and trametinib also increased the inhibition of tumor growth in pancreatic cancer patient-derived orthotopic xenografts in nude mice compared to trametinib alone[20]. Moreover, the combination of the MEK inhibitors, trametinib and cobimetinib, prevented tumor growth in gemcitabine-resistant pancreatic cancer patient-derived orthotopic xenografts in nude mice[21]. These results suggest that such combinations have therapeutic potential against pancreatic cancer.

Gemcitabine and autophagy inhibitor

Gemcitabine has significantly been shown to increase autophagy induction in human pancreatic cancer cells, and combined treatment with gemcitabine and chloroquine, an autophagy inhibitor, triggered a marked boost in reactive oxygen species (ROS) levels and increased lysosomal membrane permeability [22]. Consequently, proteases, including cathepsins, are released from lysosomes into the cytoplasm, leading to apoptosis. Thus, the combination of gemcitabine and chloroquine has an anti-tumor effect on pancreatic cancer cells through the apoptotic pathway by lysosomal dysfunction *via* a marked boost of ROS[22]. Cancer stem cells are considered to be responsible for the recurrence and chemoresistance of cancer. The expression of the markers of cancer stem cells, aldehyde dehydrogenase 1, CD44, and CD133, was found to be positively correlated with the expression of LC3 type II, an autophagy marker, in pancreatic cancer tissues[23]; this suggests an association between autophagy and cancer stem cells. Indeed, autophagy inhibition decreased the activity of sphere formation of pancreatic cancer stem cells, and gemcitabine and autophagy inhibition markedly reduced the populations of cancer stem cells[23].

COMBINATIONS OF TARGETED DRUGS

Recent studies have demonstrated that combinations of targeted drugs have potential for developing novel and effective therapy for pancreatic cancer. In this section and Figure 1, combinations of targeted drugs for PDAC therapy are summarized.

ERK and autophagy inhibitors

KRAS suppression or ERK inhibition was shown to decrease both glycolytic and mitochondrial functions and to increase autophagic flux in PDAC, suggesting that ERK inhibition enhances dependence on autophagy[24]. The combination of ERK and autophagy inhibitors synergistically enhanced anti-tumor activity in KRAS-driven PDAC *via* the dysfunction of the energy pathways consisting of glycolysis and autophagy[24]. It has been reported that inhibition of the KRAS/RAF/MEK/ERK signaling pathway elicits autophagy, resulting in protection of PDAC cells from cytotoxic effects[25]. The combination of MEK1/2 and autophagy inhibitors showed synergistic anti-tumor effects against PDAC cells *in vitro* and promoted the regression of patient-derived xenografts of PDAC in mice[25]. Furthermore, the effect of the combination of trametinib and chloroquine was not limited to PDAC and resulted in similar responses in patient-derived xenografts of *BRAF*-mutated colorectal cancer and *NRAS*-mutated melanoma[25].

ERK, Chk1, and autophagy inhibitors

Screening of druggable genes by genetic loss-of-function using CRISPR-Cas9 and small interfering RNA revealed that components of the ATR-Chk1 DNA damage response pathway were modulators of sensitivity to ERK inhibitor treatment in *KRAS-mutant* PDAC[26]. Chk1 inhibition suppressed the growth of both PDAC cell lines and organoids and activated ERK signaling and autophagy, suggesting that Chk1 inhibition enhances dependence on ERK signaling and autophagy[26]. These findings provide a mechanistic basis for the effectiveness of the inhibition of Chk1, ERK, and autophagy. Indeed, this triple combination of inhibitors synergistically enhanced the anti-tumor effect in *KRAS-mutant* PDAC [26].

2-deoxyglucose and MEK inhibitor

Pooled shRNA library screening was used in an orthotopic xenograft model to identify multiple glycolysis genes as potential targets that may sensitize PDAC cells to MEK inhibition[27]. Apoptosis in KrasG12D-driven PDAC cells was synergistically induced, *in vitro*, *via* the combination of 2-deoxyglucose, a glycolysis inhibitor, and a MEK inhibitor; the same also inhibited tumor growth of PDAC xenografts, leading to prolonged overall survival in a genetically engineered PDAC mouse model[27]. Molecular and metabolic analyses revealed that the combined inhibition of glycolysis and ERK signaling synergistically caused apoptosis by inducing lethal stress in the endoplasmic reticulum. These results indicate that the combination of 2-deoxyglucose and a MEK inhibitor may be an effective approach for targeting KRAS-driven PDAC[27].

Replication stress response and autophagy inhibitors

PDAC exhibits high basal lysosomal activity and relies on lysosome-dependent recycling pathways, such as autophagy, to generate substrates for metabolism[28]. Kinase inhibitor screening revealed that the replication stress response inhibitor and chloroquine, an autophagy inhibitor that works *via* the functional inhibition of lysosomes, were synthetically lethal in PDAC cells[28]. Chloroquine induces replication stress due to aspartate depletion, and a replication stress response inhibitor and chloroquine synergistically inhibit tumor growth in PDAC[28].

Immune checkpoint and autophagy inhibitors

Major histocompatibility complex class I (MHC-I) molecules are selectively degraded *via* autophagy in PDAC[29]. Consequently, the expression of MHC-I at the cell surface is reduced, and MHC-I is localized predominantly within autophagosomes and lysosomes. Autophagy inhibition was shown to restore the expression of MHC-I at the cell surface and improve antigen presentation[29]. Furthermore, autophagy inhibition synergizes with dual immune checkpoint blockade therapy (anti-PD1 and anti-CTLA4 antibodies) to enhance the anti-tumor immune response and reduce tumor growth in syngeneic host mice[29].

COMBINATIONS OF NATURAL PRODUCTS AND ANTI-CANCER AGENTS, INCLUDING GEMCITABINE

The use of natural products as adjunctive therapies for pancreatic cancer has a great potential due to the anti-cancer efficacy and low toxicity. Yue *et al*[30] summarized combinations of natural products and anti-cancer agents, including gemcitabine, and combinations among natural products. They focused on the following: combinations of natural products and gemcitabine (for example, cucurbitacin B and gemcitabine[31], glaucarubinone and gemcitabine[32], escin and gemcitabine[33], and gum mastic and gemcitabine[34]); combinations of natural products and other agents, such as all-trans retinoic acid and sulindac (for example, 12-O-tetradecanoylphorbol-13-acetate and all-trans retinoic acid[35], parthenolide and sulindac[36], and triptolide and hydroxycamptothecin[37]); and combinations among natural products (for example, sulforaphane and quercetin[38], wogonin, apigenin, and chrysin[39], and

metformin and aspirin[40]).

While agents from purified chemical compounds generally target single molecules, natural products mostly consist of multiple components that concurrently act on various molecular targets. Therefore, natural products are expected to have various functions, including improvement of anti-cancer efficacy, enhancement of immune system, and reduction of side effects[41].

CONCLUSION

In general, it is widely accepted that combination therapy is more effective than monotherapy. In this minireview, combinations of gemcitabine and targeted drugs, combinations of targeted drugs, combinations of natural products and anti-cancer agents, including gemcitabine, and combinations among natural products are described. Hereafter, preclinical and clinical studies are needed to examine the possibility for clinical applications. Concurrently, additional basic studies that attempt to identify combinations that synergize anti-cancer effects are needed to find the better treatment options.

FOOTNOTES

Author contributions: Nishimoto A wrote the manuscript.

Conflict-of-interest statement: There is no conflict of interest related to this minireview manuscript.

Open-Access: This article is an open-access article that was selected by an in-house editor and fully peer-reviewed by external reviewers. It is distributed in accordance with the Creative Commons Attribution NonCommercial (CC BY-NC 4.0) license, which permits others to distribute, remix, adapt, build upon this work non-commercially, and license their derivative works on different terms, provided the original work is properly cited and the use is non-commercial. See: https://creativecommons.org/Licenses/by-nc/4.0/

Country/Territory of origin: Japan

ORCID number: Arata Nishimoto 0000-0002-7406-0247.

S-Editor: Ma YJ
L-Editor: A
P-Editor: Ma YJ

REFERENCES

1 **Siegel RL**, Miller KD, Fuchs HE, Jemal A. Cancer statistics, 2022. *CA Cancer J Clin* 2022; **72**: 7-33 [PMID: 35020204 DOI: 10.3322/caac.21708]

2 **Rahib L**, Smith BD, Aizenberg R, Rosenzweig AB, Fleshman JM, Matrisian LM. Projecting cancer incidence and deaths to 2030: the unexpected burden of thyroid, liver, and pancreas cancers in the United States. *Cancer Res* 2014; **74**: 2913-2921 [PMID: 24840647 DOI: 10.1158/0008-5472.CAN-14-0155]

3 **Neoptolemos JP**, Palmer DH, Ghaneh P, Psarelli EE, Valle JW, Halloran CM, Faluyi O, O'Reilly DA, Cunningham D, Wadsley J, Darby S, Meyer T, Gillmore R, Anthoney A, Lind P, Glimelius B, Falk S, Izbicki JR, Middleton GW, Cummins S, Ross PJ, Wasan H, McDonald A, Crosby T, Ma YT, Patel K, Sherriff D, Soomal R, Borg D, Sothi S, Hammel P, Hackert T, Jackson R, Büchler MW; European Study Group for Pancreatic Cancer. Comparison of adjuvant gemcitabine and capecitabine with gemcitabine monotherapy in patients with resected pancreatic cancer (ESPAC-4): a multicentre, open-label, randomised, phase 3 trial. *Lancet* 2017; **389**: 1011-1024 [PMID: 28129987 DOI: 10.1016/S0140-6736(16)32409-6]

4 **Ouyang G**, Liu Z, Huang S, Li Q, Xiong L, Miao X, Wen Y. Gemcitabine plus cisplatin versus gemcitabine alone in the treatment of pancreatic cancer: a meta-analysis. *World J Surg Oncol* 2016; **14**: 59 [PMID: 26927942 DOI: 10.1186/s12957-016-0813-9]

5 **Conroy T**, Desseigne F, Ychou M, Bouché O, Guimbaud R, Bécouarn Y, Adenis A, Raoul JL, Gourgou-Bourgade S, de la Fouchardière C, Bennouna J, Bachet JB, Khemissa-Akouz F, Péré-Vergé D, Delbaldo C, Assenat E, Chauffert B, Michel P, Montoto-Grillot C, Ducreux M; Groupe Tumeurs Digestives of Unicancer; PRODIGE Intergroup. FOLFIRINOX versus gemcitabine for metastatic pancreatic cancer. *N Engl J Med* 2011; **364**: 1817-1825 [PMID: 21561347 DOI: 10.1056/NEJMoa1011923]

6 **Peixoto RD**, Ho M, Renouf DJ, Lim HJ, Gill S, Ruan JY, Cheung WY. Eligibility of Metastatic Pancreatic Cancer Patients for First-Line Palliative Intent nab-Paclitaxel Plus Gemcitabine Versus FOLFIRINOX. *Am J Clin Oncol* 2017; **40**: 507-511 [PMID: 25844823 DOI: 10.1097/COC.0000000000000193]

7 **Waters AM**, Der CJ. KRAS: The Critical Driver and Therapeutic Target for Pancreatic Cancer. *Cold Spring Harb Perspect Med* 2018; **8** [PMID: 29229669 DOI: 10.1101/cshperspect.a031435]

8 **Bannoura SF**, Uddin MH, Nagasaka M, Fazili F, Al-Hallak MN, Philip PA, El-Rayes B, Azmi AS. Targeting KRAS in pancreatic cancer: new drugs on the horizon. *Cancer Metastasis Rev* 2021; **40**: 819-835 [PMID: 34499267 DOI:

10.1007/s10555-021-09990-2]
9 **Mann KM**, Ying H, Juan J, Jenkins NA, Copeland NG. KRAS-related proteins in pancreatic cancer. *Pharmacol Ther* 2016; **168**: 29-42 [PMID: 27595930 DOI: 10.1016/j.pharmthera.2016.09.003]
10 **Neuzillet C**, Tijeras-Raballand A, de Mestier L, Cros J, Faivre S, Raymond E. MEK in cancer and cancer therapy. *Pharmacol Ther* 2014; **141**: 160-171 [PMID: 24121058 DOI: 10.1016/j.pharmthera.2013.10.001]
11 **Raufi AG**, Liguori NR, Carlsen L, Parker C, Hernandez Borrero L, Zhang S, Tian X, Louie A, Zhou L, Seyhan AA, El-Deiry WS. Therapeutic Targeting of Autophagy in Pancreatic Ductal Adenocarcinoma. *Front Pharmacol* 2021; **12**: 751568 [PMID: 34916936 DOI: 10.3389/fphar.2021.751568]
12 **Piffoux M**, Eriau E, Cassier PA. Autophagy as a therapeutic target in pancreatic cancer. *Br J Cancer* 2021; **124**: 333-344 [PMID: 32929194 DOI: 10.1038/s41416-020-01039-5]
13 **Miller AL**, Garcia PL, Yoon KJ. Developing effective combination therapy for pancreatic cancer: An overview. *Pharmacol Res* 2020; **155**: 104740 [PMID: 32135247 DOI: 10.1016/j.phrs.2020.104740]
14 **Jiang Z**, Zhao Y, Liu Y, Tao L. Pristimerin synergizes with gemcitabine through abrogating Chk1/53BP1-mediated DNA repair in pancreatic cancer cells. *Food Chem Toxicol* 2021; **147**: 111919 [PMID: 33301843 DOI: 10.1016/j.fct.2020.111919]
15 **Engelke CG**, Parsels LA, Qian Y, Zhang Q, Karnak D, Robertson JR, Tanska DM, Wei D, Davis MA, Parsels JD, Zhao L, Greenson JK, Lawrence TS, Maybaum J, Morgan MA. Sensitization of pancreatic cancer to chemoradiation by the Chk1 inhibitor MK8776. *Clin Cancer Res* 2013; **19**: 4412-4421 [PMID: 23804422 DOI: 10.1158/1078-0432.CCR-12-3748]
16 **Venkatesha VA**, Parsels LA, Parsels JD, Zhao L, Zabludoff SD, Simeone DM, Maybaum J, Lawrence TS, Morgan MA. Sensitization of pancreatic cancer stem cells to gemcitabine by Chk1 inhibition. *Neoplasia* 2012; **14**: 519-525 [PMID: 22787433 DOI: 10.1593/neo.12538]
17 **Kawamura D**, Takemoto Y, Nishimoto A, Ueno K, Hosoyama T, Shirasawa B, Tanaka T, Kugimiya N, Harada E, Hamano K. Enhancement of cytotoxic effects of gemcitabine by Dclk1 inhibition through suppression of Chk1 phosphorylation in human pancreatic cancer cells. *Oncol Rep* 2017; **38**: 3238-3244 [PMID: 29048622 DOI: 10.3892/or.2017.5974]
18 **Kang YW**, Lee JE, Jung KH, Son MK, Shin SM, Kim SJ, Fang Z, Yan HH, Park JH, Han B, Cheon MJ, Woo MG, Lim JH, Kim YS, Hong SS. KRAS targeting antibody synergizes anti-cancer activity of gemcitabine against pancreatic cancer. *Cancer Lett* 2018; **438**: 174-186 [PMID: 30217561 DOI: 10.1016/j.canlet.2018.09.013]
19 **Lee JE**, Kang YW, Jung KH, Son MK, Shin SM, Kim JS, Kim SJ, Fang Z, Yan HH, Park JH, Yoon YC, Han B, Cheon MJ, Woo MG, Seo MS, Lim JH, Kim YS, Hong SS. Intracellular KRAS-specific antibody enhances the anti-tumor efficacy of gemcitabine in pancreatic cancer by inducing endosomal escape. *Cancer Lett* 2021; **507**: 97-111 [PMID: 33744388 DOI: 10.1016/j.canlet.2021.03.015]
20 **Kawaguchi K**, Igarashi K, Miyake K, Lwin TM, Miyake M, Kiyuna T, Hwang HK, Murakami T, Delong JC, Singh SR, Clary B, Bouvet M, Unno M, Hoffman RM. MEK inhibitor trametinib in combination with gemcitabine regresses a patient-derived orthotopic xenograft (PDOX) pancreatic cancer nude mouse model. *Tissue Cell* 2018; **52**: 124-128 [PMID: 29857821 DOI: 10.1016/j.tice.2018.05.003]
21 **Kawaguchi K**, Igarashi K, Murakami T, Kiyuna T, Lwin TM, Hwang HK, Delong JC, Clary BM, Bouvet M, Unno M, Hoffman RM. MEK inhibitors cobimetinib and trametinib, regressed a gemcitabine-resistant pancreatic-cancer patient-derived orthotopic xenograft (PDOX). *Oncotarget* 2017; **8**: 47490-47496 [PMID: 28537897 DOI: 10.18632/oncotarget.17667]
22 **Fu Z**, Cheng X, Kuang J, Feng H, Chen L, Liang J, Shen X, Yuen S, Peng C, Shen B, Jin Z, Qiu W. CQ sensitizes human pancreatic cancer cells to gemcitabine through the lysosomal apoptotic pathway *via* reactive oxygen species. *Mol Oncol* 2018; **12**: 529-544 [PMID: 29453806 DOI: 10.1002/1878-0261.12179]
23 **Yang MC**, Wang HC, Hou YC, Tung HL, Chiu TJ, Shan YS. Blockade of autophagy reduces pancreatic cancer stem cell activity and potentiates the tumoricidal effect of gemcitabine. *Mol Cancer* 2015; **14**: 179 [PMID: 26458814 DOI: 10.1186/s12943-015-0449-3]
24 **Bryant KL**, Stalnecker CA, Zeitouni D, Klomp JE, Peng S, Tikunov AP, Gunda V, Pierobon M, Waters AM, George SD, Tomar G, Papke B, Hobbs GA, Yan L, Hayes TK, Diehl JN, Goode GD, Chaika NV, Wang Y, Zhang GF, Witkiewicz AK, Knudsen ES, Petricoin EF 3rd, Singh PK, Macdonald JM, Tran NL, Lyssiotis CA, Ying H, Kimmelman AC, Cox AD, Der CJ. Combination of ERK and autophagy inhibition as a treatment approach for pancreatic cancer. *Nat Med* 2019; **25**: 628-640 [PMID: 30833752 DOI: 10.1038/s41591-019-0368-8]
25 **Kinsey CG**, Camolotto SA, Boespflug AM, Guillen KP, Foth M, Truong A, Schuman SS, Shea JE, Seipp MT, Yap JT, Burrell LD, Lum DH, Whisenant JR, Gilcrease GW 3rd, Cavalieri CC, Rehbein KM, Cutler SL, Affolter KE, Welm AL, Welm BE, Scaife CL, Snyder EL, McMahon M. Protective autophagy elicited by RAF→MEK→ERK inhibition suggests a treatment strategy for RAS-driven cancers. *Nat Med* 2019; **25**: 620-627 [PMID: 30833748 DOI: 10.1038/s41591-019-0367-9]
26 **Klomp JE**, Lee YS, Goodwin CM, Papke B, Klomp JA, Waters AM, Stalnecker CA, DeLiberty JM, Drizyte-Miller K, Yang R, Diehl JN, Yin HH, Pierobon M, Baldelli E, Ryan MB, Li S, Peterson J, Smith AR, Neal JT, McCormick AK, Kuo CJ, Counter CM, Petricoin EF 3rd, Cox AD, Bryant KL, Der CJ. CHK1 protects oncogenic KRAS-expressing cells from DNA damage and is a target for pancreatic cancer treatment. *Cell Rep* 2021; **37**: 110060 [PMID: 34852220 DOI: 10.1016/j.celrep.2021.110060]
27 **Yan L**, Tu B, Yao J, Gong J, Carugo A, Bristow CA, Wang Q, Zhu C, Dai B, Kang Y, Han L, Feng N, Jin Y, Fleming J, Heffernan TP, Yao W, Ying H. Targeting Glucose Metabolism Sensitizes Pancreatic Cancer to MEK Inhibition. *Cancer Res* 2021; **81**: 4054-4065 [PMID: 34117030 DOI: 10.1158/0008-5472.CAN-20-3792]
28 **Elliott IA**, Dann AM, Xu S, Kim SS, Abt ER, Kim W, Poddar S, Moore A, Zhou L, Williams JL, Capri JR, Ghukasyan R, Matsumura C, Tucker DA, Armstrong WR, Cabebe AE, Wu N, Li L, Le TM, Radu CG, Donahue TR. Lysosome inhibition sensitizes pancreatic cancer to replication stress by aspartate depletion. *Proc Natl Acad Sci U S A* 2019; **116**: 6842-6847 [PMID: 30894490 DOI: 10.1073/pnas.1812410116]
29 **Yamamoto K**, Venida A, Yano J, Biancur DE, Kakiuchi M, Gupta S, Sohn ASW, Mukhopadhyay S, Lin EY, Parker SJ,

Banh RS, Paulo JA, Wen KW, Debnath J, Kim GE, Mancias JD, Fearon DT, Perera RM, Kimmelman AC. Autophagy promotes immune evasion of pancreatic cancer by degrading MHC-I. *Nature* 2020; **581**: 100-105 [PMID: 32376951 DOI: 10.1038/s41586-020-2229-5]

30 **Yue Q**, Gao G, Zou G, Yu H, Zheng X. Natural Products as Adjunctive Treatment for Pancreatic Cancer: Recent Trends and Advancements. *Biomed Res Int* 2017; **2017**: 8412508 [PMID: 28232946 DOI: 10.1155/2017/8412508]

31 **Thoennissen NH**, Iwanski GB, Doan NB, Okamoto R, Lin P, Abbassi S, Song JH, Yin D, Toh M, Xie WD, Said JW, Koeffler HP. Cucurbitacin B induces apoptosis by inhibition of the JAK/STAT pathway and potentiates antiproliferative effects of gemcitabine on pancreatic cancer cells. *Cancer Res* 2009; **69**: 5876-5884 [PMID: 19605406 DOI: 10.1158/0008-5472.CAN-09-0536]

32 **Yeo D**, Huynh N, Beutler JA, Christophi C, Shulkes A, Baldwin GS, Nikfarjam M, He H. Glaucarubinone and gemcitabine synergistically reduce pancreatic cancer growth *via* down-regulation of P21-activated kinases. *Cancer Lett* 2014; **346**: 264-272 [PMID: 24491405 DOI: 10.1016/j.canlet.2014.01.001]

33 **Wang YW**, Wang SJ, Zhou YN, Pan SH, Sun B. Escin augments the efficacy of gemcitabine through down-regulation of nuclear factor-κB and nuclear factor-κB-regulated gene products in pancreatic cancer both in vitro and in vivo. *J Cancer Res Clin Oncol* 2012; **138**: 785-797 [PMID: 22270965 DOI: 10.1007/s00432-012-1152-z]

34 **Huang XY**, Wang HC, Yuan Z, Li A, He ML, Ai KX, Zheng Q, Qin HL. Gemcitabine combined with gum mastic causes potent growth inhibition and apoptosis of pancreatic cancer cells. *Acta Pharmacol Sin* 2010; **31**: 741-745 [PMID: 20523344 DOI: 10.1038/aps.2010.54]

35 **Avila GE**, Zheng X, Cui XX, Ryan AD, Hansson A, Suh J, Rabson AB, Chang RL, Shih WJ, Lin Y, Crowell P, Lu YP, Lou YR, Conney AH. Inhibitory effects of 12-O-tetradecanoylphorbol-13-acetate alone or in combination with all-trans retinoic acid on the growth of cultured human pancreas cancer cells and pancreas tumor xenografts in immunodeficient mice. *J Pharmacol Exp Ther* 2005; **315**: 170-187 [PMID: 15976015 DOI: 10.1124/jpet.105.087585]

36 **Yip-Schneider MT**, Nakshatri H, Sweeney CJ, Marshall MS, Wiebke EA, Schmidt CM. Parthenolide and sulindac cooperate to mediate growth suppression and inhibit the nuclear factor-kappa B pathway in pancreatic carcinoma cells. *Mol Cancer Ther* 2005; **4**: 587-594 [PMID: 15827332 DOI: 10.1158/1535-7163.MCT-04-0215]

37 **Yang SW**, Wang W, Xie XY, Zhu WP, Li FQ. In vitro synergistic cytotoxic effect of triptolide combined with hydroxycamptothecin on pancreatic cancer cells. *Am J Chin Med* 2011; **39**: 121-134 [PMID: 21213403 DOI: 10.1142/S0192415X11008695]

38 **Srivastava RK**, Tang SN, Zhu W, Meeker D, Shankar S. Sulforaphane synergizes with quercetin to inhibit self-renewal capacity of pancreatic cancer stem cells. *Front Biosci (Elite Ed)* 2011; **3**: 515-528 [PMID: 21196331 DOI: 10.2741/e266]

39 **Ding J**, Polier G, Köhler R, Giaisi M, Krammer PH, Li-Weber M. Wogonin and related natural flavones overcome tumor necrosis factor-related apoptosis-inducing ligand (TRAIL) protein resistance of tumors by down-regulation of c-FLIP protein and up-regulation of TRAIL receptor 2 expression. *J Biol Chem* 2012; **287**: 641-649 [PMID: 22086925 DOI: 10.1074/jbc.M111.286526]

40 **Yue W**, Zheng X, Lin Y, Yang CS, Xu Q, Carpizo D, Huang H, DiPaola RS, Tan XL. Metformin combined with aspirin significantly inhibit pancreatic cancer cell growth in vitro and in vivo by suppressing anti-apoptotic proteins Mcl-1 and Bcl-2. *Oncotarget* 2015; **6**: 21208-21224 [PMID: 26056043 DOI: 10.18632/oncotarget.4126]

41 **Li L**, Leung PS. Use of herbal medicines and natural products: an alternative approach to overcoming the apoptotic resistance of pancreatic cancer. *Int J Biochem Cell Biol* 2014; **53**: 224-236 [PMID: 24875648 DOI: 10.1016/j.biocel.2014.05.021]

World Journal of Gastroenterology

Submit a Manuscript: https://www.f6publishing.com

World J Gastroenterol 2022 July 28; 28(28): 3644-3665

DOI: 10.3748/wjg.v28.i28.3644

ISSN 1007-9327 (print) ISSN 2219-2840 (online)

ORIGINAL ARTICLE

Basic Study

Mechanism of electroacupuncture and herb-partitioned moxibustion on ulcerative colitis animal model: A study based on proteomics

Qin Qi, Rui Zhong, Ya-Nan Liu, Chen Zhao, Yan Huang, Yuan Lu, Zhe Ma, Han-Dan Zheng, Lu-Yi Wu

Specialty type: Gastroenterology and hepatology

Provenance and peer review: Unsolicited article; Externally peer reviewed.

Peer-review model: Single blind

Peer-review report's scientific quality classification

Grade A (Excellent): A
Grade B (Very good): 0
Grade C (Good): C, C
Grade D (Fair): 0
Grade E (Poor): 0

P-Reviewer: Moldogazieva NT, Russia; Saleem S, Pakistan

Received: September 3, 2021
Peer-review started: September 3, 2021
First decision: November 7, 2021
Revised: November 19, 2021
Accepted: June 24, 2022
Article in press: June 24, 2022
Published online: July 28, 2022

Qin Qi, Ya-Nan Liu, Yan Huang, Yuan Lu, Zhe Ma, Han-Dan Zheng, Lu-Yi Wu, Yueyang Hospital of Integrated Traditional Chinese and Western Medicine, Shanghai University of Traditional Chinese Medicine, Shanghai 200437, China

Rui Zhong, Shanghai QiGong Research Institute, Shanghai University of Traditional Chinese Medicine, Shanghai 200030, China

Chen Zhao, School of Acupuncture, Moxibustion and Tuina, Shanghai University of Traditional Chinese Medicine, Shanghai 201203, China

Corresponding author: Lu-Yi Wu, PhD, Associate Professor, Yueyang Hospital of Integrated Traditional Chinese and Western Medicine, Shanghai University of Traditional Chinese Medicine, No. 110 Ganhe Road, Hongkou District, Shanghai 200437, China.
luyitcm@163.com

Abstract

BACKGROUND

Ulcerative colitis (UC) is a chronic, nonspecific intestinal inflammatory disease. Acupuncture and moxibustion is proved effective in treating UC, but the mechanism has not been clarified. Proteomic technology has revealed a variety of biological markers related to immunity and inflammation in UC, which provide new insights and directions for the study of mechanism of acupuncture and moxibustion treatment of UC.

AIM

To investigate the mechanism of electroacupuncture (EA) and herb-partitioned moxibustion (HM) on UC rats by using proteomics technology.

METHODS

Male Sprague-Dawley rats were randomly divided into the normal (N) group, the dextran sulfate sodium (DSS)-induced UC model (M) group, the HM group, and the EA group. UC rat model was prepared with 3% DSS, and HM and EA interventions at the bilateral Tianshu and Qihai acupoints were performed in HM or EA group. Haematoxylin and eosin staining was used for morphological evaluation of colon tissues. Isotope-labeled relative and absolute quantification (iTRAQ) and liquid chromatography-tandem mass spectrometry were performed for proteome analysis of the colon tissues, followed by bioinformatics analysis and protein-protein interaction networks establishment of differentially expressed

proteins (DEPs) between groups. Then western blot was used for verification of selected DEPs.

RESULTS

The macroscopic colon injury scores and histopathology scores in the HM and EA groups were significantly decreased compared to the rats in the M group ($P < 0.01$). Compared with the N group, a total of 202 DEPs were identified in the M group, including 111 up-regulated proteins and 91 down-regulated proteins, of which 25 and 15 proteins were reversed after HM and EA interventions, respectively. The DEPs were involved in various biological processes such as biological regulation, immune system progression and in multiple pathways including natural killer cell mediated cytotoxicity, intestinal immune network for immunoglobulin A (IgA) production, and FcγR-mediated phagocytosis. The Kyoto Encyclopedia of Genes and Genomes pathways of DEPs between HM and M groups, EA and M groups both included immune-associated and oxidative phosphorylation. Network analysis revealed that multiple pathways for the DEPs of each group were involved in protein-protein interactions, and the expression of oxidative phosphorylation pathway-related proteins, including ATP synthase subunit g (ATP5L), ATP synthase beta subunit precursor (Atp5f), cytochrome c oxidase subunit 4 isoform 1 (Cox4i1) were down-regulated after HM and EA interventions. Subsequent verification of selected DEPs (Synaptic vesicle glycoprotein 2A; nuclear cap binding protein subunit 1; carbamoyl phosphate synthetase 1; Cox4i1; ATP synthase subunit b, Atp5f1; doublecortin like kinase 3) by western blot confirmed the reliability of the iTRAQ data, HM and EA interventions can significantly down-regulate the expression of oxidative phosphorylation-associated proteins (Cox4i1, Atp5f1) ($P < 0.01$).

CONCLUSION

EA and HM could regulate the expression of ATP5L, Atp5f1, Cox4i1 that associated with oxidative phosphorylation, then might regulate immune-related pathways of intestinal immune network for IgA production, FcγR-mediated phagocytosis, thereby alleviating colonic inflammation of DSS-induced UC rats.

Key Words: Proteomics; Ulcerative colitis; Moxibustion; Electroacupuncture; Differential proteins

©The Author(s) 2022. Published by Baishideng Publishing Group Inc. All rights reserved.

Core Tip: Ulcerative colitis (UC) is a nonspecific inflammatory bowel disease with unclear etiology. Acupuncture and moxibustion are benefit to UC by improving colonic mucosa damage, regulating inflammatory cytokines. In recent years, proteomic technology has been widely used in the study of UC, revealing a variety of biological markers related to immunity and inflammation in UC. We applied isotope-labeled relative and absolute quantification proteomics technology to identify UC-relevant protein targets and further explore the mechanism of acupuncture and moxibustion. It was found that electroacupuncture and herb-partitioned moxibustion could regulate the expression of multiple proteins, such as ATP synthase subunit g, ATP synthase beta subunit precursor 1, cytochrome c oxidase subunit 4 isoform 1 that associated with oxidative phosphorylation, that might regulate immune-related pathways, thereby alleviating colonic inflammation of dextran sulfate sodium-induced UC rats.

Citation: Qi Q, Zhong R, Liu YN, Zhao C, Huang Y, Lu Y, Ma Z, Zheng HD, Wu LY. Mechanism of electroacupuncture and herb-partitioned moxibustion on ulcerative colitis animal model: A study based on proteomics. *World J Gastroenterol* 2022; 28(28): 3644-3665
URL: https://www.wjgnet.com/1007-9327/full/v28/i28/3644.htm
DOI: https://dx.doi.org/10.3748/wjg.v28.i28.3644

INTRODUCTION

Ulcerative colitis (UC) is a chronic, nonspecific inflammatory disease, with lesions are mainly confined to the large intestinal mucosa and submucosal layer. Mucosal inflammation at the affected site is characterized by a diffuse distribution and its clinical manifestations mainly include abdominal pain, diarrhoea, mucus pus and blood in stool[1]. UC has a prolonged disease course, which can lead to the development of colorectal cancer, accounting for 10% to 15% of deaths among patients with UC, and is listed as one of the refractory diseases by the World Health Organization. Epidemiological data show that the prevalence of UC in Asia has increased exponentially in recent years, and the growth rate of UC

in some East Asian countries including China has increased in multiples over the past decade[2,3].

The pathogenesis of UC is not yet clear, but it is believed to be related to genetic susceptibility, epithelial barrier deficiency, immune disorders, and environmental factors[4]. The modern treatment methods for UC mainly include glucocorticoids, immunosuppressants, 5-aminosalicylic acid, and biological agents (monoclonal antibodies), but it is prone to relapse after drug withdrawal, and multiple drugs have adverse side effects. Therefore, active exploration of the pathogenesis of UC, identification of disease biomarkers, and screening of specific therapeutic targets are important for the diagnosis and treatment of UC. As one of the unique treatments of traditional Chinese medicine, acupuncture and moxibustion have significant efficacy and advantages in the treatment of UC[5-7], but the specific mechanism requires further clarification.

In recent years, proteomic technology has been widely used in the study of UC[8,9], revealing a variety of biological markers related to immunity and inflammation in UC[10]. The activity of mitochondrial oxidative phosphorylation complex in intestinal tissues of UC patients decreases, and the dysfunction of mitochondrial oxidative phosphorylation may be involved in the pathogenesis of UC, but it is not clear whether acupuncture and moxibustion have a regulatory effect on it. Therefore, our study used isotope-labeled relative and absolute quantification (iTRAQ) proteomics technology to quantitatively analyse proteins in the colon tissues of UC rats, to analyse the biological functions of differentially expressed proteins (DEPs) and observe changes of immune and oxidative phosphorylation-associated protein expression profiles in colon tissues of UC rats and regulatory effect of acupuncture and moxibustion, in order to identify UC-relevant protein targets and further explore the mechanism of effects of acupuncture and moxibustion on UC.

MATERIALS AND METHODS

Animals

Healthy clean grade naïve male Sprague-Dawley (SD) rats, aged 6 wk, with body weight of 180 ± 20 g were purchased from Shanghai Slac Laboratory Animal Co., Ltd. [Laboratory Animal Use Permit No. SYXK (Shanghai) 2014-0008] and housed in the Experimental Animal Center of Shanghai University of Traditional Chinese Medicine. The animal protocol was designed to minimize pain or discomfort to the animals. The housing environment was a 12 h circadian rhythm, with a room temperature of 20 ± 2 °C and 50%-70% indoor humidity, 4 rats per cage, and rats were free to standard food and pure water. This study was approved by the Ethics Committee of the Experimental Animal Center of Shanghai University of Traditional Chinese Medicine. We tried all efforts to minimize animal suffering.

Dextran sulfate sodium-induced UC model preparation

For preparing the UC rat model, the rats received 3% dextran sulfate sodium (DSS, molecular weight: 36000-50000, MP Biomedicals, United States) in drinking water by oral for 7 d, and then were switched to pure water for 7 d, and the same procedures were repeated once (drinking 3% DSS solution for 7 d, followed by drinking pure water for 7 d)[11]. After modeling, rats were anaesthetized *via* intraperitoneal injection with 2% pentobarbital sodium (30-40 mg/kg) (P3761, Sigma, United States) for tissue collection, the gross injury and hematoxylin and eosin (HE) staining were used to evaluate whether the model was successfully established.

Grouping and interventions

After one week of adaptive feeding, 32 rats were randomly divided into the normal (N) group, the DSS-induced UC model (M) group, the herb-partitioned moxibustion (HM) group, and the electroacupuncture (EA) group, with 8 rats in each group. UC rat model was prepared by DSS except for the N group. After model establishment, the rats in the HM and EA group were treated with corresponding treatment at Tianshu (ST25, bilateral) and Qihai (CV6) acupoints[12]. In the HM group, Chinese medicine powder containing Coptis chinensis, Radix aconiti lateralis, Cortex Cinnamomi, Radix aucklandiae, Flos carthami, Salvia miltiorrhiza, and Angelica sinensis was mixed and stirred with yellow wine to make herbal cake, then an herbal cake was prepared with a thickness of 0.5 cm and a diameter of 1 cm using a specific mould, and conical moxa cones weighing approximately 90 mg were made with moxa (Nanyang Hanyi Moxa Co., Ltd., Nanyang, China) by a mould. The rats were supine immobilized on a self-made fixator, the prepared moxa cone was placed on the top of herbal cake, and the herbal cake was placed at the ST25 and CV6 acupoints, then the moxa cone was ignited using line incense, 2 moxa cones per acupoint per time, once a day for 7 d (Figure 1)[13]. In the EA group, the rats were also supine immobilized on the self-made fixator, a 0.25 mm × 25 mm acupuncture needle was inserted into the ST25 and CV6 acupoints for 5 mm, then the needle handle was connected to a Han's-200 acupoint nerve stimulator, with a frequency of 2/100 Hz and a current of 1 mA. The needle was kept for 10 min per time, once a day for a total of 7 d[14]. The rats in the N group and the M group did not receive any treatment, but only the same grasping fixation as that in the treatment groups at 10 o'clock every day for a total of 7 d.

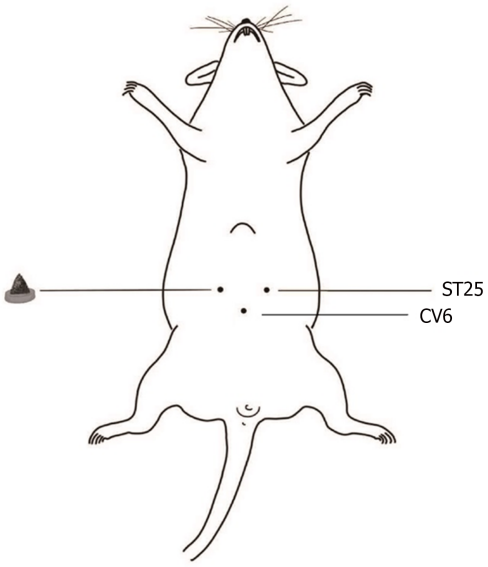


Figure 1 Schematic diagram of herb-partitioned moxibustion at the rat Tianshu (ST25, bilateral) and Qihai (CV6) acupoints.

Collection of colon tissue and macroscopic scoring of colon injury

After the intervention, rats were anaesthetized with intraperitoneal injection of 2% pentobarbital sodium. The abdominal cavity was exposed and the entire colon from the pubic symphysis to the distal cecum was collected, and the length of the colon was recorded. The distal colon with a length of 6-8 cm was collected and cut longitudinally along the mesentery, observed the gross morphology, the macroscopic scoring of the colon was performed according to the following parameters: Hyperemia, wall thickening, ulceration, inflammation extension, and damage no damage, score 0; hyperemia without ulcers, score 1; hyperemia and wall thickening without ulcers, score 2; one ulceration site without wall thickening, score 3; two or more ulceration sites, score 4; 0.5 cm extension of inflammation or major damage, score 5; 1 cm extension of inflammation or severe damage, score 6[15]. Then was cut into two parts transversely, one part was fixed in 4% paraformaldehyde for morphological observation, and the remaining part was placed in liquid nitrogen for 1 h and transferred to a -80 °C freezer for future detection.

Morphological observation of the colon

Colon tissues fixed in 4% paraformaldehyde fixative solution were dehydrated, embedded in paraffin, and sliced into 4 μm sections for HE staining with the following steps: Dewaxing in xylene I and II solutions for 20 min each; elution in 100%, 95%, 90%, 80%, and 70% ethanol for 5 min each; rinsing with double distilled water for 5 min × 2 times; haematoxylin staining for 2-3 min; rinsing with running water for 10 min; 1% hydrochloric acid ethanol differentiation solution for 1-2 s; rinsing with running water for 5 min; eosin dye staining for 2-3 min; dehydration in 70%, 80%, 90%, and 100% ethanol for 1-2 s each; xylene I and II solutions for 15 min each. After drying and sealing, the colon sections were observed under a light microscope and microscopic scoring of the colon was performed according to the following parameters: Damage/necrosis, inflammatory cell infiltration, submucosal edema, and hemorrhage of mucosa. Colonic gross damage scores were recorded according to the severity of changes: No change, score 0; mild, score 1; moderate, score 2; severe, score 3[16].

Proteomic analysis

Protein extraction and enzymatic digestion: Colon samples from 3 rats in each group were randomly collected and ground into powder, and an appropriate amount of radioimmunoprecipitation assay (RIPA) protein lysis buffer (R0010, Solarbio, United States) was added (150 μL RIPA was add to 20 mg colon tissue), high-abundance protein in the sample was removed, a 5-fold volume of 10% trichloroacetic acid/cold acetone was added to the sample and precipitated at -20 °C overnight. The precipitated proteins were centrifuged at 4 °C, 15000 g for 20 min, the supernatant was removed, and samples were air-dried and precipitated after repeating the above steps several times. After lysis, samples were centrifuged at 25000 g for 20 min at 4 °C, and the supernatant was the protein solution. A total of 100 μg of protein solution was collected from each sample, and trypsin (2.5 μg) was added to the protein solution at a ratio of 40: 1 of protein: Enzyme, enzymolysis at 37 °C for 4 h. Trypsin was then added according to the above ratio and continue enzymolysis at 37 °C for 8 h.

Peptide labelling and separation: The digested peptide fragments were desalted using a Strata X column and vacuum-dried. The peptide samples were dissolved in 0.5 M triethylammonium

bicarbonate, and then were were labeled with iTRAQ (iTRAQ8-plexreagent kit, Sigma, United States) and maintained at room temperature for 2 h. The Shimadzu LC-20AB liquid chromatography system (separation column: 5 μm, 4.6 mm × 250 mm Gemini C18) was used for liquid phase separation of samples. Dried peptide samples were redissolved in 2 mL of mobile phase A (5% ACN, pH 9.8), the solution was loaded, and gradient elution was performed at a flow rate of 1 mL/min as follows: 5% mobile phase B (95% ACN, pH 9.8) for 10 min, 5%-35% mobile phase B for 40 min, 35%-95% mobile phase B for 1 min, mobile phase B for 3 min, and equilibration with 5% mobile phase B for 10 min. The elution peak was monitored at a wavelength of 214 nm, and 1 fractionated peptide was collected every minute. The chromatographic elution peaks were combined with the samples to obtain 20 fractionated peptides, which were then freeze-dried.

High-performance liquid chromatography: The dried peptide samples were redissolved using mobile phase A (2% ACN, 0.1% FA) and centrifuged at 20000 g for 10 min. The supernatant was collected and loaded onto the column, and samples were separated by a Prominence nano LC (LC-20AD, Shimadzu, Japan). The sample was first enriched in a trap column and desalted, and the tandem self-assembled C18 column (75-μm inner diameter, 3.6-μm pore size, 15-cm length) was used. Separation was performed at a flow rate of 300 nL/min through an effective gradient: at 0-8 min, 5% mobile phase B (98% ACN, 0.1% FA); at 8-43 min, mobile phase B increased linearly from 8% to 35%; at 43-48 min, mobile phase B increased from 35% to 60%; at 48-50 min, mobile phase B increased from 60% to 80%; at 50-55 min, 80% mobile phase B; and at 55-65 min, 5% mobile phase B.

Mass spectrometric detection: The separated peptides were transferred into an electrospray ionization tandem mass spectrometer: TripleTOF 5600 (SCIEX, Framingham, United States) and theion source was Nanospray III source (SCIEX, Framingham, United States). During data collection, the parameters of the mass spectrometer were set as follows: An ion source spray voltage of 2300 V, a nitrogen pressure of 30 psi, atomizer 15, and a spray interface temperature of 150 °C. High-sensitivity mode was used for scanning. The cumulative time of primary mass spectrometry scanning was 250 ms, and the cumulative of secondary mass spectrometry scanning time was 100 ms.

iTRAQ quantification and bioinformatics analysis

ITRAQ quantification was performed using IQuant software. The selection of significantly DEPs in a single experiment were as follows: Fold change (FC) ≥ 1.2 was set as up-regulation and FC ≤ 0.83 as down-regulation, as well as Q-value < 0.05. The Gene Ontology (GO) database was used for functional annotation analysis of DEPs. The Kyoto Encyclopedia of Genes and Genomes (KEGG) pathway database was used for pathway enrichment analysis of DEPs. The protein-protein interaction network was performed using STRING software with an interaction confidence of 0.7 (the maximum confidence was 1). Cytoscape (v.3.7.1) software was used to visualize the enrichment analysis results. Figure 2 showed the process of proteomics detection and analysis.

Western blot analysis

We selected DEPs in UC that were reversed by HM and EA for verification by using western blot method. Total proteins were extracted from colon tissues using RIPA buffer supplemented with protease and phosphatase inhibitors. Protein concentration was measured with the bicinchoninic acid protein concentration assay kit. The proteins were separated by polyacrylamide gelelectrophoresis method, with the voltage of concentrated glue was 90 V and that of separating glue was 120 V (BIO-RAD, 1645050), then the separated proteins were transferred to polyvinylidene fluoride membranes. The modified membranes were blocked with 5% bovine serum albumin in TBST, and then was incubated overnight at 4 °C with primary antibody. The antibody dilutions were prepared according to the instructions [Synaptic vesicle glycoprotein 2A (Sv2a), 1: 1000; nuclear cap binding protein subunit 1 (Ncbp1), 1: 800; Cps, 1: 5000; cytochrome c oxidase subunit 4 isoform 1 (Cox4i1), 1: 2000; ATP synthase beta subunit precursor 1 (Atp5f1), 1: 1000; doublecortin like kinase 3 (Dclk3), 1: 800)]. The membranes were washed with western detergent at room temperature for 6 times, 5 min each and then were incubated with secondary antibodies at room temperature for 1 h. Followed by washed with western detergent at room temperature for 6 times, 5 min each. The membranes were stained with enhanced chemiluminescence solution and visualized in a gel imager system (Tanon, 4600).

Statistical analysis

The western blot analysis data were analyzed with SPSS 20.0 statistical software. Data that consistent with the normal distribution were presented as mean ± SD, and one-way analysis of variance was used for comparison between groups, followed by the Fisher's Least significant difference method if data met the homogeneity of variance. For data that did not meet the normal distribution were presented as medians (P_{25}, P_{75}), and nonparametric test was used for comparison. $P < 0.05$ was considered statistically significance.

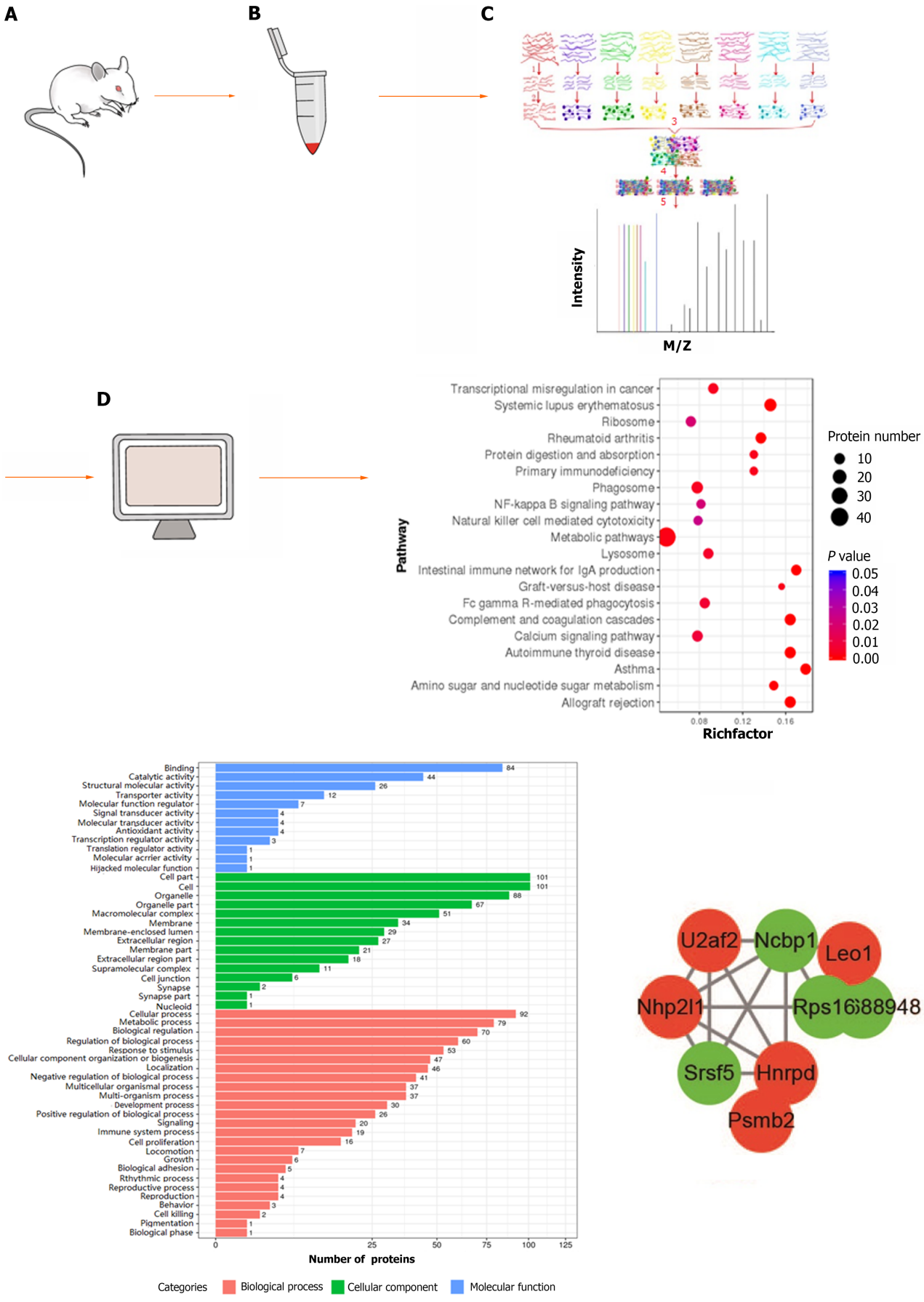


Figure 2 Flow chart of proteomics detection and analysis. A: Sprague-Dawley rat; B: Protein extraction of colon tissue; C: Protein enzymatic digestion, peptide labelling, separation, and high-performance liquid chromatography analysis; D: Bioinformatics analysis.

RESULTS

Effects of HM and EA on DSS induced UC rats

In the N group, rats were active and energetic, and their feces were moderately hard and soft. The rats in the M group had loose, bloody stools and decreased activities. Compared with the M group, the activity of rats in the HM and EA groups was obviously improved, and the stool gradually took shape without obvious mucus and blood. We found that the colon in the N group did not exhibit adhesion or bleeding points; the colonic mucosal surfaces were clean and smooth. In contracts, the colon in the M group exhibited significant adhesion and multiple bleeding points; the inner wall was not smooth, and partially visible scattered ulcers and thickened intestinal walls were observed. In the HM and EA groups, the adhesion and the bleeding points were decreased (Figure 3A).

The morphological changes of colon tissues were observed using HE staining. The colonic mucosal epithelium of the normal group was intact, with clear tissue structure, regular arranged glands, and no congestion, oedema or ulcers were evident. While the mucosal epithelium of UC rats was absent, ulcers had formed, with a loss or reduction of glands and goblet cells, and substantial inflammatory cells were infiltrated in mucosa and submucosa. After HM and EA interventions, the mucosal epithelium was restored, with healed ulcer, increased glands and goblet cells, decreased mucosal and submucosal inflammatory cell infiltration and congestion (Figure 3B).

The macroscopic colon injury scores and histopathology scores in the M group were significantly increased than that in the N group ($P < 0.01$). Conversely, the macroscopic colon injury scores and histopathology scores in the HM and EA groups were significantly decreased compared to the rats in the M group ($P < 0.01$) (Figures 3C and D). The colonic length of the rats in the M group were significantly decreased compared with the N group, the colonic length of the rats in the HM and EA groups were significantly increased compared with the M group ($P < 0.01$) (Figure 3E).

iTRAQ quantification of DEPs

The volcano plot in Figure 4 described the DEPs between the groups. The quantitative results showed that 202 DEPs were identified in DSS-induced UC rats compared with the N group, of which 111 were up-regulated and 91 were down-regulated; 117 DEPs were identified in HM group compared with the M group, of which 41 were up-regulated and 76 were down-regulated; 145 DEPs were identified in EA group compared with the M model group, of which 59 were up-regulated and 86 were down-regulated (Table 1, Figure 5).

Comparison of the M/N and HM/M groups showed that among these proteins, 25 DEPs were common to N, M and HM groups, with 17 [Sv2a, Igkv13-85, Ncbp1, Aldo-keto reductase family 1 member B8, Rathemoglobin beta-chain, Ribosomal protein S8 (RpS8), Fga, Rps2-ps6, carbamoyl phosphate synthetase 1 (Cps1), Txn, ATP synthase subunit g (ATP5L), Cox4i1, Atp5h, Necap2, Atp5f1, Papss2, Acly] up-regulated in UC but were down-regulated by HM, and 8 [Spout1, calcium-activated chloride channel regulator 1 (CLCA1), Sval1, Hspb7, Peptidyl-prolyl cis-trans isomerase, Aldh1a1, Lyz2, Dclk3] down-regulated in UC but were up-regulated by HM (Figure 5A, Table 2). Comparison of the M/N and EA/M groups showed that 15 DEPs were common to N, M and EA groups, with 9 (Sv2a, Ncbp1, Rat hemoglobin beta-chain, Fga, Cps1, ATP5L, Cox4i1, Atp5f1, Lmod1) up-regulated in UC but were down-regulated by EA, and 6 (Spout1, Sh3bgrl3, Peptidyl-prolyl cis-trans isomerase, MHC class I RT1.Aw3 protein, Tkt, Dclk3) down-regulated in UC but were up-regulated by EA (Figure 5B, Table 3).

GO enrichment analysis for DEPs

GO annotation of DEPs between groups describes the characteristics of genes and gene products in terms of molecular functions, cellular components and biological processes. 53 GO functions were significantly differentiated between the M and the N group, 52 GO functions are significantly differentiated between the M group and the HM group, and 51 GO functions are significantly differentiated between the M group and the EA group. The GO functional annotations of DEPs in the M/N, HM/M, and EA/M comparisons were basically similar. Biological process was the most favorable enrichment component, in which DEGs were significantly enriched in cellular process, metabolic process, biological regulation and so on. Cellular component analysis was enriched in cell part, cell, organelles, macromolecular complexes, *etc.* Molecular functions mainly included binding, synaptic activity, structural molecule activity, molecular function regulation, molecular sensor activity, and transcriptional regulation activity (Figure 6).

KEGG pathway enrichment analysis for DEPs

KEGG pathway enrichment analysis was performed for DEPs between the groups, we found that these DEPs were mainly enriched in inflammation responses and immune-related pathways. The pathways in which DEPs between the N and M groups mainly enriched included primary immunodeficiency, the noncanonical nuclear factor-kappaB (NF-κB) signalling pathway, natural killer cells mediated cytotoxicity, intestinal immune network for immunoglobulin A (IgA) production, FcγR-mediated phagocytosis, and complement and coagulation cascades (Figure 7A, Table 4). The pathways in which DEPs between the HM and the M groups mainly enriched included primary immunodeficiency,

Table 1 List of differential protein numbers

Compare group	Up-regulated	Down-regulated	All-regulated
M/N	111	91	202
HM/M	41	76	117
EA/M	59	86	145

N: Normal group; M: Dextran sulfate sodium-induced ulcerative colitis model group; HM: Herb-partitioned moxibustion group; EA: Electroacupuncture group.

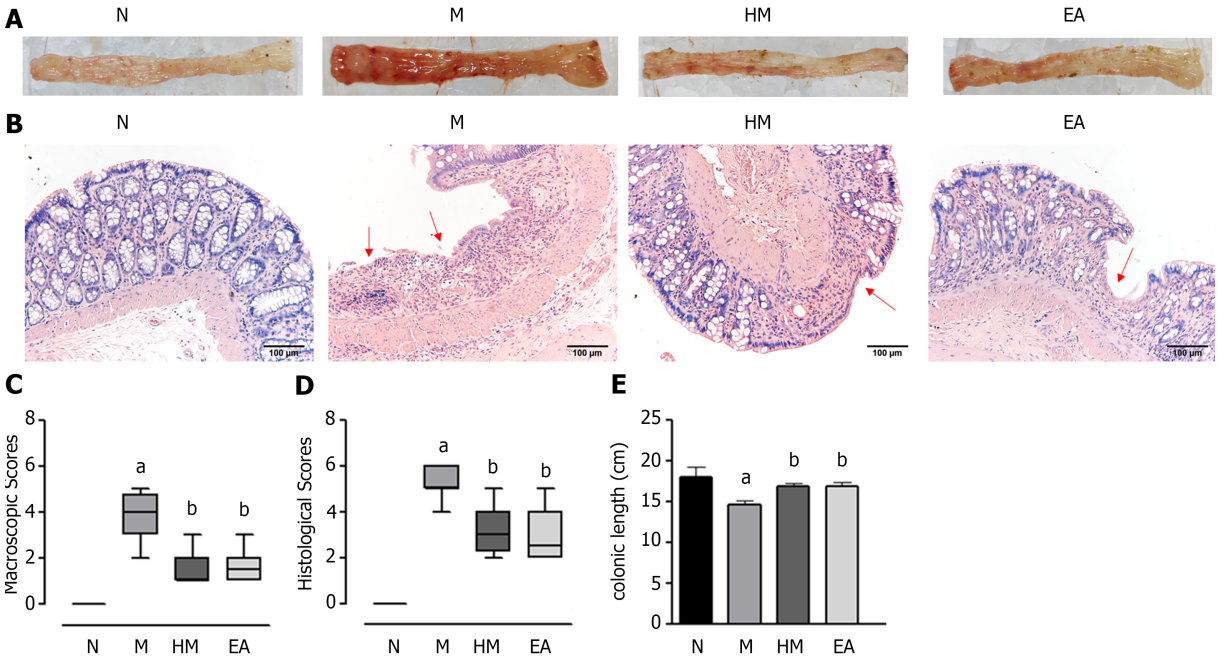


Figure 3 Colon tissue injuries in each group. A: Gross structure; B: Histopathological observation (hematoxylin and eosin, × 200); C: Macroscopic scores; D: Histopathological scores; E: Colonic length. $^{a}P < 0.01$ *vs* N group; $^{b}P < 0.01$ *vs* M group. N: Normal group; M: Dextran sulfate sodium-induced ulcerative colitis model group; HM: Herb-partitioned moxibustion group; EA: Electroacupuncture group.

oxidative phosphorylation, nitrogen metabolism, natural killer cells mediated cytotoxicity, the intestinal immune network for IgA production, FcγR-mediated phagocytosis, complement and coagulation cascades, and B cell receptor signalling pathway (Figure 7B, Table 5). The pathways in which DEPs between the EA and the M groups mainly enriched included the phosphoinositol-3 kinase (PI3K)-protein kinase B (Akt) signalling pathway, oxidative phosphorylation, intestinal immune network for IgA production, and the calcium signalling pathway (Figure 7C, Table 6).

Protein-protein interactions analysis

The STRING database (v.11.0) was used to construct the protein-protein interactions (PPIs) network for the transcription factors with an interaction score > 0.7 (high confidence) among the groups. Cytoscape (v.3.7.1) software was used to visualize the enrichment results. The statistical significance was set as $P < 0.05$. The analysis showed extensive interactions among the DEPs between groups (Figure 8). A total of 100 DEPs (63 up-regulated proteins and 37 down-regulated proteins) were included in the PPI network constructed by DEPs between the N and M groups, and Nme2 served as the junction point of two pathways, indicating that it was important for screening key candidate proteins. 38 DEPs (8 up-regulated proteins and 30 down-regulated proteins) were included in the PPI network constructed from DEPs between the M and HM groups, in which ribosomal pathway-related proteins were all down-regulated, and oxidative phosphorylation pathway-related proteins, including Atp5o, ATP5L, Atp5f, Atp5h, Cox4i1 were also down-regulated. 55 DEPs (19 up-regulated proteins and 36 down-regulated proteins) were included in the PPI network constructed from DEPs between the EA and M groups. In addition, proteins involved in inflammation regulation such as serpins were identified (serpinb6 in M/N comparisons, serpinc1 in HM/M and EA/M comparisons).

Table 2 Differentially expressed proteins in dextran sulfate sodium-induced ulcerative colitis model group rats that regulated by herb-partitioned moxibustion

Protein ID	Description	Symbol	M/N		HM/M	
			Mean ratio	Q value	Mean ratio	Q value
Q02563	Synaptic vesicle glycoprotein 2A	Sv2a	4.42	0.024	0.25	0.021
A0A0G2JZN1	Immunoglobulin kappa chain variable 13-85	Igkv13-85	4.07	0.020	0.37	0.028
Q56A27	Nuclear cap-binding protein subunit 1	Ncbp1	2.47	0.018	0.56	0.004
Q91W30	Aldose reductase-like protein	Akr1b8	1.85	0.006	0.63	0.017
Q63223	Rat hemoglobin beta-chain (Fragment)	Rat hemoglobin beta-chain (Fragment)	1.57	0.005	0.46	0.004
P62243	40S ribosomal protein S8	Rps8	1.56	0.006	0.83	0.023
P06399	Fibrinogen alpha chain	Fga	1.51	0.003	0.75	0.004
O55215	Ribosomal protein S2	Rps2-ps6	1.45	0.003	0.80	0.004
P07756	Carbamoyl-phosphate synthase (ammonia), mitochondrial	Cps1	1.33	0.009	0.70	0.004
P11232	Thioredoxin	Txn	1.28	0.002	0.74	0.004
Q6PDU7	ATP synthase subunit g, mitochondrial	ATP5L	1.27	0.028	0.76	0.004
P10888	Cytochrome c oxidase subunit 4 isoform 1, mitochondrial	Cox4i1	1.26	0.002	0.80	0.004
P31399	ATP synthase subunit d, mitochondrial	Atp5h	1.34	0.003	0.77	0.004
Q6P756	Adaptin ear-binding coat-associated protein 2	Necap2	1.48	0.011	0.83	0.023
P19511	ATP synthase F (0) complex subunit B1, mitochondrial	Atp5f1	1.24	0.003	0.83	0.004
A0A0G2K950	3′-phosphoadenosine 5′-phospho-sulfate synthase 2	Papss2	1.27	0.002	0.74	0.004
A0A0G2K5E7	ATP-citrate synthase	Acly	1.35	0.017	0.83	0.030
A0A0G2QC59	RCG45649, isoform CRA_a	Spout1	0.54	0.013	2.13	0.011
A0A0G2JWX9	Chloride channel accessory 1	Clca1	0.50	0.002	1.25	0.004
Q99N82	Colon SVA-like protein	Sval1	0.73	0.028	6.82	0.004
B5DFG4	Heat shock 27kD protein family, member 7 (cardiovascular)	Hspb7	0.76	0.016	1.24	0.050
D3ZSF3	Peptidyl-prolyl cis-trans isomerase	-	0.75	0.003	1.40	0.013
P51647	Retinal dehydrogenase 1	Aldh1a1	0.81	0.002	1.22	0.004
Q05820	Putative lysozyme C-2	Lyz2	0.67	0.013	1.48	0.050
F1LWF2	Doublecortin-like kinase 3	Dclk3	0.24	0.005	4.67	0.011

N: Normal group; M: Dextran sulfate sodium-induced ulcerative colitis model group; HM: Herb-partitioned moxibustion group; ATP5L: ATP synthase subunit g; Atp5f1: ATP synthase beta subunit precursor; Sv2a: Synaptic vesicle glycoprotein 2A; Ncbp1: Nuclear cap binding protein subunit 1; Cps1: Carbamoyl phosphate synthetase 1; Cox4i1: Cytochrome c oxidase subunit 4 isoform 1; Dclk3: Doublecortin like kinase 3; Akr1b8: Aldo-keto reductase family 1 member B8; RpS8: Ribosomal protein S8.

Western blot verification

We verified the expression of some DEPs that could be regulated by HM and EA. The western blot results showed that, compared with the N group, the expression of Sv2a, Ncbp1, Cps1, Cox4i1, Atp5f1 proteins were increased in the colon of UC rats, while the expression of Dclk3 protein was decreased ($P < 0.01$). HM and EA interventions can significantly down-regulate the expression of Sv2a, Ncbp1, Cps1, Cox4i1, Atp5f1 proteins and up-regulate Dclk3 protein ($P < 0.01$). It indicated that the western blot

Table 3 Differentially expressed proteins in dextran sulfate sodium-induced ulcerative colitis model group rats that regulated by electroacupuncture

Protein ID	Description	Symbol	M/N		EA/M	
			Mean ratio	Q value	Mean ratio	Q value
Q02563	Synaptic vesicle glycoprotein 2A	Sv2a	4.42	0.024	0.15	0.013
Q56A27	Nuclear cap-binding protein subunit 1	Ncbp1	2.47	0.018	0.55	0.003
Q63223	Rat hemoglobin beta-chain (Fragment)	-	1.57	0.005	0.38	0.002
P06399	Fibrinogen alpha chain	Fga	1.51	0.003	0.76	0.002
P07756	Carbamoyl-phosphate synthase (ammonia), mitochondrial	Cps1	1.33	0.009	0.69	0.004
Q6PDU7	ATP synthase subunit g, mitochondrial	ATP5L	1.27	0.028	0.82	0.002
P10888	Cytochrome c oxidase subunit 4 isoform 1, mitochondrial	Cox4i1	1.26	0.002	0.74	0.002
P19511	ATP synthase F (0) complex subunit B1, mitochondrial	Atp5f1	1.51	0.003	0.81	0.002
A0A0G2K0D3	Leiomodin-1	Lmod1	1.13	0.003	0.77	0.002
A0A0G2QC59	RCG45649, isoform CRA_a	Spout1	0.54	0.013	1.88	0.002
B2RZ27	SH3 domain binding glutamic acid-rich protein-like 3	Sh3bgrl3	0.74	0.027	1.31	0.027
D3ZSF3	Peptidyl-prolyl cis-trans isomerase	-	0.75	0.003	1.47	0.003
Q31266	MHC class I RT1.Aw3 protein	-	0.81	0.029	1.44	0.005
G3V826	Transketolase OS = rattus norvegicus	Tkt	0.71	0.003	1.23	0.002
F1LWF2	Doublecortin-like kinase 3	Dclk3	0.24	0.005	4.09	0.002

N: Normal group; M: Dextran sulfate sodium-induced ulcerative colitis model group; EA: Electroacupuncture group; ATP5L: ATP synthase subunit g; Atp5f1: ATP synthase beta subunit precursor; Sv2a: Synaptic vesicle glycoprotein 2A; Ncbp1: Nuclear cap binding protein subunit 1; Cps1: Carbamoyl phosphate synthetase 1; Cox4i1: Cytochrome c oxidase subunit 4 isoform 1; Dclk3: Doublecortin like kinase 3.

verification results were consistent with the iTRAQ results (Figure 9).

DISCUSSION

UC is a type of inflammatory bowel disease (IBD) characterized by chronic recurrent, and the specific aetiology and pathogenesis of UC are still not clear. Proteomics is a discipline that systematically quantifies all the proteins in cells or organisms and elucidates their biological functions, it has enormous potential for early diagnosis, prevention, and prognosis prediction of diseases[17,18]. In recent years, proteomics has gradually been applied to the study of UC, providing strong support for the research of pathogenesis, clinical diagnosis, and treatment of UC. A study has been found that 7 protein genes were differentially expressed in the intestinal tissues of UC patients using proteomics, including prohibitin, heat shock proteins, alpha-1 antitrypsin, ventralis intermedius, caspase-1, cytokeratin 20, Filamin Ainteracting protein 1, FLNa[19]. Another study analysed the transcriptome and proteome characteristics of the colon of UC patients, and found that the expression of genes and proteins related to immune and inflammatory responses in UC patients were dysregulated. At the same time, the complement cascade, metabolic processes, and peroxisome proliferator-activated receptor signal transduction were inhibited[20]. Therefore, iTRAQ proteomic technology can also be a feasible method to reveal potential targets for UC drug therapy[8].

In the present study, we performed proteomic analysis using iTRAQ labelling combined with mass spectrometry technology to identify DEPs in colon of DSS-induced UC rats, and selected DEPs that could be reversed by HM and EA. DSS has been widely used to prepare experimental colitis to study the new drug therapy, immunity and mechanism of action[21-23]. Our results showed that HM and EA improved the colonic mucosal injury of UC rats. At the same time, we have compared the normal and

Table 4 The Kyoto Encyclopedia of Genes and Genomes pathway related to immunity and inflammation with differentially expressed proteins between normal group and dextran sulfate sodium-induced ulcerative colitis model group

Pathway name	Protein ID	Number	*P* value
Primary immunodeficiency	M0RDF2, IGG2B, M0RA79, Q4QQW0, F1LXY6, Q569B3	6	0.003
Nuclear factor-kappa B signalling pathway	M0RDF2, IGG2B, M0RA79, Q4QQW0, F1LXY6, Q569B3, B2RZB2	7	0.021
Natural killer cell mediated cytotoxicity	GRZ2, M0RDF2, IGG2B, M0RA79, Q4QQW0, F1LXY6, Q569B3	7	0.025
Intestinal immune network for IgA production	M0RDF2, IGG2B, HB2B, M0RA79, Q8VI32, Q4QQW0, F1LXY6, Q569B3, B2RZB2	9	4.25E-05
Fc gamma R-mediated phagocytosis	M0RDF2, Q6AYB2, IGG2B, E9PU64, M0RA79, Q4QQW0, F1LXY6, B2GV73, Q569B3	9	0.007
Complement and coagulation cascades	CFAI, FIBB, M0RBJ7, PLMN, A1L114, CO9, A1M, FIBG, FIBA, Q99N82, A0A0G2JY31	11	8.29E-06

N: Normal group; M: Dextran sulfate sodium-induced ulcerative colitis model group; IgA: Immunoglobulin A.

Table 5 The Kyoto Encyclopedia of Genes and Genomes pathway related to immunity, inflammation and oxidative phosphorylation with differentially expressed proteins between herb-partitioned moxibustion group and dextran sulfate sodium-induced ulcerative colitis model group

Pathway name	Protein ID	Number	*P* value
Primary immunodeficiency	IGG2C, Q5BJZ2, F1LXY6, Q569B3	4	0.009
Oxidative phosphorylation	ATP5H, ATPO, COX41, AT5F1, Q5UAJ5, NMES1, ATP5L	7	0.002
Nitrogen metabolism	CAH1, CAH3, CPSM	3	0.001
Natural killer cell mediated cytotoxicity	GRZ2, IGG2C, Q5U1Y2, Q5BJZ2, F1LXY6, Q569B3	6	0.005
Intestinal immune network for IgA production	IGG2C, Q5BJZ2, Q6MG98, F1LXY6, Q569B3	5	0.002
Fc gamma R-mediated phagocytosis	IGG2C, Q5U1Y2, Q5BJZ2, F1LXY6, Q569B3	5	0.040
Complement and coagulation cascades	Q5M7T5, Q99N82, Q7TQ70, FIBA	4	0.031
B cell receptor signalling pathway	IGG2C, Q5U1Y2, Q5BJZ2, F1LXY6, Q569B3	5	0.020

M: Dextran sulfate sodium-induced ulcerative colitis model group; HM: Herb-partitioned moxibustion group; IgA: Immunoglobulin A; ATP5L: ATP synthase subunit g.

Table 6 The Kyoto Encyclopedia of Genes and Genomes pathway related to immunity, inflammation and oxidative phosphorylation with differentially expressed proteins between electroacupuncture group and dextran sulfate sodium-induced ulcerative colitis model group

Pathway name	Protein ID	Number	*P* value
PI3K-Akt signalling pathway	F1M6Q3, D4A3K7, P70570, Q5M7V3, A0A096P6L8, Q5BJZ2, F1LPR6, GBB4, PCKGC	9	0.042
Oxidative phosphorylation	B2RYT5, CX7A2, D4A565, CX6C2, COX41, M0RA24, AT5F1, B2RYS8, G3V8S4, D3ZFQ8, NMES1, ATP5L, ATPK	13	3.42E-07
Intestinal immune network for IgA production	Q5M7V3, Q5BJZ2, F1LPR6, Q6MG98	4	0.032
Calcium signalling pathway	GNAS2, Q5M7V3, A0A0G2K059, Q5BJZ2, F1LPR6, A0A0G2JSR0, ADT2	7	0.027

M: Dextran sulfate sodium-induced ulcerative colitis model group; EA: Electroacupuncture group; IgA: Immunoglobulin A; ATP5L: ATP synthase subunit g; PI3K-Akt: Phosphatidylinositol 3-kinase protein kinase B; COX41: Cytochrome c oxidase subunit IV isoform 1; PCKGC: Phosphoenolpyruvate carboxykinase 1; ATPK: ATP synthase membrane subunit F; ADT2: Arogenate dehydratase 2.

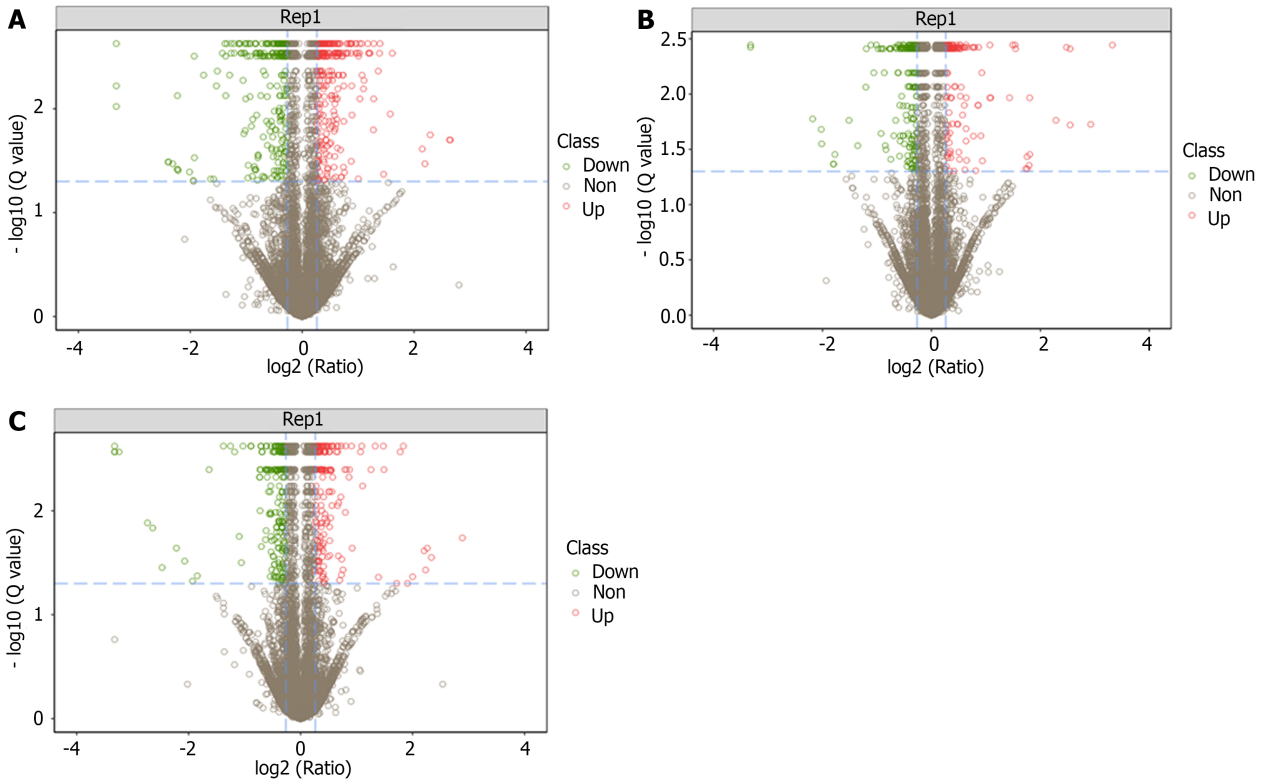


Figure 4 Volcano plot of differentially expressed proteins between groups. A: Volcano plot of differentially expressed proteins (DEPs) between the normal and dextran sulfate sodium-induced ulcerative colitis model group; B: Volcano plot of DEPs between the dextran sulfate sodium-induced ulcerative colitis model and herb-partitioned moxibustion group; C: Volcano plot of DEPs between the dextran sulfate sodium-induced ulcerative colitis model and electroacupuncture group.

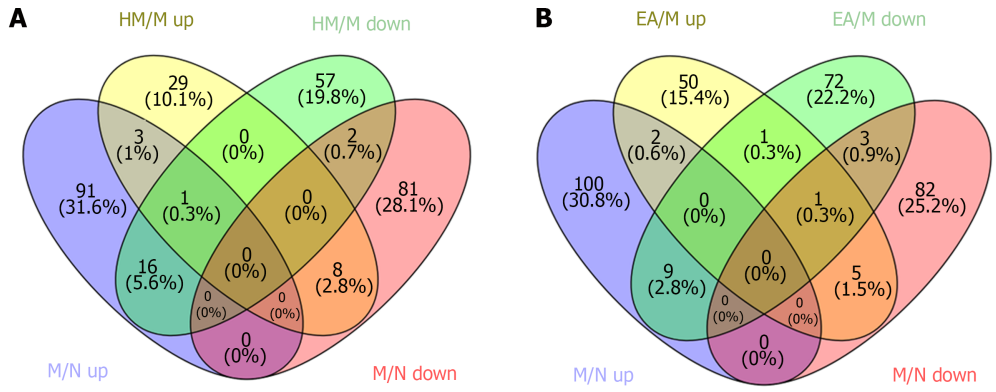
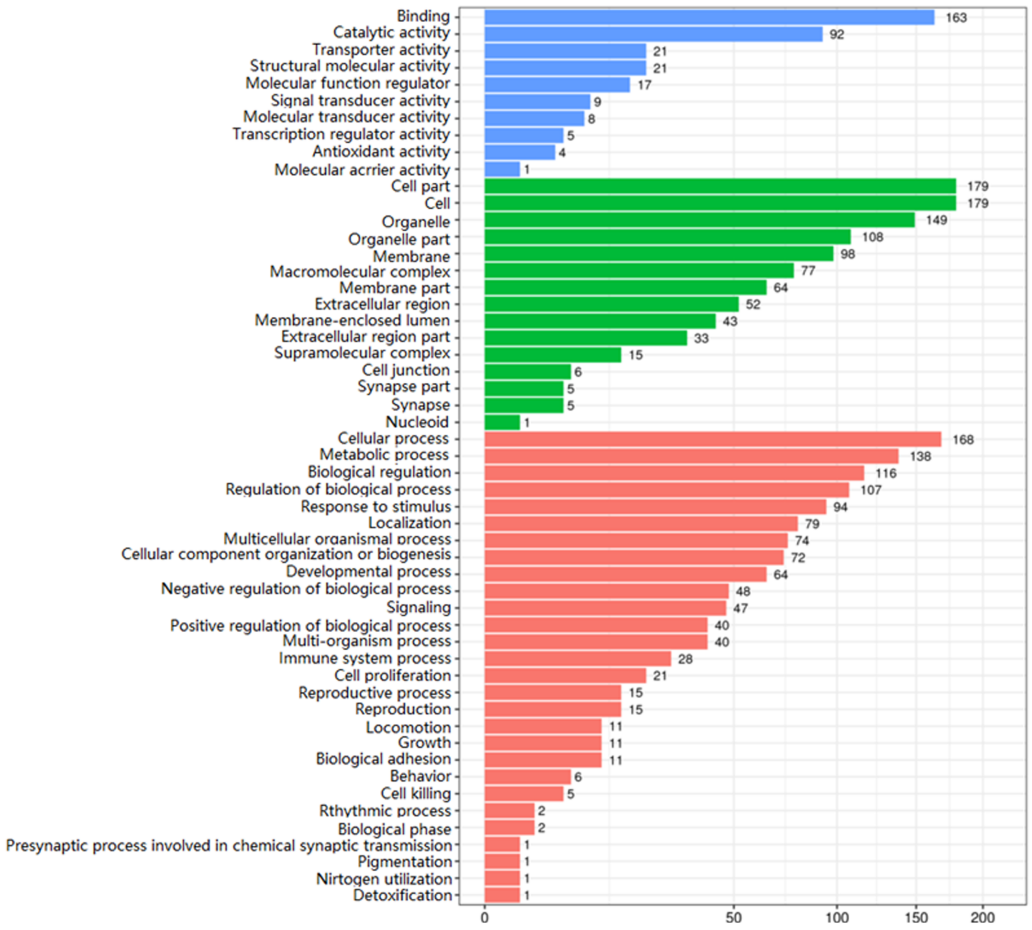


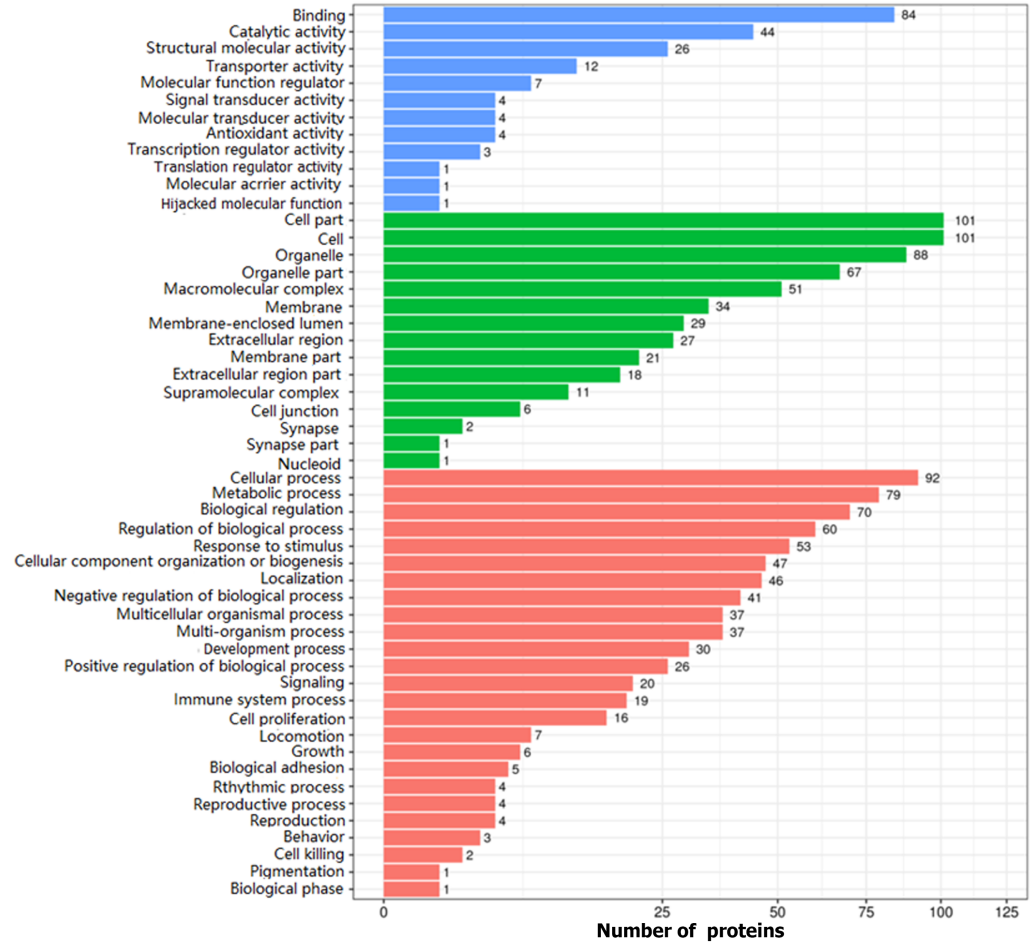
Figure 5 Venn diagram of differentially expressed proteins among groups. A: Venn diagram of differentially expressed proteins (DEPs) in dextran sulfate sodium-induced ulcerative colitis model group that can be regulated by herb-partitioned moxibustion; B: Venn diagram of DEPs in dextran sulfate sodium-induced ulcerative colitis model group that can be regulated by electroacupuncture. N: Normal group; M: Dextran sulfate sodium-induced ulcerative colitis model group; HM: Herb-partitioned moxibustion group; EA: Electroacupuncture group.

DSS-induced UC rats using iTRAQ labelling and found that 202 protein genes were differentially expressed between the two group. Among them, galectin-3, an up-regulated protein, is an endogenous lectin with extensive immunomodulatory functions, and can promote the inflammatory response in DSS-induced colitis by activating the NLR family pyrin domain containing 3 inflammasome[24]. Moreover, galectin-3 has also been shown to be a key regulator of inflammation and can be a potential biomarker for IBD[25]. s100a9 is a subunit of calprotectin with pro-inflammatory activity, and the level of s100a9 was significantly increased in the faeces of DSS-induced colitis mice compared with normal mice[26,27]. This is consistent with the upregulation of s100a9 in UC colon tissue in our study. Guanylate cyclase activator 2A (GUCA2A) is the ligand of guanylate cyclase C, which is mainly expressed in intestinal epithelial cells, and can regulate intestinal barrier function and intestinal homeostasis through the cyclic guanosine monophosphate-dependent signalling pathway[28]. The

A


Binding 163
Catalytic activity 92
Transporter activity 21
Structural molecular activity 21
Molecular function regulator 17
Signal transducer activity 9
Molecular transducer activity 8
Transcription regulator activity 5
Antioxidant activity 4
Molecular acrrier activity 1
Cell part 179
Cell 179
Organelle 149
Organelle part 108
Membrane 98
Macromolecular complex 77
Membrane part 64
Extracellular region 52
Membrane-enclosed lumen 43
Extracellular region part 33
Supramolecular complex 15
Cell junction 6
Synapse part 5
Synapse 5
Nucleoid 1
Cellular process 168
Metabolic process 138
Biological regulation 116
Regulation of biological process 107
Response to stimulus 94
Localization 79
Multicellular organismal process 74
Cellular component organization or biogenesis 72
Developmental process 64
Negative regulation of biological process 48
Signaling 47
Positive regulation of biological process 40
Multi-organism process 40
Immune system process 28
Cell proliferation 21
Reproductive process 15
Reproduction 15
Locomotion 11
Growth 11
Biological adhesion 11
Behavior 6
Cell killing 5
Rthythmic process 2
Biological phase 2
Presynaptic process involved in chemical synaptic transmission 1
Pigmentation 1
Nirtogen utilization 1
Detoxification 1
0
50
100
150
200

B


Binding 84
Catalytic activity 44
Structural molecular activity 26
Transporter activity 12
Molecular function regulator 7
Signal transducer activity 4
Molecular transducer activity 4
Antioxidant activity 4
Transcription regulator activity 3
Translation regulator activity 1
Molecular acrrier activity 1
Hijacked molecular function 1
Cell part 101
Cell 101
Organelle 88
Organelle part 67
Macromolecular complex 51
Membrane 34
Membrane-enclosed lumen 29
Extracellular region 27
Membrane part 21
Extracellular region part 18
Supramolecular complex 11
Cell junction 6
Synapse 2
Synapse part 1
Nucleoid 1
Cellular process 92
Metabolic process 79
Biological regulation 70
Regulation of biological process 60
Response to stimulus 53
Cellular component organization or biogenesis 47
Localization 46
Negative regulation of biological process 41
Multicellular organismal process 37
Multi-organism process 37
Development process 30
Positive regulation of biological process 26
Signaling 20
Immune system process 19
Cell proliferation 16
Locomotion 7
Growth 6
Biological adhesion 5
Rthythmic process 4
Reproductive process 4
Reproduction 4
Behavior 3
Cell killing 2
Pigmentation 1
Biological phase 1
0
25
50
75
100
125
Number of proteins

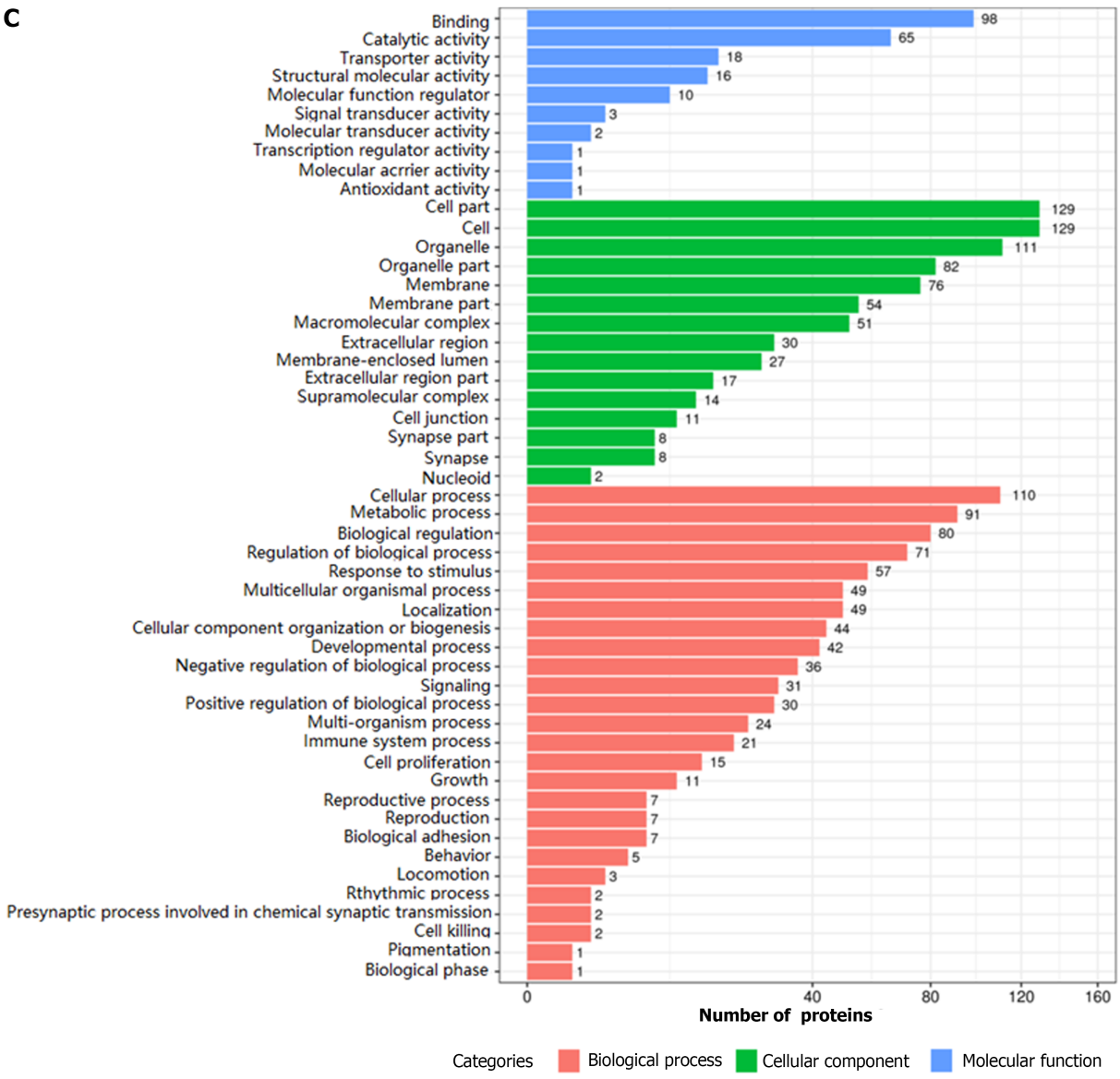
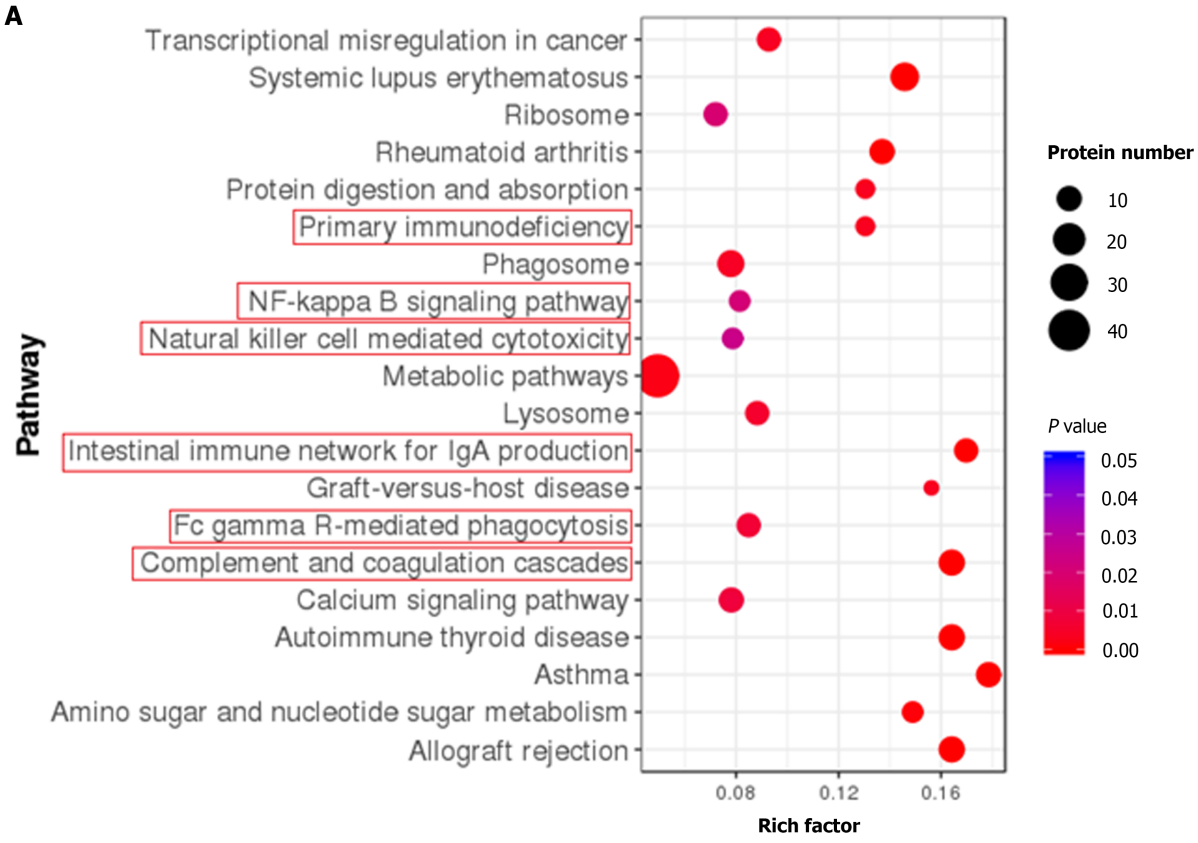
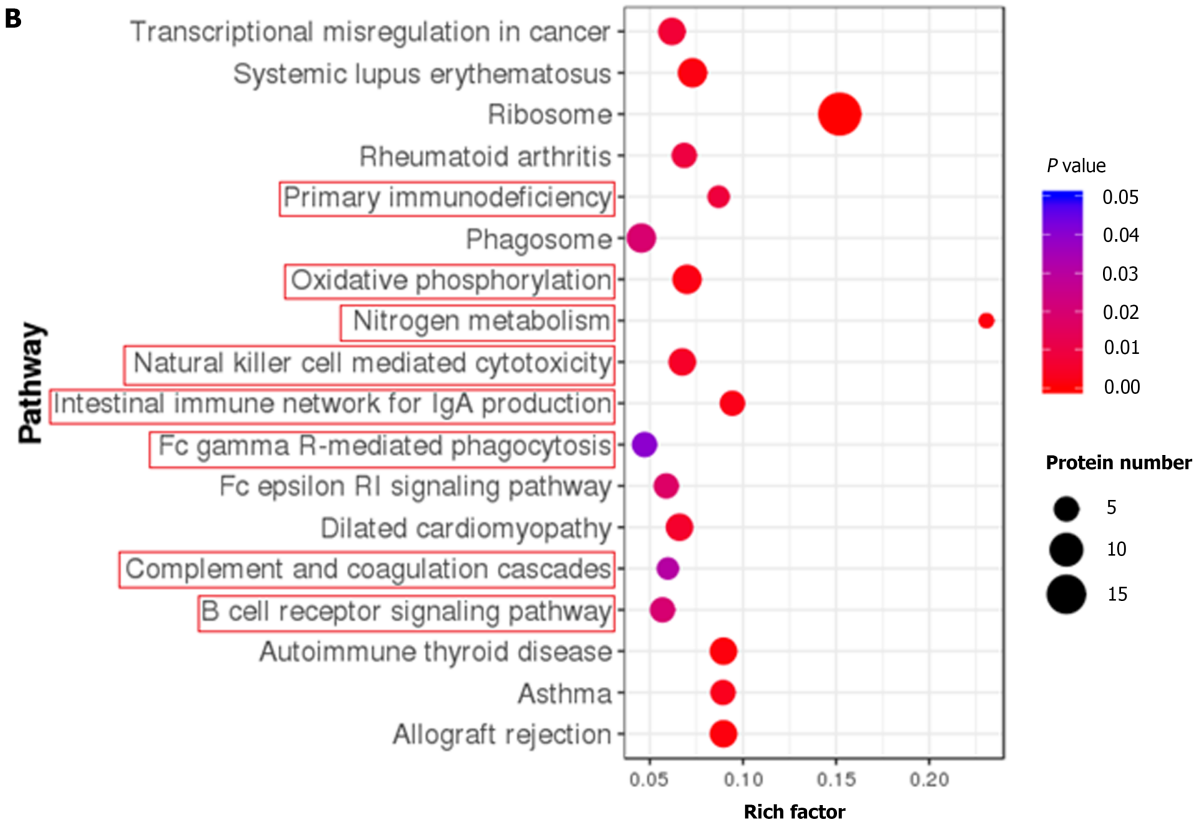


Figure 6 Biological function annotation of differentially expressed proteins between groups. A: Biological function annotation of differentially expressed proteins (DEPs) between the normal and dextran sulfate sodium-induced ulcerative colitis model group; B: Biological function annotation of DEPs between the dextran sulfate sodium-induced ulcerative colitis model and herb-partitioned moxibustion group; C: biological function annotation of DEPs between the dextran sulfate sodium-induced ulcerative colitis model and electroacupuncture group.

down-regulation of GUCA2A can injure the intestinal mucosa barrier and affect the growth and repair of intestinal epithelial cells in IBD patients[29]. Interestingly, we found that the expression of GUCA2A was down-regulated in UC colon tissue, which was consistent with previous findings. These results suggest that galectin-3, s100a9 and GUCA2A may be potential biomarkers of UC.

After receiving the HM intervention, a total of 117 DEPs were identified, of which 25 proteins were reversely regulated by HM, including 17 proteins up-regulated in UC but were down-regulated by HM, and 8 down-regulated in UC but were up-regulated by HM. Among the 17 proteins down-regulated by HM, ATP5L, Atp5f, and Atp5h are the subunits of ATP synthase that involved in energy metabolism and oxidative phosphorylation; Cox4i1 is an important regulatory subunit of cytochrome c oxidase and is mainly associated with mitochondrial oxidative phosphorylation; Cps1, the carbamyl phosphate synthetase 1, was over-expressed in the non-dysplastic tissue of UC progressors[30]; RpS8 is a small subunit protein of ribosomes that plays a critical role in regulation of protein translation. Although it is unclear whether these proteins play a role in UC, ATP-induced energy metabolism disorders and intestinal epithelial mitochondrial damage are important pathogenesis of UC[31]. Therefore, changes in the expression of these proteins may be related to the occurrence of UC and the therapeutic effect of HM. Further studies should be performed to clarify the exact mechanisms of these oxidative phosphorylation proteins. Among the 8 proteins up-regulated by HM, CLCA1 is one of the major non-mucinous proteins in intestinal mucus, which is normally expressed in the gastrointestinal tract and is most abundant in the intestinal mucosa. Studies have shown that CLCA1 regulates the structural


A
Transcriptional misregulation in cancer
Systemic lupus erythematosus
Ribosome
Rheumatoid arthritis
Protein digestion and absorption
Primary immunodeficiency
Phagosome
NF-kappa B signaling pathway
Natural killer cell mediated cytotoxicity
Metabolic pathways
Lysosome
Intestinal immune network for IgA production
Graft-versus-host disease
Fc gamma R-mediated phagocytosis
Complement and coagulation cascades
Calcium signaling pathway
Autoimmune thyroid disease
Asthma
Amino sugar and nucleotide sugar metabolism
Allograft rejection
Pathway
0.08
0.12
0.16
Rich factor
Protein number
10
20
30
40
P value
0.05
0.04
0.03
0.02
0.01
0.00


B
Transcriptional misregulation in cancer
Systemic lupus erythematosus
Ribosome
Rheumatoid arthritis
Primary immunodeficiency
Phagosome
Oxidative phosphorylation
Nitrogen metabolism
Natural killer cell mediated cytotoxicity
Intestinal immune network for IgA production
Fc gamma R-mediated phagocytosis
Fc epsilon RI signaling pathway
Dilated cardiomyopathy
Complement and coagulation cascades
B cell receptor signaling pathway
Autoimmune thyroid disease
Asthma
Allograft rejection
Pathway
0.05
0.10
0.15
0.20
Rich factor
P value
0.05
0.04
0.03
0.02
0.01
0.00
Protein number
5
10
15

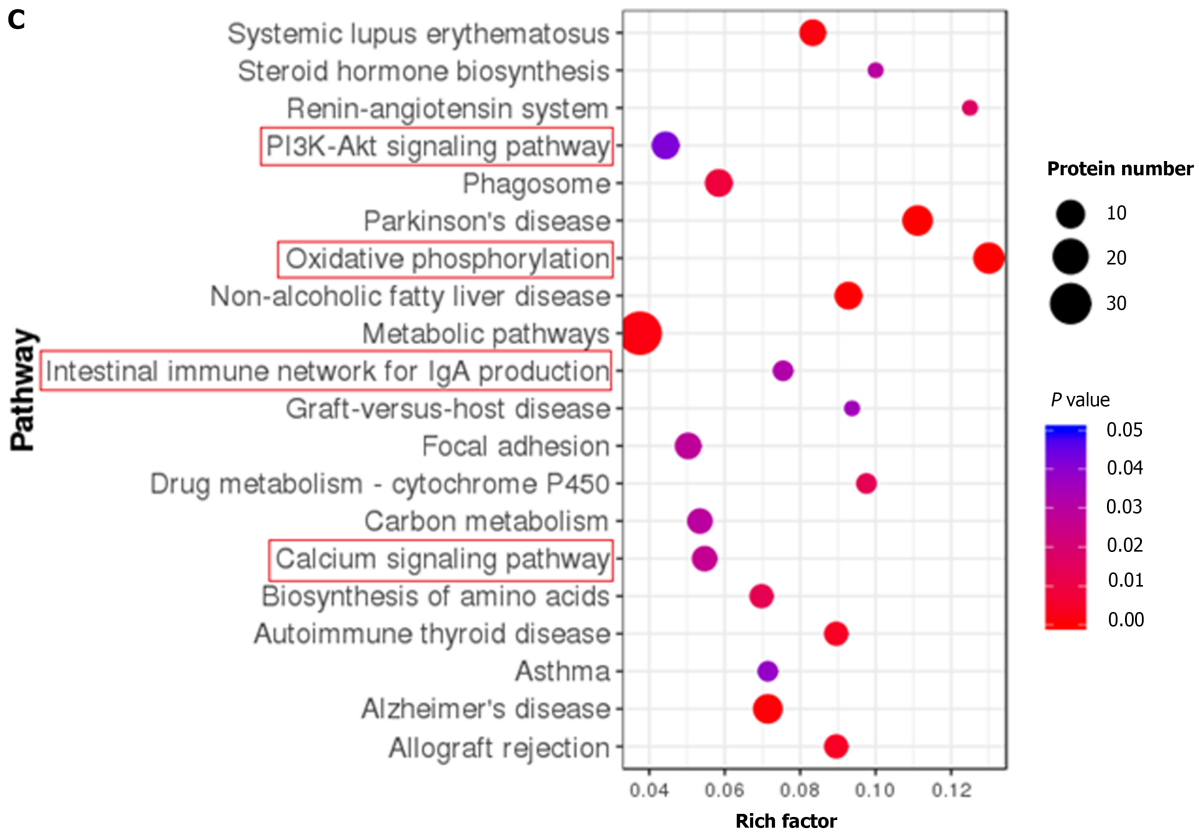


Figure 7 Kyoto Encyclopedia of Genes and Genomes pathway enrichment of differentially expressed proteins between groups. A: Kyoto Encyclopedia of Genes and Genomes (KEGG) pathway enrichment of differentially expressed proteins (DEPs) between the normal and dextran sulfate sodium-induced ulcerative colitis model group; B: KEGG pathway enrichment of DEPs between the dextran sulfate sodium-induced ulcerative colitis model and herb-partitioned moxibustion group; C: KEGG pathway enrichment of DEPs between the dextran sulfate sodium-induced ulcerative colitis model and electroacupuncture group. Each point in the KEGG pathway enrichment plot represents a KEGG pathway, with the left axis showing the pathway name and the abscissa showing the enrichment factor, which represents the ratio of the number of DEPs annotated to that pathway to the number of proteins annotated to that pathway for that species' protein. A larger enrichment factor indicates more reliable enrichment of DEPs in the pathway.

arrangement of mucus, participate in the mucus processing, and plays an important role in regulating intestinal homeostasis and intestinal inflammation[32-34]. CLCA1 can also exert a tumor suppressor effect in colorectal cancer (CRC) by inhibiting the Wnt/β-catenin signalling pathway and epithelial-mesenchymal transition process[35]. The serum concentration and mRNA expression of CLCA1 in CRC tissues were negatively correlated with metastasis and tumor staging[36,37]. These findings suggest that CLCA1 may play an important role in moxibustion in inhibiting the development and carcinogenesis of UC. While 15 proteins were reversely regulated by EA, of which 9 up-regulated in UC but were down-regulated by EA, and 6 down-regulated in UC but were up-regulated by EA. We found EA could also regulate the expression of Atp5f, Cox4i1, Cps1 that explained above, but the functions of other reversely regulated proteins in UC and immune inflammation remain unknown and require further validation and study.

We further explored the potential functions of DEPs by GO and KEGG functional enrichment analyses. GO analysis revealed that the majority of the DEPs were primarily involved in cellular process, metabolic process, biological regulation in biological processes, cell part, cell, organelles, macromolecular complexes in cellular component, and binding, synaptic activity, structural molecule activity, molecular function regulation, molecular sensor activity, and transcriptional regulation activity in molecular function. The results indicated that most differentially abundant proteins were associated with cell structure and catalytic activity which play an important role in cell function. For KEGG analysis, we found that these DEPs were mainly enriched in inflammation responses and immune-related pathways, such as primary immunodeficiency, NF-κB signalling pathway, natural killer cells mediated cytotoxicity, intestinal immune network for IgA production and so on. It has been confirmed that inflammatory response and immune response play an important role in UC. Numerous literature evidence that NF-κB pathway plays an essential role in pathogenic development of UC[38]. In addition, PPI network analysis showed that DEPs related to ribosomal pathways and oxidative phosphorylation pathways were all down-regulated by HM. As we all know that classical signalling pathways, such as the NF-κB signalling pathway, PI3K-Akt signalling pathway, have been confirmed to be associated with UC[39-42], and IgG receptor FcγR also plays an important role in UC intestinal immunity and inflam-

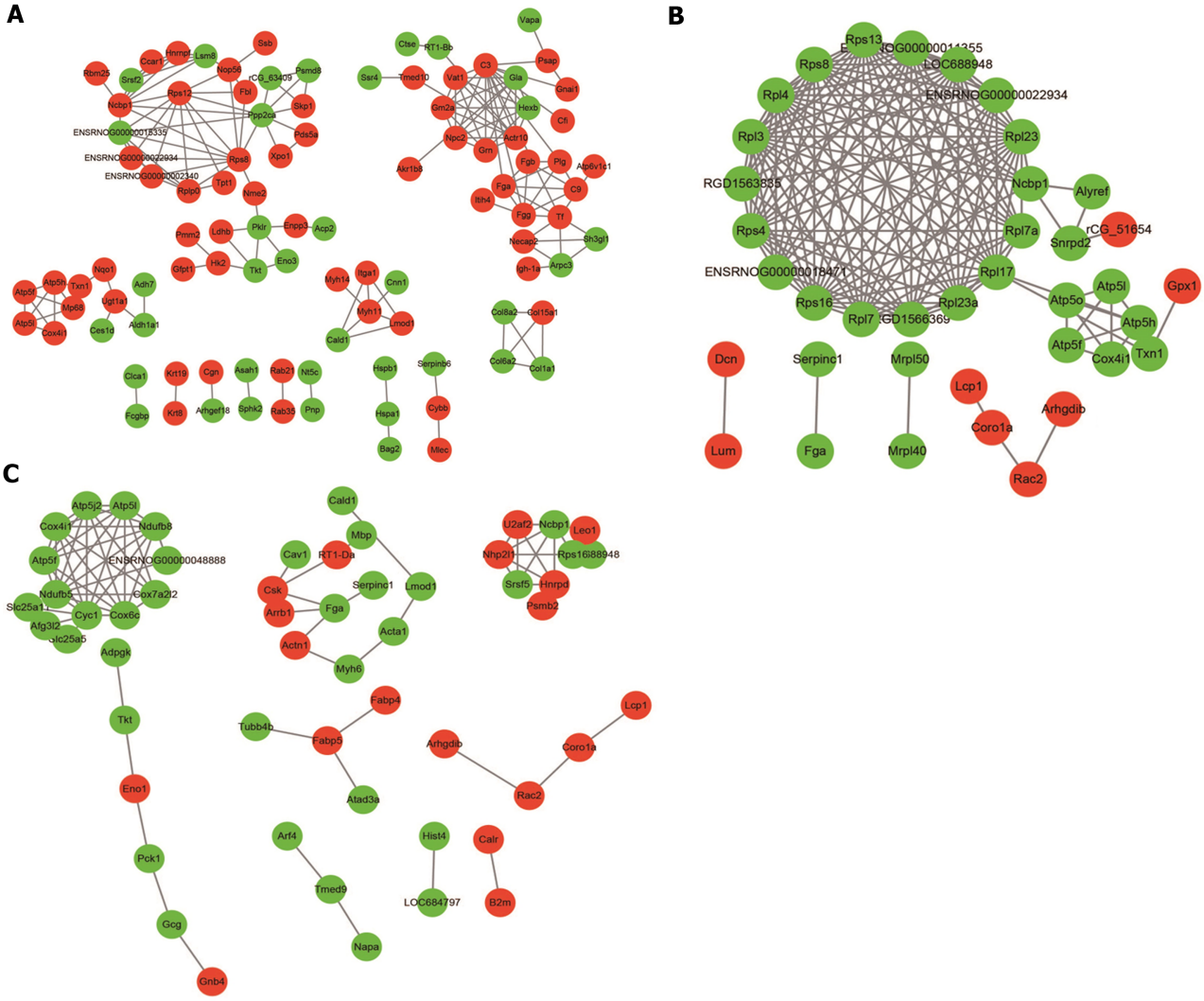


Figure 8 Protein-protein interaction network of differentially expressed proteins between groups. A: Protein-protein interaction (PPI) network of differentially expressed proteins (DEPs) between the normal and dextran sulfate sodium-induced ulcerative colitis model group; B: PPI network of DEPs between the dextran sulfate sodium-induced ulcerative colitis model and herb-partitioned moxibustion group; C: PPI network of DEPs between the dextran sulfate sodium-induced ulcerative colitis model and electroacupuncture group. Circle colours indicate changes in protein expression, with red indicating up-regulation and green indicating down-regulation, and line thickness indicates interaction intensity.

mation[43,44]. The intestinal immune network for IgA production and Fc epsilon RI signalling pathway may also the UC-specific signalling pathway. A study on pathway enrichment analysis of differentially expressed genes between IBD and healthy individuals revealed that primary immunodeficiency, complement and coagulation cascades, and nitrogen metabolism pathways may also play a key role in the progression of IBD[45]. Multiple algorithm analysis found that calcium signalling pathway was involved in the process of UC[46]. This is consistent with our findings at the protein level. Therefore, the abnormality of above pathways may be the key to the pathogenesis of UC, and HM and EA may play the therapeutic role in UC through the regulation of key molecules in these pathways. In addition, we found that proteins involved in inflammation regulation such as serpins were identified (serpinb6 in M/N comparisons, serpinc1 in HM/M and EA/M comparisons). Serpins are the largest known family of serine proteinase inhibitors, which regulate innate immunity by inhibiting the serine proteinase cascades that initiate immune responses such as melanization and antimicrobial peptide production [47]. Several human serpins have been shown to regulate serine proteases associated with processes such as inflammation and immune responses[48]. And increased activity of serine proteases is demonstrated in IBD patients and may contribute to the onset and the maintenance of the disease[49]. This appears to be a novel finding that will require additional research.

We also found that both HM and EA reversed the expression of Sv2a, Ncbp1, Rat hemoglobin beta-chain (Fragment), Fga, Cps1, ATP5L, Cox4i1, Atp5f1, Spout1, Peptidyl-prolyl cis-trans isomerase, Dclk3 proteins, while the rest is what they can reverse individually. The KEGG pathways of DEPs between HM and M groups, EA and M groups were also partly different. These results may reflect the commonness and characteristics of the therapeutic effects of HM and EA. So, the effects of HM and EA on UC may involve the differently regulating proteins and pathways. In addition, based on the results

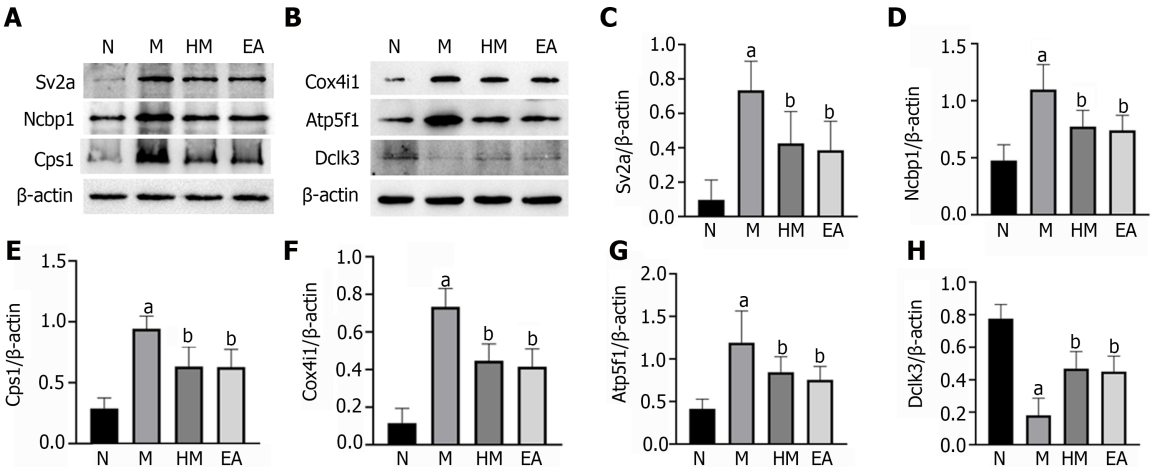


Figure 9 Verification of differentially expressed proteins expressions by western blot. A and B: Band diagrams of protein expressions. All data are expressed as mean ± SD; C: Synaptic vesicle glycoprotein 2A; D: Nuclear cap binding protein subunit 1; E: Carbamoyl phosphate synthetase 1; F: Cytochrome c oxidase subunit 4 isoform 1; G: ATP synthase beta subunit precursor 1; H: Doublecortin like kinase 3. [a]*P* < 0.01 *vs* normal group; [b]*P* < 0.01 *vs* dextran sulfate sodium-induced ulcerative colitis model group. N: Normal group; M: Dextran sulfate sodium-induced ulcerative colitis model group; HM: Herb-partitioned moxibustion group; EA: Electroacupuncture group; Sv2a: Synaptic vesicle glycoprotein 2A; Ncbp1: Nuclear cap binding protein subunit 1; Cps1: Carbamoyl phosphate synthetase 1; Cox4i1: Cytochrome c oxidase subunit 4 isoform 1; Atp5f1: ATP synthase beta subunit precursor; Dclk3: Doublecortin like kinase 3.

of proteomics, we selected 6 DEPs that could be reversed by HM and EA for verification. We found that both HM and EA decreased the expression of Sv2a, Ncbp1, Cps1, Cox4i1, Atp5f1 and increased the expression of Dclk3, which were consistent with the iTRAQ results, confirming the reliability of the iTRAQ results. Cox4i1 is the main subunit of cytochrome c oxidase, a key enzyme in energy metabolism, and plays an important role in mitochondrial oxidative phosphorylation. Defects in oxidative phosphorylation leads to a decrease in cellular ATP production. Studies have reported that the activity of mitochondrial respiratory chain complexes in UC patients is reduced, and mucosal ATP is absent[50, 51]. Atp5f1 is a nuclear gene responsible for encoding the F0 subunit of ATP synthase, which is closely related to energy metabolism. Studies have found that the high expression of Cps1 plays an important role in the formation stage from UC to colitis associated cancer[52]. The intestinal mucosa of UC patients has been under chronic stress for a long time. The dynamic balance between oxidation and antioxidant defense mechanisms in the body is broken, causing mitochondrial damage, weakened oxidative phosphorylation, and reduced energy supply, which in turn causes cell apoptosis and colonic mucosal barrier dysfunction. The above results showed that HM and EA play a therapeutic effect on UC for mitochondrial function and energy metabolism. However, the role of Sv2a, Ncbp1 and Dclk3 in UC or mitochondrial oxidative phosphorylation has not been reported yet, and further research is needed.

In summary, iTRAQ proteomics was used in this study to identify DEPs in the colon of DSS-induced UC rats, as well as proteins that could be regulated by EA and HM, and analysed the function of these DEPs. However, the specific mechanisms of these DEPs were still unclear. They may be involved in one or more regulatory pathways, thus participate in the pathogenesis of UC and the mechanism of EA and HM treatments. The underlying mechanisms may require further study through animal and cell experiments.

CONCLUSION

In conclusion, our study used proteomics to provide evidence that EA and HM might regulate immune-related pathways by regulating the expression of ATP5L, Atp5f1, Cox4i1 that associated with oxidative phosphorylation, thereby alleviating colonic inflammation of DSS-induced UC rats. Further investigations at the role of these proteins in UC will be helpful for revealing the pathogenesis and the mechanism of acupuncture and moxibustion on UC.

ARTICLE HIGHLIGHTS

Research background

Ulcerative colitis (UC) is a chronic, nonspecific intestinal inflammatory disease with unclear etiology. Our previous studies have confirmed that acupuncture and moxibustion is effective in treating UC, but the mechanisms of treatment is still not completely clarified. Proteomic technology has revealed a

variety of biological markers related to immunity and inflammation in UC, which provide new insights and directions for the study of mechanism of acupuncture and moxibustion treatment of UC.

Research motivation

The mechanisms of UC and the therapeutic targets of acupuncture and moxibustion treatment are complicated, and whether acupuncture and moxibustion play a therapeutic role in UC by regulating proteome changes remains unclear.

Research objectives

The present study aims to investigate the underlying mechanism of electroacupuncture (EA) and moxibustion on UC rats by using isotope-labeled relative and absolute quantification (iTRAQ) proteomics technology.

Research methods

Male Sprague-Dawley rats were randomly divided into the normal (N) group, the DSS-induced UC model (M) group, the herb-partitioned moxibustion (HM) group, and the EA group. 3% DSS was used to establish the UC rat model except for the N group, and HM and EA at the Tianshu (bilateral) and Qihai acupoints were performed respectively. Haematoxylin and eosin staining was used for morphological evaluation of colon tissues. iTRAQ and liquid chromatography-tandem mass spectrometry were performed for proteome analysis of the colon tissues, followed by bioinformatics analysis and protein-protein interaction networks establishment of differentially expressed proteins (DEPs) between groups. Then western blot was used for verification of selected DEPs.

Research results

Our study revealed that HM and EA could regulate the expression of multiple proteins in colon of DSS-induced UC model rat. The DEPs were involved in various biological processes such as biological regulation, immune system progression and in multiple pathways including natural killer cell mediated cytotoxicity, intestinal immune network for immunoglobulin A production, and FcγR-mediated phagocytosis. Network analysis revealed that multiple pathways for the DEPs of each group were involved in protein-protein interactions. Subsequent verification of selected DEPs [synaptic vesicle glycoprotein 2A, nuclear cap binding protein subunit 1, carbamoyl phosphate synthetase 1, cytochrome c oxidase subunit 4 isoform 1 (Cox4i1), ATP synthase beta subunit precursor (Atp5F1), doublecortin like kinase 3] by western blot confirmed the reliability of the iTRAQ data.

Research conclusions

HM and EA might regulate immune-related pathways by regulating the expression of ATP5L, Atp5f1, Cox4i1 that associated with oxidative phosphorylation pathways, thereby alleviating colonic inflammation of DSS-induced UC rats.

Research perspectives

The present study revealed the possible molecular mechanisms of acupuncture and moxibustion treatment on UC, it may provide new light on clinical therapy of acupuncture and moxibustion treatment of UC.

ACKNOWLEDGEMENTS

The authors would like to acknowledge the Experimental Animal Center of Shanghai University of Traditional Chinese Medicine for providing the animals, acknowledge the Beijing Genomics Institute for technical services and support of proteomics testings.

FOOTNOTES

Author contributions: Wu LY, Huang Y and Qi Q conceived and designed this study; Zhong R, Liu YN, Ma Z and Zheng HD performed the animal experiments, acquired and analyzed the data; Qi Q wrote the main manuscript; Liu YN and Ma Z prepared the figures and tables; Lu Y gave guidance to the manuscript writing; Zhao C, Huang Y and Wu LY revised and improved the manuscript; and all authors reviewed and approved the final version of this manuscript.

Supported by the National Natural Science Foundation of China No. 81973955, 82004475 and 82174501; Shanghai Clinical Research Center for Acupuncture and Moxibustion No. 20MC1920500; Clinical Key Specialty Construction Foundation of Shanghai No. shslczdzk04701; Natural Science Foundation of Shanghai No. 21ZR1460200.

Institutional animal care and use committee statement: All animal experiments were performed according to the protocols approved by the Animal Ethics Committee of the Experimental Animal Center of Shanghai University of Traditional Chinese Medicine.

Conflict-of-interest statement: All the authors report no relevant conflicts of interest for this article.

Data sharing statement: No additional data are available.

ARRIVE guidelines statement: The authors have read the ARRIVE guidelines, and the manuscript has been prepared and revised according to the ARRIVE guidelines.

Open-Access: This article is an open-access article that was selected by an in-house editor and fully peer-reviewed by external reviewers. It is distributed in accordance with the Creative Commons Attribution NonCommercial (CC BY-NC 4.0) license, which permits others to distribute, remix, adapt, build upon this work non-commercially, and license their derivative works on different terms, provided the original work is properly cited and the use is non-commercial. See: https://creativecommons.org/Licenses/by-nc/4.0/

Country/Territory of origin: China

ORCID number: Qin Qi 0000-0002-0563-1560; Rui Zhong 0000-0002-5136-335X; Ya-Nan Liu 0000-0002-3290-9206; Chen Zhao 0000-0002-2872-6626; Yan Huang 0000-0002-5588-0274; Yuan Lu 0000-0001-7584-5727; Zhe Ma 0000-0003-0956-4438; Han-Dan Zheng 0000-0002-8640-9194; Lu-Yi Wu 0000-0001-8888-1698.

S-Editor: Wang JJ
L-Editor: A
P-Editor: Cai YX

REFERENCES

1 **Ungaro R**, Mehandru S, Allen PB, Peyrin-Biroulet L, Colombel JF. Ulcerative colitis. *Lancet* 2017; **389**: 1756-1770 [PMID: 27914657 DOI: 10.1016/S0140-6736(16)32126-2]
2 **Ng WK**, Wong SH, Ng SC. Changing epidemiological trends of inflammatory bowel disease in Asia. *Intest Res* 2016; **14**: 111-119 [PMID: 27175111 DOI: 10.5217/ir.2016.14.2.111]
3 **Wei SC**, Sollano J, Hui YT, Yu W, Santos Estrella PV, Llamado LJQ, Koram N. Epidemiology, burden of disease, and unmet needs in the treatment of ulcerative colitis in Asia. *Expert Rev Gastroenterol Hepatol* 2021; **15**: 275-289 [PMID: 33107344 DOI: 10.1080/17474124.2021.1840976]
4 **Du L**, Ha C. Epidemiology and Pathogenesis of Ulcerative Colitis. *Gastroenterol Clin North Am* 2020; **49**: 643-654 [PMID: 33121686 DOI: 10.1016/j.gtc.2020.07.005]
5 **Ji J**, Huang Y, Wang XF, Ma Z, Wu HG, Im H, Liu HR, Wu LY, Li J. Review of Clinical Studies of the Treatment of Ulcerative Colitis Using Acupuncture and Moxibustion. *Gastroenterol Res Pract* 2016; **2016**: 9248589 [PMID: 27885326 DOI: 10.1155/2016/9248589]
6 **Yang L**, Zhao JM, Guan X, Wang XM, Zhao C, Liu HR, Wu LY, Ji J, Cheng F, Liu XR, Wu HG. Observation on the effects of different partitioned moxibustion in treating ulcerative colitis. *J Acupunct Tuina Sci* 2016; **14**: 231-241 [DOI: 10.1007/s11726-016-0931-5]
7 **Lin YY**, Zhao JM, Ji YJ, Ma Z, Zheng HD, Huang Y, Cui YH, Lu Y, Wu HG. Typical ulcerative colitis treated by herbs-partitioned moxibustion: A case report. *World J Clin Cases* 2020; **8**: 1515-1524 [PMID: 32368545 DOI: 10.12998/wjcc.v8.i8.1515]
8 **Li YH**, Sun W, Zhou BJ, Rosenstein A, Zhao J, Wang J, Bian ZX. iTRAQ-based pharmacoproteomics reveals potential targets of berberine, a promising therapy for ulcerative colitis. *Eur J Pharmacol* 2019; **850**: 167-179 [PMID: 30771347 DOI: 10.1016/j.ejphar.2019.02.021]
9 **Schniers A**, Goll R, Pasing Y, Sørbye SW, Florholmen J, Hansen T. Ulcerative colitis: functional analysis of the in-depth proteome. *Clin Proteomics* 2019; **16**: 4 [PMID: 30718987 DOI: 10.1186/s12014-019-9224-6]
10 **Pisani LF**, Moriggi M, Gelfi C, Vecchi M, Pastorelli L. Proteomic insights on the metabolism in inflammatory bowel disease. *World J Gastroenterol* 2020; **26**: 696-705 [PMID: 32116417 DOI: 10.3748/wjg.v26.i7.696]
11 **Liu W**, Chen Y, Golan MA, Annunziata ML, Du J, Dougherty U, Kong J, Musch M, Huang Y, Pekow J, Zheng C, Bissonnette M, Hanauer SB, Li YC. Intestinal epithelial vitamin D receptor signaling inhibits experimental colitis. *J Clin Invest* 2013; **123**: 3983-3996 [PMID: 23945234 DOI: 10.1172/JCI65842]
12 **Yu SG**. Experimental Acupuncture. Beijing: People's medical publishing house, 2012
13 **Huang Y**, Ma Z, Cui YH, Dong HS, Zhao JM, Dou CZ, Liu HR, Li J, Wu HG. Effects of Herb-Partitioned Moxibustion on the miRNA Expression Profiles in Colon from Rats with DSS-Induced Ulcerative Colitis. *Evid Based Complement Alternat Med* 2017; **2017**: 1767301 [PMID: 28246536 DOI: 10.1155/2017/1767301]
14 **Li H**, Li KS, Wu LY, Zhou ZG, Huang RJ, Wu HG, Liu YN, Huang Y, Ma XP, Liu HR, Lu Y. Study on the Regulatory Effects of Acupuncture on Vitamin D Receptor and p53 Signal Pathway in Ulcerative Colitis Rats. *World Chinese Med* 2020; **15**: 2259-63+70 [DOI: 10.3969/j.issn.1673-7202.2020.15.012]
15 **Wang L**, Xie H, Xu L, Liao Q, Wan S, Yu Z, Lin D, Zhang B, Lv Z, Wu Z, Sun X. rSj16 Protects against DSS-Induced

Colitis by Inhibiting the PPAR-α Signaling Pathway. *Theranostics* 2017; **7**: 3446-3460 [PMID: 28912887 DOI: 10.7150/thno.20359]

16 **Lu Y**, Ding G, Zheng H, Lü T, Ma Z, Wu H, Weng Z, Zhang F, Wu L, Liu H, Xu M, Feng H. Effect of herb-partitioned moxibustion on dopamine levels and dopamine receptor 1 expression in the colon and central nervous system in rats with Crohn's disease. *J Tradit Chin Med* 2019; **39**: 356-363 [PMID: 32186008]

17 **Li N**, Xu Z, Zhai L, Li Y, Fan F, Zheng J, Xu P, He F. Rapid development of proteomics in China: from the perspective of the Human Liver Proteome Project and technology development. *Sci China Life Sci* 2014; **57**: 1162-1171 [PMID: 25119674 DOI: 10.1007/s11427-014-4714-2]

18 **Lees T**, Nassif N, Simpson A, Shad-Kaneez F, Martiniello-Wilks R, Lin Y, Jones A, Qu X, Lal S. Recent advances in molecular biomarkers for diabetes mellitus: a systematic review. *Biomarkers* 2017; **22**: 604-613 [PMID: 28074664 DOI: 10.1080/1354750X.2017.1279216]

19 **Zhang YF**. Differential proteomics analysis of tissues from ulcerative colitis patients and the establishment of acute damaged models with ulcerative colitis. Medical College of the Chinese People's Liberation Army, 2012

20 **Jin L**, Li L, Hu C, Paez-Cortez J, Bi Y, Macoritto M, Cao S, Tian Y. Integrative Analysis of Transcriptomic and Proteomic Profiling in Inflammatory Bowel Disease Colon Biopsies. *Inflamm Bowel Dis* 2019; **25**: 1906-1918 [PMID: 31173627 DOI: 10.1093/ibd/izz111]

21 **Ahmad A**, Ansari MM, Mishra RK, Kumar A, Vyawahare A, Verma RK, Raza SS, Khan R. Enteric-coated gelatin nanoparticles mediated oral delivery of 5-aminosalicylic acid alleviates severity of DSS-induced ulcerative colitis. *Mater Sci Eng C Mater Biol Appl* 2021; **119**: 111582 [PMID: 33321628 DOI: 10.1016/j.msec.2020.111582]

22 **Mishra RK**, Ahmad A, Kumar A, Vyawahare A, Raza SS, Khan R. Lipid-based nanocarrier-mediated targeted delivery of celecoxib attenuate severity of ulcerative colitis. *Mater Sci Eng C Mater Biol Appl* 2020; **116**: 111103 [PMID: 32806257 DOI: 10.1016/j.msec.2020.111103]

23 **Lo Sasso G**, Phillips BW, Sewer A, Battey JND, Kondylis A, Talikka M, Titz B, Guedj E, Peric D, Bornand D, Dulize R, Merg C, Corciulo M, Ouadi S, Yanuar R, Tung CK, Ivanov NV, Peitsch MC, Hoeng J. The reduction of DSS-induced colitis severity in mice exposed to cigarette smoke is linked to immune modulation and microbial shifts. *Sci Rep* 2020; **10**: 3829 [PMID: 32123204 DOI: 10.1038/s41598-020-60175-3]

24 **Simovic Markovic B**, Nikolic A, Gazdic M, Bojic S, Vucicevic L, Kosic M, Mitrovic S, Milosavljevic M, Besra G, Trajkovic V, Arsenijevic N, Lukic ML, Volarevic V. Galectin-3 Plays an Important Pro-inflammatory Role in the Induction Phase of Acute Colitis by Promoting Activation of NLRP3 Inflammasome and Production of IL-1β in Macrophages. *J Crohns Colitis* 2016; **10**: 593-606 [PMID: 26786981 DOI: 10.1093/ecco-jcc/jjw013]

25 **Papa Gobbi R**, De Francesco N, Bondar C, Muglia C, Chirdo F, Rumbo M, Rocca A, Toscano MA, Sambuelli A, Rabinovich GA, Docena GH. A galectin-specific signature in the gut delineates Crohn's disease and ulcerative colitis from other human inflammatory intestinal disorders. *Biofactors* 2016; **42**: 93-105 [PMID: 26891020 DOI: 10.1002/biof.1252]

26 **Simard JC**, Cesaro A, Chapeton-Montes J, Tardif M, Antoine F, Girard D, Tessier PA. S100A8 and S100A9 induce cytokine expression and regulate the NLRP3 inflammasome *via* ROS-dependent activation of NF-κB(1.). *PLoS One* 2013; **8**: e72138 [PMID: 23977231 DOI: 10.1371/journal.pone.0072138]

27 **Sekiya S**, Murata M, Arai S, Murayama H, Kawasaki A, Ashida N, Okada K, Ikemoto M. Enzyme-linked immunosorbent assay for S100A9 in the stool of rats with dextran sulfate sodium-induced colitis. *J Immunol Methods* 2016; **439**: 44-49 [PMID: 27693389 DOI: 10.1016/j.jim.2016.09.009]

28 **Steinbrecher KA**, Harmel-Laws E, Garin-Laflam MP, Mann EA, Bezerra LD, Hogan SP, Cohen MB. Murine guanylate cyclase C regulates colonic injury and inflammation. *J Immunol* 2011; **186**: 7205-7214 [PMID: 21555532 DOI: 10.4049/jimmunol.1002469]

29 **Brenna Ø**, Furnes MW, Munkvold B, Kidd M, Sandvik AK, Gustafsson BI. Cellular localization of guanylin and uroguanylin mRNAs in human and rat duodenal and colonic mucosa. *Cell Tissue Res* 2016; **365**: 331-341 [PMID: 27044258 DOI: 10.1007/s00441-016-2393-y]

30 **Brentnall TA**, Pan S, Bronner MP, Crispin DA, Mirzaei H, Cooke K, Tamura Y, Nikolskaya T, Jebailey L, Goodlett DR, McIntosh M, Aebersold R, Rabinovitch PS, Chen R. Proteins That Underlie Neoplastic Progression of Ulcerative Colitis. *Proteomics Clin Appl* 2009; **3**: 1326 [PMID: 20098637 DOI: 10.1002/prca.200900061]

31 **Wang D**, Zhang Y, Yang S, Zhao D, Wang M. A polysaccharide from cultured mycelium of Hericium erinaceus relieves ulcerative colitis by counteracting oxidative stress and improving mitochondrial function. *Int J Biol Macromol* 2019; **125**: 572-579 [PMID: 30543884 DOI: 10.1016/j.ijbiomac.2018.12.092]

32 **Nyström EEL**, Arike L, Ehrencrona E, Hansson GC, Johansson MEV. Calcium-activated chloride channel regulator 1 (CLCA1) forms non-covalent oligomers in colonic mucus and has mucin 2-processing properties. *J Biol Chem* 2019; **294**: 17075-17089 [PMID: 31570526 DOI: 10.1074/jbc.RA119.009940]

33 **Nyström EEL**, Birchenough GMH, van der Post S, Arike L, Gruber AD, Hansson GC, Johansson MEV. Calcium-activated Chloride Channel Regulator 1 (CLCA1) Controls Mucus Expansion in Colon by Proteolytic Activity. *EBioMedicine* 2018; **33**: 134-143 [PMID: 29885864 DOI: 10.1016/j.ebiom.2018.05.031]

34 **Erickson NA**, Mundhenk L, Giovannini S, Glauben R, Heimesaat MM, Gruber AD. Role of goblet cell protein CLCA1 in murine DSS colitis. *J Inflamm (Lond)* 2016; **13**: 5 [PMID: 26855614 DOI: 10.1186/s12950-016-0113-8]

35 **Li X**, Hu W, Zhou J, Huang Y, Peng J, Yuan Y, Yu J, Zheng S. CLCA1 suppresses colorectal cancer aggressiveness *via* inhibition of the Wnt/beta-catenin signaling pathway. *Cell Commun Signal* 2017; **15**: 38 [PMID: 28974231 DOI: 10.1186/s12964-017-0192-z]

36 **Bian Q**, Chen J, Qiu W, Peng C, Song M, Sun X, Liu Y, Ding F, Zhang L. Four targeted genes for predicting the prognosis of colorectal cancer: A bioinformatics analysis case. *Oncol Lett* 2019; **18**: 5043-5054 [PMID: 31612015 DOI: 10.3892/ol.2019.10866]

37 **Hu D**, Ansari D, Bauden M, Zhou Q, Andersson R. The Emerging Role of Calcium-activated Chloride Channel Regulator 1 in Cancer. *Anticancer Res* 2019; **39**: 1661-1666 [PMID: 30952704 DOI: 10.21873/anticanres.13271]

38 **Lu PD**, Zhao YH. Targeting NF-κB pathway for treating ulcerative colitis: comprehensive regulatory characteristics of Chinese medicines. *Chin Med* 2020; **15**: 15 [PMID: 32063999 DOI: 10.1186/s13020-020-0296-z]

39 **Wang Y**, Tang Q, Duan P, Yang L. Curcumin as a therapeutic agent for blocking NF-κB activation in ulcerative colitis. *Immunopharmacol Immunotoxicol* 2018; **40**: 476-482 [PMID: 30111198 DOI: 10.1080/08923973.2018.1469145]

40 **Huang XL**, Xu J, Zhang XH, Qiu BY, Peng L, Zhang M, Gan HT. PI3K/Akt signaling pathway is involved in the pathogenesis of ulcerative colitis. *Inflamm Res* 2011; **60**: 727-734 [PMID: 21442372 DOI: 10.1007/s00011-011-0325-6]

41 **Wei J**, Feng J. Signaling pathways associated with inflammatory bowel disease. *Recent Pat Inflamm Allergy Drug Discov* 2010; **4**: 105-117 [PMID: 20001899 DOI: 10.2174/187221310791163071]

42 **Atreya I**, Atreya R, Neurath MF. NF-kappaB in inflammatory bowel disease. *J Intern Med* 2008; **263**: 591-596 [PMID: 18479258 DOI: 10.1111/j.1365-2796.2008.01953.x]

43 **Castro-Dopico T**, Clatworthy MR. IgG and Fcγ Receptors in Intestinal Immunity and Inflammation. *Front Immunol* 2019; **10**: 805 [PMID: 31031776 DOI: 10.3389/fimmu.2019.00805]

44 **Castro-Dopico T**, Dennison TW, Ferdinand JR, Mathews RJ, Fleming A, Clift D, Stewart BJ, Jing C, Strongili K, Labzin LI, Monk EJM, Saeb-Parsy K, Bryant CE, Clare S, Parkes M, Clatworthy MR. Anti-commensal IgG Drives Intestinal Inflammation and Type 17 Immunity in Ulcerative Colitis. *Immunity* 2019; **50**: 1099-1114.e10 [PMID: 30876876 DOI: 10.1016/j.immuni.2019.02.006]

45 **Xie D**, Zhang Y, Qu H. Crucial genes of inflammatory bowel diseases explored by gene expression profiling analysis. *Scand J Gastroenterol* 2018; **53**: 685-691 [PMID: 29909694 DOI: 10.1080/00365521.2018.1461923]

46 **Shi W**, Zou R, Yang M, Mai L, Ren J, Wen J, Liu Z, Lai R. Analysis of Genes Involved in Ulcerative Colitis Activity and Tumorigenesis Through Systematic Mining of Gene Co-expression Networks. *Front Physiol* 2019; **10**: 662 [PMID: 31214045 DOI: 10.3389/fphys.2019.00662]

47 **Wang F**, Song Z, Chen J, Wu Q, Zhou X, Ni X, Dai J. The immunosuppressive functions of two novel tick serpins, HlSerpin-a and HlSerpin-b, from Haemaphysalis longicornis. *Immunology* 2020; **159**: 109-120 [PMID: 31606893 DOI: 10.1111/imm.13130]

48 **Lucas A**, Yaron JR, Zhang L, Ambadapadi S. Overview of Serpins and Their Roles in Biological Systems. *Methods Mol Biol* 2018; **1826**: 1-7 [PMID: 30194590 DOI: 10.1007/978-1-4939-8645-3_1]

49 **Mkaouar H**, Mariaule V, Rhimi S, Hernandez J, Kriaa A, Jablaoui A, Akermi N, Maguin E, Lesner A, Korkmaz B, Rhimi M. Gut Serpinome: Emerging Evidence in IBD. *Int J Mol Sci* 2021; **22** [PMID: 34200095 DOI: 10.3390/ijms22116088]

50 **Sifroni KG**, Damiani CR, Stoffel C, Cardoso MR, Ferreira GK, Jeremias IC, Rezin GT, Scaini G, Schuck PF, Dal-Pizzol F, Streck EL. Mitochondrial respiratory chain in the colonic mucosal of patients with ulcerative colitis. *Mol Cell Biochem* 2010; **342**: 111-115 [PMID: 20440543 DOI: 10.1007/s11010-010-0474-x]

51 **Santhanam S**, Rajamanickam S, Motamarry A, Ramakrishna BS, Amirtharaj JG, Ramachandran A, Pulimood A, Venkatraman A. Mitochondrial electron transport chain complex dysfunction in the colonic mucosa in ulcerative colitis. *Inflamm Bowel Dis* 2012; **18**: 2158-2168 [PMID: 22374887 DOI: 10.1002/ibd.22926]

52 **Lee YY**, Li CF, Lin CY, Lee SW, Sheu MJ, Lin LC, Chen TJ, Wu TF, Hsing CH. Overexpression of CPS1 is an independent negative prognosticator in rectal cancers receiving concurrent chemoradiotherapy. *Tumour Biol* 2014; **35**: 11097-11105 [PMID: 25099619 DOI: 10.1007/s13277-014-2425-8]

World Journal of Gastroenterology

Submit a Manuscript: https://www.f6publishing.com

World J Gastroenterol 2022 July 28; 28(28): 3666-3681

DOI: 10.3748/wjg.v28.i28.3666

ISSN 1007-9327 (print) ISSN 2219-2840 (online)

ORIGINAL ARTICLE

Retrospective Study

How has the disease course of pediatric ulcerative colitis changed throughout the biologics era? A comparison with the IBSEN study

Yiyoung Kwon, Eun Sil Kim, Yon Ho Choe, Mi Jin Kim

Specialty type: Gastroenterology and hepatology

Provenance and peer review: Unsolicited article; Externally peer reviewed.

Peer-review model: Single blind

Peer-review report's scientific quality classification

Grade A (Excellent): 0
Grade B (Very good): B
Grade C (Good): C
Grade D (Fair): 0
Grade E (Poor): 0

P-Reviewer: Iizuka M, Japan; Nakaji K, Japan

Received: September 28, 2021
Peer-review started: September 28, 2021
First decision: November 18, 2021
Revised: November 21, 2021
Accepted: June 30, 2022
Article in press: June 30, 2022
Published online: July 28, 2022

Yiyoung Kwon, Yon Ho Choe, Mi Jin Kim, Department of Pediatrics, Samsung Medical Center, Seoul 06351, South Korea

Eun Sil Kim, Department of Pediatrics, Kangbuk Samsung Medical Center, Seoul 03181, South Korea

Corresponding author: Mi Jin Kim, MD, PhD, Associate Professor, Department of Pediatrics, Samsung Medical Center, Ilwon-ro 81, Gangnam-gu, Seoul 06351, South Korea.
mijin1217.kim@samsung.com

Abstract

BACKGROUND

In Korea, infliximab was approved for use in children with ulcerative colitis (UC) in October 2012.

AIM

To compare the clinical course of UC before and after the introduction of biological agents, and to compare with the IBSEN study.

METHODS

Patients under 18 years of age, who were diagnosed with UC and followed from January 2003 to October 2020, were included in the study. Group A (n = 48) was followed for at least 2 years between January 2003 and October 2012, and Group B (n = 62) was followed for at least 2 years between November 2012 and October 2020. We compared endoscopic remission, drug composition, relapse rate, steroid-free period, and the quality of life of each group. We plotted the clinical course of the included patients using the pediatric UC activity index score, and compared our patients with those in the IBSEN study.

RESULTS

After 2 years of treatment, colonoscopy evaluation revealed different outcomes in the two treatment groups. Remission was confirmed in 14 patients (29.2%) of Group A, and in 31 patients (50.0%) of Group B (P < 0.012). The median cumulative corticosteroid-free period was 3.0 years in Group A and 4.4 years in Group B. Steroid-free period of Group B was significantly longer than that of Group A (P < 0.001). There was a statistically significant difference between the two groups in evaluation of the relapse rate during the observation period (P < 0.001). The plotted clinical course graphs of Group A showed similar proportions to the

graphs in the IBSEN study. However, in Group B, the proportion of patients corresponding to curve 1 (remission or mild severity after initial high activity) was high at 76% (47/62).

CONCLUSION

The incidence of relapse has decreased and the steroid-free period has increased after the introduction of the biological agent. The clinical course also showed a different pattern from that of IBSEN study. The active use of biological agents may change the long-term disease course in moderate to severe pediatric UC.

Key Words: Colitis; Ulcerative; Children; Infliximab; Relapse; Steroid

©The Author(s) 2022. Published by Baishideng Publishing Group Inc. All rights reserved.

Core Tip: This was a retrospective study that assessed how the introduction of biological agents has altered the disease course over time in pediatric ulcerative colitis (UC). Endoscopic remission, relapse rate, steroid-free period, and the quality of life of each group were evaluated as outcomes. Clinical course was plotted with the pediatric UC activity index score, and compared to that of the IBSEN study. The incidence of relapse has decreased and the steroid-free period has increased after the introduction of biological agents. The clinical course also showed a different pattern from the IBSEN study.

Citation: Kwon Y, Kim ES, Choe YH, Kim MJ. How has the disease course of pediatric ulcerative colitis changed throughout the biologics era? A comparison with the IBSEN study. *World J Gastroenterol* 2022; 28(28): 3666-3681

URL: https://www.wjgnet.com/1007-9327/full/v28/i28/3666.htm

DOI: https://dx.doi.org/10.3748/wjg.v28.i28.3666

INTRODUCTION

Ulcerative colitis (UC) is a chronic inflammatory bowel disease (IBD) that was first described in 1875 by two English physicians. Although it has been the subject of many studies over the years, the etiology remains unknown[1]. The potential causes explained in the literature include immune system dysfunction, genetics, changes in normal intestinal bacteria, environmental factors, and a combination of any or all of these variables[2]. The incidence of UC is higher in developed countries than in less developed ones, which is thought to be the result of reduced exposure to intestinal infections and a Western-style diet and lifestyle[3]. As people in Asia adopt more Westernized dietary habits, the incidence rate is gradually increasing in that part of the world[4].

The age of onset of UC can be anywhere from 15 to 30 to > 60 years, and the incidence of UC is lower than that of Crohn's disease in children[5]. For this reason, the number of large-scale studies and long-term follow-up studies for pediatric patients with UC is insufficient, and more studies are needed to evaluate the clinical course of UC in such patients. The IBSEN study evaluated the long-term clinical course and outcomes of 423 adult patients with UC during the first 10 years. Mortality risk and cumulative colorectal resection were evaluated as clinical outcomes. The proportion of patients who relapsed and who remain in remission was evaluated as a clinical course. In addition, the authors divided the disease course of UC into four types and showed them in graphs, which became a representative figure of this paper[6]. However, this study was done before any biological agents were approved as treatments. No studies have compared the clinical course of UC before and after the introduction of biological agents in a single cohort.

Infliximab was first introduced in Europe in 1999 for the treatment of Crohn's disease[7]. Since the introduction of infliximab, several studies have reported improvements in clinical outcomes with infliximab treatment[8-11]. Nevertheless, relapse has been observed in patients treated with infliximab, and many studies have been conducted on factors that can predict relapse in these patients[12-14]. Therefore, we assessed what changes have occurred in the long-term clinical course of UC since the introduction of biological agents as treatment.

In Korea, infliximab was approved for use in adults with UC in May 2007, and in children in October 2012. Since long-term follow up is possible due to the characteristics of pediatric patients, the aim of this study was to compare the clinical course of UC before and after the introduction of biological agents. Another goal of this study was to compare the clinical course of our patients to that in the IBSEN study.

MATERIALS AND METHODS

Patients

Patients under 18 years of age, who were diagnosed with UC and had been followed from January 2003 to October 2020, were included in this study. Initially, the total number of patients was 138, but patients who had been observed for less than 2 years were eliminated. Finally, 110 patients were selected as the study group (Figure 1). All patients were children and adolescents under 18 years of age at the time of diagnosis, but some patients became adults during the follow-up period. UC was diagnosed in accordance with the guidelines of the European Society for Pediatric Gastroenterology, Hepatology and Nutrition (the Porto criteria)[15]. This study was approved by the institutional review board of Samsung Medical Center (IRB File No. SMC 2020-12-005).

Study design

This was a retrospective study. The first goal was to evaluate how the active use of biological agents causes a change in the clinical course of UC. This was done using data from patients who were treated after the approval of infliximab in October 2012. With the cut-off date of October 2012, the patients were divided into two groups, A and B. Group A had been followed for at least 2 years between January 2003 and October 2012, and Group B had been followed for at least 2 years between November 2012 and October 2020. Since the two groups were classified according to a time difference, we first checked whether there was any difference in the baseline characteristics of the patients, and then conducted a comparative analysis.

Both patient groups were evaluated by laboratory tests (including hemoglobin, albumin, erythrocyte sedimentation rate [ESR], and C-reactive protein [CRP]), colonoscopy, abdominal computed tomography (CT), and pediatric UC activity index (PUCAI) score at the time of diagnosis. Laboratory tests were performed and a PUCAI score questionnaire was submitted at each outpatient follow-up visit, which took place at intervals of 1-3 mo. We confirmed that there were no clinical differences between the two groups in terms of demographic characteristics, the extent and severity of disease according to the laboratory test and colonoscopy results, or the PUCAI score at the time of diagnosis. The fecal calprotectin test has only been available in Korea since 2017 and thus could not be included as a comparative test. Based on the colonoscopy findings, disease extent was classified into E1 (proctitis), E2 (left colitis), E3 (right colitis), and E4 (pancolitis) according to the Paris classification[16], and severity was classified from 0 to 3 using the Mayo endoscopic subscore (MES)[17].

Evaluation of clinical course including relapse and clinical outcome

Colonoscopy was performed at the time of initial diagnosis and at intervals of 1 to 2 years during the follow-up period. The colonoscopy was performed with a CF scope after sedation with midazolam and pethidine. All procedures reached the cecum and the entire colon was examined. Characteristic endoscopic findings of UC such as peri-appendiceal patches, demarcation line, mucosal edema, decreased vascularity of loss of vascularity, and superficial tiny ulcers were observed and described. We reviewed the colonoscopy findings at 2 and 5 years after the start of treatment. Remission was defined as endoscopic mucosal healing, which means that no lesion was observed and the MES was 0 with histological healing (Geboes grade 0-1). The reason for excluding MES 1 is that the authors aimed at deep remission because they experienced cases of MES 1 that relapsed easily. In addition, we investigated the drugs prescribed to both groups of patients during the follow-up period.

To compare the clinical course between the groups, the number of relapses that occurred during the follow-up period was investigated, along with the time interval at which the first relapse occurred (from the time of diagnosis) and the time interval of each relapse when multiple relapses occurred in the same patient. Since the follow-up period was different for each patient, the relapse rate was finally evaluated between the two groups. Clinical relapse was defined as a PUCAI score > 10 with modification of treatment (addition of steroids or biologic agents). To evaluate the clinical risk factors for relapse, age, PUCAI score, disease extent, MES, and initial use of corticosteroids were statistically analyzed. Situations in which symptoms temporarily worsened due to infections such as gastroenteritis were excluded.

In addition, the corticosteroid-free period, cumulative colectomy, and changes in PUCAI score during the follow-up period were evaluated as clinical outcomes of both groups. As another quality of life-related factor, patients who did not experience relapse but were hospitalized or admitted to the emergency room for antibiotic use or blood transfusions were also investigated and the rates of such patients were compared between the groups.

The second goal of this study was to actually draw a clinical course using PUCAI score in these two patient groups and compare these distributions to the four predefined curves, depicting different clinical courses of UC, as published in the IBSEN study[6].

Statistical analyses

The demographic and clinical characteristics of the study groups at initial diagnosis and the clinical outcomes of the study groups were compared using the χ^2 test and Mann-Whitney test. Steroid-free

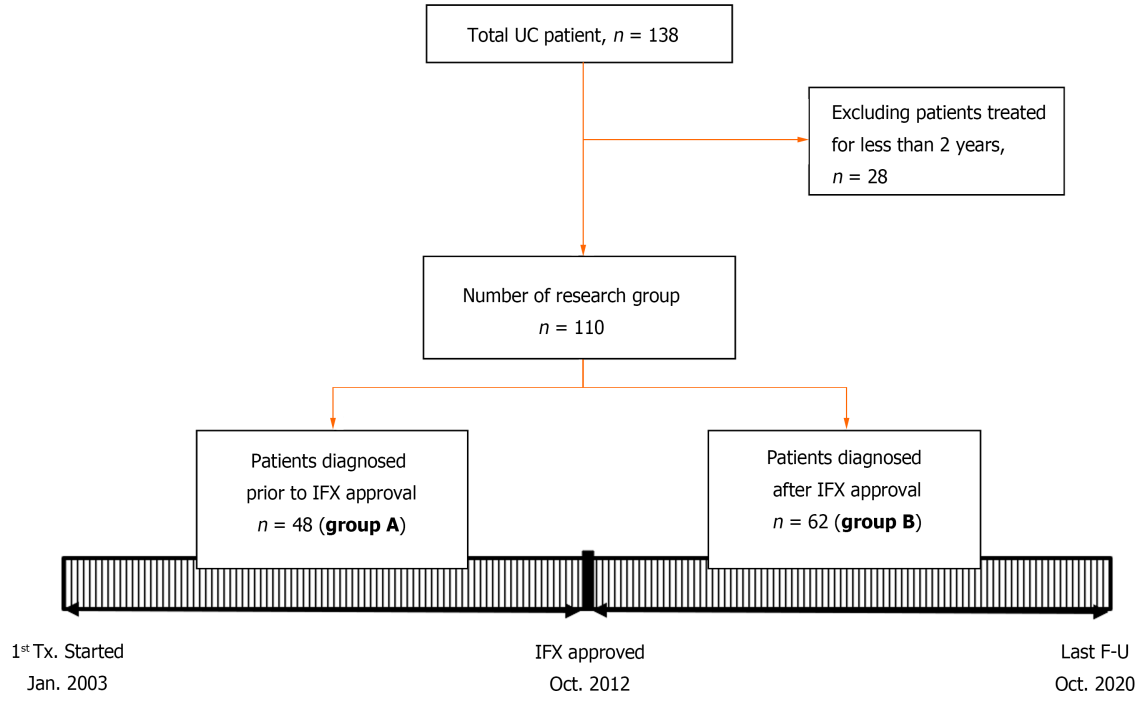


Figure 1 Patient group classification. F-U: Follow-up; IFX: Infliximab; Jan: January; *n*: Number; UC: Ulcerative colitis; Oct: October; Tx: Treatment.

survival curves were presented for the whole cohort using the Kaplan-Meier method. Differences in survival curves between the two groups were evaluated using the log-rank test. Repeated event data for relapses were exhibited by estimating mean cumulative function (MCF), which is the average number of cumulative events experienced by an individual in the study at each point in time since the start of follow-up[18,19]. Univariable/multivariable analyses of the associations between relapse rate and other factors were analyzed by Cox's proportional hazard regression using count process[20] because of multiple events for relapse. Multivariable analysis was performed by selecting variables with $P < 0.1$ in univariate analysis. The 95% confidence intervals (CIs) of the hazard ratio (HR) using robust sandwich covariance estimate to account the within subject correlation[21] were estimated. All of the above statistical analyses were conducted using SAS version 9.4. MCF was analyzed using reReg 1.4.0 package in R 4.0.4 (Vienna, Austria; http://www.R-project.org/. $P < 0.05$ was considered statistically significant.

RESULTS

Baseline characteristics

Table 1 shows the patient characteristics and disease severity information of Group A (n = 48) and Group B (n = 62) at the time of diagnosis, as well as information on the medications that were used for treatment. The median age at the time of diagnosis of UC was 14.4 years for Group A and 15.8 years for Group B. There was no significant difference between the two groups. The median value of the total follow-up period was 3.3 years in Group A and 4.5 years in Group B, and there was no significant difference between the two groups. Serum hemoglobin, albumin, ESR, and CRP levels confirmed by laboratory tests at the time of diagnosis also did not show any significant difference between the two groups.

Based on the results of endoscopy performed at the time of diagnosis, the disease extents of the two groups were classified according to the Paris classification, and severity was evaluated using the endoscopy subscore. There was no difference in disease severity between the two groups, but regarding disease extent, Group B patients had a higher rate of pancolitis and lower rate of proctitis. In Group A, 18 patients (37.5%) had proctitis and 16 (33.3%) had pancolitis, but in Group B, 13 (21%) had proctitis and 34 (54.8%) had pancolitis.

Within 3 mo of diagnosis, most patients in both groups were treated with 5-aminosalicylate and immunosuppressants, primarily azathioprine. In both groups, about 50% of patients used corticosteroids to reduce disease activity at the time of diagnosis. Among the 21 patients who used corticosteroids in Group A, 8 (38.1%) showed dependence and 1 (4.8%) showed refractory findings. In Group B, 9/30 (30.0%) of patients were corticosteroid-dependent and 1/30 (3.3%) was corticosteroid-refractory. There was no statistical difference between the two groups.

Table 1 Demographic and clinical features of the two groups before and after infliximab approval

	Group A (*n* = 48)	Group B (*n* = 62)	*P* value
Age at diagnosis, yr	14.4 (12.2-17.1)	15.8 (13.1-16.5)	0.574[c]
Total duration of follow up with treatment, yr	4.0 (4.0-5.0)	5.5 (3.0-6.9)	0.073[c]
PUCAI[a] at diagnosis	35 (30-65)	45 (35-55)	0.969[c]
Hemoglobin at diagnosis, g/dL	12.3 (10.5-14.1)	12.1 (9.6-13.5)	0.245[c]
Albumin at diagnosis, g/dL	4.3 (4.0-4.6)	4.2 (3.9-4.6)	0.702[c]
ESR at diagnosis, mm/h	14.5 (7-31.3)	20 (7.5-39)	0.249[c]
CRP at diagnosis, mg/dL	0.04 (0.03-0.13)	0.12 (0.03-0.56)	0.791[c]
Disease extent of Paris classification at diagnosis			0.018[d]
E1 proctitis	18 (37.5)	13 (21)	
E2 left colitis	8 (16.7)	8 (12.9)	
E3 right colitis	6 (12.5)	7 (11.3)	
E4 pancolitis	16 (33.3)	34 (54.8)	
Mayo endoscopic subscore at diagnosis[b]			0.310[d]
0 normal or inactive	0	0	
1 mild	12 (25.0)	7 (11.3)	
2 moderate	26 (54.2)	43 (69.4)	
3 severe	10 (20.8)	12 (19.4)	
Corticosteroid use at baseline	21 (43.8)	30 (48.4)	0.630[d]
Corticosteroid-dependent	8/21 (38.1)	9/30 (30.0)	0.550[d]
Corticosteroid-refractory	1/21 (4.8)	1/30 (3.3)	0.360[d]
Cumulative number receiving medication by			0.211[d]
3 mo after diagnosis			0.453[d]
5-aminosalicylate	48 (100)	60 (96.8)	
Azathioprine	42 (87.5)	51 (82.3)	
Methotrexate	0 (0)	1 (1.6)	
Cyclosporine	1 (2.1)	0 (0)	

[a]Pediatric Ulcerative Colitis Activity Index (PUCAI) is a 6-item disease activity index intended for use in pediatric UC clinical trials with a score ranging from 0-85.
[b]Mayo endoscopy subscores were as follows: 0: Normal or inactive disease; 1: Mild disease; 2: Moderate disease; and 3: Severe disease.
[c]χ^2 test.
[d]Mann-Whitney test.
Values are *n* (percentage) or median (interquartile range); *n*: Number of patients; PUCAI: Pediatric Ulcerative Colitis Activity Index.

Comparison of drug composition after 2 and 5 years of treatment

When the drugs that were used for treatment were investigated at the 2-year follow-up visits, 5 patients in Group B did not use any drugs, but no patient in Group A terminated drug treatment (Supplementary Figure 1). In Group A, most patients were still using 5-aminosalicylate (97.9%) and azathioprine (89.6%). In Group B, 96.8% of patients used 5-aminosalicylate as an initial treatment, but at 2 years, some patients had discontinued the use of drugs and 74% of patients were still using the drugs. Also, only 58.1% of the patients in Group B maintained azathioprine treatment at 2 years. In the case of infliximab, on the other hand, more than half of patients in Group B started infliximab treatment within 2 years of diagnosis, and 34 patients were maintaining infliximab. In line with the above results, a statistically significant difference was found between the two groups in the composition of the treatment drugs at the time of the 2-year follow-up visits.

After 5 years, drug composition was re-evaluated in patients who were treated for more than 5 years (Group A = 24 patients, Group B = 31 patients). The same 5 patients in Group B continued to not use any drugs, and 2 patients in Group A also terminated drug treatment. In Group A, mesalazine (87.5%)

and azathioprine (58.3%) use had been tapered and discontinued in many patients. Nevertheless, the proportion of patients using oral drugs was still high compared to Group B (mesalazine: 48.4%, azathioprine: 45.2%). In Group B, the percentage of patients taking infliximab and other biological agents increased (67.7%) after 5 years. In terms of drug composition, the rate of use of mesalazine and infliximab was significantly different, with *P* values of 0.003 and 0.001, respectively (Supplementary Figure 1).

Comparison of disease states after 2 and 5 years of treatment

The patients underwent colonoscopy to re-evaluate disease extent and severity after 2 years of treatment (Table 2). In Group A, remission was confirmed in 14 patients and the proportion of each category of disease extent decreased slightly in comparison to the time of diagnosis, but the differences were small and pancolitis patients still accounted for 27.1% of the total. On the other hand, although the incidence of pancolitis was significantly higher in Group B at the time of diagnosis, 50% of the patients reached remission, and the number of pancolitis patients was significantly reduced to 4 (6.5%). In addition, severity according to the MES also showed a significant difference between the two groups ($P = 0.037$). A large percentage of patients in both groups had moderately severe disease at the time of diagnosis, but after 2 years of treatment, more had mildly severe disease; this was especially true in Group B, in which the percentage of patients with subscores of 0 or 1 was high. In Group B, 53.2% of cases was evaluated as normal or inactive.

Colonoscopy findings were analyzed again after 5 years of treatment (Table 2). As with year 2, the proportion of patients who reached remission at 5 years was greater in Group B (41.9%) than in Group A (12.5%). Overall, a higher proportion of cases in Group B was evaluated as E1 or E2, so disease severity in Group B was still milder than that in Group A ($P = 0.016$). Regarding MES, 41.9% of patients in Group B maintained an inactive disease state, whereas 12.5% of patients in Group B remained low. In Group A, 58.3% of cases was evaluated as moderate, and evidence of the disease was often difficult to see as it was well controlled. In Group B, 51.6% of patients had mild disease. The difference in disease severity between the two groups was statistically significant ($P < 0.001$).

Comparison of clinical outcomes during the total follow-up period

Disease relapse occurred in 23 patients (47.9%) in Group A and 16 (25.8%) in Group B, which was a significant difference ($P = 0.027$) (Table 3). The total cumulative number of relapses was also significantly higher in Group A (40 in Group A *vs* 22 in Group B; $P = 0.006$). In addition, although the difference was not significant, the number of relapses that occurred per person per year was also higher in Group A, with a ratio of 0.44 (Group A) *vs* 0.25 (Group B). The first relapse occurred at a median of 1.2 years after diagnosis in Group A, but in Group B, relapse occurred after a median interval of 1.95 years; thus, first relapse seemed to be delayed in Group B. The time interval between each relapse was investigated in patients who experienced multiple relapses. In Group A, relapse occurred approximately every 1.3 years, whereas relapse took about 1.7 years in Group B, showing that the interval between relapses was relatively wide in Group B. Since each patient's follow-up period was different, we also evaluated the relapse rate by comparing the cumulative hazard rate up to a specific point in time. There were statistically significant differences ($P < 0.001$) between the two groups, as shown in Figure 2.

The PUCAI scores at each outpatient visit during maintenance treatment (excluding times at which the patients had relapsed) were significantly lower in Group B than in Group A ($P < 0.001$) (Table 3). The PUCAI score at the time of relapse was also compared, which showed that the PUCAI score was significantly lower in Group B than in Group A ($P < 0.001$).

Because Group B patients were treated with infliximab, the frequency of steroid use was lower in that group (Table 3). The corticosteroid-free period was compared between the two groups. The median value of the cumulative corticosteroid-free period was 3.0 years in Group A and 4.4 years in Group B. The steroid-free period of Group B was significantly longer than that of Group A ($P < 0.001$). Figure 3 shows the analysis of corticosteroid-free survival curve after initiation of treatment using the Kaplan-Meier method. Over the course of 2 years, the likelihood of remaining corticosteroid-free in Group A was 21%, while it was 88% in Group B ($P = 0.003$).

Only 1 patient underwent colectomy in Group A. At the time of colectomy, the patient used mesalazine, azathioprine, methylprednisolone, and antibiotics. The patient finally underwent total proctocolectomy due to persistent uncontrolled hematochezia at 3 years after diagnosis.

Evaluation of risk factors related to relapse

Since relapse was often observed in both Group A and Group B, the risk factors associated with an increase in relapse rate were investigated in all patients who experienced relapse using Cox's proportional hazard regression for counting processes (Table 4). Since all patients were not followed up for the same period of time, the relapse rate was evaluated but not simply the number of relapses. All factors that were analyzed reflected the status at the time of diagnosis. Young age (> 10 years), PUCAI score over 45, disease extent according to the Paris classification, MES, and initial corticosteroid use were investigated as potential risk factors. In univariable analysis, MES, and initial corticosteroid use were identified as clinical risk factors with statistical significance ($P = 0.010$ and < 0.001) In multivariable

Table 2 Comparison of composition of drugs for treatment and disease states according to colonoscopy findings 2 and 5 yr after diagnosis before (group A) and after (group B) infliximab approval

	Group A (*n* = 48)	Group B (*n* = 62)	*P* value
Maintenance treatment 2 year after diagnosis			
None	0	5 (8.1)	0.045
5-Aminosalicylate	47 (97.9)	46 (74.2)	0.001
Azathioprine	43 (89.6)	36 (58.1)	0.001
Infliximab	0	34 (54.8)	< 0.001
Adalimumab	0	0	
Vedolizumab	0	0	
Ustekinumab	0	0	
Tofacitinib	0	0	
Disease extent of Paris classification 2 years after diagnosis			0.012[b]
Remission	14 (29.2)	31 (50.0)	
E1 proctitis	13 (27.1)	11 (17.7)	
E2 left colitis	2 (4.2)	8 (12.9)	
E3 right colitis	6 (12.5)	8 (12.9)	
E4 pancolitis	13 (27.1)	4 (6.5)	
Mayo endoscopic subscore 2 years after diagnosis[a]			0.037[b]
0 normal or inactive	15 (24.2)	33 (53.2)	
1 mild	24 (50.0)	21 (33.9)	
2 moderate	8 (16.7)	8 (12.9)	
3 severe	1 (2.1)	0	
	Group A (*n* = 24)	**Group B (*n* = 31)**	***P* value**
Maintenance treatment 5 year after diagnosis			
None	2 (8.3)	5 (16.1)	0.394
5-aminosalicylate	21 (87.5)	15 (48.4)	0.003
Azathioprine	14 (58.3)	14 (45.2)	0.337
Infliximab	0	18 (58.1)	< 0.001
Adalimumab	0	2 (6.5)	
Vedolizumab	0	1 (3.2)	
Ustekinumab	0	0	
Tofacitinib	0	0	
Disease extent of Paris classification 5 years after diagnosis			0.016[b]
Remission	3 (12.5)	13 (41.9)	
E1 proctitis	9 (37.5)	9 (29.0)	
E2 left colitis	3 (12.5)	4 (12.9)	
E3 right colitis	2 (8.3)	2 (6.5)	
E4 pancolitis	7 (29.2)	3 (9.7)	
Mayo endoscopic subscore 5 years after diagnosis[a]			< 0.001[b]
0 normal or inactive	3 (12.5)	13 (41.9)	
1 mild	6 (25.0)	16 (51.6)	
2 moderate	14 (58.3)	2 (6.5)	

3 severe	1 (4.2)	0

[a]Mayo endoscopy subscores were as follows: 0: Normal or inactive disease; 1: Mild disease; 2: Moderate disease; and 3: Severe disease.
[b]Mann-Whitney test.
Values are *n* (percentage).

Table 3 Clinical outcomes during the total follow-up period before (group A) and after (group B) infliximab approval

	Group A (*n* = 48)	Group B (*n* = 62)	*P* value
Number of relapsed patients	23 (47.9)	16 (25.8)	0.027[b]
Cumulative total relapses	40	22	0.006[b]
Number of relapses per person	1.74	1.38	
Number of relapses per person per year	0.44	0.25	
First relapse interval from diagnosis, yr	1.20 (0.60-2.50)	1.95 (1.35-3.93)	0.194[b]
Each relapse interval, yr	1.30 (0.60-3.55)	1.70 (1.00-4.20)	0.943[b]
Initial disease extent of relapsed patients			0.080[c]
E1 proctitis	7 (30.4)	0	
E2 left colitis	2 (8.7)	0	
E3 right colitis	3 (13.0)	2 (12.5)	
E4 pancolitis	11 (47.8)	14 (87.5)	
Number of hospitalizations per person	0.13	0.18	0.964[b]
Median PUCAI[a] during treatment period	10 (5-20)	5 (3.75-15)	< 0.001[b]
Median PUCAI[a] at the time of relapse	65 (52.5-75)	45 (45-55)	< 0.001[b]
Median cumulative corticosteroid free period	3.0 (2.6-3.7)	4.4 (3.1-6.0)	< 0.001[b]
Number of cumulative colectomies[1]	1	0	

[a]Pediatric Ulcerative Colitis Activity Index (PUCAI) is a 6-item disease activity index intended for use in pediatric UC clinical trials with a score ranging from 0-85.
[b]χ^2 test.
[c]Mann-Whitney test.
[1]Statistical analysis was not performed as there was only one patient who underwent colectomy.
Values are *n* (percentage) or median (interquartile range); *n*: Number of patients; PUCAI: Pediatric Ulcerative Colitis Activity Index.

analysis, only severe status remained an independent risk factor with statistical significance (P = 0.015).

Supplementary Figure 2 shows a comparison of the timing of the start of infliximab treatment after diagnosis among non-relapsed and relapsed patients who used infliximab. In the group of 29 non-relapsed patients, the majority (22, 75.9%) of them began infliximab treatment within 3 mo. On the other hand, in the group that experienced relapse, there were many patients who first used oral drugs or steroids and then began to use infliximab after 6 mo as the disease progressed.

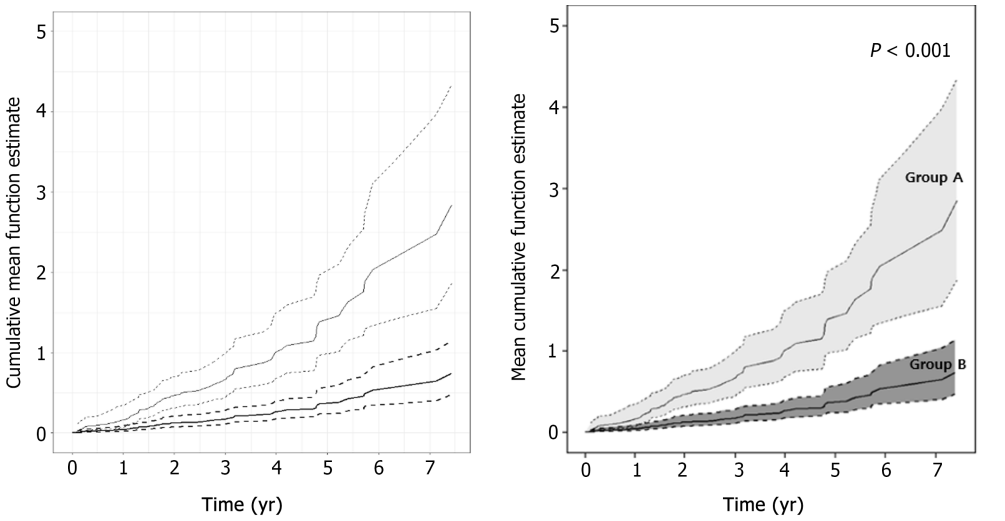
Clinical course curve: Comparison with the IBSEN study

In the IBSEN study, patients were asked to choose which of four predefined patterns best reflected their clinical course (Figure 4A). The predefined patterns were as follows: remission or mild severity of intestinal symptoms after initial high activity, increase in the severity of intestinal symptoms after an initial period of low activity, chronic continuous symptoms, or chronic intermittent symptoms[6]. These curves do not include the curve of the patients whose disease is consistently well controlled after showing mild disease activity at the time of diagnosis; they were probably included in curve 1 in the IBSEN study. In the current study, we plotted the clinical courses of all patients in both groups using the PUCAI score at each outpatient visit and the PUCAI score at relapse. We separated the patients with mild initial disease activity (PUCAI < 35) from the group with good disease control after treatment and drew a new curve (curve 5). Therefore, the proportion of patients corresponding to curve 1 was different from the IBSEN study. In this study, 27.1% of patients in Group A were included in curve 5, and 29.2% of patients showed moderate to severe initial disease activity and maintained well after treatment; they were included in curve 1 (Figure 4B). When these two were combined, it was 56%, which was similar to

Table 4 Univariable and multivariable analysis of the association between relapse rate and other factors

Parameter	Univariable analysis[b]				Multivariable analysis[b]			
	Pr > ChiSq	HR	95%CI[c] of HR		Pr > ChiSq	HR	95%CI[c] of HR	
Age at diagnosis, yr (< 10 yr)	0.063	0.434	0.642	3.714				
Disease extent at diagnosis	0.317							
E2	1	0.786	0.194	3.185[a]				
E3	1	1.097	0.555	2.166[a]				
E4	0.374	1.758	1.058	2.921[a]				
Corticosteroid uses at baseline (Yes)	**0.010**	2.111	1.201	3.712	0.109	1.682	0.890	3.176
Mayo endoscopic subscore at diagnosis (> 2 Moderate)	**< 0.001**	2.496	1.478	4.217	**0.015**	2.108	1.157	3.843
PUCAI[d] at diagnosis (> 45)	0.558	1.202	0.650	2.222				

[a]*P* value and 95%CI for hazard ratio were corrected by Bonferroni's method due to multiple testing.
[b]Cox's proportional hazard regression using counting process.
[c]The robust sandwich covariance estimate was used to account for the within-subject correlation.
[d]Pediatric Ulcerative Colitis Activity Index (PUCAI) is a 6-item disease activity index intended for use in pediatric UC clinical trials with a score ranging from 0-85.
CI: Confidence interval; HR: Hazard ratio.



Number of relapse events		Group A		Group B		Relapse Events Model	
		Number of events	Average time to event	Number of events	Average time to event	HR (95%CI[a])	P value[b]
1	41	24	1.89	17	3.13		
2	17	12	2.869	5	4.81	0.26 (0.16-0.43)	<0.01
3	3	3	3.619	0			
4	1	1	3.94				

Figure 2 Mean cumulative function for multiple relapses over time. The Y-axis is a cumulative relapse rate, which represents the cumulative hazard rate up to a specific point in time. The dotted line represents the 95% confidence interval for the cumulative risk rate. Group A: Thin black line; Group B: Thick black line.

the ratio of curve 1 in the IBSEN study. In the case of Group B, 27.4% of patients were included in curve 5 and the proportion was similar to Group A (Figure 4C). The patients of curve 1 in Group B were 48.4%, showing an increase in the proportion of patients compared to Group A. When combined with patients with mild disease initial activity, it was 76%, which was higher than that of curve 1 patients in the IBSEN study.

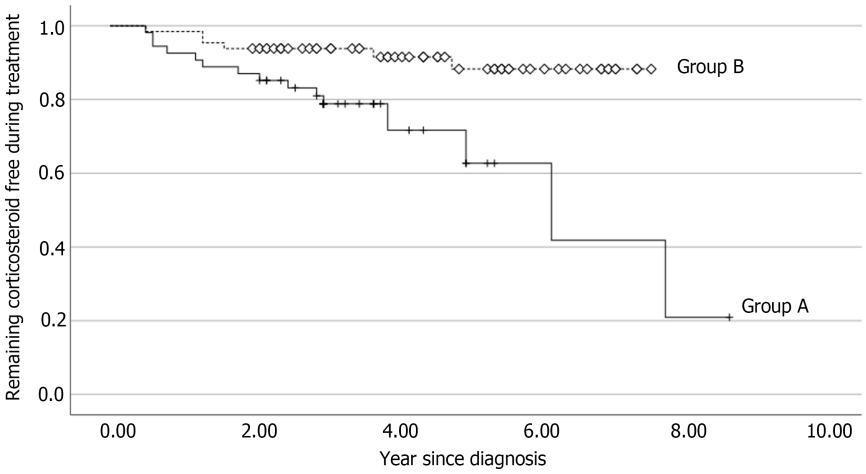


Figure 3 Analysis of corticosteroid-free survival curve after initiation of treatment using Kaplan-Meier method. The solid line represents the proportion of patients who were treated from January 2003 to September 2012 and did not receive corticosteroids. The dotted line represents the same proportion among patients who were treated from October 2012 to October 2020. In the former group, the 2-yr corticosteroid-free retention rate is 21%; in the latter group, the rate is 88% (log-rank test, $P = 0.003$).

The other clinical courses were also classified among patients with similar types and compared with the predefined curves of the IBSEN study. Patients in Group A were distributed among the four types in similar proportions as patients in the IBSEN study (Figure 4B). However, in Group B, the percentage of patients corresponding to curve 4 was relatively small (16%) (Figure 4C).

DISCUSSION

Many previous papers have cited young age at diagnosis as a risk factor for poor clinical outcomes such as relapse and colectomy in pediatric UC patients[22-25]. Thus, research on children with UC is vital. This study evaluated the ways in which the clinical course of children and adolescents with UC changed when the treatment options were diversified after the introduction of biological agents. Infliximab was approved in Korea in 2012 and is now widely used in patients with moderate to severe UC, but many patients who exhibit a good response to oral medication continue to be treated with oral medication only. Here, we compared the clinical course of patients before and after approval of the biological agent according to the passage of time, rather than directly comparing patients who used infliximab to those who did not, as was done in previous studies[8,26,27].

Table 1 shows the characteristics of the included patients. It is evident that the two groups had similar characteristics and differed only in terms of the initial disease extent. The difference in initial disease extent is thought to be due to the rise in incidence of IBD over time as dietary habits become more Westernized; accordingly, the severity of the disease is increasing in newly diagnosed patients[28-30]. Since all patients in this study were followed for at least 2 years, drug and endoscopic evaluation were performed in every patient at 2 years post-diagnosis; it was thus possible to assess changes in the disease extent after 2 years to follow up on this difference in initial disease extent. Only half of all included patients were followed for more than 5 years, but the two groups still exhibited a statistically significant difference in disease extent and severity at 5 years. Despite the high proportion of pancolitis at initial diagnosis, many patients in Group B reached remission. This finding indicates that, in patients with broad disease extent and severity, there is an active and ongoing need for biological agents such as infliximab.

The number of patients who relapsed, the total number of relapses, and the relapse rate were significantly lower in Group B than in Group A. Though both measures significantly differed between the two groups, because every patient had a different follow-up period, we assume that the relapse rate is a more relevant outcome than the total number of relapses (Figure 2). We believe that the higher relapse rate in Group A is attributable to the differences in treatment. Most of the patients with relapse in Group B initially showed pancolitis. Many previous studies have identified disease extent as a risk factor for relapse[23,31,32]. Our risk factor analysis also demonstrated that the initial disease severity (MES) was a significant risk factor for relapse, with P values of 0.006 in the univariate analysis and 0.0149 in the multivariate analysis (Table 4). The worse the initial disease state, the worse the prognosis; this relationship may be taken for granted, but it is important information to keep in mind when establishing a treatment strategy. We thought it was strange that disease extent was not significantly associated with relapse, so we delved a bit deeper into the issue. As a result, pancolitis at initial diagnosis was identified as a risk factor in the univariate analysis in Group A. In Group B, the relapse

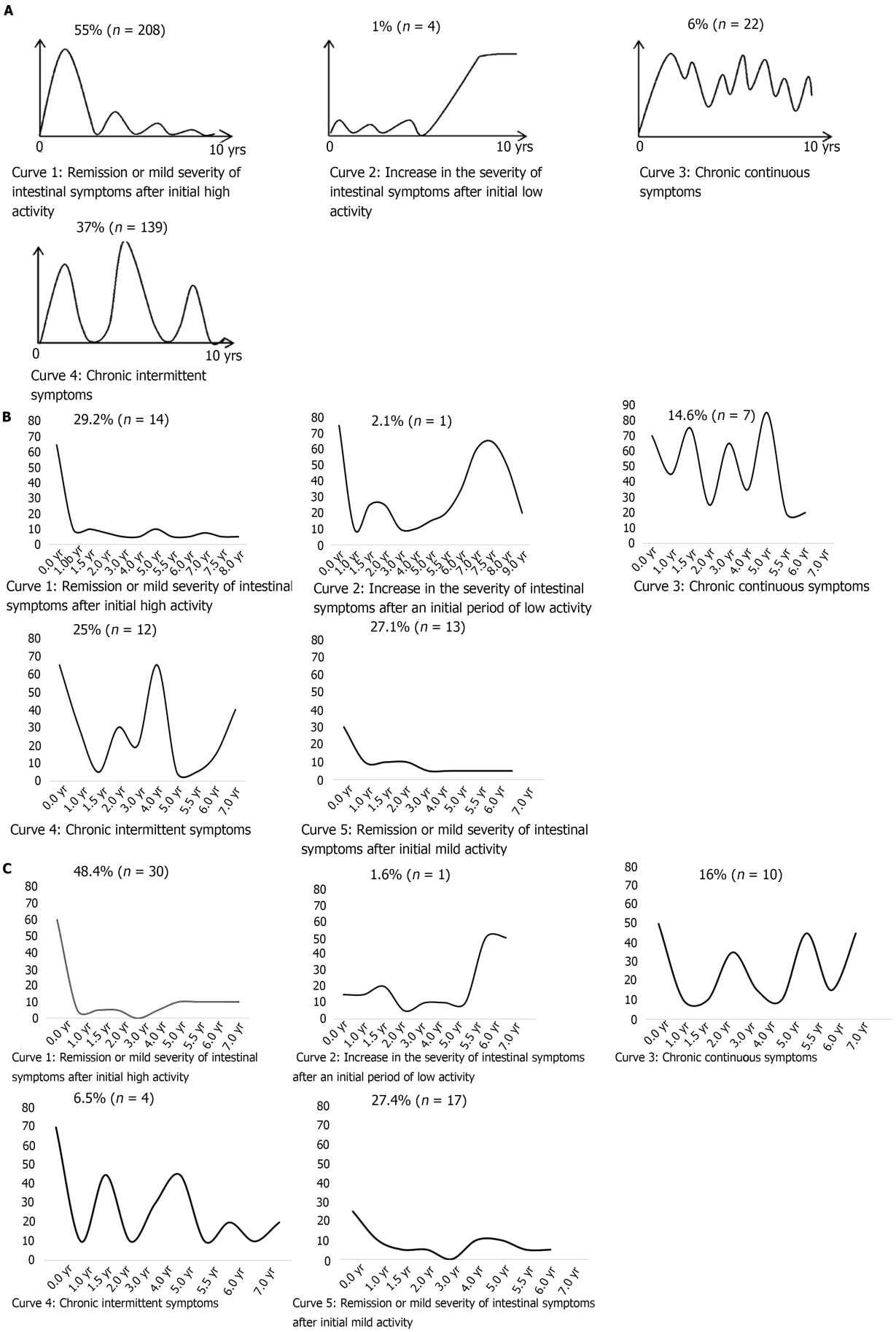


Figure 4 Comparison of clinical course curves of the IBSEN study. A: Graphs of self-identified clinical course in the IBSEN study[6]; B: Actual clinical

course according to pediatric ulcerative colitis activity index prior to the introduction of infliximab (Group A); C: Actual clinical course according to pediatric ulcerative colitis activity index after the introduction of infliximab (Group B). *n*: Number.

rate was relatively low, so statistical evaluation was not possible. In our opinion, disease extent can indicate how long a patient has been suffering from the disease without appropriate treatment. Therefore, it is less likely to be related to relapse rate than disease severity.

As with the endoscopic findings, a high PUCAI score and the use of corticosteroids, which indirectly indicate greater initial disease severity, were also identified as risk factors for relapse. We wondered whether the time at which the patients started infliximab treatment would change the clinical course in relapsed patients even in Group B. Rapid use of infliximab can be expected to reduce the risk of relapse in patients with severe disease, as shown in Supplementary Figure 2. In the non-relapsed group, there were 16 patients with pancolitis at the time of diagnosis, but no relapse occurred among those who received infliximab within 3 mo of diagnosis (Supplementary Figure 2). Since all of our patients were treated with mesalazine and azathioprine for severe disease before receiving additional treatments such as corticosteroids and infliximab, they received similar medications at similar times with the exception of infliximab. Therefore, we propose that the active use of infliximab for initial treatment of moderate to severe UC is important.

As the field of IBD research has expanded and more treatments have been developed, there have been many studies on the quality of life of IBD patients[33-35]. The average PUCAI score during maintenance treatment can be considered an important factor in terms of improving quality of life and preventing relapse. The PUCAI scores during maintenance treatment and at the time of relapse were significantly lower in Group B, indicating that the daily lives of patients in Group B may have been more enriching.

Perhaps the most important factors in evaluating the clinical outcome of treatment are how long the steroid-free period was maintained and whether colectomy was performed[31]. As children and adolescents are not yet finished growing, using steroids more sparingly can prevent osteoporosis and slow growth, which are the typical side effects of steroids[36]. It can also prevent hirsutism, moon face, and buffalo hump in adolescent patients, who tend to be sensitive to appearance. We confirmed that steroid dependency could be avoided through the use of biological agents in patients with high-severity UC (Figure 3). Since colectomy, like the length of the steroid-free period, is an important factor when evaluating long-term outcomes, other studies have also reported on colectomy rates according to treatment[37-39]. In this study, only 1 patient in Group A underwent colectomy due to uncontrolled hematochezia, so it was not possible to compare colectomy as a long-term outcome.

The IBSEN study has been cited in several papers because it is a representative paper that evaluated the clinical course of UC on a large scale[40,41]. The IBSEN study developed predefined curves to represent the clinical course of the disease (Figure 4A). Each patient was asked to choose which predefined graph was most similar to their clinical course. We wondered whether the actual clinical course is represented by these curves and whether the clinical course differs between adults and children. We also wondered whether the clinical course changed after the introduction of biological agents. Therefore, we plotted the clinical course using PUCAI scores. The PUCAI score was chosen because laboratory results such as ESR and CRP are only weakly correlated with symptoms in patients with UC. The shapes of our graphs are similar to the four curves of the IBSEN study. However, there are some differences. The biggest difference is that we separated the patients whose initial disease activity was mild and disease was well controlled from curve 1, which was not shown in the IBSEN study. We believe that patients with such clinical features were also included in curve 1 in the IBSEN study. What was newly confirmed in the process of dividing into curves 1 and 5 is that the proportion of patients in curve 5 was similar in Group A and Group B. It is an epidemiologically convincing finding that the proportion of mild cases is similar over time.

In Group A, if the patients in curve 1 and those in curve 5 were combined, the ratio was similar to that of curve 1 in the IBSEN study. Since the patients of Group A received treatments that were similar to those given in the IBSEN study, the proportion of patients corresponding to each curve was similar. In the case of curve 2, the relapse that occurred in the second half did not persist as relapses tended to do in the IBSEN study, and instead showed a trend towards improvement with treatment. In addition, curve 3 differed in that it showed a lower baseline than the IBSEN curve when disease was partially controlled.

When comparing the graphs of the two groups, fewer patients in Group B than Group A corresponded to curves 3 and 4, and more corresponded to curve 1, indicating that the disease course of patients in Group B was better controlled. Therefore, the proportion of Group B patients corresponding to each curve was also different from the IBSEN study. As mentioned above, the relapse rate dropped after the introduction of infliximab and patients showed improved clinical outcomes. Similarly, the disease course appeared to be changing due to the change in treatment. Taken together, this study suggests that the course of chronic diseases may change over time due to the expanded availability of different types of therapeutic drugs.

The main limitation of this study is that the time difference between the two groups may have introduced some degree of bias. The diagnostic environment and degree of training of the clinicians may have improved over time. To minimize this bias, we evaluated the patients' baseline characteristics using objective indicators and found that there were no significant differences between the two groups. Also, when assessing disease extent and Mayo subscore from the colonoscopy findings, the same experts evaluated all patients using the same criteria. Another limitation is that it was conducted at a single center. However, this hospital is one of the biggest pediatric IBD centers in Korea and has the advantage of having a steady patient cohort through long-term care.

CONCLUSION

As patients with moderate and severe UC have been treated with infliximab since its introduction almost a decade ago, the rate of relapse has decreased and the steroid-free period has increased. In addition, based on the PUCAI score and objective colonoscopy results, the disease is better controlled and patients' quality of life has improved. Before the introduction of the biological agent, the clinical course of pediatric patients showed patterns that resembled those in the IBSEN study, but since its introduction, the proportion of patients who have reached remission has significantly increased. The current goal of treatment for IBD is to change the disease course for a better quality of life, and appropriate treatment with biologic agents may be an option for achieving that goal.

ARTICLE HIGHLIGHTS

Research background

There are many articles comparing the clinical outcomes of patients treated with biological agents *vs* those who did not use biological agents, but no studies have compared the disease course of UC by era before and after the introduction of biological agents. The authors assessed how introduction of new treatment altered disease course over time.

Research motivation

The number of large-scale and long-term follow-up studies for pediatric patients with ulcerative colitis (UC) is insufficient. A representative paper dealing with the clinical course of adult UC is the IBSEN study. This paper dealt with the clinical course before the introduction of biological agents. If the use of biological agents in pediatric UC changed the clinical course of UC, it would be helpful in future treatment decisions.

Research objectives

The aim of this study was to compare the clinical course of pediatric UC by era before and after the introduction of biological agents, and to compare them with clinical course curve of the IBSEN study.

Research methods

Infliximab was approved for use in children in October 2012 in Korea. Group A (n = 48) was followed between January 2003 and October 2012, and Group B (n = 62) was followed between November 2012 and October 2020. Endoscopic remission, drug composition, relapse rate, steroid-free period, and the quality of life of the groups were evaluated as outcomes. Clinical course was plotted with the pediatric UC activity index score, and compared to the curve of the IBSEN study.

Research results

Despite a higher rate of pancolitis, patients in Group B had a higher rate of achieving endoscopic remission, longer steroid-free periods and reduced relapse rate. Unlike the clinical course curve of the IBSEN study, we drew one more independent curve (curve 5), and the proportion of the patients in Group B corresponding to curve 1 (remission or mild severity after initial high activity) was higher. In terms of quality of life, the number of hospitalizations and emergency room visits have improved after the introduction of biological agents. Comparison of treatment costs is also an important issue that needs future research.

Research conclusions

The active use of biological agents may change the long-term disease course in moderate to severe pediatric UC. Growth can also be achieved by reducing the use of steroids.

Research perspectives

Because biological agents are an expensive treatment option, whether there is a difference in economic

quality of life caused by treatment with biological agents is also an important topic for future research.

FOOTNOTES

Author contributions: Kwon Y designed and performed the research and wrote the paper; Kim MJ designed the research and supervised the report; Kim ES and Choe YH designed the research and contributed to the analysis.

Institutional review board statement: This study was reviewed and approved by the Ethics Committee of the Samsung Medical Center (IRB File No. SMC 2020-12-005).

Informed consent statement: Patients were not required to give informed consent to the study because the analysis used anonymous clinical data that were obtained after each patient agreed to treatment by written consent.

Conflict-of-interest statement: The authors have no conflict of interests to declare.

Data sharing statement: No additional data are available.

Open-Access: This article is an open-access article that was selected by an in-house editor and fully peer-reviewed by external reviewers. It is distributed in accordance with the Creative Commons Attribution NonCommercial (CC BY-NC 4.0) license, which permits others to distribute, remix, adapt, build upon this work non-commercially, and license their derivative works on different terms, provided the original work is properly cited and the use is non-commercial. See: https://creativecommons.org/Licenses/by-nc/4.0/

Country/Territory of origin: South Korea

ORCID number: Yiyoung Kwon 0000-0001-5600-2070; Eun sil Kim 0000-0003-2012-9867; Yon Ho Choe 0000-0003-1525-7688; Mi Jin Kim 0000-0002-4505-4083.

S-Editor: Wu YXJ
L-Editor: Filipodia
P-Editor: Cai YX

REFERENCES

1 **Wilks S**. Morbid appearances in the intestine of Miss Bankes. *Med Times Gazette* 1859; **2**: 264-265
2 **Akiho H**, Yokoyama A, Abe S, Nakazono Y, Murakami M, Otsuka Y, Fukawa K, Esaki M, Niina Y, Ogino H. Promising biological therapies for ulcerative colitis: A review of the literature. *World J Gastrointest Pathophysiol* 2015; **6**: 219-227 [PMID: 26600980 DOI: 10.4291/wjgp.v6.i4.219]
3 **Malesza IJ**, Malesza M, Walkowiak J, Mussin N, Walkowiak D, Aringazina R, Bartkowiak-Wieczorek J, Mądry E. High-Fat, Western-Style Diet, Systemic Inflammation, and Gut Microbiota: A Narrative Review. *Cells* 2021; **10** [PMID: 34831387 DOI: 10.3390/cells10113164]
4 **Rizzello F**, Spisni E, Giovanardi E, Imbesi V, Salice M, Alvisi P, Valerii MC, Gionchetti P. Implications of the Westernized Diet in the Onset and Progression of IBD. *Nutrients* 2019; **11** [PMID: 31072001 DOI: 10.3390/nu11051033]
5 **Kugathasan S**, Cohen S. Searching for new clues in inflammatory bowel disease: tell tales from pediatric IBD natural history studies. *Gastroenterology* 2008; **135**: 1038-1041 [PMID: 18786536 DOI: 10.1053/j.gastro.2008.08.030]
6 **Solberg IC**, Lygren I, Jahnsen J, Aadland E, Høie O, Cvancarova M, Bernklev T, Henriksen M, Sauar J, Vatn MH, Moum B; IBSEN Study Group. Clinical course during the first 10 years of ulcerative colitis: results from a population-based inception cohort (IBSEN Study). *Scand J Gastroenterol* 2009; **44**: 431-440 [PMID: 19101844 DOI: 10.1080/00365520802600961]
7 **Cornillie F**. Ten years of infliximab (remicade) in clinical practice: the story from bench to bedside. *Eur J Pharmacol* 2009; **623** Suppl 1: S1-S4 [PMID: 19837054 DOI: 10.1016/j.ejphar.2009.10.023]
8 **Colombel JF**, Rutgeerts P, Reinisch W, Esser D, Wang Y, Lang Y, Marano CW, Strauss R, Oddens BJ, Feagan BG, Hanauer SB, Lichtenstein GR, Present D, Sands BE, Sandborn WJ. Early mucosal healing with infliximab is associated with improved long-term clinical outcomes in ulcerative colitis. *Gastroenterology* 2011; **141**: 1194-1201 [PMID: 21723220 DOI: 10.1053/j.gastro.2011.06.054]
9 **Hyams JS**, Lerer T, Griffiths A, Pfefferkorn M, Stephens M, Evans J, Otley A, Carvalho R, Mack D, Bousvaros A, Rosh J, Grossman A, Tomer G, Kay M, Crandall W, Oliva-Hemker M, Keljo D, LeLeiko N, Markowitz J; Pediatric Inflammatory Bowel Disease Collaborative Research Group. Outcome following infliximab therapy in children with ulcerative colitis. *Am J Gastroenterol* 2010; **105**: 1430-1436 [PMID: 20104217 DOI: 10.1038/ajg.2009.759]
10 **Ferrante M**, Vermeire S, Fidder H, Schnitzler F, Noman M, Van Assche G, De Hertogh G, Hoffman I, D'Hoore A, Van Steen K, Geboes K, Penninckx F, Rutgeerts P. Long-term outcome after infliximab for refractory ulcerative colitis. *J Crohns Colitis* 2008; **2**: 219-225 [PMID: 21172214 DOI: 10.1016/j.crohns.2008.03.004]
11 **Oussalah A**, Evesque L, Laharie D, Roblin X, Boschetti G, Nancey S, Filippi J, Flourié B, Hebuterne X, Bigard MA, Peyrin-Biroulet L. A multicenter experience with infliximab for ulcerative colitis: outcomes and predictors of response, optimization, colectomy, and hospitalization. *Am J Gastroenterol* 2010; **105**: 2617-2625 [PMID: 20736936 DOI:

10.1038/ajg.2010.345]
12 **Farkas K**, Lakatos PL, Nagy F, Szepes Z, Miheller P, Papp M, Palatka K, Bálint A, Bor R, Wittmann T, Molnár T. Predictors of relapse in patients with ulcerative colitis in remission after one-year of infliximab therapy. *Scand J Gastroenterol* 2013; **48**: 1394-1398 [PMID: 24131338 DOI: 10.3109/00365521.2013.845906]
13 **Fiorino G**, Cortes PN, Ellul P, Felice C, Karatzas P, Silva M, Lakatos PL, Bossa F, Ungar B, Sebastian S, Furfaro F, Karmiris K, Katsanos KH, Muscat M, Christodoulou DK, Maconi G, Kopylov U, Magro F, Mantzaris GJ, Armuzzi A, Boscà-Watts MM, Ben-Horin S, Bonovas S, Danese S. Discontinuation of Infliximab in Patients With Ulcerative Colitis Is Associated With Increased Risk of Relapse: A Multinational Retrospective Cohort Study. *Clin Gastroenterol Hepatol* 2016; **14**: 1426-1432.e1 [PMID: 27317850 DOI: 10.1016/j.cgh.2016.05.044]
14 **De Vos M**, Louis EJ, Jahnsen J, Vandervoort JG, Noman M, Dewit O, D'haens GR, Franchimont D, Baert FJ, Torp RA, Henriksen M, Potvin PM, Van Hootegem PP, Hindryckx PM, Moreels TG, Collard A, Karlsen LN, Kittang E, Lambrecht G, Grimstad T, Koch J, Lygren I, Coche JC, Mana F, Van Gossum A, Belaiche J, Cool MR, Fontaine F, Maisin JM, Muls V, Neuville B, Staessen DA, Van Assche GA, de Lange T, Solberg IC, Vander Cruyssen BJ, Vermeire SA. Consecutive fecal calprotectin measurements to predict relapse in patients with ulcerative colitis receiving infliximab maintenance therapy. *Inflamm Bowel Dis* 2013; **19**: 2111-2117 [PMID: 23883959 DOI: 10.1097/MIB.0b013e31829b2a37]
15 **IBD Working Group of the European Society for Paediatric Gastroenterology Hepatology and Nutrition**. Inflammatory bowel disease in children and adolescents: recommendations for diagnosis--the Porto criteria. *J Pediatr Gastroenterol Nutr* 2005; **41**: 1-7 [PMID: 15990620 DOI: 10.1097/01.mpg.0000163736.30261.82]
16 **Levine A**, Griffiths A, Markowitz J, Wilson DC, Turner D, Russell RK, Fell J, Ruemmele FM, Walters T, Sherlock M, Dubinsky M, Hyams JS. Pediatric modification of the Montreal classification for inflammatory bowel disease: the Paris classification. *Inflamm Bowel Dis* 2011; **17**: 1314-1321 [PMID: 21560194 DOI: 10.1002/ibd.21493]
17 **Mazzuoli S**, Guglielmi FW, Antonelli E, Salemme M, Bassotti G, Villanacci V. Definition and evaluation of mucosal healing in clinical practice. *Dig Liver Dis* 2013; **45**: 969-977 [PMID: 23932331 DOI: 10.1016/j.dld.2013.06.010]
18 **Nelson WB**. Recurrent events data analysis for product repairs, disease recurrences, and other applications: SIAM, 2003 [DOI: 10.1137/1.9780898718454]
19 **Lawless JF**, Nadeau C. Some simple robust methods for the analysis of recurrent events. *Technometrics* 1995; **37**: 158-168 [DOI: 10.1080/00401706.1995.10484300]
20 **Andersen PK**, Borgan O, Gill RD, Keiding N. Statistical models based on counting processes: Springer Science & Business Media, 2012
21 **Lin DY**, Wei LJ. The robust inference for the Cox proportional hazards model. *J Am Stat Assoc* 1989; **84**: 1074-1078 [DOI: 10.1080/01621459.1989.10478874]
22 **Jang ES**, Lee DH, Kim J, Yang HJ, Lee SH, Park YS, Hwang JH, Kim JW, Jeong SH, Kim N, Jung HC, Song IS. Age as a clinical predictor of relapse after induction therapy in ulcerative colitis. *Hepatogastroenterology* 2009; **56**: 1304-1309
23 **Bitton A**, Peppercorn MA, Antonioli DA, Niles JL, Shah S, Bousvaros A, Ransil B, Wild G, Cohen A, Edwardes MD, Stevens AC. Clinical, biological, and histologic parameters as predictors of relapse in ulcerative colitis. *Gastroenterology* 2001; **120**: 13-20 [PMID: 11208709 DOI: 10.1053/gast.2001.20912]
24 **Lee JH**, Cheon JH, Moon CM, Park JJ, Hong SP, Kim TI, Kim WH. Do patients with ulcerative colitis diagnosed at a young age have more severe disease activity than patients diagnosed when older? *Digestion* 2010; **81**: 237-243 [PMID: 20110709 DOI: 10.1159/000253850]
25 **Leo S**, Leandro G, Di Matteo G, Caruso ML, Lorusso D. Ulcerative colitis in remission: it is possible to predict the risk of relapse? *Digestion* 1989; **44**: 217-221 [PMID: 2561106 DOI: 10.1159/000199914]
26 **Rutgeerts P**, Sandborn WJ, Feagan BG, Reinisch W, Olson A, Johanns J, Travers S, Rachmilewitz D, Hanauer SB, Lichtenstein GR, de Villiers WJ, Present D, Sands BE, Colombel JF. Infliximab for induction and maintenance therapy for ulcerative colitis. *N Engl J Med* 2005; **353**: 2462-2476 [PMID: 16339095 DOI: 10.1056/NEJMoa050516]
27 **Guo C**, Wu K, Liang X, Liang Y, Li R. Infliximab clinically treating ulcerative colitis: A systematic review and meta-analysis. *Pharmacol Res* 2019; **148**: 104455 [PMID: 31562896 DOI: 10.1016/j.phrs.2019.104455]
28 **Kim BJ**, Song SM, Kim KM, Lee YJ, Rhee KW, Jang JY, Park SJ, Yoon CH. Characteristics and trends in the incidence of inflammatory bowel disease in Korean children: a single-center experience. *Dig Dis Sci* 2010; **55**: 1989-1995 [PMID: 19763825 DOI: 10.1007/s10620-009-0963-5]
29 **Jung YS**, Han M, Kim WH, Park S, Cheon JH. Incidence and Clinical Outcomes of Inflammatory Bowel Disease in South Korea, 2011-2014: A Nationwide Population-Based Study. *Dig Dis Sci* 2017; **62**: 2102-2112 [PMID: 28593437 DOI: 10.1007/s10620-017-4640-9]
30 **Kim HJ**, Hann HJ, Hong SN, Kim KH, Ahn IM, Song JY, Lee SH, Ahn HS. Incidence and natural course of inflammatory bowel disease in Korea, 2006-2012: a nationwide population-based study. *Inflamm Bowel Dis* 2015; **21**: 623-630 [PMID: 25647154 DOI: 10.1097/MIB.0000000000000313]
31 **Farmer RG**, Easley KA, Rankin GB. Clinical patterns, natural history, and progression of ulcerative colitis. A long-term follow-up of 1116 patients. *Dig Dis Sci* 1993; **38**: 1137-1146 [PMID: 8508710 DOI: 10.1007/BF01295733]
32 **Qiu Y**, Chen B, Li Y, Xiong S, Zhang S, He Y, Zeng Z, Ben-Horin S, Chen M, Mao R. Risk factors and long-term outcome of disease extent progression in Asian patients with ulcerative colitis: a retrospective cohort study. *BMC Gastroenterol* 2019; **19**: 7 [PMID: 30630426 DOI: 10.1186/s12876-018-0928-2]
33 **Guthrie E**, Jackson J, Shaffer J, Thompson D, Tomenson B, Creed F. Psychological disorder and severity of inflammatory bowel disease predict health-related quality of life in ulcerative colitis and Crohn's disease. *Am J Gastroenterol* 2002; **97**: 1994-1999 [PMID: 12190166 DOI: 10.1111/j.1572-0241.2002.05842.x]
34 **Carcamo L**, Miranda P, Zúñiga A, Alexander E, Molina ME, Urrejola G, Larach T, Miguieles R, Bellolio F. Ileal pouch-anal anastomosis in ulcerative colitis: outcomes, functional results, and quality of life in patients with more than 10-year follow-up. *Int J Colorectal Dis* 2020; **35**: 747-753 [PMID: 32067061 DOI: 10.1007/s00384-020-03529-7]
35 **Hagelund LM**, Elkjær Stallknecht S, Jensen HH. Quality of life and patient preferences among Danish patients with ulcerative colitis - results from a survey study. *Curr Med Res Opin* 2020; **36**: 771-779 [PMID: 31944145 DOI: 10.1080/03007995.2020.1716704]

36 **Ali T**, Lam D, Bronze MS, Humphrey MB. Osteoporosis in inflammatory bowel disease. *Am J Med* 2009; **122**: 599-604 [PMID: 19559158 DOI: 10.1016/j.amjmed.2009.01.022]

37 **Abou Khalil M**, Boutros M, Nedjar H, Morin N, Ghitulescu G, Vasilevsky CA, Gordon P, Rahme E. Incidence Rates and Predictors of Colectomy for Ulcerative Colitis in the Era of Biologics: Results from a Provincial Database. *J Gastrointest Surg* 2018; **22**: 124-132 [PMID: 28808892 DOI: 10.1007/s11605-017-3530-y]

38 **Aratari A**, Papi C, Clemente V, Moretti A, Luchetti R, Koch M, Capurso L, Caprilli R. Colectomy rate in acute severe ulcerative colitis in the infliximab era. *Dig Liver Dis* 2008; **40**: 821-826 [PMID: 18472316 DOI: 10.1016/j.dld.2008.03.014]

39 **Worley G**, Almoudaris A, Bassett P, Segal J, Akbar A, Ghosh S, Aylin P, Faiz O. Colectomy rates for ulcerative colitis in England 2003-2016. *Aliment Pharmacol Ther* 2021; **53**: 484-498 [PMID: 33264468 DOI: 10.1111/apt.16202]

40 **Ossum AM**, Palm Ø, Lunder AK, Cvancarova M, Banitalebi H, Negård A, Høie O, Henriksen M, Moum BA, Høivik ML; IBSEN Study Group. Ankylosing Spondylitis and Axial Spondyloarthritis in Patients With Long-term Inflammatory Bowel Disease: Results From 20 Years of Follow-up in the IBSEN Study. *J Crohns Colitis* 2018; **12**: 96-104 [PMID: 28961700 DOI: 10.1093/ecco-jcc/jjx126]

41 **Monstad IL**, Solberg IC, Cvancarova M, Hovde O, Henriksen M, Huppertz-Hauss G, Gunther E, Moum BA, Stray N, Vatn M, Hoie O, Jahnsen J. Outcome of Ulcerative Colitis 20 Years after Diagnosis in a Prospective Population-based Inception Cohort from South-Eastern Norway, the IBSEN Study. *J Crohns Colitis* 2021; **15**: 969-979 [PMID: 33367569 DOI: 10.1093/ecco-jcc/jjaa232]

World Journal of Gastroenterology

Submit a Manuscript: https://www.f6publishing.com

World J Gastroenterol 2022 July 28; 28(28): 3682-3694

DOI: 10.3748/wjg.v28.i28.3682

ISSN 1007-9327 (print) ISSN 2219-2840 (online)

ORIGINAL ARTICLE

Retrospective Study

Gastric mucosal precancerous lesions in *Helicobacter pylori*-infected pediatric patients in central China: A single-center, retrospective investigation

Miao Yu, Jing Ma, Xiao-Xia Song, Qiao-Qiao Shao, Xue-Chun Yu, Muhammad Noman Khan, Ya-Bin Qi, Ruo-Bing Hu, Pei-Ru Wei, Wei Xiao, Bai-Ling Jia, Yan-Bo Cheng, Ling-Fei Kong, Chuan-Liang Chen, Song-Ze Ding

Specialty type: Gastroenterology and hepatology

Provenance and peer review: Unsolicited article; Externally peer reviewed.

Peer-review model: Single blind

Peer-review report's scientific quality classification

Grade A (Excellent): 0
Grade B (Very good): 0
Grade C (Good): C, C
Grade D (Fair): 0
Grade E (Poor): 0

P-Reviewer: Kirkik D, Turkey; Miftahussurur M, Indonesia

Received: January 9, 2022
Peer-review started: January 9, 2022
First decision: March 8, 2022
Revised: April 2, 2022
Accepted: June 21, 2022
Article in press: June 21, 2022
Published online: July 28, 2022

Miao Yu, Jing Ma, Qiao-Qiao Shao, Xue-Chun Yu, Muhammad Noman Khan, Ya-Bin Qi, Ruo-Bing Hu, Pei-Ru Wei, Wei Xiao, Bai-Ling Jia, Song-Ze Ding, Department of Gastroenterology and Hepatology, People's Hospital of Zhengzhou University, Henan Provincial People's Hospital, Zhengzhou 450003, Henan Province, China

Xiao-Xia Song, Ling-Fei Kong, Department of Pathology, People's Hospital of Zhengzhou University, Henan Provincial People's Hospital, Zhengzhou 450003, Henan Province, China

Yan-Bo Cheng, Department of Pediatrics, People's Hospital of Zhengzhou University, Henan Provincial People's Hospital, Zhengzhou 450003, Henan Province, China

Chuan-Liang Chen, Department of Medical Imaging, People's Hospital of Zhengzhou University, Henan Provincial People's Hospital, Zhengzhou 450003, Henan Province, China

Corresponding author: Song-Ze Ding, MD, PhD, Professor, Department of Gastroenterology and Hepatology, People's Hospital of Zhengzhou University, Henan Provincial People's Hospital, No. 7 Weiwu Road, Jinshui District, Zhengzhou 450003, Henan Province, China. dingsongze@hotmail.com

Abstract

BACKGROUND

Helicobacter pylori (*H. pylori*) infects about 50% of the world population and is the major cause of chronic gastritis, peptic ulcers, and gastric cancer. Chronic *H. pylori* infection induces gastric mucosal precancerous lesions mostly in adulthood, and it is debatable whether these pathological conditions can occur in childhood and adolescents as well. Since this is a critical issue to determine if intervention should be offered for this population group, we investigated the gastric mucosal precancerous lesions in pediatric patients in an area in central China with a high prevalence of *H. pylori* and gastric cancer.

AIM

To investigate the relationship of *H. pylori* infection and gastric mucosal precancerous lesions in children and adolescents in central China.

METHODS

We screened 4258 ward-admitted children and adolescent patients with upper gastrointestinal symptoms, and finally enrolled 1015 pediatric patients with *H. pylori* infection and endoscopic and histological data. *H. pylori* infection status was determined by rapid urease test and histopathological examination. Both clinical and pathological data were collected and analyzed retrospectively. Occurrence of gastric mucosal precancerous lesions, inflammatory activity and degree of inflammatory cell infiltration between *H. pylori*-positive and -negative groups were compared.

RESULTS

Among the 1015 eligible children and adolescents, the overall *H. pylori* infection rate was 84.14% (854/1015). The infection rate increased with age. The incidence of gastric mucosal precancerous lesions in *H. pylori*-infected children was 4.33% (37/854), which included atrophic gastritis (17 cases), intestinal metaplasia (11 cases) and dysplasia (9 cases). In *H. pylori*-negative patients, only 1 atrophic gastritis case [0.62%, (1/161)] was found ($P < 0.05$). Active inflammation in *H. pylori*-infected patients was significantly higher than that in non-infected patients, and the *H. pylori*-infected group showed more severe lymphocyte and neutrophil granulocyte infiltration ($P < 0.001$). In addition, endoscopy revealed that the most common findings in *H. pylori*-positive patients were antral nodularity, but in *H. pylori*-negative patients only superficial gastritis was observed.

CONCLUSION

In children and adolescents, gastric mucosal precancerous lesions occurred in 4.33% of *H. pylori*-infected patients in central China. These cases included atrophic gastritis, intestinal metaplasia, and dysplasia. The data revealed an obvious critical issue requiring future investigation and intervention for this population group.

Key Words: *Helicobacter pylori*; Gastric cancer; Precancerous lesions; Inflammation; Children and adolescents

©The Author(s) 2022. Published by Baishideng Publishing Group Inc. All rights reserved.

Core Tip: *Helicobacter pylori* (*H. pylori*) infection induces gastric mucosal precancerous lesions mostly in adulthood. Whether these lesions can also occur in children and adolescents remains controversial. Our study showed that in a region in central China with a high prevalence of *H. pylori* and gastric cancer, the incidence of gastric mucosal precancerous lesions was 4.33% among *H. pylori*-infected children and adolescents, which is significantly higher than the non-infected pediatric patients. The precancerous lesions included atrophic gastritis, intestinal metaplasia, and dysplasia. These data provide an alarming alert and call for further investigation and intervention for this population group.

Citation: Yu M, Ma J, Song XX, Shao QQ, Yu XC, Khan MN, Qi YB, Hu RB, Wei PR, Xiao W, Jia BL, Cheng YB, Kong LF, Chen CL, Ding SZ. Gastric mucosal precancerous lesions in *Helicobacter pylori*-infected pediatric patients in central China: A single-center, retrospective investigation. *World J Gastroenterol* 2022; 28(28): 3682-3694

URL: https://www.wjgnet.com/1007-9327/full/v28/i28/3682.htm

DOI: https://dx.doi.org/10.3748/wjg.v28.i28.3682

INTRODUCTION

Helicobacter pylori (*H. pylori*) has infected about 50% of the Chinese population and is responsible for 90% of non-cardia gastric cancer incidences. It is reported that one-third of asymptomatic or healthy children have serologically-confirmed *H. pylori* infection worldwide[1-3]. Although most *H. pylori*-infected children do not have obvious clinical symptoms, studies have shown that children with gastrointestinal symptoms have a higher rate of *H. pylori* infection, and the infection rates are affected by socioeconomic status, living habit, sanitary conditions, geographic region, *etc.*[4,5]. Despite the overall infection rate has slowly declined in China, the infection rate in rural areas is still much higher over that of city residents [6,7].

A recent meta-analysis in China in 2022 has indicated that *H. pylori* prevalence in children and adolescents is 28%[7]. Infection by *H. pylori* is closely associated with gastric mucosal inflammation and extra-gastrointestinal diseases[8-10]. A small portion of infected patients will follow Correa's cascade

and develop severe gastric mucosal lesions, such as atrophic gastritis, intestinal metaplasia (IM), and gastric cancer[11]. *H. pylori* CagA has been shown to be associated with gastric mucosal precancerous lesions in several epidemiological studies[5,12].

One 2006 review summarized the prevalence of gastric mucosal precancerous lesions in children and adolescents, ranging from 0% to 72% in *H. pylori*-infected patients[13]. Prevalence of gastric atrophy in different populations may also vary depending on different geographic/genetic origins or environmental factors in the pediatric population. For example, one Tunisian study in 2009 found that atrophic gastritis accounted for 9.3% (32/354) of enrolled children; of the 32 children with atrophic gastritis, 30 were infected with *H. pylori*[14]. In 2014, a Mexican study of 82 children with chronic gastritis found that 8.5% (7/82) children had antral atrophy and 6.1% (5/82) had IM; among the 7 children with atrophy, 6 had *H. pylori* infection[15]. Other studies carried out in different countries reported gastric atrophy was present in 4.4% to 10.7% of *H. pylori*-positive children[16,17]. However, large-scale investigation is lacking in this area.

H. pylori has the characteristics of family cluster infection and is transmissible among family members, including spouses and siblings[8,9,18]. The infected parents, especially mothers, play a major role in its transmission[19-21]. Most *H. pylori* infection is acquired during childhood and adolescents, and the infection will persist for decades unless proper treatment is offered. Because *H. pylori* infection usually does not cause or only causes mild gastric mucosal lesions in children and adolescents[22-24], the consequences were thought not to be as important as they were in adulthood. Hence, very few studies have focused on the relationships between *H. pylori* infection and gastric mucosa precancerous lesions in children and adolescents. Recent reports have begun to show that gastric mucosal atrophy and IM are also found in children and even in very young children, as mentioned above[13-15].

In this work, we retrospectively investigated a cohort of *H. pylori*-infected symptomatic pediatric inpatients on gastric mucosal inflammation status, incidence and pattern of gastric mucosal precancerous lesions in a major hospital in central China, which is an area with a high prevalence of *H. pylori* and gastric cancer (*H. pylori* infection rate is 49.6%[6], and gastric cancer incidence is 42.52/100000[25]). Studies in this area will be helpful to understand the pattern and prevalence of gastric mucosal precancerous lesions in pediatric patients and provide evidence for future *H. pylori* eradication recommendation and related disease prevention.

MATERIALS AND METHODS

Study population and patient enrollment

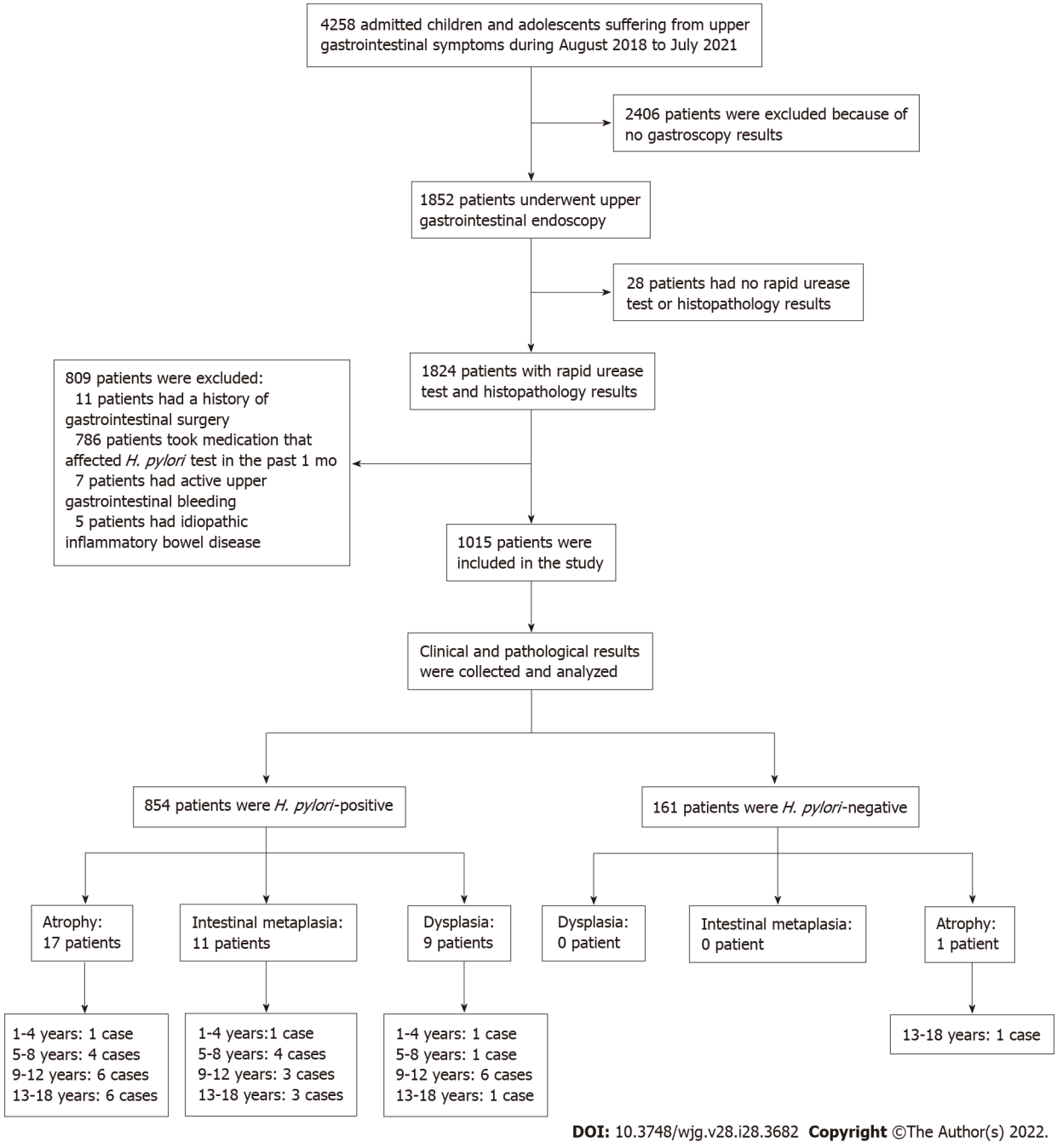
From August 1, 2018 to July 31, 2021, 4258 pediatric patients with an age less than 18-years-old who had upper gastrointestinal symptoms were admitted to the Department of Pediatrics, People's Hospital of Zhengzhou University; among them, 1852 underwent upper gastrointestinal endoscopy examination due to disease complaints, such as abdominal pain, abdominal distension, nausea, vomiting, hiccups, heartburn, *etc*. Patients who had taken biopsy specimens from the gastric mucosa for histopathological examination and rapid urease test were enrolled into the study. Exclusion criteria were as follows: (1) Use of antibiotics, bismuth salts, proton pump inhibitors, H2-receptor blockers, immunosuppressants and steroids over the past 1 mo; (2) History of gastrointestinal surgery; (3) Active upper gastrointestinal bleeding; and (4) Idiopathic inflammatory bowel disease.

The study finally enrolled 1015 eligible children and adolescents. Patient information was collected only for the purpose of disease analysis and were kept confidential. As this is a retrospective study, no informed consent was required. The research protocol was approved by the Ethics Committee of People's Hospital of Zhengzhou University (2019-KY-No. 10). The flow chart of study design and patients' enrollment is shown in Figure 1. Patients were classified into four groups according to age: (1) 1-4 years; (2) 5-8 years; (3) 9-12 years; and (4) 13-18 years.

Endoscopic and histological evaluation of patients

At least two biopsy specimens were collected from the antrum or angulus during endoscopic examination. One biopsy sample was used for immediate rapid urease test. The other was oriented, fixed in formalin and embedded in paraffin blocks. After samples were sectioned, hematoxylin and eosin staining was applied for histological analysis. *H. pylori* infection was detected by immunohistochemical staining. Due to technique limitations, all patients were not given ^{13}C-urea breath test, serological *H. pylori* antibody test or stool antigen test to determine *H. pylori* infection status at the time of their tests. Therefore, a patient was considered *H. pylori*-infected if either histological staining or rapid urease test was positive or if both were positive. Conversely, a patient was considered to be *H. pylori*-uninfected if either histological staining or rapid urease test was negative or if both were negative.

Histological variables (the activity of inflammation, lymphocyte and neutrophil granulocyte infiltration, glandular atrophy, IM and hyperplasia) were analyzed according to visual analog scale of the updated Sydney system[26]. Gastric mucosa changes were classified into absent, mild, moderate and severe levels according to the histological situation of each sample. Severity of lesions was determined by the most severe lesion in each patient. Atrophy of gastric mucosa was indicated by the destruction



DOI: 10.3748/wjg.v28.i28.3682 **Copyright** ©The Author(s) 2022.

Figure 1 Flow chart of patient enrollment on gastric mucosal precancerous lesions in children and adolescents in central China. There were 4258 patients with upper gastrointestinal symptoms under 18 year of age, 2406 patients were excluded for no gastroscopy examination, and the remaining 1852 children had underwent upper gastrointestinal endoscopy. Among these patients, 809 were excluded due to either surgery, medication, bleeding or idiopathic inflammatory bowel disease, and 28 patients were excluded due to no rapid urease test or histopathology test; the final enrolled patient number was 1015. In 854 *Helicobacter pylori* (*H. pylori*)-positive patients, 17 patients had atrophy, 11 patients had intestinal metaplasia and 9 patients had dysplasia, and only 1 of the 161 *H. pylori*-uninfected patients had atrophic gastritis. *H. pylori*: *Helicobacter pylori*.

and reduction in gastric glands of the stomach. IM is a condition in which cells that create the lining of the stomach are changed or replaced by intestinal cells. In many cases, when gastric atrophy and IM coexist, they were allocated into either the atrophy or IM category based on the major pathological presentations of the specific patients. Dysplasia refers to a proliferative lesion, abnormal hyperplasia of the gastric gland basement membrane epithelium and abnormal changes in morphology and structure. These specimens were evaluated by two pathologists in a blinded fashion.

Statistical analyses

Data were analyzed using SPSS for Windows version 25 (IBM Corp., Armonk, NY, United States). Continuous variables were described as mean ± SD or median (interquartile range), while categorical variables were described as percentages or frequencies. The χ^2 test or Fisher's exact test were used to

compare pathological changes of gastric mucosa, including activity of inflammation, presence of precancerous lesions and endoscopic pattern of gastric mucosa between patients with *H. pylori* infection and those without *H. pylori* infection. Grade data were analyzed using Wilcoxon signed-rank test, including degrees of inflammatory cell infiltration. A P value less than 0.05 (derived from two-tailed tests) was considered statistically significant.

RESULTS

Patients' demographic characteristics and clinical data

A total of 1852 selected patients were further examined from a pool of 4258 pediatric ward patients (Figure 1). Then, 809 patients were excluded due to surgery, medication, idiopathic inflammatory bowel disease or bleeding, and 28 more patients were excluded because of no rapid urease test or histopathological test. The remaining 1015 eligible patients were enrolled and analyzed. Patient demographic data were summarized in Table 1. Among the 1015 enrolled patients, 604 were males and 411 were females, with median age of 11-years-old, and 854 patients were infected by *H. pylori*, while 161 patients were not infected. The mean age of *H. pylori*-infected patients was significantly older than those of non-infected subjects (11 years *vs* 9 years, $P < 0.05$). There were no significant differences in sex distribution between the *H pylori*-infected and non-infected groups.

The clinical characteristics of patients are also presented in Table 1. For endoscopic manifestations, superficial gastritis was observed in 255 (29.86%) cases among the *H. pylori*-positive patients and 76 (47.20%) cases among the *H. pylori*-negative patients ($P < 0.05$). There was no significant difference in the proportion of superficial gastritis with erosion, superficial gastritis with bile reflux and esophagitis regardless of the status of *H. pylori* infection ($P > 0.05$). Antral nodularity was observed in 131 (15.34%) *H. pylori*-positive patients and 4 (2.48%) *H. pylori*-negative patients ($P < 0.05$). In both *H. pylori*-infected and non-infected patients, most patients were clinically diagnosed with non-atrophic gastritis, and only a small percentage of patients developed atrophic gastritis or peptic ulcers.

H. pylori infection status in different age groups

In the 1-4 years, 5-8 years, 9-12 years and 13-18 years age groups (Table 2), the *H. pylori* infection rates were 40.74%, 78.39%, 88.05% and 89.60%, respectively. The trend of infection rate increasing as age increased was noted. Patient infection rates of the 5-8 years, 9-12 years and 13-18 years age groups were significantly higher than that of the 1-4 years age group. Infection rates of the 9-12 years and 13-18 years age groups were also significantly higher than that of the 5-8 years age group, but the infection rates had no significant difference between the 9-12 and 13-18 years age groups.

Gastric mucosal precancerous lesions in different age groups

Patient gastric mucosal precancerous lesions are shown in Table 3. Among the 854 *H. pylori*-infected patients, 4.33% (37/854) had gastric mucosa precancerous lesions; among which, 17 patients had atrophy, 11 patients had IM, and 9 patients had dysplasia. Only 1 of the 161 *H. pylori*-uninfected patients (0.62%) had atrophic gastritis. The incidence of precancerous lesions of gastric mucosa in *H. pylori*-infected patients was significantly more than those uninfected patients ($\chi^2 = 5.178$, $P = 0.023$). Among the *H. pylori*-positive patients, there were gastric mucosal precancerous lesions in each age group, whereas among the *H. pylori*-negative patients, only 1 patient with atrophic gastritis was found in the 13-18 years age group. Representative pictures of normal, gastritis, and gastric mucosal precancerous lesions are shown in Figure 2.

Active inflammation in H. pylori-infected and -uninfected patients

As described in Table 4, active inflammation was observed in 16.04% (137/854) of the *H. pylori*-infected patients and only 3.73% (6/161) of the -uninfected patients. A significant difference was noticed between these two groups ($\chi^2 = 16.975$, $P < 0.001$). But in the 1-4 years age group, there was no significant difference in inflammatory activity between the *H. pylori*-infected and -uninfected patients (13.64% *vs* 6.25%, $\chi^2 = 0.196$, $P = 0.658$). Whereas in the 5-8 years, 9-12 years and 13-18 years age groups, the proportion of active inflammation in the *H. pylori*-positive patients was significantly higher than that in the *H. pylori*-negative patients ($\chi^2 = 4.901$, $P = 0.027$; $\chi^2 = 3.987$, $P = 0.046$; $\chi^2 = 6.012$, $P = 0.014$).

Characteristics of inflammatory cell infiltration in H. pylori-infected and -uninfected groups

The degree of neutrophil granulocyte infiltration with different *H. pylori* infection status is shown in Table 5. For the 854 infected patients, the proportions of absent, mild and moderate neutrophil granulocyte infiltration were 83.96%, 13.58% and 2.46%, respectively. While for the -uninfected patients, they were 96.27%, 3.73% and 0%, respectively. Compared with *H. pylori*-infected patients, the prevalence of neutrophil granulocyte infiltration in gastric mucosa was significantly higher than that in uninfected patients ($Z = 4.319$, $P < 0.001$). This difference between *H. pylori*-positive and -negative patients was also indicated in different age groups, with the exception of the 1-4 years age group.

Table 1 Demographic and clinical data of patients

Variables	Total	*H. pylori*+	*H. pylori*-	*P* value
Patients, *n*	1015	854	161	
Age in year, median (IQR)	11 (9-13)	11 (9-13)	9 (6-12)	< 0.001[a]
Sex, *n* (%)				
Female	411 (40.49)	346 (40.52)	65 (40.37)	
Male	604 (59.51)	508 (59.48)	96 (59.63)	0.973
Endoscopic pattern, *n* (%)				
Esophagitis	28 (2.76)	23 (2.69)	5 (3.11)	0.975
Superficial gastritis	331 (32.61)	255 (29.86)	76 (47.20)	< 0.001[b]
Superficial gastritis with erosion	236 (23.25)	200 (23.42)	36 (22.36)	0.77
Superficial gastritis with bile reflux	295 (29.06)	251 (29.39)	44 (27.33)	0.597
Antral nodularity	135 (13.30)	131 (15.34)	4 (2.48)	< 0.001[b]
Peptic ulcer	90 (8.87)	80 (9.37)	10 (6.21)	0.196
Atrophic gastritis	18 (1.77)	17 (1.99)	1 (0.62)	0.378
Clinical diagnosis, *n* (%)				
Esophagitis	28 (2.76)	23 (2.69)	5 (3.11)	0.975
Non atrophic gastritis	997 (98.23)	837 (98.01)	160 (99.38)	0.378
Atrophic gastritis	18 (1.77)	17 (1.99)	1 (0.62)	0.378
Gastric ulcer	18 (1.77)	16 (1.87)	2 (1.24)	0.817
Duodenal ulcer	72 (7.09)	64 (7.49)	8 (4.97)	0.252

[a]$P < 0.05$: Median age was compared between *Helicobacter pylori* (*H. pylori*)-positive and -negative groups.
[b]$P < 0.05$: When compared between *H. pylori*–positive and –negative within each disease group.
IQR: Interquartile range; *H. pylori*: *Helicobacter pylori*.

Table 2 *Helicobacter pylori* infection status in different age groups

Age group	Sex, *n* (male/female)	*H. pylori*+, *n* (%)	*H. pylori*-, *n* (%)
1-4	54 (29/25)	22 (40.74)	32 (59.26)
5-8	199 (111/88)	156 (78.39)[a]	43 (21.61)
9-12	435 (286/149)	383 (88.05)[a,b]	52 (11.95)
13-18	327 (178/149)	293 (89.60)[a,b]	34 (10.40)
Total	1015 (604/411)	854 (84.14)	161 (15.86)

[a]$P < 0.05$: When *Helicobacter pylori* (*H. pylori*) infection rates were compared with the 1-4 years age group.
[b]$P < 0.05$: When *H. pylori* infection rates were compared with the 5-8 years age group.
H. pylori: *Helicobacter pylori*.

As for lymphocyte infiltration, patients with *H. pylori* infection had more severe lymphocyte infiltration than uninfected patients ($Z = 3.997$, $P < 0.001$). In the *H. pylori*-positive group, 40.98%, 50.59% and 8.43% of mild, moderate and marked lymphocyte infiltration, respectively, were found, while in the *H. pylori*-negative group, the rates were 56.52%, 40.99% and 2.48%, respectively. In *H. pylori*-infected patients, the 9-12 years and 13-18 years age groups also showed more severe lymphocyte infiltration compared to the uninfected patients ($Z = 2.539$, $P = 0.011$; $Z = 2.164$, $P = 0.030$), but this difference was not significant between the 1-4 years and 5-8 years age groups ($Z = 0.570$, $P = 0.569$; $Z = 1.737$, $P = 0.082$) (Table 6). Representative pictures of gastric mucosal inflammatory cell infiltration are shown in Figure 2.

Table 3 Precancerous lesions in the gastric mucosa in children and adolescents

Age group	*H. pylori*+				Subtotal	*H. pylori*-				Subtotal
	n	Atrophy	IM	Dysplasia		*n*	Atrophy	IM	Dysplasia	
1-4	22	1	1	1	3	32	0	0	0	0
5-8	156	4	4	1	9	43	0	0	0	0
9-12	383	6	3	6	15	52	0	0	0	0
13-18	293	6	3	1	10	34	1	0	0	1
Total	854	37 (4.33%)[a]				161	1 (0.62%)			

[a]$P < 0.05$: The incidence of gastric mucosal precancerous lesions was compared between *Helicobacter pylori* (*H. pylori*)-positive and *H. pylori*-negative patients.
IM: Intestinal metaplasia; *H. pylori*: *Helicobacter pylori*.

Table 4 Comparison of active inflammation between *Helicobacter pylori*-positive and -negative patients

Age group	*H. pylori*+			*H. pylori*-		
	n	Active inflammation	Non-active inflammation	*n*	Active inflammation	Non-active inflammation
1-4	22	3 (13.64)	19 (86.36)	32	2 (6.25)	30 (93.75)
5-8	156	23 (14.74)[a]	133 (85.26)	43	1 (2.33)	42 (97.67)
9-12	383	52 (13.58)[b]	331 (86.42)	52	2 (3.85)	50 (96.15)
13-18	293	59 (20.14)[c]	234 (79.86)	34	1 (2.94)	33 (97.06)
Total	854	137 (16.04)[d]	717 (83.96)	161	6 (3.73)	155 (96.27)

[a]$P < 0.05$: Active inflammation in *Helicobacter pylori* (*H. pylori*)-positive patients were compared with -negative patients in the 5-8 years age group.
[b]$P < 0.05$: Active inflammation in *H. pylori*-positive patients was compared with -negative patients in the 9-12 years age group.
[c]$P < 0.05$: Active inflammation in *H. pylori*-positive patients was compared with -negative patients in the 13-18 years age group.
[d]$P < 0.05$: Active inflammation was compared between the *H. pylori*-positive and -negative groups.
Data are *n* (%), unless otherwise indicated. *H. pylori*: *Helicobacter pylori*.

Table 5 Degree of neutrophil granulocyte infiltration in *Helicobacter pylori*-positive and -negative patients

Age group	*H. pylori*+				*H. pylori*+				*Z*	*P* value
	n	Absent	Mild	Moderate	*n*	Absent	Mild	Moderate		
1-4	22	19 (86.36)	3 (13.64)	0 (0)	32	30 (93.75)	2 (6.25)	0 (0)	0.912	0.362
5-8	156	133 (85.26)	21 (13.46)	2 (1.28)	43	42 (97.67)	1 (2.33)	0 (0)	2.212	0.027[a]
9-12	383	331 (86.42)	44 (11.49)	8 (2.09)	52	50 (96.15)	2 (3.85)	0 (0)	2.009	0.045[b]
13-18	293	234 (79.86)	48 (16.38)	11 (3.76)	34	33 (97.06)	1 (2.94)	0 (0)	2.456	0.014[c]
Total	854	717 (83.96)	116 (13.58)	21 (2.46)	161	155 (96.27)	6 (3.73)	0 (0)	4.319	< 0.001[d]

[a]$P < 0.05$: Degree of neutrophil granulocyte infiltration in *Helicobacter pylori* (*H. pylori*)-positive patients were compared with -negative patients in the 5-8 years age group.
[b]$P < 0.05$: Degree of neutrophil granulocyte infiltration in *H. pylori*-positive patients was compared with -negative patients in the 9-12 years age group.
[c]$P < 0.05$: Degree of neutrophil granulocyte infiltration in *H. pylori*-positive patients was compared with -negative patients in the 13-18 years age group.
[d]$P < 0.05$: Degree of neutrophil granulocyte infiltration was compared between *H. pylori*-positive and -negative groups.
Data are *n* (%), unless otherwise indicated. *H. pylori*: *Helicobacter pylori*.

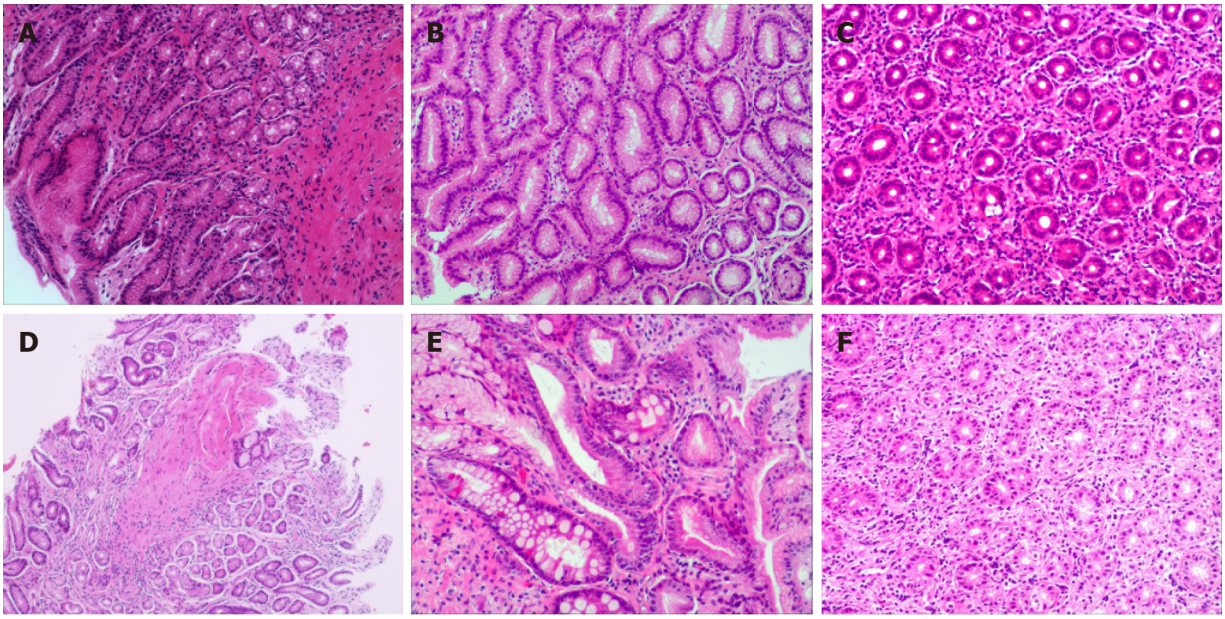
DISCUSSION

In the current study, we investigated gastric mucosal inflammation and precancerous lesions in pediatric patients who were hospitalized for gastrointestinal symptoms. Among the 1015 children in our study who underwent upper gastrointestinal endoscopy, gastric mucosa precancerous lesions occurred

Table 6 Degree of lymphocyte infiltration in *Helicobacter pylori*-positive and -negative patients

Age group	*H. pylori*+				*H. pylori*-				*Z*	*P* value
	n	Mild	Moderate	Marked	*n*	Mild	Moderate	Marked		
1-4	22	10 (45.45)	11 (50)	1 (4.55)	32	17 (53.12)	14 (43.75)	1 (3.13)	0.57	0.569
5-8	156	67 (42.95)	75 (48.08)	14 (8.97)	43	24 (55.81)	18 (41.86)	1 (2.33)	1.737	0.082
9-12	383	161 (42.04)	195 (50.91)	27 (7.05)	52	31 (59.62)	20 (38.46)	1 (1.92)	2.539	0.01[a]
13-18	293	112 (38.23)	151 (51.54)	30 (10.24)	34	19 (55.88)	14 (41.18)	1 (2.94)	2.164	0.03[b]
Total	854	350 (40.98)	432 (50.59)	72 (8.43)	161	91 (56.52)	66 (40.99)	4 (2.48)	3.997	< 0.00[c]

[a]$P < 0.05$: Degree of lymphocyte infiltration in *Helicobacter pylori* (*H. pylori*)-positive patients were compared with -negative patients in 9-12 years age group.
[b]$P < 0.05$: Degree of lymphocyte infiltration in *H. pylori*-positive patients were compared with -negative patients in 13-18 years age group.
[c]$P < 0.05$: Degree of lymphocyte infiltration was compared between *H. pylori*-positive and -negative groups.
Data are *n* (%), unless otherwise indicated. *H. pylori*: *Helicobacter pylori*.



DOI: 10.3748/wjg.v28.i28.3682 **Copyright** ©The Author(s) 2022.

Figure 2 Representative pictures of normal and pathological gastric mucosa manifestations in children and adolescents. A: Normal gastric mucosa; B: Chronic inflammation of the gastric mucosa; C: Active inflammation of the gastric mucosa; D: Gastric mucosal atrophy; E: Intestinal metaplasia; F: Mild dysplasia. Hematoxylin and eosin, × 400.

in 4.33% of *H. pylori*-infected children, in which the proportions of atrophy, IM and dysplasia were 1.99%, 1.29%, 1.05%, respectively, significantly higher than findings from *H. pylori*-negative patients.

Under endoscopy evaluation, *H. pylori*-positive children presented more nodular gastritis, which is an important feature of *H. pylori* infection in children. But, the proportions of esophagitis, chronic superficial gastritis with erosions, chronic superficial gastritis with bile reflux and esophagitis were not significantly different between the infected and non-infected groups. The results also showed that children with *H. pylori* infection had a significantly higher incidence of gastric mucosal inflammation, and the degrees of neutrophil and lymphocyte infiltration were also much more serious than in *H. pylori*-negative children. These results are in line with previous studies that showed various degrees of inflammation in *H. pylori*-infected pediatric patients. For example, in 2017, Broide *et al*[27] showed that monocyte and neutrophil infiltration was more severe in the infected children group with chronic gastritis in Israel. One retrospective study of 196 children in Japan in 2006 also reached a similar conclusion[17].

The above results indicate that *H. pylori* infection is closely related to gastric mucosal inflammation, which might be the basis for development of gastric precancerous lesions, as both basic experiments and clinical investigations have confirmed that certain bacterial components, such as CagA and VacA, have detrimental effects on gastric epithelial cells. In addition, CagA is a bacterial oncoprotein, which can cause epithelial cell oncogenic transformation *in vivo*[28-30]. Therefore, future experiments for more

detailed analysis of the *H. pylori* component on the pathogenesis of gastric precancerous lesions in children will be very helpful to understand the carcinogenesis and provide more rational for precise intervention and prevention.

The significance of this study is that it provides evidence to demonstrate that *H. pylori* infection is associated with the occurrence of precancerous lesions in pediatric patients, and these lesions increase with increase in age. Furthermore, the pediatric population might present in a similar way to adults with *H. pylori* infection, suggesting a healthcare threat to the pediatric patients. As eradication of *H. pylori* has been shown to prevent the development of atrophic gastritis, IM and gastric malignancy in adults[31,32], it is expected that proper intervention in pediatric patients could prevent the development of future diseases. Future investigation on the rationale and health economic evaluation would be required to provide more supporting evidence.

These results are also in line with previous reports. For example, in 2006, a study of 131 *H. pylori*-infected children in Japan showed that the proportion of gastric antrum atrophy was 10.7%[17]. In a 2020 study in Romania, the *H. pylori* infection rate was 33.06% (82/248); among 82 infected children, 9 (11%) had atrophic gastritis and 2 (2.4%) had IM[33]. A survey of 1634 children in China in 2014 found that atrophic gastritis accounted for 4.4% (23/524 cases) of the *H. pylori*-infected children[16]. However, one Austrian study in 2011 found gastric atrophy was rare (1/84) in children infected with *H. pylori*[34]. In addition, no gastric atrophy was found in 66 French children infected with *H. pylori* in 2009[35], and no precancerous lesions were found in 132 gastric biopsies from 22 symptomatic *H. pylori*-infected children in a 2009 study in Brazil[36].

As *H. pylori*-induced disease presentations are mostly present in adulthood, the presence of precancerous lesions in children unveiled a critical issue that was largely neglected previously[13,15,37]. Although there are still controversies on the significance and consequence of *H. pylori*-induced serious gastric mucosal lesions in children[13], current consensus reports from the Asia-Pacific region[38], China[8,39] and Japan[18] have indicated that *H. pylori* should be eradicated when such conditions are present, and their family members should also receive screening and treatment if confirmed positive. It is hypothesized that gastric mucosal atrophy and IM in children and adolescents might be present in a similar way to adult *H. pylori* infection and is probably more common in areas with high *H. pylori* infection rates than previously thought.

One of the major shortfalls of this retrospective study is that the rapid urease test was the primary test used to detect *H. pylori* infection because ^{13}C-urea breath test, serological *H. pylori* antibody tests and stool antigen tests were not available for more accurate diagnosis. This could result in the underestimation of *H. pylori* infection rates or have false negative results in the uninfected children group. Two perplexing results might be attributed to these drawbacks as there are 8 duodenal ulcer patients (Table 1) and few patients had active gastric inflammation (Tables 4 and 5) in the *H. pylori*-negative group. Due to the strong relationship of *H. pylori* in causing these diseases, it is unlikely these patients were not infected by *H. pylori*. Furthermore, it is likely because of the limitation of the rapid urease test, which is unable to detect patchy distribution of *H. pylori* in the stomach. Therefore, future studies will be required to confirm these discrepancies. Even with these drawbacks, the overall conclusions and significance of the investigation were not affected.

Although the current work provides novel points on *H. pylori*-induced gastric mucosal precancerous lesions in children, due to its retrospective nature, the investigation has limitations. First, this study only discussed the relationship between *H. pylori* infection and gastric mucosa precancerous lesions and was unable to analyze the effects of different genotypes of infected *H. pylori* strains. Therefore, more detailed information on *H. pylori* strains are not available. Nonetheless, our previous work demonstrated that type I *H. pylori* (CagA- and VacA-positive) is the primary type of *H. pylori* infection in this region[40]. It is expected that the pediatric population is similar to the adult population. Second, not all cases had biopsy specimens from both the gastric antrum and body. Some of the precancerous lesions and *H. pylori* infection may have been missed due to histopathological presentation of the stomach, and patchy *H. pylori* infection status in other places of the stomach were unable to be examined. In the future, multiple biopsies might be helpful to overcome these drawbacks. Third, this was a single-center, retrospective analysis, and all the children were hospitalized due to gastrointestinal symptoms, which may be the reason why the infection rate was much higher than among the general population. In the future, large-scale investigations in the general public and multi-center, prospective and randomized control analyses are needed to comprehensively assess the risk of *H. pylori* infection and precancerous lesions in children and adolescents in order to understand the overall precancerous lesions of *H. pylori*-infected pediatric patients.

CONCLUSION

Our results show that *H. pylori*-infected children have more active inflammation and inflammatory cell infiltration in the gastric mucosa, and infection rate increases with patient age. The incidence of precancerous lesions in *H. pylori*-infected patients is also significantly higher compared to that in -uninfected patients. Although the percentage is only 4.33%, it provides an alarming alert and call for further invest-

igation and intervention for this population group.

ARTICLE HIGHLIGHTS

Research background

Chronic *Helicobacter pylori* (*H. pylori*) infection causes gastric mucosal precancerous lesions and gastric cancer in adult patients. It remains to be determined, however, whether gastric mucosal precancerous lesions may also occur in children and adolescents, as this remains an important issue for clinical intervention.

Research motivation

Investigating the relationship between *H. pylori* infection and gastric mucosal precancerous lesions in pediatric patients will provide important evidence on whether intervention should be offered to prevent related disease development in this population group.

Research objectives

H. pylori infection status, gastric mucosal inflammation and gastric precancerous lesions in hospitalized pediatric patients were investigated in central China.

Research methods

We retrospectively enrolled 1015 symptomatic pediatric patients to analyze their clinical and pathological data. The endoscopic and histological findings, occurrence of gastric mucosal precancerous lesions, inflammatory activity and degree of inflammatory cell infiltration were analyzed between *H. pylori*-positive and -negative patient groups.

Research results

The overall *H. pylori* infection rate was 84.14% for the 1015 enrolled pediatric patients, and infection rate increased with age. The incidence of gastric mucosal precancerous lesions in *H. pylori*-infected children was 4.33%, which was significantly higher than that in *H. pylori*-negative children. Infected patients showed more active inflammation as well as more severe inflammatory cell infiltration compared to the non-infected patients. Additionally, endoscopy revealed that the most common presentation was antral nodularity in *H. pylori*-positive patients, whereas superficial gastritis was a marked feature for *H. pylori*-negative patients.

Research conclusions

In children and adolescents, gastric mucosal precancerous lesions occurred in 4.33% of *H. pylori*-infected patients in central China. The data revealed an obvious critical issue that requires future investigation and intervention for this population group.

Research perspectives

The results provide insights on *H. pylori* infection status and its relationship with gastric mucosal precancerous in symptomatic pediatric patients in central China. Further investigation and intervention for related disease prevention are required in this population group.

ACKNOWLEDGEMENTS

The authors are grateful to the staff of the Department of Gastroenterology and Hepatology, People's Hospital of Zhengzhou University for their valuable assistance in this work.

FOOTNOTES

Author contributions: Yu M, Cheng YB, Jia BL, Kong LF, Chen CL and Ding SZ designed the research; Yu M, Song XX, Ma J, Shao QQ, Yu XC, Khan MN, Qi YB, Hu RB, Wei PR and Xiao W collected the clinical data and performed the experiments; Yu M analyzed the data; Yu M and Ding SZ wrote the paper; Ding SZ revised the article; all authors approved the final version of the manuscript.

Supported by the National Natural Science Foundation of China, No. U1604174; Henan Provincial Government-Health and Family Planning Commission, No. 20170123 and No. SBGJ202002004; and Henan Provincial Government-Health and Family Planning Commission Research Innovative Talents Project, No. 51282.

Institutional review board statement: This study was reviewed and approved by the Ethics Committee of People's Hospital of Zhengzhou University (2019-KY-No. 10).

Informed consent statement: The study was performed retrospectively. Patients were not required to give informed consent for the study because the analysis used anonymous clinical data that were obtained after each patient agreed to treatment by written consent.

Conflict-of-interest statement: All authors declare that there are no conflicts of interests related to this work.

Data sharing statement: No additional data are available.

Open-Access: This article is an open-access article that was selected by an in-house editor and fully peer-reviewed by external reviewers. It is distributed in accordance with the Creative Commons Attribution NonCommercial (CC BY-NC 4.0) license, which permits others to distribute, remix, adapt, build upon this work non-commercially, and license their derivative works on different terms, provided the original work is properly cited and the use is non-commercial. See: https://creativecommons.org/Licenses/by-nc/4.0/

Country/Territory of origin: China

ORCID number: Miao Yu 0000-0002-3587-2760; Jing Ma 0000-0003-1172-527X; Xiao-Xia Song 0000-0003-4633-9862; Qiao-Qiao Shao 0000-0002-4900-9394; Xue-Chun Yu 0000-0003-4425-6019; Muhammad Noman Khan 0000-0003-4814-7768; Ya-Bin Qi 0000-0002-7736-4043; Ruo-Bing Hu 0000-0003-4735-1310; Pei-Ru Wei 0000-0001-6306-590X; Wei Xiao 0000-0002-6814-9261; Bai-Ling Jia 0000-0002-2920-2322; Yan-Bo Cheng 0000-0003-3203-4603; Ling-Fei Kong 0000-0003-1710-8344; Chuan-Liang Chen 0000-0002-5566-7297; Song-Ze Ding 0000-0002-4589-6942.

S-Editor: Yan JP
L-Editor: A
P-Editor: Yan JP

REFERENCES

1 **Yuan C**, Adeloye D, Luk TT, Huang L, He Y, Xu Y, Ye X, Yi Q, Song P, Rudan I; Global Health Epidemiology Research Group. The global prevalence of and factors associated with Helicobacter pylori infection in children: a systematic review and meta-analysis. *Lancet Child Adolesc Health* 2022; **6**: 185-194 [PMID: 35085494 DOI: 10.1016/S2352-4642(21)00400-4]
2 **Park JS**, Jun JS, Seo JH, Youn HS, Rhee KH. Changing prevalence of Helicobacter pylori infection in children and adolescents. *Clin Exp Pediatr* 2021; **64**: 21-25 [PMID: 32668822 DOI: 10.3345/cep.2019.01543]
3 **Li XC**, Wang HD, Zhang N, Wang YP, Zhou YN. Systematic review and meta-analysis of epidemiological investigation of Helicobacter pylori infection in children and adolescents in China. *Linchuang Erke Zazhi* 2017; **35**: 782-787 [DOI: 10.3969/j.issn.1000-3606.2017.10.016]
4 **Seo JH**, Bortolin K, Jones NL. Review: Helicobacter pylori infection in children. *Helicobacter* 2020; **25** Suppl 1: e12742 [PMID: 32918353 DOI: 10.1111/hel.12742]
5 **Subsomwong P**, Miftahussurur M, Uchida T, Vilaichone RK, Ratanachu-Ek T, Mahachai V, Yamaoka Y. Prevalence, risk factors, and virulence genes of Helicobacter pylori among dyspeptic patients in two different gastric cancer risk regions of Thailand. *PLoS One* 2017; **12**: e0187113 [PMID: 29084246 DOI: 10.1371/journal.pone.0187113]
6 **Li M**, Sun Y, Yang J, de Martel C, Charvat H, Clifford GM, Vaccarella S, Wang L. Time trends and other sources of variation in Helicobacter pylori infection in mainland China: A systematic review and meta-analysis. *Helicobacter* 2020; **25**: e12729 [PMID: 32686261 DOI: 10.1111/hel.12729]
7 **Ren S**, Cai P, Liu Y, Wang T, Zhang Y, Li Q, Gu Y, Wei L, Yan C, Jin G. Prevalence of Helicobacter pylori infection in China: A systematic review and meta-analysis. *J Gastroenterol Hepatol* 2022; **37**: 464-470 [PMID: 34862656 DOI: 10.1111/jgh.15751]
8 **Liu WZ**, Xie Y, Lu H, Cheng H, Zeng ZR, Zhou LY, Chen Y, Wang JB, Du YQ, Lu NH; Chinese Society of Gastroenterology, Chinese Study Group on Helicobacter pylori and Peptic Ulcer. Fifth Chinese National Consensus Report on the management of Helicobacter pylori infection. *Helicobacter* 2018; **23**: e12475 [PMID: 29512258 DOI: 10.1111/hel.12475]
9 **Malfertheiner P**, Megraud F, O'Morain CA, Gisbert JP, Kuipers EJ, Axon AT, Bazzoli F, Gasbarrini A, Atherton J, Graham DY, Hunt R, Moayyedi P, Rokkas T, Rugge M, Selgrad M, Suerbaum S, Sugano K, El-Omar EM; European Helicobacter and Microbiota Study Group and Consensus panel. Management of Helicobacter pylori infection-the Maastricht V/Florence Consensus Report. *Gut* 2017; **66**: 6-30 [PMID: 27707777 DOI: 10.1136/gutjnl-2016-312288]
10 **Jones NL**, Koletzko S, Goodman K, Bontems P, Cadranel S, Casswall T, Czinn S, Gold BD, Guarner J, Elitsur Y, Homan M, Kalach N, Kori M, Madrazo A, Megraud F, Papadopoulou A, Rowland M; ESPGHAN, NASPGHAN. Joint ESPGHAN/NASPGHAN Guidelines for the Management of Helicobacter pylori in Children and Adolescents (Update 2016). *J Pediatr Gastroenterol Nutr* 2017; **64**: 991-1003 [PMID: 28541262 DOI: 10.1097/MPG.0000000000001594]
11 **Correa P**. A human model of gastric carcinogenesis. *Cancer Res* 1988; **48**: 3554-3560 [PMID: 3288329]
12 **Miftahussurur M**, Sharma RP, Shrestha PK, Maharjan RK, Shiota S, Uchida T, Sato H, Yamaoka Y. Helicobacter pylori Infection and Gastric Mucosal Atrophy in Two Ethnic Groups in Nepal. *Asian Pac J Cancer Prev* 2015; **16**: 7911-7916

[PMID: 26625820 DOI: 10.7314/apjcp.2015.16.17.7911]
13 **Dimitrov G**, Gottrand F. Does gastric atrophy exist in children? *World J Gastroenterol* 2006; **12**: 6274-6279 [PMID: 17072948 DOI: 10.3748/wjg.v12.i39.6274]
14 **Boukthir S**, Mrad SM, Kalach N, Sammoud A. Gastric atrophy and Helicobacter pylori infection in children. *Trop Gastroenterol* 2009; **30**: 107-109 [PMID: 19760998]
15 **Villarreal-Calderon R**, Luévano-González A, Aragón-Flores M, Zhu H, Yuan Y, Xiang Q, Yan B, Stoll KA, Cross JV, Iczkowski KA, Mackinnon AC Jr. Antral atrophy, intestinal metaplasia, and preneoplastic markers in Mexican children with Helicobacter pylori-positive and Helicobacter pylori-negative gastritis. *Ann Diagn Pathol* 2014; **18**: 129-135 [PMID: 24656654 DOI: 10.1016/j.anndiagpath.2014.02.003]
16 **Yu Y**, Su L, Wang X, Xu C. Association between Helicobacter pylori infection and pathological changes in the gastric mucosa in Chinese children. *Intern Med* 2014; **53**: 83-88 [PMID: 24429445 DOI: 10.2169/internalmedicine.53.0918]
17 **Kato S**, Nakajima S, Nishino Y, Ozawa K, Minoura T, Konno M, Maisawa S, Toyoda S, Yoshimura N, Vaid A, Genta RM. Association between gastric atrophy and Helicobacter pylori infection in Japanese children: a retrospective multicenter study. *Dig Dis Sci* 2006; **51**: 99-104 [PMID: 16416219 DOI: 10.1007/s10620-006-3091-5]
18 **Sugano K**, Tack J, Kuipers EJ, Graham DY, El-Omar EM, Miura S, Haruma K, Asaka M, Uemura N, Malfertheiner P; faculty members of Kyoto Global Consensus Conference. Kyoto global consensus report on Helicobacter pylori gastritis. *Gut* 2015; **64**: 1353-1367 [PMID: 26187502 DOI: 10.1136/gutjnl-2015-309252]
19 **Osaki T**, Konno M, Yonezawa H, Hojo F, Zaman C, Takahashi M, Fujiwara S, Kamiya S. Analysis of intra-familial transmission of Helicobacter pylori in Japanese families. *J Med Microbiol* 2015; **64**: 67-73 [PMID: 25351712 DOI: 10.1099/jmm.0.080507-0]
20 **Rothenbacher D**, Winkler M, Gonser T, Adler G, Brenner H. Role of infected parents in transmission of Helicobacter pylori to their children. *Pediatr Infect Dis J* 2002; **21**: 674-679 [PMID: 12237602 DOI: 10.1097/00006454-200207000-00014]
21 **Kienesberger S**, Perez-Perez GI, Olivares AZ, Bardhan P, Sarker SA, Hasan KZ, Sack RB, Blaser MJ. When is Helicobacter pylori acquired in populations in developing countries? *Gut Microbes* 2018; **9**: 252-263 [PMID: 29494270 DOI: 10.1080/19490976.2017.1421887]
22 **Jaramillo-Rodríguez Y**, Nares-Cisneros J, Martínez-Ordaz VA, Velasco-Rodríguez VM, Márquez FC, Manríquez-Covarrubias LE. Chronic gastritis associated with Helicobacter pylori in Mexican children: histopathological patterns. *Pediatr Dev Pathol* 2011; **14**: 93-98 [PMID: 20658934 DOI: 10.2350/09-12-0754-OA.1]
23 **Okuda M**, Lin Y, Kikuchi S. Helicobacter pylori Infection in Children and Adolescents. *Adv Exp Med Biol* 2019; **1149**: 107-120 [PMID: 31037557 DOI: 10.1007/5584_2019_361]
24 **Whitney AE**, Guarner J, Hutwagner L, Gold BD. Helicobacter pylori gastritis in children and adults: comparative histopathologic study. *Ann Diagn Pathol* 2000; **4**: 279-285 [PMID: 11073332 DOI: 10.1053/adpa.2000.17871]
25 **Liu S**, Chen Q, Quan P, Zhang M, Zhang S, Guo L, Sun X, Wang C. Cancer incidence and mortality in Henan province, 2012. *Chin J Cancer Res* 2016; **28**: 275-285 [PMID: 27478313 DOI: 10.21147/j.issn.1000-9604.2016.03.02]
26 **Dixon MF**, Genta RM, Yardley JH, Correa P. Classification and grading of gastritis. The updated Sydney System. International Workshop on the Histopathology of Gastritis, Houston 1994. *Am J Surg Pathol* 1996; **20**: 1161-1181 [PMID: 8827022 DOI: 10.1097/00000478-199610000-00001]
27 **Broide E**, Richter V, Mendlovic S, Shalem T, Eindor-Abarbanel A, Moss SF, Shirin H. Lymphoid follicles in children with *Helicobacter pylori*-negative gastritis. *Clin Exp Gastroenterol* 2017; **10**: 195-201 [PMID: 28860835 DOI: 10.2147/CEG.S133421]
28 **Hatakeyama M**. Helicobacter pylori and gastric carcinogenesis. *J Gastroenterol* 2009; **44**: 239-248 [PMID: 19271114 DOI: 10.1007/s00535-009-0014-1]
29 **Myint T**, Miftahussurur M, Vilaichone RK, Ni N, Aye TT, Subsomwong P, Uchida T, Mahachai V, Yamaoka Y. Characterizing *Helicobacter pylori cagA* in Myanmar. *Gut Liver* 2018; **12**: 51-57 [PMID: 29069889 DOI: 10.5009/gnl17053]
30 **Hatakeyama M**. Linking epithelial polarity and carcinogenesis by multitasking Helicobacter pylori virulence factor CagA. *Oncogene* 2008; **27**: 7047-7054 [PMID: 19029944 DOI: 10.1038/onc.2008.353]
31 **Kong YJ**, Yi HG, Dai JC, Wei MX. Histological changes of gastric mucosa after Helicobacter pylori eradication: a systematic review and meta-analysis. *World J Gastroenterol* 2014; **20**: 5903-5911 [PMID: 24914352 DOI: 10.3748/wjg.v20.i19.5903]
32 **Ford AC**, Forman D, Hunt RH, Yuan Y, Moayyedi P. Helicobacter pylori eradication therapy to prevent gastric cancer in healthy asymptomatic infected individuals: systematic review and meta-analysis of randomised controlled trials. *BMJ* 2014; **348**: g3174 [PMID: 24846275 DOI: 10.1136/bmj.g3174]
33 **Domșa AT**, Lupușoru R, Gheban D, Șerban R, Borzan CM. *Helicobacter pylori* Gastritis in Children-The Link between Endoscopy and Histology. *J Clin Med* 2020; **9** [PMID: 32183130 DOI: 10.3390/jcm9030784]
34 **Hoepler W**, Hammer K, Hammer J. Gastric phenotype in children with Helicobacter pylori infection undergoing upper endoscopy. *Scand J Gastroenterol* 2011; **46**: 293-298 [PMID: 21073375 DOI: 10.3109/00365521.2010.533383]
35 **Kalach N**, Papadopoulos S, Asmar E, Spyckerelle C, Gosset P, Raymond J, Dehecq E, Decoster A, Creusy C, Dupont C. In French children, primary gastritis is more frequent than Helicobacter pylori gastritis. *Dig Dis Sci* 2009; **54**: 1958-1965 [PMID: 19003529 DOI: 10.1007/s10620-008-0553-y]
36 **Langner M**, Machado RS, Patrício FR, Kawakami E. Evaluation of gastric histology in children and adolescents with Helicobacter pylori gastritis using the Update Sydney System. *Arq Gastroenterol* 2009; **46**: 328-332 [PMID: 20232015 DOI: 10.1590/s0004-28032009000400015]
37 **Kara N**, Urganci N, Kalyoncu D, Yilmaz B. The association between Helicobacter pylori gastritis and lymphoid aggregates, lymphoid follicles and intestinal metaplasia in gastric mucosa of children. *J Paediatr Child Health* 2014; **50**: 605-609 [PMID: 24925694 DOI: 10.1111/jpc.12609]
38 **Mahachai V**, Vilaichone RK, Pittayanon R, Rojborwonwitaya J, Leelakusolvong S, Maneerattanaporn M, Chotivitayatarakorn P, Treeprasertsuk S, Kositchaiwat C, Pisespongsa P, Mairiang P, Rani A, Leow A, Mya SM, Lee YC,

Vannarath S, Rasachak B, Chakravuth O, Aung MM, Ang TL, Sollano JD, Trong Quach D, Sansak I, Wiwattanachang O, Harnsomburana P, Syam AF, Yamaoka Y, Fock KM, Goh KL, Sugano K, Graham D. Helicobacter pylori management in ASEAN: The Bangkok consensus report. *J Gastroenterol Hepatol* 2018; **33**: 37-56 [PMID: 28762251 DOI: 10.1111/jgh.13911]

39 **Ding SZ**, Du YQ, Lu H, Wang WH, Cheng H, Chen SY, Chen MH, Chen WC, Chen Y, Fang JY, Gao HJ, Guo MZ, Han Y, Hou XH, Hu FL, Jiang B, Jiang HX, Lan CH, Li JN, Li Y, Li YQ, Liu J, Li YM, Lyu B, Lu YY, Miao YL, Nie YZ, Qian JM, Sheng JQ, Tang CW, Wang F, Wang HH, Wang JB, Wang JT, Wang JP, Wang XH, Wu KC, Xia XZ, Xie WF, Xie Y, Xu JM, Yang CQ, Yang GB, Yuan Y, Zeng ZR, Zhang BY, Zhang GY, Zhang GX, Zhang JZ, Zhang ZY, Zheng PY, Zhu Y, Zuo XL, Zhou LY, Lyu NH, Yang YS, Li ZS; National Clinical Research Center for Digestive Diseases (Shanghai), Gastrointestinal Early Cancer Prevention & Treatment Alliance of China (GECA), Helicobacter pylori Study Group of Chinese Society of Gastroenterology, and Chinese Alliance for Helicobacter pylori Study. Chinese Consensus Report on Family-Based *Helicobacter pylori* Infection Control and Management (2021 Edition). *Gut* 2022; **71**: 238-253 [PMID: 34836916 DOI: 10.1136/gutjnl-2021-325630]

40 **Yuan L**, Zhao JB, Zhou YL, Qi YB, Guo QY, Zhang HH, Khan MN, Lan L, Jia CH, Zhang YR, Ding SZ. Type I and type II *Helicobacter pylori* infection status and their impact on gastrin and pepsinogen level in a gastric cancer prevalent area. *World J Gastroenterol* 2020; **26**: 3673-3685 [PMID: 32742135 DOI: 10.3748/wjg.v26.i25.3673]

World Journal of Gastroenterology

Submit a Manuscript: https://www.f6publishing.com

World J Gastroenterol 2022 July 28; 28(28): 3695-3705

DOI: 10.3748/wjg.v28.i28.3695

ISSN 1007-9327 (print) ISSN 2219-2840 (online)

ORIGINAL ARTICLE

Observational Study

Secular trends of intrahepatic cholangiocarcinoma in a high endemic area: A population-based study

Chun-Ru Lin, Yu-Kwang Lee, Chun-Ju Chiang, Ya-Wen Yang, Hung-Chuen Chang, San-Lin You

Specialty type: Gastroenterology and hepatology

Provenance and peer review: Unsolicited article; Externally peer reviewed.

Peer-review model: Single blind

Peer-review report's scientific quality classification

Grade A (Excellent): 0
Grade B (Very good): B
Grade C (Good): C
Grade D (Fair): 0
Grade E (Poor): 0

P-Reviewer: Coppola A, Italy; Li JT, China

Received: April 6, 2022
Peer-review started: April 6, 2022
First decision: May 29, 2022
Revised: May 30, 2022
Accepted: June 30, 2022
Article in press: June 30, 2022
Published online: July 28, 2022

Chun-Ru Lin, School of Medicine, College of Medicine, Fu Jen Catholic University, New Taipei City 242008, Taiwan

Yu-Kwang Lee, Department of Surgery, National Taiwan University Hospital, Taipei 100229, Taiwan

Chun-Ju Chiang, Ya-Wen Yang, Graduate Institute of Epidemiology and Preventive Medicine, College of Public Health, National Taiwan University, Taipei 10055, Taiwan

Hung-Chuen Chang, Division of Gastroenterology, Department of Internal Medicine, Shin Kong Wu Ho-Su Memorial Hospital, Taipei 111045, Taiwan

San-Lin You, School of Medicine and Data Science Center, Fu Jen Catholic University, New Taipei City 242008, Taiwan

Corresponding author: San-Lin You, PhD, Assistant Professor, School of Medicine and Data Science Center, Fu Jen Catholic University, No. 510 Zhongzheng Road, Xinzhuang District, New Taipei City 242008, Taiwan. yousanlin@gmail.com

Abstract

BACKGROUND

Intrahepatic cholangiocarcinoma (ICC) is one of the most aggressive malignancies. However, because of its scarcity there are limited population-based data available for investigations into its epidemiologic characteristics. In Taiwan, we have a national cancer registry database that can be used to evaluate the secular trends of ICC.

AIM

To evaluate secular trends of ICC according to age, sex, and risk factors in Taiwan.

METHODS

In this population-based study, we used the national Taiwan Cancer Registry database. Age-standardized and relative percent changes in incidence rates were used to describe secular trends in incidence rates and sex ratios of ICC in Taiwan.

RESULTS

The age-standardized ICC incidence rate among males increased from 1.51 per 100000 in 1993-1997 to 4.07 per 100000 in 2013-2017 and among female from 1.73

per 100000 to 2.95 per 100000. The incidence in females tended to plateau after 2008-2012. For males, the ICC incidence increased as age increased. In the long-term incidence trend of ICC in females, the incidence of the four age groups (40-44, 45-49, 50-54 and 55-59 years) remained stable in different years; although, the incidence of the 60-64 group had a peak in 2003-2007, and the peak incidence of the 65-69 and 70-74 groups occurred in 2008-2012. Among males, beginning at the age of 65, there were increases in the incidence of ICC for the period of 2003-2017 as compared with females in the period of 2003-2017.

CONCLUSION

Increased incidence of ICC occurred in Taiwan over the past two decades. The increased incidence has progressively shifted toward younger people for both males and females.

Key Words: Intrahepatic cholangiocarcinoma; Incidence; Secular trend; Sex ratio; Risk factor

©The Author(s) 2022. Published by Baishideng Publishing Group Inc. All rights reserved.

Core Tip: It is important to evaluate the secular trends of intrahepatic cholangiocarcinoma (ICC) incidence and to determine insightful etiological clues in a population with a high incidence of liver cancer. Using the national Taiwan Cancer Registry, we observed an increased incidence of ICC for both males and females. Our observations should be taken in the context of other studies conducted on secular trends of ICC.

Citation: Lin CR, Lee YK, Chiang CJ, Yang YW, Chang HC, You SL. Secular trends of intrahepatic cholangiocarcinoma in a high endemic area: A population-based study. *World J Gastroenterol* 2022; 28(28): 3695-3705

URL: https://www.wjgnet.com/1007-9327/full/v28/i28/3695.htm

DOI: https://dx.doi.org/10.3748/wjg.v28.i28.3695

INTRODUCTION

Intrahepatic cholangiocarcinoma (ICC) is one of the most aggressive malignancies, and its mortality rates are 1–2 per 100000[1]. After surgery, patients with ICC have 5-year survival rates of approximately 60%, and the rates of recurrence are 60%-65%[2]. In the United States, there were 1.18 new cases per 100000 in 2012[3]. ICC is the second most commonly diagnosed liver cancer[4], and the incidence of ICC continues to increase[5]. Florio *et al*[5] reported that the incidence rate of ICC has regional differences. For example, the incidence rate of ICC in 2008-2012 was 2.80 per 100000 in South Korea [95% confidence interval (CI): 2.68 to 2.93], 2.19 per 100000 in Thailand (95%CI: 2.01-2.36), 0.58 per 100000 in Italy (95%CI: 0.48-0.69), 0.78 per 100000 in the United States (95%CI: 0.74-0.82), and 1.15 per 100000 in the United Kingdom (95%CI: 1.12-1.18)[5]. The average annual percent change (AAPC) of ICC in 2008-2012 also exhibits regional differences. In particular, the AAPC of ICC in 2008-2012 was 4.5% in South Korea (95%CI: 3.0-5.9), -1.0% in Thailand (95%CI: -3.8-1.9), 3.3% in Italy (95%CI: 1.5-5.2), 2.0% in the United States (95%CI: -2.3-6.5), and 4.6% in the United Kingdom (95%CI: 3.2-6.1)[5]. Although these previous studies show that the threat of ICC is rising in many parts of the world[4,5], few studies have used nationwide incidence data to study the epidemiology of ICC.

Moreover, this population-based data facilitates an unbiased estimate of the burden of ICC into the near future. We aimed to evaluate the current trends of ICC in Taiwan. We investigated secular trends in the incidence of ICC to provide insightful etiological analyses, particularly for the variations by age and sex.

MATERIALS AND METHODS

Incidence data from 1993–2017 were obtained from the Taiwan Cancer Registry (TCR). We extracted incidence data on ICC [topography code of International Classification of Diseases for Oncology (ICD-O-FT: T-155.1 before 2002 and ICD-O-3: C22.1, M code 9590-9993 was excluded)]. TCR is organized and funded by the Health Promotion Administration, Ministry of Health and Welfare, Taiwan. In 1979, TCR began to register all cancers nationwide[6,7].

Statistical analysis

In 1995, Taiwan launched the National Health Insurance system[8]. Since that time, the health status of the Taiwanese population has been fully registered[7]. The incidence data were grouped into 17 5-year age groups (0-4, 5-9, 10-14, 15-19, … to 80+ years) and 5 periods (1993–1997, 1998–2002, …, and 2013–2017). Therefore, the data design comprised 14 birth cohorts (the oldest: 1908-1912 to the youngest: 1973-1977). In this study, we reasoned the choice of 1993-1997 as the beginning of the analytical year to avoid incomplete records of incidence data, and the quality of diagnosis in 1993 was similar to that after 1995.

We calculated the incidence rates by sex for each age group by dividing the number of cases by the corresponding population size[9]. Age-standardized incidence rates by sex were calculated using the direct method with the 2000 world standard population as reference[10]. The male-to-female incidence ratios were calculated by dividing the rate in males by that in females for each age group.

All statistical analyses were performed using SAS version 9.4 (SAS Institute Inc., Cary, NC, United States). The research protocol was approved by the Institutional Review Board of Fu-Jen Catholic University (No. C107099).

RESULTS

Age-standardized incidence rates

Figure 1 shows the trend of age-standardized rate (ASR) of ICC in men and women in Taiwan from 1993-1997 to 2013-2017. The incidence of ICC in men increased linearly. The ASR increased from 1.51 per 100000 in 1993-1997 to 4.07 per 100000 in 2013-2017, and its relative percent change was 169%. The incidence of ICC in women tended to plateau after 2008-2012. The ASR increased from 1.73 per 100000 population in 1993-1997 to 2.95 per 100000 in 2008-2012. The relative percentage change was 70%. From 1993-1997 to 2013-2017, the ASR incidence of ICC in men increased more rapidly than that in women.

Age-specific incidence rates

Figure 2A showed the age-specific rates of ICC per 100000 men in Taiwan. For males, the incidence of ICC increased as age increased. The age-specific rate of ICC in seven age groups (40-44, 45-49, 50-54, 55-59, 60-64, 65-69, and 70-74) increased steadily between 1993-1997 and 2013-2017. The respective relative percent changes were 372%, 265%, 156%, 124%, 153%, 231%, and 139%. The 70-74 age group had a larger growth between 1993-1997 and 2003-2007, and its relative percent change was 114%. Then, it increased more slowly between 2003-2007 and 2013-2017, and its relative percent change was only 5%. The 80+ age group showed a trend from rising to declining, with peaks occurring in 2008-2012. Compared to 1993-1997, its relative percent change was 175%. From 2008-2007 to 2013-2017, the incidence decreased 4%.

Figure 2B shows the age-specific rates of ICC per 100000 women in Taiwan. The age-specific rates of the four age groups of 40-44, 45-49, 50-54, and 55-59 remained stable in different years. The incidence of the 60-64 age group had a peak in 2003-2007, and the incidence increased by 69% compared with 1993-1997. The peak incidence of the 65-69 and 70-74 age groups occurred in 2008-2012 compared with the incidence of 1993-1997. The respective relative percent change was 111% and 136%. The incidence of the 75-79 age group increased steadily from 1993-1997 to 2013-2017, with an increase of 121%. The incidence of the 80+ age group peaked in 2008-2012 compared with that in 1993-1997, and the relative percentage change was 227%. Then, the incidence decreased by 11% between 2008-2012 and 2013-2017.

Figure 3 showed the age-specific rates of men and women in different birth cohorts. The incidence of ICC increased as the birth year increased for both males and females. For example, in the 70-74 age group, the incidence of males born in 1943-1947 was 8.41 times of those born in 1913-1917, and the incidence of women born in 1943-1947 was 16.11 times of those born in 1913-1917.

Sex ratios of age-standardized incidence rates

Figure 4 shows the sex ratio of the ASR of ICC in Taiwan from 1993 to 2017. A turning point was apparent at 1998-2002. Before that period, the incidence of ICC in women was higher than that in men. In 1998-2002, the sex ratio of the incidence of ICC was 1.02, which means that the incidence of ICC in men and women was almost the same. After 2002, the incidence of ICC in men was higher than that of women. From 1993-1997 to 2013-2017, the sex ratio of the incidence of ICC increased from 0.87 to 1.52, and the relative percent change was 75%, which indicates a trend of an increasing gap in the incidence of ICC between men and women.

Sex ratios of age-specific incidence rates

Figure 5 shows the sex ratio of the age-specific rates of ICC in Taiwan by diagnostic period. For ICC patients younger than 70-year-old, the sex ratio of age-specific rates increased with year. For example, in the 40-44 age group, the sex ratio was 0.72 in 1993-1997 and 2.98 in 2013-2017. Its relative percent change was 314% from 1993-1997 to 2013-2017. In the age group over 70-years-old, the sex ratio showed a stable

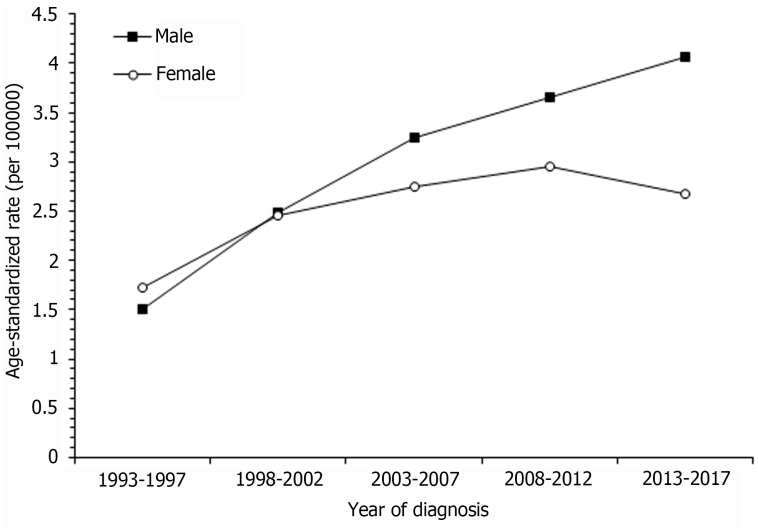


Figure 1 Secular trend in age-standardized incidence rates of intrahepatic cholangiocarcinoma in Taiwan, 1993–2017.

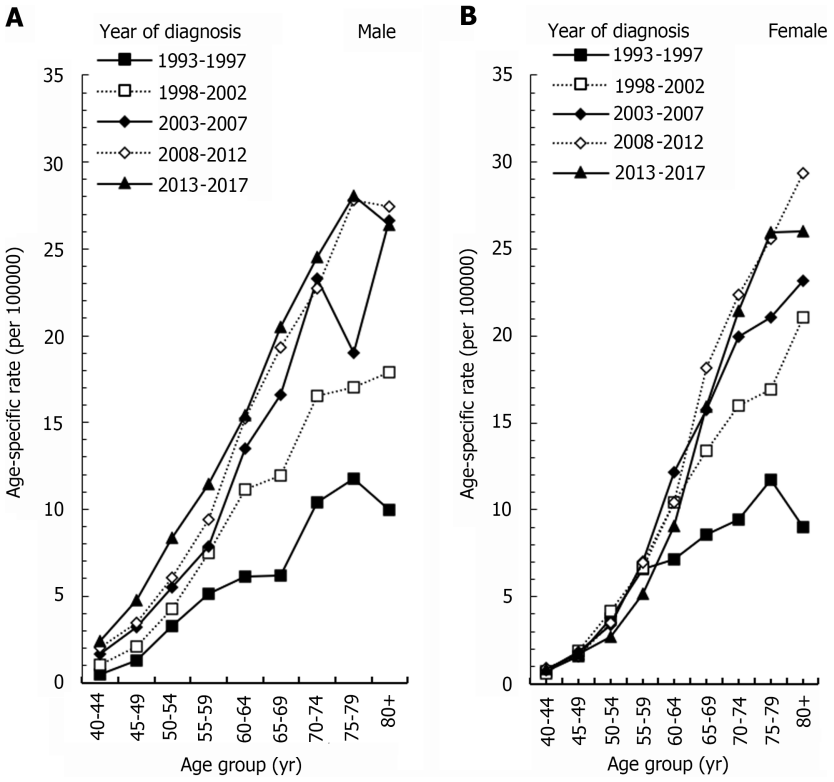


Figure 2 Age-specific incidence rates of intrahepatic cholangiocarcinoma by year of diagnosis and sex. A: Male age-specific rate; B: Female age-specific rate.

baseline in different years, which meant that the incidence of ICC was similar in men and women.

DISCUSSION

This population-based study showed that the incidence of ICC has rapidly increased in Taiwan. This increase remained after stratification by age, sex, diagnosis period, and birth cohort. These results, which highlight the current and projected incidence of ICC, suggest that there is a need for more research to prevent the burden of this cancer in Asian countries.

The incidence rate of ICC varies among different regions of the world[4]. Globally, the ASR is 0.85 per 100000[11]. In Asia, the highest ASR was 2.80 per 100000 in South Korea, and the lowest was 0.26 per 100000 in Israel during 2008-2012[5]. According to our result, the ASR in Taiwan was about 3.3 per

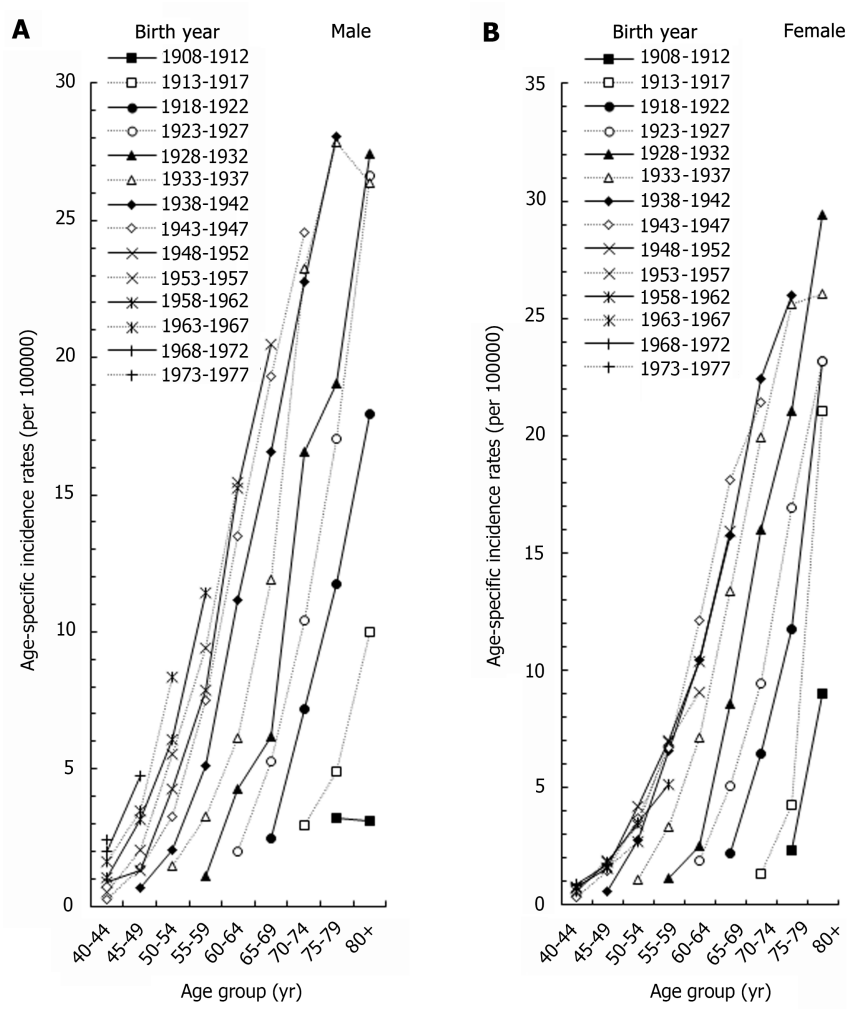


Figure 3 Age-specific incidence rates of intrahepatic cholangiocarcinoma by birth year and sex.

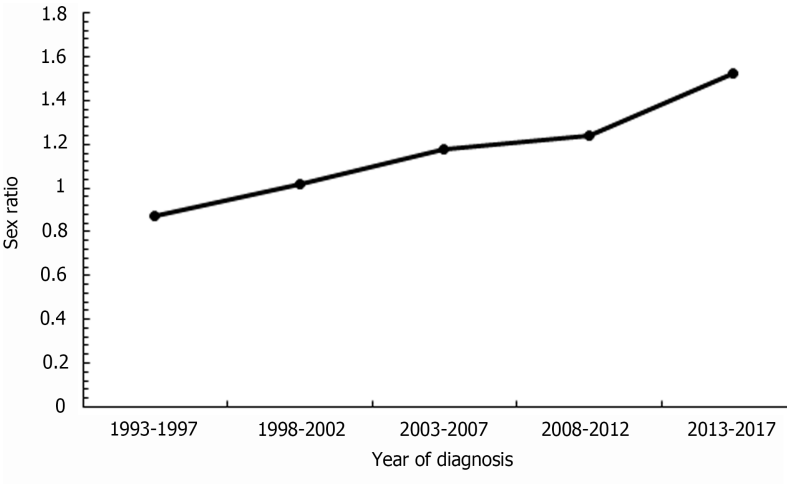


Figure 4 Sex ratio for age-standardized incidence rate of intrahepatic cholangiocarcinoma by year of diagnosis.

100000 during 2008-2012, which means that Taiwan is a high-risk region of ICC. Higher incidence of ICC in Asian countries is likely due to the presence of more risk factors[4,12].

Changes in the incidence of ICC also differs among different countries[5]. Overall, the incidence of ICC has increased in most of the countries in the world[5]. However, the incidence of ICC was higher in Asia, and the increase-rate was higher in Europe and North America[13]. The AAPC of ICC incidence from 1993 to 2012 was 5.0% in Canada, 6.1% in Costa Rica, 6.5% in France, 7.5% in Germany, 8.7% in Poland, 10.5% in Ireland, and 20.1% in Latvia[5]. In Asian countries, the AAPC of ICC incidence was -

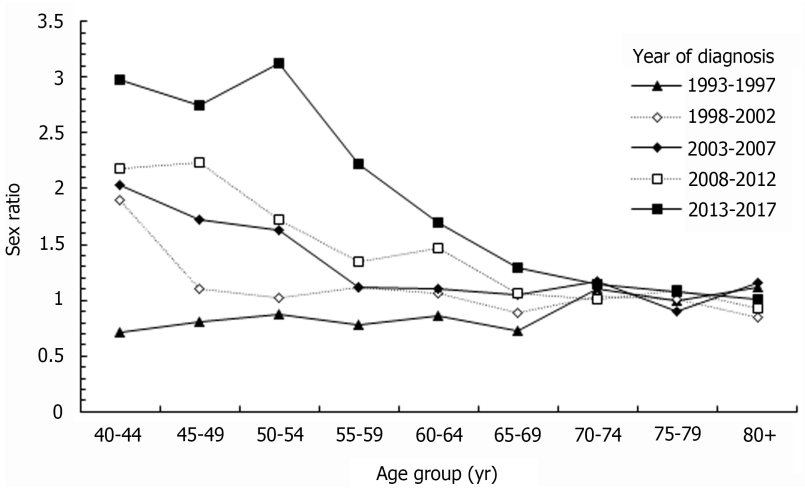


Figure 5 Age-specific sex ratio of intrahepatic cholangiocarcinoma by year of diagnosis and age groups.

0.7% in Japan, -1.0% in Thailand, -2.4% in Philippines, 4.5% in South Korea, and 11.1% in China[5]. In some Asian countries, such as Philippines, Thailand, and Japan, the incidence of ICC showed a nonsignificant decline[5]. In contrast to other studies, our results indicate a rising burden of ICC in the Asia-Pacific area.

A previous study attempted to report the population-based incidence rate of ICC[14]. A study conducted in the United States found that ICC incidence increased from 0.44 per 100000 in 1973 to 1.8 per 100000 in 2012. The AAPC from 2001 to 2012 was 2.3%, and AAPC was 4.36% from 2003 to 2012[3]. In this study, we used the national registry system, which provides comprehensive coverage of the entire population, to make an unbiased estimation of ICC incidence. We found that the incidence of ICC in Taiwan increased from 1.04 per 100000 to 3.36 per 100000 from 1988-1992 to 2013-2017.

An expert consensus document reported that ICC has several risk factors, such as aging of the population, smoking, obesity, diabetes mellitus (DM), hepatitis B virus (HBV) infection, and hepatitis C virus (HCV) infection[4], which may account for this projected increasing incidence. However, due to the number of risk factors of ICC, the phenomenon of the increasing trend of the ICC incidence in Taiwan cannot be explained by a single risk factor.

Aging is an established risk factor for ICC[4]. A study published in 2016 found that the median age at diagnosis among patients in the United States diagnosed with ICC was 67 years between 2008 and 2012 [3]. More than 73% of those patients with ICC were older than 60 years[15], which was similar to our results. We found that the incidence rate was low before age 60 and increased dramatically thereafter. The proportion of people in the population aged 60 and above increased from 13.6% in 2007 to 23.2% in 2020 in Taiwan[9]. A previous study found that the aging of populations in developed countries contributes to the increasing incidence of ICC[15]. Nevertheless, we found the age-adjusted incidence increased gradually over time, and the trend remained consistently elevated, even after stratification by age. This implies that population aging has contributed to the increasing ICC incidence in Taiwan.

A previous meta-analysis showed that DM significantly increased the risk of ICC independent of various confounding factors (relative risk: 1.97, 95%CI: 1.57-2.46; P = 0.025 for heterogeneity)[16]. A previous study reported an increasing prevalence of DM for both sexes in Taiwan from 1992 to 1996 [17], while the incidence remained stable at 6.9–7.7 per 1000 person-years from 1999 to 2004[18]. From 2000 to 2007, the ASR of type 2 DM remained high, at 8.7–9.8 per 1000[19]. In the elderly age group (≥ 65 years), the incidence rate in women (873.2/100000) was higher than that in men (721.4/100000)[20].

Smoking is the most comprehensive environmental factor responsible for ICC. A study based on the National Cancer Institute's SEER 18 database reported that smoking increases the risk of ICC by 46% (95%CI: 1.28-1.66)[20]. A cohort study that included 1518741 individuals showed that current smokers have a 47% greater risk of ICC compared to non-smokers (95%CI: 1.07-2.02)[21]. Taiwan has a high prevalence of smoking. The smoking rate among adult men increased from 59% in 1986 to 63% in 1990, which resulted from the cigarette market opening[22]. A study based on the National Health Interview Survey of Taiwan was conducted in 2001. The prevalence of smokers was 46.8% and the prevalence of ex-smokers was 6.8% in Taiwanese adult males in 2001. The prevalence of smoking was 4.3% and the prevalence of ex-smokers was 0.5% in Taiwanese adult females in 2001[23]. In 2009, a new anti-smoking law was established in Taiwan. Despite the efforts of the Taiwan government, a cross-sectional study that included 961 adults found that up to 42% of sampled Taiwanese adults had smoked cigarettes after that new law had been implemented[24]. The high prevalence of smoking among the early birth cohort in Taiwan may partly explain its high incidence of ICC and seemed to have a cohort effect on ICC.

Obesity was found to increase the risk of ICC by a previous meta-analysis [odds ratio (OR): 1.56, 95%CI: 1.26-1.94][25]. Recently, the prevalence of obesity in Taiwan has increased rapidly. More specifically, a study based on the Nutrition and Health Surveys in Taiwan reported that the prevalence of obesity in men increased from 10.5% in 1993–1996 to 17.0% in 2005. The prevalence of obesity tripled for elementary school boys from 1993 to 2002. Due to the consumption of high-fat foods and lack of physical activity, the prevalence of obesity is likely to increase further in Taiwan[26]. The aforementioned phenomenon may contribute to the increasing prevalence of ICC.

A previous study reported that ICC incidence rates were higher in males than in females in most countries in the world[5]. The sex ratio of the incidence of ICC was 2.9 in Malta, 1.9 in South Korea, 1.9 in Thailand, 1.9 in Japan, 1.9 in Spain, 1.6 in Slovakia, and 1.6 in France[5]. A study based on the SEER database reported that the incidence of ICC was higher in males than in females, and the sex ratio of the age-specific rates of ICC decreased in the aging group[27]. Our results also showed similar outcomes, and this phenomenon may be due to the different hormone profiles of males and females[28]. A study reported that estrogen may modulate cholangiocyte proliferation in nude mice[29]. A previous study used chromatography-tandem mass spectrometry and competitive electrochemiluminescence immunoassay to analyze the relationship between sex steroid hormones and ICC. In that study, a high level of estradiol was found to increase the risk of ICC (OR: 1.40, 95%CI: 1.05-1.89)[30]. A previous study in Taiwan reported that women born in younger cohorts had a later age at natural menopause (hazard ratio: 0.87 per 10-year difference, 95%CI: 0.81-0.95)[31]. The lower ICC incidence of females in our study may be attributed to decreasing estrogen levels in elderly and postmenopausal women. The lower prevalence of smoking among women (4%-8%) than men (47% in 2001)[22] may also contribute to their lower incidence of ICC.

A previous study found that hepatitis B surface antigen (HBsAg) and HCV antibodies had a high association with ICC[32]. A meta-analysis reported that HBV and HCV infection increased the risk of ICC (OR: 3.17, 95%CI: 1.88-5.34 and OR: 3.42, 95%CI: 1.96-5.99, respectively)[33]. Previously, Taiwan was classified as a high-risk region for HBsAg[34]. A study found that HBV DNA could interrupt seven genes (*TERT*, *CEACAM20*, *SPATA18*, *TRERF1*, *ZNF23*, *LINC01449*, and *LINC00486*) in ICC tissue, which may indicate a potential mechanism for the increased risk of ICC in HBV carriers[35].

A retrospective multicenter study in Taiwan reported that the HBsAg prevalence in hepatocellular carcinoma from 1981 to 2001 decreased from 81.5% to 61.2% in males and decreased from 66.7% to 41.4% in females[36]. The sex ratio of HBsAg prevalence of hepatocellular carcinoma increased from 1.22 to 1.61[36], which was consistent with the increasing trend of the sex ratio of the ICC incidence in our study. A previous review hypothesized that HCV could induce the transformation of hepatocytes into cholangiocyte precursors[37]. The HCV antibody prevalence in hepatocellular carcinoma was 31.5% (95%CI: 30.4%-32.6%) in Taiwanese males and 56.7% (95%CI: 54.4%-59.0%) in Taiwanese females[36]. A retrospective cross-sectional study in Taiwan reported that in patients with HCV infection, visceral obesity was significantly associated with waist-to-height ratio, body fat percentage, fat-free mass/body weight, and muscle mass/body weight[38]. Thus, we assumed that HBV and/or HCV infection may be at least partially explain why the incidence of ICC in Taiwan was high.

We found that the sex ratio of the incidence of ICC increased as the diagnostic year increased. In the group over the age of 70 years, the sex ratio of the incidence of ICC between men and women was close to 1, which meant that there was almost no difference in the incidence of ICC between men and women. The proportion of women with ICC increases with age. Another population-based study in the United States showed the proportion of females with ICC was 38.9% for those aged 40-59 years, 45.8% for those aged 60-79 years, and 56.3% for those aged ≥ 80 years[27]. The aforementioned research results are consistent with our study outcome. However, another study based on the Italian National Institute of Statistics A in Italy, another country with a high risk of ICC, reported that the incidence of ICC in males was always higher than that in females[39], which was different from our study outcome. Due to the variety of risk factors of ICC, it is difficult to identify the cause of this difference. A study based on the Netherlands Cancer Registry reported that the incidence of ICC in a low endemic area significantly increased in older populations, especially in in the 45–59 years age group[40]. Interestingly, we also found a similar pattern.

Assessing the temporal trends in the sex difference of ICC incidence has useful implications. Any temporal changes in the sex difference reflect the contributions from environmental and extrinsic risk factors, while a stable sex difference indicates the role of intrinsic exposures or environmental risk. The increase of the sex difference in the incidence of ICC may be explained by the decreasing prevalence of smoking, particularly in men with a historically higher prevalence[23,24]. The decline in smoking prevalence in Taiwan, which has been more rapid for men than for women, may have also contributed to the decreased sex difference in ICC[23,24]. In addition, we noted an increased sex difference in the incidence of ICC since 2008, which warrants confirmation through continued monitoring and investigations.

We found that the gap in the sex ratio between the 40-44 age group and the 80+ age group increased as the diagnostic year increased. In age groups younger than 70 years, the sex ratio increased as the diagnostic year increased. However, in the age groups over 70 years, the sex ratio was similar during each diagnostic period. In our cohort, we found that the incidence of ICC in males and females was higher in the elder birth cohort, which resulted in the aforementioned phenomenon.

Surgery is the only curative treatment for ICC[4]. A previous study found the incidence of sarcopenia among ICC patients following receipt of liver resection to be 50%. Preoperative nutritional evaluation is important for ICC[41]. In addition, nutritional factors may affect the disease incidence. Indeed, a population-based cohort study found that regular use of oil supplement lowered the risk of total liver cancer to 44% (95%CI: 25%-59%) and risk of ICC to 40% (95%CI: 7%-61%)[42]. A meta-analysis suggested that vegetable and fruit consumption may reduce the risk of ICC; specifically, the reported ORs of mixed vegetables, mixed fruits, and combined fruits and vegetables were 0.61 (95%CI: 0.50-0.75), 0.79 (95%CI: 0.65-0.96), and 0.68 (95%CI: 0.57-0.80), respectively[43]. A multi-center study determined that high dietary fiber intake could be associated with a lower risk of intrahepatic bile duct cancer[44]. Finally, an animal model-based study in Taiwan provided further evidence of a relationship between ICC and nutrition; vitamin D supplementation lead to significant suppression of ICC initiation and progression in the rat model *via* regulation of gene expression (*e.g.*, of lipocalin 2)[45].

This study has several limitations. As seen in other studies based on cancer registry databases[46], a substantial portion of cases did not receive histological verification. Old age and advanced tumor stage at presentation likely prohibited this verification. Nevertheless, integrity of the TCR database was 98.4% [47]. The morphological verification percentage of the TCR database is 93.0%[47], which minimizes the misdiagnosis of cancer incidence. In addition, quality and accuracy of clinical diagnosis in our databases has been validated, and the percentage of death certificate-only data is 1%[47]. In addition, we extracted the ICD-O-FT: T-155.1 before 2002 and ICD-O-3: C22.1 from 2003–2017, which may misclassify some diagnostic cases. However, due to the rarity of ICC cases in Taiwan, this deviation did not affect the statistical trend outcomes in our study. In addition, restriction to cases with histological proof would have introduced selection bias. Ultimately, although our study found that there are various risks associated with ICC, including sex, age, DM, HBV and/or HCV infection, obesity, nutritional factors, and smoking, the results need to be validated in larger cohorts, exploring the risk of ICC development in a high incidence area in particular.

CONCLUSION

The incidence of ICC continues to rise in Asia. The etiological role of ICC is still unclear. However, future prospective evaluations are warranted to explore potential risk factors of ICC. The assessment of their independent and/or interactive effects are suggested, which could lead to prevention of ICC, development of early detection methods for early curative surgery, and identification of potential prognostic factors related to improved therapy and outcomes.

ARTICLE HIGHLIGHTS

Research background

Intrahepatic cholangiocarcinoma (ICC) is one of the most aggressive malignancies. However, because of its scarcity few population-based studies have explored its epidemiology. In Taiwan, we have a national cancer registry database, which can be used to evaluate the epidemiology of ICC.

Research motivation

To discover the secular incidence trends and associated risk factors of ICC in Taiwan.

Research objectives

To observe secular trends in ICC incidence according to age, sex, and risk factors in Taiwan.

Research methods

In this population-based study, we used the national Taiwan Cancer Registry database. Relative percent change in incidence rates were used to describe secular trends in incidence rates and sex ratios of ICC in Taiwan.

Research results

The age-standardized ICC incidence rate among males increased from 1.51 per 100000 in 1993-1997 to 4.07 per 100000 in 2013-2017 and among females from 1.73 per 100000 to 2.95 per 100000. ICC incidence rates in females tended to plateau after 2008-2012. For males, the incidence of ICC increased as age increased. In the long-term incidence trend of ICC in females, the incidence of the four age groups of 40-44, 45-49, 50-54, and 55-59 years remained stable in different years, the incidence of the 60-64 age group had a peak in 2003-2007, and the peak incidence in the 65-69 and 70-74 age groups occurred in 2008-2012.

Research conclusions

An increased incidence of ICC has occurred in Taiwan over the past two decades. The increased sex ratios has progressively shifted toward younger people.

Research perspectives

Further long-term cohort studies are needed to investigate the relationship between ICC and its risk factors.

ACKNOWLEDGEMENTS

The authors would like to express their gratitude to the Fu Jen University Foundation.

FOOTNOTES

Author contributions: Lin CR, Lee YK, Chang HC and You SL conceived of and designed the study; Chiang CJ and You SL acquired the data; Lin CR, Lee YK and Yang YW performed the data analyses; Lin CR and You SL drafted the manuscript; Lin RC, Lee YK and You SL assisted in interpretation of the data; Lin RC, Lee YK, Chiang CJ, Yang YW and You SL critically revised the manuscript for important intellectual content.

Institutional review board statement: The study was reviewed and approved by Fu Jen Catholic University Institutional Review Board (No. C107099).

Informed consent statement: The data used in this study is from Taiwan Cancer Registry, a governmental database established by the Health Promotion Administration, Ministry of Health and Welfare, Taiwan. This study was approved by Taiwan Ministry of Health and Welfare, so the informed consent statement was not needed. The related authorization documents would be supplied in the supplement.

Conflict-of-interest statement: All authors report no relevant conflicts of interest for this article.

Data sharing statement: No additional data are available.

STROBE statement: The authors have read the STROBE statement, and manuscript was prepared and revised according to the STROBE statement.

Open-Access: This article is an open-access article that was selected by an in-house editor and fully peer-reviewed by external reviewers. It is distributed in accordance with the Creative Commons Attribution NonCommercial (CC BY-NC 4.0) license, which permits others to distribute, remix, adapt, build upon this work non-commercially, and license their derivative works on different terms, provided the original work is properly cited and the use is non-commercial. See: https://creativecommons.org/Licenses/by-nc/4.0/

Country/Territory of origin: Taiwan

ORCID number: Chun-Ru Lin 0000-0001-5530-304X; Yu-Kwang Lee 0000-0002-0308-7653; Chun-Ju Chiang 0000-0002-1330-5319; Ya-Wen Yang 0000-0001-6330-6830; San-Lin You 0000-0002-3192-3356.

S-Editor: Ma YJ
L-Editor: A
P-Editor: Cai YX

REFERENCES

1 **Bertuccio P**, Malvezzi M, Carioli G, Hashim D, Boffetta P, El-Serag HB, La Vecchia C, Negri E. Global trends in mortality from intrahepatic and extrahepatic cholangiocarcinoma. *J Hepatol* 2019; **71**: 104-114 [PMID: 30910538 DOI: 10.1016/j.jhep.2019.03.013]
2 **Rizvi S**, Gores GJ. Pathogenesis, diagnosis, and management of cholangiocarcinoma. *Gastroenterology* 2013; **145**: 1215-1229 [PMID: 24140396 DOI: 10.1053/j.gastro.2013.10.013]
3 **Saha SK**, Zhu AX, Fuchs CS, Brooks GA. Forty-Year Trends in Cholangiocarcinoma Incidence in the U.S.: Intrahepatic Disease on the Rise. *Oncologist* 2016; **21**: 594-599 [PMID: 27000463 DOI: 10.1634/theoncologist.2015-0446]
4 **Banales JM**, Cardinale V, Carpino G, Marzioni M, Andersen JB, Invernizzi P, Lind GE, Folseraas T, Forbes SJ, Fouassier L, Geier A, Calvisi DF, Mertens JC, Trauner M, Benedetti A, Maroni L, Vaquero J, Macias RI, Raggi C, Perugorria MJ, Gaudio E, Boberg KM, Marin JJ, Alvaro D. Expert consensus document: Cholangiocarcinoma: current knowledge and future perspectives consensus statement from the European Network for the Study of Cholangiocarcinoma (ENS-CCA).

Nat Rev Gastroenterol Hepatol 2016; **13**: 261-280 [PMID: 27095655 DOI: 10.1038/nrgastro.2016.51]

5 **Florio AA**, Ferlay J, Znaor A, Ruggieri D, Alvarez CS, Laversanne M, Bray F, McGlynn KA, Petrick JL. Global trends in intrahepatic and extrahepatic cholangiocarcinoma incidence from 1993 to 2012. *Cancer* 2020; **126**: 2666-2678 [PMID: 32129902 DOI: 10.1002/cncr.32803]

6 **Taiwan Cancer Registry**, Health Promotion Administration, Ministry of Health and Welfare, Taiwan. Available: http://tcr.cph.ntu.edu.tw/main.php?Page=A1. Accessed 5 April 2013 [DOI: 10.1038/s41598-021-87770-2]

7 **Chiang CJ**, You SL, Chen CJ, Yang YW, Lo WC, Lai MS. Quality assessment and improvement of nationwide cancer registration system in Taiwan: a review. *Jpn J Clin Oncol* 2015; **45**: 291-296 [PMID: 25601947 DOI: 10.1093/jjco/hyu211]

8 **Cheng TM**. Taiwan's new national health insurance program: genesis and experience so far. *Health Aff (Millwood)* 2003; **22**: 61-76 [PMID: 12757273 DOI: 10.1377/hlthaff.22.3.61]

9 **Department of Household Registration**, MOI. Table-3. Population by Age, Sex and Marital Status and Marriage Type. 2021 [DOI: 10.4324/9781315829821-23]

10 **Ahmad OB**, Boschi-Pinto C, Lopez AD, Murray CJ, Inoue M. Age Standardization of Rates: A New WHO Standard. GPE Discussion Paper Series: No.31. EIP/GPE/EBD. World Health Organization 2001 [DOI: 10.1037/e571982006-001]

11 **Dodson RM**, Weiss MJ, Cosgrove D, Herman JM, Kamel I, Anders R, Geschwind JF, Pawlik TM. Intrahepatic cholangiocarcinoma: management options and emerging therapies. *J Am Coll Surg* 2013; **217**: 736-750.e4 [PMID: 23890842 DOI: 10.1016/j.jamcollsurg.2013.05.021]

12 **Khan SA**, Tavolari S, Brandi G. Cholangiocarcinoma: Epidemiology and risk factors. *Liver Int* 2019; **39** Suppl 1: 19-31 [PMID: 30851228 DOI: 10.1111/liv.14095]

13 **Blechacz B**. Cholangiocarcinoma: Current Knowledge and New Developments. *Gut Liver* 2017; **11**: 13-26 [PMID: 27928095 DOI: 10.5009/gnl15568]

14 **Al Mahjoub A**, Bouvier V, Menahem B, Bazille C, Fohlen A, Alves A, Mulliri A, Launoy G, Lubrano J. Epidemiology of intrahepatic, perihilar, and distal cholangiocarcinoma in the French population. *Eur J Gastroenterol Hepatol* 2019; **31**: 678-684 [PMID: 30633038 DOI: 10.1097/MEG.0000000000001337]

15 **Welzel TM**, Mellemkjaer L, Gloria G, Sakoda LC, Hsing AW, El Ghormli L, Olsen JH, McGlynn KA. Risk factors for intrahepatic cholangiocarcinoma in a low-risk population: a nationwide case-control study. *Int J Cancer* 2007; **120**: 638-641 [PMID: 17109384 DOI: 10.1002/ijc.22283]

16 **Jing W**, Jin G, Zhou X, Zhou Y, Zhang Y, Shao C, Liu R, Hu X. Diabetes mellitus and increased risk of cholangiocarcinoma: a meta-analysis. *Eur J Cancer Prev* 2012; **21**: 24-31 [PMID: 21857525 DOI: 10.1097/CEJ.0b013e3283481d89]

17 **Tseng CH**, Tseng CP, Chong CK, Huang TP, Song YM, Chou CW, Lai SM, Tai TY, Cheng JC. Increasing incidence of diagnosed type 2 diabetes in Taiwan: analysis of data from a national cohort. *Diabetologia* 2006; **49**: 1755-1760 [PMID: 16788802 DOI: 10.1007/s00125-006-0314-4]

18 **Chang CH**, Shau WY, Jiang YD, Li HY, Chang TJ, Sheu WH, Kwok CF, Ho LT, Chuang LM. Type 2 diabetes prevalence and incidence among adults in Taiwan during 1999-2004: a national health insurance data set study. *Diabet Med* 2010; **27**: 636-643 [PMID: 20546280 DOI: 10.1111/j.1464-5491.2010.03007.x]

19 **Lin CC**, Li CI, Hsiao CY, Liu CS, Yang SY, Lee CC, Li TC. Time trend analysis of the prevalence and incidence of diagnosed type 2 diabetes among adults in Taiwan from 2000 to 2007: a population-based study. *BMC Public Health* 2013; **13**: 318 [PMID: 23570503 DOI: 10.1186/1471-2458-13-318]

20 **Petrick JL**, Yang B, Altekruse SF, Van Dyke AL, Koshiol J, Graubard BI, McGlynn KA. Risk factors for intrahepatic and extrahepatic cholangiocarcinoma in the United States: A population-based study in SEER-Medicare. *PLoS One* 2017; **12**: e0186643 [PMID: 29049401 DOI: 10.1371/journal.pone.0186643]

21 **Petrick JL**, Campbell PT, Koshiol J, Thistle JE, Andreotti G, Beane-Freeman LE, Buring JE, Chan AT, Chong DQ, Doody MM, Gapstur SM, Gaziano JM, Giovannucci E, Graubard BI, Lee IM, Liao LM, Linet MS, Palmer JR, Poynter JN, Purdue MP, Robien K, Rosenberg L, Schairer C, Sesso HD, Sinha R, Stampfer MJ, Stefanick M, Wactawski-Wende J, Zhang X, Zeleniuch-Jacquotte A, Freedman ND, McGlynn KA. Tobacco, alcohol use and risk of hepatocellular carcinoma and intrahepatic cholangiocarcinoma: The Liver Cancer Pooling Project. *Br J Cancer* 2018; **118**: 1005-1012 [PMID: 29520041 DOI: 10.1038/s41416-018-0007-z]

22 **Wen CP**, Tsai SP, Chen CJ, Cheng TY, Tsai MC, Levy DT. Smoking attributable mortality for Taiwan and its projection to 2020 under different smoking scenarios. *Tob Control* 2005; **14** Suppl 1: i76-i80 [PMID: 15923454 DOI: 10.1136/tc.2004.007955]

23 **Wen CP**, Levy DT, Cheng TY, Hsu CC, Tsai SP. Smoking behaviour in Taiwan, 2001. *Tob Control* 2005; **14** Suppl 1: i51-i55 [PMID: 15923450 DOI: 10.1136/tc.2004.008011]

24 **Wu IH**, Essien EJ, Sansgiry SS, Peters RJ, Yang M, Abughosh SM. Cigarette Smoking among Taiwanese Adults. *Epidemiol* 2011; **1**: 107 [DOI: 10.4172/2161-1165.1000107]

25 **Palmer WC**, Patel T. Are common factors involved in the pathogenesis of primary liver cancers? *J Hepatol* 2012; **57**: 69-76 [PMID: 22420979 DOI: 10.1016/j.jhep.2012.02.022]

26 **Pan WH**, Lee MS, Chuang SY, Lin YC, Fu ML. Obesity pandemic, correlated factors and guidelines to define, screen and manage obesity in Taiwan. *Obes Rev* 2008; **9** Suppl 1: 22-31 [PMID: 18307695 DOI: 10.1111/j.1467-789X.2007.00434.x]

27 **Mosadeghi S**, Liu B, Bhuket T, Wong RJ. Sex-specific and race/ethnicity-specific disparities in cholangiocarcinoma incidence and prevalence in the USA: An updated analysis of the 2000-2011 Surveillance, Epidemiology and End Results registry. *Hepatol Res* 2016; **46**: 669-677 [PMID: 26508039 DOI: 10.1111/hepr.12605]

28 **Antwi SO**, Patel T. Increasing mortality of intrahepatic cholangiocarcinoma in the US: are gender-specific risk factors important? *Hepatobiliary Surg Nutr* 2019; **8**: 635-636 [PMID: 31929993 DOI: 10.21037/hbsn.2019.10.10]

29 **Singsuksawat E**, Thuwajit C, Charngkaew K, Thuwajit P. Increased ETV4 expression correlates with estrogen-enhanced proliferation and invasiveness of cholangiocarcinoma cells. *Cancer Cell Int* 2018; **18**: 25 [PMID: 29467595 DOI: 10.1186/s12935-018-0525-z]

30 **Petrick JL**, Florio AA, Zhang X, Zeleniuch-Jacquotte A, Wactawski-Wende J, Van Den Eeden SK, Stanczyk FZ, Simon

TG, Sinha R, Sesso HD, Schairer C, Rosenberg L, Rohan TE, Purdue MP, Palmer JR, Linet MS, Liao LM, Lee IM, Koshiol J, Kitahara CM, Kirsh VA, Hofmann JN, Guillemette C, Graubard BI, Giovannucci E, Gaziano JM, Gapster SM, Freedman ND, Engel LS, Chong DQ, Chen Y, Chan AT, Caron P, Buring JE, Bradwin G, Beane Freeman LE, Campbell PT, McGlynn KA. Associations Between Prediagnostic Concentrations of Circulating Sex Steroid Hormones and Liver Cancer Among Postmenopausal Women. *Hepatology* 2020; **72**: 535-547 [PMID: 31808181 DOI: 10.1002/hep.31057]

31 **Shen TY**, Chen HJ, Pan WH, Yu T. Secular trends and associated factors of age at natural menopause in Taiwanese women. *Menopause* 2019; **26**: 499-505 [PMID: 30672884 DOI: 10.1097/GME.0000000000001307]

32 **Matsumoto K**, Onoyama T, Kawata S, Takeda Y, Harada K, Ikebuchi Y, Ueki M, Miura N, Yashima K, Koda M, Sakamoto T, Endo M, Horie Y, Murawaki Y. Hepatitis B and C virus infection is a risk factor for the development of cholangiocarcinoma. *Intern Med* 2014; **53**: 651-654 [PMID: 24694471 DOI: 10.2169/internalmedicine.53.1410]

33 **Zhou Y**, Zhao Y, Li B, Huang J, Wu L, Xu D, Yang J, He J. Hepatitis viruses infection and risk of intrahepatic cholangiocarcinoma: evidence from a meta-analysis. *BMC Cancer* 2012; **12**: 289 [PMID: 22799744 DOI: 10.1186/1471-2407-12-289]

34 **Beasley RP**. Rocks along the road to the control of HBV and HCC. *Ann Epidemiol* 2009; **19**: 231-234 [PMID: 19344859 DOI: 10.1016/j.annepidem.2009.01.017]

35 **Li M**, Du M, Cong H, Gu Y, Fang Y, Li J, Gan Y, Tu H, Gu J, Xia Q. Characterization of hepatitis B virus DNA integration patterns in intrahepatic cholangiocarcinoma. *Hepatol Res* 2021; **51**: 102-115 [PMID: 33037855 DOI: 10.1111/hepr.13580]

36 **Lu SN**, Su WW, Yang SS, Chang TT, Cheng KS, Wu JC, Lin HH, Wu SS, Lee CM, Changchien CS, Chen CJ, Sheu JC, Chen DS, Chen CH. Secular trends and geographic variations of hepatitis B virus and hepatitis C virus-associated hepatocellular carcinoma in Taiwan. *Int J Cancer* 2006; **119**: 1946-1952 [PMID: 16708389 DOI: 10.1002/ijc.22045]

37 **Navas MC**, Glaser S, Dhruv H, Celinski S, Alpini G, Meng F. Hepatitis C Virus Infection and Cholangiocarcinoma: An Insight into Epidemiologic Evidences and Hypothetical Mechanisms of Oncogenesis. *Am J Pathol* 2019; **189**: 1122-1132 [PMID: 30953604 DOI: 10.1016/j.ajpath.2019.01.018]

38 **Tsao YC**, Chen JY, Yeh WC, Peng YS, Li WC. Association between visceral obesity and hepatitis C infection stratified by gender: a cross-sectional study in Taiwan. *BMJ Open* 2017; **7**: e017117 [PMID: 29133317 DOI: 10.1136/bmjopen-2017-017117]

39 **Alvaro D**, Crocetti E, Ferretti S, Bragazzi MC, Capocaccia R; AISF Cholangiocarcinoma committee. Descriptive epidemiology of cholangiocarcinoma in Italy. *Dig Liver Dis* 2010; **42**: 490-495 [PMID: 20022823 DOI: 10.1016/j.dld.2009.10.009]

40 **Witjes CD**, Karim-Kos HE, Visser O, de Vries E, IJzermans JN, de Man RA, Coebergh JW, Verhoef C. Intrahepatic cholangiocarcinoma in a low endemic area: rising incidence and improved survival. *HPB (Oxford)* 2012; **14**: 777-781 [PMID: 23043667 DOI: 10.1111/j.1477-2574.2012.00536.x]

41 **Ardito F**, Coppola A, Rinninella E, Razionale F, Pulcini G, Carano D, Cintoni M, Mele MC, Barbaro B, Giuliante F. Preoperative Assessment of Skeletal Muscle Mass and Muscle Quality Using Computed Tomography: Incidence of Sarcopenia in Patients with Intrahepatic Cholangiocarcinoma Selected for Liver Resection. *J Clin Med* 2022; **11** [PMID: 35329856 DOI: 10.3390/jcm11061530]

42 **Jiang W**, Li FR, Yang HH, Chen GC, Hua YF. Relationship Between Fish Oil Use and Incidence of Primary Liver Cancer: Findings From a Population-Based Prospective Cohort Study. *Front Nutr* 2021; **8**: 771984 [PMID: 35036409 DOI: 10.3389/fnut.2021.771984]

43 **Songserm N**, Woradet S, Charoenbut P. Fruit and Vegetables Consumption: A Pointer for Cholangiocarcinoma Prevention in Northeast Thailand, the Highest Incidence Area in the World. *Nutr Cancer* 2016; **68**: 1289-1294 [PMID: 27682423 DOI: 10.1080/01635581.2016.1225101]

44 **Fedirko V**, Lukanova A, Bamia C, Trichopolou A, Trepo E, Nöthlings U, Schlesinger S, Aleksandrova K, Boffetta P, Tjønneland A, Johnsen NF, Overvad K, Fagherazzi G, Racine A, Boutron-Ruault MC, Grote V, Kaaks R, Boeing H, Naska A, Adarakis G, Valanou E, Palli D, Sieri S, Tumino R, Vineis P, Panico S, Bueno-de-Mesquita HBA, Siersema PD, Peeters PH, Weiderpass E, Skeie G, Engeset D, Quirós JR, Zamora-Ros R, Sánchez MJ, Amiano P, Huerta JM, Barricarte A, Johansen D, Lindkvist B, Sund M, Werner M, Crowe F, Khaw KT, Ferrari P, Romieu I, Chuang SC, Riboli E, Jenab M. Glycemic index, glycemic load, dietary carbohydrate, and dietary fiber intake and risk of liver and biliary tract cancers in Western Europeans. *Ann Oncol* 2013; **24**: 543-553 [PMID: 23123507 DOI: 10.1093/annonc/mds434]

45 **Chiang KC**, Yeh CN, Lin KJ, Su LJ, Yen TC, Pang JH, Kittaka A, Sun CC, Chen MF, Jan YY, Chen TC, Juang HH, Yeh TS. Chemopreventive and chemotherapeutic effect of dietary supplementation of vitamin D on cholangiocarcinoma in a Chemical-Induced animal model. *Oncotarget* 2014; **5**: 3849-3861 [PMID: 24939880 DOI: 10.18632/oncotarget.2000]

46 **Kreng VB**, Yang CT. The equality of resource allocation in health care under the National Health Insurance System in Taiwan. *Health Policy* 2011; **100**: 203-210 [PMID: 21112116 DOI: 10.1016/j.healthpol.2010.08.003]

47 **Chiang CJ**, Wang YW, Lee WC. Taiwan's Nationwide Cancer Registry System of 40 years: Past, present, and future. *J Formos Med Assoc* 2019; **118**: 856-858 [PMID: 30773272 DOI: 10.1016/j.jfma.2019.01.012]

World Journal of Gastroenterology

Submit a Manuscript: https://www.f6publishing.com

World J Gastroenterol 2022 July 28; 28(28): 3706-3719

DOI: 10.3748/wjg.v28.i28.3706

ISSN 1007-9327 (print) ISSN 2219-2840 (online)

ORIGINAL ARTICLE

Observational Study

Family-based *Helicobacter pylori* infection status and transmission pattern in central China, and its clinical implications for related disease prevention

Xue-Chun Yu, Qiao-Qiao Shao, Jing Ma, Miao Yu, Chen Zhang, Lei Lei, Yang Zhou, Wen-Chao Chen, Wei Zhang, Xin-Hui Fang, Yuan-Zeng Zhu, Gang Wu, Xue-Mei Wang, Shuang-Yin Han, Pei-Chun Sun, Song-Ze Ding

Specialty type: Gastroenterology and hepatology

Provenance and peer review: Unsolicited article; Externally peer reviewed.

Peer-review model: Single blind

Peer-review report's scientific quality classification

Grade A (Excellent): A
Grade B (Very good): B
Grade C (Good): 0
Grade D (Fair): 0
Grade E (Poor): 0

P-Reviewer: Kotelevets SM, Russia; Tilahun M, Ethiopia

Received: April 18, 2022
Peer-review started: April 18, 2022
First decision: May 29, 2022
Revised: June 9, 2022
Accepted: June 24, 2022
Article in press: June 24, 2022
Published online: July 28, 2022

Xue-Chun Yu, Qiao-Qiao Shao, Jing Ma, Miao Yu, Lei Lei, Xin-Hui Fang, Shuang-Yin Han, Song-Ze Ding, Department of Gastroenterology and Hepatology, People's Hospital of Zhengzhou University, Henan Provincial People's Hospital, Zhengzhou 450003, Henan Province, China

Chen Zhang, Department of Gastroenterology and Hepatology, Henan University People's Hospital, Henan Provincial People's Hospital, Zhengzhou 450003, Henan Province, China

Yang Zhou, Wen-Chao Chen, Wei Zhang, Yuan-Zeng Zhu, Gang Wu, Pei-Chun Sun, Department of Gastrointestinal Surgery, People's Hospital of Zhengzhou University, Henan Provincial People's Hospital, Zhengzhou 450003, Henan Province, China

Xue-Mei Wang, Department of Traditional Chinese Medicine, People's Hospital of Zhengzhou University, Henan Provincial People's Hospital, Zhengzhou 450003, Henan Province, China

Corresponding author: Song-Ze Ding, MD, PhD, Professor, Department of Gastroenterology and Hepatology, People's Hospital of Zhengzhou University, Henan Provincial People's Hospital, No. 7 Weiwu Road, Jin Shui District, Zhengzhou 450003, Henan Province, China. dingsongze@hotmail.com

Abstract

BACKGROUND

Helicobacter pylori (*H. pylori*) has characteristics of family cluster infection; however, its family-based infection status, related factors, and transmission pattern in central China, a high-risk area for *H. pylori* infection and gastric cancer, have not been evaluated. We investigated family-based *H. pylori* infection in healthy households to understand its infection status, related factors, and patterns of transmission for related disease prevention.

AIM

To investigate family-based *H. pylori* infection status, related factors, and patterns of transmission in healthy households for related disease prevention.

METHODS

Blood samples and survey questionnaires were collected from 282 families

including 772 individuals. The recruited families were from 10 selected communities in the greater Zhengzhou area with different living standards, and the family members' general data, *H. pylori* infection status, related factors, and transmission pattern were analyzed. *H. pylori* infection was confirmed primarily by serum *H. pylori* antibody arrays; if patients previously underwent *H. pylori* eradication therapy, an additional ^{13}C-urea breath test was performed to obtain their current infection status. Serum gastrin and pepsinogens (PGs) were also analyzed.

RESULTS

Among the 772 individuals examined, *H. pylori* infection rate was 54.27%. These infected individuals were from 246 families, accounting for 87.23% of all 282 families examined, and 34.55% of these families were infected by the same strains. In 27.24% of infected families, all members were infected, and 68.66% of them were infected with type I strains. Among the 244 families that included both husband and wife, spouse co-infection rate was 34.84%, and in only 17.21% of these spouses, none were infected. The infection rate increased with duration of marriage, but annual household income, history of smoking, history of alcohol consumption, dining location, presence of gastrointestinal symptoms, and family history of gastric disease or GC did not affect infection rates; however, individuals who had a higher education level showed lower infection rates. The levels of gastrin-17, PGI, and PGII were significantly higher, and PGI/II ratio was significantly lower in *H. pylori*-infected groups than in *H. pylori*-negative groups.

CONCLUSION

In our study sample from the general public of central China, *H. pylori* infection rate was 54.27%, but in 87.23% of healthy households, there was at least 1 *H. pylori*-infected person; in 27.24% of these infected families, all members were infected. Type I *H. pylori* was the dominant strain in this area. Individuals with a higher education level showed significantly lower infection rates; no other variables affected infection rates.

Key Words: *Helicobacter pylori*; Atrophic gastritis; Family clustering infection; Gastric cancer; Gastrin; Pepsinogen

©The Author(s) 2022. Published by Baishideng Publishing Group Inc. All rights reserved.

Core Tip: *Helicobacter pylori* (*H. pylori*) has characteristics of family cluster infection. However, few studies have investigated family-based infection status and pattern of intrafamilial transmission in the general public of central China. In our study, *H. pylori* infection rate was 54.27%, but in 87.23% of healthy households, there was at least 1 *H. pylori*-infected person; in 27.24% of these infected families, all members were infected. Type I *H. pylori* was the dominant strain in this area. Intrafamilial infection status and patterns of transmission represent one important source of *H. pylori* spread, indicating the urgent need for family-based infection control and related disease prevention.

Citation: Yu XC, Shao QQ, Ma J, Yu M, Zhang C, Lei L, Zhou Y, Chen WC, Zhang W, Fang XH, Zhu YZ, Wu G, Wang XM, Han SY, Sun PC, Ding SZ. Family-based *Helicobacter pylori* infection status and transmission pattern in central China, and its clinical implications for related disease prevention. *World J Gastroenterol* 2022; 28(28): 3706-3719

URL: https://www.wjgnet.com/1007-9327/full/v28/i28/3706.htm

DOI: https://dx.doi.org/10.3748/wjg.v28.i28.3706

INTRODUCTION

Chronic *Helicobacter pylori* (*H. pylori*) infection is the major cause of chronic gastritis, peptic ulcers, and gastric cancer (GC), and is also closely associated with a number of extra-gastrointestinal (GI) diseases [1-3]. *H. pylori* infection rate in China is about 50%, but the infection rate varies widely in different regions due to economic development, age, lifestyle habit, and sanitary conditions[4-6]. *H. pylori* has characteristics of family cluster infection[7]. Most *H. pylori* infections are acquired during childhood and adolescence, and infection will persist for decades unless proper treatment is offered.

Mounting evidence has demonstrated that transmission of *H. pylori* is mainly by oral-oral and fecal-oral routes, and water sources[8,9], and intra-familial spread is the major source of *H. pylori* transmission[10-12]. The infected parent, especially the mother, is thought to play an important role in its transmission[9,11]. When parents are infected with *H. pylori*, the infection rates of their children

markedly increase; spread has also been demonstrated between spouses and among siblings[13-17]. Therefore, diagnosis and treatment of the whole family have important clinical implications for preventing related diseases[18]. Recently, the notion of "family-based *H. pylori* infection control and management" has been introduced to China as a practical strategy to curb *H. pylori* intra-familial transmission[3]. However, relatively few studies have been performed to investigate the family-based infection status, related factors, and pattern of intrafamilial transmission in the general population.

Type I [cytotoxin-associated protein-positive (CagA+), vacuolating cytotoxin-positive (VacA+)] *H. pylori* infection causes severe gastric inflammation and is prone to induce carcinogenesis[19,20]. Our previous study of 3572 patients admitted to the hospital showed that the *H. pylori* infection rate was 75.9% in this area of central China. The infection rate was further confirmed by investigation of 523 endoscopy-confirmed patients (76.9%), of whom 72.4% (291/402) had type I *H. pylori* infection and 27.5% had type II *H. pylori* infection. Importantly, 88.4% of GC patients were *H. pylori*-positive, of whom 84.2% had type I infection; only 11.6% of GC patients were *H. pylori*-negative[21]. At present, the genotype of family based-*H. pylori* infection in the healthy household is unclear, as well as its relationship with GC epidemiological markers such as gastrin-17 (G-17), pepsinogen (PG) level, and PG I/II ratio (PGR).

Henan province in central China is one of the high-risk areas for *H. pylori* and GC, with an *H. pylori* infection rate of 49.6%[22] and GC incidence of 42.52/100000[23]. The capital city, Zhengzhou, has a population of 12 million, but there has been no large-scale family-based *H. pylori* intrafamilial transmission survey, and the factors that affect *H. pylori* spread and cause disease are also unclear.

Therefore, we investigated family-based *H. pylori* infection status, factors related to bacteria spread, bacteria genotype, and patterns of transmission for the residents in this area, and analyzed their impact on GC epidemiological markers including G-17, PGI, PGII, and PGR. The results of this study will provide information on *H. pylori* infection status in the household and help to refine eradication strategies for the prevention of related diseases.

MATERIALS AND METHODS

Study population and data collection

From September 2020 to April 2021, blood samples and questionnaires were collected from family members of 10 selected communities in greater Zhengzhou area; each community enrolled 20-30 families, with all members participating. The 10 communities were selected based on high, middle, and low living standards to prevent biased selection of the population; these included two high-income communities, six middle-class communities, and two communities originating from rural areas. Specifically, the study included two communities located in Guancheng District, namely Lufu Pavilion and Houjiadong Street communities; three communities located in Jinshui District, namely Chengbei Road, Jiagang, and Huilong Digital City communities; four communities in New East Zhengzhou District, namely Hanhai Qingyu, Zhengzhou Academy of Aviation Administration, Henan University of Finance, Economics and Law, and Nanxi Fudi communities; and one community in Central Zhengzhou District, namely Kowloon City community.

A total of 282 families (family size ≥ 2 persons) including 772 individuals participated in the survey. Inclusion criteria were: Family members being long-term residents living in Zhengzhou area, with no age limit; all family members being willing to participate by providing blood samples and filling out the questionnaire; at least 2 people composing the family unit, but with no limitation on how many people are living in the same household; and all family members being willing to provide written informed consent. An infected family was defined as a household with various family members infected with *H. pylori*, ranging from only 1 person to all family members being infected, and a family could be composed of only a couple, with or without children. Exclusion criteria were: Pregnant and breast-feeding females; people with mental illness; or people who refused to fill out the questionnaire or sign the consent form.

This study was approved by the Ethics Committee of People's Hospital of Zhengzhou University (No. 53, 2021). All subjects provided written informed consent; for minor subjects, written informed consent was given by their legal guardian. This study was registered in the China Clinical Trial Registry (www.chictr.org.cn; No. ChiCTR2100052950), and the protocol is freely available from the website after registration.

Subject enrollment and questionnaire

Before and during enrollment, an introduction brochure or information booklet for the study was distributed to the community center staff, who were responsible for distributing and helping recruit community family members for onsite registration. A registration website was also open to community members for whole family-based registration; registration for only a single individual was declined. A questionnaire was filled out either online or onsite by each of the participating family members. Blood samples were collected from each participating member for *H. pylori*, gastrin, and PG analyses; if necessary, ^{13}C-urea breath test (UBT) was subsequently performed by appointment.

Based on the purpose of this study, questionnaire included the following 17 items: Age; sex; family ethic; number of family members; professions; marriage status; socioeconomic data; dining history; living habits; lifestyle; disease history; medication history; presence of GI symptoms; *H. pylori* eradication history; history of gastroscopy; infection history of other family members; and treatment history (Table 1).

H. pylori infection status, gastrin, and PG analyses

Three milliliters of fasting venous blood were collected from all subjects in the morning. Blood samples were centrifuged at 1000 × *g* for 10 min, (80-2 centrifuge; Jiangsu Zhongda Instrument Technology Co., Ltd., Jiangsu, China), and samples were either analyzed on ice on the same day or stored at -80 °C for subsequent analyses. Serum anti-*H. pylori* antibodies [detecting CagA, VacA, UreA, UreB *via H. pylori* enzyme-linked immunosorbent assay (ELISA) kit (Blot Biotech Co., Ltd., Shenzhen, Guangdong, China)] and G-17, PGI, PGII levels, as well as PGR (*via* PGI, PGII, G-17 ELISA kits; Biohit Biotechnology, Helsinki, Finland) were measured by an ELISA kit following manufacturer's instructions as previously reported[22]. If patients had previously undergone *H. pylori* eradication therapy, an additional ^{13}C-UBT was performed to obtain their current infection status (^{13}C-UBT Diagnostic Kit; Beijing Boran Pharmaceutical Co., Ltd., Beijing, China).

Statistical analyses

Data were analyzed using SPSS for Windows version 25 (IBM Corp, Armonk, NY, United States). Continuous variables are expressed as mean ± SD, whereas categorical variables are described as percentages or frequencies. The measurement data were compared by *t*-test, and the enumeration data were compared by χ^2 test or Fisher's exact test. $P < 0.05$ was considered statistically significant.

RESULTS

Demographic information of the enrolled families

As shown in Table 1, a total of 282 families including 772 members participated in this study. Among them, 419 had *H. pylori* infection, giving an overall infection rate of 54.27% (419/772); among the infected individuals, 328 (42.49%, 328/772) were infected with type I strains and 91 (11.79%, 91/772) were infected with type II strains. Type I strains accounted for 78.28% (328/419) of cases, and type II strains accounted for 21.7% (91/419) of infected individuals (Figure 1A).

In total, 330 (42.75%) of the study participants were male, with an average age of 44.56 ± 20.19 years, and 442 (57.25%) were female, with an average age of 45.95 ± 18.74 years ($P > 0.05$). The age range of the enrolled individuals was 3 years to 90 years, with the youngest and oldest infected individuals aged 5 years and 87 years, respectively.

As shown in Figure 2, stratified age and *H. pylori* genotype infection were further analyzed, type I strains was the dominant strains for all age groups. The infection rates of individuals under the age of 18 were 23.26% (20/86), and the age groups of 51-60 and 61-70 years had the highest infection rates of 63.01% (92/146) and 65.95% (93/141), respectively. Compared with age groups under 18-years-old, the infection rate was significantly higher in groups above 18-years-old ($P < 0.05$), but there was no difference in infection rates among groups above 18-years-old ($P > 0.05$).

Among questionnaire variables (Table 1), annual household income, history of smoking, history of alcohol consumption, dining location, presence of GI symptoms, and family history of gastric disease and GC did not affect infection rates ($P > 0.05$), but individuals with a higher education level showed significantly lower infection rates ($P < 0.05$).

H. pylori infection status of the enrolled families

The average family size of the study cohort was 2.74 persons *per* households, and family size ranged from as few as 2 persons *per* family to as many as 6 *per* family (Figure 1B). In this survey, 2- and 3-person households accounted for 80.85% (228/282) of the families enrolled.

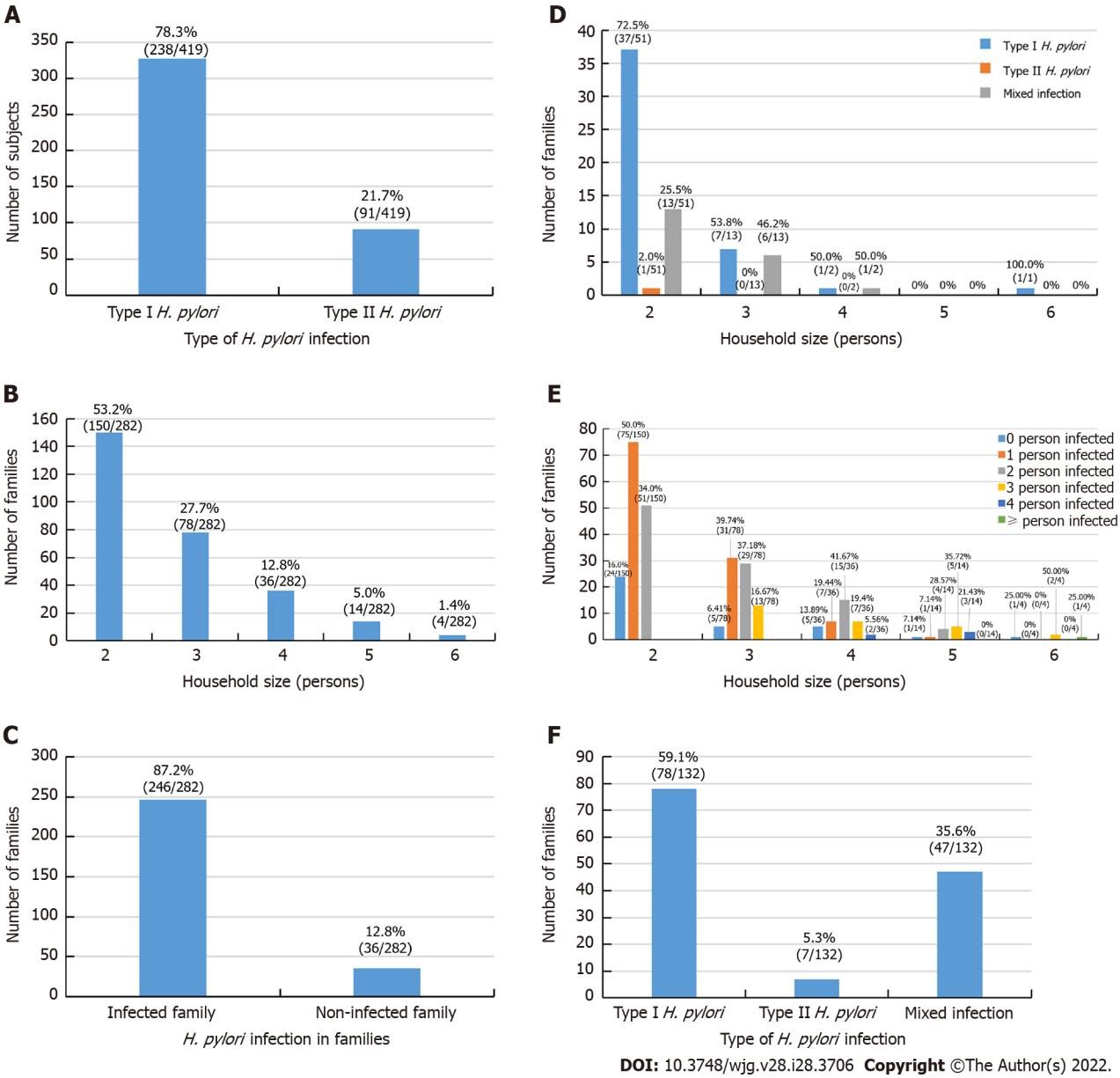
As shown in Figure 1C-F, *H. pylori*-infected individuals were distributed in 246 of the 282 families with varying numbers of members infected, ranging from only 1 person to all family members infected. The family infection rate was 87.23% with at least 1 person infected in a family unit (246/282), in 12.77% of the 282 households, no family members were infected (36/282) (Figure 1C). In 67 of the 246 infected families, all members were infected (27.24%, 67/246), among these 67 all member-infected households, 46 households were infected with the same type I strains (68.66%, 46/67), 1 household was infected with type II strains (1.49%, 1/67), and 20 households had mixed type I and II strain infection (29.85%, 20/67) (Figure 1D). The data of the stratified family member infection rate of 282 households were shown in Figure 1E. In 53.66% (132/246) of families with at least 2 members infected, 59.09% (78/132) of these families were infected with type I strains, 5.30% (7/132) were infected with type II strains, and 35.61% (47/132) were infected with mixed type I and II strains (Figure 1F).

Table 1 Demography information and *Helicobacter pylori* infection status of 772 subjects

Variables items, *n*	*H. pylori* positive			*H. pylori* negative, *n*	Infection rate (%)	*P* value
	Sub total, *n*	Type I, *n*	Type II, *n*			
Total (772)	419	328	91	353	54.27	
Gender						
Male (330)	173	130	43	157	52.42	
Female (442)	246	198	48	196	55.66	0.373
Age (yr) (mean ± SD)[1]						
Total (45.36 ± 19.38)	49.38 ± 16.92	49.59 ± 17.04	48.65 ± 16.47	40.58 ± 20.97		0.000[a]
Male (44.56 ± 20.19)	49.62 ± 18.06	49.21 ± 18.53	50.86 ± 16.50	38.98 ± 20.93		
Female (45.95 ± 18.74)	49.22 ± 16.06	49.83 ± 15.97	46.67 ± 16.20	41.86 ± 20.92		0.240[b]
Family annual income[2] **(10000 RMB)**						
< 10 (287)	171	142	29	116	59.58	
10-20 (209)	119	86	33	90	56.94	0.555[c]
20-30 (84)	47	36	11	37	55.95	0.552[c]
> 30 (59)	34	27	7	25	57.63	0.781[c]
Unknown (47)	28	20	8	19	59.57	
Cigarette smoking[2]						
Yes (158)	91	64	27	67	57.59	
No (520)	302	242	60	218	58.08	0.914
Unknown (8)	6	5	1	2	75.00	
Alcohol drinking[2]						
Yes (149)	86	64	22	63	57.72	
No (511)	297	233	64	214	58.12	0.930
Unknown (26)	16	14	2	10	61.54	
Gastrointestinal symptoms[2]						
Yes (311)	183	145	38	128	58.84	
No (339)	193	148	45	146	56.93	0.622
Unknown (36)	23	18	5	13	63.89	
Dining location[2]						
Home (472)	276	215	61	196	58.47	
Restaurant (186)	106	83	23	80	56.99	0.728
Unknown (28)	17	13	4	11	60.71	
Family history of stomach disease[3]						
Yes (167)	92	65	27	75	55.09	
No (430)	256	205	51	174	59.53	0.323
Unknown (89)	51	41	10	38	57.30	
Family history of gastric cancer[3]						
Yes (41)	23	20	3	18	56.10	
No (576)	335	260	75	241	58.16	0.796
Unknown (69)	41	31	10	28	59.42	
Education level[2]						
Senior and below (286)	180	142	38	106	62.94	

University or above (376)	199	155	44	177	52.93	0.010[a]
Unknown (24)	20	14	6	4	83.33	

[a]$P < 0.05$, when *Helicobacter pylori* (*H. pylori*)-positive groups were compared with *H. pylori*-negative groups.
[b]$P > 0.05$, when male *H. pylori*-positive groups were compared with female *H. pylori*-positive groups.
[c]$P > 0.05$, when *H. pylori* infection rate in the annual income < 100000 RMB group was compared with other income groups.
[1]Data are presented as the mean ± SD.
[2]Data only included adults, and children and adolescents age ≤ 18 yr were not included.
[3]Data only included history of gastric disease or gastric cancer in families across three consecutive generations.
H. pylori: *Helicobacter pylori*.



DOI: 10.3748/wjg.v28.i28.3706 **Copyright** ©The Author(s) 2022.

Figure 1 *Helicobacter pylori* infection status of the 282 enrolled families. Values above each column are the case number and percentages of each group. A: Genotype pattern of the 419 infected subjects in the enrolled families; B: Distribution pattern of the 282 enrolled families ranged from 2-6 people; C: General *Helicobacter pylori* (*H. pylori*) infection status of 282 families; D: Genotype pattern of the 67 all member-infected families from the enrolled 282 families; E: Distribution pattern of the *H. pylori* infection status of the 282 enrolled families; F: Genotype pattern of the 132 *H. pylori*-infected families with ≥ 2 persons infected from the 282 enrolled families. Infected family: At least 1 person in a family was infected; Non-infected family: All members in a family were not infected; Type I *H. pylori*: *H. pylori* infection with type I strains; Type II *H. pylori*: *H. pylori* infection with type II strains; Mixed infection: *H. pylori* infection with type I and type II strains.

H. pylori infection status between couples

H. pylori infection status between couples is shown in Figure 3. In all, 244 of the 282 families had both spouses, and infection rate of both spouses was 34.84% (85/244); further, 17.21% (42/244) couples were not infected, and 47.95% (117/244) had only a single spouse infection (Figure 3A). Among 117 families with infection of only 1 spouse, 75.21% (88/117) were infected with type I strains and 24.79% (29/117) were infected with type II strains (Figure 3B). Of these spouses, the husband was infected in 49.57% (58/117) of cases and the wife was infected in 50.53% (59/117) of cases ($P > 0.05$), they were further stratified into type I and type II strains infections (Figure 3C). Furthermore, among the 85 families with both husband and wife co-infected with *H. pylori*, 68.24% (58/85) were infected with the same type of strain, of whom 63.53% (54/85) were infected with type I strains, 4.71% (4/85) were infected with type II strains, and 31.76% (27/85) had mixed type I and type II infection (Figure 3D). Significantly more couples were infected with the same type of strain than with mixed strains ($P < 0.05$). In addition, with the increase in marriage duration, infection rate of both husband and wife was significantly increased ($r = 0.98$, $P < 0.05$; Figure 3E).

Parental infection and infection status of children and adolescents

In 51 families with both parents and children younger than 18 years of age, as shown in Table 2, the infection rate of children was 23.08% (6/26) when both parents were *H. pylori*-infected; however, when both parents were not infected, the infection rate of children was 18.18% (2/11) ($P > 0.05$). When only mother was infected, the infection rate of children was 45.45% (5/11); no child was infected (0/9) when only father was infected ($P > 0.05$).

Table 3 shows infection status of the 51 families comprising both parents and children, for a total of 190 individuals. Among these family members, the infection rates were as follows: Father, 62.75% (32/51); mother, 62.75% (32/51); grandfather, 50.00% (2/4); grandmother, 66.67% (8/12); maternal grandfather, 25.00% (1/4); maternal grandmother, 37.50% (3/8); and other relatives, 66.67% (2/3).

Comparison of G-17, PGI, and PGII levels, and PGR with different types of *H. pylori* infection

To determine the impact of *H. pylori* infection on common GC epidemiological markers (*e.g.*, G-17, PGI, PGII, and PGR) in healthy households, we assayed their levels during *H. pylori* infection. As shown in Table 4, compared to *H. pylori*-negative groups, PGI levels were significantly higher and PGR was significantly lower in *H. pylori* type I infections compared with *H. pylori*-negative groups ($P < 0.05$). However, there were no differences in G-17, PGII level, and PGR between type II *H. pylori* infection and *H. pylori*-negative groups ($P > 0.05$). The levels of G-17, PGI, and PGII were significantly higher, and PGR was significantly lower in *H. pylori*-infected groups than in *H. pylori*-negative groups ($P < 0.05$).

DISCUSSION

H. pylori infection rates vary greatly among different countries and regions[24]. Although numerous studies have demonstrated that intrafamilial transmission is one of the most important sources of *H. pylori* spread[2,18,24], there are few studies on the characteristics and pattern of family-based *H. pylori* infection for disease prevention and control[9,25,26]. Therefore, focusing on family-based *H. pylori* infection control and management would be a novel approach to reduce the related diseases and GC burden in a society.

In this work, we analyzed *H. pylori* infection status in a total of 772 individuals from 282 families in the Zhengzhou area. The results showed that despite an overall infection rate of only 54.27%, in as high as 87.23% of the surveyed families (246/282), there was at least 1 person infected, and in 27.07% (67/246) of these infected families, all family members were infected; further, 34.55% (85/246) of these families were infected with the same type of strain. Therefore, this study provides new evidence showing the importance of family-based *H. pylori* infection control, which has substantive public health implications, and suggests that intrafamilial infection is a major source of *H. pylori* transmission. Thus, preventing intrafamilial spread is critical to eliminate the source of infection in order to prevent the related diseases.

Over the past several decades, the social and family structure in China has changed dramatically. The latest national statistics[27] (2020) revealed that the nation has a population of 1.41 billion and 492 million families with an average family size of 2.62 persons/family, which is much smaller than it was in 1990, when China had 1.13 billion citizens and 278.6 million families, with an average family size of 4.05 persons/family[27]. Due to the previous nationwide "one-children-per-family policy" (between 1982 and 2016), most families in China only have 1 child and two generations. As these children do not have siblings, transmission among siblings within a family unit did not appear to be the major route of transmission in the current analysis. *H. pylori* spread from parent or grandparent to children is probably more important for bacteria transmission. Although the current results provide a snapshot of *H. pylori* infection status in the general public, a nationwide large-scale investigation is needed to explore the nationwide infection status and develop policies for related disease prevention.

Table 2 Parental infection and infection status of children and adolescents in 51 families

Parental infection (Household numbers)	Children infection (57)		Infection rate (%)	*P* value
	H. pylori+ (*n*)	*H. pylori*- (*n*)		
Neither parent infected (11)	2	9	18.18	
Both parent infected (21)	6	20	23.08	0.109[a]
Only father infected (9)	0	9	0	
Only mother infected (10)	5	6	45.45	
Total (51)	13	44	22.81	

[a]*P* > 0.05 when both parents infected group were compared with neither parent infected group.
n: Person *per* group; Infection rate (%): Infection rate of children in different groups; *H. pylori*+: *H. pylori*-positive; *H. pylori*-: *H. pylori*-negative.

Table 3 *Helicobacter pylori* infection status in 51 families with children and other relatives

Family members (N)	*H. pylori* positive			*H. pylori* negative, *n*	Infection rate (%)
	Sub total, *n*	Type I *H. pylori*, *n*	Type II *H. pylori*, *n*		
Total (190)	93	66	27	97	48.95
Father (51)	32	23	9	19	62.75
Mother (51)	32	22	10	19	62.75
Grandfather (4)	2	1	1	2	50.00
Grandmother (12)	8	6	2	4	66.67
Maternal grandfather (4)	1	0	1	3	25.00
Maternal grandmother (8)	3	2	1	5	37.50
Other relatives (3)	2	2	0	1	66.67
Child (57)	13	10	3	45	22.81

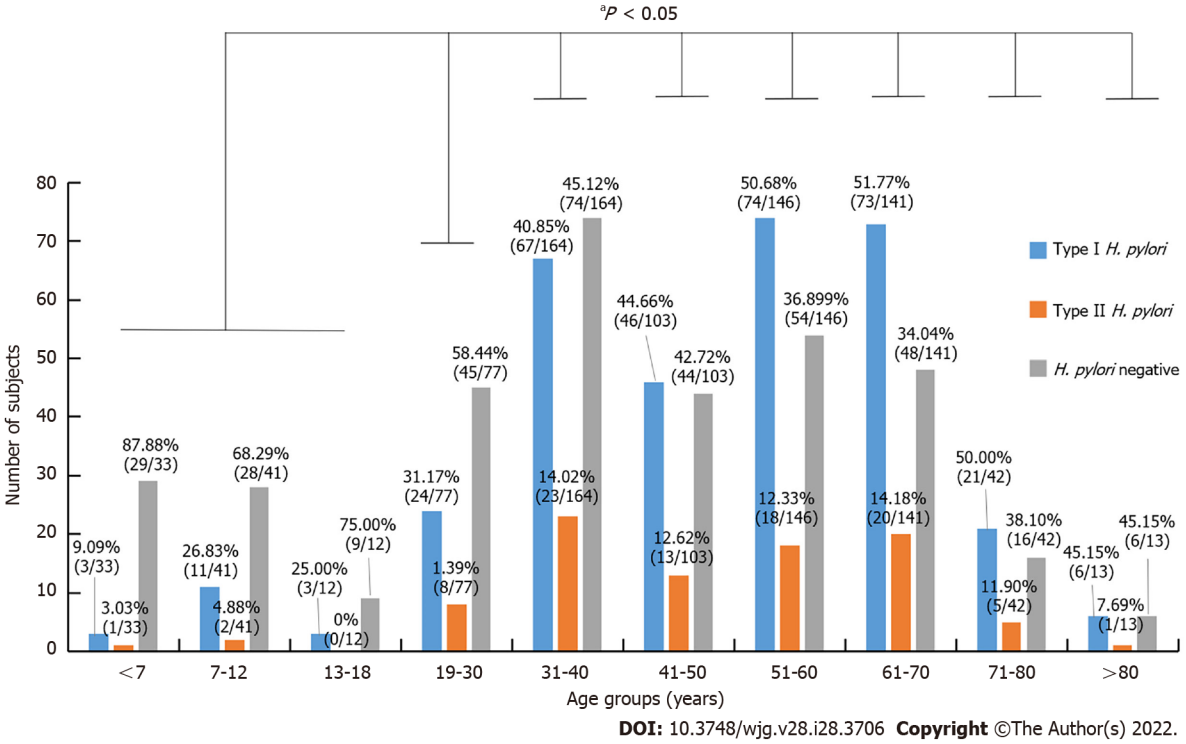
N: Number of family members in 51 families; *n*: Person *per* group; Type I *H. pylori*: *H. pylori* infection with type I strains; Type II *H. pylori*: *H. pylori* infection with type II strains; *H. pylori*: *Helicobacter pylori*; Infection rate: Number of *H. pylori*-positive family members/number of family members.

Table 4 Serum gastrin-17, pepsinogen I, pepsinogen II and pepsinogen I/II ratio levels in *Helicobacter pylori*-infected population

	H. pylori+	Type I *H. pylori*	Type II *H. pylori*	*H. pylori*-
G-17 (pmol/L)	8.95 ± 14.53	9.87 ± 15.60	5.62 ± 9.10[c]	4.90 ± 9.21[a,d]
PGI (μg/L)	117.90 ± 55.99	123.12 ± 57.11	99.10 ± 47.45	91.13 ± 38.29[a,b,d]
PGII (μg/L)	12.66 ± 10.41	13.83 ± 11.07	8.43 ± 5.91[c]	7.39 ± 6.82[a,d]
PGR	12.16 ± 6.39	11.64 ± 6.40	14.05 ± 6.04[c]	15.58 ± 7.97[a,d]

[a]*P* < 0.05 when type I *Helicobacter pylori* (*H. pylori*)-infected groups were compared with *H. pylori*-negative groups.
[b]*P* < 0.05 when type II *H. pylori*-infected groups were compared with *H. pylori*-negative groups.
[c]*P* < 0.05 when type I *H. pylori*-infected groups were compared with type II *H. pylori*-infected groups.
[d]*P* < 0.05 when *H. pylori*-infected groups were compared with *H. pylori*-negative groups.
Data are presented as mean ± SD. G-17: Gastrin-17; PG: Pepsinogen; PGR: PG I/II ratio; Type I *H. pylori*: *H. pylori* infection with type I strains; Type II *H. pylori*: *H. pylori* infection with type II strains; *H. pylori*: *Helicobacter pylori*; *H. pylori*+: *H. pylori*-positive; *H. pylori*-: *H. pylori*-negative.

In single factor analysis, we noted that the highly infected age groups were between 31 years and 70 years, and infection rates increased along with age and duration of marriage. Annual household income, history of smoking, history of alcohol consumption, dining location, and family history of gastric disease or GC were not different between the infected and non-infected groups, but individuals with a higher education level showed a lower infection rate. A 2020 all-ages population-based cross-sectional study[28] in Wuwei county in northwestern China showed that the prevalence of *H. pylori*



DOI: 10.3748/wjg.v28.i28.3706 **Copyright** ©The Author(s) 2022.

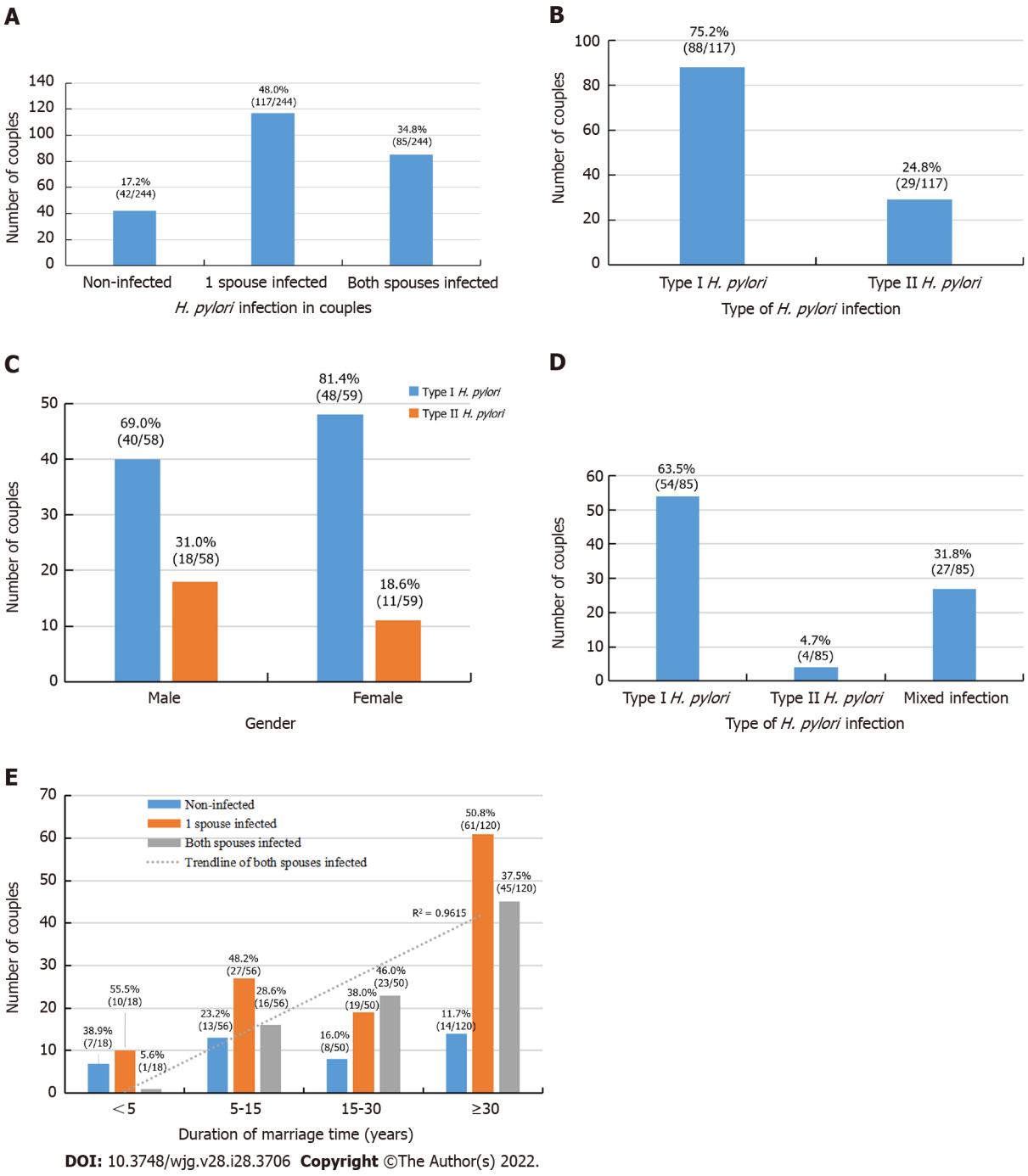
Figure 2 *Helicobacter pylori* infection status of 772 subjects in different age groups. Values above each column are the case number and its percentages in each specific age group. $^aP < 0.05$ when *Helicobacter pylori* (*H. pylori*) infection rate in the age group of ≤ 18 yr was compared with other age groups. Type I *H. pylori*: *H. pylori* infection with type I strains; Type II *H. pylori*: *H. pylori* infection with type II strains.

infection was closely associated with socioeconomic conditions, sanitary situations, dietary habits of the participants in the city. Boarding, eating at school, and drinking untreated water were main factors explaining the rising infection rate in junior-senior high school students. The results indicated that close contact is associated with increased infection risk. In addition, differences in geographic location, study population, lifestyle habit, and sanitary conditions are important factors that greatly contribute to *H. pylori* infection[22,29,30].

Similar results were obtained from other regions, such as one community-based study[31] in Vietnam in 2017 on familial clustering in a multiple-generation population. The study showed that high monthly income, not regularly being fed chewed food, and being breastfed were protective factors against *H. pylori* infection. Risk factors for *H. pylori* infection in children were not regularly handwashing after defecation, *H. pylori*-infected mother and grandfather, father's occupation, mother's education, and household size. Other factors such as number of siblings, infected fathers, regularly sharing a bed, group living, and antibiotic use were not found to be significant risk factors for infection.

H. pylori-infected family members are a possible source of continued transmission, which is an important health threat for uninfected family members[7,32,33]. A 2003 study[9] in the Stockholm area of Sweden using bacterial isolates for family-based DNA fingerprinting technique demonstrated a high proportion of shared strains among siblings, and between spouses, but also showed different strains in a portion of subjects (8%). Similar results were also reported by a 2009 study in Bangladesh[26]. In the current analysis, we found that among the 67 all member-infected households (Figure 1F), 68.66% (46/67) were infected with *H. pylori* type I strains, 1.49% (1/67) were infected with type II strains, and 29.85% (20/67) had mixed type I and II strain infection. These data support the notion that intrafamilial transmission is the primary transmission route, but exogenous infection outside the family can occur, indicating that there may be multiple sources of transmission. In 244 couples comprising both husband and wife, 34.84% (85/244) of them were co-infected, and 68.24% (58/85) of households were infected with the same strain. With an increase of marriage duration, the infection rate of both husband and wife was significantly increased, suggesting that there was also cross-infection between husband and wife.

One unexpected result was that when both parents were infected, the infection rate of children was 23.08% (6/21), whereas when both parents were not infected, the infection rate of children was 18.18% (2/11), and the difference did not reach statistical significance. This result was slightly different from our previous concept that parental *H. pylori* infection is an independent factor for infection in young children, and that mothers play an important role in *H. pylori* transmission to their descendent[13-15,26]. However, the current results likely reflect the current infection status in this region, as the gradually improved living standard, sanitary condition, use of tap water, and avoiding chewing food to feed children over the past several decades in China's urban family have resulted in a reduced infection rate. This is in line with the fact that the overall *H. pylori* infection rate is declining in most of China's urban



DOI: 10.3748/wjg.v28.i28.3706 **Copyright** ©The Author(s) 2022.

Figure 3 *Helicobacter pylori* infection status between 244 couples. Values above each column are the case number and percentages of each group. A: *Helicobacter pylori* (*H. pylori*) infection status of 244 couples; B: Type I and II *H. pylori* genotype status of the 117 couples with 1 spouse infected; C: *H. pylori* genotype and sex of 117 couples with 1 spouse infected; D: *H. pylori* genotype status in 85 couples with both spouses infected; E: Relationship between infection and marriage duration in 244 couples. The dashed line across the figure is the trendline of both spouses infected, $r = 0.98$. Non-infected: All members in a couple were not infected; one spouse infected: Only 1 in a couple was infected; Type I *H. pylori*: *H. pylori* infection with type I strains; Type II *H. pylori*: *H. pylori* infection with type II strains; Mixed infection: *H. pylori* infection with type I and type II strains.

areas[3,22]. Another possibility is that the current cohort had relatively small numbers of children and adolescents, which may not have generated enough power for statistical significance. In addition, we were unable to perform bacterial DNA fingerprinting to confirm if the strains were identical, so the genotype that precise bacterial strains transmit within a family unit has yet to be determined. Future large-scale investigations are needed to confirm the current conclusion.

Type I *H. pylori* strain accounted for 78.28% of the infected population in this survey, similar to the results of our previous study in patients admitted to the hospital, which showed that type I *H. pylori* infection accounted for 72.4% (291/402) of the infected patients, and type II was 27.6%[21]. When compared to *H. pylori*-negative groups, G-17, PGI, and PGII levels were higher in *H. pylori*-infected groups. G-17, PGI, and PGII levels were significantly higher and PGR was significantly lower in the

type I *H. pylori*-infected groups than in *H. pylori*-negative groups. The levels of G-17 and PG II were significantly higher, and PGR was significantly lower in type I *H. pylori*-infected groups than in type II-infected groups. These results are in line with our previous endoscopy results from inpatients, and indicate that both type I and type II *H. pylori* strains increase G-17 Level, whereas only type I *H. pylori* infection affects PGI and PGII levels and the PGR in this geographic area[21].

Type I infection and reduced PGR are risk factors for gastric mucosal precancerous lesions and GC [19,21]. Therefore, these results have important clinical implications, as the abnormal expression of gastric markers was noted in a portion of individuals in healthy households infected with *H. pylori* before they sought medical examinations. It was unclear if this group of individuals had gastric mucosal precancerous lesions; thus, further examinations by endoscopy may be required for confirmation. The results of this study also provide another line of support showing that family-based *H. pylori* infection control and management would be an important strategy for infection control and related disease prevention[3,18,34,35].

Although this pilot work provides novel information regarding family-based *H. pylori* infection status, it had some limitations. First, the investigation was performed with a relatively small number of families, and in some groups, especially children and adolescents, the number of samples was not large enough to reach statistical significance; thus, future large-scale, multiple region sampling would provide more convincing data. Second, this was a cross-sectional study without data from endoscopy to confirm *H. pylori* infection-related disease status and pathological changes in gastric mucosa; therefore, some in-depth information was missing, and the work was performed in a Chinese setting, which may not be suitable to other areas. Third, type I and II *H. pylori* genotype concordance through antibody array analysis only provided a very general evaluation. As we did not obtain bacteria strain culture and DNA fingerprinting data, *H. pylori* intrafamilial transmission was unable to be evaluated precisely to assess the heterogeneity of *H. pylori* strains within families. Thus, future studies are needed to evaluate the *H. pylori* DNA fingerprinting pattern for more precise evaluation. Even with these limitations, this study provides novel points and information on family-based *H. pylori* infection characteristics, which merit further large-scale exploration.

CONCLUSION

The current results provide snapshots of family-based *H. pylori* infection status in central China. The high infection rate and coincidence of people infected with *H. pylori* within a family unit indicate the status and pattern of intrafamilial transmission, which provide a novel option for family-based *H. pylori* infection control and related disease prevention. The concept is applicable not only to Chinese residents but also to other communities with high infection rates.

ARTICLE HIGHLIGHTS

Research background

Helicobacter pylori (*H. pylori*) has characteristics of family cluster infection; however, its family-based infection status, related factors, and transmission pattern in central China have not been evaluated.

Research motivation

We evaluated family-based *H. pylori* infection status, related factors, and interfamilial transmission pattern in healthy households in central China, a high-risk area for *H. pylori* and gastric cancer (GC).

Research objectives

To investigate family-based *H. pylori* infection and identify a better approach for *H. pylori* infection control and related disease prevention.

Research methods

H. pylori infection was confirmed primarily by serum antibody arrays in 282 enrolled families, including a total of 772 family members. If patients previously underwent *H. pylori* eradication therapy, an additional ^{13}C-urea breath test was performed to obtain their current infection status. Serum levels of gastrin and pepsinogens (PGs) were also analyzed.

Research results

In our study sample from the general public of central China, *H. pylori* infection rate was 54.27%. In 87.23% of healthy households, there was at least 1 *H. pylori*-infected person, and in 27.24% of these infected families, all members were infected. Type I *H. pylori* was the dominant strain in this geographic area. Among many variables, only individuals with a higher education level showed lower infection

rates. *H. pylori* infection was also correlated with abnormal gastrin-17, PGI, and PGII levels and PGI/PGII ratio.

Research conclusions

H. pylori infection in healthy households is very common in central China, and poses an important health threat to uninfected family members. The intrafamilial infection status and patterns of transmission represent one important source of *H. pylori* spread, and indicate the urgent need for family-based infection control and related disease prevention.

Research perspectives

The results of this study provide new information on family-based *H. pylori* infection status in central China, and support the novel concept of family-based *H. pylori* infection control and management. This notion is also likely to benefit other *H. pylori* and GC prevalent areas.

ACKNOWLEDGEMENTS

The authors are grateful to the staff of the Department of Gastroenterology and Hepatology, People's Hospital of Zhengzhou University, for their valuable assistance in this work.

FOOTNOTES

Author contributions: Ding SZ, Wu G, Wang XM, Han SY and Sun PC conceived and designed the study; Yu XC, Shao QQ, Zhang C and Yu M searched and screened related literature; Yu XC, Shao QQ, Ma J, Lei L and Zhou Y performed the data extraction and quality assessment; Yu XC, Zhou Y, Chen WC, Zhang W, Fang XH and Zhu YZ analyzed the data; Yu XC and Ding SZ wrote the manuscript; all authors critically revised and approved the final version of the manuscript.

Supported by National Natural Science Foundation of China, No. U1604174; Henan Provincial Government-Health and Family Planning Commission, No. 20170123 and No. SBGJ202002004; and Henan Provincial Government-Health and Family Planning Commission Research Innovative Talents Project, No. 51282.

Institutional review board statement: This study was reviewed and approved by the Ethics Committee of People's Hospital of Zhengzhou University, 2021, No. 53.

Informed consent statement: All study participants or their legal guardian provided informed written consent about personal and medical data collection prior to study enrolment.

Conflict-of-interest statement: All the authors report no relevant conflicts of interest for this article.

Data sharing statement: No additional data are available.

STROBE statement: The authors have read the STROBE Statement—checklist of items, and the manuscript was prepared and revised according to the STROBE Statement—checklist of items.

Open-Access: This article is an open-access article that was selected by an in-house editor and fully peer-reviewed by external reviewers. It is distributed in accordance with the Creative Commons Attribution NonCommercial (CC BY-NC 4.0) license, which permits others to distribute, remix, adapt, build upon this work non-commercially, and license their derivative works on different terms, provided the original work is properly cited and the use is non-commercial. See: https://creativecommons.org/Licenses/by-nc/4.0/

Country/Territory of origin: China

ORCID number: Xue-Chun Yu 0000-0003-4425-6019; Qiao-Qiao Shao 0000-0002-4900-9394; Jing Ma 0000-0003-1172-527X; Miao Yu 0000-0002-3587-2760; Chen Zhang 0000-0002-8810-6875; Lei Lei 0000-0002-6109-4229; Yang Zhou 0000-0002-5398-7764; Wen-Chao Chen 0000-0002-0642-0060; Wei Zhang 0000-0003-4620-6517; Xin-Hui Fang 0000-0001-5044-1320; Yuan-Zeng Zhu 0000-0001-9594-0916; Gang Wu 0000-0002-6627-0690; Xue-Mei Wang 0000-0003-0825-434X; Shuang-Yin Han 0000-0002-9907-7256; Pei-Chun Sun 0000-0001-7063-9537; Song-Ze Ding 0000-0002-4589-6942.

S-Editor: Fan JR
L-Editor: A
P-Editor: Li X

REFERENCES

1 **Malfertheiner P**, Megraud F, O'Morain CA, Gisbert JP, Kuipers EJ, Axon AT, Bazzoli F, Gasbarrini A, Atherton J, Graham DY, Hunt R, Moayyedi P, Rokkas T, Rugge M, Selgrad M, Suerbaum S, Sugano K, El-Omar EM; European Helicobacter and Microbiota Study Group and Consensus panel. Management of Helicobacter pylori infection-the Maastricht V/Florence Consensus Report. *Gut* 2017; **66**: 6-30 [PMID: 27707777 DOI: 10.1136/gutjnl-2016-312288]

2 **Fallone CA**, Chiba N, van Zanten SV, Fischbach L, Gisbert JP, Hunt RH, Jones NL, Render C, Leontiadis GI, Moayyedi P, Marshall JK. The Toronto Consensus for the Treatment of Helicobacter pylori Infection in Adults. *Gastroenterology* 2016; **151**: 51-69.e14 [PMID: 27102658 DOI: 10.1053/j.gastro.2016.04.006]

3 **Ding SZ**, Du YQ, Lu H, Wang WH, Cheng H, Chen SY, Chen MH, Chen WC, Chen Y, Fang JY, Gao HJ, Guo MZ, Han Y, Hou XH, Hu FL, Jiang B, Jiang HX, Lan CH, Li JN, Li Y, Li YQ, Liu J, Li YM, Lyu B, Lu YY, Miao YL, Nie YZ, Qian JM, Sheng JQ, Tang CW, Wang F, Wang HH, Wang JB, Wang JT, Wang JP, Wang XH, Wu KC, Xia XZ, Xie WF, Xie Y, Xu JM, Yang CQ, Yang GB, Yuan Y, Zeng ZR, Zhang BY, Zhang GY, Zhang GX, Zhang JZ, Zhang ZY, Zheng PY, Zhu Y, Zuo XL, Zhou LY, Lyu NH, Yang YS, Li ZS; National Clinical Research Center for Digestive Diseases (Shanghai), Gastrointestinal Early Cancer Prevention & Treatment Alliance of China (GECA), Helicobacter pylori Study Group of Chinese Society of Gastroenterology, and Chinese Alliance for Helicobacter pylori Study. Chinese Consensus Report on Family-Based *Helicobacter pylori* Infection Control and Management (2021 Edition). *Gut* 2022; **71**: 238-253 [PMID: 34836916 DOI: 10.1136/gutjnl-2021-325630]

4 **Liu WZ**, Xie Y, Lu H, Cheng H, Zeng ZR, Zhou LY, Chen Y, Wang JB, Du YQ, Lu NH; Chinese Society of Gastroenterology, Chinese Study Group on Helicobacter pylori and Peptic Ulcer. Fifth Chinese National Consensus Report on the management of Helicobacter pylori infection. *Helicobacter* 2018; **23**: e12475 [PMID: 29512258 DOI: 10.1111/hel.12475]

5 **Sugano K**, Tack J, Kuipers EJ, Graham DY, El-Omar EM, Miura S, Haruma K, Asaka M, Uemura N, Malfertheiner P; faculty members of Kyoto Global Consensus Conference. Kyoto global consensus report on Helicobacter pylori gastritis. *Gut* 2015; **64**: 1353-1367 [PMID: 26187502 DOI: 10.1136/gutjnl-2015-309252]

6 **Brown LM**, Thomas TL, Ma JL, Chang YS, You WC, Liu WD, Zhang L, Pee D, Gail MH. Helicobacter pylori infection in rural China: demographic, lifestyle and environmental factors. *Int J Epidemiol* 2002; **31**: 638-645 [PMID: 12055167 DOI: 10.1093/ije/31.3.638]

7 **Drumm B**, Perez-Perez GI, Blaser MJ, Sherman PM. Intrafamilial clustering of Helicobacter pylori infection. *N Engl J Med* 1990; **322**: 359-363 [PMID: 2300088 DOI: 10.1056/NEJM199002083220603]

8 **Kato M**, Ota H, Okuda M, Kikuchi S, Satoh K, Shimoyama T, Suzuki H, Handa O, Furuta T, Mabe K, Murakami K, Sugiyama T, Uemura N, Takahashi S. Guidelines for the management of Helicobacter pylori infection in Japan: 2016 Revised Edition. *Helicobacter* 2019; **24**: e12597 [PMID: 31111585 DOI: 10.1111/hel.12597]

9 **Kivi M**, Tindberg Y, Sörberg M, Casswall TH, Befrits R, Hellström PM, Bengtsson C, Engstrand L, Granström M. Concordance of Helicobacter pylori strains within families. *J Clin Microbiol* 2003; **41**: 5604-5608 [PMID: 14662948 DOI: 10.1128/JCM.41.12.5604-5608.2003]

10 **Georgopoulos SD**, Mentis AF, Spiliadis CA, Tzouvelekis LS, Tzelepi E, Moshopoulos A, Skandalis N. Helicobacter pylori infection in spouses of patients with duodenal ulcers and comparison of ribosomal RNA gene patterns. *Gut* 1996; **39**: 634-638 [PMID: 9026475 DOI: 10.1136/gut.39.5.634]

11 **Rothenbacher D**, Winkler M, Gonser T, Adler G, Brenner H. Role of infected parents in transmission of helicobacter pylori to their children. *Pediatr Infect Dis J* 2002; **21**: 674-679 [PMID: 12237602 DOI: 10.1097/00006454-200207000-00014]

12 **Perry S**, de la Luz Sanchez M, Yang S, Haggerty TD, Hurst P, Perez-Perez G, Parsonnet J. Gastroenteritis and transmission of Helicobacter pylori infection in households. *Emerg Infect Dis* 2006; **12**: 1701-1708 [PMID: 17283620 DOI: 10.3201/eid1211.060086]

13 **Rocha GA**, Rocha AM, Silva LD, Santos A, Bocewicz AC, Queiroz Rd Rde M, Bethony J, Gazzinelli A, Corrêa-Oliveira R, Queiroz DM. Transmission of Helicobacter pylori infection in families of preschool-aged children from Minas Gerais, Brazil. *Trop Med Int Health* 2003; **8**: 987-991 [PMID: 14629764 DOI: 10.1046/j.1360-2276.2003.01121.x]

14 **Yang YJ**, Sheu BS, Lee SC, Yang HB, Wu JJ. Children of Helicobacter pylori-infected dyspeptic mothers are predisposed to H. pylori acquisition with subsequent iron deficiency and growth retardation. *Helicobacter* 2005; **10**: 249-255 [PMID: 15904483 DOI: 10.1111/j.1523-5378.2005.00317.x]

15 **Konno M**, Yokota S, Suga T, Takahashi M, Sato K, Fujii N. Predominance of mother-to-child transmission of Helicobacter pylori infection detected by random amplified polymorphic DNA fingerprinting analysis in Japanese families. *Pediatr Infect Dis J* 2008; **27**: 999-1003 [PMID: 18845980 DOI: 10.1097/INF.0b013e31817d756e]

16 **Nguyen VB**, Nguyen GK, Phung DC, Okrainec K, Raymond J, Dupond C, Kremp O, Kalach N, Vidal-Trecan G. Intra-familial transmission of Helicobacter pylori infection in children of households with multiple generations in Vietnam. *Eur J Epidemiol* 2006; **21**: 459-463 [PMID: 16826451 DOI: 10.1007/s10654-006-9016-y]

17 **Chen XX**, Ou BY, Shang SQ, Wu XY, Zhang XP, Chen LQ, Qu YP. The correlation between family aggregation and eradication therapy in children with Helicobacter pylori infection. *Zhongguo Shiyong Erke* 2003; **18**: 475-477 [DOI: 10.3969/j.issn.1005-2224.2003.08.011]

18 **Sari YS**, Can D, Tunali V, Sahin O, Koc O, Bender O. H pylori: Treatment for the patient only or the whole family? *World J Gastroenterol* 2008; **14**: 1244-1247 [PMID: 18300351 DOI: 10.3748/wjg.14.1244]

19 **Matos JI**, de Sousa HA, Marcos-Pinto R, Dinis-Ribeiro M. Helicobacter pylori CagA and VacA genotypes and gastric phenotype: a meta-analysis. *Eur J Gastroenterol Hepatol* 2013; **25**: 1431-1441 [PMID: 23929249 DOI: 10.1097/MEG.0b013e328364b53e]

20 **Ding SZ**, Goldberg JB, Hatakeyama M. Helicobacter pylori infection, oncogenic pathways and epigenetic mechanisms in gastric carcinogenesis. *Future Oncol* 2010; **6**: 851-862 [PMID: 20465395 DOI: 10.2217/fon.10.37]

21 **Yuan L**, Zhao JB, Zhou YL, Qi YB, Guo QY, Zhang HH, Khan MN, Lan L, Jia CH, Zhang YR, Ding SZ. Type I and type II *Helicobacter pylori* infection status and their impact on gastrin and pepsinogen level in a gastric cancer prevalent area.

World J Gastroenterol 2020; **26**: 3673-3685 [PMID: 32742135 DOI: 10.3748/wjg.v26.i25.3673]

22 **Li M**, Sun Y, Yang J, de Martel C, Charvat H, Clifford GM, Vaccarella S, Wang L. Time trends and other sources of variation in Helicobacter pylori infection in mainland China: A systematic review and meta-analysis. *Helicobacter* 2020; **25**: e12729 [PMID: 32686261 DOI: 10.1111/hel.12729]

23 **Liu S**, Chen Q, Quan P, Zhang M, Zhang S, Guo L, Sun X, Wang C. Cancer incidence and mortality in Henan province, 2012. *Chin J Cancer Res* 2016; **28**: 275-285 [PMID: 27478313 DOI: 10.21147/j.issn.1000-9604.2016.03.02]

24 **Zamani M**, Ebrahimtabar F, Zamani V, Miller WH, Alizadeh-Navaei R, Shokri-Shirvani J, Derakhshan MH. Systematic review with meta-analysis: the worldwide prevalence of Helicobacter pylori infection. *Aliment Pharmacol Ther* 2018; **47**: 868-876 [PMID: 29430669 DOI: 10.1111/apt.14561]

25 **Nahar S**, Kibria KM, Hossain ME, Sultana J, Sarker SA, Engstrand L, Bardhan PK, Rahman M, Endtz HP. Evidence of intra-familial transmission of Helicobacter pylori by PCR-based RAPD fingerprinting in Bangladesh. *Eur J Clin Microbiol Infect Dis* 2009; **28**: 767-773 [PMID: 19190943 DOI: 10.1007/s10096-008-0699-8]

26 **Kivi M**, Johansson AL, Reilly M, Tindberg Y. Helicobacter pylori status in family members as risk factors for infection in children. *Epidemiol Infect* 2005; **133**: 645-652 [PMID: 16050509 DOI: 10.1017/s0950268805003900]

27 **National Bureau of Statistics of China**. China statistical Yearbook 2020. China Statistical Press, 2020

28 **Wang X**, Shu X, Li Q, Li Y, Chen Z, Wang Y, Pu K, Zheng Y, Ye Y, Liu M, Ma L, Zhang Z, Wu Z, Zhang F, Guo Q, Ji R, Zhou Y. Prevalence and risk factors of *Helicobacter pylori* infection in Wuwei, a high-risk area for gastric cancer in northwest China: An all-ages population-based cross-sectional study. *Helicobacter* 2021; **26**: e12810 [PMID: 33904635 DOI: 10.1111/hel.12810]

29 **Ding Z**, Zhao S, Gong S, Li Z, Mao M, Xu X, Zhou L. Prevalence and risk factors of Helicobacter pylori infection in asymptomatic Chinese children: a prospective, cross-sectional, population-based study. *Aliment Pharmacol Ther* 2015; **42**: 1019-1026 [PMID: 26271484 DOI: 10.1111/apt.13364]

30 **Ito LS**, Oba-Shinjo SM, Shinjo SK, Uno M, Marie SK, Hamajima N. Community-based familial study of Helicobacter pylori infection among healthy Japanese Brazilians. *Gastric Cancer* 2006; **9**: 208-216 [PMID: 16952040 DOI: 10.1007/s10120-006-0384-5]

31 **Nguyen TV**, Phan TT, Nguyen VB, Hoang TT, Le TL, Nguyen TT, Vu SN. Prevalence and risk factors of Helicobacter pylori infection in Muong children in Vietnam. *Ann Clin Lab Res* 2017; **5**: 1-9 [DOI: 10.21767/2386-5180.1000159]

32 **Garg PK**, Perry S, Sanchez L, Parsonnet J. Concordance of Helicobacter pylori infection among children in extended-family homes. *Epidemiol Infect* 2006; **134**: 450-459 [PMID: 16283949 DOI: 10.1017/S0950268805005352]

33 **Osaki T**, Konno M, Yonezawa H, Hojo F, Zaman C, Takahashi M, Fujiwara S, Kamiya S. Analysis of intra-familial transmission of Helicobacter pylori in Japanese families. *J Med Microbiol* 2015; **64**: 67-73 [PMID: 25351712 DOI: 10.1099/jmm.0.080507-0]

34 **Zhao JB**, Yuan L, Yu XC, Shao QQ, Ma J, Yu M, Wu Y, Qi YB, Hu RB, Wei PR, Jia BL, Zhang LZ, Zhang YR, Ding SZ. Whole family-based Helicobacter pylori eradication is a superior strategy to single-infected patient treatment approach: A systematic review and meta-analysis. *Helicobacter* 2021; **26**: e12793 [PMID: 33675089 DOI: 10.1111/hel.12793]

35 **Zhou G**. *Helicobacter pylori* Recurrence after Eradication Therapy in Jiangjin District, Chongqing, China. *Gastroenterol Res Pract* 2020; **2020**: 7510872 [PMID: 32328098 DOI: 10.1155/2020/7510872]

World Journal of Gastroenterology

Submit a Manuscript: https://www.f6publishing.com

World J Gastroenterol 2022 July 28; 28(28): 3720-3731

DOI: 10.3748/wjg.v28.i28.3720

ISSN 1007-9327 (print) ISSN 2219-2840 (online)

SCIENTOMETRICS

Global research on *Clostridium difficile*-associated diarrhoea: A visualized study

Sa'ed H Zyoud

Specialty type: Gastroenterology and hepatology

Provenance and peer review: Invited article; Externally peer reviewed.

Peer-review model: Single blind

Peer-review report's scientific quality classification

Grade A (Excellent): 0
Grade B (Very good): 0
Grade C (Good): C, C, C
Grade D (Fair): 0
Grade E (Poor): 0

P-Reviewer: Abdelkreem E, Egypt; He XX, China; Sintusek P, Thailand

Received: February 15, 2022
Peer-review started: February 16, 2022
First decision: March 9, 2022
Revised: March 12, 2022
Accepted: June 22, 2022
Article in press: June 22, 2022
Published online: July 28, 2022

Sa'ed H Zyoud, Department of Clinical and Community Pharmacy, College of Medicine and Health Sciences, An-Najah National University, Nablus 44839, Palestine

Sa'ed H Zyoud, Poison Control and Drug Information Center, College of Medicine and Health Sciences, An-Najah National University, Nablus 44839, Palestine

Sa'ed H Zyoud, Clinical Research Centre, An-Najah National University Hospital, Nablus 44839, Palestine

Corresponding author: Sa'ed H Zyoud, PhD, Associate Professor, Department of Clinical and Community Pharmacy, College of Medicine and Health Sciences, An-Najah National University, Academic Street, Nablus 44839, Palestine. saedzyoud@yahoo.com

Abstract

BACKGROUND

Clostridioides (Clostridium) difficile (*C. difficile*) is still the most common cause of healthcare-associated diarrhoea and is increasing in prevalence as a community-acquired infection. In addition, the emergence of antibiotic resistance in *C. difficile* can increase the likelihood of the disease developing and/or spreading.

AIM

To provide an up-to-date picture of the trends in publications related to *C. difficile* infection, together with specific insights into hot-button issues in this field.

METHODS

Publications on *C. difficile* infections in the field of microbiology between 2001 and 2020 were identified from the Scopus database and Reference Citation Analysis. Bibliometric indicators were determined, including the number and type of publications, countries, affiliations, funding agencies, journals and citation patterns. VOSviewer was used to determine research areas and hot-button issues by identifying recurring terms with a high relative occurrence in the title and abstract.

RESULTS

A total of 8127 documents on '*C. difficile*-associated diarrhoea' published between 2001 and 2020 were retrieved from the Scopus database. In the last decade, there has been a significant almost fourfold increase in the number of published papers on this topic. The United States was among the countries (44.11%) with the most publications, and the most involved institution was the *University of Leeds* in the

United Kingdom (2.50%). Three clusters of research were identified and included 'illness spectrum and severity, as well as the signs, symptoms and clinical pathogenesis of *C. difficile*'; 'laboratory diagnosis and characterization of *C. difficile*' and 'risk factors for *C. difficile* infection'.

CONCLUSION

This study contains the most up-to-date and comprehensive data ever compiled in this field. More international research and cross-institutional collaborations are needed to address more global *C. difficile* concerns and to benefit from greater sharing of expertise, which will result in higher quality or more effective studies in the future. Promising research avenues in the near future may draw the attention of relevant scientists and funding organizations and open up novel *C. difficile* infection–based diagnosis and treatment approaches.

Key Words: *Clostridioides*; *Clostridium difficile*; Bibliometric; Scopus; VOSviewer; Diarrhoea

©The Author(s) 2022. Published by Baishideng Publishing Group Inc. All rights reserved.

Core Tip: The significance of this study lies in the fact that, to our best knowledge, there are no previous bibliometric studies on *Clostridioides (Clostridium) difficile* (*C. difficile*) infection research. This study presents the evolution of *C. difficile* infection-related publications over time. This bibliometric study will provide clinicians and researchers in gastroenterology and microbiology with a quantitative and timely summary of *C. difficile* infection-related publications. Promising research avenues in the near future may draw the attention of relevant scientists and funding organizations and open up novel *C. difficile* infection–based diagnosis and treatment approaches.

Citation: Zyoud SH. Global research on *Clostridium difficile*-associated diarrhoea: A visualized study. *World J Gastroenterol* 2022; 28(28): 3720-3731
URL: https://www.wjgnet.com/1007-9327/full/v28/i28/3720.htm
DOI: https://dx.doi.org/10.3748/wjg.v28.i28.3720

INTRODUCTION

Clostridium difficile (*C. difficile*) has been reclassified as *Clostridioides difficile*, although the preferred term remains *C. difficile*. *C. difficile* infections are increasing in prevalence and are among the most common healthcare-associated illnesses globally[1-3]. *C. difficile* infections, also known as *C. difficile*-associated diarrhoea, are the most common signs of clinical infection and can range from mild diarrhoea to fulminant colitis[4]. *C. difficile* is frequently linked to the use of antibiotics. *C. difficile* was once thought to be predominantly a nosocomial illness; however, community-acquired *C. difficile* has already been identified[3].

Metronidazole and vancomycin have been the primary treatments for *C. difficile* infections for more than three decades. However, the low number of sustained cures and the rising incidence of *C. difficile* infections, as well as the accompanying morbidity and death, have necessitated the development and investigation of novel treatment approaches[1,5]. Despite ongoing attempts to enhance *C. difficile* prevention and treatment, *C. difficile* continues to be a major public health concern. In both hospitals and the community, *C. difficile* infection is still a prevalent and dangerous problem. In recent years, faecal microbial transplantation has been developed as a safe and successful method of treatment for recurrent infections[6-11]. Therefore, faecal microbial transplantation will most likely become the standard therapy for recurrent infection as a novel technique[6-11].

Bibliometrics and research performance assessments have been performed in a broad range of health areas[12,13], particularly to address environmental[14-17], and toxicological[18] issues. Yet, to our knowledge, a large number of bibliometric studies noticeably focused on microbiology[19-23] have been conducted by using different databases for data analysis. Because of these studies[19-23], microbiology research has recently been given increased scientific attention worldwide. Still, more research efforts are needed to thoroughly review and identify the existing literature related to *C. difficile* infection from different aspects, including authorships, country, affiliation, journals, citation patterns, and content analysis, to determine the research areas that are hot-button issues in this field.

C. difficile infection is considered one of the most debated topics in this era. Using the bibliometric approach to *C. difficile* infection would affect how scientists design and conduct studies and the selection of models that estimate risk. Using a bibliometric analysis of publications in Scopus, this study provides an up-to-date picture of the trends in publications related to *C. difficile* infection, together with specific insights into hot-button issues in this field. The significance of this study lies in the fact that, to our best

knowledge, there are no previous bibliometric studies on *C. difficile* infection research. Therefore, this study presents the evolution of *C. difficile* infection-related publications over time. This bibliometric study will provide clinicians and researchers in gastroenterology and microbiology with a quantitative and timely summary of *C. difficile* infection-related publications. Furthermore, it aims to provide clinicians and researchers with a resource for principles and current evidence. A detailed understanding of the historical trends in this field of research and its obstacles may help to establish a framework for future gastroenterology scholarship.

MATERIALS AND METHODS

Data acquisition

The research data were taken from the Scopus bibliographic database and Reference Citation Analysis (RCA) (https://www.referencecitationanalysis.com/). Scopus was chosen because it has a larger number of indexed journals than other databases (*e.g.* PubMed or Web of Science) and is completely inclusive of all journals in Medline[24-26]. Scopus is the most popular set of scientific publications used in bibliometric and scientometric studies, together with PubMed or Web of Science[27]. In addition, Scopus contains indexed journals in the health, social, physical and life sciences. This enhances the likelihood of retrieving as many relevant publications as is feasible. Baishideng Publishing Group Inc. owns RCA, which is an open transdisciplinary citation analysis database (Pleasanton, CA 94566, United States)[28].

Search strategy

To identify studies related to *C. difficile*-associated diarrhoea, we took the following steps.

Step 1: Data extraction was performed on July 25, 2021 and the results obtained within one day to avoid potential bias due to the regular updating of the database. The terms used in the search engines were applied in Title ((TITLE (Clostrid* difficile) OR TITLE('C. diff*') OR TITLE('Cl. diff*')))) AND Title/Abstract (TITLE-ABS(diarrh*) OR TITLE-ABS(Antibiotic) OR TITLE-ABS(infection) OR TITLE-ABS(AAD)). More precisely, in the results, the search strategy for research related to *Clostridium difficile* terms was limited to the title only to eliminate false-negative results. Search terms with different suffixes were truncated using an asterisk (*). The keywords used were chosen because they are commonly used in the literature related to *C. difficile*-associated diarrhoea[3,29-31].

Step 2: The year 2021 was omitted because the database records for this year would not have been completed at the time of the search.

Step 3: All retrieved documents were reviewed and analysed with respect to the following different bibliometric indicators, as in previous bibliometric studies[13,32-34]: (1) The annual number of publications on *C. difficile*-associated diarrhoea indexed in Scopus and published from 2001 to 2020; (2) Prolific countries, journals, and authors in this field in relation to the number of publications; (3) Research collaboration among the most productive countries; (4) The most frequently cited publications. It is likely that certain articles were cited more frequently than others due to the considerable period that had passed since their publication. Therefore, a citation index was generated for each article to overcome the bias caused by the period that had passed since publication. The citation index is derived by dividing the average number of citations by the number of years since the article was first published; (5) Hot-button issues in this field; and (6) RCA was used to determine the impact index *per* article for the top ten most-cited publications.

Step 4: A network visualization map based on the publications retrieved from the Scopus database was created using VOSviewer (version 1.6.16) software (www.vosviewer.com). The output results from VOSviewer are displayed in clusters. The existing connections between the bibliometric data can be clearly visualized to analyse collaboration between countries. Furthermore, it illustrated the terms widely used in the titles and abstracts of the publications collected, showing the hot research topics.

RESULTS

General description of the retrieved publications

A total of 8127 documents on '*C. difficile*-associated diarrhoea' published between 2001 and 2020 were retrieved from the Scopus database. From these publications, articles (n = 6062) were the most often published documents, comprising 74.59% of the total, followed by reviews (n = 1016; 12.50%) and letters (n = 384; 4.72%).

The trend of global publications

As shown in Figure 1, there was a growing trend in the number of publications on *C. difficile*-associated diarrhoea in the Scopus database between 2001 and 2020. It is obvious that there was an increasing number of publications mostly during two periods: From 2006 to 2013 and from 2014 to 2020. Since 2006, the number of relevant articles grew significantly, which is notable. Papers published during the last seven years (2014 to 2020) accounted for 60.16% of the total publications. As a result of these findings, the number of yearly publications grew progressively from 2014 to 2020, showing that the amount of research output increased steadily over that period.

Contributions by country

Table 1 shows that the United States was the most prolific country, whose authors published the most documents (n = 3585), followed by the United Kingdom (n = 1013), Canada (n = 556), and Germany (n = 434). The first 10 countries in Table 1 produced 89.84% of the documents published related to *C. difficile*-associated diarrhoea. Analysis of international collaboration was conducted on the downloaded data based on co-authorship relationships between countries (Figure 2).

Contributions by institution

The top 10 most productive institutes in terms of total papers are listed in Table 2. The major academic contributions mainly originated from *University of Leeds* (2.50%), *Leiden University Medical Center* (2.35%) and *Harvard Medical School* (2.25%).

Contributions by funding agency

Table 3 lists the top 10 global funding agencies that sponsored research output on *C. difficile*-associated diarrhoea. Among them, eight agencies were from the United States, and two were from the United Kingdom. The *National Institutes of Health* ranked first, supporting the highest number of studies at 884. The *U.S. Department of Health and Human Services* ranked second (n = 841), and the *National Institute of Allergy and Infectious Diseases* ranked third (n = 539).

Most active journals

The 10 most prolific journals are presented in Table 4. The most productive journal was *Infection Control and Hospital Epidemiology* (n = 304), followed by *Anaerobe* (n = 276), *Clinical Infectious Diseases* (n = 251) and *Journal of Hospital Infection* (n = 212). Thus, the first 10 journals in Table 4 produced 23.97% of the documents published related to *C. difficile*-associated diarrhoea.

Most cited documents

Table 5 presents the 10 most often cited articles published on *C. difficile*-associated diarrhoea[35-44]. Furthermore, the ten most cited articles have an impact index *per* article of 45.6 to 313.9 (Table 5).

Most frequent topics

We studied the distribution of co-occurrence terms using VOSviewer software (the minimum number of occurrences of a term in all publications is 100 times in titles and abstracts) to detect directions and topics in *C. difficile*-associated diarrhoea research and understand the growth of this discipline. The size of the circle or node of a term equals that particular term's number of occurrences. For example, in Figure 3, of the 84961 terms, 385 terms occurred at least 100 times, distributed in three clusters: Cluster 1, shown by green dots, includes those terms commonly found in studies related to clinical features of *C. difficile*, including the illness spectrum and severity, as well as the signs, symptoms and clinical pathogenesis of *C. difficile*. Cluster 2, shown by blue dots, includes those terms commonly found in laboratory diagnosis and characterization studies of *C. difficile*. Cluster 3, indicated by red dots, includes terms commonly found in studies related to risk factors for *C. difficile* infections. To investigate the changes in hotspots over time, a network visualization map of the most frequent terms in the titles/abstracts of the retrieved documents was generated using VOSviewer software, and the results revealed that the topic 'risk factors for *C. difficile* infection' began to appear more frequently in the last five years (Figure 4).

DISCUSSION

The current study was a descriptive study on global research output of publications related to *C. difficile* infection. It is important to examine the quantity and quality of research in this field, given the changing epidemiology of *C. difficile* morbidity and mortality, worldwide escalation of antibiotic resistance and limited alternative preventive strategies for *C. difficile* infection. This bibliometric analysis will aid in revealing key milestones and progressions in this field, detecting current shortages and developing trends and directing the field's future research path. The current study showed a fourfold increase in publications in the last decade. These results reflect those of Balsells *et al*[45] and Ofosu[46], who also

Table 1 Top 10 countries published *Clostridium difficile*-associated diarrhea between 2001 and 2020

Position	Country	No. of publication	%
1st	United States	3585	44.11
2nd	United Kingdom	1013	12.46
3rd	Canada	556	6.84
4th	Germany	434	5.34
5th	France	383	4.71
6th	China	315	3.88
7th	Netherlands	273	3.36
8th	Australia	261	3.21
9th	Italy	244	3.00
10th	Spain	238	2.93

Table 2 Ten most productive and influential institutions in *Clostridium difficile*-associated diarrhea between 2001 and 2020

Position	Institution	Country	No. of publication	%
1st	*University of Leeds*	United Kingdom	203	2.50
2nd	*Leiden University Medical Center-LUMC*	Netherlands	191	2.35
3rd	*Harvard Medical School*	United States	183	2.25
4th	*VA Medical Center*	United States	173	2.13
5th	*Leeds Teaching Hospitals NHS Trust*	United Kingdom	160	1.97
6th	*Beth Israel Deaconess Medical Center*	Israel	135	1.66
7th	*Washington University School of Medicine in St. Louis*	United States	118	1.45
8th	*Edward Hines Jr. VA Hospital*	United States	115	1.42
9th	*The University of Western Australia*	Australia	109	1.34
10th	*Baylor College of Medicine*	United States	108	1.33

Table 3 Top 10 related funding agencies in *Clostridium difficile*-associated diarrhea between 2001 and 2020

Position	Funding agencies	Country	No. of publication	%
1st	*National Institutes of Health*	United States	884	10.88
2nd	*U.S. Department of Health and Human Services*	United States	841	10.35
3rd	*National Institute of Allergy and Infectious Diseases*	United States	539	6.63
4th	*National Institute of Diabetes and Digestive and Kidney Diseases*	United States	239	2.94
5th	*Merck*	United States	171	2.10
6th	*National Center for Advancing Translational Sciences*	United States	154	1.89
7th	*Medical Research Council*	United Kingdom	150	1.85
8th	*National Institute of General Medical Sciences*	United States	146	1.80
9th	*Pfizer*	United States	137	1.69
10th	*United Kingdom Research and Innovation*	United Kingdom	132	1.62

stated that in recent years, there had been a growing understanding of the principle of *C. difficile* infection, the risk factors associated *with C. difficile* infection, the pathogenesis and clinical manifestation, prevention, diagnosis and *C. difficile* infection treatment, including new emerging therapies and faecal microbiota transplantation.

Table 4 Ten most productive and influential journals in *Clostridium difficile*-associated diarrhea between 2001 and 2020

Position	Journal	*n*	%	IF[1]
1st	*Infection Control and Hospital Epidemiology*	304	3.74	3.254
2nd	*Anaerobe*	276	3.4	3.331
3rd	*Clinical Infectious Diseases*	251	3.09	9.097
4th	*Journal of Hospital Infection*	212	2.61	3.926
5th	*Journal of Clinical Microbiology*	183	2.25	5.948
6th	*Plos One*	181	2.23	3.240
7th	*American Journal of Infection Control*	169	2.08	2.918
8th	*Antimicrobial Agents and Chemotherapy*	130	1.6	5.191
9th	*Journal of Antimicrobial Chemotherapy*	124	1.53	5.790
10th	*Clinical Microbiology and Infection*	117	1.44	8.067

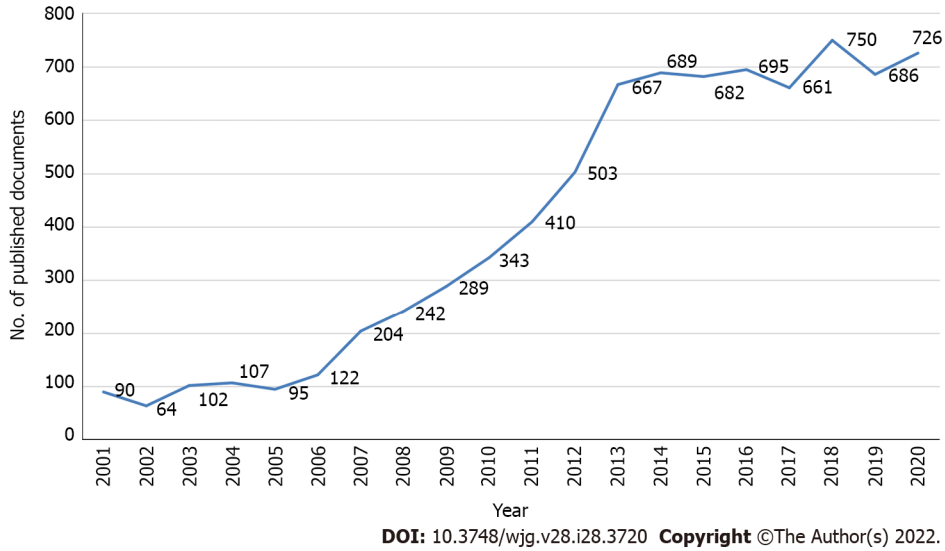
[1]Impact factor (IF) based on Journal Citation Reports (JCR) 2020 from Clarivate Analytics.

Table 5 Ten most cited publications and authors between 2001 and 2020 in in *Clostridium difficile*-associated diarrhea

Ref.	Title	Year	Source title	Cited by	Citation index	Impact index *per* article[1]
Cohen *et al* [35]	"Clinical practice guidelines for Clostridium difficile infection in adults: 2010 update by the Society for Healthcare Epidemiology of America (SHEA) and the Infectious Diseases Society of America (IDSA)"	2010	*Infection Control and Hospital Epidemiology*	2370	237.0	313.9
van Nood *et al*[42]	"Duodenal infusion of donor feces for recurrent clostridium difficile"	2013	*New England Journal of Medicine*	2140	305.7	241.3
Loo *et al*[37]	"A predominantly clonal multi-institutional outbreak of Clostridium difficile - Associated diarrhea with high morbidity and mortality"	2005	*New England Journal of Medicine*	1601	106.7	88.6
Lessa *et al* [44]	"Burden of Clostridium difficile infection in the United States"	2015	*New England Journal of Medicine*	1430	286.0	234.3
Surawicz *et al*[41]	"Guidelines for diagnosis, treatment, and prevention of clostridium difficile infections"	2013	*American Journal of Gastroenterology*	1087	155.3	116.8
Louie *et al* [38]	"Fidaxomicin versus vancomycin for Clostridium difficile infection"	2011	*New England Journal of Medicine*	1074	119.3	91.4
Kelly and LaMont[36]	"Clostridium difficile - More difficult than ever"	2008	*New England Journal of Medicine*	1019	84.9	68.1
Rupnik *et al* [40]	"Clostridium difficile infection: New developments in epidemiology and pathogenesis"	2009	*Nature Reviews Microbiology*	985	89.5	73.4
Zar *et al*[43]	"A comparison of vancomycin and metronidazole for the treatment of Clostridium difficile-associated diarrhea, stratified by disease severity"	2007	*Clinical Infectious Diseases*	935	71.9	58.9
Pépin *et al* [39]	"Clostridium difficile-associated diarrhea in a region of Quebec from 1991 to 2003: A changing pattern of disease severity"	2004	*CMAJ*	916	57.3	45.6

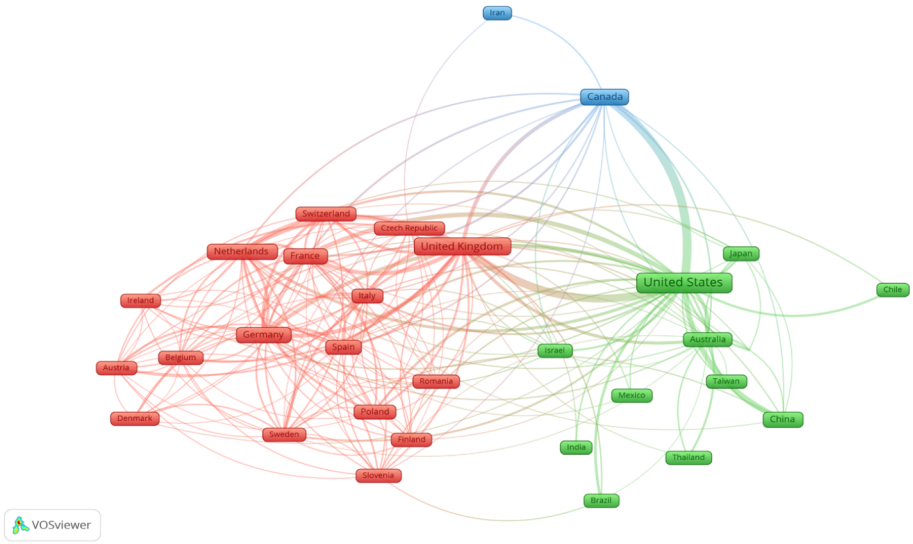
[1]The impact index *per* article is presented based on Reference Citation Analysis [Source: Baishideng Publishing Group Inc. (Pleasanton, CA 94566, United States)].

The United States was the leading country in *C. difficile* infection-related publications, contributing about half of all Scopus publications in this field. This is presumably due to economic prosperity and population growth, and the large number of microbiology researchers[47,48]. The economic basis plays an essential part in supporting scientific research in the current study. The majority of the top 10 funding agencies were based in the United States. High-income countries have published most *C. difficile* infection-related publications, with limited input from low- and middle-income countries. An analysis of the countries that generated the most *C. difficile* infection-related publications indicates that



DOI: 10.3748/wjg.v28.i28.3720 **Copyright** ©The Author(s) 2022.

Figure 1 Annual number of publications on *Clostridium difficile*-associated diarrhea indexed in Scopus and published from 2001 to 2020.



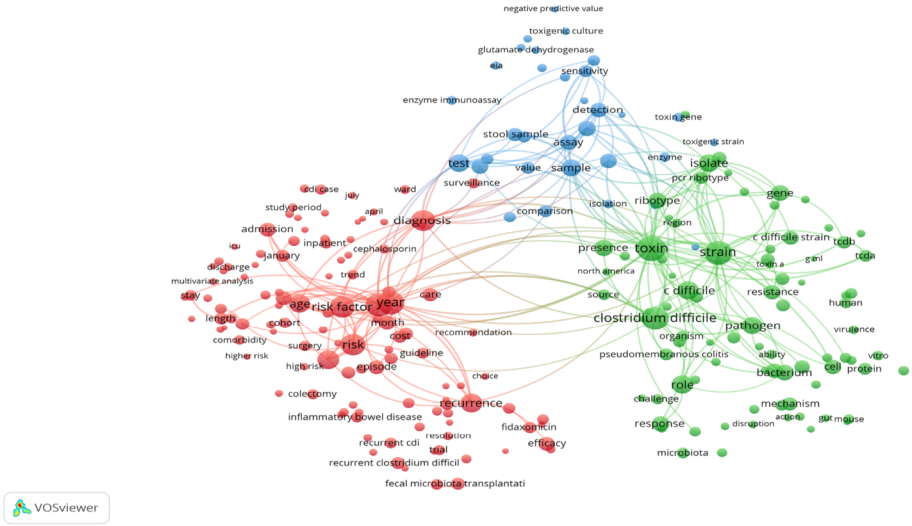
DOI: 10.3748/wjg.v28.i28.3720 **Copyright** ©The Author(s) 2022.

Figure 2 Network visualization map of country co-authorships. Of the 103 countries, 31 had at least 50 publications.

countries with economic power indicators have the greatest say in this field. This finding broadly supports the work of other studies in different areas linking scientific research output with geographical location and financial growth[12,49,50]. Various bibliometric analysis studies have also shown that the United States is the most prolific country in microbiology research output[19,20,23,51].

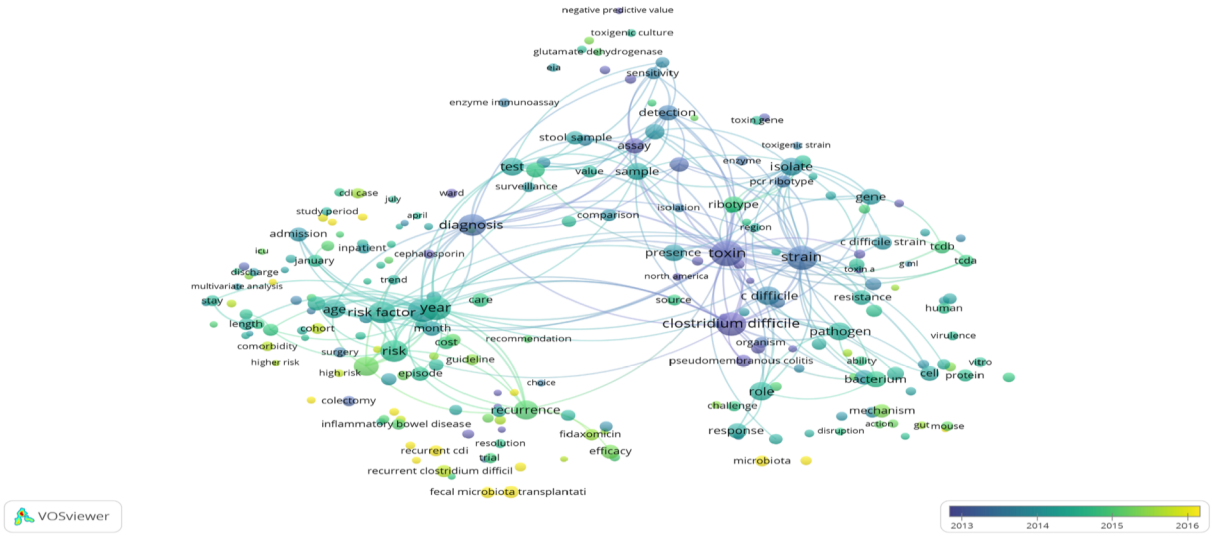
The current study showed that the most frequently cited article on *C. difficile*-associated diarrhoea, written by Cohen *et al*[35] and published in 2010, with 2370 citations, is a guideline that updates the recommendations for epidemiology, diagnostics, therapeutics, infection control, and environmental management. The second most frequently cited paper has 2140 citations and addresses the effect of duodenal infusion of donor faeces in patients with recurrent *C. difficile* infection; this article, published in 2013, was written by van Nood *et al*[42]. These two papers receive approximately 237 and 305.7 citations *per* year on average, respectively. However, the article with the second-highest number of citations *per* year, placed fourth in the ranking, was published in 2015 and was written by Lessa *et al* [44]. This paper aimed to produce more accurate national estimates the burden of illness, incidence, recurrence and death by collecting data from a variety of health care delivery and community contexts. Note that five papers published after 2010 appear in the top 10 most cited publications between 2001 and 2020 in *C. difficile*-associated diarrhoea.

Although it is challenging to reveal the quality or impact of publications through bibliometric analysis, to some degree, citations are considered an indirect measure of an article's contribution to the knowledge generated in the field, *i.e.* the connection between the research finding and its significance



DOI: 10.3748/wjg.v28.i28.3720 **Copyright** ©The Author(s) 2022.

Figure 3 Network visualization map of the most frequent terms in the titles/abstracts of the retrieved documents. Of the 84961 terms, 385 had at least 100 publications. Terms with the same color represent a separate cluster (research theme).



DOI: 10.3748/wjg.v28.i28.3720 **Copyright** ©The Author(s) 2022.

Figure 4 Overlay network visualization map of the most frequent terms in the titles/abstracts of the retrieved documents. The colors on the map reflected the period of emergence in the literature, with yellow representing terms that were relatively recent in the literature.

for science[52,53]. However, these analyses of the top 10 most cited publications will guide microbiologists interested in further studies by updating knowledge of current developments in *C. difficile* infection-related publications and potential future directions for study.

Analysis of the frequencies of occurrence of terms in publications can offer insights into certain fields' main and hot topics[54]. The current study found that highly cited literature focused on the signs, symptoms and clinical pathogenesis of *C. difficile* concepts and risk factors for *C. difficile* infections. A clear theme to emerge from the results is that the most frequently cited publications on *C. difficile* infections highlighted a range of subtopics similar to the hot research topics. A recent bibliometric study [55] was defined to assess global research activity on antimicrobial stewardship as one measure for efforts dedicated to containing antimicrobial resistance. This study found that *C. difficile* was frequently encountered as author keywords in the retrieved literature on antimicrobial stewardship. The United States Centers for Disease Control and Prevention has considered *C. difficile* infection an urgent danger in its 2019 Antibiotic Resistance Threats Report[56]. In a European point prevalence study, *C. difficile* was rated sixth among bacteria responsible for healthcare-associated illnesses[57]. The majority of *C. difficile* infections in the United States are considered hospital acquired[58].

Strengths and limitations

This study offered the first bibliometric analysis of *C. difficile* infections from the unique perspective of its research hotspots to determine the influential scientific areas and global trends. *C. difficile* infection-based publications in microbiology were collected in the online Scopus database and analysed comprehensively, thoroughly and objectively. As with all previous bibliometric studies[13,31,32,59], the current study has some limitations. First, we preferentially selected English articles from the database but lost some articles that were not in English. Second, we chose Scopus alone as the data source for *C. difficile* infection research because it presented the most reliable and credible information. Inevitably, any useful information from other medical sources such as PubMed and Web of Science would be overlooked. On the other hand, Scopus remains the best database available for analysing research activity and identifying research hotspots on a certain topic. Given these limitations, we believe that this study offers a qualified global view of *C. difficile* infection-based publications in the field of microbiology from 2001 to 2020.

CONCLUSION

The current study used a bibliometric analysis of *C. difficile* infection-based publications in the fields of microbiology and gastroenterology during the period 2001–2020 to determine research hotspots for possible future directions. The results showed that *C. difficile*-based publications have grown rapidly since 2006. Research activity on *C. difficile* infections has been an emerging topic during the last two decades and has been developed predominantly by scientists from the United States of America, the United Kingdom, Canada, Germany, France and China. Risk factors for *C. difficile* infection, laboratory diagnosis and characterization of *C. difficile*, signs, symptoms and clinical pathogenesis of *C. difficile* concepts were the main research hotspots in *C. difficile* infection, and related studies should pioneer these fields in the future. Promising research avenues in the near future may draw the attention of relevant scientists and funding organizations and open up novel *C. difficile* infection–based diagnosis and treatment approaches.

ARTICLE HIGHLIGHTS

Research background

Clostridioides (Clostridium) difficile (*C. difficile*) infections are growing more prevalent and are now one of the most often encountered healthcare-associated infections worldwide.

Research motivation

To our best knowledge, however, a large number of bibliometric studies notably focused on microbiology have been undertaken by using various databases for data analysis. More research efforts are still required to thoroughly analyse and identify the existing literature related to *C. difficile* infection from many perspectives in order to identify study area hot issues in this field.

Research objectives

This study gives an up-to-date picture of the trends in publications linked to *C. difficile* infection, as well as unique insights into hot topics in this field.

Research methods

This study was based on a bibliometric analysis of Scopus and Reference Citation Analysis publications.

Research results

Three clusters of research were highlighted as hot topics: 'illness spectrum and severity, as well as signs, symptoms and clinical pathogenesis of *C. difficile*'; 'laboratory diagnosis and characterization of *C. difficile*' and 'risk factors for *C. difficile* infection'.

Research conclusions

The current study conducted a bibliometric analysis of *C. difficile*-related publications in the disciplines of microbiology and gastroenterology from 2001 to 2020 to identify research hotspots for potential future directions. Results revealed that the topic 'risk factors for *C. difficile* infection' began to appear more frequently in the last five years.

Research perspectives

This bibliometric study will provide clinicians and researchers in gastroenterology and microbiology with a quantitative and timely summary of publications linked to *C. difficile* infection. It also intends to

be a resource for clinicians and researchers on principles and current evidence.

FOOTNOTES

Author contributions: Zyoud S developed the concept for the manuscript, reviewed the literature, formulated research questions, collected the data, conducted analyses and interpreted the data, and wrote the manuscript, the author read and approved the final manuscript.

Conflict-of-interest statement: All the authors report no relevant conflicts of interest for this article.

PRISMA 2009 Checklist statement: The author has read the PRISMA 2009 Checklist, and the manuscript was prepared and revised according to the PRISMA 2009 Checklist.

Open-Access: This article is an open-access article that was selected by an in-house editor and fully peer-reviewed by external reviewers. It is distributed in accordance with the Creative Commons Attribution NonCommercial (CC BY-NC 4.0) license, which permits others to distribute, remix, adapt, build upon this work non-commercially, and license their derivative works on different terms, provided the original work is properly cited and the use is non-commercial. See: https://creativecommons.org/Licenses/by-nc/4.0/

Country/Territory of origin: Palestine

ORCID number: Sa'ed H Zyoud 0000-0002-7369-2058.

S-Editor: Fan JR
L-Editor: A
P-Editor: Fan JR

REFERENCES

1 **Beinortas T**, Burr NE, Wilcox MH, Subramanian V. Comparative efficacy of treatments for Clostridium difficile infection: a systematic review and network meta-analysis. *Lancet Infect Dis* 2018; **18**: 1035-1044 [PMID: 30025913 DOI: 10.1016/S1473-3099(18)30285-8]
2 **Burke KE**, Lamont JT. Clostridium difficile infection: a worldwide disease. *Gut Liver* 2014; **8**: 1-6 [PMID: 24516694 DOI: 10.5009/gnl.2014.8.1.1]
3 **Curcio D**, Cané A, Fernández FA, Correa J. Clostridium difficile-associated Diarrhea in Developing Countries: A Systematic Review and Meta-Analysis. *Infect Dis Ther* 2019; **8**: 87-103 [PMID: 30659481 DOI: 10.1007/s40121-019-0231-8]
4 **Leffler DA**, Lamont JT. Clostridium difficile infection. *N Engl J Med* 2015; **372**: 1539-1548 [PMID: 25875259 DOI: 10.1056/NEJMra1403772]
5 **DuPont HL**. Search for the optimal antimicrobial therapy of Clostridium difficile infection. *Lancet Infect Dis* 2018; **18**: 936-937 [PMID: 30025912 DOI: 10.1016/S1473-3099(18)30308-6]
6 **Haifer C**, Paramsothy S, Borody TJ, Clancy A, Leong RW, Kaakoush NO. Long-Term Bacterial and Fungal Dynamics following Oral Lyophilized Fecal Microbiota Transplantation in Clostridioides difficile Infection. *mSystems* 2021; **6** [PMID: 33531405 DOI: 10.1128/mSystems.00905-20]
7 **Hourigan SK**, Nicholson MR, Kahn SA, Kellermayer R. Updates and Challenges in Fecal Microbiota Transplantation for Clostridioides difficile Infection in Children. *J Pediatr Gastroenterol Nutr* 2021; **73**: 430-432 [PMID: 34238831 DOI: 10.1097/MPG.0000000000003229]
8 **Khoruts A**, Staley C, Sadowsky MJ. Faecal microbiota transplantation for Clostridioides difficile: mechanisms and pharmacology. *Nat Rev Gastroenterol Hepatol* 2021; **18**: 67-80 [PMID: 32843743 DOI: 10.1038/s41575-020-0350-4]
9 **Li Y**, Honda K. Toward the development of defined microbial therapeutics. *Int Immunol* 2021; **33**: 761-766 [PMID: 34232990 DOI: 10.1093/intimm/dxab038]
10 **D Goldenberg S**, Merrick B. The role of faecal microbiota transplantation: looking beyond *Clostridioides difficile* infection. *Ther Adv Infect Dis* 2021; **8**: 2049936120981526 [PMID: 33614028 DOI: 10.1177/2049936120981526]
11 **Sehgal K**, Khanna S. Gut microbiome and *Clostridioides difficile* infection: a closer look at the microscopic interface. *Therap Adv Gastroenterol* 2021; **14**: 1756284821994736 [PMID: 33747125 DOI: 10.1177/1756284821994736]
12 **Liu H**, Chen H, Hong R, Liu H, You W. Mapping knowledge structure and research trends of emergency evacuation studies. *Safety Sci* 2020; **121**: 348-361 [DOI: 10.1016/j.ssci.2019.09.020]
13 **Al-Jabi SW**. Arab world's growing contribution to global leishmaniasis research (1998-2017): a bibliometric study. *BMC Public Health* 2019; **19**: 625 [PMID: 31118003 DOI: 10.1186/s12889-019-6969-9]
14 **Briganti M**, Delnevo CD, Brown L, Hastings SE, Steinberg MB. Bibliometric Analysis of Electronic Cigarette Publications: 2003-2018. *Int J Environ Res Public Health* 2019; **16**: E320 [DOI: 10.3390/ijerph16030320]
15 **Olisah C**, Okoh OO, Okoh AI. Global evolution of organochlorine pesticides research in biological and environmental matrices from 1992 to 2018: A bibliometric approach. *Emerg Contam* 2019; **5**: 157-167 [DOI: 10.1016/j.emcon.2019.05.001]
16 **Yang B**, Huang K, Sun D, Zhang Y. Mapping the scientific research on non-point source pollution: a bibliometric analysis.

Environ Sci Pollut Res Int 2017; **24**: 4352-4366 [PMID: 27928755 DOI: 10.1007/s11356-016-8130-y]
17 **Zheng T**, Li P, Shi Z, Liu J. Benchmarking the scientific research on wastewater-energy nexus by using bibliometric analysis. *Environ Sci Pollut Res Int* 2017; **24**: 27613-27630 [PMID: 29134520 DOI: 10.1007/s11356-017-0696-5]
18 **Zyoud SH**, Waring WS, Al-Jabi SW, Sweileh WM, Rahhal B, Awang R. Intravenous Lipid Emulsion as an Antidote for the Treatment of Acute Poisoning: A Bibliometric Analysis of Human and Animal Studies. *Basic Clin Pharmacol Toxicol* 2016; **119**: 512-519 [PMID: 27098056 DOI: 10.1111/bcpt.12609]
19 **Sweileh WM**. Global research activity on antimicrobial resistance in food-producing animals. *Arch Public Health* 2021; **79**: 49 [PMID: 33849636 DOI: 10.1186/s13690-021-00572-w]
20 **Ahmad T**, Haroon, Khan M, Murad MA, Baig M, Murtaza BN, Khan MM, Harapan H, Hui J. Research trends in rabies vaccine in the last three decades: a bibliometric analysis of global perspective. *Hum Vaccin Immunother* 2021; **17**: 3169-3177 [PMID: 33945433 DOI: 10.1080/21645515.2021.1910000]
21 **Dehghanbanadaki H**, Aazami H, Keshavarz Azizi Raftar S, Ashrafian F, Ejtahed HS, Hashemi E, Hoseini Tavassol Z, Ahmadi Badi S, Siadat SD. Global scientific output trend for Akkermansia muciniphila research: a bibliometric and scientometric analysis. *BMC Med Inform Decis Mak* 2020; **20**: 291 [PMID: 33167984 DOI: 10.1186/s12911-020-01312-w]
22 **Zhong H**, Chen F, Li YJ, Zhao XY, Zhang ZL, Gu ZC, Yu YT. Global trends and hotspots in research of carbapenem-resistant Enterobacteriaceae (CRE): a bibliometric analysis from 2010 to 2020. *Ann Palliat Med* 2021; **10**: 6079-6091 [PMID: 34237952 DOI: 10.21037/apm-21-87]
23 **Zhu Y**, Li JJ, Reng J, Wang S, Zhang R, Wang B. Global trends of Pseudomonas aeruginosa biofilm research in the past two decades: A bibliometric study. *Microbiologyopen* 2020; **9**: 1102-1112 [PMID: 32120451 DOI: 10.1002/mbo3.1021]
24 **Falagas ME**, Pitsouni EI, Malietzis GA, Pappas G. Comparison of PubMed, Scopus, Web of Science, and Google Scholar: strengths and weaknesses. *FASEB J* 2008; **22**: 338-342 [PMID: 17884971 DOI: 10.1096/fj.07-9492LSF]
25 **Kokol P**, Vošner HB. Discrepancies among Scopus, Web of Science, and PubMed coverage of funding information in medical journal articles. *J Med Libr Assoc* 2018; **106**: 81-86 [PMID: 29339937 DOI: 10.5195/jmla.2018.181]
26 **Barqawi A**, Abushamma FA, Akkawi M, Al-Jabi SW, Shahwan MJ, Jairoun AA, Zyoud SH. Global trends in research related to sleeve gastrectomy: A bibliometric and visualized study. *World J Gastrointest Surg* 2021; **13**: 1509-1522 [PMID: 34950437 DOI: 10.4240/wjgs.v13.i11.1509]
27 **Mongeon P**, Paul-Hus A. The journal coverage of Web of Science and Scopus: a comparative analysis. *Scientometrics* 2016; **106**: 213-228 [DOI: 10.1007/s11192-015-1765-5]
28 **Baishideng Publishing Group Inc**. Reference Citation Analysis. 2022. [cited 10 June 2022]. Available from: https://www.referencecitationanalysis.com/
29 **Nasiri MJ**, Goudarzi M, Hajikhani B, Ghazi M, Goudarzi H, Pouriran R. Clostridioides (Clostridium) difficile infection in hospitalized patients with antibiotic-associated diarrhea: A systematic review and meta-analysis. *Anaerobe* 2018; **50**: 32-37 [PMID: 29408016 DOI: 10.1016/j.anaerobe.2018.01.011]
30 **Lau CS**, Chamberlain RS. Probiotics are effective at preventing Clostridium difficile-associated diarrhea: a systematic review and meta-analysis. *Int J Gen Med* 2016; **9**: 27-37 [PMID: 26955289 DOI: 10.2147/IJGM.S98280]
31 **Sholeh M**, Krutova M, Forouzesh M, Mironov S, Sadeghifard N, Molaeipour L, Maleki A, Kouhsari E. Antimicrobial resistance in Clostridioides (Clostridium) difficile derived from humans: a systematic review and meta-analysis. *Antimicrob Resist Infect Control* 2020; **9**: 158 [PMID: 32977835 DOI: 10.1186/s13756-020-00815-5]
32 **Al-Jabi SW**. Global Trends in Aspirin Resistance-Related Research from 1990 to 2015: A Bibliometric Analysis. *Basic Clin Pharmacol Toxicol* 2017; **121**: 512-519 [PMID: 28667787 DOI: 10.1111/bcpt.12840]
33 **Al-Jabi SW**. Global research trends in West Nile virus from 1943 to 2016: a bibliometric analysis. *Global Health* 2017; **13**: 55 [PMID: 28774315 DOI: 10.1186/s12992-017-0284-y]
34 **Zyoud SH**, Smale S, Waring WS, Sweileh WM, Al-Jabi SW. Global research trends in microbiome-gut-brain axis during 2009-2018: a bibliometric and visualized study. *BMC Gastroenterol* 2019; **19**: 158 [PMID: 31470803 DOI: 10.1186/s12876-019-1076-z]
35 **Cohen SH**, Gerding DN, Johnson S, Kelly CP, Loo VG, McDonald LC, Pepin J, Wilcox MH; Society for Healthcare Epidemiology of America; Infectious Diseases Society of America. Clinical practice guidelines for Clostridium difficile infection in adults: 2010 update by the society for healthcare epidemiology of America (SHEA) and the infectious diseases society of America (IDSA). *Infect Control Hosp Epidemiol* 2010; **31**: 431-455 [PMID: 20307191 DOI: 10.1086/651706]
36 **Kelly CP**, LaMont JT. Clostridium difficile--more difficult than ever. *N Engl J Med* 2008; **359**: 1932-1940 [PMID: 18971494 DOI: 10.1056/NEJMra0707500]
37 **Loo VG**, Poirier L, Miller MA, Oughton M, Libman MD, Michaud S, Bourgault AM, Nguyen T, Frenette C, Kelly M, Vibien A, Brassard P, Fenn S, Dewar K, Hudson TJ, Horn R, René P, Monczak Y, Dascal A. A predominantly clonal multi-institutional outbreak of Clostridium difficile-associated diarrhea with high morbidity and mortality. *N Engl J Med* 2005; **353**: 2442-2449 [PMID: 16322602 DOI: 10.1056/NEJMoa051639]
38 **Louie TJ**, Miller MA, Mullane KM, Weiss K, Lentnek A, Golan Y, Gorbach S, Sears P, Shue YK; OPT-80-003 Clinical Study Group. Fidaxomicin *vs* vancomycin for Clostridium difficile infection. *N Engl J Med* 2011; **364**: 422-431 [PMID: 21288078 DOI: 10.1056/NEJMoa0910812]
39 **Pépin J**, Valiquette L, Alary ME, Villemure P, Pelletier A, Forget K, Pépin K, Chouinard D. Clostridium difficile-associated diarrhea in a region of Quebec from 1991 to 2003: a changing pattern of disease severity. *CMAJ* 2004; **171**: 466-472 [PMID: 15337727 DOI: 10.1503/cmaj.1041104]
40 **Rupnik M**, Wilcox MH, Gerding DN. Clostridium difficile infection: new developments in epidemiology and pathogenesis. *Nat Rev Microbiol* 2009; **7**: 526-536 [PMID: 19528959 DOI: 10.1038/nrmicro2164]
41 **Surawicz CM**, Brandt LJ, Binion DG, Ananthakrishnan AN, Curry SR, Gilligan PH, McFarland LV, Mellow M, Zuckerbraun BS. Guidelines for diagnosis, treatment, and prevention of Clostridium difficile infections. *Am J Gastroenterol* 2013; **108**: 478-98; quiz 499 [PMID: 23439232 DOI: 10.1038/ajg.2013.4]
42 **van Nood E**, Vrieze A, Nieuwdorp M, Fuentes S, Zoetendal EG, de Vos WM, Visser CE, Kuijper EJ, Bartelsman JF, Tijssen JG, Speelman P, Dijkgraaf MG, Keller JJ. Duodenal infusion of donor feces for recurrent Clostridium difficile. *N*

Engl J Med 2013; **368**: 407-415 [PMID: 23323867 DOI: 10.1056/NEJMoa1205037]

43 **Zar FA**, Bakkanagari SR, Moorthi KM, Davis MB. A comparison of vancomycin and metronidazole for the treatment of Clostridium difficile-associated diarrhea, stratified by disease severity. *Clin Infect Dis* 2007; **45**: 302-307 [PMID: 17599306 DOI: 10.1086/519265]

44 **Lessa FC**, Mu Y, Bamberg WM, Beldavs ZG, Dumyati GK, Dunn JR, Farley MM, Holzbauer SM, Meek JI, Phipps EC, Wilson LE, Winston LG, Cohen JA, Limbago BM, Fridkin SK, Gerding DN, McDonald LC. Burden of Clostridium difficile infection in the United States. *N Engl J Med* 2015; **372**: 825-834 [PMID: 25714160 DOI: 10.1056/NEJMoa1408913]

45 **Balsells E**, Shi T, Leese C, Lyell I, Burrows J, Wiuff C, Campbell H, Kyaw MH, Nair H. Global burden of *Clostridium difficile* infections: a systematic review and meta-analysis. *J Glob Health* 2019; **9**: 010407 [PMID: 30603078 DOI: 10.7189/jogh.09.010407]

46 **Ofosu A**. Clostridium difficile infection: a review of current and emerging therapies. *Ann Gastroenterol* 2016; **29**: 147-154 [PMID: 27065726 DOI: 10.20524/aog.2016.0006]

47 **Elsevier**. Gender in the Global Research Landscape: Analysis of Research Performance Through a Gender Lens Across 20 Years, 12 Geographies, and 27 Subject Ares. Amsterdam, the Netherlands: Elsevier B.V, 2017

48 **Dehdarirad T**, Sotudeh H, Freer J. Bibliometric mapping of microbiology research topics (2012-16): a comparison by socioeconomic development and infectious disease vulnerability values. *FEMS Microbiol Lett* 2019; **366** [PMID: 30629167 DOI: 10.1093/femsle/fnz004]

49 **Demir E**, Yaşar E, Özkoçak V, Yıldırım E. The evolution of the field of legal medicine: A holistic investigation of global outputs with bibliometric analysis. *J Forensic Leg Med* 2020; **69**: 101885 [PMID: 31733463 DOI: 10.1016/j.jflm.2019.101885]

50 **Clarke A**, Gatineau M, Grimaud O, Royer-Devaux S, Wyn-Roberts N, Le Bis I, Lewison G. A bibliometric overview of public health research in Europe. *Eur J Public Health* 2007; **17** Suppl 1: 43-49 [PMID: 17666422 DOI: 10.1093/eurpub/ckm063]

51 **Akintunde TY**, Musa TH, Musa HH, Chen S, Ibrahim E, Muhideen S, Kawuki J. Mapping the global research output on Ebola vaccine from research indexed in web of science and scopus: a comprehensive bibliometric analysis. *Hum Vaccin Immunother* 2021; **17**: 4246-4258 [PMID: 34270380 DOI: 10.1080/21645515.2021.1948785]

52 **Durieux V**, Gevenois PA. Bibliometric indicators: quality measurements of scientific publication. *Radiology* 2010; **255**: 342-351 [PMID: 20413749 DOI: 10.1148/radiol.09090626]

53 **Joshi MA**. Bibliometric indicators for evaluating the quality of scientifc publications. *J Contemp Dent Pract* 2014; **15**: 258-262 [PMID: 25095854 DOI: 10.5005/jp-journals-10024-1525]

54 **van Eck NJ**, Waltman L. Software survey: VOSviewer, a computer program for bibliometric mapping. *Scientometrics* 2010; **84**: 523-538 [PMID: 20585380 DOI: 10.1007/s11192-009-0146-3]

55 **Sweileh WM**. Bibliometric analysis of peer-reviewed literature on antimicrobial stewardship from 1990 to 2019. *Global Health* 2021; **17**: 1 [PMID: 33397377 DOI: 10.1186/s12992-020-00651-7]

56 **Centers for Disease Control and Prevention**. Antibiotic/Antimicrobial Resistance (AR/AMR). 2020. [cited 9 August 2021]. Available from: https://www.cdc.gov/DrugResistance/biggest-threats.html

57 **Suetens C**, Latour K, Kärki T, Ricchizzi E, Kinross P, Moro ML, Jans B, Hopkins S, Hansen S, Lyytikäinen O, Reilly J, Deptula A, Zingg W, Plachouras D, Monnet DL; The Healthcare-Associated Infections Prevalence Study Group. Prevalence of healthcare-associated infections, estimated incidence and composite antimicrobial resistance index in acute care hospitals and long-term care facilities: results from two European point prevalence surveys, 2016 to 2017. *Euro Surveill* 2018; **23** [PMID: 30458912 DOI: 10.2807/1560-7917.ES.2018.23.46.1800516]

58 **Lessa FC**, Winston LG, McDonald LC; Emerging Infections Program C. difficile Surveillance Team. Burden of Clostridium difficile infection in the United States. *N Engl J Med* 2015; **372**: 2369-2370 [PMID: 26061850 DOI: 10.1056/NEJMc1505190]

59 **Al-Jabi SW**. Current global research landscape on COVID-19 and depressive disorders: Bibliometric and visualization analysis. *World J Psychiatry* 2021; **11**: 253-264 [PMID: 34168972 DOI: 10.5498/wjp.v11.i6.253]

World Journal of Gastroenterology

Submit a Manuscript: https://www.f6publishing.com

World J Gastroenterol 2022 July 28; 28(28): 3732-3738

DOI: 10.3748/wjg.v28.i28.3732

ISSN 1007-9327 (print) ISSN 2219-2840 (online)

CASE REPORT

Delayed immune-related sclerosing cholangitis after discontinuation of pembrolizumab: A case report

Takeshi Tanaka, Arata Sakai, Masahiro Tsujimae, Yasutaka Yamada, Takashi Kobayashi, Atsuhiro Masuda, Yuzo Kodama

Specialty type: Gastroenterology and hepatology

Provenance and peer review: Unsolicited article; Externally peer reviewed.

Peer-review model: Single blind

Peer-review report's scientific quality classification

Grade A (Excellent): 0
Grade B (Very good): B, B
Grade C (Good): 0
Grade D (Fair): 0
Grade E (Poor): 0

P-Reviewer: Chen YH, China; Martin M

Received: April 7, 2022
Peer-review started: April 7, 2022
First decision: May 9, 2022
Revised: May 21, 2022
Accepted: June 30, 2022
Article in press: June 30, 2022
Published online: July 28, 2022

Takeshi Tanaka, Arata Sakai, Masahiro Tsujimae, Yasutaka Yamada, Takashi Kobayashi, Atsuhiro Masuda, Yuzo Kodama, Division of Gastroenterology, Department of Internal Medicine, Kobe University Graduate School of Medicine, Kobe 650-0017, Hyogo, Japan

Corresponding author: Arata Sakai, PhD, Doctor, Division of Gastroenterology, Department of Internal Medicine, Kobe University Graduate School of Medicine, 7-5-1 Kusunoki-cho, Chuo-ku, Kobe 650-0017, Hyogo, Japan. asakai@med.kobe-u.ac.jp

Abstract

BACKGROUND

Secondary sclerosing cholangitis, characterized by biliary obstruction, can be caused by drugs such as immune checkpoint inhibitors (ICIs). While there a few reports of sclerosing cholangitis after immune checkpoint inhibitor administration, no case has been reported after discontinuation of such drugs.

CASE SUMMARY

A 68-year-old man who underwent chemotherapy for lung adenocarcinoma with bone metastasis presented with abdominal pain and fever 4 mo after the final administration of pembrolizumab. Computed tomography revealed thickening of the gallbladder wall and dilatation of the common bile duct. Endoscopic retrograde cholangiopancreatography revealed an irregularly narrowed intrahepatic bile duct. Biopsy of the bile duct demonstrated that $CD8^+$ T cells were predominant over $CD4^+$T cells. Liver biopsy showed dominant infiltration of $CD8^+$T in the portal tract, but onion-skin lesions were not observed. The patient was diagnosed with immune-related sclerosing cholangitis induced by pembrolizumab. Administration of methylprednisolone and endoscopic nasobiliary drainage were performed, but the cholangiography and laboratory test findings did not improve. No further treatment was administered due to disease progression, and the patient was referred for palliative care.

CONCLUSION

Immune-related sclerosing cholangitis may have a late onset, and such cases occurring after discontinuation of ICIs should be carefully managed.

Key Words: Immune-related adverse events; Sclerosing cholangitis; Delayed immune-related events; Case report

©The Author(s) 2022. Published by Baishideng Publishing Group Inc. All rights reserved.

Core Tip: Immune checkpoint inhibitors have become a new standard in cancer treatment, but have often been reported to induce adverse events, called immune-related adverse events (irAEs). Biliary system complications, such as irAEs, remain rare, and the management strategy remains unclear. We present herein, a rare case of delayed immune-related sclerosing cholangitis (SC) after discontinuation of pembrolizumab. Our case emphasizes that immune-related SC can occur later, but the mechanisms have not yet been elucidated. As such, our case contributes to new knowledge in the hopes of being able to establish proper diagnostic criteria and management strategies for similar patients.

Citation: Tanaka T, Sakai A, Tsujimae M, Yamada Y, Kobayashi T, Masuda A, Kodama Y. Delayed immune-related sclerosing cholangitis after discontinuation of pembrolizumab: A case report. *World J Gastroenterol* 2022; 28(28): 3732-3738
URL: https://www.wjgnet.com/1007-9327/full/v28/i28/3732.htm
DOI: https://dx.doi.org/10.3748/wjg.v28.i28.3732

INTRODUCTION

Secondary sclerosing cholangitis (SC) is a chronic disease characterized by biliary obstruction and can be caused by a variety of specific etiologies such as infections, immune-related factors, toxicity, obstruction, ischemic injury, or drugs, including immune checkpoint inhibitors (ICIs)[1]. ICIs have transformed the treatment landscape for patients with many advanced malignancies but have often been reported to induce adverse events, called immune-related adverse events (irAEs)[2]. The irAEs differ from toxicities caused by cytotoxic or molecularly targeted agents, and the time to toxicity may be delayed and not follow a cyclical pattern, as observed with conventional cytotoxic agents[3]. Biliary system complications, such as irAEs, remain rare, and the management strategy remains unclear. There are a few reports of SC induced by ICIs; however, no cases developed immune-related SC after discontinuation of ICIs. Herein, we report a case of delayed immune-related SC caused by pembrolizumab.

CASE PRESENTATION

Chief complaints

A 68-year-old male patient was admitted to our hospital with abdominal pain and fever.

Imaging examinations

Contrast-enhanced computed tomography and endoscopic ultrasonography revealed swelling and wall thickening of the gallbladder and dilatation of the common bile duct without obstruction (Figure 1A-D). Endoscopic retrograde cholangiopancreatography revealed a dilated common bile duct and irregularly narrowed right intrahepatic bile duct (Figure 1E). Intraductal ultrasonography demonstrated diffuse wall thickening from the right bile duct to the common bile duct (Figure 1F).

Laboratory examinations

Laboratory tests revealed increased levels of white blood cells [10100/μL (3300-8600/μL)], C-reactive protein [4.88 mg/dL (0.00-0.18 mg/dL)], aspartate transaminase [31 U/L (13–30 U/L)], alanine transaminase (ALT) [50 U/L (7–23 U/L)], gamma-glutamyl transpeptidase [205 U/L (13-64 U/L)], and alkaline phosphatase (ALP) [996 U/L (38-113 U/L)]. Total bilirubin was within the normal range [0.7 mg/dL (0.4-1.5 mg/dL)], and blood cultures showed no bacterial infection. The serum immunological markers, including antinuclear antibody, antimitochondrial antibody, and anti-smooth muscle antibody were negative, and the immunoglobulin G4 Level (59 mg/dL) was within the normal range.

Physical examination

The patient's body temperature was 38.9 °C, but the other vital signs were stable. Regarding the pulmonary and cardiac examination, no obvious abnormality was observed. Physical examination revealed epigastric tenderness without rebound tenderness or Murphy's sign. No jaundice or palpable masses were observed.



DOI: 10.3748/wjg.v28.i28.3732 **Copyright** ©The Author(s) 2022.

Figure 1 Imaging examinations of the gallbladder and common bile duct. A, B: Contrast-enhanced computed tomography shows swelling and wall thickness of the gallbladder and common bile duct; C, D: Endoscopic ultrasonography shows dilatation of the common bile duct without obstruction and wall thickness of the gallbladder; E: Endoscopic retrograde cholangiopancreatography shows a dilated common bile duct and irregularly narrowed right intrahepatic bile duct (white arrow); F: Intraductal ultrasonography shows the wall thickness from the right bile duct to the common bile duct (white arrowhead).

Personal and family history

No information was available regarding his family history.

History of past illness

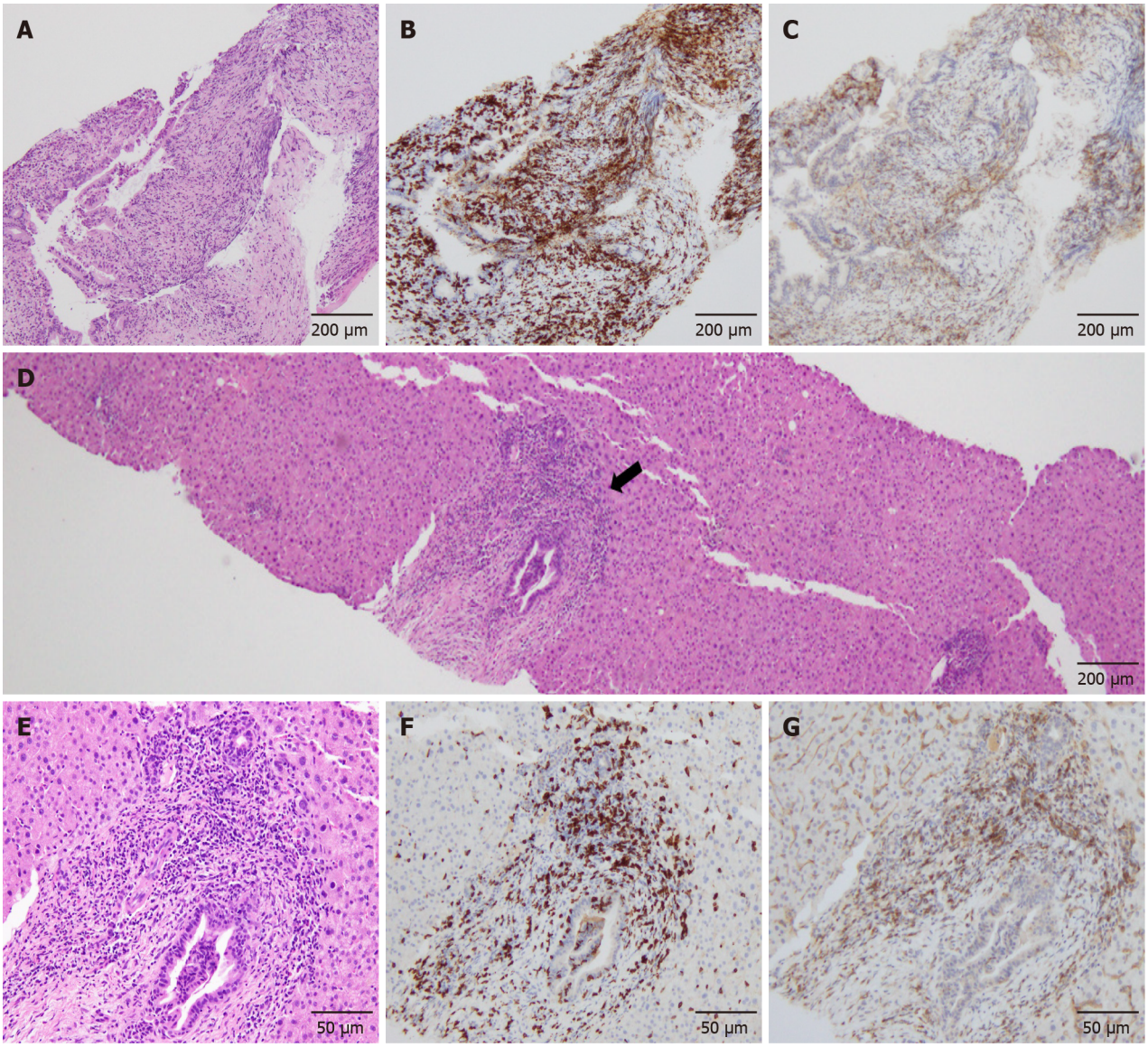
The patient has laparoscopic inguinal hernia repair twenty years ago.

History of present illness

The patient was diagnosed with stage IV lung adenocarcinoma (wild-type epidermal growth factor receptor and anaplastic lymphoma kinase, programmed death ligand 1 positive expression) and received first-line treatment with cisplatin and pemetrexed sodium hydrate. Four months after the initiation of first-line chemotherapy, the patient received second-line treatment with pembrolizumab because of disease progression. Three months later (three cycles of pembrolizumab), carboplatin and nab-paclitaxel were administered as third-line treatments. Four months after discontinuation of pembrolizumab (3 mo after initiation of third-line chemotherapy), the patient was admitted to our hospital with abdominal pain and fever.

FINAL DIAGNOSIS

The common bile duct biopsy showed intraepithelial infiltration of lymphocytes, and $CD8^+$ T cells were more predominant in the biliary epithelium than $CD4^+$ T cells (Figure 2A-C). Percutaneous ultrasonography-guided liver biopsy was also performed for differential diagnosis of other liver diseases. The liver biopsy showed infiltration of predominantly $CD8^+$ T cells in the portal area, but the periductal "onion-skin" fibrosis characteristic of primary sclerosing cholangiopathies, and panlobular hepatitis or isolated central zonal necrosis characteristic of acute hepatitis were not detected (Figure 2D-G). According to these imaging and pathological findings, the patient was diagnosed with immune-related SC induced by pembrolizumab.



DOI: 10.3748/wjg.v28.i28.3732 **Copyright** ©The Author(s) 2022.

Figure 2 Pathological findings of the common bile duct and liver. A: Hematoxylin–eosin staining (× 40): Intraepithelial infiltrations of lymphocytes are observed; B and C: CD8 (B) and CD4 (C) staining (× 40): Infiltration of $CD8^+$ T cells are predominant in the biliary epithelium compared to $CD4^+$ T cells; D and E: Hematoxylin–eosin staining: On liver biopsy, inflammation of the hepatic parenchyma is not observed. The periductal "onion-skin" fibrosis is not observed in the portal area (black arrow); F and G: CD8 (F) and CD4 (G) staining (× 200): In a zoomed-in view of the portal area, predominant infiltration of $CD8^+$ T cells, compared with $CD4^+$ T cells, is observed.

TREATMENT

Endoscopic nasobiliary drainage was performed and administration of 25 mg (0.5 mg/kg) of methylprednisolone was initiated. However, grade 3 elevation of ALP and grade 1 elevation of ALT were still present, and the cholangiography findings did not improve.

OUTCOME AND FOLLOW-UP

Because of disease progression, no further treatment was administered, and the patient was referred for palliative care.

DISCUSSION

ICIs enhance antitumor immunity by blocking negative regulators of T cell function that exist on both

immune and tumor cells. Although these agents can lead to remarkable responses, their use may also be associated with irAEs. A previous study showed that most irAEs occur in the first few months of treatment, but late-onset toxicity even after ICI discontinuation is also possible[4]. To the best of our knowledge, no case of immune-related SC after pembrolizumab discontinuation has been reported.

Kawakami *et al*[5] revealed that immune-related cholangitis was characterized by: (1) Localized extrahepatic bile duct dilation without obstruction; (2) Diffuse hypertrophy of the extrahepatic bile duct wall; (3) A dominant increase in the biliary tract enzymes ALP and gamma-glutamyl transpeptidase relative to the hepatic enzymes aspartate and alanine aminotransferase; (4) Normal or reduced levels of the serum immunological markers antinuclear antibody, antimitochondrial antibody, smooth muscle antibody, and immunoglobulin G4; (5) Pathological findings of biliary tract cluster of differentiation $CD8^+$ T cell infiltration from liver biopsy; and (6) A moderate to poor response to steroid therapy. The present case met all these characteristics of immune-related cholangitis.

In contrast, SC developed while carboplatin and nab-paclitaxel were administered. Previous studies reported that chemotherapy-induced SC and drug-induced SC appeared to be one or more strictures of the large bile ducts, mainly the common hepatic duct and the right and left hepatic ducts, usually sparing the common bile duct and smaller intrahepatic ducts[6,7]. Histologically, Weber *et al*[8] showed that a shift in the $CD4^+/CD8^+$ cell ratio in favor of $CD8^+$ cytotoxic T lymphocytes is useful in discriminating irAEs from other conditions (*e.g.*, autoimmune diseases and drug-induced injury). In our case, an irregularly narrowed right intrahepatic bile duct and infiltration of predominantly $CD8^+$ T cells were observed. Therefore, we diagnosed the patient with SC induced by pembrolizumab on the basis of the imaging and pathological findings of previous reports.

Recently, new reports of irAEs emerging after discontinuation of immunotherapy, a clinical diagnostic complex termed delayed immune-related events (DIRE), have surfaced[9]. The first case of DIRE after discontinuation of pembrolizumab was reported in 2013[10], and various late-onset irAEs have also been reported in the literature[11]. Anti-PD-1 antibodies continue to bind to lymphocytes several weeks after the last infusion of PD-1 inhibitors, which explains the development of irAEs after discontinuation of ICI therapy[12]. Although there have been some reports of DIRE after discontinuation of pembrolizumab, no cases of delayed immune-related SC induced by pembrolizumab have been reported.

Previous studies showed that steroid therapy was recommended for the treatment of irAEs, but was not useful for the treatment of immune-related SC[4,13]. Ursodeoxycholic acid (UDCA) and other anti-inflammatory agents, including immunomodulators and infliximab, have been considered for the treatment of irAEs, but their efficacy and response have been reported to be insufficient for the treatment of immune-related SC[14,15], and more cases may be needed to evaluate the usefulness of these drugs for immune-related SC. Biliary drainage has been reported to be ineffective for immune-related SCs[5,16,17]. It remains uncertain why there is a poor response to steroid therapy and biliary drainage for immune-related SC, and further studies are necessary to establish the treatment for immune-related SC.

This indicates that immune-related SC can occur later, similar to other hepatic irAEs. The imaging features and pathological findings of immune-related SC have become almost clear, but the mechanism and onset time of immune-related SC have not been elucidated. Further studies and accumulation of cases are necessary to establish appropriate diagnostic criteria and management strategies, and caution should be exercised for late-onset irAEs after discontinuation of ICIs.

CONCLUSION

Immune-related sclerosing cholangitis may have a late onset, and such cases occurring after discontinuation of immune checkpoint inhibitors should be carefully managed.

FOOTNOTES

Author contributions: All authors contributed to the study conception and design; Tanaka T, Tsujimae M, Yamada Y, and Kobayashi T performed the material preparation, data collection and analysis; Tanaka T wrote the first draft of the manuscript; Sakai A designed the study concept; Masuda A and Kodama Y were involved in study supervision and revised the manuscript; All authors commented on previous versions of the manuscript, read and approved the final manuscript.

Supported by JSPS KAKENHI, No. JP19K07938.

Informed consent statement: Informed consent was obtained from the patient presented in this article.

Conflict-of-interest statement: The authors declare that they have no conflicts of interest.

CARE Checklist (2016) statement: The authors have read the CARE Checklist (2016), and the manuscript was

prepared and revised according to the CARE Checklist (2016).

Open-Access: This article is an open-access article that was selected by an in-house editor and fully peer-reviewed by external reviewers. It is distributed in accordance with the Creative Commons Attribution NonCommercial (CC BY-NC 4.0) license, which permits others to distribute, remix, adapt, build upon this work non-commercially, and license their derivative works on different terms, provided the original work is properly cited and the use is non-commercial. See: https://creativecommons.org/Licenses/by-nc/4.0/

Country/Territory of origin: Japan

ORCID number: Takeshi Tanaka 0000-0003-0490-3453; Arata Sakai 0000-0003-1072-5243; Takashi Kobayashi 0000-0002-9202-7643; Atsuhiro Masuda 0000-0002-2138-1207; Yuzo Kodama 0000-0003-1223-7147.

S-Editor: Ma YJ
L-Editor: A
P-Editor: Ma YJ

REFERENCES

1 **Brooling J**, Leal R. Secondary Sclerosing Cholangitis: a Review of Recent Literature. *Curr Gastroenterol Rep* 2017; **19**: 44 [PMID: 28752474 DOI: 10.1007/s11894-017-0583-8]
2 **Hofmann L**, Forschner A, Loquai C, Goldinger SM, Zimmer L, Ugurel S, Schmidgen MI, Gutzmer R, Utikal JS, Göppner D, Hassel JC, Meier F, Tietze JK, Thomas I, Weishaupt C, Leverkus M, Wahl R, Dietrich U, Garbe C, Kirchberger MC, Eigentler T, Berking C, Gesierich A, Krackhardt AM, Schadendorf D, Schuler G, Dummer R, Heinzerling LM. Cutaneous, gastrointestinal, hepatic, endocrine, and renal side-effects of anti-PD-1 therapy. *Eur J Cancer* 2016; **60**: 190-209 [PMID: 27085692 DOI: 10.1016/j.ejca.2016.02.025]
3 **Khoja L**, Day D, Wei-Wu Chen T, Siu LL, Hansen AR. Tumour- and class-specific patterns of immune-related adverse events of immune checkpoint inhibitors: a systematic review. *Ann Oncol* 2017; **28**: 2377-2385 [PMID: 28945858 DOI: 10.1093/annonc/mdx286]
4 **de La Rochefoucauld J**, Noël N, Lambotte O. Management of immune-related adverse events associated with immune checkpoint inhibitors in cancer patients: a patient-centred approach. *Intern Emerg Med* 2020; **15**: 587-598 [PMID: 32144552 DOI: 10.1007/s11739-020-02295-2]
5 **Kawakami H**, Tanizaki J, Tanaka K, Haratani K, Hayashi H, Takeda M, Kamata K, Takenaka M, Kimura M, Chikugo T, Sato T, Kudo M, Ito A, Nakagawa K. Imaging and clinicopathological features of nivolumab-related cholangitis in patients with non-small cell lung cancer. *Invest New Drugs* 2017; **35**: 529-536 [PMID: 28317087 DOI: 10.1007/s10637-017-0453-0]
6 **Sandrasegaran K**, Alazmi WM, Tann M, Fogel EL, McHenry L, Lehman GA. Chemotherapy-induced sclerosing cholangitis. *Clin Radiol* 2006; **61**: 670-678 [PMID: 16843750 DOI: 10.1016/j.crad.2006.02.013]
7 **Visentin M**, Lenggenhager D, Gai Z, Kullak-Ublick GA. Drug-induced bile duct injury. *Biochim Biophys Acta Mol Basis Dis* 2018; **1864**: 1498-1506 [PMID: 28882625 DOI: 10.1016/j.bbadis.2017.08.033]
8 **Weber JS**, Yang JC, Atkins MB, Disis ML. Toxicities of Immunotherapy for the Practitioner. *J Clin Oncol* 2015; **33**: 2092-2099 [PMID: 25918278 DOI: 10.1200/JCO.2014.60.0379]
9 **Couey MA**, Bell RB, Patel AA, Romba MC, Crittenden MR, Curti BD, Urba WJ, Leidner RS. Delayed immune-related events (DIRE) after discontinuation of immunotherapy: diagnostic hazard of autoimmunity at a distance. *J Immunother Cancer* 2019; **7**: 165 [PMID: 31269983 DOI: 10.1186/s40425-019-0645-6]
10 **Hanrahan P**, Van Der Westhuizen A, Collins S, Owens D, Hersey P. Delayed autoimmune effects in patients treated with antibodies against the checkpoint inhibitor PD1. *J Dtsch Dermatol Ges* 2013; **11**: 16 [DOI: 10.1111/ddg.12015_4]
11 **Kanaoka K**, Moriizumi K, Okada H, Iwahashi K, Tsuji H, Yasuoka H, Minami S. Pembrolizumab-Induced Delayed-Onset Hepatitis. *Case Rep Gastroenterol* 2020; **14**: 586-592 [PMID: 33250701 DOI: 10.1159/000509953]
12 **Osa A**, Uenami T, Koyama S, Fujimoto K, Okuzaki D, Takimoto T, Hirata H, Yano Y, Yokota S, Kinehara Y, Naito Y, Otsuka T, Kanazu M, Kuroyama M, Hamaguchi M, Koba T, Futami Y, Ishijima M, Suga Y, Akazawa Y, Machiyama H, Iwahori K, Takamatsu H, Nagatomo I, Takeda Y, Kida H, Akbay EA, Hammerman PS, Wong KK, Dranoff G, Mori M, Kijima T, Kumanogoh A. Clinical implications of monitoring nivolumab immunokinetics in non-small cell lung cancer patients. *JCI Insight* 2018; **3** [PMID: 30282824 DOI: 10.1172/jci.insight.59125]
13 **Onoyama T**, Takeda Y, Yamashita T, Hamamoto W, Sakamoto Y, Koda H, Kawata S, Matsumoto K, Isomoto H. Programmed cell death-1 inhibitor-related sclerosing cholangitis: A systematic review. *World J Gastroenterol* 2020; **26**: 353-365 [PMID: 31988594 DOI: 10.3748/wjg.v26.i3.353]
14 **Zhu GQ**, Shi KQ, Huang GQ, Wang LR, Lin YQ, Braddock M, Chen YP, Zhou MT, Zheng MH. A network meta-analysis of the efficacy and side effects of UDCA-based therapies for primary sclerosing cholangitis. *Oncotarget* 2015; **6**: 26757-26769 [PMID: 26378046 DOI: 10.18632/oncotarget.5610]
15 **Puzanov I**, Diab A, Abdallah K, Bingham CO 3rd, Brogdon C, Dadu R, Hamad L, Kim S, Lacouture ME, LeBoeuf NR, Lenihan D, Onofrei C, Shannon V, Sharma R, Silk AW, Skondra D, Suarez-Almazor ME, Wang Y, Wiley K, Kaufman HL, Ernstoff MS; Society for Immunotherapy of Cancer Toxicity Management Working Group. Managing toxicities associated with immune checkpoint inhibitors: consensus recommendations from the Society for Immunotherapy of Cancer (SITC) Toxicity Management Working Group. *J Immunother Cancer* 2017; **5**: 95 [PMID: 29162153 DOI: 10.1186/s40425-017-0300-z]

16 **Kashima J**, Okuma Y, Shimizuguchi R, Chiba K. Bile duct obstruction in a patient treated with nivolumab as second-line chemotherapy for advanced non-small-cell lung cancer: a case report. *Cancer Immunol Immunother* 2018; **67**: 61-65 [PMID: 28913619 DOI: 10.1007/s00262-017-2062-3]

17 **Koya Y**, Shibata M, Shinohara N, Nebuya S, Oe S, Honma Y, Senju M, Sato N, Harada M. Secondary sclerosing cholangitis with hemobilia induced by pembrolizumab: Case report and review of published work. *Hepatol Res* 2019; **49**: 950-956 [PMID: 30861263 DOI: 10.1111/hepr.13329]

World Journal of Gastroenterology

Submit a Manuscript: https://www.f6publishing.com

World J Gastroenterol 2022 July 28; 28(28): 3739-3742

DOI: 10.3748/wjg.v28.i28.3739

ISSN 1007-9327 (print) ISSN 2219-2840 (online)

LETTER TO THE EDITOR

Prednisolone induced pneumatosis coli and pneumoperitoneum

Serene S N Goh, Vishal Shelat

Specialty type: Gastroenterology and hepatology

Provenance and peer review: Unsolicited article; Externally peer reviewed.

Peer-review model: Single blind

Peer-review report's scientific quality classification

Grade A (Excellent): 0
Grade B (Very good): 0
Grade C (Good): 0
Grade D (Fair): D
Grade E (Poor): 0

P-Reviewer: Lassandro F, Italy

Received: October 30, 2021
Peer-review started: October 30, 2021
First decision: April 16, 2022
Revised: May 4, 2022
Accepted: July 11, 2022
Article in press: July 11, 2022
Published online: July 28, 2022



Serene S N Goh, Vishal Shelat, Department of General Surgery, Tan Tock Seng Hospital, Singapore 308433, Singapore

Corresponding author: Serene S N Goh, MMed, Doctor, Department of General Surgery, Tan Tock Seng Hospital, 11 Jln Tan Tock Seng, Singapore 308433, Singapore.
serene.goh@mohh.com.sg

Abstract

Pneumatosis intestinalis (PI) is defined as the presence of gas within the submucosal or subserosal layer of the gastrointestinal tract. It is a radiologic sign suspicious for bowel ischemia, hence non-viable bowel must be ruled out in patients with PI. However, up to 15% of cases with PI are not associated with bowel ischemia or acute abdomen. We described an asymptomatic patient with prednisolone-induced PI and modified the Naranjo score to aid in a surgeon's decision-making for emergency laparotomy *vs* non-operative management with serial assessment in patients who are immunocompromised due to long-term steroid use.

Key Words: Benign pneumatosis; Pneumatosis coli; Pneumatosis intestinalis; Prednisolone

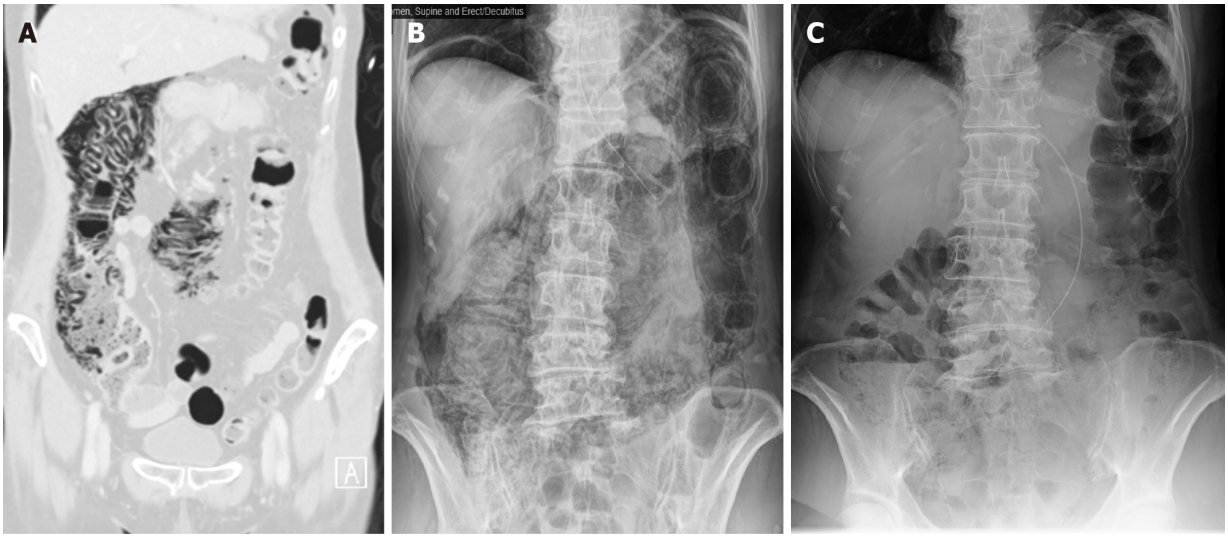
©The Author(s) 2022. Published by Baishideng Publishing Group Inc. All rights reserved.

Core Tip: We described an asymptomatic patient with prednisolone-induced pneumatosis intestinalis and modified the Naranjo score to aid in a surgeon's decision-making for emergency laparotomy *vs* non-operative management with serial assessment in patients who are immunocompromised due to long-term steroid use.

Citation: Goh SSN, Shelat V. Prednisolone induced pneumatosis coli and pneumoperitoneum. *World J Gastroenterol* 2022; 28(28): 3739-3742
URL: https://www.wjgnet.com/1007-9327/full/v28/i28/3739.htm
DOI: https://dx.doi.org/10.3748/wjg.v28.i28.3739

TO THE EDITOR

We read with interest the report by Azzaroli *et al*[1], who conservatively managed two patients with benign pneumatosis intestinalis (PI). We would like to share a similar



DOI: 10.3748/wjg.v28.i28.3739 **Copyright** ©The Author(s) 2022.

Figure 1 Computed tomography of abdomen and pelvis and serial erect abdominal radiographs showing interval improvement in pneumatosis coli and resolution of pneumoperitoneum. A: First admission day. Pneumatosis coli from cecum to transverse colon; B: 2 wk after admission. Progression of pneumatosis coli and pneumoperitoneum; C: 2 wk Post-hyperbaric oxygen therapy. Resolution of pneumoperitoneum and pneumatosis coli.

clinical case with prednisolone-induced pneumatosis coli and propose a modified Naranjo score for prednisolone-induced pneumatosis.

A 71-year-old lady with dysphagia and diplopia symptoms was diagnosed with Neuromyelitis Optica (NMO). Treatment with prednisolone 20 mg once daily improved her diplopia. Nasogastric tube (NGT) feeding was commenced due to malnourishment from dysphagia. The chest radiograph for NGT placement showed pneumoperitoneum, and she was referred urgently to the surgical unit. She was asymptomatic, afebrile with normal hemodynamics. Abdomen was soft and non-tender. Leukocyte count, procalcitonin, lactate, and arterial blood gas were normal. A computed tomography of abdomen and pelvis (CTAP) with intravenous and NGT contrast confirmed pneumoperitoneum and pneumatosis coli from cecum to splenic flexure (Figure 1). There was no contrast extravasation, portal venous gas, inflammatory pathology, or mesenteric ischemia. Non-operative management with nil enteral feeding, serial abdominal examination, serum tests, and abdominal radiographs (AXR) was done. The patient remained asymptomatic with normal serum tests. A repeat CTAP showed minimal improvement of pneumoperitoneum. A follow-up AXR two weeks later showed worsening of pneumatosis coli. Hyperbaric oxygen therapy (HBOT) was arranged. Five HBOT sessions were performed at 2.2 atmospheric pressure for 90 min. Her abdominal girth reduced from 79 to 73 cm with minimal AXR improvement. Prednisolone was weaned over next five days and she was discharged well on oral diet. At two-weeks outpatient follow-up, AXR showed improvement (Figure 1).

Corticosteroid therapy remains the cornerstone for the treatment of autoimmune diseases. The true incidence of benign PI as an ADR secondary to corticosteroids is unknown[2,3]. The hypothesis is due to atrophy of lymphoid follicles in the bowel wall. Although PI occurred after prednisolone's commencement in our patient, we did not initially stop prednisolone in balancing risk *vs* benefits for NMO therapy. When PI worsened, HBOT was offered due to concerns for secondary bowel ischemia from PI. The HBOT regimen was similar to that described by Feuerstein *et al*[4], who suggested at least three sessions. As our patient's PI improved but did not resolve fully after 5 HBOT sessions, we reduced prednisolone dose. After two weeks of cessation, PI resolved, similar to a report described by Choi *et al* [5].

According to the Naranjo score (adverse drug reaction probability scale) of 6, PI was probably caused by prednisolone in our patient. Naranjo score recommends isolation of drug in toxic concentrations in body fluid, response to placebo administration, and drug rechallenge to evaluate for the occurrence of symptoms. These three criteria are not routinely done due to practical and safety reasons[6]. We propose a modified Naranjo score (Tables 1 and 2) for prednisolone-induced pneumatosis which replaces these three criteria with the following: (1) No symptoms or signs of abdominal pathology; (2) Serum investigations for inflammatory markers (*e.g.*, C-reactive protein and procalcitonin) must be normal; and (3) Imaging studies should rule out hollow viscus perforation or inflammatory abdominal pathology as a cause for PI. With the modified Naranjo score, the causal link of PI due to prednisolone becomes definite. We propose validation of modified Naranjo score.

Table 1 Modified Naranjo score-pneumatosis intestinalis specific score

Question	Yes/No/Do not know	Score
Are there previous conclusive reports on this reaction?	Yes	1
Did the adverse event appear after the suspected drug was administered?	Yes	2
Did the adverse reaction improve when the drug was discontinued, or a specific antagonist was administered?	Yes	1
Are there alternative causes (other than the drug) that could on their own have caused the reaction?	No	0
Was the reaction more severe when the dose was increased or less severe when the dose was decreased?	Yes	1
Did the patient have a similar reaction to the same or similar drugs in any previous exposure?	No	0
Did any objective evidence confirm the adverse event?	Yes	1
Were there any symptoms or signs of abdominal pathology? (instead of isolation of drug in toxic concentrations in body fluid)	No	1
Were the serum inflammatory markers normal? (instead of drug rechallenge to evaluate for reoccurrence of symptoms)	Yes	1
Did imaging studies rule out hollow viscus perforation or inflammatory abdominal organ pathology? (instead of response to placebo administration)	Yes	1
Total score		**9 (definite)**

Table 2 Interpretation of scores

Total score	Interpretation of scores
≥ 9	Definite
5 to 8	Probable
1 to 4	Possible
≤ 0	Doubtful

FOOTNOTES

Author contributions: Goh SSN wrote the letter; Shelat V revised the letter.

Conflict-of-interest statement: All the authors report no relevant conflicts of interest for this article.

Open-Access: This article is an open-access article that was selected by an in-house editor and fully peer-reviewed by external reviewers. It is distributed in accordance with the Creative Commons Attribution NonCommercial (CC BY-NC 4.0) license, which permits others to distribute, remix, adapt, build upon this work non-commercially, and license their derivative works on different terms, provided the original work is properly cited and the use is non-commercial. See: https://creativecommons.org/Licenses/by-nc/4.0/

Country/Territory of origin: Singapore

ORCID number: Serene S N Goh 0000-0003-4916-2142; Vishal Shelat 0000-0003-3988-8142.

S-Editor: Fan JR
L-Editor: A
P-Editor: Fan JR

REFERENCES

1 **Azzaroli F**, Turco L, Ceroni L, Galloni SS, Buonfiglioli F, Calvanese C, Mazzella G. Pneumatosis cystoides intestinalis. *World J Gastroenterol* 2011; **17**: 4932-4936 [PMID: 22171137 DOI: 10.3748/wjg.v17.i44.4932]
2 **Berritto D**, Crincoli R, Iacobellis F, Iasiello F, Pizza NL, Lassandro F, Musto L, Grassi R. Primary pneumatosis intestinalis of small bowel: a case of a rare disease. *Case Rep Surg* 2014; **2014**: 350312 [PMID: 25478280 DOI: 10.1155/2014/350312]
3 **Paradkar S**. Reported Adverse Drug Reactions During the Use of Corticosteroids in a Tertiary Care Hospital. *Ther Innov Regul Sci* 2019; **53**: 128-131 [PMID: 29759019 DOI: 10.1177/2168479018776262]

4 **Feuerstein JD**, White N, Berzin TM. Pneumatosis intestinalis with a focus on hyperbaric oxygen therapy. *Mayo Clin Proc* 2014; **89**: 697-703 [PMID: 24797647 DOI: 10.1016/j.mayocp.2014.01.026]
5 **Choi JY**, Cho SB, Kim HH, Lee IH, Lee HY, Kang HS, Lee SY. Pneumatosis intestinalis complicated by pneumoperitoneum in a patient with asthma. *Tuberc Respir Dis (Seoul)* 2014; **77**: 219-222 [PMID: 25473410 DOI: 10.4046/trd.2014.77.5.219]
6 **Shelat VG**. Sulfasalazine induced acute pancreatitis in a patient with prior cholecystectomy. *Postgrad Med J* 2021; **97**: 738-739 [PMID: 32848081 DOI: 10.1136/postgradmedj-2020-138648]

World Journal of Gastroenterology

Submit a Manuscript: https://www.f6publishing.com

World J Gastroenterol 2022 July 28; 28(28): 3743-3746

DOI: 10.3748/wjg.v28.i28.3743

ISSN 1007-9327 (print) ISSN 2219-2840 (online)

LETTER TO THE EDITOR

Is patient satisfaction sufficient to validate endoscopic anti-reflux treatments?

Mauro Bortolotti

Specialty type: Gastroenterology and hepatology

Provenance and peer review: Invited article; Externally peer reviewed.

Peer-review model: Single blind

Peer-review report's scientific quality classification

Grade A (Excellent): 0
Grade B (Very good): B, B, B
Grade C (Good): 0
Grade D (Fair): 0
Grade E (Poor): 0

P-Reviewer: Chen SY, China; Jing X, China; Rogers MP, United States

Received: February 21, 2022
Peer-review started: February 21, 2022
First decision: May 29, 2022
Revised: June 8, 2022
Accepted: July 8, 2022
Article in press: July 8, 2022
Published online: July 28, 2022

Mauro Bortolotti, Department of Internal Medicine and Gastroenterology, S. Orsola-Malpighi Polyclinic, University of Bologna, Bologna 40138, Italy

Corresponding author: Mauro Bortolotti, MD, Via Massarenti 48, Bologna 40138, Italy. bormau@tin.it

Abstract

Endoscopic anti-reflux treatment is emerging as a new option for gastro-esophageal reflux disease (GERD) treatment in patients with the same indications as for laparoscopic fundoplication. There are many techniques, the first of which are transoral incisionless fundoplication (TIF) and nonablative radio-frequency (STRETTA) that have been tested with comparative studies and randomized controlled trials, whereas the other more recent ones still require a deeper evaluation. The purpose of the latter is to verify whether reflux is abolished or significantly reduced after intervention, whether there is a valid high pressure zone at the gastroesophageal junction, and whether esophagitis, when present, has disappeared. Unfortunately in a certain number of cases, and especially in the more recently introduced ones, the evaluation has been based almost exclusively on subjective criteria, such as improvement in the quality of life, remission of heartburn and regurgitation, and reduction or suspension of antacid and antisecretory drug consumption. However, with the most studied techniques such as TIF and STRETTA, an improvement in symptoms better than that of laparoscopic fundoplication can often be observed, whereas the number of acid episodes and acid exposure time are similar or higher, as if the acid refluxes are better tolerated by these patients. The suspicion of a local hyposensitivity taking place after anti-reflux endoscopic intervention seems confirmed by a Bernstein test at least for STRETTA. This examination should be done for all the other techniques, both old and new, to identify the ones that reassure rather than cure. In conclusion, the evaluation of the effectiveness of the endoscopic anti-reflux techniques should not be based exclusively on subjective criteria, but should also be confirmed by objective examinations, because there might be a gap between the improvement in symptoms declared by the patient and the underlying pathophysiologic alterations of GERD.

Key Words: Endoscopic anti-reflux treatment; Transoral incisionless fundoplication; Nonablative radio-frequency; Anti-reflux mucosectomy; Gastro-esophageal reflux disease; Laparoscopic Nissen fundoplication

©The Author(s) 2022. Published by Baishideng Publishing Group Inc. All rights reserved.

Core Tip: Endoscopic anti-reflux treatments are being increasingly used instead of anti-reflux surgery. However, most of them have been evaluated only on the ground of subjective symptoms, without performing any objective examination. Furthermore, some also appear to be more effective than surgery in improving acid reflux symptoms, even if their acid exposure is worse, suggesting a reduced sensitivity. The Bernstein test performed after nonablative radio-frequency seems to confirm this hypothesis. Hence, to verify the effectiveness of these esophageal anti-reflux interventions, in addition to evaluating the symptoms before and after the intervention, it is necessary to perform objective examinations.

Citation: Bortolotti M. Is patient satisfaction sufficient to validate endoscopic anti-reflux treatments? *World J Gastroenterol* 2022; 28(28): 3743-3746
URL: https://www.wjgnet.com/1007-9327/full/v28/i28/3743.htm
DOI: https://dx.doi.org/10.3748/wjg.v28.i28.3743

TO THE EDITOR

In the past few years, endoscopic anti-reflux treatments have increasingly caught the attention of many gastroenterological centers, as they offer a minimally invasive option for patients with gastroesophageal reflux disease (GERD) who show refractoriness or intolerance to proton pump inhibitors (PPI), or who refuse to take lifelong medication, but want to avoid a surgical intervention, such as the classical laparoscopic fundoplication (LF). A recent article[1] has provided an up-to-date review of the technical aspects, clinical effectiveness, and safety of the main endoscopic anti-reflux procedures including transoral incisionless fundoplication (TIF), nonablative radio-frequency (STRETTA), and Medigus ultrasonic surgical endostapler (MUSE), together with the following still experimental techniques, such as full-thickness endoscopic plication device, anti-reflux mucosectomy (ARMS), anti-reflux mucosal ablation, and band-assisted ligation techniques. However, two observations can be made after consulting the literature studies on the effectiveness of these systems.

First, in most studies the efficacy of an endoscopic anti-reflux technique has been evaluated almost exclusively considering subjective symptoms, such as the improvement in quality of life, remission of heartburn and regurgitation, and reduction or suspension of antacid and antisecretory drugs consumption, to the extent that it has been deemed a success when the patient halved the dose of PPI used prior to intervention.

Second, in most studies where these endoscopic interventions are compared with LF or PPI therapy, symptom improvement after endoscopic treatments is frequently greater than that obtained with LF, even when the 24 h pH recording shows a worse result.

This statement can be easily verified in the systematic review and network meta-analysis of Richter *et al*[2] from seven randomized controlled trials (RCTs) with a total of 1128 patients, concerning a comparison of laparoscopic Nissen fundoplication (LNF) *vs* TIF or PPI treatment. The results indicate that TIF has the highest likelihood of increasing the patient's health-related quality of life (HRQL) followed by LNF, whereas the LNF has the highest likelihood of increasing the percentage of time with distal esophageal pH > 4, followed by PPI and then by TIF, which, in addition, has a higher likelihood than LNF for persistent esophagitis.

Also in the randomized controlled trial of Witteman *et al*[3] performed in 60 patients to evaluate the effectiveness of TIF in comparison with the PPI treatment, GERD symptoms after 6 mo are significantly more improved in the TIF group than in the PPI group, despite the similar improvement in distal esophageal acid exposure, whereas the pH normalization for TIF group is 50% with respect to 63% for the PPI group.

A systematic review and network meta-analysis[4] comprising 516 patients from 10 RCTs compared the anti-reflux efficacy of Stretta, TIF, and PPI. Both STRETTA and TIF are significantly superior to PPI in improving GERD-HRQL and heartburn scores, whereas PPI is better in decreasing the percentage of time with pH < 4.0 when compared with TIF.

Also in the study of He *et al*[5], the symptom score improvement was significantly higher in the STRETTA group of 26 patients compared with the PPI group of 21 patients after 6 mo, whereas both interventions improved, without significant differences, the 24 h pH parameters, including the number of acid episodes, acid exposure time, and DeMeester score.

Furthermore, the absence of correlation between the improvement in GER symptoms and the decrease in acid reflux in patients treated with STRETTA is highlighted by the following two studies.

Coron *et al*[6] in an article comparing the results in 20 patients undergoing STRETTA and 16 patients treated with PPI report that GERD-HRQL scores do not differ between groups, whereas no significant

change in esophageal acid exposure is noted between baseline and 6 mo after STRETTA treatment. So they came to the conclusion that the efficacy of the STRETTA treatment does not seem to be related to a decrease in esophageal acid exposure. In addition, the study of Arts *et al*[7] shows that 3 mo after STRETTA procedure on 11 patients, the symptom score was significantly improved, whereas no changes were observed in esophageal acid exposure.

In view of all these results, we may be led to believe that the greater improvements in GER symptoms observed after TIF and STRETTA applications as compared with LF and PPI treatments, despite the scarce improvement in GER objective parameters, likely depend on another factor, that could be identified with a decreased visceral sensitivity. The hypothesis that symptom improvement in these patients depends on a decreased esophageal acid sensitivity is confirmed, at least for STRETTA, by the study of Arts *et al*[8]. They found that 6 mo after the STRETTA procedure in 13 patients, the mean time needed to induce heartburn during esophageal acid perfusion of the Bernstein test increased from 9.5 ± 2.3 (mean ± SD) to 18.1 ± 4.4 min ($P < 0.01$) , whereas five had become insensitive to 30 min acid perfusion, *vs* none at baseline ($P = 0.04$).

Also in the case of TIF, the dissociation between symptoms and objective parameters, if compared with those of LF and PPI, suggests the post-intervention appearance of a hyposensitive condition, similar to that of STRETTA, although a Bernstein test is necessary to confirm this supposition.

The cause of this local hyposensitivity could lie in an effect of radiofrequency (RF) energy of STRETTA on the myenteric and submucosal nervous plexuses carrying sensory receptors, acetylcholine stimulatory and non-adrenergic, non-cholinergic (NANC) inhibitory neurons, as well as on the two branches of the vagus nerve, which pass in the subadventitial space at the esophagogastric junction level. RF energy inducing a thermal injury promoting submucosal fibrosis and muscularis propria hypertrophy, should also act on nervous tissues impairing the inhibitory NANC neurons with a decrease in transient LES relaxations, while increasing its yield pressures[9]. It is likely that RF energy could also act on sensitive neurons of the esophageal wall. In addition, a slight excess of RF energy or a tissue weakness may also cause damage to the vagus nerve passing below, causing delayed gastric emptying and gastroparesis reported by some authors[10-13]. With regard to the other endoscopic procedures, there are no appropriate comparative studies with LNF and PPI treatments, except for the study of Wong *et al*[14], who compared Nissen fundoplication with ARMS. But they did not perform objective measurements for reflux and only evaluated GERD-HRQL and reflux symptoms up to 2 years, without observing any difference between the two groups.

In conclusion, the evaluation of the effectiveness of any endoscopic anti-reflux technique should not be based exclusively on subjective criteria, such as a good response to PPI suspension, remission of heartburn, and GERD-HRQL improvement, but should also be established with objective examinations, such as 24 h pH monitoring, and, if possible, manometric measurement of the high pressure zone in the distal esophagus, besides endoscopy for the assessment of esophagitis. The good capacity of TIF and STRETTA to improve the reflux symptoms and the quality of life more than LF and PPI treatments, is a double-edged weapon, because a scarce prevention of acid reflux in the long term may expose the patient to the risk that more or less serious alterations will pass unnoticed. This risk could also be taken with the other more recent endoscopic techniques, which, as previously mentioned, should be compared with LF or PPI treatments and possibly examined by the Bernstein test.

ACKNOWLEDGEMENTS

The author thanks Henry Monaco BA (Hons) for the assistance for the English language.

FOOTNOTES

Author contributions: Bortolotti M wrote the paper.

Conflict-of-interest statement: No conflict of interest exists.

Open-Access: This article is an open-access article that was selected by an in-house editor and fully peer-reviewed by external reviewers. It is distributed in accordance with the Creative Commons Attribution NonCommercial (CC BY-NC 4.0) license, which permits others to distribute, remix, adapt, build upon this work non-commercially, and license their derivative works on different terms, provided the original work is properly cited and the use is non-commercial. See: https://creativecommons.org/Licenses/by-nc/4.0/

Country/Territory of origin: Italy

ORCID number: Mauro Bortolotti 0000-0002-5273-9013.

S-Editor: Zhang H

L-Editor: Wang TQ
P-Editor: Zhang H

REFERENCES

1 **Rodríguez de Santiago E**, Albéniz E, Estremera-Arevalo F, Teruel Sanchez-Vegazo C, Lorenzo-Zúñiga V. Endoscopic anti-reflux therapy for gastroesophageal reflux disease. *World J Gastroenterol* 2021; **27**: 6601-6614 [PMID: 34754155 DOI: 10.3748/wjg.v27.i39.6601]
2 **Richter JE**, Kumar A, Lipka S, Miladinovic B, Velanovich V. Efficacy of Laparoscopic Nissen Fundoplication vs Transoral Incisionless Fundoplication or Proton Pump Inhibitors in Patients With Gastroesophageal Reflux Disease: A Systematic Review and Network Meta-analysis. *Gastroenterology* 2018; **154**: 1298-1308.e7 [PMID: 29305934 DOI: 10.1053/j.gastro.2017.12.021]
3 **Witteman BP**, Conchillo JM, Rinsma NF, Betzel B, Peeters A, Koek GH, Stassen LP, Bouvy ND. Randomized controlled trial of transoral incisionless fundoplication vs. proton pump inhibitors for treatment of gastroesophageal reflux disease. *Am J Gastroenterol* 2015; **110**: 531-542 [PMID: 25823768 DOI: 10.1038/ajg.2015.28]
4 **Xie P**, Yan J, Ye L, Wang C, Li Y, Chen Y, Li G. Efficacy of different endoscopic treatments in patients with gastroesophageal reflux disease: a systematic review and network meta-analysis. *Surg Endosc* 2021; **35**: 1500-1510 [PMID: 33650003 DOI: 10.1007/s00464-021-08386-1]
5 **He S**, Xu F, Xiong X, Wang H, Cao L, Liang N, Jing X, Liu T. Stretta procedure versus proton pump inhibitors for the treatment of nonerosive reflux disease: A 6-month follow-up. *Medicine (Baltimore)* 2020; **99**: e18610 [PMID: 32011441 DOI: 10.1097/MD.0000000000018610]
6 **Coron E**, Sebille V, Cadiot G, Zerbib F, Ducrotte P, Ducrot F, Pouderoux P, Arts J, Le Rhun M, Piche T, Bruley des Varannes S, Galmiche JP; Consortium de Recherche Indépendant sur le Traitement et L'exploration du Reflux Gastro-oesophagien et de L'endobrachyoesophage (CRITERE). Clinical trial: Radiofrequency energy delivery in proton pump inhibitor-dependent gastro-oesophageal reflux disease patients. *Aliment Pharmacol Ther* 2008; **28**: 1147-1158 [PMID: 18616516 DOI: 10.1111/j.1365-2036.2008.03790.x]
7 **Arts J**, Bisschops R, Blondeau K, Farré R, Vos R, Holvoet L, Caenepeel P, Lerut A, Tack J. A double-blind sham-controlled study of the effect of radiofrequency energy on symptoms and distensibility of the gastro-esophageal junction in GERD. *Am J Gastroenterol* 2012; **107**: 222-230 [PMID: 22108449 DOI: 10.1038/ajg.2011.395]
8 **Arts J**, Sifrim D, Rutgeerts P, Lerut A, Janssens J, Tack J. Influence of radiofrequency energy delivery at the gastroesophageal junction (the Stretta procedure) on symptoms, acid exposure, and esophageal sensitivity to acid perfusion in gastroesophagal reflux disease. *Dig Dis Sci* 2007; **52**: 2170-2177 [PMID: 17436101 DOI: 10.1007/s10620-006-9695-y]
9 **Sowa P**, Samarasena JB. Nonablative Radiofrequency Treatment for Gastroesophageal Reflux Disease (STRETTA). *Gastrointest Endosc Clin N Am* 2020; **30**: 253-265 [PMID: 32146945 DOI: 10.1016/j.giec.2019.12.006]
10 **Richards WO**, Scholz S, Khaitan L, Sharp KW, Holzman MD. Initial experience with the stretta procedure for the treatment of gastroesophageal reflux disease. *J Laparoendosc Adv Surg Tech A* 2001; **11**: 267-273 [PMID: 11642661 DOI: 10.1089/109264201317054546]
11 **Dughera L**, Navino M, Cassolino P, De Cento M, Cacciotella L, Cisarò F, Chiaverina M. Long-Term Results of Radiofrequency Energy Delivery for the Treatment of GERD: Results of a Prospective 48-Month Study. *Diagn Ther Endosc* 2011; **2011**: 507157 [PMID: 22110288 DOI: 10.1155/2011/507157]
12 **Houston H**, Khaitan L, Holzman M, Richards WO. First year experience of patients undergoing the Stretta procedure. *Surg Endosc* 2003; **17**: 401-404 [PMID: 12436238 DOI: 10.1007/s00464-002-8923-6]
13 **Aziz AM**, El-Khayat HR, Sadek A, Mattar SG, McNulty G, Kongkam P, Guda MF, Lehman GA. A prospective randomized trial of sham, single-dose Stretta, and double-dose Stretta for the treatment of gastroesophageal reflux disease. *Surg Endosc* 2010; **24**: 818-825 [PMID: 19730952 DOI: 10.1007/s00464-009-0671-4]
14 **Wong HJ**, Su B, Attaar M, Kuchta K, Stearns S, Linn JG, Haggerty SP, Denham W, Ujiki MB. Anti-reflux mucosectomy (ARMS) results in improved recovery and similar reflux quality of life outcomes compared to laparoscopic Nissen fundoplication. *Surg Endosc* 2021; **35**: 7174-7182 [PMID: 33237465 DOI: 10.1007/s00464-020-08144-9]

World Journal of Gastroenterology

Submit a Manuscript: https://www.f6publishing.com

World J Gastroenterol 2022 July 28; 28(28): 3747-3752

DOI: 10.3748/wjg.v28.i28.3747

ISSN 1007-9327 (print) ISSN 2219-2840 (online)

LETTER TO THE EDITOR

Endoluminal vacuum-assisted therapy as a treatment for anastomotic leakage in colorectal surgery

Maria Michela Chiarello, Valentina Bianchi, Pietro Fransvea, Giuseppe Brisinda

Specialty type: Gastroenterology and hepatology

Provenance and peer review: Unsolicited article; Externally peer reviewed.

Peer-review model: Single blind

Peer-review report's scientific quality classification
Grade A (Excellent): A
Grade B (Very good): 0
Grade C (Good): C, C
Grade D (Fair): 0
Grade E (Poor): 0

P-Reviewer: Ghareeb WM, China; Kayano H, Japan; Li J, China

Received: April 16, 2022
Peer-review started: April 16, 2022
First decision: May 11, 2022
Revised: May 13, 2022
Accepted: June 22, 2022
Article in press: June 22, 2022
Published online: July 28, 2022

Maria Michela Chiarello, Department of Surgery, Azienda Sanitaria Provinciale di Cosenza, Cosenza 87100, Italy

Valentina Bianchi, Pietro Fransvea, Emergency Surgery and Trauma Center, Fondazione Policlinico Universitario A Gemelli IRCCS, Rome 00168, taly

Giuseppe Brisinda, Medical and Surgical Sciences, Fondazione Policlinico Universitario A Gemelli IRCCS, Rome 00168, Italy

Corresponding author: Giuseppe Brisinda, MD, Professor, Surgeon, Medical and Surgical Sciences, Fondazione Policlinico Universitario A Gemelli IRCCS, Largo Agostino Gemelli 8, Rome 00168, Italy. gbrisin@tin.it

Abstract

Anastomotic leakage (AL) has a wide range of clinical features ranging from radiological only findings to peritonitis and sepsis with multiorgan failure. An early diagnosis of AL is essential in order to establish the most appropriate treatment for this complication. Despite AL continues to be a dreadful complication after colorectal surgery, there has been no consensus on its management. However, based on patient's presentation and timing of the AL, there has been a gradual shift to a more conservative management, keeping surgery as the last option Reoperation for sepsis control is rarely necessary especially in those patients who already have a diverting stoma at the time of the leak. A nonoperative management is usually preferred in these patients. There are several treatment options, also for patients without a stoma who do not require a reoperation for a contained pelvic leak, including recently developed endoscopic procedures, such as clip placement or endoluminal vacuum-assisted therapy. More conservative treatments could be an option in patients who are clinically stable or in presence of a small defect.

Key Words: Anastomotic leakage; Colorectal cancer; Colorectal surgery; Mortality; Morbidity

©The Author(s) 2022. Published by Baishideng Publishing Group Inc. All rights reserved.

Core Tip: The authors of the review have a remarkable clinical experience and scientific authority in colorectal surgery and related complications. The authors focus their attention on endoluminal vacuum therapy to treat anastomotic leakage in colorectal surgery. The authors highlight that most studies are heterogeneous in term of success rate definition, salvage and long-term results. Furthermore, there is paucity of comparative studies and thus definitive conclusions are not warranted at present time, as pointed out by the authors in their narrative review.

Citation: Chiarello MM, Bianchi V, Fransvea P, Brisinda G. Endoluminal vacuum-assisted therapy as a treatment for anastomotic leakage in colorectal surgery. *World J Gastroenterol* 2022; 28(28): 3747-3752
URL: https://www.wjgnet.com/1007-9327/full/v28/i28/3747.htm
DOI: https://dx.doi.org/10.3748/wjg.v28.i28.3747

TO THE EDITOR

We were pleased to read the high-level article on treatment of colorectal anastomotic leakage (AL) with endoluminal vacuum therapy (EVT), published by Vignali and De Nardi[1]. The authors have a remarkable clinical experience and scientific authority in colorectal surgery and related complications[2-4].

We agree with the authors that AL is still the worst complication of colorectal surgery today. The consequences of AL can severely alter functional outcomes and oncological results[5]. In the case of AL, the severity of the clinical picture is extremely variable. Some AL have no impact on the patient, while others present with sepsis and can be fatal[6-8].

The incidence of AL is variable[1,5,9]. We believe that this variability in incidence is related to several factors. In accordance with the literature data, we believe that variables such as neoplastic or inflammatory disease, timing of the operation, the distance of the tumor from the anal merge, the clinical presentation with signs of visceral perforation or intestinal obstruction, the local characteristics of the tumor and the surgery performed are important for the postoperative onset of AL. In this context, the need for a common definition appears to be fundamental. AL occurs when a surgical anastomosis fails. In this circumstance, the intestinal contents leak out of the surgical connection. A pelvic abscess close to the anastomosis must be considered as AL. The classification of severity degrees proposed by the International Study Group of Rectal Cancer (ISREC)[10] is the most widely adopted. ISREC[10] proposes a classification of AL into three types (A, B and C) of increasing severity according to the therapeutic management it requires (conservative management in type A; non-surgical management in type B; surgical treatment in type C).

We believe that the onset of AL is important. The time to onset of AL affects both the severity of the complication and also the treatment of the complication itself. Colonic or rectal stump ischemia due to excessive preparation of the stump itself with consequent interruption of the perianastomotic supply of microvascular blood or tension in the anastomotic site is usually responsible for the early onset of AL [11]. On the other hand, the late presentation of AL is not linked to surgical technique problems but rather to clinical conditions of impaired tissue healing, such as local sepsis, malnutrition, the intake of immunosuppressive drugs, severe obesity and exposure to radiation[9,12]. In most patients, AL that occurs early is associated with more severe clinical symptoms. Faecal contamination of the peritoneum is frequently observed in these patients and the incidence of emergency laparotomies is higher. In conditions of worsening sepsis, mortality rates increase. By contrast, in late forms of AL, clinical manifestations will be characterized by the appearance of a pelvic abscess[13,14].

Furthermore, we believe that early diagnosis of AL is essential in order to establish the most appropriate treatment for this complication[15]. Despite AL continues to be a dreadful complication after colorectal surgery, there has been no consensus on its management[5]. Today, however, there is an increasing use of more conservative management. It is preferred to keep surgery as a last resort. Obviously this attitude is related to the presentation of the patient and the timing of the AL[16-18]. In agreement with Vignali and De Nardi[1], we believe that saving the anastomosis through the use of conservative treatments represents a valid therapeutic option to be used especially in clinically stable patients or in the presence of a small defect.

The authors focus their attention on EVT. Its principle is based on the application of topic negative pressure to drain the cavity and to prevent the development of chronic sinus. The paragraph on the description of the device is interesting and exhaustive, too. We agree with Vignali and De Nardi[1] that several reviews, and meta-analyses have been published so far with promising results. Nevertheless, the analysis of most documents yields mixed results, especially when the success rate, anastomosis salvage rates, and long-term outcomes are taken into account. Furthermore, the paucity of comparative studies does not allow definitive conclusions to be drawn, as pointed out by the authors in their narrative review.

There are several treatment options, including recently developed endoscopic procedures, such as stent or clip placement or EVT. These procedures can be used primarily in patients who already have a diverting stoma at the time of the leak. These treatments also find application in patients with extraperitoneal anastomosis and in those without ostomy who do not require further surgery due to a contained pelvic loss (type B of the ISREC classification). EVT is performed endoscopically. An open-pored polyurethane sponge is positioned in the leakage cavity through the anastomotic defect. The main advantages of the treatment are represented by a less invasive approach and continuous drainage. Treatment favors granulation and vascularity; furthermore, it determines a mechanical reduction in the size of the abscess cavity[19-21]. The main indication for the use of the EVT are extraperitoneal, low leaks that are difficult to drain. A disadvantage to the systematic adoption of EVT is the fact that the sponges must be periodically changed, usually more than 8 times in 4-6 wk. Anastomotic necrosis and stricture are the most common complications of the procedure.

The AL treatment should be tailored taking into consideration many factors, giving that there is no universally accepted management flowchart for the optimal treatment of this complication. Non-operative management is usually preferred in patients with extraperitoneal anastomosis without sepsis and peritonitis and in those who underwent proximal faecal diversion at the initial operation[5]. Excluding complications directly related to the endoluminal device, the factors associated with the failure of a conservative approach using EVT are mainly represented by neoadjuvant therapy, lack of a protective stoma before treatment and male sex. However, it must be emphasized that most of these are well known risk factors for AL in general. The timing of EVT can influence success, significantly. A high success rate occurs when endoluminal therapy is started early (within 6 wk) after the onset of AL[22, 23]. Riss *et al*[24] found that 25% of patients assessed after primary successful EVT in a multicentre study developed recurrent abscesses after a median follow-up of 17 mo. No study in the literature has focused attention on oncological and functional outcomes.

It seems obvious to us that in case of AL it is better to prevent its complications rather than treat them once they have arisen. Unfortunately, we believe that complications after colorectal surgery are still inevitable. We are sure that also Vignali and De Nardi[1] agree with our orientation.

Moreover, surgeons have employed several intraoperative techniques to assess integrity of the colorectal anastomoses in order to minimize the risks of postoperative complications. Basic mechanic patency tests (traditional air leak testing, saline leak, and methylene blue leak tests), endoscopic visualization techniques, and more recently, micro perfusion assessment technology are the most commonly used methods. Other methods commonly adopted to evaluate the blood perfusion of the intestinal segments to be used for the creation of the anastomosis are the visual evaluation of the color of the intestinal wall, the presence of visible peristalsis and bleeding from the marginal arteries. These tests are limited. None of these tests allow viewing of the lumen. The anastomosis is assessed by occluding the proximal lumen and then filling the intraluminal cavity with air or fluid and checking for leakage[2,25].

Intraoperative endoscopy was used to visualize the anastomosis. However, the use of the method is not so widespread. Furthermore, the results of intraoperative endoscopy are not of univocal interpretation. A recent systematic review evaluating the results of five non-randomized controlled trials, in which a total of over 900 patients were enrolled, documented an incidence rate of AL of 7.7% in patients with documented AL at intraoperative endoscopy, with no significant difference in postoperative AL rate compared to patients with negative intraoperative endoscopy for AL[26].

Nowadays, a promising and increasingly used new technology is intra-operative fluorescence angiography with indocyanine green[2,27-29]. Evidence for the impact of intraoperative fluorescence angiography in reducing AL after colorectal anastomosis is growing. The procedure allows direct visualization of tissue perfusion. It may help to prevent AL. The use of indocyanine green fluorescence angiography leads to a significant reduction in AL compared to standard intraoperative methods to assess anastomotic blood perfusion in colorectal surgery. Moreover, especially in patients with low or ultra-low rectal resection, the use of indocyanine green fluorescence decreases the need for surgical reintervention for AL.

A diverting stoma ideally protects a low colorectal anastomosis. However, there is a lot of controversy surrounding the use of a protective stoma. The first controversy is certainly about which is the most optimal type of ostomy, an ileostomy or a colostomy[30]. We believe that ostomy is useful to reduce clinical symptoms of AL by increasing the percentage of sub-clinical dehiscence, but not modifying the overall percentage. Moreover, no significant benefit of a diverting stoma for reducing the risk of AL has been showed in some large-volume studies. Usually, we tend to protect with an ostomy the patients who underwent neoadjuvant radiotherapy and those with an ultralow colorectal anastomosis. In recent years, this dogma has been challenged. Several authors questioning the need of an ostomy for all patients with an ultralow anastomosis.

We believe that the use of a transanastomotic drainage tube (TDT) may be useful in preventing the onset of AL. Regarding the TDT, several studies showed no difference in AL rate between patients with and without one[31]. Other literature observations, instead, have documented a reduction in frequency of AL in patients with TDT[32-35]. Prophylactic TDT presents fewer risks of complication than derivative stoma. It was thought to lower the risk of AL, *per* as documented in a systematic review and meta-analysis pooling 1772 patients undergoing rectal anterior resection[36]. The same conclusions were obtained in another systematic review and meta-analysis, including patients with diverting stoma[37].

Therefore, prophylactic TDT could constitute an efficient method to prevent AL in high-risk patients without exposing them to the complications of a diverting stoma. However, it is necessary to conduct an RCT on a large number of patients in order to obtain definitive results from the comparison of the two techniques.

AL after rectal surgery is a fearsome complication with considerable mortality and morbidity. Many factors are related to the onset of AL in the postoperative period. Some of these factors cannot be changed in the least by medical intervention. It is paramount to identify leaks early to minimize the potential morbidities of this complication. Despite advances in combating surgical infections, new devices for bowel reapproximation, better understanding of risk factors for anastomotic complications, and improved perioperative care, we continue to struggle with the occurrence and management of this complication. Technology will likely never be developed that would allow surgeons to prevent the onset of AL in the postoperative period. The use of the TDT prevents the formation of AL. This is a simple method that could avoid performing diverting ileostomies. AL can be further reduced by fluorescence angiography. This method, while bringing significant intraoperative changes in surgical strategies, allows the direct evaluation of the vascularization of the intestinal segments. In the meantime, it's necessary promptly diagnose AL. Likewise, the knowledge of all the therapeutic possibilities, from the least invasive ones to surgery, is necessary in order to treat AL and improve patient outcomes by reducing the incidence of functional disorders or the impact on survival.

FOOTNOTES

Author contributions: Chiarello MM and Brisinda G conceived the original idea; Fransvea P and Bianchi V performed a comprehensive review of all available literature and summarized the data; Brisinda G and Chiarello MM meet the criteria for authorship established by the International Committee of Medical Journal Editors and verify the validity of the results reported; all authors read and approved the final manuscript.

Conflict-of-interest statement: All the authors report no relevant conflicts of interest for this article.

Open-Access: This article is an open-access article that was selected by an in-house editor and fully peer-reviewed by external reviewers. It is distributed in accordance with the Creative Commons Attribution NonCommercial (CC BY-NC 4.0) license, which permits others to distribute, remix, adapt, build upon this work non-commercially, and license their derivative works on different terms, provided the original work is properly cited and the use is non-commercial. See: https://creativecommons.org/Licenses/by-nc/4.0/

Country/Territory of origin: Italy

ORCID number: Maria Michela Chiarello 0000-0003-3455-0062; Valentina Bianchi 0000-0002-8817-3760; Pietro Fransvea 0000-0003-4969-3373; Giuseppe Brisinda 0000-0001-8820-9471.

S-Editor: Fan JR
L-Editor: A
P-Editor: Fan JR

REFERENCES

1 **Vignali A**, De Nardi P. Endoluminal vacuum-assisted therapy to treat rectal anastomotic leakage: A critical analysis. *World J Gastroenterol* 2022; **28**: 1394-1404 [PMID: 35582677 DOI: 10.3748/wjg.v28.i14.1394]
2 **De Nardi P**, Elmore U, Maggi G, Maggiore R, Boni L, Cassinotti E, Fumagalli U, Gardani M, De Pascale S, Parise P, Vignali A, Rosati R. Intraoperative angiography with indocyanine green to assess anastomosis perfusion in patients undergoing laparoscopic colorectal resection: results of a multicenter randomized controlled trial. *Surg Endosc* 2020; **34**: 53-60 [PMID: 30903276 DOI: 10.1007/s00464-019-06730-0]
3 **Vignali A**, De Nardi P. Multidisciplinary treatment of rectal cancer in 2014: where are we going? *World J Gastroenterol* 2014; **20**: 11249-11261 [PMID: 25170209 DOI: 10.3748/wjg.v20.i32.11249]
4 **Vignali A**, Ghirardelli L, Di Palo S, Orsenigo E, Staudacher C. Laparoscopic treatment of advanced colonic cancer: a case-matched control with open surgery. *Colorectal Dis* 2013; **15**: 944-948 [PMID: 23398664 DOI: 10.1111/codi.12170]
5 **Chiarello MM**, Fransvea P, Cariati M, Adams NJ, Bianchi V, Brisinda G. Anastomotic leakage in colorectal cancer surgery. *Surg Oncol* 2022; **40**: 101708 [PMID: 35092916 DOI: 10.1016/j.suronc.2022.101708]
6 **Paun BC**, Cassie S, MacLean AR, Dixon E, Buie WD. Postoperative complications following surgery for rectal cancer. *Ann Surg* 2010; **251**: 807-818 [PMID: 20395841 DOI: 10.1097/SLA.0b013e3181dae4ed]
7 **Alves A**, Panis Y, Lelong B, Dousset B, Benoist S, Vicaut E. Randomized clinical trial of early *vs* delayed temporary stoma closure after proctectomy. *Br J Surg* 2008; **95**: 693-698 [PMID: 18446781 DOI: 10.1002/bjs.6212]
8 **Fazio VW**, Zutshi M, Remzi FH, Parc Y, Ruppert R, Fürst A, Celebrezze J Jr, Galanduik S, Orangio G, Hyman N, Bokey L, Tiret E, Kirchdorfer B, Medich D, Tietze M, Hull T, Hammel J. A randomized multicenter trial to compare long-term functional outcome, quality of life, and complications of surgical procedures for low rectal cancers. *Ann Surg* 2007; **246**:

481-8; discussion 488 [PMID: 17717452 DOI: 10.1097/SLA.0b013e3181485617]
9 **Brisinda G**, Vanella S, Cadeddu F, Civello IM, Brandara F, Nigro C, Mazzeo P, Marniga G, Maria G. End-to-end *vs* end-to-side stapled anastomoses after anterior resection for rectal cancer. *J Surg Oncol* 2009; **99**: 75-79 [PMID: 18985633 DOI: 10.1002/jso.21182]
10 **Rahbari NN**, Weitz J, Hohenberger W, Heald RJ, Moran B, Ulrich A, Holm T, Wong WD, Tiret E, Moriya Y, Laurberg S, den Dulk M, van de Velde C, Büchler MW. Definition and grading of anastomotic leakage following anterior resection of the rectum: a proposal by the International Study Group of Rectal Cancer. *Surgery* 2010; **147**: 339-351 [PMID: 20004450 DOI: 10.1016/j.surg.2009.10.012]
11 **Park JS**, Choi GS, Kim SH, Kim HR, Kim NK, Lee KY, Kang SB, Kim JY, Kim BC, Bae BN, Son GM, Lee SI, Kang H. Multicenter analysis of risk factors for anastomotic leakage after laparoscopic rectal cancer excision: the Korean laparoscopic colorectal surgery study group. *Ann Surg* 2013; **257**: 665-671 [PMID: 23333881 DOI: 10.1097/SLA.0b013e31827b8ed9]
12 **Sparreboom CL**, van Groningen JT, Lingsma HF, Wouters MWJM, Menon AG, Kleinrensink GJ, Jeekel J, Lange JF; Dutch ColoRectal Audit group. Different Risk Factors for Early and Late Colorectal Anastomotic Leakage in a Nationwide Audit. *Dis Colon Rectum* 2018; **61**: 1258-1266 [PMID: 30239395 DOI: 10.1097/DCR.0000000000001202]
13 **Lim SB**, Yu CS, Kim CW, Yoon YS, Park IJ, Kim JC. Late anastomotic leakage after low anterior resection in rectal cancer patients: clinical characteristics and predisposing factors. *Colorectal Dis* 2016; **18**: O135-O140 [PMID: 26888300 DOI: 10.1111/codi.13300]
14 **Lim SB**, Yu CS, Kim CW, Yoon YS, Park IJ, Kim JC. The types of anastomotic leakage that develop following anterior resection for rectal cancer demonstrate distinct characteristics and oncologic outcomes. *Int J Colorectal Dis* 2015; **30**: 1533-1540 [PMID: 26260482 DOI: 10.1007/s00384-015-2359-7]
15 **Chiarello MM**, Brisinda G. A Commentary on "Diagnostic accuracy of procalcitonin on POD3 for the early diagnosis of anastomotic leakage after colorectal surgery: A meta-analysis and systematic review" (Int. J. Surg. 2022; 100: 106592). *Int J Surg* 2022; **101**: 106624 [PMID: 35472516 DOI: 10.1016/j.ijsu.2022.106624]
16 **Ahmad NZ**, Abbas MH, Khan SU, Parvaiz A. A meta-analysis of the role of diverting ileostomy after rectal cancer surgery. *Int J Colorectal Dis* 2021; **36**: 445-455 [PMID: 33064212 DOI: 10.1007/s00384-020-03771-z]
17 **Hüser N**, Michalski CW, Erkan M, Schuster T, Rosenberg R, Kleeff J, Friess H. Systematic review and meta-analysis of the role of defunctioning stoma in low rectal cancer surgery. *Ann Surg* 2008; **248**: 52-60 [PMID: 18580207 DOI: 10.1097/SLA.0b013e318176bf65]
18 **Wang Z**, Yang YS, Zhao XF. A novel multi-modal approach for prevention and treatment of anastomotic leakage after low anterior resection in rectal cancer patients. *Asian J Surg* 2022; **45**: 539-541 [PMID: 34642051 DOI: 10.1016/j.asjsur.2021.09.008]
19 **Bobkiewicz A**, Krokowicz L, Banasiewicz T, Borejsza-Wysocki M. Endoscopic vacuum therapy with instillation (iEVT) - a novel endoscopic concept for colorectal anastomotic leak and perianal complications. *Wideochir Inne Tech Maloinwazyjne* 2020; **15**: 560-566 [PMID: 33294070 DOI: 10.5114/wiitm.2020.93204]
20 **Kühn F**, Wirth U, Zimmermann J, Beger N, Hasenhütl SM, Drefs M, Heiliger C, Burian M, Werner J, Schiergens TS. Endoscopic vacuum therapy for in- and outpatient treatment of colorectal defects. *Surg Endosc* 2021; **35**: 6687-6695 [PMID: 33259019 DOI: 10.1007/s00464-020-08172-5]
21 **Shalaby M**, Emile S, Elfeki H, Sakr A, Wexner SD, Sileri P. Systematic review of endoluminal vacuum-assisted therapy as salvage treatment for rectal anastomotic leakage. *BJS Open* 2019; **3**: 153-160 [PMID: 30957061 DOI: 10.1002/bjs5.50124]
22 **Weidenhagen R**, Gruetzner KU, Wiecken T, Spelsberg F, Jauch KW. Endoscopic vacuum-assisted closure of anastomotic leakage following anterior resection of the rectum: a new method. *Surg Endosc* 2008; **22**: 1818-1825 [PMID: 18095024 DOI: 10.1007/s00464-007-9706-x]
23 **van Koperen PJ**, van Berge Henegouwen MI, Rosman C, Bakker CM, Heres P, Slors JF, Bemelman WA. The Dutch multicenter experience of the endo-sponge treatment for anastomotic leakage after colorectal surgery. *Surg Endosc* 2009; **23**: 1379-1383 [PMID: 19037698 DOI: 10.1007/s00464-008-0186-4]
24 **Riss S**, Stift A, Meier M, Haiden E, Grünberger T, Bergmann M. Endo-sponge assisted treatment of anastomotic leakage following colorectal surgery. *Colorectal Dis* 2010; **12**: e104-e108 [PMID: 19508536 DOI: 10.1111/j.1463-1318.2009.01885.x]
25 **Rausa E**, Zappa MA, Kelly ME, Turati L, Russo A, Aiolfi A, Bonitta G, Sgroi LG. A standardized use of intraoperative anastomotic testing in colorectal surgery in the new millennium: is technology taking over? *Tech Coloproctol* 2019; **23**: 625-631 [PMID: 31302816 DOI: 10.1007/s10151-019-02034-6]
26 **Hirst NA**, Tiernan JP, Millner PA, Jayne DG. Systematic review of methods to predict and detect anastomotic leakage in colorectal surgery. *Colorectal Dis* 2014; **16**: 95-109 [PMID: 23992097 DOI: 10.1111/codi.12411]
27 **Amagai H**, Miyauchi H, Muto Y, Uesato M, Ohira G, Imanishi S, Maruyama T, Tochigi T, Okada K, Maruyama M, Matsubara H. Clinical utility of transanal indocyanine green near-infrared fluorescence imaging for evaluation of colorectal anastomotic perfusion. *Surg Endosc* 2020; **34**: 5283-5293 [PMID: 31820154 DOI: 10.1007/s00464-019-07315-7]
28 **Benčurik V**, Škrovina M, Martínek L, Bartoš J, Macháčková M, Dosoudil M, Štěpánová E, Přibylová L, Briš R, Vomáčková K. Intraoperative fluorescence angiography and risk factors of anastomotic leakage in mini-invasive low rectal resections. *Surg Endosc* 2021; **35**: 5015-5023 [PMID: 32970211 DOI: 10.1007/s00464-020-07982-x]
29 **Mangano A**, Gheza F, Chen LL, Minerva EM, Giulianotti PC. Indocyanine Green (Icg)-Enhanced Fluorescence for Intraoperative Assessment of Bowel Microperfusion During Laparoscopic and Robotic Colorectal Surgery: The Quest for Evidence-Based Results. *Surg Technol Int* 2018; **32**: 101-104 [PMID: 29611153]
30 **Güenaga KF**, Lustosa SA, Saad SS, Saconato H, Matos D. Ileostomy or colostomy for temporary decompression of colorectal anastomosis. *Cochrane Database Syst Rev* 2007; CD004647 [PMID: 17253517 DOI: 10.1002/14651858.CD004647.pub2]
31 **Zhao S**, Zhang L, Gao F, Wu M, Zheng J, Bai L, Li F, Liu B, Pan Z, Liu J, Du K, Zhou X, Li C, Zhang A, Pu Z, Li Y, Feng B, Tong W. Transanal Drainage Tube Use for Preventing Anastomotic Leakage After Laparoscopic Low Anterior Resection in Patients With Rectal Cancer: A Randomized Clinical Trial. *JAMA Surg* 2021; **156**: 1151-1158 [PMID:

34613330 DOI: 10.1001/jamasurg.2021.4568]
32 **Choy KT**, Yang TWW, Heriot A, Warrier SK, Kong JC. Does rectal tube/transanal stent placement after an anterior resection for rectal cancer reduce anastomotic leak? *Int J Colorectal Dis* 2021; **36**: 1123-1132 [PMID: 33515307 DOI: 10.1007/s00384-021-03851-8]
33 **Wang Z**, Liang J, Chen J, Mei S, Liu Q. Effectiveness of a Transanal Drainage Tube for the Prevention of Anastomotic Leakage after Laparoscopic Low Anterior Resection for Rectal Cancer. *Asian Pac J Cancer Prev* 2020; **21**: 1441-1444 [PMID: 32458653 DOI: 10.31557/APJCP.2020.21.5.1441]
34 **Kawada K**, Takahashi R, Hida K, Sakai Y. Impact of transanal drainage tube on anastomotic leakage after laparoscopic low anterior resection. *Int J Colorectal Dis* 2018; **33**: 337-340 [PMID: 29270785 DOI: 10.1007/s00384-017-2952-z]
35 **Matsuda M**, Tsuruta M, Hasegawa H, Okabayashi K, Kondo T, Shimada T, Yahagi M, Yoshikawa Y, Kitagawa Y. Transanal drainage tube placement to prevent anastomotic leakage following colorectal cancer surgery with double stapling reconstruction. *Surg Today* 2016; **46**: 613-620 [PMID: 26231480 DOI: 10.1007/s00595-015-1230-3]
36 **Yang Y**, Shu Y, Su F, Xia L, Duan B, Wu X. Prophylactic transanal decompression tube *vs* non-prophylactic transanal decompression tube for anastomotic leakage prevention in low anterior resection for rectal cancer: a meta-analysis. *Surg Endosc* 2017; **31**: 1513-1523 [PMID: 27620910 DOI: 10.1007/s00464-016-5193-2]
37 **Chen H**, Cai HK, Tang YH. An updated meta-analysis of transanal drainage tube for prevention of anastomotic leak in anterior resection for rectal cancer. *Surg Oncol* 2018; **27**: 333-340 [PMID: 30217286 DOI: 10.1016/j.suronc.2018.05.018]



Published by **Baishideng Publishing Group Inc**
7041 Koll Center Parkway, Suite 160, Pleasanton, CA 94566, USA
Telephone: +1-925-3991568
E-mail: bpgoffice@wjgnet.com
Help Desk: https://www.f6publishing.com/helpdesk
https://www.wjgnet.com



© 2022 Baishideng Publishing Group Inc. All rights reserved.

ISSN 1007-9327 (print)
ISSN 2219-2840 (online)

World Journal of *Gastroenterology*

World J Gastroenterol 2022 August 7; 28(29): 3753-4018



Published by Baishideng Publishing Group Inc

World Journal of Gastroenterology

Contents

Weekly Volume 28 Number 29 August 7, 2022

REVIEW

3753 Mechanistic and functional extrapolation of SET and MYND domain-containing protein 2 to pancreatic cancer

Alshammari E, Zhang YX, Yang Z

MINIREVIEWS

3767 Clinical challenge for gastroenterologists–Gastrointestinal manifestations of systemic mastocytosis: A comprehensive review

Elvevi A, Elli EM, Lucà M, Scaravaglio M, Pagni F, Ceola S, Ratti L, Invernizzi P, Massironi S

3780 Structural changes of proteins in liver cirrhosis and consequential changes in their function

Gligorijević N, Minić S, Nedić O

3793 Epidemiologic and socioeconomic factors impacting hepatitis B virus and related hepatocellular carcinoma

Gnyawali B, Pusateri A, Nickerson A, Jalil S, Mumtaz K

3803 Endoscopic salvage therapy after failed biliary cannulation using advanced techniques: A concise review

Tsou YK, Pan KT, Lee MH, Lin CH

3814 Enhanced endoscopic ultrasound imaging for pancreatic lesions: The road to artificial intelligence

Spadaccini M, Koleth G, Emmanuel J, Khalaf K, Facciorusso A, Grizzi F, Hassan C, Colombo M, Mangiavillano B, Fugazza A, Anderloni A, Carrara S, Repici A

ORIGINAL ARTICLE

Basic Study

3825 Qingyi decoction attenuates intestinal epithelial cell injury *via* the calcineurin/nuclear factor of activated T-cells pathway

Wang GY, Shang D, Zhang GX, Song HY, Jiang N, Liu HH, Chen HL

3838 High-fat diet aggravates colitis *via* mesenteric adipose tissue derived exosome metastasis-associated lung adenocarcinoma transcript 1

Chen D, Lu MM, Wang JH, Ren Y, Xu LL, Cheng WX, Wang SS, Li XL, Cheng XF, Gao JG, Kalyani FS, Jin X

3854 Involvement of nitrergic neurons in colonic motility in a rat model of ulcerative colitis

Li YR, Li Y, Jin Y, Xu M, Fan HW, Zhang Q, Tan GH, Chen J, Li YQ

3869 N-linked glycoproteomic profiling in esophageal squamous cell carcinoma

Liu QW, Ruan HJ, Chao WX, Li MX, Jiao YL, Ward DG, Gao SG, Qi YJ

3886 HP0953 - hypothetical virulence factor overexpresion and localization during *Helicobacter pylori* infection of gastric epithelium

Arteaga-Resendiz NK, Rodea GE, Ribas-Aparicio RM, Olivares-Cervantes AL, Castelán-Vega JA, Olivares-Trejo JJ, Mendoza-Elizalde S, López-Villegas EO, Colín C, Aguilar-Rodea P, Reyes-López A, Salazar García M, Velázquez-Guadarrama N

3903 Involvement of toll-like receptor 5 in mouse model of colonic hypersensitivity induced by neonatal maternal separation

Mallaret G, Lashermes A, Meleine M, Boudieu L, Barbier J, Aissouni Y, Gelot A, Chassaing B, Gewirtz AT, Ardid D, Carvalho FA

Case Control Study

3917 Comprehensive evaluation of microRNA as a biomarker for the diagnosis of hepatocellular carcinoma

Malik J, Klammer M, Rolny V, Chan HLY, Piratvisuth T, Tanwandee T, Thongsawat S, Sukeepaisarnjaroen W, Esteban JI, Bes M, Köhler B, Swiatek-de Lange M

Retrospective Cohort Study

3934 Optimal timing of biliary drainage based on the severity of acute cholangitis: A single-center retrospective cohort study

Lu ZQ, Zhang HY, Su CF, Xing YY, Wang GX, Li CS

Retrospective Study

3946 Incidence and clinical characteristics of hypertriglyceridemic acute pancreatitis: A retrospective single-center study

Lin XY, Zeng Y, Zhang ZC, Lin ZH, Chen LC, Ye ZS

3960 Radiomics for differentiating tumor deposits from lymph node metastasis in rectal cancer

Zhang YC, Li M, Jin YM, Xu JX, Huang CC, Song B

3971 Effects of microwave ablation on serum Golgi protein 73 in patients with primary liver cancer

Xu ZJ, Wei MJ, Zhang XM, Liu HG, Wu JP, Huang JF, Li YF, Huang ZJ, Yan YY

Observational Study

3981 Evaluating the best treatment for multifocal hepatocellular carcinoma: A propensity score-matched analysis

Risaliti M, Bartolini I, Campani C, Arena U, Xodo C, Adotti V, Rosi M, Taddei A, Muiesan P, Amedei A, Batignani G, Marra F

3994 Structure of the myenteric plexus in normal and diseased human ileum analyzed by X-ray virtual histology slices

Veress B, Peruzzi N, Eckermann M, Frohn J, Salditt T, Bech M, Ohlsson B

META-ANALYSIS

4007 Recurrence rates after endoscopic resection of large colorectal polyps: A systematic review and meta-analysis

Rotermund C, Djinbachian R, Taghiakbari M, Enderle MD, Eickhoff A, von Renteln D

World Journal of Gastroenterology

Weekly Volume 28 Number 29 August 7, 2022

Contents

ABOUT COVER

Editorial Board Member of *World Journal of Gastroenterology*, Nikolaos Papadopoulos, MD, PhD, Consultant, The First Department of Internal Medicine, 417 Army Share Fund Hospital, Monis Petraki 10-12, Athens 11521, Greece. nipapmed@gmail.com

AIMS AND SCOPE

The primary aim of *World Journal of Gastroenterology* (*WJG*, *World J Gastroenterol*) is to provide scholars and readers from various fields of gastroenterology and hepatology with a platform to publish high-quality basic and clinical research articles and communicate their research findings online. *WJG* mainly publishes articles reporting research results and findings obtained in the field of gastroenterology and hepatology and covering a wide range of topics including gastroenterology, hepatology, gastrointestinal endoscopy, gastrointestinal surgery, gastrointestinal oncology, and pediatric gastroenterology.

INDEXING/ABSTRACTING

The *WJG* is now abstracted and indexed in Science Citation Index Expanded (SCIE, also known as SciSearch®), Current Contents/Clinical Medicine, Journal Citation Reports, Index Medicus, MEDLINE, PubMed, PubMed Central, Scopus, Reference Citation Analysis, China National Knowledge Infrastructure, China Science and Technology Journal Database, and Superstar Journals Database. The 2022 edition of Journal Citation Reports® cites the 2021 impact factor (IF) for *WJG* as 5.374; IF without journal self cites: 5.187; 5-year IF: 5.715; Journal Citation Indicator: 0.84; Ranking: 31 among 93 journals in gastroenterology and hepatology; and Quartile category: Q2. The *WJG*'s CiteScore for 2021 is 8.1 and Scopus CiteScore rank 2021: Gastroenterology is 18/149.

RESPONSIBLE EDITORS FOR THIS ISSUE

Production Editor: *Ying-Yi Yuan*; **Production Department Director:** *Xiang Li*; **Editorial Office Director:** *Jia-Ru Fan.*

NAME OF JOURNAL
World Journal of Gastroenterology

ISSN
ISSN 1007-9327 (print) ISSN 2219-2840 (online)

LAUNCH DATE
October 1, 1995

FREQUENCY
Weekly

EDITORS-IN-CHIEF
Andrzej S Tarnawski

EDITORIAL BOARD MEMBERS
http://www.wjgnet.com/1007-9327/editorialboard.htm

PUBLICATION DATE
August 7, 2022

COPYRIGHT
© 2022 Baishideng Publishing Group Inc

INSTRUCTIONS TO AUTHORS
https://www.wjgnet.com/bpg/gerinfo/204

GUIDELINES FOR ETHICS DOCUMENTS
https://www.wjgnet.com/bpg/GerInfo/287

GUIDELINES FOR NON-NATIVE SPEAKERS OF ENGLISH
https://www.wjgnet.com/bpg/gerinfo/240

PUBLICATION ETHICS
https://www.wjgnet.com/bpg/GerInfo/288

PUBLICATION MISCONDUCT
https://www.wjgnet.com/bpg/gerinfo/208

ARTICLE PROCESSING CHARGE
https://www.wjgnet.com/bpg/gerinfo/242

STEPS FOR SUBMITTING MANUSCRIPTS
https://www.wjgnet.com/bpg/GerInfo/239

ONLINE SUBMISSION
https://www.f6publishing.com

© 2022 Baishideng Publishing Group Inc. All rights reserved. 7041 Koll Center Parkway, Suite 160, Pleasanton, CA 94566, USA
E-mail: bpgoffice@wjgnet.com https://www.wjgnet.com

World Journal of Gastroenterology

Submit a Manuscript: https://www.f6publishing.com

World J Gastroenterol 2022 August 7; 28(29): 3753-3766

DOI: 10.3748/wjg.v28.i29.3753

ISSN 1007-9327 (print) ISSN 2219-2840 (online)

REVIEW

Mechanistic and functional extrapolation of SET and MYND domain-containing protein 2 to pancreatic cancer

Eid Alshammari, Ying-Xue Zhang, Zhe Yang

Specialty type: Oncology

Provenance and peer review: Invited article; Externally peer reviewed.

Peer-review model: Single blind

Peer-review report's scientific quality classification

Grade A (Excellent): 0
Grade B (Very good): B, B
Grade C (Good): 0
Grade D (Fair): 0
Grade E (Poor): 0

P-Reviewer: Trna J, Czech Republic; Zafari N, Iran

Received: January 18, 2022
Peer-review started: January 18, 2022
First decision: April 11, 2022
Revised: April 24, 2022
Accepted: July 5, 2022
Article in press: July 5, 2022
Published online: August 7, 2022

Eid Alshammari, Ying-Xue Zhang, Department of Biochemistry, Microbiology, and Immunology, Wayne State University, Detroit, MI 48201, United States

Zhe Yang, Department of Biochemistry, Microbiology, and Immunology, Wayne State University School of Medicine, Detroit, MI 48201, United States

Corresponding author: Zhe Yang, PhD, Associate Professor, Department of Biochemistry, Microbiology, and Immunology, Wayne State University School of Medicine, 540 E Canfield St, Detroit, MI 48201, United States. zyang@med.wayne.edu

Abstract

Pancreatic ductal adenocarcinoma (PDAC) is one of the most lethal neoplasms worldwide and represents the vast majority of pancreatic cancer cases. Understanding the molecular pathogenesis and the underlying mechanisms involved in the initiation, maintenance, and progression of PDAC is an urgent need, which may lead to the development of novel therapeutic strategies against this deadly cancer. Here, we review the role of SET and MYND domain-containing protein 2 (SMYD2) in initiating and maintaining PDAC development through methylating multiple tumor suppressors and oncogenic proteins. Given the broad substrate specificity of SMYD2 and its involvement in diverse oncogenic signaling pathways in many other cancers, the mechanistic extrapolation of SMYD2 from these cancers to PDAC may allow for developing new hypotheses about the mechanisms driving PDAC tumor growth and metastasis, supporting a proposition that targeting SMYD2 could be a powerful strategy for the prevention and treatment of PDAC.

Key Words: Pancreatic ductal adenocarcinoma; Protein lysine methyltransferase; Histone/non-histone methylation; Oncogenic signaling pathways; Methyltransferase inhibitors

©The Author(s) 2022. Published by Baishideng Publishing Group Inc. All rights reserved.

Core Tip: The broad substrate specificity of SET and MYND domain-containing protein 2 (SMYD2) and its involvement in diverse oncogenic signaling pathways in numerous cancers have provided a wealth of information that could be extrapolated to the pancreatic ductal adenocarcinoma (PDAC) research field to expand our understanding of SMYD2 in PDAC development. This review not only discusses the known roles of SMYD2 in PDAC initiation and progression, but also aims to capitalize on a rich body of knowledge with respect to SMYD2's involvement in various signaling cascades to develop new hypotheses about the mechanisms of driving PDAC tumor growth and metastasis.

Citation: Alshammari E, Zhang YX, Yang Z. Mechanistic and functional extrapolation of SET and MYND domain-containing protein 2 to pancreatic cancer. *World J Gastroenterol* 2022; 28(29): 3753-3766
URL: https://www.wjgnet.com/1007-9327/full/v28/i29/3753.htm
DOI: https://dx.doi.org/10.3748/wjg.v28.i29.3753

INTRODUCTION

Pancreatic cancer is one of the top ten leading causes of cancer-related mortality worldwide, accounting for about 448000 new cases and 441000 deaths in 2017[1]. Pancreatic cancer comprises several types of tumors that arise from the endocrine or exocrine components of the pancreas. The vast majority of pancreatic tumors arise from the exocrine cells, which make up the exocrine gland and the ducts of the pancreas. Pancreatic ductal adenocarcinoma (PDAC) is the most common and aggressive form of pancreatic cancer, which represents about 85% of pancreatic cancer cases[2]. The incidence and mortality rates of pancreatic cancer have dramatically increased over the past few decades and vary considerably across regions and populations, with the highest trends being recorded in developed countries[3]. Although the causes and mechanisms that initiate the formation and development of pancreatic cancer are still largely unknown, the variation in regions and populations may be attributed to the variance in some of the risk factors and the socioeconomic lifestyle identified for this disease, such as obesity, diabetes, and smoking. In the United States, the incidence of pancreatic cancer continues to increase, with an estimation of 60430 new cases and 48200 deaths in 2021, and it has become the fourth leading cause of cancer-related mortality[4]. Pancreatic cancer has the poorest prognosis among the top ten common cancers, with the current 5-year survival (OS) rate of just 10%[4], and it is expected to be the second most common cause of cancer death by 2030[5].

Diagnosis and treatment of PDAC are still challenging due to its multifactorial nature. It is predominantly diagnosed in advanced stages with unresectable tumors due to several reasons, including the lack of early detection methods, the lack of specific PDAC biomarkers and simple examinations, the retroperitoneal location of the pancreas, and the nonspecific symptoms due to its highly metastatic nature early in the disease course[6]. Also, PDAC incidence is significantly associated with age, with the highest incidence rates being in elderly people[1]. Given the poor overall health of the elderly, the surgical resection is not feasible for the majority of elderly PDAC patients, especially for those who have metastatic cancers that have spread to the nearby abdominal vessels and critical organs at diagnosis[7]. Only a small fraction of PDAC patients diagnosed in the early stage have resectable tumors. Although the surgery in combination with adjuvant therapy remains the only cure for PDAC patients, the overall survival rate of PDAC patients is poor, even for those PDAC populations who have undergone surgery [8-10]. PDAC patients, after surgical resection, usually develop acquired chemoresistance, with a high rate of recurrence due to the very heterogeneous biology of PDAC and the aggressive clinical behavior of this disease[6]. These factors may explain the high mortality in PDAC patients; therefore, it is of great importance to identify the molecular mechanism of PDAC pathogenesis and the involved signaling pathways in order to discover novel targets and potential biomarkers for PDAC diagnosis and therapy.

SET and MYND domain-containing protein 2 (SMYD2) has been linked with tumor progression, poor prognosis, or a worse malignant outcome in multiple human cancers including PDAC[11-16]. This protein belongs to a special class of protein lysine methyltransferases and is characterized by a conserved catalytic SET domain split by an MYND domain[11]. The MYND domain of SMYD2 is a zinc finger motif that facilitates the protein-protein interaction, while the SET domain, an evolutionarily conserved motif, catalyzes the transfer of methyl groups to lysine residues of target proteins using S-adenosylmethionine (SAM) as a donor substrate[12]. The carcinogenic potential of SMYD2 is exemplified by its ability to methylate a broad spectrum of proteins involved in cellular signaling, cell cycle control, and cell differentiation and proliferation[17-20]. SMYD2 is an epigenetic regulator that has histone lysine methyltransferase activity and can methylate histones H3K36 and H3K4[11,12]. Through the dimethylation of histone H3 at Lys36 (H3K36me2), SMYD2 was reported to downregulate gene transcription, which is further enhanced by Sin3A-mediated deacetylation to suppress cell proliferation [11]. On the other hand, methylation of histone H3K4 by SMYD2 is usually associated with gene activation, yet the exact underlying mechanism by which this SMYD2-mediated methylation regulates

cell proliferation is not well understood[12,21]. Several investigations revealed multiple nonhistone substrates of SMYD2, including the tumor suppressor p53, retinoblastomaassociated protein (RB), ERα, HSP90, PARP1, and PTEN (Table 1)[22-27]. For instance, the tumor suppressor p53 is an important nonhistone target that is monomethylated by SMYD2 at Lys370 located in the regulatory domain of p53, repressing the p53's transcriptional regulatory activity and promoting cancer initiation and growth[22]. It has also been shown that through its broad methyltransferase activity on nonhistone proteins, SMYD2 impacts various signaling pathways required for the development and progression of the malignancies [17,28-32]. These pathways include the critical signaling cascade RTK/Ras, the downstream signaling cascades of the RTK/Ras pathway, such as the mitogen-activated protein kinase (MAPK) pathway, and the PI3K/AKT pathway[16,27,28,30,31]. As dysregulation of these signaling pathways is an almost universal phenomenon in cancer, it is not surprising that SMYD2 overexpression has been linked with tumor development and progression in multiple human cancers, such as gastric cancer[33], esophageal squamous cell carcinoma[34], breast cancer[30], bladder cancer[23], colon cancer[31,35], colorectal cancer[36], hepatocellular carcinoma[14], acute lymphoblastic leukemia[37,38], hematopoietic leukemias [39], head and neck squamous cell carcinoma[15], lung adenocarcinoma[13], papillary thyroid carcinoma[40], cervical cancer[41,42], ovarian clear cell carcinoma[43,44], and renal cell carcinoma[45,46] (Table 2).

Because of SMYD2 overexpression in numerous human tumors (Figure 1A), understanding the molecular mechanisms of SMYD2 in cancer initiation and development, and validating its therapeutic potential as a drug target to inhibit abnormal cell proliferation, have gained increasing interest in recent years; currently, SMYD2 is one of the most extensively studied protein lysine methyltransferases in the context of cancer. However, the involvement of SMYD2 in PDAC initiation and progression has not yet been fully explored. The overexpression of SMYD2 has been reported in PDAC by a study that showed methylation of the human MAPK activated protein kinase 3 (MAPKAPK3) by SMYD2 promotes tumor growth and progression[16]. Another investigation identified that the SMYD2 Locus is among the active chromatin sites unique to the genomes of the adenosquamous cancer of the pancreas (ASCP) and is associated with the active H3K4me1 histone mark[47]. These pioneering works, despite being limited in scope, demonstrate that SMYD2-mediated methylation of both histone and nonhistone proteins could also be an important tumorigenic event contributing to PDAC initiation and development. On the other hand, a rich body of knowledge available in many other human cancers with respect to the roles of SMYD2 in cell cycle control and various signaling cascades provides a wealth of information that could be extrapolated to the PDAC research field to expand our understanding of SMYD2 in PDAC development. Here, we review the known roles of SMYD2 in PDAC initiation and progression, and through capitalizing on the current knowledge about its known cancer-related functions in other human cancers, we propose there existing additional SMYD2-mediated methylation events involved in diverse signaling pathways that control and coordinate different cellular processes in PDAC.

CURRENT EVIDENCE OF SMYD2 INVOLVEMENT IN PANCREATIC CANCER

One study aimed to investigate the function of SMYD2 in PDAC using mouse and cellular models found evidence that SMYD2 plays a pivotal role in the development of this deadly pancreatic cancer[16] (Figure 1B). In other human cancers, SMYD2 usually exerts its tumorigenic effects through methylating cell signaling-related proteins and through the effect of such methylation on the targets' activity, stability, or subcellular localization[13,27,42,48]. Such a methylation-oriented mechanism has been instrumental for the initial development of a mechanistic hypothesis of SMYD2 involvement in PDAC and for the subsequent success of establishing a novel link of SMYD2 to promoting PDAC growth and progression[16]. Using an *in vitro* protein-array system, which consists of about 9500 human proteins, 159 proteins were identified as SMYD2 substrates in this study. Among these hits, MAPKAPK3 was selected for further analysis due to being implicated in cancer and being linked to Ras signaling, a key driver of PDAC[16,49-52]. Although the roles of MAPKAPK3, like those of SMYD2, in PDAC were unknown at the time of the study, MAPKAPK3 has been known as a mediator in the MAPK/ERK cascade that is responsible for regulating a wide variety of stimulated cellular processes[53-55]. It has also been shown that MAPKAPK3, phosphorylated by ERK1/2, p38 kinase, and SAPK/JNK, plays a role in inflammation and stress responses[56-59]. Therefore, the identification of MAPKAPK3 as a new SMYD2 substrate suggested a novel regulatory axis in PDAC progression.

Further characterization confirmed that the SMYD2-MAPKAPK3 axis is required for efficient PDAC development and that SMYD2-mediated methylation of MAPKAPK3 is a key event during the K-Ras-driven transformation of PDAC cells *in vivo*[16]. Lys355 of MAPKAPK3 was identified as a site of methylation targeted by SMYD2 using a mutagenesis approach and an LC-MS/MS analysis. Specificity analyses using an MS approach showed that the related protein MAPKAPK2, which shares about 75% sequence identity with MAPKAPK3, as well as other MAPKAPK proteins, are not substrates of SMYD2. On the other hand, none of the eight active lysine methyltransferases, including SMYD3 and SET8, could methylate MAPKAPK3 *in vitro*. Co-expression of SMYD2 and MAPKAPK3 in PDAC cells identified MAPKAPK3-K355me1 in a SMYD2-dependent manner, demonstrating that only SMYD2 can

Table 1 Major SET and MYND domain-containing protein 2 nonhistone substrates

Substrate	Methylation site	Methylation effect	Affected pathways	Role of substrates in PDAC	Ref.
ALK	K1451; K1455; K1610	Promotes EML4-ALK phosphorylation and NSCLC cell growth	PI3K/AKT; JAK/STAT; RTK/Ras	ALK rearrangement-positive cancer correlates with better response to chemotherapy	[28, 96]
β-catenin	K133	Promotes β-catenin nuclear translocation	Wnt/β-catenin/TCF	Mediates EMT; promotes cell proliferation, migration, and invasion	[48, 97]
BMPR2	Kinase domain	Stimulates BMPR2 kinase activity; SMAD1/5 phosphorylation; BMP pathway activation	BMP	Promotes tumor growth *via* GRB2/PI3K/AKT pathway	[98, 99]
ERα	K266	Suppresses ERα target gene activation	PI3K/AKT; MAPK-ERK	ERα expression correlates with tumor progression; endocrine therapies	[100, 101]
EZH2	K307	Promotes EZH2 stability; cell proliferation; EMT;invasion in BC	RB-E2F	Linked to an aggressive phenotype	[102, 103]
HSP90AB1	K531; K574	Enhances dimerization; chaperone complex formation of HSP90AB1; promotes cancer cell proliferation	PI3K/AKT	Targeting HSP90 decreases GEM chemores-istance	[25, 104]
MAPKAPK3	K355	Promotes pancreatic ductal adenocarcinoma	RTK/Ras; MAPK-ERK	Interacts with HSP27; mediates gemcitabine toxicity	[16]
p53	K370	Inhibits p53 and p53-mediated transcrip-tional regulation	p53	p53 methylation correlates with aggressive tumors; poor prognosis	[16, 22]
PARP1	K528	Enhances poly (ADP-ribosyl) ation enzymatic activity; promotes apoptotic escape of cancer cells	Base excision repair	Promotes tumorigenesis and resistance	[26, 105]
PTEN	K313	Inactivates PTEN; promotes BC cell prolif-eration	PI3K-AKT	Loss of PTEN enhances activation of PI3K-AKT; NF-κB and MYC; promotes tumor cell growth and survival	[27, 74]
RB	K810; K860	Enhances Ser 807/811 phosphorylation of RB1; enhances E2F transcriptional activity; cell cycle progression	RB-E2F pathway	Reduced expression of RB correlates with cancer progression	[23, 76,78]
STAT3	K685	Activates and phosphorylates STAT3; promotes cell proliferation and survival in triple-negative BC	JAK2/STAT3	Suppress apoptosis *via* regulation of BCL-2 family; promotes tumorigenesis	[30, 106]
P65	K310	Activates and phosphorylation p65; represses tumor cell apoptosis in triple-negative BC	NF-κB pathway	-	[30]

PDAC: Pancreatic ductal adenocarcinoma; MAPKAPK3: Mitogen-activated protein kinase activated protein kinase 3; RB: Retinoblastomaassociated protein; BC: Breast cancer; STAT3: Signal transducer and activator of transcription 3; BCL-2: B cell lymphoma-2.

monomethylate MAPKAPK3 at Lys355 both *in vitro* and *in vivo*. Moreover, depletion of SMYD2 led to a decreased expression of endogenous methylation of MAPKAPK3 at Lys355 in the human SW1990 PDAC cell line, indicating that SMYD2 is required for the physiological levels of MAPKAPK3-K355me1 in these cells. Additional experiments further confirmed MAPKAPK3 as a cancer-relevant cytoplasmic target of SMYD2, as determined by a decreased stromal response and a diminished inflammation in *K-Ras* mutant mice, as well as by the cytoplasmic co-localization of SMYD2 and MAPKAPK3 in human and murine PDAC cell lines[16].

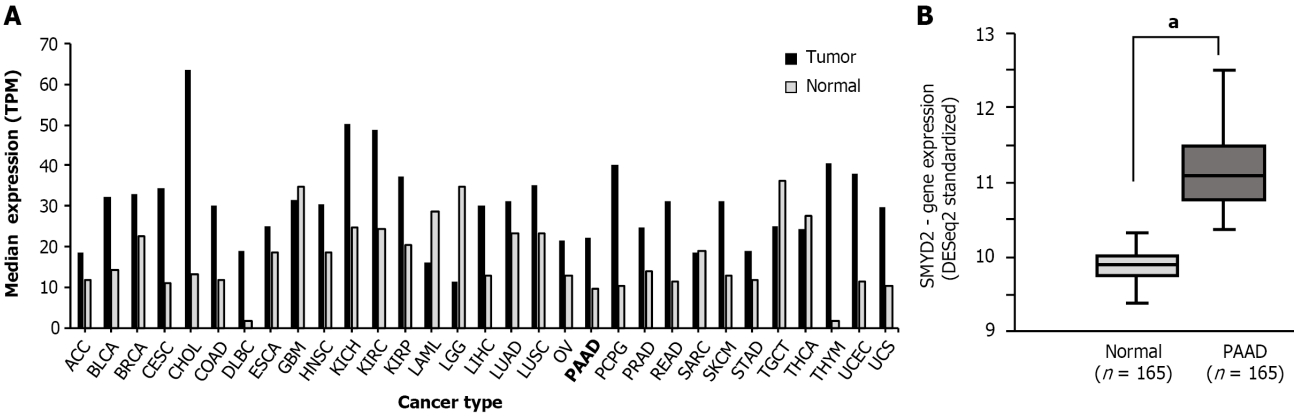
PDAC is one of the Ras-driven carcinomas, where *K-Ras* mutation is a key player in triggering the pancreatic intraepithelial neoplasia (PanIN) and tumor development[16,52]. The overexpression of SMYD2 in PDAC samples, as well as the methylation of the Ras-signaling kinase MAPKAPK3, support the idea that targeting the catalytic activity of SMYD2, or the SMYD2-MAPKAPK3 axis, may be therapeutic in the Ras-driven PDAC. SMYD2 expression was not detectable in normal pancreas tissue sections, while sections from murine and human PanIN and PDAC specimens revealed elevated expression of SMYD2[16]. Notably, an increase in the expression of SMYD2 is correlated with the cancer progression in samples from *K-Ras* mutant mice. Loss of SMYD2 resulted in a reduction in the acinar-to-ductal metaplasia (ADM)[16], an early event in PDAC development triggered by the activation of the RTK/Ras signaling pathway[60]. Consistently, a reduction in the development of the precancerous lesions PanINs and a decreased proliferation ability were also observed upon depletion of SMYD2, as determined by using MUC5AC, pERK1/2, Ki67, cleaved-Caspase-3, and αSMA as markers for PanIN lesions, Ras pathway activation, proliferation, apoptosis, and stromal response, respectively. These

Table 2 SET and MYND domain-containing protein 2 involvement in human cancers

Cancer type	Findings	Ref.
Acute lymphoblastic leukemia	SMYD2 overexpression; worse OS and EFS; higher WBC counts; a higher percentage of high-risk disease; prognostic factor	[38]
Bladder cancer	Higher expression of SMYD2; promotes cell cycle progression of cancer cells; methylation of RB	[23]
Breast cancer	SMYD2 overexpression; worse RFS; prognostic factor	[107]
	SMYD2 overexpression; poor survival	[30]
Cervical cancer	Higher expression of SMYD2; worse OS; advanced FIGO stage; larger tumor size; poor prognosis	[41]
Chronic lymphocytic leukemia	Higher expression of SMYD2; high WBC counts; complex karyotype; tumor progression	[108]
Clear cell renal cell carcinoma	SMYD2 overexpression; worse OS and DFS; high TNM stage; early tumor relapse	[46]
Colon cancer	SMYD2 overexpression; upregulation MDR1/P-glycoprotein; poor prognosis; enhances oxaliplatin resistance	[31]
Colorectal cancer	SMYD2 overexpression; activates the Wnt/β-catenin pathway; worse OS and DFS; worse oncologic outcomes	[36]
Esophageal squamous cell carcinoma	Higher expression of SMYD2; worse OS; enhances venous invasion; higher pT category and recurrence	[34]
Gastric cancer	SMYD2 overexpression correlates with larger tumor size; aggressive invasion; more lymph node metastasis; recurrence; poor OS	[33]
Hematopoietic leukemias	Higher expression of SMYD2; promote Wnt-β-Catenin signaling; poor OS	[39]
Hepatocellular carcinoma	SMYD2 overexpression correlates with tumor size; vascular invasion; differentiation; TNM stage; worse OS; poor prognosis	[14]
HPV-unrelated, non-multiple head and neck cancer	Higher expression of SMYD2; worse OS; prognostic biomarker	[15]
Lower-grade gliomas	Poor OS; prognostic biomarker	[109]
Lung adenocarcinoma	Overexpressed SMYD2 correlates with shorter OS and DFS; promotes proliferation, migration, and invasion of cancer cells	[13]
Non-small cell lung cancer	Overexpressed SMYD2 enhances cisplatin resistance; downregulates the p53 pathway	[32]
Ovarian clear cell carcinoma	Shorter OS and DSS; prognostic biomarker	[43]
Pancreatic cancer	SMYD2 overexpression; methylation of MAPKAPK3; enhances precancerous lesions; poor OS	[16]
Papillary thyroid carcinoma	SMYD2 overexpression correlates with PTC progression; poor prognosis and DFS; worse clinical outcomes	[40]
Renal cell tumor	Low expression of SMYD2 correlates with shorter DSS and DFS; prognostic biomarker	[45]

SMYD2: SET and MYND domain-containing protein 2; OS: Overall survival; EFS: Event-free survival; DFS: Disease-free survival; DSS: Disease-specific survival.

results have led to pharmacological inhibition experiments aimed to evaluate the therapeutic potential of targeting the SMYD2-MAPKAPK3 axis in Ras-driven pancreatic cancer[16]. The compound PF-3644022, which inhibits the kinase activity of MAPKAPK3, was found to suppress the expansion of PDAC cells in culture[16]. Also, treatment with PF-3644022 caused inhibition of PDAC growth in *K-Ras* mutant mice, as well as resulted in fewer PanIN, reduced cell proliferation, an elevated level of apoptosis, attenuation of the Ras pathway, and a reduced level of inflammatory cytokines. Treatment with the SMYD2 small molecule inhibitor BAY598[61] inhibited the methylation of MAPKAPK3 by SMYD2 and decreased the growth of *K-Ras*/*TP53* mutant PDAC cells, whereas the growth of *K-Ras*/*TP53*/*SMYD2* mutant cells was not significantly impacted. On the other hand, the chemotherapeutic gemcitabine had a stronger inhibitory effect on the clonal expansion of *K-Ras*/*TP53* mutant PDAC cells when combined with BAY598[16]. Gemcitabine also inhibits the growth of *K-Ras*/*TP53*/*SMYD2* mutant cells, suggesting that SMYD2 inhibition along with chemotherapy treatment cooperate to target PDAC cells. Such a notion was further supported by the fact that co-treatment of gemcitabine with either SMYD2 inhibition or its deletion resulted in much greater suppression of the growth of PDAC xenografts in mice when compared with any single-agent treatments. Another combination treatment with low-dose doxorubicin and BAY598 revealed similar results in inhibiting PDAC cell growth[16]. These studies together demonstrated that the efficacy of chemotherapy for the treatment of PDAC patients could be significantly improved by a combination of SMYD2 inhibition and effective chemotherapy agents, underscoring the therapeutic potential of targeting the SMYD2-MAPKAPK3 axis



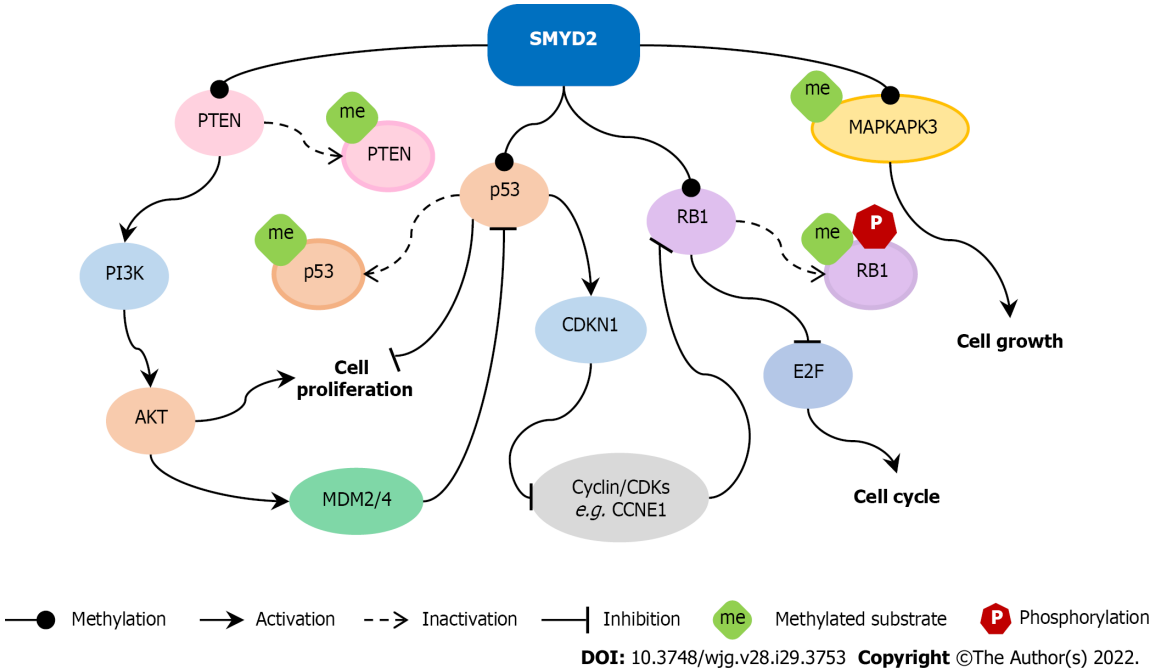
DOI: 10.3748/wjg.v28.i29.3753 **Copyright** ©The Author(s) 2022.

Figure 1 SET and MYND domain-containing protein 2 gene expression in cancer. A: The gene expression profiles of SET and MYND domain-containing protein 2 (SMYD2) across 31 types of tumor samples and paired normal tissues from the Cancer Genome Atlas (TCGA) and the Genotype-Tissue Expression (GTEx) project, the analysis was performed using the Gene Expression Profiling Interactive Analysis (GEPIA2); B: Differences in SMYD2 expression between pancreatic ductal adenocarcinoma tissues and paired normal tissues. TPM: Transcripts per kilobase of exon per million mapped reads; ACC: Adrenocortical carcinoma; BLCA: Bladder urothelial carcinoma; BRCA: Breast invasive carcinoma; CESC: Cervical squamous cell carcinoma and endocervical adenocarcinoma; CHOL: Cholangiocarcinoma; COAD: Colon adenocarcinoma; DLBC: Lymphoid neoplasm diffuse large B-cell lymphoma; ESCA: Esophageal carcinoma; GBM: Glioblastoma multiforme; HNSC: Head and neck squamous cell carcinoma; KICH: Kidney chromophobe; KIRC: Kidney renal clear cell carcinoma; KIRP: Kidney renal papillary cell carcinoma; LAML: Acute myeloid leukemia; LGG: Lower grade glioma; LIHC: Liver hepatocellular carcinoma; LUAD: Lung adenocarcinoma; LUSC: Lung squamous cell carcinoma; OV: Ovarian serous cystadenocarcinoma; PAAD/PDAC: Pancreatic ductal adenocarcinoma; PCPG: Pheochromocytoma and paraganglioma; PRAD: Prostate adenocarcinoma; READ: Rectum adenocarcinoma; SARC: Sarcoma; SKCM: Skin cutaneous melanoma; STAD: Stomach adenocarcinoma; TGCT: Testicular germ cell tumors; THCA: Thyroid carcinoma; THYM: Thymoma; UCEC: Uterine corpus endometrial carcinoma; UCS: Uterine carcinosarcoma; *n*: Number of samples. [a]$P < 0.001$ is indicated by three asterisks.

in PDAC.

FUNCTIONAL EXTRAPOLATION OF SMYD2 FROM OTHER CANCERS TO PANCREATIC CANCER

SMYD2 involvement in many other human cancers (Table 2) through regulating the oncogenic signaling pathways provides a conceptual foundation for extrapolating the known functions of SMYD2 to the less studied pancreatic cancer. SMYD2 is highly expressed in breast tumor tissues relative to normal breast tissues[30]. Inhibition of SMYD2 by RNAi-mediated knockdown or through the specific inhibitor AZ505 significantly decreased tumor growth *in vivo*, indicating that SMYD2 may be involved in the initiation and development of breast cancer (BC) *via* methylation of proteins required for BC cell survival. Indeed, the contribution of SMYD2 to BC development depends on its ability to methylate four protein targets including the NF-κB p65 subunit, signal transducer and activator of transcription 3 (STAT3), histone H3, and PTEN; the activation/inactivation of these protein targets by the methylation affects a wide range of cancer cell behaviors, including cell proliferation, migration, invasion, and survival (Figure 2). SMYD2-mediated methylation of the NF-κB p65 subunit resulted in NF-κB activation and repressed apoptosis of human breast cancer cells[30]. SMYD2-mediated methylation of STAT3 contributes to STAT3 activation in triple-negative breast cancer cells, which in turn increases SMYD2 expression, leading to increased methylation of H3K4 and H3K36 by SMYD2, thereby linking SMYD2 to several BC-associated signaling cascades, including JAK2/STAT3, ERK, and AKT signaling[11,27,30,62]. SMYD2-mediated methylation of PTEN at Lys313 was shown to downregulate the expression of PTEN and to suppress PTEN activity through inducing phosphorylation at serine 380 of PTEN[27,30]. PTEN is a dual lipid and protein phosphatase; as a negative regulator of PI3K/AKT signaling, it downregulates signal transduction initiated by growth factors and hormones through dephosphorylating phosphatidylinositol 3,4,5-triphosphate (PIP3) produced by PI3K[63]. Since PI3K/AKT signaling is a crucial intracellular pathway in human cancers and is frequently upregulated in multiple types of cancer including PDAC[64], the link of SMYD2 to this signaling pathway *via* the methylation-induced repression of PTEN activity suggests a possible new mechanism by which SMYD2 contributes to PDAC development. Several reports have shown the constitutive activation of Ras/ERK and PI3K/AKT signaling and PTEN downregulation being involved in the pathogenesis and progression of pancreatic cancer[65-70]. PTEN was shown to be abundantly expressed in the cytoplasm of non-tumor pancreatic tissues but to be significantly downregulated in PDAC tissues[71]. The downregulation of PTEN has been associated with a high rate of tumorigenesis and a poor prognosis for PDAC patients[71-73]. One important mechanism by which aberrant PTEN expression contributes to PDAC development is the activation of



DOI: 10.3748/wjg.v28.i29.3753 **Copyright** ©The Author(s) 2022.

Figure 2 A schematic model for SET and MYND domain-containing protein 2 driving pancreatic cancer development *via* methylation of nonhistone proteins. SET and MYND domain-containing protein 2 (SMYD2) can methylate several nonhistone proteins that may be involved in pancreatic cancer tumorigenesis, including p53, PTEN, retinoblastomaassociated protein (RB), and mitogen-activated protein kinase activated protein kinase 3 (MAPKAPK3). SMYD2 methylates and inactivates p53 to promote cell proliferation. PTEN is downregulated by SMYD2-mediated methylation, which promotes cell proliferation through activation of PI3K signaling. Methylation of RB by SMYD2 enhances RB phosphorylation, which allows E2F to disassociate from the RB-E2F complex and enhances E2F activity to promote cell cycle progression. SMYD2 impacts the RTK/Ras pathway through methylation of MAPKAPK3 to promote cell growth. MAPKAPK3: Mitogen-activated protein kinase activated protein kinase 3; RB: Retinoblastoma-associated protein.

the PI3K/AKT signaling pathway, which promotes PDAC cell growth, survival, and angiogenesis[74,75]. Therefore, in addition to promoting PDAC growth *via* methylation of MAPKAPK3, it is possible that the tumor-promoting activity of SMYD2 in PDAC is attributable to its methyltransferase activity on PTEN, which subsequently causes the activation of the oncogenic PI3K/AKT signaling pathway. In order to prove this hypothesis, future investigation should be directed towards assessing whether Lys313 of PTEN, which is methylated by SMYD2 in BC, can be methylated by SMYD2 in the context of PDAC, and whether such methylation represses the tumor-suppressor activity of PTEN, leading to the activation of PI3K/AKT signaling.

Methylation of RB by SMYD2[76], which is involved in the development of bladder cancer[77], suggests another potential mechanism by which SMYD2 contributes to PDAC progression. SMYD2 is overexpressed in bladder cancer cell lines and primary bladder tumor samples and plays a role in promoting bladder cancer cell proliferation[23]. One mechanism for the SMYD2's bladder cancer-promoting role is the methylation of the tumor suppressor RB, which contributes to the hyperphosphorylation of RB, leading to RB inactivation, and thereby bypassing the regulatory action of RB on cell proliferation[23]. In the case of pancreatic cancer, RB protein levels were significantly lower in PDAC tumor tissues than those in adjacent normal tissues; the low protein levels of RB have been associated with PDAC progression[78]. Another study showed that RB depletion promotes PanIN and rapid malignant transformation in *K-Ras*-induced PDAC, being associated with an impaired p53 activity[79]. This result suggests the importance of RB function in suppressing PDAC progression through mediating the cellular senescence and enhancing p53 function. However, little is known about the methylation status of RB in pancreatic cancer, how such posttranslational modification regulates RB activity, and what are the downstream effects of the methylation on cellular functions and PDAC progression. Given the role of the SMYD2-mediated RB methylation in bladder cancer, one can speculate that there might exist an analogous cancer-promoting mechanism, where SMYD2 mediates the inactivation of RB through direct methylation of RB, resulting in bypassing cell cycle restrictions and promoting PDAC cell growth.

Because of the broad substrate specificity of SMYD2 (Table 1), with most of its substrates being tumor suppressors or oncogenic proteins, the mechanistic link of SMYD2 to PDAC proliferation is expected to be complex, involving the interconnected signaling pathways that regulate the cell cycle, apoptosis, as well as energy metabolism. The tumor suppressor p53 is another important methylation target of SMYD2[22], and this methylation has been shown to promote the tumorigenesis of cervical cancer through an alternative metabolic strategy, shifting the major production of cellular metabolism to lactate production[42]. p53 exerts its tumor-suppressive function in response to severe DNA damage and

inhibits the onset and progression of tumors[80]. p53 is a master regulator of the cell cycle and apoptosis and is involved in the regulation of metabolic pathways to maintain the metabolic homeostasis of cells [81,82]. It has been reported that SMYD2 monomethylates p53 at Lys370, which led to p53 inactivation by decreasing the binding activity of p53 to its target genes[22]. Loss-of-function and gain-of-function experiments revealed that SMYD2 depletion not only significantly reduced the p53K370me level but also increased the p53 reporter activity in cervical cancer cell lines; in contrast, overexpression of SMYD2 in the same cell lines led to an increased level of p53K370me[42]. It has also been shown that the knockdown of p53 in SMYD2-overexpressing cervical cancer cells compromised the increase in glucose uptake and lactate production induced by SMYD2[42]. Moreover, hijacking tumor glycolysis by the glucose analog 2-deoxy-D-glucose (2-DG) significantly repressed SMYD2-dependent tumor growth. These findings together indicate that SMYD2 is a positive glycolytic mediator and plays a promoting role in enhancing tumor growth in a glycolysis-dependent manner, likely through SMYD2-mediated methylation of p53 to promote aerobic glycolysis and tumorigenesis in cervical cancer[42]. Although the role of SMYD2-mediated p53 methylation in PDAC has not yet been explored, dysregulation of the p53 pathway is one of the primary molecular pathological events in PDAC, which promotes the development and progression of pancreatic tumors[83]. In a cohort of 272 PDAC patients, an aberrant alteration rate of the *TP53* gene was about 38%[84], consistent with earlier reports demonstrating 40% and 47% of PDAC samples having p53 mutations[85,86]. It was shown that the inactivation of p53 occurs during the progression of PanIN to invasive tumors[87], while activation of the mitochondrial p53 was shown to restore the apoptotic pathway and inhibit PDAC growth *in vitro* and *in vivo*[88]. These studies demonstrate that p53 dysfunction has a strong association with the progression of pancreatic cancer. As an upstream regulator of the p53 pathway, SMYD2 monomethylates p53 and deactivates the transcriptional activity of p53, and it is thus possible that its ability to block the p53-tumor suppressor activity is another mechanism by which SMYD2 contributes to PDAC progression. It would also be interesting to investigate whether SMYD2-mediated silencing of p53 is also involved in the metabolic reprogramming of pancreatic tumors and promotes the aerobic glycolysis of cancer cells.

CURRENT CHALLENGES IN THE MOLECULAR THERAPEUTIC TARGETING OF SMYD2

Because of the tumor-promoting role of SMYD2 in numerous cancers including PDAC, the development of selective small-molecule inhibitors against SMYD2 could offer a substantial opportunity for targeted medicine with a broad therapeutic benefit. Great progress in crystal structure analysis of SMYD2 has allowed for the development of multiple selective and potent SMYD2 inhibitors over the past decade [89]. The first SMYD2 inhibitor AZ505 was identified in 2011 after screening over one million-compound library[90]. AZ505 is a competitive inhibitor and has high selectivity for SMYD2, with an inhibitory potency at IC_{50} of 0.12 μM. This landmark discovery opened avenues for structure-based drug discovery for SMYD2 and led to the development of more potent SMYD2 inhibitors. A systematic structure-activity relationships (SAR) study on the AZ505 structure has identified the small molecule A893 as a highly selective SMYD2 inhibitor and being more potent in inhibiting p53 methylation than AZ505[91]. LLY507, another selective SMYD2 inhibitor, was developed and validated not only by a biochemical assay but also by the cell-based assays, and this inhibitor was found to strongly inhibit SMYD2-mediated p53 methylation in several cancer cell lines[92]. Using a modified high-throughput binding assay, BAY598 was identified as one of the most selective and potent SMYD2 inhibitors, with promising pharmacokinetic properties and capable of inducing SMYD2 inhibition *in vivo*[61]. BAY598 showed more than 100-fold selectivity towards SMYD2 relative to other SMYD proteins, and it had a preferred binding to the SMYD2-SAM substrate complex. In cell-based assays, BAY598 was able to inhibit the methylation of p53 by SMYD2, and it can also lead to a slight reduction of tumor area in mice[61]. Further studies identified additional potent and selective inhibitors with suitable pharmacokinetic properties, namely AZ931 and AZ506, though these inhibitors showed no effect on the proliferation of either *TP53* wild-type or *TP53*-deficient cell lines[93]. Recent studies presented new SMYD2 inhibitors, including EPZ033294, EPZ032597, MTF1497, and MTF9975[89,94]. It is noteworthy that EPZ033294 was the first SMYD2 inhibitor acting as a non-competitive inhibitor for the substrate peptide, with a low nanomolar inhibitory activity[94]. However, all these SMYD2 inhibitors are still at a research level and have not undergone clinical trials as therapeutic agents against tumors.

It is widely accepted that the cancer-promoting role of SMYD2 is dependent on its ability to methylate histone and nonhistone proteins, which has significant functions in the development and progression of malignancies. However, targeting the methyltransferase activity of SMYD2 has not yet achieved great outcomes in current cancer studies. This lack of success may be attributed to traditional SMYD2 inhibitors that usually inhibit the evolutionarily conserved cofactor binding site, as well as the complexity of the SMYD2 broad substrate specificity and its involvement in multiple signaling pathways that are essential for both normal and cancerous cells. Targeting the cofactor binding site of SMYD2 is a straightforward strategy, as the methyltransferase activity of SMYD2 relies on the methyl donor SAM being bound at the cofactor binding site. However, the highly conserved nature of this SAM binding site across the entire SET domain-containing protein lysine methyltransferase superfamily

makes designing a highly selective inhibitor with minimum cross-reactivity a challenge. Although a great selectivity has been achieved by some SMYD2 inhibitors, the current specificity analysis is limited to a handful number of SET domain-containing proteins that are closely related to SMYD2, and the full spectrum of the specificity profiles of these inhibitors across the genome is unknown. Consequently, some reports pointed out a potent inhibition of cell proliferation by some of the SMYD2 inhibitors, such as LLY507, being independent of SMYD2 inhibition, rather targeting several other unrelated enzymes to exert their inhibitory effects[94]. Similar conflicting data was also obtained about the effect of the SMYD2 inhibitor BAY598[61]. As a result of these conflicting data, some reports concluded that SMYD2 might not be required for *in vitro* cell line proliferation, though such a claim needs to be further studied [94]. The broad substrate specificity of SMYD2 represents another significant challenge in targeting SMYD2 for cancer therapy. In the past two decades, many nonhistone substrates of SMYD2 have been reported, suggesting that the functional impact of inhibiting SMYD2 will be very complex, involving different mechanisms and affecting various cellular pathways in both normal and pathological conditions. The lack of understanding of how SMYD2 inhibition affects the physiological behavior of normal cells is a major issue of current SMYD2 inhibitors. Another issue is that, for example, SMYD2 inhibition leading to the restoration of the p53 tumor suppressor activity has been well characterized, but how this inhibition affects the function of p53 gain-of-function mutants is unknown. Many mutant p53 proteins promote tumorigenesis through the gain-of-function mechanism[95]. The activity of such p53 mutants could be enhanced by targeting SMYD2 in a similar way as it does to wild-type p53, leading to unwanted outcomes and adverse effects. This is consistent with the evidence that SMYD2 is not always a poor prognostic marker for cancer patients, and the overexpression of SMYD2 has been shown to be a favorable prognostic marker for patients with renal cell tumors[45]. Nonetheless, given that the cancer-promoting role of SMYD2 has been confirmed in multiple types of cancers, it is worthwhile to continue to exploit SMYD2 as a drug target for cancer treatment, with more attention being paid to new inhibition strategies, such as targeting protein-protein interactions and targeting additional functional sites that are less conserved but have substrate-specific functions.

CONCLUSION

In the past few decades, there have been huge improvements in our understanding of the complex molecular nature of pancreatic cancer and progress in the available therapy options, including surgery, chemotherapy, radiotherapy, immunotherapy, and targeted therapies. Although these therapy options have resulted in a slight improvement in the overall 5-year survival rate of patients, pancreatic cancer remains a difficult disease to treat. SMYD2 could be a promising target for the development of a novel PDAC therapy, given its involvement in diverse oncogenic signaling pathways to control multiple cellular processes like cell proliferation, apoptosis, and energy metabolism (Figure 2). SMYD2 is overexpressed in PDAC and serves as an important regulatory molecule through the interplay with the RTK/Ras signaling pathway and the PI3K-AKT signaling pathway to drive PDAC cell growth and metastasis. The projected role of SMYD2 in repressing the activity of the tumor suppressors p53 and PTEN in PDAC development further implies that SMYD2 is a key player in promoting the cell cycle, cell growth, and cell survival. Therefore, targeting SMYD2 could be a powerful strategy for the prevention and treatment of PDAC, in particular with consideration of tumor subtypes and genetic backgrounds.

ACKNOWLEDGEMENTS

Thanks to Jacob Sobota for proofreading the article.

FOOTNOTES

Author contributions: Alshammari E performed the majority of the writing, prepared the figures and tables; Zhang YX provided the input in writing the paper; Yang Z coordinated the writing of the paper and performed writing.

Conflict-of-interest statement: There are no conflicts of interest to report.

Open-Access: This article is an open-access article that was selected by an in-house editor and fully peer-reviewed by external reviewers. It is distributed in accordance with the Creative Commons Attribution NonCommercial (CC BY-NC 4.0) license, which permits others to distribute, remix, adapt, build upon this work non-commercially, and license their derivative works on different terms, provided the original work is properly cited and the use is non-commercial. See: https://creativecommons.org/Licenses/by-nc/4.0/

Country/Territory of origin: United States

ORCID number: Eid Alshammari 0000-0002-8676-9480; Ying-Xue Zhang 0000-0001-8099-4225; Zhe Yang 0000-0001-9406-9516.

S-Editor: Chen YL
L-Editor: A
P-Editor: Chen YL

REFERENCES

1 **GBD 2017 Pancreatic Cancer Collaborators**. The global, regional, and national burden of pancreatic cancer and its attributable risk factors in 195 countries and territories, 1990-2017: a systematic analysis for the Global Burden of Disease Study 2017. *Lancet Gastroenterol Hepatol* 2019; **4**: 934-947 [PMID: 31648972 DOI: 10.1016/S2468-1253(19)30347-4]
2 **Ryan DP**, Hong TS, Bardeesy N. Pancreatic adenocarcinoma. *N Engl J Med* 2014; **371**: 1039-1049 [PMID: 25207767 DOI: 10.1056/NEJMra1404198]
3 **Ilic M**, Ilic I. Epidemiology of pancreatic cancer. *World J Gastroenterol* 2016; **22**: 9694-9705 [PMID: 27956793 DOI: 10.3748/wjg.v22.i44.9694]
4 **Siegel RL**, Miller KD, Fuchs HE, Jemal A. Cancer Statistics, 2021. *CA Cancer J Clin* 2021; **71**: 7-33 [PMID: 33433946 DOI: 10.3322/caac.21654]
5 **Rahib L**, Smith BD, Aizenberg R, Rosenzweig AB, Fleshman JM, Matrisian LM. Projecting cancer incidence and deaths to 2030: the unexpected burden of thyroid, liver, and pancreas cancers in the United States. *Cancer Res* 2014; **74**: 2913-2921 [PMID: 24840647 DOI: 10.1158/0008-5472.CAN-14-0155]
6 **Oberstein PE**, Olive KP. Pancreatic cancer: why is it so hard to treat? *Therap Adv Gastroenterol* 2013; **6**: 321-337 [PMID: 23814611 DOI: 10.1177/1756283X13478680]
7 **Stathis A**, Moore MJ. Advanced pancreatic carcinoma: current treatment and future challenges. *Nat Rev Clin Oncol* 2010; **7**: 163-172 [PMID: 20101258 DOI: 10.1038/nrclinonc.2009.236]
8 **Ferrone CR**, Pieretti-Vanmarcke R, Bloom JP, Zheng H, Szymonifka J, Wargo JA, Thayer SP, Lauwers GY, Deshpande V, Mino-Kenudson M, Fernández-del Castillo C, Lillemoe KD, Warshaw AL. Pancreatic ductal adenocarcinoma: long-term survival does not equal cure. *Surgery* 2012; **152**: S43-S49 [PMID: 22763261 DOI: 10.1016/j.surg.2012.05.020]
9 **Stark AP**, Sacks GD, Rochefort MM, Donahue TR, Reber HA, Tomlinson JS, Dawson DW, Eibl G, Hines OJ. Long-term survival in patients with pancreatic ductal adenocarcinoma. *Surgery* 2016; **159**: 1520-1527 [PMID: 26847803 DOI: 10.1016/j.surg.2015.12.024]
10 **Strobel O**, Lorenz P, Hinz U, Gaida M, König AK, Hank T, Niesen W, Kaiser JÖR, Al-Saeedi M, Bergmann F, Springfeld C, Berchtold C, Diener MK, Schneider M, Mehrabi A, Müller-Stich BP, Hackert T, Jager D, Büchler MW. Actual Five-year Survival After Upfront Resection for Pancreatic Ductal Adenocarcinoma: Who Beats the Odds? *Ann Surg* 2022; **275**: 962-971 [PMID: 32649469 DOI: 10.1097/SLA.0000000000004147]
11 **Brown MA**, Sims RJ 3rd, Gottlieb PD, Tucker PW. Identification and characterization of Smyd2: a split SET/MYND domain-containing histone H3 lysine 36-specific methyltransferase that interacts with the Sin3 histone deacetylase complex. *Mol Cancer* 2006; **5**: 26 [PMID: 16805913 DOI: 10.1186/1476-4598-5-26]
12 **Abu-Farha M**, Lambert JP, Al-Madhoun AS, Elisma F, Skerjanc IS, Figeys D. The tale of two domains: proteomics and genomics analysis of SMYD2, a new histone methyltransferase. *Mol Cell Proteomics* 2008; **7**: 560-572 [PMID: 18065756 DOI: 10.1074/mcp.M700271-MCP200]
13 **Wu L**, Kou F, Ji Z, Li B, Zhang B, Guo Y, Yang L. SMYD2 promotes tumorigenesis and metastasis of lung adenocarcinoma through RPS7. *Cell Death Dis* 2021; **12**: 439 [PMID: 33935284 DOI: 10.1038/s41419-021-03720-w]
14 **Zuo SR**, Zuo XC, He Y, Fang WJ, Wang CJ, Zou H, Chen P, Huang LF, Huang LH, Xiang H, Liu SK. Positive Expression of SMYD2 is Associated with Poor Prognosis in Patients with Primary Hepatocellular Carcinoma. *J Cancer* 2018; **9**: 321-330 [PMID: 29344279 DOI: 10.7150/jca.22218]
15 **Ohtomo-Oda R**, Komatsu S, Mori T, Sekine S, Hirajima S, Yoshimoto S, Kanai Y, Otsuji E, Ikeda E, Tsuda H. SMYD2 overexpression is associated with tumor cell proliferation and a worse outcome in human papillomavirus-unrelated nonmultiple head and neck carcinomas. *Hum Pathol* 2016; **49**: 145-155 [PMID: 26826421 DOI: 10.1016/j.humpath.2015.08.025]
16 **Reynoird N**, Mazur PK, Stellfeld T, Flores NM, Lofgren SM, Carlson SM, Brambilla E, Hainaut P, Kaznowska EB, Arrowsmith CH, Khatri P, Stresemann C, Gozani O, Sage J. Coordination of stress signals by the lysine methyltransferase SMYD2 promotes pancreatic cancer. *Genes Dev* 2016; **30**: 772-785 [PMID: 26988419 DOI: 10.1101/gad.275529.115]
17 **Weirich S**, Schuhmacher MK, Kudithipudi S, Lungu C, Ferguson AD, Jeltsch A. Analysis of the Substrate Specificity of the SMYD2 Protein Lysine Methyltransferase and Discovery of Novel Non-Histone Substrates. *Chembiochem* 2020; **21**: 256-264 [PMID: 31612581 DOI: 10.1002/cbic.201900582]
18 **Olsen JB**, Cao XJ, Han B, Chen LH, Horvath A, Richardson TI, Campbell RM, Garcia BA, Nguyen H. Quantitative Profiling of the Activity of Protein Lysine Methyltransferase SMYD2 Using SILAC-Based Proteomics. *Mol Cell Proteomics* 2016; **15**: 892-905 [PMID: 26750096 DOI: 10.1074/mcp.M115.053280]
19 **Ahmed H**, Duan S, Arrowsmith CH, Barsyte-Lovejoy D, Schapira M. An Integrative Proteomic Approach Identifies Novel Cellular SMYD2 Substrates. *J Proteome Res* 2016; **15**: 2052-2059 [PMID: 27163177 DOI: 10.1021/acs.jproteome.6b00220]
20 **Yi X**, Jiang XJ, Fang ZM. Histone methyltransferase SMYD2: ubiquitous regulator of disease. *Clin Epigenetics* 2019; **11**: 112 [PMID: 31370883 DOI: 10.1186/s13148-019-0711-4]
21 **Sims RJ 3rd**, Nishioka K, Reinberg D. Histone lysine methylation: a signature for chromatin function. *Trends Genet* 2003; **19**: 629-639 [PMID: 14585615 DOI: 10.1016/j.tig.2003.09.007]

22 **Huang J**, Perez-Burgos L, Placek BJ, Sengupta R, Richter M, Dorsey JA, Kubicek S, Opravil S, Jenuwein T, Berger SL. Repression of p53 activity by Smyd2-mediated methylation. *Nature* 2006; **444**: 629-632 [PMID: 17108971 DOI: 10.1038/nature05287]

23 **Cho HS**, Hayami S, Toyokawa G, Maejima K, Yamane Y, Suzuki T, Dohmae N, Kogure M, Kang D, Neal DE, Ponder BA, Yamaue H, Nakamura Y, Hamamoto R. RB1 methylation by SMYD2 enhances cell cycle progression through an increase of RB1 phosphorylation. *Neoplasia* 2012; **14**: 476-486 [PMID: 22787429 DOI: 10.1593/neo.12656]

24 **Jiang Y**, Trescott L, Holcomb J, Zhang X, Brunzelle J, Sirinupong N, Shi X, Yang Z. Structural insights into estrogen receptor α methylation by histone methyltransferase SMYD2, a cellular event implicated in estrogen signaling regulation. *J Mol Biol* 2014; **426**: 3413-3425 [PMID: 24594358 DOI: 10.1016/j.jmb.2014.02.019]

25 **Hamamoto R**, Toyokawa G, Nakakido M, Ueda K, Nakamura Y. SMYD2-dependent HSP90 methylation promotes cancer cell proliferation by regulating the chaperone complex formation. *Cancer Lett* 2014; **351**: 126-133 [PMID: 24880080 DOI: 10.1016/j.canlet.2014.05.014]

26 **Piao L**, Kang D, Suzuki T, Masuda A, Dohmae N, Nakamura Y, Hamamoto R. The histone methyltransferase SMYD2 methylates PARP1 and promotes poly(ADP-ribosyl)ation activity in cancer cells. *Neoplasia* 2014; **16**: 257-264, 264.e2 [PMID: 24726141 DOI: 10.1016/j.neo.2014.03.002]

27 **Nakakido M**, Deng Z, Suzuki T, Dohmae N, Nakamura Y, Hamamoto R. Dysregulation of AKT Pathway by SMYD2-Mediated Lysine Methylation on PTEN. *Neoplasia* 2015; **17**: 367-373 [PMID: 25925379 DOI: 10.1016/j.neo.2015.03.002]

28 **Wang R**, Deng X, Yoshioka Y, Vougiouklakis T, Park JH, Suzuki T, Dohmae N, Ueda K, Hamamoto R, Nakamura Y. Effects of SMYD2-mediated EML4-ALK methylation on the signaling pathway and growth in non-small-cell lung cancer cells. *Cancer Sci* 2017; **108**: 1203-1209 [PMID: 28370702 DOI: 10.1111/cas.13245]

29 **Jiang Y**, Holcomb J, Spellmon N, Yang Z. Purification of Histone Lysine Methyltransferase SMYD2 and Co-Crystallization with a Target Peptide from Estrogen Receptor α. *Methods Mol Biol* 2016; **1366**: 207-217 [PMID: 26585137 DOI: 10.1007/978-1-4939-3127-9_16]

30 **Li LX**, Zhou JX, Calvet JP, Godwin AK, Jensen RA, Li X. Lysine methyltransferase SMYD2 promotes triple negative breast cancer progression. *Cell Death Dis* 2018; **9**: 326 [PMID: 29487338 DOI: 10.1038/s41419-018-0347-x]

31 **Ren H**, Wang Z, Chen Y, Liu Y, Zhang S, Zhang T, Li Y. SMYD2-OE promotes oxaliplatin resistance in colon cancer through MDR1/P-glycoprotein *via* MEK/ERK/AP1 pathway. *Onco Targets Ther* 2019; **12**: 2585-2594 [PMID: 31040701 DOI: 10.2147/OTT.S186806]

32 **Shang L**, Wei M. Inhibition of SMYD2 Sensitized Cisplatin to Resistant Cells in NSCLC Through Activating p53 Pathway. *Front Oncol* 2019; **9**: 306 [PMID: 31106145 DOI: 10.3389/fonc.2019.00306]

33 **Komatsu S**, Ichikawa D, Hirajima S, Nagata H, Nishimura Y, Kawaguchi T, Miyamae M, Okajima W, Ohashi T, Konishi H, Shiozaki A, Fujiwara H, Okamoto K, Tsuda H, Imoto I, Inazawa J, Otsuji E. Overexpression of SMYD2 contributes to malignant outcome in gastric cancer. *Br J Cancer* 2015; **112**: 357-364 [PMID: 25321194 DOI: 10.1038/bjc.2014.543]

34 **Komatsu S**, Imoto I, Tsuda H, Kozaki KI, Muramatsu T, Shimada Y, Aiko S, Yoshizumi Y, Ichikawa D, Otsuji E, Inazawa J. Overexpression of SMYD2 relates to tumor cell proliferation and malignant outcome of esophageal squamous cell carcinoma. *Carcinogenesis* 2009; **30**: 1139-1146 [PMID: 19423649 DOI: 10.1093/carcin/bgp116]

35 **Lai Y**, Yang Y. SMYD2 facilitates cancer cell malignancy and xenograft tumor development through ERBB2-mediated FUT4 expression in colon cancer. *Mol Cell Biochem* 2020 [PMID: 32342276 DOI: 10.1007/s11010-020-03738-2]

36 **Meng F**, Liu X, Lin C, Xu L, Liu J, Zhang P, Zhang X, Song J, Yan Y, Ren Z, Zhang Y. SMYD2 suppresses APC2 expression to activate the Wnt/β-catenin pathway and promotes epithelial-mesenchymal transition in colorectal cancer. *Am J Cancer Res* 2020; **10**: 997-1011 [PMID: 32266106]

37 **Sakamoto LH**, Andrade RV, Felipe MS, Motoyama AB, Pittella Silva F. SMYD2 is highly expressed in pediatric acute lymphoblastic leukemia and constitutes a bad prognostic factor. *Leuk Res* 2014; **38**: 496-502 [PMID: 24631370 DOI: 10.1016/j.leukres.2014.01.013]

38 **Zhang P**, Ruan J, Weng W, Tang Y. Overexpression of SET and MYND domain-containing protein 2 (*SMYD2*) is associated with poor prognosis in pediatric B lineage acute lymphoblastic leukemia. *Leuk Lymphoma* 2020; **61**: 437-444 [PMID: 31612757 DOI: 10.1080/10428194.2019.1675875]

39 **Brown MA**, Edwards MA, Alshiraihi I, Geng H, Dekker JD, Tucker HO. The lysine methyltransferase SMYD2 is required for normal lymphocyte development and survival of hematopoietic leukemias. *Genes Immun* 2020; **21**: 119-130 [PMID: 32115575 DOI: 10.1038/s41435-020-0094-8]

40 **Xu W**, Chen F, Fei X, Yang X, Lu X. Overexpression of SET and MYND Domain-Containing Protein 2 (SMYD2) Is Associated with Tumor Progression and Poor Prognosis in Patients with Papillary Thyroid Carcinoma. *Med Sci Monit* 2018; **24**: 7357-7365 [PMID: 30319138 DOI: 10.12659/MSM.910168]

41 **Sun JJ**, Li HL, Ma H, Shi Y, Yin LR, Guo SJ. SMYD2 promotes cervical cancer growth by stimulating cell proliferation. *Cell Biosci* 2019; **9**: 75 [PMID: 31548876 DOI: 10.1186/s13578-019-0340-9]

42 **Wang Y**, Jin G, Guo Y, Cao Y, Niu S, Fan X, Zhang J. SMYD2 suppresses p53 activity to promote glucose metabolism in cervical cancer. *Exp Cell Res* 2021; **404**: 112649 [PMID: 34015314 DOI: 10.1016/j.yexcr.2021.112649]

43 **Engqvist H**, Parris TZ, Kovács A, Rönnerman EW, Sundfeldt K, Karlsson P, Helou K. Validation of Novel Prognostic Biomarkers for Early-Stage Clear-Cell, Endometrioid and Mucinous Ovarian Carcinomas Using Immunohistochemistry. *Front Oncol* 2020; **10**: 162 [PMID: 32133296 DOI: 10.3389/fonc.2020.00162]

44 **Kojima M**, Sone K, Oda K, Hamamoto R, Kaneko S, Oki S, Kukita A, Kawata A, Honjoh H, Kawata Y, Kashiyama T, Sato M, Taguchi A, Miyamoto Y, Tanikawa M, Tsuruga T, Nagasaka K, Wada-Hiraike O, Osuga Y, Fujii T. The histone methyltransferase SMYD2 is a novel therapeutic target for the induction of apoptosis in ovarian clear cell carcinoma cells. *Oncol Lett* 2020; **20**: 153 [PMID: 32934721 DOI: 10.3892/ol.2020.12014]

45 **Pires-Luís AS**, Vieira-Coimbra M, Vieira FQ, Costa-Pinheiro P, Silva-Santos R, Dias PC, Antunes L, Lobo F, Oliveira J, Gonçalves CS, Costa BM, Henrique R, Jerónimo C. Expression of histone methyltransferases as novel biomarkers for renal cell tumor diagnosis and prognostication. *Epigenetics* 2015; **10**: 1033-1043 [PMID: 26488939 DOI: 10.1080/15592294.2015.1103578]

46 **Zhang Y**, Li C, Yang Z. Is MYND Domain-Mediated Assembly of SMYD3 Complexes Involved in Calcium Dependent Signaling? *Front Mol Biosci* 2019; **6**: 121 [PMID: 31737645 DOI: 10.3389/fmolb.2019.00121]

47 **Lenkiewicz E**, Malasi S, Hogenson TL, Flores LF, Barham W, Phillips WJ, Roesler AS, Chambers KR, Rajbhandari N, Hayashi A, Antal CE, Downes M, Grandgenett PM, Hollingsworth MA, Cridebring D, Xiong Y, Lee JH, Ye Z, Yan H, Hernandez MC, Leiting JL, Evans RM, Ordog T, Truty MJ, Borad MJ, Reya T, Von Hoff DD, Fernandez-Zapico ME, Barrett MT. Genomic and Epigenomic Landscaping Defines New Therapeutic Targets for Adenosquamous Carcinoma of the Pancreas. *Cancer Res* 2020; **80**: 4324-4334 [PMID: 32928922 DOI: 10.1158/0008-5472.CAN-20-0078]

48 **Deng X**, Hamamoto R, Vougiouklakis T, Wang R, Yoshioka Y, Suzuki T, Dohmae N, Matsuo Y, Park JH, Nakamura Y. Critical roles of SMYD2-mediated β-catenin methylation for nuclear translocation and activation of Wnt signaling. *Oncotarget* 2017; **8**: 55837-55847 [PMID: 28915556 DOI: 10.18632/oncotarget.19646]

49 **Dai S**, Xu S, Ye Y, Ding K. Identification of an Immune-Related Gene Signature to Improve Prognosis Prediction in Colorectal Cancer Patients. *Front Genet* 2020; **11**: 607009 [PMID: 33343640 DOI: 10.3389/fgene.2020.607009]

50 **Ren J**, Sun J, Li M, Zhang Z, Yang D, Cao H. MAPK Activated Protein Kinase 3 Is a Prognostic-Related Biomarker and Associated With Immune Infiltrates in Glioma. *Front Oncol* 2021; **11**: 793025 [PMID: 34938665 DOI: 10.3389/fonc.2021.793025]

51 **Tront JS**, Hoffman B, Liebermann DA. Gadd45a suppresses Ras-driven mammary tumorigenesis by activation of c-Jun NH2-terminal kinase and p38 stress signaling resulting in apoptosis and senescence. *Cancer Res* 2006; **66**: 8448-8454 [PMID: 16951155 DOI: 10.1158/0008-5472.CAN-06-2013]

52 **Waters AM**, Der CJ. KRAS: The Critical Driver and Therapeutic Target for Pancreatic Cancer. *Cold Spring Harb Perspect Med* 2018; **8** [PMID: 29229669 DOI: 10.1101/cshperspect.a031435]

53 **Shiryaev A**, Moens U. Mitogen-activated protein kinase p38 and MK2, MK3 and MK5: ménage à trois or ménage à quatre? *Cell Signal* 2010; **22**: 1185-1192 [PMID: 20227494 DOI: 10.1016/j.cellsig.2010.03.002]

54 **Djakiew D**. The p38 MAPK Pathway in Prostate Cancer. In: Tindall DJ, editor. Prostate Cancer: Biochemistry, Molecular Biology and Genetics. New York: Springer New York, 2013: 243-255 [DOI: 10.1007/978-1-4614-6828-8_8]

55 **Sun Y**, Liu WZ, Liu T, Feng X, Yang N, Zhou HF. Signaling pathway of MAPK/ERK in cell proliferation, differentiation, migration, senescence and apoptosis. *J Recept Signal Transduct Res* 2015; **35**: 600-604 [PMID: 26096166 DOI: 10.3109/10799893.2015.1030412]

56 **Ludwig S**, Engel K, Hoffmeyer A, Sithanandam G, Neufeld B, Palm D, Gaestel M, Rapp UR. 3pK, a novel mitogen-activated protein (MAP) kinase-activated protein kinase, is targeted by three MAP kinase pathways. *Mol Cell Biol* 1996; **16**: 6687-6697 [PMID: 8943323 DOI: 10.1128/MCB.16.12.6687]

57 **McLaughlin MM**, Kumar S, McDonnell PC, Van Horn S, Lee JC, Livi GP, Young PR. Identification of mitogen-activated protein (MAP) kinase-activated protein kinase-3, a novel substrate of CSBP p38 MAP kinase. *J Biol Chem* 1996; **271**: 8488-8492 [PMID: 8626550 DOI: 10.1074/jbc.271.14.8488]

58 **Ronkina N**, Menon MB, Schwermann J, Tiedje C, Hitti E, Kotlyarov A, Gaestel M. MAPKAP kinases MK2 and MK3 in inflammation: complex regulation of TNF biosynthesis *via* expression and phosphorylation of tristetraprolin. *Biochem Pharmacol* 2010; **80**: 1915-1920 [PMID: 20599781 DOI: 10.1016/j.bcp.2010.06.021]

59 **Kyriakis JM**, Avruch J. Mammalian MAPK signal transduction pathways activated by stress and inflammation: a 10-year update. *Physiol Rev* 2012; **92**: 689-737 [PMID: 22535895 DOI: 10.1152/physrev.00028.2011]

60 **Beel S**, Kolloch L, Apken LH, Jürgens L, Bolle A, Sudhof N, Ghosh S, Wardelmann E, Meisterernst M, Steinestel K, Oeckinghaus A. κB-Ras and Ral GTPases regulate acinar to ductal metaplasia during pancreatic adenocarcinoma development and pancreatitis. *Nat Commun* 2020; **11**: 3409 [PMID: 32641778 DOI: 10.1038/s41467-020-17226-0]

61 **Eggert E**, Hillig RC, Koehr S, Stöckigt D, Weiske J, Barak N, Mowat J, Brumby T, Christ CD, Ter Laak A, Lang T, Fernandez-Montalvan AE, Badock V, Weinmann H, Hartung IV, Barsyte-Lovejoy D, Szewczyk M, Kennedy S, Li F, Vedadi M, Brown PJ, Santhakumar V, Arrowsmith CH, Stellfeld T, Stresemann C. Discovery and Characterization of a Highly Potent and Selective Aminopyrazoline-Based in Vivo Probe (BAY-598) for the Protein Lysine Methyltransferase SMYD2. *J Med Chem* 2016; **59**: 4578-4600 [PMID: 27075367 DOI: 10.1021/acs.jmedchem.5b01890]

62 **Marotta LL**, Almendro V, Marusyk A, Shipitsin M, Schemme J, Walker SR, Bloushtain-Qimron N, Kim JJ, Choudhury SA, Maruyama R, Wu Z, Gönen M, Mulvey LA, Bessarabova MO, Huh SJ, Silver SJ, Kim SY, Park SY, Lee HE, Anderson KS, Richardson AL, Nikolskaya T, Nikolsky Y, Liu XS, Root DE, Hahn WC, Frank DA, Polyak K. The JAK2/STAT3 signaling pathway is required for growth of $CD44^+CD24^-$ stem cell-like breast cancer cells in human tumors. *J Clin Invest* 2011; **121**: 2723-2735 [PMID: 21633165 DOI: 10.1172/JCI44745]

63 **Blanco-Aparicio C**, Renner O, Leal JF, Carnero A. PTEN, more than the AKT pathway. *Carcinogenesis* 2007; **28**: 1379-1386 [PMID: 17341655 DOI: 10.1093/carcin/bgm052]

64 **Manning BD**, Cantley LC. AKT/PKB signaling: navigating downstream. *Cell* 2007; **129**: 1261-1274 [PMID: 17604717 DOI: 10.1016/j.cell.2007.06.009]

65 **Chow JY**, Quach KT, Cabrera BL, Cabral JA, Beck SE, Carethers JM. RAS/ERK modulates TGFbeta-regulated PTEN expression in human pancreatic adenocarcinoma cells. *Carcinogenesis* 2007; **28**: 2321-2327 [PMID: 17638924 DOI: 10.1093/carcin/bgm159]

66 **Kennedy AL**, Adams PD, Morton JP. Ras, PI3K/Akt and senescence: Paradoxes provide clues for pancreatic cancer therapy. *Small GTPases* 2011; **2**: 264-267 [PMID: 22292129 DOI: 10.4161/sgtp.2.5.17367]

67 **Wong MH**, Xue A, Baxter RC, Pavlakis N, Smith RC. Upstream and Downstream Co-inhibition of Mitogen-Activated Protein Kinase and PI3K/Akt/mTOR Pathways in Pancreatic Ductal Adenocarcinoma. *Neoplasia* 2016; **18**: 425-435 [PMID: 27435925 DOI: 10.1016/j.neo.2016.06.001]

68 **Ebrahimi S**, Hosseini M, Shahidsales S, Maftouh M, Ferns GA, Ghayour-Mobarhan M, Hassanian SM, Avan A. Targeting the Akt/PI3K Signaling Pathway as a Potential Therapeutic Strategy for the Treatment of Pancreatic Cancer. *Curr Med Chem* 2017; **24**: 1321-1331 [PMID: 28176634 DOI: 10.2174/0929867324666170206142658]

69 **Ma J**, Sawai H, Matsuo Y, Ochi N, Yasuda A, Takahashi H, Wakasugi T, Funahashi H, Sato M, Takeyama H. IGF-1 mediates PTEN suppression and enhances cell invasion and proliferation *via* activation of the IGF-1/PI3K/Akt signaling

pathway in pancreatic cancer cells. *J Surg Res* 2010; **160**: 90-101 [PMID: 19560785 DOI: 10.1016/j.jss.2008.08.016]
70 **Si W**, Liu X, Wei R, Zhang Y, Zhao Y, Cui L, Hong T. MTA2-mediated inhibition of PTEN leads to pancreatic ductal adenocarcinoma carcinogenicity. *Cell Death Dis* 2019; **10**: 206 [PMID: 30814496 DOI: 10.1038/s41419-019-1424-5]
71 **Ni S**, Wang H, Zhu X, Wan C, Xu J, Lu C, Xiao L, He J, Jiang C, Wang W, He Z. CBX7 suppresses cell proliferation, migration, and invasion through the inhibition of PTEN/Akt signaling in pancreatic cancer. *Oncotarget* 2017; **8**: 8010-8021 [PMID: 28030829 DOI: 10.18632/oncotarget.14037]
72 **Chen S**, He Z, Zhu C, Liu Y, Li L, Deng L, Wang J, Yu C, Sun C. TRIM37 Mediates Chemoresistance and Maintenance of Stemness in Pancreatic Cancer Cells *via* Ubiquitination of PTEN and Activation of the AKT-GSK-3β-β-Catenin Signaling Pathway. *Front Oncol* 2020; **10**: 554787 [PMID: 33194618 DOI: 10.3389/fonc.2020.554787]
73 **Zhang Q**, Li X, Li Y, Chen S, Shen X, Dong X, Song Y, Zhang X, Huang K. Expression of the PTEN/FOXO3a/PLZF signalling pathway in pancreatic cancer and its significance in tumourigenesis and progression. *Invest New Drugs* 2020; **38**: 321-328 [PMID: 31087222 DOI: 10.1007/s10637-019-00791-7]
74 **Asano T**, Yao Y, Zhu J, Li D, Abbruzzese JL, Reddy SA. The PI 3-kinase/Akt signaling pathway is activated due to aberrant Pten expression and targets transcription factors NF-kappaB and c-Myc in pancreatic cancer cells. *Oncogene* 2004; **23**: 8571-8580 [PMID: 15467756 DOI: 10.1038/sj.onc.1207902]
75 **Ma J**, Sawai H, Ochi N, Matsuo Y, Xu D, Yasuda A, Takahashi H, Wakasugi T, Takeyama H. PTEN regulates angiogenesis through PI3K/Akt/VEGF signaling pathway in human pancreatic cancer cells. *Mol Cell Biochem* 2009; **331**: 161-171 [PMID: 19437103 DOI: 10.1007/s11010-009-0154-x]
76 **Saddic LA**, West LE, Aslanian A, Yates JR 3rd, Rubin SM, Gozani O, Sage J. Methylation of the retinoblastoma tumor suppressor by SMYD2. *J Biol Chem* 2010; **285**: 37733-37740 [PMID: 20870719 DOI: 10.1074/jbc.M110.137612]
77 **Malekzadeh K**, Sobti RC, Nikbakht M, Shekari M, Hosseini SA, Tamandani DK, Singh SK. Methylation patterns of Rb1 and Casp-8 promoters and their impact on their expression in bladder cancer. *Cancer Invest* 2009; **27**: 70-80 [PMID: 19160091 DOI: 10.1080/07357900802172085]
78 **Yue H**, Na YL, Feng XL, Ma SR, Song FL, Yang B. Expression of p57kip2, Rb protein and PCNA and their relationships with clinicopathology in human pancreatic cancer. *World J Gastroenterol* 2003; **9**: 377-380 [PMID: 12532471 DOI: 10.3748/wjg.v9.i2.377]
79 **Carrière C**, Gore AJ, Norris AM, Gunn JR, Young AL, Longnecker DS, Korc M. Deletion of Rb accelerates pancreatic carcinogenesis by oncogenic Kras and impairs senescence in premalignant lesions. *Gastroenterology* 2011; **141**: 1091-1101 [PMID: 21699781 DOI: 10.1053/j.gastro.2011.05.041]
80 **Lane DP**. Cancer. p53, guardian of the genome. *Nature* 1992; **358**: 15-16 [PMID: 1614522 DOI: 10.1038/358015a0]
81 **Oren M**. Decision making by p53: life, death and cancer. *Cell Death Differ* 2003; **10**: 431-442 [PMID: 12719720 DOI: 10.1038/sj.cdd.4401183]
82 **Liu J**, Zhang C, Hu W, Feng Z. Tumor suppressor p53 and metabolism. *J Mol Cell Biol* 2019; **11**: 284-292 [PMID: 30500901 DOI: 10.1093/jmcb/mjy070]
83 **Ansari D**, Del Pino Bellido C, Bauden M, Andersson R. Centrosomal Abnormalities in Pancreatic Cancer: Molecular Mechanisms and Clinical Implications. *Anticancer Res* 2018; **38**: 1241-1245 [PMID: 29491046 DOI: 10.21873/anticanres.12345]
84 **Shin SH**, Kim SC, Hong SM, Kim YH, Song KB, Park KM, Lee YJ. Genetic alterations of K-ras, p53, c-erbB-2, and DPC4 in pancreatic ductal adenocarcinoma and their correlation with patient survival. *Pancreas* 2013; **42**: 216-222 [PMID: 23344532 DOI: 10.1097/MPA.0b013e31825b6ab0]
85 **DiGiuseppe JA**, Hruban RH, Goodman SN, Polak M, van den Berg FM, Allison DC, Cameron JL, Offerhaus GJ. Overexpression of p53 protein in adenocarcinoma of the pancreas. *Am J Clin Pathol* 1994; **101**: 684-688 [PMID: 8209852 DOI: 10.1093/ajcp/101.6.684]
86 **Casey G**, Yamanaka Y, Friess H, Kobrin MS, Lopez ME, Buchler M, Beger HG, Korc M. p53 mutations are common in pancreatic cancer and are absent in chronic pancreatitis. *Cancer Lett* 1993; **69**: 151-160 [PMID: 8513440 DOI: 10.1016/0304-3835(93)90168-9]
87 **Norfadzilah MY**, Pailoor J, Retneswari M, Chinna K, Noor LM. P53 expression in invasive pancreatic adenocarcinoma and precursor lesions. *Malays J Pathol* 2011; **33**: 89-94 [PMID: 22299208]
88 **Cheng J**, Okolotowicz KJ, Ryan D, Mose E, Lowy AM, Cashman JR. Inhibition of invasive pancreatic cancer: restoring cell apoptosis by activating mitochondrial p53. *Am J Cancer Res* 2019; **9**: 390-405 [PMID: 30906636]
89 **Fabini E**, Manoni E, Ferroni C, Rio AD, Bartolini M. Small-molecule inhibitors of lysine methyltransferases SMYD2 and SMYD3: current trends. *Future Med Chem* 2019; **11**: 901-921 [PMID: 30998113 DOI: 10.4155/fmc-2018-0380]
90 **Ferguson AD**, Larsen NA, Howard T, Pollard H, Green I, Grande C, Cheung T, Garcia-Arenas R, Cowen S, Wu J, Godin R, Chen H, Keen N. Structural basis of substrate methylation and inhibition of SMYD2. *Structure* 2011; **19**: 1262-1273 [PMID: 21782458 DOI: 10.1016/j.str.2011.06.011]
91 **Sweis RF**, Wang Z, Algire M, Arrowsmith CH, Brown PJ, Chiang GG, Guo J, Jakob CG, Kennedy S, Li F, Maag D, Shaw B, Soni NB, Vedadi M, Pappano WN. Discovery of A-893, A New Cell-Active Benzoxazinone Inhibitor of Lysine Methyltransferase SMYD2. *ACS Med Chem Lett* 2015; **6**: 695-700 [PMID: 26101576 DOI: 10.1021/acsmedchemlett.5b00124]
92 **Nguyen H**, Allali-Hassani A, Antonysamy S, Chang S, Chen LH, Curtis C, Emtage S, Fan L, Gheyi T, Li F, Liu S, Martin JR, Mendel D, Olsen JB, Pelletier L, Shatseva T, Wu S, Zhang FF, Arrowsmith CH, Brown PJ, Campbell RM, Garcia BA, Barsyte-Lovejoy D, Mader M, Vedadi M. LLY-507, a Cell-active, Potent, and Selective Inhibitor of Protein-lysine Methyltransferase SMYD2. *J Biol Chem* 2015; **290**: 13641-13653 [PMID: 25825497 DOI: 10.1074/jbc.M114.626861]
93 **Cowen SD**, Russell D, Dakin LA, Chen H, Larsen NA, Godin R, Throner S, Zheng X, Molina A, Wu J, Cheung T, Howard T, Garcia-Arenas R, Keen N, Pendleton CS, Pietenpol JA, Ferguson AD. Design, Synthesis, and Biological Activity of Substrate Competitive SMYD2 Inhibitors. *J Med Chem* 2016; **59**: 11079-11097 [PMID: 28002961 DOI: 10.1021/acs.jmedchem.6b01303]
94 **Thomenius MJ**, Totman J, Harvey D, Mitchell LH, Riera TV, Cosmopoulos K, Grassian AR, Klaus C, Foley M, Admirand EA, Jahic H, Majer C, Wigle T, Jacques SL, Gureasko J, Brach D, Lingaraj T, West K, Smith S, Rioux N,

Waters NJ, Tang C, Raimondi A, Munchhof M, Mills JE, Ribich S, Porter Scott M, Kuntz KW, Janzen WP, Moyer M, Smith JJ, Chesworth R, Copeland RA, Boriack-Sjodin PA. Small molecule inhibitors and CRISPR/Cas9 mutagenesis demonstrate that SMYD2 and SMYD3 activity are dispensable for autonomous cancer cell proliferation. *PLoS One* 2018; **13**: e0197372 [PMID: 29856759 DOI: 10.1371/journal.pone.0197372]

95 **Oren M**, Rotter V. Mutant p53 gain-of-function in cancer. *Cold Spring Harb Perspect Biol* 2010; **2**: a001107 [PMID: 20182618 DOI: 10.1101/cshperspect.a001107]

96 **Ou K**, Liu X, Li W, Yang Y, Ying J, Yang L. ALK Rearrangement-Positive Pancreatic Cancer with Brain Metastasis Has Remarkable Response to ALK Inhibitors: A Case Report. *Front Oncol* 2021; **11**: 724815 [PMID: 34568053 DOI: 10.3389/fonc.2021.724815]

97 **Zhou P**, Li Y, Li B, Zhang M, Liu Y, Yao Y, Li D. NMIIA promotes tumor growth and metastasis by activating the Wnt/β-catenin signaling pathway and EMT in pancreatic cancer. *Oncogene* 2019; **38**: 5500-5515 [PMID: 30967633 DOI: 10.1038/s41388-019-0806-6]

98 **Gao S**, Wang Z, Wang W, Hu X, Chen P, Li J, Feng X, Wong J, Du JX. The lysine methyltransferase SMYD2 methylates the kinase domain of type II receptor BMPR2 and stimulates bone morphogenetic protein signaling. *J Biol Chem* 2017; **292**: 12702-12712 [PMID: 28588028 DOI: 10.1074/jbc.M117.776278]

99 **Wang Y**, Guo H, Zhang Z, Wang Q, Tian X, Yang Y. Inhibition of bone morphogenetic protein receptor 2 suppresses pancreatic ductal adenocarcinoma growth by regulating GRB2/PI3K/AKT axis. *Ann Transl Med* 2021; **9**: 557 [PMID: 33987255 DOI: 10.21037/atm-20-2194]

100 **Zhang X**, Tanaka K, Yan J, Li J, Peng D, Jiang Y, Yang Z, Barton MC, Wen H, Shi X. Regulation of estrogen receptor α by histone methyltransferase SMYD2-mediated protein methylation. *Proc Natl Acad Sci U S A* 2013; **110**: 17284-17289 [PMID: 24101509 DOI: 10.1073/pnas.1307959110]

101 **Xue J**, Yao Y, Yao Q, Tian X, Feng Y, Su H, Kong D, Cui C, Yan L, Hao C, Zhou T. Important roles of estrogen receptor alpha in tumor progression and anti-estrogen therapy of pancreatic ductal adenocarcinoma. *Life Sci* 2020; **260**: 118302 [PMID: 32827543 DOI: 10.1016/j.lfs.2020.118302]

102 **Zeng Y**, Qiu R, Yang Y, Gao T, Zheng Y, Huang W, Gao J, Zhang K, Liu R, Wang S, Hou Y, Yu W, Leng S, Feng D, Liu W, Zhang X, Wang Y. Regulation of EZH2 by SMYD2-Mediated Lysine Methylation Is Implicated in Tumorigenesis. *Cell Rep* 2019; **29**: 1482-1498.e4 [PMID: 31693890 DOI: 10.1016/j.celrep.2019.10.004]

103 **Patil S**, Forster T, Reutlinger K, Kopp W, Versemann L, Spitalieri J, Gaedcke J, Ströbel P, Singh SK, Ellenrieder V, Neesse A, Hessmann E. Chromatin-Independent Interplay of NFATc1 and EZH2 in Pancreatic Cancer. *Cells* 2021; **10** [PMID: 34943970 DOI: 10.3390/cells10123463]

104 **Giessrigl B**, Krieger S, Rosner M, Huttary N, Saiko P, Alami M, Messaoudi S, Peyrat JF, Maciuk A, Gollinger M, Kopf S, Kazlauskas E, Mazal P, Szekeres T, Hengstschläger M, Matulis D, Jäger W, Krupitza G. Hsp90 stabilizes Cdc25A and counteracts heat shock-mediated Cdc25A degradation and cell-cycle attenuation in pancreatic carcinoma cells. *Hum Mol Genet* 2012; **21**: 4615-4627 [PMID: 22843495 DOI: 10.1093/hmg/dds303]

105 **Xu F**, Sun Y, Yang SZ, Zhou T, Jhala N, McDonald J, Chen Y. Cytoplasmic PARP-1 promotes pancreatic cancer tumorigenesis and resistance. *Int J Cancer* 2019; **145**: 474-483 [PMID: 30614530 DOI: 10.1002/ijc.32108]

106 **Huang C**, Xie K. Crosstalk of Sp1 and Stat3 signaling in pancreatic cancer pathogenesis. *Cytokine Growth Factor Rev* 2012; **23**: 25-35 [PMID: 22342309 DOI: 10.1016/j.cytogfr.2012.01.003]

107 **Song J**, Liu Y, Chen Q, Yang J, Jiang Z, Zhang H, Liu Z, Jin B. Expression patterns and the prognostic value of the SMYD family members in human breast carcinoma using integrative bioinformatics analysis. *Oncol Lett* 2019; **17**: 3851-3861 [PMID: 30930987 DOI: 10.3892/ol.2019.10054]

108 **Oliveira-Santos W**, Rabello DA, Lucena-Araujo AR, de Oliveira FM, Rego EM, Pittella Silva F, Saldanha-Araujo F. Residual expression of SMYD2 and SMYD3 is associated with the acquisition of complex karyotype in chronic lymphocytic leukemia. *Tumour Biol* 2016; **37**: 9473-9481 [PMID: 26790435 DOI: 10.1007/s13277-016-4846-z]

109 **Yu H**, Zhang D, Lian M. Identification of an epigenetic prognostic signature for patients with lower-grade gliomas. *CNS Neurosci Ther* 2021; **27**: 470-483 [PMID: 33459509 DOI: 10.1111/cns.13587]

World Journal of Gastroenterology

Submit a Manuscript: https://www.f6publishing.com

World J Gastroenterol 2022 August 7; 28(29): 3767-3779

DOI: 10.3748/wjg.v28.i29.3767

ISSN 1007-9327 (print) ISSN 2219-2840 (online)

MINIREVIEWS

Clinical challenge for gastroenterologists–Gastrointestinal manifestations of systemic mastocytosis: A comprehensive review

Alessandra Elvevi, Elena Maria Elli, Martina Lucà, Miki Scaravaglio, Fabio Pagni, Stefano Ceola, Laura Ratti, Pietro Invernizzi, Sara Massironi

Specialty type: Gastroenterology and hepatology

Provenance and peer review: Invited article; Externally peer reviewed.

Peer-review model: Single blind

Peer-review report's scientific quality classification

Grade A (Excellent): 0
Grade B (Very good): B, B
Grade C (Good): C
Grade D (Fair): 0
Grade E (Poor): 0

P-Reviewer: Bairwa DBL, India; Guo F, China; Piris-Villaespesa M, Spain

Received: December 3, 2021
Peer-review started: December 3, 2021
First decision: May 29, 2022
Revised: June 6, 2022
Accepted: July 11, 2022
Article in press: July 11, 2022
Published online: August 7, 2022

Alessandra Elvevi, Martina Lucà, Miki Scaravaglio, Laura Ratti, Pietro Invernizzi, Sara Massironi, Gastroenterology Division, San Gerardo Hospital, University of Milano – Bicocca School of Medicine, Monza 20900, Italy

Elena Maria Elli, Hematology Division and Bone Marrow Transplant Unit, San Gerardo Hospital, Monza 20900, Italy

Fabio Pagni, Stefano Ceola, Department of Medicine and Surgery, Section of Pathology, San Gerardo Hospital, University of Milano – Bicocca School of Medicine, Monza 20900, Italy

Corresponding author: Sara Massironi, MD, PhD, Gastroenterology Division, San Gerardo Hospital, University of Milano – Bicocca School of Medicine, Via G.B. Pergolesi 33, Monza 20900, Italy. sara.massironi@libero.it

Abstract

Mastocytosis is a rare and heterogeneous disease characterized by various clinical and biological features that affect different prognoses and treatments. The disease is usually divided into 2 principal categories: cutaneous and systemic disease (SM). Clinical features can be related to mast cell (MC) mediator release or pathological MC infiltration. SM is a disease often hard to identify, and the diagnosis is based on clinical, biological, histological, and molecular criteria with different specialists involved in the patient's clinical work-up. Among all manifestations of the disease, gastrointestinal (GI) symptoms are common, being present in 14%-85% of patients, and can significantly impair the quality of life. Here we review the data regarding GI involvement in SM, in terms of clinical presentations, histological and endoscopic features, the pathogenesis of GI symptoms, and their treatment.

Key Words: Systemic mastocytosis; Gastrointestinal involvement; Gastrointestinal symptoms

©The Author(s) 2022. Published by Baishideng Publishing Group Inc. All rights reserved.

Core Tip: Gastrointestinal (GI) involvement is frequent in systemic disease (SM); GI symptoms are frequent (second in frequency only to itching), being the main culprits of chronic disorders, and are a major determinant of quality of life. GI symptoms could be secondary both to mast cell (MC) mediator release and MC infiltration in the GI tract, causing organ dysfunction. Diagnosis of GI involvement in SM is based on clinical and endoscopic suspicion and histologic demonstration of MC infiltration in GI mucosa, using immunohistochemistry (*i.e.,* CD117, tryptase, CD25). Symptomatic treatment is used to control mediators-release symptoms while cytoreductive therapies are necessary to reduce organ dysfunction secondary to MC infiltration and proliferation.

Citation: Elvevi A, Elli EM, Lucà M, Scaravaglio M, Pagni F, Ceola S, Ratti L, Invernizzi P, Massironi S. Clinical challenge for gastroenterologists–Gastrointestinal manifestations of systemic mastocytosis: A comprehensive review. *World J Gastroenterol* 2022; 28(29): 3767-3779
URL: https://www.wjgnet.com/1007-9327/full/v28/i29/3767.htm
DOI: https://dx.doi.org/10.3748/wjg.v28.i29.3767

INTRODUCTION

Mastocytosis is a rare type of myeloid neoplasm characterized by clonal expansion and accumulation of morphologically and immune-phenotypically abnormal mast cells (MCs) in one or more organ systems [1]. Clinical presentation in mastocytosis patients is heterogeneous[1,2]. Cutaneous mastocytosis (CM) is the skin-limited presentation; it is most common in children, who experience spontaneous regression of skin lesions during their growth. Systemic mastocytosis (SM) is, on the contrary, a condition of MCs proliferation associated with extra-cutaneous involvement, and it is more frequent in adult patients. Neoplastic MCs form focal and/or diffuse infiltrates in various internal organs, including the bone marrow (BM), spleen, liver, and gastrointestinal (GI) tract[2-4]. Regardless of the type of SM, the BM is involved in virtually all patients.

In 2016, the World Health Organization (WHO) classification of SM identified 5 clinical variants with different prognoses: indolent SM (ISM), smoldering SM (SSM), aggressive SM (ASM), SM with associated hematological neoplasm (SM-AHN), and mast cell leukemia (MCL)[5,6]. Advanced SM (ASM, SM-AHN, and MCL) is generally associated with a poor outcome, whereas ISM patients usually have a comparable life expectancy in comparison with the general population[1,2].

In recent years, knowledge of the pathophysiology of mastocytosis has improved. Particularly, research has found that a recurrent activating D816V KIT mutation, located in the phosphor-transferase domain (PTD) of the receptor, is detectable in more than 80% of adult patients with SM[7,8]. Further genetic alterations, usually involved in myeloid malignances pathogenesis, are often found in advanced forms of SM. These mutations are associated with aggressive disease and poor prognosis[9].

For many years, mastocytosis has been considered an orphan disease, and this might be an explanation for the difficulty in estimating its prevalence. The reported prevalence of SM of 9.56 per 100000 persons[10] is probably underestimated; in the last few years, improved knowledge of the disease and availability of diagnostic tests suggested a higher prevalence, with the newer prevalence reported to be 21 per 100000 inhabitants in the adult population[11].

Mastocytosis diagnosis is based on the identification of atypical MCs in the affected tissue, according to the well-established WHO criteria, based on morphological, histological, cytofluorimetric, and molecular features[5,6] (Table 1). When the major and at least one minor SM criterion or three minor SM criteria are detected, the diagnosis SM is established. SM patients can be further sub-classified depending on the presence of B (organ involvement without organ failure) or C (organ involvement with organ dysfunction) findings, defining MCs burden or disease aggressiveness, respectively[1,5,6] (Table 2).

The severity of the symptoms associated with mastocytosis may vary from mild to life-threatening [2]. In general, symptoms occurring in SM are mainly due to the release of chemical mediators from the MCs, such as histamine, heparin, and eosinophil chemotactic factor, and thus produce symptoms associated with an allergic reaction, although a true allergic trigger may not be identified. In ASM, where MCs infiltration occurs, a decrease in blood cells (cytopenia), break-down of bones (osteolysis), swelling of the lymph nodes (lymphadenopathy), swelling of the liver (hepatomegaly), impaired liver function, ascites or portal hypertension, and malabsorption may occur[1,12,13].

Symptom-directed treatment should be considered in all SM patients[2]. Supportive therapies for SM are directed at MC's degranulation symptoms [histamine-receptors 1 (H1) and 2 (H2) antagonists, proton pump inhibitors (PPI), leukotriene antagonist, sodium cromolyn, corticosteroid], symptomatic skin disease (Psolaren plus ultraviolet A photo-chemotherapy, corticosteroids), and/or osteopenia/osteoporosis/pathologic fractures (bisphosphonate, cytokine/ immunomodulatory drugs) [2,14,15]. Treatment goals for ISM patients are primarily directed towards anaphylaxis prevention and

Table 1 Systemic mastocytosis criteria according to World Health Organization 2016

Major SM criterion	Multifocal dense infiltrates of MCs (≥ 15 MCs in aggregates) in BM biopsies and/or in sections of other extracutaneous organ(s)
Minor SM criteria	(a) > 25% of all MCs are atypical cells (type I or type II) on BM smears or are spindle-shaped in MC infiltrates detected on sections of visceral organs
	(b) KIT point mutation at codon 816 in the BM or another extracutaneous organ
	(c) MCs in BM or blood or another extracutaneous organ exhibit CD2 and/or CD25
	(d) Baseline serum tryptase level >20 ng/mL (in case of an unrelated myeloid neoplasm, item d is not valid as an SM criterion)

If at least 1 major and 1 minor or 3 minor systemic mastocytosis (SM) criteria are fulfilled, the diagnosis of SM can be established. BM: Bone marrow; MCs: Mast cells; SM: Systemic mastocytosis.

Table 2 B and C Findings in systemic mastocytosis

B and C Findings in systemic mastocytosis
B Findings
BM biopsy showing > 30% infiltration by MCs (focal, dense aggregates) and serum total tryptase level > 200 ng/mL
Myeloproliferation or signs of dysplasia in non-MC lineage(s), no prominent cytopenias; criteria for AHN not met
Hepatomegaly and/or splenomegaly on palpation without impairment of organ function and/or lymphadenopathy on palpation/imaging (> 2 cm)
C Findings[1]
Cytopenia(s): ANC < 1 × 10^9/L, Hb < 10 g/dL, or platelets < 100 × 10^9/L
Hepatomegaly on palpation with impairment of liver function, ascites, and/or portal hypertension
Skeletal lesions: Osteolyses and/or pathologic fractures
Palpable splenomegaly with hypersplenism
Malabsorption with weight loss from gastrointestinal tract MC infiltrates

[1]Must be attributable to the mast cell infiltrate. AHN: Associated hematological neoplasm; ANC: Absolute neutrophilic count; BM: Bone marrow; MCs: Mast cells.

symptom control/osteoporosis treatment. Patients with advanced SM frequently need MCs cytoreductive therapy to ameliorate disease-related organ dysfunction[2]. High response rates have been seen with small-molecules inhibitors that target mutant-KIT, including midostaurin (Food and Drug Administration and European Medicine Agency approved) or avapritinib (Food and Drug Administration approved)[2,16-19].

In this review, we sought to focus on clinical, pathophysiological, histological, and therapeutic aspects of GI tract involvement in SM.

GI CLINICAL MANIFESTATIONS OF SM

GI involvement in the clinical presentation of SM has been reported to vary from 15% to 85%. The wide range of variability is probably due to variable definitions of GI symptoms and differences in the attention on GI involvement in the case series available in the literature[20]. However, among all clinical manifestations, GI symptoms appear to be second in frequency only to itching[21] and are the main culprits of chronic disorders being a major determinant of quality of life (QoL)[20-22].

GI symptoms can be varied and may be independent of a clear GI involvement with mastocytes' infiltration[23]. In addition, GI manifestations may occur in the absence of typical cutaneous manifestations, with GI dysfunction being observed in both cutaneous mastocytosis and SM[24]. Although the gastro-enteric tract involvement has been described in all SM variants, both the frequency and the type of GI symptoms vary according to the SM subtype.

GI symptoms associated with SM are often non-specific and mimic common conditions, such as irritable bowel syndrome, inflammatory bowel disease, or celiac disease, with recurrent abdominal pain, nausea, vomiting, gastro-esophageal reflux disease, diarrhea, and bloating, until more severe pictures characterized by long-standing, persistent, and intractable diarrhea with malabsorption occurs[23]. Also, peptic ulcer disease represents a GI manifestation of SM, causing gastro-duodenal ulceration in up

to 50% of cases[25], with possible severe GI bleeding sustained by the large amount of histamine released by mast cells (Table 3).

PATHOPHYSIOLOGY OF GI INVOLVEMENT

From the pathophysiological point of view, these symptoms are caused by several mechanisms. Activation of MCs causes alteration in epithelial and neuromuscular function. MCs represent 2% of the cells present on the intestinal mucosa of the GI tract[26]: They are responsible for a series of regulatory functions concerning the barrier functions and vascular mucosal permeability, regulating the secretion of GI hormones, modulating peristalsis and the pain perception threshold, and regulating the endothelial barrier and chemotaxis of immune cells. They, therefore, intervene in the regulation of the inflammatory response and, as recently described, they drive the immune response by attracting both granulocytes and lymphocytes and triggering innate defense mechanisms, such as enhanced epithelial secretion, peristalsis, and alarm programs of the enteric nervous system[26,27].

Activated MCs release various inflammatory mediators, which determine intestinal motility alteration, visceral sensitivity alteration, and mucosal and epithelial gut barrier function alteration. Furthermore, MCs inflammatory mediators determine hypersecretion and increased motility, causing diarrhea and abdominal pain. In the more advanced and aggressive stages, there is a direct MC infiltration of the GI tract and the pathogenic mechanisms change. The GI tract can be involved in any phase of SM and the pathophysiological mechanisms are different. As well as reported for other extra-hematological manifestations of SM, in the initial and indolent forms of SM, the gut is a target of mediators released by MCs and functional disorders are more expressed, with mediator-related functional diarrhea, abdominal pain, and motor dyspepsia.

Thereafter, with the massive and persistent mediators' release, organic lesions appear, such as peptic disease. The main mediator released by MCs is histamine which exerts different effects on both the upper and lower gastrointestinal tract. Histamine interacts with H2 receptors, promoting the secretion of hydrochloric acid, resulting in gastroesophageal reflux disease, gastritis, and peptic ulcer.

The peptic ulcer due to the increase in histamine-related acid secretion is a condition not rarely observed in SM, and it is largely underestimated: It is reported in up to 40% of patients with SM. It does not correlate with circulating markers, in particular with circulating histamine; therefore, it has to be hypothesized with a low threshold of suspicion and then investigated with gastroscopy. Moreover, peptic ulcer bleeding in MS is also reported in up to 11% of patients[25]. Histamine also interacts with the H1 receptors, regulating the gut smooth muscle contraction, causing impaired peristalsis and motility disorders, clinically resulting in the dysmotility-like dyspepsia and functional diarrhea observed in patients in the early stages of SM.

Besides the GI effects of histamine, other transmitters are released in the course of SM, including prostaglandins and serotonin, which have various effects, including effects mainly on the neuromuscular junction of the GI tract, with consequently impaired motility and visceral hypersensitivity. Again, patients present with nausea, vomiting, and abdominal pain worsened by the reduction of the pain threshold. In the course of mastocytosis, diarrhea is often associated with flushing. Therefore, is important to distinguish "wet flushing", associated with profuse sweating, and "dry flushing", without sweating (Table 3). In SM, dry flushing is observed, whereas "wet flushing" is more related to physiological or para-physiological causes.

In the more advanced and aggressive stages of MS, the manifestations are mainly related to the gut MC infiltration of the GI wall, which impairs both the barrier functions and the absorbing functions, and the pathogenic mechanisms of diarrhea change from a functional to organic diarrhea. As the disease progresses, the clinical picture evolves into malabsorption, progressive caloric-protein malnutrition, vitamin deficiency, deterioration of the patient's condition, worsening of osteoporosis (already present in these patients), and finally anasarca, due to a complete impaired gut absorption and barrier function.

Mast cell mediators-related GI abnormalities

The release of a great amount of histamine and other peptides contained in MC granules has been implicated in the pathogenesis of a variety of functional GI manifestations in SM, including diarrhea, bloating, nausea, vomiting, abdominal pain, peptic ulcer disease, and related GI bleeding.

A recent multicenter French study analyzing a cohort of 83 patients affected by SM has demonstrated that GI symptoms are more frequent in SM patients compared to matched healthy subjects. Moreover, SM is correlated with a significantly greater risk of developing peptic ulcer disease, especially duodenal ulcers[28]. Diarrhea, bloating and abdominal pain have been reported as the most frequent SM-associated GI disturbances in several studies[20,22,25,29].

Abdominal pain has been described in different case series with a wide range of frequency from 12% to 100%. Of note, Cherner and colleagues[25] identified two different types of abdominal pain. The majority of SM patients suffered from an abdominal pain of dyspeptic nature, defined as an epigastric pain responsive to antacids and histamine type 2 receptor antagonists and with a high incidence of peptic disease on upper gastrointestinal endoscopic examination. A minority of patients complained of

Table 3 Differential diagnosis between systemic mastocytosis and gastrointestinal diseases

Symptoms	Differential diagnosis
Chronic diarrhea	Irritable bowel syndrome; Inflammatory bowel disease; Celiac disease; Thyreopathies (*i.e.* hyperthyroidism, medullary thyroid cancer); Pancreatopathyes
Epigastric pain, dyspepsia, heartburn	Functional dyspepsia; Peptic ulcer; Gastroesophageal reflux disease; H. pylori related gastritis; Zollinger-Ellison Syndrome
Flushing	Neuroendocrine neoplasms
Hepato-splenomegaly, portal hypertension	Cirrhosis; Non cirrhotic portal hypertension

non-dyspeptic pain associated with bloating that does not benefit from histamine 2 receptor antagonists and antacids and was associated with normal endoscopic investigations. While the pathogenesis of the first pain type may be easily correlated to increased acid secretion, the non-dyspeptic pain type is more likely related to intestinal motility disturbances and a lower pain threshold caused not only by an increased release of histamine but also by other mediators, such as serotonin, prostaglandins, and neuropeptides.

Functional diarrhea has been reported in several series of SM patients with a range from 14% to 100%. The presence of diarrhea has been described as an episodic increase in bowel movements with subsequent emission of liquid stool that may or may not be associated with a fecal weight > 200 g/d [20]. It may be related to increased gastric acid secretion with mechanisms similar to Zollinger Ellison syndrome and/or to increased bowel motility induced by prostaglandin D2 secretion, as there is evidence of cases of diarrhea responsive to aspirin administration[30]. In contrast, the presence of steatorrhea has been correlated with a condition of malabsorption characteristic of advanced mastocytosis with extensive mucosal and submucosal infiltration with MCs.

Nausea and vomiting have been described less frequently and usually as components of syndromic disorders that also include palpitations, flushing, abdominal cramps, and diarrhea, generally exacerbated by the ingestion of certain substances, such as alcohol and medications, or contact with inflammatory mediators, which stimulate MCs degranulation. The absence of specific colonic symptoms does not mean that the colon or rectum are not involved. In particular, rectal manometric studies show a lower distention threshold to induce pain or rectal urgency; patients complain of reduced rectal compliance or overactive rectal contractility.

Peptic ulcer disease

One of the most common mediator-related clinical signs, which over time can generate organic lesions and GI organic damage, is related to gastric acid hypersecretion secondary to the hyper-histaminic state, which leads to dyspeptic pain and digestive ulcer disease.

A prospective study shows that peptic ulcers in SM are common, present in up to 50% of patients [25]. It is usually symptomatic and associated with gastric acid hypersecretion and elevated basal acid output (BAO)[31]. In some patients, BAO can reach the Zollinger-Ellison range, so that may even cause the signs and symptoms of the syndrome itself[20]. Of interest, a particular form of CM, the so-called *telangiectasia macularis eruptiva perstans*, also known as paucicellular mastocytosis, has been associated with peptic giant gastro-duodenal ulcers[32]. Other acid-related complications have been reported, such as ulcer perforation and severe esophagitis. Moreover, up to 11% of SM-affected patients will manifest peptic ulcer bleeding during the disease course. However, so far there has been no evidence of a consistent relationship between the level of serum histamine and the presence of ulcer disease or gastric acid output. However, despite the increased circulating histamine level, many patients have normal acid secretion and in some cases, even achlorhydria has been observed[31]. The variability in the response to circulating histamine may relate to partial inactivity of circulating histamine, differences between circulating histamine and gastric tissue histamine, and the intervention of unknown cofactors in the stimulation of oxyntic cells, as well as the theory of possible desensitization of parietal cells that can justify the rare cases of complete achlorhydria[20].

Mast cell infiltration-related GI abnormalities

In patients with advanced SM, the B and C findings (Table 2) become prevalent to functional GI symptoms. B GI findings indicate organ involvement without organ dysfunction, while C GI-findings refer to the advanced stage where both organ infiltration and dysfunction coexist, being associated with a poor prognosis[6]. They include malabsorption, weight loss, and organomegaly (spleen, liver) until full-blown organ dysfunction leads to hepatic failure and ascites.

Malabsorption based on quantitative stool fat analysis, D-xylose, and Schilling tests has been found to occur in one-third of SM patients and is usually mild[32]. Thus, it is important to consider mastocytosis in the diagnostic work-up of chronic and intractable diarrhea, especially when the endoscopic presentation seems to be suggestive. Both the small and the large intestine can undergo permanent

alterations, which contribute to the genesis of diarrhea and malabsorption. Over time, patients could develop real intestinal malabsorption syndrome with vitamins A and D deficiency, overt osteomalacia and osteoporosis, protein-energy malnutrition, and anasarca. The whole gastrointestinal tract may be involved in SM with varying degrees.

Liver involvement in SM can range from an abnormal liver function test alone to hepatomegaly due to MC and eosinophil infiltrates in portal triads. Initial fibrosis can evolve in cirrhosis with worsening portal hypertension sustained by simultaneous splenomegaly, with or without hypersplenism, and ultimately ascites and upper digestive bleeding from esophageal varices. Of note, mastocytosis is one of the causes of non-cirrhotic portal hypertension[33], sustained by pre-sinusoidal and sinusoidal mechanisms through the infiltration of inflammatory mast cells within the portal vein and obstruction of the sinusoids[34]. In this setting, we can also observe vascular alterations, like portal hypertension, veno-occlusive disease (8%), and Budd-Chiari syndrome.

No studies have identified how many patients with SM develop portal hypertension, but in real medical practice, clinicians have to keep in mind that it can occur without associated advanced liver disease, further increasing the risk of upper GI bleeding. A study of 24 cases of SM involving the GI tract found only 3 patients with liver involvement; however, liver involvement correlates with more aggressive disease[23]. Moreover, as liver failure occurs, it contributes to worsening malnutrition and hypoalbuminemia that are already determined by intestinal insufficiency.

ENDOSCOPIC FINDINGS IN SM

Even though no remarkable endoscopic findings could be found[4], there are several endoscopic pictures described in SM, and endoscopic findings could be secondary both to MC mediator release and to MC infiltration in the GI wall or liver.

Upper gastrointestinal endoscopy

At upper GI endoscopy, peptic disease (esophagitis, esophageal strictures, peptic ulcer) is one of the most frequent findings in patients with SM[21].

According to the literature, upper GI involvement could be found in up to 40% of SM patients undergoing endoscopy[25] and may be sustained by chlorhydric acid hypersecretion. However, its pathogenesis is still uncertain: Peptic disease is thought to be secondary to gastric acid hypersecretion sustained by elevated histamine plasma levels, but data from literature are controversial: Hypersecretion-n of gastric acid does not seem to be consistently related to the level of serum histamine levels measured. It may, however, be possible that a relationship between tissue concentration of histamine and GI manifestations can exist[25].

While esophagitis and, when untreated, esophageal strictures are thought to be secondary to mediator release, esophageal varices could be accounted for SM endoscopic findings when liver infiltration is present; this infiltration determines intrahepatic portal hypertension with esophageal and gastric varices development[33-35].

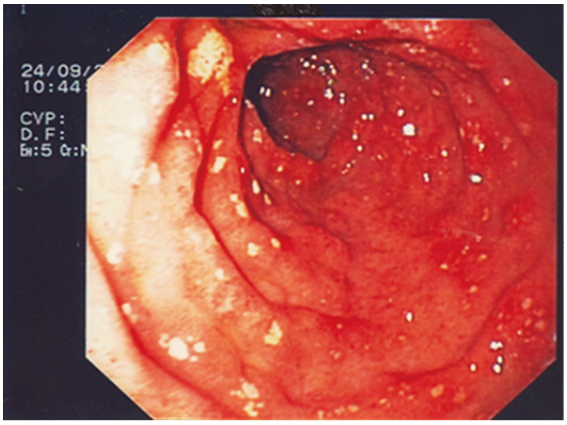
Exploration of the stomach and duodenum could show urticaria-like lesions in the antrum of the stomach, diffuse telangiectasia, multiple erosions of gastric and/or duodenal mucosa (Figure 1) and peptic ulcer; these findings are thought to be secondary to MCs mediators' release (*i.e.*, histamine, serotonin, prostaglandins, and neurotensin). When atypical mastocyte infiltration occurs, nodular mucosal lesion of the stomach and/or duodenum can be found[21,36,37].

Small bowel endoscopy and colonoscopy

Small bowel, as well as other digestive tract components, could be involved by SM. From the review of literature, the most common findings during small bowel exploration are diffuse telangiectasia, thickened jejunal folds, scalloped folds, and diffuse nodularity[21,36]. As for the upper GI tract, diffuse telangiectasia and thickened jejunal folds are thought to be secondary to MC mediator release, while scalloped folds and diffuse nodularity are thought to be secondary to MC infiltration in the GI wall[21].

Colonoscopy in patients with SM can reveal diffuse telangiectasia and/or urticarial lesion, patchy mucosal erythema, as well as mucosal edema, mucosal friability, loss of vascular patterns, and diffuse nodularity. Moreover, adding indigo carmine dye spraying could be useful to enhance yellowish-white polypoid lesions and yellowish-white nodular or granular mucosal lesions[36,38,39].

As for the other GI tracts, mucosal erythema and edema, mucosal friability are thought to be secondary to MC mediator release, while loss of vascular patterns and nodular and /or polypoid lesions are thought to be secondary to MCs infiltration into the bowel wall[21]. Unfortunately, none of these endoscopic signs is specific for GI involvement of SM; hence, biopsy specimens of the GI wall should always be performed in order to have histological diagnostic confirmation of GI involvement.



DOI: 10.3748/wjg.v28.i29.3767 **Copyright** ©The Author(s) 2022.

Figure 1 Endoscopic pictures of second portion of the duodenum. The mucosa appears to be erythematous, hyperemic, and covered with diffuse erosions.

HISTOPATHOLOGICAL ASPECT IN SM

Mast cells (MCs) are unique granulated cells (approximately 20 μm) that are absent in peripheral blood. They develop *in situ* from CD34-positive or c-Kit– positive progenitor cells[40]. MCs are distributed throughout many tissues, including the gastrointestinal mucosa. They enable an immune function in response to a diversity of exogenous substances in the gut lumen[41].

Within the gut, two subpopulations can be distinguished: the mucosal reactive MCs, which may dramatically increase in response to immune stimuli and are dependent on T lymphocytes[42,43], and the submucosal MCs, which can act in the regulation of intestinal permeability, secretion, peristalsis, nociception, immunity, and angiogenesis[44]. The histologic appearances of the GI mucosa in SM patients are incompletely described[45]. Results of mucosal mast cell quantitation have similarly been mixed with some studies reporting increased, decreased, and normal numbers of mucosal mast cells in patients with SM compared with controls[46].

The mean normal value of MCs count in normal GI mucosa is yet to be validated in large patient cohorts; most studies consider a cutoff of 20 MCs per high-power field within the lamina propria, this value being 2 standard deviations above that found in the general population[47,48]. As MC infiltrate can be focal and mild, the diagnosis of mastocytosis in GI mucosal biopsies can be challenging; hence, multiple biopsies are necessary in order to improve diagnostic yield[28].

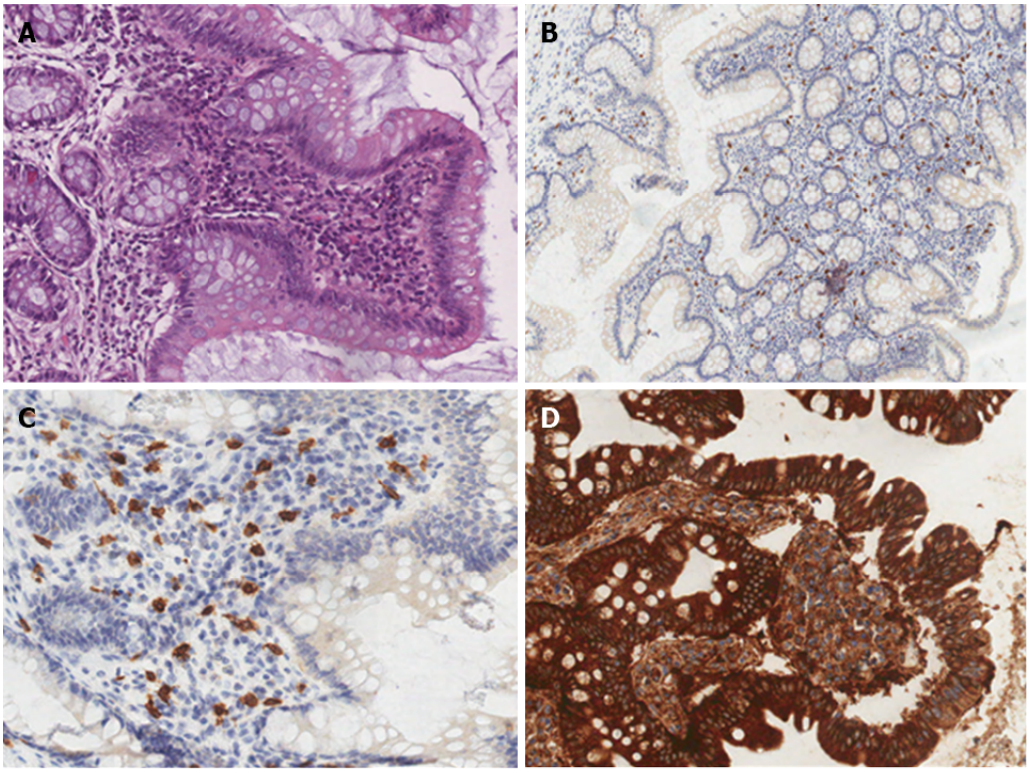
In almost all cases of SM involving the GI tract, the number of intramucosal MCs is substantially increased[23], and MCs group together forming pathognomonic compact micronodular or band-like infiltrate. Tiny clusters of cells, with a predominant sub-epithelial distribution, appear in different shapes, varying from rounded cells with a moderate amount of pale and eosinophilic cytoplasm to ovoid and spindle-shaped cells with scant cytoplasm. Those diagnostic infiltrates may be small but should consist at least of 15 clusterings[23].

Hematoxylin and eosin staining are not a definitive method for MCs detection, hence special staining is required, such as toluidine blue staining and immuno-histo-chemical panels using tryptase, CD117, and CD25[49]. Comparison between these techniques confirmed a stem cell factor receptor kit (testing for c-kit and CD117) is the most accurate technique[50]. CD117 is expressed on all types of MCs independent off maturation and activation status; in SM, c-Kit is often expressed in MCs in a mutated and constitutively activated form. In these patients, MCs aberrantly display CD25, a diagnostic marker of neoplastic MCs in all SM variants[51]. Therefore, CD117 is sensitive, but not specific for MCs; tryptase is less sensitive but more specific. Both CD117 and tryptase are not diagnostic of the neoplastic nature, whereas CD25 expression is considered a hallmark of MCs atypia[4] (Figure 2).

SM may involve other GI organs like the liver. The main site of liver involvement is the portal tract, where MCs may form groups of dense infiltrates within the fibrotic portal triads; because MCs are normally absent in the sinusoid, the presence of scattered MCs in liver sinusoids is also consistent with SM (Figure 3).

TREATMENT OF GI SYMPTOMS

Symptom-directed treatments should be considered in all SM patients and are directed at MC degranulation symptoms (*i.e.* nausea, vomiting, abdominal pain, peptic disease, diarrhea)[2].



DOI: 10.3748/wjg.v28.i29.3767 **Copyright** ©The Author(s) 2022.

Figure 2 Spectrum of histologic findings in patients with intestinal involvement of systemic mastocytosis. A: A mild initial finding with mast cells arranged in sheets and micro aggregates (hematoxylin-eosin, × 10). A heavy eosinophil infiltrate frequently dominates the picture. Crypt architectural distortion, without any other evidence of inflammatory bowel disease. Scattered lymphocytes and plasma cells often accompanied the mast cell and eosinophil infiltrates; B-C: The mast cells show expression of c-kit (B; CD117, × 2) and tryptase (C; × 10); D: CD25 positive cells in a clearcut and spread duodenal mastocytosis (CD25, × 10).

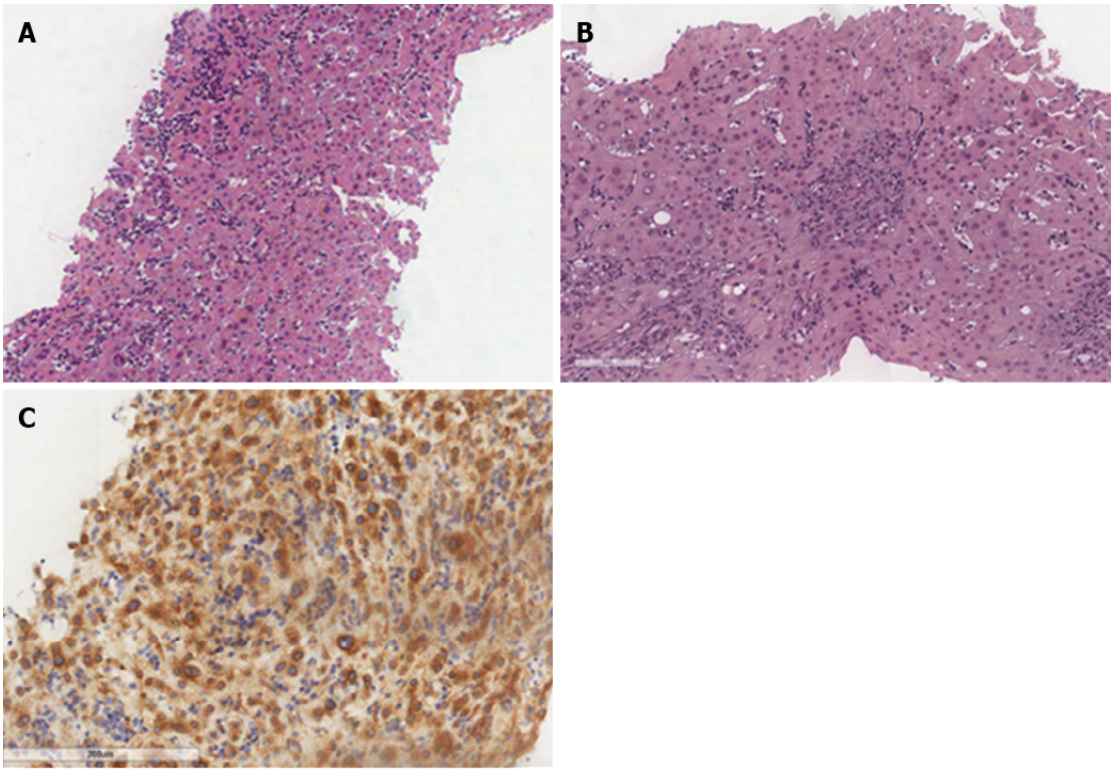
As first step, patients must recognize and avoid general and specific individual factors that trigger symptoms. These can commonly include physical factors such as heat, temperature changes, some forms of exercise, emotions, stress, sleep deprivation; diagnostic and therapeutic agents (such as opiates, NSAIDs, succinylcholine, and agents with tetrahydroisoquinoline, atracuronium, rocuronium, and quinolones), foods, alcohol and Hymenoptera venoms[52].

Different symptomatic drugs have been proposed for the control of GI symptoms: H2- antagonists (*i.e.*, Famotidine 10 mg BID, Cimetidine 400 mg BID) are the first-line therapy[2]. They act as inverse agonists that combine with and stabilize the inactive conformation of the histamine-receptor, shifting the equilibrium toward the inactive state; in a concentration-dependent manner, they inhibit MC activation and histamine release. However, although,the mechanisms involved have not yet been delineated fully, downregulation of intracellular calcium ion accumulation seems to play a role[53]. Inactivation of histamine receptors reduces the histamine effect along the GI tract, hence reducing histamine-related symptoms (*i.e.*, diarrhea, abdominal pain, peptic disease).

When histamine-receptor blockers are poorly effective or ineffective, proton pump inhibitors (PPIs, *i.e.*, Omeprazole 20 mg/d, Rabeprazole 20 mg/d, Pantoprazole 40 mg/d) represent second-line therapy [2]. Hydrochloric acid is secreted by parietal cells in the oxyntic mucosa that lines the body and the fundus of the stomach as a response to different mediators (*i.e.*, histamine, gastrin, acetylcholine), that activate H+/K+ ATP-ase (*i.e.*, the proton pump) that pumps hydrogen ions (protons) into the lumen in exchange for potassium ions. PPIs block this final step in gastric acid secretion by blocking H+/K+ ATP-ase irreversibly. They are remarkably effective in the inhibition of gastric acid secretion[54]. Considering SM as a hypersecretory condition, it is clear that reducing hydrochloric acid secretion is beneficial in SM patients because it reduces peptic symptoms, peptic disease, and/or diarrhea.

Sodium cromolyn (100-200 mg QID 30 minutes before meals and bedtime) represents the third-line therapy when H-2 antagonists and PPIs are ineffective[2]. It works as an inhibitor of histamine release and cell membrane stabilizer: cromolyn sodium caused weak inhibition of histamine release. However, different studies have shown its action on other mediators involved in mast cells' degranulation by inhibiting prostaglandin D2 release and TNFα release from mast cells, hence reducing MC degranulation and mediator release[55]. Reducing mediator release should help reduce GI symptoms.

Pardanani[2] has proposed systemic corticosteroid (*i.e.* prednisone 0.5-1 mg/kg/d starting dose; taper as feasible based on response/tolerance), as the fourth line of therapy for GI symptoms resistant to previous symptomatic therapies. Corticosteroids are potent anti-inflammatory drugs widely used in the treatment of allergic and inflammatory diseases. They also showed an in-vitro inhibition of MCs



DOI: 10.3748/wjg.v28.i29.3767 **Copyright** ©The Author(s) 2022.

Figure 3 Frustules of hepatic parenchyma with substantially preserved structure, with trabeculae with 2-cell spinnerets with no significant steatosis, but focal balloon-like degeneration associated with biliary stasis phenomena. A: Biliary spaces with preserved ducts, with ductular regeneration and bilio-hepatocyte metaplasia (hematoxylin-eosin, × 4); B: Some phenomena of hepatitis with aggression of the biliary epithelium are observed (hematoxylin-eosin, × 20). Portal spaces enlarged due to the presence of mixed inflammatory infiltrates, mainly consisting of T lymphocytes (CD3 +) with initial fibrotic expansion and formation of porto-portal bridges; C: In this context, scattered CD117 +, tryptase + cells (× 20) referable to mast cells.

mediators' release. Systemic administration of corticosteroids has been used in patients with mastocytosis. While this treatment appears to improve control of some mediator-release symptoms, it has not been proven to reduce MC numbers significantly in patients with mastocytosis[56]. Of note, systemic corticosteroids have been useful in decreasing the malabsorption and ascites in some of these patients[57].

In advanced SM, treatments interfering with MC proliferation and survival are used[2]. GI symptoms secondary to organ infiltration could also benefit from cytoreductive therapies, such as 2-chlorodeoxy-adenosine (cladribine or 2-CdA) or interferon-alfa[58]. In young and otherwise healthy ASM patients, allo-SCT is the only option for a sustained response[59]. Promising effects have been seen with the use of targeted therapy on mutated-KIT, which occurs in most SM patients[2]. Midostaurin (PKC412) is the first kit-inhibitor recent approved by the United States Food and Drug Administration (FDA) and European Medicines Agency (EMA) for the treatment of Advanced SM[16,17]. It has *in vitro* activity against kinase domain KIT mutants (D816Y and D816V). In the global Phase 2 CPKC412D2201 trial[18], 116 patients with advanced SM were enrolled; patients were treated with PKC412 at 100 mg BID. The overall response rate (ORR) per conventional criteria was 60% with 45% having a major response and 15% having a partial response, but it is often not sustained. In particular, concerning GI involvement, reversal of organ damage was reflected by normalization of hypoalbuminemia (58%), improvement in liver function test abnormalities (44%-58%), and/or reversion of weight loss (25%). Patients reported improvement of disease-related symptoms with treatment. Therefore, the most common drug side effects (all grades/grades 3-4) were nausea (79%/6%), vomiting (66%/6%), diarrhea (54%/3%), and fatigue (28%/9%), in addition to hematological toxicity, in terms of grade 3-4 of neutropenia, anemia, and thrombocytopenia, occurring in 24%, 41%, and 29% of patients, respectively.

Avapritinib[19], a KIT and PDGFRA inhibitor, showed promising results; other medications potentially effective for SM patients are under investigation[2]. Further optimization of treatment with tyrosine-kinase inhibitors in order to improve patients' quality of life is still needed.

CONCLUSION

Mastocytosis is a rare and heterogeneous disease characterized by various biological and clinical

features with different prognosis and treatments. The disease is usually divided into 2 principal categories: CM and SM. Clinical features can be related to MCs mediators release or pathological MCs infiltration. The diagnosis of SM is based on clinical, biological, histological, and molecular criteria, according to WHO 2016 classification. A proper patient's workup requires a multidisciplinary approach including gastroenterologists, endoscopists, hematologists, and pathologists. Among all manifestations of the disease, GI symptoms are common, being present in 15%-85% of the patients and can significantly impair the quality of life. Here, we review the data regarding GI involvement in SM, in terms of clinical presentations, histological features, pathogenesis of GI symptoms and their treatment. The most frequent GI symptoms are abdominal pain, diarrhea, nausea, and vomiting. GI lesions may involve all the digestive tract, from the esophagus to the rectum. The histological diagnosis of GI involvement is difficult. The treatment of GI symptoms aims to prevent and limit MCs degranulation and/or its consequences and more rarely to control tumoral mast cells infiltration. The diagnosis of mastocytosis should be considered in the case of unexplained severe GI disorders.

ACKNOWLEDGEMENTS

Massironi S and Invernizzi P are members of the European Reference Network on Hepatological Diseases (ERN RARE LIVER) and they thank AMAF Monza Onlus and AIRCS.

FOOTNOTES

Author contributions: Elvevi A, Elli EM, and Massironi S designed the study; Elvevi A, Elli EM, Lucà M, and Scaravaglio M wrote the first draft of the paper; Pagni F, Ceola S, and Ratti L revised the paper and wrote the final version; Massironi S and Invernizzi P reviewed the paper for important intellectual content; all authors have read and approved the final manuscript.

Conflict-of-interest statement: All authors report no relevant conflict of interest for this article.

Open-Access: This article is an open-access article that was selected by an in-house editor and fully peer-reviewed by external reviewers. It is distributed in accordance with the Creative Commons Attribution NonCommercial (CC BY-NC 4.0) license, which permits others to distribute, remix, adapt, build upon this work non-commercially, and license their derivative works on different terms, provided the original work is properly cited and the use is non-commercial. See: https://creativecommons.org/Licenses/by-nc/4.0/

Country/Territory of origin: Italy

ORCID number: Alessandra Elvevi 0000-0001-9841-2051; Elena Maria Elli 0000-0001-5576-5412; Martina Lucà 0000-0003-3787-6973; Miki Scaravaglio 0000-0003-2914-4908; Fabio Pagni 0000-0001-9625-1637; Stefano Ceola 0000-0002-5815-987X; Laura Ratti 0000-0003-0198-6433; Pietro Invernizzi 0000-0003-3262-1998; Sara Massironi 0000-0003-3214-8192.

S-Editor: Wu YXJ
L-Editor: Filipodia
P-Editor: Wu YXJ

REFERENCES

1 **Horny H**, Akin C, Arber D, Peterson L, Tefferi A, Metcalfe D, Bennet J, Bain B, Escribano L, Valent P. WHO Classification of Tumours of Haematopoietic and Lymphoid Tissues. Revised 4th Ed. Lyon, France: IARC, 2017
2 **Pardanani A**. Systemic mastocytosis in adults: 2021 Update on diagnosis, risk stratification and management. *Am J Hematol* 2021; **96**: 508-525 [PMID: 33524167 DOI: 10.1002/ajh.26118]
3 **Valent P**, Akin C, Escribano L, Födinger M, Hartmann K, Brockow K, Castells M, Sperr WR, Kluin-Nelemans HC, Hamdy NA, Lortholary O, Robyn J, van Doormaal J, Sotlar K, Hauswirth AW, Arock M, Hermine O, Hellmann A, Triggiani M, Niedoszytko M, Schwartz LB, Orfao A, Horny HP, Metcalfe DD. Standards and standardization in mastocytosis: consensus statements on diagnostics, treatment recommendations and response criteria. *Eur J Clin Invest* 2007; **37**: 435-453 [PMID: 17537151 DOI: 10.1111/j.1365-2362.2007.01807.x]
4 **Zanelli M**, Pizzi M, Sanguedolce F, Zizzo M, Palicelli A, Soriano A, Bisagni A, Martino G, Caprera C, Moretti M, Masia F, De Marco L, Froio E, Foroni M, Bernardelli G, Alvarez de Celis MI, Giunta A, Merli F, Ascani S. Gastrointestinal Manifestations in Systemic Mastocytosis: The Need of a Multidisciplinary Approach. *Cancers (Basel)* 2021; **13** [PMID: 34282774 DOI: 10.3390/cancers13133316]
5 **Arber DA**, Orazi A, Hasserjian R, Thiele J, Borowitz MJ, Le Beau MM, Bloomfield CD, Cazzola M, Vardiman JW. The 2016 revision to the World Health Organization classification of myeloid neoplasms and acute leukemia. *Blood* 2016; **127**: 2391-2405 [PMID: 27069254 DOI: 10.1182/blood-2016-03-643544]

6 **Valent P**, Horny HP, Escribano L, Longley BJ, Li CY, Schwartz LB, Marone G, Nuñez R, Akin C, Sotlar K, Sperr WR, Wolff K, Brunning RD, Parwaresch RM, Austen KF, Lennert K, Metcalfe DD, Vardiman JW, Bennett JM. Diagnostic criteria and classification of mastocytosis: a consensus proposal. *Leuk Res* 2001; **25**: 603-625 [PMID: 11377686 DOI: 10.1016/s0145-2126(01)00038-8]

7 **Li Z**. New Insights into the Pathogenesis of Systemic Mastocytosis. *Int J Mol Sci* 2021; **22** [PMID: 34063170 DOI: 10.3390/ijms22094900]

8 **Garcia-Montero AC**, Jara-Acevedo M, Teodosio C, Sanchez ML, Nunez R, Prados A, Aldanondo I, Sanchez L, Dominguez M, Botana LM, Sanchez-Jimenez F, Sotlar K, Almeida J, Escribano L, Orfao A. KIT mutation in mast cells and other bone marrow hematopoietic cell lineages in systemic mast cell disorders: a prospective study of the Spanish Network on Mastocytosis (REMA) in a series of 113 patients. *Blood* 2006; **108**: 2366-2372 [PMID: 16741248 DOI: 10.1182/blood-2006-04-015545]

9 **Pardanani A**, Lasho T, Elala Y, Wassie E, Finke C, Reichard KK, Chen D, Hanson CA, Ketterling RP, Tefferi A. Next-generation sequencing in systemic mastocytosis: Derivation of a mutation-augmented clinical prognostic model for survival. *Am J Hematol* 2016; **91**: 888-893 [PMID: 27214377 DOI: 10.1002/ajh.24426]

10 **Cohen SS**, Skovbo S, Vestergaard H, Kristensen T, Møller M, Bindslev-Jensen C, Fryzek JP, Broesby-Olsen S. Epidemiology of systemic mastocytosis in Denmark. *Br J Haematol* 2014; **166**: 521-528 [PMID: 24761987 DOI: 10.1111/bjh.12916]

11 **Zanotti R**, Tanasi I, Bernardelli A, Orsolini G, Bonadonna P. Bone Marrow Mastocytosis: A Diagnostic Challenge. *J Clin Med* 2021; **10** [PMID: 33915965 DOI: 10.3390/jcm10071420]

12 **Alto WA**, Clarcq L. Cutaneous and systemic manifestations of mastocytosis. *Am Fam Physician* 1999; **59**: 3047-3054, 3059

13 **Nedoszytko B**. Mastocytosis in children and adults: clinical disease heterogeneity. Archives of medical science: AMS (e-pub ahead of print 20 November 2021)

14 **Orsolini G**, Viapiana O, Rossini M, Bonifacio M, Zanotti R. Bone Disease in Mastocytosis. *Immunol Allergy Clin North Am* 2018; **38**: 443-454 [PMID: 30007462 DOI: 10.1016/j.iac.2018.04.013]

15 **Brazzelli V**, Grassi S, Merante S, Grasso V, Ciccocioppo R, Bossi G, Borroni G. Narrow-band UVB phototherapy and psoralen-ultraviolet A photochemotherapy in the treatment of cutaneous mastocytosis: a study in 20 patients. *Photodermatol Photoimmunol Photomed* 2016; **32**: 238-246 [PMID: 27353865 DOI: 10.1111/phpp.12248]

16 **Growney JD**, Clark JJ, Adelsperger J, Stone R, Fabbro D, Griffin JD, Gilliland DG. Activation mutations of human c-KIT resistant to imatinib mesylate are sensitive to the tyrosine kinase inhibitor PKC412. *Blood* 2005; **106**: 721-724 [PMID: 15790786 DOI: 10.1182/blood-2004-12-4617]

17 **Gleixner KV**, Mayerhofer M, Aichberger KJ, Derdak S, Sonneck K, Böhm A, Gruze A, Samorapoompichit P, Manley PW, Fabbro D, Pickl WF, Sillaber C, Valent P. PKC412 inhibits in vitro growth of neoplastic human mast cells expressing the D816V-mutated variant of KIT: comparison with AMN107, imatinib, and cladribine (2CdA) and evaluation of cooperative drug effects. *Blood* 2006; **107**: 752-759 [PMID: 16189265 DOI: 10.1182/blood-2005-07-3022]

18 **Gotlib J**, Berubé C, Growney JD, Chen CC, George TI, Williams C, Kajiguchi T, Ruan J, Lilleberg SL, Durocher JA, Lichy JH, Wang Y, Cohen PS, Arber DA, Heinrich MC, Neckers L, Galli SJ, Gilliland DG, Coutré SE. Activity of the tyrosine kinase inhibitor PKC412 in a patient with mast cell leukemia with the D816V KIT mutation. *Blood* 2005; **106**: 2865-2870 [PMID: 15972446 DOI: 10.1182/blood-2005-04-1568]

19 **Bose P**, Verstovsek S. Avapritinib for Systemic Mastocytosis. *Expert Rev Hematol* 2021; **14**: 687-696 [PMID: 34289787 DOI: 10.1080/17474086.2021.1959315]

20 Jensen RT. Gastrointestinal abnormalities and involvement in systemic mastocytosis. *Hematol Oncol Clin North Am* 2000; **14**: 579-623 [DOI: 10.1016/S0889-8588(05)70298-7]

21 **Lee JK**, Whittaker SJ, Enns RA, Zetler P. Gastrointestinal manifestations of systemic mastocytosis. *World J Gastroenterol* 2008; **14**: 7005-7008 [PMID: 19058339 DOI: 10.3748/wjg.14.7005]

22 **Horan RF**, Austen KF. Systemic mastocytosis: retrospective review of a decade's clinical experience at the Brigham and Women's Hospital. *J Invest Dermatol* 1991; **96**: 5S-13S; discussion 13S [PMID: 16799602 DOI: 10.1111/1523-1747.ep12468899]

23 **Doyle LA**, Sepehr GJ, Hamilton MJ, Akin C, Castells MC, Hornick JL. A clinicopathologic study of 24 cases of systemic mastocytosis involving the gastrointestinal tract and assessment of mucosal mast cell density in irritable bowel syndrome and asymptomatic patients. *Am J Surg Pathol* 2014; **38**: 832-843 [PMID: 24618605 DOI: 10.1097/PAS.0000000000000190]

24 **Hamera L**, Santos AM, Prince SA, Chandrupatla S, Jordan J. Systemic Mastocytosis: A Rare Cause of Diarrhea. *Cureus* 2020; **12**: e9112 [PMID: 32670731 DOI: 10.7759/cureus.9112]

25 **Cherner JA**, Jensen RT, Dubois A, O'Dorisio TM, Gardner JD, Metcalfe DD. Gastrointestinal Dysfunction in Systemic Mastocytosis. *Gastroenterology* 1988; **95**: 657-667 [DOI: 10.1016/S0016-5085(88)80012-X]

26 **Bischoff SC**. Physiological and pathophysiological functions of intestinal mast cells. *Semin Immunopathol* 2009; **31**: 185-205 [PMID: 19533134 DOI: 10.1007/s00281-009-0165-4]

27 **Ciriza de Los Ríos C**, Castel de Lucas I, Canga Rodríguez-Valcárcel F, Diéguez Pastor MDC, de Las Cuevas Moreno N, Rey Díaz-Rubio E. Irritable bowel syndrome and basal serum tryptase: the correlation between subtype, severity and comorbidities. a pilot study. *Rev Esp Enferm Dig* 2021 [DOI: 10.17235/reed.2021.7697/2020]

28 **Sokol H**, Georgin-Lavialle S, Canioni D, Barete S, Damaj G, Soucie E, Bruneau J, Chandesris MO, Suarez F, Launay JM, Aouba A, Grandpeix-Guyodo C, Lanternier F, Grosbois B, de Gennes C, Cathébras P, Fain O, Hoyeau-Idrissi N, Dubreuil P, Lortholary O, Beaugerie L, Ranque B, Hermine O. Gastrointestinal manifestations in mastocytosis: a study of 83 patients. *J Allergy Clin Immunol* 2013; **132**: 866-73.e1 [PMID: 23890756 DOI: 10.1016/j.jaci.2013.05.026]

29 **Kirsch R**, Geboes K, Shepherd NA, de Hertogh G, Di Nicola N, Lebel S, Mickys U, Riddell RH. Systemic mastocytosis involving the gastrointestinal tract: clinicopathologic and molecular study of five cases. *Mod Pathol* 2008; **21**: 1508-1516 [PMID: 18931652 DOI: 10.1038/modpathol.2008.158]

30 **Poynard T**, Nataf C, Messing B, Modigliani R, Lecompte T, Nicolas P, Dray F, Ferme C. Secretory diarrhea and

prostaglandin D2 overproduction in systemic mastocytosis. *N Engl J Med* 1982; **307**: 186 [DOI: 10.1056/NEJM198207153070315]
31 **Cherner JA**. Gastric acid secretion in systemic mastocytosis. *N Engl J Med* 1989; **320**: 1562 [PMID: 2725591 DOI: 10.1056/NEJM198906083202320]
32 **Arguedas MR**, Ferrante D. Systemic mastocytosis and giant gastroduodenal ulcer. *Gastrointest Endosc* 2001; **54**: 530-533 [PMID: 11577328 DOI: 10.1067/mge.2001.115320]
33 **McCarty TR**, Hung A, Mohanty A, Allen JI. Systemic Mastocytosis Complicated by Non-Cirrhotic Portal Hypertension and Variceal Bleeding. *ACG Case Rep J* 2017; **4**: e30 [PMID: 28286795 DOI: 10.14309/crj.2017.30]
34 **Narayanan MN**, Liu Yin JA, Azzawi S, Warnes TW, Turck WP. Portal hypertension and ascites in systemic mastocytosis. *Postgrad Med J* 1989; **65**: 394-396 [PMID: 2608581 DOI: 10.1136/pgmj.65.764.394]
35 **Grundfest S**, Cooperman AM, Ferguson R, Benjamin S. Portal hypertension associated with systemic mastocytosis and splenomegaly. *Gastroenterology* 1980; **78**: 370-373 [DOI: 10.1016/0016-5085(80)90591-0]
36 **Scolapio JS**, Wolfe J 3rd, Malavet P, Woodward TA. Endoscopic findings in systemic mastocytosis. *Gastrointest Endosc* 1996; **44**: 608-610 [PMID: 8934172 DOI: 10.1016/s0016-5107(96)70019-6]
37 **Mickys U**, Barakauskiene A, De Wolf-Peeters C, Geboes K, De Hertogh G. Aggressive systemic mastocytosis complicated by protein-losing enteropathy. *Dig Liver Dis* 2007; **39**: 693-697 [PMID: 16843741 DOI: 10.1016/j.dld.2006.06.003]
38 **Bedeir A**, Jukic DM, Wang L, Mullady DK, Regueiro M, Krasinskas AM. Systemic mastocytosis mimicking inflammatory bowel disease: A case report and discussion of gastrointestinal pathology in systemic mastocytosis. *Am J Surg Pathol* 2006; **30**: 1478-1482 [PMID: 17063092 DOI: 10.1097/01.pas.0000213310.51553.d7]
39 **Chrysakopoulos G**, Demonakou M, Papasavvas S, Koutsoumpas A, Mylonas G, Tzias V. Indolent systemic mastocytosis in a patient with ileocolitis. *Ann Gastroenterol* 2014; **27**: 270-272
40 **Okayama Y**, Kawakami T. Development, migration, and survival of mast cells. *Immunol Res* 2006; **34**: 97-115 [PMID: 16760571 DOI: 10.1385/IR:34:2:97]
41 **Shakoory B**, Fitzgerald SM, Lee SA, Chi DS, Krishnaswamy G. The role of human mast cell-derived cytokines in eosinophil biology. *J Interferon Cytokine Res* 2004; **24**: 271-281 [PMID: 15153310 DOI: 10.1089/107999004323065057]
42 **Irani AA**, Schechter NM, Craig SS, DeBlois G, Schwartz LB. Two types of human mast cells that have distinct neutral protease compositions. *Proc Natl Acad Sci USA* 1986; **83**: 4464-4468 [PMID: 3520574 DOI: 10.1073/pnas.83.12.4464]
43 **Irani AM**, Craig SS, DeBlois G, Elson CO, Schechter NM, Schwartz LB. Deficiency of the tryptase-positive, chymase-negative mast cell type in gastrointestinal mucosa of patients with defective T lymphocyte function. *J Immunol* 1987; **138**: 4381-4386
44 **Irani AM**, Goldstein SM, Wintroub BU, Bradford T, Schwartz LB. Human mast cell carboxypeptidase. Selective localization to MCTC cells. *J Immunol* 1991; **147**: 247-253
45 **Ammann RW**, Vetter D, Deyhle P, Tschen H, Sulser H, Schmid M. Gastrointestinal involvement in systemic mastocytosis. *Gut* 1976; **17**: 107-112 [PMID: 1261881 DOI: 10.1136/gut.17.2.107]
46 **Kleinschmidt S**, Harder J, Nolte I, Marsilio S, Hewicker-Trautwein M. Phenotypical characterization, distribution and quantification of different mast cell subtypes in transmural biopsies from the gastrointestinal tract of cats with inflammatory bowel disease. *Vet Immunol Immunopathol* 2010; **137**: 190-200 [PMID: 20646765 DOI: 10.1016/j.vetimm.2010.05.005]
47 **Jakate S**, Demeo M, John R, Tobin M, Keshavarzian A. Mastocytic enterocolitis: increased mucosal mast cells in chronic intractable diarrhea. *Arch Pathol Lab Med* 2006; **130**: 362-367 [PMID: 16519565 DOI: 10.5858/2006-130-362-MEIMMC]
48 **Akhavein M A**, Patel NR, Muniyappa PK, Glover SC. Allergic mastocytic gastroenteritis and colitis: an unexplained etiology in chronic abdominal pain and gastrointestinal dysmotility. *Gastroenterol Res Pract* 2012; **2012**: 950582 [PMID: 22577375 DOI: 10.1155/2012/950582]
49 **Shukla SA**, Veerappan R, Whittimore JS, Ellen Miller L, Youngberg GA. Mast cell ultrastructure and staining in tissue. *Methods Mol Biol* 2006; **315**: 63-76 [PMID: 16110149 DOI: 10.1385/1-59259-967-2:063]
50 **Ramsay DB**, Stephen S, Borum M, Voltaggio L, Doman DB. Mast cells in gastrointestinal disease. *Gastroenterol Hepatol* 2010; **6**: 772-777
51 **Valent P**, Cerny-Reiterer S, Herrmann H, Mirkina I, George TI, Sotlar K, Sperr WR, Horny HP. Phenotypic heterogeneity, novel diagnostic markers, and target expression profiles in normal and neoplastic human mast cells. *Best Pract Res Clin Haematol* 2010; **23**: 369-378 [PMID: 21112036 DOI: 10.1016/j.beha.2010.07.003]
52 **Castells M**, Butterfield J. Mast Cell Activation Syndrome and Mastocytosis: Initial Treatment Options and Long-Term Management. *J Allergy Clin Immunol Pract* 2019; **7**: 1097-1106 [PMID: 30961835 DOI: 10.1016/j.jaip.2019.02.002]
53 **Simons FE**, Simons KJ. Histamine and H1-antihistamines: celebrating a century of progress. *J Allergy Clin Immunol* 2011; **128**: 1139-1150.e4 [PMID: 22035879 DOI: 10.1016/j.jaci.2011.09.005]
54 **Spechler SJ**. Proton Pump Inhibitors: What the Internist Needs to Know. *Med Clin North Am* 2019; **103**: 1-14 [PMID: 30466666 DOI: 10.1016/j.mcna.2018.08.001]
55 **Leung KB**, Flint KC, Brostoff J, Hudspith BN, Johnson NM, Lau HY, Liu WL, Pearce FL. Effects of sodium cromoglycate and nedocromil sodium on histamine secretion from human lung mast cells. *Thorax* 1988; **43**: 756-761 [PMID: 2462755 DOI: 10.1136/thx.43.10.756]
56 **Marone G**, Spadaro G, Granata F, Triggiani M. Treatment of mastocytosis: pharmacologic basis and current concepts. *Leukemia Research* 2001; **25**: 583-594 [DOI: 10.1016/S0145-2126(01)00039-X]
57 **Metcalfe DD**. Classification and diagnosis of mastocytosis: current status. *J Invest Dermatol* 1991; **96**: 2S-4S; discussion 4S, 60S [PMID: 16799601 DOI: 10.1111/1523-1747.ep12468882]
58 **Lim KH**, Pardanani A, Butterfield JH, Li CY, Tefferi A. Cytoreductive therapy in 108 adults with systemic mastocytosis: Outcome analysis and response prediction during treatment with interferon-alpha, hydroxyurea, imatinib mesylate or 2-chlorodeoxyadenosine. *Am J Hematol* 2009; **84**: 790-794 [PMID: 19890907 DOI: 10.1002/ajh.21561]
59 **Ustun C**, Gotlib J, Popat U, Artz A, Litzow M, Reiter A, Nakamura R, Kluin-Nelemans HC, Verstovsek S, Gajewski J, Perales MA, George T, Shore T, Sperr W, Saber W, Kota V, Yavuz AS, Pullarkat V, Rogosheske J, Hogan W, Van Besien K, Hagglund H, Damaj G, Arock M, Horny HP, Metcalfe DD, Deeg HJ, Devine S, Weisdorf D, Akin C, Valent P.

Consensus Opinion on Allogeneic Hematopoietic Cell Transplantation in Advanced Systemic Mastocytosis. *Biol Blood Marrow Transplant* 2016; **22**: 1348-1356 [PMID: 27131865 DOI: 10.1016/j.bbmt.2016.04.018]

World Journal of Gastroenterology

Submit a Manuscript: https://www.f6publishing.com

World J Gastroenterol 2022 August 7; 28(29): 3780-3792

DOI: 10.3748/wjg.v28.i29.3780

ISSN 1007-9327 (print) ISSN 2219-2840 (online)

MINIREVIEWS

Structural changes of proteins in liver cirrhosis and consequential changes in their function

Nikola Gligorijević, Simeon Minić, Olgica Nedić

Specialty type: Biochemistry and molecular biology

Provenance and peer review: Invited article; Externally peer reviewed.

Peer-review model: Single blind

Peer-review report's scientific quality classification

Grade A (Excellent): A
Grade B (Very good): B, B
Grade C (Good): 0
Grade D (Fair): 0
Grade E (Poor): 0

P-Reviewer: Costache RS, Romania; El-Shabrawi MH, Egypt; Pan Y, China

Received: January 13, 2022
Peer-review started: January 13, 2022
First decision: May 29, 2022
Revised: May 30, 2022
Accepted: June 30, 2022
Article in press: June 30, 2022
Published online: August 7, 2022

Nikola Gligorijević, Olgica Nedić, Department of Metabolism, University of Belgrade-Institute for the Application of Nuclear Energy, Belgrade 11080, Serbia

Simeon Minić, Centre of Excellence for Molecular Food Sciences and Department of Biochemistry, University of Belgrade-Faculty of Chemistry, Belgrade 11000, Serbia

Corresponding author: Nikola Gligorijević, PhD, Research Associate, Department of Metabolism, University of Belgrade-Institute for the Application of Nuclear Energy, Banatska 31b, Belgrade 11080, Serbia. nikolag@inep.co.rs

Abstract

The liver is the site of synthesis of the majority of circulating proteins. Besides initial polypeptide synthesis, sophisticated machinery is involved in the further processing of proteins by removing parts of them and/or adding functional groups and small molecules tailoring the final molecule to suit its physiological purpose. Posttranslational modifications (PTMs) design a network of molecules with the common protein ancestor but with slightly or considerably varying activity/localization/purpose. PTMs can change under pathological conditions, giving rise to aberrant or overmodified proteins. Undesired changes in the structure of proteins most often accompany undesired changes in their function, such as reduced activity or the appearance of new effects. Proper protein processing is essential for the reactions in living beings and crucial for the overall quality control. Modifications that occur on proteins synthesized in the liver whose PTMs are cirrhosis-related are oxidation, nitration, glycosylation, acetylation, and ubiquitination. Some of them predominantly affect proteins that remain in liver cells, whereas others predominantly occur on proteins that leave the liver or originate from other tissues and perform their function in the circulation. Altered PTMs of certain proteins are potential candidates as biomarkers of liver-related diseases, including cirrhosis. This review will focus on PTMs on proteins whose structural changes in cirrhosis exert or are suspected to exert the most serious functional consequences.

Key Words: Liver cirrhosis; Post-translational modifications; Circulation; Protein function; Protein structure; Chronic liver disease

©The Author(s) 2022. Published by Baishideng Publishing Group Inc. All rights reserved.

Core Tip: Chronic liver diseases and cirrhosis are accompanied by various metabolic disorders, some of which affect proteins. Besides changes in the concentration, structural alterations of proteins occur, mostly at the level of posttranslational modifications (PTMs). Five frequent cirrhosis-related PTMs are oxidation, nitration, glycosylation, acetylation, and ubiquitination. Some are more specific for the circulating proteins, whereas others are more specific for liver tissue-residing proteins. PTMs influence folding, stability, half-life, aggregation, and function of proteins. Modified proteins with altered function contribute to further progression of liver pathology. An overview of cirrhosis-related alterations of PTMs of specific proteins is the topic of this article.

Citation: Gligorijević N, Minić S, Nedić O. Structural changes of proteins in liver cirrhosis and consequential changes in their function. *World J Gastroenterol* 2022; 28(29): 3780-3792
URL: https://www.wjgnet.com/1007-9327/full/v28/i29/3780.htm
DOI: https://dx.doi.org/10.3748/wjg.v28.i29.3780

INTRODUCTION

Liver cirrhosis is an end-stage condition of chronic liver disease[1]. The speed of progression from chronic disease to cirrhosis depends on multiple factors. Cirrhosis may develop due to toxic, infectious, immunopathological, or vascular processes. Alcoholic fatty liver disease (AFLD) and non-AFLD (NAFLD), and hepatitis B- and hepatitis C-induced diseases are the most common causes of cirrhosis, with AFLD being the most frequent.

The liver is the site of synthesis of the majority of circulating proteins. Besides initial polypeptide synthesis, sophisticated machinery is involved in the further processing of proteins by removing parts of them and/or adding functional groups and small molecules tailoring the final molecule to suit its physiological purpose. Changes that occur after formation of the polypeptide chain are known as cotranslations and posttranslational modifications (PTMs). PTMs enlarge the genome coding capacity by several orders of magnitude, designing a network of molecules with the common protein ancestor but with slightly or considerably varying activity/Localization/purpose. According to review articles of Ramazi and Zahiri[2] and Khoury *et al*[3], more than 400 different PTMs have been discovered to date.

When talking about PTMs, one should bear in mind the dynamic nature of the protein structure, which can be seen, among other ways, in different modifications at different moments of the protein lifespan. Each modification is expected to suit or respond to certain (patho)physiological needs of an organism. Furthermore, one protein can have more than one type of PTM simultaneously and at several molecular sites. Multiple PTMs are highly dependent on conformational and steric factors. A vast number of PTMs on proteins have been experimentally detected, but in the era of computational omics and bioinformatics, the prediction of PTMs based on the structure of proteins is an additional tool in the investigation of PTMs and their consequences on protein function.

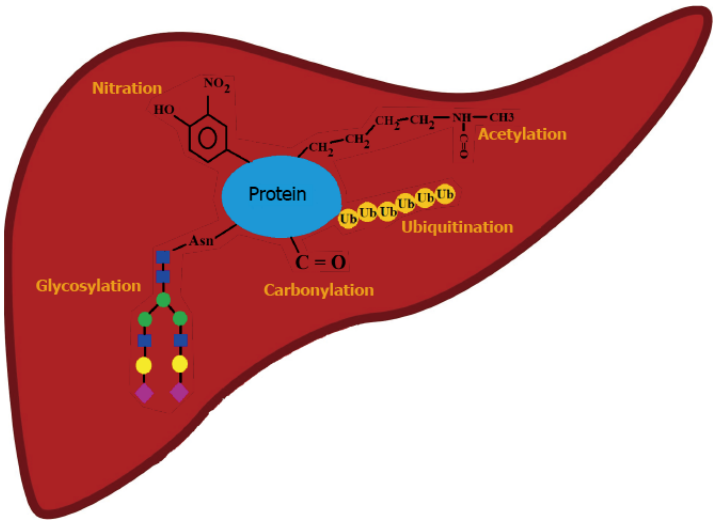
PTMs that occur under physiological conditions regulate the proper functioning of the organism. PTMs can, however, change under pathological conditions giving rise to aberrant or overmodified proteins. Undesired changes in protein structure most often accompany undesired changes in their function. Such modifications can reduce the initial activity of proteins or their lifespan with an overall outcome experienced as a decreased effect. Other modifications can, however, contribute to the appearance of new effects; these include misfolded proteins, previously unseen interactions, unusual molecular trafficking and localization, altered gene expression, creation of neoantigens, and stimulation of the immune system (which may lead to autoimmunity), protein aggregation followed by tissue deposition, prolonged half-life, impaired clearance and initiation of additional pathological processes. Thus, PTMs are essential for the reactions in living beings and crucial for the overall quality control.

Huang *et al*[4] reported more than 80 modification sites in proteins that were experimentally confirmed and named 24 major PTMs. Phosphorylation of the amino acid serine (Ser) is the most frequent modification, followed by phosphorylation of other amino acids, and then acetylation and ubiquitination. Lysine (Lys) is the amino acid that can be modified in the greatest number of different ways, resulting in as many as 15 types of altered species. Modifications that occur on proteins synthesized in the liver whose PTMs were found to be cirrhosis-related (Figure 1) are oxidation, nitration, glycosylation, acetylation, and ubiquitination[5-8].

MECHANISMS UNDERLYING PTMS IN CIRRHOSIS

Oxidation

Oxidative stress plays a major role in the development of liver pathology, regardless of etiology. The



DOI: 10.3748/wjg.v28.i29.3780 **Copyright** ©The Author(s) 2022.

Figure 1 Modifications that occur on proteins synthesized in the liver with evidence of cirrhosis-related posttranslational modifications.

liver, being a central organ of homeostasis, regulates metabolism, biosynthesis, and storage of carbohydrates, proteins, lipids, and vitamins. Due to such performances, it has intensive metabolic activity and is a site of a considerable free radical generation[9]. Any molecule possessing an unpaired electron is a free radical and is highly reactive. The most important free radicals produced by living organisms are reactive oxygen species (ROS) and reactive nitrogen species (RNS). Kupffer cells, neutrophils, and hepatocytes (mitochondria and cytochrome P450 enzymes) are involved in ROS generation during processes such as signal transduction, apoptosis, proliferation, growth, and defense against microorganisms[10]. Excessive quantities of ROS and RNS are toxic. They can induce tissue damage and are generally recognized as oxidative/nitrosative stress initiators. Cell type, intensity, and duration of the stress govern the outcome, which may be positive (beneficial) or negative (damaging). Some products of protein oxidation are chemically stable and present in large quantities, thus enabling their consideration as potential biomarkers of oxidative damage to be applied in clinical practice[11].

As mentioned before, cirrhosis usually occurs due to AFLD, NAFLD, and viral infection. The intersection point of all these conditions is oxidative stress. Alcohol in the case of AFLD, fatty acids in the case of NAFLD, and viral proteins in the case of hepatitis are the initiators of oxidative stress in these diseases. Different cellular compartments including mitochondria, cytoplasm, and endoplasmic reticulum are the sites of ROS production. Alterations in signaling pathways also play an important role in free radical induction. Detailed mechanisms underlining or assisting in oxidative stress generation in AFLD, NAFLD, and hepatitis B and C are reviewed in several papers[12-14]. Oxidation damages liver tissue by modifying proteins, DNA, and lipids. Once modified, these biomolecules gain altered structure, their function may be reduced to a different extent, their clearance rate may be increased or decreased, modified molecules may be involved in the activation of the immune system, or they alter signaling pathways contributing to further liver damage. Oxidative stress plays a role in both the initiation and progression of liver diseases[15].

Nitration

Nitric oxide (NO) is a signaling molecule that can be synthesized in either enzymatically or non-enzymatically driven reactions in many cells. NO itself is not very reactive and has a short half-life. However, highly reactive peroxynitrite ion (NO_3^-) may form in the reaction of NO with ROS. This ion can further react with tyrosine (Tyr) residues in a process called nitration, creating 3-nitroTyr[16], and with cysteine (Cys) residues in a reaction called S-nitrosylation, creating nitrosothiols[17]. Interaction with tryptophan (Trp) also occurs[18]. These nitration modifications affect not only proteins but also DNA and lipids. If not controlled, RNS may cause progressive damage to cells, tissues, and organs. Both ROS and RNS levels increase in liver diseases, as does the activity of inducible nitric oxide synthase. Mitochondria are particularly sensitive to nitro-oxidative damage since they have lower anti-oxidative capacity than the cytoplasm[19], rendering mitochondrial proteins and DNA vulnerable to nitration. Prolonged exposure of mitochondria to nitro-oxidation deteriorates their function, affecting both mitochondrial proteins and DNA[20-22].

When immunohistochemical detection of nitroproteins was performed in liver sections from patients with cirrhosis, a significant increase in nitrated proteins was observed[23]. Changes were more significant in patients with grade C (according to Child-Pugh classification) cirrhosis than in patients with grade A or B. A positive correlation was found between the level of nitrite and the level of nitroproteins with the progression of cirrhosis.

Glycosylation

Glycosylation is one of the major posttranslational modifications that affects most secretory proteins. This modification introduces a higher level of diversity in the protein population due to the covalent addition of specific sugar moieties. Glycosylation influences both structural and functional properties of proteins. The overall glycome is affected by genetic and environmental factors, and changes may suggest the presence of inflammatory or other pathological events in the organism[24]. Glycosylation is an enzymatically regulated process that depends on several glycosyltransferases and glycosidases. Many factors including the activity of enzymes involved, substrate availability, and localization of enzymes within organelles affect the final glycosylation pattern of the protein. Unlike the genome and proteome, glycome is produced without a template. In the O-glycosylation of proteins, glycan attachment occurs at amino acid residues Ser and threonine (Thr). N-glycosylation involves asparagine (Asn) residues but only in a specific sequence, Asn-X-Ser/Thr, where X represents any amino acid except proline[25].

Several liver diseases are accompanied by alterations in protein glycosylation: NAFLD, liver fibrosis, cirrhosis, and hepatocellular carcinoma (HCC)[7,26-28]. A number of common glycosylation changes were noted as a general pattern in liver diseases, regardless of the disease type. They include increased fucosylation (Fuc), increased branching, and an appearance of a bisecting N-acetylglucosamine (GlcNAc). Additional analyses of the responsible glycosyltransferases documented that their levels were altered, underlining the mechanism of detected changes[7]. When the overall N-glycan structure was examined in immunoglobulin (Ig)G-deprived sera from patients with cirrhosis, two general trends emerged: an increase in bisecting GlcNAc structures and a decrease in fully galactosylated (Gal) bi- and triantennary N-glycans. The ratios of certain glycans were suggested to serve as potential biomarkers of a specific stage of liver fibrosis or cirrhosis[27]. Data reported in that study confirmed the correlation between the detected glycan changes and the levels of the corresponding glycosyltransferases.

Acetylation

Acetylation is one of the key PTMs involved in the regulation of many proteins. It influences their stability, activity, localization, and interactions with other proteins. Metabolic pathways, including fatty acid metabolism and the Krebs cycle, are regulated by protein acetylation. This modification assumes the addition of an acetyl group from acetyl-coenzyme A on Lys residues[29]. Acetylation seems to play a significant role in liver diseases, as the pattern of protein acetylation in fatty liver is significantly different from the pattern in the healthy liver[30].

Ubiquitination

Ubiquitin and its related pathways are closely connected to chronic liver disease. Dysfunctional ubiquitination was detected in liver tissue in different stages of chronic liver disease. Ubiquitin is a protein that consists of 76 amino acids and has seven Lys and N-terminal methionine (Met) residues that can form *iso*-peptide-linked ubiquitin chains. It binds to substrates by a three-step enzymatic mechanism involving activating enzyme (E1), conjugating enzyme (E2) and ligase (E3)[31]. Receptors with ubiquitin-binding domains can recognize ubiquitinated substrates[32]. On the other hand, deubiquitinases remove ubiquitin from modified molecules, making this PTM a reversible, dynamic process with a plethora of diverse cellular effects[33]. Ubiquitinated proteins may be taken by proteasome which destroys them, thus controlling their lifespan and activity.

Some of the aforementioned PTMs predominantly affect proteins that remain in liver cells (ubiquitination, acetylation, and nitration), whereas others predominantly occur on proteins that leave the liver and exert their functions in the circulation (oxidation and glycosylation). Additionally, there are proteins not originating from the liver whose structure changes in cirrhosis. Some of these modifications have the potential to serve as biomarkers of liver-related diseases.

This review mostly focuses on PTMs on the circulating proteins originating from the liver whose structural changes in cirrhosis exert the most serious functional consequences. Modifications of Igs and liver tissue proteins will be also briefly mentioned.

PROTEINS FROM THE CIRCULATION AFFECTED BY SPECIFIC PTMS IN CIRRHOSIS

Fibrinogen

Fibrinogen is a large, fibrillar glycoprotein with a molecular mass of 340 kDa. This protein is involved both in primary (interaction with platelets) and secondary hemostasis (fibrin formation). N-glycosylation analysis using lectin microarray with 15 Lectins demonstrated that cirrhosis induces changes in its glycans[34]. Based on the interactions with lectins *Pholiota squarrosa* (PhoSL), *Maackia amurensis* lectin I (MAL-I), *Maackia amurensis* lectin II (MAL-II), *Galanthus nivalis* lectin (GNL), *Phaseolus vulgaris* leucoagglutinin (PHA-L), and *Phaseolus vulgaris* lectin E (PHA-E), an increased content of the following carbohydrate moieties was observed: terminal α-2,3 sialic acid (Sia) and α-1,3 mannose (Man), a disaccharide composed of Gal and N-acetyl galactosamine (Galβ-1,4GlcNAc) and tri/tetra-antennary

N-glucan structures. Core α-1,6 (Fuc) and bi-antennary galactosylated N-glycans with the bisecting GlcNAc were, on the other hand, reduced. An increase in the number of Sia residues on fibrinogen as a consequence of cirrhosis was confirmed by several researchers[35,36]. Sialic acid is negatively charged and is a weak binding site for calcium ions[37]. Taking into consideration that advanced chronic liver disease is characterized by hypercalcemia[38], interactions between calcium ions and an increased number of Sia residues may be seen as a modulator of fibrinogen action in cirrhosis[37]. "Proper" glycosylation of fibrinogen is essential for its function. Alterations in this PTM may even lead to complete dysfunction of the protein[39-42].

Increased oxidation of fibrinogen from patients with cirrhosis was detected as well[34,43]. Dinitrophenyl-hydrazide (DNP)-reactive sites on fibrinogen were investigated using anti-DNP antibodies to analyze protein carbonyls and it was discovered that the Aα-chain was dominantly carbonylated, followed by the Bβ-chain. It seems that the γ-chain of fibrinogen is not carbonylated in patients with cirrhosis. Carbonylation affects the function of fibrinogen[44-46], as both Aα- and Bβ-chains contain cleavage sites for thrombin action. Oxidation of αC domains on Aα-chains also affects their mutual interaction and lateral association of fibrin monomers[47]. Generally, residues that may be affected by oxidation/carbonylation are located in all structural elements of fibrinogen. Thus, alterations in the secondary and tertiary structures of fibrinogen also accompany cirrhosis[34]. Reduced content of its α-helical subunits was observed, which coincided with the formation of denser clots[46]. Although the structure of fibrinogen is altered in cirrhosis, Hugenholtz *et al*[43] did not detect significant structural changes in fibrin clots, even though clots formed from samples originating from patients with cirrhosis had reduced porosity. Subtle alterations, not visible by scanning electron microscopy, are most likely sufficient to influence porosity. Furthermore, carbonylated sites on fibrinogen are hydrophobic regions which prevent efficient liquid flow through the fibrin clot, increasing its resistance towards lysis by plasmin[36]. Overall, changes in fibrinogen structure due to cirrhosis are complex and lead to the formation of a molecule acquiring thrombogenic characteristics. Other factors that participate in coagulation or fibrinolysis are altered as well, defining a general pro-coagulant state in liver cirrhosis [48].

Albumin

Albumin is the major plasma protein, constituting approximately 50% of the total protein content. It is a globular, single-chain, α-helicoidal protein, organized into three domains. This protein exhibits many physiological roles, such as maintenance of osmotic pressure and transport of various metal ions and biomolecules (fatty acids, metabolites, and drugs), providing anti-oxidative, anti-inflammatory, and hemostatic activities[49].

Cirrhosis is accompanied by reduced albumin concentration and its significant structural changes [49]. Oxidation of free Cys-34 residue is one of the most notable changes in albumin structure due to cirrhosis. This residue strongly contributes to the anti-oxidative capacity of albumin. Oxidized albumin differs from the native molecule pharmacokinetically and conformationally, negatively influencing its function[50]. Quantities of albumin oxidative forms, assessed by measuring the level of carbonyl groups and oxidation of free Cys-34 residue, correlate with the severity of liver failure[51]. Oxidative stress triggers the dimerization of albumin molecules (through free Cys residues) in patients with cirrhosis, with significant reduction in native albumin required for the physiological functions[52]. Furthermore, matrix-assisted laser desorption/ionization time of flight (MALDI-TOF) mass spectrometry (MS) detects cysteinylation of Cys-34 in cirrhosis, followed by other molecular changes, such as truncation of N-terminal portion and glycosylation[53]. Oxidative stress also induces structural changes of the N-terminus and the reduced capacity of albumin to bind cobalt ions. Albumin modified in that way is called ischemia-modified albumin (IMA)[50]. The cobalt-binding assay revealed increased IMA levels in patients with advanced cirrhosis[54]. Additionally, the electron paramagnetic resonance study, using 16-doxyl stearic acid as a spin probe, confirmed that the ligand-binding capacity of albumin is significantly reduced in cirrhosis[55]. A small-angle X-ray scattering study demonstrated that albumin in patients with liver disease has an altered, more open conformation compared to control samples[56]. To summarize, posttranslational alternations of albumin in cirrhosis influence its conformation, which further decreases its ligand binding.

Therefore, reduced level of serum albumin in patients with cirrhosis, as well as its substantial structural change, have important and clinically relevant consequences, such as alterations in the redox balance, hemostatic disorders, modifications in the transport of endogenous and exogenous ligands, acid-base imbalance, reduced detoxification capacity, and antioxidant activity[49].

Transferrin

Human transferrin (Tf), an iron-binding protein, is a 76-kDa glycoprotein produced in the liver[57,58]. The Tf molecule contains two lobes at the N- and C-termini, and each binds one Fe^{3+} ion[58]. Tf is stabilized by 19 intrachain disulfide bonds and is modified by three carbohydrate side chains; two of them are N-linked (Asn-413 and Asn-611) and the third one is O-linked (Ser-32)[57]. The glycosylation profile of Tf changes significantly in liver diseases. A carbohydrate-deficient Tf (CDT) is found in AFLD, and it is characterized by a loss of terminal sialic acids[59]. Lectin affinity electrophoresis of CDT also confirmed the absence of Asn-linked oligosaccharides in AFLD and cirrhosis[60]. Both Tf and iron

uptake capacity of deglycosylated Tf are significantly reduced by the human hepatoma cell line PLC/PRF/5[61], suggesting impaired function of Tf in liver cirrhosis. A less advanced liver disease can be discriminated from cirrhosis by studying disialotransferrin isoforms. Poor chromatographic resolution of disialotransferrin from trisialotransferrin (the so-called "di-tri bridging") was seen for samples originating from patients with cirrhosis[62,63]. This abnormal pattern could be ascribed to the presence of higher mass disialotransferrin isoforms due to an increased branching and fucosylation of the carbohydrate moiety[64]. This phenomenon was not seen in less-advanced liver diseases[63].

Besides changes in the glycosylation profile, the lower concentration of Tf is also related to cirrhosis, and it represents a good indicator of the survival rate of patients[65]. Lower serum Tf concentration is accompanied by higher hepatic iron concentration and lipid peroxidation levels compared to healthy subjects. In this context, Tf exerts a protective role in maintaining liver function[66].

Hemopexin

Hemopexin (HPX) is secreted mainly by hepatocytes and binds free heme in the circulation. The formed complex is cleared from the circulation by a hepatocyte-specific membrane receptor. The serum concentration of HPX does not significantly vary in liver diseases[67]. However, significant alterations in the glycosylation profile of HPX occur in patients with cirrhosis. Lectin chemiluminescence-linked immunosorbent assay demonstrated a higher level of N-glycosylation (fucosylation) in samples from patients with cirrhosis and HCC than in samples from patients with hepatitis and healthy individuals [68]. A study using liquid chromatography-tandem MS with multiple reaction monitoring (LC-MS/MS MRM) assay revealed a nearly five-fold increase in the sialylation of site-specific Oglycoforms of HPX in cirrhosis[67]. Since HPX is an important anti-oxidative protein, its altered N-glycosylation in cirrhosis possibly interferes with the redox balance in organisms.

Haptoglobin

Haptoglobin (Hp) is a glycoprotein secreted by the liver into the plasma. Its major biological role is to capture released hemoglobin during intravascular hemolysis and prevent kidney damage by the released iron[69]. Hp is composed of two α and two β chains linked by disulfide bonds in a quaternary structure[70,71]. All four N-glycosylation sites are located in the β subunit and glycoforms are known to create additional phenotypic variants[69,72]. Many studies have reported glycan changes of Hp in diseases. MALDI-TOF MS analyses revealed N-linked glycan alterations (increased fucosylation) of serum Hp β chain in patients with cirrhosis[69,71]. Zhu *et al*[73] applied a similar approach to distinguish the N-glycan profile of Hp in patients with cirrhosis from those with hypophosphatasia. A degree of bifucosylation was higher in samples from patients with an early-stage HCC than in samples from patients with cirrhosis, regardless of the etiology. Thus, monitoring alterations in the glycosylation profile of the Hp β chain may become a valuable approach for detection and distinction between HCC and cirrhosis. The observed changes of Hp at the N-glycosylation level most likely affect its functional properties, including interactions with binding partners, as was suggested in the case of progressive liver diseases[69].

Ferritin

Ferritin plays an important role in storing intracellular iron and its segregation in a non-toxic form[74, 75]. It is a 24-mer globular protein that is made up of heavy (H) and light (L) subunits, with molecular masses of 21 kDa and 19 kDa, respectively[74]. Subunits surround the central hollow core, capable of binding up to 4500 iron ions[76]. Ferritin concentration in the circulation is relatively low (< 1 μg/mL) [74]. However, it is increased in conditions such as iron overload, infection, inflammation, malignancy, diabetes and liver diseases, including NAFLD and cirrhosis[77]. Besides changes in ferritin concentration, liver cirrhosis is also accompanied by the derangement of the ordered secondary structure of the protein[78].

Approximately 50%-80% of serum ferritin is glycosylated[79]. There is no strong evidence of the connection between ferritin glycosylation and cirrhosis. Some studies have reported a decrease in glycosylated ferritin in liver necrosis[79]. On the other hand, Chapman *et al*[80] demonstrated that the measurement of the fraction of glycosylated serum ferritin does not provide any advantage over the estimation of the total serum ferritin concentration in the assessment of iron stores in patients with liver cirrhosis.

Insulin-like growth factor binding protein 3

Insulin-like growth factors (IGFs), namely IGF-I and IGF-II, are peptides that exert growth-promoting, endocrine and cytokine effects[81,82]. They are synthesized in many tissues locally, but the liver is the origin of IGFs that enter the circulation. IGF-I is the mediator of the growth hormone (GH) action. The activity of IGFs is regulated by a network of insulin-like growth factor binding proteins (IGFBPs) and is most often inhibited when IGFs are in complexes with IGFBPs. To perform their physiological roles, IGFs need to be released from complexes and interact with IGF receptors, which are predominantly found on cell membranes. IGFs are liberated from complexes by the proteolysis of IGFBPs. The synthesis of several IGFBPs occurs in the liver, under the control of GH. IGFBP-3 is the major binding

protein in the circulation and is synthesized in Kupffer cells. It forms ternary complexes with IGFs, which also contain an acid-labile subunit. These complexes are large (150 kDa), remain within blood vessels, and bind 75%-90% of the circulating IGFs, serving both as a reservoir and a guardian of the IGF activity.

IGFBP-3 has three N-glycosylation and two phosphorylation sites[83,84]. It is present in the circulation as two major glycoforms of 40 kDa and 44 kDa, although a non-glycosylated form (29 kDa) can also be detected. Diethylaminoethyl ion-exchange chromatography was shown to fractionate at least 12 IGFBP-3 species that are isoforms with different charges due to PTMs[85]. Three of these isoforms exhibited significant reactivity with lectin concanavalin A (Con A), specific for Man residues and to a lesser extent for glucose (Glc) and GlcNAc residues. In patients with alcoholic liver cirrhosis, two of these glycoforms had an increased reactivity with Con A, whereas the third one had decreased reactivity, compared to molecules originating from healthy persons. Furthermore, some differences were also detected between different stages of liver cirrhosis. IGFBP-3 from patients with Child score A stage exhibited similar isoform distribution and reactivity as in healthy persons. Child score B seems to be the turning point in the progression of cirrhosis, after which considerable changes in the concentration of IGFBP-3 and its structure occur. A reduced reactivity of IGFBP-3 due to cirrhosis was also noted with wheat germ agglutinin, specific for GlcNAc, and breadfruit lectin, specific for Gal and GalNAc residues[86]. These alterations affect the conformation of IGFBP-3 and its susceptibility to proteolytic cleavage, thus influencing its half-life and the entire mechanism that controls IGFs' activity. Since IGFBP-3 can also perform IGF-independent roles after binding to its cell surface or nuclear receptors, changes in IGFBP-3 glycosylation can contribute to the pathophysiology of several diseases such as diabetes, obesity, NAFLD, and cancer[87,88].

Sex hormone-binding globulin

Sex hormone-binding globulin (SHBG) is a 90-kDa to 100-kDa homodimeric glycoprotein, mainly produced by the liver[89]. It is a transporter of sex hormones, capable of binding to them with high affinity[90]. SHBG is both N- and mucin-type O-glycosylated[90,91]. Comprehensive LC-MS/MS analysis revealed that fucosylation of N-glycoforms increases in liver cirrhosis. Additionally, the same pathology was related to an increase of the α-2−6 sialylated glycoform of the O-glycopeptide of SHBG [67]. Glycosylation of SHBG does not seem to influence binding of steroid hormones[92]. However, it is suspected that higher content of sialic acid increases the half-life of SHBG[93], elevating the total concentration of this protein in patients with cirrhosis[94]. An increased concentration of SHBG may influence the equilibrium between protein-bound and free, physiologically active steroid hormones, particularly testosterone. Consequently, SHBG seems to play an important role in the occurrence of feminization in male non-alcoholic liver cirrhosis by reducing free testosterone level[95]. On the other hand, higher concentrations of this protein were reported to possibly exert protection against NAFLD [96]. The exact effect of altered glycosylation of SHBG on is function is still not known.

IgG

Igs are principle components of the defense system known as immunity. Although Ig are not synthetized in the liver, their aberrant glycosylation has been linked to various liver diseases[97]. A study combining LC-MS/MS analysis with lectin fluorophore-linked immunosorbent assay identified changes in the glycosylation of anti-Gal IgG molecules in the sera of hepatitis C virus-infected individuals with fibrosis and cirrhosis[98]. The most prominent change was agalactosylation of heavy chains of anti-Gal IgG. The same study also revealed that truncation of Gal residues induced alterations in the tertiary structure of IgG molecules originating from patients with cirrhosis[98]. Yuan *et al*[97] confirmed agalactosylation of IgG molecules in cirrhosis and reported an increased degree of fucosylation in IgG1 and IgG3 glycoforms. Cirrhosis is also accompanied by Gal deficiency and decreased sialylation of IgA molecules, as well as by an increased amounts of abnormally glycosylated polymeric IgA molecules[99]. Furthermore, concentrations of IgG and IgA are increased in the circulation of patients with cirrhosis[97]. Altered glycosylation could influence the ability of IgG to bind and activate complement system. It was discovered that alpha-Gal IgG antibodies from patients with cirrhosis have reduced complement-mediated killing ability[100]. This issue is important since bacterial infection in one of the major complications in patients with cirrhosis and alpha-Gal epitope is abundantly synthetized by bacteria.

LIVER TISSUE PROTEINS AFFECTED BY SPECIFIC PTMS IN CIRRHOSIS

Proteins remaining in liver cells are mostly modified by ubiquitination, nitration and acetylation. Ubiquitination and associated processes play important roles in the development of cirrhosis affecting many proteins. E3 ubiquitin ligase promotes, for example, NF-E2-related factor 2 ubiquitination and degradation, disrupting the anti-oxidative pathway. The same ligase promotes the accumulation of extracellular matrix by inducing ubiquitination of procollagen1 to mature collagen1[101,102]. Sumoylation and neddylation, ubiquitin-like modifications, also play roles in liver cirrhosis. It was

discovered that *in vivo* reduction of neddylation ameliorates liver fibrosis[103]. Sumoylation affects, for example, promyelocytic leukemia protein and nuclear factor-kappa B (NF-kB)[104]. Modification of these proteins leads to cell proliferation and fibrosis in the liver. A detailed overview of ubiquitination and its implications in chronic liver disease is given in the 2021 review paper of Park *et al*[33].

Transcription factors, sterol regulatory element-binding transcription factor (SREBP), and carbohydrate-response element-binding protein (ChREBP) regulate fatty acid metabolism in the liver, promoting lipogenesis. These factors are active when acetylated. Sirtuins 1 and 3 (SIRT1 and SIRT3) are deacetylases that regulate their activity. High-fat diet and obesity reduce the expression of SIRT 1 and SIRT 3, thus promoting acetylation and activation of ChREBP and SREBP, followed by an increase in the uptake of fatty acids by the liver. Liver lipid load induces inflammation and the NF-kappa B pathway, and reduces mitophagy, altogether leading to mitochondrial and liver damage and advancement towards NAFLD. Calorie restriction and exercise upregulate SIRT1 and SIRT3, thus, preventing and ameliorating NAFLD[29]. ATP-citrate lyase, microtubules, heat shock protein 90 and CCAAT/enhancer binding protein α are differently modified by acetylation in different liver diseases preceding cirrhosis. Aberrant acetylation of the mentioned proteins leads to their functional alterations and subsequently different metabolic responses, further contributing to the liver pathology[105-108].

There are many hepatic proteins with confirmed nitration status in liver diseases, whose functions are either augmented or reduced[109]. Decreased function of glutamine synthetase, 3-ketoacyl-CoA thiolase, aldehyde dehydrogenase 2, complexes I and V of oxidative phosphorylation, cytochrome p450 2E1 and B6, superoxide dismutase 1 and 2, and cluster of differentiation 95 contribute to decreased energy production, ROS leakage, steatosis, decreased anti-oxidant defense capacity, ethanol- and drug-induced toxicity, apoptosis and necrosis. Nitration of glutathione-S-transferase, however, potentiates the function of this enzyme, leading to an increased hepatic anti-oxidative defense capacity[110].

CONCLUSION

Liver disease can progress from mild damage, over moderate with a certain degree of compensation, to severe, which cannot be compensated and may lead to organ failure. While still able to compensate for tissue damage, the liver produces scars of fibrotic tissue, which reduce its function. The persistent presence of agents and/or events that cause liver damage leads to decompensated cirrhosis, resulting in several pathological outcomes, including liver cancer, and finally, functional arrest.

Early diagnosis of chronic liver disease is critical since the etiology of the disease can be discovered in this stage. When cirrhosis progresses, the etiology of a disease is very hard to determine. Appropriate treatment administered on time can prevent and reverse the progression of cirrhosis which leads to irreversible changes. Avoiding or minimizing contributing harmful factors is recommended[1]. For example, persons with chronic liver disease should avoid alcohol intake and smoking[111]. On the other hand, consumption of coffee is associated with a slower progression of liver fibrosis[112]. There are no specific curative strategies targeting alterations in PTMs in cirrhosis.

Since oxidative stress is one of the causes involved in the etiology and development of liver diseases, supplementation of vitamins and minerals, which act as anti-oxidants and/or cofactors of enzymes and other molecules that participate in anti-oxidant defense, may be recommended. However, one should bear in mind that some substances are stored in the liver and may act as pro-disease agents[113]. For example, lipophilic vitamin A is stored in liver stellate cells. If overloaded with vitamin A, these cells start to produce collagen, leading to liver fibrosis. The beta-carotene form, however, causes no such effects and is safe to consume. Iron ions can induce oxidative stress by participation in the generation of free radicals. As already said, the liver is the site of iron storage, in association with the protein ferritin. Patients with alcoholic liver cirrhosis often have an increased intrahepatic iron concentration, which is highly correlated with mortality rates[114]. Thus, when considering management strategies to treat cirrhosis, one should have in mind the complexity and limitations of interconnected metabolic pathways.

FOOTNOTES

Author contributions: Gligorijevic N performed the literature search, writing and prepared the figure; Minic S performed the literature search and writing; Nedic O designed the outline, performed the literature search and coordinated the writing of the paper.

Supported by the Ministry of Education, Science and Technological Development of the Republic of Serbia, No. 451-03-9/2021-14/200019.

Conflict-of-interest statement: All authors report no relevant conflict of interest for this article.

Open-Access: This article is an open-access article that was selected by an in-house editor and fully peer-reviewed by

external reviewers. It is distributed in accordance with the Creative Commons Attribution NonCommercial (CC BY-NC 4.0) license, which permits others to distribute, remix, adapt, build upon this work non-commercially, and license their derivative works on different terms, provided the original work is properly cited and the use is non-commercial. See: https://creativecommons.org/Licenses/by-nc/4.0/

Country/Territory of origin: Serbia

ORCID number: Nikola Gligorijević 0000-0002-8691-2486; Simeon Minić 0000-0002-7053-1216; Olgica Nedić 0000-0003-2042-0056.

S-Editor: Wu YXJ
L-Editor: A
P-Editor: Wu YXJ

REFERENCES

1 **Wiegand J**, Berg T. The etiology, diagnosis and prevention of liver cirrhosis: part 1 of a series on liver cirrhosis. *Dtsch Arztebl Int* 2013; **110**: 85-91 [PMID: 23451000 DOI: 10.3238/arztebl.2013.0085]
2 **Ramazi S**, Zahiri J. Posttranslational modifications in proteins: resources, tools and prediction methods. *Database (Oxford)* 2021; **2021** [PMID: 33826699 DOI: 10.1093/database/baab012]
3 **Khoury GA**, Baliban RC, Floudas CA. Proteome-wide post-translational modification statistics: frequency analysis and curation of the swiss-prot database. *Sci Rep* 2011; **1** [PMID: 22034591 DOI: 10.1038/srep00090]
4 **Huang KY**, Lee TY, Kao HJ, Ma CT, Lee CC, Lin TH, Chang WC, Huang HD. dbPTM in 2019: exploring disease association and cross-talk of post-translational modifications. *Nucleic Acids Res* 2019; **47**: D298-D308 [PMID: 30418626 DOI: 10.1093/nar/gky1074]
5 **Osna NA**, Carter WG, Ganesan M, Kirpich IA, McClain CJ, Petersen DR, Shearn CT, Tomasi ML, Kharbanda KK. Aberrant post-translational protein modifications in the pathogenesis of alcohol-induced liver injury. *World J Gastroenterol* 2016; **22**: 6192-6200 [PMID: 27468209 DOI: 10.3748/wjg.v22.i27.6192]
6 **Karve TM**, Cheema AK. Small changes huge impact: the role of protein posttranslational modifications in cellular homeostasis and disease. *J Amino Acids* 2011; **2011**: 207691 [PMID: 22312457 DOI: 10.4061/2011/207691]
7 **Ramachandran P**, Xu G, Huang HH, Rice R, Zhou B, Lindpaintner K, Serie D. Serum Glycoprotein Markers in Nonalcoholic Steatohepatitis and Hepatocellular Carcinoma. *J Proteome Res* 2022; **21**: 1083-1094 [PMID: 35286803 DOI: 10.1021/acs.jproteome.1c00965]
8 **Lachiondo-Ortega S**, Mercado-Gómez M, Serrano-Maciá M, Lopitz-Otsoa F, Salas-Villalobos TB, Varela-Rey M, Delgado TC, Martínez-Chantar ML. Ubiquitin-Like Post-Translational Modifications (Ubl-PTMs): Small Peptides with Huge Impact in Liver Fibrosis. *Cells* 2019; **8** [PMID: 31817258 DOI: 10.3390/cells8121575]
9 **Arauz J**, Ramos-Tovar E, Muriel P. Redox state and methods to evaluate oxidative stress in liver damage: From bench to bedside. *Ann Hepatol* 2016; **15**: 160-173 [PMID: 26845593 DOI: 10.5604/16652681.1193701]
10 **Taub R**. Liver regeneration: from myth to mechanism. *Nat Rev Mol Cell Biol* 2004; **5**: 836-847 [PMID: 15459664 DOI: 10.1038/nrm1489]
11 **Kehm R**, Baldensperger T, Raupbach J, Höhn A. Protein oxidation - Formation mechanisms, detection and relevance as biomarkers in human diseases. *Redox Biol* 2021; **42**: 101901 [PMID: 33744200 DOI: 10.1016/j.redox.2021.101901]
12 **Galicia-Moreno M**, Gutiérrez-Reyes G. The role of oxidative stress in the development of alcoholic liver disease. *Rev Gastroenterol Mex* 2014; **79**: 135-144 [PMID: 24861526 DOI: 10.1016/j.rgmx.2014.03.001]
13 **Ivanov AV**, Valuev-Elliston VT, Tyurina DA, Ivanova ON, Kochetkov SN, Bartosch B, Isaguliants MG. Oxidative stress, a trigger of hepatitis C and B virus-induced liver carcinogenesis. *Oncotarget* 2017; **8**: 3895-3932 [PMID: 27965466 DOI: 10.18632/oncotarget.13904]
14 **Masarone M**, Rosato V, Dallio M, Gravina AG, Aglitti A, Loguercio C, Federico A, Persico M. Role of Oxidative Stress in Pathophysiology of Nonalcoholic Fatty Liver Disease. *Oxid Med Cell Longev* 2018; **2018**: 9547613 [PMID: 29991976 DOI: 10.1155/2018/9547613]
15 **Li S**, Tan HY, Wang N, Zhang ZJ, Lao L, Wong CW, Feng Y. The Role of Oxidative Stress and Antioxidants in Liver Diseases. *Int J Mol Sci* 2015; **16**: 26087-26124 [PMID: 26540040 DOI: 10.3390/ijms161125942]
16 **Radi R**. Protein tyrosine nitration: biochemical mechanisms and structural basis of functional effects. *Acc Chem Res* 2013; **46**: 550-559 [PMID: 23157446 DOI: 10.1021/ar300234c]
17 **Lamotte O**, Bertoldo JB, Besson-Bard A, Rosnoblet C, Aimé S, Hichami S, Terenzi H, Wendehenne D. Protein S-nitrosylation: specificity and identification strategies in plants. *Front Chem* 2014; **2**: 114 [PMID: 25750911 DOI: 10.3389/fchem.2014.00114]
18 **Nuriel T**, Hansler A, Gross SS. Protein nitrotryptophan: formation, significance and identification. *J Proteomics* 2011; **74**: 2300-2312 [PMID: 21679780 DOI: 10.1016/j.jprot.2011.05.032]
19 **Fernández-Checa JC**, Kaplowitz N, García-Ruiz C, Colell A. Mitochondrial glutathione: importance and transport. *Semin Liver Dis* 1998; **18**: 389-401 [PMID: 9875556 DOI: 10.1055/s-2007-1007172]
20 **Campello S**, Scorrano L. Mitochondrial shape changes: orchestrating cell pathophysiology. *EMBO Rep* 2010; **11**: 678-684 [PMID: 20725092 DOI: 10.1038/embor.2010.115]
21 **Mansouri A**, Fromenty B, Berson A, Robin MA, Grimbert S, Beaugrand M, Erlinger S, Pessayre D. Multiple hepatic mitochondrial DNA deletions suggest premature oxidative aging in alcoholic patients. *J Hepatol* 1997; **27**: 96-102 [PMID:

9252080 DOI: 10.1016/s0168-8278(97)80286-3]
22 **Mansouri A**, Gaou I, De Kerguenec C, Amsellem S, Haouzi D, Berson A, Moreau A, Feldmann G, Lettéron P, Pessayre D, Fromenty B. An alcoholic binge causes massive degradation of hepatic mitochondrial DNA in mice. *Gastroenterology* 1999; **117**: 181-190 [PMID: 10381926 DOI: 10.1016/s0016-5085(99)70566-4]
23 **Annie-Jeyachristy S**, Geetha A, Surendran R, Sundaram A, Lavanya K, Kumar SJ, Prakash SA. Level of nitrated proteins in the plasma, platelets and liver of patients with liver cirrhosis. *Redox Rep* 2009; **14**: 259-266 [PMID: 20003711 DOI: 10.1179/135100009X12525712409616]
24 **Verhelst X**, Dias AM, Colombel JF, Vermeire S, Van Vlierberghe H, Callewaert N, Pinho SS. Protein Glycosylation as a Diagnostic and Prognostic Marker of Chronic Inflammatory Gastrointestinal and Liver Diseases. *Gastroenterology* 2020; **158**: 95-110 [PMID: 31626754 DOI: 10.1053/j.gastro.2019.08.060]
25 **Reily C**, Stewart TJ, Renfrow MB, Novak J. Glycosylation in health and disease. *Nat Rev Nephrol* 2019; **15**: 346-366 [PMID: 30858582 DOI: 10.1038/s41581-019-0129-4]
26 **Vanderschaeghe D**, Laroy W, Sablon E, Halfon P, Van Hecke A, Delanghe J, Callewaert N. GlycoFibroTest is a highly performant liver fibrosis biomarker derived from DNA sequencer-based serum protein glycomics. *Mol Cell Proteomics* 2009; **8**: 986-994 [PMID: 19181623 DOI: 10.1074/mcp.M800470-MCP200]
27 **Callewaert N**, Van Vlierberghe H, Van Hecke A, Laroy W, Delanghe J, Contreras R. Noninvasive diagnosis of liver cirrhosis using DNA sequencer-based total serum protein glycomics. *Nat Med* 2004; **10**: 429-434 [PMID: 15152612 DOI: 10.1038/nm1006]
28 **Malaguarnera G**, Bertino G, Vacante M, Malaguarnera M. Hepatocellular carcinoma markers in the omics era: the glycomic analysis. *Hepatobiliary Surg Nutr* 2014; **3**: 407-409 [PMID: 25568863 DOI: 10.3978/j.issn.2304-3881.2014.07.04]
29 Nassir F. Role of acetylation in nonalcoholic fatty liver disease: a focus on SIRT1 and SIRT3. Explor Med 2020; 1: 248-258. [DOI: 10.37349/emed.2020.00017]
30 **Le-Tian Z**, Cheng-Zhang H, Xuan Z, Zhang Q, Zhen-Gui Y, Qing-Qing W, Sheng-Xuan W, Zhong-Jin X, Ran-Ran L, Ting-Jun L, Zhong-Qu S, Zhong-Hua W, Ke-Rong S. Protein acetylation in mitochondria plays critical functions in the pathogenesis of fatty liver disease. *BMC Genomics* 2020; **21**: 435 [PMID: 32586350 DOI: 10.1186/s12864-020-06837-y]
31 **Ciechanover A**. The unravelling of the ubiquitin system. *Nat Rev Mol Cell Biol* 2015; **16**: 322-324 [PMID: 25907614 DOI: 10.1038/nrm3982]
32 **Dikic I**, Wakatsuki S, Walters KJ. Ubiquitin-binding domains - from structures to functions. *Nat Rev Mol Cell Biol* 2009; **10**: 659-671 [PMID: 19773779 DOI: 10.1038/nrm2767]
33 **Park JS**, Ma H, Roh YS. Ubiquitin pathways regulate the pathogenesis of chronic liver disease. *Biochem Pharmacol* 2021; **193**: 114764 [PMID: 34529948 DOI: 10.1016/j.bcp.2021.114764]
34 **Gligorijević N**, Minić S, Križáková M, Katrlík J, Nedić O. Structural changes of fibrinogen as a consequence of cirrhosis. *Thromb Res* 2018; **166**: 43-49 [PMID: 29655002 DOI: 10.1016/j.thromres.2018.04.005]
35 **Martinez J**, Palascak JE, Kwasniak D. Abnormal sialic acid content of the dysfibrinogenemia associated with liver disease. *J Clin Invest* 1978; **61**: 535-538 [PMID: 621288 DOI: 10.1172/JCI108964]
36 **Lisman T**, Ariëns RA. Alterations in Fibrin Structure in Patients with Liver Diseases. *Semin Thromb Hemost* 2016; **42**: 389-396 [PMID: 27071046 DOI: 10.1055/s-0036-1572327]
37 **Dang CV**, Shin CK, Bell WR, Nagaswami C, Weisel JW. Fibrinogen sialic acid residues are low affinity calcium-binding sites that influence fibrin assembly. *J Biol Chem* 1989; **264**: 15104-15108 [PMID: 2549051 DOI: 10.1016/S0021-9258(18)63817-7]
38 **Kuchay MS**, Mishra SK, Farooqui KJ, Bansal B, Wasir JS, Mithal A. Hypercalcemia of advanced chronic liver disease: a forgotten clinical entity! *Clin Cases Miner Bone Metab* 2016; **13**: 15-18 [PMID: 27252737 DOI: 10.11138/ccmbm/2016.13.1.015]
39 **Marchi R**, Arocha-Piñango CL, Nagy H, Matsuda M, Weisel JW. The effects of additional carbohydrate in the coiled-coil region of fibrinogen on polymerization and clot structure and properties: characterization of the homozygous and heterozygous forms of fibrinogen Lima (Aalpha Arg141-->Ser with extra glycosylation). *J Thromb Haemost* 2004; **2**: 940-948 [PMID: 15140130 DOI: 10.1111/j.1538-7836.2004.00730.x]
40 **Maekawa H**, Yamazumi K, Muramatsu S, Kaneko M, Hirata H, Takahashi N, Arocha-Piñango CL, Rodriguez S, Nagy H, Perez-Requejo JL. Fibrinogen Lima: a homozygous dysfibrinogen with an A alpha-arginine-141 to serine substitution associated with extra N-glycosylation at A alpha-asparagine-139. Impaired fibrin gel formation but normal fibrin-facilitated plasminogen activation catalyzed by tissue-type plasminogen activator. *J Clin Invest* 1992; **90**: 67-76 [PMID: 1634621 DOI: 10.1172/JCI115857]
41 **Yamazumi K**, Shimura K, Terukina S, Takahashi N, Matsuda M. A gamma methionine-310 to threonine substitution and consequent N-glycosylation at gamma asparagine-308 identified in a congenital dysfibrinogenemia associated with posttraumatic bleeding, fibrinogen Asahi. *J Clin Invest* 1989; **83**: 1590-1597 [PMID: 2496144 DOI: 10.1172/JCI114056]
42 **Sugo T**, Nakamikawa C, Takano H, Mimuro J, Yamaguchi S, Mosesson MW, Meh DA, DiOrio JP, Takahashi N, Takahashi H, Nagai K, Matsuda M. Fibrinogen Niigata with impaired fibrin assembly: an inherited dysfibrinogen with a Bbeta Asn-160 to Ser substitution associated with extra glycosylation at Bbeta Asn-158. *Blood* 1999; **94**: 3806-3813 [PMID: 10572095 DOI: 10.1182/blood.V94.11.3806]
43 **Hugenholtz GC**, Macrae F, Adelmeijer J, Dulfer S, Porte RJ, Lisman T, Ariëns RA. Procoagulant changes in fibrin clot structure in patients with cirrhosis are associated with oxidative modifications of fibrinogen. *J Thromb Haemost* 2016; **14**: 1054-1066 [PMID: 26833718 DOI: 10.1111/jth.13278]
44 **Martinez M**, Weisel JW, Ischiropoulos H. Functional impact of oxidative posttranslational modifications on fibrinogen and fibrin clots. *Free Radic Biol Med* 2013; **65**: 411-418 [PMID: 23851017 DOI: 10.1016/j.freeradbiomed.2013.06.039]
45 **Xu YJ**, Qiang M, Zhang JL, Liu Y, He RQ. Reactive carbonyl compounds (RCCs) cause aggregation and dysfunction of fibrinogen. *Protein Cell* 2012; **3**: 627-640 [PMID: 22836718 DOI: 10.1007/s13238-012-2057-y]
46 **Becatti M**, Marcucci R, Bruschi G, Taddei N, Bani D, Gori AM, Giusti B, Gensini GF, Abbate R, Fiorillo C. Oxidative modification of fibrinogen is associated with altered function and structure in the subacute phase of myocardial infarction.

Arterioscler Thromb Vasc Biol 2014; **34**: 1355-1361 [PMID: 24790138 DOI: 10.1161/ATVBAHA.114.303785]
47 **Rosenfeld MA**, Vasilyeva AD, Yurina LV, Bychkova AV. Oxidation of proteins: is it a programmed process? *Free Radic Res* 2018; **52**: 14-38 [PMID: 29284315 DOI: 10.1080/10715762.2017.1402305]
48 **Zermatten MG**, Fraga M, Moradpour D, Bertaggia Calderara D, Aliotta A, Stirnimann G, De Gottardi A, Alberio L. Hemostatic Alterations in Patients With Cirrhosis: From Primary Hemostasis to Fibrinolysis. *Hepatology* 2020; **71**: 2135-2148 [PMID: 32090357 DOI: 10.1002/hep.31201]
49 **Bernardi M**, Ricci CS, Zaccherini G. Role of human albumin in the management of complications of liver cirrhosis. *J Clin Exp Hepatol* 2014; **4**: 302-311 [PMID: 25755577 DOI: 10.1016/j.jceh.2014.08.007]
50 **Carvalho JR**, Verdelho Machado M. New Insights About Albumin and Liver Disease. *Ann Hepatol* 2018; **17**: 547-560 [PMID: 29893696 DOI: 10.5604/01.3001.0012.0916]
51 **Oettl K**, Stadlbauer V, Petter F, Greilberger J, Putz-Bankuti C, Hallström S, Lackner C, Stauber RE. Oxidative damage of albumin in advanced liver disease. *Biochim Biophys Acta* 2008; **1782**: 469-473 [PMID: 18498776 DOI: 10.1016/j.bbadis.2008.04.002]
52 **Baldassarre M**, Domenicali M, Naldi M, Laggetta M, Giannone FA, Biselli M, Patrono D, Bertucci C, Bernardi M, Caraceni P. Albumin Homodimers in Patients with Cirrhosis: Clinical and Prognostic Relevance of a Novel Identified Structural Alteration of the Molecule. *Sci Rep* 2016; **6**: 35987 [PMID: 27782157 DOI: 10.1038/srep35987]
53 **Domenicali M**, Baldassarre M, Giannone FA, Naldi M, Mastroroberto M, Biselli M, Laggetta M, Patrono D, Bertucci C, Bernardi M, Caraceni P. Posttranscriptional changes of serum albumin: clinical and prognostic significance in hospitalized patients with cirrhosis. *Hepatology* 2014; **60**: 1851-1860 [PMID: 25048618 DOI: 10.1002/hep.27322]
54 **Giannone FA**, Domenicali M, Baldassarre M, Bartoletti M, Naldi M, Laggetta M, Bertucci C, Colecchia A, Viale P, Bernardi M, Caraceni P. Ischaemia-modified albumin: a marker of bacterial infection in hospitalized patients with cirrhosis. *Liver Int* 2015; **35**: 2425-2432 [PMID: 25939693 DOI: 10.1111/liv.12860]
55 **Baldassarre M**, Naldi M, Zaccherini G, Bartoletti M, Antognoli A, Laggetta M, Gagliardi M, Tufoni M, Domenicali M, Waterstradt K, Paterini P, Baldan A, Leoni S, Bartolini M, Viale P, Trevisani F, Bernardi M, Caraceni P. Determination of Effective Albumin in Patients With Decompensated Cirrhosis: Clinical and Prognostic Implications. *Hepatology* 2021; **74**: 2058-2073 [PMID: 33710623 DOI: 10.1002/hep.31798]
56 **Paar M**, Fengler VH, Rosenberg DJ, Krebs A, Stauber RE, Oettl K, Hammel M. Albumin in patients with liver disease shows an altered conformation. *Commun Biol* 2021; **4**: 731 [PMID: 34127764 DOI: 10.1038/s42003-021-02269-w]
57 **Gomme PT**, McCann KB, Bertolini J. Transferrin: structure, function and potential therapeutic actions. *Drug Discov Today* 2005; **10**: 267-273 [PMID: 15708745 DOI: 10.1016/S1359-6446(04)03333-1]
58 **Kawabata H**. Transferrin and transferrin receptors update. *Free Radic Biol Med* 2019; **133**: 46-54 [PMID: 29969719 DOI: 10.1016/j.freeradbiomed.2018.06.037]
59 **Stibler H**. Carbohydrate-deficient transferrin in serum: a new marker of potentially harmful alcohol consumption reviewed. *Clin Chem* 1991; **37**: 2029-2037 [PMID: 1764777 DOI: 10.1093/clinchem/37.12.2029]
60 **Inoue T**, Yamauchi M, Ohkawa K. Structural studies on sugar chains of carbohydrate-deficient transferrin from patients with alcoholic liver disease using lectin affinity electrophoresis. *Electrophoresis* 1999; **20**: 452-457 [PMID: 10217151 DOI: 10.1002/(SICI)1522-2683(19990301)20:3<452::AID-ELPS452>3.0.CO;2-R]
61 **Hoefkens P**, Huijskes-Heins MI, de Jeu-Jaspars CM, van Noort WL, van Eijk HG. Influence of transferrin glycans on receptor binding and iron-donation. *Glycoconj J* 1997; **14**: 289-295 [PMID: 9111147 DOI: 10.1023/a:1018510309524]
62 **Arndt T**, van der Meijden BB, Wielders JP. Atypical serum transferrin isoform distribution in liver cirrhosis studied by HPLC, capillary electrophoresis and transferrin genotyping. *Clin Chim Acta* 2008; **394**: 42-46 [PMID: 18442477 DOI: 10.1016/j.cca.2008.03.033]
63 **Stewart SH**, Reuben A, Anton RF. Relationship of Abnormal Chromatographic Pattern for Carbohydrate-Deficient Transferrin with Severe Liver Disease. *Alcohol Alcohol* 2017; **52**: 24-28 [PMID: 27998920 DOI: 10.1093/alcalc/agw069]
64 **Landberg E**, Åström E, Kågedal B, Påhlsson P. Disialo-trisialo bridging of transferrin is due to increased branching and fucosylation of the carbohydrate moiety. *Clin Chim Acta* 2012; **414**: 58-64 [PMID: 22902807 DOI: 10.1016/j.cca.2012.07.026]
65 **Viveiros A**, Finkenstedt A, Schaefer B, Mandorfer M, Scheiner B, Lehner K, Tobiasch M, Reiberger T, Tilg H, Edlinger M, Zoller H. Transferrin as a predictor of survival in cirrhosis. *Liver Transpl* 2018; **24**: 343-351 [PMID: 29149510 DOI: 10.1002/lt.24981]
66 **Yu Y**, Jiang L, Wang H, Shen Z, Cheng Q, Zhang P, Wang J, Wu Q, Fang X, Duan L, Wang S, Wang K, An P, Shao T, Chung RT, Zheng S, Min J, Wang F. Hepatic transferrin plays a role in systemic iron homeostasis and liver ferroptosis. *Blood* 2020; **136**: 726-739 [PMID: 32374849 DOI: 10.1182/blood.2019002907]
67 **Sanda M**, Benicky J, Wu J, Wang Y, Makambi K, Ahn J, Smith CI, Zhao P, Zhang L, Goldman R. Increased sialylation of site specific O-glycoforms of hemopexin in liver disease. *Clin Proteomics* 2016; **13**: 24 [PMID: 27688741 DOI: 10.1186/s12014-016-9125-x]
68 **Morota K**, Nakagawa M, Sekiya R, Hemken PM, Sokoll LJ, Elliott D, Chan DW, Dowell BL. A comparative evaluation of Golgi protein-73, fucosylated hemopexin, α-fetoprotein, and PIVKA-II in the serum of patients with chronic hepatitis, cirrhosis, and hepatocellular carcinoma. *Clin Chem Lab Med* 2011; **49**: 711-718 [PMID: 21231906 DOI: 10.1515/CCLM.2011.097]
69 **Pompach P**, Brnakova Z, Sanda M, Wu J, Edwards N, Goldman R. Site-specific glycoforms of haptoglobin in liver cirrhosis and hepatocellular carcinoma. *Mol Cell Proteomics* 2013; **12**: 1281-1293 [PMID: 23389049 DOI: 10.1074/mcp.M112.023259]
70 **Bensi G**, Raugei G, Klefenz H, Cortese R. Structure and expression of the human haptoglobin locus. *EMBO J* 1985; **4**: 119-126 [PMID: 4018023 DOI: 10.1002/j.1460-2075.1985.tb02325.x]
71 **Zhang S**, Shu H, Luo K, Kang X, Zhang Y, Lu H, Liu Y. N-linked glycan changes of serum haptoglobin β chain in liver disease patients. *Mol Biosyst* 2011; **7**: 1621-1628 [PMID: 21380457 DOI: 10.1039/c1mb05020f]
72 **Polticelli F**, Bocedi A, Minervini G, Ascenzi P. Human haptoglobin structure and function--a molecular modelling study. *FEBS J* 2008; **275**: 5648-5656 [PMID: 18959750 DOI: 10.1111/j.1742-4658.2008.06690.x]

73 **Zhu J**, Lin Z, Wu J, Yin H, Dai J, Feng Z, Marrero J, Lubman DM. Analysis of serum haptoglobin fucosylation in hepatocellular carcinoma and liver cirrhosis of different etiologies. *J Proteome Res* 2014; **13**: 2986-2997 [PMID: 24807840 DOI: 10.1021/pr500128t]

74 **Orino K**, Watanabe K. Molecular, physiological and clinical aspects of the iron storage protein ferritin. *Vet J* 2008; **178**: 191-201 [PMID: 17764995 DOI: 10.1016/j.tvjl.2007.07.006]

75 **Wang W**, Knovich MA, Coffman LG, Torti FM, Torti SV. Serum ferritin: Past, present and future. *Biochim Biophys Acta* 2010; **1800**: 760-769 [PMID: 20304033 DOI: 10.1016/j.bbagen.2010.03.011]

76 **Fletcher LM**, Halliday JW, Powell LW. Interrelationships of alcohol and iron in liver disease with particular reference to the iron-binding proteins, ferritin and transferrin. *J Gastroenterol Hepatol* 1999; **14**: 202-214 [PMID: 10197487 DOI: 10.1046/j.1440-1746.1999.01836.x]

77 **Czaja AJ**. Review article: iron disturbances in chronic liver diseases other than haemochromatosis - pathogenic, prognostic, and therapeutic implications. *Aliment Pharmacol Ther* 2019; **49**: 681-701 [PMID: 30761559 DOI: 10.1111/apt.15173]

78 **Domschke W**, Meyer-Bertenrath JG. -Helical structures and iron contents of the ribosomal ferritin from normal, cirrhotic and cancerous human livers. *Digestion* 1971; **4**: 321-325 [PMID: 4329888 DOI: 10.1159/000197136]

79 **Cullis JO**, Fitzsimons EJ, Griffiths WJ, Tsochatzis E, Thomas DW; British Society for Haematology. Investigation and management of a raised serum ferritin. *Br J Haematol* 2018; **181**: 331-340 [PMID: 29672840 DOI: 10.1111/bjh.15166]

80 **Chapman RW**, Gorman A, Laulicht M, Hussain MA, Sherlock S, Hoffbrand AV. Binding of serum ferritin to concanavalin A in patients with iron overload and with chronic liver disease. *J Clin Pathol* 1982; **35**: 481-486 [PMID: 7085891 DOI: 10.1136/jcp.35.5.481]

81 **Annunziata M**, Granata R, Ghigo E. The IGF system. *Acta Diabetol* 2011; **48**: 1-9 [PMID: 21042815 DOI: 10.1007/s00592-010-0227-z]

82 **Jogie-Brahim S**, Feldman D, Oh Y. Unraveling insulin-like growth factor binding protein-3 actions in human disease. *Endocr Rev* 2009; **30**: 417-437 [PMID: 19477944 DOI: 10.1210/er.2008-0028]

83 **Firth SM**, Baxter RC. Characterisation of recombinant glycosylation variants of insulin-like growth factor binding protein-3. *J Endocrinol* 1999; **160**: 379-387 [PMID: 10076184 DOI: 10.1677/joe.0.1600379]

84 **Coverley JA**, Martin JL, Baxter RC. The effect of phosphorylation by casein kinase 2 on the activity of insulin-like growth factor-binding protein-3. *Endocrinology* 2000; **141**: 564-570 [PMID: 10650937 DOI: 10.1210/endo.141.2.7306]

85 **Nedić O**, Nikolić JA, Prisić S, Acimovic J, hajdukovic-Dragojlovic L. Reactivity of IGF binding protein-3 isoforms towards concanavalin A in healthy adults and subjects with cirrhosis. *Addict Biol* 2003; **8**: 81-88 [PMID: 12745420 DOI: 10.1080/1355621031000069927]

86 **Nedić O**, Nikolić JA, Hajduković-Dragojlović L, Todorović V, Masnikosa R. Alterations of IGF-binding proteins in patients with alcoholic liver cirrhosis. *Alcohol* 2000; **21**: 223-229 [PMID: 11091025 DOI: 10.1016/s0741-8329(00)00090-2]

87 **Cai Q**, Dozmorov M, Oh Y. IGFBP-3/IGFBP-3 Receptor System as an Anti-Tumor and Anti-Metastatic Signaling in Cancer. *Cells* 2020; **9** [PMID: 32443727 DOI: 10.3390/cells9051261]

88 **Arab JP**, Cabrera D, Sehrawat TS, Jalan-Sakrikar N, Verma VK, Simonetto D, Cao S, Yaqoob U, Leon J, Freire M, Vargas JI, De Assuncao TM, Kwon JH, Guo Y, Kostallari E, Cai Q, Kisseleva T, Oh Y, Arrese M, Huebert RC, Shah VH. Hepatic stellate cell activation promotes alcohol-induced steatohepatitis through Igfbp3 and SerpinA12. *J Hepatol* 2020; **73**: 149-160 [PMID: 32087348 DOI: 10.1016/j.jhep.2020.02.005]

89 **Luo J**, Chen Q, Shen T, Wang X, Fang W, Wu X, Yuan Z, Chen G, Ling W, Chen Y. Association of sex hormone-binding globulin with nonalcoholic fatty liver disease in Chinese adults. *Nutr Metab (Lond)* 2018; **15**: 79 [PMID: 30455723 DOI: 10.1186/s12986-018-0313-8]

90 **Yuan W**, Benicky J, Wei R, Goldman R, Sanda M. Quantitative Analysis of Sex-Hormone-Binding Globulin Glycosylation in Liver Diseases by Liquid Chromatography-Mass Spectrometry Parallel Reaction Monitoring. *J Proteome Res* 2018; **17**: 2755-2766 [PMID: 29972295 DOI: 10.1021/acs.jproteome.8b00201]

91 **Thaler MA**, Seifert-Klauss V, Luppa PB. The biomarker sex hormone-binding globulin - from established applications to emerging trends in clinical medicine. *Best Pract Res Clin Endocrinol Metab* 2015; **29**: 749-760 [PMID: 26522459 DOI: 10.1016/j.beem.2015.06.005]

92 **Luppa PB**, Thaler M, Schulte-Frohlinde E, Schreiegg A, Huber U, Metzger J. Unchanged androgen-binding properties of sex hormone-binding globulin in male patients with liver cirrhosis. *Clin Chem Lab Med* 2006; **44**: 967-973 [PMID: 16879062 DOI: 10.1515/CCLM.2006.186]

93 **Brenta G**, Bedecarras P, Schnitman M, Gurfinkiel M, Damilano S, Campo S, Pisarev MA. Characterization of sex hormone-binding globulin isoforms in hypothyroid women. *Thyroid* 2002; **12**: 101-105 [PMID: 11916278 DOI: 10.1089/105072502753522329]

94 **Kaymakoğlu S**, Okten A, Cakaloğlu Y, Boztaş G, Beşişik F, Taşçioğlu C, Yalçin S. Hypogonadism is not related to the etiology of liver cirrhosis. *J Gastroenterol* 1995; **30**: 745-750 [PMID: 8963392 DOI: 10.1007/BF02349641]

95 **Maruyama Y**, Adachi Y, Aoki N, Suzuki Y, Shinohara H, Yamamoto T. Mechanism of feminization in male patients with non-alcoholic liver cirrhosis: role of sex hormone-binding globulin. *Gastroenterol Jpn* 1991; **26**: 435-439 [PMID: 1916151 DOI: 10.1007/BF02782811]

96 **Price JC**, Wang R, Seaberg EC, Brown TT, Budoff MJ, Kingsley LA, Palella FJ Jr, Witt MD, Post WS, Lake JE, Thio CL. Sex Hormone-Binding Globulin Levels Are Inversely Associated With Nonalcoholic Fatty Liver Disease in HIV-Infected and -Uninfected Men. *Open Forum Infect Dis* 2019; **6**: ofz468 [PMID: 32128321 DOI: 10.1093/ofid/ofz468]

97 **Yuan W**, Sanda M, Wu J, Koomen J, Goldman R. Quantitative analysis of immunoglobulin subclasses and subclass specific glycosylation by LC-MS-MRM in liver disease. *J Proteomics* 2015; **116**: 24-33 [PMID: 25582524 DOI: 10.1016/j.jprot.2014.12.020]

98 **Mehta AS**, Long RE, Comunale MA, Wang M, Rodemich L, Krakover J, Philip R, Marrero JA, Dwek RA, Block TM. Increased levels of galactose-deficient anti-Gal immunoglobulin G in the sera of hepatitis C virus-infected individuals with fibrosis and cirrhosis. *J Virol* 2008; **82**: 1259-1270 [PMID: 18045939 DOI: 10.1128/JVI.01600-07]

99 **Tissandié E**, Morelle W, Berthelot L, Vrtovsnik F, Daugas E, Walker F, Lebrec D, Trawalé JM, Francoz C, Durand F, Moura IC, Paradis V, Moreau R, Monteiro RC. Both IgA nephropathy and alcoholic cirrhosis feature abnormally glycosylated IgA1 and soluble CD89-IgA and IgG-IgA complexes: common mechanisms for distinct diseases. *Kidney Int* 2011; **80**: 1352-1363 [PMID: 21866091 DOI: 10.1038/ki.2011.276]

100 **Lamontagne A**, Long RE, Comunale MA, Hafner J, Rodemich-Betesh L, Wang M, Marrero J, Di Bisceglie AM, Block T, Mehta A. Altered functionality of anti-bacterial antibodies in patients with chronic hepatitis C virus infection. *PLoS One* 2013; **8**: e64992 [PMID: 23750224 DOI: 10.1371/journal.pone.0064992]

101 **Wu T**, Zhao F, Gao B, Tan C, Yagishita N, Nakajima T, Wong PK, Chapman E, Fang D, Zhang DD. Hrd1 suppresses Nrf2-mediated cellular protection during liver cirrhosis. *Genes Dev* 2014; **28**: 708-722 [PMID: 24636985 DOI: 10.1101/gad.238246.114]

102 **Hasegawa D**, Fujii R, Yagishita N, Matsumoto N, Aratani S, Izumi T, Azakami K, Nakazawa M, Fujita H, Sato T, Araya N, Koike J, Tadokoro M, Suzuki N, Nagata K, Senoo H, Friedman SL, Nishioka K, Yamano Y, Itoh F, Nakajima T. E3 ubiquitin ligase synoviolin is involved in liver fibrogenesis. *PLoS One* 2010; **5**: e13590 [PMID: 21049091 DOI: 10.1371/journal.pone.0013590]

103 **Zou T**, Zhang J. Diverse and pivotal roles of neddylation in metabolism and immunity. *FEBS J* 2021; **288**: 3884-3912 [PMID: 33025631 DOI: 10.1111/febs.15584]

104 **Dai J**, Hu Y, Niu Q, Song G, Wang H, Li S. Role of PML SUMOylation in arsenic trioxide-induced fibrosis in HSCs. *Life Sci* 2020; **251**: 117607 [PMID: 32240679 DOI: 10.1016/j.lfs.2020.117607]

105 **Guo L**, Guo YY, Li BY, Peng WQ, Chang XX, Gao X, Tang QQ. Enhanced acetylation of ATP-citrate lyase promotes the progression of nonalcoholic fatty liver disease. *J Biol Chem* 2019; **294**: 11805-11816 [PMID: 31197036 DOI: 10.1074/jbc.RA119.008708]

106 **Groebner JL**, Girón-Bravo MT, Rothberg ML, Adhikari R, Tuma DJ, Tuma PL. Alcohol-induced microtubule acetylation leads to the accumulation of large, immobile lipid droplets. *Am J Physiol Gastrointest Liver Physiol* 2019; **317**: G373-G386 [PMID: 31373507 DOI: 10.1152/ajpgi.00026.2019]

107 **Yang Y**, Sangwung P, Kondo R, Jung Y, McConnell MJ, Jeong J, Utsumi T, Sessa WC, Iwakiri Y. Alcohol-induced Hsp90 acetylation is a novel driver of liver sinusoidal endothelial dysfunction and alcohol-related liver disease. *J Hepatol* 2021; **75**: 377-386 [PMID: 33675874 DOI: 10.1016/j.jhep.2021.02.028]

108 **Ding D**, Chen LL, Zhai YZ, Hou CJ, Tao LL, Lu SH, Wu J, Liu XP. Trichostatin A inhibits the activation of Hepatic stellate cells by Increasing C/EBP-α Acetylation in vivo and in vitro. *Sci Rep* 2018; **8**: 4395 [PMID: 29535398 DOI: 10.1038/s41598-018-22662-6]

109 **Abdelmegeed MA**, Song BJ. Functional roles of protein nitration in acute and chronic liver diseases. *Oxid Med Cell Longev* 2014; **2014**: 149627 [PMID: 24876909 DOI: 10.1155/2014/149627]

110 **Ji Y**, Neverova I, Van Eyk JE, Bennett BM. Nitration of tyrosine 92 mediates the activation of rat microsomal glutathione s-transferase by peroxynitrite. *J Biol Chem* 2006; **281**: 1986-1991 [PMID: 16314419 DOI: 10.1074/jbc.M509480200]

111 **Charatcharoenwitthaya P**, Karaketklang K, Aekplakorn W. Cigarette Smoking Increased Risk of Overall Mortality in Patients With Non-alcoholic Fatty Liver Disease: A Nationwide Population-Based Cohort Study. *Front Med (Lausanne)* 2020; **7**: 604919 [PMID: 33365321 DOI: 10.3389/fmed.2020.604919]

112 **Corrao G**, Zambon A, Bagnardi V, D'Amicis A, Klatsky A; Collaborative SIDECIR Group. Coffee, caffeine, and the risk of liver cirrhosis. *Ann Epidemiol* 2001; **11**: 458-465 [PMID: 11557177 DOI: 10.1016/s1047-2797(01)00223-x]

113 **Herrera JL**, Rodríguez R. Medical Care of the Patient With Compensated Cirrhosis. *Gastroenterol Hepatol (N Y)* 2006; **2**: 124-133 [PMID: 28286440]

114 **Harrison-Findik DD**. Role of alcohol in the regulation of iron metabolism. *World J Gastroenterol* 2007; **13**: 4925-4930 [PMID: 17854133 DOI: 10.3748/wjg.v13.i37.4925]

World Journal of Gastroenterology

Submit a Manuscript: https://www.f6publishing.com

World J Gastroenterol 2022 August 7; 28(29): 3793-3802

DOI: 10.3748/wjg.v28.i29.3793

ISSN 1007-9327 (print) ISSN 2219-2840 (online)

MINIREVIEWS

Epidemiologic and socioeconomic factors impacting hepatitis B virus and related hepatocellular carcinoma

Bipul Gnyawali, Antoinette Pusateri, Ashley Nickerson, Sajid Jalil, Khalid Mumtaz

Specialty type: Gastroenterology and hepatology

Provenance and peer review: Invited article; Externally peer reviewed.

Peer-review model: Single blind

Peer-review report's scientific quality classification

Grade A (Excellent): 0
Grade B (Very good): B, B
Grade C (Good): 0
Grade D (Fair): 0
Grade E (Poor): 0

P-Reviewer: Liu DF, China; Venegas M, Chile

Received: January 18, 2022
Peer-review started: January 18, 2022
First decision: March 8, 2022
Revised: April 10, 2022
Accepted: July 11, 2022
Article in press: July 11, 2022
Published online: August 7, 2022

Bipul Gnyawali, Department of Medicine, Kettering Medical Center, Dayton, OH 45342, United States

Antoinette Pusateri, Ashley Nickerson, Sajid Jalil, Khalid Mumtaz, Department of Medicine, The Ohio State University, Columbus, OH 43210, United States

Corresponding author: Khalid Mumtaz, MBBS, MSc, Associate Professor, Department of Medicine, The Ohio State University, 395 W. 12th Avenue, 262 Suite, Columbus, OH 43210, United States. khalid.mumtaz@osumc.edu

Abstract

Chronic Hepatitis B is a highly prevalent disease worldwide and is estimated to cause more than 800000 annual deaths from complications such as cirrhosis and hepatocellular carcinoma (HCC). Although universal hepatitis B vaccination programs may have reduced the incidence and prevalence of chronic hepatitis B and related HCC, the disease still imposes a significant healthcare burden in many endemic regions such as Africa and the Asia-Pacific region. This is especially concerning given the global underdiagnosis of hepatitis B and the limited availability of vaccination, screening, and treatment in low-resource regions. Demographics including male gender, older age, ethnicity, and geographic location as well as low socioeconomic status are more heavily impacted by chronic hepatitis B and related HCC. Methods to mitigate this impact include increasing screening in high-risk groups according to national guidelines, increasing awareness and health literacy in vulnerable populations, and developing more robust vaccination programs in under-served regions.

Key Words: Hepatitis B; Epidemiology; Hepatocellular carcinoma; Socioeconomic status; Healthcare disparity; Hepatitis B vaccine

©The Author(s) 2022. Published by Baishideng Publishing Group Inc. All rights reserved.

Core Tip: While many studies in the past have analyzed the impact of various epidemiological and socioeconomic factors on viral hepatitis and hepatocellular carcinoma (HCC), this minireview is the first to adopt a global perspective in highlighting the impact of both epidemiologic and socioeconomic factors on current trends in chronic hepatitis B and related HCC. We highlight trends in incidence, prevalence and mortality of chronic hepatitis B seen throughout the world in the past few decades and the disparity in healthcare distribution and outcomes between different populations.

Citation: Gnyawali B, Pusateri A, Nickerson A, Jalil S, Mumtaz K. Epidemiologic and socioeconomic factors impacting hepatitis B virus and related hepatocellular carcinoma. *World J Gastroenterol* 2022; 28(29): 3793-3802
URL: https://www.wjgnet.com/1007-9327/full/v28/i29/3793.htm
DOI: https://dx.doi.org/10.3748/wjg.v28.i29.3793

INTRODUCTION

In 2019, the World Health Organization (WHO) estimated the worldwide prevalence of chronic hepatitis B virus (HBV) to be around 296 million with the incidence of new HBV infection to be 1.5 million each year. HBV is more prevalent with high burden of disease in the regions of Africa, Western Pacific and South-East Asia compared to North America and Europe. Furthermore, fewer people in the African and South-East Asian regions knew about their HBV status and had access to treatment compared to the latter regions[1].

Hepatocellular carcinoma (HCC) in unsuspected HBV patients is a major cause of increased morbidity and mortality in low-income countries with limited resources[2,3]. While it may be too early to see the true impact of the global HBV vaccination initiative led by the WHO or treatment efforts for HBV-related HCC, evidence thus far demonstrates decreased burden of HBV and HCC in children and suggests treatment with antivirals can reduce HCC risk in some patients[4-8]. There continues to be great disparity in access to vaccines, treatment, and screening programs worldwide, however. Even where there is access, the risk of HCC in treated chronic HBV is not fully mitigated[9,10]. While concomitant liver diseases are certainly at play including co-infection with hepatitis C, aflatoxin exposure, metabolic syndrome, and alcohol use disorder, chronic HBV-related HCC has a significant global disease burden that disproportionately impacts people of different regions and demographics[9,11]. The aim of this review is to examine the impact of epidemiologic and socioeconomic factors on chronic HBV-related HCC from a global perspective. Strategies to address the resulting disparities in disease outcomes will also be discussed.

DEMOGRAPHIC FACTORS

Geographic variations

There is significant global variation in the prevalence of chronic HBV between regions. As a result, the incidence and prevalence of HBV related HCC are also quite variable between regions and correlate with rate of HBV infection[12]. About 50%-80% of HCC can be linked to HBV worldwide, and the high-risk HCC regions represent 80% of the global burden of HCC[13]. Regions such as Africa, Southeast Asia, and the Western Pacific, are considered high-risk HCC regions owed partially due to high seroprevalence of chronic HBV which is estimated at 5%-10%. On the contrary, North America and Western Europe are low-risk HCC regions with an HBV prevalence of < 1%. The Middle East and the Indian subcontinent are intermediate-risk regions with HBV prevalence of 2%-5%[14]. Data illustrating the geographic distribution of chronic HBV by prevalence is seen in Table 1 and Figure 1.

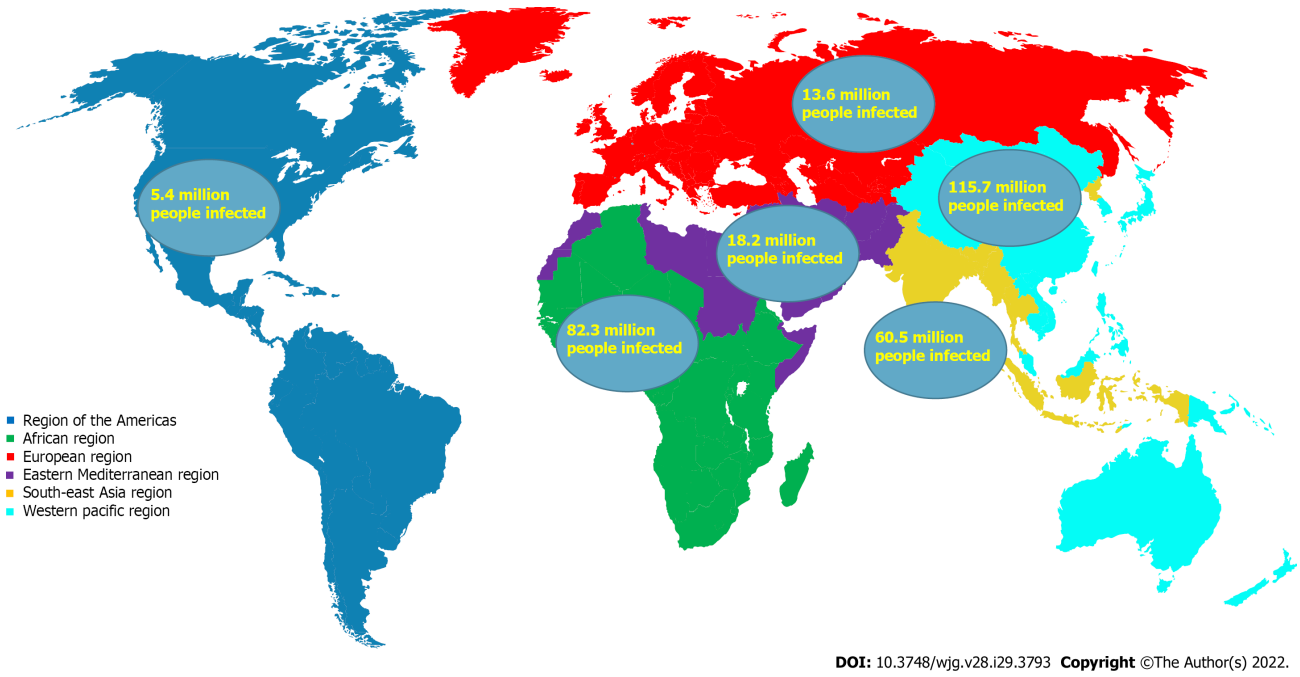
Asia and Africa

Prevalence of HBV in Asia and Africa within high-risk regions is not uniform. In Africa, particularly West Africa and Sub-Saharan Africa, complications of chronic HBV including cirrhosis and HCC are frequent and fatal due to a relative lack of vaccination, surveillance and treatment[15]. Sub Saharan Africa had an estimated vaccination rate of less than 10% and fewer than 1% of HBV infections were diagnosed in 2019[9].

In East Asia, China has a high prevalence of HBV-related HCC, estimated to be 50% of the world's burden of HCC. Mongolia has the highest incidence rate of HCC in the world at 93.7 per 100000 with HBV being the predominant risk factor[9]. However, countries of low HCC incidence also exist in the Asia-Pacific region such as Japan, India, Singapore, and Pakistan. Interestingly, Japan has a low incidence of HBV where hepatitis C virus (HCV) is the major contributor of HCC, estimated to account for 80%-90% of cases[11,14,16].

Table 1 Geographic distribution of Chronic hepatitis B virus by estimated disease burden in 2019

Geographic region[22,40]	People living with hepatitis B infection
African region	82.3 million (62.1-114.7 million)
Region of the Americas	5.4 million (3.1-12.0 million) (2.1 million in Latin America and the Caribbean)
Eastern Mediterranean region	18.2 million (14.4-23.8 million)
European region	13.6 million (10.2-22.1 million)
South-East Asia region	60.5 million (45.3-120.9 million)
Western Pacific region	115.7 million (95.2-141.9 million)



DOI: 10.3748/wjg.v28.i29.3793 **Copyright** ©The Author(s) 2022.

Figure 1 Geographic distribution of chronic hepatitis B virus.

Data from Asian nations such as India, China, Thailand and Nepal show that there are evident disparities in HBV prevalence within population sub-groups[17,18]. Surveys of the Tibetan population in Nepal's Kathmandu valley showed prevalence of chronic HBV of 10%-20% compared to the overall prevalence of 0.9% in Nepal[18]. The general population of China has an estimated HBV prevalence of 6.89% while Western provinces have a higher prevalence at 8.92%[19]. The hill tribe of Chiang Rai province in Thailand see a significantly higher prevalence of chronic HBV at 26.6% while the overall prevalence in Thailand is 5.1%[17,20]. Although Southeast Asia as a region has a higher prevalence of HBV infection at 3.0%, there are variations in prevalence between ethnicities within the region. Given the relatively high prevalence rate of chronic HBV infection in Southeast Asia compared to Europe and the Americas, the incidence of liver cancer being highest in these regions is not surprising[11,21]. Some explanations for the disparities seen in the various regions and ethnic groups include unequal access to vaccines, limited health care programs, lack of health literacy, and elements of culture and religion that also serve a role[17,19,21].

United States

Immigration from endemic countries is the main contributor to chronic HBV cases in the United States, which has a prevalence rate of 0.5% compared to 3.8% globally[21]. An estimated 70% of HBV infections in the United States are among foreign-born individuals with an estimated 730000 to 2.2 million living with chronic HBV[22]. Screening studies of foreign-born immigrants from Africa, the Middle East, and Asia have shown a higher chronic HBV prevalence rate of 10%-15% compared to 0.27%-0.50% for the general population[11,12,23,24]. Chronic HBV infection is disproportionately higher amongst Asian Americans in the United States[25]. Asian Americans comprise roughly 5%-6% of the population in the United States but 50% of the cases of chronic HBV[22].

Studies have also shown ethnic variation in HBV-related HCC within the United States, owing to differing sizes of immigrant populations from endemic countries. While rates of HCC in Asian and Pacific Islanders, once elevated are now declining, the incidence of HCC in Hispanics, Whites and African Americans continues to increase, driven mainly by HCV and non-alcoholic steatohepatitis (NASH) related cirrhosis[7,23,26-28]. Southern and Western states have the highest incidence rates of HCC in the United States[28]. While Asian Americans have the lowest mortality rates from HCC of all ethnicities, the highest mortality rates are seen in African Americans[29,30]. This apparent disparity may be partially explained by the etiology of HCC which include alcohol use disorder and HCV related cirrhosis, as well as health care disparities and access to quality care among African Americans. Recent studies show a disparity even after liver transplantation in patients with HCC, with African Americans consistently having worse survival than Asian Americans and White American patients[31].

Europe

Western Europe, like the United States, has a growing diversity in its population. Most chronic HBV infections in Western European countries are due to migrant populations, with an HBV prevalence estimated to be around 4% for migrant populations and < 1% for the general population[23,27]. There is also a greater prevalence of cirrhosis and HCC in the foreign-born population[32]. A population-based study of HCC in England found a higher proportion of HCC in non-white ethnicities, particularly due to viral hepatitis-related HCC[33]. Similar findings are reported in studies of other low HCC risk countries such as Austria, Finland, Netherlands, Germany, the United Kingdom and Denmark in which migrant populations are over-represented in cases of chronic HBV and HCC[32,34].

Latin America

There is a reported heterogeneous distribution in chronic HBV prevalence amongst Latin American countries. Owed to variation in the endemicity of HBV and underreporting, some studies report an estimated 7-12 million people infected in Central and South America and the Caribbean[35]. In contrast, a report by the Pan American Health Organization and the WHO in 2016 suggested chronic HBV seroprevalence in Latin America being 0.33% with an estimated 2.1 million infected in the general population. However, the variation in HBV serum antigen (HBsAg) seroprevalence ranged from 0.20% to 13.55% among the numerous countries[36].

In the majority of Latin America, HCV and alcoholic liver disease are the leading causes of HCC. HBV is more endemic to certain countries such as Brazil, Argentina, and Peru.

Systematic reviews and retrospective studies have shown HBV-related HCC accounting for 12%-14% of HCC in South and Central America with the countries Peru and Brazil having 20%-60% of their HCC cases related to HBV infection[37-39].

Although Latin American countries are more varied in HBV prevalence and range from low to high prevalence, overall HCC risk and burden is similarly as low as the rest of the Americas in a global context[11,36].

Gender

Chronic HBV has a greater prevalence in males than females across all geographic regions[13]. Males also have a greater incidence, prevalence, and mortality from HCC than females across geographic location and age; studies have reported a 2 to 3 times increased risk of developing HCC in males compared to females[26,27,40,41].

Regions of higher chronic HBV prevalence such as sub-Saharan Africa and Southeast Asia, tend to also have a higher male to female ratio of HCC incidence. In the United States, both sexes have shown a trend of rising incidence rates of HCC since 1975, with HBV estimated to account for 10%-15% of HCC cases[42]. The gender disparity is not completely understood but is believed to be partially due to many overlapping risk factors that are more common in males, including alcoholism, diabetes, viral hepatitis, and tobacco use[43]. In the United States, heavy alcohol usage and tobacco use is much more common in males with both being independent risk factors for incidence of HCC[43,44]. In contrast, metabolic syndrome is more common in women, with one retrospective study reporting it accountable for 32% of HCC burden in the United States[27,44].

Despite controlling for other risk factors, male sex continues to remain an independent risk factor for HCC. Studies have linked higher testosterone levels to greater incidence of HCC in chronic HBV patients and estrogen replacement therapy to reduced risk of developing HCC[42,45,46]. Serum testosterone level has been associated with upregulated inflammatory activity while estrogen has shown to have an anti-inflammatory effect by inhibition of the NF-kB pathway[46-48]. Estrogen may be protective against development of HBV-related HCC through decreasing HBV RNA transcription which could explain higher viral loads seen in male carriers of HBV[12,47]. However, studies have failed to demonstrate a benefit in survival from hormonal therapy such as flutamide, an anti-androgen, and leuprorelin, a gonadotropin-releasing hormone agonist which has anti-androgen effects[48].

Age

The average age of chronic HBV patients has continued to increase over time. A study comparing

chronic HBV patients derived from an insurance claims database of Medicaid and Medicare patients found that the median age had risen from 44.1 to 50.2 years for Medicaid patients and 48.1 to 51.8 for Medicare patients[49]. This trend has also been seen in studies from other countries. A large territory-wide cohort study conducted in Hong Kong found the mean age for Chronic HBV had increased from 41 in 2000-2004 to 55 in 2014-2017[50]. Chronic HBV is now presenting at an older median age due to longer life expectancy, under diagnosis of HBV, under screening, and delayed treatment[21,51]. There is also improved vaccine-induced immunity in the 20-49 years age group which is predicted to cause a continual upward shift in the median age of diagnosis[49].

In populations at low risk for HBV infection, such as in Western Europe and the United States where HBV in not endemic, HCC is rarely seen before the fourth decade of life with a mean age of diagnosis around 65 years[12]. In contrast, endemic regions such as Southeast Asia and sub-Saharan Africa, where > 80% of HCC cases occur, have mean ages of diagnosis about one decade earlier[42]. China has a mean age of diagnosis of HCC around 55-59 years[12]. In countries in Sub-Saharan Africa, mean age of diagnosis of HCC is 35-50 years, and found to be almost 20 years later in those Black Africans who migrate from a rural to city setting[12,52].

With the advent of the HBV vaccine in 1981, and the universal vaccination programs that began in the 1990s, there was a new focus on vaccination of newborns. As of 2020, 190 WHO member countries vaccinated newborns as part of their routine vaccination schedules, and global coverage with all 3 doses of HBV vaccine was estimated to be 83%[53]. This campaign also included recommendations to vaccinate high-risk adult populations, adolescents who had missed immunization, and advocated for societal awareness of the risks and consequences of HBV[22]. Asian males who are HBV carriers continue to present with HCC at a relatively young age[54]. This may be related to viral factors such as genotype. Genotype B is more commonly seen in the Asian demographic and has been associated with onset of HCC in patients under 50 years of age, with one study from Taiwan finding that more than 90% under 35 years of age had genotype B HBV[47,55]. Genotype C is associated with the highest risk of developing HCC in patients aged > 50 years[56]. Genotype F has been seen in Alaskan Native populations to have the greatest risk of developing HCC at a lower median age, with the annual incidence rate amongst men at 387/100000 and 63/100000 for women[57]. In contrast, genotypes A, D are less frequently associated with development of HCC and more common in North American and European populations[58].

Socioeconomic status

Patients belonging to low socio-economic status are at significant disadvantage due to low health literacy, limited healthcare resources and access-including lack of insurance or ability to pay for care, especially for care of preventable diseases such as HBV. Hepatitis B is very infectious as it can be transmitted by contact with blood or bodily fluids, sexual intercourse and vertically from mother to baby. Vertical transmission is the most common mode of transmission in the developing world and can be dramatically reduced by HBV vaccination and use of anti-viral medications during third trimester [7]. Horizontal transmission seems to be more common in low prevalence regions[13,22]. While Hepatitis B viral load is considered one of the strongest predictors of HCC risk and can be managed with anti-viral medications, unfortunately, even in low-risk regions such as United States, roughly 3% of people currently living with chronic HBV are on treatment[14,21]. Several studies have shown the impact of socioeconomic status (SES) on health outcomes in cancer with populations of lower SES and less wealthy nations having significantly lower survival rates[32,59-61]. One retrospective analysis of European nations found nearly 20% variation in all-cancer relative survival between the least wealthy and most wealthy nations[61]. Similarly, low SES groups are associated with a variety of risk factors for poor outcomes in chronic HBV-related HCC. Despite 5-year survival rate for HCC in the United States increasing to 18% in 2019, the greatest benefits in survival and mortality are seen in groups with higher SES, while higher HCC incidence, later stage of diagnosis, and lower survival rates are seen in low-SES status groups[28,40]. Disadvantaged groups are typically minority ethnic groups such as African Americans and Hispanics as they tend to live in areas with the highest rates of family poverty, unemployment and high-school dropouts and thus may be associated with greater risk for HCC due to less access to screening and treatment[62].

Among patients with Medicaid insurance, the presence of comorbidities such as obesity, diabetes, alcohol, and tobacco use disorders combined with lower educational attainment contribute to liver disease such as alcoholic and NASH (ASH/NASH) and significantly overlap with liver disease from chronic HBV[63,64].

METHODS TO ADDRESS DISPARITIES

Targeted screening and prevention

Globally, chronic HBV and HCC cases are underdiagnosed. The 2016 Polaris Observatory study estimated that only 10% of infected people were diagnosed with HBV[51]. Chronic HBV infection is often asymptomatic and requires greater emphasis on screening, especially considering that HBV can

lead to HCC in patients without cirrhosis[13,42,65]. There is a geographic disparity in screening: About 2% of people with HBV knew their status in 2019 in Africa *vs* 22% in the Americas and 19% in the European region[21]. Additionally, there is likely underestimation of the true number of chronic HBV in the United States and other regions because high-risk populations have historically been under-represented in national surveys and surveillance studies, especially considering the large influx of yearly immigration to the US[24].

Early detection of tumors from screening in chronic HBV improves overall survival. A Randomized Controlled Trial study in Shanghai found that biannual screening in chronic HBV patients reduced HCC mortality by 37%[66]. An estimated 70% of liver cancer cases are preventable with risk factor modification and screening, thus judicious screening of high-risk populations with use of evidence-based guidelines can significantly reduce mortality from chronic HBV-related HCC[40]. The the American Association for the Study of Liver Diseases (AASLD) recommends HCC surveillance with ultrasound with or without AFP for all patients with diagnosed cirrhosis, and chronic HBV carriers who are high risk including African Americans older than 20 years, Asians older than 40 years, and those with family history of HCC. However, less than 1 in 5 high-risk patients are regularly screened[67]. Although greater than 90% of patients with acute HBV experience resolution of disease and the small minority develop chronic HBV infection, 40% of chronic HBV patients go on to develop cirrhosis, liver failure and HCC, and up to 25% of patients with chronic HBV end up dying from cirrhosis or HCC; thus HCC screening has been found cost-effective in patients with HBV even without cirrhosis when incidence of HCC is greater than 0.2% per year[67,68].

Health literacy

Lack of health literacy is particularly apparent in vulnerable and underserved populations such as immigrant populations, Mexican Americans, and African Americans, who already disproportionately bear the burden of chronic HBV and HCC[69,70]. Increasing social awareness of risk factors and protective factors of chronic HBV can be an avenue to improve health literacy. Social media is used by much of the developed world. For example, World Hepatitis Day is an annual health education campaign led by the WHO in July that heavily utilizes social media to make a call to action to bolster efforts in prevention, screening, treatment and to spread awareness of viral hepatitis[71]. Culturally sensitive approaches are necessary with an increasingly diverse population of the United States, to effectively communicate with various ethnic groups. One such example is "photo novels" developed to cater to specific cultures which have been shown to be effective in increasing HBV awareness and screening in underserved populations[72].

In many developing countries, such as those in Sub-Saharan Africa and the Asia-Pacific region where the majority of global chronic HBV and HCC cases occur, there is limited knowledge of hepatitis B and the benefits of the HBV vaccine[1,11,12,73]. Only two percent of the patients in African and Southeast Asian regions were aware of their chronic HBV status in 2019[1]. There is a dire need for informational campaigns in these endemic regions to increase awareness and health education amongst vulnerable populations in addition to the national immunization programs that must be initiated at the federal level with support from international health organizations.

CONCLUSION

Chronic HBV infection continues to have significant impact globally despite escalating vaccine coverage, screening techniques and availability of anti-viral medications. The close geographic relationship between endemic chronic HBV and increased burden of HCC remains to this day in Africa and the Asia-Pacific regions comprising the vast majority of HBV-related HCC in the world. HBV and HCC disproportionately affect certain ethnic groups within the United States and worldwide, many of which are of low SES. Men and the elderly are disproportionally affected at greater rates. To mitigate this largely preventable disease, enhanced access to screening, vaccinations, surveillance, and treatment must be achieved to reduce the burden of chronic HBV and HCC worldwide.

FOOTNOTES

Author contributions: Gnyawali B and Mumtaz K contributed to the conception of the review; Gnyawali B and Pusateri A performed a review of the current literature; Gnyawali B drafted the manuscript; Pusateri A, Nickerson A, Mumtaz K, and Jalil S added key information and revised the manuscript; all authors read and approved the final manuscript.

Conflict-of-interest statement: There are no conflicts of interest to report.

Open-Access: This article is an open-access article that was selected by an in-house editor and fully peer-reviewed by external reviewers. It is distributed in accordance with the Creative Commons Attribution NonCommercial (CC BY-

NC 4.0) license, which permits others to distribute, remix, adapt, build upon this work non-commercially, and license their derivative works on different terms, provided the original work is properly cited and the use is non-commercial. See: https://creativecommons.org/Licenses/by-nc/4.0/

Country/Territory of origin: United States

ORCID number: Bipul Gnyawali 0000-0003-4745-2787; Antoinette Pusateri 0000-0002-8458-7827; Ashley Nickerson 0000-0002-4494-9985; Sajid Jalil 0000-0001-6123-153X; Khalid Mumtaz 0000-0001-7868-6514.

S-Editor: Chen YL
L-Editor: A
P-Editor: Chen YL

REFERENCES

1 **World Health Organization**. Global progress report on HIV, viral hepatitis and sexually transmitted infections, 2021: accountability for the global health sector strategies 2016–2021: actions for impact: web annex 2: data methods. July 15, 2021. [Cited 2 January 2022]. Available from: https://www.who.int/publications/i/item/9789240027077 [DOI: 10.1093/med/9780198816805.003.0070]
2 **Beasley RP**. Rocks along the road to the control of HBV and HCC. *Ann Epidemiol* 2009; **19**: 231-234 [PMID: 19344859 DOI: 10.1016/j.annepidem.2009.01.017]
3 **Schweitzer A**, Horn J, Mikolajczyk RT, Krause G, Ott JJ. Estimations of worldwide prevalence of chronic hepatitis B virus infection: a systematic review of data published between 1965 and 2013. *Lancet* 2015; **386**: 1546-1555 [PMID: 26231459 DOI: 10.1016/S0140-6736(15)61412-X]
4 **Chang MH**, Chen CJ, Lai MS, Hsu HM, Wu TC, Kong MS, Liang DC, Shau WY, Chen DS. Universal hepatitis B vaccination in Taiwan and the incidence of hepatocellular carcinoma in children. Taiwan Childhood Hepatoma Study Group. *N Engl J Med* 1997; **336**: 1855-1859 [PMID: 9197213 DOI: 10.1056/nejm199706263362602]
5 **McMahon BJ**, Bulkow LR, Singleton RJ, Williams J, Snowball M, Homan C, Parkinson AJ. Elimination of hepatocellular carcinoma and acute hepatitis B in children 25 years after a hepatitis B newborn and catch-up immunization program. *Hepatology* 2011; **54**: 801-807 [PMID: 21618565 DOI: 10.1002/hep.24442]
6 **Ni YH**, Chen DS. Hepatitis B vaccination in children: the Taiwan experience. *Pathol Biol (Paris)* 2010; **58**: 296-300 [PMID: 20116181 DOI: 10.1016/j.patbio.2009.11.002]
7 **Petrick JL**, McGlynn KA. The changing epidemiology of primary liver cancer. *Curr Epidemiol Rep* 2019; **6**: 104-111 [PMID: 31259140 DOI: 10.1007/s40471-019-00188-3]
8 **Kuang XJ**, Jia RR, Huo RR, Yu JJ, Wang JJ, Xiang BD, Li LQ, Peng Z, Zhong JH. Systematic review of risk factors of hepatocellular carcinoma after hepatitis B surface antigen seroclearance. *J Viral Hepat* 2018; **25**: 1026-1037 [PMID: 29624821 DOI: 10.1111/jvh.12905]
9 **Petrick JL**, Florio AA, Znaor A, Ruggieri D, Laversanne M, Alvarez CS, Ferlay J, Valery PC, Bray F, McGlynn KA. International trends in hepatocellular carcinoma incidence, 1978-2012. *Int J Cancer* 2020; **147**: 317-330 [PMID: 31597196 DOI: 10.1002/ijc.32723]
10 **Vallet-Pichard A**, Pol S. Review article: immunisation against hepatitis B virus infection and the prevention of hepatocellular carcinoma. *Aliment Pharmacol Ther* 2021; **53**: 1166-1182 [PMID: 33909923 DOI: 10.1111/apt.16356]
11 **Bray F**, Ferlay J, Soerjomataram I, Siegel RL, Torre LA, Jemal A. Global cancer statistics 2018: GLOBOCAN estimates of incidence and mortality worldwide for 36 cancers in 185 countries. *CA Cancer J Clin* 2018; **68**: 394-424 [PMID: 30207593 DOI: 10.3322/caac.21492]
12 **El-Serag HB**. Epidemiology of viral hepatitis and hepatocellular carcinoma. *Gastroenterology* 2012; **142**: 1264-1273.e1 [PMID: 22537432 DOI: 10.1053/j.gastro.2011.12.061]
13 **Petruzziello A**. Epidemiology of Hepatitis B Virus (HBV) and Hepatitis C Virus (HCV) Related Hepatocellular Carcinoma. *Open Virol J* 2018; **12**: 26-32 [PMID: 29541276 DOI: 10.2174/1874357901812010026]
14 **Ringelhan M**, McKeating JA, Protzer U. Viral hepatitis and liver cancer. *Philos Trans R Soc Lond B Biol Sci* 2017; **372** [PMID: 28893941 DOI: 10.1098/rstb.2016.0274]
15 **Lemoine M**, Thursz MR. Battlefield against hepatitis B infection and HCC in Africa. *J Hepatol* 2017; **66**: 645-654 [PMID: 27771453 DOI: 10.1016/j.jhep.2016.10.013]
16 **Altekruse SF**, McGlynn KA, Reichman ME. Hepatocellular carcinoma incidence, mortality, and survival trends in the United States from 1975 to 2005. *J Clin Oncol* 2009; **27**: 1485-1491 [PMID: 19224838 DOI: 10.1200/JCO.2008.20.7753]
17 **Upala P**, Apidechkul T, Tamornpark R, Chomchoei C, Yeemard F. Seroprevalence and factors associated with hepatitis B infection among the hill tribe adult population in Thailand: a cross-sectional study. *BMC Infect Dis* 2020; **20**: 494 [PMID: 32650741 DOI: 10.1186/s12879-020-05221-1]
18 **Naveira MCM**, Badal K, Dhakal J, Mayer NA, Pokharel B, Del Prado RF. Seroprevalence of hepatitis B and C in Nepal: a systematic review (1973-2017). *Hepatol Med Policy* 2018; **3**: 10 [PMID: 30288333 DOI: 10.1186/s41124-018-0039-2]
19 **Wang H**, Men P, Xiao Y, Gao P, Lv M, Yuan Q, Chen W, Bai S, Wu J. Hepatitis B infection in the general population of China: a systematic review and meta-analysis. *BMC Infect Dis* 2019; **19**: 811 [PMID: 31533643 DOI: 10.1186/s12879-019-4428-y]
20 **Leroi C**, Adam P, Khamduang W, Kawilapat S, Ngo-Giang-Huong N, Ongwandee S, Jiamsiri S, Jourdain G. Prevalence of chronic hepatitis B virus infection in Thailand: a systematic review and meta-analysis. *Int J Infect Dis* 2016; **51**: 36-43

[PMID: 27580678 DOI: 10.1016/j.ijid.2016.08.017]

21 **World Health Organization**. Global progress report on HIV, viral hepatitis and sexually transmitted infections. July 15, 2021. [Cited 2 January 2022]. Available from: http://apps.who.int/iris/bitstream/handle/10665/342808/9789240030985-eng.pdf

22 **Nelson NP**, Easterbrook PJ, McMahon BJ. Epidemiology of Hepatitis B Virus Infection and Impact of Vaccination on Disease. *Clin Liver Dis* 2016; **20**: 607-628 [PMID: 27742003 DOI: 10.1016/j.cld.2016.06.006]

23 **Chang ET**, Keegan TH, Gomez SL, Le GM, Clarke CA, So SK, Glaser SL. The burden of liver cancer in Asians and Pacific Islanders in the Greater San Francisco Bay Area, 1990 through 2004. *Cancer* 2007; **109**: 2100-2108 [PMID: 17385214 DOI: 10.1002/cncr.22642]

24 **Cohen C**, Evans AA, London WT, Block J, Conti M, Block T. Underestimation of chronic hepatitis B virus infection in the United States of America. *J Viral Hepat* 2008; **15**: 12-13 [PMID: 18088239 DOI: 10.1111/j.1365-2893.2007.00888.x]

25 **Kim HS**, Rotundo L, Yang JD, Kim D, Kothari N, Feurdean M, Ruhl C, Unalp-Arida A. Racial/ethnic disparities in the prevalence and awareness of Hepatitis B virus infection and immunity in the United States. *J Viral Hepat* 2017; **24**: 1052-1066 [PMID: 28581638 DOI: 10.1111/jvh.12735]

26 **Petrick JL**, Kelly SP, Altekruse SF, McGlynn KA, Rosenberg PS. Future of Hepatocellular Carcinoma Incidence in the United States Forecast Through 2030. *J Clin Oncol* 2016; **34**: 1787-1794 [PMID: 27044939 DOI: 10.1200/JCO.2015.64.7412]

27 **Ajayi F**, Jan J, Singal AG, Rich NE. Racial and Sex Disparities in Hepatocellular Carcinoma in the USA. *Curr Hepatol Rep* 2020; **19**: 462-469 [PMID: 33828937 DOI: 10.1007/s11901-020-00554-6]

28 **Flores YN**, Datta GD, Yang L, Corona E, Devineni D, Glenn BA, Bastani R, May FP. Disparities in Hepatocellular Carcinoma Incidence, Stage, and Survival: A Large Population-Based Study. *Cancer Epidemiol Biomarkers Prev* 2021; **30**: 1193-1199 [PMID: 33737301 DOI: 10.1158/1055-9965.EPI-20-1088]

29 **Li J**, Hansen BE, Peppelenbosch MP, De Man RA, Pan Q, Sprengers D. Factors associated with ethnical disparity in overall survival for patients with hepatocellular carcinoma. *Oncotarget* 2017; **8**: 15193-15204 [PMID: 28122352 DOI: 10.18632/oncotarget.14771]

30 **Ren F**, Zhang J, Gao Z, Zhu H, Chen X, Liu W, Xue Z, Gao W, Wu R, Lv Y, Hu L. Racial disparities in the survival time of patients with hepatocellular carcinoma and intrahepatic cholangiocarcinoma between Chinese patients and patients of other racial groups: A population-based study from 2004 to 2013. *Oncol Lett* 2018; **16**: 7102-7116 [PMID: 30546445 DOI: 10.3892/ol.2018.9550]

31 **Njei B**, Ditah I, Lim JK. Persistent racial disparities in survival among u.s. Adults with hepatocellular carcinoma after liver transplantation: the paradox of all-cause and cause-specific mortality. *Gastrointest Cancer Res* 2013; **6**: 73-74 [PMID: 23936546]

32 **Koc ÖM**, Robaeys G, Yildirim B, Posthouwer D, Hens N, Koek GH. The influence of ethnicity on disease outcome in patients with chronic hepatitis B infection. *J Med Virol* 2019; **91**: 623-629 [PMID: 30381836 DOI: 10.1002/jmv.25353]

33 **Burton A**, Balachandrakumar VK, Driver RJ, Tataru D, Paley L, Marshall A, Alexander G, Rowe IA; HCC-UK/BASL/NCRAS Partnership, Palmer DH, Cross TJS. Regional variations in hepatocellular carcinoma incidence, routes to diagnosis, treatment and survival in England. *Br J Cancer* 2022; **126**: 804-814 [PMID: 34837073 DOI: 10.1038/s41416-021-01509-4]

34 **Chu JJ**, Wörmann T, Popp J, Pätzelt G, Akmatov MK, Krämer A, Reintjes R. Changing epidemiology of hepatitis B and migration--a comparison of six Northern and North-Western European countries. *Eur J Public Health* 2013; **23**: 642-647 [PMID: 23132874 DOI: 10.1093/eurpub/cks067]

35 **Roman S**, Jose-Abrego A, Fierro NA, Escobedo-Melendez G, Ojeda-Granados C, Martinez-Lopez E, Panduro A. Hepatitis B virus infection in Latin America: a genomic medicine approach. *World J Gastroenterol* 2014; **20**: 7181-7196 [PMID: 24966588 DOI: 10.3748/wjg.v20.i23.7181]

36 **Organization PAH**. Hepatitis B and C in the Spotlight: A public health response in the Americas. 2016. [Cited 2 January 2022]. Available from: https://iris.paho.org/bitstream/handle/10665.2/31449/9789275119297-eng.pdf?sequence=5&isAllowed=y

37 **de Martel C**, Maucort-Boulch D, Plummer M, Franceschi S. World-wide relative contribution of hepatitis B and C viruses in hepatocellular carcinoma. *Hepatology* 2015; **62**: 1190-1200 [PMID: 26146815 DOI: 10.1002/hep.27969]

38 **Debes JD**, Chan AJ, Balderramo D, Kikuchi L, Gonzalez Ballerga E, Prieto JE, Tapias M, Idrovo V, Davalos MB, Cairo F, Barreyro FJ, Paredes S, Hernandez N, Avendaño K, Diaz Ferrer J, Yang JD, Carrera E, Garcia JA, Mattos AZ, Hirsch BS, Gonçalves PT, Carrilho FJ, Roberts LR. Hepatocellular carcinoma in South America: Evaluation of risk factors, demographics and therapy. *Liver Int* 2018; **38**: 136-143 [PMID: 28640517 DOI: 10.1111/liv.13502]

39 **Chan AJ**, Balderramo D, Kikuchi L, Ballerga EG, Prieto JE, Tapias M, Idrovo V, Davalos MB, Cairo F, Barreyro FJ, Paredes S, Hernandez N, Avendaño K, Ferrer JD, Yang JD, Carrera E, Mattos AZ, Hirsch BS, Gonçalves PT, Carrilho FJ, Roberts LR, Debes JD. Early Age Hepatocellular Carcinoma Associated With Hepatitis B Infection in South America. *Clin Gastroenterol Hepatol* 2017; **15**: 1631-1632 [PMID: 28532694 DOI: 10.1016/j.cgh.2017.05.015]

40 **American Cancer Society**. Cancer Facts and Figures 2019. 2019. [cited 14 Jan 2022]. Available from: https://www.cancer.org/ [DOI: 10.1080/15398285.2012.701177]

41 **Cook MB**, Dawsey SM, Freedman ND, Inskip PD, Wichner SM, Quraishi SM, Devesa SS, McGlynn KA. Sex disparities in cancer incidence by period and age. *Cancer Epidemiol Biomarkers Prev* 2009; **18**: 1174-1182 [PMID: 19293308 DOI: 10.1158/1055-9965.EPI-08-1118]

42 **Mittal S**, El-Serag HB. Epidemiology of hepatocellular carcinoma: consider the population. *J Clin Gastroenterol* 2013; **47** Suppl: S2-S6 [PMID: 23632345 DOI: 10.1097/MCG.0b013e3182872f29]

43 **Wu EM**, Wong LL, Hernandez BY, Ji JF, Jia W, Kwee SA, Kalathil S. Gender differences in hepatocellular cancer: disparities in nonalcoholic fatty liver disease/steatohepatitis and liver transplantation. *Hepatoma Res* 2018; **4** [PMID: 30687780 DOI: 10.20517/2394-5079.2018.87]

44 **Welzel TM**, Graubard BI, Quraishi S, Zeuzem S, Davila JA, El-Serag HB, McGlynn KA. Population-attributable fractions of risk factors for hepatocellular carcinoma in the United States. *Am J Gastroenterol* 2013; **108**: 1314-1321 [PMID:

23752878 DOI: 10.1038/ajg.2013.160]
45 **Yip TC**, Wong GL, Chan HL, Tse YK, Liang LY, Hui VW, Lee HW, Lui GC, Kong AP, Wong VW. Elevated testosterone increases risk of hepatocellular carcinoma in men with chronic hepatitis B and diabetes mellitus. *J Gastroenterol Hepatol* 2020; **35**: 2210-2219 [PMID: 32343449 DOI: 10.1111/jgh.15079]
46 **Hassan MM**, Botrus G, Abdel-Wahab R, Wolff RA, Li D, Tweardy D, Phan AT, Hawk E, Javle M, Lee JS, Torres HA, Rashid A, Lenzi R, Hassabo HM, Abaza Y, Shalaby AS, Lacin S, Morris J, Patt YZ, Amos CI, Khaderi SA, Goss JA, Jalal PK, Kaseb AO. Estrogen Replacement Reduces Risk and Increases Survival Times of Women With Hepatocellular Carcinoma. *Clin Gastroenterol Hepatol* 2017; **15**: 1791-1799 [PMID: 28579181 DOI: 10.1016/j.cgh.2017.05.036]
47 **Liu CJ**, Kao JH. Hepatitis B virus-related hepatocellular carcinoma: epidemiology and pathogenic role of viral factors. *J Chin Med Assoc* 2007; **70**: 141-145 [PMID: 17475593 DOI: 10.1016/S1726-4901(09)70346-6]
48 **Zhang H**, Spencer K, Burley SK, Zheng XFS. Toward improving androgen receptor-targeted therapies in male-dominant hepatocellular carcinoma. *Drug Discov Today* 2021; **26**: 1539-1546 [PMID: 33561464 DOI: 10.1016/j.drudis.2021.02.001]
49 **Nguyen MH**, Lim JK, Burak Ozbay A, Fraysse J, Liou I, Meyer N, Dusheiko G, Gordon SC. Advancing Age and Comorbidity in a US Insured Population-Based Cohort of Patients With Chronic Hepatitis B. *Hepatology* 2019; **69**: 959-973 [PMID: 30175482 DOI: 10.1002/hep.30246]
50 **Lai JC**, Wong VW, Yip TC, Hui VW, Tse YK, Lee HW, Liang LY, Lui GC, Chan HL, Wong GL. Secular trend of treatment uptake in patients with chronic hepatitis B: A territory-wide study of 135 395 patients from 2000 to 2017. *J Gastroenterol Hepatol* 2021; **36**: 3487-3499 [PMID: 34404113 DOI: 10.1111/jgh.15664]
51 **Lim JK**, Nguyen MH, Kim WR, Gish R, Perumalswami P, Jacobson IM. Prevalence of Chronic Hepatitis B Virus Infection in the United States. *Am J Gastroenterol* 2020; **115**: 1429-1438 [PMID: 32483003 DOI: 10.14309/ajg.0000000000000651]
52 **Kew MC**. Epidemiology of hepatocellular carcinoma in sub-Saharan Africa. *Ann Hepatol* 2013; **12**: 173-182 [PMID: 23396727]
53 **World Health Organization**. Immunization coverage. 15 July 2021. [cited 11 Jan 2022]. Available from: https://www.who.int/publications [DOI: 10.2471/blt.10.020910]
54 **Goh MJ**, Kang W, Kim KM, Sinn DH, Gwak GY, Paik YH, Choi MS, Lee JH, Koh KC, Paik SW. Incidence and risk factors for development of hepatocellular carcinoma at young age in patients with chronic hepatitis B. *Scand J Gastroenterol* 2022; **57**: 70-77 [PMID: 34731072 DOI: 10.1080/00365521.2021.1988700]
55 **Gomaa AI**, Khan SA, Toledano MB, Waked I, Taylor-Robinson SD. Hepatocellular carcinoma: epidemiology, risk factors and pathogenesis. *World J Gastroenterol* 2008; **14**: 4300-4308 [PMID: 18666317 DOI: 10.3748/wjg.14.4300]
56 **Zhu RX**, Seto WK, Lai CL, Yuen MF. Epidemiology of Hepatocellular Carcinoma in the Asia-Pacific Region. *Gut Liver* 2016; **10**: 332-339 [PMID: 27114433 DOI: 10.5009/gnl15257]
57 **Livingston SE**, Simonetti JP, McMahon BJ, Bulkow LR, Hurlburt KJ, Homan CE, Snowball MM, Cagle HH, Williams JL, Chulanov VP. Hepatitis B virus genotypes in Alaska Native people with hepatocellular carcinoma: preponderance of genotype F. *J Infect Dis* 2007; **195**: 5-11 [PMID: 17152003 DOI: 10.1086/509894]
58 **Wong GL**, Chan HL, Yiu KK, Lai JW, Chan VK, Cheung KK, Wong EW, Wong VW. Meta-analysis: The association of hepatitis B virus genotypes and hepatocellular carcinoma. *Aliment Pharmacol Ther* 2013; **37**: 517-526 [PMID: 23305043 DOI: 10.1111/apt.12207]
59 **Ohikere K**, Chitnis AS, Hahambis TA, Singal A, Wong RJ. Ethnic Minorities and Low Socioeconomic Status Patients With Chronic Liver Disease Are at Greatest Risk of Being Uninsured. *Gastroenterology Res* 2021; **14**: 313-323 [PMID: 35059065 DOI: 10.14740/gr1439]
60 **Quaglia A**, Lillini R, Mamo C, Ivaldi E, Vercelli M; SEIH (Socio-Economic Indicators, Health) Working Group. Socio-economic inequalities: a review of methodological issues and the relationships with cancer survival. *Crit Rev Oncol Hematol* 2013; **85**: 266-277 [PMID: 22999326 DOI: 10.1016/j.critrevonc.2012.08.007]
61 **Verdecchia A**, Baili P, Quaglia A, Kunkler I, Ciampichini R, Berrino F, Micheli A. Patient survival for all cancers combined as indicator of cancer control in Europe. *Eur J Public Health* 2008; **18**: 527-532 [PMID: 18417498 DOI: 10.1093/eurpub/ckn022]
62 **Shebl FM**, Capo-Ramos DE, Graubard BI, McGlynn KA, Altekruse SF. Socioeconomic status and hepatocellular carcinoma in the United States. *Cancer Epidemiol Biomarkers Prev* 2012; **21**: 1330-1335 [PMID: 22669949 DOI: 10.1158/1055-9965.EPI-12-0124]
63 **Yuan JM**, Govindarajan S, Arakawa K, Yu MC. Synergism of alcohol, diabetes, and viral hepatitis on the risk of hepatocellular carcinoma in blacks and whites in the U.S. *Cancer* 2004; **101**: 1009-1017 [PMID: 15329910 DOI: 10.1002/cncr.20427]
64 **Flores YN**, Yee HF Jr, Leng M, Escarce JJ, Bastani R, Salmerón J, Morales LS. Risk factors for chronic liver disease in Blacks, Mexican Americans, and Whites in the United States: results from NHANES IV, 1999-2004. *Am J Gastroenterol* 2008; **103**: 2231-2238 [PMID: 18671818 DOI: 10.1111/j.1572-0241.2008.02022.x]
65 **Stewart SL**, Kwong SL, Bowlus CL, Nguyen TT, Maxwell AE, Bastani R, Chak EW, Chen MS Jr. Racial/ethnic disparities in hepatocellular carcinoma treatment and survival in California, 1988-2012. *World J Gastroenterol* 2016; **22**: 8584-8595 [PMID: 27784971 DOI: 10.3748/wjg.v22.i38.8584]
66 **Zhang BH**, Yang BH, Tang ZY. Randomized controlled trial of screening for hepatocellular carcinoma. *J Cancer Res Clin Oncol* 2004; **130**: 417-422 [PMID: 15042359 DOI: 10.1007/s00432-004-0552-0]
67 **Frenette CT**, Isaacson AJ, Bargellini I, Saab S, Singal AG. A Practical Guideline for Hepatocellular Carcinoma Screening in Patients at Risk. *Mayo Clin Proc Innov Qual Outcomes* 2019; **3**: 302-310 [PMID: 31485568 DOI: 10.1016/j.mayocpiqo.2019.04.005]
68 **Chang MS**, Nguyen MH. Epidemiology of hepatitis B and the role of vaccination. *Best Pract Res Clin Gastroenterol* 2017; **31**: 239-247 [PMID: 28774405 DOI: 10.1016/j.bpg.2017.05.008]
69 **Samant H**, Amiri HS, Zibari GB. Addressing the worldwide hepatocellular carcinoma: epidemiology, prevention and management. *J Gastrointest Oncol* 2021; **12**: S361-S373 [PMID: 34422400 DOI: 10.21037/jgo.2020.02.08]
70 **Hyun S**, Ko O, Kim S, Ventura WR. Sociocultural barriers to hepatitis B health literacy in an immigrant population: a focus group study in Korean Americans. *BMC Public Health* 2021; **21**: 404 [PMID: 33632203 DOI:

10.1186/s12889-021-10441-4]
71 World Hepatitis Day - July 28, 2018. *MMWR Morb Mortal Wkly Rep* 2018; **67**: 773 [PMID: 30024865 DOI: 10.15585/mmwr.mm6728a1]
72 **Lee S**, Yoon H, Chen L, Juon HS. Culturally appropriate photonovel development and process evaluation for hepatitis B prevention in Chinese, Korean, and Vietnamese American communities. *Health Educ Behav* 2013; **40**: 694-703 [PMID: 23372031 DOI: 10.1177/1090198112474003]
73 **Machmud PB**, Glasauer S, Gottschick C, Mikolajczyk R. Knowledge, Vaccination Status, and Reasons for Avoiding Vaccinations against Hepatitis B in Developing Countries: A Systematic Review. *Vaccines (Basel)* 2021; **9** [PMID: 34207829 DOI: 10.3390/vaccines9060625]

World Journal of Gastroenterology

Submit a Manuscript: https://www.f6publishing.com

World J Gastroenterol 2022 August 7; 28(29): 3803-3813

DOI: 10.3748/wjg.v28.i29.3803

ISSN 1007-9327 (print) ISSN 2219-2840 (online)

MINIREVIEWS

Endoscopic salvage therapy after failed biliary cannulation using advanced techniques: A concise review

Yung-Kuan Tsou, Kuang-Tse Pan, Mu Hsien Lee, Cheng-Hui Lin

Specialty type: Gastroenterology and hepatology

Provenance and peer review: Invited article; Externally peer reviewed.

Peer-review model: Single blind

Peer-review report's scientific quality classification
Grade A (Excellent): 0
Grade B (Very good): B
Grade C (Good): C
Grade D (Fair): 0
Grade E (Poor): 0

P-Reviewer: Hou XH, China; Martino A, Italy

Received: February 13, 2022
Peer-review started: February 13, 2022
First decision: April 5, 2022
Revised: April 15, 2022
Accepted: July 5, 2022
Article in press: July 5, 2022
Published online: August 7, 2022

Yung-Kuan Tsou, Mu Hsien Lee, Cheng-Hui Lin, Department of Gastroenterology and Hepatology, Chang Gung Memorial Hospital, Taoyuan 333, Taiwan

Yung-Kuan Tsou, Kuang-Tse Pan, Mu Hsien Lee, Cheng-Hui Lin, Department of Medicine, Chang Gung University, Taoyuan 333, Taiwan

Kuang-Tse Pan, Department of Medical Imaging and Intervention, Chang Gung Memorial Hospital, Taoyuan 333, Taiwan

Corresponding author: Cheng-Hui Lin, MD, Doctor, Department of Gastroenterology and Hepatology, Chang Gung Memorial Hospital, No. 5 Fu-Shin Street, Kweishan, Taoyuan 333, Taiwan. linchehui@adm.cgmh.org.tw

Abstract

Therapeutic endoscopic retrograde cholangiopancreatography (ERCP) begins with successful biliary cannulation. However, it is not always be successful. The failure of the initial ERCP is attributed to two main aspects: the papilla/biliary orifice is endoscopically accessible, or it is inaccessible. When the papilla/biliary orifice is accessible, bile duct cannulation failure can occur even with advanced cannulation techniques, including double guidewire techniques, transpancreatic sphincterotomy, needle-knife precut papillotomy, or fistulotomy. There is currently no consensus on the next steps of treatment in this setting. Therefore, this review aims to propose and discuss potential endoscopic options for patients who have failed ERCP due to difficult bile duct cannulation. These options include interval ERCP, percutaneous-transhepatic-endoscopic rendezvous procedures (PTE-RV), and endoscopic ultrasound-assisted rendezvous procedures (EUS-RV). The overall success rate for interval ERCP was 76.3% (68%-79% between studies), and the overall adverse event rate was 7.5% (0-15.9% between studies). The overall success rate for PTE-RV was 88.7% (80.4%-100% between studies), and the overall adverse event rate was 13.2% (4.9%-19.2% between studies). For EUS-RV, the overall success rate was 82%-86.1%, and the overall adverse event rate was 13%-15.6%. Because interval ERCP has an acceptably high success rate and lower adverse event rate and does not require additional expertise, facilities, or other specialists, it can be considered the first choice for salvage therapy. EUS-RV can also be considered if local experts are available. For patients in urgent need of biliary drainage, PTE-RV should be considered.

Key Words: Difficult biliary cannulation; Endoscopic ultrasound; Rendezvous; Endoscopic retrograde cholangiopancreatography; Percutaneous transhepatic biliary drainage; Interval

©The Author(s) 2022. Published by Baishideng Publishing Group Inc. All rights reserved.

Core Tip: Three endoscopic salvage therapies are available for endoscopic retrograde cholangiopancreatography (ERCP) cannulation failure, but consensus is lacking. This review found that interval ERCP had an overall success rate of 76.3% and an adverse event rate of 7.5%. Percutaneous-transhepatic-endoscopic rendezvous procedure (PTE-RV) had an overall success rate of 88.7% and an adverse event rate of 13.2%. Endoscopic ultrasound-assisted rendezvous procedures (EUS-RV) had an overall success rate of 82%-86.1% and an adverse event rate of 13%-15.6%. Interval ERCP may be preferred, but EUS-RV may also be considered if a local expert is available. PTE-RV is reserved for patients requiring urgent biliary drainage.

Citation: Tsou YK, Pan KT, Lee MH, Lin CH. Endoscopic salvage therapy after failed biliary cannulation using advanced techniques: A concise review. *World J Gastroenterol* 2022; 28(29): 3803-3813
URL: https://www.wjgnet.com/1007-9327/full/v28/i29/3803.htm
DOI: https://dx.doi.org/10.3748/wjg.v28.i29.3803

INTRODUCTION

Endoscopic retrograde cholangiopancreatography (ERCP) has become the treatment of choice for biliary tract diseases in recent decades. Selective biliary cannulation (SBC) is a critical step in the success of therapeutic ERCP; however, it is not always successful, even for experienced endoscopists[1]. The failure to achieve SBC during the initial ERCP can be attributed to two main aspects: an endoscopically inaccessible papilla/biliary orifice; and an endoscopically accessible papilla/biliary orifice but failed SBC with available cannulation methods. Management of initial ERCP failure constitutes a major clinical challenge for endoscopists. This review focuses on the endoscopic management of initial SBC failure in patients with an accessible papilla/biliary orifice.

When the major papilla is accessible, SBC typically begins with standard cannulation methods through a cannula or sphincterotome using either guidewire-assisted or contrast-guided techniques[2]. Using standard cannulation techniques, SBC fails in approximately 5% to 15% of cases[3]. This condition is often referred to as difficult biliary cannulation, although definitions have varied widely between endoscopists or studies[4,5]. In this case, depending on the experience or preference of the endoscopist, a variety of advanced techniques can be applied as a means of rescue. In general, when unintentional pancreatic guidewire insertion has been achieved, a double guidewire cannulation approach can be attempted[1]. Alternately or sequentially, transpancreatic sphincterotomy can be performed[6]. However, some endoscopists might prefer to perform needle-knife precut papillotomy (NKP) or needle-knife fistulotomy (NKF), especially after the placement of a pancreatic stent[2,7]. If the pancreatic duct is not cannulated, however, only NKP or NKF can be applied[4]. The application of these advanced technologies does not require additional facilities. Today, most qualified ERCP endoscopists can master at least some of these advanced cannulation techniques, so these procedures can often be performed by the same endoscopist during the same endoscopic session[8]. Despite these rescue techniques, failed biliary cannulation can occur[9]. Therefore, in this review, difficult biliary cannulation was defined as failure to achieve SBC using the advanced techniques described above[10,11]. In the setting of difficult bile duct cannulation, there is currently no consensus on the next steps in treatment[9]. Because endoscopic therapy has the advantage of a broader range of treatment options and no need for external drainage, this review aims to propose and discuss potential endoscopic options, alone or in combination with the percutaneous procedure, for patients who have failed initial ERCP due to difficult bile duct cannulation. These endoscopic options include interval ERCP, percutaneous-transhepatic-endoscopic rendezvous procedures (PTE-RV), and endoscopic ultrasound (EUS)-guided procedures. We also propose a potential treatment algorithm to provide practical advice.

INTERVAL ERCP

In a literature search in early 2022, we were only able to find 7 studies (371 patients in total) reporting interval ERCP[9,12-17]. All of these studies were retrospective. There were no review/meta-analysis articles on this topic. However, when SBC cannot be achieved by advanced cannulation techniques,

Table 1 Summary of studies on reporting interval endoscopic retrograde cholangiopancreatography

Ref.	Study design (patient number)	Percentage[1]	Median time interval[2] (range)	Pre-cut during interval ERCP	Technical success rate	Factors associated with success	Overall complication rate
Kevans *et al*[12] (2010)	Retrospective (*n* = 19)	53% (19/36)	6 d (1-21 d)	0%	68% (13/19)	NA	0
Donnellan *et al*[13] (2012)	Retrospective (*n* = 51)	68% (51/75)	8 d (1-28 d)	NA	75% (38/51)	3 d *vs* 6 d (failure *vs* success)	3.9% (2/51)
Kim *et al*[14] (2012)	Retrospective (*n* = 69)	76% (69/91)	NA (1-3 d)	16% (11/69)	77% (53/69)	1 d *vs* 2-3 d (66% *vs* 88%)	15.9% (11/69)
Pavlides *et al*[15] (2014)	Retrospective (*n* = 89)	82% (89/108)	4 d (IQR 3-6 d)	NA	78% (69/89)	NA	-
Colan-Hernandez *et al*[16] (2017)	Retrospective (*n* = 72)	64% (72/112)	7 d (IQR 5-11 d)	NA	75% (54/72)	≤ 4 d *vs* > 4 d (44% *vs* 79%)	4.2% (3/72)
Narayan *et al*[17] (2017)	Retrospective (*n* = 28)	76% (28/37)	3 d (3-4 d)	NA	79% (22/28)	NA	-
Lo *et al*[9] (2021)	Retrospective (*n* = 43)	38% (43/114)	4 d (1-20 d)	28% (12/43)	79% (34/43)	None	7.0% (3/43)
Overall	*n* = 371	-	-	-	76.3% (281/371)	-	7.5% (19/254)

[1]Number of study cases as a percentage of initial endoscopic retrograde cholangiopancreatography (ERCP) failures.
[2]Time interval between initial and interval ERCP.
ERCP: Endoscopic retrograde cholangiopancreatography; NA: Not available; IQR: Interquartile range.

such as NKP or NKF, these studies have shown that interval ERCP is a viable treatment option (Table 1) [9,12-17]. The overall success rate of interval ERCP was 76.3% (68%-79% between studies). The time interval between the initial ERCP and the interval ERCP varies greatly from study to study (median, 3-8 d)[9,12,13,15-17]. Three studies reported that 0%, 16%, and 28% of patients required a second precut procedure during the interval ERCP, respectively[9,12,14].

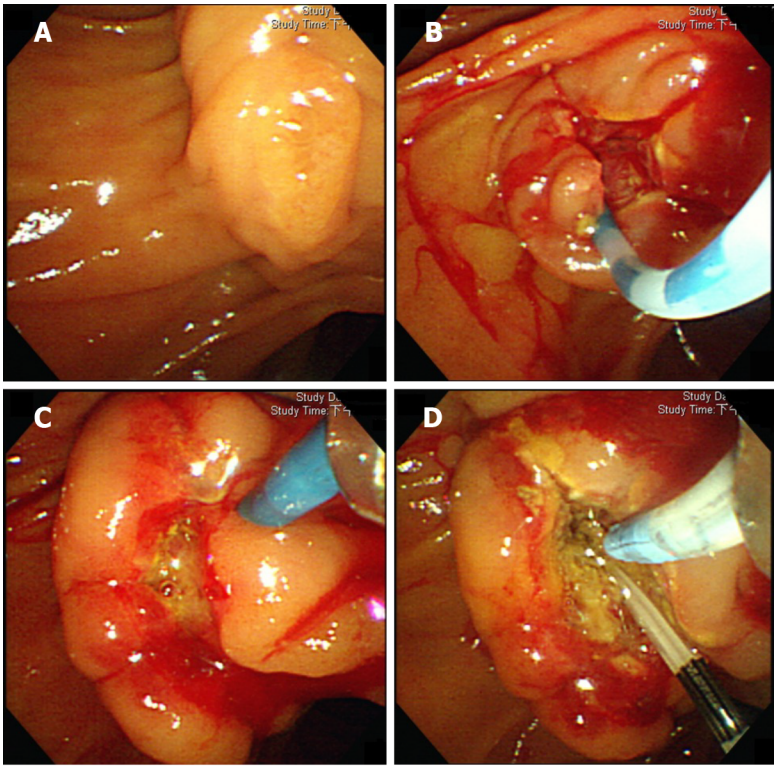
Interestingly, the timing to perform interval ERCP appeared to affect the success rate of interval ERCP[9,13,14,16]. The edema, tissue necrosis, and even bleeding of the major papilla caused by cannulation and/or NKP/F improved over time, resulting in an open and easily accessible papilla (Figures 1 and 2). Therefore, the success rate of interval ERCP could increase if it could be delayed for a couple of days. Donnellan *et al*[13] reported a significantly longer median time interval between initial and interval ERCP in the successful cannulation group compared to the failed cannulation group (6.0, 1-28 d *vs* 3.0, 1-8 d; $P = 0.02$). Kim *et al*[14] studied only patients who received interval ERCP within 3 d [14]. They reported that the success rate of interval ERCP after one day was significantly lower than after 2-3 d (65.7% *vs* 88.2%, $P = 0.027$). Except for the time interval, no other factor was significantly associated with the success of interval ERCP in their study. Colan-Hernandez *et al*[16] performed univariate and multivariate analyses of factors associated with interval ERCP cannulation failure. They found that the ERCP interval within 4 d after the initial precut was the only significant factor (cannulation success rate of 44.4% *vs* 79.4%, $P = 0.024$ for univariate and 0.026 for multivariate analysis). However, in our study, we did not find any factors associated with interval ERCP failure in either the univariate or multivariate analysis[9].

Adverse events of interval ERCP were reported in five studies involving a total of 254 patients[9,12-14,16]. These adverse events included pancreatitis, bleeding, perforation, and cholangitis. The overall adverse event rate was 7.5% (0-15.9% between studies). Pancreatitis occurred in 1.6% (0-2.9%); all cases were mild. The bleeding rate was 2.8% (0-5.8%). Approximately half of the bleeding was mild, and the other half was moderate. The perforation rate was 1.2% (0-2.9%); all cases were mild. The cholangitis rate was 2.0% (0-4.7%). Two studies compared adverse event rates for initial and interval ERCP and found no significant difference[14,15].

In these studies, only 38%-82% of patients received interval ERCP when initial NKP/F failed to achieve SBC[9,12-17]. This result could reflect that some other salvage treatments, such as percutaneous or EUS-guided drainage, are still applicable in this situation[18].

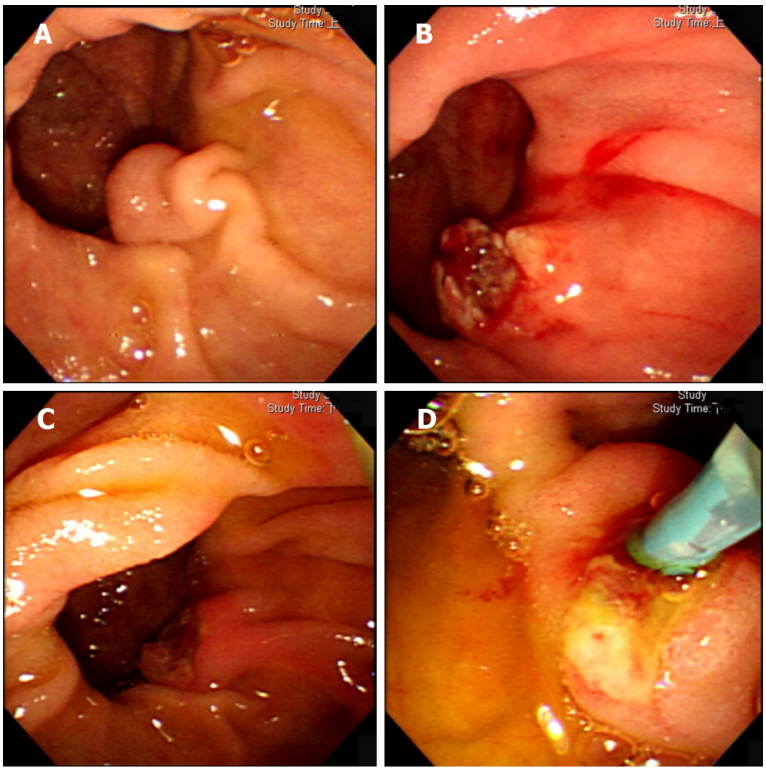
PERCUTANEOUS-TRANSHEPATIC-ENDOSCOPIC RENDEZVOUS PROCEDURES

Percutaneous transhepatic biliary drainage (PTBD) remains possibly the most widely used salvage



DOI: 10.3748/wjg.v28.i29.3803 **Copyright** ©The Author(s) 2022.

Figure 1 Interval endoscopic retrograde cholangiopancreatography, 1 d after the initial procedure. A: The original papilla in the initial endoscopic retrograde cholangiopancreatography (ERCP); B: Post-precut papilla, at the end of initial ERCP; C: post-precut papilla, at the beginning of interval ERCP. The papilla is swollen, edematous, and with mild oozing; D: Deep bile duct cannulation is unsuccessful during the interval ERCP, even after the placement of a pancreatic stent.



DOI: 10.3748/wjg.v28.i29.3803 **Copyright** ©The Author(s) 2022.

Figure 2 Interval endoscopic retrograde cholangiopancreatography, 3 d after the initial procedure. A: The original papilla in the initial endoscopic retrograde cholangiopancreatography (ERCP); B: Post-precut papilla, at the end of initial ERCP; C: post-precut papilla, at the beginning of interval ERCP. Papillary edema due to pre-cut has disappeared; D: Deep bile duct cannulation is successful during the interval ERCP.

therapy in the setting of initial ERCP failure[19]. However, PTBD has some drawbacks, including a high rate of adverse events, decreased patient quality of life, and most importantly, providing of somewhat limited options for therapeutic maneuvers[3]. In addition, external drainage can cause discomfort and pain and often requires reintervention[20]. Therefore, an improved technique combining percutaneous and endoscopic approaches, known as percutaneous-transhepatic-endoscopic rendezvous procedures (PTE-RV), seems preferable to PTBD[21]. PTE-RV have been around for more than three decades[22]. They have several advantages over PTBD alone: (1) PTE-RV allow for transhepatic puncture using only small-caliber catheters, thereby reducing complications. Bokemeyer *et al*[21] reported significantly fewer complications with PTE-RV than in PTBD (16.6% *vs* 26.4%; $P = 0.037$); (2) PTE-RV allow endoscopists to perform therapeutic ERCP in the usual manner through rendezvous access; and (3) Although PTBD is part of PTE-RV, once the biliary obstruction is resolved, the percutaneous access is closed[23].

PTE-RV can be executed as a one-stage procedure or a two-stage procedure[23]. The advantage of the one-stage procedure is that there is no need to insert a PTBD catheter. The two-stage procedure includes PTBD during the first session and internalization of the drain using an endoscope during the second session. These two steps are usually separated by a few hours to a few days[24]. Wayman *et al*[25] compared one-stage ($n = 19$) and two-stage PTE-RV ($n = 22$) and found that the technical success rates were comparable (94.7% *vs* 95.5%), but adverse events were more common in the two-stage group (37% *vs* 73%, $P < 0.05$), mainly due to complications related to external drainage.

For the following purposes, we recommend the insertion of a percutaneously placed hydrophilic-coated catheter (*e.g.*, angiocatheter) before the endoscopic rendezvous procedure (Figure 3A). First, the hepatic capsule and parenchyma, which could be damaged by the antegrade-introduced guidewire (AGW), were protected. Second, to ensure percutaneous access, once the AGW is lost incidentally during PTE-RV, it can be reintroduced into the biliary tree. Third, to facilitate the movements of AGW. After the AGW is introduced into the duodenum, there are several ways to achieve SBC[23,26]. The first and most classic technique is to grasp the distal end of the AGW with a snare and then pull the wire through the working channel of the endoscope. Retrograde bile duct cannulation can then be achieved over the wire (Figure 3B). This technique is particularly useful for patients with tight biliary strictures since the guidewire can be secured at both sides of percutaneous and endoscopic routes to facilitate retrograde passage of a catheter or stent through the stricture (push-pull technique). However, this technique might be limited by the difficult capture of the AGW and laborious guidewire manipulation, the potential for kinking or accidental loss of the AGW during withdrawal, and the risk of hepatic capsule/parenchymal tearing during AGW manipulation. The second and parallel technique is to use a standard ERCP cannulation method alongside the AGW or the percutaneously introduced catheter (Figure 3C). The advantage of this technique is that it is simple and perhaps time saving while avoiding the limitations of classical techniques. However, in some cases, it can be difficult. In such cases, retrograde biliary cannulation can be performed after antegrade balloon dilation of the biliary orifice. The other adjunctive maneuvers include insertion of a retrograde guidewire into a percutaneously placed catheter exiting the ampulla or insertion of a sphincterotome into the AGW exiting the ampulla [26].

PTE-RV has been relatively less investigated. In a literature search in early 2022, we found no review/meta-analysis articles on this topic. We were only able to find six studies (441 patients in total) over the past decade; all of them were retrospective (Table 2)[21,23,24,26-28]. The reason for PTE-RV in the searched studies was the failure of the initial ERCP. All but one study on the management of biliary strictures after living-donor liver transplantation included patients with malignant biliary strictures[28], ranging from 38% to 100% of study patients. PTE-RV is effective, with a technical success rate of 88.7% (80.4%-100% between studies). PTE-RV is also safe, with an overall adverse event rate of 13.2% (4.9%-19.2% between studies). Most studies reported no deaths from procedure-related mortality, except for one study that reported a 3.5% mortality rate possibly related to the PTE-RV procedure[23,24,27,28].

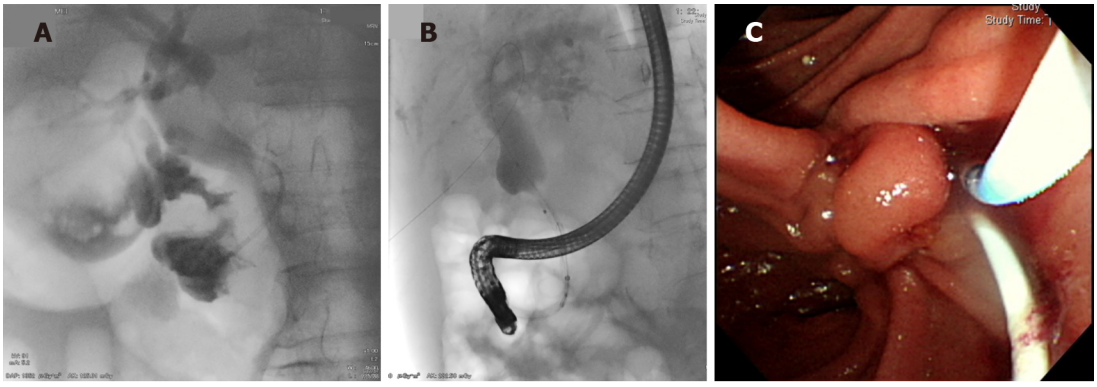
EUS-ASSISTED OR GUIDED BILIARY DRAINAGE

EUS-assisted or guided biliary drainage (EUS-BD) includes the EUS-assisted rendezvous technique (EUS-RV), EUS-guided choledochoduodenostomy (EUS-CDS), EUS-guided hepaticogastrostomy (EUS-HGS) and other procedures[29]. EUS-RV is designed to facilitate ERCP and does not involve tract dilation or stent placement and is therefore more physiologically and minimally invasive among the existing EUS-guided procedures[30]. Indications for EUS-RV include benign or potentially resectable malignant cases and unresectable malignant cases not suitable for other EUS-BD methods[31,32]. EUS-CDS and EUS-HGS involve direct transmural biliary drainage, so there could be some serious adverse events[33]. Therefore, both techniques are currently indicated for unresectable malignant cases[29-31, 33]. EUS-HGS and EUS-CDS are mainly used in patients in whom access to the papilla is not possible, such as in cases of duodenal obstruction or surgically altered anatomy. Therefore, they are beyond the scope of this review and are not included. However, indications for EUS-BD might change over time as technology advances, and improvements in devices/stents could increase technical success rates and reduce adverse event rates[34-37].

Table 2 Summary of studies on reporting percutaneous-transhepatic-endoscopic rendezvous procedures

Ref.	Study design (patient number)	Malignant biliary obstruction	One-stage *vs* two-stage	Technical success rate	Adverse events	PTE-RV related mortality
Chivot *et al*[23] (2021)	Retrospective (*n* = 84)	78.5%	One-stage	95.2% (80/84)	19% (16/84); Cholangitis: 9.5%; Pancreatitis: 3.5%; Hemorrhage: 2.3%; Pneumoperitoneum: 3.5%	3.5%
Bokemeyer *et al*[21] (2019)	Retrospective (*n* = 163)	71.3%	NA	80.4% (131/163)	16.6% (27/163); Procedure-related complications: 8.6%; Drainage-related complications: 8%	NA
Yang *et al*[26] (2017)	Retrospective (*n* = 42)	38%	Two-stage	92.9% (39/42)	7.1% (3/42)	NA
Tomizawa *et al*[24] (2014)	Retrospective (*n* = 26)	91%	One-stage (73%) or two-stage	88% (23/26)	19.2% (5/26)	0
Neal *et al*[27] (2010)	Retrospective (*n* = 106)	100%	Two-stage	92.5% (98/106)	4.9% (5/106)	0
Chang *et al*[28] (2010)	Retrospective (*n* = 20)	0	Two-stage	100% (20/20)	10% (2/20); Pancreatitis: 5%; Cholangitis: 5%	0
Overall	441	-	-	88.7% (391/441)	13.2% (58/441)	-

PTE-RV: Percutaneous-transhepatic-endoscopic rendezvous procedures; NA: Not available.



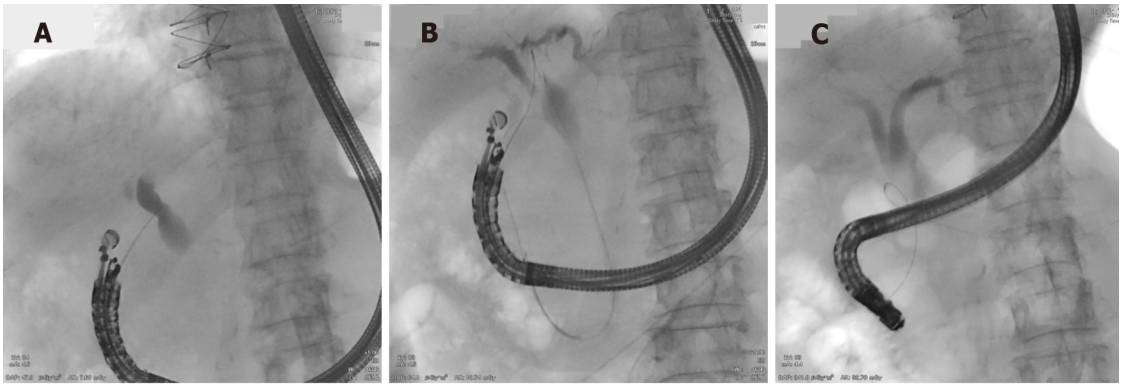
DOI: 10.3748/wjg.v28.i29.3803 **Copyright** ©The Author(s) 2022.

Figure 3 Percutaneous-transhepatic-endoscopic rendezvous procedures. A: Placement of an angiocatheter to protect the liver capsule and parenchyma from guidewire damage; B: A metal stent is passed through the distal biliary stricture over the antegrade-introduced guidewire; C: Cannulation alongside the antegrade-introduced angiocatheter.

EUS-assisted rendezvous technique

In EUS-RV, the bile duct is punctured under EUS guidance, followed by the introduction of an AGW into the duodenum (Figure 4). The EUS endoscope is then switched to a duodenoscope, with eventual ERCP (SBC is achieved over the AGW or in parallel to the AGW). There are three puncture routes for EUS-RV[11,31,38]: (1) The intrahepatic bile duct (IHBD) route: Either transesophageal puncture of B2 or transgastric puncture of B2 or B3 can be performed. If the target is the right IHBD, it can be punctured from the duodenal bulb (D1). Transgastric puncture of B2 is most frequently performed; (2) The extrahepatic bile duct (EHBD)/D1 route, with puncture from D1: In this route, the endoscope is usually in the push position (long position), and the proximal EHBD is punctured; and (3) The EHBD/second portion of the duodenum (D2) route, with puncture from D2. In this route, the endoscope is usually in a short position, and the distal EHBD is punctured.

Two studies proposing treatment algorithms suggested using the EHBD/D2 route as a first-line approach[10,31]. They reported that the EHBD/D2 route was feasible in 50%-62.5% of patients, with EUS-RV success rates of 100% in both studies. Iwashita *et al*[10] found that the EUS-RV success rate *via* the EHBD/D1 and IHBD routes was only 66.7%. Matsubara *et al*[31] found that the time between puncture and guidewire placement with the DEHBD/D2 route was significantly shorter than that with other methods (3.5 min *vs* 14.0 min, P = 0.014). Therefore, EUS-RV *via* the EHBD/D2 route can be



DOI: 10.3748/wjg.v28.i29.3803 **Copyright** ©The Author(s) 2022.

Figure 4 Endoscopic ultrasound-assisted rendezvous procedures. A: Under endoscopic ultrasound, the proximal extrahepatic bile duct is punctured through the duodenal bulb. The sonoendoscope is in a long position; B: The guidewire is delivered antegradely to the duodenum through the puncture route; C: Switch to a duodenoscope to grasp the antegradely introduced guidewire.

considered a first-line approach when feasible, although the route of access should be chosen on a patient-by-patient basis[10,31,32]. In the case of the IHBD approach, Iwashita *et al*[39] reported a hybrid rendezvous technique, in which a 6-French dilator was inserted into the biliary system for better guidewire manipulation, which could improve the technical success rate.

EUS-RV has been increasingly used in patients with SBC failure in initial ERCP[11,30]. A review by Tsuchiya *et al*[11] in 2016 (15 studies, 382 patients) reported that EUS-RV had an overall success rate of 82% (50%-100% between studies) and a complication rate of 13% (0-23% between studies). They also found that the IHBD puncture route had a lower success rate than the EHBD route (76% *vs* 85%). Therefore, in this review, we performed a literature search in Medline and included studies published after 2015 (7 studies, 177 patients; Table 3)[10,31,32,40-43]. The proportion of patients with malignant biliary obstruction was 43.5% (0-68.8% between studies). The results showed an overall EUS-RV success rate of 84.4% (78.6%-100% between studies) and a complication rate of 15.6% (6.3%-23.3% between studies) for EUS-RV. These results are similar to those in the aforementioned review article. Furthermore, we found that the IHBD puncture route also had a lower success rate than the EHBD route (74.2% *vs* 84.9%). The associated complications included pancreatitis (6.7%), cholangitis (1.7%), bile leak/peritonitis (3.3%), hematoma (0.6%), perforation (0.6%), pneumomediastinum (1.7%), aspiration pneumonia (0.6%), and gastric mucosal laceration (0.6%). In a recent meta-analysis (12 studies, 342 patients), Klair *et al*[30] further reported that, if only patients with normal anatomy (without surgical alterations) were included in the analysis, the technical success rate would have improved from 86.1% to 88.3%. The pooled clinical success rate was 80.8% (95%CI: 64.1-90.8). The pooled overall adverse event rate was 14% (95%CI: 10.5-18.4), including pancreatitis (7.2%), cholangitis (2.3%), bile leak (3.3%), bleeding (2.1%), perforation (2.7%), and peritonitis (2.3%). However, all of the studies included in this meta-analysis were retrospective.

Some unanswered questions remain; for example, does early switching to EUS-RV without spending too much time on advanced cannulation techniques improve technical success rates and reduce complication rates[44]? Further studies are required to clarify this issue.

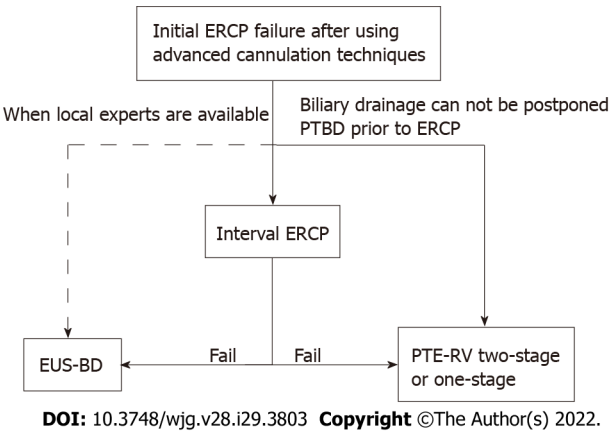
CONCLUSION

Based on this review, interval ERCP appears to have the lowest technical success rate and overall complication rate of the three endoscopic salvage methods. Given the acceptably high success rates and low complication rates, and without the need for additional expertise, facilities (*e.g.*, EUS), or other specialists (*e.g.*, radiologists), interval ERCP can be considered the first choice when SBC is not feasible with advanced cannulation techniques[4]. In this way, more invasive alternative interventions can be avoided in approximately three-quarters of patients. However, the main limitation of interval ERCP is that it must be delayed by a few days to improve the success rate. Therefore, patients in urgent need of biliary drainage (*e.g.*, uncontrolled cholangitis) should undergo other, more invasive therapies. In this setting, since percutaneous biliary puncture is a more widespread technique than EUS-BD, and most ERCP endoscopists can perform rendezvous procedures, two-stage PTE-RV can be considered because PTBD can achieve early bile drainage. Of course, if both interventional radiologists and endoscopists are available, one-stage PTE-RV is welcome because it reduces complication rates. Another situation in which PTE-RV can be considered a first choice is when the patient has a PTBD drainage tube before the initial ERCP. EUS-BD is a relatively new technique and requires additional technical expertise/facilities, and as such, its use has been limited to some ERCP endoscopists at some advanced endoscopy centers.

Table 3 Summary of studies on reporting endoscopic ultrasound-guided rendezvous procedures

Ref.	Study design (patient number)	Malignant biliary obstruction	Success rate *via* EHBD	Success rate *via* IHBD	Overall technical success rate	Overall complication rate
Iwashita *et al* [10] (2016)	Prospective (*n* = 20)	60% (12/20)	86.7% (13/15)	75% (3/4)	80% (16/20)	15% (3/20); Hematoma (5%); Pancreatitis (10%)
Tang *et al* [40] (2016)	Retrospective (*n* = 25)	52% (13/25)	83.3% (20/24)	0 (0/1)	80% (20/25)	16% (4/25); Pancreatitis (12%); Cholangitis (4%)
Okuno *et al* [32] (2017)	Retrospective (*n* = 39)	62.5% (24/39)	84.6% (22/26)	68.8% (11/16)	78.6% (33/42)	16.7% (7/42); Pneumomediastinum (4.8%); Retroperitoneal perforation (2.4%); Cholangitis (2.4%); Peritonitis (4.8%); Pancreatitis (2.4%)
Nakai *et al* [41] (2017)	Retrospective (*n* = 30)	30% (9/30)	NA	NA	93.3% (28/30)	23.3% (7/30); Pancreatitis (10.0 %); Bile peritonitis (3.3 %); Cholangitis (3.3 %); Aspiration pneumonia (3.3 %); Gastric mucosa laceration (3.3 %)
Shiomi *et al* [42] (2018)	Prospective (*n* = 20)	40% (8/20)	83.3% (10/12)	87.5% (7/8)	85% (17/20)	15% (3/20); Biliary peritonitis (10%); Pancreatitis (5%)
Martínez *et al*[43] (2019)	Retrospective (*n* = 27)	0	81.5 % (22/27)	-	81.5 % (22/27)	11.1% (3/27); Pneumomediastinum (3.7%); Bile leak (3.7%); Pancreatitis (3.7%)
Matsubara *et al*[31] (2020)	Retrospective (*n* = 16)	68.8% (11/16)	93.3% (14/15)	100% (2/2[1])	100% (16/16)	6.3% (1/16); Pancreatitis (6.3%)
Overall	*n* = 177	43.5% (77/177)	84.9% (101/119)	74.2% (23/31)	84.4% (152/180)	15.6% (28/180); Pancreatitis (6.7%); Bile leak/peritonitis (3.3%); Cholangitis (1.7%); Pneumomediastinum (1.7%); Retroperitoneal perforation (0.6%); Hematoma (0.6%); Aspiration pneumonia (0.6%); Gastric mucosa laceration (0.6%)

[1]Including one patient had initial extrahepatic bile duct approach attempt.
NA: Not available; IHBD: Intrahepatic bile duct; EHBD: Extrahepatic bile duct.



DOI: 10.3748/wjg.v28.i29.3803 **Copyright** ©The Author(s) 2022.

Figure 5 The proposed treatment algorithm. ERCP: Endoscopic retrograde cholangiopancreatography; PTBD: Percutaneous transhepatic biliary drainage; PTE-RV: Percutaneous-transhepatic-endoscopic rendezvous procedure; EUS-BD: Endoscopic ultrasound-assisted or guided biliary drainage.

When local experts are available, EUS-BD could serve as a first-line salvage technique before considering PTBD, as recommended by recently issued ESGE guidelines[29]. If not, it might be performed in a second endoscopic session by another endoscopist with dual endoscopic techniques. Based on the current review, we propose a treatment algorithm to provide practical recommendations, as shown in Figure 5. Since there have been no comparative studies between treatments, the suggested practice should be validated by further studies.

FOOTNOTES

Author contributions: Tsou YK conceptualized and designed the review and wrote the manuscript; Pan KT was

responsible for the data acquisition/analysis of the percutaneous-transhepatic-endoscopic rendezvous procedures; Lee MH was responsible for the data acquisition/analysis of the endoscopic ultrasound-assisted or guided procedures; Lin CH contributed to revising and validating the manuscript.

Conflict-of-interest statement: There is no conflict of interest associated with any of the authors contributing their efforts to this manuscript.

Open-Access: This article is an open-access article that was selected by an in-house editor and fully peer-reviewed by external reviewers. It is distributed in accordance with the Creative Commons Attribution NonCommercial (CC BY-NC 4.0) license, which permits others to distribute, remix, adapt, build upon this work non-commercially, and license their derivative works on different terms, provided the original work is properly cited and the use is non-commercial. See: https://creativecommons.org/Licenses/by-nc/4.0/

Country/Territory of origin: Taiwan

ORCID number: Yung-Kuan Tsou 0000-0002-7254-7369; Mu Hsien Lee 0000-0003-3664-5313; Cheng-Hui Lin 0000-0002-7856-2585.

S-Editor: Yan JP
L-Editor: A
P-Editor: Yan JP

REFERENCES

1 **Berry R**, Han JY, Tabibian JH. Difficult biliary cannulation: Historical perspective, practical updates, and guide for the endoscopist. *World J Gastrointest Endosc* 2019; **11**: 5-21 [PMID: 30705728 DOI: 10.4253/wjge.v11.i1.5]
2 **Reddy DN**, Nabi Z, Lakhtakia S. How to Improve Cannulation Rates During Endoscopic Retrograde Cholangiopancreatography. *Gastroenterology* 2017; **152**: 1275-1279 [PMID: 28366733 DOI: 10.1053/j.gastro.2017.03.041]
3 **Chen Q**, Jin P, Ji X, Du H, Lu J. Management of difficult or failed biliary access in initial ERCP: A review of current literature. *Clin Res Hepatol Gastroenterol* 2019; **43**: 365-372 [PMID: 30314736 DOI: 10.1016/j.clinre.2018.09.004]
4 **Testoni PA**, Mariani A, Aabakken L, Arvanitakis M, Bories E, Costamagna G, Devière J, Dinis-Ribeiro M, Dumonceau JM, Giovannini M, Gyokeres T, Hafner M, Halttunen J, Hassan C, Lopes L, Papanikolaou IS, Tham TC, Tringali A, van Hooft J, Williams EJ. Papillary cannulation and sphincterotomy techniques at ERCP: European Society of Gastrointestinal Endoscopy (ESGE) Clinical Guideline. *Endoscopy* 2016; **48**: 657-683 [PMID: 27299638 DOI: 10.1055/s-0042-108641]
5 **Liao WC**, Angsuwatcharakon P, Isayama H, Dhir V, Devereaux B, Khor CJ, Ponnudurai R, Lakhtakia S, Lee DK, Ratanachu-Ek T, Yasuda I, Dy FT, Ho SH, Makmun D, Liang HL, Draganov PV, Rerknimitr R, Wang HP. International consensus recommendations for difficult biliary access. *Gastrointest Endosc* 2017; **85**: 295-304 [PMID: 27720741 DOI: 10.1016/j.gie.2016.09.037]
6 **Zou XP**, Leung JW, Li YH, Yao YL, Pei QS, Wu YL, He QB, Cao J, Ding XW. Comparison of sequential pancreatic duct guidewire placement technique and needle knife precut sphincterotomy for difficult biliary cannulation. *J Dig Dis* 2015; **16**: 741-746 [PMID: 26562073 DOI: 10.1111/1751-2980.12300]
7 **Kubota K**, Sato T, Kato S, Watanabe S, Hosono K, Kobayashi N, Hisatomi K, Matsuhashi N, Nakajima A. Needle-knife precut papillotomy with a small incision over a pancreatic stent improves the success rate and reduces the complication rate in difficult biliary cannulations. *J Hepatobiliary Pancreat Sci* 2013; **20**: 382-388 [PMID: 22993078 DOI: 10.1007/s00534-012-0552-4]
8 **Barakat MT**, Girotra M, Thosani N, Kothari S, Banerjee S. Escalating complexity of endoscopic retrograde cholangiopancreatography over the last decade with increasing reliance on advanced cannulation techniques. *World J Gastroenterol* 2020; **26**: 6391-6401 [PMID: 33244200 DOI: 10.3748/wjg.v26.i41.6391]
9 **Lo MH**, Lin CH, Wu CH, Tsou YK, Lee MH, Sung KF, Liu NJ. Management of biliary diseases after the failure of initial needle knife precut sphincterotomy for biliary cannulation. *Sci Rep* 2021; **11**: 14968 [PMID: 34294788 DOI: 10.1038/s41598-021-94361-8]
10 **Iwashita T**, Yasuda I, Mukai T, Iwata K, Ando N, Doi S, Nakashima M, Uemura S, Mabuchi M, Shimizu M. EUS-guided rendezvous for difficult biliary cannulation using a standardized algorithm: a multicenter prospective pilot study (with videos). *Gastrointest Endosc* 2016; **83**: 394-400 [PMID: 26089103 DOI: 10.1016/j.gie.2015.04.043]
11 **Tsuchiya T**, Itoi T, Sofuni A, Tonozuka R, Mukai S. Endoscopic ultrasonography-guided rendezvous technique. *Dig Endosc* 2016; **28** Suppl 1: 96-101 [PMID: 26786389 DOI: 10.1111/den.12611]
12 **Kevans D**, Zeb F, Donnellan F, Courtney G, Aftab AR. Failed biliary access following needle knife fistulotomy: is repeat interval ERCP worthwhile? *Scand J Gastroenterol* 2010; **45**: 1238-1241 [PMID: 20553113 DOI: 10.3109/00365521.2010.495418]
13 **Donnellan F**, Enns R, Kim E, Lam E, Amar J, Telford J, Byrne MF. Outcome of repeat ERCP after initial failed use of a needle knife for biliary access. *Dig Dis Sci* 2012; **57**: 1069-1071 [PMID: 22147249 DOI: 10.1007/s10620-011-1982-6]
14 **Kim J**, Ryu JK, Ahn DW, Park JK, Yoon WJ, Kim YT, Yoon YB. Results of repeat endoscopic retrograde cholangiopancreatography after initial biliary cannulation failure following needle-knife sphincterotomy. *J Gastroenterol Hepatol* 2012; **27**: 516-520 [PMID: 21913986 DOI: 10.1111/j.1440-1746.2011.06914.x]
15 **Pavlides M**, Barnabas A, Fernandopulle N, Bailey AA, Collier J, Phillips-Hughes J, Ellis A, Chapman R, Braden B. Repeat endoscopic retrograde cholangiopancreaticography after failed initial precut sphincterotomy for biliary cannulation. *World J*

Gastroenterol 2014; **20**: 13153-13158 [PMID: 25278710 DOI: 10.3748/wjg.v20.i36.13153]
16 **Colan-Hernandez J**, Aldana A, Concepción M, Chavez K, Gómez C, Mendez-Bocanegra A, Martínez-Guillen M, Sendino O, Villanueva C, Llach J, Guarner-Argente C, Cárdenas A, Guarner C. Optimal timing for a second ERCP after failure of initial biliary cannulation following precut sphincterotomy: an analysis of experience at two tertiary centers. *Surg Endosc* 2017; **31**: 3711-3717 [PMID: 28127713 DOI: 10.1007/s00464-016-5410-z]
17 **Narayan KS**, Gupta GK, Nijhawan S, Pandey S, Dhandhu BS, Puri S, Kumar A, Sharma D. Is it Worth to Repeat Endoscopic Retrograde Cholangiopancreaticography after Failed Precut? *J Digest Endosc* 2017; **8**: 129-131
18 **Téllez-Ávila FI**, Herrera-Mora D, Duarte-Medrano G, Lopez-Arce G, Lindoro-Barraza D, Casanova I, Elizondo-Rivera J, Ramírez-Luna M, Valdovinos-Andraca F. Biliary Drainage in Patients With Failed ERCP: Percutaneous Versus EUS-guided Drainage. *Surg Laparosc Endosc Percutan Tech* 2018; **28**: 183-187 [PMID: 29683996 DOI: 10.1097/SLE.0000000000000528]
19 **Gupta K**, Mallery S, Hunter D, Freeman ML. Endoscopic ultrasound and percutaneous access for endoscopic biliary and pancreatic drainage after initially failed ERCP. *Rev Gastroenterol Disord* 2007; **7**: 22-37 [PMID: 17392627 DOI: 10.1111/j.1365-2982.2007.00981.x]
20 **Nennstiel S**, Weber A, Frick G, Haller B, Meining A, Schmid RM, Neu B. Drainage-related Complications in Percutaneous Transhepatic Biliary Drainage: An Analysis Over 10 Years. *J Clin Gastroenterol* 2015; **49**: 764-770 [PMID: 25518004 DOI: 10.1097/MCG.0000000000000275]
21 **Bokemeyer A**, Müller F, Niesert H, Brückner M, Bettenworth D, Nowacki T, Beyna T, Ullerich H, Lenze F. Percutaneous-transhepatic-endoscopic rendezvous procedures are effective and safe in patients with refractory bile duct obstruction. *United European Gastroenterol J* 2019; **7**: 397-404 [PMID: 31019708 DOI: 10.1177/2050640619825949]
22 **Robertson DA**, Ayres R, Hacking CN, Shepherd H, Birch S, Wright R. Experience with a combined percutaneous and endoscopic approach to stent insertion in malignant obstructive jaundice. *Lancet* 1987; **2**: 1449-1452 [PMID: 2447457 DOI: 10.1016/s0140-6736(87)91141-x]
23 **Chivot C**, Yzet C, Bouzerar R, Brazier F, Hakim S, Le Mouel JP, Nguyen-Khac E, Delcenserie R, Yzet T. Safety and efficacy of percutaneous transhepatic-endoscopic rendezvous procedure in a single session. *Surg Endosc* 2021; **35**: 3534-3539 [PMID: 32710212 DOI: 10.1007/s00464-020-07812-0]
24 **Tomizawa Y**, Di Giorgio J, Santos E, McCluskey KM, Gelrud A. Combined interventional radiology followed by endoscopic therapy as a single procedure for patients with failed initial endoscopic biliary access. *Dig Dis Sci* 2014; **59**: 451-458 [PMID: 24271117 DOI: 10.1007/s10620-013-2913-5]
25 **Wayman J**, Mansfield JC, Matthewson K, Richardson DL, Griffin SM. Combined percutaneous and endoscopic procedures for bile duct obstruction: simultaneous and delayed techniques compared. *Hepatogastroenterology* 2003; **50**: 915-918 [PMID: 12845949 DOI: 10.5172/rsj.351.15.2.119]
26 **Yang MJ**, Kim JH, Hwang JC, Yoo BM, Kim SS, Lim SG, Won JH. Usefulness of combined percutaneous-endoscopic rendezvous techniques after failed therapeutic endoscopic retrograde cholangiography in the era of endoscopic ultrasound guided rendezvous. *Medicine (Baltimore)* 2017; **96**: e8991 [PMID: 29310413 DOI: 10.1097/MD.0000000000008991]
27 **Neal CP**, Thomasset SC, Bools D, Sutton CD, Garcea G, Mann CD, Rees Y, Newland C, Robinson RJ, Dennison AR, Berry DP. Combined percutaneous-endoscopic stenting of malignant biliary obstruction: results from 106 consecutive procedures and identification of factors associated with adverse outcome. *Surg Endosc* 2010; **24**: 423-431 [PMID: 19565296 DOI: 10.1007/s00464-009-0586-0]
28 **Chang JH**, Lee IS, Chun HJ, Choi JY, Yoon SK, Kim DG, You YK, Choi MG, Choi KY, Chung IS. Usefulness of the rendezvous technique for biliary stricture after adult right-lobe living-donor liver transplantation with duct-to-duct anastomosis. *Gut Liver* 2010; **4**: 68-75 [PMID: 20479915 DOI: 10.5009/gnl.2010.4.1.68]
29 **van der Merwe SW**, van Wanrooij RLJ, Bronswijk M, Everett S, Lakhtakia S, Rimbas M, Hucl T, Kunda R, Badaoui A, Law R, Arcidiacono PG, Larghi A, Giovannini M, Khashab MA, Binmoeller KF, Barthet M, Perez-Miranda M, van Hooft JE. Therapeutic endoscopic ultrasound: European Society of Gastrointestinal Endoscopy (ESGE) Guideline. *Endoscopy* 2022; **54**: 185-205 [PMID: 34937098 DOI: 10.1055/a-1717-1391]
30 **Klair JS**, Zafar Y, Ashat M, Bomman S, Murali AR, Jayaraj M, Law J, Larsen M, Singh DP, Rustagi T, Irani S, Ross A, Kozarek R, Krishnamoorthi R. Effectiveness and Safety of EUS Rendezvous After Failed Biliary Cannulation With ERCP: A Systematic Review and Proportion Meta-analysis. *J Clin Gastroenterol* 2021 [PMID: 34009843 DOI: 10.1097/MCG.0000000000001543]
31 **Matsubara S**, Nakagawa K, Suda K, Otsuka T, Isayama H, Nakai Y, Oka M, Nagoshi S. A Proposed Algorithm for Endoscopic Ultrasound-Guided Rendezvous Technique in Failed Biliary Cannulation. *J Clin Med* 2020; **9** [PMID: 33260305 DOI: 10.3390/jcm9123879]
32 **Okuno N**, Hara K, Mizuno N, Hijioka S, Tajika M, Tanaka T, Ishihara M, Hirayama Y, Onishi S, Niwa Y, Yamao K. Endoscopic Ultrasound-guided Rendezvous Technique after Failed Endoscopic Retrograde Cholangiopancreatography: Which Approach Route Is the Best? *Intern Med* 2017; **56**: 3135-3143 [PMID: 28943555 DOI: 10.2169/internalmedicine.8677-16]
33 **Ogura T**, Higuchi K. Technical Review of Developments in Endoscopic Ultrasound-Guided Hepaticogastrostomy. *Clin Endosc* 2021; **54**: 651-659 [PMID: 33896154 DOI: 10.5946/ce.2021.020-KDDW]
34 **Nakai Y**, Kogure H, Isayama H, Koike K. Endoscopic Ultrasound-Guided Biliary Drainage for Benign Biliary Diseases. *Clin Endosc* 2019; **52**: 212-219 [PMID: 30866611 DOI: 10.5946/ce.2018.188]
35 **Han SY**, Kim SO, So H, Shin E, Kim DU, Park DH. EUS-guided biliary drainage versus ERCP for first-line palliation of malignant distal biliary obstruction: A systematic review and meta-analysis. *Sci Rep* 2019; **9**: 16551 [PMID: 31719562 DOI: 10.1038/s41598-019-52993-x]
36 **Ginestet C**, Sanglier F, Hummel V, Rouchaud A, Legros R, Lepetit H, Dahan M, Carrier P, Loustaud-Ratti V, Sautereau D, Albouys J, Jacques J, Geyl S. EUS-guided biliary drainage with electrocautery-enhanced lumen-apposing metal stent placement should replace PTBD after ERCP failure in patients with distal tumoral biliary obstruction: a large real-life study. *Surg Endosc* 2022; **36**: 3365-3373 [PMID: 34606007 DOI: 10.1007/s00464-021-08653-1]
37 **Karagyozov PI**, Tishkov I, Boeva I, Draganov K. Endoscopic ultrasound-guided biliary drainage-current status and future

perspectives. *World J Gastrointest Endosc* 2021; **13**: 607-618 [PMID: 35070022 DOI: 10.4253/wjge.v13.i12.607]

38 **Dhir V**, Artifon EL, Gupta K, Vila JJ, Maselli R, Frazao M, Maydeo A. Multicenter study on endoscopic ultrasound-guided expandable biliary metal stent placement: choice of access route, direction of stent insertion, and drainage route. *Dig Endosc* 2014; **26**: 430-435 [PMID: 23941261 DOI: 10.1111/den.12153]

39 **Iwashita T**, Uemura S, Yoshida K, Mita N, Tezuka R, Yasuda I, Shimizu M. EUS-guided hybrid rendezvous technique as salvage for standard rendezvous with intra-hepatic bile duct approach. *PLoS One* 2018; **13**: e0202445 [PMID: 30133542 DOI: 10.1371/journal.pone.0202445]

40 **Tang Z**, Igbinomwanhia E, Elhanafi S, Othman MO. Endoscopic Ultrasound Guided Rendezvous Drainage of Biliary Obstruction Using a New Flexible 19-Gauge Fine Needle Aspiration Needle. *Diagn Ther Endosc* 2016; **2016**: 3125962 [PMID: 27822005 DOI: 10.1155/2016/3125962]

41 **Nakai Y**, Isayama H, Matsubara S, Kogure H, Mizuno S, Hamada T, Takahara N, Nakamura T, Sato T, Takeda T, Hakuta R, Ishigaki K, Saito K, Tada M, Koike K. A novel "hitch-and-ride" deep biliary cannulation method during rendezvous endoscopic ultrasound-guided ERCP technique. *Endoscopy* 2017; **49**: 983-988 [PMID: 28732390 DOI: 10.1055/s-0043-113444]

42 **Shiomi H**, Yamao K, Hoki N, Hisa T, Ogura T, Minaga K, Masuda A, Matsumoto K, Kato H, Kamada H, Goto D, Imai H, Takenaka M, Noguchi C, Nishikiori H, Chiba Y, Kutsumi H, Kitano M. Endoscopic Ultrasound-Guided Rendezvous Technique for Failed Biliary Cannulation in Benign and Resectable Malignant Biliary Disorders. *Dig Dis Sci* 2018; **63**: 787-796 [PMID: 29349694 DOI: 10.1007/s10620-018-4908-8]

43 **Martínez B**, Martínez J, Casellas JA, Aparicio JR. Endoscopic ultrasound-guided rendezvous in benign biliary or pancreatic disorders with a 22-gauge needle and a 0.018-inch guidewire. *Endosc Int Open* 2019; **7**: E1038-E1043 [PMID: 31404452 DOI: 10.1055/a-0918-5931]

44 **Yoon WJ**, Brugge WR. EUS-guided biliary rendezvous: EUS to the rescue. *Gastrointest Endosc* 2012; **75**: 360-361 [PMID: 22248604 DOI: 10.1016/j.gie.2011.09.024]

World Journal of Gastroenterology

Submit a Manuscript: https://www.f6publishing.com

World J Gastroenterol 2022 August 7; 28(29): 3814-3824

DOI: 10.3748/wjg.v28.i29.3814

ISSN 1007-9327 (print) ISSN 2219-2840 (online)

MINIREVIEWS

Enhanced endoscopic ultrasound imaging for pancreatic lesions: The road to artificial intelligence

Marco Spadaccini, Glenn Koleth, James Emmanuel, Kareem Khalaf, Antonio Facciorusso, Fabio Grizzi, Cesare Hassan, Matteo Colombo, Benedetto Mangiavillano, Alessandro Fugazza, Andrea Anderloni, Silvia Carrara, Alessandro Repici

Specialty type: Gastroenterology and hepatology

Provenance and peer review: Invited article; Externally peer reviewed.

Peer-review model: Single blind

Peer-review report's scientific quality classification

Grade A (Excellent): 0
Grade B (Very good): B, B
Grade C (Good): 0
Grade D (Fair): 0
Grade E (Poor): 0

P-Reviewer: Pausawasdi N, Thailand; Tsoulfas G, Greece

Received: April 9, 2022
Peer-review started: April 9, 2022
First decision: May 9, 2022
Revised: June 7, 2022
Accepted: July 5, 2022
Article in press: July 5, 2022
Published online: August 7, 2022

Marco Spadaccini, Glenn Koleth, Kareem Khalaf, Cesare Hassan, Matteo Colombo, Alessandro Fugazza, Andrea Anderloni, Silvia Carrara, Alessandro Repici, Digestive Endoscopy Unit, Division of Gastroenterology, Humanitas Research Hospital and University, Milan 20800, Italy

James Emmanuel, Department of Gastroenterology and Hepatology, Queen Elizabeth, Kota Kinabalu 88200, Sabah, Malaysia

Antonio Facciorusso, Section of Gastroenterology, Department of Medical Sciences, University of Foggia, Foggia 71122, Italy

Fabio Grizzi, Department of Immunology and Inflammation, Humanitas Clinical and Research Hospital, Rozzano 20089, Italy

Benedetto Mangiavillano, Digestive Endoscopy Unit, Division of Gasteroenterology, Humanitas Mater Domini, Castellanza 21053, Italy

Corresponding author: Marco Spadaccini, MD, Associate Specialist, Senior Researcher, Digestive Endoscopy Unit, Division of Gastroenterology, Humanitas Research Hospital and University, Via Manzoni 56, Milan 20800, Italy. marco.spadaccini@humanitas.it

Abstract

Early detection of pancreatic cancer has long eluded clinicians because of its insidious nature and onset. Often metastatic or locally invasive when symptomatic, most patients are deemed inoperable. In those who are symptomatic, multi-modal imaging modalities evaluate and confirm pancreatic ductal adenocarcinoma. In asymptomatic patients, detected pancreatic lesions can be either solid or cystic. The clinical implications of identifying small asymptomatic solid pancreatic lesions (SPLs) of < 2 cm are tantamount to a better outcome. The accurate detection of SPLs undoubtedly promotes higher life expectancy when resected early, driving the development of existing imaging tools while promoting more comprehensive screening programs. An imaging tool that has matured in its reiterations and received many image-enhancing adjuncts is endoscopic ultrasound (EUS). It carries significant importance when risk stratifying cystic lesions and has substantial diagnostic value when combined with fine needle aspiration/biopsy (FNA/FNB). Adjuncts to EUS imaging include contrast-enhanced harmonic EUS and EUS-elastography, both having improved

the specificity of FNA and FNB. This review intends to compile all existing enhancement modalities and explore ongoing research around the most promising of all adjuncts in the field of EUS imaging, artificial intelligence.

Key Words: Pancreatic ductal adenocarcinoma; Pancreatic cancer; Endoscopic ultrasound; Contrast-enhanced endoscopic ultrasound; Endoscopic ultrasound contrast agents; Endoscopic ultrasound elastography; Artificial intelligence; Fractal analysis; Endoscopy; Imaging

©The Author(s) 2022. Published by Baishideng Publishing Group Inc. All rights reserved.

Core Tip: Several reviews have evaluated the use of contrast-enhanced endoscopic ultrasound (CE-EUS), EUS-elastography (EUS-E), and artificial intelligence in separation. Not many have reviewed all three modalities' strengths in a single article. This article elaborates on current methods and outcomes of CE-EUS and EUS-E while reviewing the impact of artificial intelligence on the field of EUS imaging.

Citation: Spadaccini M, Koleth G, Emmanuel J, Khalaf K, Facciorusso A, Grizzi F, Hassan C, Colombo M, Mangiavillano B, Fugazza A, Anderloni A, Carrara S, Repici A. Enhanced endoscopic ultrasound imaging for pancreatic lesions: The road to artificial intelligence. *World J Gastroenterol* 2022; 28(29): 3814-3824
URL: https://www.wjgnet.com/1007-9327/full/v28/i29/3814.htm
DOI: https://dx.doi.org/10.3748/wjg.v28.i29.3814

INTRODUCTION

Pancreatic ductal adenocarcinoma (PDAC) is the 5th most fatal cancer globally, and those receiving a diagnosis have only a 6% 5-year survival rate[1]. Fortunately, early detection of a PDAC, especially when smaller than 1 cm, along with timely resection can aggrandize 5-year survival rates by up to 80.4% [2]. This disease's increasing incidence and mortality trend have brought different specialists (*i.e.* radiologists and gastroenterologists) together to create a framework to enhance early detection. Computed tomography (CT), magnetic resonance imaging (MRI), and endoscopic ultrasound (EUS) have all emerged as essentials in the multidisciplinary diagnostic approach of PDAC. EUS images of the pancreas are distinct from all modalities above because of their increased spatial resolution, making it 94% sensitive for PDAC detection[3]. Successive generations of EUS imaging transducers and post-processing software have markedly improved the spatial resolution of conventional B-mode EUS images. When used alone, it boasts a superior diagnostic accuracy over multidetector CT and MRI, singularly for solid pancreatic lesions (SPLs), but a meager specificity when differentiating pancreatic cancer from other pathologies[3,4]. However, with the advent of image-enhancing technologies such as contrast-enhanced EUS (CE-EUS) and EUS-elastography (EUS-E), there is evidence to suggest that even smaller SPLs are now detectable with good sensitivity and specificity[5-7]. Although promising, these advances' overarching impact in the face of early pancreatic cancer detection and diagnosing benign pancreatic diseases is still largely underwhelming. Pancreatic cancer remains a leading cause of death in industrialized populations, and the new case burden is estimated to grow steadily for the next 20 years [8]. Thus far, we know that the diagnostic accuracy of EUS, when coupled with EUS-guided tissue sampling, holds good outcomes, but reproducing its performance with ease remains a global challenge. The learning curve to master and competently perform an EUS examination is steep[9,10]. In this context, the introduction of artificial intelligence (AI), alone or in combination with existing enhanced EUS imaging technologies, may contribute to filling the gaps in accurately and consistently diagnosing pancreatic diseases[11]. This commentary highlights existing enhanced EUS imaging technologies while paving the way for AI, postulating its possible role in this arena.

EUS-E

Elastography is an ultrasonographic tool to measure the stiffness of the desired study area. The desired study area for a suspicious pancreatic lesion is also known as a region of interest (ROI). Akin to the clinical aspect of palpating a mass by hand and describing its characteristics, elastography does this similarly, but instead for deeper structures[12]. The two types of elastography include strain elastography (SE) and sheer wave elastography (SWE). However, SWE is still unstable in its use to measure the elasticity of SPLs and will not be discussed further in this article[13].

The type of elastography used in EUS is quasi-static or SE. It measures tissue displacement from a compressive force generated internally by the patient's physiology like breathing and vascular pulsations or externally by the tip of the echoendoscope pressing against the GI wall[14]. The compressive force deforms the tissue momentarily. The amount the tissue deforms or the degree to which it gets displaced is known as strain. Softer or more elastic tissue, *i.e.* more benign, will have more displacement while stiffer, inelastic, and generally more malignant tissue, will have less strain[15]. The images can be seen side by side on the EUS display, with the EUS-E overlayed on the B mode image.

We present examples for PDAC (Figure 1A and B) and for a metastatic lymph node (Figure 1C). The color spectrum represents a qualitative measurement, blue being the hardest and red being the softest. Quantitative measurements are seen on the strain histogram or valued as the strain ratio (SR; the strain of the larger round-shaped ROI area A divided by the strain of smaller round-shaped region of surrounding normal tissue area B). Suggested surrounding normal homogenous tissue to be used as reference include either healthy surrounding pancreatic parenchyma (pSR) or healthy GI tract wall (wSR). Suggested elastography SR values are automatically computed and estimated using the built-in software found in the Olympus EU-ME2 processor and the Hitachi United States machines. However, the reference areas have yet to be standardized.

Outcomes

One of the earliest prospective multicenter studies by Giovannini[16] evaluated the elastography of pancreatic masses from 121 patients on initial EUS referenced against final histological diagnoses. Elastography successfully demonstrated "intense blue" on qualitative measurement for all PDAC, endocrine tumors, pancreatic metastasis, and pancreatic sarcomas. According to his scoring system of 1 through 5 (5 being the stiffest and most intense blue), scores 1 and 2 had a negative predictive value (NPV) of 77.4%, whilst scores 3 and 4 had a positive predictive value (PPV) for malignancy of 92.8%[16].

In the interest of detecting smaller ductal adenocarcinomas (< 15 mm), which if resected earlier, have shown a 5-year survival mark in PDAC survivors to exceed 30%-60%, Ignee *et al*[7] evaluated SRs for SPLs of < 15 mm from 218 patients across 13 international centers. They found that EUS-E patterns of a small lesion (average size 11 ± 3 mm), if found to be soft, could confidently rule out malignancy (NPV 98%). Although PDAC was diagnosed in these small lesions with a sensitivity of 96%, elevated stiffness in a detected lesion had a specificity of only 67% with a PPV of 56% when diagnosing malignancy[7]. These small lesions' final etiological percentage breakdown was 66% benign, while 52% were neuroendocrine tumors (NETs). Notably, 36% of the NETs were stiff lesions, while 64% were soft compared to surrounding tissue. The remaining 23% were PDAC, 17% other entities, and 8% metastasis (which showed stiffness only 59% of the time)[7].

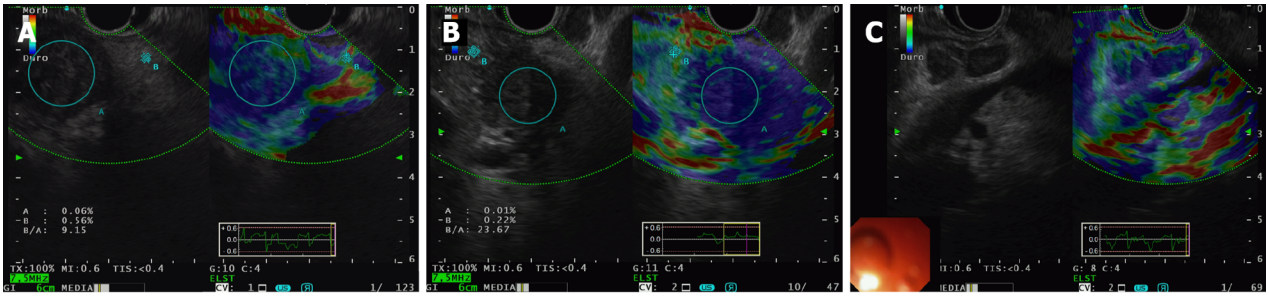
In 2012, Pei *et al*[17] and in 2013, Ying *et al*[18], the Asian groups conducted separate metanalyses, but with additions to pooled data on the subject matter of EUS-E's diagnostic accuracy, a more recent meta-analysis of 17 studies analyzing 1544 lesions from 1537 patients was conducted in 2017. From their pooled results, EUS-E reported an accumulated sensitivity of 97% (95%CI: 95%-99%) and a sensitivity of 67% (95%CI: 59%-74%) for qualitative methods; 97% sensitivity (95%CI: 95%-98%) and 67% specificity (95%CI: 61%-73%) for Strain Histograms, and lastly, 98% specificity (95%CI: 96%-99%) and 62% sensitivity (95%CI: 56%-68%) for strain ratios, suggesting its value as a complement to EUS-guided tissue sampling, *i.e.* EUS-FNA[19].

Similarly, guidelines proposed by the European Federation of Societies for Ultrasound in Medicine and Biology (EFSUMB) advocate using elastography as a complementary tool for focal pancreatic lesion characterization[20]. When a EUS-FNA sample is negative, but the index of suspicion for malignancy remains, the EFSUMB recommends using elastography and CE-EUS for repeat tissue sampling or referring the patient directly to the surgeons for operative intervention without further delay[20]. We demonstrate the clinical application of EUS-E (with CE-EUS) to target FNB sampling in a patient with a degenerated intraductal papillary mucinous neoplasm (IPMN) under our surveillance (Figure 2). This patient had positive cytology, warranting early surgery. Although documented to be helpful in the diagnosis of early autoimmune pancreatitis due to an idiosyncratic distribution of tissue stiffness, the guidelines cannot recommend the use of elastography in differentiating advanced chronic pancreatitis from pancreatic cancer[20].

One of EUS-E's many inherent limitations is evident here: Its low specificity and inability to consistently distinguish between pancreatic diseases (inflammatory *vs* neoplastic) or even types of pancreatic malignancies.

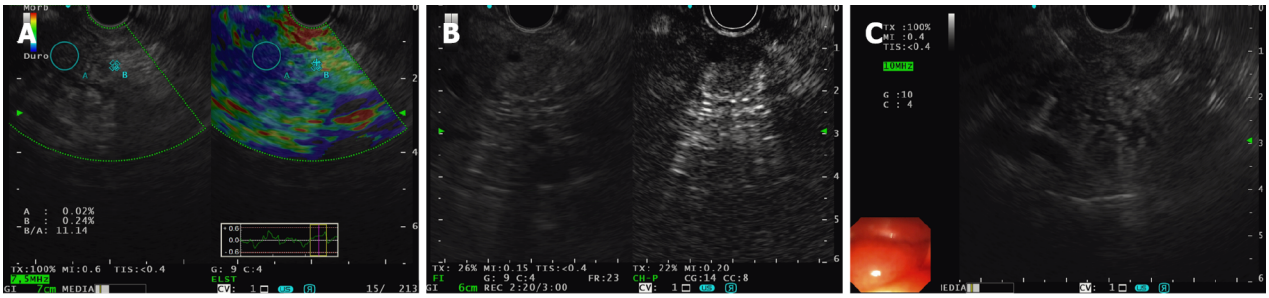
Inbuilt elastography software reduces intra-observer variability by overcoming the selection bias of images by providing the operator with a real-time movie of all recorded frames. However, there remains significant inter-observer variability when differentiating NETs from normal pancreatic parenchyma, as both may appear green *i.e.* soft.

Here are a few other scenarios where misdiagnoses occur: (1) If the endoscopist places too much compressive pressure between the probe and the examined tissue; and (2) False image reconstruction due to the heterogeneity of the examined tissue *i.e.* in the case of pancreatic cancer where some areas within the lesion are either necrotic, fibrous from desmoplasia, or have become inhomogeneous from vessel infiltration.



DOI: 10.3748/wjg.v28.i29.3814 **Copyright** ©The Author(s) 2022.

Figure 1 Endoscopic ultrasound-elastography. A and B: Endoscopic ultrasound-elastography (EUS-E) use in demonstrating stiffness of pancreatic ductal adenocarcinoma tissue (encircled A) against normal pancreatic parenchyma (encircled B); C: EUS-E use in demonstrating stiffness of metastatic lymph nodes in patient from B. The nodes in B-mode when seen with elastography are blue, indicating that it's hard and potentially malignant.



DOI: 10.3748/wjg.v28.i29.3814 **Copyright** ©The Author(s) 2022.

Figure 2 The clinical application of endoscopic ultrasound-elastography (with contrast-enhanced endoscopic ultrasound) to target fine needle biopsy sampling in a patient with a degenerated intraductal papillary mucinous neoplasm under our surveillance. A: Case demonstration of a degenerated intraductal papillary mucinous neoplasm and combination use of endoscopic ultrasound-elastography (EUS-E) to direct fine needle biopsy (FNB) sampling. Pre-EUS-E, the area of concern was iso-echoic, resembling normal parenchyma; however, under EUS-E, the area is stiff (blue); B: Contrast use post-FNB showing hypo-enhancement of the area of concern, confirming the area previously highlighted by EUS-E; C: Post-EUS-E and contrast-enhanced EUS guided FNB sampling in the same patient, allowing targeted sampling of the hard area.

Other pitfalls include: (1) A lack of standardization for cut-off values for strain ratios, although some experts propose using parenchyma-to-lesion SR of > 9.10 (PPV 89.7%; NPV 76.9%) or the gastric wall-to-lesion SR of > 16.2 (PPV 86.5%; NPV 80%)[21]; (2) Border delineation once the lesion becomes larger [22]; (3) Inability to measure strain if the lesion is too far away from the probe, and lastly; and (4) Image acquisition when fluid is present, *i.e.* with cysts[22].

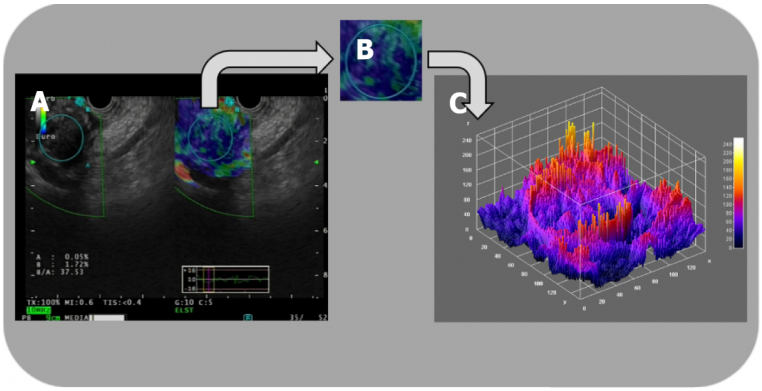
Carrara *et al*[21] demonstrated the use of fractal geometry analysis (Figure 3) to quantify the surface roughness of 2 tissues that share the same mechanical properties on elastography, and in doing so, overcome a significant limitation of EUS-E, but further trials are required[21]. Studies are also underway to evaluate the use of EUS-E in differentiating actual vessel wall infiltration by tumor tissue from that caused by an inflammatory reaction. The European Elastography Group, amongst others, is also designing and training deep learning platforms for future use in reducing inter-operator variability.

CE-EUS IMAGING

CE-EUS imaging is a non-invasive technique that utilizes a contrast agent during a EUS examination to improve diagnostic imaging. Contrast use in ultrasound imaging was first pioneered in 1986 by Matsuda and Yabuuchi with the infusion of CO_2 as a medium. Kato heralded its subsequent application into EUS in 1991, confined only to angiographic examinations[23]. In the mid-1990s, the use of Doppler function and sonicated serum albumin expanded the application of CE-EUS beyond the premise of angiographic studies[24].

In CE-EUS, the mechanical index (MI) alludes to the reaction of microbubbles in response to a stimulus in the form of an acoustic wave[25]. From this response, CE-EUS is typed into two: (1) Contrast-enhanced high-MI EUS (CEHMI-EUS), not requiring specific interpretive software; and (2) Contrast-enhanced low-MI EUS (CELMI-EUS), requiring a contrast-specific software mode.

A significant advantage of CELMI-EUS over CEHMI-EUS is its higher resolution and visibility of the contrast enhancer bubbles. In contrast, CEHMI-EUS's ability to display pancreatic macro-vessels (vessels with a diameter of approximately 0.2 mm and higher) comes at the expense of microbubble destruction



DOI: 10.3748/wjg.v28.i29.3814 **Copyright** ©The Author(s) 2022.

Figure 3 Three-dimensional surface fractal dimension estimate. A and B: Endoscopic ultrasound-elastography images (A) are used to highlight representative parenchymal regions (B) of solid pancreatic lesions; C: A computer-aided image analysis system generates an irregularly-shaped three-dimensional surface as a "shape matrix" of points with the column and row numbers proportional to the x and y coordinates and with the depth information z (x, y) stored as a matrix element. The three-dimensional fractal dimension, which is an index of the "surface roughness", is automatically determined using the box-counting algorithm. The fractal dimension of a surface is expressed by a real number greater than 2 (the Euclidean dimension of a two-dimensional surface) and less than 3 (the Euclidean dimension of a solid). A surface with a higher surface fractal dimension is wrinkled than one with a lower dimension.

and, as a result, CEHMI-EUS's use for Doppler enhancement is preferred[26].

In collaboration with European experts in a recently issued guideline, the Asian Federation of Societies for Ultrasound in Medicine and Biology (AFSUMB) concluded that the MI should be between 0.2 and 0.4. They added that the 0.1 to 0.4 range used in published reports was influenced by several factors, including EUS probe type (radial or linear), image processing hardware, and software, phase-inversion harmonics, amplitude modulations, and focal points[27].

Contrast-enhanced harmonic EUS imaging

Tissue harmonic imaging (THI) is an ultrasonographic technique, first introduced in 1997, that utilizes nonlinear propagation of ultrasound (US) waves to generate images that are superior in quality to the fundamental B-mode imaging mode[28]. This tool was incorporated into the EUS imaging arsenal approximately a decade later[29].

The two image processing techniques developed to generate harmonic images were the band filtering method and phase inversion method. The ability of harmonic imaging to improve signal-to-noise ratio and reduce artifacts produced by side lobes, grating lobes, and reverberation allowed it to outperform earlier imaging applications, such as Color Doppler and power Doppler, which were susceptible to motion artifacts[30]. Furthermore, this modality allowed for visualization of parenchymal perfusion and microvasculature of the pancreas[31].

AFSUMB, in their summary recommendations, alluded to the benefit of contrast-enhanced harmonic EUS (CH-EUS) for characterization of solid pancreatic masses, pancreatic cancer staging in patients with suspected major vessel involvement, identification of mural nodules in cystic pancreatic lesions, and detection of subtle pancreatic lesions[27].

Nevertheless, THI is saddled with certain intrinsic technical limitations. The narrow bandwidth decreases axial resolution when applying the band filtering method. This limitation gave rise to the conception of the phase inversion method. However, the latter method necessitates the transmission of two US pulses, thus decreasing the frame rate and raising the possibility of motion artifacts[30].

Contrast agents

The first reported use of intravenous ultrasound contrast agents (UCAs) in ultrasonography was for image enhancement during echocardiography. Its adoption followed this in transabdominal ultrasonography before it was eventually introduced in EUS[32]. EFSUMB's recommendation on contrast for CE-EUS in non-liver applications highlighted its similarity to its use in transabdominal CEUS[33]. Worth noting is that the modalities, as mentioned earlier, represent the only imaging techniques that allow a dynamic observation of the CE phases[34]. UCAs are used to augment their ability in lesion characterization and intervention guidance.

During the evolutionary phase of CE-EUS, various agents were explored to advance the diagnostic performance of this modality. To render stability and durability, all commercially available agents are composed of gas-filled microbubbles encapsulated by a phospholipid or albumin shell. Each agent is aptly categorized based on its half-life and ability for transpulmonary passage[32].

The AFSUMB working group strongly recommends the following for use as UCAs: SonoVue (Lumason, sulfur hexafluoride micro-bubbles; Bracco, Milan, Italy; available in Europe, China, India, Korea, Hong Kong, New Zealand, Singapore, and Brazil); Definity (octafluoropropane microbubbles;

Bristol- Myers Squibb Medical Imaging, New York, NY, United States; available in the United States, Canada, and Australia), and Sonazoid (perfluorobutane microbubbles; GE Healthcare, Chicago, IL, United States; Daiichi Sankyo, Tokyo, Japan; available in Japan, South Korea, Taiwan and Norway). They further stated that neither of the agents had a superior diagnostic ability over the other[27].

Outcomes

A significant emphasis has been placed on researching the adjunctive role of CE-EUS in evaluating solid pancreatic masses. The result is a wealth of data that supports its use in assessing the pancreas and related pathologies[33]. Mei *et al*[35] affirmed this in a recent meta-analysis (n = 1497) to evaluate the accuracy of CE-EUS in discriminating between benign and malignant pancreatic masses with a reported pooled sensitivity, specificity, and diagnostic odds ratio of 0.91, 0.86, and 69.50, respectively[35].

Another meta-analysis that included 1139 patients across 12 studies highlighted that both high and low MI techniques had a 94% sensitivity and 89% specificity in differentiating pancreatic adenocarcinoma from other pathologies, with an area under the receiver operating characteristic curve of 0.9732. Subgroup analysis by excluding the outliers provided a sensitivity and specificity of 93%[36].

Săftoiu *et al*[37] analyzed the diagnostic accuracy of combining CE-EUS and elastography to differentiate focal pancreatic masses and highlighted its influence in decision making when confronted with a negative EUS-FNB result with a strong clinical suspicion of malignancy. A similar study by the same authors assessed the "synergistic" performance of CE-EUS with EUS-EG in 50 patients with a negative FNA of pancreatic masses. The results determined 19 to be pancreatic adenocarcinoma and 31 to be pseudo-tumoral chronic pancreatitis. CE-EUS reported a specificity of 100% and an accuracy of 93% in the cohort of 25 patients where EUS-EG demonstrated high lesion stiffness, diagnosing malignancy[38].

Buxbaum *et al*[39], in a prospective tandem-controlled trial involving 101 cases of focal pancreatic lesions, concluded that CE-EUS increased the diagnostic yield compared to conventional B-mode EUS with an odds ratio of 7.8 (95%CI: 2.7-30.2). Ninety-one percent of lesions were correctly characterized in the validation cohort, with an improved yield compared to unenhanced EUS[39]. In a real-life clinical setting, we demonstrate its use in a case of a degenerated IPMN showing how its use allows differentiation of tumor vegetation from mucus within a cyst (Figure 4).

AI

AI can level the playing field for endoscopists globally by making this highly sensitive and specific, but technically challenging, diagnostic tool we know as EUS more user-friendly and quicker to master.

The existing image enhancing techniques, CH-EUS and EUS-E, are available to the endoscopist currently as stand-alone software plug-ins. They require prior training before use with a low to moderate learning curve to master given that the user is already proficient with an echoendoscope.

The potential of AI is seen here in its ability to harness the diagnostic power of EUS while unifying all existing and future image-enhancing techniques "under one roof." This unifying software can aid the endoscopist by highlighting areas of concern while prompting suitable image-enhancing methods.

This added edge of diagnostic confidence can help overcome lesion ambiguity and improve lesion specificity, regardless of the years of prior endosonographic training.

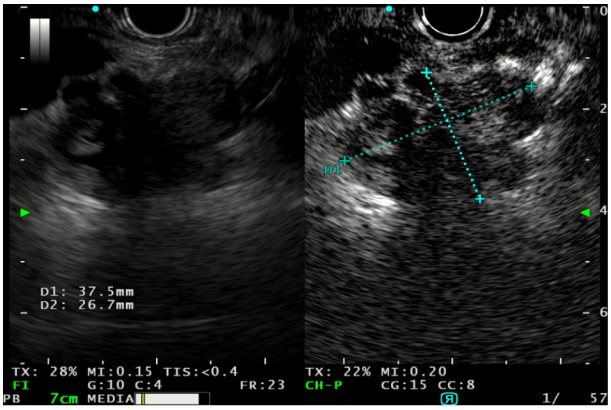
Principle of AI

AI is a divaricate under the broader umbrella of computing methodology and information sciences. It utilizes autonomous properties from rapidly advancing technological developments in deep learning as a segue to mimic human behavior ultimately. Over the last decade, AI applications have quickly matured. Their iterations in the daily practice of various fields within medicine are expanding with success.

The development and training of computer-aided diagnosis (CAD) systems revolve around the aim of autonomously distinguishing features that the human eye and mind may unintentionally miss. Identifying and interpreting changes of varying subtleties, particularly in medical images, has been the high point of AI. The objectivity of a trained CAD system could potentially seek to overcome one of the most significant limitations of any physician or endoscopist: The lack of an intra- and inter-observer agreement. Suppose an AI system can distinguish between neoplastic and non-neoplastic lesions with near perfection after training, it would seem reasonable to imagine that the burden from pathological examinations may be considerably relieved very soon. Thus far, colonic adenoma detection and differentiation have gained tremendous attention from several CAD systems utilizing deep learning and Artificial Neural networks. Due to their promising results, these systems have gained popularity in day-to-day endoscopy usage[40-43].

AI and EUS

The most common application of AI in EUS is creating machine learning architectures that extract EUS images and analyze them for their textures (boasting accuracy of up to 93%-94%) to create an artificial neural network that can ultimately serve as a clinical decision support tool. It can do one of 2 things: (1)



DOI: 10.3748/wjg.v28.i29.3814 **Copyright** ©The Author(s) 2022.

Figure 4 Use of contrast-enhanced endoscopic ultrasound to study the evolution of a degenerated intraductal papillary mucinous neoplasm and the vegetations within, allowing differentiate between mucus and vegetations as only tumor vegetations will show inhomogeneous enhancement.

Using the station approach to familiarize the endoscopist with normal anatomy, as demonstrated by Kanno *et al*[44]; and (2) Non-invasively differentiating pancreatic parenchymal pathologies when EUS-FNB may not be clinically feasible or have a poor diagnostic yield in the case of cysts or AIP[40].

In 2008, two studies emerged providing the diagnostic ability of AI integrated EUS in reporting pancreatic diseases. Săftoiu *et al*[45] reported 68 cases in a prospective study using a neural network EUS to compare PDAC and chronic pancreatitis. The authors reported 95% accuracy in the system's diagnostic ability. In the second study, Das *et al*[46] reviewed 319 images with a neural network system and performed a principal component analysis to compare acute and chronic pancreatitis, from pancreatic carcinoma. The study reported the area under the curve indicating the systems' diagnostic ability to be 93%. In 2013, Zhu *et al*[47] studied 288 cases retrospectively with a support vector machine and reached an accuracy of 94%.

Additionally, Săftoiu *et al*[48], in a prospective multicenter study, reported 167 cases using a neural network system, reaching a diagnostic accuracy of 94%. Ozkan *et al*[49] reported an accuracy of 93% in reviewing 332 images in retrospect using a neural network. A deep learning architecture specific to EUS noteworthy of mentioning is one used to differentiate high-grade dysplasia *vs* malignancy for IPMN with an accuracy of 94%[42]. In a single-center retrospective study that trained a deep learning algorithm using 3970 still images, deep learning was superior to human ability in its diagnostic accuracy (95% *vs* 56%), proving an objective method such as is this is more accurate in diagnosing malignancies of IPMN origin in comparison to conventional EUS features[42].

AI demonstrates its usefulness again in increasing diagnostic specificity using occlusion heatmap analysis to differentiate AIP from PDAC. The result is overcoming a delay in diagnosis, initiating immunosuppressive or chemoradiotherapy early, and preventing unwarranted resections (90% sensitive, 85% specific)[50]. It is worth mentioning that these studies use a cross-validation method with an internal control check, thus inflating the actuality of the diagnostic accuracy. In its applications to actual EUS fine-needle biopsy histopathological samples, AI was able to bring diagnostic clarity to difficult-to-analyze samples with an accuracy of 94.1% despite cellular paucity and contamination.

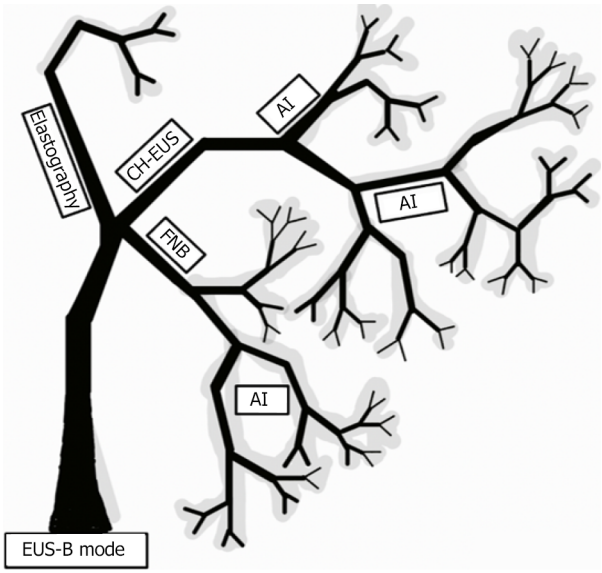
In centers with a lack of dedicated GI pathologists, AI software can quickly close this gap of diagnostic delay and eliminate repeat sampling at second or third centers[11]. One setback of AI is the black-box phenomenon, which can cause judgment errors without an explanatory basis. That said, a trained convolutional neural network model with extracted visual features from various pancreatic diseases, namely chronic pseudo-tumoral pancreatitis, NET, and PDAC, can accurately produce a real-time diagnosis[51].

SUMMARY RECOMMENDATIONS

For a suspected pancreatic mass, we propose utilizing both EUS-E and CE-EUS to augment conventional B-mode imaging (Figure 5).

Their advantages in defining nodules and ambiguous ROIs allow FNA/FNB sampling precision, making them crucial adjuncts in day-to-day practice, whether for first encounters or follow-up visits.

Validation studies are still underway to evaluate promising non-contrast-based high-definition imaging modalities. The modalities are in-built into the echo processor for ease of microvasculature study. They carry great potential in supplementing and possibly surrogating UCAs in conditions, such as pregnancy or compromised cardiopulmonary status[52]. However, until then, EUS-E and CE-EUS



DOI: 10.3748/wjg.v28.i29.3814 **Copyright** ©The Author(s) 2022.

Figure 5 Graphical representation of existing diagnostic applications to endoscopic ultrasound imaging in the form of a fractal tree, fractal analysis with artificial intelligence being the possible future of enhanced endoscopic ultrasound imaging. AI: Artificial intelligence; CH-EUS: Contrast-enhanced harmonic endoscopic ultrasound; FNB: Fine needle biopsy.

coupled with B-mode imaging will remain the choice stratagem in improving the early detection of pancreatic cancer.

CONCLUSION

In the EUS world of greys, colors emerged from elastography and patterns from contrast use, improving the overall accuracy of pancreatic mass differentiation. AI could be the rainbow that bridges us to a more precise diagnosis.

FOOTNOTES

Author contributions: Spadaccini M provided the outline; Koleth G with Spadaccini M performed most of the writing and equally contributed to this paper; Emmanuel J wrote on contrast-enhanced endoscopic ultrasound; Carrara S provided valuable oversight, all EUS pictures, and concluded the manuscript; Grizzi F provided the picture for fractal analysis; Khalaf K, Colombo M, Mangiavillano B, Fugazza A, Anderloni A, Facciorusso A, and Repici A provided input in writing the paper.

Conflict-of-interest statement: All the authors report no relevant conflicts of interest for this article.

Open-Access: This article is an open-access article that was selected by an in-house editor and fully peer-reviewed by external reviewers. It is distributed in accordance with the Creative Commons Attribution NonCommercial (CC BY-NC 4.0) license, which permits others to distribute, remix, adapt, build upon this work non-commercially, and license their derivative works on different terms, provided the original work is properly cited and the use is non-commercial. See: https://creativecommons.org/Licenses/by-nc/4.0/

Country/Territory of origin: Italy

ORCID number: Marco Spadaccini 0000-0003-3909-9012; Glenn Koleth 0000-0002-2939-6876; James Emmanuel 0000-0001-7154-461X; Kareem Khalaf 0000-0002-5534-7533; Antonio Facciorusso 0000-0002-2107-2156; Fabio Grizzi 0000-0003-0925-742X; Cesare Hassan 0000-0001-7167-1459; Matteo Colombo 0000-0003-0715-8233; Benedetto Mangiavillano 0000-0003-0611-7448; Alessandro Fugazza 0000-0003-0485-4903; Andrea Anderloni 0000-0002-1021-0031; Silvia Carrara 0000-0003-4206-9463; Alessandro Repici 0000-0002-1621-6450.

S-Editor: Fan JR
L-Editor: Filipodia
P-Editor: Fan JR

REFERENCES

1 **McGuigan A**, Kelly P, Turkington RC, Jones C, Coleman HG, McCain RS. Pancreatic cancer: A review of clinical diagnosis, epidemiology, treatment and outcomes. *World J Gastroenterol* 2018; **24**: 4846-4861 [PMID: 30487695 DOI: 10.3748/wjg.v24.i43.4846]

2 **Egawa S**, Toma H, Ohigashi H, Okusaka T, Nakao A, Hatori T, Maguchi H, Yanagisawa A, Tanaka M. Japan Pancreatic Cancer Registry; 30th year anniversary: Japan Pancreas Society. *Pancreas* 2012; **41**: 985-992 [PMID: 22750974 DOI: 10.1097/MPA.0b013e318258055c]

3 **Kitano M**, Yoshida T, Itonaga M, Tamura T, Hatamaru K, Yamashita Y. Impact of endoscopic ultrasonography on diagnosis of pancreatic cancer. *J Gastroenterol* 2019; **54**: 19-32 [PMID: 30406288 DOI: 10.1007/s00535-018-1519-2]

4 **Müller MF**, Meyenberger C, Bertschinger P, Schaer R, Marincek B. Pancreatic tumors: evaluation with endoscopic US, CT, and MR imaging. *Radiology* 1994; **190**: 745-751 [PMID: 8115622 DOI: 10.1148/radiology.190.3.8115622]

5 **Dietrich CF**, Ignee A, Frey H. Contrast-enhanced endoscopic ultrasound with low mechanical index: a new technique. *Z Gastroenterol* 2005; **43**: 1219-1223 [PMID: 16267707 DOI: 10.1055/s-2005-858662]

6 **Dietrich CF**, Sahai AV, D'Onofrio M, Will U, Arcidiacono PG, Petrone MC, Hocke M, Braden B, Burmester E, Möller K, Săftoiu A, Ignee A, Cui XW, Iordache S, Potthoff A, Iglesias-Garcia J, Fusaroli P, Dong Y, Jenssen C. Differential diagnosis of small solid pancreatic lesions. *Gastrointest Endosc* 2016; **84**: 933-940 [PMID: 27155592 DOI: 10.1016/j.gie.2016.04.034]

7 **Ignee A**, Jenssen C, Arcidiacono PG, Hocke M, Möller K, Saftoiu A, Will U, Fusaroli P, Iglesias-Garcia J, Ponnudurai R, Petrone MC, Braden B, Burmester E, Dong Y, Atkinson NS, Dietrich CF. Endoscopic ultrasound elastography of small solid pancreatic lesions: a multicenter study. *Endoscopy* 2018; **50**: 1071-1079 [PMID: 29689572 DOI: 10.1055/a-0588-4941]

8 **Rawla P**, Sunkara T, Gaduputi V. Epidemiology of Pancreatic Cancer: Global Trends, Etiology and Risk Factors. *World J Oncol* 2019; **10**: 10-27 [PMID: 30834048 DOI: 10.14740/wjon1166]

9 **Elfanagely Y**, Tse CS, Rich H, Hyder SM. Learning curves for EUS: single operators, endoscopy teams, and institutions. *Gastrointest Endosc* 2021; **93**: 989 [PMID: 33741097 DOI: 10.1016/j.gie.2020.10.031]

10 **Gonzalez JM**, Cohen J, Gromski MA, Saito K, Loundou A, Matthes K. Learning curve for endoscopic ultrasound-guided fine-needle aspiration (EUS-FNA) of pancreatic lesions in a novel ex-vivo simulation model. *Endosc Int Open* 2016; **4**: E1286-E1291 [PMID: 27995190 DOI: 10.1055/s-0042-118176]

11 **Tonozuka R**, Mukai S, Itoi T. The Role of Artificial Intelligence in Endoscopic Ultrasound for Pancreatic Disorders. *Diagnostics (Basel)* 2020; **11** [PMID: 33374181 DOI: 10.3390/diagnostics11010018]

12 **Faruk T**, Islam MK, Arefin S, Haq MZ. The Journey of Elastography: Background, Current Status, and Future Possibilities in Breast Cancer Diagnosis. *Clin Breast Cancer* 2015; **15**: 313-324 [PMID: 25858446 DOI: 10.1016/j.clbc.2015.01.002]

13 **Ohno E**, Kawashima H, Ishikawa T, Iida T, Suzuki H, Uetsuki K, Yashika J, Yamada K, Yoshikawa M, Gibo N, Aoki T, Kataoka K, Mori H, Yamamura T, Furukawa K, Nakamura M, Hirooka Y, Fujishiro M. Diagnostic performance of endoscopic ultrasonography-guided elastography for solid pancreatic lesions: Shear-wave measurements *vs* strain elastography with histogram analysis. *Dig Endosc* 2021; **33**: 629-638 [PMID: 32662150 DOI: 10.1111/den.13791]

14 **Sigrist RMS**, Liau J, Kaffas AE, Chammas MC, Willmann JK. Ultrasound Elastography: Review of Techniques and Clinical Applications. *Theranostics* 2017; **7**: 1303-1329 [PMID: 28435467 DOI: 10.7150/thno.18650]

15 **Giovannini M**. Endoscopic ultrasound elastography. *Pancreatology* 2011; **11** Suppl 2: 34-39 [PMID: 21464585 DOI: 10.1159/000323496]

16 **Giovannini M**. Contrast-enhanced endoscopic ultrasound and elastosonoendoscopy. *Best Pract Res Clin Gastroenterol* 2009; **23**: 767-779 [PMID: 19744639 DOI: 10.1016/j.bpg.2009.05.004]

17 **Pei Q**, Zou X, Zhang X, Chen M, Guo Y, Luo H. Diagnostic value of EUS elastography in differentiation of benign and malignant solid pancreatic masses: a meta-analysis. *Pancreatology* 2012; **12**: 402-408 [PMID: 23127527 DOI: 10.1016/j.pan.2012.07.013]

18 **Ying L**, Lin X, Xie ZL, Hu YP, Tang KF, Shi KQ. Clinical utility of endoscopic ultrasound elastography for identification of malignant pancreatic masses: a meta-analysis. *J Gastroenterol Hepatol* 2013; **28**: 1434-1443 [PMID: 23731128 DOI: 10.1111/jgh.12292]

19 **Lu Y**, Chen L, Li C, Chen H, Chen J. Diagnostic utility of endoscopic ultrasonography-elastography in the evaluation of solid pancreatic masses: a meta-analysis and systematic review. *Med Ultrason* 2017; **19**: 150-158 [PMID: 28440348 DOI: 10.11152/mu-987]

20 **Cosgrove D**, Piscaglia F, Bamber J, Bojunga J, Correas JM, Gilja OH, Klauser AS, Sporea I, Calliada F, Cantisani V, D'Onofrio M, Drakonaki EE, Fink M, Friedrich-Rust M, Fromageau J, Havre RF, Jenssen C, Ohlinger R, Săftoiu A, Schaefer F, Dietrich CF; EFSUMB. EFSUMB guidelines and recommendations on the clinical use of ultrasound elastography. Part 2: Clinical applications. *Ultraschall Med* 2013; **34**: 238-253 [PMID: 23605169 DOI: 10.1055/s-0033-1335375]

21 **Carrara S**, Di Leo M, Grizzi F, Correale L, Rahal D, Anderloni A, Auriemma F, Fugazza A, Preatoni P, Maselli R, Hassan C, Finati E, Mangiavillano B, Repici A. EUS elastography (strain ratio) and fractal-based quantitative analysis for the diagnosis of solid pancreatic lesions. *Gastrointest Endosc* 2018; **87**: 1464-1473 [PMID: 29329992 DOI: 10.1016/j.gie.2017.12.031]

22 **Hirche TO**, Ignee A, Barreiros AP, Schreiber-Dietrich D, Jungblut S, Ott M, Hirche H, Dietrich CF. Indications and limitations of endoscopic ultrasound elastography for evaluation of focal pancreatic lesions. *Endoscopy* 2008; **40**: 910-917 [PMID: 19009483 DOI: 10.1055/s-2008-1077726]

23 **Kato T**, Tsukamoto Y, Naitoh Y, Hirooka Y, Furukawa T, Hayakawa T. Ultrasonographic and endoscopic ultrasonographic angiography in pancreatic mass lesions. *Acta Radiol* 1995; **36**: 381-387 [PMID: 7619616]

24 **Hirooka Y**, Naitoh Y, Goto H, Ito A, Taki T, Hayakawa T. Usefulness of contrast-enhanced endoscopic ultrasonography with intravenous injection of sonicated serum albumin. *Gastrointest Endosc* 1997; **46**: 166-169 [PMID: 9283869 DOI: 10.1016/s0016-5107(97)70067-1]

25 **Mohamed RM**, Yan BM. Contrast enhanced endoscopic ultrasound: More than just a fancy Doppler. *World J Gastrointest Endosc* 2010; **2**: 237-243 [PMID: 21160613 DOI: 10.4253/wjge.v2.i7.237]

26 **Hocke M**, Dietrich CF. Advanced EUS Imaging for Pancreatic Diseases: CE-EUS (Low-MI, High-MI) and Real-Time Elastography, 3D. *Video J Encyc GI Endos* 2013; **1**: 537-539 [DOI: 10.1016/s2212-0971(13)70235-8]

27 **Kitano M**, Yamashita Y, Kamata K, Ang TL, Imazu H, Ohno E, Hirooka Y, Fusaroli P, Seo DW, Napoléon B, Teoh AYB, Kim TH, Dietrich CF, Wang HP, Kudo M; Working group for the International Consensus Guidelines for Contrast-Enhanced Harmonic Endoscopic Ultrasound. The Asian Federation of Societies for Ultrasound in Medicine and Biology (AFSUMB) Guidelines for Contrast-Enhanced Endoscopic Ultrasound. *Ultrasound Med Biol* 2021; **47**: 1433-1447 [PMID: 33653627 DOI: 10.1016/j.ultrasmedbio.2021.01.030]

28 **Anvari A**, Forsberg F, Samir AE. A Primer on the Physical Principles of Tissue Harmonic Imaging. *Radiographics* 2015; **35**: 1955-1964 [PMID: 26562232 DOI: 10.1148/rg.2015140338]

29 **Alvarez-Sánchez MV**, Napoléon B. Contrast-enhanced harmonic endoscopic ultrasound imaging: basic principles, present situation and future perspectives. *World J Gastroenterol* 2014; **20**: 15549-15563 [PMID: 25400439 DOI: 10.3748/wjg.v20.i42.15549]

30 **Ohno E**, Kawashima H, Hashimoto S, Goto H, Hirooka Y. Current status of tissue harmonic imaging in endoscopic ultrasonography (EUS) and EUS-elastography in pancreatobiliary diseases. *Dig Endosc* 2015; **27** Suppl 1: 68-73 [PMID: 25630752 DOI: 10.1111/den.12433]

31 **Kitano M**, Sakamoto H, Matsui U, Ito Y, Maekawa K, von Schrenck T, Kudo M. A novel perfusion imaging technique of the pancreas: contrast-enhanced harmonic EUS (with video). *Gastrointest Endosc* 2008; **67**: 141-150 [PMID: 18155437 DOI: 10.1016/j.gie.2007.07.045]

32 **Reddy NK**, Ioncică AM, Săftoiu A, Vilmann P, Bhutani MS. Contrast-enhanced endoscopic ultrasonography. *World J Gastroenterol* 2011; **17**: 42-48 [PMID: 21218082 DOI: 10.3748/wjg.v17.i1.42]

33 **Saftoiu A**, Vilmann P, Bhutani MS. The role of contrast-enhanced endoscopic ultrasound in pancreatic adenocarcinoma. *Endosc Ultrasound* 2016; **5**: 368-372 [PMID: 28000627 DOI: 10.4103/2303-9027.190932]

34 **D'Onofrio M**, Biagioli E, Gerardi C, Canestrini S, Rulli E, Crosara S, De Robertis R, Floriani I. Diagnostic performance of contrast-enhanced ultrasound (CEUS) and contrast-enhanced endoscopic ultrasound (ECEUS) for the differentiation of pancreatic lesions: a systematic review and meta-analysis. *Ultraschall Med* 2014; **35**: 515-521 [PMID: 25226455 DOI: 10.1055/s-0034-1385068]

35 **Mei S**, Wang M, Sun L. Contrast-Enhanced EUS for Differential Diagnosis of Pancreatic Masses: A Meta-Analysis. *Gastroenterol Res Pract* 2019; **2019**: 1670183 [PMID: 30962802 DOI: 10.1155/2019/1670183]

36 **Gong TT**, Hu DM, Zhu Q. Contrast-enhanced EUS for differential diagnosis of pancreatic mass lesions: a meta-analysis. *Gastrointest Endosc* 2012; **76**: 301-309 [PMID: 22703697 DOI: 10.1016/j.gie.2012.02.051]

37 **Săftoiu A**, Iordache SA, Gheonea DI, Popescu C, Maloş A, Gorunescu F, Ciurea T, Iordache A, Popescu GL, Manea CT. Combined contrast-enhanced power Doppler and real-time sonoelastography performed during EUS, used in the differential diagnosis of focal pancreatic masses (with videos). *Gastrointest Endosc* 2010; **72**: 739-747 [PMID: 20674916 DOI: 10.1016/j.gie.2010.02.056]

38 **Iordache S**, Costache MI, Popescu CF, Streba CT, Cazacu S, Săftoiu A. Clinical impact of EUS elastography followed by contrast-enhanced EUS in patients with focal pancreatic masses and negative EUS-guided FNA. *Med Ultrason* 2016; **18**: 18-24 [PMID: 26962549 DOI: 10.11152/mu.2013.2066.181.ich]

39 **Buxbaum J**, Ko C, Varghese N, Lee A, Sahakian A, King K, Serna J, Lee H, Tchelepi H, Van Dam J, Duddalwar V. Qualitative and Quantitative Contrast-enhanced Endoscopic Ultrasound Improves Evaluation of Focal Pancreatic Lesions. *Clin Gastroenterol Hepatol* 2020; **18**: 917-925.e4 [PMID: 31499247 DOI: 10.1016/j.cgh.2019.08.054]

40 **Kuwahara T**, Hara K, Mizuno N, Haba S, Okuno N, Koda H, Miyano A, Fumihara D. Current status of artificial intelligence analysis for endoscopic ultrasonography. *Dig Endosc* 2021; **33**: 298-305 [PMID: 33098123 DOI: 10.1111/den.13880]

41 **Murakami D**, Yamato M, Arai M, Nishino T. Artificial intelligence in colonoscopy. *Lancet Gastroenterol Hepatol* 2021; **6**: 984-985 [PMID: 34774156 DOI: 10.1016/S2468-1253(21)00379-4]

42 **Marya NB**, Powers PD, Chari ST, Gleeson FC, Leggett CL, Abu Dayyeh BK, Chandrasekhara V, Iyer PG, Majumder S, Pearson RK, Petersen BT, Rajan E, Sawas T, Storm AC, Vege SS, Chen S, Long Z, Hough DM, Mara K, Levy MJ. Utilisation of artificial intelligence for the development of an EUS-convolutional neural network model trained to enhance the diagnosis of autoimmune pancreatitis. *Gut* 2021; **70**: 1335-1344 [PMID: 33028668 DOI: 10.1136/gutjnl-2020-322821]

43 **Zhang J**, Zhu L, Yao L, Ding X, Chen D, Wu H, Lu Z, Zhou W, Zhang L, An P, Xu B, Tan W, Hu S, Cheng F, Yu H. Deep learning-based pancreas segmentation and station recognition system in EUS: development and validation of a useful training tool (with video). *Gastrointest Endosc* 2020; **92**: 874-885.e3 [PMID: 32387499 DOI: 10.1016/j.gie.2020.04.071]

44 **Kanno A**, Masamune A, Fujishima F, Iwashita T, Kodama Y, Katanuma A, Ohara H, Kitano M, Inoue H, Itoi T, Mizuno N, Miyakawa H, Mikata R, Irisawa A, Sato S, Notohara K, Shimosegawa T. Diagnosis of autoimmune pancreatitis by EUS-guided FNA using a 22-gauge needle: a prospective multicenter study. *Gastrointest Endosc* 2016; **84**: 797-804.e1 [PMID: 27068878 DOI: 10.1016/j.gie.2016.03.1511]

45 **Săftoiu A**, Vilmann P, Gorunescu F, Gheonea DI, Gorunescu M, Ciurea T, Popescu GL, Iordache A, Hassan H, Iordache S. Neural network analysis of dynamic sequences of EUS elastography used for the differential diagnosis of chronic pancreatitis and pancreatic cancer. *Gastrointest Endosc* 2008; **68**: 1086-1094 [PMID: 18656186 DOI: 10.1016/j.gie.2008.04.031]

46 **Das A**, Nguyen CC, Li F, Li B. Digital image analysis of EUS images accurately differentiates pancreatic cancer from chronic pancreatitis and normal tissue. *Gastrointest Endosc* 2008; **67**: 861-867 [PMID: 18179797 DOI: 10.1016/j.gie.2007.08.036]

47 **Zhu M**, Xu C, Yu J, Wu Y, Li C, Zhang M, Jin Z, Li Z. Differentiation of pancreatic cancer and chronic pancreatitis using computer-aided diagnosis of endoscopic ultrasound (EUS) images: a diagnostic test. *PLoS One* 2013; **8**: e63820 [PMID: 23704940 DOI: 10.1371/journal.pone.0063820]

48 **Săftoiu A**, Vilmann P, Dietrich CF, Iglesias-Garcia J, Hocke M, Seicean A, Ignee A, Hassan H, Streba CT, Ioncică AM,

Gheonea DI, Ciurea T. Quantitative contrast-enhanced harmonic EUS in differential diagnosis of focal pancreatic masses (with videos). *Gastrointest Endosc* 2015; **82**: 59-69 [PMID: 25792386 DOI: 10.1016/j.gie.2014.11.040]

49 **Ozkan M**, Cakiroglu M, Kocaman O, Kurt M, Yilmaz B, Can G, Korkmaz U, Dandil E, Eksi Z. Age-based computer-aided diagnosis approach for pancreatic cancer on endoscopic ultrasound images. *Endosc Ultrasound* 2016; **5**: 101-107 [PMID: 27080608 DOI: 10.4103/2303-9027.180473]

50 **Naito Y**, Tsuneki M, Fukushima N, Koga Y, Higashi M, Notohara K, Aishima S, Ohike N, Tajiri T, Yamaguchi H, Fukumura Y, Kojima M, Hirabayashi K, Hamada Y, Norose T, Kai K, Omori Y, Sukeda A, Noguchi H, Uchino K, Itakura J, Okabe Y, Yamada Y, Akiba J, Kanavati F, Oda Y, Furukawa T, Yano H. A deep learning model to detect pancreatic ductal adenocarcinoma on endoscopic ultrasound-guided fine-needle biopsy. *Sci Rep* 2021; **11**: 8454 [PMID: 33875703 DOI: 10.1038/s41598-021-87748-0]

51 **Udriștoiu AL**, Cazacu IM, Gruionu LG, Gruionu G, Iacob AV, Burtea DE, Ungureanu BS, Costache MI, Constantin A, Popescu CF, Udriștoiu Ș, Săftoiu A. Real-time computer-aided diagnosis of focal pancreatic masses from endoscopic ultrasound imaging based on a hybrid convolutional and long short-term memory neural network model. *PLoS One* 2021; **16**: e0251701 [PMID: 34181680 DOI: 10.1371/journal.pone.0251701]

52 **Hwang JS**, Seo DW, So H, Ko SW, Joo HD, Oh D, Song TJ, Park DH, Lee SS, Lee SK, Kim MH. Clinical utility of directional eFLOW compared with contrast-enhanced harmonic endoscopic ultrasound for assessing the vascularity of pancreatic and peripancreatic masses. *Pancreatology* 2022; **22**: 130-135 [PMID: 34753658 DOI: 10.1016/j.pan.2021.11.002]

World Journal of Gastroenterology

Submit a Manuscript: https://www.f6publishing.com

World J Gastroenterol 2022 August 7; 28(29): 3825-3837

DOI: 10.3748/wjg.v28.i29.3825

ISSN 1007-9327 (print) ISSN 2219-2840 (online)

ORIGINAL ARTICLE

Basic Study

Qingyi decoction attenuates intestinal epithelial cell injury *via* the calcineurin/nuclear factor of activated T-cells pathway

Guan-Yu Wang, Dong Shang, Gui-Xin Zhang, Hui-Yi Song, Nan Jiang, Huan-Huan Liu, Hai-Long Chen

Specialty type: Gastroenterology and hepatology

Provenance and peer review: Unsolicited article; Externally peer reviewed.

Peer-review model: Single blind

Peer-review report's scientific quality classification

Grade A (Excellent): 0
Grade B (Very good): B, B
Grade C (Good): C
Grade D (Fair): D
Grade E (Poor): 0

P-Reviewer: Exbrayat JM, France; Ma W, China; Surbatovic M, Serbia

Received: September 18, 2021
Peer-review started: September 18, 2021
First decision: December 4, 2021
Revised: December 15, 2021
Accepted: July 8, 2022
Article in press: July 8, 2022
Published online: August 7, 2022

Guan-Yu Wang, Dong Shang, Gui-Xin Zhang, Hai-Long Chen, Department of General Surgery, The First Affiliated Hospital of Dalian Medical University, Dalian 116011, Liaoning Province, China

Guan-Yu Wang, Dong Shang, Gui-Xin Zhang, Nan Jiang, Huan-Huan Liu, Hai-Long Chen, Institute of Integrative Medicine of Dalian Medical University, Dalian 116044, Liaoning Province, China

Hui-Yi Song, Laboratory of Integrative Medicine, The First Affiliated Hospital of Dalian Medical University, Dalian 116011, Liaoning Province, China

Corresponding author: Hai-Long Chen, PhD, Chief Physician, Department of General Surgery, The First Affiliated Hospital of Dalian Medical University, No. 222 Zhongshan Road, Dalian 116011, Liaoning Province, China. hailongchen2014@yeah.net

Abstract

BACKGROUND

Recent studies have demonstrated that dysfunction of the intestinal barrier is a significant contributing factor to the development of severe acute pancreatitis (SAP). A stable intestinal mucosa barrier functions as a major anatomic and functional barrier, owing to the balance between intestinal epithelial cell (IEC) proliferation and apoptosis. There is some evidence that calcium overload may trigger IEC apoptosis and that calcineurin (CaN)/nuclear factor of activated T-cells (NFAT) signaling might play an important role in calcium-mediated apoptosis.

AIM

To investigate the potential mechanisms underlying the therapeutic effect of Qingyi decoction (QYD) in SAP.

METHODS

A rat model of SAP was created *via* retrograde infusion of sodium deoxycholate. Serum levels of amylase, tumor necrosis factor (TNF-α), interleukin (IL)-6, D-lactic acid, and diamine oxidase (DAO); histological changes; and apoptosis of IECs were examined in rats with or without QYD treatment. The expression of the two subunits of CaN and NFAT in intestinal tissue was measured *via* quantitative real-time polymerase chain reaction and western blotting. For *in vitro* studies, Caco-2 cells were treated with lipopolysaccharide (LPS) and QYD serum, and then cell

viability and intracellular calcium levels were detected.

RESULTS

Retrograde infusion of sodium deoxycholate increased the severity of pancreatic and intestinal pathology and the levels of serum amylase, TNF-α, and IL-6. Both the indicators of intestinal mucosa damage (D-lactic acid and DAO) and the levels of IEC apoptosis were elevated in the SAP group. QYD treatment reduced the serum levels of amylase, TNF-α, IL-6, D-lactic acid, and DAO and attenuated the histological findings. IEC apoptosis associated with SAP was ameliorated under QYD treatment. In addition, the protein expression levels of the two subunits of CaN were remarkably elevated in the SAP group, and the NFATc3 gene was significantly upregulated at both the transcript and protein levels in the SAP group compared with the control group. QYD significantly restrained CaN and NFATc3 gene expression in the intestine, which was upregulated in the SAP group. Furthermore, QYD serum significantly decreased the LPS-induced elevation in intracellular free Ca^{2+} levels and inhibited cell death.

CONCLUSION

QYD can exert protective effects against intestinal mucosa damage caused by SAP and the protective effects are mediated, at least partially, by restraining IEC apoptosis *via* the CaN/NFATc3 pathway.

Key Words: Severe acute pancreatitis; Intestinal epithelial cell; Apoptosis; Calcineurin/nuclear factor of activated T-cells pathway; Qingyi decoction

©The Author(s) 2022. Published by Baishideng Publishing Group Inc. All rights reserved.

Core Tip: This manuscript investigated the role of the calcineurin (CaN)/nuclear factor of activated T-cells (NFATc3) pathway in the apoptosis of intestinal epithelial cells (IECs) in severe acute pancreatitis (SAP) and the potential mechanisms underlying the therapeutic effect of Qingyi decoction (QYD). QYD significantly restrained CaN and NFATc3 gene expression in the intestine, ameliorated IEC apoptosis associated with SAP, and decreased the lipopolysaccharide-induced elevation in intracellular free Ca^{2+} levels and cell death. These findings suggest that the protective effects of QYD might be mediated, at least partially, by downregulating IEC apoptosis *via* the CaN/NFATc3 pathway.

Citation: Wang GY, Shang D, Zhang GX, Song HY, Jiang N, Liu HH, Chen HL. Qingyi decoction attenuates intestinal epithelial cell injury *via* the calcineurin/nuclear factor of activated T-cells pathway. *World J Gastroenterol* 2022; 28(29): 3825-3837

URL: https://www.wjgnet.com/1007-9327/full/v28/i29/3825.htm

DOI: https://dx.doi.org/10.3748/wjg.v28.i29.3825

INTRODUCTION

Severe acute pancreatitis (SAP) is a severe acute abdominal disease characterized by high morbidity and mortality that can occur as a consequence of systemic inflammatory response syndrome (SIRS) and multiple organ dysfunction syndrome (MODS)[1]. A considerable amount of literature has been published on SAP. These studies have demonstrated that dysfunction of the intestinal barrier is a significant contributing factor to the development of SAP. Disruption of the intestinal barrier can give rise to gut bacteria and endotoxin translocation, thus creating secondary infections, SIRS, and MODS, leading to SAP[2]. A stable intestinal mucosa barrier functions as a major anatomic and functional barrier, owing to the balance between intestinal epithelial cell (IEC) proliferation and apoptosis. Recent research has revealed that IEC apoptosis plays an essential role in the development of SAP, and increased IEC apoptosis has been confirmed to contribute to intestinal injury, mucosal atrophy, bacterial translocation, and barrier dysfunction in SAP[3-5].

As a ubiquitous second messenger, Ca^{2+} has a significant impact on a variety of cellular processes in nearly all cell types. Calcineurin (CaN), a unique calcium-activated serine/threonine phosphatase, is a dominant factor in calcium-dependent signal transduction pathways. Nuclear factor of activated T-cells (NFAT) is a substrate phosphorylated by CaN, that is completely dependent on Ca^{2+}/CaN signaling; thus, NFAT is remarkably responsive to intracellular Ca^{2+} oscillations[6]. There is some evidence that calcium overload may trigger IEC apoptosis and that CaN/NFAT signaling might play an important role in calcium-mediated apoptosis[7,8].

Qingyidecoction (QYD), a Chinese herbal medicine consisting of Radix Bupleuri (Chaihu, *Bupleurum scorzonerifolium* Willd.), Scutellariae Radix (Huangqin, *Scutellaria baicalensis* Georgi.), Aucklandiae Radix (Muxiang, *Aucklandia lappa* Decne.), Rhizoma Corydalis (Yanhusuo, *Corydalis acropteryx* Fedde), Coptidis Rhizoma (Huanglian, *Coptis chinensis* Franch.), Radix Paeoniae Alba (Baishao, *Paeonia lactiflora* Pall.), Rhei Radix Et Rhizoma (Dahuang, *Rheum palmatum* L.) and Natrii Sulfas (Mangxiao, *Mirabilite*) has been widely utilized for several decades in the treatment of acute pancreatitis in China[9]. QYD, as an organic combination of many effective components, plays a multitarget role in acute pancreatitis treatment through multiple pathways, including protecting the intestinal barrier. The efficacy of QYD has been demonstrated to involve its ability to moderate endotoxin generation, restrict excessive neutrophil activation, minimize the release of inflammatory cytokines, and inhibit IEC apoptosis[10]. The present study aimed to investigate the role of the CaN/NFATc3 pathway in the apoptosis of IECs in SAP and explore the potential mechanisms underlying the therapeutic effect of QYD.

MATERIALS AND METHODS

Animal preparation and experimental protocols

Male Sprague-Dawley (SD) rats, 180-220 g, were obtained from the specific-pathogen-free Animal Center of Dalian Medical University. This study was approved by the Ethics Committee of Dalian Medical University. Thirty male SD rats were randomly divided into an SAP group, a QYD treatment group, and a control group, with ten rats per group. The SAP model was established using a method previously described[9]. The rats in the QYD group were gavaged with three doses of QYD (10 mL/kg body weight/dose, the First Affiliated Hospital of Dalian Medical University, Dalian, China) 0.5 h before and 6 and 12 h after surgery. The rats in the control group received only sham surgery[9]. The rats were anesthetized with 10% chloralhydrate *via* intraperitoneal injection at 3 mL per kg bodyweight 24 h post operation. Abdominal aorta blood samples and tissue samples were collected immediately.

Measurement of serum amylase, interleukin-6, tumor necrosis factor-α, D-lactic acid, and diamine oxidase

Serum amylase was detected using a spectrophotometric method with a commercial kit (Jiancheng, Nanjing, China). Briefly, 0.5 mL of starch reagent and 0.10 mL of serum samples were added to a 5 mL graduated tube. After incubating for 7.5 min at 37 °C, 0.5 mL of iodine reagent and 3.0 mL water were added immediately. The absorbance was measured at 660 nm. Enzyme-linked immunosorbent assay (ELISA) kits for tumor necrosis factor (TNF-α) (Lengton, Shanghai, China), D-lactic acid (Goybio, Shanghai, China), diamine oxidase (DAO) (Jiancheng, Nanjing, China), interleukin (IL)-6 (Lengton, Shanghai, China) were used to evaluate the levels in rat serum according to the manufacturer's instructions.

Histological examination

Pancreatic and intestinal tissues were fixed in 10% formaldehyde. After dehydration in gradient alcohol and transparentizing in xylene, the tissues were embedded in paraffin and cut into 5 μm thick slices. The slices were stained with hematoxylin and eosin for histological examination. The tissues were scored under an optical microscope (Leica, Solms, Germany) by a pathologist blinded to the experimental design. Five histopathological parameters (edema, inflammatory infiltration, hemorrhage, and acinar necrosis) of the pancreatic tissue were evaluated, each on a scale of 0-4 using a previously described method[11]. Mucosal injury, inflammatory infiltration, and hemorrhage were graded, each on a scale of 0-5, using a method described in a previous article to assess intestinal tissue[12].

Apoptosis detection

Fixed rat intestinal sections with 10% formaldehyde were deparaffinized in xylene and rehydrated through a graded ethanol series. A terminal deoxynucleotidyl transferase-mediated dUTP nick-end labeling (TUNEL) assay kit (Keygen, Nanjing, China) was applied to assess apoptosis in intestinal tissue. Briefly, rat intestinal sections were treated with 50 μL of the TUNEL reaction mixture and then incubated at 37 °C for 60 min. After rinsing with phosphate buffer solution, tissue sections were stained with 4′,6-diamidino-2-phenylindole (DAPI) and observed with fluorescence microscopy.

Immunofluorescence analysis

For immunofluorescence analysis, intestinal sections were incubated in a xylol-ethanol gradient to remove the paraffin. The slides were incubated with primary antibody against NFATc3 (Santa Cruz, CA, United States) and subsequently incubated with Alexa Fluor goat anti-rabbit immunoglobulin G (Life Technologies), and then observed using fluorescence microscopy following staining of the nuclei with DAPI (Sigma-Aldrich, St. Louis, MO). The specificity of the signals was monitored by blank staining without primary antibodies.

Western blot analysis

Western blotting was performed as previously described[13]. Total protein from intestinal tissue was extracted with a protein extraction kit (KeyGen, Nanjing, China). Protein was separated by sodium dodecyl sulfate-polyacrylamide gel electrophoresis and then transferred onto a nitrocellulose membrane. After nonspecific binding was blocked, the membranes were incubated with primary antibodies against calcineurin A (CnA, 1:2000, Abcam, United Kingdom), calcineurin B (CnB, 1:500, Abcam, United Kingdom), and β-actin (1:1000). Immunoreactive proteins were visualized using enhanced chemiluminescence detection (Bioworld Technology, Nanjing, China). ImageJ software was used for statistical analyses of the band intensities normalized to β-actin.

Quantitative real-time polymerase chain reaction

Total RNA extraction from intestinal tissue was performed with NAiso Plus (TaKaRa, Dalian, China), and then a PrimeScriptTMRT MasterMix kit (TaKaRa, Dalian, China) was used to synthesize cDNA. Quantitative real-time polymerase chain reaction (qRT-PCR) was carried out in a 7300 Real-time PCR System using a SYBR® Premix Ex Taq™IIKit (TaKaRa). The primer sequences were as follows: NFATC3 forward 5′-GGTGGCCATCCTGTTGTGAA-3′ and reverse 5′-CAGTAATGCGATGCACCTGGTAA-3′; β-actin forward 5′- GGAGATTACTGCCCTGGCTCCTA-3′ and reverse 5′-GACTCATCGTACTCCT-GCTTGCTG-3′. The $2^{-\Delta\Delta Ct}$ method was used for statistical analyses of the mRNA levels normalized to β-actin.

Preparation of QYD serum

Drug-containing serum was prepared as described previously[14]. Ten SD rats were divided into two groups: A normal group and a QYD serum group. In the QYD serum group, QYD (the First Affiliated Hospital of Dalian Medical University, Dalian, China) was administered to SD rats *via* gavage at 10 mL/dose/kg body weight twice per day for 5 d. The rats in the normal group were treated with the same volume of saline. After 5 d of treatment, blood samples were extracted from the abdominal arteries. Under anesthesia, serum was isolated from both the normal group and the QYD group based on a previously described method[15].

Cell experimental design

Caco-2 cells were randomly divided into the following groups: The rat serum group, in which the cells were treated with 10% normal rat serum for 24 h; the rat serum + lipopolysaccharide (LPS) group, in which the cells were exposed to 100 ng/mL LPS and 10% normal rat serum for 24 h; and the QYD serum + LPS group, in which the cells were treated with 100 ng/mL LPS and 10% QYD serum for 24 h.

Cell viability analysis

Caco-2 cell viability was assessed using MTT assays (Sigma, St Louis, MO, United States). After incubation with MTT dye (5 mg/mL) for 4 h at 37 °C, DMSO (150 μL/well) was added. The optical absorbance was evaluated with a microplate reader at 490 nm to measure cell viability.

Measurement of intracellular calcium levels

Intracellular Ca^{2+} levels were monitored using the Ca^{2+}-sensitive fluorescent indicator Fluo-3. Flou-3 can enter cells through the medium of lipophilic AM and combine with intracellular free Ca^{2+}. The fluorescence intensity of Flou-3 is positively correlated with the concentration of intracellular free Ca^{2+}. Caco-2 cells were seeded in HBSS buffer with Fluo-3/AM at 5 μmol/L for 30 min. The cells were washed twice in fresh HBSS and then treated with 0.5 mL of HBSS buffer. Finally, a confocal laser scanning microscope (BioRad Radiance 2100) was used to assess the fluorescence intensity.

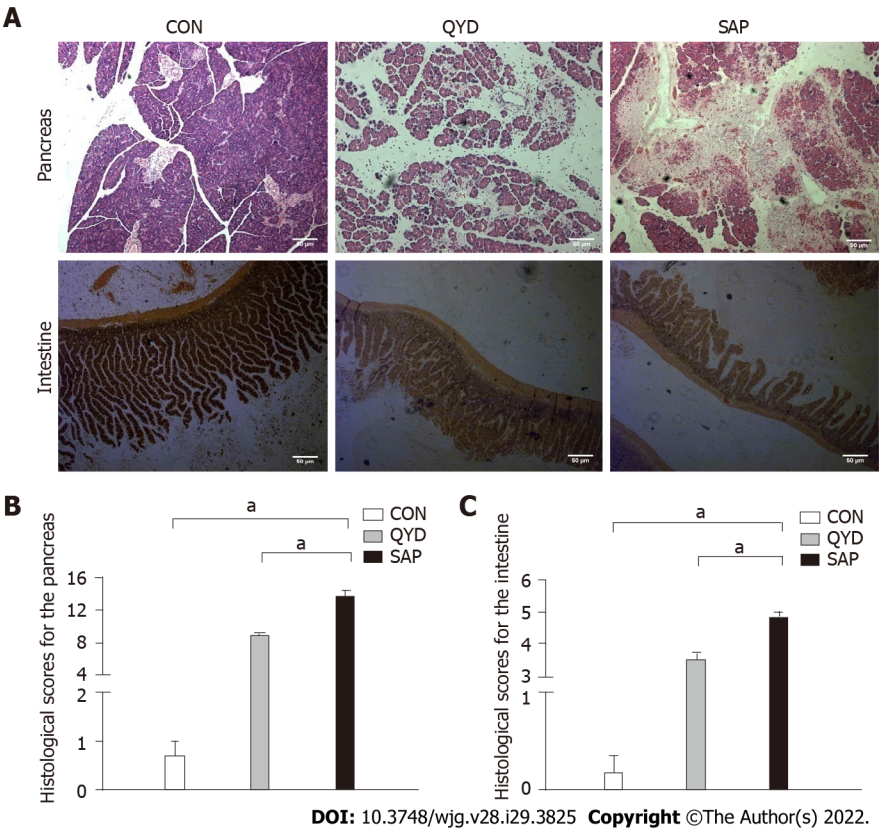
Statistical analysis

Data are expressed as the mean ± SD. SPSS v16.0 software was used for data analysis. One-way ANOVA was applied to assess significant differences between groups; $P < 0.05$ was considered to indicate a statistically significant difference.

RESULTS

Histological changes in the pancreas and intestine

As shown in Figure 1A, edema, inflammatory infiltration, hemorrhage, and acinar necrosis were observed in the pancreas as the characteristic morphological features of SAP. Interstitial edema, irregular villi, mucosal erosion, and inflammatory infiltration were exhibited in the SAP group, with necrosis and shedding of the intestinal epithelium. The pancreatic and intestinal histological scores were significantly higher according to the standards of Anthony and Chiu, respectively. However, QYD treatment significantly ameliorated the pancreatic and intestinal pathology caused by SAP (Figures 1B and 1C).



DOI: 10.3748/wjg.v28.i29.3825 **Copyright** ©The Author(s) 2022.

Figure 1 Histological changes in pancreatic and intestinal tissues. A: Slight edema was detected [pancreas control (CON) group]; broad necrosis of acinar cells and interstitial edema were observed [pancreas severe acute pancreatitis (SAP) group]; only local necrosis, slight interstitial edema, and few inflammatory cell infiltrates were observed [pancreas Qingyi decoction (QYD) group]. Slight interstitial edema was detected (intestine CON group); irregular villi, mucosal erosion, and inflammatory infiltration were observed (intestine SAP group); edema and mild mucosal erosion were observed (intestine QYD group); B: Histological scores for the pancreas; C: Histological scores for the intestine. The histological scores for the pancreas and intestine were significantly ameliorated in the QYD treatment group compared with the SAP group. $^{a}P < 0.05$, 100 ×. CON: Control; QYD: Qingyi decoction; SAP: Severe acute pancreatitis.

Serum levels of amylase, IL-6, TNF-α, D-lactic acid and DAO

It can be seen from the data in Figure 2 that the serum levels of amylase (Figure 2A), IL-6 (Figure 2B), and TNF-α (Figure 2C) were increased significantly in the SAP group compared with the control group. Consistent with previous research results, QYD treatment ameliorated the increases in amylase, IL-6, and TNF-α serum levels observed in the SAP group. D-lactic acid and DAO, which can serve as markers of intestinal barrier dysfunction and tissue injury, were significantly increased in the SAP group compared with the control group. However, the levels of serum D-lactic acid and DAO in the QYD group were significantly decreased compared with those in the SAP group (Figures 3A and 3B).

CnA and CnB expression in intestine

Following QYD treatment, the expression levels of CnA and CnB were detected *via* western blot analysis. The results, shown in Figure 4A, demonstrated that the expression levels of CnA and CnB were increased in the SAP group. The band intensities of CnA and CnB in the SAP group were 2.78 and 1.24, respectively, normalized to β-actin. QYD treatment significantly reduced the protein expression levels of CnA and CnB (Figures 4B and 4C).

NFATc3 expression in the intestine

Furthermore, we examined NFATc3 protein expression in intestinal tissues using immunofluorescence. NFATc3 was highly expressed in the SAP group compared with the control group but significantly downregulated under QYD treatment (Figure 5A). Semiquantitative analysis showed that the relative integral optical density (IOD) value was higher in the SAP group than in the control group. However, the relative IOD value was lower in the QYD group than in the SAP group (Figure 5B).

Transcription of NFATc3 mRNA in intestinal tissue

Compared with the control group, qRT-PCR analysis revealed that the level of NFATc3 mRNA transcription was obviously increased in the SAP group. QYD treatment decreased the mRNA level compared with that in the SAP group (Figure 6).

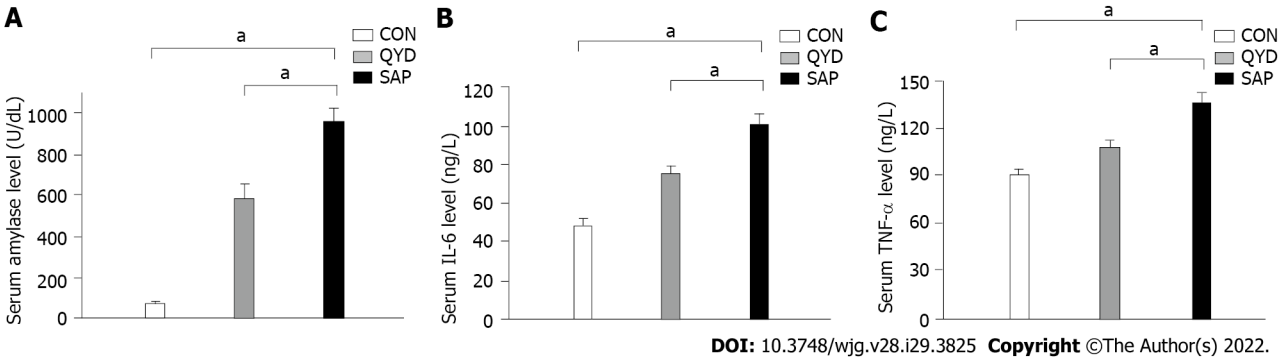


Figure 2 Serum levels in the different experimental groups. A: Amylase; B: Interleukin-6; C: Tumor necrosis factor-α. $^{a}P < 0.05$. CON: Control; QYD: Qingyi decoction; SAP: Severe acute pancreatitis; TNF: Tumor necrosis factor; IL: Interleukin.

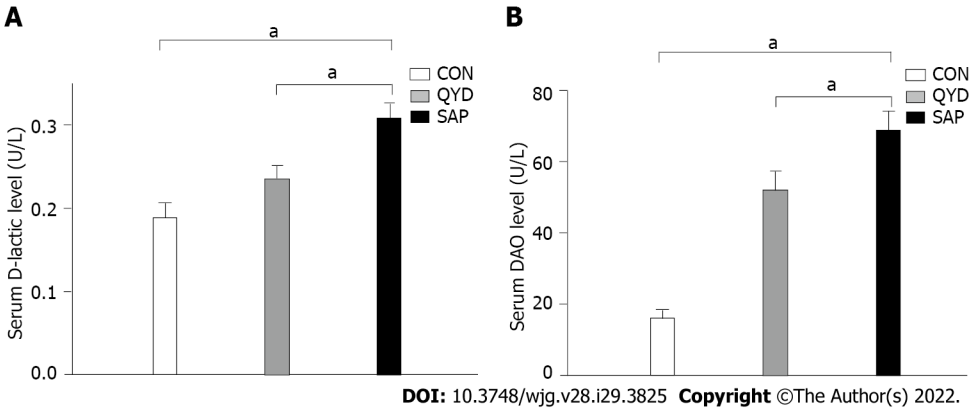


Figure 3 Effect of Qingyi decoction on serum. A: D-lactic acid; B: Diamine oxidase. $^{a}P < 0.05$. CON: Control; QYD: Qingyi decoction; SAP: Severe acute pancreatitis; DAO: Diamine oxidase.

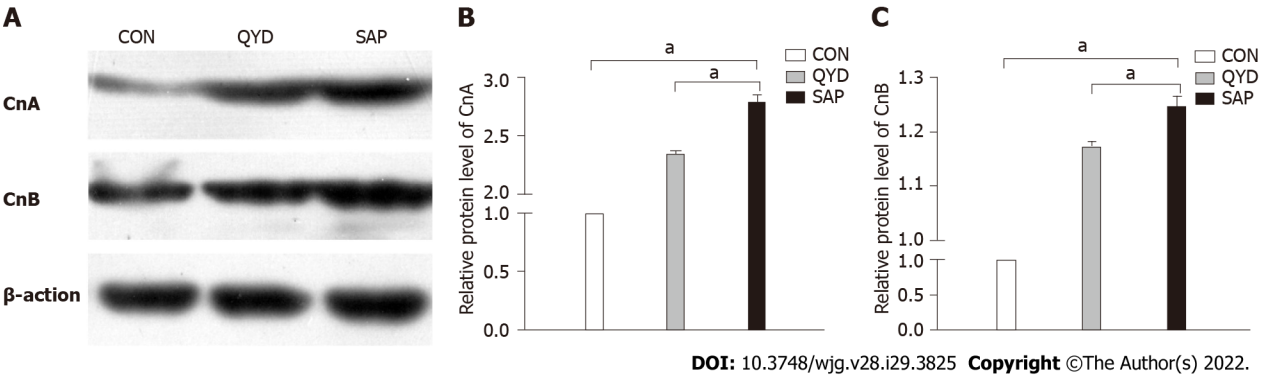


Figure 4 Expression of calcineurin subunits in the intestine. A: Calcineurin A (can) and calcineurin B (CnB) protein expression in the intestine; B: Qingyi decoction (QYD) treatment significantly inhibited the elevatcanCnA protein expression in the intestine observed in the severe acute pancreatitis (SAP) group; C: QYD treatment significantly inhibited the elevated CnB protein expression in the intestine observed in the SAP group. $^{a}P < 0.05$. CON: Control; QYD: Qingyi decoction; SAP: Severe acute pancreatitis; CnA: Calcineurin A; CnB: Calcineurin B.

ICE apoptosis

TUNEL staining results of rat intestinal tissue slices revealed that retrograde infusion of sodium deoxycholate increased ICE apoptosis compared with the control rats (Figure 7). However, compared with that in the SAP group, the level of ICE apoptosis in the QYD groups was significantly lower.

Effect of QYD serum on cell viability and intracellular calcium

A significant decline in cell viability after LPS treatment was verified by MTT assays (Figure 8), but QYD serum inhibited LPS-induced cell death. LPS induced a significant increase in Ca^{2+} levels. Treatment with QYD serum significantly attenuated the increase in Ca^{2+} levels caused by LPS-induced

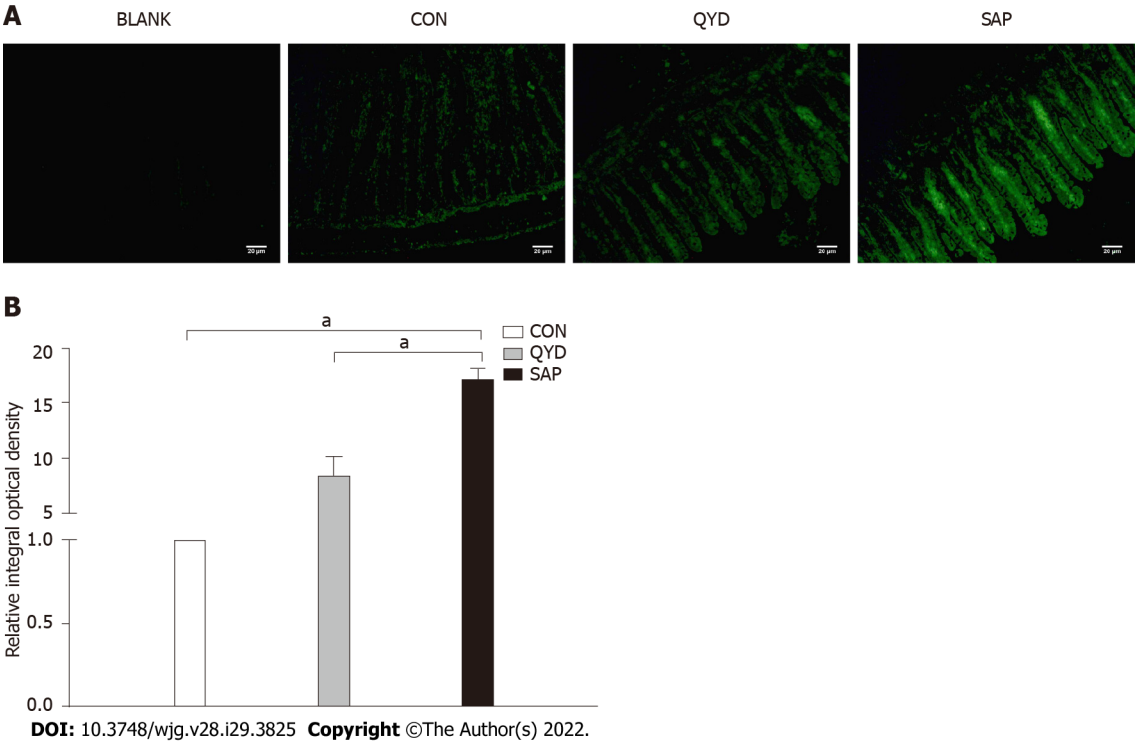


Figure 5 Immunofluorescence and semiquantitative analysis of nuclear factor of activated T-cells c3 expression. A: Immunofluorescence of nuclear factor of activated T-cells c3 (NFATc3) expression; B: Semiquantitative analysis of NFATc3 expression. NFATc3 was highly expressed in the severe acute pancreatitis group compared with the control group but significantly downregulated under Qingyi decoction treatment. $^{a}P < 0.05$. BLANK: Control without primary antibody; CON: Control; QYD: Qingyi decoction; SAP: Severe acute pancreatitis.

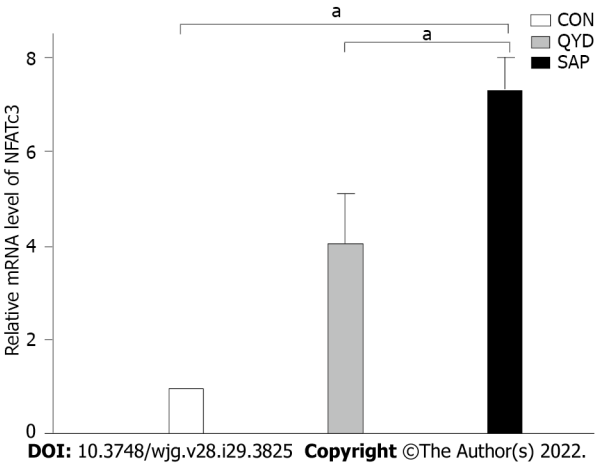
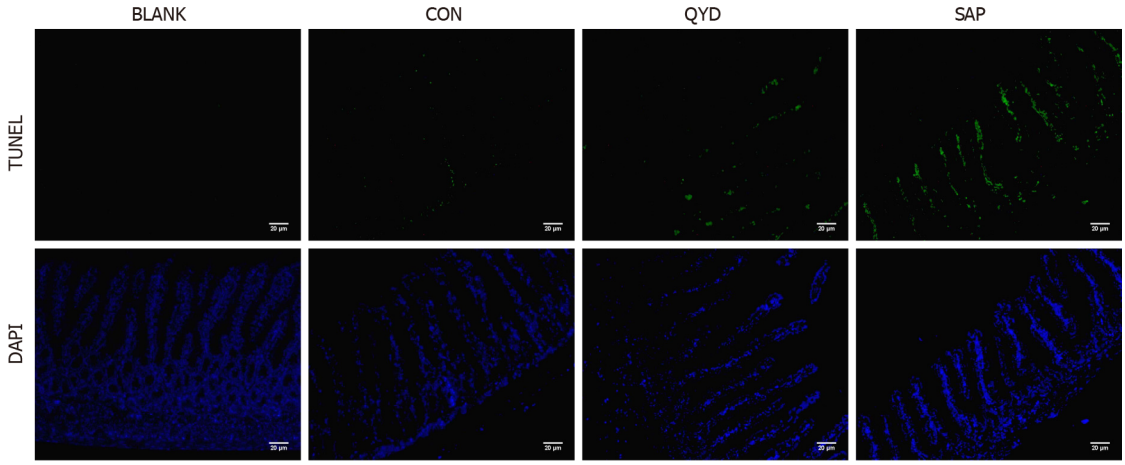


Figure 6 The level of nuclear factor of activated T-cells c3 mRNA transcription in intestinal tissue. $^{a}P < 0.05$. CON: Control; QYD: Qingyi decoction; SAP: Severe acute pancreatitis; NFATc3: Nuclear factor of activated T-cells c3.

injury (Figure 9A). The relative mean optical density value was higher in the LPS group than in the control group, but QYD serum treatment decreased the relative mean optical density induced by LPS (Figure 9B).

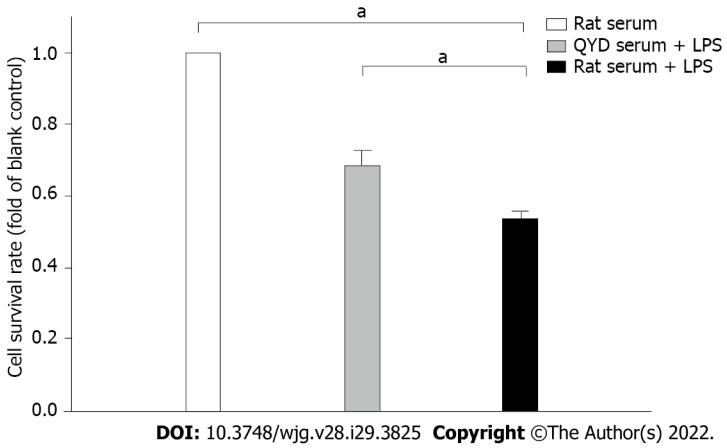
DISCUSSION

SAP refers to an acute abdominal disease characterized by rapid onset, rapid progression, and a high fatality rate. Prior studies have noted the importance of the intestinal barrier in the progression of SAP, which involves alterations in its mechanical, immune, chemical, and biological barriers[16]. Bacterial and/or endotoxin translocation from the gut lumen caused by intestinal barrier functional disturbance has a major influence on the prognosis of SAP[17]. The intestinal epithelium functions as the first barrier



DOI: 10.3748/wjg.v28.i29.3825 **Copyright** ©The Author(s) 2022.

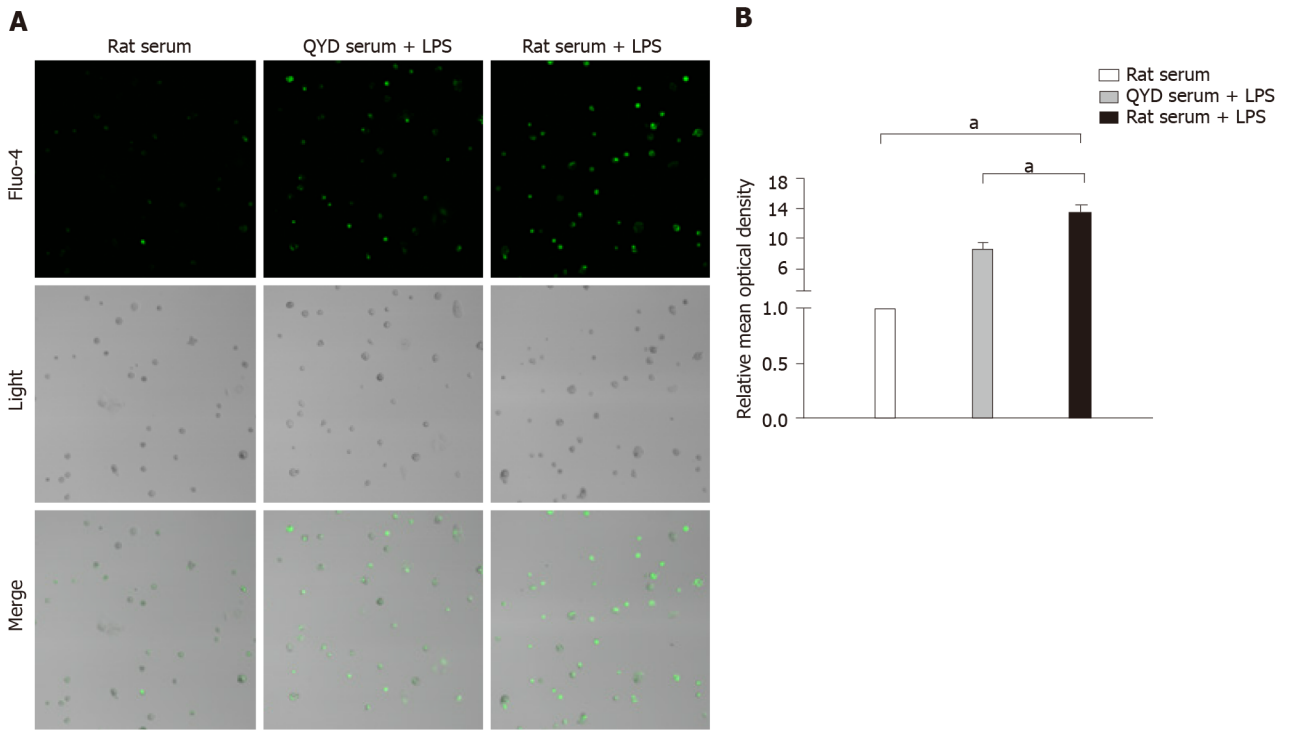
Figure 7 Transferase-mediated dUTP nick-end labeling assay to assess intestinal epithelial cell apoptosis. Compared with that in the severe acute pancreatitis group, the level of intestinal epithelial cell apoptosis in the Qingyi decoction groups was significantly lower. 200 ×. BLANK: Control without primary antibody; CON: Control; QYD: Qingyi decoction; SAP: Severe acute pancreatitis. TUNEL: Transferase-mediated dUTP nick-end labeling; DAPI: 4',6-diamidino-2-phenylindole.



DOI: 10.3748/wjg.v28.i29.3825 **Copyright** ©The Author(s) 2022.

Figure 8 Effect of Qingyi decoction serum on lipopolysaccharide-induced cell viability. $^{a}P < 0.05$. QYD: Qingyi decoction; LPS: Lipopolysaccharide.

to defend against the invasion of overcrowded intestinal bacteria owing to intestinal motor dysfunction in SAP. Therefore, conservation and renovation of the intestinal epithelial function may have a positive effect on SAP and reduce SAP-mediated septic morbidity and mortality[18]. As a specific form of cell death in terms of its morphology and biochemistry, apoptosis has been thought of as a key factor in the physiological processes of IEC biology[19]. Recently, investigators have examined the effects of IEC apoptosis on intestinal integrity[18]. TNF-α, secreted from pancreatic acinar cells, monocytes and macrophages, not only mediates primary inflammation directly but also contributes to the occurrence of secondary inflammation[20,21]. High concentrations of TNF-α can be detected in serum as well as in pancreatic parenchyma, ascitic fluid, and lymphatic drainage in the early stages of AP. Many studies have confirmed that high serum levels of TNF-α are related to the severity of AP[22,23]. IL-6 is a phosphorylated glycoprotein of 185 amino acids encoded by the human IL-6 gene. The IL-6 gene has been mapped to human chromosome 7p21-24[24]. Current evidence has clarified that IL-6 is a vital cytokine in AP development; moreover, the serum level of IL-6 is associated with AP severity[25]. DAO is an intestinal mucosal enzyme that plays a key role in digestion and absorption and maintenance of the mucosal barrier. DAO activity in the mature upper villus cells of the intestinal mucosa is high, but it is very low in all other tissues under normal physiological conditions. However, DAO activity increases in the blood plasma and intestinal lumen when the intestinal mucosa is damaged[26,27]. D-lactic acid is a metabolite produced by the fermentation of intestinal bacteria. When the permeability of the intestinal mucosa increases as a result of infection with bacteria, D-lactic acid can enter the blood circulation and be detected in the peripheral blood. Consequently, D-lactic acid can be used as an early indicator of intestinal mucosa damage with high specificity[28]. In accordance with previous studies, the present results confirmed that retrograde infusion of sodium deoxycholate successfully created a rat model of SAP. Retrograde infusion of sodium deoxycholate increased the severity of pancreatic and intestinal



DOI: 10.3748/wjg.v28.i29.3825 **Copyright** ©The Author(s) 2022.

Figure 9 Fluorescence images of [Ca^{2+}]i changes and the relative mean optical density. A: Fluorescence images of Ca^{2+} changes measured using a confocal microscope; B: The relative mean optical density. Treatment with Qingyi decoction serum significantly attenuated the increase in Ca^{2+} levels observed in response to lipopolysaccharide-induced injury. $^{a}P < 0.05$. QYD: Qingyi decoction; LPS: Lipopolysaccharide.

pathology and the levels of serum amylase, TNF-α, and IL-6. Moreover, both the indicators of intestinal mucosa damage (D-lactic acid and DAO) and the levels of IEC apoptosis were elevated in the SAP group.

CaN, a serine/threonine phosphatase, can be defined as a central calcium-responsive signaling molecule that has a significant impact on immune responses. CaN contains two subunits, CnA (the large catalytic subunit) and CnB (the smaller regulatory subunit). As a result, the formation of a heterodimer determines the activity of CaN[29]. It is now well established based on a variety of studies that CaN is a significant contributing factor to the development of acute pancreatitis as a unique target of aberrant calcium signaling[30-32]. For example, bile acid-induced pancreatic injury, transient high ductal pressure-induced pancreatic inflammation, and pancreatic inflammation caused by radiocontrast agents are all dependent on CaN activation[31,33]. CaN can dephosphorylate several substrates; one of the most important of these substrates is NFATc[34]. CaN/NFAT signaling can accurately adjust gene expression to alter cell differentiation and development, dependent on its remarkable ability to sense Ca^{2+} oscillations in cells[35]. When phosphorylated, all NFAT members reside in the cytosol of resting cells. However, upon dephosphorylation in response to high intracellular levels of Ca^{2+}, cytosolic CaN binds to NFAT, leading to nuclear translocation and transcription. The calcium-CaN-activated NFAT family contains four members (NFATc1, NFATc2, NFATc3, and NFATc4), among which the NFATc3 gene has been identified to be expressed in mammalian intestinal tissues[36]. The effects of NFATc3 in AP were described in a report by Awla *et al*[37]. Their results demonstrated that NFATc3 could adjust to trypsinogen activation, inflammation, and pancreatic tissue damage during the process of AP. Consequently, NFATc3 activity might be a therapeutic target[37]. In this study, we found that the protein expression levels of the two subunits of CaN were remarkably elevated in the SAP group. Furthermore, we examined NFATc3 expression using qRT-PCR and immunofluorescence analyses. The results suggested that the NFATc3 gene was significantly upregulated at both the transcript and protein levels in the SAP group compared with the control group.

The therapeutic effects and associated mechanisms of QYD may lie in clearing fever, detoxifying, soothing the liver, regulating the flow of vital energy and removing obstructions, invigorating the circulation of blood, dissipating blood stasis, and dredging urination and defecation, according to traditional Chinese medicine's holistic thoughts[38]. QYD, as an organic combination of many effective components, plays a multitarget role in acute pancreatitis treatment through multiple pathways, including defending the intestinal barrier. It has been proven that QYD can suppress intestinal bacterial translocation, moderate inflammatory factor release, and prohibit intestinal mucosa destruction by inhibiting the expression of intestinal secreted phospholipase A2[39], suppressing the Toll-like receptor 4/nuclear factor-kappa B signaling pathway and stimulating Zona occludens 1 expression[9]. Serum

pharmacology, first brought forward by the famous Japanese medical scientist Masakazu Tashiro, was introduced into the field of TCM medical research in 1997[40]. Serum pharmacology can broadly be defined as a new experimental method in which the target drug is administered orally to experimental animals, and then the serum is separated for *in vitro* pharmacological testing after a certain period[41]. Currently, rabbits and rats are mainly chosen for the preparation of drug-containing serum as a result of their biological characteristics similar to those of humans[42]. After investigation of many of the pharmacokinetic parameters of TCM, an optimal medication plan (medicating 2 times a day, 3 d to 5 d continuously, and exsanguination 1 h after the last medication) was proven feasible. Owing to better reflecting the metabolism of TCM in the human body, serum pharmacology can provide new directions for pharmacological analysis of TCM[43]. In this study, the severity of SAP in the QYD group was attenuated compared with that in the untreated SAP group. In addition, the levels of IEC apoptosis declined in the QYD group relative to the untreated group. QYD significantly alleviated the upregulation of CaN and NFATc3 gene expression in the intestine in the SAP group. Further study indicated that QYD serum significantly decreased the LPS-induced elevation of intracellular free Ca^{2+} levels and cell death.

CONCLUSION

In summary, the results of this research demonstrated that the CaN/NFATc3 pathway might play a key role in IEC injury caused by SAP and that QYD can exert protective effects. Moreover, QYD can regulate CaN and NFATc3 gene expression. The findings suggest that the protective effects of QYD might be mediated, at least partially, by restraining IEC apoptosis *via* the CaN/NFATc3 pathway.

ARTICLE HIGHLIGHTS

Research background

Severe acute pancreatitis (SAP) is a severe acute abdominal disease characterized by high morbidity and mortality. A considerable amount of literature has demonstrated that intestinal barrier dysfunction is a significant contributory factor to SAP development. Qingyi decoction (QYD) has been used to treat acute pancreatitis in China for many years.

Research motivation

The protective functions of QYD against intestinal mucosa injuries caused by SAP will provide new therapeutic information on SAP.

Research objectives

To research the function and mechanism of QYD in treating intestinal mucosa injuries caused by SAP.

Research methods

A rat model of SAP was created. Hematoxylin and eosin staining of pancreatic and intestinal tissue was performed. Enzyme-linked immunosorbent assay was used to estimate the concentrations of tumor necrosis factor (TNF-α), interleukin (IL)-6, D-lactic acid, and diamine oxidase (DAO). Terminal deoxynucleotidyl transferase dUTP nick-end labeling was carried out to assess intestinal epithelial cell (IEC) apoptosis. Quantitative real-time polymerase chain reaction, western blotting, and immunofluorescence were used to determine the expression of calcineurin (CaN) and nuclear factor of activated T-cells (NFATc3). MTT and confocal laser scanning microscope were used to detect cell viability and intracellular calcium levels *in vitro* studies.

Research results

In this study, the severity of SAP in the QYD group was attenuated. In addition, the levels of IEC apoptosis declined in the QYD group. QYD significantly restrained CaN and NFATc3 gene expression in the intestine. Further study indicated that QYD serum significantly decreased the lipopolysaccharide-induced elevation in intracellular free Ca^{2+} levels and cell death.

Research conclusions

This research demonstrated that the CaN/NFATc3 pathway might play a key role in IEC injury caused by SAP and that QYD can exert protective effects, at least partially, by restraining IEC apoptosis *via* the CaN/NFATc3 pathway.

Research perspectives

This study provides insight into the function and mechanism of QYD in the treatment of intestinal

mucosa injuries caused by SAP *in vivo* and *in vitro* experiments, thereby providing theoretical support for the clinical application of QYD.

FOOTNOTES

Author contributions: Wang GY, Shang D, and Chen HL designed the research; Wang GY, Jiang N, and Liu HH performed the research; Song HY, Wang GY and Zhang GX analyzed the data; Wang GY and Chen HL wrote the paper.

Supported by the National Key R and D Program of China, No. 2019YFE0119300; National Natural Science Foundation of China, No. 82074158; Project funded by China Postdoctoral Science Foundation, No. 2018M631793; Natural Science Foundation of Liaoning Province, No. 2019-ZD-0624; and Dalian Traditional Chinese Medicine-Related Scientific Research Project, No. 18Z2002.

Institutional animal care and use committee statement: This study was approved by the Animal Experimental Ethics Committee of Dalian Medical University (No. AEE19003).

Conflict-of-interest statement: All the authors report no relevant conflicts of interest for this article.

Data sharing statement: No additional data are available.

ARRIVE guidelines statement: The authors have read the ARRIVE guidelines, and the manuscript was prepared and revised according to the ARRIVE guidelines.

Open-Access: This article is an open-access article that was selected by an in-house editor and fully peer-reviewed by external reviewers. It is distributed in accordance with the Creative Commons Attribution Non Commercial (CC BY-NC 4.0) license, which permits others to distribute, remix, adapt, build upon this work non-commercially, and license their derivative works on different terms, provided the original work is properly cited and the use is non-commercial. See: https://creativecommons.org/Licenses/by-nc/4.0/

Country/Territory of origin: China

ORCID number: Guan-Yu Wang 0000-0002-9982-8785; Dong Shang 0000-0001-6156-5214; Gui-Xin Zhang 0000-0003-0125-6609; Hui-Yi Song 0000-0003-3415-9223; Nan Jiang 0000-0002-0613-5729; Huan-Huan Liu 0000-0002-2023-8708; Hai-Long Chen 0000-0001-5547-5837.

S-Editor: Wang JJ
L-Editor: A
P-Editor: Wang JJ

REFERENCES

1 **Zerem E**. Treatment of severe acute pancreatitis and its complications. *World J Gastroenterol* 2014; **20**: 13879-13892 [PMID: 25320523 DOI: 10.3748/wjg.v20.i38.13879]
2 **Zhang JX**, Dang SC, Yin K, Jiang DL. Protective effect of clodronate-containing liposomes on intestinal mucosal injury in rats with severe acute pancreatitis. *Hepatobiliary Pancreat Dis Int* 2011; **10**: 544-551 [PMID: 21947731 DOI: 10.1016/s1499-3872(11)60092-1]
3 **Yasuda T**, Takeyama Y, Ueda T, Shinzeki M, Sawa H, Nakajima T, Kuroda Y. Breakdown of intestinal mucosa *via* accelerated apoptosis increases intestinal permeability in experimental severe acute pancreatitis. *J Surg Res* 2006; **135**: 18-26 [PMID: 16603187 DOI: 10.1016/j.jss.2006.02.050]
4 **Yasuda T**, Takeyama Y, Ueda T, Shinzeki M, Kishi S, Sawa H, Nakajima T, Kuroda Y. Protective effect of caspase inhibitor on intestinal integrity in experimental severe acute pancreatitis. *J Surg Res* 2007; **138**: 300-307 [PMID: 17292420 DOI: 10.1016/j.jss.2006.09.022]
5 **McCarthy KM**, Skare IB, Stankewich MC, Furuse M, Tsukita S, Rogers RA, Lynch RD, Schneeberger EE. Occludin is a functional component of the tight junction. *J Cell Sci* 1996; **109** (Pt 9): 2287-2298 [PMID: 8886979 DOI: 10.1242/jcs.109.9.2287]
6 **Sommerer C**, Meuer S, Zeier M, Giese T. Calcineurin inhibitors and NFAT-regulated gene expression. *Clin Chim Acta* 2012; **413**: 1379-1386 [PMID: 21996081 DOI: 10.1016/j.cca.2011.09.041]
7 **Jia Z**, Chen Q, Qin H. Ischemia-induced apoptosis of intestinal epithelial cells correlates with altered integrin distribution and disassembly of F-actin triggered by calcium overload. *J Biomed Biotechnol* 2012; **2012**: 617539 [PMID: 22701305 DOI: 10.1155/2012/617539]
8 **Shati AA**. Doxorubicin-induces NFAT/Fas/FasL cardiac apoptosis in rats through activation of calcineurin and P38 MAPK and inhibition of mTOR signalling pathways. *Clin Exp PharmacolPhysiol* 2020; **47**: 660-676 [PMID: 31811646 DOI: 10.1111/1440-1681.13225]
9 **Zhang JW**, Zhang GX, Chen HL, Liu GL, Owusu L, Wang YX, Wang GY, Xu CM. Therapeutic effect of Qingyi

decoction in severe acute pancreatitis-induced intestinal barrier injury. *World J Gastroenterol* 2015; **21**: 3537-3546 [PMID: 25834318 DOI: 10.3748/wjg.v21.i12.3537]
10 **Yang DY**, Duan SB, Aili JT. [Effect of qingyi decoction in treating severe acute pancreatitis and its impacts on blood level of tumor necrosis factor-alpha, interleukin-6 and inteleukin-8]. *Zhongguo Zhong Xi Yi Jie He Za Zhi* 2009; **29**: 1122-1124 [PMID: 20214338]
11 **Rongione AJ**, Kusske AM, Kwan K, Ashley SW, Reber HA, McFadden DW. Interleukin 10 reduces the severity of acute pancreatitis in rats. *Gastroenterology* 1997; **112**: 960-967 [PMID: 9041259 DOI: 10.1053/gast.1997.v112.pm9041259]
12 **Chiu CJ**, Scott HJ, Gurd FN. Intestinal mucosal lesion in low-flow states. II. The protective effect of intraluminal glucose as energy substrate. *Arch Surg* 1970; **101**: 484-488 [PMID: 5311679 DOI: 10.1001/archsurg.1970.01340280036010]
13 **Wang G**, Zhang J, Xu C, Han X, Gao Y, Chen H. Inhibition of SOCs Attenuates Acute Lung Injury Induced by Severe Acute Pancreatitis in Rats and PMVECs Injury Induced by Lipopolysaccharide. *Inflammation* 2016; **39**: 1049-1058 [PMID: 27025854 DOI: 10.1007/s10753-016-0335-1]
14 **Guo SG**, Zhang W, Jiang T, Dai M, Zhang LF, Meng YC, Zhao LY, Niu JZ. Influence of serum collected from rat perfused with compound Biejiaruangan drug on hepatic stellate cells. *World J Gastroenterol* 2004; **10**: 1487-1494 [PMID: 15133859 DOI: 10.3748/wjg.v10.i10.1487]
15 **Zhang GX**, Zhan C, Wang K, Han J, Shang D, Chen HI. Qingyi Decoction amerliorates acute biliary pancreatitis by targeting Gpbar1/NF-kb pathway. *Front Biosci (Landmark Ed)* 2019; **24**: 833-848 [PMID: 30844716 DOI: 10.2741/4754]
16 **Nusrat A**, Parkos CA, Verkade P, Foley CS, Liang TW, Innis-Whitehouse W, Eastburn KK, Madara JL. Tight junctions are membrane microdomains. *J Cell Sci* 2000; **113** (Pt 10): 1771-1781 [PMID: 10769208 DOI: 10.1242/jcs.113.10.1771]
17 **Chen X**, Zhao HX, Fu XS, Li CP, Zhong XL. Glucagonlike peptide 2 protects intestinal barrier in severe acute pancreatitis through regulating intestinal epithelial cell proliferation and apoptosis. *Pancreas* 2012; **41**: 1080-1085 [PMID: 22481288 DOI: 10.1097/MPA.0b013e31824966b0]
18 **Wang X**, Wang B, Wu K, Xu M, Gong Z. Growth hormone downregulated the excessive apoptosis of ileal intestinal epithelial cells in rats during the early course of acute necrotizing pancreatitis. *Pancreas* 2002; **25**: 205-209 [PMID: 12142747 DOI: 10.1097/00006676-200208000-00016]
19 **Jones BA**, Gores GJ. Physiology and pathophysiology of apoptosis in epithelial cells of the liver, pancreas, and intestine. *Am J Physiol* 1997; **273**: G1174-G1188 [PMID: 9435542 DOI: 10.1152/ajpgi.1997.273.6.G1174]
20 **Malleo G**, Mazzon E, Siriwardena AK, Cuzzocrea S. TNF-alpha as a therapeutic target in acute pancreatitis--lessons from experimental models. *ScientificWorldJournal* 2007; **7**: 431-448 [PMID: 17450307 DOI: 10.1100/tsw.2007.98]
21 **Wendling D**, Prati C. Paradoxical effects of anti-TNF-α agents in inflammatory diseases. *Expert Rev Clin Immunol* 2014; **10**: 159-169 [PMID: 24325385 DOI: 10.1586/1744666X.2014.866038]
22 **Shen Y**, Cui N, Miao B, Zhao E. Immune dysregulation in patients with severe acute pancreatitis. *Inflammation* 2011; **34**: 36-42 [PMID: 20405190 DOI: 10.1007/s10753-010-9205-4]
23 **Pooran N**, Indaram A, Singh P, Bank S. Cytokines (IL-6, IL-8, TNF): early and reliable predictors of severe acute pancreatitis. *J Clin Gastroenterol* 2003; **37**: 263-266 [PMID: 12960727 DOI: 10.1097/00004836-200309000-00013]
24 **Talar-Wojnarowska R**, Gasiorowska A, Smolarz B, Romanowicz-Makowska H, Kulig A, Malecka-Panas E. Clinical significance of interleukin-6 (IL-6) gene polymorphism and IL-6 serum level in pancreatic adenocarcinoma and chronic pancreatitis. *Dig Dis Sci* 2009; **54**: 683-689 [PMID: 18661238 DOI: 10.1007/s10620-008-0390-z]
25 **Hansen M**, Nielsen AR, Vilsbøll T, Lund A, Krarup T, Knop FK, Vestergaard H. Increased levels of YKL-40 and interleukin 6 in patients with chronic pancreatitis and secondary diabetes. *Pancreas* 2012; **41**: 1316-1318 [PMID: 22647735 DOI: 10.1097/MPA.0b013e31824d9b93]
26 **Thompson JS**, Vaughan WP, Forst CF, Jacobs DL, Weekly JS, Rikkers LF. The effect of the route of nutrient delivery on gut structure and diamine oxidase levels. *JPEN J Parenter Enteral Nutr* 1987; **11**: 28-32 [PMID: 3102778 DOI: 10.1177/014860718701100128]
27 **Bragg LE**, Thompson JS, West WW. Intestinal diamine oxidase levels reflect ischemic injury. *J Surg Res* 1991; **50**: 228-233 [PMID: 1900339 DOI: 10.1016/0022-4804(91)90183-m]
28 **Smith SM**, Eng RH, Buccini F. Use of D-lactic acid measurements in the diagnosis of bacterial infections. *J Infect Dis* 1986; **154**: 658-664 [PMID: 3528318 DOI: 10.1093/infdis/154.4.658]
29 **Rusnak F**, Mertz P. Calcineurin: form and function. *Physiol Rev* 2000; **80**: 1483-1521 [PMID: 11015619 DOI: 10.1152/physrev.2000.80.4.1483]
30 **Orabi AI**, Wen L, Javed TA, Le T, Guo P, Sanker S, Ricks D, Boggs K, Eisses JF, Castro C, Xiao X, Prasadan K, Esni F, Gittes GK, Husain SZ. Targeted inhibition of pancreatic acinar cell calcineurin is a novel strategy to prevent post-ERCP pancreatitis. *Cell Mol Gastroenterol Hepatol* 2017; **3**: 119-128 [PMID: 28090570 DOI: 10.1016/j.jcmgh.2016.08.006]
31 **Muili KA**, Wang D, Orabi AI, Sarwar S, Luo Y, Javed TA, Eisses JF, Mahmood SM, Jin S, Singh VP, Ananthanaravanan M, Perides G, Williams JA, Molkentin JD, Husain SZ. Bile acids induce pancreatic acinar cell injury and pancreatitis by activating calcineurin. *J Biol Chem* 2013; **288**: 570-580 [PMID: 23148215 DOI: 10.1074/jbc.M112.428896]
32 **Shah AU**, Sarwar A, Orabi AI, Gautam S, Grant WM, Park AJ, Shah AU, Liu J, Mistry PK, Jain D, Husain SZ. Protease activation during *in vivo* pancreatitis is dependent on calcineurin activation. *Am J Physiol Gastrointest Liver Physiol* 2009; **297**: G967-G973 [PMID: 20501444 DOI: 10.1152/ajpgi.00181.2009]
33 **Wen L**, Javed TA, Yimlamai D, Mukherjee A, Xiao X, Husain SZ. Transient High Pressure in Pancreatic Ducts Promotes Inflammation and Alters Tight Junctions *via* Calcineurin Signaling in Mice. *Gastroenterology* 2018; **155**: 1250-1263.e5 [PMID: 29928898 DOI: 10.1053/j.gastro.2018.06.036]
34 **Macian F**. NFAT proteins: key regulators of T-cell development and function. *Nat Rev Immunol* 2005; **5**: 472-484 [PMID: 15928679 DOI: 10.1038/nri1632]
35 **Müller MR**, Rao A. NFAT, immunity and cancer: a transcription factor comes of age. *Nat Rev Immunol* 2010; **10**: 645-656 [PMID: 20725108 DOI: 10.1038/nri2818]
36 **Angulo C**, Alamillo E, Ascencio F, Reyes-Becerril M. Characterization of nuclear factor of activated T-cells-c3 (NFATc3) and gene expression of upstream-downstream signaling molecules in response to immunostimulants in Pacific red snapper

cells. *Dev Comp Immunol* 2018; **78**: 149-159 [PMID: 28986213 DOI: 10.1016/j.dci.2017.10.001]

37 **Awla D**, Zetterqvist AV, Abdulla A, Camello C, Berglund LM, Spégel P, Pozo MJ, Camello PJ, Regnér S, Gomez MF, Thorlacius H. NFATc3 regulates trypsinogen activation, neutrophil recruitment, and tissue damage in acute pancreatitis in mice. *Gastroenterology* 2012; **143**: 1352-1360.e7 [PMID: 22841788 DOI: 10.1053/j.gastro.2012.07.098]

38 **HanSL**. Efficacy of Qingyi decoction in the treatment of severe acute pancreatitis: systematic review and meta-analysis. *J Pract Med* 2008

39 **Su S**, Liang T, Zhou X, He K, Li B, Xia X. Qingyi decoction attenuates severe acute pancreatitis in rats *via* inhibition of inflammation and protection of the intestinal barrier. *J Int Med Res* 2019; **47**: 2215-2227 [PMID: 30700190 DOI: 10.1177/0300060518809289]

40 **Zhang WX**, Feng M, Mao YL, Zhang WZ, Ni Y. Review on the Application of Serum Pharmacochemistry of Traditional Chinese Medicine. *Drug Evaluation Res* 2019; **42**: 1448-1453

41 **Wu XW**, Hao YY, Nie CX, Ni Y, Hao XL, Liu C. An overview of methodology and research progress on application of serum pharmacochemistry of traditional Chinese medicine. *Chin J Exp Tradit Med Form* 2019; **24**: 173-179

42 **Tao S**. Research on rapid discovery method of Chinese medicine effective substances based on chemometrics and immobilized enzyme. Zhejiang University, 2015

43 **Chen Q**, Huang L, Wang R, Pang C. Research Status of Serum Pharmacology and Serum Pharmacochemistry of Traditional Chinese Medicine. *Agric Biotechnol* 2021; **10**: 126-128

World Journal of Gastroenterology

Submit a Manuscript: https://www.f6publishing.com

World J Gastroenterol 2022 August 7; 28(29): 3838-3853

DOI: 10.3748/wjg.v28.i29.3838

ISSN 1007-9327 (print) ISSN 2219-2840 (online)

ORIGINAL ARTICLE

Basic Study

High-fat diet aggravates colitis *via* mesenteric adipose tissue derived exosome metastasis-associated lung adenocarcinoma transcript 1

Dong Chen, Miao-Miao Lu, Jin-Hai Wang, Yue Ren, Ling-Ling Xu, Wei-Xin Cheng, Sai-Sai Wang, Xiao-Lin Li, Xiao-Fei Cheng, Jian-Guo Gao, Farhin Shaheed Kalyani, Xi Jin

Specialty type: Gastroenterology and hepatology

Provenance and peer review: Unsolicited article; Externally peer reviewed.

Peer-review model: Single blind

Peer-review report's scientific quality classification

Grade A (Excellent): 0
Grade B (Very good): B, B
Grade C (Good): 0
Grade D (Fair): D
Grade E (Poor): 0

P-Reviewer: Chiu CC, Taiwan; Kao JT, Taiwan; Senousy M, Egypt

Received: December 4, 2021
Peer-review started: December 4, 2021
First decision: April 16, 2022
Revised: April 28, 2022
Accepted: July 6, 2022
Article in press: July 6, 2022
Published online: August 7, 2022

Dong Chen, Jin-Hai Wang, Sai-Sai Wang, Xiao-Fei Cheng, Department of Colorectal Surgery, The First Affiliated Hospital, College of Medicine, Zhejiang University, Hangzhou 310003, Zhejiang Province, China

Miao-Miao Lu, Yue Ren, Ling-Ling Xu, Wei-Xin Cheng, Farhin Shaheed Kalyani, Department of Medicine, Zhejiang University School of Medicine, Hangzhou 310003, Zhejiang Province, China

Xiao-Lin Li, Department of Emergency, The First Affiliated Hospital, College of Medicine, Zhejiang University, Hangzhou 310003, Zhejiang Province, China

Jian-Guo Gao, Xi Jin, Department of Gastroenterology, The First affiliated Hospital, College of Medicine, Zhejiang University, Hangzhou 310003, Zhejiang Province, China

Corresponding author: Xi Jin, MD, PhD, Doctor, Professor, Department of Gastroenterology, The First Affiliated Hospital, College of Medicine, Zhejiang University, No. 79 Qingchun Road, Hangzhou 310003, Zhejiang Province, China. jxfl007@zju.edu.cn

Abstract

BACKGROUND

Obesity is associated with an increased risk of developing Crohn's disease (CD), higher disease activity, and comparatively worse clinical outcomes.

AIM

To investigate the role of mesenteric adipose tissue-derived exosomes in the pathogenesis of CD aggravation in obese individuals.

METHODS

First, we induced colitis in mice initiated on high-fat and normal diets and compared the severity of colitis. We then extracted and identified exosomes from mesenteric adipose tissue and determined the levels of metastasis-associated lung adenocarcinoma transcript 1 (MALAT1) in mesenteric adipose tissue-derived exosomes and the colon. Next, we demonstrated an interaction between MALAT1 and the miR-15a-5p/activating transcription factor 6 (ATF6) axis. Finally, we explored the effects of mesenteric adipose tissue-derived exosomes extracted from mice fed a high-fat or normal diet on the severity of 2,4,6-trinitrobe-nzenesulfonic acid (TNBS)-induced colitis and ATF6-related endoplasmic reticulum stress

pathways.

RESULTS

High-fat diet was found to aggravate TNBS-induced colitis in mice. The expression of MALAT1 in mesenteric adipose tissue-derived exosomes of high-fat diet-fed mice increased. The increased expression of MALAT1 in colon tissue exacerbated TNBS-induced colitis and activated the ATF6 endoplasmic reticulum stress pathway. This effect was partially reversed by the reduced expression of MALAT1 and overexpression of miR-15a-5p.

CONCLUSION

Mesenteric adipose tissue-derived exosome-encapsulated long noncoding RNAs MALAT1 targets the colon and aggravates TNBS-induced colitis in obese mice, which may potentially act on the miR-15a-5p/ATF6 axis and activate endoplasmic reticulum stress.

Key Words: Metastasis-associated lung adenocarcinoma transcript; Crohn's disease; miR-15a-5p; Mesenteric adipose tissue; Obesity; Colitis; Inflammatory bowel disease

©The Author(s) 2022. Published by Baishideng Publishing Group Inc. All rights reserved.

Core Tip: A higher visceral adipose tissue ratio has been associated with increased disease activity in patients with Crohn's disease. However, the mechanisms underlying this effect remain unclear. Our study indicates that a high-fat diet increases the mesenteric adipose tissue content and aggravates colitis in mice. Mesenteric adipose tissue-derived exosome long noncoding RNAs metastasis-associated lung adenocarcinoma transcript 1 can be absorbed by the colon, leading to the activation of the endoplasmic reticulum stress pathway by targeting the miR-15a-5p/activating transcription factor 6 axis to aggravate colitis.

Citation: Chen D, Lu MM, Wang JH, Ren Y, Xu LL, Cheng WX, Wang SS, Li XL, Cheng XF, Gao JG, Kalyani FS, Jin X. High-fat diet aggravates colitis *via* mesenteric adipose tissue derived exosome metastasis-associated lung adenocarcinoma transcript 1. *World J Gastroenterol* 2022; 28(29): 3838-3853
URL: https://www.wjgnet.com/1007-9327/full/v28/i29/3838.htm
DOI: https://dx.doi.org/10.3748/wjg.v28.i29.3838

INTRODUCTION

Crohn's disease (CD) is a chronic relapsing inflammatory disease of the gastrointestinal tract that results from the interplay between genetic susceptibility and various environmental exposures[1]. The incidence of CD is higher in developed countries and urban areas than in developing and rural areas[2]. Similarly, the prevalence of CD is increasing in areas with rapid urbanization[3], paralleling the obesity epidemic, possibly in conjunction with western-style diets characterized by high fat content.

The conventional understanding is that CD is a chronic disease characterized by wasting, low weight, and malnutrition. Nevertheless, based on real world data, 15%-40% of patients with inflammatory bowel disease (IBD), including CD and ulcerative colitis (UC), are obese and 20%-40% are overweight [4]. Several studies have shown that obesity is associated with an increased risk of developing CD[5,6], a higher disease activity, and comparatively worse clinical outcomes[7]. For instance, Jain *et al*[8] observed that obesity was not only associated with an increased risk of persistent disease activity and relapse in patients with IBD but also with higher rates of anxiety, depression, fatigue, pain, and inferior social function scores. Although these studies on the association between obesity and the course of CD have some limitations, and the above-mentioned outcomes have not been observed consistently, accumulating evidence indicates that visceral adiposity better captures the association between obesity and CD than body mass index[4]. A higher baseline visceral adipose tissue/total fat mass ratio was found to be associated with increased disease activity[9]. Although the influence of obesity on the course of CD has been confirmed, the underlying mechanism remains elusive.

Significant expansion of adipose tissue is a common phenomenon in obese individuals. In addition to storing energy, adipose tissue is an endocrine organ that secretes various adipokines, lipokines, and exosomes, contributing to the state of chronic inflammation in obese individuals[10]. Localized mesenteric fat accumulation in CD patients, known as creeping fat, is not only related to overall obesity but also has a systemic pro-inflammatory effect[11]. Adipose tissue and visceral adipose tissue-derived endocrine hormones are involved in multiple diseases, including cancer[12], cardiovascular disease[13], and nonalcoholic steatohepatitis (NASH)[14]. Exosomes are extracellular vesicles secreted by various cells, including adipocytes[15]. Visceral adipose tissue-derived exosomes display tissue affinity, prefer-

entially targeting the colonic lamina propria[16]. Mesenteric adipose tissue can directly invade the lamina propria. Therefore, we hypothesized that obesity exacerbates IBD, partially due to mesenteric adipose tissue-derived exosomes.

Previous studies have indicated that exosomes contain multiple non-coding RNAs such as circular RNAs, long noncoding RNAs (lncRNAs), and microRNAs, which serve as messengers in cell-to-cell communication. Among these, lncRNAs are non-coding RNAs containing more than 200 nucleotides [17]. LncRNAs can interact with transcription factors to regulate transcription, bind to proteins to promote the formation of ribonucleoproteins, guide chromatin-modifying protein complexes targeting genes, and act as sponges for downstream microRNAs, participating in a variety of pathophysiological processes[18]. To our knowledge, few studies have explored the potential functions and mechanisms of adipocyte-derived exosomal lncRNAs in the exacerbation of CD.

The present study aimed to investigate the role of lncRNAs transferred by mesenteric adipose tissue-derived exosomes in obesity aggravated CD, and thereby assess the potential of these lncRNAs as therapeutic targets for the treatment of CD in this subpopulation.

MATERIALS AND METHODS

Construction of obesity mouse model and colitis mouse model

C57BL/6 mice (6-8 wk old) were purchased from Chengdu Dossy Experimental Animals Co.,Ltd. and fed either a normal diet (ND) (#D12451, Research Diets, United States) or a high-fat diet (HFD) (#D12492, Research Diets, United States) for 12 wk. To induce acute experimental colitis, 2,4,6-trinitrobenzenesulfonic acid (TNBS) (Beyotime, China; 100 μg/g, 175 μL) was injected into the colon for 4 d. The daily disease activity index (DAI) score was calculated in mice in accordance with a well-established method[19]. The body weight of the mice in each group was also recorded. On day 8, the mice were sacrificed for colon and mesenteric adipose tissue collection. Rectum tissue, 3 cm away from the anal margin, was collected for hematoxylin and eosin (HE) staining and inflammatory pathological score determination using the following steps. Briefly, mouse colon tissue was fixed in 10% formaldehyde, embedded in paraffin, sectioned, and stained with HE. Details of histological scoring have been described previously[20]. The remaining colon tissue was placed in liquid nitrogen for subsequent analyses. Mice were randomly divided into the following four groups (n = 6 each): ND + control, HFD + control, normal diet + TNBS, and HFD + TNBS.

RNA Extraction and real-time reverse transcription-PCR

Total RNA was isolated using Trizol (Invitrogen, United States) and reverse-transcribed into cDNA using the First Strand cDNA Synthesis Kit (TransGen, China), in accordance with the manufacturer's instructions. Real-time reverse transcription-PCR (qRT-PCR) was performed using the SYBR Premix Ex Taq qPCR kit (TaKaRa, Japan). Primer sequences used are listed in Supplementary Table 1.

Enzyme linked immunosorbent assay and Western blotting

The concentrations of mouse interleukin 1β (IL-1β), tumor necrosis factor α (TNF-α), and interleukin 6 (IL-6) were detected using enzyme linked immunosorbent assay (ELISA) kits (Elabscience, China) according to the manufacturer's instructions. Additionally, total protein was isolated using radioimmune precipitation assay (RIPA) buffer (TaKaRa, Japan) supplemented with a protease inhibitor (Roche, Switzerland). After quantification using the BCA Protein Assay Kit (Thermo, United States), the proteins were separated by SDS-PAGE and transferred onto polyvinylidene fluoride (PVDF) membranes. The membranes were blocked and incubated overnight with antibodies against activating transcription factor 6 (ATF6) (ab227830, Abcam, United Kingdom), p-PERK (MA5-15033, Thermo, United States), p-IRE1 (CSB-RA00,7795A724phHU, CUSABIO, China), GRP78 (MA5-27687, Thermo, United States), p-EIF2α (51995, CST, United States), CHOP (5554T, CST, United States), and GAPDH (ab8245, Abcam, United Kingdom) at 4 °C. The membranes were then incubated with HRP-conjugated secondary antibodies (Multi Sciences, China). Finally, the protein bands were detected using enhanced chemiluminescence (ECL) kits (Thermo, United States).

Isolation and primary culture of adipocytes

Mesenteric adipose tissue (25 g) was isolated and placed into a sterile 50 mL polypropylene test tube containing 15 mL of collagenase [1 mg collagenase/1 mL phosphate belanced solution (PBS); 3 mL solution/1 g tissue]. After grinding, the solution was swirled for 20 s and the test tube was incubated at 37 °C in a rocking water bath at 100 rpm for 40 min. The solution was vortexed and filtered through a funnel containing a double gauze. Thereafter, the homogenate was centrifuged at 1000 rpm for 10 min, followed by collection of the top fat layer, which was washed three times with PBS. The precipitate was then resuspended in 10 mL of RBC lysis buffer (154 mmol/L NH_4Cl, 10 mmol/L $KHCO_3$, 1 mmol/L EDTA) in a water bath at 37 °C and 100 rpm for 5 min, followed by centrifugation at 1000 rpm for 10 min. The precipitates were resuspended in 10 mL of plate culture medium (DMEM, 0.1 mmol/L

penicillin, 0.06 mmol/L streptomycin, 10% HI-FBS, pH 7.4), swirled, spread on 100 mm culture dishes, and incubated at 37 °C. After 20 h, the cells were washed with 10 mL of PBS three times, and supplemented with 1 mL of trypsin. Finally, the cells were resuspended and subcultured for further analysis.

Isolation and confirmation of exosomes

The supernatant of adipocytes was collected and centrifuged at 2000 × g for 30 min, followed by filtration through a 0.22 μm membrane to remove apoptotic cells, debris, and large particles. Exosomes were extracted from the filtrate according to the manufacturer's instructions as described previously [21]. For further confirmation, the diluted exosomes were subjected to NanoFCM (China) for transmission electron microscopy and size distribution analysis.

Luciferase reporter assay and RNA pull-down assay

The luciferase reporter assay was performed using the Dual-Luciferase Reporter Assay System (Promega, United States), as described previously[22]. The RNA pulldown assay was performed using the Pierce Magnetic RNA-Protein Pull-Down Kit (Thermo, United States). Briefly, miR-15a-5p was biotinylated and transfected into the Caco-2 cells. Cultured cells were collected for lysis 48 h later. Thereafter, the RNA bound to miR-15a-5p was captured using Pierce nucleic acid-compatible streptavidin magnetic beads. Finally, qRT-PCR was performed to determine the expression of metastasis-associated lung adenocarcinoma transcript 1 (MALAT1).

Transfection of shMALAT1 and miR-15a-5p mimic

Adipocytes were transfected with shMALAT1 and miR-15a-5p using Plko.1-EGFP-puro. ShMALAT1 was designed based on information from Thermo Fisher (http://rnaidesigner.thermofisher.com/rnaiexpress/). The sequence of shMALAT1 was 5'-TGTACTATCCCATCACTGAAG-3'.

Statistical analysis

All data are presented as mean ± SD. Differences between two groups were analyzed using the Student's *t*-test. Two-way analysis of variance was used to compare the differences between multiple groups with two factors. All statistical analyses were performed using GraphPad 9.0.2 software, and $P < 0.05$ was considered to indicate a significant difference between groups.

RESULTS

High-fat diet aggravated TNBS-induced colitis

Accumulating evidence has shown that CD is more severe in obese individuals. We established a model of obesity in mice fed a HFD for 12 wk, while mice on a ND were used as controls. Thereafter, TNBS was used to induce colitis in the mice (Figure 1A). Compared with the control group, colon length was significantly shortened in the TNBS treatment group and the effect was further exacerbated by HFD (Figure 1B). To determine the degree of colitis activity index in different groups of mice, the DAI score was calculated daily for 8 d after starting TNBS treatment. HFD mice had a higher DAI score than the ND mice (Figure 1C). In addition, HFD significantly aggravated the TNBS-induced weight loss in mice (Figure 1D). To observe the degree of tissue damage in the mouse colon more intuitively, we used the colon tissue for HE staining and determined the histological injury scores (Figure 1E and F), which showed that HFD aggravated TNBS-induced colitis and tissue damage.

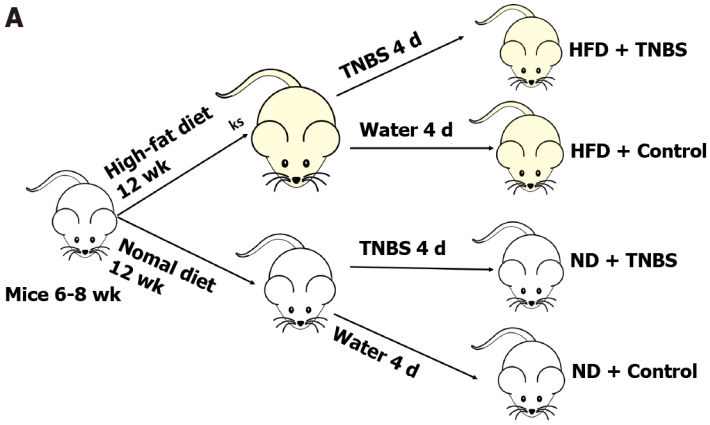
In addition, we measured the expression levels of pro-inflammatory cytokines in the colon tissues of mice in each group. The expression of TNF-α, IL-1β, and IL-6 in the colon of HFD mice treated with TNBS was significantly higher than that in ND mice treated with TNBS (Figure 1G-I). Notably, HFD itself increased the levels of pro-inflammatory cytokines in the colon of mice, which may be related to chronic inflammatory states in the body caused by obesity. These results suggest that HFD aggravates the severity of TNBS-induced colitis.

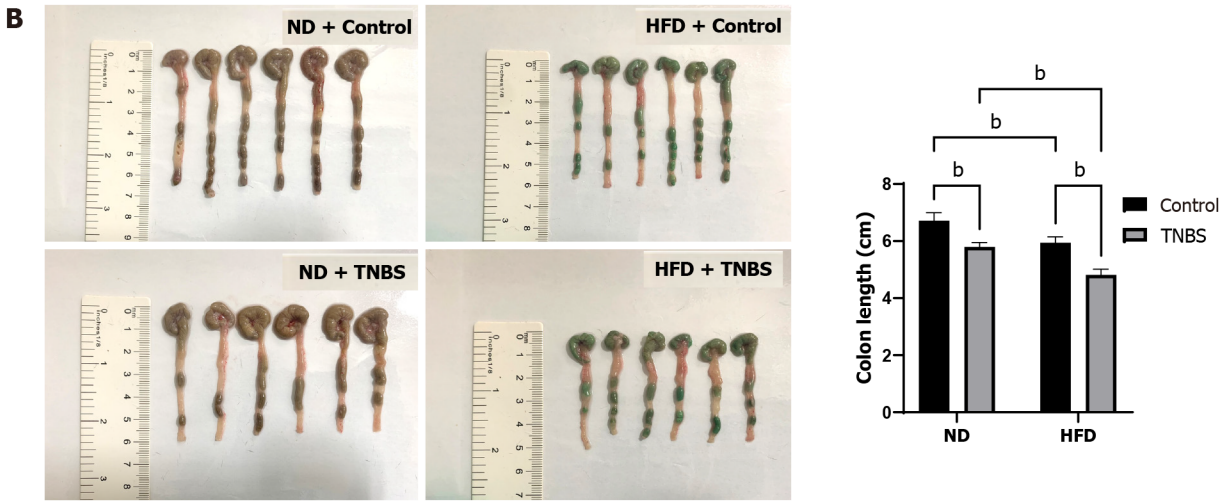
Successful extraction and identification of mesenteric adipose tissue derived exosomes (MAT-Exos)

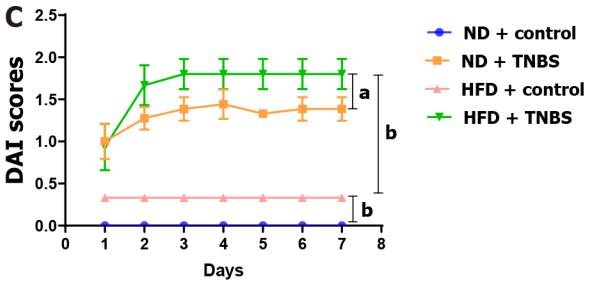
The mesenteric adipose tissue index was significantly increased in HFD mice (Figure 2A). MAT-Exos were isolated from mesenteric adipose tissue cultured in vitro, and the typical mitochondrial morphology was observed using transmission electron microscopy (Figure 2B). Using Western blotting, we demonstrated that the isolated exosomes expressed exosomal marker proteins CD63 and TSG101 and the adipocyte exosomal membrane protein HSP70 (Figure 2C). The properties of exosomes were further demonstrated by particle size analysis (Figure 2D). In summary, we successfully harvested and identified exosomes from mesenteric adipose tissue.

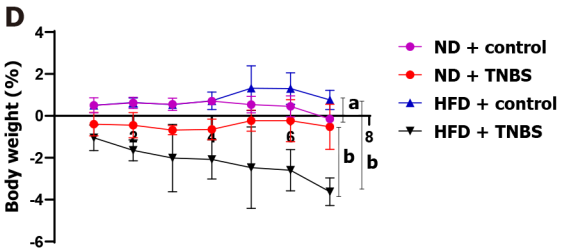
Partial contribution of MAT-Exo to increased colon lncRNA MALAT1 Levels in HRD-fed mice

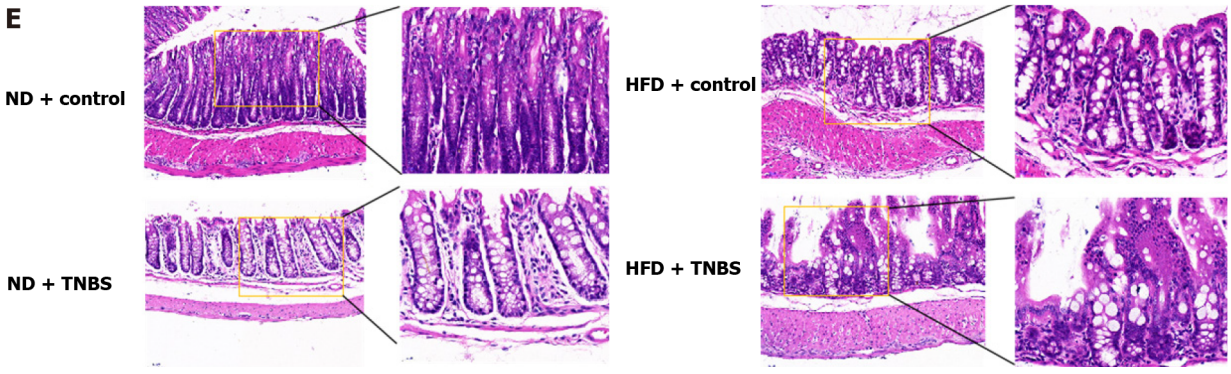
Existing literature indicates increased levels of lncRNA MALAT1 in HFD-fed mice[23]. In this study, the expression of lncRNA MALAT1 in MAT-Exos was found to be significantly increased in HFD-fed mice


A
High-fat diet 12 wk
Nomal diet 12 wk
Mice 6-8 wk
TNBS 4 d
Water 4 d
TNBS 4 d
Water 4 d
HFD + TNBS
HFD + Control
ND + TNBS
ND + Control


B
ND + Control
HFD + Control
ND + TNBS
HFD + TNBS
Colon length (cm)
Control
TNBS
ND
HFD


C
DAI scores
Days
ND + control
ND + TNBS
HFD + control
HFD + TNBS


D
Body weight (%)
ND + control
ND + TNBS
HFD + control
HFD + TNBS


E
ND + control
ND + TNBS
HFD + control
HFD + TNBS

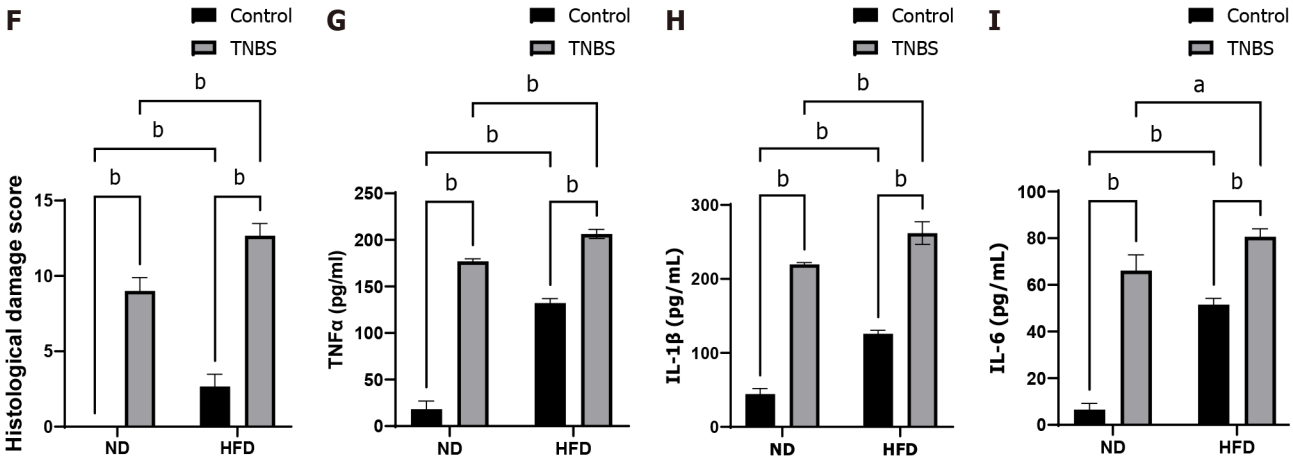


Figure 1 High-fat diet aggravated colitis. A: Experimental grouping process; B: Colon length of mice in each group; C: Disease activity index of mice in each group; D: Body weight change trend of mice in each group; E: Hematoxylin and eosin staining images of colon tissue; F: Histological damage score of colon tissue; G: Expression of tumor necrosis factor-α in colon tissue by enzyme linked immunosorbent assay (ELISA); H: Expression of interleukin-1β in colon tissue by ELISA; I: Expression of interleukin-6 (IL-6) in colon tissue by ELISA. DAI: Disease activity index; TNBS: 2,4,6-trinitrobe-nzenesulfonic acid; HFD: High-fat diet; ND: Normal diet; TNF-α: Tumor necrosis factor-α; IL-1β: Interleukin-1β. $^{a}P < 0.05$, $^{b}P < 0.01$.

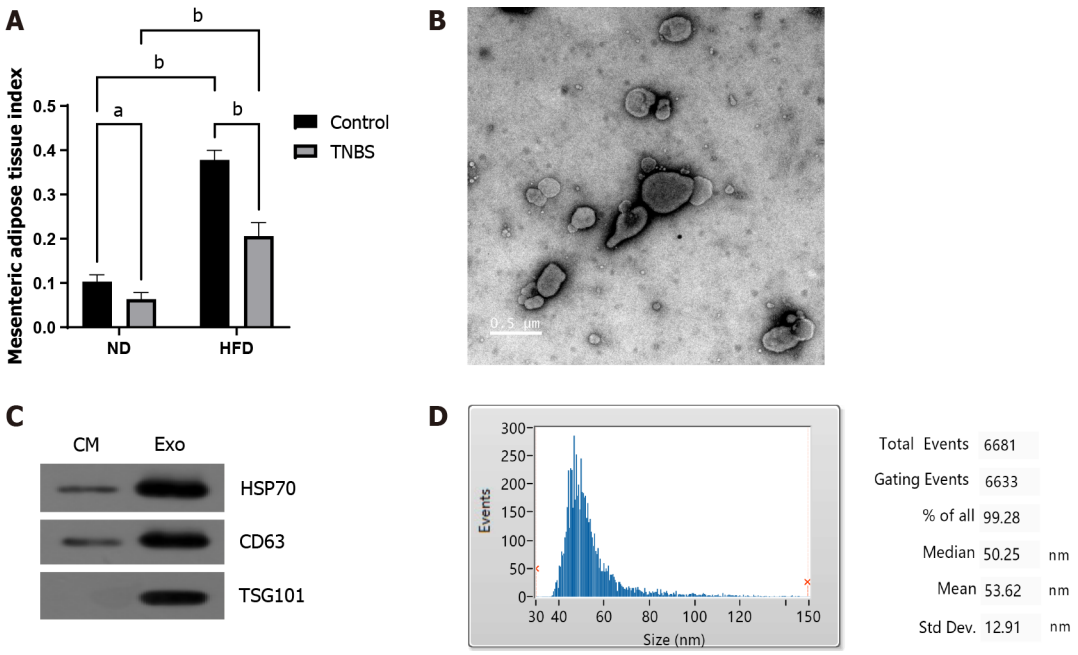


Figure 2 Extraction and identification of exosomes derived from mesenteric adipose tissue. A: Mesenteric adipose index of mice in each group; B: Images of exosomes observed under transmission electron microscopy; C: Western blotting to detect exosome marker proteins; D: Exosome particle size analysis. TNBS: 2,4,6-trinitrobe-nzenesulfonic acid; HFD: High-fat diet; ND: Normal diet. $^{a}P < 0.05$, $^{b}P < 0.01$.

using qRT-PCR (Figure 3A). The relative expression of lncRNA MALAT1 in mesenteric adipose and colon tissue in HFD mice treated with TNBS was significantly increased compared to that in ND mice treated with TNBS (Figure 3B and C). Therefore, we focused our attention on lncRNA MALAT1 and speculated that the increase in the relative expression of MALAT1 in the colon tissue of HFD mice may be partially attributed to exosomes from the mesenteric adipose tissue.

For further verification, MAT-Exos labeled with a PKH26 marker were incubated with Caco2 cells in vitro. PKH26 fluorescence in Caco2 cells was detected using a laser scanning confocal microscope, indicating that Caco2 cells can absorb MAT-Exos (Supplementary Figure 1). In addition, exosomes isolated from the mesenteric adipose tissue of HFD-fed and ND mice were injected into the mice *via* the tail vein, followed by lncRNA MALAT1 detection in the mouse colon tissue. MAT-Exos of HFD-fed mice increased the relative expression of lncRNA MALAT1 in the colon tissues of recipient mice (Figure 3D). We speculate that in HFD mice, the MAT-Exos-encapsulated lncRNA MALAT1 might target the colon to increase its local expression.

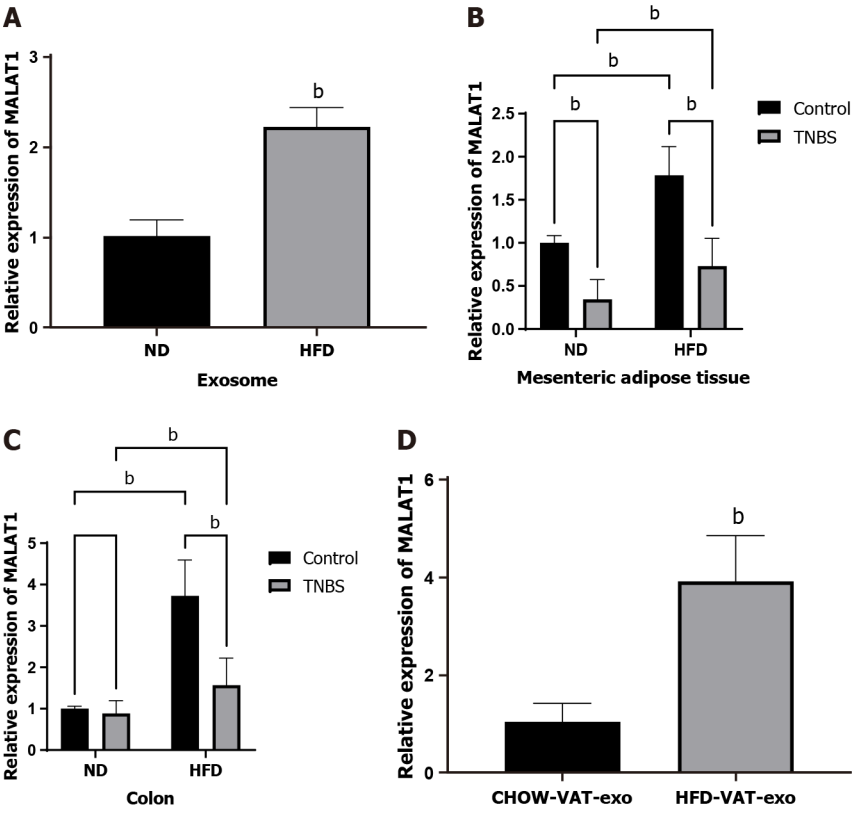


Figure 3 Mesenteric adipose tissue derived exosomes from high-fat diet-fed mice increase the expression of long noncoding RNAs metastasis-associated lung adenocarcinoma transcript 1 in colon. A: Expression of metastasis-associated lung adenocarcinoma transcript 1 (MALAT1) in mesenteric adipose tissue derived exosomes (MAT-Exos) in each group; B: Expression of MALAT1 in mesenteric adipose tissue in each group; C: Expression of MALAT1 in colon in each group; D: Expression of MALAT1 in colon of normal mice after treated with MAT-Exos extracted from higt-fat diet mice or normal diet mice. MALAT1: Metastasis-associated lung adenocarcinoma transcript 1; TNBS: 2,4,6-trinitrobe-nzenesulfonic acid; HFD: High-fat diet; ND: Normal diet. $^{b}P < 0.01$.

LncRNA MALAT1 targetes the miR-15a-5p/ATF6 axis

Numerous miRNAs with the ability to interact with lncRNA MALAT1 have been reported in literature [24], among which miR-15a-5p has attracted our attention. After searching miRDB (http://mirdb.org) [25] and TargetScan, we identified many potential mRNAs downstream of miR-15a-5p. Combining the literature review and bioinformatic prediction (Figure 4A), we chose ATF6 as the target mRNA of miR-15a-5p. ATF6 is an important molecule associated with endoplasmic reticulum (ER) stress[26] involved in gut homeostasis and IBD processes[27-29]. Western blotting was used to detect ATF6 expression in the colon tissues of mice in each group. The ATF6 Levels in the colon tissues of ND mice treated with TNBS were higher than those in ND mice without TNBS treatment. In addition, HFD was found to upregulate the expression of ATF6 in the colon tissues (Figure 4B). Subsequently, we used a dual-luciferase assay to confirm the interaction between ATF6 and miR-15a-5p. Compared with the control group, miR-15a-5p reduced the relative expression of ATF6 when placed downstream of the wild-type 3′ untranslated regions (3′ UTRs), but not when it was downstream of the mutant 3′ UTR, indicating a regulatory relationship between miR-15a-5p and ATF6 (Figure 4C). We then verified the interaction between miR-15a-5p and MALAT1 using RNA pull-down assays. We found that miR-15a-5p could bind to MALAT1, whereas the mutant miR-15a-5p could not pull down MALAT1 (Figure 4D). Based on these direct and indirect evidences, we can conclude that lncRNA MALAT1 can act on the miR-15a-5p/ATF6 axis.

LncRNA MALAT1 binds miR-15a-5p to aggravate TNBS-induced colitis in HFD-fed mice

We designed animal experiments to further demonstrate that mesenteric adipose tissue derived exosomes and their encapsulated lncRNA-MALAT1 can aggravate TNBS-induced colitis in HFD mice. First, MAT-Exos from HFD mice were isolated, and treated with either a short hairpin RNA targeting MALAT1 (shMALAT) or a miR-15a-5p mimic before injection. MAT-Exos from ND mice were used as a control. Thereafter, the mice were randomly divided into four groups and treated with ND-MAT-Exos, HFD-MAT-Exos, HFD-MAT-Exos + shMALAT1, or HFD-MAT-Exos + miR-15a-5p mimic, *i.e.*, A, B, C, and D groups, respectively. Mice were injected with MAT-Exos (100 μg/mouse) *via* the tail vein on days 1, 4, and 8. On day 3, TNBS was administered to induce colitis. On day 9, the mice were sacrificed and the colon tissue was collected. Compared to MAT-Exos from ND mice, MAT-EXOSs from HFD mice significantly increased the body weight loss (Figure 5A), DAI (Figure 5D), and histological damage

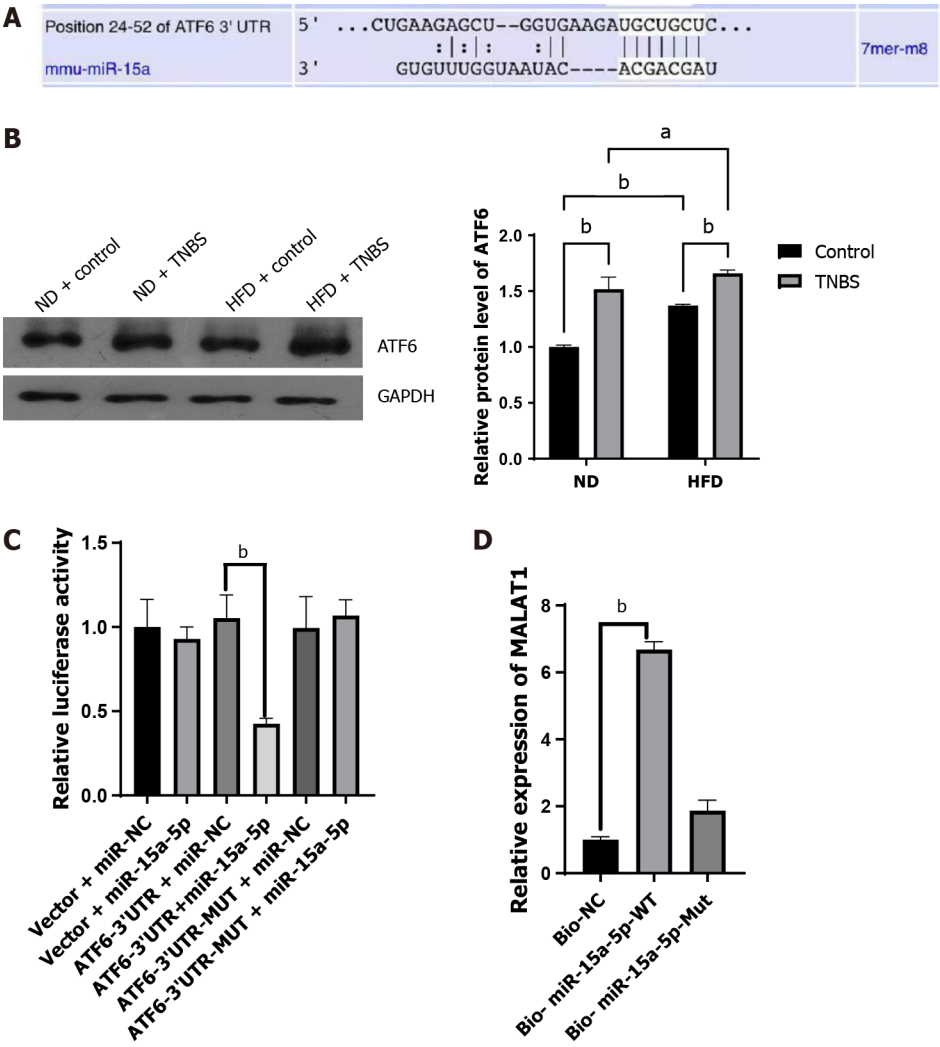


Figure 4 Associations between metastasis-associated lung adenocarcinoma transcript 1 and miR-15a-5p/activating transcription factor 6.
A: Prediction of miR-15a-5p binding site on the 3' untranslated region of activating transcription factor 6 (ATF6); B: Western blotting to detect ATF6 protein; C: Dual luciferase report of miR-15a-5p and ATF6; D: RNA pull down analysis of miR-15a-5p and metastasis-associated lung adenocarcinoma transcript 1. ATF6: Activating transcription factor 6; TNBS: 2,4,6-trinitrobe-nzenesulfonic acid; HFD: High-fat diet; ND: Normal diet; 3' UTR: 3' untranslated region; WT: Wild type; Mut: Mutant. $^{a}P < 0.05$, $^{b}P < 0.01$.

score (Figure 5E and F), and decreased colon length (Figure 5B and C). Transfection with shMALAT1 to knockdown the expression of MALAT1 or treatment with the miR-15a-5p mimic to enhance the function of miR-15a-5p partially reversed the effects of MAT-Exos on HFD mice. In conclusion, lncRNA MALAT1 may sponge miR-15a-5p and aggravate TNBS-induced colitis in HFD mice.

LncRNA MALAT1 acted on the miR-15a-5p/ATF6 axis to exacerbate colitis in response to ER stress

To further investigate whether lncRNA MALAT1 encapsulated within MAT-Exos of HFD mice aggravated TNBS-induced colitis *via* the miR-15a-5p/ATF6 axis, we detected the protein content of ATF6 in the colon tissue of mice in each group. MAT-Exos of HFD mice increased ATF6 expression in the colon tissue, whereas transfection with shMALAT1 or (A6) treatment with the miR-15a-5p mimic resulted in reduced expression of ATF6 in the colon tissue (Figure 6A). ATF6 is involved in IBD that develops in response to ER stress[30]. We further examined the expression of proteins associated with the ATF6-related ER stress pathway in the colon tissue. The expression of GRP78 and XBP-1 was increased in the colon of mice injected with MAT-Exos from HFD mice, a phenomenon that was antagonized by shMALAT1 and the miR-15a-5p mimic (Figure 6B; Supplementary Figure 2). In addition, the expression of other ER stress pathway related proteins, such as p-PERK, p-IRE1, p-eIF2α, and CHOP, also increased upon injecting MAT-Exos into HFD mice (Figure 6B). Previous studies have shown that ER stress activates NF-κB signaling to induce an inflammatory response[31,32]. Therefore, we also detected inflammatory factors associated with the NF-κB pathway (Figure 6C) using ELISA. The observed changes were consistent with the expression of proteins associated with the ATF6-related ER stress pathway.

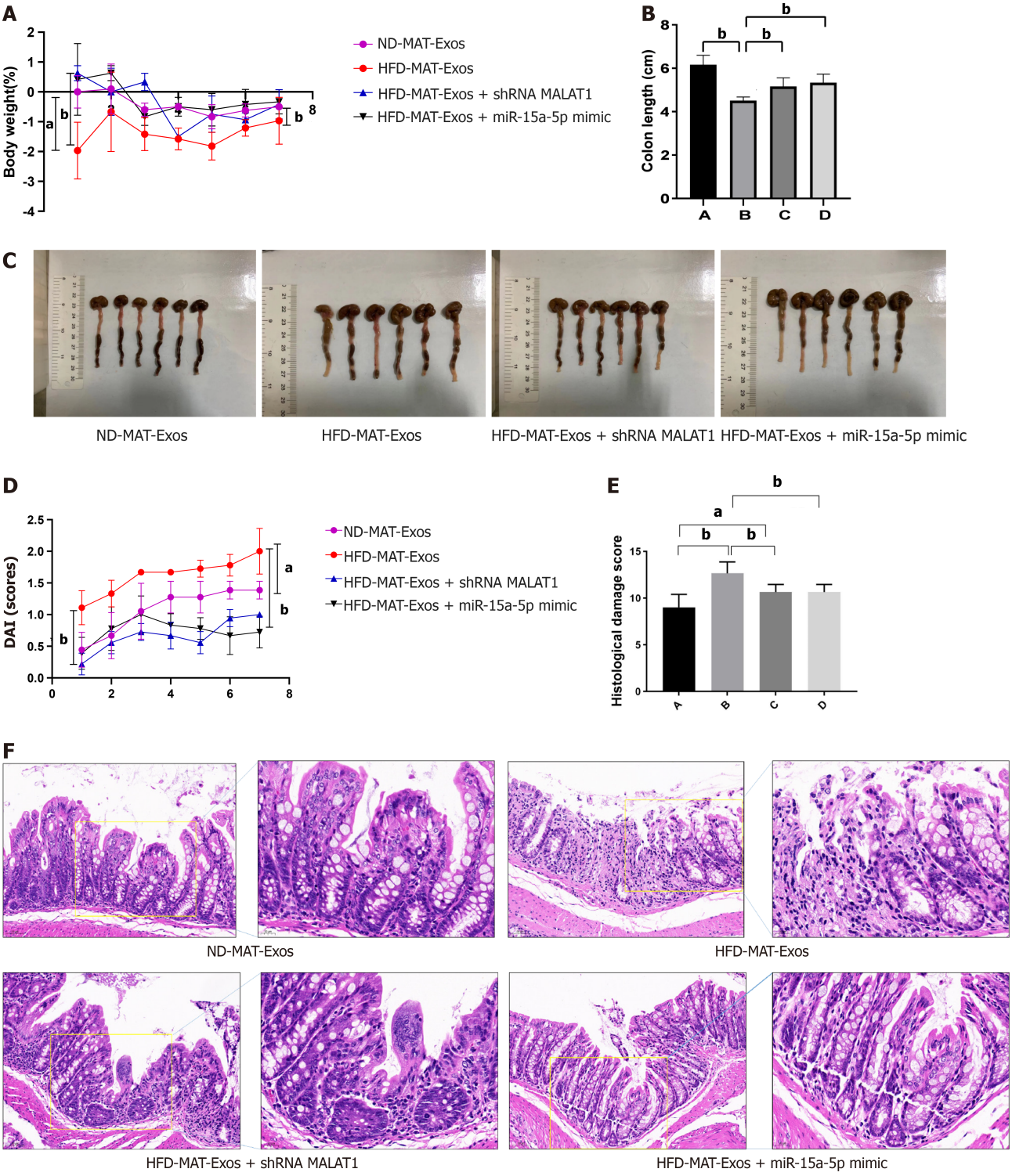


Figure 5 Mesenteric adipose tissue derived exosomes of high-fat diet-fed mice aggravate 2,4,6-trinitrobe-nzenesulfonic acid solution-induced colitis, reversed by shMALAT1 and miR-15a-5p mimic. A: Body weight change trend of mice in each group; B: Colon length of mice in each group; ND-MAT-Exos, HFD-MAT-Exos, HFD-MAT-Exos + shMALAT1, and HFD-MAT-Exos + miR-15a-5p mimic are labelled as A, B, C, and D groups, respectively; C: Colon image of mice in each group; D: Disease activity index of mice in each group; E: Histological damage score of colon tissue, ND-MAT-Exos, HFD-MAT-Exos, HFD-MAT-Exos + shMALAT1, and HFD-MAT-Exos + miR-15a-5p mimic are labelled as A, B, C, and D groups, respectively; F: Hematoxylin and eosin staining images of colon tissue. HFD: High-fat diet; ND: Normal diet; MAT-Exos: Mesenteric adipose tissue derived exosomes; MALAT1: Metastasis-associated lung adenocarcinoma transcript 1. $^{a}P < 0.05$, $^{b}P < 0.01$.

DISCUSSION

Currently, almost one-third of the patients with IBD are obese and have a poor quality of life[8], great difficulty in inducing remission[33-35], increased risk of disease recurrence[8], and a higher burden of hospitalization and disease expenditure[36]. Therefore, it is necessary to explore the mechanism by

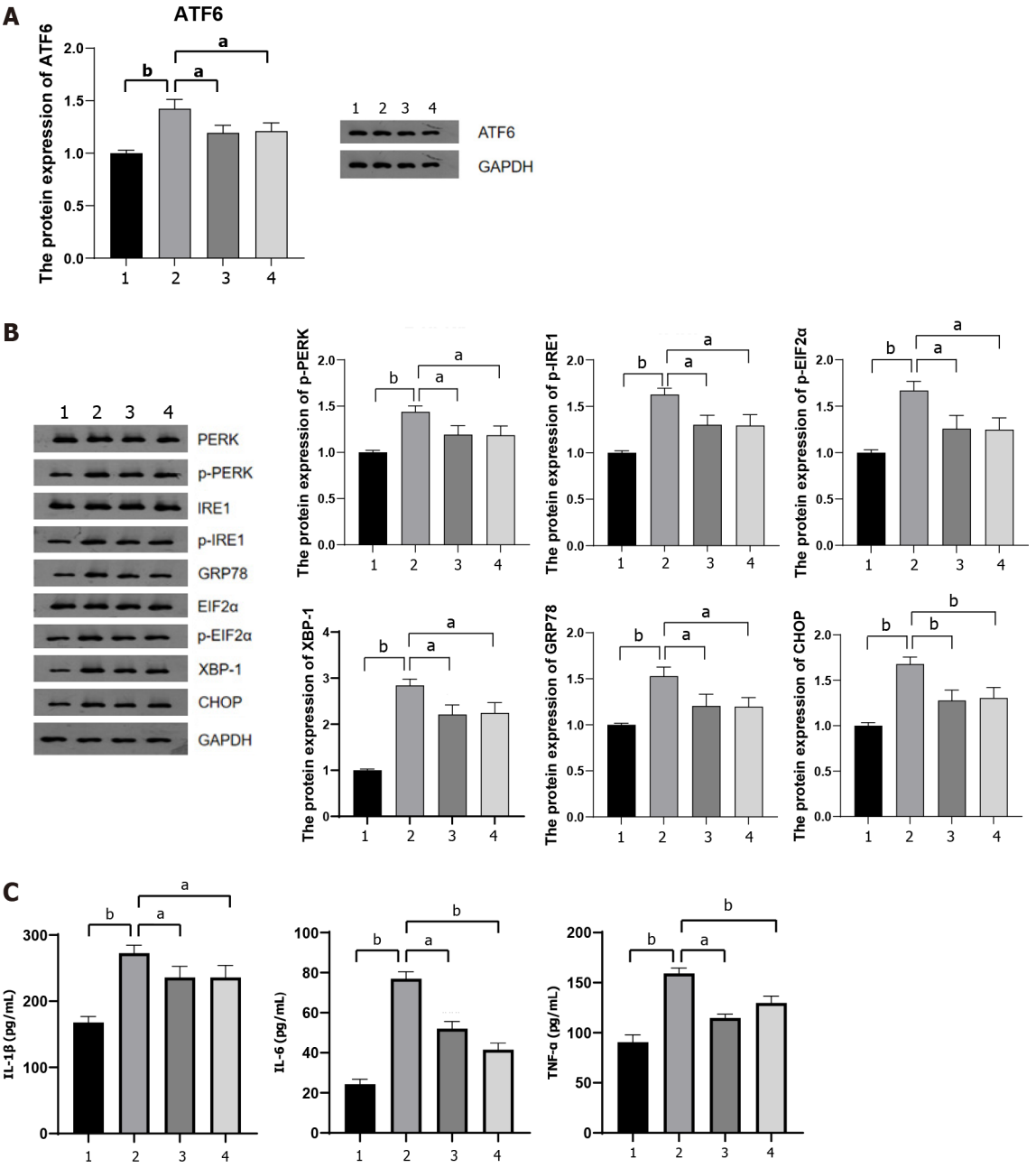


Figure 6 Long noncoding RNAs metastasis-associated lung adenocarcinoma transcript 1 acted on the miR-15a-5p/activating transcription factor 6 axis to activate the endoplasmic reticulum stress signaling pathway. ND-MAT-Exos, HFD-MAT-Exos, HFD-MAT-Exos + shMALAT1, and HFD-MAT-Exos + miR-15a-5p mimic are labelled as 1, 2, 3, and 4 groups, respectively. A: The expression level of activating transcription factor 6 in colon tissue; B: The expression level of endoplasmic reticulum stress related proteins in colon tissue detected by Western blotting; C: The expression level of interleukin (IL)-β, tumor necrosis factor α, IL-6 in the colon tissue detected by enzyme linked immunosorbent assay. ATF-6: Activating transcription factor 6; IL: Interleukin; TNF-α: Tumor necrosis factor α. $^{a}P < 0.05$, $^{b}P < 0.01$.

which obesity is induced in IBD to improve its treatment. Previous studies have shown that the increased severity of IBD in obese patients is related to increased intestinal permeability, intestinal microflora translocation, and changes in the intestinal microflora spectrum[37,38]. In addition, the increase in plasma leptin levels and decrease in adiponectin levels were also found to be involved in obesity-mediated IBD aggravation, but the mechanisms underlying these processes need further exploration[39]. In this study, we propose a novel mechanism through which obesity aggravates IBD *via* exosome-secreted lncRNAs.

First, we demonstrated that a high-fat diet could aggravate TNBS-induced colitis in mice and explored the underlying mechanisms. One of the main characteristics of obesity is the accumulation of adipose tissue. As adipose tissue is an endocrine organ, it plays an important role in a variety of metabolism-related diseases, especially visceral adipose tissue[40]. We focused our attention on the mesenteric adipose tissue, a type of visceral adipose tissue, as it is closest to the colon tissue and can communicate with the colon in various ways. In patients with CD, the lesion is often surrounded by a

special type of mesenteric adipose tissue called creeping fat, which is associated with the translocation of gut microbiota[41]. These findings suggest that the mesenteric adipose tissue may play an important role in IBD progression. We further found that TNBS treatment reduced the content of the mesenteric adipose tissue. However, the content of the mesenteric adipose tissue in HFD mice treated with TNBS was still significantly higher than that in ND mice treated with TNBS.

Exosomes serve as important means of intercellular communication. Previous reports have shown that exosomes secreted by visceral fat could target the colon tissue[16]. Therefore, we hypothesized that mesenteric-derived exosomes in obese mice may aggravate TNBS-induced colitis. Exosomes from the mesenteric adipose tissue were isolated and identified. Subsequently, exosomes extracted from the mesenteric adipose tissue of HFD and ND mice were separately injected into TNBS-treated ND mice *via* the tail vein. The results showed that exosomes from the mesenteric adipose tissue of HFD mice aggravated TNBS-induced colitis.

We then investigated the molecular mechanism by which exosomes derived from the mesenteric adipose tissue of HFD mice aggravated TNBS-induced colitis. A recent study indicated that visceral adipose tissue-derived exosomes can exacerbate colitis severity through proinflammatory noncoding RNAs such as miR-155[16]. In this study, we focused on the lncRNAs in exosomes. Using qRT-PCR, we identified that lncRNA expression is strongly associated with HFD in mesenteric adipose exosomes, as well as mesenteric adipose and colon tissues. In the same structures or tissues, the expression of MALAT1 was higher in TNBS-treated HFD mice than in TNBS-treated ND mice. An additional injection of MAT-Exos from HFD mice *via* the tail vein increased the relative expression of MALAT1 in the colon tissue, indicating that the increased expression of lncRNA MALAT1 in the colon tissue can be partially attributed to MAT-Exos arising from increased creeping fat. In fact, shMALAT1 partially reversed the effect of exosomes derived from the mesenteric adipose tissue in HFD mice, suggesting that exosomes derived from the mesenteric adipose tissue in HFD mice aggravated TNBS-induced enteritis in part due to the high expression of lncRNA MALAT1 in exosomes.

The mechanism by which lncRNA aggravates colitis was further investigated. We revealed that lncRNA MALAT1 could bind miR-15a-5p in vivo, and that the miR-15a-5p mimic could reverse the aggravation of colitis. Furthermore, the miR-15a-5p mimic and sh-MALAT1 reversed the HFD mice MAT-Exos-induced increase in the expression of ER stress-related proteins, including ATF6. We further verified the interaction between miR-15-15p and ATF6 using a dual-luciferase reporter assay. These results indicate that lncRNA MALAT1 may activate the ATF6-related ER stress signaling pathway by binding miR-15a-5p.

MALAT1 is abundantly expressed and highly conserved in 33 species of mammals, with the earliest study linking it to metastasis in non-small cell lung cancer[42]. However, recent studies have shown that MALAT1 plays an important role in a variety of tumors[18] as well as in a variety of autoimmune[43], infectious[44,45], and metabolism-related diseases[46]. Previous studies have shown that MALAT1 Levels are reduced in the plasma of patients with CD[47], suggesting that MALAT1 may be a protective factor with respect to the occurrence and development of CD. The results of our study indicated that TNBS treatment decreased the expression of MALAT1, in accordance with finding of previous reports, but the differences were not significant. Moreover, Li *et al*[48] indicated that MALAT1 targets intestinal epithelial cells and enhances the intestinal epithelial barrier, which plays a protective role by sequestering miR-146b-5p and maintaining the expression of AJC proteins, NUMB, and CLDN11 in IBD. However, they did not demonstrate an effect of MALAT1 overexpression on colitis in vivo.

Intriguingly, our study showed that obesity-induced increases in MALAT1 expression in colon tissue can aggravate colitis, suggesting that MALAT1 may be a double-edged sword with respect to IBD. Mechanistically, the contrary effect of MALAT1 in colitis was mainly due to the fact that exosomes derived from the mesenteric adipose tissue targeted the lamina propria of the colon rather than intestinal epithelial cells[16]. Many immune cells are distributed within the lamina propria of the colon, including dendritic cells, macrophages, and lymphoid cells, which supplement the barrier function of intestinal epithelial cells[49]. In addition, many adaptive immune system-related lymphocytes are recruited from peripheral circulation to the lamina propria and are involved in the onset and progression of IBD. LncRNA MALAT1 encapsulated in exosomes from the mesenteric adipose tissue may act on the abovementioned immune cells in the lamina propria and activate the ATF6-related ER stress pathway to promote the release of pro-inflammatory cytokines[50].

ER stress plays a role in the occurrence and development of metabolic syndrome-related diseases in the obese population[51]. Our study demonstrates that ER stress is one of the potential mechanisms by which obesity aggravates IBD, thereby highlighting the importance of weight loss in obese patients with IBD and the treatment of metabolic syndrome-related diseases. In addition, we preliminarily identified a new signaling pathway, namely, the MALAT1-miR-15a-5p/ATF6 axis, revealing a new regulatory mechanism, *i.e.*, the ATF6-related ER stress signaling pathway. Whether this signaling pathway plays a role in other tissues or diseases requires further investigation.

This study has several limitations that should be acknowledged. First, the effect of exosomes derived from the mesenteric adipose tissue was only studied in the colon as a whole, and the specific target cell types remain unclear and require further elucidation. Second, it would be more beneficial if the regulation of the lncRNAMALAT1-miR-15a-5p-ATF6 pathway could be confirmed in a more in-depth investigation. Finally, we speculated that the divergent effect of lncRNA MALAT1 on IBD severity may

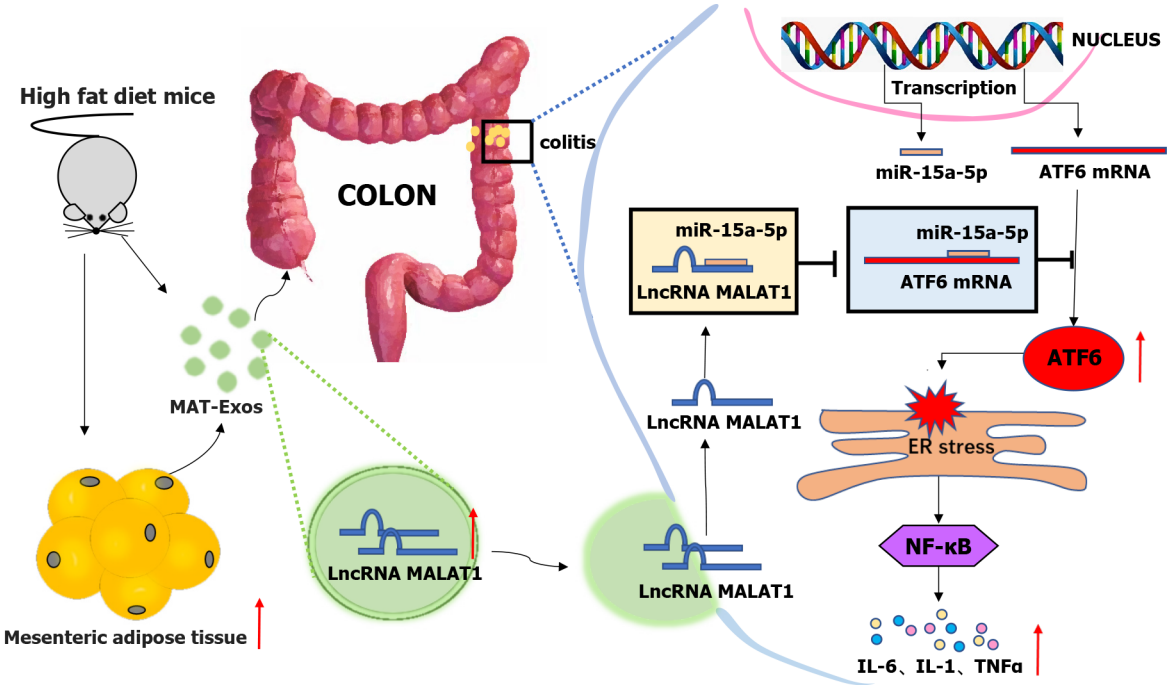


Figure 7 Long non-coding RNA metastasis-associated lung adenocarcinoma transcript 1 encapsulated by mesenteric adipose tissue-derived exosomes targets the colon to aggravate colitis *via* the microRNA-15a-5p/activating transcription factor 6 axis in response to endoplasmic reticulum stress. ATF-6: Activating transcription factor 6; LnRNA: Long non-coding RNA; IL: Interleukin; TNF-α: Tumor necrosis factor-α; ER: Endoplasmic reticulum; MAT-Exos: Mesenteric adipose tissue derived exosomes; MALAT1: Metastasis-associated lung adenocarcinoma transcript 1.

be due to its various targeting areas, where endogenous MALAT1 may exert its effect on intestinal epithelial cells, while extrinsic mesenteric adipose tissue-derived EXO-MALAT1 may act on the intestinal lamina propria through its gut-homing property. However, this theory requires further exploration in the future.

Overall, HFD increased the content of the mesenteric adipose tissue and associated EXO lncRNA MALAT1, which was then absorbed by the colon where it targeted the miR-15a-5p/ATF6 axis, thereby leading to the activation of the ER stress pathway. Further, downstream activation of the inflammatory factor signaling pathway may partially contribute to the aggravation of colitis in obese IBD patients.

CONCLUSION

A higher visceral adipose-tissue ratio was associated with an increased disease activity in CD patients. But the underlining mechanism still remains elusive. Our study indicated that high-fat diet increased the content of mesenteric adipose tissue and aggravated colitis in mice. Mesenteric adipose tissue derived exosome lncRNA metastasis-associated lung adenocarcinoma transcript 1 can be absorbed by the colon leading to activation of the endoplasmic reticulum stress pathway by way of targeting the miR-15a-5p/ATF6 axis to aggravate colitis (Figure 7).

ARTICLE HIGHLIGHTS

Research background

Obesity is associated with an increased risk of developing Crohn's disease (CD), higher disease activity, and comparatively worse clinical outcomes, especially in CD patients with a high visceral adipose tissue ratio. However, the underlying mechanisms remain unclear.

Research motivation

Exosomes contain multiple non-coding RNAs such as long non-coding RNAs (lncRNAs), which serve as messengers in cell-cell communication. Visceral adipose tissue derived exosomes display tissue affinity and preferentially target the colonic lamina propria. We hypothesized that obesity exacerbates inflammatory bowel disease, partially through mesenteric adipose tissue-derived exosomes.

Research objectives

To investigate the role of mesenteric adipose tissue-derived exosomes in CD aggravation through obesity, thereby providing a potential therapeutic target for CD in this subpopulation.

Research methods

A 2,4,6-trinitrobe-nzenesulfonic acid (TNBS) was used to induce colitis in mice fed a high-fat diet (HFD) and normal diet (ND). Exosomes from the mesenteric adipose tissue were extracted and identified, followed by the investigation of lncRNA metastasis-associated lung adenocarcinoma transcript 1 (MALAT1) expression. Luciferase reporter and RNA pull-down assays were performed to verify the interaction between MALAT1 and miR-15a-5p/activating transcription factor 6 (ATF6) axis. Finally, mesenteric adipose tissue-derived exosomes extracted from HFD-fed mice were isolated and treated with either a short hairpin RNA targeting MALAT1 (shMALAT) or an miR-15a-5p mimic before being injected into mice to explore their influence on TNBS-induced colitis.

Research results

HFD can aggravate TNBS-induced colitis in mice, and increase the expression of MALAT1 in mesenteric adipose tissue-derived exosomes. Increased expression of MALAT1 in the colon tissue exacerbated TNBS-induced colitis and activated the ATF6-related endoplasmic reticulum stress pathway. Moreover, this effect was partially reversed by the reduced expression of MALAT1 and overexpression of miR-15a-5p.

Research conclusions

Mesenteric adipose tissue-derived exosome-encapsulated lncRNA MALAT1 targets the colon and aggravates TNBS-induced colitis in obese mice, which may potentially act on the miR-15a-5p/ATF6 axis and indice endoplasmic reticulum stress.

Research perspectives

Obesity-mediated aggravation of colitis might involve the mesenteric adipose tissue-derived exosome lncRNA MALAT1, but the specific cells of the intestine targeted by MALAT1 deserve further exploration.

FOOTNOTES

Author contributions: Jin X designed the report; Chen D performed experiments and statistical analysis; Lu MM wrote the paper and assisted to design the report; Wang JH, Ren Y, Wang SS, Xu LL, Cheng XF, Cheng WX, Gao JG, and Li XL assisted to perform experiments and analyzed data; Kalyani FS assisted with paper writing; all authors had access to the study data and reviewed and approved the final manuscript.

Supported by the National Natural Science Foundation of China, No. 81770574; and the Natural Science Foundation of Zhejiang Province, No. LZ21H030002 and No. LY21H030005.

Institutional animal care and use committee statement: The study was reviewed and approved by the institutional review board of the Tab of Animal Experimental Ethical Inspection of the First Affiliated Hospital of Zhejiang University, NO. 2020-1101.

Conflict-of-interest statement: There are no conflicts of interest to report.

Data sharing statement: All the data included in this study are available upon request by contact with the corresponding author.

ARRIVE guidelines statement: The authors have read the ARRIVE guidelines, and the manuscript was prepared and revised according to the ARRIVE guidelines.

Open-Access: This article is an open-access article that was selected by an in-house editor and fully peer-reviewed by external reviewers. It is distributed in accordance with the Creative Commons Attribution NonCommercial (CC BY-NC 4.0) license, which permits others to distribute, remix, adapt, build upon this work non-commercially, and license their derivative works on different terms, provided the original work is properly cited and the use is non-commercial. See: https://creativecommons.org/Licenses/by-nc/4.0/

Country/Territory of origin: China

ORCID number: Dong Chen 0000-0003-3892-9248; Miao-Miao Lu 0000-0002-9328-8239; Jin-Hai Wang 0000-0002-4640-7661; Yue Ren 0000-0001-9071-2738; Ling-Ling Xu 0000-0002-6668-3057; Wei-Xin Cheng 0000-0003-1764-0779; Sai-Sai Wang 0000-0002-5436-5385; Xiao-Lin Li 0000-0003-3682-3237; Xiao-Fei Cheng 0000-0003-3336-0996; Jian-Guo Gao 0000-

0002-9414-5395; Farhin Shaheed Kalyani 0000-0001-8276-8125; Xi Jin 0000-0001-9985-3035.

S-Editor: Chen YL
L-Editor: A
P-Editor: Yuan YY

REFERENCES

1 **Torres J**, Mehandru S, Colombel JF, Peyrin-Biroulet L. Crohn's disease. *Lancet* 2017; **389**: 1741-1755 [PMID: 27914655 DOI: 10.1016/S0140-6736(16)31711-1]
2 **Molodecky NA**, Soon IS, Rabi DM, Ghali WA, Ferris M, Chernoff G, Benchimol EI, Panaccione R, Ghosh S, Barkema HW, Kaplan GG. Increasing incidence and prevalence of the inflammatory bowel diseases with time, based on systematic review. *Gastroenterology* 2012; **142**: 46-54.e42; quiz e30 [PMID: 22001864 DOI: 10.1053/j.gastro.2011.10.001]
3 **Ng SC**, Tang W, Ching JY, Wong M, Chow CM, Hui AJ, Wong TC, Leung VK, Tsang SW, Yu HH, Li MF, Ng KK, Kamm MA, Studd C, Bell S, Leong R, de Silva HJ, Kasturiratne A, Mufeena MNF, Ling KL, Ooi CJ, Tan PS, Ong D, Goh KL, Hilmi I, Pisespongsa P, Manatsathit S, Rerknimitr R, Aniwan S, Wang YF, Ouyang Q, Zeng Z, Zhu Z, Chen MH, Hu PJ, Wu K, Wang X, Simadibrata M, Abdullah M, Wu JC, Sung JJY, Chan FKL; Asia–Pacific Crohn's and Colitis Epidemiologic Study (ACCESS) Study Group. Incidence and phenotype of inflammatory bowel disease based on results from the Asia-pacific Crohn's and colitis epidemiology study. *Gastroenterology* 2013; **145**: 158-165.e2 [PMID: 23583432 DOI: 10.1053/j.gastro.2013.04.007]
4 **Singh S**, Dulai PS, Zarrinpar A, Ramamoorthy S, Sandborn WJ. Obesity in IBD: epidemiology, pathogenesis, disease course and treatment outcomes. *Nat Rev Gastroenterol Hepatol* 2017; **14**: 110-121 [PMID: 27899815 DOI: 10.1038/nrgastro.2016.181]
5 **Khalili H**, Ananthakrishnan AN, Konijeti GG, Higuchi LM, Fuchs CS, Richter JM, Chan AT. Measures of obesity and risk of Crohn's disease and ulcerative colitis. *Inflamm Bowel Dis* 2015; **21**: 361-368 [PMID: 25563694 DOI: 10.1097/MIB.0000000000000283]
6 **Harpsøe MC**, Basit S, Andersson M, Nielsen NM, Frisch M, Wohlfahrt J, Nohr EA, Linneberg A, Jess T. Body mass index and risk of autoimmune diseases: a study within the Danish National Birth Cohort. *Int J Epidemiol* 2014; **43**: 843-855 [PMID: 24609069 DOI: 10.1093/ije/dyu045]
7 **Pringle PL**, Stewart KO, Peloquin JM, Sturgeon HC, Nguyen D, Sauk J, Garber JJ, Yajnik V, Ananthakrishnan AN, Chan AT, Xavier RJ, Khalili H. Body Mass Index, Genetic Susceptibility, and Risk of Complications Among Individuals with Crohn's Disease. *Inflamm Bowel Dis* 2015; **21**: 2304-2310 [PMID: 26181430 DOI: 10.1097/MIB.0000000000000498]
8 **Jain A**, Nguyen NH, Proudfoot JA, Martin CF, Sandborn WJ, Kappelman MD, Long MD, Singh S. Impact of Obesity on Disease Activity and Patient-Reported Outcomes Measurement Information System (PROMIS) in Inflammatory Bowel Diseases. *Am J Gastroenterol* 2019; **114**: 630-639 [PMID: 30865012 DOI: 10.14309/ajg.0000000000000197]
9 **Büning C**, von Kraft C, Hermsdorf M, Gentz E, Wirth EK, Valentini L, Haas V. Visceral Adipose Tissue in Patients with Crohn's Disease Correlates with Disease Activity, Inflammatory Markers, and Outcome. *Inflamm Bowel Dis* 2015; **21**: 2590-2597 [PMID: 26222339 DOI: 10.1097/MIB.0000000000000527]
10 **Scheja L**, Heeren J. The endocrine function of adipose tissues in health and cardiometabolic disease. *Nat Rev Endocrinol* 2019; **15**: 507-524 [PMID: 31296970 DOI: 10.1038/s41574-019-0230-6]
11 **Siegmund B**. Mesenteric fat in Crohn's disease: the hot spot of inflammation? *Gut* 2012; **61**: 3-5 [PMID: 22068165 DOI: 10.1136/gutjnl-2011-301354]
12 **Deng T**, Lyon CJ, Bergin S, Caligiuri MA, Hsueh WA. Obesity, Inflammation, and Cancer. *Annu Rev Pathol* 2016; **11**: 421-449 [PMID: 27193454 DOI: 10.1146/annurev-pathol-012615-044359]
13 **Packer M**. Epicardial Adipose Tissue May Mediate Deleterious Effects of Obesity and Inflammation on the Myocardium. *J Am Coll Cardiol* 2018; **71**: 2360-2372 [PMID: 29773163 DOI: 10.1016/j.jacc.2018.03.509]
14 **Schuster S**, Cabrera D, Arrese M, Feldstein AE. Triggering and resolution of inflammation in NASH. *Nat Rev Gastroenterol Hepatol* 2018; **15**: 349-364 [PMID: 29740166 DOI: 10.1038/s41575-018-0009-6]
15 **Sun Z**, Yang S, Zhou Q, Wang G, Song J, Li Z, Zhang Z, Xu J, Xia K, Chang Y, Liu J, Yuan W. Emerging role of exosome-derived long non-coding RNAs in tumor microenvironment. *Mol Cancer* 2018; **17**: 82 [PMID: 29678180 DOI: 10.1186/s12943-018-0831-z]
16 **Wei M**, Gao X, Liu L, Li Z, Wan Z, Dong Y, Chen X, Niu Y, Zhang J, Yang G. Visceral Adipose Tissue Derived Exosomes Exacerbate Colitis Severity *via* Pro-inflammatory MiRNAs in High Fat Diet Fed Mice. *ACS Nano* 2020; **14**: 5099-5110 [PMID: 32275391 DOI: 10.1021/acsnano.0c01860]
17 **Djebali S**, Davis CA, Merkel A, Dobin A, Lassmann T, Mortazavi A, Tanzer A, Lagarde J, Lin W, Schlesinger F, Xue C, Marinov GK, Khatun J, Williams BA, Zaleski C, Rozowsky J, Röder M, Kokocinski F, Abdelhamid RF, Alioto T, Antoshechkin I, Baer MT, Bar NS, Batut P, Bell K, Bell I, Chakrabortty S, Chen X, Chrast J, Curado J, Derrien T, Drenkow J, Dumais E, Dumais J, Duttagupta R, Falconnet E, Fastuca M, Fejes-Toth K, Ferreira P, Foissac S, Fullwood MJ, Gao H, Gonzalez D, Gordon A, Gunawardena H, Howald C, Jha S, Johnson R, Kapranov P, King B, Kingswood C, Luo OJ, Park E, Persaud K, Preall JB, Ribeca P, Risk B, Robyr D, Sammeth M, Schaffer L, See LH, Shahab A, Skancke J, Suzuki AM, Takahashi H, Tilgner H, Trout D, Walters N, Wang H, Wrobel J, Yu Y, Ruan X, Hayashizaki Y, Harrow J, Gerstein M, Hubbard T, Reymond A, Antonarakis SE, Hannon G, Giddings MC, Ruan Y, Wold B, Carninci P, Guigó R, Gingeras TR. Landscape of transcription in human cells. *Nature* 2012; **489**: 101-108 [PMID: 22955620 DOI: 10.1038/nature11233]
18 **Amodio N**, Raimondi L, Juli G, Stamato MA, Caracciolo D, Tagliaferri P, Tassone P. MALAT1: a druggable long non-coding RNA for targeted anti-cancer approaches. *J Hematol Oncol* 2018; **11**: 63 [PMID: 29739426 DOI:

10.1186/s13045-018-0606-4]
19 **Camuesco D**, Comalada M, Rodríguez-Cabezas ME, Nieto A, Lorente MD, Concha A, Zarzuelo A, Gálvez J. The intestinal anti-inflammatory effect of quercitrin is associated with an inhibition in iNOS expression. *Br J Pharmacol* 2004; **143**: 908-918 [PMID: 15533892 DOI: 10.1038/sj.bjp.0705941]
20 **Wirtz S**, Popp V, Kindermann M, Gerlach K, Weigmann B, Fichtner-Feigl S, Neurath MF. Chemically induced mouse models of acute and chronic intestinal inflammation. *Nat Protoc* 2017; **12**: 1295-1309 [PMID: 28569761 DOI: 10.1038/nprot.2017.044]
21 **Gao J**, Li X, Wang Y, Cao Y, Yao D, Sun L, Qin L, Qiu H, Zhan X. Adipocyte-derived extracellular vesicles modulate appetite and weight through mTOR signalling in the hypothalamus. *Acta Physiol (Oxf)* 2020; **228**: e13339 [PMID: 31278836 DOI: 10.1111/apha.13339]
22 **Xie L**, Chen Z, Liu M, Huang W, Zou F, Ma X, Tao J, Guo J, Xia X, Lyu F, Wang H, Zheng C, Jiang J. MSC-Derived Exosomes Protect Vertebral Endplate Chondrocytes against Apoptosis and Calcification *via* the miR-31-5p/ATF6 Axis. *Mol Ther Nucleic Acids* 2020; **22**: 601-614 [PMID: 33230460 DOI: 10.1016/j.omtn.2020.09.026]
23 **Liu SX**, Zheng F, Xie KL, Xie MR, Jiang LJ, Cai Y. Exercise Reduces Insulin Resistance in Type 2 Diabetes Mellitus *via* Mediating the lncRNA MALAT1/MicroRNA-382-3p/Resistin Axis. *Mol Ther Nucleic Acids* 2019; **18**: 34-44 [PMID: 31479923 DOI: 10.1016/j.omtn.2019.08.002]
24 **Ji Q**, Cai G, Liu X, Zhang Y, Wang Y, Zhou L, Sui H, Li Q. MALAT1 regulates the transcriptional and translational levels of proto-oncogene RUNX2 in colorectal cancer metastasis. *Cell Death Dis* 2019; **10**: 378 [PMID: 31097689 DOI: 10.1038/s41419-019-1598-x]
25 **Chen Y**, Wang X. miRDB: an online database for prediction of functional microRNA targets. *Nucleic Acids Res* 2020; **48**: D127-D131 [PMID: 31504780 DOI: 10.1093/nar/gkz757]
26 **Hetz C**. The unfolded protein response: controlling cell fate decisions under ER stress and beyond. *Nat Rev Mol Cell Biol* 2012; **13**: 89-102 [PMID: 22251901 DOI: 10.1038/nrm3270]
27 **Powell N**, Pantazi E, Pavlidis P, Tsakmaki A, Li K, Yang F, Parker A, Pin C, Cozzetto D, Minns D, Stolarczyk E, Saveljeva S, Mohamed R, Lavender P, Afzali B, Digby-Bell J, Tjir-Li T, Kaser A, Friedman J, MacDonald TT, Bewick GA, Lord GM. Interleukin-22 orchestrates a pathological endoplasmic reticulum stress response transcriptional programme in colonic epithelial cells. *Gut* 2020; **69**: 578-590 [PMID: 31792136 DOI: 10.1136/gutjnl-2019-318483]
28 **Ma X**, Dai Z, Sun K, Zhang Y, Chen J, Yang Y, Tso P, Wu G, Wu Z. Intestinal Epithelial Cell Endoplasmic Reticulum Stress and Inflammatory Bowel Disease Pathogenesis: An Update Review. *Front Immunol* 2017; **8**: 1271 [PMID: 29118753 DOI: 10.3389/fimmu.2017.01271]
29 **Kaser A**, Lee AH, Franke A, Glickman JN, Zeissig S, Tilg H, Nieuwenhuis EE, Higgins DE, Schreiber S, Glimcher LH, Blumberg RS. XBP1 Links ER stress to intestinal inflammation and confers genetic risk for human inflammatory bowel disease. *Cell* 2008; **134**: 743-756 [PMID: 18775308 DOI: 10.1016/j.cell.2008.07.021]
30 **Stengel ST**, Fazio A, Lipinski S, Jahn MT, Aden K, Ito G, Wottawa F, Kuiper JWP, Coleman OI, Tran F, Bordoni D, Bernardes JP, Jentzsch M, Luzius A, Bierwirth S, Messner B, Henning A, Welz L, Kakavand N, Falk-Paulsen M, Imm S, Hinrichsen F, Zilbauer M, Schreiber S, Kaser A, Blumberg R, Haller D, Rosenstiel P. Activating Transcription Factor 6 Mediates Inflammatory Signals in Intestinal Epithelial Cells Upon Endoplasmic Reticulum Stress. *Gastroenterology* 2020; **159**: 1357-1374.e10 [PMID: 32673694 DOI: 10.1053/j.gastro.2020.06.088]
31 **Deng J**, Lu PD, Zhang Y, Scheuner D, Kaufman RJ, Sonenberg N, Harding HP, Ron D. Translational repression mediates activation of nuclear factor kappa B by phosphorylated translation initiation factor 2. *Mol Cell Biol* 2004; **24**: 10161-10168 [PMID: 15542827 DOI: 10.1128/MCB.24.23.10161-10168.2004]
32 **Hu P**, Han Z, Couvillon AD, Kaufman RJ, Exton JH. Autocrine tumor necrosis factor alpha links endoplasmic reticulum stress to the membrane death receptor pathway through IRE1alpha-mediated NF-kappaB activation and down-regulation of TRAF2 expression. *Mol Cell Biol* 2006; **26**: 3071-3084 [PMID: 16581782 DOI: 10.1128/MCB.26.8.3071-3084.2006]
33 **Puig L**. Obesity and psoriasis: body weight and body mass index influence the response to biological treatment. *J Eur Acad Dermatol Venereol* 2011; **25**: 1007-1011 [PMID: 21492252 DOI: 10.1111/j.1468-3083.2011.04065.x]
34 **Bhalme M**, Sharma A, Keld R, Willert R, Campbell S. Does weight-adjusted anti-tumour necrosis factor treatment favour obese patients with Crohn's disease? *Eur J Gastroenterol Hepatol* 2013; **25**: 543-549 [PMID: 23337170 DOI: 10.1097/MEG.0b013e32835d1f15]
35 **Harper JW**, Sinanan MN, Zisman TL. Increased body mass index is associated with earlier time to loss of response to infliximab in patients with inflammatory bowel disease. *Inflamm Bowel Dis* 2013; **19**: 2118-2124 [PMID: 23863401 DOI: 10.1097/MIB.0b013e31829cf401]
36 **Flores A**, Burstein E, Cipher DJ, Feagins LA. Obesity in Inflammatory Bowel Disease: A Marker of Less Severe Disease. *Dig Dis Sci* 2015; **60**: 2436-2445 [PMID: 25799938 DOI: 10.1007/s10620-015-3629-5]
37 **Martinez-Medina M**, Denizot J, Dreux N, Robin F, Billard E, Bonnet R, Darfeuille-Michaud A, Barnich N. Western diet induces dysbiosis with increased E coli in CEABAC10 mice, alters host barrier function favouring AIEC colonisation. *Gut* 2014; **63**: 116-124 [PMID: 23598352 DOI: 10.1136/gutjnl-2012-304119]
38 **Lam YY**, Ha CW, Campbell CR, Mitchell AJ, Dinudom A, Oscarsson J, Cook DI, Hunt NH, Caterson ID, Holmes AJ, Storlien LH. Increased gut permeability and microbiota change associate with mesenteric fat inflammation and metabolic dysfunction in diet-induced obese mice. *PLoS One* 2012; **7**: e34233 [PMID: 22457829 DOI: 10.1371/journal.pone.0034233]
39 **Bilski J**, Mazur-Bialy AI, Brzozowski B, Magierowski M, Jasnos K, Krzysiek-Maczka G, Urbanczyk K, Ptak-Belowska A, Zwolinska-Wcislo M, Mach T, Brzozowski T. Moderate exercise training attenuates the severity of experimental rodent colitis: the importance of crosstalk between adipose tissue and skeletal muscles. *Mediators Inflamm* 2015; **2015**: 605071 [PMID: 25684862 DOI: 10.1155/2015/605071]
40 **Kahn CR**, Wang G, Lee KY. Altered adipose tissue and adipocyte function in the pathogenesis of metabolic syndrome. *J Clin Invest* 2019; **129**: 3990-4000 [PMID: 31573548 DOI: 10.1172/JCI129187]
41 **Spencer SP**, Sonnenburg JL. When Gut Microbiota Creep into Fat, the Fat Creeps Back. *Cell* 2020; **183**: 589-591 [PMID: 33125887 DOI: 10.1016/j.cell.2020.10.008]

42 **Ji P**, Diederichs S, Wang W, Böing S, Metzger R, Schneider PM, Tidow N, Brandt B, Buerger H, Bulk E, Thomas M, Berdel WE, Serve H, Müller-Tidow C. MALAT-1, a novel noncoding RNA, and thymosin beta4 predict metastasis and survival in early-stage non-small cell lung cancer. *Oncogene* 2003; **22**: 8031-8041 [PMID: 12970751 DOI: 10.1038/sj.onc.1206928]

43 **Li GQ**, Fang YX, Liu Y, Meng FR, Wu X, Zhang CW, Zhang Y, Liu D, Gao B. MALAT1-Driven Inhibition of Wnt Signal Impedes Proliferation and Inflammation in Fibroblast-Like Synoviocytes Through CTNNB1 Promoter Methylation in Rheumatoid Arthritis. *Hum Gene Ther* 2019; **30**: 1008-1022 [PMID: 30909750 DOI: 10.1089/hum.2018.212]

44 **Gu H**, Zhu Y, Zhou Y, Huang T, Zhang S, Zhao D, Liu F. LncRNA MALAT1 Affects *Mycoplasma pneumoniae* Pneumonia *via* NF-κB Regulation. *Front Cell Dev Biol* 2020; **8**: 563693 [PMID: 33134293 DOI: 10.3389/fcell.2020.563693]

45 **Yong H**, Wu G, Chen J, Liu X, Bai Y, Tang N, Liu L, Wei J. lncRNA MALAT1 Accelerates Skeletal Muscle Cell Apoptosis and Inflammatory Response in Sepsis by Decreasing BRCA1 Expression by Recruiting EZH2. *Mol Ther Nucleic Acids* 2020; **19**: 97-108 [PMID: 31830649 DOI: 10.1016/j.omtn.2019.10.028]

46 **Cremer S**, Michalik KM, Fischer A, Pfisterer L, Jaé N, Winter C, Boon RA, Muhly-Reinholz M, John D, Uchida S, Weber C, Poller W, Günther S, Braun T, Li DY, Maegdefessel L, Perisic Matic L, Hedin U, Soehnlein O, Zeiher A, Dimmeler S. Hematopoietic Deficiency of the Long Noncoding RNA MALAT1 Promotes Atherosclerosis and Plaque Inflammation. *Circulation* 2019; **139**: 1320-1334 [PMID: 30586743 DOI: 10.1161/CIRCULATIONAHA.117.029015]

47 **Yarani R**, Mirza AH, Kaur S, Pociot F. The emerging role of lncRNAs in inflammatory bowel disease. *Exp Mol Med* 2018; **50**: 1-14 [PMID: 30523244 DOI: 10.1038/s12276-018-0188-9]

48 **Li Y**, Zhu L, Chen P, Wang Y, Yang G, Zhou G, Li L, Feng R, Qiu Y, Han J, Chen B, He Y, Zeng Z, Chen M, Zhang S. MALAT1 Maintains the Intestinal Mucosal Homeostasis in Crohn's Disease *via* the miR-146b-5p-CLDN11/NUMB Pathway. *J Crohns Colitis* 2021; **15**: 1542-1557 [PMID: 33677577 DOI: 10.1093/ecco-jcc/jjab040]

49 **Ramos GP**, Papadakis KA. Mechanisms of Disease: Inflammatory Bowel Diseases. *Mayo Clin Proc* 2019; **94**: 155-165 [PMID: 30611442 DOI: 10.1016/j.mayocp.2018.09.013]

50 **So JS**. Roles of Endoplasmic Reticulum Stress in Immune Responses. *Mol Cells* 2018; **41**: 705-716 [PMID: 30078231 DOI: 10.14348/molcells.2018.0241]

51 **Shan B**, Wang X, Wu Y, Xu C, Xia Z, Dai J, Shao M, Zhao F, He S, Yang L, Zhang M, Nan F, Li J, Liu J, Jia W, Qiu Y, Song B, Han JJ, Rui L, Duan SZ, Liu Y. The metabolic ER stress sensor IRE1α suppresses alternative activation of macrophages and impairs energy expenditure in obesity. *Nat Immunol* 2017; **18**: 519-529 [PMID: 28346409 DOI: 10.1038/ni.3709]

World Journal of Gastroenterology

Submit a Manuscript: https://www.f6publishing.com

World J Gastroenterol 2022 August 7; 28(29): 3854-3868

DOI: 10.3748/wjg.v28.i29.3854

ISSN 1007-9327 (print) ISSN 2219-2840 (online)

ORIGINAL ARTICLE

Basic Study

Involvement of nitrergic neurons in colonic motility in a rat model of ulcerative colitis

Yan-Rong Li, Yan Li, Yuan Jin, Mang Xu, Hong-Wei Fan, Qian Zhang, Guo-He Tan, Jing Chen, Yun-Qing Li

Specialty type: Gastroenterology and hepatology

Provenance and peer review: Unsolicited article; Externally peer reviewed.

Peer-review model: Single blind

Peer-review report's scientific quality classification

Grade A (Excellent): 0
Grade B (Very good): B
Grade C (Good): C
Grade D (Fair): 0
Grade E (Poor): 0

P-Reviewer: Bernstein HG, Germany; Sahin Y, Turkey

Received: December 16, 2021
Peer-review started: December 16, 2021
First decision: April 16, 2022
Revised: April 27, 2022
Accepted: July 6, 2022
Article in press: July 6, 2022
Published online: August 7, 2022

Yan-Rong Li, Yun-Qing Li, Department of Human Anatomy, Basic Medical College, Guangxi Medical University, Nanning 530000, Guangxi Zhuang Autonomous Region, China

Yan-Rong Li, Department of Gastroenterology, The First Affiliated Hospital of Jinzhou Medical University, Jinzhou 121000, Liaoning Province, China

Yan Li, Yuan Jin, Qian Zhang, Yun-Qing Li, Department of Human Anatomy, Basic Medical College, Zunyi Medical University, Zunyi 563006, Guizhou Province, China

Mang Xu, Department of Anatomy, Basic Medical College, Dali University, Dali 671000, Yunnan Province, China

Hong-Wei Fan, Department of Anatomy, Histology and Embryology, Xuzhou Medical University, Xuzhou 221000, Jiangsu Province, China

Guo-He Tan, Key Lab of Longevity and Aging-related Diseases of Chinese Ministry of Education, Guangxi Medical University, Nanning 530000, Guangxi Zhuang Autonomous Region, China

Guo-He Tan, School of Basic Medical Sciences and Center for Translational Medicine, Guangxi Medical University, Nanning 530000, Guangxi Zhuang Autonomous Region, China

Jing Chen, Yun-Qing Li, Department of Anatomy, Histology and Embryology and K. K. Leung Brain Research Centre, The Fourth Military Medical University, Xi'an 710032, Shaanxi Province, China

Yun-Qing Li, Department of Human Anatomy, College of Preclinical Medical Sciences, Zhengzhou University, Zhengzhou 450001, Henan Province, China

Yun-Qing Li, Key Laboratory of Brain Science Research and Transformation in Tropical Environment of Hainan Province, Hainan Medical University, Haikou 571199, Hainan Province, China

Corresponding author: Yun-Qing Li, PhD, Professor, Department of Human Anatomy, Basic Medical College, Guangxi Medical University, No. 22 Shuang-Yong Road, Nanning 530000, Guangxi Zhuang Autonomous Region, China. deptanat@fmmu.edu.cn

Abstract

BACKGROUND

The mechanisms underlying gastrointestinal (GI) dysmotility with ulcerative colitis (UC) have not been fully elucidated. The enteric nervous system (ENS) plays an essential role in the GI motility. As a vital neurotransmitter in the ENS, the gas neurotransmitter nitric oxide (NO) may impact the colonic motility. In this study, dextran sulfate sodium (DSS)-induced UC rat model was used for investigating the effects of NO by examining the effects of rate-limiting enzyme nitric oxide synthase (NOS) changes on the colonic motility as well as the role of the ENS in the colonic motility during UC.

AIM

To reveal the relationship between the effects of NOS expression changes in NOS-containing nitrergic neurons and the colonic motility in a rat UC model.

METHODS

Male rats (n = 8/each group) were randomly divided into a control (CG), a UC group (EG1), a UC + thrombin derived polypeptide 508 trifluoroacetic acid (TP508TFA; an NOS agonist) group (EG2), and a UC + NG-monomethyl-L-arginine monoacetate (L-NMMA; an NOS inhibitor) group (EG3). UC was induced by administering 5.5% DSS in drinking water without any other treatment (EG1), while the EG2 and EG3 were gavaged with TP508 TFA and L-NMMA, respectively. The disease activity index (DAI) and histological assessment were recorded for each group, whereas the changes in the proportion of colonic nitrergic neurons were counted using immunofluorescence histochemical staining, Western blot, and enzyme linked immunosorbent assay, respectively. In addition, the contractile tension changes in the circular and longitudinal muscles of the rat colon were investigated *in vitro* using an organ bath system.

RESULTS

The proportion of NOS-positive neurons within the colonic myenteric plexus (MP), the relative expression of NOS, and the NOS concentration in serum and colonic tissues were significantly elevated in EG1, EG2, and EG3 compared with CG rats. In UC rats, stimulation with agonists and inhibitors led to variable degrees of increase or decrease for each indicator in the EG2 and EG3. When the rats in EGs developed UC, the mean contraction tension of the colonic smooth muscle detected *in vitro* was higher in the EG1, EG2, and EG3 than in the CG group. Compared with the EG1, the contraction amplitude and mean contraction tension of the circular and longitudinal muscles of the colon in the EG2 and EG3 were enhanced and attenuated, respectively. Thus, during UC, regulation of the expression of NOS within the MP improved the intestinal motility, thereby favoring the recovery of intestinal functions.

CONCLUSION

In UC rats, an increased number of nitrergic neurons in the colonic MP leads to the attenuation of colonic motor function. To intervene NOS activity might modulate the function of nitrergic neurons in the colonic MP and prevent colonic motor dysfunction. These results might provide clues for a novel approach to alleviate diarrhea symptoms of UC patients.

Key Words: Nitrergic neurons; Nitric oxide; Nitric oxide synthase; Ulcerative colitis; Colonic motility; Colonic myenteric plexus

©The Author(s) 2022. Published by Baishideng Publishing Group Inc. All rights reserved.

Core Tip: This study focused on the effects of nitrergic neurons in the myenteric plexus (MP) on colonic motor function in rats with ulcerative colitis (UC). The results suggest that an increased number of nitrergic neurons in the colonic MP of the UC rats leads to reduced colon contractile function. Therefore, the regulation of the activity of nitrergic neurons in the colonic MP through interference with the activities of nitric oxide synthase might be a novel potential and prospective way to reduce the diarrhea symptoms in UC patients.

Citation: Li YR, Li Y, Jin Y, Xu M, Fan HW, Zhang Q, Tan GH, Chen J, Li YQ. Involvement of nitrergic neurons in colonic motility in a rat model of ulcerative colitis. *World J Gastroenterol* 2022; 28(29): 3854-3868
URL: https://www.wjgnet.com/1007-9327/full/v28/i29/3854.htm
DOI: https://dx.doi.org/10.3748/wjg.v28.i29.3854

INTRODUCTION

Ulcerative colitis (UC) is a nonspecific inflammatory disorder of the intestine that primarily involves the rectum, sigmoid colon, and/or, the whole colon, in severe cases. Clinical features include recurrent episodes of abdominal pain, diarrhea, and mucopurulent stools[1]. Unfortunately, the disease course is permanent and causes great suffering to the patients. UC can occur at any age (mainly in young adults), and in recent years, its incidence has increased worldwide[2]. The etiology of UC is complex, and its pathogenesis might be related to genetics[3], immunological factors, psychiatric depression and anxiety [4], environmental factors[5], dietary allergy, intestinal flora[6], and other factors. Therefore, it leads to treatment difficulty and a prolonged treatment course, and recurs easily. Although current pharmacological treatments in the clinic might improve patient's symptoms, they still cannot achieve satisfactory results. In recent years, the research on the aspects of gastrointestinal (GI) motility disorders in UC patients has advanced, and the abnormal intestinal dynamics has become a focus of research on the pathogenesis of UC [7-9].

The enteric nervous system (ENS), including the submucous plexus (SP) and myenteric plexus (MP) [10,11], as an essential component of the peripheral nervous system (PNS), is independent of the central nervous system (CNS) and is involved in the regulation of intestinal secretion, absorption, and motility [12]. Neurons in the ENS, depending on their neurotransmission function, are divided into sensory neurons, motor neurons, and interneurons. Further, motor neurons are divided into excitatory and inhibitory ones, regulating the systolic and diastolic function of the intestine, respectively. Typically, the ENS plays a vital role in maintaining gut homeostasis; however, gut motility gets impaired once the relaxation and contraction functions of the gut become imbalanced.

As the primary inhibitory gas neurotransmitter within the ENS, nitric oxide (NO) regulates several GI functions, such as vascular permeability, mucosal defense, immune regulation, and GI motility[13]. Nitric oxide synthase (NOS), the rate-limiting enzyme of NO synthesis, is widely distributed in endothelial cells, macrophages, neuro-phagocytes, and neuronal cells. NOS can be divided into neural NOS (nNOS), endothelial NOS (eNOS), and inducible NOS (iNOS). Out of these, nNOS is located within the nervous tissue of both the CNS and PNS. NO is one of the major inhibitory neurotransmitters of non-adrenergic noncholinergic (NANC) nerves in the ENS and its release by NOS-positive neurons plays an essential role in stimulating GI secretion and relaxing GI smooth muscle. Changes in the NOS expression level cause alterations in GI motility; however, the impact of such changes in UC on colonic motility has not been clearly defined. Therefore, this study aimed to observe the changes of NOS within the colonic MP in dextran sulfate sodium (DSS)-induced UC rats, to further understand the underlying mechanisms of colonic motility in UC for delineating a new direction for the treatment of UC.

MATERIALS AND METHODS

Reagents

Dextran sulfate sodium (DSS; PC-99017), NG-monomethyl-L-arginine monoacetate (L-NMMA; PC-45273), and thrombin derived polypeptide 508 trifluoroacetic acid (TP508TFA; PC-50991) were purchased from PlantChemMed Co., Ltd (Shanghai, China). Rabbit Anti-HuD + HuC (ab184267) and Goat Anti-nNOS (ab1376) were purchased from Abcam (Cambridge, United Kingdom). Donkey Anti-Goat Alexa Fluor 488 (a11055) and Donkey Anti-Rabbit Alexa Fluor 594 (A21207) were purchased from Invitrogen Co., Ltd (Carlsbad, United States). Mouse Anti-β-Actin monoclonal antibody (A1978) and Immobilon Forte western HRP substrate (Cat. No. WBLUF0020) were purchased from Merck KGaA (Darmstadt, Germany). HRP-Labeled Goat Anti-Rabbit IgG (H + L) (ZB-2306) and HRP-Labeled Goat Anti-Mouse IgG (H + L) (ZB-2305) were purchased from ZhongShan GoldBridge Biotechnology Co., Ltd (Beijing, China). SDS-PAGE Gel Preparation Kit (P0012A) was purchased from Beyotime Biotechnology Co., Ltd (Shanghai, China). BCA Protein Concentration Assay Kit (AR0146) was purchased from BOSTER Biological Technology Co., Ltd (Wuhan, China). NOS1/nNOS ELISA Kit (E-EL-R1438C) were purchased from Elabscience Biotechnology Co., Ltd (Wuhan, China). All other reagents and chemicals used in this study are commercially available.

Animals and animal tests

Thirty-two 8-wk-old male Sprague-Dawley rats weighing 200 ± 20 g were housed in a specific pathogen-free animal house. The animals were kept at a standard room temperature of 24 °C, with 40%-60% relative humidity, 12 h light-dark alternation, and a standard laboratory diet containing 23% protein and water. All animals were provided by the Animal Center of the Fourth Military Medical University and divided into four major groups. All experimental procedures were conducted in accordance with the Principles of Laboratory Animal Care and approved by the University Ethics Committee and performed as per institutional guidelines. Efforts were made to minimize the number of animals used.

The rats were randomly divided into four groups (n = 8/each group), including the control (CG), UC (EG1), UC + NOS agonist TP508TFA (EG2), and UC + NOS inhibitor L-NMMA (EG3) groups. The CG group was housed as described above, whereas the animals in the three experimental groups (EG1-3)

were given tap water containing 5.5% DSS. The CG group was fed in the same way as the experimental groups except that DSS was not added in the tap water. All animals were given free access to water for 7 d, and the water was changed to tap water at day 15. Further, EG2 rats were treated with 3 mL of 0.01 mmol/L TP508 TFA i.g. daily for 15 d and EG3 rats were treated with 3 mL of 0.01 mmol/L L-NMMA i.g. daily for 15 d. Animals were regularly monitored for the general conditions, body weight, stool characteristics, occult blood, and hematochezia for the evaluation of the disease condition. The scoring criteria of the disease activity index (DAI) were as follows[14]: Body weight: No loss, 0 points; loss by 1%-5%, 1 point; loss by 6%-10%, 2 points; loss by 11%-15%, 3 points; loss by more than 15%, 4 points; stool characteristics: Normal (well-shaped), 0 points; bondless (mushy and semi-formed stool that does not adhere to the anus), 2 points; loose (watery stool that can adhere to the anus), 4 points; fecal occult blood or macroscopic hematochezia: Normal, 0 points; occult blood (+), 2 points; macroscopic hematochezia, 4 points. DAI score was calculated as equal to the average value of the sum of the above scores.

Rats in each group were individually subjected to the open field test on day 14 of the experiment. The rats were randomly placed into boxes with a height of 30-40 cm and a length of 100 cm on the bottom side. The box's inner walls were darkened, and the bottom surface was divided on the average 25 squares (4 cm × 4 cm) with a digital camera set 2 m above each side. The data was acquired automatically and recorded for 15 min. This technique was used to test the spontaneous activity of the animals and their anxious behavior in an open environment.

On the 15th day of the experiment, rats in each group were anesthetized with an intraperitoneal injection of 7% chloral hydrate (0.4 mL/100 g). The whole colon was removed to compare the colon length for rats in each group.

Histological evaluation of the colon

Eight rats in each group were used for histological evaluation of the colon. Following the whole colon removal, the intestinal lumen was flushed using 0.01 mmol/L PBS buffer, and transected 6-9 cm from the anus. Colons were fixed in 4% paraformaldehyde, dehydrated in graded alcohols, and then embedded in the paraffin. The block was cut into 5 μm thick sections and hematoxylin-eosin stained. Afterwards, the slides were mounted with neutral gum and dried at 37 °C overnight. A whole slide was observed under a scanning biomicroscope (SLIDEVIEW VS200, Olympus, Tokyo, Japan). Histological changes were recorded based on the staining results, and the histological index (HI) scoring was performed, with the following criteria[15]: 0 points for no damage; 1 point for disappearance of basal 1/3 crypts; 2 points for disappearance of basal 2/3 crypts; 3 points disappearance of crypts with intact epithelial cells; and 4 points for crypt and epithelial cell disappearance.

Immunofluorescence histochemical staining

The distal colons of eight rats in each group were dissected separately. The intestinal lumens were flushed in 0.01 mol/L PBS buffer, then a colonic strip with a width of approximately 0.5-1.0 cm was cut along the travel direction of the circular muscle (CM). Afterwards, the dissected colon was fixed in 4% paraformaldehyde. The mucosal layer was fixed upward and horizontally in PBS buffer (pH = 7.4). The mucosal, submucosal, and CM layers were removed with the help of filament forceps to preserve the longitudinal muscle (LM) layer. The tissues were blocked in 10% donkey serum for 30 min and then incubated with Rabbit-Anti-HuD + HuC (1: 500) and Goat-Anti-nNOS (1: 300) in a shaker overnight at 4 °C. Slides were incubated with Donkey Anti-Goat Alexa Fluor 488 (1: 500) and Donkey Anti-Rabbit Alexa Fluor 594 (1: 500) for 4 h. Eight different fields (approximately 1.0 cm × 1.0 cm) of the specimens were observed using confocal microscopy (FV-1000, Olympus, Tokyo, Japan) with the appropriate laser beams and filter settings for Alexa 488 (excitation, 488 nm; emission, 510-530 nm) and Alexa 594 (excitation, 543 nm; emission, 590-615 nm). Digital images were captured with an FV10-ASW 4.2 from Olympus, and these images eventually saved as TIFF files to calculate changes in the proportion of colon nitrergic neurons.

Western blot analysis

Four rats in each group were anesthetized and perfused with pre-cooled PBS buffer, and the terminal colon was transected. The mucosa and submucosa were separated with silk tweezers. The muscle layer was put into a pre-cooled EP tube. The tissue was homogenized using an ultrasonic grinder, in the lysis buffer (RIPA: protease inhibitor: phosphatase inhibitors = 100:1:1). After standing for 10 min on ice, the supernatant was centrifuged at 12000 rpm (10008 × *g*) for 10 min. The protein concentration was measured using a BCA protein concentration assay kit and FC microplate reader (1410101, Thermo Fisher Scientific, Shanghai, China). The protein samples were kept at -80 °C for further use.

Gels were made using the SDS-PAGE gel preparation kit, and the samples were electrophoresed at a constant voltage of 80 and 120 V. Membrane transfer was achieved at a constant current of 300 mA. First, the PVDF membranes were blocked with Western blocking solution (P0252, Beyotime Biotechnology Co., Ltd., Shanghai, China) for 15 min and then incubated with Rabbit Anti-nNOS (1:1000) and Anti-β-Actin antibody (mouse monoclonal; 1:5000) on a shaker overnight at 4 °C. The PVDF membranes were then incubated with HRP-labeled Rabbit Anti-Goat IgG (H + L) (1:10000) and HRP-labeled Goat

Anti-Mouse IgG (H + L) (1:10000) for 2 h. After three rinses (10 min each) in TBST, the membranes were probed by Immobilon™ Western chemiluminescent HRP substrate (WBKLS0050, Merck KGaA, Darmstadt, Germany) and placed into ECL for the detection. The proteins were analyzed using Image-Pro Plus software (Image-Pro Plus Version 6.0, Media Cybernetics, Maryland, United States).

ELISA

Whole blood from four rats in each group were kept for 2 h at room temperature and then centrifuged at 3800 rpm (1000 × *g*) for 20 min, followed by the removal of supernatant. Next, the terminal colon tissues were grounded and disrupted with an appropriate volume of PBS (usually at a weight to volume ratio of 1:9), homogenized using a glass homogenizer, and then centrifuged at 8460 rpm (5000 × *g*) for 5 to 10 min. Afterwards, the supernatant was collected. The NOS1/nNOS ELISA kit was used to determine the concentration of NOS in the colon as well as in the serum.

In vitro gut colonic tension detection

Four rats in each group were used to explore the changes of *in vitro* gut colonic tension, including eight circular and eight longitudinal colon muscle strips. Rats were anesthetized, and the abdominal cavity was exposed. Then, the intestinal tube was carefully separated with the forceps and quickly freed. The colon was excised and placed in Krebs' fluid at 37 °C with a continuous supply of 95% O_2 and 5% CO_2 mixture. Then, 3 mm × 10 mm circular and LM strips were cut, where both ends were anchored to tension receptors and platinum rings at the lower end, respectively. The signals acquired by the tension receptors were recorded and processed with a multi-channel physiological signal acquisition and processing system (RM6240E, INSTRUMENT FACTORY, Chengdu, China). The mean amplitude of spontaneous contractions was recorded in circular and LM strips obtained from control and UC rats at rest, when the muscle strips were allowed to rest in the incubation solution for 30 min. After 10 min of recording, TP508TFA (1×10^{-4} mol/L) was added to the bath of the UC group, and the mean amplitude changes of circular and LM strips were recorded, respectively. The liquid in the bath was replaced after 10 min, and the bath was washed. After resting for 30 min, L-NMMA (1×10^{-4} mol/L) was added, and the corresponding mean amplitude changes were re-recorded.

Statistical analysis

SPSS version 23.0 statistical software (SPSS Inc, Chicago, United States) was used for statistical analyses. Data are expressed as the mean ± SD, and comparisons between groups were performed by one-way ANOVA. A P value of < 0.05 was considered statistically significant.

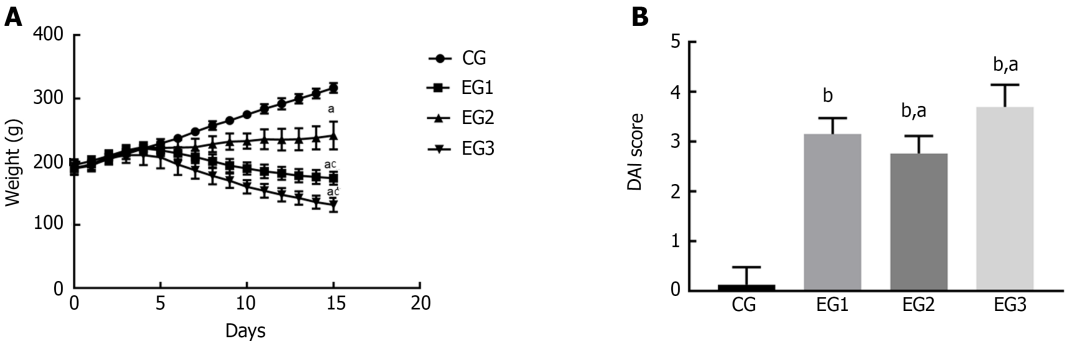
RESULTS

DAI scores

Sloth, anorexia, emaciation, decreased fur gloss, and higher stool frequency were found in all EG rats, with some developing mucopurulent bloody stools. From days 0 to 5, animals in all groups gained weight (CG group: 28.90 ± 2.43 g; EG1 group: 18.10 ± 3.23 g; EG2 group: 17.00 ± 6.17 g; EG3 group: 21.80 ± 3.63 g). The body weight of rats in each group was not significantly different ($P > 0.05$); however, the body weight of rats in the EG1-3 groups began to decrease from day 6. Until day 15, the CG group (116.60 ± 2.76 g) and EG2 group (58.60 ± 7.79 g) gained weight, while the EG1 group (26.00 ± 3.69 g) and EG3 group (60.40 ± 3.99 g) lost weight. The decrease in body weight was statistically significantly different between the EG groups and CG group ($P < 0.05$); the differences in weight change between the EG2-3 groups and EG1 group were also statistically significant ($P < 0.05$) (Figure 1A). As for the stool profiles of all the groups, two rats in the CG group exhibited bondless and loose stools without hematochezia. For the EG1 group, it took 3.25 ± 0.31 d to the occurrence of loose stools, 3.37 ± 0.37 d to fecal occult blood, and 4.1 2 ± 0.39 d to macroscopic hematochezia; the corresponding values in the EG2 and EG3 groups were 3.85 ± 0.50 d, 4.00 ± 0.37 d, and 4.62 ± 0.41 d, and 2.87 ± 0.29 d, 2.62 ± 0.26 d, and 3.37 ± 0.32 d, respectively. Regarding the DAI scores, no statistically significant differences was found from day 0 to day 5 for any group ($P > 0.05$). After day 5, the intergroup differences in DAI scores were significantly increased. The DAI scores were (0.12 ± 0.12), (3.15 ± 0.11), (2.67 ± 0.12), and (3.69 ± 0.15) for the CG, EG1, EG2 and EG3 groups, respectively, at day 15. Moreover, the scores were significantly different between the EG groups and CG group ($P < 0.0001$), and between the EG2-3 groups and EG1 group ($P < 0.05$) (Figure 1B).

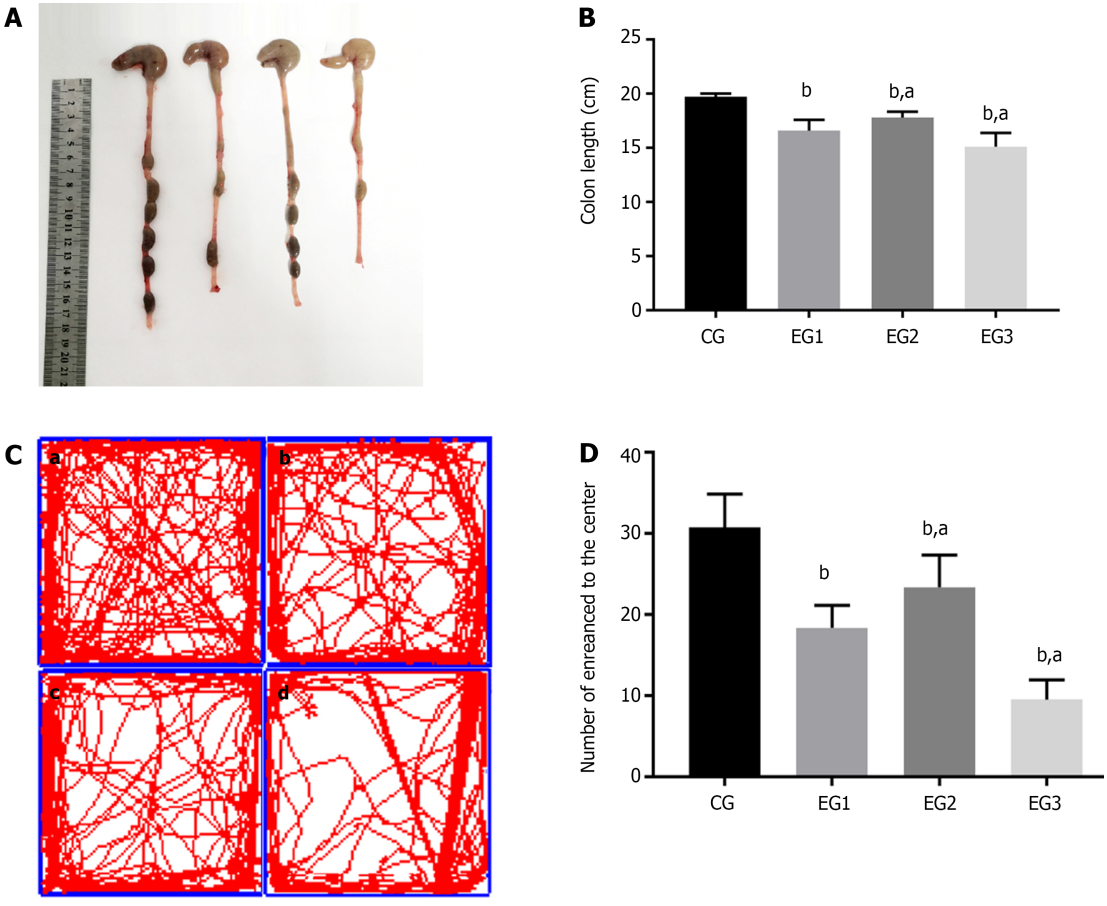
Comparison of colon length and behavior

The colonic morphology of rats from each group was compared during the dissection (Figure 2A). Compared with the CG group, the colon length in the EG groups showed various degrees of shortening, and the differences were statistically significant ($P < 0.0001$). The difference was also significant between the EG2-3 groups and EG1 group ($P < 0.05$) (Figure 2B).



DOI: 10.3748/wjg.v28.i29.3854 **Copyright** ©The Author(s) 2022.

Figure 1 Disease activity of animals in each group. A: Body weight changes of rats. The differences in body weight were statistically significant between EG groups and CG group ($^{a}P < 0.05$), and between EG2-3 groups and EG1 group ($^{c}P < 0.05$); B: Disease activity index scores. The differences were significant between EG groups and CG group ($^{b}P < 0.0001$), and between EG2-3 groups and EG1 group ($^{a}P < 0.05$). CG: Control group; UC: Ulcerative colitis; NOS: Nitric oxide synthase; L-NMMA: NG-monomethyl-L-arginine monoacetate; EG1: UC group; EG2: UC + NOS agonist TP508TFA group; EG3: UC + NOS inhibitor L-NMMA group; DAI: Disease activity index.



DOI: 10.3748/wjg.v28.i29.3854 **Copyright** ©The Author(s) 2022.

Figure 2 Colon length in each group and results of the open field test. A: Colon length of rats in the four groups; B: Comparison of colon length in CG (19.71 ± 0.11 cm), EG1 (16.59 ± 0.35 cm), EG2 (17.80 ± 0.19 cm), and EG3 (15.11 ± 0.44 cm) groups. There were statistically significant differences between EG groups and CG group ($^{b}P < 0.0001$), and between EG2-3 groups and EG1 group ($^{a}P < 0.05$); C: Movement trajectories of rats. a: CG; b: EG1; c: EG2; d: EG3; D: Results of the open field test. There were statistically significant differences between EG groups and CG group ($^{b}P < 0.0001$), and between EG2-3 groups and EG1 group ($^{a}P < 0.05$). CG: Control group; UC: Ulcerative colitis; NOS: Nitric oxide synthase; L-NMMA: NG-monomethyl-L-arginine monoacetate; EG1: UC group; EG2: UC + NOS agonist TP508TFA group; EG3: UC + NOS inhibitor L-NMMA group.

On the 14th day of the experiment, the behavior of rats was examined using an open field test. The number of times that the rats passed through the center of an open box within 15 min period is shown as follows: 30.75 ± 1.46 for the CG, 18.38 ± 0.98 for EG1, 23.38 ± 1.40 for EG2, and 9.50 ± 0.86 for EG3 group. Differences were statistically significant between the EG groups and CG group ($P < 0.0001$).

Additionally, the EG2-3 groups showed statistically significant differences compared with the EG1 group ($P < 0.05$) (Figure 2C and D).

Colonic histological damage assessment

The results of HE staining indicated that the colonic tissue structure of CG rats was normal, with the mucosal layer showing a well-arranged monolayer of columnar epithelial cells, clear intestinal glands, morphologically normal goblet cells, and no inflammatory cell infiltration. In the colon of EG1 rats, most crypts disappeared, with some broken or disappearing epithelia, accompanied by inflammatory cell infiltration. In the colon of EG2 rats, 1/3-2/3 of basal crypts disappeared, with the occasional destruction of epithelial cells. In the colon of EG3 rats, crypts completely disappeared, with some broken or disappearing epithelia, accompanied by massive inflammatory cell infiltration (Figure 3A). The HI scores for the colons of the rats in the CG, EG1, EG2, and EG3 groups were 0.00 ± 0.00, 3.07 ± 0.25, 2.22 ± 0.17, and 3.71 ± 0.14, respectively. The differences were statistically significant between the EG groups and CG group ($P < 0.0001$), and between the EG2-3 groups and EG1 group ($P < 0.05$) (Figure 3B).

Changes in proportion of NOS-positive colonic myenteric neurons

The distal rat colons were double-stained by immunofluorescence histochemistry to observe the distribution and expression of NOS-positive neurons within the colonic MP. Within the colonic MP of rats, the proportion of these neurons in each group was counted. Enteric neurons exhibited a reticular distribution in the colonic MP (Figure 4B). NOS-positive neurons accounted for 31.38 ± 0.94% in the CG group (Figure 4C) but were more distributed within the marginal side of the ganglia (Figure 4A). They were fusiform or star-shaped, and their nuclei were round with several elongated protrusions. The protrusions of these neurons were interconnected with each other to form a dense and complex neural network. In the EG1 group, the percentage of NOS-positive neurons in colonic neurons (Figure 4E) increased to 42.25% ± 0.88% under disease conditions (Figure 4F). The distribution of these neurons was no longer confined to the edges of the ganglia and began to appear elsewhere within the ganglia (Figure 4D). Moreover, the proportion of NOS-positive neurons in the EG2 group increased to 51.75% ± 1.22% (Figure 4I and H). These neurons in the ganglia were disorganized and widely distributed within the ganglia (Figure 4G). Compared with the EG1 group, the proportion of NOS-positive neurons in the EG3 group decreased to 37.25% ± 1.09% (Figure 4L and K), with their distribution within the ganglia being predominantly marginal (Figure 4J). The changes in the proportion of NOS-positive neurons to colonic neurons in the EG groups were statistically significant in comparison to the CG group ($P < 0.0001$); however, the EG2 and EG3 groups were also significantly different from the EG1 group ($P < 0.05$) (Figure 4M).

NOS protein expression level in colonic MP

The expression level of NOS protein in the colonic MP of EG1 rats was higher than that in the CG group. The NOS expression in the EG2 rat colon was further increased, while the expression in the EG3 rat colon was lower than that in the EG1 group. The differences were statistically significant between the EG groups and CG group ($P < 0.0001$) and between the EG2-3 groups and EG1 group ($P < 0.05$) (Figure 5A and B).

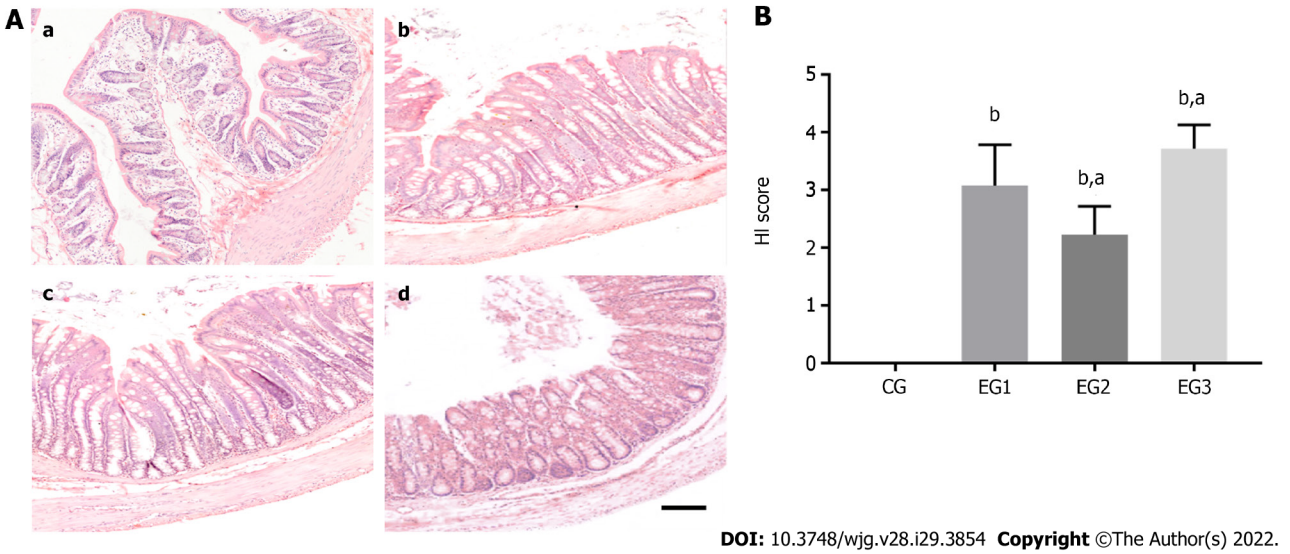
Concentration of NOS in colonic myenteric tissue and serum

The concentration of NOS was significantly increased in the colonic myenteric tissue in the EG groups compared with the CG group ($P < 0.0001$); the EG2 group had a higher NOS concentration, whereas the EG3 group had a lower concentration than the EG1 group, and the difference between the EG2-3 groups and EG1 group was also statistically significant ($P < 0.05$) (Figure 6A). In addition, serum concentrations of NOS were significantly increased in the EG group compared with the CG group ($P < 0.0001$); however, the EG2 group had a significantly higher NOS concentration, whereas the EG3 group had a significantly lower concentration than the EG1 group ($P < 0.05$) (Figure 6B).

Comparison of contraction tension of isolated rat colonic smooth muscle

At rest, the contraction of the LM in the colon of CG rats appeared as a regular and sine wave-like curve with relatively neat amplitude (Figure 7A). In EGs rats, the contraction was significantly more frequent, with the increased amplitude (Figure 7B-D). The contraction tension of the LM of the colon was considerably more significant in EG rats than in CG rats ($P < 0.0001$). However, the contraction tensions of the colonic LM were significantly weakened and increased in EG2 and EG3 rats, respectively, when compared with EG1 rats ($P < 0.001$) (Figure 7E).

At rest, the contraction of the colonic CM in CG rats appeared as a regular and triangular wave-like curve. The amplitude was neat, with a contraction interval between the adjacent two waves (Figure 8A). In EGs rats, contraction of the CM of the colon was significantly accelerated, and its amplitude was increased (Figure 8B-D). The contraction tension of the colonic CM was significantly larger in EG rats than in CG rats ($P < 0.0001$). The contraction tension of the colonic CM appeared significantly weakened and increased in EG1 rats compared with EG2 and EG3 rats, respectively ($P < 0.0001$) (Figure 8E).



DOI: 10.3748/wjg.v28.i29.3854 **Copyright** ©The Author(s) 2022.

Figure 3 Histological evaluation. A: HE stained rat colon tissues. a: CG; b: EG1; c: EG2; d: EG3. Scale bar = 100 μm; B: Comparison of colonic histological index scores showing statistically significant differences between EG groups and CG group ($^{b}P < 0.0001$) and between EG2-3 groups and EG1 group ($^{a}P < 0.05$). CG: Control group; UC: Ulcerative colitis; NOS: Nitric oxide synthase; L-NMMA: NG-monomethyl-L-arginine monoacetate; EG1: UC group; EG2: UC + NOS agonist TP508TFA group; EG3: UC + NOS inhibitor L-NMMA group; HI: Histological index.

DISCUSSION

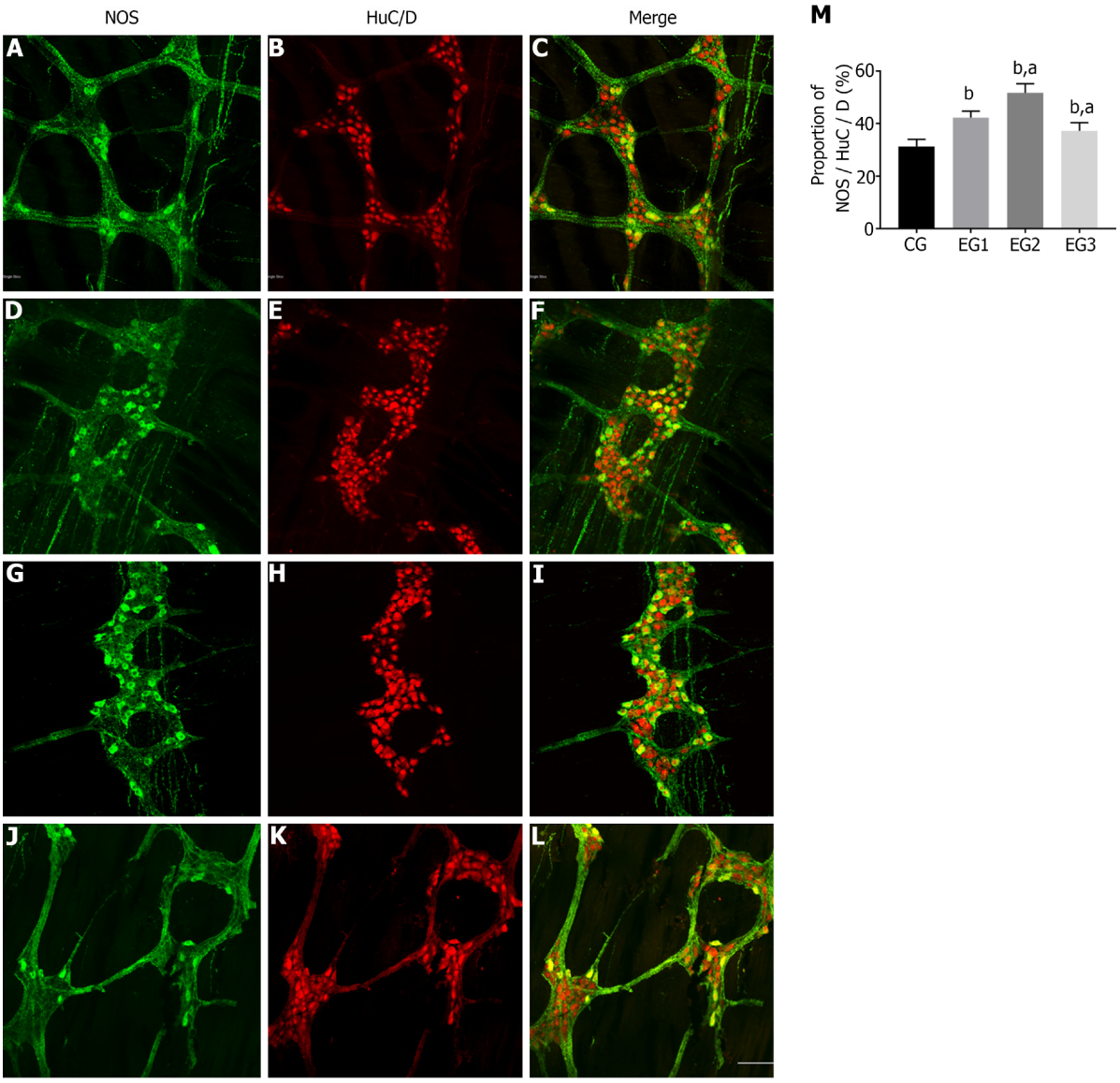
An increase or decrease in the number of neurons and/or neuronal degeneration in the ENS can lead to various diseases. For instance, congenital dysplasia of the ENS leads to congenital megacolon (Hirschsprung disease) and primary achalasia, whereas neurodegenerative ENS alterations can lead to the disorders such as Alzheimer, Huntington, and Parkinson diseases[16,17]. The secondary alterations in the ENS also result in inflammatory infiltrates or immune system pathologies such as irritable bowel syndrome[18], idiopathic enteric gangliosidosis[19], paraneoplastic syndrome[20], slow transit constipation[21], severe acute pancreatitis[22], diabetes mellitus[23,24], and UC[25].

The different types of ENS neurons have significantly different morphology and structure associated with the synthesis and secretion of neurotransmitters. However, by forming complex synaptic connections, these neurons participate in the structural basis that mainly underlies the relatively independent reflex activity of the gut and can also regulate the diverse motor and sensory activities of the digestive tract.

Despite the unclear etiology of UC, numerous studies have shown that its pathogenesis might be associated with the interactions between genetic susceptibility, environmental provoking factors, and immune-mediated tissue damage. Additionally, the relationship between abnormal intestinal motility and UC has also gained attention. Abnormal ENS is an important mechanism contributing to the abnormal colonic motility of UC, which is an important factor causing diarrhea in UC patients.

The onset of UC has a complex genetic background. Based on the gene polymorphism and heterogeneity, the impaired local barrier function of the intestinal mucosa can be the result of a combination of factors, such as altered epithelial permeability, neuroendocrine regulation, and intestinal flora translocation[26]. This, in turn, provokes the inflammatory response with symptoms such as abdominal pain, diarrhea, and colonic motor dysfunction. As the rate-limiting enzyme of NO synthesis in the body, NOS has three sub-types: iNOS, eNOS, and nNOS. Histological studies have identified intense focal iNOS expression by the inflamed bowel epithelium and in the mononuclear cell infiltrate in the intestinal tissues of both Crohn's disease and UC patients[27]. A great number of studies suggest that iNOS in the ENS may play a part in preventing activation of mast cells, reducing leukocyte adhesion to the endothelium and protecting the host from being invaded by colonic bacteria[28-30]. In normal and UC states, eNOS expression is limited to colonic vascular endothelium[31]. Baker *et al*[32] confirmed that during DSS-induced UC, eNOS KO mice suffered less tissue damage and inflammation than wild-type mice, suggesting that eNOS is essential for maintaining the integrity of the GI mucosa. nNOS is one of the specific markers for nitrergic neurons within the ENS, the primary inhibitory neurons of the colonic MP[33]. By releasing inhibitory neurotransmitter NO, nitrergic neurons can regulate GI motility. The changes in expression of nNOS in the colonic MP of UC rats indicate that nitrergic neurons may be involved in NO-based neurotransmission and regulate GI motility in UC state.

Research has shown that NO is the second messenger in the smooth muscle cells (SMCs) or interstitial cells of Cajal (ICCs)[34]. NO is highly lipid-soluble and reaches target ICCs in a freely diffusible manner after synthesis. It binds to the soluble guanylyl cyclase in the cells to increase the enzymatic activity by altering its spatial configuration, which further leads to an increase in cyclic guanosine monophosphate

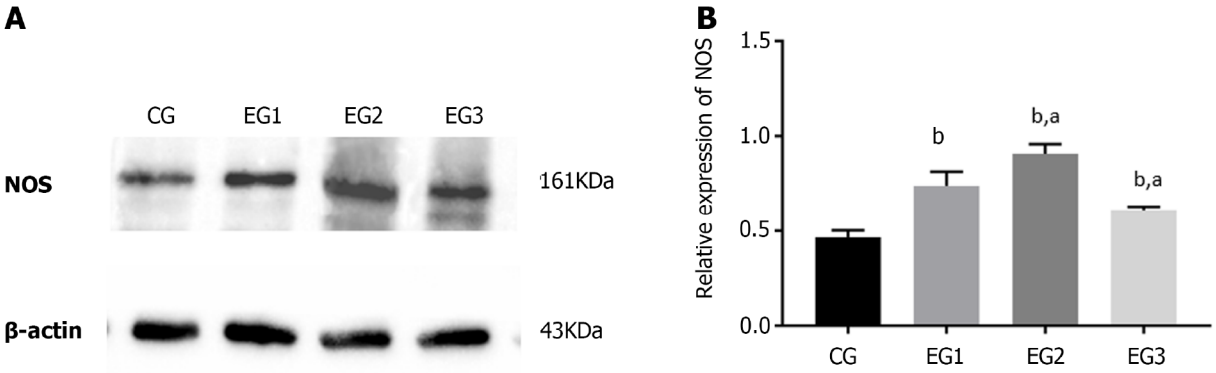


DOI: 10.3748/wjg.v28.i29.3854 **Copyright** ©The Author(s) 2022.

Figure 4 Changes in the number of nitric oxide synthase-positive neurons in the colonic myenteric plexus. A-L: Immunofluorescent histochemical double-staining of the rat colonic myenteric plexus (MP) for nitric oxide synthase (NOS; green) and HuC/D (red) in CG (A-C), EG1 (D-F), EG2 (G-I), and EG3 (J-L) rats. Scale bar = 30 μm; M: Comparison of the proportion of NOS-positive neurons in the colonic MP showing statistically significant differences between EG groups and CG group ($^{b}P < 0.0001$), and between EG2-3 groups and EG1 group ($^{a}P < 0.05$). CG: Control group; UC: Ulcerative colitis; NOS: Nitric oxide synthase; L-NMMA: NG-monomethyl-L-arginine monoacetate; EG1: UC group; EG2: UC + NOS agonist TP508TFA group; EG3: UC + NOS inhibitor L-NMMA group; MP: myenteric plexus.

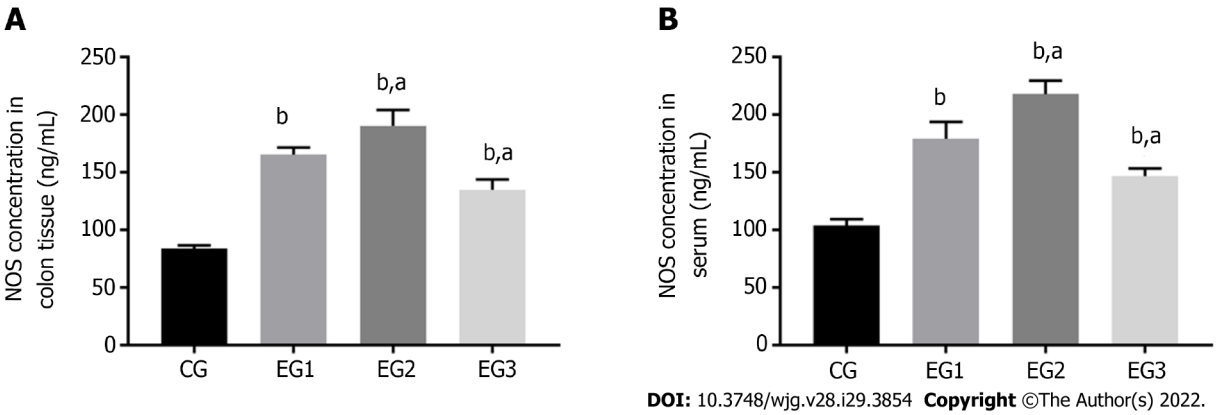
(cGMP) within the cells, activating the cGMP protein kinase-dependent calcium pumps, and therefore finally participates in intercellular information transmission[35]. Therefore, it could be concluded that as a messenger of information transmission between the NOS-positive neurons and GI SMCs, increased NO can reduce the Ca^{2+} influx and directly promotes smooth muscle relaxation. In addition, studies have confirmed that NO can inhibit muscle contraction by inhibiting the release of excitatory transmitters[23,36]. Therefore, NO-mediated reduced contractility of the intestinal smooth muscle might be one of the important mechanisms contributing to colonic dysmotility[9,37].

In the present study, DSS was applied to induce the UC rat model successfully. For the first time, the finding of a secondary increase in NOS expression in the colonic MP of UC rats, combined with altered *in vitro* colonic contraction tension, suggests that the increased NOS expression is associated with the altered colonic motility in UC rats. Increasing (or decreasing) the number of NOS-positive neurons might enhance (or attenuate) the diastolic function of the colonic smooth muscle regulated by these neurons. However, the change in the number of NOS-positive neurons is often due to changes in the concentration and release of neurotransmitters caused by changes in the amount of NOS contained in neurons under pathological conditions, rather than caused by neuronal degeneration and regeneration. The results of *in vitro* studies of the colon using both agonists and inhibitors of NOS further confirmed that the altered NOS expression regulate the colonic motility in UC. A previous similar study



DOI: 10.3748/wjg.v28.i29.3854 **Copyright** ©The Author(s) 2022.

Figure 5 Relative nitric oxide synthase protein expression in the colonic myenteric plexus. A: Western blot analysis of expression of nitric oxide synthase (NOS) in the colonic myenteric plexus (MP) of rats in the four groups; B: Comparison of the relative expression of NOS protein in the colonic MP of rats in the four groups showing statistically significant differences between EG groups and CG group ($^bP < 0.0001$), and between EG2-3 groups and EG1 group ($^aP < 0.05$). CG: Control group; UC: Ulcerative colitis; NOS: Nitric oxide synthase; L-NMMA: NG-monomethyl-L-arginine monoacetate; EG1: UC group; EG2: UC + NOS agonist TP508TFA group; EG3: UC + NOS inhibitor L-NMMA group; NOS: Nitric oxide synthase; MP: Myenteric plexus.



DOI: 10.3748/wjg.v28.i29.3854 **Copyright** ©The Author(s) 2022.

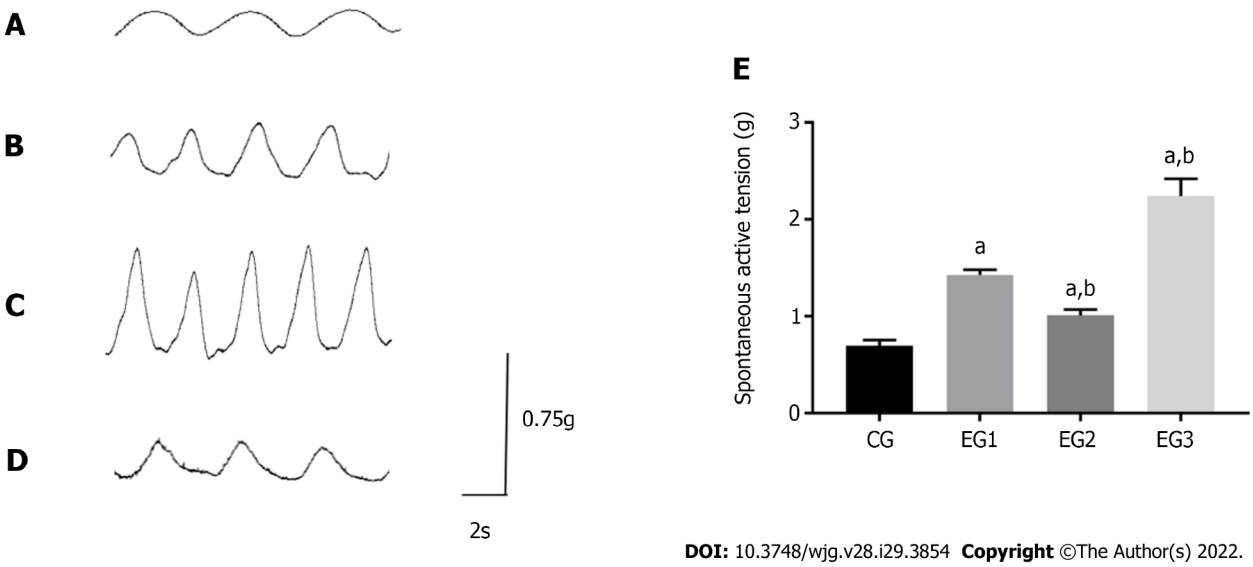
Figure 6 Changes in nitric oxide synthase concentration in colonic myenteric tissue and serum. A: Comparison of nitric oxide synthase (NOS) concentration in colonic myenteric tissue of rats in the four groups showing statistically significant differences between EG groups and CG group ($^bP < 0.0001$), and between EG2-3 groups and EG1 group ($^aP < 0.05$); B: Comparison of NOS concentrations in the serum of rats in the four groups showing statistically significant differences between EG groups and CG group ($^bP < 0.0001$), and between EG2-3 groups and CG group ($^aP < 0.05$). CG: Control group; UC: Ulcerative colitis; NOS: Nitric oxide synthase; L-NMMA: NG-monomethyl-L-arginine monoacetate; EG1: UC group; EG2: UC + NOS agonist TP508TFA group; EG3: UC + NOS inhibitor L-NMMA group; NOS: Nitric oxide synthase.

demonstrated that the NOS expression and NO concentration within the muscular layer of the stomach and small intestine were increased in an animal model of chronic pancreatitis[38]. These results suggest that the reduced contractility of the gastric CM because of NO inhibition might be an important mechanism underlying gastric motor dysfunction in chronic pancreatitis[36,38]. Moreover, these findings can provide an interesting insight into the role of the ENS during GI dysmotility.

The initiation of colonic dysmotility in UC may be related to the structural alterations and abnormal number of ICCs, disturbed intestinal electrophysiology, changes in colonic pressure, and abnormal expression of gut-related neurotransmitters. Our present results have demonstrated that the increased NOS expression inhibits the contraction motility of the colonic smooth muscle. Therefore, appropriate adjustment of NOS levels can alter the expression of nitrergic neurons, control the motor movement of the intestinal smooth muscle, and improve the UC colonic motor function. Of note, this could improve the symptoms of UC patients, providing a basis for the screening of novel agents against UC.

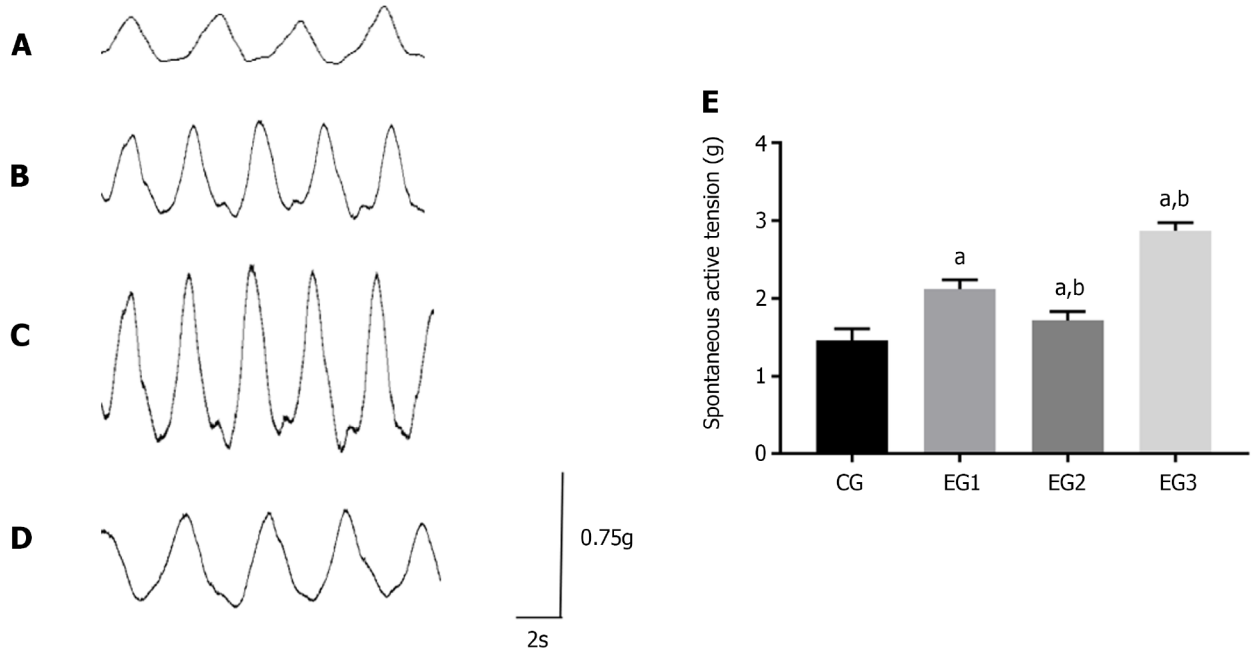
CONCLUSION

The increased number of nitrergic neurons in the colonic MP of UC rats, both *in vitro* and *in vivo*, diminishes the colonic motor function. In contrast, activation and inhibition of NOS activity could induce and diminish the colon motor function, respectively. Further, an increased number of nitrergic neurons in the colonic MP of UC rats leads to reduced colon contractile function. Therefore, the



DOI: 10.3748/wjg.v28.i29.3854 **Copyright** ©The Author(s) 2022.

Figure 7 Comparison of isolated colonic longitudinal muscle contraction tension. A-D: Contraction amplitude of the colonic longitudinal muscle of CG (A), EG1 (B), EG2 (C), and EG3 (D) rats; E: Comparison of the contraction tension of the colonic longitudinal muscle among rats from the four groups: CG (0.69 ± 0.02 g), EG1 (1.4 2 ± 0.02 g), EG2 (2.24 ± 0.07 g), and EG3 (1.01 ± 0.02 g). All differences were statistically significant between EG groups and CG group (^aP < 0.0001) and between EG2-3 groups and EG1 group (^bP < 0.001). CG: Control group; UC: Ulcerative colitis; NOS: Nitric oxide synthase; L-NMMA: NG-monomethyl-L-arginine monoacetate; EG1: UC group; EG2: UC + NOS agonist TP508TFA group; EG3: UC + NOS inhibitor L-NMMA group; LM: Longitudinal muscle.



DOI: 10.3748/wjg.v28.i29.3854 **Copyright** ©The Author(s) 2022.

Figure 8 Comparison of isolated colonic circular muscle contraction tension. A-D: Contraction amplitude of the colonic circular muscle of CG (A), EG1 (B), EG2 (C), and EG3 (D) rats; E: Comparison of the contraction tension of the rat colonic circular muscle among the four groups: CG (1.46 ± 0.06 g), EG1 (2.12 ± 0.49 g), EG2 (2.87 ± 0.04 g), and EG3 (1.72 ± 0.04 g). All differences were statistically significant between EG groups and CG group (^aP < 0.0001) and between EG2-3 groups and EG1 group (^bP < 0.0001). CG: Control group; UC: Ulcerative colitis; NOS: Nitric oxide synthase; L-NMMA: NG-monomethyl-L-arginine monoacetate; EG1: UC group; EG2: UC + NOS agonist TP508TFA group; EG3: UC + NOS inhibitor L-NMMA group; CM: Circular muscle.

regulation of nitrergic neurons in the colonic MP through interference with the activity of NOS might be a novel potential and prospective way to reduce diarrhea symptoms in UC patients.

ARTICLE HIGHLIGHTS

Research background

Ulcerative colitis (UC) is a nonspecific inflammatory intestinal disorder with a complex etiology and poorly understood pathogenesis. The association between abnormal intestinal motility and UC has gained increasing attention over the past years. The enteric nervous system (ENS) regulates gut motility and based on their functions, has been divided into inhibitory and excitatory neurons, which mainly regulate the gut motility in terms of relaxation and contraction *via* different neurotransmitters. Nitrergic neurons are typical inhibitory neurons in the ENS and act through the neurotransmitter nitric oxide, which is synthetized by the rate-limiting enzyme nitric oxide synthase (NOS), whose expression changes might affect the motor function of the gut.

Research motivation

UC is an intestinal disease with abdominal pain and diarrhea as the main symptoms, which are associated with abnormal gastrointestinal motility. Alterations in the amount of enteric neurotransmitters may change the number of enteric neurons. Nitrergic neurons are well-established enteric inhibitory neurons, and modification of its expression may interfere with its regulatory effect on intestinal motility and improve the symptoms of abdominal pain and diarrhea in UC.

Research objectives

This study aimed to investigate the relationship between colonic NOS expression changes and colonic motility in dextran sulfate sodium (DSS)-induced UC rats, and to explore the effects of nitrergic neurons on colonic motility in UC rats to discover the potential mechanisms for the treatment of UC.

Research methods

UC was induced in adult male rats with 5.5% DSS, and part of them were administered with NOS agonists and inhibitors. The rats were divided into control (CG), UC (EG1), UC + agonist (EG2), and UC + inhibitor (EG3) groups. The changes in tissue expression, relative protein expression, and concentration of NOS in rats were detected by immunofluorescence histochemical double staining, Western blot, and ELISA techniques, respectively. The effect of nitrergic neurons on colonic motility was examined by the changes in colonic circular muscle (CM) and longitudinal muscle (LM) contraction tension *in vitro*.

Research results

Compared with CG rats, the proportion of NOS positive neurons within the colonic myenteric plexus (MP), the relative expression of NOS, and the concentration of NOS in both serum and colonic tissue were significantly higher in EG rats. After administration of NOS agonists and inhibitors, various degrees of increase and decrease were observed in EG2 and EG3 rats, respectively. The contraction amplitude and mean contraction tension of the CM and LM in rat colon after administration of agonists and inhibitors were attenuated and enhanced *in vitro*, respectively. For UC, regulating the expression of NOS within the MP may improve intestinal motility, thereby favoring the recovery of intestinal function.

Research conclusions

Nitrergic neurons within the rat colonic MP are involved in the regulation of colonic motility. Increased NOS in the colonic MP of UC rats causes nitrergic neurons amplification, leading to decreased colonic contraction function. Modulation of NOS levels within colonic MP can alter nitrergic neuron expression and adjust the motor activity of the intestinal smooth muscle, which can further improve colonic motor function, moderate UC symptoms, and provide evidence for the development of new drugs against UC.

Research perspectives

This study demonstrated increased NOS expression in the colonic MP of UC rats, with a possible corresponding increase in nitrergic neuron expression and a decrease in colonic contraction function in UC rats. Thus, by regulating the expression of NOS in the colonic MP, colonic motor function and interruption in the pathogenesis of UC can be achieved, thus providing a novel insight into the treatment of UC.

FOOTNOTES

Author contributions: Li YQ and Chen J designed the study and edited the manuscript; Li YR, Li Y, Xu M, Jin Y, and Fan HW conducted the experiments; Li YR and Li Y completed the data analysis; Zhang Q and Tan GH provided language modification; Li YR and Li Y wrote the manuscript; all authors read and approved the final manuscript; and Li YR and Li Y contributed equally in carrying out this study and writing the manuscript.

Supported by National Natural Science Foundation of China, No. 31971112; Natural Science Foundation of Liaoning Province, No. 2021-MS-330; and Innovation Capability Support Program of Shaanxi, No. 2021TD-57.

Institutional animal care and use committee statement: All animal experiments conformed to the internationally accepted principles for the care and use of laboratory animals (licence No. SCXK (Shan) 2019-001, Animal Experiment Center, The Fourth Military Medical University, China; protocol No. IACUC-20211101, The Laboratory Animal Welfare and Ethics Committee at The Fourth Military Medical University, China).

Conflict-of-interest statement: All authors report no relevant conflicts of interest for this article.

Data sharing statement: No additional data are available.

ARRIVE guidelines statement: The authors have read the ARRIVE guidelines, and the manuscript was prepared and revised according to the ARRIVE guidelines.

Open-Access: This article is an open-access article that was selected by an in-house editor and fully peer-reviewed by external reviewers. It is distributed in accordance with the Creative Commons Attribution NonCommercial (CC BY-NC 4.0) license, which permits others to distribute, remix, adapt, build upon this work non-commercially, and license their derivative works on different terms, provided the original work is properly cited and the use is non-commercial. See: https://creativecommons.org/Licenses/by-nc/4.0/

Country/Territory of origin: China

ORCID number: Yan-Rong Li 0000-0001-7830-1055; Yan Li 0000-0001-5089-8574; Yuan Jin 0000-0001-7184-2844; Mang Xu 0000-0003-1017-1455; Hong-Wei Fan 0000-0002-9546-593X; Qian Zhang 0000-0001-7249-4191; Guo-He Tan 0000-0002-1101-207X; Jing Chen 0000-0001-9971-1053; Yun-Qing Li 0000-0002-3707-3348.

S-Editor: Ma YJ
L-Editor: Wang TQ
P-Editor: Cai YX

REFERENCES

1 **Kuehn F**, Hodin RA. Impact of Modern Drug Therapy on Surgery: Ulcerative Colitis. *Visc Med* 2018; **34**: 426-431 [PMID: 30675487 DOI: 10.1159/000493492]
2 **Hoffmann P**, Krisam J, Stremmel W, Gauss A. Real-World Outcomes of Vedolizumab Therapy in Ulcerative Colitis and Crohn's Disease at a Tertiary Referral Center. *Dig Dis* 2019; **37**: 33-44 [PMID: 30134234 DOI: 10.1159/000492322]
3 **Ponder A**, Long MD. A clinical review of recent findings in the epidemiology of inflammatory bowel disease. *Clin Epidemiol* 2013; **5**: 237-247 [PMID: 23922506 DOI: 10.2147/CLEP.S33961]
4 **Higuchi LM**, Khalili H, Chan AT, Richter JM, Bousvaros A, Fuchs CS. A prospective study of cigarette smoking and the risk of inflammatory bowel disease in women. *Am J Gastroenterol* 2012; **107**: 1399-1406 [PMID: 22777340 DOI: 10.1038/ajg.2012.196]
5 **Santana PT**, Rosas SLB, Ribeiro BE, Marinho Y, de Souza HSP. Dysbiosis in Inflammatory Bowel Disease: Pathogenic Role and Potential Therapeutic Targets. *Int J Mol Sci* 2022; **23** [PMID: 35408838 DOI: 10.3390/ijms23073464]
6 **Sundin J**, Aziz I, Nordlander S, Polster A, Hu YOO, Hugerth LW, Pennhag AAL, Engstrand L, Törnblom H, Simrén M, Öhman L. Evidence of altered mucosa-associated and fecal microbiota composition in patients with Irritable Bowel Syndrome. *Sci Rep* 2020; **10**: 593 [PMID: 31953505 DOI: 10.1038/s41598-020-57468-y]
7 **Bassotti G**, Antonelli E, Villanacci V, Nascimbeni R, Dore MP, Pes GM, Maconi G. Abnormal gut motility in inflammatory bowel disease: an update. *Tech Coloproctol* 2020; **24**: 275-282 [PMID: 32062797 DOI: 10.1007/s10151-020-02168-y]
8 **Li H**, Fan C, Lu H, Feng C, He P, Yang X, Xiang C, Zuo J, Tang W. Protective role of berberine on ulcerative colitis through modulating enteric glial cells-intestinal epithelial cells-immune cells interactions. *Acta Pharm Sin B* 2020; **10**: 447-461 [PMID: 32140391 DOI: 10.1016/j.apsb.2019.08.006]
9 **Głąbska D**, Guzek D, Grudzińska D, Lech G. Influence of dietary isoflavone intake on gastrointestinal symptoms in ulcerative colitis individuals in remission. *World J Gastroenterol* 2017; **23**: 5356-5363 [PMID: 28839435 DOI: 10.3748/wjg.v23.i29.5356]
10 **Costa M**, Spencer NJ, Brookes SJH. The role of enteric inhibitory neurons in intestinal motility. *Auton Neurosci* 2021; **235**: 102854 [PMID: 34329834 DOI: 10.1016/j.autneu.2021.102854]
11 **Schemann M**. Control of gastrointestinal motility by the "gut brain"--the enteric nervous system. *J Pediatr Gastroenterol Nutr* 2005; **41** Suppl 1: S4-S6 [PMID: 16131964 DOI: 10.1097/01.scs.0000180285.51365.55]
12 **Saldana-Morales FB**, Kim DV, Tsai MT, Diehl GE. Healthy Intestinal Function Relies on Coordinated Enteric Nervous System, Immune System, and Epithelium Responses. *Gut Microbes* 2021; **13**: 1-14 [PMID: 33929291 DOI: 10.1080/19490976.2021.1916376]
13 **Tse JKY**. Gut Microbiota, Nitric Oxide, and Microglia as Prerequisites for Neurodegenerative Disorders. *ACS Chem Neurosci* 2017; **8**: 1438-1447 [PMID: 28640632 DOI: 10.1021/acschemneuro.7b00176]

14 **Sánchez-Fidalgo S**, Cárdeno A, Sánchez-Hidalgo M, Aparicio-Soto M, de la Lastra CA. Dietary extra virgin olive oil polyphenols supplementation modulates DSS-induced chronic colitis in mice. *J Nutr Biochem* 2013; **24**: 1401-1413 [PMID: 23337347 DOI: 10.1016/j.jnutbio.2012.11.008]

15 **Murano M**, Maemura K, Hirata I, Toshina K, Nishikawa T, Hamamoto N, Sasaki S, Saitoh O, Katsu K. Therapeutic effect of intracolonically administered nuclear factor kappa B (p65) antisense oligonucleotide on mouse dextran sulphate sodium (DSS)-induced colitis. *Clin Exp Immunol* 2000; **120**: 51-58 [PMID: 10759763 DOI: 10.1046/j.1365-2249.2000.01183.x]

16 **Drossman DA**, Tack J, Ford AC, Szigethy E, Törnblom H, Van Oudenhove L. Neuromodulators for Functional Gastrointestinal Disorders (Disorders of Gut-Brain Interaction): A Rome Foundation Working Team Report. *Gastroenterology* 2018; **154**: 1140-1171.e1 [PMID: 29274869 DOI: 10.1053/j.gastro.2017.11.279]

17 **Filpa V**, Moro E, Protasoni M, Crema F, Frigo G, Giaroni C. Role of glutamatergic neurotransmission in the enteric nervous system and brain-gut axis in health and disease. *Neuropharmacology* 2016; **111**: 14-33 [PMID: 27561972 DOI: 10.1016/j.neuropharm.2016.08.024]

18 **Niesler B**, Kuerten S, Demir IE, Schäfer KH. Disorders of the enteric nervous system - a holistic view. *Nat Rev Gastroenterol Hepatol* 2021; **18**: 393-410 [PMID: 33514916 DOI: 10.1038/s41575-020-00385-2]

19 **Fornai M**, Pellegrini C, Antonioli L, Segnani C, Ippolito C, Barocelli E, Ballabeni V, Vegezzi G, Al Harraq Z, Blandini F, Levandis G, Cerri S, Blandizzi C, Bernardini N, Colucci R. Enteric Dysfunctions in Experimental Parkinson's Disease: Alterations of Excitatory Cholinergic Neurotransmission Regulating Colonic Motility in Rats. *J Pharmacol Exp Ther* 2016; **356**: 434-444 [PMID: 26582732 DOI: 10.1124/jpet.115.228510]

20 **Li S**, Fei G, Fang X, Yang X, Sun X, Qian J, Wood JD, Ke M. Changes in Enteric Neurons of Small Intestine in a Rat Model of Irritable Bowel Syndrome with Diarrhea. *J Neurogastroenterol Motil* 2016; **22**: 310-320 [PMID: 26645247 DOI: 10.5056/jnm15082]

21 **De Giorgio R**, Barbara G, Stanghellini V, De Ponti F, Salvioli B, Tonini M, Velio P, Bassotti G, Corinaldesi R. Clinical and morphofunctional features of idiopathic myenteric ganglionitis underlying severe intestinal motor dysfunction: a study of three cases. *Am J Gastroenterol* 2002; **97**: 2454-2459 [PMID: 12358272 DOI: 10.1111/j.1572-0241.2002.06002.x]

22 **Lin Z**, Liu Y, Zheng Q, Hu Q. Increased proportion of nitric oxide synthase immunoreactive neurons in rat ileal myenteric ganglia after severe acute pancreatitis. *BMC Gastroenterol* 2011; **11**: 127 [PMID: 22111589 DOI: 10.1186/1471-230X-11-127]

23 **Dai Y**, Haque MM, Stuehr DJ. Restricting the conformational freedom of the neuronal nitric-oxide synthase flavoprotein domain reveals impact on electron transfer and catalysis. *J Biol Chem* 2017; **292**: 6753-6764 [PMID: 28232486 DOI: 10.1074/jbc.M117.777219]

24 **Anitha M**, Gondha C, Sutliff R, Parsadanian A, Mwangi S, Sitaraman SV, Srinivasan S. GDNF rescues hyperglycemia-induced diabetic enteric neuropathy through activation of the PI3K/Akt pathway. *J Clin Invest* 2006; **116**: 344-356 [PMID: 16453021 DOI: 10.1172/JCI26295]

25 **Gracie DJ**, Guthrie EA, Hamlin PJ, Ford AC. Bi-directionality of Brain-Gut Interactions in Patients With Inflammatory Bowel Disease. *Gastroenterology* 2018; **154**: 1635-1646.e3 [PMID: 29366841 DOI: 10.1053/j.gastro.2018.01.027]

26 **Leonardi I**, Paramsothy S, Doron I, Semon A, Kaakoush NO, Clemente JC, Faith JJ, Borody TJ, Mitchell HM, Colombel JF, Kamm MA, Iliev ID. Fungal Trans-kingdom Dynamics Linked to Responsiveness to Fecal Microbiota Transplantation (FMT) Therapy in Ulcerative Colitis. *Cell Host Microbe* 2020; **27**: 823-829.e3 [PMID: 32298656 DOI: 10.1016/j.chom.2020.03.006]

27 **Singer II**, Kawka DW, Scott S, Weidner JR, Mumford RA, Riehl TE, Stenson WF. Expression of inducible nitric oxide synthase and nitrotyrosine in colonic epithelium in inflammatory bowel disease. *Gastroenterology* 1996; **111**: 871-885 [PMID: 8831582 DOI: 10.1016/s0016-5085(96)70055-0]

28 **Kolios G**, Rooney N, Murphy CT, Robertson DA, Westwick J. Expression of inducible nitric oxide synthase activity in human colon epithelial cells: modulation by T lymphocyte derived cytokines. *Gut* 1998; **43**: 56-63 [PMID: 9771406 DOI: 10.1136/gut.43.1.56]

29 **Kubes P**. Inducible nitric oxide synthase: a little bit of good in all of us. *Gut* 2000; **47**: 6-9 [PMID: 10861252 DOI: 10.1136/gut.47.1.6]

30 **Vallance BA**, Deng W, De Grado M, Chan C, Jacobson K, Finlay BB. Modulation of inducible nitric oxide synthase expression by the attaching and effacing bacterial pathogen citrobacter rodentium in infected mice. *Infect Immun* 2002; **70**: 6424-6435 [PMID: 12379723 DOI: 10.1128/IAI.70.11.6424-6435.2002]

31 **Vallance BA**, Dijkstra G, Qiu B, van der Waaij LA, van Goor H, Jansen PL, Mashimo H, Collins SM. Relative contributions of NOS isoforms during experimental colitis: endothelial-derived NOS maintains mucosal integrity. *Am J Physiol Gastrointest Liver Physiol* 2004; **287**: G865-G874 [PMID: 15217783 DOI: 10.1152/ajpgi.00187.2004]

32 **Beck PL**, Xavier R, Wong J, Ezedi I, Mashimo H, Mizoguchi A, Mizoguchi E, Bhan AK, Podolsky DK. Paradoxical roles of different nitric oxide synthase isoforms in colonic injury. *Am J Physiol Gastrointest Liver Physiol* 2004; **286**: G137-G147 [PMID: 14665440 DOI: 10.1152/ajpgi.00309.2003]

33 **Luo CX**, Zhu DY. Research progress on neurobiology of neuronal nitric oxide synthase. *Neurosci Bull* 2011; **27**: 23-35 [PMID: 21270901 DOI: 10.1007/s12264-011-1038-0]

34 **Bulc M**, Palus K, Dąbrowski M, Całka J. Hyperglycaemia-Induced Downregulation in Expression of nNOS Intramural Neurons of the Small Intestine in the Pig. *Int J Mol Sci* 2019; **20** [PMID: 30987291 DOI: 10.3390/ijms20071681]

35 **Lalatta-Costerbosa G**, Clavenzani P, Petrosino G, Mazzoni M. An immunohistochemical study of the distribution of nitric oxide synthase-immunoreactive neurons and fibers in the reticular groove of suckling lambs. *J Anat* 2011; **218**: 439-448 [PMID: 21323665 DOI: 10.1111/j.1469-7580.2011.01345.x]

36 **Tomuschat C**, O'Donnell AM, Coyle D, Dreher N, Kelly D, Puri P. NOS-interacting protein (NOSIP) is increased in the colon of patients with Hirschsprungs's disease. *J Pediatr Surg* 2017; **52**: 772-777 [PMID: 28196663 DOI: 10.1016/j.jpedsurg.2017.01.046]

37 **Huber A**, Saur D, Kurjak M, Schusdziarra V, Allescher HD. Characterization and splice variants of neuronal nitric oxide synthase in rat small intestine. *Am J Physiol* 1998; **275**: G1146-G1156 [PMID: 9815045 DOI: 10.1152/ajpgi.1998.275.5.G1146]

38 **Chen L**, Yu B, Luo D, Lin M. Enteric motor dysfunctions in experimental chronic pancreatitis: Alterations of myenteric neurons regulating colonic motility in rats. *Neurogastroenterol Motil* 2018; **30**: e13301 [PMID: 29520975 DOI: 10.1111/nmo.13301]

World Journal of Gastroenterology

Submit a Manuscript: https://www.f6publishing.com

World J Gastroenterol 2022 August 7; 28(29): 3869-3885

DOI: 10.3748/wjg.v28.i29.3869

ISSN 1007-9327 (print) ISSN 2219-2840 (online)

ORIGINAL ARTICLE

Basic Study

N-linked glycoproteomic profiling in esophageal squamous cell carcinoma

Qi-Wei Liu, Hao-Jie Ruan, Wei-Xia Chao, Meng-Xiang Li, Ye-Lin Jiao, Douglas G Ward, She-Gan Gao, Yi-Jun Qi

Specialty type: Medicine, research and experimental

Provenance and peer review: Unsolicited article; Externally peer reviewed.

Peer-review model: Single blind

Peer-review report's scientific quality classification

Grade A (Excellent): 0
Grade B (Very good): 0
Grade C (Good): C, C
Grade D (Fair): 0
Grade E (Poor): 0

P-Reviewer: Chen X, United States; Kashyap MK, India

Received: January 14, 2022
Peer-review started: January 14, 2022
First decision: April 12, 2022
Revised: April 26, 2022
Accepted: July 6, 2022
Article in press: July 6, 2022
Published online: August 7, 2022

Qi-Wei Liu, Hao-Jie Ruan, Wei-Xia Chao, Meng-Xiang Li, She-Gan Gao, Yi-Jun Qi, Henan Key Laboratory of Microbiome and Esophageal Cancer Prevention and Treatment; Henan Key Laboratory of Cancer Epigenetics; Cancer Hospital, The First Affiliated Hospital, College of Clinical Medicine, Henan University of Science and Technology, Luoyang 471003, Henan Province, China

Ye-Lin Jiao, Department of Pathology, The First People's Hospital of Luo Yang, Luoyang 471000, Henan Province, China

Douglas G Ward, Institute of Cancer and Genomic Sciences, College of Medical and Dental Sciences, University of Birmingham, Birmingham B15 2TT, United Kingdom

Corresponding author: Yi-Jun Qi, MD, PhD, Professor, Henan Key Laboratory of Microbiome and Esophageal Cancer Prevention and Treatment; Henan Key Laboratory of Cancer Epigenetics; Cancer Hospital, The First Affiliated Hospital, College of Clinical Medicine, Henan University of Science and Technology, No. 29 Jinghua Road, Luoyang 471003, Henan Province, China. qiyijun@haust.edu.cn

Abstract

BACKGROUND

Mass spectrometry-based proteomics and glycomics reveal post-translational modifications providing significant biological insights beyond the scope of genomic sequencing.

AIM

To characterize the N-linked glycoproteomic profile in esophageal squamous cell carcinoma (ESCC) *via* two complementary approaches.

METHODS

Using tandem multilectin affinity chromatography for enrichment of N-linked glycoproteins, we performed N-linked glycoproteomic profiling in ESCC tissues by two-dimensional gel electrophoresis (2-DE)-based and isobaric tags for relative and absolute quantification (iTRAQ) labeling-based mass spectrometry quantitation in parallel, followed by validation of candidate glycoprotein biomarkers by Western blot.

RESULTS

2-DE-based and iTRAQ labeling-based quantitation identified 24 and 402 differentially expressed N-linked glycoproteins, respectively, with 15 in common, demonstrating the outperformance of iTRAQ labeling-based quantitation over 2-DE and complementarity of these two approaches. Proteomaps showed the distinct compositions of functional categories between proteins and glycoproteins with differential expression associated with ESCC. Western blot analysis validated the up-regulation of total procathepsin D and high-mannose procathepsin D, and the down-regulation of total haptoglobin, high-mannose clusterin, and GlcNAc/sialic acid-containing fraction of 14-3-3ζ in ESCC tissues. The serum levels of glycosylated fractions of clusterin, proline-arginine-rich end leucine-rich repeat protein, and haptoglobin in patients with ESCC were remarkably higher than those in healthy controls.

CONCLUSION

Our study provides insights into the aberrant N-linked glycoproteome associated with ESCC, which will be a valuable resource for future investigations.

Key Words: Esophageal squamous cell carcinoma; N-linked glycoprotein; Post-translational modification; Lectin; Cathepsin D; Haptoglobin; 14-3-3ζ

©The Author(s) 2022. Published by Baishideng Publishing Group Inc. All rights reserved.

Core Tip: The N-linked glycoproteome was comprehensively profiled by two-dimensional gel electrophoresis-based and isobaric tags for relative and absolute quantification (iTRAQ) labeling-based mass spectrometry quantitation in parallel after N-linked glycoprotein enrichment by a tandem of multilectin affinity chromatography. The iTRAQ labeling-based quantitative proteomic profiling outperformed protein spot intensity quantification used by two-dimensional gel electrophoresis. A total of 411 N-linked glycoproteins were identified, including 128 up-regulated and 283 down-regulated glycoproteins with differential expression, which provide the scientific community with a dataset of glycoproteins associated with esophageal squamous cell carcinoma for in-depth investigation.

Citation: Liu QW, Ruan HJ, Chao WX, Li MX, Jiao YL, Ward DG, Gao SG, Qi YJ. N-linked glycoproteomic profiling in esophageal squamous cell carcinoma. *World J Gastroenterol* 2022; 28(29): 3869-3885
URL: https://www.wjgnet.com/1007-9327/full/v28/i29/3869.htm
DOI: https://dx.doi.org/10.3748/wjg.v28.i29.3869

INTRODUCTION

Esophageal cancer is a severe global health issue with 572000 new cases and 509000 deaths in 2018, half of which occur in China[1]. The two most common histological subtypes of esophageal cancer are esophageal squamous cell carcinoma (ESCC) and esophageal adenocarcinoma, with ESCC being the predominant histological subtype both in China and worldwide[2,3]. The long-term outcome of ESCC is correlated with clinical stage at diagnosis with the best outcome in the early stages[4-6]. Unfortunately, the current endoscopic screening for ESCC suffers from low patient compliance and high cost despite the fact that an early detection rate of 70% was achieved in a high-risk region in northern central China [7]. Furthermore, serum biomarkers for ESCC, including squamous cell carcinoma antigen, carcinoembryonic antigen, CYFRA21-1, and carbohydrate antigen 19-9, lack sufficient sensitivity and specificity for early detection[8-11]. The overall 5-year survival rate ranges from 15% to 25% because most cases of ESCC present at an advanced stage[6,12]. It is well accepted that novel biomarkers would hold great promise to improve the clinical outcome of ESCC.

Recent large-scale "omics" studies in ESCC have identified a myriad of aberrations at the levels of genome, epigenome, transcriptome, proteome, *etc*., revealing the high molecular heterogeneity of ESCC [13-17]. Beyond the scope of other techniques, mass spectrometry (MS)-based proteomics has the ability to measure post-translational modifications that provide additional significant biological insights, for example, therapeutically targetable signaling proteins and pathways[18,19]. To date, comprehensive glycoproteomic studies of ESCC are lacking. Glycosylation is present on more than 50% of human proteins and aberrant glycosylation has been implicated in the development and progression of various cancers[20-24]. The sugar chains of glycoproteins are involved in numerous physiological and pathological functions including cell growth, adhesion, differentiation, migration, signal regulation, immune responses, and tumor invasion[20,25,26]. Notably, the clinical prognosis of cancer has been correlated with certain structures of glycans attached to proteins[27,28]. The bisecting GlcNAc structure

catalyzed by N-acetylglucosaminyltransferase III plays crucial roles in suppression of cancer metastasis, which contrasts with the tumor-promoting role of β1, 6-branched N-glycan catalyzed by N-acetylglucosaminyltransferase V[29]. It has been reported that E-cadherin modified by complex N-glycans exhibits weakened adherens junctions, whereas high mannose or less N-glycans attached to E-cadherin produces stable adherens junctions[30]. Furthermore, N-acetylglucosaminyltransferase III modified α3β1 integrin suppresses cell spreading and migration and focal adhesion kinase activity[31]. The fraction of ConA-binding procathepsin D in the serum of hepatocellular carcinoma patients is significantly increased and shows a sensitivity of 85% and specificity of 80% for hepatocellular carcinoma diagnosis [24]. Not surprisingly, over 50% of current cancer biomarkers are glycoproteins, such as AFP, AFP-L3, CA19-9, CA125, and CEA[32-35].

In this study, we used MS-based proteomic analysis to identify N-linked glycoproteins associated with ESCC after isolation of N-linked glycoproteins using tandem multilectin affinity chromatography. Our study unraveled a comprehensive landscape of N-linked glycosylation dysregulation associated with ESCC and bioinformatics analysis provided insights into the functional significance of such aberrant glycosylation. The glycosylated fractions of procathepsin D, clusterin, 14-3-3ζ, proline-arginine-rich end leucine-rich repeat protein (PRELP), and haptoglobin may play important roles in malignant progression of ESCC and are potential diagnostic biomarkers for ESCC, suggesting that N-linked glycosylation aberrations may promote the malignant progression of ESCC.

MATERIALS AND METHODS

Clinical samples

All patients provided written informed consent, and the study was approved by the Ethics Committee of the Medical School, Henan University, China (ethics ref: 108) and conducted in accordance with the ethical guidelines of the 1975 Declaration of Helsinki. Forty-seven pairs of resected ESCC and adjacent normal esophageal mucosa tissue samples, and ten pre-operative serum samples were collected at Linzhou Cancer Hospital, Henan, China between 2010 and 2011 and stored in liquid nitrogen or at -70 ℃ prior to protein extraction. Among the tissue samples, 15 pairs served as a discovery set and the other 32 pairs as a validation set. All tissues were histopathologically confirmed as normal esophageal mucosa or ESCC. The adjacent non-cancerous samples were at least 3 cm distant from the edge of neoplastic mass. No patient in this study had received preoperative radiotherapy or chemotherapy.

Isolation of N-linked glycoproteins by lectin affinity chromatography

Extraction of total tissue proteins and N-linked glycoproteins was performed as previously reported with modifications[24]. Briefly, the esophageal tissue was homogenized in lysis buffer (50 mmol/L Tris, 150 mmol/L NaCl, 1% NP-40, pH 7.2) supplemented with complete proteinase inhibitor cocktail (Roche Diagnostics GmbH, Mannheim, Germany) followed by centrifugation and supernatant collection. Enrichment of N-linked glycoproteins for three pairs of pooled protein samples from 15 ESCC and adjacent non-tumor tissues (five samples for each pair) was performed by tandem lectin affinity chromatography. The multilectin affinity chromatography used a combination of three agarose-bound lectins, Con A (Vector Laboratories, AL-1003), lentil lectin (LCH, Vector Laboratories, AL-1043), and snowdrop lectin (GNA, Vector Laboratories, AL-1243), and a combination of wheat germ agglutitin lectin (WGA, Vector Laboratories, AL-1023) and elderberry lectin (SNA, Vector Laboratories, AL-1303) for the first and second affinity chromatography, respectively. Sixty milligrams of pooled proteins were diluted with binding buffer (30 mmol/L Bis-Tris, 150 mmol/L NaCl, 1 mmol/L $CaCl_2$, 1 mmol/L $MnCl_2$, pH 7.2) and incubated with the lectins in the first affinity chromatography columns at room temperature for 2 h. After incubation, 200 mmol/L methyl-α-D-mannopyranoside was used for elution of high-mannose N-linked glycoproteins. The flowthrough of the first three-lectin column was subjected to the second chromatography for isolation of GlcNAc/sialic acid-containing N-linked glycoproteins using 200 mmol/L N-Acetyl-D-glucosamine as elution buffer. The eluted samples were desalted and concentrated by acetone precipitation.

Two-dimensional gel electrophoresis and image analysis

Two-dimensional gel electrophoresis (2-DE) was performed as previously reported[24,36]. Fifty micrograms of glycoproteins were used for the first-dimension isoelectrofocusing electrophoresis using IPG strips with a linear pH range of 3-10, followed by the second dimension separation using 15% SDS-PAGE gels. Silver stained gels were scanned with an ImageScanner. Image analysis was carried out with ImageMaster 2-D Elite software 4.01.

In-gel digestion and MS identification

The excised protein spots with differential expression were reduced with DTT, alkylated with iodoacetamide, dried in a speedvac, and digested with trypsin (12.5 μg/mL in 50 mmol/L ammonium bicarbonate). LC-MS/MS analysis of tryptic peptides was performed using a Maxis Impact Q-TOF mass

spectrometer (BrukerDaltonics, Bremen, Germany). The MS/MS data were searched against the SwissProt human sequence database using MASCOT *via* Proteinscape (BrukerDaltonics, Bremen, Germany) and reverse database searching was used for estimating the false discovery rate. All proteins were identified by ≥ 2 unique peptides.

Isobaric tags for relative and absolute quantification labeling and MS identification

Isobaric tags for relative and absolute quantification (iTRAQ) labeling of tryptic peptides was performed according to the protocol provided by the supplier. The iTRAQ labeled peptides derived from pooled protein samples of ten ESCC and adjacent non-tumor tissues as previously described in duplicate[37] were separated into 16 fractions by mixed-mode anion exchange/reverse-phase chromatography. Each fraction was dried, dissolved in 0.1% formic acid, and analyzed by LC-MS/MS using a Maxis Impact Q-TOF mass spectrometer (BrukerDaltonics, Bremen, Germany). Data were searched against the SwissProt human sequence database using MASCOT and expression ratios calculated by WARP-LC *via* Proteinscape (BrukerDaltonics, Bremen, Germany). The false discovery rate was estimated using a reverse database search strategy. All proteins were identified by ≥ 2 unique peptides. The data have been deposited at https://www.iprox.cn/ with Project ID IPX0004371000.

Functional enrichment analysis

Gene-set enrichment analyses of differentially expressed glycoproteins (DEGs) and previously identified differentially expressed proteins (DEPs)[37] were performed using Enrichment Map, which organizes the enriched gene-sets into a network with links representing the overlap of member genes [38]. The gene-sets with a P value < 0.001 and false discovery rate < 5% were selected for display in the enrichment map. To gain an insight into the functional makeup of DEGs and DEPs, Proteomap was used to visualize the functional distribution of DEGs or DEPs in cellular processes, including genetic information processing, metabolism, cellular processes, signaling, and others[39].

Western blot analysis

Total tissue proteins were extracted using radioimmunoprecipitation assay lysis buffer, and glycoproteins were isolated by lectin affinity chromatography. Total proteins or glycoproteins were separated by SDS-PAGE and then transferred to PVDF membranes. The blots were blocked in 5% non-fat milk, incubated with primary antibodies and then corresponding secondary antibodies, and visualized using Supersignal West chemiluminescent substrate (Pierce Biotechnology, Rockford, IL, United States). Semi-quantitation of the band intensity was performed using image analysis software and corrected by reference to GAPDH. The antibodies used in this study were: Haptoglobin (1:2000, 16665-1-AP, Proteintech), cathepsin D (1:2500, ab75852, Abcam), clusterin (1:5000, 12289-1-AP, Proteintech), SOD3 (1:1500, T1799, Epitomics), PRELP (1:2000, AP6665b, Abgent), and 14-3-3-ζ (1:2500, ab85268, Abcam).

Statistical analysis

All statistical analyses were performed with SPSS 24.0 software (SPSS, Chicago, IL, United States). Comparisons of quantitated protein band density between ESCC and adjacent non-cancerous tissues were done by paired Student's t-tests or Wilcoxon signed-rank sum tests. All statistical tests were two-sided, and P < 0.05 was considered statistically significant.

RESULTS

N-linked glycoprotein profiling by two-dimensional gel electrophoresis

This study utilized two rounds of multilectin affinity chromatography to isolate N-linked glycoproteins. The first multilectin affinity column comprised Con A, LCH, and GNA lectins to isolate high-mannose N-linked glycoproteins, and the second affinity column included WGA and SNA lectins for GlcNAc/sialic acid-containing glycoprotein enrichment. 2-DE was used to separate the isolated N-linked glycoproteins. Figure 1A and B shows the representative 2-DE images of high-mannose glycoproteins isolated from ESCC and non-cancerous tissues. An average of 742 ± 45 protein spots could be detected on each 2-DE gel analyzed by Image Master 2-D Elite. A total of 35 differential protein spots with ≥ 1.5 fold-changes in protein spot intensities (P < 0.05) were identified, including 20 up-regulated and 15 down-regulated protein spots in ESCC compared with corresponding non-cancerous tissues, respectively. For GlcNAc/sialic acid-containing glycoprotein profiling, the patterns of protein spots on 2-DE gels were markedly different compared with those of high-mannose glycoproteins (Figure 1C and D). There were 23 protein spots with differential expression, including 5 up-regulated and 18 down-regulated protein spots in ESCC compared to non-cancerous tissues.

These protein spots were identified by LC-MS/MS of the trypsin-digested spots excised from preparative gels. The identities of proteins are shown in Tables 1 and 2, in which 22 proteins and 23 proteins were derived from the first and second lectin affinity chromatography, respectively. There

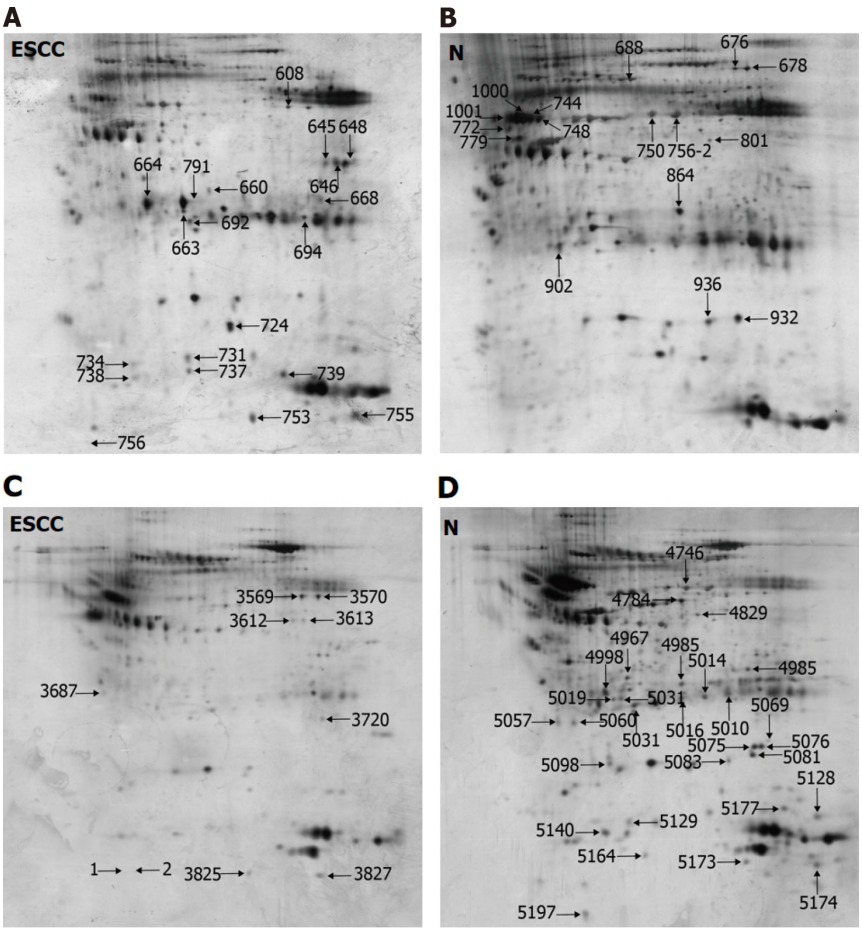
Table 1 Summary of high-mannose N-linked glycoproteins in esophageal squamous cell carcinoma by 2-dimensional gel electrophoresis

Spot No.	Accession	Protein identity (Theoretical MW/pI)	Ratio	*P* value	Scores	Unique Peptides	N-glycosylation sites
608	ENOA_HUMAN	Alpha-enolase (47.1/7.7)	2.2 (↑)	0.008	2050.2 (M:2050.2)	33	1 (102)
638	CATD_HUMAN	Cathepsin D (44.5/6.1)	2.6 (↑)	0.009	1351.8 (M:1351.8)	20	2 (134, 263)
645	G3P_HUMAN	Glyceraldehyde-3-phosphate dehydrogenase (36/9.3)	3.2 (↑)	0.009	319.9 (M:319.9)	4	0
646	G3P_HUMAN	Glyceraldehyde-3-phosphate dehydrogenase (36/9.3)	5.2 (↑)	0.002	611.5 (M:611.5)	10	0
648	G3P_HUMAN	Glyceraldehyde-3-phosphate dehydrogenase (36/9.3)	8.9 (↑)	0.009	730.1 (M:730.1)	14	0
660	CO1A2_HUMAN	Collagen alpha-2(I) chain (129.2/9.7)	1.7 (↑)	0.008	1207.8 (M:1207.8)	20	1 (207)
664	CATD_HUMAN	Cathepsin D (44.5/6.1)	12.5 (↑)	0.005	1337.1 (M:1337.1)	18	2 (134, 263)
668	ALDOA_HUMAN	Fructose-bisphosphate aldolase A (39.4/9.2)	1.6 (↑)	0.004	182.0 (M:182.0)	4	0
692	HSPB1_HUMAN	Heat shock protein beta-1 (22.8/6)	1.6 (↑)	0.009	1015.9 (M:1015.9)	15	0
694	TPIS_HUMAN	Triosephosphate isomerase (26.7/6.5)	1.8 (↑)	0.004	1277.6 (M:1277.6)	19	1 (233)
724	FABP5_HUMAN	Fatty acid-binding protein, epidermal (15.2/7.5)	2 (↑)	0.002	818.4 (M:818.4)	14	0
731	HPT_HUMAN	Haptoglobin (45.2/6.1)	2.1 (↑)	0.006	418.7 (M:418.7)	11	2 (207, 241)
734	HSPB1_HUMAN	Heat shock protein beta-1 (22.8/6)	1.5 (↑)	0.009	464.0 (M:464.0)	7	0
737	APOA1_HUMAN	Apolipoprotein A-I (30.8/5.5)	1.6 (↑)	0.002	200.4 (M:200.4)	4	0
738	COF1_HUMAN	Cofilin-1 (18.5/9.1)	1.5 (↑)	0.009	381.8 (M:381.8)	7	0
739	HBB_HUMAN	Hemoglobin subunit beta (16/6.9)	2.7 (↑)	0.008	720.5 (M:720.5)	10	0
753	CATD_HUMAN	Cathepsin D (44.5/6.1)	4.6 (↑)	0.009	702.0 (M:702.0)	13	2 (134, 263)
755	HBA_HUMAN	Hemoglobin subunit alpha (15.2/9.4)	3.9 (↑)	0.005	377.6 (M:377.6)	7	0
756	FIBB_HUMAN	Fibrinogen beta chain (55.9/9.3)	1.8 (↑)	0.009	3911.9 (M:3911.9)	55	0
791	FIBG_HUMAN	Fibrinogen gamma chain precursor (51.5/5.3)	1.5 (↑)	0.009	1356.7 (M:1356.7)	26	1 (78)
676	FIBB_HUMAN	Fibrinogen beta chain (55.9/9.3)	4.5 (↓)	0.006	1071.8 (M:1071.8)	18	0
678	CO3_HUMAN	Complement C3 (187/6)	6.2 (↓)	0.009	383.9 (M:383.9)	12	2 (85, 939)
688	HEMO_HUMAN	Hemopexin (51.6/6.6)	5.3 (↓)	0.002	698.2 (M:698.2)	13	2 (64, 240)
744	A1AT_HUMAN	Alpha-1-antitrypsin (46.7/5.3)	12.7 (↓)	0.009	784.8 (M:784.8)	14	3 (70, 107, 271)
748	HPT_HUMAN	Haptoglobin (45.2/6.1)	7.5 (↓)	0.008	1067.0 (M:1067.0)	19	2 (207, 241)
750	FIBB_HUMAN	Fibrinogen beta chain (55.9/9.3)	4.9 (↓)	0.009	3276.7 (M:3276.7)	48	0
772	A1AT_HUMAN	Alpha-1-antitrypsin (46.7/5.3)	1.8 (↓)	0.005	678.2 (M:678.2)	12	3 (70, 107, 271)
779	CLUS_HUMAN	Clusterin (52.5/5.9)	2.9 (↓)	0.009	619.3 (M:619.3)	10	3 (86, 103, 291)
801	FIBB_HUMAN	Fibrinogen beta chain (55.9/9.3)	2.1 (↓)	0.009	714.1 (M:714.1)	13	0
864	SODE_HUMAN	Extracellular superoxide dismutase [Cu-Zn] (25.8/6.2)	6.4 (↓)	0.004	798.6 (M:798.6)	12	1 (107)
902	APOA1_HUMAN	Apolipoprotein A-I (30.8/5.5)	4.3 (↓)	0.002	1206.2	24	0

					(M:1206.2)		
932	TRFE_HUMAN	Serotransferrin precursor (77/7)	3.8 (↓)	0.004	187.0 (M:187.0)	4	1 (630)
936	HPTR_HUMAN	Haptoglobin-related protein (39/6.7)	1.5 (↓)	0.002	226.4 (M:226.4)	4	1 (149)
1000	A1AT_HUMAN	Alpha-1-antitrypsin (46.7/5.3)	15.2 (↓)	0.006	1091.2 (M:1091.2)	20	3 (70, 107, 271)
1001	HPT_HUMAN	Haptoglobin (45.2/6.1)	9.8 (↓)	0.009	1054.6 (M:1054.6)	18	2 (207, 241)

Table 2 Summary of sialic N-linked glycoproteins identified in esophageal squamous cell carcinoma by 2-dimensional gel electrophoresis

Spot No.	Accession	Protein identity (Theoretical MW/pI)	Ratio	*P* value	Scores	Unique Peptides	N-glycosylation sites
3569	ENOA_HUMAN	Alpha-enolase (47.1/7.7)	2 (↑)	0.002	802.0 (M:802.0)	18	2 (17, 102)
3570	IGKC_HUMAN	Ig kappa chain C region (11.6/5.5)	2.4 (↑)	0.006	54.4 (M:54.4)	2	0
3612	TRFE_HUMAN	Serotransferrin (77/7)	1.5 (↑)	0.004	927.5 (M:927.5)	25	1 (630)
3687	KV305_HUMAN	Ig kappa chain V-III region WOL (11.7/9.5)	1.7 (↑)	0.009	125.4 (M:125.4)	2	0
3720	A1AT_HUMAN	Alpha-1-antitrypsin (46.7/5.3)	1.9 (↑)	0.002	49.3 (M:49.3)	2	3 (70, 107, 271)
4746	FIBB_HUMAN	Fibrinogen beta chain (55.9/9.3)	2.8 (↓)	0.004	817.3 (M:817.3)	17	0
4784	ACTB_HUMAN	Actin, cytoplasmic 1 (41.7/5.2)	3.4 (↓)	0.002	43.6 (M:43.6)	2	1 (12)
4948	HBB_HUMAN	Hemoglobin subunit beta (16/6.9)	1.8 (↓)	0.006	129.3 (M:129.3)	4	0
4967	ACTA_HUMAN	Actin, aortic smooth muscle (42/5.1)	1.7 (↓)	0.009	402.1 (M:402.1)	9	1 (14)
4985	FHR2_HUMAN	Complement factor H-related protein 2 (30.6/6)	2 (↓)	0.002	271.1 (M:271.1)	5	0
4998	1433Z_HUMAN	14-3-3 protein zeta/delta (27.7/4.6)	6.6 (↓)	0.009	62.1 (M:62.1)	2	2 (173, 224)
5010	FIBA_HUMAN	Fibrinogen alpha chain (94.9/5.6)	2.1 (↓)	0.002	83.3 (M:83.3)	3	3 (288, 419, 831)
5019	ACTH_HUMAN	Actin, gamma-enteric smooth muscle (41.8/5.2)	1.6 (↓)	0.009	92.7 (M:92.7)	3	1 (13)
5031	KV204_HUMAN	Ig kappa chain V-II region TEW (12.3/5.6)	1.5 (↓)	0.008	84.9 (M:84.9)	2	0
5057	CATB_HUMAN	Cathepsin B (37.8/5.9)	1.6 (↓)	0.009	84.8 (M:84.8)	2	2 (192, 289)
5069	FABP5_HUMAN	Fatty acid-binding protein, epidermal (15.2/7.5)	1.5 (↓)	0.005	88.7 (M:88.7)	2	0
5076	CRYAB_HUMAN	Alpha-crystallin B chain (20.1/6.9)	3.8 (↓)	0.009	240.1 (M:240.1)	6	0
5081	TAGL_HUMAN	Transgelin (22.6/9.4)	4.1 (↓)	0.009	134.7 (M:134.7)	3	0
5083	HSP71_HUMAN	Heat shock 70 kDa protein 1A/1B (70/5.4)	1.9 (↓)	0.004	105.8 (M:105.8)	3	1 (432)
5098	K1C17_HUMAN	Keratin, type I cytoskeletal 17 (48.1/4.8)	2.2 (↓)	0.002	198.2 (M:198.2)	5	0
5128	CYC_HUMAN	Cytochrome c (11.7/10.1)	2.6 (↓)	0.006	97.4 (M:97.4)	3	0
5164	S10A9_HUMAN	Protein S100-A9 (13.2/5.7)	1.7 (↓)	0.009	85.7 (M:85.7)	3	0
5173	S10A8_HUMAN	Protein S100-A8 (10.8/6.6)	1.5 (↓)	0.002	421.3 (M:421.3)	8	0



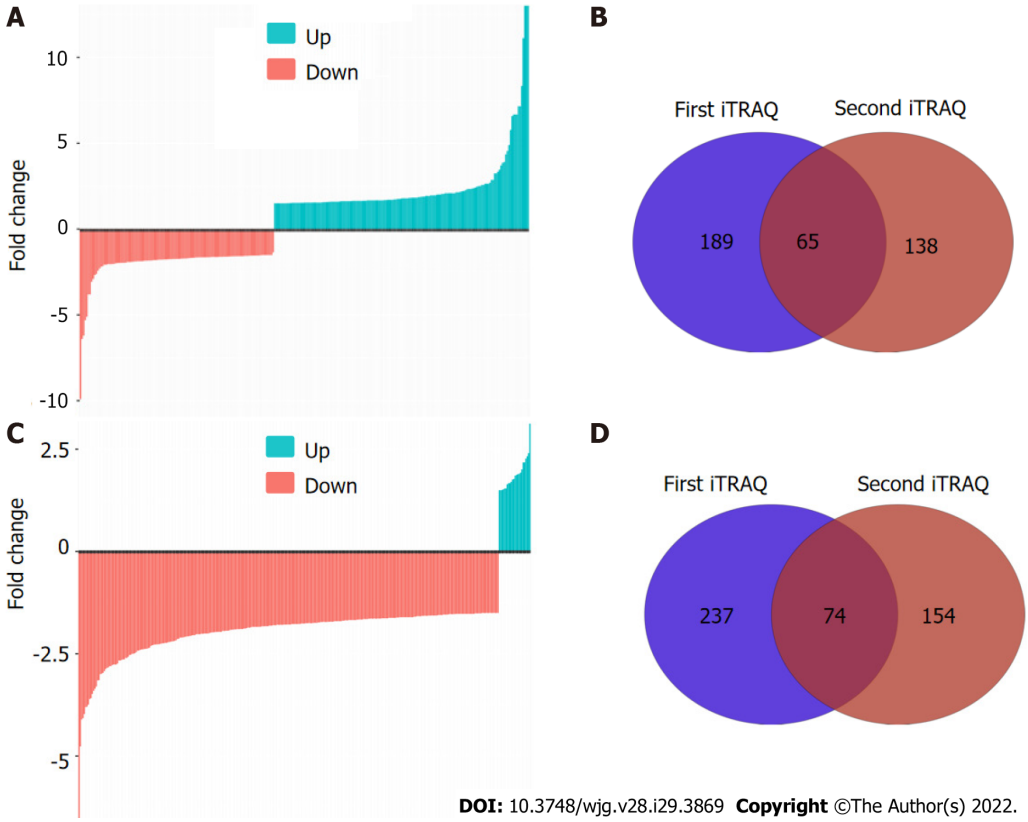
DOI: 10.3748/wjg.v28.i29.3869 **Copyright** ©The Author(s) 2022.

Figure 1 Representative two-dimensional gel electrophoresis images of N-linked glycoproteins from esophageal squamous cell carcinoma (ESCC) and adjacent non-cancerous tissues (N), in which the denoted numbers represent protein spots with differential expression. A and B: Representative two-dimensional gel electrophoresis (2-DE) images of high-mannose glycoproteins from ESCC (A) and N (B); C and D: Representative 2-DE images of GlcNAc/sialic acid-containing glycoproteins from ESCC (C) and N (D). ESCC: Esophageal squamous cell carcinoma; N: Non-cancerous tissues.

were six proteins in common between these two isolated fractions. In agreement with our previous reports[24,36], many gel spots were identified as the same protein, indicating the presence of different proteoforms due to post-translational modifications. Using NetNGlyc (http://www.cbs.dtu.dk/services/NetNGlyc) to predict the glycosylation sites on proteins, 72.7% (16/22) of high-mannose N-linked glycoproteins and 56.5% (13/23) of GlcNAc/sialic acid-containing glycoproteins were found to have potential glycosylation sites, indicating some non-specific binding to lectins by non-glycosylated proteins.

N-linked glycoprotein profiling by iTRAQ labeling

To comprehensively characterize the N-linked glycoproteome in ESCC, we further performed iTRAQ-based analysis of the N-linked glycoproteome in ESCC and non-cancerous tissues. One pair of protein pools from ten ESCC and matched non-cancerous tissues, respectively, were subjected to tandem lectin affinity chromatography enrichment, in-solution digestion with trypsin, iTRAQ labeling, and LC-MS/MS identification in duplicate. In total, 1464 and 1298 proteins from the first affinity column were identified in the two technical replicates (Figure 2A, Supplementary Tables 1 and 2). Using the cut-off criteria of ≥ 2 unique peptides and a fold-change of 1.5, 189 and 138 proteins with differential expression were identified from the first and second independent pools, respectively, with 65 proteins in common, resulting in identification of 262 differentially expressed proteins in total from the high-mannose binding lectin affinity chromatography, of which 203 (77.5%) have predicted N-linked glycosylation sites (Figure 2B). For N-linked glycoproteins enriched by the downstream GlcNAc/sialic acid binding lectin chromatography, two independent iTRAQ-labeled pools produced 1174 and 936 proteins following isolation of high-mannose glycoproteins (Figure 2C, Supplementary Tables 3 and 4). There were 237 of 1174 and 154 of 936 proteins with differential expression, respectively, with 74 proteins in common (Figure 2D). A total of 317 unique proteins, of which 246 (77.6%) were predicted to be N-linked glycoproteins, were identified from the GlcNAc/sialic acid binding lectin chromatography enrichment.



DOI: 10.3748/wjg.v28.i29.3869 **Copyright** ©The Author(s) 2022.

Figure 2 N-linked glycoprotein profiling by isobaric tags for relative and absolute quantification labeling and liquid chromatography electrospray ionisation tandem mass spectrometry/mass spectrometry identification. A: Waterfall plot shows the differentially expressed high-mannose glycoproteins; B: Venn diagram depicts the unique and overlapped high-mannose glycoproteins identified from two independent replicates; C: Waterfall plot shows the differentially expressed GlcNAc/sialic acid-containing glycoproteins; D: Venn diagram depicts the unique and overlapped GlcNAc/sialic acid-containing glycoproteins identified from two independent replicates. iTRAQ: Isobaric tags for relative and absolute quantification.

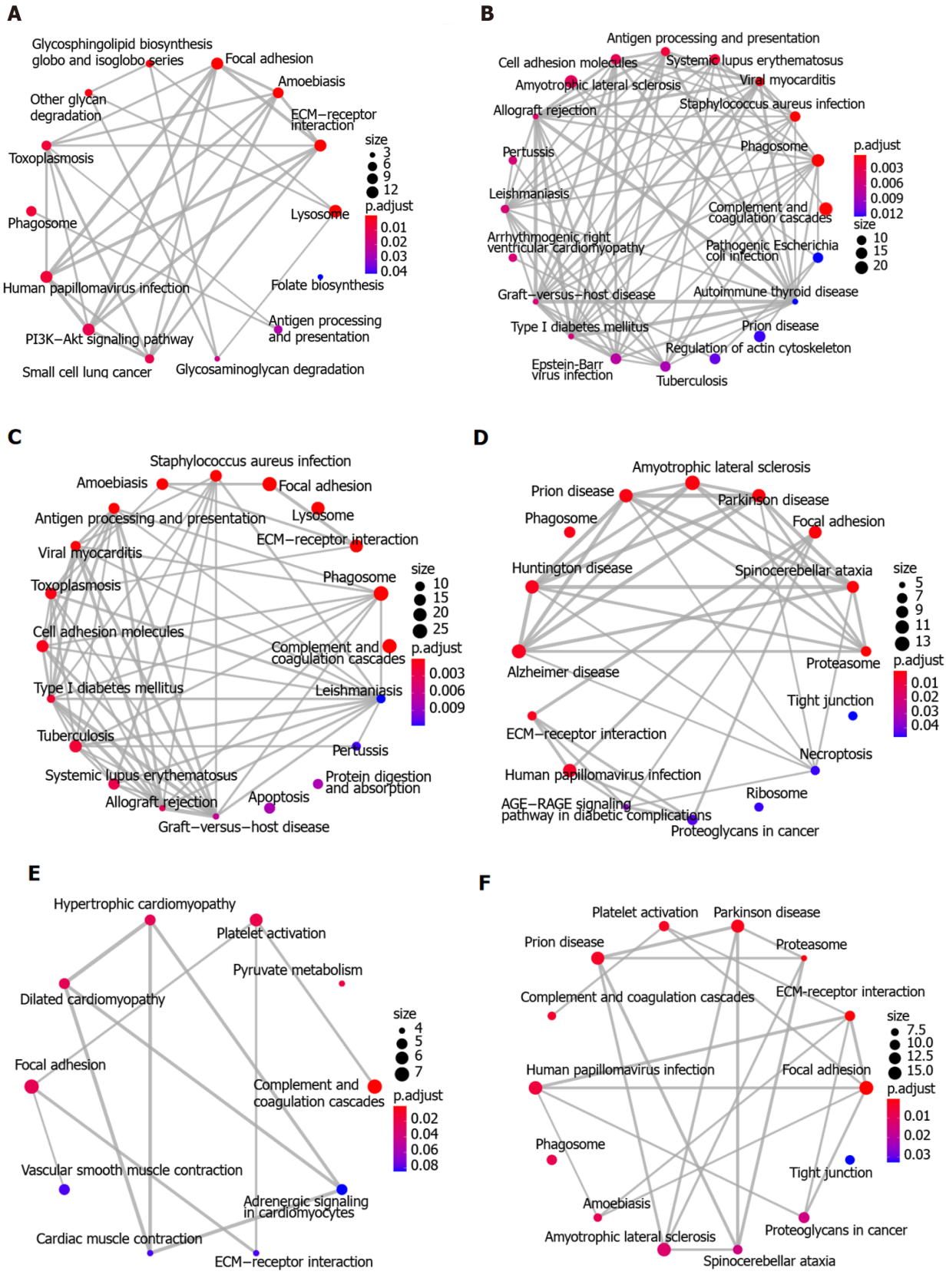
There were 58 overlapping glycoproteins found between 262 high-mannose glycoproteins and 317 GlcNAc/sialic acid-containing glycoproteins.

Comparison of two-dimensional gel electrophoresis-based and iTRAQ labeling-based profiling

In this study, two protocols for identifying N-linked glycoproteins based on different quantitative methods yielded quite different results. There were only 11 high-mannose glycoproteins and 4 GlcNAc/sialic acid-containing glycoproteins in common between 2-DE-based and iTRAQ-based glycoproteomic profiling. Our results demonstrate that iTRAQ-based quantitative proteomic profiling outperformed protein spot intensity quantification by 2-DE. There were, however, common glycoproteins found by both approaches. Therefore, the combination of these four fractions produced 411 unique N-linked glycoproteins. These findings indicate that a combination of these two complementary protocols could generate a more comprehensive landscape of N-linked glycoproteome implicated in ESCC because iTRAQ-based and 2-DE-based methods were able to isolate unique glycoproteins, thus providing a good representation of the N-linked glycoproteome.

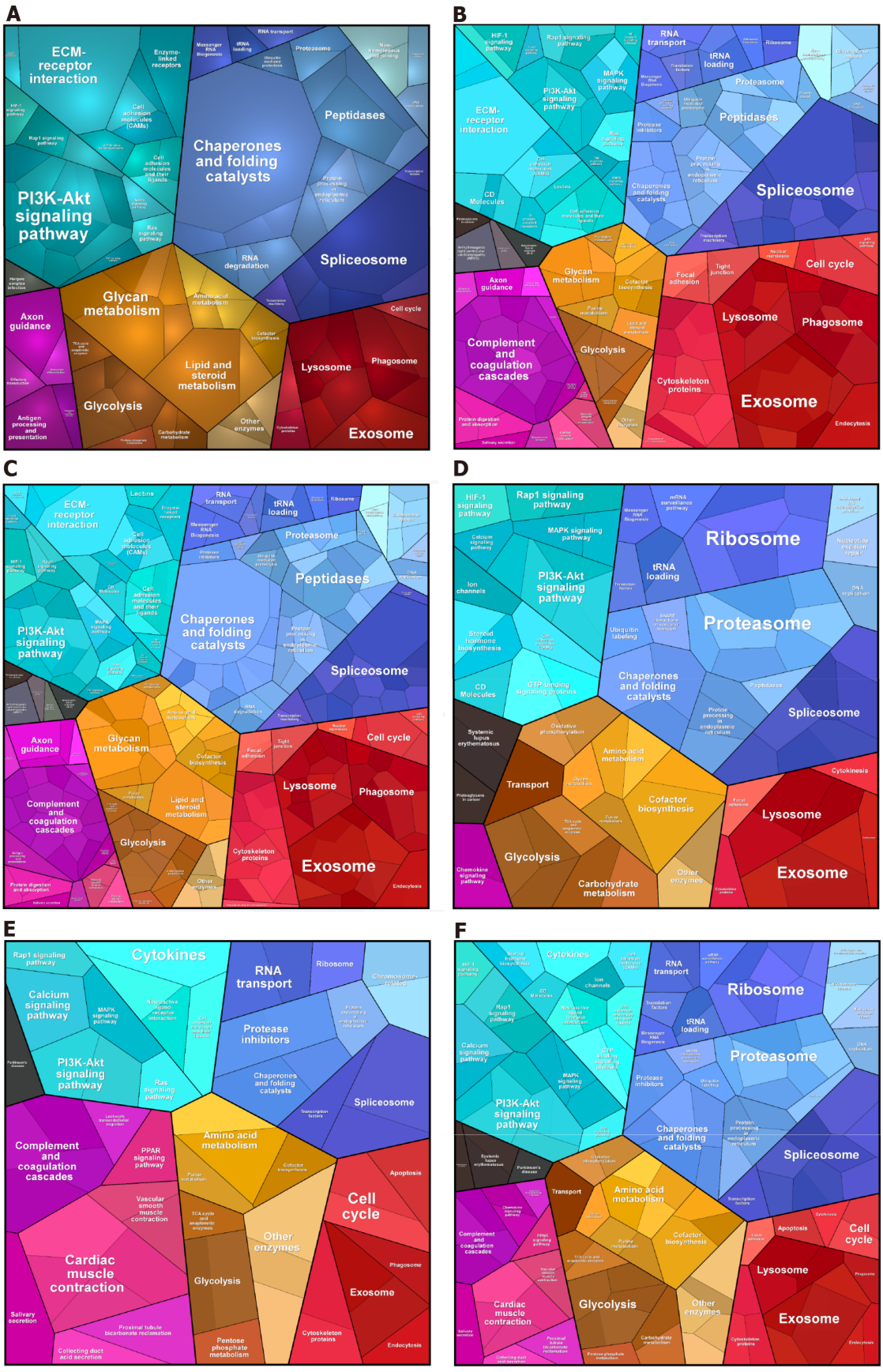
Functional analysis of differentially expressed glycoproteins

To explore the biological function of the 411 DEGs associated with ESCC, KEGG pathway enrichment analysis was initially performed using Enrichment Map. Figure 3A-C shows the 64 enriched pathways, which include complement and coagulation cascades, focal adhesion, ECM-receptor interaction, cellular interactions, immune response and infection, metabolism of fructose and mannose, glycolysis and gluconeogenesis, splicesome, and PI3K-Akt and HIF-1 signaling pathways. In addition, proteomaps were constructed to visualize the composition of these DEGs in the five functional categories, which comprise genetic information processing, environmental information processing, cellular processes, metabolism, and organismal systems. Figure 4A-C shows that the genetic information processing accounts for the largest component of the DEGs, with protein processing, translation, and transcription being the biggest contributors to this functional category. In the category of signaling events, both the up-regulated and down-regulated DEGs were involved in PI3K-Akt, MAPK, Ras, Rap1, and HIF-1 signaling pathways (Figure 4A and B). The layouts of cellular process between up-regulated and down-regulated DEGs were different, with common components of exosome, lysosome, phagosome, cytoskeleton, and cell cycle, whereas the down-regulated DEGs are implicated in focal adhesion, tight



DOI: 10.3748/wjg.v28.i29.3869 **Copyright** ©The Author(s) 2022.

Figure 3 Functional analyses of proteins and glycoproteins with differential expression using enrichment map. A-C: Kyoto encyclopedia of genes and genomes (KEGG) pathway enrichment analysis using enrichment map shows the significantly enriched biological pathways of up-regulated differentially expressed glycoproteins (DEGs), down-regulated DEGs, and total DEGs, respectively; D-F: KEGG pathway enrichment analysis using enrichment map shows the significantly enriched biological pathways of up-regulated DEPs, down-regulated DEPs, and total DEPs, respectively. KEGG: Kyoto encyclopedia of genes and genomes; DEGs: Differentially expressed glycoproteins; DEPs: Differentially expressed proteins.



DOI: 10.3748/wjg.v28.i29.3869 **Copyright** ©The Author(s) 2022.

Figure 4 Functional analyses of proteins and glycoproteins with differential expression using Proteomap. A-C: Kyoto encyclopedia of genes and genomes (KEGG) pathway enrichment analysis using Proteomap shows the significantly enriched biological pathways of up-regulated differentially expressed glycoproteins (DEGs), down-regulated DEGs, and total DEGs, respectively; D-F: KEGG pathway enrichment analysis using Proteomap shows the significantly enriched biological pathways of up-regulated DEPs, down-regulated DEPs, and total DEPs, respectively. KEGG: Kyoto encyclopedia of genes and genomes; DEGs:

Differentially expressed glycoproteins; DEPs: Differentially expressed proteins.

junction, endocytosis, and p53 signaling pathway (Figure 4A and B). In glycolysis, there were more up-regulated than down-regulated DEGs. Notably, the complement and coagulation cascades in the immune system include exclusively down-regulated DEGs (Figure 4A and B).

Functional comparison between glycoproteins and proteins with differential expression

Because there were only 82 overlapping proteins between DEGs and DEPs, the distinct subproteomes in each functional category may affect the structure of proteomaps. As shown in Figure 4, the compositions of proteomaps differ. In the category of genetic information processing, the chaperones, spliceosome, and peptidases are the predominant components in DEGs whereas the spliceosome, proteasome, and ribosome are the main contributors in DEPs. Although there are some signaling pathways (PI3K/Akt, MAPK, HIF1, Ras, and Rap1) in common in DEGs and DEPs, distinct components (neuroactive ligand-receptor interaction, calcium signaling pathway, GPT-binding signaling proteins, steroid hormone biosynthesis, and cytokines in DEPs *vs* NF kappa B pathway, FoxO pathway, ECM-receptor interaction, CD molecules, lectins, and enzyme-linked receptors in DEGs) are present in environment interaction (Figure 4C and F). Along with these differences, distinct compositions of the other three categories were found as well, in agreement with uniquely characterized proteomes. Likewise, Enrichment Map analysis showed that marked differences were found between DEGs and DEPs (Figure 3C and F). In the same line, there were remarkable distinctions between DEGs and DEPs identified using iTRAQ-based quantitation of Indian ESCC samples (data not shown)[40].

Validation of potential glycoprotein biomarkers

Western blot analysis was performed to validate the differential expression of potential glycoprotein biomarkers for ESCC, including haptoglobin, cathepsin D, clusterin, superoxide dismutase 3 (SOD3), PRELP, and 14-3-3ζ. Consistent with the corresponding protein spots of 748 and 1001 on 2-DE images, haptoglobin expression in ESCC was significantly down-regulated in tumor compared with adjacent non-cancerous tissues (Figure 5A). In contrast, the expression of procathepsin D instead of mature cathepsin D was remarkably enhanced in ESCC compared with the corresponding non-cancerous tissues (Figure 5B). There were no significant differences in the expression levels of the other four selected proteins (Supplementary Figure 1). These data suggest that the differential expression of glycoproteins identified in this study could be caused by up-regulation of protein expression, or up-regulation of N-linked glycosylation due to aberrant expression or activities of certain glycosyltransfereases.

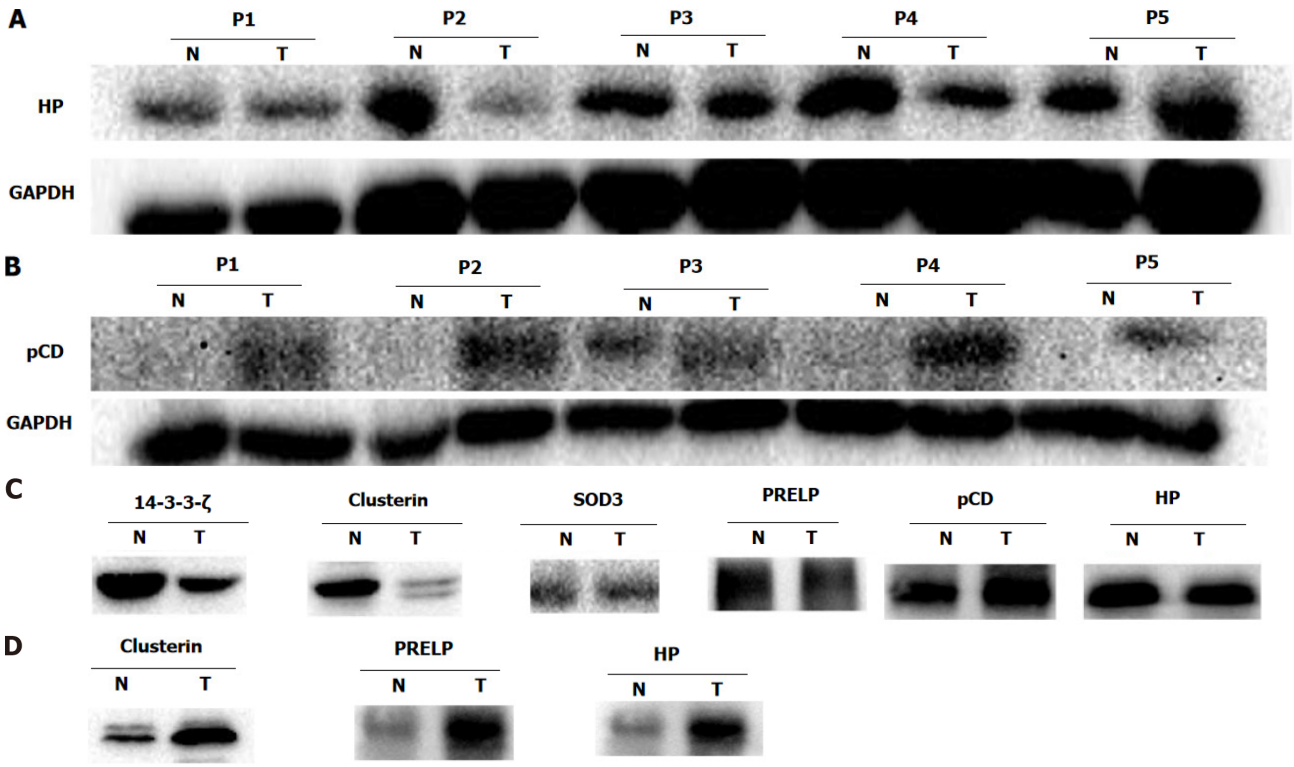
To assess the contribution of high-mannose or GlcNAc/sialic acid components attached to the selected glycoproteins, enrichment of corresponding glycoproteins *via* glycan chain binding to specific lectins was performed followed by Western blot detection. Consistent with the up-regulation of procathepsin D protein, the high-mannose subtype of procathepsin D was pronouncedly increased in ESCC as well (Figure 5C). In contrast to the expression pattern of total clusterin protein, the high-mannose fraction of clusterin was markedly down-regulated in ESCC as compared with non-cancerous tissues (Figure 5C). However, the glycosylated fractions of SOD3, PRELP, and haptoglobin did not show significant differences between ESCC and non-cancerous tissues after enrichment of high-mannose glycan structure of glycoproteins using lectin affinity chromatography. In agreement with the quantitative result of glycosylated 14-3-3ζ, the GlcNAc/sialic acid-containing fraction of 14-3-3ζ was strongly reduced in ESCC (Figure 5C).

Serum levels of potential glycoprotein biomarkers

As isolation of N-linked glycoproteins from serum reduces the high-complexity of the serum proteome, we characterized the serum levels of potential glycoprotein biomarkers in patients with ESCC. As expected, the total protein levels of the six selected proteins were not significantly different in the serum of ESCC patients and healthy controls (Supplementary Figure 2). In contrast, the serum levels of glycosylated forms of clusterin, PRELP, and haptoglobin in ESCC patients were much higher than those of healthy controls (Figure 5D).

DISCUSSION

Aberrant glycosylation of proteins, which is not correlated with mRNA levels, has been linked to a variety of cancers and reflects disease status and progression[20,41-44]. MS-based proteomics and glycomics hold considerable potential to identify novel glycosylation-based biomarkers. To the best of our knowledge, this study is the first to use tandem lectin affinity chromatography to enrich N-linked glycoproteins, followed by 2-DE-based and iTRAQ labeling-based proteomic quantitative profiling, and protein identification by MS. In total, 411 differentially expressed N-linked glycoproteins were



DOI: 10.3748/wjg.v28.i29.3869 **Copyright** ©The Author(s) 2022.

Figure 5 Western blot validations of potential glycoprotein biomarkers. A and B: Representative Western blot results show haptoglobin (HP) (A) and procathepsin D (pCD) (B) with differential expression between esophageal squamous cell carcinoma (ESCC/T) and adjacent non-cancerous tissues (N); C: Representative Western blot results show the N-linked glycosylated fraction of HP, pCD, clusterin, superoxide dismutase 3 (SOD3), proline-arginine-rich end leucine-rich repeat protein (PRELP), and 14-3-3ζ in ESCC/T and N enriched by corresponding lectins; D: Representative Western blot results show the N-linked glycosylated fractions of clusterin, PRELP, and HP in serum of patients with ESCC/T and healthy controls. The results are representative of three independent experiments. ESCC/T: Esophageal squamous cell carcinoma; HP: Haptoglobin; pCD: Procathepsin D; SOD3: Superoxide dismutase 3; PRELP: Proline-arginine-rich end leucine-rich repeat protein.

identified, including 128 up-regulated and 283 down-regulated DEGs. These DEGs provide the scientific community a dataset of glycoproteins associated with ESCC for in-depth investigation.

Depending on the linkage of carbohydrate to the protein backbone, glycoproteins fall into two main types, N-glycosylated and O-glycosylated, in which glycans are covalently attached to the amide nitrogen of asparagine residues and to the hydroxyl group of serine or threonine residues, respectively [45]. Lectins are defined as proteins that bind to the particular oligosaccharide epitope structures attached to proteins or lipids *via* selective affinities[46]. Due to these natural features, lectins are frequently used to isolate glycoproteins from a variety of origins, in particular from blood, to reduce sample complexity and to enrich low-abundance proteins. Using three lectins in parallel, *i.e.*, ConA, WGA, and Jacalin, a total of 423 proteins were fractionated from membrane proteins, among which 202 (71%) have predicted N-linked glycosylation sites[47]. As expected, there were unique and shared proteins enriched by these three lectins. To comprehensively isolate N-linked glycoproteins involved in ESCC, five lectins allocated to two sequential affinity chromatographies were used in this study to increase the coverage of captured N-linked glycoproteins. In addition, two complementary methods for quantitative profiling of enriched glycoproteins were used. In total, 262 and 317 nonredundant DEPs were identified by iTRAQ labeling-based profiling from the first and second lectin affinity chromatography, respectively. 2-DE-based MS/MS profiling led to fewer DEPs being identified compared with the iTRAQ labeling-based approach. Under a high stringency of selection criteria (foldchange ≥ 1.5, unique peptides ≥ 2), 519 proteins were identified in total, of which 402 (77.5%) carry predicted N-linked glycosylation sites. Identification of a large number of proteins without predicated glycosylation sites indicates the existence of non-specific binding to certain lectins needing further in-depth study to elucidate.

Functional analysis based on KEGG pathway annotations by Proteomap revealed that there were striking differences in the compositions of DEGs distributed in five functional entities. In line with previous findings, the DEGs in genetic information processing account for the largest fraction of N-linked glycoproteome, supporting the survival and rapid growth of cancer cells[39]. In further support of this, a number of signaling pathways, including PI3K-Akt, MAPK, Rap1, and HIF-1 pathways, which play important roles in oncogenesis and progression, were significantly enriched. In metabolism, glycolysis was significantly enriched in DEGs identified in this study. The increased rate of glucose

metabolism and aerobic glycolysis, also known as the Warburg effect, are recognized hallmarks of cancer[48]. In agreement with this, HIF signaling proteins were over-represented in ESCC and may contribute to increased glycolysis. Besides energy generation, aerobic glycolysis enhances rapid growth and unlimited proliferation of cancer cells through providing precursors for certain biosynthetic processes as well as alteration of the tumor microenvironment[49]. Moreover, extracellular lactate has inhibitory effects on human cytotoxic T lymphocytes[50,51]. Furthermore, metabolic phenotype of cancer stem cell seems distinct from bulk cancer cells and is characterized by glycolysis and/or XoPhos [49]. The increased expression of fructose-bisphosphate aldolase A, triosephosphate isomerase, alpha-enolase, all-trans-retinol dehydrogenase [NAD(+)] ADH1B, and glyceraldehyde-3-phosphate dehydrogenase in ESCC may contribute to the progression of ESCC *via* increased glycolysis and could serve as therapeutic targets for the management of ESCC. All together, these distinct functional categories and related effector molecules may represent potential therapeutic targets in ESCC.

Cathepsin D, a lysosomal protease, is expressed in nearly all cells and tissues of mammals. However, pro-cathepsin D but not mature cathepsin D is reportedly associated with the development and progression of a variety of cancers[52]. In line with up-regulation of ConA-binding cathepsin D and procathepsin D, glycosylated procathepsin D was increased in ESCC as well, suggesting it as a potential biomarker for ESCC. In addition, we also demonstrated that both total haptoglobin and N-linked haptoglobin in serum were differentially expressed in ESCC, as seen in other malignancies[41,53,54]. Although there were no alterations in the levels of total protein expression, the high-mannose clusterin and sialic acid glycoforms of 14-3-3ζ were down-regulated in ESCC but need further study to characterize their glycan moieties. After probing the serum levels of these candidate biomarkers, we provide several potential biomarkers for ESCC diagnosis. Additionally, our findings reveal that differential protein expression is a confounding factor for identification of aberrant glycosylation.

The current study has several limitations. First, the main limitation is that sample pooling used in this study may cause a loss of inter-individual information. However, this is partly compensated by the validation of candidate biomarkers using individual tissue samples. Second, affinity chromatography comprising multiple lectins for glycoprotein isolation yielded different subglycoproteomes. Further studies should characterize the composition and structure of glycans associated with proteins. Nevertheless, our study represents, to our knowledge, the first study to characterize the glycoproteome associated with ESCC, and thus provides the scientific community a resource of glycoproteins for in-depth investigation.

CONCLUSION

In conclusion, this study catalogued a total of 411 N-linked glycoproteins implicated in ESCC after glycoprotein enrichment using two stage multilectin affinity chromatography and MS/MS identification. Proteomap analysis revealed the distribution of differential glycoproteins in five functional categories. A preliminary validation demonstrated the differential expression of glycoprotein biomarker candidates, including total procathepsin D and haptoglobin in ESCC, high-mannose fractions of procathepsin D, clusterin and sialiated 14-3-3ζ in ESCC, and glycosylated fractions of clusterin, PRELP, and haptoglobin in serum. Consequently, this study yielded a comprehensive landscape of N-linked glycoproteome associated with ESCC for further characterization.

ARTICLE HIGHLIGHTS

Research background

Recent large-scale "omics" studies in esophageal squamous cell carcinoma (ESCC) have identified a myriad of aberrations at the levels of genome, epigenome, transcriptome, proteome, *etc*., revealing the high molecular heterogeneity of ESCC. However, protein post-translational modifications, such as glycosylation and phosphorylation, which provide additional significant biological insights, are missing.

Research motivation

The sugar chains of glycoproteins are involved in numerous physiological and pathological conditions. More than 50% of current cancer biomarkers are glycoproteins.

Research objectives

To identify N-linked glycoproteins associated with ESCC after isolation of N-linked glycoproteins using tandem multilectin affinity chromatography.

Research methods

N-linked glycoproteins were isolated from ESCC and adjacent non-tumor tissue samples using multilectin affinity chromatography. Two-dimensional gel electrophoresis (2-DE)-based and isobaric tags for relative and absolute quantification (iTRAQ) labeling-based mass spectrometry quantitation were performed in parallel to profile the N-linked glycoproteome in ESCC, followed by validation of candidate glycoprotein biomarkers using Western blot.

Research results

A total of 411 differentially expressed N-linked glycoproteins (DEGs) with potential glycosylation sites on proteins were identified by 2-DE-based and iTRAQ labeling-based quantitation, demonstrating the outperformance of iTRAQ labeling-based quantitation over 2-DE. These DEGs exhibited distinctive compositions in functional categories from differentially expressed proteins in ESCC. Western blot analysis validated the up-regulation of total procathepsin D and high-mannose procathepsin D, and the down-regulation of total haptoglobin, high-mannose clusterin, and GlcNAc/sialic acid-containing fraction of 14-3-3ζ in ESCC tissues. The serum levels of glycosylated fractions of clusterin, proline-arginine-rich end leucine-rich repeat protein, and haptoglobin in patients with ESCC were remarkably higher than those in healthy controls.

Research conclusions

This study identified the aberrant N-linked glycoproteome associated with ESCC, which will be a valuable resource for future investigations.

Research perspectives

In-depth characterization of the composition and structure of glycans associated with proteins can shed more lights on biological insights and clinical relevance of the identified DEGs in ESCC.

FOOTNOTES

Author contributions: Qi YJ and Gao SG designed and coordinated the study; Liu QW, Ruan HJ, Chao WX, Li MX, Jiao YL, and Ward DG performed the experiments, and acquired and analyzed the data; Qi YJ and Ward DG wrote the manuscript; and all authors approved the final version of the article.

Supported by National Natural Science Foundation of China, No. 81072039 and No. 81872037.

Institutional review board statement: The study was approved by the Ethics Committee of the Medical School, Henan University, China (ethics ref: 108) and conducted in accordance with the ethical guidelines of the 1975 Declaration of Helsinki.

Conflict-of-interest statement: All authors report no relevant conflicts of interest for this article.

Data sharing statement: No additional data are available.

Open-Access: This article is an open-access article that was selected by an in-house editor and fully peer-reviewed by external reviewers. It is distributed in accordance with the Creative Commons Attribution NonCommercial (CC BY-NC 4.0) license, which permits others to distribute, remix, adapt, build upon this work non-commercially, and license their derivative works on different terms, provided the original work is properly cited and the use is non-commercial. See: https://creativecommons.org/Licenses/by-nc/4.0/

Country/Territory of origin: China

ORCID number: Qi-Wei Liu 0000-0002-7874-4056; Hao-Jie Ruan 0000-0002-3201-3864; Wei-Xia Chao 0000-0003-0700-658X; Meng-Xiang Li 0000-0002-6987-545X; Ye-Lin Jiao 0000-0002-4920-0738; Douglas G Ward 0000-0002-2328-1445; She-Gan Gao 0000-0002-7720-8729; Yi-Jun Qi 0000-0003-0239-5862.

S-Editor: Ma YJ
L-Editor: Wang TQ
P-Editor: Qi WW

REFERENCES

1 **Bray F**, Ferlay J, Soerjomataram I, Siegel RL, Torre LA, Jemal A. Global cancer statistics 2018: GLOBOCAN estimates of incidence and mortality worldwide for 36 cancers in 185 countries. *CA Cancer J Clin* 2018; **68**: 394-424 [PMID: 30207593 DOI: 10.3322/caac.21492]

2 **Abnet CC**, Arnold M, Wei WQ. Epidemiology of Esophageal Squamous Cell Carcinoma. *Gastroenterology* 2018; **154**: 360-373 [PMID: 28823862 DOI: 10.1053/j.gastro.2017.08.023]

3 **Song Y**, Li L, Ou Y, Gao Z, Li E, Li X, Zhang W, Wang J, Xu L, Zhou Y, Ma X, Liu L, Zhao Z, Huang X, Fan J, Dong L, Chen G, Ma L, Yang J, Chen L, He M, Li M, Zhuang X, Huang K, Qiu K, Yin G, Guo G, Feng Q, Chen P, Wu Z, Wu J, Zhao J, Luo L, Fu M, Xu B, Chen B, Li Y, Tong T, Wang M, Liu Z, Lin D, Zhang X, Yang H, Zhan Q. Identification of genomic alterations in oesophageal squamous cell cancer. *Nature* 2014; **509**: 91-95 [PMID: 24670651 DOI: 10.1038/nature13176]

4 **Zeng H**, Zheng R, Guo Y, Zhang S, Zou X, Wang N, Zhang L, Tang J, Chen J, Wei K, Huang S, Wang J, Yu L, Zhao D, Song G, Shen Y, Yang X, Gu X, Jin F, Li Q, Li Y, Ge H, Zhu F, Dong J, Guo G, Wu M, Du L, Sun X, He Y, Coleman MP, Baade P, Chen W, Yu XQ. Cancer survival in China, 2003-2005: a population-based study. *Int J Cancer* 2015; **136**: 1921-1930 [PMID: 25242378 DOI: 10.1002/ijc.29227]

5 **Wang GQ**, Jiao GG, Chang FB, Fang WH, Song JX, Lu N, Lin DM, Xie YQ, Yang L. Long-term results of operation for 420 patients with early squamous cell esophageal carcinoma discovered by screening. *Ann Thorac Surg* 2004; **77**: 1740-1744 [PMID: 15111177 DOI: 10.1016/j.athoracsur.2003.10.098]

6 **Pennathur A**, Gibson MK, Jobe BA, Luketich JD. Oesophageal carcinoma. *Lancet* 2013; **381**: 400-412 [PMID: 23374478 DOI: 10.1016/S0140-6736(12)60643-6]

7 **He Z**, Liu Z, Liu M, Guo C, Xu R, Li F, Liu A, Yang H, Shen L, Wu Q, Duan L, Li X, Zhang C, Pan Y, Cai H, Ke Y. Efficacy of endoscopic screening for esophageal cancer in China (ESECC): design and preliminary results of a population-based randomised controlled trial. *Gut* 2019; **68**: 198-206 [PMID: 29306867 DOI: 10.1136/gutjnl-2017-315520]

8 **Kosugi S**, Nishimaki T, Kanda T, Nakagawa S, Ohashi M, Hatakeyama K. Clinical significance of serum carcinoembryonic antigen, carbohydrate antigen 19-9, and squamous cell carcinoma antigen levels in esophageal cancer patients. *World J Surg* 2004; **28**: 680-685 [PMID: 15383868 DOI: 10.1007/s00268-004-6865-y]

9 **Mealy K**, Feely J, Reid I, McSweeney J, Walsh T, Hennessy TP. Tumour marker detection in oesophageal carcinoma. *Eur J Surg Oncol* 1996; **22**: 505-507 [PMID: 8903494 DOI: 10.1016/s0748-7983(96)92998-4]

10 **Shimada H**, Nabeya Y, Okazumi S, Matsubara H, Miyazawa Y, Shiratori T, Hayashi H, Gunji Y, Ochiai T. Prognostic significance of CYFRA 21-1 in patients with esophageal squamous cell carcinoma. *J Am Coll Surg* 2003; **196**: 573-578 [PMID: 12691934 DOI: 10.1016/s1072-7515(02)01905-1]

11 **Zheng X**, Xing S, Liu XM, Liu W, Liu D, Chi PD, Chen H, Dai SQ, Zhong Q, Zeng MS, Liu WL. Establishment of using serum YKL-40 and SCCA in combination for the diagnosis of patients with esophageal squamous cell carcinoma. *BMC Cancer* 2014; **14**: 490 [PMID: 25001061 DOI: 10.1186/1471-2407-14-490]

12 **Enzinger PC**, Mayer RJ. Esophageal cancer. *N Engl J Med* 2003; **349**: 2241-2252 [PMID: 14657432 DOI: 10.1056/NEJMra035010]

13 **Cui Y**, Chen H, Xi R, Cui H, Zhao Y, Xu E, Yan T, Lu X, Huang F, Kong P, Li Y, Zhu X, Wang J, Zhu W, Ma Y, Zhou Y, Guo S, Zhang L, Liu Y, Wang B, Xi Y, Sun R, Yu X, Zhai Y, Wang F, Yang J, Yang B, Cheng C, Liu J, Song B, Li H, Wang Y, Zhang Y, Cheng X, Zhan Q, Liu Z. Whole-genome sequencing of 508 patients identifies key molecular features associated with poor prognosis in esophageal squamous cell carcinoma. *Cell Res* 2020; **30**: 902-913 [PMID: 32398863 DOI: 10.1038/s41422-020-0333-6]

14 **Gao YB**, Chen ZL, Li JG, Hu XD, Shi XJ, Sun ZM, Zhang F, Zhao ZR, Li ZT, Liu ZY, Zhao YD, Sun J, Zhou CC, Yao R, Wang SY, Wang P, Sun N, Zhang BH, Dong JS, Yu Y, Luo M, Feng XL, Shi SS, Zhou F, Tan FW, Qiu B, Li N, Shao K, Zhang LJ, Xue Q, Gao SG, He J. Genetic landscape of esophageal squamous cell carcinoma. *Nat Genet* 2014; **46**: 1097-1102 [PMID: 25151357 DOI: 10.1038/ng.3076]

15 **Li J**, Chen Z, Tian L, Zhou C, He MY, Gao Y, Wang S, Zhou F, Shi S, Feng X, Sun N, Liu Z, Skogerboe G, Dong J, Yao R, Zhao Y, Sun J, Zhang B, Yu Y, Shi X, Luo M, Shao K, Li N, Qiu B, Tan F, Chen R, He J. LncRNA profile study reveals a three-lncRNA signature associated with the survival of patients with oesophageal squamous cell carcinoma. *Gut* 2014; **63**: 1700-1710 [PMID: 24522499 DOI: 10.1136/gutjnl-2013-305806]

16 **Cancer Genome Atlas Research Network**; Analysis Working Group: Asan University; BC Cancer Agency; Brigham and Women's Hospital; Broad Institute; Brown University; Case Western Reserve University; Dana-Farber Cancer Institute; Duke University; Greater Poland Cancer Centre; Harvard Medical School; Institute for Systems Biology; KU Leuven; Mayo Clinic; Memorial Sloan Kettering Cancer Center; National Cancer Institute; Nationwide Children's Hospital; Stanford University; University of Alabama; University of Michigan; University of North Carolina; University of Pittsburgh; University of Rochester; University of Southern California; University of Texas MD Anderson Cancer Center; University of Washington; Van Andel Research Institute; Vanderbilt University; Washington University; Genome Sequencing Center: Broad Institute; Washington University in St. Louis; Genome Characterization Centers: BC Cancer Agency; Broad Institute; Harvard Medical School; Sidney Kimmel Comprehensive Cancer Center at Johns Hopkins University; University of North Carolina; University of Southern California Epigenome Center; University of Texas MD Anderson Cancer Center; Van Andel Research Institute; Genome Data Analysis Centers: Broad Institute; Brown University:; Harvard Medical School; Institute for Systems Biology; Memorial Sloan Kettering Cancer Center; University of California Santa Cruz; University of Texas MD Anderson Cancer Center; Biospecimen Core Resource: International Genomics Consortium; Research Institute at Nationwide Children's Hospital; Tissue Source Sites: Analytic Biologic Services; Asan Medical Center; Asterand Bioscience; Barretos Cancer Hospital; BioreclamationIVT; Botkin Municipal Clinic; Chonnam National University Medical School; Christiana Care Health System; Cureline; Duke University; Emory University; Erasmus University; Indiana University School of Medicine; Institute of Oncology of Moldova; International Genomics Consortium; Invidumed; Israelitisches Krankenhaus Hamburg; Keimyung University School of Medicine; Memorial Sloan Kettering Cancer Center; National Cancer Center Goyang; Ontario Tumour Bank; Peter MacCallum Cancer Centre; Pusan National University Medical School; Ribeirão Preto Medical School; St. Joseph's Hospital &Medical Center; St. Petersburg Academic University; Tayside Tissue Bank; University of Dundee; University of Kansas Medical Center; University of Michigan; University of North Carolina at Chapel Hill; University of Pittsburgh School of Medicine; University of Texas MD Anderson Cancer Center; Disease Working Group: Duke University; Memorial Sloan Kettering Cancer Center; National Cancer Institute; University of Texas MD Anderson Cancer Center; Yonsei University College of

Medicine; Data Coordination Center: CSRA Inc; Project Team: National Institutes of Health. Integrated genomic characterization of oesophageal carcinoma. *Nature* 2017; **541**: 169-175 [PMID: 28052061 DOI: 10.1038/nature20805]

17 **Cao W**, Lee H, Wu W, Zaman A, McCorkle S, Yan M, Chen J, Xing Q, Sinnott-Armstrong N, Xu H, Sailani MR, Tang W, Cui Y, Liu J, Guan H, Lv P, Sun X, Sun L, Han P, Lou Y, Chang J, Wang J, Gao Y, Guo J, Schenk G, Shain AH, Biddle FG, Collisson E, Snyder M, Bivona TG. Multi-faceted epigenetic dysregulation of gene expression promotes esophageal squamous cell carcinoma. *Nat Commun* 2020; **11**: 3675 [PMID: 32699215 DOI: 10.1038/s41467-020-17227-z]

18 **Zhang B**, Whiteaker JR, Hoofnagle AN, Baird GS, Rodland KD, Paulovich AG. Clinical potential of mass spectrometry-based proteogenomics. *Nat Rev Clin Oncol* 2019; **16**: 256-268 [PMID: 30487530 DOI: 10.1038/s41571-018-0135-7]

19 **Gao Q**, Zhu H, Dong L, Shi W, Chen R, Song Z, Huang C, Li J, Dong X, Zhou Y, Liu Q, Ma L, Wang X, Zhou J, Liu Y, Boja E, Robles AI, Ma W, Wang P, Li Y, Ding L, Wen B, Zhang B, Rodriguez H, Gao D, Zhou H, Fan J. Integrated Proteogenomic Characterization of HBV-Related Hepatocellular Carcinoma. *Cell* 2019; **179**: 561-577.e22 [PMID: 31585088 DOI: 10.1016/j.cell.2019.08.052]

20 **Ohtsubo K**, Marth JD. Glycosylation in cellular mechanisms of health and disease. *Cell* 2006; **126**: 855-867 [PMID: 16959566 DOI: 10.1016/j.cell.2006.08.019]

21 **Mechref Y**, Hussein A, Bekesova S, Pungpapong V, Zhang M, Dobrolecki LE, Hickey RJ, Hammoud ZT, Novotny MV. Quantitative serum glycomics of esophageal adenocarcinoma and other esophageal disease onsets. *J Proteome Res* 2009; **8**: 2656-2666 [PMID: 19441788 DOI: 10.1021/pr8008385]

22 **Sethi MK**, Hancock WS, Fanayan S. Identifying N-Glycan Biomarkers in Colorectal Cancer by Mass Spectrometry. *Acc Chem Res* 2016; **49**: 2099-2106 [PMID: 27653471 DOI: 10.1021/acs.accounts.6b00193]

23 **Li CW**, Lim SO, Xia W, Lee HH, Chan LC, Kuo CW, Khoo KH, Chang SS, Cha JH, Kim T, Hsu JL, Wu Y, Hsu JM, Yamaguchi H, Ding Q, Wang Y, Yao J, Lee CC, Wu HJ, Sahin AA, Allison JP, Yu D, Hortobagyi GN, Hung MC. Glycosylation and stabilization of programmed death ligand-1 suppresses T-cell activity. *Nat Commun* 2016; **7**: 12632 [PMID: 27572267 DOI: 10.1038/ncomms12632]

24 **Qi YJ**, Ward DG, Pang C, Wang QM, Wei W, Ma J, Zhang J, Lou Q, Shimwell NJ, Martin A, Wong N, Chao WX, Wang M, Ma YF, Johnson PJ. Proteomic profiling of N-linked glycoproteins identifies ConA-binding procathepsin D as a novel serum biomarker for hepatocellular carcinoma. *Proteomics* 2014; **14**: 186-195 [PMID: 24259486 DOI: 10.1002/pmic.201300226]

25 **Alper J**. Glycobiology. Turning sweet on cancer. *Science* 2003; **301**: 159-160 [PMID: 12855785 DOI: 10.1126/science.301.5630.159]

26 **Varki A**. Biological roles of oligosaccharides: all of the theories are correct. *Glycobiology* 1993; **3**: 97-130 [PMID: 8490246 DOI: 10.1093/glycob/3.2.97]

27 **Hakomori S**. Tumor malignancy defined by aberrant glycosylation and sphingo(glyco)lipid metabolism. *Cancer Res* 1996; **56**: 5309-5318 [PMID: 8968075 DOI: 10.1097/00002820-199612000-00006]

28 **Kobata A**. A retrospective and prospective view of glycopathology. *Glycoconj J* 1998; **15**: 323-331 [PMID: 9613818 DOI: 10.1023/a:1006961532182]

29 **Xu Q**, Isaji T, Lu Y, Gu W, Kondo M, Fukuda T, Du Y, Gu J. Roles of N-acetylglucosaminyltransferase III in epithelial-to-mesenchymal transition induced by transforming growth factor β1 (TGF-β1) in epithelial cell lines. *J Biol Chem* 2012; **287**: 16563-16574 [PMID: 22451656 DOI: 10.1074/jbc.M111.262154]

30 **Liwosz A**, Lei T, Kukuruzinska MA. N-glycosylation affects the molecular organization and stability of E-cadherin junctions. *J Biol Chem* 2006; **281**: 23138-23149 [PMID: 16682414 DOI: 10.1074/jbc.M512621200]

31 **Zhao Y**, Nakagawa T, Itoh S, Inamori K, Isaji T, Kariya Y, Kondo A, Miyoshi E, Miyazaki K, Kawasaki N, Taniguchi N, Gu J. N-acetylglucosaminyltransferase III antagonizes the effect of N-acetylglucosaminyltransferase V on alpha3beta1 integrin-mediated cell migration. *J Biol Chem* 2006; 281: 32122-32130 [PMID: 16940045 DOI: 10.1074/jbc.M607274200]

32 **Kim JH**, Jun KH, Jung H, Park IS, Chin HM. Prognostic Value of Preoperative Serum Levels of Five Tumor Markers (Carcinoembryonic Antigen, CA19-9, Alpha-fetoprotein, CA72-4, and CA125) in Gastric Cancer. *Hepatogastroenterology* 2014; **61**: 863-869 [PMID: 26176088 DOI: 10.5754/hge131018]

33 **Terzi H**, Kale E, Kale A, Turkay U, Chong GO, Lee YS. New method: Are tumor markers in vaginal-washing fluid significant in the diagnosis of primary ovarian carcinoma? *Eur J Gynaecol Oncol* 2015; **36**: 560-563 [PMID: 26513883 DOI: 10.12892/ejgo2743.2015]

34 **Zhang D**, Yu M, Xu T, Xiong B. Predictive value of serum CEA, CA19-9 and CA125 in diagnosis of colorectal liver metastasis in Chinese population. *Hepatogastroenterology* 2013; **60**: 1297-1301 [PMID: 23933921 DOI: 10.5754/hge121125]

35 **Kumada T**, Nakano S, Takeda I, Kiriyama S, Sone Y, Hayashi K, Katoh H, Endoh T, Sassa T, Satomura S. Clinical utility of Lens culinaris agglutinin-reactive alpha-fetoprotein in small hepatocellular carcinoma: special reference to imaging diagnosis. *J Hepatol* 1999; **30**: 125-130 [PMID: 9927159 DOI: 10.1016/s0168-8278(99)80016-6]

36 **Qi Y**, Chiu JF, Wang L, Kwong DL, He QY. Comparative proteomic analysis of esophageal squamous cell carcinoma. *Proteomics* 2005; **5**: 2960-2971 [PMID: 15986332 DOI: 10.1002/pmic.200401175]

37 **Gao SG**, Liu RM, Zhao YG, Wang P, Ward DG, Wang GC, Guo XQ, Gu J, Niu WB, Zhang T, Martin A, Guo ZP, Feng XS, Qi YJ, Ma YF. Integrative topological analysis of mass spectrometry data reveals molecular features with clinical relevance in esophageal squamous cell carcinoma. *Sci Rep* 2016; **6**: 21586 [PMID: 26898710 DOI: 10.1038/srep21586]

38 **Merico D**, Isserlin R, Stueker O, Emili A, Bader GD. Enrichment map: a network-based method for gene-set enrichment visualization and interpretation. *PLoS One* 2010; **5**: e13984 [PMID: 21085593 DOI: 10.1371/journal.pone.0013984]

39 **Liebermeister W**, Noor E, Flamholz A, Davidi D, Bernhardt J, Milo R. Visual account of protein investment in cellular functions. *Proc Natl Acad Sci U S A* 2014; **111**: 8488-8493 [PMID: 24889604 DOI: 10.1073/pnas.1314810111]

40 **Pawar H**, Kashyap MK, Sahasrabuddhe NA, Renuse S, Harsha HC, Kumar P, Sharma J, Kandasamy K, Marimuthu A, Nair B, Rajagopalan S, Maharudraiah J, Premalatha CS, Kumar KV, Vijayakumar M, Chaerkady R, Prasad TS, Kumar RV, Pandey A. Quantitative tissue proteomics of esophageal squamous cell carcinoma for novel biomarker discovery. *Cancer Biol Ther* 2011; **12**: 510-522 [PMID: 21743296 DOI: 10.4161/cbt.12.6.16833]

41 **Zhang Y**, Zhu J, Yin H, Marrero J, Zhang XX, Lubman DM. ESI-LC-MS Method for Haptoglobin Fucosylation Analysis

in Hepatocellular Carcinoma and Liver Cirrhosis. *J Proteome Res* 2015; **14**: 5388-5395 [PMID: 26503433 DOI: 10.1021/acs.jproteome.5b00792]

42 **Darebna P**, Novak P, Kucera R, Topolcan O, Sanda M, Goldman R, Pompach P. Changes in the expression of N- and O-glycopeptides in patients with colorectal cancer and hepatocellular carcinoma quantified by full-MS scan FT-ICR and multiple reaction monitoring. *J Proteomics* 2017; **153**: 44-52 [PMID: 27646713 DOI: 10.1016/j.jprot.2016.09.004]

43 **Ahn JM**, Sung HJ, Yoon YH, Kim BG, Yang WS, Lee C, Park HM, Kim BJ, Lee SY, An HJ, Cho JY. Integrated glycoproteomics demonstrates fucosylated serum paraoxonase 1 alterations in small cell lung cancer. *Mol Cell Proteomics* 2014; **13**: 30-48 [PMID: 24085812 DOI: 10.1074/mcp.M113.028621]

44 **Lin Z**, Yin H, Lo A, Ruffin MT, Anderson MA, Simeone DM, Lubman DM. Label-free relative quantification of alpha-2-macroglobulin site-specific core-fucosylation in pancreatic cancer by LC-MS/MS. *Electrophoresis* 2014; **35**: 2108-2115 [PMID: 24285556 DOI: 10.1002/elps.201300376]

45 **Christiansen MN**, Chik J, Lee L, Anugraham M, Abrahams JL, Packer NH. Cell surface protein glycosylation in cancer. *Proteomics* 2014; **14**: 525-546 [PMID: 24339177 DOI: 10.1002/pmic.201300387]

46 **Ghosh D**, Krokhin O, Antonovici M, Ens W, Standing KG, Beavis RC, Wilkins JA. Lectin affinity as an approach to the proteomic analysis of membrane glycoproteins. *J Proteome Res* 2004; **3**: 841-850 [PMID: 15359739 DOI: 10.1021/pr049937f]

47 **Lee A**, Kolarich D, Haynes PA, Jensen PH, Baker MS, Packer NH. Rat liver membrane glycoproteome: enrichment by phase partitioning and glycoprotein capture. *J Proteome Res* 2009; **8**: 770-781 [PMID: 19125615 DOI: 10.1021/pr800910w]

48 **Hanahan D**, Weinberg RA. Hallmarks of cancer: the next generation. *Cell* 2011; **144**: 646-674 [PMID: 21376230 DOI: 10.1016/j.cell.2011.02.013]

49 **Ganapathy-Kanniappan S**. Molecular intricacies of aerobic glycolysis in cancer: current insights into the classic metabolic phenotype. *Crit Rev Biochem Mol Biol* 2018; **53**: 667-682 [PMID: 30668176 DOI: 10.1080/10409238.2018.1556578]

50 **Fischer K**, Hoffmann P, Voelkl S, Meidenbauer N, Ammer J, Edinger M, Gottfried E, Schwarz S, Rothe G, Hoves S, Renner K, Timischl B, Mackensen A, Kunz-Schughart L, Andreesen R, Krause SW, Kreutz M. Inhibitory effect of tumor cell-derived lactic acid on human T cells. *Blood* 2007; **109**: 3812-3819 [PMID: 17255361 DOI: 10.1182/blood-2006-07-035972]

51 **Kumagai S**, Koyama S, Itahashi K, Tanegashima T, Lin YT, Togashi Y, Kamada T, Irie T, Okumura G, Kono H, Ito D, Fujii R, Watanabe S, Sai A, Fukuoka S, Sugiyama E, Watanabe G, Owari T, Nishinakamura H, Sugiyama D, Maeda Y, Kawazoe A, Yukami H, Chida K, Ohara Y, Yoshida T, Shinno Y, Takeyasu Y, Shirasawa M, Nakama K, Aokage K, Suzuki J, Ishii G, Kuwata T, Sakamoto N, Kawazu M, Ueno T, Mori T, Yamazaki N, Tsuboi M, Yatabe Y, Kinoshita T, Doi T, Shitara K, Mano H, Nishikawa H. Lactic acid promotes PD-1 expression in regulatory T cells in highly glycolytic tumor microenvironments. *Cancer Cell* 2022; **40**: 201-218.e9 [PMID: 35090594 DOI: 10.1016/j.ccell.2022.01.001]

52 **Choi H**, Ko Y, Lee CY. Pro-cathepsin D as a diagnostic marker in differentiating malignant from benign pleural effusion: a retrospective cohort study. *BMC Cancer* 2020; **20**: 825 [PMID: 32867726 DOI: 10.1186/s12885-020-07327-w]

53 **Okuyama N**, Ide Y, Nakano M, Nakagawa T, Yamanaka K, Moriwaki K, Murata K, Ohigashi H, Yokoyama S, Eguchi H, Ishikawa O, Ito T, Kato M, Kasahara A, Kawano S, Gu J, Taniguchi N, Miyoshi E. Fucosylated haptoglobin is a novel marker for pancreatic cancer: a detailed analysis of the oligosaccharide structure and a possible mechanism for fucosylation. *Int J Cancer* 2006; **118**: 2803-2808 [PMID: 16385567 DOI: 10.1002/ijc.21728]

54 **Park SY**, Yoon SJ, Jeong YT, Kim JM, Kim JY, Bernert B, Ullman T, Itzkowitz SH, Kim JH, Hakomori SI. N-glycosylation status of beta-haptoglobin in sera of patients with colon cancer, chronic inflammatory diseases and normal subjects. *Int J Cancer* 2010; **126**: 142-155 [PMID: 19551866 DOI: 10.1002/ijc.24685]

World Journal of Gastroenterology

Submit a Manuscript: https://www.f6publishing.com

World J Gastroenterol 2022 August 7; 28(29): 3886-3902

DOI: 10.3748/wjg.v28.i29.3886

ISSN 1007-9327 (print) ISSN 2219-2840 (online)

ORIGINAL ARTICLE

Basic Study

HP0953 - hypothetical virulence factor overexpresion and localization during *Helicobacter pylori* infection of gastric epithelium

Nancy K Arteaga-Resendiz, Gerardo E Rodea, Rosa María Ribas-Aparicio, Alma L Olivares-Cervantes, Juan Arturo Castelán-Vega, José de Jesús Olivares-Trejo, Sandra Mendoza-Elizalde, Edgar O López-Villegas, Christian Colín, Pamela Aguilar-Rodea, Alfonso Reyes-López, Marcela Salazar García, Norma Velázquez-Guadarrama

Specialty type: Gastroenterology and hepatology

Provenance and peer review: Invited article; Externally peer reviewed

Peer-review model: Single blind

Peer-review report's scientific quality classification

Grade A (Excellent): 0
Grade B (Very good): B
Grade C (Good): C, C
Grade D (Fair): 0
Grade E (Poor): 0

P-Reviewer: Keikha M, Iran; Kirkik D, Turkey; Mi Y, China

Received: January 29, 2022
Peer-review started: January 29, 2022
First decision: April 10, 2022
Revised: April 26, 2022
Accepted: July 11, 2022
Article in press: July 11, 2022
Published online: August 7, 2022

Nancy K Arteaga-Resendiz, Gerardo E Rodea, Alma L Olivares-Cervantes, Sandra Mendoza-Elizalde, Christian Colín, Pamela Aguilar-Rodea, Norma Velázquez-Guadarrama, Laboratorio de Investigación en Enfermedades Infecciosas, Hospital Infantil de México Federico Gómez, Mexico City 06720, Mexico

Nancy K Arteaga-Resendiz, Rosa María Ribas-Aparicio, Juan Arturo Castelán-Vega, Posgrado en Biomedicina y Biotecnología Molecular, Laboratorio de Producción y Control de Biológicos, Escuela Nacional de Ciencias Biológicas, Instituto Politécnico Nacional, Mexico City 11340, Mexico

José de Jesús Olivares-Trejo, Laboratorio de Adquisición de Hierro, Universidad Autónoma de la Ciudad México, Posgrado Ciencias Genómica, Mexico City 03100, Mexico

Edgar O López-Villegas, Laboratorio Central de Microscopía, Escuela Nacional de Ciencias Biol ógicas, Instituto Politécnico Nacional, Mexico City 11340, Mexico

Alfonso Reyes-López, Centro de estudios económicos y sociales en salud, Hospital Infantil de M éxico Federico Gómez, Mexico City 06720, Mexico

Marcela Salazar García, Laboratorio de Investigación en Biología del Desarrollo y Teratogénesis Experimental, Hospital Infantil de México Federico Gómez, Mexico City 06720, Mexico

Corresponding author: Norma Velázquez-Guadarrama, PhD, Research Scientist, Laboratorio de Investigación en Enfermedades Infecciosas, Hospital Infantil de México Federico Gómez, Dr. Márquez 162, Col. Doctores, Alcaldía Cuauhtémoc, Mexico City 06720, Mexico.
normave@himfg.edu.mx

Abstract

BACKGROUND

The high prevalence and persistence of *Helicobacter pylori* (*H. pylori*) infection, as well as the diversity of pathologies related to it, suggest that the virulence factors used by this microorganism are varied. Moreover, as its proteome contains 340 hypothetical proteins, it is important to investigate them to completely understand the mechanisms of its virulence and survival. We have previously

reported that the hypothetical protein HP0953 is overexpressed during the first hours of adhesion to inert surfaces, under stress conditions, suggesting its role in the environmental survival of this bacterium and perhaps as a virulence factor.

AIM

To investigate the expression and localization of HP0953 during adhesion to an inert surface and against gastric (AGS) cells.

METHODS

Expression analysis was performed for *HP0953* during *H. pylori* adhesion. *HP0953* expression at 0, 3, 12, 24, and 48 h was evaluated and compared using the Kruskal-Wallis equality-of-populations rank test. Recombinant protein was produced and used to obtain polyclonal antibodies for immunolocalization. Immunogold technique was performed on bacterial sections during adherence to inert surfaces and AGS cells, which was analyzed by transmission electron microscopy. HP0953 protein sequence was analyzed to predict the presence of a signal peptide and transmembrane helices, both provided by the ExPASy platform, and using the GLYCOPP platform for glycosylation sites. Different programs, *via*, I-TASSER, RaptorX, and HHalign-Kbest, were used to perform three-dimensional modeling.

RESULTS

HP0953 exhibited its maximum expression at 12 h of infection in gastric epithelium cells. Immunogold technique revealed HP0953 localization in the cytoplasm and accumulation in some peripheral areas of the bacterial body, with greater expression when it is close to AGS cells. Bioinformatics analysis revealed the presence of a signal peptide that interacts with the transmembrane region and then allows the release of the protein to the external environment. The programs also showed a similarity with the Tip-alpha protein of *H. pylori*. Tip-alpha is an exotoxin that penetrates cells and induces tumor necrosis factor alpha production, and HP0953 could have a similar function as posttranslational modification sites were found; modifications in turn require enzymes located in eukaryotic cells. Thus, to be functional, HP0953 may necessarily need to be translocated inside the cell where it can trigger different mechanisms producing cellular damage.

CONCLUSION

The location of HP0953 around infected cells, the probable posttranslational modifications, and its similarity to an exotoxin suggest that this protein is a virulence factor.

Key Words: Hypothetical protein HP0953; Adherence; *Helicobacter pylori*; Glycocalyx; Virulence factor; Persistence

©The Author(s) 2022. Published by Baishideng Publishing Group Inc. All rights reserved.

Core Tip: The high prevalence and persistence of *Helicobacter pylori* infection and the diverse pathologies associated with it suggest that the virulence factors of this microorganism are varied. Moreover, its proteome contains 340 hypothetical proteins, so it is crucial to investigate them to elucidate the mechanisms of its virulence and survival. We studied the hypothetical protein HP0953, its location around infected cells, and the probable posttranslational modifications. Its similarity to an exotoxin suggests that HP0953 is a virulence factor.

Citation: Arteaga-Resendiz NK, Rodea GE, Ribas-Aparicio RM, Olivares-Cervantes AL, Castelán-Vega JA, Olivares-Trejo JJ, Mendoza-Elizalde S, López-Villegas EO, Colín C, Aguilar-Rodea P, Reyes-López A, Salazar García M, Velázquez-Guadarrama N. HP0953 - hypothetical virulence factor overexpresion and localization during *Helicobacter pylori* infection of gastric epithelium. *World J Gastroenterol* 2022; 28(29): 3886-3902
URL: https://www.wjgnet.com/1007-9327/full/v28/i29/3886.htm
DOI: https://dx.doi.org/10.3748/wjg.v28.i29.3886

INTRODUCTION

The estimated prevalence of *Helicobacter pylori* (*H. pylori*) infection is 70% in developing countries and 30%-40% in the United States and other industrialized countries[1]. However, not all people infected with this bacterium have symptoms. *H. pylori* has been associated with gastroduodenal diseases and it is

considered the major risk factor for the development of gastric cancer[2]. *H. pylori* colonizes the gastric mucosa, adhering to the mucous epithelial cells and to the mucous layer that covers the gastric epithelium. Adherence to gastric cells is the first step in establishing an infection and for successful colonization, the bacterium releases various effector proteins/toxins[3-5].

Upon colonization, the pathogenic mechanism of *H. pylori* is mediated by virulence factors such as flagella and the ability to form a biofilm (both *in vitro* and *in vivo*)[6]. Biofilm formation enhances the ability of microorganisms to survive in a hostile environment, which would cause and exacerbate infections, rather than extend them, resulting in chronicity[7]. The glycocalyx participates in adhesion to inert surfaces, allowing biofilm formation but also participates in cell attachment; the major components of the glycocalyx are glycans and may contain digestive proteins or secreted virulence factors[8,9]. *H. pylori* secretes various virulence factors, including urease, cag pathogenicity island proteins, hemagglutinin, Lewis antigens (Le^x and Le^y), BabA CagA, and VacA[10-12]. All these virulence factors have been extensively investigated elsewhere.

Furthermore, *H. pylori* contains hypothetical proteins, some of which are secreted particularly in the context of interactions with the host. The bacterium uses a set of secreted and translocated proteins to adapt itself to the mucosal environment[13]. *H. pylori* possesses a relatively small genome of < 1.6 Mb [14,15] compared with other gram-negative prokaryotes, such as *Escherichia coli*, whose genome is > 4.5 Mb[16]. Despite its small size, an ineligible fraction of *H. pylori* proteins, possibly 30%-40%, are annotated as "hypothetical proteins". Using bioinformatics tools, Naqvi *et al*[17] and Zanotti and Cendron[18] respectively analyzed 340 hypothetical proteins of *H. pylori* 26695. The function of some of these proteins can be hypothesized based on a weak homology with proteins of other bacteria, whereas most proteins do not exhibit similarities with others, and their function cannot be predicted[17,18].

HP0953 is a hypothetical and uncharacterized protein of *H. pylori* secretome; it lacks conserved domains but, interestingly, is present in all *H. pylori* strains whose genomes have been sequenced, as well as in *H. acinonychis* that colonizes the gastric mucosa of large felines. The closely related *H. hepaticus* and *Campylobacter jejuni* lack HP0953 homologs, suggesting that HP0953 is unique to the gastric *Helicobacter* species[11]. Moreover, we previously observed that this protein is overexpressed during adhesion to inert surfaces under stress conditions. Most of the possible effects of secreted proteins on the host have yet to be discovered. In addition, secreted factors represent eligible proteins for identifying promising targets for the development of new antimicrobial drugs[17,18].

In recent years, there has been an increasing importance on *H. pylori*; on the one hand when it is present, it is associated with gastric disease, and on the other hand, it is associated with gastroduodenal reflux, food allergy, and asthma when it is absent[19]. This dual role in the human microbiota emphasizes the need for further characterization of the hypothetical proteins already described. In this study, the location of the protein is determined for the first time, inside and outside the bacterium, and we predict some biochemical characteristics, through *in silico* analysis that contribute toward understanding the importance of this hypothetical protein to the microorganism in the establishment of infection, its role in such infection, or colonization of the host.

MATERIALS AND METHODS

In silico analysis of HP0953 protein

We obtained the amino acid sequence of HP0953 (accession number NP_207745) from the National Center for Biotechnology Information database[20]. Then, we used the Pfam database to analyze the HP0953 sequence and search for conserved domains or homologous regions present in other proteins [21].

Signal peptide prediction

The amino acid sequence of HP0953 was analyzed using the SignalP-4.1 tool provided by the ExPASy platform to predict the presence of a signal peptide[22].

Prediction of transmembrane helices and glycosylation sites

The amino acid sequence previously obtained was analyzed to predict transmembrane helices using the TM pred tool provided by the ExPASy platform[23,24]. The glycosylation sites were investigated using the GLYCOPP platform[25].

Three-dimensional modeling of HP0953 protein

To explore the remote homologs that could be used as a template for modeling, we used the HHpred tool that uses the HMM comparison[26]. Different programs such as I-TASSER[27], RaptorX[28], and HHalign-Kbest[29] were used to perform three-dimensional (3D) modeling.

Strain, cell culture, and extraction of genomic DNA from H. pylori

H. pylori strain 26695 was cultured on Casman agar (Dibico; Mexico) supplemented with 5% sheep

erythrocytes and incubated in an atmosphere of 50 mL/L CO_2 and 37 °C for 48 h. The culture was harvested for infected human against gastric (AGS) cell-line assay and genomic DNA extraction. Genomic DNA extraction was performed according to the protocol established for the Wizard kit (Promega; United States) by its manufacturer.

Amplification and purification of HP0953

HP0953 was amplified by polymerase chain reaction (PCR) using *H. pylori* genomic DNA as the template. To amplify the complete gene, 50 µL of reaction mixture was prepared as follows: 1.25 U polymerase GoTaq®, 0.2 mmol/L dATP, 0.2 mmol/L dGTP, 0.2 mmol/L dCTP, 0.2 mmol/L dTTP, 1.5 mmol/L $MgCl_2$ (Promega), HP0953F oligonucleotide (25 pmol) (5'-GGGGGATCCATG-GTTTTAATCGCTCTTTTAGGGGTG-3'), HP0953R oligonucleotide (25 pmol) (5'-GGGGTCGACCCT-TAACGCACAAACGCTACC-3'), and *H. pylori* 26695 DNA (250 ng). For amplification of the gene without the signal peptide, the same PCR was performed substituting the oligonucleotide HP0953F by HP095WSPF (5'-GGGGGATCCGTCTCTGATTTAAAGGGCATG-3'). The amplification cycle consisted of 94 °C for 1 min, followed by 30 cycles at 94 °C for 30 s, 68.4 °C for 30 s, 72 °C for 1 min, and a final step at 72 °C for 7 min. Both PCR products (555 and 474 bp) were purified using the protocol established by Promega for using the Wizard® SV gel and the PCR Clean-Up System (Promega).

Cloning of the complete and without-signal peptide hp0953

Complete *HP0953* and its version without the signal peptide were inserted into the vector pJET1.2 (Thermo Scientific; Lithuania) according to the manufacturer's instructions to obtain the recombinant pJET-HP0953 and pJET-HP0953WSP plasmids, respectively. Chemically competent DH5α cells of *Escherichia coli* (*E. coli*) were transformed with each plasmid by thermal shock[30,31]. The recombinant colonies were selected in LB agar (Sigma-Aldrich; MO) containing 100 µg/mL ampicillin. The plasmids were extracted using the illustra™ plasmidPrep Mini Spin Kit (GE Healthcare; United Kingdom).

The pJET-HP0953 and pJET-HP0953WSP plasmids were digested with the fast restriction enzymes BamHI and Sal I according to the manufacturer's instructions (Thermo Scientific) to free both versions of *HP0953*. Restriction products were purified using the protocol established by Promega for the Wizard® SV gel and the PCR Clean-Up System. DNA fragments were ligated into the expression vectors pET28a(+) (Novagen, United States) for the complete *HP0953* and pGEX-6p-2 (GE Healthcare) for the version without the signal peptide. The vectors were digested with the same enzymes and treated with alkaline phosphatase (Thermo Scientific). The Rapid DNA Ligation Kit (Thermo Scientific) was used to obtain the recombinant pET-HP0953 and pGEX-HP0953WSP plasmids. Chemically competent DH5α cells of *E. coli* were transformed with each plasmid by thermal shock. The recombinant colonies were selected in LB agar containing 50 µg/mL kanamycin for pET-HP0953 or 100 µg/mL ampicillin for pGEX-HP0953WSP. The plasmids were extracted using the illustra™ plasmidPrep Mini Spin Kit (GE Healthcare) and analyzed by PCR. DNA inserts in the recombinant plasmids were characterized by sequencing; for this purpose, PCRs were performed as described earlier using the following primers: T7F (5'-TAATACGACTCACTATAGGG-3') and T7R (5'-GCTAGTTATTGCTCAGCG-3') for pET-HP0953 and HP095WSPF (5'-GGGGGATCCGTCTCTGATTTAAAGGGCATG-3') and HP0953R (5'-GGGGTCGACCCTTAACGCACAAACGCTACC-3') for pGEX-HP0953WSP. The annealing temperature was 68.4 °C for pET-HP0953 and 60 °C for pGEX-HP0953WSP. The PCR products were purified as described earlier and sequenced by Synthesis and Sequencing Unit, Institute of Biotechnology, Universidad Nacional Autónoma de México. Chemically competent BL21 pLysS cells of *E. coli* were transformed with each recombinant plasmid and the empty plasmids by thermal shock[31]. The recombinant colonies were selected in LB agar containing the corresponding antibiotic.

Expression and purification of HP0953 protein

The HP0953 protein was expressed according to the manufacturer's instructions for pET28a(+) and pGEX-6p-2 vectors using 1 mmol/L IPTG (Sigma-Aldrich) and incubating the *E. coli* pET28a(+)/pET-HP0953-transformed cells for 16 h at 30 °C to obtain the recombinant protein His-HP0953 and the *E. coli* pGEX-6p-2/pGEX-HP0953WSP-transformed cells for 3 h at 37 °C to obtain the recombinant protein GST-HP0953WSP. The inclusion bodies were extracted as described in the inclusion body preparation method without solubilizing the inclusion bodies in a denaturing agent[32]. The cell pellet was resuspended in 1 mL of 4 × sample buffer. Aliquots were collected throughout the process and analyzed by sodium dodecyl sulfate-polyacrylamide gel electrophoresis (SDS-PAGE) and western blot assays. The inclusion bodies were electrophoresed on SDS-PAGE, and the recombinant protein band was purified by electroelution. The glutathione-S-transferase (GST)-HP0953WSP recombinant protein was used to produce polyclonal antibodies, as described later, and the His-HP0953 protein was used to purify antibodies.

Production of polyclonal anti-GST-HP0953WSP

Anti-GST-HP0953WSP antibodies were obtained by immunization of a New Zealand rabbit (2 mo age) according to the Howard and Bethell method[33] (approved by the Bioethics Committee of the Hospital Infantil de México Federico Gómez).

Purification of polyclonal anti-HP0953

Purification of polyclonal antibody was performed by immunoadsorption. The His-HP0953 protein was subjected to SDS-PAGE on preparative gels. The bands were transferred onto a polyvinylidene fluoride (PVDF) membrane (Millipore; United States), which was blocked with 0.5% bovine serum albumin (BSA) and washed with phosphate buffer solution (PBS)-Tween. Serum was diluted 1:100 in PBS-Tween, incubated with the membrane for 2 h under stirring at room temperature, and washed with PBS-Tween; then, the membrane was incubated with 0.02 M glycine-HCl (pH 2.2) for 10 min at room temperature. Finally, 1 M Tris base (pH 9.1) was added. The antibody was recovered and stored at -20 °C. Nonpurified antisera and purified antibodies were tested against a total extract of *H. pylori*, and the two purified recombinant proteins were evaluated by western blotting using the same PVDF membrane, which was stripped between each test[34].

Construction of plasmid pBlue-5CM3 for site-directed mutagenesis of the HP0953 gene in H. pylori

The chloramphenicol resistance gene was obtained from the pLysS plasmid of the *E. coli* BL21 (DE3) pLysS strain by PCR, for which 50 µL of reaction mix was prepared, consisting of 1 × HF Fusion buffer (Thermo Scientific); 0.2 mmol/L each of dATP, dGTP, dCTP, and dTTP (Promega); 6 pmol each of primer CMF (5′-GGG AGATCTTTACGCCCCGCCCTG-3′) and CMR (5′-GGGCATATGATG-GAGAAAAAAATCACTGG-3′); plasmid pLysS (250 ng); and Phusion DNA Polymerase (1 U) (Thermo Scientific). The CMF and CMR primers contain restriction sites for *Bgl*II and *Nde*I, respectively. The amplification program consisted of initial denaturation at 98 °C for 30 s; 35 cycles of denaturation at 98 °C for 10 s, primer annealing at 65 °C for 30 s, and extension at 72 °C for 1 min; and a final extension at 72 °C for 7 min.

The 5′ and 3′ fragments of the *HP0953* gene were obtained from the plasmid pJET-HP0953, constructed above by PCR. To amplify the 5′ fragment, 50 µL of the reaction mixture was prepared, consisting of GoTaq DNA polymerase (Promega) (1.25 U); 0.2 mmol/L each of dATP, dGTP, dCTP, and dTTP; 1.5 mmol/L $MgCl_2$ (Promega); primer HP0953F (25 pmol) (5′-GGGGGATCCATG-GTTTTAATCGCTCTTTTAGGGGTG-3′); primer HP0953R (5′-GGGAGATCTCATGGAATTGCTCCAT-GAAGCG-3′); and plasmid DNA from pJET-HP0953 (250 ng). The amplification program consisted of initial denaturation at 94 °C for 1 min; 35 cycles of denaturation at 94 °C for 30 s, primer annealing at 68.4 °C for 30 s, and extension at 72 °C for 30 s; and a final extension at 72 °C for 7 min. To amplify the 3′ fragment, PCR was performed under the same conditions but using the primers HP0953F (5′-GGGCATATGAGTCCGAGCAGACGACTACG-3′) and HP0953R (5′-GGGGTCGACCTACCT-TAACGCACAAACGCTACC-3′). Amplicons of 304 and 248 bp were obtained, respectively.

We subjected 5 µL of each amplification product to 1.5% agarose gel electrophoresis at 85 volts for 75 min. Then, we stained the gel with ethidium bromide (Sigma-Aldrich) and observed the bands under ultraviolet light. Upon confirmation of the amplified product, the remainder was purified using a Wizard SV Gel and PCR Clean-up System, as per the manufacturer's protocol. Each fragment was inserted into a pJET1.2 vector. The ligation reaction of each fragment in the pJET1.2 vector consisted of 1 × reaction buffer, 0.15 pmol purified PCR product (5′ fragment, 3′ fragment, or chloramphenicol resistance gene; 0.15 pmol), pJET1.2/Blunt Cloning Vector (0.05 pmol), and T4 DNA ligase (5 U). The reaction mixture was incubated at 22 °C for 20 min.

After ligation, we used heat shock treatment to transform 50 µL of competent *E. coli* DH5α cells with each plasmid[31]. Then, they were centrifuged at 5000 × g for 1 min, the supernatant was decanted, and the pellet was resuspended in the residual medium. Subsequently, the bacterial suspension was seeded on LB agar plates containing ampicillin (100 µg/mL; Sigma-Aldrich) and incubated at 37 °C for 18-24 h to select the recombinant clones. Following incubation, we selected five colonies from the plate and resuspended them in 2 mL of LB broth (Sigma-Aldrich) containing ampicillin (100 µg/mL), and the plasmid was extracted using the alkaline lysis method[35]. We quantified the plasmid DNA using an Epoch microplate spectrophotometer (Biotek Instruments, Inc.; United States) and stored it at -20 °C.

We performed three PCR assays to verify the sequence of the cloned fragments. Each PCR reaction was performed in a final volume of 20 µL, consisting of 1 × HF Fusion buffer (Thermo Scientific); 0.2 mmol/L each of dATP, dGTP, dCTP, and dTTP (Thermo Scientific); primer pJET1.2F (0.2 µM) (5′-CGACTCACTATAGGGAGAGCGGC-3′) (Thermo Scientific); primer pJET1.2R (0.2 µM) (5′-AAGAACATCGATTTTCCATGGCAG-3′) (Thermo Scientific); plasmid DNA (100 ng/µL) (pJET-CM, pJET-5′ or pJET-3′); and Phusion DNA polymerase (Thermo Scientific) (0.4 U). The amplification program consisted of initial denaturation at 98 °C for 30 s; 35 cycles of 98 °C for 10 s, 68 °C for 30 s, and 72 °C for 30 s; and a final extension at 72 °C for 7 min. The PCR products were sequenced by Macrogen (Seoul, Korea).

The 5′ fragments, 3′ fragments, and the chloramphenicol resistance gene were obtained from the plasmids previously constructed by enzymatic digestion. *Bam*HI and *Bgl*II were used for the 5′ fragment, *Nde*I and *Sal*I for the 3′ fragment, and *Bgl*II and *Nde*I for the chloramphenicol resistance gene, according to the above-described digestion protocols. The fragments were inserted into the pBluescript II KS+ vector (Agilent Technologies, Inc.; United States), which allows for the synthesis of ssDNA and has an ampicillin resistance gene to facilitate selection following the above-described protocols.

E. coli XL1-blue MRF' cells were transformed with the constructed vector (pBlue-5CM3) using heat shock treatment and selected following culture on LB agar plates (Sigma-Aldrich) with 100 μg/mL of ampicillin[31]. The plasmid was extracted using alkaline lysis[35], and fragment insertion was verified by automated sequencing. *H. pylori* was transformed with the plasmid using electroporation[36]. The mutant *H. pylori* strain was cultured on Casman agar supplemented with 5% sheep erythrocytes and incubated in an atmosphere of 50 mL/L CO_2 at 37 °C for 48 h.

Identification of HP0953 in H. pylori

The purified antibody was used for identifying the protein HP0953 in *H. pylori* 26695 by western blotting. A total extract obtained from *H. pylori* adhesion test (see below) was used, and soluble and insoluble fractions were separated according to the inclusion body preparation method[32]. These fractions were subjected to SDS-PAGE (50 mg of protein) and transferred onto a PVDF membrane, where western blotting was performed using the purified antibody diluted 1:2 in PBS-Tween and incubated overnight under stirring at 4 °C and the secondary antibody diluted 1:10000 [anti-rabbit immunoglobulin G (IgG) horseradish peroxidase (HRP)-conjugated antibody] (Santa Cruz Biotechnology; United States)[34]. Washing was done with TBST (2 mmol/L Tris, 15 mmol/L NaCl, 0.1% Tween 20, pH 7.6). Finally, the membrane was visualized using Immobilon Western Chemiluminescent HRP substrate (Millipore).

Adhesion test of H. pylori

A suspension (6×10^8) of *H. pylori* 26695 culture in Brucella broth (Dibico) supplemented with 1% yeast extract was prepared. Next, 50 mL of the suspension was placed in cell culture bottles and incubated at 37 °C in an atmosphere of 50 mL/L CO_2 for 0, 1, 3, 12, and 24 h; these time points are the first hours of biofilm formation where adherence occurs. After the incubation period, the supernatant was removed, and the bottle walls were scraped to obtain adherent cells, which were resuspended in 1 mL of sterile 1 × PBS.

Thawing and seeding of AGS cells

First, 1 mL of AGS cell suspension was placed in a 15 mL conical tube. Subsequently, 2 mL of DMEM-F12 (Gibco, Life Technologies; United States) medium was added for washing by centrifugation at 1500 rpm for 5 min. A second washing step was performed, and the cells were resuspended again in DMEM-F12 medium. Next, 1 mL of the cell suspension was taken to seed into cell culture bottles. The bottles were incubated in a CO_2 chamber for 24 h at 37 °C.

AGS cell infection assay by H. pylori

The gene expression assay during biofilm formation was performed in duplicate in ten cell culture bottles of 225 mL each. A suspension of *H. pylori* (strain 26695, previously cultured for 24 h in a plate with Casman medium) was prepared in DMEM-F12 culture medium. The cells were washed by centrifugation at 3000 rpm for 15 min. After washing, the cell pellet was used to prepare a bacterial suspension in 300 mL of DMEM-F12 culture medium inside a flask until the growth level reached similar to that in tube number 2 on the McFarland scale. To each bottle, 30 mL of the bacterial suspension similar to McFarland tube 2 suspension was added, and then 20 mL of DMEM-F12 medium without the bacteria was added to complete 50 mL. One bottle was not infected with the bacterial strain and was used as the control for the transmission electron microscopy (TEM) assay. The bottles were incubated at 3, 12, 24, and 48 h post-infection. Time 0 was taken as the culture of the bacterial strain with no contact with AGS cells for the expression assay. After each time point of incubation, the supernatant was discarded, and 1 mL of sterile 1 × PBS was added for washing the cells. Subsequently, the wall of the bottle was scraped with a gendarme to detach the cells and remove the adhered biofilm. Each sample was processed for RNA extraction assay. An aliquot was taken for use in TEM, and the remainder was centrifuged at 7000 rpm for 15 min. The test was conducted in triplicate.

Immunogold technique for TEM

First, 500 μL of the samples obtained from the adhesion test was centrifuged at 2500 rpm for 10 min and fixed with 4% paraformaldehyde (MP Biomedicals; United States) in 1 × PBS (pH 7.4) for 1 h at 4 °C. Then, three washes were performed with 1 × PBS (pH 7.4), and the sample was dehydrated by adding 50% ethanol (Merck; IRL) for 10 min, followed by two washes with 70% ethanol for 15 min at room temperature. The inclusion was done using the LR-White method as described by Vázquez and Echeverría[37], and ultrathin sections of 60-90 nm were obtained. The sections were placed on nickel grids, blocked with 5% BSA for 20 min, and incubated with the purified polyclonal antibody overnight at 4 °C. The sample was then washed with TBST and incubated with the secondary antibody (goat anti-rabbit IgG coupled to 10-nm colloidal gold particles, 1:5, Sigma-Aldrich) diluted in deionized water for 1 h at room temperature. The grids were rinsed with TBST. Finally, they were observed under a transmission electron microscope (JEM 1010 JEOL Ltd. Japan) equipped with a TEM Imaging Systems AMT (Woburn; United States).

Table 1 Prediction of glycosylation sites

Position		Residue score	Prediction
Probable N-linked glycosylation sites			
68	NNK	-0.20374993	Non-glycosylated
69	NKY	-0.11718906	Non-glycosylated
80	NAK	-0.46398761	Non-glycosylated
113	NIS	0.031759513	Potentially glycosylated
120	NYL	-0.12578944	Non-glycosylated
130	NTY	-0.42088241	Non-glycosylated
134	NLK	-0.028092183	Non-glycosylated
164	NLN	0.45527702	Potentially glycosylated
166	NDN	-0.14904342	Non-glycosylated
168	NEI	0.2906731	Potentially glycosylated
Probable O-linked glycosylation sites			
15	S	0.3493683	Potentially glycosylated
16	S	-0.20711247	Non-glycosylated
18	S	-0.033164353	Non-glycosylated
20	S	-0.066886402	Non-glycosylated
23	S	0.33910492	Potentially glycosylated
33	S	-0.58418843	Non-glycosylated
40	S	-0.76207501	Non-glycosylated
43	S	0.16899016	Potentially glycosylated
78	T	-0.75721234	Non-glycosylated
84	S	-0.20144186	Non-glycosylated
107	S	-0.2527357	Non-glycosylated

There are three probable N-linked and six probable O-linked glycosylation sites.

Quantitative SYBR-Green real time-PCR analysis for hp0953 expression during H. pylori infection of AGS cells

Expression analysis was performed by real time-PCR (RT-qPCR). The glutamate racemase (*glmM)* gene was used as an internal control for the bacterial cell, and the *β-globin* gene was used as an internal control for human AGS cells. *HP0953* expression was evaluated at different time points (0, 3, 12, 24, and 48 h). Time 0 was taken as the culture of the bacterial strain with no contact with AGS cells.

Gene-specific primers were developed for *HP0953* and *glmM* using the Primer3 software, v.0.4.0[38, 39]. The sequences of all the primers were as follows: *HP0953* (5′-CATATGCCGAGCAGACGACTACG-3′; 5′-GTCGACCTACCTTAACGCACAAACGCTACC-3′), *glmM* (5′-ACCGACGCTCTCACCCACTT-3′; 5′-AGCGCGAGCCACAACCCTTT-3′). Total RNA was isolated from the AGS cell cultures with and without *H. pylori* at a multiplicity of infection of 1:100. RNA was extracted using TRIzol® Reagent (Ambion RNA, Life Technologies; United States), followed by phenol:chloroform extraction. The quality and amount of the resulting RNA were evaluated using a Nano-Drop spectrophotometer (The Epoch™ Multi-Volume Spectrophotometer System; United States) at 260 and 280 nm, respectively.

Reverse transcription reaction and SYBR-Green PCR were performed as described below. To initiate the first-strand cDNA synthesis, 1 mg of total RNA was treated with 500 μL of DNAse I (10 U/mL; Invitrogen; United States). Then, it was incubated for 30 min at 37 °C and 5 min at 75 °C with 4 μL of 5 × RT buffer, 2 μL of 25 mmol/L $MgCl_2$, 2 μL of 10 mmol/L dNTP mix, 2 μL of 50 mmol/L random hexamer primers, 1 μL of RNAse inhibitor (20 U/μL), and sufficient H_2O for a final volume of 20 μL. The mixture was then incubated for 10 min at 25 °C and 30 min at 48 °C with 2 μL of MultiScribe reverse transcriptase (50 U/mL; Applied Biosystems; United States). The reaction was terminated by heating the sample at 95 °C for 10 min. Aliquots of 200 ng of cDNA were used in the SYBR-Green PCR analysis according to the manufacturer's protocol. RT-PCR amplification was performed in triplicate under the

following conditions: 2 min at 50 °C (for UNG activation) and 10 min at 95 °C (for polymerase activation), followed by 40 cycles of denaturation and alignment/extension at 95 °C for 15 s and 60 °C for 1 min, respectively, using the Stratagene Mx3005p qPCR System and MxPro-Mx3005p software (Santa Clara; United States). Relative quantification of HP0953 RNA expression was performed using the comparative CT method. The Δ Ct (difference in CT values) between HP0953 and the *glmM* internal control and the Δ Δ Ct were calculated to normalize the differences in cDNA concentrations for each reaction. The RNA expression level was calculated using the equation $2^{-(\Delta\Delta Ct)}$[40]. The Kruskal-Wallis equality-of-populations rank test was used to compare the expression of the gene at all study time points. Differences were considered to be significant when the *P* value was < 0.05.

RESULTS

In silico analysis of HP0953 protein features

In silico analyses allow us to foresee probable protein maturation. The analysis conducted using the SignalP 4.1 tool revealed that HP0953 protein loses a signal peptide after excision between amino acids 21 and 22 which could lead to extracellular release (Figure 1). This region is also believed to present a transmembrane helix (Figure 2). The protein modifications provided us an insight into their probable function. Tables 1 and 2 show the predicted modification sites for HP0953. There are three predicted N-linked glycosylation sites in amino acid positions 113, 164, and 168 and six predicted O-linked glycosylation sites in positions 15, 23, 43, 111, 115, and 183. Moreover, there are four predicted myristoylation sites in positions 12-17, 29-34, 73-78, and 182-187 and one predicted prenylation site in the position 185-188.

To predict the structural model, we used different programs such as I-TASSER, RaptorX, and HHalign-Kbest, the latter being the one that generated a better quality model (Figures 3 and 4). The HHpred program disclosed a similarity with the Tip-alpha protein of *H. pylori*; thus, it was used as a template for modeling. Additionally, no conserved domains were found or matches with other proteins.

Site-directed mutagenesis of HP0953 gene

Plasmid pBlue-5CM3 was constructed for *HP0953* site-directed mutagenesis (Supplementary Figure 1). Sequencing the D*hp0953::Cm* Blue-5CM3 construction multiple cloning site corresponded to inserted *HP0953* and *Cm* cassette. However, we were unable to propagate the *H. pylori*-transformed strain.

HP0953 is detected in the insoluble fraction of H. pylori protein extract

For *H. pylori* HP0953 protein identification, insoluble and soluble fractions were obtained and resolved by SDS-PAGE assay. HP0953 protein was not detected in the soluble fraction, and its total concentration was very low in the insoluble fraction (data not shown). Interestingly, HP0953 was expressed constitutively at all the tested time points (Figure 5).

HP0953 is located in the cytoplasm and the peripheral zone of H. pylori

Protein location is indicative of its function. HP0953 was identified in the insoluble fraction of *H. pylori* lysates, which probably implies that the function of HP0953 is elicited in the vicinity of the outer membrane. To examine this hypothesis, we performed the immunogold technique on bacterial sections that were analyzed by TEM. The micrographs showed that HP0953 protein is located in the cytoplasm and accumulated in some peripheral areas of the bacterial body (Figure 6A), as well as in bacteria-bacteria contact areas (Figures 6B, 6C and 6D). Furthermore, there was a large accumulation of the protein in the bacterial debris (Figure 6E). Interestingly, the presence of this protein was also observed in the area of the glycocalyx that covers *H. pylori* (Figure 7), and accumulated where said coating spreads, producing a type of net, perhaps indicating the formation of a biofilm. Interestingly, a large amount of HP0953 protein was secreted during the infection of gastric cells because it was found in the *H. pylori*-AGS cell contact area (Figure 8).

Higher expression of HP0953 is required in the early stages of H. pylori-AGS cell interaction

RT-qPCR was performed to elucidate the behavior of *HP0953* during the contact of *H. pylori* with AGS cells. Figure 9 shows a comparison of the expression ratios of the treated and untreated cultures. *HP0953* expression was observed at all the tested time points; however, higher expression values were observed after 12 h of infection. *glmM* was the prokaryotic constitutive gene that was used as an internal control (Figure 9).

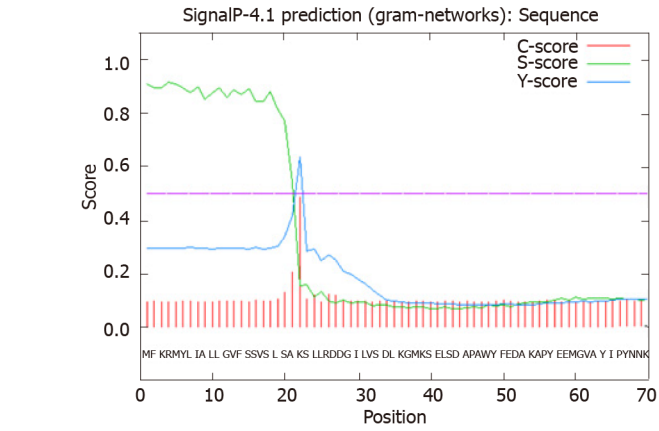
DISCUSSION

The high prevalence of *H. pylori* infection and its significant persistence in the gastrointestinal tract in the population with limited economic resources, as well as the diversity of related pathologies, the

Table 2 Prediction of posttranslational modification sites

Position	Residue	Prediction
PS00008 MYRISTYL N-myristoylation site		
12-17	GVfsSV	N-myristoylation site
29-34	GilvSD	N-myristoylation site
73-78	GIeqAT	N-myristoylation site
182-187	GSvcAL	N-myristoylation site
PS00005 PKC_PHOSPHO_SITE Protein Kinase C phosphorylation site		
20-22	SaK	MOD_RES 20 phosphoserine [condition: S]
PS00001 ASN_GLYCOSYLATION N-glycosylation site		
113-116	NISY	CARBOHYD 113 N-linked (GlcNAc) asparagine [condition: N]
PS00294 PRENYLATION Prenyl group binding site (CAAX box)		
185-188	CALr	Prenyl group binding site (CAAX box)

There are four predicted myristoylation sites, one predicted protein kinase C phosphorylation site, one predicted glycosylation site, and one predicted prenylation site.



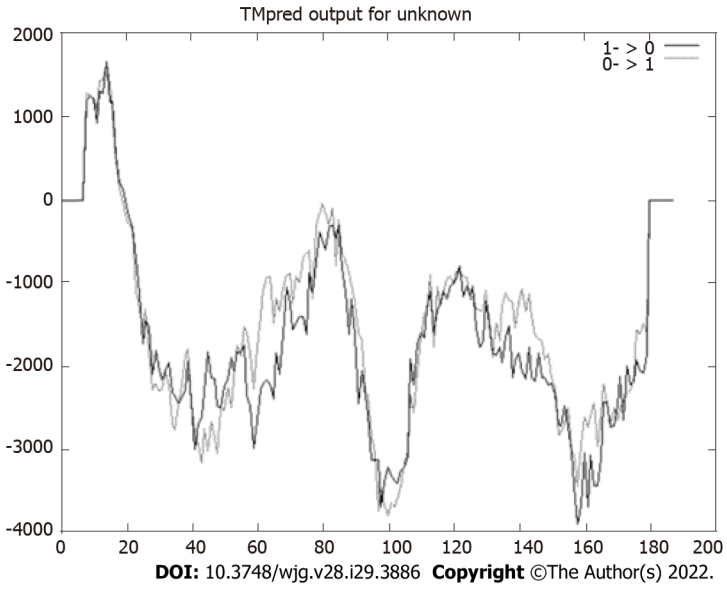
# Measure	Position	Value	Cutoff	signal peptide?
max. C	22	0.486		
max. Y	22	0.635		
max. S	4	0.916		
mean S	1-21	0.858		
D	1-21	0.740	0.570	YES

Name = Sequence SP = 'YES' Cleavage site between pos. 21 and 22: LSA-KS D = 0.740 D-cutoff = 0.570 Network = Signal1P-noTM

DOI: 10.3748/wjg.v28.i29.3886 **Copyright** ©The Author(s) 2022.

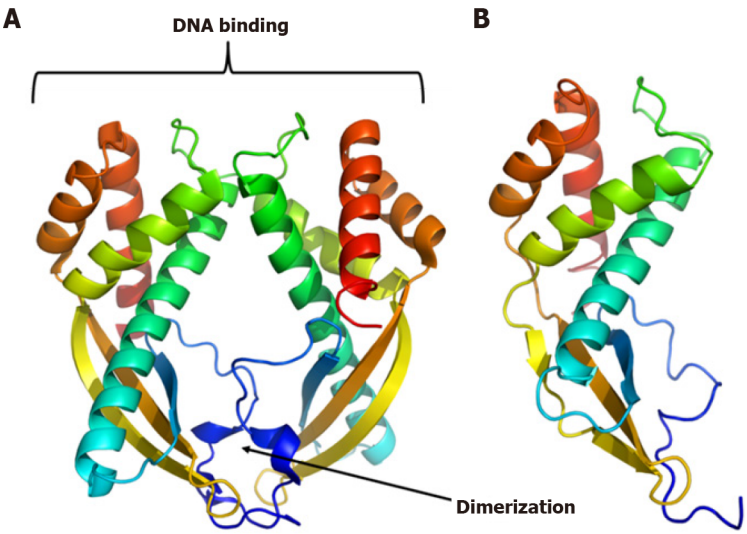
Figure 1 Prediction of a signal peptide for HP0953 protein. The green line that represents the S-score indicates a high probability that the first 20 amino acids conform a signal peptide that can be removed by a cut between amino acids 20 and 21, as marked by the tallest red line indicating the C-score.

environment, and the genetics of the host, suggest that the pathogenicity mechanisms used by this microorganism are numerous. The different bacterial strains express variations in their virulence factors, including those associated with the colonization process (*e.g.*, urease, flagella, a chemotaxis system, and adhesins), immune response evaders (*e.g.*, lipopolysaccharide and flagella; CagA and the type IV secretion system, VacA; gamma-glutamyl transpeptidase, and catalase superoxide dismutase), and disease inducers (*e.g.*, VacA, BabA, IceA, HtrA, CagA, and the type IV secretion system, DupA, and OipA)[41]. Furthermore, the *H. pylori* proteome consists of 340 proteins that are described as hypothetical, implying that their structure or function is unknown, thus indicating that some proteins may be related to pathogenicity mechanisms or are important to adapt to the surrounding environment. The HP0953 protein exhibited its maximum expression at the first 12 h of infection in a culture of gastric epithelium cells; this finding along with its location near the infected cells and the predicted prenylation and myristoylation sites suggest that it is an important protein during the bacterium's colonization phase of the gastric epithelium.



DOI: 10.3748/wjg.v28.i29.3886 **Copyright** ©The Author(s) 2022.

Figure 2 Prediction of transmembrane helices. Values > 0 indicate the probable presence of transmembrane helices, as observed in the region constituted by the first 25 amino acids. The HP0953 protein could be anchored to the membrane to be subsequently secreted.

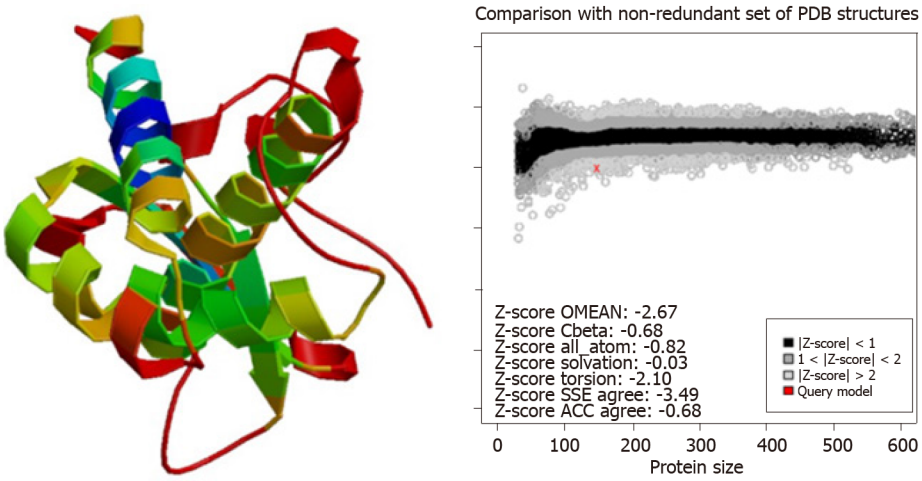


DOI: 10.3748/wjg.v28.i29.3886 **Copyright** ©The Author(s) 2022.

Figure 3 Three-dimensional models of proteins. A: Tip-alpha protein from *Helicobacter pylori* (*H. pylori*); B: HP0953 protein from *H. pylori*. Tip-alpha acquires a dimer arrangement that could also be present in the HP0953 protein due to its structural similarity in the position of the alpha helices and beta sheets.

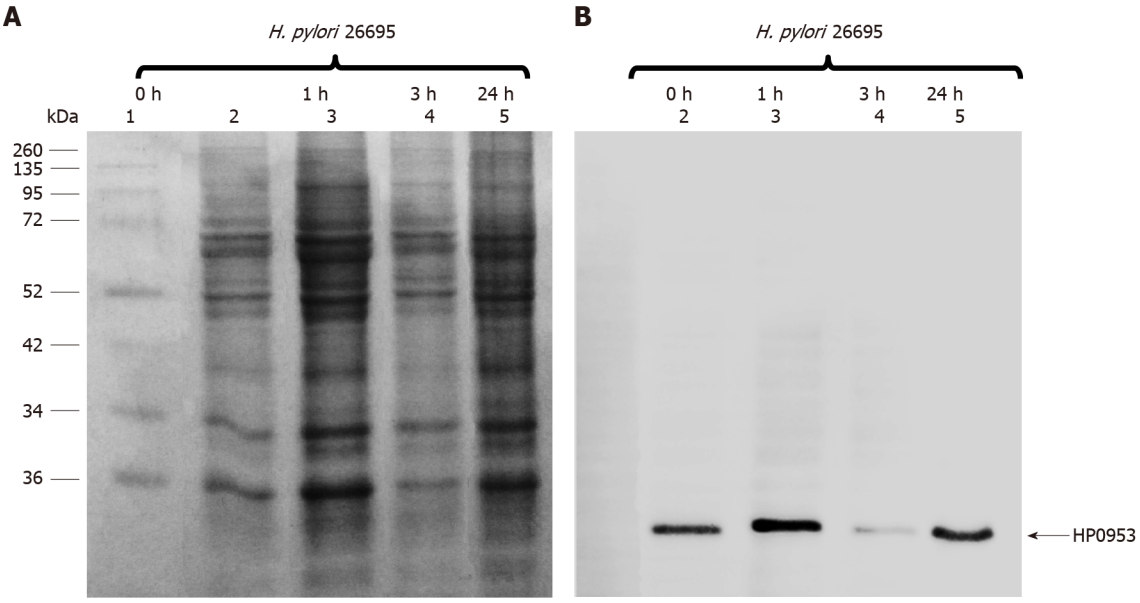
Although various studies, such as those conducted by Naqvi *et al*[17] in 2016 and Park *et al*[42] in 2012, have performed *in silico* analyses to determine the probable structures and functions of the hypothetical proteins of *H. pylori*, none of them evaluated the probable function of HP0953[17,42]. Furthermore, the bioinformatics analysis performed in this study highlighted the presence of a signal peptide that may anchor at the transmembrane region and then allow the release of the protein to the external environment after its excision. The analyses also revealed some probable glycosylation sites, which suggests that HP0953 is a protein from the glycocalyx. The glycocalyx is defined as any glycoprotein-associated polysaccharide that contains bacterial surface structures and is distant from the outer membrane or cell wall surface[43]. Bacterial glycocalyx generally has protection functions that allow bacterial survival and persistence in the natural environment and cell attachment[44].

Different modification patterns are found within the HP0953 sequence, such as the myristoylation pattern. This modification is essential for the removal of membrane proteins[45]; the existence of these putative sites provides an idea about its pathogenicity. Importantly, these bacteria lack the enzyme N-myristoyl transferase (NMT) required for producing this modification; hence, the proteins that are myristoylated are processed by the NMT of their eukaryotic hosts[46]. NMT is a suitable therapeutic target in opportunistic infections in humans; in fact, it has been associated with carcinogenesis, in



DOI: 10.3748/wjg.v28.i29.3886 **Copyright** ©The Author(s) 2022.

Figure 4 Evaluation of the modeling quality of HP0953. The QMEAN for this protein was 0.498, which indicates that the obtained model is acceptable. PDB: Protein Data Bank; SSE: Secondary Structure Element; ACC: Solvent Accessibility.

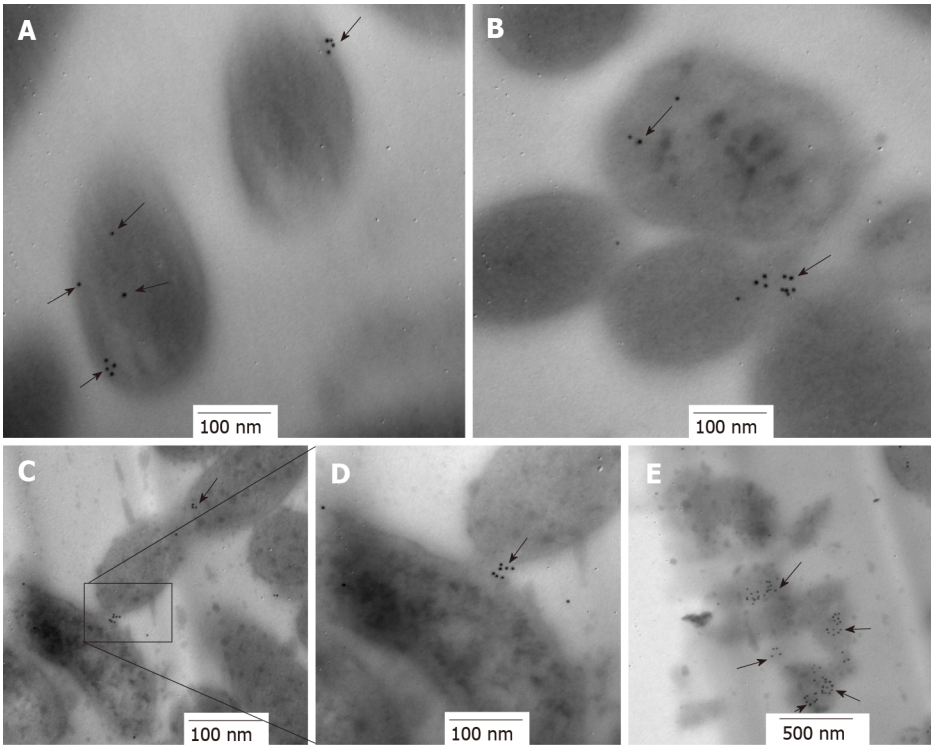


DOI: 10.3748/wjg.v28.i29.3886 **Copyright** ©The Author(s) 2022.

Figure 5 Location of the hypothetical protein HP0953 in the insoluble fraction of *Helicobacter pylori* 26695. A: Sulfate-polyacrylamide gel electrophoresis 16% gel stained with Coomassie blue; B: Western blot with an arrow showing the band corresponding to the expected molecular weight. Lanes: (1) Molecular weight marker and (2-5) insoluble fractions of *Helicobacter pylori* 26695 from samples collected at 0, 1, 3, and 24 h of incubation during biofilm formation. The arrow indicates the presence of the native HP0953 protein. *H. pylori*: *Helicobacter pylori*.

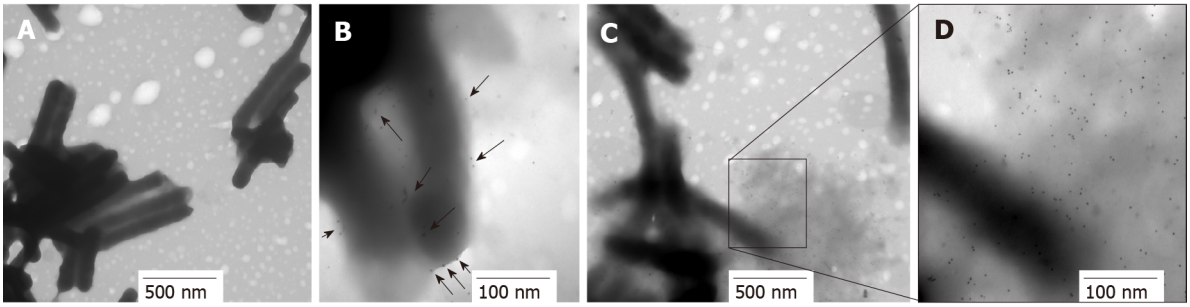
particular colon cancer[47]. Myristoylation has been suggested to occur as part of the secretory machinery[48,49]. Hypothetical patterns of prenylation were also detected, which is a class of modification involving the addition of isoprenoids or geranylgeranyl, and it is involved in membrane interactions due to the hydrophobicity of these lipids[50]. This modification is often a step to target the affected proteins to specific membranes[51]. As this modification was predicted in HP0953 by the ProtComB tool, it could be relevant for its function.

Extracellular proteins can play a vital role in bacterial pathogenesis[11], which correlates with our findings of the similarity between the HP0953 protein and the Tip-alpha protein, which is described as the only virulence factor secreted by all *H. pylori* strains[52]. Moreover, its overexpression has been related to the development of gastric cancer. Tip-alpha is an exotoxin that penetrates cells and induces the production of tumor necrosis factor alpha[53]. HP053 protein could have a similar function because probable posttranslational modification sites related to bacterial pathogenesis were also found. It has been reported that some bacteria secrete effectors through the type III or type IV secretion systems, mimicking the functions of eukaryotic proteins to evade the defense systems. Subsequently, they



DOI: 10.3748/wjg.v28.i29.3886 **Copyright** ©The Author(s) 2022.

Figure 6 Immunolocation of HP0953 protein in *Helicobacter pylori* bacterial transmission electron microscopy sections. A and B: 100000 ×; C: 75000 ×; D: 150000 ×; E: 60000 ×. The black arrows show the location of HP0953 protein. Immunogold technique, primary antibody (polyclonal rabbit anti-HP0953), secondary antibody (goat anti-rabbit immunoglobulin G coupled to 10-nm colloidal gold particles). (JEM 1010 JEOL Ltd. Tokyo, Japan) microscope equipped with a TEM Imaging Systems AMT (Woburn, MA, United States).



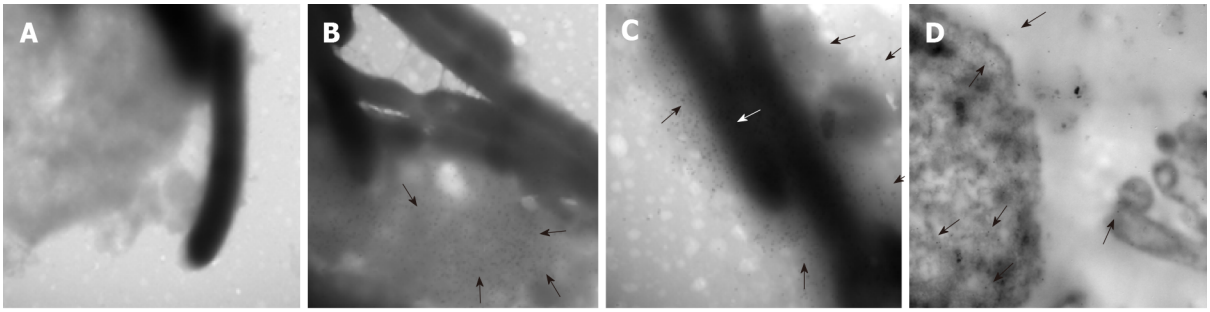
DOI: 10.3748/wjg.v28.i29.3886 **Copyright** ©The Author(s) 2022.

Figure 7 Immunolocation of HP0953 protein in whole bacteria. A: *Helicobacter pylori* (*H. pylori*) incubated with the secondary antibody alone, 20000 ×; B-D: Complete immunogold technique for *H. pylori*; B: 100000 ×; C: 30000 ×; D: 100000 ×. Black arrows indicate the location of HP0953 protein. Immunogold technique, primary antibody (polyclonal rabbit anti-HP0953), secondary antibody (goat anti-rabbit immunoglobulin G coupled to 10-nm colloidal gold particles).

undergo a posttranslational modification mediated by the same host enzymes to become biologically active[54], stimulating or inhibiting the immune response, interfering signaling pathways, affecting T-cell activation, or whatever their function may be[55]. Among these posttranslational modifications are myristoylation and prenylation[56,57], which were also detected in the *in silico* analysis conducted in this study. These modifications added lipid residues that allow the protein to anchor to the cell membrane to exert some unknown function.

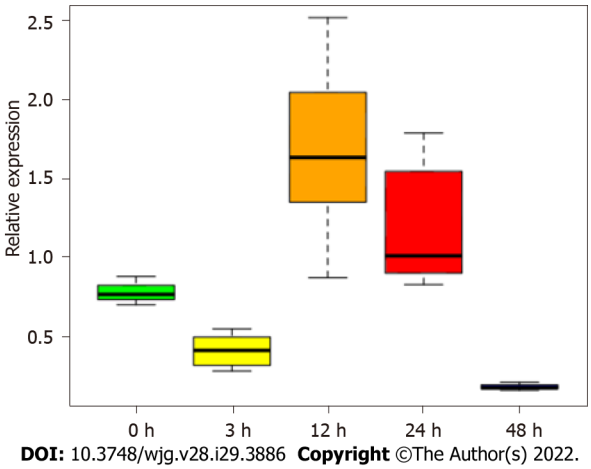
HP0953 lacks homologous proteins outside *H. pylori*, and this absence limits comparisons and the elucidation of its potential role. X-ray crystallography analysis can be performed to determine its 3D structure, which could then be used in comparisons with other proteins in the database. However, it was observed that HP0953 is an insoluble protein, which makes it difficult to purify in its native form.

The persistence of *H. pylori* in an environment where there are peristaltic movements and cell shedding is mediated by a variety of adhesins present on the bacterial surface[10,58], and the adhesion of *H. pylori* can be achieved by a connection of the plasma membrane through filamentous materials. However, it is known that glycocalyx preferentially adheres to the surfaces of biomaterials and compromised tissues, forming biofilms[55]. Research on biofilm composition has shown that a



DOI: 10.3748/wjg.v28.i29.3886 **Copyright** ©The Author(s) 2022.

Figure 8 Location of HP0953 protein during against gastric cell infection by *Helicobacter pylori*. A: Against gastric (AGS) cell at 3 h of infection by *Helicobacter pylori* (*H. pylori*), incubated with the secondary antibody alone, 40000 ×; B: Complete immunogold technique for AGS cells at 3 h of infection by *H. pylori*, 40000 ×; C: Complete immunogold technique for AGS cells at 3 h of infection by *H. pylori*, 50000 ×; D: Complete immunogold technique for AGS cells at 12 h of infection by *H. pylori*, 40000 ×. White arrows indicate the location of HP0953 protein.



DOI: 10.3748/wjg.v28.i29.3886 **Copyright** ©The Author(s) 2022.

Figure 9 Expression of HP0953 increases significantly after 12 h of infection of against gastric cells. The Kruskal-Wallis equality-of-populations rank test was used to compare the expression of the gene at all study time points. $P = 0.0006$.

pericellular matrix, also known as the glycocalyx, develops to preserve and concentrate the lytic enzymes secreted by bacteria, which, in turn, increases their metabolic efficiency[8]. This suggests that the hypothetical protein HP0953 could be involved in lytic processes by being present in the glycocalyx and concentrated in the bacterial debris; however, functionality studies are still required to elucidate the role of this protein in the persistence of *H. pylori* in the human stomach. Smith *et al*[11] suggested that this protein could be involved in the survival of the bacterium in the gastric environment based on their finding that it is also present in *H. acinonychis*, which colonizes the gastric mucosa of felines. Nevertheless, other closely related ε-proteobacteria, such as *H. hepaticus* and *C. jejuni*, lack sequences that are homologous to HP0953, thus suggesting that this protein is unique to the gastric *Helicobacter* species[11], suggesting an important role of HP0953 in *H. pylori* gastric pathogenesis.

In our previous study, we observed the overexpression of HP0953 protein during the first hours of adherence to inert surfaces and AGS cells[59], suggesting its involvement in the survival of *H. pylori* in the environment or in its pathogenic mechanisms. In the present study, we found that initial levels of *HP0953* expression become diminished, perhaps as a result of the adaptation of *H. pylori* to its environment. The levels of HP0953 rise after 3 h, indicating that this protein is required for the interaction of *H. pylori* with AGS cells, and the maximum level of *HP0953* expression occurred 12 h after the infection of AGS cells. Genetic regulation in pathogens allows for fluctuation in the expression of constitutive genes following initial contact with the target cells[60,61]. The immunogold assay demonstrated that HP0953 protein was located in the cytoplasm, accumulated in some peripheral areas of the bacterial body, and exhibited a greater expression when it is close to AGS cells. These data suggest that HP0953 protein is synthesized in the cytoplasm and subsequently exported to the outer membrane, where it is involved in adhesion functions as its agglomeration was detected at the binding sites between the bacterium and in the space between the bacterium and gastric cells. Similarly, the immunogold assay of HP0953 protein in the whole bacterium revealed that the protein was primarily located in the bacterial coat or glycocalyx, which is consistent with the finding reported by Smith *et al*[11], who investigated the proteins secreted by *H. pylori* and found that HP0953 protein was a

component of this set of proteins.

Furthermore, we altered *HP0953* to obtain a mutant strain. Unfortunately, we were unable to propagate the resultant *HP0953* mutant clone, but we are continuing with our efforts to modify the methodology to obtain a mutant strain that can be successfully propagated. Further studies are necessary to determine the structure and function of hypothetical proteins of *H. pylori*, such as HP0953, which may be associated with the disease pathology.

CONCLUSION

HP0953 protein exhibited its maximum expression during the first 12 h of infection in a culture of gastric epithelium cells. This finding indicated its location surrounding the infected cells, and the predicted presence of prenylation and myristoylation sites suggests that HP0953 is a relevant protein during the bacterium's colonization phase of the gastric epithelium. HP0953 was also found to be strikingly similar to an exotoxin, possibly associating it with the development of gastric cancer.

ARTICLE HIGHLIGHTS

Research background

Helicobacter pylori (*H. pylori*) is a bacterium of clinical relevance. Approximately 50% of the worldwide human population is colonized by this bacterium, where up to 3% can develop gastric cancer. Several environmental conditions such as the genetic predisposition of the host, and bacterial virulence factors are directly associated.

Research motivation

H. pylori is a bacterium associated with gastric diseases. This microorganism owns more than 200 hypothetical proteins with functions yet unknown. Some of them could be related to the disease or adaptation to gastric microenvironment. However, in a short-term future, they can be considered as therapeutic targets.

Research objectives

The objective was to characterize the hypothetical protein HP0953, such as structure, location, and expression, to determine if it is a virulence factor employed by *H. pylori* during infection of against gastric (AGS) cells.

Research methods

Several bioinformatic platforms (SignalP, Expasy, GLYCOPP, I-Tasser) were employed to predict some features of the hypothetical protein HP0953, such as peptide-signaling, three-dimensional structure, and possible post-translational modifications. HP0953 was located during *H. pylori* infection to AGS cells by transmission electron microscopy, employing a specific antibody for said protein and immunogold technique. The expression of HP0953 during the infection of AGS cell cultures by the bacterium was evaluated by real-time polymerase chain reaction.

Research results

The hypothetical protein HP0953 was observed in the cytoplasm and embedded in the glycocalyx secreted by the bacterium, as well as in the space between the bacterium and the AGS cell. The overexpression of the protein was observed at 12 h of infection. HP0953 was predicted to possess a signal peptide, which can interact with transmembranal regions for its secretion. Additionally, the HP0953 protein acts as like an exotoxin, which can then undergo post-translational modifications, which might then require the eukaryotic cell to be carried out.

Research conclusions

The hypothetical protein HP0953 is a protein located in the periphery of infected cells. It is overexpressed during infection. The *in silico* analysis revealed prenylation and myristoylation sites. These findings suggest that the protein has a relevant function during the colonization or infection of *H. pylori* into gastric epithelium.

Research perspectives

Propagate a *H. pylori* modified strain, which lacks the HP0953 protein. The study will define its functions and establish a new precedent for the study of the pathogenesis of the disease, and its relevance in the adaptation process in the gastric microenvironment.

ACKNOWLEDGEMENTS

The authors would like to acknowledge Alejandra S Rodríguez for her skillful technical assistance.

FOOTNOTES

Author contributions: Arteaga-Resendiz NK, Rodea GE, Olivares-Cervantes AL, and Colín C performed the experiments, and acquired and analyzed data; Arteaga-Resendiz NK, Rodea GE, Colín C, Olivares-Cervantes AL, Aguilar-Rodea P, Ribas-Aparicio RM, López-Villegas EO, Olivares-Trejo JJ, and Velázquez-Guadarrama N interpreted the data; Reyes-López A and Arteaga-Resendiz NK statistical data analyzed; Rodea GE, Ribas-Aparicio RM, Mendoza-Elizalde S, Salazar García M and Velázquez-Guadarrama N wrote the manuscript; and all authors approved the final version of the article.

Supported by the Federal Funds, HIM/2009/037. SSA851 and HIM / 2014/012. SSA 1098; the grant from Secretaría de Investigación y Posgrado, SIP 20161878; and the Instituto Politécnico Nacional by Consejo Nacional de Ciencia y Tecnología, CB-222180.

Institutional review board statement: The study was reviewed and approved by the Ethics, Biosafety and Scientific committees at the Health Institute approved the experiment (HIM/2009/037. SSA851 and HIM/2014/012. SSA 1098).

Institutional animal care and use committee statement: Animal care was performed under national and institutional policies (NOM-062-ZOO-1999).

Conflict-of-interest statement: All the authors report no relevant conflicts of interest for this article.

Data sharing statement: No additional data are available.

ARRIVE guidelines statement: The authors have read the ARRIVE guidelines, and the manuscript was prepared and revised according to them.

Open-Access: This article is an open-access article that was selected by an in-house editor and fully peer-reviewed by external reviewers. It is distributed in accordance with the Creative Commons Attribution NonCommercial (CC BY-NC 4.0) license, which permits others to distribute, remix, adapt, build upon this work non-commercially, and license their derivative works on different terms, provided the original work is properly cited and the use is non-commercial. See: https://creativecommons.org/Licenses/by-nc/4.0/

Country/Territory of origin: Mexico

ORCID number: Nancy K Arteaga-Resendiz 0000-0003-0777-4212; Gerardo E Rodea 0000-0003-1165-0511; Rosa María Ribas-Aparicio 0000-0002-1141-2794; Alma L Olivares-Cervantes 0000-0001-8209-4896; Juan Arturo Castelán-Vega 0000-0003-1102-2101; José de Jesús Olivares-Trejo 0000-0002-4225-4493; Sandra Mendoza-Elizalde 0000-0002-0255-4125; Edgar O López-Villegas 0000-0002-9995-2145; Christian Colín 0000-0002-8796-9978; Pamela Aguilar-Rodea 0000-0002-1522-2138; Alfonso Reyes-López 0000-0002-6249-3678; Marcela Salazar García 0000-0001-5318-8148; Norma Velázquez-Guadarrama 0000-0002-3620-7260.

Corresponding Author's Membership in Professional Societies: Hospital Infantil de México Federico Gómez, 11217.

S-Editor: Wang JJ
L-Editor: A
P-Editor: Wang JJ

REFERENCES

1 **Connor BA**. Helicobacter pylori. In: Centers for Disease Control and Prevention. CDC Yellow Book 2020: Health Information for International Travel. New York: Oxford University Press, 2017
2 **Cheok YY**, Lee CYQ, Cheong HC, Vadivelu J, Looi CY, Abdullah S, Wong WF. An Overview of Helicobacter pylori Survival Tactics in the Hostile Human Stomach Environment. *Microorganisms* 2021; **9** [PMID: 34946105 DOI: 10.3390/microorganisms9122502]
3 **Huang Y**, Wang QL, Cheng DD, Xu WT, Lu NH. Adhesion and Invasion of Gastric Mucosa Epithelial Cells by Helicobacter pylori. *Front Cell Infect Microbiol* 2016; **6**: 159 [PMID: 27921009 DOI: 10.3389/fcimb.2016.00159]
4 **Wizenty J**, Tacke F, Sigal M. Responses of gastric epithelial stem cells and their niche to Helicobacter pylori infection. *Ann Transl Med* 2020; **8**: 568 [PMID: 32775369 DOI: 10.21037/atm.2020.02.178]
5 **Sharndama HC**, Mba IE. Helicobacter pylori: an up-to-date overview on the virulence and pathogenesis mechanisms. *Braz J Microbiol* 2022; **53**: 33-50 [PMID: 34988937 DOI: 10.1007/s42770-021-00675-0]
6 **Yonezawa H**, Osaki T, Kamiya S. Biofilm Formation by Helicobacter pylori and Its Involvement for Antibiotic Resistance.

Biomed Res Int 2015; **2015**: 914791 [PMID: 26078970 DOI: 10.1155/2015/914791]
7 **Percival SL**, Suleman L. Biofilms and Helicobacter pylori: Dissemination and persistence within the environment and host. *World J Gastrointest Pathophysiol* 2014; **5**: 122-132 [PMID: 25133015 DOI: 10.4291/wjgp.v5.i3.122]
8 **Gristina AG**, Costerton JW. Bacterial adherence and the glycocalyx and their role in musculoskeletal infection. *Orthop Clin North Am* 1984; **15**: 517-535 [PMID: 6472832]
9 **Argüeso P**, Woodward AM, AbuSamra DB. The Epithelial Cell Glycocalyx in Ocular Surface Infection. *Front Immunol* 2021; **12**: 729260 [PMID: 34497615 DOI: 10.3389/fimmu.2021.729260]
10 **Liu Y**, Hidaka E, Kaneko Y, Akamatsu T, Ota H. Ultrastructure of Helicobacter pylori in human gastric mucosa and H. pylori-infected human gastric mucosa using transmission electron microscopy and the high-pressure freezing-freeze substitution technique. *J Gastroenterol* 2006; **41**: 569-574 [PMID: 16868805 DOI: 10.1007/s00535-006-1813-2]
11 **Smith TG**, Lim JM, Weinberg MV, Wells L, Hoover TR. Direct analysis of the extracellular proteome from two strains of Helicobacter pylori. *Proteomics* 2007; **7**: 2240-2245 [PMID: 17533641 DOI: 10.1002/pmic.200600875]
12 **Chmiela M**, Kupcinskas J. Review: Pathogenesis of Helicobacter pylori infection. *Helicobacter* 2019; **24** Suppl 1: e12638 [PMID: 31486234 DOI: 10.1111/hel.12638]
13 **Alzahrani S**, Lina TT, Gonzalez J, Pinchuk IV, Beswick EJ, Reyes VE. Effect of Helicobacter pylori on gastric epithelial cells. *World J Gastroenterol* 2014; **20**: 12767-12780 [PMID: 25278677 DOI: 10.3748/wjg.v20.i36.12767]
14 **Tomb JF**, White O, Kerlavage AR, Clayton RA, Sutton GG, Fleischmann RD, Ketchum KA, Klenk HP, Gill S, Dougherty BA, Nelson K, Quackenbush J, Zhou L, Kirkness EF, Peterson S, Loftus B, Richardson D, Dodson R, Khalak HG, Glodek A, McKenney K, Fitzegerald LM, Lee N, Adams MD, Hickey EK, Berg DE, Gocayne JD, Utterback TR, Peterson JD, Kelley JM, Cotton MD, Weidman JM, Fujii C, Bowman C, Watthey L, Wallin E, Hayes WS, Borodovsky M, Karp PD, Smith HO, Fraser CM, Venter JC. The complete genome sequence of the gastric pathogen Helicobacter pylori. *Nature* 1997; **388**: 539-547 [PMID: 9252185 DOI: 10.1038/41483]
15 **Baltrus DA**, Amieva MR, Covacci A, Lowe TM, Merrell DS, Ottemann KM, Stein M, Salama NR, Guillemin K. The complete genome sequence of Helicobacter pylori strain G27. *J Bacteriol* 2009; **191**: 447-448 [PMID: 18952803 DOI: 10.1128/JB.01416-08]
16 **Blattner FR**, Plunkett G 3rd, Bloch CA, Perna NT, Burland V, Riley M, Collado-Vides J, Glasner JD, Rode CK, Mayhew GF, Gregor J, Davis NW, Kirkpatrick HA, Goeden MA, Rose DJ, Mau B, Shao Y. The complete genome sequence of *Escherichia coli* K-12. *Science* 1997; **277**: 1453-1462 [PMID: 9278503 DOI: 10.1126/science.277.5331.1453]
17 **Naqvi AA**, Anjum F, Khan FI, Islam A, Ahmad F, Hassan MI. Sequence Analysis of Hypothetical Proteins from Helicobacter pylori 26695 to Identify Potential Virulence Factors. *Genomics Inform* 2016; **14**: 125-135 [PMID: 27729842 DOI: 10.5808/GI.2016.14.3.125]
18 **Zanotti G**, Cendron L. Structural and functional aspects of the Helicobacter pylori secretome. *World J Gastroenterol* 2014; **20**: 1402-1423 [PMID: 24587618 DOI: 10.3748/wjg.v20.i6.1402]
19 **Otero LL**, Ruiz VE, Perez Perez GI. Helicobacter pylori: the balance between a role as colonizer and pathogen. *Best Pract Res Clin Gastroenterol* 2014; **28**: 1017-1029 [PMID: 25439068 DOI: 10.1016/j.bpg.2014.09.003]
20 **National Center of Biotechnology Information**. Protein. [cited 8 July 2021]. Available from: https://www.ncbi.nlm.nih.gov/protein
21 **Mistry J**, Chuguransky S, Williams L, Qureshi M, Salazar GA, Sonnhammer ELL, Tosatto SCE, Paladin L, Raj S, Richardson LJ, Finn RD, Bateman A. Pfam: The protein families database in 2021. *Nucleic Acids Res* 2021; **49**: D412-D419 [PMID: 33125078 DOI: 10.1093/nar/gkaa913]
22 **Petersen TN**, Brunak S, von Heijne G, Nielsen H. SignalP 4.0: discriminating signal peptides from transmembrane regions. *Nat Methods* 2011; **8**: 785-786 [PMID: 21959131 DOI: 10.1038/nmeth.1701]
23 **Siss Institute of Bioinformatics**. ExPASy. [cited 8 July 2021]. Available from: https://www.expasy.org/
24 **Hofmann K**, Stoffel W. TMbase - A database of membrane spanning proteins segments. *Biol Chem* 1993; **374**: 166
25 GlycoPP V2.0 A webserver for glycosites prediction in procaryotes. [cited 8 July 2021]. Available from: https://datascience.imtech.res.in/alkarao/glycopp2/
26 **Zimmermann L**, Stephens A, Nam SZ, Rau D, Kübler J, Lozajic M, Gabler F, Söding J, Lupas AN, Alva V. A Completely Reimplemented MPI Bioinformatics Toolkit with a New HHpred Server at its Core. *J Mol Biol* 2018; **430**: 2237-2243 [PMID: 29258817 DOI: 10.1016/j.jmb.2017.12.007]
27 **Zhang Lab**. I-TASSER Protein Structure α Function Predctions. [cited 9 May 2021]. Available from: https://zhanggroup.org/I-TASSER/
28 **RaptorX**. RaptorX: Protein Structure and Function Prediction Powered by Deep Learning. [cited 4 November 2016]. Available from: http://raptorx.uchicago.edu/
29 HHalign-Kbest: A service for optimized model generation through sub optimal HMM-HMM sequence alignment. [cited 4 November 2016]. Available from: https://bioserv.rpbs.univ-paris-diderot.fr/services/HHalign-Kbest/
30 **Vosshall L**. Hanahan competent cell protocol. [cited 8 July 2021]. Available from: https://www.rockefeller.edu/research/uploads/www.rockefeller.edu/sites/8/2018/10/Hanahan.pdf
31 **Froger A**, Hall JE. Transformation of plasmid DNA into E. coli using the heat shock method. *J Vis Exp* 2007; 253 [PMID: 18997900 DOI: 10.3791/253]
32 **Hyvonen M**. Inclusion body preparation. [cited 8 July 2021]. Available from: https://hyvonen.bioc.cam.ac.uk/wp-content/uploads/2017/09/ib.pdf
33 **Howard GC**, Bethell DR. Polyclonal antibodies, In: Basic Methods in Antibody Production and Characterization. Florida, USA: CRC Press, 2000: 31-48
34 **Abcam**. Western blot membrane stripping for restaining protocol. [cited 8 July 2021]. Available from: https://docs.abcam.com/pdf/protocols/western-blot-membrane-stripping-for-restaining-protocol.pdf
35 **Birnboim HC**, Doly J. A rapid alkaline extraction procedure for screening recombinant plasmid DNA. *Nucleic Acids Res* 1979; **7**: 1513-1523 [PMID: 388356 DOI: 10.1093/nar/7.6.1513]
36 **Ge Z**, Taylor DE. H. pylori DNA Transformation by Natural Competence and Electroporation. In: Clayton CL, Mobley

HLT. Helicobacter pylori Protocols. New Jersey: Humana Press, 1997: 145-152
37 **Vázquez NG**, Echeverría O. Introducción a la microscopía Electrónica Aplicada a las Ciencias Biológicas. Facultad de Ciencias de la Universidad Nacional Autónoma de México. México: Fondo de Cultura Económica, 2000: 148-151
38 **Untergasser A**, Cutcutache I, Koressaar T, Ye J, Faircloth BC, Remm M, Rozen SG. Primer3--new capabilities and interfaces. *Nucleic Acids Res* 2012; **40**: e115 [PMID: 22730293 DOI: 10.1093/nar/gks596]
39 **Koressaar T**, Remm M. Enhancements and modifications of primer design program Primer3. *Bioinformatics* 2007; **23**: 1289-1291 [PMID: 17379693 DOI: 10.1093/bioinformatics/btm091]
40 **Pfaffl MW**. A new mathematical model for relative quantification in real-time RT-PCR. *Nucleic Acids Res* 2001; **29**: e45 [PMID: 11328886 DOI: 10.1093/nar/29.9.e45]
41 **Chang WL**, Yeh YC, Sheu BS. The impacts of *H. pylori* virulence factors on the development of gastroduodenal diseases. *J Biomed Sci* 2018; **25**: 68 [PMID: 30205817 DOI: 10.1186/s12929-018-0466-9]
42 **Park SJ**, Son WS, Lee BJ. Structural analysis of hypothetical proteins from Helicobacter pylori: an approach to estimate functions of unknown or hypothetical proteins. *Int J Mol Sci* 2012; **13**: 7109-7137 [PMID: 22837682 DOI: 10.3390/ijms13067109]
43 **Luong P**, Dube DH. Dismantling the bacterial glycocalyx: Chemical tools to probe, perturb, and image bacterial glycans. *Bioorg Med Chem* 2021; **42**: 116268 [PMID: 34130219 DOI: 10.1016/j.bmc.2021.116268]
44 **Ogata M**, Araki K, Ogata T. An electron microscopic study of Helicobacter pylori in the surface mucous gel layer. *Histol Histopathol* 1998; **13**: 347-358 [PMID: 9589892 DOI: 10.14670/HH-13.347]
45 **Hayashi N**, Titani K. N-myristoylated proteins, key components in intracellular signal transduction systems enabling rapid and flexible cell responses. *Proc Jpn Acad Ser B Phys Biol Sci* 2010; **86**: 494-508 [PMID: 20467215 DOI: 10.2183/pjab.86.494]
46 **Maurer-Stroh S**, Eisenhaber F. Myristoylation of viral and bacterial proteins. *Trends Microbiol* 2004; **12**: 178-185 [PMID: 15051068 DOI: 10.1016/j.tim.2004.02.006]
47 **Wright MH**, Heal WP, Mann DJ, Tate EW. Protein myristoylation in health and disease. *J Chem Biol* 2010; **3**: 19-35 [PMID: 19898886 DOI: 10.1007/s12154-009-0032-8]
48 **Simon SM**, Aderem A. Myristoylation of proteins in the yeast secretory pathway. *J Biol Chem* 1992; **267**: 3922-3931 [PMID: 1740440]
49 **Yuan M**, Song ZH, Ying MD, Zhu H, He QJ, Yang B, Cao J. N-myristoylation: from cell biology to translational medicine. *Acta Pharmacol Sin* 2020; **41**: 1005-1015 [PMID: 32203082 DOI: 10.1038/s41401-020-0388-4]
50 **Palsuledesai CC**, Distefano MD. Protein prenylation: enzymes, therapeutics, and biotechnology applications. *ACS Chem Biol* 2015; **10**: 51-62 [PMID: 25402849 DOI: 10.1021/cb500791f]
51 **Hildebrandt D**. Heterogeneous Prenyl Processing of the Heterotrimeric G protein Gamma Subunits. *The Enzymes* 2011; **29**: 97-124 [DOI: 10.1016/B978-0-12-381339-8.00006-8]
52 **Tosi T**, Cioci G, Jouravleva K, Dian C, Terradot L. Structures of the tumor necrosis factor alpha inducing protein Tipalpha: a novel virulence factor from Helicobacter pylori. *FEBS Lett* 2009; **583**: 1581-1585 [PMID: 19401200 DOI: 10.1016/j.febslet.2009.04.033]
53 **Mahant S**, Chakraborty A, Som A, Mehra S, Das K, Mukhopadhyay AK, Gehlot V, Bose S, Das R. The Synergistic Role of Tip α, Nucleolin and Ras in Helicobacter pylori Infection Regulates the Cell Fate Towards Inflammation or Apoptosis. *Curr Microbiol* 2021; **78**: 3720-3732 [PMID: 34468852 DOI: 10.1007/s00284-021-02626-2]
54 **Al-Quadan T**, Price CT, London N, Schueler-Furman O, AbuKwaik Y. Anchoring of bacterial effectors to host membranes through host-mediated lipidation by prenylation: a common paradigm. *Trends Microbiol* 2011; **19**: 573-579 [PMID: 21983544 DOI: 10.1016/j.tim.2011.08.003]
55 **Ismail S**, Hampton MB, Keenan JI. Helicobacter pylori outer membrane vesicles modulate proliferation and interleukin-8 production by gastric epithelial cells. *Infect Immun* 2003; **71**: 5670-5675 [PMID: 14500487 DOI: 10.1128/IAI.71.10.5670-5675.2003]
56 **Popa CM**, Tabuchi M, Valls M. Modification of Bacterial Effector Proteins Inside Eukaryotic Host Cells. *Front Cell Infect Microbiol* 2016; **6**: 73 [PMID: 27489796 DOI: 10.3389/fcimb.2016.00073]
57 **Hicks SW**, Galán JE. Exploitation of eukaryotic subcellular targeting mechanisms by bacterial effectors. *Nat Rev Microbiol* 2013; **11**: 316-326 [PMID: 23588250 DOI: 10.1038/nrmicro3009]
58 **Vázquez-Jiménez FE**, Torres J, Flores-Luna L, Cerezo SG, Camorlinga-Ponce M. Patterns of Adherence of Helicobacter pylori Clinical Isolates to Epithelial Cells, and its Association with Disease and with Virulence Factors. *Helicobacter* 2016; **21**: 60-68 [PMID: 25908566 DOI: 10.1111/hel.12230]
59 **Arteaga-Resendiz NK**, Velázquez-Guadarrama N, Rivera-Gutiérrez S, Olivares Trejo J J, Méndez-Tenorio A, Valencia Mayoral P, López-Villegas E O, Rodríguez-Leviz A, Vigueras J C, Arellano-Galindo J, Girón J, Torres-López J. In silico analysis of proteins potentially involved in fimbrial biogenesis in Helicobacter pylori. *Bol Med Hosp Infant Mex* 2013; **70**: 78-88
60 **De la Cruz MA**, Ares MA, von Bargen K, Panunzi LG, Martínez-Cruz J, Valdez-Salazar HA, Jiménez-Galicia C, Torres J. Gene Expression Profiling of Transcription Factors of *Helicobacter pylori* under Different Environmental Conditions. *Front Microbiol* 2017; **8**: 615 [PMID: 28443084 DOI: 10.3389/fmicb.2017.00615]
61 **Kitamoto S**, Nagao-Kitamoto H, Kuffa P, Kamada N. Regulation of virulence: the rise and fall of gastrointestinal pathogens. *J Gastroenterol* 2016; **51**: 195-205 [PMID: 26553054 DOI: 10.1007/s00535-015-1141-5]

World Journal of Gastroenterology

Submit a Manuscript: https://www.f6publishing.com

World J Gastroenterol 2022 August 7; 28(29): 3903-3916

DOI: 10.3748/wjg.v28.i29.3903

ISSN 1007-9327 (print) ISSN 2219-2840 (online)

ORIGINAL ARTICLE

Basic Study

Involvement of toll-like receptor 5 in mouse model of colonic hypersensitivity induced by neonatal maternal separation

Geoffroy Mallaret, Amandine Lashermes, Mathieu Meleine, Ludivine Boudieu, Julie Barbier, Youssef Aissouni, Agathe Gelot, Benoit Chassaing, Andrew T Gewirtz, Denis Ardid, Frederic Antonio Carvalho

Specialty type: Gastroenterology and hepatology

Provenance and peer review: Unsolicited article; Externally peer reviewed.

Peer-review model: Single blind

Peer-review report's scientific quality classification

Grade A (Excellent): 0
Grade B (Very good): B
Grade C (Good): C
Grade D (Fair): 0
Grade E (Poor): 0

P-Reviewer: Ghannam WM, Egypt; Plaza MA, Spain

Received: March 15, 2022
Peer-review started: March 15, 2022
First decision: May 29, 2022
Revised: June 9, 2022
Accepted: July 5, 2022
Article in press: July 5, 2022
Published online: August 7, 2022

Geoffroy Mallaret, Mathieu Meleine, Ludivine Boudieu, Julie Barbier, Youssef Aissouni, Agathe Gelot, Denis Ardid, Department of Pharmacology, UMR 1107 NeuroDol, University of Clermont Auvergne, Clermont-Ferrand 63000, France

Amandine Lashermes, Department of Microbiology, Université Paris-Saclay, National Research Institute for Agriculture, Food and the Environment, AgroParisTech, Micalis Institute, Jouy-en-Josas 78350, France

Benoit Chassaing, Team "Mucosal Microbiota in Chronic Inflammatory Diseases", INSERM U1016, CNRS UMR 8104, Université Paris Cité, Paris 75014, France

Andrew T Gewirtz, Center for Inflammation, Institute for Biomedical Sciences, Georgia State University, Atlanta, GA30033, United States

Frederic Antonio Carvalho, Department of Pharmacology, INSERM 1107 NeuroDOL/University of Clermont Auvergne, Clermont-Ferrand 63000, France

Corresponding author: Frederic Antonio Carvalho, PhD, Academic Research, Department of Pharmacology, INSERM 1107 NeuroDOL/University of Clermont Auvergne, 28 Place Henri Dunant, Clermont-Ferrand 63000, France. frederic.carvalho@inserm.fr

Abstract

BACKGROUND

Chronic abdominal pain is the most common cause for gastroenterology consultation and is frequently associated with functional gastrointestinal disorders including irritable bowel syndrome and inflammatory bowel disease. These disorders present similar brain/gut/microbiota trialogue alterations, associated with abnormal intestinal permeability, intestinal dysbiosis and colonic hypersensitivity (CHS). Intestinal dysbiosis can alter colon homeostasis leading to abnormal activation of the innate immunity that promotes CHS, perhaps involving the toll-like receptors (TLRs), which play a central role in innate immunity.

AIM

To understand the mechanisms between early life event paradigm on intestinal permeability, fecal microbiota composition and CHS development in mice with TLRs expression in colonocytes.

METHODS
Maternal separation model (NMS) CHS model, which mimics deleterious events in childhood that can induce a wide range of chronic disorders during adulthood were used. Colonic sensitivity of NMS mice was evaluated by colorectal distension (CRD) coupled with intracolonic pressure variation (IPV) measurement. Fecal microbiota composition was analyzed by 16S rRNA sequencing from weaning to CRD periods. TLR mRNA expression was evaluated in colonocytes. Additionally, the effect of acute intrarectal instillation of the TLR5 agonist flagellin (FliC) on CHS in adult naive wildtype mice was analyzed.

RESULTS
Around 50% of NMS mice exhibited increased intestinal permeability and CHS associated with intestinal dysbiosis, characterized by a significant decrease of species richness, an alteration of the core fecal microbiota and a specific increased relative abundance of flagellated bacteria. Only TLR5 mRNA expression was increased in colonocytes of NMS mice with CHS. Acute intrarectal instillation of FliC induced transient increase of IPV, reflecting transient CHS appearance.

CONCLUSION
Altogether, these data suggest a pathophysiological continuum between intestinal dysbiosis and CHS, with a role for TLR5.

Key Words: Chronic abdominal pain; Colonic hypersensitivity; Toll-like receptors; Intestinal microbiota; Early life events

©The Author(s) 2022. Published by Baishideng Publishing Group Inc. All rights reserved.

Core Tip: Neonatal maternal separation (NMS) model mimic deleterious events in childhood, which can induce a wide range of chronic disorders during adulthood. Herein, around 50% of NMS mice exhibited increased intestinal permeability and colonic hypersensitivity (CHS) associated with intestinal dysbiosis. Only toll-like receptor 5 (TLR5) mRNA expression was increased in colonocytes of NMS mice with CHS and acute intrarectal instillation of flagellin transiently increased intracolonic pressure variations, reflecting transient CHS appearance. Together, those findings suggest a pathophysiological continuum between intestinal permeability, intestinal dysbiosis and CHS, with a previously undescribed role for TLR5 in CHS.

Citation: Mallaret G, Lashermes A, Meleine M, Boudieu L, Barbier J, Aissouni Y, Gelot A, Chassaing B, Gewirtz AT, Ardid D, Carvalho FA. Involvement of toll-like receptor 5 in mouse model of colonic hypersensitivity induced by neonatal maternal separation. *World J Gastroenterol* 2022; 28(29): 3903-3916
URL: https://www.wjgnet.com/1007-9327/full/v28/i29/3903.htm
DOI: https://dx.doi.org/10.3748/wjg.v28.i29.3903

INTRODUCTION

Irritable bowel syndrome (IBS) is one of the major chronic gastrointestinal disorders, strongly related to stress. It is characterized by abdominal pain, changes in bowel habits and increased intestinal permeability without macroscopic organic alterations. Such changes has been hypothesized to trigger impairment of life's quality and the development of comorbidities such as anxiety and depression[1]. A worldwide prevalence of 3%-5% has been reported and today, efficient pharmacological treatments are limited to relieve symptoms[2]. Colonic hypersensitivity (CHS), frequently associated with abdominal pain, has been described as the main cause of medical consultation in IBS patients with a prevalence ranging from 33% to 90%[3]. This symptom is defined by an altered sensation in response to colorectal stimuli and is clinically revealed by enhanced perception of mechanical triggers applied to the bowel. The common hypothesis is that CHS may result from colonic homeostasis changes and/or alterations of the brain-gut connection. In fact, the brain-gut axis has been shown to be impacted by inflammation and immunological factors, psychological factors, dysregulation of the hypothalamic-pituitary-adrenal (HPA) axis, abnormal activation of the vagus nerve and the enteric nervous system and intestinal dysbiosis[4].

Qualitative and/or quantitative alterations of the intestinal microbiota has been characterized in most of the functional gastrointestinal disorders including IBS[5]. Despite the numerous studies carried out, data on specific bacterial groups altered in IBS patients are still inconclusive. However, *Enterobacteriaceae*

family, *Lactobacillaceae* family, and *Bacteroides* genus seem to be increased in patients with IBS compared with controls, whereas uncultured *Clostridiales* I, *Faecalibacterium* and *Bifidobacterium* genus were decreased in IBS patients[6]. Furthermore, it has been described that some IBS patients with chronic abdominal pain present specific intestinal microbiota dysbiosis, allowing considerations of the gut microbiota as a potential therapeutic target[7].

In healthy conditions, the interaction between gut microbiota and pattern recognition receptors (PRRs), especially local toll-like receptors (TLRs), allow maintenance of intestinal barrier in a homeostatic state. Indeed, TLRs, mostly present on the membrane of immune and epithelial cells, identify pathogen-associated molecular patterns (PAMPs) and induce intracellular signaling cascade resulting in the production of cytokines and chemokines important for colonic homeostasis. The mammalian TLRs family consists of 13 members (TLR1-10 in humans, TLR1-9 and TLR11-13 in mice) and each TLR responds to distinct PAMPs leading to the activation of specific signaling pathway. For example, TLR4 recognizes lipopolysaccharide (LPS) and TLR5, which is expressed in the basolateral membrane of the intestinal epithelium, detects flagellin (FliC)[8]. In a dysbiotic state, alterations in the signature of microbial molecules sensed by the host can lead to abnormal activation state of the immune system and induce a low-grade intestinal inflammation[9].

The breakdown of the symbiotic relationship between TLRs and gut microbiota could contribute to the development of various multifactorial intestinal diseases, such as IBS. Previous studies have reported modifications of TLRs expression and activation in intestinal biopsies of IBS patients[10-15]. Furthermore, a preclinical study assessed the effect of neonatal maternal separation (NMS) in rats on TLRs expression, showing an upregulation of TLRs in colonic mucosa[16]. In this context, because of correlation between IBS and early life adverse events[17], this study investigated the impact of NMS paradigm on intestinal permeability, fecal microbiota composition and CHS development in mice as well as the association with TLRs expression.

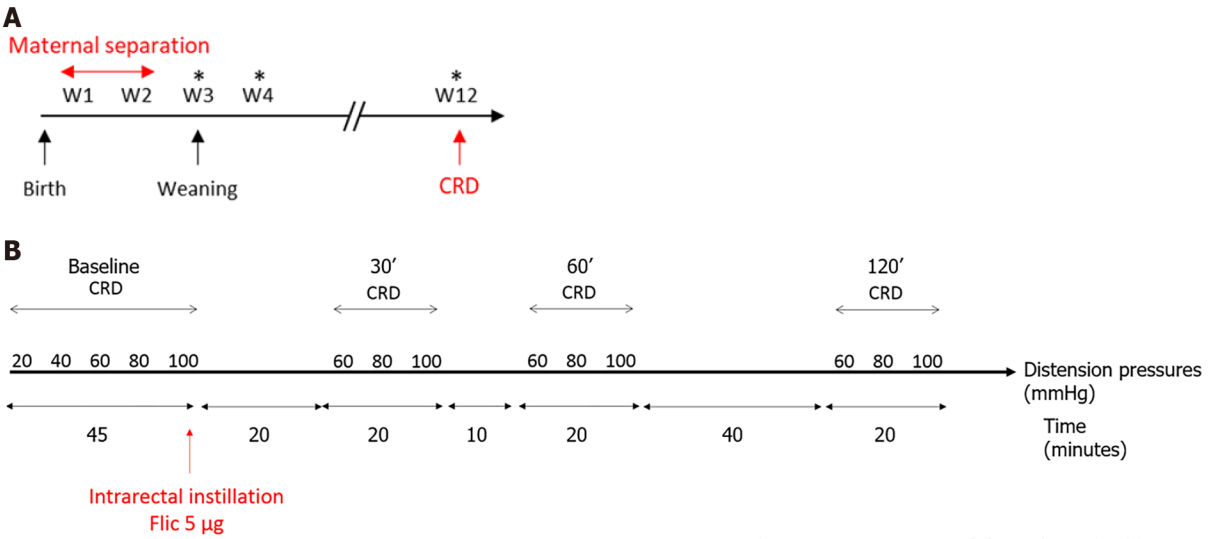
MATERIALS AND METHODS

Animals

Seven-week-old wild type C57Bl/6J males and females mice were purchased from Janvier Laboratories (Le Genest Saint Isle, France). They were mated to obtain male pups for the NMS protocol. After birth, wild-type C57Bl/AJ pups were isolated from their mother from post-natal days P2 to P14, three hours per day (from 9:00 a.m. to 12:00 p.m.). These mice were named NMS mice. Pups were then left with their mothers up to weaning (P21) (Figure 1A). Control wild-type C57Bl/AJ pups were co-housed in the animal facility and were called non-handled (NH) mice. In addition, ten-week-old wild type C57Bl/6J males were purchased from Janvier Laboratories and used for FliC intrarectal instillation experiment. Animals were given access to food and water *ad libitum* and housed with a 12 h light-dark cycle. All experiments were performed on twelve-week-old male mice and were performed according to the ethical guidelines set out by the International Association for the Study of Pain (IASP), complied with the European Union regulation and were approved by ethics committees: The local committees C2EA-02 of Clermont-Ferrand (approvals CE110-12 and CE111-12).

Colorectal distension test

Colorectal distension test (CRD) was performed using the non-invasive manometric method described [18]. A miniaturized pressure transducer catheter (Mikro-Tip SPR-254; Millar Instruments, Houston, TX, United States) equipped with a custom-made balloon (length: 1.5 cm) prepared from a polyethylene plastic bag which avoid any colonic compliance effect. On the day of the experiment, the mice were accustomed to the holding device for 1 h before the CRD. Then, under mild anesthetic (2.5% isoflurane), the balloon was inserted into the rectum such that the distal end of the balloon was 5 mm from the anal margin. Subsequently, the animals were placed in the holding device and allowed to recover for 30 min prior to CRD. The balloon was connected to an electronic barostat (Distender Series II, G&J Electronics, Toronto, Canada) and a preamplifier (PCU-2000 Dual Channel Pressure Control Unit, Millar Instruments, Houston, TX, United States) connected to the PowerLab interface (AD Instruments, Dunedin, New Zealand). The barostat enabled the control of the balloon pressure. The distension protocol consisted of a set of increasing distension pressures (20, 40, 60, 80 and 100 mmHg), each of which was repeated twice, which was applied for 20 s with a 4 min inter-pressure interval. The signal was acquired and analyzed using LabChart 7 software (ADInstruments, Dunedin, New Zealand). After intracolonic pressure recording for each animals along the CRD protocols and signal treatment as previously described[18], intracolonic pressure variation (IPV), reflecting the colonic sensitivity, was calculated as previously described[19] for each distension pressure. Briefly, IPV was calculated by subtracting the integral (area under the curve) of the treated signal corresponding to the 20 s preceding the CRD from the integral (area under the curve) of the treated signal during the 20 s of CRD stimulation. Therefore, two groups of NMS mice were defined: NMS non-sensitized (NMS NS) and NMS sensitized (NMS S) mice. The NMS S animals are distinguished according to the area under the curve (AUC) value in response to the distention pressures from 60 to 100 mmHg during CRD procedure



DOI: 10.3748/wjg.v28.i29.3903 **Copyright** ©The Author(s) 2022.

Figure 1 Time course protocols used in this study. A: Time course protocol for neonatal maternal separation experiment; B: Time course protocol for flagellin intrarectal instillation experiment. ∗Feces sample collection for Next Generation Sequencing; CRD: Colorectal distention test.

[20]. Briefly, if this value is higher than the average AUC of the NH control animals plus twice the SEM value ($AUC_{NMS\,S} \geq AUC_{NH} + 2 \times SEM_{NH}$), this mouse is considered as hypersensitive and are placed in the NMS S group. Others are considered as NMS NS. For FliC intrarectal instillation experiment, the distension protocol was the same before intrarectal instillation and, only a set of distension pressure 60, 80 and 100 mmHg was used 30 min, 60 min and 120 min after intrarectal instillation.

In vivo intestinal permeability

In vivo intestinal permeability was assessed using fluorescein dextran (FITC- dextran 3000-5000 Da, TdB Consultancy AB, Uppsala, Sweden) as previously described[21]. Briefly, before CRD, NMS and NH mice were orally gavaged with 0.6 g/g body weight of FITC-dextran and blood samples were obtained from the retro-orbital venous plexus 3 h after this administration. Plasma FITC levels were determined by fluorometry at 488 nm using a microplate reader (Tecan, Lyon, France).

Fecal pellets collection, DNA extraction and microbiota sequencing

Fecal pellets were collected from mice at week 3, 4 and 12 and stored at -80 °C prior to DNA extraction. Bacterial DNA was extracted from fecal bacteria following the protocol of NucleoSpin® Soil kit (Macherey-Nagel, Düren, Germany). DNA concentrations and purity were then assessed using Take3 micro-volume plate and Epoch Microplate Spectrophotometer (BioTek, Winooski, VT, United States). The 16S rRNA gene V4 variable region polymerase chain reaction (PCR) primers 515/806 with barcode on the forward primer were used in a 30 cycles PCR using the HotStarTaq Plus Master Mix Kit (Qiagen®, Germantown, MD, United States). Next generation sequencing (NGS) was performed at Molecular Research DNA (MR DNA - Shallowater, TX, United States) on a MiSeq following the manufacturer's guidelines. Sequences data analysis was performed using the quantitative insights into microbial ecology pipeline (QIIME)[22]. The analysis was carried out on the core microbiota *i.e.* the operational taxonomic units (OTUs) present in the fecal microbiota of 90% of the mice.

FliC intrarectal instillation

FliC from wildtype *Salmonella enterica* serovar typhimurium (SL3201, fljB−) was provided by Pr. A. Gewirtz (Center for Inflammation, Georgia State University, Atlanta, GA, United States). Briefly, FliC was purified through sequential cation- and anion-exchange chromatography and purity was verified as described previously[8]. Intrarectal instillation was performed under mild anesthetic (2.5% isoflurane) using orogastric feeding tube and inserted 2.5 cm up the colon (Figure 1B). At this point, 50 µL of FliC diluted in PBS, corresponding to 5 µg was slowly administered over 30 s while pressure was applied to the anal area to prevent leakage. Following the injection of the solution, the tube was slowly removed and the rectal pressure was maintained for a further 30 s.

Colonocytes extraction

Following mice euthanasia, fragments of colon (3-4 cm) were flushed and opened longitudinally along the mesentery and homogenized in cold PBS to remove feces. Then, these fragments were incubated into HBSS containing EDTA solution (2 mmol/L) 30 min at 37 °C with strong agitation every 10 min. After HBSS/EDTA incubation, colons were removed and samples were centrifuged at 2000 g for 10 min.

Then, HBSS/EDTA was removed and colonocytes were deep-frozen in liquid nitrogen and stored at -80 °C for further analysis.

RNA extraction, reverse transcription and quantitative PCR

Total RNA from mice colonocytes was extracted using the RNeasy Plus Mini Kit (Qiagen®, Germantown, MD, United States) according to the manufacturer's protocol. After RNA extraction, reverse transcription was performed with the High Capacity cDNA RT Kit (Applied Biosystems, Foster City, CA, United States) with 500 ng of RNA, followed by a qPCR using LightCycler FastStart DNA Master SYBR Green Kit (Roche Applied Science, Penzberg, Germany). The primers used for TLRs expression analysis are described in Table 1. All results were normalized to the *HPRT* gene. Samples were tested in duplicate, and the average values were used for quantification by using 2-ΔΔCt method.

Fecal FliC and LPS load quantification

FliC and LPS were quantified using human embryonic kidney (HEK)-Blue-mTLR5 and HEK-Blue-mTLR4 cells, respectively (Invivogen, San Diego, California, United States). Fecal material was resuspended in PBS to a final concentration of 100 mg/mL and homogenized for 10 s using a Mini-Beadbeater-24 without the addition of beads to avoid bacteria disruption. The samples were then centrifuged at 8000 g for 2 min and the resulting supernatant was serially diluted and applied to mammalian cells. Purified *Escherichia coli* FliC and LPS (Sigma, St Louis, Missouri, United States) were used for standard curve determination using HEK-Blue-mTLR5 and HEK-Blue-mTLR4 cells, respectively. After 24 h of stimulation, cell culture supernatant was applied to QUANTI-Blue medium (Invivogen, San Diego, California, United States) and alkaline phosphatase activity was measured at 620 nm after 30 min.

Statistical analysis

Statistical analyses were performed with Prism 7 software (GraphPad, La Jolla, CA, United States). The Kolmogorov-Smirnov test has been used to check if data follow a normal distribution. One-way ANOVA, Kruskal-Wallis test or two-way ANOVA (more than two groups) were used for intergroup-comparisons with Tukey's, Dunn's and Dunnett's test for the post-hoc analysis. Correlation was assessed using Pearson's test. ANOSIM method followed by Monte-Carlo permutation test was performed to assess the significativity of beta-diversity analysis of fecal microbiota using the QIIME. A P value ≤ 0.05 was considered statistically significant.

RESULTS

NMS paradigm induces CHS and intestinal permeability increase in a subset of mice

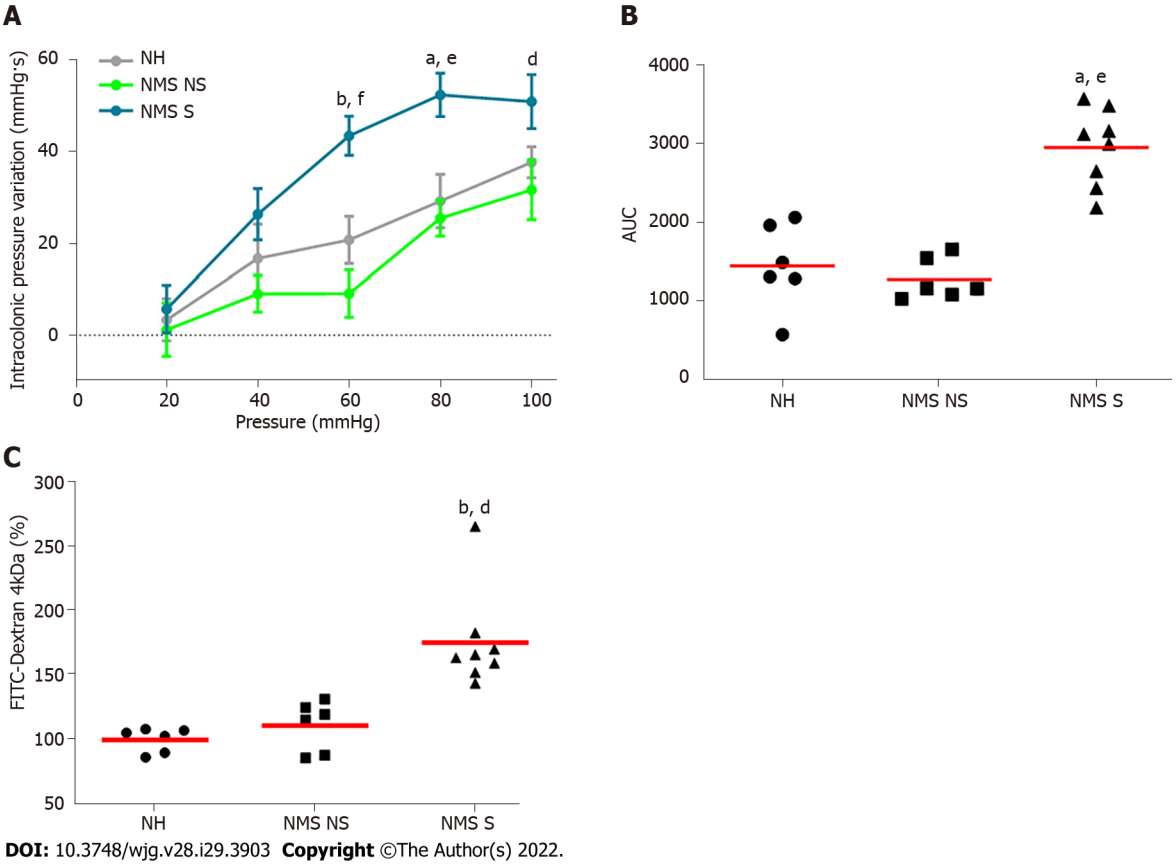
In order to evaluate colonic sensitivity, a CRD test was performed on twelve-week-old NH or NMS mice (Figure 1A). As previously described[23], among NMS mice only a subset developed CHS in comparison to NH mice Therefore, two groups of NMS mice were defined: NMS NS and NMS S mice. In fact, colorectal distension assessment revealed significant increase of IPV for the highest distension pressures 60, 80 and 100 mmHg in the NMS S group in comparison to NMS NS and NH groups (Figure 2A). Analysis of the areas under the curve (AUC) for each mouse confirmed this significant difference between NH, NMS NS and NMS S groups (Figure 2B). Intestinal permeability assessment revealed significant increase of FITC-Dextran plasma levels in the NMS S group compared to NH and NMS NS groups (Figure 2C).

Fecal microbiota dysbiosis is associated with CHS in neonatal maternal separated mice

Illumina sequencing of the 16S rRNA gene was performed on fecal pellets DNA extracts from NH, NMS NS and NMS S mice at W3, W4 and W12 (just before the CRD test) according to the time course protocol for NMS experiment (Figure 1A). Alpha-diversity analysis (number of observed OTUs) of the core fecal microbiota revealed no statistical difference between NH, NMS NS and NMS S animals at week 3, before weaning (Figure 3A-left panel). However, a significant decrease of species richness appeared at W4 in NMS S mice in comparison to NH or NMS NS animals and persisted at adulthood (W12, time point of CRD test), even if NMS NS and NMS S mice were co-housed in the same cage during all the experiment (Figure 3A-middle and right panels). In addition, a significant decrease of the observed OTUs number was present in NMS NS at adulthood (W12) in comparison to NH mice. Principal coordinates analysis based on unweighted UniFrac distances confirmed the alteration of the core fecal microbiota. It enabled to significantly (ANOSIM method followed by the Monte-Carlo permutation test, $P < 0.05$) identify the three animals' groups from W3 to W12 (Figure 3B). The taxonomic analysis of the fecal core microbiota composition in the NMS S group revealed in twelve weeks old mice a decreased relative abundance of bacteria belonging to the phylum *Bacteroidetes* and an increase in *Firmicutes* in comparison to the NMS NS group (Figure 3C). At lower taxonomic levels, NMS S mice were characterized by a decreased abundance of bacteria from the genera *Allobaculum* and *Barnesiella* compared to

Table 1 Primers used for toll-like receptors expression analysis

Gene	5'-3' Forward	5'-3' Reverse
tlr2	ACCAAGATCCAGAAGAGCCA	CATCACCGGTCAGAAAACAA
tlr3	GCGTTGCGAAGTGAAGAACT	TTCAAGAGGAGGGCGAATAA
tlr4	TTCAGAACTTCAGTGGCTGG	TGTTAGTCCAGAGAAACTTCCTG
tlr5	GCAGGATCATGGCATGTCAAC	ATCTGGGTGAGGTTACAGCCT
tlr9	AACCGCCACTTCTATAACCAG	GTAAGACAGAGCAAGGCAGG
hprt	TTGCTGACCTGCTGGATTA	AGTTGAGAGATCATGTCCAC



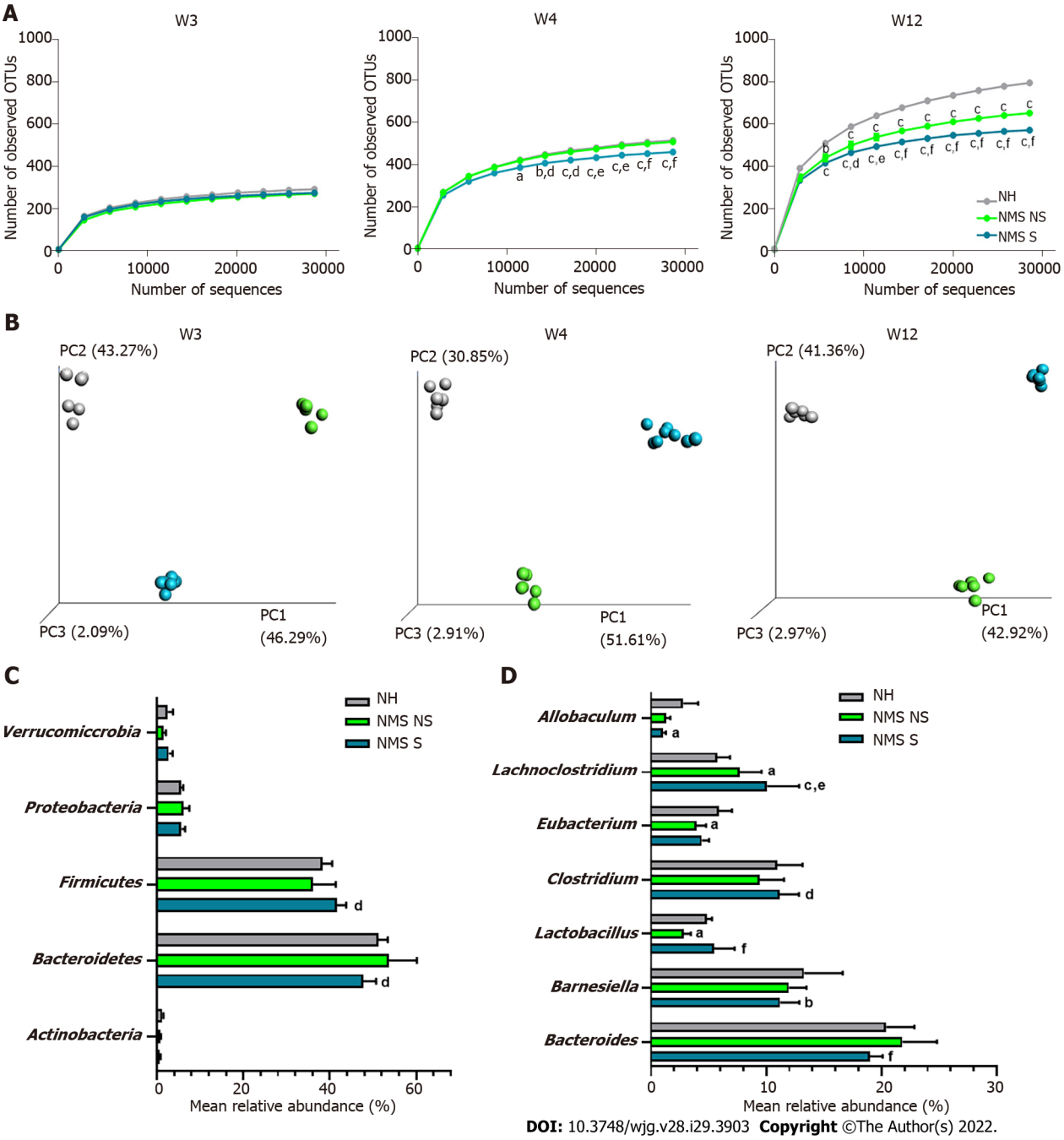
DOI: 10.3748/wjg.v28.i29.3903 **Copyright** ©The Author(s) 2022.

Figure 2 Neonatal maternal separation induces colonic hypersensitivity and increases intestinal permeability in mice. A: Intracolonic pressure variation (IPV) in response to colorectal distension in non-handled (NH), neonatal maternal separated non-sensitized (NMS NS) and neonatal maternal separated sensitized (NMS S) mice; B: Area under the curve (AUC) of the IPV relative to colorectal distension for each NH, NMS NS and NMS S mouse; C: FITC-dextran 4 kDa plasmatic concentrations, 3 h after oral gavage with 15 mg of FITC-dextran of NH, NMS NS and NMS S mice. Values are expressed as a percentage of FITC-dextran per mL of plasma in comparison to the NH group mean. NH: $n = 6$; NMS NS: $n = 6$; NMS S: $n = 8$. $^{a}P < 0.05$ and $^{b}P < 0.01$ *vs* NH group; and $^{d}P < 0.05$, $^{e}P < 0.01$ and $^{f}P < 0.001$ *vs* NMS NS group. For IPV to CRD test, dots represent means and error bars represent SEM. For AUC and FITC-dextran, each dot represents one mouse and red lines represent means.

control NH mice, and a decreased abundance of bacteria from the genera *Bacteroides* compared to NMS NS mice. The relative abundances of *Lachnoclostridium, Clostridium* and *Lactobacillus* were increased in these NMS animals with CHS in comparison to NMS mice without CHS. Surprisingly, the relative abundance of *Lactobacillus* was decreased in NMS NS animals compared to NH group (Figure 3D).

CHS induced by NMS exposure increased fecal level of FliC and is related to TLR5 overexpression in colonocytes

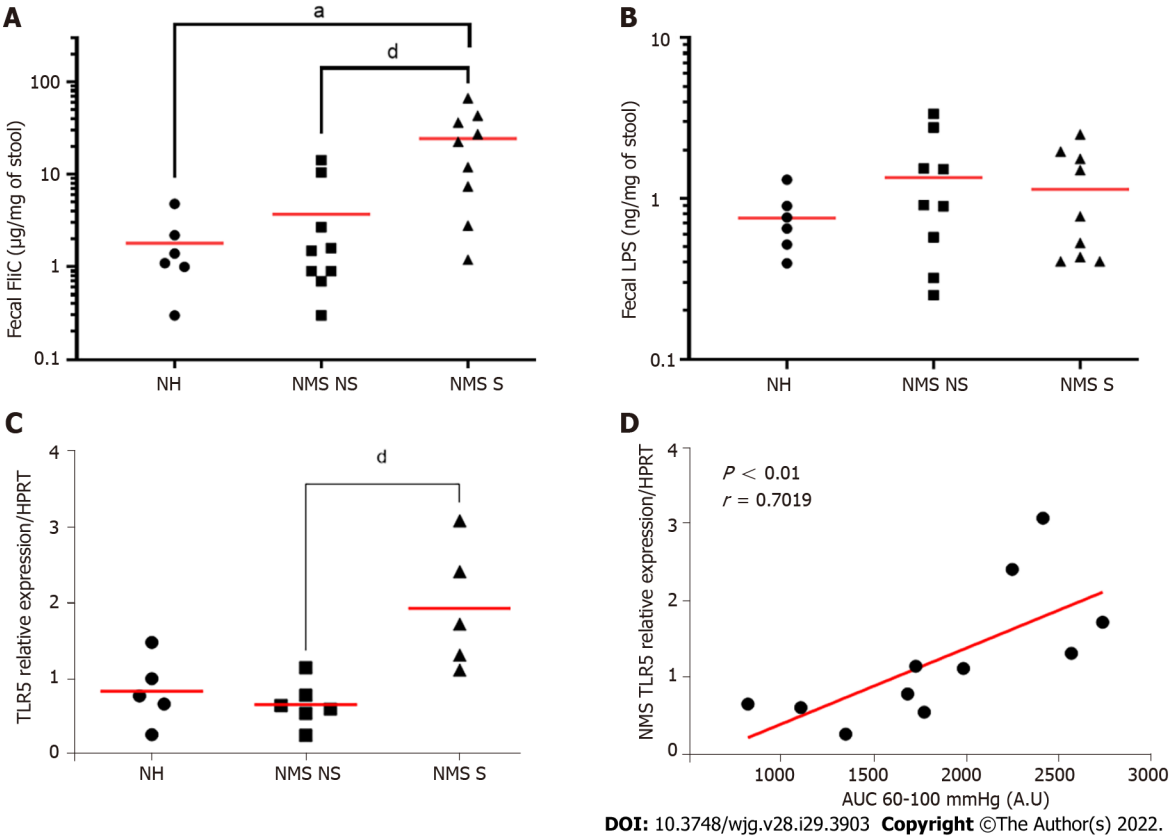
To understand potential mechanisms between fecal microbiota dysbiosis and CHS induced by NMS, quantification of two different PAMPs, FliC and LPS, was performed in feces from twelve-week-old NH, NM NS and NMS S mice. Exposure to NMS paradigm increased significantly fecal level of FliC (Figure 4A) rather than fecal LPS which is not significant better between different animal (Figure 4B).



DOI: 10.3748/wjg.v28.i29.3903 **Copyright** ©The Author(s) 2022.

Figure 3 Neonatal maternal separation paradigm induces alterations of core fecal microbiota related to colonic hypersensitivity. A: Alpha-diversity analysis of the core microbiota. Number of observed operational taxonomic units according to the number of sequences per samples of fecal samples from non-handled (NH), neonatal maternal separated non-sensitized (NMS NS) and neonatal maternal separated sensitized (NMS S) at week 3 (W3), week 4 (W4) and week 12 (W12); B: Beta-diversity analysis of the core microbiota. Principal coordinates analysis (PCoA) of unweighted UniFrac distances of NH, NMS NS and NMS S mice at W3, W4 and W12; C and D: Mean relative abundances of bacterial phyla (C) and genera (D) significantly altered by the NMS paradigm between NH, NMS NS and NMS S mice at W12. NH: n = 6; NMS NS: n = 6; NMS S: n = 8. $^{a}P < 0.05$, $^{b}P < 0.01$ and $^{c}P < 0.001$ *vs* NH or $^{d}P < 0.05$, $^{e}P < 0.01$ and $^{f}P < 0.001$ *vs* NMS NS groups respectively. For alpha-diversity analysis, dots represent means and error bars represent SEM. For PCoA analysis each dot represents one mouse.

As TLRs are the main receptors of PAMPs, the TLRs mRNA expression in colonocytes from NH, NMS NS and NMS S mice was quantified in adult (W12) mice. As previously described, three mouse groups were defined, based on the CHS (Supplementary Figure 1A and B). In those mouse groups, the TLR2, 3, 4 and 9 mRNA were not modified between NH, NMS NS and NMS S animals (Supplementary Figure 1C), whereas TLR5 mRNA expression is significantly increased only in NMS S subgroup (NH: 0.836 ± 0.200, NMS NS: 0.662 ± 0.120, NMS S: 1.925 ± 0.363, $P < 0.05$ *vs* NMS NS) (Figure 4C). AUC corresponding to the IPV for highest colorectal distension pressures (60, 80 and 100 mmHg) significantly correlated with the mRNA expression level of TLR5 in colonocytes of NMS mice ($P < 0.01$) (Figure 4D).



DOI: 10.3748/wjg.v28.i29.3903 **Copyright** ©The Author(s) 2022.

Figure 4 Neonatal maternal separation induced colonic hypersensitivity is associated with increased flagellin fecal content and colonocytes toll-like receptor 5 expression. A: Levels of fecal flagellin (FliC) assayed with toll-like receptor 5 (TLR5) reporter cells; B: Levels of fecal lipopolysaccharide assayed with TLR4 reporter cells; C: Colonocytes mRNA expression of TLR5 in non-handled (NH), neonatal maternal separated non-sensitized (NMS NS) and neonatal maternal separated sensitized (NMS S) mice at week 12. Values are expressed as relative expression of TLR5 mRNA compared to *HPRT* expression; D: Correlation between NMS colonocytes TLR5 expression and area under the curve (AUC) corresponding of the intracolonic pressure variation (IPV) for highest colorectal distension pressures (60, 80 and 100 mmHg). A and B: NH: $n = 6$; NMS NS: $n = 9$; NMS S: $n = 9$. $^{a}P < 0.05$ *vs* NH group; and $^{d}P < 0.05$ *vs* NMS NS group. C and D: NH: $n = 5$; NMS NS: $n = 6$; NMS S: $n = 5$. $^{d}P < 0.05$ *vs* NMS NS. For FliC quantification TLR5 mRNA relative expression, each dot represents one mouse and red lines represent means and for correlation between TLR5 expression and AUC of IPV, each dot represents one mouse and red line represents the linear regression curve.

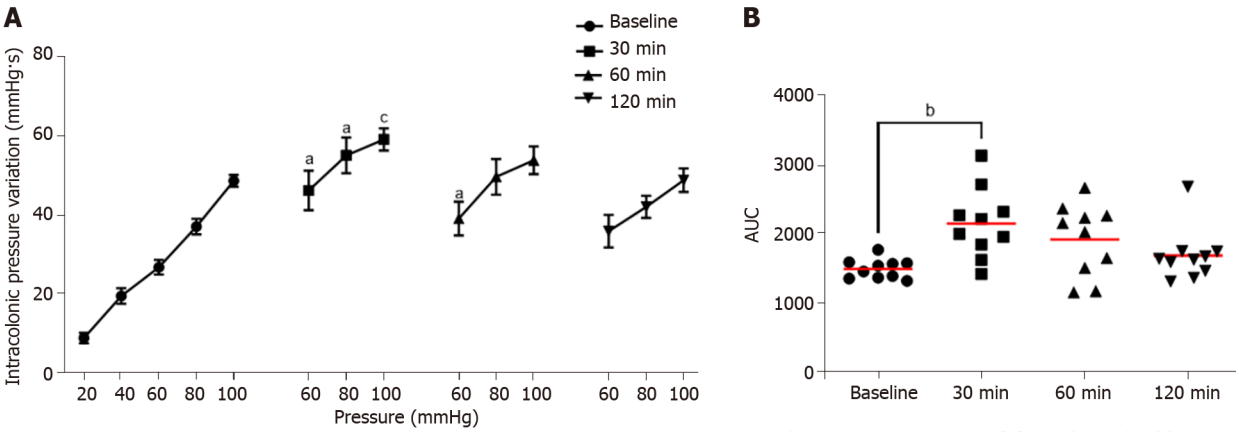
FliC intrarectal instillation is associated with a transient increase of colonic sensitivity

Intrarectal instillation of FliC, agonist of the receptor TLR5, significantly increased IPV at the 60, 80 and 100 mmHg distension pressure 30 min and 60 min post-instillation (Figure 5A). The increase in the response to CRD test was transient and did not persist 120 min after FliC instillation. AUC confirmed this significant increase of IPV 30 min after intrarectal instillation of FliC (Figure 5B).

DISCUSSION

Abdominal pain, frequently associated with CHS, has been shown to be a common feature of IBS patients. It also strongly impacts on patient's quality of life, leading to an important rate of consultation in Gastroenterology[24]. According to clinical studies, 33% to 90% of IBS patients exhibit CHS[3,25]. IBS presents a poorly first line treatment efficacy, especially regarding the treatment of abdominal pain[26]. Thus, in accordance with the aim of our study, a better characterization of mechanisms associated with CHS is important for the establishment of new potential pharmacological targets.

The etiology of this condition, resulting in various symptoms, remains unclear even if biological, psychological and social factors seem to be involved. Indeed, several studies reported an increased risk of IBS associated with early adverse life events[17,27-29]. These events refer to traumatic experience during childhood such as physical, sexual or emotional abuse as well as discordant relationship with primary caretaker. Using NMS stress animal model[30], our study demonstrates the impact of early adverse life events on colonic sensitivity of adult mice. Interestingly, only a subset of NMS mice presented CHS, revealed by CRD test, compared to control non-handled mice. These results were consistent with data obtained in previous studies carried out in both rats and mice[23,31,32].



DOI: 10.3748/wjg.v28.i29.3903 **Copyright** ©The Author(s) 2022.

Figure 5 Evaluation of the impact of intrarectal instillation of flagellin on colonic sensitivity. A: Intracolonic pressure variation (IPV) in response to colorectal distension in males mice before (Baseline) and after (30, 60 and 120 min) intrarectal instillation of flagellin (5 µg); B: Area under the curve (AUC) of the IPV relative to highest colorectal distension pressures (60, 80 and 100 mmHg). For each mouse and each time point, $n = 10$. $^{a}P < 0.05$, $^{b}P < 0.01$ and $^{c}P < 0.001$ respect to Baseline. For IPV to colorectal distension test, dots represent means and error bars represent SEM. For AUC, each dot represents one mouse and red lines represent means.

Many studies reported an association between activation of the HPA axis, the major neuroendocrine system regulating various bodily processes in response to psychological or physical stressors, and intestinal permeability increase[33,34]. Furthermore, alteration of the intestinal barrier is a key clinical feature of IBS and it has been related to CHS[35]. In our study, assessment of intestinal permeability was carried out by measurement of FITC-dextran plasma level. Only NMS animals with CHS exhibited high plasmatic levels of FITC-dextran, suggesting that NMS paradigm induced CHS is associated with altered intestinal barrier. This result is in accordance with previous reports showing increased intestinal permeability following NMS paradigm or chronic stress exposure[34,36,37]. In addition, the link between the weakness of the intestinal mucosa barrier and CHS has been demonstrated in a mouse model of post-infectious IBS[20].

Consistent studies reported intestinal dysbiosis in IBS patients[6]. The main distinguishing feature of IBS patients compared to heathy volunteers is on one hand the increased abundance of bacteria belonging to the *Firmicutes* phylum and on the other hand, the decreases abundance of bacteria belongs to the *Bacteroidetes* phylum. Implication of the intestinal microbiota in CHS and associated chronic abdominal pain was also suggested[38]. In the present study, the characterization of the fecal microbiota composition using high-throughput sequencing of the 16S rRNA revealed the presence of a dysbiotic state making it possible to discriminate NH, NMS NS and NMS S mice. Indeed, the beta-diversity analyses showed that the composition of the fecal microbiota is different between NMS and NH control mice but also between NMS NS and NMS S mice while these animals came from the same litters and were co-housed. Changes in intestinal microbiota composition associated with NMS and CHS appeared very early, before weaning the animals (week 3) and persisted over time up to 12 wk. These alterations in the fecal microbiota composition were also characterized by a decreased bacterial richness in NMS S mice from week 4 to week 12. In general, this decrease was associated with a physiological disorder in the host, which seemed to be in agreement with the results obtained in this model[39]. A reduction in the bacterial diversity of the intestinal microbiota has notably been demonstrated in IBD and IBS patients but also in stress animal models[40-44]. *Clostridium* and *Lachnoclostridium*, flagellated bacteria, are among the genera whose abundance was increased in NMS S mice, at W12, the time of colonic sensitivity assessment, compared to NMS mice without CHS. Studies carried out in animals subjected to stress during the neonatal period have also shown an increase in the relative abundance of the *Clostridium* genus[43,45,46]. Furthermore and interestingly, Luna *et al*[47] highlighted an increased relative abundance of different species of *Clostridium* and *Lachnoclostridium* within the mucosa-associated microbiota in children with an autistic disorder associated with functional gastrointestinal disorders and in particular abdominal pain. These findings suggest an implication of the intestinal microbiota in the development of CHS in the NMS model.

In a dysbiotic state, particularly associated with an increase in intestinal permeability, alterations in the signature of microbial molecules sensed by the host can lead to a different activation state of the immune system[9]. Indeed, PAMPs, such as LPS or FliC, are sensed by PRRs including TLRs, which are expressed on the host cell surface or in the cytosolic compartment of numerous cell types. In this context, the aim of our study was to characterize the expression of different TLRs in colonocytes from our different animal subgroups after NMS paradigm. It is important to note that NMS paradigm is not associated with a modification of the intestinal inflammation status[23,36]. An increased TLR5 expression was observed only in animals presenting CHS after NMS paradigm, moreover, correlation

between gene expression of TLR5 and AUC from 60 to 100 mmHg (corresponding to nociceptive stimulation) in NMS mice. These findings are in line with some reports showing upregulation of TLRs in IBS patient's colonic biopsies[10-12,15]. An increased expression of some TLRs was also observed in NMS model but without association with visceral pain[11]. Few publications have indicated TLRs implication in animal pain model, especially inflammatory and neuropathic pain[48,49]. In visceral pain context, Tramullas *et al*[50] in 2014 demonstrated involvement of TLR4 in visceral sensitivity in a chronic stress model. Furthermore, Luczynski *et al*[51] demonstrated increased colonic sensitivity to colorectal distention in germ free mice, associated with an increase of TLRs expression in spinal cord. Finally, in 2018, a study published by Zhou *et al*[52] established TLR4 implication in inflammatory visceral pain in animals with high-fat diet. Following the demonstration of FliC increase in NMS S mice fecal content and the upregulation of TLR5 expression in the NMS S mouse colonocytes, the effect of FliC was assessed on visceral sensitivity in naïve animals. We highlighted a transient increase of colonic sensitivity between 30 min and 60 min after FliC intra-rectal instillation. These results are the first to demonstrate potential FliC and TLR5 involvement in CHS in a non-inflammatory IBS-like animal model. Indeed, only Das *et al*[53] have shown that TLR5 signaling mediates hypersensitivity in a model of allodynia and that sensitivity was reversed by blocking TLR5 with a specific antagonist. Moreover, Dlugosz *et al*[54] has found a significantly higher serum level of antibodies to FliC patients with IBS. Our data, associated with the results of previous studies suggest that TLR5, through its activation by FliC, could play a key role in CHS induced by dysbiosis related to the NMS paradigm and more generally, in the pathophysiology of IBS.

CONCLUSION

In conclusion, our results demonstrated the association of fecal dysbiosis, characterized especially by an increased abundance of flagellated bacteria, with impaired intestinal permeability, increased TLR5 expression and induced CHS. Taken together, TLR5 signaling upon recognition of FliC is relevant in visceral pain through both direct and indirect mechanisms, and application of TLR5-specific antagonists could potentially reversed CHS in non-inflammatory visceral pain context[23,36].

ARTICLE HIGHLIGHTS

Research background

Chronic abdominal pain associated to irritable bowel syndrome (IBS) is strongly related to stress and is the most common cause for gastroenterology consultation. Brain/gut/microbiota trialogue alterations are suspected to be involved in colonic hypersensitivity (CHS), responsible for chronic abdominal pain. It is also associated with abnormal intestinal permeability and intestinal dysbiosis, which can alter colon homeostasis leading to abnormal activation of the innate immunity that promotes CHS, perhaps involving the toll-like receptors (TLRs), which play a central role in innate immunity.

Research motivation

The breakdown of the relationship between TLRs and gut microbiota could contribute to the development of IBS. Thus, because of correlation between IBS and early life adverse events, our study investigated the impact of neonatal maternal separation (NMS) paradigm on intestinal homeostasis, fecal microbiota composition and CHS development in mice as well as the association with TLRs expression.

Research objectives

A better characterization of mechanisms associated with CHS is important for the establishment of new potential pharmacological targets.

Research methods

In our study, we used a referenced CHS animal model, the NMS paradigm, which mimics deleterious events in childhood that can induce a wide range of chronic disorders during adulthood. In addition, we have evaluated colonic sensitivity of NMS mice by colorectal distension (CRD) coupled with intracolonic pressure variation measurement. Fecal microbiota composition was analyzed by 16S rRNA sequencing from weaning to CRD periods. TLR mRNA expression was evaluated in colonocytes.

Research results

This study, based on the preclinical mouse model of NMS, demonstrated that around 50% of NMS mice exhibited increased intestinal permeability and CHS associated with intestinal dysbiosis. In particular, a significant increased amount of flagellated bacteria was observed in the NMS mice with CHS. In

association, only tlr5 mRNA expression was increased in colonocytes of NMS mice with CHS.

Research conclusions

Taken together, our results suggest a pathophysiological continuum between intestinal dysbiosis and CHS, with a role for TLR5.

Research perspectives

TLR5 signaling upon recognition of flagellin is relevant in visceral pain through both direct and indirect mechanisms, and application of TLR5-specific antagonists could potentially reversed CHS in non-inflammatory visceral pain context.

ACKNOWLEDGEMENTS

The authors would like to acknowledge Abdelkrim Alloui (Animal facilities) for animal care.

FOOTNOTES

Author contributions: Mallaret G and Lashermes A contributed equally to this article; Study concept and design done by Mallaret G, Lashermes A, Ardid D and Carvalho FA; Acquisition of data done by Mallaret G, Lashermes A, Barbier J, Aissouni Y, Chassaing B; Analysis and interpretation of data done by Mallaret G, Lashermes A, Chassaing B, Gewirtz AT, Ardid D and Carvalho FA; Drafting of the manuscript done by Mallaret G, Lashermes A Meleine M, Boudieu L and Carvalho FA; Obtained funding done by Ardid D and Carvalho FA; Study supervision done by Gewirtz AT, Ardid D and Carvalho FA.

Supported by the Region Auvergne-Rhône-Alpes and FEDER, No. Thématiques émergentes and Pack Ambition Recherche; the French Government IDEX-ISITE Initiative, No. 16-IDEX-0001-CAP 20-25; the Ministère de la Recherche et de la Technologie, INSERM and University of Clermont Auvergne, No. UMR1071.

Institutional animal care and use committee statement: All experiments were performed according to the ethical guidelines set out by the International Association for the Study of Pain, complied with the European Union regulation and were approved by ethics committees: the local committees C2EA-02 of Clermont-Ferrand (approvals CE110-12 and CE111-12).

Conflict-of-interest statement: All authors have nothing to disclose.

Data sharing statement: All sequencing raw data have been deposited in European Nucleotide Archive (ENA) under accession number PRJEB50651.

ARRIVE guidelines statement: The authors have read the ARRIVE guidelines, and the manuscript was prepared and revised according to the ARRIVE guidelines.

Open-Access: This article is an open-access article that was selected by an in-house editor and fully peer-reviewed by external reviewers. It is distributed in accordance with the Creative Commons Attribution NonCommercial (CC BY-NC 4.0) license, which permits others to distribute, remix, adapt, build upon this work non-commercially, and license their derivative works on different terms, provided the original work is properly cited and the use is non-commercial. See: https://creativecommons.org/Licenses/by-nc/4.0/

Country/Territory of origin: France

ORCID number: Geoffroy Mallaret 0000-0002-3658-3418; Amandine Lashermes 0000-0002-8241-464X; Mathieu Meleine 0000-0002-0925-087X; Ludivine Boudieu 0000-0002-4774-9313; Julie Barbier 0000-0001-7177-3236; Youssef Aissouni 0000-0002-9264-7690; Agathe Gelot 0000-0002-7884-6968; Benoit Chassaing 0000-0002-4285-769X; Andrew T Gewirtz 0000-0002-6338-7578; Denis Ardid 0000-0003-4320-7338; Frederic Antonio Carvalho 0000-0003-1592-2369.

S-Editor: Zhang H
L-Editor: A
P-Editor: Yu HG

REFERENCES

1 **Kopczyńska M**, Mokros Ł, Pietras T, Małecka-Panas E. Quality of life and depression in patients with irritable bowel syndrome. *Prz Gastroenterol* 2018; **13**: 102-108 [PMID: 30002768 DOI: 10.5114/pg.2018.75819]

2 **Sperber AD**, Bangdiwala SI, Drossman DA, Ghoshal UC, Simren M, Tack J, Whitehead WE, Dumitrascu DL, Fang X, Fukudo S, Kellow J, Okeke E, Quigley EMM, Schmulson M, Whorwell P, Archampong T, Adibi P, Andresen V, Benninga MA, Bonaz B, Bor S, Fernandez LB, Choi SC, Corazziari ES, Francisconi C, Hani A, Lazebnik L, Lee YY, Mulak A, Rahman MM, Santos J, Setshedi M, Syam AF, Vanner S, Wong RK, Lopez-Colombo A, Costa V, Dickman R, Kanazawa M, Keshteli AH, Khatun R, Maleki I, Poitras P, Pratap N, Stefanyuk O, Thomson S, Zeevenhooven J, Palsson OS. Worldwide Prevalence and Burden of Functional Gastrointestinal Disorders, Results of Rome Foundation Global Study. *Gastroenterology* 2021; **160**: 99-114.e3 [PMID: 32294476 DOI: 10.1053/j.gastro.2020.04.014]

3 **Farzaei MH**, Bahramsoltani R, Abdollahi M, Rahimi R. The Role of Visceral Hypersensitivity in Irritable Bowel Syndrome: Pharmacological Targets and Novel Treatments. *J Neurogastroenterol Motil* 2016; **22**: 558-574 [PMID: 27431236 DOI: 10.5056/jnm16001]

4 **Watanabe S**, Radman-Livaja M, Rando OJ, Peterson CL. A histone acetylation switch regulates H2A.Z deposition by the SWR-C remodeling enzyme. *Science* 2013; **340**: 195-199 [PMID: 23580526 DOI: 10.1126/science.1229758]

5 **Enck P**, Mazurak N. Dysbiosis in Functional Bowel Disorders. *Ann Nutr Metab* 2018; **72**: 296-306 [PMID: 29694952 DOI: 10.1159/000488773]

6 **Pittayanon R**, Lau JT, Yuan Y, Leontiadis GI, Tse F, Surette M, Moayyedi P. Gut Microbiota in Patients With Irritable Bowel Syndrome-A Systematic Review. *Gastroenterology* 2019; **157**: 97-108 [PMID: 30940523 DOI: 10.1053/j.gastro.2019.03.049]

7 **Jalanka-Tuovinen J**, Salonen A, Nikkilä J, Immonen O, Kekkonen R, Lahti L, Palva A, de Vos WM. Intestinal microbiota in healthy adults: temporal analysis reveals individual and common core and relation to intestinal symptoms. *PLoS One* 2011; **6**: e23035 [PMID: 21829582 DOI: 10.1371/journal.pone.0023035]

8 **Gewirtz AT**, Navas TA, Lyons S, Godowski PJ, Madara JL. Cutting edge: bacterial flagellin activates basolaterally expressed TLR5 to induce epithelial proinflammatory gene expression. *J Immunol* 2001; **167**: 1882-1885 [PMID: 11489966 DOI: 10.4049/jimmunol.167.4.1882]

9 **Levy M**, Kolodziejczyk AA, Thaiss CA, Elinav E. Dysbiosis and the immune system. *Nat Rev Immunol* 2017; **17**: 219-232 [PMID: 28260787 DOI: 10.1038/nri.2017.7]

10 **Brint EK**, MacSharry J, Fanning A, Shanahan F, Quigley EM. Differential expression of toll-like receptors in patients with irritable bowel syndrome. *Am J Gastroenterol* 2011; **106**: 329-336 [PMID: 21102570 DOI: 10.1038/ajg.2010.438]

11 **McKernan DP**, Gaszner G, Quigley EM, Cryan JF, Dinan TG. Altered peripheral toll-like receptor responses in the irritable bowel syndrome. *Aliment Pharmacol Ther* 2011; **33**: 1045-1052 [PMID: 21453321 DOI: 10.1111/j.1365-2036.2011.04624.x]

12 **Belmonte L**, Beutheu Youmba S, Bertiaux-Vandaële N, Antonietti M, Lecleire S, Zalar A, Gourcerol G, Leroi AM, Déchelotte P, Coëffier M, Ducrotté P. Role of toll like receptors in irritable bowel syndrome: differential mucosal immune activation according to the disease subtype. *PLoS One* 2012; **7**: e42777 [PMID: 23028414 DOI: 10.1371/journal.pone.0042777]

13 **Dlugosz A**, Zakikhany K, Acevedo N, D'Amato M, Lindberg G. Increased Expression of Toll-Like Receptors 4, 5, and 9 in Small Bowel Mucosa from Patients with Irritable Bowel Syndrome. *Biomed Res Int* 2017; **2017**: 9624702 [PMID: 28246611 DOI: 10.1155/2017/9624702]

14 **Koçak E**, Akbal E, Köklü S, Ergül B, Can M. The Colonic Tissue Levels of TLR2, TLR4 and Nitric Oxide in Patients with Irritable Bowel Syndrome. *Intern Med* 2016; **55**: 1043-1048 [PMID: 27150852 DOI: 10.2169/internalmedicine.55.5716]

15 **Shukla R**, Ghoshal U, Ranjan P, Ghoshal UC. Expression of Toll-like Receptors, Pro-, and Anti-inflammatory Cytokines in Relation to Gut Microbiota in Irritable Bowel Syndrome: The Evidence for Its Micro-organic Basis. *J Neurogastroenterol Motil* 2018; **24**: 628-642 [PMID: 30347939 DOI: 10.5056/jnm18130]

16 **McKernan DP**, Nolan A, Brint EK, O'Mahony SM, Hyland NP, Cryan JF, Dinan TG. Toll-like receptor mRNA expression is selectively increased in the colonic mucosa of two animal models relevant to irritable bowel syndrome. *PLoS One* 2009; **4**: e8226 [PMID: 20011045 DOI: 10.1371/journal.pone.0008226]

17 **Bradford K**, Shih W, Videlock EJ, Presson AP, Naliboff BD, Mayer EA, Chang L. Association between early adverse life events and irritable bowel syndrome. *Clin Gastroenterol Hepatol* 2012; **10**: 385-90.e1 [PMID: 22178460 DOI: 10.1016/j.cgh.2011.12.018]

18 **Larauche M**, Gourcerol G, Million M, Adelson DW, Taché Y. Repeated psychological stress-induced alterations of visceral sensitivity and colonic motor functions in mice: influence of surgery and postoperative single housing on visceromotor responses. *Stress* 2010; **13**: 343-354 [PMID: 20536336 DOI: 10.3109/10253891003664166]

19 **Picard E**, Carvalho FA, Agosti F, Bourinet E, Ardid D, Eschalier A, Daulhac L, Mallet C. Inhibition of $Ca_v3.2$ calcium channels: A new target for colonic hypersensitivity associated with low-grade inflammation. *Br J Pharmacol* 2019; **176**: 950-963 [PMID: 30714145 DOI: 10.1111/bph.14608]

20 **Lashermes A**, Boudieu L, Barbier J, Sion B, Gelot A, Barnich N, Ardid D, Carvalho FA. Adherent-Invasive E. coli enhances colonic hypersensitivity and P2X receptors expression during post-infectious period. *Gut Microbes* 2018; **9**: 26-37 [PMID: 28806140 DOI: 10.1080/19490976.2017.1361091]

21 **Tambuwala MM**, Cummins EP, Lenihan CR, Kiss J, Stauch M, Scholz CC, Fraisl P, Lasitschka F, Mollenhauer M, Saunders SP, Maxwell PH, Carmeliet P, Fallon PG, Schneider M, Taylor CT. Loss of prolyl hydroxylase-1 protects against colitis through reduced epithelial cell apoptosis and increased barrier function. *Gastroenterology* 2010; **139**: 2093-2101 [PMID: 20600011 DOI: 10.1053/j.gastro.2010.06.068]

22 **Caporaso JG**, Bittinger K, Bushman FD, DeSantis TZ, Andersen GL, Knight R. PyNAST: a flexible tool for aligning sequences to a template alignment. *Bioinformatics* 2010; **26**: 266-267 [PMID: 19914921 DOI: 10.1093/bioinformatics/btp636]

23 **Meleine M**, Boudieu L, Gelot A, Muller E, Lashermes A, Matricon J, Silberberg C, Theodorou V, Eschalier A, Ardid D, Carvalho FA. Comparative effects of α2δ-1 ligands in mouse models of colonic hypersensitivity. *World J Gastroenterol* 2016; **22**: 7111-7123 [PMID: 27610021 DOI: 10.3748/wjg.v22.i31.7111]

24 **Lovell RM**, Ford AC. Effect of gender on prevalence of irritable bowel syndrome in the community: systematic review and meta-analysis. *Am J Gastroenterol* 2012; **107**: 991-1000 [PMID: 22613905 DOI: 10.1038/ajg.2012.131]

25 **Kanazawa M**, Palsson OS, Thiwan SI, Turner MJ, van Tilburg MA, Gangarosa LM, Chitkara DK, Fukudo S, Drossman DA, Whitehead WE. Contributions of pain sensitivity and colonic motility to IBS symptom severity and predominant bowel habits. *Am J Gastroenterol* 2008; **103**: 2550-2561 [PMID: 18684175 DOI: 10.1111/j.1572-0241.2008.02066.x]

26 **Camilleri M**, Boeckxstaens G. Dietary and pharmacological treatment of abdominal pain in IBS. *Gut* 2017; **66**: 966-974 [PMID: 28232472 DOI: 10.1136/gutjnl-2016-313425]

27 **Ju T**, Naliboff BD, Shih W, Presson AP, Liu C, Gupta A, Mayer EA, Chang L. Risk and Protective Factors Related to Early Adverse Life Events in Irritable Bowel Syndrome. *J Clin Gastroenterol* 2020; **54**: 63-69 [PMID: 30575634 DOI: 10.1097/MCG.0000000000001153]

28 **Park SH**, Videlock EJ, Shih W, Presson AP, Mayer EA, Chang L. Adverse childhood experiences are associated with irritable bowel syndrome and gastrointestinal symptom severity. *Neurogastroenterol Motil* 2016; **28**: 1252-1260 [PMID: 27061107 DOI: 10.1111/nmo.12826]

29 **Whitehead WE**, Crowell MD, Robinson JC, Heller BR, Schuster MM. Effects of stressful life events on bowel symptoms: subjects with irritable bowel syndrome compared with subjects without bowel dysfunction. *Gut* 1992; **33**: 825-830 [PMID: 1624167 DOI: 10.1136/gut.33.6.825]

30 **Moloney RD**, O'Mahony SM, Dinan TG, Cryan JF. Stress-induced visceral pain: toward animal models of irritable-bowel syndrome and associated comorbidities. *Front Psychiatry* 2015; **6**: 15 [PMID: 25762939 DOI: 10.3389/fpsyt.2015.00015]

31 **Botschuijver S**, Welting O, Levin E, Maria-Ferreira D, Koch E, Montijn RC, Seppen J, Hakvoort TBM, Schuren FHJ, de Jonge WJ, van den Wijngaard RM. Reversal of visceral hypersensitivity in rat by Menthacarin®, a proprietary combination of essential oils from peppermint and caraway, coincides with mycobiome modulation. *Neurogastroenterol Motil* 2018; **30**: e13299 [PMID: 29383802 DOI: 10.1111/nmo.13299]

32 **Yi L**, Zhang H, Sun H, Zhou L, Chen Y, Xuan L, Jiang Y, Xu S. Maternal Separation Induced Visceral Hypersensitivity from Childhood to Adulthood. *J Neurogastroenterol Motil* 2017; **23**: 306-315 [PMID: 28238254 DOI: 10.5056/jnm16089]

33 **de Punder K**, Pruimboom L. Stress induces endotoxemia and low-grade inflammation by increasing barrier permeability. *Front Immunol* 2015; **6**: 223 [PMID: 26029209 DOI: 10.3389/fimmu.2015.00223]

34 **Kelly JR**, Kennedy PJ, Cryan JF, Dinan TG, Clarke G, Hyland NP. Breaking down the barriers: the gut microbiome, intestinal permeability and stress-related psychiatric disorders. *Front Cell Neurosci* 2015; **9**: 392 [PMID: 26528128 DOI: 10.3389/fncel.2015.00392]

35 **Camilleri M**, Madsen K, Spiller R, Greenwood-Van Meerveld B, Verne GN. Intestinal barrier function in health and gastrointestinal disease. *Neurogastroenterol Motil* 2012; **24**: 503-512 [PMID: 22583600 DOI: 10.1111/j.1365-2982.2012.01921.x]

36 **Miquel S**, Martín R, Lashermes A, Gillet M, Meleine M, Gelot A, Eschalier A, Ardid D, Bermúdez-Humarán LG, Sokol H, Thomas M, Theodorou V, Langella P, Carvalho FA. Anti-nociceptive effect of Faecalibacterium prausnitzii in non-inflammatory IBS-like models. *Sci Rep* 2016; **6**: 19399 [PMID: 26775847 DOI: 10.1038/srep19399]

37 **Rincel M**, Olier M, Minni A, Monchaux de Oliveira C, Matime Y, Gaultier E, Grit I, Helbling JC, Costa AM, Lépinay A, Moisan MP, Layé S, Ferrier L, Parnet P, Theodorou V, Darnaudéry M. Pharmacological restoration of gut barrier function in stressed neonates partially reverses long-term alterations associated with maternal separation. *Psychopharmacology (Berl)* 2019; **236**: 1583-1596 [PMID: 31147734 DOI: 10.1007/s00213-019-05252-w]

38 **Moloney RD**, Johnson AC, O'Mahony SM, Dinan TG, Greenwood-Van Meerveld B, Cryan JF. Stress and the Microbiota-Gut-Brain Axis in Visceral Pain: Relevance to Irritable Bowel Syndrome. *CNS Neurosci Ther* 2016; **22**: 102-117 [PMID: 26662472 DOI: 10.1111/cns.12490]

39 **Mosca A**, Leclerc M, Hugot JP. Gut Microbiota Diversity and Human Diseases: Should We Reintroduce Key Predators in Our Ecosystem? *Front Microbiol* 2016; **7**: 455 [PMID: 27065999 DOI: 10.3389/fmicb.2016.00455]

40 **Frank DN**, St Amand AL, Feldman RA, Boedeker EC, Harpaz N, Pace NR. Molecular-phylogenetic characterization of microbial community imbalances in human inflammatory bowel diseases. *Proc Natl Acad Sci U S A* 2007; **104**: 13780-13785 [PMID: 17699621 DOI: 10.1073/pnas.0706625104]

41 **Lepage P**, Häsler R, Spehlmann ME, Rehman A, Zvirbliene A, Begun A, Ott S, Kupcinskas L, Doré J, Raedler A, Schreiber S. Twin study indicates loss of interaction between microbiota and mucosa of patients with ulcerative colitis. *Gastroenterology* 2011; **141**: 227-236 [PMID: 21621540 DOI: 10.1053/j.gastro.2011.04.011]

42 **Pozuelo M**, Panda S, Santiago A, Mendez S, Accarino A, Santos J, Guarner F, Azpiroz F, Manichanh C. Reduction of butyrate- and methane-producing microorganisms in patients with Irritable Bowel Syndrome. *Sci Rep* 2015; **5**: 12693 [PMID: 26239401 DOI: 10.1038/srep12693]

43 **Moussaoui N**, Jacobs JP, Larauche M, Biraud M, Million M, Mayer E, Taché Y. Chronic Early-life Stress in Rat Pups Alters Basal Corticosterone, Intestinal Permeability, and Fecal Microbiota at Weaning: Influence of Sex. *J Neurogastroenterol Motil* 2017; **23**: 135-143 [PMID: 27829577 DOI: 10.5056/jnm16105]

44 **Tap J**, Derrien M, Törnblom H, Brazeilles R, Cools-Portier S, Doré J, Störsrud S, Le Nevé B, Öhman L, Simrén M. Identification of an Intestinal Microbiota Signature Associated With Severity of Irritable Bowel Syndrome. *Gastroenterology* 2017; **152**: 111-123.e8 [PMID: 27725146 DOI: 10.1053/j.gastro.2016.09.049]

45 **Zhou XY**, Li M, Li X, Long X, Zuo XL, Hou XH, Cong YZ, Li YQ. Visceral hypersensitive rats share common dysbiosis features with irritable bowel syndrome patients. *World J Gastroenterol* 2016; **22**: 5211-5227 [PMID: 27298564 DOI: 10.3748/wjg.v22.i22.5211]

46 **Murakami T**, Kamada K, Mizushima K, Higashimura Y, Katada K, Uchiyama K, Handa O, Takagi T, Naito Y, Itoh Y. Changes in Intestinal Motility and Gut Microbiota Composition in a Rat Stress Model. *Digestion* 2017; **95**: 55-60 [PMID: 28052282 DOI: 10.1159/000452364]

47 **Luna RA**, Oezguen N, Balderas M, Venkatachalam A, Runge JK, Versalovic J, Veenstra-VanderWeele J, Anderson GM, Savidge T, Williams KC. Distinct Microbiome-Neuroimmune Signatures Correlate With Functional Abdominal Pain in Children With Autism Spectrum Disorder. *Cell Mol Gastroenterol Hepatol* 2017; **3**: 218-230 [PMID: 28275689 DOI: 10.1016/j.jcmgh.2016.11.008]

48 **Lacagnina MJ**, Watkins LR, Grace PM. Toll-like receptors and their role in persistent pain. *Pharmacol Ther* 2018; **184**: 145-158 [PMID: 28987324 DOI: 10.1016/j.pharmthera.2017.10.006]

49 **Nicotra L**, Loram LC, Watkins LR, Hutchinson MR. Toll-like receptors in chronic pain. *Exp Neurol* 2012; **234**: 316-329 [PMID: 22001158 DOI: 10.1016/j.expneurol.2011.09.038]

50 **Tramullas M**, Finger BC, Moloney RD, Golubeva AV, Moloney G, Dinan TG, Cryan JF. Toll-like receptor 4 regulates chronic stress-induced visceral pain in mice. *Biol Psychiatry* 2014; **76**: 340-348 [PMID: 24331544 DOI: 10.1016/j.biopsych.2013.11.004]

51 **Luczynski P**, Tramullas M, Viola M, Shanahan F, Clarke G, O'Mahony S, Dinan TG, Cryan JF. Microbiota regulates visceral pain in the mouse. *Elife* 2017; **6**: e25887 [PMID: 28629511 DOI: 10.7554/eLife.25887]

52 **Zhou SY**, Gillilland M 3rd, Wu X, Leelasinjaroen P, Zhang G, Zhou H, Ye B, Lu Y, Owyang C. FODMAP diet modulates visceral nociception by lipopolysaccharide-mediated intestinal inflammation and barrier dysfunction. *J Clin Invest* 2018; **128**: 267-280 [PMID: 29202473 DOI: 10.1172/JCI92390]

53 **Das N**, Dewan V, Grace PM, Gunn RJ, Tamura R, Tzarum N, Watkins LR, Wilson IA, Yin H. HMGB1 Activates Proinflammatory Signaling *via* TLR5 Leading to Allodynia. *Cell Rep* 2016; **17**: 1128-1140 [PMID: 27760316 DOI: 10.1016/j.celrep.2016.09.076]

54 **Dlugosz A**, Nowak P, D'Amato M, Mohammadian Kermani G, Nyström J, Abdurahman S, Lindberg G. Increased serum levels of lipopolysaccharide and antiflagellin antibodies in patients with diarrhea-predominant irritable bowel syndrome. *Neurogastroenterol Motil* 2015; **27**: 1747-1754 [PMID: 26387872 DOI: 10.1111/nmo.12670]

World Journal of Gastroenterology

Submit a Manuscript: https://www.f6publishing.com

World J Gastroenterol 2022 August 7; 28(29): 3917-3933

DOI: 10.3748/wjg.v28.i29.3917

ISSN 1007-9327 (print) ISSN 2219-2840 (online)

ORIGINAL ARTICLE

Case Control Study

Comprehensive evaluation of microRNA as a biomarker for the diagnosis of hepatocellular carcinoma

Juliane Malik, Martin Klammer, Vinzent Rolny, Henry Lik-Yuen Chan, Teerha Piratvisuth, Tawesak Tanwandee, Satawat Thongsawat, Wattana Sukeepaisarnjaroen, Juan Ignacio Esteban, Marta Bes, Bruno Köhler, Magdalena Swiatek-de Lange

Specialty type: Oncology

Provenance and peer review: Unsolicited article; Externally peer reviewed.

Peer-review model: Single blind

Peer-review report's scientific quality classification

Grade A (Excellent): A
Grade B (Very good): 0
Grade C (Good): C
Grade D (Fair): 0
Grade E (Poor): 0

P-Reviewer: Elkady N, Egypt; Sahin TT, Turkey

Received: January 28, 2022
Peer-review started: January 28, 2022
First decision: April 10, 2022
Revised: May 20, 2022
Accepted: July 11, 2022
Article in press: July 11, 2022
Published online: August 7, 2022

Juliane Malik, Martin Klammer, Vinzent Rolny, Magdalena Swiatek-de Lange, Roche Diagnostics GmbH, Penzberg 82377, Germany

Henry Lik-Yuen Chan, Faculty of Medicine, The Chinese University of Hong Kong, Hong Kong 999077, China

Teerha Piratvisuth, NKC Institute of Gastroenterology and Hepatology, Songklanagarind Hospital, Hat Yai 90112, Thailand

Tawesak Tanwandee, Division of Gastroenterology, Faculty of Medicine, Siriraj Hospital, Mahidol University, Bangkok 10700, Thailand

Satawat Thongsawat, Department of Internal Medicine, Maharaj Nakorn Chiang Mai Hospital, Chiang Mai University, Chiang Mai 50200, Thailand

Wattana Sukeepaisarnjaroen, Faculty of Medicine, Srinagarind Hospital, Khon Kaen University, Khon Kaen 40000, Thailand

Juan Ignacio Esteban, Liver Unit, Vall d'Hebron University Hospital, Barcelona 08035, Spain

Marta Bes, Transfusion Safety Laboratory, Banc de Sang i Teixits, Barcelona 08005, Spain

Bruno Köhler, Department of Medical Oncology, National Center for Tumor Diseases, University Hospital Heidelberg, Heidelberg 69120, Germany

Bruno Köhler, Liver Cancer Center Heidelberg, University Hospital Heidelberg, Heidelberg 69120, Germany

Corresponding author: Juliane Malik, PhD, Roche Diagnostics GmbH, Nonnenwald 2, Penzberg 82377, Germany. juliane.malik@roche.com

Abstract

BACKGROUND

Hepatocellular carcinoma (HCC) is the most common type of primary liver cancer. Current guidelines for HCC management recommend surveillance of high-risk patients every 6 mo using ultrasonography. Serum biomarkers, like alpha-fetoprotein (AFP), protein induced by vitamin K absence/antagonist-II

(PIVKA-II) and lectin-reactive AFP, show suboptimal performance for detection of HCC, which is crucial for successful resection or treatment. Thus, there is a significant need for new biomarkers to aid early diagnosis of HCC. Studies have shown that the expression level of human microRNAs (miRNAs), a small, non-coding RNA species released into the blood, can serve as an early marker for various diseases, including HCC.

AIM

To evaluate the diagnostic role of miRNAs in HCC as single markers, signatures or in combination with known protein biomarkers.

METHODS

Our prospective, multicenter, case-control study recruited 660 participants (354 controls with chronic liver disease and 306 participants with HCC) and employed a strategy of initial screening by two independent methods, real-time quantitative PCR (n = 60) and next-generation sequencing (n = 100), to assess a large number of miRNAs. The results from the next-generation sequencing and real-time quantitative PCR screening approaches were then combined to select 26 miRNAs (including two putative novel miRNAs). Those miRNAs were analyzed for their diagnostic potential as single markers or in combination with other miRNAs or established protein biomarkers AFP and PIVKA-II *via* real-time quantitative PCR in training (n = 200) and validation cohorts (n = 300).

RESULTS

We identified 26 miRNAs that differentiated chronic liver disease controls from (early) HCC *via* two independent discovery approaches. Three miRNAs, miR-21-5p (miR-21), miR-320a and miR-186-5p, were selected by both methods. In the training cohort, only miR-21, miR-320d and miR-423 could significantly distinguish (Q < 0.05) between the HCC and chronic liver disease control groups. In the multivariate setting, miR-21 with PIVKA-II was selected as the best combination, resulting in an area under the curve of 0.87 for diagnosis and area under the curve of 0.74 for early diagnosis of HCC. In the validation cohort, only miR-21 and miR-423 could be confirmed as potential HCC biomarkers. A combination of miRNAs did not perform better than any single miRNA. Improvement of PIVKA-II performance through combination with miRNAs could not be confirmed in the validation panel. Two putative miRs, put-miR-6 and put-miR-99, were tested in the training and validation panels, but their expression could only be detected in very few samples and at a low level (cycle threshold between 31.24 and 34.97).

CONCLUSION

miRNAs alone or as a signature in combination with protein biomarkers AFP and PIVKA-II do not improve the diagnostic performance of the protein biomarkers.

Key Words: Carcinoma; Hepatocellular; MicroRNAs; Biomarkers; Alpha-fetoprotein; Protein induced by vitamin K absence-II; Diagnosis

©The Author(s) 2022. Published by Baishideng Publishing Group Inc. All rights reserved.

Core Tip: Hepatocellular carcinoma (HCC) is the most common type of primary liver cancer and has a high mortality rate, making early diagnosis essential for better treatment outcomes. Studies have shown microRNAs to be early markers for HCC; we evaluated the potential diagnostic role of microRNAs alone and in combination with known protein biomarkers (alpha-fetoprotein, protein induced by vitamin K absence/antagonist-II) in samples from HCC-affected individuals and controls using real-time quantitative PCR and next-generation sequencing. MiR-21 and miR-423 demonstrated significant differential expression between the HCC and control groups. MicroRNAs alone or as a signature in combination with protein biomarkers did not improve diagnostic performance of the protein biomarkers.

Citation: Malik J, Klammer M, Rolny V, Chan HLY, Piratvisuth T, Tanwandee T, Thongsawat S, Sukeepaisarnjaroen W, Esteban JI, Bes M, Köhler B, Swiatek-de Lange M. Comprehensive evaluation of microRNA as a biomarker for the diagnosis of hepatocellular carcinoma. *World J Gastroenterol* 2022; 28(29): 3917-3933

URL: https://www.wjgnet.com/1007-9327/full/v28/i29/3917.htm

DOI: https://dx.doi.org/10.3748/wjg.v28.i29.3917

INTRODUCTION

According to the World Health Organization report of cancer cases worldwide, hepatocellular carcinoma (HCC) was the sixth most common cancer in terms of new cases and the fourth most common cause of cancer-related deaths in 2018[1]. HCC accounts for 85%-90% of all primary liver cancers[2], and in most cases develops in cirrhotic livers. Cirrhosis arises as a consequence of chronic liver injury and inflammation caused by viral and non-viral factors. About 70% of all HCC cases are caused by viral liver infections like hepatitis B virus (HBV) and hepatitis C virus (HCV)[3]. Approximately 80% of HCC cases occur in eastern Asia and sub-Saharan Africa, where the dominant risk factor is chronic infection with HBV and exposure to aflatoxin B1. In contrast, the main risk factors for HCC development in North America, Europe and Japan are infection with HCV or alcohol misuse, diabetes and obesity[4]. The mortality rate of HCC is high, with 5-year overall survival rates of 19.5%[5].

Limited treatment options exist for patients with HCC when diagnosed at advanced stages, so early detection is crucial to reduce mortality. If diagnosed early, treatment options such as resection, local ablation and liver transplantation are available and increase the 5-year overall survival rate for very early HCC [Barcelona-Clinic Liver Cancer (BCLC) stage 0] to 70%-90% and for early HCC (BCLC stage A) to 50%-70%. Intermediate to end-stage HCCs are unresectable and have a median survival of 16 mo for intermediate HCC (BCLC stage B), 6 mo for advanced HCC (BCLC stage C) and 3-4 mo for end-stage HCC (BCLC stage D)[6].

HCC is often asymptomatic, making its early diagnosis challenging. Major international guidelines recommend surveillance of high-risk patients [patients with severe chronic liver disease (CLD) such as chronic HBV or HCV infections, alcohol abuse or non-alcoholic steatohepatitis, leading to cirrhosis of the liver) at 6-mo intervals using abdominal ultrasound (US) with (The Asian Pacific Association for the Study of the Liver, American Association for the Study of Liver Diseases) or without (European Association for the Study of the Liver-European Organisation for Research and Treatment of Cancer) measurement of alpha-fetoprotein (AFP) levels in serum[7-9]. Japanese guidelines on HCC management propose the use of US and measurement of AFP, lectin-reactive AFP and protein induced by vitamin K absence/antagonist-II (PIVKA-II; also known as des-gamma-carboxy prothrombin) for routine follow-up in patients at high risk for developing HCC[10]. Other recommended imaging methods are computed tomography (CT) and magnetic resonance imaging; however, these are very cost-intensive, not easily accessible and have potential adverse effects like radiation exposure (CT)[6-8,11]. US use is also not without problems, as its performance is operator-dependent[12] and is limited in the setting of non-alcoholic steatohepatitis[13]. Adjunctive use of AFP may improve HCC detection rates. Although it has limited sensitivity for early-stage HCC, its addition to US improved sensitivity from 45% to 63% (P = 0.002)[11,14]. PIVKA-II is more sensitive but less specific than AFP for diagnosis of HCC in patients affected by chronic HCV infection[15]. Thus, there is a great need for new, non-invasive diagnostic tools to improve the detection of early HCC and eliminate operator-dependent variability.

MicroRNAs (miRNAs) are small (approximately 22 nucleotides), non-coding RNA molecules that post-transcriptionally modify gene regulation by base-pairing to mRNA[16]. The target mRNA is then either degraded (complementary or near-perfect complementary binding) or the translation is inhibited (partial complementarity), thus inhibiting protein expression[17].

In the cancer research field, the role of miRNAs has been discussed extensively. In the context of human cancers, miRNAs are associated with cell proliferation, genomic instability, tissue invasion, metastasis, angiogenesis, evasion of apoptosis and immune response. They can also act as oncogenes or tumor suppressor genes[18]. Clinical applications of miRNAs have been studied in various malignant tumors, such as lung, breast and prostate cancers[19]. Primarily, miRNAs from serum and plasma are of particular interest for diagnosis of cancer and the study of disease prognosis. The main advantage of miRNA-based diagnosis is the high stability of these molecules in blood and other biological fluids that can be easily sampled[20-22].

In HCC, the role of miRNAs for diagnosis and therapy has been exhaustively analyzed, although with contradictory results[23]. The expression of several miRNAs in different HCC tumor tissue samples was both elevated and decreased compared with a control group (non-tumorous tissue) in different studies[24]. Additionally, numerous circulating miRNA candidates or signatures composed of several miRNAs have been published as biomarker candidates for HCC (*e.g.*, hsa-miR-206, hsa-miR-141-3p and hsa-miR-433-3p)[25]. In some cases, both increases and decreases in the expression of the same miRNA (*e.g.*, hsa-miR-143, hsa-miR-155, hsa-miR-195) have been reported[26]. While previous studies have given some indication that miRNAs may be useful biomarkers for HCC, no miRNA has been found as a reliable biomarker in the diagnosis of early-stage HCC. To date, studied cohorts have been small, or control cohorts contained only one group of patients with a disease having a high risk for HCC [27], only healthy individuals[28] or did not include patients with early HCC[29]. A large cohort is necessary to obtain statistically significant results[30], and an HCC biomarker should show high sensitivity and specificity in patients at risk for HCC (including those with HBV, HCV and cirrhosis).

The aim of this study was to identify and clinically validate potential miRNAs for the early detection of HCC in human plasma samples through a comprehensive, prospective, multicenter, case-control study. To this end, a large cohort including 660 HCC (early and late stage) and CLD patients was studied. The potential improvement of the diagnostic performance of already established protein

biomarkers for HCC (AFP and PIVKA-II) in combination with miRNA biomarkers was also assessed.

MATERIALS AND METHODS

Patient sample collection

Between 2014 and 2016, EDTA-plasma samples from 354 CLD controls, including HBV and HCV with and without cirrhosis, and 306 HCC (early and late stage) patients were provided by the following institutions: Maharaj Nakorn Chiang Mai Hospital, Chiang Mai, Thailand; Siriraj Hospital, Bangkok, Thailand; Songklanagarind Hospital, Hat Yai, Thailand; Srinagarind Hospital, Khon Kaen, Thailand; Prince of Wales Hospital, Shatin, Hong Kong; NCT University Hospital Heidelberg, Heidelberg, Germany; and Vall d'Hebron University Hospital, Barcelona, Spain. Full inclusion and exclusion criteria have been previously described[31].

Written informed consent was obtained from all participants. The study was conducted in full conformance with the principles of the Declaration of Helsinki and with approval of independent ethics committees. Plasma samples were collected before treatment (surgery, percutaneous ethanol injection, chemotherapy, radiotherapy) according to the appropriate standard operating procedures and stored at -70 °C until analysis. Repeated freeze-thaw cycles were avoided. HCC diagnosis was verified using imaging (ultrasonography, CT, magnetic resonance imaging) or biopsy, followed by histopathological analysis.

Description and clinical data of patients

The demographic and clinical characteristics of the study participants are presented in Supplementary Table 1. All diagnosed HCC cases were classified according to BCLC guidelines upon sample collection. Early-stage HCC was defined as BCLC 0 and A and late-stage HCC as BCLC B, C and D. CLD controls were individuals with HBV or HCV with or without cirrhosis. Some patients had additional underlying diseases, which were not considered when distributing them into the four groups. All clinical data, including the patients' diagnoses, were blinded to laboratory operators to avoid measurement bias.

Study design

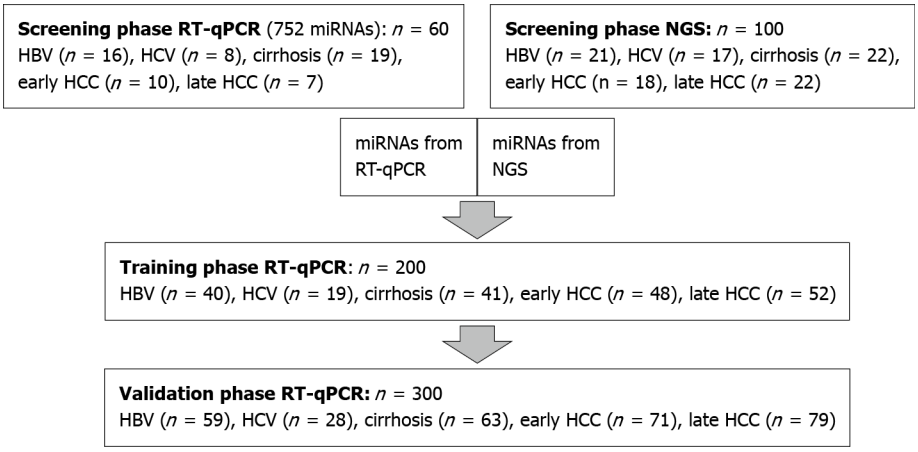
CLD and HCC patient samples were randomly distributed into four panels: a screening panel for real-time quantitative (RT-q) PCR (n = 60), a screening panel for next-generation sequencing (NGS) (n = 100), a training panel (n = 200) and a validation panel (n = 300) (Supplementary Table 1). Comparisons were made for: (1) All HCC (early + late stages) *vs* controls (HBV and HCV, with and without cirrhosis); (2) Early HCC *vs* controls; and (3) Early HCC *vs* cirrhosis (Figure 1).

miRNA isolation

The following methods for miRNA isolation from plasma were validated: TaqMan miRNA ABC Purification Kit, mirVana PARIS Kit (both LifeTechnologies, Carlsbad, CA, United States) and the miRCURY RNA Isolation Kit-Biofluids (Exiqon, Vedbaek, Denmark). The best performance for the isolation of small RNA was found using the last method; therefore, all isolation experiments were performed using the miRCURY RNA Isolation Kit-Biofluids. The starting material was 250 µL of EDTA-plasma per patient. Handling was according to the manufacturer's protocol with the following adaption: after adding the protein precipitation solution and subsequent centrifugation, only 200 µL of supernatant was transferred into a new tube; the remaining volume was discarded. For quality control, spike-ins UniSp2, UniSp4 and UniSp5 from the miRCURY Universal RT microRNA PCR, RNA Spike-in kit (Exiqon) were added to all samples prior to isolation. Isolated small RNA (including miRNA) was stored at -80 °C until analysis.

NGS

NGS of miRNAs from EDTA-plasma samples was performed by Exiqon. Briefly, RNA was isolated following quality control by RT-qPCR. Next, the miRNA library was prepared, followed by quality control *via* RT-qPCR and bioanalyzer. Finally, miRNAs were sequenced on a Nextseq500 (Illumina, San Diego, CA, United States) with 10 million reads per sample and 50 nucleotide single-end read. The annotation reference used was miRBase 20 (http://mirbase.org/). In the following data analyses, the reads were mapped and classified based on their sequence as: (1) Known miRNA; (2) Predicted (putative) miRNA; (3) Outmapped; (4) Unmapped; (5) Genome; and (6) Small RNA. In the NGS report from Exiqon, putative miRNAs were described as miRNAs predicted from the sequences that do not map to any organism found in miRBase or to other known RNA sequences. miRPara was used to analyze the potential folding of these sequences[32]. These results were combined to identify putative novel miRNAs. The differential expression analyses were done using the trimmed mean of M-value normalization method in the EdgeR statistical software package.



DOI: 10.3748/wjg.v28.i29.3917 **Copyright** ©The Author(s) 2022.

Figure 1 Overview of study design. HBV: Hepatitis B virus; HCC: Hepatocellular carcinoma; HCV: Hepatitis C virus; miRNA: Micro ribonucleic acid; NGS: Next-generation sequencing; RT-qPCR: Real-time quantitative PCR.

Putative miRNA primer design

For the evaluation of the putative miRNA (put-miRs), the following RT-qPCR primers were designed using the Exiqon tool for primer design: put-miR-25, put-miR-46, put-miR-56, put-miR-66, put-miR-79, put-miR-99, put-miR-83, put-miR-86, put-miR-91, put-miR-100, put-miR-118 and put-miR-128. Three primer sets for each put-miR were tested in the three EDTA-plasma samples that had shown the highest expression for the respective put-miR in NGS. The put-miRs that showed a cycle threshold (Ct) lower than 35 were selected for clinical validation. The primer set with the lowest Ct of all three primer sets was used for the following RT-qPCR analyses. Details on the put-miRs and their corresponding chromosome location, chromosome strand, start and stop position, sequence and primer design-IDs from Exiqon can be found in the Supplementary materials (Supplementary Table 2).

Reverse transcription and RT-qPCR

Reverse transcription and RT-qPCR were carried out using the Universal complementary DNA synthesis kit II for reverse transcription and the ExiLENT SYBR Green master mix kit for RT-qPCR (Exiqon) according to the manufacturer's protocol. For quality control, spike-ins UniSp6 and cel-miR-39-3p from the miRCURY LNA Universal RT microRNA PCR, RNA Spike-in kit were added to all samples prior to reverse transcription. RT-qPCR analysis was performed for: (1) Individual miRNA primer sets; (2) Commercially available predefined ready-to-use panels: Human miRNome panel I and II, V4 which included primers for 752 known miRNAs; and (3) Customized ready-to-use panels [all primer sets and panels from miRCURY LNA Universal RT microRNA PCR Biofluids (Exiqon)]. RT-qPCR was performed on a LightCycler® 480 (Roche Diagnostics International Ltd, Rotkreuz, Switzerland). The following modifications to the manufacturer's protocol were made: (1) In both customized and predefined ready-to-use panels the amount of complementary DNA was doubled; and (2) After adding the PCR mastermix-complementary DNA mix to each well and centrifuging the plate, the reagents in the plate were mixed on a shaker for 20 s and then centrifuged again.

Normalization and miRNA expression

Pre-processing of RT-qPCR data from the ready-to-use and customized panels was done using GenEx (MultiD Analyses AB, Gothenburg, Sweden) following the Exiqon Data Analysis Guide for the miRCURY LNA Universal RT microRNA Ready-to-Use PCR panels, V3. All Ct values < 35 were considered valid and included in further analyses. Normalization was done by applying the global mean (Human miRNome panel I and II, V4) or by normalizing to the expression of reference genes (customized panels). When conducting RT-qPCR analysis with only a small number of miRNAs, global mean normalization was not applicable. Therefore, a normalization to endogenous control miRNAs that show equal expression throughout all sample groups was necessary. Reference genes for normalization of customized panels were selected with GenEx NormFinder software by comparing their standard deviation (SD) and accumulated SD (accumulated SD = $\frac{1}{n}\sqrt{\sum_{i=1}^{n} SD_i^2}$. Relative miRNA expression was calculated using a $2^{-\Delta\Delta Ct}$ method.

Serum protein assays measurements

AFP and PIVKA-II were measured using microchip capillary electrophoresis and a liquid-phase binding assay on the uTASWako i30 automated analyzer (Fujifilm Wako Pure Chemical Industries, Osaka, Japan).

Biostatistical analyses

The statistical methods and analyses of this study were performed and reviewed by biostatisticians Dr. Martin Klammer and Vinzent Rolny of Roche Diagnostics GmbH.

Univariate analysis

For each miRNA, two-sample Wilcoxon rank-sum testing was performed, and the *P* value was reported. Subsequently, the *P* values were corrected by means of Benjamini-Hochberg false discovery rate correction to account for multiple hypothesis testing (referred to as '*Q*-values' in the tables).

In the initial global discovery of differentially expressed miRNAs, the raw *P* values (without false discovery rate correction) were used. Here, a higher false-positive rate was deliberately accepted for the sake of minimizing the risk of missing a potential biomarker candidate (*i.e.*, minimizing the false-negative rate).

Multivariate analysis

To discover the optimal bivariate biomarker combination and reliably estimate its performance in future samples, a two-tier cross-validation workflow employing logistic regression was established. In the first (outer) tier with 200 Monte-Carlo cross-validation runs, the data set was randomly split into training and test set (80% and 20%, respectively) in each run, while maintaining the ratio of cases and controls. The optimal feature combination was then searched for in the second (inner) tier with five-fold cross-validation, where the training data were again split into an inner training and an inner test set. All possible two-marker combinations (exhaustive search) were then assessed by training a logistic regression model on the inner training data containing only information of the respective two markers (inner selected training data) and testing their performances by means of area under the curve (AUC) of the receiver operating characteristics curve with the respective inner test set (inner selected test data). The combination showing the best inner cross-validation results (*i.e.*, maximum mean AUC across the five cross-validation runs) was then selected and used to train a model in the outer tier. As with the inner tier, logistic regression was used, and the performance of the test set (selected test data) for each of the 200 Monte-Carlo cross-validation runs was then assessed; the mean AUC represented the estimated overall performance.

Since the feature selection procedure was part of the outer cross-validation tier, it was possible that different marker pairs were selected in the 200 Monte-Carlo cross-validation runs. However, it was necessary to select the one pair that would be used to train a model to predict future samples. This was achieved by subjecting the entire data set to the inner cross-validation tier (not only the training data, as was done for the performance evaluation) and receiving the final biomarker pair, which was subsequently used to train the final logistic regression model on the entire data set (Figure 2).

In the case of searching for a miRNA that best complements the protein marker (AFP or PIVKA-II), the protein marker itself was fixed as first feature in the feature selection process, and the optimal partner was determined as described above.

RESULTS

Analysis of differentially expressed miRNAs yielded 26 potential biomarker candidates

To find a suitable biomarker for the (early) diagnosis of HCC, a large number of miRNAs were screened, using two independent methods: RT-qPCR (752 predefined miRNAs) and NGS (resulting in 244 miRNAs). We analyzed whether miRNAs were differentially expressed between a group with (early stage) HCC and a control group with CLD (including patients with hepatitis B, hepatitis C and cirrhosis). The miRNAs identified in the screening were then analyzed as potential biomarkers for (early) diagnosis of HCC in an independent training panel using RT-qPCR and validated in an independent panel.

Global miRNome analysis of miRNAs by NGS and human miRNA panels

Compared with RT-qPCR, NGS can identify all known and unknown miRNAs. First, miRNA was isolated from the plasma of 60 patients from the CLD control group (HBV, HCV and cirrhosis; see Supplementary Table 1) and 40 patients from the HCC groups (early and late stages), followed by a quality control *via* RT-qPCR. Six control samples did not pass the quality control and were excluded from NGS. Illumina Nextseq500 sequencing of the prepared library produced an average of 10.9 million accepted reads per sample. After data analysis, two additional outlier control samples were identified and excluded from further analysis. The miRNA expression was compared for the following groups: all HCC *vs* CLD and early HCC *vs* CLD, for known and unknown miRNAs, respectively (Supplementary Table 3). The 13 miRNAs with the smallest *P* value, highest AUC and largest fold change (approximately 1.2 or higher) were selected for validation *via* RT-qPCR (Table 1).

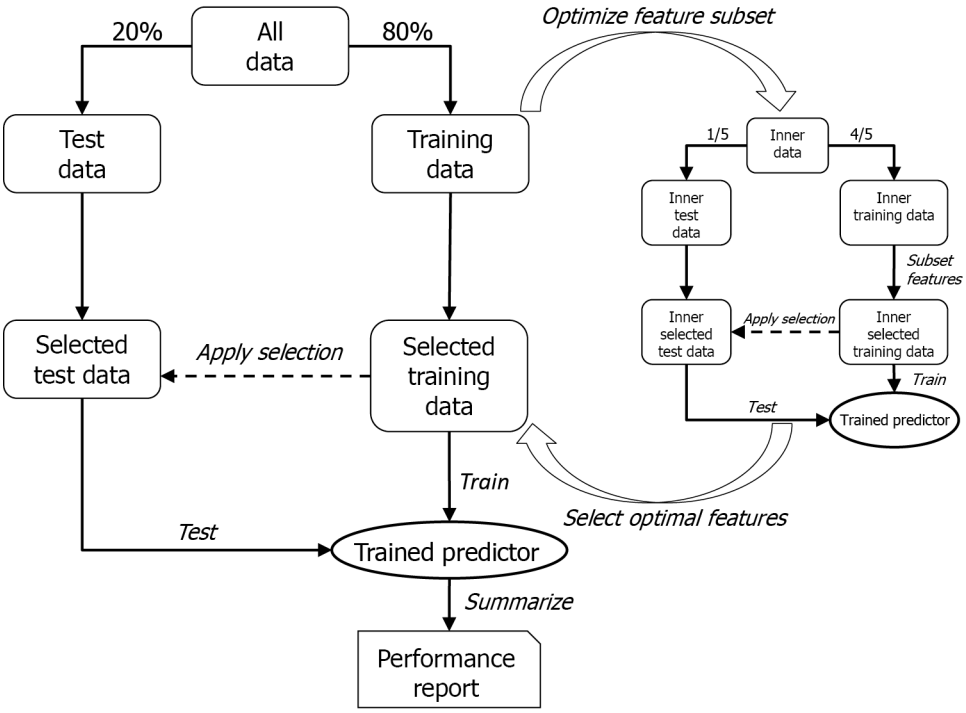
In the second discovery approach, RT-qPCR panels of preassigned assays for 752 known human miRNAs were applied for the screening of miRNA expression. miRNAs were investigated in the

Table 1 Overview of the 26 selected known and putative microRNA candidates from next-generation sequencing and real-time quantitative PCR

Known miRNA	Fold change	AUC	*P* value (Wilcoxon)	Method	Comparison
hsa-miR-185-5p	2.01	0.77	0.000099[c]	NGS	All HCC *vs* CLD
hsa-miR-320a[1]	1.52	0.74	0.000335[c]		
hsa-miR-423-5p	-1.22	0.69	0.004126[b]		
hsa-miR-664a-5p	1.38	0.69	0.005695[b]		
hsa-miR-203a	-2.73	0.67	0.01167[a]		
hsa-miR-320d	2.56	0.66	0.017151[a]		
hsa-miR-21-5p[1]	1.34	0.66	0.020486[a]		
hsa-miR-28-5p	-1.65	0.80	0.0004[c]	RT-qPCR	
hsa-miR-21-5p[1]	1.59	0.79	0.0006[c]		
hsa-miR-103a-3p	-1.65	0.78	0.012[a]		
hsa-miR-301a-3p	-1.50	0.78	0.013[a]		
hsa-miR-30b-5p	-1.63	0.75	0.0033[b]		
hsa-miR-495-3p	-1.50	0.73	0.0068[b]		
hsa-miR-320a[1]	1.37	0.72	0.0093[b]		
hsa-miR-30a-3p	-1.60	0.72	0.008145[b]	NGS	Early HCC *vs* CLD
hsa-miR-25-3p	1.75	0.71	0.01019[a]		
hsa-miR-7706	1.67	0.69	0.02002[a]		
hsa-miR-186-5p[1]	1.68	0.68	0.02364[a]		
hsa-miR-15b-5p	4.21	0.97	< 0.0001[c]	RT-qPCR	
hsa-miR-339-3p	-2.73	0.87	0.0006[c]		
hsa-miR-10b-5p	2.81	0.86	0.0007[c]		
hsa-miR-151a-5p	-2.25	0.85	0.0011[b]		
hsa-miR-652-3p	-2.22	0.85	0.001[b]		
hsa-miR-32-5p	2.03	0.85	0.001[b]		
hsa-miR-221-3p	-2.96	0.83	0.0021[b]		
hsa-miR-486-5p	2.43	0.82	0.0034[b]		
hsa-miR-186-5p[1]	1.46	0.75	0.0215[a]		
Putative miRNA	Fold change	AUC	*P* value (Wilcoxon)	Method	Comparison
put-miR-6	3.63	0.68	0.001956[b]	NGS	All HCC *vs* CLD
put-miR-99	1.83	0.6	0.188		Early HCC *vs* CLD

[1]MicroRNAs detected in both next-generation sequencing and real-time quantitative PCR.
[a]$P < 0.05$.
[b]$P < 0.01$.
[c]$P < 0.001$.
AUC: Area under the curve; CLD: Chronic liver disease; HCC: Hepatocellular carcinoma; miRNA: MicroRNA; NGS: Next-generation sequencing; RT-qPCR: Real-time quantitative PCR; miR: MicroRNA; put-miR: Putative microRNA.

independent sample panel (n = 60, see Supplementary Table 1). After global mean normalization, the miRNA expression was compared between the following groups: (1) All HCC *vs* CLD; and (2) Early HCC *vs* CLD (Supplementary Table 4). The 16 miRNAs with the smallest *P* value, highest AUC and largest fold change were selected for further analysis *via* RT-qPCR (Table 1). The AUCs and fold changes for the comparison of early HCC *vs* CLD were generally higher than the AUCs and fold changes when comparing all HCC *vs* CLD. Twenty-six miRNAs with the highest AUCs and fold changes, resulting from both discovery methods, were selected for further evaluation. Three miRNAs,



DOI: 10.3748/wjg.v28.i29.3917 **Copyright** ©The Author(s) 2022.

Figure 2 Overview of the two-tier cross-validation workflow employing logistic regression.

hsa-miR-320a (miR-320a), hsa-miR-421 (miR-421) and hsa-miR-21-5p (miR-21-5p), were identified by both independent methods (Supplementary Table 3).

Selection of five endogenous control miRNAs for normalization

The 26 selected miRNAs were then analyzed by RT-qPCR in an independent sample panel. As the number of examined miRNAs was very small, the normalization could not be based on the global mean value, which was used for the screening. To select endogenous miRNAs that could be used for normalization, GenEx software (MultiD) was used. Five miRNAs with the lowest SD and SDacc, hsa-let-7i-5p, hsa-miR-222-3p, hsa-miR-23a-3p, hsa-miR-30e-5p and hsa-miR-191-5p, were selected as endogenous controls for normalization (Table 2).

Putative miRNA primer selection

During NGS, sequences that could be potential miRNAs based on their length and structure were identified (= put-miR; Supplementary Table 2). Some showed different expression between the all/early-stage HCC and CLD groups. The 15 potential miRNAs with the smallest *P* values, highest AUCs and largest fold changes detected in the NGS were validated by RT-qPCR in an independent sample panel. For all 15 put-miRs identified, the three plasma samples with the highest expression of the respective put-miR in the NGS were selected, and RNA was isolated with the miRCURY isolation kit and subject to RT-qPCR analysis. In the RT-qPCR, two put-miRs (put-miR-6 and put-miR-99) reached Cts below the cut-off of 35, and their best primer pairs showed a mean Ct of 33.54 (put-miR-6) and 34.17 (put-miR-99). The remaining 13 put-miRs showed no expression. Put-miR-6 and put-miR-99 were further analyzed in the training and validation cohorts (Table 1).

RT-qPCR analysis of training cohort: univariate analysis

The 26 (24 known and 2 putative) miRNAs showing the best diagnostic performance and expression fold change in the NGS and RT-qPCR analysis (Table 1) were further validated by RT-qPCR in two independent sample panels: training cohort (200 samples) and validation cohort (300 samples). From the 24 previously selected known miRNAs, only three candidates (miR-21-5p, miR-320a and miR-186-5p) revealed themselves as potential biomarkers through both NGS and RT-qPCR analysis. miRNAs were analyzed alone (univariate) and as a combination of several miRNAs (signature, multivariate). miRNAs were also combined with known protein markers PIVKA-II and AFP (multivariate).

The training cohort consisted of the following plasma samples: HCC group (48 early stage and 52 late stage) and control group (100 HCV and HBV patients with and without cirrhosis). When comparing all HCC *vs* CLD controls in a univariate analysis, three miRNAs, namely miR-21-5p, hsa-miR-320d (miR-320d) and hsa-miR-423-5p (miR-423), could significantly distinguish ($Q < 0.05$) between those two groups (Table 3, Supplementary Figure 1).

Table 2 Individual standard deviation and accumulated standard deviation for consecutive microRNA reference genes

miRNA	SD	SD_{acc}
hsa-let-7i-5p	0.49	0.49
hsa-miR-222-3p	0.57	0.37
hsa-miR-23a-3p	0.63	0.33
hsa-miR-30e-5p	0.65	0.29
hsa-miR-191-5p	0.79	0.28

The lower the standard deviation/accumulated standard deviation, the more applicable microRNA/microRNA combination was as reference gene. These miRNAs were used as endogenous controls for the normalization of real-time quantitative PCR data. SD: Standard deviation; SD_{acc}: Accumulated standard deviation; miRNA: MicroRNA; miR: MicroRNA.

For the comparison of early HCC *vs* CLD, none of the 26 miRNAs could significantly distinguish between early HCC and the control group. After a refined analysis of the control groups, hsa-miR-652-3p (miR-652) demonstrated itself to be a marker significantly distinguishing early HCC from the cirrhosis group (mixed HBV and HCV) (Table 3, Supplementary Figure 1).

RT-qPCR analysis of training cohort: multivariate analysis and combination with protein biomarkers

A combination of several miRNAs did not perform better than the single miRNAs (data not shown). MiRNA marker candidates from the univariate analysis of all HCC *vs* CLD were then combined with the protein marker PIVKA-II, which is a widely used marker for HCC[33]. As a result, two-tier cross-validation workflow (see Methods for details) was established, which employed logistic regression and combined two features (PIVKA-II and one of the 26 miRNAs) repeatedly to investigate the potential improvement of the diagnostic performance of PIVKA-II alone. The combined approach resulted in a higher AUC and specificity at 90% sensitivity than PIVKA-II or miR-21-5p alone (Table 4, Supplementary Figure 2A). miR-21-5p was selected as the best PIVKA-II partner in 86% of the cross-validation runs (Table 5), and PIVKA-II + miR-21-5p was selected as the final biomarker pair.

In the next step, the specificity of the combined approach was tested for early HCC *vs* CLD. The three best partners for PIVKA-II were miR-21-5p in 60%, miR-320d in 18% and miR-652 in 16% of the cross-validation runs (Table 5, Supplementary Figure 2B), and PIVKA-II + miR-21-5p was selected as the final biomarker pair.

For the differentiation between early HCC and cirrhotic control patients, the AUC and specificity at 90% sensitivity of the combination PIVKA-II with miRNAs was higher than for single markers (Table 4, Supplementary Figure 2C). The two best miRNA partners for PIVKA-II were miR-652 in 64% and hsa-miR-221 in 26% of the cross-validation runs (Table 5), and PIVKA-II + miR-652 was selected as the final biomarker pair.

The multivariate analyses of the miRNA marker candidates combined with protein marker AFP did not show any improvement in diagnostic performance (Supplementary Figure 3).

RT-qPCR analysis of validation cohort: univariate analysis

The validation cohort consisted of the following plasma samples: all HCC group (71 early stage and 79 late stage) and CLD control group [63 cirrhosis (HBV, HCV), 59 HBV and 28 HCV). When comparing all HCC *vs* CLD, miR-21-5p and miR-423 were confirmed as possible biomarker candidates for the diagnosis of HCC. The performance of miR-21-5p was slightly worse in the validation cohort compared with the training cohort; miR-423 performance remained almost unchanged. The results from the training cohort for miR-320d could not be confirmed (Table 6, Supplementary Figure 4).

For the comparison of early HCC *vs* CLD with cirrhosis, miR-652 could not be confirmed as a possible biomarker, as seen in the training cohort (Table 6, Supplementary Figure 4).

RT-qPCR analysis of validation cohort: multivariate analysis and combination with protein biomarkers

As no combination of miRNAs could be identified in the training analysis, only PIVKA-II + miRNA combinations were validated here. However, the performance of PIVKA-II as a single marker could not be improved through combination with miRNAs selected in the training cohort for all data sets (Figure 3).

No confirmation of put-miRs as potential biomarkers for HCC

Put-miRs (put-miR-6 and put-miR-99) were tested in the training and validation panels. Put-miR-6 could only be detected in 2 samples, with a Ct of 31.24 in 1 of 200 samples in the training panel and a Ct of 34.00 in 1 of 300 samples in the validation panel. Put-miR-99 Cts between 34.00 and 34.97 (mean value

Table 3 Univariate analysis of real-time quantitative PCR results for comparison

miRNA	Wilcoxon *Q*-value	AUC	Specificity at 90% sensitivity
All HCC *vs* CLD			
hsa-miR-21-5p	0.000003[a]	0.71	0.24
hsa-miR-320d	0.010872[b]	0.63	0.25
hsa-miR-423-5p	0.046214[b]	0.61	0.26
hsa-miR-221-3p	0.099403	0.60	0.27
hsa-miR-320a	0.109399	0.60	0.28
hsa-miR-339-3p	0.154338	0.58	0.29
hsa-miR-301a-3p	0.160690	0.57	0.30
hsa-miR-652-3p	0.160690	0.56	0.31
hsa-miR-30b-5p	0.160690	0.56	0.32
hsa-miR-25-3p	0.186436	0.57	0.33
Early HCC *vs* CLD			
hsa-miR-21-5p	0.113812	0.64	0.20
hsa-miR-320d	0.302365	0.61	0.16
hsa-miR-652-3p	0.382238	0.60	0.23
hsa-miR-320a	0.432100	0.58	0.01
hsa-miR-423-5p	0.432100	0.56	0.06
hsa-miR-301a-3p	0.432100	0.57	0.09
hsa-miR-15b-5p	0.432100	0.57	0.07
hsa-miR-186-5p	0.432100	0.57	0.15
hsa-miR-221-3p	0.432100	0.56	0.24
hsa-miR-25-3p	0.432100	0.56	0.15
Early HCC *vs* cirrhosis			
hsa-miR-652-3p	0.038792[b]	0.69	0.34
hsa-miR-221-3p	0.094025	0.66	0.29
hsa-miR-151a-5p	0.201979	0.63	0.15
hsa-miR-21-5p	0.201979	0.63	0.24
hsa-miR-15b-5p	0.217324	0.61	0.10
hsa-miR-25-3p	0.217324	0.61	0.15
hsa-miR-320a	0.306457	0.59	0.00
hsa-miR-423-5p	0.306457	0.59	0.07
hsa-miR-320d	0.306457	0.59	0.15
hsa-miR-28-5p	0.306457	0.59	0.20

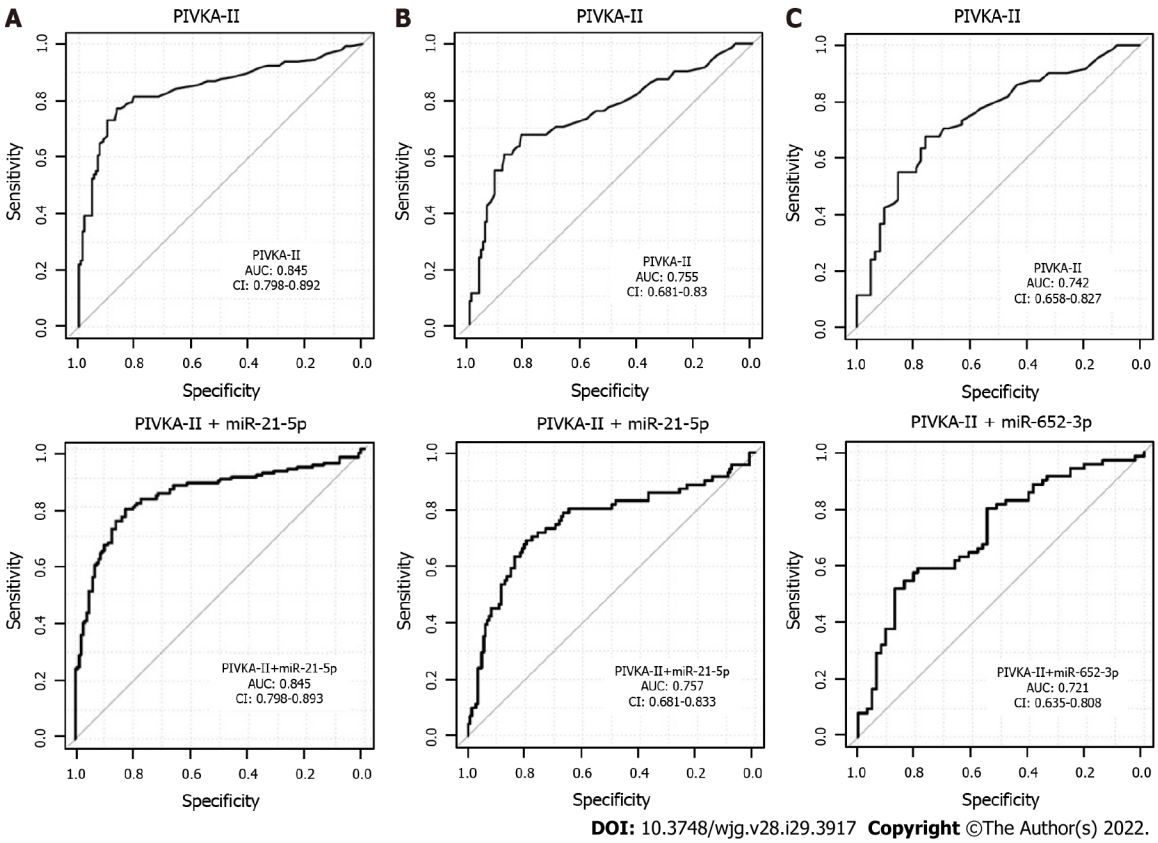
[a]*Q*-value < 0.001.
[b]*Q*-value < 0.05.
AUC: Area under the curve; CLD: Chronic liver disease; HCC: Hepatocellular carcinoma; miRNA: MicroRNA; miR: MicroRNA.

Ct = 34.41) could be detected in 3 of 200 samples in the training panel and Cts between 33.85 and 34.89 (mean Ct = 34.42) in 5 of 300 samples in the validation panel. All other samples showed no put-miR-6 and put-miR-99 expression, thus both put-miRs were excluded from further analysis.

Table 4 Multivariate analysis of real-time quantitative PCR results for comparison

Marker	AUC	Specificity at 90% sensitivity	Comparison
PIVKA-II	0.83	34	All HCC *vs* CLD
PIVKA-II + miRNAs	0.87	48	
PIVKA-II	0.70	15	Early HCC *vs* CLD
PIVKA-II + miRNAs	0.74	29	
PIVKA-II	0.64	12	Early HCC *vs* cirrhosis
PIVKA-II + miRNAs	0.71	42	

Area under the curve and specificity at 90% sensitivity for Protein induced by vitamin K absence/antagonist-II alone and in combination with the 26 selected miRNAs, resulting from the logistic regression model. AUC: Area under the curve; CLD: Chronic liver disease; HCC: Hepatocellular carcinoma; miRNA: MicroRNA; PIVKA-II: Protein induced by vitamin K absence/antagonist-II.



DOI: 10.3748/wjg.v28.i29.3917 **Copyright** ©The Author(s) 2022.

Figure 3 Receiver operating characteristics curves and area under the curve for multivariate analysis of real-time quantitative PCR results. A: Comparison of all hepatocellular carcinoma *vs* chronic liver disease; B: Early hepatocellular carcinoma *vs* chronic liver disease; C: Early hepatocellular carcinoma *vs* cirrhosis. Analyses were for the validation cohort. Upper panel: Protein induced by vitamin K absence/antagonist-II alone; Lower panel: Protein induced by vitamin K absence/antagonist-II in combination with the best miRNA (selected as final pair in the training analysis). AUC: Area under the curve; CI: Confidence interval; CLD: Chronic liver disease; HCC: Hepatocellular carcinoma; miR: MicroRNA; PIVKA-II: Protein induced by vitamin K absence/antagonist-II.

DISCUSSION

HCC is a severe disease of the liver and one of the leading causes of cancer-related deaths worldwide [5]. As with all other cancers, early detection is crucial for successful treatment. Recommended detection methods include US, CT, magnetic resonance imaging and measurement of AFP and PIVKA-II. However, these methods are either cost-intensive, operator-dependent or not suitable for the detection of early HCC[6-8,11-13,15]. Previous publications show that single miRNAs, like miR-21, hsa-miR-26a and hsa-miR-101[34,35], as well as miRNA signatures (*e.g.*, hsa-miR-3677, miR-421, hsa-miR-326, hsa-miR-424 and hsa-miR-511-2)[36,37] can improve detection of HCC. While these results are promising, the studies were conducted in small cohorts and/or the control group included healthy individuals who were not being screened regularly for HCC.

Table 5 Fractions of characteristics (feature) selected during internal cross-validation for evaluating the two-marker combination performance

Feature	Fraction selected in cross-validation
All HCC *vs* CLD	
PIVKA-II	1.00
hsa-miR-21-5p	0.86
hsa-miR-320d	0.10
hsa-miR-339-3p	0.02
hsa-miR-320a	0.01
hsa-miR-423-5p	0.00
Early HCC *vs* CLD	
PIVKA-II	1.00
hsa-miR-21-5p	0.60
hsa-miR-320d	0.18
hsa-miR-652-3p	0.16
hsa-miR-339-3p	0.02
hsa-miR-221-3p	0.01
hsa-miR-30b-5p	0.01
hsa-miR-10b-5p	0.00
hsa-miR-15b-5p	0.00
Early HCC *vs* cirrhosis	
PIVKA-II	1.00
hsa-miR-652-3p	0.64
hsa-miR-221-3p	0.26
hsa-miR-21-5p	0.05
hsa-miR-423-5p	0.04
hsa-miR-320a	0.01
hsa-miR-339-3p	0.01
hsa-miR-320d	0.00

CLD: Chronic liver disease; HCC: Hepatocellular carcinoma; PIVKA-II: Protein induced by vitamin K absence/antagonist-II; miR: MicroRNA.

Therefore, we carried out a comprehensive, prospective, multicenter, case-control study including patient samples with early-stage (n = 147) and late-stage HCC (n = 160), HBV (n = 136), HCV (n = 72) and cirrhosis with HBV and HCV (n = 145). We analyzed plasma samples to evaluate the utility of circulating miRNAs alone and in combination with two established protein markers, PIVKA-II and AFP, as biomarkers for detection (including early detection) of HCC and performed multivariate analysis on the included miRNAs. When compared with other studies of circulating miRNAs, our study is unique for the following reasons. First, we screened a large number of plasma miRNAs *via* NGS and RT-qPCR, which enabled us to identify potential diagnostic markers independently of the detection method. Second, we included early-stage and late-stage HCC and for the control cohort included HBV and HCV patients with and without cirrhosis to find a miRNA that can diagnose HCC at an early stage and to validate a biomarker that would be applicable for most of the at-risk population. Third, we used a large sample size of 660 samples with four different independent sample panels to increase statistical power. Finally, we employed an empirically validated set of endogenous reference genes for the normalization of our data.

To find reliable miRNA biomarkers for HCC that were unbiased with respect to the detection method, we followed two different screening approaches (RT-qPCR and NGS) to assess a large number of miRNAs isolated from patient plasma. For each method, we used a different set of plasma samples to receive reproducible results by two independent techniques in a large set of samples. These factors

Table 6 Univariate analysis of real-time quantitative PCR results for comparison

miRNA	Wilcoxon *Q*-value	AUC	Specificity at 90% sensitivity	Comparison
hsa-miR-21-5p	0.00025[a]	0.65	0.17	All HCC *vs* CLD
hsa-miR-423-5p	0.037[b]	0.59	0.11	
hsa-miR-320d	0.078	0.57	0.11	
hsa-miR-652-3p	0.25	0.59	0.13	Early HCC *vs* cirrhosis

[a]*Q*-value < 0.001.
[b]*Q*-value < 0.05.
AUC: Area under the curve; CLD: Chronic liver disease; HCC: Hepatocellular carcinoma; miRNA: MicroRNA; miR: MicroRNA.

could explain why we obtained only three miRNAs (miR-21-5p, miR-320a and miR-421) that showed high potential as diagnostic biomarkers for HCC in both screening approaches.

The 26 best miRNAs selected by both screening methods, including the three overlapping miRNAs, were then analyzed in two different sample panels (training and validation) and combined with the established protein markers PIVKA-II and AFP. In the training panel, miR-21-5p, miR-320d and miR-423 were the best single markers for distinguishing between the HCC and CLD groups. For the early detection of HCC, our data showed that miR-21-5p has the potential to improve the diagnostic performance of PIVKA-II. In the validation panel, the results from the training panel for the comparison of HCC *vs* CLD for miR-21-5p (AUC = 0.65) and miR-423 (AUC = 0.59) could be confirmed. However, the hypothesis of finding a miRNA signature specific for the detection of early HCC could not be confirmed, and the combination of all 26 miRNAs and AFP did not reveal greater diagnostic potential than AFP alone.

MiR-21-5p was one of the two miRNAs with significantly higher expression in the HCC group compared with the CLD group in both the training and validation cohorts. Other publications have shown similar results. Amr *et al*[38] demonstrated that the expression of serum miR-21 was increased in HCC compared with chronic hepatitis, while Gedawya *et al*[39] revealed overexpression of plasma miR-21 in an HCC group ($P < 0.05$) compared with both CLD and healthy subjects from a cohort in Egypt. However, miR-21 was also reported as a circulating diagnostic biomarker for various other cancers[40] such as breast cancer[41], glioma[42] and non-small cell lung cancer[43]. MiR-21 has been described as an oncogene, targeting tumor suppressors like TP63, TP53, TGF-β and PTEN, leading to the inhibition of apoptosis[44,45]. Furthermore, miR-21 contributes to the epithelial-to-mesenchymal transition in cervical cancer by modulating the expression of the *Rasa1* gene (RAS p21 protein activator 1). Therefore, by indirectly influencing the activity of Ras, miR-21 contributes to the migration potential of these cells. Another described oncogenic effect is that miR-21 modulates angiogenesis in prostate cancer cells[46]. Thus, the underlying biology of miR-21 supports its role in HCC development and its potential diagnostic value in HCC as well as other cancers.

MiR-423 also showed differential expression when comparing HCC and CLD in both the training and validation groups. Previously, it was revealed that the expression of miR-423 was significantly increased in HCC tissues compared with adjacent normal tissues[47,48]. In serum samples from HCC patients, miR-423 was also found to be significantly upregulated compared with a control group consisting of patients with cirrhosis or chronic hepatitis[49]. In the training and validation panels (total of 500 independent samples), miR-423 levels were elevated in the HCC group. MiR-423 expression has also been found to be upregulated in breast cancer tissue[50], human prostate cancer tissues and prostate cancer PC3 cells[51] and plasma of patients with oral squamous cell carcinoma[52]. This indicates that miR-423 is not limited to the detection of HCC and can also detect several other cancer types. It can act as an oncogene by enhancing the proliferation and migration of gastric cancer cells *in vitro* and *in vivo* when overexpressed[53]. Furthermore, when knocking down miR-423, proliferation of PC3 cells was inhibited, and apoptosis was promoted[51]. In summary, although miR-21 and miR-423 are upregulated in several diseases, their overexpression in a high-risk population could be indicative of early HCC development.

Our results indicate that miR-320d and miR-652 might not be robust biomarkers to diagnose (early) HCC as the results from the training cohort could not be validated. However, they seem to play a role in the development of cancer in general, which requires further investigation.

The 15 putative miRNAs detected by NGS in the screening phase that were differentially expressed between HCC and CLD could not be confirmed as potential biomarkers by RT-qPCR in the training and validation panel. Nonetheless, they could be detected in a small number of samples by both NGS and RT-qPCR. Though the putative miRNAs only showed a relatively low expression, they could be novel miRNAs and should be considered in further investigations.

In the training panel, the combination of the HCC biomarker PIVKA-II with the 26 miRNAs selected in the screening phase improved diagnostic capability, and AUC was increased compared with PIVKA-

II alone. However, this could not be confirmed in the validation panel, which included more samples than the training panel. The combination of AFP and miRNA also did not show any improvement in AFP diagnostic capability in the training panel and was therefore not analyzed in the validation panel. We observed that individual miRNAs identified the same set of patients as those identified by AFP, thus the miRNAs did not add any significant value in this case. However, as the performance of PIVKA-II in the same cohort was between 5% and 20% lower than the performance of AFP, the miRNAs therefore had higher additive value when combined with PIVKA-II. Our results demonstrate that the protein markers AFP and PIVKA-II are more robust biomarkers for HCC than miRNAs.

CONCLUSION

In conclusion, our study found that two miRNAs (miR-21-5p and miR-423) demonstrated significant differential expression between the HCC group and CLD control group. However, the combination of miRNAs with established protein biomarkers (AFP and PIVKA-II) did not improve diagnostic performance of either protein. Further investigation of the molecular mechanisms by which miRNAs, specifically miR-21-5p and miR-423, support HCC development may help in diagnosing and treating this highly malignant tumor.

ARTICLE HIGHLIGHTS

Research background

Hepatocellular carcinoma (HCC) is the sixth most common cancer worldwide and a leading cause of cancer-related mortality. Current guidelines recommend the surveillance of high-risk patients every 6 mo using ultrasonography, but early-stage HCC detection is limited.

Research motivation

Previous reports show that the expression level of human microRNAs (miRNAs) can serve as an early marker for HCC, even outperforming established biomarkers like alpha-fetoprotein (AFP) and protein induced by vitamin K absence/antagonist-II (PIVKA-II).

Research objectives

To evaluate the diagnostic role of miRNAs in HCC as single markers, signatures or in combination with known protein biomarkers AFP and PIVKA-II in a prospective, multicenter, case-control study.

Research methods

We employed two independent methods, real-time quantitative PCR and next-generation sequencing, to investigate miRNAs levels in the discovery cohort of 160 HCC and control patients. Selected miRNAs were subsequently analyzed for their univariate and multivariate performance in independent training (n = 200) and validation cohorts (n = 300).

Research results

Real-time quantitative PCR and next-generation sequencing identified 26 miRNAs differentiating between HCC and chronic liver disease controls. Three miRNAs (miR-21, miR-320a and miR-186-5p) were selected by both methods. In the training cohort, only miR-21, miR-320d and miR-423 could significantly distinguish (Q < 0.05) between the HCC and control groups. In the multivariate setting, miR-21 with PIVKA-II was selected as the best combination, resulting in an area under the curve of 0.87 for diagnosis and 0.74 for early diagnosis of HCC. miR-21 and miR-423 were confirmed as potential HCC biomarkers in the validation cohort. A combination of miRNAs did not perform better than any single miRNA. Improvement of AFP or PIVKA-II performance through combination with miRNAs was not confirmed in the validation panel.

Research conclusions

Selected miRNA candidates in standalone or signature settings or in combination with biomarkers AFP and PIVKA-II did not improve the diagnostic performance of the protein biomarkers in identification of early-stage HCC.

Research perspectives

Diagnostic superiority of microRNAs for detection of early HCC could not be confirmed, which was primarily due to the excellent and robust performance of the protein biomarkers AFP and PIVKA-II for this intended use. Therefore, miRNAs still carry diagnostic potential for application in other oncological diseases.

ACKNOWLEDGEMENTS

The authors would like to acknowledge Heike Wegmeyer for her help with study protocol design and sample collection and Gloria Tabares for her help with study design and interpretation. LightCycler 480 is a trademark of Roche. All other product names and trademarks are the property of their respective owners.

FOOTNOTES

Author contributions: Swiatek-de Lange M provided study supervision; Malik J and Swiatek-de Lange M contributed to project development; Chan HL-Y, Piratvisuth T, Tanwandee T, Thongsawat S, Sukeepaisarnjaroen W, Esteban JI, Bes M and Köhler B contributed to sample collection; Malik J contributed to development of methodology and collection of data; Malik J, Klammer M and Rolny V contributed to the biostatistical analysis of the data; Malik J, Klammer M, Rolny V and Swiatek-de Lange M contributed to the interpretation of the data; Malik J, Klammer M and Swiatek-de Lange wrote the manuscript; Malik J and Swiatek-de Lange M provided critical review and editing of the manuscript; All authors have read and approved the final manuscript.

Institutional review board statement: The study was approved by the following review boards: Siriraj Institutional Review Board; Research Ethics Committee of the Faculty of Medicine, Chiang Mai University; Joint Chinese University of Hong Kong – New Territories East Cluster Clinical Research Ethics Committee; Ethikkommission Medizinische Fakultät Heidelberg; Research Ethics Committee, Faculty of Medicine, Prince of Songkla University; Clinical Research Ethics Committee of Vall d'Hebron University Hospital; and Khon Kaen University Ethics Committee for Human Research.

Informed consent statement: Written informed consent was obtained from all participants.

Conflict-of-interest statement: Malik J, Klammer M, Rolny V and Swiatek-de Lange M are employees of Roche Diagnostics GmbH and shareholders in Roche Diagnostics.

Data sharing statement: No additional data are available.

STROBE statement: The authors have read the STROBE Statement—checklist of items, and the manuscript was prepared and revised according to the STROBE Statement—checklist of items.

Open-Access: This article is an open-access article that was selected by an in-house editor and fully peer-reviewed by external reviewers. It is distributed in accordance with the Creative Commons Attribution NonCommercial (CC BY-NC 4.0) license, which permits others to distribute, remix, adapt, build upon this work non-commercially, and license their derivative works on different terms, provided the original work is properly cited and the use is non-commercial. See: https://creativecommons.org/Licenses/by-nc/4.0/

Country/Territory of origin: Germany

ORCID number: Juliane Malik 0000-0003-2306-3920; Martin Klammer 0000-0001-6426-0029; Vinzent Rolny 0000-0001-8229-0002; Henry Lik-Yuen Chan 0000-0002-7790-1611; Teerha Piratvisuth 0000-0002-5249-9208; Tawesak Tanwandee 0000-0001-7634-0843; Satawat Thongsawat 0000-0003-3302-3930; Wattana Sukeepaisarnjaroen 0000-0001-5065-9397; Juan Ignacio Esteban 0000-0001-5085-917X; Marta Bes 0000-0001-6103-072X; Bruno Köhler 0000-0002-7308-0377; Magdalena Swiatek-de Lange 0000-0003-1406-3232.

S-Editor: Chang KL
L-Editor: Filipodia
P-Editor: Chang KL

REFERENCES

1 International Agency for Research on Cancer. Cancer today. [cited 1 January 2022]. Available from: http://gco.iarc.fr/today/
2 **El-Serag HB**, Rudolph KL. Hepatocellular carcinoma: epidemiology and molecular carcinogenesis. *Gastroenterology* 2007; **132**: 2557-2576 [PMID: 17570226 DOI: 10.1053/j.gastro.2007.04.061]
3 **Sherman M**. Hepatocellular carcinoma: epidemiology, surveillance, and diagnosis. *Semin Liver Dis* 2010; **30**: 3-16 [PMID: 20175029 DOI: 10.1055/s-0030-1247128]
4 **El-Serag HB**. Hepatocellular carcinoma. *N Engl J Med* 2011; **365**: 1118-1127 [PMID: 21992124 DOI: 10.1056/NEJMra1001683]
5 **Wang CY**, Li S. Clinical characteristics and prognosis of 2887 patients with hepatocellular carcinoma: A single center 14 years experience from China. *Medicine (Baltimore)* 2019; **98**: e14070 [PMID: 30681563 DOI:

10.1097/MD.0000000000014070]
6 **European Association For The Study Of The Liver**; European Organisation For Research And Treatment Of Cancer. EASL-EORTC clinical practice guidelines: management of hepatocellular carcinoma. *J Hepatol* 2012; **56**: 908-943 [PMID: 22424438 DOI: 10.1016/j.jhep.2011.12.001]
7 **Omata M**, Cheng AL, Kokudo N, Kudo M, Lee JM, Jia J, Tateishi R, Han KH, Chawla YK, Shiina S, Jafri W, Payawal DA, Ohki T, Ogasawara S, Chen PJ, Lesmana CRA, Lesmana LA, Gani RA, Obi S, Dokmeci AK, Sarin SK. Asia-Pacific clinical practice guidelines on the management of hepatocellular carcinoma: a 2017 update. *Hepatol Int* 2017; **11**: 317-370 [PMID: 28620797 DOI: 10.1007/s12072-017-9799-9]
8 **Heimbach JK**, Kulik LM, Finn RS, Sirlin CB, Abecassis MM, Roberts LR, Zhu AX, Murad MH, Marrero JA. AASLD guidelines for the treatment of hepatocellular carcinoma. *Hepatology* 2018; **67**: 358-380 [PMID: 28130846 DOI: 10.1002/hep.29086]
9 **European Association for the Study of the Liver**. EASL Clinical Practice Guidelines: Management of hepatocellular carcinoma. *J Hepatol* 2018; **69**: 182-236 [PMID: 29628281 DOI: 10.1016/j.jhep.2018.03.019]
10 **Kokudo N**, Takemura N, Hasegawa K, Takayama T, Kubo S, Shimada M, Nagano H, Hatano E, Izumi N, Kaneko S, Kudo M, Iijima H, Genda T, Tateishi R, Torimura T, Igaki H, Kobayashi S, Sakurai H, Murakami T, Watadani T, Matsuyama Y. Clinical practice guidelines for hepatocellular carcinoma: The Japan Society of Hepatology 2017 (4th JSH-HCC guidelines) 2019 update. *Hepatol Res* 2019; **49**: 1109-1113 [PMID: 31336394 DOI: 10.1111/hepr.13411]
11 **Singal A**, Volk ML, Waljee A, Salgia R, Higgins P, Rogers MA, Marrero JA. Meta-analysis: surveillance with ultrasound for early-stage hepatocellular carcinoma in patients with cirrhosis. *Aliment Pharmacol Ther* 2009; **30**: 37-47 [PMID: 19392863 DOI: 10.1111/j.1365-2036.2009.04014.x]
12 **Jeong WK**. Surveillance of hepatocellular carcinoma: is only ultrasound enough? *Clin Mol Hepatol* 2017; **23**: 222-223 [PMID: 28942623 DOI: 10.3350/cmh.2017.0046]
13 **Li Q**, Dhyani M, Grajo JR, Sirlin C, Samir AE. Current status of imaging in nonalcoholic fatty liver disease. *World J Hepatol* 2018; **10**: 530-542 [PMID: 30190781 DOI: 10.4254/wjh.v10.i8.530]
14 **Tzartzeva K**, Obi J, Rich NE, Parikh ND, Marrero JA, Yopp A, Waljee AK, Singal AG. Surveillance Imaging and Alpha Fetoprotein for Early Detection of Hepatocellular Carcinoma in Patients With Cirrhosis: A Meta-analysis. *Gastroenterology* 2018; **154**: 1706-1718.e1 [PMID: 29425931 DOI: 10.1053/j.gastro.2018.01.064]
15 **Gentile I**, Buonomo AR, Scotto R, Zappulo E, Carriero C, Piccirillo M, Izzo F, Rizzo M, Cerasuolo D, Borgia G, Cavalcanti E. Diagnostic Accuracy of PIVKA-II, Alpha-Fetoprotein and a Combination of both in Diagnosis of Hepatocellular Carcinoma in Patients Affected by Chronic HCV Infection. *In Vivo* 2017; **31**: 695-700 [PMID: 28652441 DOI: 10.21873/invivo.11115]
16 **Bushati N**, Cohen SM. microRNA functions. *Annu Rev Cell Dev Biol* 2007; **23**: 175-205 [PMID: 17506695 DOI: 10.1146/annurev.cellbio.23.090506.123406]
17 **Wienholds E**, Plasterk RH. MicroRNA function in animal development. *FEBS Lett* 2005; **579**: 5911-5922 [PMID: 16111679 DOI: 10.1016/j.febslet.2005.07.070]
18 **Ruan K**, Fang X, Ouyang G. MicroRNAs: novel regulators in the hallmarks of human cancer. *Cancer Lett* 2009; **285**: 116-126 [PMID: 19464788 DOI: 10.1016/j.canlet.2009.04.031]
19 **Nana-Sinkam SP**, Croce CM. Clinical applications for microRNAs in cancer. *Clin Pharmacol Ther* 2013; **93**: 98-104 [PMID: 23212103 DOI: 10.1038/clpt.2012.192]
20 **Mitchell PS**, Parkin RK, Kroh EM, Fritz BR, Wyman SK, Pogosova-Agadjanyan EL, Peterson A, Noteboom J, O'Briant KC, Allen A, Lin DW, Urban N, Drescher CW, Knudsen BS, Stirewalt DL, Gentleman R, Vessella RL, Nelson PS, Martin DB, Tewari M. Circulating microRNAs as stable blood-based markers for cancer detection. *Proc Natl Acad Sci U S A* 2008; **105**: 10513-10518 [PMID: 18663219 DOI: 10.1073/pnas.0804549105]
21 **Li L**, Zhu D, Huang L, Zhang J, Bian Z, Chen X, Liu Y, Zhang CY, Zen K. Argonaute 2 complexes selectively protect the circulating microRNAs in cell-secreted microvesicles. *PLoS One* 2012; **7**: e46957 [PMID: 23077538 DOI: 10.1371/journal.pone.0046957]
22 **Lässer C**. Exosomal RNA as biomarkers and the therapeutic potential of exosome vectors. *Expert Opin Biol Ther* 2012; **12** Suppl 1: S189-S197 [PMID: 22506888 DOI: 10.1517/14712598.2012.680018]
23 **Huang JT**, Liu SM, Ma H, Yang Y, Zhang X, Sun H, Xu J, Wang J. Systematic Review and Meta-Analysis: Circulating miRNAs for Diagnosis of Hepatocellular Carcinoma. *J Cell Physiol* 2016; **231**: 328-335 [PMID: 26291451 DOI: 10.1002/jcp.25135]
24 **Murakami Y**, Yasuda T, Saigo K, Urashima T, Toyoda H, Okanoue T, Shimotohno K. Comprehensive analysis of microRNA expression patterns in hepatocellular carcinoma and non-tumorous tissues. *Oncogene* 2006; **25**: 2537-2545 [PMID: 16331254 DOI: 10.1038/sj.onc.1209283]
25 **Tan Y**, Ge G, Pan T, Wen D, Chen L, Yu X, Zhou X, Gan J. A serum microRNA panel as potential biomarkers for hepatocellular carcinoma related with hepatitis B virus. *PLoS One* 2014; **9**: e107986 [PMID: 25238238 DOI: 10.1371/journal.pone.0107986]
26 **Borel F**, Konstantinova P, Jansen PL. Diagnostic and therapeutic potential of miRNA signatures in patients with hepatocellular carcinoma. *J Hepatol* 2012; **56**: 1371-1383 [PMID: 22314424 DOI: 10.1016/j.jhep.2011.11.026]
27 **Yang W**, Zhou C, Luo M, Shi X, Li Y, Sun Z, Zhou F, Chen Z, He J. MiR-652-3p is upregulated in non-small cell lung cancer and promotes proliferation and metastasis by directly targeting Lgl1. *Oncotarget* 2016; **7**: 16703-16715 [PMID: 26934648 DOI: 10.18632/oncotarget.7697]
28 **Sun X**, Dongol S, Qiu C, Xu Y, Sun C, Zhang Z, Yang X, Zhang Q, Kong B. miR-652 Promotes Tumor Proliferation and Metastasis by Targeting *RORA* in Endometrial Cancer. *Mol Cancer Res* 2018; **16**: 1927-1939 [PMID: 30093563 DOI: 10.1158/1541-7786.MCR-18-0267]
29 **Li LM**, Hu ZB, Zhou ZX, Chen X, Liu FY, Zhang JF, Shen HB, Zhang CY, Zen K. Serum microRNA profiles serve as novel biomarkers for HBV infection and diagnosis of HBV-positive hepatocarcinoma. *Cancer Res* 2010; **70**: 9798-9807 [PMID: 21098710 DOI: 10.1158/0008-5472.CAN-10-1001]
30 **Zhou J**, Yu L, Gao X, Hu J, Wang J, Dai Z, Wang JF, Zhang Z, Lu S, Huang X, Wang Z, Qiu S, Wang X, Yang G, Sun H,

Tang Z, Wu Y, Zhu H, Fan J. Plasma microRNA panel to diagnose hepatitis B virus-related hepatocellular carcinoma. *J Clin Oncol* 2011; **29**: 4781-4788 [PMID: 22105822 DOI: 10.1200/JCO.2011.38.2697]

31 **Piratvisuth T**, Tanwandee T, Thongsawat S, Sukeepaisarnjaroen W, Esteban JI, Bes M, Köhler B, He Y, Swiatek-de Lange M, Morgenstern D, Chan HL. Multimarker Panels for Detection of Early Stage Hepatocellular Carcinoma: A Prospective, Multicenter, Case-Control Study. *Hepatol Commun* 2022; **6**: 679-691 [PMID: 34796691 DOI: 10.1002/hep4.1847]

32 **Wu Y**, Wei B, Liu H, Li T, Rayner S. MiRPara: a SVM-based software tool for prediction of most probable microRNA coding regions in genome scale sequences. *BMC Bioinformatics* 2011; **12**: 107 [PMID: 21504621 DOI: 10.1186/1471-2105-12-107]

33 **Sengupta S**, Parikh ND. Biomarker development for hepatocellular carcinoma early detection: current and future perspectives. *Hepat Oncol* 2017; **4**: 111-122 [PMID: 30191058 DOI: 10.2217/hep-2017-0019]

34 **Qu KZ**, Zhang K, Li H, Afdhal NH, Albitar M. Circulating microRNAs as biomarkers for hepatocellular carcinoma. *J Clin Gastroenterol* 2011; **45**: 355-360 [PMID: 21278583 DOI: 10.1097/MCG.0b013e3181f18ac2]

35 **Zhuang C**, Jiang W, Huang D, Xu L, Yang Q, Zheng L, Wang X, Hu L. Serum miR-21, miR-26a and miR-101 as potential biomarkers of hepatocellular carcinoma. *Clin Res Hepatol Gastroenterol* 2016; **40**: 386-396 [PMID: 26669589 DOI: 10.1016/j.clinre.2015.11.002]

36 **Wen Y**, Han J, Chen J, Dong J, Xia Y, Liu J, Jiang Y, Dai J, Lu J, Jin G, Wei Q, Shen H, Sun B, Hu Z. Plasma miRNAs as early biomarkers for detecting hepatocellular carcinoma. *Int J Cancer* 2015; **137**: 1679-1690 [PMID: 25845839 DOI: 10.1002/ijc.29544]

37 **Lu M**, Kong X, Wang H, Huang G, Ye C, He Z. A novel microRNAs expression signature for hepatocellular carcinoma diagnosis and prognosis. *Oncotarget* 2017; **8**: 8775-8784 [PMID: 28060739 DOI: 10.18632/oncotarget.14452]

38 **Amr KS**, Ezzat WM, Elhosary YA, Hegazy AE, Fahim HH, Kamel RR. The potential role of miRNAs 21 and 199-a in early diagnosis of hepatocellular carcinoma. *Gene* 2016; **575**: 66-70 [PMID: 26302751 DOI: 10.1016/j.gene.2015.08.038]

39 **Gedawya GE**, Obada M, Kelani A, El-Saida H, Ghanayem NM. Circulating MiRNA-21 and programed cell death (PDCD) 4 gene expression in hepatocellular carcinoma (HCC) in Egyptian patients. *Egypt J Med Hum Genet* 2017; **18**: 137-145 [DOI: 10.1016/j.ejmhg.2016.04.007]

40 **Wu K**, Li L, Li S. Circulating microRNA-21 as a biomarker for the detection of various carcinomas: an updated meta-analysis based on 36 studies. *Tumour Biol* 2015; **36**: 1973-1981 [PMID: 25527152 DOI: 10.1007/s13277-014-2803-2]

41 **Asaga S**, Kuo C, Nguyen T, Terpenning M, Giuliano AE, Hoon DS. Direct serum assay for microRNA-21 concentrations in early and advanced breast cancer. *Clin Chem* 2011; **57**: 84-91 [PMID: 21036945 DOI: 10.1373/clinchem.2010.151845]

42 **Ivo D'Urso P**, Fernando D'Urso O, Damiano Gianfreda C, Mezzolla V, Storelli C, Marsigliante S. miR-15b and miR-21 as Circulating Biomarkers for Diagnosis of Glioma. *Curr Genomics* 2015; **16**: 304-311 [PMID: 27047250 DOI: 10.2174/1389202916666150707155610]

43 **Zhao W**, Zhao JJ, Zhang L, Xu QF, Zhao YM, Shi XY, Xu AG. Serum miR-21 Level: a potential diagnostic and prognostic biomarker for non-small cell lung cancer. *Int J Clin Exp Med* 2015; **8**: 14759-14763 [PMID: 26628958]

44 **Buscaglia LE**, Li Y. Apoptosis and the target genes of microRNA-21. *Chin J Cancer* 2011; **30**: 371-380 [PMID: 21627859 DOI: 10.5732/cjc.011.10132]

45 **Papagiannakopoulos T**, Shapiro A, Kosik KS. MicroRNA-21 targets a network of key tumor-suppressive pathways in glioblastoma cells. *Cancer Res* 2008; **68**: 8164-8172 [PMID: 18829576 DOI: 10.1158/0008-5472.CAN-08-1305]

46 **Bica-Pop C**, Cojocneanu-Petric R, Magdo L, Raduly L, Gulei D, Berindan-Neagoe I. Overview upon miR-21 in lung cancer: focus on NSCLC. *Cell Mol Life Sci* 2018; **75**: 3539-3551 [PMID: 30030592 DOI: 10.1007/s00018-018-2877-x]

47 **Sun X**, Wang M, Liu H, Wang J. MicroRNA-423 enhances the invasiveness of hepatocellular carcinoma *via* regulation of BRMS1. *Am J Transl Res* 2017; **9**: 5576-5584 [PMID: 29312509]

48 **Yu Z**, Zhao H, Feng X, Li H, Qiu C, Yi X, Tang H, Zhang J. Long Non-coding RNA FENDRR Acts as a miR-423-5p Sponge to Suppress the Treg-Mediated Immune Escape of Hepatocellular Carcinoma Cells. *Mol Ther Nucleic Acids* 2019; **17**: 516-529 [PMID: 31351327 DOI: 10.1016/j.omtn.2019.05.027]

49 **An Y**, Gao S, Zhao WC, Qiu BA, Xia NX, Zhang PJ, Fan ZP. Novel serum microRNAs panel on the diagnostic and prognostic implications of hepatocellular carcinoma. *World J Gastroenterol* 2018; **24**: 2596-2604 [PMID: 29962816 DOI: 10.3748/wjg.v24.i24.2596]

50 **Sun X**, Huang T, Zhang C, Zhang S, Wang Y, Zhang Q, Liu Z. Long non-coding RNA LINC00968 reduces cell proliferation and migration and angiogenesis in breast cancer through up-regulation of PROX1 by reducing hsa-miR-423-5p. *Cell Cycle* 2019; **18**: 1908-1924 [PMID: 31213129 DOI: 10.1080/15384101.2019.1632641]

51 **Lin H**, Lin T, Lin J, Yang M, Shen Z, Liu H, Zou Z, Zheng Z. Inhibition of miR-423-5p suppressed prostate cancer through targeting GRIM-19. *Gene* 2019; **688**: 93-97 [PMID: 30415005 DOI: 10.1016/j.gene.2018.11.021]

52 **Chang YA**, Weng SL, Yang SF, Chou CH, Huang WC, Tu SJ, Chang TH, Huang CN, Jong YJ, Huang HD. A Three-MicroRNA Signature as a Potential Biomarker for the Early Detection of Oral Cancer. *Int J Mol Sci* 2018; **19** [PMID: 29518940 DOI: 10.3390/ijms19030758]

53 **Yang H**, Fu H, Wang B, Zhang X, Mao J, Li X, Wang M, Sun Z, Qian H, Xu W. Exosomal miR-423-5p targets SUFU to promote cancer growth and metastasis and serves as a novel marker for gastric cancer. *Mol Carcinog* 2018; **57**: 1223-1236 [PMID: 29749061 DOI: 10.1002/mc.22838]

World Journal of Gastroenterology

Submit a Manuscript: https://www.f6publishing.com

World J Gastroenterol 2022 August 7; 28(29): 3934-3945

DOI: 10.3748/wjg.v28.i29.3934

ISSN 1007-9327 (print) ISSN 2219-2840 (online)

ORIGINAL ARTICLE

Retrospective Cohort Study

Optimal timing of biliary drainage based on the severity of acute cholangitis: A single-center retrospective cohort study

Zhao-Qing Lu, Han-Yu Zhang, Chen-Fen Su, Yue-Yan Xing, Guo-Xing Wang, Chun-Sheng Li

Specialty type: Gastroenterology and hepatology

Provenance and peer review: Unsolicited article; Externally peer reviewed.

Peer-review model: Single blind

Peer-review report's scientific quality classification

Grade A (Excellent): 0
Grade B (Very good): 0
Grade C (Good): C, C, C
Grade D (Fair): 0
Grade E (Poor): 0

P-Reviewer: Badessi G, Italy; Emran TB, Bangladesh; Maieron A, Austria

Received: March 17, 2022
Peer-review started: March 17, 2022
First decision: April 11, 2022
Revised: April 25, 2022
Accepted: July 5, 2022
Article in press: July 5, 2022
Published online: August 7, 2022

Zhao-Qing Lu, Han-Yu Zhang, Chen-Fen Su, Yue-Yan Xing, Guo-Xing Wang, Department of Emergency Medicine, Beijing Friendship Hospital, Capital Medical University, Beijing 100050, China

Chun-Sheng Li, Emergency and Critical Care Center, Beijing Friendship Hospital, Capital Medical University, Beijing 100050, China

Corresponding author: Chun-Sheng Li, PhD, Professor, Emergency and Critical Care Center, Beijing Friendship Hospital, Capital Medical University, No. 95 Yongan Road, Xicheng District, Beijing 100050, China. lcscyyy@163.com

Abstract

BACKGROUND

Biliary decompression is well known to greatly decrease the risks of mortality in acute cholangitis (AC). Although early biliary drainage is recommended by the treatment guidelines for AC, the best time for performing this procedure is yet to be established. Furthermore, since the clinical outcomes of patients with severe AC vary dramatically, screening for patients that could benefit the most from early drainage would be more beneficial than the drainage performed based on the severity grade criteria.

AIM

To investigate the optimal drainage timing for AC patients with each disease severity grade and organ dysfunction.

METHODS

In this retrospective monocenter cohort analysis, we reviewed 1305 patients who were diagnosed with AC according to the Tokyo guidelines 2018 at a Chinese tertiary hospital between July 2016 and December 2020. Demographic characteristics including age and sex, clinical and laboratory characteristics, and imaging findings of each patient were obtained from electronic medical records. We investigated the all-cause in-hospital mortality (IHM), hospital length of stay (LOS), and hospitalization costs associated with the timing of biliary drainage according to the severity grading and different dysfunctioning organs and predictors [age, white blood cell (WBC) count, total bilirubin, albumin, lactate, malignant obstruction, and Charlton comorbidity index (CCI)].

RESULTS

Biliary drainage within 24 or 48 h in Grade III AC patients could dramatically decrease IHM (3.9% *vs* 9.0%, $P = 0.041$; 4% *vs* 9.9%, $P = 0.018$, respectively), while increasing LOS and hospitalization costs. Multivariate logistic analysis revealed that neurological, respiratory, renal, and cardiovascular dysfunctions, hypoalbuminemia, and malignant obstruction were significantly associated with IHM (odds ratio = 5.32, 2.541, 6.356, 4.021, 5.655, and 7.522; $P < 0.001$, $P = 0.016$, $P < 0.001$, $P = 0.012$, $P < 0.001$, and $P < 0.001$; respectively). Biliary decompression performed within 12 h of admission significantly decreased the IHM in AC patients with neurological dysfunction (0% *vs* 17.3%, $P = 0.041$) or with serum lactate > 2 mmol/L (0% *vs* 5.4%, $P = 0.016$). In the subgroup of AC patients with renal dysfunction, abnormal WBC count, hyperbilirubinemia, or hypoalbuminemia, early drainage (< 24 h) reduced the IHM (3.6% *vs* 33.3%, $P = 0.004$; 1.9% *vs* 5.8%, $P = 0.031$; 1.7% *vs* 5.0%, $P = 0.019$; 0% *vs* 27%, $P = 0.026$; respectively). The IHM was lower in patients with AC combined with hepatic dysfunction, malignant obstruction, or a CCI > 3 who had undergone biliary drainage within 48 h (2.6% *vs* 20.5%, $P = 0.016$; 3.0% *vs* 13.5%, $P = 0.006$; 3.4% *vs* 9.6%, $P = 0.021$; respectively).

CONCLUSION

Biliary drainage within 12 h is beneficial for AC patients with neurological or cardiovascular dysfunction, while complete biliary decompression within 24 h of admission is recommended for treating patients with Grade III AC.

Key Words: Acute cholangitis; Endoscopic retrograde cholangiopancreatography; Mortality; Biliary drainage; Organ dysfunction

©The Author(s) 2022. Published by Baishideng Publishing Group Inc. All rights reserved.

Core Tip: This study aimed to investigate the optimal timing of drainage for patients with acute cholangitis (AC) with each grade and organ dysfunction. We first attempted to study whether AC patients with different organ dysfunction should undergo biliary drainage at distinct times. We believe that our study makes a significant contribution to the literature because we found that patients with severe AC should complete biliary decompression within 24 h of admission, while biliary drainage within 12 h was beneficial for AC patients with neurological or cardiovascular dysfunction.

Citation: Lu ZQ, Zhang HY, Su CF, Xing YY, Wang GX, Li CS. Optimal timing of biliary drainage based on the severity of acute cholangitis: A single-center retrospective cohort study. *World J Gastroenterol* 2022; 28(29): 3934-3945

URL: https://www.wjgnet.com/1007-9327/full/v28/i29/3934.htm

DOI: https://dx.doi.org/10.3748/wjg.v28.i29.3934

INTRODUCTION

Acute cholangitis (AC) is a life-threatening condition that occurs in the presence of biliary obstruction. Although growing evidence confirms that biliary decompression can dramatically decrease the mortality rates associated with AC, the optimal time for biliary drainage remains controversial[1-3]. Most experts agree that the timeframe for biliary decompression is distinct for different severity grades based on the Tokyo guidelines 2018/2013 (TG18/13), which recommend early biliary drainage for Grade II AC and urgent biliary drainage for Grade III AC; however, the exact timeframe is unclear[4]. Moreover, the 2019 European Society of Gastrointestinal Endoscopy guidelines recommend biliary drainage as soon as possible in patients with Grade III AC and within 12 h for patients with septic shock, while within 48–72 h for patients with Grade II AC[2]. Meanwhile, the 2021 American Society of Gastrointestinal Endoscopy (ASGE) guidelines suggest endoscopic retrograde cholangiopancreatography (ERCP) within 48 h in AC patients, regardless of severity[1]. Some studies have demonstrated a "the earlier, the better" approach for the management of AC cases[5-8]. They deemed urgent biliary decompression necessary in severe cases. However, other studies have shown that ERCP can be safely delayed to allow for sufficient resuscitation[9-11]. In our clinical experience, the severity of Grade III AC varies dramatically, and we have observed that the optimal timing of biliary decompression may vary for different organ injuries.

So far, no relevant study has determined whether the clinical outcomes of Grade III AC patients vary with different organ injuries and whether AC patients with different organ dysfunction should undergo biliary drainage at distinct times. Consequently, this single-center retrospective study aimed to

investigate the relationship between drainage timing and in-hospital mortality (IHM) in patients with AC of different severities, and attempted to stratify patients with AC to identify the best decompression time.

MATERIALS AND METHODS

Patients

Ethical compliance: This retrospective cohort study was conducted according to the tenets of the Declaration of Helsinki, and approved by the Bioethics Committee of Beijing Friendship Hospital, Capital Medical University (Certification No. 2020-P2-224-01). After the review conducted by the Ethics Committee, the need for informed consent was waived.

Sample size: Based on the pre-experimental results, which revealed a 0.87% and 3% mortality rates for patients who did and did not undergo biliary drainage, respectively, we calculated the sample size using PASS 15.0 with Power = 0.8, Alpha = 0.05, and N1 = N2. The resultant sample size was 1306. On this basis, we expanded the sample size by 15% to exclude the reduction caused by data deficiency or diagnostic errors.

Enrollment: We searched the electronic medical record database of the Beijing Friendship Hospital for all adult (> 18 years) non-pregnant patients visiting the Emergency Department (ED) between July 2016 and December 2020 who were discharged with a diagnosis of AC. A total of 1498 patients were included in the study. All the medical records were reviewed and a diagnosis of AC was confirmed according to the TG18 diagnostic criteria[12]. Besides pregnant women and patients aged < 18 years, we also excluded patients transferred to other hospitals or outpatient departments for treatment and patients whose medical data were incomplete or missing. Finally, 1305 patients were enrolled (Figure 1).

Data collection

Demographic data, including age and sex, were obtained for each patient. Clinical data, laboratory characteristics, and imaging findings were obtained from the electronic medical records. Clinical data included vital signs, fluid output, Glasgow coma score, the vasoactive drug dose, history of biliary disease, Charlton comorbidity index (CCI), etiology of AC, registration time at the ED, time and type of drainage, discharge time, complications of drainage, hospitalization cost, and IHM. Laboratory findings included white blood cell (WBC) count, platelet count, total bilirubin, albumin, aspartate transaminase, alanine transaminase, creatinine, amylase, prothrombin time-international normalized ratio, arterial blood oxygen pressure, and lactate. Computed tomography, magnetic resonance cholangiopancreatography, or ERCP findings were reviewed to determine the etiology of cholangitis. The time interval for biliary drainage was calculated as the difference between ED registration time and the time of ERCP or percutaneous transhepatic biliary drainage (PTBD). We used the TG18 severity criteria for grading the severity[12].

Definition and indications

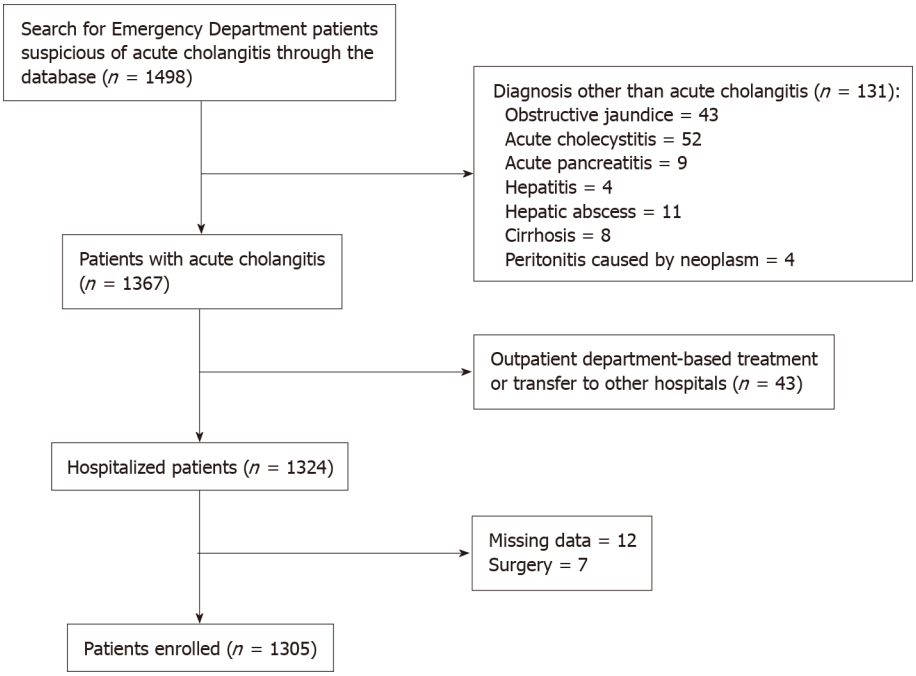
Benign stenosis was defined as stenosis in the biliary ducts without radiological findings of metastasis or malignant cells on histological examination. The indications of ERCP were AC combined with persistent extrahepatic biliary obstruction, and cases of anatomical derangement, failed ERCP, intrahepatic biliary obstruction underwent PTBD. The contraindications of ERCP included acute coronary syndrome, acute heart failure (New York Heart Association class III-IV), acute stroke occurring within 2 wk prior to enrollment, and acute pulmonary embolism complicated with the arterial PaO_2 <60 mmHg, while the contraindications of PTBD were platelet count < 50000/mm^3 or prothrombin activity < 60%. The adverse effects after drainage were based on the lexicon guidelines of the ASGE[13]. The second treatment included a second ERCP and a second PTBD for stone removal or stent placement. The need for a second therapeutic ERCP was assessed per the discretion of the experienced operators who performed the intervention and based on 2018 ERCP Guidelines for China[14]. All of the endoscopists had independently completed 300 ERCP interventions per year for 3 years.

Study outcomes

Our primary outcome was IHM, and the secondary outcomes were hospital length of stay (LOS) and hospitalization costs. When analyzing the survivors' LOS and entailed cost, we excluded patients who died or were transferred to other hospitals. We investigated the primary and secondary outcomes relevant to the timing of biliary drainage according to severity grading and some predictors based on TG18 and other previous studies.

Statistical analysis

Continuous variables were reported as medians with interquartile ranges (IQR) for not normally distributed; categorical variables were expressed as numbers and percentages. Comparisons between



DOI: 10.3748/wjg.v28.i29.3934 **Copyright** ©The Author(s) 2022.

Figure 1 A flowchart of the study population.

groups for continuous variables were evaluated using the Kruskal–Wallis test and Mann–Whitney *U* test, and for categorical variables, Fisher's exact test was used. Univariate logistic regression analysis and multivariate logistic regression with stepwise variable selection were used to analyze the relationship between organ dysfunction or predictors and IHM. Odds ratios (ORs) and 95% confidence intervals were calculated. Statistical significance was set at $P < 0.05$. Statistical analyses were conducted using SPSS v22.

RESULTS

The characteristics of the study population are shown in Tables 1 and 2. This cohort included 1305 patients, the majority of whom were men (60%). The median age of the group was 74 years (IQR, 63-82 years), and patients with Grade I AC were significantly younger ($P < 0.001$). The CCI of individuals with Grade III cholangitis was significantly higher than that of patients with Grade I or II cholangitis ($P < 0.001$). Choledocholithiasis (69.4%) was the most common cause of cholangitis, followed by malignant obstruction (18.5%). Among patients with cholangitis caused by malignancy, the number of patients with Grade II cholangitis was higher than that of patients with Grade I or III cholangitis. More patients with Grade II AC underwent biliary decompression ($P = 0.006$), while the IHM and hospitalization costs were significantly higher in the Grade III AC group than in the Grade I and II AC groups (IHM: $P < 0.001$, hospitalization costs: $P < 0.001$). Deaths tended to occur earlier in the disease course in patients with Grade III AC (median time 6 d).

A total of 915 patients in this cohort (70.1%) underwent biliary decompression, most of whom underwent endoscopic interventions (90.7%), while more patients underwent PTBD in the severe AC groups (Grade II: 37 cases, Grade III: 35 cases *vs* Grade I: 13 cases, $P = 0.001$). One hundred and sixty patients with Grade III were treated with antibiotics and fluid infusion only (disagreement about procedures = 35 cases, including two of mortality; with contraindications = 24 cases, including five of death; not tolerable conditions = 14 cases, including eight of death; obstruction spontaneous relief = 67 cases, including seven of mortality; not persistent biliary obstruction with high risk to stone removal by ERCP = 15 cases without death; not persistent biliary obstruction with selective cholecystectomy = five cases without death). The median drainage time was 24 h. Nearly half of the patients underwent biliary drainage within 24 h (445/915, 48%), while 89 patients with Grade III underwent drainage within 12 h (29%), which was significantly higher than that in Grades I and II ($P = 0.04$). Among the patients who underwent biliary drainage, more patients in Grade III underwent biliary drainage outside regular working hours (31.9%) and 478 patients (52.2%) required a second intervention for stone removal or stent placement, which exhibited no relationship with severity ($P = 0.688$). Post-ERCP pancreatitis was the major adverse event (8.2%), and the incidence of adverse events was not significantly different among the three severity grades.

Table 1 Characteristics data for all patients

Characteristics, *n* (%)	Total (*n* = 1305)	Grade I (*n* = 433)	Grade II (*n* = 405)	Grade III (*n* = 467)	*P* value
Age (yr)-median (IQR)	74 (63-82)	66 (59-72.5)	79 (69-84)	77 (66-83)	< 0.001
Male, *n* (%)	783 (60)	276 (63.7)	240 (59.3)	267 (57.2)	0.123
CCI- median (IQR)	2 (1-4)	2 (1-3)	2 (1-4)	3 (1-5)	< 0.001
Etiology, *n* (%)					< 0.001
Choledocholithiasis	906 (69.4)	315 (72.7)	252 (62.2)	339 (72.6)	
Malignant obstruction	242 (18.5)	73 (16.9)	97 (24.0)	72 (15.4)	
Benign stenosis	94 (7.2)	27 (6.2)	42 (10.4)	25 (5.4)	
Others	63 (4.8)	18 (4.2)	14 (3.5)	31 (6.6)	
Biliary drainage, *n* (%)	915 (70.1)	302 (69.7)	306 (75.6)	307 (65.7)	0.006
LOS (d)-median (IQR)	11 (8-14)	11 (8-14)	11 (7.5-14)	12 (7-15)	0.110
Hospitalization cost (CNY)-median (IQR)	38784.37 (22744.31-53278.63)	36536.36 (20851.37-47274.77)	38308.33 (23452.14-52847.29)	41832.19 (23355.98-58145.52)	< 0.001
IHM, *n* (%)	41 (3.1)	1 (0.2)	7 (1.7)	33 (7.1)	< 0.001
Survival time of dead (d)-median (IQR)	8 (3-23.5)	9	23 (13-46)	6 (3-17)	0.024
Organ dysfunction					
Neurological dysfunction	126	0	0	126	< 0.001
Respiratory dysfunction	227	0	0	227	< 0.001
Renal dysfunction	64	0	0	64	< 0.001
Cardiovascular dysfunction	39	0	0	39	< 0.001
Hematological dysfunction	149	0	0	149	< 0.001
Hepatic dysfunction	83	0	0	83	< 0.001
Temperature (°C)-median (IQR)	37.0 (36.6-38)	36.8 (36.6-37.8)	37 (36.6-38.25)	37.2 (36.6-38.3)	0.001
Laboratory values					
WBC (/mm^3)-median (IQR)	10560 (7705-14305)	9120 (7160-11165)	12700 (8897-18441)	11140 (7870-15810)	< 0.001
T-Bil (mg/dL)-median (IQR)	99.81 (62.43-155.76)	69.28 (49.625-120.975)	121.74 (88.97-184.41)	1041.2 (67.74-156.31)	< 0.001
Albumin (g/L)-median (IQR)	35.4 (31.2-39.2)	37.5 (34.2-40.4)	34.9 (30.8-38.1)	33.6 (29.2-37.8)	< 0.001
Lactate (mmol/L)-median (IQR)	2.15 (1.6-3.4)	1.8 (1.4-2.7)	2.1 (1.5-2.8)	2.4 (1.7-4.1)	< 0.001

IQR: Interquartile range; CCI: Charlton Comorbidity Index; LOS: Length of stay; CNY: Chinese Yuan; IHM: In-hospital mortality; WBC: White blood cell count; T-Bil: Total bilirubin.

The association of the IHM, LOS, and hospitalization costs with the timing of biliary drainage in each severity grade has been presented in Table 3. Biliary drainage significantly decreased the IHM in all AC patients (13/915 *vs* 28/390, $P < 0.001$). Among individuals with Grade III cholangitis, the IHM rate was significantly decreased in patients who had biliary drainage within 24 h or 48 h ($P = 0.041$, $P = 0.018$), while the LOS was significantly increased among those patients who underwent drainage within 12 h, 24 h, or 48 h ($P < 0.001$, $P < 0.001$, and $P < 0.001$, respectively). Hospitalization costs significantly increased for all patients with biliary drainage, regardless of severity criteria. For patients with Grade I AC, IHM was not affected by the timing of drainage and there was no relationship between LOS and the timing of biliary drainage for the survivors, but LOS was significantly extended in all the patients who underwent biliary drainage within 24 h or 48 h ($P = 0.004$, $P = 0.002$).

Univariate and multivariate analyses of predictors, including TG18 severity grading factors, lactate, CCI, and etiology of malignant obstruction, are shown in Table 4. In the univariate analysis, organ dysfunction, abnormal WBC count, hypoalbuminemia, CCI > 3, and etiology of malignancy were significantly associated with IHM. In a multivariate analysis of organ dysfunction, only neurological, respiratory, renal, and cardiovascular dysfunction, hypoalbuminemia, and malignant obstruction were significantly positively associated with IHM (OR = 5.32, 2.541, 6.356, 4.021, 5.655, and 7.522; $P < 0.001$, $P = 0.016$, $P < 0.001$, $P = 0.012$, $P < 0.001$, and $P < 0.001$, respectively).

Table 2 Characteristics data for patients with drainage

Characteristics, *n* (%)	Total (*n* = 915)	Grade I (*n* = 302)	Grade II (*n* = 306)	Grade III (*n* = 307)	*P* value
Drainage method, *n* (%)					0.001
ERCP	830 (90.7)	289 (95.7)	269 (87.9)	272 (88.6)	
PTBD	85 (9.3)	13 (4.3)	37 (12.1)	35 (11.4)	
Timing of drainage (hours)- median (IQR), *n* (%)	24.0 (60.0)	26.4 (62.4)	26.4 (62.4)	21.6 (45.6)	0.001
Biliary drainage within, *n* (%)					0.001
12 h	212 (23.2)	54 (17.9)	69 (22.5)	89 (29.0)	
12-24 h	233 (25.5)	74 (24.5)	70 (22.9)	89 (29.0)	
24-48 h	172 (18.8)	71 (23.5)	54 (17.6)	47 (15.3)	
> 48 h	298 (32.6)	103 (34.1)	113 (36.9)	82 (26.7)	
Second intervention, *n* (%)	478 (52.2)	159 (52.6)	154 (50.3)	165 (53.7)	0.688
Drainage outside working hours, *n* (%)	207 (22.6)	49 (16.2)	60 (19.6)	98 (31.9)	< 0.001
Adverse events, *n* (%)					
Pancreatitis	75 (8.2)	23 (7.6)	23 (7.5)	29 (9.4)	0.643
Cholangitis	8 (0.9)	2 (0.7)	2 (0.7)	4 (1.3)	0.742
Perforation	7 (0.8)	1 (0.3)	2 (0.7)	0 (0)	0.440
Bile leak	4 (0.4)	2 (0.7)	1 (0.3)	1 (0.3)	0.701
Myocardial infarction	5 (0.5)	0 (0)	3 (1.0)	2 (0.7)	0.339

IQR: Interquartile range; ERCP: Endoscopic retrograde cholangiopancreatography; PTBD: Percutaneous transhepatic biliary drainage.

From the data presented in Table 4, the association between IHM and the timing of biliary drainage for each clinical predictor is reflected. Among patients with AC complicated with neurological dysfunction or hyperlactatemia, the IHM rate was significantly decreased in individuals who underwent biliary decompression within 12 h (P = 0.041, P = 0.016), while those patients complicated with neurological dysfunction who had drainage within 24 h or 48 h could not improve prognosis compared with those who underwent drainage after 24 or 48 h, as well as those who did not undergo biliary drainage after admission (P = 0.175, P = 0.304). In patients with renal dysfunction, abnormal WBC count, hyperbilirubinemia, hypoalbuminemia, or hyperlactatemia, who had biliary decompression within 24 h or 48 h, there were significantly lower IHM rates than those of the remaining patients in each subgroup. Among patients with AC complicated with hepatic dysfunction, higher CCI (> 3), or malignancy, a lower IHM rate was significantly associated with early drainage (< 48 h) (P = 0.016, P = 0.006, P = 0.021).

DISCUSSION

In this retrospective monocenter cohort analysis including 1305 AC patients stratified according to TG18 severity criteria, early drainage (< 24 h) in Grade III AC patients had the greatest benefit, which could significantly reduce the all-cause IHM. It is worth noting that, in this subgroup, patients complicated with neurological dysfunction should be drained as early as possible (< 12 h). Moreover, early drainage was also required for AC patients with lactate more than 2 mmol/L, abnormal WBC count, hyperbilirubinemia, or hypoalbuminemia. Although these patients may have no severe cholangitis, early drainage could significantly reduce IHM and benefit the most. However, it should be noted that our results did not prove that drainage reduced hospitalization costs compared to conservative treatment. Furthermore, early drainage increased hospitalization costs and LOS.

AC is a clinically heterogeneous disease with recent mortality rates ranging from 2.7% to 10%, which is considered as an improvement since these rates were as high as 50%-60% in severe cases[15,16]. Although it is well-accepted that biliary decompression can significantly decrease the mortality of AC, it is highly debatable as to what the optimal strategy is for performing biliary drainage procedures. Should drainage occur as early as possible or should the procedure be delayed until stabilization after adequate resuscitation, especially for Grade III AC patients? Our study showed that biliary drainage could significantly decrease the IHM of AC patients (1.4% *vs* 7.2%, P < 0.001), and AC patients of Grade

Table 3 Association of the clinical outcomes in relation to the timing of biliary drainage and severity grading by Tokyo guidelines 2018

Severity of AC	Characteristic-median (IQR)	Drainage	Absence of drainage	*P* value	Drainage < 12 h	Drainage > 12 h or absence	*P* value	Drainage < 24 h	Drainage > 24 h or absence	*P* value	Drainage < 48 h	Drainage > 48 h or absence	*P* value
Grade I	IHM	0/302	1/131	0.303	0/54	1/379	1.000	0/128	1/305	1.000	0/199	1/234	1.000
	LOS (d)	11 (9-15)	7 (4-10)	< 0.001	11 (8-13.25)	10 (8-14)	0.778	11 (8-14)	10 (7-14)	0.004	11 (8-14)	10 (6-14)	0.002
	Survivors' LOS (d) (*n* = 387)	12 (9-15)	8 (5-11)	< 0.001	11 (8-13.25)	11 (8-14)	0.794	11 (9-14)	11 (8-14)	0.065	11 (9-14)	10 (8-14)	0.101
	Hospitalization cost (CNY)	42845.67 (33734.18-52209.23)	15763.10 (7737.32-23680.31)	< 0.001	43328.59 (32863.61-49384.19)	35317.71 (18848.59-46850.08	0.001	44154.19 (35638.76-52219.56)	31292.68 (16269.75-44599.67)	< 0.001	42908.34 (33358.44-50564.68)	25519.43 (12347.06-42424.96)	< 0.001
	Survivors' hospitalization cost (CNY) (*n* = 387)	42957.18 (33973.58-52224.73)	16596.85 (9096.73-24755.65	< 0.001	43462.72 (36174.00-49384.19)	36604.86 (21962.98-47554.27)	0.003	44443.3 (35988.02-52237.14)	33492.6 (46019.17-18880.26)	< 0.001	43264.07 (34606.54-51093.62)	29762.32 (16376.75-44463.21)	< 0.001
Grade II	IHM	2/306	5/99	0.011	0/69	7/336	0.608	0/139	7/266	0.101	1/193	6/212	0.125
	LOS (d)	11 (9-15)	7 (4-12)	< 0.001	11 (8-14)	11 (7-14)	0.684	11 (9-14)	10 (7-14)	0.122	11 (8-14)	10 (7-14.8)	0.190
	Survivors' LOS (d) (*n* = 349)	12 (9-15)	7.5 (4.75-11.25)	< 0.001	11.5 (9-14)	11 (8-14)	0.367	12 (10-14)	11 (7-14)	0.024	12 (9-14)	11 (7-14)	0.050
	Hospitalization cost (CNY)	44033.13 (31071.05-56134.72)	17626.20 (10037.69-25587.43)	< 0.001	45832.44 (36061.53-56949.37)	36132.93 (21795.89-51453.62)	< 0.001	46789.09 (35989.59-57723.15)	31505.72 (19948.31-47463.61)	< 0.001	45489.74 (33858.99-57600.43)	29275.30 (16928.45-46255.47)	< 0.001
	Survivors' hospitalization cost (CNY) (*n* = 349)	45004.20 (32631.09-56660.62)	16342.15 (10300.68-25017.80)	< 0.001	47938.00 (37937.29-58046.02)	36629.15 (22828.93-51509.37)	< 0.001	48254.61 (37937.29-58929.51)	31589.96 (20386.80-47062.76)	< 0.001	46564.37 (36191.07-57998.63)	29338.38 (17687.02-45685.12)	< 0.001
Grade III	IHM	11/307	22/160	< 0.001	3/89	30/378	0.168	7/178	26/289	0.041	9/225	24/242	0.018
	LOS (d)	13 (9-17)	8 (3-12)	< 0.001	13 (11-19)	11 (6-15)	< 0.001	13 (10-17)	10 (6-14)	< 0.001	13 (9-17)	9.5 (5-14)	< 0.001
	Survivors' LOS (d) (*n* = 351)	13 (11-18)	9.5 (7-13.25)	<0.001	13 (12-19)	12 (9-16)	0.001	13 (11-17.75)	12 (9-15)	< 0.001	13 (11-17.75)	11 (8-15)	< 0.001
	Hospitalization cost	51583.64 (38985.47-64886.01)	20183.58 (11317.37-29525.99)	< 0.001	56599.94 (43260.73-70300.00)	38527.58 (21034.79-55279.53)	< 0.001	55121.49 (40428.29-67707.01)	31832.99 (17933.81-50037.89)	< 0.001	54295.52 (39252.57-65638.57)	28165.23 (15708.29-45478.26)	< 0.001
	Survivors' hospitalization cost (CNY) (*n* = 351)	53507.33 (41027.94-65312.29)	22909.77 (15594.93-31845.39)	< 0.001	57976.4 (50131.44-70333.71)	43241.54 (28347.56-57860.29)	< 0.001	55873.84 (46654.40-69946.73)	38973.06 (24292.41-53090.85)	< 0.001	55782.38 (43994.26-66493.67)	34748.29 (21379.37-50147.24)	< 0.001

AC: Acute cholangitis; IQR: Interquartile range; IHM: In-hospital mortality; LOS: Length of stay; CNY: Chinese Yuan.

Table 4 Univariate and multivariate analysis of predictors of mortality, and relationship of mortality with the timing of drainage for each predictor

Predictors (*n* = 1305)	Univariate analysis		Multivariate analysis		Mortality to the timing of drainage								
	OR (95%CI)	*P* value	OR (95%CI)	*P* value	< 12 h	> 12 h or absence	*P* value	< 24 h	> 24 h or absence	*P* value	< 48 h	> 48 h or absence	*P* value
Neurological dysfunction	8.377 (4.384-16.007)	< 0.001	5.32 (2.373-11.931)	< 0.001	0/22	18/104	0.041	3/42	15/84	0.175	5/51	13/75	0.304
Respiratory dysfunction	2.886 (1.491-5.497)	0.003	2.541 (1.189-5.43)	0.016	1/44	14/183	0.314	4/91	11/136	0.414	6/117	9/110	0.428
Renal dysfunction	11.043 (5.402-22.573)	< 0.001	6.356 (2.623-15.397)	< 0.001	1/15	12/49	0.269	1/28	12/36	0.004	1/31	12/33	0.001
Cardiovascular dysfunction	11.569 (5.078-26.357)	< 0.001	4.021 (1.361-11.88)	0.012	0/7	9/32	0.169	2/16	7/23	0.262	2/18	7/21	0.139
Hematological dysfunction	2.611 (1.253-5.441)	0.02	N/A		2/37	8/104	1	3/61	7/88	0.527	3/74	7/75	0.327
Hepatic dysfunction	5.263 (2.484-11.152)	< 0.001	N/A		0/15	10/68	0.196	1/30	9/53	0.086	1/39	9/44	0.016
Age (≥ 75 yr)	1.432 (0.765-2.680)	0.261	N/A		2/88	21/531	0.759	4/196	19/423	0.172	7/267	16/352	0.284
Temperature (≥ 39 ℃)	0.390 (0.093-1.631)	0.197	N/A		0/43	2/106	1	1/75	1/74	1	1/85	1/64	1
WBC (> 12000/mm^3, < 4000/mm^3)	1.962 (1.043-3.688)	0.036	N/A		1/107	23/445	0.063	4/207	20/342	0.031	6/278	18/275	0.012
T-Bil (≥ 5 mg/dL)	1.711 (0.865-3.385)	0.123	N/A		3/143	26/626	0.333	5/292	24/477	0.019	8/407	21/362	0.007
Albumin (< STD*0.7)	10.715 (5.147-22.303)	< 0.001	5.655 (2.398-13.335)	< 0.001	0/8	12/51	0.188	0/15	12/44	0.026	1/24	11/35	0.018
Lactate (≥ 2 mmol/L)	1.450 (0.766-2.747)	0.254	N/A		0/105	16/298	0.016	2/186	14/217	0.008	4/227	12/176	0.018
Malignant obstruction	5.495 (2.924-10.325)	< 0.001	7.522 (3.504-16.149)	< 0.001	1/26	21/216	0.483	2/59	20/183	0.116	3/101	19/141	0.006
CCI (> 3)	4.080 (2.153-7.7340)	< 0.001	N/A		2/57	23/318	0.397	4/127	21/248	0.052	6/177	19/198	0.021

WBC: White blood cell count; T-Bil: Total bilirubin; STD: Lower limit of normal value; CCI: Charlton Comorbidity Index; OR: Odds ratio; CI: Confidence interval; N/A: Not applicable.

III underwent decompression within 24 h or 48 h had lower IHM (3.9% *vs* 9.0%, $P = 0.041$; 4% *vs* 9.9%, $P = 0.018$). These findings are in line with the results of a large sample size retrospective study, which showed that drainage within 48 h was associated with improved IHM (3.4% *vs* 10.2%, $P = 0.019$)[17], although it did not discuss drainage within 24 h. Another retrospective study of 6063 patients with AC conducted by Kiriyama *et al*[3] reported a distinct result: decompression within 24 h or 48 h improved the 30-d mortality rate only among Grade II patients (drainage within 24 h *vs*. after 24 h or no drainage: 1.7% *vs* 3.4%, $P < 0.05$; drainage within 48 h *vs* after 48 h or no drainage: 2.0% *vs* 3.7%, $P < 0.05$), and the drainage timing did not influence 30-d mortality in patients with Grade I and Grade III. This dissimilarity may be because we reviewed the all-cause IHM, while Kiriyama *et al*'s study observed 30-d cholangitis-caused mortality, and the mortality rate of Grade III AC patients was lower than that in our study (5.1% *vs* 9.4%), especially for subgroups of delayed decompression in which more patients died from malignancy[3]. In addition, as the number and grade of patients without drainage were not shown in the results of Kiriyama *et al*[3], the proportion of patients without drainage in our study may be different from the group studied by Kiriyama *et al*[3]. Since then, few researchers have tried to examine

the possibility of improving the prognosis of Grade III AC patients by undergoing biliary drainage more immediately[6,8]. Unfortunately, consistent with our results, there was no evidence that earlier decompression (within 12 h) benefited these severe patients.

Another multicenter retrospective net cohort study reported a novel finding in which delayed biliary decompression (> 12 h) was significantly associated with increased mortality in AC patients combined with septic shock [OR 3.40 (1.12-10.31)][7]. These results suggest that it may be necessary to approach each organ's failure separately and that different types of organ dysfunction should be considered when determining the optimal drainage timing. This was verified by our multivariable analysis which showed that neurological, respiratory, renal, and cardiovascular dysfunction were significantly associated with IHM (OR = 5.32, 2.541, 6.356, 4.021, respectively), whereas hepatic and hematological dysfunction did not influence IHM. In addition to indicators affecting mortality recommended in TG18, we also analyzed CCI, malignancy, and lactate levels, which were previously reported to have an impact on the death rate[5,7,18]. Multivariate regression analysis showed that, in addition to organ dysfunction, hypoproteinemia and malignant obstruction significantly increased IHM. These outcomes were similar to those reported in a previous review[3].

In this study, we first attempted to stratify Grade III AC patients according to organ dysfunction to identify patients whose prognosis could most likely be improved by earlier decompression. According to our clinical experience, neurological dysfunction was the most severe complication and might affect drainage operation; therefore, AC patients with altered mental status require immediate biliary decompression. This was verified by our data that only undergoing drainage within 12 h could greatly improve IHM in this subgroup of individuals (0% *vs* 17.3%, P = 0.041). For AC patients with renal dysfunction, performing drainage within 24 h could decrease the IHM. As a result, the renal injury was not only caused by infection but also induced by hypovolemia, which was provoked by fever, decreased appetite, early initiation of antibiotics, and aggressive fluid resuscitation to improve renal flow were more valuable for these patients. Unlike previous studies[7], we did not observe an association between drainage and IHM in AC patients with cardiovascular dysfunction. This may be because only 39 patients were included in this subgroup. Drainage within 12 h significantly reduced mortality in AC patients with increased lactate levels (≥ 2 mmol/L), suggesting that decompression within 12 h might be beneficial for patients with cardiovascular dysfunction. Performing drainage within 48 h greatly reduced mortality in AC patients with hepatic dysfunction, because the amelioration of biliary stasis after drainage could directly rescue hepatic function and diminish inflammatory reaction, even if no significant association between hepatic injury and IHM was observed.

The influence of abnormal WBC count and hyperbilirubinemia on outcomes in AC has been previously described[9]. The underlying pathophysiologic mechanisms are known to result from sepsis; therefore, abnormal WBC count and hyperbilirubinemia are linked with an increased likelihood of poor prognosis. Hypoalbuminemia refers to malnutrition, which is linked to life-threatening infections and poor outcomes. For individuals in these subgroups, undergoing drainage within 24 h indicated a lower IHM.

Decompression within 12, 24, or 48 h in Grade III AC patients would extend the LOS, which was contrary to the findings of Aboelsoud *et al*[19] who demonstrated that drainage within 24 h or 48 h could decrease the LOS, compared with drainage after 24 h or 48 h (drainage within 24 h *vs* after 24 h: mean 7.71 *vs* 13.57 d, P = 0.001; drainage within 48 h *vs* after 48 h: mean 8.61 *vs* 14.24 d, P = 0.002). This was because their study only reviewed patients who underwent drainage, whereas our study included both patients who underwent drainage and those who did not. In addition, most of the Grade II and Grade III patients in this study received only endoscopic nasobliary drainage or endoscopic retrograde biliary drainage treatment at the first ERCP intervention because of their serious condition, and 52.2% of them received a second endoscopic intervention for biliary stone removal or stent placement when their condition stabilized, thus increasing the LOS. Drainage within 12, 24, or 48 h was associated with increased hospital costs despite the severity of AC since endoscopic operation itself was expensive, and the delayed-drainage group contained non-drainage ones who spent little.

Limits of study

Our analysis had certain limitations. First, it was retrospective in design, and as such, was susceptible to record bias and incomplete data. Second, because it is a single-center study, the study results only reflect the clinical status of our center and cannot represent the situation of all hospitals. Third, due to the limited sample size, especially the limited number of patients with cardiovascular dysfunction who underwent drainage within 48 h, some results were not statistically significant. In addition, the time from onset to initial treatment and the antibiotics and fluid resuscitation before admission to our hospital were not evaluated, which may have an impact on the outcome. A prospective multicenter study will be conducted to further explore a precise stratified model to guide drainage timing rather than TG18.

CONCLUSION

To our knowledge, this is the first study to stratify patients with Grade III AC according to different organ dysfunctions and to recommend the optimal timing of biliary drainage accordingly. Biliary decompression significantly decreases the all-cause IHM rates in AC, and early biliary drainage (< 24 h) was shown to be beneficial for AC patients with Grade III severity. Severe cases with different organ dysfunctions have distinct prognoses, and cases complicated with either neurological or cardiovascular dysfunction should undergo drainage within 12 h of admission. For patients with mild or moderate cholangitis, early drainage increases the probability of a second treatment and increases the patients' injury, hospitalization cost, and LOS. A further multicenter prospective cohort study will be conducted to verify the result and investigate whether the optimal timing of drainage based on different organ dysfunctions can increase the 30-d mortality rates and decrease the readmission rate.

ARTICLE HIGHLIGHTS

Research background

Acute cholangitis (AC) is a life-threatening condition that occurs in the presence of biliary obstruction. Biliary decompression is well known to greatly decrease the risks of mortality in AC. Although early biliary drainage is recommended by the treatment guidelines for AC, the exact timeframe is yet to be established.

Research motivation

We have observed that the clinical outcomes of severe AC patients vary dramatically. So, we first attempted to study whether AC patients with different organ dysfunction should undergo biliary drainage at distinct times and try to screen out patients that could benefit the most from earlier drainage.

Research objectives

To investigate the optimal drainage timing for AC patients with each disease severity grade and organ dysfunction.

Research methods

In this retrospective monocenter cohort analysis, we reviewed 1305 patients who were diagnosed with AC according to the Tokyo guidelines 2018 at a Chinese tertiary hospital for four years. We investigated the all-cause in-hospital mortality (IHM), hospital length of stay (LOS), and hospitalization costs associated with the timing of biliary drainage according to the severity grading and different dysfunctioning organs and critical predictors [age, white blood cell (WBC) count, total bilirubin, albumin, lactate, malignant obstruction, and Charlton comorbidity index (CCI)].

Research results

Biliary drainage within 24 h in Grade III AC patients had the greatest benefit, which could significantly reduce the all-cause IHM, while increasing LOS and hospitalization costs. Multivariate logistic analysis revealed that neurological, respiratory, renal, and cardiovascular dysfunctions, hypoalbuminemia, and malignant obstruction were significantly associated with IHM. Furthermore, AC patients complicated with neurological dysfunction or with serum lactate > 2 mmol/L should be drained as early as possible (< 12 h) for it could significantly decrease the IHM. In the subgroup of AC patients with renal dysfunction, abnormal WBC count, hyperbilirubinemia, or hypoalbuminemia, drainage within 24 h reduced the IHM, while in the subgroup of AC patients with hepatic dysfunction, malignant obstruction, or a CCI > 3, biliary drainage should be performed within 48 h.

Research conclusions

Biliary drainage within 12 h is beneficial for AC patients with neurological or cardiovascular dysfunction, while complete biliary decompression within 24 h of admission is recommended for treating patients with Grade III AC.

Research perspectives

A further multicenter prospective cohort study will be conducted to verify the result and investigate whether the optimal timing of drainage based on different organ dysfunctions can increase the 30-d mortality rates and decrease the readmission rate.

FOOTNOTES

Author contributions: Li CS designed the research study and made critical revisions to the article; Lu ZQ, Zhang HY, Xing YY, Su CF, and Wang GX performed the research and analyzed the data; Lu ZQ drafted the article; all authors have read and approved the final manuscript.

Institutional review board statement: This retrospective cohort study was conducted according to the tenets of the Declaration of Helsinki, and approved by the Bioethics Committee of Beijing Friendship Hospital, Capital Medical University (Certification No. 2020-P2-224-01).

Informed consent statement: Since we conducted a retrospective review of patient data obtained from the electronic medical records of our hospital, and as stated by the ethical standards of China, the Ethics Committee exempted the need for obtaining informed consent.

Conflict-of-interest statement: All the Authors have no conflict of interest related to the manuscript.

Data sharing statement: The datasets used during the current study are available from the corresponding author on reasonable request at lcscyyy@163.com.

STROBE statement: The authors have read the STROBE Statement—checklist of items, and the manuscript was prepared and revised according to the STROBE Statement—checklist of items.

Open-Access: This article is an open-access article that was selected by an in-house editor and fully peer-reviewed by external reviewers. It is distributed in accordance with the Creative Commons Attribution NonCommercial (CC BY-NC 4.0) license, which permits others to distribute, remix, adapt, build upon this work non-commercially, and license their derivative works on different terms, provided the original work is properly cited and the use is non-commercial. See: https://creativecommons.org/Licenses/by-nc/4.0/

Country/Territory of origin: China

ORCID number: Zhao-Qing Lu 0000-0001-8895-1596; Han-Yu Zhang 0000-0001-5181-4619; Chen-Fen Su 0000-0002-7882-6975; Yue-Yan Xing 0000-0002-6162-3098; Guo-Xing Wang 0000-0003-1379-5749; Chun-Sheng Li 0000-0002-3161-4457.

S-Editor: Yan JP
L-Editor: A
P-Editor: Yan JP

REFERENCES

1 **Buxbaum JL**, Buitrago C, Lee A, Elmunzer BJ, Riaz A, Ceppa EP, Al-Haddad M, Amateau SK, Calderwood AH, Fishman DS, Fujii-Lau LL, Jamil LH, Jue TL, Kwon RS, Law JK, Lee JK, Naveed M, Pawa S, Sawhney MS, Schilperoort H, Storm AC, Thosani NC, Qumseya BJ, Wani S. ASGE guideline on the management of cholangitis. *Gastrointest Endosc* 2021; **94**: 207-221.e14 [PMID: 34023065 DOI: 10.1016/j.gie.2020.12.032]

2 **Manes G**, Paspatis G, Aabakken L, Anderloni A, Arvanitakis M, Ah-Soune P, Barthet M, Domagk D, Dumonceau JM, Gigot JF, Hritz I, Karamanolis G, Laghi A, Mariani A, Paraskeva K, Pohl J, Ponchon T, Swahn F, Ter Steege RWF, Tringali A, Vezakis A, Williams EJ, van Hooft JE. Endoscopic management of common bile duct stones: European Society of Gastrointestinal Endoscopy (ESGE) guideline. *Endoscopy* 2019; **51**: 472-491 [PMID: 30943551 DOI: 10.1055/a-0862-0346]

3 **Kiriyama S**, Takada T, Hwang TL, Akazawa K, Miura F, Gomi H, Mori R, Endo I, Itoi T, Yokoe M, Chen MF, Jan YY, Ker CG, Wang HP, Wada K, Yamaue H, Miyazaki M, Yamamoto M. Clinical application and verification of the TG13 diagnostic and severity grading criteria for acute cholangitis: an international multicenter observational study. *J Hepatobiliary Pancreat Sci* 2017; **24**: 329-337 [PMID: 28419764 DOI: 10.1002/jhbp.458]

4 **Miura F**, Okamoto K, Takada T, Strasberg SM, Asbun HJ, Pitt HA, Gomi H, Solomkin JS, Schlossberg D, Han HS, Kim MH, Hwang TL, Chen MF, Huang WS, Kiriyama S, Itoi T, Garden OJ, Liau KH, Horiguchi A, Liu KH, Su CH, Gouma DJ, Belli G, Dervenis C, Jagannath P, Chan ACW, Lau WY, Endo I, Suzuki K, Yoon YS, de Santibañes E, Giménez ME, Jonas E, Singh H, Honda G, Asai K, Mori Y, Wada K, Higuchi R, Watanabe M, Rikiyama T, Sata N, Kano N, Umezawa A, Mukai S, Tokumura H, Hata J, Kozaka K, Iwashita Y, Hibi T, Yokoe M, Kimura T, Kitano S, Inomata M, Hirata K, Sumiyama Y, Inui K, Yamamoto M. Tokyo Guidelines 2018: initial management of acute biliary infection and flowchart for acute cholangitis. *J Hepatobiliary Pancreat Sci* 2018; **25**: 31-40 [PMID: 28941329 DOI: 10.1002/jhbp.509]

5 **Navaneethan U**, Gutierrez NG, Jegadeesan R, Venkatesh PG, Butt M, Sanaka MR, Vargo JJ, Parsi MA. Delay in performing ERCP and adverse events increase the 30-day readmission risk in patients with acute cholangitis. *Gastrointest Endosc* 2013; **78**: 81-90 [PMID: 23528654 DOI: 10.1016/j.gie.2013.02.003]

6 **Khamaysi I**, Taha R. ERCP for severe acute cholangitis: The earlier, the better. *Turk J Gastroenterol* 2020; **31**: 78-79 [PMID: 32009619 DOI: 10.5152/tjg.2020.19103]

7 **Karvellas CJ**, Abraldes JG, Zepeda-Gomez S, Moffat DC, Mirzanejad Y, Vazquez-Grande G, Esfahani EK, Kumar A; Cooperative Antimicrobial Therapy of Septic Shock (CATSS) Database Research Group. The impact of delayed biliary

decompression and anti-microbial therapy in 260 patients with cholangitis-associated septic shock. *Aliment Pharmacol Ther* 2016; **44**: 755-766 [PMID: 27506331 DOI: 10.1111/apt.13764]

8 **Becq A**, Chandnani M, Bartley A, Nuzzo A, Bilal M, Bharadwaj S, Cohen J, Gabr M, Berzin TM, Pleskow DK, Sawhney MS. ERCP within 6 or 12 h for acute cholangitis: a propensity score-matched analysis. *Surg Endosc* 2022; **36**: 2418-2429 [PMID: 33977378 DOI: 10.1007/s00464-021-08523-w]

9 **Schwed AC**, Boggs MM, Pham XD, Watanabe DM, Bermudez MC, Kaji AH, Kim DY, Plurad DS, Saltzman DJ, de Virgilio C. Association of Admission Laboratory Values and the Timing of Endoscopic Retrograde Cholangiopancreatography With Clinical Outcomes in Acute Cholangitis. *JAMA Surg* 2016; **151**: 1039-1045 [PMID: 27557050 DOI: 10.1001/jamasurg.2016.2329]

10 **Tabibian JH**, Yang JD, Baron TH, Kane SV, Enders FB, Gostout CJ. Weekend Admission for Acute Cholangitis Does Not Adversely Impact Clinical or Endoscopic Outcomes. *Dig Dis Sci* 2016; **61**: 53-61 [PMID: 26391268 DOI: 10.1007/s10620-015-3853-z]

11 **Inamdar S**, Sejpal DV, Ullah M, Trindade AJ. Weekend vs. Weekday Admissions for Cholangitis Requiring an ERCP: Comparison of Outcomes in a National Cohort. *Am J Gastroenterol* 2016; **111**: 405-410 [PMID: 26782818 DOI: 10.1038/ajg.2015.425]

12 **Kiriyama S**, Kozaka K, Takada T, Strasberg SM, Pitt HA, Gabata T, Hata J, Liau KH, Miura F, Horiguchi A, Liu KH, Su CH, Wada K, Jagannath P, Itoi T, Gouma DJ, Mori Y, Mukai S, Giménez ME, Huang WS, Kim MH, Okamoto K, Belli G, Dervenis C, Chan ACW, Lau WY, Endo I, Gomi H, Yoshida M, Mayumi T, Baron TH, de Santibañes E, Teoh AYB, Hwang TL, Ker CG, Chen MF, Han HS, Yoon YS, Choi IS, Yoon DS, Higuchi R, Kitano S, Inomata M, Deziel DJ, Jonas E, Hirata K, Sumiyama Y, Inui K, Yamamoto M. Tokyo Guidelines 2018: diagnostic criteria and severity grading of acute cholangitis (with videos). *J Hepatobiliary Pancreat Sci* 2018; **25**: 17-30 [PMID: 29032610 DOI: 10.1002/jhbp.512]

13 **Cotton PB**, Eisen GM, Aabakken L, Baron TH, Hutter MM, Jacobson BC, Mergener K, Nemcek A Jr, Petersen BT, Petrini JL, Pike IM, Rabeneck L, Romagnuolo J, Vargo JJ. A lexicon for endoscopic adverse events: report of an ASGE workshop. *Gastrointest Endosc* 2010; **71**: 446-454 [PMID: 20189503 DOI: 10.1016/j.gie.2009.10.027]

14 **ERCP group of Digestive Endoscopy Branch of Chinese Medical Association**; Biliopancreology Group of Gastroenterologist Branch of Chinese Medical Association, National Clinical Research Center for Digestive Diseases. ERCP Guidelines for China (2018). *Zhonghua Xiaohua Neijing Zazhi* 2018; **35**: 777-813

15 **Andrew DJ**, Johnson SE. Acute suppurative cholangitis, a medical and surgical emergency. A review of ten years experience emphasizing early recognition. *Am J Gastroenterol* 1970; **54**: 141-154 [PMID: 5458220]

16 **Shimada H**, Nakagawara G, Kobayashi M, Tsuchiya S, Kudo T, Morita S. Pathogenesis and clinical features of acute cholangitis accompanied by shock. *Jpn J Surg* 1984; **14**: 269-277 [PMID: 6436560 DOI: 10.1007/bf02469641]

17 **Mulki R**, Shah R, Qayed E. Early *vs* late endoscopic retrograde cholangiopancreatography in patients with acute cholangitis: A nationwide analysis. *World J Gastrointest Endosc* 2019; **11**: 41-53 [PMID: 30705731 DOI: 10.4253/wjge.v11.i1.41]

18 **Lee F**, Ohanian E, Rheem J, Laine L, Che K, Kim JJ. Delayed endoscopic retrograde cholangiopancreatography is associated with persistent organ failure in hospitalised patients with acute cholangitis. *Aliment Pharmacol Ther* 2015; **42**: 212-220 [PMID: 25997554 DOI: 10.1111/apt.13253]

19 **Aboelsoud M**, Siddique O, Morales A, Seol Y, Al-Qadi M. Early biliary drainage is associated with favourable outcomes in critically-ill patients with acute cholangitis. *Prz Gastroenterol* 2018; **13**: 16-21 [PMID: 29657606 DOI: 10.5114/pg.2018.74557]

World Journal of Gastroenterology

Submit a Manuscript: https://www.f6publishing.com

World J Gastroenterol 2022 August 7; 28(29): 3946-3959

DOI: 10.3748/wjg.v28.i29.3946

ISSN 1007-9327 (print) ISSN 2219-2840 (online)

ORIGINAL ARTICLE

Retrospective Study

Incidence and clinical characteristics of hypertriglyceridemic acute pancreatitis: A retrospective single-center study

Xue-Yan Lin, Yi Zeng, Zheng-Chao Zhang, Zhi-Hui Lin, Lu-Chuan Chen, Zai-Sheng Ye

Specialty type: Gastroenterology and hepatology

Provenance and peer review: Invited article; Externally peer reviewed.

Peer-review model: Single blind

Peer-review report's scientific quality classification

Grade A (Excellent): A
Grade B (Very good): B, B
Grade C (Good): C, C, C
Grade D (Fair): D
Grade E (Poor): 0

P-Reviewer: Cho E, South Korea; Fujimori N, Japan; Gupta R, India; Kitamura K, Japan; Trna J, Czech Republic

Received: December 6, 2021
Peer-review started: December 6, 2021
First decision: April 16, 2022
Revised: April 25, 2022
Accepted: June 30, 2022
Article in press: June 30, 2022
Published online: August 7, 2022

Xue-Yan Lin, Zhi-Hui Lin, Department of Gastroenterology, Fujian Provincial Hospital, Fujian Medical University Provincial of Clinical Medicine, Fuzhou 350001, Fujian Province, China

Yi Zeng, Lu-Chuan Chen, Zai-Sheng Ye, Department of Gastrointestinal Surgical Oncology, Fujian Cancer Hospital, Fujian Medical University Cancer Hospital, Fuzhou 350014, Fujian Province, China

Zheng-Chao Zhang, Department of Emergency Surgery, Fujian Provincial Hospital, Fujian Medical University Provincial of Clinical Medicine, Fuzhou 350001, Fujian Province, China

Corresponding author: Zai-Sheng Ye, PhD, Attending Doctor, Surgical Oncologist, Teacher, Department of Gastrointestinal Surgical Oncology, Fujian Cancer Hospital, Fujian Medical University Cancer Hospital, No. 420 Fuma Road, Fuzhou 350014, Fujian Province, China. flyingengel@sina.cn

Abstract

BACKGROUND

The incidence of hypertriglyceridemic acute pancreatitis (HTG-AP) has increased yearly, but updated population-based estimates on the incidence of HTG-AP are lacking. Reducing serum triglyceride (TG) levels quickly is crucial in the early treatment of HTG-AP. Decreased serum TG levels are treated by non-invasive methods, which include anti-lipidemic agents, heparin, low-molecular weight heparin, and insulin, and invasive methods, such as blood purification including hemoperfusion (HP), plasmapheresis, and continuous renal replacement therapy. However, authoritative guidelines have not been established. Early selection of appropriate treatment is important and beneficial in controlling the development of HTG-AP.

AIM

To evaluate the effect between patients treated with intravenous insulin (INS) and HP to guide clinical treatment.

METHODS

We retrospectively reviewed 371 patients with HTG-AP enrolled in the Department of Fujian Provincial Hospital form April 2012 to March 2021. The inpatient medical and radiologic records were reviewed to determine clinical features, severity, complications, mortality, recurrence rate, and treatment. Multivariate logistic regression analyses were used to analyze risk factors for

severe HTG-AP. Propensity score matching was used to compare the clinical outcomes of INS and HP.

RESULTS

A total of 371 patients met the HTG-AP criteria. The incidence of HTG-AP was increased by approximately 2.6 times during the 10 years (8.4% in April 2012-March 2013 and 22.3% in April 2020-March 2021). The highest incidence rate of acute pancreatitis was observed for men in the age group of 30-39 years. The amylase level was elevated in 80.1% of patients but was only three times the normal value in 46.9% of patients. The frequency of severe acute pancreatitis (26.9%), organ failure (31.5%), rate of recurrence (32.9%), and mortality (3.0%) of HTG-AP was high. Improved Marshall score, modified computed tomography severity index score, baseline TG, baseline amylase, C-reactive protein (CRP), albumin, aspartate aminotransferase, low-density lipoprotein cholesterol, urea nitrogen, creatinine, calcium, hemoglobin, free triiodothyronine, admission to intensive care unit, and mortality were significantly different between patients with different grades of severity ($P < 0.050$). Multivariate logistic regression analysis confirmed that high CRP [$P = 0.005$, odds ratio (OR) = 1.011, 95%CI: 1.003-1.019], low calcium ($P = 0.003$, OR = 0.016, 95%CI: 0.001-0.239), and low albumin ($P = 0.023$, OR = 0.821, 95%CI: 0.693-0.973) were risk factors of severe HTG-AP. After propensity score matching adjusted by sex, age, severity of HTG-AP, and baseline TG, the serum TG significantly decreased in patients treated with INS ($P < 0.000$) and HP ($P < 0.000$) within 48 h. However, the clearance rate of TG (57.24 ± 33.70% *vs* 56.38 ± 33.61%, $P = 0.927$) and length of stay (13.04 ± 7.92 d *vs* 12.35 ± 6.40 d, $P = 0.730$) did not differ between the two groups.

CONCLUSION

The incidence of HTG-AP exhibited a significant increase, remarkable severity, and recurrent trend. Patients with mild and moderately severe acute pancreatitis can be treated effectively with INS safely and effectively without HP.

Key Words: Hypertriglyceridemic acute pancreatitis; Triglyceride; Improved Marshall score; Severity of acute pancreatitis; Intravenous insulin; Hemoperfusion

©The Author(s) 2022. Published by Baishideng Publishing Group Inc. All rights reserved.

Core Tip: We assessed the clinical characteristics of hypertriglyceridemic acute pancreatitis, determined factors related to grades of severity, and evaluated differences in clinical outcomes between patients treated with intravenous insulin and hemoperfusion to guide clinical diagnosis and treatment.

Citation: Lin XY, Zeng Y, Zhang ZC, Lin ZH, Chen LC, Ye ZS. Incidence and clinical characteristics of hypertriglyceridemic acute pancreatitis: A retrospective single-center study. *World J Gastroenterol* 2022; 28(29): 3946-3959

URL: https://www.wjgnet.com/1007-9327/full/v28/i29/3946.htm

DOI: https://dx.doi.org/10.3748/wjg.v28.i29.3946

INTRODUCTION

Acute pancreatitis (AP) is an inflammatory condition of the pancreas that originates within the pancreatic acinar cells and causes pancreatic necrosis, systemic inflammatory response syndrome, and multiple organ failure[1], with a mortality rate for severe cases as high as 20%-25%[2]. The great majority of AP is driven by gallstones (40%-70%) and alcohol (25%-35%)[3]. With the change of people's diet structure and lifestyle, the incidence and mortality of hypertriglyceridemic (HTG)-AP are increasing year by year and has surpassed alcohol as the second leading cause of AP in China[4]. The standardized incidence rate of HTG-AP increased from 0.7 to 1.7 per 100000 person-years from 2008 to 2019 in Denmark[5], and the incidence has increased by 2.4 times in 10 years. However, the increasing number of HTG-AP incidence remains unclear in China.

The mechanism by which severe HTG precipitates to AP remains unknown. Studies have shown that pancreatic lipase hydrolyses excess triglyceride (TG) with accumulation of free fatty acids, thereby inducing the production of acinar cell and pancreatic capillary injury; chylomicrons lead to increased blood viscosity and local tissue ischemia[6,7]. Therefore, early detection of serum TG and active treatment measures to reduce serum TG are crucial for the prognosis of AP. Some scholars believe that

rapid reduction of serum triglyceride levels within 48 h before the onset of HTG-AP is the key to treatment[8]. Effective treatments of reducing serum TG levels include anti-lipidemic agents, insulin, heparin, low-molecular weight heparin, and blood purification, such as hemoperfusion (HP), plasmapheresis (PE), and continuous renal replacement therapy[6,9]; however, no HTG-AP treatment guideline has been established. At present, selecting routine treatment or blood purification for patients with HTG-AP after admission remains controversial.

In view of the increasing incidence of HTG-AP in recent years and its short and long-term harmful effects on patients, families, and society, scholars have focused on preventing and effectively blocking HTG-AP as well as on its diagnosis and treatment. However, the causes remain unknown[10-12]; the low elevation of amylase (AMY) levels[13] and other characteristics[14] lead to the early misdiagnosis of HTG-AP. In addition, HTG-AP is prone to young age of onset[10], many complications[15], higher chance of systemic inflammatory response syndrome and cardiopulmonary and renal insufficiency[16], severe tendency[17], and lack of unified clinical treatment standards, which bring some difficulties to clinical treatment.

This study aims to improve the clinical diagnosis rate of HTG-AP by summarizing the clinical characteristics of HTG-AP and developing appropriate and cost-effective treatments for patients with HTG-AP.

MATERIALS AND METHODS

Patients

From April 2012 to March 2021, AP was diagnosed in 2206 patients in the Fujian Provincial Hospital. A total of 371 hospitalized patients who met the diagnostic criteria of HTG-AP were retrospectively studied, and 219 patients met the inclusion and exclusion criteria that were used to explore risk factors for severe HTG-AP. Fifty-two patients were included after propensity score matching (PSM) was adjusted by sex, age, grades of severity, and baseline TG. Clinical outcomes were compared between the 52 patients treated with intravenous insulin (INS) and HP (Figure 1). The Ethics Committee of Fujian Provincial Hospital approved the study (K2021-02-007).

The inclusion criteria were as follows: (1) Diagnosis of HTG-AP; (2) Admission within 72 h after onset; (3) Age older than 18 years; (4) Assessment of the first episode (for patients with multiple episodes of AP); and (5) Serum TG detected within 24 h after admission.

The exclusion criteria were as follows: (1) Did not undergo serum lipid detection within 48 h after treatment upon hospitalization; (2) AP due to other etiologies (including gallstones, alcohol, autoimmune, drug-induced, hypercalcemia, hyperparathyroidism, pancreatic tumor-related etiology of AP); (3) Treatment in another hospital; and (4) Incomplete information.

Grouping methods

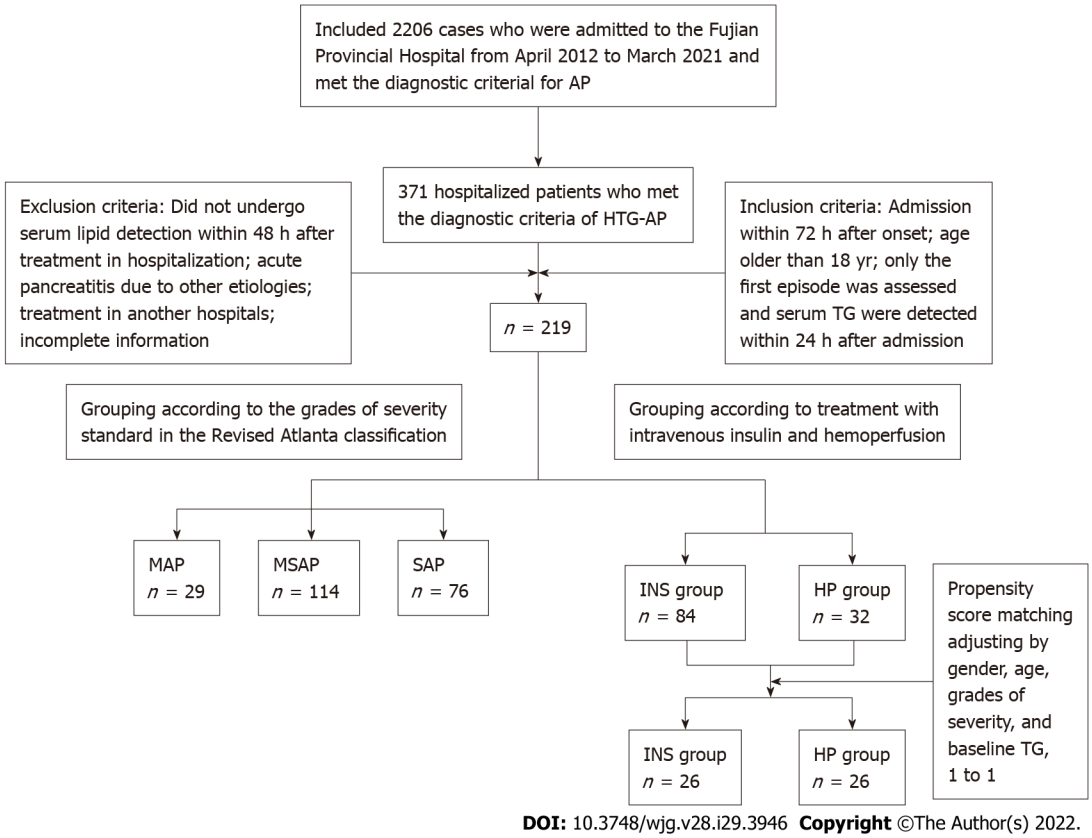
According to the grades of severity standard in the Revised Atlanta Classification, patients were classified into the mild acute pancreatitis (MAP) group, moderately severe acute pancreatitis (MSAP) group, and severe acute pancreatitis (SAP) groups.

Patients were divided into the INS group and HP group according to treatment method. All patients were given basic support treatment including abrosia, gastrointestinal decompression, enema, fluid resuscitation, water maintenance, electrolyte and acid-base balance, lactulose to improve intestinal function, low molecular weight heparin, proton pump inhibitors for gastric acid secretion, and somatostatin/octreotide inhibitor pancreatic secretion. The INS group was given INS. The HP group was treated with HP. Blood access was established by puncture of the femoral vein or internal jugular vein. HP was performed with a resin irrigator (HA330, Zhuhai Lizhu Group, Biological Material Co, Ltd., China) for 2 h every 24 h with a blood flow of 150-250 mL/min. During the procedure, heparin was used to flush the infusion tube. After the procedure, coagulation markers were monitored. For those with prolonged coagulation times, 10-15 mg protamine was given to neutralize the effect of heparin. For patients with bleeding tendency, low molecular weight heparin was chosen, or the dose of heparin was appropriately reduced.

Definition

The diagnosis of AP was in accordance with the Revised Atlanta Definitions[18]. AP was diagnosed when two of the following three characteristics were met: (1) Abdominal pain consistent with AP (acute onset of a persistent, severe, epigastric pain often radiating to the back); (2) At least three times higher levels of AMY and/or lipase above the upper limit of the normal value; and (3) Abdominal imaging (including computed tomography, magnetic resonance imaging, or transabdominal ultrasonography) consistent with changes in AP.

HTG-AP was considered in patients with AP when the level of serum TG was: (1) Over 1000 mg/dL; and (2) Between 500 and 1000 mg/dL with lactescent serum at admission[19].



DOI: 10.3748/wjg.v28.i29.3946 **Copyright** ©The Author(s) 2022.

Figure 1 Research sample screening and grouping process. HTG-AP: Hypertriglyceridemic acute pancreatitis; MAP: Mild acute pancreatitis; MSAP: Moderately severe acute pancreatitis; SAP: Severe acute pancreatitis; TG: Triglyceride; INS: Insulin; HP: Hemoperfusion; AP: Acute pancreatitis.

The severity of AP was graded according to the Revised Atlanta Definitions[18]: MAP, MSAP, and SAP. MAP was defined by the absence of organ failure and the absence of local or systemic complications. MSAP was defined by the presence of transient (< 48 h) organ failure or local or systemic complications in the absence of persistent organ failure. SAP was defined by persistent (> 48 h) organ failure.

Organ failure was determined according to the improved Marshall score standard in the Revised Atlanta classification[18]. Three organ systems were assessed to define organ failure: respiratory, cardiovascular, and renal. For respiratory (PaO_2/FiO_2), 301 mmHg ≤ PaO_2/FiO_2 ≤ 400 mmHg was scored as 1 point, 201 mmHg ≤ PaO_2/FiO_2 ≤ 300 mmHg was scored as 2 points, 101 mmHg ≤ PaO_2/FiO_2 ≤ 200 mmHg was scored as 3 points, and PaO_2/FiO_2 ≤ 101 mmHg was scored as 4 points. For renal serum creatinine (SCR), 134 μmol/L ≤ SCR ≤ 169 μmol/L was scored as 1 point, 170 μmol/L ≤ SCR ≤ 310 μmol/L was scored as 2 points, 311 μmol/L ≤ SCR ≤ 439 μmol/L was scored as 3 points, and SCR > 439 μmol/L was scored as 4 points. For cardiovascular systolic blood pressure (BP), BP < 90 mmHg and fluid responsive was scored as 1 point, BP < 90 mmHg without fluid responsive was scored as 2 points, BP < 90 mmHg and pH < 7.3 was scored as 3 points, and BP < 90 mmHg and pH < 7.2 was scored as 4 points. A score of 2 or more in any system defined the presence of organ failure.

Data collection

Data were obtained from the patients' medical records and hospital electronic database records. Sex, age, and comorbidities were collected. Clinical manifestations, improved Marshall score[18], modified computed tomography severity index (MCTSI) score[20], organ failure[18], laboratory and imaging data, treatments, intensive care unit admission, length of stay, and prognosis during hospitalization were recorded. All laboratory data were measured within 24 h after admission. Baseline TG and serum AMY were measured using the first tested values since onset. Serum lipids were reviewed within 48 h after administering lipid-lowering treatment.

Statistical analysis

SPSS 25.0 (IBM Corp., Armonk, NY, United States) was used for data analysis, and GraphPad Prism7.0 was used for mapping. Measurement data in normal distribution were expressed as mean ± SD and analyzed with Student's *t*-test or analysis of variance. Otherwise, variables were described as medians and interquartile ranges and analyzed by Mann-Whitney *U* test or Kruskal-Wallis test. Categorical variables were presented as absolute numbers and proportions and tested by χ^2 or Fisher's exact test.

Paired *t* test was used for continuous variables before and after treatment. Multivariate logistic regression analysis was used to identify independent risk factors with odds ratios (ORs) and 95%CIs. In addition, 1-1 PSM was performed, followed by univariate analysis. $P < 0.05$ was considered statistically significant.

RESULTS

Trends in incidence of HTG-AP

For nearly a decade, 371 patients were diagnosed with HTG-AP in Fujian Provincial Hospital. The total number of patients with HTG-AP in our hospital increased, and the incidence of HTG-AP was increased by approximately 2.6 times over the past 10 years and ranged from 8.4% to 22.3% (Figure 2).

Clinical characteristics of HTG-AP

A total of 371 patients were diagnosed with HTG-AP, the mean age of the patients with HTG-AP was 39.86 ± 10.20 years, and most of the patients (approximately 93.8%) were young and middle-aged individuals, with a male/female ratio of 2.0 (247/124). The highest incidence rate of AP was observed for men in the age group of 30-39 years (Figure 3).

The mean serum baseline TG values in HTG-AP were significantly high (2544.59 ± 2305.37 mg/dL). The serum AMY elevated levels were higher than normal in 80.1% of the patients with HTG-AP but only three times greater than normal in 46.9% of patients (Table 1).

About 90.6% of patients with HTG-AP had comorbidity with fatty liver disease, and 11 women (3.0%) had an HTG-AP attack during pregnancy. About 54.7% of the cases were related to diet (high fatty acid) and/or drinking (beer). Patients with HTG-AP had a high frequency of SAP (100, 26.9%), organ failure (117, 31.5%), recurrence (122, 32.9%), and high MCTSI score (5.00 ± 1.83). Eleven patients (3.0%) died during hospitalization (Table 1).

Comparisons of different grades of severity of HTG-AP

A total of 219 patients met the inclusion and exclusion criteria divided into the MAP group ($n = 29$), MSAP group ($n = 114$), and SAP group ($n = 76$).

Table 2 shows that the more severe HTG-AP was, the more frequent blood purification was used. Improved Marshall score ($P < 0.000$), MCTSI score ($P < 0.000$), baseline TG ($P = 0.035$), baseline AMY ($P < 0.000$), CRP ($P < 0.000$), albumin ($P < 0.000$), aspartate aminotransferase ($P < 0.000$), low-density lipoprotein-cholesterol ($P = 0.003$), urea nitrogen ($P < 0.000$), creatinine ($P < 0.000$), calcium ($P < 0.000$), hemoglobin ($P = 0.010$), free triiodothyronine ($P = 0.018$), admission to the intensive care unit ($P < 0.000$), and mortality ($P < 0.000$) were significantly different between patients with different grades of severity.

Multivariate logistic regression analysis confirmed that high CRP ($P = 0.005$, OR = 1.011, 95%CI: 1.003-1.019), low calcium ($P = 0.003$, OR = 0.016, 95%CI: 0.001-0.239), and low albumin ($P = 0.023$, OR = 0.821, 95%CI: 0.693-0.973) were risk factors of severe HTG-AP (Table 3).

Comparisons between INS and HP treatments

Of the 219 patients, 84 patients were treated with INS in the INS group and 32 patients were treated with HP in the HP group. The entire cohort showed that the grades of severity of HTG-AP ($P = 0.002$) and baseline TG ($P = 0.037$) were significantly different between patients treated with INS and HP (Table 4).

Given the large severity and baseline TG gap between the two groups, patients were selected for further analysis using PSM, adjusted by sex, age, grades of severity, and baseline TG. After matching, 26 patients were in the INS group and 26 patients were in the HP group (1:1, match tolerance = 0.02). No significant differences in sex ($P = 0.184$), age ($P = 0.895$), grades of severity ($P = 0.755$), improved Marshall score ($P = 0.186$), MCTSI score ($P = 0.127$), and baseline TG ($P = 0.734$) were found between the two groups (Table 4).

In patients with MAP and MSAP, the serum TG level significantly decreased in patients treated with INS ($P < 0.000$) and HP ($P < 0.000$) within 48 h (Figure 4). The clearance rates of TG were 57.24% ± 33.70% and 56.38% ± 33.61%, respectively ($P = 0.927$). However, the clearance rate of TG ($P = 0.927$) and length of stay (13.04 ± 7.92 d *vs* 12.35 ± 6.40 d, $P = 0.730$) did not differ between the two groups (Table 4).

DISCUSSION

Trends in incidence of HTG-AP

AP has many etiologies, and previous studies reported that HTG as an etiologic factor is between 1.3% and 6.9%[21,22]. However, HTG-AP increased at a fast rate in the Asian region during recent years. Taiwan reported that the frequency of HTG as an etiologic factor in patients with AP ranged from 6.3% to 12.3%[23]. A study reported that the incidence of HTG-AP reached 25.6% in 2013[14]. Zheng *et al*[24]

Table 1 Clinical characteristics of hypertriglyceridemic acute pancreatitis

Characteristic	All (*n* = 371)
Sex, *n* (%)	
Male	247 (66.6)
Female	124 (33.4)
Age, yr	39.86 ± 10.20
BMI (kg/m^2)	25.99 ± 3.18
Causes, *n* (%)	203 (54.7)
Diet (high fatty acid)	127 (34.2)
Drinking (beer)	55 (14.8)
Mixed	21 (5.7)
Complications, *n* (%)	
Diabetes mellitus	115 (31.0)
Hypertension	62 (16.7)
Fatty liver disease	336 (90.6)
Pregnancy	11 (3.0)
Recurrence, *n* (%)	122 (32.9)
Grades of severity, *n* (%)	
MAP	63 (17.0)
MSAP	208 (56.1)
SAP	100 (26.9)
Improved Marshall score	1.30 ± 1.77
Organ failure, *n* (%)	117 (31.5)
MCTSI score	5.00 ± 1.83
Lipid-lowering treatment, *n* (%)	
Intravenous insulin	144 (38.8)
HP	32 (8.6)
CRRT/HP + CRRT	77 (20.8)
Only anti-lipemic	118 (31.8)
Baseline TG, mg/dL	2544.59 ± 2305.37
Baseline AMY (nUNL)	5.00 ± 6.47
> UNL, *n* (%)	297 (80.1)
≥ 3UNL, *n* (%)	174 (46.9)
Admission to ICU, *n* (%)	126 (34.0)
Death, *n* (%)	11 (3.0)

BMI: Body mass index; MAP: Mild acute pancreatitis; MSAP: Moderately severe acute pancreatitis; SAP: Severe acute pancreatitis; MCTSI: Modified computed tomography severity index; HP: Hemoperfusion; CRRT: Continuous renal replacement therapy; TG: Triglyceride; AMY: Amylase; UNL: Upper limit of normal; ICU: Intensive care unit.

retrospectively analyzed 2461 patients with AP in Beijing during a 5-year period and reported that the causes of AP included biliary (55.75%), alcoholism (10%), hypertriglyceridemia (10.36%), and others (23.89%); however, this work did not mention the rate of increase in HTG-AP.

The standardized incidence rate of HTG-AP increased from 0.7 to 1.7 per 100000 person-years from 2008 to 2019 in Denmark, and the incidence has increased by 2.4 times over the past 10 years[5]. Another study from Guangdong showed that the incidence of HTG-AP in 2000 to 2005 was 2.6 times higher than that in 1990 to 1994 (8.9% *vs* 3.4%, $P < 0.05$)[25]. Based on recent observations from China[26], the

Table 2 Comparisons of clinical characteristics and laboratory parameters with different grades of severity of hypertriglyceridemic acute pancreatitis

Characteristic	All (*n* = 219)	MAP group (*n* = 29)	MSAP group (*n* = 114)	SAP group (*n* = 76)	*P* value
Sex, *n* (%)					0.111
Male	140 (63.9)	23 (79.3)	67 (58.8)	50 (65.8)	
Female	79 (36.1)	6 (20.7)	47 (41.2)	26 (34.2)	
Age, yr	38.92 ± 10.02	38.66 ± 9.73	38.96 ± 10.12	38.96 ± 10.12	0.941
BMI (kg/m^2)	26.13 ± 3.30	26.20 ± 1.56	25.58 ± 3.54	28.51 ± 2.97	0.097
Complications, *n* (%)					
Diabetes mellitus	109 (49.8)	14 (48.3)	58 (50.9)	37 (48.7)	0.982
Fatty liver disease	205 (93.6)	25 (86.2)	106 (93.0)	74 (97.4)	0.112
Lipid-lowering treatment, *n* (%)					< 0.001
Intravenous insulin	84 (38.4)	14 (48.3)	69 (60.5)	1 (1.3)	
HP	32 (14.6)	1 (3.4)	26 (22.8)	5 (6.6)	
CRRT/HP + CRRT	60 (27.4)	0 (0.0)	1 (0.9)	59 (77.6)	
Only anti-lipemic	43 (19.6)	14 (48.3)	18 (15.8)	11 (14.5)	
Improved Marshall score	1.00 (0.00, 3.00)	0.00 (0.00, 0.00)	0.00 (0.00, 1.00)	3.00 (3.00, 4.75)	< 0.001
MCTSI score	5.11 ± 1.70	2.14 ± 0.92	5.14 ± 1.06	6.18 ± 1.35	< 0.001
Baseline TG, mg/dL	2713.82 ± 2458.65	1895.15 ± 1685.17	2480.80 ± 2040.458	3386.29 ± 3081.51	0.035
Baseline AMY (nUNL)	2.92 (1.43, 6.41)	2.81 (1.47, 5.21)	2.22 (0.98, 5.08)	5.28 (2.21, 8.66)	< 0.001
CRP, mg/L	196.36 ± 121.97	143.17 ± 97.51	178.65 ± 103.25	247.12 ± 143.73	< 0.001
Albumin, g/L	32.66 ± 5.99	36.48 ± 4.96	34.46 ± 5.16	28.49 ± 5.16	< 0.001
TBIL, mmol/L	16.60 (10.80, 22.90)	18.91 (13.02, 23.68)	15.35 (10.69, 22.46)	16.57 (10.60, 24.92)	0.511
ALT, U/L	20.00 (13.60, 30.70)	21.30 (14.90, 35.75)	20.25 (13.00, 31.93)	19.75 (14.03, 27.30)	0.648
AST, U/L	25.00 (17.50, 39.50)	21.30 (17.00, 28.05)	20.00 (16.08, 30.63)	36.55 (25.00, 56.80)	< 0.001
Total cholesterol, mmol/L	8.58 ± 4.56	7.47 ± 2.96	8.82 ± 4.53	8.64 ± 5.06	0.522
HDL-C, mmol/L	0.82 (0.61, 1.10)	0.88 (0.75, 1.17)	0.86 (0.66, 1.16)	0.69 (0.52, 0.99)	0.241
LDL-C, mmol/L	2.92 ± 1.55	3.77 ± 1.41	2.91 ± 1.58	2.62 ± 1.46	0.003
Glucose, mmol/L	10.50 ± 3.64	9.47 ± 3.70	10.34 ± 3.54	11.13 ± 3.69	0.100
Urea nitrogen, mmol/L	4.73 ± 3.31	4.56 ± 1.63	3.66 ± 1.76	6.40 ± 4.64	< 0.001
Creatinine, μmol/L	83.03 ± 66.48	71.90 ± 18.03	65.46 ± 19.11	113.63 ± 103.46	< 0.001
Calcium, mmol/L	1.93 ± 0.31	2.16 ± 0.18	2.00 ± 0.21	1.75 ± 0.37	< 0.001
WBC, × 10^9/L	11.67 ± 4.10	11.22 ± 3.64	11.99 ± 4.06	11.37 ± 4.33	0.351
PLT, × 10^9/L	200.19 ± 69.19	194.69 ± 73.58	208.67 ± 65.17	189.57 ± 72.51	0.159
Hb, g/L	141.11 ± 24.52	143.69 ± 19.12	136.87 ± 22.76	146.49 ± 27.78	0.010
STSH, mIU/L	0.28 (0.16, 0.65)	0.49 (0.28, 0.98)	0.28 (0.14, 0.66)	0.24 (0.16, 0.62)	0.188
FT3, pmol/L	2.29 ± 1.00	2.90 ± 0.77	2.36 ± 0.86	2.89 ± 1.18	0.018
FT4, pmol/L	12.56 ± 3.70	12.83 ± 2.10	12.88 ± 3.95	12.11 ± 3.68	0.302
Admission to ICU, *n* (%)	98 (44.7)	1 (3.4)	27 (23.7)	70 (92.1)	< 0.001
Death, *n* (%)	9 (4.1)	0 (0.0)	0 (0.0)	9 (11.8)	< 0.001

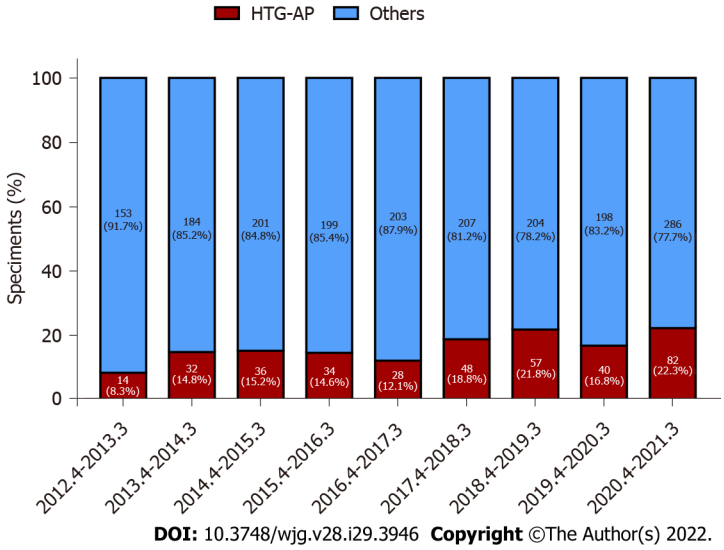
MAP: Mild acute pancreatitis; MSAP: Moderately severe acute pancreatitis; SAP: Severe acute pancreatitis; BMI: Body mass index; HP: Hemoperfusion; CRRT: Continuous renal replacement therapy; MCTSI: Modified computed tomography severity index; TG: Triglyceride; AMY: Amylase; UNL: Upper

limit of normal; CRP: C-reactive protein; TBIL: Total bilirubin; ALT: Alanine aminotransferase; AST: Aspartate transaminase; HDL-C: High-density lipoprotein cholesterol; LDL-C: Low-density lipoprotein cholesterol; WBC: White blood cell; PLT: Blood platelet; Hb: Hemoglobin; STSH: Sensitive thyrotropin; FT3: Free triiodothyronine; FT4: Free thyroxine; ICU: Intensive care unit.

Table 3 Factors associated with severe hypertriglyceridemic acute pancreatitis according to multivariate logistic regression analysis

Variable	B	OR	OR (95%CI)	*P* value
Baseline TG	0.023	1.023	(0.991-1.056)	0.159
Baseline AMY	0.345	1.412	(0.916-2.175)	0.118
CRP	0.110	1.011	(1.003-1.019)	0.005
Albumin	-0.197	0.821	(0.693-0.973)	0.023
AST	0.018	1.018	(0.975-1.063)	0.423
LDL-C	-0.173	0.814	(0.556-1.272)	0.412
Urea nitrogen	-0.334	0.709	(0.462-1.086)	0.114
Creatinine	0.025	1.026	(0.988-1.065)	0.186
Calcium	-4.152	0.016	(0.001-0.239)	0.003
Hb	0.008	1.008	(0.975-1.043)	0.621
FT3	-1.324	0.266	(0.055-1.281)	0.099

OR: Odds ratio; TG: Triglyceride; AMY: Amylase; CRP: C-reactive protein; AST: Aspartate transaminase; LDL-C: Low-density lipoprotein cholesterol; Hb: Hemoglobin; FT3: Free triiodothyronine.



DOI: 10.3748/wjg.v28.i29.3946 **Copyright** ©The Author(s) 2022.

Figure 2 The total number of patients with hypertriglyceridemic acute pancreatitis and other acute pancreatitis in Fujian Provincial Hospital increased significantly during nearly 10 years. HTG-AP: Hypertriglyceridemic acute pancreatitis.

proportion of patients with HTG-AP increased from 14.0% to 34.0% during a 16-year period in a tertiary hospital setting. Our study found that the incidence of HTG-AP increased by approximately 2.6 times and ranged from 8.4% to 22.3% during nearly 10 years, with a significant increase detected after 2017. Our results are similar to previously reported data.

At present, updated population-based estimates on the incidence of HTG-AP are lacking. Some studies have shown that the incidence and mortality of HTG-AP were increasing year by year, which was related to the change of people's diet structure and lifestyle[4]. At the same time, the availability of the detection of serum TG also improved the diagnosis of HTG-AP. For example, the emergency of our hospital began testing serum TG in 2017, and Figure 1 shows the incidence of HTG-AP has increased since 2017.

Table 4 Comparisons of clinical characteristics and laboratory parameters with different treatment between intravenous insulin and hemoperfusion before and after propensity score matching

Characteristic	Entire cohort		*P* value	PSM		*P* value
	INS group (*n* = 84)	HP Group (*n* = 32)		INS group (*n* = 26)	HP group (*n* = 26)	
Sex, *n* (%)			0.626			0.184
Male	51 (60.7)	21 (65.6)		20 (76.9)	16 (61.5)	
Female	33 (39.3)	11 (34.4)		6 (23.1)	10 (38.5)	
Age, yr	39.99 ± 10.36	36.44 ± 11.60	0.965	36.81 ± 10.79	36.42 ± 10.10	0.895
Grades of severity, *n* (%)			0.002			0.755[a]
MAP	14 (16.7)	1 (3.1)		1 (3.8)	1 (3.8)	
MSAP	69 (82.1)	26 (81.3)		25 (96.2)	25 (96.2)	
SAP	1 (1.2)	5 (15.6)		0 (0.0)	0 (0.0)	
Improved Marshall score	0.00 (0.00, 1.00)	1.00 (1.00, 2.00)	< 0.001	0.00 (0.00, 1.00)	1.00 (0.00, 1.00)	0.186[a]
MCTSI score	4.67 ± 1.59	5.75 ± 0.84	< 0.001	5.15 ± 1.29	5.62 ± 0.80	0.127[a]
Baseline TG, mg/dL	2493.20 ± 1958.06	3443.88 ± 1676.31	0.037	3484.64 ± 2275.248	3264.91 ± 2375.37	0.734[a]
Treated TG within 48 h, mg/dL	946.25 ± 769.05	1145.60 ± 699.05	0.205	1108.39 ± 856.76	1040.16 ± 686.65	0.753
Clearance rate of TG within 48 h, %	47.65 ± 34.64	63.91 ± 23.32	0.005	57.24 ± 33.70	56.38 ± 33.61	0.927[a]
CRP, mg/L	184.75 ± 99.84	198.43 ± 94.00	0.552	214.612 ± 119.22	198.28 ± 97.09	0.629
Albumin, g/L	34.05 ± 4.81	32.50 ± 6.39	0.219	34.56 ± 5.03	32.53 ± 6.58	0.218
TBIL, mmol/L	17.80 ± 8.96	19.83 ± 13.61	0.439	18.70 ± 9.38	20.87 ± 14.41	0.523
ALT, U/L	24.55 ± 17.77	23.15 ± 18.15	0.705	24.58 ± 16.69	21.81 ± 16.47	0.550
AST, U/L	25.70 ± 14.23	30.85 ± 26.87	0.187	24.84 ± 12.40	32.10 ± 29.44	0.252
Total cholesterol, mmol/L	8.38 ± 3.89	8.93 ± 4.37	0.511	9.84 ± 4.91	8.52 ± 4.58	0.318
Glucose, mmol/L	11.08 ± 3.65	10.83 ± 3.42	0.739	11.71 ± 2.74	10.07 ± 3.22	0.057
Urea nitrogen, mmol/L	4.02 ± 1.86	3.83 ± 2.27	0.652	3.54 ± 1.76	3.34 ± 1.94	0.688
Creatinine, mmol/L	63.73 ± 18.23	67.72 ± 24.01	0.338	65.00 ± 12.33	67.00 ± 23.36	0.702
Calcium, mmol/L	1.98 ± 0.25	1.90 ± 0.28	0.100	2.03 ± 0.23	1.89 ± 0.31	0.063
WBC, × 10^9/L	11.79 ± 4.20	12.33 ± 4.37	0.541	12.40 ± 4.00	12.51 ± 4.44	0.920
PLT, × 10^9/L	205.39 ± 68.44	204.34 ± 65.98	0.941	201.66 ± 59.77	197.38 ± 57.91	0.795
Hb, g/L	137.48 ± 23.67	138.12 ± 27.60	0.902	143.44 ± 19.50	135.38 ± 27.50	0.230
Length of stay, d	11.88 ± 6.37	11.93 ± 6.01	0.965	13.04 ± 7.92	12.35 ± 6.40	0.730
Death, *n* (%)	0 (0.0)	0 (0.0)		0 (0.0)	0 (0.0)	

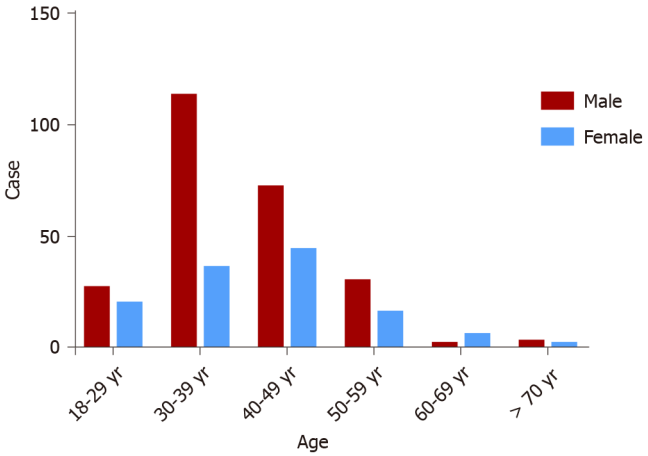
[a]*P* value changed after propensity score matching.

PSM: Propensity score matching; INS: Intravenous insulin; HP: Hemoperfusion; MAP: Mild acute pancreatitis; MSAP: Moderately severe acute pancreatitis; SAP: Severe acute pancreatitis; MCTSI: Modified computed tomography severity index; TG: Triglyceride; CRP: C-reactive protein; TBIL: Total bilirubin; ALT: Alanine aminotransferase; AST: Aspartate transaminase; WBC: White blood cell; PLT: Blood platelet; Hb: Hemoglobin.

Figure 1 showed the decrease in the incidence of HTG-AP from April 2016 to March 2017 and from April 2019 to March 2020, which coincided with the opening of the South Hospital of Fujian Provincial Hospital and the outbreak of coronavirus disease 2019 in China, leading to the diversion and reduction of the number of patients with AP and HTG-AP.

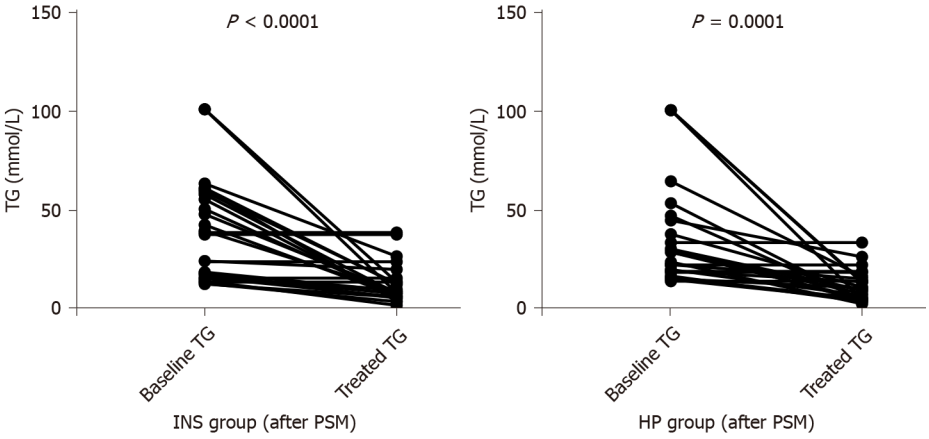
Clinical feature of HTG-AP

This study also found that the clinical manifestations of patients with HTG-AP included the most common abdominal pain and abdominal distension as well as nausea, vomiting, and anhelation without



DOI: 10.3748/wjg.v28.i29.3946 **Copyright** ©The Author(s) 2022.

Figure 3 Incidence rates of hypertriglyceridemic acute pancreatitis stratified by age and sex.



DOI: 10.3748/wjg.v28.i29.3946 **Copyright** ©The Author(s) 2022.

Figure 4 Changes of serum triglyceride levels in both groups before and after treatment. TG: Triglyceride; INS: Insulin; PSM: Propensity score matching; HP: Hemoperfusion.

specificity. However, patients with HTG-AP have some clinical characteristics, such as serum TG level (2544.59 ± 2305.37 mg/dL) that was significantly higher than normal values at the onset of disease. Hence, serum TG level ≥ 1000 mg/dL is the most important characteristic of HTG-AP[19]. Thus, we can improve the diagnosis rate of HTG-AP by improving the early detection rate of serum TG in clinical work.

We found that the mean age of patients with HTG-AP was 39.86 ± 10.20 years. The highest incidence rate of AP was observed for men in the age group of 30-39 years, and the male/female ratio was 2.0 (247/124). Li *et al*[10] reported that patients with HTG-AP were younger (40 *vs* 51, $P < 0.01$) and were mostly males (214/91 *vs* 242/183, $P < 0.01$) compared with patients with biliary AP.

Sekimoto *et al*[27] stated that the average age for HTG-AP was lower than that for other causes. Zheng *et al*[24] reported a higher proportion of alcoholic and HTG-AP in men than in women and in patients younger than 50 years. Olesen *et al*[5] reported that the highest incidence rate of severe HTG was observed for men in the age group of 40-49 years, and severe HTG is a well-known risk factor for AP. Therefore, HTG-AP is becoming more prevalent among younger individuals.

AMY was elevated to levels higher than the normal value in 80.1% of patients but only three times higher than the normal in 46.9% of patients. About 50% of patients with HTG-AP showed no significant increase in serum and urine AMY levels[13], which may be due to the presence of AMY activity inhibitors in their plasma; these inhibitors can enter the urine through the kidneys and inhibit urinary AMY activity. In addition, increased TG levels directly affected the determination of AMY. Therefore, the early diagnosis of HTG-AP is more difficult. The diagnostic accuracy of lipase for HTG-AP was 91.83%, while that of AMY was only 40.38%[14]. Thus, we can improve the diagnosis rate of HTG-AP by combining serum AMY and lipase.

In this study, the frequency of SAP (26.9%), organ failure (31.5%), rate of recurrence (32.9%), and mortality (3.0%) of HTG-AP was high. A large multicenter study in China showed higher incidences of

local complication (34.13% *vs* 15.72%, $P < 0.000$) and MSAP (28.85% *vs* 12.95%, $P < 0.000$) in patients with HTG-AP than in patients without HTG-AP[14]. HTG-AP varied in severity between mild (41%), moderate (26%), and severe (33%)[17]. A foreign study showed that patients with HTG-AP had significantly higher percentages of multiple organ dysfunction syndrome (24.1% *vs* 12.1%, $P = 0.009$) and cardiovascular failure (17.6% *vs* 4.6%, $P < 0.001$) compared with biliary AP[26].

Some reports showed a more severe course of AP induced by HTG compared with other causes, whereas other scholars seemed to favor no significant difference in disease severity[28]. Vipperla *et al* [17] reported that the risk of recurrent AP attacks was 32%, often in patients with poorly controlled diabetes, alcoholism, and TG levels. Our study showed that the recurrence rate of MSAP was higher than that of SAP, which may be due to insufficient attention and medical care. Different studies reported that the mortality rate of HTG-AP ranged from 0.48% to 7.9%[10,14,26], but the mortality rate for severe cases reached as high as 20%-25%[2].

The high frequency rates of fatty liver disease, diabetes mellitus, and hypertension were found in patients with HTG-AP, with values of 90.6%, 31.0%, and 16.7%, respectively. Patients with HTG-AP were often complicated with metabolic diseases such as diabetes mellitus and obesity, and patients with type 2 diabetes mellitus had an elevated risk of AP compared with patients without diabetes[15].

Comparisons of different grades of severity of HTG-AP

A comparison was conducted among patients with MAP, MSAP, and SAP to investigate the association of the severity of HTG-AP with clinical data and laboratory indicators. Table 2 showed that age and sex had no difference among the three groups (all $P > 0.050$). Improved Marshall score, MCTSI score, baseline TG, baseline AMY, CRP, albumin, aspartate aminotransferase, low-density lipoprotein-cholesterol, urea nitrogen, creatinine, calcium, hemoglobin, and free triiodothyronine were significantly different among patients with different grades of severity of HTG-AP (all $P < 0.050$). Multivariate logistic regression analysis confirmed that high CRP ($P = 0.005$, OR = 1.011, 95%CI: 1.003-1.019), low calcium ($P = 0.003$, OR = 0.016, 95%CI: 0.001-0.239), and low albumin ($P = 0.023$, OR = 0.821, 95%CI: 0.693-0.973) were risk factors of severe HTG-AP.

CRP, serum calcium, and serum albumin are well-known predictors of severe AP with non-HTG-AP and are widely used in its early detection. Experts suggested that CRP levels > 150 mg/L 48 h after the onset of symptoms have a high sensitivity for predicting the severity of AP[29]. Yu *et al*[30] reported that patients with HTG-AP had lower serum ionized calcium associated with a higher risk of developing SAP. Chen *et al*[31] confirmed that low serum albumin ($P = 0.004$, OR = 3.362, 95%CI: 1.492–8.823) and high CRP ($P = 0.005$, OR = 3.061, 95%CI: 1.407–6.659) were risk factors of moderately severe to severe HTG-AP.

Our study showed that the predictors of SAP with HTG-AP were similar to those of AP with other etiologies including alcoholic and biliary AP.

Comparisons among different treatments

Reducing serum TG levels quickly is crucial in the early treatment of HTG-AP. This method mainly includes two categories of routine treatment, and blood purification had been implemented for the patients with HTG-AP. Currently, the TG levels should be reduced to below 500 mg/dL as soon as possible; when follow-up TG levels were < 500 mg/dL, an associated reduction in the risk of clinical events and decrease in health care resource use and costs were observed[32]. However, selecting routine treatment or blood purification for patients with HTG-AP after admission to obtain economic cost effectiveness remains controversial. Routine treatments, such as insulin, heparin, and anti-HTG drugs, are effective in reducing TG and have the advantages of non-invasiveness and low cost.

Blood purification includes HP, PE, and continuous renal replacement therapy, which have the disadvantages of invasiveness and expensive. Compared with HP and PE, continuous renal replacement therapy can not only reduce TG rapidly but also remove inflammatory mediators and is more accurate for systemic inflammatory response syndrome control[9]. However, selecting routine treatment or blood purification for patients with HTG-AP after admission in order to obtain economic cost effectiveness remains controversial. Therefore, this study mainly compared the effect of INS and HP on lowering serum TG.

Among patients with MAP and MSAP, a significant decrease in serum TG was found in patients treated with INS ($P < 0.000$) and HP ($P < 0.000$) within 48 h. The clearance rates of TG were 57.24% ± 33.70% and 56.38% ± 33.61%, respectively ($P = 0.927$). This rate of decline was similar to a report[33] wherein 22 episodes of HTG-AP had a calculated fall in serum TG of 69.8% within 48 h by conservative management. This finding is also similar to that reported in an HP case series, which demonstrated 49%-80% reductions in serum TG after a single session[34,35]. These reports showed no difference in the rate of TG decline between patients managed with or without HP. This study also showed that length of stay (13.04 ± 7.92 d *vs* 12.35 ± 6.40 d, $P = 0.730$) did not differ between the two treatments. A large multicenter retrospective study collected 1159 patients with SAP, which included 30 patients with HTG-AP, and 10 patients treated with PE compared with 20 patients treated with routine therapy; no additional reduction in TG levels and no improvement in clinical outcomes were detected[36].

Study strengths and limitations

The strengths of this study are the high accuracy of data due to the strict inclusion and exclusion criteria and the use of PSM to avoid test errors. At present, few studies have reported on how to choose the treatment mode of HTG-AP, which is the innovation of this study.

Our study has some important limitations. This study adopted a single-center retrospective design. The incidence of HTG-AP is not universal and can only reflect the situation of our hospital. Data such as body mass index, urine AMY, blood lipase, and blood gas analysis were missing. The choice of treatment had selection bias.

CONCLUSION

The incidence of HTG-AP exhibited a significant increase, remarkable severity, and recurrent trend. By understanding the characteristics of HTG-AP, we can improve the clinical diagnosis rate and identify patients who are likely to develop severe disease early. Patients with MAP and MSAP can be treated with INS safely and effectively without HP. This work provides a basis for doctors to choose an appropriate treatment plan for patients.

ARTICLE HIGHLIGHTS

Research background

The incidence of hypertriglyceridemic acute pancreatitis (HTG-AP) has increased yearly, but updated population-based estimates on the incidence of HTG-AP are lacking. Reducing serum triglyceride (TG) levels quickly is crucial in the early treatment of HTG-AP. Currently, there are many treatments to reduce TG levels, but there is still a lack of authoritative guidelines.

Research motivation

We wanted to explore appropriate treatments to block the progression of HTG-AP.

Research objectives

To explore the clinical characteristics to reduce the missed diagnosis rate of HTG-AP and to identify the patients who would develop severe acute pancreatitis early. To compare the clinical outcomes of intravenous insulin (INS) and hemoperfusion (HP) and guide the choice of treatment for patients.

Research methods

We retrospectively reviewed the incidence and clinical characteristics of 371 patients with HTG-AP in our hospital from the past 10 years. Then, 219 patients who met the inclusion and exclusion criteria were further screened and divided to different groups according to grades of severity of HTG-AP and treatments. Multivariate logistic regression analyses were used to identify the independent risk factors for severe HTG-AP. Propensity score matching was used to compare the clinical outcomes of INS and HP.

Research results

The incidence of HTG-AP increased by approximately 2.6 times during the 10 years and ranged from 8.4% to 22.3% (8.4% in April 2012–March 2013 and 22.3% in April 2020–March 2021). Multivariate logistic regression analysis confirmed that high C-reactive protein [P = 0.005, odds ratio (OR) = 1.011, 95%CI: 1.003-1.019], low calcium (P = 0.003, OR = 0.016, 95%CI: 0.001-0.239), and low albumin (P = 0.023, OR = 0.821, 95%CI: 0.693-0.973) were risk factors of severe HTG-AP. After propensity score matching with sex, age, grades of severity, and baseline TG, there was a significant decrease in serum TG in patients treated with INS (P < 0.0001) and HP (P = 0.0001) within 48 h. However, the clearance rate of TG and length of stay did not differ between the two groups.

Research conclusions

The incidence of HTG-AP exhibited a significant increase. Patients with mild and moderately severe acute pancreatitis can be treated with INS safely and effectively without HP.

Research perspectives

Identifying patients with a severe tendency at the early stage of HTG-AP and choosing cost-effective treatments is the future direction of this research.

FOOTNOTES

Author contributions: Lin XY, Zeng Y, and Zhang ZC contributed equally to the work; Lin XY, Zeng Y, and Zhang ZC designed the study, collected and analyzed the data, and wrote the manuscript; Lin ZH, Chen LC, and Ye ZS made contributions to conception, design, and coordination of the study and gave final approval of the version to be published; All authors read and approved the final manuscript.

Institutional review board statement: The Ethics Committee of Fujian Provincial Hospital approved the study (K2021-02-007).

Informed consent statement: Informed written consent was obtained from the patient for publication of this report and any accompanying images.

Conflict-of-interest statement: The authors declare that they have no conflict of interest.

Data sharing statement: Participants gave informed consent for data sharing.

Open-Access: This article is an open-access article that was selected by an in-house editor and fully peer-reviewed by external reviewers. It is distributed in accordance with the Creative Commons Attribution NonCommercial (CC BY-NC 4.0) license, which permits others to distribute, remix, adapt, build upon this work non-commercially, and license their derivative works on different terms, provided the original work is properly cited and the use is non-commercial. See: https://creativecommons.org/Licenses/by-nc/4.0/

Country/Territory of origin: China

ORCID number: Xue-Yan Lin 0000-0002-3397-0498; Yi Zeng 0000-0001-9144-8414; Zheng-Chao Zhang 0000-0003-3291-2947; Zhi-Hui Lin 0000-0001-6595-7952; Lu-Chuan Chen 0000-0003-3362-447x; Zai-Sheng Ye 0000-0001-9881-6400.

S-Editor: Zhang H
L-Editor: Filipodia CL
P-Editor: Zhang H

REFERENCES

1 **Crockett SD**, Wani S, Gardner TB, Falck-Ytter Y, Barkun AN; American Gastroenterological Association Institute Clinical Guidelines Committee. American Gastroenterological Association Institute Guideline on Initial Management of Acute Pancreatitis. *Gastroenterology* 2018; **154**: 1096-1101 [PMID: 29409760 DOI: 10.1053/j.gastro.2018.01.032]
2 **Johnson CD**, Abu-Hilal M. Persistent organ failure during the first week as a marker of fatal outcome in acute pancreatitis. *Gut* 2004; **53**: 1340-1344 [PMID: 15306596 DOI: 10.1136/gut.2004.039883]
3 **Khatua B**, El-Kurdi B, Singh VP. Obesity and pancreatitis. *Curr Opin Gastroenterol* 2017; **33**: 374-382 [PMID: 28719397 DOI: 10.1097/MOG.0000000000000386]
4 **Carr RA**, Rejowski BJ, Cote GA, Pitt HA, Zyromski NJ. Systematic review of hypertriglyceridemia-induced acute pancreatitis: A more virulent etiology? *Pancreatology* 2016; **16**: 469-476 [PMID: 27012480 DOI: 10.1016/j.pan.2016.02.011]
5 **Olesen SS**, Harakow A, Krogh K, Drewes AM, Handberg A, Christensen PA. Hypertriglyceridemia is often under recognized as an aetiologic risk factor for acute pancreatitis: A population-based cohort study. *Pancreatology* 2021; **21**: 334-341 [PMID: 33608229 DOI: 10.1016/j.pan.2021.02.005]
6 **Tsuang W**, Navaneethan U, Ruiz L, Palascak JB, Gelrud A. Hypertriglyceridemic pancreatitis: presentation and management. *Am J Gastroenterol* 2009; **104**: 984-991 [PMID: 19293788 DOI: 10.1038/ajg.2009.27]
7 **Ewald N**, Hardt PD, Kloer HU. Severe hypertriglyceridemia and pancreatitis: presentation and management. *Curr Opin Lipidol* 2009; **20**: 497-504 [PMID: 19770656 DOI: 10.1097/MOL.0b013e3283319a1d]
8 **Dominguez-Muñoz JE**, Malfertheiner P, Ditschuneit HH, Blanco-Chavez J, Uhl W, Büchler M, Ditschuneit H. Hyperlipidemia in acute pancreatitis. Relationship with etiology, onset, and severity of the disease. *Int J Pancreatol* 1991; **10**: 261-267 [PMID: 1787337]
9 **Guo YY**, Li HX, Zhang Y, He WH. Hypertriglyceridemia-induced acute pancreatitis: progress on disease mechanisms and treatment modalities. *Discov Med* 2019; **27**: 101-109 [PMID: 30939294]
10 **Li X**, Ke L, Dong J, Ye B, Meng L, Mao W, Yang Q, Li W, Li J. Significantly different clinical features between hypertriglyceridemia and biliary acute pancreatitis: a retrospective study of 730 patients from a tertiary center. *BMC Gastroenterol* 2018; **18**: 89 [PMID: 29914404 DOI: 10.1186/s12876-018-0821-z]
11 **Devlin JW**, Lau AK, Tanios MA. Propofol-associated hypertriglyceridemia and pancreatitis in the intensive care unit: an analysis of frequency and risk factors. *Pharmacotherapy* 2005; **25**: 1348-1352 [PMID: 16185179 DOI: 10.1592/phco.2005.25.10.1348]
12 **Durval A**, Zamidei L, Bettocchi D, Luzzio MG, Consales G. Hyperlipidemic acute pancreatitis: a possible role of antiretroviral therapy with entecavir. *Minerva Anestesiol* 2011; **77**: 1018-1021 [PMID: 21242955]
13 **Yadav D**, Pitchumoni CS. Issues in hyperlipidemic pancreatitis. *J Clin Gastroenterol* 2003; **36**: 54-62 [PMID: 12488710 DOI: 10.1097/00004836-200301000-00016]

14 **Yin G**, Cang X, Yu G, Hu G, Ni J, Xiong J, Hu Y, Xing M, Chen C, Huang Y, Tang M, Zhao Y, Cheng G, Wan R, Wang S, Wang X. Different Clinical Presentations of Hyperlipidemic Acute Pancreatitis: A Retrospective Study. *Pancreas* 2015; **44**: 1105-1110 [PMID: 26348469 DOI: 10.1097/MPA.0000000000000403]

15 **Girman CJ**, Kou TD, Cai B, Alexander CM, O'Neill EA, Williams-Herman DE, Katz L. Patients with type 2 diabetes mellitus have higher risk for acute pancreatitis compared with those without diabetes. *Diabetes Obes Metab* 2010; **12**: 766-771 [PMID: 20649628 DOI: 10.1111/j.1463-1326.2010.01231.x]

16 **Bosques-Padilla FJ**, Vázquez-Elizondo G, González-Santiago O, Del Follo-Martínez L, González OP, González-González JA, Maldonado-Garza HJ, Garza-González E. Hypertriglyceridemia-induced pancreatitis and risk of persistent systemic inflammatory response syndrome. *Am J Med Sci* 2015; **349**: 206-211 [PMID: 25545390 DOI: 10.1097/MAJ.0000000000000392]

17 **Vipperla K**, Somerville C, Furlan A, Koutroumpakis E, Saul M, Chennat J, Rabinovitz M, Whitcomb DC, Slivka A, Papachristou GI, Yadav D. Clinical Profile and Natural Course in a Large Cohort of Patients With Hypertriglyceridemia and Pancreatitis. *J Clin Gastroenterol* 2017; **51**: 77-85 [PMID: 27322530 DOI: 10.1097/MCG.0000000000000579]

18 **Banks PA**, Bollen TL, Dervenis C, Gooszen HG, Johnson CD, Sarr MG, Tsiotos GG, Vege SS; Acute Pancreatitis Classification Working Group. Classification of acute pancreatitis--2012: revision of the Atlanta classification and definitions by international consensus. *Gut* 2013; **62**: 102-111 [PMID: 23100216 DOI: 10.1136/gutjnl-2012-302779]

19 **Wang Q**, Wang G, Qiu Z, He X, Liu C. Elevated Serum Triglycerides in the Prognostic Assessment of Acute Pancreatitis: A Systematic Review and Meta-Analysis of Observational Studies. *J Clin Gastroenterol* 2017; **51**: 586-593 [PMID: 28682990 DOI: 10.1097/MCG.0000000000000846]

20 **Zhao K**, Adam SZ, Keswani RN, Horowitz JM, Miller FH. Acute Pancreatitis: Revised Atlanta Classification and the Role of Cross-Sectional Imaging. *AJR Am J Roentgenol* 2015; **205**: W32-W41 [PMID: 26102416 DOI: 10.2214/AJR.14.14056]

21 **Fortson MR**, Freedman SN, Webster PD 3rd. Clinical assessment of hyperlipidemic pancreatitis. *Am J Gastroenterol* 1995; **90**: 2134-2139 [PMID: 8540502]

22 **Gullo L**, Migliori M, Oláh A, Farkas G, Levy P, Arvanitakis C, Lankisch P, Beger H. Acute pancreatitis in five European countries: etiology and mortality. *Pancreas* 2002; **24**: 223-227 [PMID: 11893928 DOI: 10.1097/00006676-200204000-00003]

23 **Chen CH**, Dai CY, Hou NJ, Chen SC, Chuang WL, Yu ML. Etiology, severity and recurrence of acute pancreatitis in southern taiwan. *J Formos Med Assoc* 2006; **105**: 550-555 [PMID: 16877234 DOI: 10.1016/S0929-6646(09)60149-2]

24 **Zheng Y**, Zhou Z, Li H, Li J, Li A, Ma B, Zhang T, Liao Q, Ye Y, Zhang Z, Yang Y, Wang Z, Yang J, Li F. A multicenter study on etiology of acute pancreatitis in Beijing during 5 years. *Pancreas* 2015; **44**: 409-414 [PMID: 25438072 DOI: 10.1097/MPA.0000000000000273]

25 **Huang YX**, Jia L, Jiang SM, Wang SB, Li MX, Yang BH. Incidence and clinical features of hyperlipidemic acute pancreatitis from Guangdong, China: a retrospective multicenter study. *Pancreas* 2014; **43**: 548-552 [PMID: 24717803 DOI: 10.1097/MPA.0000000000000069]

26 **Jin M**, Bai X, Chen X, Zhang H, Lu B, Li Y, Lai Y, Qian J, Yang H. A 16-year trend of etiology in acute pancreatitis: The increasing proportion of hypertriglyceridemia-associated acute pancreatitis and its adverse effect on prognosis. *J Clin Lipidol* 2019; **13**: 947-953.e1 [PMID: 31735687 DOI: 10.1016/j.jacl.2019.09.005]

27 **Sekimoto M**, Takada T, Kawarada Y, Hirata K, Mayumi T, Yoshida M, Hirota M, Kimura Y, Takeda K, Isaji S, Koizumi M, Otsuki M, Matsuno S; JPN. JPN Guidelines for the management of acute pancreatitis: epidemiology, etiology, natural history, and outcome predictors in acute pancreatitis. *J Hepatobiliary Pancreat Surg* 2006; **13**: 10-24 [PMID: 16463207 DOI: 10.1007/s00534-005-1047-3]

28 **Scherer J**, Singh VP, Pitchumoni CS, Yadav D. Issues in hypertriglyceridemic pancreatitis: an update. *J Clin Gastroenterol* 2014; **48**: 195-203 [PMID: 24172179 DOI: 10.1097/01.mcg.0000436438.60145.5a]

29 **Dervenis C**. Assessments of severity and management of acute pancreatitis based on the Santorini Consensus Conference report. *JOP* 2000; **1**: 178-182 [PMID: 11856859]

30 **Yu S**, Wu D, Jin K, Yin L, Fu Y, Liu D, Zhang L, Yu X, Xu J. Low Serum Ionized Calcium, Elevated High-Sensitivity C-Reactive Protein, Neutrophil-Lymphocyte Ratio, and Body Mass Index (BMI) Are Risk Factors for Severe Acute Pancreatitis in Patients with Hypertriglyceridemia Pancreatitis. *Med Sci Monit* 2019; **25**: 6097-6103 [PMID: 31413252 DOI: 10.12659/MSM.915526]

31 **Chen L**, Huang Y, Yu H, Pan K, Zhang Z, Man Y, Hu D. The association of parameters of body composition and laboratory markers with the severity of hypertriglyceridemia-induced pancreatitis. *Lipids Health Dis* 2021; **20**: 9 [PMID: 33573658 DOI: 10.1186/s12944-021-01443-7]

32 **Christian JB**, Arondekar B, Buysman EK, Johnson SL, Seeger JD, Jacobson TA. Clinical and economic benefits observed when follow-up triglyceride levels are less than 500 mg/dL in patients with severe hypertriglyceridemia. *J Clin Lipidol* 2012; **6**: 450-461 [PMID: 23009781 DOI: 10.1016/j.jacl.2012.08.007]

33 **Berberich AJ**, Ziada A, Zou GY, Hegele RA. Conservative management in hypertriglyceridemia-associated pancreatitis. *J Intern Med* 2019; **286**: 644-650 [PMID: 31077464 DOI: 10.1111/joim.12925]

34 **Galán Carrillo I**, Demelo-Rodriguez P, Rodríguez Ferrero ML, Anaya F. Double filtration plasmapheresis in the treatment of pancreatitis due to severe hypertriglyceridemia. *J Clin Lipidol* 2015; **9**: 698-702 [PMID: 26350817 DOI: 10.1016/j.jacl.2015.07.004]

35 **Valdivielso P**, Ramírez-Bueno A, Ewald N. Current knowledge of hypertriglyceridemic pancreatitis. *Eur J Intern Med* 2014; **25**: 689-694 [PMID: 25269432 DOI: 10.1016/j.ejim.2014.08.008]

36 **Miyamoto K**, Horibe M, Sanui M, Sasaki M, Sugiyama D, Kato S, Yamashita T, Goto T, Iwasaki E, Shirai K, Oe K, Sawano H, Oda T, Yasuda H, Ogura Y, Hirose K, Kitamura K, Chiba N, Ozaki T, Oshima T, Yamamoto T, Nagata K, Mine T, Saito K, Sekino M, Furuya T, Matsuda N, Hayakawa M, Kanai T, Mayumi T. Plasmapheresis therapy has no triglyceride-lowering effect in patients with hypertriglyceridemic pancreatitis. *Intensive Care Med* 2017; **43**: 949-951 [PMID: 28233051 DOI: 10.1007/s00134-017-4722-3]

World Journal of Gastroenterology

Submit a Manuscript: https://www.f6publishing.com

World J Gastroenterol 2022 August 7; 28(29): 3960-3970

DOI: 10.3748/wjg.v28.i29.3960

ISSN 1007-9327 (print) ISSN 2219-2840 (online)

ORIGINAL ARTICLE

Retrospective Study

Radiomics for differentiating tumor deposits from lymph node metastasis in rectal cancer

Yong-Chang Zhang, Mou Li, Yu-Mei Jin, Jing-Xu Xu, Chen-Cui Huang, Bin Song

Specialty type: Radiology, nuclear medicine and medical imaging

Provenance and peer review: Unsolicited article; Externally peer reviewed.

Peer-review model: Single blind

Peer-review report's scientific quality classification

Grade A (Excellent): 0
Grade B (Very good): B, B
Grade C (Good): 0
Grade D (Fair): 0
Grade E (Poor): 0

P-Reviewer: Gnetti L, Italy; Hwang KH, South Korea

Received: December 29, 2021
Peer-review started: December 29, 2021
First decision: March 10, 2022
Revised: March 28, 2022
Accepted: July 6, 2022
Article in press: July 6, 2022
Published online: August 7, 2022

Yong-Chang Zhang, Department of Radiology, Chengdu Seventh People's Hospital, Chengdu 610213, Sichuan Province, China

Yong-Chang Zhang, Mou Li, Yu-Mei Jin, Bin Song, Department of Radiology, West China Hospital, Sichuan University, Chengdu 610041, Sichuan Province, China

Jing-Xu Xu, Chen-Cui Huang, Department of Research Collaboration, R&D center, Beijing Deepwise & League of PHD Technology Co., Ltd, Beijing 100080, China

Corresponding author: Bin Song, MD, PhD, Chief Doctor, Professor, Department of Radiology, West China Hospital, Sichuan University, No. 37 Guoxue Alley, Chengdu 610041, Sichuan Province, China. songlab_radiology@163.com

Abstract

BACKGROUND

Tumor deposits (TDs) are not equivalent to lymph node (LN) metastasis (LNM) but have become independent adverse prognostic factors in patients with rectal cancer (RC). Although preoperatively differentiating TDs and LNMs is helpful in designing individualized treatment strategies and achieving improved prognoses, it is a challenging task.

AIM

To establish a computed tomography (CT)-based radiomics model for preoperatively differentiating TDs from LNM in patients with RC.

METHODS

This study retrospectively enrolled 219 patients with RC [TDs^+LNM^- (n = 89); LNM^+ TDs^- (n = 115); TDs^+LNM^+ (n = 15)] from a single center between September 2016 and September 2021. Single-positive patients (*i.e.*, TDs^+LNM^- and LNM^+TDs^-) were classified into the training (n = 163) and validation (n = 41) sets. We extracted numerous features from the enhanced CT (region 1: The main tumor; region 2: The largest peritumoral nodule). After deleting redundant features, three feature selection methods and three machine learning methods were used to select the best-performing classifier as the radiomics model (Rad-score). After validating Rad-score, its performance was further evaluated in the field of diagnosing double-positive patients (*i.e.*, TDs^+LNM^+) by outlining all peritumoral nodules with diameter (short-axis) > 3 mm.

RESULTS

Rad-score 1 (radiomics signature of the main tumor) had an area under the curve (AUC) of 0.768 on the training dataset and 0.700 on the validation dataset. Rad-score 2 (radiomics signature of the largest peritumoral nodule) had a higher AUC (training set: 0.940; validation set: 0.918) than Rad-score 1. Clinical factors, including age, gender, location of RC, tumor markers, and radiological features of the largest peritumoral nodule, were excluded by logistic regression. Thus, the combined model was comprised of Rad-scores of 1 and 2. Considering that the combined model had similar AUCs with Rad-score 2 (P = 0.134 in the training set and 0.594 in the validation set), Rad-score 2 was used as the final model. For the diagnosis of double-positive patients in the mixed group [TDs^+LNM^+ (n = 15); single-positive (n = 15)], Rad-score 2 demonstrated moderate performance (sensitivity, 73.3%; specificity, 66.6%; and accuracy, 70.0%).

CONCLUSION

Radiomics analysis based on the largest peritumoral nodule can be helpful in preoperatively differentiating between TDs and LNM.

Key Words: Radiomics; Tumor deposits; Lymph node metastasis; Rectal cancer; Computed tomography; Differential diagnosis

©The Author(s) 2022. Published by Baishideng Publishing Group Inc. All rights reserved.

Core Tip: In this study, a radiomics model based on the largest peritumoral nodule was developed to preoperatively differentiate tumor deposits (TDs) from lymph node (LN) metastasis in patients with rectal cancer. This model demonstrated good performance in both the training and validation cohorts. However, its performance decreased with the diagnosis of the double-positive patients. In summary, this model can be helpful for differentiating TDs from LN metastasis.

Citation: Zhang YC, Li M, Jin YM, Xu JX, Huang CC, Song B. Radiomics for differentiating tumor deposits from lymph node metastasis in rectal cancer. *World J Gastroenterol* 2022; 28(29): 3960-3970
URL: https://www.wjgnet.com/1007-9327/full/v28/i29/3960.htm
DOI: https://dx.doi.org/10.3748/wjg.v28.i29.3960

INTRODUCTION

Colorectal cancer (CRC) ranks third in terms of incidence and second in terms of mortality[1], and RC accounts for approximately 30% of CRC[2]. Tumor deposits (TDs) in RC are defined as discontinuous extramural extensions or focal aggregates of adenocarcinoma located in the perirectal region, without histological evidence of residual lymph node (LN) or vascular/neural structures[3,4]. As a factor for poor prognosis, TDs have attracted widespread attention in recent years[4,5]. A review published in 2017 confirmed that TDs were independently associated with lower overall and disease-free survival according to data available in the literature[4].

Clearly, TDs are not equivalent to LN metastasis (LNM) in terms of biology and prognosis. Among patients with LNM, the occurrence of TDs can lead to a worse prognosis[4,5], strongly indicating that their impact on prognosis is independent and additive. Therefore, TDs must be reported separately from LNM[6]. However, TDs and LNM can only be determined through pathological examinations of surgical specimens[7]. Presently, it is difficult to preoperatively differentiate TDs from LNM using computed tomography (CT).

Radiomics is a rapidly developing field of research that involves the extraction of numerous quantitative features from medical images. These features can capture characteristics of volume of interest (VOI), such as heterogeneity, and it may, alone or in combination with other data, be used to solve clinical problems[8]. Recently, some studies have reported the involvement of TDs in RC[6,9,10]. However, some previous studies did not focus on the differentiation of TDs from LNM[9,10], and Atre *et al*[6] used only texture analysis and lacked the construction and validation of a model. Therefore, we aimed to establish a CT-based radiomics model to preoperatively differentiate TDs from LNM in patients with RC.

MATERIALS AND METHODS

Patients

This retrospective study was approved by the institutional review board (No. 1159) of the authors' hospital. Given the retrospective design and use of anonymized patient data, requirements for informed consent were waived.

Patient data collected between September 2016 and September 2021 were reviewed by searching radiological and pathological databases. A total of 219 patients [single-positive, 112 male, 92 female; mean ± SD age, 60 ± 12 years (range, 32-92 years); double-positive, 6 male, 9 female; mean age, 60 ± 13 years (range, 37-83 years)] were enrolled. The inclusion criteria were as follows: Diagnosis of rectal adenocarcinoma on pathology; single positive result (*i.e.*, TDs^+ or LNM^+); and 15 randomly selected patients who were TDs^+LNM^+. The exclusion criteria were as follows: No peritumoral nodules with short-axis diameter > 3 mm on enhanced CT images (n = 22); incomplete clinical data, such as tumor markers (n = 36); patients who did not undergo surgery (n = 5); treatment before CT examination (n = 2); and poor-quality CT images (n = 4). Figure 1 shows the flow diagram of patient recruitment. Figure 2 shows the workflow of this radiomics study. Clinical characteristics, including age, gender, location of RC, tumor markers, pTN stage, extramural vascular invasion (EMVI), histological grade, and radiological features of the largest peritumoral nodule, are summarized in Table 1.

Reference standard

Pathological confirmation reports based on surgically resected specimens were obtained from the hospital's electronic medical database. From these reports, pathological information about the main tumor and peritumoral nodules (status and number of TDs and LNMs) were obtained.

Image acquisition and evaluation

Chest-abdomen-pelvis enhanced CT can detect not only the primary tumor but also suspected metastases. The main scanning parameters of CT are described in the Supplementary Table 1.

Two experiential radiologists reviewed the CT images and recorded the radiological features while blinded to clinical and pathological information. As shown in Table 1, the tumor location and radiological features of the largest peritumoral nodule, such as size, morphology, spiculation, and CT value, was confirmed by summarizing the results of these two radiologists (disagreements were resolved by consensus discussion).

Feature extraction and model-building

The reliability of the radiomics features was tested in twenty patients. The features with intra-/inter-class correlation coefficients (ICCs) > 0.75 were considered stable[11]. Thereafter, the radiologists independently segmented the main tumor and largest peritumoral nodule by manually drawing three-dimensional VOI (Figure 2). All images were resampled to pixel spacing of 1 mm in all three dimensions. Several transformation methods, such as wavelet filter and Laplace of Gaussian filter, were applied to the original images. PyRadiomics was used to extract features from the original and filtered images[12]. Figure 2 shows the types of the features. The correlation analysis was performed to remove redundant features. In detail, if the correlation coefficient between two features was > 0.4, the one with a lower coefficient was removed. Subsequently, three feature selection methods and three machine learning methods were tested to select the best performing classifier as the radiomics model (*i.e.*, Rad-score). Statistically significant factors from univariate and multivariate logistic regression analyses were used to develop the combined model.

Model evaluation

Receiver operating characteristic (ROC) curves of the models were performed to assess and compare their performance in identifying TDs^+LNM^- patients. Moreover, the performance of the models in diagnosing double-positive (*i.e.*, TDs^+LNM^+) patients were further evaluated by outlining all peritumoral nodules with short-axis diameters > 3 mm in the mixed group [TDs^+LNM^+ (n = 15); randomly selected single-positive patients from the training or validation sets (n = 15)]. If there were two different results (TD^+ or LNM^+) in all the outlined peritumoral nodules of each patient, double-positive patients were considered to be diagnosed correctly.

Statistical analysis

Statistical analyses were performed using SPSS (IBM Corporation, Armonk, NY, United States), Stata (StataCorp LP, College Station, TX, United States), and MedCalc software. In Table 1, continuous variables were analyzed using t-test or Mann-Whitney U test, and categorical variables were compared using the chi-squared test or Fisher's exact test. The areas under the curve (AUCs) of the models were compared using DeLong's test.

Table 1 Baseline and clinical characteristics of the included patients

Characteristics	TDs^+LNM^- (n = 89)	LNM^+TDs^- (n = 115)	P value	Training set (n = 163)	Validation set (n = 41)	P value
Age (mean ± SD, yr)	59 ± 12	61 ± 12	0.268	60 ± 12	60 ± 11	0.965
Gender (man/woman)	49/40	63/52	0.969	94/69	18/23	0.113
Location (middle-low/high)	65/24	74/41	0.187	107/56	32/9	0.128
Neoadjuvant therapy (+/-)	34/55	43/72	0.906	62/101	15/26	0.864
CEA (+/-) (positive ≥ 5 ng/mL)	42/47	43/72	0.159	75/88	10/31	0.012
CA19-9 (+/-) (positive ≥ 30 U/mL)	23/66	18/97	0.072	34/129	7/34	0.589
CA125 (+/-) (positive ≥ 24 U/mL)	13/76	14/101	0.611	21/142	6/35	0.767
pT stage (T1/T2/T3/T4)	0/9/70/10	4/12/93/6	0.063	4/17/127/15	0/4/36/1	0.894
pN stage (1a/1b/1c/2a/2b)	0/0/89/0/0	52/39/0/15/9	< 0.001	37/33/71/13/9	15/6/18/2/0	0.115
Histologic EMVI (+/-)	33/56	16/99	< 0.001	41/122	8/33	0.450
Histologic grade (G1/G2/G3)	1/63/25	0/76/39	0.299	0/113/50	1/26/14	0.901
Peritumoral nodule						
Shape (irregular/regular)	12/77	2/113	0.003	11/152	3/38	0.898
Spiculation (+/-)	7/82	2/113	0.077	7/156	2/39	0.871
Size (mm^2) (median)	72.7	41.2	< 0.001	54	43	0.886
CT value (HU)	61 ± 22	65 ± 23	0.258	64 ± 23	63 ± 23	0.858
Rad-score 1 (median)	0.71	0.39	< 0.001	0.44	0.71	0.002
Rad-score 2 (median)	0.89	0.13	< 0.001	0.39	0.62	0.561

Rad-score 1: Rad-score of the main tumor; Rad-score 2: Rad-score of the largest peritumoral nodule; CT: Computed tomography; TDs: Tumor deposits; LNM: Lymph node metastasis; CEA: Carcinoembryonic antigen; CA19-9: Carbohydrate antigen 19-9; CA125: Carbohydrate antigen 125; pT stage: Pathological T stage; pN stage: Pathological N stage; EMVI: Extramural vascular invasion.

RESULTS

Patient characteristics

A total of 219 patients with RC [TDs^+LNM^- (n = 89); LNM^+TDs^- (n = 115); TDs^+LNM^+ (n = 15)] were enrolled in this study. Clinical factors, including pathological N stage, pathological EMVI, and the size and shape of the largest peritumoral nodule, were found significantly different between the TDs^+LNM^- group and LNM^+TDs^- group. No statistical differences were found in age, gender, location of RC, tumor markers, pathological T stage, histological grade, and other features of the peritumoral nodule (spiculation and CT values) between the TDs^+LNM^- group and LNM^+TDs^- group. The patients were classified into a training set (n = 163) and a validation set (n = 41). Except for carcinoembryonic antigen (P = 0.012), no significant differences were found in the other clinical factors between the training and validation sets (Table 1).

Feature selection and model building

After evaluating the reliability, a large number of radiomics features remained (n = 1490 extracted from the tumor and 1252 from the largest peritumoral nodule), with ICCs of > 0.75. After excluding redundant radiomics features, we selected features using the L1-based method and established Rad-score using a logistic regression analysis. Features included in Rad-score are reported in the Supplementary Tables 2 and 3. Rad-score of the main tumor (Rad-score 1) and that of the largest peritumoral nodule (Rad-score 2) were independent risk factors for differentiating TDs from LNM [odds ratio (OR) = 3.267 and 14.396, respectively]. Regarding clinical factors, although the size and shape of the largest peritumoral nodule had significant difference between the TDs^+ group and LNM^+ group, they were all deleted in the logistic regression (P = 0.314 and 0.948, respectively; Table 2). Furthermore, a combined model integrating Rad-scores of 1 and 2 was established using the logistic regression.

Table 2 Univariate and multivariate logistic regression analysis

Variables	Univariate		Multivariate	
	OR	*P* value	OR	*P* value
Age	0.995	0.693	-	-
Gender	0.820	0.534	-	-
Location	0.819	0.282	-	-
CEA	1.546	0.171	-	-
CA19-9	1.613	0.217	-	-
CA125	1.503	0.384	-	-
Peritumoral nodule				
Shape	14.918	0.011	0.915	0.948
Spiculated (+/-)	8.400	0.051	-	-
Size (mm^2)	1.009	0.001	0.999	0.314
CT value (HU)	0.994	0.364	-	-
Rad-score 1	2.946	< 0.001	3.267	< 0.001
Rad-score 2	11.979	< 0.001	14.396	< 0.001

Rad-score 1: Rad-score of the main tumor; Rad-score 2: Rad-score of the largest peritumoral nodule; CEA: Carcinoembryonic antigen; CA19-9: Carbohydrate antigen 19-9; CA125: Carbohydrate antigen 125; CT: Computed tomography; OR: Odds ratio.

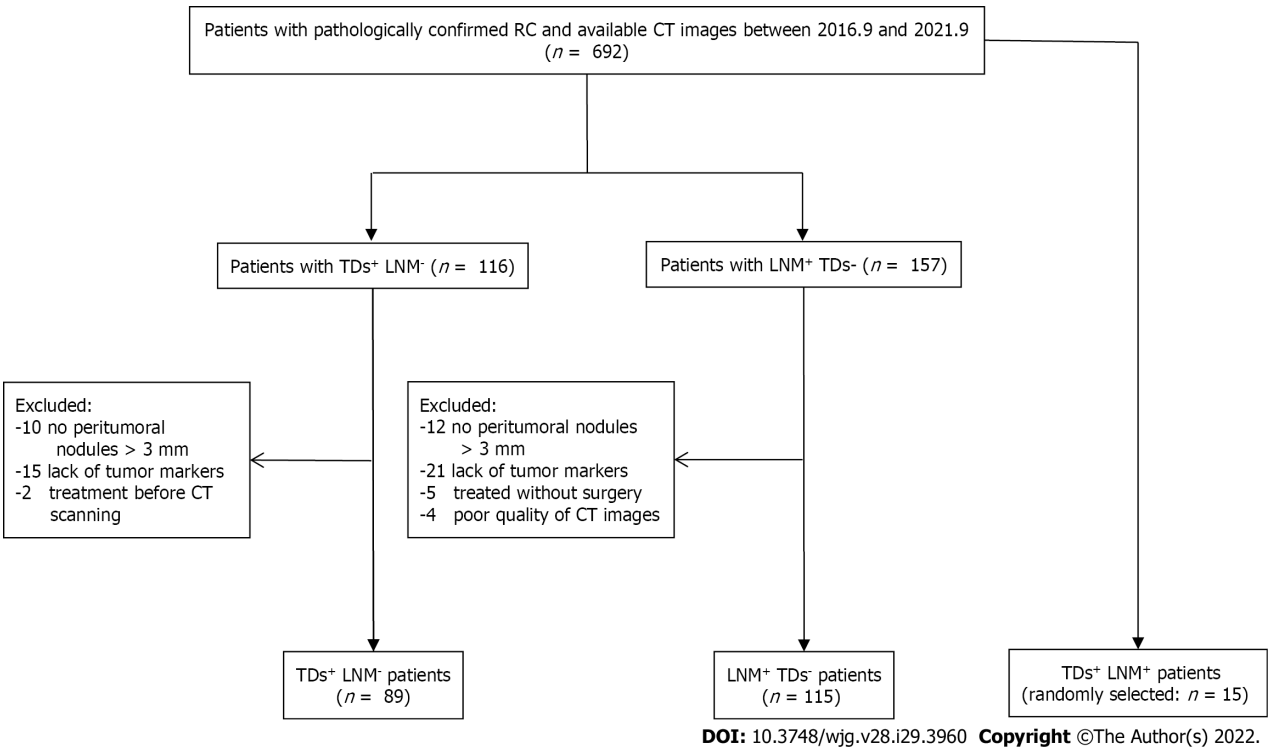


Figure 1 Flowchart of patients' recruitment pathway. RC: Rectal cancer; CT: Computed tomography; TDs: Tumor deposits; LNM: Lymph node metastasis.

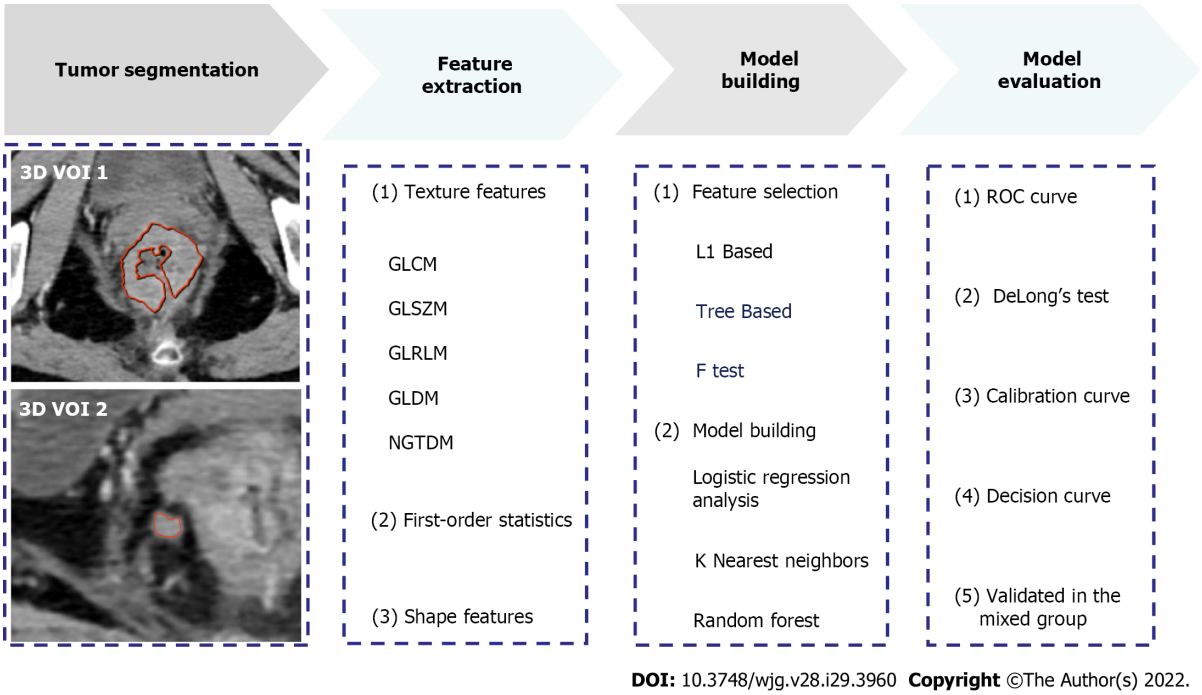
Model evaluation

For classification results, the AUC for Rad-score 1 was 0.768 [95% confidence interval (CI): 0.695-0.830] in the training set and 0.700 (95%CI: 0.537-0.833) in the validation set. Rad-score 2 achieved improved performance, with an AUC of 0.940 (95%CI: 0.892-0.971) in the training set and 0.918 (95%CI: 0.789-0.981) in the validation set. The combined model (Rad-scores 1 + 2) had similar AUCs to Rad-score 2 in both the training and validation sets, as shown in Table 3 and Figure 3A and B. Thus, Rad-score 2 (Rad-

Table 3 Comparisons of the models in the training, validation, and mixed groups

	Training set				Validation set				Mixed group		
	AUC	SEN	SPE	*P* value	AUC	SEN	SPE	*P* value	SEN	SPE	Accuracy
Rad-score 1	0.768 (95%CI: 0.695-0.830)	66.2%	70.7%	< 0.001	0.700 (95%CI: 0.537-0.833)	77.8%	47.8%	0.032	-	-	-
Combined model	0.955 (95%CI: 0.910-0.981)	83.1%	88.0%	0.134	0.930 (95%CI: 0.805-0.986)	94.4%	82.6%	0.594	66.6%	73.3%	70.0%
Rad-score 2	0.940 (95%CI: 0.892-0.971)	83.1%	84.8%		0.918 (95%CI: 0.789-0.981)	83.3%	82.6%		73.3%	66.6%	70.0%

The mixed group consisted of 15 double-positive (TDs^+LNM^+) and 15 single-positive (11 TDs^+LNM^- and 4 LNM^+TDs^-) patients. *P* value: compared with Rad-score 2 by DeLong's test. Rad-score 1: Rad-score of the main tumor; Rad-score 2: Rad-score of the largest peritumoral nodule; TDs: Tumor deposits; LNM: Lymph node metastasis; AUC: Area under the curve; SEN: Sensitivity; SPE: Specificity.



DOI: 10.3748/wjg.v28.i29.3960 **Copyright** ©The Author(s) 2022.

Figure 2 Radiomics workflow. 3D VOI: Three-dimensional volume of interest; GLCM: Gray level co-occurrence matrix; GLSZM: Gray level size zone matrix; GLRLM: Gray level run length matrix; GLDM: Gray level dependence matrix; NGTDM: Neighbouring gray tone difference matrix; ROC: Receiver operating characteristic curve.

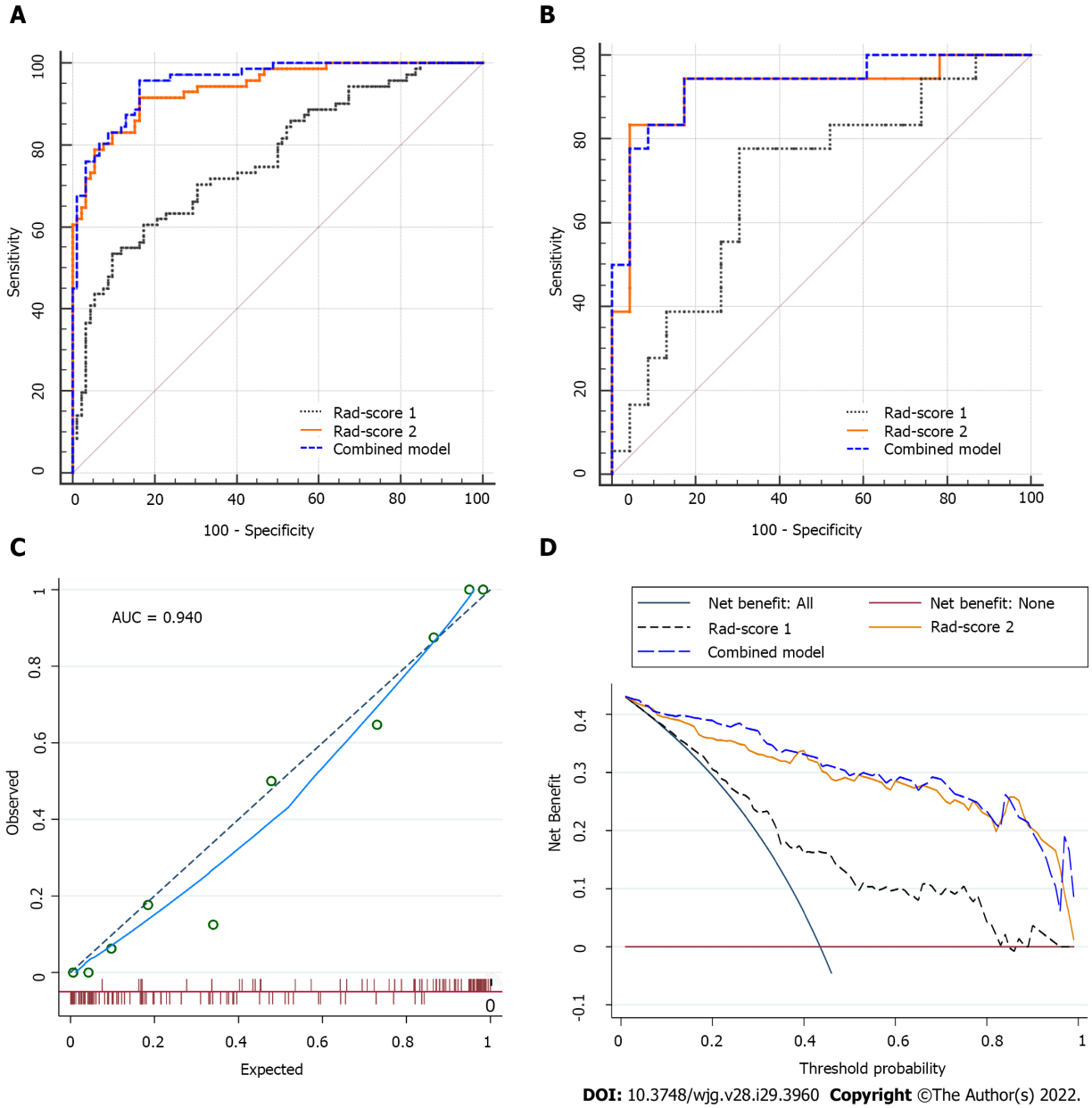
score of the largest peritumoral nodule) was used as the final model owing to its simplicity.

In the calibration curve for Rad-score 2, the solid line was close to the reference line (dotted line), indicating that Rad-score 2 demonstrated good agreement between the prediction (x-axis) and observation (y-axis) (Figure 3C). However, Rad-score 2 still overestimated the actual risk for TDs^+ (approximately 10%, at most). A decision curve was constructed to evaluate the clinical utility of Rad-score 2 in differentiating TDs from LNM. The net benefit can be measured along the y-axis. Figure 3D shows that Rad-score 2 yielded more benefit than "treat all", "treat none", and Rad-score 1. A case example is shown in Figure 4.

Moreover, all peritumoral nodules with short-axis diameter > 3 mm were delineated in each patient in the mixed group [TDs^+LNM^+ (n = 15); single-positive (n = 15)] to evaluate the performance of the models in predicting double-positive (*i.e.*, TDs^+LNM^+) patients. Of the 30 patients, 134 peritumoral nodules were delineated. Rad-score 2 had a moderate accuracy of 70% (sensitivity, 73.3%; specificity, 66.6%). Because the combined model had the same accuracy of 70% as Rad-score 2, it confirmed the use of Rad-score 2 as the final model.

Subgroup analysis

In view of the prognostic difference between the upper and middle-lower RC[13], we performed a subgroup analysis indicating that Rad-score 2 had high AUCs in both the upper [0.941 (95%CI: 0.853-



DOI: 10.3748/wjg.v28.i29.3960 **Copyright** ©The Author(s) 2022.

Figure 3 Comparisons of the receiver operating characteristic curves, and fit and usefulness evaluation of Rad-score 2. A: In the training set: Area under the curve (AUC) = 0.768 for Rad-score 1, 0.955 for the combined model, and 0.940 for Rad-score 2; B: In the validation set: AUC = 0.700 for Rad-score 1, 0.930 for the combined model, and 0.918 for Rad-score 2; C: The calibration curve of Rad-score 2 shows good agreement between the predicted and observed risks in the training cohort; D: The decision curve demonstrates that Rad-score 2 obtains more benefit than "treat all", "treat none", and Rad-score 1. Rad-score 1: Rad-score of the main tumor; Rad-score 2: Rad-score of the largest peritumoral nodule; AUC: Area under the curve.

0.984)] and middle-lower [0.931 (95%CI: 0.875-0.967)] RC groups. For patients receiving neoadjuvant chemoradiotherapy (nCRT), Rad-score 2 also had high AUCs, as shown in Table 4. In these subgroup analyses, Rad-score 2 outperformed Rad-score 1.

The American Joint Committee on Cancer (AJCC) tumor-node-metastasis (TNM) staging system has not correlated a higher number of TDs with staging, unlike LNs (*e.g.*, N1, 1-3 and N2, ≥ 4 regional LNs) [14]. Several authors have found that patients with ≥ 3 TDs have a significantly worse prognosis than those with 1-2 TDs[15]. However, in this study, the values of Rad-scores 1 and 2 were not significantly different between the ≥ 3 TDs group and the 1-2 TDs group (P = 0.838 for Rad-score 1, and P = 0.309 for Rad-score 2) (Table 4).

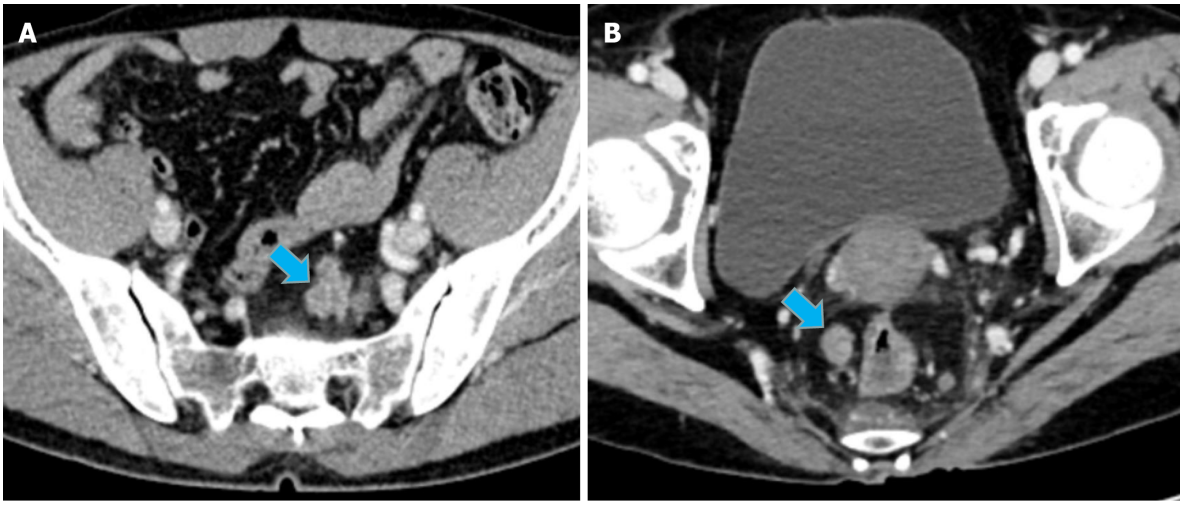
DISCUSSION

Our study established a new radiomics signature (Rad-score 2) based on 11 features extracted from the largest peritumoral nodule, demonstrating the potential for preoperatively differentiating TDs from

Table 4 Subgroup analyses of the models in single-positive patients

	Rad-score 1			Rad-score 2			*P* value
Subgroups	**AUC**	**SEN (%)**	**SPE (%)**	**AUC**	**SEN (%)**	**SPE (%)**	
nCRT							
With (n = 77)	0.740 (95%CI: 0.628-0.833)	73.5%	74.4%	0.897 (95%CI: 0.806-0.954)	73.5%	90.7%	0.014
Without (n = 127)	0.753 (95%CI: 0.668-0.825)	60%	86.1%	0.957 (95%CI: 0.905-0.985)	89.1%	93.1%	< 0.001
Location							
Mid-low (n = 139)	0.782 (95%CI: 0.704-0.848)	75.4%	62.2%	0.931 (95%CI: 0.875-0.967)	86.2%	82.4%	< 0.001
High (n = 65)	0.643 (95%CI: 0.515-0.758)	54.2%	73.2%	0.941 (95%CI: 0.853-0.984)	83.3%	85.4%	< 0.001
Number of TDs	1-2 (n = 50)	≥ 3 (n = 39)	P = 0.838	1-2 (n = 50)	≥ 3 (n = 39)	P = 0.309	
Value	0.64 ± 0.24	0.65 ± 0.22		0.83 ± 0.22	0.77 ± 0.26		

Rad-score 1: Rad-score of the main tumor; Rad-score 2: Rad-score of the largest peritumoral nodule; TDs: Tumor deposits; AUC: Area under the curve; SEN: Sensitivity; SPE: Specificity; nCRT: Neoadjuvant chemoradiotherapy.



DOI: 10.3748/wjg.v28.i29.3960 **Copyright** ©The Author(s) 2022.

Figure 4 Case presentation. A: A 56-year-old man with upper RC, the nodule of TDs (size: 24 mm × 16 mm) had an irregular shape; B: A 44-year-old man with lower RC, the nodule of TDs (size: 14 mm × 11 mm) had a regular oval shape. It is difficult to distinguish TDs and LNM from conventional imaging findings. For these two patients, Rad-score of the largest peritumoral nodule achieved correct diagnosis (values = 0.98 and 0.97, respectively). RC: Rectal cancer; TDs: Tumor deposits; LNM: Lymph node metastasis.

LNM. Moreover, Rad-score 2 outperformed Rad-score 1 (based on the main tumor) in this field [0.918 *vs* 0.700 (P = 0.032) in the validation set]. However, this model had a minor overestimation of TDs^+ probability for most of the included patients.

The 8th AJCC TNM staging system incorporates a N1c category for RC patients with TDs^+LNM^-. The N1c category represents 5% to 10% of RC with TDs (TDs^+LNM^- and TDs^+LNM^+) observed in approximately 20% of all rectal adenocarcinomas[5]. Although many authors have speculated on the origin of TDs, the phenomenon remains unclear. However, some authors have found that a significant proportion of TDs cannot be traced back to the LN[16]. Goldstein *et al*[17] reported that, after performing experiments on deeper sections, most TDs (up to 90%) exhibited signs of > 1 origin. Currently, the only method to determine the status of peritumoral nodules is the histopathologic examination of the resected specimens. The preoperative differentiation of TDs and LNM facilitates the design of individualized treatment strategies and evaluation of prognosis.

Unlike CT and magnetic resonance imaging (MRI), radiomics may solve clinical problems by extracting an enormous number of features which can quantify invisible differences in tissues for the human eye. Several radiomics studies investigating TDs[6,9,10] and LNM[18-21] have been reported in

RC. There were, however, some differences in our study. First, in contrast to most previous models (predicting single factor positive TDs[9,10] or LNM[18-21]), our model can be used to predict the status of both TDs and LNM. When a peritumoral nodule with a short-axis diameter > 3 mm was found on CT images, we could then use our model to predict the classification of this nodule (TDs^+ or LNM^+) and further identify the patient as TDs^+ only, LNM^+ only, or double positive. Second, we delineated the main tumor and the largest peritumoral nodule, while previous authors delineated the tumor and whole peritumoral fat[10] or only the main tumor[9]. Third, our study included a larger sample size of TDs^+ patients (n = 89) and had a higher AUC (0.918 in the validation set) than those reported by Chen *et al*[10] [TDs^+ (n = 40); AUC 0.795], Yang *et al*[9] [TDs^+ (n = 23); AUC 0.820], and Atre *et al*[6] [TDs^+ (n = 25); AUC 0.810]. Finally, although Atre *et al*[6] could also predict both TDs^+ and LNM^+, they only performed texture analysis, which was clearly different from the analysis in our study.

Notably, double-positive patients had a worse prognosis than those with TDs^+ or LNM^+ only. One positive LN 5-year survival rate was 62% without TDs, *vs* 44% with TDs[4]. Thus, preoperative diagnosis of double-positive patients is of great clinical significance. However, the performance of the model decreased (accuracy, 70%) when used to diagnose double-positive patients. We speculated that this may be related to the following factors. First, we established a model based on the largest peritumoral nodule. When diagnosing double-positive patients, we used all peritumoral nodules (> 3 mm). Thus, the mean size in the mixed group was smaller than that in the training set. Second, the sample size of the mixed group was small. Third, among the double-positive patients, some LNMs were incorrectly evaluated as TDs. In these lesions, the value of wavelet-HLH_firstorder_Median (a radiomics feature) decreased. In the future, we will include a larger sample to improve the applicability of the model in double-positive patients.

Nevertheless, the nature of TDs after neoadjuvant therapy remains unclear. Regarding the 77 patients who underwent nCRT in our study, the AUC for the Rad-score 2 did not decrease significantly (0.897), indicating that the model was stable. Regarding the tumor location, the AUCs of the model were also similar between the upper and middle-lower RC. Our model failed to differentiate between groups with ≥ 3 TDs and 1-2 TDs (P = 0.309).

Our study had several limitations. Firstly, because this was a retrospective study, selection bias may have been introduced. Secondly, to directly compare peritumoral nodules, we especially selected a sample comprising TDs^+LNM^- and LNM^+TDs^- and outlined the largest peritumoral nodule. However, it was still possible to identify benign peritumoral nodules. Thirdly, this was a single-center analysis. In the future, it will be necessary to conduct an external validation to confirm the versatility of the model.

CONCLUSION

A radiomics signature based on the largest peritumoral nodule is established in this article. This signature can facilitate the preoperative differentiation of TDs from LNM.

ARTICLE HIGHLIGHTS

Research background

Tumor deposits (TDs) are not equivalent to lymph node (LN) metastasis (LNM) but have become independent adverse prognostic factors in patients with rectal cancer (RC). If TDs can be differentiated from LNM before therapy, individualized treatment and patient prognosis may greatly improve.

Research motivation

Currently, preoperative differentiation of TDs and LNM can be challenging.

Research objectives

To establish a radiomics model for preoperatively differentiating between TDs and LNM in patients with RC.

Research methods

The present study retrospectively enrolled 219 patients with RC [TDs^+LNM^- (n = 89); LNM^+TDs^- (n = 115); TDs^+LNM^+ (n = 15)] from a single center between September 2016 and September 2021. Single-positive patients (TDs^+LNM^- and LNM^+TDs^-) were classified into training (n = 163) and validation (n = 41) sets. Rad-scores were established based on the main tumor and largest peritumoral nodule. After validating Rad-score, we further evaluated its performance for diagnosing double-positive patients (*i.e.*, TDs^+LNM^+) by outlining all peritumoral nodules with diameters > 3 mm (short axis).

Research results

Rad-score 1 (radiomics signature of the main tumor) had an area under the curve (AUC) of 0.768 on the training dataset and 0.700 on the validation dataset. Rad-score 2 (radiomics signature of the largest peritumoral nodule) had a higher AUC (training set: 0.940; validation set: 0.918) than Rad-score 1. For the diagnosis of double-positive patients in the mixed group [TDs^+LNM^+ (n = 15); single-positive (n = 15)], Rad-score 2 demonstrated moderate performance (sensitivity, 73.3%; specificity, 66.6%; and accuracy, 70%).

Research conclusions

The radiomics signature of the largest peritumoral nodule could provide individualized preoperative differentiation of TDs and LNM. Moreover, it was helpful in diagnosing patients who were TDs^+LNM^+.

Research perspectives

To improve the model, surgeons, radiologists, and pathologists should collaborate through prospective research to achieve node-to-node correspondence between CT images and pathological examinations in the future.

FOOTNOTES

Author contributions: Song B designed the research; Zhang YC and Jin YM collected the data; Li M, Xu JX, and Huang CC analyzed the data; Zhang YC and Li M wrote the paper; all authors have read and approved the final manuscript.

Institutional review board statement: This study was reviewed and approved by the Ethics Committee of West China Hospital of Sichuan University, No. 1159.

Informed consent statement: Patients were not required to give informed consent to the study because the analysis used anonymous clinical data that were obtained after each patient agreed to treatment by written consent.

Conflict-of-interest statement: Authors Jing-Xu Xu and Chen-Cui Huang are employed by the company Beijing Deepwise & League of PHD Technology Co., Ltd; the remaining authors declare no conflicts-of-interest related to this article.

Data sharing statement: No additional data are available.

Open-Access: This article is an open-access article that was selected by an in-house editor and fully peer-reviewed by external reviewers. It is distributed in accordance with the Creative Commons Attribution NonCommercial (CC BY-NC 4.0) license, which permits others to distribute, remix, adapt, build upon this work non-commercially, and license their derivative works on different terms, provided the original work is properly cited and the use is non-commercial. See: https://creativecommons.org/Licenses/by-nc/4.0/

Country/Territory of origin: China

ORCID number: Yong-Chang Zhang 0000-0003-0402-2525; Mou Li 0000-0002-7101-5942; Yu-Mei Jin 0000-0001-6606-8049; Jing-Xu Xu 0000-0003-1079-7378; Chen-Cui Huang 0000-0003-3307-6872; Bin Song 0000-0002-7269-2101.

S-Editor: Chen YL
L-Editor: A
P-Editor: Chen YL

REFERENCES

1 **Sung H**, Ferlay J, Siegel RL, Laversanne M, Soerjomataram I, Jemal A, Bray F. Global Cancer Statistics 2020: GLOBOCAN Estimates of Incidence and Mortality Worldwide for 36 Cancers in 185 Countries. *CA Cancer J Clin* 2021; **71**: 209-249 [PMID: 33538338 DOI: 10.3322/caac.21660]
2 **Bailey CE**, Hu CY, You YN, Bednarski BK, Rodriguez-Bigas MA, Skibber JM, Cantor SB, Chang GJ. Increasing disparities in the age-related incidences of colon and rectal cancers in the United States, 1975-2010. *JAMA Surg* 2015; **150**: 17-22 [PMID: 25372703 DOI: 10.1001/jamasurg.2014.1756]
3 **Maguire A**, Sheahan K. Controversies in the pathological assessment of colorectal cancer. *World J Gastroenterol* 2014; **20**: 9850-9861 [PMID: 25110416 DOI: 10.3748/wjg.v20.i29.9850]
4 **Lord AC**, D'Souza N, Pucher PH, Moran BJ, Abulafi AM, Wotherspoon A, Rasheed S, Brown G. Significance of extranodal tumour deposits in colorectal cancer: A systematic review and meta-analysis. *Eur J Cancer* 2017; **82**: 92-102 [PMID: 28651160 DOI: 10.1016/j.ejca.2017.05.027]

5 **Benoit O**, Svrcek M, Creavin B, Bouquot M, Challine A, Chafai N, Debove C, Voron T, Parc Y, Lefevre JH. Prognostic value of tumor deposits in rectal cancer: A monocentric series of 505 patients. *J Surg Oncol* 2020; **122**: 1481-1489 [PMID: 32789859 DOI: 10.1002/jso.26165]

6 **Atre ID**, Eurboonyanun K, Noda Y, Parakh A, O'Shea A, Lahoud RM, Sell NM, Kunitake H, Harisinghani MG. Utility of texture analysis on T2-weighted MR for differentiating tumor deposits from mesorectal nodes in rectal cancer patients, in a retrospective cohort. *Abdom Radiol (NY)* 2021; **46**: 459-468 [PMID: 32700214 DOI: 10.1007/s00261-020-02653-w]

7 **Jin M**, Frankel WL. Lymph Node Metastasis in Colorectal Cancer. *Surg Oncol Clin N Am* 2018; **27**: 401-412 [PMID: 29496097 DOI: 10.1016/j.soc.2017.11.011]

8 **Mayerhoefer ME**, Materka A, Langs G, Häggström I, Szczypiński P, Gibbs P, Cook G. Introduction to Radiomics. *J Nucl Med* 2020; **61**: 488-495 [PMID: 32060219 DOI: 10.2967/jnumed.118.222893]

9 **Yang YS**, Feng F, Qiu YJ, Zheng GH, Ge YQ, Wang YT. High-resolution MRI-based radiomics analysis to predict lymph node metastasis and tumor deposits respectively in rectal cancer. *Abdom Radiol (NY)* 2021; **46**: 873-884 [PMID: 32940755 DOI: 10.1007/s00261-020-02733-x]

10 **Chen LD**, Li W, Xian MF, Zheng X, Lin Y, Liu BX, Lin MX, Li X, Zheng YL, Xie XY, Lu MD, Kuang M, Xu JB, Wang W. Preoperative prediction of tumour deposits in rectal cancer by an artificial neural network-based US radiomics model. *Eur Radiol* 2020; **30**: 1969-1979 [PMID: 31828415 DOI: 10.1007/s00330-019-06558-1]

11 **Benchoufi M**, Matzner-Lober E, Molinari N, Jannot AS, Soyer P. Interobserver agreement issues in radiology. *Diagn Interv Imaging* 2020; **101**: 639-641 [PMID: 32958434 DOI: 10.1016/j.diii.2020.09.001]

12 **van Griethuysen JJM**, Fedorov A, Parmar C, Hosny A, Aucoin N, Narayan V, Beets-Tan RGH, Fillion-Robin JC, Pieper S, Aerts HJWL. Computational Radiomics System to Decode the Radiographic Phenotype. *Cancer Res* 2017; **77**: e104-e107 [PMID: 29092951 DOI: 10.1158/0008-5472.CAN-17-0339]

13 **Clancy C**, Flanagan M, Marinello F, O'Neill BD, McNamara D, Burke JP. Comparative Oncologic Outcomes of Upper Third Rectal Cancers: A Meta-analysis. *Clin Colorectal Cancer* 2019; **18**: e361-e367 [PMID: 31445919 DOI: 10.1016/j.clcc.2019.07.004]

14 **Amin MB**, Greene FL, Edge SB, Compton CC, Gershenwald JE, Brookland RK, Meyer L, Gress DM, Byrd DR, Winchester DP. The Eighth Edition AJCC Cancer Staging Manual: Continuing to build a bridge from a population-based to a more "personalized" approach to cancer staging. *CA Cancer J Clin* 2017; **67**: 93-99 [PMID: 28094848 DOI: 10.3322/caac.21388]

15 **Puppa G**, Maisonneuve P, Sonzogni A, Masullo M, Capelli P, Chilosi M, Menestrina F, Viale G, Pelosi G. Pathological assessment of pericolonic tumor deposits in advanced colonic carcinoma: relevance to prognosis and tumor staging. *Mod Pathol* 2007; **20**: 843-855 [PMID: 17491597 DOI: 10.1038/modpathol.3800791]

16 **Wünsch K**, Müller J, Jähnig H, Herrmann RA, Arnholdt HM, Märkl B. Shape is not associated with the origin of pericolonic tumor deposits. *Am J Clin Pathol* 2010; **133**: 388-394 [PMID: 20154277 DOI: 10.1309/AJCPAWOLX7ADZQ2K]

17 **Goldstein NS**, Turner JR. Pericolonic tumor deposits in patients with T3N+MO colon adenocarcinomas: markers of reduced disease free survival and intra-abdominal metastases and their implications for TNM classification. *Cancer* 2000; **88**: 2228-2238 [PMID: 10820343]

18 **Chen LD**, Liang JY, Wu H, Wang Z, Li SR, Li W, Zhang XH, Chen JH, Ye JN, Li X, Xie XY, Lu MD, Kuang M, Xu JB, Wang W. Multiparametric radiomics improve prediction of lymph node metastasis of rectal cancer compared with conventional radiomics. *Life Sci* 2018; **208**: 55-63 [PMID: 29990485 DOI: 10.1016/j.lfs.2018.07.007]

19 **Zhou X**, Yi Y, Liu Z, Zhou Z, Lai B, Sun K, Li L, Huang L, Feng Y, Cao W, Tian J. Radiomics-Based Preoperative Prediction of Lymph Node Status Following Neoadjuvant Therapy in Locally Advanced Rectal Cancer. *Front Oncol* 2020; **10**: 604 [PMID: 32477930 DOI: 10.3389/fonc.2020.00604]

20 **Li J**, Zhou Y, Wang X, Zhou M, Chen X, Luan K. An MRI-based multi-objective radiomics model predicts lymph node status in patients with rectal cancer. *Abdom Radiol (NY)* 2021; **46**: 1816-1824 [PMID: 33241428 DOI: 10.1007/s00261-020-02863-2]

21 **Zhu H**, Zhang X, Li X, Shi Y, Zhu H, Sun Y. Prediction of pathological nodal stage of locally advanced rectal cancer by collective features of multiple lymph nodes in magnetic resonance images before and after neoadjuvant chemoradiotherapy. *Chin J Cancer Res* 2019; **31**: 984-992 [PMID: 31949400 DOI: 10.21147/j.issn.1000-9604.2019.06.14]

World Journal of Gastroenterology

Submit a Manuscript: https://www.f6publishing.com

World J Gastroenterol 2022 August 7; 28(29): 3971-3980

DOI: 10.3748/wjg.v28.i29.3971

ISSN 1007-9327 (print) ISSN 2219-2840 (online)

ORIGINAL ARTICLE

Retrospective Study

Effects of microwave ablation on serum Golgi protein 73 in patients with primary liver cancer

Zheng-Ju Xu, Mei-Juan Wei, Xiao-Man Zhang, Hui-Guo Liu, Jin-Piao Wu, Jin-Fa Huang, Yong-Fei Li, Zhi-Jie Huang, Yan-Yan Yan

Specialty type: Gastroenterology and hepatology

Provenance and peer review: Unsolicited article; Externally peer reviewed.

Peer-review model: Single blind

Peer-review report's scientific quality classification

Grade A (Excellent): 0
Grade B (Very good): 0
Grade C (Good): C, C, C
Grade D (Fair): 0
Grade E (Poor): 0

P-Reviewer: Koganti S, United States; Sultana N, Bangladesh; Zhang X, United States

Received: February 21, 2022
Peer-review started: February 21, 2022
First decision: April 16, 2022
Revised: April 30, 2022
Accepted: July 5, 2022
Article in press: July 5, 2022
Published online: August 7, 2022

Zheng-Ju Xu, Hui-Guo Liu, Jin-Piao Wu, Jin-Fa Huang, Yong-Fei Li, Zhi-Jie Huang, Yan-Yan Yan, The Liver Disease Center, The 910th Hospital of the PLA Joint Logistics Support Force, Quanzhou 362000, Fujian Province, China

Mei-Juan Wei, Central Laboratory, Decheng Hospital, Quanzhou 362104, Fujian Province, China

Xiao-Man Zhang, Central Laboratory of Clinical Hepatology, The 910th Hospital of the PLA Joint Logistics Support Force, Quanzhou 362000, Fujian Province, China

Corresponding author: Zheng-Ju Xu, MD, Chief Doctor, The Liver Disease Center, The 910th Hospital of the PLA Joint Logistics Support Force, No. 180 Huayuan Road, Fengze District, Quanzhou 362000, Fujian Province, China. h180@163.com

Abstract

BACKGROUND

Microwave ablation (MWA) is an effective treatment option for patients with primary liver cancer. However, it has been reported that the MWA procedure induces a hepatic inflammatory response and injury, which may negatively affect the efficacy of MWA. As such, the discovery of reliable markers to monitor the patient's response to MWA is needed. Golgi protein 73 (GP73) has been shown to be associated with chronic liver disease. To date, the potential value of serum GP73 in the dynamic monitoring during MWA of liver cancer remains unclear.

AIM

To examine the effects of MWA on the serum levels of GP73 in patients with primary liver cancer.

METHODS

A total of 150 primary liver cancer patients with a single small lesion (≤ 3 cm in diameter) were retrospectively enrolled spanning the period between January 2016 and October 2018. All of the patients received MWA for the treatment of primary liver cancer. Serum GP73, alpha-fetoprotein (AFP), and widely used liver biochemical indicators [serum albumin, total bilirubin (TBIL), alanine aminotransferase (ALT), and aspartate aminotransferase (AST)] were compared before MWA and at different time points, including 1, 2, and 4 wk following the ablation procedure.

RESULTS

Complete tumor ablation was achieved in 95.33% of the patients at 1 mo after MWA. The 1-, 2-, and 3-year disease-free survival rates were 74.67%, 59.33%, and 54.00%, respectively. The serum AFP levels were significantly decreased at 1, 2, and 4 wk after MWA; they returned to the normal range at 12 wk after MWA; and they remained stable thereafter during follow-up in those cases without recurrence. In contrast, the serum GP73 levels were significantly increased at 1 and 2 wk after MWA. The serum GP73 levels reached the peak at 2 wk after MWA, started to decline after hepatoprotective treatment with glycyrrhizin and reduced glutathione, and returned to the pretreatment levels at 12 and 24 wk after MWA. Notably, the changes of serum GP73 in response to MWA were similar to those of TBIL, ALT, and AST.

CONCLUSION

Serum GP73 is markedly increased in response to MWA of liver cancer. Thus, serum GP73 holds potential as a marker to monitor MWA-induced inflammatory liver injury in need of amelioration.

Key Words: Liver cancer; Microwave ablation; Ablation therapy; Golgi protein 73; Biomarker; Liver injury

©The Author(s) 2022. Published by Baishideng Publishing Group Inc. All rights reserved.

Core Tip: Microwave ablation (MWA) has become an effective modality of cancer treatment, including primary liver cancer. However, the MWA procedure induces a hepatic inflammatory response and injury, which may diminish the efficacy of MWA. Therefore, the discovery of reliable markers to monitor the response to MWA is still needed. In this study, we examined the effects of MWA on the serum levels of Golgi protein 73 (GP73). The resulting data suggest that serum GP73 is markedly elevated in response to the MWA procedure. Importantly, our novel findings may have the clinical implication that serum GP73 could be a potential marker to monitor MWA-induced inflammatory liver injury.

Citation: Xu ZJ, Wei MJ, Zhang XM, Liu HG, Wu JP, Huang JF, Li YF, Huang ZJ, Yan YY. Effects of microwave ablation on serum Golgi protein 73 in patients with primary liver cancer. *World J Gastroenterol* 2022; 28(29): 3971-3980

URL: https://www.wjgnet.com/1007-9327/full/v28/i29/3971.htm

DOI: https://dx.doi.org/10.3748/wjg.v28.i29.3971

INTRODUCTION

Liver cancer is one of the most common malignant tumors throughout the world, and its incidence is relatively high in Asian countries and Pacific islands[1,2]. In China, nearly 500000 cases of primary liver cancer are newly diagnosed annually, accounting for approximately 50% of all new primary liver cancer cases worldwide, mainly due to a particularly high prevalence of hepatitis B virus (HBV) infection[1-3]. Primary liver cancer mainly includes hepatocellular carcinoma (HCC), intrahepatic cholangiocarcinoma (ICC), and combined hepatocellular-cholangiocarcinoma, of which HCC makes up 75%-85% and ICC accounts for 10%-15% of all primary liver cancer cases[4]. For patients with primary liver cancer at an early stage, ablation therapy has been shown to be an effective treatment option. Microwave ablation (MWA) is an ablation modality that destroys cancer cells by using heat from microwave energy. Over the last decade, extensive studies have shown that MWA is effective and safe for treating small primary liver cancer, which is usually less than 3 cm in diameter[5-9]. However, it has been reported that the MWA procedure induces a hepatic inflammatory response and injury, which may negatively affect its efficacy[10]. Therefore, the discovery of reliable markers to monitor the patient's response to MWA is still needed.

Golgi protein 73 (GP73) is a transmembrane glycoprotein with a molecular weight of 73 kDa. Under normal conditions in the liver, GP73 is mainly expressed in the epithelial cells of the bile duct, while its expression in hepatocytes is considerably lower[11]. Previous studies have shown that hepatic GP73 expression is upregulated in a variety of acute and chronic liver diseases[12]. Our previous study also has demonstrated that GP73 is expressed in the cytoplasm of hepatocytes, but not in the infiltrating inflammatory cells in patients with chronic HBV infection, and that changes in the hepatic and serum levels of GP73 are positively correlated with hepatic necroinflammatory activity in CHB patients[13]. Few hepatocytes expressed GP73, and the serum GP73 levels were low in patients with chronic HBV infection but without indications of liver injury. However, once hepatic necrosis was triggered, the affected hepatocytes started to release more GP73 into the blood, resulting in elevated hepatic and

serum levels of GP73. Our previous study also found that elevated serum GP73 levels were positively associated with a higher hepatic necroinflammatory activity grade[14]. To date, the potential value of serum GP73 in the dynamic monitoring and assessment of patient response to MWA during the treatment of liver cancer remains to be further investigated.

Intrigued by our previous findings, we aimed to examine the effects of MWA of liver cancer on the serum GP73 levels before and at different time points after ablation therapy in patients with primary liver cancer. The findings may help to identify potential markers to be used in the dynamic monitoring of the response to MWA for the treatment of primary liver cancer.

MATERIALS AND METHODS

Study subjects

A total of 150 patients with primary liver cancer were retrospectively enrolled from the Liver Disease Center at the 910th Hospital of the PLA Logistics Support Force between January 2016 and October 2018. All of the study subjects were diagnosed as having primary liver cancer, in accordance with the Guidelines for the Diagnosis and Treatment of Primary Liver Cancer in China (2019 edition) issued by the National Health and Health Commission of the People's Republic of China[15], and fulfilled the following inclusion criteria: (1) Age > 18 years old; (2) A single lesion ≤ 3 cm in diameter; and (3) No invasion into the portal vein, hepatic vein, or extrahepatic distant metastasis on imaging examinations [*e.g.*, color Doppler ultrasound, computed tomography (CT), or magnetic resonance imaging (MRI)]. All of the 150 patients with primary liver cancer had a history of HBV infection. Chronic hepatitis B (CHB) and CHB-associated liver cirrhosis were diagnosed in accordance with the diagnostic criteria as reported in the Guidelines of Prevention and Treatment for Chronic Hepatitis B (2019 version)[16]. The exclusion criteria were as follows: (1) Age ≤ 18 years old; (2) The number of lesions ≥ 2 or the size > 3 cm in diameter; (3) The tumor invaded adjacent organs or extrahepatic metastases occurred; (4) Child–Pugh score of grade C; (5) Uncorrectable coagulation dysfunction; (6) Complicated with active infection; (7) Massive ascites and cachexia; (8) Major organ failure (heart, brain, lung, kidney, or other important organs); (9) Eastern Cooperative Oncology Group (ECOG) score > 2; and (10) Disorders of consciousness or inability to cooperate with medical treatments. Among the 150 patients with primary liver cancer, 143 patients with space-occupying lesions with typical imaging features of liver cancer did not receive a liver biopsy, and the remaining 7 patients underwent a liver biopsy and had a pathological diagnosis of primary HCC. In terms of the status of the background liver, 115 patients had background liver cirrhosis, and 35 patients showed no clinical signs of liver cirrhosis.

This study was approved by the Ethics Committee of the 910th Hospital of the PLA Joint Logistics Support Force (Quanzhou, Fujian Province, China). All of the patients provided a signed informed consent.

MWA of liver cancer

All of the patients refused liver resection surgery and were willing to undergo MWA of liver cancer on a microwave therapeutic apparatus (Nanjing, Jiangsu Province, China). The procedure was performed under the guidance of CT or color Doppler ultrasound. The power and ablation time were designed for each patient based on the size of the liver cancer and the surrounding tissues. The ablation zone size was 0.5-1 cm to the margin of the tumor.

Effectiveness of MWA and follow-up

Enhanced CT or MRI examinations were performed on the patients at 1 mo after MWA to determine the complete or partial tumor ablation rate. The patients were followed up for more than 3 years, during which the patients were scheduled for enhanced CT or MRI to determine the cumulative recurrence rate, survival time, local tumor progression, presence of new tumors, disease-free survival (DFS), and overall survival (OS). Complete tumor ablation was defined as no residual tumor on enhanced CT or MRI within the ablation zone and adequate ablation margins of 0.5-1.0 cm. Partial tumor ablation was defined as the presence of a residual tumor on enhanced CT or MRI in the zone of ablation.

Quantitative enzyme-linked immunosorbent assay of serum GP73 levels

Enzyme-linked immunosorbent assay (ELISA) was performed to determine the serum GP73 levels at the Laboratory of Liver Diseases, the 910th Hospital of the PLA Joint Logistics Support Force. The GP73 ELISA detection kit was purchased from Hotgen Biotech Co. Ltd. (Beijing, China) and used for the determination of serum GP73 levels on a Model 680 Microplate Reader (BIO-RAD, United States), according to the manufacturer's protocol. A serum GP73 concentration of 45 mg/L was used as a cut-off value for the general healthy population.

Serum alpha-fetoprotein and liver biochemical tests

Serum alpha-fetoprotein (AFP) was examined using an AFP detection kit (Roche Diagnostics, Basel,

Switzerland), and a value of < 7 mg/L was considered to be normal. Liver biochemical tests, including serum albumin (ALB), total bilirubin (TBIL), alanine aminotransferase (ALT), and aspartate aminotransferase (AST), were determined on a TBA120FR automatic biochemistry analyzer (Toshiba Medical System Co., Ltd., Japan) in the Clinical Laboratory of the 910th Hospital of the PLA Joint Logistics Support Force (Quanzhou, Fujian Province, China).

Statistical analysis

Statistical analysis was performed using GraphPad Prism 5.0 software (Graphpad Software Inc., La Jolla, CA, United States). Count data were expressed as percentages (%). Continuous variables were presented as the median (25%, 75%). For paired data following a normal distribution, a paired *t*-test was used to evaluate differences between the pairs. For non-normally distributed data, a paired Wilcoxon signed-rank test was applied to determine the difference between matched samples. The Kaplan–Meier method was used for survival analysis. $P < 0.05$ indicated that the difference was statistically significant. The statistical methods of this study were reviewed by Zhu YL from the Department of Medical Statistics, Huaqiao University.

RESULTS

Characteristics of the enrolled patients with primary liver cancer

The study cohort was comprised of 150 primary liver cancer patients with one small lesion (average size, 2.03 cm in diameter; range, 0.7-3 cm), including 130 men (86.67%) and 20 women (13.33%), and the median age was 56.00 years old. All of the enrolled patients had a medical history of chronic HBV infection, of which 97 patients (97/150, 64.7%) were positive for the HBV e antigen. Of note, 91 patients (91/150, 60.7%) received antiviral treatment with entecavir or tenofovir disoproxil fumarate for more than 1 year before undergoing MWA and had an HBV DNA concentration of < 500 IU/L, while the remaining 59 patients (59/150, 39.33%) who did not receive the antiviral treatment had an average HBV DNA level of 6.32 (4.52, 7.15) log10 IU/L. Of the enrolled primary liver cancer patients, 115 patients had compensated liver cirrhosis, accounting for 76.7% of the study subjects. Prior to MWA, the 150 patients with primary liver cancer had an ECOG Performance Status score of 0 and a Child–Pugh classification of Class A. The majority of the patients with primary liver cancer had abnormally high levels of AFP, accounting for 68.00% (102/150) of the study subjects. The liver biochemical characteristics, including serum ALB, TBIL, ALT, and AST, as well as the AFP and serum GP73 Levels of the study subjects before MWA are summarized in Table 1.

All of the patients received MWA for primary liver cancer, and the effectiveness was evaluated, including the complete tumor ablation rate at 1 mo after MWA, recurrence rate, and survival time. At 1 month after MWA, enhanced CT/MRI examinations showed that 143 patients (143/150, 95.33%) achieved complete tumor ablation. A small proportion of the patients (7/150, 4.67%) who had partial tumor ablation underwent reablation treatment with MWA and achieved complete tumor ablation. All of the 150 patients were followed up for more than 3 years, and the results were as follows: 134 patients (134/150, 89.33%) survived and 16 patients (16/150, 10.67%) died due to gastrointestinal bleeding in 5 patients (5/150, 3.33%) and liver failure in 11 patients (11/150, 7.33%). The OS rates at 1, 2, and 3 years after MWA were 100.00%, 96.00%, and 89.33%, respectively. In terms of tumor recurrence, cumulative recurrence occurred in 69 patients (69/150, 46.00%) at 3 years after MWA, including 13 patients (13/150, 8.67%) with local tumor progression and 57 patients (57/150, 37.33%) with a new tumor. Among the 69 patients with tumor recurrence, the overall 1-, 2-, and 3-year recurrence rates after MWA were 55.07% (38/150), 33.33% (23/150), and 11.59% (8/150), respectively. As presented in Figure 1, the 1-, 2-, and 3-year DFS rates after MWA were 74.67%, 59.33%, and 54.00%, respectively, in the patients with MWA treatment of primary liver cancer.

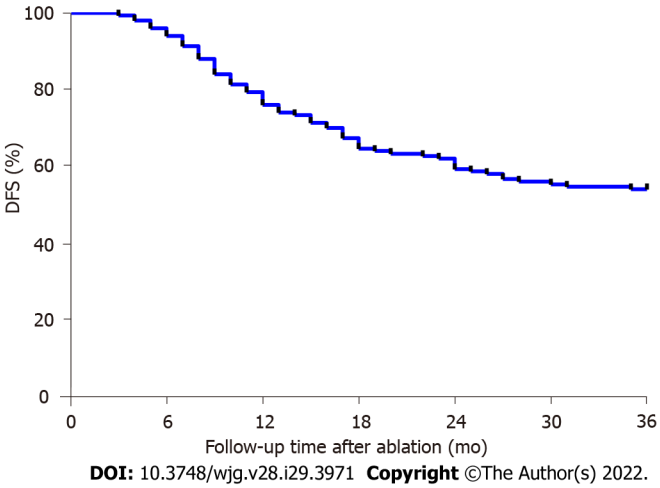
Changes of liver biochemical indicators before and after MWA in the enrolled patients with primary liver cancer

MWA for primary liver cancer may cause some adverse effects, including inflammatory injury in the liver. We analyzed the effects of MWA treatment on the widely used liver biochemical indicators ALB, TBIL, ALT, and AST by comparing their values of the enrolled patients before MWA and at different time points (1, 2, and 4 wk) after the treatment procedure. As shown in Table 1, the serum levels of ALB were significantly decreased, while the levels of serum TBIL, ALT, and AST were significantly increased at 1 wk after MWA treatment compared with those levels prior to MWA as a control (all $P < 0.001$). We found that increases in the biochemical indicators (TBIL, ALT, and AST) were related to the hepatocyte injury in response to MWA treatment. There were no significant differences in ALB, TBIL, ALT, or AST between before and at 2 or 4 wk after the MWA treatment (Table 1), which was mainly attributed to the implementation of hepatoprotective therapy using the active compounds glycyrrhizin and reduced glutathione for nearly 2 wk.

Table 1 Liver biochemical tests in the primary liver cancer patients before and after microwave ablation treatment

	ALB (g/L)	TBIL (μmol/L)	ALT (U/L)	AST (U/L)	GP73 (mg/L)	AFP (mg/L)
Cases	150	150	150	150	150	102[1]
Before MWA	42.10 (38.83, 45.20)	16.20 (12.70, 23.35)	30.10 (20.55, 41.55)	28.30 (22.05, 35.40)	90.83 (54.49, 110.60)	110.40 (32.71, 267.30)
1 wk after MWA	38.40 (36.65, 41.15)[a]	24.80(16.25, 30.60)[a]	102.20(88.65, 166.30)[a]	81.70(68.25, 91.30)[a]	127.10(84.66, 175.50)[a]	37.61(23.30, 95.48)[a]
2 wk after MWA	40.30 (38.36, 42.00)	15.00 (12.90, 18.05)	29.40 (25.65, 36.85)	29.00 (24.10, 36.05)	130.70 (88.39, 163.60)	27.34 (6.32, 81.59)[b]
4 wk after MWA	43.75 (37.12, 47.31)	17.35 (13.62, 25.76)	33.21 (21.57, 43.82)	26.29 (19.70, 40.61)	102.20 (59.15, 121.90)	7.32 (3.87, 16.25)[c]
[a]*t*/*W*	7.037 (*t*)	3.991 (*t*)	6.703 (*t*)	5.768 (*t*)	5.150 (*t*)	-157 (*W*)
[a]*P*	< 0.001	< 0.001	< 0.001	< 0.001	< 0.001	< 0.001

[1]Cases with significantly elevated alpha-fetoprotein.
[a]$P < 0.001$ *vs* before microwave ablation (MWA) as a control.
[b]$P < 0.001$ ($W = -190$) versus before MWA as a control.
[c]$P < 0.001$ ($W = -253$) versus before MWA as a control.
t from the paired *t*-test for normally distributed data and *W* from the paired Wilcoxon signed-rank test for non-normally distributed data.
MWA: Microwave ablation; ALB: Serum albumin; TBIL: Total bilirubin; ALT: Alanine aminotransferase; AST: Aspartate aminotransferase; AFP: Alpha-fetoprotein; GP73: Golgi protein 73.

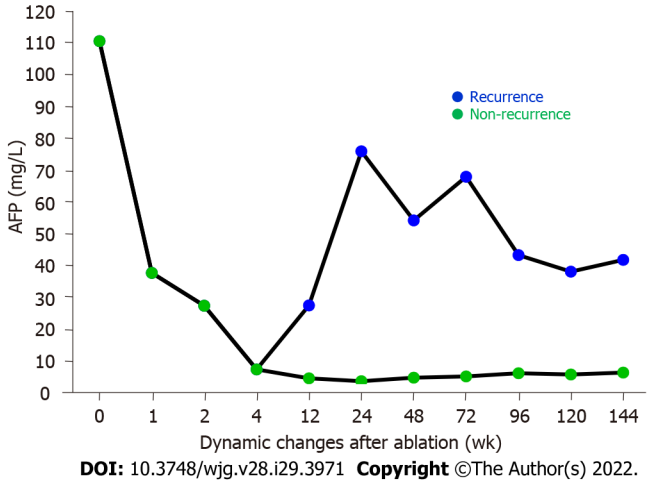


DOI: 10.3748/wjg.v28.i29.3971 **Copyright** ©The Author(s) 2022.

Figure 1 Disease-free survival rates of the patients with primary liver cancer after treatment with microwave ablation. The disease-free survival (DFS) rates were analyzed at 6, 12, 18, 24, 30, and 36 mo after microwave ablation (MWA) for primary liver cancer in the patients. The 1-, 2-, and 3-year DFS rates after MWA were 74.67%, 59.33%, and 54.00%, respectively. DFS: Disease-free survival.

Changes of serum AFP before and after MWA treatment in the enrolled patients with primary liver cancer

We examined the effects of MWA on the serum AFP levels before and after MWA treatment in the enrolled patients with primary liver cancer. As illustrated in Figure 2 and Table 1, the patients had an abnormally high AFP level of 110.40 (32.71, 267.30) mg/L before MWA treatment (pre-MWA), which was decreased sharply to 37.61 (23.30, 95.48) mg/L at 1 wk after MWA treatment. Notably, the AFP level continued to decrease at 2 and 4 wk, returned to the normal range at 12 wk after MWA, and remained stable thereafter during follow-up in those cases without recurrence (Figure 2, Table 1). Statistical analysis revealed that the serum AFP levels at all time points after the MWA treatment were significantly lower compared with the value prior to MWA treatment as a control (all $P < 0.001$). For the recurrent cases with primary liver cancer, however, the serum AFP levels started to increase at 12 wk post MWA; the values were 75.85 mg/L (range, 38.32-86.70 mg/L), 54.17 mg/L (range, 37.83-82.60 mg/L), 67.80 mg/L (range, 37.67-97.32 mg/L), 43.20 mg/L (range, 29.80-58.96 mg/L), 38.05 mg/L (range, 30.85-93.93 mg/L), and 66.73 mg/L (range, 51.90-81.56 mg/L) at 24, 48, 72, 96, 120, and 144 wk following the MWA treatment, respectively (Figure 2).



DOI: 10.3748/wjg.v28.i29.3971 **Copyright** ©The Author(s) 2022.

Figure 2 Effects of microwave ablation treatment on the serum alpha-fetoprotein levels in patients with primary liver cancer. The serum alpha-fetoprotein (AFP) levels were examined in the primary liver cancer patients before microwave ablation (MWA) treatment and at different time points after the treatment. The average serum AFP level was 110.4 mg/L before MWA treatment (pre-MWA), decreased sharply to 37.61 mg/L at 1 wk after MWA treatment, continued to decrease, returned to the normal range at 12 wk after MWA, and remained stable thereafter during follow-up in those cases without recurrence. For the recurrent cases with primary liver cancer, however, the serum AFP levels started to increase at 12 wk following the MWA treatment. AFP: Alpha-fetoprotein.

Comparison of serum GP73 levels in the primary liver cancer patients with or without liver cirrhosis

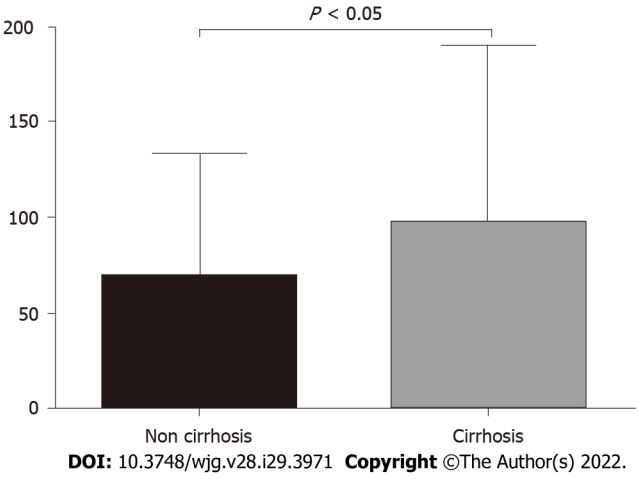
We compared the serum GP73 levels in the enrolled liver cancer patients with *vs* without background liver cirrhosis. As shown in Figure 3, the average level of serum GP73 in the 115 patients with liver cirrhosis was 97.76 mg/L (range, 70.65-133.10 mg/L), which was significantly greater than 69.02 mg/L (range, 45.48-101.40 mg/L) in the 35 patients without liver cirrhosis ($t = 2.477$, $P < 0.05$) (Figure 3).

Changes of serum GP73 before and after MWA treatment in the enrolled patients with primary liver cancer

To evaluate the potential value of serum GP73 measurement for inflammatory injury associated with MWA treatment, we analyzed the serum GP73 levels in the primary liver cancer patients before and at different times after the MWA treatment. As shown in Figure 4 and Table 1, the average serum GP73 level was 90.83 mg/L (range, 54.49-110.6 mg/L) before MWA, which was increased to 127.1 mg/L (range, 84.66-175.50 mg/L) and 130.70 mg/L (range, 88.39-163.60 mg/L) at 1 and 2 wk following the MWA treatment, respectively. Notably, the serum GP73 level started to decline after hepatoprotective treatment with glycyrrhizin and reduced glutathione at 4 wk post MWA; the values were 102.20 mg/L (range, 59.15-121.90 mg/L), 85.73 mg/L (range, 61.42-105.70 mg/L), and 76.09 mg/L (range, 59.26-102.66 mg/L) at 8, 12, and 24 wk following the MWA treatment, respectively (Figure 4). Statistical analysis revealed that the serum GP73 levels were significantly greater at 1 and 2 wk after the MWA procedure *vs* before MWA (1 wk after MWA *vs* before MWA: $t = 5.150$, $P < 0.001$; 2 wk after MWA *vs* before MWA: $t = 6.182$, $P < 0.001$) (Figure 4). It is worth noting that the serum GP73 level reached the peak at 2 wk after MWA and then started to decline at 4 wk after MWA (Figure 4). During the follow-up of the patients at 12 and 24 wk following the MWA treatment, the serum GP73 levels were similar to the pretreatment level (Figure 4).

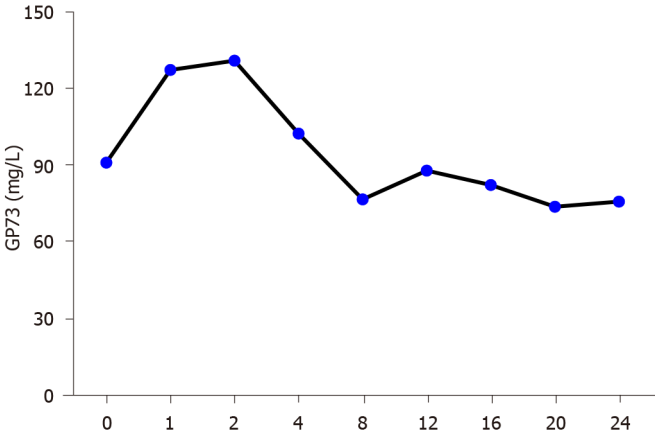
DISCUSSION

This retrospective study has the following major findings: (1) MWA was highly efficacious in treating patients with small primary liver cancer, with as high as 95.33% of the patients achieving complete tumor ablation at 1 mo after MWA; (2) The serum AFP level was significantly decreased following the MWA treatment and returned to the normal range at 3 mo after MWA, which was in agreement with the observation for the complete tumor ablation rate; (3) The serum GP73 levels were significantly elevated at 1 and 2 wk following MWA, with the peak reached at 2 wk after completion of the treatment; (4) The serum GP73 level declined starting at 4 wk after MWA and continued to decrease to the pretreatment level at 12 and 24 wk after MWA; and (5) The effect of MWA on the serum GP73 level was similar to those of TBIL, ALT, and AST. These findings suggest that measurement of the serum GP73 level has the potential to monitor MWA-mediated inflammatory injury in patients with primary liver cancer.



DOI: 10.3748/wjg.v28.i29.3971 **Copyright** ©The Author(s) 2022.

Figure 3 Comparison of serum Golgi protein 73 levels in the primary liver cancer patients with *vs* without liver cirrhosis. The serum Golgi protein 73 levels were examined in the primary liver cancer patients with compensated liver cirrhosis (n = 115) *vs* those without liver cirrhosis (n = 35). P < 0.05. GP73: Golgi protein 73.



DOI: 10.3748/wjg.v28.i29.3971 **Copyright** ©The Author(s) 2022.

Figure 4 Effects of microwave ablation treatment on serum Golgi protein 73 levels in the enrolled patients with primary liver cancer. The serum Golgi protein 73 (GP73) levels were examined in the primary liver cancer patients before and after microwave ablation (MWA) treatment. The serum GP73 levels were increased 1 and 2 wk after MWA. The serum GP73 levels reached the peak at 2 wk after MWA, then progressively decreased, and returned to the pretreatment levels 12 and 24 wk following the MWA treatment. GP73: Golgi protein 73.

In the last decade, percutaneous ablation therapy has been used as a radical treatment method for treating patients with liver cancer[6,17]. In contrast to other types of ablation therapy, MWA has a number of advantages (*e.g.*, a faster ablation time, the capability of simultaneous ablation of multiple lesions, and larger tumor ablation volumes)[18]. Compared with traditional radiofrequency ablation for the treatment of small primary liver cancer nodules, MWA is less affected by the heat sink effect[19-21]. Therefore, MWA is widely accepted as an effective nonsurgical treatment option for liver cancer of a small size and at an early stage[19-23]. Of note, MWA has been demonstrated to completely destroy tumor cells and has been proposed as a radical treatment for small primary liver cancer (≤ 3 cm in diameter) with a single lesion[6,22,24]. In addition, Zhang *et al*[25] performed a meta-analysis of 1480 patients and showed that the therapeutic effectiveness of MWA was superior to that of surgical resection for the treatment of small liver cancer (< 3 cm in diameter). There were no significant differences in the OS, DFS rate, and recurrence rate between MWA and surgical resection for small liver cancer. Our results revealed a high therapeutic effectiveness of MWA for primary liver cancer as supported by several lines of evidence, including 95.33% of patients reaching complete tumor ablation at 1 mo after MWA, high OS rates (1- and 3-year OS rates of 100.00% and 89.33%, respectively), and high DFS rates (1-, 2-, and 3-year DFS rates of 74.67%, 59.33%, and 54.00%, respectively), which were similar to those values previously reported for surgical resection[26]. Despite the high therapeutic effectiveness of MWA for small primary liver cancer, the procedure may trigger an inflammatory response and cause liver injury, which will need to be monitored and alleviated properly.

It merits attention that the serum GP73 level in the present study was significantly elevated at 1 wk after MWA, reached the peak at 2 wk after completion of the procedure, and then declined at 4 wk following MWA. During follow-up of the patients with primary liver cancer at 12 and 24 wk after MWA, the serum GP73 levels nearly returned to the pretreatment level. Consistent with the increase of the serum GP73 levels at 2 and 4 wk after MWA, the serum TBIL, ALT, and AST levels were also significantly increased. Moreover, previous studies have reported that MWA is associated with liver injury due to the high temperature generated in the procedure, induction of hepatocyte apoptosis, and stimulation of the intrahepatic macrophage-related inflammatory response[10,21]. After the MWA-mediated liver injury was alleviated with the implementation of hepatoprotective therapy using the active compounds glycyrrhizin and reduced glutathione for nearly 2 wk, the serum GP73 level was significantly decreased and returned to a level similar to that before MWA. The change of the serum GP73 level in the early response to MWA as well as anti-inflammatory and hepatoprotective therapy using glycyrrhizin and reduced glutathione suggests that serum GP73 is related to the aseptic inflammatory injury of hepatocytes after MWA. The results of this study are also in agreement with those of our previous study demonstrating that the serum GP73 level is increased in liver inflammatory injury [13,14]. Therefore, these findings suggest that the serum GP73 level could be a useful diagnostic approach to monitor the liver inflammatory injury caused by MWA during the treatment of primary liver cancer.

This study does have some limitations that must be addressed. For instance, this was a retrospective study that selected liver cancer patients with one small lesion (≤ 3 cm); therefore, bias in patient selection may have occurred. In addition, due to the retrospective nature of this study, we were unable to examine the correlation between the initial level of GP73 after MWA and the AFP level, recurrence rate, or survival rate. Further prospective studies are needed in the future to validate the interesting findings and to assess the diagnostic accuracy of serum GP73 for monitoring liver injury following MWA treatment for primary liver cancer.

CONCLUSION

Taken together, this study demonstrated that serum GP73 is markedly elevated in response to MWA treatment for primary liver cancer. Therefore, the findings have a clinical implication that measurement of serum GP73 holds promise for monitoring MWA-induced inflammatory liver injury that requires alleviation.

ARTICLE HIGHLIGHTS

Research background

Microwave ablation (MWA) has been proven to be highly effective in treatment of small primary liver cancer. However, the procedure may trigger an inflammatory response and cause liver injury in primary liver cancer patients undergoing MWA. As such, it is needed to find reliable markers to monitor and evaluate patient response to MWA. Previous studies have shown that Golgi protein 73 (GP73) are associated with liver inflammatory injury.

Research motivation

This study was designed to test our hypothesis that serum GP73 levels altered in response to MWA in patients with primary liver cancer, and thereby could be used as a potential marker for MWA-induced liver inflammation and injury.

Research objectives

The main objective of this study was to examine effects of MWA on the serum levels of GP73 before and at different time points after the ablation procedure in patients with primary liver cancer.

Research methods

Patients with primary liver cancer (≤ 3 cm in diameter) receiving MWA were retrospectively enrolled in this study. Serum GP73 levels were compared before and 1, 2, and 4 wk after the ablation procedure.

Research results

The serum GP73 levels were significantly elevated at 1 and 2 wk after MWA with the peak at 2 wk after completion of the treatment. The serum GP73 levels decreased starting at 4 wk after MWA and continued to decline to the pretreatment level at 12 and 24 wk after MWA. It was worthy to note that the alterations of serum GP73 levels in response to MWA were similar to those of liver biochemical indicators.

Research conclusions

The findings of this study have demonstrated that serum GP73 levels altered in response to MWA in patients with primary liver cancer, and thereby measurement of serum GP73 level holds potential as a biomarker for monitoring and assessment of MWA-mediated inflammatory injury in patients with primary liver cancer.

Research perspectives

Future prospective studies are needed to validate the findings and to assess the diagnostic accuracy of serum GP73 for monitoring liver injury following MWA treatment for primary liver cancer.

FOOTNOTES

Author contributions: Xu ZJ carried out the design, coordination of experimental work, manuscript writing, and also performed the microwave ablation procedure; Wei MJ and Zhang XM participated in the study design and data analysis; Liu HG, Wu JP, Huang JF, Li YF, Huang ZJ, and Yan YY participated in data collection and analysis; all authors read and approved the final manuscript.

Supported by the Military Medical Science and Technology Committee of China, No. 14MS095; and the Quanzhou Science and Technology Planning Project, No. 2017Z018.

Institutional review board statement: The study was reviewed and approved by the 910th Hospital of the PLA Joint Logistics Support Force Institutional Review Board.

Informed consent statement: All study participants or their legal guardian provided informed written consent about personal and medical data collection prior to study enrolment.

Conflict-of-interest statement: Xu ZJ has received research funding from the Military Medical Science and Technology Committee of China, No. 14MS095, and grants from the Quanzhou Science and Technology Planning Project, No. 2017Z018, during the conduct of the study.

Data sharing statement: Technical appendix and dataset available from the corresponding author at " h180@163.com". Participants gave informed consent for data sharing.

Open-Access: This article is an open-access article that was selected by an in-house editor and fully peer-reviewed by external reviewers. It is distributed in accordance with the Creative Commons Attribution NonCommercial (CC BY-NC 4.0) license, which permits others to distribute, remix, adapt, build upon this work non-commercially, and license their derivative works on different terms, provided the original work is properly cited and the use is non-commercial. See: https://creativecommons.org/Licenses/by-nc/4.0/

Country/Territory of origin: China

ORCID number: Zheng-Ju Xu 0000-0002-2250-5013; Mei-Juan Wei 0000-0003-1639-7244; Xiao-Man Zhang 0000-0001-7525-2972; Hui-Guo Liu 0000-0003-4314-9836; Jin-Piao Wu 0000-0001-5160-2894; Jin-Fa Huang 0000-0001-5287-1607; Yong-Fei Li 0000-0002-7742-8203; Zhi-Jie Huang 0000-0002-3479-5791; Yan-Yan Yan 0000-0002-6164-8260.

S-Editor: Yan JP
L-Editor: A
P-Editor: Yan JP

REFERENCES

1 **Sung H**, Ferlay J, Siegel RL, Laversanne M, Soerjomataram I, Jemal A, Bray F. Global Cancer Statistics 2020: GLOBOCAN Estimates of Incidence and Mortality Worldwide for 36 Cancers in 185 Countries. *CA Cancer J Clin* 2021; **71**: 209-249 [PMID: 33538338 DOI: 10.3322/caac.21660]

2 **Bosch FX**, Ribes J, Díaz M, Cléries R. Primary liver cancer: worldwide incidence and trends. *Gastroenterology* 2004; **127**: S5-S16 [PMID: 15508102 DOI: 10.1053/j.gastro.2004.09.011]

3 **Fung J**, Lai CL, Yuen MF. Hepatitis B and C virus-related carcinogenesis. *Clin Microbiol Infect* 2009; **15**: 964-970 [PMID: 19874379 DOI: 10.1111/j.1469-0691.2009.03035.x]

4 **Bray F**, Ferlay J, Soerjomataram I, Siegel RL, Torre LA, Jemal A. Global cancer statistics 2018: GLOBOCAN estimates of incidence and mortality worldwide for 36 cancers in 185 countries. *CA Cancer J Clin* 2018; **68**: 394-424 [PMID: 30207593 DOI: 10.3322/caac.21492]

5 **Hasegawa K**, Aoki T, Ishizawa T, Kaneko J, Sakamoto Y, Sugawara Y, Kokudo N. Comparison of the therapeutic outcomes between surgical resection and percutaneous ablation for small hepatocellular carcinoma. *Ann Surg Oncol* 2014; **21** Suppl 3: S348-S355 [PMID: 24566865 DOI: 10.1245/s10434-014-3585-x]

6 **Liang P**, Yu J, Lu MD, Dong BW, Yu XL, Zhou XD, Hu B, Xie MX, Cheng W, He W, Jia JW, Lu GR. Practice guidelines for ultrasound-guided percutaneous microwave ablation for hepatic malignancy. *World J Gastroenterol* 2013; **19**: 5430-5438 [PMID: 24023485 DOI: 10.3748/wjg.v19.i33.5430]

7 **Shibata T**, Iimuro Y, Yamamoto Y, Maetani Y, Ametani F, Itoh K, Konishi J. Small hepatocellular carcinoma: comparison of radio-frequency ablation and percutaneous microwave coagulation therapy. *Radiology* 2002; **223**: 331-337 [PMID: 11997534 DOI: 10.1148/radiol.2232010775]

8 **Vogl TJ**, Nour-Eldin NA, Hammerstingl RM, Panahi B, Naguib NNN. Microwave Ablation (MWA): Basics, Technique and Results in Primary and Metastatic Liver Neoplasms - Review Article. *Rofo* 2017; **189**: 1055-1066 [PMID: 28834968 DOI: 10.1055/s-0043-117410]

9 **Shiina S**, Sato K, Tateishi R, Shimizu M, Ohama H, Hatanaka T, Takawa M, Nagamatsu H, Imai Y. Percutaneous Ablation for Hepatocellular Carcinoma: Comparison of Various Ablation Techniques and Surgery. *Can J Gastroenterol Hepatol* 2018; **2018**: 4756147 [PMID: 29974040 DOI: 10.1155/2018/4756147]

10 **Zhou H**, Sun Y, Wang Q, Li Z, Zhong W, Wang X, Dai X, Kong L. N-acetylcysteine alleviates liver injury by suppressing macrophage-mediated inflammatory response post microwave ablation. *Int Immunopharmacol* 2020; **85**: 106580 [PMID: 32438077 DOI: 10.1016/j.intimp.2020.106580]

11 **Kladney RD**, Bulla GA, Guo L, Mason AL, Tollefson AE, Simon DJ, Koutoubi Z, Fimmel CJ. GP73, a novel Golgi-localized protein upregulated by viral infection. *Gene* 2000; **249**: 53-65 [PMID: 10831838 DOI: 10.1016/s0378-1119(00)00136-0]

12 **Liu X**, Wan X, Li Z, Lin C, Zhan Y, Lu X. Golgi protein 73(GP73), a useful serum marker in liver diseases. *Clin Chem Lab Med* 2011; **49**: 1311-1316 [PMID: 21663469 DOI: 10.1515/CCLM.2011.640]

13 **Xu Z**, Liu L, Pan X, Wei K, Wei M, Yang H, Liu Q. Serum Golgi protein 73 (GP73) is a diagnostic and prognostic marker of chronic HBV liver disease. *Medicine (Baltimore)* 2015; **94**: e659 [PMID: 25816035 DOI: 10.1097/MD.0000000000000659]

14 **Xu Z**, Shen J, Pan X, Wei M, Liu L, Wei K, Yang H, Huang J. Predictive value of serum Golgi protein 73 for prominent hepatic necroinflammation in chronic HBV infection. *J Med Virol* 2018; **90**: 1053-1062 [PMID: 29424455 DOI: 10.1002/jmv.25045]

15 **Department of Medical Administration**, National Health and Health Commission of the People's Republic of China. . [Guidelines for diagnosis and treatment of primary liver cancer in China (2019 edition)]. *Zhonghua Gan Zang Bing Za Zhi* 2020; **28**: 112-128 [PMID: 32164061 DOI: 10.3760/cma.j.issn.1007-3418.2020.02.004]

16 **Chinese Society of Infectious Diseases**; Chinese Medical Association. ; Chinese Society of Hepatology, Chinese Medical Association. [The guidelines of prevention and treatment for chronic hepatitis B (2019 version)]. *Zhonghua Gan Zang Bing Za Zhi* 2019; **27**: 938-961 [PMID: 31941257 DOI: 10.3760/cma.j.issn.1007-3418.2019.12.007]

17 **Hinshaw JL**, Lubner MG, Ziemlewicz TJ, Lee FT Jr, Brace CL. Percutaneous tumor ablation tools: microwave, radiofrequency, or cryoablation--what should you use and why? *Radiographics* 2014; **34**: 1344-1362 [PMID: 25208284 DOI: 10.1148/rg.345140054]

18 **Poulou LS**, Botsa E, Thanou I, Ziakas PD, Thanos L. Percutaneous microwave ablation *vs* radiofrequency ablation in the treatment of hepatocellular carcinoma. *World J Hepatol* 2015; **7**: 1054-1063 [PMID: 26052394 DOI: 10.4254/wjh.v7.i8.1054]

19 **Ierardi AM**, Giorlando F, Piacentino F, Fontana F, Novario R, Angileri SA, Duka E, Carrafiello G. Factors predicting outcomes of microwave ablation of small hepatocellular carcinoma. *Radiol Med* 2017; **122**: 81-87 [PMID: 27744607 DOI: 10.1007/s11547-016-0694-6]

20 **Poggi G**, Tosoratti N, Montagna B, Picchi C. Microwave ablation of hepatocellular carcinoma. *World J Hepatol* 2015; **7**: 2578-2589 [PMID: 26557950 DOI: 10.4254/wjh.v7.i25.2578]

21 **Bhardwaj N**, Dormer J, Ahmad F, Strickland AD, Gravante G, West K, Dennison AR, Lloyd DM. Microwave ablation of the liver: a description of lesion evolution over time and an investigation of the heat sink effect. *Pathology* 2011; **43**: 725-731 [PMID: 22027742 DOI: 10.1097/PAT.0b013e32834c356c]

22 **Luo W**, Zhang Y, He G, Yu M, Zheng M, Liu L, Zhou X. Effects of radiofrequency ablation versus other ablating techniques on hepatocellular carcinomas: a systematic review and meta-analysis. *World J Surg Oncol* 2017; **15**: 126 [PMID: 28693505 DOI: 10.1186/s12957-017-1196-2]

23 **Wang ZL**, Liang P, Dong BW, Yu XL, Yu DJ. Prognostic factors and recurrence of small hepatocellular carcinoma after hepatic resection or microwave ablation: a retrospective study. *J Gastrointest Surg* 2008; **12**: 327-337 [PMID: 17943391 DOI: 10.1007/s11605-007-0310-0]

24 **Rao Z**, Ling W, Dai X, Zhang H, Pu L, Wu J, Zhu D, Yang X, Li Z, Lu L, Wang X, Zhou H, Kong L. Precoagulation with microwave ablation for hepatic parenchymal transection during liver partial resection. *Int J Hyperthermia* 2019; **36**: 146-150 [PMID: 30484720 DOI: 10.1080/02656736.2018.1540799]

25 **Zhang M**, Ma H, Zhang J, He L, Ye X, Li X. Comparison of microwave ablation and hepatic resection for hepatocellular carcinoma: a meta-analysis. *Onco Targets Ther* 2017; **10**: 4829-4839 [PMID: 29042794 DOI: 10.2147/OTT.S141968]

26 **Zhang EL**, Yang F, Wu ZB, Yue CS, He TY, Li KY, Xiao ZY, Xiong M, Chen XP, Huang ZY. Therapeutic efficacy of percutaneous microwave coagulation *vs* liver resection for single hepatocellular carcinoma ≤3 cm with Child-Pugh A cirrhosis. *Eur J Surg Oncol* 2016; **42**: 690-697 [PMID: 26995115 DOI: 10.1016/j.ejso.2016.02.251]

World Journal of Gastroenterology

Submit a Manuscript: https://www.f6publishing.com

World J Gastroenterol 2022 August 7; 28(29): 3981-3993

DOI: 10.3748/wjg.v28.i29.3981

ISSN 1007-9327 (print) ISSN 2219-2840 (online)

ORIGINAL ARTICLE

Observational Study

Evaluating the best treatment for multifocal hepatocellular carcinoma: A propensity score-matched analysis

Matteo Risaliti, Ilenia Bartolini, Claudia Campani, Umberto Arena, Carlotta Xodo, Valentina Adotti, Martina Rosi, Antonio Taddei, Paolo Muiesan, Amedeo Amedei, Giacomo Batignani, Fabio Marra

Specialty type: Gastroenterology and hepatology

Provenance and peer review: Invited article; Externally peer reviewed.

Peer-review model: Single blind

Peer-review report's scientific quality classification

Grade A (Excellent): 0
Grade B (Very good): B
Grade C (Good): C
Grade D (Fair): 0
Grade E (Poor): 0

P-Reviewer: Gorrell MD, Australia; Nakano M, Japan

Received: February 1, 2022
Peer-review started: February 1, 2022
First decision: February 24, 2022
Revised: March 9, 2022
Accepted: July 6, 2022
Article in press: July 6, 2022
Published online: August 7, 2022

Matteo Risaliti, Ilenia Bartolini, Claudia Campani, Umberto Arena, Carlotta Xodo, Valentina Adotti, Martina Rosi, Antonio Taddei, Paolo Muiesan, Amedeo Amedei, Giacomo Batignani, Fabio Marra, Department of Experimental and Clinical Medicine, AOU Careggi, Florence 50134, Italy

Corresponding author: Fabio Marra, MD, Professor, Department of Experimental and Clinical Medicine, AOU Careggi, Largo Brambilla 3, Florence 50134, Italy. fabio.marra@unifi.it

Abstract

BACKGROUND

Hepatocellular carcinoma (HCC) is a common tumour often diagnosed with a multifocal presentation. Patients with multifocal HCC represent a heterogeneous group. Although Trans-Arterial ChemoEmbolization (TACE) is the most frequently employed treatment for these patients, previous data suggested that liver resection (LR) could be a safe and effective procedure.

AIM

To compare LR and TACE in patients with multifocal HCC in terms of procedure-related morbidity and oncologic outcomes.

METHODS

All patients with multifocal HCC who underwent LR or TACE as the first procedure between May 2011 and March 2021 were enrolled. The decision to perform surgery or TACE was made after a multidisciplinary team evaluation. Only patients in Child-Pugh class A or B7 and stage B (according to the Barcelona Clinic Liver Cancer staging system, without severe portal hypertension, vascular invasion, or extrahepatic spread) were included in the final analysis. Propensity score matching was used to adjust the baseline differences between patients undergoing LR and the TACE group [number and diameter of lesions, presence of cirrhosis, alpha-fetoprotein (AFP) levels, and Model for End-Stage Liver Disease score]. The Kaplan-Meier method was used to estimate overall survival (OS) and disease-free survival (DFS). The outcomes of LR and TACE were compared using the log-rank test.

RESULTS

After matching, 30 patients were eligible for the final analysis, 15 in each group. Morbidity rates were 42.9% and 40% for LR and TACE, respectively (P = 0.876).

Median OS was not different in the LR and TACE groups (53 mo *vs* 18 mo, $P = 0.312$), while DFS was significantly longer with LR (19 mo *vs* 0 mo, $P = 0.0001$). Subgroup analysis showed that patients in the Italian Liver Cancer (ITA.LI.CA) B2 stage, with AFP levels lower than 400 ng/mL, less than 3 lesions, and lesions bigger than 41 mm, benefited more from LR in terms of DFS. Patients classified as ITA.LI.CA B3, with AFP levels higher than 400 ng/mL and with more than 3 lesions, appeared to receive more benefit from TACE in terms of OS.

CONCLUSION

In a small cohort of patients with multifocal HCC, LR confers longer DFS compared with TACE, with similar OS and post-procedural morbidity.

Key Words: Hepatocellular carcinoma; Multifocal hepatocellular carcinoma; Liver resection; Trans-arterial chemoembolization; Guidelines; Liver tumour management

©The Author(s) 2022. Published by Baishideng Publishing Group Inc. All rights reserved.

Core Tip: Hepatocellular carcinoma (HCC) is a leading cause of death and often presents in a multifocal form. Trans-Arterial ChemoEmbolization (TACE) is the most frequently employed treatment for this patient category. As patients with multifocal HCC are a heterogeneous group, previous data suggested that liver resection (LR) could be a safe and effective procedure. A propensity score-matched analysis has been performed to compare LR and TACE in terms of post-procedure morbidity and survival. Despite the limited number of patients, LR conferred longer disease-free survival with similar overall survival compared to TACE. Subgroup analyses identified the patients benefiting more from a specific treatment.

Citation: Risaliti M, Bartolini I, Campani C, Arena U, Xodo C, Adotti V, Rosi M, Taddei A, Muiesan P, Amedei A, Batignani G, Marra F. Evaluating the best treatment for multifocal hepatocellular carcinoma: A propensity score-matched analysis. *World J Gastroenterol* 2022; 28(29): 3981-3993
URL: https://www.wjgnet.com/1007-9327/full/v28/i29/3981.htm
DOI: https://dx.doi.org/10.3748/wjg.v28.i29.3981

INTRODUCTION

Hepatocellular carcinoma (HCC) is the most frequent primary liver cancer worldwide, accounting for approximately 90% of cases[1]. HCC incidence has grown over the last two decades, with more than 900.000 new cases *per* year. Moreover, it is expected to further increase in the next few years due to the exponential growth in nonalcoholic fatty liver disease[2]. Despite the improvements in diagnosis and management, HCC is detected in a multinodular form in 35%-40% of cases[3,4] with a reported 5-year survival rate of 19.5%[5].

Over the years, various staging systems have been proposed to overcome the limitations of the tumour-node-metastasis system, which only considers tumour burden[6]. Currently, the Barcelona Clinic Liver Classification (BCLC) is one of the most widely used staging systems for HCC, and includes variables related to tumour status, liver function, and performance status (PS), and recommends one or more specific treatment modalities for each disease stage[7].

Several additional efforts have been made to deal with the heterogeneity of the BCLC-B or intermediate stage of this classification. The Italian Liver Cancer (ITA.LI.CA) group recently proposed a new staging system and prognostic score, based on the BCLC staging system, which includes tumour burden, liver function, and other patient-related variables, and provides a subclassification of this stage [8].

Surgical treatments, including liver resection (LR) and liver transplantation, are considered the best choice for survival and quality of life whenever feasible, while Trans-Arterial ChemoEmbolization (TACE) is not a curative treatment and should be used for patients with well-defined, multifocal HCC, a preserved portal flow, and adequate liver function and PS. TACE outcomes are poor, and several lines of information about the safety and effectiveness of surgery in selected patients for whom TACE is usually recommended have been reported[9-12]. Finally, liver transplantation could also have a central role for these patients, especially after successful downstaging[7], but organ shortage and increased demand for organ transplantation could lead to high drop-out rates.

The debate concerning whether selected patients with multinodular HCC may benefit from surgery rather than TACE remains unsolved.

In this study, a propensity-score matching analysis was used to compare procedure-related morbidity and oncological outcomes in multifocal HCC patients classified as BCLC-B who underwent LR or TACE to determine if one treatment should be given priority over the other.

MATERIALS AND METHODS

Study design and patients

A retrospective analysis was conducted on patients with multifocal HCC who had undergone surgical resection or TACE as first-line treatment between May 2011 and March 2021. The following exclusion criteria were considered: Age < 18 years, Child-Pugh score > 7, vascular invasion or extrahepatic spread, and hepatic venous pressure gradient > 15 mmHg. HCC was diagnosed histologically or by imaging techniques [magnetic resonance imaging and/or triphasic computed tomography (CT)] according to the available EASL guidelines version. Before LR or TACE, an evaluation of age, comorbidities, blood chemistry, tumour number and size (major radiological diameter of the largest lesion from the last available imaging test), ITA.LI.CA. stage and Eastern Cooperative Oncology Group PS.

The decision to perform surgery or TACE was taken by the local multidisciplinary team who considered patients and tumour features, including lesion location and relation with the pedicles, and the volume of the future liver remnant. During surgery, intraoperative ultrasound sonography (IOUS) was routinely performed to confirm preoperative planning. Whenever feasible, anatomic resections were preferred. Both conventional, lipiodol-based TACE and TACE with drug-eluting beads were included. The patients' response was evaluated one month after the procedure with a CT scan. For patients who did not achieve a complete response, data and the effectiveness of each subsequent TACE were also recorded.

Post-treatment morbidity was evaluated according to the Clavien-Dindo (CD) classification[13].

All patients underwent a standardised follow-up programme that included blood tests with alpha-fetoprotein (AFP), and a triple phase-contrast enhanced CT scan every three months for the first year and then biannually for 5 years after surgery (starting 3 mo after surgery or 1 mo after TACE). Recurrence was diagnosed in the case of radiological evidence of HCC.

Statistical analysis

Quantitative data were expressed as mean ± SD or median and range, as appropriate. Qualitative data are reported as absolute and relative frequencies. Satterthwait's test or the Mann-Whitney test was used according to the Shapiro-Wilk test and F-Test, respectively, for normality distribution and homoscedasticity to assess the difference in quantitative variables between treatment groups t-test. The chi-square test or Fisher's test were used as appropriate to verify the association between qualitative variables and treatment groups. The propensity score matching (PSM) method was used to compare similar treatment groups for known prognostic factors (AFP levels as a dichotomous variable with a cut-off set at 400 ng/dL, presence or not of cirrhosis, Child-Pugh and Model for End-Stage Liver Disease (MELD) score, number, and diameter of lesions). An AFP level > 400 ng/mL was considered a prognostic factor of poor outcome, as suggested by recent guidelines[14]. A diagnosis of cirrhosis was established based on the presence of one or more of the following: Compatible histology, imaging showing compatible hepatic morphology, liver stiffness > 15 kPa by vibration-controlled transient elastography, clinical or endoscopic or imaging signs of portal hypertension. The propensity score was calculated by a multiple logistic regression model with a backward selection method. The nearest neighbour method was used to match the two groups with a 1:1 ratio.

Overall survival (OS) was calculated from the date of the first treatment to death of any cause or the last follow-up. As TACE patients could need more than one treatment to achieve a complete response, disease-free survival (DFS) was calculated from the date of the effective treatment to the date of first radiological recurrence. Survival was expressed as the median and 95% confidence interval.

The Kaplan-Meier curve method and the log-rank test were used to evaluate the difference in OS and DFS between the groups.

Subgroup survival analyses were performed comparing the results of the different treatment modalities and stratifying patients by the different grades of the ITA.LI.CA classification, the AFP levels (using 400 ng/mL as cut-off), and by the different number and size of HCC (dividing them into two groups using the median value as a cut-off). A P value < 0.05 was considered statistically significant.

All the analyses were conducted using SAS, version 9.2 (SAS Corporation, Cary, NC, United States), and revised by a biomedical statistician.

RESULTS

Patient clinical characteristics

A total of 50 patients with multifocal HCC were included in the study, 25 underwent LR while 25

underwent TACE. The distribution of the factors used for the PSM in the general population is reported in Table 1. All patients belonging to the TACE group had cirrhosis, whereas, among those who underwent LR, cirrhosis was absent in 36% of cases (P = 0.002). The number of lesions was higher among patients who underwent TACE, whereas resected patients usually had more extensive tumours. No significant differences were found between the two groups regarding Child-Pugh score and AFP levels. In contrast, the MELD score tended to be higher in patients who underwent TACE compared with the resected patients. After the PSM, only 30 patients were eligible for the final analysis, 15 from each subgroup.

The general baseline clinical characteristics are shown in Table 2, while data regarding liver function aspects, tumour characteristics, and patient distribution according to the Up-to-7 criteria[15] and ITA.LI.CA classification are reported in Table 3. No statistical differences were found in baseline characteristics. The median age was 69 years, and more than two/thirds of patients were male. The most common cause of liver disease was viral hepatitis, followed by NASH and alcohol use disorder. Lower platelet counts and higher bilirubin levels were present in the TACE group. There was also a trend towards a higher presence of varices in the TACE group. No significant differences across the Up-to-7 criteria in or out and ITA.LI.CA. staging distribution were found.

Postoperative short-term outcomes and survival analysis

Patients in the TACE group received a significantly higher number of treatments (Table 4, P = 0.001). Post-procedure complications were not significantly different between patients who underwent LR and TACE (Table 4). In the surgery group, complications classified as grade 1 and 2 of CD included fever, pneumonia, or the need for blood transfusion. Only one patient developed bile leakage classified as grade 3 according to CD and was treated with percutaneous drainage.

In the TACE group, complications classified as grade 1 and 2 of CD included mostly transient alterations in liver biochemistry and/or fever. Only one patient developed temporary liver failure and required percutaneous drainage due to an abdominal effusion.

The median follow-up was 19 mo (range 3-62). The estimated global median OS and DFS were 31 and 5 mo, respectively (Figure 1). There were no significant differences in OS and DFS for the global population stratified by the ITA.LI.CA classification. Median OS for B1, B2, and B3 groups were 31, 31, and 14 mo, respectively (P = 0.803), while median DFS for B1, B2, and B3 groups were 5, 14.5, and 1.5 mo, respectively (P = 0.516).

No differences in OS were observed when the two treatment groups were compared. A significantly longer DFS was found in resected patients compared with those undergoing TACE (19 mo *vs* 0 mo, respectively, P = 0.0001) (Figure 2).

Subgroup analyses were also performed to evaluate the possible differences in OS or DFS according to AFP levels, size, lesion number, Up-to-7 criteria, and ITA.LI.CA staging between each treatment group.

A significant difference was found in both OS and DFS (P < 0.0001 and P = 0.0001, respectively, Figure 3A), with patients presenting with lower levels of AFP showing the best prognosis, in both treatment groups. Furthermore, patients with AFP levels higher than 400 ng/mL and receiving surgery showed a poor OS compared to the TACE group.

No difference in OS was found when comparing treatment modalities in patients stratified according to the Up-to-7 criteria. On the contrary, DFS was higher in the LR group (P = 0.002) (Figure 3B).

The results of different treatment modalities for patients stratified by the ITA.LI.CA classification are reported in Figure 3C. Similar to the previous analysis, a significant difference was found in both OS and DFS (P = 0.047 and P = 0.001, respectively), with patients classified as B2 and receiving resection, showing the best prognosis, while those classified as B3 and receiving resection had the worst prognosis.

Although no significant differences were found in OS, the 4 patients with more than 3 lesions receiving TACE showed a 1, 3, and 5-year OS of 75%, 25%, and 25%, respectively. Among the surgery group, patients with less than 3 lesions had a significantly higher DFS compared with those with 3 or more lesions (P = 0.001). Conversely, no differences in terms of OS and DFS were found in the TACE group stratified by the number of lesions (Figure 3D). Similar results were obtained when the treatment groups were stratified according to the size of the more extensive lesion (Figure 3E). Patients with smaller lesions in the surgery group had a better DFS.

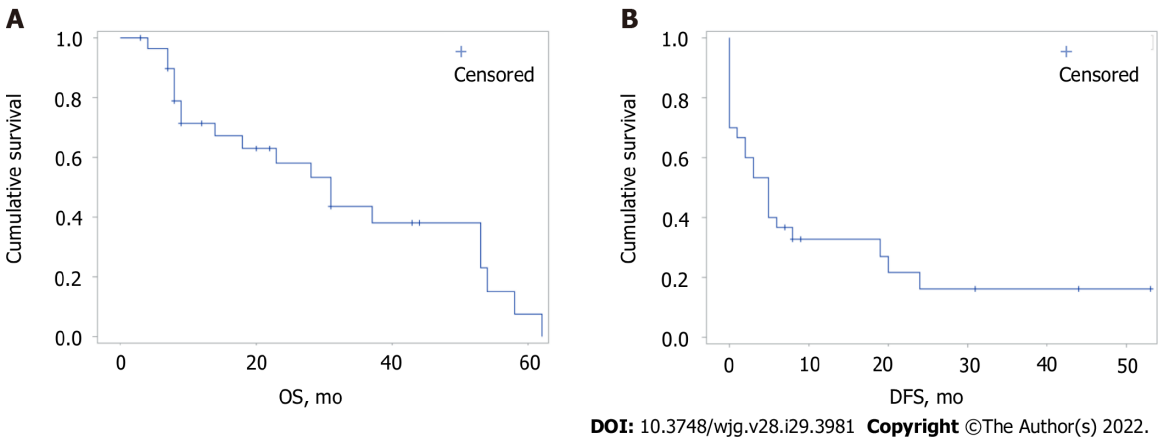
DISCUSSION

HCC is the most common primary liver tumour. Despite recent advantages in terms of follow-up, early diagnosis, and treatment, a considerable percentage of patients are still diagnosed in multiple or advanced forms and global mortality remains high with poor long-term prognosis[16]. The term multifocal HCC comprises patients presenting with a broad disease spectrum, ranging from small, oligonodular tumours to diffuse disease. The accompanying liver cirrhosis, portal hypertension, and liver function impairment should be considered, as they are related to high post-procedure morbidity

Table 1 Distribution of the factors used in the propensity score matching in the general population (*n* = 50), *n* (%)

	Resection, *n* = 25	TACE, *n* = 25	Total, *n* = 50	*P* value
AFP, *n* (%)				0.243
< 400 ng/mL	20 (90.9)	17 (73.9)	37 (82.2)	
> 400 ng/mL	2 (9.1)	6 (26.1)	8 (17.8)	
Missing	3	2	5	
Cirrhosis, *n* (%)				0.002
No	9 (36)	0	9 (18)	
Yes	16 (64)	25 (100)	41 (82)	
Child-Pugh score, *n* (%)				0.840
A5	12 (48)	10 (40)	22 (44)	
A6	9 (36)	11 (44)	20 (40)	
B7	4 (16)	4 (16)	8 (16)	
MELD	8.4 ± 2.7	9.7 ± 2.2	9 ± 2.5	0.069
Number of lesions	2 (2-10)	4 (2-7)	2.5 (2-10)	0.008
Tumor diameter (mm)	69.5 ± 52.2	41.9 ± 17	55.7 ± 40.9	0.018

TACE: Trans-Arterial ChemoEmbolization; AFP: Alpha-fetoprotein; MELD: Model for End-Stage Liver Disease.



DOI: 10.3748/wjg.v28.i29.3981 **Copyright** ©The Author(s) 2022.

Figure 1 Kaplan–Meier curves of global overall survival and disease-free survival. The median overall survival (OS) and disease-free survival (DFS) were 31 mo [95% confidence interval (CI): 14-53] and 5 mo (95%CI: 1-8), respectively. 1, 3 and 5-yr OS rates were 71.4%, 43.6%, and 7.6%, respectively. 1-, and 3-yr DFS rates were 32.6%, and 16.3%, respectively. A: OS; B: DFS. OS: Overall survival; DFS: Disease-free survival.

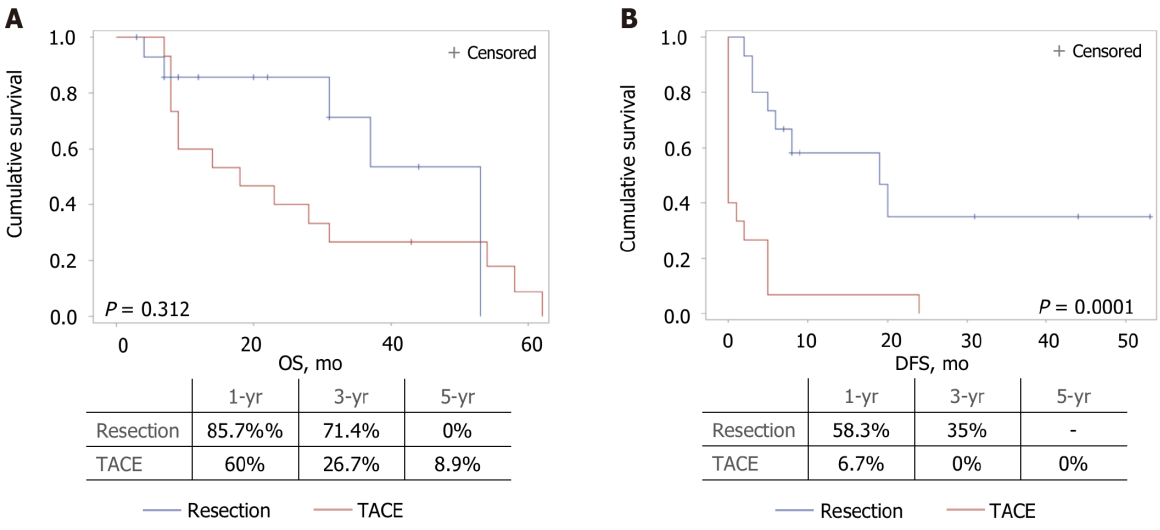
and mortality. Therefore, a tailored approach is mandatory for each patient, and the decisional role of a specialised multidisciplinary team has been highlighted and encouraged in the last version of the BCLC classification[7].

The BCLC algorithm recommends TACE as the primary treatment modality for multinodular HCC, but whether a subset of patients may benefit from a surgical approach remains unestablished. We conducted a retrospective analysis using the PSM, a method that may provide high-quality evidence in conditions when randomised clinical trials are unethical or unfeasible. For the PSM analysis, both indicators of liver function and tumour burden and aggressiveness were used. Although the Child-Pugh and MELD scores could be considered outdated after the last published version of the BCLC staging system[7], these data are still commonly used in clinical practice. Wang *et al*[5] showed that patients with gradual deterioration in CP score had shorter survival times and worse prognosis (5-year OS rates of 31.1%, 2.4%, and 0.9% for CP A, B, and C, respectively). AFP is a well-established independent risk factor for survival in HCC patients and levels greater than 400 ng/mL are generally considered diagnostic for HCC, in the presence of appropriate radiologic findings[5,17]. Finally, the number and dimension of the nodules are two of the major prognostic factors, and the most used guidelines underscore their importance in treatment allocation[7,8,14,18].

Table 2 General baseline characteristics after propensity score matching (*n* = 30)

	Resection, *n* = 15	TACE, *n* = 15	Total, *n* = 30	*P* value
Age (yr)	68.9 ± 9.2	70.5 ± 9.9	69.7 ± 9.5	0.651
Gender, *n* (%)				0.651
Male	13 (86.7)	11 (73.3)	24 (80)	
Female	2 (13.3)	4 (26.7)	6 (20)	
BMI (kg/m^2)	26.1 ± 4.3	26.3 ± 7.7	26.2 ± 5.9	0.927
Hepatitis Etiology, *n* (%)				0.300
Viral	4 (28.6)	9 (60)	13 (44.8)	
Alcoholic	0	1 (6.7)	1 (3.5)	
Dysmetabolic	3 (21.4)	1 (6.7)	4 (13.8)	
Mixed	3 (21.4)	1 (6.7)	4 (13.8)	
Other	4 (28.6)	3 (20)	7 (24.1)	
Missing	1	-	1	
Diabetes, *n* (%)				0.700
No	9 (60)	11 (73.3)	20 (66.7)	
Yes	6 (40)	4 (26.7)	10 (33.3)	
Heart disease, *n* (%)				0.330
No	11 (73.3)	14 (93.3)	25 (83.3)	
Yes	4 (26.7)	1 (6.7)	5 (16.7)	

TACE: Trans-Arterial ChemoEmbolization; BMI: Body mass index.



DOI: 10.3748/wjg.v28.i29.3981 **Copyright** ©The Author(s) 2022.

Figure 2 Kaplan–Meier curves of overall and disease-free survival comparing the results of the different treatment modalities (*P* = 0.312 and *P* = 0.0001, respectively). Median overall survival (OS) and disease-free survival (DFS) for the resection group were 53 [95% confidence interval (CI): 31-53] and 19 mo (95%CI: 3-Not Evaluable), respectively. Median OS and DFS for the Trans-Arterial ChemoEmbolization group were 18 (95%CI: 8-31) and 0 (95%CI: 0-2) months, respectively. A: OS; B: DFS. OS: Overall survival; DFS: Disease-free survival; TACE: Trans-Arterial ChemoEmbolization.

TACE is considered the standard treatment for BCLC-B patients, as evidence from randomised clinical trials and meta-analyses indicates that TACE provides better survival outcomes compared to the best supportive care with a 1-year mortality rate of 34.1%[19-21]. On the other hand, guidelines do not recommend LR for BCLC-B patients, due to the unfavourable prognostic impact of multinodular presentation and high postoperative morbidity[18]. Moreover, LR for multifocal HCC is a challenging

Table 3 Liver function test and disease burden after propensity score matching (*n* = 30)

	Resection, *n* = 15	TACE, *n* = 15	Total, *n* = 30	*P* value
INR	1.2 ± 0.1	1.3 ± 0.3	1.2 ± 0.2	0.185
Bilirubin (mg/dL)	0.75 ± 0.5	1.2 ± 0.6	0.99 ± 0.6	0.026
Platelets (10^3/μL)	245 ± 118	95 ± 31	163 ± 111	0.003
Creatinine (mg/dL)	1.37 ± 0.8	0.78 ± 0.2	1.08 ± 1.19	0.188
AFP, *n* (%)				1.000
< 400 ng/mL	13 (86.7)	12 (80)	25 (83.3)	
> 400 ng/mL	2 (13.3)	3 (20)	5 (16.7)	
Varices, *n* (%)				0.081
No	8 (80)	4 (36.4)	12 (57.1)	
Yes	2 (20)	7 (63.6)	9 (42.9)	
Missing	5	4	9	
Cirrhosis, *n* (%)				0.100
No	4 (26.7)	0	4 (13.3)	
Yes	11 (73.3)	15 (100)	26 (86.7)	
Child-Pugh score, *n* (%)				0.556
A5	8 (53.3)	5 (33.3)	13 (43.3)	
A6	6 (40)	7 (46.7)	13 (43.3)	
B7	1 (6.7)	3 (20)	4 (13.4)	
MELD score	9.1 ± 3.2	9.9 ± 2.4	9.5 ± 2.8	0.473
Number of lesions	2 (2-5)	3 (2-5)	2 (2-5)	0.101
Diameter (mm)	46.3 ± 3	47 ± 5	46.9 ± 12.9	0.793
Up-to-7 criteria, *n* (%)				0.456
In	10 (66.7)	8 (53.3)	18 (60)	
Out	5 (33.3)	7 (46.7)	12 (40)	
ITA.LI.CA classification, *n* (%)				0.868
B1	10 (66.7)	8 (53.3)	18 (60)	
B2	3 (20)	5 (33.3)	8 (26.7)	
B3	2 (13.3)	2 (13.3)	4 (13.3)	

TACE: Trans-Arterial ChemoEmbolization; INR: International normalized ratio; AFP: Alpha-fetoprotein; MELD: Model for End-Stage Liver Disease.

surgery as wide and/or multiple resections are needed, possibly leading to bile leaks and/or postoperative liver failure.

Advances in surgical techniques, including extensive use of IOUS, better coagulation devices, and wider application of minimally invasive surgery, together with better perioperative management, have contributed to improving the results of LR in this difficult-to-treat population. Remarkably, the comparison between different studies is limited by variations in the modalities of detection and reporting of post-procedural complications.

In the present series, we did not find any differences in post-procedure morbidity when comparing resection and TACE. According to the CD classification, only three patients undergoing LR and one patient in the TACE group had a clinically relevant event. However, it should be documented that TACE patients often required more than one treatment to achieve the best response, thus partially explaining the lower morbidity rate of the procedure. Conflicting results on morbidity were previously reported. Zhong *et al*[22] showed a complication rate of 35% and 21% for resection and TACE, respectively[22]. On the contrary, a meta-analysis did not find any difference in post-procedure morbidity between these two treatment modalities[23].

Table 4 Postoperative morbidity and recurrence status (*n* = 30)

	Resection, *n* = 15	TACE, *n* = 15	Total, *n* = 30	*P* value
Number of treatments	1 ± 0	2.4 ± 1.1	1.7 ± 1.1	0.001
Complications, *n* (%)				0.876
No	8 (57.1)	9 (60)	17 (58.6)	
Yes	6 (42.9)	6 (40)	12 (41.4)	
Missing	1	-	1	
Complications, *n* (%)				0.545
CD 1-2	5 (83.3)	5 (83.3)	10	
CD 3-4	1 (16.7)	1 (16.7)	2 (16.7)	
Hospital stay (days)	7 ± 3	5 ± 5	6 ± 4.3	0.224
Recurrence, *n* (%)				0.006
No	7 (46.7)	0	7 (23.3)	
Yes	8 (53.3)	15 (100)	23 (76.7)	

TACE: Trans-Arterial ChemoEmbolization; CD: Clavien-Dindo classification grade.

While only a nonsignificant trend towards better OS was observed with surgery, we found that DFS was significantly longer in resected patients. These results confirm and extend previous studies conducted on patients with multinodular HCC. Favourable results with surgery were originally reported by non-controlled studies[10,24]. In a multicentric study including 736 BCLC-B patients, Torzilli *et al*[24] reported a 5-year survival rate of 57% and a DFS of 27%. The survival benefit of LR compared with TACE in BCLC-B patients has been previously reported in the meta-analysis by Liu *et al*[23], and similar conclusions were reached in a randomised controlled trial enrolling 173 patients[25].

Considering the marked population heterogeneity of patients with multinodular HCC, subgroup analyses may provide additional clues for better selection of the treatment modality. Not surprisingly, patients with lower AFP levels had the best prognosis. An exciting result was the observation that patients with high AFP levels benefit more from TACE in terms of OS, and further studies are needed to confirm these data and investigate the possible mechanisms thereof. Another aspect which deserves further investigation is to what extent some of these patients with multinodular HCC could benefit from new systemic combination treatments which include the use of immunotherapy with excellent results [26].

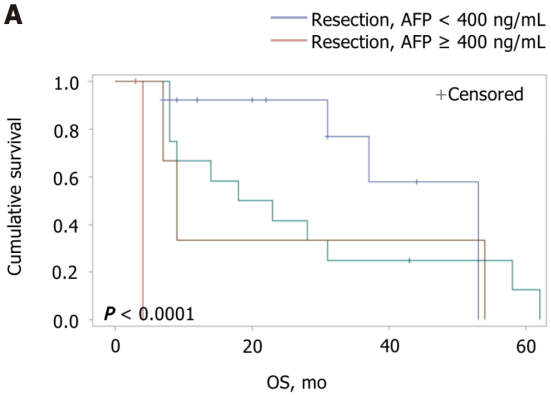
Interesting results were also provided by patient stratification according to the ITA.LI.CA classification. Patients in the B2 subgroup, characterised by nodules of smaller size or lower number, showed the best prognosis when receiving LR. In contrast, those classified as B3, *i.e.*, with larger nodules and higher numbers, had the worst prognosis when resected. Patients with two HCC nodules had a more significant benefit from LR compared with TACE in terms of DFS. These data emphasise the relevance of the number of nodules, which is considered a poor prognostic factor and a predictor of early recurrence.

Nonetheless, a clear cut-off value for the number of nodules beyond which resection is contraindicated has not been determined[10,12,25,27]. Furthermore, although using the same parameters of the Up-to-7 criteria (number of lesions and a maximum diameter of the bigger lesions), the ITA.LI.CA. classification showed better ability in patient stratification.

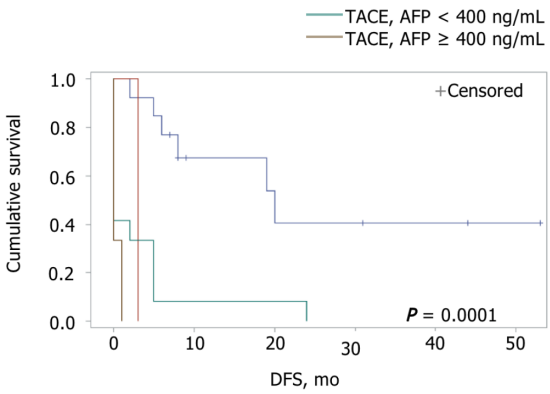
We also evaluated the impact of nodule size on survival in our series. Interestingly, patients with lesions larger than 41 mm had an even more significant benefit from LR in terms of DFS. Previously published studies reported that patients with large solitary HCC had better survival rates when treated with resection than TACE[28,29]. Furthermore, conflicting results have been reported regarding the potential role of tumour diameter as a prognostic factor. While some studies indicated that tumour size alone was not a predictor of poor prognosis[24,30], other reports mentioned tumour dimension as a predictor of survival[31-33]. In particular, in the analysis of 2887 HCC patients, tumour size was an independent prognostic factor of poor survival at multivariate analysis[5], and Wada *et al*[12] concluded that while size alone was not a contraindication for resection, a diameter lower than 5 cm was a favourable factor[12].

Several limitations of this study must be acknowledged, including its retrospective nature with the inherent selection bias. Moreover, the fact that a limited number of patients from a single centre were enrolled should lead to caution in the general applicability of the results. In addition, the relatively long period of enrollment could have been associated with differences due to modifications in the HCC

A

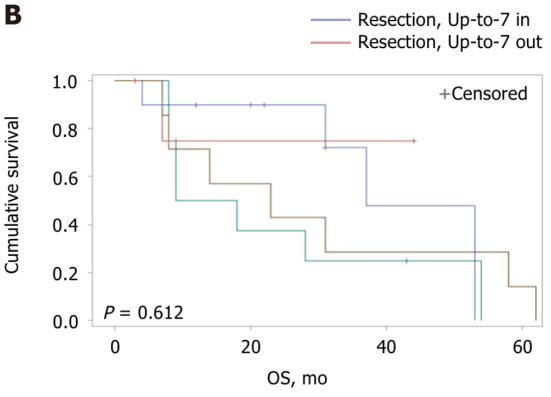


	1-yr	3-yr	5-yr	Median OS (m)
Resection				
AFP < 400 ng/mL (n = 13)	92.3%	76.9%	0%	53 (31-53)
AFP ≥ 400 ng/mL (n = 2)	0%	0%	0%	4 (N.E.-N.E.)
TACE				
AFP < 400 ng/mL (n = 12)	66.7%	25%	12.5%	21 (8-58)
AFP ≥ 400 ng/mL (n = 3)	55.6%	11.1%	0%	9 (7-54)

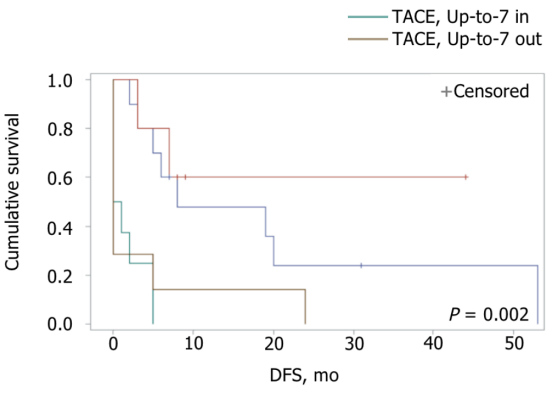


	1-yr	3-yr	5-yr	Median DFS (m)
Resection				
AFP < 400 ng/mL (n = 13)	67.3%	40.4%	-	20 (6-N.E.)
AFP ≥ 400 ng/mL (n = 2)	0%	0%	0%	3 (N.E.-N.E.)
TACE				
AFP < 400 ng/mL (n = 12)	8.3%	0%	0%	0 (0-24)
AFP ≥ 400 ng/mL (n = 3)	0%	0%	0%	0 (0-1)

B

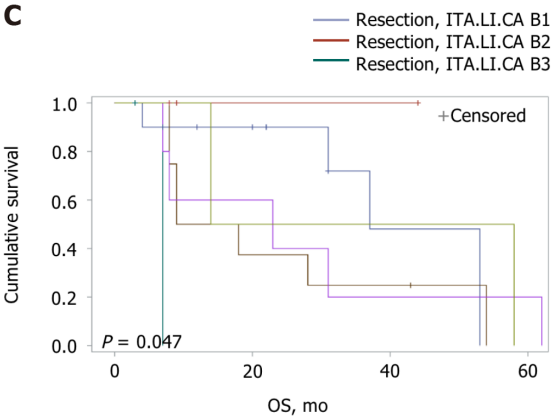


	1-yr	3-yr	5-yr	Median OS (m)
Resection				
In (n = 10)	90%	72%	0%	37 (4-53)
Out (n = 5)	75%	75%	-	N.E.
TACE				
In (n = 8)	50%	25%	0%	14 (8-54)
Out (n = 7)	71%	29%	14%	23 (7-58)

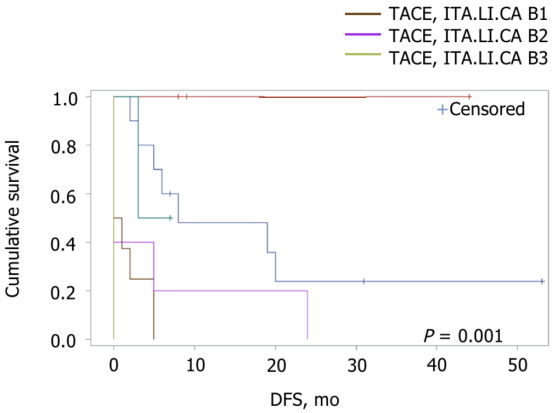


	1-yr	3-yr	5-yr	Median DFS (m)
Resection				
In (n = 10)	48%	24%	-	8 (2-N.E.)
Out (n = 5)	60%	60%	-	N.E. (3-N.E.)
TACE				
In (n = 8)	0%	0%	0%	0.5 (0-5)
Out (n = 7)	14%	0%	0%	0 (0-5)

C

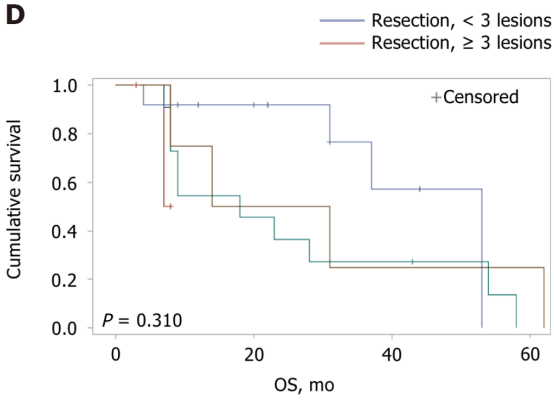


	1-yr	3-yr	5-yr	Median OS (m)
Resection				
ITA.LI.CA B1 (n = 10)	90%	72%	0%	37 (4-53)
ITA.LI.CA B2 (n = 3)	100%	100%	-	N.E.
ITA.LI.CA B3 (n = 2)	0%	0%	0%	7 (N.E.-N.E.)
TACE				
ITA.LI.CA B1 (n = 8)	50%	25%	0%	14 (8-54)
ITA.LI.CA B2 (n = 5)	60%	20%	20%	23 (7-62)
ITA.LI.CA B3 (n = 2)	100%	50%	0%	36 (14-58)

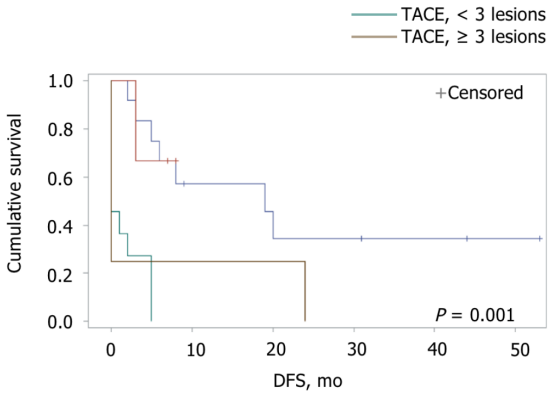


	1-yr	3-yr	5-yr	Median DFS (m)
Resection				
ITA.LI.CA B1 (n = 10)	48%	24%	-	8 (2-N.E.)
ITA.LI.CA B2 (n = 3)	100%	100%	-	N.E.
ITA.LI.CA B3 (n = 2)	-	-	-	N.E.
TACE				
ITA.LI.CA B1 (n = 8)	0%	0%	0%	0.5 (0-5)
ITA.LI.CA B2 (n = 5)	20%	0%	0%	0 (0-24)
ITA.LI.CA B3 (n = 2)	0%	0%	0%	0 (N.E.-N.E.)

D

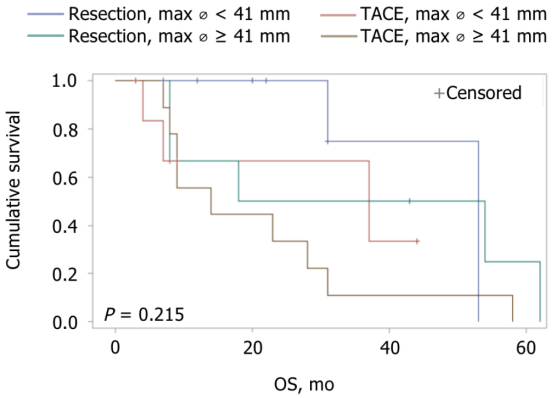


	1-yr	3-yr	5-yr	Median OS (m)
Resection				
2 lesions (n = 12)	91.7%	76.4%	0%	53 (31-53)
≥ 3 lesions (n = 3)	-	-	-	N.E. (7-N.E.)
TACE				
2 lesions (n = 11)	54.6%	27.2%	0%	18 (8-54)
≥ 3 lesions (n = 4)	75%	25%	25%	23 (8-62)

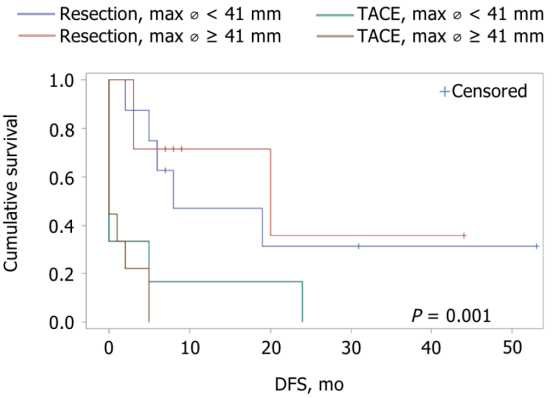


	1-yr	3-yr	5-yr	Median DFS (m)
Resection				
2 lesions (n = 12)	57.1%	34.3%	-	19 (3-N.E.)
≥ 3 lesions (n = 3)	-	-	-	N.E. (3-N.E.)
TACE				
2 lesions (n = 11)	0%	0%	0%	0 (0-5)
≥ 3 lesions (n = 4)	25%	0%	0%	0 (0-24)

E



	1-yr	3-yr	5-yr	Median OS (m)
Resection				
Max ⌀ < 41 mm (n = 8)	100%	75%	0%	53 (31-53)
Max ⌀ ≥ 41 mm (n = 7)	66.7%	66.7%	-	37 (4-N.E.)
TACE				
Max ⌀ < 41 mm (n = 6)	66.7%	50%	25%	36 (8-62)
Max ⌀ ≥ 41 mm (n = 9)	55.6%	11.1%	0%	14 (7-31)



	1-yr	3-yr	5-yr	Median DFS (m)
Resection				
Max ⌀ < 41 mm (n = 8)	46.9%	31.2%	-	8 (2-N.E.)
Max ⌀ ≥ 41 mm (n = 7)	71.4%	35.7%	-	20 (3-N.E.)
TACE				
Max ⌀ < 41 mm (n = 6)	16.7%	0%	0%	0 (0-24)
Max ⌀ ≥ 41 mm (n = 9)	0%	0%	0%	0 (0-5)

DOI: 10.3748/wjg.v28.i29.3981 **Copyright** ©The Author(s) 2022.

Figure 3 Kaplan–Meier curves of overall and disease-free survival comparing the results of the different treatment modalities for patients stratified by different parameters (n = 30). A: Stratification by alpha-fetoprotein levels, lower or higher than 400 ng/mL [overall survival (OS): P < 0.0001 and disease-free survival (DFS): P = 0.0001]; B: Stratification by the Up-to-7 criteria, in or out (OS: P = 0.612 and DFS: P =0.002); C: Stratification by the ITA.LI.CA classification (OS: P = 0.047 and DFS: P = 0.001); D: Stratification by the number of lesions, 2 lesions or more than 3 lesions (OS: P = 0.310 and DFS: P = 0.001); E: Stratification by the maximum diameter of the lesion, smaller or bigger than 41 mm (OS: P = 0.215 and DFS: P = 0.001). Median survival is expressed as months and 95% confidence interval. OS: Overall survival; DFS: Disease-free survival; AFP: Alpha-fetoprotein; N.E.: Not Evaluable; TACE: Trans-Arterial ChemoEmbolization.

management. On the other hand, we performed a rigorous matching using a powerful statistical tool such as the propensity score, although some additional variables not included in the score could have influenced the outcomes.

CONCLUSION

Although the small sample analysed should lead to careful interpretation of the results, after a propensity score matching analysis, patients with multinodular HCC appear to significantly benefit from a surgical approach over TACE in terms of DFS. These results are more evident in the sub-population belonging to the less advanced B2 subgroup according to the ITA.LI.CA. classification, with AFP levels lower than 400 ng/mL, 2 lesions, and with lesions bigger than 41 mm. Patients classified as

ITA.LI.CA B3, with AFP levels higher than 400 ng/mL, and more than 3 lesions had higher benefits from TACE in terms of OS. Future studies are needed to confirm these results in a larger population and to identify other HCC subgroups of patients who would benefit from personalised treatment.

ARTICLE HIGHLIGHTS

Research background

Hepatocellular carcinoma (HCC) is the most frequent primary liver tumour and a leading cause of death. Despite follow-up programmes for cirrhotic patients, HCC is diagnosed in a multifocal form in up to 40% of the patients. Although being a heterogeneous group, the existing classifications consider together the patients with multifocal HCC and generally recommend Trans-Arterial ChemoEmbolization (TACE) as the main treatment. Considering the progress in perioperative care, a growing body of literature has started to propose liver resection (LR) in selected cases, which has shown the best long-term oncological results.

Research motivation

A consensus and detailed guidelines that also consider LR for these patients have not yet been proposed. Moreover, the characteristics of the patients that could benefit more from LR have still to be determined. Defining these aspects could help clinicians in patient management and potentially improve their prognosis.

Research objectives

A comparison between LR and TACE as the first main treatment in terms of post-procedural results and long-term oncological outcomes was performed in patients with multifocal HCC.

Research methods

To reduce the influence of the well-known prognostic factors [*i.e.*, Alpha-fetoprotein (AFP) levels as a dichotomous variable with a cut-off set at 400 ng/dL, presence or absence of cirrhosis, Child-Pugh and Model for End-Stage Liver Disease score, number, and diameter of lesions], a propensity score-matched analysis was performed. Two homogeneous groups (with a 1:1 ratio) were compared to assess the difference in short- and long-term post-procedural results.

Research results

After matching, 30 patients were eligible for the final analysis. Morbidity rates were 42.9% and 40% for LR and TACE, respectively (P = 0.876). Median overall survival (OS) was not different when comparing LR and TACE (53 mo *vs* 18 mo, P = 0.312), while disease-free survival (DFS) was significantly longer with LR (19 mo *vs* 0 mo, P = 0.0001). Subgroup analysis showed that patients in the Italian Liver Cancer (ITA.LI.CA) B2 stage, with AFP levels lower than 400 ng/mL, 2 lesions, and lesions bigger than 41 mm benefited more from LR in terms of DFS. Patients classified as ITA.LI.CA B3, with AFP levels higher than 400 ng/mL and more than 3 lesions appeared to receive more benefit from TACE in terms of OS. However, not all patients with multifocal HCC are amenable to treatment with LR or TACE. Consequently, only a small sample of patients resulted in being eligible for the analysis. Therefore, these results should be considered with caution and further studies are needed.

Research conclusions

There are subgroups of patients with multifocal HCC that seem to benefit more from LR than TACE.

Research perspectives

Further studies are needed to include LR in the guidelines as a potential treatment to be offered to specific subgroups of patients with multifocal HCC.

FOOTNOTES

Author contributions: All authors contributed to the conceptualization and design of the study; Risaliti M, Bartolini I and Campani C wrote the original draft; all authors contributed to critical revision of the article and final approval of the version to be published; Amedei A, Batignani G and Marra F supervised the work.

Institutional review board statement: The study was approved by the Ethical Committee Area Vasta Centro (Florence), No. 12254/22.

Informed consent statement: All study participants or their legal guardian provided informed written consent for

personal and medical data collection prior to study enrolment.

Conflict-of-interest statement: All the authors report no relevant conflicts of interest for this article.

Data sharing statement: No additional data are available.

STROBE statement: The authors have read the STROBE Statement—checklist of items, and the manuscript was prepared and revised according to the STROBE Statement—checklist of items.

Open-Access: This article is an open-access article that was selected by an in-house editor and fully peer-reviewed by external reviewers. It is distributed in accordance with the Creative Commons Attribution NonCommercial (CC BY-NC 4.0) license, which permits others to distribute, remix, adapt, build upon this work non-commercially, and license their derivative works on different terms, provided the original work is properly cited and the use is non-commercial. See: https://creativecommons.org/Licenses/by-nc/4.0/

Country/Territory of origin: Italy

ORCID number: Matteo Risaliti 0000-0001-8476-2536; Ilenia Bartolini 0000-0003-0387-2042; Claudia Campani 0000-0003-3842-782X; Umberto Arena 0000-0002-8839-1506; Carlotta Xodo 0000-0002-7975-5865; Valentina Adotti 0000-0003-3639-0509; Martina Rosi 0000-0001-6601-4737; Antonio Taddei 0000-0003-2963-4085; Paolo Muiesan 0000-0002-7389-6691; Amedeo Amedei 0000-0002-6797-9343; Giacomo Batignani 0000-0001-8369-6418; Fabio Marra 0000-0001-8629-0878.

S-Editor: Fan JR
L-Editor: Webster JR
P-Editor: Chen YX

REFERENCES

1 **Llovet JM**, Kelley RK, Villanueva A, Singal AG, Pikarsky E, Roayaie S, Lencioni R, Koike K, Zucman-Rossi J, Finn RS. Hepatocellular carcinoma. *Nat Rev Dis Primers* 2021; **7**: 6 [PMID: 33479224 DOI: 10.1038/s41572-020-00240-3]
2 **Younossi ZM**, Henry L. Epidemiology of non-alcoholic fatty liver disease and hepatocellular carcinoma. *JHEP Rep* 2021; **3**: 100305 [PMID: 34189448 DOI: 10.1016/j.jhepr.2021.100305]
3 **Fukami Y**, Kaneoka Y, Maeda A, Kumada T, Tanaka J, Akita T, Kubo S, Izumi N, Kadoya M, Sakamoto M, Nakashima O, Matsuyama Y, Kokudo T, Hasegawa K, Yamashita T, Kashiwabara K, Takayama T, Kokudo N, Kudo M; Liver Cancer Study Group of Japan. Liver Resection for Multiple Hepatocellular Carcinomas: A Japanese Nationwide Survey. *Ann Surg* 2020; **272**: 145-154 [PMID: 30672806 DOI: 10.1097/SLA.0000000000003192]
4 **Roayaie S**, Jibara G, Tabrizian P, Park JW, Yang J, Yan L, Schwartz M, Han G, Izzo F, Chen M, Blanc JF, Johnson P, Kudo M, Roberts LR, Sherman M. The role of hepatic resection in the treatment of hepatocellular cancer. *Hepatology* 2015; **62**: 440-451 [PMID: 25678263 DOI: 10.1002/hep.27745]
5 **Wang CY**, Li S. Clinical characteristics and prognosis of 2887 patients with hepatocellular carcinoma: A single center 14 years experience from China. *Medicine (Baltimore)* 2019; **98**: e14070 [PMID: 30681563 DOI: 10.1097/MD.0000000000014070]
6 **Brierley JD**, Gospodarowicz MK, Wittekind C. TNM Classification of Malignant Tumours, 8 th edition due December 2016. *J Clin Pathol* 1998; **1**: 84 [DOI: 10.1136/jcp.43.4.350-e]
7 **Reig M**, Forner A, Rimola J, Ferrer-Fàbrega J, Burrel M, Garcia-Criado Á, Kelley RK, Galle PR, Mazzaferro V, Salem R, Sangro B, Singal AG, Vogel A, Fuster J, Ayuso C, Bruix J. BCLC strategy for prognosis prediction and treatment recommendation: The 2022 update. *J Hepatol* 2022; **76**: 681-693 [PMID: 34801630 DOI: 10.1016/j.jhep.2021.11.018]
8 **Farinati F**, Vitale A, Spolverato G, Pawlik TM, Huo TL, Lee YH, Frigo AC, Giacomin A, Giannini EG, Ciccarese F, Piscaglia F, Rapaccini GL, Di Marco M, Caturelli E, Zoli M, Borzio F, Cabibbo G, Felder M, Sacco R, Morisco F, Biasini E, Foschi FG, Gasbarrini A, Svegliati Baroni G, Virdone R, Masotto A, Trevisani F, Cillo U; ITA. LI.CA study group. Development and Validation of a New Prognostic System for Patients with Hepatocellular Carcinoma. *PLoS Med* 2016; **13**: e1002006 [PMID: 27116206 DOI: 10.1371/journal.pmed.1002006]
9 **Ruzzenente A**, Capra F, Pachera S, Iacono C, Piccirillo G, Lunardi M, Pistoso S, Valdegamberi A, D'Onofrio M, Guglielmi A. Is liver resection justified in advanced hepatocellular carcinoma? *J Gastrointest Surg* 2009; **13**: 1313-1320 [PMID: 19418103 DOI: 10.1007/s11605-009-0903-x]
10 **Ishizawa T**, Hasegawa K, Aoki T, Takahashi M, Inoue Y, Sano K, Imamura H, Sugawara Y, Kokudo N, Makuuchi M. Neither multiple tumors nor portal hypertension are surgical contraindications for hepatocellular carcinoma. *Gastroenterology* 2008; **134**: 1908-1916 [PMID: 18549877 DOI: 10.1053/j.gastro.2008.02.091]
11 **Kamiyama T**, Orimo T, Wakayama K, Shimada S, Nagatsu A, Yokoo H, Kamachi H, Yamashita K, Shimamura T, Taketomi A. Survival outcomes of hepatectomy for stage B Hepatocellular carcinoma in the BCLC classification. *World J Surg Oncol* 2017; **15**: 156 [PMID: 28830473 DOI: 10.1186/s12957-017-1229-x]
12 **Wada H**, Eguchi H, Noda T, Ogawa H, Yamada D, Tomimaru Y, Tomokuni A, Asaoka T, Kawamoto K, Gotoh K, Marubashi S, Umeshita K, Nagano H, Doki Y, Mori M. Selection criteria for hepatic resection in intermediate-stage (BCLC stage B) multiple hepatocellular carcinoma. *Surgery* 2016; **160**: 1227-1235 [PMID: 27395761 DOI: 10.1016/j.surg.2016.05.023]
13 **Clavien PA**, Barkun J, de Oliveira ML, Vauthey JN, Dindo D, Schulick RD, de Santibañes E, Pekolj J, Slankamenac K,

Bassi C, Graf R, Vonlanthen R, Padbury R, Cameron JL, Makuuchi M. The Clavien-Dindo classification of surgical complications: five-year experience. *Ann Surg* 2009; **250**: 187-196 [PMID: 19638912 DOI: 10.1097/SLA.0b013e3181b13ca2]

14 **European Association for the Study of the Liver**. EASL Clinical Practice Guidelines: Management of hepatocellular carcinoma. *J Hepatol* 2018; **69**: 182-236 [PMID: 29628281 DOI: 10.1016/j.jhep.2018.03.019]

15 **Mazzaferro V**, Llovet JM, Miceli R, Bhoori S, Schiavo M, Mariani L, Camerini T, Roayaie S, Schwartz ME, Grazi GL, Adam R, Neuhaus P, Salizzoni M, Bruix J, Forner A, De Carlis L, Cillo U, Burroughs AK, Troisi R, Rossi M, Gerunda GE, Lerut J, Belghiti J, Boin I, Gugenheim J, Rochling F, Van Hoek B, Majno P; Metroticket Investigator Study Group. Predicting survival after liver transplantation in patients with hepatocellular carcinoma beyond the Milan criteria: a retrospective, exploratory analysis. *Lancet Oncol* 2009; **10**: 35-43 [PMID: 19058754 DOI: 10.1016/S1470-2045(08)70284-5]

16 **Pecorelli A**, Lenzi B, Gramenzi A, Garuti F, Farinati F, Giannini EG, Ciccarese F, Piscaglia F, Rapaccini GL, Di Marco M, Caturelli E, Zoli M, Borzio F, Sacco R, Cabibbo G, Felder M, Morisco F, Gasbarrini A, Baroni GS, Foschi FG, Biasini E, Masotto A, Virdone R, Bernardi M, Trevisani F; Italian LiverCancer (ITA. LI.CA) group. Curative therapies are superior to standard of care (transarterial chemoembolization) for intermediate stage hepatocellular carcinoma. *Liver Int* 2017; **37**: 423-433 [PMID: 27566596 DOI: 10.1111/liv.13242]

17 **Bai DS**, Zhang C, Chen P, Jin SJ, Jiang GQ. The prognostic correlation of AFP level at diagnosis with pathological grade, progression, and survival of patients with hepatocellular carcinoma. *Sci Rep* 2017; **7**: 12870 [PMID: 28993684 DOI: 10.1038/s41598-017-12834-1]

18 **Llovet JM**, Brú C, Bruix J. Prognosis of hepatocellular carcinoma: the BCLC staging classification. *Semin Liver Dis* 1999; **19**: 329-338 [PMID: 10518312 DOI: 10.1055/s-2007-1007122]

19 **Llovet JM**, Bruix J. Systematic review of randomized trials for unresectable hepatocellular carcinoma: Chemoembolization improves survival. *Hepatology* 2003; **37**: 429-442 [PMID: 12540794 DOI: 10.1053/jhep.2003.50047]

20 **Llovet JM**, Real MI, Montaña X, Planas R, Coll S, Aponte J, Ayuso C, Sala M, Muchart J, Solà R, Rodés J, Bruix J; Barcelona Liver Cancer Group. Arterial embolisation or chemoembolisation *vs* symptomatic treatment in patients with unresectable hepatocellular carcinoma: a randomised controlled trial. *Lancet* 2002; **359**: 1734-1739 [PMID: 12049862 DOI: 10.1016/S0140-6736(02)08649-X]

21 **Lo CM**, Ngan H, Tso WK, Liu CL, Lam CM, Poon RT, Fan ST, Wong J. Randomized controlled trial of transarterial lipiodol chemoembolization for unresectable hepatocellular carcinoma. *Hepatology* 2002; **35**: 1164-1171 [PMID: 11981766 DOI: 10.1053/jhep.2002.33156]

22 **Zhong JH**, Peng NF, You XM, Ma L, Li LQ. Hepatic resection is superior to transarterial chemoembolization for treating intermediate-stage hepatocellular carcinoma. *Liver Int* 2017; **37**: 1083-1084 [PMID: 27797424 DOI: 10.1111/liv.13290]

23 **Liu W**, Zhou JG, Sun Y, Zhang L, Xing BC. Hepatic Resection Improved the Long-Term Survival of Patients with BCLC Stage B Hepatocellular Carcinoma in Asia: a Systematic Review and Meta-Analysis. *J Gastrointest Surg* 2015; **19**: 1271-1280 [PMID: 25943910 DOI: 10.1007/s11605-015-2811-6]

24 **Torzilli G**, Belghiti J, Kokudo N, Takayama T, Capussotti L, Nuzzo G, Vauthey JN, Choti MA, De Santibanes E, Donadon M, Morenghi E, Makuuchi M. A snapshot of the effective indications and results of surgery for hepatocellular carcinoma in tertiary referral centers: is it adherent to the EASL/AASLD recommendations? *Ann Surg* 2013; **257**: 929-937 [PMID: 23426336 DOI: 10.1097/SLA.0b013e31828329b8]

25 **Yin L**, Li H, Li AJ, Lau WY, Pan ZY, Lai EC, Wu MC, Zhou WP. Partial hepatectomy vs. transcatheter arterial chemoembolization for resectable multiple hepatocellular carcinoma beyond Milan Criteria: a RCT. *J Hepatol* 2014; **61**: 82-88 [PMID: 24650695 DOI: 10.1016/j.jhep.2014.03.012]

26 **Finn RS**, Qin S, Ikeda M, Galle PR, Ducreux M, Kim TY, Kudo M, Breder V, Merle P, Kaseb AO, Li D, Verret W, Xu DZ, Hernandez S, Liu J, Huang C, Mulla S, Wang Y, Lim HY, Zhu AX, Cheng AL; IMbrave150 Investigators. Atezolizumab plus Bevacizumab in Unresectable Hepatocellular Carcinoma. *N Engl J Med* 2020; **382**: 1894-1905 [PMID: 32402160 DOI: 10.1056/NEJMoa1915745]

27 **Donadon M**, Fontana A, Procopio F, Del Fabbro D, Cimino M, Viganò L, Palmisano A, Torzilli G. Dissecting the multinodular hepatocellular carcinoma subset: is there a survival benefit after hepatectomy? *Updates Surg* 2019; **71**: 57-66 [PMID: 30852806 DOI: 10.1007/s13304-019-00626-3]

28 **Liu PH**, Su CW, Hsu CY, Hsia CY, Lee YH, Huang YH, Lee RC, Lin HC, Huo TI. Solitary Large Hepatocellular Carcinoma: Staging and Treatment Strategy. *PLoS One* 2016; **11**: e0155588 [PMID: 27176037 DOI: 10.1371/journal.pone.0155588]

29 **Hong SK**, Lee KW, Hong SY, Suh S, Hong K, Han ES, Lee JM, Choi Y, Yi NJ, Suh KS. Efficacy of Liver Resection for Single Large Hepatocellular Carcinoma in Child-Pugh A Cirrhosis: Analysis of a Nationwide Cancer Registry Database. *Front Oncol* 2021; **11**: 674603 [PMID: 33996606 DOI: 10.3389/fonc.2021.674603]

30 **Chang WT**, Kao WY, Chau GY, Su CW, Lei HJ, Wu JC, Hsia CY, Lui WY, King KL, Lee SD. Hepatic resection can provide long-term survival of patients with non-early-stage hepatocellular carcinoma: extending the indication for resection? *Surgery* 2012; **152**: 809-820 [PMID: 22766361 DOI: 10.1016/j.surg.2012.03.024]

31 **Delis SG**, Bakoyiannis A, Tassopoulos N, Athanassiou K, Kelekis D, Madariaga J, Dervenis C. Hepatic resection for hepatocellular carcinoma exceeding Milan criteria. *Surg Oncol* 2010; **19**: 200-207 [PMID: 19500972 DOI: 10.1016/j.suronc.2009.05.003]

32 **Truant S**, Boleslawski E, Duhamel A, Bouras AF, Louvet A, Febvay C, Leteurtre E, Huet G, Zerbib P, Dharancy S, Hebbar M, Pruvot FR. Tumor size of hepatocellular carcinoma in noncirrhotic liver: a controversial predictive factor for outcome after resection. *Eur J Surg Oncol* 2012; **38**: 1189-1196 [PMID: 22863304 DOI: 10.1016/j.ejso.2012.07.112]

33 **Bartolini I**, Nelli T, Russolillo N, Cucchetti A, Pesi B, Moraldi L, Ferrero A, Ercolani G, Grazi G, Batignani G. Multiple hepatocellular carcinoma: Long-term outcomes following resection beyond actual guidelines. An Italian multicentric retrospective study. *Am J Surg* 2021; **222**: 599-605 [PMID: 33546852 DOI: 10.1016/j.amjsurg.2021.01.023]

World Journal of Gastroenterology

Submit a Manuscript: https://www.f6publishing.com

World J Gastroenterol 2022 August 7; 28(29): 3994-4006

DOI: 10.3748/wjg.v28.i29.3994

ISSN 1007-9327 (print) ISSN 2219-2840 (online)

ORIGINAL ARTICLE

Observational Study

Structure of the myenteric plexus in normal and diseased human ileum analyzed by X-ray virtual histology slices

Bela Veress, Niccolò Peruzzi, Marina Eckermann, Jasper Frohn, Tim Salditt, Martin Bech, Bodil Ohlsson

Specialty type: Gastroenterology and hepatology

Provenance and peer review: Unsolicited article; Externally peer reviewed.

Peer-review model: Single blind

Peer-review report's scientific quality classification

Grade A (Excellent): 0
Grade B (Very good): B
Grade C (Good): C
Grade D (Fair): 0
Grade E (Poor): 0

P-Reviewer: Goldstein AM, United States; Natale G, Italy

Received: April 28, 2022
Peer-review started: April 28, 2022
First decision: May 11, 2022
Revised: May 18, 2022
Accepted: July 11, 2022
Article in press: July 11, 2022
Published online: August 7, 2022

Bela Veress, Department of Pathology, Skåne Universiity Hospital, Malmö 205 02, Sweden

Niccolò Peruzzi, Martin Bech, Medical Radiation Physics, Department of Clinical Sciences, Lund University, Lund 221 00, Sweden

Marina Eckermann, Jasper Frohn, Tim Salditt, Institute for X-Ray Physics, University of Göttingen, Göttingen 37077, Germany

Marina Eckermann, Tim Salditt, Cluster of Excellence "Multiscale Bioimaging: from Molecular Machines to Networks of Excitable Cells" (MBExC), University of Göttingen, Göttingen 37077, Germany

Marina Eckermann, ESRF, The European Synchrotron, Grenoble 38043, France

Bodil Ohlsson, Department of Internal Medicine, Skåne University Hospital, Lund University, Malmö S-205 02, Sweden

Corresponding author: Bodil Ohlsson, MD, PhD, Full Professor, Department of Internal Medicine, Skåne University Hospital, Lund University, 15 Jan Waldenströms Street, Malmö S-205 02, Sweden. bodil.ohlsson@med.lu.se

Abstract

BACKGROUND

The enteric nervous system (ENS) is situated along the entire gastrointestinal tract and is divided into myenteric and submucosal plexuses in the small and large intestines. The ENS consists of neurons, glial cells, and nerves assembled into ganglia, surrounded by telocytes, interstitial cells of Cajal, and connective tissue. Owing to the complex spatial organization of several interconnections with nerve fascicles, the ENS is difficult to examine in conventional histological sections of 3-5 μm.

AIM

To examine human ileum full-thickness biopsies using X-ray phase-contrast nanotomography without prior staining to visualize the ENS.

METHODS

Six patients were diagnosed with gastrointestinal dysmotility and neuropathy based on routine clinical and histopathological examinations. As controls, full-thickness biopsies were collected from healthy resection ileal regions after

hemicolectomy for right colon malignancy. From the paraffin blocks, 4-μm thick sections were prepared and stained with hematoxylin and eosin for localization of the myenteric ganglia under a light microscope. A 1-mm punch biopsy (up to 1 cm in length) centered on the myenteric plexus was taken and placed into a Kapton® tube for mounting in the subsequent investigation. X-ray phase-contrast tomography was performed using two custom-designed laboratory setups with micrometer resolution for overview scanning. Subsequently, selected regions of interest were scanned at a synchrotron-based end-station, and high-resolution slices were reported. In total, more than 6000 virtual slices were analyzed from nine samples.

RESULTS

In the overview scans, the general architecture and quality of the samples were studied, and the myenteric plexus was localized. High-resolution scans revealed details, including the ganglia, interganglional nerve fascicles, and surrounding tissue. The ganglia were irregular in shape and contained neurons and glial cells. Spindle-shaped cells with very thin cellular projections could be observed on the surface of the ganglia, which appeared to build a network. In the patients, there were no alterations in the general architecture of the myenteric ganglia. Nevertheless, several pathological changes were observed, including vacuolar degeneration, autophagic activity, the appearance of sequestosomes, chromatolysis, and apoptosis. Furthermore, possible expulsion of pyknotic neurons and defects in the covering cellular network could be observed in serial slices. These changes partly corresponded to previous light microscopy findings.

CONCLUSION

The analysis of serial virtual slices could provide new information that cannot be obtained by classical light microscopy. The advantages, disadvantages, and future possibilities of this method are also discussed.

Key Words: Enteric nervous system; Immunohistochemistry; Neuropathy; Synchrotron; Virtual histology; X-ray phase-contrast nanotomography

©The Author(s) 2022. Published by Baishideng Publishing Group Inc. All rights reserved.

Core Tip: Full-thickness biopsies of 1 mm diameter and up to 1 cm length from the human ileum were scanned using two laboratory-based μ-computed tomography setups to study the architecture of the enteric nervous system (ENS) and further scanned by a synchrotron-based end-station for histopathological studies, without any staining. Several pathological neuronal changes, such as vacuolar degeneration, autophagic activity, appearance of sequestosomes, chromatolysis, and apoptosis, were identified in diseased patients. Phenomena that were undetectable by light microscopy were observed. The relationships among various tissue components could be followed in all directions. Thus, this method provides a unique analysis of the ENS.

Citation: Veress B, Peruzzi N, Eckermann M, Frohn J, Salditt T, Bech M, Ohlsson B. Structure of the myenteric plexus in normal and diseased human ileum analyzed by X-ray virtual histology slices. *World J Gastroenterol* 2022; 28(29): 3994-4006

URL: https://www.wjgnet.com/1007-9327/full/v28/i29/3994.htm

DOI: https://dx.doi.org/10.3748/wjg.v28.i29.3994

INTRODUCTION

The neurons of the enteric nervous system (ENS) assemble into ganglia, forming the submucosal and myenteric plexuses[1]. The ganglia, which also contain glial cells, are connected by nerve fascicles and are surrounded by telocytes and interstitial cells of Cajal (ICC), as well as by other cells and fibers of connective tissue. Various diseases of the ENS may lead to severe bowel motility dysfunction in the form of chronic intestinal pseudo-obstruction (CIPO) and enteric dysmotility (ED)[2,3]. Enteric neuropathy is seldom studied because only a few centers are available for the evaluation of gastrointestinal motility, access to the myenteric plexus requires full-thickness bowel biopsies, and pathologists subspecializing in neuromuscular diseases of the ENS are scarce. Subsequently, the neuropathy diagnosis may be ignored or delayed for several years, which prevents proper healthcare of the patients[4].

We recently presented a methodology to use X-ray phase-contrast nanotomography to study the volume and structure of the ENS[5]. Neurons and surrounding structures are visible using this method without any prior staining, allowing the possibility to study large sample volumes[5,6]. The aim of the present qualitative analysis of virtual slices was to describe in detail the structure of human ileal myenteric ganglia in the normal human ileum as well as in patients with CIPO or ED.

MATERIALS AND METHODS

Patients and samples

Six patients with severe gastrointestinal pain and dysmotility were examined using esophageal manometry, gastric emptying scintigraphy, antroduodenojejunal manometry, and colonic transit time, after exclusion of organic disease. Patients were diagnosed with CIPO when they fulfilled the following three criteria: a medical history compatible with pseudo-obstruction, documented events or chronic signs mimicking mechanical obstruction (bowel dilatation and/or air/fluid levels), and absence of mechanical obstruction or other organic causes for these symptoms and findings[3]. The criteria for ED were documented abnormal contractile activity, but no history of episodes or current signs mimicking mechanical obstruction and the absence of any medication that could lead to the observed motor abnormalities[2].

A previously described laparoscopy-assisted technique for ileal full-thickness biopsies and the preparation of biopsies was used[4,7]. Briefly, 1.0 cm × 1.5 cm large full-thickness biopsies were cut from the ileum and embedded in paraffin. Transversal and horizontal 3-5-mm thick serial sections were stained according to the protocol for CIPO analysis[8]. Histopathological findings were evaluated by a pathologist (B.V.) and classified as previously described[9]. The criteria for neuropathies were based on criteria suggested by the Gastro 2009 International Working Group for Gastrointestinal Neuromuscular Pathology[10]. The histopathological diagnoses and various stains, such as CD117 for ICC, CD34 for telocytes, S100 for Schwann cells, periodic acid-Schiff (PAS) with or without diastase (PAS-D) for carbohydrates or their compounds (*e.g.*, glycogen and mucin), and p62 for sequestosome, were obtained from the medical records (Table 1). For all patients, the disease initially presented when they were adults without any known heredity. Genetic analysis was not performed. There was no correlation between the varying histopathological findings described in Table 1 and the clinical presentation or other functional findings of patients (data not shown).

Three men aged 45, 54, and 82 years were used as controls, all of whom had undergone hemicolectomy due to malignancy in the right colon. A full-thickness biopsy specimen was collected and stained from the healthy resection region of the ileum. The sample size was adopted based on the beam time available in the laboratory.

Sample preparation

From the paraffin blocks of these nine individuals, 4-μm thick sections were prepared and stained with hematoxylin and eosin (H&E) for the localization of the myenteric ganglia under a light microscope. A biopsy punch of 1 mm diameter and up to 1 cm in length centered on the myenteric plexus was taken from the paraffin blocks of patients and controls and placed into a Kapton® tube (Paramount, Indiana, United States) for mounting in the subsequent tomographic investigation[11].

X-ray phase-contrast tomography

X-ray phase-contrast tomography was performed on two custom-designed laboratory setups with micrometer resolution, located at the Institute for X-Ray Physics, University of Göttingen, Göttingen, Germany[11] and a Gottingen Instrument for Nano-Imaging with X-rays (GINIX), installed at the P10/PETRAIII beamline (Hamburg, Germany) with sub-micron resolution[12]. All setups used propagation-based, phase-contrast methods, in which the sample is placed between the source and detector, and the phase information is obtained by free-space propagation and self-interference of the coherent X-ray beam without the need for additional optical elements. Phase retrieval is necessary to correctly extract phase information before tomographic reconstruction[13-15].

The two laboratory setups were installed at a liquid metal jet source (Excillum, Kista, Sweden) or a microfocus rotating anode (mm007, Rigaku, Austin, TX, United States). Both setups used high-resolution scintillator-based detectors (Xsight, Rigaku) and employed broad bandpass radiation peaking at the characteristic lines of Ga Ka (9.25 keV) and Cu (8.05 keV) for the liquid jet and rotating anode sources, respectively. Phase retrieval was performed using the Bronnikov-aided correction algorithm[11,15,16]. As a result, these home-built setups allowed us to image the whole 1-mm wide and several-mm long sample with an isotropic effective voxel size of approximately 1 μm (approximately 15 h scan time per sample), enabling identification of the neural tissue structure (further information about the experimental parameters is provided in (Table 2). The two systems could run in parallel and were used to optimize time consumption.

Table 1 Basic characteristics of subjects

Age, sex	Disease (years)	Clinical diagnosis	Histopathological findings	Histopathological diagnosis	X-ray
45, M	NA	Control	Normal neurons	Healthy	Healthy
54, M	NA	Control	Normal neurons	Healthy	Healthy
82, M	NA	Control	Normal neurons	Healthy	Healthy
27, W	4	ED/type 1 diabetes	Vacuolated, apoptotic neurons, chromatolysis	Lymphocytic ganglioneuritis	Vacuolated, shrunken neurons, chromatolysis, autophagia
27, W	6	Idiopathic ED	Vacuolated neurons, chromatolysis	Degenerative neuropathy	Pre-apoptotic and dead nucleus
32, W	2	Drug-induced CIPO	Vacuolated, shrunken, chromatolysis, hyperplasia ICC	Visceral degenerative neuropathy with axon vacuolization, hyperplasia, and vacuolization of ICCs, and hypertrophy of the longitudinal and internal circular muscle layers	Only fascicle, no ganglia for evaluation
43, W	3	Idiopathic ED	Amphophilic shrunken neurons, Vacuolated neurons, chromatolysis	Lymphocytic ganglioneuritis with neurondegeneration	Amphophilic degeneration, vacuolated neurons
52, W	4	Idiopathic ED	Vacuolated, shrunken neurons, hypoplasia of ICC	Lymphocytic ganglioneuritis	Vacuolated, shrunken neurons, chromatolysis
56, W	50	ED/Ehlers-Danlos	Vacuolated neurons, chromatolysis, hyperplasia ICC	Lymphocytic ganglioneuritis with vacuolar neurodegeneration and hyperplasia of the ICC	Severe atrophy with reduced volume

Data obtained from the medical records; disease duration assessed in years. CIPO: Chronic intestinal pseudo-obstruction; ED: Enteric dysmotility; ICC: Interstitial cells of Cajal; M: Man; W: Woman; NA: Not available.

Table 2 Experimental and reconstruction parameters

Scan configuration	Effective pixel size (μm)	Energy (keV)	Number of projections[1]	Phase retrieval scheme	Phase retrieval parameter	Ring removal algorithm
Laboratory setup (liquid metal jet)	0.920[2]	9.25 (Kα)	1 × 1000 (50 s) or 1 × 700 (40 s)	BAC	α = 0.008, β = 0.160	Wavelet
Laboratory setup (rotating anode)	1.072	8.05 (Kα)	1 × 1000 (50 s) or 1 × 700 (40 s)	BAC	α = 0.07, β = 0.16	Wavelet
GINIX waveguide (all samples except for ED/Ehlers-Danlos patient)	0.169	8.00	4 × 1500 (1 s) or 3 × 1500 (1 s)	Non-linear Tikhonov[3]	δ/β = 50, lim1 = 8e-3, lim2 = 0.5	Additive
GINIX waveguide (ED/Ehlers-Danlos patient)	0.176	7.50	4 × 1000 (2 s)	Non-linear Tikhonov[3]	δ/β = 50, lim1 = 1e-4, lim2 = 0.1	Additive

[1]Due to time constraints, some samples were scanned with a lower number of projections and shorter exposure times (in the overview scans) or with less distances (in the high-resolution scans of the drug-induced chronic intestinal pseudo-obstruction patient and of the 40 years old control).
[2]After voxel binning of 2 × 2 × 2.
[3]No support, no restriction on phase shift.
GINIX: Gottingen Instrument for Nano-Imaging with X-rays; ED: Enteric dysmotility.

Selected regions of interest (ROIs) of 320 μm × 320 μm × 320 μm were scanned with an isotropic effective voxel size of 169 nm at the synchrotron-based end-station (approximately 2.5-3.0 h scan time), using inline holography based on a coherent divergent beam [8 keV, Si (111) monochromator] exiting from an X-ray waveguide[11,12]. Holographic phase retrieval based on contrast-transfer-function (CTF) approach, ring removal, and tomographic reconstructions were performed using in-house reconstruction pipelines[16]. Further details can be found in Table 2.

Complete information regarding the experimental setups and reconstruction pipelines, which were performed by physicists unaware of the diagnosis, is provided in a previous publication[5]. The analysis of the slices reported in this paper was performed on the data acquired at the synchrotron end-station, on the high-resolution scans.

Image analysis

All the obtained volumetric datasets were digitally sectioned along any arbitrary slicing plane, enabling virtual histology of the samples. In the histological evaluation, the term "spindle-shaped cells" was used to describe the cells around the ganglia, which represented either telocytes, ICCs, or fibroblasts/cytes because no differentiation could be made without immunohistochemistry. In cases where identification can be made from double immunohistochemical staining of the same regions[17], the cells are called telocytes or ICC. In total, more than 6000 virtual slices were analyzed from the nine samples.

RESULTS

In the overview scans performed with the laboratory setup, the general architecture of the bowel samples was examined with respect to the quality of the sample and the presence and localization of the myenteric plexus. High-resolution scans revealed details of the myenteric plexus, including the ganglia, interganglional nerve fascicles, and surrounding tissue.

Normal structure of the ileal myenteric plexus

Ganglion: The shape of the ganglia was uneven toward both the muscle layers and interganglional nerve fascicles. The smaller or larger irregularities contained one or more neurons and glial cells (Figures 1, 2A, 4A-D, and 5).

In the surface view of the ganglia, a parallel arrangement of telocytes with long thin "primary" telopodes originating directly from the cellular bodies could be observed, from which shorter "secondary" telopodes radiated sidewise, building up a network (Figures 1A-C, 3B, 4A and B). Occasionally, at the optimal transverse view of the ganglion, a double layer of thin cytoplasmic projections was present (Figure 2B), corresponding to the immunohistochemical demonstration of telocytes and ICCs[17].

Both larger and smaller neurons had mostly rounded nuclei and nucleoli, where larger neurons had finely granulated cytoplasm with a paler network between the granules, whereas the smaller neurons had slightly denser and more homogeneous cytoplasm (Figures 2B and 3B-D). Axons were occasionally observed (Figure 2A). Small glial cells were present around and between the neurons (Figures 2A, 3C and D). No degenerating neurons were found in either of the two younger individuals. In the 82-year-old control, however, one neuron with a shrunken, dark body, pyknotic small almost black nucleus and larger autophagic vacuoles could be observed in addition to numerous normal neurons (not shown).

Nerve fascicles and spindle-shaped cell layer

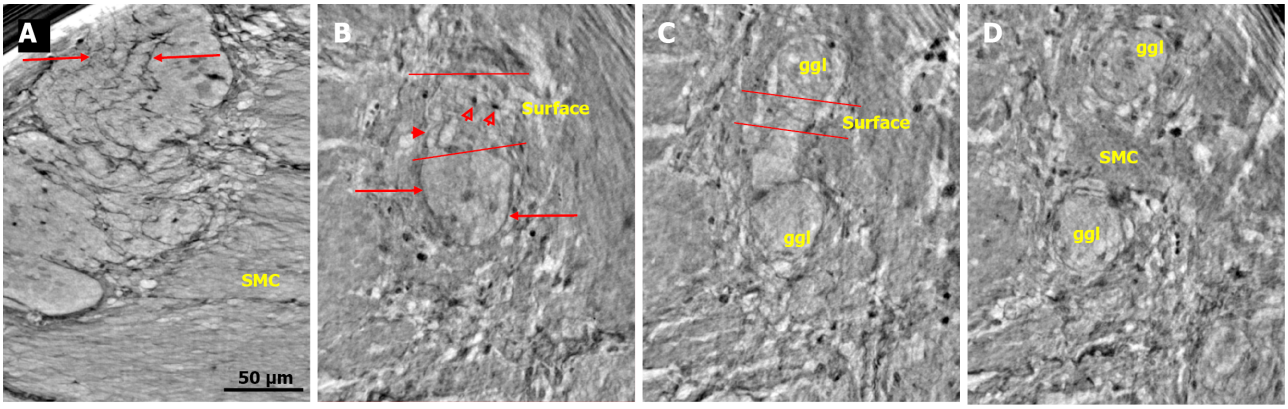
The nerve fascicles had normal architecture. Parallel thin telopodes separated the individual axons (Figures 2C and 3A-C). Some spindle-shaped cells had very thin, dark nuclei, whereas the nuclei of others were larger and cigar-like.

Pathological findings of the ileal myenteric plexus

Four patients had lymphocytic ganglioneuritis or lymphocytic neuritis, and two patients had only visceral degenerative neuropathy. No alterations were observed in the general architecture of the myenteric ganglia. Nevertheless, several pathological changes could be observed, partly corresponding to the light microscopic findings, as shown in the insets of the figures. Cellular changes occurred in all six patients with dysmotility. Suspected lymphocytes were found within the ganglion only in one patient. The lack of lymphocytic attack on the ganglion in other patients can be explained by the focal nature of inflammation.

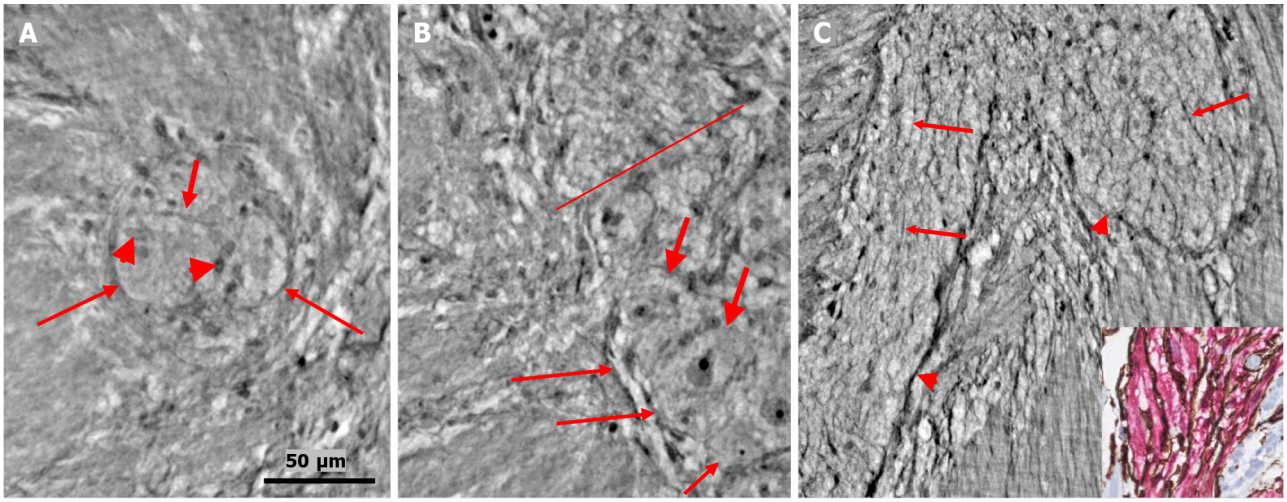
Pathological neuronal changes

The cytoplasm of several neurons contained vacuoles. Many of the vacuoles contained small dark granules (Figure 5A, C, and D) (autophagic vacuoles/Lipofuscin; 5D-inset: PAS-D$^+$). In one patient, several neurons exhibited pale cytoplasm (Figure 4A-D) (chromatolysis), and a large homogeneous irregular dark area was present (Figure 4F) (4F-inset: Sequestosome p62$^+$). Apoptotic shrunken neurons had compact, dark cytoplasm with small, irregular, pyknotic nuclei (Figures 4C-E, 5B and 6) (4E-inset H&E; 5B-inset: Apoptosis H&E). These neurons were observed in three patients at the ganglion border without telopodes in a few virtual slices (Figure 4B-D), possibly representing the ejection of a dead neuron (Figures 4B-D and 6). Very dense dark inclusions with similar substructures were found in two patients, which are foreign structures for the normal ganglion; one of these bodies is shown in serial virtual slices (Figure 4A-C) (4A-C: Hyaline bodies; 4A and B-insets: PAS-D$^+$). At 6.8 μm in Figure 4A, an inner structure with a central pale area surrounded by an irregular dark ring can be seen within the body (Figure 4B). When viewing 4.0 μm deeper, there is a semi-dense "half-moon" at the edge of the hyaline body (Figure 4C).



DOI: 10.3748/wjg.v28.i29.3994 **Copyright** ©The Author(s) 2022.

Figure 1 Ganglion from healthy human ileum. A: Part of the myenteric ganglion in two portions. Quite regular, almost parallel, thin cytoplasmic projections of telocytes (telopodes) with short, thin "spines" on the surface are observed (between arrows). The scale bar (50 µm) was applied to all subfigures; B: A small portion of the ganglion containing two neurons. On the surface of the ganglion (between the two lines), the cellular nuclei of the two telocytes were observed as dark spots (empty arrowheads). Telopodes radiate from their body. Arrows indicate the telopodes around the ganglion. A telopode can be followed toward the surface (arrowhead); C: 16.9 µm deeper from Figure B, two portions appeared with thin telopodes on the surface; D: 10.1 µm deeper from Figure C, SMCs are observed between the two portions. B-D are representative virtual slices from a series covering 27.0 µm thickness of the ganglion. Ggl: Ganglion; SMC: Smooth muscle cells.



DOI: 10.3748/wjg.v28.i29.3994 **Copyright** ©The Author(s) 2022.

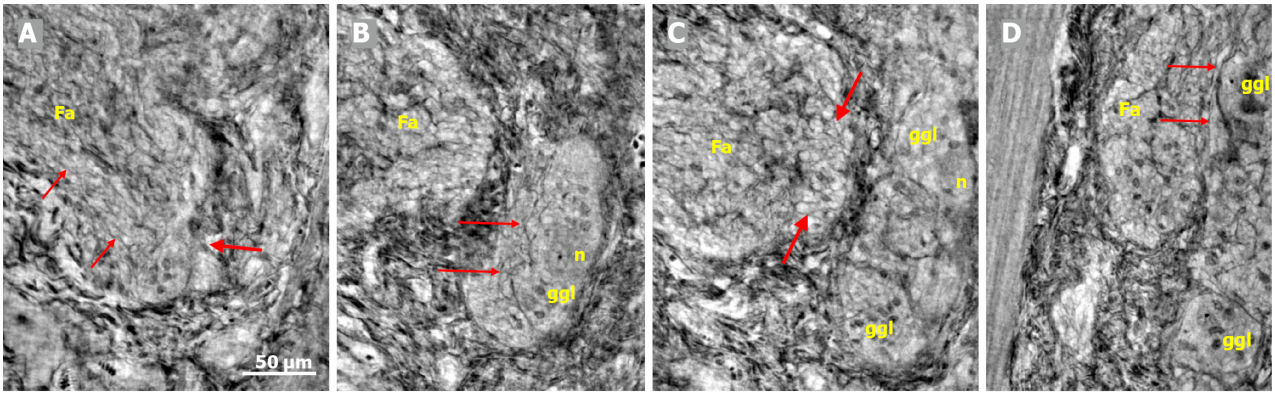
Figure 2 Ganglion and fascicle from healthy human ileum. A: Within a portion of the ganglion, there is a neuron with an axon (thick arrow). Arrowheads indicate glial cells. Thin arrows indicate a single layer of telopodes at the border of the ganglion. The scale bar (50 µm) was applied to all subfigures; B: Part of a ganglion with several large (thick arrows) and medium-large (short thin arrow) neurons. The nuclei contain dark nucleoli. The cytoplasm is slightly granulated. Above the straight line, a small area of the neuropil was observed. Long thin arrows indicate the double-cell layer at the border; C: Normal nerve fascicle and thicker nerve with telopodes separating axons (arrows). Note the single layer of telopodes around the fascicle and nerve (arrowheads). Inset: Normal nerve fascicles stained with double immunohistochemistry. Telocytes run parallel to Schwann cells (light microscopy; S100: Schwann cells red; CD34: Telocytes brown).

Pathological change of the nerve fascicles and perigangliональ spindle-shaped cell layer

In one patient who was diagnosed with lymphocytic ganglioneuritis, a segment of the perigangliональ spindle-shaped cell layer showed vacuolization and/or was absent within a 19.9 µm distance along the length axis of the bowel sample (Figure 5). The largest window in this absence was 16.1 µm in the virtual slices (Figure 5B). At a 7.8 µm deeper level (Figure 5C), a double layer of thin cellular projections appeared at the border of the defect, whereas at an additionally 4.7 µm deeper, one intact layer of cellular projections was again present between the ganglion and the surrounding tissue (Figure 5D).

Video-film

In the video film from one patient, more than one dozen neurons and glial cells could be observed (Supplementary material). Almost all the neurons showed various types of degeneration. Furthermore, one pre-apoptotic neuron in the lower part of the ganglion was probably in contact with the tip of the incomplete septum, and hence, extended into the surrounding tissue (Supplementary material).



DOI: 10.3748/wjg.v28.i29.3994 **Copyright** ©The Author(s) 2022.

Figure 3 Series of virtual slices covering 113.6 µm thickness at the border between the nerve fascicle and the ganglion. A: Thick fascicle with parallel telopodes (thin arrows). There is a small peripheral part of the ganglion (thick arrow); B: 62.2 µm deeper from Figure A. Connective tissue cells between the fascicle and the superficial part of the ganglion. Normal large neurons and nuclei of several glial cells in the ganglion. A network of telopodes is present on the surface of the ganglion (arrows); C: 11.5 µm deeper from Figure B. The thickness of the connective tissue is diminished between the fascicle and the periphery of the ganglion, with two neurons and small glial cells. Transversally cut vesicle-like axons (between the arrows) on the right end of the fascicle; D: 39.9 µm deeper from Figure C, the fascicle and ganglion are united. Thin arrows show telopodes. The scale bar (50 µm) applies to all the subfigures. Fa: Fascicle; ggl: Ganglion; n: Neuron.

DISCUSSION

The main qualitative finding in the present study was that X-ray phase-contrast nanotomography could analyze the different cellular components of the myenteric plexus in more than 6000 serial virtual slices, which could reveal minor changes not seen under the light microscope. We could image large volumes with finer sampling resolution with shorter distances between sections along the sample direction, that is, below the standard thickness of a histological scan.

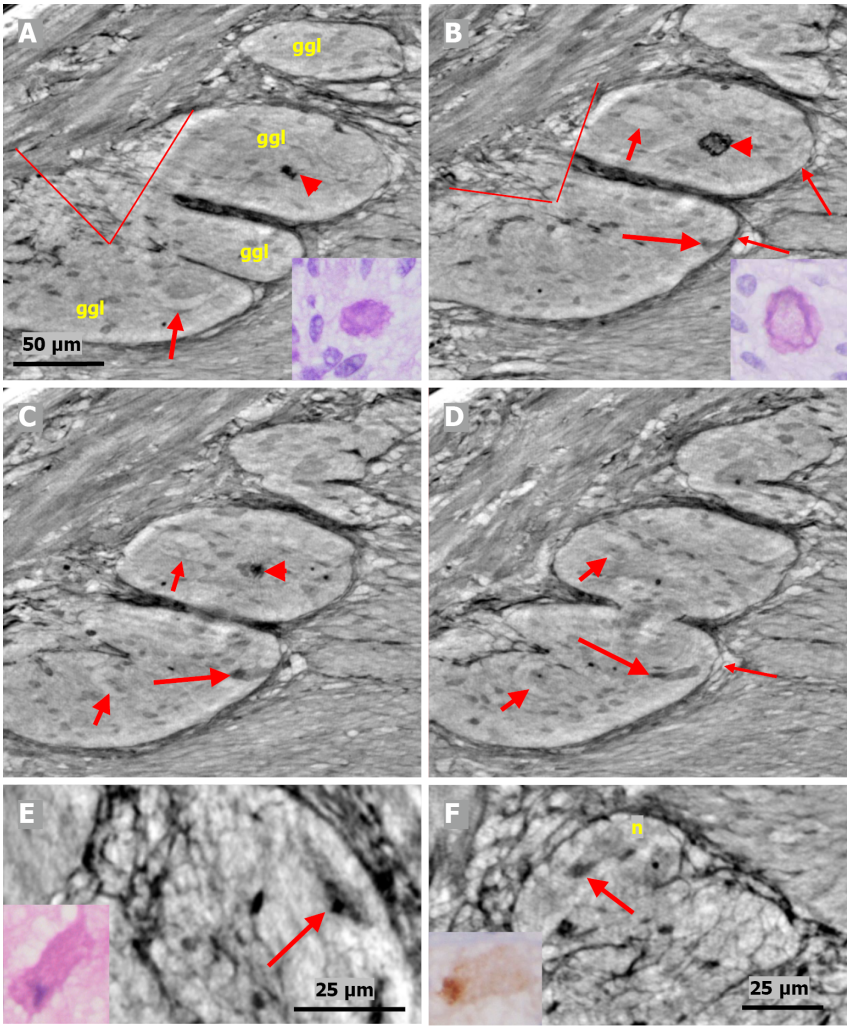
A study of the normal ganglia revealed that their shape is not usually seen in the transverse sections under a light microscope with a well-defined border. In serial virtual slices, the ganglia have smaller or larger irregularities, with one or a few neurons and glial cells protruding into the muscle layers or the intermyenteric connective tissue. Within the ganglia, neurons of various sizes and glial cells could be clearly differentiated. The absence of thin cytoplasmic projections in the neuropil corroborates our previous finding in the ileal ganglia, namely the lack of telopodes in the ileum in contrast to the colon [17]. The presence of one degenerating neuron in the 82-year-old control may be the result of aging starting at around 40-50 years of age[18].

The optimal transverse sections showed two clear layers of cellular projections surrounding the ganglion, in accordance with our previous immunohistochemical findings[17]. The inner layer consisted of cytoplasmic projections of telocytes called telopodes, which were situated almost parallel to each other, in agreement with immunohistochemical observations[17]. The outer layer is composed of an ICC [17].

Pathological changes from the patients revealed different types of neuronal degeneration (vacuolization, autophagic vacuoles/Lipofuscin, chromatolysis, and apoptosis) and the presence of a hyaline body within the ganglion, as observed under a light microscope by the golden standard of various staining techniques[8]. Furthermore, p62+ sequestosomes were also observed in accordance with the findings of Alafuzoff *et al*[19].

Three new phenomena were discovered with the present phase-contrast nanotomography, which cannot be observed under a light microscope because of the thickness of the paraffin sections. First, the presence of a semi-dense "half-moon" attached to the hyaline body could hypothetically be one of the end stages of cellular death. Second, the phenomenon of a probable expulsion of dead neurons could be followed in the virtual serial slices because of the occurrence of a short "opening" of the telopode-layer between the surrounding connective tissue and shrunken apoptotic neurons. Third, the total absence of the single telopode layer within the 16.1 µm "window" could possibly have negatively affected the stability of the ganglion.

The virtual histology of the myenteric ganglion using X-ray nanotomography has advantages, disadvantages, and future possibilities. The main advantage is that the method can exactly measure the volumes of chosen tissue components following segmentation, as have been previously published[5]. The second advantage is the possibility to analyze several hundred serial virtual slices at subcellular, isotropic resolution, and through this, discover "nano-changes" which cannot be seen using the light microscope. Because the neuron size is 15-40 µm, the ENS is difficult to examine in conventional histological sections of 3-5 µm. Slow videos make it possible to follow the relationships between the various tissue components. The third advantage is the flexibility in sample preparation; samples can be examined with or without paraffin embedding (*e.g.*, in liquid or epoxy resin) or staining. Thus, the

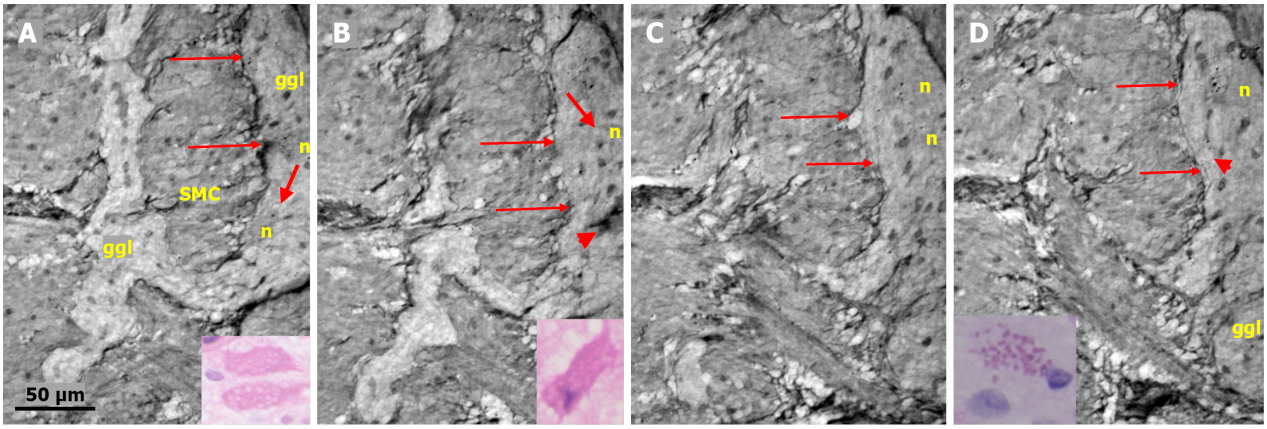


DOI: 10.3748/wjg.v28.i29.3994 **Copyright** ©The Author(s) 2022.

Figure 4 Series of virtual slices covering 17.2 µm thickness of the ganglion from one patient. A: Four portions of the ganglion. There is a dark body at the center of one of these areas (arrowheads). An arrow indicates a neuron with a very pale homogeneous cytoplasm below the nucleus. Between the straight lines, a network of telopodes is observed on the ganglion surface. Incomplete septa between portions. Scale bar (50 µm) is applied to subfigures A-D. Inset: Hyaline body in the ganglion [1st level of serial sections; light microscopy; periodic acid-Schiff with diastase (PAS-D) staining]; B: 6.8 µm from Figure A., three portions of the ganglia are completely separated, and the surface area is smaller (between straight lines). The central dark body shows an irregular dense outer layer and central light area (arrowhead). A new neuron with pale cytoplasm is seen in the middle portion (short arrow). Intact telopodes form the border between the ganglion and the periganglional connective tissue rim (thin arrows). An almost triangle-shaped moderately dense area is seen below the telopode telopode corresponding to an apoptotic neuron (long arrow; see also C and D). Inset: The central region of the hyaline body is negative, whereas the outer layer is positive with PAS-D staining (2nd level of serial sections, light microscopy; PAS-D); C: 4.0 µm from Figure B. The hyaline body is without a central pale area (arrowhead), with a semi-dense irregular half-moon to the left. The two neurons had a pale cytoplasm (short arrows). A dark pyknotic nucleus appeared in the semi-dense cytoplasm at the border showing an apoptotic neuron corresponding to the "dark triangle" in Figure B (long arrow); D: 6.4 µm deeper from Figure C. Two of the portions are united. Nuclei are present in neurons with pale cytoplasm (short arrows). Intact telopodes are present between the degenerated apoptotic cells (long arrow) and the periganglional space (thin arrow); E: Digital magnification of a shrunken neuron with a darker cytoplasm, small vacuoles, and enlarged nucleolus. Scale bar: 25 µm Inset: Pre-apoptotic neurons with pyknotic nucleus and vacuole-containing amphophilic cytoplasm (light microscopy; H&E staining); F: There is a homogeneous circumscribed "inclusion" in the neuron, suggesting a sequestosome, as seen in the inset (arrow). Scale bar: 25 µm. Inset: Large p62+ aggregates in neurons (arrow; light microscopy; p62 immunohistochemistry). Scales bars of 50 or 25 µm included. Ggl: Ganglion; n: Neuron; PAS-D: Periodic acid-schiff with diastase.

samples require less handling and fewer preparation steps[20].

The current established method to diagnose enteric neuropathy uses immunohistochemistry with a wide range of staining according to a standardized protocol[8,21]. The strength of this method lies in the exact identification of different cell types and tissue structures. The weakness is that there is a wide range of different molecules and structures that can vary in abundance among different patients with the same diagnosis. We do not know whether these changes are causal or primary, or whether they are secondary or compensatory. Due to the large variation between patients, no uniform pattern has been determined for the diagnosis of enteric neuropathy, and thus, some of the information did not add substantial value to the examination. The current description of neurons, glial cells, and spindle-shaped cells appears to be sufficient for diagnosis.



DOI: 10.3748/wjg.v28.i29.3994 **Copyright** ©The Author(s) 2022.

Figure 5 Series of virtual slices covering 19.9 µm thickness of the ganglion from one patient. A: Two portions of the ganglion with smooth muscle cells between them. Long arrows indicate the continuous layer of telopodes with tiny vesicles bordering the ganglion. A string of glial cell nuclei was present within the left portion. The thick arrow shows the vacuole above the nucleus of the neuron. Four small dark granules were present in the other neurons. Inset: Several vacuoles fill the cytoplasm of the two degenerating neurons (light microscopy and H&E staining); B: 7.4 µm deeper from Figure A. Between the thin arrows there is no continuous layer of telopodes, instead some vesicles are seen. The left portion has disappeared. The remaining portion is part of a pre-apoptotic neuron with a dark cytoplasm and pyknotic nucleus (arrowhead). Above this neuron is the nuclei of normal glial cells. The thick arrow indicates a vacuole in the neuron. Inset: Apoptotic neurons with strongly amphophilic cytoplasm and rest of the pyknotic nuclei (light microscopy; H&E staining); C: 7.8 µm deeper from Figure B. The defect of the telopodes (between the thin arrows) was shorter. Double layer of telopodes below the defect. In the upper part of the ganglion, there is a large neuron with a few small dark, dense dots, whereas the pre-apoptotic neuron from the middle of the ganglion is no longer present; D: 4.7 µm deeper from Figure C. There is a continuous layer of telopodes (between arrows) with a "remnant" of the double layer, as shown in Figure C. The dark granules in the neurons were larger and more numerous. Arrowhead shows a neuron with both dark granules and vacuoles. Inset: The cytoplasm of the neurons was filled with diastase-resistant PAS+ lipofuscin granules (light microscopy; PAS-D staining). The scale bar (50 µm) applies to all the subfigures. Ggl: Ganglion; H&E: Hematoxylin & eosin; n: Neuron; PAS: Periodic acid-Schiff; PAS-D: Periodic acid-Schiff with diastase; SMC: Smooth muscle cells.

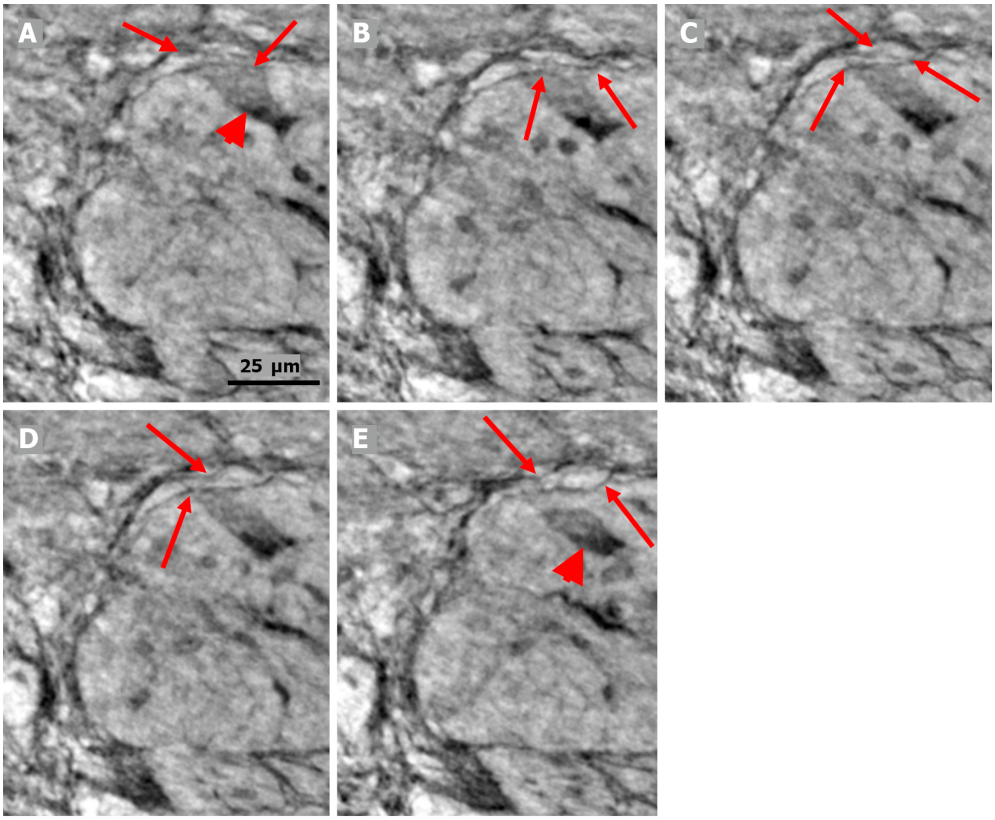
Fluorescence confocal microscopy has been performed with serial sectioning to mimic three-dimensional (3D) imaging; however, the maximal thickness of viewing is still limited, and the space between sections is larger[22-25]. Recently, another method using immunohistochemistry and confocal microscopy was developed for the quantitative analysis of full-thickness bowel biopsies[26]. These different efforts to improve the analysis of ENS prove the importance of clinicians obtaining more information about the function and dysfunction of the gastrointestinal tract.

Among the disadvantages were the limited access to synchrotron beamtime and the cost of the entire process in terms of money and manpower. Furthermore, because the ganglia of the ENS are very sparse, especially in patients with dysmotility, and the myenteric plexus can fold and curve beneath what is visible on the surface of the block, it is very difficult to correctly punch the tissue of interest based on a histological section. Hence, multi-scale X-ray phase-contrast tomography, which involves scanning a tissue block with a mm-sized field-of-view at µm-resolution and then imaging specific features of interest in greater detail using local nanotomography on the full block (instead of extracting biopsy punches as in this work), would be preferable and has been proven to be feasible at different synchrotron beamlines, such as TOMCAT[27,28] and P10/GINIX[29-31].

In the future, the combination of immunohistochemistry with X-ray phase-contrast nanotomography, such as immuno-electron microscopy[32], or with joint X-ray phase-contrast tomography and focused ion beam scanning electron microscopy (FIB-SEM) could provide unique possibilities to study targeted cells and their internal and external relationships[33]. In addition, this technique can determine the exact volume of the target tissue components[5].

CONCLUSION

Virtual sectioning by X-ray phase-contrast nanotomography is a method that provides a unique analysis of the myenteric ganglion, revealing minor pathological changes that cannot be discovered using light microscopy or other two-dimensional scanning methods to study the relationship between various tissue components.



DOI: 10.3748/wjg.v28.i29.3994 **Copyright** ©The Author(s) 2022.

Figure 6 Series of virtual slices covering 6.4 μm thickness of the ganglion from one patient. A: Neuron with shrunken pyknotic nucleus and dark cytoplasm containing vacuoles at the edge of the ganglion (arrowhead). A part of the cytoplasm of the pre-apoptotic neuron is present between the telopodes (arrows); B: 2.0 μm deeper from Figure A. The lower telopode was discontinuous (arrows); C: 0.7 μm deeper from Figure B. The two telopodes are intact, and almost all of the cytoplasm between them has disappeared; D: 0.7 μm deeper from Figure C. Pre-apoptotic neurons seem to be in contact with the lower telopode; E: 3.0 μm deeper from Figure D. The pre-apoptotic neuron (arrowhead) lies within the ganglion, without contact with the telopodes. Arrows point to two telopodes on the figures. The scale bar (25 μm) applies to all the subfigures.

ARTICLE HIGHLIGHTS

Research background

The enteric nervous system (ENS) is difficult to study because of its deep localization in the intestinal wall. The limited sections visualized by light microscopy cannot show the size of the neurons or the interconnection between different parts of the ENS or different cell types.

Research motivation

Since the ENS is difficult to examine, patients with gastrointestinal dysmotility are not properly examined, diagnosed, and treated. They can experience symptoms for several years before a proper diagnosis is established.

Research objectives

The main objective of this study was to examine whether X-ray phase-contrast tomography could improve the visualization of the ENS. We realized that the ENS could be visualized without any prior staining, and the information provided was superior to conventional light microscopy in some respects. Thus, this method should be further evaluated in future studies.

Research methods

Full-thickness biopsies from the ileum of patients with dysmotility and controls were examined using X-ray phase-contrast tomography. For comparison, the same samples were examined using immunohistochemistry. This is the first time that bowel biopsies have been examined using X-ray tomography, and the histopathology has been described in detail.

Research results

This study showed that X-ray phase-contrast tomography can be used to study the ENS in detail to describe normal and pathological cells and tissue structures. The interconnections between the cells and

structures can be visualized. Some new findings could not have been observed using conventional light microscopy.

Research conclusions

Virtual sectioning by X-ray phase-contrast nanotomography provides a unique analysis of the myenteric ganglion, revealing minor pathological changes that cannot be discovered by light microscopy, to follow the relationship between various tissue components.

Research perspectives

This method needs to be further studied in larger cohorts, with scanning of whole paraffin blocks combined with different staining methods to try to improve the identification of different cell types and tissue structures. More healthy controls should be examined to obtain reference values for health and disease.

ACKNOWLEDGEMENTS

The authors thank Maria Teresa Moreira Jara and Maria Nilsson for their technical assistance and the pathologists for control sample collection. The valuable discussion with Anca Dragomir, MD, PhD, Uppsala University, regarding possible artifacts, is greatly appreciated.

FOOTNOTES

Author contributions: Veress B performed the histochemical and pathological analyses of the X-ray data and wrote the initial draft together with Ohlsson B; Peruzzi N, Eckermann M, and Frohn J scanned the samples; Peruzzi N analyzed the technical data; all authors planned and designed the study, contributed to intellectual analysis of the results, and approved the final version of the manuscript.

Supported by the Development Foundation of Region Skåne, No. REGSKANE-818781 and No. 2018-Projekt0024; and the Foundation Skåne University Hospital, No. 2020-0000028.

Institutional review board statement: The study was reviewed and approved by the Regional Ethics Review Board at Lund University (2009/209, Date of approval 28/04/2009; 2012/527, Date of approval 16/10/2012 and 2018/132, Date of approval 02/08/2018) and the Swedish Biobank Act.

Informed consent statement: All study participants provided informed written consent prior to study enrollment.

Conflict-of-interest statement: There are no conflicts of interest to report.

Data sharing statement: No additional data is available.

STROBE statement: The authors have read the STROBE Statement—checklist of items, and the manuscript was prepared and revised according to the STROBE Statement—checklist of items.

Open-Access: This article is an open-access article that was selected by an in-house editor and fully peer-reviewed by external reviewers. It is distributed in accordance with the Creative Commons Attribution NonCommercial (CC BY-NC 4.0) license, which permits others to distribute, remix, adapt, build upon this work non-commercially, and license their derivative works on different terms, provided the original work is properly cited and the use is non-commercial. See: https://creativecommons.org/Licenses/by-nc/4.0/

Country/Territory of origin: Sweden

ORCID number: Bela Veress 0000-0001-9529-6809; Niccolò Peruzzi 0000-0002-2929-4247; Marina Eckermann 0000-0001-6418-4310; Jasper Frohn 0000-0003-3849-6032; Tim Salditt 0000-0003-4636-0813; Bodil Ohlsson 0000-0002-9142-5244.

Corresponding Author's Membership in Professional Societies: UEG; Swedish Society of Gastroenterology.

S-Editor: Chen YL
L-Editor: A
P-Editor: Chen YL

REFERENCES

1 **Furness JB**, Callaghan BP, Rivera LR, Cho HJ. The enteric nervous system and gastrointestinal innervation: integrated local and central control. *Adv Exp Med Biol* 2014; **817**: 39-71 [PMID: 24997029 DOI: 10.1007/978-1-4939-0897-4_3]

2 **Wingate D**, Hongo M, Kellow J, Lindberg G, Smout A. Disorders of gastrointestinal motility: towards a new classification. *J Gastroenterol Hepatol* 2002; **17** Suppl: S1-14 [PMID: 12000590 DOI: 10.1046/j.1440-1746.17.s1.7.x]

3 **Keller J**, Bassotti G, Clarke J, Dinning P, Fox M, Grover M, Hellström PM, Ke M, Layer P, Malagelada C, Parkman HP, Scott SM, Tack J, Simren M, Törnblom H, Camilleri M; International Working Group for Disorders of Gastrointestinal Motility and Function. Expert consensus document: Advances in the diagnosis and classification of gastric and intestinal motility disorders. *Nat Rev Gastroenterol Hepatol* 2018; **15**: 291-308 [PMID: 29622808 DOI: 10.1038/nrgastro.2018.7]

4 **Hammar O**, Ohlsson B, Veress B, Alm R, Fredrikson GN, Montgomery A. Depletion of enteric gonadotropin-releasing hormone is found in a few patients suffering from severe gastrointestinal dysmotility. *Scand J Gastroenterol* 2012; **47**: 1165-1173 [PMID: 22835010 DOI: 10.3109/00365521.2012.706826]

5 **Peruzzi N**, Veress B, Dahlin LB, Salditt T, Andersson M, Eckermann M, Frohn J, Robisch AL, Bech M, Ohlsson B. 3D analysis of the myenteric plexus of the human bowel by X-ray phase-contrast tomography - a future method? *Scand J Gastroenterol* 2020; **55**: 1261-1267 [PMID: 32907418 DOI: 10.1080/00365521.2020.1815079]

6 **Eckermann M**, Peruzzi N, Frohn J, Bech M, Englund E, Veress B, Salditt T, Dahlin LB, Ohlsson B. 3d phase-contrast nanotomography of unstained human skin biopsies may identify morphological differences in the dermis and epidermis between subjects. *Skin Res Technol* 2021; **27**: 316-323 [PMID: 33022848 DOI: 10.1111/srt.12974]

7 **Törnblom H**, Lindberg G, Nyberg B, Veress B. Full-thickness biopsy of the jejunum reveals inflammation and enteric neuropathy in irritable bowel syndrome. *Gastroenterology* 2002; **123**: 1972-1979 [PMID: 12454854 DOI: 10.1053/gast.2002.37059]

8 **Lindberg G**, Törnblom H, Iwarzon M, Nyberg B, Martin JE, Veress B. Full-thickness biopsy findings in chronic intestinal pseudo-obstruction and enteric dysmotility. *Gut* 2009; **58**: 1084-1090 [PMID: 19136514 DOI: 10.1136/gut.2008.148296]

9 **Knowles CH**, Veress B, Kapur RP, Wedel T, Farrugia G, Vanderwinden JM, Geboes K, Smith VV, Martin JE, Lindberg G, Milla PJ, De Giorgio R. Quantitation of cellular components of the enteric nervous system in the normal human gastrointestinal tract--report on behalf of the Gastro 2009 International Working Group. *Neurogastroenterol Motil* 2011; **23**: 115-124 [PMID: 21175997 DOI: 10.1111/j.1365-2982.2010.01657.x]

10 **Knowles CH**, De Giorgio R, Kapur RP, Bruder E, Farrugia G, Geboes K, Lindberg G, Martin JE, Meier-Ruge WA, Milla PJ, Smith VV, Vandervinden JM, Veress B, Wedel T. The London Classification of gastrointestinal neuromuscular pathology: report on behalf of the Gastro 2009 International Working Group. *Gut* 2010; **59**: 882-887 [PMID: 20581236 DOI: 10.1136/gut.2009.200444]

11 **Töpperwien M**, van der Meer F, Stadelmann C, Salditt T. Three-dimensional virtual histology of human cerebellum by X-ray phase-contrast tomography. *Proc Natl Acad Sci U S A* 2018; **115**: 6940-6945 [PMID: 29915047 DOI: 10.1073/pnas.1801678115]

12 **Salditt T**, Osterhoff M, Krenkel M, Wilke RN, Priebe M, Bartels M, Kalbfleisch S, Sprung M. Compound focusing mirror and X-ray waveguide optics for coherent imaging and nano-diffraction. *J Synchrotron Radiat* 2015; **22**: 867-878 [PMID: 26134789 DOI: 10.1107/S1600577515007742]

13 **Cloetens P**, Ludwig W, Baruchel J, Van Dyck D, Landuyt JV, Guigay JP, Schlenker M. Holotomography: Quantitative phase tomography with micrometer resolution using hard synchrotron radiation x rays. *Appl Phys Lett* 1999; **75**: 2912 [DOI: 10.1063/1.125225]

14 **Groso A**, Stampanoni M, Abela R, Schneider P, Linga S, Müller R. Phase contrast tomography: An alternative approach. *Appl Phys Lett* 2006; **88**: 214104 [DOI: 10.1063/1.2207221]

15 **De Witte Y**, Boone M, Vlassenbroeck J, Dierick M, Van Hoorebeke L. Bronnikov-aided correction for x-ray computed tomography. *J Opt Soc Am A Opt Image Sci Vis* 2009; **26**: 890-894 [PMID: 19340263 DOI: 10.1364/josaa.26.000890]

16 **Lohse LM**, Robisch AL, Töpperwien M, Maretzke S, Krenkel M, Hagemann J, Salditt T. A phase-retrieval toolbox for X-ray holography and tomography. *J Synchrotron Radiat* 2020; **27**: 852-859 [PMID: 32381790 DOI: 10.1107/S1600577520002398]

17 **Veress B**, Ohlsson B. Spatial relationship between telocytes, interstitial cells of Cajal and the enteric nervous system in the human ileum and colon. *J Cell Mol Med* 2020; **24**: 3399-3406 [PMID: 31983076 DOI: 10.1111/jcmm.15013]

18 **Hanewinckel R**, Drenthen J, van Oijen M, Hofman A, van Doorn PA, Ikram MA. Prevalence of polyneuropathy in the general middle-aged and elderly population. *Neurology* 2016; **87**: 1892-1898 [PMID: 27683845 DOI: 10.1212/WNL.0000000000003293]

19 **Alafuzoff I**, Popova SN, Veress B. Neuronal protein alteration in enteric dysmotility syndrome. *J Alzheimers Dis Parkinsonism* 2016; **6**: 212-216 [DOI: 10.4172/2161-0460.1000212]

20 **Eckermann M**, van der Meer F, Cloetens P, Ruhwedel T, Möbius W, Stadelmann C, Salditt T. Three-dimensional virtual histology of the cerebral cortex based on phase-contrast X-ray tomography. *Biomed Opt Express* 2021; **12**: 7582-7598 [PMID: 35003854 DOI: 10.1364/BOE.434885]

21 **Lehtonen HJ**, Sipponen T, Tojkander S, Karikoski R, Järvinen H, Laing NG, Lappalainen P, Aaltonen LA, Tuupanen S. Segregation of a missense variant in enteric smooth muscle actin γ-2 with autosomal dominant familial visceral myopathy. *Gastroenterology* 2012; **143**: 1482-1491.e3 [PMID: 22960657 DOI: 10.1053/j.gastro.2012.08.045]

22 **Vanderwinden JM**, Rumessen JJ, De Laet MH, Vanderhaeghen JJ, Schiffmann SN. CD34+ cells in human intestine are fibroblasts adjacent to, but distinct from, interstitial cells of Cajal. *Lab Invest* 1999; **79**: 59-65 [PMID: 9952111]

23 **Toma H**, Nakamura K, Kuraoka A, Tanaka M, Kawabuchi M. Three-dimensional structures of c-Kit-positive cellular networks in the guinea pig small intestine and colon. *Cell Tissue Res* 1999; **295**: 425-436 [PMID: 10022963 DOI: 10.1007/s004410051249]

24 **Cobine CA**, Hennig GW, Kurahashi M, Sanders KM, Ward SM, Keef KD. Relationship between interstitial cells of Cajal, fibroblast-like cells and inhibitory motor nerves in the internal anal sphincter. *Cell Tissue Res* 2011; **344**: 17-30 [PMID: 21337122 DOI: 10.1007/s00441-011-1138-1]

25 **Grover M**, Bernard CE, Pasricha PJ, Parkman HP, Abell TL, Nguyen LA, Snape W, Shen KR, Sarr M, Swain J, Kendrick M, Gibbons S, Ordog T, Farrugia G. Platelet-derived growth factor receptor α (PDGFRα)-expressing "fibroblast-like cells" in diabetic and idiopathic gastroparesis of humans. *Neurogastroenterol Motil* 2012; **24**: 844-852 [PMID: 22650155 DOI: 10.1111/j.1365-2982.2012.01944.x]

26 **Graham KD**, López SH, Sengupta R, Shenoy A, Schneider S, Wright CM, Feldman M, Furth E, Valdivieso F, Lemke A, Wilkins BJ, Naji A, Doolin EJ, Howard MJ, Heuckeroth RO. Robust, 3-Dimensional Visualization of Human Colon Enteric Nervous System Without Tissue Sectioning. *Gastroenterology* 2020; **158**: 2221-2235.e5 [PMID: 32113825 DOI: 10.1053/j.gastro.2020.02.035]

27 **Norvik C**, Westöö CK, Peruzzi N, Lovric G, van der Have O, Mokso R, Jeremiasen I, Brunnström H, Galambos C, Bech M, Tran-Lundmark K. Synchrotron-based phase-contrast micro-CT as a tool for understanding pulmonary vascular pathobiology and the 3-D microanatomy of alveolar capillary dysplasia. *Am J Physiol Lung Cell Mol Physiol* 2020; **318**: L65-L75 [PMID: 31596108 DOI: 10.1152/ajplung.00103.2019]

28 **Westöö C**, Norvik C, Peruzzi N, van der Have O, Lovric G, Jeremiasen I, Tran PK, Mokso R, de Jesus Perez V, Brunnström H, Bech M, Galambos C, Tran-Lundmark K. Distinct types of plexiform lesions identified by synchrotron-based phase-contrast micro-CT. *Am J Physiol Lung Cell Mol Physiol* 2021; **321**: L17-L28 [PMID: 33881927 DOI: 10.1152/ajplung.00432.2020]

29 **Frohn J**, Pinkert-Leetsch D, Missbach-Güntner J, Reichardt M, Osterhoff M, Alves F, Salditt T. 3D virtual histology of human pancreatic tissue by multiscale phase-contrast X-ray tomography. *J Synchrotron Radiat* 2020; **27**: 1707-1719 [PMID: 33147198 DOI: 10.1107/S1600577520011327]

30 **Reichardt M**, Frohn J, Khan A, Alves F, Salditt T. Multi-scale X-ray phase-contrast tomography of murine heart tissue. *Biomed Opt Express* 2020; **11**: 2633-2651 [PMID: 32499949 DOI: 10.1364/BOE.386576]

31 **Eckermann M**, Schmitzer B, van der Meer F, Franz J, Hansen O, Stadelmann C, Salditt T. Three-dimensional virtual histology of the human hippocampus based on phase-contrast computed tomography. *Proc Natl Acad Sci U S A* 2021; **118** [PMID: 34819378 DOI: 10.1073/pnas.2113835118]

32 **Goodarzi N**, Akbari Bazm M, Poladi S, Rashidi F, Mahmoudi B, Abumandour MMA. Histology of the small intestine in the common pheasant (Phasianus colchicus): A scanning electron microscopy, histochemical, immunohistochemical, and stereological study. *Microsc Res Tech* 2021; **84**: 2388-2398 [PMID: 33908129 DOI: 10.1002/jemt.23794]

33 **Eckermann M**, Ruhwedel T, Möbus W, Salditt T. Towards correlative imaging of neuronal tissue by phase-contrast x-ray tomography and SEM. *Proceedings of the SPIE* 2021; **11840**: 29-36 [DOI: 10.1117/12.2596133]

World Journal of Gastroenterology

Submit a Manuscript: https://www.f6publishing.com

World J Gastroenterol 2022 August 7; 28(29): 4007-4018

DOI: 10.3748/wjg.v28.i29.4007

ISSN 1007-9327 (print) ISSN 2219-2840 (online)

META-ANALYSIS

Recurrence rates after endoscopic resection of large colorectal polyps: A systematic review and meta-analysis

Carola Rotermund, Roupen Djinbachian, Mahsa Taghiakbari, Markus D Enderle, Axel Eickhoff, Daniel von Renteln

Specialty type: Gastroenterology and hepatology

Provenance and peer review: Invited article; Externally peer reviewed.

Peer-review model: Single blind

Peer-review report's scientific quality classification
Grade A (Excellent): A
Grade B (Very good): 0
Grade C (Good): C
Grade D (Fair): 0
Grade E (Poor): 0

P-Reviewer: Gao W, China; Yu T, China

Received: March 30, 2022
Peer-review started: March 30, 2022
First decision: April 25, 2022
Revised: May 11, 2022
Accepted: July 8, 2022
Article in press: July 8, 2022
Published online: August 7, 2022

Carola Rotermund, Markus D Enderle, Research and Basic Technologies, ERBE Elektromedizin GmbH, Tuebingen 72072, Germany

Roupen Djinbachian, Division of Internal Medicine, Montreal University Hospital Center, Montreal QC H2X 3E4, Canada

Mahsa Taghiakbari, Daniel von Renteln, Montreal University Hospital Research Center, Montreal University Hospital Center, Montreal QC H2X 3E4, Canada

Axel Eickhoff, Department of Internal Medicine II, Klinikum Hanau, Hanau 63450, Germany

Corresponding author: Daniel von Renteln, MD, Associate Professor, Montreal University Hospital Research Center, Montreal University Hospital Center, 1051 Rue Sanguinet, Montreal QC H2X 3E4, Canada. danielrenteln@gmail.com

Abstract

BACKGROUND

Complete polyp resection is the main goal of endoscopic removal of large colonic polyps. Resection techniques have evolved in recent years and endoscopic submucosal dissection (ESD), endoscopic mucosal resection (EMR) with margin ablation, cold snare polypectomy (CSP), cold EMR, and underwater EMR have been introduced. Yet, efficacy of these techniques with regard to local recurrence rates (LRRs) *vs* traditional hot snare polypectomy and standard EMR remains unclear.

AIM

To analyze LRR of large colonic polyps in a systematic review and meta-analysis.

METHODS

MEDLINE, EMBASE, EBM Reviews, and CINAHL were searched for prospective studies reporting LRR or incomplete resection rate (IRR) after colonic polypectomy of polyps ≥ 10 mm, published between January 2011 and July 2021. Primary outcome was LRR for polyps ≥ 10 mm.

RESULTS

Six thousand nine hundred and twenty-eight publications were identified, of which 34 prospective studies were included. LRR for polyps ≥ 10 mm at up to 12 mo' follow-up was 11.0% (95%CI, 7.1%-14.8%; 15 studies; 4904 polyps). ESD

(1.7%; 95%CI, 0%-3.4%; 3 studies, 221 polyps) and endoscopic mucosal resection with margin ablation (3.3%; 95%CI, 2.2%-4.5%; 2 studies, 947 polyps) significantly reduced LRR *vs* standard EMR without (15.2%; 95%CI, 12.5%-18.0%; 4 studies, 650 polyps) or with unsystematic margin ablation (16.5%; 95%CI, 15.2%-17.8%; 6 studies, 3031 polyps).

CONCLUSION
LRR is significantly lower after ESD or EMR with routine margin ablation; thus, these techniques should be considered standard for endoscopic removal of large colorectal polyps. Other techniques, such as CSP, cold EMR, and underwater EMR require further evaluation in prospective studies before their routine implementation in clinical practice can be recommended.

Key Words: Colonoscopy; Adenoma; Polyp; Endoscopic mucosal resection; Colorectal cancer

©The Author(s) 2022. Published by Baishideng Publishing Group Inc. All rights reserved.

Core Tip: Complete polyp resection is the main goal of endoscopic removal of large colonic polyps. Resection techniques have evolved in recent years and endoscopic submucosal dissection, endoscopic mucosal resection (EMR) with margin ablation, cold snare polypectomy, cold EMR, and underwater EMR have been introduced. Yet, efficacy of these techniques with regard to local recurrence rates (LRRs) *vs* traditional hot snare polypectomy and standard EMR remains unclear. We aimed to analyze LRR of large colonic polyps in a systematic review and meta- analysis.

Citation: Rotermund C, Djinbachian R, Taghiakbari M, Enderle MD, Eickhoff A, von Renteln D. Recurrence rates after endoscopic resection of large colorectal polyps: A systematic review and meta-analysis. *World J Gastroenterol* 2022; 28(29): 4007-4018
URL: https://www.wjgnet.com/1007-9327/full/v28/i29/4007.htm
DOI: https://dx.doi.org/10.3748/wjg.v28.i29.4007

INTRODUCTION

Complete endoscopic polyp removal is especially important for large colorectal polyps in order to prevent local polyp recurrence and progression to colorectal cancer[1]. Evidence is growing that polyp removal is frequently incomplete, putting patients at risk of developing post-colonoscopy cancer[2-4]. A meta-analysis published in 2020 found that after snare resection, 15.9% of diminutive and small polyps and 20.8% of polyps 10–19 mm are removed incompletely[5]. For polyps 20 mm or larger, a meta-analysis published in 2014 demonstrated a recurrence rate of 15% after endoscopic mucosal resection (EMR)[6].

In recent years, different techniques for endoscopic resection of large colorectal polyps have evolved or been developed. Cold snare polypectomy (CSP) has been introduced and its use expanded to include the removal of large colorectal polyps[7]. Endoscopic submucosal dissection (ESD) has gained traction in Western countries and EMR has undergone technical modifications by introducing margin ablation or underwater EMR[8,9].

These developments have sparked our interest in providing an up-to-date meta-analysis of local recurrence rates (LRRs) and incomplete resection rates (IRRs) for large (≥ 10 mm) colorectal polyps, and to evaluate the impact of the novel or modified endoscopic resection techniques on LRRs.

MATERIALS AND METHODS

The analysis was conducted adhering to the Preferred Reporting Items for Systematic Reviews and Meta-analysis statement[10].

Literature search

A systematic literature search was performed within MEDLINE, EMBASE, EBM Reviews, and CINAHL databases. All articles published between January 2011 and July 2021 reporting on IRR and/or LRR for colorectal polyps 10 mm or larger removed by endoscopic resection techniques were included in the search. For specific search terms, see Supplementary Table 1. Additionally, a secondary search was performed to identify further records using article reference crosscheck, manual searching, and expert contact.

Article selection

Articles retrieved by the systematic search were collected and duplicates removed. Two researchers (Rotermund C and Taghiakbari M) assessed all articles independently and decided upon inclusion and exclusion. In cases of disagreement, a third researcher (von Renteln D) was consulted.

Inclusion criteria were full-text articles of prospectively performed clinical studies reporting on either LRR or IRR evaluated by margin assessment or margin biopsy of endoscopically removed polyps ≥ 10 mm. Even though often of larger sample size, publications with retrospective study design were excluded from the analysis, as risk for selection bias and risk for missed data is usually higher.

Exclusion criteria were retrospective study design, polyps < 10 mm, IRR evaluated by visual margin assessment, data from first follow-up that exceeded 12 mo, publications solely evaluating difficult polypectomies, publication languages other than English, articles reporting on training of a certain technique, and articles in which results from different polypectomy techniques were not clearly distinguishable.

Data extraction

Relevant data retrieved from the evaluated study included author, year of publication, country, study type, study quality, polyp size, polyp morphology, polyp histology, polyp resection method and adjunct therapy, LRR, IRR, IRR assessment method, submucosal injection rate and solution, *en bloc* resection rate, and endoscopist number and experience level. For analyses, polyps were subdivided according to size: 10–19 mm, ≥ 20 mm (not including polyps < 20 mm), and all polyps ≥ 10 mm (including polyps ≥ 20 mm). Data were retrieved by one author (Rotermund C) and correct retrieval confirmed by a second author (Djinbachian R).

Outcomes

Primary outcome was LRR for polyps ≥ 10 mm. Local recurrence was defined as the presence of recurrent polyp at the resection site, detected during follow-up examination. Publications, in which the appointments for follow-up examinations exceeded 12 mo between the different patients, were excluded from the analysis. Secondary outcomes were IRR evaluated by either margin assessment or margin biopsy for polyps ≥ 10 mm, as well as factors influencing LRR and IRR, including polyp resection technique [hot snare polypectomy (HSP), CSP, hot and cold EMR, underwater EMR, ESD], adjunct therapy, margin assessment method, submucosal injection status, polyp size, polyp morphology and histology, endoscopist experience and number of endoscopists involved. IRR assessment method was defined as (1) Biopsy from the resection margin (="margin biopsy"); (2) Histologic assessment of polyp margin (= "margin assessment"); and (3) *En bloc* resection and histologic assessment of polyp margin (= "*en bloc* and margin assessment"). Endoscopist experience was defined as (1) Less experienced for EMR, when a fellow was included in the study or < 2000 colonoscopies had been performed by the endoscopist; (2) Experienced for EMR, when only expert endoscopists (> 2000 colonoscopies) were involved; (3) Less experienced for ESD, when fellows for ESD (< 200 cases) were included in the study; and (4) Experts for ESD (> 200 cases).

Quality assessment and publication bias

Study quality was assessed independently by two researchers (Taghiakbari M and Rotermund C). In cases of disagreement, a third researcher (von Renteln D) was consulted. For evaluation, National Institutes of Health quality assessment forms for case series and randomized controlled trials (RCTs) were used[11]. For RCTs (maximum score: 14), a score of 11–14 was rated as good, a score of 8–10 as fair, and a score below 8 as poor quality. For prospective case series (maximum score: 9), a score of 7–9 was rated as good, a score of 4–6 as fair, and a score below 4 as poor quality. Detailed information on criteria for low and high quality are given in Supplementary Tables 2 and 3.

A sensitivity analysis was performed to determine the effects of excluding poor-quality studies and publication bias was assessed using funnel plots (Supplementary Figure 1). The graph was plotted as proportion vs. sample size instead of log odds *vs* 1/standard error, as this method has been shown to be more accurate in predicting risk of publication bias for meta-analyses of proportions[12].

Statistical analysis

Proportions were meta-analyzed using the metaprop command of Stata version 16 (StataCorp, College Station, TX, United States), and tests of heterogeneity were performed using the I^2 statistic. Either a random-effects model or a fixed-effect model was used for the analyses. Proportions were reported with their associated 95% confidence intervals (CIs) with an alpha level of < 0.05 used for statistical significance.

RESULTS

Literature search and study characteristics

Systematic literature search yielded 6922 hits and 6 additional records were identified through reference crosscheck, manual search, and expert contact (Figure 1, Supplementary Table 1). After removal of duplicates, 5010 publications remained. Of these, 4070 were excluded based on title and 672 based on abstract, so that 268 full-text records were evaluated for eligibility. Ultimately, 34 publications were included in the analysis, with 19 reporting on IRR, 13 on LRR, and 2 on both (Figure 1). All studies were prospective and 14 were RCTs.

Quality assessment and publication bias

Included studies showed symmetrical distribution for both assessments of LRR and IRR, with no publication bias detected (Supplementary Figure 1). Quality assessment revealed 23 studies of good quality, 10 studies of fair quality, and 1 study of poor quality (Supplementary Tables 2 and 3). Sensitivity analyses did not show statistically different results or decreased heterogeneity when excluding poor- or fair-quality studies (Supplementary Figures 2 and 3).

Local recurrence rate

A total of 15 studies reported on LRR after removal of large colonic polyps ≥ 10 mm. Of these, 15 studies stated LRR obtained during follow-up examinations up to 12 mo, 7 during follow-up up to 24 mo, and 3 from follow-up after more than 24 mo (Supplementary Table 4). Definitions of LRR given in the original studies are presented in Supplementary Table 5. Mean overall LRR at up to 12 mo' follow-up was 11.0% (95%CI, 7.1%–14.8%; 4904 polyps) (Figure 2A). Overall LRR for follow-up up to 24 mo was 14.6% (95%CI, 8.4%–20.8%; 7 studies) (Supplementary Figure 4).

Local recurrence rate up to 12 mo' follow-up: Influence of resection method: Resection method was found to exhibit major influence on LRR of polyps ≥ 10 mm (Figure 2B, Table 1). ESD (1.7%; 95%CI, 0–3.4%; 3 studies) and EMR with margin ablation (3.3%; 95%CI, 2.2%–4.5%; 2 studies) significantly reduced LRR compared with EMR in which margin ablation was not performed (15.2%; 95%CI, 12.5%–18.0%; 4 studies) or only used in some cases (16.5%; 95%CI, 15.2%–17.8%; 6 studies). No prospective studies were found evaluating LRR after HSP, CSP, or cold EMR within the search period. Two studies evaluated LRR after underwater EMR; however, heterogeneity between studies was high, so that a valid analysis could not be performed.

Similarly, when only results for polyps ≥ 20 mm were evaluated, ESD and EMR with margin ablation yielded lower LRRs compared with EMR without margin ablation (Table 1). No prospective studies were found evaluating HSP, CSP, or cold EMR.

Local recurrence rate up to 12 mo' follow-up: further influencing factors: Polyp size did not influence LRR (≥ 10 mm: 11.0%; 95%CI, 7.1%–14.8%; 15 studies *vs* ≥ 20 mm: 11.2%; 95%CI, 6.8%–15.6%; 12 studies) (Table 1). Similarly, expert status of the endoscopist was not found to influence LRR (Table 1); however, as only two expert studies were found, the data set was small. The data set was also insufficient for analysis of the influence of polyp morphology or histology on LRR. Only one study included pedunculated polyps (12.1% of all resected polyps); however, the reported LRR was comparable to the rate observed in other studies[13]. Most studies included sessile serrated adenoma/polyps (SSA/Ps). One study compared LRR after EMR removal of SSA/Ps *vs* conventional adenomas and reported significantly reduced LRR for SSA/Ps[14].

Incomplete resection rate

A total of 21 studies reported on IRR after removal of large colonic polyps ≥ 10 mm, using either margin assessment or margin biopsy for evaluation (Supplementary Table 6). Mean overall IRR for all polyps ≥ 10 mm was 14.9% (95%CI, 11.4%–18.4%; 21 studies; 3563 polyps) (Figure 3). Twelve studies indicated IRR for polyps 10–19 mm, resulting in a mean IRR of 16.0% (95%CI, 10.4-21.7%) (Supplementary Figure 5), and 14 studies reported IRR for polyps ≥20 mm, yielding a mean IRR of 11.7% (95%CI, 7.5%–15.8%; 1739 polyps) (Supplementary Figure 6).

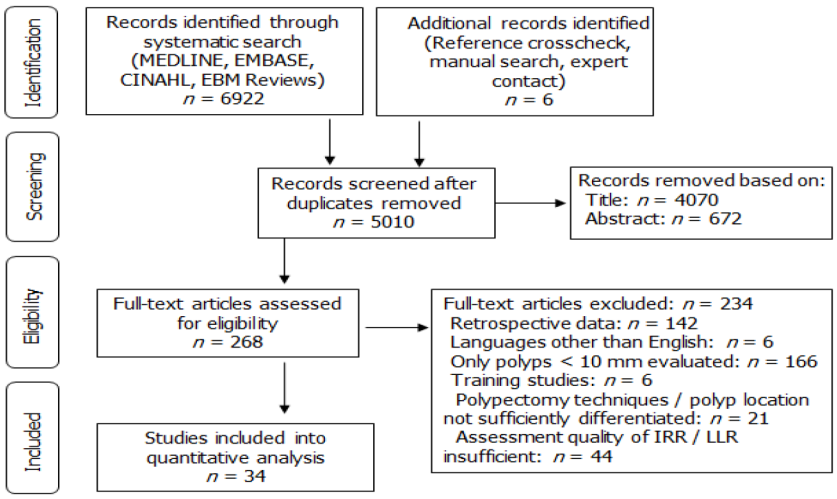
Incomplete resection rate: Influence of resection method: Resection method was not found to significantly influence IRR of polyps 10–19 mm, comparing hot EMR (18.5%; 95%CI, 8.9%–28.1%; 8 studies), HSP (16.2%; 95%CI, 10.6%–21.7%; 2 studies), underwater EMR (25.5%; 95%CI, 18.9%–32.2%; 2 studies), and cold EMR (14.0%; 95%CI, 1.8%–26.3%; 3 studies), with studies on cold EMR exhibiting high variability (Table 2). Only two studies evaluated CSP, showing high heterogeneity, so that a valid analysis could not be performed.

Comparison of ESD and EMR for polyps ≥ 20 mm showed a lower IRR for ESD (12.5%; 95%CI, 6.2%–18.8%; 9 studies) than for EMR (29.3%; 95%CI, 19.3%–39.2%; 3 studies) (Table 2). Only two studies evaluated IRR for polyps ≥ 20 mm with HSP, yielding high heterogeneity, so that a valid analysis could not be performed. No data were found reporting IRR after CSP or cold EMR for polyps ≥ 20 mm.

Table 1 Factors influencing local recurrence for polyps ≥ 10 mm at 0–12 mo' follow-up

Subgroups	LRR % (95%CI)	I^2 %	Studies, *n*	Polyps, *n*
Resection method, polyps ≥ 10 mm				
Hot EMR, no margin ablation	15.2 (12.5–18.0)	0	4	650
Hot EMR, some margin ablation	16.5 (15.2–17.8)	0	6	3013
Hot EMR, with margin ablation	3.3 (2.2–4.5)	NA	2	947
ESD	1.7 (0.0–3.4)	NA	3	221
Resection method, polyps ≥ 20 mm				
Hot EMR, no margin ablation	14.8 (11.0–18.5)	NA	2	334
Hot EMR, some margin ablation	16.5 (15.2–17.8)	0	6	3013
Hot EMR, with margin ablation	3.3 (2.2–4.5)	NA	2	947
ESD	2.4 (0–5.7)	NA	2	83
Polyp size				
≥ 10 mm	11.0 (7.1–14.8)	95.6	15	4904
≥ 20 mm	11.2 (6.8–15.6)	95.8	12	4431
Expert level				
Only expert endoscopists	13.3 (11.1–15.6)	NA	2	3712
Including non-expert endoscopists	11.8 (6.8–16.8)	95.8	9	837
Not defined	9.2 (1.5–16.9)	93.7	4	524

NA: Number of studies insufficient for estimation; EMR: Endoscopic mucosal resection; ESD: Endoscopic submucosal dissection; LRR: Local recurrence rate.



DOI: 10.3748/wjg.v28.i29.4007 **Copyright** ©The Author(s) 2022.

Figure 1 Literature search strategy.

Incomplete resection rate: Further influencing factors: For polyps sized 10–19 mm, submucosal injection status did not influence IRR. Mean IRR after resection with submucosal injection was 20.0% (95%CI, 11.9%–28.0%; 10 studies) compared with 14.4% (95%CI, 5.4%–23.3%; 6 studies) after resection without submucosal injection (Table 2). For polyps ≥20 mm, IRR was lower after resection with prior submucosal injection (Table 2). Mean IRR after submucosal injection was 12.6% (95%CI 7.7–17.6; 13 studies), compared to 32.4% (95%CI, 0-76.3%; 3 studies) after resection without injection.

The solution used for submucosal injection was not found to influence IRR, yielding comparable results for saline solution (15.8%, 95%CI, 7.1%–24.8%; 6 studies) and hyaluronic acid (16.3%, 95%CI, 8.5%–24.1%; 8 studies) (Table 2).

Table 2 Factors influencing incomplete resection

Subgroups	IRR % (95%CI)	I^2 %	Studies, *n*	Polyps, *n*
Resection method, polyps 10–19 mm				
Hot EMR	18.5 (8.9–28.1)	93.2	8	655
HSP	16.2 (10.6–21.7)	NA	2	167
U-EMR	25.5 (18.9–32.2)	NA	2	160
Cold EMR[1]	14.0[1] (1.8–26.3)	NA	3	334
Resection method, polyps ≥ 20 mm				
ESD	12.5 (6.2–18.8)	95.0	9	1452
Hot EMR	29.3 (19.3–39.2)	NA	3	88
Submucosal injection, polyps 10–19 mm				
No injection	14.4 (5.4–23.3)	95.8	6	836
Injection	20.0 (11.9–28.0)	93.9	10	989
Submucosal injection, polyps ≥ 20 mm				
No injection	32.4 (0–76.3)	96.2	3	124
Injection	12.6 (7.7–17.6)	94.4	13	1614
Injection solution, polyps ≥ 10 mm				
Saline solution	15.8 (7.1–24.6)	95. 6	6	774
Hyaluronic acid	16.3 (8.5–24.1)	95.1	8	916
Expert level				
Only expert endoscopists	7.0 (3.5, 10.4)	93. 7	8	1451
Including non-expert endoscopists	20.3 (13.5–27.1)	96.0	13	2092
Method of margin evaluation, polyps 10–19 mm				
Margin assessment	18.6 (10.9, 26.2)	75.1	5	380
Margin biopsy	5.7 (1.1, 10.3)	95.1	5	1150
Method of margin evaluation, polyps ≥ 20 mm				
Margin assessment	21.8 (9.4–34.2)	92.1	4	429
Margin assessment and *en bloc* resection	14.1 (5.7–22.6)	96.0	7	1106
Margin biopsy	0.4 (0–2.5)	55.8	3	203

[1]Data exhibit high variance; calculated mean should be handled with care.

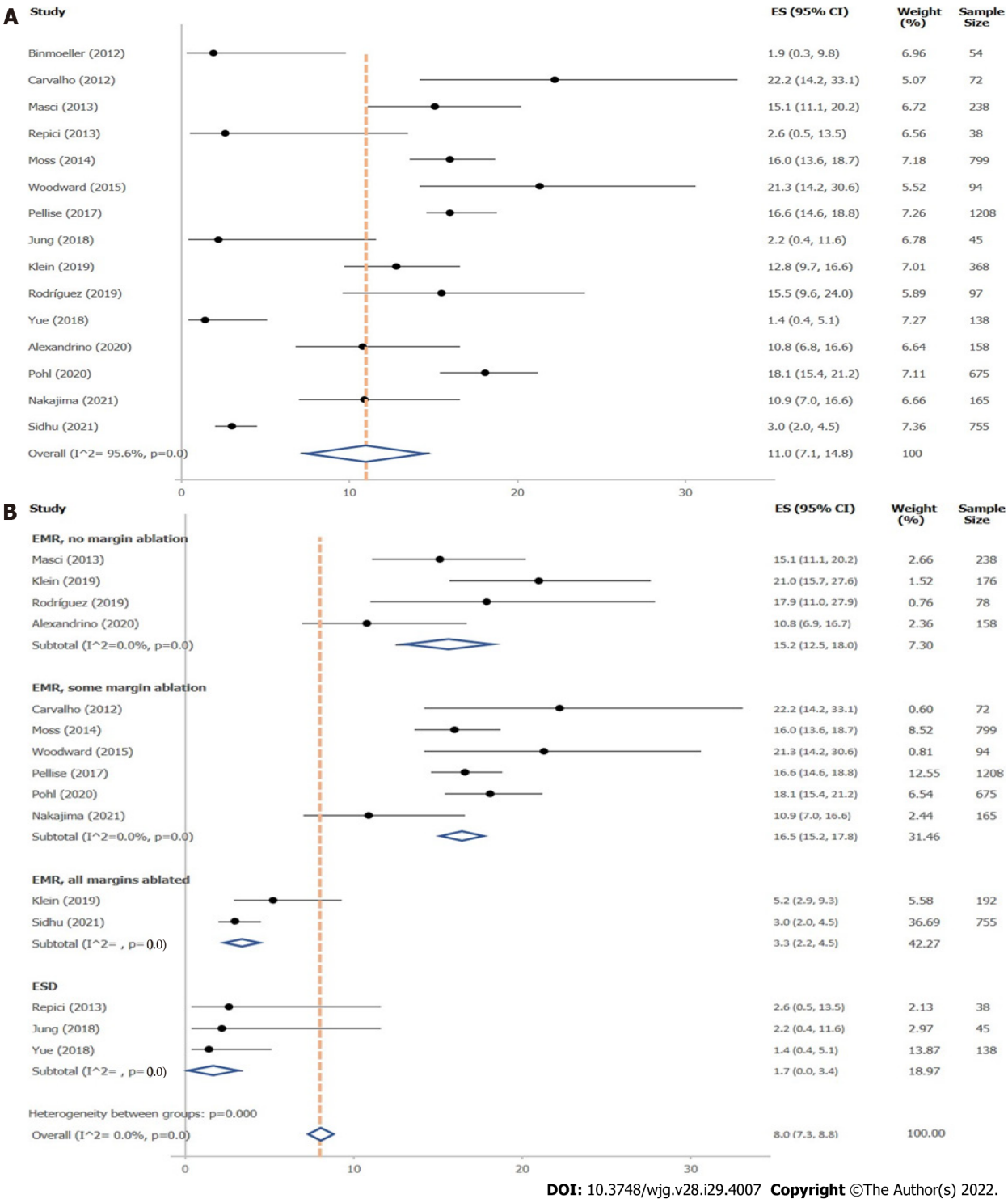
NA: Number of studies insufficient for estimation; EMR: Endoscopic mucosal resection; ESD: Endoscopic submucosal dissection; HSP: Hot snare polypectomy; IRR: Incomplete resection rate; U-EMR: Underwater endoscopic mucosal resection.

There was a strong trend toward lower IRR when considering endoscopist experience (Table 2, Supplementary Figure 7). The mean IRR was 7.0% (95%CI, 3.5%–10.4%; 8 studies) when only expert endoscopists were involved in the study, and 20.3% (95%CI, 13.5%–27.1%; 13 studies) when non-experts were included.

Insufficient data were available for analysis of the influence of polyp morphology or histology on IRR. Three studies included around 50% or more pedunculated polyps; two analyzed hot EMR[15,16] , and the third analyzed hot and cold EMR and CSP[17]. Three further studies included smaller numbers of pedunculated polyps, using cold EMR[18], ESD[19], and underwater EMR[20]. Most studies included 10% or less SSA/Ps, while two studies investigating CSP and cold EMR evaluated results from SSA/Ps only[21,22]. The latter two studies reported exceptionally low IRR of less than 1.5%.

DISCUSSION

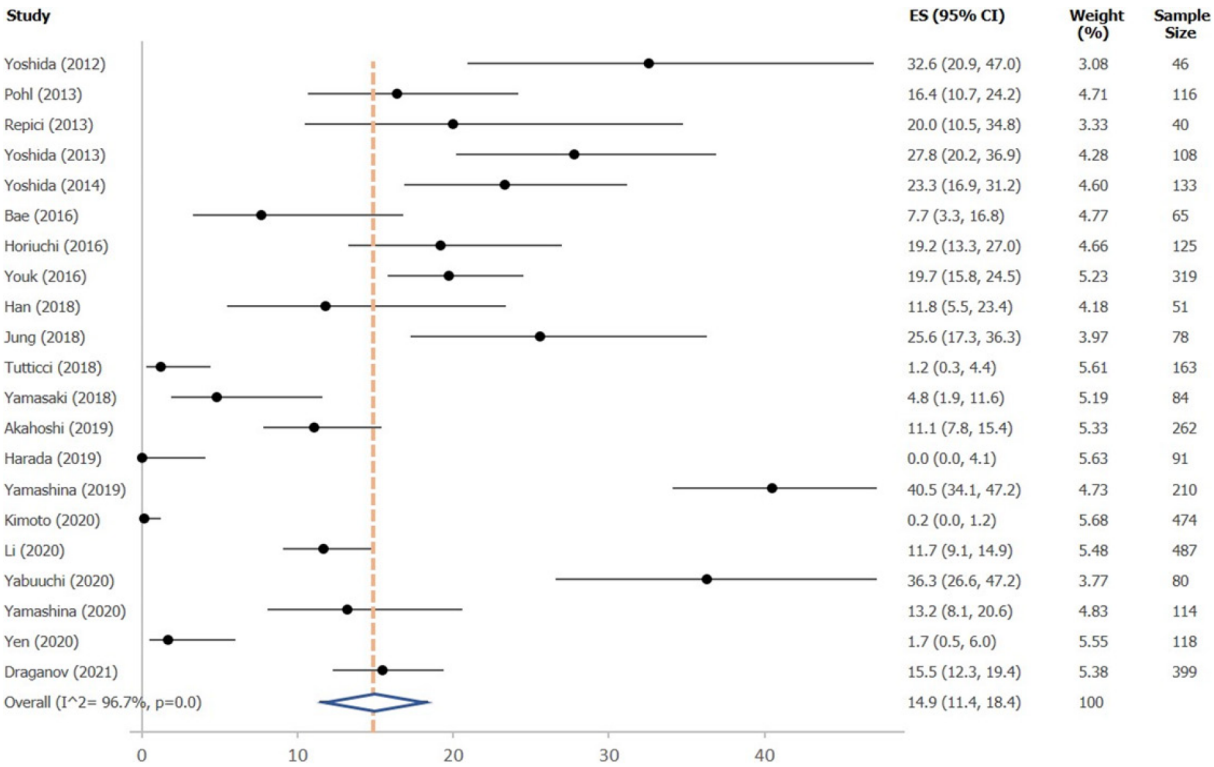
This meta-analysis confirms the high risk for recurrence after standard EMR resection of large colonic



DOI: 10.3748/wjg.v28.i29.4007 **Copyright** ©The Author(s) 2022.

Figure 2 Local recurrence rate at < 12 mo' follow-up. A: For polyps ≥ 10 mm; B: For polyps ≥ 10 mm, stratified by resection method.

polyps. When standard EMR without routine margin ablation is used, we found a 12-month recurrence rate of 15.2%. This is comparable to the results found in the two available meta-analyses published in 2014 and 2021, which reported recurrence rates of 15%[6] and 10%[23], respectively. However, since then, many new or modified endoscopic removal techniques have been developed. These novel developments include cold EMR, hot snare with margin ablation, and an increasing body of literature on ESD for colorectal polyps coming from Asian, European and North American centers. We found that two of these modalities resulted in significantly lower LRRs compared with standard EMR. ESD was associated with an LRR of only 1.7%, and the LRR after EMR with routine ablation of the complete margin was 3.3%. However, ESD requires advanced endoscopy skills, adequate training, and the technique is associated with an increased risk for complications[24-26]. Furthermore, significant differences in safety and efficacy of ESD have been shown between Asian and non-Asian countries[27], so that EMR has remained the standard for large polyp resection in Western countries to date.



DOI: 10.3748/wjg.v28.i29.4007 **Copyright** ©The Author(s) 2022.

Figure 3 Incomplete resection rate for polyps ≥ 10 mm, independent of resection method.

The other modality that shows significantly reduced recurrence rates is the combination of hot EMR with routine margin ablation[9,28]. Thus, ESD or EMR with routine margin ablation currently seem to be the best approaches for endoscopic removal of large colorectal polyps in order to avoid recurrence. We found that systematic margin ablation after EMR can reduce the LRR to rates similar to those of ESD. These results originate from two recent Australian prospective studies, in which snare tip soft coagulation (STSC) was routinely performed after EMR[9,28]. As these studies included only polyps ≥ 20 mm further studies evaluating the effect of margin ablation on polyps sized 10-19 mm may be of additional value. The positive effect of margin ablation has also been shown in a retrospective US study, evaluating systematic application of argon plasma coagulation (APC) after EMR in 246 patients[29]. The authors found an LRR of 5% at < 12 mo FU, which is comparable to the rates found by Klein (5%) [9] and Sidhu (3%)[28]. However, the results for using APC margin ablation still need to be confirmed by prospective studies. A recently completed prospective, multicenter study evaluating resection of large colonic lesions ≥ 20 mm in 76 patients using EMR and hybrid APC for margin and base ablation found a LRR of 2.2%[30]. This indicates that APC ablation can reduce local recurrence comparable to ESD and EMR with STSC.

Importantly, margin ablation should be performed systematically and completely, as visual margin assessment may underestimate incomplete resection[4]. This is confirmed by our analysis, which showed that studies using unsystematic or incomplete margin ablation were not able to reduce the LRR [9,14,31].

Notably, even though use of cold snare resection techniques for large colonic polyps is increasingly reported, at present no prospective studies have been published reporting LRR for CSP or cold EMR for large colorectal polyps. Furthermore, recent retrospective studies have indicated that these techniques might potentially increase the risk for local recurrence. In the largest retrospective series published to date, Suresh *et al*[32] reported an LRR of 34.8% after cold EMR. Therefore, caution is warranted for routine use of cold EMR outside of clinical studies until data from ongoing RCTs comparing hot with cold EMR become available.

For polyps 10–19 mm, follow-up examination is often performed years after the index colonoscopy. Therefore, data on LRR for 10–19 mm colorectal polyps are sparse, and we used IRR to estimate the risk of local recurrence for this subgroup. In our analysis, overall IRR for polyps sized 10–19 mm was 16.0%. This rate was similar to the IRR found in a previous meta-analysis (20.8%)[5] and in one of the landmark studies on IRR (CARE study)[4]. The CARE study reported that even though endoscopists rated resection as complete by visual assessment, 10.1% of cases showed residual tissue on margin biopsy. Compared with the previous meta-analysis, our analysis included more data, especially regarding cold snare resection techniques[5]. However, adding the recently published data on cold snare resection did not significantly alter overall IRR of polyps 10–19 mm. Furthermore, IRR of EMR, cold EMR, HSP, and

underwater EMR were similar[17,18,21]. Only two prospective studies evaluated IRR for large colonic polyps after CSP resection[17,21]. These studies showed high variability in IRR, and while one study found rates comparable to those obtained with other techniques[17], rates reported in the second were extremely low[21]. This is likely based on the fact that in this study only expert endoscopists were involved and only SSA/Ps were removed by wide-field style cold snare resection. A previous meta-analysis has already demonstrated that expert endoscopists achieve lower IRRs[5], and this was confirmed in our analysis, with an IRR of 7.0% for expert endoscopists and 20.3% for those studies in which less experienced endoscopists were included. Furthermore, the exclusive inclusion of SSA/Ps introduced a further bias into the study, as removal of SSA/Ps generally yields better results[14]. This renders the generalizability of CSP to general clinical practice difficult, and more prospective studies are needed to establish IRR, and especially LRR risk, after CPS and cold EMR removal of large colorectal polyps including all pathology types.

For polyps ≥ 20 mm, the mean IRR was 11.7% in this analysis. Interestingly, this rate is lower than the results obtained for polyps sized 10–19 mm (16.0%). This effect was based on the good results obtained with ESD, and is most likely also associated with the fact that 10–19 mm polyps are usually resected in general endoscopic practice, whereas polyps ≥ 20 mm are often referred for expert resection.

Recent guidelines recommend HSP, EMR [European Society of Gastrointestinal Endoscopy, American Gastroenterological Association (AGA)][33,34] and CSP (AGA)[34] for resection of 10–19 mm polyps. Our data show that EMR with margin ablation is an important new development that warrants further study. For lesions ≥ 20 mm, guidelines recommend ESD in specific cases, and the need for a skilled endoscopist to perform the procedure is highlighted[25,26,35]. The importance of endoscopist skill level is also supported by our data. Furthermore, our data suggest that EMR with systematic and complete margin ablation may be an appropriate alternative to ESD, especially considering the low complication rates reported in the available studies[9,28,29].

However, safety profiles should also be taken into account when evaluating different polypectomy techniques. Known complications occurring during and after polypectomy are immediate and delayed bleeding as well as perforation and post-coagulation syndrome[33,34]. A meta-analysis from 2016 evaluating endoscopic resection of polyps ≥ 20 mm found perforation occurring in 1.5% and bleeding in 6.5% of polyps. Mortality was indicated as 0.08%[36]. Yet, an up-to-date analysis comparing safety profiles of CSP, HSP, EMR with and without margin ablation, underwater EMR, and ESD still has to be performed.

Our analysis has several strengths, including the robustness of the literature search with a large number of publications screened (6928 publications). Of these, 34 prospective studies with a total of 10268 polyp resections were included. As only prospective data were evaluated, we were able to perform a high-quality analysis, as retrospective studies reporting on LRR and IRR are unsystematic in the ascertainment of the main outcomes, thus having a high likelihood of bias. Furthermore, the retrieval of granular data allowed us to perform multiple analyses.

The main limitation of the study is that by exclusion of retrospective studies, the data set was reduced. Furthermore, publications were excluded in which IRR was determined by visual assessment or in which appointments for follow-up examinations for LRR assessment exceeded 12 mo. While this reduced the amount of studies included into the analysis, it ensured a better overview of the high-quality data available in the literature. Additionally, it shows that for some techniques data of sufficient quality is sparse and that there is a need for further studies. Second, expert endoscopist status was difficult to determine, as there is no published consensus definition, and some studies do not clarify the expertise of the involved endoscopists. However, expert and non-expert status were systematically assessed and discussed for this meta-analysis. Third, as assessment for IRR is not standardized, different methods, including margin assessment and margin biopsy, are used for its estimation. However, margin assessment is likely to overestimate IRR, as lesions resected in piecemeal fashion may be resected completely, but will appear with positive resection margins. Margin biopsy, on the other hand, is likely to underestimate IRR, as only sample parts of the margins are examined[37]. Therefore, true IRR will be located somewhere in between the values found with margin biopsy and margin assessment. Another limitation is the elevated heterogeneity in some reported outcomes. For LRR, most of the observed heterogeneity was due to combining different resection techniques into the same analysis. When stratifying for resection technique and use of margin ablation, we found very low heterogeneity in the reported outcomes. For IRR, the differing use of wide field resection before biopsies and the number of margin biopsies taken could explain some of the heterogeneity reported.

CONCLUSION

In conclusion, we found that local recurrence after resection of large colonic polyps occurs frequently when standard EMR is used. Local polyp recurrence can be reduced by performing ESD or EMR with routine and complete margin ablation. Other techniques, such as CSP, cold EMR, and underwater EMR require further evaluation in prospective studies before their routine implementation in clinical practice can be recommended.

ARTICLE HIGHLIGHTS

Research background

Complete resection is the aim of endoscopic therapy for large colonic polyps. Endoscopic mucosal resection (EMR) is the most common endoscopic treatment for such polyps. In recent years, endoscopic resection techniques have evolved, including cold snare polypectomy (CSP), cold EMR, EMR with margin ablation, underwater EMR, and endoscopic submucosal dissection (ESD).

Research motivation

Efficacy of these newer polypectomy techniques with regard to local recurrence rates (LRRs) *vs* traditional hot snare polypectomy and standard EMR remains unclear.

Research objectives

These developments have sparked our interest in providing an up-to-date meta-analysis of LRRs and incomplete resection rates (IRRs) for large (≥ 10 mm) colorectal polyps, and to evaluate the impact of the novel or modified endoscopic resection techniques on LRRs.

Research methods

A systematic literature search was performed within MEDLINE, EMBASE, EBM Reviews, and CINAHL databases. All articles published between January 2011 and July 2021 reporting on IRR and/or LRR for colorectal polyps 10 mm or larger removed by endoscopic resection techniques were included in the search.

Research results

LRR were lowest when EMR with systematic margin ablation (3.3%) or ESD (1.7%) were used for endoscopic removal of large (> 10 mm) colorectal polyps. When standard EMR (without margin ablation) or with partial margin ablation were used, LRRs were high (15.2% and 16.5%, respectively).

Research conclusions

Local recurrence after resection of large colonic polyps occurs frequently when standard EMR is used, but can be reduced by performing ESD or EMR with routine and complete margin ablation. Other techniques, such as CSP, cold EMR, and underwater EMR require further evaluation in prospective studies before their routine implementation in clinical practice can be recommended.

Research perspectives

ESD or EMR with margin ablation should be considered standard of care for endoscopic removal of large colorectal polyps in order to avoid recurrence. At present, cold snare resection techniques or underwater EMR should only be performed within clinical trials, pending the availability of high-quality evidence.

FOOTNOTES

Author contributions: von Renteln D designed the research study; von Renteln D, Rotermund C, Djinbachian R, Taghiakbari M, Enderle MD, and Eickhoff A performed the research; von Renteln D, Rotermund C, Djinbachian R, and Taghiakbari M analyzed the data; and von Renteln D, Rotermund C, and Djinbachian R wrote the manuscript; and All authors have read and approve the final manuscript.

Conflict-of-interest statement: All authors report no relevant conflicts of interest for this article.

PRISMA 2009 Checklist statement: The authors have read the PRISMA 2009 Checklist, and the manuscript was prepared and revised according to the PRISMA 2009 Checklist.

Open-Access: This article is an open-access article that was selected by an in-house editor and fully peer-reviewed by external reviewers. It is distributed in accordance with the Creative Commons Attribution NonCommercial (CC BY-NC 4.0) license, which permits others to distribute, remix, adapt, build upon this work non-commercially, and license their derivative works on different terms, provided the original work is properly cited and the use is non-commercial. See: https://creativecommons.org/Licenses/by-nc/4.0/

Country/Territory of origin: Canada

ORCID number: Daniel von Renteln 0000-0002-6125-0068.

S-Editor: Ma YJ

L-Editor: A
P-Editor: Ma YJ

REFERENCES

1 **Pohl H**, Anderson JC, Aguilera-Fish A, Calderwood AH, Mackenzie TA, Robertson DJ. Recurrence of Colorectal Neoplastic Polyps After Incomplete Resection. *Ann Intern Med* 2021; **174**: 1377-1384 [PMID: 34370514 DOI: 10.7326/M20-6689]
2 **Hassan C**, Antonelli G, Dumonceau JM, Regula J, Bretthauer M, Chaussade S, Dekker E, Ferlitsch M, Gimeno-Garcia A, Jover R, Kalager M, Pellisé M, Pox C, Ricciardiello L, Rutter M, Helsingen LM, Bleijenberg A, Senore C, van Hooft JE, Dinis-Ribeiro M, Quintero E. Post-polypectomy colonoscopy surveillance: European Society of Gastrointestinal Endoscopy (ESGE) Guideline - Update 2020. *Endoscopy* 2020; **52**: 687-700 [PMID: 32572858 DOI: 10.1055/a-1185-3109]
3 **Gupta S**, Lieberman D, Anderson JC, Burke CA, Dominitz JA, Kaltenbach T, Robertson DJ, Shaukat A, Syngal S, Rex DK. Recommendations for Follow-Up After Colonoscopy and Polypectomy: A Consensus Update by the US Multi-Society Task Force on Colorectal Cancer. *Gastrointest Endosc* 2020; **91**: 463-485.e5 [PMID: 32044106 DOI: 10.1016/j.gie.2020.01.014]
4 **Pohl H**, Srivastava A, Bensen SP, Anderson P, Rothstein RI, Gordon SR, Levy LC, Toor A, Mackenzie TA, Rosch T, Robertson DJ. Incomplete polyp resection during colonoscopy-results of the complete adenoma resection (CARE) study. *Gastroenterology* 2013; **144**: 74-80.e1 [PMID: 23022496 DOI: 10.1053/j.gastro.2012.09.043]
5 **Djinbachian R**, Iratni R, Durand M, Marques P, von Renteln D. Rates of Incomplete Resection of 1- to 20-mm Colorectal Polyps: A Systematic Review and Meta-Analysis. *Gastroenterology* 2020; **159**: 904-914.e12 [PMID: 32437747 DOI: 10.1053/j.gastro.2020.05.018]
6 **Belderbos TD**, Leenders M, Moons LM, Siersema PD. Local recurrence after endoscopic mucosal resection of nonpedunculated colorectal lesions: systematic review and meta-analysis. *Endoscopy* 2014; **46**: 388-402 [PMID: 24671869 DOI: 10.1055/s-0034-1364970]
7 **Thoguluva Chandrasekar V**, Spadaccini M, Aziz M, Maselli R, Hassan S, Fuccio L, Duvvuri A, Frazzoni L, Desai M, Fugazza A, Jegadeesan R, Colombo M, Dasari CS, Hassan C, Sharma P, Repici A. Cold snare endoscopic resection of nonpedunculated colorectal polyps larger than 10 mm: a systematic review and pooled-analysis. *Gastrointest Endosc* 2019; **89**: 929-936.e3 [PMID: 30639542 DOI: 10.1016/j.gie.2018.12.022]
8 **Binmoeller KF**, Weilert F, Shah J, Bhat Y, Kane S. "Underwater" EMR without submucosal injection for large sessile colorectal polyps (with video). *Gastrointest Endosc* 2012; **75**: 1086-1091 [PMID: 22365184 DOI: 10.1016/j.gie.2011.12.022]
9 **Klein A**, Tate DJ, Jayasekeran V, Hourigan L, Singh R, Brown G, Bahin FF, Burgess N, Williams SJ, Lee E, Sidhu M, Byth K, Bourke MJ. Thermal Ablation of Mucosal Defect Margins Reduces Adenoma Recurrence After Colonic Endoscopic Mucosal Resection. *Gastroenterology* 2019; **156**: 604-613.e3 [PMID: 30296436 DOI: 10.1053/j.gastro.2018.10.003]
10 **Page MJ**, McKenzie JE, Bossuyt PM, Boutron I, Hoffmann TC, Mulrow CD, Shamseer L, Tetzlaff JM, Akl EA, Brennan SE, Chou R, Glanville J, Grimshaw JM, Hróbjartsson A, Lalu MM, Li T, Loder EW, Mayo-Wilson E, McDonald S, McGuinness LA, Stewart LA, Thomas J, Tricco AC, Welch VA, Whiting P, Moher D. The PRISMA 2020 statement: An updated guideline for reporting systematic reviews. *J Clin Epidemiol* 2021; **134**: 178-189 [PMID: 33789819 DOI: 10.1016/j.jclinepi.2021.03.001]
11 **National Institutes of Health**. NIH Study Quality Assessment Tool 2021. Available from: https://www.nhlbi.nih.gov/health-topics/study-quality-assessment-tools
12 **Hunter JP**, Saratzis A, Sutton AJ, Boucher RH, Sayers RD, Bown MJ. In meta-analyses of proportion studies, funnel plots were found to be an inaccurate method of assessing publication bias. *J Clin Epidemiol* 2014; **67**: 897-903 [PMID: 24794697 DOI: 10.1016/j.jclinepi.2014.03.003]
13 **Woodward T**, Crook JE, Raimondo M, Wallace M. Improving complete EMR of colorectal neoplasia: a randomized trial comparing snares and injectate in the resection of large sessile colon polyps. *Gastrointest Endosc* 2015; **81**: 673-681 [PMID: 25708754 DOI: 10.1016/j.gie.2014.10.010]
14 **Pellise M**, Burgess NG, Tutticci N, Hourigan LF, Zanati SA, Brown GJ, Singh R, Williams SJ, Raftopoulos SC, Ormonde D, Moss A, Byth K, P'Ng H, Mahajan H, McLeod D, Bourke MJ. Endoscopic mucosal resection for large serrated lesions in comparison with adenomas: a prospective multicentre study of 2000 lesions. *Gut* 2017; **66**: 644-653 [PMID: 26786685 DOI: 10.1136/gutjnl-2015-310249]
15 **Han SJ**, Jung Y, Cho YS, Chung IK, Kim JY, Eun JY, Lee SH, Ko GB, Lee TH, Park SH, Cho HD, Kim SJ. Clinical Effectiveness of Submucosal Injection with Indigo Carmine Mixed Solution for Colon Endoscopic Mucosal Resection. *Dig Dis Sci* 2018; **63**: 775-780 [PMID: 29383606 DOI: 10.1007/s10620-018-4918-6]
16 **Yoshida N**, Saito Y, Hirose R, Ogiso K, Inada Y, Yagi N, Naito Y, Otake Y, Nakajima T, Matsuda T, Yanagisawa A, Itoh Y. Endoscopic mucosal resection for middle and large colorectal polyps with a double-loop snare. *Digestion* 2014; **90**: 232-239 [PMID: 25532080 DOI: 10.1159/000368044]
17 **Li D**, Wang W, Xie J, Liu G, Wang R, Jiang C, Ye Z, Xu B, He X, Hong D. Efficacy and safety of three different endoscopic methods in treatment of 6-20 mm colorectal polyps. *Scand J Gastroenterol* 2020; **55**: 362-370 [PMID: 32150478 DOI: 10.1080/00365521.2020.1732456]
18 **Yabuuchi Y**, Imai K, Hotta K, Ito S, Kishida Y, Yoshida M, Kawata N, Kakushima N, Takizawa K, Ishiwatari H, Matsubayashi H, Aizawa D, Oishi T, Imai T, Ono H. Efficacy and safety of cold-snare endoscopic mucosal resection for colorectal adenomas 10 to 14 mm in size: a prospective observational study. *Gastrointest Endosc* 2020; **92**: 1239-1246 [PMID: 32464143 DOI: 10.1016/j.gie.2020.05.019]

19 **Draganov PV**, Aihara H, Karasik MS, Ngamruengphong S, Aadam AA, Othman MO, Sharma N, Grimm IS, Rostom A, Elmunzer BJ, Jawaid SA, Westerveld D, Perbtani YB, Hoffman BJ, Schlachterman A, Siegel A, Coman RM, Wang AY, Yang D. Endoscopic Submucosal Dissection in North America: A Large Prospective Multicenter Study. *Gastroenterology* 2021; **160**: 2317-2327.e2 [PMID: 33610532 DOI: 10.1053/j.gastro.2021.02.036]

20 **Yamashina T**, Uedo N, Akasaka T, Iwatsubo T, Nakatani Y, Akamatsu T, Kawamura T, Takeuchi Y, Fujii S, Kusaka T, Shimokawa T. Comparison of Underwater vs Conventional Endoscopic Mucosal Resection of Intermediate-Size Colorectal Polyps. *Gastroenterology* 2019; **157**: 451-461.e2 [PMID: 30981791 DOI: 10.1053/j.gastro.2019.04.005]

21 **Kimoto Y**, Sakai E, Inamoto R, Kurebayashi M, Takayanagi S, Hirata T, Suzuki Y, Ishii R, Konishi T, Kanda K, Negishi R, Takita M, Ono K, Minato Y, Muramoto T, Ohata K. Safety and Efficacy of Cold Snare Polypectomy Without Submucosal Injection for Large Sessile Serrated Lesions: A Prospective Study. *Clin Gastroenterol Hepatol* 2022; **20**: e132-e138 [PMID: 33152541 DOI: 10.1016/j.cgh.2020.10.053]

22 **Tutticci NJ**, Hewett DG. Cold EMR of large sessile serrated polyps at colonoscopy (with video). *Gastrointest Endosc* 2018; **87**: 837-842 [PMID: 29133196 DOI: 10.1016/j.gie.2017.11.002]

23 **Lim XC**, Nistala KRY, Ng CH, Lin SY, Tan DJH, Ho KY, Chong CS, Muthiah M. Endoscopic submucosal dissection *vs* endoscopic mucosal resection for colorectal polyps: A meta-analysis and meta-regression with single arm analysis. *World J Gastroenterol* 2021; **27**: 3925-3939 [PMID: 34321855 DOI: 10.3748/wjg.v27.i25.3925]

24 **Fuccio L**, Hassan C, Ponchon T, Mandolesi D, Farioli A, Cucchetti A, Frazzoni L, Bhandari P, Bellisario C, Bazzoli F, Repici A. Clinical outcomes after endoscopic submucosal dissection for colorectal neoplasia: a systematic review and meta-analysis. *Gastrointest Endosc* 2017; **86**: 74-86.e17 [PMID: 28254526 DOI: 10.1016/j.gie.2017.02.024]

25 **Tanaka S**, Kashida H, Saito Y, Yahagi N, Yamano H, Saito S, Hisabe T, Yao T, Watanabe M, Yoshida M, Saitoh Y, Tsuruta O, Sugihara KI, Igarashi M, Toyonaga T, Ajioka Y, Kusunoki M, Koike K, Fujimoto K, Tajiri H. Japan Gastroenterological Endoscopy Society guidelines for colorectal endoscopic submucosal dissection/endoscopic mucosal resection. *Dig Endosc* 2020; **32**: 219-239 [PMID: 31566804 DOI: 10.1111/den.13545]

26 **Draganov PV**, Wang AY, Othman MO, Fukami N. AGA Institute Clinical Practice Update: Endoscopic Submucosal Dissection in the United States. *Clin Gastroenterol Hepatol* 2019; **17**: 16-25.e1 [PMID: 30077787 DOI: 10.1016/j.cgh.2018.07.041]

27 **Daoud DC**, Suter N, Durand M, Bouin M, Faulques B, von Renteln D. Comparing outcomes for endoscopic submucosal dissection between Eastern and Western countries: A systematic review and meta-analysis. *World J Gastroenterol* 2018; **24**: 2518-2536 [PMID: 29930473 DOI: 10.3748/wjg.v24.i23.2518]

28 **Sidhu M**, Shahidi N, Gupta S, Desomer L, Vosko S, Arnout van Hattem W, Hourigan LF, Lee EYT, Moss A, Raftopoulos S, Heitman SJ, Williams SJ, Zanati S, Tate DJ, Burgess N, Bourke MJ. Outcomes of Thermal Ablation of the Mucosal Defect Margin After Endoscopic Mucosal Resection: A Prospective, International, Multicenter Trial of 1000 Large Nonpedunculated Colorectal Polyps. *Gastroenterology* 2021; **161**: 163-170.e3 [PMID: 33798525 DOI: 10.1053/j.gastro.2021.03.044]

29 **Raju GS**, Lum P, Abu-Sbeih H, Ross WA, Thirumurthi S, Miller E, Lynch P, Lee J, Bhutani MS, Shafi M, Weston B, Rashid A, Wang Y, Chang GJ, Carlson R, Hagan K, Davila M, Stroehlein J. Cap-fitted endoscopic mucosal resection of ≥ 20 mm colon flat lesions followed by argon plasma coagulation results in a low adenoma recurrence rate. *Endosc Int Open* 2020; **8**: E115-E121 [PMID: 32010742 DOI: 10.1055/a-1012-1811]

30 **Motchum L**, Levenick J, Djinbachian R, Moyer M, Bouchard S, Taghiakbari M, Repici A, Deslandres E, Renteln D von. Endoscopic mucosal resection combined with hybrid argon plasma coagulation to prevent recurrence of large nonpedunculated colorectal polyps. Gastrointestinal Endoscopy, under Revision 2022 [PMID: 35724695 DOI: 10.1016/j.gie.2022.06.018]

31 **Pohl H**, Grimm IS, Moyer MT, Hasan MK, Pleskow D, Elmunzer BJ, Khashab MA, Sanaei O, Al-Kawas FH, Gordon SR, Mathew A, Levenick JM, Aslanian HR, Antaki F, von Renteln D, Crockett SD, Rastogi A, Gill JA, Law RJ, Elias PA, Pellise M, Mackenzie TA, Rex DK. Effects of Blended (Yellow) vs Forced Coagulation (Blue) Currents on Adverse Events, Complete Resection, or Polyp Recurrence After Polypectomy in a Large Randomized Trial. *Gastroenterology* 2020; **159**: 119-128.e2 [PMID: 32173478 DOI: 10.1053/j.gastro.2020.03.014]

32 **Suresh S**, Zhang J, Ahmed A, Abu Ghanimeh M, Elbanna A, Kaur R, Isseh M, Watson A, Dang DT, Chathadi KV, Pompa R, Singla S, Piraka C, Zuchelli T. Risk factors associated with adenoma recurrence following cold snare endoscopic mucosal resection of polyps ≥ 20 mm: a retrospective chart review. *Endosc Int Open* 2021; **9**: E867-E873 [PMID: 34079869 DOI: 10.1055/a-1399-8398]

33 **Ferlitsch M**, Moss A, Hassan C, Bhandari P, Dumonceau JM, Paspatis G, Jover R, Langner C, Bronzwaer M, Nalankilli K, Fockens P, Hazzan R, Gralnek IM, Gschwantler M, Waldmann E, Jeschek P, Penz D, Heresbach D, Moons L, Lemmers A, Paraskeva K, Pohl J, Ponchon T, Regula J, Repici A, Rutter MD, Burgess NG, Bourke MJ. Colorectal polypectomy and endoscopic mucosal resection (EMR): European Society of Gastrointestinal Endoscopy (ESGE) Clinical Guideline. *Endoscopy* 2017; **49**: 270-297 [PMID: 28212588 DOI: 10.1055/s-0043-102569]

34 **Kaltenbach T**, Anderson JC, Burke CA, Dominitz JA, Gupta S, Lieberman D, Robertson DJ, Shaukat A, Syngal S, Rex DK. Endoscopic Removal of Colorectal Lesions-Recommendations by the US Multi-Society Task Force on Colorectal Cancer. *Gastroenterology* 2020; **158**: 1095-1129 [PMID: 32122632 DOI: 10.1053/j.gastro.2019.12.018]

35 **Pimentel-Nunes P**, Dinis-Ribeiro M, Ponchon T, Repici A, Vieth M, De Ceglie A, Amato A, Berr F, Bhandari P, Bialek A, Conio M, Haringsma J, Langner C, Meisner S, Messmann H, Morino M, Neuhaus H, Piessevaux H, Rugge M, Saunders BP, Robaszkiewicz M, Seewald S, Kashin S, Dumonceau JM, Hassan C, Deprez PH. Endoscopic submucosal dissection: European Society of Gastrointestinal Endoscopy (ESGE) Guideline. *Endoscopy* 2015; **47**: 829-854 [PMID: 26317585 DOI: 10.1055/s-0034-1392882]

36 **Hassan C**, Repici A, Sharma P, Correale L, Zullo A, Bretthauer M, Senore C, Spada C, Bellisario C, Bhandari P, Rex DK. Efficacy and safety of endoscopic resection of large colorectal polyps: a systematic review and meta-analysis. *Gut* 2016; **65**: 806-820 [PMID: 25681402 DOI: 10.1136/gutjnl-2014-308481]

37 **Djinbachian R**, Renteln DV. Endoscopic Polypectomy: How Should We Determine Complete Resection Status? *Clin Gastroenterol Hepatol* 2022; **20**: 242-243 [PMID: 33309986 DOI: 10.1016/j.cgh.2020.12.006]



Published by **Baishideng Publishing Group Inc**
7041 Koll Center Parkway, Suite 160, Pleasanton, CA 94566, USA
Telephone: +1-925-3991568
E-mail: bpgoffice@wjgnet.com
Help Desk: https://www.f6publishing.com/helpdesk
https://www.wjgnet.com



© 2022 Baishideng Publishing Group Inc. All rights reserved.

ISSN 1007-9327 (print)
ISSN 2219-2840 (online)

World Journal of *Gastroenterology*

World J Gastroenterol 2022 August 14; 28(30): 4019-4234



Published by Baishideng Publishing Group Inc

World Journal of Gastroenterology

Contents

Weekly Volume 28 Number 30 August 14, 2022

REVIEW

4019 Role of one-step nucleic acid amplification in colorectal cancer lymph node metastases detection

Crafa F, Vanella S, Catalano OA, Pomykala KL, Baiamonte M

MINIREVIEWS

4044 Current perspectives on the role of liver transplantation for Langerhans cell histiocytosis: A narrative review

Menon J, Rammohan A, Vij M, Shanmugam N, Rela M

4053 Gut microbiota, inflammatory bowel disease and colorectal cancer

Quaglio AEV, Grillo TG, De Oliveira ECS, Di Stasi LC, Sassaki LY

4061 Thrombocytopenia in chronic liver disease: Physiopathology and new therapeutic strategies before invasive procedures

Gallo P, Terracciani F, Di Pasquale G, Esposito M, Picardi A, Vespasiani-Gentilucci U

ORIGINAL ARTICLE

Basic Study

4075 P2X7 receptor blockade decreases inflammation, apoptosis, and enteric neuron loss during *Clostridioides difficile* toxin A-induced ileitis in mice

Santos AAQA, Costa DVS, Foschetti DA, Duarte ASG, Martins CS, Soares PMG, Castelucci P, Brito GAC

Case Control Study

4089 Serological profiling of Crohn's disease and ulcerative colitis patients reveals anti-microbial antibody signatures

Shome M, Song L, Williams S, Chung Y, Murugan V, Park JG, Faubion W, Pasha SF, Leighton JA, LaBaer J, Qiu J

Retrospective Cohort Study

4102 Trends in medication use and treatment patterns in Chinese patients with inflammatory bowel disease

Yao LY, Shao BL, Tian F, Ye M, Li YQ, Wang XL, Wang L, Yang SQ, Lv XP, Jia Y, Wang XH, Zhang XQ, Wei YL, Cao Q

Retrospective Study

4120 Salivary *Fusobacterium nucleatum* serves as a potential diagnostic biomarker for gastric cancer

Chen WD, Zhang X, Zhang MJ, Zhang YP, Shang ZQ, Xin YW, Zhang Y

4133 Development and validation of a nomogram for predicting overall survival in cirrhotic patients with acute kidney injury

Wan YP, Wang AJ, Zhang W, Zhang H, Peng GH, Zhu X

World Journal of Gastroenterology

Weekly Volume 28 Number 30 August 14, 2022

Contents

4152 Cumulative incidence and risk factors for pouch adenomas associated with familial adenomatous polyposis following restorative proctocolectomy

Ryu HS, Yu CS, Kim YI, Lee JL, Kim CW, Yoon YS, Park IJ, Lim SB, Kim JC

4163 Changes in the esophagogastric junction outflow obstruction manometric feature based on the Chicago Classification updates

Li YY, Lu WT, Liu JX, Wu LH, Chen M, Jiao HM

Observational Study

4174 Epidemiology of inflammatory bowel diseases in the state of Rio Grande do Sul, Brazil

Cassol OS, Zabot GP, Saad-Hossne R, Padoin A

4182 Hepatocellular carcinoma, decompensation, and mortality based on hepatitis C treatment: A prospective cohort study

Choi GH, Jang ES, Kim YS, Lee YJ, Kim IH, Cho SB, Lee HC, Jang JW, Ki M, Choi HY, Baik D, Jeong SH

META-ANALYSIS

4201 Network meta-analysis of randomized controlled trials on esophagectomies in esophageal cancer: The superiority of minimally invasive surgery

Szakó L, Németh D, Farkas N, Kiss S, Dömötör RZ, Engh MA, Hegyi P, Eross B, Papp A

CASE REPORT

4211 Contrast-enhanced ultrasound of a traumatic neuroma of the extrahepatic bile duct: A case report and review of literature

Yuan ZQ, Yan HL, Li JW, Luo Y

LETTER TO THE EDITOR

4221 Prognostic role of expression of angiogenesis markers in hepatocellular carcinoma: A bioinformatics analysis

Miao YD, Tang XL, Wang JT, Mi DH

4227 Benefits of minimally invasive surgery in the treatment of gastric cancer

Sibio S, La Rovere F, Di Carlo S

4231 Alcohol-related diseases and liver metastasis: Role of cell-free network communication

Muro M, Collados-Ros A, Legaz I

Contents

ABOUT COVER

Associate Editor of *World Journal of Gastroenterology*, Ming-Lung Yu, MD, PhD, Chair Professor, Chief, Hepatitis Research Center, Kaohsiung Medical University, No. 100 Tzyou 1st Road, Kaohsiung 807, Taiwan. fish6069@gmail.com

AIMS AND SCOPE

The primary aim of *World Journal of Gastroenterology* (*WJG*, *World J Gastroenterol*) is to provide scholars and readers from various fields of gastroenterology and hepatology with a platform to publish high-quality basic and clinical research articles and communicate their research findings online. *WJG* mainly publishes articles reporting research results and findings obtained in the field of gastroenterology and hepatology and covering a wide range of topics including gastroenterology, hepatology, gastrointestinal endoscopy, gastrointestinal surgery, gastrointestinal oncology, and pediatric gastroenterology.

INDEXING/ABSTRACTING

The *WJG* is now abstracted and indexed in Science Citation Index Expanded (SCIE, also known as SciSearch®), Current Contents/Clinical Medicine, Journal Citation Reports, Index Medicus, MEDLINE, PubMed, PubMed Central, Scopus, Reference Citation Analysis, China National Knowledge Infrastructure, China Science and Technology Journal Database, and Superstar Journals Database. The 2022 edition of Journal Citation Reports® cites the 2021 impact factor (IF) for *WJG* as 5.374; IF without journal self cites: 5.187; 5-year IF: 5.715; Journal Citation Indicator: 0.84; Ranking: 31 among 93 journals in gastroenterology and hepatology; and Quartile category: Q2. The *WJG*'s CiteScore for 2021 is 8.1 and Scopus CiteScore rank 2021: Gastroenterology is 18/149.

RESPONSIBLE EDITORS FOR THIS ISSUE

Production Editor: *Hua-Ge Yu*; **Production Department Director:** *Xu Guo*; **Editorial Office Director:** *Jia-Ru Fan*.

NAME OF JOURNAL
World Journal of Gastroenterology

ISSN
ISSN 1007-9327 (print) ISSN 2219-2840 (online)

LAUNCH DATE
October 1, 1995

FREQUENCY
Weekly

EDITORS-IN-CHIEF
Andrzej S Tarnawski

EDITORIAL BOARD MEMBERS
http://www.wjgnet.com/1007-9327/editorialboard.htm

PUBLICATION DATE
August 14, 2022

COPYRIGHT
© 2022 Baishideng Publishing Group Inc

INSTRUCTIONS TO AUTHORS
https://www.wjgnet.com/bpg/gerinfo/204

GUIDELINES FOR ETHICS DOCUMENTS
https://www.wjgnet.com/bpg/GerInfo/287

GUIDELINES FOR NON-NATIVE SPEAKERS OF ENGLISH
https://www.wjgnet.com/bpg/gerinfo/240

PUBLICATION ETHICS
https://www.wjgnet.com/bpg/GerInfo/288

PUBLICATION MISCONDUCT
https://www.wjgnet.com/bpg/gerinfo/208

ARTICLE PROCESSING CHARGE
https://www.wjgnet.com/bpg/gerinfo/242

STEPS FOR SUBMITTING MANUSCRIPTS
https://www.wjgnet.com/bpg/GerInfo/239

ONLINE SUBMISSION
https://www.f6publishing.com

© 2022 Baishideng Publishing Group Inc. All rights reserved. 7041 Koll Center Parkway, Suite 160, Pleasanton, CA 94566, USA
E-mail: bpgoffice@wjgnet.com https://www.wjgnet.com

World Journal of Gastroenterology

Submit a Manuscript: https://www.f6publishing.com

World J Gastroenterol 2022 August 14; 28(30): 4019-4043

DOI: 10.3748/wjg.v28.i30.4019

ISSN 1007-9327 (print) ISSN 2219-2840 (online)

REVIEW

Role of one-step nucleic acid amplification in colorectal cancer lymph node metastases detection

Francesco Crafa, Serafino Vanella, Onofrio A Catalano, Kelsey L Pomykala, Mario Baiamonte

Specialty type: Surgery

Provenance and peer review: Invited article; Externally peer reviewed.

Peer-review model: Single blind

Peer-review report's scientific quality classification

Grade A (Excellent): 0
Grade B (Very good): B, B
Grade C (Good): C, C, C, C
Grade D (Fair): 0
Grade E (Poor): 0

P-Reviewer: Gao W, China; Hamaya Y, Japan; Liu Z, China; Luo ZW, China; Skok P, Slovenia; Wan XH, China

Received: February 26, 2022
Peer-review started: February 26, 2022
First decision: May 9, 2022
Revised: June 3, 2022
Accepted: July 20, 2022
Article in press: July 20, 2022
Published online: August 14, 2022

Francesco Crafa, Serafino Vanella, Mario Baiamonte, Division of General and Surgical Oncology, St. Giuseppe Moscati Hospital, Center of National Excellence and High Specialty, Avellino 83100, Italy

Onofrio A Catalano, Department of Radiology, Athinoula A. Martinos Center for Biomedical Imaging, Massachusetts General Hospital, Harvard Medical School, Boston, MA 02114, United States

Kelsey L Pomykala, Department of Nuclear Medicine, Department of Radiological Sciences, David Geffen School of Medicine at University of California, Los Angeles, University Hospital Essen, University of Duisburg-Essen, Essen 45141, Germany

Corresponding author: Francesco Crafa, MD, Director, Division of General and Surgical Oncology, St. Giuseppe Moscati Hospital, Center of National Excellence and High Specialty, C/da Amoretta, Avellino 83100, Italy. crafa@tiscali.it

Abstract

Current histopathological staging procedures in colorectal cancer (CRC) depend on midline division of the lymph nodes (LNs) with one section of hematoxylin and eosin staining. Cancer cells outside this transection line may be missed, which could lead to understaging of Union for International Cancer Control Stage II high-risk patients. The one-step nucleic acid amplification (OSNA) assay has emerged as a rapid molecular diagnostic tool for LN metastases detection. It is a molecular technique that can analyze the entire LN tissue using a reverse-transcriptase loop-mediated isothermal amplification reaction to detect tumor-specific cytokeratin 19 mRNA. Our findings suggest that the OSNA assay has a high diagnostic accuracy in detecting metastatic LNs in CRC and a high negative predictive value. OSNA is a standardized, observer-independent technique, which may lead to more accurate staging. It has been suggested that in stage II CRC, the upstaging can reach 25% and these patients can access postoperative adjuvant chemotherapy. Moreover, intraoperative OSNA sentinel node evaluation may allow early CRC to be treated with organ-preserving surgery, while in more advanced-stage disease, a tailored lymphadenectomy can be performed considering the presence of aberrant lymphatic drainage and skip metastases.

Key Words: Colorectal malignancies; One-step nucleic acid amplification; Diagnostic accuracy; Negative predictive value; Upstaging; Organ-sparing surgery; Tailored lymphadenectomy

©The Author(s) 2022. Published by Baishideng Publishing Group Inc. All rights reserved.

Core Tip: Our findings suggest that the one-step nucleic acid amplification (OSNA) assay has high diagnostic accuracy and negative predictive value in detecting metastatic lymph nodes in colorectal cancer (CRC). The short turnaround time renders OSNA an attractive intra-operative method. OSNA results in upstaging in about 25% of stage II CRC cases. Moreover, organ-sparing surgery in early CRC and tailored lymphadenectomy, in more advanced cases, can be performed.

Citation: Crafa F, Vanella S, Catalano OA, Pomykala KL, Baiamonte M. Role of one-step nucleic acid amplification in colorectal cancer lymph node metastases detection. *World J Gastroenterol* 2022; 28(30): 4019-4043
URL: https://www.wjgnet.com/1007-9327/full/v28/i30/4019.htm
DOI: https://dx.doi.org/10.3748/wjg.v28.i30.4019

INTRODUCTION

Of the gastrointestinal cancers, the colorectal cancer (CRC) is the most represented. Among the indication criteria for chemotherapy, lymph node (LN) positivity (stage III) is the most important[1]. The histopathological study of the LNs is performed on one or at most two sections of each LN with hematoxylin and eosin (HE). Therefore the conventional study presents the possibility of not detecting micro-metastases (MMs) or macro-metastases leading to an "understaging". The high relapse rates (20%–25%) in patients with negative LNs could be due to this "understaging"[2]. Multilevel LN sectioning combined with immunohistochemistry (IHC) can improve the detection rate of small nodal tumor infiltrates [*i.e.* isolated tumor cells (ITCs) and MMs], although it is a costly and protracted process [3-6].

Tsujimoto *et al*[7] were the first to describe the one-step nucleic acid amplification (OSNA) assay for detecting LN metastases (LNMs) in patients with breast cancer (BC). Numerous studies have followed which have confirmed the high sensitivity of OSNA in detecting LNMs of breast, gastric and CRCs[8-15]. Other studies[16-18] have underlined the usefulness of the OSNA assay as a complementary tool for diagnosing LNMs and upstaging in histologically node-negative stage II CRC.

The sentinel LN (SLN) is gaining more and more consensus because it allows to perform a more conservative surgery with considerable advantages, when applicable for the patient and for the operating times. Obviously in the early stages of CRCs this could play an important role, allowing to realize, in case of absence of lymph node metastases on SLNs, an organ preserving surgery.

In this review, we analyzed the use of OSNA in detecting LNMs in CRC.

LITERATURE SEARCH

Search strategy

After developing and piloting search terms, MEDLINE, SCOPUS, ClinicalTrials.gov, and Cochrane Database were used to conduct a comprehensive computerized literature search for articles pertaining to OSNA use in detecting LNMs in CRC. Medical subject headings terms and keywords were combined: colorectal malignant, cancer, colorectal tumor, colorectal neoplasm, carcinoma, lymph node metastasis, SLN, one-step nucleic acid amplification, OSNA, cytokeratin 19, CK-19, predictive value, upstaging, organ-sparing surgery, and tailored lymphadenectomy. The electronic search was supplemented by reviewing reference lists of included studies and previous systematic reviews. No time limitation was stipulated for the search, which was last updated December 20, 2021. In addition, we retrieved and cited high-quality references using the Reference Citation Analysis database (https://www.referencecitation-analysis.com/).

Study selection, data extraction, and quality assessment

The retrieval of articles was completed in three consecutive stages. Following reduplication of the sum of collected articles, their titles and abstracts underwent further screening and those deemed ineligible were removed. For duplicates, the most recent or complete publication was chosen. The remaining papers were evaluated in full text. Two reviewers (MB, SV) extracted data in duplicate using a standardized data extraction sheet.

LYMPHATIC DRAINAGE IN CRC

The American Joint Committee on Cancer/Union for International Cancer Control (AJCC/UICC) staging score divides the stages according to how many metastatic lymph nodes are present. Based on the location of the primary tumor, those with a course adjacent to the main vascular branches near the affected colon are considered regional lymph nodes. In particular, starting from the rectum up to the right colon, in addition to the peri-colic lymph nodes, regional lymph nodes are considered, those adjacent to the rectal arteries, the sigmoid arteries, the left colonic artery, the inferior mesenteric artery, the middle colic artery, the right colic artery, the ileocolic artery[19].

In AJCC/UICC tumor-node-metastasis (TNM) staging system[20-22], patients with no metastatic LNs are N0, cases with one to three metastatic LNs are N1, and cases with more than three positive LNs are N2. Moreover, the N1 category is subdivided into N1a (1 metastatic LN), N1b (2–3 metastatic LNs), and N1c (no regional LNs are positive but there are tumor deposits in the subserosa, mesentery or non-peritonealized pericolic or perirectal/mesorectal tissues), whereas the N2 category is subdivided into N2a (4–6 metastatic LNs) and N2b (7 or more metastatic LNs). The minimum number of examined LNs needed for adequate staging should not be less than 12 to minimize the possibility of stage migration[19, 23-27].

The Japanese Society for Cancer of the Colon and Rectum (JSCCR) staging score classifies the involved LNs based on location and number. This system divides the regional LNs into three groups: main, intermediate and peri-colic. Regional LNs depend on their adjacency to the blood vessels following the primary tumor site. LNs adjacent to the marginal arcade are pericolic nodes, the LNs along the course of the main vessels of the colon are intermediate nodes (sigmoid arteries, the left colonic artery, the inferior mesenteric artery, the right and left middle colic artery, the right colic artery, the ileocolic artery). Lymph nodes located proximal to the origin of the main colonic vascular branches of the inferior and superior mesenteric artery are the main nodes. LNMs are classified as N1 if up to 3 peri-colic or intermediate LNs are involved, N2 if they are ≥ 4, N3 when the main LNs are involved[28, 29].

ITCs and MMs

When single or few tumor cells smaller than 0.2 mm are found, these are called ITCs, if instead the deposits have a diameter between 0.2 and 2.0 mm these are called MMs. When ITCs or MMs with HE or IHC are found, they are classified as pN0 (i +), if instead the deposits are diagnosed only by reverse transcriptase polymerase chain reaction (RT-PCR), they are classified as pN0 (mol +)[19,20]. MMs, ITCs, and occult metastasis have been reported in 4.2%, 19.3%, and 5% of patients with stage I and II CRC, respectively, and attracted interest as prognostic factors[30-33].

Tumor deposits

In the literature, tumor deposits (TDs) are defined as foci of tumor separated from the main neoplasm and found in peri-rectal or peri-colonic adipose tissue or in mesocolon in the lymphatic drainage area, in the absence of identifiable LN tissue.

It is postulated that they are produced either by discontinuous dissemination of the tumor or by vascular/perineural dissemination. TDs can be found in 10.2%–22% of CRC cases and it has been suggested that TDs may represent a LN, a vascular structure, or a nerve completely replaced by carcinoma[34].

Several studies[35,36] have shown decreased disease-specific survival and overall survival (OS) in the presence of TDs. Moreover, the survival outcomes worsen when TDs occur concomitantly with LNMs. Other studies confirmed this evidence in CRC. It has been suggested that TDs have negative prognostic value but are not sufficiently categorized in the current TNM staging and the number and/or presence of the TD should be added to the number of LNMs to define the final N stage creating a specific category for TDs with LNM, which could be called category N2c or N3[37-41].

CLINICAL STAGE OF NODAL METASTASES

Diagnostic imaging

Diagnostic imaging assessment of lymphadenopathy in CRCs is challenging. Individual imaging modalities face specific intrinsic limitations, for example, transrectal ultrasound is operator-dependent, detrimentally affected by a small field of view, and cannot be employed in stenosing or rectal cancers. Computed tomography (CT) is hampered by its low soft tissue contrast resolution which, besides negatively impacting detection, precludes evaluation of fine LN details and therefore must rely only on LN size for assessing lymphadenopathy. Magnetic resonance imaging (MRI) requires long acquisition times and is prone to artifacts in the case of poor patient cooperation. Fluorodeoxyglucose (FDG)-positron emission tomography (PET)/CT and PET/MRI necessitate exposure to radiation, and its yields are influenced by the amount of metabolically avid cells in the affected LNs.

Size

Lymphadenopathy is also intrinsically challenging. Despite malignant LNs tending to be larger than their benign counterparts, there is wide size superimposition between malignant and benign LNs. In one study that evaluated only LNs ≥ 5 mm, short axis range was 6-12 mm for malignant LNs and 5-13 mm for benign LNs[42,43]. Moreover, the size of metastatic LNs is often at the lower limits of imaging spatial resolution. In a study, median LN short axis was 3.2 mm for malignant LNs and 2.8 mm for benign LNs[44]. Additionally, 30%-94% of metastatic LNs from rectal cancer are < 5 mm in short axis [45-48]. To make things even more challenging, some benign etiologies, especially inflammation, might increase LNs size.

MRI

Due its superior anatomic layout and high soft tissue contrast resolution, MRI can explore LN nature trough size and morphologic criteria. LN size criteria have yielded different results in different studies. However, across studies, the bigger the short axis threshold, the higher the specificity and lower the sensitivity; a 3 mm short axis has been associated with 92% sensitivity, 3% specificity, and 40% accuracy; a short axis threshold of 9 mm has been associated with the opposite trend, giving 8% sensitivity, 100% specificity, and 62% accuracy[42]. Short axis thresholds of 7.2-7.5 mm have reached 32%-87% sensitivity and 70%-94% specificity, with 68% of accuracy[42,43]. However, the most accepted short axis cut off for lymphadenopathy in rectal cancer is 5 mm, yielding sensitivities of 50%-72%, specificities of 46%-60%, and an accuracy of 57%[42,46-50].

Beside size, several other MRI criteria can be used, with diffusion weighted imaging (DWI) believed to be one of the most promising tools. However, DWI has proven inadequate for this purpose so far. High b-value DWI is a powerful tool for LN detection. However, DWI and even apparent diffusion coefficient values[43,51,52] are unable to discriminate benign from malignant LNs (accuracy 40%). Therefore, in our practice, we use DWI just to detect all LNs, relegating the differentiation of benign from malignant ones to morphologic, size and/or metabolic criteria.

Chemical shift effect (CSE) refers to a black or bright border outlining organ contours, including LNs. In the case of neoplastic growth in the subcapsular sinus, the resonance frequencies of hydrogen protons in the subcapsular sinus and in the adjacent fat are similar, resulting in the loss of CSE.

Four patterns of LN CSE have been described: continuous and smooth, continuous, and irregular, discontinuous, and irregular, or absent[44]. Once neoplastic cells have colonized the subcapsular sinus, they easily spread outside of the LN, likely more rapidly than toward the medulla. This results in irregular or obscure LN contours, reported in 60%-65% of malignant LNs and in 16%-20% of benign LNs, leading to sensitivity of 88%, specificity of 23%, and accuracy of 50% in one study. On the other hand, a smooth external contour has been described in 80%-84% of benign LNs and in 34%-40% of malignant LNs[42-44].

The internal structure of LNs may be heterogenous in the settings of metastases; this has been reported in 26%-52% of benign and 54%-91% of malignant LNs, with a sensitivity of 84%, specificity of 31%, and accuracy of 53%; on the other hand, homogeneous internal structure, has been observed in 48%-73% of benign and 8%-46% of malignant LNs[42-44]. The combination of inhomogeneous signal intensity and indistinct/irregular borders has been shown to yield sensitivity, specificity, and accuracy of 56%, 91%, and 77%, respectively[42].

Currently, LN size is the most used criterion to discriminate between malignant and benign LNs on MRI, but given the previously discussed inherent limitations, it is often integrated with the morphologic criteria described above. According to the European Society of Abdominal and Gastrointestinal Radiology (ESGAR) guidelines, a LN is considered metastatic in the case of[53]: Short axis diameter ≥ 9 mm, short axis 5-8 mm plus ≥ 2 morphologic criteria, short axis < 5 mm plus 3 morphologic criteria, or mucinous LN regardless of the size. Morphologic criteria chosen by ESGAR are round shape, irregular borders, and heterogenous signal.

However, despite all of the above efforts, even MRI, the most promising imaging modality for LN evaluation is still inadequate for the scope. A recent study that explored the staging performance of MRI in rectal cancer, using surgical pathology as a standard of reference, showed that MRI LN status was correctly assigned in 68% of cases, overstaged in 28%, and understaged in 4%. Moreover, only 40% of MRI-positive LN cases were pathologically confirmed[54]. These results are in line with a FDG-PET/MRI study where N status was overstaged by MRI in 22.6% of patients and by PET/MRI in 8% of cases; correct N status was assigned by MRI in 58% of patients and by PET/MRI in 79% of patients[55].

PET

FDG-PET, in addition to structural information, includes the advantage of assessing the metabolic activity of colorectal patient LNs. However, even with metabolic information, sensitivity is limited. A recent meta-analysis including 13 studies published between 2007 and 2019 evaluated the pretreatment ability of 18F-FDG PET/CT as a staging modality to detect metastatic LNs in CRC[15]. The pooled sensitivity, specificity, positive and negative likelihood ratios were 65%, 75%, 4.57, and 0.37, respectively. Prospective studies have demonstrated higher sensitivity and specificity compared to retrospective studies, and studies with sample sizes greater than 100 and that used a cut off value of

maximum standardized uptake value (SUV) ≤ 2.5 revealed better accuracy. An older meta-analysis of CRC patients found an even lower pooled sensitivity of 42.9% for detecting LN metastasis, but a higher specificity of 87.9%[56,57]. Differences in meta-analysis outcomes are thought to be due to the heterogeneity of baseline patient characteristics and included article methodologies. Regardless of the variances between the two meta-analyses, FDG-PET has limitations in sensitivity[58-61], likely due to a partial volume effect when assessing the SUV of small LNs (< 10 mm), as well as limitations in spatial resolution when differentiating between extension of primary tumor and adjacent positive LNs[62-64]. Specificity on the other hand is limited by false positives seen most often in reactive LNs.

Innovations

Advancements in the imaging evaluation of LNs in CRC are going to happen in the very near future due to innovative scanning technologies such as PET/MRI, which can investigate tumor biology, phenotypes, improve diagnosis, and impact the management of several solid organ malignancies including CRC[55,65-72], innovative radiopharmaceuticals such as fibroblast activation protein inhibitor (FAPI), which is already outperforming FDG in several settings[73,74], and due to the endless possibilities opened by artificial intelligence. Regarding FAPI, a study[74] comparing 68Ga-FAPI and 18F-FDG uptake in 35 patients with gastric, duodenal, and CRCs, showed a significantly higher sensitivity with 68Ga-FAPI PET/CT compared to 18F-FDG PET/CT (79% *vs* 54%) but an equivalent specificity (82% *vs* 89%). Artificial intelligence is going to play a major role in diagnostic imaging evaluation of LNs. A recently published metanalysis, which focused on LN staging in CRC, showed that deep learning and radiomics outperform radiologists, with deep learning also being superior to radiomics. In rectal cancer, on a per patient basis, pooled area under receiver operator characteristic curve was 0.017 for deep learning, 0.808 for radiomics, and 0.727 for radiologists; and sensitivity and specificity were 89% and 94% for deep learning, 78% and 73% for radiomics, and 68% and 70% for radiologists respectively[75].

CONTROVERSIES IN LN DISSECTION IN CRC

Several studies have shown that in more than 80% of cases, the first metastatic LN in CRC is a paracolic LN located 5 cm or less from the tumor[76-81]. Besides this classic lymphatic drainage, aberrant drainage within the regional LNs can exist. Such drainage leads directly to main LN stations near the superior and inferior mesenteric vessels or to colic and paracolic LNs located a significant distance from the tumor. The prevalence of aberrant lymphatic drainage is reportedly up to 20%[82,83]. Drainage of this nature influences the scope of lymphadenectomy since "aberrant" LNs are potential locations for "skip metastases"[76,77,84-86].

In some individual studies, a higher rate of aberrant lymphatic drainage reaching up to 29% has been observed in patients undergoing lymphatic mapping[87]. There are some different points of view on the resection type between East and West. The Japanese concept is partial resection of the bowel according feeding artery (short bowel specimen, long lymph vascular pedicle), and the opposite European concept is wide resection of the bowel such as hemicolectomy or extended hemicolectomy.

European Society of Medical Oncology (ESMO) recommends that local excision could be considered in the early colon cancer (CC) Stage 0 (Tis) and in selected T1N0M0 (G1-2, N0). ESMO and National Comprehensive Cancer Network (NCCN) recommend wide surgical resection with a safe margin (ESMO suggests at least 5 cm from the tumor), and en bloc removal of LNs with the feeding arterial arcade (regional nodes). NCCN suggests removing only suspicious LNs that are not contained in the arcade[25,26,88,89].

The best results in terms of prognosis after the introduction of the TME concept in the treatment of rectal cancer led to the Hohenberger *et al*[90] hypothesis in which surgical dissection according to embryological planes could lead to a similar improvement also in surgery of the. On this hypothesis is based the complete mesocolic excision (CME) associated with the concept of central vascular ligation (CVL) in which the main blood vessels are tied at the origin after a dissection according to the embryological planes (*i.e.* removing the surgical trunk of Gillot in right-sided CC)[90].

JSCCR provides a detailed description of the extent of surgical lymphadenectomy, based on tumor stage. In brief, JSCCR advocates central (D3) lymphadenectomy in selected T2 and in all T3-T4 cancers, as well as in all N-positive patients.

In the study by West *et al*[91] the CME with CVL does not show significant differences with the Japanese D3 as regards the quality of the mesocolon surgical plan and the free margins. In the Japanese school, as indicated in the JSCCR guidelines, the longitudinal extension is less important; consequently the number of lymph nodes and the mesenteric surface were lower. Even if the operative pieces in western countries have a greater longitudinal extension than in the Asian ones, the TNM system does not include in its nomenclature the localization of regional lymph nodes. The indications to D3 Lymphadenectomy with CVL in the Western countries are still a subject of debate.

CONTROVERSIES IN LN DISSECTION IN RECTAL CANCER

Rectal cancer surgery is based on[92-94] TME or tumor-specific mesorectal excision (TSME). TME is a procedure that resects all of the mesorectum just above the anal canal[92]. TSME is a procedure for partially resecting the mesorectum according to the location of the tumor[94]. In Western countries, in the rectal cancer, lateral LNM is generally considered a metastatic disease and neoadjuvant chemoradiotherapy combined with TME is widely used. By contrast, the Japanese Classification of Colorectal Carcinoma[95-98] defines lateral LNs as regional LNs in the internal iliac, obturator and common iliac subregions. The JSCCR Guidelines for the treatment of CRC[28,29] consider mesorectal excision as D1 resection and recommend a D3 procedure (TME with lateral LN dissection) as standard treatment for T3 or more middle and lower located rectal cancer.

Some studies have shown that extensive lymphadenectomy is associated with improved prognosis in patients with more advanced stage CRC, even though numerous postoperative complications related to this extensive surgery are described.

Among colorectal surgeons, it is now accepted that "one size does not fit all", and there is increasing agreement regarding the need for a more targeted surgery and a tailored lymphadenectomy[98-100]. The real challenge is careful patient selection.

HYSTOPATHOLOGICAL DIAGNOSIS OF LNMs IN CRC

A relevant clinical finding is the fact that up to 30% of patients with CRC diagnosed as pN0 following surgery will die within 5 years due to regional recurrence or distant metastases[87,101-104].

A discussion to establish criteria for defining high-risk stage II patients who could benefit from adjuvant therapy was undertaken by the Multicenter International Study of Oxaliplatin/5-Fluorouracil/Leucovorin in the Adjuvant Treatment of Colon Cancer and National Surgical Adjuvant Breast and Bowel Project studies. Presently, the high-risk group, according to ESMO and NCCN treatment standards, comprises patients with T4 tumors (especially T4b), a high grade of histological malignancy, infiltration of vessels and perineural tissue, tumor budding (TB), a small number of removed LNs (< 12), and emergency surgery[101,105,106]. Several studies have identified prognostic genes that may select high-risk patients for adjuvant treatment[107-112], but only a few are routinely used in clinical practice.

Mismatch repair (MMR) genes act in DNA repair pathways. MMR deficiency results from the loss of function of their products (MMR-D), leading to microsatellite instability (MSI). MSI increases CRC risk by increasing tumor mutational burden and the number of tumor-infiltrating lymphocytes (TILs). There are two categories of CRC with MSI: MSI-high (MSI-H) and MSI-low (MSI-L). Instability in more than 30% of the markers as detected by PCR is defined as MSI-H, and alteration in 10%–30% of the markers is considered MSI-L. The MSI-H is associated with a high mutational burden in DNA.

Frameshift mutations can create antigenic epitopes that make MSI-H/MMR-D tumors more immunogenic compared with microsatellite-stable tumors. MSI-induced frameshift mutations produce a significant number of neoantigens. Accordingly, MSI-H/MMR-D tumors manifest a great number of TILs, many of which can be directed against tumor-related neoantigens[107].

Despite this, the most important risk factor is the presence of unidentified LN MMs and macrometastases. Rahbari *et al*[113] concluded that the presence of LN MMs is associated with poor OS and shorter disease-free survival (DFS) in stage II CRC patients. Therefore, the problem is to identify diagnostic methods that can improve selection based on this criterion in terms of both cost and effectiveness[101,114,115]. The relevant literature shows that examination of only one LN slide using HE staining leaves up to 33% of metastases unidentified. A single slide with HE staining through the center of a node 1 cm in diameter provides information on < 1% of its volume[114-118].

Additional HE histopathologic analyses of serial sections allows for the identification of micrometastatic disease in up to 20% of LNs determined to be negative by standard HE methods[119]. However, performing HE histopathologic analyses of sections can be technically challenging and time consuming, as well as entailing significantly greater cost. Other histopathologic methods utilized for more accurate assessment of the status of the regional LNs, such as IHC using antibodies against human cytokeratin (CK) or RT-PCR, require even more time and incur an even higher cost.

IDENTIFICATION OF AN OPTIMAL mRNA MARKER FOR THE OSNA ASSAY IN CRC METASTATIC NODES

Yamamoto *et al*[13] reported the background for the identification of CK19 mRNA as an optimal marker for the OSNA assay in CRC. Yamamoto *et al*[13] examined 98 candidate mRNA genetic markers, which were from a genome-wide database, by comparing an expression frequency in CC. After four sequencing phases, CK19, carcinoembryonic antigen (CEA), and CK20 mRNAs were evaluated using

the OSNA assay. The expression of CK19 mRNA was observed in all pathologically positive LNs; however, CEA and CK20 mRNAs were not found in metastatic nodes.

DIAGNOSTIC PERFORMANCE OF THE OSNA ASSAY IN CRC

A novel technique for pathological examination, OSNA, uses the reverse transcription loop-mediated isothermal amplification method to amplify CK19 mRNA. In contrast to the current routine histopathological examination, it can examine whole LNs and detect metastases in a sufficiently short time (Table 1). A standard curve previously determined with three calibrators containing different CK19 mRNA copy numbers was used to calculate the amount of CK19 mRNA. Positive and negative control samples were used to ensure the quality of the assay.

A limit value of 250 copies/mL of CK19 mRNA copy had been choosed. A value less than 250 copies/mL was considered negative for metastasis, on the contrary, a value ≥ 250 copies/mL was considered positive. Previous studies defined this by the logarithmic midpoint between the maximum value of the CK19 mRNA copy number in non-metastatic patients and minus 2 or 3 standard deviations (SDs) from the average of CK19 mRNA copy number in node-positive patients. These studies also defined the MM threshold between 250 and 4999 CK19 mRNA copies/mL. LNs with 5000 or more mRNA copies/mL were considered macrometastases[7,120,121]. The utility of conventional OSNA as a molecular staging method has been demonstrated for various cancers[9,17,122-124].

Although most of the studies evaluated in this review were prospective in design, none was a randomized controlled trial (Table 1). The studies comparing the diagnostic performance between OSNA and pathological examination for the detection of LNMs in CRC are shown in Tables 2 and 3. Our review on OSNA and CRC shows high sensitivity, few false negatives results, and a concordance rate with pathological findings ranging from 61.8% to 98.7% (Table 2). Moreover, studies have shown that OSNA results in upstaging in about 25% of initially nodal-negative CRC patients after conventional HE analysis (Table 3). With the OSNA approach, the lymph node is homogenized without the need for other preparations and the results are ready in less than 40 min for 3 or 4 LNs, 20 min for a single LN. The stage of the tumor and the number of lymph nodes analyzed correlates with upstaging. Notably, the OSNA upstaging rate in Croner's investigation for stage UICC I and II patients was 16.2% and 30.3%, respectively. Therefore, it was suggested that stage UICC I and II patients, who suffer from recurrent disease, were understaged by conventional HE analyses[9,124-126].

In a study of Yamamoto *et al*[13] OSNA-positive patients (2.0% of stage I CRC and 17.6% of stage II CRC) had more advanced features of CRC, such as deeper invasion to the colonic wall and severe invasion to lymphatic invasion compared with OSNA-negative cases. They found a 95% concordance rate between OSNA and classical histological analyses with HE and IHC. Yamamoto *et al*[13] concluded that OSNA is comparable to a 2-mm interval histopathological examination in its ability to detect LNMs.

In our previous published study[127], OSNA was superior to HE in identifying LNMs, with a false negative rate of 0% *vs* 44.4% and accuracy of 100% *vs* 76.4%, respectively (Table 2). As represented in Tables 2 and 3, few studies evaluated HE and IHC, few performed multi-sliced tissue sections using HE and the remaining single slice HE tissue section *vs* OSNA[11,128-131]. While the detection of small metastatic foci in LNs is influenced by the skill and experience of the pathologists, the advantage of the OSNA assay is the possibility to perform standard evaluations without being influenced by operator skill or experience. This explains the reason why the use of OSNA has recently garnered interest for detecting MMs[9,16,17,128].

Methods of LN division and pooled OSNA

Previous reports have detailed three major methods to compare LN status between pathological examination and the OSNA assay (Table 3). The first method[14,125] involves dividing LNs in half and sending each 50% portion for pathology and OSNA (half-division method). The second method[11,12,15] involves dividing LNs into four equal sections and sending two of these sections (50%) for pathology and OSNA (four-section method). In the third method[14,124], only 1 mm from the center of LNs are sent for pathological examination and the rest are used for OSNA measurement (center-cut method). The latter two methods described above are thought to be technically difficult for evaluating small LNs. By contrast, dividing in half and sending each 50% portion for pathology and OSNA is the simplest method.

In previous studies using classic OSNA (cOSNA), 50% of each LN was submitted for pathologic examination, followed by evaluation of each remaining half by OSNA. The obstacles for clinical applications of cOSNA include a need to simplify the procedure for halving the dissected LNs and reducing the operating costs associated with the equipment used for OSNA analyses.

Rakislova *et al*[125] conducted a study comparing two methods of LN evaluation by OSNA in CRC: an individual analysis of each LN (cOSNA) and a new approach involving pooling several LNs, known as the "pooling method". The diagnostic performance of pooled OSNA (pOSNA) was comparable to that of cOSNA. In the pOSNA method, the LNs are pooled together in a test tube for OSNA analysis. The weight limitation for the LNs per tube was ≤ 600 mg, with those exceeding this limit placed in another

Table 1 Characteristics of one-step nucleic acid amplification studies in colorectal cancer patients

Ref.	Nation	Type of study	Patients number (sample number)	Tumor type	Purpose of the OSNA analysis
Croner *et al*[11], 2010	Germany	Prospective study	184 (184)	Colorectal	Diagnosis of LN metastasis
Yamamoto *et al*[16], 2011	Japan	Prospective multicenter study	85 (385)	Colorectal	Diagnosis of LN metastasis
Güller *et al*[12], 2012	Switzerland	Prospective study	22 (313)	Colon	Diagnosis of LN metastasis
Yamamoto *et al*[13], 2013	Japan	Not shown	30 (66)	Colorectal	Identification of CK19
Croner *et al*[14], 2014	Germany	Prospective multicenter study	103 (1594)	Colon	Pathologically nodenegative CC
Vogelaar *et al*[15], 2014	Switzerland	Prospective multicenter study	128 (325)	Colon	Diagnosis of SLN metastasis
Yamamoto *et al*[17], 2016	Japan	Prospective multicenter study	204 (1925)	Colorectal	Diagnosis of LN metastasis
Aldecoa *et al*[133], 2016	Spain	Prospective multicenter study	149 (1940)	Colorectal	Correlation between TTL and tumor's characteristics
Rakislova *et al*[125], 2017	Spain	Observational study	188 (3206)	Colon	Diagnosis of pooled LN metastasis
Miyake *et al*[193], 2017	Japan	Prospective study	25 (306)	Rectum	Indication of LPLN dissection
Marhic *et al*[184], 2017	France	Prospective study	17	Colon	Diagnosis of SLN metastasis
Colling *et al*[129], 2-17	United Kingdom	Prospective study	19 (82)	Colorectal	Diagnosis of LN metastasis
Aldecoa *et al*[124], 2017	Spain	Prospective study	71 (936)	Colon	OSNA with endoscopic tattooing
Yeung *et al*[130], 2018	United Kingdom	Prospective study	16 (78)	Colorectal	OSNA with ICG detection
Brito *et al*[126], 2018	Portugal	Prospective multicenter study	59 (753)	Colon	Pathologically node negative CRC
Esposito *et al*[127], 2019	Italy	Prospective study	34 (51)	Colorectal	Diagnosis of SLN metastasis
Diaz-Mercedes *et al* [109], 2019	Spain	Prospective study	17 (980)	Colorectal	Budget impact analysis
Itabashi *et al*[18], 2020	Japan	Prospective multicenter study	195	Colorectal	Prognostic value of the OSNA assay for pStage IICRC patients
Archilla *et al*[145], 2021	Spain	Retrospective multicenter study	342 (5931)	Colorectal	Correlation between the TTL with patient outcome
Weixler *et al*[147], 2021	Netherlands, Germany, Switzerland	Retrospective multicenter study	87	Colon	Prognostic value of OSNA
Tani *et al*[33], 2021	Japan	Prospective multicenter study	92	Colon	Diagnosis of pooled LN metastasis
Numata *et al*[188], 2021	Japan	Prospective study	34	Rectum	Indication of LPLN dissection

CRC: Colorectal cancer; ICG: Indocyanine green; LPLN: Lateral pelvic lymph node; OSNA: One-step nucleic acid amplification; SLN: Sentinel lymph node; TTL: Total tumor load.

tube for measurement. In the study by Tani *et al*[33], pOSNA and the half-division method were combined and used in the diagnosis of pericolic LNMs and applied in clinical practice[33]. These results revealed that the pOSNA with the half-division method might be useful as a clinical molecular staging method.

In this study, the upstaging rate for early-stage CC patients was 9.1% (6/66). The upstaging rates of the study by Tani *et al*[33] were slightly lower than those previously reported (Table 3).

Table 2 A comparison of the diagnostic accuracy of the one-step nucleic acid amplification assay in colorectal cancer patients

Ref.	Pathological evaluation	IHC	LN number inspected by OSNA, mean	Sensitivity, %	Specificity, %	Concordance, %	PPV, %	NPV, %
Croner *et al*[11]	Multi-slice	CK19	1.0	92.5	96.5	93.6	88.1	97.9
Yamamoto *et al*[16]	Multi-slice	CK19	4.5	95.2	97.7	97.1	91.9	98.7
Güller *et al*[12]	Multi-slice	CK19	14.2	94.5	97.6	97.1	89.7	98.8
Yamamoto *et al*[17]	Single-slice	None	9.4	86.2	96.5	95.7	66.5	98.8
Colling *et al*[129]	Single-slice	None	4.3	92.9	97.1	96.3	86.7	98.5
Yeung *et al*[130]	Single-slice	None	4.9	100	98.4	98.7	94.1	100
Esposito *et al*[127]	Multi-slice	None	1.5	69.2	100	88.2	100	84.0
Rakislova *et al*[125]	Not shown	None	20.5 (pOSNA)	88.9	79.2	80.2	33.3	98.4
Vogelaar *et al*[15]	Multi-slice	Anti pan-cytokeratin	15.3	51.6	84.1	67.7	76.7	63.1
Miyake *et al*[193]	Single-slice	CEA	11	100	86	88	57	100
Marhic *et al*[184]	Not shown	None	Not shown	50	100	70.6	100	58
Numata *et al*[188] (predictive value for pathological LatLNM testing OSNA-MesLNM)	Not shown	None	17	100	55	61.8	28	100
Tani *et al*[33]	Not shown	CK19	6.9 (pOSNA)	84.6	90.9	89.1%	78.6	93.7

CEA: Carcinoembryonic antigen; CK19: Cytokeratin 19; IHC: Immunohistochemistry; LatLNM: Lateral lymph node metastasis; MesLNM: Mesorectal lymph node metastasis; NPV: Negative predictive value; OSNA: One-step nucleic acid amplification; pOSNA: Pooled one-step nucleic acid amplification; PPV: Positive predictive value.

COMPARISON OF THE NUMBER OF POSITIVE NODES AND QUANTITATIVE OSNA RESULTS

The OSNA assay of retrieved LNs does not allow the number of involved LNs typically used for TNM staging, and therefore cannot be used for conventional cancer staging. Nevertheless, the OSNA assay can potentially be used to infer the size of metastatic foci based on the detected copy numbers[113,132]. Patient's total tumor load (TTL) resulted from the sum of all CK19 mRNA tumor copies/μL of each positive LN from the colectomy specimen. Yamamoto *et al*[17] found that the sum of CK19 mRNA increased as the number of histologically positive LNs increased. Indeed, the median value of CK19 mRNA was significantly smaller in patients with < 3 regional LNMs than in those with ≥ 4 regional LNMs. The median TTL values of pN0, pN1 (1-3 positive LNs), and pN2 (4 or more positive LNs) were 1550 copies/mL (300-320000 copies/mL), 24050 copies/mL (250-890000 copies/mL), and 90600 copies/mL (7700-1635100 copies/mL), respectively. The TTL significantly increased as the node status increased.

In the study of Aldecoa *et al*[133] the TTL was related to pT stage ($P = 0.01$) and tumor size ($P < 0.01$) in low-grade tumors. In that study TTL, correlated with classical high-risk factors in stage I–II CC patients. These findings indicate that the sum of CK19 mRNA assessed by OSNA displays a trend compatible to the current pathological diagnosis system. These findings suggest the future possibility of novel molecular staging using OSNA, based on metastasis volume (amount of CK19 mRNA) rather than the number of LNMs. It has been suggested a correlation between CRC risk factors[11,12,16,18,122,126,134] such as pN, pT, tumor grade, male sex, tumor size, lymph vascular invasion (LVI), poor prognosis, worse DFS and TTL.

Correlation of node TTL with TB and poorly differentiated clusters

The physiological process that can lead epithelial cells to acquire mesenchymal properties and the potential for migration and stromal invasion, essential for the development of metastases, is the morphological manifestation of the epithelial-mesenchymal transition phenotype that can lead to the formation of TB and clusters poorly differentiated (PDCs). The presence of isolated tumor cells or cell clusters of ≤ 4 cells on the invasive front of the tumor is termed tuberculosis[134]. 5 or more neoplastic cells in the tumor stroma not organized into glandular structures constitute the PDCs. In stage II CC, both PDCs and TB are independent prognostic factors[134-136], associated with LNMs, distant

Table 3 Differences in lymph node processing methods and upstage rates of previous reports

Ref.	Subject (patients)	OSNA method	Harvested LN, *n*	Harvested LN, median	Dividing method of LN	Pathological staining	Measured LN by OSNA, *n*	Measured LN by OSNA, median	Upstage rate (pStage I and II)
Yamamoto *et al*[16]	Stage 0, I (85)	cOSNA	434	N/A[a]	Four[b]; 4 mm over diameter of LN	HE and IHC	385	4.5	16.5% (2/16)
Güller *et al* [12]	Stage I, II, III (22)	cOSNA	313	30 (16–60)	Four[b]; 3 mm over diameter of LN	HE and IHC	56	13 (6–24)	15.3% (2/13)
Croner *et al* [14]	Stage I, II (103)	cOSNA	N/A[a]	N/A[a]	Center[c]; 6 mm over half[d]; 4 mm to 6 mm diameter of LN	HE	1594	14 (1–46)	25.2% (26/103)
Vogelaar *et al*[15]	Stage I, II (128)	cOSNA	N/A[a]	N/A[a]	Four[b]; 10 mm over half[d]; 10 or less than 10 mm diameter of LN	HE and IHC	317	Mean 15.3 (4–40)	20.2% (20/90)
Yamamoto *et al*[17]	Stage I, II, III (204)	cOSNA	4324	19 (3–25)	Half[d]	HE	1925	8 (2–25)	17.6% (13/74)
Aldecoa *et al*[133]	Stage I, II (149)	cOSNA	2483	15	Center[c]	HE	1940	12	51% (76/149)
Rakislova *et al*[125]	Stage I, II, III (188)	cOSNA, pOSNA	cOSNA 1828, pOSNA 1992	cOSNA 17 (13-22), pOSNA 20.5 (17-27)	Center[c]	HE	cOSNA 1757, pOSNA 1449	cOSNA 13 (10-18), pOSNA 18 (13-25)	cOSNA 55.4% (51/92), pOSNA 20.7% (16/77)
Brito *et al* [126]	Stage I, II (59)	cOSNA	1046	13 (9-19)	Center[c]; 5 mm over half[d]; 4 or less diameter of LN	HE	753	12 (7-16)	28.8% (17/59)
Itabashi *et al*[18]	Stage I, II, III (195)	cOSNA	Not shown	19 (1-75)	Half[d]; 4 mm over diameter of LN	HE	Not shown	8 (2-25)	15.7% (11/70) in stage II patients
Tani *et al* [33]	Stage II, IIIA (92)	pOSNA	2236	24.3 (5–66)	Half[d]; 4 mm over diameter of LN	HE	636	6.9 (1–35)	9.1% (6/66)

[a]Not applicable.
[b]Four section method: dividing lymph nodes into four equal sections and sending two of these sections (50%) for pathology and one-step nucleic acid amplification (OSNA) measurement.
[c]Center-cut method: 1 mm from the center of lymph nodes are sent for pathological examination and the rest are used for OSNA.
[d]Half-division method divides lymph nodes in half and sends each 50% portion for pathology and OSNA.
HE: Hematoxylin and eosin; IHC: Immunohistochemistry; LN: Lymph node; OSNA: One-step nucleic acid amplification; pOSNA: Pooled one-step nucleic acid amplification.

metastases, extramural vascular invasion, LVI, perineural invasion (PNI), tumor grade and high pT stage[136-142].

International Consortium on TB Recommendations indicates how to count the number of TB at the invasive front of the tumor[135]. The classification for TB was as follows: Bd1/low (≤ 4 buds), Bd2/intermediate (5–9 buds), and Bd3/high (10 one more buds). The classification for PDCs evaluated [143] at the invasive front or in the center of the tumor was as follows: G1 (≤ 4 clusters), G2 (5–9 clusters), and G3 (10 or more clusters). Barresi *et al*[144] suggested not classifying tumor cells within mucin pools in mucinous carcinomas as TB, considering only tumor cells infiltrating the stroma with minimal extracellular mucin. While, the PDCs were evaluated within mucin lakes.

Recently Archilla *et al*[145] suggested the correlation of the TTL with patient outcome, TB, and PDC. The use of molecular methods to assess LN status, together with other pathological risk factors, could help improve risk stratification and management of patients with early-stage CRC.

Indeed, OSNA positivity was found in 38.3% of the cases (131/342) with a mean TTL of 36662 copies/mL among positive cases. The TTL present in the LNs evaluated by the OSNA test correlated positively, with both PDC (r = 0.266 by IHC; r = 0.257 by HE) and TB (r = 0.249 by IHC; r = 0.243 by HE) (P = 0.001). Low and intermediate TB had similar mean TTL (Bd1: 3292 copies/mL and Bd2: 18002 copies/mL), with no significant differences between both groups (*P* = 0.154). The mean TTL of high-Bd3

TB was 45331 copies/mL, and. it was significantly different from Bd1 and Bd2. Likewise, the mean TTL of PDC G1, with 4962 copies/mL and G2, with 13146 copies/mL did not show significant differences (P = 0.068), while PDC G3 had 61108 copies/mL, significantly different than low and intermediate grades. Thus, the authors grouped low and intermediate grades of TB and PDC into one category, obtaining two groups with significant differences for both TB and PDC (P < 0.001) as well. The authors also concluded that TTL can be used as an alternative method to to better stage patients compared to the classic HE because it is able to identify real stage II or III patients, thereby selecting those who are candidates for adjuvant therapy[145].

SURVIVAL ANALYSES

In the meta-analysis of Wild *et al*[146] it is emphasized that long-term outcomes and the use of adjuvant therapy in those upstaged by OSNA should be clarified before routine use of OSNA test.

Itabashi *et al*[18] showed that pStage II patients with OSNA positive LN had a lower 3-year DFS than negative patients (55% *vs* 86%; P = 0.005), with no significant differences in 3-year OS (P = 0.914). In this study, the upstaging occurred for patients with pStage II, of whom 11 of 70 patients (15.7%) were OSNA-positive. Most of the OSNA positive LNs were located in the peri-colic or peri-rectal area (10 out of 11 OSNA-positive stage II CRC patients).

Weixler *et al*[147] showed that the detection of positive LN by HE staining but not by OSNA as significant predictors of cancer-specific survival, cancer-specific and recurrence-free survival, and DFS. He concluded that in patients with CC, OSNA offers no prognostic advantage compared to conventional LN staging with HE contrasting findings in other cancers. It is important to highlight that the methodology of the histopathological evaluation for detection of the LNMs differed among studies. In Weixler's multicenter study[147] all harvested LNs > 3 mm in greatest dimension or a short axis ≥ 10 mm was cut into four slices: two were stored for later OSNA analysis and two were allocated to conventional standard HE staining, multilevel HE staining, and IHC for CK19. Multilevel sectioning with IHC leads to relevant upstaging of 15.4%-26% of otherwise negatively classified patients[148,149]. In addition, stage I-III patients were included in this study, whereas most of the OSNA studies focused on stage I-II patients. Therefore this HE + IHC *vs* OSNA study including stage I-III patients, although well conducted and of great value and interest, is not amenable to a comparison with studies in which HE *vs* OSNA in stage I-II patients are evaluated.

ORGAN-PRESERVING SURGERY

CC

Early CRC can be treated by endoscopic mucosal resection or endoscopic submucosal dissection (ESD). In determining the indication for endoscopic treatment and the treatment method, information on the depth of invasion and morphology of the tumor is essential. Colorectal ESD is an "endoscopic resection technique, which enables en bloc resection of a tumor, regardless of size" and avoids piecemeal resection. It is of great importance to differentiate Tis and T1a cancers from T1b cancers (T1 cancer with ≥ 1000 μm submucosal invasion depth), as the former can be treated by endoscopy while the latter requires surgical operation with nodal status assessment[29,150-154]. Moreover, innovative organ-preserving procedures such as endoscopic full-thickness resection or transanal minimally invasive surgery have been proposed to perform high-quality resections with decreased incidence of specimen fragmentation without resorting to demolitive interventions[155]. Nevertheless, it is estimated that overall 10%–20% of patients in stage T1 will have LNMs, and such patients subjected to a localized resection are undertreated[151].

Laparoscopic endoscopic cooperative surgery (LECS) can also lead to full thickness local resection by means of combined use of laparoscope and endoscope. The development of modified LECS procedures, such as non-exposed endoscopic wall-inversion surgery and closed LECS has almost resolved these drawbacks. This has led to a recent increase in the indication of modified LECS to include patients with gastric epithelial neoplasms. The LECS concept is also beginning to be applied in other organs such as the duodenum, colon and rectum. Further evolution of LECS procedures is expected in the future. SLN mapping could also be combined with LECS, resulting in a portion of early gastrointestinal cancers being treated by LECS with SLN mapping[156].

Rectal cancer

TEM, first described by Gerhard Buess[157-161], due to its ability to perform high-quality resections with decreased incidence of fragmentation, is superior to standard transanal excision for treating benign and malignant rectal lesions, most notably[162,163].

Transanal minimally invasive surgery (TAMIS) was initially born as a fusion between trans anal endoscopic microsurgery (TEM) and single-site laparoscopy. This technique was designed as a cost-

effective and easily reproducible alternative to TEM without specialized equipment.

The indications for TAMIS are similar to standard transanal resection for benign and malignant lesions determined by EUS or MRI[164,165]. TAMIS is also indicated for early malignant neoplasms confined to the submucosa[166]. T1 neoplasms of the rectum can still be divided into low-risk lesions [167] and at high risk for poor histopathological features (TB, poor differentiation, LVI or perineural invasion). Studies[155,168-170] identified a higher risk of LN metastasis in T1 sessile tumors with deeper submucosal invasion (sm^2 or sm^3).

THE OSNA ASSAY FOR THE DETECTION OF CRC METASTASIS IN SLN

LN status plays a crucial role in oncologic therapeutic strategies, and despite the use of increasingly sophisticated imaging techniques, pre-operative metastatic LN identification in patients with CRC is unsatisfactory[171,172].

The study of the SLN is gaining more and more popularity because it can avoid extensive lymphadenectomies, reduce operating times and morbidity. This can change the surgical strategy in patients with an apparent early stage of CRC, as patients with intraoperative positive SLN are submitted, during the same surgical procedure, to an adequate lymphadenectomy, whereas those with negative SLN can be treated with an organ-preserving surgery, avoiding unnecessary lymphadenectomy. The extemporaneous intraoperative examination performed on frozen specimen has a lower sensitivity than the classic postoperative analysis. The problem is mainly due to the low detection rate of MMs and ITC[173,174]. The disease detection rate increased with the technique of multi-step formalin-fixed tissue sections (FFTS) stained by HE with or without IHC[6,175-179]. Nonetheless, a significant number of MMs can still be overlooked, as during histological workup usually only small parts of LNs are screened.

Therefore, there are two methods for SLN mapping: staining and radioguided[180]. Three tracers have been used to detect SLNs: Dye, radioisotope, and indocyanine green (ICG). Each tracer has its respective disadvantages. The use of the ICG fluorescence method has officially been approved in Japan for LNs of BC and malignant melanoma; thus, it appears that ICG can be an acceptable tracer for the detection of LNs in gastric and CC.

ICG tattooing method is very useful for the marking of early gastric and CCs, especially when using a laparoscopic approach[181]. It has been suggested that SLN mapping with fluorescent dye can play an important role in the treatment of CC, particularly those at early stages, and can lead to ultraconservative surgery[182]. Because the results of OSNA are available in a relatively short time compared to the conventional technique, intraoperative OSNA analysis of SLNs may be employed easily in clinical practice.

In the study by Vogelaar *et al*[15] OSNA proved to be a promising method for the detection of SLN metastases in CC patients after *ex vivo* SLN mapping. OSNA appeared to outperform routine pathological examination with HE-stained slides with an upstaging rate of 20.2%. In the study by Yeung *et al*[130] OSNA was used intraoperatively, together with the technique of retrieving colorectal LNs by fluorescence imaging, to analyze the status of these specific LNs. In this study, OSNA is highly concordant with standard histology.

The results of the meta-analysis by Tranoulis *et al*[183] indicate that the the use of OSNA can allow to identify the status of the LNs even when applied intraoperatively. Marhic *et al*[184] proposed that the OSNA technique may be a new method to reduce time to adjuvant chemotherapy after surgery for CC. In this study, SLN status was determined intraoperatively with the OSNA assay; when positive, a port-a-cath was placed during the procedure for upcoming adjuvant chemotherapy. In this study, there was no difference between the groups regarding cancer staging, duration of hospitalization, and major morbidities but the time interval between surgery and adjuvant chemotherapy was significantly shorter in the OSNA group at 35 ± 8 d *vs* 67 ± 36 d ($P = 0.021$).

In our previous study[127], we showed that SLN analysis with OSNA in combination with ICG-near infrared (NIR) lymphangiography is feasible and may allow intraoperative prediction of LN status in patients with CRC (Table 4). Patients with SLN positive by the OSNA method were considered pN-positive and subjected to adjuvant chemotherapy. The time to start chemotherapy was lower in OSNA (+) patients [39.1 ± 1.9 d *vs* 50.2 ± 4.1 d in the OSNA (−) group; $P = 0.01$].

Both *ex vivo* and *in vivo* ICG fluorescence imaging are feasible for the detection of SLNs in CRC. The submucosal injection technique and subserosal were both used. A NIR 30° laparoscope (Olympus, Tokyo, Japan) was used to inspect the mesocolon. The LNs found using fluorescence were considered SLNs and analyzed intraoperatively. More work needs to be done to define protocols, indications for its use, a standard number of LNs that need to be removed and to test its efficacy in larger patient populations.

Implementation SLN analysis with OSNA in combination with ICG-NIR lymphangiography could allow more precise staging, reducing the delay between surgery and the onset of adjuvant chemotherapy. SLN evaluation by intraoperative OSNA analysis combined with a LECS approach may allow, in case of OSNA-negative early CRC, to apply an organ-preserving surgery avoiding the complic-

Table 4 Studies analyzing colorectal cancer metastasis in sentinel lymph nodes with one-step nucleic acid amplification

Author	Patients (samples), *n*	Injected dye	Intraoperative OSNA assay	Examined SLNs, *n*
Vogelaar *et al*[15]	128 (325)	Patent blue dye V or indocyanine green	No	3.0 (median)
Marhic *et al*[184]	17	Blue dye	Yes	Not shown
Yeung *et al*[130]	16 (78)	Indocyanine green	No	4.9 (mean)
Esposito *et al*[127]	34 (51)	Indocyanine green	Yes	1.0 (median)

OSNA: One-step nucleic acid amplification; SLN: Sentinel lymph node.

ations related to an unnecessary lymphadenectomy.

By contrast, in intraoperative OSNA-positive early CRC, a colorectal resection associated with selective lymphadenectomy can be performed, also taking into consideration the presence of aberrant lymphatic drainage and skip metastases. Despite the attractiveness of the previously exposed concept, studies in this field are lacking or very few (Table 4). However, several studies underline the role of OSNA SLN evaluation in more advanced stages and in case of positivity, the consequent upstaging and access to adjuvant treatment (Table 4).

LATERAL PELVIC LNs AND OSNA

There is disagreement in the international literature regarding the use of prophylactic lymphadenectomy in comparison with preoperative radiochemotherapy to improve prognosis in patients with locally advanced rectal cancer, due in part to the complex anatomy of the pelvic floor which makes diagnosis of lateral pelvic LNs (LPLNs) metastasis difficult. In Japan, the evolution in the surgical oncology approach has been toward LN clearance and, as a result, LPLNs have been considered local-regional disease from the outset[185].

Nevertheless, the rate of pathological lateral (Lat) LNM (p-LatLNM) in patients without clinical LatLNM (c-LatLNM) remained low at 7%, and lateral LN dissection (LatLND) is generally considered technically demanding and can prolong the operative time[186-188]. As Sammour *et al*[189] proposed, patients who are candidates for curative-intent treatment should be stratified depending on their risk to have LPLN metastasis in high, moderate, and low risk in order to select the best option to manage the pelvic compartment. Nevertheless, with preoperative images or traditional criteria, it is difficult to predict LatLNM. Obtaining a preoperative or intraoperative diagnosis is essential to select patients with LatLNM.

If SLN navigation surgery could be applied in cases of middle and lower rectal cancer, unnecessary LatLND procedures could be avoided. SLN anlysis may be useful in deciding both the indication of LatLND and which side of the lateral pelvic wall should be dissected[190]. In the study of Noura *et al*[191] the existence of a lateral pelvic region SLN in 53 lower rectal cancer patients was investigated. The lateral pelvic region was observed using a NIR camera system (photodynamic eye) after the ICG has been injected into the submucosa along the dentate line. If SLNs were positive for metastasis a Bilateral LatLND was performed, if instead SLNs were negative for metastasis mesorectal excision only was performed. In 49 (92.5%) of the 53 patients the lateral SLNs were successfully identified, 4 of these patients (8.2%) had lymph node metastases; the mean number of lateral SLNs per patient was 2.0 (range, 1–4).

The results of Yasui *et al*[192] suggested the potential use of SLN with ICG strategy to identify cases with non-metastatic LPLN, and to omit LatLND in such cases, and thereby avoid both LatLND-related surgical complications and radiation-induced adverse events. Moreover, the author suggested that further studies are needed to shorten the required time and improve the accuracy of SLN biopsy by the intraoperative rapid diagnosis with different methods such as molecular biological diagnosis.

Miyake *et al*[193] attempted to perform an intraoperative OSNA assay to detect perirectal LNMs to predict LPLN metastasis in rectal cancer patients undergoing surgical resection plus LatLND. In their study, LPLN metastases were present in 16% of patients (4/25), and all of these patients were positive on an OSNA for perirectal LNMs. The sensitivity of OSNA was 100%, specificity 86%, positive predictive value 57%, and negative predictive value 100% for predicting LPLN metastasis, and the authors concluded that the OSNA of perirectal LNs might be useful for selecting candidates for omission of LatLND in rectal cancer surgery. OSNA can be associated with SLN to intraoperatively identify foci of metastasis in LPLNs.

With respect to risk factors for p-LatLNM, three previous studies reported that pathological mesorectal LN (MesLN) metastasis (p-MesLNM) is a consistent risk factor for p-LatLNM[194-196]. Furthermore, previous studies have shown that p-LatLNM rarely occurs without p-MesLNM[16,197].

Negative OSNA diagnosis for mesorectal LNM (MesLNM) (OSNA-MesLNM) is highly correlated with negative p-LatLNM; hence, negative confirmation of OSNA-MesLNM may be useful in selecting patients in whom LatLND can be omitted[189].

In conclusion, the role of LatLND is still under discussion. Nevertheless, it has been suggested a selective and mono- or bilateral LatLND in advanced low and middle rectal cancer, based on OSNA positive mesorectal nodes or OSNA-positive ICG-stained sentinel LPLNs.

COSTS

A disadvantage of cOSNA is that it is more costly than pathologic examination. Depending on the number of samples analyzed in each lot, there is a variation in the cost of consumables and additional reagents. For example, a 12 LN analysis would have an indicative cost of single use products is £ 550–£ 590 per patient [excluding value added tax (VAT)]. If consumables are maximized and samples from more than 1 patient are tested in one batch, the cost could be as high as £ 33.50 per LN. The annual maintenance contract for the system (which would apply from the 2nd year after installation) is priced at £ 6628.48 (excluding VAT) with a 12 mo warranty.

The lifespan of the OSNA system declared by the manufacturer is at least 6 years. The duration of the analysis is approximately 90 min for 12 LNs, therefore it is possible to analyze samples of approximately 5 patients per day (7.5 h), and 1200 in 1 year (considering 240 annual working days). Average cost per patient (including capital, maintenance and disposable costs) ranges from £ 568 to £ 608, using the standard annuity method with a 3.5% discount rate[198]. Nonetheless, the OSNA use may reduce the reinterventions and allow earlier commencement of adjuvant treatment. The financial implications of OSNA have been previously investigated in BC, with an estimated saving between 400 and 700 £ per patient[199,200].

With pOSNA, only one measurement is required, at a cost of $ 225 (¥ 24000). In contrast, cOSNA requires three or more measurements, at a cost of $ 670 (¥ 72000) or more. In pOSNA, multiple LNs can be measured in one tube, taking into consideration the upper limit of the LN weight that can be assayed in one tube by the OSNA method is 600 mg. However, in cOSNA, only one LN can be measured in a single tube (max 50 mg). Using cOSNA to measure 12 or more halved LNs would require at least 12 tubes and three or more measurements per tube, whereas if 12 pericolic LNs are measured, pOSNA would require only one or two tubes for each case. The OSNA measuring device can measure up to four tubes at once; however, because pOSNA requires only one or two measurements per case, this allows the device to take measurements for two cases simultaneously depending on the number and weight of the removed LNs.

Diaz-Mercedes *et al*[109] analyzed the budget impact of introducing an OSNA assay in early-stage CRC patients and suggested that OSNA might have not only an economic benefit but also a clinical benefit in CRC patients, since it enabled more accurate staging, thereby avoiding unnecessary treatment. The results of Diaz-Mercedes *et al*[109] indicate that the Spanish National Health System would have saved over € 19 million from 2017 to 2019 if OSNA had been introduced in clinical practice for surgically treated CRC patients. In this study, HE-positive patients and OSNA-positive patients, both underwent adjuvant therapy. Savings are explained by the fact that OSNA ensures a more accurate diagnosis in CRC patients, allowing a reduction in treatment costs after initial surgery, as well as costs of adjuvant treatments and surgery after recurrence, compared with HE techniques. Although patients' LN staging is more expensive with OSNA than with HE, savings regarding treatment costs after surgery and treatment costs due to recurrence are high enough to justify the investment in OSNA analysis.

Although the costs of OSNA are high, the speed, simplicity, and reproducibility could allow a reduction in the hours of work of individual pathologists. Furthermore, two cases can be studied during a single procedure using the pOSNA method. Adding, as demonstrated by Diaz-Mercedes *et al*[109], the reduction in treatment costs after surgery and the reduction in costs relating to the treatment of recurrences, this method could be also attractive for developing countries.

ADVANTAGES AND DISADVANTAGES

Advantages

The innovative aspects of OSNA are that unlike standard histopathology, OSNA can analyze the whole LN as well as partial LNs. This may improve cancer staging accuracy. It can detect metastatic foci regardless of their size or location. It is seemingly superior to conventional FFTS in detecting MMs and ITC, as it can identify metastatic foci as small as 0.35 mm[201]. Yamamoto *et al*[17] found that the sum of CK19 mRNA increased as the number of histologically positive LNs increased. Indeed, the median value of CK19 mRNA was significantly smaller in patients with < 3 regional LNMs than in those with ≥ 4 regional LNMs. In the study of Aldecoa *et al*[133], the TTL was related to pT stage (P = 0.01) and tumor size (P < 0.01) in low-grade tumors. In this study, TTL correlates with classical high-risk factors in stage

I–II CC patients. These findings indicate that the sum of CK19 mRNA assessed by OSNA displays a trend compatible to the current pathological diagnosis system. These findings suggest the future possibility of novel molecular staging using OSNA, based on metastasis volume (amount of CK19 mRNA) rather than the number of LNMs.

Archilla *et al*[145] have suggested the correlation of TTL with TB and PDCs. TTL could be used as a new prognostic factor in CRC as it is related to the outcome and. The combination of the TTL as a new prognostic factor, TB and PDC, could help to better stratify and manage patients with early-stage CRC at risk of recurrence.

The application of OSNA in addition to the current standard pathology would likely provide an additional risk factor for disease recurrence regarding patients with stage II CRC. LNM is a reliable prognostic marker of CRC; it is used as the ''gold standard'' for post adjuvant chemotherapy after curative surgery. One may question whether OSNA-positive CRC patients should receive post-adjuvant chemotherapy after curative surgery. Further clinical trials are needed to determine if adjuvant therapy is beneficial in this upstaged group. On the other hand, the short turnaround time renders OSNA an attractive intra-operative method. Based upon the BC accumulated experience, the turnaround time is less than 40 min for one LN, whereas it ranges from 50 to 62 min for assessing four LNs[7]. The OSNA rapid turnover time may potentially be useful in circumventing the major issues associated with SLN biopsy. Moreover, OSNA is automated and the results are quantifiable; hence, easily reproducible, less operator-dependent with short learning curve[201-203]. Therefore, implementation of OSNA in routine clinical practice may ease the burden on pathologists.

Finally, it is laborious and rather expensive to perform molecular tests. Nonetheless, the OSNA use may reduce the re-interventions and could allow earlier commencement of adjuvant treatment. The financial implications of OSNA have been previously investigated in BC[199,200]. The results showed that pOSNA can simplify the process of cutting harvested LNs in half while reducing the equipment-related costs associated with OSNA assays used in clinical practice. Additionally, pOSNA demonstrated an upstaging rate for pNNCC equivalent to that reported in previous studies, suggesting its feasibility for molecular staging in clinical practice. With pOSNA, the possibility of fewer measurements per patient and of studying more cases simultaneously with the same panel further reduces costs[33,125]. In an era of stringent economics, health systems should undergo cost-effectiveness analyses upon which a progressive integration of OSNA in their daily clinical practice could be based on[109,200].

Limitations

The few OSNA limitations should be acknowledged. OSNA can be used to analyze LNs more than 50 mg; if the LN diameter is inferior to 3-4 mm, it cannot be divided and analyzed with OSNA and conventional histology (Table 3). The examination of the whole LN by OSNA inevitably precludes FFTS examination. One limitation of all OSNA studies performed in CRC, is that the analysis has been performed using only a part of the LNs, while using the rest of the LN tissue for conventional histological analysis and pN staging[145].

The technique of nodal division must be taken into account when evaluating the results because it can vary widely between different studies. Discordant results between OSNA and FFTS were reported. The three main reasons for these discrepancies are: tissue allocation bias, low CK19 expression, and tissue contamination. Moreover, discordances may also arise from the presence of metastases from primary tumors that do not express CK19[147]. The latter is considered an important limitation of OSNA. The accuracy of OSNA is seemingly higher amongst CK19 positive primary tumors by IHC compared to those with CK19-negative primary tumors[183]. As such, the positive CK19 IHC in primary tumors has been proposed as a prerequisite for the OSNA use by some authors[183]. An additional challenge is the fact that 36% and 49% of CK19-negative primary tumors have CK19-positive LNs[183]. Peigné *et al*[203] also reported that CK19 mRNA can also be detected by OSNA even in cases with CK19-negative primary lesion.

The tendency toward a loss of CK19 expression in poorly differentiated cancers may represent a challenge for assays using CK19 IHC or PCR for detecting MMs. It is of note that upregulation of CK19 in tumors derived from cells that are CK19-negative can also be linked to unfavorable tumor features. CK19 is highly expressed in positive LNs from BC patients even when its expression is not observed in primary tumors. Targeted studies on the upregulation of CK19 mRNA in LNM of CRC are needed[13].

In light of the potential for false-negative results, the incorporation of additional markers would be a possible direction in improving the diagnostic performance of OSNA. The cut-off point of 250 copies/mL is established in BC and seemingly sensitive in CRC while the optimal diagnostic cut-off point is a matter of debate[184]. The aforementioned pitfalls remain to date a field of contention necessitating a shift in the focus of future research into incorporation of novel biomarkers and evaluation of the optimal diagnostic cut-off point.

At this time there is no exact definition of true LN positives or negatives, cancer-related relapse and death were used as real positive LN indicators, disease-free survival as negative real LN[147]. The false-negative rate of pOSNA is a point to be considered when applying OSNA in clinical practice (Table 2). However, Aldecoa *et al*[133] observed that high-grade (G3) tumors or tumors with vascular invasion presented lower levels of TTL making it not a reliable prognostic tool for these specific pathologic features.

Finally, in this review, we found few reports dealing with CRC and SLN evaluation and there is obviously the need for future research in this field.

CONCLUSION

OSNA analysis is potentially more accurate than conventional pathologic methods for identifying metastasis because it solubilizes the entire LN and analyzes CK19 mRNA levels in the resulting sample. The advantages of OSNA include a short analysis time of approximately 30–40 min from start to completion, and the ability to automate the OSNA assay eliminates interlaboratory differences based on pathologist skill and experience. The short turnaround time renders OSNA an attractive intra-operative method. Patients with pN0 OSNA-positive CRC might also need chemotherapy after curative surgery. To achieve this goal, it needs several studies to compare the recurrence rate between the groups of no treatment or adjuvant chemotherapy after surgery both in OSNA-positive pStage II CRC patients. The result would clarify whether adjuvant chemotherapy is beneficial to patients with OSNA-positive pStage II CRC. Anyway, it can be suggested that OSNA may be considered as the route to tailormade surgery.

ACKNOWLEDGEMENTS

We thank the members of the Department of Surgery at San Giuseppe Moscati Hospital for carefully reading and examining the manuscript.

FOOTNOTES

Author contributions: Crafa F wrote and edited the manuscript and collected the clinical data; Vanella S reviewed the discussion section of the manuscript; Baiamonte M, Catalano OA and Pomykala KL revised the manuscript and provided recommendations for the clinical diagnosis paragraph.

Conflict-of-interest statement: Dr Crafa has nothing to disclose.

Open-Access: This article is an open-access article that was selected by an in-house editor and fully peer-reviewed by external reviewers. It is distributed in accordance with the Creative Commons Attribution NonCommercial (CC BY-NC 4.0) license, which permits others to distribute, remix, adapt, build upon this work non-commercially, and license their derivative works on different terms, provided the original work is properly cited and the use is non-commercial. See: https://creativecommons.org/Licenses/by-nc/4.0/

Country/Territory of origin: Italy

ORCID number: Francesco Crafa 0000-0002-2038-625X; Serafino Vanella 0000-0002-6599-8225; Onofrio A Catalano 0000-0001-7733-4138; Kelsey L Pomykala 0000-0001-8922-9597; Mario Baiamonte 0000-0001-8323-8118.

S-Editor: Zhang H
L-Editor: A
P-Editor: Zhang H

REFERENCES

1 **André T**, de Gramont A, Vernerey D, Chibaudel B, Bonnetain F, Tijeras-Raballand A, Scriva A, Hickish T, Tabernero J, Van Laethem JL, Banzi M, Maartense E, Shmueli E, Carlsson GU, Scheithauer W, Papamichael D, Möehler M, Landolfi S, Demetter P, Colote S, Tournigand C, Louvet C, Duval A, Fléjou JF. Adjuvant Fluorouracil, Leucovorin, and Oxaliplatin in Stage II to III Colon Cancer: Updated 10-Year Survival and Outcomes According to BRAF Mutation and Mismatch Repair Status of the MOSAIC Study. *J Clin Oncol* 2015; **33**: 4176-4187 [PMID: 26527776 DOI: 10.1200/JCO.2015.63.4238]

2 **Compton CC**. Optimal pathologic staging: defining stage II disease. *Clin Cancer Res* 2007; **13**: 6862s-6870s [PMID: 18006791 DOI: 10.1158/1078-0432.CCR-07-1398]

3 **Choi HK**, Law WL, Poon JT. The optimal number of lymph nodes examined in stage II colorectal cancer and its impact of on outcomes. *BMC Cancer* 2010; **10**: 267 [PMID: 20529352 DOI: 10.1186/1471-2407-10-267]

4 **Maguire A**, Sheahan K. Controversies in the pathological assessment of colorectal cancer. *World J Gastroenterol* 2014; **20**: 9850-9861 [PMID: 25110416 DOI: 10.3748/wjg.v20.i29.9850]

5 **Meyer JE**, Cohen SJ, Ruth KJ, Sigurdson ER, Hall MJ. Young Age Increases Risk of Lymph Node Positivity in Early-Stage Rectal Cancer. *J Natl Cancer Inst* 2016; **108** [PMID: 26719881 DOI: 10.1093/jnci/djv284]

6 **Resch A**, Langner C. Lymph node staging in colorectal cancer: old controversies and recent advances. *World J Gastroenterol* 2013; **19**: 8515-8526 [PMID: 24379568 DOI: 10.3748/wjg.v19.i46.8515]

7 **Tsujimoto M**, Nakabayashi K, Yoshidome K, Kaneko T, Iwase T, Akiyama F, Kato Y, Tsuda H, Ueda S, Sato K, Tamaki Y, Noguchi S, Kataoka TR, Nakajima H, Komoike Y, Inaji H, Tsugawa K, Suzuki K, Nakamura S, Daitoh M, Otomo Y, Matsuura N. One-step nucleic acid amplification for intraoperative detection of lymph node metastasis in breast cancer patients. *Clin Cancer Res* 2007; **13**: 4807-4816 [PMID: 17699859 DOI: 10.1158/1078-0432.CCR-06-2512]

8 **Hunter-Smith AE**, Rayter Z. One-step nucleic acid amplification: the possible value in assessing sentinel lymph node metastasis during mastectomy. *Breast Cancer (Dove Med Press)* 2018; **10**: 13-21 [PMID: 29416374 DOI: 10.2147/BCTT.S113737]

9 **Kumagai K**, Yamamoto N, Miyashiro I, Tomita Y, Katai H, Kushima R, Tsuda H, Kitagawa Y, Takeuchi H, Mukai M, Mano M, Mochizuki H, Kato Y, Matsuura N, Sano T. Multicenter study evaluating the clinical performance of the OSNA assay for the molecular detection of lymph node metastases in gastric cancer patients. *Gastric Cancer* 2014; **17**: 273-280 [PMID: 23743877 DOI: 10.1007/s10120-013-0271-9]

10 **Hayama M**, Chida M, Karube Y, Tamura M, Kobayashi S, Oyaizu T, Honma K. One-step nucleic acid amplification for detection of lymph node metastasis in lung cancer. *Ann Thorac Cardiovasc Surg* 2014; **20**: 181-184 [PMID: 23603642 DOI: 10.5761/atcs.oa.12.02224]

11 **Croner RS**, Schellerer V, Demund H, Schildberg C, Papadopulos T, Naschberger E, Stürzl M, Matzel KE, Hohenberger W, Schlabrakowski A. One step nucleic acid amplification (OSNA) - a new method for lymph node staging in colorectal carcinomas. *J Transl Med* 2010; **8**: 83 [PMID: 20819209 DOI: 10.1186/1479-5876-8-83]

12 **Güller U**, Zettl A, Worni M, Langer I, Cabalzar-Wondberg D, Viehl CT, Demartines N, Zuber M. Molecular investigation of lymph nodes in colon cancer patients using one-step nucleic acid amplification (OSNA): a new road to better staging? *Cancer* 2012; **118**: 6039-6045 [PMID: 22684906 DOI: 10.1002/cncr.27667]

13 **Yamamoto N**, Daito M, Hiyama K, Ding J, Nakabayashi K, Otomo Y, Tsujimoto M, Matsuura N, Kato Y. An optimal mRNA marker for OSNA (One-step nucleic acid amplification) based lymph node metastasis detection in colorectal cancer patients. *Jpn J Clin Oncol* 2013; **43**: 264-270 [PMID: 23293371 DOI: 10.1093/jjco/hys227]

14 **Croner RS**, Geppert CI, Bader FG, Nitsche U, Späth C, Rosenberg R, Zettl A, Matias-Guiu X, Tarragona J, Güller U, Stürzl M, Zuber M. Molecular staging of lymph node-negative colon carcinomas by one-step nucleic acid amplification (OSNA) results in upstaging of a quarter of patients in a prospective, European, multicentre study. *Br J Cancer* 2014; **110**: 2544-2550 [PMID: 24722182 DOI: 10.1038/bjc.2014.170]

15 **Vogelaar FJ**, Reimers MS, van der Linden RL, van der Linden JC, Smit VT, Lips DJ, van de Velde CJ, Bosscha K. The diagnostic value of one-step nucleic acid amplification (OSNA) for sentinel lymph nodes in colon cancer patients. *Ann Surg Oncol* 2014; **21**: 3924-3930 [PMID: 24912612 DOI: 10.1245/s10434-014-3820-5]

16 **Yamamoto H**, Sekimoto M, Oya M, Yamamoto N, Konishi F, Sasaki J, Yamada S, Taniyama K, Tominaga H, Tsujimoto M, Akamatsu H, Yanagisawa A, Sakakura C, Kato Y, Matsuura N. OSNA-based novel molecular testing for lymph node metastases in colorectal cancer patients: results from a multicenter clinical performance study in Japan. *Ann Surg Oncol* 2011; **18**: 1891-1898 [PMID: 21290195 DOI: 10.1245/s10434-010-1539-5]

17 **Yamamoto H**, Tomita N, Inomata M, Furuhata T, Miyake Y, Noura S, Kato T, Murata K, Hayashi S, Igarashi S, Itabashi M, Kameoka S, Matsuura N. OSNA-Assisted Molecular Staging in Colorectal Cancer: A Prospective Multicenter Trial in Japan. *Ann Surg Oncol* 2016; **23**: 391-396 [PMID: 26438440 DOI: 10.1245/s10434-015-4880-x]

18 **Itabashi M**, Yamamoto H, Tomita N, Inomata M, Murata K, Hayashi S, Miyake Y, Igarashi S, Kato T, Noura S, Furuhata T, Ozawa H, Takemasa I, Yasui M, Takeyama H, Okamura S, Ohno Y, Matsuura N. Lymph Node Positivity in One-Step Nucleic Acid Amplification is a Prognostic Factor for Postoperative Cancer Recurrence in Patients with Stage II Colorectal Cancer: A Prospective, Multicenter Study. *Ann Surg Oncol* 2020; **27**: 1077-1083 [PMID: 31722072 DOI: 10.1245/s10434-019-07971-y]

19 **Weiser MR**. AJCC 8th Edition: Colorectal Cancer. *Ann Surg Oncol* 2018; **25**: 1454-1455 [PMID: 29616422 DOI: 10.1245/s10434-018-6462-1]

20 **Hari DM**, Leung AM, Lee JH, Sim MS, Vuong B, Chiu CG, Bilchik AJ. AJCC Cancer Staging Manual 7th edition criteria for colon cancer: do the complex modifications improve prognostic assessment? *J Am Coll Surg* 2013; **217**: 181-190 [PMID: 23768788 DOI: 10.1016/j.jamcollsurg.2013.04.018]

21 **Hashiguchi Y**, Hase K, Kotake K, Ueno H, Shinto E, Mochizuki H, Yamamoto J, Sugihara K. Evaluation of the seventh edition of the tumour, node, metastasis (TNM) classification for colon cancer in two nationwide registries of the United States and Japan. *Colorectal Dis* 2012; **14**: 1065-1074 [PMID: 22176600 DOI: 10.1111/j.1463-1318.2011.02917.x]

22 **Shida D**, Kanemitsu Y, Hamaguchi T, Shimada Y. Introducing the eighth edition of the tumor-node-metastasis classification as relevant to colorectal cancer, anal cancer and appendiceal cancer: a comparison study with the seventh edition of the tumor-node-metastasis and the Japanese Classification of Colorectal, Appendiceal, and Anal Carcinoma. *Jpn J Clin Oncol* 2019; **49**: 321-328 [PMID: 30608547 DOI: 10.1093/jjco/hyy198]

23 **Namm J**, Ng M, Roy-Chowdhury S, Morgan JW, Lum SS, Wong JH. Quantitating the impact of stage migration on staging accuracy in colorectal cancer. *J Am Coll Surg* 2008; **207**: 882-887 [PMID: 19183535 DOI: 10.1016/j.jamcollsurg.2008.08.019]

24 **Li J**, Guo BC, Sun LR, Wang JW, Fu XH, Zhang SZ, Poston G, Ding KF. TNM staging of colorectal cancer should be reconsidered by T stage weighting. *World J Gastroenterol* 2014; **20**: 5104-5112 [PMID: 24803826 DOI: 10.3748/wjg.v20.i17.5104]

25 **Benson AB**, Venook AP, Al-Hawary MM, Arain MA, Chen YJ, Ciombor KK, Cohen S, Cooper HS, Deming D, Farkas L, Garrido-Laguna I, Grem JL, Gunn A, Hecht JR, Hoffe S, Hubbard J, Hunt S, Johung KL, Kirilcuk N, Krishnamurthi S, Messersmith WA, Meyerhardt J, Miller ED, Mulcahy MF, Nurkin S, Overman MJ, Parikh A, Patel H, Pedersen K, Saltz L, Schneider C, Shibata D, Skibber JM, Sofocleous CT, Stoffel EM, Stotsky-Himelfarb E, Willett CG, Gregory KM, Gurski LA. Colon Cancer, Version 2.2021, NCCN Clinical Practice Guidelines in Oncology. *J Natl Compr Canc Netw* 2021; **19**: 329-359 [PMID: 33724754 DOI: 10.6004/jnccn.2021.0012]

26 **Benson AB**, Venook AP, Al-Hawary MM, Arain MA, Chen YJ, Ciombor KK, Cohen S, Cooper HS, Deming D, Garrido-

Laguna I, Grem JL, Gunn A, Hoffe S, Hubbard J, Hunt S, Kirilcuk N, Krishnamurthi S, Messersmith WA, Meyerhardt J, Miller ED, Mulcahy MF, Nurkin S, Overman MJ, Parikh A, Patel H, Pedersen K, Saltz L, Schneider C, Shibata D, Skibber JM, Sofocleous CT, Stoffel EM, Stotsky-Himelfarb E, Willett CG, Johnson-Chilla A, Gurski LA. NCCN Guidelines Insights: Rectal Cancer, Version 6.2020. *J Natl Compr Canc Netw* 2020; **18**: 806-815 [PMID: 32634771 DOI: 10.6004/jnccn.2020.0032]

27 **Ueno H**, Mochizuki H, Akagi Y, Kusumi T, Yamada K, Ikegami M, Kawachi H, Kameoka S, Ohkura Y, Masaki T, Kushima R, Takahashi K, Ajioka Y, Hase K, Ochiai A, Wada R, Iwaya K, Shimazaki H, Nakamura T, Sugihara K. Optimal colorectal cancer staging criteria in TNM classification. *J Clin Oncol* 2012; **30**: 1519-1526 [PMID: 22430272 DOI: 10.1200/JCO.2011.39.4692]

28 **Japanese Society for Cancer of the Colon and Rectum**. Japanese Classification of Colorectal, Appendiceal, and Anal Carcinoma: the 3d English Edition [Secondary Publication]. *J Anus Rectum Colon* 2019; **3**: 175-195 [PMID: 31768468 DOI: 10.23922/jarc.2019-018]

29 **Hashiguchi Y**, Muro K, Saito Y, Ito Y, Ajioka Y, Hamaguchi T, Hasegawa K, Hotta K, Ishida H, Ishiguro M, Ishihara S, Kanemitsu Y, Kinugasa Y, Murofushi K, Nakajima TE, Oka S, Tanaka T, Taniguchi H, Tsuji A, Uehara K, Ueno H, Yamanaka T, Yamazaki K, Yoshida M, Yoshino T, Itabashi M, Sakamaki K, Sano K, Shimada Y, Tanaka S, Uetake H, Yamaguchi S, Yamaguchi N, Kobayashi H, Matsuda K, Kotake K, Sugihara K; Japanese Society for Cancer of the Colon and Rectum. Japanese Society for Cancer of the Colon and Rectum (JSCCR) guidelines 2019 for the treatment of colorectal cancer. *Int J Clin Oncol* 2020; **25**: 1-42 [PMID: 31203527 DOI: 10.1007/s10147-019-01485-z]

30 **Bilchik AJ**, Hoon DS, Saha S, Turner RR, Wiese D, DiNome M, Koyanagi K, McCarter M, Shen P, Iddings D, Chen SL, Gonzalez M, Elashoff D, Morton DL. Prognostic impact of micrometastases in colon cancer: interim results of a prospective multicenter trial. *Ann Surg* 2007; **246**: 568-75; discussion 575 [PMID: 17893493 DOI: 10.1097/SLA.0b013e318155a9c7]

31 **Sloothaak DAM**, van der Linden RLA, van de Velde CJH, Bemelman WA, Lips DJ, van der Linden JC, Doornewaard H, Tanis PJ, Bosscha K, van der Zaag ES, Buskens CJ. Prognostic implications of occult nodal tumour cells in stage I and II colon cancer: The correlation between micrometastasis and disease recurrence. *Eur J Surg Oncol* 2017; **43**: 1456-1462 [PMID: 28576463 DOI: 10.1016/j.ejso.2017.04.012]

32 **Park SJ**, Lee KY, Kim SY. Clinical significance of lymph node micrometastasis in stage I and II colon cancer. *Cancer Res Treat* 2008; **40**: 75-80 [PMID: 19688052 DOI: 10.4143/crt.2008.40.2.75]

33 **Tani K**, Itabashi M, Okuya K, Okita K, Takemasa I, Tomita N, Ogawa S, Nagashima Y, Yamamoto M. Feasibility of Pooled One-Step Nucleic Acid Amplification for Molecular Staging of Pathologically Node-Negative Colon Cancer: A Prospective Multicenter Study. *Ann Surg Oncol* 2021; **28**: 8804-8812 [PMID: 34086123 DOI: 10.1245/s10434-021-10140-9]

34 **Lino-Silva LS**, Xinaxtle DL, Salcedo-Hernández RA. Tumor deposits in colorectal cancer: the need for a new "pN" category. *Ann Transl Med* 2020; **8**: 733 [PMID: 32647658 DOI: 10.21037/atm.2020.03.175]

35 **Nagtegaal ID**, Knijn N, Hugen N, Marshall HC, Sugihara K, Tot T, Ueno H, Quirke P. Tumor Deposits in Colorectal Cancer: Improving the Value of Modern Staging-A Systematic Review and Meta-Analysis. *J Clin Oncol* 2017; **35**: 1119-1127 [PMID: 28029327 DOI: 10.1200/JCO.2016.68.9091]

36 **Mirkin KA**, Kulaylat AS, Hollenbeak CS, Messaris E. Prognostic Significance of Tumor Deposits in Stage III Colon Cancer. *Ann Surg Oncol* 2018; **25**: 3179-3184 [PMID: 30083832 DOI: 10.1245/s10434-018-6661-9]

37 **Yamano T**, Semba S, Noda M, Yoshimura M, Kobayashi M, Hamanaka M, Beppu N, Yano A, Tsukamoto K, Matsubara N, Tomita N. Prognostic significance of classified extramural tumor deposits and extracapsular lymph node invasion in T3-4 colorectal cancer: a retrospective single-center study. *BMC Cancer* 2015; **15**: 859 [PMID: 26545360 DOI: 10.1186/s12885-015-1885-6]

38 **Nagayoshi K**, Ueki T, Nishioka Y, Manabe T, Mizuuchi Y, Hirahashi M, Oda Y, Tanaka M. Tumor deposit is a poor prognostic indicator for patients who have stage II and III colorectal cancer with fewer than 4 lymph node metastases but not for those with 4 or more. *Dis Colon Rectum* 2014; **57**: 467-474 [PMID: 24608303 DOI: 10.1097/DCR.0000000000000059]

39 **Li J**, Yang S, Hu J, Liu H, Du F, Yin J, Liu S, Li C, Xing S, Yuan J, Lv B, Fan J, Leng S, Zhang X, Wang B. Tumor deposits counted as positive lymph nodes in TNM staging for advanced colorectal cancer: a retrospective multicenter study. *Oncotarget* 2016; **7**: 18269-18279 [PMID: 26934317 DOI: 10.18632/oncotarget.7756]

40 **Basnet S**, Lou QF, Liu N, Rana R, Shah A, Khadka M, Warrier H, Sigdel S, Dhakal S, Devkota A, Mishra R, Sapkota G, Zheng L, Ge HY. Tumor deposit is an independent prognostic indicator in patients who underwent radical resection for colorectal cancer. *J Cancer* 2018; **9**: 3979-3985 [PMID: 30410602 DOI: 10.7150/jca.27475]

41 **Athanasakis E**, Xenaki S, Venianaki M, Chalkiadakis G, Chrysos E. Newly recognized extratumoral features of colorectal cancer challenge the current tumor-node-metastasis staging system. *Ann Gastroenterol* 2018; **31**: 525-534 [PMID: 30174388 DOI: 10.20524/aog.2018.0284]

42 **Gröne J**, Loch FN, Taupitz M, Schmidt C, Kreis ME. Accuracy of Various Lymph Node Staging Criteria in Rectal Cancer with Magnetic Resonance Imaging. *J Gastrointest Surg* 2018; **22**: 146-153 [PMID: 28900855 DOI: 10.1007/s11605-017-3568-x]

43 **Kim MJ**, Hur BY, Lee ES, Park B, Joo J, Kim MJ, Park SC, Baek JY, Chang HJ, Kim DY, Oh JH. Prediction of lateral pelvic lymph node metastasis in patients with locally advanced rectal cancer with preoperative chemoradiotherapy: Focus on MR imaging findings. *PLoS One* 2018; **13**: e0195815 [PMID: 29649321 DOI: 10.1371/journal.pone.0195815]

44 **Zhang H**, Zhang C, Zheng Z, Ye F, Liu Y, Zou S, Zhou C. Chemical shift effect predicting lymph node status in rectal cancer using high-resolution MR imaging with node-for-node matched histopathological validation. *Eur Radiol* 2017; **27**: 3845-3855 [PMID: 28168369 DOI: 10.1007/s00330-017-4738-7]

45 **Choi J**, Oh SN, Yeo DM, Kang WK, Jung CK, Kim SW, Park MY. Computed tomography and magnetic resonance imaging evaluation of lymph node metastasis in early colorectal cancer. *World J Gastroenterol* 2015; **21**: 556-562 [PMID: 25593474 DOI: 10.3748/wjg.v21.i2.556]

46 **Kaur H**, Choi H, You YN, Rauch GM, Jensen CT, Hou P, Chang GJ, Skibber JM, Ernst RD. MR imaging for

preoperative evaluation of primary rectal cancer: practical considerations. *Radiographics* 2012; **32**: 389-409 [PMID: 22411939 DOI: 10.1148/rg.322115122]

47 **Koh DM**, Brown G, Husband JE. Nodal staging in rectal cancer. *Abdom Imaging* 2006; **31**: 652-659 [PMID: 16897279 DOI: 10.1007/s00261-006-9021-3]

48 **Wang C**, Zhou Z, Wang Z, Zheng Y, Zhao G, Yu Y, Cheng Z, Chen D, Liu W. Patterns of neoplastic foci and lymph node micrometastasis within the mesorectum. *Langenbecks Arch Surg* 2005; **390**: 312-318 [PMID: 16049726 DOI: 10.1007/s00423-005-0562-7]

49 **Hadfield MB**, Nicholson AA, MacDonald AW, Farouk R, Lee PW, Duthie GS, Monson JR. Preoperative staging of rectal carcinoma by magnetic resonance imaging with a pelvic phased-array coil. *Br J Surg* 1997; **84**: 529-531 [PMID: 9112909]

50 **Kim NK**, Kim MJ, Yun SH, Sohn SK, Min JS. Comparative study of transrectal ultrasonography, pelvic computerized tomography, and magnetic resonance imaging in preoperative staging of rectal cancer. *Dis Colon Rectum* 1999; **42**: 770-775 [PMID: 10378601 DOI: 10.1007/BF02236933]

51 **Roy C**, Bierry G, Matau A, Bazille G, Pasquali R. Value of diffusion-weighted imaging to detect small malignant pelvic lymph nodes at 3 T. *Eur Radiol* 2010; **20**: 1803-1811 [PMID: 20182732 DOI: 10.1007/s00330-010-1736-4]

52 **Zhou J**, Zhan S, Zhu Q, Gong H, Wang Y, Fan D, Gong Z, Huang Y. Prediction of nodal involvement in primary rectal carcinoma without invasion to pelvic structures: accuracy of preoperative CT, MR, and DWIBS assessments relative to histopathologic findings. *PLoS One* 2014; **9**: e92779 [PMID: 24695111 DOI: 10.1371/journal.pone.0092779]

53 **Beets-Tan RGH**, Lambregts DMJ, Maas M, Bipat S, Barbaro B, Curvo-Semedo L, Fenlon HM, Gollub MJ, Gourtsoyianni S, Halligan S, Hoeffel C, Kim SH, Laghi A, Maier A, Rafaelsen SR, Stoker J, Taylor SA, Torkzad MR, Blomqvist L. Magnetic resonance imaging for clinical management of rectal cancer: Updated recommendations from the 2016 European Society of Gastrointestinal and Abdominal Radiology (ESGAR) consensus meeting. *Eur Radiol* 2018; **28**: 1465-1475 [PMID: 29043428 DOI: 10.1007/s00330-017-5026-2]

54 **Fritz S**, Killguss H, Schaudt A, Lazarou L, Sommer CM, Richter GM, Küper-Steffen R, Feilhauer K, Köninger J. Preoperative versus pathological staging of rectal cancer-challenging the indication of neoadjuvant chemoradiotherapy. *Int J Colorectal Dis* 2021; **36**: 191-194 [PMID: 32955607 DOI: 10.1007/s00384-020-03751-3]

55 **Catalano OA**, Lee SI, Parente C, Cauley C, Furtado FS, Striar R, Soricelli A, Salvatore M, Li Y, Umutlu L, Cañamaque LG, Groshar D, Mahmood U, Blaszkowsky LS, Ryan DP, Clark JW, Wo J, Hong TS, Kunitake H, Bordeianou L, Berger D, Ricciardi R, Rosen B. Improving staging of rectal cancer in the pelvis: the role of PET/MRI. *Eur J Nucl Med Mol Imaging* 2021; **48**: 1235-1245 [PMID: 33034673 DOI: 10.1007/s00259-020-05036-x]

56 **Dahmarde H**, Parooie F, Salarzaei M. Is ^{18}F-FDG PET/CT an Accurate Way to Detect Lymph Node Metastasis in Colorectal Cancer: A Systematic Review and Meta-Analysis. *Contrast Media Mol Imaging* 2020; **2020**: 5439378 [PMID: 32733174 DOI: 10.1155/2020/5439378]

57 **Kijima S**, Sasaki T, Nagata K, Utano K, Lefor AT, Sugimoto H. Preoperative evaluation of colorectal cancer using CT colonography, MRI, and PET/CT. *World J Gastroenterol* 2014; **20**: 16964-16975 [PMID: 25493009 DOI: 10.3748/wjg.v20.i45.16964]

58 **Lu YY**, Chen JH, Ding HJ, Chien CR, Lin WY, Kao CH. A systematic review and meta-analysis of pretherapeutic lymph node staging of colorectal cancer by 18F-FDG PET or PET/CT. *Nucl Med Commun* 2012; **33**: 1127-1133 [PMID: 23000829 DOI: 10.1097/MNM.0b013e328357b2d9]

59 **Abdel-Nabi H**, Doerr RJ, Lamonica DM, Cronin VR, Galantowicz PJ, Carbone GM, Spaulding MB. Staging of primary colorectal carcinomas with fluorine-18 fluorodeoxyglucose whole-body PET: correlation with histopathologic and CT findings. *Radiology* 1998; **206**: 755-760 [PMID: 9494497 DOI: 10.1148/radiology.206.3.9494497]

60 **Furukawa H**, Ikuma H, Seki A, Yokoe K, Yuen S, Aramaki T, Yamagushi S. Positron emission tomography scanning is not superior to whole body multidetector helical computed tomography in the preoperative staging of colorectal cancer. *Gut* 2006; **55**: 1007-1011 [PMID: 16361308 DOI: 10.1136/gut.2005.076273]

61 **Mukai M**, Sadahiro S, Yasuda S, Ishida H, Tokunaga N, Tajima T, Makuuchi H. Preoperative evaluation by whole-body 18F-fluorodeoxyglucose positron emission tomography in patients with primary colorectal cancer. *Oncol Rep* 2000; **7**: 85-87 [PMID: 10601597]

62 **Shin SS**, Jeong YY, Min JJ, Kim HR, Chung TW, Kang HK. Preoperative staging of colorectal cancer: CT vs. integrated FDG PET/CT. *Abdom Imaging* 2008; **33**: 270-277 [PMID: 17610107 DOI: 10.1007/s00261-007-9262-9]

63 **Bae SU**, Won KS, Song BI, Jeong WK, Baek SK, Kim HW. Accuracy of F-18 FDG PET/CT with optimal cut-offs of maximum standardized uptake value according to size for diagnosis of regional lymph node metastasis in patients with rectal cancer. *Cancer Imaging* 2018; **18**: 32 [PMID: 30217167 DOI: 10.1186/s40644-018-0165-5]

64 **Rahmim A**, Qi J, Sossi V. Resolution modeling in PET imaging: theory, practice, benefits, and pitfalls. *Med Phys* 2013; **40**: 064301 [PMID: 23718620 DOI: 10.1118/1.4800806]

65 **Catalano OA**, Coutinho AM, Sahani DV, Vangel MG, Gee MS, Hahn PF, Witzel T, Soricelli A, Salvatore M, Catana C, Mahmood U, Rosen BR, Gervais D. Colorectal cancer staging: comparison of whole-body PET/CT and PET/MR. *Abdom Radiol (NY)* 2017; **42**: 1141-1151 [PMID: 27891551 DOI: 10.1007/s00261-016-0985-3]

66 **Amorim BJ**, Hong TS, Blaszkowsky LS, Ferrone CR, Berger DL, Bordeianou LG, Ricciardi R, Clark JW, Ryan DP, Wo JY, Qadan M, Vangel M, Umutlu L, Groshar D, Cañamaques LG, Gervais DA, Mahmood U, Rosen BR, Catalano OA. Clinical impact of PET/MR in treated colorectal cancer patients. *Eur J Nucl Med Mol Imaging* 2019; **46**: 2260-2269 [PMID: 31359108 DOI: 10.1007/s00259-019-04449-7]

67 **Ferrone C**, Goyal L, Qadan M, Gervais D, Sahani DV, Zhu AX, Hong TS, Blaszkowsky LS, Tanabe KK, Vangel M, Amorim BJ, Wo JY, Mahmood U, Pandharipande PV, Catana C, Duenas VP, Collazo YQ, Canamaque LG, Domachevsky L, Bernstine HH, Groshar D, Shih TT, Li Y, Herrmann K, Umutlu L, Rosen BR, Catalano OA. Management implications of fluorodeoxyglucose positron emission tomography/magnetic resonance in untreated intrahepatic cholangiocarcinoma. *Eur J Nucl Med Mol Imaging* 2020; **47**: 1871-1884 [PMID: 31705172 DOI: 10.1007/s00259-019-04558-3]

68 **Furtado FS**, Suarez-Weiss KE, Vangel M, Clark JW, Cusack JC, Hong T, Blaszkowsky L, Wo J, Striar R, Umutlu L, Daldrup-Link HE, Groshar D, Rocco R, Bordeianou L, Anderson MA, Mojtahed A, Qadan M, Ferrone C, Catalano OA.

Clinical impact of PET/MRI in oligometastatic colorectal cancer. *Br J Cancer* 2021; **125**: 975-982 [PMID: 34282295 DOI: 10.1038/s41416-021-01494-8]

69 **Catalano OA**, Daye D, Signore A, Iannace C, Vangel M, Luongo A, Catalano M, Filomena M, Mansi L, Soricelli A, Salvatore M, Fuin N, Catana C, Mahmood U, Rosen BR. Staging performance of whole-body DWI, PET/CT and PET/MRI in invasive ductal carcinoma of the breast. *Int J Oncol* 2017; **51**: 281-288 [PMID: 28535000 DOI: 10.3892/ijo.2017.4012]

70 **Incoronato M**, Grimaldi AM, Cavaliere C, Inglese M, Mirabelli P, Monti S, Ferbo U, Nicolai E, Soricelli A, Catalano OA, Aiello M, Salvatore M. Relationship between functional imaging and immunohistochemical markers and prediction of breast cancer subtype: a PET/MRI study. *Eur J Nucl Med Mol Imaging* 2018; **45**: 1680-1693 [PMID: 29696443 DOI: 10.1007/s00259-018-4010-7]

71 **Nensa F**, Beiderwellen K, Heusch P, Wetter A. Clinical applications of PET/MRI: current status and future perspectives. *Diagn Interv Radiol* 2014; **20**: 438-447 [PMID: 25010371 DOI: 10.5152/dir.2014.14008]

72 **Lambregts DM**, Maas M, Cappendijk VC, Prompers LM, Mottaghy FM, Beets GL, Beets-Tan RG. Whole-body diffusion-weighted magnetic resonance imaging: current evidence in oncology and potential role in colorectal cancer staging. *Eur J Cancer* 2011; **47**: 2107-2116 [PMID: 21664810 DOI: 10.1016/j.ejca.2011.05.013]

73 **Chen H**, Zhao L, Ruan D, Pang Y, Hao B, Dai Y, Wu X, Guo W, Fan C, Wu J, Huang W, Lin Q, Sun L, Wu H. Usefulness of [68Ga]Ga-DOTA-FAPI-04 PET/CT in patients presenting with inconclusive [18F]FDG PET/CT findings. *Eur J Nucl Med Mol Imaging* 2021; **48**: 73-86 [PMID: 32588089 DOI: 10.1007/s00259-020-04940-6]

74 **Pang Y**, Zhao L, Luo Z, Hao B, Wu H, Lin Q, Sun L, Chen H. Comparison of ^{68}Ga-FAPI and ^{18}F-FDG Uptake in Gastric, Duodenal, and Colorectal Cancers. *Radiology* 2021; **298**: 393-402 [PMID: 33258746 DOI: 10.1148/radiol.2020203275]

75 **Bedrikovetski S**, Dudi-Venkata NN, Kroon HM, Seow W, Vather R, Carneiro G, Moore JW, Sammour T. Artificial intelligence for pre-operative lymph node staging in colorectal cancer: a systematic review and meta-analysis. *BMC Cancer* 2021; **21**: 1058 [PMID: 34565338 DOI: 10.1186/s12885-021-08773-w]

76 **Wood TF**, Nora DT, Morton DL, Turner RR, Rangel D, Hutchinson W, Bilchik AJ. One hundred consecutive cases of sentinel lymph node mapping in early colorectal carcinoma: detection of missed micrometastases. *J Gastrointest Surg* 2002; **6**: 322-9; discussion 229 [PMID: 12022982 DOI: 10.1016/s1091-255x(02)00013-6]

77 **Saha S**, Monson KM, Bilchik A, Beutler T, Dan AG, Schochet E, Wiese D, Kaushal S, Ganatra B, Desai D. Comparative analysis of nodal upstaging between colon and rectal cancers by sentinel lymph node mapping: a prospective trial. *Dis Colon Rectum* 2004; **47**: 1767-1772 [PMID: 15622567 DOI: 10.1007/s10350-004-0661-5]

78 **Cahill RA**, Bembenek A, Sirop S, Waterhouse DF, Schneider W, Leroy J, Wiese D, Beutler T, Bilchik A, Saha S, Schlag PM. Sentinel node biopsy for the individualization of surgical strategy for cure of early-stage colon cancer. *Ann Surg Oncol* 2009; **16**: 2170-2180 [PMID: 19472012 DOI: 10.1245/s10434-009-0510-9]

79 **Tiffet O**, Kaczmarek D, Chambonnière ML, Guillan T, Baccot S, Prévot N, Bageacu S, Bourgeois E, Cassagnau E, Lehur PA, Dubois F. Combining radioisotopic and blue-dye technique does not improve the false-negative rate in sentinel lymph node mapping for colorectal cancer. *Dis Colon Rectum* 2007; **50**: 962-970 [PMID: 17468975 DOI: 10.1007/s10350-007-0236-3]

80 **Bianchi PP**, Petz W, Casali L. Laparoscopic lymphatic roadmapping with blue dye and radioisotope in colon cancer. *Colorectal Dis* 2011; **13** Suppl 7: 67-69 [PMID: 22098523 DOI: 10.1111/j.1463-1318.2011.02786.x]

81 **Tan KY**, Kawamura YJ, Mizokami K, Sasaki J, Tsujinaka S, Maeda T, Nobuki M, Konishi F. Distribution of the first metastatic lymph node in colon cancer and its clinical significance. *Colorectal Dis* 2010; **12**: 44-47 [PMID: 19438890 DOI: 10.1111/j.1463-1318.2009.01924.x]

82 **Bilchik AJ**, Saha S, Wiese D, Stonecypher JA, Wood TF, Sostrin S, Turner RR, Wang HJ, Morton DL, Hoon DS. Molecular staging of early colon cancer on the basis of sentinel node analysis: a multicenter phase II trial. *J Clin Oncol* 2001; **19**: 1128-1136 [PMID: 11181678 DOI: 10.1200/JCO.2001.19.4.1128]

83 **Saha S**, Johnston G, Korant A, Shaik M, Kanaan M, Johnston R, Ganatra B, Kaushal S, Desai D, Mannam S. Aberrant drainage of sentinel lymph nodes in colon cancer and its impact on staging and extent of operation. *Am J Surg* 2013; **205**: 302-5; discussion 305 [PMID: 23414953 DOI: 10.1016/j.amjsurg.2012.10.029]

84 **Iddings D**, Bilchik A. The biologic significance of micrometastatic disease and sentinel lymph node technology on colorectal cancer. *J Surg Oncol* 2007; **96**: 671-677 [PMID: 18081169 DOI: 10.1002/jso.20918]

85 **Bianchi PP**, Ceriani C, Rottoli M, Torzilli G, Roncalli M, Spinelli A, Montorsi M. Laparoscopic lymphatic mapping and sentinel lymph node detection in colon cancer: technical aspects and preliminary results. *Surg Endosc* 2007; **21**: 1567-1571 [PMID: 17285373 DOI: 10.1007/s00464-006-9152-1]

86 **Wiese DA**, Saha S, Badin J, Ng PS, Gauthier J, Ahsan A, Yu L. Pathologic evaluation of sentinel lymph nodes in colorectal carcinoma. *Arch Pathol Lab Med* 2000; **124**: 1759-1763 [PMID: 11100053 DOI: 10.5858/2000-124-1759-PEOSLN]

87 **Bilchik AJ**, Trocha SD. Lymphatic mapping and sentinel node analysis to optimize laparoscopic resection and staging of colorectal cancer: an update. *Cancer Control* 2003; **10**: 219-223 [PMID: 12794620 DOI: 10.1177/107327480301000305]

88 **Argilés G**, Tabernero J, Labianca R, Hochhauser D, Salazar R, Iveson T, Laurent-Puig P, Quirke P, Yoshino T, Taieb J, Martinelli E, Arnold D; ESMO Guidelines Committee. Electronic address: clinicalguidelines@esmo.org. Localised colon cancer: ESMO Clinical Practice Guidelines for diagnosis, treatment and follow-up. *Ann Oncol* 2020; **31**: 1291-1305 [PMID: 32702383 DOI: 10.1016/j.annonc.2020.06.022]

89 **Shinagawa T**, Tanaka T, Nozawa H, Emoto S, Murono K, Kaneko M, Sasaki K, Otani K, Nishikawa T, Hata K, Kawai K, Watanabe T. Comparison of the guidelines for colorectal cancer in Japan, the USA and Europe. *Ann Gastroenterol Surg* 2018; **2**: 6-12 [PMID: 29863118 DOI: 10.1002/ags3.12047]

90 **Hohenberger W**, Weber K, Matzel K, Papadopoulos T, Merkel S. Standardized surgery for colonic cancer: complete mesocolic excision and central ligation--technical notes and outcome. *Colorectal Dis* 2009; **11**: 354-64; discussion 364 [PMID: 19016817 DOI: 10.1111/j.1463-1318.2008.01735.x]

91 **West NP**, Kobayashi H, Takahashi K, Perrakis A, Weber K, Hohenberger W, Sugihara K, Quirke P. Understanding optimal colonic cancer surgery: comparison of Japanese D3 resection and European complete mesocolic excision with

central vascular ligation. *J Clin Oncol* 2012; **30**: 1763-1769 [PMID: 22473170 DOI: 10.1200/JCO.2011.38.3992]
92 **Heald RJ**, Husband EM, Ryall RD. The mesorectum in rectal cancer surgery--the clue to pelvic recurrence? *Br J Surg* 1982; **69**: 613-616 [PMID: 6751457 DOI: 10.1002/bjs.1800691019]
93 **MacFarlane JK**, Ryall RD, Heald RJ. Mesorectal excision for rectal cancer. *Lancet* 1993; **341**: 457-460 [PMID: 8094488 DOI: 10.1016/0140-6736(93)90207-w]
94 **Lowry AC**, Simmang CL, Boulos P, Farmer KC, Finan PJ, Hyman N, Killingback M, Lubowski DZ, Moore R, Penfold C, Savoca P, Stitz R, Tjandra JJ. Consensus statement of definitions for anorectal physiology and rectal cancer: report of the Tripartite Consensus Conference on Definitions for Anorectal Physiology and Rectal Cancer, Washington, D.C., May 1, 1999. *Dis Colon Rectum* 2001; **44**: 915-919 [PMID: 11496067 DOI: 10.1007/BF02235475]
95 **Fujita S**, Mizusawa J, Kanemitsu Y, Ito M, Kinugasa Y, Komori K, Ohue M, Ota M, Akazai Y, Shiozawa M, Yamaguchi T, Bandou H, Katsumata K, Murata K, Akagi Y, Takiguchi N, Saida Y, Nakamura K, Fukuda H, Akasu T, Moriya Y; Colorectal Cancer Study Group of Japan Clinical Oncology Group. Mesorectal Excision With or Without Lateral Lymph Node Dissection for Clinical Stage II/III Lower Rectal Cancer (JCOG0212): A Multicenter, Randomized Controlled, Noninferiority Trial. *Ann Surg* 2017; **266**: 201-207 [PMID: 28288057 DOI: 10.1097/SLA.0000000000002212]
96 **Sakai Y**, Hida K. Real-World Situation of Lateral Lymph Node Dissection for Rectal Cancer in Japan. *Dis Colon Rectum* 2019; **62**: e29 [PMID: 31094963 DOI: 10.1097/DCR.0000000000001369]
97 **Yokoyama S**, Takifuji K, Hotta T, Matsuda K, Watanabe T, Mitani Y, Ieda J, Yamaue H. Survival benefit of lateral lymph node dissection according to the region of involvement and the number of lateral lymph nodes involved. *Surg Today* 2014; **44**: 1097-1103 [PMID: 24370948 DOI: 10.1007/s00595-013-0815-y]
98 **Cahill RA**, Leroy J, Marescaux J. Localized resection for colon cancer. *Surg Oncol* 2009; **18**: 334-342 [PMID: 18835772 DOI: 10.1016/j.suronc.2008.08.004]
99 **Creavin B**, Ryan E, Martin ST, Hanly A, O'Connell PR, Sheahan K, Winter DC. Organ preservation with local excision or active surveillance following chemoradiotherapy for rectal cancer. *Br J Cancer* 2017; **116**: 169-174 [PMID: 27997526 DOI: 10.1038/bjc.2016.417]
100 **Augestad KM**, Merok MA, Ignatovic D. Tailored Treatment of Colorectal Cancer: Surgical, Molecular, and Genetic Considerations. *Clin Med Insights Oncol* 2017; **11**: 1179554917690766 [PMID: 28469509 DOI: 10.1177/1179554917690766]
101 **Saha S**, Sehgal R, Patel M, Doan K, Dan A, Bilchik A, Beutler T, Wiese D, Bassily N, Yee C. A multicenter trial of sentinel lymph node mapping in colorectal cancer: prognostic implications for nodal staging and recurrence. *Am J Surg* 2006; **191**: 305-310 [PMID: 16490536 DOI: 10.1016/j.amjsurg.2005.10.028]
102 **Wright FC**, Law CH, Berry S, Smith AJ. Clinically important aspects of lymph node assessment in colon cancer. *J Surg Oncol* 2009; **99**: 248-255 [PMID: 19235179 DOI: 10.1002/jso.21226]
103 **van der Zaag ES**, Bouma WH, Tanis PJ, Ubbink DT, Bemelman WA, Buskens CJ. Systematic review of sentinel lymph node mapping procedure in colorectal cancer. *Ann Surg Oncol* 2012; **19**: 3449-3459 [PMID: 22644513 DOI: 10.1245/s10434-012-2417-0]
104 **Quadros CA**, Lopes A, Araujo I, Fregnani JH, Fahel F. Upstaging benefits and accuracy of sentinel lymph node mapping in colorectal adenocarcinoma nodal staging. *J Surg Oncol* 2008; **98**: 324-330 [PMID: 18618578 DOI: 10.1002/jso.21112]
105 **André T**, Boni C, Mounedji-Boudiaf L, Navarro M, Tabernero J, Hickish T, Topham C, Zaninelli M, Clingan P, Bridgewater J, Tabah-Fisch I, de Gramont A; Multicenter International Study of Oxaliplatin/5-Fluorouracil/Leucovorin in the Adjuvant Treatment of Colon Cancer (MOSAIC) Investigators. Oxaliplatin, fluorouracil, and leucovorin as adjuvant treatment for colon cancer. *N Engl J Med* 2004; **350**: 2343-2351 [PMID: 15175436 DOI: 10.1056/NEJMoa032709]
106 **Kuebler JP**, Wieand HS, O'Connell MJ, Smith RE, Colangelo LH, Yothers G, Petrelli NJ, Findlay MP, Seay TE, Atkins JN, Zapas JL, Goodwin JW, Fehrenbacher L, Ramanathan RK, Conley BA, Flynn PJ, Soori G, Colman LK, Levine EA, Lanier KS, Wolmark N. Oxaliplatin combined with weekly bolus fluorouracil and leucovorin as surgical adjuvant chemotherapy for stage II and III colon cancer: results from NSABP C-07. *J Clin Oncol* 2007; **25**: 2198-2204 [PMID: 17470851 DOI: 10.1200/JCO.2006.08.2974]
107 **Sahin IH**, Akce M, Alese O, Shaib W, Lesinski GB, El-Rayes B, Wu C. Immune checkpoint inhibitors for the treatment of MSI-H/MMR-D colorectal cancer and a perspective on resistance mechanisms. *Br J Cancer* 2019; **121**: 809-818 [PMID: 31607751 DOI: 10.1038/s41416-019-0599-y]
108 **Gray RG**, Quirke P, Handley K, Lopatin M, Magill L, Baehner FL, Beaumont C, Clark-Langone KM, Yoshizawa CN, Lee M, Watson D, Shak S, Kerr DJ. Validation study of a quantitative multigene reverse transcriptase-polymerase chain reaction assay for assessment of recurrence risk in patients with stage II colon cancer. *J Clin Oncol* 2011; **29**: 4611-4619 [PMID: 22067390 DOI: 10.1200/JCO.2010.32.8732]
109 **Diaz-Mercedes S**, Archilla I, Camps J, de Lacy A, Gorostiaga I, Momblan D, Ibarzabal A, Maurel J, Chic N, Bombí JA, Balaguer F, Castells A, Aldecoa I, Borras JM, Cuatrecasas M. Budget Impact Analysis of Molecular Lymph Node Staging Versus Conventional Histopathology Staging in Colorectal Carcinoma. *Appl Health Econ Health Policy* 2019; **17**: 655-667 [PMID: 31115896 DOI: 10.1007/s40258-019-00482-7]
110 **Salazar R**, Roepman P, Capella G, Moreno V, Simon I, Dreezen C, Lopez-Doriga A, Santos C, Marijnen C, Westerga J, Bruin S, Kerr D, Kuppen P, van de Velde C, Morreau H, Van Velthuysen L, Glas AM, Van't Veer LJ, Tollenaar R. Gene expression signature to improve prognosis prediction of stage II and III colorectal cancer. *J Clin Oncol* 2011; **29**: 17-24 [PMID: 21098318 DOI: 10.1200/JCO.2010.30.1077]
111 **Nitsche U**, Rosenberg R, Balmert A, Schuster T, Slotta-Huspenina J, Herrmann P, Bader FG, Friess H, Schlag PM, Stein U, Janssen KP. Integrative marker analysis allows risk assessment for metastasis in stage II colon cancer. *Ann Surg* 2012; **256**: 763-71; discussion 771 [PMID: 23095620 DOI: 10.1097/SLA.0b013e318272de87]
112 **Maak M**, Simon I, Nitsche U, Roepman P, Snel M, Glas AM, Schuster T, Keller G, Zeestraten E, Goossens I, Janssen KP, Friess H, Rosenberg R. Independent validation of a prognostic genomic signature (ColoPrint) for patients with stage II colon cancer. *Ann Surg* 2013; **257**: 1053-1058 [PMID: 23295318 DOI: 10.1097/SLA.0b013e31827c1180]
113 **Rahbari NN**, Bork U, Motschall E, Thorlund K, Büchler MW, Koch M, Weitz J. Molecular detection of tumor cells in regional lymph nodes is associated with disease recurrence and poor survival in node-negative colorectal cancer: a

systematic review and meta-analysis. *J Clin Oncol* 2012; **30**: 60-70 [PMID: 22124103 DOI: 10.1200/JCO.2011.36.9504]

114 **Broderick-Villa G**, Ko A, O'Connell TX, Guenther JM, Danial T, DiFronzo LA. Does tumor burden limit the accuracy of lymphatic mapping and sentinel lymph node biopsy in colorectal cancer? *Cancer J* 2002; **8**: 445-450 [PMID: 12500853 DOI: 10.1097/00130404-200211000-00008]

115 **Bembenek A**, String A, Gretschel S, Schlag PM. Technique and clinical consequences of sentinel lymph node biopsy in colorectal cancer. *Surg Oncol* 2008; **17**: 183-193 [PMID: 18571920 DOI: 10.1016/j.suronc.2008.05.003]

116 **Bilchik AJ**, DiNome M, Saha S, Turner RR, Wiese D, McCarter M, Hoon DS, Morton DL. Prospective multicenter trial of staging adequacy in colon cancer: preliminary results. *Arch Surg* 2006; **141**: 527-33; discussion 533 [PMID: 16785352 DOI: 10.1001/archsurg.141.6.527]

117 **Bilchik AJ**, Nora DT, Sobin LH, Turner RR, Trocha S, Krasne D, Morton DL. Effect of lymphatic mapping on the new tumor-node-metastasis classification for colorectal cancer. *J Clin Oncol* 2003; **21**: 668-672 [PMID: 12586804 DOI: 10.1200/JCO.2003.04.037]

118 **Esser S**, Reilly WT, Riley LB, Eyvazzadeh C, Arcona S. The role of sentinel lymph node mapping in staging of colon and rectal cancer. *Dis Colon Rectum* 2001; **44**: 850-4; discussion 854 [PMID: 11391147 DOI: 10.1007/BF02234707]

119 **Dionigi G**, Castano P, Rovera F, Boni L, Annoni M, Villa F, Bianchi V, Carrafiello G, Bacuzzi A, Dionigi R. The application of sentinel lymph node mapping in colon cancer. *Surg Oncol* 2007; **16** Suppl 1: S129-S132 [PMID: 18023573 DOI: 10.1016/j.suronc.2007.10.024]

120 **Notomi T**, Okayama H, Masubuchi H, Yonekawa T, Watanabe K, Amino N, Hase T. Loop-mediated isothermal amplification of DNA. *Nucleic Acids Res* 2000; **28**: E63 [PMID: 10871386 DOI: 10.1093/nar/28.12.e63]

121 **Mori Y**, Nagamine K, Tomita N, Notomi T. Detection of loop-mediated isothermal amplification reaction by turbidity derived from magnesium pyrophosphate formation. *Biochem Biophys Res Commun* 2001; **289**: 150-154 [PMID: 11708792 DOI: 10.1006/bbrc.2001.5921]

122 **Yamamoto H**, Murata K, Fukunaga M, Ohnishi T, Noura S, Miyake Y, Kato T, Ohtsuka M, Nakamura Y, Takemasa I, Mizushima T, Ikeda M, Ohue M, Sekimoto M, Nezu R, Matsuura N, Monden M, Doki Y, Mori M. Micrometastasis Volume in Lymph Nodes Determines Disease Recurrence Rate of Stage II Colorectal Cancer: A Prospective Multicenter Trial. *Clin Cancer Res* 2016; **22**: 3201-3208 [PMID: 26831719 DOI: 10.1158/1078-0432.CCR-15-2199]

123 **Kosťun J**, Pešta M, Sláma J, Slunéčko R, Vlasák P, Bouda J, Novotný Z, Topolčan O, Kučera R, Kulda V, Houfková K, Berezovskiy D, Bartáková A, Presl J. One-step nucleic acid amplification vs ultrastaging in the detection of sentinel lymph node metastasis in endometrial cancer patients. *J Surg Oncol* 2019; **119**: 361-369 [PMID: 30508294 DOI: 10.1002/jso.25322]

124 **Aldecoa I**, Montironi C, Planell N, Pellise M, Fernandez-Esparrach G, Gines A, Delgado S, Momblan D, Moreira L, Lopez-Ceron M, Rakislova N, Martinez-Palli G, Balust J, Bombi JA, de Lacy A, Castells A, Balaguer F, Cuatrecasas M. Endoscopic tattooing of early colon carcinoma enhances detection of lymph nodes most prone to harbor tumor burden. *Surg Endosc* 2017; **31**: 723-733 [PMID: 27324339 DOI: 10.1007/s00464-016-5026-3]

125 **Rakislova N**, Montironi C, Aldecoa I, Fernandez E, Bombi JA, Jimeno M, Balaguer F, Pellise M, Castells A, Cuatrecasas M. Lymph node pooling: a feasible and efficient method of lymph node molecular staging in colorectal carcinoma. *J Transl Med* 2017; **15**: 14 [PMID: 28088238 DOI: 10.1186/s12967-016-1114-3]

126 **Brito MJ**, Honavar M, Cipriano MA, Lopes J, Coelho H, Silva AR, Silva M, Guimarães S, Frutuoso A, Gomes A, Barbosa E, Carlos S. Molecular Staging of Patients with Colon Cancer. The C-Closer-II Study: A Multicentre Study in Portugal. *Acta Med Port* 2018; **31**: 661-669 [PMID: 30521460 DOI: 10.20344/amp.9696]

127 **Esposito F**, Noviello A, Moles N, Coppola Bottazzi E, Baiamonte M, Macaione I, Ferbo U, Lepore M, Miro A, Crafa F. Sentinel Lymph Node Analysis in Colorectal Cancer Patients Using One-Step Nucleic Acid Amplification in Combination With Fluorescence and Indocyanine Green. *Ann Coloproctol* 2019; **35**: 174-180 [PMID: 31487764 DOI: 10.3393/ac.2018.07.21.1]

128 **Tiernan JP**, Verghese ET, Nair A, Pathak S, Kim B, White J, Thygesen H, Horgan K, Hanby AM. Systematic review and meta-analysis of cytokeratin 19-based one-step nucleic acid amplification versus histopathology for sentinel lymph node assessment in breast cancer. *Br J Surg* 2014; **101**: 298-306 [PMID: 24536007 DOI: 10.1002/bjs.9386]

129 **Colling R**, Yeung T, Hompes R, Kraus R, Cahill R, Mortensen N, Wang LM. OSNA testing for lymph node staging in colorectal cancer. *J Clin Pathol* 2017; **70**: 638-639 [PMID: 28348048 DOI: 10.1136/jclinpath-2016-204299]

130 **Yeung TM**, Wang LM, Colling R, Kraus R, Cahill R, Hompes R, Mortensen NJ. Intraoperative identification and analysis of lymph nodes at laparoscopic colorectal cancer surgery using fluorescence imaging combined with rapid OSNA pathological assessment. *Surg Endosc* 2018; **32**: 1073-1076 [PMID: 28643063 DOI: 10.1007/s00464-017-5644-4]

131 **Hiyoshi Y**, Akiyoshi T, Fukunaga Y. The advantage of one-step nucleic acid amplification for the diagnosis of lymph node metastasis in colorectal cancer patients. *Ann Gastroenterol Surg* 2021; **5**: 60-66 [PMID: 33532681 DOI: 10.1002/ags3.12392]

132 **Iddings D**, Ahmad A, Elashoff D, Bilchik A. The prognostic effect of micrometastases in previously staged lymph node negative (N0) colorectal carcinoma: a meta-analysis. *Ann Surg Oncol* 2006; **13**: 1386-1392 [PMID: 17009147 DOI: 10.1245/s10434-006-9120-y]

133 **Aldecoa I**, Atares B, Tarragona J, Bernet L, Sardon JD, Pereda T, Villar C, Mendez MC, Gonzalez-Obeso E, Elorriaga K, Alonso GL, Zamora J, Planell N, Palacios J, Castells A, Matias-Guiu X, Cuatrecasas M. Molecularly determined total tumour load in lymph nodes of stage I-II colon cancer patients correlates with high-risk factors. A multicentre prospective study. *Virchows Arch* 2016; **469**: 385-394 [PMID: 27447172 DOI: 10.1007/s00428-016-1990-1]

134 **Lugli A**, Kirsch R, Ajioka Y, Bosman F, Cathomas G, Dawson H, El Zimaity H, Fléjou JF, Hansen TP, Hartmann A, Kakar S, Langner C, Nagtegaal I, Puppa G, Riddell R, Ristimäki A, Sheahan K, Smyrk T, Sugihara K, Terris B, Ueno H, Vieth M, Zlobec I, Quirke P. Recommendations for reporting tumor budding in colorectal cancer based on the International Tumor Budding Consensus Conference (ITBCC) 2016. *Mod Pathol* 2017; **30**: 1299-1311 [PMID: 28548122 DOI: 10.1038/modpathol.2017.46]

135 **Koelzer VH**, Zlobec I, Lugli A. Tumor budding in colorectal cancer--ready for diagnostic practice? *Hum Pathol* 2016; **47**: 4-19 [PMID: 26476568 DOI: 10.1016/j.humpath.2015.08.007]

136 **Lee VWK**, Chan KF. Tumor budding and poorly-differentiated cluster in prognostication in Stage II colon cancer. *Pathol Res Pract* 2018; **214**: 402-407 [PMID: 29487008 DOI: 10.1016/j.prp.2017.12.019]

137 **Ryan É**, Khaw YL, Creavin B, Geraghty R, Ryan EJ, Gibbons D, Hanly A, Martin ST, O'Connell PR, Winter DC, Sheahan K. Tumor Budding and PDC Grade Are Stage Independent Predictors of Clinical Outcome in Mismatch Repair Deficient Colorectal Cancer. *Am J Surg Pathol* 2018; **42**: 60-68 [PMID: 29112018 DOI: 10.1097/PAS.0000000000000931]

138 **Backes Y**, Elias SG, Groen JN, Schwartz MP, Wolfhagen FHJ, Geesing JMJ, Ter Borg F, van Bergeijk J, Spanier BWM, de Vos Tot Nederveen Cappel WH, Kessels K, Seldenrijk CA, Raicu MG, Drillenburg P, Milne AN, Kerkhof M, Seerden TCJ, Siersema PD, Vleggaar FP, Offerhaus GJA, Lacle MM, Moons LMG; Dutch T1 CRC Working Group. Histologic Factors Associated With Need for Surgery in Patients With Pedunculated T1 Colorectal Carcinomas. *Gastroenterology* 2018; **154**: 1647-1659 [PMID: 29366842 DOI: 10.1053/j.gastro.2018.01.023]

139 **Mitrovic B**, Schaeffer DF, Riddell RH, Kirsch R. Tumor budding in colorectal carcinoma: time to take notice. *Mod Pathol* 2012; **25**: 1315-1325 [PMID: 22790014 DOI: 10.1038/modpathol.2012.94]

140 **Grizzi F**, Celesti G, Basso G, Laghi L. Tumor budding as a potential histopathological biomarker in colorectal cancer: hype or hope? *World J Gastroenterol* 2012; **18**: 6532-6536 [PMID: 23236225 DOI: 10.3748/wjg.v18.i45.6532]

141 **Barresi V**, Reggiani Bonetti L, Branca G, Di Gregorio C, Ponz de Leon M, Tuccari G. Colorectal carcinoma grading by quantifying poorly differentiated cell clusters is more reproducible and provides more robust prognostic information than conventional grading. *Virchows Arch* 2012; **461**: 621-628 [PMID: 23093109 DOI: 10.1007/s00428-012-1326-8]

142 **Barresi V**, Branca G, Ieni A, Reggiani Bonetti L, Baron L, Mondello S, Tuccari G. Poorly differentiated clusters (PDCs) as a novel histological predictor of nodal metastases in pT1 colorectal cancer. *Virchows Arch* 2014; **464**: 655-662 [PMID: 24771119 DOI: 10.1007/s00428-014-1580-z]

143 **Ueno H**, Kajiwara Y, Shimazaki H, Shinto E, Hashiguchi Y, Nakanishi K, Maekawa K, Katsurada Y, Nakamura T, Mochizuki H, Yamamoto J, Hase K. New criteria for histologic grading of colorectal cancer. *Am J Surg Pathol* 2012; **36**: 193-201 [PMID: 22251938 DOI: 10.1097/PAS.0b013e318235edee]

144 **Barresi V**, Reggiani Bonetti L, Ieni A, Domati F, Tuccari G. Prognostic significance of grading based on the counting of poorly differentiated clusters in colorectal mucinous adenocarcinoma. *Hum Pathol* 2015; **46**: 1722-1729 [PMID: 26344416 DOI: 10.1016/j.humpath.2015.07.013]

145 **Archilla I**, Díaz-Mercedes S, Aguirre JJ, Tarragona J, Machado I, Rodrigo MT, Lopez-Prades S, Gorostiaga I, Landolfi S, Alén BO, Balaguer F, Castells A, Camps J, Cuatrecasas M. Lymph Node Tumor Burden Correlates With Tumor Budding and Poorly Differentiated Clusters: A New Prognostic Factor in Colorectal Carcinoma? *Clin Transl Gastroenterol* 2021; **12**: e00303 [PMID: 33939382 DOI: 10.14309/ctg.0000000000000303]

146 **Wild JB**, Iqbal N, Francombe J, Papettas T, Sanders DS, Ramcharan S. Is it time for one-step nucleic acid amplification (OSNA) in colorectal cancer? *Tech Coloproctol* 2017; **21**: 693-699 [PMID: 28887714 DOI: 10.1007/s10151-017-1690-0]

147 **Weixler B**, Teixeira da Cunha S, Warschkow R, Demartines N, Güller U, Zettl A, Vahrmeijer A, van de Velde CJH, Viehl CT, Zuber M. Molecular Lymph Node Staging with One-Step Nucleic Acid Amplification and its Prognostic Value for Patients with Colon Cancer: The First Follow-up Study. *World J Surg* 2021; **45**: 1526-1536 [PMID: 33512566 DOI: 10.1007/s00268-020-05949-6]

148 **Viehl CT**, Guller U, Cecini R, Langer I, Ochsner A, Terracciano L, Riehle HM, Laffer U, Oertli D, Zuber M. Sentinel lymph node procedure leads to upstaging of patients with resectable colon cancer: results of the Swiss prospective, multicenter study sentinel lymph node procedure in colon cancer. *Ann Surg Oncol* 2012; **19**: 1959-1965 [PMID: 22322951 DOI: 10.1245/s10434-012-2233-6]

149 **Weixler B**, Rickenbacher A, Raptis DA, Viehl CT, Guller U, Rueff J, Zettl A, Zuber M. Sentinel Lymph Node Mapping with Isosulfan Blue or Indocyanine Green in Colon Cancer Shows Comparable Results and Identifies Patients with Decreased Survival: A Prospective Single-Center Trial. *World J Surg* 2017; **41**: 2378-2386 [PMID: 28508233 DOI: 10.1007/s00268-017-4051-2]

150 **Tanaka S**, Oka S, Chayama K. Colorectal endoscopic submucosal dissection: present status and future perspective, including its differentiation from endoscopic mucosal resection. *J Gastroenterol* 2008; **43**: 641-651 [PMID: 18807125 DOI: 10.1007/s00535-008-2223-4]

151 **Sakuragi M**, Togashi K, Konishi F, Koinuma K, Kawamura Y, Okada M, Nagai H. Predictive factors for lymph node metastasis in T1 stage colorectal carcinomas. *Dis Colon Rectum* 2003; **46**: 1626-1632 [PMID: 14668587 DOI: 10.1007/BF02660767]

152 **Kudo S**. Endoscopic mucosal resection of flat and depressed types of early colorectal cancer. *Endoscopy* 1993; **25**: 455-461 [PMID: 8261988 DOI: 10.1055/s-2007-1010367]

153 **Tanaka S**, Oka S, Kaneko I, Hirata M, Mouri R, Kanao H, Yoshida S, Chayama K. Endoscopic submucosal dissection for colorectal neoplasia: possibility of standardization. *Gastrointest Endosc* 2007; **66**: 100-107 [PMID: 17591481 DOI: 10.1016/j.gie.2007.02.032]

154 **Kouyama Y**, Kudo SE, Miyachi H, Ichimasa K, Hisayuki T, Oikawa H, Matsudaira S, Kimura YJ, Misawa M, Mori Y, Kodama K, Kudo T, Hayashi T, Wakamura K, Katagiri A, Hidaka E, Ishida F, Hamatani S. Practical problems of measuring depth of submucosal invasion in T1 colorectal carcinomas. *Int J Colorectal Dis* 2016; **31**: 137-146 [PMID: 26428364 DOI: 10.1007/s00384-015-2403-7]

155 **deBeche-Adams T**, Hassan I, Haggerty S, Stefanidis D. Transanal Minimally Invasive Surgery (TAMIS): a clinical spotlight review. *Surg Endosc* 2017; **31**: 3791-3800 [PMID: 28656337 DOI: 10.1007/s00464-017-5636-4]

156 **Hiki N**, Nunobe S. Laparoscopic endoscopic cooperative surgery (LECS) for the gastrointestinal tract: Updated indications. *Ann Gastroenterol Surg* 2019; **3**: 239-246 [PMID: 31131352 DOI: 10.1002/ags3.12238]

157 **Buess G**, Kipfmüller K, Hack D, Grüssner R, Heintz A, Junginger T. Technique of transanal endoscopic microsurgery. *Surg Endosc* 1988; **2**: 71-75 [PMID: 3413659 DOI: 10.1007/BF00704356]

158 **Buess G**, Mentges B, Manncke K, Starlinger M, Becker HD. Technique and results of transanal endoscopic microsurgery in early rectal cancer. *Am J Surg* 1992; **163**: 63-9; discussion 69 [PMID: 1733375 DOI: 10.1016/0002-9610(92)90254-o]

159 **Saclarides TJ**, Smith L, Ko ST, Orkin B, Buess G. Transanal endoscopic microsurgery. *Dis Colon Rectum* 1992; **35**:

1183-1191 [PMID: 1473424 DOI: 10.1007/BF02251975]
160 **Lev-Chelouche D**, Margel D, Goldman G, Rabau MJ. Transanal endoscopic microsurgery: experience with 75 rectal neoplasms. *Dis Colon Rectum* 2000; **43**: 662-7; discussion 667 [PMID: 10826428 DOI: 10.1007/BF02235583]
161 **Cataldo PA**. Transanal endoscopic microsurgery. *Surg Clin North Am* 2006; **86**: 915-925 [PMID: 16905416 DOI: 10.1016/j.suc.2006.06.004]
162 **de Graaf EJ**, Burger JW, van Ijsseldijk AL, Tetteroo GW, Dawson I, Hop WC. Transanal endoscopic microsurgery is superior to transanal excision of rectal adenomas. *Colorectal Dis* 2011; **13**: 762-767 [PMID: 20345967 DOI: 10.1111/j.1463-1318.2010.02269.x]
163 **Moore JS**, Cataldo PA, Osler T, Hyman NH. Transanal endoscopic microsurgery is more effective than traditional transanal excision for resection of rectal masses. *Dis Colon Rectum* 2008; **51**: 1026-30; discussion 1030 [PMID: 18481147 DOI: 10.1007/s10350-008-9337-x]
164 **Nascimbeni R**, Burgart LJ, Nivatvongs S, Larson DR. Risk of lymph node metastasis in T1 carcinoma of the colon and rectum. *Dis Colon Rectum* 2002; **45**: 200-206 [PMID: 11852333 DOI: 10.1007/s10350-004-6147-7]
165 **Heidary B**, Phang TP, Raval MJ, Brown CJ. Transanal endoscopic microsurgery: a review. *Can J Surg* 2014; **57**: 127-138 [PMID: 24666451 DOI: 10.1503/cjs.022412]
166 **Kikuchi R**, Takano M, Takagi K, Fujimoto N, Nozaki R, Fujiyoshi T, Uchida Y. Management of early invasive colorectal cancer. Risk of recurrence and clinical guidelines. *Dis Colon Rectum* 1995; **38**: 1286-1295 [PMID: 7497841 DOI: 10.1007/BF02049154]
167 **Choi PW**, Yu CS, Jang SJ, Jung SH, Kim HC, Kim JC. Risk factors for lymph node metastasis in submucosal invasive colorectal cancer. *World J Surg* 2008; **32**: 2089-2094 [PMID: 18553050 DOI: 10.1007/s00268-008-9628-3]
168 **Borschitz T**, Heintz A, Junginger T. Transanal endoscopic microsurgical excision of pT2 rectal cancer: results and possible indications. *Dis Colon Rectum* 2007; **50**: 292-301 [PMID: 17252286 DOI: 10.1007/s10350-006-0816-7]
169 **Hahnloser D**, Wolff BG, Larson DW, Ping J, Nivatvongs S. Immediate radical resection after local excision of rectal cancer: an oncologic compromise? *Dis Colon Rectum* 2005; **48**: 429-437 [PMID: 15747069 DOI: 10.1007/s10350-004-0900-9]
170 **Serra-Aracil X**, Badia-Closa J, Pallisera-Lloveras A, Mora-López L, Serra-Pla S, Garcia-Nalda A, Navarro-Soto S. Management of intra- and postoperative complications during TEM/TAMIS procedures: a systematic review. *Minerva Surg* 2021; **76**: 343-349 [PMID: 33433070 DOI: 10.23736/S2724-5691.20.08405-9]
171 **Dighe S**, Purkayastha S, Swift I, Tekkis PP, Darzi A, A'Hern R, Brown G. Diagnostic precision of CT in local staging of colon cancers: a meta-analysis. *Clin Radiol* 2010; **65**: 708-719 [PMID: 20696298 DOI: 10.1016/j.crad.2010.01.024]
172 **Choi AH**, Nelson RA, Schoellhammer HF, Cho W, Ko M, Arrington A, Oxner CR, Fakih M, Wong J, Sentovich SM, Garcia-Aguilar J, Kim J. Accuracy of computed tomography in nodal staging of colon cancer patients. *World J Gastrointest Surg* 2015; **7**: 116-122 [PMID: 26225194 DOI: 10.4240/wjgs.v7.i7.116]
173 **Slama J**, Dundr P, Dusek L, Cibula D. High false negative rate of frozen section examination of sentinel lymph nodes in patients with cervical cancer. *Gynecol Oncol* 2013; **129**: 384-388 [PMID: 23395889 DOI: 10.1016/j.ygyno.2013.02.001]
174 **Balasubramanian SP**, Harrison BJ. Systematic review and meta-analysis of sentinel node biopsy in thyroid cancer. *Br J Surg* 2011; **98**: 334-344 [PMID: 21246517 DOI: 10.1002/bjs.7425]
175 **Hyslop T**, Waldman SA. Molecular staging of node negative patients with colorectal cancer. *J Cancer* 2013; **4**: 193-199 [PMID: 23459453 DOI: 10.7150/jca.5830]
176 **Melfi FM**, Lucchi M, Davini F, Viti A, Fontanini G, Boldrini L, Boni G, Mussi A. Intraoperative sentinel lymph node mapping in stage I non-small cell lung cancer: detection of micrometastases by polymerase chain reaction. *Eur J Cardiothorac Surg* 2008; **34**: 181-186 [PMID: 18502662 DOI: 10.1016/j.ejcts.2008.03.059]
177 **Miyashiro I**, Hiratsuka M, Sasako M, Sano T, Mizusawa J, Nakamura K, Nashimoto A, Tsuburaya A, Fukushima N; Gastric Cancer Surgical Study Group (GCSSG) in the Japan Clinical Oncology Group (JCOG). High false-negative proportion of intraoperative histological examination as a serious problem for clinical application of sentinel node biopsy for early gastric cancer: final results of the Japan Clinical Oncology Group multicenter trial JCOG0302. *Gastric Cancer* 2014; **17**: 316-323 [PMID: 23933782 DOI: 10.1007/s10120-013-0285-3]
178 **Daraï E**, Dubernard G, Bats AS, Heitz D, Mathevet P, Marret H, Querleu D, Golfier F, Leblanc E, Rouzier R, Ballester M. Sentinel node biopsy for the management of early stage endometrial cancer: long-term results of the SENTI-ENDO study. *Gynecol Oncol* 2015; **136**: 54-59 [PMID: 25450151 DOI: 10.1016/j.ygyno.2014.09.011]
179 **Zhou M**, Wang X, Jiang L, Chen X, Bao X. The diagnostic value of one step nucleic acid amplification (OSNA) in differentiating lymph node metastasis of tumors: A systematic review and meta-analysis. *Int J Surg* 2018; **56**: 49-56 [PMID: 29753955 DOI: 10.1016/j.ijsu.2018.05.010]
180 **Balagué C**, Pallarés JL. Preoperative and Intraoperative Lymphatic Mapping for Radioguided Sentinel Node Biopsy in Cancers of the Gastrointestinal Tract. In: Mariani G, Manca G, Orsini F, Vidal-Sicart S, Valdés Olmos RA. Atlas of Lymphoscintigraphy and Sentinel Node Mapping. Milano: Springer, 2013 [DOI: 10.1007/978-88-470-2766-4_13]
181 **Kusano M**, Ono H, Danjo Y, Kawamata F, Tajima Y, Ohtsubo S, Shimada S, Koyanagi K. Fluorescent Navigation Surgery for Gastrointestinal Tract Cancers: Detection of Sentinel Nodes, Tumor Tattooing, and Harvesting of Lymph Nodes. In: Kusano M, Kokudo N, Toi M, Kaibori M. ICG Fluorescence Imaging and Navigation Surger. Tokyo: Springer, 2016 [DOI: 10.1007/978-4-431-55528-5_14]
182 **Carrara A**, Motter M, Amabile D, Pellecchia L, Moscatelli P, Pertile R, Barbareschi M, Decarli NL, Ferrari M, Tirone G. Predictive value of the sentinel lymph node procedure in the staging of non-metastatic colorectal cancer. *Int J Colorectal Dis* 2020; **35**: 1921-1928 [PMID: 32556650 DOI: 10.1007/s00384-020-03654-3]
183 **Tranoulis A**, Georgiou D, Yap J, Attard-Montalto S, Twigg J, Elattar A, Singh K, Balega J, Kehoe S. The evolving role of one-step nucleic acid amplification (OSNA) for the intra-operative detection of lymph node metastases: A diagnostic accuracy meta-analysis. *Eur J Surg Oncol* 2021; **47**: 1233-1243 [PMID: 33309549 DOI: 10.1016/j.ejso.2020.12.001]
184 **Marhic A**, Tremblay JF, Kaci R, André T, Eveno C, Pocard M. Molecular analysis of sentinel lymph node in colon carcinomas by one-step nucleic acid amplification (OSNA) reduces time to adjuvant chemotherapy interval. *Dig Liver Dis* 2017; **49**: 924-928 [PMID: 28668271 DOI: 10.1016/j.dld.2017.05.017]

185 **Otero de Pablos J**, Mayol J. Controversies in the Management of Lateral Pelvic Lymph Nodes in Patients With Advanced Rectal Cancer: East or West? *Front Surg* 2019; **6**: 79 [PMID: 32010707 DOI: 10.3389/fsurg.2019.00079]

186 **Sugihara K**, Kobayashi H, Kato T, Mori T, Mochizuki H, Kameoka S, Shirouzu K, Muto T. Indication and benefit of pelvic sidewall dissection for rectal cancer. *Dis Colon Rectum* 2006; **49**: 1663-1672 [PMID: 17041749 DOI: 10.1007/s10350-006-0714-z]

187 **Akiyoshi T**, Watanabe T, Miyata S, Kotake K, Muto T, Sugihara K; Japanese Society for Cancer of the Colon and Rectum. Results of a Japanese nationwide multi-institutional study on lateral pelvic lymph node metastasis in low rectal cancer: is it regional or distant disease? *Ann Surg* 2012; **255**: 1129-1134 [PMID: 22549752 DOI: 10.1097/SLA.0b013e3182565d9d]

188 **Numata M**, Shiozawa M, Godai T, Kazama K, Okamoto H, Kato A, Katayama Y, Sato S, Sugano N, Kohmura T, Higuchi A, Saito K, Iguchi K, Atsumi Y, Aoyama T, Tamagawa H, Mushiake H, Saeki H, Yukawa N, Taguri M, Sato M, Rino Y. Prediction of lateral lymph node metastasis using OSNA method for mesorectal lymph nodes in low rectal cancer: A prospective study by the Kanagawa Yokohama Colorectal Cancer Study Group (KYCC1801). *J Surg Oncol* 2022; **125**: 457-464 [PMID: 34704609 DOI: 10.1002/jso.26730]

189 **Sammour T**, Chang GJ. Lateral pelvic lymph node dissection and radiation treatment for rectal cancer: Mutually exclusive or mutually beneficial? *Ann Gastroenterol Surg* 2018; **2**: 348-350 [PMID: 30238075 DOI: 10.1002/ags3.12197]

190 **Yanagita S**, Uenosono Y, Arigami T, Kita Y, Mori S, Natsugoe S. Utility of the sentinel node concept for detection of lateral pelvic lymph node metastasis in lower rectal cancer. *BMC Cancer* 2017; **17**: 433 [PMID: 28629335 DOI: 10.1186/s12885-017-3408-0]

191 **Noura S**, Ohue M, Miyoshi N. Sentinel Node Navigation Surgery for Rectal Cancer: Indications for Lateral Node Dissection. In: Kusano M, Kokudo N, Toi M, Kaibori M. ICG Fluorescence Imaging and Navigation Surgery. Tokyo: Springer, 2016 [DOI: 10.1007/978-4-431-55528-5_15]

192 **Yasui M**, Ohue M, Noura S, Miyoshi N, Takahashi Y, Matsuda C, Nishimura J, Haraguchi N, Ushigome H, Nakai N, Fujino S, Sugimura K, Wada H, Takahashi H, Omori T, Miyata H. Exploratory analysis of lateral pelvic sentinel lymph node status for optimal management of laparoscopic lateral lymph node dissection in advanced lower rectal cancer without suspected lateral lymph node metastasis. *BMC Cancer* 2021; **21**: 911 [PMID: 34380428 DOI: 10.1186/s12885-021-08480-6]

193 **Miyake Y**, Mizushima T, Hata T, Takahashi H, Hanada H, Shoji H, Nomura M, Haraguchi N, Nishimura J, Matsuda C, Takemasa I, Doki Y, Maeda I, Mori M, Yamamoto H. Inspection of Perirectal Lymph Nodes by One-Step Nucleic Acid Amplification Predicts Lateral Lymph Node Metastasis in Advanced Rectal Cancer. *Ann Surg Oncol* 2017; **24**: 3850-3856 [PMID: 28924845 DOI: 10.1245/s10434-017-6069-y]

194 **Glynne-Jones R**, Wyrwicz L, Tiret E, Brown G, Rödel C, Cervantes A, Arnold D; ESMO Guidelines Committee. Rectal cancer: ESMO Clinical Practice Guidelines for diagnosis, treatment and follow-up. *Ann Oncol* 2017; **28**: iv22-iv40 [PMID: 28881920 DOI: 10.1093/annonc/mdx224]

195 **Ogawa S**, Hida J, Ike H, Kinugasa T, Ota M, Shinto E, Itabashi M, Okamoto T, Sugihara K. The important risk factor for lateral pelvic lymph node metastasis of lower rectal cancer is node-positive status on magnetic resonance imaging: study of the Lymph Node Committee of Japanese Society for Cancer of the Colon and Rectum. *Int J Colorectal Dis* 2016; **31**: 1719-1728 [PMID: 27576475 DOI: 10.1007/s00384-016-2641-3]

196 **Takahashi T**, Ueno M, Azekura K, Ohta H. Lateral node dissection and total mesorectal excision for rectal cancer. *Dis Colon Rectum* 2000; **43**: S59-S68 [PMID: 11052480 DOI: 10.1007/BF02237228]

197 **Numata M**, Yamaguchi T, Kinugasa Y, Shiomi A, Kagawa H, Yamakawa Y, Furutani A, Manabe S, Yamaoka Y. Index of Estimated Benefit from Lateral Lymph Node Dissection for Middle and Lower Rectal Cancer. *Anticancer Res* 2017; **37**: 2549-2555 [PMID: 28476826 DOI: 10.21873/anticanres.11598]

198 OSNA for colon cancer staging-medtech innovation briefing (MIB77). 2016 Aug 24 [cited 26 February 2022]. In: National Institute for Health and Care Excellence. Available from: https://www.nice.org.uk/advice/mib77

199 **Guillén-Paredes MP**, Carrasco-González L, Cháves-Benito A, Campillo-Soto A, Carrillo A, Aguayo-Albasini JL. [One-step nucleic acid amplification (OSNA) assay for sentinel lymph node metastases as an alternative to conventional postoperative histology in breast cancer: A cost-benefit analysis]. *Cir Esp* 2011; **89**: 456-462 [PMID: 21664607 DOI: 10.1016/j.ciresp.2011.04.013]

200 **Cutress RI**, McDowell A, Gabriel FG, Gill J, Jeffrey MJ, Agrawal A, Wise M, Raftery J, Cree IA, Yiangou C. Observational and cost analysis of the implementation of breast cancer sentinel node intraoperative molecular diagnosis. *J Clin Pathol* 2010; **63**: 522-529 [PMID: 20439323 DOI: 10.1136/jcp.2009.072942]

201 **Yaguchi Y**, Sugasawa H, Tsujimoto H, Takata H, Nakabayashi K, Ichikura T, Ono S, Hiraki S, Sakamoto N, Horio T, Kumano I, Otomo Y, Mochizuki H, Yamamoto J, Hase K. One-step nucleic acid amplification (OSNA) for the application of sentinel node concept in gastric cancer. *Ann Surg Oncol* 2011; **18**: 2289-2296 [PMID: 21301968 DOI: 10.1245/s10434-011-1591-9]

202 **Cserni G**. Intraoperative analysis of sentinel lymph nodes in breast cancer by one-step nucleic acid amplification. *J Clin Pathol* 2012; **65**: 193-199 [PMID: 22090341 DOI: 10.1136/jclinpath-2011-200301]

203 **Peigné L**, Godey F, Le Gallo M, Le Gall F, Fautrel A, Morcet J, Jégoux F. One-step nucleic acid amplification for detecting lymph node metastasis of head and neck squamous cell carcinoma. *Oral Oncol* 2020; **102**: 104553 [PMID: 32004908 DOI: 10.1016/j.oraloncology.2019.104553]

World Journal of Gastroenterology

Submit a Manuscript: https://www.f6publishing.com

World J Gastroenterol 2022 August 14; 28(30): 4044-4052

DOI: 10.3748/wjg.v28.i30.4044

ISSN 1007-9327 (print) ISSN 2219-2840 (online)

MINIREVIEWS

Current perspectives on the role of liver transplantation for Langerhans cell histiocytosis: A narrative review

Jagadeesh Menon, Ashwin Rammohan, Mukul Vij, Naresh Shanmugam, Mohamed Rela

Specialty type: Transplantation

Provenance and peer review: Invited article; Externally peer reviewed.

Peer-review model: Single blind

Peer-review report's scientific quality classification

Grade A (Excellent): A
Grade B (Very good): 0
Grade C (Good): C, C
Grade D (Fair): 0
Grade E (Poor): 0

P-Reviewer: Guo WZ, China; Hashimoto K, Japan; Saito R, Japan

Received: January 9, 2022
Peer-review started: January 9, 2022
First decision: March 8, 2022
Revised: March 30, 2022
Accepted: July 19, 2022
Article in press: July 19, 2022
Published online: August 14, 2022

Jagadeesh Menon, Ashwin Rammohan, Mukul Vij, Naresh Shanmugam, Mohamed Rela, Institute of Liver Disease & Transplantation, Dr. Rela Institute & Medical Centre, Bharath Institute of Higher Education & Research, Chennai 600044, India

Corresponding author: Ashwin Rammohan, FACS, FRCS, MCh, Attending Doctor, Institute of Liver Disease & Transplantation, Dr. Rela Institute & Medical Centre, Bharath Institute of Higher Education & Research, CLC Works Road, Chromepet, Chennai 600044, India. ashwinrammohan@gmail.com

Abstract

Langerhans cell histiocytosis (LCH) is a malignant disease of the histiocytes involving various organ systems. The spectrum of liver involvement in LCH ranges from mild transaminitis to end-stage liver disease. The hallmark of hepatic LCH is secondary sclerosing cholangitis, which manifests due to a progressive destruction of the biliary tree by malignant histiocytes. Chemotherapy remains the mainstay of treatment for active LCH. Early recognition, diagnosis and a systematic approach to the management of LCH can ameliorate the disease process. Nonetheless, the liver involvement in these patients may progress despite the LCH being in remission. Liver transplantation (LT) remains central in the management of such patients. Various facets of the management of LCH, especially those with liver involvement remain unclear. Furthermore, aspects of LT in LCH with regards to the indication, timing and post-LT management, including immunosuppression and adjuvant therapy, remain undefined. This review summarises the current evidence and discusses the practical aspects of the role of LT in the management of LCH.

Key Words: Langerhans cell histiocytosis; Liver transplantation; Outcomes; Management; Chemotherapy; Ethics

©The Author(s) 2022. Published by Baishideng Publishing Group Inc. All rights reserved.

Core Tip: Involvement of the liver in Langerhans cell histiocytosis (LCH) is considered a high-risk disease and the management algorithm needs to factor in the malignancy and the severity of liver disease. Liver transplantation (LT) is usually offered to LCH patients in remission with decompensated liver disease. However, given the paucity of currently available literature, the role of LT in LCH remains undefined. There is hence a need for large collaborative, multicentre studies to provide recommendations on the management algorithm for LCH.

Citation: Menon J, Rammohan A, Vij M, Shanmugam N, Rela M. Current perspectives on the role of liver transplantation for Langerhans cell histiocytosis: A narrative review. *World J Gastroenterol* 2022; 28(30): 4044-4052
URL: https://www.wjgnet.com/1007-9327/full/v28/i30/4044.htm
DOI: https://dx.doi.org/10.3748/wjg.v28.i30.4044

INTRODUCTION

Langerhans cell histiocytosis (LCH) is a malignant disease of the histiocytes involving various organ systems including the liver, spleen, skin, bone, lymph nodes, lung, and the gastrointestinal tract[1]. Involvement of the liver in LCH occurs in many ways. The spectrum ranges from mild transaminitis to end-stage liver disease (ESLD). The hallmark of hepatic LCH is secondary sclerosing cholangitis (SSC), which manifests due to a progressive destruction of the biliary tree by malignant histiocytes[2]. Chemotherapy remains the mainstay of treatment for active LCH[3]. However, conventionally used vinblastine-based chemotherapy may not be tolerated by patients with concomitant liver involvement and modified regimens which balance the risk of liver decompensation with the oncological efficacy need to be instituted[3,4].

By the time the bile duct injury presents clinically, the primary disease is usually burnt out and the characteristic histiocytes are absent. ESLD and portal hypertension develop as a sequalae of SSC[5]. These patients are offered liver transplantation (LT) with an intent to cure the liver damage[6,7]. Various facets of the management of LCH, especially those with a liver involvement remain unclear. Furthermore, aspects of LT in LCH with regards to the indication, timing and post-LT management, including immunosuppression and adjuvant therapy, remain undefined. This review summaries the current evidence and discuss the practical aspects of the role of LT in the management of LCH.

LIVER INVOLVEMENT IN LCH

Liver is involved in 20%-60% of patients with LCH and is more common when there is multiorgan involvement[2]. LCH-related liver disease is conventionally divided into two stages: Early infiltrative and late sclerosis[8]. The early stage is characterised by reactions elicited by the malignant histiocytes and other inflammatory cells, manifesting as periportal infiltration and hepatic nodular lesions. In the late fibrous stage, progressive destruction of biliary tree occurs resulting in cirrhosis and portal hypertension[8,9].

Hepatic involvement as defined by the European Consortium for Histiocytosis includes a palpable liver 3 cm below the coastal margin confirmed by ultrasound and liver dysfunction as defined by hyperbilirubinemia (at least 3 times the upper limit of normal) hypoalbuminemia (< 30 g/dL) , alanine transaminase (ALT) and/or aspartate transaminase (AST) (more than 3 times the upper limit of normal), -glutamyl transpeptidase (GGT) over twice the upper limit of normal, ascites, oedema, or intrahepatic nodular mass[3]. Sclerosing cholangitis in LCH is defined as involvement of extrahepatic/intrahepatic biliary tree with strictures, dilatation, pruning detected on imaging (computed tomography or magnetic resonance imaging) and/or on liver biopsy with or without elevated GGT[10,11]. The characteristic features of bile duct injury can be detected by magnetic resonance cholangiopancreatography. It is noteworthy that despite resolution of active malignancy, the biliary injury continues to progress. The major site of LCH involvement is the large bile duct, and hence sites of active disease may be missed on liver biopsy[8].

With a mortality risk of over three times that of patients without liver involvement, hepatic LCH is considered a high-risk disease. In a study of patients with LCH, liver involvement drastically reduced survival from 97% to 52%[12]. SSC may be observed in up to 20%, which invariably progress to ESLD requiring LT[13]. It is noteworthy that an acute hepatic involvement by active LCH may be reversible with timely instituted chemotherapy[12]. Later stages and/or burnt out disease on the other hand may continue to have worsening liver injury. Furthermore, this progression of SSC is more rapid than what is observed in primary sclerosing cholangitis[14]. In a series of adults with LCH, nearly 30% died due to complications of SSC and ESLD[14].

LIVER PATHOLOGY IN LCH

LCH exhibit diverse morphological features in the liver, which vary depending on the phase, stage and activity of the disease. Aggregates of LCs having lobulated, coffee-bean-shaped or contorted nuclei with a fine chromatin pattern and abundant eosinophilic cytoplasm admixed with eosinophils, polymorphs, lymphocytes, plasma cells, non-Langerhans histiocytes and rare multinucleated giant cells forming masses of variable sizes have been described (Figure 1A). Most cases with hepatic infiltration show marked tropism of the bile ducts. Active infiltrations of the bile ducts cause mucosal injury and fibrosis that lead to a progressive pattern of SSC, ultimately resulting in biliary cirrhosis[11,15,16]. There is destruction of the walls of bile ducts which may lead to cystic dilatation with intraluminal biliary sludge and rupture (Figure 1B). LCs can be identified within the basement membrane of the bile ducts, displacing the epithelial cells off the wall. Many cases demonstrate concentric periductal fibrosis. Cholangiopathy causes periportal bile ductular proliferation (Figure 1C), duct loss (Figure 1D), and features of chronic cholestasis with periportal cholestasis and stainable granules of copper and copper-binding protein. It is important to note that, despite evidence of biliary damage, the characteristic LCs may not be detected on liver biopsy. The diagnosis then rests on the presence of a concomitant infiltrate in other sites. Reassuringly, examination of liver explants in patients with LCH-induced biliary cirrhosis usually shows no evidence of active disease[17].

CHEMOTHERAPEUTIC AGENTS IN LCH

Liver, bone marrow and spleen are defined as the high-risk organs and their involvement makes the prognosis worse in patients with LCH[3]. The standard chemotherapy regimen for high-risk LCH as per the LCH IV protocol includes an induction phase of 6 wk with vinblastine (6 mg/m^2) once weekly for 6 wk and prednisolone (40 mg/m^2/d) daily for 4 wk, tapered over the next 2 wk[3,18]. LCH is invariably avid on positron emission tomography (PET), and presence of active disease can easily be ascertained. At the end of 6 wk, a PET scan is recommended, and the maintenance phase of therapy is commenced only after confirmed remission of LCH. Nonresponders conventionally receive another 6-wk cycle of the same regimen. If after the second cycle, remission is not achieved, second-line salvage chemotherapeutic agents are used[3,18].

Maintenance-phase therapy consists of vinblastine (6 mg/m^2) given once in 3 wk along with prednisolone (40 mg/m^2/d) for 5 d in the same week for 1 year. A few other drugs have been tried with doubtful benefit. These include methotrexate, fludarabine, 6-mercaptopurine, cyclophosphamide and etoposide[17,19]. Clinical trials have shown that newer targeted agents like BRAF inhibitors (see below) have shown promise in achieving remission in patients with refractory disease[20].

LT FOR LCH

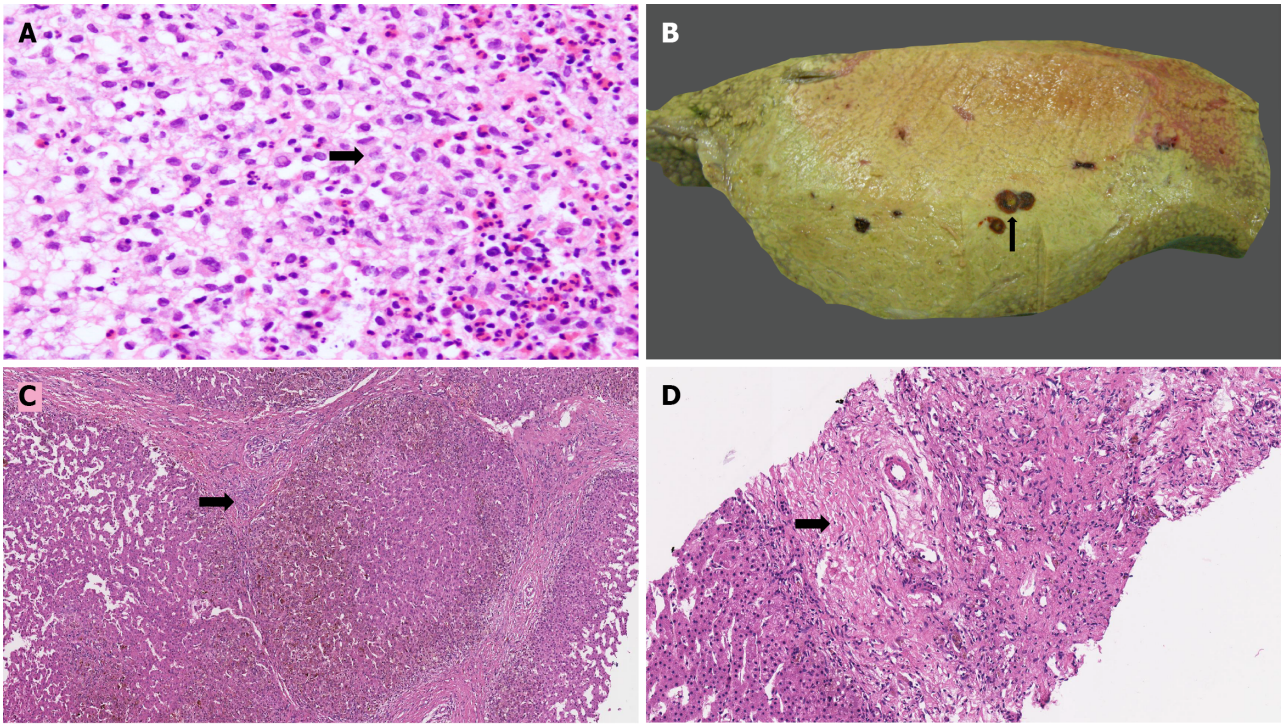
In contrast to other hepatic malignancies like hepatoblastomas or haematological cancers, hepatic involvement in LCH is unique. While the latter result in cirrhosis progressing to ESLD, the former do not. Hence management of LCH with liver involvement needs a meticulous balance of two major decision domains, *i.e.*, malignancy and ESLD.

In patients who have normal liver function, standard chemotherapeutic regimens (vinca alkaloids and steroids) can be safely used. However, in those with features of decompensated liver disease (DCLD) and/or synthetic failure, these drugs can result in serious adverse effects. Vinblastine is inherently hepatotoxic and can worsen liver dysfunction[16,21,22]. Also, since vinblastine is metabolised in the liver, a failing liver could lead to severe drug-related toxicity (peripheral neuropathy, myelosuppression, *etc.*)[16,21,22]. Nonetheless, a delay in initiating chemotherapy for the fear of compromising liver function potentially worsens the malignant process. Deferring LT may result in morbidity and morbidity from cirrhosis and decompensation[13]. However, premature LT in the presence of active malignancy is not a standard recommended practice, and risks recurrent LCH in the graft.

The oncologist and the transplant clinician are faced with four clinical scenarios in patients who have LCH with liver involvement. These include patients with CLD and LCH in remission, patients with DCLD and LCH in remission, those with CLD and active LCH, and lastly, those with DCLD and active LCH.

Compensated liver disease with LCH in remission

These are a subset of patients who have completed chemotherapy and have the disease in remission. As mentioned above, they could still have progressive liver disease as sequalae of LCH. It could be many years before they present with symptoms of liver disease, which may be in the form of cirrhosis and/portal hypertension[23]. LT is offered to these patients independent of their previous history of LCH. Apart from decompensation, other indications for LT in these patients include, portal



DOI: 10.3748/wjg.v28.i30.4044 **Copyright** ©The Author(s) 2022.

Figure 1 Langerhans cell histiocytosis exhibit diverse morphological features in the liver. A: Aggregates of Langerhans cells admixed with inflammatory cells (arrow, H&E, 40 ×); B: Explant liver with dilated bile ducts and sludge (arrow); C: Liver wedge biopsy with evolving biliary cirrhosis and mild peripheral bile ductular proliferation (arrow, H&E, 20 ×); D: Liver biopsy with ductopenia (arrow, H&E, 40 ×).

hypertension, intractable pruritus and growth retardation. Nonetheless, irrespective of the lag-time between LCH remission and LT, prior to LT, a PET scan is performed to confirm the absence of active LCH.

Decompensated liver disease with LCH in remission

When indicated, LT may be performed in these patients. Evidence shows that the post-LT outcomes including disease-free survival in these patients is similar to those who have undergone LT for other indications[7].

Compensated liver disease with active LCH

Standard chemotherapeutic regimens (vinca alkaloid based) directed at LCH treatment should be initiated after appropriate staging workup for the disease. If the liver does not show signs of decompensation, patients should complete the full course of chemotherapy (induction and maintenance)[3]. They should however remain on close follow-up for LCH remission, signs of worsening of the liver disease and consequently the need for LT. The total duration of 12 mo chemotherapy is recommended in patients with LCH and an LT is offered after a minimum interval of 3 wk, when indicated[3]. The need for adjuvant chemotherapy in these patients is debatable, and a decision is usually made on a case-by-case basis. There may be a situation wherein the liver decompensates after initiating chemotherapy. In these patients, the severity of liver decompensation and the state of LCH remission guides further course of management.

In patients where the liver decompensation can be managed supportively, chemotherapy is continued with an aim to achieve remission. In this case however, the chemotherapy needs to be switched to relatively nonhepatoxic agents like cytarabine[24]. Once remission is confirmed following induction chemotherapy, these patients may be offered LT. It is nonetheless imperative to complete the full chemotherapeutic course. A chemotherapy-free interval of at least 3 wk is recommended prior to LT. This helps reduce the risk of chemotherapy-related damage to the liver allograft. Evidence is divisive with regards to the timing, dosing and regimen of post-LT chemotherapy. It is nonetheless unequivocally clear that the maintenance phase of chemotherapy needs to be completed. The agents are reintroduced usually 3 wk following LT. This allows for the transplanted liver to cope with the toxic agents better. Furthermore, it is advisable to reintroduce vinca alkaloids when the bilirubin is near normal (< 3 mg/dL)[22].

Decompensated liver disease with active LCH

Striking the balance between achieving remission with chemotherapy, abating worsening liver dysfunction and postponing LT remains a challenge in the management of these patients. The prudent approach would be to attempt achieving remission with relatively nonhepatotoxic, low-dose chemotherapy. Should this be achieved, as mentioned above, LT may be offered following a negative PET scan. A rarer and unfortunate situation is when a patient with active LCH requires LT. While LT may not be justified as per protocol, these are exceptional situations requiring a multi-disciplinary team decision.

ETHICS OF LT IN LCH

LCH is a malignancy; therefore, before offering these patients LT, the ethical aspects need to be debated. Immunosuppressants mute the native immune system's antitumour action, potentially resulting in a higher risk of recurrence. Furthermore, the ideal latency period between disease remission and LT remains undefined. There are also data to suggest that in patients with DCLD, delaying LT may result in worse outcomes[9]. Hence, for selected patients with DCLD, potential benefit and risk must be evaluated on an individual basis[25]. It does however, seem reasonable to indicate LT only when the oncological probability of survival disregarding immunosuppression is at least 50% at 5 years. The caveat in these cases is that the LCH should be amenable to sustained remission prior to LT and there should always remain the option of post-LT adjuvant therapy. Living donor LT (LDLT), especially in regions where deceased donor LT (DDLT) is uncommonly performed, permits optimal timing of the LT and avoidance of delays between the end of chemotherapy and LT.

LCH is a relatively rare oncological condition, and despite advances in medical oncology, there are few approved chemotherapeutic agents and even fewer clinical trials in this regard. An ethical dilemma also arises when despite chemotherapy, disease remission cannot be achieved in patients with DCLD. This subgroup of patients along with those who have active LCH and urgently require LT are outliers who need to have their management tailored according to the disease state; ideally in a clinical trial setting.

Nonetheless, prior to offering LT, it is imperative to satisfy the time-tested tenets of justice, utility and normal feasance for DDLT, and that of balancing the donor risk *versus* recipient benefit (principle of double equipoise) in living donor LT.

OUTCOMES OF LT IN LCH

Paediatric transplant oncology is a niche area that aims at optimising post-LT oncological outcomes. Given that LCH is a rare oncological condition, the literature remains sparse. Earlier series of LCH noted a recurrence of 30%-55% with a patient survival of 60%–67%[26,27]. With advances in immunosuppression, chemotherapeutic agents, and a better understanding of the oncopathology, more recent series including ours, have shown remarkably improved outcomes which are on par with LT for other indications[7,28] (Table 1). In a recent meta-analysis of 60 LT recipients with LCH, the 1-year, 3-year and 5-year patient survival rates were 86.6%, 82.4%, and 82.4%, respectively[25]. Furthermore, a cumulative recurrence of LCH in the grafts was 8%[25].

OUR UNIT POLICY AND OUTCOMES

We offer LT in patients with acute decompensation, portal hypertension with sclerosing cholangitis or growth retardation or intractable pruritus. If any patient decompensates in between chemotherapy, a LT is offered, following which the chemotherapy cycles are completed. A 18-fluorodeoxyglucose (FDG)-PET scan is mandatorily done before considering a LT in these patients. Patients who do not tolerate the full course of chemotherapy are also considered for LT during mid-cycle if the FDG-PET shows disease in remission. An interval of 2-3 wk is considered between the chemotherapy cycle and LT. This is followed by restarting of chemotherapy (if the cycles are not completed prior to surgery) after 3 wk.

Our unit's protocol includes the use of standard chemotherapy regimen in patients who are likely to withstand the full course. We use a modified chemotherapy in patients with liver dysfunction. This regimen includes low-dose cytarabine (100 mg/m^2) every 3 wk along with prednisolone (40 mg/m^2/d) daily for 4 wk tapered over the next 2 wk (each cycle is of 6 wk duration). Maintenance chemotherapy includes the same dose of cytarabine and prednisolone as the standard regimen, administered for 1 year. In our experience of six patients who underwent a LDLT, all are alive after mean follow up 36 mo (18-80 mo).

Table 1 Liver transplantation for Langerhan cell histiocytosis

Author (year)	No. of patients	Age at diagnosis (mo)	Age at transplant (mo)	Immunosuppression (No. of patients)	Surgical complications (No. of patients)	Medical complications (No. of patients)	Survival (follow-up in mo)
Stieber (1990)	3 (1adult/2 paediatric)	-	-	Cyclosporine, steroid	-	Recurrent rejection (3); retransplant (2)	66% (1 adult died of long bone fracture)
Whitington (1992)	2 (paediatric)	36 & 19	60 & 30	Cyclosporine, steroid	Roux-en Y anastomotic leak	CMV hepatitis (2); rejection (2); GI bleed (1)	100% (30-34)
Zandi (1995)	5 (paediatric)	23 ± 13	151 ± 43	Cyclosporine, steroid, azathioprine (3); cyclosporine, steroid (1); OKT3, steroid (1)	-	Rejection (4); CMV infection (2); GI bleed (1); Kidney injury (1)	60% (0.25-88.00)
Newell (1997)	6 (paediatric)	15 (12-30)	36	Cyclosporine, steroid, azathioprine (6)	Nil	PTLD (4); rejection (6); retransplantation (4); recurrence (2)	67% (24-74)
Hazdic (2000)	2 (paediatric)	16 & 17	34 & 14	Cyclosporine, steroid, MMF (1); tacrolimus, steroid (1)	Bowel perforation due to PTLD (1); PVT (1)	Recurrence (2); PTLD (1); rejection (2)	100% (5 & 60)
Braier (2002)	5 (paediatric)	-	-	Cyclosporine, steroid, azathioprine (5)	HAT & Retransplant (1)	CMV (1); rejection (1)	60% (14-37)
Chen (2020)	5 (paediatric)	15 (13-28)	53 (24-81)	Tacrolimus, steroid, MMF (5)	HAT (1)	EBV (4), CMV (1); LCH recurrence (1); DILI (1)	100%: 32 (2-67)
Our experience	6 (paediatric)	25 (9-48)	52.5 (33-204)	Tacrolimus, steroid (6)	Nil	Nil	100%: 36 (18-80)

CMV: Cytomegalovirus; GI: Gastrointestinal; MMF: Mycophenolate mofetil; EBV: Epstein–Barr virus; HAT: Hepatic artery thrombosis.

POST-LT COMPLICATIONS

Patients transplanted for LCH are known to have a higher incidence of rejections and post-transplant lymphoproliferative disorder (PTLD) (0%-67%)[7,8,27]. A purported theory is that of increased release of proinflammatory cytokines from the neoplastic cells predisposing to rejection. There remain concerns that immunosuppression could potentially increase risk an early recurrence of the index cancer, making LT futile. Hence the relative hesitancy at increasing immunosuppression in the early experiences of LT in LCH. There is no evidence till for the role of the mechanistic target of rapamycin inhibitors like sirolimus for preventing the occurrence of PTLD in these patients.

FUTURE DIRECTIONS

There is some encouraging evidence on the use of targeted therapy in LCH refractory to standard chemotherapy. *BRAF* gene mutations are observed in up to 67% of patients with LCH[29]. Vemurafenib and dabrafenib are two such agents that have shown potential in the clinical trial settings. Vemurafenib showed 83% response rate in refractory LCH[30]. In another trial of children with refractory LCH, 65% showed a remission with dabrafenib[31]. While vemurafenib may be hepatotoxic, dabrafenib is safe in patients with liver disease[32]. The authors concluded, that these agents may be used as the second- or third-line therapy for patients with refractory LCH and DCLD.

Another target for such novel therapy is the MEK1 mutation. It is observed in 19% of patients with LCH. Cobimetinib and trametinib are MEK1 inhibitors, and have shown some promise in clinical trials [33]. There however, remains a need for further research especially in those with concomitant liver disease to assess the true efficacy of these novel agents.

There have been studies evaluating the role of PD-1 (programmed cell death-1)/PD-L1 (programmed cell death ligand-1) check points in pathogenesis of LCH, especially when it involves the musculoskeletal system[34]. Hence anti PD-1 immunotherapy (pembrolizumab/nivolumab) may have a role in treating patients of LCH if there is an active musculoskeletal disease[35,36]. The role of anti-PD-1-based immunotherapy in the post-LT population remains a matter of intense debate. Given that these drugs act primarily by potentiating the native immune response, there have been studies demonstrating a high likelihood of rejections and allograft loss[37]. Therefore, the indications of anti PDL-1 therapy in the LCH patients who are likely to need LT remains undefined.

CONCLUSION

Early recognition, diagnosis and a systematic approach to the management of LCH can ameliorate the disease process. Nonetheless, the liver involvement in these patients may progress despite the LCH in remission. LT remains the mainstay in the management of such patients. Over the last decade significant advances in immunosuppression protocols, and availability of effective chemotherapeutic agents, have translated into better long-term allograft and recurrence-free patient survival. The post-LT outcomes are now comparable with those for other indications. However, given the rarity of the disease and the paucity of currently available literature, there is a need for large collaborative international, multicentre, society-based studies to provide recommendations on evidence-based algorithm for LCH, especially in patients with liver involvement.

FOOTNOTES

Author contributions: Menon J, Rammohan A, and Shanmugam N contributed to conception and design; Rammohan A, Menon J, and Rela M contributed to the acquisition, analysis, and interpretation of data; Menon J, Rammohan A, Vij M, and Shanmugam N drafted the article, and revised it critically for important intellectual content; Rela M gave the final approval of the version to be published.

Conflict-of-interest statement: There are no conflicts of interest to report.

Open-Access: This article is an open-access article that was selected by an in-house editor and fully peer-reviewed by external reviewers. It is distributed in accordance with the Creative Commons Attribution NonCommercial (CC BY-NC 4.0) license, which permits others to distribute, remix, adapt, build upon this work non-commercially, and license their derivative works on different terms, provided the original work is properly cited and the use is non-commercial. See: https://creativecommons.org/Licenses/by-nc/4.0/

Country/Territory of origin: India

ORCID number: Jagadeesh Menon 0000-0002-2649-0058; Ashwin Rammohan 0000-0001-9528-8892; Mukul Vij 0000-0003-0149-0294; Naresh Shanmugam 0000-0001-9644-9838; Mohamed Rela 0000-0003-4282-4676.

S-Editor: Chen YL
L-Editor: Kerr C
P-Editor: Chen YL

REFERENCES

1 **Allen CE**, Merad M, McClain KL. Langerhans-Cell Histiocytosis. *N Engl J Med* 2018; **379**: 856-868 [PMID: 30157397 DOI: 10.1056/NEJMra1607548]
2 **Yi X**, Han T, Zai H, Long X, Wang X, Li W. Liver involvement of Langerhans' cell histiocytosis in children. *Int J Clin Exp Med* 2015; **8**: 7098-7106 [PMID: 26221247]
3 **Haupt R**, Minkov M, Astigarraga I, Schäfer E, Nanduri V, Jubran R, Egeler RM, Janka G, Micic D, Rodriguez-Galindo C, Van Gool S, Visser J, Weitzman S, Donadieu J; Euro Histio Network. Langerhans cell histiocytosis (LCH): guidelines for diagnosis, clinical work-up, and treatment for patients till the age of 18 years. *Pediatr Blood Cancer* 2013; **60**: 175-184 [PMID: 23109216 DOI: 10.1002/pbc.24367]
4 **Floyd J**, Mirza I, Sachs B, Perry MC. Hepatotoxicity of chemotherapy. *Semin Oncol* 2006; **33**: 50-67 [PMID: 16473644 DOI: 10.1053/j.seminoncol.2005.11.002]
5 **Fu Z**, Li H, Arslan ME, Ells PF, Lee H. Hepatic Langerhans cell histiocytosis: A review. *World J Clin Oncol* 2021; **12**: 335-341 [PMID: 34131565 DOI: 10.5306/wjco.v12.i5.335]
6 **Stieber AC**, Sever C, Starzl TE. Liver transplantation in patients with Langerhans' cell histiocytosis. *Transplantation* 1990; **50**: 338-340 [PMID: 2382301]
7 **Chen C**, Gu G, Zhou T, Huang M, Xia Q. Combination of Neoadjuvant Therapy and Liver Transplantation in Pediatric Multisystem Langerhans Cell Histiocytosis With Liver Involvement. *Front Oncol* 2020; **10**: 566987 [PMID: 33117696 DOI: 10.3389/fonc.2020.566987]
8 **Jaffe R**. Liver involvement in the histiocytic disorders of childhood. *Pediatr Dev Pathol* 2004; **7**: 214-225 [PMID: 15022067 DOI: 10.1007/s10024-003-9876-z]
9 **Braier J**, Ciocca M, Latella A, de Davila MG, Drajer M, Imventarza O. Cholestasis, sclerosing cholangitis, and liver transplantation in Langerhans cell Histiocytosis. *Med Pediatr Oncol* 2002; **38**: 178-182 [PMID: 11836717 DOI: 10.1002/mpo.1306]
10 **Haas S**, Theuerkauf I, Kühnen A, Wickesberg A, Fischer HP. [Langerhans' cell histiocytosis of the liver. Differential diagnosis of a rare chronic destructive sclerosing cholangitis]. *Pathologe* 2003; **24**: 119-123 [PMID: 12673501 DOI: 10.1007/s00292-002-0565-x]
11 **Kaplan KJ**, Goodman ZD, Ishak KG. Liver involvement in Langerhans' cell histiocytosis: a study of nine cases. *Mod*

Pathol 1999; **12**: 370-378 [PMID: 10229501]
12 **Henter JI**, Tondini C, Pritchard J. Histiocyte disorders. *Crit Rev Oncol Hematol* 2004; **50**: 157-174 [PMID: 15157664 DOI: 10.1016/j.critrevonc.2004.01.002]
13 **Khanna R**, Pawaria A, Alam S, Rawat D. Liver Transplantation in LCH: Risk Reactivation or Wait Till Decompensation? *J Pediatr Hematol Oncol* 2016; **38**: 664-665 [PMID: 27271811 DOI: 10.1097/MPH.0000000000000599]
14 **Abdallah M**, Généreau T, Donadieu J, Emile JF, Chazouillères O, Gaujoux-Viala C, Cabane J. Langerhans' cell histiocytosis of the liver in adults. *Clin Res Hepatol Gastroenterol* 2011; **35**: 475-481 [PMID: 21550330 DOI: 10.1016/j.clinre.2011.03.012]
15 **Li H**, Ells P, Arslan ME, Robstad KA, Lee H. Hepatic Langerhans Cell Histiocytosis (LCH) Presenting as a Harbinger of Multisystem LCH. *Cureus* 2020; **12**: e8591 [PMID: 32676232 DOI: 10.7759/cureus.8591]
16 **Tang Y**, Zhang Z, Chen M, Ju W, Wang D, Ji F, Ren Q, Guo Z, He X. Severe sclerosing cholangitis after Langerhans cell histiocytosis treated by liver transplantation: An adult case report. *Medicine (Baltimore)* 2017; **96**: e5994 [PMID: 28248858 DOI: 10.1097/MD.0000000000005994]
17 **Jezierska M**, Stefanowicz J, Romanowicz G, Kosiak W, Lange M. Langerhans cell histiocytosis in children - a disease with many faces. Recent advances in pathogenesis, diagnostic examinations and treatment. *Postepy Dermatol Alergol* 2018; **35**: 6-17 [PMID: 29599667 DOI: 10.5114/pdia.2017.67095]
18 **Allen CE**, Ladisch S, McClain KL. How I treat Langerhans cell histiocytosis. *Blood* 2015; **126**: 26-35 [PMID: 25827831 DOI: 10.1182/blood-2014-12-569301]
19 **Aricò M**. Langerhans cell histiocytosis in children: from the bench to bedside for an updated therapy. *Br J Haematol* 2016; **173**: 663-670 [PMID: 26913480 DOI: 10.1111/bjh.13955]
20 **Abla O**, Weitzman S. Treatment of Langerhans cell histiocytosis: role of BRAF/MAPK inhibition. *Hematology Am Soc Hematol Educ Program* 2015; **2015**: 565-570 [PMID: 26637773 DOI: 10.1182/asheducation-2015.1.565]
21 **Grigorian A**, O'Brien CB. Hepatotoxicity Secondary to Chemotherapy. *J Clin Transl Hepatol* 2014; **2**: 95-102 [PMID: 26357620 DOI: 10.14218/JCTH.2014.00011]
22 **Bahirwani R**, Reddy KR. Drug-induced liver injury due to cancer chemotherapeutic agents. *Semin Liver Dis* 2014; **34**: 162-171 [PMID: 24879981 DOI: 10.1055/s-0034-1375957]
23 **Bansal D**, Marwaha RK, Trehan A, Poddar U, Radotra BD. Portal hypertension secondary to Langerhans cell histiocytosis. *Indian J Gastroenterol* 2001; **20**: 201-202 [PMID: 11676337]
24 **Simko SJ**, McClain KL, Allen CE. Up-front therapy for LCH: is it time to test an alternative to vinblastine/prednisone? *Br J Haematol* 2015; **169**: 299-301 [PMID: 25400231 DOI: 10.1111/bjh.13208]
25 **Ziogas IA**, Kakos CD, Wu WK, Montenovo MI, Matsuoka LK, Zarnegar-Lumley S, Alexopoulos SP. Liver Transplantation for Langerhans Cell Histiocytosis: A US Population-Based Analysis and Systematic Review of the Literature. *Liver Transpl* 2021; **27**: 1181-1190 [PMID: 33484600 DOI: 10.1002/lt.25995]
26 **Zandi P**, Panis Y, Debray D, Bernard O, Houssin D. Pediatric liver transplantation for Langerhans' cell histiocytosis. *Hepatology* 1995; **21**: 129-133 [PMID: 7806145]
27 **Newell KA**, Alonso EM, Kelly SM, Rubin CM, Thistlethwaite JR Jr, Whitington PF. Association between liver transplantation for Langerhans cell histiocytosis, rejection, and development of posttransplant lymphoproliferative disease in children. *J Pediatr* 1997; **131**: 98-104 [PMID: 9255199 DOI: 10.1016/s0022-3476(97)70131-8]
28 **Hadzic N**, Pritchard J, Webb D, Portmann B, Heaton ND, Rela M, Dhawan A, Baker AJ, Mieli-Vergani G. Recurrence of Langerhans cell histiocytosis in the graft after pediatric liver transplantation. *Transplantation* 2000; **70**: 815-819 [PMID: 11003364 DOI: 10.1097/00007890-200009150-00019]
29 **Feng S**, Han L, Yue M, Zhong D, Cao J, Guo Y, Sun Y, Zhang H, Cao Z, Cui X, Liu R. Frequency detection of BRAF V600E mutation in a cohort of pediatric langerhans cell histiocytosis patients by next-generation sequencing. *Orphanet J Rare Dis* 2021; **16**: 272 [PMID: 34116682 DOI: 10.1186/s13023-021-01912-3]
30 **Donadieu J**, Larabi IA, Tardieu M, Visser J, Hutter C, Sieni E, Kabbara N, Barkaoui M, Miron J, Chalard F, Milne P, Haroche J, Cohen F, Hélias-Rodzewicz Z, Simon N, Jehanne M, Kolenova A, Pagnier A, Aladjidi N, Schneider P, Plat G, Lutun A, Sonntagbauer A, Lehrnbecher T, Ferster A, Efremova V, Ahlmann M, Blanc L, Nicholson J, Lambilliote A, Boudiaf H, Lissat A, Svojgr K, Bernard F, Elitzur S, Golan M, Evseev D, Maschan M, Idbaih A, Slater O, Minkov M, Taly V, Collin M, Alvarez JC, Emile JF, Héritier S. Vemurafenib for Refractory Multisystem Langerhans Cell Histiocytosis in Children: An International Observational Study. *J Clin Oncol* 2019; **37**: 2857-2865 [PMID: 31513482 DOI: 10.1200/JCO.19.00456]
31 **Yang Y**, Wang D, Cui L, Ma HH, Zhang L, Lian HY, Zhang Q, Zhao XX, Zhang LP, Zhao YZ, Li N, Wang TY, Li ZG, Zhang R. Effectiveness and Safety of Dabrafenib in the Treatment of 20 Chinese Children with BRAFV600E-Mutated Langerhans Cell Histiocytosis. *Cancer Res Treat* 2021; **53**: 261-269 [PMID: 32972045 DOI: 10.4143/crt.2020.769]
32 **Spengler EK**, Kleiner DE, Fontana RJ. Vemurafenib-induced granulomatous hepatitis. *Hepatology* 2017; **65**: 745-748 [PMID: 27335285 DOI: 10.1002/hep.28692]
33 **Diamond EL**, Durham BH, Ulaner GA, Drill E, Buthorn J, Ki M, Bitner L, Cho H, Young RJ, Francis JH, Rampal R, Lacouture M, Brody LA, Ozkaya N, Dogan A, Rosen N, Iasonos A, Abdel-Wahab O, Hyman DM. Efficacy of MEK inhibition in patients with histiocytic neoplasms. *Nature* 2019; **567**: 521-524 [PMID: 30867592 DOI: 10.1038/s41586-019-1012-y]
34 **Hashimoto K**, Nishimura S, Sakata N, Inoue M, Sawada A, Akagi M. Characterization of PD-1/PD-L1 immune checkpoint expression in the pathogenesis of musculoskeletal Langerhans cell histiocytosis: A retrospective study. *Medicine (Baltimore)* 2021; **100**: e27650 [PMID: 34713856 DOI: 10.1097/MD.0000000000027650]
35 **Hashimoto K**, Nishimura S, Sakata N, Inoue M, Sawada A, Akagi M. Treatment Outcomes of Langerhans Cell Histiocytosis: A Retrospective Study. *Medicina (Kaunas)* 2021; **57** [PMID: 33917120 DOI: 10.3390/medicina57040356]
36 **Hashimoto K**, Nishimura S, Ito T, Akagi M. Characterization of PD-1/PD-L1 immune checkpoint expression in soft tissue sarcomas. *Eur J Histochem* 2021; **65** [PMID: 34218652 DOI: 10.4081/ejh.2021.3203]
37 **Rammohan A**, Reddy MS, Farouk M, Vargese J, Rela M. Pembrolizumab for metastatic hepatocellular carcinoma

following live donor liver transplantation: The silver bullet? *Hepatology* 2018; **67**: 1166-1168 [PMID: 29023959 DOI: 10.1002/hep.29575]

World Journal of Gastroenterology

Submit a Manuscript: https://www.f6publishing.com

World J Gastroenterol 2022 August 14; 28(30): 4053-4060

DOI: 10.3748/wjg.v28.i30.4053

ISSN 1007-9327 (print) ISSN 2219-2840 (online)

MINIREVIEWS

Gut microbiota, inflammatory bowel disease and colorectal cancer

Ana Elisa Valencise Quaglio, Thais Gagno Grillo, Ellen Cristina Souza De Oliveira, Luiz Claudio Di Stasi, Ligia Yukie Sassaki

Specialty type: Gastroenterology and hepatology

Provenance and peer review: Invited article; Externally peer reviewed.

Peer-review model: Single blind

Peer-review report's scientific quality classification

Grade A (Excellent): 0
Grade B (Very good): B, B
Grade C (Good): 0
Grade D (Fair): 0
Grade E (Poor): 0

P-Reviewer: Budin C, Romania; Houston KV, United States

Received: January 18, 2022
Peer-review started: January 18, 2022
First decision: March 8, 2022
Revised: March 16, 2022
Accepted: July 18, 2022
Article in press: July 18, 2022
Published online: August 14, 2022

Ana Elisa Valencise Quaglio, Luiz Claudio Di Stasi, Departament of Biophysics and Pharmacology, São Paulo State University (Unesp), Institute of Biosciences, Botucatu 18618-689, São Paulo State, Brazil

Thais Gagno Grillo, Ellen Cristina Souza De Oliveira, Ligia Yukie Sassaki, Department of Internal Medicine, São Paulo State University (Unesp), Medical School, Botucatu 18618-686, São Paulo State, Brazil

Corresponding author: Ligia Yukie Sassaki, MD, PhD, Assistant Professor, Ligia Yukie Sassaki, MD, PhD, Assistant Professor, Department of Internal Medicine, São Paulo State University (Unesp), Medical School, s/n. Bairro Rubião Junior, Botucatu 18618-686, São Paulo State, Brazil. ligia.sassaki@unesp.br

Abstract

The gut microbiota is a complex community of microorganisms that inhabit the digestive tracts of humans, living in symbiosis with the host. Dysbiosis, characterized by an imbalance between the beneficial and opportunistic gut microbiota, is associated with several gastrointestinal disorders, such as irritable bowel syndrome (IBS); inflammatory bowel disease (IBD), represented by ulcerative colitis and Crohn's disease; and colorectal cancer (CRC). Dysbiosis can disrupt the mucosal barrier, resulting in perpetuation of inflammation and carcinogenesis. The increase in some specific groups of harmful bacteria, such as *Escherichia coli* (*E. coli*) and enterotoxigenic *Bacteroides fragilis* (ETBF), has been associated with chronic tissue inflammation and the release of pro-inflammatory and carcinogenic mediators, increasing the chance of developing CRC, following the inflammation-dysplasia-cancer sequence in IBD patients. Therefore, the aim of the present review was to analyze the correlation between changes in the gut microbiota and the development and maintenance of IBD, CRC, and IBD-associated CRC. Patients with IBD and CRC have shown reduced bacterial diversity and abundance compared to healthy individuals, with enrichment of *Firmicute* sand *Bacteroidetes*. Specific bacteria are also associated with the onset and progression of CRC, such as *Fusobacterium nucleatum*, *E. coli*, *Enterococcus faecalis*, *Streptococcus gallolyticus*, and ETBF. Future research can evaluate the advantages of modulating the gut microbiota as preventive measures in CRC high-risk patients, directly affecting the prognosis of the disease and the quality of life of patients.

Key Words: Gut microbiota; Dysbiosis; Ulcerative colitis; Crohn's disease; Inflammatory bowel disease; Colorectal cancer

©**The Author(s) 2022.** Published by Baishideng Publishing Group Inc. All rights reserved.

Core Tip: Dysbiosis is present in patients with inflammatory bowel disease (IBD) and colorectal cancer (CRC). Dysbiosis can lead to a disruption of the mucosal barrier of the digestive tract lining, resulting in the perpetuation of inflammation and carcinogenesis, thus increasing the risk of developing CRC in IBD patients. Therefore, the aim of this review was to analyze the correlation between changes in gut microbiota and the development of IBD, CRC, and IBD-associated CRC. Further studies should be carried out to identify bacterial species that cause imbalances in the gut microbiota, enabling the development of prevention strategies or treatment of IBD-associated CRC.

Citation: Quaglio AEV, Grillo TG, De Oliveira ECS, Di Stasi LC, Sassaki LY. Gut microbiota, inflammatory bowel disease and colorectal cancer. *World J Gastroenterol* 2022; 28(30): 4053-4060
URL: https://www.wjgnet.com/1007-9327/full/v28/i30/4053.htm
DOI: https://dx.doi.org/10.3748/wjg.v28.i30.4053

INTRODUCTION

The human microbiome is composed of several types of microbes that colonize different niches of the human body, such as the skin, lungs, vagina, and gastrointestinal tract[1]. Of these, the gut microbiota is the most studied, due to the presence of greater diversity and number of microbial species compared to other parts of the body[1,2]. The gut microbiota is a complex community of approximately 100 trillion microorganisms, such as fungi, viruses, and protists, that inhabit the digestive tracts of humans, living in symbiosis with the host[3,4].

Alterations in the gut microbiota are associated with several diseases, including inflammatory bowel disease (IBD) and colorectal cancer (CRC)[2]. Thus, studies aimed at elucidating the role of the microbiota in each phase of each disease are necessary. Based on changes in the intestinal microbiota, new diagnostic tools and possible treatments can be developed. Further, studies aiming to correlate alterations in the microbiota or in specific bacterial populations with the diagnosis, prognosis, and/or treatment of diseases are necessary. Therefore, this mini-review was conducted to determine the correlation between changes in the gut microbiota and IBD, CRC, and IBD-associated CRC.

At birth, the intestinal tract is sterile[2], with bacterial colonization beginning as early as during the passage of the baby through the birth canal[5]. Colonization continues through feeding and other environmental contacts. Several factors are known to influence colonization, including gestational age, mode of delivery (vaginal birth *vs* cesarean delivery), diet (breast milk *vs* formula) and exposure to antibiotics, and sanitation[2].

During the first year of life, the microbial composition of the mammalian intestine is relatively simple and characterized by low diversity with relative dominance of species from the phyla *Proteobacteria* and *Actinobacteria*[2,5]. Over time, the microbiota becomes more diverse, with the *Firmicutes* and *Bacteroidetes* phyla later emerging as the predominant microbes characterizing the adult microbiota[2,6-8].

In an adult individual, over 90% of intestinal bacteria belong to *Firmicutes*, *Bacteroidetes*, *Proteobacteria*, or *Actinobacteria* phyla[4,7]. The gut microbiota can be differentiated into beneficial bacteria and opportunistic bacteria, the latter of which can cause infection[8]. *Lactobacillus*, *Bifidobacterium*, *Enterococci*, and *Propionobacteria* are some of the beneficial microbes, while the opportunistic groups include *Bacteriodes*, *Bacilli*, *Clostridia*, *Enterobacteria*, *Actinobacteria*, *Peptococci*, *Staphylococci*, and *Streptococci*[8].

The benefits of the gut microbiota to the host's physiology are vast, including nutrition, immune development, and host defense[4,7]. In the field of nutrition, some bacterial species, such as *Bifidobacterium*, participate in the biosynthesis of several components as vitamin K and vitamin B[7]. In addition, some can provide short-chain fatty acids (SCFAs) by fermenting dietary fibers[7,9]. SCFAs are a group of small fatty acids (2 to 5 carbons) produced by anaerobic microorganisms that, after absorption, have systemic immunomodulatory and anti-inflammatory properties[9].

The most abundant SCFAs in the colon are acetate, propionate, and butyrate[7,9,10], which promote the proliferation of beneficial bacteria and stimulate regulatory T cells to reduce inflammatory mediators, associated with an increase in colonic oxygen consumption by epithelial cells, and enhancing immune regulation, and gut barrier function[9-11].

Imbalance between the beneficial and opportunistic groups causes dysbiosis, which is associated with gastrointestinal disorders such as IBS, IBD, and CRC[4,7,8].

IBD AND GUT MICROBIOTA

IBD, a heterogeneous chronic and relapsing inflammatory illnesses of the digestive system, is traditionally classified into ulcerative colitis (UC) and Crohn's disease (CD)[4,12,13]. Both UC and CD can cause several symptoms like diarrhea, rectal bleeding, and abdominal pain. However, inflammation in CD is transmural and can involve any part of the gastrointestinal tract. In contrast, inflammation in UC is more superficial and limited to the colon[14].

Although the cause of IBD is not fully known, genetic history is likely involved in the pathophysiology of IBD, thus, several studies have identified a number of susceptible genes[12]. However, environmental factors, such as stress, sleeping patterns, antibiotic use, hygiene, diet, and smoking, are also associated with the development of IBD[4].

While IBD is a disease with the highest rates in industrialized countries, its incidence varies considerably worldwide, and newly industrialized areas such as India and South America presented a rapid increase in case numbers[7,13,14]. This enhancement can be related to dietary habits such as increased consumption of processed foods, sugars, and fats; overutilization of antibiotics; and an overall improvement in sanitary conditions and hygiene[13].

Nevertheless, the exact factors that trigger the first episode of inflammation and subsequent relapse remain unknown, it is now know that inflammatory episodes can result, in genetically predisposed people, from an immune response against intestinal microbial antigens under several environmental conditions[14]. Several IBD-associated susceptible genes are correlated with host responses to gut bacteria, suggesting that the gut microbiota also participate in the pathogenesis of IBD[7]. Dysbiosis is a reduction in microbial diversity, or a combination of the loss of beneficial bacteria and an increase in pathogenic bacteria[15], that may influence the pathogenesis of IBD.

The most prominent changes in the microbiota of IBD patients are the decreased diversity in bacteria species associated with decreased abundance of *Bacteroidetes* and *Firmicutes*[4,7] alongside an increase in the abundance of *Proteobacteria*[4].

In patients with IBD, the mucus layer is compromised, allowing luminal bacteria to penetrate and invade the submucosal layers, leading to the proliferative and inflammatory processes[4,13]. Then, mucosal destruction due to inflammatory injury further exposes the submucosa to more bacteria, leading to a vicious, positive feedback cycle of antigenic exposure and mucosal damage[13].

Faecalibacterium prausnitzii is one of the most abundant human gut bacteria and can be used as synonym of the gut health because of its anti-inflammatory and immunoregulatory properties[14]. One of the its products is butyrate, which is associated with an anti-inflammatory effect[7]. Several authors have correlated decreases in *Faecalibacterium prausnitzii* (*F. prausnitzii*) abundance with CD development [7,14,16] and in UC patients, a decrease was also observed during remission, being the recovery of the *F. prausnitzii* population associated with the maintenance of clinical remission[17].

Roseburia spp, including *Roseburia faecis*, *Roseburia intestinalis* (*R. intestinalis*), *and Roseburia hominis* (*R. hominis*), another genus of butyrate-producing bacteria, were significantly lower in healthy individuals with a high genetic risk for IBD compared to healthy individuals with low genetic risk[7]. *R. hominis*, specifically, was significantly reduced in UC patients, and an inverse correlation was observed between *R hominis* and disease severity[18]. In contrast, *R. intestinalis* supernatant suppressed the expression of interleukin (IL)-6 as well as the signal transducer and activator of transcription 3 (STAT3) *via* macrophage regulation in an *in vitro* experiment. Additionally, in dextran sodium sulfate- and 2,4,6-trinitrobenzene sulfonic acid-induced intestinal inflammation models, *R. intestinalis* supernatant reduced macrophages and Th17 cells in the colon, which was associated with the downregulation of IL-6 and STAT3[19].

In the field of pathogenic bacteria, several authors have described a relative increase in *Proteobacteria*, mainly *Escherichia coli* (*E. coli*), in IBD patients[7,20-22]. The exact mechanisms that lead to an increase in *Proteobacteria* during inflammation are not completely understood; however, Rizzatti *et al*[20] proposed two mechanisms: The oxygen hypothesis and the presence of nitrate. In a normal colon, epithelial cells deplete oxygen in the lumen through beta oxidation, creating an anaerobic environment[23]. In contrast, during an inflammatory episode, the beta oxidation capacity of colonic cells is decreased, thus increasing oxygen availability, which promotes dysbiosis and *Proteobacteria* growth[24]. Nitrate generated as a by-product during the inflammatory process conferred a growth advantage to the commensal bacteria *E. coli* in the large intestine, which then became predominant[25].

The increase in pathogenic bacteria in the digestive tract that can adhere to the colonic mucosa could alters the gut permeability, modifying the diversity and composition of intestinal microbiota, and ultimately leading to intestinal inflammation by regulating inflammatory genes expression[7].

Dysbiosis can further alter bacterial metabolites; decreased concentration of SCFAs has been reported as a result of a diminish in butyrate-producing bacteria like *F. prausnitzii*, in patients with IBD and in animal models of intestinal inflammation[7,9,10]. Decreased levels of SCFAs affects the differentiation and expansion of Treg cells and the growth of epithelial cells[26], leading to the loss of intestinal homeostasis.

CRC AND GUT MICROBIOTA

CRC is the third most common cancer, and the second most frequent cause of cancer deaths worldwide being more common in developed than in developing countries[27,28]. Notwithstanding cases in all countries are on the rise, most CRC cases occur in Western countries, where there is an increase in incidence[28]. CRC rates in older adults in the United States have declined in recent years probably due to increased screening, but rates in younger adults have been rising, which may be correlated with higher incidence of obesity and other diet and lifestyle trends in the western hemisphere[29].

The exact mechanism for CRC onset and progression has not been fully elucidated, but it is generally believed to be the result of extensive and complex interactions between genetic and environmental factors[30]. According to Olovo *et al*[28], the progression of adenoma to carcinoma could be linked to the gut microbiota and conversely, a healthy microbiota is correlated with a minor risk of advanced adenoma[28].

Several factors that affect the gut microbiota are thought to be related to colon carcinogenesis, such as obesity, a high-fat diet, smoking, and frequent consumption of alcohol[30].

Patients with CRC have shown reduced bacterial diversity and abundance compared to healthy individuals, with enrichment of *Firmicutes* and *Bacteroidetes*[31]. Specific bacteria are also associated with the onset and progression of CRC, such as *Fusobacterium nucleatum*, *E. coli*, *Enterococcus faecalis*, *Streptococcus gallolyticus*, and enterotoxigenic *Bacteroides fragilis* (ETBF)[32].

The abundance of *Fusobacterium nucleatum*, an opportunistic pathogen found normally in the oral cavity, is correlated with age and tumor diameter in CRC patients[31,33,34]. Additionally, an overabundance of *F. nucleatum* is associated with poor prognosis in metastatic CRC[32]; thus, *F. nucleatum* could be considered a potential biomarker for predicting the prognosis in patients with proximal colon cancer[34].

There is plenty of evidence of the tumor-promoting effects of *Streptococcus gallolyticus* in colon cells [35-37]. Colonic cells incubated with *Streptococcus gallolyticus* (*S. gallolyticus*) presented increased levels of β-catenin, c-Myc, and proliferating cell nuclear antigen (PCNA), all of which are transcription factors associated with cancer development[35]. In addition, in mice, administration of *S. gallolyticus* leads to more tumors, higher tumor burden, and dysplasia grade, and increased cell proliferation and β-catenin staining in colonic crypts compared to mice incubated with control bacteria[35]. Furthermore, CRC patients present high levels of this bacterium compared to healthy individuals[37]. However, CRC-specific conditions, such as the increased concentration of bile acids, could also promote *S. gallolyticus* colonization, creating a maintenance cycle for high levels of this bacterium in the gut[37].

ETBF is the most frequent anaerobe isolated from cases of diarrhea, peritonitis, intra-abdominal abscesses, and sepsis, and there is a positive correlation between the presence of ETBF and active IBD and CRC[38]. According to Appunni *et al*[39], co-colonization of toxigenic *E. coli* and ETBF in mice resulted in increased production of pro-inflammatory IL-17 and subsequent DNA damage, which could accelerate the development of CRC[39]. In addition, the toxin in ETBF could induce c-myc expression and IL-8 secretion causing oxidative DNA and epithelial barrier damage, and STAT3/Th17 immune responses activation, which are further correlated with an increased risk of CRC[38].

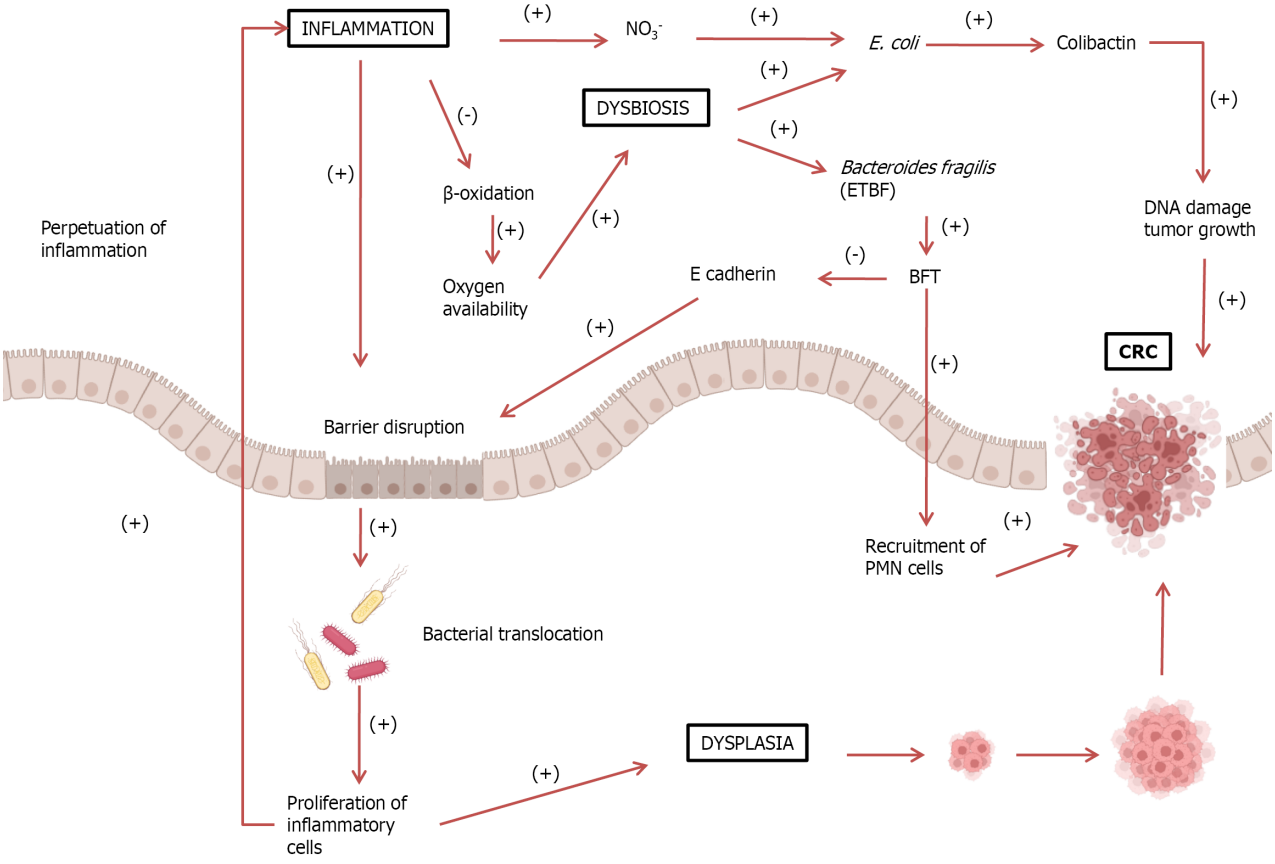
IBD-ASSOCIATED CRC AND GUT MICROBIOTA

Intestinal inflammation is one of the most common risk factors for developing CRC. Besides being two to six times more likely to develop CRC than healthy people, IBD patients with cancer are affected younger than sporadic CRC patients[40]. Disease duration, extension of the lesions, inflammation, sclerosing cholangitis, age at onset and onset in childhood are factors linking IBD with an increased incidence of CRC[41,42].

Chronic inflammation initiates and drives tumorigenesis[42], leading to an "inflammation-dysplasia-carcinoma" sequence, not the "adenoma-sequence" classically described in sporadic CRC[40].

Popov *et al*[43]proposed the three main theories about bacterial involvement in the development of IBD-associated CRC: The alpha-bug hypothesis, driver-passenger hypothesis, and common ground hypothesis. In the alpha-bug hypothesis, a single bacterium (normally ETBF) is thought to cause all modifications and damage that lead to carcinogenesis. The driver-passenger hypothesis is similar, but after the attack by the first bacteria, other opportunistic bacteria start to grow and contribute to cancer development. Finally, in the common ground hypothesis, endogenous and exogenous factors form a "leaky gut," allowing the passage of bacteria into the submucosal tissue, leading to chronic inflammation and the consequent emergence of cancer[43].

It is known that bacteria, through pathogen-associated molecular patterns (PAMPs), are capable of communicating with the tool-like receptors (TLRs), retinoic acid-inducible gene I-like receptors (RLRs), and nucleotide binding oligomerization domain-receptors (NLRs), and trigger an immune response [42]. Nuclear factor kB (NF-kB) can be activated by the TLR and tumor necrosis factor-α (TNF-α), inducing the transcription of several tumorigenesis genes such as COX-2, which then leads to the apoptosis of intestinal epithelial cells *via* tumor suppressor p53 pathways[40] and consequent



DOI: 10.3748/wjg.v28.i30.4053 **Copyright** ©The Author(s) 2022.

Figure 1 Increased inflammatory response can lead to barrier disruption, allowing bacterial translocation into the intestinal lumen. These pathogens trigger an immune and inflammatory response, perpetuating the inflammatory process. Inflammatory cells can also cause dysplasia, leading to the development of colorectal cancer (CRC). Under normal conditions, epithelial cells, during β-oxidation, decrease oxygen availability, thus creating an anaerobic environment. During chronic inflammation, β-oxidation decreases, enhancing oxygen availability. This also leads to an increase in nitrate (NO3-) formation, leading to dysbiosis and growth of proteobacteria such as *Escherichia coli* (*E. coli*). *E. coli* produces colibactin, which could damage DNA and stimulate tumor growth. The growth of Bacteroidetes fragilis may also occur, which produces Bacteroides fragilis toxin (BFT). This toxin cleaves E-cadherin, a major constituent of the zonula adherens, which is responsible for cell adhesion, leading to further barrier disruption. Additionally, BFT also stimulates epithelial cells to recruit polymorphonuclear leukocytes (PMN) cells, promoting the development of CRC. BFT: Bacteroides fragilis toxin; ETBF: Enterotoxigenic *Bacteroides fragilis*; CRC: Colorectal cancer; PMN: Polymorphonuclear leukocytes.

breakdown of the intestinal barrier, allowing microbial translocation.

Increased quantities of *Proteobacteria* are associated with decreased levels of SCFAs and increased colonic inflammation[43]. In addition, intestinal Dysbiosis and barrier defects, associated with alterations in mucin secretion may happen even in the absence of active inflammation[43], perpetuating a favorable environment for the emergence of CRC.

Several studies have demonstrated the participation of bacteria such as *E. coli*, ETBF, and *Fusobacterium nucleatum* in chronic inflammation and cancer development in IBD patients[40,42-45].

A review by Yu *et al*[44] concluded that commensal bacteria, *E. coli* and *E. faecalis*, isolated from healthy subjects are capable of initiating intestinal inflammation in genetically deficient mice, suggesting that opportunistic commensal bacteria may become pathogenic only in genetically predisposed hosts[44]. Nevertheless, some types of *E. coli* can produce colibactin, a genotoxic compound capable of promoting tumor growth, alkylating DNA, and inducing tumorigenic double-stranded breaks[45]. According to Yang *et al*[45], inflammation may upregulate bacterial virulence genes, such as colibactin, and facilitate colonization of the mucosa, leading to increased colibactin-induced DNA damage in colonic epithelial cells, allowing this bacterial strain to exert its carcinogenic activity[42].

The enterotoxin produced by ETBF known as bacteroides fragilis toxin, acted as a metalloprotease cleaving E-cadherin, a major constituent of the zonula adherens, which is responsible for cell adhesion [46]. This toxin can trigger an inflammatory, pro-tumoral signaling caspase in colonic epithelial cells that cause the recruitment of polymorphonuclear immature myeloid cells to promote colon cancers[44].

CONCLUSION

There is a consensus that dysbiosis is present in both IBD and CRC, and that dysbiosis could lead to a disruption of the mucosal barrier with perpetuation of inflammation and carcinogenesis. Dysbiosis with a consequent increase in bacteria, such as *E. coli* and ETBF, is believed to lead to a breakdown of the intestinal mucosal barrier, allowing the translocation of more bacteria from the lumen to the interior of the tissue. This condition leads to chronic tissue inflammation, with the release of inflammatory and pro-carcinogenic mediators increasing the risk of developing CRC. This positive feedback loop of dysbiosis could be the basis for the inflammation-dysplasia-cancer sequence (Figure 1).

Further studies should be carried out to identify which bacteria or which set of bacteria may be responsible for this feedback cycle. Understanding the mechanism behind dysbiosis cycles may be the basis for preventing or treating IBD-associated CRC and CRC. Future research should evaluate the advantages of modulating the intestinal microbiota as a protective factor for the development of IBD-associated CRC; thus, the use of prebiotics, probiotics, or diet-based treatment can be used as preventive measures in CRC high-risk patients, directly affecting the prognosis of the disease and the quality of life of patients living with IBD.

FOOTNOTES

Author contributions: Quaglio AEV, Grillo TG, and De Oliveira ECS performed the majority of the writing; Di Stasi LC and Sassaki LY designed the outline and coordinated the writing of the paper; all authors critically revised the manuscript for important intellectual content and approved the final version.

Conflict-of-interest statement: There are no conflicts of interest to report.

Open-Access: This article is an open-access article that was selected by an in-house editor and fully peer-reviewed by external reviewers. It is distributed in accordance with the Creative Commons Attribution Non Commercial (CC BY-NC 4.0) license, which permits others to distribute, remix, adapt, build upon this work non-commercially, and license their derivative works on different terms, provided the original work is properly cited and the use is non-commercial. See: https://creativecommons.org/Licenses/by-nc/4.0/

Country/Territory of origin: Brazil

ORCID number: Ana Elisa Valencise Quaglio 0000-0002-5998-2382; Thais Gagno Grillo 0000-0002-4351-5034; Ellen Cristina Souza De Oliveira 0000-0001-5357-3468; Luiz Claudio Di Stasi 0000-0002-7864-1073; Ligia Yukie Sassaki 0000-0002-7319-8906.

S-Editor: Chen YL
L-Editor: A
P-Editor: Chen YL

REFERENCES

1 **Michaudel C**, Sokol H. The Gut Microbiota at the Service of Immunometabolism. *Cell Metab* 2020; **32**: 514-523 [PMID: 32946809 DOI: 10.1016/j.cmet.2020.09.004]
2 **Quigley EM**. Gut bacteria in health and disease. *Gastroenterol Hepatol (N Y)* 2013; **9**: 560-569 [PMID: 24729765]
3 **Kc D**, Sumner R, Lippmann S. Gut microbiota and health. *Postgrad Med* 2020; **132**: 274 [PMID: 31566046 DOI: 10.1080/00325481.2019.1662711]
4 **Gomaa EZ**. Human gut microbiota/microbiome in health and diseases: a review. *Antonie Van Leeuwenhoek* 2020; **113**: 2019-2040 [PMID: 33136284 DOI: 10.1007/s10482-020-01474-7]
5 **Sekirov I**, Russell SL, Antunes LC, Finlay BB. Gut microbiota in health and disease. *Physiol Rev* 2010; **90**: 859-904 [PMID: 20664075 DOI: 10.1152/physrev.00045.2009]
6 **Eckburg PB**, Bik EM, Bernstein CN, Purdom E, Dethlefsen L, Sargent M, Gill SR, Nelson KE, Relman DA. Diversity of the human intestinal microbial flora. *Science* 2005; **308**: 1635-1638 [PMID: 15831718 DOI: 10.1126/science.1110591]
7 **Nishida A**, Inoue R, Inatomi O, Bamba S, Naito Y, Andoh A. Gut microbiota in the pathogenesis of inflammatory bowel disease. *Clin J Gastroenterol* 2018; **11**: 1-10 [PMID: 29285689 DOI: 10.1007/s12328-017-0813-5]
8 **Roy Sarkar S**, Banerjee S. Gut microbiota in neurodegenerative disorders. *J Neuroimmunol* 2019; **328**: 98-104 [PMID: 30658292 DOI: 10.1016/j.jneuroim.2019.01.004]
9 **Almeida-Junior LD**, Curimbaba TFS, Chagas AS, Quaglio AEV, Di Stasi LC. Dietary intervention with green dwarf banana flour (Musa sp. AAA) modulates oxidative stress and colonic SCFAs production in the TNBS model of intestinal inflammation. *J Funct Foods* 2017; **38**: 497-504
10 **Curimbaba TFS**, Almeida-Junior LD, Chagas AS, Quaglio AEV, Herculano AM, Di Stasi LC. Prebiotic, antioxidant and anti-inflammatory properties of edible Amazon fruits. *Food Biosci* 2020; 100599
11 **Mills S**, Stanton C, Lane JA, Smith GJ, Ross RP. Precision Nutrition and the Microbiome, Part I: Current State of the

Science. *Nutrients* 2019; **11** [PMID: 31022973 DOI: 10.3390/nu11040923]
12 **Matsuoka K**, Kanai T. The gut microbiota and inflammatory bowel disease. *Semin Immunopathol* 2015; **37**: 47-55 [PMID: 25420450 DOI: 10.1007/s00281-014-0454-4]
13 **Ghouri YA**, Tahan V, Shen B. Secondary causes of inflammatory bowel diseases. *World J Gastroenterol* 2020; **26**: 3998-4017 [PMID: 32821067 DOI: 10.3748/wjg.v26.i28.3998]
14 **Ryma T**, Samer A, Soufli I, Rafa H, Touil-Boukoffa C. Role of Probiotics and Their Metabolites in Inflammatory Bowel Diseases (IBDs). *Gastroenterol Insights* 2021; **12**: 56-66 [DOI: 10.3390/gastroent12010006]
15 **Humphreys C**. Intestinal Permeability. 5th ed. Pizzorno JE, Murray, MT, editors. Textbook of Natural Medicine, 2020: 166-177 [DOI: 10.1016/B978-0-323-43044-9.00019-4]
16 **Zuo T**, Ng SC. The Gut Microbiota in the Pathogenesis and Therapeutics of Inflammatory Bowel Disease. *Front Microbiol* 2018; **9**: 2247 [PMID: 30319571 DOI: 10.3389/fmicb.2018.02247]
17 **Varela E**, Manichanh C, Gallart M, Torrejón A, Borruel N, Casellas F, Guarner F, Antolin M. Colonisation by Faecalibacterium prausnitzii and maintenance of clinical remission in patients with ulcerative colitis. *Aliment Pharmacol Ther* 2013; **38**: 151-161 [PMID: 23725320 DOI: 10.1111/apt.12365]
18 **Machiels K**, Joossens M, Sabino J, De Preter V, Arijs I, Eeckhaut V, Ballet V, Claes K, Van Immerseel F, Verbeke K, Ferrante M, Verhaegen J, Rutgeerts P, Vermeire S. A decrease of the butyrate-producing species Roseburia hominis and Faecalibacterium prausnitzii defines dysbiosis in patients with ulcerative colitis. *Gut* 2014; **63**: 1275-1283 [PMID: 24021287 DOI: 10.1136/gutjnl-2013-304833]
19 **Luo W**, Shen Z, Deng M, Li X, Tan B, Xiao M, Wu S, Yang Z, Zhu C, Tian L, Wu X, Meng X, Quan Y, Wang X. Roseburia intestinalis supernatant ameliorates colitis induced in mice by regulating the immune response. *Mol Med Rep* 2019; **20**: 1007-1016 [PMID: 31173202 DOI: 10.3892/mmr.2019.10327]
20 **Rizzatti G**, Lopetuso LR, Gibiino G, Binda C, Gasbarrini A. Proteobacteria: A Common Factor in Human Diseases. *Biomed Res Int* 2017; **2017**: 9351507 [PMID: 29230419 DOI: 10.1155/2017/9351507]
21 **Nishino K**, Nishida A, Inoue R, Kawada Y, Ohno M, Sakai S, Inatomi O, Bamba S, Sugimoto M, Kawahara M, Naito Y, Andoh A. Analysis of endoscopic brush samples identified mucosa-associated dysbiosis in inflammatory bowel disease. *J Gastroenterol* 2018; **53**: 95-106 [PMID: 28852861 DOI: 10.1007/s00535-017-1384-4]
22 **Vester-Andersen MK**, Mirsepasi-Lauridsen HC, Prosberg MV, Mortensen CO, Träger C, Skovsen K, Thorkilgaard T, Nøjgaard C, Vind I, Krogfelt KA, Sørensen N, Bendtsen F, Petersen AM. Increased abundance of proteobacteria in aggressive Crohn's disease seven years after diagnosis. *Sci Rep* 2019; **9**: 13473 [PMID: 31530835 DOI: 10.1038/s41598-019-49833-3]
23 **Rivera-Chávez F**, Lopez CA, Bäumler AJ. Oxygen as a driver of gut dysbiosis. *Free Radic Biol Med* 2017; **105**: 93-101 [PMID: 27677568 DOI: 10.1016/j.freeradbiomed.2016.09.022]
24 **Hughes ER**, Winter MG, Duerkop BA, Spiga L, Furtado de Carvalho T, Zhu W, Gillis CC, Büttner L, Smoot MP, Behrendt CL, Cherry S, Santos RL, Hooper LV, Winter SE. Microbial Respiration and Formate Oxidation as Metabolic Signatures of Inflammation-Associated Dysbiosis. *Cell Host Microbe* 2017; **21**: 208-219 [PMID: 28182951 DOI: 10.1016/j.chom.2017.01.005]
25 **Winter SE**, Winter MG, Xavier MN, Thiennimitr P, Poon V, Keestra AM, Laughlin RC, Gomez G, Wu J, Lawhon SD, Popova IE, Parikh SJ, Adams LG, Tsolis RM, Stewart VJ, Bäumler AJ. Host-derived nitrate boosts growth of E. coli in the inflamed gut. *Science* 2013; **339**: 708-711 [PMID: 23393266 DOI: 10.1126/science.1232467]
26 **Atarashi K**, Tanoue T, Oshima K, Suda W, Nagano Y, Nishikawa H, Fukuda S, Saito T, Narushima S, Hase K, Kim S, Fritz JV, Wilmes P, Ueha S, Matsushima K, Ohno H, Olle B, Sakaguchi S, Taniguchi T, Morita H, Hattori M, Honda K. Treg induction by a rationally selected mixture of Clostridia strains from the human microbiota. *Nature* 2013; **500**: 232-236 [PMID: 23842501 DOI: 10.1038/nature12331]
27 **Weitz J**, Koch M, Debus J, Höhler T, Galle PR, Büchler MW. Colorectal cancer. *Lancet* 2005; **365**: 153-165 [PMID: 15639298 DOI: 10.1016/S0140-6736(05)17706-X]
28 **Olovo CV**, Huang X, Zheng X, Xu M. Faecal microbial biomarkers in early diagnosis of colorectal cancer. *J Cell Mol Med* 2021; **25**: 10783-10797 [PMID: 34750964 DOI: 10.1111/jcmm.17010]
29 **Kehm RD**, Lima SM, Swett K, Mueller L, Yang W, Gonsalves L, Terry MB. Age-specific Trends in Colorectal Cancer Incidence for Women and Men, 1935-2017. *Gastroenterology* 2021; **161**: 1060-1062.e3 [PMID: 34058214 DOI: 10.1053/j.gastro.2021.05.050]
30 **Zhang W**, An Y, Qin X, Wu X, Wang X, Hou H, Song X, Liu T, Wang B, Huang X, Cao H. Gut Microbiota-Derived Metabolites in Colorectal Cancer: The Bad and the Challenges. *Front Oncol* 2021; **11**: 739648 [PMID: 34733783 DOI: 10.3389/fonc.2021.739648]
31 **Silva M**, Brunner V, Tschurtschenthaler M. Microbiota and Colorectal Cancer: From Gut to Bedside. *Front Pharmacol* 2021; **12**: 760280 [PMID: 34658896 DOI: 10.3389/fphar.2021.760280]
32 **Liu K**, Yang X, Zeng M, Yuan Y, Sun J, He P, Xie Q, Chang X, Zhang S, Chen X, Cai L, Xie Y, Jiao X. The Role of Fecal *Fusobacterium nucleatum* and *pks+ Escherichia coli* as Early Diagnostic Markers of Colorectal Cancer. *Dis Markers* 2021; **2021**: 1171239 [PMID: 34853619 DOI: 10.1155/2021/1171239]
33 **Brennan CA**, Garrett WS. Fusobacterium nucleatum - symbiont, opportunist and oncobacterium. *Nat Rev Microbiol* 2019; **17**: 156-166 [PMID: 30546113 DOI: 10.1038/s41579-018-0129-6]
34 **Jin M**, Shang F, Wu J, Fan Q, Chen C, Fan J, Liu L, Nie X, Zhang T, Cai K, Ogino S, Liu H. Tumor-Associated Microbiota in Proximal and Distal Colorectal Cancer and Their Relationships With Clinical Outcomes. *Front Microbiol* 2021; **12**: 727937 [PMID: 34650531 DOI: 10.3389/fmicb.2021.727937]
35 **Kumar R**, Herold JL, Schady D, Davis J, Kopetz S, Martinez-Moczygemba M, Murray BE, Han F, Li Y, Callaway E, Chapkin RS, Dashwood WM, Dashwood RH, Berry T, Mackenzie C, Xu Y. Streptococcus gallolyticus subsp. gallolyticus promotes colorectal tumor development. *PLoS Pathog* 2017; **13**: e1006440 [PMID: 28704539 DOI: 10.1371/journal.ppat.1006440]
36 **Kumar R**, Herold JL, Taylor J, Xu J, Xu Y. Variations among Streptococcus gallolyticus subsp. gallolyticus strains in connection with colorectal cancer. *Sci Rep* 2018; **8**: 1514 [PMID: 29367658 DOI: 10.1038/s41598-018-19941-7]

37 **Oehmcke-Hecht S**, Mandl V, Naatz LT, Dühring L, Köhler J, Kreikemeyer B, Maletzki C. Streptococcus gallolyticus abrogates anti-carcinogenic properties of tannic acid on low-passage colorectal carcinomas. *Sci Rep* 2020; **10**: 4714 [PMID: 32170212 DOI: 10.1038/s41598-020-61458-5]

38 **Haghi F**, Goli E, Mirzaei B, Zeighami H. The association between fecal enterotoxigenic B. fragilis with colorectal cancer. *BMC Cancer* 2019; **19**: 879 [PMID: 31488085 DOI: 10.1186/s12885-019-6115-1]

39 **Appunni S**, Rubens M, Ramamoorthy V, Tonse R, Saxena A, McGranaghan P, Kaiser A, Kotecha R. Emerging Evidence on the Effects of Dietary Factors on the Gut Microbiome in Colorectal Cancer. *Front Nutr* 2021; **8**: 718389 [PMID: 34708063 DOI: 10.3389/fnut.2021.718389]

40 **Keller DS**, Windsor A, Cohen R, Chand M. Colorectal cancer in inflammatory bowel disease: review of the evidence. *Tech Coloproctol* 2019; **23**: 3-13 [PMID: 30701345 DOI: 10.1007/s10151-019-1926-2]

41 **Olén O**, Erichsen R, Sachs MC, Pedersen L, Halfvarson J, Askling J, Ekbom A, Sørensen HT, Ludvigsson JF. Colorectal cancer in ulcerative colitis: a Scandinavian population-based cohort study. *Lancet* 2020; **395**: 123-131 [PMID: 31929014 DOI: 10.1016/S0140-6736(19)32545-0]

42 **Lucafò M**, Curci D, Franzin M, Decorti G, Stocco G. Inflammatory Bowel Disease and Risk of Colorectal Cancer: An Overview From Pathophysiology to Pharmacological Prevention. *Front Pharmacol* 2021; **12**: 772101 [PMID: 34744751 DOI: 10.3389/fphar.2021.772101]

43 **Popov J**, Caputi V, Nandeesha N, Rodriguez DA, Pai N. Microbiota-Immune Interactions in Ulcerative Colitis and Colitis Associated Cancer and Emerging Microbiota-Based Therapies. *Int J Mol Sci* 2021; **22** [PMID: 34768795 DOI: 10.3390/ijms222111365]

44 **Yu LC**. Microbiota dysbiosis and barrier dysfunction in inflammatory bowel disease and colorectal cancers: exploring a common ground hypothesis. *J Biomed Sci* 2018; **25**: 79 [PMID: 30413188 DOI: 10.1186/s12929-018-0483-8]

45 **Yang Y**, Gharaibeh RZ, Newsome RC, Jobin C. Amending microbiota by targeting intestinal inflammation with TNF blockade attenuates development of colorectal cancer. *Nat Cancer* 2020; **1**: 723-734 [PMID: 33768208 DOI: 10.1038/s43018-020-0078-7]

46 **Zamani S**, Taslimi R, Sarabi A, Jasemi S, Sechi LA, Feizabadi MM. Enterotoxigenic *Bacteroides fragilis*: A Possible Etiological Candidate for Bacterially-Induced Colorectal Precancerous and Cancerous Lesions. *Front Cell Infect Microbiol* 2019; **9**: 449 [PMID: 32010637 DOI: 10.3389/fcimb.2019.00449]

World Journal of Gastroenterology

Submit a Manuscript: https://www.f6publishing.com

World J Gastroenterol 2022 August 14; 28(30): 4061-4074

DOI: 10.3748/wjg.v28.i30.4061

ISSN 1007-9327 (print) ISSN 2219-2840 (online)

MINIREVIEWS

Thrombocytopenia in chronic liver disease: Physiopathology and new therapeutic strategies before invasive procedures

Paolo Gallo, Francesca Terracciani, Giulia Di Pasquale, Matteo Esposito, Antonio Picardi, Umberto Vespasiani-Gentilucci

Specialty type: Gastroenterology and hepatology

Provenance and peer review: Invited article; Externally peer reviewed.

Peer-review model: Single blind

Peer-review report's scientific quality classification

Grade A (Excellent): A
Grade B (Very good): 0
Grade C (Good): C
Grade D (Fair): 0
Grade E (Poor): 0

P-Reviewer: Ishikawa T, Japan; Jiang W, China

Received: January 24, 2022
Peer-review started: January 24, 2022
First decision: April 10, 2022
Revised: April 21, 2022
Accepted: July 18, 2022
Article in press: July 18, 2022
Published online: August 14, 2022

Paolo Gallo, Francesca Terracciani, Giulia Di Pasquale, Matteo Esposito, Antonio Picardi, Umberto Vespasiani-Gentilucci, Clinical Medicine and Hepatology Unit, Campus Bio-Medico University, Roma 00128, Italy

Corresponding author: Paolo Gallo, MD, Associate Research Scientist, Doctor, Clinical Medicine and Hepatology Unit, Campus Bio-Medico University, *Via* Alvaro del Portillo, 200, Roma 00128, Italy. paolo.gallo@policlinicocampus.it

Abstract

Chronic liver disease is characterized by several hematological derangements resulting in a complex and barely rebalanced haemostatic environment. Thrombocytopenia is the most common abnormality observed in these patients and recent advances have led to researchers focus the attention on the multifactorial origin of thrombocytopenia and on the key role of thrombopoietin (TPO) in its physiopathology. Severe thrombocytopenia (platelet count < 50000/μL) complicates the management of patients with chronic liver disease by increasing the potential risk of bleeding for invasive procedures, which may be therefore delayed or canceled even if lifesaving. In the very last years, the development of new drugs which exceed the limits of the current standard of care (platelet transfusions, either immediately before or during the procedure) paves the way to a new scenario in the management of this population of patients. Novel agents, such as the TPO-receptor agonists avatrombopag and lusutrombopag, have been developed in order to increase platelet production as an alternative to platelet transfusions. These agents have demonstrated a good profile in terms of efficacy and safety and will hopefully allow reducing limitations and risks associated with platelet transfusion, without any delay in scheduled interventions. Altogether, it is expected that patients with chronic liver disease will be able to face invasive procedures with one more string in their bow.

Key Words: Thrombocytopenia; Chronic liver disease; Thrombopoietin agonists; Platelet transfusions; Avatrombopag; Lusutrombopag

©The Author(s) 2022. Published by Baishideng Publishing Group Inc. All rights reserved.

Core Tip: Recent advances have shed light on the pathophysiology of thrombocytopenia in chronic liver disease and on the key role of thrombopoietin (TPO). Severe thrombocytopenia complicates the management of patients with liver disease by increasing the potential risk of bleeding for invasive procedures, possibly delaying lifesaving interventions. In the very last years, novel agents such as the TPO-receptor agonists avatrombopag and lusutrombopag have been developed in order to increase platelet production as an alternative to platelet transfusions, with positive efficacy and safety outcomes.

Citation: Gallo P, Terracciani F, Di Pasquale G, Esposito M, Picardi A, Vespasiani-Gentilucci U. Thrombocytopenia in chronic liver disease: Physiopathology and new therapeutic strategies before invasive procedures. *World J Gastroenterol* 2022; 28(30): 4061-4074
URL: https://www.wjgnet.com/1007-9327/full/v28/i30/4061.htm
DOI: https://dx.doi.org/10.3748/wjg.v28.i30.4061

INTRODUCTION

Thrombocytopenia, usually defined as any decrease in platelet count below the lower normal limit of 150000/μL, is the most common haematological abnormality in patients with chronic liver disease[1]. Current data report a prevalence ranging from 6% to 78%, which progressively increases from patients with compensated to those with decompensated cirrhosis[2]. The clinical significance of mild (100000/μL-150000/μL) and moderate (50000/μL-100000/μL) thrombocytopenia is minimal and does not interfere with the regular clinical practice. Otherwise, severe thrombocytopenia (< 50000/μL) can be associated with many sequelae and could have a negative impact on the management of patients with advanced chronic liver disease.

PHYSIOPATHOLOGY OF THROMBOCYTOPENIA IN CHRONIC LIVER DISEASE

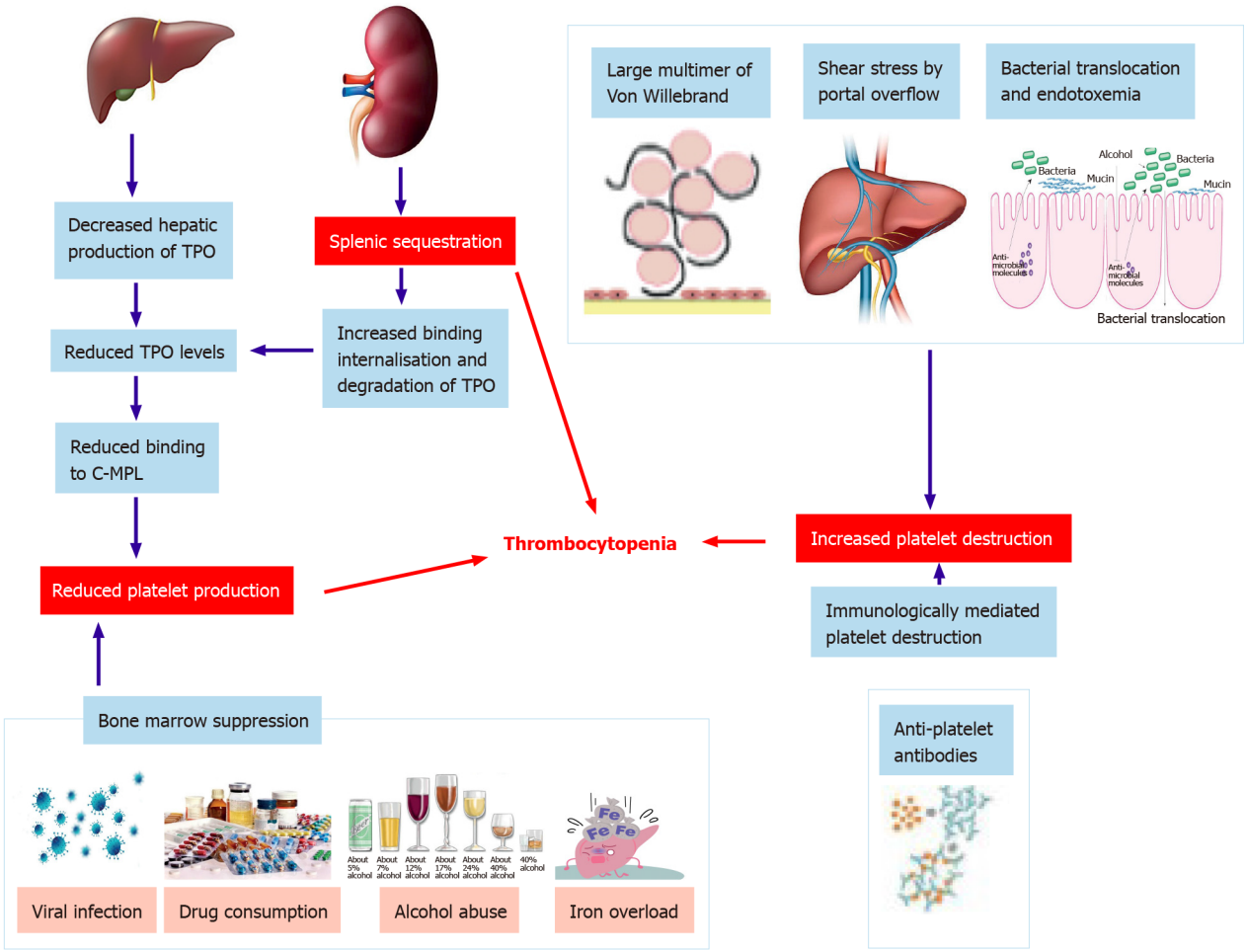
In chronic liver disease, thrombocytopenia has been classically attributed to hypersplenism[1,3]. Over the last decades, however, advances in the understanding of thrombopoiesis have led to a wider and better understanding of its physiopathology. As a result, thrombocytopenia is considered a more complex and multifactorial process involving multiple different mechanisms. These are generically divided into those leading to decreased production or increased destruction of thrombocytes and splenic sequestration[1] (Figure 1).

Decreased platelet production

Decreased platelet production is a consequence of decreased production of thrombopoietin (TPO) and direct bone marrow suppression. Currently, the production of TPO is believed to play a pivotal role in thrombopoiesis. TPO is primarily produced in the liver and, after being secreted into the circulation, it binds to the surface of platelets and megakaryocytes through the c-MPL receptor[4]. TPO-receptor ligation activates a number of intracellular signalling pathways *via* Janus kinase type 2 and tyrosine kinase 2[5], which ultimately lead to the differentiation of bone marrow stem cells into mature megakaryocytes and to the production of platelets which are released into the peripheral circulation[6]. Of note, after binding to its receptor, TPO is internalized and destroyed in order to reduce further platelet and megakaryocyte exposure[4]. Platelet production is therefore mainly regulated by platelet levels in the blood through a negative feedback circuit[1]. The role of a decreased hepatic production of TPO in the development of thrombocytopenia in chronic liver disease is supported by the immediate increase in TPO levels and platelet production after liver transplantation[7]. Animal models and human clinical studies have confirmed decreased expression of *TPO* mRNA in liver tissue with the progression of cirrhosis[8], which is probably associated with specific regulatory mechanisms for the expression of *TPO* gene and is not regulated by bone marrow[9]. Moreover, a correlation between reduced c-MPL expression and the progression of liver cirrhosis has been demonstrated and may play an additional role in the development of thrombocytopenia[10]. Some chronic liver diseases may also cause decreased platelet production through direct bone marrow suppression or toxicity, as observed during viral infection (particularly hepatitis C virus (HCV) infection[11], alcohol abuse[12], iron overload[12], and drug consumption[1,13]).

Increased platelet destruction

Increased platelet destruction is a multifactorial process that may involve decreased levels of A disintegrin-like and metalloprotease with thrombospondin type 1 motif 13 (ADAMTS13), immunologically mediated platelet destruction, and bacterial activity. ADAMTS13 is a metalloproteinase



DOI: 10.3748/wjg.v28.i30.4061 **Copyright** ©The Author(s) 2022.

Figure 1 Pathophysiology of thrombocytopenia. TPO: Thrombopoietin.

produced by hepatic stellate cells, whose physiological role is to cleave large von Willebrand factor (vWF) multimers[14]. In cirrhosis, decreased levels and activity of ADAMTS13 drive the accumulation of vWF multimers, which mediates an enhancement of shear-stress induced platelet aggregation[14]. Additionally, anti-platelet antibodies are a frequent finding in patients with liver cirrhosis, being detectable in up to 64% of cases[15]. The inverse relationship between platelet-associated immunoglobulin G (IgG) levels and platelet count evidences that immunologic destruction contributes to the genesis of thrombocytopenia at least in some chronic liver diseases[16]. Immune-mediated thrombocytopenia is most likely to occur in the course of autoimmune liver diseases (particularly primary biliary cholangitis) and HCV infection[1,17].

HCV can cause immune-mediated thrombocytopenia through multiple mechanisms[1]. First, it can be associated with idiopathic thrombocytopenic purpura (ITP), as supported by a prevalence of anti-HCV antibodies of approximately 10% in patients with ITP[18]. The virus can also directly bind to platelets interacting with multiple surface receptors, leading to the attachment of anti-HCV antibodies to platelets. This will ultimately determine either platelet phagocytosis by the reticuloendothelial system or alterations in the platelet membrane epitopes that induce the production of anti-platelet antibodies[19]. Finally, HCV infection can be associated with the production of cryoglobulins, which can accelerate platelet clearance by the reticuloendothelial system[20]. Thrombocytopenia can be found in about 48% of patients with bacterial infection and sepsis[21], confirming that the inflammatory cascade plays a role in the development of thrombocytopenia. This is confirmed in the hospitalized cirrhotic population[22]. In sepsis, thrombocytopenia is mainly dependent on the increased activation of the coagulative system, resulting in clot formation and platelet consumption[23].

Splenic sequestration

Hypersplenism has been classically considered the main determinant of thrombocytopenia during chronic liver disease[1,3], even after that many other physiopathologic mechanisms have been progressively identified. During chronic liver disease, the inception of portal hypertension causes a redistribution of splanchnic venous blood flow, ultimately responsible for congestion of the spleen and consequent enlargement of the organ, leading to a significant increase of the splenic pool of platelets

[24]. Actually, hypersplenism is the clinical syndrome in which splenomegaly is associated with splenic hyperactivity, *i.e.*, a reduction in one or more peripheral blood cell types, in patients with an appropriate proliferative bone marrow response. This syndrome can be reverted with splenectomy[1,24].

COAGULOPATHY AND HAEMORRHAGIC RISK ASSESSMENT IN CHRONIC LIVER DISEASE

Chronic liver disease is characterized by alterations of the entire hemostatic system[25]. Thrombocytopenia is just one face of a wider coagulation disorder whose relevance is mirrored by the inclusion of coagulation indices in all functional and prognostic scores of liver disease[26]. Traditionally, coagulopathy in cirrhosis was considered as a bleeding diathesis disorder[27], alongside the well-known thrombocytopenia, and the impaired coagulation tests were perceived as indicators of hemorrhagic risk [28]. In the last decades, several studies led to significant changes in knowledge, with a renewed vision concerning the coagulopathy of liver cirrhosis. A new paradigm of a balanced, *albeit* precarious, hemostatic state has emerged and the net effect is a rebalanced equilibrium[26,27], which can be easily disturbed by many different clinical events, alternatively leading to hemorrhagic as well as to thrombotic manifestations, with the latter being even more frequent indeed[27] (Figure 2).

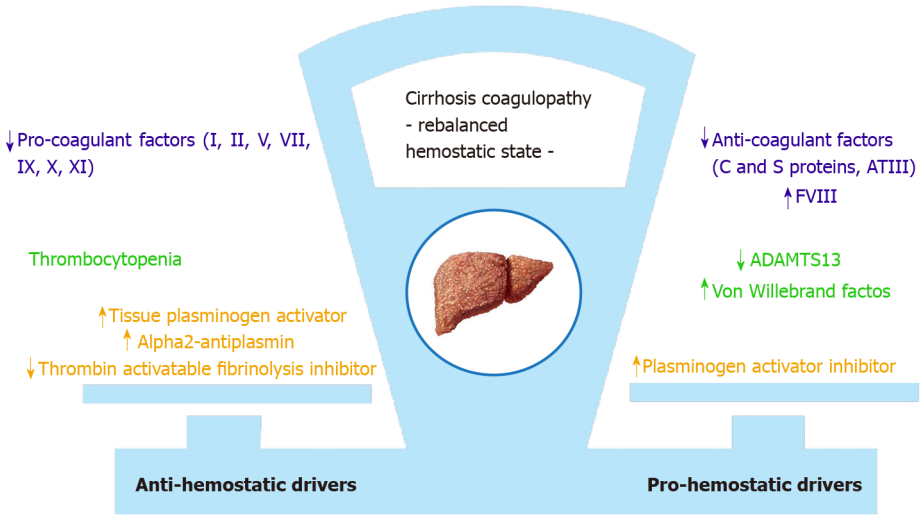
It has been shown that the reduction in liver-derived pro-coagulant factors is counteracted by the concomitant decrease of the liver-derived anti-coagulant ones, especially protein C[28,29]. Thrombocytopenia and platelet abnormal function are offset by increased vWF and decreased ADAMTS13 levels. In cirrhosis, even if diminished in number, platelets are able to support normal thrombin generation at least until they are in the range 50-60000/mL, therefore assuring a normal primary hemostasis. This is possible thanks to the compensatory action of vWF and to the upregulation of intracellular activating signalling pathways[27], leading to an enhanced thrombocyte response. Furthermore, decreased clearance of tissue plasminogen activator and plasminogen activator inhibitor, and decreased synthesis of alpha 2-antiplasmin and thrombin activable fibrinolysis inhibitor are all factors contributing to hyperfibrinolysis. The latter is observed in up to 30% of patients with advanced liver disease[1], confirming a re-arrangement of the whole hemostatic system.

In cirrhotic patients, even though reduced in number, platelets are still able to ensure an adequate haemostatic function. Consequently, the sole platelet count is not able to predict bleeding risk in liver cirrhosis. Actually, for patients with cirrhosis undergoing invasive diagnostic or therapeutic procedures, the risk of procedure-related bleeding remains a clinical issue[30], and risk stratification is a great challenge. This is mainly due to the inaccuracy, in the context of cirrhosis, of the laboratory tests that are routinely used for the assessment of the hemocoagulative system[25,27,30]. Indeed, it is now well established that the standard clotting tests do not reflect the actual bleeding risk[30-32], and current evidence does not support prothrombin time (PT)/international normalized ratio (INR) as clinical targets[25,33]. Conversely, assessing platelet count and fibrinogen levels before high-risk procedures is recommended, as well as it is the pre-procedural correction of these parameters, having these laboratory parameters been proposed as more reliable indicators of the bleeding risk in patients with cirrhosis[34].

Moreover, many studies have shown that cirrhotic portal hypertension and kidney injury are more essential in determining the risk of bleeding[25,35]. As a matter of fact, renal failure can lead to platelet impairment resulting from reduced adhesive and aggregative capacities *via* alterations of serotonin concentration, of calcium flow and of thromboxane metabolism[25]. Patient with cirrhosis can also develop accelerated intravascular coagulation and fibrinolysis, described as a bleeding entity similar to disseminated intravascular coagulation, but different for the imbalance between pro- and anti-fibrinolytic factors, resulting in hyper-fibrinolysis with an increased bleeding risk[35]. Despite all such evidence, most current guidelines still recommend correcting elevated PT/INR values through plasma transfusions, while tests capable of better capturing the hemostatic function of cirrhotic patients (thrombin generation tests, thromboelastography, *etc.*) are not readily available in everyday clinical practice[25].

NON-PHARMACOLOGICAL TREATMENT OPTIONS FOR MANAGEMENT OF THROMBOCYTOPENIA

The management of thrombocytopenia in chronic liver disease has been a primary and challenging endpoint for decades. In the 1960s, surgical splenorenal shunts were performed with this purpose, but they were soon abandoned due to high mortality rates and the risk of liver decompensation[36]. Total and partial splenectomy were therefore developed. They gained popularity in the 1990s thanks to limited complication rates, mainly after the introduction of the laparoscopic technique. Later, less invasive techniques, namely, splenic artery embolization or spleen radiofrequency ablation, opened new scenarios[36].



DOI: 10.3748/wjg.v28.i30.4061 **Copyright** ©The Author(s) 2022.

Figure 2 Pathophysiology of coagulopathy. ATIII: Antithrombin III; FVIII: Coagulation factor VIII; ADAMTS13: A disintegrin-like and metalloprotease with thrombospondin type 1 motif 13.

Splenectomy

In the past, open splenectomy has been considered among the strategies for treating thrombocytopenia. Actually, this procedure was associated with a high risk of bleeding and consequent hepatic decompensation, particularly following the open technique. For these reasons, subsequent studies supported the laparoscopic technique over open surgical splenectomy or the shunt techniques over splenectomy[37,38]. Overall, also with less invasive procedures, the rate of complications range from 2.5% to 17%, and the risk of portal and splenic vein thrombosis is elevated (about 10%)[39]. Altogether, due to their invasive nature and to the high risk of complications, these strategies are restricted to rare and specific cases, while they have been virtually abandoned in the ordinary clinical practice.

Splenic artery embolization

Splenic artery embolization has been introduced since the 1970s as an alternative to splenectomy in surgically unfit patients. For the increased risk of developing splenic abscesses after total embolization, partial splenic embolization has become the preferred option for candidate patients[40], with a lower risk of complications, sepsis and mortality compared to total splenectomy[36,41]. Unfortunately, the extent of the beneficial effect on platelet count depends on the amount of the splenic mass embolized, which is proportional to the complications observed.

Radiofrequency ablation of the spleen

Radiofrequency ablation of the spleen is a minimally invasive procedure with promising results in patients with cirrhosis and severe thrombocytopenia[36]. The main benefits of this minimally invasive procedure are cost-effectiveness and lower complication rates over other invasive procedures. The major side effects are hemorrhagic shock and intra-abdominal bleeding, while complications such as splenic abscess or rupture are not a concern with this procedure[42]. Besides, to date, more clinical trials with longer follow-up would be needed to estimate the effectiveness of this strategy.

Shunt procedures

Shunt procedures [portocaval shunt, splenorenal shunt, and transjugular intrahepatic portosystemic shunt (TIPS)] are other possible techniques which have been experimented in chronic liver disease. They are aimed at decreasing splenic congestion and, therefore, platelet sequestration[36]. To date, however, these approaches are not supported by available studies; indeed, there is an absence of clear benefits on the platelet number and well-known complications. Actually, the use of these procedures, in particular TIPS, is currently restricted to selected cases where the aim is not to increase platelet levels, but to control bleeding from oesophageal varices or to manage refractory ascites[43].

Platelet transfusion

Platelet transfusion has become the mainstay of treatment in patients with chronic liver disease and severe thrombocytopenia who require an invasive procedure[44]. The choice to transfuse platelets is variable and controversial, depending upon patient comorbidities and the risk of bleeding. Most data suggest that invasive procedures may be performed without a significantly increased risk of bleeding in patients with more than 50000/μL platelets, while there is less consensus about the risk in patients with

a lower count, as reflected also in the latest guidelines and a recent retrospective study[45,46]. In a sub-analysis of 2740 liver biopsies from the Hepatitis C Antiviral Long-term Treatment against Cirrhosis trial, there were only 16 bleeding events (0.6%), and the highest bleeding risk (5.3%) was recognized for platelet counts less than 60000/μL[47]. Conversely, in another study evaluating the safety of liver biopsies (177 patients), the frequency of bleeding in patients with a platelet count lower than 50000/μL was not significantly different from that in those with a normal platelet count, and the only independent risk factor for bleeding was an underlying malignancy[32].

Guidelines vary as to the threshold below which periprocedural bleeding risk justifies intervening to treat thrombocytopenia; however, transfusions are more frequently indicated with a platelet threshold < 50000/μL[48]. Although platelet transfusion has been the standard of care for correcting thrombocytopenia for a long time, relevant side effects limit its use. The most common issues include febrile or allergic reactions, risk of infection (even if very low), hemolysis, transfusion-related graft-*versus*-host disease, and alloimmunization[41,49]. Even the procedure of transfusion itself may be critical. Potential risks include errors in patient identification, in blood typing, and in cross-matching[50]. Concerning efficacy, platelet transfusions determine an overall modest increase in platelet count, without a significant impact on the risk of bleeding[51], and treatment effect has a limited duration. Moreover, up to 70% of patients receiving repeated platelet transfusions become refractory to subsequent ones. Finally, platelet transfusions are limited by donor supply, and the reduced availability may have a great impact on the management and clinical outcomes of these patients.

NEW THERAPEUTIC OPTIONS FOR THRMBOCYTOPENIA IN CHRONIC LIVER DISEASE

Recent advances in understanding the physiopathology of thrombocytopenia in chronic liver disease, with the discovery of the central role of TPO in thrombocytopoiesis, has led to the development of many drugs with TPO activity.

Recombinant TPO and human cytokines

Two recombinant TPOs that stimulate platelet production in humans and showed potential promise were recombinant human TPO and pegylated recombinant megakaryocyte growth and development factor[52,53]. They have shown clinical benefits in clinical trials of haematological patients without safety concerns, but have been withdrawn from clinical development for the induction of neutralizing antibodies[53]. Similarly, the use of recombinant human cytokines was limited because of side effects and the occurrence of toxicities as observed after the subcutaneous injection of the recombinant human interleukin-1, approved by the Food and Drug Administration (FDA) for the treatment of the thrombocytopenia induced by chemotherapy for solid tumors, which can cause cardiovascular side effects and flu-like symptoms[54].

TPO agonists

Activation of thrombopoiesis through TPO receptor agonists is an alternative method to stimulate platelet production with the use of drugs, which are not homologous to endogenous TPO but activate the same receptor working on a different site. These drugs have been primarily investigated in patients with chronic ITP and subsequently in chronic liver disease for treating thrombocytopenia before invasive procedures. The effect of TPO agonists is mediated by the interaction with TPO receptors on megakaryocytes, specifically c-MPL ligand-mediated activation of Janus kinases and signal transducer and activator of transcription proteins and mitogen-activated protein kinase pathways[55].

Romiplostin: Romiplostin is a polypeptide linked to an IgG heavy-chain Fc molecule and has no amino acid sequence homology to endogenous TPO. It acts by competing with the same site of the TPO-receptor and activating intracellular transcriptional pathways aimed to increase platelet production[55]. Due to a different molecular structure, its use has not been associated with antibodies reacting against endogenous TPO. This drug is administered subcutaneously once a week, but it is currently approved only for treatment of ITP when refractory to other drugs[54,56].

Indeed, most of the experience with romiplostin was derived from clinical studies in patients with refractory ITP[57], while only anecdotal case reports and small series involved patients with chronic liver disease[58-61]. A single-centre study in Egypt involved 35 patients with HCV-related cirrhosis and severe thrombocytopenia who required elective surgery[60]. Patients received romiplostin once weekly for a maximum of 4 wk. The primary endpoint - achieving a threshold of platelet count of 70000/μL - was reached in 94% of patients, and 20% of them had maintained a count > 50000/μL 3 mo after the last injection. Headache was reported as the only adverse event. In another single centre, prospective, randomized, double-blind study, 65 subjects with chronic liver disease and thrombocytopenia (less than 60000/μL) undergoing percutaneous liver biopsy received a TPO agonist or platelet transfusion[61]. Romiplostin determined significantly higher pre-biopsy and post-biopsy platelet counts compared to eltrombopag and platelet transfusion, and it was cost-effective and safe.

Eltrombopag: Eltrombopag is an orally available, small non-peptide TPO mimetic molecule more largely studied for use in liver disease. Its binding to a specific human transmembrane domain of TPO-receptor induces proliferation and differentiation of megakaryocytes and precursor cells[62]. It is taken orally once daily and is approved for thrombocytopenia: (1) In chronic ITP refractory to other treatments; (2) In HCV chronic hepatitis candidates for treatment with interferon-based regimens; and (3) In patients with severe aplastic anaemia[63].

Eltrombopag safely increased platelet number in patients with cirrhosis and HCV infection[64]. In a phase II multicentre randomized trial, eltrombopag was effective in increasing platelet count to more than 100000/μL at week 4 in 75%-95% of patients, compared to 0% of patients in the placebo group. Consequently, these patients were significantly more likely to initiate and complete 12 wk of antiviral treatment with respect to those on placebo (36%-65% *vs* 6%). In a phase II trial in Japan on 38 patients with chronic liver disease, eltrombopag increased platelet count in a dose-dependent manner[65].

The most recently published data in chronic liver disease are derived from the Eltrombopag Evaluated for Its Ability to Overcome Thrombocytopenia and Enable Procedures study, a phase 3 double-blind, placebo controlled trial that assessed the utility of this drug to increase platelet count and reduce the need for transfusion in patients undergoing elective procedures[66]. In this trial, 86% of patients recruited had liver cirrhosis with a platelet count less than 50000/μL. Patients were randomized to receive 75 mg eltrombopag daily or placebo in the 2 wk preceding the invasive procedure performed within 5 d from the last dose. Primary endpoint was the number of subjects who did not require a platelet transfusion before, during, and up to 7 d after the procedure. This was achieved in 72% (104/145) of subjects who received eltrombopag, compared to 19% (28/147) in the placebo group (P < 0.001). However, this study was prematurely terminated since six patients in the treatment group developed thrombotic events (2 patients in placebo, odds ratio for eltrombopag 3.04, 95% confidence interval: 0.62-14.82). *Post-hoc* analysis suggested an association of platelet count > 200000/μL with the occurrence of portal vein thrombosis[66].

The other two international phase III trials included patients with chronic hepatitis C and platelet counts less than 75000/μL[67]. Eltrombopag to Initiate and Maintain Interferon Antiviral Treatment to Benefit Subjects with Hepatitic C-Related Liver Disease (ENABLE)-1 and ENABLE-2 assessed the ability of eltrombopag to increase platelet count and, so, allow subjects to initiate and maintain antiviral treatment with pegylated interferon and ribavirin. In both trials, significantly more patients on eltrombopag achieved a sustained virological response at 24 wk of antiviral therapy, with similar adverse events. However, the absolute benefit over placebo was less than 10% and the use of this drug was associated with an increased risk of hepatic decompensation (10% *vs* 5% placebo) and thromboembolic events (3% *vs* 1% placebo). The most frequent adverse events reported were anaemia, pyrexia, and neutropenia.

Avatrombopag: Avatrombopag is an orally available drug that has a similar mode of action to eltrombopag, and it does not compete with endogenous TPO for its receptor site-binding. It is taken once daily with food for 5 d a week, with the dose adjusted according to baseline platelet count. Differently from eltrombopag, it exhibits significant drug-drug interactions based on the cytochrome P450 2C9 (CYP2C9) and CYP3A cytochrome systems[68]. In a phase II study, 130 patients with chronic liver disease and platelet count less than 60000/μL received two different formulations of the drug 1 wk prior to an elective invasive procedure, and both groups of avatrombopag-treated patients achieved the primary endpoint of an platelet increase of > 20000/μL from baseline, and to > 50000/μL, at least once during the treatment days 4-8.

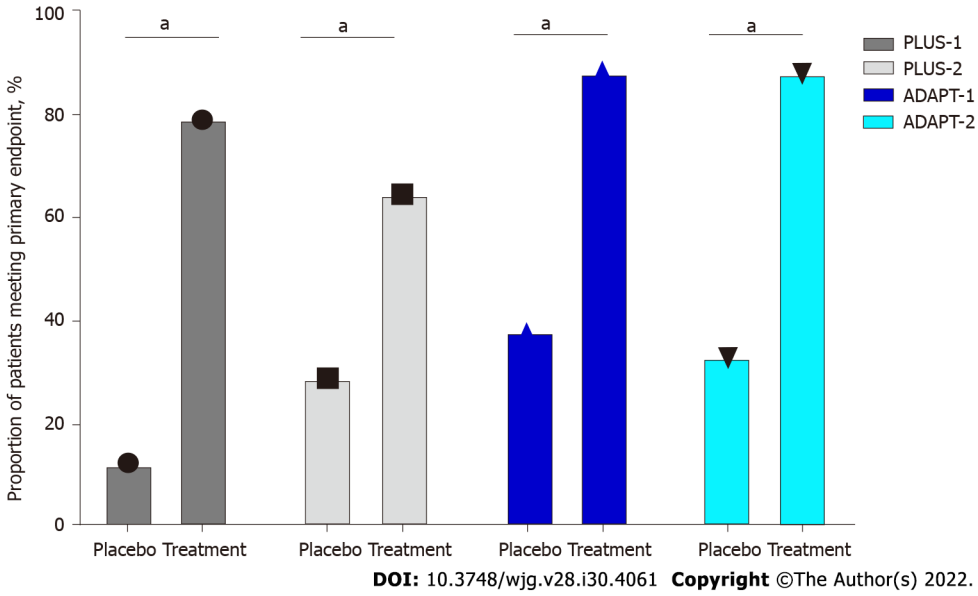
After that, avatrombopag was approved by the FDA in 2018 and the European Medicines Agency (EMA) in 2019 for the treatment of severe thrombocytopenia in patients with chronic liver disease undergoing invasive procedures, with the recommendation to take it 10-13 d before the procedure scheduled within 5-8 d from the last dose administration[69]. The safety and efficacy were evaluated in two pivotal randomized phase 3 studies[69]. ADAPT-1 and ADAPT-2 (Table 1) randomized 430 patients with cirrhosis and severe thrombocytopenia undergoing scheduled procedures to receive avatrombopag at different doses (according to platelet baseline count) or placebo for 5 d. The primary endpoint was the need for platelet transfusion or rescue procedures for bleeding in the 7 d after the procedures[70]. Significantly more patients met this endpoint in avatrombopag groups: In ADAPT-1, 65.6% and 88.1% compared to 22.9% and 38.2% of patients receiving placebo; in ADAPT-2, 68.6% and 87.9% compared to 34.9% and 33.3% (P < 0.001 for both) (Figure 3). Overall, the safety profile was similar to placebo and the most frequent adverse events were nausea, fatigue, abdominal pain, pyrexia, and headache. Serious adverse events occurred in 16%-19% of patients with avatrombopag and 6%-14% of those with placebo, including one patient who developed portal vein thrombosis during post-treatment follow-up. Finally, the safety and efficacy of avatrombopag were recently confirmed in a real-world setting, where cirrhotic patients mainly undergoing esophageal varices band ligation received the drug without requiring platelet transfusion, and with a good profile of adverse events[71,72].

Lusutrombopag: Lusutrombopag is an orally administered synthetic small molecule that acts as an agonist of human TPO, activating the signal transduction pathways to upregulate platelet production. Earlier studies have demonstrated that lusutrombopag raises platelet count and is a manageable drug

Table 1 ADAPT 1-2 key characteristics

Key characteristic	ADAPT 1-2
Key inclusion criteria	Chronic liver disease (MELD score ≤ 24) and thrombocytopenia (platelet counts < 50000/μL). Age ≥ 18 yr
Key exclusion criteria	ADAPT-1/2: History of thrombosis or hematologic disorders. Significant cardiovascular disease. Portal or splenic mesenteric system thrombosis at screening; portal vein blood flow < 10 cm/s at screening. Platelet transfusion within 7 d of screening. Use of heparin, warfarin, FANS, aspirin, verapamil, or antiplatelet therapy with ticlopidine or glycoprotein IIb/IIIa antagonists, or erythropoietin-stimulating agents within 7 d of screening. Advanced hepatocellular carcinoma (BCLC C or D)
Dosing	Low baseline platelet count cohort (≤ 40000/μL): 60 mg avatrombopag or placebo once daily with a meal on days 1-5. High baseline platelet count cohort (40000-50000/μL): 40 mg avatrombopag or placebo once daily with a meal on days 1-5
Type of study	ADAPT-1/2: Global, multicenter, randomized, double-blind, placebo- controlled, phase 3 studies
Patients number	ADAPT-1: 231; ADAPT-2: 204
Endpoints	Efficacy assessment: (1) Primary: Proportion of patients not requiring a platelet transfusion or rescue procedure for bleeding bleeding in the 7 d after the procedures; and (2) Secondary: Proportion of patients achieving the target platelet count of 50000/μL on procedure day; the change in platelet count from baseline to procedure day. Safety assessment: The incidence of adverse events adverse drug reactions, treatment-emergent adverse events

MELD: Model for end-stage liver disease.



DOI: 10.3748/wjg.v28.i30.4061 **Copyright** ©The Author(s) 2022.

Figure 3 Overview of primary endpoints of phase 3 studies (ADAPT-1, ADAPT-2, L-PLUS 1, and L-PLUS 2). [a]*P* ≤ 0.0001.

that does not require food restrictions, and has no clinically significant drug-drug interactions[73,74]. Furthermore, it has demonstrated a dose-proportional pharmacokinetic with no clinically significant differences in the pharmacokinetic grounded on age, liver function (Child-Pugh classes A and B), and renal function (creatinine clearance greater than 30 mL/min)[75]. It is primarily metabolized by CPY4 enzymes, including CYP4A11, and it is mainly excreted by the faecal route (83% of dose). Moreover, it has a low potential to inhibit or induce transporter systems and CYP enzymes[73]. The recommended dose of the drug is 3 mg once daily for 7 d, beginning 8-14 d prior to the scheduled procedure.

Lusutrombopag was approved in Japan in 2015 for use in patients with thrombocytopenia and chronic liver disease who needed invasive procedures and received a positive opinion from the EMA Committee for Medicinal Products for Human Use in 2018[76]. The approval of this drug was based on the results of Lusutrombopag for the Treatment of Thrombocytopenia in Patients with Chronic Liver Disease Undergoing Invasive Procedures trial (L-PLUS-1), a phase 3 double-blind study, carried out in Japan with 96 patients with chronic liver disease and severe thrombocytopenia (platelet count < 50000/μL) undergoing invasive procedures[77] (Table 2). In this study, the proportion of patients that did not require pre-operative platelet transfusions was significantly greater in the lusutrombopag group *vs* placebo (79.2 % *vs* 12.5%, respectively, $P < 0.0001$) (Figure 3). The median platelet count reached more than 50000/μL after 5 d in the drug group, with the greatest value observed after a mean of 13.4 d.

Table 2 Lusutrombopag for the Treatment of Thrombocytopenia in Patients with Chronic Liver Disease Undergoing Invasive Procedures trial 1-2 key characteristics

Key characteristic	L-PLUS 1-2
Key inclusion criteria	Chronic liver disease (Child Pugh A or B) and thrombocytopenia (platelet counts < 50000/μL). Age ≥ 18 yr (≥ 20 yr in L-PLUS 2)
Key exclusion criteria	L-PLUS 1: (1) Hematopoietic tumors; aplastic anemia, myelodysplastic syndrome, myelofibrosis, congenital, immune, or drug-induced thrombocytopenia; (2) Splenectomy, any other causes of thrombocytopenia; (3) History of portal vein thrombosis; (4) Active malignant tumor other than primary hepatic cancer; (5) Therapies that could influence platelet count (L-PLUS 1); (6) Chronic liver disease with Child-Pugh C; (7) Portal vein tumor embolism; and (8) Past or present thrombosis or prothrombotic condition. L-PLUS 2: (1) Hematopoietic tumors; aplastic anemia, myelodysplastic syndrome, myelofibrosis, congenital, immune, or drug-induced thrombocytopenia; (2) Portal vein thrombosis within 28 d prior to randomization or a history of portal vein thrombosis; absence of hepatopetal blood flow in the main trunk of the portal vein as demonstrated by doppler ultrasonography within 28 d prior to randomization; (3) Chronic liver disease with Child-Pugh C; (4) Portal vein tumor embolism; and (5) Past or present thrombosis or prothrombotic condition, history of splenectomy
Dosing	3 mg lusutrombopag or placebo once daily for up to 7 d
Type of study	L-PLUS 1: Double-blind, parallel-group, phase 3 study; L-PLUS 2: Global, phase 3, randomized, double-blind, placebo-controlled study
Patients number	L-PLUS 1: 96; L-PLUS 2: 215
Endpoints	Efficacy assessment: (1) Primary: Proportion of patients who required no platelet transfusions before the primary invasive procedure and no rescue therapy for bleeding; and (2) Secondary: Rate of response (defined as proportion of patients who achieved platelet count of more than 50000/μL with an increase of ≥ 20000/μL from baseline at any time during the study); the duration of sustained platelet count increase; time courses of changes in platelet count. Safety assessment: The incidence of adverse effects, adverse drug reactions, treatment-emergent adverse effects, bleeding-related adverse effects, and thrombotic events

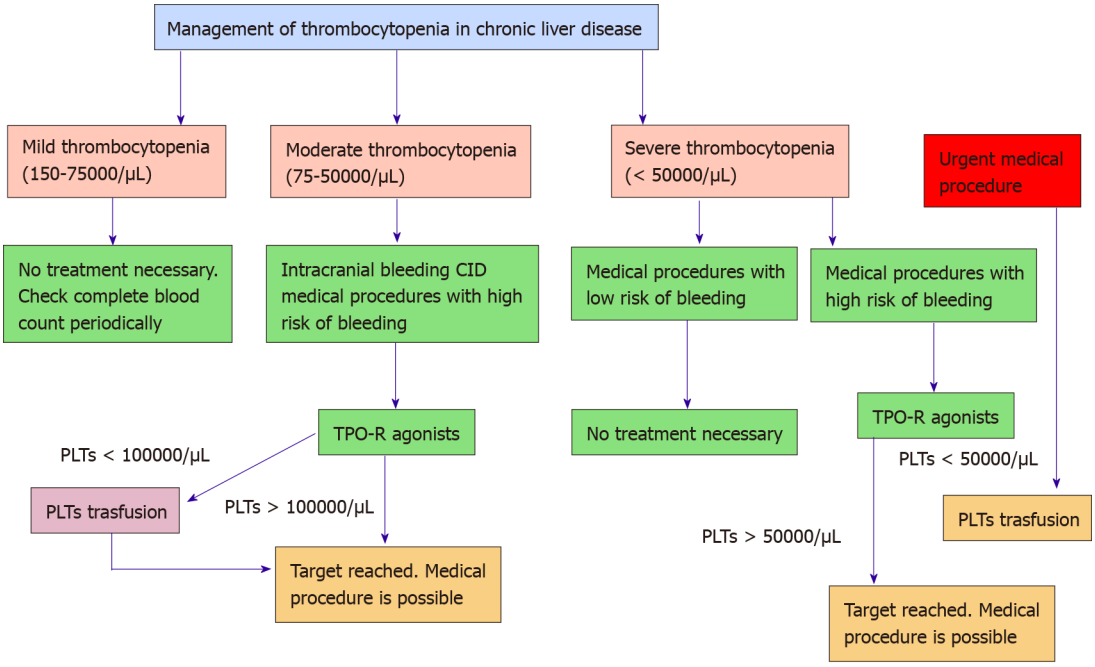
L-PLUS: Lusutrombopag for the Treatment of Thrombocytopenia in Patients with Chronic Liver Disease Undergoing Invasive Procedures trial.

Moreover, no significant concerns were raised in this study, and no significant adverse drug reactions were observed.

The safety and efficacy of this drug were confirmed in a larger study, the L-PLUS-2[78]: 215 patients with chronic liver disease and a platelet count < 50000/μL were randomly assigned to once-daily lusutrombopag at a dosage of 3 mg or placebo for ≤ 7 d before an invasive procedure. The procedure was performed within 7 d after the last dose. In the intention to treat analysis, significantly more patients in the lusutrombopag group (64.8%) met this endpoint compared with placebo (29%, $P < 0001$). This percentage was greater in the per-protocol analysis, with the endpoint reached in 72.5% of patients in the active drug group *vs* 20% in the placebo group ($P < 0.0001$). The median duration of the achievement of a target of platelet count > 50000/μL was 19.2 d in the lusutrombopag group *vs* 0 d for the patients who received placebo. Moreover, the median maximum change in platelets from baseline was over 4 times higher for patients treated with the active drug, who did not receive platelet transfusions, compared with patients who did receive transfusions (45000 *vs* 11000/μL)[78]. Finally, 47.7% of patients in the lusutrombopag group and 48.6% in the placebo group had at least one adverse event. These side effects were mainly mild or moderate in severity and the most common were headache, abdominal pain, fatigue, peripheral edema, and nausea. There were only three mild bleeding events in three patients in the lusutrombopag group (2.8%) *vs* seven bleeding events (4 moderate and 1 severe; 5.6%) with placebo. Only three thromboembolic events were recorded (1 in the lusutrombopag group), which were not related to platelet count.

The first real-life study in Japan enrolled 25 patients with cirrhosis, who were treated with lusutrombopag prior to invasive treatments (radiofrequency ablation, transarterial chemoembolization, and endoscopic variceal ligation)[79]. In this group, platelet count significantly increased compared with baseline (82000 ± 26000 *vs* 41000 ± 11000 /μL). The proportion of patients who needed platelet transfusions before procedures was very low (only 4, 16%) compared to those not treated with lusutrombopag (69 patients, 54%). Moreover, platelet counts after treatment and before invasive procedures were lower in patients with a count less than 30000/μL, and this cut-off, together with a spleen index > 40 cm^2, was predictive of a lower response rate to the drug[80]. This was probably due to a larger number of platelets sequestered in the spleen in this subgroup of patients. No haemorrhagic complications were observed, and only a single case of recurrent portal vein thrombosis was observed and successfully treated.

Another real-life setting retrospective study was carried out in patients with chronic liver disease and severe thrombocytopenia. In this study[81], 74.2% of patients who received treatment did not require platelet transfusion before invasive procedures. This percentage increased to 82.1% of treatments if patients who repeated lusutrombopag use more times were included, thus demonstrating the efficacy of repeated use of the drug. Furthermore, only one serious adverse event was observed during/after treatment, *i.e.*, one case of portal thrombosis disappearing after anticoagulation. Notably, this study



DOI: 10.3748/wjg.v28.i30.4061 **Copyright** ©The Author(s) 2022.

Figure 4 Operative flow chart for management of thrombocytopenia in chronic liver disease. TPO-R: Thrombopoietin receptor; PLTs: Platelets; CID: Disseminated intravascular coagulation.

confirmed that a lower platelet count at baseline was a predictive factor for failure to reach the target of > 50000/μL platelets. Indeed, median basal platelet count was higher in responders *vs* non-responders (38000/μL *vs* 12000/μL).

Moreover, the safety and efficacy of repeated use of lusutrombopag have been confirmed also in 66 patients who underwent radiofrequency ablation for recurrence of hepatocellular carcinoma[82]. Later, others reports have confirmed the efficacy and safety of lusutrombopag in real life in patients with thrombocytopenia due to chronic liver disease. In a case report, Kaneko *et al*[83] showed lusutrombopag to be a successful substitute for platelet transfusion in a patient with chronic liver disease undergoing endoscopic spinal surgery. Kawata *et al*[84] reported three patients treated with lusutrombopag before tooth extraction: Platelet count increased, preventing the need for transfusion in two of three cases. There were no adverse events. In addition, the efficacy and safety of the drug have been confirmed in a retrospective Japanese study based on hospital administrative databases. Here the incidence of bleeding events was lower in the lusutrombopag group than in the platelet transfusion group (3.7% *vs* 8.2%, $P < 0.001$), with a consequently lower average medical cost[85]. Finally, real-world data for adverse events (spontaneously reported by healthcare professionals and consumers in a database including about 4000 patients exposed to lusutrombopag from December 2015 to April 2018) confirm the efficacy and the safety of the drug (93% of patients did not require pre-procedural platelet transfusion; 1.2% of serious adverse events, with 0.4% cases of portal vein thrombosis)[86].

CONCLUSION

Thrombocytopenia represents one of the main coagulation disorders in patients with chronic liver disease. Recent awareness in its physiopathology shed light on the central role of TPO. The development of TPO receptor agonists has opened a new scenario in the management of patients with liver disease who need invasive procedures (Figure 4). Avatrombopag and lusutrombopag have demonstrated their efficacy and safety in increasing platelet count without an increased risk of thrombosis. Moreover, they reduce the overall clinical risk associated with platelet transfusion without any delay in the management of these patients. With careful logistical planning and coordination between drug availability and medical procedures, patients with chronic liver disease and severe thrombocytopenia should now be able to undergo more easily invasive procedures.

FOOTNOTES

Author contributions: Vespasiani-Gentilucci U and Gallo P conceived the study; Gallo P, Terracciani F, Di Pasquale

G, and Esposito M wrote the manuscript; Picardi A and Vespasiani-Gentilucci U helped in drafting and revising the manuscript.

Conflict-of-interest statement: All the authors report no relevant conflicts of interest for this article.

Open-Access: This article is an open-access article that was selected by an in-house editor and fully peer-reviewed by external reviewers. It is distributed in accordance with the Creative Commons Attribution NonCommercial (CC BY-NC 4.0) license, which permits others to distribute, remix, adapt, build upon this work non-commercially, and license their derivative works on different terms, provided the original work is properly cited and the use is non-commercial. See: https://creativecommons.org/Licenses/by-nc/4.0/

Country/Territory of origin: Italy

ORCID number: Paolo Gallo 0000-0001-8292-1134; Francesca Terracciani 0000-0002-4778-4194; Giulia Di Pasquale 0000-0001-8872-6815; Matteo Esposito 0000-0003-0609-6333; Antonio Picardi 0000-0002-0230-218X; Umberto Vespasiani-Gentilucci 0000-0002-1138-1967.

S-Editor: Wang JJ
L-Editor: A
P-Editor: Wang JJ

REFERENCES

1 **Mitchell O**, Feldman DM, Diakow M, Sigal SH. The pathophysiology of thrombocytopenia in chronic liver disease. *Hepat Med* 2016; **8**: 39-50 [PMID: 27186144 DOI: 10.2147/HMER.S74612]
2 **Bashour FN**, Teran JC, Mullen KD. Prevalence of peripheral blood cytopenias (hypersplenism) in patients with nonalcoholic chronic liver disease. *Am J Gastroenterol* 2000; **95**: 2936-2939 [PMID: 11051371 DOI: 10.1111/j.1572-0241.2000.02325.x]
3 **Aster RH**. Pooling of platelets in the spleen: role in the pathogenesis of "hypersplenic" thrombocytopenia. *J Clin Invest* 1966; **45**: 645-657 [PMID: 5327481 DOI: 10.1172/JCI105380]
4 **Saur SJ**, Sangkhae V, Geddis AE, Kaushansky K, Hitchcock IS. Ubiquitination and degradation of the thrombopoietin receptor c-Mpl. *Blood* 2010; **115**: 1254-1263 [PMID: 19880496 DOI: 10.1182/blood-2009-06-227033]
5 **Sattler M**, Durstin MA, Frank DA, Okuda K, Kaushansky K, Salgia R, Griffin JD. The thrombopoietin receptor c-MPL activates JAK2 and TYK2 tyrosine kinases. *Exp Hematol* 1995; **23**: 1040-1048 [PMID: 7543416]
6 **Rouyez MC**, Boucheron C, Gisselbrecht S, Dusanter-Fourt I, Porteu F. Control of thrombopoietin-induced megakaryocytic differentiation by the mitogen-activated protein kinase pathway. *Mol Cell Biol* 1997; **17**: 4991-5000 [PMID: 9271377 DOI: 10.1128/MCB.17.9.4991]
7 **Martin TG 3rd**, Somberg KA, Meng YG, Cohen RL, Heid CA, de Sauvage FJ, Shuman MA. Thrombopoietin levels in patients with cirrhosis before and after orthotopic liver transplantation. *Ann Intern Med* 1997; **127**: 285-288 [PMID: 9265428 DOI: 10.7326/0003-4819-127-4-199708150-00005]
8 **Ishikawa T**, Ichida T, Matsuda Y, Sugitani S, Sugiyama M, Kato T, Miyazaki H, Asakura H. Reduced expression of thrombopoietin is involved in thrombocytopenia in human and rat liver cirrhosis. *J Gastroenterol Hepatol* 1998; **13**: 907-913 [PMID: 9794189 DOI: 10.1111/j.1440-1746.1998.tb00760.x]
9 **Ishikawa T**, Ichida T, Matsuda Y, Sugitani S, Sugiyama M, Kato T, Miyazaki H, Asakura H. Expression of hepatic thrombopoietin mRNA in primary cultured hepatocytes and in rats with acute liver injury or bone marrow suppression with or without cirrhosis. *J Gastroenterol Hepatol* 2000; **15**: 647-653 [PMID: 10921419 DOI: 10.1046/j.1440-1746.2000.02087.x]
10 **Ishikawa T**, Ichida T, Sugahara S, Yamagiwa S, Matsuda Y, Uehara K, Kato T, Miyazaki H, Asakura H. Thrombopoietin receptor (c-Mpl) is constitutively expressed on platelets of patients with liver cirrhosis, and correlates with its disease progression. *Hepatol Res* 2002; **23**: 115-121 [PMID: 12048065 DOI: 10.1016/s1386-6346(01)00170-x]
11 **Zeldis JB**, Mugishima H, Steinberg HN, Nir E, Gale RP. In vitro hepatitis B virus infection of human bone marrow cells. *J Clin Invest* 1986; **78**: 411-417 [PMID: 3090103 DOI: 10.1172/JCI112591]
12 **Brissot P**, Pietrangelo A, Adams PC, de Graaff B, McLaren CE, Loréal O. Haemochromatosis. *Nat Rev Dis Primers* 2018; **4**: 18016 [PMID: 29620054 DOI: 10.1038/nrdp.2018.16]
13 **Connell WR**, Kamm MA, Ritchie JK, Lennard-Jones JE. Bone marrow toxicity caused by azathioprine in inflammatory bowel disease: 27 years of experience. *Gut* 1993; **34**: 1081-1085 [PMID: 8174958 DOI: 10.1136/gut.34.8.1081]
14 **Uemura M**, Fujimura Y, Matsumoto M, Ishizashi H, Kato S, Matsuyama T, Isonishi A, Ishikawa M, Yagita M, Morioka C, Yoshiji H, Tsujimoto T, Kurumatani N, Fukui H. Comprehensive analysis of ADAMTS13 in patients with liver cirrhosis. *Thromb Haemost* 2008; **99**: 1019-1029 [PMID: 18521503 DOI: 10.1160/TH08-01-0006]
15 **Pereira J**, Accatino L, Alfaro J, Brahm J, Hidalgo P, Mezzano D. Platelet autoantibodies in patients with chronic liver disease. *Am J Hematol* 1995; **50**: 173-178 [PMID: 7485078 DOI: 10.1002/ajh.2830500305]
16 **Sanjo A**, Satoi J, Ohnishi A, Maruno J, Fukata M, Suzuki N. Role of elevated platelet-associated immunoglobulin G and hypersplenism in thrombocytopenia of chronic liver diseases. *J Gastroenterol Hepatol* 2003; **18**: 638-644 [PMID: 12753144 DOI: 10.1046/j.1440-1746.2003.03026.x]
17 **Bassendine MF**, Collins JD, Stephenson J, Saunders P, James OF. Platelet associated immunoglobulins in primary biliary cirrhosis: a cause of thrombocytopenia? *Gut* 1985; **26**: 1074-1079 [PMID: 4054707 DOI: 10.1136/gut.26.10.1074]
18 **Pawlotsky JM**, Bouvier M, Fromont P, Deforges L, Duval J, Dhumeaux D, Bierling P. Hepatitis C virus infection and

autoimmune thrombocytopenic purpura. *J Hepatol* 1995; **23**: 635-639 [PMID: 8750160 DOI: 10.1016/0168-8278(95)80027-1]

19 **Panzer S**, Seel E. Is there an increased frequency of autoimmune thrombocytopenia in hepatitis C infection? *Wien Med Wochenschr* 2003; **153**: 417-420 [PMID: 14648921 DOI: 10.1007/s10354-003-0028-x]

20 **Misiani R**, Bellavita P, Fenili D, Borelli G, Marchesi D, Massazza M, Vendramin G, Comotti B, Tanzi E, Scudeller G. Hepatitis C virus infection in patients with essential mixed cryoglobulinemia. *Ann Intern Med* 1992; **117**: 573-577 [PMID: 1326246 DOI: 10.7326/0003-4819-117-7-573]

21 **Venkata C**, Kashyap R, Farmer JC, Afessa B. Thrombocytopenia in adult patients with sepsis: incidence, risk factors, and its association with clinical outcome. *J Intensive Care* 2013; **1**: 9 [PMID: 25810916 DOI: 10.1186/2052-0492-1-9]

22 **Caly WR**, Strauss E. A prospective study of bacterial infections in patients with cirrhosis. *J Hepatol* 1993; **18**: 353-358 [PMID: 8228129 DOI: 10.1016/s0168-8278(05)80280-6]

23 **Warkentin TE**, Aird WC, Rand JH. Platelet-endothelial interactions: sepsis, HIT, and antiphospholipid syndrome. *Hematology Am Soc Hematol Educ Program* 2003; 497-519 [PMID: 14633796 DOI: 10.1182/asheducation-2003.1.497]

24 **Jandl JH**, Aster RH. Increased splenic pooling and the pathogenesis of hypersplenism. *Am J Med Sci* 1967; **253**: 383-398 [PMID: 5336447 DOI: 10.1097/00000441-196704000-00001]

25 **O'Leary JG**, Greenberg CS, Patton HM, Caldwell SH. AGA Clinical Practice Update: Coagulation in Cirrhosis. *Gastroenterology* 2019; **157**: 34-43.e1 [PMID: 30986390 DOI: 10.1053/j.gastro.2019.03.070]

26 **Under the auspices of the Italian Association for the Study of Liver Diseases (AISF) and the Italian Society of Internal Medicine (SIMI)**. Hemostatic balance in patients with liver cirrhosis: Report of a consensus conference. *Dig Liver Dis* 2016; **48**: 455-467 [PMID: 27012444 DOI: 10.1016/j.dld.2016.02.008]

27 **Tripodi A**, Primignani M, Mannucci PM, Caldwell SH. Changing Concepts of Cirrhotic Coagulopathy. *Am J Gastroenterol* 2017; **112**: 274-281 [PMID: 27801884 DOI: 10.1038/ajg.2016.498]

28 **Tripodi A**. Hemostasis abnormalities in cirrhosis. *Curr Opin Hematol* 2015; **22**: 406-412 [PMID: 26203733 DOI: 10.1097/MOH.0000000000000164]

29 **Tripodi A**, Mannucci PM. The coagulopathy of chronic liver disease. *N Engl J Med* 2011; **365**: 147-156 [PMID: 21751907 DOI: 10.1056/NEJMra1011170]

30 **Thakrar SV**, Mallett SV. Thrombocytopenia in cirrhosis: Impact of fibrinogen on bleeding risk. *World J Hepatol* 2017; **9**: 318-325 [PMID: 28293381 DOI: 10.4254/wjh.v9.i6.318]

31 **Violi F**, Ferro D. Clotting activation and hyperfibrinolysis in cirrhosis: implication for bleeding and thrombosis. *Semin Thromb Hemost* 2013; **39**: 426-433 [PMID: 23487343 DOI: 10.1055/s-0033-1334144]

32 **Giannini EG**, Greco A, Marenco S, Andorno E, Valente U, Savarino V. Incidence of bleeding following invasive procedures in patients with thrombocytopenia and advanced liver disease. *Clin Gastroenterol Hepatol* 2010; **8**: 899-902; quiz e109 [PMID: 20601131 DOI: 10.1016/j.cgh.2010.06.018]

33 **Tripodi A**, Caldwell SH, Hoffman M, Trotter JF, Sanyal AJ. Review article: the prothrombin time test as a measure of bleeding risk and prognosis in liver disease. *Aliment Pharmacol Ther* 2007; **26**: 141-148 [PMID: 17593061 DOI: 10.1111/j.1365-2036.2007.03369.x]

34 **Intagliata NM**, Argo CK, Stine JG, Lisman T, Caldwell SH, Violi F; faculty of the 7th International Coagulation in Liver Disease. Concepts and Controversies in Haemostasis and Thrombosis Associated with Liver Disease: Proceedings of the 7th International Coagulation in Liver Disease Conference. *Thromb Haemost* 2018; **118**: 1491-1506 [PMID: 30060258 DOI: 10.1055/s-0038-1666861]

35 **Joist JH**. AICF and DIC in liver cirrhosis: expressions of a hypercoagulable state. *Am J Gastroenterol* 1999; **94**: 2801-2803 [PMID: 10520824 DOI: 10.1111/j.1572-0241.1999.02801.x]

36 **Gangireddy VG**, Kanneganti PC, Sridhar S, Talla S, Coleman T. Management of thrombocytopenia in advanced liver disease. *Can J Gastroenterol Hepatol* 2014; **28**: 558-564 [PMID: 25222481 DOI: 10.1155/2014/532191]

37 **Yamamoto S**, Hidemura R. Surgical treatment of portal hypertension--with special reference to the feature of intrahepatic circulatory disturbances. *Jpn Circ J* 1964; **28**: 178-180 [PMID: 14132589 DOI: 10.1253/jcj.28.178]

38 **Shigekawa Y**, Uchiyama K, Takifuji K, Ueno M, Hama T, Hayami S, Tamai H, Ichinose M, Yamaue H. A laparoscopic splenectomy allows the induction of antiviral therapy for patients with cirrhosis associated with hepatitis C virus. *Am Surg* 2011; **77**: 174-179 [PMID: 21337875]

39 **Hassn AM**, Al-Fallouji MA, Ouf TI, Saad R. Portal vein thrombosis following splenectomy. *Br J Surg* 2000; **87**: 362-373 [PMID: 10718950 DOI: 10.1046/j.1365-2168.2000.01383-16.x]

40 **Witte CL**, Ovitt TW, Van Wyck DB, Witte MH, O'Mara RE, Woolfenden JM. Ischemic therapy in thrombocytopenia from hypersplenism. *Arch Surg* 1976; **111**: 1115-1121 [PMID: 987762 DOI: 10.1001/archsurg.1976.01360280073012]

41 **Peck-Radosavljevic M**. Thrombocytopenia in chronic liver disease. *Liver Int* 2017; **37**: 778-793 [PMID: 27860293 DOI: 10.1111/liv.13317]

42 **Liu Q**, Ma K, He Z, Dong J, Hua X, Huang X, Qiao L. Radiofrequency ablation for hypersplenism in patients with liver cirrhosis: a pilot study. *J Gastrointest Surg* 2005; **9**: 648-657 [PMID: 15862259 DOI: 10.1016/j.gassur.2004.11.006]

43 **Boyer TD**, Haskal ZJ; American Association for the Study of Liver Diseases. The Role of Transjugular Intrahepatic Portosystemic Shunt (TIPS) in the Management of Portal Hypertension: update 2009. *Hepatology* 2010; **51**: 306 [PMID: 19902484 DOI: 10.1002/hep.23383]

44 **Saab S**, Brown RS Jr. Management of Thrombocytopenia in Patients with Chronic Liver Disease. *Dig Dis Sci* 2019; **64**: 2757-2768 [PMID: 31011942 DOI: 10.1007/s10620-019-05615-5]

45 **Northup PG**, Garcia-Pagan JC, Garcia-Tsao G, Intagliata NM, Superina RA, Roberts LN, Lisman T, Valla DC. Vascular Liver Disorders, Portal Vein Thrombosis, and Procedural Bleeding in Patients With Liver Disease: 2020 Practice Guidance by the American Association for the Study of Liver Diseases. *Hepatology* 2021; **73**: 366-413 [PMID: 33219529 DOI: 10.1002/hep.31646]

46 **Ronca V**, Barabino M, Santambrogio R, Opocher E, Hodson J, Bertolini E, Birocchi S, Piccolo G, Battezzati P, Cattaneo M, Podda GM. Impact of Platelet Count on Perioperative Bleeding in Patients With Cirrhosis Undergoing Surgical Treatments of Liver Cancer. *Hepatol Commun* 2022; **6**: 423-434 [PMID: 34716696 DOI: 10.1002/hep4.1806]

47 **Seeff LB**, Everson GT, Morgan TR, Curto TM, Lee WM, Ghany MG, Shiffman ML, Fontana RJ, Di Bisceglie AM, Bonkovsky HL, Dienstag JL; HALT–C Trial Group. Complication rate of percutaneous liver biopsies among persons with advanced chronic liver disease in the HALT-C trial. *Clin Gastroenterol Hepatol* 2010; **8**: 877-883 [PMID: 20362695 DOI: 10.1016/j.cgh.2010.03.025]

48 **ASGE Standards of Practice Committee**, Ben-Menachem T, Decker GA, Early DS, Evans J, Fanelli RD, Fisher DA, Fisher L, Fukami N, Hwang JH, Ikenberry SO, Jain R, Jue TL, Khan KM, Krinsky ML, Malpas PM, Maple JT, Sharaf RN, Dominitz JA, Cash BD. Adverse events of upper GI endoscopy. *Gastrointest Endosc* 2012; **76**: 707-718 [PMID: 22985638 DOI: 10.1016/j.gie.2012.03.252]

49 **Murphy MF**, Waters AH. Clinical aspects of platelet transfusions. *Blood Coagul Fibrinolysis* 1991; **2**: 389-396 [PMID: 1893071 DOI: 10.1097/00001721-199104000-00026]

50 **Kaufman RM**, Assmann SF, Triulzi DJ, Strauss RG, Ness P, Granger S, Slichter SJ. Transfusion-related adverse events in the Platelet Dose study. *Transfusion* 2015; **55**: 144-153 [PMID: 25065959 DOI: 10.1111/trf.12791]

51 **Nuttall GA**, Stubbs JR, Oliver WC Jr. Transfusion errors: causes, incidence, and strategies for prevention. *Curr Opin Anaesthesiol* 2014; **27**: 657-659 [PMID: 25254574 DOI: 10.1097/ACO.0000000000000136]

52 **Kuter DJ**, Begley CG. Recombinant human thrombopoietin: basic biology and evaluation of clinical studies. *Blood* 2002; **100**: 3457-3469 [PMID: 12411315 DOI: 10.1182/blood.V100.10.3457]

53 **Li J**, Yang C, Xia Y, Bertino A, Glaspy J, Roberts M, Kuter DJ. Thrombocytopenia caused by the development of antibodies to thrombopoietin. *Blood* 2001; **98**: 3241-3248 [PMID: 11719360 DOI: 10.1182/blood.v98.12.3241]

54 **Demetri GD**. Targeted approaches for the treatment of thrombocytopenia. *Oncologist* 2001; **6** Suppl 5: 15-23 [PMID: 11700388 DOI: 10.1634/theoncologist.6-suppl_5-15]

55 **Miyazaki H**. Update on thrombopoietin in preclinical and clinical trials. *Curr Opin Hematol* 1998; **5**: 197-202 [PMID: 9664160 DOI: 10.1097/00062752-199805000-00009]

56 **U.S. Food and Drug Administration**. NPLATE® (romiplostim). [cited 24 December 2021]. Available from: https://www.accessdata.fda.gov/drugsatfda_docs/label/2018/125268s163lbl.pdf

57 **Kuter DJ**, Bussel JB, Lyons RM, Pullarkat V, Gernsheimer TB, Senecal FM, Aledort LM, George JN, Kessler CM, Sanz MA, Liebman HA, Slovick FT, de Wolf JT, Bourgeois E, Guthrie TH Jr, Newland A, Wasser JS, Hamburg SI, Grande C, Lefrère F, Lichtin AE, Tarantino MD, Terebelo HR, Viallard JF, Cuevas FJ, Go RS, Henry DH, Redner RL, Rice L, Schipperus MR, Guo DM, Nichol JL. Efficacy of romiplostim in patients with chronic immune thrombocytopenic purpura: a double-blind randomised controlled trial. *Lancet* 2008; **371**: 395-403 [PMID: 18242413 DOI: 10.1016/S0140-6736(08)60203-2]

58 **Voican CS**, Naveau S, Perlemuter G. Successful antiviral therapy for hepatitis C virus-induced cirrhosis after an increase in the platelet count with romiplostim: two case reports. *Eur J Gastroenterol Hepatol* 2012; **24**: 1455-1458 [PMID: 22890208 DOI: 10.1097/MEG.0b013e328357d5f2]

59 **Castellote J**, Girbau A, Arajol C, Xiol X. Romiplostim in chronic liver disease with severe thrombocytopenia undergoing an elective invasive procedure. *Rev Esp Enferm Dig* 2011; **103**: 556 [PMID: 22054278 DOI: 10.4321/s1130-01082011001000015]

60 **Moussa MM**, Mowafy N. Preoperative use of romiplostim in thrombocytopenic patients with chronic hepatitis C and liver cirrhosis. *J Gastroenterol Hepatol* 2013; **28**: 335-341 [PMID: 22849409 DOI: 10.1111/j.1440-1746.2012.07246.x]

61 **Basu P**, Nair T, Jafri M, Shah James N, Farhat S, Foustin S. Single use of romiplostim thrombopoietin analogue in severe thrombocytopenia for outpatient percutaneous liver biopsy in patients with chronic liver disease—a randomized double blinded prospective trial. *Gut* 2012; **56**: 38 [DOI: 10.1016/S0168-8278(12)60101-9]

62 **Dieterich DT**, Bernstein D, Flamm S, Pockros PJ, Reau N. Review article: a treatment algorithm for patients with chronic liver disease and severe thrombocytopenia undergoing elective medical procedures in the United States. *Aliment Pharmacol Ther* 2020; **52**: 1311-1322 [PMID: 32813292 DOI: 10.1111/apt.16044]

63 **U.S. Food and Drug Administration**. PROMACTA® (eltrombopag). [cited 24 December 2021]. Available from: https://www.novartis.us/sites/www.novartis.us/files/promacta.pdf

64 **McHutchison JG**, Dusheiko G, Shiffman ML, Rodriguez-Torres M, Sigal S, Bourliere M, Berg T, Gordon SC, Campbell FM, Theodore D, Blackman N, Jenkins J, Afdhal NH; TPL102357 Study Group. Eltrombopag for thrombocytopenia in patients with cirrhosis associated with hepatitis C. *N Engl J Med* 2007; **357**: 2227-2236 [PMID: 18046027 DOI: 10.1056/NEJMoa073255]

65 **Kawaguchi T**, Komori A, Seike M, Fujiyama S, Watanabe H, Tanaka M, Sakisaka S, Nakamuta M, Sasaki Y, Oketani M, Hattori T, Katsura K, Sata M. Efficacy and safety of eltrombopag in Japanese patients with chronic liver disease and thrombocytopenia: a randomized, open-label, phase II study. *J Gastroenterol* 2012; **47**: 1342-1351 [PMID: 22674141 DOI: 10.1007/s00535-012-0600-5]

66 **Afdhal NH**, Giannini EG, Tayyab G, Mohsin A, Lee JW, Andriulli A, Jeffers L, McHutchison J, Chen PJ, Han KH, Campbell F, Hyde D, Brainsky A, Theodore D; ELEVATE Study Group. Eltrombopag before procedures in patients with cirrhosis and thrombocytopenia. *N Engl J Med* 2012; **367**: 716-724 [PMID: 22913681 DOI: 10.1056/NEJMoa1110709]

67 **Afdhal NH**, Dusheiko GM, Giannini EG, Chen PJ, Han KH, Mohsin A, Rodriguez-Torres M, Rugina S, Bakulin I, Lawitz E, Shiffman ML, Tayyab GU, Poordad F, Kamel YM, Brainsky A, Geib J, Vasey SY, Patwardhan R, Campbell FM, Theodore D. Eltrombopag increases platelet numbers in thrombocytopenic patients with HCV infection and cirrhosis, allowing for effective antiviral therapy. *Gastroenterology* 2014; **146**: 442-52.e1 [PMID: 24126097 DOI: 10.1053/j.gastro.2013.10.012]

68 **Moore AH**. Thrombocytopenia in Cirrhosis: A Review of Pathophysiology and Management Options. *Clin Liver Dis (Hoboken)* 2019; **14**: 183-186 [PMID: 31879561 DOI: 10.1002/cld.860]

69 **U.S. Food and Drug Administration**. DOPTELET® (avatrombopag). [cited 24 December 2021]. Available from: https://doptelet.com/themes/pdf/prescribing-information.pdf

70 **Terrault N**, Chen YC, Izumi N, Kayali Z, Mitrut P, Tak WY, Allen LF, Hassanein T. Avatrombopag Before Procedures Reduces Need for Platelet Transfusion in Patients With Chronic Liver Disease and Thrombocytopenia. *Gastroenterology* 2018; **155**: 705-718 [PMID: 29778606 DOI: 10.1053/j.gastro.2018.05.025]

71 **Verma D**, Yum JJ, LeRoy K, McDaniel TK, Saab S. Real-life experience with avatrombopag. *Dig Med Res* 2021; **4** [DOI: 10.21037/dmr-21-10]

72 **Saab S**, McDaniel TK, Bau SN, Patel RP. Efficacy of repeat doses of avatrombopag: a case series. *Dig Med Res* 2019; **2** [DOI: 10.21037/dmr.2019.04.03]

73 **U.S. Food and Drug Administration**. MULPLETA® (lusutrombopag). [cited 24 December 2021]. Available from: https://doptelet.com/themes/pdf/prescribing-information.pdf

74 **Tateishi R**, Seike M, Kudo M, Tamai H, Kawazoe S, Katsube T, Ochiai T, Fukuhara T, Kano T, Tanaka K, Kurokawa M, Yamamoto K, Osaki Y, Izumi N, Imawari M. A randomized controlled trial of lusutrombopag in Japanese patients with chronic liver disease undergoing radiofrequency ablation. *J Gastroenterol* 2019; **54**: 171-181 [PMID: 30105510 DOI: 10.1007/s00535-018-1499-2]

75 **Katsube T**, Ishibashi T, Kano T, Wajima T. Population Pharmacokinetic and Pharmacodynamic Modeling of Lusutrombopag, a Newly Developed Oral Thrombopoietin Receptor Agonist, in Healthy Subjects. *Clin Pharmacokinet* 2016; **55**: 1423-1433 [PMID: 27209291 DOI: 10.1007/s40262-016-0411-6]

76 **Kim ES**. Lusutrombopag: First Global Approval. *Drugs* 2016; **76**: 155-158 [PMID: 26666417 DOI: 10.1007/s40265-015-0525-4]

77 **Hidaka H**, Kurosaki M, Tanaka H, Kudo M, Abiru S, Igura T, Ishikawa T, Seike M, Katsube T, Ochiai T, Kimura K, Fukuhara T, Kano T, Nagata T, Tanaka K, Kurokawa M, Yamamoto K, Osaki Y, Izumi N, Imawari M. Lusutrombopag Reduces Need for Platelet Transfusion in Patients With Thrombocytopenia Undergoing Invasive Procedures. *Clin Gastroenterol Hepatol* 2019; **17**: 1192-1200 [PMID: 30502505 DOI: 10.1016/j.cgh.2018.11.047]

78 **Peck-Radosavljevic M**, Simon K, Iacobellis A, Hassanein T, Kayali Z, Tran A, Makara M, Ben Ari Z, Braun M, Mitrut P, Yang SS, Akdogan M, Pirisi M, Duggal A, Ochiai T, Motomiya T, Kano T, Nagata T, Afdhal N. Lusutrombopag for the Treatment of Thrombocytopenia in Patients With Chronic Liver Disease Undergoing Invasive Procedures (L-PLUS 2). *Hepatology* 2019; **70**: 1336-1348 [PMID: 30762895 DOI: 10.1002/hep.30561]

79 **Takada H**, Kurosaki M, Nakanishi H, Takahashi Y, Itakura J, Tsuchiya K, Yasui Y, Tamaki N, Takaura K, Komiyama Y, Higuchi M, Kubota Y, Wang W, Okada M, Shimizu T, Watakabe K, Enomoto N, Izumi N. Real-life experience of lusutrombopag for cirrhotic patients with low platelet counts being prepared for invasive procedures. *PLoS One* 2019; **14**: e0211122 [PMID: 30768601 DOI: 10.1371/journal.pone.0211122]

80 **Uojima H**, Arase Y, Itokawa N, Atsukawa M, Satoh T, Miyazaki K, Hidaka H, Sung JH, Kako M, Tsuruya K, Kagawa T, Iwakiri K, Horie R, Koizumi W. Relationship between response to lusutrombopag and splenic volume. *World J Gastroenterol* 2018; **24**: 5271-5279 [PMID: 30581275 DOI: 10.3748/wjg.v24.i46.5271]

81 **Nomoto H**, Morimoto N, Miura K, Watanabe S, Takaoka Y, Maeda H, Sasaki T, Koyashiki Y, Kurata H, Numao N, Isoda N, Yamamoto H. Lusutrombopag is effective and safe in patients with chronic liver disease and severe thrombocytopenia: a multicenter retrospective study. *BMC Gastroenterol* 2020; **20**: 427 [PMID: 33317473 DOI: 10.1186/s12876-020-01573-9]

82 **Ishikawa T**, Okoshi M, Tomiyoshi K, Kojima Y, Horigome R, Imai M, Nozawa Y, Iwanaga A, Sano T, Honma T, Yoshida T. Efficacy and safety of repeated use of lusutrombopag prior to radiofrequency ablation in patients with recurrent hepatocellular carcinoma and thrombocytopenia. *Hepatol Res* 2019; **49**: 590-593 [PMID: 30602063 DOI: 10.1111/hepr.13305]

83 **Kaneko T**, Takano Y, Ishibashi K. Lusutrombopag as a substitute for platelet transfusion for thrombocytopenia associated with chronic liver disease in a patient undergoing endoscopic spinal surgery: A case report. *Medicine (Baltimore)* 2021; **100**: e24094 [PMID: 33466174 DOI: 10.1097/MD.0000000000024094]

84 **Kawata Y**, Endou M, Isozaki Y, Kitamura T, Fukushima Y, Sato T. Three cases of patients with chronic liver disease complicated by thrombocytopenia who were treated with lusutrombopag before tooth extraction. *J Oral Max Surg Med* 2021; **33**: 463-466 [DOI: 10.1016/j.ajoms.2021.02.007]

85 **Yoshida M**, Tateishi R, Hiroi S, Hongo Y, Fujiwara M, Kitanishi Y, Iwasaki K, Takeshima T, Igarashi A. Effects of Lusutrombopag on Post-invasive Procedural Bleeding in Thrombocytopenic Patients with Chronic Liver Disease. *Adv Ther* 2022; **39**: 379-390 [PMID: 34748184 DOI: 10.1007/s12325-021-01965-7]

86 **Brown RS**, Izumi N, Kano T, Ochiai T, Kurosaki M, Violi F, Shrestha P. Lusutrombopag is a safe treatment option for thrombocytopenia in patients with chronic liver disease undergoing a scheduled invasive procedure: pooled safety analysis from 3 studies. Proceedings of the 24th Congress of the European Hematology Association (EHA); 2019 Jun 13-16; Amsterdam, Netherlands. Netherlands: EHA Library

World Journal of Gastroenterology

Submit a Manuscript: https://www.f6publishing.com

World J Gastroenterol 2022 August 14; 28(30): 4075-4088

DOI: 10.3748/wjg.v28.i30.4075

ISSN 1007-9327 (print) ISSN 2219-2840 (online)

ORIGINAL ARTICLE

Basic Study

P2X7 receptor blockade decreases inflammation, apoptosis, and enteric neuron loss during *Clostridioides difficile* toxin A-induced ileitis in mice

Ana A Q A Santos, Deiziane V S Costa, Danielle A Foschetti, Antoniella S G Duarte, Conceição S Martins, Pedro M G Soares, Patricia Castelucci, Gerly A C Brito

Specialty type: Gastroenterology and hepatology

Provenance and peer review: Unsolicited article; Externally peer reviewed.

Peer-review model: Single blind

Peer-review report's scientific quality classification

Grade A (Excellent): 0
Grade B (Very good): 0
Grade C (Good): C, C, C
Grade D (Fair): D
Grade E (Poor): 0

P-Reviewer: Lin L, China; Shen ZY, China; Wang HD, China

Received: November 9, 2021
Peer-review started: November 9, 2021
First decision: April 16, 2022
Revised: May 4, 2022
Accepted: July 11, 2022
Article in press: July 11, 2022
Published online: August 14, 2022

Ana A Q A Santos, Deiziane V S Costa, Conceição S Martins, Pedro M G Soares, Department of Morphology, School of Medicine, Federal University of Ceara, Fortaleza 60430-170, Ceara, Brazil

Deiziane V S Costa, Department of Physiology and Pharmacology, School of Medicine, Federal University of Ceará, Fortaleza 60430-170, Ceara, Brazil

Danielle A Foschetti, Department of Pathology and Legal Medicine, School of Medicine, Federal University of Ceara, Fortaleza 60430-170, Ceara, Brazil

Antoniella S G Duarte, Department of Morphology (UFC), Federal University of Ceara, Fortaleza 60430-170, Ceara, Brazil

Patricia Castelucci, Department of Anatomy, Institute of Biomedical Sciences, University of São Paulo, Sao Paulo 05508-270, Brazil

Gerly A C Brito, Department of Morphology, Federal University of Ceara, Fortaleza 60140-170, Ceara, Brazil

Corresponding author: Gerly A C Brito, MD, PhD, Professor, Department of Morphology, Federal University of Ceara, Rua Delmiro de Farias, Fortaleza 60140-170, Ceara, Brazil. gerlybrito@gmail.com

Abstract

BACKGROUND

Clostridioides difficile (*C. difficile*) is the most common pathogen causing health care-associated infections. *C. difficile* TcdA and TcdB have been shown to activate enteric neurons; however, what population of these cells is more profoundly influenced and the mechanism underlying these effects remain unknown.

AIM

To characterize a specific population of TcdA-affected myenteric neurons and investigate the role of the P2X7 receptor in TcdA-induced ileal inflammation, cell death, and the changes in the enteric nervous system in mice.

METHODS
Swiss mice were used to model TcdA-induced ileitis in ileal loops exposed to TcdA (50 μg/Loop) for 4 h. To investigate the role of the P2X7 receptor, Brilliant Blue G (50 mg/kg, i.p.), which is a nonspecific P2X7 receptor antagonist, or A438079 (0.7 μg/mouse, i.p.), which is a competitive P2X7 receptor antagonist, were injected one hour prior to TcdA challenge. Ileal samples were collected to analyze the expression of the P2X7 receptor (by quantitative real-time polymerase chain reaction and immunohistochemistry), the population of myenteric enteric neurons (immunofluorescence), histological damage, intestinal inflammation, cell death (terminal deoxynucleotidyltransferase-mediated dUTP-biotin nick end labeling), neuronal loss, and S100B synthesis (immunohistochemistry).

RESULTS
TcdA upregulated ($P < 0.05$) the expression of the P2X7 receptor gene in the ileal tissues, increasing the level of this receptor in myenteric neurons compared to that in control mice. Comparison with the control mice indicated that TcdA promoted ($P < 0.05$) the loss of myenteric calretinin+ (Calr) and choline acetyltransferase+ neurons and increased the number of nitrergic+ and Calr+ neurons expressing the P2X7 receptor. Blockade of the P2X7 receptor decreased TcdA-induced intestinal damage, cytokine release [interleukin (IL)-1β, IL-6, IL-8, and tumor necrosis factor-α], cell death, enteric neuron loss, and S100B synthesis in the mouse ileum.

CONCLUSION
Our findings demonstrated that TcdA induced the upregulation of the P2X7 receptor, which promoted enteric neuron loss, S100B synthesis, tissue damage, inflammation, and cell death in the mouse ileum. These findings contribute to the future directions in understanding the mechanism involved in intestinal dysfunction reported in patients after *C. difficile* infection.

Key Words: *Clostridioides difficile*; *Clostridioides difficile* toxin A; P2X7 receptor; Enteric nervous system; Enteric neuron; Enteric glia

©The Author(s) 2022. Published by Baishideng Publishing Group Inc. All rights reserved.

Core Tip: There is a knowledge gap regarding the population of enteric neurons affected by TcdA and the role of the P2X7 receptor, which is a low-sensitivity adenosine triphosphate-gated cation channel, in TcdA-induced alterations in enteric neurons and enteric glial cell (EGC)-derived mediators, particularly S100B. The findings of the present study demonstrated the mechanism of P2X7 receptor-driven enteric neuronal loss induced by TcdA in the mouse ileum. TcdA promoted the upregulation of the P2X7 receptor, which promoted cell death in enteric neurons and induced the release of proinflammatory mediators, which in turn promoted S100B synthesis in EGCs. However, the blockade of the P2X7 receptor abrogated ileal damage induced by TcdA.

Citation: Santos AAQA, Costa DVS, Foschetti DA, Duarte ASG, Martins CS, Soares PMG, Castelucci P, Brito GAC. P2X7 receptor blockade decreases inflammation, apoptosis, and enteric neuron loss during *Clostridioides difficile* toxin A-induced ileitis in mice. *World J Gastroenterol* 2022; 28(30): 4075-4088
URL: https://www.wjgnet.com/1007-9327/full/v28/i30/4075.htm
DOI: https://dx.doi.org/10.3748/wjg.v28.i30.4075

INTRODUCTION

Clostridioides difficile (*C. difficile*) continues to be the leading cause of nosocomial diarrhea worldwide[1]. TcdA, TcdB, and *C. difficile* binary toxin are the main virulence factors of *C. difficile* infection-related intestinal damage. These toxins have been shown to play an important role in secretory diarrhea and inflammation during the infection[2,3]. The clinical disease ranges from mild diarrhea to toxic megacolon, colonic perforation, and death.

Intestinal dysfunction has been identified in patients after the acute phase of *C. difficile* infection[4-7]. Growing evidence suggests that the enteric nervous system (ENS) plays an important role in the regulation of intestinal inflammation. Alterations in the ENS components, including enteric neurons and glia, contribute to the amplification of inflammatory immune response and intestinal dysfunction under inflammatory conditions.

The P2X7 receptor is a low-sensitivity adenosine triphosphate (ATP)-gated cation channel expressed by several cell types, such as macrophages[8], EGCs[9], and enteric neurons[10]. Once activated, the P2X7 receptor increases the intracellular Ca^{2+} concentrations, which in turn promote the release of proinflammatory cytokines and neuromodulators[11,12]. Additionally, high levels of the P2X7 receptor have been reported in enteric neurons during colitis induced by dinitrobenzene sulfonic acid[13] and intestinal ischemia[10].

TcdA and TcdB have been shown to excite enteric neurons, stimulating the release of substance P and vasoactive intestinal peptide *via* the inhibition of noradrenergic transmission and the interleukin (IL)-1β pathway, respectively, resulting in neutrophil recruitment and secretory diarrhea[14-16]. However, there is a knowledge gap regarding the population of enteric neurons affected by TcdA and the role of the P2X7 receptor in TcdA-induced alterations in enteric neurons and enteric glial cell (EGC)-derived mediators, particularly S100B.

In the present study, we characterized the population of myenteric neurons affected by TcdA during ileitis in mice. In addition, we investigated the role of the P2X7 receptor in ileal damage, inflammation, and enteric glial and neuronal changes in TcdA-induced ileitis in mice. Our hypothesis was that TcdA affects specific types of neurons and induces reactive gliosis and that activation of P2RX7 is involved not only in ileal damage and inflammation but also in the activation of enteric glia and neuronal loss induced by this toxin.

MATERIALS AND METHODS

Animals

Swiss mice (8-week-old) were provided by the central vivarium of the Federal University of Ceara. All mice were maintained under standard conditions at 24 °C at a 12-h light-dark cycle, and all groups were provided water and food *ad libitum*. All mouse procedures were conducted according to current regulations regarding animal experiments approved by the local Animals Care and Use Committee (protocol no. 7028200418).

Mouse ileal loop model

A mouse model of TcdA-induced ileitis was established as described previously with[17] some modifications. Swiss mice (n = 5 *per* group) were fasted for 4 h with free access to water and deeply anesthetized with an intraperitoneal injection of ketamine (80 mg/kg) and xylazine (10 mg/kg). After a midline laparotomy, a single 4-cm ileal loop was ligated and injected with 50 μg of TcdA in 100 μL of phosphate-buffered saline (PBS). The control loops were injected with 100 μL of PBS alone. After 4 h, the mice were euthanized, and the ileal loops were removed for subsequent analysis. Alternatively, some mice were injected with Brilliant Blue G (BBG, Sigma–Aldrich, 50 mg/kg, i.p.)[10], a nonspecific P2X7 receptor antagonist, or with A438079 (Abcam, 10 μM/200 μL, i.p.), a competitive P2X7 receptor antagonist[18], one hour prior to PBS or TcdA (50 μg) injection in the ileal loops. The experimental groups were as follows: Control (loops were injected with 100 μL of PBS alone), TcdA (loops were injected with 50 μg of TcdA in 100 μL of PBS), BBG (injected with BBG one hour prior to the injection of 100 μL of PBS in the loop), A438079 (injected with A438079 one hour prior to the injection of 100 μL of PBS in the loop), TcdA + BBG (injected with BBG one hour prior to the injection of 50 μg of TcdA in 100 μL of PBS), and A438079 (injected with A438079 one hour prior to the injection of 50 μg of TcdA in 100 μL of PBS).

TcdA was provided by Prof. Carlos Quesada from the University of Costa Rica. BBG was kindly provided by Dr. Patricia Castelucci from the University of São Paulo. A43807 was kindly provided by Dr. Henning Ulrich from the University of São Paulo.

Analysis of histological damage in the ileum

The ileal samples were fixed in 10% formalin solution for 20 h and processed by the NEMPI-UFC Research Histology Core. The severity of ileal damage was measured by a blinded expert in histopathology based on a scoring system ranging from 0 to 3 as described previously with some modifications as follows: (0) Absence of alterations; (1) Mild loss of the integrity of the villi, mild edema, and neutrophil infiltration; (2) Partial loss of the villi, moderate edema, and neutrophil infiltration; and (3) Complete loss of the villi, extensive edema, and intense neutrophil infiltration[19].

Analysis of enteric neuron population

Fresh ileal samples were flushed with PBS, dissected, and opened along the mesenteric border. Then, the samples were fixed in 4% paraformaldehyde (in 0.2 M sodium phosphate buffer, pH 7.4) overnight at 4 °C. Then, the samples were washed three times with 100% dimethyl sulfoxide for 10 min, followed by three washes with PBS for 10 min each. All samples were stored at 4 °C in PBS containing 0.1% sodium azide. The fixed tissues were dissected to remove the mucosa, submucosa, and circular layers, yielding longitudinal muscle-myenteric plexus whole mounts as described previously[10].

Table 1 Primary and secondary antibodies used

Antigen	Host	Dilution	Manufacturer
nNOS	Sheep	1:2000	Millipore (AB1529/Lot 2488802)
ChAT	Goat	1:50	Millipore (AB144P/Lot 1978747)
P2X7 receptor	Rabbit	1:100	Millipore (AB5246/Lot 2361386)
Calretinin	Goat	1:100	Molecular
Donkey anti-rabbit IgG Alexa 594	Donkey	1:200	Probes (A21206/Lot 1182675)
Donkey anti-sheep IgG Alexa 488	Donkey	1:400	Molecular
			Probes (A11016/Lot93D1-1)

nNOS: Neuronal nitric oxide synthase; ChAT: Choline acetyltransferase; IgG: Immunoglobulin G.

Whole-mount preparations of the ileal myenteric samples were preincubated in 10% horse serum in PBS containing 1.5% Triton X-100 for 45 min at room temperature to reduce nonspecific binding and permeabilize the tissue. The antibodies used in the present study are described in Table 1. Double labeling was achieved using the combinations of primary antibodies (Table 1) overnight at 4 °C. Then, the samples were washed (with PBS three times for 10 min each) and incubated with secondary antibodies (Table 1). After washing with PBS, the samples were mounted in glycerol buffer (in 0.5 M sodium carbonate, pH 8.6). The immunostaining images were acquired using confocal microscopy by a Zeiss confocal scanning laser system installed on a Zeiss Axioplan 2 microscope. The images were acquired at a resolution of 512 × 512 pixels, and the thickness of each optical section was 0.5 μm. The Z-stacks of immunoreactive cells were captured as a series of optical sections with a center spacing of 0.2 μm. Confocal images were collected using Zeiss LSM 5 image processing software and further processed using Corel Photo Paint and Corel Draw software[10].

Quantitative analysis of myenteric neuron immunostaining

The antigen colocalization was determined in fluorescently labeled preparations. Initially, the neurons were identified by immunofluorescence. Then, the filter was switched, and the labeling of the second antigen was evaluated. The proportion of the neurons labeled with the antigen pairs was thus determined. The cohort size was 100 neurons, and the data were collected from the preparations obtained from five mice *per* experimental group. The percentage of double immunoreactive neurons was calculated and is expressed as the mean ± standard error of the mean (SEM). The density of the neurons immunoreactive (neurons/cm^2) to the P2X7 receptor, neuronal nitric oxide synthase (nNOS), calretinin (Calr), and choline acetyltransferase (ChaT) and neuronal morphological profiles were assessed in the whole-mount preparations at 100 × magnification. The number of the cell bodies of immunoreactive neurons in the myenteric ganglia in each visual microscopic field (0.04909 mm^2) was estimated. To quantify two whole-mount preparations (1.0 cm^2 each), the counts were estimated in 40 microscopic fields selected at random for each antigen in each animal. The perikaryon profile areas (μm^2) of 50 randomly selected neurons from each animal were obtained using a semiautomatic morphometry device and measured using the Image-Pro Plus software package.

Immunohistochemistry

Immunostaining of S100B (an enteric glia-derived mediator), HuC/D (a neuronal marker), and the P2X7 receptor was performed in paraffin-embedded ileal formalin-fixed sections (4-μm thick) using the streptavidin-biotin-peroxidase method; the sections were mounted on poly(L)-lysine-coated microscope slides as described previously[20]. Briefly, the samples were deparaffinized and rehydrated by incubation with xylene and graded alcohol solutions, respectively. Then, the samples were immersed in antigen retrieval solution (*EnVision™ FLEX target retrieval solution, pH = 6.0; Dako, Denmark A/S*) for 20 min on a PT Link system (Dako), incubated in 3% hydrogen peroxide (*EnVision™ FLEX peroxidase-blocking reagent; Dako)* to block endogenous peroxidase for 15 min at room temperature, and washed with PBS. Then, the samples were incubated with primary antibodies (rabbit anti-P2X7 receptor (Invitrogen), mouse anti-HuC/D (Invitrogen), or goat anti-S100B (Santa Cruz Biotechnology, 1:100) in antibody diluent solution (*EnVisionTM FLEX antibody diluent; Dako*) overnight at 4 °C. Then, the samples were incubated with *EnVision™ FLEX/HRP (Dako)* as recommended by the manufacturer. P2X7 receptor, HuC/D, and S100B were detected using the chromogen 3,3'-diaminobenzidine (DAB, *EnVision™ FLEX DAB+ chromogen; Dako*). The negative control sections were processed simultaneously as described above; however, the primary antibody was replaced with antibody diluent solution (*EnVision™ FLEX antibody diluent; Dako*). The slides were counterstained with Mayer's hematoxylin. The images were acquired by a Leica DM100 microscope and analyzed using Adobe Photoshop 8.0 software. The

percentages of P2X7 receptor-, S100B- and HuC/D-stained tissue sections were measured by using Adobe Photoshop as described previously[20].

Total RNA extraction, reverse transcription, and real-time polymerase chain reaction

Total RNA was isolated from the ileum using an *Aurum™ total RNA fatty and fibrous tissue* kit (Bio-Rad, CA, United States), and 1 μg of the RNA was reverse transcribed using iScript™ (Bio-Rad) according to the manufacturer's instructions. Real-time polymerase chain reaction (qPCR) was performed on a 7900HT fast real-time PCR system (Applied Biosystems) using the following specific primers (IDT, Coralville, IA): P2X7 receptor (forward: GCACGAATTATGGCACCGTC and reverse: CCCCACCCTCT-GTGACATTCT) and GAPDH (forward: TGCACCACCAACTGCTTAG and reverse: GGATGCAGG-GATGATGTTC)[21]. The reaction mixture was prepared in a final volume of 20 μL as follows: 10 μL of master mix iQTM SYBR® Green (Applied Biosystems), 2 μL of each primer (200 nM), 1 μL of cDNA, and 5 μL of nuclease-free water. The gene amplification included the following steps: 10 min at 95 °C (initial denaturation), 15 s at 95 °C and 60 s at 60 °C for 40 cycles; thus, a melting curve was obtained. Relative gene expression was determined using the 2-Δ Δ Ct method with GAPDH as a housekeeping gene.

Terminal deoxynucleotidyltransferase-mediated dUTP-biotin nick end labeling assay

Ileal samples were processed for terminal deoxynucleotidyltransferase-mediated dUTP-biotin nick end labeling (TUNEL) using an *ApopTagR S 7100* kit (Merck Millipore, Germany) to quantify apoptotic and necrotic cells. Briefly, paraffin-embedded sections were hydrated and incubated with proteinase K (Sigma, United States, 20 mg/mL) for 15 min at room temperature. Endogenous peroxidase was blocked with 3% hydrogen peroxide in PBS for 5 min at room temperature. After a washing step, the sections were incubated with TdT buffer containing TdT enzyme and reaction buffer in a humidified chamber at 37 °C for 1 h. The specimens were incubated for 10 min at room temperature with stop/wash buffer and then incubated with an anti-digoxigenin–peroxidase conjugate at room temperature in a humidified chamber for 30 min. After washing with PBS, the slides were covered with peroxidase substrate (DAB) to develop the color and were counterstained with methyl green.

Cytokine quantification by enzyme-linked immunosorbent assay

To measure inflammatory markers, the ileal samples were processed to evaluate the levels of IL-1β, IL-6, keratinocyte chemoattractant (KC, a human IL-8 analog), and tumor necrosis factor (TNF)-α by enzyme-linked immunosorbent assay (ELISA) using a mouse cytokine kit (R&D Systems) according to the manufacturer's instructions. The absorbance of the samples was detected at 450 nm using an ELISA plate reader (Biotech Epoch, United States). The data are expressed as pg *per* mg of tissue.

Statistical analysis

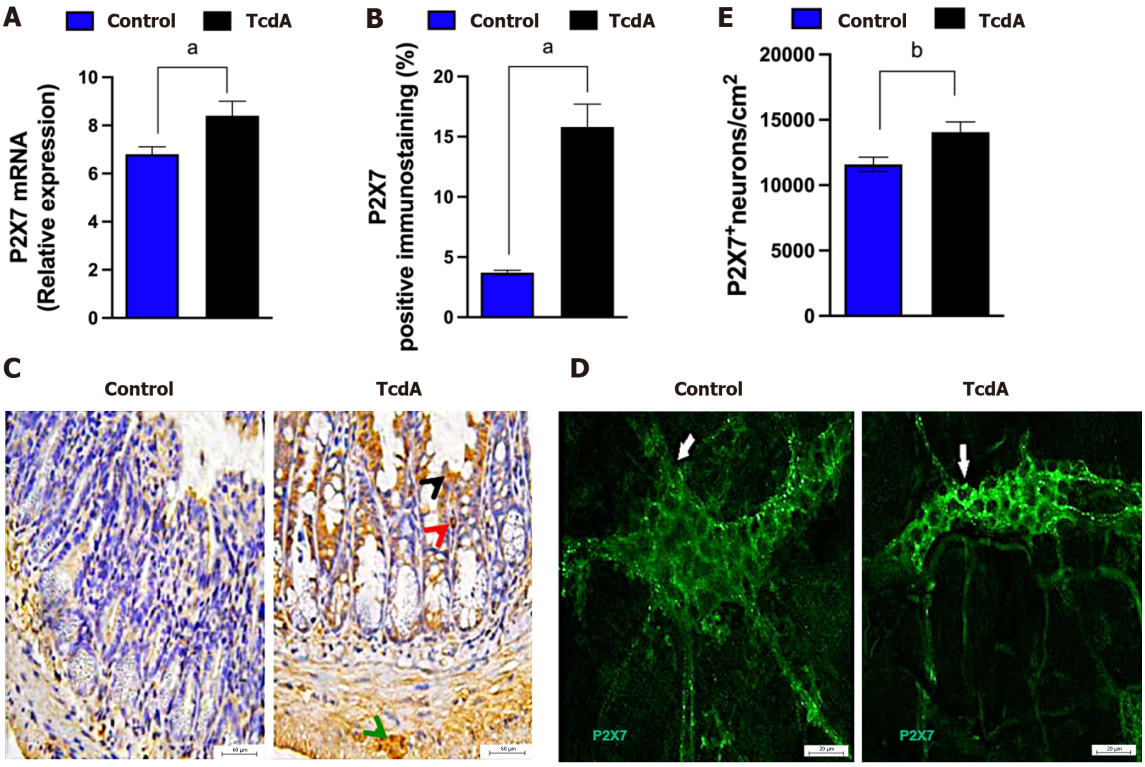
The results are expressed as the mean ± SEM calculated by GraphPad Prism version 9.0 (GraphPad Software, San Diego, CA). The differences between more than two experimental groups were evaluated using one-way analysis of variance (ANOVA) with Bonferroni's multiple comparison test. Student's t test was performed to analyze the differences between two groups. The histopathological score data were compared by using Kruskal–Wallis nonparametric test followed by Dunn's test. Statistical significance was defined as $P < 0.05$.

RESULTS

TcdA upregulates the P2X7 receptor transcripts in the ileum of mice and increases the population of myenteric enteric neurons expressing the P2X7 receptor

Initially, we investigated whether TcdA alters the expression of the *P2RX7* gene in the ileum of mice by using qPCR. We demonstrated that TcdA upregulated the P2X7 receptor in the ileum of mice compared with that in control mice ($P < 0.05$, Figure 1A). The data of the assay of the P2X7 receptor protein by immunofluorescence showed an increase in the percentage of positive P2X7 receptor immunostaining in the ileal samples of TcdA-challenged mice compared with that in the control samples ($P < 0.05$, Figure 1B). An increase in the expression of the P2X7 receptor was observed in epithelial cells, the lamina propria, and the myenteric plexus (Figure 1C).

Enteric neurons are an important component of the myenteric plexus, which is a part of the ENS; hence, we investigated whether the level of the P2X7 receptor is increased in these cells in the myenteric plexus by using immunofluorescence analysis. Comparison with the control group indicated an increase in the density of enteric neurons expressing the P2X7 receptor in the ileum myenteric plexus in mice challenged with TcdA ($P = 0.01$, Figure 1D and E).



DOI: 10.3748/wjg.v28.i30.4075 **Copyright** ©The Author(s) 2022.

Figure 1 *Clostridioides difficile* toxin A increases the expression of the P2X7 receptor in the ileum myenteric plexus of mice. A: The expression of the *P2RX7* gene [mean ± standard error of the mean (SEM)] assayed by quantitative real-time polymerase chain reaction in the ileal samples of mice injected with TcdA [TcdA, 50 μg in phosphate-buffered saline (PBS)] or PBS alone in the ileal loops (Control) (n = 4); B: Quantification of the percentage (mean ± SEM) of the P2X7 receptor-immunopositive area in the ileum from control and *TcdA*-challenged mice in 5-6 microscope fields *per* sample (n = 4 animals *per* group); C: Representative immunohistochemical images of the expression of the P2X7 receptor in the ileum of control and *TcdA*-challenged mice. Increased expression of the P2X7 receptor (arrowhead) was detected in the intestinal epithelial layer (black arrowhead), lamina propria (red arrowhead), and myenteric plexus (green arrowhead). Scale bars, 50 μm; D: Representative photomicrographs ofimmunostaining of the P2X7 receptor (arrow indicates the region stained green) in the ileum myenteric plexus from control and *TcdA*-challenged mice; E: Quantification of the number of P2RX7$^+$ neurons/cm^2 (mean ± SEM) in the ileum of control and *TcdA*-challenged mice (n = 4 animals *per* group); A, B and E: Unpaired two-tailed Student's t test ($^aP < 0.05$; $^bP = 0.01$).

TcdA decreases the density of enteric Calr+ and ChaT+ neurons in the ileum myenteric plexus of mice

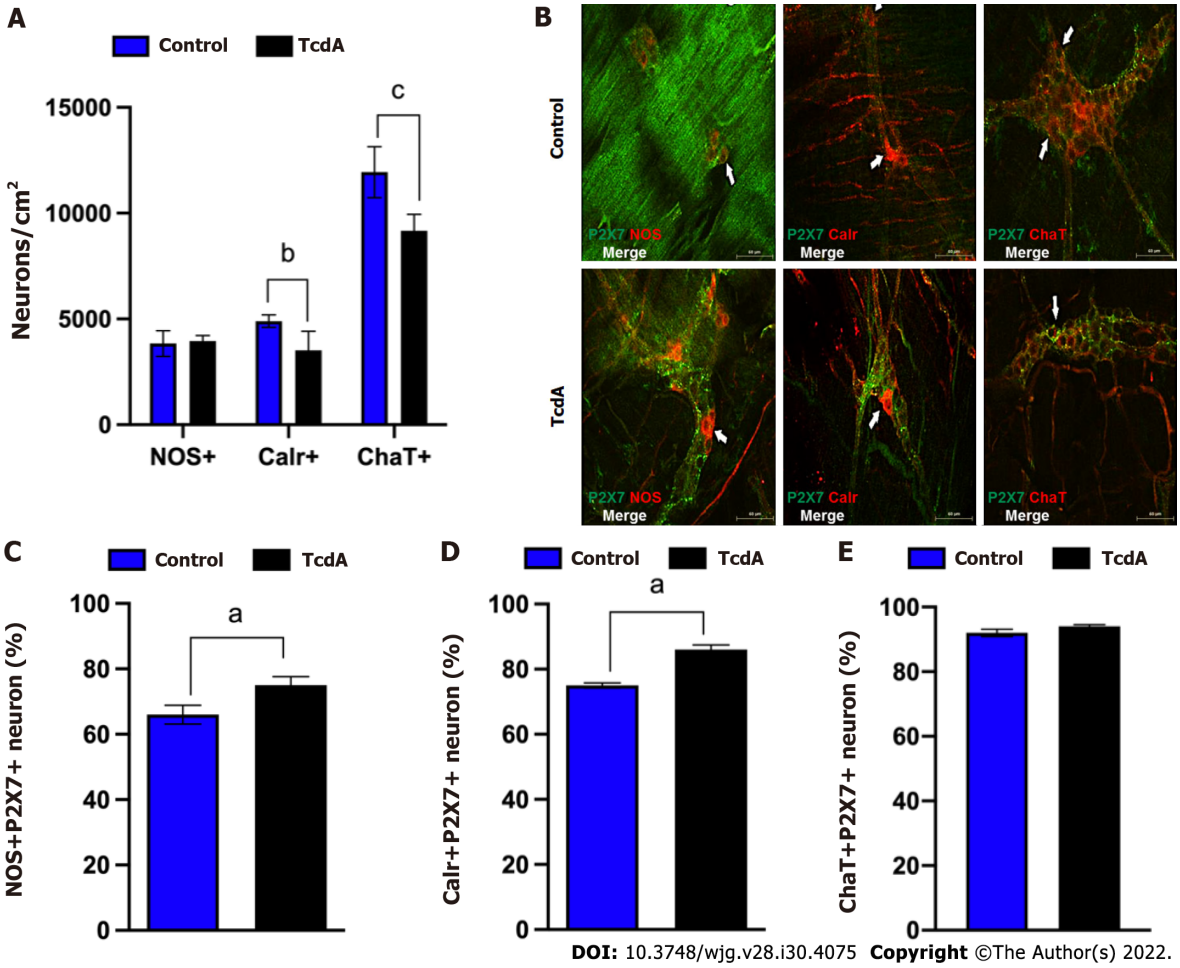
Subsequently, to better understand how TcdA affects the myenteric enteric neuron population, we immunostained the ileum myenteric plexus to detect nNOS, Calr, and ChaT, which were stained in the main population of enteric neurons. As shown in Figure 2A, the density of Calr+ ($P < 0.03$) and ChaT+ neurons ($P < 0.002$) in the ileum myenteric plexus of mice challenged with TcdA was decreased compared to that in control mice. In addition, all these subtypes of the neurons expressed the P2X7 receptor (Figure 2B).

Comparison with the control group of mice indicated that the enteric neuron population expressing the P2X7 receptor in the ileum myenteric plexus had a higher number of nNOS+P2RX7+ and Calr+P2RX7+ neurons, but not of ChaT+P2RX7+ neurons ($P < 0.05$, Figure 2C-E).

Overall, these findings indicated that TcdA decreased the enteric neuron population, specifically Calr+ and ChaT+ cells and upregulated the P2X7 receptor in a specific population (nNOS and Calr) of the neurons in the ileum myenteric plexus in mice.

Blockade of the P2X7 receptor decreases ileal damage induced by TcdA in mice

Then, we blocked the P2X7 receptor by pretreating mice using a pharmacological approach, including administration of BBG and A438079 one hour prior to the challenge with TcdA to determine whether P2X7 receptor activity is required for ileal damage induced by TcdA. Hematoxylin and eosin-stained slides of ileum samples were analyzed for evidence of epithelial damage, edema, and neutrophil infiltration, with a maximal severity score of 3 (Figure 3). TcdA induced complete epithelial disruption, extensive edema, and intense neutrophil infiltration in the ileum of mice, resulting in a high damage score (score = 3) compared with those in the undamaged ileum in control mice ($P < 0.007$, Figure 3). However, both P2X7 receptor antagonists (BBG and 438079) induced a substantial decrease in the ileal damage promoted by TcdA, resulting in a reduction in the damage score (score = 1) compared to that in untreated TcdA-challenged mice ($P < 0.04$, Figure 3).



DOI: 10.3748/wjg.v28.i30.4075 **Copyright** ©The Author(s) 2022.

Figure 2 *Clostridioides difficile* toxin A induces alterations in enteric neuronal coding in the myenteric plexus in the ileum of mice. A: Quantification of the number of neuronal nitric oxide synthase+ (nNOS+), calretinin+ (Calr+), and choline acetyltransferase+ (ChaT+) neurons/cm^2 [mean ± standard error of the mean (SEM)] in the ileum myenteric plexus in control and *TcdA*-challenged mice; B: Representative photomicrographs of the P2X7 receptor (green), nNOS (left panels, red), Calr (center panels, red), and ChaT (right panel, red) immunostaining and DAPI (blue) nuclear staining in control and *TcdA*-challenged mice. White arrows indicate positive immunostaining. Scale bars, 50 μm; C-E: Percentage of NOS$^+$P2X7$^+$ neurons (C), Calr$^+$P2RX7$^+$ neurons (D), and ChaT$^+$P2RX7$^+$ neurons (E) (mean ± SEM) in the ileum myenteric plexus of control and *TcdA*-challenged mice (n = 4); A, C, D and E: Unpaired two-tailed Student's t test ($^aP < 0.05$; $^bP < 0.03$; $^cP < 0.002$). NOS: Nitric oxide synthase; Calr: Calretinin; ChaT: Choline acetyltransferase.

Blockade of the P2X7 receptor decreases ileal inflammation and cell death induced by TcdA in mice

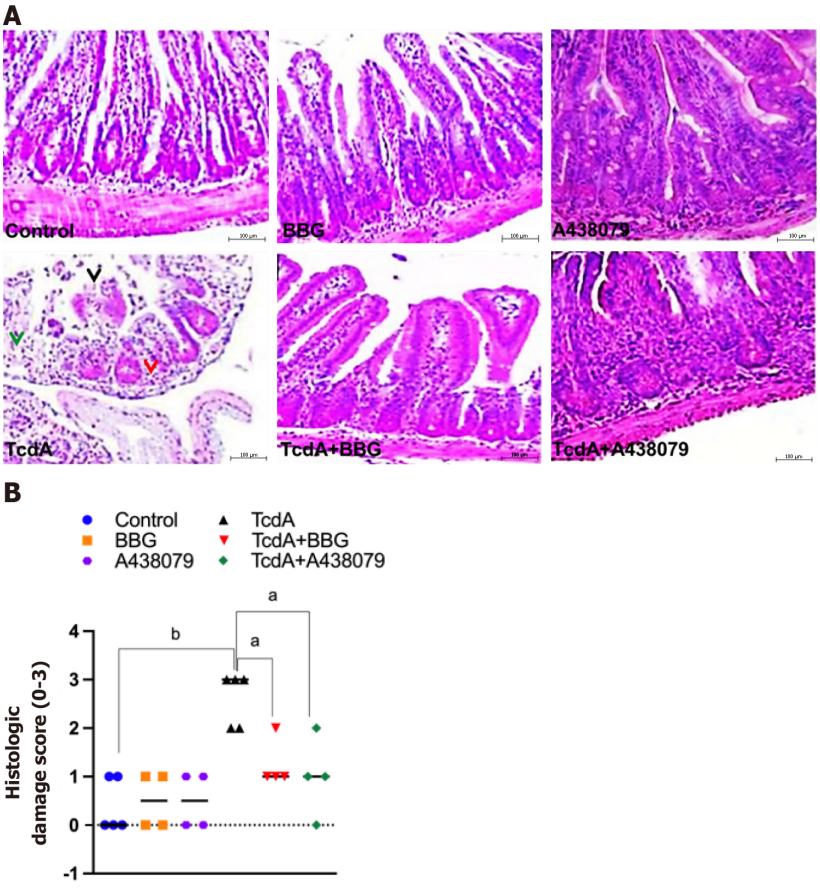
Subsequently, we evaluated whether P2X7 receptor activity is involved in ileal inflammation and cell death induced by TcdA in mice. We demonstrated that both P2X7 receptor blockers (BBG and A438079) reversed a TcdA-induced increase in IL-1β (P = 0.008 and P = 0.03, Figure 4A), TNF-α (P = 0.0002 and P = 0.0001, Figure 4B), and IL-6 (P = 0.03 and P < 0.0001, Figure 4C) in the ileal samples of mice. However, comparison with TcdA-challenged mice, which were not pretreated with the blockers, indicated that blockade of the P2X7 receptor by A438079, but not by BBG, decreased the levels of KC (P = 0.01, Figure 4D) and the number of TUNEL+ cells (P = 0.01, Figure 4E) in the ileum of mice challenged with TcdA.

Overall, these data indicated that the P2X7 receptor was involved in intestinal damage, inflammation, and cell death induced by TcdA in mice.

Blockade of the P2X7 receptor decreases enteric neuron loss and S100B synthesis induced by TcdA in mice

Since we demonstrated that TcdA promoted a decrease in ileum enteric neurons in mice, we assessed whether the P2X7 receptor accounts for this alteration. Comparison with TcdA-challenged mice, which were not pretreated with the blockers, indicated that a P2X7 receptor blocker (A438079) increased the percentage of positive immunostaining of HuC/D, which is a pan-marker of enteric neurons, in the ileum of mice challenged with TcdA (Figure 5).

Furthermore, we evaluated whether the activation of the P2X7 receptor is required to induce S100B expression in the ileum of TcdA-challenged mice; high levels of S100B are released by EGCs under inflammatory conditions. As shown in Figure 5, the P2X7 receptor antagonist A438079 induced a



DOI: 10.3748/wjg.v28.i30.4075 **Copyright** ©The Author(s) 2022.

Figure 3 Inhibition of the P2X7 receptor decreases *Clostridioides difficile* toxin A-induced ileal damage in mice. Mouse ileal loops were injected with TcdA [TcdA, 50 μg in phosphate-buffered saline (PBS)] or PBS alone (control) (n = 5), and the animals were pretreated with a P2X7 receptor antagonist [Brilliant Blue G (BBG) or A438079] one hour prior to TcdA challenge. A: Representative histological images (magnification of 200 ×) of TcdA-unchallenged (control, BBG, and A438079) and challenged (TcdA, TcdA + BBG, and TcdA + A438079) mice. TcdA induced epithelial disruption (black arrowhead), edema (green arrowhead), and neutrophil infiltration (red arrowhead); B: Histopathological score (median; 0 corresponds to-no damage and 3 corresponds to intense damage) performed by a blinded histopathological expert and based on epithelial damage, submucosal edema, and infiltration of inflammatory cells. Kruskal–Wallis nonparametric test followed by Dunn's test. $^{a}P < 0.04$; $^{b}P < 0.007$. BBG: Brilliant Blue G.

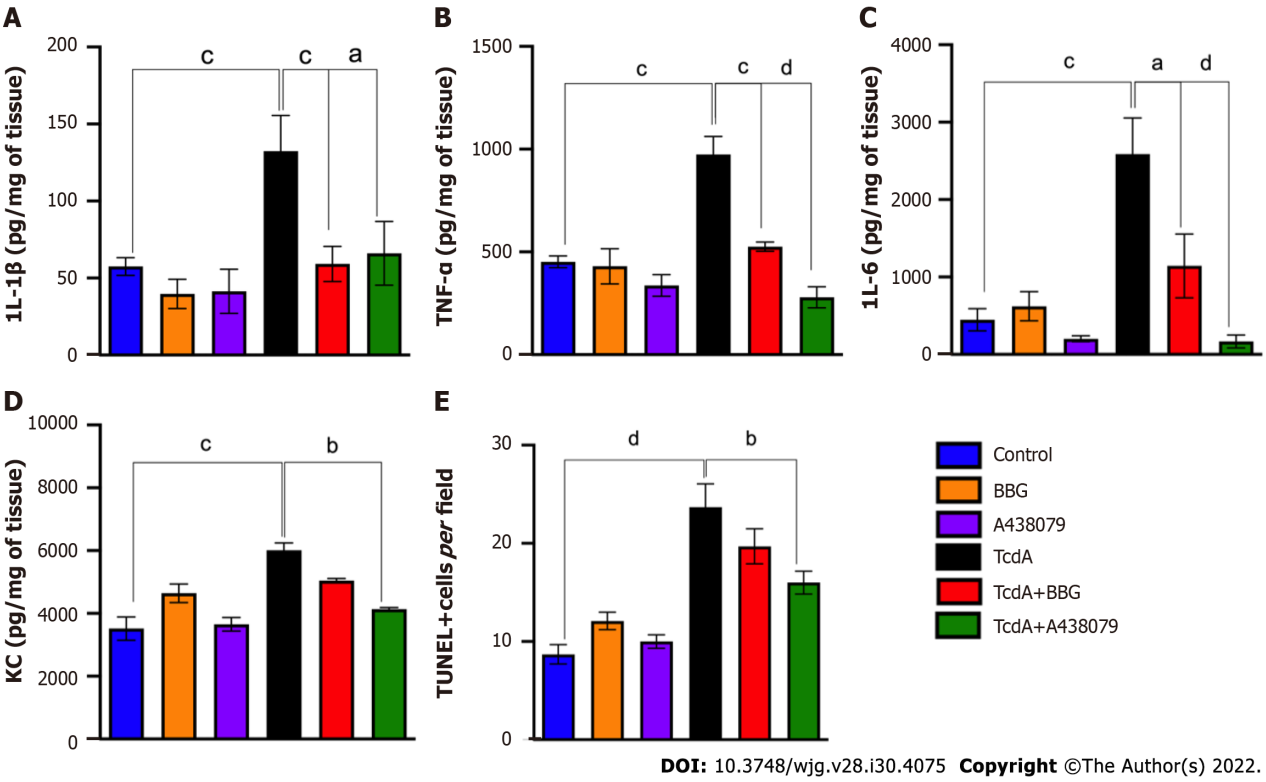
considerable decrease in the percentage of S100B-positive immunostaining in the ileum of mice challenged with TcdA compared with that in the ileum TcdA-challenged mice, which were not pretreated with the blockers (P = 0.009).

Overall, these data indicated that the P2X7 receptor was involved in enteric neuronal loss and S100B synthesis induced by TcdA in mice.

DISCUSSION

The data of the present study indicated that TcdA upregulated the P2X7 receptor in the ileum of mice. An increase in the expression of P2RX7 has been reported in colonic biopsies from Crohn's disease patients[21] and in preclinical models of intestinal inflammation, such as colitis induced by trinitrobenzene sulfonic (TNBS) acid[22] and sepsis[23]. Thus, the upregulation of the P2X7 receptor is a common phenomenon under inflammatory conditions[24].

In the present study, we also demonstrated that the level of the P2X7 receptor was increased in the epithelial layer, lamina propria, and myenteric plexus. In the myenteric plexus, we detected an increase in the density of neurons expressing the P2X7 receptor, including the nNOS+ and Calr+ subtypes. In addition to enteric neurons, other cell types can express the P2X7 receptors, such as mast cells, T cells, and dendritic cells[21]. However, we focused on enteric neurons in the myenteric plexus because this component of the ENS is a major functional unit of the system that moves the luminal contents along the intestine by coordinating muscle contraction and relaxation[25]. In addition, *C. difficile* infection is characterized by intense diarrhea in the acute phase of the disease, and the mechanism of these events is poorly understood.



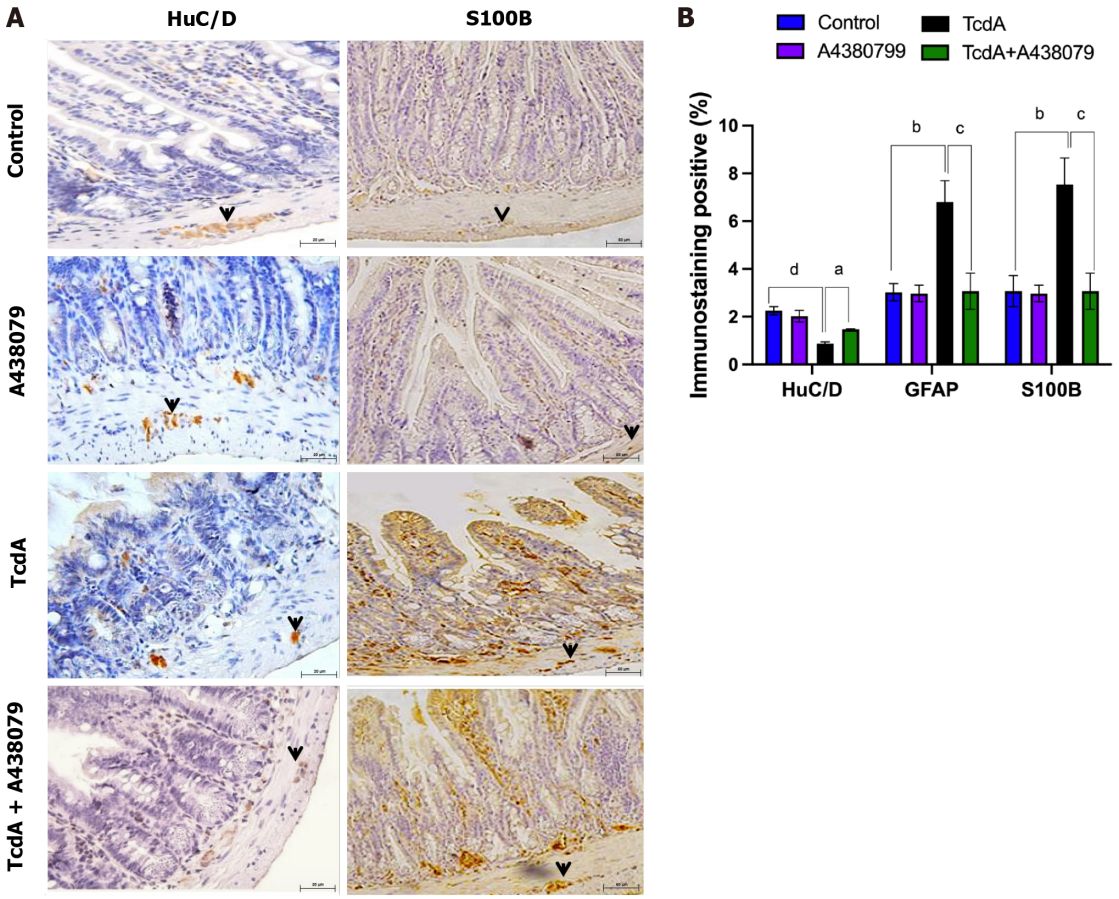
DOI: 10.3748/wjg.v28.i30.4075 **Copyright** ©The Author(s) 2022.

Figure 4 P2X7 receptor inhibition abrogates *Clostridioides difficile* toxin A-induced inflammation and cell death in mice. A-D: The levels of interleukin (IL)-1β (A), tumor necrosis factor-α (B), IL-6 (C), and keratinocyte chemoattractant (D) in the ileal samples of TcdA-unchallenged [control, Brilliant Blue G (BBG), and A438079] and challenged (TcdA, TcdA + BBG, and TcdA + A438079) mice measured by ELISA (n = 5); E: The number of TUNEL+ cells *per* field in the ileal samples of TcdA-unchallenged (control, BBG, and A438079) and challenged (TcdA, TcdA + BBG, and TcdA + A438079) mice. The data are expressed as the mean ± standard error of the mean. ANOVA followed by Tukey's test was used (^{a}P = 0.03; ^{b}P = 0.01; ^{c}P < 0.008; ^{d}P < 0.0001). IL: Interleukin; TNF: Tumor necrosis factor; BBG: Brilliant Blue G; KC: Keratinocyte chemoattractant; TUNEL: Terminal deoxynucleotidyltransferase-mediated dUTP-biotin nick end labeling.

We demonstrated that TcdA promoted neuron loss specifically by reducing the density of the Calr+ and ChaT+ neuronal populations. Acetylcholine, which is synthesized in a reaction of choline with acetyl-CoA catalyzed by ChaT, is the primary transmitter in excitatory motor neurons, intrinsic afferent neurons, and interneurons, and Calr is the primary transmitter in excitatory cholinergic neurons[26]. Excitatory motor neurons are involved in coordinated muscle contraction[25]; thus, a reduction in the density of Calr+ and ChaT+ neuronal populations induced by TcdA may be involved in the functional disorders manifested after *C. difficile* infection. Accordingly, a study performed in the United States military personnel reported functional gastrointestinal disorders (including gastroesophageal reflux disease, dyspepsia, irritable bowel syndrome, or constipation) after *C. difficile* infection recovery[6]. In the present study, alterations in the myenteric enteric neuron population induced by TcdA could have been related to these post-*C. difficile* infection-related intestinal dysfunctions. However, more studies are needed to better understand how these alterations specifically contribute to intestinal dysfunction induced by *C. difficile* infection.

In the present study, we also showed that the activation of the P2X7 receptor was involved in the TcdA-induced loss of enteric neurons because inhibition of the receptor by known P2RX7 antagonists (BBG and A438079) resulted in a substantial decrease in the loss of these ENS cells during ileitis induced by TcdA. In agreement with these data of the present study, another study demonstrated that the activation of P2RX7 promotes cell death in mucosal regulatory T cells in colitis induced by TNBS[27]. The P2X7 receptor regulates cell death pathways, such as apoptosis, pyroptosis, necrosis, and autophagy[28].

ATP released from dead cells can increase the activation of the P2X7 receptor and promote the secretion of proinflammatory cytokines, such as IL-1β, which in turn can induce the secretion of other cytokines[29,30]. In the present study, the blockade of the P2X7 receptor markedly decreased IL-1β, IL-6, KC, and TNF-α synthesis in the TcdA-challenged mouse ileum, suggesting that this receptor plays an important role in inflammation induced by *C. difficile* toxin. Similarly, in a model of TNBS-induced colitis, P2X7 receptor blockade reduces the severity of inflammation by decreasing the infiltration of macrophages in the lamina propria[31]. In contrast, deletion of P2RX7 increases the susceptibility to toxoplasmic ileitis[32], suggesting that the activation of this receptor plays a role in the response against intracellular pathogens. In contrast, *C. difficile* releases toxins, which in turn enter the cells to inhibit Rho GTPases, and the P2RX7 antagonists have positive effects in this case.



DOI: 10.3748/wjg.v28.i30.4075 **Copyright** ©The Author(s) 2022.

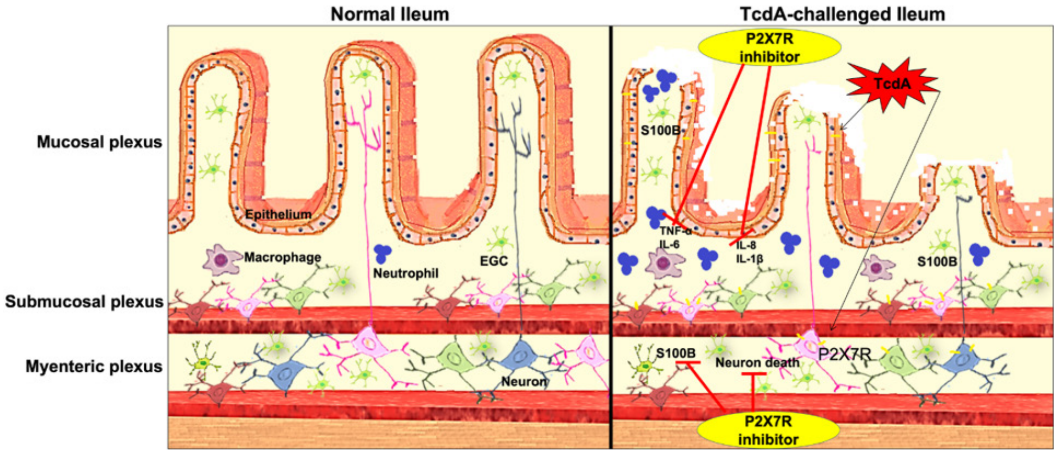
Figure 5 P2X7 receptor inhibition attenuates *Clostridioides difficile* toxin A-induced enteric neuron loss and S100B synthesis in mice. A: Representative immunohistochemical images of the expression of HuC/D (neuronal marker) and S100B (enteric glia marker) in the ileum of TcdA-unchallenged (control and A438079) and challenged (TcdA and TcdA + A438079) mice. Black arrows indicate positive immunostaining. Scale bars, 50 μm; B: Quantification of the percentage (mean ± standard error of the mean) of HuC/D- and S100B-immunopositive areas in the ileum of TcdA-unchallenged (control and A438079) and challenged (TcdA and TcdA + A438079) mice (n = 4 animals *per* group). ANOVA followed by Tukey's test was used (^aP = 0.04; ^bP = 0.01; ^cP < 0.009; ^dP < 0.0001). GFAP: Glial fibrillary acidic protein.

In addition, we demonstrated that blockade of the P2X7 receptor decreased S100B synthesis in the ileum of mice challenged with TcdA. S100B functions as a proinflammatory mediator when released at higher levels by activating the nuclear activation factor-κB[20] and is an important mediator during *C. difficile* infection[33]. In the myenteric plexus, EGCs express S100B[34] and are involved in the control of motility and epithelial barrier[35]. In a rat glioblastoma cell line, IL-6 promotes S100B synthesis[36]. In the present study, a reduction in proinflammatory cytokines related to P2X7 receptor blockade could have contributed to a decrease in S100B synthesis induced by TcdA, which in turn reduced intestinal inflammation and neuronal death.

Additional studies are needed, for example, using a *C. difficile* infection model, to explore how P2RX7 blockage can influence the *C. difficile* infection outcome and to better understand physiological benefits of this blockade for relief of intestinal permeability and dysmotility during the infection. However, it is important to emphasize that investigations of the role of this receptor in the damaging effects induced by one of the main virulence factors released by *C. difficile* will help to understand the pathogenesis of these effects and to develop alternative cotreatments to control the deleterious and exacerbated host response to the *C. difficile* toxins.

CONCLUSION

In conclusion, the results of the present study revealed the mechanism of P2X7 receptor-driven loss of enteric neurons induced by TcdA in the mouse ileum. TcdA promoted the upregulation of the P2X7 receptor, which promoted cell death in enteric neurons and induced the release of proinflammatory mediators (IL-1β, IL-6, KC, and TNF-α) in epithelial/immune cells, which in turn promoted S100B synthesis in EGCs. However, blockade of the P2X7 receptor abrogated ileal damage induced by TcdA (Figure 6). Overall, the findings of the present study open new avenues to better understand how *C.*



DOI: 10.3748/wjg.v28.i30.4075 **Copyright** ©The Author(s) 2022.

Figure 6 Scheme of the hypothetical role of the P2X7 receptor during *Clostridioides difficile* toxin A-induced ileitis. *Clostridioides difficile* TcdA promotes epithelial damage and the upregulation of the P2X7 receptor in enteric neurons, intestinal epithelial cells, and immune cells. Once activated, the P2X7 receptor promotes the death of enteric neurons and the release of proinflammatory mediators by epithelial/immune cells [interleukin (IL)-1β, IL-6, keratinocyte chemoattractant, and tumor necrosis factor-α]. These proinflammatory mediators induce S100B synthesis by enteric glial cells. Blockade of the P2X7 receptor using a pharmacological approach attenuates these deleterious effects of TcdA. IL: Interleukin; TNF: Tumor necrosis factor; EGC: Enteric glial cell.

difficile toxins promote the changes in the ENS components that can be related to intestinal dysfunction after *C. difficile* infection.

ARTICLE HIGHLIGHTS

Research background

The P2X7 receptor, a low-sensitivity adenosine triphosphate-gated cation channel, is expressed in several cell types, including enteric neurons. Once activated, the P2X7 receptor promotes the release of proinflammatory cytokines and neuromodulators. High levels of P2X7 receptor have been reported in enteric neurons during experimental colitis.

Research motivation

There is a knowledge gap regarding the population of enteric neurons affected by TcdA and the role of the P2X7 receptor in TcdA-induced alterations in enteric neurons and enteric glial cell-derived mediators, particularly S100B.

Research objectives

We characterized the population of myenteric neurons affected by TcdA during ileitis in mice. In addition, we investigated the role of the P2X7 receptor in ileal damage, inflammation, and the changes in enteric glia and neurons in TcdA-induced ileitis in mice.

Research methods

Swiss mice were used to model TcdA-induced ileitis in ileal loops exposed to TcdA (50 μg/Loop) for 4 h. To investigate the role of the P2X7 receptor Brilliant Blue G (50 mg/kg, i.p.), which is a nonspecific P2X7 receptor antagonist or A438079 (0.7 μg/mouse, i.p.), which is a competitive P2X7 receptor antagonist, were injected one hour prior to TcdA challenge. Ileum samples were collected to analyze the expression of the P2X7 receptor (quantitative real-time polymerase chain reaction and immunohistochemistry), the population of myenteric enteric neurons (immunofluorescence), histological damage, intestinal inflammation, cell death (terminal deoxynucleotidyltransferase-mediated dUTP-biotin nick end labeling), neuronal loss, and S100B synthesis (immunohistochemistry).

Research results

TcdA upregulated ($P < 0.05$) the expression of the P2RX7 gene in the ileal tissues, increasing the level of this receptor in myenteric enteric neurons compared with that in control mice. Comparison with control mice indicated that TcdA promoted ($P < 0.05$) the loss of myenteric calretinin+ (Calr) and choline acetyltransferase+ neurons and increased the number of nitrergic+ (nitric oxide synthase+) and Calr+ neurons expressing the P2X7 receptor. Blockade of the P2X7 receptor decreased TcdA-induced intestinal damage, cytokine release (interleukin (IL)-1β, IL-6, IL-8, and tumor necrosis factor-α), cell death, enteric

neuron loss, and S100B synthesis in the mouse ileum.

Research conclusions

The findings of the present study demonstrated that TcdA induced the upregulation of the P2X7 receptor, which promoted enteric neuron loss, S100B synthesis, tissue damage, inflammation, and cell death in the ileum of mice.

Research perspectives

These findings contribute to future directions in understanding the mechanism involved in intestinal dysfunction reported in patients after *Clostridioides difficile* infection.

ACKNOWLEDGEMENTS

The authors would like to thank Darlyane V S Costa for kindly drawing Figure 6 and Socorro França and Flávia A Silva for their technical assistance.

FOOTNOTES

Author contributions: Santos AAQA and Costa DVS contributions equally; Santos AAQA participated in the design and performed the experiments, analyzed the data and wrote the manuscript; Costa DVS analyzed the data and wrote the manuscript; Foschetti DA, Duarte ASG, Martins CS, and Soares PMG helped in the acquisition of the data and review of the manuscript; Castelucci P participated in the initial experimental design and helped to revise the manuscript; Brito GAC, the main investigator of the laboratory where the experiments were performed, conceptualized the main ideas, supervised the study and reviewed the manuscript.

Supported by PRONEX CNPq/FUNCAP, No. PR2-0101-00060.01.00/15; São Paulo Research Foundation (FAPESP), No. 2014/25927-2 and No. 2018/07862-1.

Institutional animal care and use committee statement: All mouse procedures were conducted according to current regulations regarding animal experiments approved by the local Animal Care and Use Committee, No. 31/2015.

Conflict-of-interest statement: All the authors report no relevant conflicts of interest for this article.

Data sharing statement: No additional data are available.

ARRIVE guidelines statement: The authors have read the ARRIVE guidelines, and the manuscript was prepared and revised according to the ARRIVE guidelines.

Open-Access: This article is an open-access article that was selected by an in-house editor and fully peer-reviewed by external reviewers. It is distributed in accordance with the Creative Commons Attribution NonCommercial (CC BY-NC 4.0) license, which permits others to distribute, remix, adapt, build upon this work non-commercially, and license their derivative works on different terms, provided the original work is properly cited and the use is non-commercial. See: https://creativecommons.org/Licenses/by-nc/4.0/

Country/Territory of origin: Brazil

ORCID number: Ana A Q A Santos 0000-0001-9512-3182; Deiziane V S Costa 0000-0001-6402-8908; Danielle A Foschetti 0000-0002-4213-9786; Antoniella S G Duarte 0000-0001-6632-6685; Conceição S Martins 0000-0001-8710-1856; Pedro M G Soares 0000-0003-0606-2539; Patricia Castelucci 0000-0002-7475-5962; Gerly A C Brito 0000-0002-8214-4379.

S-Editor: Fan JR
L-Editor: A
P-Editor: Guo X

REFERENCES

1 **Kumar R**, Goomber S, Kaur J. Engineering lipases for temperature adaptation: Structure function correlation. *Biochim Biophys Acta Proteins Proteom* 2019; **1867**: 140261 [PMID: 31401312 DOI: 10.1016/j.bbapap.2019.08.001]
2 **Jank T**, Giesemann T, Aktories K. Clostridium difficile glucosyltransferase toxin B-essential amino acids for substrate binding. *J Biol Chem* 2007; **282**: 35222-35231 [PMID: 17901056 DOI: 10.1074/jbc.M703138200]
3 **Bilverstone TW**, Garland M, Cave RJ, Kelly ML, Tholen M, Bouley DM, Kaye P, Minton NP, Bogyo M, Kuehne SA, Melnyk RA. The glucosyltransferase activity of C. difficile Toxin B is required for disease pathogenesis. *PLoS Pathog*

2020; **16**: e1008852 [PMID: 32960931 DOI: 10.1371/journal.ppat.1008852]
4 **Solomon K**. The host immune response to Clostridium difficile infection. *Ther Adv Infect Dis* 2013; **1**: 19-35 [PMID: 25165542 DOI: 10.1177/2049936112472173]
5 **Walker AS**, Eyre DW, Wyllie DH, Dingle KE, Griffiths D, Shine B, Oakley S, O'Connor L, Finney J, Vaughan A, Crook DW, Wilcox MH, Peto TE; Infections in Oxfordshire Research Database. Relationship between bacterial strain type, host biomarkers, and mortality in Clostridium difficile infection. *Clin Infect Dis* 2013; **56**: 1589-1600 [PMID: 23463640 DOI: 10.1093/cid/cit127]
6 **Gutiérrez RL**, Riddle MS, Porter CK. Increased risk of functional gastrointestinal sequelae after Clostridium difficile infection among active duty United States military personnel (1998-2010). *Gastroenterology* 2015; **149**: 1408-1414 [PMID: 26255560 DOI: 10.1053/j.gastro.2015.07.059]
7 **Grubišić V**, Verkhratsky A, Zorec R, Parpura V. Enteric glia regulate gut motility in health and disease. *Brain Res Bull* 2018; **136**: 109-117 [PMID: 28363846 DOI: 10.1016/j.brainresbull.2017.03.011]
8 **Liu YH**, Chang YC, Chen LK, Su PA, Ko WC, Tsai YS, Chen YH, Lai HC, Wu CY, Hung YP, Tsai PJ. The ATP-P2X$_7$ Signaling Axis Is an Essential Sentinel for Intracellular *Clostridium difficile* Pathogen-Induced Inflammasome Activation. *Front Cell Infect Microbiol* 2018; **8**: 84 [PMID: 29616195 DOI: 10.3389/fcimb.2018.00084]
9 **Mendes CE**, Palombit K, Tavares-de-Lima W, Castelucci P. Enteric glial cells immunoreactive for P2X7 receptor are affected in the ileum following ischemia and reperfusion. *Acta Histochem* 2019; **121**: 665-679 [PMID: 31202513 DOI: 10.1016/j.acthis.2019.06.001]
10 **Palombit K**, Mendes CE, Tavares-de-Lima W, Barreto-Chaves ML, Castelucci P. Blockage of the P2X7 Receptor Attenuates Harmful Changes Produced by Ischemia and Reperfusion in the Myenteric Plexus. *Dig Dis Sci* 2019; **64**: 1815-1829 [PMID: 30734238 DOI: 10.1007/s10620-019-05496-8]
11 **Di Virgilio F**, Dal Ben D, Sarti AC, Giuliani AL, Falzoni S. The P2X7 Receptor in Infection and Inflammation. *Immunity* 2017; **47**: 15-31 [PMID: 28723547 DOI: 10.1016/j.immuni.2017.06.020]
12 **Miras-Portugal MT**, Sebastián-Serrano Á, de Diego García L, Díaz-Hernández M. Neuronal P2X7 Receptor: Involvement in Neuronal Physiology and Pathology. *J Neurosci* 2017; **37**: 7063-7072 [PMID: 28747389 DOI: 10.1523/JNEUROSCI.3104-16.2017]
13 **Gulbransen BD**, Bashashati M, Hirota SA, Gui X, Roberts JA, MacDonald JA, Muruve DA, McKay DM, Beck PL, Mawe GM, Thompson RJ, Sharkey KA. Activation of neuronal P2X7 receptor-pannexin-1 mediates death of enteric neurons during colitis. *Nat Med* 2012; **18**: 600-604 [PMID: 22426419 DOI: 10.1038/nm.2679]
14 **Neunlist M**, Barouk J, Michel K, Just I, Oreshkova T, Schemann M, Galmiche JP. Toxin B of Clostridium difficile activates human VIP submucosal neurons, in part *via* an IL-1beta-dependent pathway. *Am J Physiol Gastrointest Liver Physiol* 2003; **285**: G1049-G1055 [PMID: 12801886 DOI: 10.1152/ajpgi.00487.2002]
15 **Xia Y**, Hu HZ, Liu S, Pothoulakis C, Wood JD. Clostridium difficile toxin A excites enteric neurones and suppresses sympathetic neurotransmission in the guinea pig. *Gut* 2000; **46**: 481-486 [PMID: 10716676 DOI: 10.1136/gut.46.4.481]
16 **Pothoulakis C**, Castagliuolo I, LaMont JT, Jaffer A, O'Keane JC, Snider RM, Leeman SE. CP-96,345, a substance P antagonist, inhibits rat intestinal responses to Clostridium difficile toxin A but not cholera toxin. *Proc Natl Acad Sci U S A* 1994; **91**: 947-951 [PMID: 7508124 DOI: 10.1073/pnas.91.3.947]
17 **Castagliuolo I**, Riegler M, Pasha A, Nikulasson S, Lu B, Gerard C, Gerard NP, Pothoulakis C. Neurokinin-1 (NK-1) receptor is required in Clostridium difficile- induced enteritis. *J Clin Invest* 1998; **101**: 1547-1550 [PMID: 9541482 DOI: 10.1172/JCI2039]
18 **Glaser T**, de Oliveira SL, Cheffer A, Beco R, Martins P, Fornazari M, Lameu C, Junior HM, Coutinho-Silva R, Ulrich H. Modulation of mouse embryonic stem cell proliferation and neural differentiation by the P2X7 receptor. *PLoS One* 2014; **9**: e96281 [PMID: 24798220 DOI: 10.1371/journal.pone.0096281]
19 **Koon HW**, Ho S, Hing TC, Cheng M, Chen X, Ichikawa Y, Kelly CP, Pothoulakis C. Fidaxomicin inhibits Clostridium difficile toxin A-mediated enteritis in the mouse ileum. *Antimicrob Agents Chemother* 2014; **58**: 4642-4650 [PMID: 24890583 DOI: 10.1128/AAC.02783-14]
20 **Costa DVS**, Bon-Frauches AC, Silva AMHP, Lima-Júnior RCP, Martins CS, Leitão RFC, Freitas GB, Castelucci P, Bolick DT, Guerrant RL, Warren CA, Moura-Neto V, Brito GAC. 5-Fluorouracil Induces Enteric Neuron Death and Glial Activation During Intestinal Mucositis *via* a S100B-RAGE-NFκB-Dependent Pathway. *Sci Rep* 2019; **9**: 665 [PMID: 30679569 DOI: 10.1038/s41598-018-36878-z]
21 **Kurashima Y**, Amiya T, Nochi T, Fujisawa K, Haraguchi T, Iba H, Tsutsui H, Sato S, Nakajima S, Iijima H, Kubo M, Kunisawa J, Kiyono H. Extracellular ATP mediates mast cell-dependent intestinal inflammation through P2X7 purinoceptors. *Nat Commun* 2012; **3**: 1034 [PMID: 22948816 DOI: 10.1038/ncomms2023]
22 **Marques CC**, Castelo-Branco MT, Pacheco RG, Buongusto F, do Rosário A Jr, Schanaider A, Coutinho-Silva R, de Souza HS. Prophylactic systemic P2X7 receptor blockade prevents experimental colitis. *Biochim Biophys Acta* 2014; **1842**: 65-78 [PMID: 24184714 DOI: 10.1016/j.bbadis.2013.10.012]
23 **Wu X**, Ren J, Chen G, Wu L, Song X, Li G, Deng Y, Wang G, Gu G, Li J. Systemic blockade of P2X7 receptor protects against sepsis-induced intestinal barrier disruption. *Sci Rep* 2017; **7**: 4364 [PMID: 28663567 DOI: 10.1038/s41598-017-04231-5]
24 **Liu Y**, Liu X. Research progress of P2X7 receptor in inflammatory bowel disease. *Scand J Gastroenterol* 2019; **54**: 521-527 [PMID: 31056977 DOI: 10.1080/00365521.2019.1609077]
25 **Drokhlyansky E**, Smillie CS, Van Wittenberghe N, Ericsson M, Griffin GK, Eraslan G, Dionne D, Cuoco MS, Goder-Reiser MN, Sharova T, Kuksenko O, Aguirre AJ, Boland GM, Graham D, Rozenblatt-Rosen O, Xavier RJ, Regev A. The Human and Mouse Enteric Nervous System at Single-Cell Resolution. *Cell* 2020; **182**: 1606-1622.e23 [PMID: 32888429 DOI: 10.1016/j.cell.2020.08.003]
26 **Fung C**, Vanden Berghe P. Functional circuits and signal processing in the enteric nervous system. *Cell Mol Life Sci* 2020; **77**: 4505-4522 [PMID: 32424438 DOI: 10.1007/s00018-020-03543-6]
27 **Figliuolo VR**, Savio LEB, Safya H, Nanini H, Bernardazzi C, Abalo A, de Souza HSP, Kanellopoulos J, Bobé P, Coutinho CMLM, Coutinho-Silva R. P2X7 receptor promotes intestinal inflammation in chemically induced colitis and triggers death

of mucosal regulatory T cells. *Biochim Biophys Acta Mol Basis Dis* 2017; **1863**: 1183-1194 [PMID: 28286160 DOI: 10.1016/j.bbadis.2017.03.004]

28 **Bidula S**, Dhuna K, Helliwell R, Stokes L. Positive allosteric modulation of P2X7 promotes apoptotic cell death over lytic cell death responses in macrophages. *Cell Death Dis* 2019; **10**: 882 [PMID: 31767863 DOI: 10.1038/s41419-019-2110-3]

29 **Oliveira-Giacomelli Á**, Petiz LL, Andrejew R, Turrini N, Silva JB, Sack U, Ulrich H. Role of P2X7 Receptors in Immune Responses During Neurodegeneration. *Front Cell Neurosci* 2021; **15**: 662935 [PMID: 34122013 DOI: 10.3389/fncel.2021.662935]

30 **Soare AY**, Freeman TL, Min AK, Malik HS, Osota EO, Swartz TH. P2RX7 at the Host-Pathogen Interface of Infectious Diseases. *Microbiol Mol Biol Rev* 2021; **85** [PMID: 33441488 DOI: 10.1128/MMBR.00055-20]

31 **Neves AR**, Castelo-Branco MT, Figliuolo VR, Bernardazzi C, Buongusto F, Yoshimoto A, Nanini HF, Coutinho CM, Carneiro AJ, Coutinho-Silva R, de Souza HS. Overexpression of ATP-activated P2X7 receptors in the intestinal mucosa is implicated in the pathogenesis of Crohn's disease. *Inflamm Bowel Dis* 2014; **20**: 444-457 [PMID: 24412990 DOI: 10.1097/01.MIB.0000441201.10454.06]

32 **Miller CM**, Zakrzewski AM, Robinson DP, Fuller SJ, Walker RA, Ikin RJ, Bao SJ, Grigg ME, Wiley JS, Smith NC. Lack of a Functioning P2X7 Receptor Leads to Increased Susceptibility to Toxoplasmic Ileitis. *PLoS One* 2015; **10**: e0129048 [PMID: 26053862 DOI: 10.1371/journal.pone.0129048]

33 **Costa DVS**, Moura-Neto V, Bolick DT, Guerrant RL, Fawad JA, Shin JH, Medeiros PHQS, Ledwaba SE, Kolling GL, Martins CS, Venkataraman V, Warren CA, Brito GAC. S100B Inhibition Attenuates Intestinal Damage and Diarrhea Severity During *Clostridioides difficile* Infection by Modulating Inflammatory Response. *Front Cell Infect Microbiol* 2021; **11**: 739874 [PMID: 34568098 DOI: 10.3389/fcimb.2021.739874]

34 **Boesmans S**, Decoster L, Schallier D. Pemetrexed-induced radiation recall dermatitis of the breast. *Anticancer Res* 2014; **34**: 1179-1182 [PMID: 24596357]

35 **Sharkey KA**. Emerging roles for enteric glia in gastrointestinal disorders. *J Clin Invest* 2015; **125**: 918-925 [PMID: 25689252 DOI: 10.1172/JCI76303]

36 **de Souza DF**, Wartchow K, Hansen F, Lunardi P, Guerra MC, Nardin P, Gonçalves CA. Interleukin-6-induced S100B secretion is inhibited by haloperidol and risperidone. *Prog Neuropsychopharmacol Biol Psychiatry* 2013; **43**: 14-22 [PMID: 23246638 DOI: 10.1016/j.pnpbp.2012.12.001]

World Journal of Gastroenterology

Submit a Manuscript: https://www.f6publishing.com

World J Gastroenterol 2022 August 14; 28(30): 4089-4101

DOI: 10.3748/wjg.v28.i30.4089

ISSN 1007-9327 (print) ISSN 2219-2840 (online)

ORIGINAL ARTICLE

Case Control Study

Serological profiling of Crohn's disease and ulcerative colitis patients reveals anti-microbial antibody signatures

Mahasish Shome, Lusheng Song, Stacy Williams, Yunro Chung, Vel Murugan, Jin G Park, William Faubion, Shabana F Pasha, Jonathan A Leighton, Joshua LaBaer, Ji Qiu

Specialty type: Gastroenterology and hepatology

Provenance and peer review: Unsolicited article; Externally peer reviewed.

Peer-review model: Single blind

Peer-review report's scientific quality classification
Grade A (Excellent): 0
Grade B (Very good): B
Grade C (Good): C
Grade D (Fair): 0
Grade E (Poor): 0

P-Reviewer: Liu G, China; Sato Y, Japan

Received: April 4, 2022
Peer-review started: April 4, 2022
First decision: May 29, 2022
Revised: June 16, 2022
Accepted: July 11, 2022
Article in press: July 11, 2022
Published online: August 14, 2022

Mahasish Shome, Lusheng Song, Stacy Williams, Yunro Chung, Vel Murugan, Jin G Park, Joshua LaBaer, Ji Qiu, Virginia G. Piper Center for Personalized Diagnostics, Biodesign Institute, Arizona State University, Tempe, AZ 85281, United States

William Faubion, Department of Internal Medicine, Mayo Clinic, Rochester, MN 55902, United States

Shabana F Pasha, Department of Internal Medicine, Division of Gastroenterology and Hepatology, Mayo Clinic Arizona, Scottsdale, AZ 85259, United States

Jonathan A Leighton, Division of Gastroenterology, Mayo Clinic School of Medicine, Scottsdale, AZ 85259, United States

Corresponding author: Ji Qiu, PhD, Research Assistant Professor, Virginia G. Piper Center for Personalized Diagnostics, Biodesign Institute, Arizona State University, 1001 S McAllister Avenue, Tempe, AZ 85281, United States. ji.qiu@asu.edu

Abstract

BACKGROUND

The healthcare burden of inflammatory bowel disease (IBD) is rising globally and there are limited non-invasive biomarkers for accurate and early diagnosis.

AIM

To understand the important role that intestinal microbiota play in IBD pathogenesis and identify anti-microbial antibody signatures that benefit clinical management of IBD patients.

METHODS

We performed serological profiling of 100 Crohn's disease (CD) patients, 100 ulcerative colitis (UC) patients and 100 healthy controls against 1173 bacterial and 397 viral proteins from 50 bacteria and 33 viruses on protein microarrays. The study subjects were randomly divided into discovery (n = 150) and validation (n = 150) sets. Statistical analysis was performed using R packages.

RESULTS

Anti-bacterial antibody responses showed greater differential prevalence among the three subject groups than anti-viral antibody responses. We identified novel

antibodies against the antigens of *Bacteroidetes vulgatus* (BVU_0562) and *Streptococcus pneumoniae* (SP_1992) showing higher prevalence in CD patients relative to healthy controls. We also identified antibodies against the antigen of *Streptococcus pyogenes* (SPy_2009) showing higher prevalence in healthy controls relative to UC patients. Using these novel antibodies, we built biomarker panels with area under the curve (AUC) of 0.81, 0.87, and 0.82 distinguishing CD *vs* control, UC *vs* control, and CD *vs* UC, respectively. Subgroup analysis revealed that penetrating CD behavior, colonic CD location, CD patients with a history of surgery, and extensive UC exhibited highest antibody prevalence among all patients. We demonstrated that autoantibodies and anti-microbial antibodies in CD patients had minimal correlation.

CONCLUSION

We have identified antibody signatures for CD and UC using a comprehensive analysis of anti-microbial antibody response in IBD. These antibodies and the source microorganisms of their target antigens improve our understanding of the role of specific microorganisms in IBD pathogenesis and, after future validation, should aid early and accurate diagnosis of IBD.

Key Words: Inflammatory bowel disease; Anti-microbial antibody; Protein microarray; Crohn's disease; Ulcerative colitis; Gut microbiome

©The Author(s) 2022. Published by Baishideng Publishing Group Inc. All rights reserved.

Core Tip: We performed the largest serological profiling of anti-microbial antibodies to date in using 100 Crohn's disease (CD) and 100 ulcerative colitis (UC) patients. We identified novel anti-microbial antibodies with differential prevalence in inflammatory bowel disease (IBD) patients compared with healthy controls. There was minimal correlation between anti-microbial antibodies and our previously reported autoantibodies in CD patients. We combined novel anti-microbial antibodies to build biomarker panels distinguishing CD *vs* control, UC *vs* control and CD *vs* UC with an area under the curve of 0.81, 0.87, and 0.82, respectively. Subgroup analysis revealed that IBD patients with severe disease had the highest antibody prevalence.

Citation: Shome M, Song L, Williams S, Chung Y, Murugan V, Park JG, Faubion W, Pasha SF, Leighton JA, LaBaer J, Qiu J. Serological profiling of Crohn's disease and ulcerative colitis patients reveals anti-microbial antibody signatures. *World J Gastroenterol* 2022; 28(30): 4089-4101
URL: https://www.wjgnet.com/1007-9327/full/v28/i30/4089.htm
DOI: https://dx.doi.org/10.3748/wjg.v28.i30.4089

INTRODUCTION

Inflammatory bowel disease (IBD) represents a group of intestinal disorders that causes chronic inflammation in the digestive tract. The two main clinical phenotypes are ulcerative colitis (UC) and Crohn's disease (CD). The public health burden of IBD is rising globally[1]. Early and accurate diagnosis is key to reducing this burden. Gastroenterologists often use a combination of relatively invasive procedures, like ileocolonoscopy with biopsy for diagnosis, and to determine the disease extent and activity. There is a need for serological biomarkers that can reveal the disease state non-invasively. Herein, our objectives were to discover anti-microbial antibody signatures in IBD patients and understand the association of microbial infection with IBD pathogenesis.

IBD is caused by a combination of genetic predisposition, faulty immune responses, and environmental factors[2]. The interaction of microbes with the gut mucosa in a genetically susceptible individual and the corresponding immune response play a pivotal role in the initiation and progression of IBD[3]. After birth, a limited diversity microbial community develops into a complex community due to the influence of diet and environmental factors[4]. During the second or third decade of life, a dysbiosis is observed in IBD patients which leads to an imbalance between commensal and potentially pathogenic microorganisms[5]. The healthy gut microbiota predominately comprises Firmicutes and Bacteroidetes, and to a lesser extent, Actinobacteria and Proteobacteria[6,7]. In IBD, dysbiosis is observed with reduced abundance of Firmicutes and either higher or similar abundance of Proteobacteria. Besides compositional changes, genetic alterations also contribute to gut dysbiosis that leads to disease initiation and progression. For example, NOD2 variants were found in 20%-40% of European and American CD patients[8,9]. NOD2 encodes an intracellular receptor for the bacterial peptidoglycan muramyl dipeptide, which helps maintain the balance of commensal bacterial flora[10].

Immune response to microbes results in the production of antibodies to microbial antigens[11]. Anti-*Saccharomyces cerevisiae* antibodies (ASCA) are associated with CD patients, with sensitivities and specificities ranging between 55% to 65% and 80% to 95%, respectively[12]. Perinuclear antineutrophil cytoplasmic antibodies (pANCA) are associated with UC patients, with sensitivities and specificities ranging between 50% to 71% and 75% to 98%, respectively[13]. Outer membrane protein of *Escherichia coli* (OmpC) and flagellin (CBir1) antibodies are prevalent in CD patients, with prevalence ranging between 24%-55% and 50%-56%[13]. The number and response magnitude of anti-microbial antibodies have previously been shown to indicate the presence of IBD, its severity and its clinical course; however, the clinical utility of available antibodies in diagnosis and clinical management of IBD patients has been limited. The techniques used to discover the known anti-microbial antibodies associated with IBD are of low throughput, and have only been applied to test on small number of candidate microorganisms or microbial antigens[14]. We have performed a large-scale comparative profiling of anti-microbial antibodies in CD and UC patients and healthy controls using an innovative protein microarray technology, namely Nucleic Acid Programmable Protein Array. We selected 1570 microbial proteins from our microbial protein collection (DNASU.org) from 50 bacteria and 33 viruses based on preliminary studies in our laboratory and a review of the literature, displayed them on microarrays and probed them against 100 CD, 100 UC and 100 healthy control serum samples.

MATERIALS AND METHODS

Patients and samples

All the serum samples were acquired from Serum Biobank at Mayo clinic with approval from institutional review board. CD patients were randomly selected, followed by age and gender matched healthy controls and UC patients. The samples (100 CD, 100 UC and 100 controls) were divided evenly into two non-overlapping discovery and validation sets randomly (Table 1). Disease status for study participants was assessed by clinicians at Mayo clinic.

Microbial protein array fabrication

We analyzed 1570 microbial proteins, of which 1173 proteins were from 50 different species of bacteria, 397 proteins were from 33 different species of viruses and the remaining proteins were autoantigens. These proteins were selected from our large collection of microbial antigens (DNASU.org) with reference to our anti-microbial antibody studies on other diseases (unpublished data). Microbial protein arrays were fabricated as described earlier[15,16]. Briefly, plasmids with genes of interest cloned in the pANT7_cGST expression vector were obtained from the DNASU plasmid repository, prepared, and printed into silicon nanowells using a piezoelectric dispensing system to produce microbial protein arrays. On the day of experiment, proteins were freshly expressed from printed plasmids using an *in-vitro* transcription and translation protein expression kit (Fisher Scientific) and captured by anti-GST antibody co-printed in each nanowell. After expression, microarrays were incubated with 1:100 diluted serum samples. We randomized the case and control serum samples while profiling on microarray to reduce bias. IgG and IgA anti-microbial protein antibodies were detected by Alexa-647 goat anti-human IgG (H+L) and Cy3 goat anti-human IgA (Jackson ImmunoResearch). After washing and drying, the microarrays were scanned in a Tecan PowerScanner and the raw fluorescence intensity data were extracted using the ArrayPro Analyzer Software. Raw fluorescence intensity of each protein on the microarray was divided by the median intensity of all the proteins on the microarray for normalization. The normalized value was termed as Median Normalized Intensity (MNI) and used for all analysis. Seropositivity of antibody for a particular antigen was defined as MNI ≥ 2 as we have done for our other studies[17,18].

Statistical analysis

Pairwise comparisons of numbers of IgG or IgA antibodies for each bacterial species among the 3 subject groups were performed using Chi-squared tests to assess statistical significance (Supplementary Figure 1). For each pairwise comparison, the Chi-squared *P* values were adjusted using the FDR (false discovery rate) method to reduce the likelihood of false positives. In addition to the multiple comparison adjustment at the antibody level, we performed adjustment at the species level.

For univariate analysis between two comparison groups, we calculated sensitivity for one group at the 96th percentile of the other group or the MNI of 2, whichever was larger. Antibodies with ≥ 14% sensitivity in the discovery set were selected as candidates for further validation. If an antibody had ≥ 14% sensitivity at 96% specificity in both discovery and validation sets, then it was considered as a "validated marker". Venn diagram for the overlap of microbial antigen targets were plotted using Venny[19].

We used a three-stage approach to build our multi-antibody panels. In the first stage, we selected all candidate biomarkers that passed the criteria above, *i.e.*, sensitivity was greater or equal than 14% at 96% specificity. Next, we applied the minimum redundancy maximum relevance algorithm to further select biomarkers that were possibly the most important and least correlated[20]. In the third stage, we

Table 1 Clinical information of the samples

	Discovery set			Validation set		
	CD	UC	HC	CD	UC	HC
N	50	50	50	50	50	50
Gender (female, male)	29, 21	29, 21	29, 21	28, 22	28, 22	28, 22
Age (median ± SD)	41 ± 17.66	44 ± 17.25	42 ± 18.47	39.5 ± 17.49	44.5 ± 17.23	39.5 ± 16.02
Disease behavior (B1/B2/B3)	9/10/6			16/8/2		
Disease location (L1/L2/L3/L4)	12/6/7/0			12/7/7/0		
Disease extent (E1/E2/E3)		0/32/18			0/34/16	
Surgery (Yes, No)	24, 25	8, 42		22, 27	7, 42	

Fischer's exact test *P* value is equal to 1 for the gender difference among CD, UC and HC in both discovery and validation set. Kruskal-Wallis test *P* value for the age difference among CD, UC and HC in discovery and validation set were 0.3159 and 0.1737 respectively. CD: Crohn's disease; UC: Ulcerative colitis; HC: Healthy control.

fit a logistic regression model using the selected biomarkers from the first two stages and generated its receiver operating characteristic curve and AUC value to evaluate the model's discriminatory performance between CD, UC, and healthy controls.

Pair-wise subgroup comparisons based on the Montreal classification were performed for the odds ratio (OR) of each antibody using the seropositivity threshold defined as the maximum of MNI 2 and the 75th percentile of all samples. Chi-squared tests were used to test global significance between all groups with a slight modification by adding 0.5 to each cell of the table to avoid zero cell counts. *P* values from the Chi-squared method were adjusted for each pair of comparisons and for all candidate biomarkers. The number of antibodies with significant difference in prevalence among classifications were counted based on OR > 1 and OR < 1 for each pair of classification of CD behavior, CD location, UC extent and the surgery history of CD patients. The difference in total number of antibodies with significant difference between classification groups were computed using two sample proportion test. We did not perform a subgroup analysis for the UC patients based on the surgery history because most (84 out of 100) had no surgeries (Table 1).

Spearman's rank correlation analysis was performed to assess the correlation between autoantibody and anti-microbial antibody reactivity for CD patients and healthy controls. The R "pheatmap" package was used to generate the heatmap for correlation coefficients.

Bioinformatics analysis

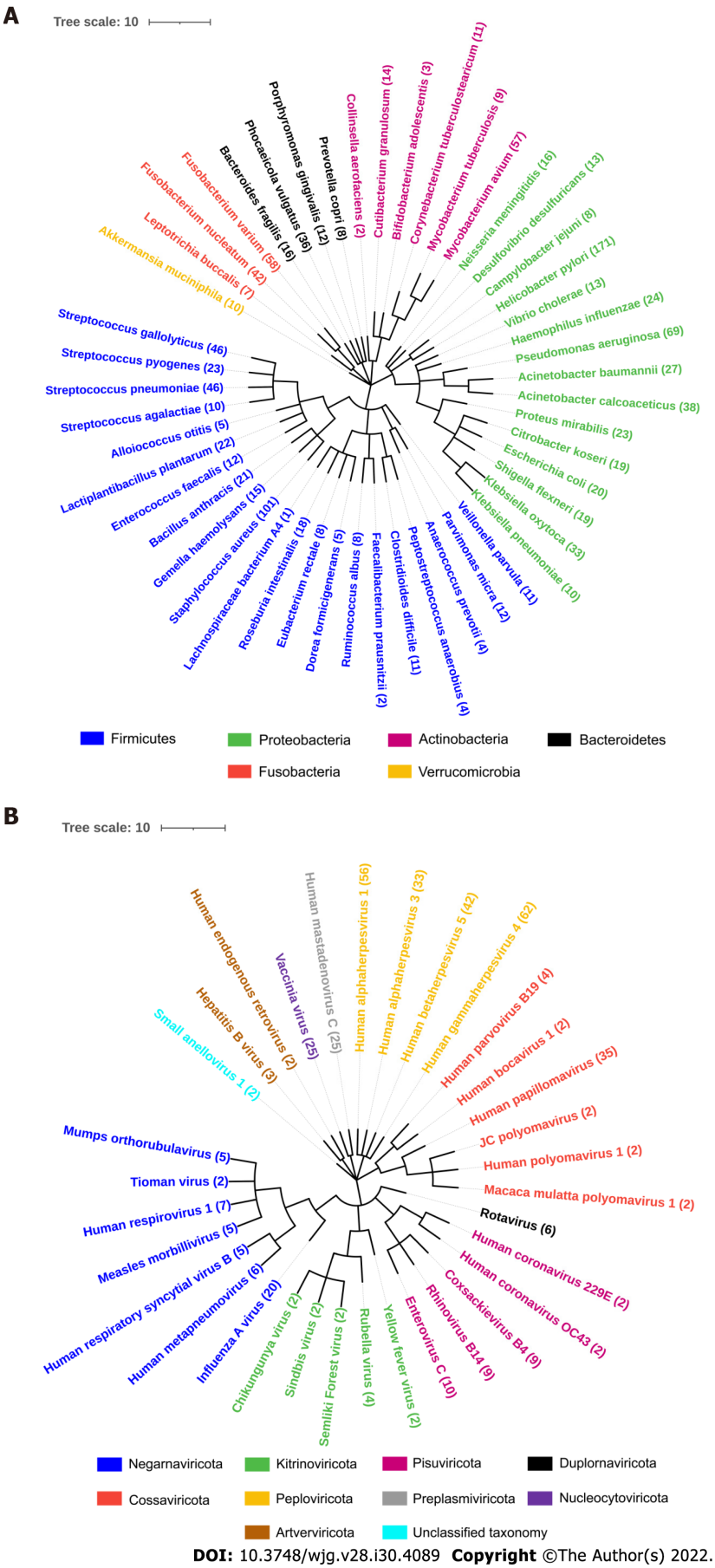
The NCBI Taxonomy browser was used to find the taxonomical details of all the bacteria and viruses used in our study. The taxa were downloaded as phylip tree file and was used as an input in interactive tree of life software. Two phylogenetic trees were created for bacteria and viruses with different colors distinguishing the phylum.

For sequence homology analysis, a pair-wise BLAST analysis was carried out on the antigen protein sequences of validated antibodies for CD *vs* healthy control analysis. E-values were used to generate a heatmap using Python Seaborn package.

RESULTS

Anti-microbial antibody profiling in IBD on microbial protein arrays

We studied IgG and IgA anti-microbial antibody profiles of 100 CD and 100 UC patients and 100 age-gender matched healthy controls (Table 1) against 1570 microbial antigens including 1173 antigens from 50 different bacteria and 397 antigens from 33 different viruses using our protein microarray platform (Figure 1, Supplementary Table 1). This study provided a representative overview of the anti-microbial antibody response in IBD patients (Supplementary Figure 1). The numbers of IgG antibodies against bacterial proteins from *Bacteroidetes vulgatus* (*B. vulgatus*) and *Citrobacter koseri* (*C. koseri*) were significantly higher in CD patients compared with those in healthy controls (Chi-square test, $P < 0.01$) (Supplementary Figure 1). On the contrary, the numbers of IgG antibodies against proteins from several bacteria, such as *Streptococcus pneumoniae* (*S. pneumoniae*), *Haemophilus influenza* (*H. influenzae*), *Staphylococcus aureus* (*S. aureus*), *Helicobacter pylori* (*H. pylori*) and *Parvimonas micra* (*P. micra*) were significantly lower in CD and UC patients compared with those in healthy controls (Chi-square test, $P < 0.05$)



DOI: 10.3748/wjg.v28.i30.4089 **Copyright** ©The Author(s) 2022.

Figure 1 Phylogenetic tree of microbes studied with their corresponding number of proteins analyzed. A: Fifty species of bacteria with 1173 proteins were segregated into 6 phyla; B: Thirty-three species of viruses with 397 proteins were segregated into 10 phyla.

(Supplementary Figure 1). Overall, fewer IgA anti-microbial antibodies were found than IgG antibodies. The numbers of IgA antibodies against *S. pneumoniae*, *H. influenzae*, *S. aureus*, and *H. pylori* were significantly lower in UC patients compared with those in healthy controls (Chi-square test, $P < 0.01$). On the other hand, anti-viral IgG and IgA antibodies showed heterogenous prevalence with no clear trend of differences among CD, UC, healthy controls (data not shown). Therefore, we focused our analysis on anti-bacterial antibodies.

Antibodies distinguishing CD from healthy controls

We compared prevalence for individual anti-microbial antibodies between CD patients and healthy controls. We randomly split samples evenly into discovery and the validation sets (Table 1). For antibodies with elevated prevalence in CD patients, 13 IgG antibodies passed the criteria (sensitivity ≥ 14% at 96% specificity) in both discovery and validation sets (Table 2). Anti-A4-Fla2_IgG, a well-studied anti-bacterial flagellin antibody in CD, had the best performance with 47% sensitivity at 96% specificity in the full sample set (Table 2). Beside the flagellins, we found antibodies to four novel target antigens from *B. vulgatus* (BVU_0562), *P. mirabilis* (PMI_RS06815), *S. flexneri* (SF_Lpp) and *S. pneumoniae* (SP_1992) (Table 2) with no significant sequence homology to flagellins (Figure 2A).

To our surprise, 12 validated IgG antibodies showed elevated prevalence in healthy controls relative to CD patients (Supplementary Table 2). Among these 12 antibodies, anti-bacterial antibodies performed better in differentiating CD patients from healthy controls than anti-viral antibodies (Supplementary Table 2). Antibody against SPy_2009, an anchoring protein located in the cell wall of *Streptococcus pyogenes* (*S. pyogenes*), had the highest sensitivity of 24% at 96% specificity in healthy controls relative to CD patients. Seven validated IgA antibodies showed higher prevalence in healthy controls relative to CD patients (Supplementary Table 4).

Antibodies distinguishing UC from healthy controls

For anti-microbial antibodies with elevated prevalence in UC patients relative to healthy controls, 4 IgG antibodies passed the criteria in both discovery and validation sets (Table 2). Antibodies to A4-Fla2_IgG and a flagellin from *C. koseri* had a sensitivity of 18% and 15% respectively. For IgG antibodies with higher prevalence in healthy controls relative to UC patients, 32 antibodies got validated (Supplementary Table 3). Source microorganisms for the target antigens of these 32 antibodies were enriched for *S. pneumoniae, S. aureus,* and *H. influenzae* (2-sample proportion test, $P < 0.05$). 2.7% of the proteins on the microbial protein microarray were from *S. pneumoniae* while 18.7% of antigens for validated antibodies were from *S. pneumoniae*, 6.1% of the proteins on the microarrays were from *S. aureus* while 18.7% of antigens for validated antibodies were from *S. aureus,* and 1.4% of the proteins on the microarrays were from *H. influenzae* while 12.5% of antigens for validated antibodies were from *H. influenzae*. Nine validated IgA antibodies showed higher prevalence in healthy controls relative to UC patients (Supplementary Table 4).

Fewer anti-viral antibodies than anti-bacterial antibodies were validated comparing CD or UC patients with healthy controls (Table 2, Supplementary Tables 2 and 3). Anti-viral antibodies to Rhinovirus B14, Enterovirus C, Influenza A virus, Human metapneumovirus had higher prevalence in healthy controls compared with CD and UC patients (Supplementary Tables 2 and 3).

Comparison of anti-microbial antibody response between CD and UC

We found 46 IgG and 22 IgA validated anti-microbial antibodies with higher prevalence in CD patients compared to UC patients while 28 IgG and 9 IgA validated anti-microbial antibodies with higher prevalence in UC patients compared to CD patients. There was minimal overlap of the target antigens of these validated IgG and IgA antibodies (Figure 2B).

Multivariate analysis to distinguish CD, UC, and healthy controls

We built multi-antibody panels that could distinguish CD *vs* control, UC *vs* control, and CD *vs* UC with an area under the curve (AUC) of 0.81, 0.87, and 0.82 respectively. For CD *vs* control, antibodies against novel flagellins (HP_0115, CK_LafA, CK_LafA.1, VC_flaD, VC_flaB, VC_flaE, VC_flaA) had an AUC of 0.73, antibodies against non-flagellins (BVU_0562, SP_1992, PMI_RS06815, and SF_Lpp) had an AUC of 0.75 and the combined AUC of antibodies against novel flagellins and non-flagellins was 0.81 (Figure 3A). For UC *vs* control, a combination of seven antibodies, four against *S. pneumoniae* and one each against *S. aureus*, *H. influenzae* and *B. vulgatus* had an AUC of 0.87 (Figure 3B). For CD *vs* UC, combination of seven antibodies, two against *H. pylori* and one each against *E. coli*, *S. pneumoniae*, *S. pyogenes*, *C. jejuni* and *L. bacterium A4* had an AUC of 0.82 (Figure 3C).

Subgroup analysis

We investigated the association of CD behavior (B1, B2, B3), CD location (L1, L2, L3), and UC extent (E1, E2, E3) based on the Montreal classification with the anti-microbial antibody prevalence. We calculated the 4th quartile odds ratio for each antibody between the two classification groups and compared the number of antibodies with significant odds ratio (P value < 0.05) in each group. We found B3 (penetrating) had the highest prevalence of antibodies followed by B2 (stricturing) and B1 (non-

Table 2 Sensitivities of validated IgG antibodies comparing Crohn's disease and ulcerative colitis with healthy controls in the discovery, validation, and the entire set at 96% specificity

		Antigen	Protein name	Organism	Discovery	Validation	Entire
Crohn's disease	Bacteria	HP_0115	Flagellin B	*H. pylori*	28	48	38
		BVU_0562	Uncharacterized protein	*B. vulgatus*	26	22	25
		CK_LafA	Lateral flagellin	*C. koseri*	20	22	21
		CK_LafA.1	Lateral flagellin	*C. koseri*	16	26	24
		A4-Fla2	Flagellin	*L. bacterium A4*	40	54	47
		PMI_RS06815	Hypothetical protein	*P. mirabilis*	14	16	15
		VC_flaD	Flagellin	*V. cholerae*	24	18	19
		VC_flaB	Flagellin	*V. cholerae*	28	22	24
		VC_flaE	Flagellin	*V. cholerae*	26	28	23
		VC_flaA	Flagellin	*V. cholerae*	20	22	21
		SF_Lpp	Outer membrane lipoprotein	*S. flexneri*	14	18	14
		SP_1992	Cell wall surface anchor	*S. pneumoniae*	20	16	18
	Virus	BILF2	Glycoprotein BILF2	Human herpesvirus 4	18	18	18
Ulcerative colitis	Bacteria	CK_flgG	Flagellar basal-body rod protein	*C. koseri*	14	16	15
		A4-Fla2	Flagellin	*L. bacterium A4*	22	16	18
	Virus	BVRF2	Capsid scaffolding protein	Human herpesvirus 4	14	16	14
		UL139	Membrane glycoprotein UL139	Human herpesvirus 5	14	20	17

stricturing, non-penetrating) (Table 3). For CD location, we found L2 had the highest prevalence of antibodies followed by L3 (ileocolonic) and L1 (Table 3). For UC extent, E3 (extensive UC) had higher prevalence of antibodies compared to E2 (left sided UC). In addition to the Montreal classification, we also performed subgroup analysis based on the surgery history of CD patients. We found that patients who had surgery possessed higher prevalence of antibodies compared to those without surgery (Table 3).

Correlation of anti-microbial antibodies and autoantibodies in CD patients

We previously reported novel autoantibodies in CD patients using the same set of CD patients and healthy controls[21]. We profiled both IgG and IgA autoantibodies and anti-microbial antibodies in all 100 CD and 100 healthy controls. It is interesting to note the antibodies showing differences for autoantibodies were mostly IgA, but the anti-microbial antibodies were mostly IgG[21]. Anti-SNRPB_IgA had the highest sensitivity of 20% at 96% specificity among all autoantibodies compared with 47% sensitivity at 96% specificity for the best performing anti-microbial antibody, anti-A4-Fla2_IgG.

We compared the novel autoantibodies and validated anti-microbial antibody profiles to determine if correlation existed between their reactivity. Overall, we did not observe high correlation between autoantibodies and anti-microbial antibodies in CD patients (Figure 4). Anti-microbial antibodies formed two clusters, one with anti-flagellin antibodies, and the other with SF_Lpp_IgG and PMI_RS06815_IgG. Five autoantibodies, PRPH_IgA, SNAI1_IgA, PPP1R13L_IgA, SNRPB_IgA and PTTG1_IgA, formed a cluster. The remaining antibodies had relatively unique reactivity patterns.

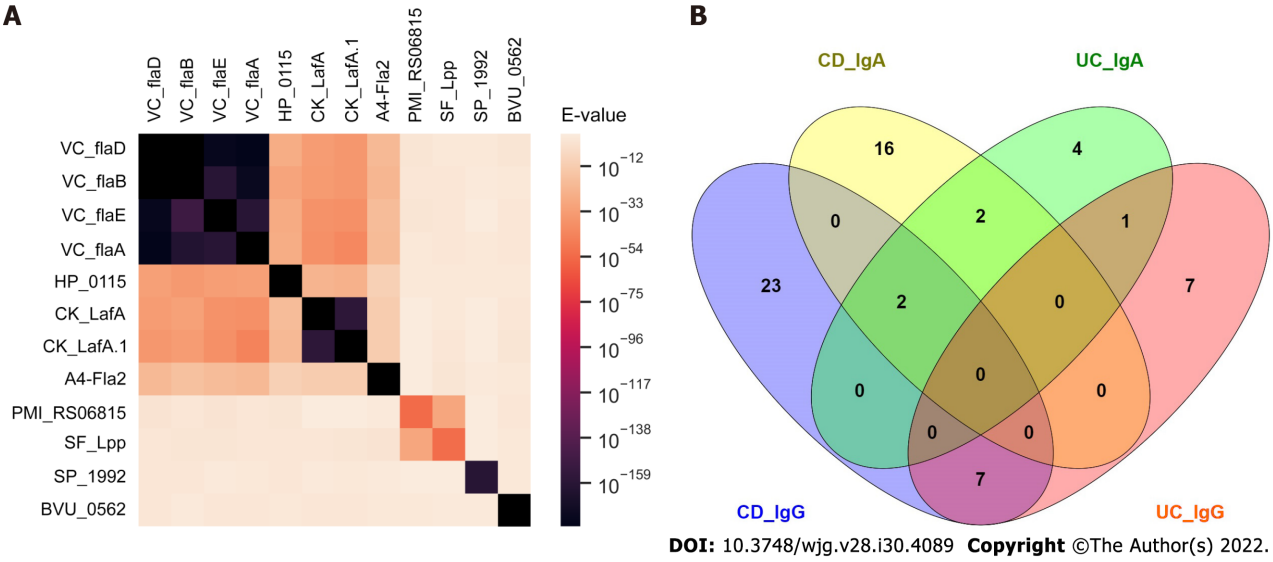
DISCUSSION

We have performed a microbiomics study to understand the connection between host anti-microbial responses and IBD and to identify antibody signatures that can aid in the accurate diagnosis of IBD. We found antibody responses to novel non-flagellin antigens with elevated prevalence in CD patients compared with healthy controls. On the contrary, we observed many anti-microbial antibodies with

Table 3 Subgroup analysis of inflammatory bowel disease patients

Classification	Comparison	Number of antibodies with		Two sample proportion test
		OR > 1	OR < 1	
Disease behavior: B1: non-stricturing, non-penetrating; B2: stricturing; B3: penetrating	B1 *vs* B2 ($P < 0.05$)	0	32	$P < 0.001$
	B2 *vs* B3 ($P < 0.05$)	0	19	$P < 0.001$
	B1 *vs* B3 ($P < 0.05$)	2	41	$P < 0.001$
Disease location: L1: ileal; L2: colonic; L3: ileocolonic	L1 *vs* L2 ($P < 0.05$)	0	38	$P < 0.001$
	L2 *vs* L3 ($P < 0.05$)	9	5	$P = 0.131$
	L1 *vs* L3 ($P < 0.05$)	5	16	$P < 0.001$
Disease extent: E2: left sided UC; E3: extensive UC	E2 *vs* E3 ($P < 0.05$)	11	39	$P < 0.001$
Surgery in CD patients	No *vs* Yes ($P < 0.05$)	6	25	$P < 0.001$

For each comparison, the number of antibodies with significant difference in prevalence between two classifications were counted based on odds ratio (OR) > 1 and OR < 1. The difference in total number of antibodies for each comparison were computed using two sample proportion test. CD: Crohn's disease; UC: Ulcerative colitis; OR: Odds ratio.

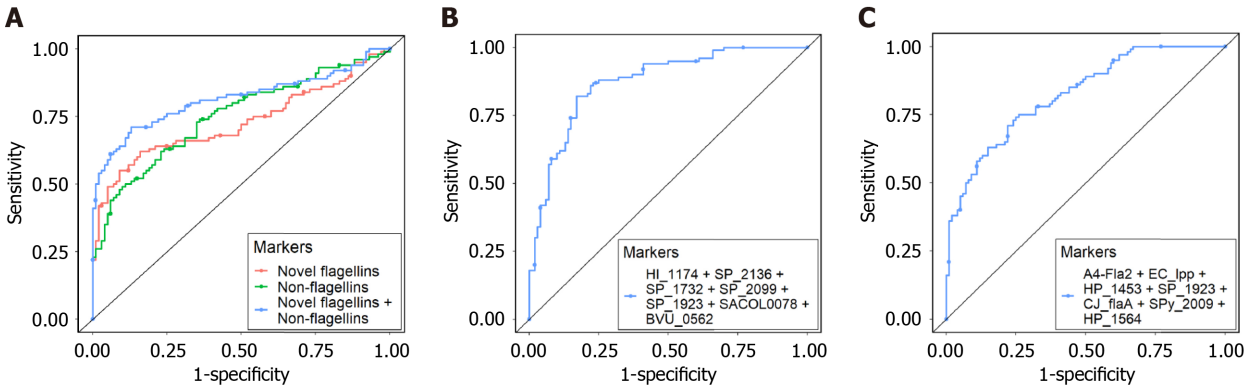


DOI: 10.3748/wjg.v28.i30.4089 **Copyright** ©The Author(s) 2022.

Figure 2 Sequence homology of target antigens of validated antibodies and overlap of antibodies among Crohn's disease and ulcerative colitis. A: Heatmap showing sequence homology among target antigens for antibodies with validated performance of ≥ 14% sensitivity at 96% specificity comparing Crohn's disease (CD) patients with healthy controls; B: CD_IgG, ulcerative colitis (UC)_IgG, CD_IgA and UC_IgG represent the overlap of anti-microbial antibodies of IgG and IgA isotypes in CD and UC patients with ≥ 14% sensitivity at 96% specificity against healthy controls in the discovery set. CD: Crohn's disease; UC: Ulcerative colitis.

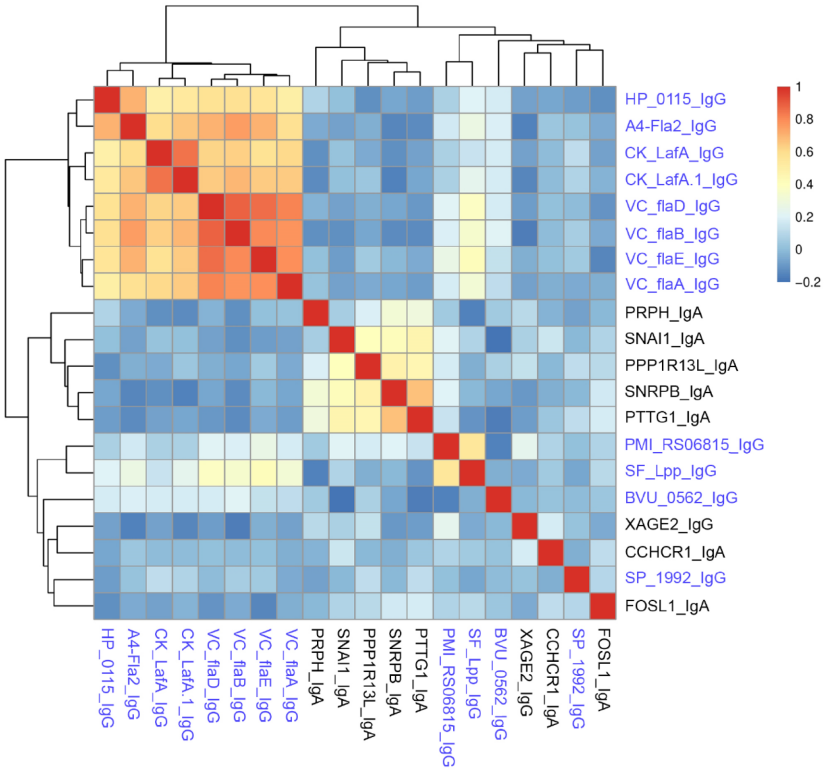
lower prevalence in UC patients relative to healthy controls. We built antibody panels that could distinguish CD *vs* control, UC *vs* control and CD *vs* UC with AUCs of 0.81, 0.87, and 0.82, respectively. Lichtenstein *et al*[22] reported an integrated serological (ASCA-IgA, ASCA-IgG, anti-OmpC, anti-CBir1, anti-I2, pANCA) and genetic (SNP8, SNP12, SNP13) marker panel with an AUC of 0.80 to distinguish CD *vs* control. A panel of serological markers (ASCA-IgA, ASCA-IgG, ANCA, pANCA, OmpC, and CBir1) built by Plevy *et al*[23] yields an AUC of 0.78 to distinguish CD *vs* UC. Our novel antibody marker panels had comparable or better performance in IBD diagnosis or distinguishing CD from UC subtypes. We observed a stronger anti-microbial antibody response with more aggressive disease in both CD and UC patients. Finally, we demonstrated that anti-microbial antibodies and autoantibodies had different reactivity patterns in CD patients.

Our comprehensive study of anti-microbial antibodies in IBD patients provided interesting insight into its pathogenesis. Antibody responses to proteins from *B. vulgatus*, *P. mirabilis*, *S. flexneri* and *S. pneumoniae* were elevated in CD patients. *B. vulgatus* has been reported to induce colitis in IBD-susceptible mice[24,25]. *P. mirabilis* in gut can induce inflammation in cells and a colitis mouse model and has been associated with CD pathogenesis[26]. Our results suggest that *B. vulgatus* and *P. mirabilis*



DOI: 10.3748/wjg.v28.i30.4089 **Copyright** ©The Author(s) 2022.

Figure 3 Receiver operating characteristic curves to discriminate Crohn's disease, ulcerative colitis, and healthy controls. A: Receiver operating characteristic (ROC) curve for Crohn's disease (CD) *vs* healthy controls. Area under the curve (AUC) values of novel anti-flagellin antibodies (HP_0115, CK_LafA, CK_LafA.1, VC_flaD, VC_flaB, VC_flaE, VC_flaA) and anti-non-flagellin antibodies (BVU_0562, SP_1992, PMI_RS06815, SF_Lpp) was 0.73 and 0.75, respectively. The AUC value obtained with a combination of novel anti-flagellin and anti-non-flagellin antibodies was 0.81; B: ROC curve for ulcerative colitis (UC) *vs* healthy controls. The AUC value obtained with a combination of 7 markers was 0.87; C: ROC curve for CD *vs* UC. The AUC value obtained with a combination of 7 markers was 0.82.



DOI: 10.3748/wjg.v28.i30.4089 **Copyright** ©The Author(s) 2022.

Figure 4 Spearman's rank correlation coefficient heatmap of anti-microbial antibodies and autoantibodies in Crohn's disease patients. The names of anti-microbial antibodies are colored in blue while autoantibodies are colored in black.

may also play a role in human CD development. We observed reduced antibody responses in UC patients to several genera of the Firmicutes phylum including *P. micra*, *S. pyogenes*, *S. aureus*, which were often reduced in abundance in UC patients' gut microbiota[27]. For several genera belonging to Proteobacteria phylum, such as *H. influenzae*, *H. pylori*, *K. oxytoca*, we observed overall reduced antibody responses; however, their abundance in the gut microbiota of UC patients has been reported to be either increased or remained the same compared with healthy controls[6,28].

Beyond exposure alone, antibody response requires functional immunological interaction between a microorganism and the host; however, anti-microbial antibodies by themselves do not prove causality. As such, source microorganisms whose antibodies show significant changes between IBD patients and healthy controls warrant future confirmation and functional assessment in causing IBD. A4-Fla2

flagellin included in our study showed IBD-specific prevalence with performance similar to that reported in the literature[14,29]. We also identified several antibodies to flagellins with higher prevalence in CD patients relative to healthy controls.

Previous studies mostly focused on antibodies with higher prevalence in IBD patients[30]. Our unbiased data-driven approach revealed the existence of many anti-microbial antibodies with higher prevalence in healthy controls relative to CD and especially UC patients (Supplementary Tables 3 and 4). The reduction observed in CD and UC patients may be attributed to the dysbiosis and reduced diversity of gut microbiota in CD and UC patients[28,31]. It is also possible that the reduction in anti-microbial antibodies in some CD and UC patients was in part because of immunosuppressive therapies they received. The greater number of antibodies having high prevalence in CD patients compared with UC patients indicates stronger anti-microbial humoral immunity in CD than in UC, which is consistent with reports in the literature that most known anti-microbial antibodies, such as ASCA, anti-OmpC, anti-Cbir1, and anti-I2, had higher prevalence in CD patients than in UC patients[30]. This agreement, together with comparable performance of anti-flagellin antibodies in our study and that reported in the literature, suggests that our results reflect the microbial association of IBD etiopathology. However, the use of samples from patients with established disease and the lack of information on immunosuppressive therapies of these patients limited the interpretation of the results.

We studied the association between anti-microbial antibody prevalence and various disease classifications based on Montreal classification and surgery history. We found more antibodies with significantly higher prevalence in patients with more aggressive disease behaviors relative to those with milder disease behavior. We also found more antibodies with significantly higher prevalence in colonic CD patients relative to those in ileal CD patients. Our results were consistent with previous reports that increasing diversity and magnitude of anti-microbial immune response was correlated with increased frequency of penetrating and/or stricturing disease behavior[13,32]. It is known that the colon has a microbial density of 10^{11}-10^{12} anaerobic bacteria/gram while the ileum is colonized by 10^{7}-10^{8} anaerobic bacteria/gram[7]. Kleessen *et al*[33] found higher percentage of bacterial invasion of mucosa in colon compared to ileum. CD patients requiring surgery usually had more severe disease compared with those who did not need surgery. Stronger anti-microbial immune response in patients with severe CD or UC suggests a higher abundance of the source microorganisms for the target antigens of the differential antibodies and/or a stronger more conducive immune microenvironment at the disease site in severe disease.

Both autoantibodies and anti-microbial antibodies associated with IBD have been reported[30]. One popular hypothesis for the autoantibody elicitation is molecular mimicry, where anti-microbial antibodies cross react with human proteins. However, we found minimal correlation between the anti-microbial antibodies and the autoantibody profiles in the same set of CD samples. The lack of correlation suggests that IBD-specific autoantibodies and anti-microbial antibodies are elicited independently through different underlying mechanisms, and cross-reactivity may play less of a role in eliciting CD-associated autoantibodies. The breakdown of immune tolerance to human proteins might have occurred due to the damaged gut epithelial cells and the faulty immunological microenvironment partly caused by microbial infections. In addition, the elicitation of autoantibodies may be associated with the infections of multiple microorganisms, and the correlation with individual anti-microbial antibodies may not be great.

Strengths of our study include the broadest analysis to date of IgG and IgA antibodies against individual antigens from many different microorganisms in both CD and UC patients and the use of a two-stage approach with discovery and independent validation of antibody markers. There are some limitations to our study. Except for a few microbes, the number of proteins studied for each species is small, which might limit our interpretation of antibody response in IBD at the species level. Furthermore, many samples used in studies were collected from patients with established disease. Future studies with access to more clinical information, such as information about the use of immunosuppressive or antibiotics treatment, could aid in the interpretation of our results. In addition, samples collected from newly diagnosed patients will strengthen our ability to identify diagnostic markers and microbial connections for IBD development.

CONCLUSION

In summary, we have demonstrated the power of a microbiomics study of anti-microbial antibodies in IBD for the identification of anti-microbial antibody signatures to improve early accurate diagnosis and help understand IBD etiology. The elucidation of the source microorganisms of the target antigens of the antibody biomarkers could lead to novel strategies for the prevention of IBD.

ARTICLE HIGHLIGHTS

Research background

Early and accurate diagnosis of inflammatory bowel disease (IBD) can benefit the clinical management of IBD patients. The clinical utility of available non-invasive biomarkers is limited.

Research motivation

The gut microbiota plays an important role in the pathogenesis of IBD. Antibody responses to microbial antigens can be exploited to identify better diagnosis markers and improve our understanding of IBD pathology.

Research objectives

This study aimed to compare anti-microbial antibody profiles in Crohn's disease (CD) and ulcerative colitis (UC) patients and healthy controls.

Research methods

We employed an innovative protein microarray platform and profiled antibodies against 1570 microbial antigens in 100 CD, 100 UC, and 100 healthy controls.

Research results

Antibodies to bacterial proteins were better in distinguishing IBD patients from healthy controls compared with antibodies to viral proteins. We identified a set of novel anti-microbial antibodies against the antigens of *Bacteroidetes vulgatus* (BVU_0562) and *Streptococcus pneumoniae* (SP_1992) elevated in CD patients relative to healthy controls. In addition, anti-microbial antibodies against the antigen of *Streptococcus pyogenes* (SPy_2009) were found to be elevated in healthy controls relative to UC patients. We constructed antibody panels that could distinguish CD *vs* control, UC *vs* control, and CD *vs* UC with an AUC of 0.81, 0.87 and 0.82 respectively. Patients with severe disease had higher prevalence of anti-microbial antibodies. There was minimal correlation among the occurrence of autoantibodies and anti-microbial antibodies in CD patients.

Research conclusions

This study discovered novel anti-microbial antibodies with differential prevalence in CD and UC patients relative to healthy controls. In addition, this study revealed the potentially different roles of gut microbiota in CD and UC pathology.

Research perspectives

Our study demonstrated the power of a microbiomics approach to identify biomarkers that could aid in the early and accurate detection of IBD non-invasively, and shed light into the role of various microbes in IBD etiology.

ACKNOWLEDGEMENTS

The authors would like to thank Jessica Friton for her help with patient sample and data acquisition. The authors would like to thank Shehzad Sheikh for helpful suggestions to improve the manuscript.

FOOTNOTES

Author contributions: Shome M and Song L designed and ran the experiment; Williams S and Chung Y performed the statistical analysis; Murugan V and Park JG helped in preparation of clones; Faubion W, Pasha SF and Leighton JA provided the serum samples and also provided intellectual guidance; LaBaer J and Qiu J supervised the project and secured funding; Shome M and Qiu J wrote the original manuscript which was then reviewed by remaining authors.

Institutional review board statement: The authors have taken appropriate steps to protect the rights and welfare of humans participating as subjects in the research (IRB Application #: 13-008267).

Informed consent statement: All study participants or their legal guardian of the study provided informed written consent about personal and medical data collection prior to study enrollment.

Conflict-of-interest statement: All the authors report no relevant conflicts of interest for this article.

Data sharing statement: Data from this study is available on request from the corresponding author.

STROBE statement: The authors have read the STROBE Statement-checklist of items, and the manuscript was prepared and revised according to the STROBE Statement-checklist of items.

Open-Access: This article is an open-access article that was selected by an in-house editor and fully peer-reviewed by external reviewers. It is distributed in accordance with the Creative Commons Attribution NonCommercial (CC BY-NC 4.0) license, which permits others to distribute, remix, adapt, build upon this work non-commercially, and license their derivative works on different terms, provided the original work is properly cited and the use is non-commercial. See: https://creativecommons.org/Licenses/by-nc/4.0/

Country/Territory of origin: United States

ORCID number: William Faubion 0000-0003-1291-5745; Ji Qiu 0000-0002-7913-9042.

S-Editor: Gong ZM
L-Editor: A
P-Editor: Gong ZM

REFERENCES

1 **GBD 2017 Inflammatory Bowel Disease Collaborators**. The global, regional, and national burden of inflammatory bowel disease in 195 countries and territories, 1990-2017: a systematic analysis for the Global Burden of Disease Study 2017. *Lancet Gastroenterol Hepatol* 2020; **5**: 17-30 [PMID: 31648971 DOI: 10.1016/S2468-1253(19)30333-4]
2 **de Souza HS**, Fiocchi C. Immunopathogenesis of IBD: current state of the art. *Nat Rev Gastroenterol Hepatol* 2016; **13**: 13-27 [PMID: 26627550 DOI: 10.1038/nrgastro.2015.186]
3 **Fakhoury M**, Negrulj R, Mooranian A, Al-Salami H. Inflammatory bowel disease: clinical aspects and treatments. *J Inflamm Res* 2014; **7**: 113-120 [PMID: 25075198 DOI: 10.2147/JIR.S65979]
4 **Zuo T**, Ng SC. The Gut Microbiota in the Pathogenesis and Therapeutics of Inflammatory Bowel Disease. *Front Microbiol* 2018; **9**: 2247 [PMID: 30319571 DOI: 10.3389/fmicb.2018.02247]
5 **Ni J**, Wu GD, Albenberg L, Tomov VT. Gut microbiota and IBD: causation or correlation? *Nat Rev Gastroenterol Hepatol* 2017; **14**: 573-584 [PMID: 28743984 DOI: 10.1038/nrgastro.2017.88]
6 **Frank DN**, St Amand AL, Feldman RA, Boedeker EC, Harpaz N, Pace NR. Molecular-phylogenetic characterization of microbial community imbalances in human inflammatory bowel diseases. *Proc Natl Acad Sci USA* 2007; **104**: 13780-13785 [PMID: 17699621 DOI: 10.1073/pnas.0706625104]
7 **Sartor RB**. Microbial influences in inflammatory bowel diseases. *Gastroenterology* 2008; **134**: 577-594 [PMID: 18242222 DOI: 10.1053/j.gastro.2007.11.059]
8 **Ahmad T**, Armuzzi A, Bunce M, Mulcahy-Hawes K, Marshall SE, Orchard TR, Crawshaw J, Large O, de Silva A, Cook JT, Barnardo M, Cullen S, Welsh KI, Jewell DP. The molecular classification of the clinical manifestations of Crohn's disease. *Gastroenterology* 2002; **122**: 854-866 [PMID: 11910336 DOI: 10.1053/gast.2002.32413]
9 **Hugot JP**, Chamaillard M, Zouali H, Lesage S, Cézard JP, Belaiche J, Almer S, Tysk C, O'Morain CA, Gassull M, Binder V, Finkel Y, Cortot A, Modigliani R, Laurent-Puig P, Gower-Rousseau C, Macry J, Colombel JF, Sahbatou M, Thomas G. Association of NOD2 leucine-rich repeat variants with susceptibility to Crohn's disease. *Nature* 2001; **411**: 599-603 [PMID: 11385576 DOI: 10.1038/35079107]
10 **Ramanan D**, Tang MS, Bowcutt R, Loke P, Cadwell K. Bacterial sensor Nod2 prevents inflammation of the small intestine by restricting the expansion of the commensal Bacteroides vulgatus. *Immunity* 2014; **41**: 311-324 [PMID: 25088769 DOI: 10.1016/j.immuni.2014.06.015]
11 **Elkadri AA**, Stempak JM, Walters TD, Lal S, Griffiths AM, Steinhart AH, Silverberg MS. Serum antibodies associated with complex inflammatory bowel disease. *Inflamm Bowel Dis* 2013; **19**: 1499-1505 [PMID: 23702714 DOI: 10.1097/MIB.0b013e318281f2a1]
12 **Vermeire S**, Joossens S, Peeters M, Monsuur F, Marien G, Bossuyt X, Groenen P, Vlietinck R, Rutgeerts P. Comparative study of ASCA (Anti-Saccharomyces cerevisiae antibody) assays in inflammatory bowel disease. *Gastroenterology* 2001; **120**: 827-833 [PMID: 11231936 DOI: 10.1053/gast.2001.22546]
13 **Kuna AT**. Serological markers of inflammatory bowel disease. *Biochem Med (Zagreb)* 2013; **23**: 28-42 [PMID: 23457764 DOI: 10.11613/bm.2013.006]
14 **Lodes MJ**, Cong Y, Elson CO, Mohamath R, Landers CJ, Targan SR, Fort M, Hershberg RM. Bacterial flagellin is a dominant antigen in Crohn disease. *J Clin Invest* 2004; **113**: 1296-1306 [PMID: 15124021 DOI: 10.1172/JCI20295]
15 **Takulapalli BR**, Qiu J, Magee DM, Kahn P, Brunner A, Barker K, Means S, Miersch S, Bian X, Mendoza A, Festa F, Syal K, Park JG, LaBaer J, Wiktor P. High density diffusion-free nanowell arrays. *J Proteome Res* 2012; **11**: 4382-4391 [PMID: 22742968 DOI: 10.1021/pr300467q]
16 **Song L**, Wallstrom G, Yu X, Hopper M, Van Duine J, Steel J, Park J, Wiktor P, Kahn P, Brunner A, Wilson D, Jenny-Avital ER, Qiu J, Labaer J, Magee DM, Achkar JM. Identification of Antibody Targets for Tuberculosis Serology using High-Density Nucleic Acid Programmable Protein Arrays. *Mol Cell Proteomics* 2017; **16**: S277-S289 [PMID: 28223349 DOI: 10.1074/mcp.M116.065953]
17 **Song L**, Song M, Rabkin CS, Williams S, Chung Y, Van Duine J, Liao LM, Karthikeyan K, Gao W, Park JG, Tang Y, Lissowska J, Qiu J, LaBaer J, Camargo MC. *Helicobacter pylori* Immunoproteomic Profiles in Gastric Cancer. *J Proteome Res* 2021; **20**: 409-419 [PMID: 33108201 DOI: 10.1021/acs.jproteome.0c00466]

18 **Song L**, Song M, Camargo MC, Van Duine J, Williams S, Chung Y, Kim KM, Lissowska J, Sivins A, Gao W, Karthikeyan K, Park J, Leja M, Cohen JI, LaBaer J, Qiu J, Rabkin CS. Identification of anti-Epstein-Barr virus (EBV) antibody signature in EBV-associated gastric carcinoma. *Gastric Cancer* 2021; **24**: 858-867 [PMID: 33661412 DOI: 10.1007/s10120-021-01170-z]

19 **Oliveros JC**. VENNY. An interactive tool for comparing lists with Venn Diagrams. Available from: https://bioinfogp.cnb.csic.es/tools/venny/index.html

20 **Ding C**, Peng H. Minimum redundancy feature selection from microarray gene expression data. *J Bioinform Comput Biol* 2005; **3**: 185-205 [PMID: 15852500 DOI: 10.1142/s0219720005001004]

21 **Wang H**, Demirkan G, Bian X, Wallstrom G, Barker K, Karthikeyan K, Tang Y, Pasha SF, Leighton JA, Qiu J, LaBaer J. Identification of Antibody Against SNRPB, Small Nuclear Ribonucleoprotein-Associated Proteins B and B', as an Autoantibody Marker in Crohn's Disease using an Immunoproteomics Approach. *J Crohns Colitis* 2017; **11**: 848-856 [PMID: 28204086 DOI: 10.1093/ecco-jcc/jjx019]

22 **Lichtenstein GR**, Targan SR, Dubinsky MC, Rotter JI, Barken DM, Princen F, Carroll S, Brown M, Stachelski J, Chuang E, Landers CJ, Stempak JM, Singh S, Silverberg MS. Combination of genetic and quantitative serological immune markers are associated with complicated Crohn's disease behavior. *Inflamm Bowel Dis* 2011; **17**: 2488-2496 [PMID: 21391291 DOI: 10.1002/ibd.21661]

23 **Plevy S**, Silverberg MS, Lockton S, Stockfisch T, Croner L, Stachelski J, Brown M, Triggs C, Chuang E, Princen F, Singh S. Combined serological, genetic, and inflammatory markers differentiate non-IBD, Crohn's disease, and ulcerative colitis patients. *Inflamm Bowel Dis* 2013; **19**: 1139-1148 [PMID: 23518807 DOI: 10.1097/MIB.0b013e318280b19e]

24 **Bloom SM**, Bijanki VN, Nava GM, Sun L, Malvin NP, Donermeyer DL, Dunne WM Jr, Allen PM, Stappenbeck TS. Commensal Bacteroides species induce colitis in host-genotype-specific fashion in a mouse model of inflammatory bowel disease. *Cell Host Microbe* 2011; **9**: 390-403 [PMID: 21575910 DOI: 10.1016/j.chom.2011.04.009]

25 **Glassner KL**, Abraham BP, Quigley EMM. The microbiome and inflammatory bowel disease. *J Allergy Clin Immunol* 2020; **145**: 16-27 [PMID: 31910984 DOI: 10.1016/j.jaci.2019.11.003]

26 **Zhang J**, Hoedt EC, Liu Q, Berendsen E, Teh JJ, Hamilton A, O' Brien AW, Ching JYL, Wei H, Yang K, Xu Z, Wong SH, Mak JWY, Sung JJY, Morrison M, Yu J, Kamm MA, Ng SC. Elucidation of Proteus mirabilis as a Key Bacterium in Crohn's Disease Inflammation. *Gastroenterology* 2021; **160**: 317-330.e11 [PMID: 33011176 DOI: 10.1053/j.gastro.2020.09.036]

27 **Zakerska-Banaszak O**, Tomczak H, Gabryel M, Baturo A, Wolko L, Michalak M, Malinska N, Mankowska-Wierzbicka D, Eder P, Dobrowolska A, Slomski R, Skrzypczak-Zielinska M. Dysbiosis of gut microbiota in Polish patients with ulcerative colitis: a pilot study. *Sci Rep* 2021; **11**: 2166 [PMID: 33495479 DOI: 10.1038/s41598-021-81628-3]

28 **Manichanh C**, Rigottier-Gois L, Bonnaud E, Gloux K, Pelletier E, Frangeul L, Nalin R, Jarrin C, Chardon P, Marteau P, Roca J, Dore J. Reduced diversity of faecal microbiota in Crohn's disease revealed by a metagenomic approach. *Gut* 2006; **55**: 205-211 [PMID: 16188921 DOI: 10.1136/gut.2005.073817]

29 **Targan SR**, Landers CJ, Yang H, Lodes MJ, Cong Y, Papadakis KA, Vasiliauskas E, Elson CO, Hershberg RM. Antibodies to CBir1 flagellin define a unique response that is associated independently with complicated Crohn's disease. *Gastroenterology* 2005; **128**: 2020-2028 [PMID: 15940634 DOI: 10.1053/j.gastro.2005.03.046]

30 **Mitsuyama K**, Niwa M, Takedatsu H, Yamasaki H, Kuwaki K, Yoshioka S, Yamauchi R, Fukunaga S, Torimura T. Antibody markers in the diagnosis of inflammatory bowel disease. *World J Gastroenterol* 2016; **22**: 1304-1310 [PMID: 26811667 DOI: 10.3748/wjg.v22.i3.1304]

31 **Furrie E**, Macfarlane S, Cummings JH, Macfarlane GT. Systemic antibodies towards mucosal bacteria in ulcerative colitis and Crohn's disease differentially activate the innate immune response. *Gut* 2004; **53**: 91-98 [PMID: 14684582 DOI: 10.1136/gut.53.1.91]

32 **Dubinsky MC**, Lin YC, Dutridge D, Picornell Y, Landers CJ, Farrior S, Wrobel I, Quiros A, Vasiliauskas EA, Grill B, Israel D, Bahar R, Christie D, Wahbeh G, Silber G, Dallazadeh S, Shah P, Thomas D, Kelts D, Hershberg RM, Elson CO, Targan SR, Taylor KD, Rotter JI, Yang H; Western Regional Pediatric IBD Research Alliance. Serum immune responses predict rapid disease progression among children with Crohn's disease: immune responses predict disease progression. *Am J Gastroenterol* 2006; **101**: 360-367 [PMID: 16454844 DOI: 10.1111/j.1572-0241.2006.00456.x]

33 **Kleessen B**, Kroesen AJ, Buhr HJ, Blaut M. Mucosal and invading bacteria in patients with inflammatory bowel disease compared with controls. *Scand J Gastroenterol* 2002; **37**: 1034-1041 [PMID: 12374228 DOI: 10.1080/003655202320378220]

World Journal of Gastroenterology

Submit a Manuscript: https://www.f6publishing.com

World J Gastroenterol 2022 August 14; 28(30): 4102-4119

DOI: 10.3748/wjg.v28.i30.4102

ISSN 1007-9327 (print) ISSN 2219-2840 (online)

ORIGINAL ARTICLE

Retrospective Cohort Study

Trends in medication use and treatment patterns in Chinese patients with inflammatory bowel disease

Ling-Ya Yao, Bu-Le Shao, Feng Tian, Mei Ye, Yu-Qin Li, Xiao-Lei Wang, Lin Wang, Shao-Qi Yang, Xiao-Ping Lv, Yan Jia, Xue-Hong Wang, Xiao-Qi Zhang, Yan-Ling Wei, Qian Cao

Specialty type: Gastroenterology and hepatology

Provenance and peer review: Unsolicited article; Externally peer reviewed.

Peer-review model: Single blind

Peer-review report's scientific quality classification

Grade A (Excellent): 0
Grade B (Very good): B, B
Grade C (Good): C
Grade D (Fair): 0
Grade E (Poor): 0

P-Reviewer: Knudsen T, Denmark; Nikolić M, Croatia

Received: April 15, 2022
Peer-review started: April 15, 2022
First decision: May 12, 2022
Revised: May 26, 2022
Accepted: July 20, 2022
Article in press: July 20, 2022
Published online: August 14, 2022

Ling-Ya Yao, Bu-Le Shao, Qian Cao, Department of Gastroenterology, Sir Run Run Shaw Hospital, College of Medicine Zhejiang University, Hangzhou 310016, Zhejiang Province, China

Feng Tian, Department of Gastroenterology, Shengjing Hospital of China Medical University, Shenyang 110000, Liaoning Province, China

Mei Ye, Department of Gastroenterology, Zhongnan Hospital of Wuhan University, Wuhan 430000, Hubei Province, China

Yu-Qin Li, Department of Gastroenterology, Bethune First Affiliated Hospital of Jilin University, Changchun 130000, Jilin Province, China

Xiao-Lei Wang, Department of Gastroenterology, Shanghai 10th People's Hospital, Tongji University, Shanghai 200072, China

Lin Wang, Department of Gastroenterology, Zhongshan Hospital Affiliated to Xiamen University, Xiamen 361000, Fujian Province, China

Shao-Qi Yang, Department of Gastroenterology, General Hospital of Ningxia Medical University, Yinchuan 750004, Ningxia Hui Autonomous Region, China

Xiao-Ping Lv, Department of Gastroenterology, The First Affiliated Hospital of Guangxi Medical University, Nanning 530000, Guangxi Zhuang Autonomous Region, China

Yan Jia, Department of Gastroenterology, The 7th Medical Center of Chinese PLA General Hospital, Beijing 100000, China

Xue-Hong Wang, Department of Gastroenterology, Second Xiangya Hospital, Changsha 410011, Hunan Province, China

Xiao-Qi Zhang, Department of Gastroenterology, Nanjing Drum Tower Hospital, Nanjing 210000, Jiangsu Province, China

Yan-Ling Wei, Department of Gastroenterology, Daping Hospital, Army Medical University, Chongqing 400000, China

Corresponding author: Qian Cao, PhD, Chief Doctor, Chief Physician, Department of Gastroenterology, Sir Run Run Shaw Hospital, College of Medicine Zhejiang University, No. 3

East Qingchun Road, Shangcheng District, Hangzhou 310016, Zhejiang Province, China. caoq@zju.edu.cn

Abstract

BACKGROUND

Medications for inflammatory bowel disease (IBD) have changed dramatically over time. However, no study on long-term medication profiles has been conducted in the Chinese population.

AIM

To evaluate temporal changes in medication use and treatment patterns for Chinese patients with IBD.

METHODS

A multicenter retrospective cohort study was conducted among Chinese patients newly diagnosed with Crohn's disease (CD) and ulcerative colitis (UC) between January 1999 and December 2019. Baseline characteristics and drug prescriptions were collected. Trends in medication use and therapeutic patterns were analyzed.

RESULTS

In total, 3610 patients were analyzed. During follow-up, 5-aminosalicylates (5-ASA) and corticosteroids (CS) prescriptions gradually decreased, accompanied by a notable increase in immunosuppressants (IMS) and infliximab (IFX) prescriptions in patients with CD. Prescription rates of 5-ASA and CS were stable, whereas IMS and IFX slightly increased since 2007 in patients with UC. Subgroup (n = 957) analyses showed a switch from conventional medications to IFX in patients with CD, while 5-ASA and CS were still steadily prescribed in patients with UC. Logistic regression analyses revealed that surgical history, disease behavior, and disease location were associated with initial therapeutic strategies in patients with CD. However, medications before diagnosis, disease location, and diagnostic year might affect initial strategies in patients with UC.

CONCLUSION

Long-term treatment strategies analyses has provided unique insight into the switch from conventional drugs to IFX in Chinese patients with CD.

Key Words: Inflammatory bowel disease; Crohn's disease; Ulcerative colitis; Medication trends; Treatment pattern; Infliximab

©The Author(s) 2022. Published by Baishideng Publishing Group Inc. All rights reserved.

Core Tip: Prescriptions of immunosuppressants and infliximab (IFX) increased in parallel with steady or decreasing prescriptions of 5-aminosalicylates and corticosteroids in Chinese patients with inflammatory bowel disease. Furthermore, a switching profile from conventional drugs to IFX was observed in patients with Crohn's disease. This is the first multicenter cohort study to depict temporal trends in long-term medication uses and periodic changes in treatment paradigms in the Chinese population, which may provide evidence for clinical practice in the foreseeable future.

Citation: Yao LY, Shao BL, Tian F, Ye M, Li YQ, Wang XL, Wang L, Yang SQ, Lv XP, Jia Y, Wang XH, Zhang XQ, Wei YL, Cao Q. Trends in medication use and treatment patterns in Chinese patients with inflammatory bowel disease. *World J Gastroenterol* 2022; 28(30): 4102-4119
URL: https://www.wjgnet.com/1007-9327/full/v28/i30/4102.htm
DOI: https://dx.doi.org/10.3748/wjg.v28.i30.4102

INTRODUCTION

Inflammatory bowel diseases (IBD), consisting of Crohn's disease (CD) and ulcerative colitis (UC), are chronic debilitating disorders characterized by alternating periods of relapse and remission[1,2]. With a growing incidence worldwide, IBD cases in China are expected to exceed 1.5 million by 2025[3]. In light of the need for lifelong medical interventions, IBD poses a global public health challenge.

Owing to the rapid development of new drugs, IBD medications have launched in succession and changed in the past few decades, especially following the discovery of infliximab (IFX), the first anti-tumor necrosis factor agent, which has revolutionized the field[4,5]. Several attempts have been made by Western and other Asian countries to provide rough medication changes. Specifically, increasing proportions of immunomodulators and biological agents have been observed, accompanied by decreasing prescription rates of 5-aminosalicylates (5-ASA) and corticosteroids (CS)[6-8]. A few studies have been carried out on annual changes in IBD medications, including 5-ASA and CS[9,10]. However, no long-term analysis of medication tendency has been conducted in a large population of Chinese patients with IBD.

Drug diversification enables treatment combinations for better therapeutic effects[11]. However, combination treatment also correlates with increasing risks of side effects[12,13]. Therefore, patients might switch treatment strategies to acquire optimal effects from IBD medications under different circumstances. Currently, minimal attention has been paid to periodic changes in IBD treatment strategies. Additionally, initial treatment strategies affect follow-up therapeutic patterns to some extent; thus, investigating the possible predictors for initial treatment strategies may help to better understand periodic changes in therapeutic patterns in patients with IBD.

Therefore, this study aimed to provide fresh insights into temporal trends in medication prescriptions among the Chinese patients with IBD for over 20 years. The study also aimed to investigate long-term periodic changes in treatment paradigms and identify the possible factors that influence initial drug strategies.

MATERIALS AND METHODS

Study design

This multicenter retrospective cohort study included 12 IBD referral centers across all seven administrative regions in China with diverse socioeconomic backgrounds. The study protocol was reviewed and approved by Sir Run Run Shaw Hospital, College of Medicine Zhejiang University Institutional Review Board (Approval No. 20210714-31) with approval for all hospitals involved in the study. The requirement for patient informed consent was waived due to the retrospective nature of this study.

Study population

Incident adult patients with a definite diagnosis of CD or UC according to the Chinese consensus on IBD diagnosis, which was similar to that of the European Crohn's and Colitis Organization (ECCO) consensus, between January 1, 1999 and December 31, 2019 were included[14,15]. Patients were excluded from analyses for medication trends if the cessation date of medications was unclear. Additionally, patients were further excluded from analyses for treatment patterns if: (1) They were followed up for < 3 years since diagnosis; or (2) No prescription of either 5-ASA, CS, immunosuppressants (IMS), or IFX was administered throughout follow-up. Cases were followed from diagnosis until loss to follow-up, or December 31, 2020, whichever came first.

Data collection and definition

Patients were identified using International Classification of Diseases 8th and 10th revision codes for CD (563.00–563.09 and K50) and UC (563.19, 569.04 and K51), respectively. Data regarding baseline characteristics and prescriptions since diagnosis were collected by reviewing medical records and digitized into the Epidata 3.0. Data quality was ensured using standardized case report forms and careful manual scrutinization.

Demographic parameters including sex, date of first IBD-related symptoms, date of initial diagnosis, smoking status, region of urbanization, occupation, and clinical parameters including disease location, disease activity, extraintestinal manifestations (EIMs), IBD family history, gastrointestinal surgical history, and medication use within six months before diagnosis were collected from patients with IBD. Additionally, disease behavior, perianal involvement, and perianal surgical history were also collected from patients with CD. Other relevant variables were calculated, including median age of onset and diagnosis, median interval from onset of symptoms to diagnosis, median follow-up duration, and body mass index (BMI) at diagnosis.

Smoking status was defined by smoking habits at diagnosis. EIMs classification originated from the 2016 ECCO consensus[9]. Disease location for IBD and CD behavior were defined according to the Montreal classification[10]. Disease activity was acquired from medical records using the Crohn's Disease Activity Index (CDAI) and Mayo score for CD and UC, respectively, and was assessed and recorded by IBD nurses when patients were first diagnosed[16,17].

Statistical analysis

Continuous variables are presented as medians with interquartile ranges (IQRs), and categorical variables as numbers with percentages. A T-test or Mann-Whitney U test was used to compare

continuous variables, and Chi-square test or Fisher's exact test was used to compare categorical variables.

The initiation date of medications (including 5-ASA, CS, IMS, and IFX) since diagnosis was set as the first prescription date, and the last date was calculated as the first prescription date plus the number of prescription days. Annual percentage of each drug used among all available patients was plotted against every calendar year to demonstrate medication trends from 1999 to 2020. To conduct subgroup analysis for periodic changes in treatment paradigms, the study period was divided according to the following time points since diagnosis: 1, 3, 6, 12, 24, and 36 mo. The frequency and percentage of different drug combination strategies were plotted against different periods to illustrate periodic changes in drug patterns with a 3-year follow-up. To investigate possible factors for initial treatment strategies, we incorporated drugs into the following combination strategies. For CD, initial medications were classified as: (1) CS (CS monotherapy or combined with 5-ASA); (2) CS + IMS (CS combined with IMS); and (3) IFX [IFX monotherapy or combined with conventional drugs (5-ASA, CS, or IMS)]. For UC, initial medications were classified as: (1) 5-ASA (5-ASA monotherapy); (2) CS (CS monotherapy or combined with 5-ASA); and (3) IFX/IMS (IFX monotherapy, IMS monotherapy, or IFX combined with IMS). Predictors for initial drug strategies were identified using logistic regression analysis and presented as odds ratios and 95% confidence intervals.

P value < 0.05 were considered a statistically significant difference. Statistical analyses were conducted using SAS 9.4 (SAS Institute, Cary NC, United States), and graphs were plotted using R software (version 4.1) with the "ggplot2" and "ggalluvial" packages[18,19].

RESULTS

Baseline characteristics

Altogether, 3610 patients were included in the analysis for temporal changes in medication use (2208 and 1402 patients with CD and UC, respectively). Furthermore, 957 patients were included in the analysis for periodic changes in treatment patterns (686 and 271 patients with CD and UC, respectively), after excluding 2452 patients who were followed up < 3 years since diagnosis, and 201 patients with no prescription of either 5-ASA, CS, IMS, or IFX throughout follow-up (Figure 1).

Patient baseline characteristics are summarized in Table 1. The median (IQR) follow-up duration was 1.6 (0.3-3.8) years, the median (IQR) age at diagnosis was 33.0 (25.0-48.0) years, and male accounted for 46.2% of patients. Similar patterns were found in the region of urbanization and IBD family history between CD and UC, except for male sex (P < 0.0001), median age of onset (P < 0.0001), median age at diagnosis (P < 0.0001), median interval from onset to diagnosis (P < 0.0001), median follow-up duration (P < 0.0001), smoking status (P < 0.0001), occupation (P < 0.0001), BMI category (P < 0.0001), EIM classification (P < 0.0001), gastrointestinal surgical history (P < 0.0001), and drug history (medication use within six months before diagnosis; P < 0.0001).

The differences in baseline characteristics between included and excluded patients in the analysis for periodic changes in treatment patterns are shown in Table 2. Briefly, patients who were included in further analysis were prone to be younger at the age of onset and diagnosis (P < 0.001), accompanied with EIMs (P = 0.0096), and underwent perianal surgeries before diagnosis (P < 0.0001). Moreover, patients with UC had a higher risk of proctitis and left-sided involvement (P = 0.0005), and patients with CD had higher proportion of moderate severity (P = 0.0002).

Temporal trends in medication use

Proportions of different prescriptions during the 20-year follow-up of patients with CD are depicted in Figure 2A and Supplementary Table 1. The prescription rate of 5-ASA showed a steady decline from 50.0% in 2002 to 5.5% in 2020, and a similar trend was observed for CS. Meanwhile, the prescription rate of IMS increased prominently from 2005 onwards, but decreased slightly between 2018 and 2020. The prescription rate of IFX has gradually increased since 2008, reaching 60.3% in 2020.

We also reported the proportions of different prescriptions among patients with UC (Figure 2B and Supplementary Table 2). 5-ASA and CS were steadily prescribed between 1999 and 2020. IMS was first prescribed in 2007, increasing slightly to 8.5% in 2020. Parallel to IMS, a gentle increase was observed in the proportion of IFX prescriptions between 2009 and 2020.

Periodic changes in treatment patterns

Therapeutic regimens were evaluated for three consecutive years after diagnosis. As IFX was first prescribed between 2008 and 2009 in China, we further divided the total cohort into Cohorts I (1999–2008) and II (2009-2020), to evaluate the potential impact of IFX availability on therapeutic strategies.

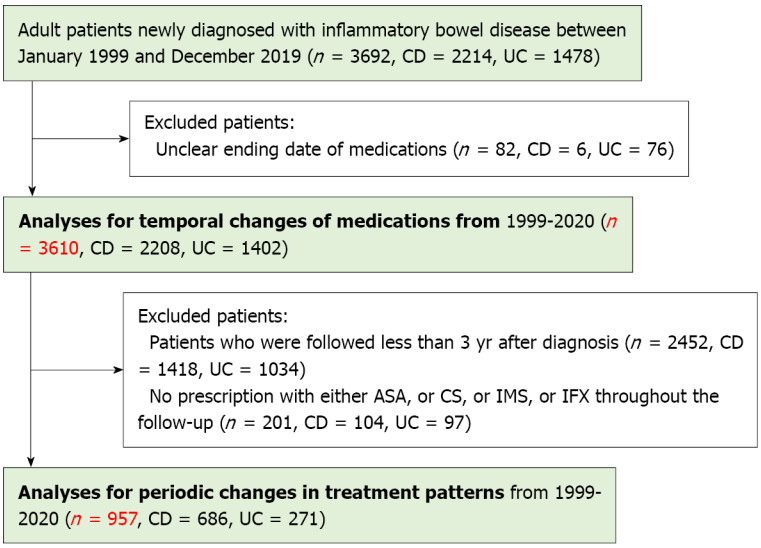
IFX (22.3%), IMS (7.1%), and IMS combined with IFX (12.0%) accounted for nearly half of initial (within the first month after diagnosis) treatment strategies for patients with CD (Figure 3A and Supplementary Table 3). Interestingly, 51.6% of patients ceased medical treatment within 1-3 mo, but 41.7% re-prescribed in the following period. Specifically, a prominent increase in monotherapy or

Table 1 Demographic and clinical characteristics of patients with inflammatory bowel disease in 1999-2020

	Total (*n* = 3610)	CD (*n* = 2208)	UC (*n* = 1402)	*P* value
Male sex, *n* (%)	1666 (46.2)	935 (42.3)	731 (52.1)	< 0.0001
Median age of onset (IQR), yr	31.0 (23.0-45.0)	27.0 (21.0-37.0)	42.0 (30.0-54.0)	< 0.0001
Median age at diagnosis (IQR), yr	33.0 (25.0-48.0)	29.0 (23.0-39.0)	45.0 (32.0-56.0)	< 0.0001
Median interval from onset to diagnosis (IQR), mo	12.2 (2.4-36.5)	12.4 (3.7-36.7)	6.17 (1.2-26.4)	< 0.0001
Median duration of follow-up (IQR), yr	1.6 (0.3-3.8)	2.0 (0.8-3.9)	0.7 (0.1-3.2)	< 0.0001
Smoking status at diagnosis, *n* (%)				< 0.0001
Non-smoker	2860 (79.2)	1828 (82.8)	1032 (73.6)	
Current smoker	356 (9.9)	198 (9.0)	158 (11.3)	
Former smoker	233 (6.4)	114 (5.2)	119 (8.5)	
Unknown	161 (4.5)	68 (3.0)	93 (6.6)	
Region of urbanization, *n* (%)				0.7918
Rural	1607 (44.5)	991 (44.9)	616 (43.9)	
Urban	1959 (54.3)	1189 (53.8)	770 (54.9)	
Unknown	44 (1.2)	28 (1.3)	16 (1.2)	
Occupation, *n* (%)				< 0.0001
Unemployed	495 (13.7)	316 (14.3)	179 (12.8)	
Employed	1851 (51.3)	1227 (55.6)	624 (44.5)	
Student	377 (10.5)	334 (15.1)	43 (3.1)	
Retire	258 (7.1)	95 (4.3)	163 (11.6)	
Unknown	629 (17.4)	236 (10.7)	393 (28.0)	
BMI category at diagnosis, *n* (%)				< 0.0001
Normal	1014 (28.1)	812 (36.8)	202 (14.4)	
Underweight	1524 (42.2)	912 (41.3)	612 (43.7)	
Overweight + Obese	379 (10.5)	183 (8.3)	196 (14.0)	
Unknown	691 (19.2)	300 (13.6)	391 (27.9)	
Disease location, *n* (%)				
L1—ileal location	-	626 (28.4)	-	
L2—colon location		224 (10.2)		
L3—ileocolon location		1142 (51.8)		
L4—including upper GI location		211 (9.6)		
E1—proctitis		-	201 (14.3)	
E2—left-sided			458 (32.7)	
E3—extensive colitis			660 (47.1)	
Unknown			83 (5.9)	
Disease activity (CDAI/Mayo), *n* (%)				
Remission	122 (3.4)	100 (4.5)	22 (1.6)	
Mild	719 (19.9)	417 (18.9)	302 (21.5)	
Moderate	1683 (46.6)	1156 (52.4)	527 (37.6)	
Severe	440 (12.2)	188 (8.5)	252 (18.0)	
Unknown	646 (17.9)	347 (15.7)	299 (21.3)	

Disease behavior, *n* (%)				
B1—inflammatory disease	-	1175 (53.3)	-	
B2—stricturing disease		690 (31.3)		
B3—penetrating disease		338 (15.4)		
Perianal involvement, *n* (%)				
Fistula	-	772 (35.0)	-	
Abscess		392 (17.8)		
Fissure		38 (1.7)		
Extraintestinal manifestations, *n* (%)	464 (12.9)	357 (16.2)	107 (7.6)	< 0.0001
Family history of IBD, *n* (%)	27 (0.7)	20 (0.9)	7 (0.5)	0.1671
History of gastrointestinal surgery, *n* (%)	594 (16.5)	524 (23.7)	70 (5.0)	< 0.0001
History of perianal surgery, *n* (%)	471 (13.0)	471 (21.3)	0 (0.0)	< 0.0001
Medication use before diagnosis (≤ 6 mo), *n* (%)	908 (25.2)	440 (19.9)	468 (33.4)	< 0.0001

The classification of body mass index: Underweight: < 18.5; Normal: 18.5-23.9; Overweight: 24-28; Obese: > 28. Disease behavior was not available in 5 patients. IBD: Inflammatory bowel disease; CD: Crohn's disease; UC: Ulcerative colitis; IQR: Interquartile ranges; BMI: Body mass index; CDAI: Crohn's Disease Activity Index.



DOI: 10.3748/wjg.v28.i30.4102 **Copyright** ©The Author(s) 2022.

Figure 1 Flowchart of inflammatory bowel disease selection and analysis. CD: Crohn's disease; UC: Ulcerative colitis; ASA: Aminosalicylates; CS: Corticosteroids; IMS: Immunosuppressants; IFX: Infliximab.

combination therapy containing IMS and IFX was observed during the subsequent 6-36 mo. Meanwhile, conventional therapies including 5-ASA, CS, and CS combined with IMS were steadily used. When comparing the two cohorts, we found that all initial prescriptions originated from conventional medications in Cohort I, while therapies comprising of IFX or IMS accounted for 45.0% of all initial prescriptions in Cohort II (Supplementary Figures 1 and 2).

Data on UC are presented in Figure 3B and Supplementary Table 4. 5-ASA (56.1%) was the most frequently prescribed medication in initial strategies, followed by CS (20.7%). Similar to CD, 60.1% of patients stopped medications within 1-3 mo, but 38.7% were put back on the same or other drugs for treatment progression, resulting in a steady increase of 5-ASA, CS, and IFX/IMS prescriptions in the following period. Compared with Cohort I in initial strategies, we still found 5-ASA and CS comprised a majority of prescriptions in Cohort II (Supplementary Figures 3 and 4).

Factors associated with initial drug strategies

Since initial therapeutic regimens may affect follow-up strategies to some extent, we further invest-

Table 2 Comparison of demographic and clinical characteristics of patients with inflammatory bowel disease included and excluded from analysis in 1999-2020

	Excluded (*n* = 2653)	Included (*n* = 957)	*P* value
Male sex, *n* (%)	1268 (47.8)	398 (41.6)	0.0009
Median age of onset (IQR), yr	32.0 (23.0-46.0)	30.0 (22.0-41.0)	< 0.001
Median age at diagnosis (IQR), yr	35.0 (25.0-49.0)	32.0 (24.0-44.0)	< 0.001
Median interval from onset to diagnosis (IQR), mo	12.2 (2.4-36.6)	12.2 (2.4-32.9)	0.3270
Smoking status at diagnosis, *n* (%)			0.0005
Non-smoker	2067 (77.9)	793 (82.8)	
Current smoker	273 (10.3)	83 (8.7)	
Former smoker	174 (6.6)	59 (6.2)	
Unknown	139 (5.2)	22 (2.3)	
Region of urbanization, *n* (%)			0.0411
City	1450 (54.7%)	509 (53.2)	
Rural	1164 (43.9)	443 (46.3)	
Unknown	39 (1.4)	5 (0.5)	
Occupation, *n* (%)			< 0.0001
Unemployed	371 (14.0)	124 (12.9)	
Employed	1226 (46.2)	625 (65.3)	
Student	272 (10.2)	105 (11.0)	
Retire	201 (7.6)	57 (6.0)	
Unknown	583 (22.0)	46 (4.8)	
BMI category at diagnosis, *n* (%)			< 0.0001
Normal	694 (26.1)	320 (33.4)	
Underweight	1100 (41.5)	424 (44.4)	
Overweight + Obese	278 (10.5)	101 (10.6)	
Unknown	580 (21.9)	111 (11.6)	
Disease location, *n* (%)			
L1—ileal location	441 (29.1)	185 (27.0)	0.3722
L2—colon location	158 (10.4)	66 (9.6)	
L3—ileocolon location	768 (50.6)	374 (54.6)	
L4—including upper GI location	151 (9.9)	60 (8.8)	
E1—proctitis	156 (13.8)	45 (16.6)	0.0005
E2—left-sided	360 (31.8)	98 (36.2)	
E3—extensive colitis	534 (47.2)	126 (46.5)	
Unknown	81 (7.2)	2 (0.7)	
Disease activity (CDAI), *n* (%)			0.0002
Remission	75 (4.9)	25 (3.6)	
Mild	314 (20.6)	103 (15.0)	
Moderate	748 (49.1)	408 (59.5)	
Severe	136 (9.0)	52 (7.6)	
Unknown	249 (16.4)	98 (14.3)	
Disease activity (Mayo), *n* (%)			< 0.0001

Remission	18 (1.6)	4 (1.5)	
Mild	231 (20.4)	71 (26.2)	
Moderate	406 (35.9)	121 (44.7)	
Severe	192 (17.0)	60 (22.1)	
Unknown	284 (25.1)	15 (5.5)	
Disease behavior (CD), *n* (%)			0.4273
B1—inflammatory disease	797 (52.5)	378 (55.2)	
B2—stricturing disease	488 (32.1)	202 (29.5)	
B3—penetrating disease	233 (15.4)	105 (15.3)	
Perianal involvement (CD), *n* (%)			0.0800
Fistula	524 (34.4)	248 (36.2)	
Abscess	262 (17.2)	130 (19.0)	
Fissure	24 (1.6)	14 (2.0)	
Extraintestinal manifestations, *n* (%)	318 (12.0)	146 (15.3)	0.0096
Family history, *n* (%)	19 (0.7)	8 (0.8)	0.7124
History of gastrointestinal surgery, *n* (%)	423 (15.9)	171 (17.9)	0.1687
History of perianal surgery, *n* (%)	263 (9.9)	208 (21.7)	< 0.0001
Medication use within 6 mo before diagnosis, *n* (%)	646 (24.3)	262 (27.4)	0.0643

The classification of body mass index: Underweight: < 18.5; Normal: 18.5-23.9; Overweight: 24-28; Obese > 28. Disease behavior was not available in 1407 patients. IQR: Interquartile ranges; BMI: Body mass index; CDAI: Crohn's disease Activity Index; CD: Crohn's Disease.

igated potential factors impacting initial drug strategies.

Table 3 presents factors for commencing different medications compared with a no prescription group among patients with CD. Specifically, variables including urban living, L3, B3, gastrointestinal surgical history, and diagnosis after 2009 yielded the most significant predictors of patients not commencing CS for initial treatment strategies. However, patients with a drug history had a higher probability of commencing CS. When compared with the no prescription group, patients of male sex, urban living, BMI ≥ 24.0 kg/m^2, B3, and gastrointestinal surgical history were less likely to be prescribed CS combined with IMS as initial treatment. In contrast, patients with L4, EIMs, drug history, and perianal surgical history were more likely to be prescribed CS combined with IMS strategy. In terms of comparison between the IFX and no prescription groups, patients who were smokers, had a BMI ≥ 24.0 kg/m^2, B2 or B3, and had a gastrointestinal surgical history had a fewer possibility to be prescribed IFX. Contrarily, patients who were students, L4, had moderate severity, and had a perianal surgical history were more likely to be prescribed IFX.

Table 4 presents the variables that determined initial therapeutic regimens in patients with UC. Particularly, patients with a drug history tended to maintain treatments after diagnosis, regardless of type (5-ASA, CS, IMS, or IFX). Variables including current smoker, severe disease activity, and diagnosis after 2009 were the most significant factors for not commencing 5-ASA, whereas variables including employed or retired and E3 were related to a higher probability of commencing 5-ASA. Likewise, patients with a BMI ≥ 24.0 kg/m^2 and diagnosed after 2009 were less likely to be prescribed CS, and those with E3 and EIMs involvement were likely to be prescribed CS. Moreover, patients with a drug history were more likely to be prescribed IFX/IMS for initial treatment.

DISCUSSION

To the best of our knowledge, no multicenter cohort study has been conducted to investigate temporal trends in long-term medication use and periodic changes in treatment paradigms in Chinese IBD patients. Our findings showed that prescriptions of IMS and IFX gradually increased in IBD over the past 20 years, paralleled by decreasing prescriptions of 5-ASA and CS for CD but not for UC. Additionally, periodic changes in treatment patterns revealed a switching profile from conventional medications to IFX in CD, while 5-ASA and CS still took irreplaceable positions in UC.

Table 3 Influencing factors of initial drug strategies in patients with Crohn's disease

	CS (*n* = 132)		CS + IMS (*n* = 203)		IFX (*n* = 728)	
	OR (95%CI)	*P* value	OR (95%CI)	*P* value	OR (95%CI)	*P* value
Sex						
Female	Ref	–	Ref	–	Ref	–
Male	0.86 (0.57-1.29)	0.4577	0.49 (0.33-0.73)	0.0005	0.89 (0.70-1.13)	0.3295
Age of onset	1.02 (0.95-1.10)	0.5165	1.01 (0.93-1.09)	0.8581	0.99 (0.95-1.02)	0.4621
Age at diagnosis	1.00 (0.93-1.08)	0.9428	0.99 (0.92-1.07)	0.8167	0.98 (0.95-1.02)	0.3752
Smoking status at diagnosis						
Non-smoker	Ref	–	Ref	–	Ref	–
Current smoker	0.91 (0.49-1.71)	0.7754	0.86 (0.48-1.54)	0.6041	0.64 (0.42-0.99)	0.0452
Former smoker	0.65 (0.26-1.62)	0.3560	0.66 (0.30-1.43)	0.2900	0.47 (0.28-0.81)	0.0062
Unknown	1.30 (0.46-3.71)	0.6211	NS	NS	1.11 (0.62-1.99)	0.7192
Region of urbanization						
Rural	Ref	–	Ref	–	Ref	–
Urban	0.60 (0.40-0.89)	0.0117	0.49 (0.34-0.69)	< 0.0001	1.07 (0.85-1.35)	0.5761
Unknown	NS	NS	NS	NS	1.84 (0.76-4.49)	0.1794
Occupation						
Unemployed	Ref	–	Ref	–	Ref	–
Employed	1.27 (0.72-2.23)	0.4031	1.01 (0.62-1.63)	0.9826	1.11 (0.78-1.58)	0.5578
Student	1.27 (0.53-3.05)	0.5960	0.98 (0.49-1.95)	0.9539	1.61 (1.02-2.53)	0.0408
Retire	0.62 (0.21-1.84)	0.3916	0.56 (0.16-1.94)	0.3619	1.74 (0.85-3.54)	0.1267
Unknown	0.46 (0.19-1.11)	0.0830	NS	NS	0.86 (0.54-1.37)	0.5216
BMI category at diagnosis						
Normal	Ref	–	Ref	–	Ref	–
Underweight	1.30 (0.83-2.04)	0.2498	0.88 (0.60-1.30)	0.5295	0.92 (0.71-1.21)	0.5645
Overweight + Obese	0.56 (0.25-1.26)	0.1601	0.42 (0.20-0.88)	0.0204	0.47 (0.30-0.73)	0.0008
Unknown	0.46 (0.23-0.94)	0.0320	0.14 (0.04-0.46)	0.0012	0.81 (0.57-1.14)	0.2241
Disease location						
L1 – ileal location	Ref	–	Ref	–	Ref	–
L2 – colon location	0.81 (0.41-1.57)	0.5317	0.74 (0.35-1.55)	0.4201	0.94 (0.63-1.43)	0.7869
L3 – ileocolon location	0.58 (0.37-0.90)	0.0162	1.05 (0.69-1.61)	0.8105	1.12 (0.85-1.46)	0.4211
L4 – including upper GI location	0.69 (0.31-1.56)	0.3708	1.91 (1.02-3.57)	0.0438	1.88 (1.20-2.96)	0.0061
Disease activity (CDAI)						
Remission	Ref	–	Ref	–	Ref	–
Mild	0.84 (0.28-2.51)	0.7498	2.17 (0.84-5.61)	0.1091	1.44 (0.79-2.63)	0.2346
Moderate	1.56 (0.57-4.33)	0.3888	2.35 (0.94-5.86)	0.0664	2.08 (1.18-3.69)	0.0118
Severe	0.77 (0.19-3.04)	0.7050	0.46 (0.08-2.53)	0.3710	1.62 (0.83-3.16)	0.1576
Unknown	1.37 (0.45-4.15)	0.5791	0.88 (0.28-2.78)	0.8290	1.05 (0.56-1.98)	0.8746
Disease behavior						
B1 – inflammatory disease	Ref	–	Ref	–	Ref	–
B2 – stricturing disease	0.82 (0.53-1.27)	0.3734	0.99 (0.67-1.47)	0.9531	0.63 (0.48-0.83)	0.0008
B3 – penetrating disease	0.22 (0.10-0.48)	< 0.001	0.12 (0.05-0.30)	< 0.0001	0.39 (0.28-0.56)	< 0.0001

Extraintestinal manifestations						
No	Ref	–	Ref	–	Ref	–
Yes	1.10 (0.65-1.87)	0.7105	1.88 (1.23-2.87)	0.0037	0.93 (0.67-1.28)	0.6605
Family history of IBD						
No	Ref	–	Ref	–	Ref	–
Yes	1.46 (0.14-15.30)	0.7514	1.70 (0.22-13.10)	0.6104	1.67 (0.37-7.62)	0.5082
History of gastrointestinal surgery						
No	Ref	–	Ref	–	Ref	–
Yes	0.35 (0.20-0.60)	0.0002	0.35 (0.20-0.59)	< 0.0001	0.55 (0.41-0.73)	< 0.0001
History of perianal surgery						
No	Ref	–	Ref	–	Ref	–
Yes	1.36 (0.77-2.40)	0.2948	1.86 (1.20-2.87)	0.0052	2.68 (1.92-3.73)	< 0.0001
Medication use before diagnosis (≤ 6 mo)						
No	Ref	–	Ref	–	Ref	–
Yes	1.94 (1.16-3.23)	0.0111	3.06 (2.04-4.58)	< 0.0001	1.33 (0.95-1.85)	0.0934
Calendar year of diagnosis						
< 2009	Ref	–	Ref	–	Ref	–
≥ 2009	0.19 (0.09-0.40)	< 0.0001	0.77 (0.25-2.33)	0.6393	NS	NS

CS: Corticosteroids; IMS: Immunosuppressants; IFX: Infliximab; OR: Odd ratio; CI: Confidence interval; BMI: Body mass index; CDAI: Crohn's Disease Activity Index; IBD: Inflammatory bowel disease; NS: Non-significant.

In China, more than 1.5 million people are expected to suffer from IBD by 2025[3]. Therefore, the study population accounted for merely 0.2% of the total estimated Chinese patients with IBD. However, because there is lack of national registries covering all IBD patients, it is difficult to acquire complete data on the diagnosis, treatment, and prognosis of all Chinese patients with IBD. A well-organized national IBD registry in the near future will help facilitate larger clinical studies in China. Besides, IBD referral centers in our study are distributed across all seven administrative regions in China with diverse socioeconomic backgrounds. To some extent, the study population represents in-patients from Chinese referral centers. Moreover, we found similar patterns in demographic and clinical characteristics by further comparing IBD patients in our study with those in other large-sample Chinese studies, which also reflects the representativeness of our study to a certain extent[20,21].

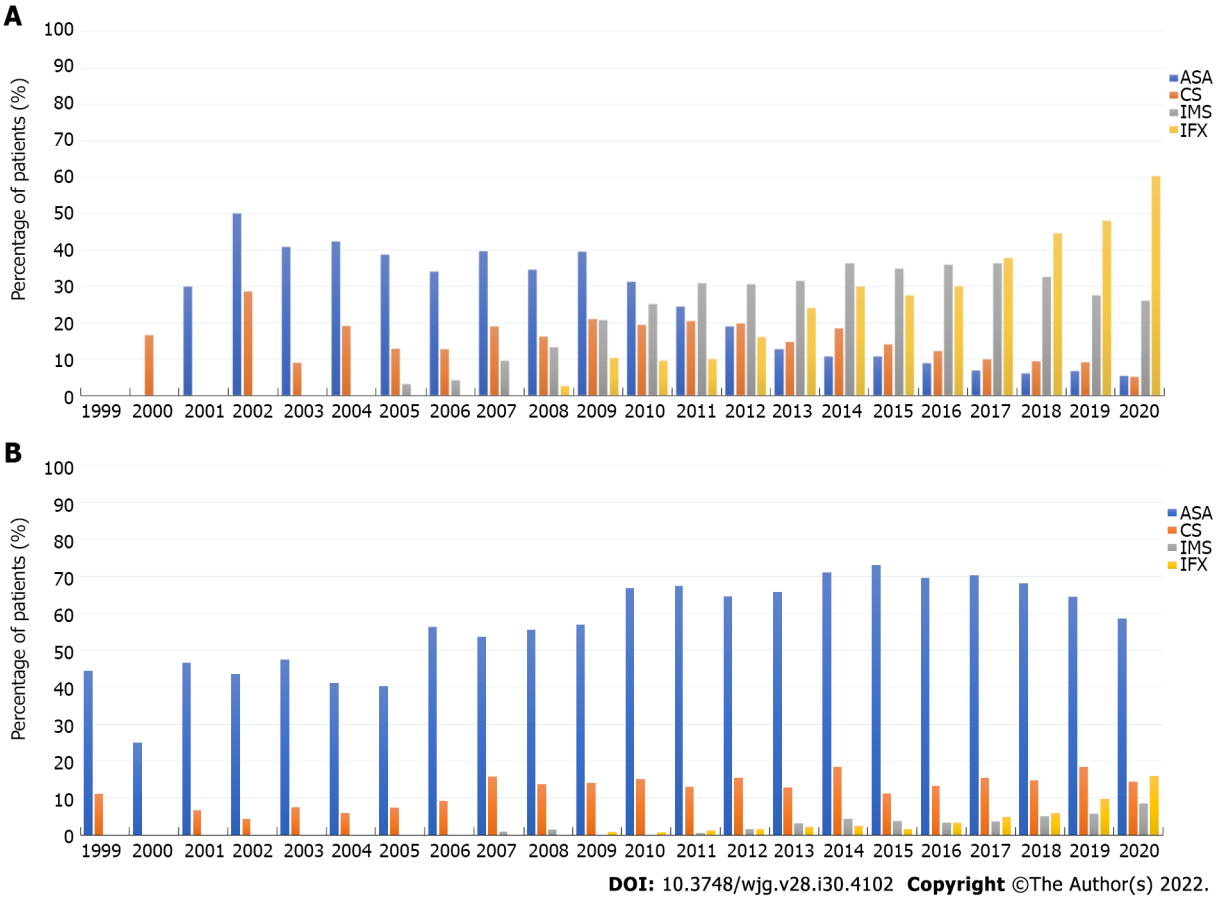
In this study, the median (IQR) age of onset and diagnosis was 31.0 (23.0–45.0) years and 33.0 (25.0–48.0) years, respectively, similar to other Asian and Western populations[22,23]. The total median duration of follow-up was short. There are two possible explanations for this. On one hand, the study population mainly stems from IBD referral centers and therefore many patients will go back to grass-roots hospitals for following treatment after acquiring definite IBD diagnosis and initial treatment strategies, which may result in loss to follow-up. On the other hand, due to the observational design of this study, most information originated from medical records or databases. It would be a huge cost to follow such a large number of patients. Despite the short follow-up period, which may affect medication trend analysis, there were still more than 1000 patients who were followed for more than three years, and our analysis towards long-term changes in treatment patterns provided a credible result, which can assist in clinical drug management. We also compared baseline characteristics between CD and UC patients. Regarding demographic differences, CD patients seemed more likely to be younger at onset or diagnosis and have longer intervals from onset to diagnosis and follow-up duration. This is possibly due to more sophisticated processes in CD diagnosis and treatment. However, UC patients were more likely to be overweight compared to those with CD. UC patients who seldom implicate small intestine that would cause malabsorption of nutrients and following weight loss might explain BMI differences. In regard to clinical discrepancies, more CD patients had EIMs involvement, family history, and gastrointestinal and perianal surgical histories than UC. Patients with CD often undergo intestinal resection for perforation, ileocecal junction inflammation, or perianal surgeries before diagnosis. Contrarily, more medications were likely prescribed for UC before diagnosis, which was probably due to the fact that 5-ASA was also prescribed for patients with undetermined intestinal ulcers before definite diagnosis. Furthermore, L3 was the most frequent disease location for CD, while B1 and B2 predominated disease behaviors, sharing similar clinical patterns with other Asian cohorts[22,24].

Table 4 Influencing factors of initial drug strategy in patients with ulcerative colitis

	5-ASA (*n* = 566)		CS (*n* = 213)		IFX/IMS (*n* = 43)	
	OR (95%CI)	*P* value	OR (95%CI)	*P* value	OR (95%CI)	*P* value
Sex						
Female	Ref	–	Ref	–	Ref	–
Male	1.02 (0.78-1.34)	0.8770	0.90 (0.63-1.27)	0.5397	0.98 (0.50-1.92)	0.9493
Age of onset	0.98 (0.95-1.02)	0.4057	1.03 (0.97-1.09)	0.3654	0.93 (0.87-0.99)	0.0233
Age at diagnosis	1.02 (0.98-1.05)	0.3876	0.96 (0.91-1.02)	0.1792	1.04 (0.98-1.10)	0.2434
Smoking status at diagnosis						
Non-smoker	Ref	–	Ref	–	Ref	–
Current smoker	0.64 (0.41-1.00)	0.0490	0.67 (0.38-1.18)	0.1651	0.94 (0.32-2.79)	0.9156
Former smoker	0.76 (0.46-1.25)	0.2812	0.87 (0.45-1.67)	0.6713	2.04 (0.72-5.78)	0.1777
Unknown	3.39 (1.83-6.27)	0.0001	1.15 (0.42-3.19)	0.7864	3.42 (0.62-18.90)	0.1583
Region of urbanization						
Rural	Ref	–	Ref	–	Ref	–
Urban	0.80 (0.60-1.07)	0.1311	0.82 (0.57-1.19)	0.2945	1.03 (0.51-2.08)	0.9245
Unknown	0.11 (0.02-0.64)	0.0138	0.23 (0.02-2.21)	0.2010	NS	NS
Occupation						
Unemployed	Ref	–	Ref	–	Ref	–
Employed	2.85 (1.79-4.55)	< 0.001	1.23 (0.74-2.06)	0.4241	0.93 (0.34-2.53)	0.8866
Student	1.06 (0.39-2.87)	0.9159	0.57 (0.19-1.71)	0.3178	0.78 (0.12-5.10)	0.7976
Retire	2.39 (1.31-4.35)	0.0043	1.14 (0.55-2.39)	0.7216	2.02 (0.52-7.91)	0.3135
Unknown	2.07 (1.15-3.70)	0.0145	0.73 (0.36-1.46)	0.3691	1.93 (0.60-6.19)	0.2697
BMI category at diagnosis						
Normal	Ref	–	Ref	–	Ref	–
Underweight	0.85 (0.55-1.31)	0.4669	1.22 (0.74-2.03)	0.4325	0.90 (0.36-2.22)	0.8136
Overweight + Obese	1.10 (0.73-1.64)	0.6532	0.52 (0.28-0.99)	0.0455	0.49 (0.14-1.77)	0.2757
Unknown	0.78 (0.55-1.12)	0.1742	0.78 (0.49-1.23)	0.2900	0.42 (0.16-1.11)	0.0785
Disease location						
E1 – proctitis	Ref	–	Ref	–	Ref	–
E2 – left-sided	1.18 (0.78-1.78)	0.4254	1.67 (0.82-3.38)	0.1585	2.57 (0.54-12.20)	0.2331
E3 – extensive colitis	1.58 (1.05-2.38)	0.0288	3.06 (1.54-6.08)	0.0014	2.93 (0.63-13.60)	0.1695
Unknown	4.41 (1.95-9.97)	0.0004	3.99 (1.23- 12.9)	0.0209	NS	NS
Disease activity (MAYO)						
Remission	Ref	–	Ref	–	Ref	–
Mild	0.65 (0.22-1.92)	0.4374	1.04 (0.11-9.97)	0.9697	0.35 (0.03-3.86)	0.3905
Moderate	0.76 (0.26-2.22)	0.6156	2.99 (0.33-27.10)	0.3292	0.57 (0.06-5.61)	0.6308
Severe	0.32 (0.10-0.97)	0.0442	6.51 (0.71-59.60)	0.0972	1.91 (0.19-19.00)	0.5798
Unknown	0.39 (0.13-1.22)	0.1061	1.57 (0.16-15.30)	0.6994	0.09 (0.01-1.24)	0.0716
Extraintestinal manifestations						
No	Ref	–	Ref	–	Ref	–
Yes	0.74 (0.41-1.31)	0.2993	1.94 (1.07-3.51)	0.0287	1.83 (0.72-4.62)	0.2025
Family history of IBD						

No	Ref	–	Ref	–	Ref	–
Yes	0.68 (0.09-4.94)	0.7041	0.87 (0.08-10.00)	0.9096	NS	NS
History of gastrointestinal surgery						
No	Ref	–	Ref	–	Ref	–
Yes	0.68 (0.36-1.26)	0.2163	0.57 (0.25-1.31)	0.1824	0.88 (0.18-4.23)	0.8683
Medication use before diagnosis (≤ 6 mo)						
No	Ref	–	Ref	–	Ref	–
Yes	10.2 (7.19-14.5)	< 0.0001	7.23 (4.71-11.10)	< 0.0001	9.88 (4.77-20.50)	< 0.0001
Calendar year of diagnosis						
< 2009	Ref	–	Ref	–	Ref	–
≥ 2009	0.31 (0.22-0.45)	< 0.0001	0.51 (0.30-0.85)	0.0097	3.12 (0.41-23.90)	0.2748

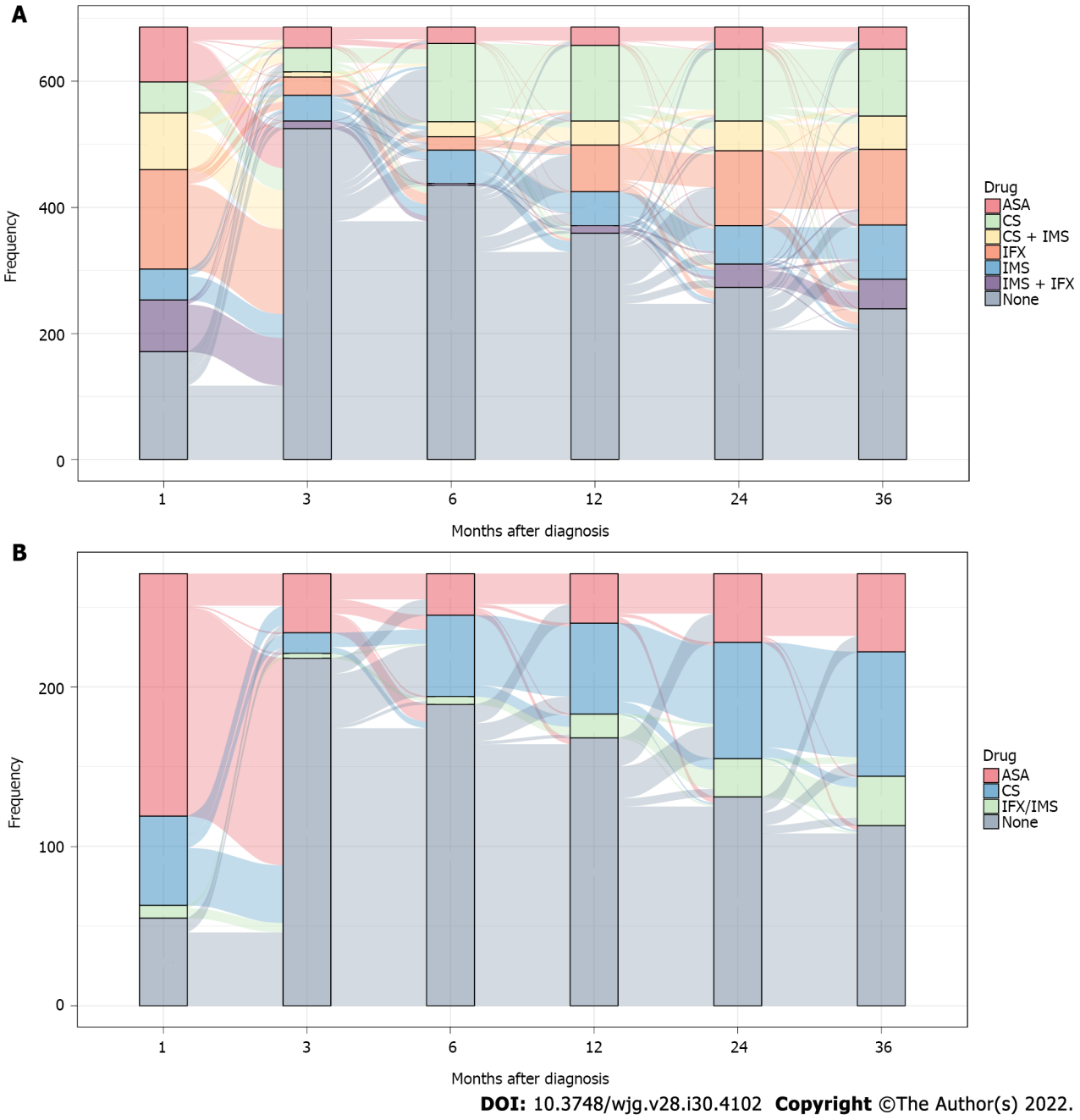
5-ASA: 5-aminosalicylates; CS: Corticosteroids; IMS: Immunosuppressants; IFX: Infliximab; OR: Odd ratio; CI: Confidence interval; BMI: Body mass index; NS: Non-significant; IBD: Inflammatory bowel disease.



DOI: 10.3748/wjg.v28.i30.4102 **Copyright** ©The Author(s) 2022.

Figure 2 Temporal trends in medication use in patients with inflammatory bowel disease. A: Trends in medication use in patients with Crohn's disease; B: Trends in medication use in patients with ulcerative colitis. ASA: Aminosalicylates; CS: Corticosteroids; IMS: Immunosuppressants; IFX: Infliximab.

Currently, IBD medications mainly include 5-ASA, CS, IMS, and biological agents. In our study, trend analysis for CD found a prominent decline in prescriptions of 5-ASA and CS in parallel to a significant increase in prescriptions of IMS and IFX from 1999 to 2020. A previous national study from the American database reported that 37.3% of patients with CD were prescribed 5-ASA between 2009 and 2014, despite the debatable effectiveness of 5-ASA[25]. Nevertheless, the latest ECCO guideline no longer recommends 5-ASA in patients with mild-to-moderate CD[26]. In our analysis, 5-ASA usage significantly decreased from 39.6% in 2009 to 5.5% in 2020, reflecting a positive trend in narrowing the



DOI: 10.3748/wjg.v28.i30.4102 **Copyright** ©The Author(s) 2022.

Figure 3 Periodic changes in treatment patterns in patients with inflammatory bowel disease. A: Crohn's disease; B: Ulcerative colitis. ASA: Aminosalicylates; CS: Corticosteroids; IMS: Immunosuppressants; IFX: Infliximab.

knowledge gap between Chinese providers and IBD consensus. We also observed an apparent reduction in CS prescription onwards, which was probably due to improved awareness of steroid-sparing, earlier treatment after diagnosis, closer surveillance for disease relapse, or more attention on adverse effect of CS[27]. Moreover, IMS emerged in 2005, and prescription rates increased strikingly afterwards, except for a slight decrease between 2018 and 2020. The effect of maintenance treatment with IMS administered to patients with CD who are steroid-dependent has been testified[28]. IFX prominently increased between 2008 and 2020. These may reflect deeper market infiltration of IFX and better treatment adherence. It is worth noting that insurance coverage of IFX was not achieved until November 28, 2019, the day IFX entered the national medical insurance. This policy will influence the decision making of Chinese IBD patients on whether to choose IFX or other IMS and may explain treatment discrepancies between Chinese patients and those from other countries. Regarding trend analysis in UC patients, 5-ASA and CS were steadily prescribed, accompanied by a modest increase in IMS and IFX, demonstrating 5-ASA as a milestone during therapeutic armamentarium extension. The American Gastroenterological Association recommends treating patients with mild-to-moderate left sided UC with mesalamine or diazo-bonded 5-ASA compounds[29]. For patients with extensive mild-to-moderate UC, ECCO recommends the addition of rectal 5-ASA to oral therapy, as combined oral and

rectal therapy delivers a greater effective dose to the affected areas of colon and leads to higher rates of remission[30]. In our study, 51.6% of CD patients and 60.1% of UC patients ceased medical treatment within 1-3 mo. We realized the contradicting results from our study with the current strategy applied worldwide. Our treatment data are mainly derived from IBD referral centers where patients may cease treatment after returning home with only one-month prescriptions. This may be explained by the following reasons which reflect the specific situation of Chinese IBD management: (1) Lack of communication between referral centers and grass-roots hospitals during the early period of IBD treatment; (2) Poor medication adherence at the patient level[31]; and (3) Knowledge gap between doctors and guidelines worldwide. Overall, we are the first to depict temporal changes in medications among a large Chinese IBD population, which has not been well elucidated before.

To further investigate long-term changes in treatment patterns, we included patients who were followed for at least three consecutive years. Our analysis showed that monotherapy or combination therapy with IFX and IMS accounted for nearly half of initial treatment strategies for CD. In fact, 12.7% were prescribed 5-ASA as the initial drug, among which nearly two-thirds ceased treatment within 1-3 mo. However, most patients switched to up-level drugs afterwards, probably reflecting the limitations of 5-ASA for disease maintenance. According to a previous study, treatment strategies for patients with moderate-to-severe CD could be listed as: (1) Conventional step-care therapy (CS and IMS are prescribed sequentially); (2) Accelerated step-care therapy (a tapering process of CS together with IMS); and (3) Top-down therapy (early combination of IMS and IFX). In our study, 7.2% of cases were prescribed CS as the initial drug, most of whom received conventional step-care therapy three months after diagnosis[32]. Another 13.1% were prescribed CS combined with IMS as the initial strategy, most of whom followed an accelerated step-care regimen. Moreover, top-down therapy was the first choice for almost half of the population. Despite short-term interruption, most patients recovered with IMS, IFX, or a minority of CS or 5-ASA. We noted that conventional medications were the main initial strategies in Cohort I, comprising mostly of two step-care therapies. By contrast, the initial approach in Cohort II was predominated by top-down therapies. Regarding therapeutic patterns in UC patients, initial treatments mainly included 5-ASA and CS. As the principal therapy in initial strategies, 5-ASA was highly effective for UC[33]. Similar to CD patterns, patients with UC who stopped treatment within 1-3 mo were re-prescribed different levels of medications afterwards, reflecting better adherence and more standardized treatment. Additionally, 5-ASA and CS were only initial strategies in Cohort I, complying with clinical settings in the early period of IBD management. In general, our analysis provides a unique insight into long-term therapeutic paradigms in Chinese population.

Since initial treatments were crucial for long-term therapeutic paradigms, we next investigated potential predictors for initial drugs. In CD patients, L3 congruously reduced the possibility of commencing CS, whereas L4 increased the possibility of commencing CS combined with IMS or commencing IFX. This is likely due to the fact that patients with upper gastrointestinal involvement are prone to behave in a more sophisticated course, requiring IMS or IFX for maintenance of remission. Intriguingly, patients with penetrating behavior and gastrointestinal surgical history appeared to have a lower likelihood of being prescribed either drug, given the intricate and drug-refractory nature, calling for short-term surgical intervention after diagnosis. We also observed an increase in CS combined with IMS or IFX in patients who underwent perianal surgeries before diagnosis. A possible explanation is that poor healing after perianal surgeries provide useful evidence for making detailed diagnosis and more appropriate selection of therapeutic strategies. Regarding factors in UC, we found an appreciable correlation between all strategies and medication history. This finding should be carefully generalized to other UC populations. Thus, future investigation elucidating detailed association between treatments before diagnosis and initial therapeutic paradigms in larger population is warranted. Interestingly, patients with E3 reflected a higher risk of 5-ASA and CS medications, possibly explained by the fact that patients with extensive colitis naturally tended to adopt medications that might relieve symptoms. Moreover, our observations indicated that patients diagnosed after 2009 were less likely to be prescribed 5-ASA or CS as initial therapies, which is mainly due to IFX insurance coverage or improved awareness of steroid-sparing medications. Generally, these results suggest that baseline characteristics probably affect initial treatment strategies to a certain extent.

There are several strengths in this study. First, patients were from IBD referral centers, which covered all the administrative regions in China. The population represented a broad spectrum of Chinese patients with IBD for over 20 years, facilitating temporal trends evaluation in medication use and drug strategies. Second, detailed baseline characteristics and prescriptions through follow-up were retrieved from consecutive medical records, which may reflect actual drug intake to some extent. Lastly, no study has analyzed periodic changes in treatment paradigms for three consecutive years and associated factors with initial drug strategies in Chinese IBD patients.

The study also has limitations. First, extrapolation of medication trends to the entire country and other Asian countries remains unproven due to lack of the national registry in China and potential differences in racial phenotypes and treatment strategies worldwide. A wholesome IBD registry system and multicenter studies among Asian populations are needed in the near future. Second, potential information and confounding bias exist due to observational design. Therefore, we assessed baseline factors thoroughly and employed multivariate logistic regression analysis to minimize bias. Moreover, outcomes, including hospitalization, surgeries, or phenotype progression were not collected, limiting

further investigation in the correlation between different drug strategies and long-term outcomes.

CONCLUSION

In conclusion, this study provides insights into temporal trends in long-term medication use and periodic changes in treatment patterns for Chinese patients with IBD. The findings suggest that prescriptions of IMS and IFX increased in parallel with steady or decreasing prescriptions of 5-ASA and CS in real-world settings. The study also shed light on periodic changes in treatment patterns, reflecting a switching profile from conventional drugs to IFX in CD. Further research into the full breadth of trends in medication use and treatment patterns should be conducted for additional compliance with guidelines for IBD management.

ARTICLE HIGHLIGHTS

Research background

Medications for inflammatory bowel disease (IBD) have changed dramatically over time, especially following market availability of infliximab (IFX). Several attempts have been made by Western and other Asian countries to provide rough medication changes.

Research motivation

No study on long-term medication profiles has been conducted in Chinese population, and minimal attention has been paid to periodic changes in IBD treatment strategies. Additionally, investigating possible predictors for initial treatment strategies may help to better understand periodic changes in therapeutic patterns in patients with IBD.

Research objectives

This study was designed to leverage the real-world evidence in Chinese referral hospitals to provide fresh insights into temporal trends in medication prescriptions among the Chinese population with IBD for over 20 years, and to investigate long-term periodic changes in treatment paradigms and identify the possible factors that influence initial drug strategies.

Research methods

A multicenter retrospective cohort study was conducted to analyze trends in medication use and therapeutic patterns. Predictors for initial drug strategies were identified using logistic regression analysis.

Research results

Of 5-aminosalicylates (5-ASA) and corticosteroids (CS) prescriptions gradually decreased, accompanied by a notable increase in immunosuppressants (IMS) and IFX prescriptions in patients with Crohn's disease (CD). Prescription rates of 5-ASA and CS were stable, whereas IMS and IFX slightly increased since 2007 in patients with ulcerative colitis (UC). Subgroup analyses showed the switch from conventional medications to IFX in patients with CD, while 5-ASA and CS were still steadily prescribed in patients with UC. Logistic regression analyses revealed that surgical history, disease behavior, and disease location were associated with initial therapeutic strategies in patients with CD. However, medications before diagnosis, disease location, and diagnostic year might affect initial strategies in patients with UC.

Research conclusions

Parallel to increasing IMS and IFX use in IBD over the past two decades, a significant decrease in 5-ASA and CS use were observed for CD but not for UC. Long-term treatment strategies analyses provided a unique insight in switching from conventional drugs to IFX in Chinese patients with CD.

Research perspectives

The study was based on IBD referral centers, therefore the study population only accounted for limited proportion of total Chinese patients with IBD. A well-organized national registry system in the near future will help facilitate larger clinical studies in China. In addition, clinical outcomes, including hospitalization, surgeries, or phenotype progression were not collected. Further investigation in the correlation between different drug strategies and long-term outcomes are needed in future studies.

ACKNOWLEDGEMENTS

We want to thank Professor Yun-Xian Yu from Zhejiang University to help with reviewing the statistical methods and proofreading the manuscript of this study.

FOOTNOTES

Author contributions: Cao Q formulated the research idea; Yao LY developed the study protocol; Yao LY, Tian F, Ye M, Li YQ, Wang XL, Wang L, Yang SQ, Lv XP, Jia Y, Wang XH, Zhang XQ and Wei YL conducted the patient identification and data collection; Shao BL and Yao LY conducted the data analysis; Yao LY, Shao BL and Cao Q developed the manuscript; and all authors have read and approve the final manuscript.

Institutional review board statement: The study protocol was reviewed and approved by Sir Run Run Shaw Hospital, College of Medicine Zhejiang University Institutional Review Board with approval for all hospitals involved in the study, No. 20210714-31.

Informed consent statement: The requirement for patient informed consent was waived due to the retrospective nature of this study.

Conflict-of-interest statement: All the authors report no relevant conflicts of interest for this article.

Data sharing statement: Technical appendix, statistical code, and dataset available from the corresponding author at caoq@zju.edu.cn.

STROBE statement: The authors have read the STROBE Statement—checklist of items, and the manuscript was prepared and revised according to the STROBE Statement—checklist of items.

Open-Access: This article is an open-access article that was selected by an in-house editor and fully peer-reviewed by external reviewers. It is distributed in accordance with the Creative Commons Attribution NonCommercial (CC BY-NC 4.0) license, which permits others to distribute, remix, adapt, build upon this work non-commercially, and license their derivative works on different terms, provided the original work is properly cited and the use is non-commercial. See: https://creativecommons.org/Licenses/by-nc/4.0/

Country/Territory of origin: China

ORCID number: Qian Cao 0000-0001-7938-7532.

S-Editor: Fan JR
L-Editor: A
P-Editor: Fan JR

REFERENCES

1 **Shanahan F**. Crohn's disease. *Lancet* 2002; **359**: 62-69 [PMID: 11809204 DOI: 10.1016/S0140-6736(02)07284-7]
2 **Ordás I**, Eckmann L, Talamini M, Baumgart DC, Sandborn WJ. Ulcerative colitis. *Lancet* 2012; **380**: 1606-1619 [PMID: 22914296 DOI: 10.1016/S0140-6736(12)60150-0]
3 **Kaplan GG**. The global burden of IBD: from 2015 to 2025. *Nat Rev Gastroenterol Hepatol* 2015; **12**: 720-727 [PMID: 26323879 DOI: 10.1038/nrgastro.2015.150]
4 **Akobeng AK**, Zachos M. Tumor necrosis factor-alpha antibody for induction of remission in Crohn's disease. *Cochrane Database Syst Rev* 2004; CD003574 [PMID: 14974022 DOI: 10.1002/14651858.CD003574.pub2]
5 **Behm BW**, Bickston SJ. Tumor necrosis factor-alpha antibody for maintenance of remission in Crohn's disease. *Cochrane Database Syst Rev* 2008; CD006893 [PMID: 18254120 DOI: 10.1002/14651858.CD006893]
6 **Jeuring SF**, van den Heuvel TR, Liu LY, Zeegers MP, Hameeteman WH, Romberg-Camps MJ, Oostenbrug LE, Masclee AA, Jonkers DM, Pierik MJ. Improvements in the Long-Term Outcome of Crohn's Disease Over the Past Two Decades and the Relation to Changes in Medical Management: Results from the Population-Based IBDSL Cohort. *Am J Gastroenterol* 2017; **112**: 325-336 [PMID: 27922024 DOI: 10.1038/ajg.2016.524]
7 **Gower-Rousseau C**, Savoye G, Colombel JF, Peyrin-Biroulet L. Are we improving disease outcomes in IBD? *Gut* 2014; **63**: 1529-1530 [PMID: 24287275 DOI: 10.1136/gutjnl-2013-306045]
8 **Cha JM**, Park SH, Rhee KH, Hong SN, Kim YH, Seo SI, Kim KH, Jeong SK, Lee JH, Park SY, Park H, Kim JS, Im JP, Yoon H, Kim SH, Jang J, Kim JH, Suh SO, Kim YK, Ye BD, Yang SK. Long-term prognosis of ulcerative colitis and its temporal changes between 1986 and 2015 in a population-based cohort in the Songpa-Kangdong district of Seoul, Korea. *Gut* 2020; **69**: 1432-1440 [PMID: 31822581 DOI: 10.1136/gutjnl-2019-319699]
9 **Harbord M**, Annese V, Vavricka SR, Allez M, Barreiro-de Acosta M, Boberg KM, Burisch J, De Vos M, De Vries AM, Dick AD, Juillerat P, Karlsen TH, Koutroubakis I, Lakatos PL, Orchard T, Papay P, Raine T, Reinshagen M, Thaci D, Tilg

H, Carbonnel F; European Crohn's and Colitis Organisation. The First European Evidence-based Consensus on Extra-intestinal Manifestations in Inflammatory Bowel Disease. *J Crohns Colitis* 2016; **10**: 239-254 [PMID: 26614685 DOI: 10.1093/ecco-jcc/jjv213]

10 **Silverberg MS**, Satsangi J, Ahmad T, Arnott ID, Bernstein CN, Brant SR, Caprilli R, Colombel JF, Gasche C, Geboes K, Jewell DP, Karban A, Loftus EV Jr, Peña AS, Riddell RH, Sachar DB, Schreiber S, Steinhart AH, Targan SR, Vermeire S, Warren BF. Toward an integrated clinical, molecular and serological classification of inflammatory bowel disease: report of a Working Party of the 2005 Montreal World Congress of Gastroenterology. *Can J Gastroenterol* 2005; **19** Suppl A: 5A-36A [PMID: 16151544 DOI: 10.1155/2005/269076]

11 **Gorelik Y**, Freilich S, Gerassy-Vainberg S, Pressman S, Friss C, Blatt A, Focht G, Weisband YL, Greenfeld S, Kariv R, Lederman N, Dotan I, Geva-Zatorsky N, Shen-Orr SS, Kashi Y, Chowers Y; IIRN. Antibiotic use differentially affects the risk of anti-drug antibody formation during anti-TNFα therapy in inflammatory bowel disease patients: a report from the epi-IIRN. *Gut* 2022; **71**: 287-295 [PMID: 34344783 DOI: 10.1136/gutjnl-2021-325185]

12 **Lemaitre M**, Kirchgesner J, Rudnichi A, Carrat F, Zureik M, Carbonnel F, Dray-Spira R. Association Between Use of Thiopurines or Tumor Necrosis Factor Antagonists Alone or in Combination and Risk of Lymphoma in Patients With Inflammatory Bowel Disease. *JAMA* 2017; **318**: 1679-1686 [PMID: 29114832 DOI: 10.1001/jama.2017.16071]

13 **Singh S**, Facciorusso A, Dulai PS, Jairath V, Sandborn WJ. Comparative Risk of Serious Infections With Biologic and/or Immunosuppressive Therapy in Patients With Inflammatory Bowel Diseases: A Systematic Review and Meta-Analysis. *Clin Gastroenterol Hepatol* 2020; **18**: 69-81.e3 [PMID: 30876964 DOI: 10.1016/j.cgh.2019.02.044]

14 **Chinese Cooperative Group For The Study on IBD**; Chinese Society of Gastroenterology, Ouyang Q, Hu PJ, Qian JM, Zheng JJ, Hu RW. Consensus on the management of inflammatory bowel disease in China in 2007. *J Dig Dis* 2008; **9**: 52-62 [PMID: 18251795 DOI: 10.1111/j.1443-9573.2007.00320.x]

15 **Maaser C**, Sturm A, Vavricka SR, Kucharzik T, Fiorino G, Annese V, Calabrese E, Baumgart DC, Bettenworth D, Borralho Nunes P, Burisch J, Castiglione F, Eliakim R, Ellul P, González-Lama Y, Gordon H, Halligan S, Katsanos K, Kopylov U, Kotze PG, Krustinš E, Laghi A, Limdi JK, Rieder F, Rimola J, Taylor SA, Tolan D, van Rheenen P, Verstockt B, Stoker J; European Crohn's and Colitis Organisation [ECCO] and the European Society of Gastrointestinal and Abdominal Radiology [ESGAR]. ECCO-ESGAR Guideline for Diagnostic Assessment in IBD Part 1: Initial diagnosis, monitoring of known IBD, detection of complications. *J Crohns Colitis* 2019; **13**: 144-164 [PMID: 30137275 DOI: 10.1093/ecco-jcc/jjy113]

16 **Best WR**, Becktel JM, Singleton JW, Kern F Jr. Development of a Crohn's disease activity index. National Cooperative Crohn's Disease Study. *Gastroenterology* 1976; **70**: 439-444 [PMID: 1248701]

17 **D'Haens G**, Sandborn WJ, Feagan BG, Geboes K, Hanauer SB, Irvine EJ, Lémann M, Marteau P, Rutgeerts P, Schölmerich J, Sutherland LR. A review of activity indices and efficacy end points for clinical trials of medical therapy in adults with ulcerative colitis. *Gastroenterology* 2007; **132**: 763-786 [PMID: 17258735 DOI: 10.1053/j.gastro.2006.12.038]

18 **R Core Team**. R: A Language and Environment for Statistical Computing. R Foundation for Statistical Computing, Vienna: Austria, 2021

19 **Wickham H**. ggplot2: Elegant Graphics for Data Analysis. Springer-Verlag: New York, 2016

20 **Liu J**, Ge X, Ouyang C, Wang D, Zhang X, Liang J, Zhu W, Cao Q. Prevalence of Malnutrition, Its Risk Factors, and the Use of Nutrition Support in Patients with Inflammatory Bowel Disease. *Inflamm Bowel Dis* 2022; **28**: S59-S66 [PMID: 34984471 DOI: 10.1093/ibd/izab345]

21 **Yang L**, Song X, Chen Y, Li Y, Gu Y, Wang X, Zhu L, Zhi M, Ouyang C, Guo H. Treatment Decision-making in Chinese Inflammatory Bowel Disease Patients. *Inflamm Bowel Dis* 2022; **28**: S76-S84 [PMID: 34894126 DOI: 10.1093/ibd/izab305]

22 **Chou JW**, Lai HC, Chang CH, Cheng KS, Feng CL, Chen TW. Epidemiology and Clinical Outcomes of Inflammatory Bowel Disease: A Hospital-Based Study in Central Taiwan. *Gastroenterol Res Pract* 2019; **2019**: 4175923 [PMID: 31312216 DOI: 10.1155/2019/4175923]

23 **Burisch J**, Kiudelis G, Kupcinskas L, Kievit HAL, Andersen KW, Andersen V, Salupere R, Pedersen N, Kjeldsen J, D'Incà R, Valpiani D, Schwartz D, Odes S, Olsen J, Nielsen KR, Vegh Z, Lakatos PL, Toca A, Turcan S, Katsanos KH, Christodoulou DK, Fumery M, Gower-Rousseau C, Zammit SC, Ellul P, Eriksson C, Halfvarson J, Magro FJ, Duricova D, Bortlik M, Fernandez A, Hernández V, Myers S, Sebastian S, Oksanen P, Collin P, Goldis A, Misra R, Arebi N, Kaimakliotis IP, Nikuina I, Belousova E, Brinar M, Cukovic-Cavka S, Langholz E, Munkholm P; Epi-IBD group. Natural disease course of Crohn's disease during the first 5 years after diagnosis in a European population-based inception cohort: an Epi-IBD study. *Gut* 2019; **68**: 423-433 [PMID: 29363534 DOI: 10.1136/gutjnl-2017-315568]

24 **Kalaria R**, Desai D, Abraham P, Joshi A, Gupta T, Shah S. Temporal Change in Phenotypic Behaviour in Patients with Crohn's Disease: Do Indian Patients Behave Differently from Western and Other Asian Patients? *J Crohns Colitis* 2016; **10**: 255-261 [PMID: 26519461 DOI: 10.1093/ecco-jcc/jjv202]

25 **Noureldin M**, Cohen-Mekelburg S, Mahmood A, Stidham R, Higgins PDR, Govani S, Deshpande AR, Waljee AK. Trends of 5-Aminosalicylate Medication Use in Patients With Crohn Disease. *Inflamm Bowel Dis* 2021; **27**: 516-521 [PMID: 32469067 DOI: 10.1093/ibd/izaa127]

26 **Torres J**, Bonovas S, Doherty G, Kucharzik T, Gisbert JP, Raine T, Adamina M, Armuzzi A, Bachmann O, Bager P, Biancone L, Bokemeyer B, Bossuyt P, Burisch J, Collins P, El-Hussuna A, Ellul P, Frei-Lanter C, Furfaro F, Gingert C, Gionchetti P, Gomollon F, González-Lorenzo M, Gordon H, Hlavaty T, Juillerat P, Katsanos K, Kopylov U, Krustins E, Lytras T, Maaser C, Magro F, Marshall JK, Myrelid P, Pellino G, Rosa I, Sabino J, Savarino E, Spinelli A, Stassen L, Uzzan M, Vavricka S, Verstockt B, Warusavitarne J, Zmora O, Fiorino G. ECCO Guidelines on Therapeutics in Crohn's Disease: Medical Treatment. *J Crohns Colitis* 2020; **14**: 4-22 [PMID: 31711158 DOI: 10.1093/ecco-jcc/jjz180]

27 **Singleton JW**, Law DH, Kelley ML Jr, Mekhjian HS, Sturdevant RA. National Cooperative Crohn's Disease Study: adverse reactions to study drugs. *Gastroenterology* 1979; **77**: 870-882 [PMID: 38177]

28 **Chande N**, Patton PH, Tsoulis DJ, Thomas BS, MacDonald JK. Azathioprine or 6-mercaptopurine for maintenance of remission in Crohn's disease. *Cochrane Database Syst Rev* 2015; CD000067 [PMID: 26517527 DOI: 10.1002/14651858.CD000067.pub3]

29 **Ko CW**, Singh S, Feuerstein JD, Falck-Ytter C, Falck-Ytter Y, Cross RK; American Gastroenterological Association Institute Clinical Guidelines Committee. AGA Clinical Practice Guidelines on the Management of Mild-to-Moderate Ulcerative Colitis. *Gastroenterology* 2019; **156**: 748-764 [PMID: 30576644 DOI: 10.1053/j.gastro.2018.12.009]

30 **Harbord M**, Eliakim R, Bettenworth D, Karmiris K, Katsanos K, Kopylov U, Kucharzik T, Molnár T, Raine T, Sebastian S, de Sousa HT, Dignass A, Carbonnel F; European Crohn's and Colitis Organisation [ECCO]. Third European Evidence-based Consensus on Diagnosis and Management of Ulcerative Colitis. Part 2: Current Management. *J Crohns Colitis* 2017; **11**: 769-784 [PMID: 28513805 DOI: 10.1093/ecco-jcc/jjx009]

31 **Tripathi K**, Dong J, Mishkin BF, Feuerstein JD. Patient Preference and Adherence to Aminosalicylates for the Treatment of Ulcerative Colitis. *Clin Exp Gastroenterol* 2021; **14**: 343-351 [PMID: 34511961 DOI: 10.2147/CEG.S237653]

32 **Ordás I**, Feagan BG, Sandborn WJ. Early use of immunosuppressives or TNF antagonists for the treatment of Crohn's disease: time for a change. *Gut* 2011; **60**: 1754-1763 [PMID: 21997558 DOI: 10.1136/gutjnl-2011-300934]

33 **Nagahori M**, Kochi S, Hanai H, Yamamoto T, Nakamura S, Omuro S, Watanabe M, Hibi T; OPTIMUM Study Group. Real life results in using 5-ASA for maintaining mild to moderate UC patients in Japan, a multi-center study, OPTIMUM Study. *BMC Gastroenterol* 2017; **17**: 47 [PMID: 28390410 DOI: 10.1186/s12876-017-0604-y]

World Journal of Gastroenterology

Submit a Manuscript: https://www.f6publishing.com

World J Gastroenterol 2022 August 14; 28(30): 4120-4132

DOI: 10.3748/wjg.v28.i30.4120

ISSN 1007-9327 (print) ISSN 2219-2840 (online)

ORIGINAL ARTICLE

Retrospective Study

Salivary *Fusobacterium nucleatum* serves as a potential diagnostic biomarker for gastric cancer

Wen-Dan Chen, Xin Zhang, Meng-Jiao Zhang, Ya-Ping Zhang, Zi-Qi Shang, Yi-Wei Xin, Yi Zhang

Specialty type: Gastroenterology and hepatology

Provenance and peer review: Unsolicited article; Externally peer reviewed.

Peer-review model: Single blind

Peer-review report's scientific quality classification

Grade A (Excellent): 0
Grade B (Very good): B, B, B, B
Grade C (Good): C
Grade D (Fair): 0
Grade E (Poor): 0

P-Reviewer: Imai Y, Japan; Mincione G, Italy; Mishra TS, India; Rahimi-Movaghar E, Iran

Received: November 26, 2021
Peer-review started: November 26, 2021
First decision: January 8, 2022
Revised: January 21, 2022
Accepted: July 18, 2022
Article in press: July 18, 2022
Published online: August 14, 2022

Wen-Dan Chen, Xin Zhang, Meng-Jiao Zhang, Ya-Ping Zhang, Zi-Qi Shang, Yi-Wei Xin, Yi Zhang, Department of Clinical Laboratory, Qilu Hospital of Shandong University, Jinan 250012, Shandong Province, China

Corresponding author: Yi Zhang, PhD, Professor, Department of Clinical Laboratory, Qilu Hospital of Shandong University, No. 107 Wenhua Xi Road, Jinan 250012, Shandong Province, China. yizhang@sdu.edu.cn

Abstract

BACKGROUND

As one of the most common tumors, gastric cancer (GC) has a high mortality rate, since current examination approaches cannot achieve early diagnosis. *Fusobacterium nucleatum* (Fn) primarily colonized in the oral cavity, has been reported to be involved in the development of gastrointestinal tumor. Until now, little is known about the relationship between salivary Fn and GC.

AIM

To determine whether salivary Fn could be a biomarker to diagnose GC and explore the influence of Fn on GC cells.

METHODS

The abundance of Fn in saliva was quantified by droplet digital polymerase chain reaction in 120 GC patients, 31 atrophic gastritis (AG) patients, 35 non-AG (NAG) patients, 26 gastric polyp (GP) patients, and 20 normal controls (NC) from Qilu Hospital of Shandong University from January 2019 to December 2020. Receiver operating characteristic (ROC) curve analysis was performed to evaluate the diagnostic value of Fn as well as traditional serum tumor markers, including carcinoembryonic antigen (CEA), carbohydrate antigen (CA) 19-9, and CA72-4. Transwell assay and wound-healing assay were conducted to assess the influence of Fn infection on GC cells. The expression of epithelial-mesenchymal transition (EMT) markers was detected using western blot assay.

RESULTS

We found that the level of salivary Fn in GC patients was significantly increased compared with those in AG, NAG, and GP patients and NC ($P < 0.001$). ROC curve analysis showed a favorable capability of Fn (73.33% sensitivity; 82.14% specificity; area under the curve: 0.813) in GC diagnosis, which was superior to that of CEA, CA19-9, CA72-4, ferritin, and sialic acid. The Fn level in saliva of GC

patients was increased as the TNM stage increased. GC patients with lymph node metastasis had higher Fn levels than those without metastasis. Both transwell and wound-healing assays indicated that Fn infection promoted the migration and invasion of GC cells. Western blot analysis showed that Fn infection decreased the expression of E-cadherin and increased the expressions of N-cadherin, vimentin, and snail.

CONCLUSION

Fn abundance in saliva could be used as a promising biomarker to diagnose GC, and Fn infection could promote GC metastasis by accelerating the EMT process.

Key Words: Gastric cancer; *Fusobacterium nucleatum*; Saliva; Prognosis; Metastasis; Epithelial-mesenchymal transition

©The Author(s) 2022. Published by Baishideng Publishing Group Inc. All rights reserved.

Core Tip: *Fusobacterium nucleatum* (Fn), known as a periodontal pathogen, is frequently detected in tissues of gastrointestinal tumor. Here, we found that the level of salivary Fn was increased in gastric cancer (GC) patients, which could be used as a potential biomarker for GC diagnosis, and its diagnostic capability was superior to that of traditional serum tumor markers. We also showed that salivary Fn level was positively associated with the GC TNM stage and lymph node metastasis. Further, experiments *in vitro* revealed that Fn could promote the migration and invasion of GC cells by promoting the epithelial-mesenchymal transition process. Our findings suggest that salivary Fn is a potential biomarker in diagnosis of GC.

Citation: Chen WD, Zhang X, Zhang MJ, Zhang YP, Shang ZQ, Xin YW, Zhang Y. Salivary *Fusobacterium nucleatum* serves as a potential diagnostic biomarker for gastric cancer. *World J Gastroenterol* 2022; 28(30): 4120-4132

URL: https://www.wjgnet.com/1007-9327/full/v28/i30/4120.htm

DOI: https://dx.doi.org/10.3748/wjg.v28.i30.4120

INTRODUCTION

Gastric cancer (GC) is one of the most common malignant tumors, with morbidity and mortality ranking fifth and third in the world, respectively, posing a great threat to global human health[1]. Although the 5-year survival rate of GC is enhanced with the combination of chemotherapy and surgery, its mortality remains high due to the diagnosis at an advanced stage with a limited therapeutic scheme to choose from. Therefore, effective early diagnosis for GC is especially important.

The microorganisms in the human body are complex and they play important roles in each part of our body. Over 700 bacterial species have been detected in the human oral cavity, and they interact with each other as well as with the host[2]. The stomach was considered a sterile organ until the discovery of *Helicobacter pylori* (*H. pylori*) in 1984[3]. Subsequently, other microorganisms were found in the gastric mucosa[4]. Although the gut microbiota ecosystem is different from that of the oral cavity, there is also a partial similarity between them, since most of the bacteria in the oral cavity enter the stomach when swallowing food and saliva.

Human saliva is a unique biofluid resource with huge clinical diagnostic and risk assessment capacity. Moreover, it is easy to acquire in non-invasive and painless approaches. Most importantly, individual oral environment basically maintains a long-term relatively stable state except for little fluctuation caused by diet, infections, or other factors, and the dominant oral floras in different individuals are host specific[5]. *Fusobacterium nucleatum* (Fn) is a Gram-negative anaerobic bacterium, which is a normal composition of the oral microenvironment[6,7]. In recent years, due to its increased detection rate in oral infectious diseases, it has been identified as an opportunistic pathogen[8]. Chronic periodontitis is caused by the ecological imbalance of the subgingival plaque biofilm communities, leading to the growth of dominant species, which destroys the host immune response and leads to inflammation[9]. Fn has been proved to be one of the pathogens that grow abnormally before periodontal disease, leading to an imbalance in the composition of oral symbiotic bacteria, which leads to the occurrence of periodontitis[10]. It forms a bridge between the early symbiotic colonizers and the late pathogenic colonizers[11]. In recent years, Fn has also been found to be associated with extra-oral infections, including adverse pregnancy outcomes, rheumatoid arthritis, respiratory tract infections, and gastrointestinal neoplasm[12-14]. Accumulating evidence has shown that Fn is associated with the occurrence, development, and metastasis of colorectal cancer (CRC). However, the information for GC is

limited. In the present study, we aimed to detect the Fn abundance in saliva using digital droplet polymerase chain reaction (ddPCR), and establish a new simple and effective diagnostic approach to improve the early diagnosis of GC.

MATERIALS AND METHODS

Study population and sample collection

Subjects with GC (n = 120), atrophic gastritis (AG) (n = 31), non-AG (NAG) (n = 35), and gastric polyps (GP) (n = 26) and normal controls (NC) (n = 20) undergoing gastroscopy examination at Qilu Hospital of Shandong University from January 2019 to December 2020 were enrolled in this study. The selection of NC mainly depended on the normal results of gastroscopy examination, biochemical indexes, and tumor marker detection. GC, AG, NAG, and GP were further confirmed based on histopathological analyses. The pathological stage of GC was assessed by the 8th edition TNM staging system. The exclusion criteria were as follows: (1) Subjects who used any antibiotics within the last 4 wk; (2) Subjects with oral inflammation; and (3) Subjects without detailed general clinical data. Whole saliva specimens were collected with Salivette® tube before brushing teeth and eating breakfast in the morning. After collection, samples were immediately transferred to the laboratory with ice gauges and centrifuged at 3000 r/min for 10 min at 4 °C. All saliva samples were stored at -80 °C until further analysis. All study participants provided informed written consent prior to study enrollment. This study was approved by the Ethics Committee of the Qilu Hospital of Shandong University (Approval No. KYLL-2019-2-013).

DNA isolation

Total genomic DNA was extracted from 200 μL saliva using the QIAamp Blood Mini Kit (cat. 51106, Qiagen, Hilden, Germany), and purified DNA was finally dissolved in 80 μL AE buffer. The concentration of DNA was determined with a Qubit 3 Fluorometer using an Equalbit 1 × dsDNA HS Assay Kit (cat. EQ121-01, Thermo Fisher Scientific, United States) according to the manufacturer's instructions.

ddPCR

ddPCR was performed on the bio-digital PCR platform (Turtle Tech Ltd., Shanghai, China) in a 35 μL reaction system consisting of 5 μL genomic DNA, 3.5 μL 10 × dPCR buffer, 1 μL dPCR enzyme, 1 μM primers, and 0.5 μM probe of Fn (forward primer: 5'-TGGTGTCATTCTTCCAAAAATATCA-3'; reverse primer: 5'-AGATCAAGAAGGACAAGTTGCTGAA-3'; probe: 5'-ACTTTAACTCTACCATGTTCA-3'). After the automatic sample loading process was completed, the chips with samples added were transferred into a nucleic acid amplification instrument (Turtle Tech Ltd., Shanghai, China). Briefly, after an initial enzyme activation step at 50 °C for 10 min and then at 90 °C for 10 min, amplification (45 cycles) of Fn DNA was carried out. After amplification, the chips were transferred to the commercial digital PCR platform (BioDigital dPCR System, Turtle Tech. Ltd., Shanghai, China) to detect fluorescence amplitude signals.

Cell culture

The GC cell lines AGS and MKN-28 were purchased from Shanghai Zhongqiao Xinzhou Biotechnology Co., Ltd. (Shanghai, China) and maintained in appropriate medium (Hyclone, United States) supplanted with 10% fetal bovine serum (Hyclone, United States) under the standard conditions (50 mL/L CO_2, 37 °C).

Bacterial strains and growth conditions

Two strains of Fn (ATCC49256 and ATCC25586) used in our assays were purchased from American Type Culture Collection. The strains were first inoculated and cultured on Columbia Blood Agar under the anaerobic condition at 37 °C for 48 h. Then a single colony was transferred to a fluid thioglycolate medium, followed by incubation at 37 °C under anaerobic conditions (90 mL/L N_2, 50 mL/L CO_2, and 50 mL/L H_2) to reach an optical density (OD_{600}) of 0.2 for each bacterial strain.

Coculture

AGS and MKN-28 cells (2 × 10^5/per well) were seeded in six-well plates with 2 mL complete RPMI-1640 medium and cultured overnight. The plates were then incubated under an anaerobic condition mentioned above for 24 h. On the next day, the cultured Fn was centrifuged (4400 × g for 5 min at room temperature), and the bottom bacteria were sedimented and then re-suspended with fresh RPMI-1640 medium after the supernatant was discarded. After the OD_{600} was determined, the resuspended Fn was added to AGS and MKN-28 cells for co-culture. Cell treated with phosphate buffer solution served as a control group. The plates were centrifuged at 250 × g for 5 min and placed back in an anaerobic incubator for 24 h. For all the experiments in this study, Fn bacteria were added to the cells at an multiplicity of infection (MOI) of 100 based on the preliminary experiments, and this value was common in the published articles.

Transwell assay

After 24 h of infection, the cells were washed and seeded into the upper chamber of an 8-μm transwell insert (Costar, Corning, New York, United States). Transwell chambers used for invasion assay were pre-coated with Matrigel (Corning), while the chambers used for migration assay were not treated. The upper chamber of the transwell contained 2×10^4 cells in a volume of 200 μL serum-free medium, and 700 μL of medium containing 10% serum was added into the lower chamber. After being cultured for 24 h, the cells in the upper chamber were wiped with the cotton tip, and the adherent cells in the lower chamber were fixed with 40 g/L formaldehyde for 10 min and stained with 0.5% crystal violet for 30 min. The images were captured with an inverted microscope (Olympus, Tokyo, Japan).

Wound-healing assay

AGS and MKN-28 cells (5×10^5 cells/ per well) were seeded in six-well plates, and the later infection process was the same as the transwell assay above-mentioned. After 24 h of Fn infection, the cells were washed with RPMI-1640 medium (by this time, the cells were grown to 100% confluence, if not, cultured continually). A 200 μL pipette tip was used to make a straight scratch, simulating a wound. Subsequently, the medium and floating cells were removed and replaced with a serum-free culture medium, and the imagines were captured (0 h). After 48 h of cell culture, images were captured again. The cell migration rate was evaluated by comparing the healing degree between 0 h and 48 h.

Western blot analysis

The AGS and MKN-28 cells with or without Fn infection were lysed in radioimmune precipitation assay buffer for 30 min on ice. Then the cell lysates were centrifuged at 12000 r/min for 10 min at 4 °C, and the supernatant was collected. The bicinchoninic acid protein assay kit (Pierce, Rockford, United States) was used to quantify protein concentrations. Subsequently, equal amounts of proteins (30 μg) were subjected to sodium dodecyl sulphate-polyacrylamide gel electrophoresis, and then electrophoretically transferred onto polyvinylidene fluoride membranes. The blots were blocked with 5% skim milk in Tris-buffered saline with tween (TBST) (BD Biosciences, San Jose, CA, United States) containing 0.1% tween-20 (Bio-Rad, Richmond, CA, United States) at room temperature for 1 h. The membranes were then incubated overnight at 4 °C with the primary antibodies against E-cadherin (1:1000, Cell Signaling, #3195S, Danvers, MA, United States), N-cadherin (1:1000, Cell Signaling, #13116T), vimentin (1:1000, Cell Signaling, #5741S, Danvers, MA, United States), Snail (1:1000, Cell Signaling, #3879S), and GAPDH (1:1000, Cell Signaling, #5174S). The membranes were washed three times with 1 × TBST buffer, followed by incubation with anti-rabbit HRP-conjugated secondary antibody (1:5000; Huaan, Hangzhou, China) at room temperature for 1.5 h. The immunoreactive bands were visualized using an Amersham Imager 680 (GE, Boston, United States). GAPDH served as a loading control.

Statistical analysis

Statistical analyses were conducted using SPSS software (SPSS Inc., Chicago, IL, United States) and graphs were prepared using GraphPad Prism 8.0 (La Jolla, CA). Statistical review was performed by a biomedical statistician. Fn abundance in different groups is expressed as the median and interquartile range. A χ^2 test was used for the comparison of categorical variables. A Kruskal-Wallis test was performed for the global comparison of multiple groups and post-hoc multiple comparisons were performed using the Mann-Whitney *U* test. Receiver operating characteristic (ROC) curve analysis was conducted *via* MedCalc15.2.2 to evaluate the diagnostic value of Fn as well as other serum tumor markers, and the best cut-off values were calculated by the Youden index. All statistical tests were two-tailed, and $P < 0.05$ was considered statistically significant.

RESULTS

Abundance of Fn in the saliva of GC patients

Our ddPCR results showed a significant difference in salivary Fn among the patients with GC, AG, NAG, and GP, and NC. And the Fn level was significantly increased in GC patients compared with patients with AG, NAG, and GP and NC while there was no difference among AG, NAG, and GP patients and NC (Figure 1A). Moreover, the Fn level was increased as the TNM stage increased (Figure 1B). Further clinical characteristic analysis showed that GC patients with lymph node metastasis had higher Fn levels than those without (Table 1). However, the Fn level in GC was not significantly associated with age, gender, tumor size, pathological differentiation, or invasion depth.

Diagnostic performance of salivary Fn in GC patients

ROC analysis indicated some diagnostic power with a fitted area under the curve (AUC) of 0.813 (95% confidence interval: 0.756-0.861) (Figure 2A). When the Youden index was used to calculate the optimal cut-off value of the Fn copy number as 67.58 copies/μL, the sensitivity and specificity were 73.33% and 82.14%, respectively. To better evaluate the diagnostic value of Fn in saliva for GC, the routine clinical

Table 1 Association of *Fusobacterium nucleatum* levels in saliva with clinicopathologic features

Feature	Number of cases	*Fusobacterium nucleatum* level	*P* value
Age (yr)			0.780
< 61	56	153.00 (39.20-542.00)	
≥ 61	64	204.00 (57.30-566.00)	
Gender			0.961
Male	99	161.00 (53.52-620.60)	
Female	21	213.60 (46.63-335.90)	
Tumor size (cm)			0.450
< 5	76	152.90 (52.21-443.80)	
≥ 5	44	239.90 (47.31-846.80)	
Pathological differentiation			0.658
Well	77	147.50 (33.98-543.90)	
Moderate	33	155.80 (84.94-754.60)	
Poor	10	280.80 (78.46-518.70)	
Invasion depth			0.227
T1	29	124.60 (32.21-415.80)	
T2	60	298.30 (76.58-666.90)	
T3	21	102.10 (68.62-385.70)	
T4	10	223.00 (66.99-790.30)	
Lymph nodes metastasis			< 0.001
N0	43	80.14 (23.98-241.80)	
N1	25	324.50 (72.43-549.10)	
N2	22	239.60 (79.36-501.70)	
N3	30	478.00 (96.09-1054.00)	

test records of traditional serum tumor markers, including CEA, CA19-9, CA72-4, ferritin, and sialic acid were assessed. The upper cut-off values of these markers were determined according to the manufacturer's directions. Table 2 shows that the Fn level was significantly higher in GC patients compared with AG, NAG, and GP patients and NC, while CEA, CA19-9, CA72-4, and ferritin did not significantly different between GC patients and the other four groups. Although sialic acid was also significantly different among the five groups, its diagnostic value was still lower than that of Fn, according to the ROC curves.

The ROC curves presented that the AUC of CEA, CA19-9, CA72-4, ferritin, and sialic acid was 0.620, 0.570, 0.541, 0.648, and 0.693, respectively (Figures 2B-F). In addition, the sensitivity of Fn was higher compared with the other traditional serum markers. As for the specificity, the value of Fn was higher than those of CEA, CA72-4, ferritin, and sialic acid, but lower than that of CA19-9. Of note, although the specificity of CA19-9 was high, its sensitivity was relatively low (Table 3). These results indicated that the diagnostic capability of Fn was superior to that of CEA, CA19-9, CA72-4, ferritin, and sialic acid.

Role of Fn in GC metastasis

To evaluate the effect of Fn infection *in vitro*, we infected AGS and MKN-28 cells with Fn. The transwell assay indicated that Fn infection significantly enhanced the invasive and migratory capacities of AGS and MKN-28 cells (Figure 3). Consistent with these results, the wound-healing assay showed that Fn infection promoted the migration of these cells (Figure 4). Since epithelial-mesenchymal transition (EMT) is an important process of metastasis, we examined the effect of Fn infection on the expression of proteins involved in the EMT process. The western blot analysis revealed that Fn infection decreased the expression of epithelial markers, such as E-cadherin, but increased the expression of mesenchymal phenotype-associated molecules, such as N-cadherin, vimentin, and snail (Figure 5).

Table 2 Characteristics and levels of biomarkers among different subjects

	Normal control	Atrophic gastritis	Non-atrophic gastritis	Gastric polyps	Gastric cancer
Cases	20	31	35	26	120
Gender (male/female)	13/7	17/14	19/16	15/11	73/47
Age (yr)[1]	56.90 ± 16.02	62.13 ± 10.56	60.80 ± 14.54	58.17 ± 15.26	61.38 ± 10.31
CEA (mg/L)[2,3]	2.03 (1.22-2.56)	1.95 (1.49-53.37)	1.72 (1.44-2.60)	1.36 (1.10-1.85)	2.46 (1.38-4.63)
CA19-9 (pg/mL)[2,3]	6.38 (3.61-11.39)	10.67 (8.68-16.35)	10.30 (7.09-15.07)	9.20 (5.68-12.09)	11.46 (6.75-20.28)
CA72-4 (U/mL)[2,3]	2.86 (0.98-6.48)	0 (0-3.18)	2.41 (1.50-4.65)	1.71 (0.15-4.63)	2.58 (0-5.69)
Ferritin (ng/mL)[2,3]	143.15 (97.04-273.98)	96.98 (69.33-206.55)	126.70 (74.49-245.30)	182.95 (101.13-263.88)	86.20 (25.99-165.75)
Sialic acid (g/L)[2,4]	54.30 (51.45-56.75)	52.50 (46.50-55.30)	53.70 (48.25-60.55)	56.2 (50.53-59.65)	59.55 (53.28-65.33)
Fusobacterium nucleatum (copies/μL)[2,4]	16.70 (2.4-26.10)	28.611 (5.99-61.50)	12.18 (0.74-35.55)	16.32 (1.59-122.234)	177.09 (53.09-547.11)

[1]Data are presented as the mean ± SD.
[2]Data are presented as the median (interquartile range).
[3]Date are compared using Kruskal-Wallis test, $P < 0.05$.
[4]Date are compared using Kruskal-Wallis test, $P < 0.001$.
CEA: Carcinoembryonic antigen; CA19-9: Carbohydrate antigen 19-9; CA72-4: Carbohydrate antigen 72-4.

Table 3 Diagnostic performance of *Fusobacterium nucleatum*, carcinoembryonic antigen, carbohydrate antigen 19-9, carbohydrate antigen 72-4, ferritin, and sialic acid for gastric cancer

Index	AUC	Cut-off value	Sensitivity (%)	Specificity (%)	PPV (%)	NPV (%)
Fn	0.813	67.58 copies/μL	73.33	82.14	81.48	74.19
CEA	0.620	5 ng/mL	55.00	69.64	66.00	59.09
CA19-9	0.570	69.2 pg/mL	26.67	86.61	68.09	52.43
CA72-4	0.541	6.9 U/mL	67.50	44.64	56.64	56.18
Ferritin	0.648	400 ng/mL	51.67	23.21	41.89	30.95
Sialic acid	0.693	75.4 mg/dL	60.83	70.54	68.87	62.70

AUC: Area under curve; PPV: Positive predictive value; NPV: Negative predictive value; Fn: *Fusobacterium nucleatum*; CEA: Carcinoembryonic antigen; CA19-9: Carbohydrate antigen 19-9; CA72-4: Carbohydrate antigen 72-4.

DISCUSSION

In the present study, we reported the relationship between the Fn level in saliva and GC development for the first time. First, a more sensitive ddPCR approach was used to determine the amount of Fn DNA in saliva, and the results showed that a higher number of Fn existed in the saliva of GC patients compared with NC and patients with benign disease. Importantly, salivary Fn had good diagnostic value for GC, which was superior to traditional serum tumor markers, such as CEA, CA19-9, CA72-4, ferritin, and sialic acid, providing a new direction for the diagnosis of GC. We also found that the Fn level was positively associated with TNM stage and lymph node metastasis. Furthermore, transwell and wound-healing assays verified the role of Fn in promoting the invasion and migration of GC cells. Subsequently, we indicated that Fn infection promoted GC metastasis by accelerating the EMT process.

It is essential to diagnose GC at an early stage. Currently, gastroscopy in combination with biopsy is considered the most accurate method to diagnose GC. However, early asymptomatic patients have poor compliance with gastroscopy due to its invasiveness, which directly reduces the rate of early diagnosis of GC. Serum tumor markers are another approach to screen GC. For example, CEA, CA19-9, and CA72-4 are widely used in clinical practice. However, serum tumor markers are not recommended for routine clinical screening due to the lack of specificity and sensitivity[15]. In a cohort consisting of 587 early GC patients, the positive rate of CA19-9, CA125, and CEA was 4.8%, 1.9%, and 4.3%, respectively[16]. For Fn in saliva, it is not only easy to obtain, but also shows a better diagnostic capacity for GC. Moreover, salivary Fn has a pleasurable tissue specificity as a diagnostic marker for GC.

H. pylori is a well-known risk factor for GC. However, other bacterial genera are also detected in the gastric mucosa, such as *Prevotella, Rothia, Fusobacterium,* and *Klebsiella*[17,18]. Fn, a resident colony of

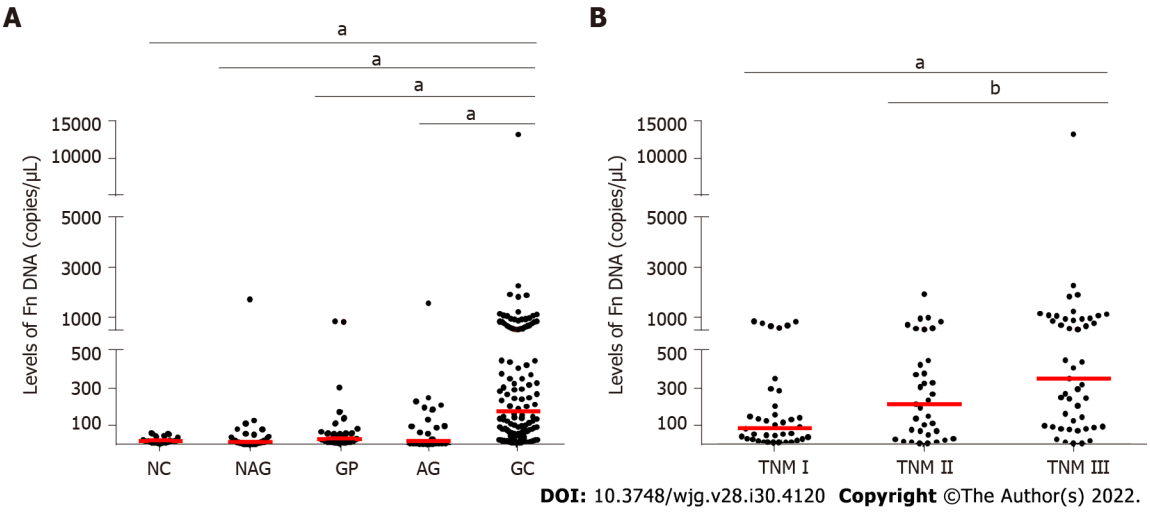


Figure 1 *Fusobacterium nucleatum* levels in different groups. A: *Fusobacterium nucleatum* (Fn) levels in normal control, atrophic gastritis (AG), non-AG, gastric polyps, and gastric cancer (GC) groups; B: Fn levels in different TNM stages of GC patients. Red lines represent the median. $^{a}P < 0.001$, $^{b}P < 0.05$ (Mann-Whitney *U* test). NC: Normal controls; NAG: Non-atrophic gastritis; GP: Gastric polyps; AG: Atrophic gastritis; GC: Gastric cancer; Fn: *Fusobacterium nucleatum*.

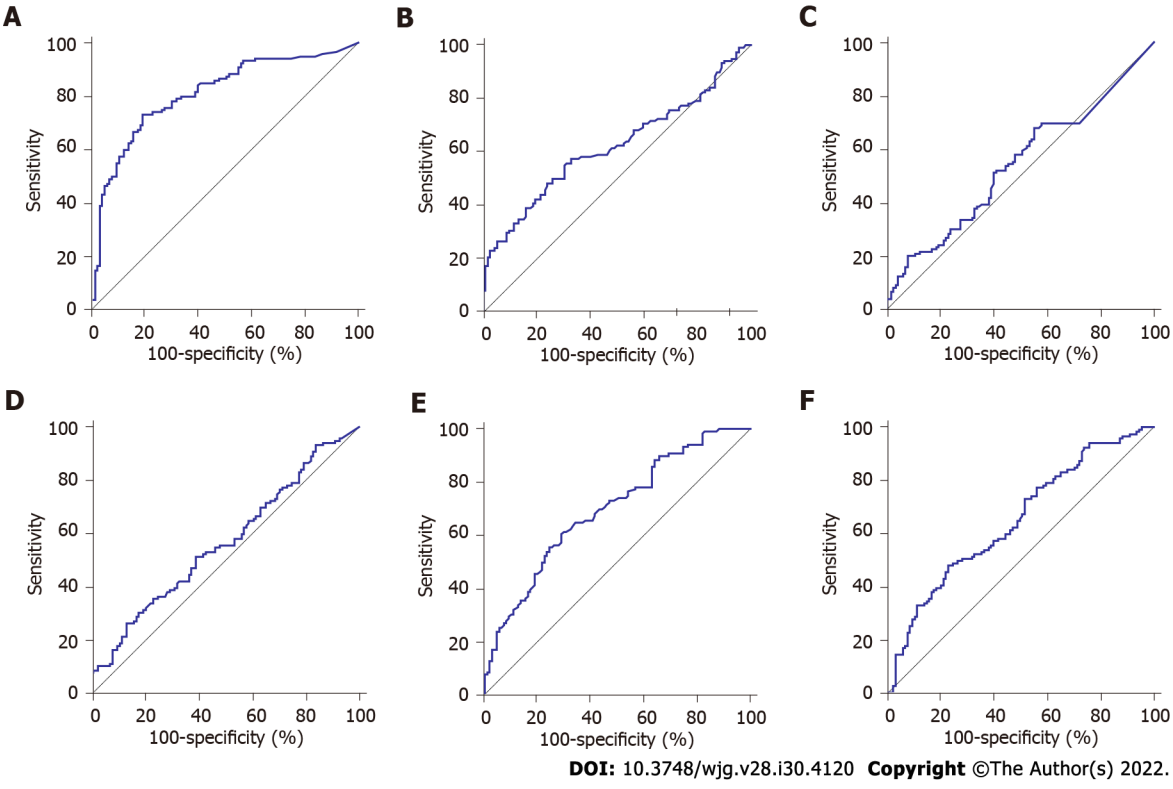
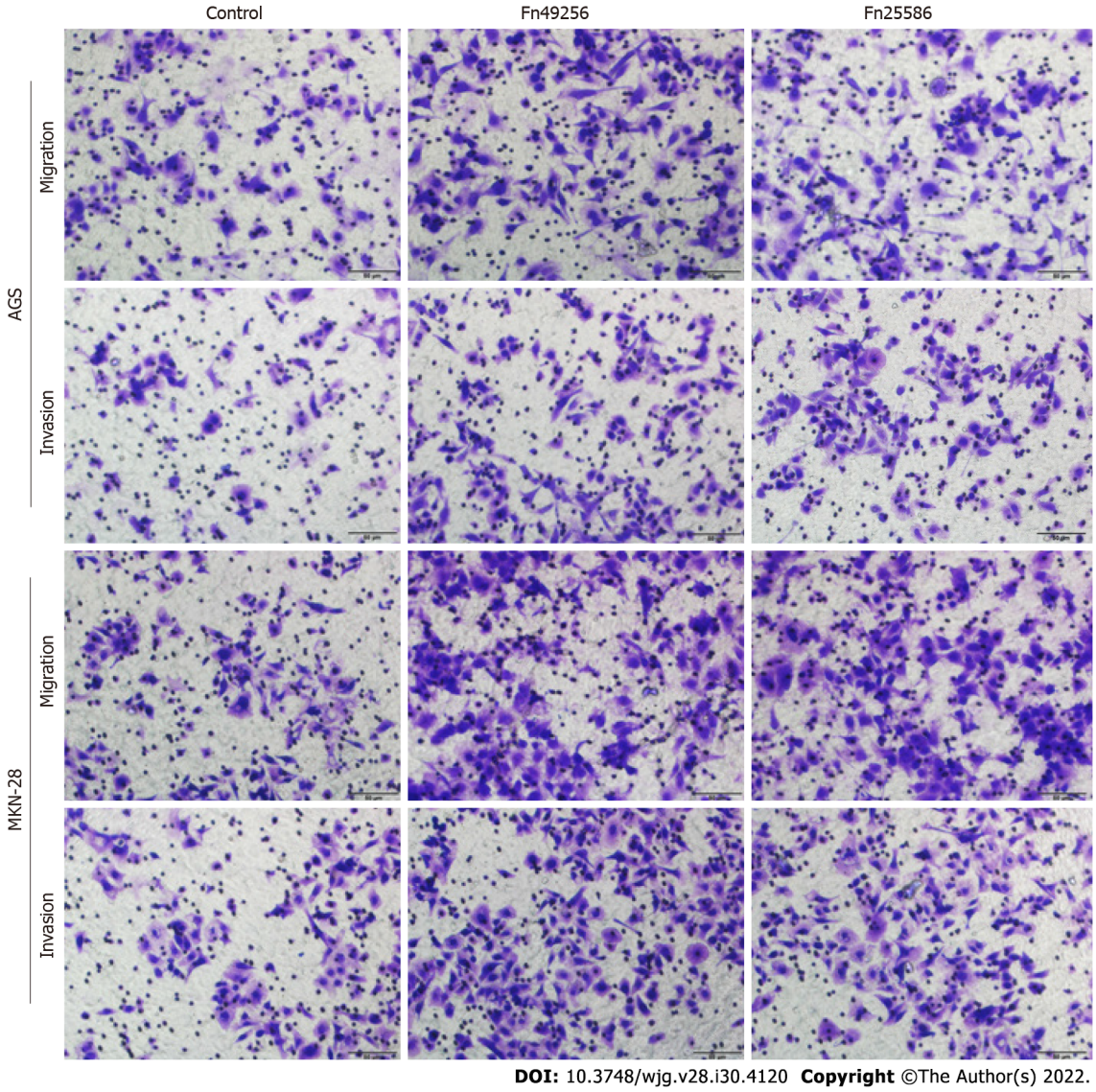


Figure 2 Diagnostic significance analysis of *Fusobacterium nucleatum* and traditional serum markers. Receiver operating characteristic curve analysis for the detection of gastric cancer. A: *Fusobacterium nucleatum*; B: Carcinoembryonic antigen; C: Carbohydrate antigen 72-4; D: Carbohydrate antigen 19-9; E: Ferritin; F: Sialic acid.

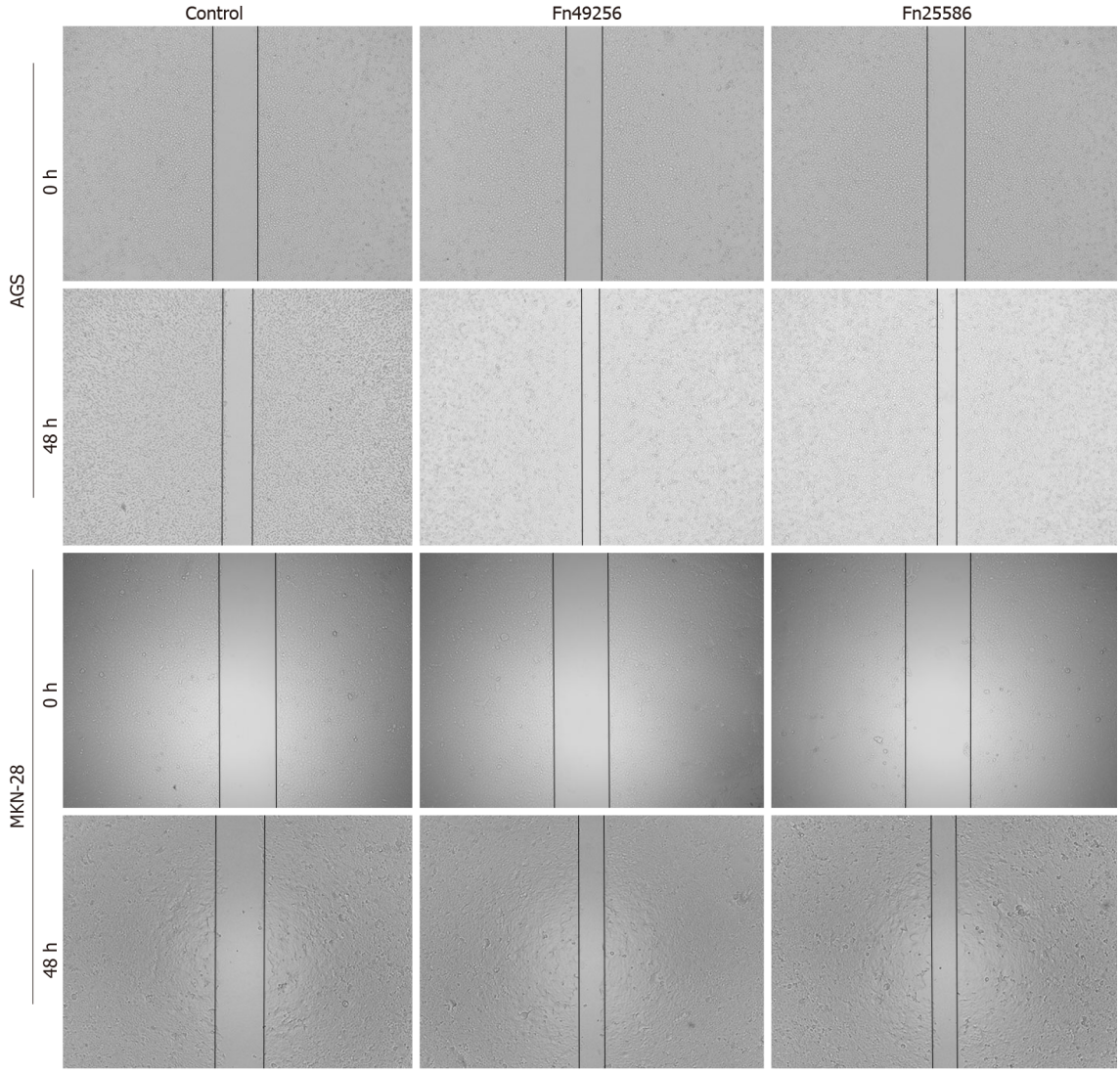
bacteria in the oral cavity, is detected significantly higher in the GC tissue compared with the para-cancerous tissue[19]. There is a microbial succession hypothesis to explain the decrease of *H. pylori* and elevation of the non-dominant flora in GC[18]. The hypothesis proposes that *H. pylori* can produce urease through the mucus layer, enhancing pH value to modify the microenvironment and triggering a strong inflammatory response. In such a process, gastric mucosal integrity is destroyed, and other secondary bacteria invade the mucus layer, causing more aggressive tumor occurrence. Therefore, Fn in the oral cavity can easily reach the stomach and colonize through the gastric mucosa barrier as the swallowing of saliva, forming an invasion focus. Thus, we think that Fn cooperates with *H. pylori* to promote GC development. Hsieh *et al*[20] have shown that Fn colonization leads to worse prognosis in GC patients with *H. pylori* positivity.



DOI: 10.3748/wjg.v28.i30.4120 **Copyright** ©The Author(s) 2022.

Figure 3 *Fusobacterium nucleatum* promotes the invasion of gastric cancer cells. Transwell assay of AGS and MKN-28 cells was performed 48 h after coculture with *Fusobacterium nucleatum*. The cells in the control group were treated with phosphate buffer solution. Fn: *Fusobacterium nucleatum*.

As a high-frequency periodontal pathogen, Fn has been confirmed to promote the initiation, proliferation, invasion, and chemoresistance of CRC in recent years. There are several suggested mechanisms, such as enhancing adhesion and evasion ability, modulating host immune evasion, and improving autophagy to cause chemoresistance[21-23]. It is worth noting that Fn is considered to play a more important role in promoting the formation of tumor, rather than its development[24]. Consistent with these findings, Fn has been confirmed to have key pathogenic characteristics, such as virulence factor FadA and characteristic adhesion protein Fap2[25-27]. In addition to promoting the occurrence and development of CRC, accumulating evidence has shown that Fn also plays an important role in promoting CRC metastasis[28,29]. In our present study, a high level of Fn was found in GC patients with lymph node metastasis. Although its impact in promoting tumor metastasis has been recognized, the role of Fn in such a process and its potential mechanism remain largely unclear. Chen *et al*[30] have detected Fn colonization in metastatic lung lesions of nude mice, and they further verified that Fn infection up-regulates KRT7 (type II cytokeratin, which plays a role in maintaining the structural integrity of the cells as well as promoting motile activities) to promote CRC metastasis. Besides, Chen *et al*[31] have identified that Fn activates autophagy to promote CRC metastasis. It is worth mentioning that EMT is the most well-validated method by which Fn promotes CRC metastasis, and it has been discovered that the effect is enhanced when the MOI is increased[32-34]. EMT is a classical pathway promoting metastasis. It is a special program that enables settled epithelial cells to gain the ability to migrate as single cells, which can enhance mobility, invasion, and resistance to apoptosis, conferring metastatic properties of cancer cells[35]. The examinations conducted in CRC both *in vivo* and *in vitro* have verified that Fn can promote the EMT process[28]. We supplemented the evidence that Fn promoted the EMT process in GC cells. Moreover, Fn infection significantly decreased the expression of



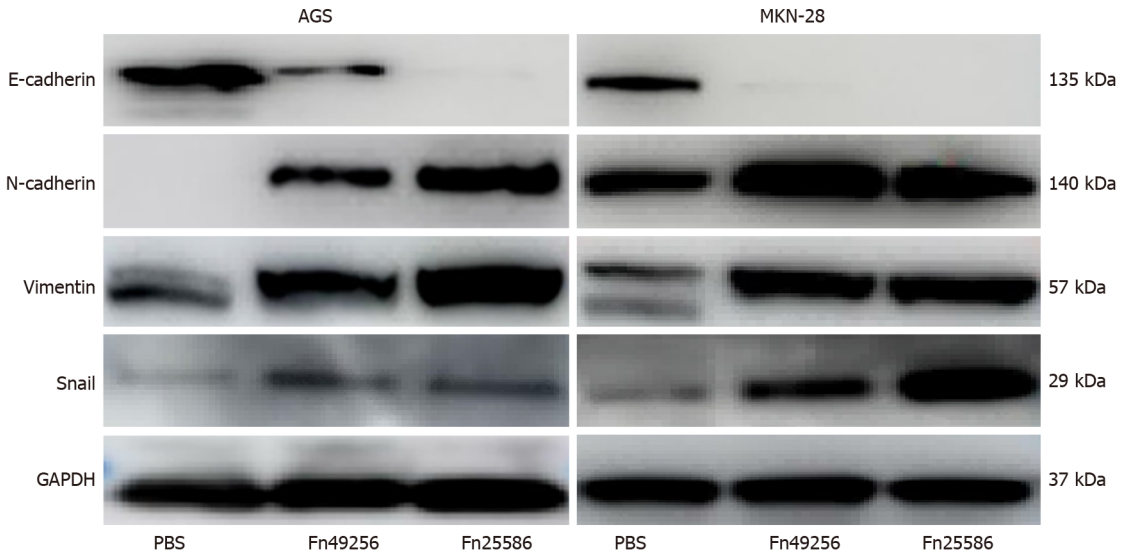
DOI: 10.3748/wjg.v28.i30.4120 **Copyright** ©The Author(s) 2022.

Figure 4 *Fusobacterium nucleatum* promotes the migration of gastric cancer cells. Wound-healing assay of AGS and MKN-28 cells was performed 48 h after coculture with *Fusobacterium nucleatum*. The cells in the control group were treated with phosphate buffer solution. Fn: *Fusobacterium nucleatum*.

cell adhesion molecules and increased the expression of mesenchymal phenotype-associated molecules, eventually resulting in GC metastasis. Taken together, we identified that Fn promoted GC metastasis by facilitating the EMT process.

Targeting Fn may reduce the progression of related cancers to ascertain the origin of Fn in cancers, and determining the route by which it reaches the tumor is of therapeutic significance. It has been found for a long time that part of Fn detected in CRC tissue is originated from the oral cavity, while how Fn in the oral cavity is transported to other body sites is also a hot topic. Initially, Fn strains with similar sequences were found in human primary CRC tissues and paired liver metastases, suggesting that these bacteria can migrate to distant sites with CRC cells[29]. Therefore, some scholars believe that Fn enters tumor tissue *via* blood circulation. The existing data have shown that Fn is detected at higher loads in GC tissue[19], and our data suggested that Fn abundance was increased in the saliva of GC patients. Could this indicate that Fn could directly enter the gastrointestinal tract, and then colonize epithelial cells? For Fn can produce a variety of adhesion factors as well as invasive factors, it is easy to adhere to the gastrointestinal mucosa, and form an inflammatory microenvironment, which is conducive to the formation of tumor. However, some evidence has also shown that Fn in the blood is more successful in CRC colonization than being gavaged, indicating that Fn the in blood (from a bleeding wound in the gum or some other way) plays a more important role in forming colonization than the ones in the digestive tract, even if there is a disadvantage in quantity[36]. Which type of Fn transmission is dominant in tumor formation (or the two work together) remains to be further studied.

There are also some limitations in our study. First, the small sample size caused by high cost led to selection bias. In follow-up studies, larger, multicenter studies are required to consolidate the findings. Second, the flora in the oral cavity is diverse. Whether other floras have an impact on the occurrence and development of GC, or whether they have interacted with Fn needs to be further explored.



DOI: 10.3748/wjg.v28.i30.4120 **Copyright** ©The Author(s) 2022.

Figure 5 *Fusobacterium nucleatum* enhances epithelial-mesenchymal transition of AGS and MKN-28 cells. Fn: *Fusobacterium nucleatum*; PBS: Phosphate buffer solution; GAPDH: Glyceraldehyde-3-phosphate dehydrogenase.

CONCLUSION

Collectively, Fn in saliva exhibits a good predictive ability and represents a promising diagnostic marker for GC. Given the tumorigenicity and metastasis-promoting properties of Fn, we suggest that the elimination of Fn could reduce the incidence of GC and improve the treatment outcomes, which is similar to triple or quadruple anti-*H. pylori* therapy.

ARTICLE HIGHLIGHTS

Research background

Gastric cancer (GC) is a common malignant tumor in the digestive tract. Although the 5-year survival rate of GC is enhanced with the combination of chemotherapy and surgery, its mortality remains high due to the diagnosis at an advanced stage. It is essential to develop a new method to diagnose GC at an early stage.

Research motivation

Fusobacterium nucleatum (Fn) primarily colonized in the oral cavity, has been detected in tissues of GC in recent years. We wondered whether there is a correlation between salivary Fn and GC.

Research objectives

The research purpose was to find a new simple and effective biomarker to diagnose GC.

Research methods

The abundance of Fn in saliva was quantified by droplet digital polymerase chain reaction in 120 GC patients, 31 atrophic gastritis (AG) patients, 35 non-AG (NAG) patients, 26 gastric polyp patients, and 20 normal controls (NC). The diagnostic value of Fn was evaluated and compared with traditional serum tumor markers, including carcinoembryonic antigen (CEA), carbohydrate antigen (CA)19-9, CA72-4, ferritin, and sialic acid. Transwell and wound-healing assays were conducted to assess the influence of Fn infection on GC cells. Western blot analysis was performed to detect the expression of epithelial-mesenchymal transition (EMT) markers.

Research results

Fn had favorable diagnostic value in classifying GC from NC and benign diseases, which was superior to those traditional serum tumor markers, such as CEA, CA19-9, CA72-4, ferritin, and sialic acid. Salivary Fn level was positively associated with the GC TNM stage and lymph node metastasis. Further, *in vitro* experiments revealed that Fn could promote the migration and invasion of GC cells. Western blot analysis indicated that Fn infection decreased the expression of epithelial marker such as E-cadherin, and increased the expression of mesenchymal markers such as N-cadherin, vimentin, and

snail.

Research conclusions

Fn in saliva could be used as a promising biomarker to diagnose GC, and Fn infection could promote GC metastasis by accelerating the EMT process.

Research perspectives

Human saliva is a unique bio-fluid resource with huge clinical diagnostic and risk assessment capacity. Salivary Fn has promising value for diagnosing GC.

FOOTNOTES

Author contributions: Chen WD and Zhang X contributed equally to this work; Chen WD performed the research; Zhang X contributed to conception and revised the manuscript; Zhang YP collected the samples; Chen WD, Zhang MJ, Zhang YP, Shang ZQ, and Xin YW performed the experiments together; Zhang Y managed and coordinated the research, and provided the financial support; and all authors approved the final version of the article.

Supported by the National Natural Science Foundation of China, No. 81972005 and 82172339; the Natural Science Foundation of Shandong Province, No. ZR2020MH238; and Shandong Medical and Health Technology Development Project, No. 2018WS327.

Institutional review board statement: The study was reviewed and approved by the Ethics Committee of the Qilu Hospital of Shandong University.

Informed consent statement: All study participants, or their legal guardian, provided informed written consent prior to study enrollment.

Conflict-of-interest statement: All the authors report no relevant conflicts of interest for this article.

Data sharing statement: No additional data are available.

Open-Access: This article is an open-access article that was selected by an in-house editor and fully peer-reviewed by external reviewers. It is distributed in accordance with the Creative Commons Attribution NonCommercial (CC BY-NC 4.0) license, which permits others to distribute, remix, adapt, build upon this work non-commercially, and license their derivative works on different terms, provided the original work is properly cited and the use is non-commercial. See: https://creativecommons.org/Licenses/by-nc/4.0/

Country/Territory of origin: China

ORCID number: Wen-Dan Chen 0000-0002-2679-3243; Xin Zhang 0000-0003-2138-5600; Meng-Jiao Zhang 0000-0002-1615-9089; Ya-Ping Zhang 0000-0003-2989-3298; Zi-Qi Shang 0000-0002-3141-2898; Yi-Wei Xin 0000-0003-2459-4205; Yi Zhang 0000-0002-0440-1798.

S-Editor: Wang JJ
L-Editor: Wang TQ
P-Editor: Wang JJ

REFERENCES

1 **Bray F**, Ferlay J, Soerjomataram I, Siegel RL, Torre LA, Jemal A. Global cancer statistics 2018: GLOBOCAN estimates of incidence and mortality worldwide for 36 cancers in 185 countries. *CA Cancer J Clin* 2018; **68**: 394-424 [PMID: 30207593 DOI: 10.3322/caac.21492]
2 **Aas JA**, Paster BJ, Stokes LN, Olsen I, Dewhirst FE. Defining the normal bacterial flora of the oral cavity. *J Clin Microbiol* 2005; **43**: 5721-5732 [PMID: 16272510 DOI: 10.1128/jcm.43.11.5721-5732.2005]
3 **Marshall BJ**, Warren JR. Unidentified curved bacilli in the stomach of patients with gastritis and peptic ulceration. *Lancet* 1984; **1**: 1311-1315 [PMID: 6145023 DOI: 10.1016/s0140-6736(84)91816-6]
4 **Alarcón T**, Llorca L, Perez-Perez G. Impact of the Microbiota and Gastric Disease Development by Helicobacter pylori. *Curr Top Microbiol Immunol* 2017; **400**: 253-275 [PMID: 28124157 DOI: 10.1007/978-3-319-50520-6_11]
5 **Rasiah IA**, Wong L, Anderson SA, Sissons CH. Variation in bacterial DGGE patterns from human saliva: over time, between individuals and in corresponding dental plaque microcosms. *Arch Oral Biol* 2005; **50**: 779-787 [PMID: 15970209 DOI: 10.1016/j.archoralbio.2005.02.001]
6 **Kabwe M**, Brown TL, Dashper S, Speirs L, Ku H, Petrovski S, Chan HT, Lock P, Tucci J. Genomic, morphological and functional characterisation of novel bacteriophage FNU1 capable of disrupting Fusobacterium nucleatum biofilms. *Sci Rep* 2019; **9**: 9107 [PMID: 31235721 DOI: 10.1038/s41598-019-45549-6]

7 **Habib AM**, Islam MS, Sohel M, Mazumder MH, Sikder MO, Shahik SM. Mining the Proteome of *Fusobacterium nucleatum* subsp. *nucleatum* ATCC 25586 for Potential Therapeutics Discovery: An *In Silico* Approach. *Genomics Inform* 2016; **14**: 255-264 [PMID: 28154519 DOI: 10.5808/GI.2016.14.4.255]

8 **Moore WE**, Moore LV. The bacteria of periodontal diseases. *Periodontol 2000* 1994; **5**: 66-77 [PMID: 9673163 DOI: 10.1111/j.1600-0757.1994.tb00019.x]

9 **Fragkioudakis I**, Riggio MP, Apatzidou DA. Understanding the microbial components of periodontal diseases and periodontal treatment-induced microbiological shifts. *J Med Microbiol* 2021; **70** [PMID: 33295858 DOI: 10.1099/jmm.0.001247]

10 **Nozawa A**, Oshima H, Togawa N, Nozaki T, Murakami S. Development of Oral Care Chip, a novel device for quantitative detection of the oral microbiota associated with periodontal disease. *PLoS One* 2020; **15**: e0229485 [PMID: 32109938 DOI: 10.1371/journal.pone.0229485]

11 **Baek K**, Ji S, Choi Y. Complex Intratissue Microbiota Forms Biofilms in Periodontal Lesions. *J Dent Res* 2018; **97**: 192-200 [PMID: 28945499 DOI: 10.1177/0022034517732754]

12 **Han YW**. Fusobacterium nucleatum: a commensal-turned pathogen. *Curr Opin Microbiol* 2015; **23**: 141-147 [PMID: 25576662 DOI: 10.1016/j.mib.2014.11.013]

13 **Han YW**, Fardini Y, Chen C, Iacampo KG, Peraino VA, Shamonki JM, Redline RW. Term stillbirth caused by oral Fusobacterium nucleatum. *Obstet Gynecol* 2010; **115**: 442-445 [PMID: 20093874 DOI: 10.1097/AOG.0b013e3181cb9955]

14 **Wang X**, Buhimschi CS, Temoin S, Bhandari V, Han YW, Buhimschi IA. Comparative microbial analysis of paired amniotic fluid and cord blood from pregnancies complicated by preterm birth and early-onset neonatal sepsis. *PLoS One* 2013; **8**: e56131 [PMID: 23437088 DOI: 10.1371/journal.pone.0056131]

15 **Sekiguchi M**, Matsuda T. Limited usefulness of serum carcinoembryonic antigen and carbohydrate antigen 19-9 levels for gastrointestinal and whole-body cancer screening. *Sci Rep* 2020; **10**: 18202 [PMID: 33097814 DOI: 10.1038/s41598-020-75319-8]

16 **Feng F**, Tian Y, Xu G, Liu Z, Liu S, Zheng G, Guo M, Lian X, Fan D, Zhang H. Diagnostic and prognostic value of CEA, CA19-9, AFP and CA125 for early gastric cancer. *BMC Cancer* 2017; **17**: 737 [PMID: 29121872 DOI: 10.1186/s12885-017-3738-y]

17 **Ianiro G**, Molina-Infante J, Gasbarrini A. Gastric Microbiota. *Helicobacter* 2015; **20** Suppl 1: 68-71 [PMID: 26372828 DOI: 10.1111/hel.12260]

18 **Hutton ML**, Kaparakis-Liaskos M, Turner L, Cardona A, Kwok T, Ferrero RL. Helicobacter pylori exploits cholesterol-rich microdomains for induction of NF-kappaB-dependent responses and peptidoglycan delivery in epithelial cells. *Infect Immun* 2010; **78**: 4523-4531 [PMID: 20713621 DOI: 10.1128/IAI.00439-10]

19 **Hsieh YY**, Tung SY, Pan HY, Yen CW, Xu HW, Lin YJ, Deng YF, Hsu WT, Wu CS, Li C. Increased Abundance of Clostridium and Fusobacterium in Gastric Microbiota of Patients with Gastric Cancer in Taiwan. *Sci Rep* 2018; **8**: 158 [PMID: 29317709 DOI: 10.1038/s41598-017-18596-0]

20 **Hsieh YY**, Tung SY, Pan HY, Chang TS, Wei KL, Chen WM, Deng YF, Lu CK, Lai YH, Wu CS, Li C. *Fusobacterium nucleatum* colonization is associated with decreased survival of *helicobacter pylori*-positive gastric cancer patients. *World J Gastroenterol* 2021; **27**: 7311-7323 [PMID: 34876791 DOI: 10.3748/wjg.v27.i42.7311]

21 **Yu T**, Guo F, Yu Y, Sun T, Ma D, Han J, Qian Y, Kryczek I, Sun D, Nagarsheth N, Chen Y, Chen H, Hong J, Zou W, Fang JY. Fusobacterium nucleatum Promotes Chemoresistance to Colorectal Cancer by Modulating Autophagy. *Cell* 2017; **170**: 548-563.e16 [PMID: 28753429 DOI: 10.1016/j.cell.2017.07.008]

22 **Zhang S**, Yang Y, Weng W, Guo B, Cai G, Ma Y, Cai S. Fusobacterium nucleatum promotes chemoresistance to 5-fluorouracil by upregulation of BIRC3 expression in colorectal cancer. *J Exp Clin Cancer Res* 2019; **38**: 14 [PMID: 30630498 DOI: 10.1186/s13046-018-0985-y]

23 **Dong G**, Wang M, Gu G, Li S, Sun X, Li Z, Cai H, Zhu Z. MACC1 and HGF are associated with survival in patients with gastric cancer. *Oncol Lett* 2018; **15**: 3207-3213 [PMID: 29435059 DOI: 10.3892/ol.2017.7710]

24 **Shang FM**, Liu HL. *Fusobacterium nucleatum* and colorectal cancer: A review. *World J Gastrointest Oncol* 2018; **10**: 71-81 [PMID: 29564037 DOI: 10.4251/wjgo.v10.i3.71]

25 **Rubinstein MR**, Wang X, Liu W, Hao Y, Cai G, Han YW. Fusobacterium nucleatum promotes colorectal carcinogenesis by modulating E-cadherin/β-catenin signaling *via* its FadA adhesin. *Cell Host Microbe* 2013; **14**: 195-206 [PMID: 23954158 DOI: 10.1016/j.chom.2013.07.012]

26 **Fardini Y**, Wang X, Témoin S, Nithianantham S, Lee D, Shoham M, Han YW. Fusobacterium nucleatum adhesin FadA binds vascular endothelial cadherin and alters endothelial integrity. *Mol Microbiol* 2011; **82**: 1468-1480 [PMID: 22040113 DOI: 10.1111/j.1365-2958.2011.07905.x]

27 **Gur C**, Ibrahim Y, Isaacson B, Yamin R, Abed J, Gamliel M, Enk J, Bar-On Y, Stanietsky-Kaynan N, Coppenhagen-Glazer S, Shussman N, Almogy G, Cuapio A, Hofer E, Mevorach D, Tabib A, Ortenberg R, Markel G, Miklić K, Jonjic S, Brennan CA, Garrett WS, Bachrach G, Mandelboim O. Binding of the Fap2 protein of Fusobacterium nucleatum to human inhibitory receptor TIGIT protects tumors from immune cell attack. *Immunity* 2015; **42**: 344-355 [PMID: 25680274 DOI: 10.1016/j.immuni.2015.01.010]

28 **Yan X**, Liu L, Li H, Qin H, Sun Z. Clinical significance of *Fusobacterium nucleatum*, epithelial-mesenchymal transition, and cancer stem cell markers in stage III/IV colorectal cancer patients. *Onco Targets Ther* 2017; **10**: 5031-5046 [PMID: 29081665 DOI: 10.2147/OTT.S145949]

29 **Bullman S**, Pedamallu CS, Sicinska E, Clancy TE, Zhang X, Cai D, Neuberg D, Huang K, Guevara F, Nelson T, Chipashvili O, Hagan T, Walker M, Ramachandran A, Diosdado B, Serna G, Mulet N, Landolfi S, Ramon Y Cajal S, Fasani R, Aguirre AJ, Ng K, Élez E, Ogino S, Tabernero J, Fuchs CS, Hahn WC, Nuciforo P, Meyerson M. Analysis of *Fusobacterium* persistence and antibiotic response in colorectal cancer. *Science* 2017; **358**: 1443-1448 [PMID: 29170280 DOI: 10.1126/science.aal5240]

30 **Chen S**, Su T, Zhang Y, Lee A, He J, Ge Q, Wang L, Si J, Zhuo W. *Fusobacterium nucleatum* promotes colorectal cancer metastasis by modulating *KRT7-AS*/KRT7. *Gut Microbes* 2020; **11**: 511-525 [PMID: 31910722 DOI: 10.1080/19490976.2019.1695494]

31 **Chen Y**, Chen Y, Zhang J, Cao P, Su W, Deng Y, Zhan N, Fu X, Huang Y, Dong W. *Fusobacterium nucleatum* Promotes Metastasis in Colorectal Cancer by Activating Autophagy Signaling *via* the Upregulation of CARD3 Expression. *Theranostics* 2020; **10**: 323-339 [PMID: 31903123 DOI: 10.7150/thno.38870]

32 **Wang Q**, Yu C, Yue C, Liu X. Fusobacterium nucleatum produces cancer stem cell characteristics *via* EMT-resembling variations. *Int J Clin Exp Pathol* 2020; **13**: 1819-1828 [PMID: 32782710]

33 **Yu MR**, Kim HJ, Park HR. *Fusobacterium nucleatum* Accelerates the Progression of Colitis-Associated Colorectal Cancer by Promoting EMT. *Cancers (Basel)* 2020; **12** [PMID: 32977534 DOI: 10.3390/cancers12102728]

34 **Duan C**, Tang X, Wang W, Qian W, Fu X, Deng X, Han C, Hou X. L-fucose ameliorates the carcinogenic properties of *Fusobacterium nucleatum* in colorectal cancer. *Oncol Lett* 2021; **21**: 143 [PMID: 33552262 DOI: 10.3892/ol.2020.12404]

35 **Yeung KT**, Yang J. Epithelial-mesenchymal transition in tumor metastasis. *Mol Oncol* 2017; **11**: 28-39 [PMID: 28085222 DOI: 10.1002/1878-0261.12017]

36 **Abed J**, Maalouf N, Manson AL, Earl AM, Parhi L, Emgård JEM, Klutstein M, Tayeb S, Almogy G, Atlan KA, Chaushu S, Israeli E, Mandelboim O, Garrett WS, Bachrach G. Colon Cancer-Associated *Fusobacterium nucleatum* May Originate From the Oral Cavity and Reach Colon Tumors *via* the Circulatory System. *Front Cell Infect Microbiol* 2020; **10**: 400 [PMID: 32850497 DOI: 10.3389/fcimb.2020.00400]

World Journal of Gastroenterology

Submit a Manuscript: https://www.f6publishing.com

World J Gastroenterol 2022 August 14; 28(30): 4133-4151

DOI: 10.3748/wjg.v28.i30.4133

ISSN 1007-9327 (print) ISSN 2219-2840 (online)

ORIGINAL ARTICLE

Retrospective Study

Development and validation of a nomogram for predicting overall survival in cirrhotic patients with acute kidney injury

Yi-Peng Wan, An-Jiang Wang, Wang Zhang, Hang Zhang, Gen-Hua Peng, Xuan Zhu

Specialty type: Gastroenterology and hepatology

Provenance and peer review: Unsolicited article; Externally peer reviewed.

Peer-review model: Single blind

Peer-review report's scientific quality classification

Grade A (Excellent): 0
Grade B (Very good): B
Grade C (Good): C, C, C, C, C, C
Grade D (Fair): D
Grade E (Poor): 0

P-Reviewer: Chen C, China; Feng J, China; Ferrarese A, Italy; Koller T, Slovakia; Kreisel W, Germany

Received: February 7, 2022
Peer-review started: February 7, 2022
First decision: April 10, 2022
Revised: April 29, 2022
Accepted: July 22, 2022
Article in press: July 22, 2022
Published online: August 14, 2022

Yi-Peng Wan, An-Jiang Wang, Wang Zhang, Hang Zhang, Gen-Hua Peng, Xuan Zhu, Department of Gastroenterology and Hepatology, The First Affiliated Hospital of Nanchang University, Nanchang 331706, Jiangxi Province, China

Xuan Zhu, Biomolecular Research Laboratory, Jiangxi Clinical Research Center for Gastroenterology, Nanchang 331706, Jiangxi Province, China

Corresponding author: Xuan Zhu, MD, Chief Doctor, Department of Gastroenterology and Hepatology, The First Affiliated Hospital of Nanchang University, No. 17 Yongwaizheng Street, Nanchang 331706, Jiangxi Province, China. waiyongtg@163.com

Abstract

BACKGROUND

Acute kidney injury (AKI) is a common and severe complication in patients with cirrhosis, and is associated with poor prognosis. Therefore, identifying cirrhotic patients with AKI who are at high risk of mortality is very important and may be helpful for providing timely medical interventions to improve the prognosis of these patients. However, studies focused on investigating the risk factors for the mortality of cirrhotic patients with AKI were scarce.

AIM

To identify risk factors for mortality and establish a nomogram for predicting the prognosis of these patients.

METHODS

Two hundred fifty consecutive patients with cirrhosis and AKI were recruited and randomly divided into training cohort (n = 173) and validation cohort (n = 77). In the training cohort, potential risk factors for death were identified by performing a Cox regression analysis, and a nomogram was established. The predictive performance of the nomogram was internally and externally validated by calculating the area under the receiver operating characteristic curve (AUROC), constructing a calibration curve and performing decision curve analysis.

RESULTS

The serum sodium level, international normalized ratio, peak serum creatinine level > 1.5 mg/dL, the presence of hepatic encephalopathy and diabetes were potential risk factors for mortality of cirrhotic patients with AKI in the training dataset. A prognostic nomogram incorporating these variables was established for

predicting the overall survival of these patients. Compared with Child-Turcotte-Pugh, the model for end-stage liver disease (MELD) and the MELD-Na scores, the nomogram in predicting 90- and 180-d mortality exhibited better discriminatory power with AUROCs of 0.792 and 0.801 for the training dataset and 0.817 and 0.862 for the validation dataset, respectively. With a nomogram score of 98, patients were divided into low- and high-risk groups, and high-risk patients had a higher mortality rate.

CONCLUSION

A prognostic nomogram displayed good performance for predicting the overall survival of cirrhotic patients with AKI, and will assist clinicians in evaluating the prognosis of these patients.

Key Words: Acute kidney injury; Cirrhosis; Nomogram; Prognosis

©The Author(s) 2022. Published by Baishideng Publishing Group Inc. All rights reserved.

Core Tip: We investigated the potential risk factors for death in cirrhotic patients with acute kidney injury (AKI). A nomogram incorporating these risk factors was developed and evaluated by calculating the area under the receiver operating characteristic curve, constructing a calibration curve and performing decision curve analysis. Compared with Child-Turcotte-Pugh, the model for end-stage liver disease (MELD) and MELD-Na score, the nomogram has a better discriminative ability in predicting the overall survival of cirrhotic patients with AKI. Moreover, the nomogram was used to select patients with a high risk of death and assist clinicians in making clinical decisions.

Citation: Wan YP, Wang AJ, Zhang W, Zhang H, Peng GH, Zhu X. Development and validation of a nomogram for predicting overall survival in cirrhotic patients with acute kidney injury. *World J Gastroenterol* 2022; 28(30): 4133-4151

URL: https://www.wjgnet.com/1007-9327/full/v28/i30/4133.htm

DOI: https://dx.doi.org/10.3748/wjg.v28.i30.4133

INTRODUCTION

Acute kidney injury (AKI) is a common and severe complication occurring in patients with cirrhosis, manifesting as an abrupt increase in serum creatinine (SCr) levels and an acute significant reduction in urine output (UO) in a short period[1,2]. Many diagnostic criteria and classifications of AKI have been developed to identify AKI and improve prognosis over the last two decades, such as the Risk, Injury, Failure, Loss of kidney function, and End-stage kidney disease (RIFLE) classification in 2004[3], the Acute Kidney Injury Network (AKIN) classification in 2007[4], and the Kidney Disease: Improving Global Outcomes (KDIGO) classification in 2012[5]. However, the concept of AKI in patients with cirrhosis was debated for many years until the International Club of Ascites (ICA) proposed a new classification of AKI in 2015[1]. These classifications are based on SCr levels and/or UO. One of the main differences between the ICA classification and other classifications is the abandonment of the UO criteria[1]. Although these criteria have been established, a single criterion that comprehensively evaluates and diagnoses AKI is still unavailable.

The incidence and mortality of AKI in patients with cirrhosis varies substantially among studies[2,6,7]. In some studies, the incidence of AKI ranges from 20%-50% in patients with cirrhosis[2,8]. Moreover, studies have reported that the mortality rate of AKI was also unacceptably high in patients with cirrhosis, reaching up to 80%[6,9]. Therefore, identifying cirrhotic patients with AKI who are at high risk of mortality is very important and may be helpful for providing timely medical interventions to improve the prognosis of these patients. Currently, many studies have investigated risk factors for mortality in patients with cirrhosis[10] and other complications, such as gastroesophageal variceal bleeding[11,12], ascites[13], bacterial infections[14] and metabolic acidosis[15]. Moreover, a number of studies have focused on identifying the risk factors for the development of AKI in patients with cirrhosis[16-19] and other conditions[20-22]. Furthermore, numerous studies have also evaluated the effect of AKI on the mortality of patients with cirrhosis[16,23-25]. A systematic review reported that the risk of death from AKI was increased more than 6-fold in patients with cirrhosis[24]. However, few studies have focused on analyzing the risk factors for mortality in patients with cirrhosis who are diagnosed with AKI. Additionally, based on clinician demand, a quantitative predictive model for determining the prognosis of cirrhotic patients with AKI also must be developed to predict the risk of mortality and distinguish patients with a high risk of mortality.

Therefore, the purpose of the present study was to investigate the risk factors for mortality of cirrhotic patients with AKI and establish a nomogram for predicting the overall survival of these patients to identify high-risk patients and guide timely treatments to improve the prognosis of these patients.

MATERIALS AND METHODS

Patients

We conducted a retrospective study at the Department of Gastroenterology and Hepatology and the Department of Infectious Diseases, The First Affiliated Hospital of Nanchang University, a tertiary care referral hospital in China, between January 2015 and December 2016. The inclusion criteria were as follows: (1) Patients who were diagnosed with cirrhosis; and (2) Patients who met the criteria for at least one of the RIFLE, AKIN, KDIGO and ICA classifications. These patients were hospitalized. The exclusion criteria were as follows: (1) Patients aged less than 18 and more than 80 years; (2) Patients with a previously history renal dysfunction or chronic kidney disease; (3) Patients who underwent liver or renal transplantation; (4) Patients who received renal replacement therapy (including hemodialysis and peritoneal dialysis) before admission; (5) Patients with malignancy or severe cardiopulmonary disease; (6) Patients who were discharged or died < 48 h after admission; (7) Pregnant patients; and (8) Patients without complete data.

According to the inclusion and exclusion criteria, 382 consecutive patients with cirrhosis who were diagnosed with AKI were screened, and 250 eligible patients were recruited and randomly divided into the training cohort (n = 173) and the validation cohort (n = 77) using the built-in random packet function of SPSS 23.0 software according at a ratio of 1:2. The flow chart for inclusion and exclusion is shown in Figure 1.

The study was approved by the Ethics Committee of The First Affiliated Hospital of Nanchang University (No. AF-SG-04-2.0).

Data collection

Demographics and clinical variables, namely, demographic data (age, sex and body weight), mean arterial pressure (MAP), underlying liver disease, cirrhosis-related complications, diabetes, biochemical analysis (routine blood tests, serum biochemical tests, coagulation function tests, *etc*.), days of the hospital stay, and comorbidities were recorded and collected from every cirrhotic patient with AKI. UO was recorded for all patients during hospitalization. The Child-Turcotte-Pugh (CTP), model for end-stage liver disease (MELD) and MELD-Na scores at admission were calculated accordingly.

Definitions

Cirrhosis was diagnosed based on the medical history, physical signs and symptoms, endoscopic signs of portal hypertension, radiological evidence of liver nodularity, and liver biopsy[26].

According to the consensus of the Asian Pacific Association for the Study of the Liver[27], acute-on-chronic liver failure (ACLF) was defined as acute hepatic insult manifesting as jaundice and coagulopathy complicated within 4 wk by ascites and/or encephalopathy in patients with previously diagnosed or undiagnosed chronic liver disease associated with high mortality.

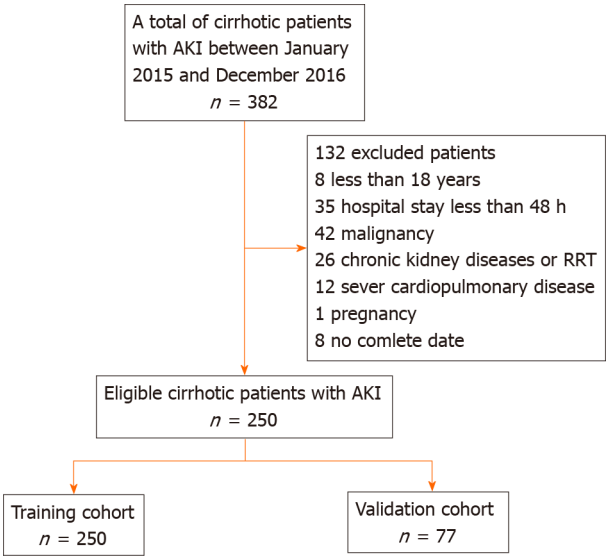
AKI was defined and classified using the RIFLE, AKIN, KDIGO or ICA classifications (Supplementary Table 1). The peak AKI stage based on the SCr level or UO criterion during hospitalization was used. For the RIFLE, KDIGO and ICA classifications, the last SCr level recorded within the previous 3 mo before admission was used as the baseline SCr level, but the SCr level at admission was used as the baseline SCr level for patients without a previous SCr measurement[1]. The SCr level at admission was also considered the baseline SCr level for the AKIN classification. The glomerular filtration rate (GFR) was used for the RIFLE classification, and the eGFR was calculated using the revised Schwartz method[28]. UO was used in the RIFLE, AKIN and KDIGO classifications.

Calculations of the CTP, MELD and MELD-Na scores

The CTP score was calculated as described in previous reports and classified as grade A (5-6 points), grade B (7-9 points), and grade C (10-15 points)[29]. The computed formula for the MELD score was 3.8 × ln (bilirubin, mg/dL) + 11.2 × ln (international normalized ratio) + 9.6 × ln (creatinine, mg/dL) + 6.4 (constant for liver disease etiology)[30,31]. The computed formula for the MELD-Na score was MELD + 1.59 × [135 – (Na, mmol/L)], and sodium ion concentrations ranged from 125 to 140 mmol/L[32].

Management of patients

A comprehensive medical intervention was administered to every patient, including supportive therapy, prevention and treatment of complications, and reduction or withdrawal of all unnecessary nephrotoxic medications. Patients also received albumin, vasoconstrictors (norepinephrine and terlipressin), intravenous antibiotics, diuretics, proton pump inhibitors or continuous renal replacement



DOI: 10.3748/wjg.v28.i30.4133 **Copyright** ©The Author(s) 2022.

Figure 1 Flow chart of patient inclusion and exclusion. AKI: Acute kidney injury; RRT: Renal replacement therapy.

therapy if required. Twenty-six patients (10.4%) received continuous replacement therapy.

Follow-up and outcomes

After the diagnosis of AKI, regular follow-up was performed for all cirrhotic patients with AKI by telephone and electronic medical records. Patients were followed for a maximum of 180 d or until death, liver or renal transplantation, or the end of the study period. Follow-up data on the prognosis were collected and evaluated. The primary endpoint of the study was the mortality rate.

Statistical analysis

All continuous variables were tested for a normal distribution using the Kolmogorov–Smirnov test. Variables that met the normal distribution are presented as the mean ± SD and were analyzed using Student's *t* test, while nonnormally distributed variables are summarized as medians and interquartile ranges and were analyzed using the Mann–Whitney *U* test. Categorical variables are presented as numbers and percentages and were analyzed using the χ^2 test or Fisher's exact test. Cumulative survival was evaluated using the Kaplan–Meier method and compared between groups using the log-rank test. The univariate analysis of risk factors of death in cirrhotic patients with AKI was performed using Cox regression analysis, and multivariate Cox analysis with the forward Wald method was subsequently performed for all variables with *P* values less than 0.2.

A nomogram was developed based on the weighted sum of each independent variable, with weights equal to the hazard ratios from the multivariate Cox model to predict the prognosis of cirrhotic patients with AKI. The area under the receiver operating characteristic curve (AUROC), calibration curve and decision curve analysis (DCA) were used to evaluate its predictive performance. All tests were two-tailed, and *P* values less than 0.05 were considered indicative of statistical significance. Data were analyzed using SPSS software, version 23.0 (SPSS Inc., Chicago, IL, Untied States) and R software, version 3.5.3.

RESULTS

Baseline characteristics of the study patients

The characteristics of the patients in the training and validation cohorts are summarized in Table 1. Among the 250 patients, the mean age was 53.6 ± 13.3 years, and most of the patients were male (190/250, 76.0%). Notably, 25.6% (64/250) of the patients presented AKI at the time of admission, and 74.4% (186/250) developed AKI during hospital stay. Only 7 (2.8%) of these patients had compensated cirrhosis, and 243 (97.2%) patients had decompensated cirrhosis. The main etiology of these patients in both datasets was hepatitis B, accounting for 69.6% (174/250) of the entire cohort. Most of the patients (239/250, 95.6%) had ascites, and 60.8% (152/250) of the patients had ACLF. The main causes of AKI were hypovolemia (136/250, 54.4%), followed by infections (54/250, 21.6%), nephrotoxicity (21/250, 8.4%) and other factors (39/250, 15.6%). In the comparison of the training cohort and validation cohort, although the MAP, albumin level and serum sodium level were significantly different (all $P < 0.05$), a significant difference in mortality was not observed between the training (75.1%) and validation (79.2%)

Table 1 Demographic and baseline clinical characteristics of cirrhotic patients with acute kidney injury

Variables	Total (*n* = 250)	Training cohort (*n* = 173)	Validation cohort (*n* = 77)	*P* value
Age (yr), mean ± SD	53.6 ± 13.3	53.3 ± 13.1	54.4 ± 13.7	0.554
Male, *n* (%)	190 (76.0)	127 (73.4)	63 (81.8)	0.199
Heart rates > 100 bpm, *n* (%)	58 (23.2)	36 (20.8)	22 (28.6)	0.120
MAP (mmHg), mean ± SD	87.8 ± 13.9	89.2 ± 13.7	84.5 ± 13.9	0.013
Duration of hospitalization (d), median (IQR)	16.0 (8.0-28.0)	16.0 (9.0-33.5)	16 (8.0-23.5)	0.180
Etiology of cirrhosis				> 0.05
Hepatitis B, *n* (%)	174 (69.6)	124 (71.7)	50 (64.9)	
Alcoholic liver disease, *n* (%)	16 (6.4)	9 (5.2)	7 (9.1)	
Hepatitis B and alcoholic, *n* (%)	20 (8.0)	14 (8.1)	6 (7.8)	
Other, *n* (%)	40 (16.0)	24 (13.9)	14 (18.2)	
Diabetes, *n* (%)	25 (10.0)	17 (9.8)	8 (10.4)	0.527
Ascites, *n* (%)	239 (95.6)	168 (97.1)	71 (92.2)	0.083
Infections, *n* (%)	62 (24.8)	42 (24.3)	20 (25.9)	0.445
HE, *n* (%)	93 (37.2)	68 (39.3)	25 (32.5)	0.187
ACLF, *n* (%)	152 (60.8)	111 (64.2)	41 (53.2)	0.068
Previous esophagogastric variceal bleeding, *n* (%)	57 (22.8)	40 (23.1)	17 (22.1)	0.497
UO (mL/kg/h), mean ± SD	0.61 ± 0.39	0.53 ± 0.38	0.61 ± 0.41	0.130
WBC count (10^9/L), mean ± SD	8.3 ± 6.2	8.0 ± 5.1	8.1 ± 6.8	0.853
Platelet count (10^9/L), median (IQR)	75.5 (48.0-123.7)	73.0 (47.5-124.0)	77.0 (48.0-124.5)	0.623
Albumin (g/L), mean ± SD	28.6 ± 5.4	29.1 ± 5.3	27.5 ± 5.4	0.029
Total bilirubin (mg/dL), mean ± SD	14.6 ± 10.8	15.4 ± 10.8	12.6 ± 10.7	0.060
AST (U/L), median (IQR)	127.5 (63.7-280.7)	130 (65.5-262.5)	118.0 (56.5-304.0)	0.842
ALT (U/L), median (IQR)	76.0 (32.7-203.5)	76.0 (37.0-206.0)	76.0 (30.0-204.0)	0.904
INR, mean ± SD	2.0 ± 0.8	2.0 ± 0.7	2.1 ± 0.9	0.361
Serum sodium (mmol/L), mean ± SD	132.9 ± 5.7	132.3 ± 6.2	133.9 ± 4.8	0.024
Admission SCr (mg/dL), (IQR)	1.17 (0.8-1.8)	1.17 (0.80-1.75)	1.26 (0.77-1.79)	0.897
Peak SCr > 1.5 mg/dL during hospitalization, *n* (%)	211 (84.4)	148 (85.5)	63 (81.8)	0.283
HDL (mmol/L), mean ± SD	0.34 ± 0.33	0.36 ± 0.33	0.37 ± 0.31	0.857
LDL (mmol/L), mean ± SD	1.2 ± 1.0	1.2 ± 0.9	1.1 ± 1.1	0.783
CTP score, mean ± SD	10.6 ± 1.8	10.7 ± 1.8	10.4 ± 1.9	0.396
MELD, mean ± SD	23.6 ± 8.8	24.0 ± 8.2	22.7 ± 9.9	0.304
MELD-Na, mean ± SD	29.0 ± 13.0	30.1 ± 12.7	26.5 ± 13.3	0.044
Mortality within 180 d, *n* (%)	191.0 (76.4)	130 (75.1)	61 (79.2)	0.298
Period of follow up (d), median (IQR)	35.0 (17.0-143.0)	38.0 (18.0-151.0)	32.0 (15.0-119.0)	0.512

MAP: Mean arterial pressure; IQR: Interquartile range; bpm: Beat per minute; SCr: Serum creatinine; HE: Hepatic encephalopathy; INR: International normalized ratio; ACLF: Acute on chronic liver failure; WBC: White blood cell; UO: Urine output; HDL: High-density lipoprotein; LDL: Low-density lipoprotein; CTP: Child-Turcotte-Pugh; MELD: The model for end-stage liver disease; AST: Aspartate aminotransferase; ALT: Alanine aminotransferase.

datasets (P = 0.298). Based on RIFLE, AKIN, KDIGO and ICA classifications, 234, 221, 241 and 211 of all 250 patients were diagnosed with AKI, respectively. No patients who underwent liver transplantation.

Mortality of cirrhotic patients with AKI

The median period of follow-up for all 250 patients after the diagnosis of AKI was 35.0 (17.0-143.0) d. The overall 30-d mortality, 90-d mortality and 180-d mortality rates were 46.4% (116/250), 68.8% (172/250) and 76.4% (191/250), respectively. Among these patients who died, the most common cause of mortality was hepatic failure (74/191, 38.7%), followed by infections (41/191, 21.5%), renal failure (34/191, 17.8%), variceal bleeding (24/191, 12.6%), and other causes (19/191, 9.9%). The median follow-up periods in the training and validation cohorts were 38.0 (18.0-151.0) and 32.0 (15.0-119.0) d, respectively. The mortality rates of the training cohort were 45.1%, 68.2% and 75.1% at 30 d, 90 d and 180 d, respectively. The mortality rates at 30 d, 90 d and 180 d were 49.4%, 70.1% and 79.2% in the validation cohort, respectively. No significant difference in mortality was observed during follow-up in either dataset (P = 0.511; Figure 2).

Potential risk factors for mortality in the training cohort

During the follow-up period, 130 cirrhotic patients with AKI in the training cohort died. We performed a Cox regression analysis to identify risk factors of death from cirrhotic patients with AKI (Table 2). The univariate Cox regression analysis showed that a heart rate > 100 bpm, UO, presence of diabetes, total bilirubin level, international normalized ratio (INR), serum sodium level, high-density lipoprotein level, admission SCr level, peak SCr level > 1.5 mg/dL, overt hepatic encephalopathy (HE) or ACLF, and CTP, MELD and MELD-Na scores were potential risk factors of mortality. Multicollinearity between CTP, MELD and MELD-Na scores and other predictors was avoided by excluding these predictive models from the multivariate analysis. Subsequently, the multivariate Cox regression analysis revealed that the presence of diabetes [Hazard ratio (HR) = 1.795; 95% confidence interval (CI): 1.048-3.076; P = 0.001], HE (HR = 1.986; 95%CI: 1.381-2.856; P < 0.001), INR (HR = 1.390; 95%CI: 1.081-1.787; P = 0.010), serum sodium level (HR = 0.964; 95%CI: 0.937-0.992; P = 0.011) and peak SCr level > 1.5 mg/dL (HR = 2.026; 95%CI: 1.109-3.702; P = 0.022) were potential risk factors for mortality in cirrhotic patients with AKI.

Establishment of a prediction nomogram in the training cohort

A nomogram incorporating these potential risk factors recorded after the diagnosis of AKI during hospitalization was constructed to predict the probability of death within 180 d for cirrhotic patients with AKI (Figure 3). Each predictor had a number with weights equal to the HR of the multivariate Cox regression model, and the estimated probability of death for cirrhotic patients with AKI was calculated by adding the scores of each predictor.

Validation of the prediction nomogram

In the training cohort, the AUROC of the nomogram in predicting mortality at 30, 90 and 180 d were 0.757 (95%CI: 0.685-0.830), 0.792 (95%CI: 0.726-0.859) and 0.801 (95%CI: 0.726-0.870), respectively, which exhibited good discrimination for the prognosis of cirrhotic patients with AKI (Figure 4A). The calibration plots of 30-, 90- and 180-d survival showed satisfactory agreement between the predicted prognosis and actual prognosis probability in the training cohort (Figure 4B-D). In the validation cohort, the nomogram also displayed good discrimination with AUROCs of 0.763 (95%CI: 0.656-0.869), 0.817 (95%CI: 0.716-0.917) and 0.862 (95%CI: 0.765-0.958) in predicting mortality at 30, 90 and 180 d, respectively (Figure 5A). The calibration plots also showed good agreement between the predicted and actual prognosis probabilities in the validation cohort (Figure 5B-D). Based on the results, the nomogram had good discrimination and calibration in predicting the prognosis of cirrhotic patients with AKI.

Performance of the nomogram in predicting mortality

We compared the performance of the nomogram with CTP, MELD and MELD-Na scores in predicting the overall survival of cirrhotic patients with AKI, and the results are shown in Table 3. There were no significant differences between the nomogram and the CTP, MELD and MELD-Na scores in predicting 30-d mortality for either the training or validation cohort (all P > 0.05; Figure 6A and B). However, the AUROC of the nomogram in predicting mortality at 90 d was significantly higher than that of the CTP, MELD and MELD-Na scores in both the training and validation cohort (all P < 0.05; Figure 6C and D). Moreover, the AUROC of the nomogram in predicting mortality at 180 d was also larger than that of the CTP, MELD and MELD-Na scores in both the training and validation cohort (all P < 0.05; Figure 6E and F). With regard to clinical usefulness, DCA of the nomogram was depicted and compared with the CTP, MELD and MELD-Na scores. Compared with the CTP, MELD and MELD-Na scores, medical intervention guided by the nomogram increased the net benefit for 90- and 180-d overall survival but nor 30-d overall survival in the training dataset (Figure 7A-C). In the validation dataset, the similar result was obtained: The nomogram showed the best net benefit for 90- and 180-d overall survival but not 30-d overall survival (Figure 7D-F). Taken together, these results showed that the nomogram better predicted the overall survival of cirrhotic patients with AKI than the CTP, MELD and MELD-Na scores.

Table 2 Cox regression analysis of predictors for death of cirrhotic patients with acute kidney injury in the training cohort

Variable	Univariate			Multivariate		
	HR	95%CI	*P* value	HR	95%CI	*P* value
Age (≤ 60 *vs* > 60 yr)	1.003	0.989-1.017	0.670			
Male (male *vs* female)	0.779	0.522-1.161	0.220			
MAP (mmHg)	0.993	0.981-1.005	0.226			
Heart rates (55 ≤ HR ≤ 100 *vs* HR > 100 bpm)	1.317	0.867-2.001	0.197			
Etiology (viral hepatitis *vs* non-viral hepatitis)	0.897	0.521-1.248	0.335			
Diabetes (absent *vs* present)	1.486	0.878-2.514	0.140	1.795	1.048-3.076	0.033
Previous esophagogastric variceal bleeding (absent *vs* present)	0.834	0.549-1.268	0.397			
Ascites, (absent *vs* present)	1.594	0.507-5.012	0.425			
Infections (absent *vs* present)	1.127	0.756-1.680	0.559			
HE (absent *vs* present)	2.308	1.627-3.276	< 0.001	1.986	1.381-2.856	< 0.001
ACLF (absent *vs* present)	1.545	1.064-2.244	0.022			
UO (mL/kg/h)	0.679	0.420-1.098	0.114			
WBC count (10^9/L)	1.018	0.987-1.050	0.264			
Platelet count (10^9/L)	1.000	0.998-1.003	0.805			
Albumin (g/L)	1.001	0.971-1.032	0.963			
Total bilirubin (≤ 4.0 *vs* > 4.0 mg/dL)	2.225	1.350-3.666	0.002			
INR	1.625	1.282-2.061	< 0.001	1.390	1.081-1.787	0.010
Serum sodium (mmol/L)	0.957	0.933-0.982	0.001	0.964	0.937-0.992	0.011
Admission SCr (mg/dL)	1.121	0.975-1.289	0.109			
Peak SCr (≤ 1.5 *vs* > 1.5 mg/dL)	2.407	1.326-4.371	0.004	2.026	1.109-3.702	0.022
HDL (mmol/L)	0.477	0.258-0.883	0.018			
LDL (mmol/L)	0.871	0.696-1.090	0.227			
CTP score	1.328	1.192-1.478	< 0.001			
MELD score	1.057	1.034-1.082	< 0.001			
MELD-Na score	1.036	1.022-1.050	< 0.001			

HR: Hazard ratio; MAP: Mean arterial pressure; bpm: Beat per minute; SCr: Serum creatinine; HE: Hepatic encephalopathy; INR: International normalized ratio; ACLF: Acute on chronic liver failure; WBC: White blood cell; UO: Urine output; HDL: High-density lipoprotein; LDL: Low-density lipoprotein; CTP: Child-Turcotte-Pugh; MELD: The model for end-stage liver disease; CI: Confidence interval.

According to the nomogram, the score of each patient was calculated and utilized for a stratified analysis. Based on the Youden index, the optimal cutoff value of the nomogram score in predicting mortality within 180 d in the training cohort was 98, with a sensitivity of 56.1% and a specificity of 90.7%. Based on the threshold of 98, patients in the training cohort were divided into two subgroups, with high risk (> 98 points, n = 77) and low risk (≤ 98 points, n = 96) of mortality. The high-risk group had a significantly higher mortality rate within 180 d than the low-risk group (94.8% *vs* 59.4%, P < 0.001; Figure 8A). In the validation cohort, the same cutoff value was used, and the sensitivity and specificity of the nomogram were 55.6% and 92.9%, respectively. Patients from the validation cohort were also stratified into a high-risk group (n = 36) and a low-risk group (n = 41), and the mortality rate was significantly different between both risk groups (97.2% *vs* 68.3%, P < 0.001; Figure 8B).

Table 3 Comparison of models in predicting the death of cirrhotic patients with acute kidney injury

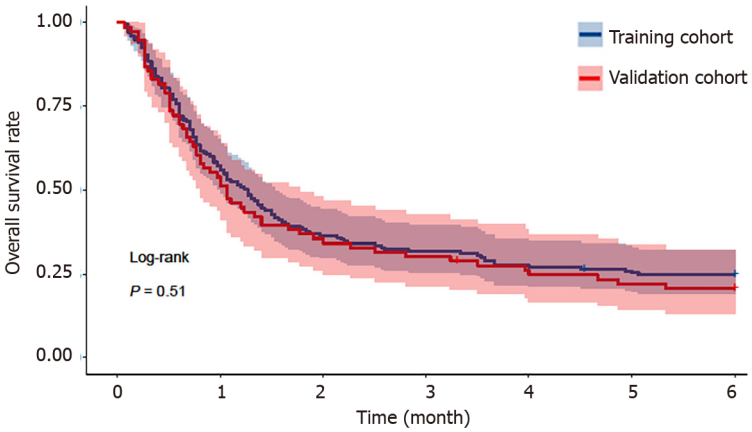
Datasets	Time of mortality	Predictive model	AUROC (95%CI)	*P* value
Training dataset	30-d	Nomogram	0.757 (0.685-0.830)	Ref.
		CTP	0.694 (0.616-0.772)	0.210
		MELD	0.669 (0.585-0.752)	0.114
		MELD-Na	0.702 (0.622-0.782)	0.332
Validation dataset	30-d	Nomogram	0.763 (0.656-0.869)	Ref.
		CTP	0.689 (0.569-0.809)	0.416
		MELD	0.745 (0.631-0.859)	0.979
		MELD-Na	0.763 (0.649-0.876)	> 0.05
Training dataset	90-d	Nomogram	0.792 (0.726-0.859)	Ref.
		CTP	0.696 (0.614 – 0.778)	0.041
		MELD	0.657 (0.574-0.740)	0.003
		MELD-Na	0.670 (0.586-0.755)	0.003
Validation dataset	90-d	Nomogram	0.817 (0.716-0.917)	Ref.
		CTP	0.667 (0.523-0.809)	0.031
		MELD	0.650 (0.515-0.785)	0.008
		MELD-Na	0.642 (0.502-0.783)	0.005
Training dataset	180-d	Nomogram	0.801 (0.726-0.870)	Ref.
		CTP	0.722 (0.630-0.814)	0.045
		MELD	0.663 (0.575-0.752)	0.008
		MELD-Na	0.680 (0.588-0.771)	0.009
Validation dataset	180-d	Nomogram	0.862 (0.765-0.958)	Ref.
		CTP	0.708 (0.540-0.878)	0.027
		MELD	0.659 (0.512-0.806)	0.002
		MELD-Na	0.652 (0.491-0.812)	0.002

CTP: Child-Turcotte-Pugh; MELD: The model for end-stage liver disease; AUROC: The area under the curve of the receiver operating characteristic curve; CI: Confidence interval.

DISCUSSION

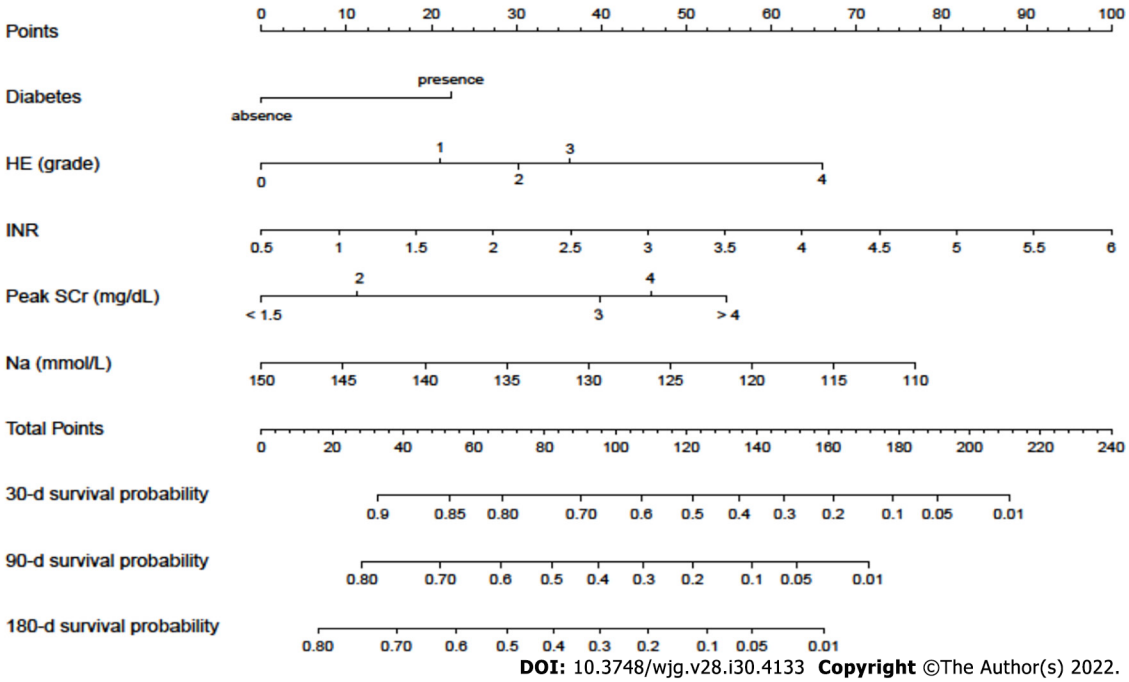
In this study, we conducted a Cox regression analysis to identify the risk factors for mortality within 180 d in cirrhotic patients with AKI, and these predictors included the presence of diabetes, HE, INR, serum sodium level and peak SCr levels. A nomogram incorporating these predictors was developed and showed good predictive discrimination and calibration for the mortality of these patients. Moreover, compared with the CTP, MELD and MELD-Na scores, the nomogram showed better performance for predicting the overall survival of cirrhotic patients with AKI. To our knowledge, this is the first to establish a quantitative nomogram based on these risk factors for the overall survival of cirrhotic patients with AKI.

AKI is a very common and life-threatening complication in patients with cirrhosis and has an unacceptably high mortality rate[33]. Therefore, many AKI criteria and classifications have been developed over the past two decades to comprehensively evaluate and diagnose AKI as early as possible and improve the prognosis. Currently, four main classifications are used: The RIFLE[3], AKIN [4], KIDGO[5] and ICA[1] criteria. SCr level and UO, which are established markers of kidney function, were the basis for the development of these AKI classifications. The use of the SCr level alone to diagnose with AKI may not be appropriate. First, SCr levels are influenced by various factors, such as age, race, sex, body weight, tubular creatinine secretion and the effect of bilirubin on creatinine assays [34,35]. Second, in patients with advanced cirrhosis in particular, the diagnostic value of SCr levels was diminished because of the reduced hepatic production of creatinine from creatine and muscle wasting[7, 36]. Finally, a greater number of AKI cases could be detected earlier using UO in combination with the



DOI: 10.3748/wjg.v28.i30.4133 **Copyright** ©The Author(s) 2022.

Figure 2 Kaplan–Meier analysis of the overall survival of cirrhotic patients with acute kidney injury within 180 d in both the training and validation cohorts.

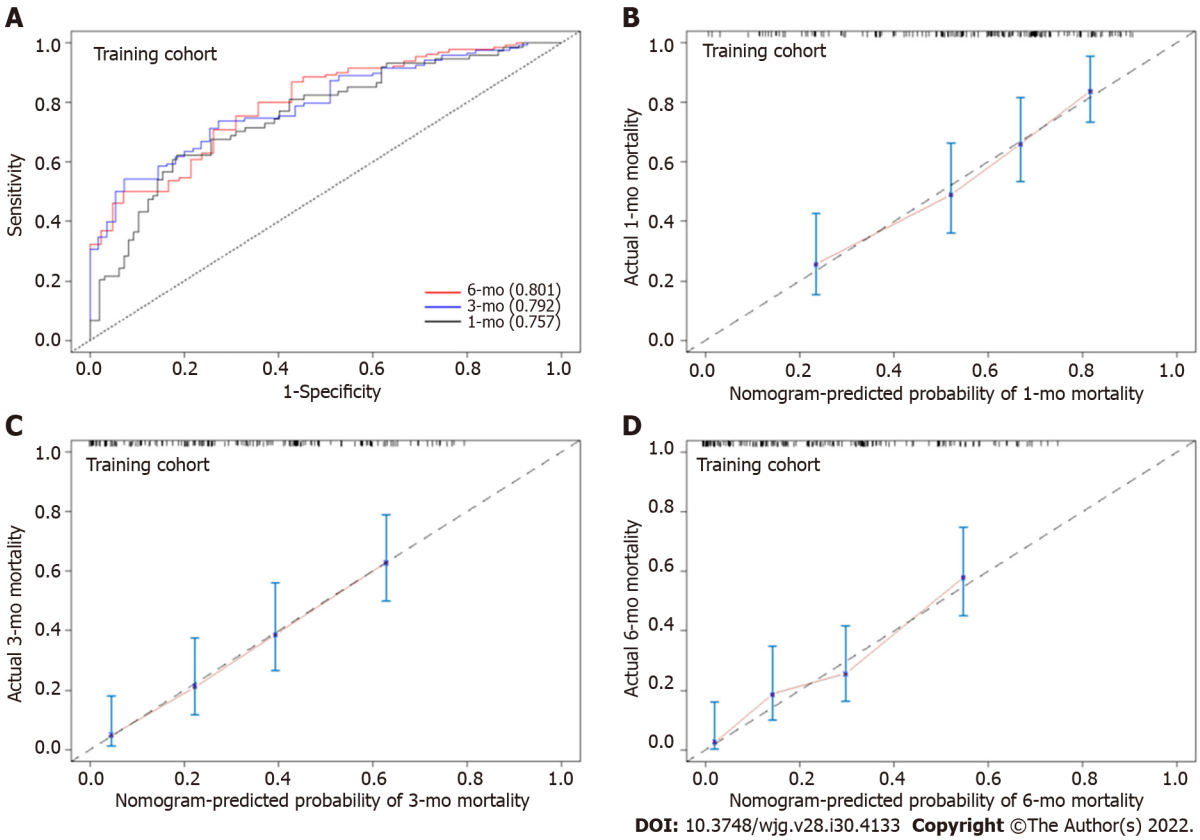


DOI: 10.3748/wjg.v28.i30.4133 **Copyright** ©The Author(s) 2022.

Figure 3 A nomogram for predicting the 30-d, 90-d and 180-d overall survival of cirrhotic patients with acute kidney injury. HE: Hepatic encephalopathy; SCr: Serum creatinine; INR: International normalized ratio.

SCr level[37-39]. Notably, UO is also affected by many factors, such as the body fluid volume of the patients and the use of diuretics, which may decrease the diagnostic and predictive value of the UO criteria for AKI[37]. As a result, any single criterion for AKI may not be able to comprehensively identify and evaluate these patients. Therefore, in the present study, patients who met the criteria for at least one of the RIFLE, AKIN, KDIGO and ICA classifications were recruited as comprehensively as possible, to analyze the clinical characteristics of cirrhotic patients with AKI and identify risk factors for mortality.

The mortality rate of cirrhotic patients with AKI displays substantial heterogeneity among studies. Xiong *et al*[9] reported that the mortality rates were 76.1% and 86.7% in-hospital and at 6 mo, respectively, for patients with cirrhosis who were diagnosed with AKI upon admission to the intensive care unit (ICU), which was consistent with the results of previous studies[7,40]. The results were significantly higher than the values reported in our present study (52.4% in-hospital mortality and 76.4% 180-d mortality). Another study conducted by Kumar *et al*[41] showed that the mortality rate at 30 d was 46.7% for cirrhotic patients with AKI, which was consistent with our result of 46.4%. A meta-analysis conducted by Tariq *et al*[42] revealed that the overall in-hospital mortality, 30-d mortality, and 90-d mortality rates of patients with liver cirrhosis were 34.6%, 42.4%, and 47.1%, respectively, which was lower than the results from our study (52.4% in-hospital mortality, 46.4% 30-d mortality, and 68.8% 90-d mortality). The heterogeneity of the mortality rate may be mainly affected by the difference in the

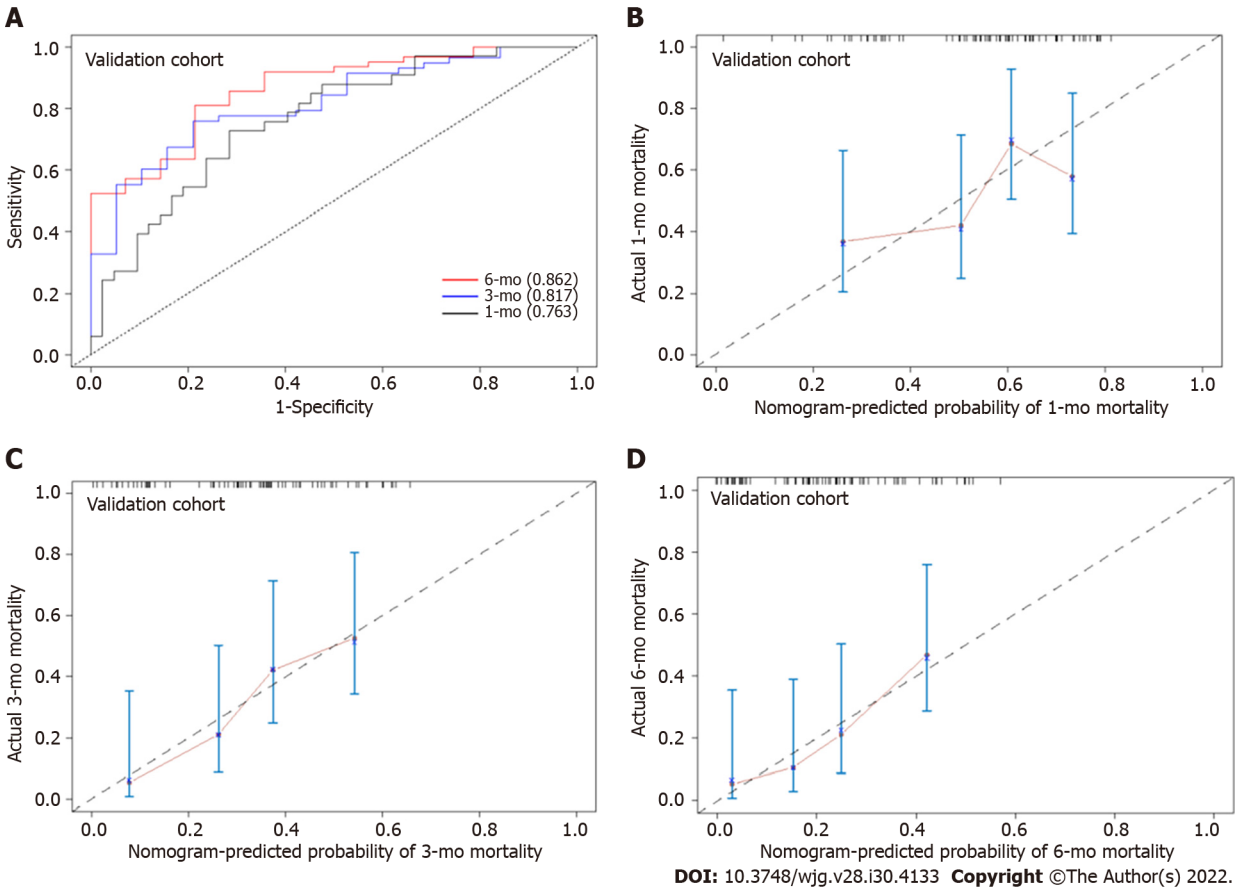


DOI: 10.3748/wjg.v28.i30.4133 **Copyright** ©The Author(s) 2022.

Figure 4 The area under the receiver operating characteristic curve and calibration curve of the nomogram for predicting the overall survival of cirrhotic patients with acute kidney injury in the training cohort. A: The area under the receiver operating characteristic curve of the nomogram for mortality at 30-, 90- and 180-d in the training cohort; B: Calibration curve of the nomogram in predicting 30-d overall survival in the training cohort; C: Calibration curve of the nomogram in predicting 90-d overall survival in the training cohort; D: Calibration curve of the nomogram in predicting 180-d overall survival in the training cohort.

severity of the patient's condition. Moreover, some serious complications of patients with cirrhosis may also contribute to the high mortality rate. For instance, in the present investigation, 60.8% (152/250) of patients had cirrhosis combined with ACLF, resulting in an increase in the AKI mortality rate, which was supported by previous studies by Zang *et al*[43] and Shi *et al*[44]. Furthermore, the literature has indicated that the mortality of AKI in patients with cirrhosis who were admitted to the ICU was significantly higher than that of patients admitted to regular wards[7,42]. In addition, the use of different AKI criteria to identify patients among studies also resulted in different the mortality rate[6,7]. Notably, the types of AKI may also affect the prognosis of these patients. AKI is usually divided into three subtypes: Prerenal AKI, acute tubular necrosis (ATN) and hepatorenal syndrome (HRS)[9]. AKI is closely associated with the prognosis of patients with cirrhosis. A retrospective study showed that compared with non-AKI patients, patients with prerenal AKI had a 2.37-fold higher risk of in-hospital death, patients with ATN had a 6.878-fold higher risk, and patients with HRS had a 12.98-fold higher risk[9]. The result seems to indicate that cirrhotic patients with HRS have a higher risk of death than those with ATN and prerenal AKI. Moreover, patients with HRS-AKI have a worse prognosis than those with non-HRS-AKI[2]. Taken together, the varying mortality of AKI in patients with cirrhosis may be influenced by the severity of the liver disease, the diversity of AKI classifications, survey populations, complications of cirrhosis, and the subtypes of AKI, making the evaluation of AKI difficult and in many cases impossible.

Considering the high mortality rate of AKI in patients with cirrhosis, the identification of risk factors for mortality in these patients is meaningful. However, few studies conducted to date have focused on investigating the risk factors for death in cirrhotic patients with AKI. A study conducted by Kumar *et al*[41] showed that the presence of jaundice, HE, SCr level > 1.5 mg/dL at admission, CTP score, and MELD score were independent predictors of mortality for cirrhotic patients with AKI. Another study by Pan *et al*[40] found that MAP, total bilirubin levels, acute respiratory failure and sepsis were closely associated with the prognosis of cirrhotic patients with AKI who were admitted to the ICU. In the present study, the serum sodium level, INR, peak SCr level > 1.5 mg/dL, the presence of diabetes and HE were considered potential risk factors for death in cirrhotic patients with AKI. Notably, the CTP, MELD and MELD-Na scores were excluded from the multivariate Cox regression analysis because of the increased probability of multicollinearity. An increase in INR is one of the manifestations of

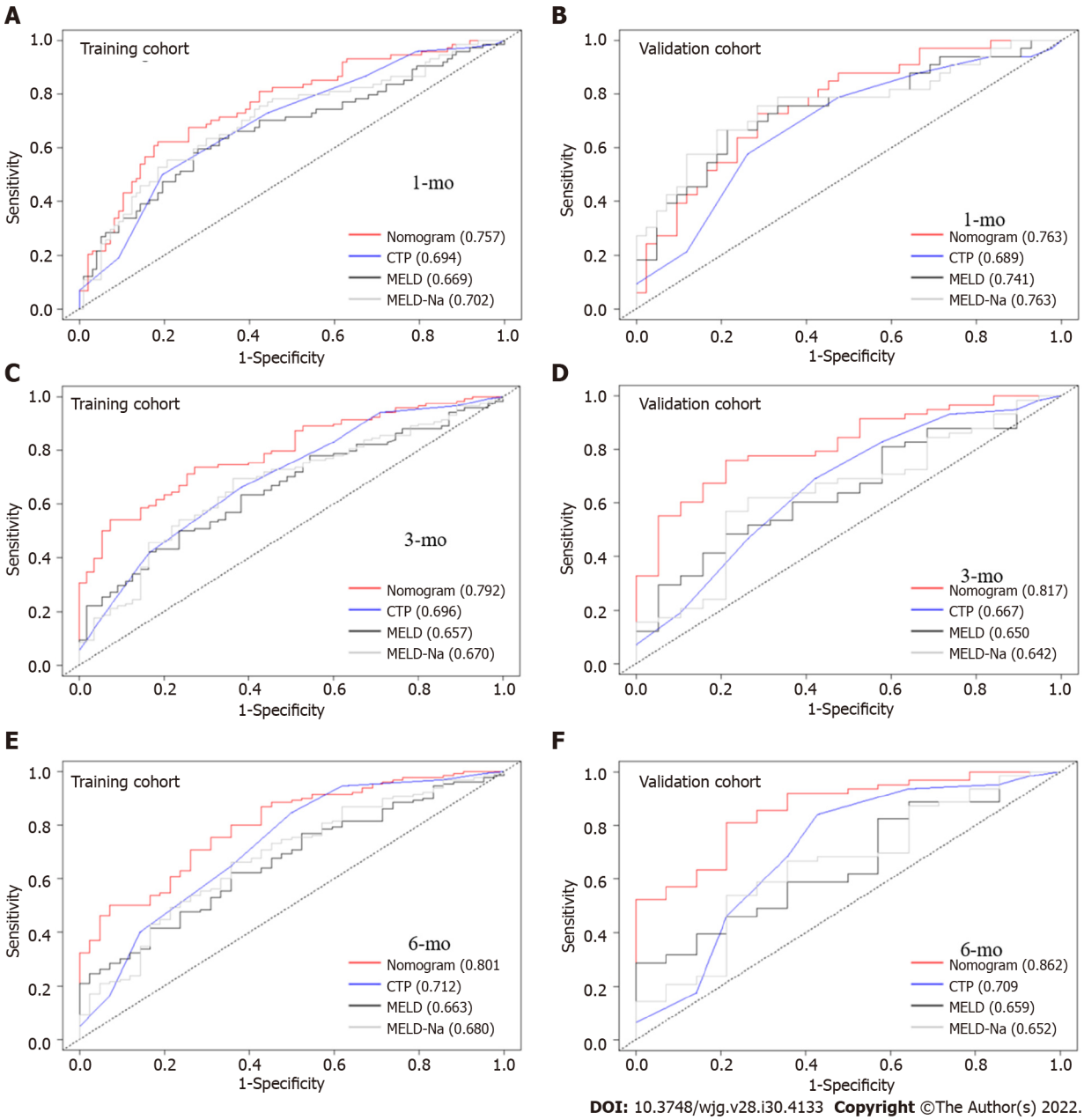


DOI: 10.3748/wjg.v28.i30.4133 **Copyright** ©The Author(s) 2022.

Figure 5 The area under the receiver operating characteristic curve and calibration curve of the nomogram for predicting the overall survival of cirrhotic patients with acute kidney injury in the validation cohort. A: The area under the receiver operating characteristic curve of the nomogram for mortality at 30-, 90- and 180-d in the validation cohort; B: Calibration curve of the nomogram in predicting 30-d overall survival in the validation cohort; C: Calibration curve of the nomogram in predicting 90-d overall survival in the validation cohort; D: Calibration curve of the nomogram in predicting 180-d overall survival in the validation cohort.

synthesis dysfunction in the liver. Similarly, HE is also an important feature of liver failure. Once HE occurs in patients with chronic liver disease, the prognosis is very poor, with a 1-year survival rate of less than 50% and a 3-year survival rate of less than 25%[46]. Studies have shown that INR is associated with the death of patients with cirrhosis[46,47]. Moreover, a serum sodium imbalance is very common in cirrhotic patients with AKI and affect the prognosis of these patients[48-50]. Furthermore, the SCr level represents the status of renal function. Patients with a peak SCr > 1.5 mg/dL had a higher short-term mortality rate than those with a peak SCr ≤ 1.5 mg/dL[51,52]. A study showed that a SCr > 1.5 mg/dL was an independent predictor of mortality in cirrhotic patients with AKI[41]. In addition, diabetes was also considered an independent risk factor for mortality in cirrhotic patients with AKI in this study. Although the mechanisms underlying the relationship between diabetes and mortality in cirrhotic patients with AKI remain unclear, several studies have documented that the presence of diabetes and poorly controlled blood glucose levels are associated with the prognosis of patients with cirrhosis[53-55]. Diabetes is an independent risk factor for the development of AKI or acute kidney disease[56,57]. Consequently, we postulate that the presence of diabetes is associated with the prognosis of cirrhotic patients with AKI. Overall, the recovery of liver and kidney function, correction of electrolyte imbalances, and monitoring and control of blood glucose levels in patients with diabetes may improve the poor prognosis of cirrhotic patients with AKI.

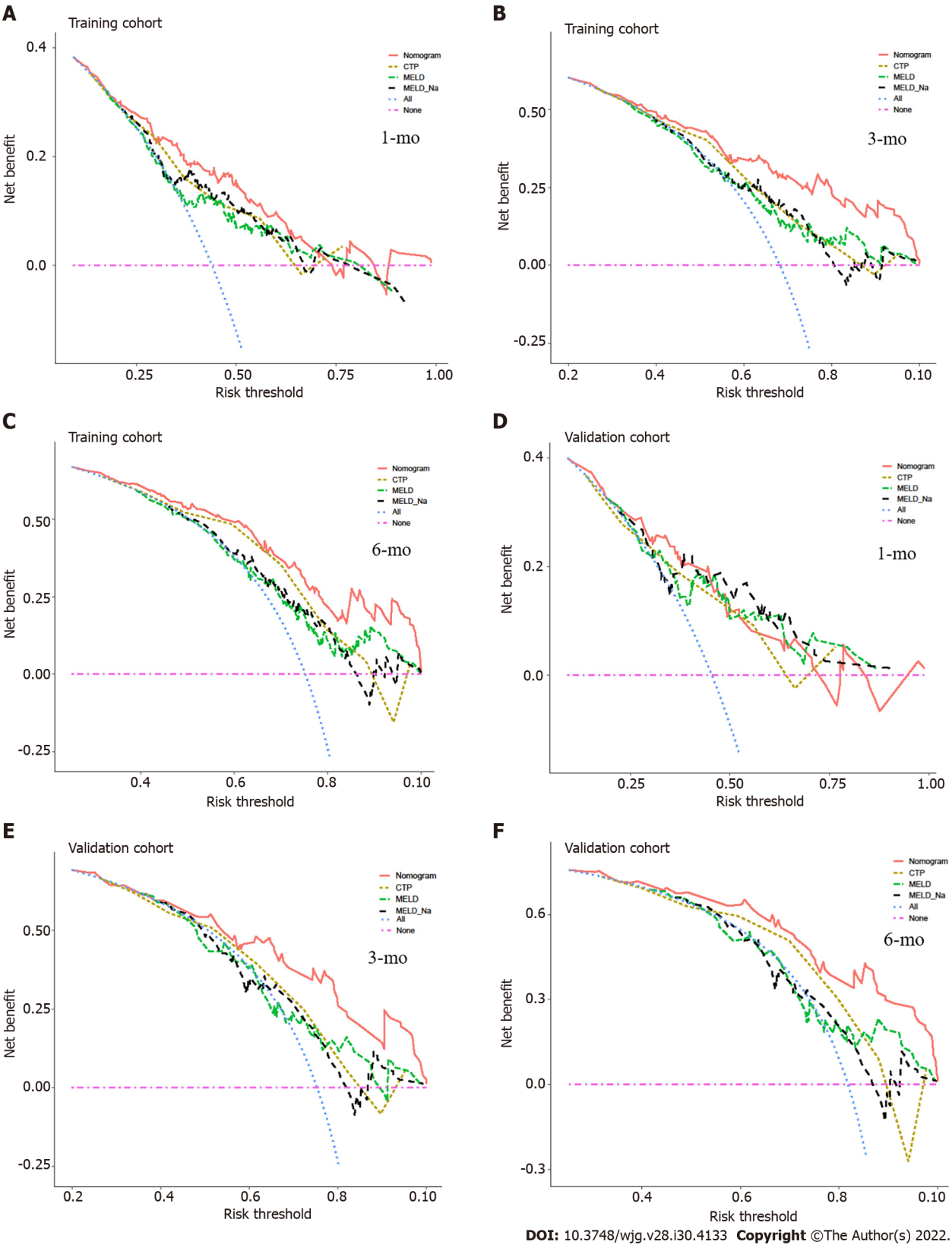
Currently, many studies have investigated the risk factors for the development of AKI in patients with numerous acute and chronic diseases, or have established a model for the development of AKI[20,58-60]. However, studies focused on predicting the prognosis of cirrhotic patients with AKI are scarce. According to Kumar *et al*[41], the AUROCs of CTP and MELD scores were 0.82 and 0.84, respectively, for predicting 30-d mortality in cirrhotic patients with AKI who met the ICA classification. Fang *et al*[45] reported that CTP and MELD scores had AUROCs of 0.61 and 0.757, respectively, for predicting in-hospital mortality of cirrhotic patients with AKI. Moreover, another prospective study conducted by Pan *et al*[40] indicated that CTP and MELD scores had AUROCs of 0.622 and 0.776, respectively, for predicting the in-hospital mortality of cirrhotic patients with AKI who met the RIFLE classification. In the present study, the AUROCs of CTP and MELD scores were 0.694 and 0.669, respectively, for predicting 30-d mortality of cirrhotic patients with AKI in the training cohort, respectively. The discrim-



DOI: 10.3748/wjg.v28.i30.4133 **Copyright** ©The Author(s) 2022.

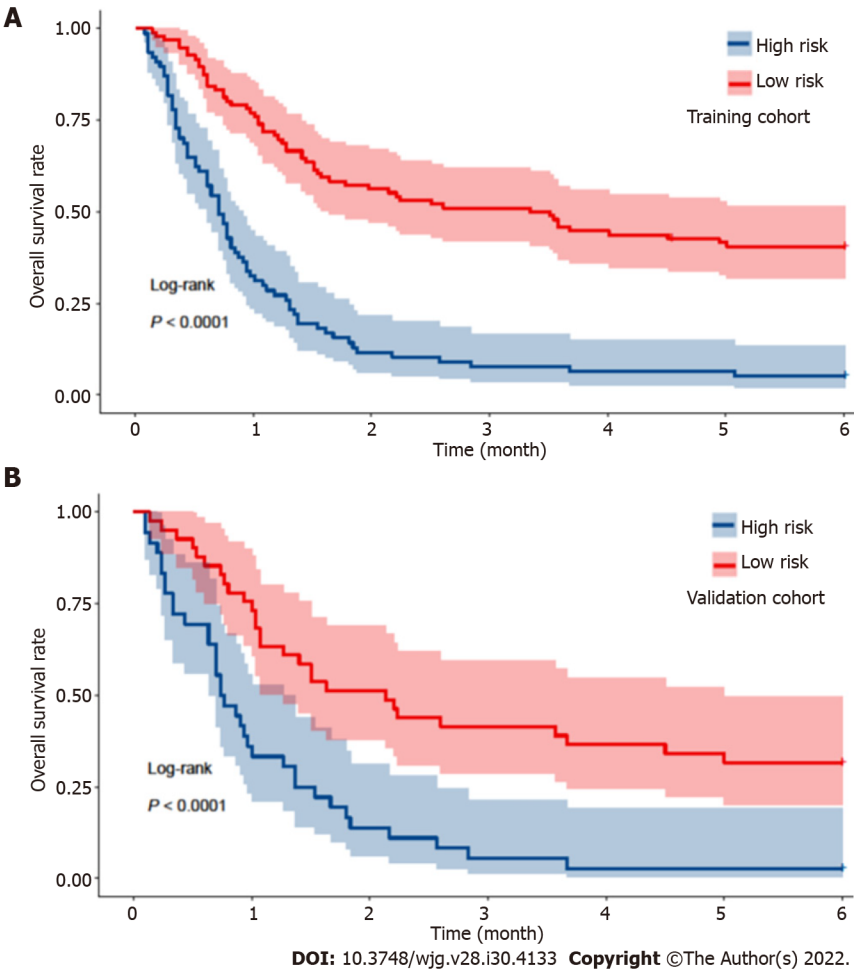
Figure 6 Comparison of the performance of the nomogram and the other scores in predicting mortality of cirrhotic patients with acute kidney injury. A: The area under the receiver operating characteristic curve (AUROC) of the nomogram and the Child-Turcotte-Pugh (CTP), model for end-stage liver disease (MELD) and MELD-Na scores in predicting 30-d mortality in the training cohort; B: The AUROCs of the nomogram and the CTP, MELD and MELD-Na scores in predicting 30-d mortality in the validation cohort; C: The AUROCs of the nomogram and the CTP, MELD and MELD-Na scores in predicting 90-d mortality in the training cohort; D: The AUROCs of the nomogram and the CTP, MELD and MELD-Na scores in predicting 90-d mortality in the validation cohort; E: The AUROCs of the nomogram and the CTP, MELD and MELD-Na scores in predicting 180-d mortality in the training cohort; F: The AUROCs of the nomogram and the CTP, MELD and MELD-Na scores in predicting 180-d mortality in the validation cohort. CTP: Child-Turcotte-Pugh; MELD: Model for end-stage liver disease.

inative ability of CTP and MELD scores differed among studies, which may be explained by the analysis of different patients. Patients with cirrhosis who were diagnosed with AKI in the study by Kumar *et al* [41] only met the ICA criteria, and those patients in the studies by Fang *et al*[45] and Pan *et al*[40] only met the RIFLE criteria, while the study population in our cohort met the criteria for at least one of the main four classifications. In addition, Fang *et al*[45] developed an MBRS (MAP + bilirubin + respiratory failure + sepsis) score (AUROC = 0.898) (including MAP, serum bilirubin level and presence of acute respiratory failure and sepsis) in 2008, a predictive model for cirrhotic patients with AKI, that had better discriminative ability than the CTP and MELD scores. Another prospective study by their team published in 2012 further validated the discrimination and calibration of the MBRS score[40]. The AUROCs and goodness-of-fit of the MBRS were 0.863 and 1.160, respectively, which were superior to the CTP and MELD scores in terms of discriminative ability[40]. Notably, the development of the MBRS score was based on patients admitted to the ICU who may suffer from multiple organ failures and comorbidities, but the authors did not clearly determine whether the MBRS score was applicable to



DOI: 10.3748/wjg.v28.i30.4133 **Copyright** ©The Author(s) 2022.

Figure 7 Comparison of the decision curve analysis curve of medical interventions in patients based on the nomogram and the other scores. A: The decision curve analysis (DCA) curve of medical interventions in patients from the training cohort based on the nomogram, Child-Turcotte-Pugh (CTP), model for end-stage liver disease (MELD) and MELD-Na scores at 30 d; B: The DCA curve of medical interventions in patients from the training cohort based on the nomogram, CTP, MELD and MELD-Na scores at 90 d; C: The DCA curve of medical interventions in patients from the training cohort based on the nomogram, CTP, MELD and MELD-Na scores at 180 d; D: The DCA curve of medical interventions in patients from the validation cohort based on the nomogram, CTP, MELD and MELD-Na scores at 30 d; E: The DCA curve of medical interventions in patients from the validation cohort based on the nomogram, CTP, MELD and MELD-Na scores at 90 d; F: The DCA curve of medical intervention in patients from the validation cohort based on the nomogram, CTP, MELD and MELD-Na scores at 180 d. CTP: Child-Turcotte-Pugh; MELD: Model for end-stage liver disease.



DOI: 10.3748/wjg.v28.i30.4133 **Copyright** ©The Author(s) 2022.

Figure 8 Kaplan–Meier analysis of the cirrhotic patients with acute kidney injury stratified into high-risk and low-risk mortality groups according to the nomogram score, with cutoff of 98. A: Overall survival rates were compared between patients with a high and low risk of mortality in the training cohort; B: Overall survival rates were compared between patients with a high and low risk of mortality in the validation cohort.

patients admitted to regular wards, which requires further validation in the future. Moreover, some clinical data incorporated in the MBRS score, such as the fraction of inspired oxygen, are difficult to obtain in the regular ward and have a complex calculation, which may result in the score not being widely used in clinical practice.

In the present study, we developed a quantitative and visual nomogram for predicting the overall survival of cirrhotic patients with AKI based on these potential risk factors of mortality. The nomogram could be used to calculate the scores corresponding to each potential risk factor, and the predicted probability corresponding to the sum of the scores represented the risk of death for patients with cirrhosis and AKI. For example, patients with cirrhosis presenting AKI and diabetes had SCr level of 2 mg/dL, INR 2, grade 1 HE and blood sodium level of 130 mmol/L. The total score of the patient was approximately 118 points (SCr level of 2 mg/dL, approximately 11 points; INR 2, approximately 26 points; grade 1 HE, approximately 21 points; diabetes, approximately 22.5 points; and blood sodium level of 130 mmol/L, approximately 37.5 points.), and the probability of the overall survival at 30, 90 and 180 d was approximately 53%, 23% and 15%, respectively. Compared with the CTP, MELD and MELD-Na scores, the nomogram had better discriminative power for mortality at 90 and 180 d in both the training and validation datasets (all $P < 0.05$). Moreover, with regard to clinical decisions, the DCA curve indicated that the nomogram had more net benefits than the CTP, MELD and MELD-Na scores for predicting mortality at 90 and 180 d in both the training and validation datasets. However, the AUROC and DCA curves were not significantly different between the nomogram and the CTP, MELD and MELD-Na scores for predicting mortality at 30 d in both the training and validation datasets. Overall, the nomogram was also superior to the CTP, MELD and MELD-Na scores in predicting the prognosis of cirrhotic patients with AKI, especially 90- and 180-d mortality. Furthermore, a score for each patient was calculated based on the nomogram and utilized for stratifing patients into two risk groups for mortality. The high-risk group had a significantly higher mortality rate within 180 d than the low-risk group (all $P < 0.001$) in both the training and validation cohorts. The mortality rates of high-risk patients were as high as 94.8% in the training cohort and 97.2% in the validation cohort. As a result, the nomogram might select patients with a high-risk mortality to allow treatments to be provided as soon as

possible, which may improve the prognosis of cirrhotic patients with AKI. In addition, compared with the MBRS score, the five variables included in the nomogram were all convenient and easily accessible in clinical practice. Since the use of nomograms for evaluation in clinical practice can be time-consuming and complicated, our next step will be to develop software that can be embedded in electronic medical systems to guide clinicians in the timely treatment of these patients and reduce patient mortality without increasing the working time and burden of clinicians.

Several limitations of the present study should also be considered. First, this study analyzed a small sample and employed a retrospective design in which selection biases were unavoidable. Second, this investigation was performed at one academic tertiary-care medical center; the results may not be extrapolated to other centers. In addition, a prospective, large-scale and multicenter study will be needed to validate the reliability of the nomogram.

CONCLUSION

In conclusion, the presence of HE and diabetes, serum sodium level, INR and peak SCr level > 1.5 mg/dL were considered potential risk factors for mortality. A nomogram based on these risk factors was established, and compared with the CTP, MELD and MELD-Na scores, the nomogram exhibited better predictive performance for the overall survival of cirrhotic patients with AKI. According to the score obtained from the nomogram, patients with a high risk of mortality could be selected for suitable individualized treatments, which may improve the prognosis of cirrhotic patients with AKI.

ARTICLE HIGHLIGHTS

Research background

Acute kidney injury (AKI) is a life-threatening complication in cirrhotic patients and is closely associated with the prognosis of these patients. The mortality of AKI in patients with cirrhosis was as high as 80%. Therefore, the identification of patients with AKI at high risk of death is necessary to improve their prognosis.

Research motivation

The majority of studies have focused on investigating the risk factors for the development of AKI or establishing a risk score model for predicting the development of AKI. However, studies focused on identifying the potential risk factors for cirrhotic patients with AKI are scarce.

Research objectives

This study aimed to identify risk factors of mortality and establish a nomogram for predicting overall survival in cirrhotic patients with AKI.

Research methods

We included 250 eligible cirrhotic patients with AKI in this study. These patients were randomly divided into a training cohort and a validation cohort at a ratio of 2:1. Potential risk factors for death were investigated by performing a Cox regression analysis of the training cohort. A prognostic nomogram was developed and evaluated by calculating the area under the curve of the receiver operating characteristic curve, constructing a calibration curve and performing decision curve analysis.

Research results

The serum sodium level, international normalized ratio, peak serum creatinine level > 1.5 mg/dL, the presence of hepatic encephalopathy and diabetes were considered potential risk factors for death in cirrhotic patients with AKI. The nomogram based on these risk factors has a good performance in predicting the short-term prognosis of cirrhotic patients with AKI. The cutoff value of 98 for the nomogram score was used to stratify patients; patients were divided into low- and high-risk groups, and high-risk patients had a higher mortality rate.

Research conclusions

The nomogram was a practical tool to predict the short-term prognosis of patients with cirrhosis who were diagnosed with AKI, and assist clinicians in making clinical decisions.

Research perspectives

The reliability and practicability of nomogram must be validated by conducting prospective, large-scale and multicenter studies. Application programs or software that can be embedded in electronic medical systems will be developed to guide clinicians in the timely evaluation and treatment of these patients.

FOOTNOTES

Author contributions: Wan YP, Wang AJ and Zhang W equally contributed to this work; Wang AJ and Zhu X contributed to the concept; Wan YP, Wang AJ and Zhang W designed this study; Wan YP performed the manuscript writing; Zhang W performed data analysis; Zhang H and Peng GH contributed to samples collection and data collection and validation; Zhu X were clinical experts and performed the manuscript revision; all authors read and approved the final version of the manuscript.

Supported by the National Natural Science Foundation of China, No. 81960120 and No. 82160115.

Institutional review board statement: This study was reviewed and approved by the Ethics Committee of The First Affiliated Hospital of Nanchang University (No. AF-SG-04-2.0).

Informed consent statement: Patients were not required to give informed consent to the study because the analysis used anonymous clinical data that were obtained after each patient agreed to treatment by written consent. For full disclosure, the details of the study are published on the home page of The First Affiliated Hospital of Nanchang University.

Conflict-of-interest statement: We have no financial relationships to disclose.

Data sharing statement: No additional data are available.

Open-Access: This article is an open-access article that was selected by an in-house editor and fully peer-reviewed by external reviewers. It is distributed in accordance with the Creative Commons Attribution NonCommercial (CC BY-NC 4.0) license, which permits others to distribute, remix, adapt, build upon this work non-commercially, and license their derivative works on different terms, provided the original work is properly cited and the use is non-commercial. See: https://creativecommons.org/Licenses/by-nc/4.0/

Country/Territory of origin: China

ORCID number: Yi-Peng Wan 0000-0002-8156-4670; An-Jiang Wang 0000-0001-6670-6645; Wang Zhang 0000-0002-8438-6718; Hang Zhang 0000-0003-3205-5455; Gen-Hua Peng 0000-0002-1369-0333; Xuan Zhu 0000-0002-1240-0947.

S-Editor: Yan JP
L-Editor: A
P-Editor: Yu HG

REFERENCES

1 **Angeli P**, Gines P, Wong F, Bernardi M, Boyer TD, Gerbes A, Moreau R, Jalan R, Sarin SK, Piano S, Moore K, Lee SS, Durand F, Salerno F, Caraceni P, Kim WR, Arroyo V, Garcia-Tsao G; International Club of Ascites. Diagnosis and management of acute kidney injury in patients with cirrhosis: revised consensus recommendations of the International Club of Ascites. *Gut* 2015; **64**: 531-537 [PMID: 25631669 DOI: 10.1136/gutjnl-2014-308874]

2 **Gupta K**, Bhurwal A, Law C, Ventre S, Minacapelli CD, Kabaria S, Li Y, Tait C, Catalano C, Rustgi VK. Acute kidney injury and hepatorenal syndrome in cirrhosis. *World J Gastroenterol* 2021; **27**: 3984-4003 [PMID: 34326609 DOI: 10.3748/wjg.v27.i26.3984]

3 **Bellomo R**, Ronco C, Kellum JA, Mehta RL, Palevsky P; Acute Dialysis Quality Initiative workgroup. Acute renal failure - definition, outcome measures, animal models, fluid therapy and information technology needs: the Second International Consensus Conference of the Acute Dialysis Quality Initiative (ADQI) Group. *Crit Care* 2004; **8**: R204-R212 [PMID: 15312219 DOI: 10.1186/cc2872]

4 **Mehta RL**, Kellum JA, Shah SV, Molitoris BA, Ronco C, Warnock DG, Levin A; Acute Kidney Injury Network. Acute Kidney Injury Network: report of an initiative to improve outcomes in acute kidney injury. *Crit Care* 2007; **11**: R31 [PMID: 17331245 DOI: 10.1186/cc5713]

5 **Kellum JA**, Lameire N, Aspelin P, Barsoum RS, Burdmann EA, Goldstein SL, Herzog CA, Joannidis M, Kribben A, Levey AS. Kidney disease: improving global outcomes (KDIGO) acute kidney injury work group. KDIGO clinical practice guideline for acute kidney injury. *Kidney Int Suppl* 2012; **2**: 1-138 [DOI: 10.1038/kisup.2012.1]

6 **Pan HC**, Chien YS, Jenq CC, Tsai MH, Fan PC, Chang CH, Chang MY, Tian YC, Fang JT, Yang CW, Chen YC. Acute Kidney Injury Classification for Critically Ill Cirrhotic Patients: A Comparison of the KDIGO, AKIN, and RIFLE Classifications. *Sci Rep* 2016; **6**: 23022 [PMID: 26983372 DOI: 10.1038/srep23022]

7 **Xiong J**, Zhang M, Guo X, Pu L, Xiong H, Xiang P, Liu J, Li A. Acute kidney injury in critically ill cirrhotic patients with spontaneous bacterial peritonitis: a comparison of KDIGO and ICA criteria. *Arch Med Sci* 2020; **16**: 569-576 [PMID: 32399104 DOI: 10.5114/aoms.2019.85148]

8 **Garcia-Tsao G**, Parikh CR, Viola A. Acute kidney injury in cirrhosis. *Hepatology* 2008; **48**: 2064-2077 [PMID: 19003880 DOI: 10.1002/hep.22605]

9 **Xiong J**, Pu L, Xiong H, Xiang P, Zhang M, Liu J, Li A. Evaluation of the criteria of hepatorenal syndrome type of acute kidney injury in patients with cirrhosis admitted to ICU. *Scand J Gastroenterol* 2018; **53**: 1590-1596 [PMID: 30621473

DOI: 10.1080/00365521.2018.1545423]

10 **John JA**, de Mattos AA, da Silva Miozzo SA, Comerlato PH, Porto M, Contiero P, da Silva RR. Survival and risk factors related to death in outpatients with cirrhosis treated in a clinic in Southern Brazil. *Eur J Gastroenterol Hepatol* 2015; **27**: 1372-1377 [PMID: 26426832 DOI: 10.1097/MEG.0000000000000480]

11 **Haukeland JW**, Småstuen MC, Pålsdatter PP, Ismail M, Konopski Z, Jørgensen KK, Lannerstedt H, Midgard H. Effect of gender on mortality and causes of death in cirrhotic patients with gastroesophageal varices. A retrospective study in Norway. *PLoS One* 2020; **15**: e0230263 [PMID: 32163489 DOI: 10.1371/journal.pone.0230263]

12 **Rakotondrainibe A**, Rahanitriniaina NMP, Randriamizao HMR, Raelison JG, Ramanampamonjy RM, Rajaonera AT, Sztark F. Clinical mortality risk factors of variceal upper gastrointestinal bleeding in a Malagasy surgical intensive care unit. *Afr J Emerg Med* 2020; **10**: 188-192 [PMID: 33299747 DOI: 10.1016/j.afjem.2020.06.004]

13 **Turco L**, Villanueva C, La Mura V, García-Pagán JC, Reiberger T, Genescà J, Groszmann RJ, Sharma BC, Merkel C, Bureau C, Alvarado E, Abraldes JG, Albillos A, Bañares R, Peck-Radosavljevic M, Augustin S, Sarin SK, Bosch J, García-Tsao G. Lowering Portal Pressure Improves Outcomes of Patients With Cirrhosis, With or Without Ascites: A Meta-Analysis. *Clin Gastroenterol Hepatol* 2020; **18**: 313-327.e6 [PMID: 31176013 DOI: 10.1016/j.cgh.2019.05.050]

14 **Xu L**, Ying S, Hu J, Wang Y, Yang M, Ge T, Huang C, Xu Q, Zhu H, Chen Z, Ma W. Pneumonia in patients with cirrhosis: risk factors associated with mortality and predictive value of prognostic models. *Respir Res* 2018; **19**: 242 [PMID: 30514312 DOI: 10.1186/s12931-018-0934-5]

15 **Gao F**, Lin MT, Yang XY, Cai MX, Nan H, Xie W, Huang ZM. Metabolic acidosis in critically ill patients with cirrhosis: Epidemiology and short-term mortality risk factors. *Turk J Gastroenterol* 2019; **30**: 883-891 [PMID: 31633484 DOI: 10.5152/tjg.2019.18813]

16 **Karagozian R**, Bhardwaj G, Wakefield DB, Verna EC. Acute kidney injury is associated with higher mortality and healthcare costs in hospitalized patients with cirrhosis. *Ann Hepatol* 2019; **18**: 730-735 [PMID: 31175020 DOI: 10.1016/j.aohep.2019.03.011]

17 **Vaz NF**, da Cunha VNR, Cunha-Silva M, Sevá-Pereira T, de Souza Almeida JR, Mazo DF. Evolution of diagnostic criteria for acute kidney injury in patients with decompensated cirrhosis: A prospective study in a tertiary university hospital. *Clin Res Hepatol Gastroenterol* 2020; **44**: 551-563 [PMID: 31427198 DOI: 10.1016/j.clinre.2019.07.004]

18 **Jeon H**, Kim JH, Lee SS, Kim HJ, Cha RR, Cho HC, Lee JM, Ha CY, Kim TH, Jung WT, Lee OJ. Impact of acute kidney injury on survival in patients with chronic hepatitis C: a retrospective cohort study. *BMC Infect Dis* 2021; **21**: 301 [PMID: 33765952 DOI: 10.1186/s12879-021-05991-2]

19 **Khatua CR**, Sahu SK, Meher D, Nath G, Singh SP. Acute kidney injury in hospitalized cirrhotic patients: Risk factors, type of kidney injury, and survival. *JGH Open* 2021; **5**: 199-206 [PMID: 33553656 DOI: 10.1002/jgh3.12467]

20 **Hu L**, Gao L, Zhang D, Hou Y, He LL, Zhang H, Liang Y, Xu J, Chen C. The incidence, risk factors and outcomes of acute kidney injury in critically ill patients undergoing emergency surgery: a prospective observational study. *BMC Nephrol* 2022; **23**: 42 [PMID: 35065624 DOI: 10.1186/s12882-022-02675-0]

21 **Yuan SM**. Acute Kidney Injury after Cardiac Surgery: Risk Factors and Novel Biomarkers. *Braz J Cardiovasc Surg* 2019; **34**: 352-360 [PMID: 31310475 DOI: 10.21470/1678-9741-2018-0212]

22 **Li D**, Gao J, Guo Y, Jia Y, An X, Liu Y, Wang L, Su P. Risk factor analysis of acute kidney injury after one-stop hybrid coronary revascularization. *Ann Palliat Med* 2021; **10**: 7398-7405 [PMID: 34263638 DOI: 10.21037/apm-21-959]

23 **Makar M**, Reja D, Chouthai A, Kabaria S, Patel AV. The impact of acute kidney injury on mortality and clinical outcomes in patients with alcoholic cirrhosis in the USA. *Eur J Gastroenterol Hepatol* 2021; **33**: 905-910 [PMID: 32976187 DOI: 10.1097/MEG.0000000000001947]

24 **Fede G**, D'Amico G, Arvaniti V, Tsochatzis E, Germani G, Georgiadis D, Morabito A, Burroughs AK. Renal failure and cirrhosis: a systematic review of mortality and prognosis. *J Hepatol* 2012; **56**: 810-818 [PMID: 22173162 DOI: 10.1016/j.jhep.2011.10.016]

25 **Kim JH**, Im CB, Lee SS, Jeon H, Choi JW, Kim HJ, Cha RR, Cho HC, Lee JM, Ha CY, Kim TH, Jung WT, Lee OJ. Impact of acute kidney injury on mortality in patients with acute variceal bleeding. *BMC Gastroenterol* 2021; **21**: 290 [PMID: 34256711 DOI: 10.1186/s12876-021-01862-x]

26 **Tsochatzis EA**, Bosch J, Burroughs AK. Liver cirrhosis. *Lancet* 2014; **383**: 1749-1761 [PMID: 24480518 DOI: 10.1016/S0140-6736(14)60121-5]

27 **Sarin SK**, Choudhury A, Sharma MK, Maiwall R, Al Mahtab M, Rahman S, Saigal S, Saraf N, Soin AS, Devarbhavi H, Kim DJ, Dhiman RK, Duseja A, Taneja S, Eapen CE, Goel A, Ning Q, Chen T, Ma K, Duan Z, Yu C, Treeprasertsuk S, Hamid SS, Butt AS, Jafri W, Shukla A, Saraswat V, Tan SS, Sood A, Midha V, Goyal O, Ghazinyan H, Arora A, Hu J, Sahu M, Rao PN, Lee GH, Lim SG, Lesmana LA, Lesmana CR, Shah S, Prasad VGM, Payawal DA, Abbas Z, Dokmeci AK, Sollano JD, Carpio G, Shresta A, Lau GK, Fazal Karim M, Shiha G, Gani R, Kalista KF, Yuen MF, Alam S, Khanna R, Sood V, Lal BB, Pamecha V, Jindal A, Rajan V, Arora V, Yokosuka O, Niriella MA, Li H, Qi X, Tanaka A, Mochida S, Chaudhuri DR, Gane E, Win KM, Chen WT, Rela M, Kapoor D, Rastogi A, Kale P, Sharma CB, Bajpai M, Singh V, Premkumar M, Maharashi S, Olithselvan A, Philips CA, Srivastava A, Yachha SK, Wani ZA, Thapa BR, Saraya A, Shalimar, Kumar A, Wadhawan M, Gupta S, Madan K, Sakhuja P, Vij V, Sharma BC, Garg H, Garg V, Kalal C, Anand L, Vyas T, Mathur RP, Kumar G, Jain P, Pasupuleti SSR, Chawla YK, Chowdhury A, Song DS, Yang JM, Yoon EL; APASL ACLF Research Consortium (AARC) for APASL ACLF working Party. Acute-on-chronic liver failure: consensus recommendations of the Asian Pacific association for the study of the liver (APASL): an update. *Hepatol Int* 2019; **13**: 353-390 [PMID: 31172417 DOI: 10.1007/s12072-019-09946-3]

28 **Schwartz GJ**, Muñoz A, Schneider MF, Mak RH, Kaskel F, Warady BA, Furth SL. New equations to estimate GFR in children with CKD. *J Am Soc Nephrol* 2009; **20**: 629-637 [PMID: 19158356 DOI: 10.1681/ASN.2008030287]

29 **Pugh RN**, Murray-Lyon IM, Dawson JL, Pietroni MC, Williams R. Transection of the oesophagus for bleeding oesophageal varices. *Br J Surg* 1973; **60**: 646-649 [PMID: 4541913 DOI: 10.1002/bjs.1800600817]

30 **Botta F**, Giannini E, Romagnoli P, Fasoli A, Malfatti F, Chiarbonello B, Testa E, Risso D, Colla G, Testa R. MELD scoring system is useful for predicting prognosis in patients with liver cirrhosis and is correlated with residual liver function: a European study. *Gut* 2003; **52**: 134-139 [PMID: 12477775 DOI: 10.1136/gut.52.1.134]

31 **Wiesner R**, Edwards E, Freeman R, Harper A, Kim R, Kamath P, Kremers W, Lake J, Howard T, Merion RM, Wolfe RA, Krom R; United Network for Organ Sharing Liver Disease Severity Score Committee. Model for end-stage liver disease (MELD) and allocation of donor livers. *Gastroenterology* 2003; **124**: 91-96 [PMID: 12512033 DOI: 10.1053/gast.2003.50016]

32 **Biggins SW**, Kim WR, Terrault NA, Saab S, Balan V, Schiano T, Benson J, Therneau T, Kremers W, Wiesner R, Kamath P, Klintmalm G. Evidence-based incorporation of serum sodium concentration into MELD. *Gastroenterology* 2006; **130**: 1652-1660 [PMID: 16697729 DOI: 10.1053/j.gastro.2006.02.010]

33 **Flamm SL**, Brown K, Wadei HM, Brown RS Jr, Kugelmas M, Samaniego-Picota M, Burra P, Poordad F, Saab S. The Current Management of Hepatorenal Syndrome-Acute Kidney Injury in the United States and the Potential of Terlipressin. *Liver Transpl* 2021; **27**: 1191-1202 [PMID: 33848394 DOI: 10.1002/lt.26072]

34 **Umemura T**, Joshita S, Shibata S, Sugiura A, Yamazaki T, Fujimori N, Matsumoto A, Tanaka E. Renal impairment is associated with increased risk of mortality in patients with cirrhosis: A retrospective cohort study. *Medicine (Baltimore)* 2019; **98**: e14475 [PMID: 30732215 DOI: 10.1097/MD.0000000000014475]

35 **Spencer K**. Analytical reviews in clinical biochemistry: the estimation of creatinine. *Ann Clin Biochem* 1986; **23**: 1-25 [PMID: 3532908 DOI: 10.1177/000456328602300101]

36 **Angeli P**, Sanyal A, Moller S, Alessandria C, Gadano A, Kim R, Sarin SK, Bernardi M; International Club of Ascites. Current limits and future challenges in the management of renal dysfunction in patients with cirrhosis: report from the International Club of Ascites. *Liver Int* 2013; **33**: 16-23 [PMID: 22507181 DOI: 10.1111/j.1478-3231.2012.02807.x]

37 **Martins CB**, De Bels D, Honore PM, Redant S. Early Prediction of Acute Kidney Injury by Machine Learning: Should We Add the Urine Output Criterion to Improve this New Tool? *J Transl Int Med* 2020; **8**: 201-202 [PMID: 33511045 DOI: 10.2478/jtim-2020-0031]

38 **Koeze J**, Keus F, Dieperink W, van der Horst IC, Zijlstra JG, van Meurs M. Incidence, timing and outcome of AKI in critically ill patients varies with the definition used and the addition of urine output criteria. *BMC Nephrol* 2017; **18**: 70 [PMID: 28219327 DOI: 10.1186/s12882-017-0487-8]

39 **Macedo E**, Malhotra R, Claure-Del Granado R, Fedullo P, Mehta RL. Defining urine output criterion for acute kidney injury in critically ill patients. *Nephrol Dial Transplant* 2011; **26**: 509-515 [PMID: 20562094 DOI: 10.1093/ndt/gfq332]

40 **Pan HC**, Jenq CC, Tsai MH, Fan PC, Chang CH, Chang MY, Tian YC, Hung CC, Fang JT, Yang CW, Chen YC. Risk models and scoring systems for predicting the prognosis in critically ill cirrhotic patients with acute kidney injury: a prospective validation study. *PLoS One* 2012; **7**: e51094 [PMID: 23236437 DOI: 10.1371/journal.pone.0051094]

41 **Kumar U**, Kumar R, Jha SK, Jha AK, Dayal VM, Kumar A. Short-term mortality in patients with cirrhosis of the liver and acute kidney injury: A prospective observational study. *Indian J Gastroenterol* 2020; **39**: 457-464 [PMID: 33175368 DOI: 10.1007/s12664-020-01086-z]

42 **Tariq R**, Hadi Y, Chahal K, Reddy S, Salameh H, Singal AK. Incidence, Mortality and Predictors of Acute Kidney Injury in Patients with Cirrhosis: A Systematic Review and Meta-analysis. *J Clin Transl Hepatol* 2020; **8**: 135-142 [PMID: 32832393 DOI: 10.14218/JCTH.2019.00060]

43 **Zang H**, Liu F, Liu H, You S, Zhu B, Wan Z, Xin S. Incidence, risk factors and outcomes of acute kidney injury (AKI) in patients with acute-on-chronic liver failure (ACLF) of underlying cirrhosis. *Hepatol Int* 2016; **10**: 807-818 [PMID: 27485174 DOI: 10.1007/s12072-016-9756-z]

44 **Shi X**, Zhu P, Yan G, Liu C, Zhang C, Huang G, Zhang Y, Yan Z, Wang Y. Clinical characteristics and long-term outcome of acute kidney injury in patients with HBV-related acute-on-chronic liver failure. *J Viral Hepat* 2016; **23**: 920-929 [PMID: 27397610 DOI: 10.1111/jvh.12566]

45 **Fang JT**, Tsai MH, Tian YC, Jenq CC, Lin CY, Chen YC, Lien JM, Chen PC, Yang CW. Outcome predictors and new score of critically ill cirrhotic patients with acute renal failure. *Nephrol Dial Transplant* 2008; **23**: 1961-1969 [PMID: 18187499 DOI: 10.1093/ndt/gfm914]

46 **Hu XP**, Gao J. International normalized ratio and Model for End-stage Liver Disease score predict short-term outcome in cirrhotic patients after the resolution of hepatic encephalopathy. *World J Gastroenterol* 2019; **25**: 3426-3437 [PMID: 31341366 DOI: 10.3748/wjg.v25.i26.3426]

47 **Ampuero J**, Montoliú C, Simón-Talero M, Aguilera V, Millán R, Márquez C, Jover R, Rico MC, Sendra C, Serra MÁ, Romero-Gómez M. Minimal hepatic encephalopathy identifies patients at risk of faster cirrhosis progression. *J Gastroenterol Hepatol* 2018; **33**: 718-725 [PMID: 28768371 DOI: 10.1111/jgh.13917]

48 **Sohn W**, Kim JH, Cho JY. Effect of acute kidney injury on long-term outcomes of spontaneous bacterial peritonitis in cirrhotic patients using the International Club of Ascites-acute kidney injury criteria. *J Gastroenterol Hepatol* 2020; **35**: 870-876 [PMID: 31816662 DOI: 10.1111/jgh.14871]

49 **Umemura T**, Shibata S, Sekiguchi T, Kitabatake H, Nozawa Y, Okuhara S, Kimura T, Morita S, Komatsu M, Matsumoto A, Tanaka E. Serum sodium concentration is associated with increased risk of mortality in patients with compensated liver cirrhosis. *Hepatol Res* 2015; **45**: 739-744 [PMID: 25163635 DOI: 10.1111/hepr.12412]

50 **Heuman DM**, Abou-Assi SG, Habib A, Williams LM, Stravitz RT, Sanyal AJ, Fisher RA, Mihas AA. Persistent ascites and low serum sodium identify patients with cirrhosis and low MELD scores who are at high risk for early death. *Hepatology* 2004; **40**: 802-810 [PMID: 15382176 DOI: 10.1002/hep.20405]

51 **Piano S**, Rosi S, Maresio G, Fasolato S, Cavallin M, Romano A, Morando F, Gola E, Frigo AC, Gatta A, Angeli P. Evaluation of the Acute Kidney Injury Network criteria in hospitalized patients with cirrhosis and ascites. *J Hepatol* 2013; **59**: 482-489 [PMID: 23665185 DOI: 10.1016/j.jhep.2013.03.039]

52 **Fagundes C**, Barreto R, Guevara M, Garcia E, Solà E, Rodríguez E, Graupera I, Ariza X, Pereira G, Alfaro I, Cárdenas A, Fernández J, Poch E, Ginès P. A modified acute kidney injury classification for diagnosis and risk stratification of impairment of kidney function in cirrhosis. *J Hepatol* 2013; **59**: 474-481 [PMID: 23669284 DOI: 10.1016/j.jhep.2013.04.036]

53 **Abdelkader RY**, Abdelrazek MA, Attallah A, Farid K, El-Far M. High blood glucose levels are associated with fibrosis/cirrhosis progression in chronic hepatitis C. *J Immunoassay Immunochem* 2021; **42**: 559-570 [PMID: 33886414 DOI: 10.1080/15321819.2021.1911813]

54 **Hsiang JC**, Gane EJ, Bai WW, Gerred SJ. Type 2 diabetes: a risk factor for liver mortality and complications in hepatitis B cirrhosis patients. *J Gastroenterol Hepatol* 2015; **30**: 591-599 [PMID: 25250942 DOI: 10.1111/jgh.12790]

55 **Garcia-Compean D**, Jaquez-Quintana JO, Gonzalez-Gonzalez JA, Maldonado-Garza H. Liver cirrhosis and diabetes: risk factors, pathophysiology, clinical implications and management. *World J Gastroenterol* 2009; **15**: 280-288 [PMID: 19140227 DOI: 10.3748/wjg.15.280]

56 **Cullaro G**, Verna EC, Duarte-Rojo A, Kappus MR, Ganger DR, Rahimi RS, Boyarsky B, Segev DL, McAdams-DeMarco M, Ladner DP, Volk ML, Hsu CY, Lai JC. Frailty and the Risk of Acute Kidney Injury Among Patients With Cirrhosis. *Hepatol Commun* 2022; **6**: 910-919 [PMID: 34676697 DOI: 10.1002/hep4.1840]

57 **Wong F**, Garcia-Tsao G, Reddy KR, O'Leary JG, Kamath PS, Tandon P, Lai JC, Vargas HE, Biggins SW, Fallon MB, Thuluvath PJ, Maliakkal BJ, Subramanian R, Thacker L, Bajaj JS. Prognosis of hospitalized patients with cirrhosis and acute kidney disease. *Liver Int* 2022; **42**: 896-904 [PMID: 35023264 DOI: 10.1111/liv.15154]

58 **Martinez DA**, Levin SR, Klein EY, Parikh CR, Menez S, Taylor RA, Hinson JS. Early Prediction of Acute Kidney Injury in the Emergency Department With Machine-Learning Methods Applied to Electronic Health Record Data. *Ann Emerg Med* 2020; **76**: 501-514 [PMID: 32713624 DOI: 10.1016/j.annemergmed.2020.05.026]

59 **Tseng PY**, Chen YT, Wang CH, Chiu KM, Peng YS, Hsu SP, Chen KL, Yang CY, Lee OK. Prediction of the development of acute kidney injury following cardiac surgery by machine learning. *Crit Care* 2020; **24**: 478 [PMID: 32736589 DOI: 10.1186/s13054-020-03179-9]

60 **Duah A**, Duah F, Ampofo-Boobi D, Addo BP, Osei-Poku F, Agyei-Nkansah A. Acute Kidney Injury in Patients with Liver Cirrhosis: Prevalence, Predictors, and In-Hospital Mortality at a District Hospital in Ghana. *Biomed Res Int* 2022; **2022**: 4589767 [PMID: 35237687 DOI: 10.1155/2022/4589767]

World Journal of Gastroenterology

Submit a Manuscript: https://www.f6publishing.com

World J Gastroenterol 2022 August 14; 28(30): 4152-4162

DOI: 10.3748/wjg.v28.i30.4152

ISSN 1007-9327 (print) ISSN 2219-2840 (online)

ORIGINAL ARTICLE

Retrospective Study

Cumulative incidence and risk factors for pouch adenomas associated with familial adenomatous polyposis following restorative proctocolectomy

Hyo Seon Ryu, Chang Sik Yu, Young Il Kim, Jong Lyul Lee, Chan Wook Kim, Yong Sik Yoon, In Ja Park, Seok-Byung Lim, Jin Cheon Kim

Specialty type: Gastroenterology and hepatology

Provenance and peer review: Unsolicited article; Externally peer reviewed.

Peer-review model: Single blind

Peer-review report's scientific quality classification

Grade A (Excellent): 0
Grade B (Very good): B, B
Grade C (Good): C, C, C
Grade D (Fair): 0
Grade E (Poor): 0

P-Reviewer: Di Leo A, Italy; M'Koma AE, United States; Roncucci L, Italy; Sulbaran MN, Brazil

Received: March 3, 2022
Peer-review started: March 3, 2022
First decision: April 11, 2022
Revised: April 24, 2022
Accepted: July 18, 2022
Article in press: July 18, 2022
Published online: August 14, 2022

Hyo Seon Ryu, Chang Sik Yu, Young Il Kim, Jong Lyul Lee, Chan Wook Kim, Yong Sik Yoon, In Ja Park, Seok-Byung Lim, Jin Cheon Kim, Division of Colon and Rectal Surgery, Department of Surgery, University of Ulsan College of Medicine, Asan Medical Center, Seoul 05505, South Korea

Corresponding author: Chang Sik Yu, MD, PhD, Professor, Division of Colon and Rectal Surgery, Department of Surgery, University of Ulsan College of Medicine, Asan Medical Center, 88 Olympic-ro 43-gil, Songpa-gu, Seoul 05505, South Korea. csyu@amc.seoul.kr

Abstract

BACKGROUND

The emergence of restorative total proctocolectomy has significantly reduced the lifetime colorectal cancer risk associated with familial adenomatous polyposis (FAP). However, adenomas may develop in the ileal pouch over time and may even progress to carcinoma. We evaluated the cumulative incidence, time to development, and risk factors associated with ileal pouch adenoma.

AIM

To evaluate the cumulative incidence, time to development, and risk factors associated with pouch adenoma.

METHODS

In this retrospective, observational study conducted at a tertiary center, 95 patients with FAP who underwent restorative proctocolectomy at our center between 1989 and 2018 were consecutively included. The mean follow-up period was 88 mo.

RESULTS

Pouch adenomas were found in 24 (25.3%) patients, with a median time of 52 mo to their first formation. Tubular adenomas were detected in most patients (95.9%). There were no high-grade dysplasia or malignancies. Of the 24 patients with pouch adenomas, 13 had all detected adenomas removed. Among the 13 patients who underwent complete adenoma removal, four (38.5%) developed recurrence. Among 11 (45.8%) patients with numerous polyps within the pouch, seven

(63.6%) exhibited progression of pouch adenoma. The cumulative risks of pouch adenoma development at 5, 10, and 15 years after pouch surgery were 15.2%, 29.6%, and 44.1%, respectively. Severe colorectal polyposis (with more than 1000 polyps) was a significant risk factor for pouch adenoma development (hazard ratio, 2.49; 95% confidence interval: 1.04-5.96; $P = 0.041$).

CONCLUSION

Pouch adenomas occur at a fairly high rate in association with FAP after restorative proctocolectomy, and a high colorectal polyp count is associated with pouch adenoma development.

Key Words: Adenomatous polyposis coli; Familial adenomatous polyposis; Adenoma; Intestinal polyps; Proctocolectomy, restorative; Ileal pouch anal anastomosis

©The Author(s) 2022. Published by Baishideng Publishing Group Inc. All rights reserved.

Core Tip: This is a retrospective study that evaluated the cumulative incidence and risk factors for pouch adenoma in association with familial adenomatous polyposis following restorative proctocolectomy. The incidence of pouch adenoma was 25.3%, and the cumulative risk 15 years after pouch surgery was 44.1%. Severe colorectal polyposis was a significant risk factor for pouch adenoma development. In our series, 62% of adenomas did not recur after endoscopic removal, but 63% of patients under observation showed progression. There was no spontaneous adenoma diminution or disappearance. Close endoscopic pouch surveillance is essential, and new pouch adenoma management guidelines are needed.

Citation: Ryu HS, Yu CS, Kim YI, Lee JL, Kim CW, Yoon YS, Park IJ, Lim SB, Kim JC. Cumulative incidence and risk factors for pouch adenomas associated with familial adenomatous polyposis following restorative proctocolectomy. *World J Gastroenterol* 2022; 28(30): 4152-4162
URL: https://www.wjgnet.com/1007-9327/full/v28/i30/4152.htm
DOI: https://dx.doi.org/10.3748/wjg.v28.i30.4152

INTRODUCTION

Familial adenomatous polyposis (FAP) is a genetic syndrome caused by an adenomatous polyposis coli (*APC*) gene mutation that has an incidence of 1 in 10000 births[1]. This genetic variation is characterized by extensive polyposis in the colon and rectum, and patients with FAP have a lifetime colorectal cancer risk of 100% by the age of 35 to 40 years[2]. Hence, prophylactic surgical intervention is required for these individuals, and the currently favorable therapeutic option is a total proctocolectomy and ileal pouch-anal anastomosis (TPC/IPAA)[2]. TPC/IPAA increases life expectancy among patients with FAP by eliminating their metachronous colorectal cancer risk[3]. The postoperative disease course is determined by extracolonic manifestations, including duodenal adenoma and carcinoma, and desmoid tumors[4].

Cancers of the terminal ileum are extremely rare, and this region thus represents a far lower disease risk than the remaining rectal mucosa after ileorectal anastomosis. Notably, however, several studies have found a 35%-57% incidence of ileal pouch adenomas associated with FAP, which can progress to malignancy[5-11]. Given that most of these prior studies involved small sample sizes and were retrospective in nature, definitive results on these cancers are lacking, and the risk factors associated with pouch adenoma development remain to be established. Although these data are limited, the pouch adenoma incidence is reported to be quite high; therefore, long-term periodic surveillance is required. Most clinical guidelines recommend annual endoscopic surveillance of the anal transition zone (ATZ) mucosa after TPC/IPAA as a surgical management strategy for FAP patients. According to the National Comprehensive Cancer Network guidelines, this surveillance interval should be shortened to 6 mo if the adenoma is large or has advanced histology. However, there are currently no specific criteria directing more frequent surveillance. Moreover, with the currently implemented management approaches for pouch adenoma, uncertainty remains regarding the specific indications for endoscopic or surgical intervention[12-14]. More information is, therefore, needed regarding the incidence, natural course, and risk factors associated with pouch adenoma.

We investigated the cumulative incidence and time to development of pouch adenomas. In an FAP cohort after TPC/IPAA, we analyzed the clinical factors associated with pouch adenoma development.

MATERIALS AND METHODS

Study sample

Data on all patients with FAP who underwent pouch surgery at Asan Medical Center, Seoul, South Korea between November 1989 and December 2018 were identified from the hospital database. The FAP patients were identified by the presence of more than 100 colorectal adenomas. The indication for TPC/IPAA was FAP with or without malignancy. We excluded patients with attenuated FAP with fewer than 100 polyps (as per histopathology reports), as well as patients who did not receive TPC/IPAA. Demographic data, surgical details, original histopathology, and details of follow-up pouch endoscopic and pathologic findings were captured retrospectively. The definition of pouch adenoma included lesions that occurred in the ileum above the anastomosis site. Pouch adenoma progression was defined as an increase in the number or size of these lesions, as well as the development of dysplasia or malignancy, evident on histopathological examination. The severity of the duodenal polyposis in each case was assessed using the Spigelman classification[15] (Table 1). The study protocol was approved by the institutional review board of Asan Medical Center (registration No. 2021-0309) in accordance with the Declaration of Helsinki.

Surgical techniques of IPAA

An anal mucosectomy leaving a short rectal muscular cuff above the dentate line and transanal hand-sewn ileoanal anastomosis were performed for 72 of our enrolled FAP patients (75.8%). The remaining 23 patients (24.2%) underwent double-stapled anastomosis adjacent to the dentate line at the ATZ. The pouch construction in all patients was J-shaped using two ileal limbs of 15 cm in length.

Follow-up protocols

The regular follow-up protocols for our study patients included clinical examinations, pouch and upper gastrointestinal endoscopy, and abdominoperineal computed tomography. Pouch endoscopy was performed within 1 postoperative year. Subsequently, for patients who underwent a mucosectomy, endoscopic examinations were performed once every 2 years in the absence of any polyps. If polyps were observed during endoscopic follow-up, they were removed regardless of size. In patients with multiple polyps, those larger than 5 mm in diameter were removed, or a biopsy specimen was collected. More intensive follow-up was performed, at intervals of 6-12 mo, if warranted by the size, number, or pathologic characteristics of identified polyps. Patients with colorectal cancer in our cohort were followed at 6-mo intervals for 5 years and annually thereafter. Additionally, testing for carcinoembryonic antigens was conducted every 6 mo, and chest computed tomography was performed annually.

Statistical analysis

The quantitative variables in this study are expressed as medians with interquartile ranges (IQRs) or ranges, and categorical variables are summarized as frequencies and percentages. The clinicopathological variables for the patients with and without pouch adenomas were compared using the Kruskal-Wallis test and Fisher's exact test. The time to pouch adenoma formation was defined as the time from the date of surgery to the date of detection of the first histologically confirmed adenoma. Pouch adenoma–free survival was calculated using the Kaplan-Meier method. Multivariate Cox regression analysis based on backward elimination was used to assess the impact of variables on pouch adenoma–free survival with adjustment for variables reported to be associated with pouch adenoma–free survival in previous reports (colorectal polyp burden, time interval after IPAA, presence of desmoid tumors, and presence of gastric polyps and duodenal adenomas) in addition to basic patient characteristics, such as age and sex. Hazard ratios (HRs) with 95% confidence intervals (CIs) were also calculated. Statistical significance was established with a two-sided test at $P < 0.05$. All statistical analyses were performed using SPSS Statistics for Windows, version 25.0 (IBM Corp., Armonk, NY, United States).

RESULTS

A total of 175 patients with FAP who underwent pouch surgery were identified from the hospital database. Among these patients, we excluded 48 with attenuated FAP with fewer than 100 polyps according to histopathology reports. We also excluded six patients who underwent total colectomy procedures with ileorectal anastomosis, two who underwent end-ileostomy without ileal pouches, and one whose pouch was removed due to postoperative bleeding. We further excluded 23 patients who did not undergo postoperative follow-up sigmoidoscopy. The final study cohort, thus, comprised 95 patients with FAP who underwent TPC/IPAA (Figure 1).

The characteristics of the 95 FAP patients enrolled in this study are summarized in Table 2. The median follow-up period after pouch surgery was 88 mo (IQR, 61-141 mo). The median age at the time of IPAA was 32 years (IQR, 24-41 years). The median number of follow-up endoscopies was 5 (IQR, 3-7).

Table 1 Characteristics of familial adenomatous polyposis patients analyzed in this study

Variable	
Age at time of IPAA [yr, median (IQR)]	32 (24-41)
Sex, *n* (%)	
Male	52 (54.7)
Female	42 (45.3)
No. of colorectal polyps [*n*, median (IQR)]	350 (150-700)
Type of anastomosis, *n* (%)	
Hand-sewn with mucosectomy	72 (75.8)
Double stapling	23 (24.2)
No. of surveillances [*n*, median (IQR)]	
Upper GI endoscopy	5 (2-8)
Sigmoidoscopy	5 (3-7)
Pouch adenomas, *n* (%)	24 (25.3)
Time to pouch adenoma onset [mo, median (IQR)]	52 (28.3-114.3)
ATZ adenomas, *n* (%)	7 (7.4)
Gastric polyps, *n* (%)	70 (73.7)
Duodenal adenomas, *n* (%)	46 (48.5)
Spigelman stage, *n* (%)	
I	24 (25.3)
II	12 (12.6)
III	10 (10.5)
IV	0
Missing data	49 (51.6)
Desmoid tumors, *n* (%)	23 (24.2)
Colorectal cancer at time of IPAA, *n* (%)	43 (45.3)
Colon	24 (55.8)
Rectum	19 (44.2)

IPAA: Ileal pouch anal anastomosis; IQR: Interquartile range; ATZ: Anal transition zone; GI: Gastrointestinal.

We observed that 24 (25.3%) of our study patients had adenomas that had been histologically confirmed in the pouch mucosa above the anastomosis. The median time to first pouch adenoma detection was 52 mo (IQR, 28.3-114.3 mo). Adenomas arising from the ATZ below the anastomosis were detected in seven (7.4%) patients. Upper gastrointestinal endoscopy was also performed for all patients. Gastric polyps were present in 70 (73.3%) patients; these were mainly fundic gland polyps (75.7%) as per biopsy results. Duodenal adenomas were confirmed in 46 (48.5%) patients. Twenty-four, 12, and 10 patients were classified as having Spigelman stages I, II, and III lesions, respectively, and there were no stage IV cases. Twenty-three (24.2%) patients developed desmoid tumors. At the time of surgery, 43 (45.3%) patients had colorectal cancer.

Mutation analysis

Information on the underlying germline mutation was available for 40 (42.1%) FAP patients, among whom 28 (70.0%) harbored *APC* mutations, most commonly within exon 15 of the *APC* gene (64.3%). No significant difference was found in terms of the distribution of germline mutations between patients with and without pouch adenomas ($P = 0.21$).

Presence and distribution of pouch adenomas

The cumulative incidences of pouch adenomas at 5, 10, and 15 years after IPAA were 15.2%, 29.6%, and 44.1% (95%CI: 7.2%-22.4%, 15.8%-41.1%, and 25.3%-58.2%), respectively (Figure 2). Among the 24

Table 2 Clinical characteristics of study patients according to presence of pouch adenomas

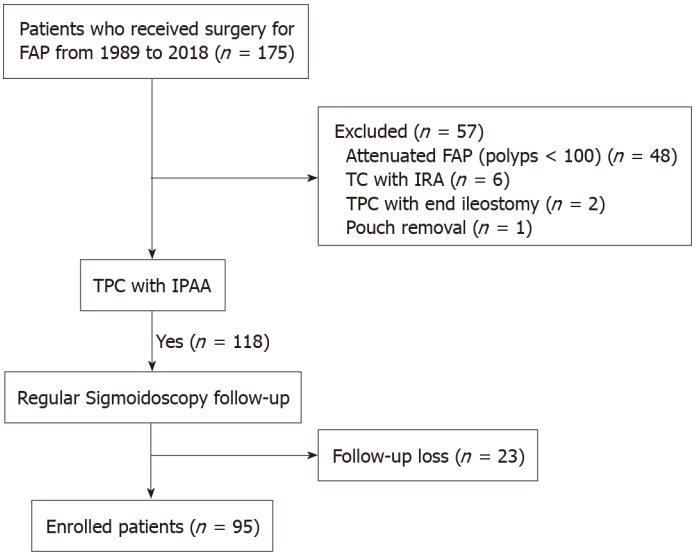
Characteristic	Presence of pouch adenomas (*n* = 24)	Absence of pouch adenomas (*n* = 71)	*P* value
Age at time of IPAA [yr, median (IQR)]	29 (20-40)	32 (26-41)	0.10
Sex (male), *n* (%)	16 (66.7)	36 (50.7)	0.17
No. of colorectal polyps [*n*, median (IQR)]	700 (325-1000)	250 (110-500)	0.001
Colorectal polyps < 1000, *n* (%)	16 (66.7)	64 (90.1)	0.006
Colorectal polyps ≥ 1000, *n* (%)	8 (33.3)	7 (9.9)	
Time interval after IPAA [mo, median (IQR)]	142 (106-199)	116 (91-175)	0.01
Mucosectomy, *n* (%)	19 (79.2)	53 (74.6)	0.66
Gastric polyps, *n* (%)	19 (79.2)	51 (71.8)	0.49
Gastric polyp burden, *n* (%)			0.31
< 20	13 (54.2)	41 (57.7)	
20-49	0	11 (15.5)	
≥ 50	6 (25.0)	0	
Duodenal adenomas, *n* (%)	16 (66.7)	30 (42.3)	0.039
Spigelman stage, *n* (%)			0.30
I	6 (37.5)	18 (60.0)	
II	6 (37.5)	6 (20)	
III	4 (25.0)	6 (20)	
Desmoid tumor, *n* (%)	4 (16.7)	19 (26.8)	0.32
NSAIDs use, *n* (%)	1 (4.2)	14 (19.7)	0.07
Colorectal cancer, *n* (%)	9 (37.5)	34 (47.9)	0.38

IPAA: Ileal pouch anal anastomosis; NSAIDs: Nonsteroidal anti-inflammatory drugs; IQR: Interquartile range.

patients with pouch adenomas, 13 (54.2%) had fewer than 12 countable lesions, whereas others had numerous polyps within the pouch. All countable adenomas were removed endoscopically regardless of size. Only one patient had to undergo a transanal excision to remove a pouch adenoma 31 mm in diameter. The median value of the maximum diameter was 3 mm (range, 2.0-31.0 mm). Tubular adenomas were detected in 23 (95.9%) patients, and tubule-villous adenomas were detected in two (8.4%) patients. There were no cases of high-grade dysplasia or malignancy in our study sample. During follow-up for the 13 patients who underwent complete removal of all detected adenomas, eight (61.5%) patients had no recurrence, and four (38.5%) developed recurrent adenomas, which were endoscopically resected. The remaining patient in this group was lost to follow-up, and the disease course after adenoma removal was not documented. For the 11 (45.8%) patients with numerous polyps within the pouch, only those larger than 5 mm were removed, and surveillance biopsy specimens were collected. In four (36.4%) patients, the adenomas remained unchanged, while seven (63.6%) patients exhibited pouch adenoma progression (Figure 3).

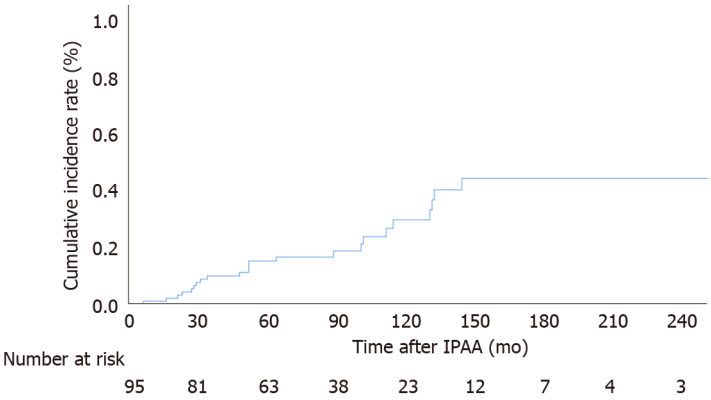
Clinical characteristics of study patients with and without pouch adenomas

Comparisons of the clinical characteristics among the FAP patients according to the presence of pouch adenomas are presented in Table 2. Compared with patients without adenomas, the pouch adenoma group had a significantly higher mean number of colorectal polyps at the time of surgery (700 *vs* 250, $P = 0.001$). Severe polyposis involving more than 1000 colorectal polyps was also significantly more common in the pouch adenoma group ($P = 0.006$). Additionally, patients with pouch adenomas (relative to those without pouch adenomas) were more likely to have duodenal adenomas (66.7% *vs* 42.3%, $P = 0.039$). There was no significant intergroup difference in the Spigelman adenoma stage distributions ($P = 0.30$) and no differences in the gastric polyp status (absent or present) or gastric polyp burden. Nonsteroidal anti-inflammatory drug (NSAID) treatment for desmoid tumors-including with celecoxib and meloxicam—was more common among patients without pouch adenomas, but this difference was not statistically significant (4.2% *vs* 19.7%, $P = 0.07$). There were no differences between the clinical characteristics of the study patients when stratified by the presence of colorectal cancer at the time of surgery ($P = 0.38$).



DOI: 10.3748/wjg.v28.i30.4152 **Copyright** ©The Author(s) 2022.

Figure 1 Patient selection flow chart. FAP: Familial adenomatous polyposis; TPC: Total proctocolectomy; IPAA: Ileal pouch-anal anastomosis; IRA: Ileorectal anastomosis.



DOI: 10.3748/wjg.v28.i30.4152 **Copyright** ©The Author(s) 2022.

Figure 2 Cumulative incidence of pouch adenomas. IPAA: Ileal pouch-anal anastomosis.

Associations between different clinical factors and pouch adenoma–free survival

Associations between different patient factors and pouch adenoma–free survival were evaluated (Table 3). Among the clinical factors analyzed, multivariate analysis revealed severe colorectal polyposis (with more than 1000 polyps) to be a significant risk factor for pouch adenoma development (HR, 2.49; 95%CI: 1.04-5.96; P = 0.041) (Figure 4). The presence of gastric polyps or a duodenal adenoma had no significant association with pouch adenoma development (P = 0.28 and 0.54, respectively).

DISCUSSION

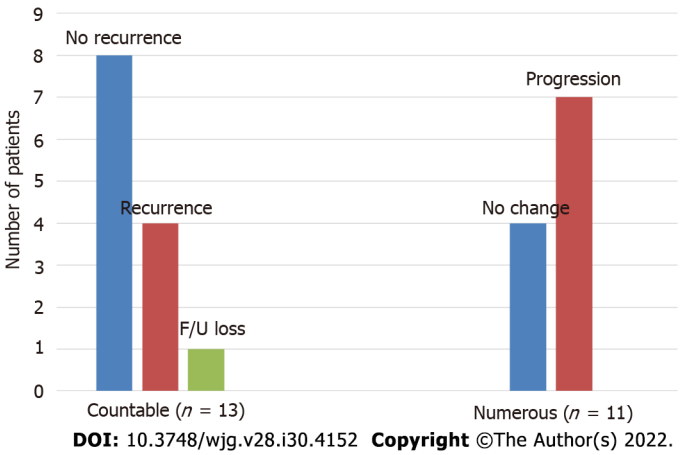
TPC/IPAA is now being implemented as a standard treatment to eliminate the risk of colorectal cancer in patients with FAP. However, the postoperative development of adenomas in the ileal pouch in these individuals has raised new concerns about appropriate postoperative surveillance and management approaches. In this study cohort, the incidence of pouch adenoma was 25.3% at a median follow-up of 88 mo (IQR, 61-141 mo) after IPAA. The cumulative risk of pouch adenoma was 15.2%, 29.6%, and 44.1% at 5, 10, and 15 years after TPC/IPAA, respectively. There were no cases of high-grade dysplasia or carcinoma in our cohort. We found that a higher colorectal polyp burden at the time of surgery was positively associated with the occurrence of pouch adenoma formation (P = 0.001). These results are consistent with the findings reported in prior studies[9,10,16-18].

Several potential risk factors associated with pouch adenoma development have been investigated previously, but they remain controversial. Consistent with the findings of Tonelli *et al*[10], we found in

Table 3 Risk factors associated with pouch adenoma-free survival

Variable	Univariate analysis		Multivariable analysis	
	HR (95%CI)	*P* value	HR (95%CI)	*P* value
Age	0.97 (0.93-1.01)	0.12		
Sex (male)	1.46 (0.62-3.44)	0.39		
No. of colorectal polyps (≥ 1000)	2.80 (1.18-6.63)	0.019	2.49 (1.04-5.96)	0.041
Time interval after IPAA	0.996 (0.99-1.003)	0.29		
Mucosectomy	1.54 (0.56-4.24)	0.40		
Gastric polyps	1.73 (0.64-4.68)	0.28		
Duodenal adenoma	2.31 (0.99-5.41)	0.54	2.08 (0.88-4.93)	0.10
Spigelman stage		0.15		
I-II	2.27 (0.92-5.55)	0.07		
III-IV	2.46 (0.73-8.25)	0.14		
Desmoid tumor	0.82 (0.28-2.44)	0.72		
NSAID use	0.29 (0.04-2.13)	0.22		
Colorectal cancer	0.58 (0.25-1.37)	0.21		

IPAA: Ileal pouch anal anastomosis; NSAIDs: Nonsteroidal anti-inflammatory drugs; HR: Hazard ratio; CI: Confidence interval.

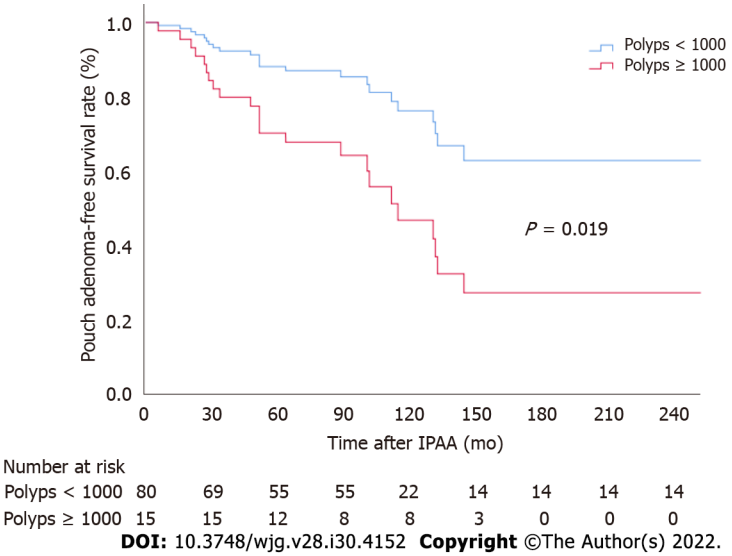


DOI: 10.3748/wjg.v28.i30.4152 **Copyright** ©The Author(s) 2022.

Figure 3 Progression of pouch adenomas. Patients in the countable group had all adenomas removed, and numerous groups were only undergoing surveillance biopsy.

our present analyses that a high colorectal polyp count at the time of IPAA was positively associated with pouch adenoma development. This result is likely to be assumed to be more aggressive disease. However, other authors have not observed an association between the severity of colonic disease and development of pouch adenoma[5].

Mutations of the *APC* gene predispose the carrier to benign polyps and malignancies in the upper gastrointestinal tract. Therefore, the risk of developing small bowel adenomas remains in these individuals even after TPC/IPAA. In this context, gastric or duodenal adenomas may be relevant to development of pouch adenoma. Ganschow *et el*[9] analyzed these variables previously and found that the presence of a gastric adenoma was a significant risk factor for developing a pouch adenoma (P = 0.0019). Several investigator groups have also reported that the presence of a duodenal adenoma is associated with pouch adenoma formation[10,16]. Tonelli *et al*[10] observed that the severity of duodenal polyposis was also relevant in this regard. As with the findings of other studies, our experience has been that patients who develop pouch adenomas are more likely to have had duodenal adenomas, although this was not observed to be a significant risk factor in our present multivariate analysis.



DOI: 10.3748/wjg.v28.i30.4152 **Copyright** ©The Author(s) 2022.

Figure 4 Pouch adenoma-free survival according to colorectal polyp burden at the time of ileal pouch-anal anastomosis. IPAA: Ileal pouch-anal anastomosis.

There has been little research conducted on the association between the site of an *APC* mutation and the occurrence of pouch adenoma. No such association has been identified in earlier studies[9,10,16], nor was such an association identified in our present analysis. However, in previous reports and in our present series, *APC* mutation data were not available for all subjects. Moreover, the low number of patients who underwent this mutation analysis in our present series and in prior study cohorts could not yield the statistical power needed to determine whether the *APC* mutation site is associated with the tendency to develop pouch adenomas. Additionally, a recently published study of genotype-phenotype associations between *APC* mutations and pouch adenomas found that patients with either indel/deletion mutations or exon 15 mutations had a higher tendency for pouch adenoma formation (P = 0.002 and 0.019, respectively)[19]. Hence, further larger-scale research is required to investigate the association between underlying germline mutations and pouch adenoma development.

Several authors have implicated colonic metaplasia of the ileal mucosa—an adaptive response of the neorectum—as a predisposing condition to the onset of ileal adenoma development[20]. Advanced adenomas with high-grade dysplasia were observed in about 18% of previous study samples[5,18]. However, no case of an advanced adenoma was detected in our present study cohort, possibly because adenomas were aggressively removed from our patients, even if small. If ileal pouch adenomas progress to carcinoma, following the classic adenoma-carcinoma sequence, a higher number and larger size of polyps may be associated with the severity of the dysplasia. Tajika *et al*[18] reported that the postoperative time interval was significantly associated with the maximum ileal pouch adenoma size (P = 0.0214). Progression of a pouch adenoma to invasive carcinoma appears to be rare, with an incidence of less than 1% in patients that undergo IPAA[8,9,19]. Moreover, the majority of carcinomas observed after IPAA arise in the residual rectal mucosa or anal canal, although several cases of carcinoma inside the ileal pouch have been described in the past few years[18]. Tonelli *et al*[10] found that the development of malignancy in the terminal ileum can present with a rapid disease course and does not seem to follow the classic adenoma-carcinoma sequence. In some patients, ileal polyps are not detected by endoscopic follow-up until the development of a pouch carcinoma, and the mean interval between pouch construction and the diagnosis of carcinoma can be very short (range, 3-16.4 years).

Clinically, the treatment of pouch adenomas depends on the number, size, shape, and histological features—as for the gastric or duodenal polyps. According to the American Society for Gastrointestinal Endoscopy and British Society of Gastroenterology guidelines, all types of gastric or duodenal polyps detected *via* endoscopy need to be sampled using biopsy forceps for evaluation[21-23]. In the case of adenomatous polyps, these guidelines recommend complete endoscopic removal when it is safe to do so, given the higher probability of malignant transformation[22,23]. Endoscopic follow-up should be repeated at 6 mo for incompletely resected polyps or for those with high-grade dysplasia; it can be conducted again at 12 mo for all other polyps[22]. Although the data are currently limited, 62% of our cohort did not develop adenoma recurrence after adenoma removal, whereas 63% of our patients under observation showed progression. There was no spontaneous diminution or disappearance of any adenoma in our study cohort. Hence, it is important to be aware of the risk of pouch neoplasia when caring for FAP patients after IPAA, and—to enable evaluation and treatment at the same time—we recommend endoscopic resection when the adenoma is detected. If numerous polyps are present, random biopsy sampling is required, and polyps larger than 5 mm should be removed.

Interestingly, our FAP patients who used NSAIDs as a treatment for desmoid tumors rarely developed pouch adenomas. This finding is presumed to be related to the chemopreventive effect of these drugs. Chemoprevention with NSAIDs is a treatment option considered to facilitate the management of the remaining rectum or pouch in selected postoperative patients[13]. In a prior randomized controlled study, patients with FAP and attenuated FAP treated with celecoxib following prophylactic surgery showed reductions in polyp number and diameter[24]. NSAIDs may thus be considered if not all of the numerous polyps within the pouch can be removed, although there are currently no Food and Drug Administration–approved drugs for this indication.

There were some limitations to this study. First, this was a retrospective cohort study with a small sample size, and there may have been unknown confounders. However, as we were investigating a rare disease, there have been few studies to date that have analyzed a substantial number of affected patients. Therefore, in relative terms, our sample size was large, and the patients were followed for a considerable length of time. A second limitation was that whereas all of the patients had a clinical phenotype of 100 or more colorectal polyps and biopsy-confirmed FAP, *APC* genetic mutation analysis was only performed for about 50% of the patients. This limited the strength of our findings related to these mutations. Additionally, there was no consistent endoscopic treatment standard in our cohort. When a polyp was countable, it was removed regardless of its size. In patients with multiple polyps, however, the individual judgment of the endoscopist determined whether to perform endoscopic resection or observation. The indications used for polyp removal were, therefore, not clear.

Overall, our study findings provide further evidence for the need for standardized endoscopic surveillance of FAP patients following TPC/IPAA. Pouch endoscopy should be performed yearly for these patients, and standardized biopsy and removal protocols are needed if pouch adenomas are observed. Furthermore, surveillance should be tailored depending on the presence and characteristics of the pouch adenoma. In the future, validation of whether an annual endoscopic interval is appropriate is required, as is an evaluation of the feasibility and effectiveness of endoscopic resection of a pouch adenoma.

CONCLUSION

In conclusion, pouch adenomas occur at a fairly high rate over time in association with FAP after IPAA. A high colorectal polyp count increases the risk of developing a pouch adenoma in this patient population. In our experience, the progression of pouch adenomas to high-grade dysplasia or carcinoma is rare. However, this risk is not negligible, and the long-term risk of this cannot presently be well quantified. Close surveillance of the pouch should thus be mandatory, and new guidelines for the management of pouch adenomas are essential.

ARTICLE HIGHLIGHTS

Research background

Restorative total proctocolectomy is now being implemented as a standard treatment to eliminate the risk of colorectal cancer in patients with familial adenomatous polyposis (FAP). However, the postoperative development of adenomas in the ileal pouch in these individuals has raised new concerns about appropriate postoperative surveillance and management approaches.

Research motivation

More information is needed regarding the incidence, natural course, and risk factors associated with pouch adenoma.

Research objectives

To investigate the cumulative incidence and time to development of pouch adenomas and analyze the clinical factors associated with pouch adenoma development among patients with FAP after restorative proctocolectomy.

Research methods

A retrospective cohort study was carried out with 95 consecutive patients with FAP who underwent restorative proctocolectomy at Asan Medical Center (Seoul, South Korea) from November 1989 to December 2018.

Research results

The cumulative risks of pouch adenoma development at 5, 10, and 15 years after pouch surgery were 15.2%, 29.6%, and 44.1%, respectively. Severe colorectal polyposis (with more than 1000 polyps) was a

significant risk factor for pouch adenoma development (hazard ratio, 2.49; 95% confidence interval: 1.04-5.96; $P = 0.041$).

Research conclusions

We recommend endoscopic resection when the adenoma is detected. If numerous polyps are present, random biopsy sampling is required, and polyps larger than 5 mm should be removed. Close surveillance of the pouch should be mandatory, and new guidelines for the management of pouch adenomas are required.

Research perspectives

In the future, validation of whether an annual endoscopic interval is appropriate is required, as is an evaluation of the feasibility and effectiveness of endoscopic resection of a pouch adenoma.

FOOTNOTES

Author contributions: Ryu HS designed and performed the research and wrote the paper; Yu CS designed the research and supervised the report; Kim YI, Lee JL, Kim CW, Yoon YS, Park IJ, Lim SB, and Kim JC provided clinical advice and supervised the report.

Institutional review board statement: The protocol for this research project has been approved by a suitably constituted ethics committee of the institution (Committee of Asan Medical Center, Approval No. 2021-0309), and it conforms to the provisions of the Declaration of Helsinki.

Informed consent statement: Patients were not required to give informed consent to the study because the analysis used anonymous clinical data that were obtained after each patient agreed to treatment by written consent.

Conflict-of-interest statement: This study did not receive a specific grant from any funding agency in the public, commercial, or not-for-profit sectors.

Data sharing statement: No additional data are available.

Open-Access: This article is an open-access article that was selected by an in-house editor and fully peer-reviewed by external reviewers. It is distributed in accordance with the Creative Commons Attribution NonCommercial (CC BY-NC 4.0) license, which permits others to distribute, remix, adapt, build upon this work non-commercially, and license their derivative works on different terms, provided the original work is properly cited and the use is non-commercial. See: https://creativecommons.org/Licenses/by-nc/4.0/

Country/Territory of origin: South Korea

ORCID number: Hyo Seon Ryu 0000-0003-2606-9973; Chang Sik Yu 0000-0001-9401-9981; Young Il Kim 0000-0002-0212-9196; Jong Lyul Lee 0000-0002-5878-8000; Chan Wook Kim 0000-0002-2382-0939; Yong Sik Yoon 0000-0002-3196-8423; In Ja Park 0000-0001-5355-3969; Seok-Byung Lim 0000-0001-8824-4808; Jin Cheon Kim 0000-0003-4823-8619.

S-Editor: Yan JP
L-Editor: Wang TQ
P-Editor: Yan JP

REFERENCES

1 **Bisgaard ML**, Fenger K, Bülow S, Niebuhr E, Mohr J. Familial adenomatous polyposis (FAP): frequency, penetrance, and mutation rate. *Hum Mutat* 1994; **3**: 121-125 [PMID: 8199592 DOI: 10.1002/humu.1380030206]
2 **Nieuwenhuis MH**, Mathus-Vliegen LM, Slors FJ, Griffioen G, Nagengast FM, Schouten WR, Kleibeuker JH, Vasen HF. Genotype-phenotype correlations as a guide in the management of familial adenomatous polyposis. *Clin Gastroenterol Hepatol* 2007; **5**: 374-378 [PMID: 17368237 DOI: 10.1016/j.cgh.2006.12.014]
3 **Koskenvuo L**, Ryynänen H, Lepistö A. Timing of prophylactic colectomy in familial adenomatous polyposis. *Colorectal Dis* 2020; **22**: 1553-1559 [PMID: 32441460 DOI: 10.1111/codi.15151]
4 **Half E**, Bercovich D, Rozen P. Familial adenomatous polyposis. *Orphanet J Rare Dis* 2009; **4**: 22 [PMID: 19822006 DOI: 10.1186/1750-1172-4-22]
5 **Friederich P**, de Jong AE, Mathus-Vliegen LM, Dekker E, Krieken HH, Dees J, Nagengast FM, Vasen HF. Risk of developing adenomas and carcinomas in the ileal pouch in patients with familial adenomatous polyposis. *Clin Gastroenterol Hepatol* 2008; **6**: 1237-1242 [PMID: 18848811 DOI: 10.1016/j.cgh.2008.06.011]
6 **Pommaret E**, Vienne A, Lefevre JH, Sogni P, Florent C, Desaint B, Parc Y. Prevalence and risk factors for adenomas in the ileal pouch and the afferent loop after restorative proctocolectomy for patients with familial adenomatous polyposis. *Surg Endosc* 2013; **27**: 3816-3822 [PMID: 23636532 DOI: 10.1007/s00464-013-2980-x]

7 **Zahid A**, Kumar S, Koorey D, Young CJ. Pouch adenomas in Familial Adenomatous Polyposis after restorative proctocolectomy. *Int J Surg* 2015; **13**: 133-136 [PMID: 25498488 DOI: 10.1016/j.ijsu.2014.11.048]

8 **Boostrom SY**, Mathis KL, Pendlimari R, Cima RR, Larson DW, Dozois EJ. Risk of neoplastic change in ileal pouches in familial adenomatous polyposis. *J Gastrointest Surg* 2013; **17**: 1804-1808 [PMID: 23949425 DOI: 10.1007/s11605-013-2319-x]

9 **Ganschow P**, Trauth S, Hinz U, Schaible A, Büchler MW, Kadmon M. Risk Factors Associated With Pouch Adenomas in Patients With Familial Adenomatous Polyposis. *Dis Colon Rectum* 2018; **61**: 1096-1101 [PMID: 30086059 DOI: 10.1097/DCR.0000000000001157]

10 **Tonelli F**, Ficari F, Bargellini T, Valanzano R. Ileal pouch adenomas and carcinomas after restorative proctocolectomy for familial adenomatous polyposis. *Dis Colon Rectum* 2012; **55**: 322-329 [PMID: 22469800 DOI: 10.1097/DCR.0b013e318241e6f2]

11 **Tajika M**, Niwa Y, Bhatia V, Tanaka T, Ishihara M, Yamao K. Risk of ileal pouch neoplasms in patients with familial adenomatous polyposis. *World J Gastroenterol* 2013; **19**: 6774-6783 [PMID: 24187452 DOI: 10.3748/wjg.v19.i40.6774]

12 **Vasen HF**, Möslein G, Alonso A, Aretz S, Bernstein I, Bertario L, Blanco I, Bülow S, Burn J, Capella G, Colas C, Engel C, Frayling I, Friedl W, Hes FJ, Hodgson S, Järvinen H, Mecklin JP, Møller P, Myrhøi T, Nagengast FM, Parc Y, Phillips R, Clark SK, de Leon MP, Renkonen-Sinisalo L, Sampson JR, Stormorken A, Tejpar S, Thomas HJ, Wijnen J. Guidelines for the clinical management of familial adenomatous polyposis (FAP). *Gut* 2008; **57**: 704-713 [PMID: 18194984 DOI: 10.1136/gut.2007.136127]

13 **National Comprehensive Cancer Network**. NCCN Genetic/Familial High-Risk Assessment: Colorectal. 2020. Available from: http://www.nccn.org/

14 **Stjepanovic N**, Moreira L, Carneiro F, Balaguer F, Cervantes A, Balmaña J, Martinelli E; ESMO Guidelines Committee. Electronic address: clinicalguidelines@esmo.org. Hereditary gastrointestinal cancers: ESMO Clinical Practice Guidelines for diagnosis, treatment and follow-up†. *Ann Oncol* 2019; **30**: 1558-1571 [PMID: 31378807 DOI: 10.1093/annonc/mdz233]

15 **Spigelman AD**, Williams CB, Talbot IC, Domizio P, Phillips RK. Upper gastrointestinal cancer in patients with familial adenomatous polyposis. *Lancet* 1989; **2**: 783-785 [PMID: 2571019 DOI: 10.1016/s0140-6736(89)90840-4]

16 **Parc YR**, Olschwang S, Desaint B, Schmitt G, Parc RG, Tiret E. Familial adenomatous polyposis: prevalence of adenomas in the ileal pouch after restorative proctocolectomy. *Ann Surg* 2001; **233**: 360-364 [PMID: 11224623 DOI: 10.1097/00000658-200103000-00009]

17 **van Duijvendijk P**, Vasen HF, Bertario L, Bülow S, Kuijpers JH, Schouten WR, Guillem JG, Taat CW, Slors JF. Cumulative risk of developing polyps or malignancy at the ileal pouch-anal anastomosis in patients with familial adenomatous polyposis. *J Gastrointest Surg* 1999; **3**: 325-330 [PMID: 10481126 DOI: 10.1016/s1091-255x(99)80075-4]

18 **Tajika M**, Tanaka T, Ishihara M, Hirayama Y, Oonishi S, Mizuno N, Kuwahara T, Okuno N, Matsumoto S, Ooshiro T, Kinoshita T, Komori K, Bhatia V, Hara K, Yatabe Y, Niwa Y. Long-term outcomes of metachronous neoplasms in the ileal pouch and rectum after surgical treatment in patients with familial adenomatous polyposis. *Endosc Int Open* 2019; **7**: E691-E698 [PMID: 31073536 DOI: 10.1055/a-0849-9465]

19 **Kariv R**, Rosner G, Fliss-Isakov N, Gluck N, Goldstein A, Tulchinsky H, Zelber-Sagi S. Genotype-Phenotype Associations of APC Mutations With Pouch Adenoma in Patients With Familial Adenomatous Polyposis. *J Clin Gastroenterol* 2019; **53**: e54-e60 [PMID: 29099467 DOI: 10.1097/MCG.0000000000000950]

20 **Corfield AP**, Warren BF, Bartolo DC, Wagner SA, Clamp JR. Mucin changes in ileoanal pouches monitored by metabolic labelling and histochemistry. *Br J Surg* 1992; **79**: 1209-1212 [PMID: 1467907 DOI: 10.1002/bjs.1800791139]

21 **Burke CA**, Beck GJ, Church JM, van Stolk RU. The natural history of untreated duodenal and ampullary adenomas in patients with familial adenomatous polyposis followed in an endoscopic surveillance program. *Gastrointest Endosc* 1999; **49**: 358-364 [PMID: 10049420 DOI: 10.1016/s0016-5107(99)70013-1]

22 **Goddard AF**, Badreldin R, Pritchard DM, Walker MM, Warren B; British Society of Gastroenterology. The management of gastric polyps. *Gut* 2010; **59**: 1270-1276 [PMID: 20675692 DOI: 10.1136/gut.2009.182089]

23 **Yang J**, Gurudu SR, Koptiuch C, Agrawal D, Buxbaum JL, Abbas Fehmi SM, Fishman DS, Khashab MA, Jamil LH, Jue TL, Law JK, Lee JK, Naveed M, Qumseya BJ, Sawhney MS, Thosani N, Wani SB, Samadder NJ. American Society for Gastrointestinal Endoscopy guideline on the role of endoscopy in familial adenomatous polyposis syndromes. *Gastrointest Endosc* 2020; **91**: 963-982.e2 [PMID: 32169282 DOI: 10.1016/j.gie.2020.01.028]

24 **Cruz-Correa M**, Hylind LM, Romans KE, Booker SV, Giardiello FM. Long-term treatment with sulindac in familial adenomatous polyposis: a prospective cohort study. *Gastroenterology* 2002; **122**: 641-645 [PMID: 11874996 DOI: 10.1053/gast.2002.31890]

World Journal of Gastroenterology

Submit a Manuscript: https://www.f6publishing.com

World J Gastroenterol 2022 August 14; 28(30): 4163-4173

DOI: 10.3748/wjg.v28.i30.4163

ISSN 1007-9327 (print) ISSN 2219-2840 (online)

ORIGINAL ARTICLE

Retrospective Study

Changes in the esophagogastric junction outflow obstruction manometric feature based on the Chicago Classification updates

Yue-Yuan Li, Wen-Ting Lu, Jian-Xiang Liu, Li-Hong Wu, Meng Chen, Hong-Mei Jiao

Specialty type: Gastroenterology and hepatology

Provenance and peer review: Unsolicited article; Externally peer reviewed.

Peer-review model: Single blind

Peer-review report's scientific quality classification

Grade A (Excellent): 0
Grade B (Very good): B
Grade C (Good): C, C, C
Grade D (Fair): 0
Grade E (Poor): 0

P-Reviewer: Herbella FAM, Brazil; Sweis R, United Kingdom

Received: March 10, 2022
Peer-review started: March 10, 2022
First decision: April 11, 2022
Revised: April 21, 2022
Accepted: July 18, 2022
Article in press: July 18, 2022
Published online: August 14, 2022

Yue-Yuan Li, Wen-Ting Lu, Meng Chen, Hong-Mei Jiao, Department of Geriatrics, Peking University First Hospital, Beijing 100034, China

Jian-Xiang Liu, Li-Hong Wu, Department of Gastroenterology and Hepatology, Peking University First Hospital, Beijing 100034, China

Corresponding author: Hong-Mei Jiao, MD, Chief Physician, Department of Geriatrics, Peking University First Hospital, No. 8 Xishiku Street, Xicheng District, Beijing 100034, China. jiaohm@139.com

Abstract

BACKGROUND

The critical diagnostic criteria for esophagogastric junction outflow obstruction (EGJOO) were published in the latest Chicago Classification version 4.0 (CCv4.0). In addition to the previous criterion [elevated integrated relaxation pressure (IRP) in supine position], manometric diagnosis of EGJOO requires meeting the criteria of elevated median-IRP during upright wet swallows and elevated intrabolus pressure. However, with the diagnostic criteria modification, the change in manometric features of EGJOO remained unclear.

AIM

To evaluate the esophageal motility characteristics of patients with EGJOO and select valuable parameters for confirming the diagnosis of EGJOO.

METHODS

We performed a retrospective analysis of 370 patients who underwent high-resolution manometry with 5 mL water swallows × 10 in supine, × 5 in upright position and the rapid drink challenge (RDC) with 200 mL water from November 2016 to November 2021 at Peking University First Hospital. Fifty-one patients with elevated integrated supine IRP and evidence of peristalsis were enrolled, with 24 patients meeting the updated manometric EGJOO diagnosis (CCv4.0) as the EGJOO group and 27 patients not meeting the updated EGJOO criteria as the isolated supine IRP elevated group (either normal median IRP in upright position or less than 20% of supine swallows with elevated IBP). Forty-six patients with normal manometric features were collected as the normal high-resolution manometry (HRM) group. Upper esophageal sphincter (UES), esophageal body, and lower esophageal sphincter (LES) parameters were compared between groups.

RESULTS

Compared with the normal HRM group, patients with EGJOO (CCv4.0) had significantly lower proximal esophageal contractile integral (PECI) and proximal esophageal length (PEL), with elevated IRP on RDC ($P < 0.05$ for each comparison), while isolated supine IRP elevated patients had no such feature. Patients with EGJOO also had more significant abnormalities in the esophagogastric junction than isolated supine IRP elevated patients, including higher LES resting pressure (LESP), intrabolus pressure, median supine IRP, median upright IRP, and IRP on RDC ($P < 0.05$ for each comparison). Patients with dysphagia had significantly lower PECI and PEL than patients without dysphagia among the fifty-one with elevated supine IRP. Further multivariate analysis revealed that PEL, LESP, and IRP on RDC are factors associated with EGJOO. The receiver-operating characteristic analysis showed UES nadir pressure, PEL, PECI, LESP, and IRP on RDC are parameters supportive for confirming the diagnosis of EGJOO.

CONCLUSION

Based on CCv4.0, patients with EGJOO have more severe esophagogastric junction dysfunction and are implicated in the proximal esophagus. Additionally, several parameters are supportive for confirming the diagnosis of EGJOO.

Key Words: Esophagogastric junction outflow obstruction; High-resolution manometry; Esophageal motility disorders; Upper esophageal sphincter; Proximal esophagus

©The Author(s) 2022. Published by Baishideng Publishing Group Inc. All rights reserved.

Core Tip: This is a retrospective study to evaluate the motility features of esophagogastric junction outflow obstruction (EGJOO). This is the first detailed study of EGJOO based on the latest Chicago Classification. Patients with EGJOO showed more substantial abnormalities at the esophagogastric junction than patients who met the previous criteria, and the motility disorder of EGJOO is implicated in the proximal esophagus. Additionally, the upper esophageal sphincter nadir pressure, proximal esophageal contractile integral, proximal esophageal length, lower esophageal sphincter resting pressure, and integrated relaxation pressure on rapid drink challenge contribute to confirming the diagnosis of EGJOO.

Citation: Li YY, Lu WT, Liu JX, Wu LH, Chen M, Jiao HM. Changes in the esophagogastric junction outflow obstruction manometric feature based on the Chicago Classification updates. *World J Gastroenterol* 2022; 28(30): 4163-4173

URL: https://www.wjgnet.com/1007-9327/full/v28/i30/4163.htm

DOI: https://dx.doi.org/10.3748/wjg.v28.i30.4163

INTRODUCTION

Esophagogastric junction outflow obstruction (EGJOO) is a common type of esophageal motility disorder in patients with dysphagia or chest pain. EGJOO includes a group of heterogeneous disorders with common manometric features for esophageal outflow obstruction. Progress has been made toward understanding the manometric features and symptoms of patients who meet the EGJOO criteria[1-5]. The Chicago Classification version 4.0 (CCv4.0) updated the critical diagnostic criteria for the manometric diagnosis of EGJOO, including increased median-integrated relaxation pressure (IRP) in supine and upright positions, ≥ 20% elevated intrabolus pressure (IBP) in the supine position, and evidence of peristalsis[1]. A clinically relevant conclusive diagnosis of EGJOO requires a manometric diagnosis of EGJOO as described above, and clinically relevant symptoms with at least one of the complementary tests, including timed barium esophagram and functional lumen imaging probe. Additional provocative tests including rapid drink challenge (RDC), solid test swallows, or pharmacologic provocation may also strengthen the confidence in an EGJOO diagnosis and helps to identify the causes of symptoms, particularly in borderline cases. Compared with the previous version (v3.0)[6], the new diagnostic criteria provided a more rigorous definition for EGJOO by adding criteria for median IRP in the secondary position, IBP, clinically relevant symptoms, and complementary tests, which aid in distinguishing pathological motility disorder and abnormal manometry caused by mechanical effect, opioid use, or other nonpathological motility disorders[7]. However, the change in manometric features of EGJOO with the diagnostic criteria modification remained unclear. This study aims to investigate the esophageal motility features of patients with the manometric diagnosis of EGJOO and to identify high-resolution manometry (HRM) parameters that are supportive for confirming the diagnosis of EGJOO.

MATERIALS AND METHODS

Patient and data selection

Patients who completed esophageal HRM and upper gastrointestinal endoscopy from November 2016 to November 2021 at Peking University First Hospital were retrospectively analyzed. Exclusion criteria included: (1) Patients under 18 years of age; (2) A history of upper gastrointestinal or mediastinal surgery; (3) Previous endoscopic treatment for esophageal motor disorders; (4) Diseases with abnormal intraabdominal pressure, such as intestinal obstruction or ascites; (5) Use of opiates; and (6) Secondary factors identified by upper gastrointestinal endoscopy or endoscopic ultrasonography, especially for hiatal hernia, infiltrative disease, mechanical obstruction, and extrinsic compression. The normal HRM group was obtained from patients who underwent HRM for mild symptoms such as dysphagia, retrosternal pain, regurgitation, or heartburn, with normal HRM results. The patients also fulfilled normal results in pH-monitoring and upper gastrointestinal endoscopy, in order to exclude the possibility of organic diseases. Demographic data, including age, gender, body mass index (BMI), previous medical and surgical history were collected, and symptoms were extracted from self-report questionnaires completed by patients before HRM. The Institutional Review Board (IRB) of the Peking University First Hospital approved the study protocol (2022-099). The IRB waived the requirement for informed consent because our retrospective analysis used completely anonymized data.

HRM protocol

HRM studies were conducted according to standard clinical protocol, using a 4.2-mm outer diameter, 36-sensor solid-state HRM catheter (ManoScan™, Medtronic, Los Angeles, CA, United States)[8]. Experienced nurses performed nasal canal anesthesia and transnasal placement of the solid-state manometry catheter with the patient sitting upright after an 8-h fast. Sensors were positioned to ensure a complete record of the hypopharynx, esophagus, and proximal stomach. The manometric protocol consisted of a landmark phase captured during a quiet rest in the supine position at the beginning, followed by ten 5-mL ambient temperature water swallows in the supine position, then five 5-mL water swallows in the upright position, with 30 s between each swallow, and finally a RDC of 200 mL water in the upright position.

HRM data analysis

HRM Clouse plots were analyzed using computerized HRM analysis software (Manoview, Medtronic). All pressure measurements were referenced to the gastric pressure.

Upper esophageal sphincter parameters[9,10]: Upper esophageal sphincter (UES) parameters were measured within the UES high-pressure zone defined by a 20-mmHg isobaric contour, consisting of UES length (UESL), UES resting pressure (UESP), nadir pressure (UESNP), and postdeglutitive UES contractile integral (PD-UESCI). PD-UESCI was measured by the smart mouse at the beginning of the deglutitive UES relaxation to the end of the proximal esophageal contraction or the beginning of the transition zone (Figure 1).

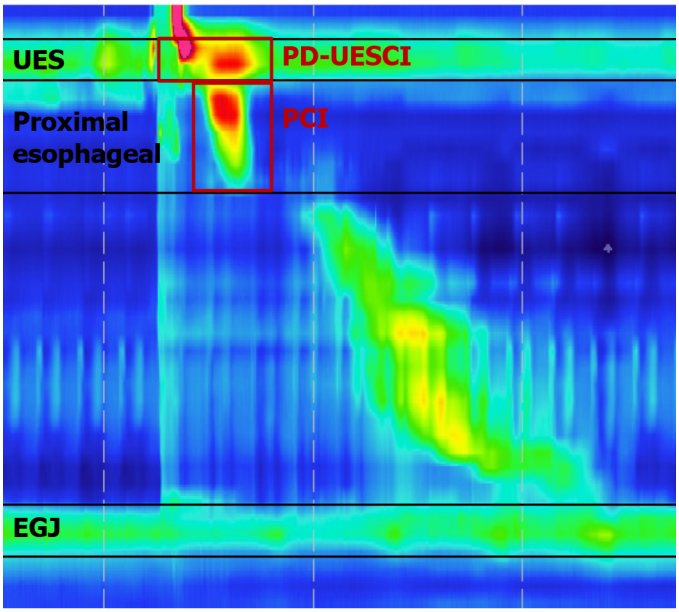
Proximal esophageal parameters[9,11]: Proximal esophageal parameters measured from the lower border of the UES to either a break between the proximal and distal segment or the area with the lowest pressure between the proximal and distal segment of the contraction in patients showed no break in the 20-mmHg isobaric contour. Measurements of the proximal esophageal segment included proximal esophageal segment length (PEL), proximal latency (PL, defined as the time interval between UES relaxation to the transition zone), and proximal esophageal contractile integral (PECI, = amplitude × duration × length, measured using a 20-mmHg pressure threshold).

Esophageal body parameters[12]: Esophageal shortening during RDC (ES-RDC) was defined as an upward lift of lower esophageal sphincter (LES) for more than 1 cm, as measured by the length variation between the baseline position of the LES before RDC and its maximal axial position during RDC or within 60 s after the start of RDC. The distal latency (DL) and distal contraction integral (DCI) were calculated automatically using the ManoView system.

Esophagogastric junction parameters[13]: The LES resting pressure (LESP), IBP were calculated automatically using the ManoView system. The median IRP in the supine and upright positions was selected from a list of IRP in each position. The IRP on RDC was assessed in the window beginning with dilatative UES relaxation to the end of esophagogastric junction (EGJ) relaxation for free drinking lasting less than 30 s, or during the first 30 s of the window for free drinking lasting longer.

Statistical analysis

Statistical analysis was performed using SPSS 25.0, and GraphPad Prism 8.0. The chi-square test was used for the comparison of categorical variables. The Student's *t*-test and analysis of variance were used to compare quantitative data with normal distribution between groups, and the results are expressed as mean ± SD. Multivariate analysis was performed with stepwise variable selection. The receiver-



DOI: 10.3748/wjg.v28.i30.4163 **Copyright** ©The Author(s) 2022.

Figure 1 Key metrics of Clouse plots used in our study. The postdeglutitive upper esophageal sphincter (UES) contractile integral was measured using a 20-mmHg pressure threshold from the beginning of the deglutitive UES relaxation to the end of the proximal esophageal contraction or the beginning of the transition zone. The proximal esophageal contractile integral was measured using a 20-mmHg pressure threshold from the lower border of the UES to either a break between the proximal and distal segment or the area with the lowest pressure between the proximal and distal segment of the contraction in patients showed no break in the 20-mmHg isobaric contour. UES: Upper esophageal sphincter; PD-UESCI: Postdeglutitive upper esophageal sphincter contractile integral; PCI: Proximal contractile integral; EGJ: Esophagogastric junction.

operating characteristics (ROC) curve was used to illustrate the diagnostic ability of the HRM parameters for EGJOO. A P value < 0.05 was considered statistically significant.

RESULTS

Patient characteristics

Fifty-one patients (33 female, 59.5 ± 1.7 years) fulfilling the criteria of EGJOO (CCv3.0) were identified, with supine IRP ≥ 15 mmHg (Medtronic) and evidence of peristalsis. Among them, 24 patients (14 female, 62.7 ± 2.7 years) met the manometric definitions of EGJOO (CCv4.0), while 27 patients (19 female, 56.6 ± 11.1 years) failed to meet the updated EGJOO criteria formed the isolated supine IRP elevated group, with either normal median IRP in upright position or less than 20% of supine swallows with elevated IBP. The normal HRM group comprised 46 patients (24 female, 50.2 ± 2.2 years) with normal HRM results (Figure 2). Patients in the EGJOO group were older than the normal HRM group. There was no difference in gender or BMI between these three groups. As for symptoms, among the 24 patients with manometric diagnosis of EGJOO (CCv4.0), there were seven with dysphagia and five with retrosternal pain that might be clinically relevant. Symptoms were also counted in isolated supine IRP elevated group and normal HRM group as shown in Table 1. The occurrence of dysphagia, retrosternal pain, and regurgitation did not differ between these three groups. Among the 24 patients with manometric diagnosis of EGJOO (CCv4.0), there were five patients with spastic features, five with hypercontractile features, two with ineffective motility, and twelve with no evidence of peristalsis disorders.

Esophageal HRM parameters

Table 2 details the differences in manometric parameters among EGJOO, isolated supine IRP elevated group, and the normal HRM group.

UES parameters: UESNP was significantly higher in the EGJOO group and the isolated supine IRP elevated group than in the normal HRM group. There was no significant difference in UESL, UESP, and PD-UESCI between the three groups.

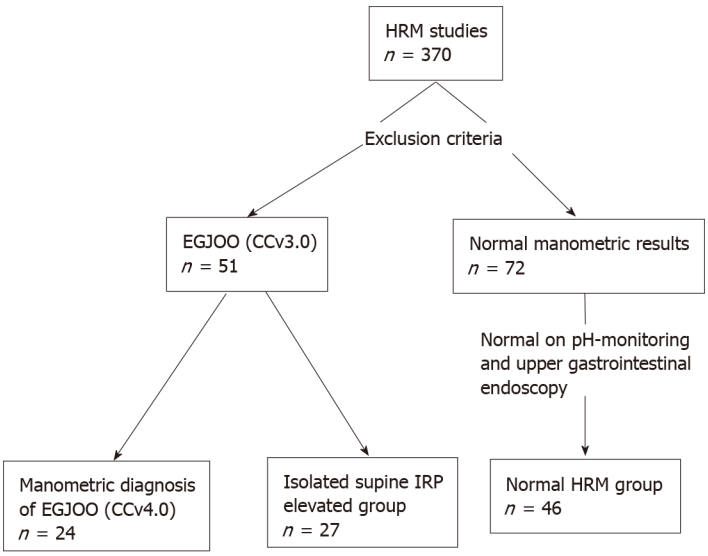
Proximal esophageal parameters: Proximal esophageal contractile function was weaker in the EGJOO group than in the normal HRM group, specifically PEL and PECI. Consistently, PEL was lower in the EGJOO group than in the isolated supine IRP elevated group. There was no difference in PL in the EGJOO group, isolated supine IRP elevated group, and the normal HRM group.

Table 1 Patient characteristics

	EGJOO (*n* = 24)	Isolated supine IRP elevated (*n* = 27)	Normal HRM (*n* = 46)	*P* value
Demographics				
Age (yr)	62.7 ± 2.7[a]	56.6 ± 11.1	50.2 ± 2.2	0.001
Female, *n* (%)	14 (58.3)	19 (70.4)	24 (52.2)	0.312
BMI (kg/m^2)	23.29 ± 0.63	21.88 ± 2.50	23.17 ± 0.68	0.300
Dominant symptom				
Dysphagia, *n* (%)	7 (29.2)	6 (22.2)	7 (15.2)	0.380
Retrosternal pain, *n* (%)	5 (20.8)	3 (11.1)	8 (17.4)	0.630
Regurgitation, *n* (%)	8 (33.3)	9 (33.3)	15 (32.6)	0.997

[a]$P < 0.05$, compared with normal high-resolution manometry group.

BMI: Body mass index; EGJOO: Esophagogastric junction outflow obstruction; IRP: Integrated relaxation pressure; HRM: High-resolution manometry.



DOI: 10.3748/wjg.v28.i30.4163 **Copyright** ©The Author(s) 2022.

Figure 2 Patient flow. HRM: High-resolution manometry; EGJOO: Esophagogastric junction outflow obstruction; CCv3.0: Chicago Classification version 3.0; CCv4.0: Chicago Classification version 4.0; IRP: Integrated relaxation pressure.

Esophageal body parameters: There was no significant difference in DL, DCI, and ES-RDC among the three groups.

EGJ parameters: Patients with EGJOO exhibited stronger contractile function in EGJ than in the isolated supine IRP elevated group and the normal HRM group, including LESP, IBP, median supine IRP, median upright IRP, and IRP on RDC.

The multivariate analysis revealed that PEL, LESP, and IRP on RDC are factors associated with EGJOO (Table 3).

Relationship between symptoms and parameters

We compared parameters based on symptoms for the 51 patients with elevated IRP. Patients with dysphagia showed significantly lower PD-UESCI (377.60 ± 36.67 *vs* 517.14 ± 30.47 mmHg·s·cm, $P = 0.017$), PECI (200.25 ± 39.18 *vs* 315.08 ± 30.24 mmHg·s·cm, $P = 0.048$) and PEL (4.43 ± 0.42 *vs* 5.75 ± 0.24 cm, $P = 0.008$) than patients without dysphagia. PEL was higher in patients with retrosternal pain, compared to patients without the symptom (6.43 ± 0.46 *vs* 5.23 ± 0.24 cm, $P = 0.046$) (Figure 3).

Predictors of EGJOO

The ROC analysis discovered HRM parameters that helped identify EGJOO (Table 4). The area under the curve (AUC) of LESP in predicting EGJOO is 0.85, with the optimal cutoff at 40.20 mmHg, yielding a

Table 2 High-resolution manometry parameters of the patients

HRM findings	EGJOO (*n* = 24)	Isolated supine IRP elevated (*n* = 27)	Normal HRM (*n* = 46)	*P* value
UES parameters				
UESL (cm)	3.13 ± 0.18	3.01 ± 0.67	3.34 ± 0.12	0.206
UESP (mmHg)	53.35 ± 5.28	68.12 ± 6.35	57.77 ± 3.35	0.123
UESNP (mmHg)	3.00 ± 1.43[a]	3.50 ± 6.57[a]	-4.08 ± 0.84	< 0.001
PD-UESCI (mmHg·s·cm)	430.01 ± 32.90	527.41 ± 37.48	534.13 ± 34.40	0.118
Proximal esophageal parameters				
PEL (cm)	4.89 ± 0.27[a]	5.89 ± 0.32[b]	6.08 ± 0.14	0.001
PL (s)	1.99 ± 0.08	2.05 ± 0.08	2.04 ± 0.07	0.872
PECI (mmHg·s·cm)	238.34 ± 35.18[a]	328.00 ± 35.15	367.99 ± 37.88	0.048
Esophageal body parameters				
DL (s)	6.14 ± 0.25	6.85 ± 0.32	6.25 ± 0.14	0.078
DCI (mmHg·s·cm)	1581.21 ± 276.20	1655.80 ± 170.33	1705.41 ± 144.27	0.897
ES-RDC (%)	37.5% (9)	18.5% (5)	13.0% (6)	0.053
EGJ parameters				
LESP (mmHg)	47.91 ± 4.05[a]	35.68 ± 1.80[a,b]	23.89 ± 1.34	< 0.001
IBP (mmHg)	12.29 ± 1.37[a]	7.41 ± 0.84[b]	5.45 ± 0.54	< 0.001
Median supine IRP (mmHg)	27.76 ± 2.39[a]	18.74 ± 0.52[a,b]	10.48 ± 0.60	< 0.001
Median upright IRP (mmHg)	23.69 ± 2.58[a]	7.32 ± 0.53[b]	5.41 ± 0.84	< 0.001
IRP on RDC (mmHg)	9.96 ± 1.78[a]	3.00 ± 0.98[b]	2.04 ± 0.58	< 0.001

[a]*P* < 0.05, compared with normal high-resolution manometry group.
[b]*P* < 0.05, compared with esophagogastric junction outflow obstruction group.
IRP: Integrated relaxation pressure; EGJOO: Esophagogastric junction outflow obstruction; UES: Upper esophageal sphincter; UESL: Upper esophageal sphincter length; UESP: Upper esophageal sphincter resting pressure; UESNP: Upper esophageal sphincter nadir pressure; PD-UESCI: Postdeglutitive upper esophageal sphincter contractile integral; PEL: Proximal esophageal length; PECI: Proximal contractile integral; PL: Proximal latency; DL: Distal latency; DCI: Distal contraction integral; ES: Esophageal shortening; RDC: Rapid drink challenge; LESP: Lower esophageal sphincter resting pressure; IBP: Intrabolus pressure; HRM: High-resolution manometry.

Table 3 Multivariate logistic regression analysis for factors associated with esophagogastric junction outflow obstruction

Effect variables	OR	95%CI	*P* value
PEL (cm)	0.543	0.30-0.99	0.044
LESP (mmHg)	1.106	1.05-1.17	0.001
IRP on RDC (mmHg)	1.197	1.02-1.41	0.028

PEL: Proximal esophageal length; LESP: Lower esophageal sphincter resting pressure; IRP: Integrated relaxation pressure; RDC: Rapid drink challenge.

sensitivity of 68.2% and specificity of 85.1%. IRP on RDC achieved an AUC value of 0.81, with the optimal cutoff at > 10.75 mmHg and sensitivity and specificity of 50.0% and 98.5%, respectively. UESNP, PEL, and PECI showed the best predictive value for EGJOO, with cutoff values of 1.15 mmHg (AUC 0.66), 4.76 cm (AUC 0.67), 312.35 mmHg·s·cm (AUC 0.67), respectively.

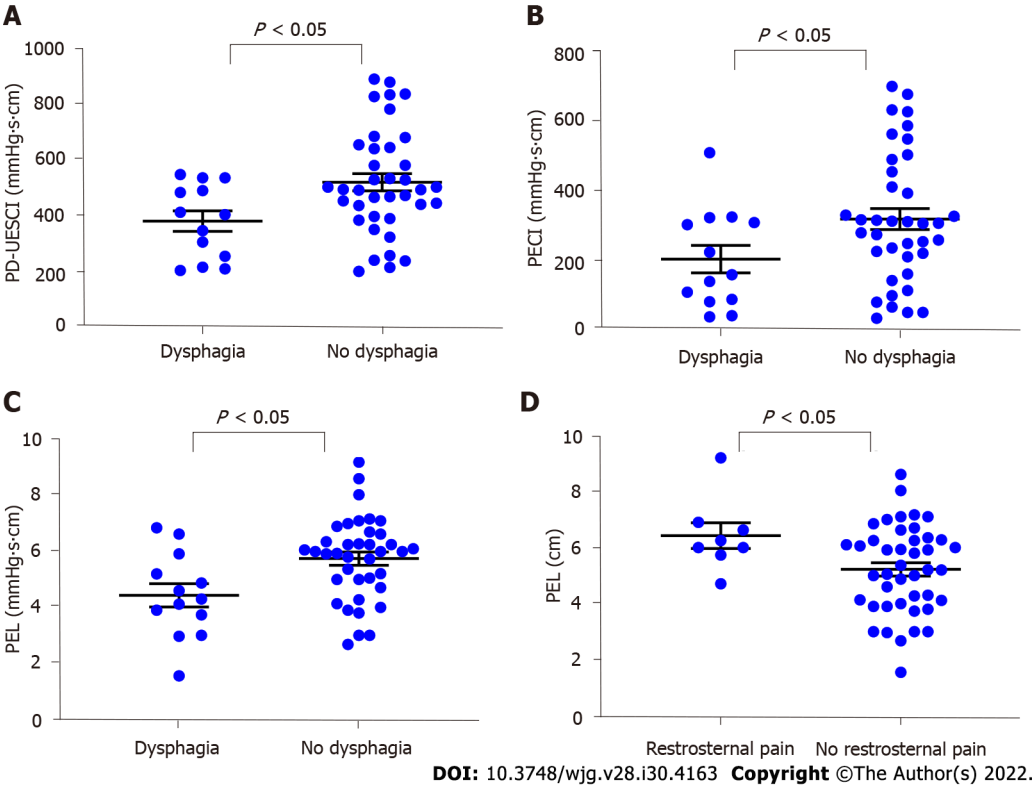
DISCUSSION

In this study, we mainly assessed the clinical and manometric characteristics of EGJOO based on the Chicago Classification version 4.0 (CCv4.0) to reveal potential changes in esophageal dynamics based on

Table 4 Receiver-operating characteristic analysis for esophagogastric junction outflow obstruction

	Cutoff	AUC	95%CI	Sensitivity (%)	Specificity (%)
UESNP (mmHg)	> 1.15	0.66	0.53-0.78	63.6	68.7
PEL (cm)	< 4.76	0.67	0.55-0.80	50.0	87.7
PECI (mmHg·s·cm)	< 312.35	0.67	0.55-0.80	83.3	46.6
LESP (mmHg)	> 40.20	0.85	0.75-0.94	68.2	85.1
IRP on RDC (mmHg)	> 10.75	0.81	0.70-0.91	50.0	98.5

UESNP: Upper esophageal sphincter nadir pressure; PEL: Proximal esophageal length; PECI: Proximal esophageal contractile integral; LESP: Lower esophageal sphincter resting pressure; IRP: Integrated relaxation pressure; RDC: Rapid drink challenge; AUC: Area under the curve.



DOI: 10.3748/wjg.v28.i30.4163 **Copyright** ©The Author(s) 2022.

Figure 3 Comparisons of parameters according to symptoms in 51 patients with elevated integrated relaxation pressure. A: Patients with dysphagia showed lower postdeglutitive upper esophageal sphincter contractile integral than patients without dysphagia; B: Patients with dysphagia showed lower proximal esophageal contractile integral than patients without dysphagia; C: Patients with dysphagia showed lower proximal esophageal length (PEL) than patients without dysphagia; D: Patients with retrosternal pain showed higher PEL than patients without retrosternal pain. PD-UESCI: Postdeglutitive upper esophageal sphincter contractile integral; PECI: Proximal esophageal contractile integral; PEL: Proximal esophageal length.

the new diagnostic criteria, and we identified parameters that help distinguish the EGJOO.

Based on our observations, older people had a higher likelihood of being diagnosed with EGJOO according to manometric results. The EGJOO group showed no significant difference in symptom distribution pattern compared with the isolated supine IRP elevated group and the normal HRM group. Therefore, more manometric features and additional examinations are required for a better understanding of EGJOO.

The nadir UES residual pressure (UESNP) was reported to be higher in EGJOO (CCv3.0) than in normal controls[2,14]. Within EGJOO, higher UESNP was observed in motor disorders compared to mechanical etiologies and was a potential predictor of symptom recurrence after myotomy, with a cutoff level of 2 mmHg[2]. Based on our initial findings, patients with EGJOO and isolated supine IRP had significantly higher UESNP than the normal HRM group. The findings support the hypothesis that the UES is hypertonic with impaired relaxation, which may serve as a protective mechanism to facilitate esophageal clearance and prevent aspiration pneumonitis under IRP elevation[15]. Further ROC analysis revealed that UESNP elevation might serve as a feature for confirming EGJOO.

Previous studies have linked proximal esophageal motility abnormalities to achalasia[9]. The PECI of type 1 achalasia patients was weaker than that of healthy volunteers, but there was no difference between EGJOO (CCv3.0) and health volunteers, and patients with aberrant PECI had more severe upper gastrointestinal symptoms than patients with normal PECI[9]. It is worth noting that EGJOO (CCv4.0) group had weaker PECI than the normal HRM group, while patients with isolated IRP elevation had no difference compared to the normal HRM group. PECI resulted in a limited value for confirming the diagnosis of EGJOO. Furthermore, our findings suggest that PEL is lower in patients with EGJOO than patients with isolated elevated supine IRP or normal HRM, which might also serve as a feature that strengthens the confidence in an EGJOO diagnosis. The above results indicate that based on the updated criteria, EGJOO dysfunction may involve the proximal esophagus, while patients with isolated supine IRP elevated had no such features. It is reasonable to speculate that patients with EGJOO have common changes in proximal esophageal dynamic features, although further studies are required to reveal the underlying pathophysiological mechanism.

With our current analysis of symptoms, postdeglutitive contraction of the UES and proximal esophagus were weaker, and PEL was significantly lower in patients with dysphagia compared to patients without the symptom, indicating that in patients with impaired EGJ relaxation, dysphagia may represent a potential dysfunction of the UES and proximal esophagus.

Esophageal shortening has been proposed as an outcome of longitudinal muscle contraction, and esophageal shortening during the rapid drink test was mainly associated with impaired EGJ relaxation or major peristalsis disorders, particularly achalasia[12]. In our study, the incidence of ES-RDC had a marginal difference between the three groups, which is comparable with the motor pattern observed in achalasia.

In this study, LESP increased progressively from normal HRM to the isolated supine IRP elevated and EGJOO groups, with significant differences between groups. LESP was critical in the evaluation of EGJ obstruction. Furthermore, ROC curve analysis revealed that LESP had the highest differential diagnostic efficacy of EGJOO, indicating that the value of LESP is helpful in the assessment of EGJOO.

CCv4.0 also highlights the role of ancillary manometric evaluations, such as RDC, to identify the causes of symptoms and elicit evidence of obstruction. Our study performed IRP on RDC, which was significantly higher in the EGJOO group than in other groups, while the isolated supine IRP elevated group showed no difference compared with the normal HRM group, indicating that Chicago Classification updates filtered out EGJ dysfunction with more severe obstruction. It is worth noting that IRP on RDC greater than 12 mmHg (Medtronic software) indicates achalasia and may correlate with symptom severity[1,13,16]. The ROC analysis revealed that a high IRP on RDC is useful for confirming the diagnosis of EGJOO with high specificity (98.5%), but low sensitivity (50.0%).

Based on CCv3.0, a significant proportion of EGJOO is associated with the effect of artifact, hiatal hernia, mechanical obstruction, opioid effect, or gastric volvulus, but not primary LES dysfunction. Hence, numerous studies focused on the identification of primary motility disorders and excluded motility patterns secondary to medication use, mechanical obstruction, previous surgery, or endoscopic interventions[3,4,17], which are critical in making appropriate therapeutic decisions. Since the morphology of LES is affected by position, the CCv4.0 defines IRP in the upright position and IBP; thus, the Chicago Classification update has reduced the number of clinically irrelevant diagnoses and improved the specificity for EGJOO diagnosis[7,17,18], enabling us to avoid irreversible treatment for these conditions. According to the results of this study, patients with EGJOO had multiple abnormalities in EGJ parameters compared with the isolated supine IRP elevated group, including LESP, IBP, median supine IRP, median upright IRP, and IRP on RDC, implying that the Chicago Classification update aids in the selection of EGJOO with more severe EGJ dysfunction.

Due to the limitations of the retrospective study, our study lacked data on treatment and outcomes of patients, larger cohorts are required to explore the prognostic value of the parameters mentioned above. Based on CCv4.0, additional provocative tests such as solid test swallows, or pharmacologic provocation were recommended, and complementary tests are required for a conclusive, actionable diagnosis of clinically relevant EGJOO, while our study did not include the tests mentioned above and mainly focused on the changes in the manometric diagnosis of EGJOO. Moreover, it is necessary to further investigate the pathophysiological mechanism of the changes in proximal esophageal motility of patients with EGJOO.

CONCLUSION

Conclusively, our current analysis revealed that patients with EGJOO had multiple changes in esophageal parameters based on Chicago Classification updates, especially more severe dysfunction at the esophagogastric junction than the previous diagnostic criteria, and showed multiple abnormalities at the proximal esophagus. The results illustrate that EGJOO is implicated in the proximal esophagus, and Chicago Classification updates improved the specificity for EGJOO diagnosis. Accordingly, we have expanded the valuable parameters for confirming the diagnosis of EGJOO based on CCv4.0, including UESNP, PEL, PECI, LESP, and IRP on RDC. With the advancement of EGJOO research, more

contributions will be provided to the diagnosis and treatment of this type of disorder.

ARTICLE HIGHLIGHTS

Research background

The critical diagnostic criteria for esophagogastric junction outflow obstruction (EGJOO) were published in the latest Chicago Classification version 4.0 (CCv4.0). However, as a result of the diagnostic criteria modifications, the changes in manometric features of EGJOO remained unclear.

Research motivation

To investigate the changes of EGJOO manometric features according to the Chicago Classification updates.

Research objectives

This study focused on evaluating the esophageal motility characteristics of patients with EGJOO, and selecting valuable parameters that are supportive for confirming the diagnosis of EGJOO.

Research methods

A total of 97 patients were enrolled, with 24 patients that met the updated manometric diagnosis of EGJOO (CCv4.0), 27 patients that only met the previous criteria, and 46 patients with normal manometric features served as the normal high-resolution manometry (HRM) group for this study. We collected clinical data, HRM parameters, and conducted comparisons among groups. Factors associated with EGJOO were illustrated by multivariate analysis. Furthermore, valuable parameters that strengthen the confidence in an EGJOO diagnosis were selected by the receiver-operating characteristic analysis.

Research results

EGJOO patients revealed significantly decreased proximal esophageal contractile integral (PECI) and proximal esophageal length (PEL) compared to the normal HRM group, and the features were related to dysphagia. EGJOO patients also had more severe dysfunction of the esophagogastric junction including lower esophageal sphincter resting pressure (LESP), intrabolus pressure, median supine integrated relaxation pressure (IRP), median upright IRP, and IRP on rapid drink challenge (RDC) than patients that only met the previous criteria. Further multivariate analysis revealed that the PEL, LESP, and IRP on RDC are factors associated with EGJOO. Additionally, the upper esophageal sphincter nadir pressure, PECI, PEL, LESP, and IRP on RDC contributes to confirming the diagnosis of EGJOO.

Research conclusions

The updates of Chicago Classification have improved the precision for identification of EGJ dysfunction that may reduce over-diagnosing for EGJOO. The motility disorder of EGJOO is implicated in the proximal esophagus, and the changes of proximal esophagus may relate to dysphagia. Additionally, there are valuable parameters that can be applied for confirming the diagnosis of EGJOO.

Research perspectives

Further investigations are required to reveal the pathophysiological mechanism of the abnormal proximal esophageal motility showed in EGJOO patients, and larger cohorts are required to explore the prognostic value of the parameters mentioned above.

FOOTNOTES

Author contributions: Li YY and Lu WT contributed equally to this work; Li YY, Lu WT, and Jiao HM conception and designed of research; Li YY and Lu WT analyzed data; Lu WT and Chen M performed the HRM and provided clinical information; Li YY, Liu JX, and Jiao HM interpreted of research; Li YY drafted manuscript; Jiao HM revised manuscript and approved the final version of manuscript; all authors approved the final version of the article.

Supported by the China Central Health Research Fund, No. W2013BJ29; and the Interdisciplinary Clinical Research Project of Peking University First Hospital, No.2019CR40.

Institutional review board statement: This study was reviewed and approved by the Institutional Review Board of the Peking University First Hospital, No. 2022-099.

Informed consent statement: A waiver of informed consent was granted by our Institutional Review Board because our retrospective analysis used completely anonymized data.

Conflict-of-interest statement: All authors have declared no conflicts of interest.

Data sharing statement: Data sharing available, please require through email.

Open-Access: This article is an open-access article that was selected by an in-house editor and fully peer-reviewed by external reviewers. It is distributed in accordance with the Creative Commons Attribution NonCommercial (CC BY-NC 4.0) license, which permits others to distribute, remix, adapt, build upon this work non-commercially, and license their derivative works on different terms, provided the original work is properly cited and the use is non-commercial. See: https://creativecommons.org/Licenses/by-nc/4.0/

Country/Territory of origin: China

ORCID number: Yue-Yuan Li 0000-0003-4973-8906; Wen-Ting Lu 0000-0002-6483-8342; Jian-Xiang Liu 0000-0003-0196-6459; Li-Hong Wu 0000-0002-2885-7482; Meng Chen 0000-0002-7882-008X; Hong-Mei Jiao 0000-0002-9139-9744.

Corresponding Author's Membership in Professional Societies: Association of Digestive Disease, Chinese Geriatrics Society.

S-Editor: Yan JP
L-Editor: A
P-Editor: Yan JP

REFERENCES

1 **Yadlapati R**, Kahrilas PJ, Fox MR, Bredenoord AJ, Prakash Gyawali C, Roman S, Babaei A, Mittal RK, Rommel N, Savarino E, Sifrim D, Smout A, Vaezi MF, Zerbib F, Akiyama J, Bhatia S, Bor S, Carlson DA, Chen JW, Cisternas D, Cock C, Coss-Adame E, de Bortoli N, Defilippi C, Fass R, Ghoshal UC, Gonlachanvit S, Hani A, Hebbard GS, Wook Jung K, Katz P, Katzka DA, Khan A, Kohn GP, Lazarescu A, Lengliner J, Mittal SK, Omari T, Park MI, Penagini R, Pohl D, Richter JE, Serra J, Sweis R, Tack J, Tatum RP, Tutuian R, Vela MF, Wong RK, Wu JC, Xiao Y, Pandolfino JE. Esophageal motility disorders on high-resolution manometry: Chicago classification version 4.0©. *Neurogastroenterol Motil* 2021; **33**: e14058 [PMID: 33373111 DOI: 10.1111/nmo.14058]

2 **Blais P**, Bennett MC, Gyawali CP. Upper esophageal sphincter metrics on high-resolution manometry differentiate etiologies of esophagogastric junction outflow obstruction. *Neurogastroenterol Motil* 2019; **31**: e13558 [PMID: 30815910 DOI: 10.1111/nmo.13558]

3 **Kahrilas PJ**, Bredenoord AJ, Fox M, Gyawali CP, Roman S, Smout AJPM, Pandolfino JE; International Working Group for Disorders of Gastrointestinal Motility and Function. Expert consensus document: Advances in the management of oesophageal motility disorders in the era of high-resolution manometry: a focus on achalasia syndromes. *Nat Rev Gastroenterol Hepatol* 2017; **14**: 677-688 [PMID: 28951579 DOI: 10.1038/nrgastro.2017.132]

4 **Lynch KL**, Yang YX, Metz DC, Falk GW. Clinical presentation and disease course of patients with esophagogastric junction outflow obstruction. *Dis Esophagus* 2017; **30**: 1-6 [PMID: 28475741 DOI: 10.1093/dote/dox004]

5 **Samo S**, Qayed E. Esophagogastric junction outflow obstruction: Where are we now in diagnosis and management? *World J Gastroenterol* 2019; **25**: 411-417 [PMID: 30700938 DOI: 10.3748/wjg.v25.i4.411]

6 **Rohof WOA**, Bredenoord AJ. Chicago Classification of Esophageal Motility Disorders: Lessons Learned. *Curr Gastroenterol Rep* 2017; **19**: 37 [PMID: 28730503 DOI: 10.1007/s11894-017-0576-7]

7 **Triggs JR**, Carlson DA, Beveridge C, Jain A, Tye MY, Kahrilas PJ, Pandolfino JE. Upright Integrated Relaxation Pressure Facilitates Characterization of Esophagogastric Junction Outflow Obstruction. *Clin Gastroenterol Hepatol* 2019; **17**: 2218-2226.e2 [PMID: 30708108 DOI: 10.1016/j.cgh.2019.01.024]

8 **Gyawali CP**, Carlson DA, Chen JW, Patel A, Wong RJ, Yadlapati RH. ACG Clinical Guidelines: Clinical Use of Esophageal Physiologic Testing. *Am J Gastroenterol* 2020; **115**: 1412-1428 [PMID: 32769426 DOI: 10.14309/ajg.0000000000000734]

9 **Jehangir A**, Tanner S, Malik Z, Parkman HP. Characterizing the proximal esophageal segment in patients with symptoms of esophageal dysmotility. *Neurogastroenterol Motil* 2020; **32**: e13888 [PMID: 32485784 DOI: 10.1111/nmo.13888]

10 **Jiao H**, Mei L, Sharma T, Kern M, Sanvanson P, Shaker R. A human model of restricted upper esophageal sphincter opening and its pharyngeal and UES deglutitive pressure phenomena. *Am J Physiol Gastrointest Liver Physiol* 2016; **311**: G84-G90 [PMID: 27198193 DOI: 10.1152/ajpgi.00145.2016]

11 **Peng L**, Patel A, Kushnir V, Gyawali CP. Assessment of upper esophageal sphincter function on high-resolution manometry: identification of predictors of globus symptoms. *J Clin Gastroenterol* 2015; **49**: 95-100 [PMID: 24492407 DOI: 10.1097/MCG.0000000000000078]

12 **Biasutto D**, Roman S, Garros A, Mion F. Esophageal shortening after rapid drink test during esophageal high-resolution manometry: A relevant finding? *United European Gastroenterol J* 2018; **6**: 1323-1330 [PMID: 30386605 DOI: 10.1177/2050640618796752]

13 **Sanagapalli S**, McGuire J, Leong RW, Patel K, Raeburn A, Abdul-Razakq H, Plumb A, Banks M, Haidry R, Lovat L, Sehgal V, Graham D, Sami SS, Sweis R. The Clinical Relevance of Manometric Esophagogastric Junction Outflow Obstruction Can Be Determined Using Rapid Drink Challenge and Solid Swallows. *Am J Gastroenterol* 2021; **116**: 280-288 [PMID: 33136563 DOI: 10.14309/ajg.0000000000000988]

14 **Chavez YH**, Ciarleglio MM, Clarke JO, Nandwani M, Stein E, Roland BC. Upper esophageal sphincter abnormalities:

frequent finding on high-resolution esophageal manometry and associated with poorer treatment response in achalasia. *J Clin Gastroenterol* 2015; **49**: 17-23 [PMID: 24859712 DOI: 10.1097/MCG.0000000000000157]

15 **Norton P**, Herbella FAM, Schlottmann F, Patti MG. The upper esophageal sphincter in the high-resolution manometry era. *Langenbecks Arch Surg* 2021; **406**: 2611-2619 [PMID: 34462811 DOI: 10.1007/s00423-021-02319-1]

16 **Woodland P**, Gabieta-Sonmez S, Arguero J, Ooi J, Nakagawa K, Glasinovic E, Yazaki E, Sifrim D. 200 mL Rapid Drink Challenge During High-resolution Manometry Best Predicts Objective Esophagogastric Junction Obstruction and Correlates With Symptom Severity. *J Neurogastroenterol Motil* 2018; **24**: 410-414 [PMID: 29969859 DOI: 10.5056/jnm18038]

17 **Patcharatrakul T**, Alkaddour A, Pitisuttithum P, Jangsirikul S, Vega KJ, Clarke JO, Gonlachanvit S. How to approach esophagogastric junction outflow obstruction? *Ann N Y Acad Sci* 2020; **1481**: 210-223 [PMID: 32557701 DOI: 10.1111/nyas.14412]

18 **Shahsavari D**, Malik Z, Parkman HP. Management of the patient with esophagogastric junction outflow obstruction. *Curr Opin Gastroenterol* 2021; **37**: 397-407 [PMID: 34059606 DOI: 10.1097/MOG.0000000000000747]

World Journal of Gastroenterology

Submit a Manuscript: https://www.f6publishing.com

World J Gastroenterol 2022 August 14; 28(30): 4174-4181

DOI: 10.3748/wjg.v28.i30.4174

ISSN 1007-9327 (print) ISSN 2219-2840 (online)

ORIGINAL ARTICLE

Observational Study

Epidemiology of inflammatory bowel diseases in the state of Rio Grande do Sul, Brazil

Ornella Sari Cassol, Gilmara Pandolfo Zabot, Rogerio Saad-Hossne, Alexandre Padoin

Specialty type: Gastroenterology and hepatology

Provenance and peer review: Unsolicited article; Externally peer reviewed.

Peer-review model: Single blind

Peer-review report's scientific quality classification

Grade A (Excellent): 0
Grade B (Very good): 0
Grade C (Good): C, C
Grade D (Fair): 0
Grade E (Poor): 0

P-Reviewer: Sharma V, India; Zhang F, China

Received: January 19, 2022
Peer-review started: January 19, 2022
First decision: April 10, 2022
Revised: April 22, 2022
Accepted: July 16, 2022
Article in press: July 16, 2022
Published online: August 14, 2022

Ornella Sari Cassol, Department of Coloproctology, IMED Medical School, Passo Fundo 99010260, RS, Brazil

Ornella Sari Cassol, Alexandre Padoin, Graduate Program in Medicine and Health Sciences, Pontifícia Universidade Católica do Rio Grande do Sul (PUCRS), Porto Alegre 90610001, RS, Brazil

Gilmara Pandolfo Zabot, Department of Coloproctology, Coloprocto Canoas Clinic, Canoas 92310205, RS, Brazil

Gilmara Pandolfo Zabot, Department of Coloproctology, Hospital Moinhos de Vento (HMV), Porto Alegre 90035000, RS, Brazil

Rogerio Saad-Hossne, Department of Surgery and Orthopaedics, Universidade Estadual Paulista (UNESP), Botucatu 18618687, SP, Brazil

Corresponding author: Ornella Sari Cassol, MSc, Professor, Coloproctology, IMED Medical School, 295 Rua Tiradentes, Passo Fundo 99010260, RS, Brazil. cassol.ornella@gmail.com

Abstract

BACKGROUND

This is the first study on the epidemiology of inflammatory bowel diseases (IBDs) in Rio Grande do Sul (RS), the southernmost state of Brazil with the country's fifth largest population. Crohn's disease (CD) and ulcerative colitis (UC) are collectively termed IBDs. They have high incidence and prevalence rates in high-income countries, although in recent years there has been a change in the classic geographical distribution of IBDs, with growing rates in traditionally low-incidence regions.

AIM

To estimate the incidence and prevalence of IBDs in the RS state, Brazil, between 2014 and 2019.

METHODS

This is a cross-sectional descriptive observational study. Patients with IBD who had initiated treatment and met the inclusion criteria of the RS state free drug distribution program were included. Data were obtained from registration or renewal records of the RS state specialty pharmacy. The male, female, and total

populations were estimated according to mid-year data from the Brazilian Institute of Geography and Statistics, which served as a reference for calculating the incidence and prevalence rates of IBDs during the study period. Results were described using mean, standard deviation, and range.

RESULTS

We included 1082 patients with IBD, of whom 57.5% were female and 42.5% were male. Patients with CD accounted for 72.45% of the sample, and those with UC accounted for 27.54%. IBD prevalence during the study period was 9.51 per 100000 population, of which 6.89 corresponded to people with CD and 2.62, to people with UC. Incidence rates per 100000 population/year were 2.54 in 2014, 2.61 in 2015, 1.91 in 2016, 0.80 in 2017, 0.83 in 2018, and 0.96 in 2019. The mean IBD incidence rate per 100000 population was 1.61, of which 1.17 corresponded to CD and 0.44, to UC. The mean age was 41 years, and patients were mostly aged 30-40 years. Prevalence by region was higher in the state capital metropolitan area: 12.69 per 100000 population.

CONCLUSION

Our results demonstrated an IBD prevalence of 9.51% and incidence of 1.61 per 100000 population. The patients were predominantly female, and CD was more prevalent than UC.

Key Words: Inflammatory bowel diseases; Crohn's disease; Ulcerative colitis; Epidemiology; Incidence; Prevalence

©The Author(s) 2022. Published by Baishideng Publishing Group Inc. All rights reserved.

Core Tip: This is the first study in the state of Rio Grande do Sul to address the epidemiology of inflammatory bowel diseases (IBDs). We assessed the incidence and prevalence of IBDs between 2014 and 2019, including 1082 patients (57.5% female and 42.5% male). Crohn's disease corresponded to 72.45% of the analyzed cases and ulcerative colitis, to 27.54%. Prevalence was 9.51% and the mean incidence rate was 1.61 per 100000 population. The mean age was 41 years, and the capital metropolitan area had the highest prevalence. This study showed a similar prevalence to other studies and a decrease in annual incidence rates.

Citation: Cassol OS, Zabot GP, Saad-Hossne R, Padoin A. Epidemiology of inflammatory bowel diseases in the state of Rio Grande do Sul, Brazil. *World J Gastroenterol* 2022; 28(30): 4174-4181
URL: https://www.wjgnet.com/1007-9327/full/v28/i30/4174.htm
DOI: https://dx.doi.org/10.3748/wjg.v28.i30.4174

INTRODUCTION

Inflammatory bowel diseases (IBDs) are characterized by a chronic inflammatory process that compromises the digestive tract. The main presentations are Crohn's disease (CD) and ulcerative colitis (UC), which are chronic idiopathic diseases causing inflammation of the gastrointestinal tract, with individual clinical and pathophysiological characteristics[1-3]. Children and young adults are more commonly affected[4]. Although uncommon, the chronicity, severity, progression, and morbidity of IBDs can significantly affect the patient's quality of life and are associated with an increased risk of hospitalizations and surgery[3,4].

IBDs are contemporary health conditions of industrialized societies. The prevalence of IBDs continues to increase steadily in Western countries, and their incidence is growing in newly industrialized countries. The global spread of IBDs seems to be associated with the Westernization of human diets and environments, affecting the gut microbiota and increasing the risk of IBDs in genetically susceptible individuals. It is therefore important to deepen our understanding of these events to delay the progression of IBDs[5].

Despite the paucity of population-based studies from low- and middle-income countries, epidemiological studies of IBDs have shown increased incidence and prevalence of CD and UC in different parts of the world. The increasing epidemiology of IBDs in newly industrialized countries in Latin America resembles that of high-income countries. Although a stabilization of incidence rates has been observed in many Western countries, the global burden of IBDs is still high, with an estimated prevalence exceeding 0.3% of the population in North America and Europe and 0.7% in Canada in 2018[6].

In newly industrialized countries, obstacles to conducting epidemiological studies of IBDs include the lack of disease surveillance systems and reliable unified health care databases, which are available in high-income countries. In countries of continental dimensions with economic problems such as Brazil,

an additional challenge is the country's generally disorganized health care system, which can result in inadequate records and, consequently, few population-based studies[6]. In this respect, Rio Grande do Sul (RS), the southernmost state of Brazil with the country's fifth largest population, still does not have a specific study on the epidemiology of IBDs. Therefore, the purpose of this study was to estimate the incidence and prevalence of IBDs in the state of RS.

MATERIALS AND METHODS

Study design

This is a cross-sectional descriptive observational study. All patients who had initiated treatment for IBD and met the inclusion criteria for the free drug distribution program of the state of RS between 2014 and 2019 were included. Drugs for the treatment of CD and UC are dispensed by the specialty pharmacy [*Farmácia de Medicamentos Especializados* (FME), or FME for short, in Portuguese] according to clinical protocols and therapeutic guidelines published by the Brazilian Ministry of Health. In Brazil, access to care is provided through private health insurance or the Unified Health System, which is a universal health care system funded by federal taxes and operated by state or municipal governments that includes the public provision of core physician and hospital services without copayments or patient charges. Approximately 22% of the population in the state of RS have private health insurance and only occasionally use the public health system. Therefore, because the FME is a government program within the Brazilian Unified Health System, it is responsible for supplying specialty medications to approximately 78% of the state population, all of them users of the public health system. Data from private health insurance companies are not included in this study.

Demographic characteristics and incidence and prevalence data were obtained from registration or renewal records of the FME. We requested from the State Health Department and its affiliated School of Public Health the data of patients included in the specialty medication distribution programs of the FME, which were provided through administrative and judicial means[7].

As variables to be analyzed, we included CD or UC diagnosis using International Classification of Diseases codes K50 and K51, date of treatment initiation, sex, and age.

Data analysis

Quantitative variables, such as age, were described using mean, standard deviation, and range. Categorical variables were expressed as counts and percentages. Disease prevalence and incidence were estimated by dividing the annual case notifications by the total estimated population of that year and presented as cases per 100000 population. Binomial distribution was used for obtaining 95% confidence intervals. All comparisons between rates assumed the binomial distribution and were based on the chi-square test. Findings with $P \leq 0.05$ were deemed statistically significant. All estimates of incidence and prevalence were calculated considering the population of the state of RS between 2014 and 2019[8]. Data analysis was conducted using IBM-SPSS, version 25.0.

Ethical considerations

This study did not involve the collection of biological material from participants. Data obtained with the data collection instrument were coded to preserve the participants' privacy and anonymity. All investigators signed a data use agreement.

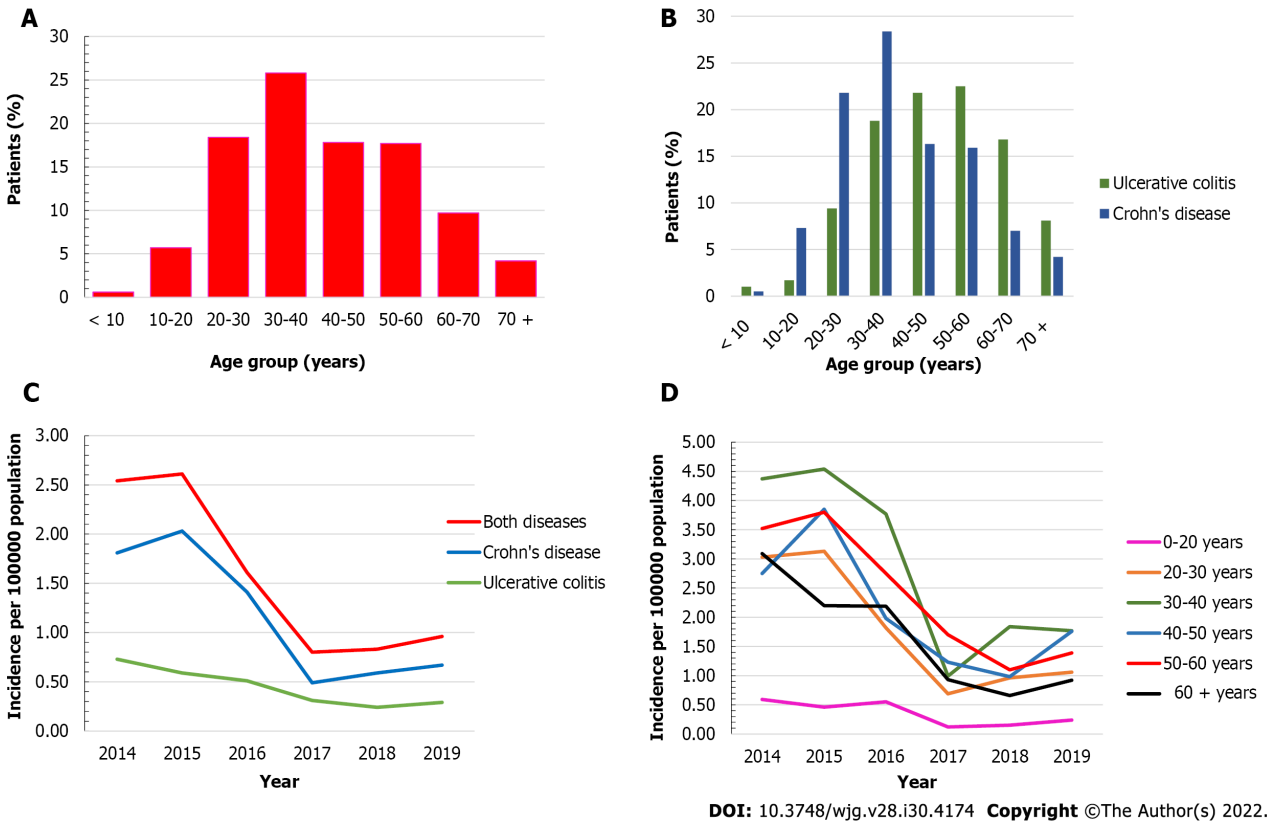
The study was conducted after approval by the Research Ethics Committees of Pontifícia Universidade Católica do Rio Grande do Sul, Certificate of Presentation for Ethical Appreciation No. 25551019 9 0000 5336, and of the State Health Department and its affiliated School of Public Health, Certificate of Presentation for Ethical Appreciation No. 25551019 9 3001 5312. The study followed the guidelines of Resolution No. 466/12 of the Brazilian National Health Council and the Brazilian General Data Protection Law No. 13709.

RESULTS

This study involved 1082 patients with IBD of a total population of 11377239 people. Of these, 784 (72.45%) had CD and 298 (27.54%) had UC.

Age

Patient age ranged from 1 to 91 years, with a mean of 41 years and standard deviation of 15 years. The highest IBD incidence was between 20 and 60 years of age, and patients were mostly aged 30-40 years (Figure 1A). The highest incidence occurred between the ages of 30 and 40 years for CD, and between the ages of 50 and 60 years for UC. UC affected a higher percentage of people aged 40 years or more ($P < 0.01$), whereas CD affected a higher percentage of people under 40 years of age ($P < 0.01$) (Figure 1B).



DOI: 10.3748/wjg.v28.i30.4174 **Copyright** ©The Author(s) 2022.

Figure 1 Age distribution and incidence rates of patients with inflammatory bowel diseases. A: Age distribution of patients with inflammatory bowel diseases (IBD) (n = 1082), state of Rio Grande do Sul, Brazil, 2014-2019; B: Age distribution of patients with Crohn's disease (n = 784) and ulcerative colitis (n = 298), state of Rio Grande do Sul, Brazil, 2014-2019; C: Annual IBD incidence rates, new cases per 100000 population/year in the state of Rio Grande do Sul (Brazil), 2014-2019; D: Annual IBD incidence rates by age group, new cases per 100000 population/year in the state of Rio Grande do Sul (Brazil), 2014-2019.

Sex

Of all patients with IBD, 622 (57.5%) were female and 460 (42.5%) were male (female-to-male ratio of 1.35:1.00; $P < 0.001$).

Considering CD only, 432 (55.10%) patients were female and 352 (44.89%) were male (female-to-male ratio of 1.23:1.00; $P < 0.001$). For UC, 190 (63.75%) were female and 108 (36.25%) were male (female-to-male ratio of 1.76:1.00; $P < 0.001$).

Incidence and prevalence

Overall, IBD prevalence was 9.51 per 100000 population during the study period (2014-2019), of which 6.89 corresponded to CD and 2.62, to UC. Table 1 shows the sex distribution of prevalence for each disease.

Figure 1C shows the annual incidence rates of IBD in the state of RS. The mean incidence rate was 1.61, of which 1.17 corresponded to CD and 0.44, to UC.

Table 2 shows annual incidence percentages. There was a 62% reduction in the accumulated incidence between 2014 and 2017 ($P < 0.015$). A statistically significant reduction in incidence was observed when comparing 2014 and 2019 ($P < 0.001$).

Figure 1D shows that, when listing annual incidence rates by age group, all groups showed reductions in 2017, with increases in the following years.

DISCUSSION

Historical data on the geographical distribution of IBDs worldwide have shown higher incidence and prevalence rates in high-income countries with predominantly White populations. More recently, IBDs have shown an increasing frequency in all continents, including low- and middle-income countries[2].

In Brazil, IBDs are not notifiable diseases. Therefore, data on the incidence and prevalence of CD and UC are scarce, and health systems lack adequate records. These data would be useful for better organization and political and economic planning of the public health system[9,6].

Table 1 Prevalence of inflammatory bowel diseases in the state of Rio Grande do Sul between 2014 and 2019 (per 100000 habitants)

Item	CD	UC	IBD
Female	7.40	3.26	10.66
Male	6.35	1.95	8.30
Total	6.89	2.62	9.51

CD: Crohn's disease; UC: Ulcerative colitis; IBD: Inflammatory bowel disease.

Table 2 Annual percentages of incidence rates

Year	Percentage
2014-2015	↑ 3%
2014-2015	↓ 26%
2014-2015	↓ 58%
2014-2015	↑ 3%
2014-2015	↑ 15%

In North America, 6.30 to 23.82 new cases per 100000 population are estimated per year for CD, and 8.8 to 23.14 new cases per 100000 population for UC. Prevalence rates are far higher than those in Brazil, with 96.3 to 318.5 cases/100000 population for CD and 139.8 to 286.3 cases/100000 population for UC[1,10].

A cohort study published in the United Kingdom reported incidence and prevalence rates much higher than those in Brazil between 2000 and 2018. The study estimated incidence rates of 28.6, 10.2, and 15.7/100000 population for IBD, CD, and UC, respectively, and prevalence rates of 725, 276, and 397/100000 population[11].

In the state of RS, we observed a predominance of CD during the study period (CD 72.54% and UC 27.54%), which differs from previous studies published in Brazil reporting a predominance of UC[2,3,12,13]. This is consistent with a study conducted in the Southeast region of Brazil by Souza *et al*[14], who reported an increase in CD cases in comparison with UC. These differences between countries and regions may reflect differences in environmental risk factors and genetic predispositions, such as those observed in Europe, where the incidence of NOD2 mutations appears to be higher in the central part of the continent, corresponding to areas with a higher proportion of CD cases[15].

According to the present study, the state of RS had a mean annual IBD incidence rate of 1.61 new cases per 100000 population/year (CD = 1.17 and UC = 0.44 new cases per 100000 population/year) between 2014 and 2019, which is consistent with the results reported by Kaplan *et al*[5] in a systematic review considering 147 studies on IBD worldwide. This comprehensive review demonstrated a CD incidence of 0-3.5 new cases per 100000 population/year, and an UC incidence of 0.19-6.76 new cases per 100000 population/year in Brazil[1]. In comparison, the systematic review by Selvaratnam *et al*[16] on the epidemiology of IBD in South America showed higher incidence rates, ranging from 4.3 to 5.3 per 100000 population/year for UC and from 0.74 to 3.5 per 100000 population/year for CD between 1990 and 2018. Similarly, a Brazilian study conducted in the state of Sao Paulo reported higher incidence rates than those found in the state of RS, with rates of 6.14 for CD and 7.16 for UC (per 100000 population/year)[3].

Regarding IBD prevalence, the mean rate observed during the study period (2014-2019) was 9.51 cases per 100000 population, of which 6.89 corresponded to CD and 2.62, to UC. Prevalence in the state of RS was higher than that reported for Brazil in a systematic review by Ng *et al*[1], with rates ranging from 0.9 to 6.75 cases/100000 population for CD and from 2.42 to 21 cases/100000 population for UC. Prevalence was also higher in a systematic review on IBD epidemiology conducted in South America, reaching 15-24.1/100000 population for UC and 2.4-14.1/100000 population for CD[16]. Similarly, in the Brazilian study by Gasparini *et al*[3], overall prevalence rates were 24.3 for CD and 28.3 for UC per 100000 population.

If we were to analyze the state of RS according to the epidemiological transition theory proposed by Gilaad G Kaplan and Joseph W Windsor in 2021, where each region of the world is at an epidemiological stage (Emergence, Acceleration in Incidence, Compounding Prevalence, and Prevalence Equilibrium), RS would be in the Compounding Prevalence stage, where a steady increase in the population living with IBD is observed despite stabilization or even a decrease in incidence[17].

Regarding patient age, studies show a clear predominance of IBD in individuals aged 20 to 50 years. In our study, the mean age was 41 years. The highest IBD incidence was between 20 and 60 years of age, and patients were mostly aged 30-40 years. The highest incidence was at 30-40 years of age for CD, and at 50-60 years of age for UC. UC showed a trend toward an increased incidence among patients aged 50 to 60 years, and these results are consistent with those of national and international studies[3,11]. A limitation of this variable is that patients were selected through the FME, which provides the age that the patients begin to receive the free specialty medications rather than their age at diagnosis.

Regarding the sex distribution of patients with IBD, we observed a predominance of female patients for both CD and UC, which is consistent with the Brazilian studies conducted by Victoria *et al*[12] in the state of Sao Paulo and Lima Martins *et al*[13] in the state of Espírito Santo. However, our findings differ from those reported in the state of Piauí by Parente *et al*[2], who found a male-to-female ratio of 1.2:1.0 for patients with CD, but with no significant association when considering sex in statistical analyses. Patients with UC, on the other hand, were mostly female (male-to-female ratio of 1.8:1.0, statistically significant)[2].

CONCLUSION

Based on the methodology used in this study, our results demonstrated an IBD prevalence of 9.51% and incidence of 1.61 per 100000 population in the state of RS between 2014 and 2019. The patients were predominantly female, and CD was more prevalent than UC. Our prevalence rate was similar to that reported in previous Brazilian studies. Mean CD and UC incidence rates were, respectively, 1.17 and 0.44 new cases per 100000 population, decreasing until 2017 and increasing afterwards. Women were more affected than men by both CD and UC. IBD occurred more frequently in major urban centers, where the referral centers that care for patients with IBD are often located. The highest IBD incidence was observed in patients aged 20 to 60 years, predominantly between the ages of 30 and 40 years; this was slightly higher than the mean values reported in previous studies.

This is the first study to estimate IBD incidence and prevalence in the state of RS. Our findings suggest that detailed studies in this field are needed to properly understand in which epidemiological stage the state of RS currently is. We believe that the difficulty in keeping accurate epidemiological records and the consequent underestimation of disease burden result from a disorganized health care system, associated with economic problems, inadequate records, lack of population-based studies, and the inaccurate diagnosis of IBD as an infectious disease before the proper knowledge of CD and UC.

ARTICLE HIGHLIGHTS

Research background

First study on the epidemiology of inflammatory bowel diseases (IBDs) in Rio Grande do Sul (RS), the southernmost state of Brazil. IBDs have high incidence and prevalence rates in high-income countries, although in recent years there has been a change in the classic geographical distribution of IBDs, with growing rates in traditionally low-incidence regions.

Research motivation

The importance of this study lies in the lack of research on the incidence and prevalence of IBDs in the state of RS. A challenge for future studies is related to access to data of all patients with IBDs, as these are not notifiable diseases in Brazil.

Research objectives

To determine the incidence and prevalence of IBD in the state of RS. The relevance of the results lies in the lack of knowledge of such data until the present study.

Research methods

This is an observational study of IBDs from the state of RS between 2014 and 2019. Drugs for the treatment of Crohn's disease (CD) and ulcerative colitis (UC) are dispensed by the specialty pharmacy. The variables analyzed were incidence, prevalence, age, sex, and CD or UC.

Research results

These are the first data on the incidence and prevalence of IBDs in the state of RS. However, these are not comprehensive data, as only patients from the public health system were included. Studies also including patients from the private health insurance sector are needed.

Research conclusions

The most relevant of the following questions should be briefly answered: What are the new theories that this study proposes? This study showed a similar IBD prevalence to other Brazilian studies and a decreasing incidence. What are the new methods that this study proposed? We propose that studies covering patients from both public and private health sectors should be conducted.

Research perspectives

Future studies should include a larger sample to provide a more reliable understanding of the real epidemiology of IBDs in the state of RS.

ACKNOWLEDGEMENTS

We thank the RS State Health Department pharmacy and its affiliated School of Public Health for making their data available, and CAPES for the funding that contributed to the improvement of higher education.

FOOTNOTES

Author contributions: Cassol OS contributed to data collection, investigation, writing-original draft, and statistical analysis; Zabot GP, Saad-Hossne R, and Padoin A contributed to writing-review and editing.

Supported by the Coordenação de Aperfeiçoamento de Pessoal de Nível Superior-Brasil (CAPES)-Finance Code 001.

Institutional review board statement: This study was performed after approval by the Research Ethics Committee of Pontifícia Universidade Católica do Rio Grande do Sul, Certificate of Presentation for Ethical Appreciation No. 25551019 9 0000 5336; and the ESP/SES/RS Research Ethics Committee, Certificate of Presentation for Ethical Appreciation 25551019 9 3001 5312; this work respected the guidelines of Resolution No. 466/12 of the National Health Council and Law No. 13709 of the General Personal Data Protection Law.

Informed consent statement: This study did not involve the collection of biological material from participants. Data obtained with the data collection instrument were codified, aiming to preserve the participants' privacy and anonymity. A data use agreement form was signed.

Conflict-of-interest statement: There are no conflicts of interest to report.

Data sharing statement: No additional data are available.

STROBE statement: The authors have read the STROBE Statement—checklist of items, and the manuscript was prepared and revised according to the STROBE Statement—checklist of items.

Open-Access: This article is an open-access article that was selected by an in-house editor and fully peer-reviewed by external reviewers. It is distributed in accordance with the Creative Commons Attribution NonCommercial (CC BY-NC 4.0) license, which permits others to distribute, remix, adapt, build upon this work non-commercially, and license their derivative works on different terms, provided the original work is properly cited and the use is non-commercial. See: https://creativecommons.org/Licenses/by-nc/4.0/

Country/Territory of origin: Brazil

ORCID number: Ornella Sari Cassol 0000-0003-0867-6593; Gilmara Pandolfo Zabot 0000-0002-1253-4945; Rogerio Saad-Hossne 0000-0002-8166-0304; Alexandre Padoin 0000-0002-9754-4818.

S-Editor: Chen YL
L-Editor: A
P-Editor: Chen YL

REFERENCES

1 **Ng SC**, Shi HY, Hamidi N, Underwood FE, Tang W, Benchimol EI, Panaccione R, Ghosh S, Wu JCY, Chan FKL, Sung JJY, Kaplan GG. Worldwide incidence and prevalence of inflammatory bowel disease in the 21st century: a systematic review of population-based studies. *Lancet* 2017; **390**: 2769-2778 [PMID: 29050646 DOI: 10.1016/S0140-6736(17)32448-0]

2 **Parente JM**, Coy CS, Campelo V, Parente MP, Costa LA, da Silva RM, Stephan C, Zeitune JM. Inflammatory bowel

disease in an underdeveloped region of Northeastern Brazil. *World J Gastroenterol* 2015; **21**: 1197-1206 [PMID: 25632193 DOI: 10.3748/wjg.v21.i4.1197]

3 **Gasparini RG**, Sassaki LY, Saad-Hossne R. Inflammatory bowel disease epidemiology in São Paulo State, Brazil. *Clin Exp Gastroenterol* 2018; **11**: 423-429 [PMID: 30464570 DOI: 10.2147/CEG.S176583]

4 **Katz JA**. Management of inflammatory bowel disease in adults. *J Dig Dis* 2007; **8**: 65-71 [PMID: 17532817 DOI: 10.1111/j.1443-9573.2007.00287.x]

5 **Kaplan GG**, Ng SC. Understanding and Preventing the Global Increase of Inflammatory Bowel Disease. *Gastroenterology* 2017; **152**: 313-321.e2 [PMID: 27793607 DOI: 10.1053/j.gastro.2016.10.020]

6 **Quaresma AB**, Kaplan GG, Kotze PG. The globalization of inflammatory bowel disease: the incidence and prevalence of inflammatory bowel disease in Brazil. *Curr Opin Gastroenterol* 2019; **35**: 259-264 [PMID: 30973356 DOI: 10.1097/MOG.0000000000000534]

7 **Brasil**. Ministério da Saúde. DATASUS. Tabnet. [cited 18 January 2022]. Available from: https://datasus.saude.gov.br/informacoes-de-saude-tabnet/

8 **Instituto Brasileiro de Geografia e Estatística (IBGE)**. Rio Grande do Sul. Cidades. [cited 18 January 2022]. Available from: https://cidades.ibge.gov.br/brasil/rs/panorama

9 **Lima LD**, Albuquerque MV, Scatena JHG, Melo ECP, Oliveira EXG, Carvalho MS, Pereira AMM, Oliveira RAD, Martinelli NL, Oliveira CF. Regional governance arrangements of the Brazilian Unified National Health System: provider diversity and spacial inequality in service provision. *Cad Saude Publica* 2019; **35Suppl** 2: e00094618 [PMID: 31215597 DOI: 10.1590/0102-311X00094618]

10 **Kaplan GG**, Bernstein CN, Coward S, Bitton A, Murthy SK, Nguyen GC, Lee K, Cooke-Lauder J, Benchimol EI. The Impact of Inflammatory Bowel Disease in Canada 2018: Epidemiology. *J Can Assoc Gastroenterol* 2019; **2**: S6-S16 [PMID: 31294381 DOI: 10.1093/jcag/gwy054]

11 **Pasvol TJ**, Horsfall L, Bloom S, Segal AW, Sabin C, Field N, Rait G. Incidence and prevalence of inflammatory bowel disease in UK primary care: a population-based cohort study. *BMJ Open* 2020; **10**: e036584 [PMID: 32690524 DOI: 10.1136/bmjopen-2019-036584]

12 **Victoria CR**, Sassak LY, Nunes HR. Incidence and prevalence rates of inflammatory bowel diseases, in midwestern of São Paulo State, Brazil. *Arq Gastroenterol* 2009; **46**: 20-25 [PMID: 19466305 DOI: 10.1590/s0004-28032009000100009]

13 **Lima Martins A**, Volpato RA, Zago-Gomes MDP. The prevalence and phenotype in Brazilian patients with inflammatory bowel disease. *BMC Gastroenterol* 2018; **18**: 87 [PMID: 29914399 DOI: 10.1186/s12876-018-0822-y]

14 **Souza MH**, Troncon LE, Rodrigues CM, Viana CF, Onofre PH, Monteiro RA, Passos AD, Martinelli AL, Meneghelli UG. [Trends in the occurrence (1980-1999) and clinical features of Crohn's disease and ulcerative colitis in a university hospital in southeastern Brazil]. *Arq Gastroenterol* 2002; **39**: 98-105 [PMID: 12612713 DOI: 10.1590/s0004-28032002000200006]

15 **Ng SC**, Bernstein CN, Vatn MH, Lakatos PL, Loftus EV Jr, Tysk C, O'Morain C, Moum B, Colombel JF; Epidemiology and Natural History Task Force of the International Organization of Inflammatory Bowel Disease (IOIBD). Geographical variability and environmental risk factors in inflammatory bowel disease. *Gut* 2013; **62**: 630-649 [PMID: 23335431 DOI: 10.1136/gutjnl-2012-303661]

16 **Selvaratnam S**, Gullino S, Shim L, Lee E, Lee A, Paramsothy S, Leong RW. Epidemiology of inflammatory bowel disease in South America: A systematic review. *World J Gastroenterol* 2019; **25**: 6866-6875 [PMID: 31885427 DOI: 10.3748/wjg.v25.i47.6866]

17 **Kaplan GG**, Windsor JW. The four epidemiological stages in the global evolution of inflammatory bowel disease. *Nat Rev Gastroenterol Hepatol* 2021; **18**: 56-66 [PMID: 33033392 DOI: 10.1038/s41575-020-00360-x]

World Journal of Gastroenterology

Submit a Manuscript: https://www.f6publishing.com

World J Gastroenterol 2022 August 14; 28(30): 4182-4200

DOI: 10.3748/wjg.v28.i30.4182

ISSN 1007-9327 (print) ISSN 2219-2840 (online)

ORIGINAL ARTICLE

Observational Study

Hepatocellular carcinoma, decompensation, and mortality based on hepatitis C treatment: A prospective cohort study

Gwang Hyeon Choi, Eun Sun Jang, Young Seok Kim, Youn Jae Lee, In Hee Kim, Sung Bum Cho, Han Chu Lee, Jeong Won Jang, Moran Ki, Hwa Young Choi, Dahye Baik, Sook-Hyang Jeong

Specialty type: Gastroenterology and hepatology

Provenance and peer review: Unsolicited article; Externally peer reviewed.

Peer-review model: Single blind

Peer-review report's scientific quality classification
Grade A (Excellent): 0
Grade B (Very good): B, B
Grade C (Good): C
Grade D (Fair): 0
Grade E (Poor): 0

P-Reviewer: Li J, China; Tamori A, Japan; Zarębska-Michaluk D, Poland

Received: March 12, 2022
Peer-review started: March 12, 2022
First decision: April 10, 2022
Revised: April 24, 2022
Accepted: July 16, 2022
Article in press: July 16, 2022
Published online: August 14, 2022

Gwang Hyeon Choi, Eun Sun Jang, Sook-Hyang Jeong, Department of Internal Medicine, Seoul National University Bundang Hospital, Seoul National University College of Medicine, Seongnam 13620, South Korea

Young Seok Kim, Department of Internal Medicine, Soonchunhyang University Bucheon Hospital, Bucheon 14584, South Korea

Youn Jae Lee, Department of Internal Medicine, Inje University Busan Paik Hospital, Busan 47392, South Korea

In Hee Kim, Department of Internal Medicine, Chonbuk National University Hospital, Jeonju 54907, Jeonbuk, South Korea

Sung Bum Cho, Department of Internal Medicine, Chonnam National University Hwasun Hospital, Hwasun 58128, South Korea

Han Chu Lee, Department of Gastroenterology, Asan Medical Center, University of Ulsan College of Medicine, Seoul 05505, South Korea

Jeong Won Jang, Department of Internal Medicine, The Catholic University of Korea, Seoul 06591, South Korea

Moran Ki, Hwa Young Choi, Dahye Baik, Cancer Control and Population Health, Graduate School of Cancer Science and Policy, National Cancer Center, Goyang 10408, South Korea

Corresponding author: Sook-Hyang Jeong, MD, PhD, Professor, Department of Internal Medicine, Seoul National University Bundang Hospital, Seoul National University College of Medicine, 82, Gumi-ro 173 Beon-gil, Bundang-gu, Seongnam 13620, South Korea.
jsh@snubh.org

Abstract

BACKGROUND

Prospective studies of the long-term outcomes of patients with hepatitis C virus (HCV) infection after treatment with interferon-based therapy (IBT) or direct-acting antivirals (DAA) are limited in many Asian countries.

AIM

To elucidate the incidences of hepatocellular carcinoma (HCC) and

death/transplantation based on treatment with IBT or DAA, to compare the outcomes of the sustained virologic response (SVR) to IBT and DAA, and to investigate outcome-determining factors after SVR.

METHODS

This cohort included 2054 viremic patients (mean age, 57 years; 46.5% male; 27.4% with cirrhosis) prospectively enrolled at seven hospitals between 2007 and 2019. They were classified as the untreated group (n = 619), IBT group (n = 578), and DAA group (n = 857). Outcomes included the incidences of HCC and death/transplantation. The incidences of the outcomes for each group according to treatment were calculated using an exact method based on the Poisson distribution. A multivariate Cox regression analysis was performed to determine the factors associated with HCC or death/transplantation, followed by propensity score matching to confirm the results.

RESULTS

During a median of 4.1 years of follow-up, HCC and death/transplantation occurred in 113 and 206 patients, respectively, in the entire cohort. Compared with the untreated group, the incidences of HCC and death/transplantation were significantly lower in the IBT group [adjusted hazard ratio (aHR) 0.47, 95%CI: 0.28-0.80 and aHR 0.28, 95%CI: 0.18-0.43, respectively] and the DAA group (aHR 0.58, 95%CI: 0.35-0.96, and aHR 0.19, 95%CI: 0.20-0.68, respectively). Among 1268 patients who attained SVR with IBT (n = 451) or DAA (n = 816), the multivariable-adjusted analysis showed no differences in the risks of HCC (HR 2.03; 95%CI: 0.76-5.43) and death/transplantation (HR 1.38; 95%CI: 0.55-3.49) between the two groups. This was confirmed by a propensity score-matching analysis. Independent factors for HCC after SVR were age, genotype 1, and the presence of cirrhosis.

CONCLUSION

Treatment and achieving SVR with either IBT or DAA significantly reduced the incidences of HCC and mortality in the Asian patients with HCV infection. The risks of HCC and mortality were not significantly different regardless of whether SVR was induced by IBT or DAA.

Key Words: Hepatitis C virus; Direct-acting antiviral; Sustained virologic response; Hepatocellular carcinoma; Mortality

©The Author(s) 2022. Published by Baishideng Publishing Group Inc. All rights reserved.

Core Tip: Treatment and sustained virologic response (SVR) with either interferon-based treatment (IBT) or direct-acting antiviral (DAA) significantly reduced the incidences of hepatocellular carcinoma and mortality in our Asian prospective cohort. The risks of HCC and all-cause of mortality were not significantly different regardless of whether SVR was induced by IBT or DAA. After achieving SVR, age, the presence of cirrhosis, and genotype 1 hepatitis C virus infection were indicators of worse clinical outcomes.

Citation: Choi GH, Jang ES, Kim YS, Lee YJ, Kim IH, Cho SB, Lee HC, Jang JW, Ki M, Choi HY, Baik D, Jeong SH. Hepatocellular carcinoma, decompensation, and mortality based on hepatitis C treatment: A prospective cohort study. *World J Gastroenterol* 2022; 28(30): 4182-4200

URL: https://www.wjgnet.com/1007-9327/full/v28/i30/4182.htm

DOI: https://dx.doi.org/10.3748/wjg.v28.i30.4182

INTRODUCTION

Hepatitis C virus (HCV) is a major cause of liver cirrhosis, hepatocellular carcinoma (HCC), and liver-related and overall mortality. In 2019, the World Health Organization estimated that 58 million people worldwide had chronic HCV infection[1]. Currently, this substantial public health burden can be reduced by active screening and treatment with highly tolerable direct-acting antivirals (DAA), which result in a cure rate of more than 95% in terms of the sustained virologic response (SVR)[2-4].

From the identification of HCV to the introduction of DAA therapy, interferon (IFN)-based therapy (IBT) was the only option for HCV treatment, with an approximate SVR rate of 50%[5]. Although IBT-induced SVR includes a wide variety of adverse effects and narrow indications, it significantly reduces the incidence of HCC and long-term mortality[6,7]. Furthermore, DAA-induced SVR has resulted in

reductions in hepatic fibrosis[8,9], portal hypertension[10], hepatic decompensation[11], HCC incidence [11,12], and liver-related and overall mortality[11,13]; however, the follow-up durations were relatively short.

To reach the HCV elimination goal of 2030, it is imperative to understand the regional epidemiology and outcomes of HCV. However, prospective studies of the long-term outcomes after treatment with IBT or DAA are limited in many Asian countries, where hepatitis B virus (HBV) is the major cause of liver-related complications. Additionally, comparative studies of the outcomes of SVR induced by IBT and DAA are scarce.

We established a prospective, nationwide, multicenter HCV cohort (the Korea HCV cohort study) funded by the Korean National Institute of Health in 2007. Using these data, we aimed to elucidate the clinical outcomes, including HCC, hepatic decompensation, and all-cause death, among Korean patients with chronic HCV infection. We compared the outcomes based on the antiviral treatments (untreated, IBT, and DAA) and analyzed patients after achieving SVR (IBT-SVR and DAA-SVR groups). Additionally, we investigated outcome-determining factors after SVR.

MATERIALS AND METHODS

Study subjects

The Korea HCV cohort is a prospective cohort of 2485 adult patients with HCV RNA positivity at seven tertiary centers nationwide enrolled from January 2007 to June 2019 in South Korea. Patients who met any of the following criteria were excluded: Positive serology for HBV surface antigen (n = 62) or HIV (n = 2); decompensated cirrhosis at enrollment (n = 79); previous antiviral treatment before cohort entry (n = 260); and less than 6 mo of follow-up (n = 28). Additionally, patients who had HCC before or at the time of cohort entry were excluded.

Therefore, 2054 viremic patients with or without compensated cirrhosis were analyzed as the entire cohort, which was further classified into three groups based on their treatment: untreated group (n = 619; 30.2%); IBT group (n = 578; 28.1%); and DAA group (n = 857; 41.7%). Patients in the untreated group did not receive IBT or DAA treatment during the entire follow-up period. Subject selection, classification, and overall outcomes are summarized in Figure 1.

In the entire cohort, 1267 patients achieved SVR (61.7%) with IBT (n = 451) or DAA (n = 816); these patients comprised the SVR cohort. Diagnostic criteria for liver cirrhosis were based on histology or at least one clinical sign of portal hypertension, such as cirrhotic features on radiological images, platelet count less than 100,000/mm^3, and documented gastroesophageal varices without hemorrhage. The study protocol was approved by the Institutional Review Board of seven hospitals, and each enrolled patient provided written informed consent.

Data collection at baseline and follow-up visits

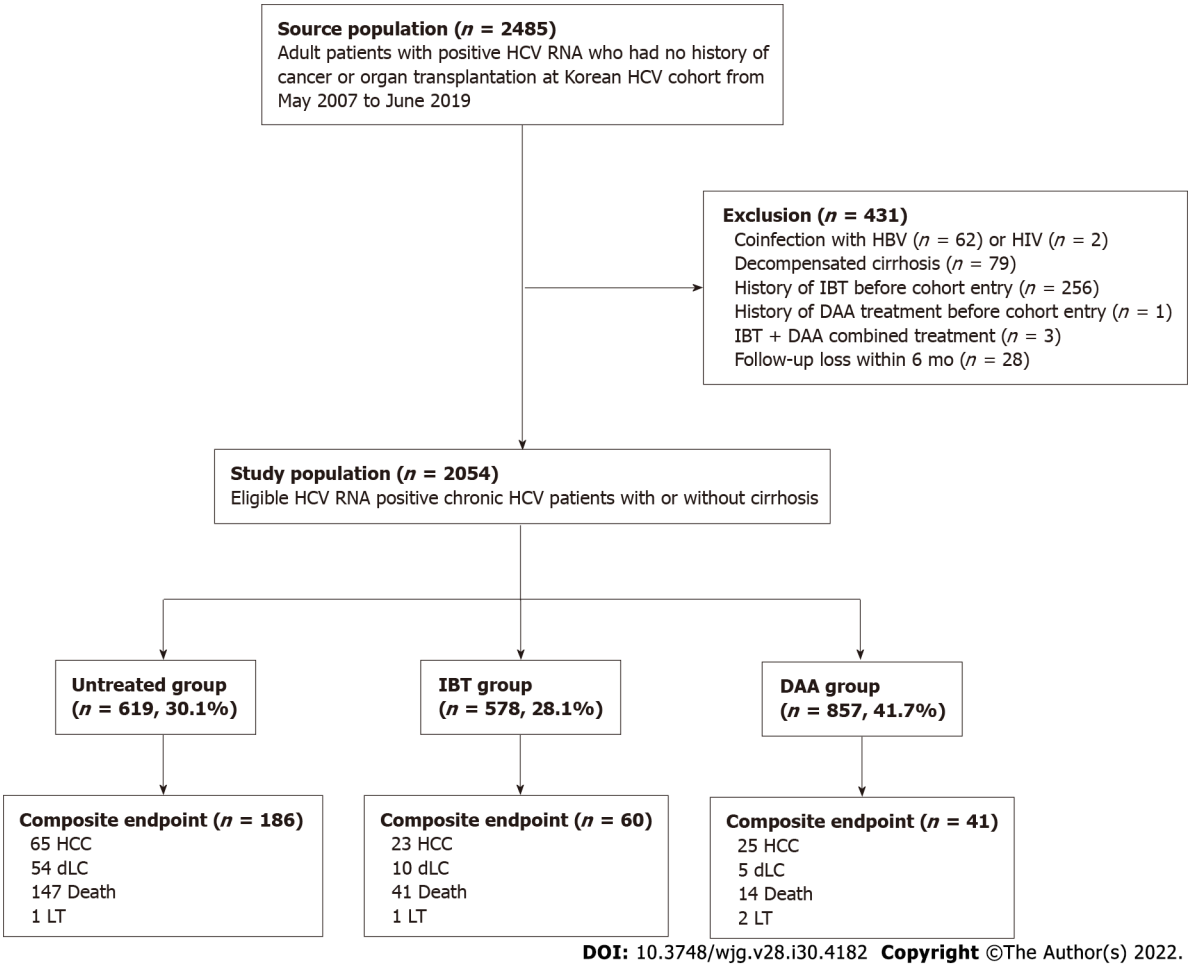
At the time of enrollment, trained research coordinators at the seven hospitals interviewed the patients using a standardized questionnaire that included demographic and socioeconomic factors (age, sex, body mass index, education level, and occupation), health behaviors (smoking and alcohol consumption), comorbidities (extrahepatic cancers, thyroid disease, psychiatric disease, diabetes, kidney disease, cerebrovascular disease, and cardiovascular disease), and lifetime exposure to risk factors for HCV infection.

Laboratory data at baseline and follow-up visits were collected from the medical records, including the anti-HCV antibody, serum HCV RNA level, HCV genotype, HBV surface antigen, HBV core antibody immunoglobulin G (anti-HBc IgG), white blood cell count, hemoglobin, platelet count, aspartate aminotransferasel (AST), alanine aminotransferase, alkaline phosphatase, total bilirubin, albumin, creatinine, prothrombin time (PT) and alpha-fetoprotein (AFP). The following three non-invasive serum fibrosis assessment scores were calculated at the index date: The fibrosis-4 (FIB-4) index [14], the AST-to-platelet ratio index (APRI) score[15], and the albumin-bilirubin (ALBI) score[16].

The results of imaging studies, such as abdominal ultrasonography or computed tomography, liver pathology, and transient elastography (FibroScan®, Echosens, Paris, France), were collected when available. Detailed information about antiviral treatment, including therapeutic regimens, duration, and achievement of SVR, was collected from the patients' medical records. These data were entered into the established electronic case report form on the authorized website of the Korean Centers for Disease Control Korea HCV cohort study (http://is.cdc.go.kr/) by the research coordinators. All input data were quality-controlled by independent statistical researchers (Baik D, Choi HY, and Ki M) at least four times per year.

Follow-up evaluations

All patients underwent regular clinical assessments every 3 to 12 mo, and HCV treatment was recommended by their attending physicians according to the treatment guidelines for HCV infection unless there were contraindications or patient's refusal. If the patients were treated, then SVR was evaluated, and regular follow-up visits every 6 to 12 mo after SVR were encouraged. HCC surveillance



DOI: 10.3748/wjg.v28.i30.4182 **Copyright** ©The Author(s) 2022.

Figure 1 Patient flow diagram. DAA: Direct-acting antivirals; dLC: Decompensated liver cirrhosis; HBV: Hepatitis B virus; HCC: Hepatocellular carcinoma; HCV: Hepatitis C virus; IBT: Interferon-based treatment; HIV: Human immunodeficiency virus; LT: Liver transplantation.

using abdominal ultrasonography and serum AFP tests every 6 to 12 mo were recommended according to the pretreatment fibrosis stage. If the patients did not adhere to the regular follow-up schedule, then research coordinators called the patients or their families to encourage them to attend the clinic and to check their survival status, disease progression to hepatic decompensation, or development of HCC. The end of follow-up was defined as the date of death/liver transplantation (LT), or the last follow-up date (June 30, 2020).

Measurement of liver-related outcomes

Outcomes included the incidences of HCC, hepatic decompensation, and death/LT. HCC was diagnosed according to pathology or typical imaging criteria observed on dynamic computed tomography and/or magnetic resonance imaging in accordance with the Korean Liver Cancer Study Group guidelines (similar to major international guidelines)[17]. Decompensated liver cirrhosis was defined as the presence of ascites, jaundice, variceal bleeding, encephalopathy, or a combination of these [18]. All-cause mortality or death/LT was directly documented or indirectly indicated as disqualification from the National Health Insurance status provided in the electronic medical records. In Korea, enrollment in the National Health Insurance is compulsory for all individuals; therefore, disqualification from the National Health Insurance indicates death or emigration in most cases[19]. To verify the survival status, physician-confirmed death certificate data, including the date and cause of death, were obtained from the Statistics Korea mortality database, which was established in 1981.

To calculate the outcomes of the entire cohort, the index date of the entire cohort was defined as the date of cohort entry when HCV RNA positivity was confirmed by the referred clinics. To compare the outcomes of patients with SVR induced by IBT and patients with SVR induced by DAA, the index date for the SVR cohort was defined as the initiation day of the antiviral treatment. SVR was evaluated using an intention-to-treat analysis; therefore, patients who received at least one dose of IBT or DAA were included.

Statistical analysis

Baseline characteristics of the patients were compared using the chi-square test for categorical variables, and a one-way analysis of variance (ANOVA) or *t*-test was used for continuous variables. For multiple comparisons, a one-way ANOVA was used followed by a Bonferroni correction. The total follow-up (in person-years) of each group was calculated by multiplying the cohort population size by the average follow-up in years. Survival time was calculated as the time from cohort entry (the entire cohort) or the start of the first treatment (SVR cohort) until the date of death/LT or the last available follow-up date. A few patients who received a second course of DAA treatment because of failure of the first DAA treatment were censored at the time of retreatment.

The incidences and 95% confidence intervals (CI) of the outcomes for each group based on treatment were calculated using an exact method based on the Poisson distribution. Cumulative incidence curves for outcome development were estimated using the pseudo-Kaplan–Meier method with a clock reset procedure for patients treated with IBT or DAA during follow-up and compared using the log-rank test. Therefore, patients who had received IBT and subsequent DAA treatment were considered as the DAA group, but the period between IBT and DAA treatment was included in the IBT group with no event.

A time-varying Cox regression model was used to determine the factors associated with outcomes, and the adjusted hazard ratio was estimated for the entire cohort and the SVR cohort. In the models, baseline variables (sex, body mass index, alcohol, smoking, HCV genotype) were adjusted, and age, antiviral treatment, laboratory data, achievement of SVR, and presence of cirrhosis were considered time-dependent variables. A multivariate Cox regression analysis was performed to determine the factors associated with HCC or death/LT, and the adjusted hazard ratio was estimated for the SVR cohort at the time of IBT or DAA initiation. Covariates with $P < 0.05$ in the univariate Cox regression model were used as covariates for the multivariate Cox regression analyses. To confirm the multivariate analysis results for the SVR cohort, significant differences in characteristics at the time of initiation of each treatment were adjusted by propensity score (PS) matching for all possible variables, including the time from cohort entry to treatment. We used nearest-neighbor matching with a caliper size of 0.1 and matched the patients using a 1:1 ratio. The covariate balance was considered to be achieved if the absolute standardized difference between the two groups was ≤ 0.1.

All *P*-values were two-sided, and $P < 0.05$ was considered significant. SPSS (version 21; IBC Corp., Armonk, NY, United States) and R (version 4.0.4; http://cran.r-project.org/) software were used for statistical analyses. The R package of *MatchIt* was used for matching analyses.

RESULTS

Baseline characteristics of the entire cohort

The demographic, clinical, and laboratory characteristics of the entire cohort ($n = 2054$), untreated group ($n = 619$; 30.1%), IBT group ($n = 578$; 28.1%), and DAA group ($n = 857$; 41.7%) at the index date are provided in Table 1. The mean age of the patients was 57 years; 46.5% were men and 27.4% had compensated cirrhosis.

Compared with the untreated and DAA groups, the IBT group was significantly younger, had a higher proportion of genotype 2, lower rates of alcohol consumption, cirrhosis and high FIB-4 index values (≥ 3.25), and fewer comorbidities.

Among the DAA group, 14.0% had been treated with an IFN-based regimen after cohort enrollment, and 86.0% were treatment-naive. DAA treatments administered were sofosbuvir plus ribavirin (32.1%), daclatasvir plus asunaprevir (26.3%), elbasvir plus grazoprevir (13.7%), glecaprevir plus pibrentasvir (13.7%), ledipasvir plus sofosbuvir (9.1%), and ombitasvir plus paritaprevir plus ritonavir plus dasabuvir (3.9%).

Incidences of HCC, decompensation, and death/LT in the entire cohort according to treatment, SVR, or the presence of liver cirrhosis

The median time periods between cohort entry (index date) and the end of follow-up were 5.6 years [interquartile range (IQR), 3.4-8.2] for the untreated group, 7.9 years (IQR, 6.1-9.7) for the IBT group, and 3.5 years (IQR, 2.0-5.5) for the DAA group (Table 1). During this period, 113 patients developed HCC, 69 patients experienced hepatic decompensation, 202 patients died (119 Liver related and 83 non-liver related), and four patients underwent LT.

As shown in Table 2, the estimated HCC incidence rates per 100 person-years for the untreated group, IBT group, and DAA group were 1.98 (95%CI: 1.56-2.52), 0.59 (95%CI: 0.39-0.89), and 1.16 (95%CI: 0.78-1.71), respectively (Table 2). The incidence rates of hepatic decompensation per 100 person-years for the untreated group, IBT group, and DAA group were 1.62 (95%CI: 1.24-2.11), 0.25 (95%CI: 0.14-0.47), and 0.23 (95%CI: 0.10-0.55), respectively. The incidence rates of death/LT per 100 person-years for the untreated group, IBT group, and DAA group were 3.33 (95%CI: 2.85-3.91), 0.87 (95%CI: 0.64-1.18), and 0.65 (95%CI: 0.40-1.06), respectively. The incidence rates of all three outcomes were significantly lower in the IBT and DAA groups compared with the untreated group. However, the

Table 1 Baseline characteristics of the entire hepatitis C virus cohort according to the treatment

Variable, *n* (%)	Untreated group (*n* = 619)	IBT group (*n* = 578)	DAA group (*n* = 857)	*P* value (3 Gr.)	*P* value (U *vs* I)	*P* value (U *vs* D)	*P* value (I *vs* D)
Age (yr)	60.4 ± 13.4	51.4 ± 10.9	59.1±11.4	< 0.001	< 0.001	0.086	< 0.001
Male sex	280 (45.2)	277 (47.9)	412 (48.1)	0.511	0.351	0.281	0.955
HCV RNA, $\log_{10}$ IU/mL	5.89 (5.08-6.45)	5.83 (4.87-6.49)	6.04 (5.27-6.53)	< 0.001	0.979	0.017	< 0.001
HCV genotype				< 0.001	< 0.001	< 0.001	< 0.001
1	256 (41.4)	242 (41.9)	491 (57.3)				
2	299 (48.3)	323 (55.9)	355 (41.4)				
Others/missing	64 (10.3)	13 (2.2)	11 (1.3)				
Diagnosis status				< 0.001	< 0.001	0.002	0.058
Chronic hepatitis	417 (67.4)	456 (78.9)	639 (74.6)				
Compensated cirrhosis	202 (32.6)	122 (21.1)	218 (25.4)				
FIB-4 index				< 0.001	< 0.001	0.142	< 0.001
≤ 1.45	112 (18.9)	191 (33.3)	164 (19.9)				
1.45-3.25	218 (36.8)	200 (34.8)	337 (40.9)				
≥ 3.25	263 (44.3)	183 (31.9)	323 (39.2)				
APRI score				0.15	0.09	0.094	0.853
≤ 2.0	480 (80.3)	485 (84.1)	708 (83.7)				
> 2.0	118 (19.7)	92 (15.9)	138 (16.3)				
ALBI score				0.004	0.04	0.001	0.313
≤ -2.60 (Grade 1)	446 (73.0)	450 (78.1)	674 (80.3)				
> -2.60 (Grade 2 or 3)	165 (27.0)	126 (21.9)	165 (19.7)				
Ever smoker	264 (42.9)	283 (49.5)	380 (44.5)	0.058	0.022	0.519	0.068
Alcohol intake				< 0.001	< 0.001	< 0.001	< 0.001
None	326 (53.0)	226 (39.4)	419 (48.9)				
Social	227 (36.9)	308 (53.7)	229 (26.7)				
Significant[1]	61 (9.9)	40 (7.0)	209 (24.4)				
Fatty liver disease on imaging study, *n* = 1389	71 (19.3), *n* = 367	86 (21.1), *n* = 408	140 (22.8), *n* = 614	0.435	0.549	0.202	0.516
Anti-HBcIgG (+), *n* = 1442	47 (11.0), *n* = 429	33 (8.4), *n* = 391	64 (10.3), *n* = 622	0.46	0.225	0.73	0.33
BMI, kg/m^2	23.4 ± 3.2	23.8 ± 3.0	23.8 ± 3.1	0.02	0.143	0.02	1
Diabetes mellitus	120 (19.4)	77 (13.3)	128 (14.9)	0.01	0.005	0.024	0.391
Hypertension	145 (23.4)	107 (18.5)	243 (28.4)	< 0.001	0.037	0.034	< 0.001
Cardiovascular disease	16 (2.6)	3 (0.5)	25 (2.9)	0.006	0.004	0.701	0.001
Cerebrovascular disease	17 (2.7)	4 (0.7)	20 (2.3)	0.026	0.007	0.617	0.017
Laboratory study							
WBC, × 10^3/mm^3	5.09 (4.29-6.50)	5.05 (3.91-6.16)	5.40 (4.40-6.61)	< 0.001	0.145	0.164	< 0.001
Hemoglobin, g/dL	13.5 (12.3-14.5)	13.7 (12.7-14.8)	13.8 (12.7-14.8)	< 0.001	0.004	< 0.001	1
Platelet, × 10^3/mm^3	162 (118-212)	174 (130-220)	172 (129-215)	0.229	0.236	0.317	1
Albumin, g/dL	4.2 (3.9-4.4)	4.2 (4.0-4.5)	4.2 (4.0-4.4)	< 0.001	< 0.001	0.001	1
Total bilirubin, mg/dL	0.8 (0.5-1.0)	0.7 (0.6-1.0)	0.7 (0.6-1.0)	0.784	1	1	1
ALP, IU/L	87 (68-136)	79 (63-112)	121 (78-250)	< 0.001	0.001	< 0.001	< 0.001

AST, IU/L	50 (30-85)	50 (31-83)	46 (30-76)	0.026	1	0.139	0.038
ALT, IU/L	42 (23-80)	52 (29-100)	36 (22-70)	< 0.001	0.013	0.176	< 0.001
Creatinine, mg/dL	0.9 (0.7-1.0)	0.8 (0.7-1.0)	0.8 (0.7-1.0)	0.857	1	1	1
PT, INR	1.06 (1.01-1.12)	1.03 (0.98-1.08)	1.03 (0.97-1.09)	< 0.001	< 0.001	0.007	0.119
AFP, ng/dL	4.3 (2.5-9.7)	3.5 (2.3-7.1)	3.8 (2.4-6.6)	0.868	1	1	1
Cohort entry time				< 0.001	< 0.001	< 0.001	< 0.001
January 2007–June 2015	488 (78.8)	561 (97.1)	49 (5.7)				
July 2015–June 2019	131 (21.2)	17 (2.9)	808 (94.3)				
SVR rate	-	67.5 (451/668)	95.3 (817/857)	-	-	< 0.001	-
Follow-up duration (yr)	5.6 (3.4-8.2)	7.9 (6.1-9.7)	3.5 (2.0-5.5)	< 0.001	< 0.001	< 0.001	< 0.001

[1]Significant alcohol intake is defined as weekly ≥ 210 g for men and ≥ 140 g for women.

Data were presented as mean ± SD, median (interquartile range), or *n* (%). AFP: Alpha-feto protein; ALBI: Albumin-bilirubin; ALP: Alkaline phosphatase; ALT: Alanine aminotransferase; APRI: Aspartate aminotransferase to platelet ratio index; AST: Aspartate aminotransferase; BMI: Body mass index; DAA: Direct acting antivirals; FIB-4: Fibrosis-4; HCV: Hepatitis C virus; IBT: Interferon-based therapy; INR: International normalized ratio; PT: Prothrombin time; WBC: White blood cell.

incidence of HCC in the non-cirrhotic group was not significantly different between the untreated and DAA groups, while the incidences of decompensation and death/LT were significantly lower in the DAA group compared with the untreated group. The cumulative outcome incidences for the untreated, IBT, and DAA groups are shown in Figure 2, and those for the non-cirrhotic and cirrhotic subgroups are shown in Supplementary Figures 1 and 2, respectively.

Multivariable analyses of factors associated with HCC, decompensation, and death/LT in the entire cohort

A multivariable time-varying Cox regression analysis with the untreated group as a reference showed that IBT [hazard ratio (HR), 0.47; 95%CI: 0.28-0.80; $P = 0.005$] and DAA groups (HR, 0.58; 95%CI: 0.35-0.96; $P = 0.035$) were independently associated with a significantly lower risk of HCC (Table 3, model 1). Other independent HCC risk factors were older age (HR, 1.06; 95%CI: 1.03-1.08; $P < 0.001$), male sex (HR, 2.50; 95%CI: 1.37-4.55; $P = 0.003$), genotype 1 (HR, 2.25; 95%CI: 1.45-3.48; $P < 0.001$), the presence of cirrhosis (HR, 3.81; 95%CI: 2.38-6.10; $P < 0.001$), significant alcohol consumption (HR, 2.20; 95%CI: 1.14-4.24; $P = 0.027$), prolonged PT (HR, 2.66; 95%CI: 1.13-6.24; $P = 0.025$), and higher AFP level (HR, 2.12; 95%CI: 1.48-3.05; $P < 0.001$) (Table 3, model 1).

The death/LT incidence decreased independently after antiviral treatment with IBT (HR, 0.28; 95%CI: 0.19-0.43; $P < 0.001$) or DAA (HR, 0.19; 95%CI: 0.10-0.35; $P < 0.001$) (Table 3, model 1). In contrast, older age (HR, 1.05; 95%CI: 1.03-1.06; $P < 0.001$), male sex (HR, 1.70; 95%CI: 1.24-2.33; $P < 0.001$), the presence of cirrhosis (HR, 1.88; 95%CI: 1.34-2.64; $P < 0.001$), lower body mass index (HR, 0.94; 95%CI: 0.89-0.99; $P = 0.019$), lower albumin level (HR, 0.35; 95%CI: 0.25-0.51; $P < 0.001$), and prolonged PT (HR, 2.34; 95%CI: 1.06-5.16; $P = 0.034$) independently increased mortality/LT rates. Antiviral treatment, cirrhosis, albumin level, and PT were independently associated with the risk of decompensation (Table 3, model 1).

We established another multivariable model (model 2) by replacing the achievement of SVR instead of IBT or DAA treatment. A multivariate time-varying Cox regression analysis of the combined outcomes of the untreated and no SVR groups as a reference showed that SVR induced by either IBT or DAA significantly decreased the risk of HCC (HR, 0.41; 95%CI: 0.26-0.65; $P < 0.001$), decompensation (HR, 0.10; 95%CI: 0.04-0.29; $P < 0.001$), and death/LT (HR, 0.26; 95%CI: 0.17-0.39; $P < 0.001$) (Table 3, model 2).

Comparison of the clinical outcomes of the IBT-SVR group and DAA-SVR group in the SVR cohort: Unadjusted and PS-matched results

The SVR cohort comprised 1,268 chronic HCV patients who achieved SVR with IBT or DAA (IBT-SVR group, $n = 451$; DAA-SVR group, $n = 817$). The SVR rates of the IBT and DAA groups were 67.5% and 95.3%, respectively. The baseline characteristics at the time of initiation of treatment of the IBT and DAA groups according to SVR are shown in Supplementary Table 1. The incidence rates of HCC, decompensation, and death/LT were significantly lower in the IBT-SVR group than in the IBT-no SVR group (Supplementary Table 2). In contrast, the incidence rate of death/LT was significantly lower in the DAA-SVR group than in the DAA-no SVR group, whereas the incidence rates of HCC and decompensation did not reach statistical significance, probably because of the short follow-up or rare incidence of decompensation (Supplementary Table 2).

Table 2 Annual incidence rates of hepatocellular carcinoma, decompensation and death/transplantation according to treatment exposure and the presence of cirrhosis

	Group	PY	No. of events	No./100 PY (95%CI)	HR (95%CI)	*P* value
Entire cohort	Hepatocellular carcinoma					
	Untreated group	3285.4	65	1.98 (1.56-2.52)	Reference	-
	IBT group	3888.9	23	0.59 (0.39-0.89)	0.31 (0.19-0.49)	< 0.001
	DAA group	2158.0	25	1.16 (0.78-1.71)	0.59 (0.37-0.95)	0.029
	Decompensation					
	Untreated group	3333.6	54	1.62 (1.24-2.11)	Reference	-
	IBT group	3950.1	10	0.25 (0.14-0.47)	0.15 (0.07-0.29)	< 0.001
	DAA group	2178.7	5	0.23 (0.10-0.55)	0.16 (0.06-0.39)	< 0.001
	Death or transplantation					
	Untreated group	4438.3	148	3.33 (2.85-3.91)	Reference	-
	IBT group	4850.1	42	0.87 (0.64-1.18)	0.22 (0.16-0.31)	< 0.001
	DAA group	2467.2	16	0.65 (0.40-1.06)	0.30 (0.17-0.51)	< 0.001
No cirrhosis	Hepatocellular carcinoma					
	Untreated group	2364.6	15	0.63 (0.38-1.05)	Reference	-
	IBT group	2971.8	6	0.20 (0.09-0.45)	0.30 (0.11-0.77)	0.012
	DAA group	1569.4	8	0.51 (0.26-1.02)	0.90 (0.37-2.18)	0.812
	Decompensation					
	Untreated group	2369.9	6	0.25 (0.11-0.56)	Reference	-
	IBT group	2992.3	1	0.03 (0.00-0.24)	0.09 (0.01-0.74)	0.026
	DAA group	1573.4	0	0.00	0.00	N/A
	Death or transplantation					
	Untreated group	3176.3	63	1.98 (4.15-7.12)	Reference	-
	IBT group	3712.3	22	0.59 (0.39-0.90)	0.26 (0.16-0.42)	< 0.001
	DAA group	1784.6	7	0.39 (0.19-0.82)	0.33 (0.15-0.75)	0.008
Cirrhosis	Hepatocellular carcinoma					
	Untreated group	919.9	50	5.44 (4.15-7.12)	Reference	-
	IBT group	917.1	17	1.85 (1.16-2.97)	0.35 (0.20-0.61)	< 0.001
	DAA group	588.6	17	2.89 (1.81-4.61)	0.53 (0.30-0.92)	0.025
	Decompensation					
	Untreated group	962.8	48	4.99 (3.78-6.57)	Reference	-
	IBT group	957.7	9	0.84 (0.49-1.80)	0.18 (0.09-0.37)	< 0.001
	DAA group	606.3	5	0.82 (0.34-1.97)	0.17 (0.07-0.44)	< 0.001
	Death or transplantation					
	Untreated group	1262.1	85	6.73 (5.48-8.27)	Reference	-
	IBT group	1137.8	20	1.76 (1.14-2.71)	0.21 (0.13-0.35)	< 0.001
	DAA group	682.6	9	1.32 (0.69-2.52)	0.28 (0.14-0.56)	< 0.001

A Cox proportional hazards model was used to determine hazards ratios and *P* values. CI: Confidence interval; DAA: Direct acting antivirals; HR: Hazard ratio; IBT: Interferon-based therapy; N/A: Not applicable; PY: Person-year.

Table 3 Multivariate time-varying Cox regression analysis for hepatocellular carcinoma and death/transplantation in entire cohort

Variable	Hepatocellular carcinoma		Decompensation		Death/transplantation	
	aHR (95%CI)	*P* value	aHR (95%CI)	*P* value	aHR (95%CI)	*P* value
Model 1						
Untreated group	Reference	-	Reference	-	Reference	-
IBT group	0.47 (0.28-0.80)	0.005	0.16 (0.08-0.33)	< 0.001	0.28 (0.18-0.43)	< 0.001
DAA group	0.58 (0.35-0.96)	0.035	0.12 (0.03-0.33)	< 0.001	0.19 (0.10-0.35)	< 0.001
Age, yr	1.06 (1.03-1.08)	< 0.001	1.00 (0.98-1.03)	0.805	1.05 (1.03-1.06)	< 0.001
Male sex	2.50 (1.37-4.55)	0.003	-	-	1.70 (1.24-2.33)	< 0.001
HCV genotype			-	-	-	-
2	Reference	-				
1	2.25 (1.45-3.48)	< 0.001				
Others/unknown	1.72 (0.66-4.48)	0.266				
Cirrhosis	3.81 (2.38-6.10)	< 0.001	9.26 (4.03-21.03)	< 0.001	1.88 (1.34-2.64)	< 0.001
Ever smoker	1.47 (0.82-2.66)	0.192	-	-	-	-
Alcohol consumption			-	-	-	-
None	Reference	-				
Social	1.20 (0.73-1.98)	0.473				
Significant	2.20 (1.14-4.24)	0.027				
BMI, kg/m^2	-	-	-	-	0.94 (0.89-0.99)	0.019
Diabetes mellitus	0.96 (0.59-1.56)	0.872	-	-	1.12 (0.77-1.62)	0.563
Albumin, g/dL	0.71 (0.44-1.15)	0.162	0.35 (0.20-0.63)	< 0.001	0.36 (0.25-0.51)	< 0.001
Total bilirubin, mg/dL	0.95 (0.80-1.12)	0.568	1.03 (0.98-1.08)	0.264	-	-
PT, INR	2.66 (1.13-6.24)	0.025	3.32 (1.08-10.19)	0.036	2.34 (1.06-5.16)	0.034
AFP, $\log_{10}$ ng/dL	2.12 (1.48-3.05)	< 0.001	1.54 (0.95-2.51)	0.08	1.29 (0.94-1.77)	0.112
Model 2						
Untreated or no SVR	Reference	-	Reference	-	Reference	-
SVR	0.41 (0.26-0.65)	< 0.001	0.10 (0.04-0.29)	< 0.001	0.26 (0.17-0.39)	< 0.001
Age, yr	1.06 (1.04- 1.08)	< 0.001	1.02 (0.99-1.04)	0.152	1.06 (1.04-1.07)	< 0.001
Male sex	2.50 (1.38-4.54)	0.003	-	-	1.68 (1.23-2.30)	0.001
HCV genotype			-	-	-	-
2	Reference	-				
1	2.25 (1.45-3.48)	< 0.001				
Others/unknown	1.57 (0.60-4.09)	0.359				
Cirrhosis	3.75 (2.35-6.01)	< 0.001	7.54 (3.32-17.15)	< 0.001	1.72 (1.23-2.41)	0.002
Ever smoker	1.53 (0.85-2.75)	0.156	-	-	-	-
Alcohol consumption			-	-	-	-
None	Reference	-				
Social	1.24 (0.75-2.04)	0.397				
Significant	2.69 (1.40-5.16)	0.003				
BMI, kg/m^2	-	-	-	-	0.94 (0.89-0.99)	0.024
Diabetes mellitus	0.99 (0.61-1.61)	0.959	-	-	1.10 (0.76-1.60)	0.612
Albumin, g/dL	0.76 (0.47-1.20)	0.238	0.42 (0.24-0.71)	0.001	0.42 (0.30-0.60)	< 0.001

Total bilirubin, mg/dL	0.96 (0.81-1.13)	0.624	1.03 (0.99-1.08)	0.156	-	-
PT, INR	2.53 (1.02-6.28)	0.044	4.42 (1.48-13.20)	0.008	2.69 (1.22-5.92)	0.014
AFP, $\log_{10}$ ng/dL	2.10 (1.46-3.02)	< 0.001	1.48 (0.90-2.44)	0.12	1.17 (0.86-1.60)	0.32

Total number of patients, 2197; number of hepatocellular carcinomas, 113; number of deaths, 202; number of transplantations, 4; number of decompensations, 69. AFP: Alpha-feto protein; aHR: Adjusted hazard ratio; BMI: Body mass index; CI: Confidence interval; DAA: Direct acting antivirals; HCV: Hepatitis C virus; IBT: Interferon-based therapy; PT: Prothrombin time; SVR: Sustained virologic response.

In the SVR cohort (5880.4 patient-years), 30 patients developed HCC, 6 patients had decompensation, 35 patients died, and no patient underwent LT during follow-up. The cumulative incidence rates of HCC at 2 and 5 years were 0.6% and 1.6%, respectively for non-cirrhotic patients with SVR (n = 985), and 4.8% and 10.1%, respectively, for cirrhotic SVR patients (n = 283). The cumulative HCC risk according to the presence of cirrhosis, FIB-4 index, APRI score, and ALBI score were significantly different (Supplementary Figure 3). However, HBcIgG positivity (HR, 0.39; 95%CI: 0.05-2.89; P = 0.358) and the presence of fatty liver disease (HR, 0.16; 95%CI: 0.02-1.18; P = 0.072) were not significant risk factors for the development HCC.

Comparisons of the clinical characteristics and outcomes of the IBT-SVR and DAA-SVR groups before and after PS matching (Table 4) yielded 213 matched pairs of patients from the IBT-SVR and DAA-SVR groups with no significant between-group differences in all baseline variables. Before PS matching, the DAA-SVR group had a significantly higher risk of HCC than the IBT-SVR group (HR, 3.53; 95%CI: 1.47-8.49; P = 0.005) (Supplementary Figure 4A), whereas the risks of decompensation (HR, 2.45; 95%CI: 0.33-18.37; P = 0.382) and death/LT (HR, 1.44; 95%CI: 0.62-3.34; P = 0.400) did not reach statistical significance (Supplementary Figure 4B and C). However, after PS matching, the DAA-SVR group showed no significant differences in the risks of HCC (HR, 2.72; 95%CI: 0.63-11.81; P = 0.179), decompensation (HR, 9.74; 95%CI: 0.42-224.81; P = 0.155), and death/LT (HR, 2.18; 95%CI: 0.47-10.15; P = 0.318) compared with the IBT-SVR group (Figure 3).

Multivariable-adjusted analyses of factors associated with outcomes of the SVR cohort

According to the multivariable-adjusted analysis, the DAA-SVR group did not show any independent differences in the development of HCC (HR, 2.03; 95%CI: 0.76-5.43; P = 0.160) or death/LT (HR, 1.38; 95%CI: 0.55-3.49; P = 0.494) compared with the IBT-SVR group (Table 5). Covariates independently associated with a higher incidence of HCC were older age (HR, 1.05; 95%CI: 1.01-1.10; P = 0.025), genotype 1 (HR, 3.02; 95%CI: 1.18-7.68; P = 0.021), and the presence of cirrhosis (HR, 3.18; 95%CI: 1.33-7.68; P = 0.009) after adjustment for the antiviral treatment regimen, sex, alcohol consumption, diabetes mellitus, albumin level, PT, and AFP level (Table 5). Additionally, covariates independently associated with death/LT risk were the presence of cirrhosis (HR, 2.97; 95%CI: 1.42-6.20; P = 0.004) and PT (HR, 5.27; 95%CI: 1.01-27.53; P = 0.049).

DISCUSSION

We analyzed the incidence rates of HCC, decompensation, and all-cause death/LT in a large, prospective, Asian cohort including 2054 patients with chronic HCV infection. During a median follow-up period of 4.1 years, the risks of HCC, decompensation, and all-cause mortality were significantly lower after treatment with IBT or DAA compared with no treatment.

After statistical adjustment, including a time-varying Cox analysis and PS-matched analysis, the risks of HCC, decompensation, and all-cause mortality were not significantly different regardless of whether SVR was achieved after IBT or DAA treatment; however, the follow-up duration of the DAA group was shorter than that of the IBT group. After achieving SVR, independent factors associated with HCC risk were no treatment, age, male sex, HCV genotype 1, cirrhosis, alcohol consumption, PT, and pretreatment AFP level, whereas independent factors associated with all-cause mortality were cirrhosis and PT.

There are limited studies of the association between antiviral treatment (IBT or DAA) and all-cause mortality, especially those involving Asian cohorts. Many studies focused on liver-related mortality rather than all-cause mortality as the primary outcome after SVR achievement. However, extrahepatic mortality should be considered for patients with HCV because HCV is associated with increased cardiovascular disease events[20] and extrahepatic malignancies such as bile duct cancers and diffuse large B-cell lymphoma[21,22]. Moreover, Tada *et al*[23] reported that IBT could reduce all-cause mortality and HCC risk even in patients who did not achieve SVR. However, the effect of DAA treatment in the absence of SVR on clinical outcomes is unknown. Therefore, this study focused on the effect of treatment on the outcomes including all-cause mortality in the entire cohort, and the effect of SVR induced by IBT and DDA on the outcomes in the SVR cohort.

Table 4 Comparison of characteristics and outcomes between the interferon-based treatment-sustained virologic response and direct-acting antivirals-sustained virologic response groups: Unadjusted and propensity score matching groups

Variable	Before adjustment				PS matched			
	IBT-SVR group (*n* = 451)	DAA-SVR group (*n* = 817)	*P* value	SMD	IBT-SVR group (*n* = 213)	DAA-SVR group (*n* = 213)	*P* value	SMD
Age, yr	51.0 ± 10.6	59.1 ± 11.4	< 0.001	0.741	53.9 ± 9.8	53.7 ± 11.4	0.823	0.022
Male sex	209 (46.3)	394 (48.2)	0.52	0.036	102 (47.9)	97 (45.5)	0.627	0.047
HCV RNA, $xlog_{10}$ IU/mL	5.72 (4.77-6.37)	6.04 (5.26-6.52)	< 0.001	0.278	5.84 (4.91-6.53)	6.07 (5.21-6.50)	0.439	0.073
HCV genotype			< 0.001	0.406			0.731	0.058
1	167 (37.0)	464 (56.8)			95 (44.6)	101 (47.4)		
2	278 (61.6)	342 (41.9)			116 (54.5)	111 (52.1)		
Others	6 (1.3)	11 (1.3)			2 (0.9)	1 (0.5)		
Entry-to-treat, year	0 (0-0.3)	0.2 (0-2.1)	< 0.001	0.654	0.1 (0-0.4)	0.1 (0-0.4)	0.78	0.125
Diagnosis status			0.001	0.192			0.901	0.012
Chronic hepatitis	373 (82.7)	612 (74.9)			174 (81.7)	173 (81.2)		
Compensated cirrhosis	78 (17.3)	205 (25.1)			39 (18.3)	40 (18.8)		
FIB-4 index			< 0.001	0.294			0.363	0.071
≤ 1.45	156 (34.8)	156 (19.9)			69 (32.7)	59 (29.1)		
1.45–3.25	155 (34.6)	326 (41.6)			74 (35.1)	85 (41.9)		
≥ 3.25	137 (30.6)	302 (38.5)			68 (32.2)	59 (29.1)		
APRI score			0.562	0.096			0.108	0.048
< 2.0	383 (85.1)	676 (83.9)			186 (87.7)	170 (82.1)		
≥ 2.0	67 (14.9)	130 (16.1)			26 (12.3)	37 (17.9)		
ALBI score			0.958	0.044			0.339	0.054
≤ -2.60 (Grade 1)	360 (80.0)	639 (79.9)			172 (81.1)	172 (82.7)		
> -2.60 (Grade 2 or 3)	90 (20.0)	161 (20.1)			40 (18.9)	36 (16.3)		
Ever smoker	228 (50.8)	15 (37.5)	0.045	0.162	95 (44.6)	93 (43.7)	0.527	0.019
Alcohol intake			< 0.001	0.669			0.816	0.058
None	171 (38.0)	19 (47.5)			98 (46.0)	104 (48.8)		
Social	245 (54.4)	13 (32.5)			88 (41.3)	85 (39.9)		
Significant[1]	34 (7.6)	8 (20.0)			27 (12.7)	24 (11.3)		
Fatty liver disease on imaging study	77 (22.8), *n* = 337	131 (22.4), *n* = 586	0.863	0.039	34 (24.3)	35 (24.8)	0.917	0.013
Anti-HBc IgG positivity	25 (8.6), *n* = 290	62 (10.5), *n* = 592	0.386	0.062	12 (7.8)	15 (9.7)	0.546	0.062
BMI, kg/m^2	23.7 ± 3.0	23.9 ± 3.1	0.429	0.047	23.9 ± 2.9	23.9 ± 3.4	0.983	0.005
Diabetes mellitus	61 (13.6)	122 (14.9)	0.495	0.049	26 (12.2)	22 (10.3)	0.54	0.055
Hypertension	80 (17.7)	236 (28.9)	< 0.001	0.267	45 (21.1)	44 (20.7)	0.905	0.012
Cardiovascular disease	3 (0.7)	24 (2.9)	0.007	0.162	2 (0.9)	3 (1.4)	0.315	0.058
Cerebrovascular disease	2 (0.4)	19 (2.3)	0.012	0.172	1 (0.5)	3 (1.4)	0.315	0.141
Laboratory study								
WBC, $\times 10^3/mm^3$	4.99 (3.90-6.10)	5.40 (4.40-6.63)	< 0.0010.297	0.24	5.26 (4.25-6.35)	5.35 (4.50-6.52)	0.787	0.027
Hemoglobin, g/dL	13.6 (12.6-14.9)	13.8 (12.8-14.8)	0.218	0.061	13.9 (12.8-14.9)	13.9 (12.8-14.9)	0.916	0.01

PLT, × 10^3/mm^3	177 (136-220)	173 (130-216)	0.178	0.055	176 (136-222)	180 (139-219)	0.401	0.083
Albumin, g/dL	4.2 (4.0-4.5)	4.2 (4.0-4.4)	0.664	0.082	4.3 (4.0-4.5)	4.3 (4.0-4.5)	0.734	0.031
Total bilirubin, mg/dL	0.7 (0.6-1.0)	0.7 (0.6-1.0)	< 0.001	0.072	0.8 (0.6-1.0)	0.7 (0.6-1.0)	0.85	0.009
ALP, IU/L	80 (63-113)	122 (78-250)	0.012	0.612	90 (65-126)	96 (72-183)	0.524	0.072
AST, IU/L	50 (30-86)	46 (30-76)	< 0.001	0.156	50 (32-83)	42 (27-85)	0.899	0.012
ALT, IU/L	54 (29-105)	36 (22-70)	0.756	0.297	49 (29-85)	37 (21-91)	0.915	0.009
Creatinine, mg/dL	0.8 (0.7-1.0)	0.8 (0.7-1.0)	0.02	0.09	0.8 (0.7-1.0)	0.8 (0.7-0.9)	0.176	0.069
PT, INR	1.03 (0.98-1.08)	1.04 (0.99-1.10)	0.434	0.111	1.03 (0.98-1.08)	1.04 (0.87-1.09)	0.67	0.038
AFP, ng/dL	3.3 (2.3-6.3)	3.8 (2.3-6.5)		0.142	5.8 (4.9-6.5)	6.1 (5.2-6.5)	0.278	0.034

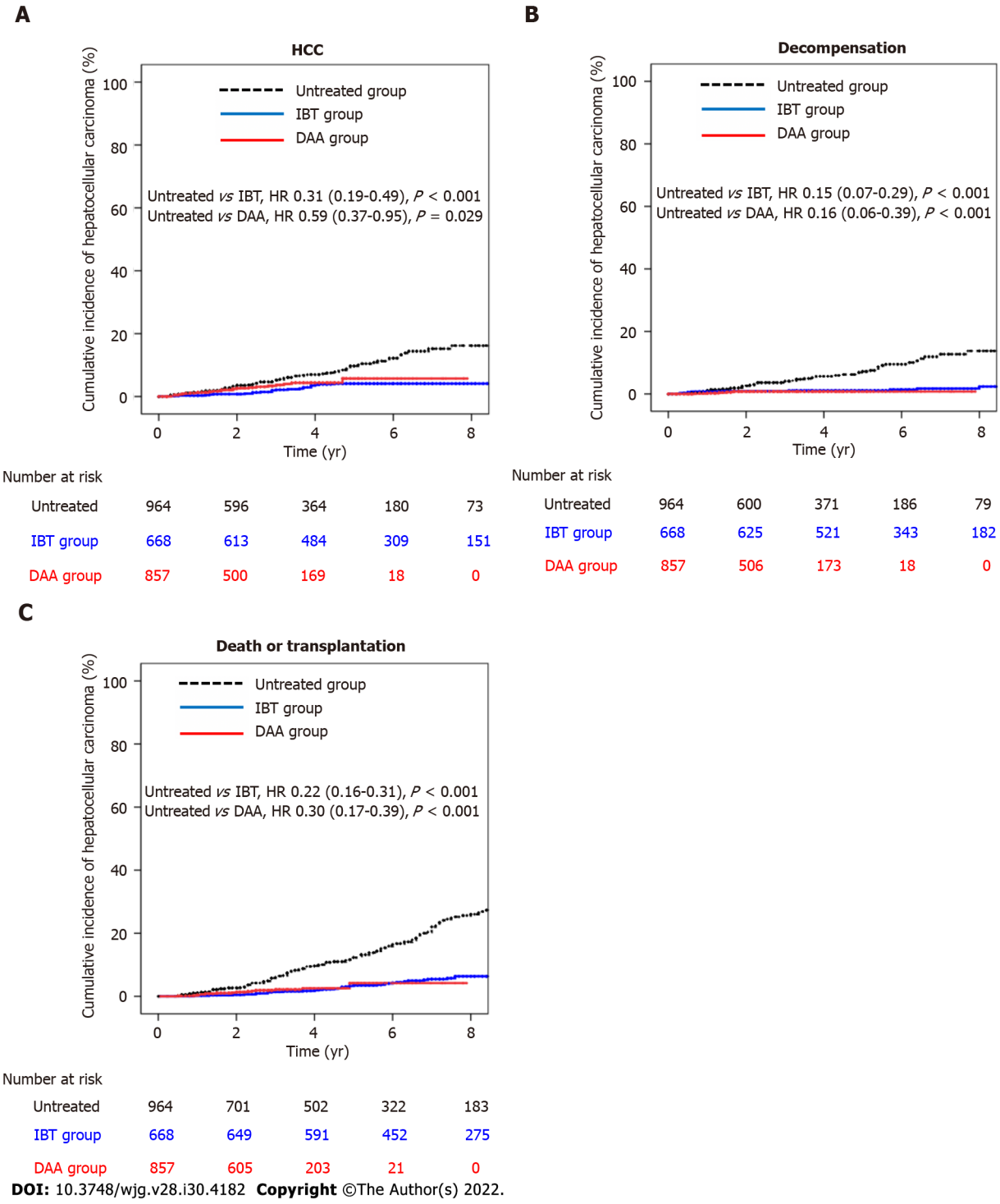
[1]Significant alcohol intake is defined as weekly alcohol consumption ≥ 210 g for men and ≥ 140 g for women.
Data were presented as mean ± SD, median (interquartile range), or *n* (%). AFP: Alpha-feto protein; ALBI: Albumin-bilirubin; ALP: Alkaline phosphatase; ALT: Alanine aminotransferase; APRI: Aspartate aminotransferase to platelet ratio index; AST: Aspartate aminotransferase; BMI: Body mass index; DAA: Direct acting antivirals; FIB-4: Fibrosis-4; HCV: Hepatitis C virus; IBT: Interferon-based therapy; MELD: Model for end-stage liver disease; PLT: Platelet; PT: Prothrombin time; WBC: White blood cell; SVR: Sustained virologic response.

Table 5 Multivariate Cox regression analysis for hepatocellular carcinoma and death/transplantation among the sustained virologic response cohort

Variable	Hepatocellular carcinoma		Death/transplantation	
	aHR (95%CI)	*P* value	aHR (95%CI)	*P* value
IBT-SVR group	Reference	-	Reference	-
DAA-SVR group	2.03 (0.76-5.43)	0.16	1.38 (0.55-3.49)	0.494
Age, yr	1.05 (1.01-1.10)	0.025	-	-
Male sex	2.89 (0.97-8.61)	0.057	-	-
HCV genotype			-	–
2	Reference	-		
1	3.02 (1.18-7.68)	0.021		
Cirrhosis	3.18 (1.33-7.68)	0.009	2.97 (1.42-6.20)	0.004
Ever smoker	0.72 (0.26-1.99)	0.545	-	-
Alcohol consumption			-	-
None	Reference	-		
Social	2.62 (0.92-7.60)	0.072		
Significant	2.51 (0.71-8.82)	0.152		
BMI, kg/m^2	-	-	-	-
Diabetes mellitus	1.03 (0.42-2.52)	0.952	2.16 (0.98-4.78)	0.057
Albumin, g/dL	0.53 (0.19-1.49)	0.228	-	-
Total bilirubin, mg/dL	-	-	-	-
PT, INR	4.12 (0.89-19.17)	0.071	5.27 (1.01-27.53)	0.049
AFP, log_{10} ng/dL	1.07 (0.49-2.34)	0.858	-	-

Total number of patients, 1250; number of hepatocellular carcinomas, 30; number of deaths, 7; number of transplantations, 3. AFP: Alpha-feto protein; aHR: Adjusted hazard ratio; BMI: Body mass index; CI: Confidence interval; DAA: Direct acting antivirals; HCV: Hepatitis C virus; IBT: Interferon-based therapy; PT: Prothrombin time; SVR: Sustained virologic response.

Recent 5-year follow-up studies after DAA treatment showed that SVR is associated with a gradual but significant reduction in liver fibrosis in terms of FIB-4, METAVIR, transient elastography, and Child-Pugh score[24,25], whereas another study showed that induced SVR was associated with a reduced risk of clinical disease progression in patients with Child-Pugh A cirrhosis but not in patients

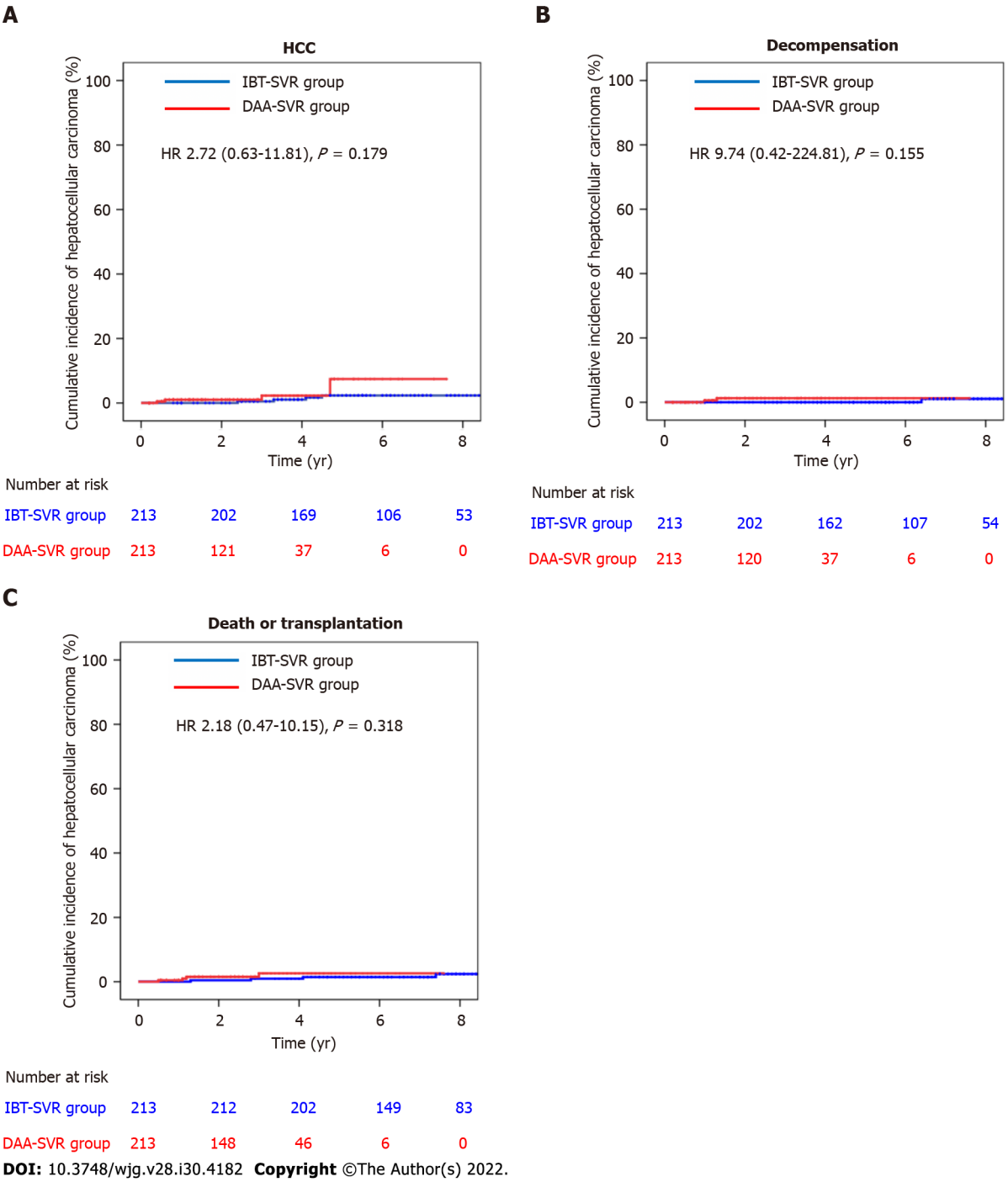


DOI: 10.3748/wjg.v28.i30.4182 **Copyright** ©The Author(s) 2022.

Figure 2 Cumulative incidences of hepatocellular carcinoma, decompensation, and death/transplantation in entire cohort. A: Cumulative incidence of hepatocellular carcinoma in the untreated, interferon-based treatment (IBT), and direct-acting antivirals (DAA) groups; B: Cumulative incidence of decompensation in the untreated, IBT, and DAA groups; C: Cumulative incidence of death/transplantation in the untreated, IBT, and DAA groups. DAA: Direct-acting antivirals; HCC: Hepatocellular carcinoma; IBT: Interferon-based treatment.

with Child-Pugh B/C cirrhosis[26]. In this context, our study showed an approximately 85% reduction in the risk of decompensation after IBT or DAA treatment in Child-Pugh A patients, with decompensated cirrhotic patients being excluded from enrollment.

This study demonstrated that treatment with IBT and DAA resulted in risk reductions of 72% (median follow-up, 94.8 mo) and 81% (median follow-up, 42 mo) for all-cause mortality, respectively, compared with no treatment after multivariate adjustment. Similar to previous studies[27], our results showed that even IBT, with its probable adverse events and lower SVR rates, had long-term beneficial effects on mortality. Regarding the benefit of DAA treatment, Butt *et al*[28] (n = 6790), using the Electronically Retrieved Cohort of HCV Infected Veterans (ERCHIVES) data in the United States in



DOI: 10.3748/wjg.v28.i30.4182 **Copyright** ©The Author(s) 2022.

Figure 3 Cumulative incidences of hepatocellular carcinoma, decompensation, and death/transplantation in the matched sustained virologic response cohort. A: Cumulative incidence of hepatocellular carcinoma in the interferon-based treatment-sustained virologic response (IBT-SVR) and direct-acting antivirals-sustained virologic response (DAA-SVR) groups; B: Cumulative incidence of decompensation in the IBT-SVR and DAA-SVR groups; C: Cumulative incidence of death/Liver transplantation in the IBT-SVR and DAA-SVR groups. DAA: Direct-acting antivirals; HCC: Hepatocellular carcinoma; IBT: Interferon-based treatment; SVR: Sustained virologic response.

2017, reported that DAA treatment and the achievement of SVR reduced all-cause mortality by 57% and 43%, respectively, within the first 18 mo of treatment. A prospective cohort study performed in France (n = 9895; follow-up, 33.4 mo) reported a 52% reduction in the risk of all-cause mortality in the DAA-treated group compared with the untreated group in 2019[11]. Compared with these studies, our results showed a higher reduction in the risk of all-cause mortality with DAA treatment. This may be related to the low proportion of patients with advanced fibrosis in the DAA group in our cohort. Additionally, the follow-up duration of this study was relatively longer than the durations used for those studies.

During this study, the achievement of SVR by IBT or by DAA resulted in a 59% reduction in the risk of HCC compared with no treatment or no SVR after multivariable adjustment, similar to previous studies[29,30]. Nonetheless, our results also showed that the HCC risk remained after SVR achievement.

Despite the achievement of SVR, the absolute risk of HCC remains high for patients with cirrhosis; therefore, according to international guidelines, they should be enrolled in an HCC surveillance program[2-4]. However, there is little evidence of the benefits of HCC surveillance for non-cirrhotic chronic HCV patients with SVR, because of the low residual HCC risk. During this study, the non-cirrhotic group had an HCC risk of 0.26 per 100 person-years (5-year cumulative incidence of 1.6%). In particular, the low FIB-4 (5-year cumulative incidence of 0.3%) group had a very low risk of HCC during this study. These results are similar to those of the retrospective REAL-C cohort study that targeted Eastern Asians (5-year cumulative incidence: 1.35 for the non-cirrhotic group and 0.13 for the low FIB-4 group)[30]. These results support the European guidelines, which do not recommend HCC surveillance for fibrosis 0 to 2[4]. However, more long-term follow-up data after achieving SVR are needed.

Identifying the risk factors associated with HCC after SVR is important to the development of a reasonable surveillance strategy. An East Asian retrospective study suggested that among the cirrhotic DAA-SVR group, age older than 60 years, ALBI scores of 2 or 3, and pretreatment AFP > 10 ng/mL were associated with HCC risk; however, among the non-cirrhotic group, only AFP > 10 ng/mL was significant[30]. Additionally, there are many factors associated with HCC risk after SVR, such as clinical factors (age, sex, presence of diabetes, HCV genotype 3, history of IBT), laboratory parameters (platelet count, AFP), and fibrosis stage (determined by histology or estimation by Fibroscan®, FIB-4, APRI, or the presence of esophageal varices) before DAA treatment and at follow-up (determined by Fibroscan®, FIB-4, APRI, alanine aminotransferase, AFP, albuminemia, or VITRO score)[31]. In our study, age, cirrhosis, and HCV genotype 1 (compared with genotype 2) were independent risk factors for HCC after SVR. Therefore, it is necessary to test the HCV genotype even in the therapeutic era of pangenotypic regimens to develop a follow-up strategy after SVR according to the regional distribution of HCV genotypes. These factors should be considered when establishing an optimal HCC prediction model.

Previous studies have suggested a similar risk of HCC development with IBT and DAA treatment [32]. Interestingly, a recent meta-analysis suggested that IBT is better than DAA for preventing the occurrence of HCC in chronic hepatitis C patients after achieving SVR[33]. Biologically, IFN family members, especially class I IFN (IFN-α, IFN-β), have important anti-HCC effects[32]. However, some investigators have suggested that the sudden decrease in viral load caused by DAA treatment causes immune distortion, thus deregulating the antitumor response and releasing precancerous foci from immune surveillance[34,35]. Although it can be explained theoretically, there is little clinical evidence regarding the difference in the HCC risk for patients with DAA-SVR and IBT-SVR. Our results showed significant clinical differences between the IBT-SVR and DAA-SVR groups. Both the multivariable analysis and PS matching analysis showed that the effect of IBT-SVR was not different from that of DAA-SVR on the HCC incidence and all-cause mortality. Recently, some studies reported different effects of IBT-SVR and DAA-SVR on the incidence of diabetes[36] and hematologic malignancies[37]. Therefore, long-term studies of the effects of DAA-SVR are warranted.

To meet the 2030 HCV elimination target of the WHO[1], active testing and enhanced linkage to treatment are important. In this study, 30.1% of patients remained untreated, and this percentage should be reduced. Indeed, the untreated group showed a higher mortality rate of 23.7% (88 Liver related deaths and 59 non-liver related deaths) during the median follow-up of 5.6 years. In the untreated group, 3 patients received IBT after HCC diagnosis, and 19 patients received DAA treatment after HCC diagnosis or a decompensation event. The majority of the untreated patients (78.8%, 457/619) were enrolled in the Korean HCV cohort before June 2015, when the first DAA was introduced, and 46.7% (289/619) died or were lost to follow-up before June 2015. Although DAA therapy is covered by the National Health Insurance System, 30% of the drug price is an out-of-pocket expense of the patients, equaling to approximately 3000 United States dollars. Even in the DAA era, the main reasons for non-treatment are the relatively high price of DAA, old age, and extrahepatic or advanced hepatic malignancy.

One of the strengths of our study was that it was a long-term study involving a prospective, Asian cohort that included both IBT and DAA groups. This study used a well-established protocol, guidelines and database, and the data, including death outcomes, were verified under government guidance. To date, few reports have evaluated and compared clinical outcomes (HCC, death, and decompensation) after IBT and DAA treatment, especially in Asia, where HCV is less prevalent than HBV.

This study had several limitations. First, because it was an observational study, the findings may show selection and confounding biases. Despite this limitation, it would be useful for comparing the effectiveness of IBT and DAA because of the relatively low incidence of clinical events. Second, we used clinical and radiological criteria to diagnose cirrhosis; therefore, some patients with advanced fibrosis may have been included in the non-cirrhotic group. However, we attempted to correct this point using a non-invasive liver fibrosis biomarker. Third, there was a disparity in the follow-up periods of the IBT and DAA groups because of the later introduction of DAA (since 2015 in Korea). Additional long-term follow-up studies evaluating the outcomes of patients with SVR are warranted. Forth, the presence of anti-HBc IgG in HCV patients has been implicated in HCC development, and a non-negligible risk of HBV inactivation during DAA treatment (0.91%)[38]. However, approximately 30% of our patients were not tested for anti-HBc IgG, and none of the anti-HBc IgG-positive patients were tested for HBV DNA during DAA treatment. Likewise, the role of fatty liver in the outcomes of HCV patients was not

completely evaluated owing to missing data. Finally, compared with the IBT era, diagnostic imaging modalities and treatment options for HCC have improved in the DAA era. Therefore, these points could have affected the clinical outcomes of the IBT and DAA groups.

CONCLUSION

This study showed that antiviral treatment significantly reduced the incidences of HCC, decompensation, and mortality in an Asian population, regardless of the use of IBT or DAA. After achieving SVR, age, the presence of cirrhosis, and HCV genotype 1 were indicators of worse clinical outcomes. Therefore, an adequate HCC surveillance strategy after SVR that considers age, the presence of cirrhosis, and genotype should be developed. Additional studies evaluating the long-term DAA outcomes of SVR patients are also warranted.

ARTICLE HIGHLIGHTS

Research background

Sustained virologic response (SVR) with either interferon-based therapy (IBT) or direct acting antivirals (DAA)-induced SVR significantly reduces the incidence of hepatocellular carcinoma (HCC) and long-term mortality in patients with hepatitis C virus (HCV) infection.

Research motivation

Prospective studies of the long-term outcomes for patients with HCV infection after treatment with IBT or DAA are limited in many Asian countries.

Research objectives

We aimed to elucidate the incidences of HCC and death/transplantation based on treatment with IBT or DAA. And, we aimed to compare the outcomes of the SVR to IBT and DAA. Finally, we aimed to investigate outcome-determining factors after SVR.

Research methods

The cohort included 2054 viremic patients (mean age, 57 years; 46.5% male; 27.4% with cirrhosis) prospectively enrolled at seven hospitals between 2007 and 2019. They were classified as the untreated group (n = 619), IBT group (n = 578), and DAA group (n = 857).

Research results

Compared to the untreated group, the incidences of HCC and death/transplantation were significantly lower in the IBT group and the DAA group. SVR induced by IBT or DAA did not show significant differences in the risk of HCC and all-cause mortality. After achieving SVR, age, presence of cirrhosis, and genotype 1 HCV infection were indicators of worse clinical outcomes.

Research conclusions

Treatment and SVR with either IBT or DAA significantly reduced the incidences of HCC and mortality in the Asian prospective cohort.

Research perspectives

This study was a long-term study involving a prospective, Asian cohort that included both IBT and DAA groups. This study used a well-established protocol, guidelines and database, and the data, including death outcomes, were verified under government guidance.

ACKNOWLEDGEMENTS

We deeply appreciate the clinical research coordinators (Lee DE, Kim NH, Jeong DH, Na SM, Kang HY, Jo AR, Han SH, Chung ES, Jeong HY, and Lee HM) for their dedication to this study and the officials of the Korea Disease Control and Prevention Agency (Lee MS, Seong JH, Lee JK, Kee MK, Chung HM, Choi BS, Kim KS, Kang C, Kim SS, and Jee YM) for their strong support of this study.

FOOTNOTES

Author contributions: Choi GH and Jang ES contributed equally to this work; Choi GH, Jang ES, and Jeong SH were responsible for the study concept and design, data acquisition, analysis and interpretation, statistical analysis, and manuscript drafting; Kim YS, Lee YJ, Kim IH, Cho SB, Lee HC, and Jang JW assisted with data acquisition and analysis; Ki M, Choi HY, and Baik D assisted with the data analysis and interpretation.

Supported by the Chronic Infectious Disease Cohort Study (Korea HCV Cohort Study) from the National Institute of Infectious Disease, National Institute of Health, Korea Disease Control and Prevention Agency, No. 2020-E5104-02.

Institutional review board statement: The study protocol was approved by the Institutional Review Board of seven hospitals.

Informed consent statement: All participants provided written informed consent prior to study enrollment.

Conflict-of-interest statement: Nothing to declare.

Data sharing statement: We are not willing to share data.

STROBE statement: The authors have read the STROBE Statement—checklist of items, and the manuscript was prepared and revised according to the STROBE Statement—checklist of items.

Open-Access: This article is an open-access article that was selected by an in-house editor and fully peer-reviewed by external reviewers. It is distributed in accordance with the Creative Commons Attribution NonCommercial (CC BY-NC 4.0) license, which permits others to distribute, remix, adapt, build upon this work non-commercially, and license their derivative works on different terms, provided the original work is properly cited and the use is non-commercial. See: https://creativecommons.org/Licenses/by-nc/4.0/

Country/Territory of origin: South Korea

ORCID number: Gwang Hyeon Choi 0000-0002-8795-8427; Eun Sun Jang 0000-0003-4274-2582; Sung Bum Cho 0000-0001-9816-3446; Han Chu Lee 0000-0002-7631-4124; Jeong Won Jang 0000-0002-0305-5846; Sook-Hyang Jeong 0000-0002-4916-7990.

S-Editor: Yan JP
L-Editor: A
P-Editor: Yan JP

REFERENCES

1 **World Health Organization**. Interim guidance for country validation of viral hepatitis elimination. World Health Organization, 2021. Available from: https://apps.who.int/iris/handle/10665/341652
2 **Korean Association for the Study of the Liver (KASL)**. 2017 KASL clinical practice guidelines management of hepatitis C: Treatment of chronic hepatitis C. *Clin Mol Hepatol* 2018; **24**: 169-229 [PMID: 30092624 DOI: 10.3350/cmh.2018.1004]
3 **Ghany MG**, Morgan TR; AASLD-IDSA Hepatitis C Guidance Panel. Hepatitis C Guidance 2019 Update: American Association for the Study of Liver Diseases-Infectious Diseases Society of America Recommendations for Testing, Managing, and Treating Hepatitis C Virus Infection. *Hepatology* 2020; **71**: 686-721 [PMID: 31816111 DOI: 10.1002/hep.31060]
4 **European Association for the Study of the Liver**; Clinical Practice Guidelines Panel: Chair; EASL Governing Board representative; Panel members. EASL recommendations on treatment of hepatitis C: Final update of the series☆. *J Hepatol* 2020; **73**: 1170-1218 [PMID: 32956768 DOI: 10.1016/j.jhep.2020.08.018]
5 **Fried MW**, Shiffman ML, Reddy KR, Smith C, Marinos G, Gonçales FL Jr, Häussinger D, Diago M, Carosi G, Dhumeaux D, Craxi A, Lin A, Hoffman J, Yu J. Peginterferon alfa-2a plus ribavirin for chronic hepatitis C virus infection. *N Engl J Med* 2002; **347**: 975-982 [PMID: 12324553 DOI: 10.1056/NEJMoa020047]
6 **Bang CS**, Song IH. Impact of antiviral therapy on hepatocellular carcinoma and mortality in patients with chronic hepatitis C: systematic review and meta-analysis. *BMC Gastroenterol* 2017; **17**: 46 [PMID: 28376711 DOI: 10.1186/s12876-017-0606-9]
7 **Lee YB**, Nam JY, Lee JH, Chang Y, Cho H, Cho YY, Cho EJ, Yu SJ, Kim HY, Lee DH, Lee JM, Hwang SG, Kim YJ, Yoon JH. Differential Effect of HCV Eradication and Fibrosis Grade on Hepatocellular Carcinoma and All-cause Mortality. *Sci Rep* 2018; **8**: 13651 [PMID: 30209336 DOI: 10.1038/s41598-018-31839-y]
8 **Dolmazashvili E**, Abutidze A, Chkhartishvili N, Karchava M, Sharvadze L, Tsertsvadze T. Regression of liver fibrosis over a 24-week period after completing direct-acting antiviral therapy in patients with chronic hepatitis C receiving care within the national hepatitis C elimination program in Georgia: results of hepatology clinic HEPA experience. *Eur J Gastroenterol Hepatol* 2017; **29**: 1223-1230 [PMID: 28857900 DOI: 10.1097/MEG.0000000000000964]
9 **Bachofner JA**, Valli PV, Kröger A, Bergamin I, Künzler P, Baserga A, Braun D, Seifert B, Moncsek A, Fehr J, Semela D, Magenta L, Müllhaupt B, Terziroli Beretta-Piccoli B, Mertens JC. Direct antiviral agent treatment of chronic hepatitis C results in rapid regression of transient elastography and fibrosis markers fibrosis-4 score and aspartate aminotransferase-

platelet ratio index. *Liver Int* 2017; **37**: 369-376 [PMID: 27678216 DOI: 10.1111/liv.13256]

10 **Afdhal N**, Everson GT, Calleja JL, McCaughan GW, Bosch J, Brainard DM, McHutchison JG, De-Oertel S, An D, Charlton M, Reddy KR, Asselah T, Gane E, Curry MP, Forns X. Effect of viral suppression on hepatic venous pressure gradient in hepatitis C with cirrhosis and portal hypertension. *J Viral Hepat* 2017; **24**: 823-831 [PMID: 28295923 DOI: 10.1111/jvh.12706]

11 **Carrat F**, Fontaine H, Dorival C, Simony M, Diallo A, Hezode C, De Ledinghen V, Larrey D, Haour G, Bronowicki JP, Zoulim F, Asselah T, Marcellin P, Thabut D, Leroy V, Tran A, Habersetzer F, Samuel D, Guyader D, Chazouilleres O, Mathurin P, Metivier S, Alric L, Riachi G, Gournay J, Abergel A, Cales P, Ganne N, Loustaud-Ratti V, D'Alteroche L, Causse X, Geist C, Minello A, Rosa I, Gelu-Simeon M, Portal I, Raffi F, Bourliere M, Pol S; French ANRS CO22 Hepather cohort. Clinical outcomes in patients with chronic hepatitis C after direct-acting antiviral treatment: a prospective cohort study. *Lancet* 2019; **393**: 1453-1464 [PMID: 30765123 DOI: 10.1016/S0140-6736(18)32111-1]

12 **Nahon P**, Layese R, Bourcier V, Cagnot C, Marcellin P, Guyader D, Pol S, Larrey D, De Lédinghen V, Ouzan D, Zoulim F, Roulot D, Tran A, Bronowicki JP, Zarski JP, Riachi G, Calès P, Péron JM, Alric L, Bourlière M, Mathurin P, Blanc JF, Abergel A, Serfaty L, Mallat A, Grangé JD, Attali P, Bacq Y, Wartelle C, Dao T, Thabut D, Pilette C, Silvain C, Christidis C, Nguyen-Khac E, Bernard-Chabert B, Zucman D, Di Martino V, Sutton A, Roudot-Thoraval F, Audureau E; ANRS CO12 CirVir Group. Incidence of Hepatocellular Carcinoma After Direct Antiviral Therapy for HCV in Patients With Cirrhosis Included in Surveillance Programs. *Gastroenterology* 2018; **155**: 1436-1450.e6 [PMID: 30031138 DOI: 10.1053/j.gastro.2018.07.015]

13 **Sahakyan Y**, Lee-Kim V, Bremner KE, Bielecki JM, Krahn MD. Impact of direct-acting antiviral regimens on mortality and morbidity outcomes in patients with chronic hepatitis c: Systematic review and meta-analysis. *J Viral Hepat* 2021; **28**: 739-754 [PMID: 33556225 DOI: 10.1111/jvh.13482]

14 **Vallet-Pichard A**, Mallet V, Nalpas B, Verkarre V, Nalpas A, Dhalluin-Venier V, Fontaine H, Pol S. FIB-4: an inexpensive and accurate marker of fibrosis in HCV infection. comparison with liver biopsy and fibrotest. *Hepatology* 2007; **46**: 32-36 [PMID: 17567829 DOI: 10.1002/hep.21669]

15 **Loaeza-del-Castillo A**, Paz-Pineda F, Oviedo-Cárdenas E, Sánchez-Avila F, Vargas-Vorácková F. AST to platelet ratio index (APRI) for the noninvasive evaluation of liver fibrosis. *Ann Hepatol* 2008; **7**: 350-357 [PMID: 19034235 DOI: 10.1152/ajpgi.90287.2008]

16 **Johnson PJ**, Berhane S, Kagebayashi C, Satomura S, Teng M, Reeves HL, O'Beirne J, Fox R, Skowronska A, Palmer D, Yeo W, Mo F, Lai P, Iñarrairaegui M, Chan SL, Sangro B, Miksad R, Tada T, Kumada T, Toyoda H. Assessment of liver function in patients with hepatocellular carcinoma: a new evidence-based approach-the ALBI grade. *J Clin Oncol* 2015; **33**: 550-558 [PMID: 25512453 DOI: 10.1200/JCO.2014.57.9151]

17 **Korean Liver Cancer Association**; National Cancer Center. 2018 Korean Liver Cancer Association-National Cancer Center Korea Practice Guidelines for the Management of Hepatocellular Carcinoma. *Gut Liver* 2019; **13**: 227-299 [PMID: 31060120 DOI: 10.5009/gnl19024]

18 **Garcia-Tsao G**, Friedman S, Iredale J, Pinzani M. Now there are many (stages) where before there was one: In search of a pathophysiological classification of cirrhosis. *Hepatology* 2010; **51**: 1445-1449 [PMID: 20077563 DOI: 10.1002/hep.23478]

19 **Lee J**, Lee JS, Park SH, Shin SA, Kim K. Cohort Profile: The National Health Insurance Service-National Sample Cohort (NHIS-NSC), South Korea. *Int J Epidemiol* 2017; **46**: e15 [PMID: 26822938 DOI: 10.1093/ije/dyv319]

20 **Chaudhari R**, Fouda S, Sainu A, Pappachan JM. Metabolic complications of hepatitis C virus infection. *World J Gastroenterol* 2021; **27**: 1267-1282 [PMID: 33833481 DOI: 10.3748/wjg.v27.i13.1267]

21 **Mahale P**, Torres HA, Kramer JR, Hwang LY, Li R, Brown EL, Engels EA. Hepatitis C virus infection and the risk of cancer among elderly US adults: A registry-based case-control study. *Cancer* 2017; **123**: 1202-1211 [PMID: 28117886 DOI: 10.1002/cncr.30559]

22 **Masarone M**, Persico M. Hepatitis C virus infection and non-hepatocellular malignancies in the DAA era: A systematic review and meta-analysis. *Liver Int* 2019; **39**: 1292-1306 [PMID: 30983083 DOI: 10.1111/liv.14119]

23 **Tada T**, Kumada T, Toyoda H, Kiriyama S, Tanikawa M, Hisanaga Y, Kanamori A, Kitabatake S, Yama T, Tanaka J. Viral eradication reduces all-cause mortality in patients with chronic hepatitis C virus infection: a propensity score analysis. *Liver Int* 2016; **36**: 817-826 [PMID: 26787002 DOI: 10.1111/liv.13071]

24 **Flisiak R**, Zarębska-Michaluk D, Janczewska E, Łapiński T, Rogalska M, Karpińska E, Mikuła T, Bolewska B, Białkowska J, Flejscher-Stępniewska K, Tomasiewicz K, Karwowska K, Pazgan-Simon M, Piekarska A, Berak H, Tronina O, Garlicki A, Jaroszewicz J. Five-Year Follow-Up of Cured HCV Patients under Real-World Interferon-Free Therapy. *Cancers (Basel)* 2021; **13** [PMID: 34359594 DOI: 10.3390/cancers13153694]

25 **Poordad F**, Castro RE, Asatryan A, Aguilar H, Cacoub P, Dieterich D, Marinho RT, Carvalho A, Siddique A, Hu YB, Charafeddine M, Bondin M, Khan N, Cohen DE, Felizarta F. Long-term safety and efficacy results in hepatitis C virus genotype 1-infected patients receiving ombitasvir/paritaprevir/ritonavir + dasabuvir ± ribavirin in the TOPAZ-I and TOPAZ-II trials. *J Viral Hepat* 2020; **27**: 497-504 [PMID: 31954087 DOI: 10.1111/jvh.13261]

26 **Krassenburg LAP**, Maan R, Ramji A, Manns MP, Cornberg M, Wedemeyer H, de Knegt RJ, Hansen BE, Janssen HLA, de Man RA, Feld JJ, van der Meer AJ. Clinical outcomes following DAA therapy in patients with HCV-related cirrhosis depend on disease severity. *J Hepatol* 2021; **74**: 1053-1063 [PMID: 33242501 DOI: 10.1016/j.jhep.2020.11.021]

27 **Yoshida H**, Arakawa Y, Sata M, Nishiguchi S, Yano M, Fujiyama S, Yamada G, Yokosuka O, Shiratori Y, Omata M. Interferon therapy prolonged life expectancy among chronic hepatitis C patients. *Gastroenterology* 2002; **123**: 483-491 [PMID: 12145802 DOI: 10.1053/gast.2002.34785]

28 **Butt AA**, Yan P, Simon TG, Abou-Samra AB. Effect of Paritaprevir/Ritonavir/Ombitasvir/Dasabuvir and Ledipasvir/Sofosbuvir Regimens on Survival Compared With Untreated Hepatitis C Virus-Infected Persons: Results From ERCHIVES. *Clin Infect Dis* 2017; **65**: 1006-1011 [PMID: 28903508 DOI: 10.1093/cid/cix364]

29 **Kanwal F**, Kramer J, Asch SM, Chayanupatkul M, Cao Y, El-Serag HB. Risk of Hepatocellular Cancer in HCV Patients Treated With Direct-Acting Antiviral Agents. *Gastroenterology* 2017; **153**: 996-1005.e1 [PMID: 28642197 DOI: 10.1053/j.gastro.2017.06.012]

30 **Tanaka Y**, Ogawa E, Huang CF, Toyoda H, Jun DW, Tseng CH, Hsu YC, Enomoto M, Takahashi H, Furusyo N, Yeh ML, Iio E, Yasuda S, Lam CP, Lee DH, Haga H, Yoon EL, Ahn SB, Wong G, Nakamuta M, Nomura H, Tsai PC, Jung JH, Song DS, Dang H, Maeda M, Henry L, Cheung R, Yuen MF, Ueno Y, Eguchi Y, Tamori A, Yu ML, Hayashi J, Nguyen MH; REAL-C Investigators. HCC risk post-SVR with DAAs in East Asians: findings from the REAL-C cohort. *Hepatol Int* 2020; **14**: 1023-1033 [PMID: 33277685 DOI: 10.1007/s12072-020-10105-2]

31 **Negro F**. Residual risk of liver disease after hepatitis C virus eradication. *J Hepatol* 2021; **74**: 952-963 [PMID: 33276027 DOI: 10.1016/j.jhep.2020.11.040]

32 **Nagaoki Y**, Imamura M, Aikata H, Daijo K, Teraoka Y, Honda F, Nakamura Y, Hatooka M, Morio R, Morio K, Kan H, Fujino H, Kobayashi T, Masaki K, Ono A, Nakahara T, Kawaoka T, Tsuge M, Hiramatsu A, Kawakami Y, Hayes CN, Miki D, Ochi H, Chayama K. The risks of hepatocellular carcinoma development after HCV eradication are similar between patients treated with peg-interferon plus ribavirin and direct-acting antiviral therapy. *PLoS One* 2017; **12**: e0182710 [PMID: 28797106 DOI: 10.1371/journal.pone.0182710]

33 **Ma L**, Liu J, Wang W, Yang F, Li P, Cai S, Zhou X, Chen X, Zhuang X, Zhang H, Cao G. Direct-acting antivirals and interferon-based therapy on hepatocellular carcinoma risk in chronic hepatitis-C patients. *Future Oncol* 2020; **16**: 675-686 [PMID: 32223423 DOI: 10.2217/fon-2019-0845]

34 **Llovet JM**, Villanueva A. Liver cancer: Effect of HCV clearance with direct-acting antiviral agents on HCC. *Nat Rev Gastroenterol Hepatol* 2016; **13**: 561-562 [PMID: 27580683 DOI: 10.1038/nrgastro.2016.140]

35 **Llorens-Revull M**, Costafreda MI, Rico A, Guerrero-Murillo M, Soria ME, Píriz-Ruzo S, Vargas-Accarino E, Gabriel-Medina P, Rodríguez-Frías F, Riveiro-Barciela M, Perales C, Quer J, Sauleda S, Esteban JI, Bes M. Partial restoration of immune response in Hepatitis C patients after viral clearance by direct-acting antiviral therapy. *PLoS One* 2021; **16**: e0254243 [PMID: 34242330 DOI: 10.1371/journal.pone.0254243]

36 **Butt AA**, Yan P, Aslam S, Shaikh OS, Abou-Samra AB. Hepatitis C Virus (HCV) Treatment With Directly Acting Agents Reduces the Risk of Incident Diabetes: Results From Electronically Retrieved Cohort of HCV Infected Veterans (ERCHIVES). *Clin Infect Dis* 2020; **70**: 1153-1160 [PMID: 30977808 DOI: 10.1093/cid/ciz304]

37 **Ioannou GN**, Green PK, Berry K, Graf SA. Eradication of Hepatitis C Virus Is Associated With Reduction in Hematologic Malignancies: Major Differences Between Interferon and Direct-Acting Antivirals. *Hepatol Commun* 2019; **3**: 1124-1136 [PMID: 31388632 DOI: 10.1002/hep4.1389]

38 **Kanda T**, Lau GKK, Wei L, Moriyama M, Yu ML, Chuang WL, Ibrahim A, Lesmana CRA, Sollano J, Kumar M, Jindal A, Sharma BC, Hamid SS, Kadir Dokmeci A, Mamun-Al-Mahtab, McCaughan GW, Wasim J, Crawford DHG, Kao JH, Ooka Y, Yokosuka O, Sarin SK, Omata M. APASL HCV guidelines of virus-eradicated patients by DAA on how to monitor HCC occurrence and HBV reactivation. *Hepatol Int* 2019; **13**: 649-661 [PMID: 31541423 DOI: 10.1007/s12072-019-09988-7]

World Journal of Gastroenterology

Submit a Manuscript: https://www.f6publishing.com

World J Gastroenterol 2022 August 14; 28(30): 4201-4210

DOI: 10.3748/wjg.v28.i30.4201

ISSN 1007-9327 (print) ISSN 2219-2840 (online)

META-ANALYSIS

Network meta-analysis of randomized controlled trials on esophagectomies in esophageal cancer: The superiority of minimally invasive surgery

Lajos Szakó, Dávid Németh, Nelli Farkas, Szabolcs Kiss, Réka Zsuzsa Dömötör, Marie Anne Engh, Péter Hegyi, Balint Eross, András Papp

Specialty type: Surgery

Provenance and peer review: Invited article; Externally peer reviewed.

Peer-review model: Single blind

Peer-review report's scientific quality classification

Grade A (Excellent): A
Grade B (Very good): 0
Grade C (Good): C, C
Grade D (Fair): 0
Grade E (Poor): 0

P-Reviewer: Liu Z, China; Scurtu RR, Romania; Tsujinaka S, Japan

Received: January 16, 2022
Peer-review started: January 16, 2022
First decision: April 12, 2022
Revised: April 26, 2022
Accepted: July 16, 2022
Article in press: July 16, 2022
Published online: August 14, 2022

Lajos Szakó, Nelli Farkas, Marie Anne Engh, Péter Hegyi, Institute of Translational Medicine, University of Pécs, Medical School, Pécs 7624, Hungary

Lajos Szakó, János Szentágothai Research Centre, University of Pécs, Medical School, Pécs 7624, Hungary

Dávid Németh, Réka Zsuzsa Dömötör, Institute for Translational Medicine, University of Pécs, Medical School, Pécs 7624, Hungary

Dávid Németh, Nelli Farkas, Institute of Bioanalysis, University of Pécs, Medical School, Pécs 7624, Hungary

Szabolcs Kiss, Insittute of Translational Medicine, University of Pécs, Medical School, Pécs 7624, Hungary

Szabolcs Kiss, Doctoral School of Clinical Medicine, University of Szeged, Medical School, Szeged 6720, Hungary

Péter Hegyi, First Department of Medicine, University of Szeged, Medical School, Szeged 6725, Hungary

Balint Eross, Institute of Translational Medicine, University of Pecs, Medical School, Pecs 7624, Hungary

András Papp, Department of Surgery, Clinical Center, University of Pécs, Medical School, Pécs 7624, Hungary

Corresponding author: András Papp, PhD, Associate Professor, Department of Surgery, Clinical Center, University of Pécs, Medical School, 13 Ifjúság útja, Pécs 7624, Hungary.
papp.andras@pte.hu

Abstract

BACKGROUND

Previous meta-analyses, with many limitations, have described the beneficial nature of minimal invasive procedures.

AIM

To compare all modalities of esophagectomies to each other from the results of randomized controlled trials (RCTs) in a network meta-analysis (NMA).

METHODS

We conducted a systematic search of the MEDLINE, EMBASE, *Reference Citation Analysis* (https://www.referencecitationanalysis.com/) and CENTRAL databases to identify RCTs according to the following population, intervention, control, outcome (commonly known as PICO): P: Patients with resectable esophageal cancer; I/C: Transthoracic, transhiatal, minimally invasive (thoracolaparoscopic), hybrid, and robot-assisted esophagectomy; O: Survival, total adverse events, adverse events in subgroups, length of hospital stay, and blood loss. We used the Bayesian approach and the random effects model. We presented the geometry of the network, results with probabilistic statements, estimated intervention effects and their 95% confidence interval (CI), and the surface under the cumulative ranking curve to rank the interventions.

RESULTS

We included 11 studies in our analysis. We found a significant difference in postoperative pulmonary infection, which favored the minimally invasive intervention compared to transthoracic surgery (risk ratio 0.49; 95%CI: 0.23 to 0.99). The operation time was significantly shorter for the transhiatal approach compared to transthoracic surgery (mean difference -85 min; 95%CI: -150 to -29), hybrid intervention (mean difference -98 min; 95%CI: -190 to -9.4), minimally invasive technique (mean difference -130 min; 95%CI: -210 to -50), and robot-assisted esophagectomy (mean difference -150 min; 95%CI: -240 to -53). Other comparisons did not yield significant differences.

CONCLUSION

Based on our results, the implication of minimally invasive esophagectomy should be favored.

Key Words: Surgery; Esophageal cancer; Esophagectomy; Network meta-analysis; Minimally invasive; Laparoscopy

©The Author(s) 2022. Published by Baishideng Publishing Group Inc. All rights reserved.

Core Tip: Minimally invasive laparoscopic techniques should be the preferred approach for the treatment of esophageal cancer, due to the lower incidence of postoperative pulmonary complications.

Citation: Szakó L, Németh D, Farkas N, Kiss S, Dömötör RZ, Engh MA, Hegyi P, Eross B, Papp A. Network meta-analysis of randomized controlled trials on esophagectomies in esophageal cancer: The superiority of minimally invasive surgery. *World J Gastroenterol* 2022; 28(30): 4201-4210
URL: https://www.wjgnet.com/1007-9327/full/v28/i30/4201.htm
DOI: https://dx.doi.org/10.3748/wjg.v28.i30.4201

INTRODUCTION

Esophageal cancer is the eighth most common type of cancer worldwide[1], with an incidence of 5.2 per 100000 for squamous cell cancer (SCC) and 0.7 per 100000 for adenocarcinoma (AC)[2]. While the prognosis varies between the two histological diagnoses, both AC and SCC are associated with poor clinical outcomes, with a 5-year survival rate of 20%[3].

Surgical therapy plays an essential role in the treatment of esophageal cancer. However, it cannot be routinely used due to the late diagnosis, as symptoms usually occur when the cancer is already unresectable[4]. Traditionally, open surgical interventions are performed, including transhiatal and transthoracic techniques. A meta-analysis comparing these two open surgical modalities did not find a significant difference in 5-year survival[5]. While both techniques are successful in terms of removing the neoplasm, open esophagectomies are associated with significant limitations, most importantly, postoperative morbidity[6,7].

A transition to non-open surgical techniques has been the trend in almost every field of surgery in recent years[8]. A wide variety of non-open techniques are available, including minimally invasive surgery (thoracolaparoscopic) surgery or even robot-assisted esophagectomy[9,10]. In the form of hybrid surgical intervention, a combination of open and non-open technique is available[11].

Previous meta-analyses have compared the different types of surgical techniques, with variable success and significant limitations[12-19]. To date, convincing evidence is missing regarding the optimal surgical approach of resectable esophageal cancer, as it is presented in a recent guideline[20].

Network meta-analysis (NMA) is a relatively novel methodology, which allows the direct and indirect comparison of multiple interventions, thus providing more information than traditional meta-analyses. Indirect comparisons can be made in the case of missing trials comparing two interventions if those are compared with a third intervention[21]. Several meta-analyses were carried out focusing on esophageal cancer surgery, but none of those addressed the problem of the wide variety of surgical techniques.

The purpose of our study was to provide objective evidence considering the surgical treatment of resectable esophageal cancer by comparing each treatment modality in the form of an NMA and possibly rank the different approaches.

MATERIALS AND METHODS

The NMA was conducted according to the Preferred Reporting Items for Systematic Reviews and Meta-Analyses-NMA guideline[22].

Protocol

The NMA protocol was registered in advance in PROSPERO under the number CRD42020160978. Analyses of the mortality and quality of life could not be carried out due to the low number of reporting articles. The risk of bias was assessed using an updated risk assessment tool.

Search strategy and inclusion criteria

We conducted a systematic search of the MEDLINE (*via* PubMed), EMBASE, *Reference Citation Analysis* (https://www.referencecitationanalysis.com/) and Cochrane Central Register of Controlled Trials (CENTRAL) from initiation until 2019 November to identify studies, comparing at least two types of esophagectomies from transthoracic, transhiatal, hybrid, laparoscopic or robot-assisted approach treating esophageal cancer without the restriction of histological subtype and an NMA was performed. The following search key was used: (((esophagus OR oesophagus OR esophageal OR oesophageal) AND (tumor OR tumour OR malign* OR cancer OR adenocarcinoma OR carcinoma)) AND (esophagectomy OR oesophagectomy OR Ivor-Lewis OR „Ivor Lewis" OR hybrid OR laparoscop* OR „minimal invasive")) AND random*. We also reviewed the reference lists of eligible articles for further studies. Only randomized controlled trials (RCTs) were included.

Selection and data extraction

After the removal of duplications, two independent reviewers (Szakó L, Engh MA) executed the selection first by title, second by abstract, last by full text following pre-discussed aspects. Data extraction was done by the same two independent reviewers (Szakó L, Engh MA) onto a pre-established Excel worksheet (Office 365, Microsoft, Redmond, WA, United States). Extracted data consisted of the year of publication, name of the first author, study design, country, applied surgical modalities, mortality, overall survival rate (referred as survival), adverse events (AEs), blood loss, length of hospitalization, length of surgical procedure, and demographic data including age, male-female ratio, and SCC/AC ratio. Disagreements regarding both selection and data extraction were resolved by consensus. If consensus could not be reached, a third reviewer (Dömötör RZ) resolved the disagree-ment.

Statistical analysis

The Bayesian method was used to perform pairwise meta-analyses and NMAs. All analyses were carried out using a random effects model. To ensure the interpretability of the NMA results (pooled of direct and indirect data), we presented the geometry of the network, the results with probabilistic statements, and estimates of intervention effects along with their corresponding 95% confidence intervals (CIs), as well as forest plots for ranking the interventions, we chose to use the surface under the cumulative ranking (SUCRA) curve, which provides a numerical summary of the rank distribution of each treatment.

Risk of bias assessment and quality of evidence

The risk of bias assessment was performed at the individual study level, according to the Revised Cochrane risk-of-bias tool for RCTs[23].

The Grading of Recommendations Assessment, Development, and Evaluation system was used to assess the certainty of evidence into four levels: high, moderate, low, and very low. The certainty of the evidence was classified into four levels: high, moderate, low, and very low. Two independent reviewers (Szakó L, Engh MA) decided the overall quality of the evidence[24]. Disagreements were resolved by consensus. If consensus could not be reached, a third reviewer (Dömötör RZ) resolved the

Table 1 Baseline characteristics of the included studies

Ref.	Year	Country	Design	Compared interventions	Number of patients	Male/female ratio	Age in yr, mean	Squamous cell cancer/adenocarcinoma ratio	Inclusion criteria
Straatman *et al*[25]	2012	Netherlands, Spain, Italy	Multicenter	MI-TT	59-56	43/16-46/17	62.3–61.8	24/35-19/36	cT1-3, N0-1, M0
van der Sluis *et al* [26]	2019	Netherlands	Single center	RA-TT	54-55	46/8-42/13	64-65	13/41-12/43	T1-4a, N0-3, M0
Mariette *et al*[27]	2019	France	Multi center	H-TT	103-104	88/15-175/32	59-61 (median)	46/57-84/123	T1-3, N0-1, M0
Guo *et al* [28]	2013	China	Single center	MI-TT	111-110	68/43-72/38	57.3-60.8	No information	T1-3, N0-1, M0
Ma *et al* [29]	2018	China	Single center	MI-TT	47-97	36/11-83/14	61-59.3	43/0-91/2	Resectable cancer
Jacobi *et al* [30]	1997	Germany	Single center	TH-TT	16-16	No information	54-55	13/3-13/3	Resectable cancer
Goldminc *et al*[31]	1993	Australia	Single center	TH-TT	32-35	31/1-33/2	57.4-57.4	32/0-35/0	Resectable squamous cell cancer
Chu *et al* [32]	1997	China	Single center	TH-TT	20-19	18/2-17/2	60.7-63.9	No information	Lower third resectable cancer
Hulscher *et al*[33]	2002	Netherlands	Multicenter	TH-TT	106-114	92/14-97/17	69-64	0/106-0/114	Resectable adenocarcinoma
Yang *et al* [35]	2016	China	Single center	MI-TT	120-120	82/38-87/33	62.5 -67.8	75/45-72/48	T1-3, N0-1, M0
Paireder *et al*[34]	2018	Austria	Single center	H-TT	14-12	10/4-10/2	64.5-62.5 (median)	4/10-1/11	Siewert I-II, resectable squamous cell cancer

Number of patients, male/female ratio, age, and ratio of squamous cell cancer and adenocarcinoma are presented according to the compared interventional arms. H: Hybrid esophagectomy; MIE: Minimally invasive esophagectomy; RA: Robot assisted esophagectomy; TH: Transhiatal esophagectomy; TT: Transthoracic esophagectomy.

disagreement.

RESULTS

Selection process

The database search yielded 3335 records, of which 2002 articles were left after removing duplicates. Twenty-one full-text articles were screened for eligibility. Finally, we included 11 RCTs (25-35), including 1525 patients, in the quantitative synthesis (Figure 1). Baseline characteristics of the enrolled studies are presented in Table 1[25-35].

Outcomes

A significant difference was found for pulmonary infection, which favored the minimally invasive intervention compared to transthoracic surgery (relative risk [RR]: 0.49, 95%CI: 0.23-0.99) (Figure 2). Operation time was significantly shorter for the transhiatal approach compared to transthoracic surgery (mean difference: -86 min, 95%CI: -150 to -29 min), hybrid intervention (mean difference -99 min, 95%CI: -190 to -9.4 min), minimally invasive technique (mean difference -130 min, 95%CI: -210 to -53 min), and robot-assisted esophagectomy (mean difference -150 min, 95%CI: -250 to -52 min) (Figure 3). We did not find significant differences regarding survival (Supplementary Figures 1-5), total AEs (Supplementary Figure 6), cardiac AEs (Supplementary Figure 7), anastomotic leakage (Supplementary Figure 8), atrial fibrillation (Supplementary Figure 9), wound infection (Supplementary Figure 10), total pulmonary AEs (Supplementary Figure 11), vocal chord paralysis (Supplementary Figure 12), length of hospital stay (Supplementary Figure 13), and blood loss (Supplementary Figure 14). The ranking and detailed results of the comparisons of the interventions are presented in the supplementary files (Supplementary Figures 1-14).

Table 2 The results of the risk of bias assessment by each domain

Ref.	Randomization process	Deviation from intended intervention	Missing outcome data	Measurement of the outcome	Selection of the reported results	Overall
Straatman *et al* [25]	Low risk	Low risk	Low risk	Low risk	Low risk	Low risk
van der Sluis *et al* [26]	Low risk	Low risk	Low risk	Low risk	Low risk	Low risk
Mariette *et al*[27]	Low risk	Low risk	Low risk	Low risk	Low risk	Low risk
Guo *et al*[28]	Unclear risk	Low risk	Low risk	Low risk	Unclear risk	Unclear risk
Ma *et al*[29]	Unclear risk	Unclear risk	Low risk	Low risk	Unclear risk	High risk
Jacobi *et al*[30]	Unclear risk	Unclear risk	Low risk	Low risk	Unclear risk	High risk
Goldminc *et al* [31]	Unclear risk	Unclear risk	Low risk	Low risk	Low risk	Unclear risk
Chu *et al*[32]	Unclear risk	Unclear risk	Low risk	Low risk	Unclear risk	High risk
Hulscher *et al*[33]	Low risk	Unclear risk	Low risk	Low risk	Unclear risk	Unclear risk
Yang *et al*[35]	Unclear risk	Unclear risk	Low risk	Low risk	Unclear risk	High risk
Paireder *et al*[34]	Low risk	Unclear risk	Low risk	Low risk	Unclear risk	Unclear risk

Risk of bias is indicated according to each domain of the Revised Cochrane risk-of-bias tool for randomized trials[23]. By the assessment of overall risk of bias, low risk of bias was given in the case of low risk of bias by every domain; if one or two domains were assessed as unclear risk of bias, unclear overall risk of bias was given, and if at least three domains were accompanied with unclear risk of bias, the overall risk of bias was assessed as high risk of bias.

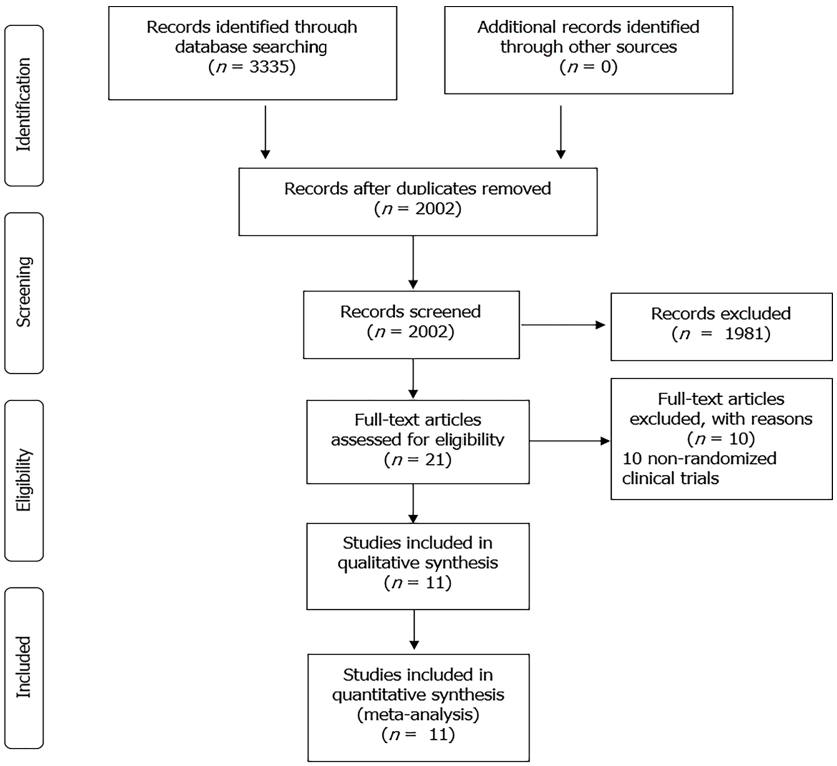
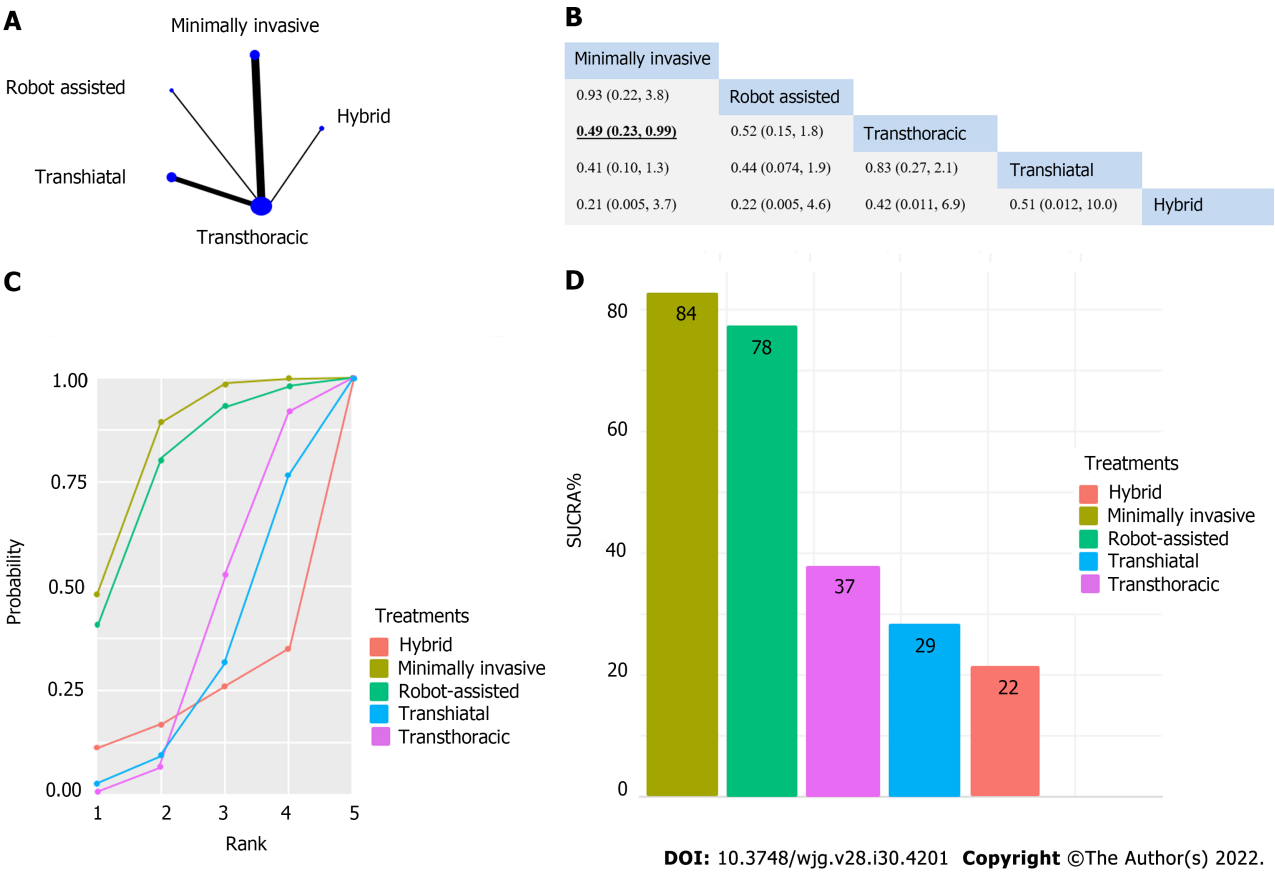


Figure 1 Results of the selection process according to the Preferred Reporting Items for Systematic Reviews and Meta-Analyses guidelines. Available from: https://prisma-statement.org//prismastatement/flowdiagram.aspx.

Risk of bias assessment and grade of evidence

Results of the risk of bias assessment for the outcome of survival were assessed following the Cochrane Risk of Bias Assessment Tool 2. Details are shown in Table 2.



DOI: 10.3748/wjg.v28.i30.4201 **Copyright** ©The Author(s) 2022.

Figure 2 A significant difference was found considering pulmonary infection, which favored the minimally invasive intervention compared to transthoracic surgery. A: The network of eligible studies for pulmonary infection (the width of the lines is proportional to the number of trials comparing every pair of treatments, and the size of every circle is proportional to the number of randomly assigned participants [sample size]); B: League table of the analysis for pulmonary infection. Comparisons should be read from left to right. The values are presented in risk ratios, with corresponding credible interval. Significant result is in TextTitle and underlined; C: Cumulative probability of treatment rank; D: Treatment rank in SUCRA% histogram.

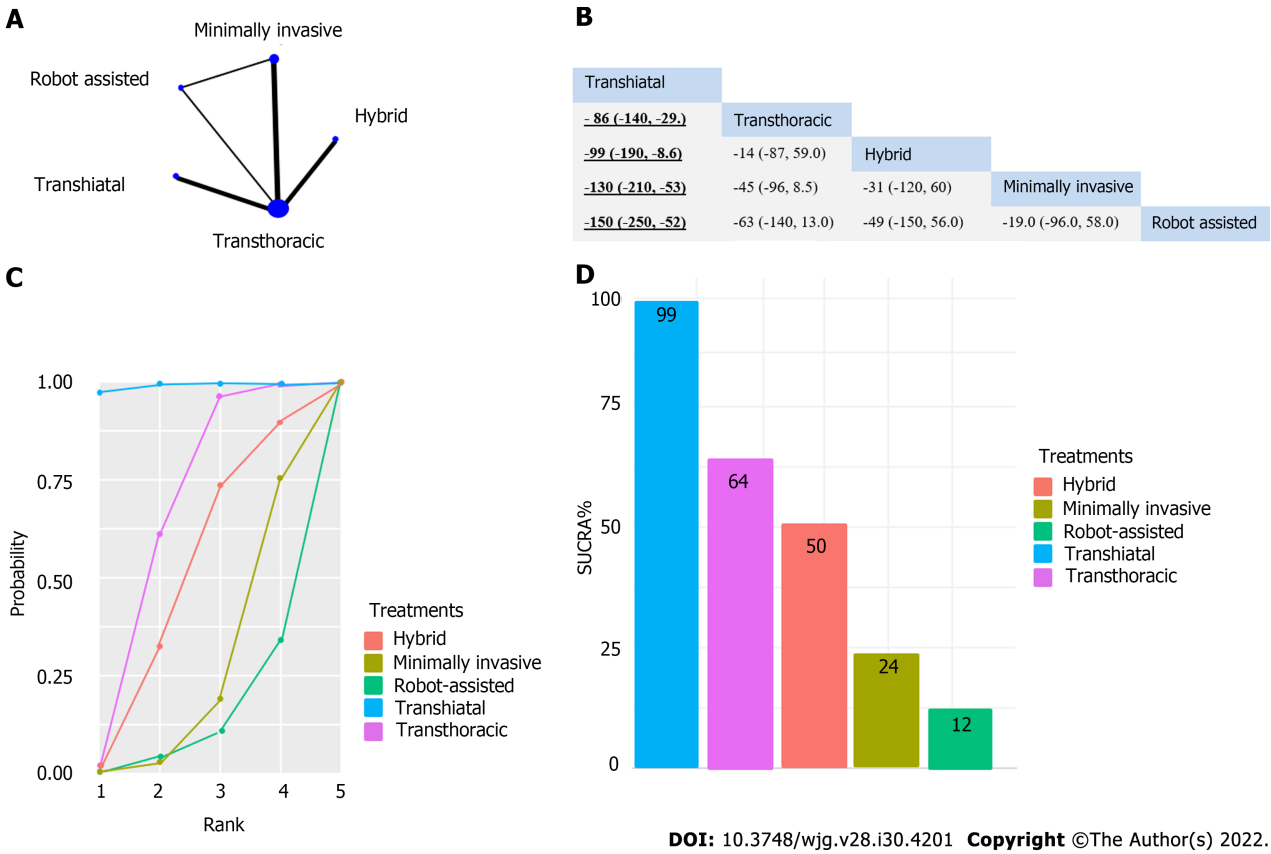
The results of the certainty of evidence are presented in Supplementary Table 1.

DISCUSSION

Our NMA confirmed the superiority of the minimally invasive esophagectomy over transthoracic open surgery regarding one of the main complications during these procedures, namely pulmonary infection. On the other hand, non-open surgical techniques require significantly more time to perform compared to open techniques. While statistically significant results were only achieved in the case of pulmonary infection, a clear tendency was demonstrated by the SUCRA curves, showing a preference for non-open techniques, which is also supported by the individual studies.

The results of previous meta-analyses and systematic reviews are not congruent regarding the comparison of minimally invasive and open surgical techniques. Kauppila *et al*[14] described the superiority of minimally invasive esophagectomy (MIE) regarding quality of life (QoL), which our work failed to analyze, as there were not enough RCTs reporting on QoL. Guo *et al*[13] also described the advantages of minimally invasive techniques regarding total complication rate, intraoperative blood loss, wound infection, and pulmonary infection, supporting our findings. MIE was also favorable in the analysis of Wang *et al*[19] considering blood loss. Besides blood loss and hospital stay, fewer respiratory complications were also shown by MIE in a meta-analysis conducted by Nagpal *et al*[15]. The work of Yibulayin *et al*[18] also supports the superiority of MIE in terms of in-hospital mortality and postoperative morbidity. By contrast, Dantoc *et al*[12] focused on oncological outcomes in their meta-analysis, where significant differences could not be proven. Sgourakis *et al*[17] showed that open surgery was more beneficial in terms of anastomotic stricture, while morbidity favored MIE. Oor *et al*[16] also described the benefit of open surgery in the case of hiatal hernia. The above comprehensive studies show that the inclusion of non-randomized studies carries a notable limitation.

Although the results of our analysis are only supportive in terms of pulmonary complication, the future perspectives are promising regarding minimally invasive esophagectomy, as the limelight shifts towards robot-assisted surgical techniques. The technique is time consuming, but with the development



DOI: 10.3748/wjg.v28.i30.4201 **Copyright** ©The Author(s) 2022.

Figure 3 Operation time was significantly shorter for transhiatal approach compared to transthoracic surgery, hybrid intervention, minimally invasive technique, and robot-assisted esophagectomy. A: The network of eligible studies for operation time [the width of the lines is proportional to the number of trials comparing every pair of treatments, and the size of every circle is proportional to the number of randomly assigned participants (sample size)]; B: League table of the analysis for operation time. Comparisons should be read from left to right. The values are presented in weighted mean difference (minutes), with corresponding credible interval. Significant results are in TextTitle and underlined; C: Cumulative probability of interventions rank; D: Intervention ranking in surface under the cumulative ranking (SUCRA)% histogram.

of new robotic platforms, the benefit of less AEs and more precise procedure will overcome this limitation[36]. The steep learning curve will be possibly managed by allowing the intervention to be carried out only in larger centers, as it has been seen in northern countries[37]. Despite the missing cumulative evidence, minimal invasive techniques have become the gold standard interventions for esophageal cancer since the TIME study. The results of this RCT provide evidence for using minimally invasive surgery for patients with resectable esophageal cancer aimed toward improving postoperative outcomes (especially pulmonary complication) and QoL with comparable oncologic results[25].

Considering the strengths of our analysis, by the inclusion of only RCTs, we managed to achieve a higher quality of evidence than previous works. Furthermore, a thorough methodology was applied. With the application of NMA, we were also able to make indirect comparisons. To date, this work is the most comprehensive review of the available RCTs.

One of the limiting factors of our study was the low number of cases and limited number of direct comparisons. Other limitations were the different enrollment criteria of the individual studies considering the histological subtype and stage of esophageal cancer. Furthermore, our analysis included many indirect comparisons, with weak direct comparisons. Additionally, we only included studies published until 2019.

We emphasize the application of MIE over open surgical techniques. Further analyses should focus on the outcomes of robot-assisted esophagectomies, and direct comparisons should be carried out between robot-assisted esophagectomy and thoracolaparoscopic intervention. Following recent trends, the centralization of upper gastrointestinal surgery is suggested, thus achieving the possibility of the implementation of such techniques without the limitation originating from the low number of cases and the learning curve of minimally invasive techniques.

CONCLUSION

While practice is already shifting towards the application of minimally invasive techniques, it should be

noted that clear evidence is still needed to form guidelines. As we aimed to fill this void, we were only able to prove the beneficial nature of these techniques regarding pulmonary infection. To further assess any other potential differences between the techniques, RCTs and systematic analysis of these trials are needed.

ARTICLE HIGHLIGHTS

Research background

The differences considering esophagectomies as the most applied curative methodology in the case of esophageal cancer are not clearly described. Minimally invasive techniques have become more popular in the belief of their superiority, although objective evidence is missing.

Research motivation

Recent guidelines are not yet clear considering the usage of minimally invasive esophagectomies. The authors wanted to provide the most objective evidence available, considering the differences between every subtype of minimally invasive and open esophagectomies.

Research objectives

The authors aimed to find every randomized controlled trial (RCT) providing comparative information about at least two types of esophagectomies, and pool the results using NMA.

Research methods

After establishing our clinical question using the population, intervention, control, outcome (commonly known as (PICO) framework a systemic search was carried out using three different databases. The results of the search were pooled, duplications were removed, suitable studies were selected, from which the data extraction was carried out onto a data sheet. With the help of biostatisticians, a network meta-analysis was performed. The quality of the included studies was assessed, as well as the grade of evidence.

Research results

Eleven articles were included in our analysis, according to which the minimally invasive surgical technique was superior compared to the transthoracic open approach in terms of pulmonary infection, while transthoracic surgery took less time to perform than any other surgical technique.

Research conclusions

The authors conclude that minimally invasive surgical techniques should be performed, whenever possible, for resectable esophageal cancer.

Research perspectives

The conduction of additional RCTs evaluating the same problem would be welcomed, while we hope that our work will help clinicians in the decision-making of the selection of the right surgical technique.

FOOTNOTES

Author contributions: Szakó L conceptualized the work, contributed to establishment of the search key, selection strategy, data extraction, interpretation of the results, and writing of the manuscript; Németh D and Farkas N performed the bio-statistical analyses, and contributed to the interpretation of the results and writing of the manuscript; Kiss S helped was involved in the conceptualization, coordination of the work, and writing the manuscript; Dömötör RZ conceptualized, wrote, and critically appraised the manuscript; Engh MA was involved in the conceptualization, data extraction, risk of bias assessment, writing of the manuscript, and language revision of the manuscript; Hegyi P contributed to the conceptualization, interpretation of the results, critical appraisal, and writing of the manuscript; Erőss BM conceptualized the work, interpreted the results, critically appraised and wrote the manuscript; Papp A provided supervision, and was involved in the conceptualization, interpretation of the results, critical appraisal, and writing of the manuscript.

Conflict-of-interest statement: All authors have no conflicts of interest to declare.

PRISMA 2009 Checklist statement: The authors have read the PRISMA 2009 Checklist, and the manuscript was prepared and revised according to the PRISMA 2009 Checklist.

Open-Access: This article is an open-access article that was selected by an in-house editor and fully peer-reviewed by external reviewers. It is distributed in accordance with the Creative Commons Attribution NonCommercial (CC BY-

NC 4.0) license, which permits others to distribute, remix, adapt, build upon this work non-commercially, and license their derivative works on different terms, provided the original work is properly cited and the use is non-commercial. See: https://creativecommons.org/Licenses/by-nc/4.0/

Country/Territory of origin: Hungary

ORCID number: Lajos Szakó 0000-0001-9783-4076; Dávid Németh 0000-0002-3258-6195; Nelli Farkas 0000-0002-5349-6527; Szabolcs Kiss 0000-0001-5032-866X; Réka Zsuzsa Dömötör 0000-0002-3561-2539; Marie Anne Engh 0000-0003-4269-5130; Péter Hegyi 0000-0003-0399-7259; Balint Eross 0000-0003-3658-8427; András Papp 0000-0002-2845-531X.

S-Editor: Ma YJ
L-Editor: Filipodia
P-Editor: Cai YX

REFERENCES

1 **Zhang Y**. Epidemiology of esophageal cancer. *World J Gastroenterol* 2013; **19**: 5598-5606 [PMID: 24039351 DOI: 10.3748/wjg.v19.i34.5598]
2 **Arnold M**, Soerjomataram I, Ferlay J, Forman D. Global incidence of oesophageal cancer by histological subtype in 2012. *Gut* 2015; **64**: 381-387 [PMID: 25320104 DOI: 10.1136/gutjnl-2014-308124]
3 **Howlader N**, Noone AM, Krapcho M, Miller D, Brest A, Yu M, Ruhl J, Tatalovich Z, Mariotto A, Lewis DR, Chen HS, Feuer EJ, Cronin K A. SEER Cancer Statistics Review, 1975-2016, National Cancer Institute. Bethesda, MD, based on November 2018 SEER data submission, posted to the SEER web site, April 2019. Available from: https://seer.cancer.gov/csr/1975_2016/
4 **Enzinger PC**, Mayer RJ. Esophageal cancer. *N Engl J Med* 2003; **349**: 2241-2252 [PMID: 14657432 DOI: 10.1056/nejmra035010]
5 **Boshier PR**, Anderson O, Hanna GB. Transthoracic versus transhiatal esophagectomy for the treatment of esophagogastric cancer: a meta-analysis. *Ann Surg* 2011; **254**: 894-906 [PMID: 21785341 DOI: 10.1097/SLA.0b013e3182263781]
6 **Alanezi K**, Urschel JD. Mortality secondary to esophageal anastomotic leak. *Ann Thorac Cardiovasc Surg* 2004; **10**: 71-75 [PMID: 15209546 DOI: 10.1308/003588413x13511609956255]
7 **Morita M**, Nakanoko T, Fujinaka Y, Kubo N, Yamashita N, Yoshinaga K, Saeki H, Emi Y, Kakeji Y, Shirabe K, Maehara Y. In-hospital mortality after a surgical resection for esophageal cancer: analyses of the associated factors and historical changes. *Ann Surg Oncol* 2011; **18**: 1757-1765 [PMID: 21207167 DOI: 10.1245/s10434-010-1502-5]
8 **Himal HS**. Minimally invasive (laparoscopic) surgery. *Surg Endosc* 2002; **16**: 1647-1652 [PMID: 12098024 DOI: 10.1007/s00464-001-8275-7]
9 **Levy RM**, Wizorek J, Shende M, Luketich JD. Laparoscopic and thoracoscopic esophagectomy. *Adv Surg* 2010; **44**: 101-116 [PMID: 20919517 DOI: 10.1016/j.yasu.2010.05.002]
10 **van Hillegersberg R**, Seesing MF, Brenkman HJ, Ruurda JP. Robot-assisted minimally invasive esophagectomy. *Chirurg* 2017; **88**: 7-11 [PMID: 27470056 DOI: 10.1007/s00104-016-0200-7]
11 **Allaix ME**, Long JM, Patti MG. Hybrid Ivor Lewis Esophagectomy for Esophageal Cancer. *J Laparoendosc Adv Surg Tech A* 2016; **26**: 763-767 [PMID: 27541591 DOI: 10.1089/lap.2016.29011.mea]
12 **Dantoc M**, Cox MR, Eslick GD. Evidence to support the use of minimally invasive esophagectomy for esophageal cancer: a meta-analysis. *Arch Surg* 2012; **147**: 768-776 [PMID: 22911078 DOI: 10.1001/archsurg.2012.1326]
13 **Guo W**, Ma X, Yang S, Zhu X, Qin W, Xiang J, Lerut T, Li H. Combined thoracoscopic-laparoscopic esophagectomy versus open esophagectomy: a meta-analysis of outcomes. *Surg Endosc* 2016; **30**: 3873-3881 [PMID: 26659248 DOI: 10.1007/s00464-015-4692-x]
14 **Kauppila JH**, Xie S, Johar A, Markar SR, Lagergren P. Meta-analysis of health-related quality of life after minimally invasive versus open oesophagectomy for oesophageal cancer. *Br J Surg* 2017; **104**: 1131-1140 [PMID: 28632926 DOI: 10.1002/bjs.10577]
15 **Nagpal K**, Ahmed K, Vats A, Yakoub D, James D, Ashrafian H, Darzi A, Moorthy K, Athanasiou T. Is minimally invasive surgery beneficial in the management of esophageal cancer? *Surg Endosc* 2010; **24**: 1621-1629 [PMID: 20108155 DOI: 10.1007/s00464-009-0822-7]
16 **Oor JE**, Wiezer MJ, Hazebroek EJ. Hiatal Hernia After Open versus Minimally Invasive Esophagectomy: A Systematic Review and Meta-analysis. *Ann Surg Oncol* 2016; **23**: 2690-2698 [PMID: 26926480 DOI: 10.1245/s10434-016-5155-x]
17 **Sgourakis G**, Gockel I, Radtke A, Musholt TJ, Timm S, Rink A, Tsiamis A, Karaliotas C, Lang H. Minimally invasive versus open esophagectomy: meta-analysis of outcomes. *Dig Dis Sci* 2010; **55**: 3031-3040 [PMID: 20186484 DOI: 10.1007/s10620-010-1153-1]
18 **Yibulayin W**, Abulizi S, Lv H, Sun W. Minimally invasive oesophagectomy versus open esophagectomy for resectable esophageal cancer: a meta-analysis. *World J Surg Oncol* 2016; **14**: 304 [PMID: 27927246 DOI: 10.1186/s12957-016-1062-7]
19 **Wang B**, Zuo Z, Chen H, Qiu B, Du M, Gao Y. The comparison of thoracoscopic-laparoscopic esophagectomy and open esophagectomy: A meta-analysis. *Indian J Cancer* 2017; **54**: 115-119 [PMID: 29199673 DOI: 10.4103/ijc.IJC_192_17]
20 **Lordick F**, Mariette C, Haustermans K, Obermannová R, Arnold D; ESMO Guidelines Committee. Oesophageal cancer: ESMO Clinical Practice Guidelines for diagnosis, treatment and follow-up. *Ann Oncol* 2016; **27**: v50-v57 [PMID: 27664261 DOI: 10.1093/annonc/mdw329]
21 **Rouse B**, Chaimani A, Li T. Network meta-analysis: an introduction for clinicians. *Intern Emerg Med* 2017; **12**: 103-111

[PMID: 27913917 DOI: 10.1007/s11739-016-1583-7]

22 **Hutton B**, Salanti G, Caldwell DM, Chaimani A, Schmid CH, Cameron C, Ioannidis JP, Straus S, Thorlund K, Jansen JP, Mulrow C, Catalá-López F, Gøtzsche PC, Dickersin K, Boutron I, Altman DG, Moher D. The PRISMA extension statement for reporting of systematic reviews incorporating network meta-analyses of health care interventions: checklist and explanations. *Ann Intern Med* 2015; **162**: 777-784 [PMID: 26030634 DOI: 10.7326/M14-2385]

23 **Sterne JAC**, Savović J, Page MJ, Elbers RG, Blencowe NS, Boutron I, Cates CJ, Cheng HY, Corbett MS, Eldridge SM, Emberson JR, Hernán MA, Hopewell S, Hróbjartsson A, Junqueira DR, Jüni P, Kirkham JJ, Lasserson T, Li T, McAleenan A, Reeves BC, Shepperd S, Shrier I, Stewart LA, Tilling K, White IR, Whiting PF, Higgins JPT. RoB 2: a revised tool for assessing risk of bias in randomised trials. *BMJ* 2019; **366**: l4898 [PMID: 31462531 DOI: 10.1136/bmj.l4898]

24 **Brozek JL**, Akl EA, Alonso-Coello P, Lang D, Jaeschke R, Williams JW, Phillips B, Lelgemann M, Lethaby A, Bousquet J, Guyatt GH, Schünemann HJ; GRADE Working Group. Grading quality of evidence and strength of recommendations in clinical practice guidelines. Part 1 of 3. An overview of the GRADE approach and grading quality of evidence about interventions. *Allergy* 2009; **64**: 669-677 [PMID: 19210357 DOI: 10.1111/j.1398-9995.2009.01973.x]

25 **Straatman J**, van der Wielen N, Cuesta MA, Daams F, Roig Garcia J, Bonavina L, Rosman C, van Berge Henegouwen MI, Gisbertz SS, van der Peet DL. Minimally Invasive Versus Open Esophageal Resection: Three-year Follow-up of the Previously Reported Randomized Controlled Trial: the TIME Trial. *Ann Surg* 2017; **266**: 232-236 [PMID: 28187044 DOI: 10.1097/SLA.0000000000002171]

26 **van der Sluis PC**, van der Horst S, May AM, Schippers C, Brosens LAA, Joore HCA, Kroese CC, Haj Mohammad N, Mook S, Vleggaar FP, Borel Rinkes IHM, Ruurda JP, van Hillegersberg R. Robot-assisted Minimally Invasive Thoracolaparoscopic Esophagectomy Versus Open Transthoracic Esophagectomy for Resectable Esophageal Cancer: A Randomized Controlled Trial. *Ann Surg* 2019; **269**: 621-630 [PMID: 30308612 DOI: 10.1097/SLA.0000000000003031]

27 **Mariette C**, Markar S, Dabakuyo-Yonli TS, Meunier B, Pezet D, Collet D, D'Journo XB, Brigand C, Perniceni T, Carrere N, Mabrut JY, Msika S, Peschaud F, Prudhomme M, Bonnetain F, Piessen G; FRENCH, FREGAT. Health-related Quality of Life Following Hybrid Minimally Invasive Versus Open Esophagectomy for Patients With Esophageal Cancer, Analysis of a Multicenter, Open-label, Randomized Phase III Controlled Trial: The MIRO Trial. *Ann Surg* 2020; **271**: 1023-1029 [PMID: 31404005 DOI: 10.1097/SLA.0000000000003559]

28 **Guo M**, Xie B, Sun X, Hu M, Yang Q, Lei Y. A comparative study of the therapeutic effect in two protocols: video-assisted thoracic surgery combined with laparoscopy versus right open transthoracic esophagectomy for esophageal cancer management. *Zhongde Linchuang Zhongliuxue Zazhi* 2013; **12**: 68-71 [DOI: 10.1007/s10330-012-0966-0]

29 **Ma G**, Cao H, Wei R, Qu X, Wang L, Zhu L, Du J, Wang Y. Comparison of the short-term clinical outcome between open and minimally invasive esophagectomy by comprehensive complication index. *J Cancer Res Ther* 2018; **14**: 789-794 [PMID: 29970654 DOI: 10.4103/jcrt.JCRT_48_18]

30 **Jacobi CA**, Zieren HU, Müller JM, Pichlmaier H. Surgical therapy of esophageal carcinoma: the influence of surgical approach and esophageal resection on cardiopulmonary function. *Eur J Cardiothorac Surg* 1997; **11**: 32-37 [PMID: 9030787 DOI: 10.1016/s1010-7940(96)01106-2]

31 **Goldminc M**, Maddern G, Le Prise E, Meunier B, Campion JP, Launois B. Oesophagectomy by a transhiatal approach or thoracotomy: a prospective randomized trial. *Br J Surg* 1993; **80**: 367-370 [PMID: 8472154 DOI: 10.1002/bjs.1800800335]

32 **Chu KM**, Law SY, Fok M, Wong J. A prospective randomized comparison of transhiatal and transthoracic resection for lower-third esophageal carcinoma. *Am J Surg* 1997; **174**: 320-324 [PMID: 9324146 DOI: 10.1016/s0002-9610(97)00105-0]

33 **Hulscher JB**, van Sandick JW, de Boer AG, Wijnhoven BP, Tijssen JG, Fockens P, Stalmeier PF, ten Kate FJ, van Dekken H, Obertop H, Tilanus HW, van Lanschot JJ. Extended transthoracic resection compared with limited transhiatal resection for adenocarcinoma of the esophagus. *N Engl J Med* 2002; **347**: 1662-1669 [PMID: 12444180 DOI: 10.1056/nejmoa022343]

34 **Paireder M**, Asari R, Kristo I, Rieder E, Zacherl J, Kabon B, Fleischmann E, Schoppmann SF. Morbidity in open versus minimally invasive hybrid esophagectomy (MIOMIE): Long-term results of a randomized controlled clinical study. *Eur Surg* 2018; **50**: 249-255 [PMID: 30546384 DOI: 10.1007/s10353-018-0552-y]

35 **Yang ZQ**, Lu HX, Zhang JH, Wang J. Comparative study on long-term survival results between minimally invasive surgery and traditional resection for esophageal squamous cell carcinoma. *Eur Rev Med Pharmacol Sci* 2016; **20**: 3368-3372 [PMID: 27608894]

36 **van Boxel GI**, Kingma BF, Voskens FJ, Ruurda JP, van Hillegersberg R. Robotic-assisted minimally invasive esophagectomy: past, present and future. *J Thorac Dis* 2020; **12**: 54-62 [PMID: 32190354 DOI: 10.21037/jtd.2019.06.75]

37 **Jeremiasen M**, Linder G, Hedberg J, Lundell L, Björ O, Lindblad M, Johansson J. Improvements in esophageal and gastric cancer care in Sweden-population-based results 2007-2016 from a national quality register. *Dis Esophagus* 2020; **33** [PMID: 31608927 DOI: 10.1093/dote/doz070]

World Journal of Gastroenterology

Submit a Manuscript: https://www.f6publishing.com

World J Gastroenterol 2022 August 14; 28(30): 4211-4220

DOI: 10.3748/wjg.v28.i30.4211

ISSN 1007-9327 (print) ISSN 2219-2840 (online)

CASE REPORT

Contrast-enhanced ultrasound of a traumatic neuroma of the extrahepatic bile duct: A case report and review of literature

Zhi-Qiang Yuan, Hua-Lin Yan, Jia-Wu Li, Yan Luo

Specialty type: Gastroenterology and hepatology

Provenance and peer review: Unsolicited article; Externally peer reviewed.

Peer-review model: Single blind

Peer-review report's scientific quality classification

Grade A (Excellent): 0
Grade B (Very good): B, B
Grade C (Good): 0
Grade D (Fair): 0
Grade E (Poor): 0

P-Reviewer: Cochior D, Romania; Koganti S, United States

Received: February 10, 2022
Peer-review started: February 10, 2022
First decision: April 5, 2022
Revised: April 17, 2022
Accepted: July 16, 2022
Article in press: July 16, 2022
Published online: August 14, 2022

Zhi-Qiang Yuan, Hua-Lin Yan, Jia-Wu Li, Yan Luo, Department of Medical Ultrasound, West China Hospital of Sichuan University, Chengdu 610041, Sichuan Province, China

Corresponding author: Yan Luo, Doctor, Professor, Department of Medical Ultrasound, West China Hospital of Sichuan University, No. 37 Guo Xue Xiang, Chengdu 610041, Sichuan Province, China. yanluo@scu.edu.cn

Abstract

BACKGROUND

Traumatic neuromas result from nerve injury after trauma or surgery but rarely occur in the bile duct. However, it is challenging to diagnose traumatic neuromas correctly preoperatively. Although some previous reports have described the imaging features of traumatic neuroma in the bile duct, no features of traumatic neuromas in the bile duct have been identified by using contrast-enhanced ultrasound (CEUS) imaging before.

CASE SUMMARY

A 55-year-old male patient presented to our hospital with a 3-mo history of abdominal distension and anorexia and history of cholecystectomy 4 years ago. Grayscale ultrasound demonstrated mild to moderate intrahepatic bile duct dilatation. Meanwhile, a hyperechoic nodule was found in the upper extrahepatic bile duct. The lesion approximately 0.8 cm × 0.6 cm with a regular shape and clear margins. The nodule of the bile duct showed slight hyperenhancement in the arterial phase and isoenhancement in the venous phase on CEUS. Laboratory tests showed that alanine aminotransferase and aspartate aminotransferase were increased significantly, while the tumor marker carbohydrate antigen 19-9 was increased slightly. Then, hilar bile duct resection and end-to-end bile ductal anastomosis were performed. The histological examination revealed traumatic neuroma of the extrahepatic bile duct. The patient had an uneventful recovery after surgery.

CONCLUSION

The current report will help enhance the current knowledge regarding identifying traumatic neuromas by CEUS imaging and review the related literature.

Key Words: Traumatic neuroma; Bile duct; Contrast-enhanced ultrasound; Enhancement; Cholangiocarcinoma; Case report

©The Author(s) 2022. Published by Baishideng Publishing Group Inc. All rights reserved.

Core Tip: A traumatic neuroma results from nerve injury after trauma or surgery but rarely occurs in the bile duct. Herein, we present some of the sonographic features of ultrasound and contrast-enhanced ultrasound in a case of a traumatic neuroma. We report this unusual case and review the related literature to improve the diagnosis and differential diagnosis of a traumatic neuroma of the bile duct and related imaging findings.

Citation: Yuan ZQ, Yan HL, Li JW, Luo Y. Contrast-enhanced ultrasound of a traumatic neuroma of the extrahepatic bile duct: A case report and review of literature. *World J Gastroenterol* 2022; 28(30): 4211-4220
URL: https://www.wjgnet.com/1007-9327/full/v28/i30/4211.htm
DOI: https://dx.doi.org/10.3748/wjg.v28.i30.4211

INTRODUCTION

A traumatic neuroma is a chronic reparative proliferative response of the nerve after trauma or surgery. It is composed of disorganized nerve fiber bundles with fibrous stroma, Schwann cells, perineural cells, axons, and endoneural fibroblasts[1]. The common sites of traumatic neuromas are the necks and extremities[2,3]. Although some studies have described traumatic neuromas in the bile duct, cases of sonographic features of contrast-enhanced ultrasound (CEUS) have not been published before. The clinical manifestation and imaging examination of a traumatic neuroma of the bile duct are not specific, which makes it challenging be accurately diagnosed preoperatively. Herein, we report a traumatic neuroma of the extrahepatic bile duct with detailed ultrasonographic imaging features. We also reviewed the literature on the imaging findings for traumatic neuromas.

CASE PRESENTATION

Chief complaints

A 55-year-old man was admitted to our hospital with unexplained abdominal distension and anorexia 3 mo ago.

History of present illness

The patient suffered from unexplained abdominal distension and anorexia for 3 mo. The patient developed darkened urine 2 mo ago. He experienced a weight loss of 5 kg over the course of the disease. He underwent contrast-enhanced computed tomography (CECT) examination at a local hospital, and a lesion was found in the extrahepatic bile duct, which was believed to be a tumor.

History of past illness

The patient underwent cholecystectomy for gallbladder stones with an uneventful postoperative recovery 4 years ago. He had a 10-year history of hypertension.

Personal and family history

There was no other personal or family history of acute or chronic disease.

Physical examination

The patient showed no tenderness, rebound tenderness or muscle tension on abdominal palpation.

Laboratory examinations

The liver function tests demonstrated increased levels of alanine aminotransferase (185 IU/L, normal range: < 50 IU/L), aspartate aminotransferase (148 IU/L, normal range: < 40 IU/L) and total bilirubin (37.0 μmol/L, normal range: 5 μmol/L to 28 μmol/L). Tumor markers included carbohydrate antigen 19-9 (98.6 U/mL, normal range: < 22 U/mL), carcinoembryonic antigen (0.97 ng/mL, normal range: < 5 ng/mL), and alpha-fetoprotein (4.67 ng/mL, normal range: < 7 ng/mL).

Imaging examinations

The patient underwent an abdominal ultrasound (US) examination by a Resona7 US system (Mindray Medical International, Shenzhen, Guangdong Province, China) equipped with an SC6-1U (1-6 MHz)

transducer. The US revealed mild to moderate dilatation of the intrahepatic bile duct, and the diameter of the upper extrahepatic bile duct was 1.2 cm (Figure 1A). A hyperechoic nodule sized 0.8 cm × 0.6 cm was found in the upper extrahepatic bile duct with an almost regular shape and slightly clear margins (Figure 1B). The patient underwent CEUS with the patient's consent for further diagnosis. A 2.4-mL US contrast agent SonoVue (Bracco, Milan, Italy) suspension was injected through the left cubital vein followed by a flush with 5 mL saline. In the arterial phase, the nodule showed slight heterogeneous hyperenhancement without rim-like enhancement (Figure 1C). The nodule appeared heterogeneous isoenhancement in the venous phase (Figure 1D). Additional CECT in our hospital showed a hypoenhancement nodule approximately 1.3 cm × 1.0 cm in size in the upper extrahepatic bile duct (Figure 2).

FINAL DIAGNOSIS

Based on the incidence of bile duct diseases, imaging findings and laboratory tests, the patient's clinical diagnosis was hilar cholangiocarcinoma. However, postoperative pathology of the common bile duct lesion showed a neoplastic proliferation of submucosal nerve tissue and fibrous tissue (Figure 3A), and an immunohistochemistry marker was positive for S-100 (Figure 3B). The above pathological findings indicated that the lesion in the bile duct was a traumatic neuroma.

TREATMENT

During the surgery, intraoperative frozen pathology showed no tumor cells within the bile duct lesion. Therefore, hilar bile duct resection and end-to-end bile ductal anastomosis (EE) were performed. The patient recovered uneventfully after surgery.

OUTCOME AND FOLLOW-UP

There was no obvious abnormality on CECT for half a year after the operation.

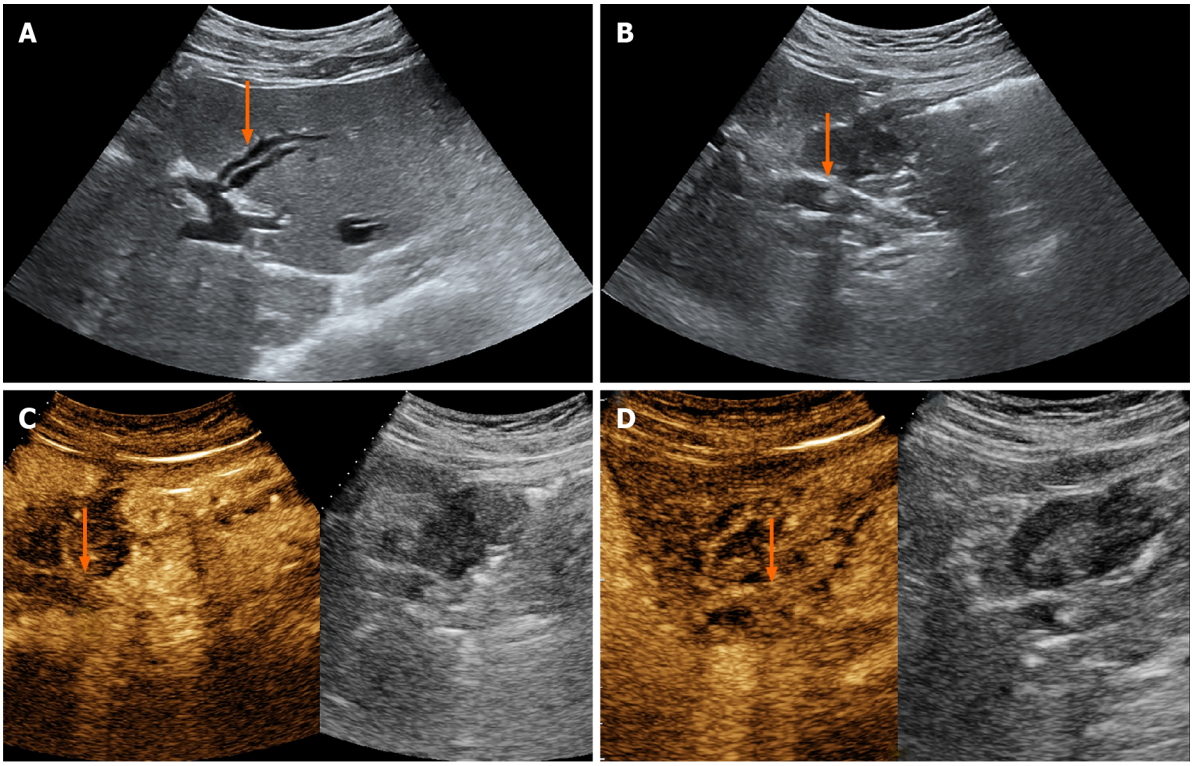
DISCUSSION

Extrahepatic bile duct masses are commonly malignant tumors, while benign tumors account for only 6%[4-7]. Consequently, the possibility that extrahepatic bile duct lesions are traumatic neuromas is easily overlooked. It has been reported that most traumatic neuromas of the biliary tract arise in the cystic duct stump after cholecystectomy[8]. If a nerve is transected and its continuity cannot be reestablished, a traumatic neuroma may develop[9].

We reviewed the literature from 2000 to 2021 and found 18 publications regarding the imaging features of traumatic neuromas in the bile ducts[2,10-26]. The clinical findings and imaging features of these 18 reported cases are summarized in Table 1. Finally, 22 patients were included in the literature review for further analysis. The age of patients ranged from 17 to 81 years of age, and there was a significant male predominance, with 15 males (68.2%), 2 females, and 5 patients of unreported sex. Most cases were secondary to cholecystectomy, but a few were secondary to liver transplantation, hepatectomy and hilar cholangiocarcinoma. The major symptoms found in these patients were jaundice, abdominal pain, and weight loss, while some patients had no apparent symptoms.

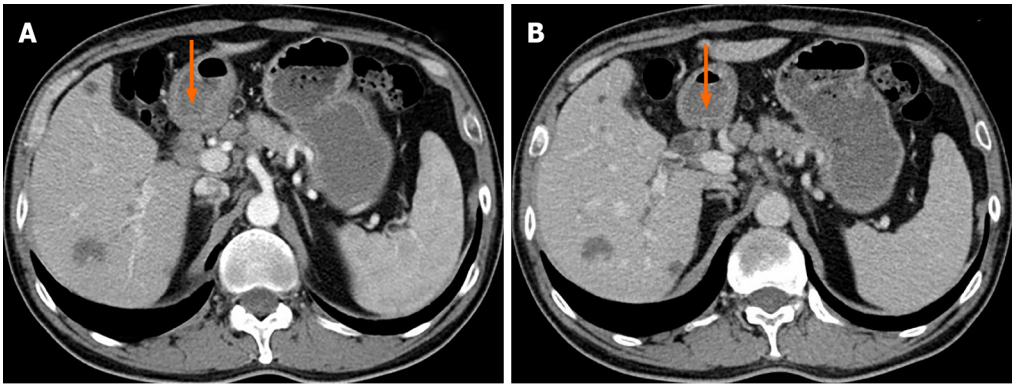
Unfortunately, no specific imaging features for traumatic neuromas of the bile duct have been found at present. Although some imaging modalities, such as US, computed tomography (CT), and nuclear magnetic resonance imaging (MRI), are valuable to some extent, it remains a challenge to diagnose traumatic bile duct neuromas preoperatively[17]. Imaging findings in these 22 patients varied from nodules or masses to localized bile duct stenosis with dilatation of the upper bile duct. It has been reported in the literature that the US imaging findings of extraabdominal nerve tumors and traumatic neuromas are generally hypoechoic masses, larger than the nerve trunk and continuous with the nerve [27]. However, the nerve injury related to cholecystectomy may be too small, so we could not find that the nerve is connected to traumatic neuroma of the bile duct. US was performed in 5 of the 22 patients, 2 of whom showed hypoechoic nodules, and the remaining 3 patients showed stenosis and dilatation of the bile ducts. However, our patient's US sonogram showed a hyperechoic nodule, indicating that the echogenicity of the nodule of traumatic neuroma was variable.

CECT was performed in 2 of the 18 cases, and an enhancing nodule was seen, which was consistent with the CECT findings of our patient. Traumatic neuromas also show enhancement on MRI when a contrast agent is used[28], which may be related to a damaged peripheral nerve blood barrier that occurred during a prior insult to the nerve[29-32]. One of these 18 cases described the enhancement



DOI: 10.3748/wjg.v28.i30.4211 **Copyright** ©The Author(s) 2022.

Figure 1 Ultrasound images of the patient. A and B: The ultrasound (US) showed mild to moderate intrahepatic bile duct dilatation (orange arrow) and a hyperechoic nodule sized 0.8 cm × 0.6 cm (orange arrow) in the extrahepatic bile duct; C and D: In the arterial phase, contrast-enhanced US (CEUS) showed slight hyperenhancement (orange arrow); in the venous phase, CEUS showed isoenhancement (orange arrow).



DOI: 10.3748/wjg.v28.i30.4211 **Copyright** ©The Author(s) 2022.

Figure 2 Contrast-enhanced computed tomography images of the patient. Contrast-enhanced computed tomography showed a hypoenhancement nodule in the upper extrahepatic bile duct (orange arrow).

pattern of traumatic neuroma on MRI in detail, which showed a marked homogeneously enhanced nodule that was iso-intense to the aorta in the atrial phase and a homogeneously enhanced nodule that was iso-intense to the aorta in the portal phase. There have been a few reports of other imaging techniques for diagnosing traumatic neuromas, such as magnetic resonance cholangiopancreatography, endoscopic US, contrast-enhanced harmonic endoscopic ultrasonography, intraductal ultrasonography and percutaneous transhepatic cholangiography. None of these imaging methods revealed specific features for traumatic neuromas.

It is challenging to distinguish bile duct traumatic neuroma from other lesions before surgery, so it is often misdiagnosed. The diagnosis of bile duct traumatic neuroma was correctly diagnosed in 1 of the 18 cases examined and confirmed by biopsy. The remaining cases were not correctly diagnosed, and it was difficult to distinguish between benign and malignant lesions in most cases. Therefore, surgery would be performed on a large proportion of patients. Once the patient underwent surgery, an intraoperative frozen section examination helped to confirm that the lesion was benign and extensive surgical

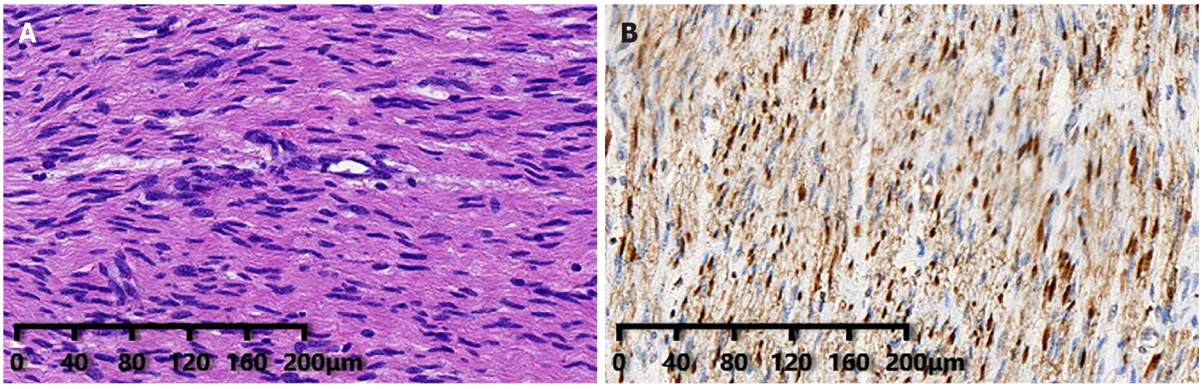
Table 1 Traumatic neuroma of the bile duct reported in the literature between 2000 and 2020

Ref.	Age	Sex	Symptoms	Location	Imaging findings	Preoperative diagnosis	Treatment
Shimura *et al*[10]	70	F	Abdominal discomfort	Extrahepatic bile duct	US: Hypoechoic tumor, bile duct slightly dilated CT: Round, hyperdense, distinct margin tumor Angiography: No encasement of the surrounding major vessels Endoscopic retrograde cholangiography: A protuberant nodule Intraductal ultrasonography: A smooth hypoechoic tumor	Did not indicate bile duct carcinoma	Bile duct excision and a Roux-en-Y hepaticojejunostomy
Watanabe *et al*[11]	48	M	Jaundice	Extrahepatic bile duct	Cholangiogram *via* the percutaneous transhepatic biliary drainage tube: The extrahepatic bile duct severely stenotic	ND	Bile duct excision and a Roux-en-Y hepaticojejunostomy
Iannelli *et al* [12]	81	M	Jaundice	Common bile duct	US: Dilatation of the intrahepatic bile ducts MRCP: A focal stricture	ND	Bile duct excision and a Roux-en-Y hepaticojejunostomy
Ueno *et al*[2]	60	M	Jaundice	Mid-common bile duct	US: Dilatation of the bile ducts, a mildly echogenic mass CT: Dilatation of the bile ducts, a markedly enhanced nodule MRI: Dilatation of the bile ducts. Homogeneous enhanced nodule with an iso-intense to the aorta, both in the arterial and portal phase Percutaneous transhepatic cholangiography: Dilatation of the bile ducts and a smooth stricture	Could not confirm benign or malignant nature	Bile duct excision and a hepatojejunal anastomosis
Choi *et al* [13]	46	M	Increased liver enzymes	Right hepatic duct	CT: A mass approximately 2 cm MRI: A mass approximately 2 cm	A bile duct cancer could not be excluded	Right hemihepatectomy
Kim *et al*[14]	76	M	ND	Mid-bile duct	CT: A small enhancing nodule MRC: Eccentric wall thickening of the bile duct consistent with a neoplasm	ND	Segmental resection with a Roux-en-Y hepaticojejunostomy
Cheng *et al* [15]	33	F	Jaundice and weight loss	Remnant choledochal cyst	MRI: A mass	Cholangiocarcinoma	Excision of the remnant choledochal cyst and a new hepaticojejunostomy
Cheng *et al*	56	M	Jaundice, abdominal	Distal	US: Dilatation of bile	Ampullary or	Pancreaticoduodenectomy

[16]			pain and weight loss	extrahepatic bile duct	duct MRI: Dilatation of bile duct, a filling-defect in the distal bile duct and a thickened biliary wall around the ampulla of Vater	periampullary carcinoma	
Cheng *et al* [17]	68	M	Progressive jaundice and abdominal pain	Bifurcation of the left and right hepatic duct	MRI: A mass with enhancement, a stricture of the hilar bile duct, dilatation of bile ducts	Cholangiocarcinoma	Excision of the mass and a new Roux-en-Y hepaticojejunostomy
Navez *et al* [18]	ND	ND	Jaundice (3 patients) or liver function test alteration (1 patient), a retro-obstructive choleperitoneum on the downstream biliary stenosis (1 patient)	Anastomotic biliary stricture	CT: Anastomotic biliary stricture (4 patients) MRI: A markedly homogeneous high intensity nodule enhanced on portal-phase (1 patient), anastomotic biliary stricture (4 patients)	ND	Traumatic biliary neuromas resection combined with hepaticojejunostomy (1 patient); traumatic biliary neuromas resection and duct-to-duct biliary reconstruction protected by a T-tube (4 patients)
Terzi *et al* [19]	17	F	Persistent elevated transaminase and bilirubin levels	Anastomotic biliary	Percutaneous transhepatic cholangiography: A biliary stricture at the anastomosis	ND	Resection of the bile duct stricture and a Roux-en-Y hepaticojejunostomy
Toyonaga *et al*[20]	76	F	A bile duct nodule	Proximal common bile duct	CT: An 8 mm, smooth, and uniformly enhanced nodule Contrast enhanced endoscopic ultrasonography: A clear boundary and a low echoic nodule, uniformly enhanced at early Cholangioscopy: A smooth elevated lesion, covered with normal mucosa	Submucosal tumor	Biopsy, observation for 1 year, no changes to the nodule
Yang *et al* [21]	65	M	Jaundice	Right bile duct	MRI: A 1.0 cm × 1.5 cm mass	Cholangiocarcinoma	Resection of the mass and Roux-en-Y hepaticojejunostomy.
Hirohata *et al*[22]	60	F	No chief complaint	Junction of the cystic duct	US: A 6 mm round tumor, surrounding lymph nodes were not swollen MRI: A slightly high signal on T2 and the periphery remnant cystic duct of the tumor presented as a high-intensity lesion on T2 EUS: A residual cystic duct tumor with enhancement ERCP: Not invade the common bile duct	Cholangiocarcinoma	Surgery
Yasuda *et al* [23]	76	M	ND	Stump of the dilatated cystic duct	EUS: A hypoechoic oval mass with a hyperechoic rim on the surface, 14 mm in	Amputation neuroma	Biopsy, observation

					diameter, hypervascularity Cholangiogram: A hemispherical defect Cholangioscopy: A hemispherical mass covered with thin normal cystic duct epithelium		
Lalchandani *et al*[24]	41	M	Epigastric pain, weight loss, tea-colored urine	Common hepatic duct	US: Dilation of the bile ducts ERCP: A 3-4 cm stricture	Acute cholangitis	First: Biliary stent Finally: Bile duct resection and hepaticojejunostomy
Kim *et al*[25]	72	M	A duodenal subepithelial tumor during a medical checkup	Near the duodenal wall and the cystic duct stump	CT: A 1.4 cm mass EUS: An 18 mm hypoechoic mass	Duodenal subepithelial tumor	Resection of the mass and duodenal wall, en-block resection of the mass and cystic duct origin
Nechi *et al*[26]	76	M	Jaundice	The transition zone between the common hepatic duct and the main bile duct	US: Dilation of the bile ducts, a 5 mm hypoechoic nodule MRI: Dilation of the common hepatic duct	Could not confirm benign or malignant nature	Resection of the main bile duct with a choledocho-duodenal anastomosis

ND: Not described; US: Grayscale ultrasound; CT: Computed tomography; CECT: Contrast-enhanced computed tomography; MRI: Magnetic resonance imaging; MRC: Magnetic resonance cholangiogram; MRCP: Magnetic resonance cholangiopancreatography; EUS: Endoscopic ultrasonography; ERCP: Endoscopic retrograde cholangiopancreatography.



DOI: 10.3748/wjg.v28.i30.4211 **Copyright** ©The Author(s) 2022.

Figure 3 Postoperative histopathological images of the patient. A: Hematoxylin and eosin staining showed proliferation of submucosal nerve tissue (magnification, × 100); B: Immunohistochemical staining displayed S100(+) (magnification, × 100).

resection of the traumatic neuroma was avoided[2,3]. The primary treatment reported in the literature consists of bile duct excision and hepaticojejunostomy (HJ). Although HJ is frequently recommended for reconstruction, the indications, surgical options and suture selection are also controversial. Some investigators also recommend EE because it is more physiological and can maintain physiological balance [33]. It is possible to achieve excellent long-term results and high quality of life using both HJ and EE when it is feasible for the proximal and distal ductal ends to permit EE[34]. Therefore, the choice of the optimum method is strictly correlated with the morphological nature of the lesion, which is different from one stage to the other, depending upon the moment of detection, and therefore have different surgical implications[35]. The surgeon found that the anastomosed edges blood supply was good and that there was no tension of the anastomosed edges in this patient. Therefore, according to the actual conditions of patients, as well as to maintain physiological balance, our hospital professor implemented EE for this patient.

In this patient, the symptoms of anorexia, weight loss and jaundice mimicked those often caused by malignant tumors of extrahepatic bile ducts. CEUS and CECT showed enhancement of the nodule. Based on the incidence of bile duct diseases and imaging findings, the surgeons misdiagnosed it as cholangiocarcinoma. Periductal infiltrative cholangiocarcinomas account for the majority of extrahepatic cholangiocarcinomas[36]. Extrahepatic cholangiocarcinomas may show hyperenhancement, isoenhancement, or hypoenhancement in the early phase of CEUS, and most of them show hypoenhancement in the late phase[37]. If we find a nodule in the bile duct, we should rule out the diagnosis of cholangiocarcinoma when the nodule does not show hypoenhancement in the late phase of CEUS. However, when traumatic neuroma presents as localized bile duct stenosis, it is relatively difficult to distinguish it from malignant lesions. When a patient has a history of biliary system surgery and the tumor markers are not significantly elevated, suspicion of traumatic neuroma increases. If conditions permit, patients can be protected from unnecessary surgeries by confirming the diagnosis with a biopsy. CEUS is beneficial for differentiating cholangiocarcinoma from traumatic neuromas, but more cases are needed to summarize the sonographic features of this disease. Recognizing of traumatic neuromas may aid in preoperative work up, planning, and patient counseling[24].

CONCLUSION

It is difficult to correctly diagnose traumatic neuroma of the bile duct before surgery. We should rule out malignant differential diagnoses, such as cholangiocarcinoma preoperatively, to avoid unnecessary surgery. The enhancement mode of CEUS may provide information to distinguish traumatic neuromas from malignant lesions. We need to combine the history of biliary tract surgery, clinical findings, imaging findings and laboratory tests to diagnose this disease.

FOOTNOTES

Author contributions: Yuan ZQ performed the literature review and wrote the manuscript; Yan HL and Li JW supported the data collection and manuscript revision; Luo Y supervised the writing and revision of the manuscript; all authors read and approved the final manuscript.

Supported by National Natural Science Foundation of China, No. 82071940.

Informed consent statement: Written informed consent for publication was obtained from the patient.

Conflict-of-interest statement: The authors declare that they have no conflicts of interest to report.

CARE Checklist (2016) statement: The authors have read the CARE Checklist (2016), and the manuscript was prepared and revised according to the CARE Checklist (2016).

Open-Access: This article is an open-access article that was selected by an in-house editor and fully peer-reviewed by external reviewers. It is distributed in accordance with the Creative Commons Attribution NonCommercial (CC BY-NC 4.0) license, which permits others to distribute, remix, adapt, build upon this work non-commercially, and license their derivative works on different terms, provided the original work is properly cited and the use is non-commercial. See: https://creativecommons.org/Licenses/by-nc/4.0/

Country/Territory of origin: China

ORCID number: Zhi-Qiang Yuan 0000-0002-3037-7576; Hua-Lin Yan 0000-0003-1338-1124; Jia-Wu Li 0000-0003-0844-5883; Yan Luo 0000-0003-2985-1768.

Corresponding Author's Membership in Professional Societies: Society of Ultrasound, Abdomen Ultrasound Subcommittee, Chinese Medical Doctor Association, No. 199174.

S-Editor: Yan JP
L-Editor: A
P-Editor: Yan JP

REFERENCES

1 **Foltán R**, Klíma K, Spacková J, Sedý J. Mechanism of traumatic neuroma development. *Med Hypotheses* 2008; **71**: 572-576 [PMID: 18599222 DOI: 10.1016/j.mehy.2008.05.010]

2 **Ueno Y**, Ikeda K, Maehara M, Sakaida N, Omura N, Kurokawa H, Sawada S. Traumatic neuroma of the bile duct. *Abdom*

Imaging 2008; **33**: 560-562 [PMID: 18360736 DOI: 10.1007/s00261-007-9318-x]
3 **Herrera L**, Martino E, Rodríguez-Sanjuán JC, Castillo J, Casafont F, González F, Figols J, Casanueva J, Cagigas M, Gómez-Fleitas M. Traumatic neuroma of extrahepatic bile ducts after orthotopic liver transplantation. *Transplant Proc* 2009; **41**: 1054-1056 [PMID: 19376425 DOI: 10.1016/j.transproceed.2009.02.032]
4 **Burhans R**, Myers RT. Benign neoplasms of the extrahepatic biliary ducts. *Am Surg* 1971; **37**: 161-166 [PMID: 5548431]
5 **Dowdy GS Jr**, Olin WG Jr, Shelton EL Jr, Waldron GW. Benign tumors of the extrahepatic bile ducts. Report of three cases and review of the literature. *Arch Surg* 1962; **85**: 503-513 [PMID: 13887615 DOI: 10.1001/archsurg.1962.01310030151024]
6 **Duncan JT Jr**, Wilson H. Benign tumor of the common bile duct. *Ann Surg* 1957; **145**: 271-274 [PMID: 13395318 DOI: 10.1097/00000658-195702000-00021]
7 **Gertsch P**, Thomas P, Baer H, Lerut J, Zimmermann A, Blumgart LH. Multiple tumors of the biliary tract. *Am J Surg* 1990; **159**: 386-388 [PMID: 2180336 DOI: 10.1016/s0002-9610(05)81278-4]
8 **Larson DM**, Storsteen KA. Traumatic neuroma of the bile ducts with intrahepatic extension causing obstructive jaundice. *Hum Pathol* 1984; **15**: 287-289 [PMID: 6698545 DOI: 10.1016/s0046-8177(84)80193-8]
9 **Shumate CR**, Curley SA, Cleary KR, Ames FC. Traumatic neuroma of the bile duct causing cholangitis and atrophy of the right hepatic lobe. *South Med J* 1992; **85**: 425-427 [PMID: 1566148 DOI: 10.1097/00007611-199204000-00021]
10 **Shimura K**, Tamada K, Asada M, Watabiki N, Wada I, Tanaka N, Suzuki Y. Intraductal ultrasonography of traumatic neuroma of the bile duct. *Abdom Imaging* 2001; **26**: 632-634 [PMID: 11907729 DOI: 10.1007/s00261-001-0016-9]
11 **Watanabe O**, Haga S, Okabe T, Kumazawa K, Shiozawa S, Tsuchiya A, Kajiwara T, Hirotani T, Aiba M. Amputation neuroma of common bile duct with obstructive jaundice. *J Gastroenterol Hepatol* 2001; **16**: 945-946 [PMID: 11555116 DOI: 10.1111/j.1440-1746.2001.2379b.x]
12 **Iannelli A**, Fabiani P, Karimdjee BS, Converset S, Saint-Paul MC, Gugenheim J. Traumatic neuroma of the cystic duct with biliary obstruction. Report of a case. *Acta Gastroenterol Belg* 2003; **66**: 28-29 [PMID: 12812146]
13 **Choi SB**, Park YN, Kim KS. Traumatic neuroma of the right hepatic duct undertaken right hemihepatectomy. *ANZ J Surg* 2009; **79**: 91-92 [PMID: 19183395 DOI: 10.1111/j.1445-2197.2008.04816.x]
14 **Kim HH**, Koh YS, Seoung JS, Hur YH, Cho CK. Education and imaging. Hepatobiliary and pancreatic: traumatic bile duct neuroma. *J Gastroenterol Hepatol* 2011; **26**: 1465 [PMID: 21884252 DOI: 10.1111/j.1440-1746.2011.06840.x]
15 **Cheng Y**, Jia Q, Xiong X, Cheng N. Traumatic bile duct neuroma developing in a remnant choledochal cyst. *Dig Liver Dis* 2014; **46**: e3 [PMID: 24290066 DOI: 10.1016/j.dld.2013.10.014]
16 **Cheng Y**, Jia Q, Xiong X, He D, Cheng NS. Hepatobiliary and pancreatic: traumatic neuroma of the ampulla of Vater. *J Gastroenterol Hepatol* 2014; **29**: 1342 [PMID: 25040619 DOI: 10.1111/jgh.12625]
17 **Cheng Y**, Jia Q, Xiong X, Cheng N. Traumatic bile duct neuroma after resection of hilar cholangiocarcinoma. *Clin Res Hepatol Gastroenterol* 2014; **38**: 127-128 [PMID: 24485597 DOI: 10.1016/j.clinre.2013.12.007]
18 **Navez J**, Golse N, Bancel B, Rode A, Ducerf C, Mezoughi S, Mohkam K, Mabrut JY. Traumatic biliary neuroma after orthotopic liver transplantation: a possible cause of "unexplained" anastomotic biliary stricture. *Clin Transplant* 2016; **30**: 1366-1369 [PMID: 27411162 DOI: 10.1111/ctr.12802]
19 **Terzi A**, Kirnap M, Sercan C, Ozdemir G, Ozdemir BH, Haberal M. Traumatic Neuroma Causing Biliary Stricture After Orthotopic Liver Transplant, Treated With Hepaticojejunostomy: A Case Report. *Exp Clin Transplant* 2017; **15**: 175-177 [PMID: 28260461 DOI: 10.6002/ect.mesot2016.P52]
20 **Toyonaga H**, Taniguchi Y, Inokuma T, Imai Y. Traumatic bile duct neuroma diagnosed by boring biopsy with cholangioscopy. *Gastrointest Endosc* 2018; **87**: 1361-1362 [PMID: 29102735 DOI: 10.1016/j.gie.2017.10.015]
21 **Yang SS**, Wu X, Lu J, Cheng NS. Jaundice 8years after left hemi-hepatectomy for hepatocellular carcinoma. *Clin Res Hepatol Gastroenterol* 2020; **44**: 622-624 [PMID: 31884001 DOI: 10.1016/j.clinre.2019.11.009]
22 **Hirohata R**, Abe T, Amano H, Kobayashi T, Shimizu A, Hanada K, Yonehara S, Nakahara M, Ohdan H, Noriyuki T. Amputation neuroma derived from a remnant cystic duct 30 years after cholecystectomy: A case report. *Int J Surg Case Rep* 2019; **64**: 184-187 [PMID: 31671354 DOI: 10.1016/j.ijscr.2019.10.011]
23 **Yasuda I**, Kobayashi S, Nagata K, Takahashi K, Entani T. Endoscopic images of amputation neuroma at the cystic duct stump. *Gastrointest Endosc* 2019; **90**: 986-987 [PMID: 31302090 DOI: 10.1016/j.gie.2019.07.006]
24 **Lalchandani P**, Korn A, Lu JG, French SW, Hou L, Chen KT. Traumatic bile duct neuroma presenting with acute cholangitis: A case report and review of literature. *Ann Hepatobiliary Pancreat Surg* 2019; **23**: 282-285 [PMID: 31501819 DOI: 10.14701/ahbps.2019.23.3.282]
25 **Kim DH**, Park JH, Cho JK, Yang JW, Kim TH, Jeong SH, Kim YH, Lee YJ, Hong SC, Jung EJ, Ju YT, Jeong CY, Kim JY. Traumatic neuroma of remnant cystic duct mimicking duodenal subepithelial tumor: A case report. *World J Clin Cases* 2020; **8**: 3821-3827 [PMID: 32953859 DOI: 10.12998/wjcc.v8.i17.3821]
26 **Nechi S**, Nakhli A, Ben Hamida W, Bani A, Khsiba A, Ben Mohamed A, Chelbi E, Hamzaoui L, Touinsi H. Traumatic neuroma of the bile duct: A case report. *Clin Case Rep* 2021; **9**: e04619 [PMID: 34457287 DOI: 10.1002/ccr3.4619]
27 **Provost N**, Bonaldi VM, Sarazin L, Cho KH, Chhem RK. Amputation stump neuroma: ultrasound features. *J Clin Ultrasound* 1997; **25**: 85-89 [PMID: 9023697 DOI: 10.1002/(sici)1097-0096(199702)25:2<85::aid-jcu7>3.0.co;2-f]
28 **Ahlawat S**, Belzberg AJ, Montgomery EA, Fayad LM. MRI features of peripheral traumatic neuromas. *Eur Radiol* 2016; **26**: 1204-1212 [PMID: 26188658 DOI: 10.1007/s00330-015-3907-9]
29 **Pindrik J**, Chhabra A, Belzberg AJ. Update on peripheral nerve surgery. *Neurosurgery* 2013; **60** Suppl 1: 70-77 [PMID: 23839355 DOI: 10.1227/01.neu.0000430772.18220.76]
30 **Seitz RJ**, Reiners K, Himmelmann F, Heininger K, Hartung HP, Toyka KV. The blood-nerve barrier in Wallerian degeneration: a sequential long-term study. *Muscle Nerve* 1989; **12**: 627-635 [PMID: 2506446 DOI: 10.1002/mus.880120803]
31 **Aagaard BD**, Lazar DA, Lankerovich L, Andrus K, Hayes CE, Maravilla K, Kliot M. High-resolution magnetic resonance imaging is a noninvasive method of observing injury and recovery in the peripheral nervous system. *Neurosurgery* 2003; **53**: 199-203; discussion 203 [PMID: 12823890 DOI: 10.1227/01.neu.0000069534.43067.28]

32 **Liao CD**, Zhang F, Guo RM, Zhong XM, Zhu J, Wen XH, Shen J. Peripheral nerve repair: monitoring by using gadofluorine M-enhanced MR imaging with chitosan nerve conduits with cultured mesenchymal stem cells in rat model of neurotmesis. *Radiology* 2012; **262**: 161-171 [PMID: 22056686 DOI: 10.1148/radiol.11110911]

33 **Górka Z**, Ziaja K, Wojtyczka A, Kabat J, Nowak J. End-to-end anastomosis as a method of choice in surgical treatment of selected cases of biliary handicap. *Pol J Surg* 1992; **64**: 977-979

34 **Jabłońska B**, Lampe P, Olakowski M, Górka Z, Lekstan A, Gruszka T. Hepaticojejunostomy vs. end-to-end biliary reconstructions in the treatment of iatrogenic bile duct injuries. *J Gastrointest Surg* 2009; **13**: 1084-1093 [PMID: 19266245 DOI: 10.1007/s11605-009-0841-7]

35 **Moldovan CA**, Ungureanu DF, Beliş V. A proposed therapeutic algorithm based on multiple case analysis regarding the repair options of iatrogenic biliary lesions following open and laparoscopic surgery. *J Mind Med Sci* 2016; **3**: 162-171

36 **Oliveira IS**, Kilcoyne A, Everett JM, Mino-Kenudson M, Harisinghani MG, Ganesan K. Cholangiocarcinoma: classification, diagnosis, staging, imaging features, and management. *Abdom Radiol (NY)* 2017; **42**: 1637-1649 [PMID: 28271275 DOI: 10.1007/s00261-017-1094-7]

37 **Xu HX**. Contrast-enhanced ultrasound in the biliary system: Potential uses and indications. *World J Radiol* 2009; **1**: 37-44 [PMID: 21160719 DOI: 10.4329/wjr.v1.i1.37]

World Journal of Gastroenterology

Submit a Manuscript: https://www.f6publishing.com

World J Gastroenterol 2022 August 14; 28(30): 4221-4226

DOI: 10.3748/wjg.v28.i30.4221

ISSN 1007-9327 (print) ISSN 2219-2840 (online)

LETTER TO THE EDITOR

Prognostic role of expression of angiogenesis markers in hepatocellular carcinoma: A bioinformatics analysis

Yan-Dong Miao, Xiao-Long Tang, Jiang-Tao Wang, Deng-Hai Mi

Specialty type: Gastroenterology and hepatology

Provenance and peer review: Invited article; Externally peer reviewed.

Peer-review model: Single blind

Peer-review report's scientific quality classification
Grade A (Excellent): 0
Grade B (Very good): 0
Grade C (Good): C
Grade D (Fair): 0
Grade E (Poor): 0

P-Reviewer: Zhong C, China

Received: July 30, 2021
Peer-review started: July 30, 2021
First decision: August 19, 2021
Revised: August 22, 2021
Accepted: July 18, 2022
Article in press: July 18, 2022
Published online: August 14, 2022

Yan-Dong Miao, Xiao-Long Tang, Jiang-Tao Wang, Deng-Hai Mi, The First Clinical Medical College, Lanzhou University, Lanzhou 730000, Gansu Province, China

Yan-Dong Miao, Jiang-Tao Wang, Yantai Affiliated Hospital of Binzhou Medical University, The Second Clinical Medical College of Binzhou Medical University, Yantai 264000, Shandong Province, China

Deng-Hai Mi, Dean's Office, Gansu Academy of Traditional Chinese Medicine, Lanzhou 730000, Gansu Province, China

Corresponding author: Deng-Hai Mi, MD, Chief Doctor, Dean, Dean's Office, Gansu Academy of Traditional Chinese Medicine, No. 418 Guazhou Road, Qilihe District, Lanzhou 730000, Gansu Province, China. mi.dh@outlook.com

Abstract

The expression of angiopoietin (ANGPT) 1, ANGPT2, vascular endothelial growth factor (VEGF) A, VEGFB, VEGFC, VEGFD, and placental growth factor (PGF) is significantly higher in tumor tissues than in normal tissues in both unpaired and paired hepatocellular carcinoma (HCC) samples. ANGPT2, VEGFB, VEGFC, and PGF are primarily involved in regulating the activation of the epithelial-mesenchymal transition pathway; ANGPT1 is primarily involved in regulating the activation of the RAS/mitogen-activated protein kinase and receptor tyrosine kinase (RTK) pathways; VEGFA is engaged in regulating the RTK activation pathway; and VEGFD is mainly involved in regulating the activation of the tuberous sclerosis protein/mammalian target of rapamycin pathway. There is a significant difference in overall survival between HCC patients with high and low expression of ANGPT2, PGF, VEGFA, and VEGFD. Disease free survival (DFS) is significantly shorter in HCC patients with high ANGPT2, PGF, and VEGFA expression than in those with low ANGPT2, PGF, and VEGFA expression.

Key Words: Hepatocellular carcinoma; Angiogenesis; Marker; Bioinformatics analysis; Pathway

©The Author(s) 2022. Published by Baishideng Publishing Group Inc. All rights reserved.

Core Tip: We found that the expression of angiogenesis markers was significantly higher in tumor tissues than in normal tissues in both unpaired and paired hepatocellular carcinoma (HCC) samples. These angiogenesis markers are mainly involved in regulating the activation of the EMT pathway, the RAS/mitogen-activated protein kinase and receptor tyrosine kinase pathways, and the tuberous sclerosis protein/mammalian target of rapamycin pathway. In addition, there was a significant difference in overall survival between HCC patients with high and low expression of angiopoietin-2 (ANGPT2), placental growth factor (PGF), vascular endothelial growth factor A (VEGFA), and VEGFD. Disease free survival was significantly shorter in HCC patients with high ANGPT2, PGF, and VEGFA expression than in those with low ANGPT2, PGF, and VEGFA expression.

Citation: Miao YD, Tang XL, Wang JT, Mi DH. Prognostic role of expression of angiogenesis markers in hepatocellular carcinoma: A bioinformatics analysis. *World J Gastroenterol* 2022; 28(30): 4221-4226
URL: https://www.wjgnet.com/1007-9327/full/v28/i30/4221.htm
DOI: https://dx.doi.org/10.3748/wjg.v28.i30.4221

TO THE EDITOR

We read with read interest the article by Choi *et al*[1], in which they initially evaluated plasma levels of angiogenesis biomarkers in hepatocellular carcinoma (HCC) patients, and then assessed their roles in forecasting overall survival (OS) and progression-free survival (PFS), indicating that the plasma level of angiopoietin (ANGPT) 2 was related to tumor stage, liver function, and cancer invasiveness, and that ANGPT2 performed better in predicting OS and PFS than alpha-fetoprotein (AFP), ANGPT1, and vascular endothelial growth factor (VEGF).

We appreciate the authors' unique perspective in exploring the prognostic role of plasma levels of ANGPT1, ANGPT2, and VEGF in HCC. However, there are some errors in the original text that may cause confusion for readers. For example, the survival curve in figure 3B in the original article should have represented the survival curve between the high and low ANGPT2 expression subgroups, which the authors incorrectly labeled as ANGPT1. Second, it is well known that the VEGF family includes VEGFA, VEGFB, VEGFC, VEGFD, VEGFE, and placental growth factor (PGF)[2,3], so to which VEGF do the authors refer in the text? Usually, VEGF refers to VEGFA, but the authors should have clarified it in the text.

Moreover, it might make the results more significant if the authors could improve the outcome by demonstrating the differential expression of ANGPT1, ANGPT2, and VEGF in normal tissues and HCC tissues as a whole, for example, the analysis of HCC samples in the Cancer Genome Atlas database using bioinformatics. We found that the expression of ANGPT1, ANGPT2, VEGFA, VEGFB, VEGFC, VEGFD, and PGF was significantly higher in cancer samples than in corresponding normal samples in both unpaired and paired HCC samples (Figures 1A and B). Detailed statistical results are reported in Tables 1 and 2.

We also found that ANGPT2, VEGFB, VEGFC, and PGF are mainly involved in regulating the activation of the EMT pathway; ANGPT1 is prominently involved in regulating the activation of the RAS/mitogen-activated protein kinase and receptor tyrosine kinase (RTK) pathways; VEGFA is engaged in regulating the activation of the RTK pathway; and VEGFD is mainly involved in regulating the activation of the tuberous sclerosis protein/mammalian target of rapamycin pathway (Figure 1C). These results are consistent with those of previously reported studies[4-7]. Our findings could be a supplement to Choi *et al*'s study[1]. In the future, the roles of ANGPT1, ANGPT2, and VEGF in the development of HCC should be further explored.

Choi *et al*[1] found that OS was significantly shorter in the high ANGPT2 and high AFP subgroups than in the low ANGPT2 and AFP subgroups, respectively, though the differences in OS rates were not significant between the high and low ANGPT1 subgroups or between the high and low VEGF subgroups. Our study found that OS was significantly shorter in patients with high ANGPT2, PGF, VEGFA, or VEGFD expression than in those with low expression, respectively (Figures 2A-D; $P < 0.05$). However, there was no significant difference in survival time between patients with high and low expression of ANGPT1, VEGFB, VEGFC, and AFP (Figures 2E-H; $P > 0.05$). Prognostic data for HCC came from Liu *et al*[8].

In addition, we also analyzed the differences in disease free survival (DFS) between patients with high and low angiogenesis marker expression. We found that DFS was significantly shorter in the high ANGPT2, PGF, and VEGFA groups than in the low ANGPT2, PGF, and VEGFA groups, respectively (Figures 3A, B and C; $P < 0.05$). However, there was no significantly difference in DFS between groups with high and low expression of AFP, ANGPT1, VEGFB, VEGFC, and VEGFD (Figures 3D-H; $P > 0.05$). The above results confirm that the study performed by Choi *et al*[1] is of great value and that our discovery could be a supplement to their research.

Table 1 Detailed statistical results of differential expression analysis of angiogenesis markers in hepatocellular carcinoma

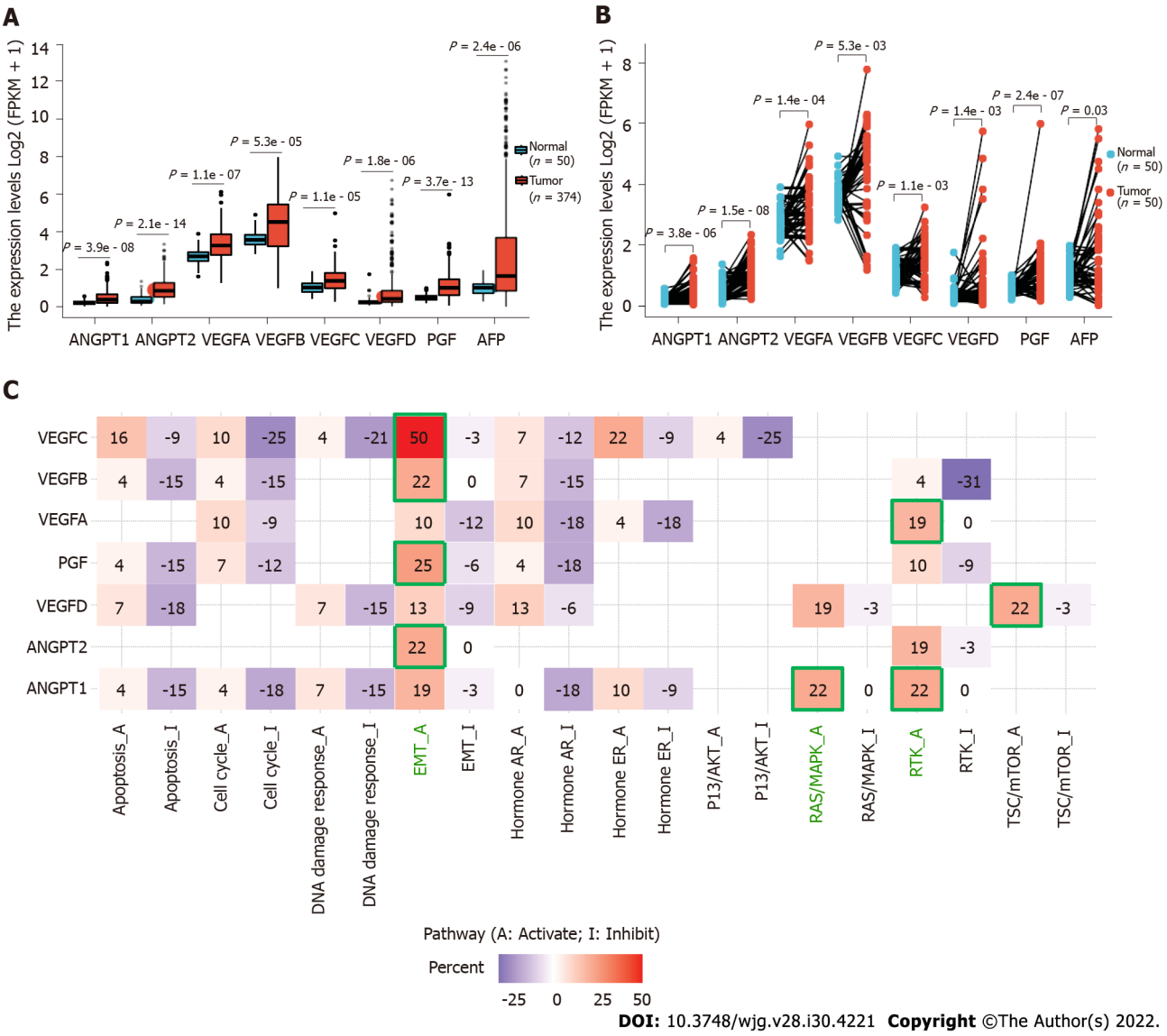
Gene	Group	Number	Minimum	Maximum	Median	IQR	Lower quartile	Upper quartile	Mean	SD	SE
ANGPT1	Normal	50	0.029	0.552	0.188	0.132	0.138	0.27	0.206	0.106	0.015
ANGPT1	Tumor	374	0	2.351	0.373	0.464	0.2	0.664	0.485	0.391	0.02
ANGPT2	Normal	50	0.043	1.351	0.278	0.33	0.195	0.525	0.394	0.289	0.041
ANGPT2	Tumor	374	0.116	3.339	0.848	0.769	0.513	1.282	0.963	0.581	0.03
VEGFA	Normal	50	1.616	3.901	2.687	0.473	2.439	2.911	2.717	0.445	0.063
VEGFA	Tumor	374	1.258	6.138	3.268	1.103	2.769	3.871	3.291	0.809	0.042
VEGFB	Normal	50	2.816	4.919	3.568	0.523	3.325	3.848	3.636	0.444	0.063
VEGFB	Tumor	374	0.978	8.003	4.532	2.234	3.223	5.458	4.292	1.521	0.079
VEGFC	Normal	50	0.408	1.901	1.019	0.453	0.787	1.239	1.057	0.355	0.05
VEGFC	Tumor	374	0.253	4.988	1.376	0.816	0.978	1.795	1.436	0.62	0.032
VEGFD	Normal	50	0.054	1.74	0.236	0.151	0.164	0.316	0.307	0.28	0.04
VEGFD	Tumor	374	0.014	6.756	0.422	0.622	0.241	0.863	0.838	1.14	0.059
PGF	Normal	50	0.182	0.992	0.471	0.204	0.37	0.575	0.501	0.188	0.027
PGF	Tumor	374	0.061	5.991	1.007	0.855	0.613	1.467	1.104	0.675	0.035
AFP	Normal	50	0.266	1.969	1.016	0.507	0.714	1.221	0.992	0.416	0.059
AFP	Tumor	374	0	13.118	1.644	2.855	0.844	3.699	2.965	3.15	0.163

ANGPT: Angiopoietin; VEGFA: Vascular endothelial growth factor; PGF: Placental growth factor; AFP: Alpha-fetoprotein; IQR: Interquartile range; SD: Standard deviation, SE: Standard error.

Table 2 Detailed statistical results of differential expression analysis of angiogenesis markers in paired samples of hepatocellular carcinoma

Gene	Group	Number	Minimum	Maximum	Median	IQR	Lower quartile	Upper quartile	Mean	SD	SE
ANGPT1	Normal	50	0.029	0.552	0.188	0.132	0.138	0.27	0.206	0.106	0.015
ANGPT1	Tumor	50	0.014	1.557	0.463	0.56	0.228	0.788	0.507	0.363	0.051
ANGPT2	Normal	50	0.043	1.351	0.278	0.33	0.195	0.525	0.394	0.289	0.041
ANGPT2	Tumor	50	0.193	2.324	1.056	0.77	0.747	1.517	1.111	0.517	0.073
VEGFA	Normal	50	1.616	3.901	2.687	0.473	2.439	2.911	2.717	0.445	0.063
VEGFA	Tumor	50	1.471	5.974	3.102	1.087	2.801	3.888	3.287	0.902	0.128
VEGFB	Normal	50	2.816	4.919	3.568	0.523	3.325	3.848	3.636	0.444	0.063
VEGFB	Tumor	50	1.164	7.789	4.833	1.993	3.323	5.317	4.328	1.575	0.223
VEGFC	Normal	50	0.408	1.901	1.019	0.453	0.787	1.239	1.057	0.355	0.05
VEGFC	Tumor	50	0.261	3.233	1.398	0.819	1.013	1.831	1.459	0.633	0.09
VEGFD	Normal	50	0.054	1.74	0.236	0.151	0.164	0.316	0.307	0.28	0.04
VEGFD	Tumor	50	0.014	5.746	0.367	0.562	0.231	0.793	0.832	1.207	0.171
PGF	Normal	50	0.182	0.992	0.471	0.204	0.37	0.575	0.501	0.188	0.027
PGF	Tumor	50	0.144	5.991	1.072	0.833	0.67	1.503	1.16	0.859	0.121
AFP	Normal	50	0.266	1.969	1.016	0.507	0.714	1.221	0.992	0.416	0.059
AFP	Tumor	50	0	5.824	1.033	1.31	0.725	2.036	1.62	1.383	0.196

ANGPT: Angiopoietin; VEGFA: Vascular endothelial growth factor; PGF: Placental growth factor; AFP: Alpha-fetoprotein; IQR: Interquartile range; SD: Standard deviation, SE: Standard error.

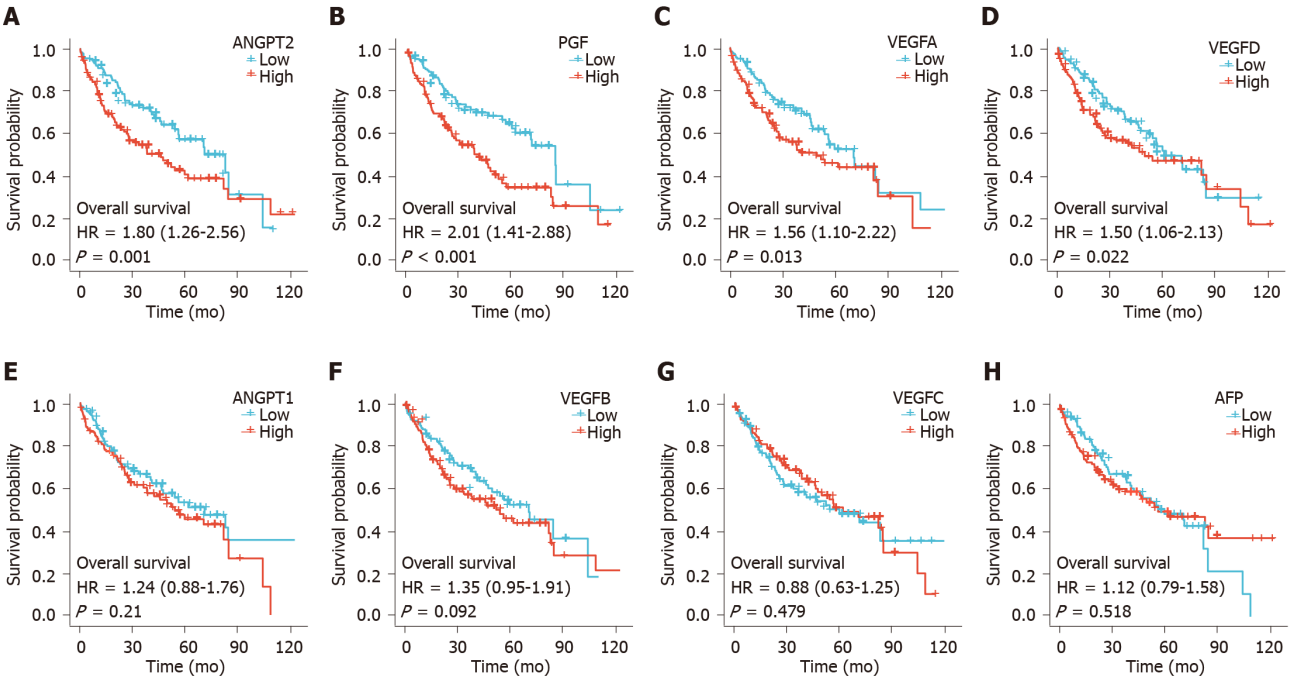


DOI: 10.3748/wjg.v28.i30.4221 **Copyright** ©The Author(s) 2022.

Figure 1 Roles of angiopoietins 1 and 2, vascular endothelial growth factors A-D, and placental growth factor in development of hepatocellular carcinoma. Data source: UCSC XENA (https://xenabrowser.net/datapages/) mRNA-Seq data of TPM format for GTEx and TCGA processed uniformly *via* the Toil process[11]. Liver hepatocellular carcinoma tissue data from TCGA and corresponding normal tissue data from GTEx were used. A: Differential expression of angiopoietin (ANGPT) 1, ANGPT2, vascular endothelial growth factor (VEGF) A, VEGFB, VEGFC, VEGFD, and placental growth factor (PGF) in hepatocellular carcinoma (HCC) and normal tissue samples; B: Differential expression of ANGPT1, ANGPT2, VEGFA, VEGFB, VEGFC, VEGFD, and PGF in paired HCC and normal samples. The expression in cancer tissues is represented in orange, and that in normal tissues is displayed in blue; C: Pathway analysis for ANGPT1, ANGPT2, VEGFA, VEGFB, VEGFC, VEGFD, and PGF in HCC. ANGPT: Angiopoietin; PGF: Placental growth factor; VEGF: Vascular endothelial growth factor; AFP: Alpha-fetoprotein; EMT: Epithelial-mesenchymal transition; AR: Androgen receptor; ER: Estrogen receptor; P13K/AKT: Phosphatidylinositol 3 kinase/AKT; RAS/MAPK: RAS/mitogen-activated protein kinase; RTK: Receptor tyrosine kinase; TSC/mTOR: TSC/mammalian target of rapamycin.

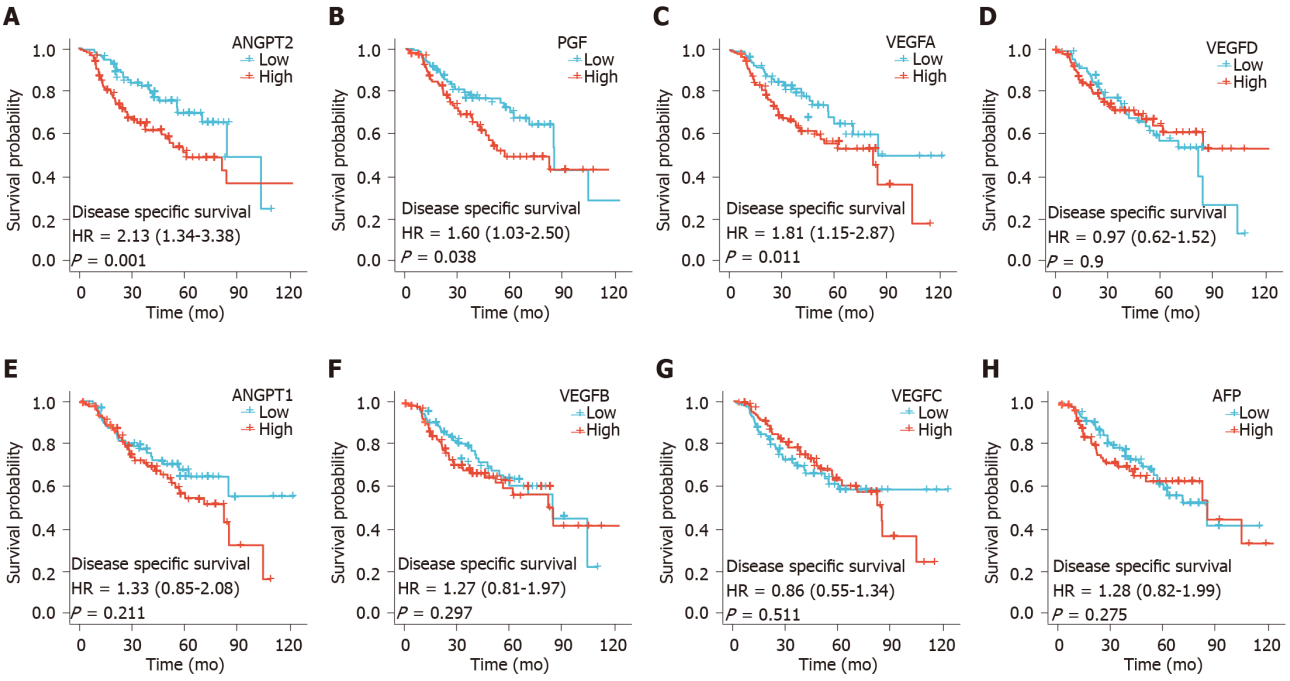
Statistical analysis

We utilized R (version 4.0.3) to perform statistical analyses and display the results. The differential expression analysis of angiogenesis markers between HCC tissues and corresponding normal tissues was performed using the Wilcoxon rank-sum test, and the results are presented by using R-package "ggplot2"[9]. Survival analysis was completed through log-rank test and COX regression. Pathway analysis was performed based on the online database GSCALite (http://bioinfo.life.hust.edu.cn/web/GSCALite/)[10].



DOI: 10.3748/wjg.v28.i30.4221 **Copyright** ©The Author(s) 2022.

Figure 2 Overall survival by angiogenesis marker expression in hepatocellular carcinoma. A: Angiopoietin (ANGPT) 2; B: Placental growth factor; C: Vascular endothelial growth factor (VEGF) A; D: VEGFD; E: ANGPT1; F: VEGFB; G: VEGFC; H: Alpha-fetoprotein. The red and blue lines indicate the survival curves of the high and low angiogenesis marker expression groups, respectively. ANGPT: Angiopoietin; PGF: Placental growth factor; VEGF: Vascular endothelial growth factor; AFP: Alpha-fetoprotein; HR: Hazard ratio.



DOI: 10.3748/wjg.v28.i30.4221 **Copyright** ©The Author(s) 2022.

Figure 3 Disease free survival by angiogenesis marker expression in hepatocellular carcinoma. A: Angiopoietin (ANGPT) 2; B: Placental growth factor; C: Vascular endothelial growth factor (VEGF) A; D: Alpha-fetoprotein; E: ANGPT1; F: VEGFB; G: VEGFC; H: VEGFD. The red and blue lines indicate the survival curves of the high and low angiogenesis marker expression groups, respectively. ANGPT: Angiopoietin; PGF: Placental growth factor; VEGF: Vascular endothelial growth factor; AFP: Alpha-fetoprotein; HR: Hazard ratio.

ACKNOWLEDGEMENTS

We are grateful to the professors at the School of Foreign Languages of Lanzhou University for their help in the language polish of this manuscript.

FOOTNOTES

Author contributions: Mi DH and Miao YD designed the research; Miao YD wrote this comment; Miao YD and Tang XL performed data analysis and prepared the tables and figures; Wang JT downloaded the data; Mi DH reviewed the manuscript; Miao YD and Tang XL contributed equally to this work; and all authors approved the final manuscript.

Supported by the Special Plan for Condition Construction of Gansu Provincial Scientific Research Institutes, No. 20JR10RA432.

Conflict-of-interest statement: All the authors report no relevant conflicts of interest for this article.

Open-Access: This article is an open-access article that was selected by an in-house editor and fully peer-reviewed by external reviewers. It is distributed in accordance with the Creative Commons Attribution NonCommercial (CC BY-NC 4.0) license, which permits others to distribute, remix, adapt, build upon this work non-commercially, and license their derivative works on different terms, provided the original work is properly cited and the use is non-commercial. See: https://creativecommons.org/Licenses/by-nc/4.0/

Country/Territory of origin: China

ORCID number: Yan-Dong Miao 0000-0002-1429-8915; Xiao-Long Tang 0000-0001-9229-6424; Jiang-Tao Wang 0000-0002-1222-164X; Deng-Hai Mi 0000-0002-8643-4496.

S-Editor: Wang JJ
L-Editor: Wang TQ
P-Editor: Wang JJ

REFERENCES

1 **Choi GH**, Jang ES, Kim JW, Jeong SH. Prognostic role of plasma level of angiopoietin-1, angiopoietin-2, and vascular endothelial growth factor in hepatocellular carcinoma. *World J Gastroenterol* 2021; **27**: 4453-4467 [PMID: 34366616 DOI: 10.3748/wjg.v27.i27.4453]
2 **Heloterä H**, Alitalo K. The VEGF family, the inside story. *Cell* 2007; **130**: 591-592 [PMID: 17719536 DOI: 10.1016/j.cell.2007.08.012]
3 **Thomas JL**, Eichmann A. The power of VEGF (vascular endothelial growth factor) family molecules. *Cell Mol Life Sci* 2013; **70**: 1673-1674 [PMID: 23475064 DOI: 10.1007/s00018-013-1276-6]
4 **Kong D**, Zhou H, Neelakantan D, Hughes CJ, Hsu JY, Srinivasan RR, Lewis MT, Ford HL. VEGF-C mediates tumor growth and metastasis through promoting EMT-epithelial breast cancer cell crosstalk. *Oncogene* 2021; **40**: 964-979 [PMID: 33299122 DOI: 10.1038/s41388-020-01539-x]
5 **Wang X**, Xing Z, Xu H, Yang H, Xing T. Development and validation of epithelial mesenchymal transition-related prognostic model for hepatocellular carcinoma. *Aging (Albany NY)* 2021; **13**: 13822-13845 [PMID: 33929972 DOI: 10.18632/aging.202976]
6 **Bi X**, Niu J, Ding W, Zhang M, Yang M, Gu Y. Angiopoietin-1 attenuates angiotensin II-induced ER stress in glomerular endothelial cells *via* a Tie2 receptor/ERK1/2-p38 MAPK-dependent mechanism. *Mol Cell Endocrinol* 2016; **428**: 118-132 [PMID: 27033326 DOI: 10.1016/j.mce.2016.03.027]
7 **Chen H**, Guan R, Lei Y, Chen J, Ge Q, Zhang X, Dou R, Chen H, Liu H, Qi X, Zhou X, Chen C. Lymphangiogenesis in gastric cancer regulated through Akt/mTOR-VEGF-C/VEGF-D axis. *BMC Cancer* 2015; **15**: 103 [PMID: 25884175 DOI: 10.1186/s12885-015-1109-0]
8 **Liu J**, Lichtenberg T, Hoadley KA, Poisson LM, Lazar AJ, Cherniack AD, Kovatich AJ, Benz CC, Levine DA, Lee AV, Omberg L, Wolf DM, Shriver CD, Thorsson V; Cancer Genome Atlas Research Network, Hu H. An Integrated TCGA Pan-Cancer Clinical Data Resource to Drive High-Quality Survival Outcome Analytics. *Cell* 2018; **173**: 400-416.e11 [PMID: 29625055 DOI: 10.1016/j.cell.2018.02.052]
9 **Walter W**, Sánchez-Cabo F, Ricote M. GOplot: an R package for visually combining expression data with functional analysis. *Bioinformatics* 2015; **31**: 2912-2914 [PMID: 25964631 DOI: 10.1093/bioinformatics/btv300]
10 **Liu CJ**, Hu FF, Xia MX, Han L, Zhang Q, Guo AY. GSCALite: a web server for gene set cancer analysis. *Bioinformatics* 2018; **34**: 3771-3772 [PMID: 29790900 DOI: 10.1093/bioinformatics/bty411]
11 **Vivian J**, Rao AA, Nothaft FA, Ketchum C, Armstrong J, Novak A, Pfeil J, Narkizian J, Deran AD, Musselman-Brown A, Schmidt H, Amstutz P, Craft B, Goldman M, Rosenbloom K, Cline M, O'Connor B, Hanna M, Birger C, Kent WJ, Patterson DA, Joseph AD, Zhu J, Zaranek S, Getz G, Haussler D, Paten B. Toil enables reproducible, open source, big biomedical data analyses. *Nat Biotechnol* 2017; **35**: 314-316 [PMID: 28398314 DOI: 10.1038/nbt.3772]

World Journal of Gastroenterology

Submit a Manuscript: https://www.f6publishing.com

World J Gastroenterol 2022 August 14; 28(30): 4227-4230

DOI: 10.3748/wjg.v28.i30.4227

ISSN 1007-9327 (print) ISSN 2219-2840 (online)

LETTER TO THE EDITOR

Benefits of minimally invasive surgery in the treatment of gastric cancer

Simone Sibio, Francesca La Rovere, Sara Di Carlo

Specialty type: Gastroenterology and hepatology

Provenance and peer review: Unsolicited article; Externally peer reviewed.

Peer-review model: Single blind

Peer-review report's scientific quality classification

Grade A (Excellent): 0
Grade B (Very good): 0
Grade C (Good): C
Grade D (Fair): D, D, D
Grade E (Poor): E

P-Reviewer: Jheng YC, Taiwan; Khaled I, Egypt; Sun Q, China; Viswanath YK, United Kingdom; Yao K, China

Received: November 17, 2021
Peer-review started: November 17, 2021
First decision: December 26, 2021
Revised: January 8, 2022
Accepted: July 22, 2022
Article in press: July 22, 2022
Published online: August 14, 2022

Simone Sibio, Francesca La Rovere, Department of Surgery P. Valdoni, Unit of Oncologic and Minimally Invasive Surgery, Sapienza University of Rome, Umberto I University Hospital, Rome 00161, Italy

Sara Di Carlo, Minimally Invasive Surgery Unit, Department of Surgery, Tor Vergata University, Rome 00133, Italy

Corresponding author: Simone Sibio, PhD, Associate Professor, Consultant Physician-Scientist, Lecturer, Surgical Oncologist, Department of Surgery P. Valdoni, Unit of Oncologic and Minimally Invasive Surgery, Sapienza University of Rome, Umberto I University Hospital, Viale del Policlinico 155, Rome 00161, Italy. simone.sibio@uniroma1.it

Abstract

We read with great interest the article that retrospectively analyzed 814 patients with primary gastric cancer, who underwent minimally invasive R0 gastrectomy between 2009 and 2014 by grouping them in laparoscopic *vs* robotic procedures. The results of the study highlighted that age, American Society of Anesthesiologists status, gastrectomy type and pathological T and N status were the main prognostic factors of minimally invasive gastrectomy and showed how the robotic approach may improve long-term outcomes of advanced gastric cancer. According to most of the current literature, robotic surgery is associated with a statistically longer operating time when compared to open and laparoscopic surgery; however, looking at the adequacy of resection, defined by negative surgical margins and number of lymph nodes removed, it seems that robotic surgery gives better results in terms of the 5-year overall survival and recurrence-free survival. The robotic approach to gastric cancer surgery aims to overcome the difficulties and technical limitations of laparoscopy in major surgery. The three-dimensional vision, articulation of the instruments and good ergonomics for the surgeon allow for accurate and precise movements which facilitate the complex steps of surgery such as lymph node dissection, esophagus-jejunal anastomosis packaging and reproducing the technical accuracy of open surgery. If the literature, as well as the analyzed study, offers us countless data regarding the short-term oncological results of robotic surgery in the treatment of gastric cancer, satisfactory data on long-term follow-up are lacking, so future studies are necessary.

Key Words: Gastric cancer; Robotic gastrectomy; Laparoscopy; D2 lymphadenectomy; Long-term outcomes; Morbidity

©**The Author(s) 2022.** Published by Baishideng Publishing Group Inc. All rights reserved.

Core Tip: Laparoscopic and robotic approaches are compared in the treatment of gastric cancer focusing on the prognostic factors as well as the oncological benefits brought about. While the long-term outcomes of laparoscopic surgery have been increasingly cited in recent years, only a few studies have analyzed the long-term results of the robotic approach, underlining the importance of future studies. A relevant aspect of robotic gastrectomy is the possibility to perform a more accurate lymph node dissection, which results in a longer survival with advanced gastric cancers.

Citation: Sibio S, La Rovere F, Di Carlo S. Benefits of minimally invasive surgery in the treatment of gastric cancer. *World J Gastroenterol* 2022; 28(30): 4227-4230
URL: https://www.wjgnet.com/1007-9327/full/v28/i30/4227.htm
DOI: https://dx.doi.org/10.3748/wjg.v28.i30.4227

TO THE EDITOR

We read with interest the Nakauchi *et al*[1] study, which retrospectively examined 814 patients with primary gastric cancer undergoing a minimally invasive R0 gastrectomy, between 2009 and 2014 in Kanazawa (Japan), comparing the laparoscopic and robotic approach and looking at the 5-year overall survival (OS) and recurrence-free survival (RFS). We were pleased to see from the results of the study that the robotic approach could improve the long-term outcomes of advanced gastric cancer. The authors observed that the robotic approach led to significantly better RFS compared to the laparoscopic one in patients with p-Stage II/III tumors, although no significant difference in OS was detected, nor in OS and RFS in p-Stage patients treated with laparoscopy or robotics.

The study also revealed that age > 65 years, American Society of Anesthesiologists physical status 3, total or proximal gastrectomy, and disease status T4 and N positive, are all independent prognostic factors[1]. Since gastric cancer is the fifth most common malignancy in the world and the third cause of cancer death, it is worth it to identify the most appropriate technical approach for this disease being minimally invasive surgery the standard approach for several GI surgery procedures[2,3].

Surgical treatment remains the only therapeutic option with curative intent. Total or subtotal gastrectomy, associated with D2 lymphadenectomy, represents the therapeutic gold standard for gastric cancer. We must acknowledge that the traditional surgical approach, open surgery, remains the most widespread surgical technique. Although, laparoscopy has become almost constant in general surgery, the use of the laparoscopic technique for gastric surgery is yet scarce in the case of malignancies. As supported by various authors, laparoscopy has several technical drawbacks and limitations, including two-dimensional vision, stiffness of instruments, limited range of motion, amplification of hand tremors and uncomfortable surgical placement which makes some fundamental surgical steps, such as D2 lymphadenectomy, extremely complex[2,4].

According to the paper discussed, the pN factor is strongly associated with survival after gastric cancer treatment, confirming the thesis that laparoscopy in gastric cancer is more adequate in the earlier stages. In contrast, the safety and oncological adequacy of laparoscopic-assisted radical D2 gastrectomy for advanced gastric cancer are still under discussion[5]. From the meta-analysis, it emerges that the main variables associated with a statistically significant advantage of laparoscopic technique over open surgery are represented by: Reduced blood loss, lower complication rate, faster recovery and reduced pain at the expense of a longer surgical time and fewer lymph nodes removed, therefore a potential worse local control of the disease[6,7].

Alongside laparoscopy, robotic technology allows us to overcome the technical difficulties of laparoscopy, thanks to the three-dimensional vision, instruments' articulation and greater ergonomics for the surgeon, offering a better therapeutic approach to the minimally invasive treatment of stomach tumors. Thus, the short and medium term results of robotic gastric surgery can be almost compared with open and laparoscopic procedure when taken into account surgeon experience and technical implementation of the robotic system.

We fully agree with the authors, who have shown a significantly lower morbidity in the group of patients treated with robotics than in the laparoscopic group, as widely discussed in many studies. A recent meta-analysis, which compared laparoscopy with robotics in the treatment of gastric cancer, highlighted that the robotic approach appears to achieve better surgical results in the short term, also thanks to the ability to recover a greater number of lymph nodes, namely lymph nodes in station n. 7, 8a, 9 and 11p, which are avowedly more difficult to reach, ensuring a more appropriate staging and chemotherapy plan[8].

A study conducted in Japan reported, among the advantages of robotic surgery, a lower intraoperative blood loss, with a consequent reduction in the dissemination of cancer cells in the peritoneal cavity during surgery and, therefore, a better prognosis. Another aspect highlighted is a lower risk of dehiscence of the esophagus-jejunal anastomosis, along with a lower incidence of internal hernias[9-11]. From the short-term results it emerges that robotic gastrectomy is a safe technique that potentially allows to extend the number of patients treatable with a minimally invasive approach, overcoming the technical difficulties of laparoscopy, offering some benefits in terms of blood loss, conversion rate, overall number of lymph nodes removed and in suprapancreatic areas, procedure-specific postoperative morbidity and shorter length of hospital stay[12].

Robotic gastrectomy is a safe and effective surgical technique when performed by experienced surgeons, however, it is associated with a longer operative time and a higher economic value than laparoscopic and open approaches[13,14]. Indeed, one of the factors that slows down the spread of robotic surgery is the particular technical expertise required while handling the robotic devices, resulting in a steeper learning curve for the specialized operator. The cost and longer timeframe of robotics make future studies necessary[15], as well as the need for randomized controlled trials comparing the two techniques with a long-term follow-up, on which publications are still scarce given the relatively recent diffusion of the technique[16].

Given the greater cost of robotics, we want to underline one of the limitations of the study discussed here, represented by possible errors in the selection of patients. The availability of robotic devices is strongly dependent on the wealth of the country and of the individual; both patients who are aware of the advantages of the robotic approach and experienced surgeons who are able to perform this novel technique could lead to an overuse of the technique. In Western countries, robotic devices are associated with longer operative time, and higher costs but fewer post-operative complications resulting in lower hospitalization costs, and shorter hospital stays[17].

In conclusion, the study discussed here provides valid results on the correct therapeutic management of patients with gastric cancer, with the aim to bridge over some of the difficulties and technical limitations that laparoscopy encounters in major surgery. Essentially, laparoscopic D2 lymphadenectomy remains a challenging procedure: In particular, the dissection of the lymph nodes along the celiac, hepatic and splenic arteries makes this approach technically complicated and time-consuming even for well-trained surgeons. It is in this context that robotic surgery is worth looking at and it represents a useful tool that overcomes some limitations of conventional laparoscopic techniques, even if greater surgical and anesthetic times and the higher costs have to be considered when compared to open surgery.

Although, in accordance with the international literature that ascribes better results to robotic surgery in perioperative outcomes in terms of blood loss, and postoperative complications, future studies of higher quality are necessary due to the lack of data on long-term results, given the relatively recent diffusion of the technique. In a long-term perspective, considering the need for further studies on larger samples of patients from Western countries, we believe that robotic technology for gastric cancer surgery, taking into account the many advantages it offers, can become a gold standard[18].

FOOTNOTES

Author contributions: La Rovere F and Di Carlo S equally contributed in writing the draft; Di Carlo S revised the English language; Sibio S revised and approved the draft.

Conflict-of-interest statement: All the authors report no relevant conflicts of interest for this article.

Open-Access: This article is an open-access article that was selected by an in-house editor and fully peer-reviewed by external reviewers. It is distributed in accordance with the Creative Commons Attribution NonCommercial (CC BY-NC 4.0) license, which permits others to distribute, remix, adapt, build upon this work non-commercially, and license their derivative works on different terms, provided the original work is properly cited and the use is non-commercial. See: https://creativecommons.org/Licenses/by-nc/4.0/

Country/Territory of origin: Italy

ORCID number: Simone Sibio 0000-0002-5694-951X; Francesca La Rovere 0000-0001-8561-1406; Sara Di Carlo 0000-0001-6519-991X.

S-Editor: Wang JJ
L-Editor: Filipodia
P-Editor: Wang JJ

REFERENCES

1 **Nakauchi M**, Suda K, Shibasaki S, Nakamura K, Kadoya S, Kikuchi K, Inaba K, Uyama I. Prognostic factors of minimally invasive surgery for gastric cancer: Does robotic gastrectomy bring oncological benefit? *World J Gastroenterol* 2021; **27**: 6659-6672 [PMID: 34754159 DOI: 10.3748/wjg.v27.i39.6659]

2 **Amelio I**, Bertolo R, Bove P, Buonomo OC, Candi E, Chiocchi M, Cipriani C, Di Daniele N, Ganini C, Juhl H, Mauriello A, Marani C, Marshall J, Montanaro M, Palmieri G, Piacentini M, Sica G, Tesauro M, Rovella V, Tisone G, Shi Y, Wang Y, Melino G. Liquid biopsies and cancer omics. *Cell Death Discov* 2020; **6**: 131 [PMID: 33298891 DOI: 10.1038/s41420-020-00373-0]

3 **Amelio I**, Bertolo R, Bove P, Candi E, Chiocchi M, Cipriani C, Di Daniele N, Ganini C, Juhl H, Mauriello A, Marani C, Marshall J, Montanaro M, Palmieri G, Piacentini M, Sica G, Tesauro M, Rovella V, Tisone G, Shi Y, Wang Y, Melino G. Cancer predictive studies. *Biol Direct* 2020; **15**: 18 [PMID: 33054808 DOI: 10.1186/s13062-020-00274-3]

4 **EuroSurg Collaborative**. Body mass index and complications following major gastrointestinal surgery: a prospective, international cohort study and meta-analysis. *Colorectal Dis* 2018; **20**: O215-O225 [PMID: 29897171 DOI: 10.1111/codi.14292]

5 **Ojima T**, Nakamura M, Nakamori M, Hayata K, Katsuda M, Kitadani J, Maruoka S, Shimokawa T, Yamaue H. Robotic versus laparoscopic gastrectomy with lymph node dissection for gastric cancer: study protocol for a randomized controlled trial. *Trials* 2018; **19**: 409 [PMID: 30064474 DOI: 10.1186/s13063-018-2810-5]

6 **Cai J**, Wei D, Gao CF, Zhang CS, Zhang H, Zhao T. A prospective randomized study comparing open versus laparoscopy-assisted D2 radical gastrectomy in advanced gastric cancer. *Dig Surg* 2011; **28**: 331-337 [PMID: 21934308 DOI: 10.1159/000330782]

7 **Lee HJ**, Hyung WJ, Yang HK, Han SU, Park YK, An JY, Kim W, Kim HI, Kim HH, Ryu SW, Hur H, Kong SH, Cho GS, Kim JJ, Park DJ, Ryu KW, Kim YW, Kim JW, Lee JH, Kim MC; Korean Laparo-endoscopic Gastrointestinal Surgery Study (KLASS) Group. Short-term Outcomes of a Multicenter Randomized Controlled Trial Comparing Laparoscopic Distal Gastrectomy With D2 Lymphadenectomy to Open Distal Gastrectomy for Locally Advanced Gastric Cancer (KLASS-02-RCT). *Ann Surg* 2019; **270**: 983-991 [PMID: 30829698 DOI: 10.1097/SLA.0000000000003217]

8 **Garbarino GM**, Costa G, Laracca GG, Castagnola G, Mercantini P, Di Paola M, Vita S, Masoni L. Laparoscopic versus open distal gastrectomy for locally advanced gastric cancer in middle-low-volume centers in Western countries: a propensity score matching analysis. *Langenbecks Arch Surg* 2020; **405**: 797-807 [PMID: 32754848 DOI: 10.1007/s00423-020-01951-7]

9 **Guerrini GP**, Esposito G, Magistri P, Serra V, Guidetti C, Olivieri T, Catellani B, Assirati G, Ballarin R, Di Sandro S, Di Benedetto F. Robotic versus laparoscopic gastrectomy for gastric cancer: The largest meta-analysis. *Int J Surg* 2020; **82**: 210-228 [PMID: 32800976 DOI: 10.1016/j.ijsu.2020.07.053]

10 **Pan HF**, Wang G, Liu J, Liu XX, Zhao K, Tang XF, Jiang ZW. Robotic Versus Laparoscopic Gastrectomy for Locally Advanced Gastric Cancer. *Surg Laparosc Endosc Percutan Tech* 2017; **27**: 428-433 [PMID: 29211699 DOI: 10.1097/SLE.0000000000000469]

11 **Sica GS**, Djapardy V, Westaby S, Maynard ND. Diagnosis and management of aortoesophageal fistula caused by a foreign body. *Ann Thorac Surg* 2004; **77**: 2217-2218 [PMID: 15172312 DOI: 10.1016/j.athoracsur.2003.06.031]

12 **Li ZY**, Zhou YB, Li TY, Li JP, Zhou ZW, She JJ, Hu JK, Qian F, Shi Y, Tian YL, Gao GM, Gao RZ, Liang CC, Shi FY, Yang K, Wen Y, Zhao YL, Yu PW; Robotic, Laparoscopic Surgery Committee of Chinese Research Hospital Association. Robotic Gastrectomy versus Laparoscopic Gastrectomy for Gastric Cancer: A Multicenter Cohort Study of 5402 Patients in China. *Ann Surg* 2021 [PMID: 34225299 DOI: 10.1097/SLA.0000000000005046]

13 **Ma J**, Li X, Zhao S, Zhang R, Yang D. Robotic versus laparoscopic gastrectomy for gastric cancer: a systematic review and meta-analysis. *World J Surg Oncol* 2020; **18**: 306 [PMID: 33234134 DOI: 10.1186/s12957-020-02080-7]

14 **Giuliani G**, Guerra F, De Franco L, Salvischiani L, Benigni R, Coratti A. Review on Perioperative and Oncological Outcomes of Robotic Gastrectomy for Cancer. *J Pers Med* 2021; **11** [PMID: 34357105 DOI: 10.3390/jpm11070638]

15 **Zhang Z**, Zhang X, Liu Y, Li Y, Zhao Q, Fan L, Zhang Z, Wang D, Zhao X, Tan B. Meta-analysis of the efficacy of Da Vinci robotic or laparoscopic distal subtotal gastrectomy in patients with gastric cancer. *Medicine (Baltimore)* 2021; **100**: e27012 [PMID: 34449473 DOI: 10.1097/MD.0000000000027012]

16 **Hu LD**, Li XF, Wang XY, Guo TK. Robotic versus Laparoscopic Gastrectomy for Gastric Carcinoma: a Meta-Analysis of Efficacy and Safety. *Asian Pac J Cancer Prev* 2016; **17**: 4327-4333 [PMID: 27797239]

17 **Caruso R**, Vicente E, Núñez-Alfonsel J, Ferri V, Diaz E, Fabra I, Malave L, Duran H, Isernia R, D'Ovidio A, Pinna E, Ielpo B, Quijano Y. Robotic-assisted gastrectomy compared with open resection: a comparative study of clinical outcomes and cost-effectiveness analysis. *J Robot Surg* 2020; **14**: 627-632 [PMID: 31620970 DOI: 10.1007/s11701-019-01033-x]

18 **Shibasaki S**, Suda K, Obama K, Yoshida M, Uyama I. Should robotic gastrectomy become a standard surgical treatment option for gastric cancer? *Surg Today* 2020; **50**: 955-965 [PMID: 31512060 DOI: 10.1007/s00595-019-01875-w]

World Journal of Gastroenterology

Submit a Manuscript: https://www.f6publishing.com

World J Gastroenterol 2022 August 14; 28(30): 4231-4234

DOI: 10.3748/wjg.v28.i30.4231

ISSN 1007-9327 (print) ISSN 2219-2840 (online)

LETTER TO THE EDITOR

Alcohol-related diseases and liver metastasis: Role of cell-free network communication

Manuel Muro, Aurelia Collados-Ros, Isabel Legaz

Specialty type: Biology

Provenance and peer review: Unsolicited article; Externally peer reviewed.

Peer-review model: Single blind

Peer-review report's scientific quality classification

Grade A (Excellent): 0
Grade B (Very good): B, B, B
Grade C (Good): 0
Grade D (Fair): 0
Grade E (Poor): 0

P-Reviewer: Chu HK, China; Luo JH, China; Qin Y, China

Received: May 12, 2022
Peer-review started: May 12, 2022
First decision: May 28, 2022
Revised: May 31, 2022
Accepted: July 18, 2022
Article in press: July 18, 2022
Published online: August 14, 2022

Manuel Muro, Immunology Service, Instituto Murciano de investigación biosanitaria (IMIB), Hospital Clínico Universitario Virgen de la Arrixaca (HCUVA), Murcia 30120, Spain

Aurelia Collados-Ros, Isabel Legaz, Department of Legal and Forensic Medicine, Biomedical Research Institute (IMIB), Regional Campus of International Excellence "Campus Mare Nostrum", Faculty of Medicine, University of Murcia, Murcia 30100, Spain

Corresponding author: Isabel Legaz, PhD, Senior Lecturer, Department of Legal and Forensic Medicine, Biomedical Research Institute (IMIB), Regional Campus of International Excellence "Campus Mare Nostrum", Faculty of Medicine, University of Murcia, Campus de Espinardo, Murcia 30100, Spain. isalegaz@um.es

Abstract

Alcohol intake is a risk factor for cancer development and metastatic disease progression. Extracellular vesicle (EV)-mediated interorgan communication is assumed to be significant in boosting tumorigenic pathways and disease progression. Recent research indicates that exosomes have a variety of roles in the development of cancer during pathophysiological conditions. The involvement of EV signaling during cancer progression in the alcohol environment is unknown. Therefore, understanding communication networks and the role of EVs as biomarkers can contribute significantly to developing strategies to address the serious public health problems associated with alcohol consumption and cancer.

Key Words: Exosomes; Liver metastasis; Alcohol-associated liver disease; Cancer

©The Author(s) 2022. Published by Baishideng Publishing Group Inc. All rights reserved.

Core Tip: In this letter to the editor, we discussed the reality that alcohol consumption is a risk factor that acts by itself to favor the appearance of the carcinogenic process and its harmful evolution towards metastatic pathology. One of the hypotheses that have been suggested as important in metastasis and communication between cells and/or organs is the traffic of extracellular vesicles/exosomes that can play or promote tumorigenesis locally and even at a distance from the primary tumor. Unraveling these communication mechanisms and therapeutic possibilities may lead to new ways to combat cancer's worsening, as metastasis, in the future.

Citation: Muro M, Collados-Ros A, Legaz I. Alcohol-related diseases and liver metastasis: Role of cell-free network communication. *World J Gastroenterol* 2022; 28(30): 4231-4234
URL: https://www.wjgnet.com/1007-9327/full/v28/i30/4231.htm
DOI: https://dx.doi.org/10.3748/wjg.v28.i30.4231

TO THE EDITOR

We have read with great attention and particular interest the review by Kuracha *et al*[1] entitled: "Role of cell-free network communication in alcohol-associated disorders and liver metastasis". The authors highlight the many implications of extracellular vesicle (EV) (exosome) communications across organs in this review, focusing on the role of EVs in alcohol-related illnesses and cancer metastasis. It is crucial to consider the impact of EV cargo and release along a multi-organ axis on tumorigenic pathways and metastatic disease.

Alcohol consumption negatively impacts people's health and quality of life, contributing to more than 5% of the global disease burden and early death[2,3]. Alcohol intake has been linked to several neoplastic diseases, including colorectal, head and neck, esophageal, liver, breast, and pancreatic cancers[4,5]. On the other hand, recent research suggests that exosomes have different functions in disease progression during pathophysiological circumstances. Exosomes from tumors have been found to operate as regulatory factors in cancer development, promoting cell migration and proliferation and creating a pre-metastatic niche for cells resistant to treatment[6,7].

Hepatocytes and non-parenchymal cells produce and release EVs at higher rates in response to alcohol-mediated stress[8]. The EVs produced can alter gene expression and target cell function, prolonging liver damage[8]. Bidirectional exosomal communication between organs, including the liver, brain, intestine, and lungs, can also happen in addition to intra-organ transmission mediated by EVs. The gut-liver axis maintains bilateral interactions in an environment where alcohol is present, which results in gut dysbiosis and the progression of liver impairment[9,10].

In addition to persistent alcoholism, endotoxin transfer during sepsis and brain inflammation are caused by loss of intestinal barrier integrity. Alcohol dependency and its regulatory consequences, such as altered immunological function and neurological and endocrine signaling, are hypothesized to be influenced by alcohol-induced gut dysbiosis[11,12]. Acute respiratory distress syndrome, bacterial infection, and hepatopulmonary syndrome are also linked to persistent alcohol exposure on the liver-lung axis (ARDS)[13,14].

The significance of alcohol-induced EV communication in cancer initiation and progression is unknown until now because of the high prevalence of alcohol drinking and cancer-related risk. The therapeutic significance of the function of these exosomes has been highlighted by identifying EVs as critical mediators of communication networks within and across organ systems[7,15,16]. Clinical evaluation of EVs in body fluids provides another measure for understanding exosomes as valid and valuable diagnostic biomarkers and therapeutic targets.

Communication between malignant and non-cancerous cells, mediated by nanometric vesicles, is thought to be an essential part of tumor growth and its subsequent spread through the body. By promoting oncogene overexpression, stromal cell remodeling, immune system regulation, and angiogenesis, tumor-derived exosomes may control the course of cancer[17]. Cancer cells' ability to grow anchorage-independently is thought to be enhanced, and their morphological changes may be modulated by the transfer of tumor-causing material through EVs[18].

Additionally, miRNA-enriched EVs have also been demonstrated in cell-cell communications and the conversion of cells into populations with enhanced motility[19]. The involvement of EV signaling during cancer progression in the alcohol environment is unknown. Recent studies have shown that the exosomal content (proteins, miRNA, non-coding RNA) can help diagnose and treat cancer[20-22]. Therefore, comprehending EVs and communication networks as biomarkers can considerably aid in developing methods to deal with the serious public health issues brought on by alcohol intake and cancer.

FOOTNOTES

Author contributions: Legaz I contrubited to conceptualization; Muro M, Collados-Ros A, and Legaz I contrubited to writing-original draft preparation; Muro M and Legaz I contrubited to writing-review and editing, writing-original draft preparation, supervision, and writing-review and editing; all authors read and approved the final manuscript, read and approved the final manuscript.

Conflict-of-interest statement: There are no conflicts of interest to report.

Open-Access: This article is an open-access article that was selected by an in-house editor and fully peer-reviewed by

external reviewers. It is distributed in accordance with the Creative Commons Attribution NonCommercial (CC BY-NC 4.0) license, which permits others to distribute, remix, adapt, build upon this work non-commercially, and license their derivative works on different terms, provided the original work is properly cited and the use is non-commercial. See: https://creativecommons.org/Licenses/by-nc/4.0/

Country/Territory of origin: Spain

ORCID number: Manuel Muro 0000-0001-9987-0994; Isabel Legaz 0000-0002-1140-4313.

S-Editor: Chen YL
L-Editor: A
P-Editor: Chen YL

REFERENCES

1 **Kuracha MR**, Thomas P, Tobi M, McVicker BL. Role of cell-free network communication in alcohol-associated disorders and liver metastasis. *World J Gastroenterol* 2021; **27**: 7080-7099 [PMID: 34887629 DOI: 10.3748/wjg.v27.i41.7080]
2 **Wallace AE**, Weeks WB. Substance abuse intensive outpatient treatment: does program graduation matter? *J Subst Abuse Treat* 2004; **27**: 27-30 [PMID: 15223090 DOI: 10.1016/j.jsat.2004.03.006]
3 **World Health Organization**. Global status report on alcohol and health 2018. July 12, 2019. [cited 3 May 2022]. Available from: https://www.who.int/publications/i/item/9789241565639
4 **Bagnardi V**, Rota M, Botteri E, Tramacere I, Islami F, Fedirko V, Scotti L, Jenab M, Turati F, Pasquali E, Pelucchi C, Galeone C, Bellocco R, Negri E, Corrao G, Boffetta P, La Vecchia C. Alcohol consumption and site-specific cancer risk: a comprehensive dose-response meta-analysis. *Br J Cancer* 2015; **112**: 580-593 [PMID: 25422909 DOI: 10.1038/bjc.2014.579]
5 **IARC Working Group on the Evaluation of Carcinogenic Risks to Humans**. Alcohol consumption and ethyl carbamate. *IARC Monogr Eval Carcinog Risks Hum* 2010; **96**: 3-1383 [PMID: 21735939]
6 **Becker A**, Thakur BK, Weiss JM, Kim HS, Peinado H, Lyden D. Extracellular Vesicles in Cancer: Cell-to-Cell Mediators of Metastasis. *Cancer Cell* 2016; **30**: 836-848 [PMID: 27960084 DOI: 10.1016/j.ccell.2016.10.009]
7 **Raposo G**, Stoorvogel W. Extracellular vesicles: exosomes, microvesicles, and friends. *J Cell Biol* 2013; **200**: 373-383 [PMID: 23420871 DOI: 10.1083/jcb.201211138]
8 **Shim YR**, Jeong WI. Recent advances of sterile inflammation and inter-organ cross-talk in alcoholic liver disease. *Exp Mol Med* 2020; **52**: 772-780 [PMID: 32457490 DOI: 10.1038/s12276-020-0438-5]
9 **Dasarathy S**, Brown JM. Alcoholic Liver Disease on the Rise: Interorgan Cross Talk Driving Liver Injury. *Alcohol Clin Exp Res* 2017; **41**: 880-882 [PMID: 28295407 DOI: 10.1111/acer.13370]
10 **Stärkel P**, Schnabl B. Bidirectional Communication between Liver and Gut during Alcoholic Liver Disease. *Semin Liver Dis* 2016; **36**: 331-339 [PMID: 27997973 DOI: 10.1055/s-0036-1593882]
11 **Leclercq S**, Matamoros S, Cani PD, Neyrinck AM, Jamar F, Stärkel P, Windey K, Tremaroli V, Bäckhed F, Verbeke K, de Timary P, Delzenne NM. Intestinal permeability, gut-bacterial dysbiosis, and behavioral markers of alcohol-dependence severity. *Proc Natl Acad Sci U S A* 2014; **111**: E4485-E4493 [PMID: 25288760 DOI: 10.1073/pnas.1415174111]
12 **Mutlu EA**, Gillevet PM, Rangwala H, Sikaroodi M, Naqvi A, Engen PA, Kwasny M, Lau CK, Keshavarzian A. Colonic microbiome is altered in alcoholism. *Am J Physiol Gastrointest Liver Physiol* 2012; **302**: G966-G978 [PMID: 22241860 DOI: 10.1152/ajpgi.00380.2011]
13 **Afshar M**, Smith GS, Terrin ML, Barrett M, Lissauer ME, Mansoor S, Jeudy J, Netzer G. Blood alcohol content, injury severity, and adult respiratory distress syndrome. *J Trauma Acute Care Surg* 2014; **76**: 1447-1455 [PMID: 24854314 DOI: 10.1097/TA.0000000000000238]
14 **Moss M**, Parsons PE, Steinberg KP, Hudson LD, Guidot DM, Burnham EL, Eaton S, Cotsonis GA. Chronic alcohol abuse is associated with an increased incidence of acute respiratory distress syndrome and severity of multiple organ dysfunction in patients with septic shock. *Crit Care Med* 2003; **31**: 869-877 [PMID: 12626999 DOI: 10.1097/01.CCM.0000055389.64497.11]
15 **Mathivanan S**, Ji H, Simpson RJ. Exosomes: extracellular organelles important in intercellular communication. *J Proteomics* 2010; **73**: 1907-1920 [PMID: 20601276 DOI: 10.1016/j.jprot.2010.06.006]
16 **Record M**, Carayon K, Poirot M, Silvente-Poirot S. Exosomes as new vesicular lipid transporters involved in cell-cell communication and various pathophysiologies. *Biochim Biophys Acta* 2014; **1841**: 108-120 [PMID: 24140720 DOI: 10.1016/j.bbalip.2013.10.004]
17 **Maia J**, Caja S, Strano Moraes MC, Couto N, Costa-Silva B. Exosome-Based Cell-Cell Communication in the Tumor Microenvironment. *Front Cell Dev Biol* 2018; **6**: 18 [PMID: 29515996 DOI: 10.3389/fcell.2018.00018]
18 **Quaglia F**, Krishn SR, Daaboul GG, Sarker S, Pippa R, Domingo-Domenech J, Kumar G, Fortina P, McCue P, Kelly WK, Beltran H, Liu Q, Languino LR. Small extracellular vesicles modulated by αVβ3 integrin induce neuroendocrine differentiation in recipient cancer cells. *J Extracell Vesicles* 2020; **9**: 1761072 [PMID: 32922691 DOI: 10.1080/20013078.2020.1761072]
19 **Baroni S**, Romero-Cordoba S, Plantamura I, Dugo M, D'Ippolito E, Cataldo A, Cosentino G, Angeloni V, Rossini A, Daidone MG, Iorio MV. Exosome-mediated delivery of miR-9 induces cancer-associated fibroblast-like properties in human breast fibroblasts. *Cell Death Dis* 2016; **7**: e2312 [PMID: 27468688 DOI: 10.1038/cddis.2016.224]
20 **Xu Z**, Chen Y, Ma L, Liu J, Guo Y, Yu T, Zhang L, Zhu L, Shu Y. Role of exosomal non-coding RNAs from tumor cells and tumor-associated macrophages in the tumor microenvironment. *Mol Ther* 2022 [PMID: 35405312 DOI:

10.1016/j.ymthe.2022.01.046]

21 **Jiang J**, Li J, Zhou X, Zhao X, Huang B, Qin Y. Exosomes Regulate the Epithelial-Mesenchymal Transition in Cancer. *Front Oncol* 2022; **12**: 864980 [PMID: 35359397 DOI: 10.3389/fonc.2022.864980]

22 **Zhang K**, Erkan EP, Jamalzadeh S, Dai J, Andersson N, Kaipio K, Lamminen T, Mansuri N, Huhtinen K, Carpén O, Hietanen S, Oikkonen J, Hynninen J, Virtanen A, Häkkinen A, Hautaniemi S, Vähärautio A. Longitudinal single-cell RNA-seq analysis reveals stress-promoted chemoresistance in metastatic ovarian cancer. *Sci Adv* 2022; **8**: eabm1831 [PMID: 35196078 DOI: 10.1126/sciadv.abm1831]



Published by **Baishideng Publishing Group Inc**
7041 Koll Center Parkway, Suite 160, Pleasanton, CA 94566, USA
Telephone: +1-925-3991568
E-mail: bpgoffice@wjgnet.com
Help Desk: https://www.f6publishing.com/helpdesk
https://www.wjgnet.com



© 2022 Baishideng Publishing Group Inc. All rights reserved.

ISSN 1007-9327 (print)
ISSN 2219-2840 (online)

World Journal of *Gastroenterology*

World J Gastroenterol 2022 August 21; 28(31): 4235-4474



Published by Baishideng Publishing Group Inc

World Journal of Gastroenterology

Contents

Weekly Volume 28 Number 31 August 21, 2022

REVIEW

4235 Early diagnosis of pancreatic cancer: What strategies to avoid a foretold catastrophe

Tonini V, Zanni M

4249 Insights into induction of the immune response by the hepatitis B vaccine

Di Lello FA, Martínez AP, Flichman DM

4263 Evidence-based pathogenesis and treatment of ulcerative colitis: A causal role for colonic epithelial hydrogen peroxide

Pravda J

MINIREVIEWS

4299 Recent advances in multidisciplinary therapy for adenocarcinoma of the esophagus and esophagogastric junction

Zheng YH, Zhao EH

ORIGINAL ARTICLE

Basic Study

4310 Exosomal glypican-1 is elevated in pancreatic cancer precursors and can signal genetic predisposition in the absence of endoscopic ultrasound abnormalities

Moutinho-Ribeiro P, Batista IA, Quintas ST, Adem B, Silva M, Morais R, Peixoto A, Coelho R, Costa-Moreira P, Medas R, Lopes S, Vilas-Boas F, Baptista M, Dias-Silva D, Esteves AL, Martins F, Lopes J, Barroca H, Carneiro F, Macedo G, Melo SA

4328 Duodenal-jejunal bypass reduces serum ceramides *via* inhibiting intestinal bile acid-farnesoid X receptor pathway

Cheng ZQ, Liu TM, Ren PF, Chen C, Wang YL, Dai Y, Zhang X

4338 Duodenal-jejunal bypass increases intraduodenal bile acids and upregulates duodenal SIRT1 expression in high-fat diet and streptozotocin-induced diabetic rats

Han HF, Liu SZ, Zhang X, Wei M, Huang X, Yu WB

Retrospective Study

4351 Approaches to reconstruction of inferior vena cava by *ex vivo* liver resection and autotransplantation in 114 patients with hepatic alveolar echinococcosis

Maimaitinijiati Y, AJi T, Jiang TM, Ran B, Shao YM, Zhang RQ, Guo Q, Wang ML, Wen H

4363 Application of computed tomography-based radiomics in differential diagnosis of adenocarcinoma and squamous cell carcinoma at the esophagogastric junction

Du KP, Huang WP, Liu SY, Chen YJ, Li LM, Liu XN, Han YJ, Zhou Y, Liu CC, Gao JB

World Journal of Gastroenterology

Weekly Volume 28 Number 31 August 21, 2022

Contents

4376 Preoperative contrast-enhanced computed tomography-based radiomics model for overall survival prediction in hepatocellular carcinoma

Deng PZ, Zhao BG, Huang XH, Xu TF, Chen ZJ, Wei QF, Liu XY, Guo YQ, Yuan SG, Liao WJ

4390 Nationwide retrospective study of hepatitis B virological response and liver stiffness improvement in 465 patients on nucleos(t)ide analogue

Ramji A, Doucette K, Cooper C, Minuk GY, Ma M, Wong A, Wong D, Tam E, Conway B, Truong D, Wong P, Barrett L, Ko HH, Haylock-Jacobs S, Patel N, Kaplan GG, Fung S, Coffin CS

Observational Study

4399 Radiomics and nomogram of magnetic resonance imaging for preoperative prediction of microvascular invasion in small hepatocellular carcinoma

Chen YD, Zhang L, Zhou ZP, Lin B, Jiang ZJ, Tang C, Dang YW, Xia YW, Song B, Long LL

4417 Prevalence and clinical characteristics of autoimmune liver disease in hospitalized patients with cirrhosis and acute decompensation in China

Shen ZX, Wu DD, Xia J, Wang XB, Zheng X, Huang Y, Li BL, Meng ZJ, Gao YH, Qian ZP, Liu F, Lu XB, Shang J, Yan HD, Zheng YB, Gu WY, Zhang Y, Wei JY, Tan WT, Hou YX, Zhang Q, Xiong Y, Zou CC, Chen J, Huang ZB, Jiang XH, Luo S, Chen YY, Gao N, Liu CY, Yuan W, Mei X, Li J, Li T, Zhou XY, Deng GH, Chen JJ, Ma X, Li H

4431 Simple cholecystectomy is an adequate treatment for grade I T1bN0M0 gallbladder carcinoma: Evidence from 528 patients

Shao J, Lu HC, Wu LQ, Lei J, Yuan RF, Shao JH

META-ANALYSIS

4442 Current standard values of health utility scores for evaluating cost-effectiveness in liver disease: A meta-analysis

Ishinuki T, Ota S, Harada K, Kawamoto M, Meguro M, Kutomi G, Tatsumi H, Harada K, Miyanishi K, Kato T, Ohyanagi T, Hui TT, Mizuguchi T

CASE REPORT

4456 Low-grade myofibroblastic sarcoma of the liver misdiagnosed as cystadenoma: A case report

Li J, Huang XY, Zhang B

LETTER TO THE EDITOR

4463 Evidence-based considerations on bowel preparation for colonoscopy

Argyriou K, Parra-Blanco A

4467 Influence of different portal vein branches on hepatic encephalopathy during intrahepatic portal shunt *via* jugular vein

Yao X, He S, Wei M, Qin JP

4471 Promising role of D-amino acids in irritable bowel syndrome

Ikeda Y, Taniguchi K, Sawamura H, Tsuji A, Matsuda S

ABOUT COVER

Editorial Board Member of *World Journal of Gastroenterology*, Mortada H F El-Shabrawi, MD, FAASLD, Professor, Department of Paediatrics, Kasr Alainy School of Medicine, Cairo University, Cairo 11562, Egypt. melshabrawi@kasralainy.edu.eg

AIMS AND SCOPE

The primary aim of *World Journal of Gastroenterology* (*WJG*, *World J Gastroenterol*) is to provide scholars and readers from various fields of gastroenterology and hepatology with a platform to publish high-quality basic and clinical research articles and communicate their research findings online. *WJG* mainly publishes articles reporting research results and findings obtained in the field of gastroenterology and hepatology and covering a wide range of topics including gastroenterology, hepatology, gastrointestinal endoscopy, gastrointestinal surgery, gastrointestinal oncology, and pediatric gastroenterology.

INDEXING/ABSTRACTING

The *WJG* is now abstracted and indexed in Science Citation Index Expanded (SCIE, also known as SciSearch®), Current Contents/Clinical Medicine, Journal Citation Reports, Index Medicus, MEDLINE, PubMed, PubMed Central, Scopus, Reference Citation Analysis, China National Knowledge Infrastructure, China Science and Technology Journal Database, and Superstar Journals Database. The 2022 edition of Journal Citation Reports® cites the 2021 impact factor (IF) for *WJG* as 5.374; IF without journal self cites: 5.187; 5-year IF: 5.715; Journal Citation Indicator: 0.84; Ranking: 31 among 93 journals in gastroenterology and hepatology; and Quartile category: Q2. The *WJG*'s CiteScore for 2021 is 8.1 and Scopus CiteScore rank 2021: Gastroenterology is 18/149.

RESPONSIBLE EDITORS FOR THIS ISSUE

Production Editor: *Yi-Xuan Cai*; **Production Department Director:** *Xiang Li*; **Editorial Office Director:** *Jia-Ru Fan.*

NAME OF JOURNAL
World Journal of Gastroenterology

ISSN
ISSN 1007-9327 (print) ISSN 2219-2840 (online)

LAUNCH DATE
October 1, 1995

FREQUENCY
Weekly

EDITORS-IN-CHIEF
Andrzej S Tarnawski

EDITORIAL BOARD MEMBERS
http://www.wjgnet.com/1007-9327/editorialboard.htm

PUBLICATION DATE
August 21, 2022

COPYRIGHT
© 2022 Baishideng Publishing Group Inc

INSTRUCTIONS TO AUTHORS
https://www.wjgnet.com/bpg/gerinfo/204

GUIDELINES FOR ETHICS DOCUMENTS
https://www.wjgnet.com/bpg/GerInfo/287

GUIDELINES FOR NON-NATIVE SPEAKERS OF ENGLISH
https://www.wjgnet.com/bpg/gerinfo/240

PUBLICATION ETHICS
https://www.wjgnet.com/bpg/GerInfo/288

PUBLICATION MISCONDUCT
https://www.wjgnet.com/bpg/gerinfo/208

ARTICLE PROCESSING CHARGE
https://www.wjgnet.com/bpg/gerinfo/242

STEPS FOR SUBMITTING MANUSCRIPTS
https://www.wjgnet.com/bpg/GerInfo/239

ONLINE SUBMISSION
https://www.f6publishing.com

© 2022 Baishideng Publishing Group Inc. All rights reserved. 7041 Koll Center Parkway, Suite 160, Pleasanton, CA 94566, USA
E-mail: bpgoffice@wjgnet.com https://www.wjgnet.com

World Journal of Gastroenterology

Submit a Manuscript: https://www.f6publishing.com

World J Gastroenterol 2022 August 21; 28(31): 4235-4248

DOI: 10.3748/wjg.v28.i31.4235

ISSN 1007-9327 (print) ISSN 2219-2840 (online)

REVIEW

Early diagnosis of pancreatic cancer: What strategies to avoid a foretold catastrophe

Valeria Tonini, Manuel Zanni

Specialty type: Oncology

Provenance and peer review: Invited article; Externally peer reviewed.

Peer-review model: Single blind

Peer-review report's scientific quality classification

Grade A (Excellent): 0
Grade B (Very good): B
Grade C (Good): C
Grade D (Fair): 0
Grade E (Poor): 0

P-Reviewer: Jeong KY, South Korea; Khalil MTASH, Egypt

Received: March 24, 2022
Peer-review started: March 24, 2022
First decision: May 9, 2022
Revised: May 18, 2022
Accepted: July 24, 2022
Article in press: July 24, 2022
Published online: August 21, 2022



Valeria Tonini, Manuel Zanni, Department of Medical and Surgical Sciences, University of Bologna, Bologna 40138, Italy

Corresponding author: Valeria Tonini, MD, PhD, Adjunct Associate Professor, Professor, Surgeon, Surgical Oncologist, Department of Medical and Surgical Sciences, University of Bologna, Via Massarenti 9, Bologna 40138, Italy. valeria.tonini@unibo.it

Abstract

While great strides in improving survival rates have been made for most cancers in recent years, pancreatic ductal adenocarcinoma (PDAC) remains one of the solid tumors with the worst prognosis. PDAC mortality often overlaps with incidence. Surgical resection is the only potentially curative treatment, but it can be performed in a very limited number of cases. In order to improve the prognosis of PDAC, there are ideally two possible ways: the discovery of new strategies or drugs that will make it possible to treat the tumor more successfully or an earlier diagnosis that will allow patients to be operated on at a less advanced stage. The aim of this review was to summarize all the possible strategies available today for the early diagnosis of PDAC and the paths that research needs to take to make this goal ever closer. All the most recent studies on risk factors and screening modalities, new laboratory tests including liquid biopsy, new imaging methods and possible applications of artificial intelligence and machine learning were reviewed and commented on. Unfortunately, in 2022 the results for this type of cancer still remain discouraging, while a catastrophic increase in cases is expected in the coming years. The article was also written with the aim of highlighting the urgency of devoting more attention and resources to this pathology in order to reach a solution that seems more and more unreachable every day.

Key Words: Pancreatic cancer; Pancreatic ductal adenocarcinoma; Early diagnosis; Liquid biopsy; Pancreatic cancer biomarkers; Artificial intelligence; Pancreatic cancer screening

©The Author(s) 2022. Published by Baishideng Publishing Group Inc. All rights reserved.

Core Tip: Pancreatic ductal adenocarcinoma is one of the solid neoplasms with the worst prognosis. Surgical resection is the only potentially curative treatment. In 80% of patients, pancreatic ductal adenocarcinoma is discovered at a stage too advanced for surgery. The aim of this review was to summarize all the possible strategies available today for the early diagnosis of pancreatic ductal adenocarcinoma and the paths that research must take to make this goal ever closer. The article highlights the urgency of devoting more attention and resources to this pathology in order to reach a solution that seems more and more unreachable every day.

Citation: Tonini V, Zanni M. Early diagnosis of pancreatic cancer: What strategies to avoid a foretold catastrophe. *World J Gastroenterol* 2022; 28(31): 4235-4248
URL: https://www.wjgnet.com/1007-9327/full/v28/i31/4235.htm
DOI: https://dx.doi.org/10.3748/wjg.v28.i31.4235

INTRODUCTION

Pancreatic ductal adenocarcinoma (PDAC) is ranked as the seventh leading cause of cancer deaths worldwide, while it ranks fourth in the Western world, just behind lung, colorectal and breast cancers. Rahib *et al*[1] estimated that it will become the second leading cause of cancer death by 2030. The 2020 global cancer statistics reported a total of nearly 496000 new cases of PDAC and more than 466000 related deaths. PDAC mortality is almost overlapping with incidence[2].

The 5-year survival rate of PDAC is less than 10%[3]. A study that included 84275 patients showed that the 5-year survival rate increased from 0.9% in 1975 to 4.2% in 2011, considering all stages of PDAC. In patients undergoing surgical resection, it increased from 1.5% to 17.4%[4], while in unresected patients by 0.8% in 1975 and 0.9% in 2011. The high mortality and poor improvement in survival rates over the years are due to several factors. First, the retroperitoneal location of the pancreas results in the appearance of symptoms only when the neoplasm has reached considerable size, and diagnosis is often made at an advanced stage of the disease. Second, PDAC is inherently characterized by a fierce biology with early metastasis, and in fact about half of patients have metastatic disease at the time of presentation. Third, PDAC drastically weakens patients, limiting the possibility of aggressive treatments. Finally, through the desmoplastic reaction, it shows resistance to many antineoplastic therapies[5,6].

The 5-year survival rate for patients with stage 0 (in situ) according to the Union for International Cancer Control classification is 85.8%, while that of patients with stage IA is 68.7%. In the early stages of the disease, therefore, the prognosis is relatively good[7,8]. Early diagnosis of the disease is therefore essential.

Our efforts should focus on recognizing risk factors that contribute to the development of the disease in order to define the population at risk that could benefit from a screening protocol and on researching new techniques for early diagnosis[9-12].

RISK FACTORS AND STRATIFICATION

Several non-modifiable and modifiable risk factors are correlated with PDAC. Non-modifiable risk factors include the patient's age, ethnicity, gender, blood type, microbiota, diabetes mellitus, family history and genetic predisposition, while modifiable risk factors include tobacco use, alcohol consumption, diet, pancreatitis, obesity and socioeconomic status[12]. According to some studies, one-third of all cancers could be prevented through lifestyle improvement. The EPIC study, for example, evaluated the association between healthy lifestyle index score and pancreatic cancer[13,14]. A three-point increase in this score, achieved through adherence to healthy behaviors, is associated with a 16%-23% lower risk[15]. No smoking, making your home/workplace smoke-free, maintaining a normal body weight, having a diet rich in grains, legumes, and vegetables and limiting alcohol intake are key factors in the prevention of PDAC.

According to several studies, the new onset of diabetes in an elderly patient should suggest PDAC, especially if such a finding is associated with unintentional weight loss[16-18]. A study by Pelaez-Luna *et al*[19] evaluated the use of computed tomography (CT) scans in asymptomatic patients at the time of diabetes diagnosis and found a higher likelihood of detecting potentially resectable tumors compared with scans performed 6 mo later. However, CT-based screening of all elderly patients with new-onset diabetes (NOD) is not feasible[18]. Screening programs and guidelines will likely be updated when the features that differentiate pancreatic cancer-associated diabetes from other cases of NOD are identified.

The creation of a pancreatic cancer risk prediction model based on the integration of multiple risk factors could contribute to its early detection[20]. Sharma *et al*[21] developed a model called Enriching New-Onset Diabetes for Pancreatic Cancer that weights the scores of three factors including weight change, blood glucose change and age at diabetes onset in patients with NOD. A score of at least three points in the Enriching New-Onset Diabetes for Pancreatic Cancer model was able to identify individuals who developed PDAC within 3 years of the onset of diabetes with good sensitivity and specificity[21].

In addition to the strictly environmental risk factors, familial pancreatic cancer and genetic syndromes (hereditary breast and ovarian cancer syndrome, Lynch syndrome, familial atypical multiple melanoma, Peutz-Jegher syndrome, Li-Fraumeni syndrome and hereditary pancreatitis) are added. Familial pancreatic cancer is defined by the occurrence of PDAC in at least two first-degree relatives and accounts for up to 10% of all cases of PDAC[22].

Patients at high risk for developing PDAC include those with inherited risk factors (both genetic syndromes and familial pancreatic cancer), those with NOD and those with cystic lesions of the pancreas.

Pancreatic cysts are found in approximately 8% of individuals over the age of 70 years[23] and include intraductal papillary mucinous neoplasms (IPMN) and mucinous cystic neoplasms, both of which are precursors to PDAC. IPMN and mucinous cystic neoplasms are collectively referred to as mucinous cystic lesions. In contrast to the third precursor lesion, pancreatic intraepithelial neoplasia, which can be identified only at surgical histopathology, mucinous cystic lesions are easy to detect and are found incidentally in 3% of CT subjects[23]. Therefore, their identification offers the potential for early diagnosis of PDAC. However, there are two problems. First, not all pancreatic cystic lesions are IPMN or mucinous cystic neoplasms. Many are cystic lesions without risk of malignant transformation, and therefore do not require surveillance. Second, most IPMN and mucinous cystic neoplasms do not progress to PDAC. Over the years, evidence has been found to predict the possibility of progression to PDAC[23].

In mucinous cystic neoplasms the presence of eggshell calcification, larger tumor size or a mural nodule on cross-sectional imaging is suggestive of malignancy[24]. Regarding IPMN, worrisome (main duct 5-9 mm, enhancing mural nodule < 5 mm, thickened, enhancing cyst wall, branch duct IPMN > 3 cm, abrupt caliber change in main duct with upstream atrophy, lymphadenopathy, pancreatitis, increased serum 19-9, cyst growth > 5 mm over 2 years) and high-risk features (main duct > 1 cm, enhancing, mural nodule > 5 mm, jaundice) have been defined[25].

However, these clinical features are still imperfect in differentiating between benign cysts and mucinous cystic lesions that harbor high-grade dysplasia or PDAC and require surgical resection and mucinous cystic lesions that have low-grade dysplasia and are safe to look at.

For the time being, a screening program is offered to individuals with a strong family history and/or genetic predisposition to develop pancreatic cancer and subjects with mucinous cystic lesions of the pancreas. The primary goals of screening are the detection of high-grade dysplastic precancerous lesions (IPMN and pancreatic intraepithelial neoplasia) and T1N0M0 pancreatic cancer that are more amenable to potentially curative resection[26].

The current recommendation is to perform endoscopic ultrasound (EUS) or magnetic resonance imaging (MRI)/magnetic resonance cholangiopancreatography. Screening is recommended at age 50 years or 10 years before the youngest relative with PDAC in familial pancreatic cancer cases. In other settings, screening is performed between the ages of 35 years and 45 years. In case the patient had a normal pancreas on imaging, it is recommended to repeat the procedure every year alternating EUS and magnetic resonance cholangiopancreatography. However, no consensus has been found on the preferred modality and optimal timing/frequency. This reflects the absence of robust data in the literature and underscores the lack of biological tools to detect precancerous lesions early.

IMAGING

There are several imaging methods that can identify pancreatic cancer at an early stage. Contrast-enhanced CT and MRI according to Japanese guidelines[27] are the first methods to be performed in patients with suspected PDAC based on clinical symptoms, serum pancreatic enzymes, tumor markers and transabdominal US. They are supplemented by EUS and endoscopic retrograde cholangiopancreatography (ERCP).

A study evaluated the diagnostic accuracy of US, CT, MRI, and EUS in 200 cases of PDAC stage 0/1. Only 20% of patients were symptomatic[28]. The diagnostic accuracy was 67.5%, 98.0%, 86.5%, and 86.5%, respectively. According to some authors, CT and US are procedures with limitations in the early detection of pancreatic cancer because only indirect signs, such as pancreatic duct dilatation, localized pancreatic atrophy or local fat changes in the pancreatic parenchyma, can be detected with these methods[20].

Two systematic reviews[29,30] evaluated the performance of EUS in the diagnosis of pancreatic cancer. In the first review, EUS was shown to have higher sensitivity than CT (91%-100% *vs* 53%-91%),

while in the second review, Kitano *et al*[30] reported that EUS was more sensitive than US and CT (94% *vs* 67% and 98% *vs* 74%, respectively).

However, conventional EUS does not distinguish carcinoma from other etiologies very well because most pancreatic tumors, including benign ones, have a hypoechogenic appearance. Contrast-enhanced EUS can improve imaging of parenchymal perfusion and microvessels in pancreatic pathology. This method has higher sensitivity (94.5% *vs* 83.1%) and specificity (84.1% *vs* 78.6%) than conventional EUS [31,32].

Endoscopic ultrasonography guided fine needle aspiration (EUS-FNA) represents the first-line method for pathological diagnosis. In relation to lesion size, the accuracy of EUS-FNA is 93.4% for lesions ≥ 20 mm, 83.5% for lesions of 10-20 mm and 82.5% for lesions of 10 mm or less[33]. Sometimes CT, MRI and EUS fail to detect early stage pancreatic tumors and it is difficult to collect specimens with EUS-FNA. In this situation, especially with regard to PDAC in situ, the only available imaging finding is localized stenosis of the main pancreatic duct. Detailed evaluation of the pancreatic duct by ERCP and subsequent cytology of pancreatic juice become extremely important for diagnosis. In this context, ERCP has a sensitivity and specificity of 57.9% and 90.6%[34]. The sensitivity of pancreatic juice cytology in the diagnosis of PDAC in situ is 72.2%-100%[28,35].

ERCP is particularly useful in distinguishing autoimmune pancreatitis from PDAC, especially in patients[36] with atypical pancreatic parenchymal findings, such as focal enlargement of the pancreas and mass formation.

Ikemoto *et al*[37] proposed a recent algorithm for early diagnosis of PDAC in stage 0 and IA, with a promising long-term prognosis. In addition to pancreatic laboratory tests, US should be performed earlier in patients with risk factors in order to identify asymptomatic patients. Patients with an obvious tumor are managed according to conventional algorithms. Patients who do not have an overt pancreatic tumor but have indirect findings, such as abnormalities of the main pancreatic duct, cystic lesions or pancreatic atrophy, should be evaluated by MRI with magnetic resonance cholangiopancreatography. If the MRI shows abnormalities suggestive for PDAC, EUS-FNA is performed[37].

ARTIFICIAL INTELLIGENCE APPLIED TO IMAGING

Great hopes are now pinned on artificial intelligence (AI) for solving the most difficult problems in medicine, and these include the early diagnosis of PDAC. AI is the ability of a computer to perform functions and reasoning typical of the human mind completely autonomously. In the deepest sense, it is the ability of a machine to learn and improve automatically based on experience, provided directly through data. In this way, AI becomes a powerful tool for discovering signals that are difficult for humans to infer or describe and for expanding the frontiers of our scientific capabilities.

Muhammad *et al*[38] used AI to predict the risk of developing PDAC. By analyzing variables such as demographic data, comorbidities and family history, they built a model capable of predicting the development of PDAC with good accuracy [area under the curve (AUC) of 0.85][38,39].

The application of AI in the field of radiology is also very promising, as AI is capable of analyzing thousands of images on a pixel-by-pixel level, does not make human errors and achieves data processing in a short time[40]. Several studies have reported the application of AI in EUS image analysis of pancreatic diseases. Das *et al*[41] evaluated the performance of AI in differentiating PDAC from normal pancreas and chronic pancreatitis. The algorithm they used identified neoplasia with an AUC of 0.93. A recent study by Zhu *et al*[42] reported an overall accuracy of 94% by AI in distinguishing pancreatic cancer from chronic inflammation. CT is the most explored medical imaging modality with AI. Liu *et al*[43] reported an AUC of 0.963 for the diagnosis of PDAC using CT with the AI platform. In addition, the time to diagnosis was 20 s/case, certainly less than the time needed by radiologists. The same authors, in more recent work, found 99% accuracy for analysis based on the use of AI. In this study, AI provided higher sensitivity than radiologists (0.983 *vs* 0.929, respectively)[44]. AI missed 3 (1.7%) of 176 PDACs (1.1-1.2 cm), while radiologists missed 12 (7%) of 168 PDACs (1.0-3.3 cm), of which 11 (92%) were correctly detected by AI.

Two important ongoing projects should be noted. Project Felix is a multidisciplinary study led by Johns Hopkins University, which compared 156 PDAC cases and 300 healthy controls using deep learning computer models with manually segmented images. In an initial report, they reported a sensitivity and specificity of 94% and 99%, respectively[45]. The analysis was subsequently expanded to 575 normal patients and 750 patients with PDAC. The second ongoing project is being conducted by the Alliance of Pancreatic Cancer Consortium Imaging Working Group[46]. The goal of the project is to create a shared repository by collecting pre- and post-diagnosis CT, MRI and US images of patients with PDAC to develop AI that can predict the onset of pancreatic cancer and/or diagnose it at an early stage [47].

LIQUID BIOPSY

Serum biomarkers

Carbohydrate antigens: The most validated serum tumor marker in terms of diagnostic, prognostic and surveillance capacity for pancreatic cancer is CA19-9. The sensitivity and specificity of elevated CA19-9 to detect PDAC are 79% and 82%, respectively[48,49].

However, the use of CA19-9 has several limitations. Approximately 10% of the Caucasian population has reduced CA19-9 production due to Lewis antigen dependence. In addition, there are several conditions that result in the increase of the biomarker, such as obstructive jaundice, liver cirrhosis, chronic pancreatitis and cholangitis. The low positive predictive value of CA19-9 limits its application as a screening tool for larger populations[48,50-52]. Other carbohydrate antigens have been evaluated for early diagnosis of pancreatic cancer, such as CA125, CA72-4[53], CA50, CA199 and CA242[48,54]. The solitary diagnostic potential of these biomarkers could not be verified; however, they could help in discriminating between benign and malignant pancreatic lesions in combination with CA19-9[48].

Circulating tumor DNA and circulating tumor cells: New and interesting diagnostic tools in the field of pancreatic cancer are circulating tumor DNA (ctDNA) and circulating tumor cells (CTCs). In patients with malignancies, cell-free circulating DNA (cfDNA) molecules are released from tumor cells by apoptosis, necrosis or active release and are called ctDNA. The ctDNA contains mutations specific to the cancer cells from which they are released[55,56]. Thanks to these DNA molecules, it is therefore possible to trace the presence or absence of cancer.

However, a recent meta-analysis evaluated the role of ctDNA in the diagnosis of PDAC and found a rather low sensitivity[57]. This happens because in the early stages the rate of necrosis and apoptosis is lower and not enough ctDNA is released into the circulation (in the early stages of PDAC, only one molecule of circulating tumor DNA can be detected for every 5 mL of plasma)[57]. This challenge could be solved with technological advances, and ctDNA could become an important tool for early diagnosis.

CtDNA has been studied together with other biomarkers to improve its sensitivity and specificity. The combination of KRAS mutations in ctDNA and CA19-9 proved to be particularly interesting. Indeed, it showed a sensitivity and specificity of 0.98 and 0.77, respectively, to differentiate PDAC from chronic pancreatitis and sensitivity and specificity of 0.82 and 0.81 to differentiate PDAC from benign pancreatic tumors[56,58]. Combining the KRAS mutation in ctDNA with four protein biomarkers (CEA, CA19-9, hepatocyte growth factor and osteopontin) identified 64% of patients with pancreatic cancer with a specificity of 0.99[59]. This strategy seems to be very promising; however, it needs validation through studies on large populations.

Analysis of epigenetic alterations in cfDNA also seems to play an important role. By assessing the methylation status of two genes (*ADAMTS1* and *BNC1*) in cfDNA, it seems possible to identify pancreatic cancer early with a sensitivity of 0.95 and specificity of 0.92[60]. In a pilot study, it was reported that a model combining changes in 5-methylcytosine and 5-hydroxymethylcytosine in cfDNA achieved a sensitivity of 0.94 and specificity of 0.95, with an AUC of 0.99 for the diagnosis of PDAC[61].

The ability of targeted cfDNA methylation analysis to detect and localize multiple cancer types at all stages was evaluated. Among patients included with PDAC at different stages, a sensitivity of 0.63 in stage I, 0.83 in stage II, 0.75 in stage III and 1.0 in stage IV was found[62]. These changes in cfDNA methylation could be very useful for monitoring risk groups[63].

CTCs can be isolated tumor cells or cells organized in a group to form a tumor microthrombus[64] and are detected in 21%-100% of patients with PDAC[65]. According to some studies, they can be detected in 75%-80% of patients with early-stage tumors[66] and up to 88% of patients with precursor lesions, predominantly IPMNs[67-69]. Notably, CTCs identify patients with high-grade dysplasia, indicating its potential to stratify high-grade IPMNs against low-grade IPMNs and other benign cysts [67]. In a meta-analysis, the sensitivity, specificity and AUC for PDAC diagnosis of ctDNA, exosomes and CTCs were evaluated. They were 0.64, 0.92 and 0.94 for ctDNA, 0.93, 0.92 and 0.98 for exosomes and 0.74, 0.83 and 0.81 for CTCs, respectively[57]. This lower AUC of CTCs is due to the possibility that CTCs become trapped in the liver when traveling through the portal vein[57]. The ability to detect CTCs by analyzing portal vein blood is greatly increased. They can be found in 100% of patients with metastatic PDAC[70] and in 58% of resectable patients[71]. As with ctDNA, the low amount of CTCs in the early stages is the main factor hindering their use as biomarkers[57].

RNA, metabolites and exosomes: The most significant microRNAs are *miR-21*, *miR-25* and *miR-233*. *miR-21* has a sensitivity for early diagnosis of 0.90 and a specificity of 0.72, while *miR-25* has a sensitivity of 0.75 and 0.93, respectively[72,73]. In contrast, *miR-233* has proven useful in the differential diagnosis between benign and malignant IPMNs[74]. The microRNAs offer a cumulative sensitivity for early-stage pancreatic cancer of 0.79 and a specificity of 0.74[75]. The combined use of CA19-9 and microRNAs can improve diagnostic accuracy, especially *miR-216*[76-77].

Potentially useful biomarkers also include long non-coding (lnc)RNAs. *SNHG15* lncRNA expression is found to be increased in patients with pancreatic cancer compared to healthy controls[78]. Permuth *et al*[79] demonstrated that the differential diagnosis between malignant and nonmalignant IPMNs can be made through the combination of eight lncRNAs. In addition, some lncRNAs (*HAND2-AS1*, *CTD-*

2033D15.2 and *lncRNA-TGF*) are early markers of IPMNs[80]. Other lncRNAs that might be useful in the early detection of pancreatic cancer and IPMN are *HOTAIR*, *MALAT1*, *MEG3*, *H19*, *PVT1*, *HOTTIP*[81], *HAND2-AS1*, *CTD-2033D15.2* and *lncRNA-TGF*[82].

The role of serum metabolites in pancreatic cancer has become of interest with the advent of metabolomic technologies involving nuclear magnetic resonance and mass spectrometry[83]. An important study was performed by Michálková *et al*[84], who developed a nuclear magnetic resonance-based model that included 12 metabolites (3-hydroxybutyrate, lactate, glutamine, alanine, valine, lysine, citrate, histidine, isoleucine, glutamate, acetone and dimethylamine). The model has 94% accuracy, 100% sensitivity and 90% specificity in distinguishing patients with PDAC from healthy individuals[84].

Another study compared the metabolomic profiles of serum samples from patients with NOD and those with PDAC and NOD[85]. This identified 62 different metabolites and found that a panel including N-succinyl-L-diaminopimelic and PE (18:2) had high sensitivity (93.3%) and specificity (93.1%). Currently, studies focusing on metabolomics are expensive and consequently rare; however, it is offering great results on the early diagnosis of PDAC. Further studies are desperately needed.

Recent studies are focusing on multimarker panels in combination with CA19-9. The combined use of eight proteins (S100A11, ITGB5, PPY, ERBB3, SCAMP3, RET, 5-NT, CEACAM1) discriminated with fair accuracy between patients with early stage I/II PDAC and healthy individuals[48,86].

A new and still much to be studied chapter in PDAC concerns the study of exosomes. Kitagawa *et al*[87] studied molecules of exosomal mRNA (*CCDC88A*, *ARF6*, *Vav3* and *WASF2*) and nucleolar RNA (*SNORA14B*, *SNORA18*, *SNORA25*, *SNORA74A* and *SNORD22*) and obtained excellent results for early-stage neoplasia. Tumor-specific expression of exosome surface proteins, the so-called tumor-specific surfaceome, can also be analyzed. Castillo *et al*[88] characterized six PDAC-specific surfaceome proteins, such as CLDN4, EPCAM, CD151, LGALS3BP, HIST2H2BE and HIST2H2BF. These proteins were suggested as promising biomarkers for PDAC diagnosis by the authors. Yu *et al*[89] developed a signature with long RNAs from plasma extracellular vesicles. This signature identified stage I/II pancreatic cancer with very high accuracy and performed better than CA19-9 in distinguishing PDAC from chronic pancreatitis (AUC 0.931 *vs* 0.873)[89]. Serum biomarkers are summarized in Table 1.

Pancreatic juice and pancreatic cyst fluid

In addition to blood, other body materials can be exploited to diagnose PDAC. For example, pancreatic juice collected during ERCP and cyst fluid obtained by EUS-FNA can be analyzed for specific markers. They include KRAS and GNAS mutants (the latter specific for IPMNs) as well as TP53, SMAD4, PIK3CA, PTEN and AKT1, which are generally related to IPMN-associated tumors[90-92].

Biomarkers still under study include mucins (MUCs). Normal pancreatic tissue expresses low levels of MUCs, whereas in branch duct IPMNs there is upregulation of the mucin gene and even more pronounced changes in PDAC[93-95]. MUC4 and MUC16 are 100% specific for pancreatic cancer but have sensitivities of 63% and 67%, respectively[95]. The combined biomarker panel consisting of MUC5AC and CA19-9 also showed excellent performance in distinguishing pancreatic cancer subjects from healthy controls[96].

It also seems possible to distinguish pancreatic cystic lesions with high-grade dysplasia or malignancy by assessing interleukins (IL-1b, IL-5 and IL-8) present in pancreatic juice or by using the monoclonal antibody Das-1. Das-1 can detect pancreatic cysts at risk of malignancy with a sensitivity of 88% and specificity of 98%[97-99].

In recent work by Majumder *et al*[100], a panel of three methylated DNA markers (C13orf18, FER1L4 and BMP3) in pancreatic juice discriminated cases from controls with good accuracy. Using a specificity cutoff value of 86%, the panel distinguished patients with any stage of pancreatic cancer from controls with a sensitivity of 83% and identified patients with stage I or II PDAC or IPMN with high-grade dysplasia with a sensitivity of 80%[100].

Saliva

Progress has also been made in saliva evaluation. A recent study[101] identified seven upregulated genes (*MBD3L2*, *KRAS*, *STIM2*, *DMXL2*, *ACRV1*, *DMD* and *CABLES1*) and five downregulated genes (*TK2*, *GLTSCR2*, *CDKL3*, *TPT1* and *DPM1*) in subjects with PDAC compared with healthy controls or those with chronic pancreatitis. It was possible to discriminate patients with pancreatic cancer with sensitivity and specificity greater than 90% by combining the mRNAs of *MBD3L2*, *KRAS*, *ACRV1* and *DPM1*[101]. Xie *et al*[102] evaluated the expression of lncRNAs and found an upregulation of *HOTAIR* and *PV1T* in the PDAC group compared with controls and benign pancreatic cancers. The combination of salivary *HOTAIR* and *PVT1* differentiated PDAC from healthy controls with a sensitivity of 78.2% and specificity of 90.9% and PDAC from benign tumors with a sensitivity of 81.8% and specificity of 95%[103].

Urine

Radon *et al*[104] used three protein biomarkers (REG1A, TFF1 and LYVE1) to form a powerful urinary panel that could detect patients with stage I-II PDAC with an accuracy of more than 90%. Brezgyte *et al*[105] found increased levels of *miR-143*, *miR-204* and *miR-223* and reduced levels of *miR-30e* in the urine

Table 1 Serum biomarkers

Carbohydrate antigens	CtDNA	miRNA	lncRNA	Metabolites
CA19-9	KRAS	*miR21*	*SNHG15*	3-hydroxybutyrate
CA125	ADAMTS1	*miR25*	*HOTAIR*	Lactate
CA72-4	BNC1	*miR233*	*MALAT1*	Glutamine
CA50	5-methylcytosine	*miR216*	*MEG3*	Alanine
CA242	5-hydroxymethylcytosine	*miR-92-a-5p*	*H19*	Valine
		miR-125b-3p	*PVT1*	Lysine
		miR-532e5p	*HOTTIP*	Citrate
		miR-663	*HAND2-AS1*	Histidine
		miR-1469	*CTD-2033D15.2*	Isoleucine
				Glutamate
				Acetone
				Dimethylamine
				N-succinyl-L-diaminopimelic
				PE (18:2)
Exosomal mRNA molecules	**Exosomal small nucleolar RNA molecules**	**Exosome surfaceome**	**Exosomal long RNAs**	**Others**
CCDC88A	*SNORA14B*	*CLDN4*	*FGA*	CTCs
ARF6	*SNORA18*	*EPCAM*	*KRT19*	ITGB5
Vav3	*SNORA25*	*CD151*	*HIST1H2BK*	PPY
WASF2	*SNORA74A*	*LGAL53BP*	*ITIH2*	ERBB3
	SNORD22	*HIST2H2BE*	*MARCH2*	SCAMP3
		HIST2H2BF	*CLDN1*	RET
			MAL2	5-NT
			TIMP1	CEACAM1
				S100A11

CtDNA: Circulation tumor DNA; miRNA: MicroRNA; lncRNA: Long non-coding RNA; CTC: Circulating tumor cells.

of patients with stage I PDAC compared with the healthy population. However, further studies are needed to validate their clinical utility.

A case-control study that included 914 PDAC patients found the superiority of a panel of metabolites (proline, sphingomyelin, phosphatidylcholine, isocitrate, sphinganine-1-phosphate, histidine, pyruvate, ceramide, sphingomyelin) over CA19-9 in discriminating early-stage PDAC from chronic pancreatitis [106]. According to the authors, the metabolic panel could result in changes in the diagnostic pathway and treatment stratification for one-third of the included patients[106]. Biomarkers of pancreatic juice and cystic fluid, saliva and urine are listed in Table 2.

ARTIFICIAL INTELLIGENCE AND BIOMARKERS

AI can be applied to the identification of biomarkers. Zhang *et al*[107] identified a nine gene pair signature that can distinguish PDAC patients from non-PDAC patients. Alizadeh Savareh *et al*[108] evaluated the best miRNAs using a machine learning method to aid in the early detection of PDAC. The final model included *miR-92a-2-5p*, *miR-125b-3p*, *miR-532e5p*, *miR-663a and miR-1469* with a high performance in differentiating PDAC from controls (accuracy, 0.93; sensitivity, 0.93 and specificity, 0.92).

Table 2 Pancreatic juice and cyst fluid biomarkers, saliva biomarkers, urine biomarkers

Pancreatic juice and cyst fluid biomarkers			
Mutant genes	**Mucins**	**Interleukins**	**Methylated DNA markers**
GNAS	MUC4	IL-1b	C13orf18
KRAS	MUC16	IL-5	FER1L4
TP53	MUC5AC	IL-8	BMP3
SMAD4			
PIK3CA			
PTEN			
AKT1			
Saliva biomarkers			
Upregulated genes	**Downregulated genes**	**LncRNA**	
MBD3L2	*TK2*	*HOTAIR*	
KRAS	*GLTSCR2*	*PVT1*	
STIM2	*CDKL3*		
DMXL2	*TPT1*		
ACRV1	*DPM1*		
DMD			
CABLES1			
Urine biomarkers			
Protein markers	**MiRNA**	**Metabolites**	
REG1A	*miR-143*	CA19.9	
TFF1	*miR-204*	Proline	
LYVE1	*miR-223*	Sphingomyelin (d18:2, C17:0)	
	miR-30e	Phosphatidylcholine	
		Isocitrate	
		Sphinganine-1-phosphate	
		Histidine	
		Pyruvate	
		Sphingomyelin (d17:1, C18:0)	

miRNA: MicroRNA; lncRNA: Long non-coding RNA.

WHAT STRATEGIES TO AVOID A FORETOLD CATASTROPHE

As we have already mentioned in the introduction, the current predictions for PDAC give us a glimpse of a catastrophe on the horizon. If the increase in annual PDAC cases continues at the current rate, we will soon have a staggering number of cases without the weapons to stem this foretold catastrophe. The only option is to arm ourselves and not arrive unprepared for this hard battle. What strategies should we adopt to prepare for this ordeal? Undoubtedly first, we need to make academia, industry and the politics/economic world understand the urgency of finding solutions quickly, trying to interact with each other according to specific competencies. On the one hand, academia and industry will have to move forward together, as quickly as possible, in those research paths that we have broadly summarized in this article. On the other hand, the political/economic world, made aware of the emergency to be faced, will have to commit itself both to allocating more funding for research in this field and to lavishing more funding on public health. If public health had sufficient funds to subject all patients of a certain age to a simple screening ultrasound of the abdomen, perhaps many patients could be saved. But at present, with current resources, this scenario remains a pipe dream.

CONCLUSION

In this article, we have summarized all the possible strategies we have available today for the early detection of PDAC and the paths that research must pursue to make this goal ever closer. Unfortunately, in 2022 the results for this type of cancer still remain discouraging, while a catastrophic increase in cases is expected in the coming years. The article has been written with the aim of highlighting the urgency of devoting more attention and resources to this pathology in order to reach a solution that seems more and more unreachable every day.

FOOTNOTES

Author contributions: Tonini V and Zanni M contributed equally to this work; Both authors designed the research study, wrote the manuscript and read and approved the final manuscript.

Conflict-of-interest statement: All authors report no relevant conflicts of interest for this article.

Open-Access: This article is an open-access article that was selected by an in-house editor and fully peer-reviewed by external reviewers. It is distributed in accordance with the Creative Commons Attribution NonCommercial (CC BY-NC 4.0) license, which permits others to distribute, remix, adapt, build upon this work non-commercially, and license their derivative works on different terms, provided the original work is properly cited and the use is non-commercial. See: https://creativecommons.org/Licenses/by-nc/4.0/

Country/Territory of origin: Italy

ORCID number: Valeria Tonini 0000-0003-3130-2928; Manuel Zanni 0000-0001-7732-7739.

S-Editor: Ma YJ
L-Editor: Filipodia
P-Editor: Ma YJ

REFERENCES

1 **Rahib L**, Smith BD, Aizenberg R, Rosenzweig AB, Fleshman JM, Matrisian LM. Projecting cancer incidence and deaths to 2030: the unexpected burden of thyroid, liver, and pancreas cancers in the United States. *Cancer Res* 2014; **74**: 2913-2921 [PMID: 24840647 DOI: 10.1158/0008-5472.CAN-14-0155]
2 **Sung H**, Ferlay J, Siegel RL, Laversanne M, Soerjomataram I, Jemal A, Bray F. Global Cancer Statistics 2020: GLOBOCAN Estimates of Incidence and Mortality Worldwide for 36 Cancers in 185 Countries. *CA Cancer J Clin* 2021; **71**: 209-249 [PMID: 33538338 DOI: 10.3322/caac.21660]
3 **Oldfield LE**, Connor AA, Gallinger S. Molecular Events in the Natural History of Pancreatic Cancer. *Trends Cancer* 2017; **3**: 336-346 [PMID: 28718411 DOI: 10.1016/j.trecan.2017.04.005]
4 **Bengtsson A**, Andersson R, Ansari D. The actual 5-year survivors of pancreatic ductal adenocarcinoma based on real-world data. *Sci Rep* 2020; **10**: 16425 [PMID: 33009477 DOI: 10.1038/s41598-020-73525-y]
5 **Siegel RL**, Miller KD, Jemal A. Cancer statistics, 2020. *CA Cancer J Clin* 2020; **70**: 7-30 [PMID: 31912902 DOI: 10.3322/caac.21590]
6 **Grasso C**, Jansen G, Giovannetti E. Drug resistance in pancreatic cancer: Impact of altered energy metabolism. *Crit Rev Oncol Hematol* 2017; **114**: 139-152 [PMID: 28477742 DOI: 10.1016/j.critrevonc.2017.03.026]
7 **Ishii Y**, Serikawa M, Tsuboi T, Kawamura R, Tsushima K, Nakamura S, Hirano T, Fukiage A, Mori T, Ikemoto J, Kiyoshita Y, Saeki S, Tamura Y, Miyamoto S, Chayama K. Role of Endoscopic Ultrasonography and Endoscopic Retrograde Cholangiopancreatography in the Diagnosis of Pancreatic Cancer. *Diagnostics (Basel)* 2021; **11** [PMID: 33557084 DOI: 10.3390/diagnostics11020238]
8 **Egawa S**, Toma H, Ohigashi H, Okusaka T, Nakao A, Hatori T, Maguchi H, Yanagisawa A, Tanaka M. Japan Pancreatic Cancer Registry; 30th year anniversary: Japan Pancreas Society. *Pancreas* 2012; **41**: 985-992 [PMID: 22750974 DOI: 10.1097/MPA.0b013e318258055c]
9 **Singhi AD**, Koay EJ, Chari ST, Maitra A. Early Detection of Pancreatic Cancer: Opportunities and Challenges. *Gastroenterology* 2019; **156**: 2024-2040 [PMID: 30721664 DOI: 10.1053/j.gastro.2019.01.259]
10 **Carreras-Torres R**, Johansson M, Gaborieau V, Haycock PC, Wade KH, Relton CL, Martin RM, Davey Smith G, Brennan P. The Role of Obesity, Type 2 Diabetes, and Metabolic Factors in Pancreatic Cancer: A Mendelian Randomization Study. *J Natl Cancer Inst* 2017; **109** [PMID: 28954281 DOI: 10.1093/jnci/djx012]
11 **Michl P**, Löhr M, Neoptolemos JP, Capurso G, Rebours V, Malats N, Ollivier M, Ricciardiello L. UEG position paper on pancreatic cancer. Bringing pancreatic cancer to the 21st century: Prevent, detect, and treat the disease earlier and better. *United European Gastroenterol J* 2021; **9**: 860-871 [PMID: 34431604 DOI: 10.1002/ueg2.12123]
12 **Hu JX**, Zhao CF, Chen WB, Liu QC, Li QW, Lin YY, Gao F. Pancreatic cancer: A review of epidemiology, trend, and risk factors. *World J Gastroenterol* 2021; **27**: 4298-4321 [PMID: 34366606 DOI: 10.3748/wjg.v27.i27.4298]
13 **Klein AP**. Pancreatic cancer epidemiology: understanding the role of lifestyle and inherited risk factors. *Nat Rev*

Gastroenterol Hepatol 2021; **18**: 493-502 [PMID: 34002083 DOI: 10.1038/s41575-021-00457-x]

14 **McKenzie F**, Biessy C, Ferrari P, Freisling H, Rinaldi S, Chajès V, Dahm CC, Overvad K, Dossus L, Lagiou P, Trichopoulos D, Trichopoulou A, Bueno-de-Mesquita HB, May A, Peeters PH, Weiderpass E, Sanchez MJ, Navarro C, Ardanaz E, Ericson U, Wirfält E, Travis RC, Romieu I. Healthy Lifestyle and Risk of Cancer in the European Prospective Investigation Into Cancer and Nutrition Cohort Study. *Medicine (Baltimore)* 2016; **95**: e2850 [PMID: 27100409 DOI: 10.1097/MD.0000000000002850]

15 **Ferrari P**, Licaj I, Muller DC, Kragh Andersen P, Johansson M, Boeing H, Weiderpass E, Dossus L, Dartois L, Fagherazzi G, Bradbury KE, Khaw KT, Wareham N, Duell EJ, Barricarte A, Molina-Montes E, Sanchez CN, Arriola L, Wallström P, Tjønneland A, Olsen A, Trichopoulou A, Benetou V, Trichopoulos D, Tumino R, Agnoli C, Sacerdote C, Palli D, Li K, Kaaks R, Peeters P, Beulens JW, Nunes L, Gunter M, Norat T, Overvad K, Brennan P, Riboli E, Romieu I. Lifetime alcohol use and overall and cause-specific mortality in the European Prospective Investigation into Cancer and nutrition (EPIC) study. *BMJ Open* 2014; **4**: e005245 [PMID: 24993766 DOI: 10.1136/bmjopen-2014-005245]

16 **Yuan C**, Babic A, Khalaf N, Nowak JA, Brais LK, Rubinson DA, Ng K, Aguirre AJ, Pandharipande PV, Fuchs CS, Giovannucci EL, Stampfer MJ, Rosenthal MH, Sander C, Kraft P, Wolpin BM. Diabetes, Weight Change, and Pancreatic Cancer Risk. *JAMA Oncol* 2020; **6**: e202948 [PMID: 32789511 DOI: 10.1001/jamaoncol.2020.2948]

17 **Roy A**, Sahoo J, Kamalanathan S, Naik D, Mohan P, Kalayarasan R. Diabetes and pancreatic cancer: Exploring the two-way traffic. *World J Gastroenterol* 2021; **27**: 4939-4962 [PMID: 34497428 DOI: 10.3748/wjg.v27.i30.4939]

18 **US Preventive Services Task Force**, Owens DK, Davidson KW, Krist AH, Barry MJ, Cabana M, Caughey AB, Curry SJ, Doubeni CA, Epling JW Jr, Kubik M, Landefeld CS, Mangione CM, Pbert L, Silverstein M, Simon MA, Tseng CW, Wong JB. Screening for Pancreatic Cancer: US Preventive Services Task Force Reaffirmation Recommendation Statement. *JAMA* 2019; **322**: 438-444 [PMID: 31386141 DOI: 10.1001/jama.2019.10232]

19 **Pelaez-Luna M**, Takahashi N, Fletcher JG, Chari ST. Resectability of presymptomatic pancreatic cancer and its relationship to onset of diabetes: a retrospective review of CT scans and fasting glucose values prior to diagnosis. *Am J Gastroenterol* 2007; **102**: 2157-2163 [PMID: 17897335 DOI: 10.1111/j.1572-0241.2007.01480.x]

20 **Yang J**, Xu R, Wang C, Qiu J, Ren B, You L. Early screening and diagnosis strategies of pancreatic cancer: a comprehensive review. *Cancer Commun (Lond)* 2021; **41**: 1257-1274 [PMID: 34331845 DOI: 10.1002/cac2.12204]

21 **Sharma A**, Kandlakunta H, Nagpal SJS, Feng Z, Hoos W, Petersen GM, Chari ST. Model to Determine Risk of Pancreatic Cancer in Patients With New-Onset Diabetes. *Gastroenterology* 2018; **155**: 730-739.e3 [PMID: 29775599 DOI: 10.1053/j.gastro.2018.05.023]

22 **Goggins M**, Overbeek KA, Brand R, Syngal S, Del Chiaro M, Bartsch DK, Bassi C, Carrato A, Farrell J, Fishman EK, Fockens P, Gress TM, van Hooft JE, Hruban RH, Kastrinos F, Klein A, Lennon AM, Lucas A, Park W, Rustgi A, Simeone D, Stoffel E, Vasen HFA, Cahen DL, Canto MI, Bruno M; International Cancer of the Pancreas Screening (CAPS) consortium. Management of patients with increased risk for familial pancreatic cancer: updated recommendations from the International Cancer of the Pancreas Screening (CAPS) Consortium. *Gut* 2020; **69**: 7-17 [PMID: 31672839 DOI: 10.1136/gutjnl-2019-319352]

23 **Pereira SP**, Oldfield L, Ney A, Hart PA, Keane MG, Pandol SJ, Li D, Greenhalf W, Jeon CY, Koay EJ, Almario CV, Halloran C, Lennon AM, Costello E. Early detection of pancreatic cancer. *Lancet Gastroenterol Hepatol* 2020; **5**: 698-710 [PMID: 32135127 DOI: 10.1016/S2468-1253(19)30416-9]

24 **European Study Group on Cystic Tumours of the Pancreas**. European evidence-based guidelines on pancreatic cystic neoplasms. *Gut* 2018; **67**: 789-804 [PMID: 29574408 DOI: 10.1136/gutjnl-2018-316027]

25 **Tanaka M**, Fernández-Del Castillo C, Kamisawa T, Jang JY, Levy P, Ohtsuka T, Salvia R, Shimizu Y, Tada M, Wolfgang CL. Revisions of international consensus Fukuoka guidelines for the management of IPMN of the pancreas. *Pancreatology* 2017; **17**: 738-753 [PMID: 28735806 DOI: 10.1016/j.pan.2017.07.007]

26 **Aslanian HR**, Lee JH, Canto MI. AGA Clinical Practice Update on Pancreas Cancer Screening in High-Risk Individuals: Expert Review. *Gastroenterology* 2020; **159**: 358-362 [PMID: 32416142 DOI: 10.1053/j.gastro.2020.03.088]

27 **Okusaka T**, Nakamura M, Yoshida M, Kitano M, Uesaka K, Ito Y, Furuse J, Hanada K, Okazaki K; Committee for Revision of Clinical Guidelines for Pancreatic Cancer of the Japan Pancreas Society. Clinical Practice Guidelines for Pancreatic Cancer 2019 From the Japan Pancreas Society: A Synopsis. *Pancreas* 2020; **49**: 326-335 [PMID: 32132516 DOI: 10.1097/MPA.0000000000001513]

28 **Kanno A**, Masamune A, Hanada K, Maguchi H, Shimizu Y, Ueki T, Hasebe O, Ohtsuka T, Nakamura M, Takenaka M, Kitano M, Kikuyama M, Gabata T, Yoshida K, Sasaki T, Serikawa M, Furukawa T, Yanagisawa A, Shimosegawa T; Japan Study Group on the Early Detection of Pancreatic Cancer (JEDPAC). Multicenter study of early pancreatic cancer in Japan. *Pancreatology* 2018; **18**: 61-67 [PMID: 29170051 DOI: 10.1016/j.pan.2017.11.007]

29 **Dewitt J**, Devereaux BM, Lehman GA, Sherman S, Imperiale TF. Comparison of endoscopic ultrasound and computed tomography for the preoperative evaluation of pancreatic cancer: a systematic review. *Clin Gastroenterol Hepatol* 2006; **4**: 717-25; quiz 664 [PMID: 16675307 DOI: 10.1016/j.cgh.2006.02.020]

30 **Kitano M**, Yoshida T, Itonaga M, Tamura T, Hatamaru K, Yamashita Y. Impact of endoscopic ultrasonography on diagnosis of pancreatic cancer. *J Gastroenterol* 2019; **54**: 19-32 [PMID: 30406288 DOI: 10.1007/s00535-018-1519-2]

31 **Bunganič B**, Laclav M, Dvořáková T, Bradáč O, Traboulsi E, Suchánek Š, Frič P, Zavoral M. Accuracy of EUS and CEH EUS for the diagnosis of pancreatic tumours. *Scand J Gastroenterol* 2018; **53**: 1411-1417 [PMID: 30394143 DOI: 10.1080/00365521.2018.1524023]

32 **Yamashita Y**, Shimokawa T, Napoléon B, Fusaroli P, Gincul R, Kudo M, Kitano M. Value of contrast-enhanced harmonic endoscopic ultrasonography with enhancement pattern for diagnosis of pancreatic cancer: A meta-analysis. *Dig Endosc* 2019; **31**: 125-133 [PMID: 30338569 DOI: 10.1111/den.13290]

33 **Haba S**, Yamao K, Bhatia V, Mizuno N, Hara K, Hijioka S, Imaoka H, Niwa Y, Tajika M, Kondo S, Tanaka T, Shimizu Y, Yatabe Y, Hosoda W, Kawakami H, Sakamoto N. Diagnostic ability and factors affecting accuracy of endoscopic ultrasound-guided fine needle aspiration for pancreatic solid lesions: Japanese large single center experience. *J Gastroenterol* 2013; **48**: 973-981 [PMID: 23090002 DOI: 10.1007/s00535-012-0695-8]

34 **Li H**, Hu Z, Chen J, Guo X. Comparison of ERCP, EUS, and ERCP combined with EUS in diagnosing pancreatic

neoplasms: a systematic review and meta-analysis. *Tumour Biol* 2014; **35**: 8867-8874 [PMID: 24891188 DOI: 10.1007/s13277-014-2154-z]

35 **Kawamura R**, Ishii Y, Serikawa M, Tsuboi T, Tsushima K, Nakamura S, Hirano T, Ikemoto J, Kiyoshita Y, Saeki S, Tamura Y, Miyamoto S, Nakamura K, Furukawa M, Ishida K, Arihiro K, Uemura K, Aikata H. Optimal indication of endoscopic retrograde pancreatography-based cytology in the preoperative pathological diagnosis of pancreatic ductal adenocarcinoma. *Pancreatology* 2022; **22**: 414-420 [PMID: 35219581 DOI: 10.1016/j.pan.2022.02.001]

36 **Kawa S**, Kamisawa T, Notohara K, Fujinaga Y, Inoue D, Koyama T, Okazaki K. Japanese Clinical Diagnostic Criteria for Autoimmune Pancreatitis, 2018: Revision of Japanese Clinical Diagnostic Criteria for Autoimmune Pancreatitis, 2011. *Pancreas* 2020; **49**: e13-e14 [PMID: 31856100 DOI: 10.1097/MPA.0000000000001443]

37 **Ikemoto J**, Serikawa M, Hanada K, Eguchi N, Sasaki T, Fujimoto Y, Sugiyama S, Yamaguchi A, Noma B, Kamigaki M, Minami T, Okazaki A, Yukutake M, Ishii Y, Mouri T, Shimizu A, Tsuboi T, Arihiro K, Chayama K. Clinical Analysis of Early-Stage Pancreatic Cancer and Proposal for a New Diagnostic Algorithm: A Multicenter Observational Study. *Diagnostics (Basel)* 2021; **11** [PMID: 33673151 DOI: 10.3390/diagnostics11020287]

38 **Muhammad W**, Hart GR, Nartowt B, Farrell JJ, Johung K, Liang Y, Deng J. Pancreatic Cancer Prediction Through an Artificial Neural Network. *Front Artif Intell* 2019; **2**: 2 [PMID: 33733091 DOI: 10.3389/frai.2019.00002]

39 **Hayashi H**, Uemura N, Matsumura K, Zhao L, Sato H, Shiraishi Y, Yamashita YI, Baba H. Recent advances in artificial intelligence for pancreatic ductal adenocarcinoma. *World J Gastroenterol* 2021; **27**: 7480-7496 [PMID: 34887644 DOI: 10.3748/wjg.v27.i43.7480]

40 **Mendoza Ladd A**, Diehl DL. Artificial intelligence for early detection of pancreatic adenocarcinoma: The future is promising. *World J Gastroenterol* 2021; **27**: 1283-1295 [PMID: 33833482 DOI: 10.3748/wjg.v27.i13.1283]

41 **Das A**, Nguyen CC, Li F, Li B. Digital image analysis of EUS images accurately differentiates pancreatic cancer from chronic pancreatitis and normal tissue. *Gastrointest Endosc* 2008; **67**: 861-867 [PMID: 18179797 DOI: 10.1016/j.gie.2007.08.036]

42 **Zhu M**, Xu C, Yu J, Wu Y, Li C, Zhang M, Jin Z, Li Z. Differentiation of pancreatic cancer and chronic pancreatitis using computer-aided diagnosis of endoscopic ultrasound (EUS) images: a diagnostic test. *PLoS One* 2013; **8**: e63820 [PMID: 23704940 DOI: 10.1371/journal.pone.0063820]

43 **Liu SL**, Li S, Guo YT, Zhou YP, Zhang ZD, Lu Y. Establishment and application of an artificial intelligence diagnosis system for pancreatic cancer with a faster region-based convolutional neural network. *Chin Med J (Engl)* 2019; **132**: 2795-2803 [PMID: 31856050 DOI: 10.1097/CM9.0000000000000544]

44 **Liu KL**, Wu T, Chen PT, Tsai YM, Roth H, Wu MS, Liao WC, Wang W. Deep learning to distinguish pancreatic cancer tissue from non-cancerous pancreatic tissue: a retrospective study with cross-racial external validation. *Lancet Digit Health* 2020; **2**: e303-e313 [PMID: 33328124 DOI: 10.1016/S2589-7500(20)30078-9]

45 **Chu LC**, Park S, Kawamoto S, Wang Y, Zhou Y, Shen W, Zhu Z, Xia Y, Xie L, Liu F, Yu Q, Fouladi DF, Shayesteh S, Zinreich E, Graves JS, Horton KM, Yuille AL, Hruban RH, Kinzler KW, Vogelstein B, Fishman EK. Application of Deep Learning to Pancreatic Cancer Detection: Lessons Learned From Our Initial Experience. *J Am Coll Radiol* 2019; **16**: 1338-1342 [PMID: 31492412 DOI: 10.1016/j.jacr.2019.05.034]

46 **Young MR**, Abrams N, Ghosh S, Rinaudo JAS, Marquez G, Srivastava S. Prediagnostic Image Data, Artificial Intelligence, and Pancreatic Cancer: A Tell-Tale Sign to Early Detection. *Pancreas* 2020; **49**: 882-886 [PMID: 32675784 DOI: 10.1097/MPA.0000000000001603]

47 **Kenner B**, Chari ST, Kelsen D, Klimstra DS, Pandol SJ, Rosenthal M, Rustgi AK, Taylor JA, Yala A, Abul-Husn N, Andersen DK, Bernstein D, Brunak S, Canto MI, Eldar YC, Fishman EK, Fleshman J, Go VLW, Holt JM, Field B, Goldberg A, Hoos W, Iacobuzio-Donahue C, Li D, Lidgard G, Maitra A, Matrisian LM, Poblete S, Rothschild L, Sander C, Schwartz LH, Shalit U, Srivastava S, Wolpin B. Artificial Intelligence and Early Detection of Pancreatic Cancer: 2020 Summative Review. *Pancreas* 2021; **50**: 251-279 [PMID: 33835956 DOI: 10.1097/MPA.0000000000001762]

48 **Sturm N**, Ettrich TJ, Perkhofer L. The Impact of Biomarkers in Pancreatic Ductal Adenocarcinoma on Diagnosis, Surveillance and Therapy. *Cancers (Basel)* 2022; **14** [PMID: 35008381 DOI: 10.3390/cancers14010217]

49 **Fahrmann JF**, Schmidt CM, Mao X, Irajizad E, Loftus M, Zhang J, Patel N, Vykoukal J, Dennison JB, Long JP, Do KA, Chabot JA, Kluger MD, Kastrinos F, Brais L, Babic A, Jajoo K, Lee LS, Clancy TE, Ng K, Bullock A, Genkinger J, Yip-Schneider MT, Maitra A, Wolpin BM, Hanash S. Lead-Time Trajectory of CA19-9 as an Anchor Marker for Pancreatic Cancer Early Detection. *Gastroenterology* 2021; **160**: 1373-1383.e6 [PMID: 33333055 DOI: 10.1053/j.gastro.2020.11.052]

50 **Luo G**, Fan Z, Cheng H, Jin K, Guo M, Lu Y, Yang C, Fan K, Huang Q, Long J, Liu L, Xu J, Lu R, Ni Q, Warshaw AL, Liu C, Yu X. New observations on the utility of CA19-9 as a biomarker in Lewis negative patients with pancreatic cancer. *Pancreatology* 2018; **18**: 971-976 [PMID: 30131287 DOI: 10.1016/j.pan.2018.08.003]

51 **Loosen SH**, Neumann UP, Trautwein C, Roderburg C, Luedde T. Current and future biomarkers for pancreatic adenocarcinoma. *Tumour Biol* 2017; **39**: 1010428317692231 [PMID: 28618958 DOI: 10.1177/1010428317692231]

52 **Lee T**, Teng TZJ, Shelat VG. Carbohydrate antigen 19-9 - tumor marker: Past, present, and future. *World J Gastrointest Surg* 2020; **12**: 468-490 [PMID: 33437400 DOI: 10.4240/wjgs.v12.i12.468]

53 **Wang Z**, Tian YP. Clinical value of serum tumor markers CA19-9, CA125 and CA72-4 in the diagnosis of pancreatic carcinoma. *Mol Clin Oncol* 2014; **2**: 265-268 [PMID: 24649344 DOI: 10.3892/mco.2013.226]

54 **Dou H**, Sun G, Zhang L. CA242 as a biomarker for pancreatic cancer and other diseases. *Prog Mol Biol Transl Sci* 2019; **162**: 229-239 [PMID: 30905452 DOI: 10.1016/bs.pmbts.2018.12.007]

55 **Buscail E**, Maulat C, Muscari F, Chiche L, Cordelier P, Dabernat S, Alix-Panabières C, Buscail L. Liquid Biopsy Approach for Pancreatic Ductal Adenocarcinoma. *Cancers (Basel)* 2019; **11** [PMID: 31248203 DOI: 10.3390/cancers11060852]

56 **Heredia-Soto V**, Rodríguez-Salas N, Feliu J. Liquid Biopsy in Pancreatic Cancer: Are We Ready to Apply It in the Clinical Practice? *Cancers (Basel)* 2021; **13** [PMID: 33924143 DOI: 10.3390/cancers13081986]

57 **Zhu Y**, Zhang H, Chen N, Hao J, Jin H, Ma X. Diagnostic value of various liquid biopsy methods for pancreatic cancer: A systematic review and meta-analysis. *Medicine (Baltimore)* 2020; **99**: e18581 [PMID: 32011436 DOI:

10.1097/MD.0000000000018581]
58 **Wang ZY**, Ding XQ, Zhu H, Wang RX, Pan XR, Tong JH. *KRAS* Mutant Allele Fraction in Circulating Cell-Free DNA Correlates With Clinical Stage in Pancreatic Cancer Patients. *Front Oncol* 2019; **9**: 1295 [PMID: 31850201 DOI: 10.3389/fonc.2019.01295]
59 **Cohen JD**, Javed AA, Thoburn C, Wong F, Tie J, Gibbs P, Schmidt CM, Yip-Schneider MT, Allen PJ, Schattner M, Brand RE, Singhi AD, Petersen GM, Hong SM, Kim SC, Falconi M, Doglioni C, Weiss MJ, Ahuja N, He J, Makary MA, Maitra A, Hanash SM, Dal Molin M, Wang Y, Li L, Ptak J, Dobbyn L, Schaefer J, Silliman N, Popoli M, Goggins MG, Hruban RH, Wolfgang CL, Klein AP, Tomasetti C, Papadopoulos N, Kinzler KW, Vogelstein B, Lennon AM. Combined circulating tumor DNA and protein biomarker-based liquid biopsy for the earlier detection of pancreatic cancers. *Proc Natl Acad Sci U S A* 2017; **114**: 10202-10207 [PMID: 28874546 DOI: 10.1073/pnas.1704961114]
60 **Eissa MAL**, Lerner L, Abdelfatah E, Shankar N, Canner JK, Hasan NM, Yaghoobi V, Huang B, Kerner Z, Takaesu F, Wolfgang C, Kwak R, Ruiz M, Tam M, Pisanic TR 2nd, Iacobuzio-Donahue CA, Hruban RH, He J, Wang TH, Wood LD, Sharma A, Ahuja N. Promoter methylation of ADAMTS1 and BNC1 as potential biomarkers for early detection of pancreatic cancer in blood. *Clin Epigenetics* 2019; **11**: 59 [PMID: 30953539 DOI: 10.1186/s13148-019-0650-0]
61 **Cao F**, Wei A, Hu X, He Y, Zhang J, Xia L, Tu K, Yuan J, Guo Z, Liu H, Xie D, Li A. Integrated epigenetic biomarkers in circulating cell-free DNA as a robust classifier for pancreatic cancer. *Clin Epigenetics* 2020; **12**: 112 [PMID: 32703318 DOI: 10.1186/s13148-020-00898-2]
62 **Liu MC**, Oxnard GR, Klein EA, Swanton C, Seiden MV; CCGA Consortium. Sensitive and specific multi-cancer detection and localization using methylation signatures in cell-free DNA. *Ann Oncol* 2020; **31**: 745-759 [PMID: 33506766 DOI: 10.1016/j.annonc.2020.02.011]
63 **Brancaccio M**, Natale F, Falco G, Angrisano T. Cell-Free DNA Methylation: The New Frontiers of Pancreatic Cancer Biomarkers' Discovery. *Genes (Basel)* 2019; **11** [PMID: 31877923 DOI: 10.3390/genes11010014]
64 **Yeo D**, Bastian A, Strauss H, Saxena P, Grimison P, Rasko JEJ. Exploring the Clinical Utility of Pancreatic Cancer Circulating Tumor Cells. *Int J Mol Sci* 2022; **23** [PMID: 35163592 DOI: 10.3390/ijms23031671]
65 **Kaczor-Urbanowicz KE**, Cheng J, King JC, Sedarat A, Pandol SJ, Farrell JJ, Wong DTW, Kim Y. Reviews on Current Liquid Biopsy for Detection and Management of Pancreatic Cancers. *Pancreas* 2020; **49**: 1141-1152 [PMID: 33003085 DOI: 10.1097/MPA.0000000000001662]
66 **Ankeny JS**, Court CM, Hou S, Li Q, Song M, Wu D, Chen JF, Lee T, Lin M, Sho S, Rochefort MM, Girgis MD, Yao J, Wainberg ZA, Muthusamy VR, Watson RR, Donahue TR, Hines OJ, Reber HA, Graeber TG, Tseng HR, Tomlinson JS. Circulating tumour cells as a biomarker for diagnosis and staging in pancreatic cancer. *Br J Cancer* 2016; **114**: 1367-1375 [PMID: 27300108 DOI: 10.1038/bjc.2016.121]
67 **Poruk KE**, Valero V 3rd, He J, Ahuja N, Cameron JL, Weiss MJ, Lennon AM, Goggins M, Wood LD, Wolfgang CL. Circulating Epithelial Cells in Intraductal Papillary Mucinous Neoplasms and Cystic Pancreatic Lesions. *Pancreas* 2017; **46**: 943-947 [PMID: 28697136 DOI: 10.1097/MPA.0000000000000869]
68 **Franses JW**, Basar O, Kadayifci A, Yuksel O, Choz M, Kulkarni AS, Tai E, Vo KD, Arora KS, Desai N, Licausi JA, Toner M, Maheswaran S, Haber DA, Ryan DP, Brugge WR, Ting DT. Improved Detection of Circulating Epithelial Cells in Patients with Intraductal Papillary Mucinous Neoplasms. *Oncologist* 2018; **23**: 121-127 [PMID: 28860411 DOI: 10.1634/theoncologist.2017-0234]
69 **Vasseur A**, Kiavue N, Bidard FC, Pierga JY, Cabel L. Clinical utility of circulating tumor cells: an update. *Mol Oncol* 2021; **15**: 1647-1666 [PMID: 33289351 DOI: 10.1002/1878-0261.12869]
70 **Catenacci DV**, Chapman CG, Xu P, Koons A, Konda VJ, Siddiqui UD, Waxman I. Acquisition of Portal Venous Circulating Tumor Cells From Patients With Pancreaticobiliary Cancers by Endoscopic Ultrasound. *Gastroenterology* 2015; **149**: 1794-1803.e4 [PMID: 26341722 DOI: 10.1053/j.gastro.2015.08.050]
71 **Tien YW**, Kuo HC, Ho BI, Chang MC, Chang YT, Cheng MF, Chen HL, Liang TY, Wang CF, Huang CY, Shew JY, Chang YC, Lee EY, Lee WH. A High Circulating Tumor Cell Count in Portal Vein Predicts Liver Metastasis From Periampullary or Pancreatic Cancer: A High Portal Venous CTC Count Predicts Liver Metastases. *Medicine (Baltimore)* 2016; **95**: e3407 [PMID: 27100430 DOI: 10.1097/MD.0000000000003407]
72 **Deng T**, Yuan Y, Zhang C, Yao W, Wang C, Liu R, Ba Y. Identification of Circulating MiR-25 as a Potential Biomarker for Pancreatic Cancer Diagnosis. *Cell Physiol Biochem* 2016; **39**: 1716-1722 [PMID: 27639768 DOI: 10.1159/000447872]
73 **Li X**, Gao P, Wang Y, Wang X. Blood-Derived microRNAs for Pancreatic Cancer Diagnosis: A Narrative Review and Meta-Analysis. *Front Physiol* 2018; **9**: 685 [PMID: 29922178 DOI: 10.3389/fphys.2018.00685]
74 **Komatsu S**, Ichikawa D, Miyamae M, Kawaguchi T, Morimura R, Hirajima S, Okajima W, Ohashi T, Imamura T, Konishi H, Shiozaki A, Ikoma H, Okamoto K, Taniguchi H, Otsuji E. Malignant potential in pancreatic neoplasm; new insights provided by circulating miR-223 in plasma. *Expert Opin Biol Ther* 2015; **15**: 773-785 [PMID: 25819175 DOI: 10.1517/14712598.2015.1029914]
75 **Peng C**, Wang J, Gao W, Huang L, Liu Y, Li X, Li Z, Yu X. Meta-analysis of the Diagnostic Performance of Circulating MicroRNAs for Pancreatic Cancer. *Int J Med Sci* 2021; **18**: 660-671 [PMID: 33437201 DOI: 10.7150/ijms.52706]
76 **Shen SY**, Singhania R, Fehringer G, Chakravarthy A, Roehrl MHA, Chadwick D, Zuzarte PC, Borgida A, Wang TT, Li T, Kis O, Zhao Z, Spreafico A, Medina TDS, Wang Y, Roulois D, Ettayebi I, Chen Z, Chow S, Murphy T, Arruda A, O'Kane GM, Liu J, Mansour M, McPherson JD, O'Brien C, Leighl N, Bedard PL, Fleshner N, Liu G, Minden MD, Gallinger S, Goldenberg A, Pugh TJ, Hoffman MM, Bratman SV, Hung RJ, De Carvalho DD. Sensitive tumour detection and classification using plasma cell-free DNA methylomes. *Nature* 2018; **563**: 579-583 [PMID: 30429608 DOI: 10.1038/s41586-018-0703-0]
77 **Cirmena G**, Dameri M, Ravera F, Fregatti P, Ballestrero A, Zoppoli G. Assessment of Circulating Nucleic Acids in Cancer: From Current Status to Future Perspectives and Potential Clinical Applications. *Cancers (Basel)* 2021; **13** [PMID: 34298675 DOI: 10.3390/cancers13143460]
78 **Guo XB**, Yin HS, Wang JY. Evaluating the diagnostic and prognostic value of long non-coding RNA SNHG15 in pancreatic ductal adenocarcinoma. *Eur Rev Med Pharmacol Sci* 2018; **22**: 5892-5898 [PMID: 30280769 DOI:

10.26355/eurrev_201809_15917]
79 **Permuth JB**, Chen DT, Yoder SJ, Li J, Smith AT, Choi JW, Kim J, Balagurunathan Y, Jiang K, Coppola D, Centeno BA, Klapman J, Hodul P, Karreth FA, Trevino JG, Merchant N, Magliocco A, Malafa MP, Gillies R. Linc-ing Circulating Long Non-coding RNAs to the Diagnosis and Malignant Prediction of Intraductal Papillary Mucinous Neoplasms of the Pancreas. *Sci Rep* 2017; **7**: 10484 [PMID: 28874676 DOI: 10.1038/s41598-017-09754-5]
80 **Satoh K**. Molecular Approaches Using Body Fluid for the Early Detection of Pancreatic Cancer. *Diagnostics (Basel)* 2021; **11** [PMID: 33671729 DOI: 10.3390/diagnostics11020375]
81 **Li Y**, Al Hallak MN, Philip PA, Azmi AS, Mohammad RM. Non-Coding RNAs in Pancreatic Cancer Diagnostics and Therapy: Focus on lncRNAs, circRNAs, and piRNAs. *Cancers (Basel)* 2021; **13** [PMID: 34439315 DOI: 10.3390/cancers13164161]
82 **Ding J**, Li Y, Zhang Y, Fan B, Li Q, Zhang J. Identification of key lncRNAs in the tumorigenesis of intraductal pancreatic mucinous neoplasm by coexpression network analysis. *Cancer Med* 2020; **9**: 3840-3851 [PMID: 32239802 DOI: 10.1002/cam4.2927]
83 **Schmidt DR**, Patel R, Kirsch DG, Lewis CA, Vander Heiden MG, Locasale JW. Metabolomics in cancer research and emerging applications in clinical oncology. *CA Cancer J Clin* 2021; **71**: 333-358 [PMID: 33982817 DOI: 10.3322/caac.21670]
84 **Michálková L**, Horník Š, Sýkora J, Habartová L, Setnička V. Diagnosis of pancreatic cancer via^{1}H NMR metabolomics of human plasma. *Analyst* 2018; **143**: 5974-5978 [PMID: 30270368 DOI: 10.1039/c8an01310a]
85 **He X**, Zhong J, Wang S, Zhou Y, Wang L, Zhang Y, Yuan Y. Serum metabolomics differentiating pancreatic cancer from new-onset diabetes. *Oncotarget* 2017; **8**: 29116-29124 [PMID: 28418859 DOI: 10.18632/oncotarget.16249]
86 **Yu J**, Ploner A, Kordes M, Löhr M, Nilsson M, de Maturana MEL, Estudillo L, Renz H, Carrato A, Molero X, Real FX, Malats N, Ye W. Plasma protein biomarkers for early detection of pancreatic ductal adenocarcinoma. *Int J Cancer* 2021; **148**: 2048-2058 [PMID: 33411965 DOI: 10.1002/ijc.33464]
87 **Kitagawa T**, Taniuchi K, Tsuboi M, Sakaguchi M, Kohsaki T, Okabayashi T, Saibara T. Circulating pancreatic cancer exosomal RNAs for detection of pancreatic cancer. *Mol Oncol* 2019; **13**: 212-227 [PMID: 30358104 DOI: 10.1002/1878-0261.12398]
88 **Castillo J**, Bernard V, San Lucas FA, Allenson K, Capello M, Kim DU, Gascoyne P, Mulu FC, Stephens BM, Huang J, Wang H, Momin AA, Jacamo RO, Katz M, Wolff R, Javle M, Varadhachary G, Wistuba II, Hanash S, Maitra A, Alvarez H. Surfaceome profiling enables isolation of cancer-specific exosomal cargo in liquid biopsies from pancreatic cancer patients. *Ann Oncol* 2018; **29**: 223-229 [PMID: 29045505 DOI: 10.1093/annonc/mdx542]
89 **Yu S**, Li Y, Liao Z, Wang Z, Qian L, Zhao J, Zong H, Kang B, Zou WB, Chen K, He X, Meng Z, Chen Z, Huang S, Wang P. Plasma extracellular vesicle long RNA profiling identifies a diagnostic signature for the detection of pancreatic ductal adenocarcinoma. *Gut* 2020; **69**: 540-550 [PMID: 31562239 DOI: 10.1136/gutjnl-2019-318860]
90 **Kanda M**, Knight S, Topazian M, Syngal S, Farrell J, Lee J, Kamel I, Lennon AM, Borges M, Young A, Fujiwara S, Seike J, Eshleman J, Hruban RH, Canto MI, Goggins M. Mutant GNAS detected in duodenal collections of secretin-stimulated pancreatic juice indicates the presence or emergence of pancreatic cysts. *Gut* 2013; **62**: 1024-1033 [PMID: 22859495 DOI: 10.1136/gutjnl-2012-302823]
91 **Kanda M**, Sadakari Y, Borges M, Topazian M, Farrell J, Syngal S, Lee J, Kamel I, Lennon AM, Knight S, Fujiwara S, Hruban RH, Canto MI, Goggins M. Mutant TP53 in duodenal samples of pancreatic juice from patients with pancreatic cancer or high-grade dysplasia. *Clin Gastroenterol Hepatol* 2013; **11**: 719-30.e5 [PMID: 23200980 DOI: 10.1016/j.cgh.2012.11.016]
92 **Singhi AD**, McGrath K, Brand RE, Khalid A, Zeh HJ, Chennat JS, Fasanella KE, Papachristou GI, Slivka A, Bartlett DL, Dasyam AK, Hogg M, Lee KK, Marsh JW, Monaco SE, Ohori NP, Pingpank JF, Tsung A, Zureikat AH, Wald AI, Nikiforova MN. Preoperative next-generation sequencing of pancreatic cyst fluid is highly accurate in cyst classification and detection of advanced neoplasia. *Gut* 2018; **67**: 2131-2141 [PMID: 28970292 DOI: 10.1136/gutjnl-2016-313586]
93 **Garcia-Carracedo D**, Chen ZM, Qiu W, Huang AS, Tang SM, Hruban RH, Su GH. PIK3CA mutations in mucinous cystic neoplasms of the pancreas. *Pancreas* 2014; **43**: 245-249 [PMID: 24518503 DOI: 10.1097/MPA.0000000000000034]
94 **Kaur S**, Kumar S, Momi N, Sasson AR, Batra SK. Mucins in pancreatic cancer and its microenvironment. *Nat Rev Gastroenterol Hepatol* 2013; **10**: 607-620 [PMID: 23856888 DOI: 10.1038/nrgastro.2013.120]
95 **Nagata K**, Horinouchi M, Saitou M, Higashi M, Nomoto M, Goto M, Yonezawa S. Mucin expression profile in pancreatic cancer and the precursor lesions. *J Hepatobiliary Pancreat Surg* 2007; **14**: 243-254 [PMID: 17520199 DOI: 10.1007/s00534-006-1169-2]
96 **Henry KE**, Shaffer TM, Mack KN, Ring J, Ogirala A, Klein-Scory S, Eilert-Micus C, Schmiegel W, Bracht T, Sitek B, Clyne M, Reid CJ, Sipos B, Lewis JS, Kalthoff H, Grimm J. Exploiting the MUC5AC Antigen for Noninvasive Identification of Pancreatic Cancer. *J Nucl Med* 2021; **62**: 1384-1390 [PMID: 33712530 DOI: 10.2967/jnumed.120.256776]
97 **Maker AV**, Katabi N, Qin LX, Klimstra DS, Schattner M, Brennan MF, Jarnagin WR, Allen PJ. Cyst fluid interleukin-1beta (IL1beta) levels predict the risk of carcinoma in intraductal papillary mucinous neoplasms of the pancreas. *Clin Cancer Res* 2011; **17**: 1502-1508 [PMID: 21266527 DOI: 10.1158/1078-0432.CCR-10-1561]
98 **Hao S**, Takahashi C, Snyder RA, Parikh AA. Stratifying Intraductal Papillary Mucinous Neoplasms by Cyst Fluid Analysis: Present and Future. *Int J Mol Sci* 2020; **21** [PMID: 32050465 DOI: 10.3390/ijms21031147]
99 **Das KK**, Geng X, Brown JW, Morales-Oyarvide V, Huynh T, Pergolini I, Pitman MB, Ferrone C, Al Efishat M, Haviland D, Thompson E, Wolfgang C, Lennon AM, Allen P, Lillemoe KD, Fields RC, Hawkins WG, Liu J, Castillo CF, Das KM, Mino-Kenudson M. Cross Validation of the Monoclonal Antibody Das-1 in Identification of High-Risk Mucinous Pancreatic Cystic Lesions. *Gastroenterology* 2019; **157**: 720-730.e2 [PMID: 31175863 DOI: 10.1053/j.gastro.2019.05.014]
100 **Majumder S**, Raimondo M, Taylor WR, Yab TC, Berger CK, Dukek BA, Cao X, Foote PH, Wu CW, Devens ME, Mahoney DW, Smyrk TC, Pannala R, Chari ST, Vege SS, Topazian MD, Petersen BT, Levy MJ, Rajan E, Gleeson FC,

Abu Dayyeh B, Nguyen CC, Faigel DO, Woodward TA, Wallace MB, Petersen G, Allawi HT, Lidgard GP, Kisiel JB, Ahlquist DA. Methylated DNA in Pancreatic Juice Distinguishes Patients With Pancreatic Cancer From Controls. *Clin Gastroenterol Hepatol* 2020; **18**: 676-683.e3 [PMID: 31323382 DOI: 10.1016/j.cgh.2019.07.017]

101 **Zhang L**, Farrell JJ, Zhou H, Elashoff D, Akin D, Park NH, Chia D, Wong DT. Salivary transcriptomic biomarkers for detection of resectable pancreatic cancer. *Gastroenterology* 2010; **138**: 949-57.e1 [PMID: 19931263 DOI: 10.1053/j.gastro.2009.11.010]

102 **Xie Z**, Yin X, Gong B, Nie W, Wu B, Zhang X, Huang J, Zhang P, Zhou Z, Li Z. Salivary microRNAs show potential as a noninvasive biomarker for detecting resectable pancreatic cancer. *Cancer Prev Res (Phila)* 2015; **8**: 165-173 [PMID: 25538087 DOI: 10.1158/1940-6207.CAPR-14-0192]

103 **Ghafouri-Fard S**, Fathi M, Zhai T, Taheri M, Dong P. LncRNAs: Novel Biomarkers for Pancreatic Cancer. *Biomolecules* 2021; **11** [PMID: 34827663 DOI: 10.3390/biom11111665]

104 **Radon TP**, Massat NJ, Jones R, Alrawashdeh W, Dumartin L, Ennis D, Duffy SW, Kocher HM, Pereira SP, Guarner posthumous L, Murta-Nascimento C, Real FX, Malats N, Neoptolemos J, Costello E, Greenhalf W, Lemoine NR, Crnogorac-Jurcevic T. Identification of a Three-Biomarker Panel in Urine for Early Detection of Pancreatic Adenocarcinoma. *Clin Cancer Res* 2015; **21**: 3512-3521 [PMID: 26240291 DOI: 10.1158/1078-0432.CCR-14-2467]

105 **Brezgyte G**, Shah V, Jach D, Crnogorac-Jurcevic T. Non-Invasive Biomarkers for Earlier Detection of Pancreatic Cancer-A Comprehensive Review. *Cancers (Basel)* 2021; **13** [PMID: 34072842 DOI: 10.3390/cancers13112722]

106 **Mayerle J**, Kalthoff H, Reszka R, Kamlage B, Peter E, Schniewind B, González Maldonado S, Pilarsky C, Heidecke CD, Schatz P, Distler M, Scheiber JA, Mahajan UM, Weiss FU, Grützmann R, Lerch MM. Metabolic biomarker signature to differentiate pancreatic ductal adenocarcinoma from chronic pancreatitis. *Gut* 2018; **67**: 128-137 [PMID: 28108468 DOI: 10.1136/gutjnl-2016-312432]

107 **Zhang ZM**, Wang JS, Zulfiqar H, Lv H, Dao FY, Lin H. Early Diagnosis of Pancreatic Ductal Adenocarcinoma by Combining Relative Expression Orderings With Machine-Learning Method. *Front Cell Dev Biol* 2020; **8**: 582864 [PMID: 33178697 DOI: 10.3389/fcell.2020.582864]

108 **Alizadeh Savareh B**, Asadzadeh Aghdaie H, Behmanesh A, Bashiri A, Sadeghi A, Zali M, Shams R. A machine learning approach identified a diagnostic model for pancreatic cancer through using circulating microRNA signatures. *Pancreatology* 2020; **20**: 1195-1204 [PMID: 32800647 DOI: 10.1016/j.pan.2020.07.399]

World Journal of Gastroenterology

Submit a Manuscript: https://www.f6publishing.com

World J Gastroenterol 2022 August 21; 28(31): 4249-4262

DOI: 10.3748/wjg.v28.i31.4249

ISSN 1007-9327 (print) ISSN 2219-2840 (online)

REVIEW

Insights into induction of the immune response by the hepatitis B vaccine

Federico Alejandro Di Lello, Alfredo Pedro Martínez, Diego Martín Flichman

Specialty type: Gastroenterology and hepatology

Provenance and peer review: Invited article; Externally peer reviewed.

Peer-review model: Single blind

Peer-review report's scientific quality classification

Grade A (Excellent): 0
Grade B (Very good): B
Grade C (Good): C, C
Grade D (Fair): 0
Grade E (Poor): 0

P-Reviewer: JAN CFJ, Taiwan; Kumar R, India; Maslennikov R, Russia

Received: January 16, 2022
Peer-review started: January 16, 2022
First decision: May 10, 2022
Revised: May 21, 2022
Accepted: July 24, 2022
Article in press: July 24, 2022
Published online: August 21, 2022

Federico Alejandro Di Lello, Microbiology, Universidad de Buenos Aires. Facultad de Farmacia y Bioquímica. Instituto de Investigaciones en Bacteriología y Virología Molecular, Buenos Aires C1113AAD, Argentina

Federico Alejandro Di Lello, Diego Martín Flichman, Consejo Nacional de Investigaciones Científicas y Técnicas, Buenos Aires C1425FQB, Argentina

Alfredo Pedro Martínez, Virology Section, Centro de Educación Médica e Investigaciones Clínicas Norberto Quirno "CEMIC", Buenos Aires C1431FWO, Argentina

Diego Martín Flichman, Microbiology, Universidad de Buenos Aires, Instituto de Investigaciones Biomédicas en Retrovirus y Síndrome de Inmunodeficiencia Adquirida, Buenos Aires C1121ABG, Argentina

Corresponding author: Diego Martín Flichman, PhD, Adjunct Professor, Research Scientist, Microbiology, Universidad de Buenos Aires, Instituto de Investigaciones Biomédicas en Retrovirus y Síndrome de Inmunodeficiencia Adquirida, Paraguay 2155, Buenos Aires C1121ABG, Argentina. dflichman@ffyb.uba.ar

Abstract

After more than four decades of hepatitis B virus (HBV) vaccine implementation, its safety and efficacy in preventing HBV infection have been proven and several milestones have been achieved. Most countries have included HBV immunization schedules in their health policies and progress has been made regarding universalization of the first HBV vaccine dose at birth. All of these actions have significantly contributed to reducing both the incidence of HBV infection and its related complications. However, there are still many drawbacks to overcome. The main concerns are the deficient coverage rate of the dose at birth and the large adult population that has not been reached timely by universal immunization. Additionally, the current most widely used second-generation vaccines do not induce protective immunity in 5% to 10% of the population, particularly in people over 40-years-old, obese (body mass index > 25 kg/m^2), heavy smokers, and patients undergoing dialysis or infection with human immunodeficiency virus. Recently developed and approved novel vaccine formulations using more potent adjuvants or multiple antigens have shown better performance, particularly in difficult settings. These advances re-launch the expectations of achieving the World Health Organization's objective of completing hepatitis control by 2030.

Key Words: Hepatitis B virus; Vaccine; Immune response; Antibodies; Neutralizing

©The Author(s) 2022. Published by Baishideng Publishing Group Inc. All rights reserved.

Core Tip: Second-generation vaccines induce the production of anti-hepatitis B surface antibodies (anti-HBs). Anti-HBs levels ≥ 10 mIU/mL prevent against infection. More than 90% of immunized persons achieve protective anti-HBs levels 1 mo after completing the three-dose vaccination schedule. Although antibody titers significantly drop during the 1st years after vaccination, memory immunity is sufficient to prevent infection regardless of the antibody levels. In some specific settings showing lower immune response rates, schemes with larger or additional doses and novel vaccine formulations are recommended.

Citation: Di Lello FA, Martínez AP, Flichman DM. Insights into induction of the immune response by the hepatitis B vaccine. *World J Gastroenterol* 2022; 28(31): 4249-4262
URL: https://www.wjgnet.com/1007-9327/full/v28/i31/4249.htm
DOI: https://dx.doi.org/10.3748/wjg.v28.i31.4249

INTRODUCTION

Hepatitis B infection has been a major public health concern for a long time. Identification of the hepatitis B virus (HBV) in the 1960s and the subsequent development of a safe and effective vaccine were the kickoff to begin to retrace the path and achieve the desired control of this health problem.

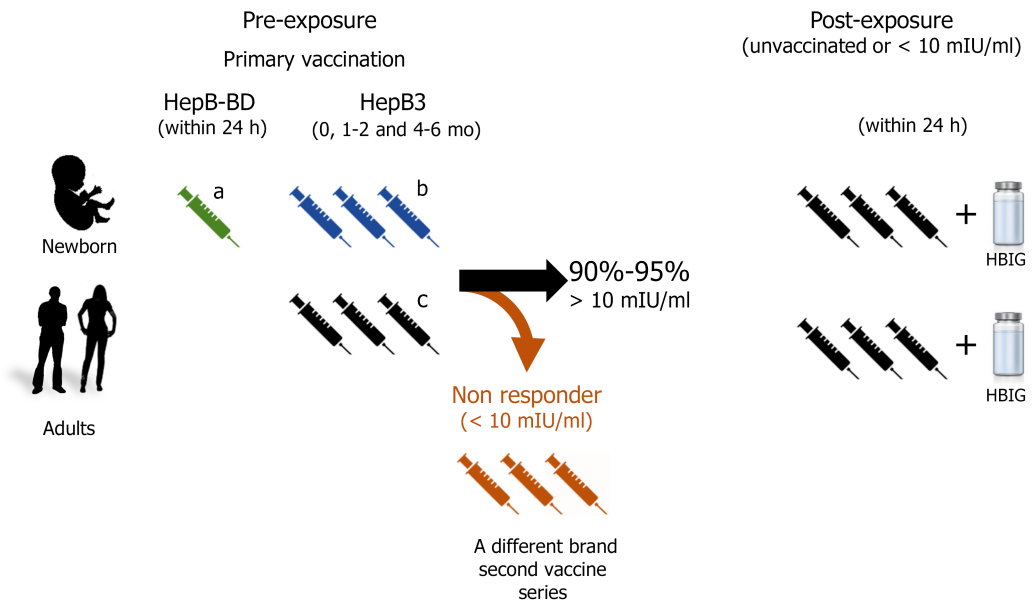
First-generation vaccines based on heat-treated plasma derived from hepatitis B surface antigen (HBsAg)-positive donors raised concerns about its safety and availability to meet the vaccine manufacturer's needs. Shortly afterwards, second-generation DNA vaccines prepared in yeast transfected with recombinant plasmids encoding small HBV surface proteins (SHBs) were developed and approved in 1986[1]. Lastly, third-generation vaccines have been produced in mammalian cells that express and secrete SHBs and middle pre-S2 proteins (MHBs) or the three HBV envelope proteins (SHBs, MHBs, and large HBs).

It is worth noting that several studies have compared the immune response to plasma-derived first-generation vaccines to the recombinant second-generation ones. Most of the studies showed that the lowering rate of anti-HBs was higher in people receiving the recombinant HBV vaccine. However, plasma-derived vaccines were replaced by the recombinant ones due to safety concerns about human blood-derived products[2-5]. In addition, it has been shown that third-generation vaccines containing the pre-S2 and pre-S1 antigens would induce a higher anti-HBs response than second-generation ones, particularly in people ≥ 45-years-old[6-8]. Moreover, compared to plasma-derived vaccines, it has been observed that the HBsAg seropositive rate drops by about 71% and that the anti-HBc seropositive rate decreases by approximately 65% when recombinant HBV vaccines are used, supporting their higher effectiveness[4].

The HBV vaccine has been introduced progressively in the national vaccination calendars. Currently, second-generation HBV vaccines have been widely implemented for newborns in most countries. The pentavalent vaccine formulation protecting against diphtheria, pertussis, tetanus, hepatitis B, and *Haemophilus influenzae* type B is administered in three doses, 4 wk apart (recommended dosing at 6, 10, and 14 postnatal wk), and aims to lessen horizontal transmission. In addition, a monovalent single dose of the HBV vaccine (HepB-BD) administered within 24 h after delivery is also recommended to reduce mother-to-child transmission (Figure 1). The advised immunization schedule for the adult population includes three vaccine doses (HepB3) according to the individuals' age. Immunocompromised adults or patients on dialysis treatment require higher or additional doses of HBV vaccines. Recently, a novel vaccine (Heplisav-B) with a different adjuvant was approved for adult immunization with a recommended schedule of two doses 1 mo apart.

Since 1990, the proportion of children receiving all three doses of the HBV vaccine has increased globally from 1% to 85%. By 2020, the HBV vaccine was introduced to 190 countries with 83% of three-dose coverage rate. Few countries with very low endemicity that consider HBV infection as a limited public health problem provide the HBV vaccine to only well-defined risk groups. Likewise, a dose of HepB-BD has been introduced in the national calendar of 113 countries. Figure 2 shows the HBV worldwide three-dose infant vaccine coverage and the HBsAg seroprevalence[2,9]. However, the at birth dose coverage rate is poor (estimated at 43%) with remarkable disparities according to region and development level[10-12].

Universal vaccination is the most effective strategy to prevent and control HBV infection. In 2016, the World Health Organization (WHO) set the goal of controlling HBV by 2030. The proposed targets include the 90% global coverage of three-dose infant vaccination by 2020, birth-dose vaccination of 50%



DOI: 10.3748/wjg.v28.i31.4249 **Copyright** ©The Author(s) 2022.

Figure 1 Recommended hepatitis B virus vaccination schemes. The hepatitis B immunization schedule is flexible, but minimal intervals and ages need to be observed. The recommended dose varies (5-40 μg of hepatitis B surface antigen protein/mL) depending on the individuals' age and the vaccine brand. [a]Monovalent hepatitis B vaccine 0.5 mL must be used for the at birth immunization (HepB-BD). Immunocompromised adults or patients under dialysis require larger or additional doses of the hepatitis B vaccine; [b]Combined hepatitis B, diphtheria, tetanus, adsorbed acellular pertussis, inactivated poliovirus vaccine. This vaccine cannot be administered at birth, before 6 postnatal weeks, or at age ≥ 7 years; [c]Heplisav-B is a vaccine recently approved for adults; it has a novel adjuvant and its recommended schedule is two doses 1 mo apart. HepB3: Three doses of hepatitis B vaccine; HepB-BD: Monovalent single dose of the hepatitis B virus vaccine; HBIG: Hepatitis B Immunoglobulin.

of infants by 2020, and of 90% of them by 2030[13].

MILESTONES ACHIEVED WITH THE HBV VACCINE

One of the goals of the strategy to achieve HBV control by 2030 is to reduce HBsAg prevalence to 0.1% in 5-year-old children and many countries are already on track to that milestone[14].

The global implementation of the HBV vaccine as part of the national health policies has contributed to directly reducing the global burden of infection, and indirectly, the HBV-related mortality. After the inclusion of HBV vaccination schedules, several surveillance studies have shown an overtime global HBsAg prevalence decrease in most countries[15], either in hyperendemic ones or in those with low or medium HBV infection prevalence[16-20].

Taiwan was the first country to implement a mass vaccination program against HBV in 1984 and it is the paradigm of its impact on the control of hepatitis. After 30 years of sustained immunization programs, the prevalence of HBsAg has decreased from 9.8% in the pre-vaccination period to 0.5% in the cohort reached by HBV vaccination protocols[21]. The main reason for Taiwan's success was its high three-dose hepatitis infant vaccine coverage rate, which increased from 88.9% in 1985[22,23] to 98.1% in 2018[21].

In the United States, since first HBV vaccine recommendations, the infection incidence has decreased by approximately 90%, from 9.6/100000 cases in 1982 to 1.0/100000 cases in 2018[24]. Similarly, in China, where the coverage of the three-dose vaccine schedule has increased from 30.0% to 93.4% and the at birth dose increased from 22.2% to 82.6%, the HBsAg prevalence decreased from 5.5% to 0.9% between 1992 and 2005[25]. In Argentina, a country with low HBV endemicity, the HBV vaccine was included in newborns' schedules in 2000 and, later in 2003, the catch-up strategy was implemented in 11-year-old adolescents. Currently, the coverage rate of protective antibodies is significantly higher in persons born after 1992 than in those born previously (Figure 3A)[26,27]. In fact, new infections generally occur in the population over 20-years-old not reached by vaccination[28]. These results emphasize the need to raise awareness among people not reached by universal HBV immunization programs and to focus vaccination campaigns on this group.

However, the most outstanding HBV preventive action impact has been detected in regions that were hyperendemic before introduction of the vaccine. In a Southern Italian area, where the vaccine was introduced in 1991, the HBsAg prevalence dropped from 13.4% in 1978 to 0.91% in 2006[29]. Likewise, in Alaska, where one of the highest HBV infection incidences has been reported, universal childhood

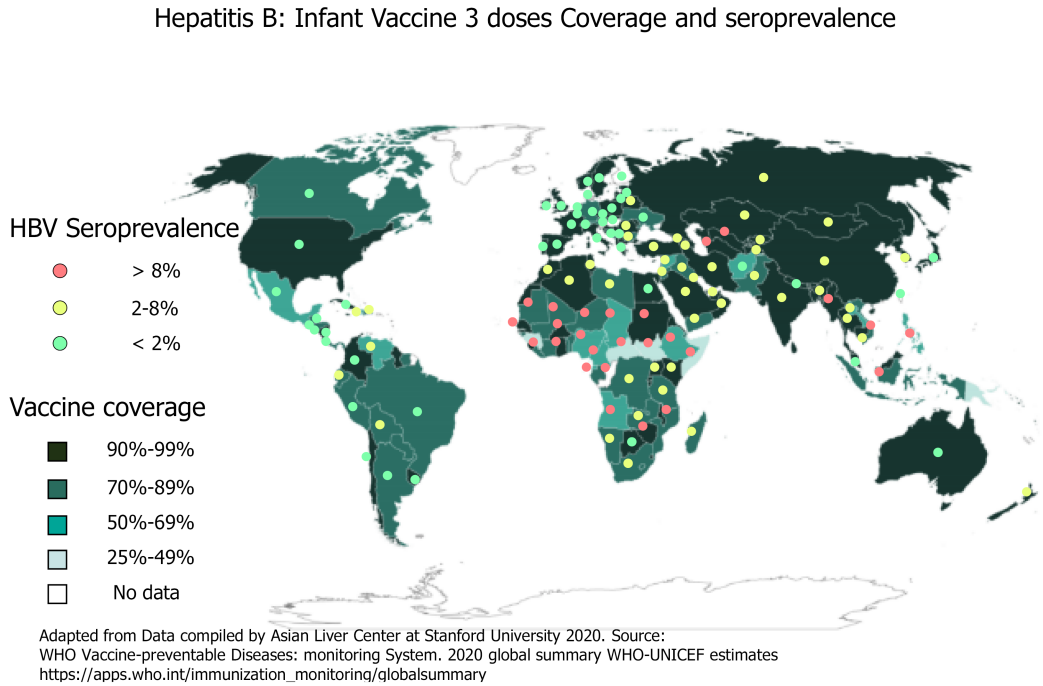
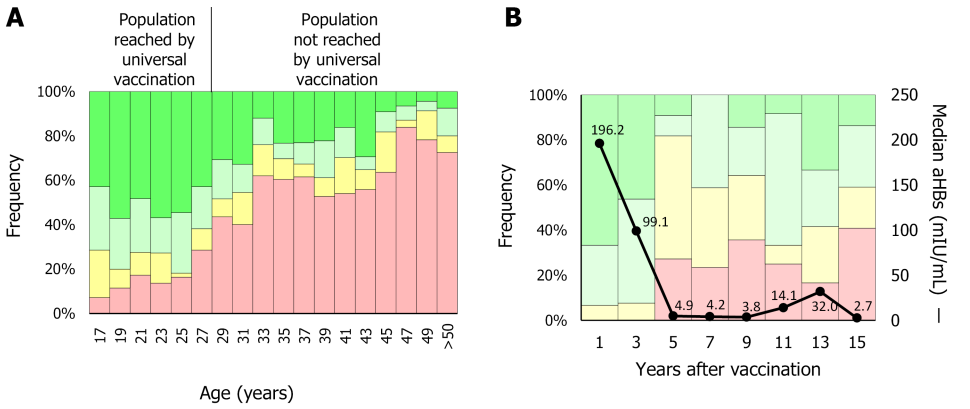


Figure 2 Hepatitis B three doses of infant vaccine coverage and seroprevalence. Hepatitis B virus seroprevalence data is from Polaris Observatory Collaborators: Global Prevalence, Treatment, and Prevention of Hepatitis B Virus Infection in 2016: A Modelling Study. Lancet Gastroenterol Hepatol 2018; 3: 383–403. HBV: Hepatitis B virus.



DOI: 10.3748/wjg.v28.i31.4249 **Copyright** ©The Author(s) 2022.

Figure 3 Anti-hepatitis B surface antibodies titers by age. A: The anti-hepatitis B surface antibodies (anti-HBs) titer was determined in 765 blood donors. In 2000, vaccination against hepatitis B virus was included in the Argentine newborns' National Vaccination Calendar. In 2003, the catch-up strategy for 11-year-old children was implemented. Therefore, individuals under 28-years-old are reached currently by the universal vaccine implementation. On average, protective levels of anti-HBs (> 10 mIU/mL) were detected in 75.2% of the population reached by universal vaccination (< 28-years-old) and in 32.2% of the not reached population (> 28-years-old); B: Anti-HBs kinetics. The anti-HBs titer was determined in 132 children born after 2000. In the first 2 years, the median anti-HBs titer fell from 196.2 mIU/mL to less than 10 mIU/mL (black line). Five years post-vaccination, about 20% of the population showed anti-HBs levels below 10 mIU/mL. aHBs: Anti-hepatitis B surface antibodies.

vaccination was implemented for newborns in 1993. The HBsAg prevalence dropped from 13% detected before the HBV vaccination program, to 0% HBsAg-positive children less than 10-years-old[30].

Although slowly and delayed, a significant reduction in the hepatocellular carcinoma annual average incidence has been observed concomitantly with the HBV infection incidence decline, particularly in those countries where early vaccine protocols have been introduced[31-33].

IMMUNITY

HBV vaccine-induced protective immunity

Several studies have shown that HBV vaccines induced both humoral and cellular immunity providing long-term protection[34,35]. On the one hand, neutralizing antibodies are elicited and two types of them have been identified. The first type targets the "a" determinant and neutralizes cell viral penetration by blocking the interaction with heparan sulfate[36], required by the virus at an early stage of hepatocyte entrance[37]. The second type targets the high-affinity receptor-binding site of the HBV pre-S1 domain and blocks the binding to the Na^+-taurocholate cotransporting polypeptide receptor preventing the infection of hepatocytes[38,39]. On the other hand, immune memory cells are generated, which upon contact with the HBV can be activated to expand rapidly. This response has been well demonstrated in studies that administered a booster dose to previously vaccinated persons whose antibody titers had fallen below protective titers[16,40-42].

Pre-exposure: Efficacy and effectiveness studies carried out in animal models first and then in human beings have shown that the HBV vaccine induces the production of neutralizing antibodies against HBV surface antigen (anti-HBs)[43]. Two main questions raised suddenly once the HBV vaccine was developed: What are the levels of antibodies that protect against infection and how long does immunity last? Soon after the release of the vaccine, several studies have shown that anti-HBs levels ≥ 10 mIU/mL, determined 1 to 3 mo after the complete three-dose vaccination scheme administration, were a surrogate marker for vaccine-induced protective immunity[44-46].

The overall response rate to the HBV vaccine, defined as individuals achieving anti-HBs levels > 10 mIU/mL, is 90% to 95% of immunized persons. Different factors such as host genetics, age, body weight, smoking, and concomitant disease have been shown to affect the response rate to the vaccine [47]. These variations probably rely on the strength of the cellular immune response. Velu *et al*[48] have characterized the cellular immune response and the cytokine profile of vaccine responders and non-responders to investigate the immunization outcome underlying mechanisms. The authors reported that HBsAg-specific interferon gamma, interleukin 10, and tumor necrosis factor alpha secretion correlated with the HBV vaccine-induced humoral immune response. Likewise, non-responders had lower levels of T helper type 1 (Th1) and Th2 cytokines. In addition, Körber *et al*[49] observed a higher frequency of regulatory B cells in HBV vaccine non-responders. Regulatory B cells suppress immunopathology by skewing T-cell differentiation. Overall, these results suggest that impaired lymphocyte activation is associated with a weak or no response to HBV vaccination.

Notably, although the HBV vaccine induces protective immunity against infection it would not be sterilizing. Consequently, vaccinated people can become infected although episodes are usually asymptomatic and self-limited[50-52]. These benign infection results are possibly due to long-lasting HBV cellular immunity induced by the vaccine despite antibody loss against HBV surface antigens[53].

Post-exposure: Immunization with HBV vaccines combined with different injection sites of HBV immunoglobulin administration, within 12 h after birth, showed a greater than 85% efficacy in preventing infection in infants born to HBsAg-positive mothers[54]. In adult persons, post-exposure prophylaxis is also recommended depending on the individual's vaccination and anti-HBs status. In unvaccinated subjects or with non-protective levels of anti-HBs, the HBV vaccine has shown high efficacy in preventing infection when administered within 24 h after percutaneous or mucosal exposure to HBV-positive blood. Additional post-exposure immunoprophylaxis is not suggested in individuals who achieved anti-HBs protective levels after vaccination.

Although, as previously mentioned, the massive implementation of the HBV vaccine substantially reduced the incidence and prevalence of the infection, few works have addressed the effectiveness of the vaccine and most of them have been carried out in high endemic countries. In general, a 70% to 94% effectiveness range has been reported, depending mainly on the follow-up time, the exposure risk rate (HBsAg prevalence of the population), and the studied cohort age[18,23,55]. A recent study showed an approximately 58% effectiveness in a birth cohort (mean age, 12 years) and 85% in participants at least 20-years-old[56]. The lower efficacy observed in the birth cohort could be a consequence of a lower level of exposure.

HOW LONG DO THE ANTIBODIES LAST?

Protective antibodies levels tend to decrease over time, especially during the 1st years after vaccination [57]. In a study carried out by our group, including 132 children born after infants' vaccine implementation, we observed that anti-HBs titers were significantly higher 1 year post-vaccination compared to the 2 years and 3 years earliest vaccinated population (Figure 3B). In addition, approximately 20% of the 5-year post-vaccination cohort showed anti-HBs levels lower than 10 mIU/mL[27]. These results are in line with a study conducted in Germany, where anti-HBs levels were determined in 106 teenagers, mean age 13.7-years-old, after primary vaccination. Forty percent of cases had anti-HBs levels < 10 mIU/mL. However, almost all (97%) teenagers who received a booster vaccine achieved anti-

HBs levels ≥ 100 mIU/mL regardless of their pre-booster levels[58]. Besides time elapsed since primary vaccination, a systematic meta-analysis including 46 studies analyzed the anti-HBs levels from 5 years to 20 years after the primary vaccination and identified the vaccination dose and the less than 6-mo interval between the last dose and the previous one as the main factors associated with anti-HBs titer loss[59]. On the other hand, the duration of antibody levels is directly correlated with the titers reached when completing the vaccination scheme[60].

Another interesting issue regarding antibodies duration refers to the subjects' age at the time of vaccination. Numerous studies have shown that vaccination in adolescence generates higher and long-lasting titers compared to children vaccinated at birth[61-64], being the age at the time of vaccination an independent variable associated with an anti-HBs titer < 10 mIU/mL. However, childhood HBV vaccination, together with other vaccines, guarantees a higher coverage rate.

Overall, it is widely accepted that a large proportion of vaccinated individuals, particularly those immunized during childhood, rapidly lose their anti-HBs titers below protective levels[40]. However, it has also been extensively described that individuals who achieved anti-HBs protective titers at the time of vaccination, show a rapid anamnestic response when boosted[41,42], suggesting that memory immunity plays a decisive role in the protection against clinical disease and the development of a carrier state regardless of anti-HBs antibody levels[35]. In this regard, it has been observed that even in the lack of anti-HBs, a significant amount of HBsAg-specific memory T and B cells are detected in vaccine responders. For this reason, although it remains a controversial issue, vaccine booster doses are not recommended currently for children and adults with normal immune status, despite the overtime drop of anti-HBs antibody titers[35,65]. Nonetheless, the anti-HBs titer decline could represent a problem for high-risk groups.

MANAGEMENT OF SPECIAL POPULATIONS

Adult persons with increased risk factors for infection are one of the WHO identified obstacles to HBV elimination as a public health problem[66,67]. These groups mainly include health care providers, illicit injected drug users, sexually active individuals (more than 1 partner in the past 6 mo), persons with diabetes, dialysis patients, and people living with human immunodeficiency virus (HIV). The last two groups, in addition to showing a higher risk of HBV infection compared to the general population[68-70] due to the frequent use of percutaneous materials and the common route of HBV and HIV transmission, have shown suboptimal responses to HBV immunization[71,72]. Patients on dialysis have also shown a diminished response to the HBV vaccine probably due to a uremic-associated suppression of the immune system that leads to a significant progressive reduction of the percentage and count of lymphocytes CD3+, CD4+, and CD8+ and a disturbance of antigen-presenting cells that results in an inability to sustain a satisfactory antibody titer over time[73-76]. In fact, in this population subset, the rate of seroprotection level ranges from 33.3% to 86%[77].

It has been reported that patients living with HIV present a poor initial HBV immunization response, lower seroconversion rates, and difficulty in maintaining immunity over time, mainly due to B-cell dysfunction[67,71,78,79]. For this group, the efficacy of the standard vaccine scheme in the era of the highly active antiretroviral therapy ranges from 17.5% to 71%[80-83].

Consequently, for patients on dialysis and/or living with HIV, other approaches are recommended to enhance the HBV vaccine immune response. For patients undergoing dialysis therapy, alternative strategies include the use of adjuvants, additional vaccination cycles, different vaccine formulations, greater number and concentration of doses, greater frequency of doses, dual vaccination, alternative administration routes, and/or use of booster vaccines[67,72,84-86]. On the other hand, for HIV-infected individuals with negative or < 10 mIU/mL anti-HBs levels after a primary vaccine series, a second HBV vaccine series using larger or additional doses is recommended[71,87]. Furthermore, revaccination should be attempted after HIV viral load suppression and CD4 cell count improvement[83].

RATE OF RESPONSE TO HBV VACCINE

As mentioned above, the average response rate to the HBV vaccine is greater than 90% with 5% to 10% vaccinated persons failing to mount a protective immunity level once the vaccination schedule is completed. The response to the vaccine ultimately relies on the individual immune system; however, different factors impairing the response rate have been identified. Response rates can drop drastically when more than one of these factors are present.

Host genetics

Several studies have addressed, through different experimental approaches, the role of genetic polymorphisms in the response to the HBV vaccine. Single nucleotide polymorphisms in HLA loci[88-92], ILs (with a key role in the cellular and humoral response interplay)[93,94], or even other genes have

been associated with the response rate to HBV vaccination[90,95,96]. However, these findings have not been widely validated in different cohorts and should be considered with caution.

Age

One of the most recognized consequences of aging is the declination of the immune function and the concomitant vaccination response reduction. The HBV vaccine response rate decreases in people 40-years-old and even more in people older than 60 years[97,98]. This highlights the need to vaccinate the population not covered by health policies before they reach 40-years-old, which will result in important cost-benefit profits.

Body weight

Overweight and obesity are a growing public health problem worldwide that affects all age groups[99]. They are caused by the deposition of lipids into the adipose tissue and are defined as a body mass index ≥ 25 kg/m.

Shortly after the HBV vaccine was developed and implemented, obesity was found to be a factor impairing the strength of the immune response[100]. This finding has been widely validated in subsequent studies[101,102]. This drawback is not only attributed to the HBV vaccine but has also been described for other vaccines[103,104]. Adipose tissue has a role in modulating the immune system through different pathways, inducing a chronic pro-inflammatory state[105,106], which in the end is associated with immune system dysfunction. This includes the chronic activation of cells of the innate immune system and consequent local and systemic inflammation[107]. In addition, Frasca *et al*[108] described a percentage decrease of switched memory and transitional B cells and an increase of late/exhausted memory B cells with the consequent impaired response to the vaccine.

Smoking

As described for obesity, the link between tobacco smoking and impaired vaccine response has been proposed to be mediated by inflammation[109]. However, data from different studies are less robust. Some studies have reported lower responses to vaccination while others showed no association[110]. This controversy could be based on the level of daily cigarette intake. A recent study reported that subjects in the non-responder group were almost exclusively 'heavy smokers' defined as consumers of ≥ 10 cigarettes per day[111]. The development of new vaccine formulations including either additional antigens or more potent adjuvants could represent a solution to improve the response rate of individuals affected by these factors as well as for dialyzed or immunosuppressed patients.

NEW FORMULATIONS

As previously mentioned, one of the main drawbacks of the second-generation vaccines is the poor induction of immune response in 5% to 10% of the general population and individuals presenting detrimental factors that impair vaccine response. Therefore, efforts have been made to find more effective formulations to overcome this limitation. Two advances have been reported in recent years. One of them is the development and evaluation of new and more powerful adjuvants to enhance immunogenicity[112,113].

Heplisav-B (HepB-CpG), a single-antigen vaccine with a novel immunostimulatory adjuvant, has been approved for its use in people at least 18-years-old. This vaccine is administered in two doses, 1 mo apart[114]. The new adjuvant is a small synthetic cytidine-phosphate-guanosine oligodeoxynucleotide containing non-methylated CpG patterns, similar to those present in microbial DNA. This structure acts as an agonist of the toll-like receptor 9 that enhances the immune response. Several studies have shown higher response rates to other second-generation vaccines both in general population[115-117] and in persons with detrimental factors for vaccination response[118-120]. In addition, the two doses-1 mo apart-simplified schedule could help increase patient compliance and raise the coverage rate.

Alternatively, third-generation vaccines derived from mammalian cells, containing the medium and large HBV envelope proteins have been developed. The advantage of this approach is that antigens display the same *in vivo* post-translational modifications and protein folding.

In 2021, Sci-B-Vac was licensed, and phase III trials showed faster seroprotection and higher response rates than the second-generation vaccines[8,121]. These data making turn Sci-B-Vac of particular interest for its use in people with poor or no response. Particularly, Sci-B-Vac has shown greater efficacy in HIV-infected individuals' immunization and in the prevention of vertical infection transmission[122,123]. Furthermore, the multiple antigen display of the third-generation vaccines would protect against HBV vaccine breakthrough infections caused by the HBV S gene mutants widely described[124-126]. The results obtained through novel vaccine formulation approaches suppose a contribution to the prophylaxis of HBV infection and represent a promising future.

CURRENT CHALLENGE

Beyond significant advances in the prevention of HBV infection, several pitfalls have been identified that need to be overcome in order to eliminate HBV as a health problem[127]. Particularly, in developing countries, sustainable financial mechanisms are required to scale up screening interventions and ensure access to vaccines.

Regarding the at birth dose, out-of-hospital deliveries, shortage of monovalent vaccine formulation in some regions, insufficient training of health care providers, weak monitoring and reporting systems, and low government commitment impair its implementation. On the other hand, in the adult population not covered by universal vaccination, promoting information, raising consciousness about risk, and finally focusing and promoting vaccination campaigns should improve immunization strategies for this group.

CONCLUSION

The worldwide application of HBV vaccines has led to a significant decrease in HBV infection incidence and its related death rates. As a general strategy, surveys are necessary to identify local constraints (in regions or countries) in order to achieve the implementation of WHO guidelines, both at the prophylaxis and diagnostic levels. Increasing efforts to improve vaccination coverage and raise awareness among populations not reached by universal vaccination will contribute significantly to achieving the WHO goals by 2030. Although HBV vaccines induce protective immunity in more than 90% of immunized people, there are particular settings where the efficacy is lower. In recent years, new formulations containing new adjuvants or other HBV antigens in addition to HBs, that could overcome the limitations of current presentations.

ACKNOWLEDGEMENTS

To Silvina Heisecke, from CEMIC-CONICET, for the copyediting of the manuscript.

FOOTNOTES

Author contributions: Di Lello FA and Flichman DM contributed to the review concept, and designed and drafted the manuscript; Martínez AP contributed to critical revisions of the manuscript for important intellectual content and gave final approval of the version to be submitted.

Conflict-of-interest statement: The authors have no conflicts of interest to declare.

Open-Access: This article is an open-access article that was selected by an in-house editor and fully peer-reviewed by external reviewers. It is distributed in accordance with the Creative Commons Attribution NonCommercial (CC BY-NC 4.0) license, which permits others to distribute, remix, adapt, build upon this work non-commercially, and license their derivative works on different terms, provided the original work is properly cited and the use is non-commercial. See: https://creativecommons.org/Licenses/by-nc/4.0/

Country/Territory of origin: Argentina

ORCID number: Federico Alejandro Di Lello 0000-0001-9771-9705; Alfredo Pedro Martínez 0000-0002-1807-0598; Diego Martín Flichman 0000-0001-5730-154X.

S-Editor: Chang KL
L-Editor: Filipodia
P-Editor: Chang KL

REFERENCES

1 **Beasley RP**. Development of hepatitis B vaccine. *JAMA* 2009; **302**: 322-324 [PMID: 19602694 DOI: 10.1001/jama.2009.1024]
2 **Kao JT**, Wang JH, Hung CH, Yen YH, Hung SF, Hu TH, Lee CM, Lu SN. Long-term efficacy of plasma-derived and recombinant hepatitis B vaccines in a rural township of Central Taiwan. *Vaccine* 2009; **27**: 1858-1862 [PMID: 19186203 DOI: 10.1016/j.vaccine.2009.01.027]
3 **Kim YJ**, Li P, Hong JM, Ryu KH, Nam E, Chang MS. A Single Center Analysis of the Positivity of Hepatitis B Antibody

after Neonatal Vaccination Program in Korea. *J Korean Med Sci* 2017; **32**: 810-816 [PMID: 28378555 DOI: 10.3346/jkms.2017.32.5.810]

4 **Hsu SH**, Chih AH, Lee YC, Huang KC, Jan CF. Higher disappearance rate of anti-HBs in Taiwanese freshers neonatally vaccinated with recombinant yeast hepatitis B vaccine. *Liver Int* 2017; **37**: 1780-1787 [PMID: 28374906 DOI: 10.1111/liv.13437]

5 **Hu YC**, Yeh CC, Chen RY, Su CT, Wang WC, Bai CH, Chan CF, Su FH. Seroprevalence of hepatitis B virus in Taiwan 30 years after the commencement of the national vaccination program. *PeerJ* 2018; **6**: e4297 [PMID: 29472994 DOI: 10.7717/peerj.4297]

6 **Shouval D**, Roggendorf H, Roggendorf M. Enhanced immune response to hepatitis B vaccination through immunization with a Pre-S1/Pre-S2/S vaccine. *Med Microbiol Immunol* 2015; **204**: 57-68 [PMID: 25557605 DOI: 10.1007/s00430-014-0374-x]

7 **Krawczyk A**, Ludwig C, Jochum C, Fiedler M, Heinemann FM, Shouval D, Roggendorf M, Roggendorf H, Lindemann M. Induction of a robust T- and B-cell immune response in non- and low-responders to conventional vaccination against hepatitis B by using a third generation PreS/S vaccine. *Vaccine* 2014; **32**: 5077-5082 [PMID: 24975813 DOI: 10.1016/j.vaccine.2014.06.076]

8 **Vesikari T**, Langley JM, Segall N, Ward BJ, Cooper C, Poliquin G, Smith B, Gantt S, McElhaney JE, Dionne M, van Damme P, Leroux-Roels I, Leroux-Roels G, Machluf N, Spaans JN, Yassin-Rajkumar B, Anderson DE, Popovic V, Diaz-Mitoma F; PROTECT Study Group. Immunogenicity and safety of a tri-antigenic *vs* a mono-antigenic hepatitis B vaccine in adults (PROTECT): a randomised, double-blind, phase 3 trial. *Lancet Infect Dis* 2021; **21**: 1271-1281 [PMID: 33989539 DOI: 10.1016/S1473-3099(20)30780-5]

9 **Polaris Observatory Collaborators**. Global prevalence, treatment, and prevention of hepatitis B virus infection in 2016: a modelling study. *Lancet Gastroenterol Hepatol* 2018; **3**: 383-403 [PMID: 29599078 DOI: 10.1016/S2468-1253(18)30056-6]

10 **World Health Organization**. Hepatitis B Control Through Immunization: A Reference Guide. [cited 5 February 2021]. In: World Health Organization [Internet]. Available from: http://iris.wpro.who.int/bitstream/handle/10665.1/10820/9789290616696_eng.pdf;jsessionid=FEDDD4672274909D7E6998B86BED45C8?sequence=3%0Ahttp://www.who.int/immunization/sage/meetings/2015/october/8_WPRO_Hepatitis_B_Prevention_Through_Immunization_Regional_R

11 **de Villiers MJ**, Nayagam S, Hallett TB. The impact of the timely birth dose vaccine on the global elimination of hepatitis B. *Nat Commun* 2021; **12**: 6223 [PMID: 34711822 DOI: 10.1038/s41467-021-26475-6]

12 **World Health Organization**. Progress Towards Global Immunization Goals – 2019. Summary presentations of key indicators, Updated July 2020. [cited 5 February 2021]. In: World Health Organization [Internet]. Available from: https://cdn.who.int/media/docs/default-source/immunization/global_monitoring/slidesglobalimmunization.pdf?sfvrsn=25385c3b_7

13 **World Health Organization**. Combating hepatitis B and C to reach elimination by 2030: advocacy brief (World Health Organization, Geneva, 2016). [cited 5 February 2021]. In: World Health Organization [Internet]. Available from: https://www.who.int/publications/i/item/combating-hepatitis-b-and-c-to-reach-elimination-by-2030

14 **World Health Organization**. Global health sector strategy on viral hepatitis 2016–2021. Towards ending viral hepatitis. [cited 5 February 2021]. In: World Health Organization [Internet]. Available from: https://www.who.int/publications/i/item/WHO-HIV-2016.06

15 **Zanetti AR**, Van Damme P, Shouval D. The global impact of vaccination against hepatitis B: a historical overview. *Vaccine* 2008; **26**: 6266-6273 [PMID: 18848855 DOI: 10.1016/j.vaccine.2008.09.056]

16 **McMahon BJ**, Dentinger CM, Bruden D, Zanis C, Peters H, Hurlburt D, Bulkow L, Fiore AE, Bell BP, Hennessy TW. Antibody levels and protection after hepatitis B vaccine: results of a 22-year follow-up study and response to a booster dose. *J Infect Dis* 2009; **200**: 1390-1396 [PMID: 19785526 DOI: 10.1086/606119]

17 **Mohaghegh Shelmani H**, Karayiannis P, Ashtari S, Mahmanzar MA, Khanabadi B, Modami N, Gholipour F, Zare F, Zali MR. Demographic changes of hepatitis B virus infection in Iran for the last two decades. *Gastroenterol Hepatol Bed Bench* 2017; **10**: S38-S43 [PMID: 29511470]

18 **Garcia D**, Porras A, Rico Mendoza A, Alvis N, Navas MC, De La Hoz F, De Neira M, Osorio E, Valderrama JF. Hepatitis B infection control in Colombian Amazon after 15 years of hepatitis B vaccination. Effectiveness of birth dose and current prevalence. *Vaccine* 2018; **36**: 2721-2726 [PMID: 29609968 DOI: 10.1016/j.vaccine.2017.11.004]

19 **Stroffolini T**, Guadagnino V, Rapicetta M, Menniti Ippolito F, Caroleo B, De Sarro G, Focà A, Liberto MC, Giancotti A, Barreca GS, Marascio N, Lombardo F, Staltari O; Sersale's Study Collaborating Group. The impact of a vaccination campaign against hepatitis B on the further decrease of hepatitis B virus infection in a southern Italian town over 14 years. *Eur J Intern Med* 2012; **23**: e190-e192 [PMID: 22981290 DOI: 10.1016/j.ejim.2012.08.009]

20 **Huynh C**, Minuk GY, Uhanova J, Baikie M, Wong T, Osiowy C. Serological and molecular epidemiological outcomes after two decades of universal infant hepatitis B virus (HBV) vaccination in Nunavut, Canada. *Vaccine* 2017; **35**: 4515-4522 [PMID: 28736196 DOI: 10.1016/j.vaccine.2017.07.040]

21 **Lu FT**, Ni YH. Elimination of Mother-to-Infant Transmission of Hepatitis B Virus: 35 Years of Experience. *Pediatr Gastroenterol Hepatol Nutr* 2020; **23**: 311-318 [PMID: 32704492 DOI: 10.5223/pghn.2020.23.4.311]

22 **Gust ID**. Immunisation against hepatitis B in Taiwan. *Gut* 1996; **38** Suppl 2: S67-S68 [PMID: 8786059 DOI: 10.1136/gut.38.suppl_2.s67]

23 **Chien YC**, Jan CF, Kuo HS, Chen CJ. Nationwide hepatitis B vaccination program in Taiwan: effectiveness in the 20 years after it was launched. *Epidemiol Rev* 2006; **28**: 126-135 [PMID: 16782778 DOI: 10.1093/epirev/mxj010]

24 **Centers for Diseases Control and Prevention**. Epidemiology and Prevention of Vaccine-Preventable Diseases, Chapter 10: Hepatitis B. [cited 5 February 2021]. Available From: https://www.cdc.gov/vaccines/pubs/pinkbook/hepb.html

25 **Liang X**, Bi S, Yang W, Wang L, Cui G, Cui F, Zhang Y, Liu J, Gong X, Chen Y, Wang F, Zheng H, Guo J, Jia Z, Ma J, Wang H, Luo H, Li L, Jin S, Hadler SC, Wang Y. Evaluation of the impact of hepatitis B vaccination among children born during 1992-2005 in China. *J Infect Dis* 2009; **200**: 39-47 [PMID: 19469708 DOI: 10.1086/599332]

26 **Stecher D**, Katz N, Vizzotti C. Hepatitis B en Argentina. Situación actual y estrategia de vacunación universal para su

control y eliminación. *Actualizaciones en Sida e Infectología* 2014; **22**: 18-21

27 **Di Lello FA**, Blejer J, Alter A, Bartoli S, Vargas F, Ruiz R, Galli C, Blanco S, Gallego S, Fernández R, Martínez AP, Flichman DM. Hepatitis B surface antibodies seroprevalence among people born before and after implementation of universal HBV vaccination. *Vaccine* 2020; **38**: 2678-2682 [PMID: 32061386 DOI: 10.1016/j.vaccine.2020.02.014]

28 **Ministerio de Salud y desarrollo Social**. Boletín sobre las Hepatitis Virales en Argentina, N 1, AÑO 1, Octubre 2019. [cited 5 February 2021]. Available from: https://bancos.salud.gob.ar/sites/default/files/2020-01/0000001592cnt-2019-10_boletin-hepatitis.pdf

29 **Da Villa G**, Romanò L, Sepe A, Iorio R, Paribello N, Zappa A, Zanetti AR. Impact of hepatitis B vaccination in a highly endemic area of south Italy and long-term duration of anti-HBs antibody in two cohorts of vaccinated individuals. *Vaccine* 2007; **25**: 3133-3136 [PMID: 17280750 DOI: 10.1016/j.vaccine.2007.01.044]

30 **Harpaz R**, McMahon BJ, Margolis HS, Shapiro CN, Havron D, Carpenter G, Bulkow LR, Wainwright RB. Elimination of new chronic hepatitis B virus infections: results of the Alaska immunization program. *J Infect Dis* 2000; **181**: 413-418 [PMID: 10669320 DOI: 10.1086/315259]

31 **Lin CL**, Kao JH. Hepatitis B: Immunization and Impact on Natural History and Cancer Incidence. *Gastroenterol Clin North Am* 2020; **49**: 201-214 [PMID: 32389359 DOI: 10.1016/j.gtc.2020.01.010]

32 **Chang MH**, Chen CJ, Lai MS, Hsu HM, Wu TC, Kong MS, Liang DC, Shau WY, Chen DS. Universal hepatitis B vaccination in Taiwan and the incidence of hepatocellular carcinoma in children. Taiwan Childhood Hepatoma Study Group. *N Engl J Med* 1997; **336**: 1855-1859 [PMID: 9197213 DOI: 10.1056/NEJM199706263362602]

33 **Chang MH**, You SL, Chen CJ, Liu CJ, Lee CM, Lin SM, Chu HC, Wu TC, Yang SS, Kuo HS, Chen DS; Taiwan Hepatoma Study Group. Decreased incidence of hepatocellular carcinoma in hepatitis B vaccinees: a 20-year follow-up study. *J Natl Cancer Inst* 2009; **101**: 1348-1355 [PMID: 19759364 DOI: 10.1093/jnci/djp288]

34 **Said ZN**, Abdelwahab KS. Induced immunity against hepatitis B virus. *World J Hepatol* 2015; **7**: 1660-1670 [PMID: 26140085 DOI: 10.4254/wjh.v7.i12.1660]

35 **Van Damme P**, Dionne M, Leroux-Roels G, Van Der Meeren O, Di Paolo E, Salaun B, Surya Kiran P, Folschweiller N. Persistence of HBsAg-specific antibodies and immune memory two to three decades after hepatitis B vaccination in adults. *J Viral Hepat* 2019; **26**: 1066-1075 [PMID: 31087382 DOI: 10.1111/jvh.13125]

36 **Sureau C**, Salisse J. A conformational heparan sulfate binding site essential to infectivity overlaps with the conserved hepatitis B virus a-determinant. *Hepatology* 2013; **57**: 985-994 [PMID: 23161433 DOI: 10.1002/hep.26125]

37 **Schulze A**, Gripon P, Urban S. Hepatitis B virus infection initiates with a large surface protein-dependent binding to heparan sulfate proteoglycans. *Hepatology* 2007; **46**: 1759-1768 [PMID: 18046710 DOI: 10.1002/hep.21896]

38 **Urban S**, Bartenschlager R, Kubitz R, Zoulim F. Strategies to inhibit entry of HBV and HDV into hepatocytes. *Gastroenterology* 2014; **147**: 48-64 [PMID: 24768844 DOI: 10.1053/j.gastro.2014.04.030]

39 **Yan H**, Zhong G, Xu G, He W, Jing Z, Gao Z, Huang Y, Qi Y, Peng B, Wang H, Fu L, Song M, Chen P, Gao W, Ren B, Sun Y, Cai T, Feng X, Sui J, Li W. Sodium taurocholate cotransporting polypeptide is a functional receptor for human hepatitis B and D virus. *Elife* 2012; **1**: e00049 [PMID: 23150796 DOI: 10.7554/eLife.00049]

40 **Lu CY**, Ni YH, Chiang BL, Chen PJ, Chang MH, Chang LY, Su IJ, Kuo HS, Huang LM, Chen DS, Lee CY. Humoral and cellular immune responses to a hepatitis B vaccine booster 15-18 years after neonatal immunization. *J Infect Dis* 2008; **197**: 1419-1426 [PMID: 18444799 DOI: 10.1086/587695]

41 **Bruce MG**, Bruden D, Hurlburt D, Zanis C, Thompson G, Rea L, Toomey M, Townshend-Bulson L, Rudolph K, Bulkow L, Spradling PR, Baum R, Hennessy T, McMahon BJ. Antibody Levels and Protection After Hepatitis B Vaccine: Results of a 30-Year Follow-up Study and Response to a Booster Dose. *J Infect Dis* 2016; **214**: 16-22 [PMID: 26802139 DOI: 10.1093/infdis/jiv748]

42 **Wang ZZ**, Gao YH, Lu W, Jin CD, Zeng Y, Yan L, Ding F, Li T, Liu XE, Zhuang H. Long-term persistence in protection and response to a hepatitis B vaccine booster among adolescents immunized in infancy in the western region of China. *Hum Vaccin Immunother* 2017; **13**: 909-915 [PMID: 27874311 DOI: 10.1080/21645515.2016.1250990]

43 **Bitter GA**, Egan KM, Burnette WN, Samal B, Fieschko JC, Peterson DL, Downing MR, Wypych J, Langley KE. Hepatitis B vaccine produced in yeast. *J Med Virol* 1988; **25**: 123-140 [PMID: 3292698 DOI: 10.1002/jmv.1890250202]

44 **Jack AD**, Hall AJ, Maine N, Mendy M, Whittle HC. What level of hepatitis B antibody is protective? *J Infect Dis* 1999; **179**: 489-492 [PMID: 9878036 DOI: 10.1086/314578]

45 **Hall AJ**. Hepatitis B vaccination: protection for how long and against what? *BMJ* 1993; **307**: 276-277 [PMID: 8374369 DOI: 10.1136/bmj.307.6899.276]

46 Immunisation against hepatitis B. *Lancet* 1988; **1**: 875-876 [PMID: 2895375]

47 **Yang S**, Tian G, Cui Y, Ding C, Deng M, Yu C, Xu K, Ren J, Yao J, Li Y, Cao Q, Chen P, Xie T, Wang C, Wang B, Mao C, Ruan B, Jiang T, Li L. Factors influencing immunologic response to hepatitis B vaccine in adults. *Sci Rep* 2016; **6**: 27251 [PMID: 27324884 DOI: 10.1038/srep27251]

48 **Velu V**, Saravanan S, Nandakumar S, Shankar EM, Vengatesan A, Jadhav SS, Kulkarni PS, Thyagarajan SP. Relationship between T-lymphocyte cytokine levels and sero-response to hepatitis B vaccines. *World J Gastroenterol* 2008; **14**: 3534-3540 [PMID: 18567083 DOI: 10.3748/wjg.14.3534]

49 **Körber N**, Pohl L, Weinberger B, Grubeck-Loebenstein B, Wawer A, Knolle PA, Roggendorf H, Protzer U, Bauer T. Hepatitis B Vaccine Non-Responders Show Higher Frequencies of $CD24^{high}CD38^{high}$ Regulatory B Cells and Lower Levels of IL-10 Expression Compared to Responders. *Front Immunol* 2021; **12**: 713351 [PMID: 34566969 DOI: 10.3389/fimmu.2021.713351]

50 **Werner JM**, Abdalla A, Gara N, Ghany MG, Rehermann B. The hepatitis B vaccine protects re-exposed health care workers, but does not provide sterilizing immunity. *Gastroenterology* 2013; **145**: 1026-1034 [PMID: 23916846 DOI: 10.1053/j.gastro.2013.07.044]

51 **Su TH**, Chen PJ. Emerging hepatitis B virus infection in vaccinated populations: a rising concern? *Emerg Microbes Infect* 2012; **1**: e27 [PMID: 26038431 DOI: 10.1038/emi.2012.28]

52 **Poovorawan Y**, Chongsrisawat V, Theamboonlers A, Leroux-Roels G, Kuriyakose S, Leyssen M, Jacquet JM. Evidence

of protection against clinical and chronic hepatitis B infection 20 years after infant vaccination in a high endemicity region. *J Viral Hepat* 2011; **18**: 369-375 [PMID: 20384962 DOI: 10.1111/j.1365-2893.2010.01312.x]

53 **Simons BC**, Spradling PR, Bruden DJ, Zanis C, Case S, Choromanski TL, Apodaca M, Brogdon HD, Dwyer G, Snowball M, Negus S, Bruce MG, Morishima C, Knall C, McMahon BJ. A Longitudinal Hepatitis B Vaccine Cohort Demonstrates Long-lasting Hepatitis B Virus (HBV) Cellular Immunity Despite Loss of Antibody Against HBV Surface Antigen. *J Infect Dis* 2016; **214**: 273-280 [PMID: 27056956 DOI: 10.1093/infdis/jiw142]

54 **Yu AS**, Cheung RC, Keeffe EB. Hepatitis B vaccines. *Clin Liver Dis* 2004; **8**: 283-300 [PMID: 15481341 DOI: 10.1016/j.cld.2004.02.010]

55 **Peto TJ**, Mendy ME, Lowe Y, Webb EL, Whittle HC, Hall AJ. Efficacy and effectiveness of infant vaccination against chronic hepatitis B in the Gambia Hepatitis Intervention Study (1986-90) and in the nationwide immunisation program. *BMC Infect Dis* 2014; **14**: 7 [PMID: 24397793 DOI: 10.1186/1471-2334-14-7]

56 **He WQ**, Guo GN, Li C. The impact of hepatitis B vaccination in the United States, 1999-2018. *Hepatology* 2022; **75**: 1566-1578 [PMID: 34855999 DOI: 10.1002/hep.32265]

57 **Jilg W**, Schmidt M, Deinhardt F. Four-year experience with a recombinant hepatitis B vaccine. *Infection* 1989; **17**: 70-76 [PMID: 2714860 DOI: 10.1007/BF01646879]

58 **Anderson CL**, Remschmidt C, Drobnitzky FP, Falkenhorst G, Zimmermann R, Wichmann O, Harder T. Hepatitis B immune status in adolescents vaccinated during infancy: A retrospective cohort study from a pediatric practice in Germany. *Hum Vaccin Immunother* 2016; **12**: 779-784 [PMID: 26633195 DOI: 10.1080/21645515.2015.1105414]

59 **Schönberger K**, Riedel C, Rückinger S, Mansmann U, Jilg W, Kries RV. Determinants of Long-term protection after hepatitis B vaccination in infancy: a meta-analysis. *Pediatr Infect Dis J* 2013; **32**: 307-313 [PMID: 23249904 DOI: 10.1097/INF.0b013e31827bd1b0]

60 **Mendy M**, Peterson I, Hossin S, Peto T, Jobarteh ML, Jeng-Barry A, Sidibeh M, Jatta A, Moore SE, Hall AJ, Whittle H. Observational study of vaccine efficacy 24 years after the start of hepatitis B vaccination in two Gambian villages: no need for a booster dose. *PLoS One* 2013; **8**: e58029 [PMID: 23533578 DOI: 10.1371/journal.pone.0058029]

61 **Coppola N**, Corvino AR, De Pascalis S, Signoriello G, Di Fiore E, Nienhaus A, Sagnelli E, Lamberti M. The long-term immunogenicity of recombinant hepatitis B virus (HBV) vaccine: contribution of universal HBV vaccination in Italy. *BMC Infect Dis* 2015; **15**: 149 [PMID: 25884719 DOI: 10.1186/s12879-015-0874-3]

62 **Trevisan A**, Mason P, Nicolli A, Maso S, Fonzo M, Scarpa B, Bertoncello C. Future Healthcare Workers and Hepatitis B Vaccination: A New Generation. *Int J Environ Res Public Health* 2021; **18** [PMID: 34360071 DOI: 10.3390/ijerph18157783]

63 **Pileggi C**, Papadopoli R, Bianco A, Pavia M. Hepatitis B vaccine and the need for a booster dose after primary vaccination. *Vaccine* 2017; **35**: 6302-6307 [PMID: 28988867 DOI: 10.1016/j.vaccine.2017.09.076]

64 **Stefanati A**, Bolognesi N, Sandri F, Dini G, Massa E, Montecucco A, Lupi S, Gabutti G. Long-term persistency of hepatitis B immunity: an observational cross-sectional study on medical students and resident doctors. *J Prev Med Hyg* 2019; **60**: E184-E190 [PMID: 31650052 DOI: 10.15167/2421-4248/jpmh2019.60.3.1315]

65 **Bauer T**, Jilg W. Hepatitis B surface antigen-specific T and B cell memory in individuals who had lost protective antibodies after hepatitis B vaccination. *Vaccine* 2006; **24**: 572-577 [PMID: 16171909 DOI: 10.1016/j.vaccine.2005.08.058]

66 World Health Organization. Hepatitis B vaccines: WHO position paper – July 2017. [cited 5 February 2021]. In: World Health Organization [Internet]. Available from: https://www.who.int/immunization/policy/position_papers/hepatitis_b/en/

67 **Schillie S**, Harris A, Link-Gelles R, Romero J, Ward J, Nelson N. Recommendations of the Advisory Committee on Immunization Practices for Use of a Hepatitis B Vaccine with a Novel Adjuvant. *MMWR Morb Mortal Wkly Rep* 2018; **67**: 455-458 [PMID: 29672472 DOI: 10.15585/mmwr.mm6715a5]

68 **Burdick RA**, Bragg-Gresham JL, Woods JD, Hedderwick SA, Kurokawa K, Combe C, Saito A, LaBrecque J, Port FK, Young EW. Patterns of hepatitis B prevalence and seroconversion in hemodialysis units from three continents: the DOPPS. *Kidney Int* 2003; **63**: 2222-2229 [PMID: 12753311 DOI: 10.1046/j.1523-1755.2003.00017.x]

69 **Thio CL**. Hepatitis B and human immunodeficiency virus coinfection. *Hepatology* 2009; **49**: S138-S145 [PMID: 19399813 DOI: 10.1002/hep.22883]

70 **Pereson MJ**, Martínez AP, Isaac K, Laham G, Ridruejo E, Garcia GH, Flichman DM, Di Lello FA. Seroprevalence of hepatitis B, hepatitis C and HIV infection among patients undergoing haemodialysis in Buenos Aires, Argentina. *J Med Microbiol* 2021; **70** [PMID: 33180017 DOI: 10.1099/jmm.0.001278]

71 **Whitaker JA**, Rouphael NG, Edupuganti S, Lai L, Mulligan MJ. Strategies to increase responsiveness to hepatitis B vaccination in adults with HIV-1. *Lancet Infect Dis* 2012; **12**: 966-976 [PMID: 23174382 DOI: 10.1016/S1473-3099(12)70243-8]

72 **Fabrizi F**, Cerutti R, Alfieri CM, Ridruejo E. An Update on Hepatocellular Carcinoma in Chronic Kidney Disease. *Cancers (Basel)* 2021; **13** [PMID: 34298832 DOI: 10.3390/cancers13143617]

73 **Fabrizi F**, Martin P. Hepatitis B virus infection in dialysis patients. *Am J Nephrol* 2000; **20**: 1-11 [PMID: 10644861 DOI: 10.1159/000013548]

74 **Cohen G**, Hörl WH. Immune dysfunction in uremia—an update. *Toxins (Basel)* 2012; **4**: 962-990 [PMID: 23202302 DOI: 10.3390/toxins4110962]

75 **Sampani E**, Vagiotas L, Daikidou DV, Nikolaidou V, Xochelli A, Kasimatis E, Lioulios G, Dimitriadis C, Fylaktou A, Papagianni A, Stangou M. End stage renal disease has an early and continuous detrimental effect on regulatory T cells. *Nephrology (Carlton)* 2022; **27**: 281-287 [PMID: 34781412 DOI: 10.1111/nep.13996]

76 **Sampani E**, Stangou M, Daikidou DV, Nikolaidou V, Asouchidou D, Dimitriadis C, Lioulios G, Xochelli A, Fylaktou A, Papagianni A. Influence of end stage renal disease on CD28 expression and T-cell immunity. *Nephrology (Carlton)* 2021; **26**: 185-196 [PMID: 32935413 DOI: 10.1111/nep.13784]

77 **Fabrizi F**, Lunghi G, Martin P. Treatment of HBV-related liver disease in the dialysis population: reality and promises. *Int J Artif Organs* 2001; **24**: 598-605 [PMID: 11693415]

78 **Kernéis S**, Launay O, Turbelin C, Batteux F, Hanslik T, Boëlle PY. Long-term immune responses to vaccination in HIV-

infected patients: a systematic review and meta-analysis. *Clin Infect Dis* 2014; **58**: 1130-1139 [PMID: 24415637 DOI: 10.1093/cid/cit937]

79 **Moretto F**, Catherine FX, Esteve C, Blot M, Piroth L. Isolated Anti-HBc: Significance and Management. *J Clin Med* 2020; **9** [PMID: 31940817 DOI: 10.3390/jcm9010202]

80 **Rey D**, Krantz V, Partisani M, Schmitt MP, Meyer P, Libbrecht E, Wendling MJ, Vetter D, Nicolle M, Kempf-Durepaire G, Lang JM. Increasing the number of hepatitis B vaccine injections augments anti-HBs response rate in HIV-infected patients. Effects on HIV-1 viral load. *Vaccine* 2000; **18**: 1161-1165 [PMID: 10649616 DOI: 10.1097/00002030-199911120-00016]

81 **Overton ET**, Sungkanuparph S, Powderly WG, Seyfried W, Groger RK, Aberg JA. Undetectable plasma HIV RNA load predicts success after hepatitis B vaccination in HIV-infected persons. *Clin Infect Dis* 2005; **41**: 1045-1048 [PMID: 16142673 DOI: 10.1086/433180]

82 **Paitoonpong L**, Suankratay C. Immunological response to hepatitis B vaccination in patients with AIDS and virological response to highly active antiretroviral therapy. *Scand J Infect Dis* 2008; **40**: 54-58 [PMID: 17852939 DOI: 10.1080/00365540701522975]

83 **Landrum ML**, Huppler Hullsiek K, Ganesan A, Weintrob AC, Crum-Cianflone NF, Barthel RV, Peel S, Agan BK. Hepatitis B vaccine responses in a large U.S. military cohort of HIV-infected individuals: another benefit of HAART in those with preserved CD4 count. *Vaccine* 2009; **27**: 4731-4738 [PMID: 19540026 DOI: 10.1016/j.vaccine.2009.04.016]

84 **Janus N**, Vacher LV, Karie S, Ledneva E, Deray G. Vaccination and chronic kidney disease. *Nephrol Dial Transplant* 2008; **23**: 800-807 [PMID: 18065804]

85 **Zhang W**, Du X, Zhao G, Jin H, Kang Y, Xiao C, Liu M, Wang B. Levamisole is a potential facilitator for the activation of Th1 responses of the subunit HBV vaccination. *Vaccine* 2009; **27**: 4938-4946 [PMID: 19549606 DOI: 10.1016/j.vaccine.2009.06.012]

86 **Haddiya I**. Current Knowledge of Vaccinations in Chronic Kidney Disease Patients. *Int J Nephrol Renovasc Dis* 2020; **13**: 179-185 [PMID: 32801834 DOI: 10.2147/IJNRD.S231142]

87 **Vargas JI**, Jensen D, Martínez F, Sarmiento V, Peirano F, Acuña P, Provoste F, Bustos V, Cornejo F, Fuster A, Acuña M, Fuster F, Soto S, Estay D, Jensen W, Ahumada R, Arab JP, Soza A. Comparative Efficacy of a High-Dose *vs* Standard-Dose Hepatitis B Revaccination Schedule Among Patients With HIV: A Randomized Clinical Trial. *JAMA Netw Open* 2021; **4**: e2120929 [PMID: 34424307 DOI: 10.1001/jamanetworkopen.2021.20929]

88 **Wang C**, Tang J, Song W, Lobashevsky E, Wilson CM, Kaslow RA. HLA and cytokine gene polymorphisms are independently associated with responses to hepatitis B vaccination. *Hepatology* 2004; **39**: 978-988 [PMID: 15057902 DOI: 10.1002/hep.20142]

89 **Davila S**, Froeling FE, Tan A, Bonnard C, Boland GJ, Snippe H, Hibberd ML, Seielstad M. New genetic associations detected in a host response study to hepatitis B vaccine. *Genes Immun* 2010; **11**: 232-238 [PMID: 20237496 DOI: 10.1038/gene.2010.1]

90 **Pan LP**, Zhang W, Zhang L, Wu XP, Zhu XL, Yan BY, Li JY, Xu AQ, Liu Y, Li H. CD3Z genetic polymorphism in immune response to hepatitis B vaccination in two independent Chinese populations. *PLoS One* 2012; **7**: e35303 [PMID: 22536368 DOI: 10.1371/journal.pone.0035303]

91 **Pan L**, Zhang L, Zhang W, Wu X, Li Y, Yan B, Zhu X, Liu X, Yang C, Xu J, Zhou G, Xu A, Li H, Liu Y. A genome-wide association study identifies polymorphisms in the HLA-DR region associated with non-response to hepatitis B vaccination in Chinese Han populations. *Hum Mol Genet* 2014; **23**: 2210-2219 [PMID: 24282030 DOI: 10.1093/hmg/ddt586]

92 **Ou G**, Liu X, Jiang Y. HLA-DPB1 alleles in hepatitis B vaccine response: A meta-analysis. *Medicine (Baltimore)* 2021; **100**: e24904 [PMID: 33832070 DOI: 10.1097/MD.0000000000024904]

93 **Cui W**, Sun CM, Deng BC, Liu P. Association of polymorphisms in the interleukin-4 gene with response to hepatitis B vaccine and susceptibility to hepatitis B virus infection: a meta-analysis. *Gene* 2013; **525**: 35-40 [PMID: 23651591 DOI: 10.1016/j.gene.2013.04.065]

94 **Höhler T**, Reuss E, Freitag CM, Schneider PM. A functional polymorphism in the IL-10 promoter influences the response after vaccination with HBsAg and hepatitis A. *Hepatology* 2005; **42**: 72-76 [PMID: 15918171 DOI: 10.1002/hep.20740]

95 **Duan Z**, Chen X, Liang Z, Zeng Y, Zhu F, Long L, McCrae MA, Zhuang H, Shen T, Lu F. Genetic polymorphisms of CXCR5 and CXCL13 are associated with non-responsiveness to the hepatitis B vaccine. *Vaccine* 2014; **32**: 5316-5322 [PMID: 25077417 DOI: 10.1016/j.vaccine.2014.07.064]

96 **Höhler T**, Reuss E, Evers N, Dietrich E, Rittner C, Freitag CM, Vollmar J, Schneider PM, Fimmers R. Differential genetic determination of immune responsiveness to hepatitis B surface antigen and to hepatitis A virus: a vaccination study in twins. *Lancet* 2002; **360**: 991-995 [PMID: 12383669 DOI: 10.1016/S0140-6736(02)11083-X]

97 **Van Der Meeren O**, Crasta P, Cheuvart B, De Ridder M. Characterization of an age-response relationship to GSK's recombinant hepatitis B vaccine in healthy adults: An integrated analysis. *Hum Vaccin Immunother* 2015; **11**: 1726-1729 [PMID: 25996260 DOI: 10.1080/21645515.2015.1039758]

98 **Weinberger B**, Haks MC, de Paus RA, Ottenhoff THM, Bauer T, Grubeck-Loebenstein B. Impaired Immune Response to Primary but Not to Booster Vaccination Against Hepatitis B in Older Adults. *Front Immunol* 2018; **9**: 1035 [PMID: 29868000 DOI: 10.3389/fimmu.2018.01035]

99 **Ng M**, Fleming T, Robinson M, Thomson B, Graetz N, Margono C, Mullany EC, Biryukov S, Abbafati C, Abera SF, Abraham JP, Abu-Rmeileh NM, Achoki T, AlBuhairan FS, Alemu ZA, Alfonso R, Ali MK, Ali R, Guzman NA, Ammar W, Anwari P, Banerjee A, Barquera S, Basu S, Bennett DA, Bhutta Z, Blore J, Cabral N, Nonato IC, Chang JC, Chowdhury R, Courville KJ, Criqui MH, Cundiff DK, Dabhadkar KC, Dandona L, Davis A, Dayama A, Dharmaratne SD, Ding EL, Durrani AM, Esteghamati A, Farzadfar F, Fay DF, Feigin VL, Flaxman A, Forouzanfar MH, Goto A, Green MA, Gupta R, Hafezi-Nejad N, Hankey GJ, Harewood HC, Havmoeller R, Hay S, Hernandez L, Husseini A, Idrisov BT, Ikeda N, Islami F, Jahangir E, Jassal SK, Jee SH, Jeffreys M, Jonas JB, Kabagambe EK, Khalifa SE, Kengne AP, Khader YS, Khang YH, Kim D, Kimokoti RW, Kinge JM, Kokubo Y, Kosen S, Kwan G, Lai T, Leinsalu M, Li Y, Liang X, Liu S, Logroscino G, Lotufo PA, Lu Y, Ma J, Mainoo NK, Mensah GA, Merriman TR, Mokdad AH, Moschandreas J,

Naghavi M, Naheed A, Nand D, Narayan KM, Nelson EL, Neuhouser ML, Nisar MI, Ohkubo T, Oti SO, Pedroza A, Prabhakaran D, Roy N, Sampson U, Seo H, Sepanlou SG, Shibuya K, Shiri R, Shiue I, Singh GM, Singh JA, Skirbekk V, Stapelberg NJ, Sturua L, Sykes BL, Tobias M, Tran BX, Trasande L, Toyoshima H, van de Vijver S, Vasankari TJ, Veerman JL, Velasquez-Melendez G, Vlassov VV, Vollset SE, Vos T, Wang C, Wang X, Weiderpass E, Werdecker A, Wright JL, Yang YC, Yatsuya H, Yoon J, Yoon SJ, Zhao Y, Zhou M, Zhu S, Lopez AD, Murray CJ, Gakidou E. Global, regional, and national prevalence of overweight and obesity in children and adults during 1980-2013: a systematic analysis for the Global Burden of Disease Study 2013. *Lancet* 2014; **384**: 766-781 [PMID: 24880830 DOI: 10.1016/S0140-6736(14)60460-8]

100 **Weber DJ**, Rutala WA, Samsa GP, Santimaw JE, Lemon SM. Obesity as a predictor of poor antibody response to hepatitis B plasma vaccine. *JAMA* 1985; **254**: 3187-3189 [PMID: 2933532]

101 **Young KM**, Gray CM, Bekker LG. Is obesity a risk factor for vaccine non-responsiveness? *PLoS One* 2013; **8**: e82779 [PMID: 24349359 DOI: 10.1371/journal.pone.0082779]

102 **Liu F**, Guo Z, Dong C. Influences of obesity on the immunogenicity of Hepatitis B vaccine. *Hum Vaccin Immunother* 2017; **13**: 1014-1017 [PMID: 28059607 DOI: 10.1080/21645515.2016.1274475]

103 **Painter SD**, Ovsyannikova IG, Poland GA. The weight of obesity on the human immune response to vaccination. *Vaccine* 2015; **33**: 4422-4429 [PMID: 26163925 DOI: 10.1016/j.vaccine.2015.06.101]

104 **Tagliabue C**, Principi N, Giavoli C, Esposito S. Obesity: impact of infections and response to vaccines. *Eur J Clin Microbiol Infect Dis* 2016; **35**: 325-331 [PMID: 26718941 DOI: 10.1007/s10096-015-2558-8]

105 **Ellulu MS**, Patimah I, Khaza'ai H, Rahmat A, Abed Y. Obesity and inflammation: the linking mechanism and the complications. *Arch Med Sci* 2017; **13**: 851-863 [PMID: 28721154 DOI: 10.5114/aoms.2016.58928]

106 **de Heredia FP**, Gómez-Martínez S, Marcos A. Obesity, inflammation and the immune system. *Proc Nutr Soc* 2012; **71**: 332-338 [PMID: 22429824 DOI: 10.1017/S0029665112000092]

107 **Thomas AL**, Alarcon PC, Divanovic S, Chougne CA, Hildeman DA, Moreno-Fernandez ME. Implications of Inflammatory States on Dysfunctional Immune Responses in Aging and Obesity. *Front Aging* 2021; **2**: 732414 [DOI: 10.3389/fragi.2021.732414]

108 **Frasca D**, Ferracci F, Diaz A, Romero M, Lechner S, Blomberg BB. Obesity decreases B cell responses in young and elderly individuals. *Obesity (Silver Spring)* 2016; **24**: 615-625 [PMID: 26857091 DOI: 10.1002/oby.21383]

109 **Younas M**, Carrat F, Desaint C, Launay O, Corbeau P; ANRS HB03 VIHVAC-B Trial Group. Immune activation, smoking, and vaccine response. *AIDS* 2017; **31**: 171-173 [PMID: 27835620 DOI: 10.1097/QAD.0000000000001311]

110 **Zimmermann P**, Curtis N. Factors That Influence the Immune Response to Vaccination. *Clin Microbiol Rev* 2019; **32** [PMID: 30867162 DOI: 10.1128/CMR.00084-18]

111 **Meier MA**, Berger CT. A simple clinical score to identify likely hepatitis B vaccination non-responders - data from a retrospective single center study. *BMC Infect Dis* 2020; **20**: 891 [PMID: 33238923 DOI: 10.1186/s12879-020-05634-y]

112 **Leroux-Roels G**. Old and new adjuvants for hepatitis B vaccines. *Med Microbiol Immunol* 2015; **204**: 69-78 [PMID: 25523196 DOI: 10.1007/s00430-014-0375-9]

113 **Lee S**, Nguyen MT. Recent advances of vaccine adjuvants for infectious diseases. *Immune Netw* 2015; **15**: 51-57 [PMID: 25922593 DOI: 10.4110/in.2015.15.2.51]

114 **Food and Drug Administration**. Product approval information: package insert. Heplisav-B. Silver Spring, MD: US Department of Health and Human Services, Food and Drug Administration; 2018. [cited 5 February 2021]. Available from: https://www.fda.gov/BiologicsBloodVaccines/Vaccines/ApprovedProducts/ucm584752.htm

115 **Jackson S**, Lentino J, Kopp J, Murray L, Ellison W, Rhee M, Shockey G, Akella L, Erby K, Heyward WL, Janssen RS; HBV-23 Study Group. Immunogenicity of a two-dose investigational hepatitis B vaccine, HBsAg-1018, using a toll-like receptor 9 agonist adjuvant compared with a licensed hepatitis B vaccine in adults. *Vaccine* 2018; **36**: 668-674 [PMID: 29289383 DOI: 10.1016/j.vaccine.2017.12.038]

116 **Splawn LM**, Bailey CA, Medina JP, Cho JC. Heplisav-B vaccination for the prevention of hepatitis B virus infection in adults in the United States. *Drugs Today (Barc)* 2018; **54**: 399-405 [PMID: 30090877 DOI: 10.1358/dot.2018.54.7.2833984]

117 **Halperin SA**, Ward B, Cooper C, Predy G, Diaz-Mitoma F, Dionne M, Embree J, McGeer A, Zickler P, Moltz KH, Martz R, Meyer I, McNeil S, Langley JM, Martins E, Heyward WL, Martin JT. Comparison of safety and immunogenicity of two doses of investigational hepatitis B virus surface antigen co-administered with an immunostimulatory phosphorothioate oligodeoxyribonucleotide and three doses of a licensed hepatitis B vaccine in healthy adults 18-55 years of age. *Vaccine* 2012; **30**: 2556-2563 [PMID: 22326642 DOI: 10.1016/j.vaccine.2012.01.087]

118 **Heyward WL**, Kyle M, Blumenau J, Davis M, Reisinger K, Kabongo ML, Bennett S, Janssen RS, Namini H, Martin JT. Immunogenicity and safety of an investigational hepatitis B vaccine with a Toll-like receptor 9 agonist adjuvant (HBsAg-1018) compared to a licensed hepatitis B vaccine in healthy adults 40-70 years of age. *Vaccine* 2013; **31**: 5300-5305 [PMID: 23727002 DOI: 10.1016/j.vaccine.2013.05.068]

119 **Halperin SA**, Ward BJ, Dionne M, Langley JM, McNeil SA, Smith B, Mackinnon-Cameron D, Heyward WL, Martin JT. Immunogenicity of an investigational hepatitis B vaccine (hepatitis B surface antigen co-administered with an immunostimulatory phosphorothioate oligodeoxyribonucleotide) in nonresponders to licensed hepatitis B vaccine. *Hum Vaccin Immunother* 2013; **9**: 1438-1444 [PMID: 23571179 DOI: 10.4161/hv.24256]

120 **Champion CR**. Heplisav-B: A Hepatitis B Vaccine With a Novel Adjuvant. *Ann Pharmacother* 2021; **55**: 783-791 [PMID: 32988213 DOI: 10.1177/1060028020962050]

121 **Vesikari T**, Finn A, van Damme P, Leroux-Roels I, Leroux-Roels G, Segall N, Toma A, Vallieres G, Aronson R, Reich D, Arora S, Ruane PJ, Cone CL, Manns M, Cosgrove C, Faust SN, Ramasamy MN, Machluf N, Spaans JN, Yassin-Rajkumar B, Anderson D, Popovic V, Diaz-Mitoma F; CONSTANT Study Group. Immunogenicity and Safety of a 3-Antigen Hepatitis B Vaccine *vs* a Single-Antigen Hepatitis B Vaccine: A Phase 3 Randomized Clinical Trial. *JAMA Netw Open* 2021; **4**: e2128652 [PMID: 34636914 DOI: 10.1001/jamanetworkopen.2021.28652]

122 **Alon D**, Stein GY, Hadas-Golan V, Tau L, Brosh T, Turner D. Immunogenicity of Sci-B-Vac (a Third-Generation Hepatitis B Vaccine) in HIV-Positive Adults. *Isr Med Assoc J* 2017; **19**: 143-146 [PMID: 28457089]

123 **Safadi R**, Khoury T, Saed N, Hakim M, Jamalia J, Nijim Y, Farah N, Nuser T, Natur N, Mahamid M, Amer J, Roppert PL, Gerlich WH, Glebe D. Efficacy of Birth Dose Vaccination in Preventing Mother-to-Child Transmission of Hepatitis B: A Randomized Controlled Trial Comparing Engerix-B and Sci-B-Vac. *Vaccines (Basel)* 2021; **9** [PMID: 33915943 DOI: 10.3390/vaccines9040331]

124 **Di Lello FA**, Ridruejo E, Martínez AP, Pérez PS, Campos RH, Flichman DM. Molecular epidemiology of hepatitis B virus mutants associated with vaccine escape, drug resistance and diagnosis failure. *J Viral Hepat* 2019; **26**: 552-560 [PMID: 30576055 DOI: 10.1111/jvh.13052]

125 **Campos-Valdez M**, Monroy-Ramírez HC, Armendáriz-Borunda J, Sánchez-Orozco LV. Molecular Mechanisms during Hepatitis B Infection and the Effects of the Virus Variability. *Viruses* 2021; **13** [PMID: 34207116 DOI: 10.3390/v13061167]

126 **Qin Y**, Liao P. Hepatitis B virus vaccine breakthrough infection: surveillance of S gene mutants of HBV. *Acta Virol* 2018; **62**: 115-121 [PMID: 29895151 DOI: 10.4149/av_2018_210]

127 **Ropero Alvarez AM**, Vilajeliu A, Magariños M, Jauregui B, Guzmán L, Whittembury A, Cain E, Garcia O, Montesanos R, Ruiz Matus C; PAHO MNI working group. Enablers and barriers of maternal and neonatal immunization programs in Latin America. *Vaccine* 2021; **39** Suppl 2: B34-B43 [PMID: 32943263 DOI: 10.1016/j.vaccine.2020.07.051]

World Journal of Gastroenterology

Submit a Manuscript: https://www.f6publishing.com

World J Gastroenterol 2022 August 21; 28(31): 4263-4298

DOI: 10.3748/wjg.v28.i31.4263

ISSN 1007-9327 (print) ISSN 2219-2840 (online)

REVIEW

Evidence-based pathogenesis and treatment of ulcerative colitis: A causal role for colonic epithelial hydrogen peroxide

Jay Pravda

Specialty type: Gastroenterology and hepatology

Provenance and peer review: Unsolicited article; Externally peer reviewed

Peer-review model: Single blind

Peer-review report's scientific quality classification

Grade A (Excellent): 0
Grade B (Very good): 0
Grade C (Good): C, C
Grade D (Fair): 0
Grade E (Poor): 0

P-Reviewer: Iizuka M, Japan; Zhao G, China

Received: January 25, 2022
Peer-review started: January 25, 2022
First decision: April 10, 2022
Revised: April 19, 2022
Accepted: July 20, 2022
Article in press: July 20, 2022
Published online: August 21, 2022

Jay Pravda, Disease Pathogenesis, Inflammatory Disease Research Centre, Palm Beach Gardens, FL 33410, United States

Corresponding author: Jay Pravda, MD, Research Scientist, Senior Researcher, Disease Pathogenesis, Inflammatory Disease Research Centre, 4371 Northlake Blvd No. 247, Palm Beach Gardens, FL 33410, United States. jay.pravda@protonmail.com

Abstract

In this comprehensive evidence-based analysis of ulcerative colitis (UC), a causal role is identified for colonic epithelial hydrogen peroxide (H_2O_2) in both the pathogenesis and relapse of this debilitating inflammatory bowel disease. Studies have shown that H_2O_2 production is significantly increased in the non-inflamed colonic epithelium of individuals with UC. H_2O_2 is a powerful neutrophilic chemo-tactic agent that can diffuse through colonic epithelial cell membranes creating an interstitial chemotactic molecular "trail" that attracts adjacent intra-vascular neutrophils into the colonic epithelium leading to mucosal inflammation and UC. A novel therapy aimed at removing the inappropriate H_2O_2 mediated chemotactic signal has been highly effective in achieving complete histologic resolution of colitis in patients experiencing refractory disease with at least one (biopsy-proven) histologic remission lasting 14 years to date. The evidence implies that therapeutic intervention to prevent the re-establishment of a pathologic H_2O_2 mediated chemotactic signaling gradient will indefinitely preclude neutrophilic migration into the colonic epithelium constituting a functional cure for this disease. Cumulative data indicate that individuals with UC have normal immune systems and current treatment guidelines calling for the suppression of the immune response based on the belief that UC is caused by an underlying immune dysfunction are not supported by the evidence and may cause serious adverse effects. It is the aim of this paper to present experimental and clinical evidence that identifies H_2O_2 produced by the colonic epithelium as the causal agent in the pathogenesis of UC. A detailed explanation of a novel therapeutic intervention to normalize colonic H_2O_2, its rationale, components, and formulation is also provided.

Key Words: Ulcerative colitis; Pathogenesis, Treatment; Hydrogen peroxide

©The Author(s) 2022. Published by Baishideng Publishing Group Inc. All rights reserved.

Core Tip: Ulcerative colitis (UC) is a chronic inflammatory bowel disease that has resisted all efforts to uncover its cause and cure. However, an evidence-based systems medicine approach has provided compelling evidence that the secretion of hydrogen peroxide (H_2O_2) from colonic epithelial cells is the etiological agent responsible for this debilitating illness. H_2O_2 is a highly potent chemotactic agent that can attract neutrophils into the colonic epithelium, and significantly elevated production of H_2O_2 has been documented in the non-inflamed colonic epithelium of individuals with UC. Treatment to normalize colonic H_2O_2 leads to long-lasting histologic remission.

Citation: Pravda J. Evidence-based pathogenesis and treatment of ulcerative colitis: A causal role for colonic epithelial hydrogen peroxide. *World J Gastroenterol* 2022; 28(31): 4263-4298
URL: https://www.wjgnet.com/1007-9327/full/v28/i31/4263.htm
DOI: https://dx.doi.org/10.3748/wjg.v28.i31.4263

INTRODUCTION

Treating ulcerative colitis (UC) has never been easy. The natural history of UC is one of worsening and progressive disease, and no currently available approved medication can cure the life-long repeating episodes of rectal bleeding, diarrhea, and abdominal pain that are experienced by individuals suffering from this illness[1]. The difficulty in choosing from currently available non-curative therapies was underscored by a recent study, which concluded that the majority of clinical guidelines for the treatment of UC are based on low or very low-quality evidence[2]. Thus, we are left with therapies that cannot cure and have a disappointing track record when it comes to treatment.

The distress engendered by the lack of effective treatment is universal with the majority of UC patients in a 10-country global survey reporting poor disease control, mental exhaustion, and adverse impact on quality of life[3]. This is consistent with other multi-country studies reporting that UC was not controlled in over 87% of participants[4]. The real-world effects of non-curative low-quality therapy are evident by the high degree of medical treatment failure that is responsible for up to a 30% colectomy rate in patients with this illness[5]. With a dismal 40% one-year clinical remission rate for current drugs that alter the immune response, and similar upcoming drugs no more effective, there is no reason to believe that any treatment focused on modifying the immune response will improve current patient outcomes[6]. We are thus left to conclude that this class of therapeutics has reached the limit of clinical effectiveness, and any hope for effective therapy or a cure can only arrive with a fundamentally new approach in our understanding and treatment of this disease.

Almost all treatments for UC consist of agents that modify, alter, or suppress the immune response[7, 8]. This is based on the belief that an underlying immune abnormality is the cause of this condition. But is this assumption evidence-based? Unfortunately not, despite extensive research conducted since the mid-20th century, no evidence of a causal antecedent immune vulnerability has been uncovered in individuals with UC or their first-degree relatives[9]. Additionally, studies in UC patients have revealed normal immune responses when compared to healthy controls[10,11]. Thus, the evidence indicates that an immune abnormality is not the cause of UC, and treatment directed against the immune response cannot bring about a cure, restore healthy colonic functionality, or a normal quality of life.

Faced with these facts, we must consider that the immune response in UC is an accompanying effect of a separate underlying phenomenon that has a causal role in the development of this disease. In other words, the immune system is doing what it's programed to do given the stimulus it is subjected to. But if there's nothing wrong with the immune system then what stimulus could cause inflammation of the colon leading to UC and how can we treat it? The next section describes a novel evidence-based pathogenesis that provides answers to these questions.

UC: AN EVIDENCE-BASED PATHOGENESIS

A causal role for colonic epithelial cell hydrogen peroxide in the pathogenesis of UC

In order to understand the pathogenesis of UC and develop an effective treatment, we need to answer several questions. Starting with what we can see, we must explain why the inflammation typically begins in the rectum and advances contiguously to more proximal regions of the colon without sparing intervening mucosa. We also need to identify the molecular mechanism that initiates the inflammation in the first place. In other words, how the inflammation begins. This raises the question of what causes this mechanism to initially appear and reappear over and over again after (apparently) successful treatment leading to life-long relapse. Finally, we need to derive the genetic predisposition that makes this all possible. Understanding the overlapping lineal sequence of events leading up to UC and the

mechanism of relapse is crucial for effective therapeutic intervention and long-term remission so as to permanently alter the natural history of disease. Stated differently, we will start with what we can see (the inflammation) and work our way upstream until we arrive at the inception of disease, which originates from the interaction of a shared genetic predisposition with exposomal elements giving rise to a final common pathway that must be present among all individuals with UC; at all times basing our conclusions on the known experimental evidence.

Neutrophils are the first responders into the colonic epithelium in UC with the formation of neutrophilic cryptitis and neutrophilic crypt abscesses, which are hallmarks of active inflammation[12-14]. This typically begins in the rectum causing mucosal inflammation, which advances proximally and contiguously (without skipping). Once in contact with bacteria in the rectal epithelium, neutrophils are activated to release large amounts of hydrogen peroxide (H_2O_2). Studies have shown that a single neutrophil can produce enough H_2O_2 to diffuse into and oxidize nearly all the hemoglobin contained in ten intact surrounding red blood cells[15].

H_2O_2 is a cell-membrane permeable, highly potent neutrophilic chemotactic factor that attracts neutrophils into the colonic epithelium[16]. Studies have demonstrated that neutrophils can respond to and migrate towards an H_2O_2 concentration variation of 100 picomolar, which is a difference of approximately five molecules of H_2O_2 between the leading and trailing halves of the neutrophil[17]. H_2O_2 is also a powerful oxidizing agent that disintegrates tight junctional proteins[18-21]. This leads to increased paracellular permeability and decreased epithelial resistance, which is characteristically observed in UC[22-25].

The resulting H_2O_2 mediated increase in paracellular permeability facilitates antigenic translocation across the colonic epithelium while simultaneously creating an H_2O_2 chemotactic gradient, both of which act cooperatively to attract other neutrophils into the advancing proximal edge of the inflammatory field thereby extending colonic inflammation from the rectum, in a contiguous fashion, to more proximal regions of the colon. The inflammation only halting upon encountering sufficient circumferential epithelial reductive capacity to neutralize the advancing wave of neutrophil released H_2O_2, resulting in a sharp demarcation between healthy and diseased tissue. This redox tug-of-war between epithelial reductive capacity and neutrophilic H_2O_2 explains the characteristic proximal migratory behavior of colonic mucosal inflammation in UC. This interpretation is supported by studies showing that neutrophil accumulation within epithelial crypts and in the intestinal mucosa directly correlates with clinical disease activity and epithelial injury in individuals with UC[26]. Stated differently, neutrophils in the crypts of Lieberkühn secrete large amounts of H_2O_2 that attracts other neutrophils into the epithelium. Continuous secretion of H_2O_2 by neutrophils overwhelms epithelial reductive (antioxidant) capacity causing additional neutrophils to enter the inflammatory field. This advances the inflammation in a proximal direction until sufficient epithelial reductive (antioxidant) capacity is encountered to stop further proximal advance.

On a cellular level, neutrophils in the colonic epithelium can be thought of as microscopic H_2O_2 factories, whose function can be replaced by exogenous H_2O_2. This interpretation is supported by rectal H_2O_2 infusion studies in mice resulting in sharp inflammatory tissue delineation from normal tissue, contiguous inflammatory proximal extension, and rectal inflammatory persistence (discussed below), which are also characteristic of human UC[27]. Additionally, the colonic introduction of H_2O_2 in humans results in classic UC[28]. Although this explains proximal extension, the next step is to explicate what causes these white blood cells (neutrophils) to move into the colonic epithelium in the first place causing inflammation and why it typically starts in the rectum?

Neutrophils are attracted into the colonic epithelium by H_2O_2 secreted by the colonic epithelium

Neutrophils are not the only cells in the body that produce H_2O_2. All living cells in the body generate H_2O_2 from metabolic reactions, including colonic epithelial cells (colonocytes)[29]. Studies have shown increased production of H_2O_2 in ascending non-inflamed colonic epithelium from patients with UC[30]. This indicates a pre-inflammatory build-up of H_2O_2 within colonocytes. In other words, H_2O_2 builds up in colonic epithelial cells prior to the appearance of inflammation satisfying the absolute requirement of chronology for the cause (H_2O_2) to precede the effect (colitis).

H_2O_2 is membrane permeable and can easily diffuse through the colonic epithelial cell membrane to the extracellular space[29]. Once outside the colonocyte, H_2O_2 initiates inflammation *via* the same mechanism as H_2O_2 secreted by neutrophils, *i.e.*, oxidative disintegration of tight junctions and neutrophilic chemotaxis. Other studies have shown that reductive capacity (ability to neutralize H_2O_2) progressively decreases from proximal to distal regions of the colon with rectal epithelial cells having the least protection against the buildup of H_2O_2[31]. This causes the rectum to be the initial location in the colonic epithelium where H_2O_2 will build up and, upon diffusion to the colonocyte extracellular space, attract neutrophils into the rectal epithelium causing inflammation and colitis. And due to its diminished reductive capacity, the rectum will be the last colonic region to heal resulting in a persistent ulcerative proctitis that is experienced by many patients.

Studies in genetically engineered mice that are unable to neutralize colonic H_2O_2 [glutathione (GSH) peroxidase knock-out mice] develop colitis analogous to human UC[32]. This indicates that colonic epithelial cells can generate enough H_2O_2, which upon extracellular diffusion, can initiate colonic inflammation and colitis. The mechanism behind the initial increase in colonocyte H_2O_2 giving rise to

human UC will be discussed below in the section on oxidative stressors.

In other words, H_2O_2 is a normal immune signaling molecule that attracts neutrophils. Neutrophils cannot determine which cell is secreting H_2O_2; whether it's another neutrophil calling for help fighting an infection or a colonic epithelial cell leaking H_2O_2. In the latter case, neutrophils are simply doing what they are programmed to do given the stimulus (H_2O_2) they are exposed to. The development of UC indicates a healthy functioning innate immune system responding to a normal immune chemotactic factor (H_2O_2) being inappropriately secreted by the colonic epithelium. The correct treatment (discussed below) is not to abrogate this normal response with drugs that suppress essential innate normal immune reactivity but to restore colonic redox homeostasis so as to prevent colonocyte secretion of H_2O_2.

In summary, H_2O_2's unique properties of cell membrane permeability, long life, potent oxidizing potential, and neutrophilic chemotactic capability combine to promote colonocyte extracellular diffusion followed by oxidative disintegration of colonic epithelial tight junctional proteins, which facilitates bacterial translocation from the colonic lumen into the sterile subjacent lamina propria while simultaneously (and chemotactically) attracting neutrophils into the colonic epithelium, both of which lead to colonic inflammation, and eventual UC (Figures 1A and 1B). H_2O_2 initially accumulates in colonocytes and diffuses to the extra-cellular space in the rectal epithelium, which has the least tissue reductive capacity of the entire colon.

Neutrophils in the subjacent epithelial vasculature migrate along the interstitial H_2O_2 concentration gradient to the source of the H_2O_2 in the rectal epithelium. Once exposed to lumenal antigens, neutrophils are activated to secrete large amounts of H_2O_2, which promotes further neutrophilic infiltration while migrating the advancing edge of the inflammatory field to more proximal regions of the colon as described above. H_2O_2 also causes vasodilation and severe damage to blood vessels with destruction of endothelial cells and disruption of endothelial cell tight junctions[33-35]. This leads to erythrocyte extravasation and bleeding into the colonic lumen as commonly observed in UC. Thus, the effects of H_2O_2 on the innate immune system and vasculature explain both the microscopic and macroscopic features that characterize UC. The next section provides an evidence-based explanation for relapse. Following this, the concept of oxidative stress is discussed, which provides an evidence-based mechanism to explicate why H_2O_2 builds up in the colonic epithelium to begin with.

Relapse: An acquired "hard-wired" vicious cycle of inflammation

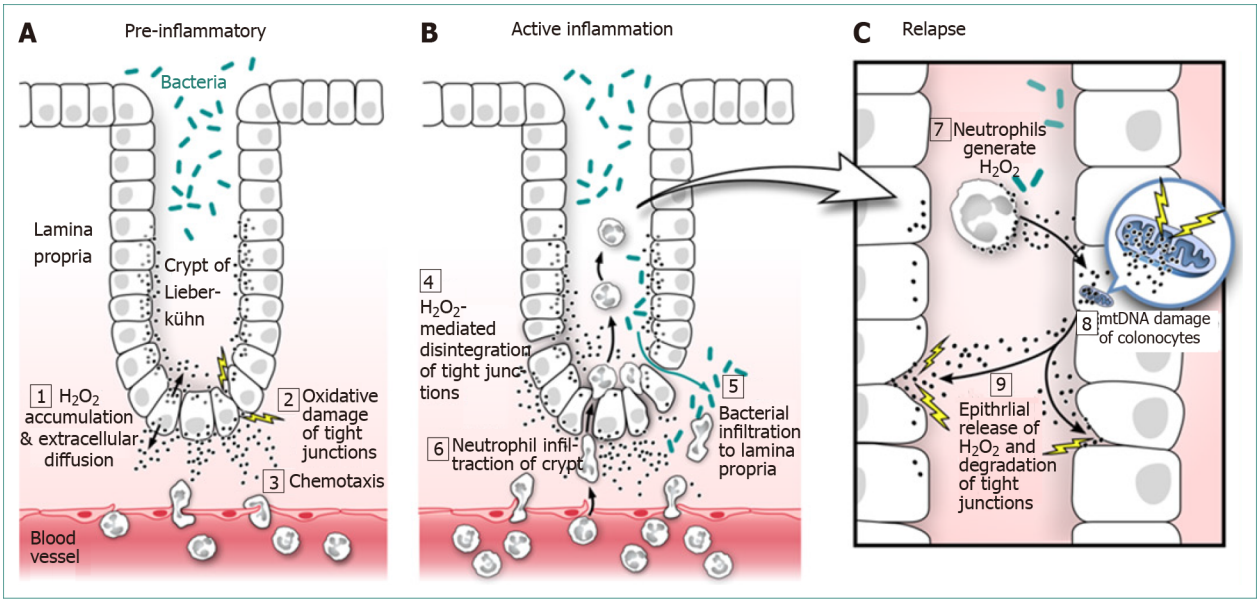
Once complete histologic remission has been achieved and the colonic epithelium is free of inflammatory cells, neutrophils can, once again, migrate back into the colonic epithelium after medication is withdrawn. This resumption of inflammation after a period of quiescent disease is called relapse, also known as a flare. Stated differently, if UC were simply a function of exposure to environmental factors, neutrophils would not migrate back into the colonic epithelium causing mucosal inflammation and relapse after exposure has ceased and medication is withdrawn.

Relapse indicates that a fundamental change has occurred in colonic epithelial cells before and/or during mucosal inflammation leading to increased production of H_2O_2, which continues to diffuse throughout the extracellular space resulting in neutrophilic chemotactic migration into the colonic epithelium and eventual relapse. This is consistent with the significantly elevated intracellular colonocyte H_2O_2 production observed in the non-involved colonic epithelium in patients with UC[30]. The question is why do colonocytes in individuals with UC produce more H_2O_2 than normal?

The answer is suggested by the susceptibility of mitochondrial DNA (mtDNA) to H_2O_2-induced oxidative damage. Due to their lack of histones, limited repair capability, and high single strand exposure time, mtDNA is highly susceptible to H_2O_2-induced oxidative damage[36,37]. H_2O_2 induced oxidative damage to mtDNA introduces base mutations into the mitochondrial genome, which miscode during transcription of electron transport chain (ETC) complexes resulting in nucleotide mispairing and the incorporation of faulty protein subunits into the ETC. These acquired mitochondrial ETC mutations cause increased ETC electron leakage that produces increased amounts of superoxide, which is converted to excess H_2O_2. The end result is a dysfunctional mitochondrial ETC that generates higher levels of cellular H_2O_2, which upon extracellular diffusion initiates a relapse of colonic inflammation (Figure 1C)[38].

The elevated colonocyte H_2O_2 resulting in mtDNA mutations originates from two sources. The initial increase in colonocyte H_2O_2 is intracellular and originates from oxidative stress exposure (discussed in the next section). This is augmented by a large exogenous source of H_2O_2 supplied by neutrophils that stream into the colonic epithelium and fill up the crypts of Lieberkühn. Being cell membrane permeable, H_2O_2 can easily diffuse into surrounding epithelial stem cells and transition amplification cells, which give rise to the surface epithelium. This "back flow" of H_2O_2 into colonocytes would ordinarily be neutralized by the cell. However, colonocyte reductive capacity has already been compromised by the initial rise in cellular H_2O_2 due to oxidative stress exposure. This allows intracellular H_2O_2 to diffuse unimpeded throughout the colonocyte into mitochondria leading to mtDNA oxidative damage and acquired mutations.

A causal role for mitochondrial ETC generated H_2O_2 in the development of relapse is consistent with the onset of impaired mitochondrial beta-oxidation in the weeks leading up to relapse, which is reported to be caused by H_2O_2 induced oxidative inhibition of mitochondrial thiolase, a necessary



DOI: 10.3748/wjg.v28.i31.4263 **Copyright** ©The Author(s) 2022.

Figure 1 Ulcerative colitis: Evidence-based pathogenesis and relapse. A: Pre-inflammatory; B: Active inflammation; C: Relapse. Hydrogen peroxide (H_2O_2) is produced by all cells of the body, mainly as a toxic by-product of cellular metabolism and must be immediately neutralized to prevent cell damage. If produced in excess by colonocytes (colonic epithelial cells), H_2O_2 easily diffuses through the cell membrane; 1: To the extracellular space where its unique properties of long life, potent oxidizing power, and the ability to attract neutrophils (neutrophilic chemotaxis) combine to promote oxidative damage of colonocyte tight junctions; 2: While attracting neutrophils into the colonic epithelium; 3: Continued H_2O_2 exposure leads to oxidative disintegration of tight junctional proteins and increased colonic epithelial paracellular permeability; 4: Increased paracellular permeability promotes bacterial translocation into the sterile lamina propria; 5: And facilitates neutrophil migration up the H_2O_2 concentration gradient into the crypts of Lieberkühn; 6: Both of which lead to colonic inflammation and eventual ulcerative colitis. Neutrophils exposed to bacteria in the crypts become activated and produce large amounts of H_2O_2 that diffuses into colonic epithelial cells; 7: Which adds to the already high colonocyte H_2O_2 load. The increased colonocyte H_2O_2 oxidizes mitochondrial DNA (mtDNA) introducing genetic mutations that miscode when transcribing for electron transport chain (ETC) proteins; 8: Faulty ETC proteins exhibit additional electron leakage leading to greater H_2O_2 production creating a vicious cycle of mtDNA damage and ever greater H_2O_2 production, which contributes to and increases the frequency and severity of relapse; 9: This amounts to a "hard-wired" genetic reprogramming that promotes colonic inflammation as discussed below. H_2O_2: Hydrogen peroxide; mtDNA: Mitochondrial DNA.

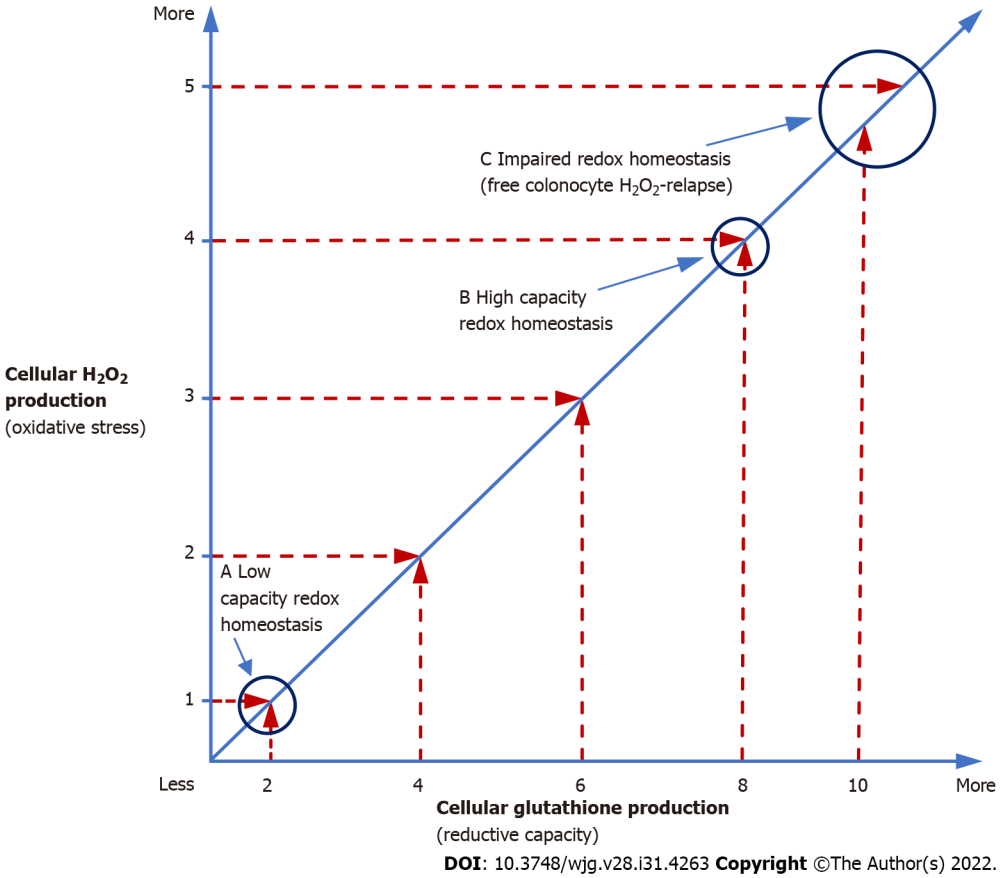
enzyme in the mitochondrial beta-oxidation pathway[39-41]. The involvement of ETC-generated H_2O_2 in UC relapse is supported by reports of intractable UC in the setting of inherited ETC disfunction[42]. At birth, all mtDNA is normally identical. This is called homoplasmy. After H_2O_2-induced base mutations are introduced into the mitochondrial genome, all mtDNA is no longer identical. The simultaneous occurrence of genetically dissimilar cellular mtDNA (normal and mutated) is called mitochondrial heteroplasmy[43]. Studies have shown a significant degree of heteroplasmic mtDNA in the colonic epithelium of individuals with UC[44,45]. The presence of colonocyte mitochondrial heteroplasmy in UC will constitutively generate higher amounts of H_2O_2 leading to additional mtDNA damage and greater H_2O_2 production creating a self-amplifying vicious cycle of ever-increasing colonocyte H_2O_2[46]. This constitutive internally reinforcing production of colonocyte H_2O_2 perpetuates mucosal inflammation leading to relapse upon withdrawal of medication. The increased basal production of colonocyte H_2O_2 promotes more frequent episodes of relapse and leads to refractory disease as colonocyte H_2O_2 increases and UC becomes less responsive to medication.

Up until now, we have an H_2O_2-based mechanism that explains how UC begins, why inflammation extends proximally throughout the colon, and how mitochondrial heteroplasmy promotes a constitutive increase in colonocyte H_2O_2 that contributes to relapse. What we are missing is why colonocyte H_2O_2 becomes elevated in the first place. To understand this, we need to discuss the concept of oxidative stress as outlined in the next section for it is exposure to oxidative stress that initiates *de novo* development (and relapse) of UC.

OXIDATIVE STRESS

The invisible force that increases H_2O_2 and leads to UC

We are all subjected to oxidative stress since the moment of conception. But what is oxidative stress? More importantly, how can we define oxidative stress in a manner that is relevant for diagnosing disease, understanding pathogenesis, and advancing therapeutic intervention. Since most biological effects of reactive oxidant species are mediated by H_2O_2[47], and since cellular GSH is principally responsible for supplying the reducing equivalents (electrons) needed to neutralize H_2O_2[48,49], a



DOI: 10.3748/wjg.v28.i31.4263 **Copyright** ©The Author(s) 2022.

Figure 2 Redox homeostasis. Redox homeostasis is more than just a balance between oxidizing [hydrogen peroxide (H_2O_2)] and reducing agents (glutathione). In the above graph, redox homeostasis (slanted line) is maintained at both low and high H_2O_2 production rates (a and b), but the cell is functioning at a higher oxidative capacity (high capacity redox homeostasis) (b), when more H_2O_2 is being produced compared to times when lesser amounts of H_2O_2 are being generated (a). Mitochondria, the site of most cellular H_2O_2 production, do not synthesize their own glutathione and only contain 10% of the total cellular supply of this vital reducing equivalent that must be generated in the cytoplasm and imported into mitochondria, which takes time[53]. Once depleted, mitochondrial glutathione can take several hours to restore to normal levels[46]. In contrast to the limited supply of mitochondrial glutathione, studies have shown that mitochondrial electron transport chain production of H_2O_2 can increase up to 15 × during periods of high metabolic demand[54]. Any increase in H_2O_2 production forces the cell to utilize additional glutathione in order to maintain redox balance which may lead to high capacity redox homeostasis (b). Since about 30% of cell thiols (*i.e.*, glutathione) normally undergo oxidation per hour[55], the additional oxidative stress imposed by high capacity redox homeostasis can, over time, deplete available glutathione and overwhelm colonocyte reductive capacity creating a state of impaired redox homeostasis (c) followed by H_2O_2 build-up and extracellular diffusion, which can lead to *de novo* ulcerative colitis or relapse. High capacity redox homeostasis is consistent with increased H_2O_2 production observed in the non-inflamed ascending colonic epithelium of individuals with ulcerative colitis[30]. H_2O_2: Hydrogen peroxide.

clinical working definition of oxidative stress can be summarized as any stimulus that increases the amount or production of H_2O_2 or elevates the risk of its occurrence by decreasing cellular reductive (antioxidant) capacity (*i.e.*, GSH). Stimuli that fulfill this definition are called oxidative stressors.

Oxidative stressors can be external (*i.e.*, environmental) or internal (originating in the body). Many oxidative stressors can be identified by the medical history and targeted for elimination by changes in diet and lifestyle. Clinically assessing the risk that oxidative stress will increase H_2O_2 leading to worsening disease requires a working understanding of redox homeostasis. Redox homeostasis refers to the balance that is achieved when there is sufficient cellular reductive capacity (GSH) to neutralize the H_2O_2 being produced. Thus, an oxidative stressor is a stimulus that places additional demands on the cell's capacity to neutralize H_2O_2 and maintain redox homeostasis. Over time, oxidative stress can disrupt the cell's ability to maintain this critical balance. When this occurs it is called impaired redox homeostasis, which can lead to the build-up of colonocyte H_2O_2 resulting in extracellular diffusion, mucosal inflammation, and UC as described above. Thus, identifying and eliminating oxidative stressors in order to assist in restoring colonic redox homeostasis is critical for the maintenance of long-term remission in UC. In order to maintain redox homeostasis, colonocytes utilize as much GSH as needed to neutralize the H_2O_2 that is being produced by the cell. In this reaction, two molecules of GSH react with one molecule of H_2O_2 *via* the action of GSH peroxidase (GPx) to yield one molecule of GSH disulfide (GSSG) and one molecule of water, as illustrated below.

$$2\,GSH + H_2O_2 \xrightarrow{GPx} GSSG + H_2O_2$$

At higher levels of H_2O_2 production significantly more GSH is consumed compared to lower levels of H_2O_2 production in order to maintain a 2 (GSH) to 1 (H_2O_2) balance or redox homeostasis. However, higher levels of GSH consumption enhance the risk of GSH depletion after which free H_2O_2 can begin to accumulate within the cell[50].

Thus, all redox homeostasis is not the same. Redox homeostasis maintained at high levels of H_2O_2 production [high capacity redox homeostasis (HCRH)] increases the risk of GSH depletion and subsequent accumulation of intracellular H_2O_2 (Figure 2). HCRH indicates that the cell has a greater capacity to oxidize substrate such as GSH and is consuming GSH at greater rates than normal. As long as the substrate being oxidized is GSH, redox homeostasis can be maintained and the cell is protected from the toxic effects of H_2O_2 buildup. However, if GSH is depleted due to excessive utilization by HCRH, H_2O_2 is free to diffuse throughout the cell and oxidize other molecules in the colonocyte such as enzymes and DNA. This can lead to metabolic disturbances such as impaired mitochondrial beta-oxidation in addition to oxidative nuclear DNA mutations in tumor suppression and oncogenes that promote colorectal cancer as well as mtDNA mutations (mitochondrial heteroplasmy) that increase cellular H_2O_2 production and facilitate disease relapse[30,51,52] (Figure 2).

Even if redox homeostasis is maintained during HCRH, the high demand for GSH may sequester this vital reducing agent away from other critical metabolic functions that depend upon GSH such as elimination of toxic xenobiotics and electrophiles, regulation of apoptosis and cell division, GSH dependent enzymes, maintenance of reduced vitamins C and E for cell membrane protection, and glutathionylation of proteins/enzymes to protect against irreversible oxidative damage[56-58]. Thus, HCRH may consume GSH needed for other cellular activity and compromise colonocyte and colonic functionality independent of the development of UC.

Exposure to multiple contemporaneous oxidative stressors facilitates progressively greater production of H_2O_2 that increases the risk of reaching HCRH, which can lead to impaired redox homeostasis with the development of symptomatic UC (Figure 2C). This explains why the initial appearance of UC can be very explosive since HCRH may lead to sudden depletion of GSH causing significant acute increases in cellular H_2O_2, which can lead to severe mucosal inflammation as large amounts of colonocyte H_2O_2 diffuse to the cell exterior. Lesser amounts of colonocyte extracellular H_2O_2 can account for the pre-symptomatic systemic inflammation observed in individuals who go on to develop UC[59]. Seemingly insignificant oxidative stressors can lead to relapse for individuals functioning at HCRH. This should prompt a search for other unrecognized oxidative stress exposures to prevent relapse. Lastly, an important distinction to keep in mind is that oxidative stress is not the same as oxidative damage. Oxidative stress appears before oxidative damage occurs, while oxidative damage always indicates previous or ongoing oxidative stress. Rectal bleeding in UC is an indication of severe concurrent oxidative (H_2O_2 induced) tissue damage caused by exposure to oxidative stress.

In summary, oxidative stress increases H_2O_2 in the body. Oxidative stressors mediate the effects of oxidative stress on the body. As H_2O_2 increases, colonocytes utilize greater amounts of GSH to maintain redox balance leading to HCRH, which can deplete cellular GSH leading to *de novo* UC or relapse. The increased H_2O_2 production rates observed in the non-inflamed colonic epithelium of individuals with UC indicate the presence of HCRH[30]. The effects of multiple oxidative stressors are additive, each contributing to the cellular H_2O_2 load. HCRH may lead to a GSH deficiency state and cellular disfunction**.** In the next section, we put it all together and derive the genetic susceptibility that predisposes to the development of UC.

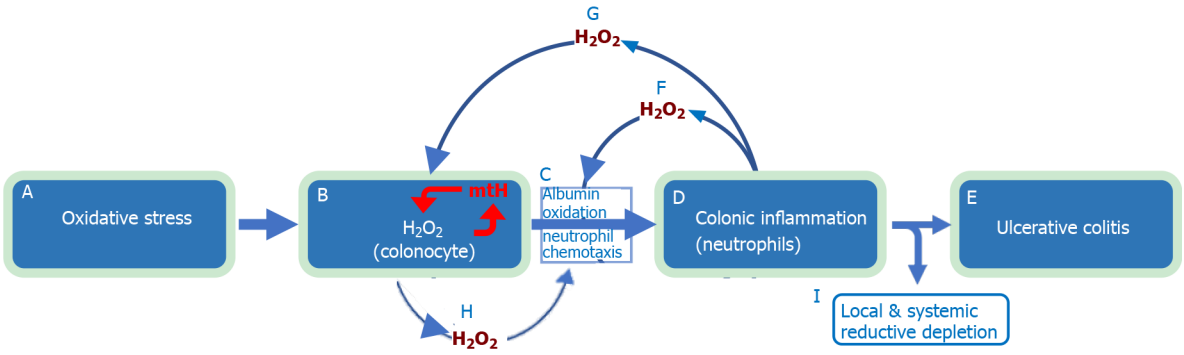
PUTTING IT ALL TOGETHER

Predisposition, pathogenesis, pathophysiology, and relapse

Based on the cumulative data, we can now construct an evidence-based natural history of UC. The disease begins with exposure to one or more oxidative stressors, which increase the production of colonocyte H_2O_2. Over time, cellular reductive capacity is overwhelmed as the colonocyte is no longer able to maintain HCRH and H_2O_2 accumulates in the cell. This is followed by H_2O_2 diffusion through the cell membrane to the extracellular space within the crypts of Lieberkühn and the surrounding cellular microenvironment. This results in oxidative damage to interepithelial tight junctions and increased paracellular permeability accompanied by the creation of an H_2O_2 diffusion gradient that envelops the subjacent microvasculature.

The combined effect of colonic epithelial antigenic translocation due to increased paracellular permeability and H_2O_2 gradient-guided neutrophilic chemotaxis results in directed migration of neutrophils from the subjacent vasculature into the crypts of Lieberkühn along with the formation of neutrophilic cryptitis and crypt abscesses. Continued neutrophilic infiltration into the colonic epithelium leads to mucosal inflammation and UC (Figures 3A-E).

The rectum, having the lowest reductive capacity of the intestinal tract, is the initial site of H_2O_2 accumulation and the first region to experience inflammation, which proceeds in a proximal direction as continuous secretion of large amounts of neutrophil released H_2O_2 overcomes colonic epithelial reductive capacity in a circumferential manner resulting in a sharp demarcation between healthy and



DOI: 10.3748/wjg.v28.i31.4263 **Copyright** ©The Author(s) 2022.

Figure 3 Natural history of ulcerative colitis. The evidence-based natural history of ulcerative colitis begins with exposure to oxidative stressors (a), which increases colonocyte hydrogen peroxide (H_2O_2) (b). The increase in colonocyte H_2O_2 facilitates extracellular diffusion which overwhelms (oxidizes) local interstitial serum albumin antioxidant defense (60% of serum albumin is interstitial), leading to directed migration of neutrophils (chemotaxis) into the colonic epithelium (c) and mucosal inflammation (d) with subsequent development of ulcerative colitis (e). Large amounts of H_2O_2 are released by neutrophils into the extracellular space (f) with further oxidation of interstitial albumin and exhaustion of tissue antioxidant capacity (c). This worsens colonic inflammation (d) leading to local and systemic reductive depletion (i) as albumin is circulated through the colonic interstitium into tissue lymphatics and back into the systemic circulation. Neutrophil released H_2O_2 "back flows" into colonocytes (g) adding to the already elevated intracellular H_2O_2 levels resulting in mitochondrial DNA damage and mitochondrial heteroplasmy (b, red mtH). Mitochondrial heteroplasmy introduces mutations into the electron transport chain protein subunits, which generate additional H_2O_2 *via* enhanced electron leakage setting up a vicious cycle of ever increasing colonocyte H_2O_2 (b, red arrows). Increased colonocyte H_2O_2 diffuses into the extracellular space (h) causing disease relapse (c, d, e). The combination of local and systemic reductive depletion along with a ready supply of H_2O_2 from colonocytes and neutrophils (b and d) creates a mucosal inflammation that is self-amplifying, forward propagating, and auto-initiating (relapsing). Elimination of neutrophilic inflammation (d) by any means (*i.e.*, immunosuppressive agents) will not stop relapse from occurring as colonocyte H_2O_2 continues to diffuse into the extracellular space (c, h). Conversely, normalizing colonocyte H_2O_2 alone will not stop the inflammation, which has become self-sustaining. This indicates that simultaneous elimination of all pathological sources contributing H_2O_2 to the inflammatory field must be achieved to ensure long-term remission and normal colonic functionality. Systemic reductive depletion may contribute to other serious health hazards as detailed below. H_2O_2: Hydrogen peroxide.

diseased tissue (epithelial cells at the same circumferential level have the same reductive capacity). Mucosal inflammation may reach more proximally and regress distally over time as a result of fluctuations in colonic epithelial reductive capacity due to changes in oxidative stress exposure (diet, stress, *etc.*) and epithelial repopulation.

The large amount of H_2O_2 released by neutrophils in the inflammatory field is chemotactic for other neutrophils in the subjacent vascular bed. This causes epithelial inflammation to become self-propagating and auto-amplifying (Figure 3F), which enables prolonged contact between neutrophils and surrounding colonocytes. This close contact facilitates the back-flow of neutrophil-derived H_2O_2 into adjacent colonocytes that adds to the already high colonocyte H_2O_2 load due to oxidative stress exposure (Figure 3G).

High intracellular colonocyte H_2O_2 promotes diffusion into mitochondria leading to mtDNA oxidation and the formation of acquired mtDNA mutations (mitochondrial heteroplasmy-mtH) (Figure 3B red arrows), which miscode during translation of ETC protein subunits. The resulting ETC mutations facilitate a higher degree of electron leakage and greater H_2O_2 formation causing additional mtDNA damage and the creation of a vicious cycle, which maintains a high intracellular colonocyte H_2O production that facilitates spontaneous relapse upon withdrawal of medication or exposure to ever-present oxidative stressors (Figure 3H).

Thus, based on the data, the derived genetic predisposition leading to UC is the inability of the colonic epithelium to cope with (neutralize) an oxidant (H_2O_2) load forcing the colonocyte into a state of impaired redox homeostasis after which free H_2O_2 begins to accumulate in the cell (Figure 2C). Pathogenesis begins with impaired colonocyte redox homeostasis leading to the intracellular accumulation of H_2O_2 after HCRH has exhausted cellular reductive capacity (Figure 2C). The pathophysiology commences with the influx of neutrophils into the colonic mucosa, which defines the beginning of what will eventually become the symptomatic phase of the illness. However, extracellular colonocyte diffusion of H_2O_2 does not inexorably lead to UC due to the presence of a secondary "back-up" system of antioxidant defense provided by human serum albumin (HSA) (Figure 3C) as discussed in the following section.

HSA: The link between colonocyte and systemic redox homeostasis

Although UC is traditionally thought of being limited to the colon, the significant decrease reported in total blood antioxidant capacity (erythrocytes and plasma) in individuals with UC suggests that excess colonic production of H_2O_2 is causing impaired systemic redox homeostasis as well[60-62]. In other words, the capacity of the blood to remove H_2O_2 in UC patients is compromised. Why would colonic production of H_2O_2 affect systemic redox homeostasis and what effect might this have on the severity of UC and overall patient health?

Systemic redox homeostasis is provided by HSA and erythrocytes, both of which are highly effective scavengers of H_2O_2. Their combined action maintains blood H_2O_2 at very low levels, in the range of 0.8-6 μM for healthy individuals[63]. HSA can directly scavenge H_2O_2 *via* a reduced surface cysteine thiol (cys34)[64]. In addition, the HSA molecule itself has a GSH-linked thiol peroxidase activity that can remove circulating H_2O_2[65]. The significant anti-oxidant scavenging ability of HSA represents approximately 70% of the free radical trapping ability of human serum[64]. Since 60% of HSA is present in the interstitial space, this indicates that HSA acts as an extracellular backup anti-oxidant defensive layer (after intracellular colonocyte GSH) that protects against the development of UC by preventing the interstitial accumulation and diffusion of colonocyte released H_2O_2 from reaching the subjacent epithelial blood vessels and attracting neutrophils into the colonic epithelium leading to colonic mucosal inflammation and UC. Interstitial albumin has a turnover of 4% per hour after which it recycles back to the systemic circulation[66]. This suggests that each day the entire blood supply of reduced albumin is exposed to excess colonic H_2O_2 with a significant portion becoming oxidized.

Red blood cells also provide a significant level of systemic anti-oxidant defense. Erythrocytes contribute up to 30% of whole blood reductive capacity. Erythrocytes are highly permeable to H_2O_2[67]. With a normal mean inter-erythrocytic distance of 3 μm, a molecule of H_2O_2 in the circulation will encounter a red blood cell before it encounters HSA[68]. Free serum H_2O_2 will diffuse into red blood cells where it is neutralized by significant anti-oxidant enzymatic defenses comprised of catalase and GSH[67]. Whereas H_2O_2 released by colonocytes or infiltrating epithelial neutrophils during active UC can oxidize HSA in the interstitial space, decreased red blood cell reductive capacity (*i.e.*, decreased erythrocyte GSH) implies that colonic H_2O_2 is diffusing directly into the systemic circulation and into erythrocytes with depletion of total blood reductive capacity. The inability of interstitial HSA to completely remove colonic H_2O_2 will lead to H_2O_2 accumulation and a greater degree of tissue damage accompanied by neutrophilic infiltration resulting in increased severity of disease, which contributes to relapse (Figure 3F). This is supported by studies showing that the loss of blood reductive capacity (inability to remove H_2O_2) is associated with worsening UC[62]. The critical role of reduced albumin for the maintenance of colonic interstitial redox homeostasis is illustrated by studies showing that the onset and progression of experimental murine colitis were prevented by reduced (reductively enhanced) albumin, which, in turn, was strongly associated with an improved systemic reductive capacity[69].

Reduced albumin also directly neutralized H_2O_2 and prevented the *in vitro* loss of tight junctional proteins in human intestinal cell tissue treated with H_2O_2[69]. This indicates that reduced albumin can act as an interstitial reducing agent (antioxidant) and delay/prevent the onset of UC by neutralizing interstitial H_2O_2 released by colonocytes before the H_2O_2 can initiate chemotactic directed migration of neutrophils into the colonic epithelium. This implies that oxidized, or decreased albumin levels would offer less protection and hasten the development of UC. This is consistent with worsening UC observed in association with anemia and hypoalbuminemia[70,71]. Other studies report a significant inverse relationship between low serum albumin and risk of colectomy[72]. Conversely, studies in UC patients have shown that mucosal healing is positively associated with high (> 4.4 mg/dL) serum albumin[73].

Although low HSA can be secondary to colonic protein loss, and improved HSA levels may follow mucosal healing, the association of high HSA levels with a protective effect in conditions without colitis such as Bell's palsy and coronary artery disease implies an independent association with an intrinsic property of HSA such as oxidation status and not just as a biomarker for worsening colitis[74,75]. Thus, it is reasonable to assume that it is not just worsening colitis that causes low albumin but low serum albumin reductive capacity causing worsening colitis that increases albumin loss. HSA oxidation status should be part of screening lab work as oxidized albumin is inherently proinflammatory and associated with the progression of other diseases in addition to UC[76,77]. The proinflammatory nature of oxidized albumin and subsequent loss of systemic reductive capacity may be reflected in the worsening health and the high healthcare resource utilization in the year leading up to the diagnosis of UC[78]. This insight provides a critical therapeutic window of opportunity to restore systemic redox homeostasis and prevent UC if HSA is found to be significantly oxidized. In summary, once symptomatic UC develops, local and systemic reductive depletion is likely. At this point, colonocytes have already been exposed to genotoxic levels of H_2O_2 for many months or years setting the stage for molecular oxidative alterations that lead to life-long relapse (Figures 3A-H). However, the oxidative nature of these changes offers the possibility of reversal with a therapeutic reducing agent (detailed in treatment section below).

HOW OXIDATIVE STRESSORS GENERATE H_2O_2 IN THE BODY

Oxidative stress: Sources, classification, and definition

H_2O_2 is produced by many different cellular enzymatic reactions. Using the advanced search option in the BRENDA enzyme database limited to "homo sapiens" as the organism and "H_2O_2" as the product in the subitem text field returned 29 different enzymes acting upon 188 distinct molecular substrates[79]. This does not include non-enzymatic reactions such as the auto-oxidation of oxyhemoglobin or subunits of the mitochondrial ETC, which is considered the principal source of H_2O_2 in the body. Oxidative stressors are extremely diverse in their mechanism of action with some increasing the substrate for a

single enzyme while others can affect every H_2O_2 generating system in the body by inhibiting critical anti-oxidant enzyme systems needed for H_2O_2 removal. Individuals with UC are usually contemporaneously affected by more than one oxidative stressor but the commonality among all oxidative stressors, however, is the production of H_2O_2. Consequently, oxidative stressors are additive since they all increase the H_2O_2 load in the body. This may cause different individuals with UC to be more or less affected by the same oxidative stressor depending on the pre-existing H_2O_2 load in the colonocyte and state of redox homeostasis, which can change over time (Figure 2).

This can also result in the individual tolerance for the same oxidative stressor to vary with age, comorbidity, lifestyle and exposure duration and intensity. Thus, based on the evidence, it is reasonable to conclude that all factors that increase the risk of relapse or developing *de novo* UC are oxidative stressors that increase H_2O_2 in the body. Conversely, all oxidative stressors are risk factors for relapse or the development of UC. A convenient method of classification is grouping oxidative stressors as exogenous (originating external to the body) or endogenous (originating inside the body). The following section details the mechanism of action for several reported and/or common oxidative stressors associated with UC.

Exogenous oxidative stressors

Diet has been implicated in the pathogenesis and pathophysiology of UC[80]. 65% of surveyed individuals with UC believe that food is a significant trigger for relapse with 50% asserting that diet contributed to the initial development of disease[81]. This suggests that dietary factors exert their effect on the pathogenesis of UC by means of a common mechanism within the molecular chain of events leading to the onset of disease.

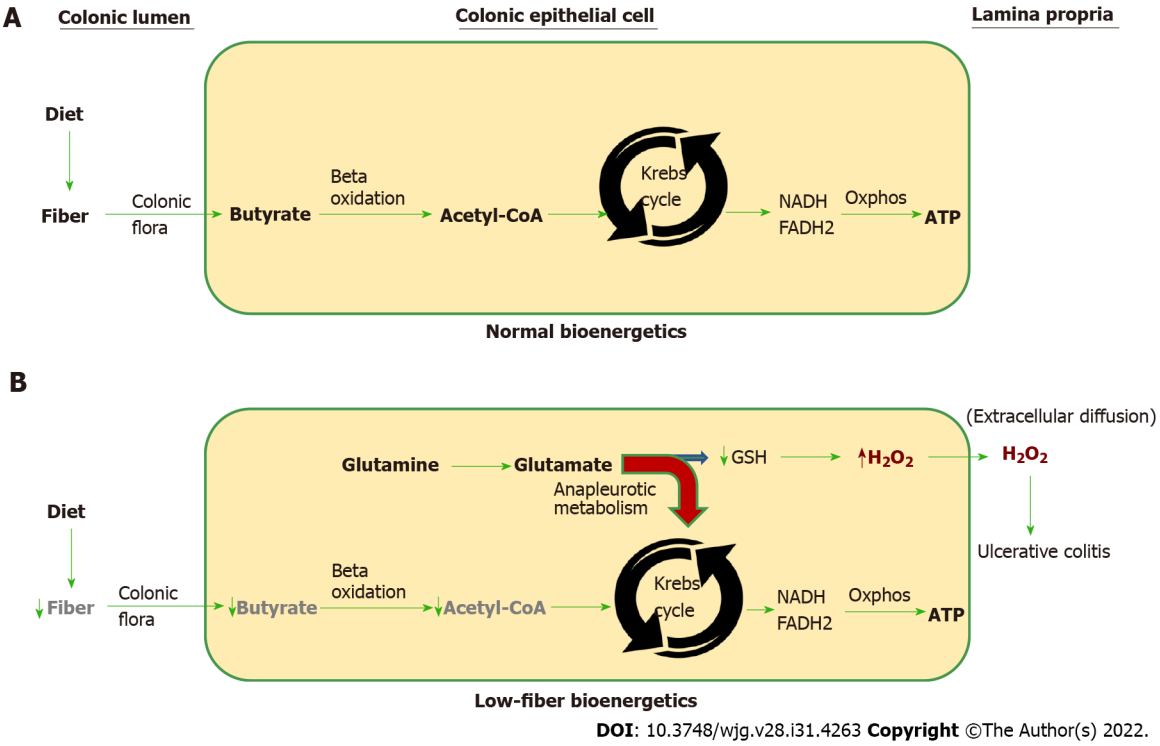
Dietary fat

Studies have shown that a high-fat low-fiber "westernized" type diet is associated with the development of UC, and high-fiber low-fat diets reduce systemic inflammatory biomarkers in patients with this illness[82,83]. Additionally, diets high in total fat and certain fatty acids are associated with exacerbation of UC[82,84,85]. But how does dietary fat initiate or worsen UC? Peroxisomes play an indispensable role in the metabolism of fatty acids obtained from dietary fat[86]. Peroxisomes are involved in the metabolism of dietary lipids such as medium chain, long chain, and very long chain fatty acids and cholesterol in addition to pristanic and phytanic acids[86,87]. Peroxisomal metabolism of fatty acids generates large amounts of H_2O_2, which is estimated to be about 35% of total cellular H_2O_2 production[88]. This is in line with data implicating peroxisomal H_2O_2 as an important source of cellular oxidative stress[89]. This implies that excess peroxisomal generated H_2O_2 can overwhelm the cell's reductive (antioxidant) capacity and accumulate to the point of causing cellular dysfunction. This is consistent with previous data ascribing a causal role for H_2O_2 in the pathogenesis of UC and implies that high fat diets contribute to the pathogenesis and relapse of UC by generating large amounts of peroxisomal H_2O_2. Excess peroxisomal generated H_2O_2 can diffuse into the cytoplasm and overwhelm the colonocyte's ability for its removal leading to extracellular diffusion and the development or relapse of UC as described above. Thus, high fat diets are risk factors for the development of UC because they are oxidative stressors that generate large amounts of peroxisomal H_2O_2[89]. Low fat diets ameliorate colonocyte oxidative stress by decreasing production of peroxisomal H_2O_2 and in so doing promote remission of UC.

Fiber

As mentioned above, low fiber diets are associated with the development and worsening of UC. But how does fiber interface with the pathogenesis and relapse of this illness? The colonic epithelium utilizes short chain fatty acids (*i.e.*, butyrate) for most of its energy requirements[90]. The production of butyrate starts with the fermentation of dietary soluble fiber by colonic bacteria. Butyrate is rapidly absorbed by colonic epithelial cells *via* passive diffusion and cell membrane transport proteins[91]. Once in the cytoplasm, butyrate is transported *via* the carnitine shuttle into mitochondria where it undergoes beta-oxidation. The resulting acetyl-coenzyme A (CoA) enters the Krebs cycle, which generates reducing equivalents (NADH, FADH2) that provide the energy for oxidative phosphorylation and ATP production[92]. This process provides up to 70% of colonocyte energy supplies (Figure 4A)[93,94].

A decrease in the available dietary soluble fiber will diminish the amount of butyrate absorbed by colonic epithelial cells and less butyrate will be available to undergo mitochondrial beta-oxidation. With decreased beta-oxidation of butyrate generating less acetyl-CoA, the colonocyte may not have enough fuel for the Krebs cycle to produce sufficient reducing equivalents (NADH, FADH2) in order to power oxidative phosphorylation and provide the energy for the biosynthesis of ATP. Without sufficient ATP to fuel critical cellular functions, the colonocyte will die. To increase ATP production, the colonocyte diverts glutamate into the Krebs cycle (*via* alpha keto-glutarate) in order to replace Krebs cycle intermediary metabolites that would otherwise be supplied by dietary fiber, which is in low supply (Figure 4B). Glutamate (an amino acid) is derived from the amino acid glutamine (the storage form of glutamate), and studies have shown cellular diversion of glutamine into the Krebs cycle as a consequence of impaired mitochondrial pyruvate transport underscoring glutamine's role as a backup



DOI: 10.3748/wjg.v28.i31.4263 **Copyright** ©The Author(s) 2022.

Figure 4 Normal *vs* low-fiber colonocyte bioenergetics. A: The normal vectorial bioenergetic flux beginning with soluble dietary fiber that is converted to short-chain fatty acids (*i.e.*, butyrate) by bacteria in the colonic lumen. Butyrate is rapidly absorbed by colonic epithelial cells (colonocytes). Once inside the colonocyte, butyrate undergoes mitochondrial beta-oxidation to generate acetyl-coenzyme A (CoA), which is processed by the Krebs cycle that produces NADH and FADH2. The high-energy electrons present in NADH and FADH2 are used to drive oxidative phosphorylation (Oxphos) resulting in the biosynthesis of ATP, which fuels most of the cell's energy needs; B: Low fiber intake decreases available butyrate needed for acetyl-CoA production. Under these energy-restricted conditions, glutamate is diverted into the Krebs cycle and away from the synthesis of glutathione (GSH). Diversion of glutamate into the Krebs cycle is called anapleurotic metabolism (red curved arrow) and is needed to replenish depleted Krebs cycle intermediary metabolites that would otherwise be supplied by dietary soluble fiber, which can no longer perform this role due to a low fiber diet. Since glutamate is needed for the synthesis of GSH, the sequestration of glutamate as a replacement energy source restricts the amount of glutathione the cell is able to synthesize. GSH is the principal reducing equivalent required to neutralize cellular hydrogen peroxide (H_2O_2). Insufficient glutathione will cause cellular H_2O_2 to increase, which upon extracellular diffusion may initiate neutrophil chemotaxis into the colonic epithelium and *de novo* ulcerative colitis or disease relapse. Interruption of colonocyte bioenergetic flux anywhere along the pathway from the microbiome to acetyl CoA will increase colonocyte anapleurotic metabolism and cellular H_2O_2, which can lead to ulcerative colitis. H_2O_2: Hydrogen peroxide; CoA: Coenzyme A.

energy supply during times of limited acetyl-CoA availability[95].

Studies on isolated colonocytes from germ-free rats (that cannot produce butyrate) report a 45% increase in glutamine use by these cells compared to conventionally reared animals[96]. Other studies using isolated colonocytes from germ-free mice demonstrated 16-fold lower NADH/NAD+ ratios as well as 56% lower ATP levels[97]. Colonization of germ-free mice with flora from conventional mice or butyrate-producing bacteria rescued the colonocyte energy deficit as did butyrate exposure to isolated colonocytes from germ-free mice[97]. This indicates that butyrate is a critical source of energy for colonocyte ATP production and colonocytes will compensate for the loss of butyrate by diverting glutamine (*via* glutamate) into the Krebs cycle to maintain the production of ATP.

However, the continued Krebs-cycle oxidation of glutamine as a backup energy source (*i.e.*, during prolonged low-fiber diets) entails significant consequences for the colonocyte. Glutamine is the precursor to glutamate, which is necessary for GSH synthesis. The diversion of glutamate into the Krebs cycle (called anapleurotic metabolism) to sustain cellular energy requirements restricts glutamate's availability for the biosynthesis of GSH, which is critical for the elimination of cellular H_2O_2[98]. Studies have shown that disrupting mitochondrial pyruvate uptake directs glutamine into the Krebs cycle and away from GSH synthesis[99]. Because GSH is critical for the elimination of cellular H_2O_2, a decrease in GSH synthesis will lead to increased colonocyte H_2O_2 and subsequent diffusion through the cell membrane to the extracellular space, which may precipitate *de novo* UC, worsen existing UC, or contribute to relapse (Figure 1B). Thus, low fiber diets are oxidative stressors because they increase the risk of colonocyte intracellular H_2O_2 buildup.

The critical importance of (soluble) dietary fiber for colonic bioenergetics and redox homeostasis is underscored by what occurs with the complete absence of colonic fiber. Diversion colitis is a reactive colonic inflammatory response in the by-passed segment of the large intestine as a result of fecal stream diversion secondary to colostomy or ileostomy. Under these circumstances, there is no dietary fiber entering the defunctioned segment of the large intestine. This results in a colitis affecting nearly all individuals undergoing this procedure within 1 to 3 years after colonic diversion[90]. Histopathology

soon after onset shows an influx of neutrophils into the colonic epithelium (analogous to UC)[100]. This suggests the alternate use of glutamate to compensate for the complete lack of lumenal butyrate decreases colonocyte GSH enough to raise cellular H_2O_2 to levels that facilitate extracellular diffusion and the development of colitis. It also implies that H_2O_2 plays a prominent causal role in the development of diversion colitis as well[101].

This interpretation is consistent with a case report of a healthy 36-year-old male who developed UC after following an extremely low carbohydrate diet for weight loss, which resolved without medication upon the institution of a semi-vegetarian diet[102]. Studies have demonstrated significant declines in fecal butyrate and butyrate-producing bacteria in individuals with reduced dietary carbohydrates[103]. The decrease in colonocyte butyrate can be reversed with butyrate enemas that significantly increased colonic epithelial GSH, which is consistent with a GSH sparing effect of butyrate inferred from Figure 4B[104].

Butyrate enemas also significantly reduced mucosal inflammation in patients with refractory UC [105]. This can be attributed to the butyrate-mediated increase in colonocyte GSH and subsequent reduction in colonic epithelial H_2O_2. This is supported by studies showing that butyrate prevents H_2O_2-induced DNA damage in isolated human colonocytes[106]. Thus, colonic butyrate has a critical role in maintaining colonocyte redox-homeostasis by preventing the anapleurotic metabolism of glutamate and subsequent decrease in colonic epithelial GSH, which leads to elevated colonocyte H_2O_2 and UC[107].

The crucial role of GSH in the elimination of cellular H_2O_2 can be seen in GPx knockout mice that lack this key enzyme needed to utilize GSH for the elimination of H_2O_2. Knockout mice lacking GPx develop colitis[32]. Colitis also occurs concomitantly with experimental beta-oxidation inhibition in mice, and in pigs subsequent to vitamin B-5 (pantothenic acid) deficiency. Vitamin B-5 is necessary for CoA synthesis, without which there is no acetyl CoA[108,109]. This suggests that disruption of bioenergetic flux at any point along the metabolic pathway from lumenal fiber to the formation of acetyl CoA will result in increased colonocyte H_2O_2 and colitis (Figure 4B).

Based on these data, we can reasonably predict that alterations in the colonic flora (microbiome dysbiosis) that lead to impaired short-chain fatty acid (*i.e.*, butyrate) production will contribute to the development and relapse of UC by increasing colonocyte H_2O_2. A diverse set of adverse environmental exposures can shift the colonic microbiome towards dysbiosis and impaired butyrate production. These include high fat/low fiber/high protein diets, food additives in processed food, smoking and alcohol ingestion[110-113]. Other diverse factors such as infant delivery and feeding methods, medications, enteric endocrine disruptors, psychological stress can also facilitate microbiome dysbiosis[114-117]. Long term dietary patterns that include soft drinks and artificial sweeteners may tip the balance towards dysbiosis[118,119]. Thus, microbiome dysbiosis is an oxidative stressor that can increase colonocyte H_2O_2 and contribute to the onset of UC[120].

Lastly, as mentioned above, H_2O_2, being membrane permeable, can diffuse into the colonocyte nucleus leading to oxidative nuclear DNA mutations in tumor suppression and oncogenes that promote colorectal cancer[51,52]. Studies have shown that mice fed a total western diet develop a neutrophil predominant colitis and colorectal cancer[121]. This is analogous to histological findings in human UC, which also carries an enhanced risk of colorectal cancer. Taken together, when the evidence supporting a causal role for H_2O_2 in UC and its associated colon cancer is viewed in light of biological mechanisms leading to increased colonocyte H_2O_2 subsequent to low-fiber high-fat diets, it is reasonable to conclude that the increased incidence of UC and colorectal cancer associated with the (low-fiber high-fat) western diet[9,97,122] is mediated through elevated colonocyte H_2O_2. This raises the possibility of primary prevention *via* changes to reduce dietary oxidative stress (*i.e.*, high fiber, low fat *etc*) and/or the administration of an oral reducing agent (detailed in the treatment section below).

Alcohol

Several studies have found that alcohol consumption increases the risk of onset, relapse, and gastrointestinal symptoms in individuals with UC[123]. Alcohol is biomembrane permeable, and after ingestion is distributed to all tissues in the body[124]. Alcohol metabolizing enzymes in the colonic epithelium can generate large amounts of H_2O_2[124]. Alcohol metabolism by alcohol dehydrogenase generates acetaldehyde, which is converted to acetic acid by aldehyde dehydrogenase. Both these reactions generate NADH, which feeds into the mitochondrial ETC causing increased electron leakage and enhanced generation of H_2O_2[124]. The increased amount of colonocyte H_2O_2 can overwhelm cellular reductive capacity and diffuse to the extracellular space leading to relapse or the onset of UC.

Cytochrome P450 2E1 (CYP2E1) is a second alcohol oxidizing enzyme that is highly expressed in the human intestine and is upregulated by chronic alcohol exposure[125]. CYP2E1 has the highest catalytic activity among the members of CYP enzymes in metabolizing ethanol[126]. CYP2E1 consumes NADPH when metabolizing ethanol to acetaldehyde and in the process generates large amounts of H_2O_2[126, 127]. NADPH is also required for the recycling of oxidized GSH (GSSG) back to reduced GSH by GSSG reductase[49]. This can reduce the availability of GSH for the elimination of H_2O_2 and contribute to increased colonocyte H_2O_2 levels. The total combined effect of alcohol metabolism is excess production of colonocyte H_2O_2 that can overwhelm cellular reductive capacity leading to extracellular H_2O_2 diffusion and *de novo* UC or relapse by the mechanisms detailed above. CYP2E1 is also upregulated by ethanol, which magnifies the oxidative stress caused by this alcohol metabolizing enzyme.

Antibiotics

Due to their widespread use, antibiotics represent a significant source of oxidative stress within the population. Studies have shown an association between antibiotic use and the development of UC[128]. Although antibiotics are administered to eradicate pathogenic bacteria they also indiscriminately kill beneficial commensal bacteria that make up the colonic microbiome leading to a decrease in species diversity including a reduction in bacterial species that produce butyrate[129]. A decrease in colonic butyrate can lead to metabolic changes favoring increased colonocyte production of H_2O_2 (Figure 4). Antibiotic-induced microbiome depletion (dysbiosis) can last for years and act cooperatively with other oxidative stressors such as a high-fat diet[130,131]. This can hasten colonocyte H_2O_2 build-up (HCRH) and the development of UC.

However, microbiome depletion is not the only mechanism by which antibiotics generate excess colonocyte H_2O_2. Studies have shown that antibiotics induce the production of significant amounts of H_2O_2 in both bacteria and human intestinal epithelial cells, which in the latter was caused by an alteration to the ETC[132-135]. Since H_2O_2 is cell membrane permeable, bacterial H_2O_2 can diffuse across epithelial cell membranes and add to the already increased antibiotic-induced colonic epithelial cell H_2O_2 load. This can lead to mtDNA oxidative damage with the formation of colonocyte mitochondrial heteroplasmy and ever-increasing production of intracellular H_2O_2 resulting in HCRH (Figure 2). Increased cellular production of H_2O_2 can overwhelm colonocyte reductive (antioxidant) capacity and lead to a buildup of colonocyte H_2O_2 that will facilitate the development of UC years later. Because virtually everyone is exposed to antibiotics at one time or another, they exert a selective oxidative pressure that can manifest as UC in individuals with a predisposing genetic makeup encoding for a diminished reductive capacity that facilitates the buildup of H_2O_2.

Psychological stress: A common oxidative stressor leading to H_2O_2 production

Stress is a significant risk factor for UC. Up to 40% of patients with UC report psychological stress as an exacerbating factor[136]. Psychological stress can cause *de novo* UC and worsen existing disease[137-141]. Psychological stress exposure is reported to induce mucosal inflammatory responses and can result in colonic hypermotility that may be sufficient to occlude the lumen[142,143]. But why is psychological stress pro-inflammatory in the colon and how does stress initiate or worsen UC?

The coordinated movement of food along the gastrointestinal (GI) tract is dependent on 5-hydroxytryptamine (serotonin) mediated regulation of smooth muscle tone, motility, and peristalsis[144]. 95% of serotonin is stored in enterochromaffin cells (EC) that are present in the GI tract mucosa[145]. Serotonin is released from EC cells and stimulates enteric nerve terminals to initiate a peristaltic wave[144,146]. However, the amount released is much more than needed and the excess serotonin is rapidly taken up by colonic epithelial cells and metabolized by colonocyte monoamine oxidase (EC#1.4.3.4)[144]. This prevents hyper-stimulation and excessive bowel motility that can lead to colonic spasms. Mono-amine oxidase catalyzes the oxidative deamination of serotonin in a process that generates H_2O_2; the reaction catalyzed is $RCH2NHR' + H_2O + O_2 \rightarrow RCHO + R'NH_2 + H_2O_2$[147].

Studies have shown that psychological stress causes prolonged increases in colonic motility[148]. Stress-induced colonic hypermobility and spasm will release large amounts of serotonin into the colonic mucosa that is metabolized to H_2O_2 within colonocytes. The excess colonocyte H_2O_2 can acutely overwhelm the enterocyte's antioxidant capacity resulting in H_2O_2 accumulation and eventual UC after extracellular diffusion. This mechanism is supported by studies showing that serotonin has a key role in the pathogenesis of experimental colitis[149].

Thus, psychological stress has a pernicious effect on the course of UC but UC is also psychologically stressful with studies reporting that patients with UC are engaged in a continuous "fight" to maintain health-related normality[150]. This sets up a self-sustaining bidirectional cycle of continuous psychological stress that contributes to increased frequency and severity of disease[151]. Although stress can cause or worsen UC, stress reduction is generally not effective at altering the activity or course of disease sufficiently to induce remission[152,153]. This is not surprising since the principal driving force behind the auto-propagating nature of inflammation in UC is H_2O_2 release by activated infiltrating mucosal neutrophils and not the metabolism of serotonin, which has its principal effect as a contributing factor in the stress-induced pathogenesis and relapse of UC[26,149].

Cigarette smoking: Releasing the brakes

Since reports in the early 1980s, numerous studies included in three meta-analyses (1989, 2006 and 2021) have established that cigarette smoking is significantly protective against the development of UC compared to non-smokers while smoking cessation is a significant risk factor for developing UC or experiencing disease relapse with increased severity of illness[154-158]. Additionally, as noted below, cigarette smoking also affects the therapeutic response after smoking cessation. But why is cigarette smoking protective against the onset of UC?

Nicotine, an addictive chemical present in tobacco, was initially considered as a possible protective factor. Nicotine is effective at inducing remission when begun at the time of or soon (up to 4 wk) after smoking cessation (early relapse)[159,160] However, nicotine is largely ineffective when therapy is administered for disease relapse several months or years after smoking cessation (late relapse) with

studies concluding that nicotine therapy is of minimal value in the treatment of UC and questions whether nicotine is the active protective component of smoking that decreases risk and inflammation in UC[161-164]. In contrast, the resumption of smoking is reported to be an effective therapy for induction and long-term maintenance of remission in patients with early or late relapse[159,160,165]. Indeed, studies have reported that resumption of smoking is highly effective for induction of remission in refractory disease years after smoking cessation; with nicotine being effective if treatment is begun at the same time as smoking cessation[160]. Thus, in ex-smokers, nicotine is effective for remission induction in early relapse while the resumption of smoking is effective in both early and late relapse.

Taken together, the data indicate that there are two distinct oxidative stressors with distinct short and long-term mechanisms of action both of which are caused by the latent and repressed effects of active smoking and are only unmasked by smoking cessation. The initial mechanism manifests soon after smoking cessation and lasts for days to under a month. In contrast, the second mechanism becomes predominant many months to years later reaching a peak of the highest risk of relapse within 2 to 5 years of smoking cessation[166].

The initial oxidative stressor is the physiological and psychological stress of nicotine withdrawal, which is manifest shortly after smoking cessation and peaks within the first week, and lasts up to one month[167]. Nicotine withdrawal symptoms can include anger, irritability, frustration, anxiety, depression, insomnia, restlessness, and constipation[167]. These same psychological emotions of anger, resentment, emotional conflict, hostility, anxiety, and psychological tension were observed under direct observation to cause significant colonic hypermotility and spasm[168]. Thus, it is reasonable to conclude that nicotine withdrawal secondary to smoking cessation can result in colonic hypermotility with increased colonic serotonin secretion and enhanced monoamine oxidase production of H_2O_2 (see above section-psychological stress). Under these circumstances, the administration of nicotine will decrease colonic hypermotility and lower colonic serotonin production, which decreases colonocyte H_2O_2 leading to remission. Resumption of cigarette smoking also provides the nicotine needed to treat early relapse due to nicotine withdrawal.

In other words, nicotine-induced remission is due to the relief of nicotine withdrawal symptoms (and accompanying colonic hypermotility) during early relapse after smoking cessation. Nicotine treatment is rendered minimally effective after nicotine withdrawal symptoms (and colonic hypermotility) have subsided. Colonic hypermotility (from any cause) is an oxidative stressor that increases colonocyte H_2O_2, which can overwhelm colonocyte reductive (antioxidant) capacity leading to extracellular diffusion and UC.

The second oxidative stressor caused by cigarette smoking cessation is due to disinhibition of the colonocyte ETC. Studies quantifying the effect of cigarette tar on mitochondrial ETC activity report an 82% inhibition rate on whole chain respiration[169]. Under normal conditions, the ETC is fueled by electron flux provided by reducing equivalents (NADH and FADH2) generated by the multi-enzyme Krebs cycle[170]. H_2O_2 is produced by spontaneous auto-oxidation of the ETC (electron leakage). These leaked electrons combine with vicinal oxygen within the mitochondrial matrix to form superoxide, which is converted to H_2O_2 by superoxide dismutase. H_2O_2 is subsequently neutralized by GPx using GSH as a reducing co-factor.

Under conditions of ETC inhibition during active smoking, less ETC-generated H_2O_2 is produced, which affords protection against the development of UC. However, while smoking, upregulation of bioenergetic enzyme systems can be expected as the colonocyte attempts to overcome the smoking-induced inhibition and restore normal mitochondrial bioenergetics[171]. Upon smoking cessation, the inhibition is slowly lifted and increased production of ETC "fuel" is metabolized producing supraphysiological amounts of H_2O_2 as a result of increased ETC auto-oxidation (electron leakage). Colonocytes respond to this oxidative stress by producing additional GSH for H_2O_2 neutralization. This creates a condition of HCRH (Figure 2) that can eventually overwhelm colonocyte reductive capacity leading to cellular H_2O_2 build-up and eventual *de novo* UC as H_2O_2 diffuses to the extracellular interstitial space attracting neutrophils into the colonic epithelium from the subjacent microvasculature.

Smoking resumption inhibits ETC activity, which decreases colonic epithelial cell H_2O_2 leading to remission. Nicotine does not inhibit the ETC and cannot induce remission of late UC relapse (years after smoking cessation). This interpretation is supported by studies that demonstrated significantly improved clinical manifestations such as bloody stool, diarrhea, and abdominal pain in UC patients treated with metformin[172]. Further, UC patients treated with metformin showed a significant decrease in histological and endoscopic disease scores in addition to significantly diminished erythrocyte sedimentation rate (a biomarker of systemic inflammation) and significantly decreased indices of colonic local oxidative stress (tissue malonaldehyde and myeloperoxidase)[172].

But how does metformin improve UC and how is it related to cigarette smoking? Metformin is a biguanide antihyperglycemic agent used to treat type 2 diabetes. Its mechanism of action includes inhibition of mitochondrial glycerol 3-phosphate dehydrogenase (of the glycerolphosphate shuttle-EC 1.1.5.3) and inhibition of ETC complex I both of which are major contributors of electrons to the ETC in mitochondria[173-175]. Inhibition of electron flux by metformin is analogous to the ETC inhibitory effects of cigarette smoking. This implies that both smoking and metformin improve UC by decreasing mitochondrial production of H_2O_2. This is supported by studies showing that targeted inhibition of glycerol 3-phosphate dehydrogenase decreases cellular production of H_2O_2[176].

In summary, the evidence supports two distinct oxidative stress mechanisms to explain the effects of smoking cessation on UC. Early relapse after smoking cessation (within days) is mediated by the oxidative stress induced by the physiological effects of nicotine withdrawal while late relapse (months to years) is mediated by a slow rise in colonocyte H_2O_2 due to disinhibition of mitochondrial H_2O_2-generating metabolic pathways. Conversely, cigarette smoking affords protection against early and late UC relapse by providing nicotine and decreasing colonocyte production of H_2O_2, respectively.

Mercury

Mercury is a major environmental contaminant and a significant source of occupational exposure[177]. Occupational inhalation of mercury vapor is reported to cause a recurrent relapse of UC[178]. Mercury forms stable bonds with thiol groups present on GSH in addition to inhibiting GPx, both of which are critical for the removal of cellular H_2O_2[179-181]. This results in the inactivation of the entire GSH-based antioxidant system. The compromise of this critical system by mercury prevents neutralization of H_2O_2, which can accumulate to excessive levels inside colonocytes leading to extracellular diffusion and UC relapse as described above. Thus, mercury is an oxidative stressor that increases cellular H_2O_2 by preventing its elimination from the cell. Mercury is a pervasive contaminating xenobiotic whose exposure is likely to be insidious, bio-accumulative, and additive to other contemporaneous oxidative stress exposures.

PERFLUOROOCTANOIC ACID

Perfluorooctanoic acid (PFOA) is a ubiquitous environmental contaminant that was used to manufacture non-stick pans in addition to other commercial products such as stain and water-resistant fabrics. Introduced into the environment in the 1950s, PFOA can be found in the serum of virtually all residents of industrialized countries. Human exposure occurs *via* many sources including contaminated drinking water, food, and house dust. Due to the high dissociation energy of its carbon-fluorine bond, PFOA is resistant to vertebrate metabolism and environmental degradation[182]. As a result, PFOA is called a "forever-chemical" because it is not biodegradable and has a long elimination half-life of 3.5 years[183].

Studies have demonstrated a significant exposure-response relationship between PFOA serum levels and subsequent UC but no association with Crohn's disease (CD)[183]. Other studies have reported significantly increased serum PFOA in UC patients compared to a combined group of CD (positive control for intestinal inflammation) and normal individuals (negative non-diseased control)[184]. The specific association of PFOA with UC suggests that PFOA's effect is acting in concert with a unique predisposing genetic makeup to select a subset of individuals for the development of UC. In other words, PFOA's mechanism of action in all exposed individuals is the same but the genetic predisposition in a subset of individuals is permissive for the development of UC.

A related halogenated chemical, 2-bromooctanoic acid, after conversion to the sodium salt 2-bromooctanoate, is reported to cause an acute murine colitis analogous to human UC after rectal installation[108]. This suggests the possibility that PFOA might be acting in the same manner as 2-bromooctanoate since halogenated carbon compounds, as a group, have a high resistance to degradation[185].

In human UC, beta-oxidation is inhibited as a secondary effect caused by rising levels of colonocyte H_2O_2[30]. Since 2-bromooctanoate causes murine UC accompanied by inhibition of beta-oxidation and the related halogenated chemical PFOA causes UC and is not biodegradable this suggests that intracellular H_2O_2 is increased as a result of the colonocyte's high expenditure of energy (ATP) in a futile attempt to metabolize and remove these non-biodegradable halogenated xenobiotics from the cell. Since almost all cellular ATP is produced as a result of mitochondrial ETC activity, which also generates most of the cell's H_2O_2, this implies that the initial buildup of H_2O_2 occurs in mitochondria where beta-oxidation is also located. Increased mitochondrial H_2O_2 will inhibit mitochondrial thiolase, the last enzyme in the beta-oxidation cascade, leading to inhibition of mitochondrial beta-oxidation[30].

In other words, the colonocyte's persistent metabolic response in an attempt to eliminate these non-biodegradable chemicals leads to increased H_2O_2 generated by the ETC, which inhibits mitochondrial beta-oxidation followed, sometime later, by UC as H_2O_2 diffuses out of the colonocyte into the extra cellular space. This mechanism is consistent with studies showing inhibition of beta-oxidation in UC patients is followed shortly after by a relapse of disease[41]. H_2O_2-induced inhibition of mitochondrial beta-oxidation (*via* mitochondrial thiolase inhibition) increases the anapleurotic metabolism of glutamine, which decreases the biosynthesis of GSH contributing to the excess colonocyte H_2O_2 load (Figure 4). This mechanism is also consistent with a genetic predisposition that impairs the colonocyte's ability to neutralize an H_2O_2 load. Within this redox framework, inhibition of colonocyte beta-oxidation is a secondary effect of colonocyte xenobiotic (PFOA or bromooctanoate) metabolism, which generates excess ETC H_2O_2 that impairs mitochondrial beta-oxidation *via* H_2O_2 induced inhibition of mitochondrial thiolase. This raises the possibility of primary prevention with an oral reducing agent for communities at risk for the adverse effects of PFOA exposure. A causal role for H_2O_2 can be tested in the

laboratory by the prevention of PFOA (or 2-bromooctanoate) induced murine colitis with an oral reducing agent (see treatment section below).

Lastly, PFOA's adverse effects are not limited to UC. Lymphocytes are highly sensitive to the toxic effects of H_2O_2 and undergo apoptosis at very low levels of H_2O_2 exposure of less than 1 μm[186]. Studies showing a significant association between PFOA serum levels and decreased antibody response to vaccination are consistent with this mechanism of action[182]. Thus, PFOA resistance to cellular metabolism and degradation is likely to result in excess H_2O_2 production in any cell contaminated by this xenobiotic.

Endogenous oxidative stressors: A look inside

In UC, lifelong episodes of relapsing inflammation affecting the same colonic regions previously inflamed indicate that inflammation has fundamentally changed the colonic epithelium compared to the pre-morbid state. Since the character of the inflammation does not change over time and neutrophils continue to be the first responders streaming into the colonic epithelium, this suggests that H_2O_2 is still the chemotactic agent involved but from a new source. The evidence points to new endogenous sources of H_2O_2 that combine with pre-existing sources of H_2O_2 to increase the likelihood of relapse.

Microbiome: An oxidative dysbiosis

Although disruption of the colonic microbiome can contribute to the onset of UC by decreasing butyrate production, which leads to increased colonocyte H_2O_2 (Figure 4), UC can also adversely affect the microbiome. Studies have shown a 10 × increase in H_2O_2 producing bacteria in biopsies of inflamed colonic tissue in individuals with UC compared to normal controls[120]. These H_2O_2-producing bacteria are adherent to the colonic mucosa. This suggests that chronically high levels of H_2O_2 in the inflammatory field create an environment that selects for bacteria that produce H_2O_2, which are those able to tolerate the abnormally high levels of lumenal oxidative stress. Over time, this oxidative dysbiosis may replace large portions of the normal microbiome, which may not be able to survive under conditions of high H_2O_2-induced oxidative stress. The H_2O_2 released by bacteria can contribute to relapse by diffusing through the epithelium to the subjacent vascular layer where it serves as a chemotactic agent to attract neutrophils into the colonic epithelium. This creates a microbiome, which is a pro-inflammatory endogenous oxidative stressor that contributes to the onset or relapse of UC by continuous H_2O_2 production. A recent analysis examining the pathogenesis of UC concluded that "*disease onset is triggered by events that alter the healthy balance of the gut microbiota, perturb the mucosal barrier, and abnormally stimulate gut immune responses*"[12]. H_2O_2 does all three.

CYP2E1 induction: A vicious cycle

As explained above CYP2E1 is an alcohol inducible enzyme that is involved in the metabolism of ethanol and other xenobiotics entering the body. H_2O_2 is within the chain of molecular events that upregulate inducible CYP2E1[187]. This implies that chronically elevated colonocyte H_2O_2 from any source (*i.e.*, ethanol or xenobiotic metabolism, oxidative stress exposure, *etc*) can upregulate CYP2E1. In other words, elevated colonocyte H_2O_2 can upregulate CYP2E1 without ethanol exposure. This can cause increased sensitivity to CYP2E1 substrates, which can lead to heightened H_2O_2 production in areas of previous inflammation when exposed to ethanol or other xenobiotics metabolized by this enzyme. Studies have shown the cells with upregulated CYP2E1 produced higher amounts of H_2O_2 that can exit the cell[188]. This can cause increased H_2O_2 production upon exposure to CYP2E1 substrates such as alcohol and other xenobiotics, which increases the risk of relapse or *de novo* UC. Under these circumstances, upregulated CYP2E1 becomes an endogenous oxidative stressor.

Mitochondrial heteroplasmy: Hard-wired for inflammation

Intracellular H_2O_2 is normally kept within a very low picomolar range to prevent oxidative damage from this very powerful oxidizing agent[186,189]. Over time, colonocytes from individuals with UC are exposed to higher levels of H_2O_2 due to multiple oxidative stressors including infiltrating epithelial neutrophils (mucosal inflammation), microbiome (oxidative dysbiosis), CYP2E1 induction (alcohol and xenobiotic exposure), peroxisomal beta-oxidation (high-fat diet) and ETC hyperactivity (smoking cessation), *etc.* The increase in colonocyte H_2O_2 can overwhelm cellular antioxidant systems resulting in mitochondrial genetic damage[44,45]. This occurs because mtDNA is highly susceptible to H_2O_2-induced oxidative damage due to a lack of introns or histones, proximity to the ETC where H_2O_2 is produced, and inefficient DNA repair mechanisms compared to nuclear DNA[37,38].

As mentioned above, H_2O_2-induced mitochondrial genetic damage introduces mutations into mtDNA resulting in a different genetic sequence for some of the hundreds of mitochondrial chromosomes present in a cell. The simultaneous occurrence of normal and mutated mtDNA is called mitochondrial heteroplasmy. The presence of mitochondrial heteroplasmy (mtDNA mutations) causes miscoding during the transcription of ETC proteins leading to the biosynthesis of faulty and mutated ETC subunits. The mutated ETC disrupts electron flow causing electron loss at a greater rate than normal (increased electron leakage). These electrons combine with vicinal molecular oxygen to form superoxide that is converted to H_2O_2 by superoxide dismutase. Since the ETC and mtDNA are both in close

proximity to each other within the mitochondrial matrix, any excess H_2O_2 produced by the ETC can easily diffuse over to any one of the 2-10 chromosomes contained within a mitochondrion leading to additional mtDNA mutations and greater H_2O_2 production[190]. This positive biofeedback mechanism establishes a vicious cycle that leads to ever-increasing levels of colonocyte H_2O_2.

The presence of mitochondrial heteroplasmy (and the resulting increase in colonocyte H_2O_2) can contribute to the tendency of UC to worsen over time with more frequent and severe episodes of relapse [7]. Relapse may occur in response to increasingly minor (oxidative) stressors due to the already high intracellular colonocyte H_2O_2. Thus, the accumulation of colonocyte H_2O_2 transforms otherwise innocuous insults into 'second hit' stimuli. The "first hit" being the pre-existing excess of colonocyte H_2O_2. For example, in individuals with inactive UC, low to moderate red wine consumption (1-3 glasses daily) increased colonic epithelial paracellular permeability in areas previously affected by mucosal inflammation[123,191]. Increased colonic paracellular permeability is characteristic of individuals with UC[24,25]. And H_2O_2 is reported to increase paracellular permeability by disrupting cellular tight junctions[20,22,192-194]. Under these circumstances, it takes less alcohol to increase colonocyte H_2O_2 to the point where it diffuses out of the cell causing oxidative damage to tight junctions with subsequent increases in colonic paracellular permeability. This explains the second hit phenomenon in UC. In summary, mitochondrial heteroplasmy is unique because it is an ever-present self-amplifying intracellular oxidative stressor that facilitates the establishment of HCRH (Figure 2), which contributes to both the increased frequency of relapse and/or severity of disease.

Homocysteine: Inhibition of GPx

Several studies have reported significantly elevated levels of tissue and serum homocysteine in children and adults with UC[195-198]. A significant positive association between elevated homocysteine and UC was confirmed by two meta-analyses in 2011 and 2018[199,200]. Homocysteine inhibits GPx, the principal antioxidant enzyme system used by the cell to remove (neutralize) H_2O_2[201,202]. Furthermore, homocysteine-induced inhibition of GPx occurs at physiologic levels of serum homocysteine[203]. Inhibition of GPx can increase cellular H_2O_2, especially during oxidative stress exposure, which acutely increases cellular H_2O_2 production. Thus, homocysteine is a significant endogenous oxidative stressor that can increase colonocyte H_2O_2 and contribute to *de novo* UC or disease relapse.

EVIDENCE-BASED TREATMENT

Therapy: Targeting H_2O_2

A causal role for H_2O_2 in the pathogenesis of UC implies that induction of remission can be achieved by eliminating extracellular colonocyte H_2O_2 while maintenance of remission is attained by normalizing intracellular levels of colonocyte H_2O_2. The overall objective is to abrogate the H_2O_2 molecular chemotactic "trail" that is guiding the directed migration of subjacent intravascular neutrophils to the source of H_2O_2 emanating from the colonic epithelium. Without an interstitial H_2O_2 gradient signal to follow, neutrophils are no longer attracted into the colonic epithelium, which effectively terminates the inflammatory response. These were the goals that guided the formulation of a novel therapy, which consists of a topical multicomponent enema (described below) administered with a systemic oral reducing agent [R-dihydrolipoic acid (RDLA)] that targets extracellular and intracellular colonocyte H_2O_2 respectively. RDLA is the reduced form of the biologically active 'R' enantiomer of lipoic acid and is the only form that should be administered as the oxidized form (described below) might worsen UC.

We administered the enema once daily (usually at bedtime) for 2 wk followed by once every other day for two weeks. Oral RDLA 300 mg twice daily was initiated when enema therapy was begun. Treatment with RDLA was continued for 4-6 mo. The components of the enema are mesalamine [5-aminosalicylic acid (5-ASA)], budesonide, sodium cromolyn, and sodium butyrate. The enema formulation and evidence-based rationale for the inclusion of each component of the entire therapy are discussed below. The severity or extension of the disease was not a consideration when initiating therapy since, in theory, all patients with UC should respond to a reduction of colonic H_2O_2. Our only consideration was whether the patient could tolerate the therapy.

Enema formulation

The enema was formulated by adding the following components to a standard 60-milliliter enema bottle containing 4 g of mesalamine (5-ASA) from which 20 milliliters were removed (and discarded): (1) 15 milliliters of 1 molar sodium butyrate (1.7 g); (2) 5 milliliters of sodium cromolyn (total 100 mg); and (3) 1 milliliter of budesonide (5 mg/mL). Gentle swirling should follow the addition of each component to ensure uniform dispersal. The total ending volume is 61 milliliters. The combination enema is easily made by a compounding pharmacist. We only used the original enema bottle containing mesalamine to formulate this therapy as other bottles may have residual chemicals that can worsen UC.

Results of treatment

The novel treatment was offered to 36 patients with refractory UC as part of the practice of medicine (average MAYO score 8.6, range 3-12) and the results were published as a case series in which 85% achieved complete histologic remission in under 8 wk[204]. Although long-term follow-up was not part of the case series, a case report was generated after I was contacted by a patient included in this case series[205]. The patient had a 39-year history of refractory UC, which had progressed to severe pancolitis at the time of treatment when he was being considered for a total colectomy. His follow-up colonoscopy, which was performed 12 years later in 2019, showed completely normal colonic biopsies with no signs of UC. To date, (14 years after treatment) the patient relates having uninterrupted completely normal bowel movements. Based on the available data, this appears to be the first documented cure of UC. The video of an in-house clinical presentation of the first five patients to receive this new therapy with before-and-after treatment histology presented by the attending physician and attending pathologist is available[206].

Within this evidence-based redox framework, the general therapeutic intervention for all UC patients is the same regardless of duration or severity of illness, course, relapsing frequency, mucosal inflammatory distribution, age of onset, previous medications, or extra intestinal manifestations. Modifications may be required for those patients who are intolerant to any of the components in the therapy. In patients who are intolerant of topical (enema) therapy, treatment can be initiated with RDLA alone, which as an amphipathic membrane-permeable antioxidant (H_2O_2 neutralizing) and reducing (cellular electron-donating) agent may restore colonocyte redox homeostasis and resolve mild-moderate cases of UC with more severe cases improving enough to begin topical (enema) therapy if needed.

Severe UC

Up to 25% of patients with UC will experience severe disease requiring hospitalization either on initial presentation or during the course of their illness[207]. Severe UC presenting with multiple daily episodes of bloody diarrhea and signs of systemic toxicity is a life-threatening emergency with significant morbidity, high risk of colectomy, and a pre- and post-operative mortality of up to 3% and 5% respectively[8,207,208]. In these individuals, oral and/or topical therapy may not be possible or advisable. The evolution of UC to this extreme degree indicates severe depletion of both colonic and systemic reductive capacity[61,62]. The exceptionally high rate of current medical treatment failure for severe UC and the observation that remission is associated with restoration of colonic redox homeostasis[208,209], suggests that patients with severe UC should be considered for therapy with an intravenous reducing agent such as sodium thiosulfate (STS) as part of their overall treatment regimen in order to rapidly reduce systemic and colonic H_2O_2, restore redox homeostasis and promote mucosal healing. Given that current management of acute severe UC is not based on high-quality evidence, the need for effective therapy is all the more pressing[210].

STS is an odorless, water-soluble, small inorganic molecule (MW-158.11 g/mol) that is normally produced in mitochondria as a product of sulfide oxidation pathways[211]. STS is on the World Health Organization's (WHO) list of essential medicines and is supplied for intravenous use due to rapid gastric degradation[211]. STS is a direct-acting reducing agent that can donate two electrons to chemically neutralize H_2O_2 upon contact[212]. STS will also reduce the oxidized form of GSH (GSSG) back to reduced GSH, which is needed to neutralize H_2O_2 and maintain cellular redox homeostasis[213]. The advantage of STS is that it does not depend upon biological antioxidant enzyme systems for its therapeutic action. This is beneficial in critical settings when rapid reduction of H_2O_2 and restoration of redox homeostasis are required.

The basic chemical reaction for the reduction of H_2O_2 with STS is: $4\ H_2O_2 + S_2O_3^{2-} \rightarrow 2\ SO_4^{2-} + 2\ H^+ + 3\ H_2O$[212]. Based on the above chemical reaction and evidence implicating a causal role for H_2O_2 in the pathogenesis of UC, STS is expected to abrogate the interstitial neutrophilic chemotactic effect being exerted by H_2O_2 and thus prevent neutrophil migration into the colonic epithelium, which perpetuates colonic inflammation. The reduction of extracellular colonic mucosal H_2O_2 by STS can act as a sink that will facilitate the diffusion of intracellular colonocyte H_2O_2 to the extracellular space where it can be neutralized by STS.

H_2O_2 can impair smooth muscle contraction and interrupt neuromuscular transmission leading to reduced colonic muscle tone and lowered colonic lumenal pressure, which is postulated to play an essential role in the development of toxic megacolon, a life-threatening complication of UC[214-218]. Thus, reducing agents such as STS or RDLA may have a role in treating or preventing toxic megacolon. Once severe UC is resolved, patients should be discharged on an oral reducing agent such as RDLA for an indefinite period of time to lower the risk of relapse.

STS is well tolerated and approved for use in cyanide poisoning with a recommended dose of 12.5 g over slow IV infusion (10-20 min) in adults and 250 mg/kg in children[219,220]. Similar dosing regimens can be considered in UC with repeat dosing guided by clinical status. STS is an accepted therapy for calciphylaxis due to chronic renal failure and is administered to mitigate the adverse effects of cisplatin toxicity during the treatment of solid tumors[213].

MAINTENANCE: TARGETING OXIDATIVE STRESSORS

Although therapeutic intervention to lower H_2O_2 and restore colonic redox homeostasis is a critical part of overall therapy, elimination of contributing lifestyle and dietary habits that increase cellular H_2O_2 (environmental oxidative stressors, Figure 3A) must be part of the long term strategy to maintain remission. A complete list of environmental oxidative stressors and their mechanisms is beyond the scope of this paper however, some general evidence-based guidelines can be made. Stress and alcohol ingestion are major oxidative stressors and should be avoided. A low-fat diet with adequate amounts of dietary fiber, especially soluble fiber, is extremely important to minimize colonic oxidative stress[83,221-223].

Eating food that is free of pesticides, chemicals and additives is critical for maintaining a healthy microbiome. High levels of iron in red meat and some tap water are oxidative stressors and should be avoided[224,225]. Certain fish contain high levels of mercury[226,227]. Mercury is an oxidative stressor and therefore it is prudent to minimize ingestion of fish containing high levels of mercury. Studies have shown that sugar and sugar-sweetened drinks are also associated with UC[228,229]. So it is best to avoid high sugar-containing foods and drinks.

Carrageenan is a non-nutritive food additive that is used as a thickening agent in many foods. Although considered safe, food-grade carrageenan can be converted to a colitis-promoting small-molecular (degraded) carrageenan when exposed to H_2O_2[230,231]. Since H_2O_2 is present in the inflammatory field it (H_2O_2) can convert food-grade carrageenan to the degraded variety in the colon of individuals with UC. Studies report that degraded carrageenan can penetrate colonocytes and generate superoxide, which is converted to H_2O_2[232]. Thus, carrageenan is an oxidative stressor that generates intracellular colonic H_2O_2 and should avoid by individuals with UC.

Smoking cessation is a strong oxidative stressor and should be undertaken very slowly in patients with UC to avoid relapse. RDLA can be administered during smoking cessation to counteract oxidative stress. Patients should be very cautious with vitamin supplementation because studies have shown that certain vitamins such as vitamin B6 (pyridoxine) have been associated with the development of UC [233]. Pyridoxine used in supplements and food fortification is converted to the biologically active pyridoxal by pyridoxine 4-oxidase (EC1.1.3.12), which produces H_2O_2 as a by-product[234]. Adequate sleep (at least 6 h) and regular moderate exercise are very important for individuals with UC to reduce stress[235,236]. Based on the data indicating a compromised reductive capacity, all UC patients should be maintained on an oral reducing agent (*i.e.*, RDLA) for an indefinite period of time. The following section provides a detailed explanation regarding the scientific basis for each component of the therapy.

Rationale for multicomponent enema therapy

As mentioned above, the compound enema contains four components: Mesalamine (5-ASA), budesonide, sodium cromolyn, and sodium butyrate. The therapeutic rationale for the compound enema is based on the mechanism of action for each component to act in an additive fashion in order to decrease colonic H_2O_2 as indicated below. The base component, 5-ASA has an anti-inflammatory effect that is limited to the specific type of inflammation present in UC and does not have a positive therapeutic action on colonic inflammation in general[237]. This suggests that 5-ASA's mechanism of action is directed at the causal agent responsible for the inflammation in UC. This is in contrast to other currently available therapeutic agents used to treat UC, which have a more general immunosuppressive action in the colon. 5-ASA's mechanism of action is that of a topically-acting extracellular tetra-valent reducing agent capable of donating up to 4 electrons per molecule for the reduction (neutralization) of H_2O_2 and other oxygen radials[238,239]. Since 5-ASA is able to induce and maintain histologic remission in active UC, this indicates that 5-ASA can neutralize extracellular neutrophil-derived H_2O_2 in the inflammatory field leading to induction of remission while the sustained topical epithelial presence of 5-ASA maintains remission by neutralizing H_2O_2 diffusing from colonocytes.

Neutralization of colonocyte-derived H_2O_2 by 5-ASA prevents the establishment of an H_2O_2 mediated neutrophilic chemotactic gradient, which attracts neutrophils into the colonic epithelium leading to relapse. This is supported by the observation that 5-ASA's histologic remission rate of nearly 45% is the highest of any currently available therapeutic approved to treat UC suggesting 5-ASA's ability to neutralize colonic H_2O_2 is interrupting a fundamental underlying biological process (*i.e.*, neutrophilic chemotaxis) in the molecular chain of events leading to UC[240].

Butyrate, a short-chain fatty acid normally produced by the colonic microbiome as a colonocyte fuel source, is the second component. Butyrate reduces the anapleurotic metabolism of glutamine, which increases colonocyte GSH. This augments the colonocyte's capacity to neutralize intracellular H_2O_2 (Figure 4). Studies have shown significantly increased colonic epithelial GSH after topical butyrate administration, and high fiber diets that generate increased fecal butyrate are reported to maintain prolonged remission in patients with UC[104,241].

The third component, cromolyn sodium, is a mast cell stabilizer that inhibits the secretion of histamine by mast cells, which accumulate in large amounts at sites of tissue injury in UC[242-244]. Mast cells are significantly activated in UC and undergo intense degranulation resulting in the secretion of significantly greater amounts of histamine that is concentrated at sites of colonic inflammation in UC [245-248]. Rectal biopsies of patients with UC contained significantly higher amounts of histamine

compared to normal controls[249,250]. Histamine is degraded by diamine oxidase (EC 1.4.3.22) whose activity is especially high in the intestinal mucosa and the inflammatory field with H_2O_2 being the product of this reaction[245,251,252]. Thus, cromolyn prevents histamine from being secreted from mucosal mast cells, which precludes its conversion to H_2O_2 that can significantly contribute to the intensity and persistence of colonic inflammation in UC. This is consistent with studies reporting that histamine drives the severity of inflammation in a murine model of experimental UC[253].

Budesonide is the fourth component and is a topically acting corticosteroid that inhibits neutrophil infiltration into the colon by down-regulating neutrophil and endothelial surface adhesion molecules, which prevents neutrophil attachment to the endothelium and subsequent directed migration into the colonic epithelium[254]. Neutrophils produce a large amount of H_2O_2 *via* surface NADPH oxidase[255]. Corticosteroids reduce the expression of neutrophil surface NADPH oxidase thus decreasing neutrophil production of H_2O_2[254]. The combination of inhibited neutrophilic epithelial migration and decreased production of H_2O_2 significantly reduces this large source of H_2O_2, which is a significant driving factor of mucosal inflammation in UC.

RATIONALE FOR RDLA

Targeting H_2O_2 with RDLA

RDLA, the oral component of the therapy, is the biologically active (dextrorotatory) reduced enantiomer of alpha-lipoic acid (the oxidized form)[256]. Alpha-lipoic acid is synthesized in mitochondria and plays an essential role as a co-factor for several multi-enzymatic complexes involved in mitochondrial energy metabolism[257]. Alpha-lipoic acid is enzymatically reduced to RDLA (the reduced form) *via* dihydrolipoamide dehydrogenase (E.C. 1.8.1.4) in mitochondria. Thus, alpha-lipoic acid acts as an oxidizing agent that may worsen colonocyte redox homeostasis and should not be administered to patients with UC (Figure 5).

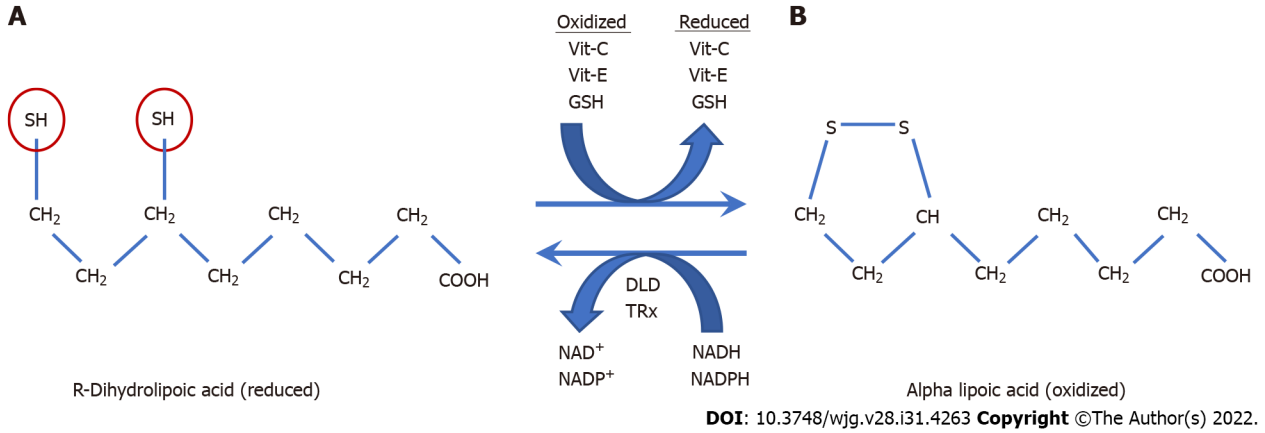
Aside from its enzymatic role in energy metabolism, RDLA is a powerful biological reducing (antioxidant) agent that can be administered orally[263]. RDLA's dithiol group can donate electrons to reduce (reactivate) oxidized forms of other cellular antioxidants such as vitamin-C, vitamin-E, and GSH [264]. RDLA is both a water and lipid-soluble (amphipathic) molecule so it is delivered *via* the bloodstream to all cells of the body where it diffuses through cell membranes to deliver needed reducing equivalents for the reduction of H_2O_2 and synthesis of GSH[265]. Studies in mice demonstrate that the recycling of GSH is critical for cell survival when exposed to oxidative stress (*i.e.*, H_2O_2)[266]. Other studies show that GSH protects rat intestinal epithelial cells from H_2O_2-induced injury[267]. RDLA's capacity to directly react with H_2O_2 combined with its ability to significantly increase cellular GSH, the principal cellular H_2O_2 reducing agent, underlie RDLA's ability to combat the high levels of colonocyte H_2O_2 in UC.

RDLA significantly increases nuclear factor E2-related factor 2, a master antioxidant transcription factor that mediates the expression of antioxidant genes, including those for GSH synthesis[268]. This significantly increases the cellular capacity to synthesize GSH and neutralize H_2O_2. RDLA is reported to reduce nuclear transcription factor-kappa B and adhesion molecule expression[268], which downregulates the inflammatory response and decreases neutrophilic infiltration into the colonic epithelium contributing to the resolution of inflammation and colitis. Thus, RDLA prevents colonocyte cell death during periods of oxidative stress (H_2O_2 exposure) and promotes *de novo* synthesis and recycling of GSH in order to keep cellular GSH high and H_2O_2 low. Hence, RDLA's mechanism of action indicates that it can significantly contribute to inducing and achieving remission in UC.

Studies have shown that restoration of depleted mitochondrial GSH can reverse oxidant (*i.e.*, H_2O_2) induced mtDNA damage, which leads to mitochondrial heteroplasmy[46]. Since RDLA is highly effective at increasing cellular GSH, this suggests that RDLA will be also effective at reversing H_2O_2 induced mtDNA oxidative damage and subsequent mitochondrial heteroplasmy that is postulated to contribute to life-long relapse. This is supported by the continuous 14-year biopsy-proven histologic remission in a patient with a 39-year history of severe refractory UC after treatment with a regimen containing RDLA[205].

RDLA is generally considered safe and is approved for the treatment of diabetic peripheral neuropathy in Europe[269]. Oral lipoic acid at doses as high as 1800 mg/d for 6 mo and 1200 mg/d for 2 years did not result in serious adverse effects when used to treat diabetic peripheral neuropathy[270,271]. Studies indicate that 40% of RDLA is quickly absorbed systemically after oral dosing and rapidly distributed to tissues[263]. RDLA undergoes renal excretion and intracellular beta-oxidation[268,272], which provides a second pathway to increase cellular GSH by decreasing the anapleurotic metabolism of glutamate (Figure 4).

RDLA is the only amphipathic orally administered therapeutic that is both an intracellular and extracellular anti-oxidant (H_2O_2 neutralizing) and reducing agent (electron-donating for maintenance of redox homeostasis). Given these highly unique and desirable therapeutic properties, which are essential for long-term remission in UC, RDLA should be made widely available and be included on the WHO's list of essential medications. STS, an intravenous reducing agent, is already on the WHO's list of



DOI: 10.3748/wjg.v28.i31.4263 Copyright ©The Author(s) 2022.

Figure 5 R-dihydrolipoic acid. A: R-dihydrolipoic acid (RDLA) is the reduced form of alpha lipoic acid (the oxidized form); B: The reducing equivalents of RDLA are provided by its two thiol groups (red circles) that are each capable of donating one electron. RDLA has a redox potential of -290 millivolts which is only exceeded by NADH and NADPH with a redox potential of -320 and -400 millivolts respectively[258]. Due to its very low (more negative) redox potential, RDLA can directly or indirectly reduce all other cellular antioxidants and many types of oxygen radicals[256]. These include vitamin-C, vitamin-E, glutathione, thioredoxin, glutaredoxin, catalase, glutathione peroxidase, and peroxiredoxin[258-261]. Alpha-lipoic acid is reduced by dehydrolipoamide dehydrogenase and Thioredoxin reductase, which use NADH and NADPH as reducing co-factors respectively[262]. The amphipathic nature of RDLA (lipid and water-soluble) allows it to diffuse throughout cellular compartments to transport reducing equivalents where needed and assist in neutralizing excess hydrogen peroxide. The elimination of excess intracellular cellular hydrogen peroxide is essential in order to restore cellular redox homeostasis and prevent ulcerative colitis relapse caused by extracellular diffusion of colonocyte hydrogen peroxide. Vit: Vitamin; DLD: Dehydrolipoamide dehydrogenase; TRx: Thioredoxin reductase; GSH: Glutathione.

essential medications and thus RDLA, a therapeutically active oral reducing agent should also be included. In addition to UC, emerging evidence suggests that RDLA (and STS) may have a preventive and/or therapeutic role in other diseases in which the evidence indicates a causal role for H_2O_2 such as systemic lupus erythematosus, sepsis, and diabetes[273-275].

In summary, an evidence-based analysis of the pathogenesis and therapy of UC indicates that treatment of inflammation is no longer the main objective of this illness. Instead, the primary goal is the restoration of colonic and systemic redox homeostasis by therapeutic normalization of colonic H_2O_2, which removes the molecular chemotactic signal that initiates and maintains colonic inflammation and is responsible for disease relapse.

DISCUSSION

The existence of an unpredictable, unexplainable, and incurable disease such as UC indicates that we are guided by the wrong theory of pathogenesis in our quest to develop effective treatment and find causes and cures. Currently, there are two, mutually exclusive, mechanisms of disease that have been put forward to explain how UC develops and guide therapeutic development. Both mechanisms attempt to answer the same question; why do white blood cells (neutrophils) suddenly leave the surrounding blood vessels and head straight into the epithelial lining of the large intestine causing inflammation, bleeding, and UC?

The first hypothesis is consensus-based, agreed upon among researchers in the field, and posits an immune abnormality as a primary event in the development of UC while the second mechanism is evidence-based and maintains that the immune system is completely normal but only appears to be "attacking" the colon due to the inappropriate secretion of a neutrophilic chemoattractant, H_2O_2, by the colonic epithelium, which draws neutrophils into the epithelial lining. Despite decades of intensive research, no evidence of any antecedent immune abnormality has ever been identified in individuals with UC or their immediate relatives, and studies of basic immune functionality in UC patients are normal[10,11]. Due to the absence of a biologically plausible mechanism, the term "immune dysregulation" has been coined to explain the presence of neutrophils in the colonic epithelium. In contrast, studies have demonstrated significantly increased H_2O_2 production in non-inflamed colonic epithelium prior to the appearance of mucosal inflammation, satisfying the absolute chronological requirement that the cause (H_2O_2) must precede the effect (inflammation). Since H_2O_2 is cell membrane permeable, once it leaves the colonocyte H_2O_2 can establish a chemotactic gradient "trail" that neutrophils can follow right into the colonic epithelium after exiting the subjacent vasculature. Hence, within this framework and in line with previous data, the immune system in UC is normal. Neutrophils are just doing what they are biologically programmed to do when exposed to H_2O_2; a normal chemotactic immune signaling agent being inappropriately secreted by the colonic epithelium.

On a clinical level, immune dysregulation cannot explain any of the basic characteristics that define UC such as why people develop this disease to begin with, what is the genetic predisposition, why it always starts in the rectum, what causes proximal inflammatory progression, why the loss of intestinal hemostasis leading to bloody diarrhea, what is the mechanism behind relapse, what causes colonic epithelial crypt abscesses, why are smoking cessation, low fiber and high-fat diets risk factors for UC, what dietary and lifestyle changes will help prevent relapse, what therapeutic intervention will provide long-lasting remission and how can we effectuate a cure, to name a few. In other words, immune dysregulation, as a mechanism of disease, has no explanatory power, which is essential for understanding a disease process. In comparison, a redox mechanism of disease based on colonocyte buildup of H_2O_2 explains these basic observations and provides a consistent and clear mechanistic foundation to understand the hereto-forth puzzling observations that characterize UC.

Despite the absence of any hard evidence for an immune abnormality, this hypothesis continues to be the main focus of ongoing investigation by "leading researchers" in the field who have issued consensus statements asserting that a "dysregulated immune response" is the "widely accepted" cause of UC[276, 277]. A consequence of leading researcher support for immune dysregulation is the near-total focus of therapeutic development on proprietary and costly drugs that alter the immune response in a limited number of commercially viable but non-curative ways[6]. As a result, induction trials for new drug development have reached an unsurpassable therapeutic ceiling of 20%-30% indicating that treatment aimed solely at modifying the immune response cannot alter the natural history of the disease, which is essential for achieving universal long-lasting remission in patients with UC[278]. In other words, immune dysregulation as a mechanism of disease has no predictive power to identify a discreet causal agent, which can be targeted for effective treatment and curative potential.

In contrast, the evidence-based identification of H_2O_2 as a causal agent in UC has guided the development of highly effective treatment with at least one documented, biopsy-proven, histologic remission lasting 14 years to date without any episodes of intervening relapse, in a patient with a 39-year history of refractory UC[205]. This is the basis of bench-to-bedside translational medicine that integrates basic science discoveries into predictable effective treatments and potential cures. A causal therapeutic target eliminates much of the "trial and error" that defines the history of current UC therapeutic development[279].

Nevertheless, what leading researchers think is highly relevant for patients with UC. A consensus mechanism of disease put forth and agreed upon among researchers means that clinicians do not have an evidence-based pathogenesis to guide clinical decision-making. This forces clinicians to rely on a variety of clinical variables including the severity of disease, colonic inflammatory distribution, age of onset, previous medication, disease duration, disease course, relapse frequency, and extra-intestinal manifestations to make bedside patient care determinations[7]. Since each one of these variables can be different for every patient, the number of treatment guidelines must be numerous enough to encompass all these different patient combinations. These treatment guidelines, in turn, are not founded on evidence that defines the pathogenesis but instead rely on an ever-growing and changing database of empirical studies incorporating one or more of these myriad clinical variables. The interpretation of these clinical studies is consensus-driven by committee and thus inherently subjective, leading to numerous clinical recommendations for UC that range in number from 32 to 124 treatment guidelines depending on the country of origin[2].

Committee members may also disagree about the relevance of any particular study for the treatment of UC leading to differences in the number of treatment guidelines between medical societies in the same country with the American Gastroenterological Association espousing 24 treatment recommendations while the American College of Gastroenterology supports 49 clinical treatment guidelines for the treatment of this highly debilitating inflammatory bowel disease[280-282]. Moreover, due to the "inconsistencies regarding recommendations" between the two societies, a "Guide to Guidelines in UC" was published in an effort to reconcile the differences among leading clinicians in the field[283]. In contrast, an evidence-based H_2O_2 mechanism of disease only has one guideline for the treatment of UC that does not change, which is to normalize colonic H_2O_2.

The current degree of therapeutic uncertainty when treating patients with UC is the inevitable result of not having an evidence-based mechanism of disease as the foundation for clinical decision-making and therapeutic development. In other words, since there is no evidence for an antecedent immune vulnerability in UC, treatment with the sole aim of suppressing the immune response is not anchored in an evidence-based pathogenesis. The end result is subjective and malleable clinical guidelines with shifting therapeutic targets generating different empirical treatments, the majority of which are based on low or very low-quality evidence while being permeated by high degrees of conflict of interest[2]. Patients ultimately bear the brunt of these fluid upstream decisions because treatments based on low-quality evidence cannot alter the natural history of disease leading to a high degree of medical treatment failure and a 30% colectomy rate[5]. The high degree of medical treatment failure, in turn, fuels endless fund-raising to pay for research in order to find a more effective therapy. And research, unfortunately, continues to be guided by the same consensus immune dysregulation hypothesis ultimately degenerating into a perpetual sisyphean iterative endeavor.

Perhaps the most relevant outcome when applying the predictive power of an H_2O_2 evidence-based mechanism of disease to UC is the expectation of indefinite remission and normal colon functionality once excess colonic H_2O_2 is neutralized. Given a causal role for H_2O_2 in UC, the elimination of excess colonic H_2O_2 would abrogate the molecular signal for directed neutrophil migration into the colonic epithelium leading to long-term histologic (and biochemical) remission. Accordingly, colonic inflammation is not the principal focus of treatment, instead, the primary therapeutic goal is to remove the H_2O_2 mediated chemotactic signal attracting neutrophils into the colonic epithelium.

This represents a functional cure as long as intracellular colonocyte H_2O_2 remains normal and unable to diffuse into the extracellular microenvironment. Treatment limited to reducing inflammation does not address H_2O_2 emanating from colonocytes, and thus cannot cure. The continued build-up of colonocyte H_2O_2 while being treated with these drugs can increase mitochondrial heteroplasmy with worsening disease and/or lead to colon cancer due to the genotoxic effects of H_2O_2[50,51].

From a redox medicine perspective, inflammation (neutrophil infiltration) is just one source of H_2O_2 that must be addressed. Other sources contributing H_2O_2 to the colonic inflammatory field in UC such as mast cells (histamine), EC (serotonin), and microbiome oxidative dysbiosis must also be considered for optimal therapeutic intervention to induce remission. Environmental oxidative stressors and mitochondrial heteroplasmy, which channel H_2O_2 *via* the colonocyte into the colonic epithelium have a crucial role in provoking relapse and must be addressed in order to achieve long-lasting remission.

Additionally, the common metabolic origin of cellular H_2O_2 suggests that H_2O_2-mediated intestinal inflammation is not solely confined to the colon. A recent analysis concluded that a shared mechanism underlies UC and UC-associated ileitis, which develops in up to 35% of patients with UC[284]. This is supported by studies in UC patients showing impaired ileal butyrate oxidation in both terminal ileum and colon, which in the latter was associated with H_2O_2 induced inhibition of mitochondrial thiolase, the last enzyme in the butyrate beta-oxidation cascade[30,285]. This suggests that excess H_2O_2 is responsible for impaired ileal butyrate oxidation in the small intestine as well. Moreover, the neutrophilic epithelial infiltration, cryptitis, and crypt abscesses that characterize UC-associated ileitis is analogous to the typical histopathological changes observed in UC[286]. This strongly implies that H_2O_2 is also elevated in the small intestine leading to mucosal inflammation and metabolic derangements. Thus, treatments that simply target colonic inflammation do not address the consequences of elevated ileal H_2O_2, which may lead to small bowel inflammation and interfere with the absorption of nutrients. In contrast, treatment with a systemic reducing agent such as RDLA has the potential of resolving UC-associated ileitis.

The interdisciplinary nature of evidence-based analysis can provide clues to understanding and effectively treating other serious conditions that are linked to UC whose medical therapy has so far been suboptimal. Studies have shown that H_2O_2 can effectively inhibit neuromuscular transmission[216]. Protection against H_2O_2-induced inhibition of neuromuscular transmission was associated with the cellular ability to eliminate H_2O_2[287]. Other studies have demonstrated that H_2O_2 contributes to motor disfunction in human UC[218]. This suggests a potential causal role for H_2O_2 in the motility dysfunction that is thought to underlie toxic mega colon and small bowel bacterial overgrowth, both of which are associated with symptomatic UC[214,288]. It also implies that therapeutic intervention with reducing agents (STS or RDLA) to reduce colonic H_2O_2 may be an effective therapeutic option in treating or preventing these serious conditions.

At the other end of the clinical spectrum, up to 2% of asymptomatic individuals undergoing screening colonoscopy were shown to have typical histologic inflammatory features of UC with two-thirds developing symptomatic disease (rectal bleeding) within 5 years[289,290]. Despite having a high probability of developing symptomatic UC and the possibility of increased risk of colon cancer, clinicians are in a quandary regarding the appropriate treatment for these asymptomatic individuals since all medications used to treat UC can have serious side effects and there are no data regarding their effectiveness at this very early asymptomatic stage[291-293]. However, the presence of preclinical neutrophilic inflammation implies that H_2O_2 has begun "leaking" out of colonocytes and is attracting neutrophils into the colonic epithelium. The use of an oral reducing agent (RDLA) to normalize colonocyte H_2O_2 and restore redox homeostasis would be a logical choice at this stage due to its recognized safety profile and ability to enhance cellular reductive capacity in order to reduce colonic H_2O_2. If future studies show that this is an effective treatment, it will be possible to prevent symptomatic disease from developing while UC is still in a preclinical asymptomatic stage.

All things considered, with current therapy and under the best of circumstances, UC patients must undergo life-long surveillance colonoscopy for colon cancer, which cannot detect all neoplastic lesions leading to a high mortality rate[29,294,295]. And although total colectomy has been touted as a cure for the approximately 30% of UC patients who fail medical therapy or develop colon cancer, studies have shown that patients who have undergone ileal pouch/anal anastomosis have higher disability scores than patients with active UC[296]. In contrast, maintenance therapy with an oral reducing agent has the potential of eliminating the need for colectomy, lifelong colonoscopies, and, by removing excess colonic H_2O_2, may significantly reduce the incidence of UC-associated colorectal cancer.

An evidence-based theory of UC identifying H_2O_2 as a causal therapeutic target not only has the potential of highly effective and inexpensive treatment that may be curative but opens the door to population-wide primary prevention by increasing total reducing equivalents (antioxidants) in our food

supply. This is supported by studies demonstrating a decreased risk of developing UC with diets high in anti-oxidants (reducing agents)[297]. Dietary intervention can be successful in reducing the incidence of UC because, in contrast to established disease with high levels of colonic H_2O_2 that require treatment with powerful reducing agents, intervention before colonocytes develop HCRH (while intracellular H_2O_2 is still low) requires much less reductive capacity, which can be supplied by increasing the amount of reducing equivalents (antioxidants) in the food supply. This public health level intervention may prevent UC from developing in the entire population before it even starts.

CONCLUSION

The evidence supports a causal role for colonocyte H_2O_2 in the pathogenesis and pathophysiology of UC. Treatment to reduce and maintain normal colonic H_2O_2 levels leads to long-term histologic remission (complete mucosal healing) in patients with refractory disease. The treatment is inexpensive and well tolerated. Lifestyle modifications to reduce oxidative stress exposure will help maintain remission. This is the first time that a causal evidence-based therapeutic target with curative potential has been identified for UC. The inclusion of multiple components to address the different sources of H_2O_2 within the colitic inflammatory field contributes to its singular effectiveness but also slows its acceptance by a healthcare system dominated by single molecular therapeutics.

H_2O_2 is a normal by-product of cellular metabolism that can accumulate within colonic epithelial cells. H_2O_2's unique properties of cell membrane permeability, long life, potent oxidizing potential, and the ability to attract white blood cells combine to promote colonocyte extracellular diffusion followed by oxidative disintegration of colonic epithelial tight junctional proteins while simultaneously attracting white blood cells into the colonic epithelium, both of which lead to colonic inflammation and eventual UC. This makes it appear as if the immune system is "attacking" the colon when in reality the immune response is behaving as it is normally programmed to respond. The abnormality is the inappropriate secretion of H_2O_2 by the colonic epithelium and not the immune response.

The pleiotropic effects of H_2O_2 have misdirected the careers of multiple generations of researchers into searching for a non-existent primary immune abnormality as the cause of UC. Extensive research since the mid-20th century has failed to uncover a primary immune vulnerability to explicate this illness. Cumulative evidence does not support any form of immune dysregulation in the pathogenesis of UC. This line of research is not evidence-based and should be abandoned. The continued search for immune dysregulation as the cause of UC leads to enormous research waste and endless fundraising that will never find the cause or cure for this disease while at the same time encouraging the treatment of UC with expensive immune altering agents that drive up healthcare costs, do not cure and are associated with lower quality of life, higher rates of colon cancer and other serious adverse effects. Continued research to uncover a primary immune abnormality as the cause of UC reinforces a false sense of hope for millions of individuals suffering from this illness who are desperately waiting for a cure that will never materialize with this line of research. Only by following the evidence can we cure disease.

Evidence-based medical research will eventually displace consensus-driven hypothesis in the highly competitive race for research funding as the National Institute of General Medical Sciences begins to shift funding priorities to grant applications that can clearly explicate falsifiable disease mechanisms that are "associated with the pathogenesis and resolution" of disease[298]. This pathogenesis initiative has begun with sepsis in July 2019 and is likely to be expanded as a requirement to obtain scarce research funding for other diseases as well. Under these guidelines, the current consensus-based immune dysregulation hypothesis invoked to explain UC does not meet this threshold for Federal research funding since it neither provides a coherent falsifiable pathogenesis nor a means of disease resolution.

A causal role for colonic H_2O_2 in the pathogenesis of UC is biologically plausible and supported by both experimental and clinical evidence. H_2O_2 satisfies all the basic requirements for an etiological agent leading to the development of UC and is worthy of continued and expanded research to confirm a potential causal role in the pathogenesis of this debilitating inflammatory bowel disease affecting millions worldwide. It is incumbent upon the research community to follow up on this highly promising line of research that raises the real possibility of targeted and highly effective treatment with curative potential.

Future directions

Complex diseases such as UC arise as an emergent systems property of its individual, *in vivo*, interacting constituent elements. The physical proximity of the colonic epithelium, innate immune system, and colonic lumenal contents gives rise to the disease phenotype we call UC in response to colonocyte extracellular diffusion of H_2O_2. Complex chronic diseases such as UC are not amenable to a reductionist analytical laboratory approach that examines each contributing element outside of its disease-producing *in vivo* context[299]. The prevalence of "incurable" complex chronic diseases continues to rise because they have slipped through the cracks of our current reductionist methodology of medical research that is not designed to detect emergent systems diseases such as UC. The shortcoming of laboratory research

to deal with chronic complex diseases can be overcome with graduate programs dedicated to theoretical (systems) medicine, which looks at the big picture to help guide laboratory researchers down a focused experimental pathway to discovering causes and cures of disease[300]. With chronic disease mortality accounting for 60% of all global deaths as well as 70% of all deaths in the United States, and 60% of Americans suffering from at least one chronic disease with 40% afflicted with two or more chronic ailments, chronic disease has become the leading driver of the United States' $3.5 trillion in annual health care cost[301-303]. We simply cannot win the war against encroaching chronic disease by experimentation alone. This underscores the critical need for collaboration between systems medicine (theoretical systems pathogenesis) and laboratory-based experimentalists (reductionist medical research) before the financial, emotional, and familial burden becomes too much to bear and society begins to destabilize under the weight of too many sick people.

FOOTNOTES

Author contributions: Pravda J is the sole author of this manuscript and solely responsible for its content; Pravda J performed all the research, collected, analyzed, and interpreted all the data; Pravda J conceived of and developed the hydrogen peroxide-based pathogenesis of ulcerative colitis; Pravda J prepared and wrote the manuscript and performed all critical revisions; Pravda J certifies that this manuscript is the product of his original research; and Pravda J has overall responsibility for this manuscript.

Conflict-of-interest statement: The author reported no relevant conflicts of interest for this article.

Open-Access: This article is an open-access article that was selected by an in-house editor and fully peer-reviewed by external reviewers. It is distributed in accordance with the Creative Commons Attribution NonCommercial (CC BY-NC 4.0) license, which permits others to distribute, remix, adapt, build upon this work non-commercially, and license their derivative works on different terms, provided the original work is properly cited and the use is non-commercial. See: https://creativecommons.org/Licenses/by-nc/4.0/

Country/Territory of origin: United States

ORCID number: Jay Pravda 0000-0001-5737-5506.

S-Editor: Wang JJ
L-Editor: A
P-Editor: Wang JJ

REFERENCES

1 **Fumery M**, Singh S, Dulai PS, Gower-Rousseau C, Peyrin-Biroulet L, Sandborn WJ. Natural History of Adult Ulcerative Colitis in Population-based Cohorts: A Systematic Review. *Clin Gastroenterol Hepatol* 2018; **16**: 343-356.e3 [PMID: 28625817 DOI: 10.1016/j.cgh.2017.06.016]
2 **Goldowsky A**, Sen R, Hoffman G, Feuerstein JD. Is there a standardized practice for the development of international ulcerative colitis and Crohn's disease treatment guidelines? *Gastroenterol Rep (Oxf)* 2021; **9**: 408-417 [PMID: 34733526 DOI: 10.1093/gastro/goab009]
3 **Rubin DT**, Hart A, Panaccione R, Armuzzi A, Suvanto U, Deuring JJ, Woolcott J, Cappelleri JC, Steinberg K, Wingate L, Schreiber S. Ulcerative Colitis Narrative Global Survey Findings: Communication Gaps and Agreements Between Patients and Physicians. *Inflamm Bowel Dis* 2021; **27**: 1096-1106 [PMID: 33057598 DOI: 10.1093/ibd/izaa257]
4 **Peyrin-Biroulet L**, Van Assche G, Sturm A, Gisbert JP, Gaya DR, Bokemeyer B, Mantzaris GJ, Armuzzi A, Sebastian S, Lara N, Lynam M, Rojas-Farreras S, Fan T, Ding Q, Black CM, Kachroo S. Treatment satisfaction, preferences and perception gaps between patients and physicians in the ulcerative colitis CARES study: A real world-based study. *Dig Liver Dis* 2016; **48**: 601-607 [PMID: 27012447 DOI: 10.1016/j.dld.2016.01.013]
5 **Wong DJ**, Roth EM, Feuerstein JD, Poylin VY. Surgery in the age of biologics. *Gastroenterol Rep (Oxf)* 2019; **7**: 77-90 [PMID: 30976420 DOI: 10.1093/gastro/goz004]
6 **Hirten RP**, Sands BE. New Therapeutics for Ulcerative Colitis. *Annu Rev Med* 2021; **72**: 199-213 [PMID: 33502898 DOI: 10.1146/annurev-med-052919-120048]
7 **Gajendran M**, Loganathan P, Jimenez G, Catinella AP, Ng N, Umapathy C, Ziade N, Hashash JG. A comprehensive review and update on ulcerative colitis. *Dis Mon* 2019; **65**: 100851 [PMID: 30837080 DOI: 10.1016/j.disamonth.2019.02.004]
8 **Kayal M**, Shah S. Ulcerative Colitis: Current and Emerging Treatment Strategies. *J Clin Med* 2019; **9** [PMID: 31905945 DOI: 10.3390/jcm9010094]
9 **Kirsner JB**. Historical origins of current IBD concepts. *World J Gastroenterol* 2001; **7**: 175-184 [PMID: 11819757 DOI: 10.3748/wjg.v7.i2.175]
10 **Jewell DP**, Truelove SC. Reaginic hypersensitivity in ulcerative colitis. *Gut* 1972; **13**: 903-906 [PMID: 4646293 DOI: 10.1136/gut.13.11.903]
11 **Triantafillidis JK**, Economidou J, Manousos ON, Efthymiou P. Cutaneous delayed hypersensitivity in Crohn's disease

and ulcerative colitis. Application of multi-test. *Dis Colon Rectum* 1987; **30**: 536-539 [PMID: 3595375 DOI: 10.1007/BF02554785]
12 **Porter RJ**, Kalla R, Ho GT. Ulcerative colitis: Recent advances in the understanding of disease pathogenesis. *F1000Res* 2020; **9** [PMID: 32399194 DOI: 10.12688/f1000research.20805.1]
13 **Petri B**, Sanz MJ. Neutrophil chemotaxis. *Cell Tissue Res* 2018; **371**: 425-436 [PMID: 29350282 DOI: 10.1007/s00441-017-2776-8]
14 **Kővári B**, Báthori Á, Friedman MS, Lauwers GY. Histologic Diagnosis of Inflammatory Bowel Diseases. *Adv Anat Pathol* 2022; **29**: 48-61 [PMID: 34879038 DOI: 10.1097/PAP.0000000000000325]
15 **Weiss SJ**. Neutrophil-mediated methemoglobin formation in the erythrocyte. The role of superoxide and hydrogen peroxide. *J Biol Chem* 1982; **257**: 2947-2953 [PMID: 6277918 DOI: 10.1016/S0021-9258(19)81056-6]
16 **Klyubin IV**, Kirpichnikova KM, Gamaley IA. Hydrogen peroxide-induced chemotaxis of mouse peritoneal neutrophils. *Eur J Cell Biol* 1996; **70**: 347-351 [PMID: 8864663]
17 **Morad H**, Luqman S, Tan CH, Swann V, McNaughton PA. TRPM2 ion channels steer neutrophils towards a source of hydrogen peroxide. *Sci Rep* 2021; **11**: 9339 [PMID: 33927223 DOI: 10.1038/s41598-021-88224-5]
18 **Gangwar R**, Meena AS, Shukla PK, Nagaraja AS, Dorniak PL, Pallikuth S, Waters CM, Sood A, Rao R. Calcium-mediated oxidative stress: a common mechanism in tight junction disruption by different types of cellular stress. *Biochem J* 2017; **474**: 731-749 [PMID: 28057718 DOI: 10.1042/BCJ20160679]
19 **Rao RK**, Baker RD, Baker SS, Gupta A, Holycross M. Oxidant-induced disruption of intestinal epithelial barrier function: role of protein tyrosine phosphorylation. *Am J Physiol* 1997; **273**: G812-G823 [PMID: 9357822 DOI: 10.1152/ajpgi.1997.273.4.G812]
20 **Parrish AR**, Catania JM, Orozco J, Gandolfi AJ. Chemically induced oxidative stress disrupts the E-cadherin/catenin cell adhesion complex. *Toxicol Sci* 1999; **51**: 80-86 [PMID: 10496679 DOI: 10.1093/toxsci/51.1.80]
21 **Grisham MB**, Gaginella TS, von Ritter C, Tamai H, Be RM, Granger DN. Effects of neutrophil-derived oxidants on intestinal permeability, electrolyte transport, and epithelial cell viability. *Inflammation* 1990; **14**: 531-542 [PMID: 2174408 DOI: 10.1007/BF00914274]
22 **Katinios G**, Casado-Bedmar M, Walter SA, Vicario M, González-Castro AM, Bednarska O, Söderholm JD, Hjortswang H, Keita ÅV. Increased Colonic Epithelial Permeability and Mucosal Eosinophilia in Ulcerative Colitis in Remission Compared With Irritable Bowel Syndrome and Health. *Inflamm Bowel Dis* 2020; **26**: 974-984 [PMID: 31944236 DOI: 10.1093/ibd/izz328]
23 **Bienert GP**, Chaumont F. Aquaporin-facilitated transmembrane diffusion of hydrogen peroxide. *Biochim Biophys Acta* 2014; **1840**: 1596-1604 [PMID: 24060746 DOI: 10.1016/j.bbagen.2013.09.017]
24 **Rao RK**, Li L, Baker RD, Baker SS, Gupta A. Glutathione oxidation and PTPase inhibition by hydrogen peroxide in Caco-2 cell monolayer. *Am J Physiol Gastrointest Liver Physiol* 2000; **279**: G332-G340 [PMID: 10915642 DOI: 10.1152/ajpgi.2000.279.2.G332]
25 **Hu JE**, Weiß F, Bojarski C, Branchi F, Schulzke JD, Fromm M, Krug SM. Expression of tricellular tight junction proteins and the paracellular macromolecule barrier are recovered in remission of ulcerative colitis. *BMC Gastroenterol* 2021; **21**: 141 [PMID: 33789594 DOI: 10.1186/s12876-021-01723-7]
26 **Naito Y**, Takagi T, Yoshikawa T. Molecular fingerprints of neutrophil-dependent oxidative stress in inflammatory bowel disease. *J Gastroenterol* 2007; **42**: 787-798 [PMID: 17940831 DOI: 10.1007/s00535-007-2096-y]
27 **Sheehan JF**, Brynjolfsson G. Ulcerative colitis following hydrogen peroxide enema: case report and experimental production with transient emphysema of colonic wall and gas embolism. *Lab Invest* 1960; **9**: 150-168 [PMID: 14445720]
28 **Meyer CT**, Brand M, DeLuca VA, Spiro HM. Hydrogen peroxide colitis: a report of three patients. *J Clin Gastroenterol* 1981; **3**: 31-35 [PMID: 7276490 DOI: 10.1097/00004836-198103000-00008]
29 **Hopkins RZ**. Hydrogen peroxide in biology and medicine: an overview. *React Oxyg Species* 2017; **3**: 26-37
30 **Santhanam S**, Venkatraman A, Ramakrishna BS. Impairment of mitochondrial acetoacetyl CoA thiolase activity in the colonic mucosa of patients with ulcerative colitis. *Gut* 2007; **56**: 1543-1549 [PMID: 17483192 DOI: 10.1136/gut.2006.108449]
31 **Hoensch H**, Peters WH, Roelofs HM, Kirch W. Expression of the glutathione enzyme system of human colon mucosa by localisation, gender and age. *Curr Med Res Opin* 2006; **22**: 1075-1083 [PMID: 16846540 DOI: 10.1185/030079906X112480]
32 **Esworthy RS**, Aranda R, Martín MG, Doroshow JH, Binder SW, Chu FF. Mice with combined disruption of Gpx1 and Gpx2 genes have colitis. *Am J Physiol Gastrointest Liver Physiol* 2001; **281**: G848-G855 [PMID: 11518697 DOI: 10.1152/ajpgi.2001.281.3.G848]
33 **Harrison GJ**, Jordan LR, Willis RJ. Deleterious effects of hydrogen peroxide on the function and ultrastructure of cardiac muscle and the coronary vasculature of perfused rat hearts. *Can J Cardiol* 1994; **10**: 843-849 [PMID: 7954020]
34 **Wittenburg AL**, Phillips SA, Gutterman DD. The role of catalase and endothelium in hydrogen peroxide induced vasodilatation of human adipose arterioles. *FASEB J* 2007; **21**
35 **Weiss SJ**, Young J, LoBuglio AF, Slivka A, Nimeh NF. Role of hydrogen peroxide in neutrophil-mediated destruction of cultured endothelial cells. *J Clin Invest* 1981; **68**: 714-721 [PMID: 6268662 DOI: 10.1172/JCI110307]
36 **Yakes FM**, Van Houten B. Mitochondrial DNA damage is more extensive and persists longer than nuclear DNA damage in human cells following oxidative stress. *Proc Natl Acad Sci U S A* 1997; **94**: 514-519 [PMID: 9012815 DOI: 10.1073/pnas.94.2.514]
37 **Wu Z**, Sainz AG, Shadel GS. Mitochondrial DNA: cellular genotoxic stress sentinel. *Trends Biochem Sci* 2021; **46**: 812-821 [PMID: 34088564 DOI: 10.1016/j.tibs.2021.05.004]
38 **Hahn A**, Zuryn S. Mitochondrial Genome (mtDNA) Mutations that Generate Reactive Oxygen Species. *Antioxidants (Basel)* 2019; **8** [PMID: 31514455 DOI: 10.3390/antiox8090392]
39 **Dlasková A**, Hlavatá L, Jezek P. Oxidative stress caused by blocking of mitochondrial complex I H(+) pumping as a link in aging/disease vicious cycle. *Int J Biochem Cell Biol* 2008; **40**: 1792-1805 [PMID: 18291703 DOI: 10.1016/j.biocel.2008.01.012]

40 **Den Hond E**, Hiele M, Evenepoel P, Peeters M, Ghoos Y, Rutgeerts P. In vivo butyrate metabolism and colonic permeability in extensive ulcerative colitis. *Gastroenterology* 1998; **115**: 584-590 [PMID: 9721155 DOI: 10.1016/S0016-5085(98)70137-4]

41 **Chapman MA**, Grahn MF, Boyle MA, Hutton M, Rogers J, Williams NS. Butyrate oxidation is impaired in the colonic mucosa of sufferers of quiescent ulcerative colitis. *Gut* 1994; **35**: 73-76 [PMID: 8307454 DOI: 10.1136/gut.35.1.73]

42 **Vanderborght M**, Nassogne MC, Hermans D, Moniotte S, Seneca S, Van Coster R, Buts JP, Sokal EM. Intractable ulcerative colitis of infancy in a child with mitochondrial respiratory chain disorder. *J Pediatr Gastroenterol Nutr* 2004; **38**: 355-357 [PMID: 15076640 DOI: 10.1097/00005176-200403000-00023]

43 **Dimauro S**, Davidzon G. Mitochondrial DNA and disease. *Ann Med* 2005; **37**: 222-232 [PMID: 16019721 DOI: 10.1080/07853890510007368]

44 **Nishikawa M**, Oshitani N, Matsumoto T, Nishigami T, Arakawa T, Inoue M. Accumulation of mitochondrial DNA mutation with colorectal carcinogenesis in ulcerative colitis. *Br J Cancer* 2005; **93**: 331-337 [PMID: 15956973 DOI: 10.1038/sj.bjc.6602664]

45 **Sifroni KG**, Damiani CR, Stoffel C, Cardoso MR, Ferreira GK, Jeremias IC, Rezin GT, Scaini G, Schuck PF, Dal-Pizzol F, Streck EL. Mitochondrial respiratory chain in the colonic mucosal of patients with ulcerative colitis. *Mol Cell Biochem* 2010; **342**: 111-115 [PMID: 20440543 DOI: 10.1007/s11010-010-0474-x]

46 **Circu ML**, Moyer MP, Harrison L, Aw TY. Contribution of glutathione status to oxidant-induced mitochondrial DNA damage in colonic epithelial cells. *Free Radic Biol Med* 2009; **47**: 1190-1198 [PMID: 19647792 DOI: 10.1016/j.freeradbiomed.2009.07.032]

47 **Martínez-Reyes I**, Cuezva JM. The H(+)-ATP synthase: a gate to ROS-mediated cell death or cell survival. *Biochim Biophys Acta* 2014; **1837**: 1099-1112 [PMID: 24685430 DOI: 10.1016/j.bbabio.2014.03.010]

48 **Schafer FQ**, Buettner GR. Redox environment of the cell as viewed through the redox state of the glutathione disulfide/glutathione couple. *Free Radic Biol Med* 2001; **30**: 1191-1212 [PMID: 11368918 DOI: 10.1016/s0891-5849(01)00480-4]

49 **Marí M**, de Gregorio E, de Dios C, Roca-Agujetas V, Cucarull B, Tutusaus A, Morales A, Colell A. Mitochondrial Glutathione: Recent Insights and Role in Disease. *Antioxidants (Basel)* 2020; **9** [PMID: 32987701 DOI: 10.3390/antiox9100909]

50 **Han D**, Canali R, Rettori D, Kaplowitz N. Effect of glutathione depletion on sites and topology of superoxide and hydrogen peroxide production in mitochondria. *Mol Pharmacol* 2003; **64**: 1136-1144 [PMID: 14573763 DOI: 10.1124/mol.64.5.1136]

51 **Lu SC**. Regulation of glutathione synthesis. *Mol Aspects Med* 2009; **30**: 42-59 [PMID: 18601945 DOI: 10.1016/j.mam.2008.05.005]

52 **Aon MA**, Stanley BA, Sivakumaran V, Kembro JM, O'Rourke B, Paolocci N, Cortassa S. Glutathione/thioredoxin systems modulate mitochondrial H2O2 emission: an experimental-computational study. *J Gen Physiol* 2012; **139**: 479-491 [PMID: 22585969 DOI: 10.1085/jgp.201210772]

53 **Seril DN**, Liao J, Yang GY, Yang CS. Oxidative stress and ulcerative colitis-associated carcinogenesis: studies in humans and animal models. *Carcinogenesis* 2003; **24**: 353-362 [PMID: 12663492 DOI: 10.1093/carcin/24.3.353]

54 **Qi L**, Wu XC, Zheng DQ. Hydrogen peroxide, a potent inducer of global genomic instability. *Curr Genet* 2019; **65**: 913-917 [PMID: 30963245 DOI: 10.1007/s00294-019-00969-9]

55 **Jones DP**. Radical-free biology of oxidative stress. *Am J Physiol Cell Physiol* 2008; **295**: C849-C868 [PMID: 18684987 DOI: 10.1152/ajpcell.00283.2008]

56 **Forman HJ**, Zhang H, Rinna A. Glutathione: overview of its protective roles, measurement, and biosynthesis. *Mol Aspects Med* 2009; **30**: 1-12 [PMID: 18796312 DOI: 10.1016/j.mam.2008.08.006]

57 **Deponte M**. The Incomplete Glutathione Puzzle: Just Guessing at Numbers and Figures? *Antioxid Redox Signal* 2017; **27**: 1130-1161 [PMID: 28540740 DOI: 10.1089/ars.2017.7123]

58 **Musaogullari A**, Chai YC. Redox Regulation by Protein S-Glutathionylation: From Molecular Mechanisms to Implications in Health and Disease. *Int J Mol Sci* 2020; **21** [PMID: 33143095 DOI: 10.3390/ijms21218113]

59 **Bergemalm D**, Andersson E, Hultdin J, Eriksson C, Rush ST, Kalla R, Adams AT, Keita ÅV, D'Amato M, Gomollon F, Jahnsen J; IBD Character Consortium, Ricanek P, Satsangi J, Repsilber D, Karling P, Halfvarson J. Systemic Inflammation in Preclinical Ulcerative Colitis. *Gastroenterology* 2021; **161**: 1526-1539.e9 [PMID: 34298022 DOI: 10.1053/j.gastro.2021.07.026]

60 **Blázovics A**, Kovács A, Lugasi A, Hagymási K, Bíró L, Fehér J. Antioxidant defense in erythrocytes and plasma of patients with active and quiescent Crohn disease and ulcerative colitis: a chemiluminescent study. *Clin Chem* 1999; **45**: 895-896 [PMID: 10351999 DOI: 10.1093/clinchem/45.6.895]

61 **Rana SV**, Sharma S, Prasad KK, Sinha SK, Singh K. Role of oxidative stress & antioxidant defence in ulcerative colitis patients from north India. *Indian J Med Res* 2014; **139**: 568-571 [PMID: 24927343]

62 **Neselioglu S**, Keske PB, Senat AA, Yurekli OT, Erdogan S, Alisik M, Ergin MS, Koseoglu H, Ersoy O, Erel O. The relationship between severity of ulcerative colitis and thiol-disulphide homeostasis. *Bratisl Lek Listy* 2018; **119**: 498-502 [PMID: 30160158 DOI: 10.4149/BLL_2018_091]

63 **Gaikwad R**, Thangaraj PR, Sen AK. Direct and rapid measurement of hydrogen peroxide in human blood using a microfluidic device. *Sci Rep* 2021; **11**: 2960 [PMID: 33536535 DOI: 10.1038/s41598-021-82623-4]

64 **Roche M**, Rondeau P, Singh NR, Tarnus E, Bourdon E. The antioxidant properties of serum albumin. *FEBS Lett* 2008; **582**: 1783-1787 [PMID: 18474236 DOI: 10.1016/j.febslet.2008.04.057]

65 **Cha MK**, Kim IH. Glutathione-linked thiol peroxidase activity of human serum albumin: a possible antioxidant role of serum albumin in blood plasma. *Biochem Biophys Res Commun* 1996; **222**: 619-625 [PMID: 8670254 DOI: 10.1006/bbrc.1996.0793]

66 **Turell L**, Botti H, Carballal S, Radi R, Alvarez B. Sulfenic acid--a key intermediate in albumin thiol oxidation. *J Chromatogr B Analyt Technol Biomed Life Sci* 2009; **877**: 3384-3392 [PMID: 19386559 DOI: 10.1016/j.jchromb.2009.03.035]

67 **Tozzi-Ciancarelli MG**, Di Massimo C, D'Orazio MC, Mascioli A, Di Giulio A, Tozzi E. Effect of exogenous hydrogen peroxide on human erythrocytes. *Cell Mol Biol* 1990; **36**: 57-64 [PMID: 2337915]

68 **Turell L**, Radi R, Alvarez B. The thiol pool in human plasma: the central contribution of albumin to redox processes. *Free Radic Biol Med* 2013; **65**: 244-253 [PMID: 23747983 DOI: 10.1016/j.freeradbiomed.2013.05.050]

69 **Yang X**, Mao Z, Huang Y, Yan H, Yan Q, Hong J, Fan J, Yao J. Reductively modified albumin attenuates DSS-Induced mouse colitis through rebalancing systemic redox state. *Redox Biol* 2021; **41**: 101881 [PMID: 33601276 DOI: 10.1016/j.redox.2021.101881]

70 **Koutroubakis IE**, Ramos-Rivers C, Regueiro M, Koutroumpakis E, Click B, Schoen RE, Hashash JG, Schwartz M, Swoger J, Baidoo L, Barrie A, Dunn MA, Binion DG. Persistent or Recurrent Anemia Is Associated With Severe and Disabling Inflammatory Bowel Disease. *Clin Gastroenterol Hepatol* 2015; **13**: 1760-1766 [PMID: 25862987 DOI: 10.1016/j.cgh.2015.03.029]

71 **Khan N**, Patel D, Shah Y, Trivedi C, Yang YX. Albumin as a prognostic marker for ulcerative colitis. *World J Gastroenterol* 2017; **23**: 8008-8016 [PMID: 29259376 DOI: 10.3748/wjg.v23.i45.8008]

72 **Tanaka M**, Takagi T, Naito Y, Uchiyama K, Hotta Y, Toyokawa Y, Kashiwagi S, Kamada K, Ishikawa T, Yasuda H, Konishi H, Itoh Y. Low serum albumin at admission is a predictor of early colectomy in patients with moderate to severe ulcerative colitis. *JGH Open* 2021; **5**: 377-381 [PMID: 33732885 DOI: 10.1002/jgh3.12506]

73 **Yagi S**, Furukawa S, Shiraishi K, Hashimoto Y, Tange K, Mori K, Ninomiya T, Suzuki S, Shibata N, Murakami H, Ohashi K, Hasebe A, Tomida H, Yamamoto Y, Takeshita E, Ikeda Y, Hiasa Y. Effect of disease duration on the association between serum albumin and mucosal healing in patients with ulcerative colitis. *BMJ Open Gastroenterol* 2021; **8** [PMID: 34099464 DOI: 10.1136/bmjgast-2021-000662]

74 **Suzuki S**, Hashizume N, Kanzaki Y, Maruyama T, Kozuka A, Yahikozawa K. Prognostic significance of serum albumin in patients with stable coronary artery disease treated by percutaneous coronary intervention. *PLoS One* 2019; **14**: e0219044 [PMID: 31269058 DOI: 10.1371/journal.pone.0219044]

75 **Shang W**, Hu H, Shen M, Wu J, Yu Z, Xuan L. Investigating the correlation between serum albumin level and the prognosis of Bell's palsy. *Medicine (Baltimore)* 2021; **100**: e26726 [PMID: 34398047 DOI: 10.1097/MD.0000000000026726]

76 **Tabata F**, Wada Y, Kawakami S, Miyaji K. Serum Albumin Redox States: More Than Oxidative Stress Biomarker. *Antioxidants (Basel)* 2021; **10** [PMID: 33804859 DOI: 10.3390/antiox10040503]

77 **Magzal F**, Sela S, Szuchman-Sapir A, Tamir S, Michelis R, Kristal B. In-vivo oxidized albumin- a pro-inflammatory agent in hypoalbuminemia. *PLoS One* 2017; **12**: e0177799 [PMID: 28542419 DOI: 10.1371/journal.pone.0177799]

78 **Rodríguez-Lago I**, Zabana Y, Barreiro-de Acosta M. Diagnosis and natural history of preclinical and early inflammatory bowel disease. *Ann Gastroenterol* 2020; **33**: 443-452 [PMID: 32879589 DOI: 10.20524/aog.2020.0508]

79 BRENDA Enzyme Database. [cited 24 December 2021]. Available from: https://www.brenda-enzymes.org/advanced.php

80 **Keshteli AH**, Madsen KL, Dieleman LA. Diet in the Pathogenesis and Management of Ulcerative Colitis; A Review of Randomized Controlled Dietary Interventions. *Nutrients* 2019; **11** [PMID: 31262022 DOI: 10.3390/nu11071498]

81 **Casanova MJ**, Chaparro M, Molina B, Merino O, Batanero R, Dueñas-Sadornil C, Robledo P, Garcia-Albert AM, Gómez-Sánchez MB, Calvet X, Trallero MDR, Montoro M, Vázquez I, Charro M, Barragán A, Martínez-Cerezo F, Megias-Rangil I, Huguet JM, Marti-Bonmati E, Calvo M, Campderá M, Muñoz-Vicente M, Merchante A, Ávila AD, Serrano-Aguayo P, De Francisco R, Hervías D, Bujanda L, Rodriguez GE, Castro-Laria L, Barreiro-de Acosta M, Van Domselaar M, Ramirez de la Piscina P, Santos-Fernández J, Algaba A, Torra S, Pozzati L, López-Serrano P, Arribas MDR, Rincón ML, Peláez AC, Castro E, García-Herola A, Santander C, Hernández-Alonso M, Martín-Noguerol E, Gómez-Lozano M, Monedero T, Villoria A, Figuerola A, Castaño-García A, Banales JM, Díaz-Hernández L, Argüelles-Arias F, López-Díaz J, Pérez-Martínez I, García-Talavera N, Nuevo-Siguairo OK, Riestra S, Gisbert JP. Prevalence of Malnutrition and Nutritional Characteristics of Patients With Inflammatory Bowel Disease. *J Crohns Colitis* 2017; **11**: 1430-1439 [PMID: 28981652 DOI: 10.1093/ecco-jcc/jjx102]

82 **Hou JK**, Abraham B, El-Serag H. Dietary intake and risk of developing inflammatory bowel disease: a systematic review of the literature. *Am J Gastroenterol* 2011; **106**: 563-573 [PMID: 21468064 DOI: 10.1038/ajg.2011.44]

83 **Fritsch J**, Garces L, Quintero MA, Pignac-Kobinger J, Santander AM, Fernández I, Ban YJ, Kwon D, Phillips MC, Knight K, Mao Q, Santaolalla R, Chen XS, Maruthamuthu M, Solis N, Damas OM, Kerman DH, Deshpande AR, Lewis JE, Chen C, Abreu MT. Low-Fat, High-Fiber Diet Reduces Markers of Inflammation and Dysbiosis and Improves Quality of Life in Patients With Ulcerative Colitis. *Clin Gastroenterol Hepatol* 2021; **19**: 1189-1199.e30 [PMID: 32445952 DOI: 10.1016/j.cgh.2020.05.026]

84 **Barnes EL**, Nestor M, Onyewadume L, de Silva PS, Korzenik JR; DREAM Investigators. High Dietary Intake of Specific Fatty Acids Increases Risk of Flares in Patients With Ulcerative Colitis in Remission During Treatment With Aminosalicylates. *Clin Gastroenterol Hepatol* 2017; **15**: 1390-1396.e1 [PMID: 28110099 DOI: 10.1016/j.cgh.2016.12.036]

85 **Gu P**, Feagins LA. Dining With Inflammatory Bowel Disease: A Review of the Literature on Diet in the Pathogenesis and Management of IBD. *Inflamm Bowel Dis* 2020; **26**: 181-191 [PMID: 31670372 DOI: 10.1093/ibd/izz268]

86 **Waterham HR**, Ferdinandusse S, Wanders RJ. Human disorders of peroxisome metabolism and biogenesis. *Biochim Biophys Acta* 2016; **1863**: 922-933 [PMID: 26611709 DOI: 10.1016/j.bbamcr.2015.11.015]

87 **Poirier Y**, Antonenkov VD, Glumoff T, Hiltunen JK. Peroxisomal beta-oxidation--a metabolic pathway with multiple functions. *Biochim Biophys Acta* 2006; **1763**: 1413-1426 [PMID: 17028011 DOI: 10.1016/j.bbamcr.2006.08.034]

88 **Jo DS**, Park NY, Cho DH. Peroxisome quality control and dysregulated lipid metabolism in neurodegenerative diseases. *Exp Mol Med* 2020; **52**: 1486-1495 [PMID: 32917959 DOI: 10.1038/s12276-020-00503-9]

89 **Nordgren M**, Fransen M. Peroxisomal metabolism and oxidative stress. *Biochimie* 2014; **98**: 56-62 [PMID: 23933092 DOI: 10.1016/j.biochi.2013.07.026]

90 **Tominaga K**, Kamimura K, Takahashi K, Yokoyama J, Yamagiwa S, Terai S. Diversion colitis and pouchitis: A mini-review. *World J Gastroenterol* 2018; **24**: 1734-1747 [PMID: 29713128 DOI: 10.3748/wjg.v24.i16.1734]

91 **Leonel AJ**, Alvarez-Leite JI. Butyrate: implications for intestinal function. *Curr Opin Clin Nutr Metab Care* 2012; **15**:

474-479 [PMID: 22797568 DOI: 10.1097/MCO.0b013e32835665fa]
92 **Houten SM**, Wanders RJ. A general introduction to the biochemistry of mitochondrial fatty acid β-oxidation. *J Inherit Metab Dis* 2010; **33**: 469-477 [PMID: 20195903 DOI: 10.1007/s10545-010-9061-2]
93 **De Preter V**, Arijs I, Windey K, Vanhove W, Vermeire S, Schuit F, Rutgeerts P, Verbeke K. Impaired butyrate oxidation in ulcerative colitis is due to decreased butyrate uptake and a defect in the oxidation pathway. *Inflamm Bowel Dis* 2012; **18**: 1127-1136 [PMID: 21987487 DOI: 10.1002/ibd.21894]
94 **McNabney SM**, Henagan TM. Short Chain Fatty Acids in the Colon and Peripheral Tissues: A Focus on Butyrate, Colon Cancer, Obesity and Insulin Resistance. *Nutrients* 2017; **9** [PMID: 29231905 DOI: 10.3390/nu9121348]
95 **Yang C**, Ko B, Hensley CT, Jiang L, Wasti AT, Kim J, Sudderth J, Calvaruso MA, Lumata L, Mitsche M, Rutter J, Merritt ME, DeBerardinis RJ. Glutamine oxidation maintains the TCA cycle and cell survival during impaired mitochondrial pyruvate transport. *Mol Cell* 2014; **56**: 414-424 [PMID: 25458842 DOI: 10.1016/j.molcel.2014.09.025]
96 **Cherbuy C**, Darcy-Vrillon B, Morel MT, Pégorier JP, Duée PH. Effect of germfree state on the capacities of isolated rat colonocytes to metabolize n-butyrate, glucose, and glutamine. *Gastroenterology* 1995; **109**: 1890-1899 [PMID: 7498654 DOI: 10.1016/0016-5085(95)90756-4]
97 **Donohoe DR**, Garge N, Zhang X, Sun W, O'Connell TM, Bunger MK, Bultman SJ. The microbiome and butyrate regulate energy metabolism and autophagy in the mammalian colon. *Cell Metab* 2011; **13**: 517-526 [PMID: 21531334 DOI: 10.1016/j.cmet.2011.02.018]
98 **Kim MH**, Kim H. The Roles of Glutamine in the Intestine and Its Implication in Intestinal Diseases. *Int J Mol Sci* 2017; **18** [PMID: 28498331 DOI: 10.3390/ijms18051051]
99 **Tompkins SC**, Sheldon RD, Rauckhorst AJ, Noterman MF, Solst SR, Buchanan JL, Mapuskar KA, Pewa AD, Gray LR, Oonthonpan L, Sharma A, Scerbo DA, Dupuy AJ, Spitz DR, Taylor EB. Disrupting Mitochondrial Pyruvate Uptake Directs Glutamine into the TCA Cycle away from Glutathione Synthesis and Impairs Hepatocellular Tumorigenesis. *Cell Rep* 2019; **28**: 2608-2619.e6 [PMID: 31484072 DOI: 10.1016/j.celrep.2019.07.098]
100 **Lane A**, Dalkie N, Henderson L, Irwin J, Rostami K. An elemental diet is effective in the management of diversion colitis. *Gastroenterol Hepatol Bed Bench* 2021; **14**: 81-84 [PMID: 33868614]
101 **Pravda J**. Diversion Colitis: A Bioenergetic Model of Pathogenesis. *Japanese J Gastroenterol Hepatol* 2019; **2**: 1-11
102 **Chiba M**, Tsuda S, Komatsu M, Tozawa H, Takayama Y. Onset of Ulcerative Colitis during a Low-Carbohydrate Weight-Loss Diet and Treatment with a Plant-Based Diet: A Case Report. *Perm J* 2016; **20**: 80-84 [PMID: 26824967 DOI: 10.7812/TPP/15-038]
103 **Duncan SH**, Belenguer A, Holtrop G, Johnstone AM, Flint HJ, Lobley GE. Reduced dietary intake of carbohydrates by obese subjects results in decreased concentrations of butyrate and butyrate-producing bacteria in feces. *Appl Environ Microbiol* 2007; **73**: 1073-1078 [PMID: 17189447 DOI: 10.1128/AEM.02340-06]
104 **Hamer HM**, Jonkers DM, Bast A, Vanhoutvin SA, Fischer MA, Kodde A, Troost FJ, Venema K, Brummer RJ. Butyrate modulates oxidative stress in the colonic mucosa of healthy humans. *Clin Nutr* 2009; **28**: 88-93 [PMID: 19108937 DOI: 10.1016/j.clnu.2008.11.002]
105 **Scheppach W**, Sommer H, Kirchner T, Paganelli GM, Bartram P, Christl S, Richter F, Dusel G, Kasper H. Effect of butyrate enemas on the colonic mucosa in distal ulcerative colitis. *Gastroenterology* 1992; **103**: 51-56 [PMID: 1612357 DOI: 10.1016/0016-5085(92)91094-k]
106 **Rosignoli P**, Fabiani R, De Bartolomeo A, Spinozzi F, Agea E, Pelli MA, Morozzi G. Protective activity of butyrate on hydrogen peroxide-induced DNA damage in isolated human colonocytes and HT29 tumour cells. *Carcinogenesis* 2001; **22**: 1675-1680 [PMID: 11577008 DOI: 10.1093/carcin/22.10.1675]
107 **Blachier F**, Boutry C, Bos C, Tomé D. Metabolism and functions of L-glutamate in the epithelial cells of the small and large intestines. *Am J Clin Nutr* 2009; **90**: 814S-821S [PMID: 19571215 DOI: 10.3945/ajcn.2009.27462S]
108 **Roediger WE**, Nance S. Metabolic induction of experimental ulcerative colitis by inhibition of fatty acid oxidation. *Br J Exp Pathol* 1986; **67**: 773-782 [PMID: 3099821]
109 **Nelson RA**. Intestinal transport, coenzyme A, and colitis in pantothenic acid deficiency. *Am J Clin Nutr* 1968; **21**: 495-501 [PMID: 5649470 DOI: 10.1093/ajcn/21.5.495]
110 **Martinez JE**, Kahana DD, Ghuman S, Wilson HP, Wilson J, Kim SCJ, Lagishetty V, Jacobs JP, Sinha-Hikim AP, Friedman TC. Unhealthy Lifestyle and Gut Dysbiosis: A Better Understanding of the Effects of Poor Diet and Nicotine on the Intestinal Microbiome. *Front Endocrinol (Lausanne)* 2021; **12**: 667066 [PMID: 34168615 DOI: 10.3389/fendo.2021.667066]
111 **Losso JN**. Food Processing, Dysbiosis, Gastrointestinal Inflammatory Diseases, and Antiangiogenic Functional Foods or Beverages. *Annu Rev Food Sci Technol* 2021; **12**: 235-258 [PMID: 33467906 DOI: 10.1146/annurev-food-062520-090235]
112 **Kamm MA**. Processed food affects the gut microbiota: The revolution has started. *J Gastroenterol Hepatol* 2020; **35**: 6-7 [PMID: 31965661 DOI: 10.1111/jgh.14976]
113 **Defois C**, Ratel J, Garrait G, Denis S, Le Goff O, Talvas J, Mosoni P, Engel E, Peyret P. Food Chemicals Disrupt Human Gut Microbiota Activity And Impact Intestinal Homeostasis As Revealed By In Vitro Systems. *Sci Rep* 2018; **8**: 11006 [PMID: 30030472 DOI: 10.1038/s41598-018-29376-9]
114 **Gálvez-Ontiveros Y**, Páez S, Monteagudo C, Rivas A. Endocrine Disruptors in Food: Impact on Gut Microbiota and Metabolic Diseases. *Nutrients* 2020; **12** [PMID: 32326280 DOI: 10.3390/nu12041158]
115 **Bajinka O**, Tan Y, Abdelhalim KA, Özdemir G, Qiu X. Extrinsic factors influencing gut microbes, the immediate consequences and restoring eubiosis. *AMB Express* 2020; **10**: 130 [PMID: 32710186 DOI: 10.1186/s13568-020-01066-8]
116 **Vich Vila A**, Collij V, Sanna S, Sinha T, Imhann F, Bourgonje AR, Mujagic Z, Jonkers DMAE, Masclee AAM, Fu J, Kurilshikov A, Wijmenga C, Zhernakova A, Weersma RK. Impact of commonly used drugs on the composition and metabolic function of the gut microbiota. *Nat Commun* 2020; **11**: 362 [PMID: 31953381 DOI: 10.1038/s41467-019-14177-z]
117 **Karl JP**, Hatch AM, Arcidiacono SM, Pearce SC, Pantoja-Feliciano IG, Doherty LA, Soares JW. Effects of Psychological, Environmental and Physical Stressors on the Gut Microbiota. *Front Microbiol* 2018; **9**: 2013 [PMID:

30258412 DOI: 10.3389/fmicb.2018.02013]
118 **Bolte LA**, Vich Vila A, Imhann F, Collij V, Gacesa R, Peters V, Wijmenga C, Kurilshikov A, Campmans-Kuijpers MJE, Fu J, Dijkstra G, Zhernakova A, Weersma RK. Long-term dietary patterns are associated with pro-inflammatory and anti-inflammatory features of the gut microbiome. *Gut* 2021; **70**: 1287-1298 [PMID: 33811041 DOI: 10.1136/gutjnl-2020-322670]
119 **Laudisi F**, Stolfi C, Monteleone G. Impact of Food Additives on Gut Homeostasis. *Nutrients* 2019; **11** [PMID: 31581570 DOI: 10.3390/nu11102334]
120 **Strus M**, Gosiewski T, Fyderek K, Wedrychowicz A, Kowalska-Duplaga K, Kochan P, Adamski P, Heczko PB. A role of hydrogen peroxide producing commensal bacteria present in colon of adolescents with inflammatory bowel disease in perpetuation of the inflammatory process. *J Physiol Pharmacol* 2009; **60** Suppl 6: 49-54 [PMID: 20224151]
121 **Benninghoff AD**, Hintze KJ, Monsanto SP, Rodriguez DM, Hunter AH, Phatak S, Pestka JJ, Wettere AJV, Ward RE. Consumption of the Total Western Diet Promotes Colitis and Inflammation-Associated Colorectal Cancer in Mice. *Nutrients* 2020; **12** [PMID: 32093192 DOI: 10.3390/nu12020544]
122 **Rizzello F**, Spisni E, Giovanardi E, Imbesi V, Salice M, Alvisi P, Valerii MC, Gionchetti P. Implications of the Westernized Diet in the Onset and Progression of IBD. *Nutrients* 2019; **11** [PMID: 31072001 DOI: 10.3390/nu11051033]
123 **White BA**, Ramos GP, Kane S. The Impact of Alcohol in Inflammatory Bowel Diseases. *Inflamm Bowel Dis* 2022; **28**: 466-473 [PMID: 33988227 DOI: 10.1093/ibd/izab089]
124 **Cederbaum AI**. Alcohol metabolism. *Clin Liver Dis* 2012; **16**: 667-685 [PMID: 23101976 DOI: 10.1016/j.cld.2012.08.002]
125 **Forsyth CB**, Voigt RM, Keshavarzian A. Intestinal CYP2E1: A mediator of alcohol-induced gut leakiness. *Redox Biol* 2014; **3**: 40-46 [PMID: 25462064 DOI: 10.1016/j.redox.2014.10.002]
126 **Abdelmegeed MA**, Ha SK, Choi Y, Akbar M, Song BJ. Role of CYP2E1 in Mitochondrial Dysfunction and Hepatic Injury by Alcohol and Non-Alcoholic Substances. *Curr Mol Pharmacol* 2017; **10**: 207-225 [PMID: 26278393 DOI: 10.2174/1874467208666150817111114]
127 **García-Suástegui WA**, Ramos-Chávez LA, Rubio-Osornio M, Calvillo-Velasco M, Atzin-Méndez JA, Guevara J, Silva-Adaya D. The Role of CYP2E1 in the Drug Metabolism or Bioactivation in the Brain. *Oxid Med Cell Longev* 2017; **2017**: 4680732 [PMID: 28163821 DOI: 10.1155/2017/4680732]
128 **Nguyen LH**, Örtqvist AK, Cao Y, Simon TG, Roelstraete B, Song M, Joshi AD, Staller K, Chan AT, Khalili H, Olén O, Ludvigsson JF. Antibiotic use and the development of inflammatory bowel disease: a national case-control study in Sweden. *Lancet Gastroenterol Hepatol* 2020; **5**: 986-995 [PMID: 32818437 DOI: 10.1016/S2468-1253(20)30267-3]
129 **Ramirez J**, Guarner F, Bustos Fernandez L, Maruy A, Sdepanian VL, Cohen H. Antibiotics as Major Disruptors of Gut Microbiota. *Front Cell Infect Microbiol* 2020; **10**: 572912 [PMID: 33330122 DOI: 10.3389/fcimb.2020.572912]
130 **Korpela K**, Salonen A, Virta LJ, Kekkonen RA, Forslund K, Bork P, de Vos WM. Intestinal microbiome is related to lifetime antibiotic use in Finnish pre-school children. *Nat Commun* 2016; **7**: 10410 [PMID: 26811868 DOI: 10.1038/ncomms10410]
131 **Lee JY**, Cevallos SA, Byndloss MX, Tiffany CR, Olsan EE, Butler BP, Young BM, Rogers AWL, Nguyen H, Kim K, Choi SW, Bae E, Lee JH, Min UG, Lee DC, Bäumler AJ. High-Fat Diet and Antibiotics Cooperatively Impair Mitochondrial Bioenergetics to Trigger Dysbiosis that Exacerbates Pre-inflammatory Bowel Disease. *Cell Host Microbe* 2020; **28**: 273-284.e6 [PMID: 32668218 DOI: 10.1016/j.chom.2020.06.001]
132 **Dwyer DJ**, Belenky PA, Yang JH, MacDonald IC, Martell JD, Takahashi N, Chan CT, Lobritz MA, Braff D, Schwarz EG, Ye JD, Pati M, Vercruysse M, Ralifo PS, Allison KR, Khalil AS, Ting AY, Walker GC, Collins JJ. Antibiotics induce redox-related physiological alterations as part of their lethality. *Proc Natl Acad Sci U S A* 2014; **111**: E2100-E2109 [PMID: 24803433 DOI: 10.1073/pnas.1401876111]
133 **Kalghatgi S**, Spina CS, Costello JC, Liesa M, Morones-Ramirez JR, Slomovic S, Molina A, Shirihai OS, Collins JJ. Bactericidal antibiotics induce mitochondrial dysfunction and oxidative damage in Mammalian cells. *Sci Transl Med* 2013; **5**: 192ra85 [PMID: 23825301 DOI: 10.1126/scitranslmed.3006055]
134 **Guillouzo A**, Guguen-Guillouzo C. Antibiotics-induced oxidative stress. *Cure Opin Tox* 2020; **20-21**: 23-28 [DOI: 10.1016/j.cotox.2020.03.004]
135 **Singh R**, Sripada L, Singh R. Side effects of antibiotics during bacterial infection: mitochondria, the main target in host cell. *Mitochondrion* 2014; **16**: 50-54 [PMID: 24246912 DOI: 10.1016/j.mito.2013.10.005]
136 **Theis MK**, Boyko EJ. Patient perceptions of causes of inflammatory bowel disease. *Am J Gastroenterol* 1994; **89**: 1920 [PMID: 7942711]
137 **Crohn BB**. The clinical use of succinyl sulfathiazole (Sulfasuxidine). *Gastroenterology* 1943; **1**: 140-146
138 **Salem SN**, Shubair KS. Non-specific ulcerative colitis in Bedouin Arabs. *Lancet* 1967; **1**: 473-475 [PMID: 4164069 DOI: 10.1016/s0140-6736(67)91094-x]
139 **Araki M**, Shinzaki S, Yamada T, Arimitsu S, Komori M, Shibukawa N, Mukai A, Nakajima S, Kinoshita K, Kitamura S, Murayama Y, Ogawa H, Yasunaga Y, Oshita M, Fukui H, Masuda E, Tsujii M, Kawai S, Hiyama S, Inoue T, Tanimukai H, Iijima H, Takehara T. Psychologic stress and disease activity in patients with inflammatory bowel disease: A multicenter cross-sectional study. *PLoS One* 2020; **15**: e0233365 [PMID: 32453762 DOI: 10.1371/journal.pone.0233365]
140 **Levenstein S**, Prantera C, Varvo V, Scribano ML, Andreoli A, Luzi C, Arcà M, Berto E, Milite G, Marcheggiano A. Stress and exacerbation in ulcerative colitis: a prospective study of patients enrolled in remission. *Am J Gastroenterol* 2000; **95**: 1213-1220 [PMID: 10811330 DOI: 10.1111/j.1572-0241.2000.02012.x]
141 **Maunder RG**, Levenstein S. The role of stress in the development and clinical course of inflammatory bowel disease: epidemiological evidence. *Curr Mol Med* 2008; **8**: 247-252 [PMID: 18537632 DOI: 10.2174/156652408784533832]
142 **Mawdsley JE**, Macey MG, Feakins RM, Langmead L, Rampton DS. The effect of acute psychologic stress on systemic and rectal mucosal measures of inflammation in ulcerative colitis. *Gastroenterology* 2006; **131**: 410-419 [PMID: 16890594 DOI: 10.1053/j.gastro.2006.05.017]
143 **Almy TP**, Tulin M. Alterations in colonic function in man under stress; experimental production of changes simulating the irritable colon. *Gastroenterology* 1947; **8**: 616-626 [PMID: 20238757]

144 **Beattie DT**, Smith JA. Serotonin pharmacology in the gastrointestinal tract: a review. *Naunyn Schmiedebergs Arch Pharmacol* 2008; **377**: 181-203 [PMID: 18398601 DOI: 10.1007/s00210-008-0276-9]

145 **Gershon MD**. 5-Hydroxytryptamine (serotonin) in the gastrointestinal tract. *Curr Opin Endocrinol Diabetes Obes* 2013; **20**: 14-21 [PMID: 23222853 DOI: 10.1097/MED.0b013e32835bc703]

146 **Nozawa K**, Kawabata-Shoda E, Doihara H, Kojima R, Okada H, Mochizuki S, Sano Y, Inamura K, Matsushime H, Koizumi T, Yokoyama T, Ito H. TRPA1 regulates gastrointestinal motility through serotonin release from enterochromaffin cells. *Proc Natl Acad Sci U S A* 2009; **106**: 3408-3413 [PMID: 19211797 DOI: 10.1073/pnas.0805323106]

147 **BRENDA**. Information on EC 1.4.3.4 - monoamine oxidase. [cited 24 December 2021]. Available from: https://www.brenda-enzymes.org/enzyme.php?ecno=1.4.3.4

148 **Rao SS**, Hatfield RA, Suls JM, Chamberlain MJ. Psychological and physical stress induce differential effects on human colonic motility. *Am J Gastroenterol* 1998; **93**: 985-990 [PMID: 9647034 DOI: 10.1111/j.1572-0241.1998.00293.x]

149 **Ghia JE**, Li N, Wang H, Collins M, Deng Y, El-Sharkawy RT, Côté F, Mallet J, Khan WI. Serotonin has a key role in pathogenesis of experimental colitis. *Gastroenterology* 2009; **137**: 1649-1660 [PMID: 19706294 DOI: 10.1053/j.gastro.2009.08.041]

150 **McMullan C**, Pinkney TD, Jones LL, Magill L, Nepogodiev D, Pathmakanthan S, Cooney R, Mathers JM. Adapting to ulcerative colitis to try to live a 'normal' life: a qualitative study of patients' experiences in the Midlands region of England. *BMJ Open* 2017; **7**: e017544 [PMID: 28827271 DOI: 10.1136/bmjopen-2017-017544]

151 **Kobayashi T**, Siegmund B, Le Berre C, Wei SC, Ferrante M, Shen B, Bernstein CN, Danese S, Peyrin-Biroulet L, Hibi T. Ulcerative colitis. *Nat Rev Dis Primers* 2020; **6**: 74 [PMID: 32913180 DOI: 10.1038/s41572-020-0205-x]

152 **Jedel S**, Hoffman A, Merriman P, Swanson B, Voigt R, Rajan KB, Shaikh M, Li H, Keshavarzian A. A randomized controlled trial of mindfulness-based stress reduction to prevent flare-up in patients with inactive ulcerative colitis. *Digestion* 2014; **89**: 142-155 [PMID: 24557009 DOI: 10.1159/000356316]

153 **Boye B**, Lundin KE, Jantschek G, Leganger S, Mokleby K, Tangen T, Jantschek I, Pripp AH, Wojniusz S, Dahlstroem A, Rivenes AC, Benninghoven D, Hausken T, Roseth A, Kunzendorf S, Wilhelmsen I, Sharpe M, Blomhoff S, Malt UF, Jahnsen J. INSPIRE study: does stress management improve the course of inflammatory bowel disease and disease-specific quality of life in distressed patients with ulcerative colitis or Crohn's disease? *Inflamm Bowel Dis* 2011; **17**: 1863-1873 [PMID: 21287660 DOI: 10.1002/ibd.21575]

154 **Harries AD**, Baird A, Rhodes J. Non-smoking: a feature of ulcerative colitis. *Br Med J (Clin Res Ed)* 1982; **284**: 706 [PMID: 6802296 DOI: 10.1136/bmj.284.6317.706]

155 **Mahid SS**, Minor KS, Soto RE, Hornung CA, Galandiuk S. Smoking and inflammatory bowel disease: a meta-analysis. *Mayo Clin Proc* 2006; **81**: 1462-1471 [PMID: 17120402 DOI: 10.4065/81.11.1462]

156 **Calkins BM**. A meta-analysis of the role of smoking in inflammatory bowel disease. *Dig Dis Sci* 1989; **34**: 1841-1854 [PMID: 2598752 DOI: 10.1007/BF01536701]

157 **Piovani D**, Pansieri C, Kotha SRR, Piazza AC, Comberg CL, Peyrin-Biroulet L, Danese S, Bonovas S. Ethnic Differences in the Smoking-related Risk of Inflammatory Bowel Disease: A Systematic Review and Meta-analysis. *J Crohns Colitis* 2021; **15**: 1658-1678 [PMID: 33721889 DOI: 10.1093/ecco-jcc/jjab047]

158 **Du L**, Ha C. Epidemiology and Pathogenesis of Ulcerative Colitis. *Gastroenterol Clin North Am* 2020; **49**: 643-654 [PMID: 33121686 DOI: 10.1016/j.gtc.2020.07.005]

159 Non-smoking: a feature of ulcerative colitis. *Br Med J (Clin Res Ed)* 1982; **285**: 440 [PMID: 6809118 DOI: 10.1136/bmj.285.6339.440-a]

160 **Calabrese E**, Yanai H, Shuster D, Rubin DT, Hanauer SB. Low-dose smoking resumption in ex-smokers with refractory ulcerative colitis. *J Crohns Colitis* 2012; **6**: 756-762 [PMID: 22398093 DOI: 10.1016/j.crohns.2011.12.010]

161 **Kannichamy V**, Antony I, Mishra V, Banerjee A, Gandhi AB, Kaleem I, Alexander J, Hisbulla M, Khan S. Transdermal Nicotine as a Treatment Option for Ulcerative Colitis: A Review. *Cureus* 2020; **12**: e11096 [PMID: 33240692 DOI: 10.7759/cureus.11096]

162 **Lunney PC**, Leong RW. Review article: Ulcerative colitis, smoking and nicotine therapy. *Aliment Pharmacol Ther* 2012; **36**: 997-1008 [PMID: 23072629 DOI: 10.1111/apt.12086]

163 **Carlens C**, Hergens MP, Grunewald J, Ekbom A, Eklund A, Höglund CO, Askling J. Smoking, use of moist snuff, and risk of chronic inflammatory diseases. *Am J Respir Crit Care Med* 2010; **181**: 1217-1222 [PMID: 20203245 DOI: 10.1164/rccm.200909-1338OC]

164 **Salih A**, Widbom L, Hultdin J, Karling P. Smoking is associated with risk for developing inflammatory bowel disease including late onset ulcerative colitis: a prospective study. *Scand J Gastroenterol* 2018; **53**: 173-178 [PMID: 29262738 DOI: 10.1080/00365521.2017.1418904]

165 **de Castella H**. Non-smoking: a feature of ulcerative colitis. *Br Med J (Clin Res Ed)* 1982; **284**: 1706 [PMID: 6805664 DOI: 10.1136/bmj.284.6330.1706]

166 **Higuchi LM**, Khalili H, Chan AT, Richter JM, Bousvaros A, Fuchs CS. A prospective study of cigarette smoking and the risk of inflammatory bowel disease in women. *Am J Gastroenterol* 2012; **107**: 1399-1406 [PMID: 22777340 DOI: 10.1038/ajg.2012.196]

167 **Hughes JR**. Effects of abstinence from tobacco: valid symptoms and time course. *Nicotine Tob Res* 2007; **9**: 315-327 [PMID: 17365764 DOI: 10.1080/14622200701188919]

168 **Grace WJ**. Life stress and chronic ulcerative colitis. *Ann of NY Acad Sci* 2006; **58**: 389-397 [DOI: 10.1111/j.1749-6632.1954.tb45851.x]

169 **Pryor WA**, Arbour NC, Upham B, Church DF. The inhibitory effect of extracts of cigarette tar on electron transport of mitochondria and submitochondrial particles. *Free Radic Biol Med* 1992; **12**: 365-372 [PMID: 1317324 DOI: 10.1016/0891-5849(92)90085-u]

170 **Murphy MP**. How mitochondria produce reactive oxygen species. *Biochem J* 2009; **417**: 1-13 [PMID: 19061483 DOI: 10.1042/BJ20081386]

171 **Miró O**, Alonso JR, Jarreta D, Casademont J, Urbano-Márquez A, Cardellach F. Smoking disturbs mitochondrial

respiratory chain function and enhances lipid peroxidation on human circulating lymphocytes. *Carcinogenesis* 1999; **20**: 1331-1336 [PMID: 10383908 DOI: 10.1093/carcin/20.7.1331]

172 **Kabel A**, Omar MS, Alotaibi SN, Baali MH. Effect of Indole-3-carbinol and/or Metformin on Female Patients with Ulcerative Colitis (Premalignant Condition): Role of Oxidative Stress, Apoptosis and Proinflammatory Cytokines. *J Cancer Res Treat* 2017; **5**: 1-8 [DOI: 10.12691/jcrt-5-1-1]

173 **Vancura A**, Bu P, Bhagwat M, Zeng J, Vancurova I. Metformin as an Anticancer Agent. *Trends Pharmacol Sci* 2018; **39**: 867-878 [PMID: 30150001 DOI: 10.1016/j.tips.2018.07.006]

174 **LaMoia TE**, Shulman GI. Cellular and Molecular Mechanisms of Metformin Action. *Endocr Rev* 2021; **42**: 77-96 [PMID: 32897388 DOI: 10.1210/endrev/bnaa023]

175 **Mráček T**, Drahota Z, Houštěk J. The function and the role of the mitochondrial glycerol-3-phosphate dehydrogenase in mammalian tissues. *Biochim Biophys Acta* 2013; **1827**: 401-410 [PMID: 23220394 DOI: 10.1016/j.bbabio.2012.11.014]

176 **Singh G**. Mitochondrial FAD-linked Glycerol-3-phosphate Dehydrogenase: A Target for Cancer Therapeutics. *Pharmaceuticals (Basel)* 2014; **7**: 192-206 [PMID: 24521925 DOI: 10.3390/ph7020192]

177 **Shirkhanloo H**, Golbabaei F, Hassani H, Eftekhar F, Kian MJ. Occupational Exposure to Mercury: Air Exposure Assessment and Biological Monitoring based on Dispersive Ionic Liquid-Liquid Microextraction. *Iran J Public Health* 2014; **43**: 793-799 [PMID: 26110150]

178 **Schmoldt A**, Benthe HF, Haberland G. Digitoxin metabolism by rat liver microsomes. *Biochem Pharmacol* 1975; **24**: 1639-1641 [PMID: 10]

179 **Bagger S**, Breddam K, Byberg BR. Binding of mercury(II) to protein thiol groups: a study of proteinase K and carboxypeptidase Y. *J Inorg Biochem* 1991; **42**: 97-103 [PMID: 1856724 DOI: 10.1016/0162-0134(91)80036-h]

180 **Franco JL**, Posser T, Dunkley PR, Dickson PW, Mattos JJ, Martins R, Bainy AC, Marques MR, Dafre AL, Farina M. Methylmercury neurotoxicity is associated with inhibition of the antioxidant enzyme glutathione peroxidase. *Free Radic Biol Med* 2009; **47**: 449-457 [PMID: 19450679 DOI: 10.1016/j.freeradbiomed.2009.05.013]

181 **Bose-O'Reilly S**, McCarty KM, Steckling N, Lettmeier B. Mercury exposure and children's health. *Curr Probl Pediatr Adolesc Health Care* 2010; **40**: 186-215 [PMID: 20816346 DOI: 10.1016/j.cppeds.2010.07.002]

182 **Liang L**, Pan Y, Bin L, Liu Y, Huang W, Li R, Lai KP. Immunotoxicity mechanisms of perfluorinated compounds PFOA and PFOS. *Chemosphere* 2022; **291**: 132892 [PMID: 34780734 DOI: 10.1016/j.chemosphere.2021.132892]

183 **Steenland K**, Zhao L, Winquist A, Parks C. Ulcerative colitis and perfluorooctanoic acid (PFOA) in a highly exposed population of community residents and workers in the mid-Ohio valley. *Environ Health Perspect* 2013; **121**: 900-905 [PMID: 23735465 DOI: 10.1289/ehp.1206449]

184 **Steenland K**, Kugathasan S, Barr DB. PFOA and ulcerative colitis. *Environ Res* 2018; **165**: 317-321 [PMID: 29777922 DOI: 10.1016/j.envres.2018.05.007]

185 **Balaban N**, Gelman F, Taylor AA, Walker SL, Bernstein A, Ronen Z. Degradation of Brominated Organic Compounds (Flame Retardants) by a Four-Strain Consortium Isolated from Contaminated Groundwater. *Applied Sci* 2021; **11**: 6263 [DOI: 10.3390/app11146263]

186 **Antunes F**, Cadenas E. Cellular titration of apoptosis with steady state concentrations of H(2)O(2): submicromolar levels of H(2)O(2) induce apoptosis through Fenton chemistry independent of the cellular thiol state. *Free Radic Biol Med* 2001; **30**: 1008-1018 [PMID: 11316581 DOI: 10.1016/s0891-5849(01)00493-2]

187 **Jin M**, Ande A, Kumar A, Kumar S. Regulation of cytochrome P450 2e1 expression by ethanol: role of oxidative stress-mediated pkc/jnk/sp1 pathway. *Cell Death Dis* 2013; **4**: e554 [PMID: 23519123 DOI: 10.1038/cddis.2013.78]

188 **Wu D**, Cederbaum AI. Oxidative stress mediated toxicity exerted by ethanol-inducible CYP2E1. *Toxicol Appl Pharmacol* 2005; **207**: 70-76 [PMID: 16019049 DOI: 10.1016/j.taap.2005.01.057]

189 **Halliwell B**, Clement MV, Long LH. Hydrogen peroxide in the human body. *FEBS Lett* 2000; **486**: 10-13 [PMID: 11108833 DOI: 10.1016/s0014-5793(00)02197-9]

190 **Fazzini F**, Schöpf B, Blatzer M, Coassin S, Hicks AA, Kronenberg F, Fendt L. Plasmid-normalized quantification of relative mitochondrial DNA copy number. *Sci Rep* 2018; **8**: 15347 [PMID: 30337569 DOI: 10.1038/s41598-018-33684-5]

191 **Swanson GR**, Tieu V, Shaikh M, Forsyth C, Keshavarzian A. Is moderate red wine consumption safe in inactive inflammatory bowel disease? *Digestion* 2011; **84**: 238-244 [PMID: 21876358 DOI: 10.1159/000329403]

192 **Seth A**, Yan F, Polk DB, Rao RK. Probiotics ameliorate the hydrogen peroxide-induced epithelial barrier disruption by a PKC- and MAP kinase-dependent mechanism. *Am J Physiol Gastrointest Liver Physiol* 2008; **294**: G1060-G1069 [PMID: 18292183 DOI: 10.1152/ajpgi.00202.2007]

193 **Chuenkitiyanon S**, Pengsuparp T, Jianmongkol S. Protective effect of quercetin on hydrogen peroxide-induced tight junction disruption. *Int J Toxicol* 2010; **29**: 418-424 [PMID: 20445016 DOI: 10.1177/1091581810366487]

194 **Katsube T**, Tsuji H, Onoda M. Nitric oxide attenuates hydrogen peroxide-induced barrier disruption and protein tyrosine phosphorylation in monolayers of intestinal epithelial cell. *Biochim Biophys Acta* 2007; **1773**: 794-803 [PMID: 17451824 DOI: 10.1016/j.bbamcr.2007.03.002]

195 **Nakano E**, Taylor CJ, Chada L, McGaw J, Powers HJ. Hyperhomocystinemia in children with inflammatory bowel disease. *J Pediatr Gastroenterol Nutr* 2003; **37**: 586-590 [PMID: 14581802 DOI: 10.1097/00005176-200311000-00016]

196 **Akbulut S**, Altiparmak E, Topal F, Ozaslan E, Kucukazman M, Yonem O. Increased levels of homocysteine in patients with ulcerative colitis. *World J Gastroenterol* 2010; **16**: 2411-2416 [PMID: 20480528 DOI: 10.3748/wjg.v16.i19.2411]

197 **Morgenstern I**, Raijmakers MT, Peters WH, Hoensch H, Kirch W. Homocysteine, cysteine, and glutathione in human colonic mucosa: elevated levels of homocysteine in patients with inflammatory bowel disease. *Dig Dis Sci* 2003; **48**: 2083-2090 [PMID: 14627359 DOI: 10.1023/A:1026338812708]

198 **Drzewoski J**, Gasiorowska A, Małecka-Panas E, Bald E, Czupryniak L. Plasma total homocysteine in the active stage of ulcerative colitis. *J Gastroenterol Hepatol* 2006; **21**: 739-743 [PMID: 16677162 DOI: 10.1111/j.1440-1746.2006.04255.x]

199 **Oussalah A**, Guéant JL, Peyrin-Biroulet L. Meta-analysis: hyperhomocysteinaemia in inflammatory bowel diseases. *Aliment Pharmacol Ther* 2011; **34**: 1173-1184 [PMID: 21967576 DOI: 10.1111/j.1365-2036.2011.04864.x]

200 **Zhong Y**, Yan F, Jie W, Zhou Y, Fang F. Correlation between serum homocysteine level and ulcerative colitis: A meta-

analysis. *Pteridines* 2019; **30**: 114-120 [DOI: 10.1515/pteridines-2019-0013]
201 **Handy DE**, Zhang Y, Loscalzo J. Homocysteine down-regulates cellular glutathione peroxidase (GPx1) by decreasing translation. *J Biol Chem* 2005; **280**: 15518-15525 [PMID: 15734734 DOI: 10.1074/jbc.M501452200]
202 **Upchurch GR Jr**, Welch GN, Fabian AJ, Freedman JE, Johnson JL, Keaney JF Jr, Loscalzo J. Homocyst(e)ine decreases bioavailable nitric oxide by a mechanism involving glutathione peroxidase. *J Biol Chem* 1997; **272**: 17012-17017 [PMID: 9202015 DOI: 10.1074/jbc.272.27.17012]
203 **Chen N**, Liu Y, Greiner CD, Holtzman JL. Physiologic concentrations of homocysteine inhibit the human plasma GSH peroxidase that reduces organic hydroperoxides. *J Lab Clin Med* 2000; **136**: 58-65 [PMID: 10882228 DOI: 10.1067/mlc.2000.107692]
204 **Pravda J**, Weickert MJ, Wruble LD. Novel Combination Therapy Induced Histological Remission in Patients with Refractory Ulcerative Colitis. *J Inflam Bowel Dis Disor* 2019; **4**: 1-8
205 **Pravda J**, Gordon R, Sylvestre P. Sustained Histologic Remission (Complete Mucosal Healing) 12 Years after One-Time Treatment of Refractory Ulcerative Colitis with Novel Combination Therapy: A Case Report. *J Inflamm Bowel Dis Disorder* 2020; **5**: 1-5 [DOI: 10.37421/2476-1958.2020.5.132]
206 Clinical presentation: Novel therapy induced Complete histologic remission in refractory ulcerative colitis. [cited 12 December 2021]. Available from: https://www.youtube.com/watch?v=oQYwUMFAraA
207 **Dong C**, Metzger M, Holsbø E, Perduca V, Carbonnel F. Systematic review with meta-analysis: mortality in acute severe ulcerative colitis. *Aliment Pharmacol Ther* 2020; **51**: 8-33 [PMID: 31821584 DOI: 10.1111/apt.15592]
208 **Rosiou K**, Selinger CP. Acute severe ulcerative colitis: management advice for internal medicine and emergency physicians. *Intern Emerg Med* 2021; **16**: 1433-1442 [PMID: 33754227 DOI: 10.1007/s11739-021-02704-0]
209 **Tsunada S**, Iwakiri R, Ootani H, Aw TY, Fujimoto K. Redox imbalance in the colonic mucosa of ulcerative colitis. *Scand J Gastroenterol* 2003; **38**: 1002-1003 [PMID: 14531541 DOI: 10.1080/00365520310005055]
210 **Holvoet T**, Lobaton T, Hindryckx P. Optimal Management of Acute Severe Ulcerative Colitis (ASUC): Challenges and Solutions. *Clin Exp Gastroenterol* 2021; **14**: 71-81 [PMID: 33727846 DOI: 10.2147/CEG.S197719]
211 **Zhang MY**, Dugbartey GJ, Juriasingani S, Sener A. Hydrogen Sulfide Metabolite, Sodium Thiosulfate: Clinical Applications and Underlying Molecular Mechanisms. *Int J Mol Sci* 2021; **22** [PMID: 34208631 DOI: 10.3390/ijms22126452]
212 **Bijarnia RK**, Bachtler M, Chandak PG, van Goor H, Pasch A. Sodium thiosulfate ameliorates oxidative stress and preserves renal function in hyperoxaluric rats. *PLoS One* 2015; **10**: e0124881 [PMID: 25928142 DOI: 10.1371/journal.pone.0124881]
213 **McGeer PL**, McGeer EG, Lee M. Medical uses of Sodium thiosulfate. *J Neurol Neuromed* 2016 [DOI: 10.29245/2572.942X/2016/3.1032]
214 **Desai J**, Elnaggar M, Hanfy AA, Doshi R. Toxic Megacolon: Background, Pathophysiology, Management Challenges and Solutions. *Clin Exp Gastroenterol* 2020; **13**: 203-210 [PMID: 32547151 DOI: 10.2147/CEG.S200760]
215 **Shi XZ**, Winston JH, Sarna SK. Differential immune and genetic responses in rat models of Crohn's colitis and ulcerative colitis. *Am J Physiol Gastrointest Liver Physiol* 2011; **300**: G41-G51 [PMID: 20947704 DOI: 10.1152/ajpgi.00358.2010]
216 **Giniatullin A**, Petrov A, Giniatullin R. Action of Hydrogen Peroxide on Synaptic Transmission at the Mouse Neuromuscular Junction. *Neuroscience* 2019; **399**: 135-145 [PMID: 30593920 DOI: 10.1016/j.neuroscience.2018.12.027]
217 **Colton CA**, Colton JS, Gilbert DL. Changes in synaptic transmission produced by hydrogen peroxide. *J Free Radic Biol Med* 1986; **2**: 141-148 [PMID: 3029210 DOI: 10.1016/s0748-5514(86)80063-0]
218 **Cao W**, Vrees MD, Kirber MT, Fiocchi C, Pricolo VE. Hydrogen peroxide contributes to motor dysfunction in ulcerative colitis. *Am J Physiol Gastrointest Liver Physiol* 2004; **286**: G833-G843 [PMID: 14670823 DOI: 10.1152/ajpgi.00414.2003]
219 **Electronic medicines compendium**. Sodium Thiosulfate Solution for Injection. [cited 24 December 2021]. Available from: https://www2.medicines.org.uk/emc/product/7354/smpc
220 US Department of Health and Human Services. Chemical Hazards emergency medical management. [cited 24 December 2021]. Available from: https://chemm.hhs.gov/
221 **De Angelis M**, Garruti G, Minervini F, Bonfrate L, Portincasa P, Gobbetti M. The Food-gut Human Axis: The Effects of Diet on Gut Microbiota and Metabolome. *Curr Med Chem* 2019; **26**: 3567-3583 [PMID: 28462705 DOI: 10.2174/0929867324666170428103848]
222 **Pituch-Zdanowska A**, Banaszkiewicz A, Albrecht P. The role of dietary fibre in inflammatory bowel disease. *Prz Gastroenterol* 2015; **10**: 135-141 [PMID: 26516378 DOI: 10.5114/pg.2015.52753]
223 **Wagenaar CA**, van de Put M, Bisschops M, Walrabenstein W, de Jonge CS, Herrema H, van Schaardenburg D. The Effect of Dietary Interventions on Chronic Inflammatory Diseases in Relation to the Microbiome: A Systematic Review. *Nutrients* 2021; **13** [PMID: 34579085 DOI: 10.3390/nu13093208]
224 **Aamodt G**, Bukholm G, Jahnsen J, Moum B, Vatn MH; IBSEN Study Group. The association between water supply and inflammatory bowel disease based on a 1990-1993 cohort study in southeastern Norway. *Am J Epidemiol* 2008; **168**: 1065-1072 [PMID: 18801890 DOI: 10.1093/aje/kwn218]
225 **Jowett SL**, Seal CJ, Pearce MS, Phillips E, Gregory W, Barton JR, Welfare MR. Influence of dietary factors on the clinical course of ulcerative colitis: a prospective cohort study. *Gut* 2004; **53**: 1479-1484 [PMID: 15361498 DOI: 10.1136/gut.2003.024828]
226 **United States Environmental Protection Agency**. EPA-FDA Advice about Eating Fish and Shellfish. [cited 26 December 2021]. Available from: https://www.epa.gov/fish-tech/epa-fda-advice-about-eating-fish-and-shellfish
227 EPA-2: Fish Advice. [cited 24 December 2021]. Available from: https://www.fda.gov/food/metals-and-your-food/mercury-levels-commercial-fish-and-shellfish-1990-2012
228 **Wang F**, Feng J, Gao Q, Ma M, Lin X, Liu J, Li J, Zhao Q. Carbohydrate and protein intake and risk of ulcerative colitis: Systematic review and dose-response meta-analysis of epidemiological studies. *Clin Nutr* 2017; **36**: 1259-1265 [PMID: 27776925 DOI: 10.1016/j.clnu.2016.10.009]
229 **Nie JY**, Zhao Q. Beverage consumption and risk of ulcerative colitis: Systematic review and meta-analysis of

epidemiological studies. *Medicine (Baltimore)* 2017; **96**: e9070 [PMID: 29245319 DOI: 10.1097/MD.0000000000009070]

230 **Benitz KF**, Golberg L, Coulston F. Intestinal effects of carrageenans in the rhesus monkey (*Macaca mulatta*). *Food Cosmet Toxicol* 1973; **11**: 565-575 [DOI: 10.1016/S0015-6264(73)80327-X]

231 **Siregar RF**, Santoso J, Uju U. Physico Chemical Characteristic of Kappa Carrageenan Degraded Using Hydrogen Peroxide. *JPHPI* 2017; **19**: 256 [DOI: 10.17844/jphpi.v19i3.14532]

232 **Bhattacharyya S**, Dudeja PK, Tobacman JK. Carrageenan-induced NFkappaB activation depends on distinct pathways mediated by reactive oxygen species and Hsp27 or by Bcl10. *Biochim Biophys Acta* 2008; **1780**: 973-982 [PMID: 18452717 DOI: 10.1016/j.bbagen.2008.03.019]

233 **Geerling BJ**, Dagnelie PC, Badart-Smook A, Russel MG, Stockbrügger RW, Brummer RJ. Diet as a risk factor for the development of ulcerative colitis. *Am J Gastroenterol* 2000; **95**: 1008-1013 [PMID: 10763951 DOI: 10.1111/j.1572-0241.2000.01942.x]

234 **BRENDA**. Information on EC 1.1.3.12 - pyridoxine 4-oxidase. [cited 24 December 2021]. Available from: https://www.brenda-enzymes.org/enzyme.php?ecno=1.1.3.12

235 **Everson CA**, Laatsch CD, Hogg N. Antioxidant defense responses to sleep loss and sleep recovery. *Am J Physiol Regul Integr Comp Physiol* 2005; **288**: R374-R383 [PMID: 15472007 DOI: 10.1152/ajpregu.00565.2004]

236 **Ananthakrishnan AN**, Khalili H, Konijeti GG, Higuchi LM, de Silva P, Fuchs CS, Richter JM, Schernhammer ES, Chan AT. Sleep duration affects risk for ulcerative colitis: a prospective cohort study. *Clin Gastroenterol Hepatol* 2014; **12**: 1879-1886 [PMID: 24780288 DOI: 10.1016/j.cgh.2014.04.021]

237 **Hauso Ø**, Martinsen TC, Waldum H. 5-Aminosalicylic acid, a specific drug for ulcerative colitis. *Scand J Gastroenterol* 2015; **50**: 933-941 [PMID: 25733192 DOI: 10.3109/00365521.2015.1018937]

238 **Couto D**, Ribeiro D, Freitas M, Gomes A, Lima JL, Fernandes E. Scavenging of reactive oxygen and nitrogen species by the prodrug sulfasalazine and its metabolites 5-aminosalicylic acid and sulfapyridine. *Redox Rep* 2010; **15**: 259-267 [PMID: 21208525 DOI: 10.1179/135100010X12826446921707]

239 **Ahnfelt-Rønne I**, Nielsen OH. The antiinflammatory moiety of sulfasalazine, 5-aminosalicylic acid, is a radical scavenger. *Agents Actions* 1987; **21**: 191-194 [PMID: 2888280 DOI: 10.1007/BF01974941]

240 **Battat R**, Duijvestein M, Guizzetti L, Choudhary D, Boland BS, Dulai PS, Parker CE, Nguyen TM, Singh S, Vande Casteele N, Pai RK, Feagan BG, Sandborn WJ, Jairath V. Histologic Healing Rates of Medical Therapies for Ulcerative Colitis: A Systematic Review and Meta-Analysis of Randomized Controlled Trials. *Am J Gastroenterol* 2019; **114**: 733-745 [PMID: 30694863 DOI: 10.14309/ajg.0000000000000111]

241 **Hallert C**, Björck I, Nyman M, Pousette A, Grännö C, Svensson H. Increasing fecal butyrate in ulcerative colitis patients by diet: controlled pilot study. *Inflamm Bowel Dis* 2003; **9**: 116-121 [PMID: 12769445 DOI: 10.1097/00054725-200303000-00005]

242 **Minutello K**, Gupta V. Cromolyn Sodium. 2022 Jan 12. In: StatPearls [Internet]. Treasure Island (FL): StatPearls Publishing; 2022 Jan- [PMID: 32491405]

243 **Chen E**, Chuang LS, Giri M, Villaverde N, Hsu NY, Sabic K, Joshowitz S, Gettler K, Nayar S, Chai Z, Alter IL, Chasteau CC, Korie UM, Dzedzik S, Thin TH, Jain A, Moscati A, Bongers G, Duerr RH, Silverberg MS, Brant SR, Rioux JD, Peter I, Schumm LP, Haritunians T, McGovern DP, Itan Y, Cho JH. Inflamed Ulcerative Colitis Regions Associated With MRGPRX2-Mediated Mast Cell Degranulation and Cell Activation Modules, Defining a New Therapeutic Target. *Gastroenterology* 2021; **160**: 1709-1724 [PMID: 33421512 DOI: 10.1053/j.gastro.2020.12.076]

244 **van Hoboken EA**, Thijssen AY, Verhaaren R, van der Veek PP, Prins FA, Verspaget HW, Masclee AA. Symptoms in patients with ulcerative colitis in remission are associated with visceral hypersensitivity and mast cell activity. *Scand J Gastroenterol* 2011; **46**: 981-987 [PMID: 21623672 DOI: 10.3109/00365521.2011.579156]

245 **Schirmer B**, Neumann D. The Function of the Histamine H4 Receptor in Inflammatory and Inflammation-Associated Diseases of the Gut. *Int J Mol Sci* 2021; **22** [PMID: 34204101 DOI: 10.3390/ijms22116116]

246 **Fox CC**, Lazenby AJ, Moore WC, Yardley JH, Bayless TM, Lichtenstein LM. Enhancement of human intestinal mast cell mediator release in active ulcerative colitis. *Gastroenterology* 1990; **99**: 119-124 [PMID: 1693122 DOI: 10.1016/0016-5085(90)91238-2]

247 **Balázs M**, Illyés G, Vadász G. Mast cells in ulcerative colitis. Quantitative and ultrastructural studies. *Virchows Arch B Cell Pathol Incl Mol Pathol* 1989; **57**: 353-360 [PMID: 2575298 DOI: 10.1007/BF02899101]

248 **Youngblood BA**, Butuci M, Davis T, Schanin J, Brock EC, Singh B, Rasmussen HS, Holman A, Drake R, Peterson K, Flynn AD. Mast Cells Are Significantly Activated In Patients with Ulcerative Colitis and Are Inhibited by an Anti-Siglec-8 Antibody, Antolimab (AK002). Proceedings of the Digestive Disease Week; 2020 May 2-5; Leeds, US. Chicago: Springer, 2020

249 **Baenkler HW**, Lux G, Günthner R, Kohlhäufl M, Matek W. Biopsy histamine in ulcerative colitis and Crohn's disease. *Hepatogastroenterology* 1987; **34**: 289-290 [PMID: 3428863]

250 **Raithel M**, Matek M, Baenkler HW, Jorde W, Hahn EG. Mucosal histamine content and histamine secretion in Crohn's disease, ulcerative colitis and allergic enteropathy. *Int Arch Allergy Immunol* 1995; **108**: 127-133 [PMID: 7549499 DOI: 10.1159/000237129]

251 **McGrath AP**, Hilmer KM, Collyer CA, Shepard EM, Elmore BO, Brown DE, Dooley DM, Guss JM. Structure and inhibition of human diamine oxidase. *Biochemistry* 2009; **48**: 9810-9822 [PMID: 19764817 DOI: 10.1021/bi9014192]

252 **Wolvekamp MC**, de Bruin RW. Diamine oxidase: an overview of historical, biochemical and functional aspects. *Dig Dis* 1994; **12**: 2-14 [PMID: 8200121 DOI: 10.1159/000171432]

253 **Wechsler JB**, Szabo A, Hsu CL, Krier-Burris RA, Schroeder HA, Wang MY, Carter RG, Velez TE, Aguiniga LM, Brown JB, Miller ML, Wershil BK, Barrett TA, Bryce PJ. Histamine drives severity of innate inflammation *via* histamine 4 receptor in murine experimental colitis. *Mucosal Immunol* 2018; **11**: 861-870 [PMID: 29363669 DOI: 10.1038/mi.2017.121]

254 **Ronchetti S**, Ricci E, Migliorati G, Gentili M, Riccardi C. How Glucocorticoids Affect the Neutrophil Life. *Int J Mol Sci* 2018; **19** [PMID: 30563002 DOI: 10.3390/ijms19124090]

255 **Winterbourn CC**, Kettle AJ, Hampton MB. Reactive Oxygen Species and Neutrophil Function. *Annu Rev Biochem* 2016; **85**: 765-792 [PMID: 27050287 DOI: 10.1146/annurev-biochem-060815-014442]

256 **Bilska A**, Włodek L. Lipoic acid - the drug of the future? *Pharmacol Rep* 2005; **57**: 570-577 [PMID: 16227639]

257 **Tort F**, Ferrer-Cortes X, Ribes A. Differential diagnosis of lipoic acid synthesis defects. *J Inherit Metab Dis* 2016; **39**: 781-793 [PMID: 27586888 DOI: 10.1007/s10545-016-9975-4]

258 **Xiao W**, Wang RS, Handy DE, Loscalzo J. NAD(H) and NADP(H) Redox Couples and Cellular Energy Metabolism. *Antioxid Redox Signal* 2018; **28**: 251-272 [PMID: 28648096 DOI: 10.1089/ars.2017.7216]

259 **Rampon C**, Volovitch M, Joliot A, Vriz S. Hydrogen Peroxide and Redox Regulation of Developments. *Antioxidants (Basel)* 2018; **7** [PMID: 30404180 DOI: 10.3390/antiox7110159]

260 **Packer L**, Kraemer K, Rimbach G. Molecular aspects of lipoic acid in the prevention of diabetes complications. *Nutrition* 2001; **17**: 888-895 [PMID: 11684397 DOI: 10.1016/s0899-9007(01)00658-x]

261 **Rochette L**, Ghibu S, Richard C, Zeller M, Cottin Y, Vergely C. Direct and indirect antioxidant properties of α-lipoic acid and therapeutic potential. *Mol Nutr Food Res* 2013; **57**: 114-125 [PMID: 23293044 DOI: 10.1002/mnfr.201200608]

262 **Arnér ES**, Nordberg J, Holmgren A. Efficient reduction of lipoamide and lipoic acid by mammalian thioredoxin reductase. *Biochem Biophys Res Commun* 1996; **225**: 268-274 [PMID: 8769129 DOI: 10.1006/bbrc.1996.1165]

263 **Smith AR**, Shenvi SV, Widlansky M, Suh JH, Hagen TM. Lipoic acid as a potential therapy for chronic diseases associated with oxidative stress. *Curr Med Chem* 2004; **11**: 1135-1146 [PMID: 15134511 DOI: 10.2174/0929867043365387]

264 **Nguyen H**, Gupta V. Alpha-Lipoic Acid. 2021 Nov 20. In: StatPearls [Internet]. Treasure Island (FL): StatPearls Publishing; 2022 Jan- [PMID: 33231971]

265 **Moura FA**, de Andrade KQ, dos Santos JC, Goulart MO. Lipoic Acid: its antioxidant and anti-inflammatory role and clinical applications. *Curr Top Med Chem* 2015; **15**: 458-483 [PMID: 25620240 DOI: 10.2174/1568026615666150114161358]

266 **Harvey CJ**, Thimmulappa RK, Singh A, Blake DJ, Ling G, Wakabayashi N, Fujii J, Myers A, Biswal S. Nrf2-regulated glutathione recycling independent of biosynthesis is critical for cell survival during oxidative stress. *Free Radic Biol Med* 2009; **46**: 443-453 [PMID: 19028565 DOI: 10.1016/j.freeradbiomed.2008.10.040]

267 **Ren H**, Meng Q, Yepuri N, Du X, Sarpong JO, Cooney RN. Protective effects of glutathione on oxidative injury induced by hydrogen peroxide in intestinal epithelial cells. *J Surg Res* 2018; **222**: 39-47 [PMID: 29273374 DOI: 10.1016/j.jss.2017.09.041]

268 **Petersen Shay K**, Moreau RF, Smith EJ, Hagen TM. Is alpha-lipoic acid a scavenger of reactive oxygen species in vivo? *IUBMB Life* 2008; **60**: 362-367 [PMID: 18409172 DOI: 10.1002/iub.40]

269 **Nguyen N**, Takemoto JK. A Case for Alpha-Lipoic Acid as an Alternative Treatment for Diabetic Polyneuropathy. *J Pharm Pharm Sci* 2018; **21**: 177s-191s [PMID: 30139425 DOI: 10.18433/jpps30100]

270 **Reljanovic M**, Reichel G, Rett K, Lobisch M, Schuette K, Möller W, Tritschler HJ, Mehnert H. Treatment of diabetic polyneuropathy with the antioxidant thioctic acid (alpha-lipoic acid): a two year multicenter randomized double-blind placebo-controlled trial (ALADIN II). Alpha Lipoic Acid in Diabetic Neuropathy. *Free Radic Res* 1999; **31**: 171-179 [PMID: 10499773 DOI: 10.1080/10715769900300721]

271 **Ziegler D**, Hanefeld M, Ruhnau KJ, Hasche H, Lobisch M, Schütte K, Kerum G, Malessa R. Treatment of symptomatic diabetic polyneuropathy with the antioxidant alpha-lipoic acid: a 7-month multicenter randomized controlled trial (ALADIN III Study). ALADIN III Study Group. Alpha-Lipoic Acid in Diabetic Neuropathy. *Diabetes Care* 1999; **22**: 1296-1301 [PMID: 10480774 DOI: 10.2337/diacare.22.8.1296]

272 **Moini H**, Packer L, Saris NE. Antioxidant and prooxidant activities of alpha-lipoic acid and dihydrolipoic acid. *Toxicol Appl Pharmacol* 2002; **182**: 84-90 [PMID: 12127266 DOI: 10.1006/taap.2002.9437]

273 **Pravda J**. Hydrogen peroxide and disease: towards a unified system of pathogenesis and therapeutics. *Mol Med* 2020; **26**: 41 [PMID: 32380940 DOI: 10.1186/s10020-020-00165-3]

274 **Elsner M**, Gehrmann W, Lenzen S. Peroxisome-generated hydrogen peroxide as important mediator of lipotoxicity in insulin-producing cells. *Diabetes* 2011; **60**: 200-208 [PMID: 20971967 DOI: 10.2337/db09-1401]

275 **Lenzen S**. The pancreatic beta cell: an intricate relation between anatomical structure, the signalling mechanism of glucose-induced insulin secretion, the low antioxidative defence, the high vulnerability and sensitivity to diabetic stress. *ChemTexts* 2021; **7**: 13 [DOI: 10.1007/s40828-021-00140-3]

276 Challenges in IBD Research. *Inflamm Bowel Dis* 2019; **25** Suppl 2: S1-S4 [PMID: 31095705 DOI: 10.1093/ibd/izz074]

277 **Pizarro TT**, Stappenbeck TS, Rieder F, Rosen MJ, Colombel JF, Donowitz M, Towne J, Mazmanian SK, Faith JJ, Hodin RA, Garrett WS, Fichera A, Poritz LS, Cortes CJ, Shtraizent N, Honig G, Snapper SB, Hurtado-Lorenzo A, Salzman NH, Chang EB. Challenges in IBD Research: Preclinical Human IBD Mechanisms. *Inflamm Bowel Dis* 2019; **25**: S5-S12 [PMID: 31095706 DOI: 10.1093/ibd/izz075]

278 **Alsoud D**, Verstockt B, Fiocchi C, Vermeire S. Breaking the therapeutic ceiling in drug development in ulcerative colitis. *Lancet Gastroenterol Hepatol* 2021; **6**: 589-595 [PMID: 34019798 DOI: 10.1016/S2468-1253(21)00065-0]

279 **Truelove SC**. Ulcerative colitis provoked by milk. *Br Med J* 1961; **1**: 154-160 [PMID: 13778258 DOI: 10.1136/bmj.1.5220.154]

280 **Ko CW**, Singh S, Feuerstein JD, Falck-Ytter C, Falck-Ytter Y, Cross RK; American Gastroenterological Association Institute Clinical Guidelines Committee. AGA Clinical Practice Guidelines on the Management of Mild-to-Moderate Ulcerative Colitis. *Gastroenterology* 2019; **156**: 748-764 [PMID: 30576644 DOI: 10.1053/j.gastro.2018.12.009]

281 **Feuerstein JD**, Isaacs KL, Schneider Y, Siddique SM, Falck-Ytter Y, Singh S; AGA Institute Clinical Guidelines Committee. AGA Clinical Practice Guidelines on the Management of Moderate to Severe Ulcerative Colitis. *Gastroenterology* 2020; **158**: 1450-1461 [PMID: 31945371 DOI: 10.1053/j.gastro.2020.01.006]

282 **Rubin DT**, Ananthakrishnan AN, Siegel CA, Sauer BG, Long MD. ACG Clinical Guideline: Ulcerative Colitis in Adults. *Am J Gastroenterol* 2019; **114**: 384-413 [PMID: 30840605 DOI: 10.14309/ajg.0000000000000152]

283 **Sandborn WJ**, Feagan BG, Hanauer SB, Lichtenstein GR. The Guide to Guidelines in Ulcerative Colitis: Interpretation

and Appropriate Use in Clinical Practice. *Gastroenterol Hepatol (N Y)* 2021; **17**: 3-13 [PMID: 34135718]
284 **Patil DT**, Odze RD. Backwash Is Hogwash: The Clinical Significance of Ileitis in Ulcerative Colitis. *Am J Gastroenterol* 2017; **112**: 1211-1214 [PMID: 28631729 DOI: 10.1038/ajg.2017.182]
285 **Chapman MA**, Grahn MF, Hutton M, Williams NS. Butyrate metabolism in the terminal ileal mucosa of patients with ulcerative colitis. *Br J Surg* 1995; **82**: 36-38 [PMID: 7881952 DOI: 10.1002/bjs.1800820115]
286 **DeRoche TC**, Xiao SY, Liu X. Histological evaluation in ulcerative colitis. *Gastroenterol Rep (Oxf)* 2014; **2**: 178-192 [PMID: 24942757 DOI: 10.1093/gastro/gou031]
287 **Shakirzyanova A**, Valeeva G, Giniatullin A, Naumenko N, Fulle S, Akulov A, Atalay M, Nikolsky E, Giniatullin R. Age-dependent action of reactive oxygen species on transmitter release in mammalian neuromuscular junctions. *Neurobiol Aging* 2016; **38**: 73-81 [PMID: 26827645 DOI: 10.1016/j.neurobiolaging.2015.10.023]
288 **Yang C**, Zhang X, Wang S, Huo X, Wang J. Small intestinal bacterial overgrowth and evaluation of intestinal barrier function in patients with ulcerative colitis. *Am J Transl Res* 2021; **13**: 6605-6610 [PMID: 34306403]
289 **Park SK**, Ye BD, Yang SK, Kim SO, Kim J, Kim JW, Park SH, Yang DH, Jung KW, Kim KJ, Byeon JS, Myung SJ, Kim JH. Clinical features and course of ulcerative colitis diagnosed in asymptomatic subjects. *J Crohns Colitis* 2014; **8**: 1254-1260 [PMID: 24662395 DOI: 10.1016/j.crohns.2014.03.002]
290 **Rodríguez-Lago I**, Ramírez C, Merino O, Azagra I, Maiz A, Zapata E, Higuera R, Montalvo I, Fernández-Calderón M, Arreba P, Carrascosa J, Iriarte A, Muñoz-Navas M, Cabriada JL, Barreiro-de Acosta M. Early microscopic findings in preclinical inflammatory bowel disease. *Dig Liver Dis* 2020; **52**: 1467-1472 [PMID: 32601034 DOI: 10.1016/j.dld.2020.05.052]
291 **Farrukh A**, Mayberry JF. Asymptomatic inflammatory bowel disease and colorectal cancer screening programs: how common is it and what should be done about it? *Gastrointest Disord* 2019; **1**: 261-265 [DOI: 10.3390/gidisord1020021]
292 **Howarth GF**, Robinson MH, Jenkins D, Hardcastle JD, Logan RF. High prevalence of undetected ulcerative colitis: data from the Nottingham fecal occult blood screening trial. *Am J Gastroenterol* 2002; **97**: 690-694 [PMID: 11926210 DOI: 10.1111/j.1572-0241.2002.05586.x]
293 **Sheriff MZ**, Mansoor E, Luther J, Ananthakrishnan AN, Abou Saleh M, Ho E, Briggs FBS, Dave M. Opportunistic Infections Are More Prevalent in Crohn's Disease and Ulcerative Colitis: A Large Population-Based Study. *Inflamm Bowel Dis* 2020; **26**: 291-300 [PMID: 31314891 DOI: 10.1093/ibd/izz147]
294 **Reznicek E**, Arfeen M, Shen B, Ghouri YA. Colorectal Dysplasia and Cancer Surveillance in Ulcerative Colitis. *Diseases* 2021; **9** [PMID: 34842672 DOI: 10.3390/diseases9040086]
295 **Narula N**, Hu A, Nguyen GC, Rangrej J, Marshall JK. Periodic Colonoscopies Are Associated with Improved Survival and Prognosis of Colorectal Cancer in Ulcerative Colitis. *Dig Dis Sci* 2021 [PMID: 34318355 DOI: 10.1007/s10620-021-07151-7]
296 **Kayal M**, Ungaro RC, Riggs A, Kamal K, Agrawal M, Cohen-Mekelburg S, Axelrad J, Faye A, Scherl E, Lawlor G, Sultan K, Lukin D, Dubinsky MC, Colombel JF; New York Crohn's and Colitis Organization (NYCCO). Ileal Pouch Anal Anastomosis for the Management of Ulcerative Colitis Is Associated With Significant Disability. *Clin Gastroenterol Hepatol* 2022; **20**: e761-e769 [PMID: 34033922 DOI: 10.1016/j.cgh.2021.05.033]
297 **Rahmani J**, Kord-Varkaneh H, Ryan PM, Rashvand S, Clark C, Day AS, Hekmatdoost A. Dietary total antioxidant capacity and risk of ulcerative colitis: A case-control study. *J Dig Dis* 2019; **20**: 636-641 [PMID: 31571400 DOI: 10.1111/1751-2980.12823]
298 **National Institutes of Health**. Notice of information: NIGMS Priorities for Sepsis Research. [cited 23 December 2021]. Available from: https://grants.nih.gov/grants/guide/notice-files/NOT-GM-19-054.html
299 **Finzer P**. How we become ill: Investigating emergent properties of biological systems could help to better understand the pathology of diseases. *EMBO Rep* 2017; **18**: 515-518 [PMID: 28242749 DOI: 10.15252/embr.201743948]
300 **Pravda J**. Can Medical Research Do Its Job? *Med Sci Ed* 2017; **27**: 1-2 [DOI: 10.1007/s40670-017-0481-6]
301 **World Health Organization**. Chronic Disease Mortality. [cited 26 December 2021]. Available from: https://www.who.int/chp/chronic_disease_report/part1/en/index1.html
302 **Raghupathi W**, Raghupathi V. An Empirical Study of Chronic Diseases in the United States: A Visual Analytics Approach. *Int J Environ Res Public Health* 2018; **15** [PMID: 29494555 DOI: 10.3390/ijerph15030431]
303 **Centers for Disease Control and Prevention**. Chronic Diseases in America. [cited 24 December 2021]. Available from: https://www.cdc.gov/chronicdisease/resources/infographic/chronic-diseases.htm

World Journal of Gastroenterology

Submit a Manuscript: https://www.f6publishing.com

World J Gastroenterol 2022 August 21; 28(31): 4299-4309

DOI: 10.3748/wjg.v28.i31.4299

ISSN 1007-9327 (print) ISSN 2219-2840 (online)

MINIREVIEWS

Recent advances in multidisciplinary therapy for adenocarcinoma of the esophagus and esophagogastric junction

Yi-Han Zheng, En-Hao Zhao

Specialty type: Gastroenterology and hepatology

Provenance and peer review: Invited article; Externally peer reviewed.

Peer-review model: Single blind

Peer-review report's scientific quality classification

Grade A (Excellent): 0
Grade B (Very good): B, B
Grade C (Good): 0
Grade D (Fair): 0
Grade E (Poor): 0

P-Reviewer: Oguma J, Japan; Ono T, Japan

Received: January 17, 2022
Peer-review started: January 17, 2022
First decision: March 8, 2022
Revised: March 22, 2022
Accepted: July 20, 2022
Article in press: July 20, 2022
Published online: August 21, 2022

Yi-Han Zheng, En-Hao Zhao, Department of Gastrointestinal Surgery, Renji Hospital, Shanghai Jiao Tong University School of Medicine, Shanghai 200127, China

Corresponding author: En-Hao Zhao, PhD, Associate Professor, Doctor, Department of Gastrointestinal Surgery, Renji Hospital, Shanghai Jiao Tong University School of Medicine, No. 160 Pujian Road, Shanghai 200127, China. microzhaoenhao@hotmail.com

Abstract

Esophageal adenocarcinoma (EAC) and adenocarcinoma of the esophagogastric junction (EGJA) have long been associated with poor prognosis. With changes in the spectrum of the disease caused by economic development and demographic changes, the incidence of EAC and EGJA continues to increase, making them worthy of more attention from clinicians. For a long time, surgery has been the mainstay treatment for EAC and EGJA. With advanced techniques, endoscopic therapy, radiotherapy, chemotherapy, and other treatment methods have been developed, providing additional treatment options for patients with EAC and EGJA. In recent decades, the emergence of multidisciplinary therapy (MDT) has enabled the comprehensive treatment of tumors and made the treatment more flexible and diversified, which is conducive to achieving standardized and individualized treatment of EAC and EGJA to obtain a better prognosis. This review discusses recent advances in EAC and EGJA treatment in the surgical-centered MDT mode in recent years.

Key Words: Multidisciplinary therapy; Esophageal adenocarcinoma; Adenocarcinoma of esophagogastric junction; Endoscopic resection; Surgery

©The Author(s) 2022. Published by Baishideng Publishing Group Inc. All rights reserved.

Core Tip: Worldwide, esophageal adenocarcinoma (EAC) and adenocarcinoma of the esophagogastric junction (EGJA) have long been associated with poor prognosis, and their incidence continues to increase. For a long time, surgery has been the mainstay treatment for EAC and EGJA. With the advent of advanced techniques, other treatment methods have been developed. In recent decades, the emergence of multidisciplinary therapy (MDT) has enabled the comprehensive treatment of tumors, which is conducive to achieving standardized and individualized treatment. This review discusses recent advances in EAC and EGJA treatment in the surgical-centered MDT mode in recent years.

Citation: Zheng YH, Zhao EH. Recent advances in multidisciplinary therapy for adenocarcinoma of the esophagus and esophagogastric junction. *World J Gastroenterol* 2022; 28(31): 4299-4309
URL: https://www.wjgnet.com/1007-9327/full/v28/i31/4299.htm
DOI: https://dx.doi.org/10.3748/wjg.v28.i31.4299

INTRODUCTION

Currently, esophageal cancer is ranked 7th in incidence and 6th in overall mortality worldwide, with approximately 70% of cases occurring in males[1]. The most common subtypes of esophageal cancer are esophageal adenocarcinoma (EAC) and esophageal squamous cell carcinoma (ESCC). The two subtypes have very different etiologies; therefore, their incidence varies greatly in different countries and regions. Although its morbidity is much lower than that of ESCC in low-income countries, EAC accounts for two-thirds of esophageal cancer cases in high-income countries. Furthermore, owing to demographic changes, the burden of EAC is expected to increase in the future[2]. Obesity, gastroesophageal reflux disease (GERD), and Barrett's esophagus are some of the main risk factors for EAC. The increasing incidences of obesity and GERD are likely responsible for the continuing increase in the incidence of EAC. Additionally, reduction in chronic *Helicobacter pylori* (*H. pylori*) infection has been shown to be negatively correlated with EAC[2].

Adenocarcinoma of the esophagogastric junction (EGJA) is a type of cancer that develops at the junction of the esophagus and stomach, and is traditionally known as cardia cancer. According to the standard set by Siewert *et al*[3] in 1987, esophagogastric carcinoma is defined as a tumor located within 5 cm of the esophagogastric junction (EGJ). Type I was defined when the tumor center was located 1-5 cm above the EGJ, Type II when located from 1 cm above to 2 cm below the EGJ, and Type III when located 2-5 cm below the EGJ. Type II is also known as "real" carcinoma of the cardia. This classification also coincides with the distribution of the cardiac glands[4]. The American Joint Committee on Cancer 8th edition suggests that when the tumor center is located 2 cm below the EGJ or within 2 cm without invasion, it should be staged according to the TNM staging of gastric cancer. When the tumor center is located within 2 cm below the EGJ or with invasion, it should be staged according to the TNM staging of esophageal cancer[5]. Siewert type I EGJA is treated as esophageal cancer, Siewert type III EGJA is classified as gastric cancer, while controversies still exist in the treatment principles for Siewert type II EGJA[6,7]. Evidence indicates that the etiology of EGJA, which is negatively related to *H. pylori* infection and correlates with obesity and GERD injury, is similar to the risk factors for EAC[8].

Currently, surgery remains the primary treatment method for EAC and EGJA. However, due to the anatomical location, gastrointestinal surgeons and thoracic surgeons have different opinions regarding the treatment options. Perioperative therapies, including neoadjuvant and adjuvant therapies, are also gaining attention in the treatment of EAC and EGJA. The importance of multidisciplinary therapy (MDT) in the diagnosis and treatment of tumors has been increasingly emphasized. Clinicians from multiple departments, including radiologists, endoscopists, surgeons, and oncologists, have joined the MDT team to participate in clinical decision making, which has been conducive to the individualization of the diagnosis and treatment of EAC and EGJA.

ENDOSCOPIC RESECTION: GROWING IN IMPORTANCE

For years, surgery has been the only radical treatment for esophageal and EGJ cancer. However, in recent decades, with the development of techniques, endoscopic therapy has gained popularity. Endoscopy has already been used for the early diagnosis of malignant tumors of the esophagus and EGJ, and in suitable patients, endoscopic treatment can be performed. However, endoscopic resection still has limitations and is more commonly used as a diagnostic method than a treatment. A retrospective cohort study demonstrated that, compared to patients who did not undergo continuous endoscopic examination, patients who underwent continuous endoscopy before the diagnosis of EAC were associated with less advanced locoregional staging, better prognosis and survival[9].

Endoscopic radical therapy includes endoscopic tumor resection and ablation of surrounding precancerous tissues to prevent recurrence. The most widely used techniques are endoscopic mucosal resection (EMR) and endoscopic submucosal dissection (ESD). EMR is a relatively safe procedure, with a low risk of postoperative complications. However, it should be noted that during EMR operations, the involved Barrett's esophagus requires treatment; otherwise, locoregional EMR operations may lead to a high rate of recurrence[10]. Research has shown that the prognosis is relatively acceptable, with approximately 96% of patients achieving complete remission, with a 10-year survival rate of 75%[11]. ESD technology is more demanding than EMR technology. Both EMR and ESD have similar postoperative adverse events, but their incidence is higher following ESD[12]. The most common complications are stenosis, perforation, and bleeding[10]. According to a study, in the postoperative assessment, the recurrence rate after radical resection at 22.9 mo of follow-up was 0.17%[13].

The risk of lymphatic metastasis is relatively low in T1a cancer, but appears to increase with the depth of submucosal infiltration[14]. For EAC, the lymphatic metastasis rate is 0-2% in T1a cancer, and 0-22%, 0-30%, 20%-70% when T1b cancers infiltrate the upper third, the middle third, and the lower third of the submucosa, respectively[15-17]. Therefore, patient selection is essential for endoscopic therapy. EAC endoscopic resection is indicated in T1 carcinomas of differentiation grade G1/G2 without lymphatic invasion, venous invasion, or ulceration. In addition to these criteria, for T1b, infiltration less than 500 μm in depth and less than 20 mm in size is required[14]. Current guidelines usually recommend that additional surgery should be performed after endoscopic resection when the risk of lymphatic metastasis or residual cancer is too high to cure[18]. Meanwhile, if the specimen resected by endoscopic therapy reveals a positive margin on histological examination, additional esophagectomy is also required. Based on some cases of T1 carcinoma that underwent esophageal endoscopic resection with additional esophagectomy, among which 17/30 were cases of EAC, researchers concluded that esophagectomy could achieve further removal of residual advanced cancer or lymphatic metastases in 13% of patients. However, postoperative severe morbidity was 43% and mortality was 7%; therefore, the benefits and risks of close follow-up *vs* surgery should be considered[19].

In addition, Barrett's esophagus has been demonstrated to be a significant risk factor for esophageal and EGJ carcinomas. The pathological basis of Barrett's esophagus is the change in mucosal cells caused by long-term exposure to gastric acid, which can develop into adenocarcinoma. Compared to the normal population, patients with Barrett's esophagus have a relative risk of 11.3 of developing adenocarcinoma[20]. Due to the relatively high rate of 25% developing into carcinoma, precursor intraepithelial neoplasia in Barrett's esophagus is usually necessary for endoscopic resection[21]. Additionally, removal of low-grade intraepithelial neoplasia is recommended[22].

SURGERY: REMAINS THE MAINSTAY OF TREATMENT

Surgical options for esophagus adenocarcinoma

According to the guidelines, the transthoracic approach is usually recommended for the treatment of esophageal carcinoma. For cancers located in the proximal one-third of the esophagus, thoracic esophagectomy can be expanded to three fields, including cervical lymph node dissection. However, controversy remains between transthoracic esophagectomy combined with intrathoracic anastomosis (Ivor-Lewis esophagectomy) and three-field esophagectomy combined with esophagogastrostomy (McKeown esophagectomy); the recommendations of concerned guidelines vary from country to country[7]. It is recommended that the absence of suspicious lymph node enlargement indicates a preference for extended two-field thoracoabdominal lymphadenectomy (conventional thoracoabdominal and upper mediastinal lymphadenectomy), whereas, suspicious lymph node enlargement supports the option of three-field cervical and thoracoabdominal lymphadenectomy (cervical and thoracoabdominal lymphadenectomy and upper mediastinal lymphadenectomy)[23]. Furthermore, to investigate the precise lymphatic staging, at least 15 Lymph nodes should be obtained[24]. In recent years, studies have compared two-field approach lymphadenectomy with three-field approach lymphadenectomy for postoperative overall survival (OS) and disease-free survival. The results suggest that there are no significant differences in prognosis between the two approaches[25].

Additionally, studies have shown that lymph node harvest during esophagectomy is associated with improved postoperative survival. A study by Lutfi *et al*[26] demonstrated that during lymphadenectomy, when 7 lymph nodes were harvested, OS improved significantly, and when 25 Lymph nodes were harvested, it showed maximum OS benefits. Other researchers also came to a similar conclusion regarding the influence of lymphadenectomy on postoperative survival after neoadjuvant therapy; when the number of lymph node dissections reached 25, postoperative life expectancy was the highest [27].

Surgical options for adenocarcinoma of EGJ

Although many studies have compared the transthoracic approach to the transhiatal approach, because of the special anatomical location of EGJA, the optimal surgical option is still under debate and recommendations are inconsistent[7]. Based on 14 studies published over the last 30 years, Tseng *et al*

[28] concluded that the Siewert classification had a significant influence on the surgical options. The transthoracic approach was recommended for Siewert type I EGJA, and extended gastrectomy for Siewert type III EGJA. Siewert type II EGJA can be resected using a transthoracic or transhiatal approach, and each approach has similar effects on surgical results and overall prognosis. The surgical method should be determined according to patient factors, such as risk factors and general condition, and also depends on the preference of the surgeon[28]. The advantages of the transthoracic approach are better mediastinal lymph node dissection and better proximal resection margin, as it has the advantages of better para-celiac and para-aortic lymph node dissection, avoidance of thoracotomy-associated morbidity, and preferable postoperative quality of life[28].

Based on the analysis of the results of the Siewert type II EGJ carcinoma surgical treatment conducted by the JCOG9502 trial, the consensus of Chinese experts suggested that the transhiatal approach is recommended for esophageal invasion < 3 cm, and the right thoracoabdominal two-incision surgical approach is preferred for esophageal invasion ≥ 3 cm[29]. Currently, surgical treatment for true EGJA in Japan is generally determined by esophageal invasion of 3 cm and gastric invasion of the upper one-third as a demarcation[4]. Ivor-Lewis esophagectomy combined with upper or middle mediastinal lymphadenectomy is recommended for esophageal invasion ≥ 3 cm. For esophageal invasion < 3 cm, an extended proximal transdiaphragmatic gastrectomy was performed for distal invasion within the upper third of the stomach, and an extended total transdiaphragmatic gastrectomy was performed for invasion that exceeded the upper third of the stomach; meanwhile, a lower mediastinal lymphadenectomy was also required[4]. Nishiwaki *et al*[30] proposed that the distance from the EGJ to the proximal margin of the primary tumor (esophageal invasion) could be an indicator of mediastinal lymph node metastasis in Siewert type II tumors. The results showed that a distance ≥ 2 cm in esophageal invasion was associated with a higher risk of mediastinal lymph node metastasis. When esophageal infiltrates reach 3 cm, the risk was even higher, and the transthoracic approach should be considered for upper and middle mediastinal lymphatic dissection[30]. These results are consistent with the guidelines and current surgical options (Figure 1).

The optimum range of lymphatic dissection has not reached a consensus. According to previous studies, for Siewert type III EGJA, the incidence of lymphatic metastasis in groups No. 1, 2, 3, and 7 was higher than 20 %, metastasis in groups No. 5, 6, 11d, and 12a was less than 5 %, and metastasis in groups No. 107, 111, and 112 was much lower and close to zero. Compared with Siewert type III EGJA, the incidence of lymphatic metastasis in Siewert type II EGJA was significantly lower in the abdominal lymph nodes and higher in the lower mediastinal lymph nodes[31].

To date, only retrospective trials have been conducted on the surgical choice of Siewert type II EGJA, and research has not indicated any difference between the two surgical approaches. The CARDIA trial is the first randomized trial to compare transthoracic esophagectomy with transhiatal extended gastrectomy for Siewert type II EGJA, and the trial is ongoing (DRKS00016923). Esophagectomy is expected to achieve better radical resection and thorough mediastinal lymphatic dissection, leading to better OS, while the quality of life is still acceptable[32].

PERIOPERATIVE CHEMOTHERAPY AND RADIOTHERAPY: EXIST CONTROVERSY

Perioperative treatment includes multiple options, among which chemotherapy (CT), radiotherapy (RT), and chemoradiotherapy (CRT) are the most commonly used regimens. Neoadjuvant therapies benefit tumors by reducing tumor volume, tumor stage, *etc*., and therefore improve the surgical resection rate and prognosis. Postoperative therapies are mainly used to eliminate tumors that have not been completely resected and possible metastases, prolong postoperative survival and reduce the recurrence rate. Over the years, many researchers have made efforts to explore the best perioperative therapy for adenocarcinoma of esophagus and EGJ (Table 1).

RT in adenocarcinoma of esophagus and EGJ

Compared to many other tumors, including gastric carcinoma, RT plays a more important role in the treatment of EAC and EGJA. A Chinese research group included 4160 patients with Siewert type II EGJA to investigate whether perioperative RT benefits patients. The results indicate that neoadjuvant RT improves prognosis in more advanced patients (T3 or with lymphatic metastases) and is more effective in T4 tumors. For stage T1-2, surgery alone is preferred[33]. Furthermore, studies have shown that CRT is superior to RT alone in many aspects, such as tumor downstaging, R0 resection, and pathological complete response (pCR)[34,35], especially in patients with fairly good tolerance for CT. A study analyzed 101 patients with esophageal cancer who underwent CRT or RT alone. The primary endpoints were OS, progression-free survival, local control rate, and toxicity. The results showed that RT was safe and feasible and could partially compensate for the absence of CT[36]. However, because many elderly patients included in the cohort were not eligible for CT, the conclusion has limitations.

CT in adenocarcinoma of esophagus and EGJ

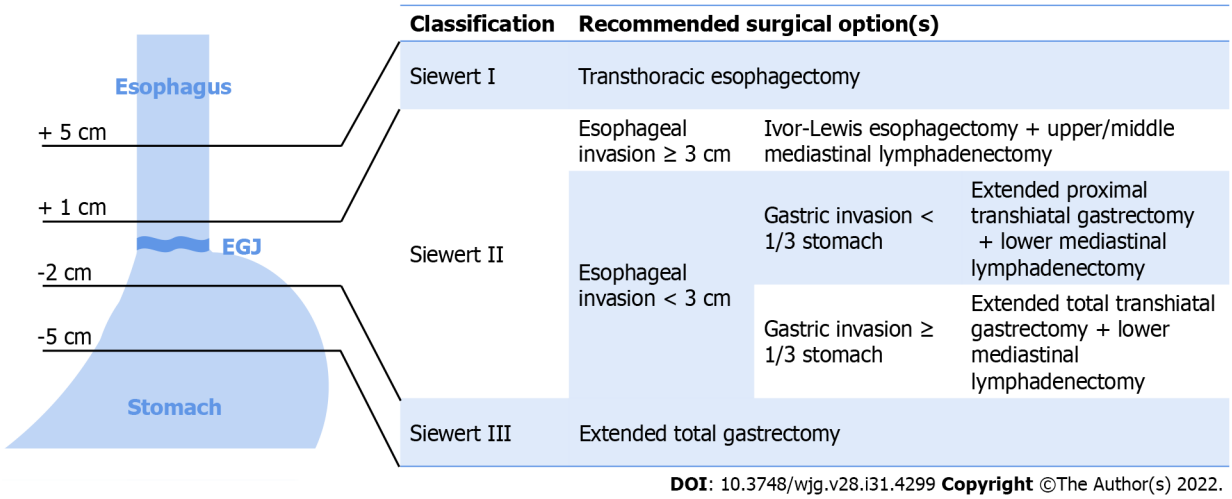
The validity of perioperative CT and concurrent CRT has been widely discussed and is considered the

Table 1 Some clinical studies of perioperative therapy in recent years

Ref.	Cancer	Cases	Groups	Conclusion
RT in EAC and EGJA				
Zhou *et al*[33], 2021	EGJA (Siewert II)	4160	nRT *vs* RT	nRT improves prognosis in patients with more advanced tumors
Klevebro *et al*[35], 2016	Esophageal or EGJ cancer	181	nCRT *vs* nCT	nCRT group had higher complete response rate, R0 resection rate, and lower lymph-node metastases, without significantly affecting survival
Ristau *et al*[36], 2021	EC	101	RT *vs* CT	RT could partially compensate for CT
CT in EAC and EGJA				
Mokdad *et al*[37], 2018	Lower EAC or EGJA	10086	CT *vs* observation	Most patients benefited from adjuvant CT for OS
Papaxoinis *et al*[38], 2019	Lower EAC or EGJA	312	nCT *vs* CT	No significant differences; only patients with postoperative microscopic residual disease benefited from postoperative CT
Davies *et al*[39], 2014	EAC or EGJA	584	Downstaging after nCT *vs* no response	Tumor stage after nCT is more closely associated with prognosis and eligibility for surgery
Bunting *et al*[41], 2018	EAC	286	Toxicity of nCT *vs* no toxicity	Toxicity can lead to adverse consequences, such as failure to complete CT, loss of opportunity for surgical resection, and poor OS
CRT in EAC and EGJA				
Shapiro *et al*[44], 2015	Esophageal or EGJ cancer	368	nCT + surgery *vs* surgery alone	Patients with resectable esophageal or EGJ carcinoma benefited more from nCRT plus surgery than surgery alone
Zafar *et al*[46], 2020	Lower EAC or EGJA	13783	nCRT *vs* nCT	nCRT group was more likely to achieve pCR; OS was not statistically different
Al-Sukhni *et al*[47], 2016	EAC or EGJA	6986	nCRT *vs* nCT	nCRT group showed no difference in improving survival in resectable tumor
Samson *et al*[48], 2016	EC	7338	nCRT *vs* nCT	nCRT lead to more downstaging of tumor, but it is not an individual prognostic factor
Li *et al*[50], 2021	EGJA (Siewert II/III)	170	nCRT *vs* nCT	nCRT provided better survival and improved R0 removal and pCR rates more than nCT in patients with locally advanced EJGA
Tian *et al*[51], 2020	Gastric or EGJ adenocarcinoma	1048	Perioperative CRT *vs* perioperative CT	Perioperative CRT was associated with a higher pCR rate but increase the risk of mortality
Noordman *et al*[52], 2018	Esophageal or EGJ cancer	368	nCRT + surgery *vs* surgery alone	Physical function and frailty remained relatively low in nCRT group, but no adverse effects on long-term HRQoL were observed
Noordman *et al*[53], 2019	Esophageal or EGJ cancer	96	nCRT	HRQoL reduced in short-term, but would return to baseline
Noordman *et al*[54], 2018	Esophageal or EGJ cancer	363	nCRT + surgery *vs* surgery alone	nCRT had no significant effect on postoperative HRQoL
Nilsson *et al*[55], 2020	Esophageal or EGJ cancer	249	Standard TTS *vs* prolonged TTS	Time to surgery (TTS) after nCRT had no significant effect on short-term prognosis

RT: Radiotherapy; EAC: Esophageal adenocarcinoma; EGJA: Adenocarcinoma of the esophagogastric junction; EGJ: Esophagogastric junction; TTS: Time to surgery; HRQoL: Health-related quality of life; CT: Chemotherapy; CRT: Chemoradiotherapy; pCR: Pathological complete response; OS: Overall survival; nRT: Neoadjuvant radiotherapy; nCT: Neoadjuvant chemotherapy; nCRT: Neoadjuvant chemoradiotherapy.

standard treatment option. Mokdad *et al*[37] included 10086 patients with EGJ cancer who received adjuvant CT or postoperative observation. Patients who underwent adjuvant CT were relatively younger and more likely to have advanced disease. In the long-term, the OS of patients who received CT was clearly better at 1 year (94% *vs* 88%), 3 years (54% *vs* 47%), and 5 years (38% *vs* 34%). In other words, most patients benefited from adjuvant CT for OS[37]. Another group included 312 patients (210 with EGJA and 102 with EAC) who underwent radical surgery after neoadjuvant CT (nCT). The experimental group received postoperative CT based on ECX (epirubicin, cisplatin, and capecitabine) regimen, while the control group did not. No significant differences were found in the primary prognostic data between the two groups. Only patients with postoperative microscopic residual disease (R1) benefited from postoperative CT[38].



DOI: 10.3748/wjg.v28.i31.4299 **Copyright** ©The Author(s) 2022.

Figure 1 Siewert classification of adenocarcinoma of the esophagogastric junction and recommended surgical options[3,4,28,29]. The tumors that centered 1-5 cm above esophagogastric junction (EGJ) are defined as Siewert type I, transthoracic esophagectomy is recommended. the tumors centered from 1 cm above to 2 cm below the EGJ are Siewert type II. For Siewert type II tumor with esophageal invasion ≥ 3 cm, Ivor-Lewis esophagectomy with upper/middle mediastinal lymphadenectomy is propriate surgical option; for esophageal invasion < 3 cm, extended proximal transhiatal gastrectomy or extended total trashiatal gastrectomy with lower mediastinal lymphadenectomy are recommended according to whether gastric invasion exceeded 1/3 of the stomach. The tumors that centered 2-5 cm below EGJ are defined as Siewert type III and extended total gastrectomy is the optimal surgical option. EGJ: Esophagogastric junction.

The purpose of nCT in tumor downstaging is to facilitate resection and improve the postoperative prognosis. Compared with the clinical stage before nCT, the tumor stage after nCT is more closely associated with prognosis and eligibility for surgery[39]. For borderline resectable cancers of the esophagus and EGJ, neoadjuvant therapy is usually recommended, followed by evaluation of the tumor stage according to the guidelines. Davies *et al*[39] reported that patients who received neoadjuvant therapy had a lower local recurrence rate (6% *vs* 13%) and systemic recurrence rate (19% *vs* 29%), along with improved survival. Predictors of postoperative survival after nCT have also been discussed. The results showed that pT staging, pN staging, and resection status were strong predictors of survival, including patients who underwent surgery alone or who received neoadjuvant therapy. Patients who achieved R1 resection or pT3/4 stage after neoadjuvant therapy had better OS than those who achieved the same outcome after surgery alone[40]. In addition, the adverse effects associated with neoadjuvant therapy, also known as toxicity, require attention. Bunting *et al*[41] reported 67 (23.4% of 286 cases) patients who experienced toxicity during nCT. Toxicity can lead to adverse consequences, such as failure to complete CT (47% *vs* 17%), loss of opportunity for surgical resection (17.9% *vs* 7.8%), and poor OS (median survival of 20.7 mo *vs* 37.8 mo). Even if patients who missed surgery were excluded, median survival was shorter in patients with toxicity responses (26.2 mo *vs* 47.8 mo)[41].

CRT in adenocarcinoma of esophagus and EGJ

Perioperative concurrent CRT is widely used to treat EAC and EGJA. The INT0116 trial, the first randomized controlled study of postoperative adjuvant CRT for gastric and EGJ carcinoma, showed that postoperative 5-FU and tetrahydrofolic acid combined with RT significantly extended OS and relapse-free survival in patients with advanced gastric and EGJ carcinoma[42]. This illustrates the importance of CRT in perioperative adjuvant therapy. Currently, adjuvant CRT is the standard treatment for gastric and EGJ carcinoma in the United States[43]. The CROSS study conducted by a Netherlands group in 2015 concluded that the OS of the long-term follow-up of 368 patients with resectable esophageal or EGJ carcinoma benefited more from neoadjuvant CRT (nCRT) followed by surgery than surgery alone. For patients with adenocarcinoma, the median OS of the group that received nCRT plus surgery was 43.2 mo, longer than 27.1 mo of the group that received surgery alone. Therefore, nCRT followed by surgery could be considered the standard treatment for patients with resectable locally advanced EAC or EGJA [44]. The importance of nCRT in the treatment of esophageal and EGJ carcinoma has been widely recognized. After sufficient evaluation of perioperative treatment options, the American Radium Society gastrointestinal expert panel established appropriate criteria that recommended nCRT for patients with resectable non-metastatic EAC or EGJA, cT3 or lymphatic metastasis, and high-risk manifestations. In patients with pathological evidence of lymphatic metastasis without neoadjuvant treatment, adjuvant CRT is recommended[45].

Compared with surgery alone, CT and CRT promote the survival of patients with EAC and EGJA. However, whether CRT is superior to CT remains under debate. Among the 13738 patients with EAC and EGJA who received nCT or nCRT and eventually underwent surgery, patients who underwent nCRT were 2.7 times more likely to achieve pCR than those who underwent nCT; however, OS was not statistically different[46]. Similarly, many studies have shown that nCRT is associated with a higher

pCR rate, higher R0 resection rate, lower lymphatic metastasis rate, and is more likely to achieve downstaging before surgery than nCT; however, previous studies have not been able to reveal the effect on postoperative survival[35,47,48]. Several studies have suggested improvements in postoperative survival in patients treated with nCRT compared with those treated with nCT. Smyth *et al*[49] showed a 4% increase in the 3-year OS in patients who received adjuvant CT after CRT plus surgery. Since most recurrent EGJAs occur within three years after surgery, this may indicate an increase in the curative ratio and that postoperative CT improves survival even after neoadjuvant therapy[49]. In another study of 170 patients with Siewert type II/III EGJA, Li *et al*[50] showed that nCRT provided better survival and improved R0 removal and pCR rates more than nCT in patients with locally advanced EJGA. However, Tian *et al*[51] drew the opposite conclusion after retrospectively reviewing 1048 patients with gastric adenocarcinoma and EGJA who underwent preoperative CT or CRT. While perioperative CRT was associated with a higher pCR rate (13.1% *vs* 8.2%), preoperative CRT appeared to increase the risk of mortality[51].

In addition to the effectiveness of nCRT, its adverse effects and impact on the postoperative quality of life are also factors that must be considered. In the postoperative follow-up, a total of 386 patients with EAC who underwent surgery alone or nCRT plus surgery were followed up for 105 mo. Although the physical function and frailty of the patients remained relatively low, no adverse effects on long-term health-related quality of life (HRQoL) were observed in patients with preoperative nCRT. This finding supports the application of nCRT in patients with EAC[52]. Other similar trials conducted by the same group showed a significant reduction in HRQoL, but eventually HRQoL returned to baseline within eight weeks[53], and nCRT had no significant effect on postoperative HRQoL compared with patients who received surgery alone[54]. That is, nCRT did not cause irreversible long-term changes in HRQoL, which confirmed the safety of nCRT.

Further, there has been some discussion regarding the timing of surgery after neoadjuvant therapy. The current routine is 4-6 wk. Nilsson *et al*[55] randomly assigned 249 patients with esophageal or EGJ cancer into two groups: standard timing of surgery (4-6 wk) or prolonged timing of surgery (10-12 wk). The primary endpoint was overall postoperative complications, and the secondary endpoints were severity of complications, 90-d mortality, and inpatient stay. Data analysis showed that the timing of surgery after nCRT had no significant effect on short-term prognosis[55], while a meta-analysis in 2018 suggested a different opinion. A total of 15086 patients from 13 studies were included. Enrolled patients were divided into two groups based on the time of surgery (shorter or longer than the 7-8 wk interval). A subgroup analysis of patients with adenocarcinoma did not show significant differences in pCR rates, and a prolonged interval was significantly associated with increased mortality. An extended interval was also detrimental to the 2-year and 5-year OS[56].

Furthermore, researchers have compared the prognosis of patients with EAC after surgery alone and in combination with neoadjuvant therapy to clarify whether current treatment strategies could obtain any benefit. Although many patients are predicted to benefit from neoadjuvant therapy, their responses to therapy vary. It is estimated that the total restricted mean survival time would have a 7% gain if optimal therapy was applied instead of actual therapy[57]. This suggests that individualized treatment could benefit patients the most, but how to select individuals with better reactions to specific treatment options and achieve such benefits remains to be further studied.

DEFINITIVE CRT: FOR UNRESECTABLE TUMORS

At diagnosis, tumors in a considerable proportion of patients are no longer indicated for surgery because of tumor invasion of vital organs, main vessels, or nerves (T4b) or the occurrence of distant metastasis (M1)[5]. Neoadjuvant therapy might achieve tumor downstaging in some cases; however, for patients who refuse surgery or have unresectable tumors, definitive CRT (dCRT) remains the only option[23]. With the improvement in concurrent CRT, the 5-year survival of patients with unresectable tumors significantly improved from 0-14% to 20%-25%, indicating that the aim was transformed from palliative to efficient treatment[58]. It was about three decades ago when dCRT first attracted attention. Early randomized trials have shown that the median survival and 5-year survival of patients who received CRT were superior to those who received RT alone[59], and subsequent research confirmed the superiority of CRT over RT[58].

Locoregional recurrence was the main cause of treatment failure in patients who underwent dCRT. In a retrospective study of 184 patients with esophageal carcinoma, locoregional recurrences occurred in 41% of the cases, mostly within 12 mo after cessation of dCRT, and almost all occurred in 24 mo. Among the cases that recurred at the primary tumor site, only 57% occurred within the scope of radiation, which suggests that RT is valid in reducing locoregional recurrences[60]. However, the therapeutic doses of dCRT are still under discussion. In a cohort study, 12638 patients with metastatic esophageal cancer were divided into three groups: CT alone, combined with palliative RT, and combined with definitive RT. The median OS of the patients treated with CRT was 11.3 mo for the definitive dose radiation group and 7.5 mo for the palliative dose group. Thus, in CRT, compared to a lower dose of radiation, patients benefit more from definitive dose radiation[61]. In contrast, another study compared

RT of standard dose with high dose in dCRT, which enrolled 260 patients with esophageal cancer. The results showed that the 3-year local progression-free survival rates were 70% and 73%, respectively, which suggested that higher doses of RT did not necessarily improve the clinical outcome, as assumed [62]. Therefore, the current recommended dose of radiation for dCRT benefits clinical outcomes more than higher or lower doses.

CONCLUSION

Surgery has long been the only radical treatment available for EAC and EGJA. In recent decades, with the development of various other techniques as well as the concept of MDT, increased treatment options could be applied in patients with EAC or EGJA. There is no doubt that surgery is always one of the most important treatments; however, it is no longer the only solution. Clinicians with MDT teams can tailor the regimens for patients. At the same time, more options face more challenges. There are still many controversies, such as the optimal treatment for specific patient groups and the proper timing for applying certain treatments. Moreover, the implementation of MDT is also problematic because not every region or medical center can perform every treatment independently. It is worth exploring and discussing how to make MDT a useful and efficient method to guide treatment. It should be clarified that the final goal is to provide a standardized, efficient, and individualized treatment to each patient to improve OS and quality of life.

FOOTNOTES

Author contributions: Zheng YH wrote the manuscript; Zhao EH reviewed and revised the manuscript; and both authors proofed the manuscript.

Conflict-of-interest statement: The authors have nothing to disclose.

Open-Access: This article is an open-access article that was selected by an in-house editor and fully peer-reviewed by external reviewers. It is distributed in accordance with the Creative Commons Attribution NonCommercial (CC BY-NC 4.0) license, which permits others to distribute, remix, adapt, build upon this work non-commercially, and license their derivative works on different terms, provided the original work is properly cited and the use is non-commercial. See: https://creativecommons.org/Licenses/by-nc/4.0/

Country/Territory of origin: China

ORCID number: Yi-Han Zheng 0000-0003-2664-0535; En-Hao Zhao 0000-0003-1112-0043.

S-Editor: Yan JP
L-Editor: A
P-Editor: Yan JP

REFERENCES

1 **Sung H**, Ferlay J, Siegel RL, Laversanne M, Soerjomataram I, Jemal A, Bray F. Global Cancer Statistics 2020: GLOBOCAN Estimates of Incidence and Mortality Worldwide for 36 Cancers in 185 Countries. *CA Cancer J Clin* 2021; **71**: 209-249 [PMID: 33538338 DOI: 10.3322/caac.21660]
2 **Arnold M**, Laversanne M, Brown LM, Devesa SS, Bray F. Predicting the Future Burden of Esophageal Cancer by Histological Subtype: International Trends in Incidence up to 2030. *Am J Gastroenterol* 2017; **112**: 1247-1255 [PMID: 28585555 DOI: 10.1038/ajg.2017.155]
3 **Siewert JR**, Hölscher AH, Becker K, Gössner W. [Cardia cancer: attempt at a therapeutically relevant classification]. *Chirurg* 1987; **58**: 25-32 [PMID: 3829805]
4 **Kumamoto T**, Kurahashi Y, Niwa H, Nakanishi Y, Okumura K, Ozawa R, Ishida Y, Shinohara H. True esophagogastric junction adenocarcinoma: background of its definition and current surgical trends. *Surg Today* 2020; **50**: 809-814 [PMID: 31278583 DOI: 10.1007/s00595-019-01843-4]
5 **Rice TW**, Ishwaran H, Hofstetter WL, Kelsen DP, Apperson-Hansen C, Blackstone EH; Worldwide Esophageal Cancer Collaboration Investigators. Recommendations for pathologic staging (pTNM) of cancer of the esophagus and esophagogastric junction for the 8th edition AJCC/UICC staging manuals. *Dis Esophagus* 2016; **29**: 897-905 [PMID: 27905172 DOI: 10.1111/dote.12533]
6 **Chevallay M**, Bollschweiler E, Chandramohan SM, Schmidt T, Koch O, Demanzoni G, Mönig S, Allum W. Cancer of the gastroesophageal junction: a diagnosis, classification, and management review. *Ann N Y Acad Sci* 2018; **1434**: 132-138 [PMID: 30138540 DOI: 10.1111/nyas.13954]
7 **Jung MK**, Schmidt T, Chon SH, Chevallay M, Berlth F, Akiyama J, Gutschow CA, Mönig SP. Current surgical treatment

standards for esophageal and esophagogastric junction cancer. *Ann N Y Acad Sci* 2020; **1482**: 77-84 [PMID: 32798235 DOI: 10.1111/nyas.14454]

8 **Kamangar F**, Dawsey SM, Blaser MJ, Perez-Perez GI, Pietinen P, Newschaffer CJ, Abnet CC, Albanes D, Virtamo J, Taylor PR. Opposing risks of gastric cardia and noncardia gastric adenocarcinomas associated with Helicobacter pylori seropositivity. *J Natl Cancer Inst* 2006; **98**: 1445-1452 [PMID: 17047193 DOI: 10.1093/jnci/djj393]

9 **Cummings LC**, Kou TD, Chak A, Schluchter MD, Margevicius S, Cooper GS. Receipt of Serial Endoscopy Procedures Prior to Esophageal Adenocarcinoma Diagnosis Is Associated with Better Survival. *Dig Dis Sci* 2022; **67**: 1036-1044 [PMID: 33881677 DOI: 10.1007/s10620-021-06927-1]

10 **Malik S**, Sharma G, Sanaka MR, Thota PN. Role of endoscopic therapy in early esophageal cancer. *World J Gastroenterol* 2018; **24**: 3965-3973 [PMID: 30254401 DOI: 10.3748/wjg.v24.i35.3965]

11 **Pech O**, May A, Manner H, Behrens A, Pohl J, Weferling M, Hartmann U, Manner N, Huijsmans J, Gossner L, Rabenstein T, Vieth M, Stolte M, Ell C. Long-term efficacy and safety of endoscopic resection for patients with mucosal adenocarcinoma of the esophagus. *Gastroenterology* 2014; **146**: 652-660.e1 [PMID: 24269290 DOI: 10.1053/j.gastro.2013.11.006]

12 **Terheggen G**, Horn EM, Vieth M, Gabbert H, Enderle M, Neugebauer A, Schumacher B, Neuhaus H. A randomised trial of endoscopic submucosal dissection *vs* endoscopic mucosal resection for early Barrett's neoplasia. *Gut* 2017; **66**: 783-793 [PMID: 26801885 DOI: 10.1136/gutjnl-2015-310126]

13 **Yang D**, Zou F, Xiong S, Forde JJ, Wang Y, Draganov PV. Endoscopic submucosal dissection for early Barrett's neoplasia: a meta-analysis. *Gastrointest Endosc* 2018; **87**: 1383-1393 [PMID: 28993137 DOI: 10.1016/j.gie.2017.09.038]

14 **Gockel I**, Hoffmeister A. Endoscopic or Surgical Resection for Gastro-Esophageal Cancer. *Dtsch Arztebl Int* 2018; **115**: 513-519 [PMID: 30149830 DOI: 10.3238/arztebl.2018.0513]

15 **Cho JW**, Choi SC, Jang JY, Shin SK, Choi KD, Lee JH, Kim SG, Sung JK, Jeon SW, Choi IJ, Kim GH, Jee SR, Lee WS, Jung HY; Korean ESD Study Group. Lymph Node Metastases in Esophageal Carcinoma: An Endoscopist's View. *Clin Endosc* 2014; **47**: 523-529 [PMID: 25505718 DOI: 10.5946/ce.2014.47.6.523]

16 **Japan Esophageal Society**. Japanese Classification of Esophageal Cancer, 11th Edition: part I. *Esophagus* 2017; **14**: 1-36 [PMID: 28111535 DOI: 10.1007/s10388-016-0551-7]

17 **Japan Esophageal Society**. Japanese Classification of Esophageal Cancer, 11th Edition: part II and III. *Esophagus* 2017; **14**: 37-65 [PMID: 28111536 DOI: 10.1007/s10388-016-0556-2]

18 **Pimentel-Nunes P**, Dinis-Ribeiro M, Ponchon T, Repici A, Vieth M, De Ceglie A, Amato A, Berr F, Bhandari P, Bialek A, Conio M, Haringsma J, Langner C, Meisner S, Messmann H, Morino M, Neuhaus H, Piessevaux H, Rugge M, Saunders BP, Robaszkiewicz M, Seewald S, Kashin S, Dumonceau JM, Hassan C, Deprez PH. Endoscopic submucosal dissection: European Society of Gastrointestinal Endoscopy (ESGE) Guideline. *Endoscopy* 2015; **47**: 829-854 [PMID: 26317585 DOI: 10.1055/s-0034-1392882]

19 **Dermine S**, Leconte M, Leblanc S, Dousset B, Terris B, Berger A, Rahmi G, Lepilliez V, Plomteux O, Leclercq P, Coriat R, Chaussade S, Prat F, Barret M. Outcomes of esophagectomy after noncurative endoscopic resection of early esophageal cancer. *Therap Adv Gastroenterol* 2019; **12**: 1756284819892556 [PMID: 31839807 DOI: 10.1177/1756284819892556]

20 **Hvid-Jensen F**, Pedersen L, Drewes AM, Sørensen HT, Funch-Jensen P. Incidence of adenocarcinoma among patients with Barrett's esophagus. *N Engl J Med* 2011; **365**: 1375-1383 [PMID: 21995385 DOI: 10.1056/NEJMoa1103042]

21 **Kastelein F**, van Olphen S, Steyerberg EW, Sikkema M, Spaander MC, Looman CW, Kuipers EJ, Siersema PD, Bruno MJ, de Bekker-Grob EW; ProBar-study group. Surveillance in patients with long-segment Barrett's oesophagus: a cost-effectiveness analysis. *Gut* 2015; **64**: 864-871 [PMID: 25037191 DOI: 10.1136/gutjnl-2014-307197]

22 **Phoa KN**, van Vilsteren FG, Weusten BL, Bisschops R, Schoon EJ, Ragunath K, Fullarton G, Di Pietro M, Ravi N, Visser M, Offerhaus GJ, Seldenrijk CA, Meijer SL, ten Kate FJ, Tijssen JG, Bergman JJ. Radiofrequency ablation *vs* endoscopic surveillance for patients with Barrett esophagus and low-grade dysplasia: a randomized clinical trial. *JAMA* 2014; **311**: 1209-1217 [PMID: 24668102 DOI: 10.1001/jama.2014.2511]

23 **Ajani JA**, D'Amico TA, Bentrem DJ, Chao J, Corvera C, Das P, Denlinger CS, Enzinger PC, Fanta P, Farjah F, Gerdes H, Gibson M, Glasgow RE, Hayman JA, Hochwald S, Hofstetter WL, Ilson DH, Jaroszewski D, Johung KL, Keswani RN, Kleinberg LR, Leong S, Ly QP, Matkowskyj KA, McNamara M, Mulcahy MF, Paluri RK, Park H, Perry KA, Pimiento J, Poultsides GA, Roses R, Strong VE, Wiesner G, Willett CG, Wright CD, McMillian NR, Pluchino LA. Esophageal and Esophagogastric Junction Cancers, Version 2.2019, NCCN Clinical Practice Guidelines in Oncology. *J Natl Compr Canc Netw* 2019; **17**: 855-883 [PMID: 31319389 DOI: 10.6004/jnccn.2019.0033]

24 **Isono K**, Sato H, Nakayama K. Results of a nationwide study on the three-field lymph node dissection of esophageal cancer. *Oncology* 1991; **48**: 411-420 [PMID: 1745490 DOI: 10.1159/000226971]

25 **Li B**, Zhang Y, Miao L, Ma L, Luo X, Ye T, Li H, Zhang J, Li Y, Zhao K, Fan M, Zhu Z, Wang J, Xu J, Deng Y, Lu Q, Pan Y, Liu S, Shao L, Sun Y, Xiang J, Hu H, Chen H. Esophagectomy With Three-Field Versus Two-Field Lymphadenectomy for Middle and Lower Thoracic Esophageal Cancer: Long-Term Outcomes of a Randomized Clinical Trial. *J Thorac Oncol* 2021; **16**: 310-317 [PMID: 33307192 DOI: 10.1016/j.jtho.2020.10.157]

26 **Lutfi W**, Martinez-Meehan D, Dhupar R, Christie N, Sarkaria I, Ekeke C, Baker N, Luketich JD, Okusanya OT. Higher lymph node harvest in patients with a pathologic complete response after neoadjuvant therapy for esophageal cancer is associated with improved survival. *J Surg Oncol* 2020; **121**: 654-661 [PMID: 31970776 DOI: 10.1002/jso.25846]

27 **Raja S**, Rice TW, Murthy SC, Ahmad U, Semple ME, Blackstone EH, Ishwaran H; Worldwide Esophageal Cancer Collaboration Investigators. Value of Lymphadenectomy in Patients Receiving Neoadjuvant Therapy for Esophageal Adenocarcinoma. *Ann Surg* 2021; **274**: e320-e327 [PMID: 31850981 DOI: 10.1097/SLA.0000000000003598]

28 **Tseng J**, Posner MC. For Gastroesophageal Junction Cancers, Does an "Esophageal" or "Gastric" Surgical Approach Offer Better Perioperative and Oncologic Outcomes? *Ann Surg Oncol* 2020; **27**: 511-517 [PMID: 31571057 DOI: 10.1245/s10434-019-07732-x]

29 **Kurokawa Y**, Yamaguchi T, Sasako M, Sano T, Mizusawa J, Nakamura K, Fukuda H. Institutional variation in short- and long-term outcomes after surgery for gastric or esophagogastric junction adenocarcinoma: correlative study of two randomized phase III trials (JCOG9501 and JCOG9502). *Gastric Cancer* 2017; **20**: 508-516 [PMID: 27568321 DOI:

10.1007/s10120-016-0636-y]
30 **Nishiwaki N**, Noma K, Matsuda T, Maeda N, Tanabe S, Sakurama K, Shirakawa Y, Fujiwara T. Risk factor of mediastinal lymph node metastasis of Siewert type I and II esophagogastric junction carcinomas. *Langenbecks Arch Surg* 2020; **405**: 1101-1109 [PMID: 33155069 DOI: 10.1007/s00423-020-02017-4]
31 **Chen XD**, He FQ, Chen M, Zhao FZ. Incidence of lymph node metastasis at each station in Siewert types II/III adenocarcinoma of the esophagogastric junction: A systematic review and meta-analysis. *Surg Oncol* 2020; **35**: 62-70 [PMID: 32835903 DOI: 10.1016/j.suronc.2020.08.001]
32 **Leers JM**, Knepper L, van der Veen A, Schröder W, Fuchs H, Schiller P, Hellmich M, Zettelmeyer U, Brosens LAA, Quaas A, Ruurda JP, van Hillegersberg R, Bruns CJ. The CARDIA-trial protocol: a multinational, prospective, randomized, clinical trial comparing transthoracic esophagectomy with transhiatal extended gastrectomy in adenocarcinoma of the gastroesophageal junction (GEJ) type II. *BMC Cancer* 2020; **20**: 781 [PMID: 32819399 DOI: 10.1186/s12885-020-07152-1]
33 **Zhou Y**, Tian M, Güngör C, Wang D. Neoadjuvant radiotherapy for locoregional Siewert type II gastroesophageal junction adenocarcinoma: A propensity scores matching analysis. *PLoS One* 2021; **16**: e0251555 [PMID: 33979405 DOI: 10.1371/journal.pone.0251555]
34 **Herskovic A**, Martz K, al-Sarraf M, Leichman L, Brindle J, Vaitkevicius V, Cooper J, Byhardt R, Davis L, Emami B. Combined chemotherapy and radiotherapy compared with radiotherapy alone in patients with cancer of the esophagus. *N Engl J Med* 1992; **326**: 1593-1598 [PMID: 1584260 DOI: 10.1056/NEJM199206113262403]
35 **Klevebro F**, Alexandersson von Döbeln G, Wang N, Johnsen G, Jacobsen AB, Friesland S, Hatlevoll I, Glenjen NI, Lind P, Tsai JA, Lundell L, Nilsson M. A randomized clinical trial of neoadjuvant chemotherapy versus neoadjuvant chemoradiotherapy for cancer of the oesophagus or gastro-oesophageal junction. *Ann Oncol* 2016; **27**: 660-667 [PMID: 26782957 DOI: 10.1093/annonc/mdw010]
36 **Ristau J**, Thiel M, Katayama S, Schlampp I, Lang K, Häfner MF, Herfarth K, Debus J, Koerber SA. Simultaneous integrated boost concepts in definitive radiation therapy for esophageal cancer: outcomes and toxicity. *Radiat Oncol* 2021; **16**: 23 [PMID: 33522923 DOI: 10.1186/s13014-021-01749-x]
37 **Mokdad AA**, Yopp AC, Polanco PM, Mansour JC, Reznik SI, Heitjan DF, Choti MA, Minter RR, Wang SC, Porembka MR. Adjuvant Chemotherapy *vs* Postoperative Observation Following Preoperative Chemoradiotherapy and Resection in Gastroesophageal Cancer: A Propensity Score-Matched Analysis. *JAMA Oncol* 2018; **4**: 31-38 [PMID: 28975352 DOI: 10.1001/jamaoncol.2017.2805]
38 **Papaxoinis G**, Kamposioras K, Weaver JMJ, Kordatou Z, Stamatopoulou S, Germetaki T, Nasralla M, Owen-Holt V, Anthoney A, Mansoor W. The Role of Continuing Perioperative Chemotherapy Post Surgery in Patients with Esophageal or Gastroesophageal Junction Adenocarcinoma: a Multicenter Cohort Study. *J Gastrointest Surg* 2019; **23**: 1729-1741 [PMID: 30671799 DOI: 10.1007/s11605-018-04087-8]
39 **Davies AR**, Gossage JA, Zylstra J, Mattsson F, Lagergren J, Maisey N, Smyth EC, Cunningham D, Allum WH, Mason RC. Tumor stage after neoadjuvant chemotherapy determines survival after surgery for adenocarcinoma of the esophagus and esophagogastric junction. *J Clin Oncol* 2014; **32**: 2983-2990 [PMID: 25071104 DOI: 10.1200/JCO.2014.55.9070]
40 **Ronellenfitsch U**, Schwarzbach M, Hofheinz R, Kienle P, Nowak K, Kieser M, Slanger TE, Burmeister B, Kelsen D, Niedzwiecki D, Schuhmacher C, Urba S, van de Velde C, Walsh TN, Ychou M, Jensen K. Predictors of overall and recurrence-free survival after neoadjuvant chemotherapy for gastroesophageal adenocarcinoma: Pooled analysis of individual patient data (IPD) from randomized controlled trials (RCTs). *Eur J Surg Oncol* 2017; **43**: 1550-1558 [PMID: 28551325 DOI: 10.1016/j.ejso.2017.05.005]
41 **Bunting D**, Berrisford R, Wheatley T, Humphreys L, Ariyarathenam A, Sanders G. Prospective cohort study of neoadjuvant therapy toxicity in the treatment of oesophageal adenocarcinoma. *Int J Surg* 2018; **52**: 126-130 [PMID: 29455047 DOI: 10.1016/j.ijsu.2018.02.023]
42 **Macdonald JS**, Smalley SR, Benedetti J, Hundahl SA, Estes NC, Stemmermann GN, Haller DG, Ajani JA, Gunderson LL, Jessup JM, Martenson JA. Chemoradiotherapy after surgery compared with surgery alone for adenocarcinoma of the stomach or gastroesophageal junction. *N Engl J Med* 2001; **345**: 725-730 [PMID: 11547741 DOI: 10.1056/NEJMoa010187]
43 **Moorcraft SY**, Smyth EC, Cunningham D. Adjuvant or neoadjuvant therapy for operable esophagogastric cancer? *Gastric Cancer* 2015; **18**: 1-10 [PMID: 24638977 DOI: 10.1007/s10120-014-0356-0]
44 **Shapiro J**, van Lanschot JJB, Hulshof MCCM, van Hagen P, van Berge Henegouwen MI, Wijnhoven BPL, van Laarhoven HWM, Nieuwenhuijzen GAP, Hospers GAP, Bonenkamp JJ, Cuesta MA, Blaisse RJB, Busch ORC, Ten Kate FJW, Creemers GM, Punt CJA, Plukker JTM, Verheul HMW, Bilgen EJS, van Dekken H, van der Sangen MJC, Rozema T, Biermann K, Beukema JC, Piet AHM, van Rij CM, Reinders JG, Tilanus HW, Steyerberg EW, van der Gaast A; CROSS study group. Neoadjuvant chemoradiotherapy plus surgery *vs* surgery alone for oesophageal or junctional cancer (CROSS): long-term results of a randomised controlled trial. *Lancet Oncol* 2015; **16**: 1090-1098 [PMID: 26254683 DOI: 10.1016/S1470-2045(15)00040-6]
45 **Anker CJ**, Dragovic J, Herman JM, Bianchi NA, Goodman KA, Jones WE 3rd, Kennedy TJ, Kumar R, Lee P, Russo S, Sharma N, Small W, Suh WW, Tchelebi LT, Jabbour SK. Executive Summary of the American Radium Society Appropriate Use Criteria for Operable Esophageal and Gastroesophageal Junction Adenocarcinoma: Systematic Review and Guidelines. *Int J Radiat Oncol Biol Phys* 2021; **109**: 186-200 [PMID: 32858113 DOI: 10.1016/j.ijrobp.2020.08.050]
46 **Zafar SN**, Blum M, Chiang YJ, Ajani JA, Estrella JS, Das P, Minsky BD, Hofstetter WL, Mansfield P, Badgwell BD, Ikoma N. Preoperative Chemoradiation Versus Chemotherapy in Gastroesophageal Junction Adenocarcinoma. *Ann Thorac Surg* 2020; **110**: 398-405 [PMID: 32289300 DOI: 10.1016/j.athoracsur.2020.03.024]
47 **Al-Sukhni E**, Gabriel E, Attwood K, Kukar M, Nurkin SJ, Hochwald SN. No Survival Difference with Neoadjuvant Chemoradiotherapy Compared with Chemotherapy in Resectable Esophageal and Gastroesophageal Junction Adenocarcinoma: Results from the National Cancer Data Base. *J Am Coll Surg* 2016; **223**: 784-792.e1 [PMID: 27641320 DOI: 10.1016/j.jamcollsurg.2016.09.002]
48 **Samson P**, Robinson C, Bradley J, Lockhart AC, Puri V, Broderick S, Kreisel D, Krupnick AS, Patterson GA, Meyers B,

Crabtree T. Neoadjuvant Chemotherapy *vs* Chemoradiation Prior to Esophagectomy: Impact on Rate of Complete Pathologic Response and Survival in Esophageal Cancer Patients. *J Thorac Oncol* 2016; **11**: 2227-2237 [PMID: 27544058 DOI: 10.1016/j.jtho.2016.07.031]

49 **Smyth EC**, Cunningham D. Adjuvant Chemotherapy Following Neoadjuvant Chemotherapy Plus Surgery for Patients With Gastroesophageal Cancer-Is There Room for Improvement? *JAMA Oncol* 2018; **4**: 38-39 [PMID: 28975190 DOI: 10.1001/jamaoncol.2017.2792]

50 **Li J**, Zhao Q, Ge X, Song Y, Tian Y, Wang S, Liu M, Qiao X. Neoadjuvant chemoradiotherapy improves survival in locally advanced adenocarcinoma of esophagogastric junction compared with neoadjuvant chemotherapy: a propensity score matching analysis. *BMC Surg* 2021; **21**: 137 [PMID: 33731072 DOI: 10.1186/s12893-021-01136-z]

51 **Tian S**, Jiang R, Madden NA, Ferris MJ, Buchwald ZS, Xu KM, Cardona K, Maithel SK, McDonald MW, Lin JY, Curran WJ, El-Rayes BF, Behera M, Patel PR. Survival outcomes in patients with gastric and gastroesophageal junction adenocarcinomas treated with perioperative chemotherapy with or without preoperative radiotherapy. *Cancer* 2020; **126**: 37-45 [PMID: 31532544 DOI: 10.1002/cncr.32516]

52 **Noordman BJ**, Verdam MGE, Lagarde SM, Shapiro J, Hulshof MCCM, van Berge Henegouwen MI, Wijnhoven BPL, Nieuwenhuijzen GAP, Bonenkamp JJ, Cuesta MA, Plukker JTM, Spillenaar Bilgen EJ, Steyerberg EW, van der Gaast A, Sprangers MAG, van Lanschot JJB; CROSS Study Group. Impact of neoadjuvant chemoradiotherapy on health-related quality of life in long-term survivors of esophageal or junctional cancer: results from the randomized CROSS trial. *Ann Oncol* 2018; **29**: 445-451 [PMID: 29126244 DOI: 10.1093/annonc/mdx726]

53 **Noordman BJ**, Verdam MGE, Onstenk B, Heisterkamp J, Jansen WJBM, Martijnse IS, Lagarde SM, Wijnhoven BPL, Acosta CMM, van der Gaast A, Sprangers MAG, van Lanschot JJB. Quality of Life During and After Completion of Neoadjuvant Chemoradiotherapy for Esophageal and Junctional Cancer. *Ann Surg Oncol* 2019; **26**: 4765-4772 [PMID: 31620943 DOI: 10.1245/s10434-019-07779-w]

54 **Noordman BJ**, Verdam MGE, Lagarde SM, Hulshof MCCM, van Hagen P, van Berge Henegouwen MI, Wijnhoven BPL, van Laarhoven HWM, Nieuwenhuijzen GAP, Hospers GAP, Bonenkamp JJ, Cuesta MA, Blaisse RJB, Busch OR, Ten Kate FJW, Creemers GM, Punt CJA, Plukker JTM, Verheul HMW, Spillenaar Bilgen EJ, van Dekken H, van der Sangen MJC, Rozema T, Biermann K, Beukema JC, Piet AHM, van Rij CM, Reinders JG, Tilanus HW, Steyerberg EW, van der Gaast A, Sprangers MAG, van Lanschot JJB. Effect of Neoadjuvant Chemoradiotherapy on Health-Related Quality of Life in Esophageal or Junctional Cancer: Results From the Randomized CROSS Trial. *J Clin Oncol* 2018; **36**: 268-275 [PMID: 29161204 DOI: 10.1200/JCO.2017.73.7718]

55 **Nilsson K**, Klevebro F, Rouvelas I, Lindblad M, Szabo E, Halldestam I, Smedh U, Wallner B, Johansson J, Johnsen G, Aahlin EK, Johannessen HO, Hjortland GO, Bartella I, Schröder W, Bruns C, Nilsson M. Surgical Morbidity and Mortality From the Multicenter Randomized Controlled NeoRes II Trial: Standard Versus Prolonged Time to Surgery After Neoadjuvant Chemoradiotherapy for Esophageal Cancer. *Ann Surg* 2020; **272**: 684-689 [PMID: 32833767 DOI: 10.1097/SLA.0000000000004340]

56 **Qin Q**, Xu H, Liu J, Zhang C, Xu L, Di X, Zhang X, Sun X. Does timing of esophagectomy following neoadjuvant chemoradiation affect outcomes? *Int J Surg* 2018; **59**: 11-18 [PMID: 30261331 DOI: 10.1016/j.ijsu.2018.09.013]

57 **Rice TW**, Lu M, Ishwaran H, Blackstone EH; Worldwide Esophageal Cancer Collaboration Investigators. Precision Surgical Therapy for Adenocarcinoma of the Esophagus and Esophagogastric Junction. *J Thorac Oncol* 2019; **14**: 2164-2175 [PMID: 31442498 DOI: 10.1016/j.jtho.2019.08.004]

58 **van Rossum PSN**, Mohammad NH, Vleggaar FP, van Hillegersberg R. Treatment for unresectable or metastatic oesophageal cancer: current evidence and trends. *Nat Rev Gastroenterol Hepatol* 2018; **15**: 235-249 [PMID: 29235549 DOI: 10.1038/nrgastro.2017.162]

59 **Cooper JS**, Guo MD, Herskovic A, Macdonald JS, Martenson JA Jr, Al-Sarraf M, Byhardt R, Russell AH, Beitler JJ, Spencer S, Asbell SO, Graham MV, Leichman LL. Chemoradiotherapy of locally advanced esophageal cancer: long-term follow-up of a prospective randomized trial (RTOG 85-01). Radiation Therapy Oncology Group. *JAMA* 1999; **281**: 1623-1627 [PMID: 10235156 DOI: 10.1001/jama.281.17.1623]

60 **Versteijne E**, van Laarhoven HW, van Hooft JE, van Os RM, Geijsen ED, van Berge Henegouwen MI, Hulshof MC. Definitive chemoradiation for patients with inoperable and/or unresectable esophageal cancer: locoregional recurrence pattern. *Dis Esophagus* 2015; **28**: 453-459 [PMID: 24725186 DOI: 10.1111/dote.12215]

61 **Guttmann DM**, Mitra N, Bekelman J, Metz JM, Plastaras J, Feng W, Swisher-McClure S. Improved Overall Survival with Aggressive Primary Tumor Radiotherapy for Patients with Metastatic Esophageal Cancer. *J Thorac Oncol* 2017; **12**: 1131-1142 [PMID: 28461255 DOI: 10.1016/j.jtho.2017.03.026]

62 **Hulshof MCCM**, Geijsen ED, Rozema T, Oppedijk V, Buijsen J, Neelis KJ, Nuyttens JJME, van der Sangen MJC, Jeene PM, Reinders JG, van Berge Henegouwen MI, Thano A, van Hooft JE, van Laarhoven HWM, van der Gaast A. Randomized Study on Dose Escalation in Definitive Chemoradiation for Patients With Locally Advanced Esophageal Cancer (ARTDECO Study). *J Clin Oncol* 2021; **39**: 2816-2824 [PMID: 34101496 DOI: 10.1200/JCO.20.03697]

World Journal of Gastroenterology

Submit a Manuscript: https://www.f6publishing.com

World J Gastroenterol 2022 August 21; 28(31): 4310-4327

DOI: 10.3748/wjg.v28.i31.4310

ISSN 1007-9327 (print) ISSN 2219-2840 (online)

ORIGINAL ARTICLE

Basic Study

Exosomal glypican-1 is elevated in pancreatic cancer precursors and can signal genetic predisposition in the absence of endoscopic ultrasound abnormalities

Pedro Moutinho-Ribeiro, Ines A Batista, Sofia T Quintas, Bárbara Adem, Marco Silva, Rui Morais, Armando Peixoto, Rosa Coelho, Pedro Costa-Moreira, Renato Medas, Susana Lopes, Filipe Vilas-Boas, Manuela Baptista, Diogo Dias-Silva, Ana L Esteves, Filipa Martins, Joanne Lopes, Helena Barroca, Fátima Carneiro, Guilherme Macedo, Sonia A Melo

Specialty type: Gastroenterology and hepatology

Provenance and peer review: Unsolicited article; Externally peer reviewed.

Peer-review model: Single blind

Peer-review report's scientific quality classification

Grade A (Excellent): A
Grade B (Very good): B
Grade C (Good): 0
Grade D (Fair): 0
Grade E (Poor): 0

P-Reviewer: Chen SY, China; Villa E, United States

Received: February 17, 2022
Peer-review started: February 17, 2022
First decision: April 16, 2022
Revised: April 30, 2022
Accepted: June 24, 2022
Article in press: June 24, 2022
Published online: August 21, 2022

Pedro Moutinho-Ribeiro, Marco Silva, Rui Morais, Armando Peixoto, Rosa Coelho, Pedro Costa-Moreira, Renato Medas, Susana Lopes, Filipe Vilas-Boas, Guilherme Macedo, Serviço de Gastrenterologia, Centro Hospitalar Universitário de São João, Porto 4200, Portugal

Pedro Moutinho-Ribeiro, Marco Silva, Rui Morais, Armando Peixoto, Rosa Coelho, Pedro Costa-Moreira, Renato Medas, Susana Lopes, Filipe Vilas-Boas, Fátima Carneiro, Guilherme Macedo, Sonia A Melo, Faculty of Medicine, University of Porto, Porto 4200, Portugal

Ines A Batista, Sofia T Quintas, Bárbara Adem, Fátima Carneiro, Sonia A Melo, Instituto de Investigação e Inovação em Saúde (i3S), Universidade do Porto, Porto 4200, Portugal

Ines A Batista, Sofia T Quintas, Fátima Carneiro, Sonia A Melo, IPATIMUP–Institute of Molecular Pathology and Immunology, University of Porto, Porto 4200, Portugal

Ines A Batista, Bárbara Adem, Instituto de Ciências Biomédicas Abel Salazar (ICBAS), University of Porto, Porto 4050, Portugal

Manuela Baptista, Serviço de Cirurgia Geral, Centro Hospitalar Universitário de São João, Porto 4200, Portugal

Diogo Dias-Silva, Ana L Esteves, Filipa Martins, Unidade de Saúde Familiar Serpa Pinto, ACeS Porto Ocidental, Porto 4250, Portugal

Joanne Lopes, Helena Barroca, Fátima Carneiro, Serviço de Anatomia Patológica, Centro Hospitalar Universitário de São João, Porto 4200, Portugal

Corresponding author: Sonia A Melo, PhD, Academic Research, Assistant Professor, Instituto de Investigação e Inovação em Saúde (i3S), Universidade do Porto, R. Alfredo Allen 208, Porto 4200, Portugal. smelo@i3s.up.pt

Abstract

BACKGROUND

Individuals within specific risk groups for pancreatic ductal adenocarcinoma

(PDAC) [mucinous cystic lesions (MCLs), hereditary risk (HR), and new-late onset diabetes mellitus (NLOD)] represent an opportunity for early cancer detection. Endoscopic ultrasound (EUS) is a premium image modality for PDAC screening and precursor lesion characterization. While no specific biomarker is currently clinically available for this purpose, glypican-1 (GPC1) is overexpressed in the circulating exosomes (crExos) of patients with PDAC compared with healthy subjects or those harboring benign pancreatic diseases.

AIM

To evaluate the capacity of GPC1$^+$ crExos to identify individuals at higher risk within these specific groups, all characterized by EUS.

METHODS

This cross-sectional study with a prospective unicentric cohort included 88 subjects: 40 patients with MCL, 20 individuals with HR, and 20 patients with NLOD. A control group (CG) was submitted to EUS for other reasons than pancreatic pathology, with normal pancreas and absence of hereditary risk factors (n = 8). The inclusion period was between October 2016 and January 2019, and the study was approved by the Ethics Committee of Centro Hospitalar Universitário de São João, Porto, Portugal. All patients provided written informed consent. EUS and blood tests for quantification of GPC1$^+$ crExos by flow cytometry and carbohydrate antigen 19-9 (CA 19-9) levels by ELISA were performed in all subjects. EUS-guided tissue acquisition was done whenever necessary. For statistical analysis, SPSS® 27.0 (IBM Corp., Armonk, NY, United States) version was used. All graphs were created using GraphPad Prism 7.00 (GraphPad Software, San Diego, CA, United States).

RESULTS

Half of MCLs harbored worrisome features (WF) or high-risk stigmata (HRS). Pancreatic abnormalities were detected by EUS in 10.0% and 35.0% in HR and NLOD individuals, respectively, all considered non-malignant and "harmless." Median levels of GPC1$^+$ crExos were statistically different: MCL [99.4%, interquartile range (IQR): 94.9%-99.8%], HR (82.0%, IQR: 28.9%-98.2%), NLOD (12.6%, IQR: 5.2%-63.4%), and CG (16.2%, IQR: 6.6%-20.1%) (P < 0.0001). Median levels of CA 19-9 were within the normal range in all groups (standard clinical cut-off of 37 U/mL). Within HR, individuals with a positive history of cancer had higher median levels of GPC1$^+$ crExos (97.9%; IQR: 61.7%-99.5%), compared to those without (59.7%; IQR: 26.3%-96.4%), despite no statistical significance (P = 0.21). Pancreatic cysts with WF/HRS were statistically associated with higher median levels of GPC1$^+$ crExos (99.6%; IQR: 97.6%-99.8%) compared to those without (96.5%; IQR: 81.3%-99.5%) (P = 0.011), presenting an area under the receiver operating characteristic curve value of 0.723 (sensitivity 75.0% and specificity 67.7%, using a cut-off of 98.5%; P = 0.012).

CONCLUSION

GPC1$^+$ crExos may act as biomarker to support the diagnosis and stratification of PDAC precursor lesions, and in signaling individuals with genetic predisposition in the absence of EUS abnormalities.

Key Words: Glypican-1; Circulating exosomes; Endoscopic ultrasound; Pancreatic cancer risk groups; Pancreatic cancer precursor lesions; Genetic predisposition

©The Author(s) 2022. Published by Baishideng Publishing Group Inc. All rights reserved.

Core Tip: Patients with mucinous cystic lesions (MCLs), hereditary risk (HR), and new-late onset diabetes mellitus represent a target for early pancreatic ductal adenocarcinoma (PDAC) detection. Within these groups, we evaluated the capacity of glypican-1 positive (GPC1$^+$) circulating exosomes (crExos) to identify individuals at higher risk, all characterized by endoscopic ultrasound (EUS). High levels of GPC1$^+$ crExos were present in MCL and in individuals with HR (predominantly in those with history of cancer), even in the absence of EUS abnormalities. GPC1 may represent a biomarker to support the diagnosis and stratification of PDAC precursor lesions, and indicate genetic predisposition.

Citation: Moutinho-Ribeiro P, Batista IA, Quintas ST, Adem B, Silva M, Morais R, Peixoto A, Coelho R, Costa-Moreira P, Medas R, Lopes S, Vilas-Boas F, Baptista M, Dias-Silva D, Esteves AL, Martins F, Lopes J, Barroca H, Carneiro F, Macedo G, Melo SA. Exosomal glypican-1 is elevated in pancreatic cancer precursors and can signal genetic predisposition in the absence of endoscopic ultrasound abnormalities. *World J Gastroenterol* 2022; 28(31): 4310-4327
URL: https://www.wjgnet.com/1007-9327/full/v28/i31/4310.htm
DOI: https://dx.doi.org/10.3748/wjg.v28.i31.4310

INTRODUCTION

Pancreatic ductal adenocarcinoma (PDAC) is considered one of the deadliest malignant diseases around the world, and is estimated to become the second leading cause of cancer-related deaths in the United States in 2030[1]. Most patients present with advanced disease at diagnosis, with only 20% being candidates for surgical treatment, the only chance for cure[2,3].

In its early stages, PDAC usually develops with few or no symptoms, and current sectional imaging modalities are inadequate to detect early small lesions[3]. Endoscopic ultrasound (EUS) is a highly accurate diagnostic technique for pancreatic lesions, with its role majored by the possibility of performing EUS-guided tissue acquisition[4-6].

Among PDAC precursor lesions are pancreatic intraepithelial neoplasias (PanINs) and mucinous cystic lesions (MCLs)[7,8]. While the former are very difficult to identify by available imaging modalities, the latter can be more clearly detected and characterized, specially by magnetic resonance imaging (MRI)/magnetic resonance cholangiopancreatography (MRCP) and EUS[5,9].

Along with the improvement of imaging diagnostic accuracy, the search for a biomarker that could adequately identify PDAC at early stages or its high-risk precursor lesions is a top research priority. The only biomarker approved for clinical use is carbohydrate antigen 19-9 (CA 19-9), but it lacks sensitivity and specificity for PDAC early detection, being mostly reserved for monitoring response to therapy and disease progression[10]. In recent years, several molecules have been tested to serve this purpose[11,12]. Among these, membrane-anchored proteoglycan glypican-1 (GPC1) has been shown to be a good candidate. We previously studied GPC1 in circulating exosomes (crExos) and found that it could identify PDAC patients among healthy individuals with perfect accuracy[13]. In addition, $GPC1^+$ crExos correlated with tumor burden and patients' survival. Moreover, in a genetically engineered mouse model of PDAC, GPC1 was overexpressed in crExos even before the tumor could be detected by MRI [13]. Finally, we also showed higher levels of $GPC1^+$ crExos in MCL compared to controls, although the number of patients was very limited[13]. Several studies have demonstrated the role of GPC1 in PDAC [14-18]. Considering the distinct methodologies that some of the studies adopted to study GPC1 in circulation, some support the potential of $GPC1^+$ crExos as a biomarker for early detection of PDAC[14, 15,19], while others only demonstrate their correlation with disease burden[16-18].

At present, while 90% of PDAC cases are sporadic, only individuals harboring increased hereditary risk (HR), either kindreds of familial pancreatic cancer (FPC) (7%) or belonging to other cancer syndromes with increased risk of PDAC (3%), are candidates for screening[20-22]. Nevertheless, there are other well-defined PDAC-associated risk groups that deserve special attention and can constitute a refined population to be surveilled in order to increase the rate of early detection and improve overall survival. One of these groups is composed by individuals older than 50 years with a recent (< 36 mo) diagnosis of type II diabetes mellitus (DM). Increasing epidemiological, clinical, and experimental evidence shows that new-onset DM can be a clinical manifestation of asymptomatic PDAC or harbinger the disease and offers the promise for early detection in these individuals[3,23-26]. In fact, although the complex and multidirectional relationship between the two entities is not fully understood, new-late onset DM (NLOD) has been recognized as an entity signaling a 6- to 8-fold increased risk of developing PDAC in 3 years[27].

We previously showed that levels of $GPC1^+$ crExos discriminate PDAC from chronic pancreatitis (CP) with high accuracy[28]. In this work, we aimed to determine the capacity of $GPC1^+$ crExos to identify individuals at higher risk of developing PDAC, comparing its levels with EUS pancreatic abnormalities (PA) within specific risk groups: MCL, HR, and NLOD.

MATERIALS AND METHODS

Design of the study and population

This cross-sectional study with a prospective unicentric cohort included 88 subjects: 40 patients with MCLs, 20 individuals with HR, 20 patients with NLOD, and 8 individuals in the control group (CG). The inclusion period was between October 2016 and January 2019, and the study was approved by the Ethics Committee of Centro Hospitalar Universitário de São João (CHUSJ) (ID No. CES 327-15), Porto,

Portugal. All patients provided written informed consent and underwent blood sample collection at the time of EUS.

In the MCL group, we considered for inclusion both intraductal papillary mucinous neoplasms (IPMNs) and mucinous cystic neoplasms (MCNs). For its diagnosis, we used both imagiological and cyst fluid analysis criteria. We have assumed IPMN etiology when EUS and/or MRCP clearly showed communication of the cyst(s) with the pancreatic ductal system. In this situation, branch-duct type (BD-IPMN) were presumed if multiple and no dominant main pancreatic duct (MPD) dilation was seen. Main-duct IPMN (MD-IPMN) was considered if a segmental or diffuse dilatation of the main duct > 5 mm was observed without any other cause of obstruction. Mixed-type IPMN (MT-IPMN) was defined when features of MD-IPMN and BD-IPMN coexisted[29]. MCN was assumed when a mucin-producing cyst forming epithelial neoplasia of the pancreas with a distinctive ovarian-type stroma was present, typically with no communication with the ductal system[30].

We performed EUS-guided fine needle aspiration (FNA) in almost all cystic lesions included. Mucinous nature was supported by a fluid carcinoembryonic antigen (CEA) > 192 ng/mL and/or fluid glucose < 50 mg/dL[31]. In relation to amylase content, if > 250 U/L, a diagnosis of IPMN was likely, whereas levels < 250 U/L suggested MCN. If the aspirated content was sufficient, a sample was also evaluated by experienced cytopathologists.

In the HR group, we considered for inclusion FPC (family history of PDAC in at least two first-degree, or in three or more first- and second-degree relatives) and PDAC susceptibility gene mutation carriers[20,22,32,33]. All of these individuals had a clinically and genetically established diagnosis and have been followed in a dedicated consultation for hereditary digestive cancers in our institution. They underwent detailed evaluation of family history, and verification of cancer diagnoses by review of medical records and genetic testing.

In the NLOD group, we included patients aged ≥ 50 years who had been diagnosed with type II DM within a period of 36 mo[23,24]. Diagnosis of type II DM was made according to the American Diabetes Association and consisted of: Fasting plasma glucose level ≥ 126 mg/dL, a 2-h plasma glucose level of ≥ 200 mg/dL during a 75-g oral glucose tolerance test, a random plasma glucose level of ≥ 200 mg/dL in a patient with classic symptoms of hyperglycemia or hyperglycemic crisis, or a hemoglobin A1c level of ≥ 6.5%[34].

In the CG, individuals who underwent EUS for other reasons than pancreatic pathology were included with a normal pancreas and absence of hereditary/familial risk factors. The exclusion criteria were patients unable or unwilling to give informed consent, individuals younger than 18 years of age, pregnancy or breast feeding, contraindications to endoscopic procedures or contrast administration, contraindications to computed tomography (CT) or MRI, coagulopathy (prothrombin time > 50% of control, activated partial thromboplastin time > 50 s, or international normalized ratio > 1.5), patients on chronic anticoagulation, platelet count < 50000/μL, and inability to tolerate sedated upper endoscopy due to cardiopulmonary instability or other contraindication to endoscopic procedures.

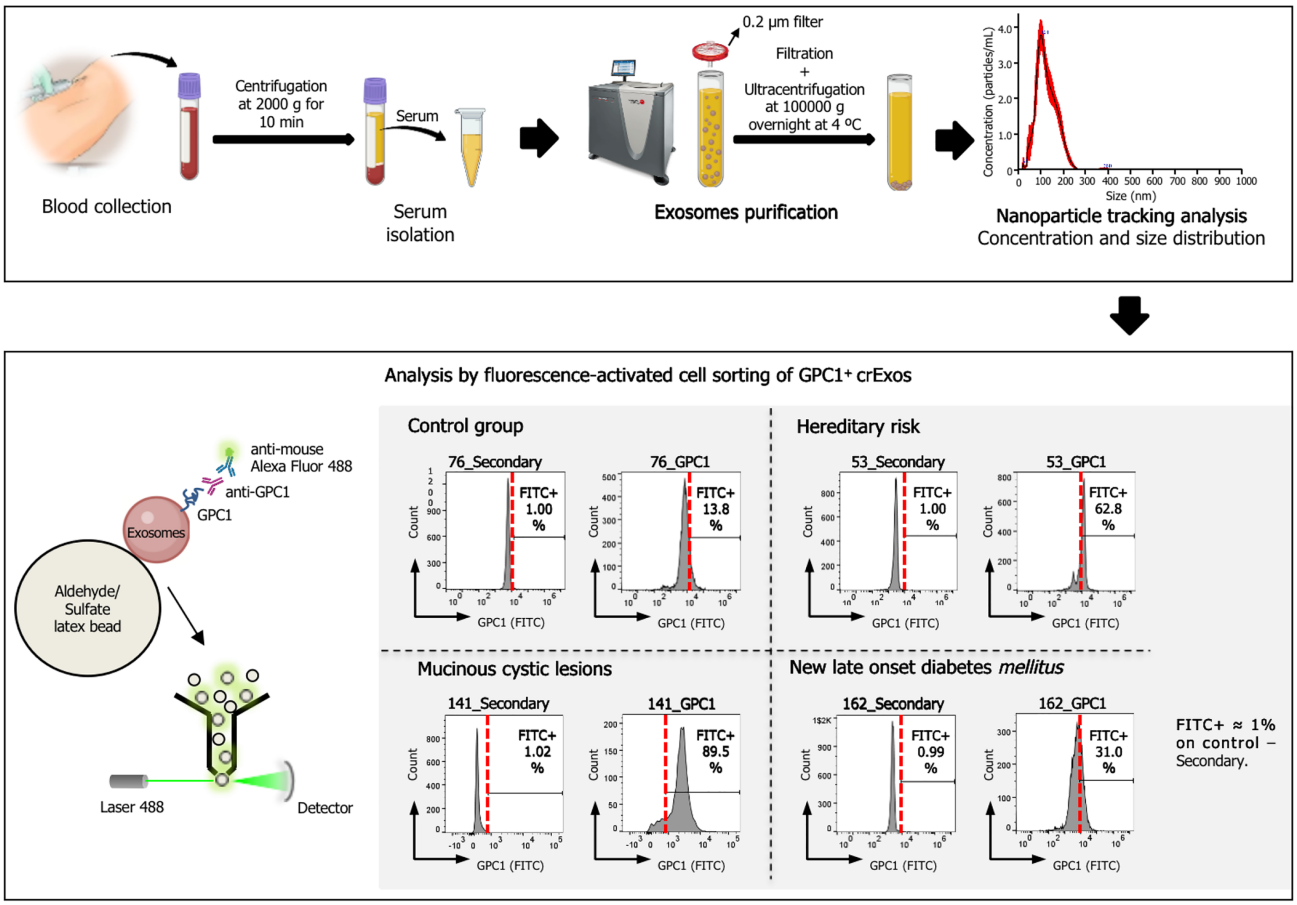
At the time of inclusion, immediately before EUS examination, a blood sample was collected for complete blood count as well as renal, liver, and pancreatic chemistry at the CHUSJ laboratory. A separate blood sample collected at the same time was used to quantify CA 19-9 serum levels (ab108642, CA 19-9 Human ELISA Kit; Abcam, Cambridge, MA, United States) and GPC1 expression in crExos by fluorescence-activated cell sorting (FACS) (Figure 1). For CA 19-9, the standard clinical cut-off of 37 U/mL was used. A complete personal and family clinical history was registered, and demographic data was recorded [age, body mass index (BMI)], previous history of pancreatic disease, smoking and drinking habits, history of diabetes and duration since diagnosis, digestive and systemic symptoms. Laboratory values and previous results of cross-sectional imaging (CT, MRI, or magnetic resonance cholangiopancreatography) were registered. The results of the EUS evaluation at the time of inclusion in the study as well as transechoendoscopic or surgically collected specimens were also recorded.

All subjects were observed, examined, and followed-up at the Department of Gastroenterology of CHUSJ (Porto, Portugal) until death or July 2021.

EUS, tissue acquisition techniques, and fluid/specimen analyses

All EUS evaluations were performed by three experienced endoscopists under deep sedation (propofol or pethidine plus midazolam as assisted by an anesthesiologist). Linear scopes from Olympus® (GT-UCT140, GT-UCT180; Tokyo, Japan) and Pentax® (EG-3670UTK, EG-3870UTK; Tokyo, Japan) along with Olympus® EU-ME2 and Hitachi Avius® (Tokyo, Japan) image processors were used.

PA were classified into major and minor changes. Major changes comprised cystic lesions, CP-like parenchymal changes, and solid lesions. Minor ones constituted changes in pancreatic echogenicity compatible with lipomatous transformation[35,36]. EUS high-risk stigmata (HRS) and worrisome features (WF) were categorized according to the International consensus of Fukuoka guidelines for the management of IPMN of the pancreas[29]. A main duct dilatation ≥ 10 mm or an enhancing mural nodule > 5 mm were classified as HRS, whereas a main duct dilatation between 5 and 9 mm, an enhancing mural nodule < 5 mm, a cyst diameter > 3 cm, the presence of thickened/enhancing cyst walls, an abrupt change in pancreatic duct caliber with distal pancreatic atrophy, and lymphadenopathy were considered WF.



DOI: 10.3748/wjg.v28.i31.4310 **Copyright** ©The Author(s) 2022.

Figure 1 Schematic representation of the workflow for the analysis of circulating exosomes from control group, mucinous cystic lesions, hereditary risk and new-late onset diabetes mellitus patients for the expression of glypican-1. Scheme illustrating the workflow of our study of the expression of glypican-1 (GPC1) on exosomes retrieved from patients' blood samples, from blood collection to the analysis by flow cytometry of GPC1$^+$ circulating exosomes (crExos). A representative histogram of the percentage of beads bound to GPC1-positive crExos (GPC1$^+$ crExos) that were isolated from the serum of a control group, composed by individuals submitted to endoscopic ultrasound for other reasons than pancreatic pathology, as well as the following pancreatic ductal adenocarcinoma risk groups: Mucinous cystic lesions, hereditary risk, and new-late onset diabetes mellitus. Red dashed lines in each histogram depict the start of the fluorescein isothiocyanate (FITC)-positive gate (anti-immunoglobulin G) Alexa Fluor 488), which was determined for each patient separately by considering FITC+ approximately 1% on control–secondary–but maintained between control and GPC1 samples. GPC1: Glypican-1; FITC: Fluorescein isothiocyanate; crExos: Circulating exosomes.

Doppler, elastography, and contrast-enhanced EUS image acquisition (sulphur hexafluoride microbubbles; SonoVue®, Bracco, Italy) were used for assistance in the characterization of mural nodules and thickened cyst walls.

EUS-FNA was performed in almost all cystic lesions, preferably with a 22 G needle (Wilson-Cook Medical, Winston, NC, United States and Boston Scientific, Natick MA, United States) in a single pass, and along with antibiotic prophylaxis (single intravenous infusion of 200 mg ciprofloxacin). The fluid collected was sent for amylase, glucose, and CEA quantification, and also, if in enough volume, for cytological examination. Solid or indeterminate lesions, mural nodules, or suspicious thickenings of the cyst wall or septa were punctured in a distinct pass, preferably with a 22 G fine needle biopsy. Adverse events related to EUS procedures were registered and monitored.

Microscopic examinations of specimens resulting from EUS-FNA/B and/or surgical resection were analyzed by experienced pathologists in pancreatic diseases and contextualized to patients' clinical history and imaging findings. Cytological evaluation was performed according to the Papanicolaou Society of Cytopathology System for Reporting Pancreaticobiliary Cytology[37].

Collection of human blood samples

At the same time of EUS performance, blood samples were collected at the Department of Gastroenterology of CHUSJ. Serum samples were obtained by centrifugation of the whole blood sample at 2000 g for 10 min at 4 °C and collection of the supernatant. The resultant serum samples were then aliquoted and stored at -80 °C prior to analysis.

Isolation of exosomes by ultracentrifugation of serum samples and nanoparticle tracking analysis

Human serum samples were allowed to thaw on ice with periodic agitation to avoid degradation. A volume of 200 µL serum was retrieved into a new tube and centrifuged at 10000 rpm for 2 min at 4 ºC. The recovered supernatant was diluted in 200 µL NaCl prior to filtration into 14 mL Open-Top Thinwall Ultra-Clear Tubes (Beckman Coulter, Inc., Brea, CA, United States) using a 0.2 µm pore filter (Whatman International Ltd., England, United Kingdom). The tubes were filled with NaCl, and the samples were ultracentrifuged at 100000 g overnight at 4 °C. The next day, the supernatant was carefully and thoroughly discarded and the exosomes' pellet was resuspended in 300 µL of 1 × phosphate-buffered saline (PBS). To determine particle concentration and size distribution, nanoparticle tracking (NTA) (NanoSight NS300) was performed using 10 µL of the exosomes sample dissolved in 1 × PBS at a 1:100 dilution. The remaining exosomes sample was saved at -20 ºC for downstream analysis.

GPC1 analysis by FACS of exosomes coupled to beads

Using the exosomes concentration previously obtained by NTA analysis as a reference, an equal number of exosomes was used for downstream FACS analysis. A total of 3.0×10^9 exosomes were coupled to 4 µm aldehyde/sulfate latex beads (A37304; Thermo Fisher Scientific, Waltham, MA, United States) that had been previously equilibrated at room temperature (through resuspension of 5 µL beads in 100 µL of 1 × PBS and rotation at room temperature for 15 min). The sample volume was adjusted to 300 µL with 1 × PBS. Upon incubation in a rotator at room temperature for 15 min and then at 4 ºC for 30 min to allow the formation of exosomes-bead complexes, 300 µL glycine 1 M in 1 × PBS was added to the sample, followed by incubation at room temperature for 1 h with continuous rotation. Samples were centrifuged at 12000 rpm for 2 min and the supernatant was discarded. The pellet containing the exosomes-bead complexes was subjected to a blocking step with 100 µL of 10% bovine serum albumin (BSA) in 1 × PBS and then incubated with continuous rotation at room temperature for 45 min. The samples were centrifuged at 12000 rpm for 2 min and divided into two tubes: Control and GPC1-incubated samples. Control samples were incubated with a solution of 2% BSA in 1 × PBS, whereas experimental samples were incubated with anti-GPC1 (1:240 dilution in a solution of 2% BSA in 1 × PBS, MAB8351; Abnova, Taipei, Taiwan) overnight in a rotator at 4 ºC. The next morning, the samples were spun at 12000 rpm for 2 min and the pellet was washed twice with 2% BSA in 1 × PBS, with centrifugation at 12000 rpm for 2 min between washes. Following incubation with an Alexa-488-tagged secondary antibody (anti-mouse A-21202; Thermo Fisher Scientific) for 30 min with continuous rotation at room temperature of both control and experimental samples, samples were washed again twice with 2% BSA in 1 × PBS. Finally, samples were resuspended in 300 µL of 2% BSA in 1 × PBS for BD Accuri C6 or BD FACS Canto II analysis (BD Biosciences, Haryana, IN, United States). Using the control samples of each patient (*i.e.* exosomes-bead complexes from each patient only incubated with secondary antibody) as a reference, the fluorescein isothiocyanate (FITC) voltage was adjusted until the percentage of FITC+ beads was 1%. Then, using the same gate and FITC voltage, the percentage of beads bound with $GPC1^+$ crExos in the experimental sample was determined for each patient separately. Data were analyzed using FlowJo software.

Statistical analyses

Categorical variables are described as absolute and relative frequencies and continuous variables as mean and standard deviation, median, percentiles, minimum, and maximum. Hypotheses were tested regarding the distribution of continuous variables *via* the independent samples *t*-test/one-way analysis of variance (ANOVA) or nonparametric Mann-Whitney and Kruskal-Wallis test depending on normal or non-normal distribution, respectively, and considering the nature of the hypothesis. The chi-squared and ANOVA tests were used for categorical variables analysis. Pearson's correlation coefficient was used to assess the statistical relationship/association between two continuous variables. The diagnostic accuracy of $GPC1^+$ crExos was assessed by receiver operating characteristic curve (ROC) considering 95% confidence intervals. Area under the ROC curve (AUROC) was calculated. SPSS® 27.0 (IBM Corp., Armonk, NY, United States) version was used. All graphs were created using GraphPad Prism 7.00 (GraphPad Software, San Diego, CA, United States). The statistical review of the study was performed by a biomedical statistician.

RESULTS

Population demographic characteristics

The baseline demographic characteristics of the 88 individuals included in the study (40 MCL, 20 HR, 20 NLOD, and 8 CG) are summarized in Table 1. The overall female:male ratio was 1.6:1 and did not differ statistically among groups. The mean age of the population was 60.3 ± 12.6 years. The older individuals belonged to the MCL group, with a median age of 67.2 ± 8.9 years, whereas the younger individuals were in the HR group, with a median age of 48.7 ± 10.8 years ($P < 0.001$). Patients in the NLOD group presented with a significantly higher BMI (29.9 ± 4.5 kg/m^2; $P < 0.001$).

Table 1 Baseline demographic characteristics of the study population, *n* = 88

Cohort characteristics	MCL, *n* = 40	HR, *n* = 20	NLOD, *n* = 20	CG, *n* = 8	Total, *n* = 88	*P* value
Sex						NS
Male	14 (35.0)	9 (45.0)	9 (45.0)	2 (25.0)	34 (38.6)	
Female	26 (65.0)	11 (55.0)	11 (55.0)	6 (75.0)	54 (61.4)	
Age in yr	67.2 ± 8.9	48.7 ± 10.8	60.8 ± 7.4	53.8 ± 18.7	60.3 ± 12.6	< 0.001
BMI in kg/m^2	24.9 ± 3.8	24.2 ± 3.9	29.9 ± 4.5	25.0 ± 4.0	25.9 ± 4.5	< 0.001
Smoking habits						NS
Never	27 (67.5)	13 (65.0)	12 (60.0)	7 (87.5)	59 (67.1)	
Ex-smoker, > 5 yr	8 (20.0)	4 (20.0)	7 (35.0)	1 (12.5)	20 (22.7)	
Active	5 (12.5)	3 (15.0)	1 (5.0)	0 (0.0)	9 (10.2)	
Alcohol habits						NS
No	22 (55.0)	11 (55.0)	10 (50.0)	7 (87.5)	50 (56.8)	
Yes	18 (45.0)	9 (45.0)	10 (50.0)	1 (12.5)	38 (43.2)	
Family history of PDAC						< 0.001
No	34 (85.0)	7 (35.0)	18 (90.0)	8 (100.0)	67 (76.1)	
Yes	6 (15.0)	13 (65.0)	2 (10.0)	0 (0.0)	21 (23.9)	

Data are presented as *n* (%) or mean ± SD. BMI: Body mass index; CG: Control group; HR: Hereditary risk; MCL: Mucinous cystic lesion; NLOD: New-late onset diabetes mellitus; NS: Non-significant; PDAC: Pancreatic ductal adenocarcinoma; SD: Standard deviation.

No statistically significant differences were observed in relation to smoking or drinking habits among the studied groups. Overall, 10.2% of the population were active smokers and 22.7% ex-smokers (more than 5 years of abstinence). In relation to alcohol consumption, 43.2% were considered active drinkers (average ingesting amounts of > 30 g or > 40 g alcohol *per* day, in case of female or male individuals, respectively).

Family history of PDAC was present in 23.9% of the entire population, with the highest proportion observed in the HR group (65.0%; $P < 0.001$). In the HR group, 17 (85.0%) individuals were diagnosed with Lynch Syndrome, 1 (5.0%) with Peutz-Jeghers syndrome, and the remaining 2 (10%) with FPC. Six individuals with Lynch Syndrome had a previous personal history of cancer, mostly colorectal ($n = 5$), but all were disease-free at the time of inclusion. Detailed information about this group, including the type of harbored mutation(s), can be found in Table 2. In the NLOD group, the mean time between inclusion in the study and establishment of DM diagnosis was 20.9 ± 8.6 mo.

EUS findings and other clinicopathological features

Main PA detected by EUS is illustrated in Figure 2A-F and constituted cystic lesions (with or without WF/HRS), CP-like parenchymal changes, and lipomatous transformation of pancreatic parenchyma. The EUS features of cystic lesions in the MCL group are described in Table 3. Of the 40 cases included, 39 (97.5%) were IPMNs, and most (89.8%) were classified as BD-IPMNs. Sixty percent of patients presented with multiple cysts, with a mean size of the dominant lesion of 28.1 ± 14.1 mm. In respect to WF and/or HRS, mural nodules, wall thickening, and a dilated MPD were identified in 10%, 7.5%, and 15% of the lesions, respectively. Nineteen of the forty MCL patients (47.5%) underwent additional study with MRCP.

The clinicopathological characteristics of the study population, particularly the type of PA found in EUS among the different groups, the results of EUS-guided tissue acquisition, surgical treatment and specimen analysis, as well as information on cancer detection during follow-up and mortality rate, are summarized in Table 4. Besides the MCL group, where PA in the form of cyst(s) were present in all patients by definition, PA were also detected during the EUS exam in 10.0% and 35.0% of the subjects belonging to HR and NLOD groups, respectively. Half of the lesions in the MCL group were considered to harbor WF or HRS, in contrast to the PA found in the other groups that were all "harmless" in terms of ultrasonographic appearance (CP-like parenchymal changes, lipomatous transformation and infracentimetric simple cystic lesions). EUS-FNA/B was performed only in the MCL group in 35 of the 40 patients (87.5%), either to confirm the diagnosis or in the presence of WF or HRS (Figure 2G and H). Malignancy was detected in 3 patients; in 1, the malignancy was detected in a subsequent EUS exam performed during follow-up (this case was previously reported by our team[38]). The result of cytological exam was considered inconclusive in 37.1% of the procedures. Of the 88 patients of the

Table 2 Characterization of hereditary risk group: Germline mutations and personal history of cancer, *n* = 20

	Lynch syndrome, *n* = 17 (85.0%)	Peutz-Jeghers syndrome, *n* = 1 (5.0%)	FPC, *n* = 2 (10.0%)
Germline mutation(s)			
MLH1	7 (41.2)	-	-
MSH2	6 (35.3)	-	-
MLH1 + *MSH2*	1 (5.9)	-	-
MSH2 + *MSH6*	2 (11.7)	-	-
MSH6	1 (5.9)	-	-
STK11	-	1 (100.0)	-
Not identified	-		2 (100.0)
Personal history of cancer			
No	11 (64.7)	1 (100.0)	2 (100.0)
Yes	6 (35.3)	0 (0.0)	0 (0.0)
Type of cancer			
Colon and rectum	5 (83.3%)	-	-
Endometrium	1 (16.7)	-	-

FPC: Familial pancreatic cancer.

Table 3 Endoscopic ultrasound features of cystic lesions among the mucinous cystic lesions group, *n* = 40

Type of mucinous cyst, *n* (%)	MCN	1 (2.5)
	IPMN	39 (97.5)
Type of IPMN, *n* (%)	MD-IPMN	2 (5.1)
	BD-IPMN	35 (89.8)
	MT-IPMN	2 (5.1)
Number of cysts, *n* (%)	Single	16 (40.0)
	Multiple	24 (60.0)
Main cyst size in mm, mean ± SD		28.1 ± 14.4
Main cyst size in mm, median (IQR)		21.5 (16.3-40.5)
Septa, *n* (%)	Absent	10 (25.0)
	Present	30 (75.0)
Mural nodules, *n* (%)	Absent	36 (90.0)
	Present	4 (10.0)
Wall thickening, *n* (%)	Absent	37 (92.5)
	Present	3 (7.5)
MPD caliber, *n* (%)	Normal	34 (85.0)
	Dilated	6 (15.0)

BD-IPMN: Branch-duct IPMN; IPMN: Intraductal papillary mucinous neoplasm; IQR: Interquartile range; MCN: Mucinous cystic neoplasm; MD-IPMN: Main-duct IPMN; MPD: Main pancreatic duct; MT-IPMN: Mixed type.

cohort, 15 (17.0%) were submitted to surgical resection, and all belonged to the MCL group. These 15 patients either harbored MD or MT-IPMNs or presented a cyst with WF/HRS with suspicious or positive cytology. Malignancy was confirmed in the surgical specimen in all 3 patients with a previous positive cytological exam, and the remaining 12 had a definitive histopathological diagnosis of a low grade dysplastic MCL.

Table 4 Clinical-pathological findings, treatment and follow-up of the study population, *n* = 88

	MCL, *n* = 40	HR, *n* = 20	NLOD, *n* = 20	CG, *n* = 8	Total, *n* = 88
PA in EUS					
No	0 (0.0)	18 (90.0)	13 (65.0)	8 (100.0)	39 (44.3)
Yes	40 (100.0)	2 (10.0)	7 (35.0)	0 (0.0)	49 (55.7)
Type of PA					
Cystic lesions	40 (100.0)	2 (100.0)	2 (28.6)	-	44 (89.8)
CP-like parenchymal changes	0 (0.0)	0 (0.0)	2 (28.6)	-	2 (4.1)
Solid lesions	0 (0.0)	0 (0.0)	0 (0.0)	-	0 (0.0)
Lipomatous transformation	0 (0.0)	0 (0.0)	3 (42.8)	-	3 (6.1)
PA with HRS / WF					
No	20 (50.0)	2 (100.0)	7 (100.0)	-	29 (59.2)
Yes	20 (50.0)	0 (0.0)	0 (0.0)	-	20 (40.8)
EUS FNA/B					
No	5 (12.5)	20 (100.0)	20 (100)	8 (100)	53 (60.2)
Yes	35 (87.5)	0 (0.0)	0 (0.0)	0 (0.0)	35 (39.8)
Inconclusive	13 (37.1)	-	-	-	13 (37.1)
Benign	19 (54.3)	-	-	-	19 (54.3)
Malignant	3 (8.6)[1]	-	-	-	3 (8.6)[1]
Surgery					
No	25 (62.5)	20 (100)	20 (100)	8 (100)	73 (83.0)
Yes	15 (37.5)	0 (0.0)	0 (0.0)	0 (0.0)	15 (17.0)
Benign/Malignant	12 (80.0)/3 (20.0)	-/-	-/-	-/-	12 (80.0)/3 (20.0)
F-up in mo	33.3 ± 12.8	34.9 ± 7.1	27.7 ± 4.7	36.1 ± 5.1	32.6 ± 10.0
Cancer detection during F-up	1 (2.5)	0 (0.0)	0 (0.0)	0 (0.0)	1 (1.1)
Mortality	5 (12.5)	0 (0.0)	0 (0.0)	0 (0.0)	5 (5.7)

Data are presented as *n* (%) or mean ± SD.

[1]One of 3 patients with malignant cytology was diagnosed during follow-up.

CG: Control group; CP: Chronic pancreatitis; EUS: Endoscopic ultrasound; FNA/B: Fine needle aspiration/biopsy; F-up: Follow up; HR: Hereditary risk; HRS: High risk stigmata; MCL: Mucinous cystic lesion; NLOD: New-late onset diabetes mellitus; NS: Non-significant; PA: Pancreatic abnormality; WF: Worrisome features.

The mean follow-up period of the entire cohort was 32 ± 8.6 mo and did not differ statistically among groups (*P* = NS). Five of the 88 individuals (5.7%) died during follow-up, but only one of these due to cancer progression. Two of the other deaths were related to post-operative complications in a 74-year-old and 75-year-old patients, one was related to a pulmonary carcinoma that developed 1 year after inclusion in a 72-year-old patient, and the remaining one corresponded to an 85-year-old patient that did not survive to an infectious respiratory insufficiency. The 2 other patients submitted to surgical resection of malignant cysts were alive and disease-free after 45 mo of follow-up.

Exosomal GPC1 levels are elevated in MCL lesions with WF/HRS and HR groups

The overall median levels of $GPC1^+$ crExos coupled to beads were statistically different among the studied groups: MCL [99.4%, interquartile range (IQR): 94.9%-99.8%], HR (82.0%, IQR: 28.9%-98.2%), and NLOD and CG groups (12.6%, IQR: 5.2%-63.4% and 16.2%, IQR: 6.6%-20.1%, respectively) ($P < 0.0001$) (Figure 3A and Table 5).

The crExos concentration and their median size were significantly higher in NLOD patients (6.05E+10/mL; IQR: 4.83-7.22 and 100.7 nm; IQR: 89.2-110.1, respectively) compared to all other groups ($P < 0.001$ and $P = 0.012$, respectively) (Figure 3B and C and Table 6).

In turn, overall median levels of CA 19-9 were 18.4 U/mL (IQR: 8.3-206) and did not differ statistically between groups: MCL: 20.4 U/mL (IQR: 14.0-35.8), HR: 16.9 U/mL (IQR: 11.7-18.1), NLOD: 18.8

Table 5 Biomarkers (glypican-1-positive circulating exosomes and carbohydrate antigen 19-9) profiles in the study groups, *n* = 88

Biomarker	MCL, *n* = 40	HR, *n* = 20	NLOD, *n* = 20	CG, *n* = 8	Total, *n* = 88	*P* value
$GPC1^+$ crExos, %						< 0.001
Median	99.4	82.0	12.6	16.2	86.8	
Min/Max	6.4/99.9	1.1/99.0	2.1/93.9	1.2/24.5	1.1/99.9	
IQR	94.9-99.8	28.9-98.2	5.2-63.4	6.6-20.1	18.6-99.4	
CA 19-9 in U/mL						NS
Median	20.4	16.9	18.8	30.6	18.4	
Min/Max	8.5/206.6	8.3/28.0	12.8-48.7	13.7-69.6	8.3/206.6	
IQR	14.0-35.8	11.7-18.1	16.6-23.4	15.0-40.8	14.2-27.7	

P value for Kruskal-Wallis test. CA 19-9: Carbohydrate antigen 19-9; CG: Control group; HR: Hereditary risk; IQR: Interquartile range; $GPC1^+$ crExos: Glypican-1 positive circulating exosomes; Max: Maximum; MCL: Mucinous cystic lesion; Min: Minimum; NLOD: New-late onset diabetes mellitus; NS: Non-significant.

Table 6 Size and concentration of exosomes according to the study groups, *n* = 88

	MCL, *n* = 40	HR, *n* = 20	NLOD, *n* = 20	CG, *n* = 8	Total, *n* = 88	*P* value
Size in nm						0.012
Median	82.5	94.7	100.7	72.8	90.5	
IQR	72.8-97.6	83.0-109.7	89.2-110.1	67.0-102.8	77.9-103.2	
Concentration as particles E + 10/mL						< 0.001
Median	3.48	3.36	6.05	3.30	4.10	
IQR	1.88-5.08	2.51-4.37	4.83-7.22	2.91-4.20	2.60-5.69	

P value for Kruskal-Wallis test. CG: Control group; HR: Hereditary risk; IQR: Interquartile range; MCL: Mucinous cystic lesion; NLOD: New-late onset diabetes mellitus.

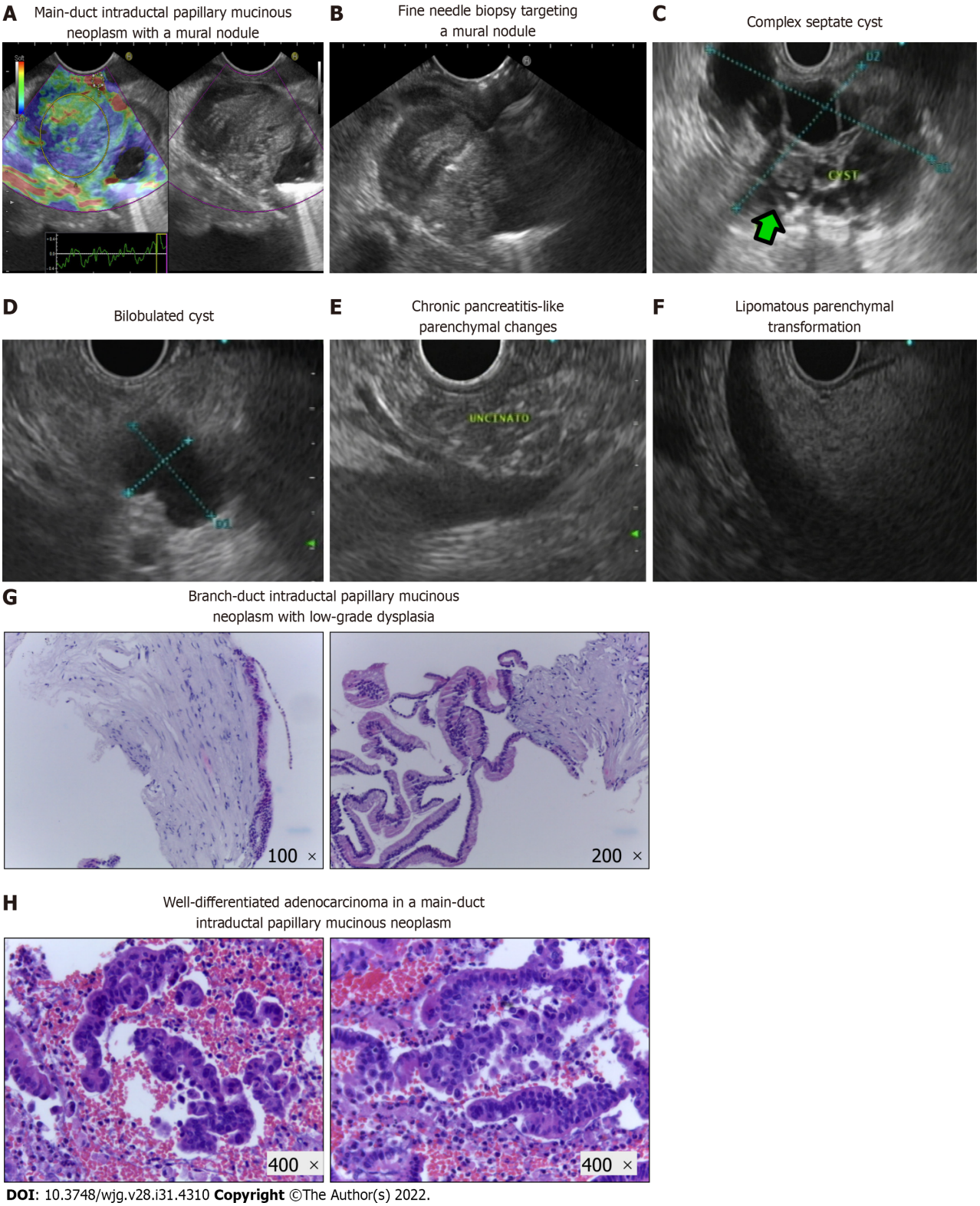
U/mL (IQR: 12.8-48.7) and CG: 30.6 U/mL (IQR: 13.7-69.6) (*P* = NS) (Figure 3D and Table 5). All CA 19-9 median levels were considered in the normal range considering the clinical standard cut-off (37 U/mL).

We further investigated the profile of both biomarkers in a sub-analysis in two distinct settings. First, among the HR group, we evaluated $GPC1^+$ crExos and CA 19-9 levels according to the presence or absence of personal cancer history (Figure 4A and B). In the individuals with a positive history of cancer (5 colorectal and 1 cancer of the endometrium), although not statistically significant, we observed higher median levels of $GPC1^+$ crExos (97.9%; IQR: 61.7%-99.5%) compared to those with a negative history (*n* = 14) (59.7%; IQR: 26.3%-96.4%) (*P* = 0.21). In relation to CA 19-9 median levels, they did not differ among these two subgroups (17.5 U/mL; IQR: 10.7%-20.1% and 16.3 U/mL; IQR: 12.2%-19.5%, respectively) (*P* = NS).

Second, in the total number of patients harboring pancreatic cystic lesions (40 in the MCL group, 2 diagnosed in the HR group, and 2 in the NLOD group), we studied the levels of $GPC1^+$ crExos and CA 19-9 according to the presence or absence of WF/HRS in the EUS examination (Figure 4C and D). When WF or HRS were present (*n* = 20), patients presented with statistically significant higher median levels of $GPC1^+$ crExos (99.6%; IQR: 97.6%-99.8%) compared to those with endosonographic "harmless" lesions (*n* = 24) (96.5%; IQR: 81.3%-99.5%) (*P* = 0.011) (Figure 4C). The levels of $GPC1^+$ crExos presented an AUROC value of 0.723 in differentiating the group of cystic lesions with WF/HRS from those without (sensitivity 75.0% and specificity 67.7% for a cut-off of 98.5% (*P* = 0.012) (Figure 4E). CA 19-9 median levels did not statistically differ between these two subgroups (22.9 U/mL; IQR: 14.1-35.8 and 17.4 U/mL; IQR: 13.7-29.8, respectively) (*P* = NS) (Figure 4D).

DISCUSSION

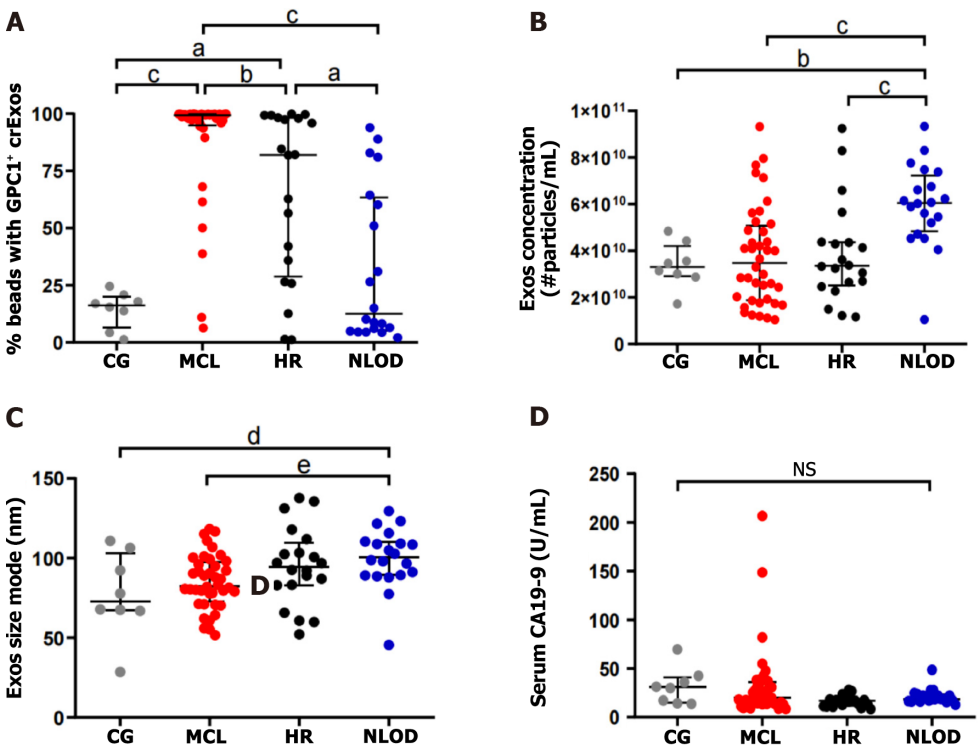
MCLs are established as PDAC precursor lesions, with different risks considering morphologic



DOI: 10.3748/wjg.v28.i31.4310 **Copyright** ©The Author(s) 2022.

Figure 2 Pancreatic abnormalities in endoscopy ultrasound examination and pathological exams of endoscopic ultrasound-guided fine needle aspiration/biopsy specimens from intraductal papillary mucinous neoplasms. A: Main-duct intraductal papillary mucinous neoplasm (MD-IPMN) with a large mural nodule, visualized in B-mode (right panel) and characterized with qualitative elastography (left panel) that revealed areas of hard consistency (blue color); B: Endoscopic ultrasound-guided fine needle biopsy with a 22 G needle targeting the harder lesions in the described mural nodule (pathological exam showed malignant degeneration); C: Complex septate cyst with areas of wall focal thickenings and a mural nodule (green arrow); D: Simple bilobulated cyst without worrisome features or high-risk stigmata; E: Chronic pancreatitis-like parenchymal changes (lobulation, hyperechoic foci, and strands); F: Homogenous hyperechogenic appearance of pancreatic parenchyma suggestive of lipomatous transformation; G: Branch-duct IPMN with low-grade dysplasia [hematoxylin and eosin (H&E)-stained cellblock]. These images show the wall of a cystic lesion, partly lined by a cylindrical mucosecretory epithelium with low-grade atypia (left: 100 ×; right: 200 ×); H: Well-differentiated adenocarcinoma originated in a MD-IPMN (H&E-stained cellblock: 400 ×). These images show an epithelial neoplasm with marked architectural disorganization and severe cytological atypia. The cells have a high nucleus-cytoplasmic ratio, with anisokaryosis, irregular nuclei

with coarse chromatin and some with an exuberant nucleolus.

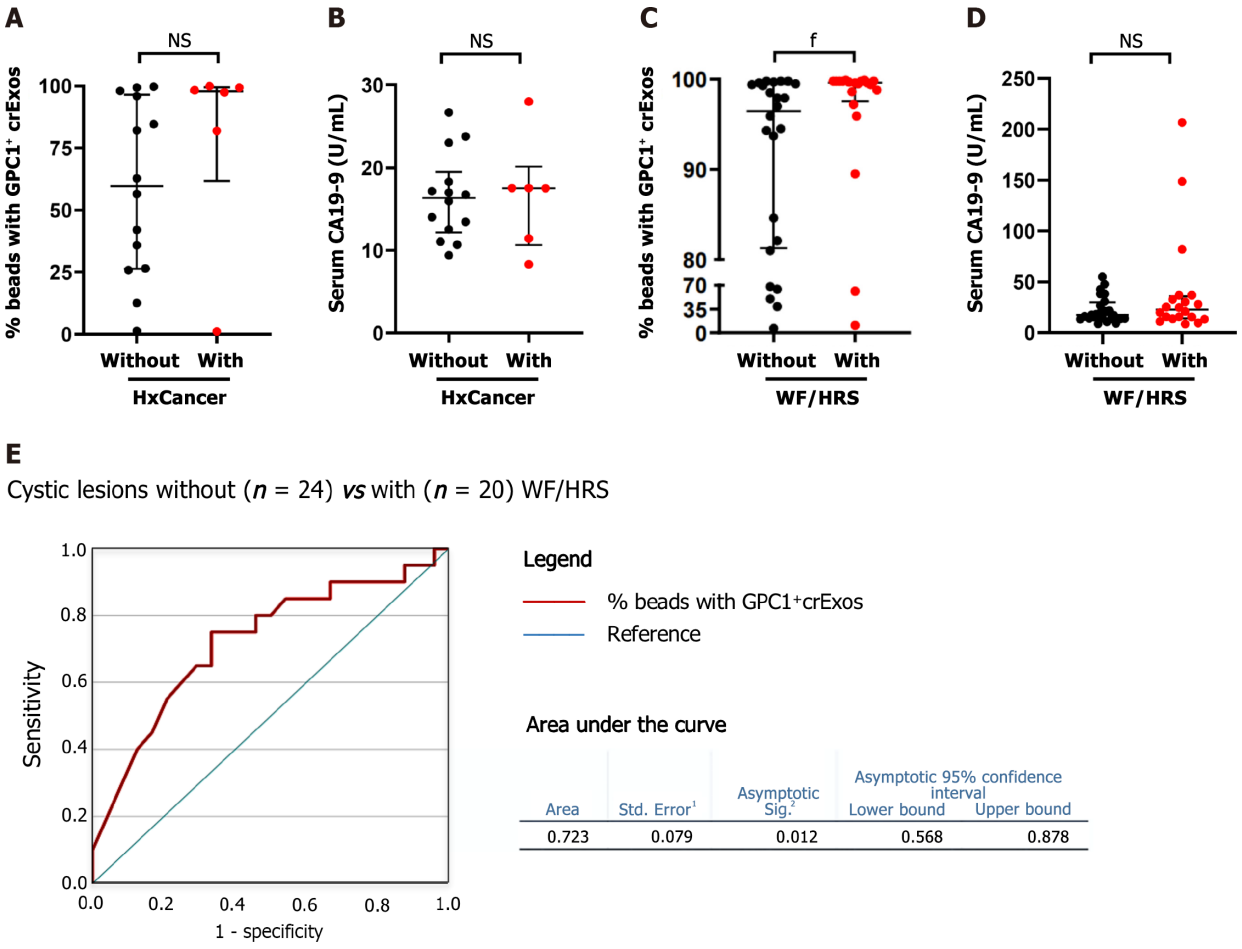


DOI: 10.3748/wjg.v28.i31.4310 **Copyright** ©The Author(s) 2022.

Figure 3 Glypican-1-positive circulating exosomes levels are different among the studied groups, whereas the levels of carbohydrate antigen 19-9 do not differ and are within the normal range in the entire population. A: Scatter dot plot representing the percentage of beads bound to glypican-1-positive exosomes (GPC1$^+$ crExos) in the control group (CG) (n = 8), mucinous cystic lesions (MCLs) (n = 40), hereditary risk (HR) (n = 20) and new-late onset diabetes mellitus (NLOD) (n = 20), (Mann-Whitney U Test, $^aP < 0.02$, $^bP = 0.005$, $^cP < 0.001$); B: Scatter dot plot representing exosomes concentration measured by nanoparticle tracking analysis depicting the number of exosomes/0.666 mL serum derived from CG (n = 8), MCL (n = 40), HR (n = 20), and NLOD (n = 20) donors (Mann-Whitney U Test, $^bP = 0.005$, $^cP < 0.001$); C: Scatter dot plot representing exosomes mode size distribution determined by nanoparticle tracking analysis from CG (n = 8), MCL (n = 40), HR (n = 20), and NLOD (n = 20) donors (Mann-Whitney U Test, $^dP = 0.018$, $^eP = 0.04$); D: Scatter dot plot representing the serum carbohydrate antigen 19-9 concentration (U/mL) as determined by enzyme-linked immunoassay in CG (n = 8), MCL (n = 40), HR (n = 20), and NLOD (n = 20), (Kruskal-Wallis Test, P = NS). Data are shown as the median ± interquartile range. NS: Non-significant; GPC1: Glypican-1; CA 19-9: Carbohydrate antigen 19-9; crExos: Circulating exosomes.

appearance as well as cytological findings resulting from guided tissue acquisition. While the diagnostic and management of pancreatic cysts differs between international guidelines[29,39-42], they all agree that the risk of malignancy should be based, essentially, in the assessment of the classical WF/HRS, which was initially defined in the Fukuoka consensus[43].

Our cohort mainly constituted IPMNs, most of which were BD-IPMN type and half of the lesions presented with WF and/or HRS[29]. Malignancy was suspected by EUS in two advanced lesions with main duct involvement, which were confirmed by cytology. Interestingly, the third confirmed malignant cyst corresponded to a case we have previously reported[38], and was diagnosed during a follow-up examination of an apparently "inoffensive" cystic lesion in the index EUS. Our results have confirmed the limited utility of the use of cytology alone for cyst etiological characterization[44,45], as 37% of the results of EUS-FNA of the cyst fluid were considered inconclusive by pathologists. This limitation of cyst fluid cytological analysis tends to be overwhelmed by the referral for surgical resection of indeterminate suspicious lesions. In fact, 15 of the 40 patients with MCL proposed for surgical treatment, after evaluation by a multidisciplinary team, corresponded to 3 cases with a positive cytology for malignancy and 12 patients with indeterminate/inconclusive results of EUS-FNA. The surgical specimen confirmed malignancy in all 3 cases with previous diagnosis and in the remaining 12 revealed benign IPMNs with low grade dysplasia. The overtreatment of some of these patients is an important issue, as the morbidity and mortality of pancreatic surgery is not negligible[46,47]. In the present cohort, 2 of the 5 deaths recorded were precisely due to complications after surgery, both in patients harboring benign lesions. This observation supports the drive of research, justifying the need to evaluate the role of upcoming biomarkers, like exosomal GPC1, in complement with EUS evaluation, for the stratification of MCL, ultimately contributing to refine the criteria for surgical treatment or continued surveillance. In



DOI: 10.3748/wjg.v28.i31.4310 **Copyright** ©The Author(s) 2022.

Figure 4 Glypican-1-positive circulating exosomes are higher in individuals with personal history of cancer within the hereditary risk group, and among patients harboring pancreatic cystic lesions when worrisome features/high-risk stigmata are present. A: Scatter dot plot representing the percentage of beads bound to glypican-1 (GPC1)-positive circulating exosomes (GPC1⁺ crExos) in subjects in the hereditary risk (HR) group, without (n = 14) and with (n = 6) a personal history of cancer (HxCancer) [Mann-Whitney U Test, P = non-significant (NS)]; B: Scatter dot plot representing the serum carbohydrate antigen 19-9 (CA 19-9) concentration (U/mL) as determined by enzyme-linked immunoassay (ELISA) in subjects in the HR group, without (n = 14) and with (n = 6) HxCancer (Mann-Whitney U Test, P = 0.21); C: Scatter dot plot representing the percentage of GPC1⁺ crExos coupled to beads in subjects harboring pancreatic cystic lesions, without (n = 24) and with (n = 20) worrisome features (WF) or high-risk stigmata (HRS) (Mann-Whitney U Test, [f]P = 0.011); D: Scatter dot plot representing the serum CA 19-9 concentration (U/mL) as determined by ELISA in subjects harboring pancreatic cystic lesions, without (n = 24) and with (n = 20) WF/HRS (Mann-Whitney U Test, P = NS); E: Receiver operating characteristic curve of the cohort of pancreatic cystic lesions without (n = 24) or with (n = 20) WF/HRS, regarding the GPC1⁺ crExos levels (% beads with GPC1⁺ crExos). [1]Under nonparametric assumption; [2]Null hypothesis: True area = 0.5. Data are shown as the median ± interquartile range. NS: Non-significant; GPC1: Glypican-1; crExos: Circulating exosomes; WF: Worrisome features; HRS: High-risk stigmata.

this setting, our preliminary results initially reported were promising, as the levels of GPC1⁺ crExos were equally elevated in patients with PDAC and with MCLs[48,49]. The findings in the present study confirm these observations, as the median levels of GPC1⁺ crExos observed in the MCL group (significantly higher than in the other studied groups) were in the same magnitude as the ones registered for PDAC patients, that we have recently reported using the same methodology[28]. Moreover, when we analyzed the levels GPC1⁺ crExos among all pancreatic cystic lesions (MCL group plus those detected in the screening EUS in HR and NLOD groups), we found that they were statistically more elevated when WF/HRS were present, suggesting that this biomarker can, in fact, have a role in the risk stratification of these PDAC precursor lesions.

This is the first study to access the profile of GPC1⁺ crExos in HR and NLOD individuals, and our results showed that the median levels of this biomarker were statistically more elevated among the HR group when compared to NLOD patients and controls. Considering our previous published observations[28], these levels of GPC1⁺ crExos in HR individuals were also higher than those registered among patients with CP (28.4%), but not as elevated as in those with PDAC (99.7%). Interestingly, our results also showed a tendency of the individuals with a history of previous cancer (mainly colorectal) to present higher levels of GPC1⁺ crExos when compared to those without. While PA were detected in only 10% among HR individuals, all representing simple cystic lesions, these observations may suggest a potential role of GPC1⁺ crExos as a marker of genetically determined predisposition for cancer development, even in the absence of "harmful" pancreatic lesions.

Important studies have recently been published[24-26] and prospective investigational projects are ongoing[50] demonstrating the importance to access the magnitude of the risk to develop PDAC among NLOD patients and to define PDAC incidence during long-term follow-up. This justified the inclusion of NLOD patients in our investigation cohort. We found PA in EUS in 35% of the NLOD patients, comprising simple cystic lesions, CP-like changes and lipomatous parenchymal transformations, all of them considered "harmless", not requiring further investigation. Despite the highest median values of exosomes' size and particle concentration being registered in this group, the percentage of crExos positive for GPC1 was low and not statistically different from the CG. This finding is in accordance with the lack of sufficient evidence, at the present, to include these patients in regular screening programs for PDAC early detection.

Some limitations of this study should be pointed out, namely the sample size, the possibility of a referral bias giving the nature of our tertiary center, the relatively short period of patients' follow-up, and the cut-off found to stratify patients with cystic lesions and WF/HRS from those without. Also, the impossibility to include PanIN lesions in the study that would certainly power the analysis of GPC1 profile among PDAC pathological precursors. Lastly, the technique of exosomes isolation and analysis can still hamper its translation to clinical use. Despite these restraints, our results open the door for future studies to determine the value of this biomarker in the stratification of risk groups.

CONCLUSION

In summary, we demonstrate that GPC1$^+$ crExos levels are elevated in MCL, in the same magnitude of PDAC patients. These levels were statistically higher in cysts harboring WF/HRS. High levels were also registered among individuals with HR for PDAC (predominantly in those with history of previous cancer). Longitudinal studies will clarify the potential of exosomal GPC1 as a biomarker for the diagnosis and stratification of PDAC precursor lesions, as well as in signaling individuals with genetic predisposition for this neoplasia, ultimately contributing to refine screening and surveillance strategies.

ARTICLE HIGHLIGHTS

Research background

Most of the patients with pancreatic ductal adenocarcinoma (PDAC) are diagnosed with advanced disease at which stage treatment is inefficient. In order to improve survival, new strategies to identify and stratify individuals at risk of developing PDAC [*i.e.* individuals with hereditary risk (HR), mucinous cystic lesions (MCLs) and new-late onset diabetes mellitus (NLOD)] are urgently needed. Endoscopic ultrasound (EUS) is one of the imaging modalities with better performance for the study of the pancreas. In turn, carbohydrate antigen 19-9 (CA 19-9), the only biomarker approved for clinical use, is still imperfect as it lacks sensitivity and specificity. Glypican-1 (GPC1) represents a promising candidate since it has been demonstrated to be overexpressed in circulating exosomes (crExos) of patients with PDAC, possibly allowing early detection.

Research motivation

To contribute to further evaluate the capacity of GPC1$^+$ crExos to act as a potential biomarker for the investigation of individuals at risk for PDAC development, allowing for the early detection of the disease or its high-grade precursor lesions. Ultimately, we aim to contribute to improve patient's survival.

Research objectives

We aimed to determine the capacity of GPC1$^+$ crExos to identify individuals at higher risk to develop PDAC by comparing EUS pancreatic abnormalities (PA) with its levels within specific risk groups: HR, MCL and NLOD.

Research methods

We conducted a cross-sectional study with a prospective unicentric cohort including individuals with HR, MCL and NLOD, along with a control group (CG). All subjects were submitted to EUS at time of inclusion, with detailed characterization of detected PA. At the same time, blood samples were analyzed for GPC1$^+$ crExos and CA 19-9 by flow cytometry and ELISA, respectively. EUS-guided tissue acquisition was performed whenever necessary. SPSS® 27.0 version was used for statistical analysis and all graphs were created using GraphPad Prism 7.

Research results

We found that: Individuals harboring MCL globally presented with the highest levels of GPC1$^+$ crExos;

these levels were increased in the presence of worrisome features and or high-risk stigmata characterized by EUS; GPC1$^+$ crExos levels were also elevated among individuals with HR for PDAC (predominantly in those with personal history of cancer), even in absence of harmful PA in EUS examination; and NLOD patients presented with GPC1$^+$ crExos levels as low as those observed in the CG.

Research conclusions

Our study supports the role of GPC1$^+$ crExos in the diagnosis and stratification of PDAC precursor lesions, namely MCL, and its eventual capacity in signaling individuals with genetic predisposition for this neoplasia, even when no harmful PA are detected by EUS.

Research perspectives

Our data encourage longitudinal studies to confirm the potential of exosomal GPC1 as a biomarker to be used in the future in the management of individuals at risk for PDAC.

ACKNOWLEDGEMENTS

The authors acknowledge the support of the Translational Cytometry i3S Scientific Platform and the collaboration of Catarina Meireles MD, Elvira Sampaio MD, Liliana Silva MD and Mariana Santos MD in patient management.

FOOTNOTES

Author contributions: Moutinho-Ribeiro P was the main project investigator, was responsible for patient selection and sample collection, performed pancreatic endoscopic ultrasound, and wrote the initial manuscript; Batista IA participated in the sample processing, supervised and collected the data, performed the data analyses, and supported the manuscript writing; Quintas ST participated in the sample processing, data collection and analyses, assembled the figures, and supported the manuscript writing; Adem B participated in the sample processing and supported the data analyses; Silva M participated in the data collection and performed the statistical analyses; Morais R, Peixoto A, Coelho R, Costa-Moreira P, and Medas R participated in patient observation, data collection, and database management; Medas R performed the statistical analyses; Lopes S and Vilas-Boas F performed the pancreatic endoscopic ultrasound; Baptista M, Dias-Silva D, Esteves AL, and Martins F participated in patient observation and data collection; Lopes J, Barroca H, and Carneiro F performed the cytological and histological examination of the pancreatic specimens; Macedo G conceived and designed the study, interpreted the data analyses, and critically reviewed the manuscript; Melo SA conceived and designed the study, supervised the data analyses, and critically reviewed the manuscript; All authors approved the final version to be published.

Supported by Guilherme Macedo team was supported by the Portuguese Society of Digestive Endoscopy (SPED) 2017 Research Grant, No. SG/CHSJ-A2017; Norte Portugal Regional Programme (NORTE 2020) under the PORTUGAL 2020 Partnership Agreement through the European Regional Development Fund (ERDF) to Sonia A Melo, No. NORTE-01-0145-FEDER-000029; National Funds through Foundation for Science and Technology (FCT) to Sonia A Melo, No. POCI-01-0145-FEDER-32189; and Foundation for Science and Technology (FCT) to Bárbara Adem and Ines A Batista, No. PD/BD/135546/2018 and No. SFRH/BD/144854/2019.

Institutional review board statement: This study was reviewed and approved by the Ethics Committee of *Centro Hospitalar Universitário de São João* (CHUSJ), Porto, Portugal, No. CES 327-15.

Informed consent statement: All study participants or their legal guardian provided informed written consent about personal and medical data collection prior to study enrolment.

Conflict-of-interest statement: Sónia A Melo holds patents in the field of exosomes biology and are licensed to Codiak Biosciences, Inc. All other authors have no conflicts of interest to declare.

Data sharing statement: No additional data are available.

Open-Access: This article is an open-access article that was selected by an in-house editor and fully peer-reviewed by external reviewers. It is distributed in accordance with the Creative Commons Attribution NonCommercial (CC BY-NC 4.0) license, which permits others to distribute, remix, adapt, build upon this work non-commercially, and license their derivative works on different terms, provided the original work is properly cited and the use is non-commercial. See: https://creativecommons.org/Licenses/by-nc/4.0/

Country/Territory of origin: Portugal

ORCID number: Pedro Moutinho-Ribeiro 0000-0002-4782-6489; Ines A Batista 0000-0003-0321-7902; Sofia T Quintas 0000-0002-4190-3527; Bárbara Adem 0000-0003-0398-1185; Marco Silva 0000-0001-8215-1213; Rui Morais 0000-0003-1293-3353;

Armando Peixoto 0000-0003-3994-2882; Rosa Coelho 0000-0003-2706-2351; Pedro Costa-Moreira 0000-0003-0981-2497; Renato Medas 0000-0002-1892-2666; Susana Lopes 0000-0002-0407-6016; Filipe Vilas-Boas 0000-0001-7041-0863; Manuela Baptista 0000-0002-4306-769X; Diogo Dias-Silva 0000-0001-7367-6915; Ana L Esteves 0000-0001-8844-7939; Filipa Martins 0000-0002-5753-9811; Joanne Lopes 0000-0002-2339-2823; Helena Barroca 0000-0001-5684-3523; Fátima Carneiro 0000-0002-1964-1006; Guilherme Macedo 0000-0002-9387-9872; Sonia A Melo 0000-0002-2291-4263.

S-Editor: Fan JR
L-Editor: Filipodia
P-Editor: Fan JR

REFERENCES

1 **Sung H**, Ferlay J, Siegel RL, Laversanne M, Soerjomataram I, Jemal A, Bray F. Global Cancer Statistics 2020: GLOBOCAN Estimates of Incidence and Mortality Worldwide for 36 Cancers in 185 Countries. *CA Cancer J Clin* 2021; **71**: 209-249 [PMID: 33538338 DOI: 10.3322/caac.21660]
2 **Moutinho-Ribeiro P**, Coelho R, Giovannini M, Macedo G. Pancreatic cancer screening: Still a delusion? *Pancreatology* 2017; **17**: 754-765 [PMID: 28739291 DOI: 10.1016/j.pan.2017.07.001]
3 **Singhi AD**, Koay EJ, Chari ST, Maitra A. Early Detection of Pancreatic Cancer: Opportunities and Challenges. *Gastroenterology* 2019; **156**: 2024-2040 [PMID: 30721664 DOI: 10.1053/j.gastro.2019.01.259]
4 **Moutinho-Ribeiro P**, Iglesias-Garcia J, Gaspar R, Macedo G. Early pancreatic cancer - The role of endoscopic ultrasound with or without tissue acquisition in diagnosis and staging. *Dig Liver Dis* 2019; **51**: 4-9 [PMID: 30337098 DOI: 10.1016/j.dld.2018.09.027]
5 **Bhutani MS**, Koduru P, Joshi V, Saxena P, Suzuki R, Irisawa A, Yamao K. The role of endoscopic ultrasound in pancreatic cancer screening. *Endosc Ultrasound* 2016; **5**: 8-16 [PMID: 26879161 DOI: 10.4103/2303-9027.175876]
6 **Luz LP**, Al-Haddad MA, Sey MS, DeWitt JM. Applications of endoscopic ultrasound in pancreatic cancer. *World J Gastroenterol* 2014; **20**: 7808-7818 [PMID: 24976719 DOI: 10.3748/wjg.v20.i24.7808]
7 **Hruban RH**, Maitra A, Kern SE, Goggins M. Precursors to pancreatic cancer. *Gastroenterol Clin North Am* 2007; **36**: 831-849, vi [PMID: 17996793 DOI: 10.1016/j.gtc.2007.08.012]
8 **Pereira SP**, Oldfield L, Ney A, Hart PA, Keane MG, Pandol SJ, Li D, Greenhalf W, Jeon CY, Koay EJ, Almario CV, Halloran C, Lennon AM, Costello E. Early detection of pancreatic cancer. *Lancet Gastroenterol Hepatol* 2020; **5**: 698-710 [PMID: 32135127 DOI: 10.1016/S2468-1253(19)30416-9]
9 **Al-Hawary MM**, Francis IR, Chari ST, Fishman EK, Hough DM, Lu DS, Macari M, Megibow AJ, Miller FH, Mortele KJ, Merchant NB, Minter RM, Tamm EP, Sahani DV, Simeone DM. Pancreatic ductal adenocarcinoma radiology reporting template: consensus statement of the society of abdominal radiology and the american pancreatic association. *Gastroenterology* 2014; **146**: 291-304.e1 [PMID: 24355035 DOI: 10.1053/j.gastro.2013.11.004]
10 **Ballehaninna UK**, Chamberlain RS. The clinical utility of serum CA 19-9 in the diagnosis, prognosis and management of pancreatic adenocarcinoma: An evidence based appraisal. *J Gastrointest Oncol* 2012; **3**: 105-119 [PMID: 22811878 DOI: 10.3978/j.issn.2078-6891.2011.021]
11 **Yadav DK**, Bai X, Yadav RK, Singh A, Li G, Ma T, Chen W, Liang T. Liquid biopsy in pancreatic cancer: the beginning of a new era. *Oncotarget* 2018; **9**: 26900-26933 [PMID: 29928492 DOI: 10.18632/oncotarget.24809]
12 **Buscail E**, Maulat C, Muscari F, Chiche L, Cordelier P, Dabernat S, Alix-Panabières C, Buscail L. Liquid Biopsy Approach for Pancreatic Ductal Adenocarcinoma. *Cancers (Basel)* 2019; **11** [PMID: 31248203 DOI: 10.3390/cancers11060852]
13 **Melo SA**, Luecke LB, Kahlert C, Fernandez AF, Gammon ST, Kaye J, LeBleu VS, Mittendorf EA, Weitz J, Rahbari N, Reissfelder C, Pilarsky C, Fraga MF, Piwnica-Worms D, Kalluri R. Glypican-1 identifies cancer exosomes and detects early pancreatic cancer. *Nature* 2015; **523**: 177-182 [PMID: 26106858 DOI: 10.1038/nature14581]
14 **Lewis JM**, Vyas AD, Qiu Y, Messer KS, White R, Heller MJ. Integrated Analysis of Exosomal Protein Biomarkers on Alternating Current Electrokinetic Chips Enables Rapid Detection of Pancreatic Cancer in Patient Blood. *ACS Nano* 2018; **12**: 3311-3320 [PMID: 29570265 DOI: 10.1021/acsnano.7b08199]
15 **Xiao D**, Dong Z, Zhen L, Xia G, Huang X, Wang T, Guo H, Yang B, Xu C, Wu W, Zhao X, Xu H. Combined Exosomal GPC1, CD82, and Serum CA19-9 as Multiplex Targets: A Specific, Sensitive, and Reproducible Detection Panel for the Diagnosis of Pancreatic Cancer. *Mol Cancer Res* 2020; **18**: 300-310 [PMID: 31662449 DOI: 10.1158/1541-7786.MCR-19-0588]
16 **Qian JY**, Tan YL, Zhang Y, Yang YF, Li XQ. Prognostic value of glypican-1 for patients with advanced pancreatic cancer following regional intra-arterial chemotherapy. *Oncol Lett* 2018; **16**: 1253-1258 [PMID: 29963198 DOI: 10.3892/ol.2018.8701]
17 **Zhou CY**, Dong YP, Sun X, Sui X, Zhu H, Zhao YQ, Zhang YY, Mason C, Zhu Q, Han SX. High levels of serum glypican-1 indicate poor prognosis in pancreatic ductal adenocarcinoma. *Cancer Med* 2018; **7**: 5525-5533 [PMID: 30358133 DOI: 10.1002/cam4.1833]
18 **Frampton AE**, Prado MM, López-Jiménez E, Fajardo-Puerta AB, Jawad ZAR, Lawton P, Giovannetti E, Habib NA, Castellano L, Stebbing J, Krell J, Jiao LR. Glypican-1 is enriched in circulating-exosomes in pancreatic cancer and correlates with tumor burden. *Oncotarget* 2018; **9**: 19006-19013 [PMID: 29721179 DOI: 10.18632/oncotarget.24873]
19 **Lucien F**, Lac V, Billadeau DD, Borgida A, Gallinger S, Leong HS. Glypican-1 and glycoprotein 2 bearing extracellular vesicles do not discern pancreatic cancer from benign pancreatic diseases. *Oncotarget* 2019; **10**: 1045-1055 [PMID: 30800217 DOI: 10.18632/oncotarget.26620]
20 **Canto MI**, Harinck F, Hruban RH, Offerhaus GJ, Poley JW, Kamel I, Nio Y, Schulick RS, Bassi C, Kluijt I, Levy MJ,

Chak A, Fockens P, Goggins M, Bruno M; International Cancer of Pancreas Screening (CAPS) Consortium. International Cancer of the Pancreas Screening (CAPS) Consortium summit on the management of patients with increased risk for familial pancreatic cancer. *Gut* 2013; **62**: 339-347 [PMID: 23135763 DOI: 10.1136/gutjnl-2012-303108]

21 **Goggins M**, Overbeek KA, Brand R, Syngal S, Del Chiaro M, Bartsch DK, Bassi C, Carrato A, Farrell J, Fishman EK, Fockens P, Gress TM, van Hooft JE, Hruban RH, Kastrinos F, Klein A, Lennon AM, Lucas A, Park W, Rustgi A, Simeone D, Stoffel E, Vasen HFA, Cahen DL, Canto MI, Bruno M; International Cancer of the Pancreas Screening (CAPS) consortium. Management of patients with increased risk for familial pancreatic cancer: updated recommendations from the International Cancer of the Pancreas Screening (CAPS) Consortium. *Gut* 2020; **69**: 7-17 [PMID: 31672839 DOI: 10.1136/gutjnl-2019-319352]

22 **Aslanian HR**, Lee JH, Canto MI. AGA Clinical Practice Update on Pancreas Cancer Screening in High-Risk Individuals: Expert Review. *Gastroenterology* 2020; **159**: 358-362 [PMID: 32416142 DOI: 10.1053/j.gastro.2020.03.088]

23 **Pannala R**, Leirness JB, Bamlet WR, Basu A, Petersen GM, Chari ST. Prevalence and clinical profile of pancreatic cancer-associated diabetes mellitus. *Gastroenterology* 2008; **134**: 981-987 [PMID: 18395079 DOI: 10.1053/j.gastro.2008.01.039]

24 **Sharma A**, Smyrk TC, Levy MJ, Topazian MA, Chari ST. Fasting Blood Glucose Levels Provide Estimate of Duration and Progression of Pancreatic Cancer Before Diagnosis. *Gastroenterology* 2018; **155**: 490-500.e2 [PMID: 29723506 DOI: 10.1053/j.gastro.2018.04.025]

25 **Sharma A**, Kandlakunta H, Nagpal SJS, Feng Z, Hoos W, Petersen GM, Chari ST. Model to Determine Risk of Pancreatic Cancer in Patients With New-Onset Diabetes. *Gastroenterology* 2018; **155**: 730-739.e3 [PMID: 29775599 DOI: 10.1053/j.gastro.2018.05.023]

26 **Boursi B**, Finkelman B, Giantonio BJ, Haynes K, Rustgi AK, Rhim AD, Mamtani R, Yang YX. A Clinical Prediction Model to Assess Risk for Pancreatic Cancer Among Patients With New-Onset Diabetes. *Gastroenterology* 2017; **152**: 840-850.e3 [PMID: 27923728 DOI: 10.1053/j.gastro.2016.11.046]

27 **Chari ST**, Leibson CL, Rabe KG, Ransom J, de Andrade M, Petersen GM. Probability of pancreatic cancer following diabetes: a population-based study. *Gastroenterology* 2005; **129**: 504-511 [PMID: 16083707 DOI: 10.1016/j.gastro.2005.05.007]

28 **Moutinho-Ribeiro P**, Adem B, Batista I, Silva M, Silva S, Ruivo CF, Morais R, Peixoto A, Coelho R, Costa-Moreira P, Lopes S, Vilas-Boas F, Durães C, Lopes J, Barroca H, Carneiro F, Melo SA, Macedo G. Exosomal glypican-1 discriminates pancreatic ductal adenocarcinoma from chronic pancreatitis. *Dig Liver Dis* 2021 [PMID: 34840127 DOI: 10.1016/j.dld.2021.10.012]

29 **Tanaka M**, Fernández-Del Castillo C, Kamisawa T, Jang JY, Levy P, Ohtsuka T, Salvia R, Shimizu Y, Tada M, Wolfgang CL. Revisions of international consensus Fukuoka guidelines for the management of IPMN of the pancreas. *Pancreatology* 2017; **17**: 738-753 [PMID: 28735806 DOI: 10.1016/j.pan.2017.07.007]

30 **Reddy RP**, Smyrk TC, Zapiach M, Levy MJ, Pearson RK, Clain JE, Farnell MB, Sarr MG, Chari ST. Pancreatic mucinous cystic neoplasm defined by ovarian stroma: demographics, clinical features, and prevalence of cancer. *Clin Gastroenterol Hepatol* 2004; **2**: 1026-1031 [PMID: 15551256 DOI: 10.1016/s1542-3565(04)00450-1]

31 **McCarty TR**, Garg R, Rustagi T. Pancreatic cyst fluid glucose in differentiating mucinous from nonmucinous pancreatic cysts: a systematic review and meta-analysis. *Gastrointest Endosc* 2021; **94**: 698-712.e6 [PMID: 33964311 DOI: 10.1016/j.gie.2021.04.025]

32 **Overbeek KA**, Levink IJM, Koopmann BDM, Harinck F, Konings ICAW, Ausems MGEM, Wagner A, Fockens P, van Eijck CH, Groot Koerkamp B, Busch ORC, Besselink MG, Bastiaansen BAJ, van Driel LMJW, Erler NS, Vleggaar FP, Poley JW, Cahen DL, van Hooft JE, Bruno MJ; Dutch Familial Pancreatic Cancer Surveillance Study Group. Long-term yield of pancreatic cancer surveillance in high-risk individuals. *Gut* 2022; **71**: 1152-1160 [PMID: 33820756 DOI: 10.1136/gutjnl-2020-323611]

33 **DaVee T**, Coronel E, Papafragkakis C, Thaiudom S, Lanke G, Chakinala RC, Nogueras González GM, Bhutani MS, Ross WA, Weston BR, Lee JH. Pancreatic cancer screening in high-risk individuals with germline genetic mutations. *Gastrointest Endosc* 2018; **87**: 1443-1450 [PMID: 29309780 DOI: 10.1016/j.gie.2017.12.019]

34 **American Diabetes Association**. 2. Classification and Diagnosis of Diabetes: *Standards of Medical Care in Diabetes-2021 . Diabetes Care* 2021; **44**: S15-S33 [PMID: 33298413 DOI: 10.2337/dc21-S002]

35 **Lorenzo D**, Rebours V, Maire F, Palazzo M, Gonzalez JM, Vullierme MP, Aubert A, Hammel P, Lévy P, de Mestier L. Role of endoscopic ultrasound in the screening and follow-up of high-risk individuals for familial pancreatic cancer. *World J Gastroenterol* 2019; **25**: 5082-5096 [PMID: 31558858 DOI: 10.3748/wjg.v25.i34.5082]

36 **Canto MI**, Hruban RH, Fishman EK, Kamel IR, Schulick R, Zhang Z, Topazian M, Takahashi N, Fletcher J, Petersen G, Klein AP, Axilbund J, Griffin C, Syngal S, Saltzman JR, Mortele KJ, Lee J, Tamm E, Vikram R, Bhosale P, Margolis D, Farrell J, Goggins M; American Cancer of the Pancreas Screening (CAPS) Consortium. Frequent detection of pancreatic lesions in asymptomatic high-risk individuals. *Gastroenterology* 2012; **142**: 796-804; quiz e14 [PMID: 22245846 DOI: 10.1053/j.gastro.2012.01.005]

37 **Pitman MB**, Centeno BA, Ali SZ, Genevay M, Stelow E, Mino-Kenudson M, Castillo CF, Schmidt CM, Brugge WR, Layfield LJ. Standardized terminology and nomenclature for pancreatobiliary cytology: The Papanicolaou Society of Cytopathology Guidelines. *Cytojournal* 2014; **11**: 3 [PMID: 25191517 DOI: 10.4103/1742-6413.133343]

38 **Moutinho-Ribeiro P**, Costa-Moreira P, Adem B, Batista I, Almeida M, Barroca H, Lopes J, Carneiro F, Melo SA, Macedo G. Exosomal glypican-1 for risk stratification of pancreatic cystic lesions: A case of pathological progression in the absence of any suspicious imaging finding. *Pancreatology* 2020; **20**: 571-575 [PMID: 32024605 DOI: 10.1016/j.pan.2020.01.015]

39 **Vege SS**, Ziring B, Jain R, Moayyedi P; Clinical Guidelines Committee; American Gastroenterology Association. American gastroenterological association institute guideline on the diagnosis and management of asymptomatic neoplastic pancreatic cysts. *Gastroenterology* 2015; **148**: 819-22; quize12 [PMID: 25805375 DOI: 10.1053/j.gastro.2015.01.015]

40 **Elta GH**, Enestvedt BK, Sauer BG, Lennon AM. ACG Clinical Guideline: Diagnosis and Management of Pancreatic Cysts. *Am J Gastroenterol* 2018; **113**: 464-479 [PMID: 29485131 DOI: 10.1038/ajg.2018.14]

41 **Megibow AJ**, Baker ME, Morgan DE, Kamel IR, Sahani DV, Newman E, Brugge WR, Berland LL, Pandharipande PV. Management of Incidental Pancreatic Cysts: A White Paper of the ACR Incidental Findings Committee. *J Am Coll Radiol*

2017; **14**: 911-923 [PMID: 28533111 DOI: 10.1016/j.jacr.2017.03.010]

42 **European Study Group on Cystic Tumours of the Pancreas**. European evidence-based guidelines on pancreatic cystic neoplasms. *Gut* 2018; **67**: 789-804 [PMID: 29574408 DOI: 10.1136/gutjnl-2018-316027]

43 **Tanaka M**, Fernández-del Castillo C, Adsay V, Chari S, Falconi M, Jang JY, Kimura W, Levy P, Pitman MB, Schmidt CM, Shimizu M, Wolfgang CL, Yamaguchi K, Yamao K; International Association of Pancreatology. International consensus guidelines 2012 for the management of IPMN and MCN of the pancreas. *Pancreatology* 2012; **12**: 183-197 [PMID: 22687371 DOI: 10.1016/j.pan.2012.04.004]

44 **Thornton GD**, McPhail MJ, Nayagam S, Hewitt MJ, Vlavianos P, Monahan KJ. Endoscopic ultrasound guided fine needle aspiration for the diagnosis of pancreatic cystic neoplasms: a meta-analysis. *Pancreatology* 2013; **13**: 48-57 [PMID: 23395570 DOI: 10.1016/j.pan.2012.11.313]

45 **Brugge WR**, Lewandrowski K, Lee-Lewandrowski E, Centeno BA, Szydlo T, Regan S, del Castillo CF, Warshaw AL. Diagnosis of pancreatic cystic neoplasms: a report of the cooperative pancreatic cyst study. *Gastroenterology* 2004; **126**: 1330-1336 [PMID: 15131794 DOI: 10.1053/j.gastro.2004.02.013]

46 **Nimptsch U**, Krautz C, Weber GF, Mansky T, Grützmann R. Nationwide In-hospital Mortality Following Pancreatic Surgery in Germany is Higher than Anticipated. *Ann Surg* 2016; **264**: 1082-1090 [PMID: 26978570 DOI: 10.1097/SLA.0000000000001693]

47 **Kimura W**, Miyata H, Gotoh M, Hirai I, Kenjo A, Kitagawa Y, Shimada M, Baba H, Tomita N, Nakagoe T, Sugihara K, Mori M. A pancreaticoduodenectomy risk model derived from 8575 cases from a national single-race population (Japanese) using a web-based data entry system: the 30-day and in-hospital mortality rates for pancreaticoduodenectomy. *Ann Surg* 2014; **259**: 773-780 [PMID: 24253151 DOI: 10.1097/SLA.0000000000000263]

48 **Moutinho-Ribeiro P**, Santos A, Batista I, Adem B, Silva S, Morais R, Coelho R, Lopes S, Vilas-Boas F, Baptista M, Barroca H, Machado J, Carneiro F, Melo SA, Macedo G. Exosomal Glypican-1 and Pancreatic Adenocarcinoma: Prime Time for Early Diagnosis? *Am J Gastroenterol* 2018; **113**: S44 [DOI: 10.14309/00000434-201810001-00079]

49 **Moutinho-Ribeiro P**, Silva S, Adem B, Silva M, Lopes S, Vilas-Boas F, Melo S, Macedo G. Glipican-1 circulating exosomes levels are higher in pancreatic adenocarcinoma and cystic mucinous neoplasms than in other associated risk groups for pancreatic cancer: Clues for early diagnosis? *Pancreatology* 2017; **17**: S63-S64 [DOI: 10.1016/j.pan.2017.07.219]

50 **Maitra A**, Sharma A, Brand RE, Van Den Eeden SK, Fisher WE, Hart PA, Hughes SJ, Mather KJ, Pandol SJ, Park WG, Feng Z, Serrano J, Rinaudo JAS, Srivastava S, Chari ST; Consortium for the Study of Chronic Pancreatitis, Diabetes, and Pancreatic Cancer (CPDPC). A Prospective Study to Establish a New-Onset Diabetes Cohort: From the Consortium for the Study of Chronic Pancreatitis, Diabetes, and Pancreatic Cancer. *Pancreas* 2018; **47**: 1244-1248 [PMID: 30325864 DOI: 10.1097/MPA.0000000000001169]

World Journal of Gastroenterology

Submit a Manuscript: https://www.f6publishing.com

World J Gastroenterol 2022 August 21; 28(31): 4328-4337

DOI: 10.3748/wjg.v28.i31.4328

ISSN 1007-9327 (print) ISSN 2219-2840 (online)

ORIGINAL ARTICLE

Basic Study

Duodenal-jejunal bypass reduces serum ceramides *via* inhibiting intestinal bile acid-farnesoid X receptor pathway

Zhi-Qiang Cheng, Tong-Ming Liu, Peng-Fei Ren, Chang Chen, Yan-Lei Wang, Yong Dai, Xiang Zhang

Specialty type: Gastroenterology and hepatology

Provenance and peer review: Unsolicited article; Externally peer reviewed

Peer-review model: Single blind

Peer-review report's scientific quality classification

Grade A (Excellent): 0
Grade B (Very good): B, B, B
Grade C (Good): 0
Grade D (Fair): 0
Grade E (Poor): 0

P-Reviewer: Becchetti C, Switzerland; Cereatti F, Italy; Pazos F, Spain

Received: March 11, 2022
Peer-review started: March 11, 2022
First decision: May 10, 2022
Revised: May 12, 2022
Accepted: July 25, 2022
Article in press: July 25, 2022
Published online: August 21, 2022

Zhi-Qiang Cheng, Chang Chen, Yan-Lei Wang, Yong Dai, Xiang Zhang, Department of General Surgery, Qilu Hospital of Shandong University, Jinan 250012, Shandong Province, China

Tong-Ming Liu, Department of Colorectal and Anal Surgery, Feicheng Hospital Affiliated to Shandong First Medical University, Feicheng 271600, Shandong Province, China

Peng-Fei Ren, Department of General Surgery, Lincheng People's Hospital, Dezhou 253500, Shandong Province, China

Corresponding author: Xiang Zhang, MD, PhD, Surgeon, Surgical Oncologist, Department of General Surgery, Qilu Hospital of Shandong University, No. 107 West Wenhua Road, Jinan 250012, Shandong Province, China. xiang.zhang02@hotmail.com

Abstract

BACKGROUND

Bile acids play an important role in the amelioration of type 2 diabetes following duodenal-jejunal bypass (DJB). Serum bile acids are elevated postoperatively. However, the clinical relevance is not known. Bile acids in the peripheral circulation reflect the amount of bile acids in the gut. Therefore, a further investigation of luminal bile acids following DJB is of great significance.

AIM

To investigate changes of luminal bile acids following DJB.

METHODS

Salicylhydroxamic acid (SHAM), DJB, and DJB with oral chenodeoxycholic acid (CDCA) supplementation were performed in a high-fat-diet/streptozotocin-induced diabetic rat model. Body weight, energy intake, oral glucose tolerance test, luminal bile acids, serum ceramides and intestinal ceramide synthesis were analyzed at week 12 postoperatively.

RESULTS

Compared to SHAM, DJB achieved rapid and durable improvement in glucose tolerance and led to increased total luminal bile acid concentrations with preferentially increased proportion of farnesoid X receptor (FXR) - inhibitory bile acids within the common limb. Intestinal ceramide synthesis was repressed with decreased serum ceramides, and this phenomenon could be partially antagonized by luminal supplementation of FXR activating bile acid CDCA.

CONCLUSION
DJB significantly changes luminal bile acid composition with increased proportion FXR-inhibitory bile acids and reduces serum ceramide levels. There observations suggest a novel mechanism of bile acids in metabolic regulation after DJB.

Key Words: Bariatric surgery; Duodenal-jejunal bypass; Farnesoid X receptor; Ceramide; Bile acids; Liver fat accumulation

©The Author(s) 2022. Published by Baishideng Publishing Group Inc. All rights reserved.

Core Tip: Bile acids play an important role in the amelioration of type 2 diabetes following duodenal-jejunal bypass (DJB), and are elevated significantly in the serum postoperatively. Bile acids in the peripheral circulation reflect the amount of bile acids in the gut. Therefore, a further investigation of luminal bile acids following DJB is of great significance. Here we performed DJB in a high-fat diet/streptozotocin-induced diabetic rat model and demonstrated that DJB achieved rapid and durable improvement in glucose tolerance and led to increased total luminal bile acid concentrations with preferentially increased proportion of farnesoid X receptor (FXR) - inhibitory bile acids within the common limb. Intestinal ceramide synthesis was repressed with decreased serum ceramides, and this phenomenon could be partially antagonized by luminal supplementation of FXR activating bile acid (chenodeoxycholic acid). There observations suggest a novel mechanism of bile acids in metabolic regulation after DJB.

Citation: Cheng ZQ, Liu TM, Ren PF, Chen C, Wang YL, Dai Y, Zhang X. Duodenal-jejunal bypass reduces serum ceramides *via* inhibiting intestinal bile acid-farnesoid X receptor pathway. *World J Gastroenterol* 2022; 28(31): 4328-4337
URL: https://www.wjgnet.com/1007-9327/full/v28/i31/4328.htm
DOI: https://dx.doi.org/10.3748/wjg.v28.i31.4328

INTRODUCTION

Duodenal-jejunal bypass (DJB) can induce rapid and durable amelioration of type 2 diabetes mellitus[1-3]. The underlying mechanisms remain incompletely understood. Our previous research has proved that bile acids play an important role in the amelioration of type 2 diabetes following DJB[4], and found that serum taurine-conjugated bile acids are preferentially elevated postoperatively[5]. However, the clinical relevance of the specific alterations of serum bile acids is still not known. Bile acids in the peripheral circulation reflect the amount of bile acids that could not be totally reabsorbed by hepatocytes during the enterohepatic circulation[6]. Therefore, the alterations of serum bile acids might be a secondary change of the bile acids within the gut, and a further investigation of luminal bile acids following DJB is of great significance.

Bile acids are traditionally known as lipid absorption-facilitating agents. It was not until recent years that the role of bile acids as signaling molecules in modulating metabolism has be unveiled. The intestinal lumina, where bile acid concentrations are high, is the main place for bile acid signaling. Two major receptors, including Takeda G-protein-coupled receptor 5 (TGR5) and nuclear farnesoid X receptor (FXR) are responsible for luminal bile acid sensing. TGR5 expression is detected in a variety of enteroendocrine cells and acute exposure of TGR5 to luminal bile acids lead to significant secretion of glucagon-like peptide 1 (GLP-1), which is a vital hormone for maintaining normal incretin effect in type 2 diabetes[7,8]. The interaction between bile acids and FXR is more complicated, as different subtypes of bile acids have distinct effect on the downstream pathway of FXR[9]. Chenodeoxycholic acid (CDCA) represents the most potent FXR stimulator while ursodeoxycholic acid (UDCA) and β-muricholic acid (β MCA) are FXR inhibitors[9-11]. Therefore, the net effect of luminal bile acids on FXR depends on the proportion of FXR-stimulating bile acids rather than the total amount of bile acids.

Intestinal FXR could affect lipid metabolism and this process is closely related to ceramide synthesis. Intestine-selective FXR inhibition downregulates the expression of ceramide synthesis-related genes sphingomyelin phosphodiesterase 3 (Smpd3) and serine palmitoyltransferase long chain base subunit 2 (Sptlc2), resulting in decreased concentrations of ceramides within the small intestine, portal system and peripheral circulation[12]. Decreased ceramides inhibit the expression of sterol regulatory element binding protein-1 (SREBP-1) in the liver[12], which is a key enzyme in the process of hepatic fat accumulation. Coincidentally, the changes in lipid metabolism after intestine-selective FXR inhibition is similar to the changes following DJB that hepatic fat accumulation is alleviated and the key transcriptional regulators and enzymes involved in hepatic *de novo* lipogenesis are downregulated[13]. Therefore, we

hypothesized that the net effect of luminal bile acids on intestinal FXR might be inhibitory after DJB which leads to decreased ceramide synthesis. To test this hypothesis, we measure the changes of individual luminal bile acid and ceramide concentrations within the enterohepatic circulation after DJB in a high-fat diet (HFD)/streptozotocin (STZ)-induced diabetic rat model.

MATERIALS AND METHODS

Animals and surgical procedures

Eight-week-old male Wistar rats (220 g on average, purchased from Huafukang Biotech, China) were individually housed with a 12 h light/dark cycle under constant temperature (24-26 °C) and humidity (50%-70%). All rats were fed with HFD (42% carbohydrate, 18% protein and 40% fat, as a total percentage of calories, Huafukang Biotech, China) with no restriction to tap water for 1 mo to induce insulin resistance. After fasting for 12 h, 30 mg/kg STZ (Sigma Aldrich, United States) dissolved in sodium citrate buffer (pH 4.2) was injected into the peritoneal cavity. Random blood glucose concentrations were measured with a glucometer (Roche Diagnostics, Germany) from tail veins 72 h later. Thirty rats with random blood glucose ≥ 16.7 mmol/L were considered diabetic and were matched into salicylhydroxamic acid (SHAM) group (n = 10), DJB group (n = 10) and DJB + CDCA group (n = 10). One month later, surgery was performed as we previously reported[5]. Body weight and calorie intake were recorded daily. All rats were sacrificed after 12 h fasting at week 12 postoperatively. All procedures involving animals were reviewed and approved by the Ethics Committee on Animal Experiment of Shandong University Qilu Hospital.

CDCA gavage

Without fasting, rats in the DJB + CDCA group were administrated with CDCA suspension (100 mg/kg suspended in 3 mL tap water) by intragastric gavage three times a week since week 5 postoperatively. The gavage procedure ceased after week 11.

Oral glucose tolerance test

At week 4 and week 12, after 12 h fasting, the rats were administrated with 20% of glucose (1 g/kg) by intragastric gavage. Blood glucose concentrations were measured at t = 0, 10, 30, 60 and 120 min.

Blood sample preparation

Peripheral blood samples were collected from the retrobulbar venous plexus after 12 h fasting before sacrificing. Portal venous blood samples were collected directly from the portal vein. After centrifugation, the supernatant was stored at -80 °C until analysis.

Luminal bile acid detection

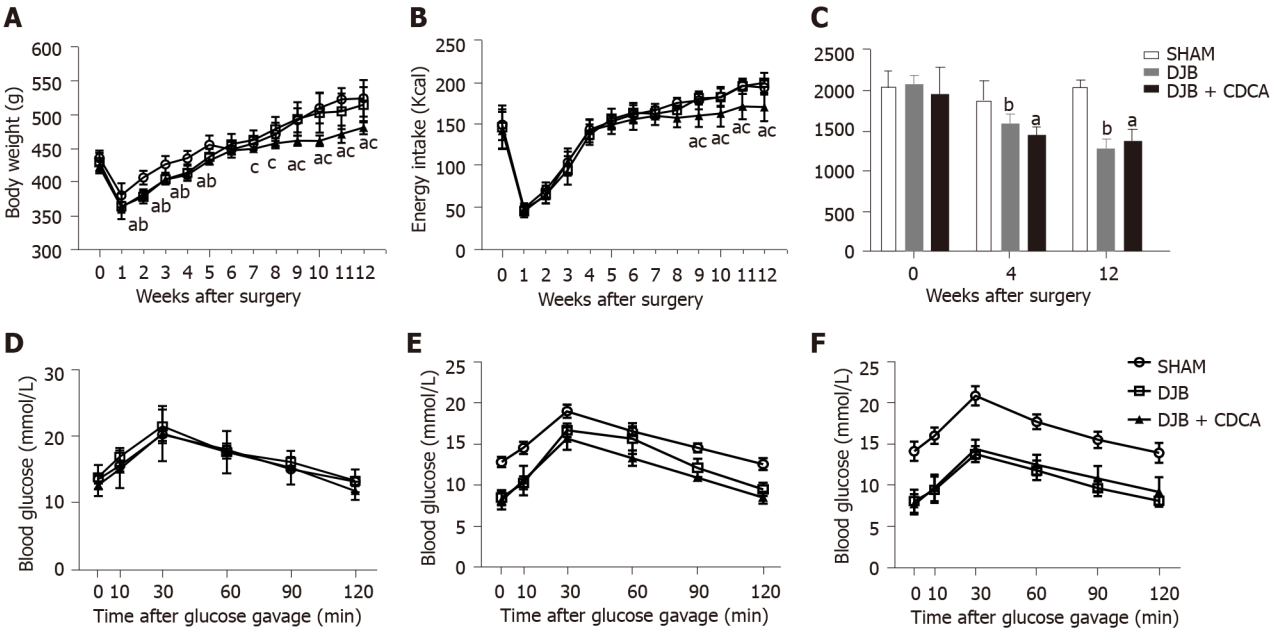
Three independent intestinal segments (3 cm each) was excised at the proximal, medium and distal sites within the common limb, respectively, without prior flushing. The control intestinal segments from SHAM group were excised at the corresponding anatomic location. Total luminal bile acids from intestinal segments were extracted by 9 mL 50 % tert-butyl alcohol for 1 h at 37 °C. After centrifugation, the supernatant was collected for bile acid analysis. Total bile acids were measured by Roche Cobas 8000 system using enzyme cycling method and individual bile acid species was measured using high-pressure liquid chromatography coupled with tandem mass spectrometry as we previously described [5].

Western blot

Small intestinal mucosa were flushed with saline and then scratched. Total protein was extracted by RIPA lysis buffer (KeyGEN, China) with protease and phosphatase inhibitor cocktail (KeyGEN, China) and was quantified using bicinchoninic acid protein assay kit (Beyotime, China). Equivalent amount of small intestinal mucosal protein were loaded on 10% sodium dodecyl sulfate-polyacrylamide gel electrophoresis gels (Bio-Rad, United States) and separated by electrophoresis. Then, proteins were transferred onto 0.45 μm polyvinylidene fluoride membranes (Millipore, Ireland). After being blocked in 5 % skim milk powder (Beyotime, China) for 2 h, the membranes were incubated with primary antibodies to Smpd3 (Abcam, United Kingdom) and Sptlc2 (Invitrogen, United States) overnight, followed by incubation in horseradish peroxidase-conjugated secondary antibodies (Proteintech, China) for 60 min. The protein bands were visualized by ECL solution (Millipore, United States) and their density was assessed with LI-COR Odyssey Imager (LI-COR Biosciences, United States).

RNA analysis

The expression of smpd3 and sptlc2 in the small intestine was analyzed by real-ime quantitative polymerase chain reaction (RT-qPCR). RNA was isolated using Trizol reagent (Invitrogen, United States), and the concentration of RNA was measured using the NanoDrop spectrophotometer



DOI: 10.3748/wjg.v28.i31.4328 **Copyright** ©The Author(s) 2022.

Figure 1 Body weight and energy intake from baseline to week 12 after operations as well as oral glucose tolerance test and the corresponding areas under the curves at baseline, week 4 and week 12 after operations. A: Body weight; B: Energy intake; C: Area under the curve of oral glucose tolerance test; D: Oral glucose tolerance test at baseline; E: Oral glucose tolerance test at week 4; F: Oral glucose tolerance test at week 12. $^{a}P < 0.05$, salicylhydroxamic acid *vs* duodenal-jejunal bypass + chenodeoxycholic acid; $^{b}P < 0.05$, salicylhydroxamic acid *vs* duodenal-jejunal bypass. SHAM: Salicylhydroxamic acid; DJB: Duodenal-jejunal bypass; CDCA: Chenodeoxycholic acid.

(NanoDrop Technologies, United States). RNA was then reverse transcribed into complementary DNA (cDNA) using a ReverTra Ace qPCR RT Kit (TOYOBO, Japan). Amplification of messenger RNA (mRNA) was carried out using SYBR Green Real-time PCR Master Mix Kit (TOYOBO, Japan) at a range of temperatures in a Roche Lightcycle 2.0 system (Roche, Switzerland). The housekeeping gene gapdh was used as an internal reference, and mRNA levels for each target were then calculated by the $2^{-\Delta\Delta Ct}$ method. The primers were smpd3 (forward primer: 5′-ACTCGCTCGCAAGGCTCAATAATG-3′, reverse primer: 5′-CTGAAGCTGGCTGCACTGATGG-3′), sptlc2 (forward primer: 5′-CGCCTTCCT-GAAGTGATTGCTCTC-3′, reverse primer: 5′-AGTCTACTACACCACGCCCTGAAG-3′), and gapdh (forward primer: 5′-ACCCTGTTGCTGTAGCCATATTC-3′; reverse primer: 5′-ACCCTGTTGCTGTAGC-CATATTC-3′).

Ceramide detection

Ceramide concentrations peripheral circulation and the portal vein were measured as previously described using Ceramide LIPIDOMIX Mass Spec Standard (#330712X-1EA, Avanti, United States) as standards[14].

Statistical analysis

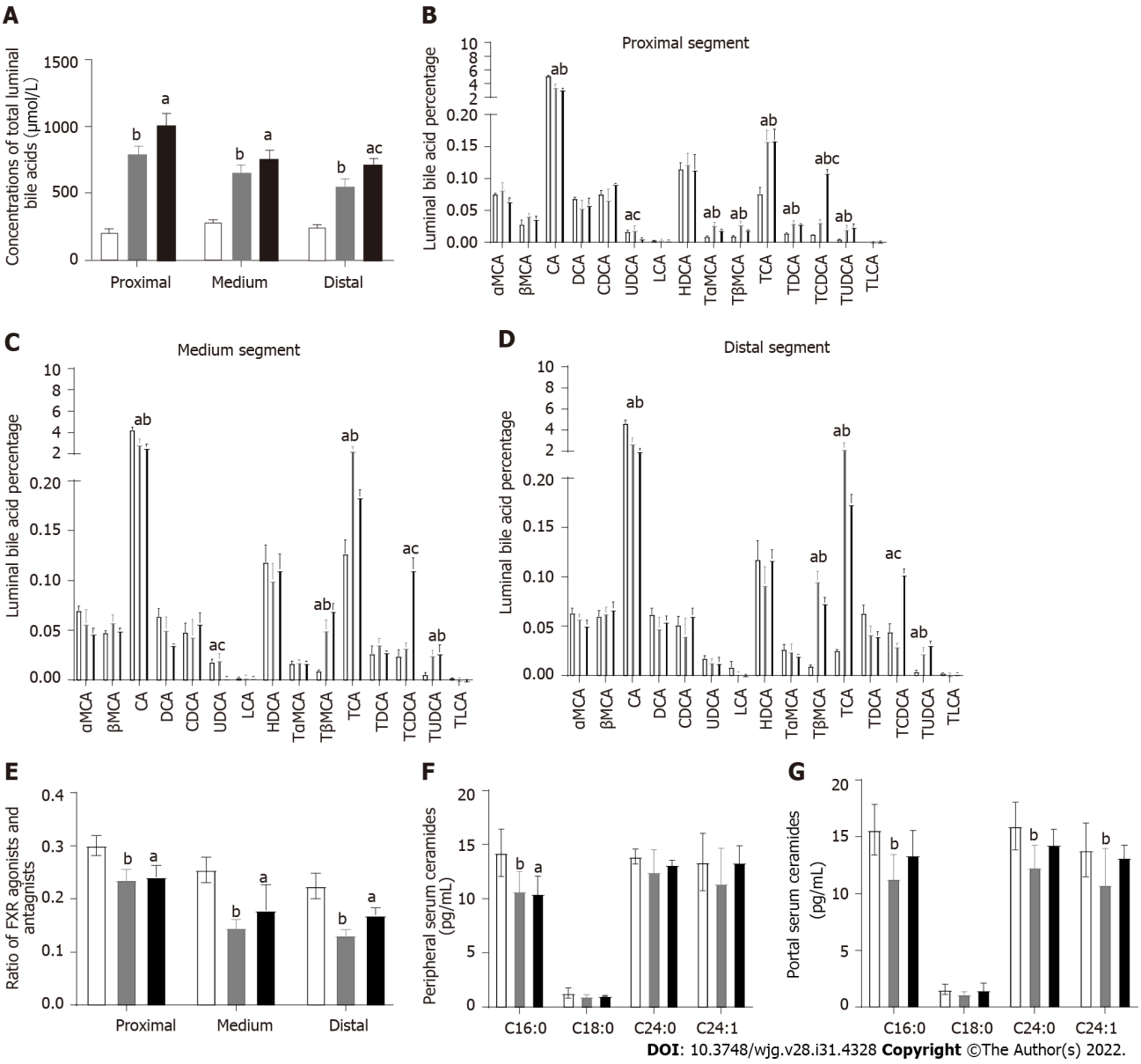
Data are mean ± SEM. Area under the curve (AUC) for oral glucose tolerance test (OGTT) was calculated by trapezoidal integration. Intergroup comparisons were performed by one-way analysis of variance followed by Bonferroni *post hoc* comparisons. $P < 0.05$ was considered statistically significant. All calculations were performed using SPSS version 25.0.

RESULTS

One rat in SHAM group died of intestinal obstruction. Two rats in DJB group and 2 rats in DJB + CDCA group died of anastomotic leak. At the end of the study, the number of rats alive in SHAM, DJB and DJB + CDCA groups were 9, 8 and 8, respectively.

Body weight and energy intake

At baseline, both body weight and energy intake were comparable between three groups. After surgery, both body weight and energy intake decreased sharply in all three groups and increased gradually thereafter. At week 2-5 postoperatively, body weight of the rats in DJB and DJB + CDCA groups was significantly less than that in SHAM group ($P < 0.05$ all). At week 7-12 postoperatively, body weight of



DOI: 10.3748/wjg.v28.i31.4328 **Copyright** ©The Author(s) 2022.

Figure 2 Luminal total and individual bile acid concentrations and ceramide concentrations within the peripheral and portal circulations.
A: Total amount of luminal bile acids; B: Luminal individual bile acid percentage in the proximal; C: Medium segment within the common limb; D: Distal segment within the common limb; E: Ratio of farnesoid X receptor agonist and antagnist within the common limb; F: Peripheral serum ceramides; G: Portal serum ceramides. $^{a}P < 0.05$, salicylhydroxamic acid *vs* duodenal-jejunal bypass + chenodeoxycholic acid; $^{b}P < 0.05$, salicylhydroxamic acid *vs* duodenal-jejunal bypass; $^{c}P < 0.05$, duodenal-jejunal bypass *vs* duodenal-jejunal bypass + chenodeoxycholic acid. FXR: Farnesoid X receptor; SHAM: Salicylhydroxamic acid; DJB: Duodenal-jejunal bypass; CDCA: Chenodeoxycholic acid; αMCA: α-muricholic acid; UDCA: Ursodeoxycholic acid; LCA: Lithocholic acid; HDCA: Hyocholic acid; TLCA: Taurine-conjugated lithocholic acid.

the rats in DJB + CDCA group was significantly less than that in DJB group ($P < 0.05$ all) (Figure 1A). At week 9-12 postoperatively, body weight of the rats in DJB + CDCA group was significantly less than that in SHAM group ($P < 0.05$ all). At week 9-12 postoperatively, energy intake of the rats in DJB + CDCA group was significantly less than that in SHAM and DJB groups ($P < 0.05$ all) (Figure 1B).

OGTT

There was no difference in glucose tolerance between three groups at baseline based on AUC_{OGTT}. At week 4 and 12, glucose tolerance was significantly improved with DJB and DJB + CDCA groups compared to SHAM group based on AUC_{OGTT} ($P < 0.05$ each). There was no difference between DJB and DJB + CDCA groups, or between week 4 and week 12 within each group (Figures 1C-F).

Luminal bile acids

Total luminal bile acid concentrations were significantly less with SHAM group compared to both DJB and DJB + CDCA groups in either proximal, medium or distal segment in the common limb ($P < 0.05$ all). In the distal segment, luminal total bile acid concentrations were significantly greater with DJB +

CDCA group than DJB group ($P < 0.05$), while this difference was not significant in the proximal or medium segment (Figure 2A).

In the proximal segment (Figure 2B), CA accounted for over 20% of the total luminal bile acids in all three groups, and was significantly greater with SHAM group than DJB and DJB + CDCA groups ($P < 0.05$). The percentages of α-muricholic acid (αMCA), βMCA, deoxycholic acid, CDCA, lithocholic acid (LCA), hyocholic acid (HDCA), and taurine-conjugated LCA (TLCA) were comparable between all three groups. The percentage of UDCA was less with DJB + CDCA group compared to SHAM and DJB groups ($P < 0.05$). The percentages of taurine-conjugated forms of αMCA, βMCA, CA, DCA, CDCA and UDCA were all greater with DJB and DJB + CDCA groups compared to SHAM group ($P < 0.05$). The percentage of TCDCA was greater with DJB + CDCA group than DJB group ($P < 0.05$).

In the medium segment (Figure 2C), the difference in TαMCA and TDCA between three groups was no longer significant compared to the proximal segment. The percentage of TβMCA increased to more than 5% in DJB and DJB + CDCA groups which was significantly greater than SHAM group ($P < 0.05$). The percentage of TCDCA was comparable between SHAM and DJB groups, which was significantly less than DJB + CDCA group ($P < 0.05$).

In the distal segment (Figure 2D), the percentage of TβMCA, TCA and TUDCA was significantly greater with DJB and DJB + CDCA groups compared to SHAM group ($P < 0.05$), without any difference between the former two groups. The percentage of CA was significantly less with DJB and DJB + CDCA groups compared to SHAM group ($P < 0.05$). There was no difference in the percentage of UDCA between three groups. The percentage of other individual bile acids was comparable to that in the medium segment. The ratio of FXR agonists (including CA, TCA, DCA, TDCA, CDCA, TCDCA, LCA, and TLCA) and antagonists (including αMCA, TαMCA, βMCA, TβMCA, UDCA, TUDCA and HDCA) in DJB and DJB + CDCA groups was decreased compared to SHAM group in either proximal, medium or distal segment ($P < 0.05$). No difference was observed between DJB group and DJB + CDCA group (Figure 2E).

Ceramides

At week 12, in the peripheral circulation, serum C16:0 ceramide concentrations were lower with DJB and DJB + CDCA groups compared to SHAM group ($P < 0.05$); no difference in C18:0, C24:0 or C24:1 ceramides between three groups (Figure 2F). In the portal vein, serum C16:0, C24:0 and C24:1 ceramide concentrations were lower with DJB group compared to SHAM group ($P < 0.05$); there was no difference in either ceramide species between DJB and DJB + CDCA groups or between DJB + CDCA and SHAM groups (Figure 2G).

Expression of Smpd3 and Sptlc2

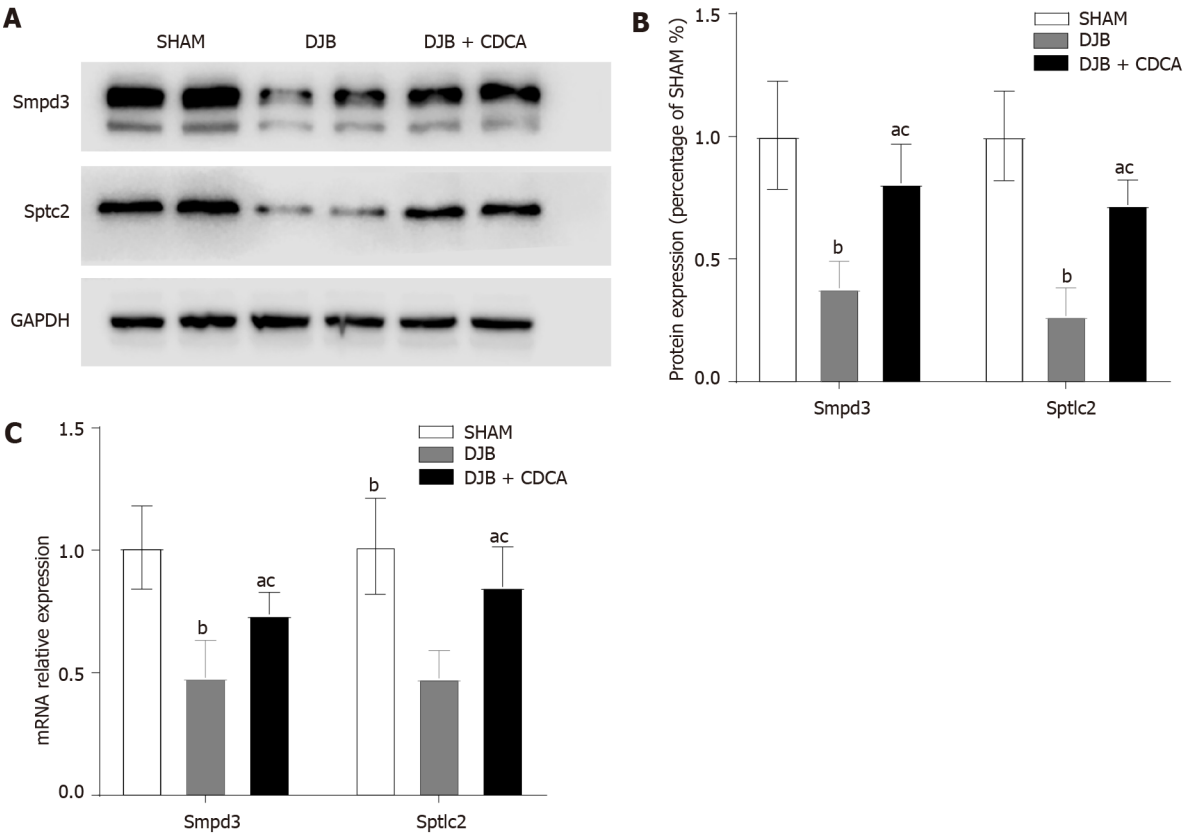
At week 12, the expression of Smpd3 and Sptlc2 were lower with DJB and DJB + CDCA groups than SHAM group at both protein and mRNA levels ($P < 0.05$). Compared to DJB + CDCA group, the expression of Smpd3 and Sptlc2 with DJB group were even lower at both protein and mRNA levels ($P < 0.05$) (Figures 3A, 3B and 3C).

DISCUSSION

In the present study, we performed SHAM, DJB and DJB + CDCA procedures in a HFD/STZ induced diabetic rat model, and for the first time, demonstrated the changes of luminal individual bile acids in the distal small intestine. We also found that the subsequent changes of the bile acids within the distal common limb after DJB elicited inhibitory effect on regional ceramide synthesis and this phenomenon could be partially antagonized by luminal supplementation of FXR activating bile acid CDCA.

DJB was initially designed to investigate the weight loss independent mechanisms of bariatric surgery[3]. This procedure has no effect on weight loss but could induce fast and sustainable amelioration of type 2 diabetes[4]. Consistent with other bariatric procedures[15,16], serum bile acid concentrations were also increased following DJB, and this phenomenon is clearly related to reconstruction of the gastrointestinal tract[5]. *Via* the biliopancreatic limb, bile acids contact the distal small intestine, where luminal bile acid reabsorption mainly occurs, more rapidly and lead to early and increased reabsorption of luminal bile acids in the small intestine. A recent study has proved that in the biliopancreatic limb, increased reabsorption of luminal bile acids has already commenced as a result of highly concentrated bile acids as well as lack of lipids[17]. While in the alimentary limb, only trace amount of luminal bile acids could be detected[4]. Decreased luminal bile acids lead to marked luminal sodium insufficiency, and hence, intestinal uptake of glucose in the alimentary limb is significantly decreased[18], which represents another mechanism in controlling postprandial glucose excursion. The common limb is where food and bile mix up and the major place for intestinal FXR expression. Therefore, we concentrated on bile acid milieu within the common limb rather than the biliopancreatic or alimentary limb because the common limb is the place mostly close to physiological conditions.

To our knowledge, the present study is the first study reporting luminal bile acid changes after DJB. Most clinical and animal studies concentrated on serum or fecal bile acids, as the intestinal lumen is



DOI: 10.3748/wjg.v28.i31.4328 **Copyright** ©The Author(s) 2022.

Figure 3 Expression of ceramide synthesis-related enzyme sphingomyelin phosphodiesterase 3 and serine palmitoyltransferase long chain base subunit 2 at protein and mRNA levels. A: Expression of sphingomyelin phosphodiesterase 3 (Smpd3), serine palmitoyltransferase long chain base subunit 2 (Sptlc2) and GAPDH; B: Expression of Smpd3, Sptlc2 at protein; C: Expression of Smpd3, Sptlc2 mRNA levels. $^{a}P < 0.05$, salicylhydroxamic acid *vs* duodenal-jejunal bypass + chenodeoxycholic acid; $^{b}P < 0.05$, salicylhydroxamic acid *vs* duodenal-jejunal bypass; $^{c}P < 0.05$, duodenal-jejunal bypass *vs* duodenal-jejunal bypass + chenodeoxycholic acid. SHAM: Salicylhydroxamic acid; DJB: Duodenal-jejunal bypass; CDCA: Chenodeoxycholic acid; Smpd3: Sphingomyelin phosphodiesterase 3; Sptlc2: Serine palmitoyltransferase long chain base subunit 2.

deep inside and *in vivo* study of luminal contents, particularly in the small intestine, is technically difficult and ethically challenging. Consistent with our previous findings of serum bile acid changes after DJB, the total amount of luminal bile acids and the proportion of FXR-inhibitory bile acids were both increased. These specific changes have at least two clinical relevance. First, concentrated luminal bile acids stimulate TRG5 on the surface of enteroendocrine cells and leads to potentiated GLP-1 secretion[4]; second, increased proportion of FXR-inhibitory bile acids has inhibited expression of FXR downstream pathways and reduced biosynthesis of intestinal-derived ceramides[12]. Compared to TGR5, FXR appears to be a more important and complicated receptor in metabolic regulation; in the absence of FXR, the ability of bariatric surgery to reduce body weight and improve glucose tolerance is substantially reduced while these metabolic benefits are largely preserved when TGR5 is deficient[19-20]. Whole body FXR knock-out mice were associated with elevated serum triglycerides, cholesterols, free fatty acids and severe liver fat accumulation, but were protected from diet- or genetically- induced obesity[21]. In contrast, liver-specific FXR knock-out mice were not protected from diet-induced obesity and insulin resistance[22], suggesting the distinct role of hepatic and intestinal FXR activation in improving glucose tolerance and insulin resistance. In the small intestine, the role of FXR is controversial. After bariatric surgery, increased serum fibroblast growth factor 19 (FGF19) concentrations have been thought to play a role in the remission of human diabetes[15]. And intestinal FXR activation by luminal bile acids has been thought as a major source of increased serum FGF19. However, no direct evidence was available to confirm the state of intestinal FXR activation, and other tissues may also be sources of FGF19. In contrast, more studies support that intestinal FXR activation would damage metabolic homeostasis by reducing energy expenditure and impairing glucose tolerance[12,14,23]. To investigate the direct influence of bile acids on intestinal FXR, bile diversion procedure was reported by three separate studies[4,24,25], including one from our group[4]. Surprisingly, all three studies showed activated intestinal FXR in response to direct bile acid stimulation. However, in contrast, in DJB, the effect of bile acids on intestinal FXR within the common limb was inhibitory. The discrepancy suggests the biliopancreatic limb may have altered the luminal bile acid composition by premature bile acid reabsorption.

Consistent with our hypothesis, both ceramides in the portal vein and in the peripheral circulation were decreased in response to increased proportion of luminal FXR-inhibitory bile acids. Ceramides are signaling molecules and are associated with obesity and insulin resistance at high concentrations[26]. Decreased ceramides inhibits the expression of SREBP-1 in the liver and alleviates hepatic fat accumulation, thus increasing hepatic insulin sensitivity[12]. Our previous study found that DJB suppressed hepatic *de novo* lipogenesis and alleviates liver fat accumulation by inhibiting SREBP-1. However, the mechanisms underlying were unknown. Based on results from the present study, we have unveiled at least one mechanism accounting for alleviated hepatic fat accumulation. Therefore, manipulation of luminal bile acid composition towards FXR-inhibitory trend may have metabolic beneficial effects.

The present study has several limitations. First, bile acids are mixture with a variety of individual bile acids. As bile acids are mainly conjugated with taurine in rodents[27], we only tested luminal unconjugated and taurine-conjugated bile acids. Second, CDCA is not dissolved in water and we used CDCA suspension for gavage, which may have compromised CDCA absorption to a certain degree. Third, the results from the present study were based on a diabetic rat model and should be interpreted with caution due to species gap.

CONCLUSION

In conclusion, DJB significantly changes luminal bile acid composition with increased proportion of FXR-inhibitory bile acids and reduce serum ceramide levels. There observations suggest a novel mechanism of bile acids in metabolic regulation after DJB.

ARTICLE HIGHLIGHTS

Research background

Bile acids have proved to be signaling molecules in mediating metabolic benefits and circulating bile acids were found to be increased following duodenal-jejunal bypass (DJB). However, whether and how the bile acids take effect in the amelioration of metabolic disorders after DJB remain unknown.

Research motivation

Circulating bile acids reflect the amount of bile acids within the gut. It has been proved that luminal bile acids take effect *via* Takeda G-protein-coupled receptor 5 and nuclear farnesoid X receptor (FXR). However, different subtypes of bile acids have distinct effect on the downstream pathway of FXR and hence, a further investigation of luminal bile acids after DJB is of great significance.

Research objectives

To investigate changes and mechanisms of luminal bile acids in mediating metabolic benefits following DJB.

Research methods

Salicylhydroxamic acid (SHAM), DJB, and DJB with oral chenodeoxycholic acid (CDCA) supplementation were performed in a high-fat-diet/streptozotocin-induced diabetic rat model. Body weight, energy intake, oral glucose tolerance test, luminal bile acids, serum ceramides and intestinal ceramide synthesis were analyzed at week 12 postoperatively.

Research results

Compared to SHAM, DJB achieved rapid and durable improvement in glucose tolerance and led to increased total luminal bile acid concentrations with preferentially increased proportion of FXR - inhibitory bile acids within the common limb. Intestinal ceramide synthesis was repressed with decreased serum ceramides, and this phenomenon could be partially antagonized by luminal supplementation of FXR activating bile acid CDCA.

Research conclusions

DJB significantly changes luminal bile acid composition with increased proportion FXR-inhibitory bile acids and reduces serum ceramide levels. There observations suggest a novel mechanism of bile acids in metabolic regulation after DJB.

Research perspectives

Mechanisms of bile acids in mediating metabolic benefits after bariatric surgery.

FOOTNOTES

Author contributions: Cheng ZQ and Liu TM were involved in animal surgery, data collection, interpretation, statistical analysis, and writing of the manuscript; Ren PF, Chen C, Wang YL and Dai Y were involved in animal surgery, experimental analysis and assist in writing; Cheng ZQ, Dai Y and Zhang X were involved in conception, design, and coordination of the work; Dai Y and Zhang X are the guarantors of this work; and all authors critically reviewed the manuscript and have approved the publication of this final version of the manuscript.

Institutional animal care and use committee statement: All procedures involving animals were reviewed and approved by the Ethics Committee on Animal Experiment of Shandong University Qilu Hospital (KYLL-2017(ZM)-156).

Conflict-of-interest statement: All the authors report no relevant conflicts of interest for this article.

Data sharing statement: No additional data are available.

ARRIVE guidelines statement: The authors have read the ARRIVE guidelines, and the manuscript was prepared and revised according to the ARRIVE guidelines.

Open-Access: This article is an open-access article that was selected by an in-house editor and fully peer-reviewed by external reviewers. It is distributed in accordance with the Creative Commons Attribution NonCommercial (CC BY-NC 4.0) license, which permits others to distribute, remix, adapt, build upon this work non-commercially, and license their derivative works on different terms, provided the original work is properly cited and the use is non-commercial. See: https://creativecommons.org/Licenses/by-nc/4.0/

Country/Territory of origin: China

ORCID number: Zhi-Qiang Cheng 0000-0002-6916-747X; Yan-Lei Wang 0000-0002-4227-0274; Yong Dai 0000-0001-6163-8022; Xiang Zhang 0000-0001-7417-6082.

S-Editor: Wang JJ
L-Editor: A
P-Editor: Wang JJ

REFERENCES

1 **Cohen R**, Caravatto PP, Correa JL, Noujaim P, Petry TZ, Salles JE, Schiavon CA. Glycemic control after stomach-sparing duodenal-jejunal bypass surgery in diabetic patients with low body mass index. *Surg Obes Relat Dis* 2012; **8**: 375-380 [PMID: 22410638 DOI: 10.1016/j.soard.2012.01.017]
2 **Ramos AC**, Galvão Neto MP, de Souza YM, Galvão M, Murakami AH, Silva AC, Canseco EG, Santamaría R, Zambrano TA. Laparoscopic duodenal-jejunal exclusion in the treatment of type 2 diabetes mellitus in patients with BMI<30 kg/m^2 (LBMI). *Obes Surg* 2009; **19**: 307-312 [PMID: 18987919 DOI: 10.1007/s11695-008-9759-5]
3 **Rubino F**, Forgione A, Cummings DE, Vix M, Gnuli D, Mingrone G, Castagneto M, Marescaux J. The mechanism of diabetes control after gastrointestinal bypass surgery reveals a role of the proximal small intestine in the pathophysiology of type 2 diabetes. *Ann Surg* 2006; **244**: 741-749 [PMID: 17060767 DOI: 10.1097/01.sla.0000224726.61448.1b]
4 **Zhang X**, Liu T, Wang Y, Zhong M, Zhang G, Liu S, Wu T, Rayner CK, Hu S. Comparative Effects of Bile Diversion and Duodenal-Jejunal Bypass on Glucose and Lipid Metabolism in Male Diabetic Rats. *Obes Surg* 2016; **26**: 1565-1575 [PMID: 26464241 DOI: 10.1007/s11695-015-1925-y]
5 **Zhang X**, Wang Y, Zhong M, Liu T, Han H, Zhang G, Liu S, Wei M, Wu Q, Hu S. Duodenal-Jejunal Bypass Preferentially Elevates Serum Taurine-Conjugated Bile Acids and Alters Gut Microbiota in a Diabetic Rat Model. *Obes Surg* 2016; **26**: 1890-1899 [PMID: 26715331 DOI: 10.1007/s11695-015-2031-x]
6 **Angelin B**, Björkhem I, Einarsson K, Ewerth S. Hepatic uptake of bile acids in man. Fasting and postprandial concentrations of individual bile acids in portal venous and systemic blood serum. *J Clin Invest* 1982; **70**: 724-731 [PMID: 7119112 DOI: 10.1172/jci110668]
7 **Goldspink DA**, Lu VB, Billing LJ, Larraufie P, Tolhurst G, Gribble FM, Reimann F. Mechanistic insights into the detection of free fatty and bile acids by ileal glucagon-like peptide-1 secreting cells. *Mol Metab* 2018; **7**: 90-101 [PMID: 29167062 DOI: 10.1016/j.molmet.2017.11.005]
8 **Wu T**, Bound MJ, Standfield SD, Gedulin B, Jones KL, Horowitz M, Rayner CK. Effects of rectal administration of taurocholic acid on glucagon-like peptide-1 and peptide YY secretion in healthy humans. *Diabetes Obes Metab* 2013; **15**: 474-477 [PMID: 23181598 DOI: 10.1111/dom.12043]
9 **Makishima M**, Okamoto AY, Repa JJ, Tu H, Learned RM, Luk A, Hull MV, Lustig KD, Mangelsdorf DJ, Shan B. Identification of a nuclear receptor for bile acids. *Science* 1999; **284**: 1362-1365 [PMID: 10334992 DOI: 10.1126/science.284.5418.1362]
10 **Mueller M**, Thorell A, Claudel T, Jha P, Koefeler H, Lackner C, Hoesel B, Fauler G, Stojakovic T, Einarsson C, Marschall HU, Trauner M. Ursodeoxycholic acid exerts farnesoid X receptor-antagonistic effects on bile acid and lipid metabolism in morbid obesity. *J Hepatol* 2015; **62**: 1398-1404 [PMID: 25617503 DOI: 10.1016/j.jhep.2014.12.034]

11 **Sayin SI**, Wahlström A, Felin J, Jäntti S, Marschall HU, Bamberg K, Angelin B, Hyötyläinen T, Orešič M, Bäckhed F. Gut microbiota regulates bile acid metabolism by reducing the levels of tauro-beta-muricholic acid, a naturally occurring FXR antagonist. *Cell Metab* 2013; **17**: 225-235 [PMID: 23395169 DOI: 10.1016/j.cmet.2013.01.003]

12 **Jiang C**, Xie C, Lv Y, Li J, Krausz KW, Shi J, Brocker CN, Desai D, Amin SG, Bisson WH, Liu Y, Gavrilova O, Patterson AD, Gonzalez FJ. Intestine-selective farnesoid X receptor inhibition improves obesity-related metabolic dysfunction. *Nat Commun* 2015; **6**: 10166 [PMID: 26670557 DOI: 10.1038/ncomms10166]

13 **Han H**, Hu C, Wang L, Zhang G, Liu S, Li F, Sun D, Hu S. Duodenal-jejunal bypass surgery suppresses hepatic de novo lipogenesis and alleviates liver fat accumulation in a diabetic rat model. *Obes Surg* 2014; **24**: 2152-2160 [PMID: 24898720 DOI: 10.1007/s11695-014-1308-9]

14 **Jiang C**, Xie C, Li F, Zhang L, Nichols RG, Krausz KW, Cai J, Qi Y, Fang ZZ, Takahashi S, Tanaka N, Desai D, Amin SG, Albert I, Patterson AD, Gonzalez FJ. Intestinal farnesoid X receptor signaling promotes nonalcoholic fatty liver disease. *J Clin Invest* 2015; **125**: 386-402 [PMID: 25500885 DOI: 10.1172/JCI76738]

15 **Gerhard GS**, Styer AM, Wood GC, Roesch SL, Petrick AT, Gabrielsen J, Strodel WE, Still CD, Argyropoulos G. A role for fibroblast growth factor 19 and bile acids in diabetes remission after Roux-en-Y gastric bypass. *Diabetes Care* 2013; **36**: 1859-1864 [PMID: 23801799 DOI: 10.2337/dc12-2255]

16 **Myronovych A**, Kirby M, Ryan KK, Zhang W, Jha P, Setchell KD, Dexheimer PJ, Aronow B, Seeley RJ, Kohli R. Vertical sleeve gastrectomy reduces hepatic steatosis while increasing serum bile acids in a weight-loss-independent manner. *Obesity (Silver Spring)* 2014; **22**: 390-400 [PMID: 23804416 DOI: 10.1002/oby.20548]

17 **Ueno T**, Tanaka N, Imoto H, Maekawa M, Kohyama A, Watanabe K, Motoi F, Kamei T, Unno M, Naitoh T. Mechanism of Bile Acid Reabsorption in the Biliopancreatic Limb After Duodenal-Jejunal Bypass in Rats. *Obes Surg* 2020; **30**: 2528-2537 [PMID: 32291708 DOI: 10.1007/s11695-020-04506-3]

18 **Baud G**, Daoudi M, Hubert T, Raverdy V, Pigeyre M, Hervieux E, Devienne M, Ghunaim M, Bonner C, Quenon A, Pigny P, Klein A, Kerr-Conte J, Gmyr V, Caiazzo R, Pattou F. Bile Diversion in Roux-en-Y Gastric Bypass Modulates Sodium-Dependent Glucose Intestinal Uptake. *Cell Metab* 2016; **23**: 547-553 [PMID: 26924216 DOI: 10.1016/j.cmet.2016.01.018]

19 **Ryan KK**, Tremaroli V, Clemmensen C, Kovatcheva-Datchary P, Myronovych A, Karns R, Wilson-Pérez HE, Sandoval DA, Kohli R, Bäckhed F, Seeley RJ. FXR is a molecular target for the effects of vertical sleeve gastrectomy. *Nature* 2014; **509**: 183-188 [PMID: 24670636 DOI: 10.1038/nature13135]

20 **Hao Z**, Leigh Townsend R, Mumphrey MB, Gettys TW, Yu S, Münzberg H, Morrison CD, Berthoud HR. Roux-en-Y Gastric Bypass Surgery-Induced Weight Loss and Metabolic Improvements Are Similar in TGR5-Deficient and Wildtype Mice. *Obes Surg* 2018; **28**: 3227-3236 [PMID: 29770924 DOI: 10.1007/s11695-018-3297-6]

21 **Wang W**, Cheng Z, Wang Y, Dai Y, Zhang X, Hu S. Role of Bile Acids in Bariatric Surgery. *Front Physiol* 2019; **10**: 374 [PMID: 31001146 DOI: 10.3389/fphys.2019.00374]

22 **Watanabe M**, Houten SM, Wang L, Moschetta A, Mangelsdorf DJ, Heyman RA, Moore DD, Auwerx J. Bile acids lower triglyceride levels *via* a pathway involving FXR, SHP, and SREBP-1c. *J Clin Invest* 2004; **113**: 1408-1418 [PMID: 15146238 DOI: 10.1172/JCI21025]

23 **Watanabe M**, Horai Y, Houten SM, Morimoto K, Sugizaki T, Arita E, Mataki C, Sato H, Tanigawara Y, Schoonjans K, Itoh H, Auwerx J. Lowering bile acid pool size with a synthetic farnesoid X receptor (FXR) agonist induces obesity and diabetes through reduced energy expenditure. *J Biol Chem* 2011; **286**: 26913-26920 [PMID: 21632533 DOI: 10.1074/jbc.M111.248203]

24 **Flynn CR**, Albaugh VL, Cai S, Cheung-Flynn J, Williams PE, Brucker RM, Bordenstein SR, Guo Y, Wasserman DH, Abumrad NN. Bile diversion to the distal small intestine has comparable metabolic benefits to bariatric surgery. *Nat Commun* 2015; **6**: 7715 [PMID: 26197299 DOI: 10.1038/ncomms8715]

25 **Goncalves D**, Barataud A, De Vadder F, Vinera J, Zitoun C, Duchampt A, Mithieux G. Bile Routing Modification Reproduces Key Features of Gastric Bypass in Rat. *Ann Surg* 2015; **262**: 1006-1015 [PMID: 25575265 DOI: 10.1097/SLA.0000000000001121]

26 **Bikman BT**, Summers SA. Ceramides as modulators of cellular and whole-body metabolism. *J Clin Invest* 2011; **121**: 4222-4230 [PMID: 22045572 DOI: 10.1172/JCI57144]

27 **Shonsey EM**, Wheeler J, Johnson M, He D, Falany CN, Falany J, Barnes S. Synthesis of bile acid coenzyme a thioesters in the amino acid conjugation of bile acids. *Methods Enzymol* 2005; **400**: 360-373 [PMID: 16399360 DOI: 10.1016/S0076-6879(05)00021-2]

World Journal of Gastroenterology

Submit a Manuscript: https://www.f6publishing.com

World J Gastroenterol 2022 August 21; 28(31): 4338-4350

DOI: 10.3748/wjg.v28.i31.4338

ISSN 1007-9327 (print) ISSN 2219-2840 (online)

ORIGINAL ARTICLE

Basic Study

Duodenal-jejunal bypass increases intraduodenal bile acids and upregulates duodenal SIRT1 expression in high-fat diet and streptozotocin-induced diabetic rats

Hai-Feng Han, Shao-Zhuang Liu, Xiang Zhang, Meng Wei, Xin Huang, Wen-Bin Yu

Specialty type: Gastroenterology and hepatology

Provenance and peer review: Unsolicited article; Externally peer reviewed.

Peer-review model: Single blind

Peer-review report's scientific quality classification

Grade A (Excellent): 0
Grade B (Very good): B, B, B
Grade C (Good): 0
Grade D (Fair): 0
Grade E (Poor): 0

P-Reviewer: Kim M, South Korea; Madadi-Sanjani O, Germany; Nio M, Japan

Received: May 26, 2022
Peer-review started: May 26, 2022
First decision: June 19, 2022
Revised: June 28, 2022
Accepted: July 25, 2022
Article in press: July 25, 2022
Published online: August 21, 2022

Hai-Feng Han, Shao-Zhuang Liu, Xiang Zhang, Meng Wei, Xin Huang, Wen-Bin Yu, Department of General Surgery, Qilu Hospital, Cheeloo College of Medicine, Shandong University, Jinan 250012, Shandong Province, China

Corresponding author: Wen-Bin Yu, MD, PhD, Chief Doctor, Professor, Department of General Surgery, Qilu Hospital, Cheeloo College of Medicine, Shandong University, No. 107 West Wenhua Road, Jinan 250012, Shandong Province, China. wenbin_yu2003@163.com

Abstract

BACKGROUND

The mechanisms underlying diabetes remission after duodenal-jejunal bypass (DJB) remain elusive. In DJB surgery, the duodenum is excluded. However, the duodenum has emerged as an important regulator of glucose homeostasis, and elevated duodenal SIRT1 leads to improved hepatic insulin sensitivity. After DJB, bile acids (BAs) in the duodenum are not mixed and diluted by the ingested food. And activation of BA receptors promotes SIRT1 expression in many tissues. We hypothesized that BA-mediated upregulation of SIRT1 may contribute to diabetic control after DJB.

AIM

To investigate the surgical effects of DJB on duodenal SIRT1 expression and uncover the potential crosslinks between BAs and SIRT1.

METHODS

Twenty diabetic rats were randomly allocated to the sham (n = 10) and DJB (n = 10) groups. Body weight, food intake, fasting blood glucose (FBG), serum and intraduodenal total BA (TBA) levels were measured accordingly. Oral glucose tolerance test (OGTT) and intraperitoneal pyruvate tolerance test (ipPTT) were performed to evaluate the effects of surgeries on systemic glucose disposal and hepatic gluconeogenesis. The key genes of BA signaling pathway in the duodenal mucosa, including farnesoid X receptor (FXR), small heterodimer partner (SHP), and Takeda G-protein-coupled receptor 5 (TGR5) were evaluated by real-time quantitative polymerase chain reaction 8 wk postoperatively. The duodenal SIRT1, AMPK, and phosphorylated AMPK (p-AMPK) levels were evaluated by western blotting. Rat small intestine epithelial IEC-6 cells were treated with

GW4064 and INT-777 to verify the effects of BAs on SIRT1 expression in enterocytes.

RESULTS

The DJB group exhibited body weight and food intake comparable to those of the sham group at all postoperative time points. The FBG level and area under the curve for the OGTT and ipPTT were significantly lower in the DJB group. The DJB group exhibited higher fasting and postprandial serum TBA levels than the sham group at both 2 and 8 wk postoperatively. At 8 wk after surgery, the DJB group showed higher intraluminal TBA concentration, upregulated mRNA expression of FXR and SHP, and elevated protein expression of SIRT1 and p-AMPK in the descending and horizontal segments of the duodenum. Activation of FXR and TGR5 receptors by GW4064 and INT-777 increased the mRNA and protein expression of SIRT1 and promoted the phosphorylation of AMPK in IEC-6 cells.

CONCLUSION

DJB elevates intraduodenal BA levels and activates the duodenal BA signaling pathway, which may upregulate duodenal SIRT1 and further contribute to improved glucose homeostasis after DJB.

Key Words: Duodenal-jejunal bypass; Diabetes mellitus; Bile acids; Sirtuin 1; Duodenum; High-fat diet

©The Author(s) 2022. Published by Baishideng Publishing Group Inc. All rights reserved.

Core Tip: The intrinsic mechanisms of diabetes remission after duodenal-jejunal bypass (DJB) surgery are complicated. Duodenal SIRT1 is a novel therapeutic target for diabetes, and increased duodenal SIRT1 is linked to improved hepatic insulin sensitivity and decreased hepatic glucose output. The animal study demonstrated that DJB increased intraduodenal bile acid (BA) levels, activated the BA signaling pathway, and upregulated SIRT1 expression in the duodenal mucosa. Our cell experiments proved that farnesoid X receptor and Takeda G-protein-coupled receptor 5 activation increased SIRT1 expression in rat small intestine epithelial cells, indicating that increased intraluminal BAs and activation of BA receptors contributed to increased duodenal SIRT1 after DJB.

Citation: Han HF, Liu SZ, Zhang X, Wei M, Huang X, Yu WB. Duodenal-jejunal bypass increases intraduodenal bile acids and upregulates duodenal SIRT1 expression in high-fat diet and streptozotocin-induced diabetic rats. *World J Gastroenterol* 2022; 28(31): 4338-4350

URL: https://www.wjgnet.com/1007-9327/full/v28/i31/4338.htm

DOI: https://dx.doi.org/10.3748/wjg.v28.i31.4338

INTRODUCTION

Diabetes is one of the fastest-growing global health issues. The International Diabetes Federation reported that the global prevalence of diabetes in adults was approximately 10.5% in 2021, expected to rise to 12.2% in 2045[1]. Bariatric surgery is much more effective and persistent in diabetes control than conventional medical therapy[2]. Duodenal-jejunal bypass (DJB) is a well-designed experimental procedure investigating the weight-independent anti-diabetic mechanisms of Roux-en-Y gastric bypass (RYGB). It can improve glucose homeostasis in both diabetic rats and patients[3-5], however, the underlying mechanisms remain unclear. A critical anatomical alteration of DJB is the exclusion of the duodenum. In addition, DJB liner, which mimics the duodenal-jejunal exclusion effects of RYGB, also improves glucose homeostasis[6]. Duodenal mucosal resurfacing, an endoscopic procedure that involves circumferential hydrothermal ablation and subsequent regeneration of the duodenal mucosa, elicits dramatic and durable glycemic improvements in patients with type 2 diabetes mellitus (T2DM)[7]. These findings suggest that the bypassed duodenum may play an important role in diabetic control after DJB.

The duodenum was primarily viewed as a digestive organ. However, accumulating evidence demonstrates that the duodenum has emerged as a key regulator of metabolic diseases, including diabetes[8]. The duodenal mucosa is exposed to various endogenous and exogenous chemical stimuli, such as macro- and micronutrients, gastric acid, bile acids (BAs), digestive enzymes, microorganisms, and drugs[9,10]. The duodenum is densely innervated by the enteric autonomous nervous system (ENS). Through chemical sensors located in the mucosa and ENS, the duodenum detects changes in luminal contents and further triggers a gut-brain negative feedback loop to inhibit exogenous nutrient intake and endogenous liver nutrient production[10,11]. In healthy rats, short-term intraduodenal

intralipid infusion inhibits hepatic glucose production (HGP) *via* the gut-brain-liver neural axis. However, this suppressive effect is negated in insulin-resistant rats[12]. Metformin and resveratrol, two well-known anti-diabetic drugs, can activate specific duodenal energy sensors (AMPK and SIRT1, respectively) even before being absorbed into the systemic circulation, and further trigger the gut-brain-liver network to reverse insulin resistance and inhibit HGP[13,14].

SIRT1 is a conserved mammalian nicotinamide adenine dinucleotide (NAD+)-dependent protein deacetylase that acts as a key metabolic sensor in various metabolic tissues, including the liver, skeletal muscle, adipose tissue, and pancreas. It directly links the cellular metabolic status to the regulation of gene expression, thus modulating various cellular processes, such as glucose metabolism, inflammation, and stress response[15,16]. SIRT1 is also expressed in the duodenal mucosa, which is significantly inhibited in high-fat diet (HFD)-fed insulin-resistant rats. Duodenum-specific knockdown of SIRT1 is sufficient to induce hepatic insulin resistance and increase hepatic glucose output in normal chow-fed rats[14]. To the best of our knowledge, the anti-diabetic effects of DJB surgery that could be linked to duodenal SIRT1 have not been investigated.

DJB hinders the duodenum from contacting the ingested chyme, therefore, the BAs released into the duodenum will not be mixed and diluted by food. In addition to their widely known roles in facilitating lipid absorption, BAs have recently been recognized as novel endocrine molecules that modulate glucose, lipids, and energy metabolism[17,18]. Activation of BA receptors, including the nuclear farnesoid X receptor (FXR) and membrane Takeda G-protein-coupled receptor 5 (TGR5), upregulates SIRT1 expression in the liver and brain, respectively[19,20]. These findings raise the possibility that DJB might upregulate duodenal SIRT1 by increasing intraluminal BAs, which might further contribute to the improved glucose homeostasis after DJB. Therefore, this study aimed to investigate the impact of DJB on duodenal BA signaling and SIRT1 expression in HFD and streptozotocin (STZ)-induced diabetic rats, and further explore the roles of BAs in modulating SIRT1 expression.

MATERIALS AND METHODS

Animals

Eight-week-old male Wistar rats were purchased from the Laboratory Animal Center of Shandong University (Jinan, China) and individually housed in ventilated cages in a controlled environment (12 h light/dark cycle, 24 ± 2 °C, humidity 50%-60%). The rats had *ad libitum* access to rodent chow and water. The diabetic rat model was established by HFD (40% fat, Huafukang Biotech, China) feeding for 4 wk to induce insulin resistance, followed by subsequent intraperitoneal injection of low-dose STZ (35 mg/kg, Sigma, United States) to induce mild insulin deficiency and hyperglycemia. After 72 h of STZ administration, 20 diabetic rats with random blood glucose ≥ 16.7 mmol/L were selected and randomly allocated to the sham (n = 10) and DJB (n = 10) groups. All animal protocols were approved by the Ethics Committee on Experimental Animals of Cheeloo College of Medicine, Shandong University.

Surgical procedures

The rats were deprived of solid food but were given free access to water and 10% enteral nutrition powder (Ensure, Abbott Laboratories B.V., Netherlands) two days preoperatively. Complete fasting was initiated 12 h preoperatively. All operations were conducted under anesthesia with 10% chloral hydrate (3 mL/kg). DJB and sham surgeries were performed as previously described[21].

DJB: First, a midline incision was made in the upper abdomen and the duodenum was then transected 1 cm distal to the pylorus and the stump was sealed. Next, the jejunum was transected approximately 10 cm distal to the ligament of Treitz, and the distal limb of the jejunum was anastomosed to the proximal duodenum in an end-to-end manner. Finally, the biliopancreatic limb was anastomosed to the jejunum 15 cm distal to the duodenojejunal anastomosis in a Roux-en-Y manner.

Sham: Sham surgery was performed *via* an incision comparable to that of the DJB group. The intestines were transected at the same sites where enterotomies were performed in DJB, and re-anastomosis was made *in situ*. The operation time was prolonged equally to that of the DJB group to achieve similar surgical and anesthetic stress.

The rats were only given access to water during the first 24 h postoperatively, followed by 10% enteral nutrition powder for three days, and thereafter a standard rodent chow until the end of this study. Body weight and food intake were recorded preoperatively and once a week postoperatively. Fasting blood glucose (FBG) levels were measured at baseline and at 1, 2, 4, 6, and 8 wk postoperatively.

Oral glucose tolerance test

Oral glucose tolerance test (OGTT) was performed 2 and 8 wk postoperatively. The rats were administered with 20% glucose (1 g/kg body weight) by oral gavage after overnight fasting. Blood samples were collected from the tail vein at baseline and at 15, 30, 60, 120, and 180 min after glucose administration to measure blood glucose levels. The area under the curve for the OGTT (AUC_{OGTT}) was

calculated by trapezoidal integration.

Intraperitoneal pyruvate tolerance test

The intraperitoneal pyruvate tolerance test (ipPTT) was conducted 2 and 8 wk postoperatively to evaluate hepatic gluconeogenic capacity and hepatic insulin resistance. After 12 h of fasting, 10% pyruvate solution (1 g/kg body weight) was administered intraperitoneally into conscious rats. Blood glucose levels were monitored at baseline and at 15, 30, 60, and 120 min after injection. The AUC for ipPTT (AUC_{ipPTT}) was calculated using trapezoidal integration.

Systemic and duodenal BAs parameters

Fasting and postprandial systemic total BAs (TBAs) were measured 2 and 8 wk postoperatively. The rats were fasted for 12 h and then administered with 10% Ensure (10 mL/kg body weight) *via* intragastric gavage. Blood samples were collected from the retrobulbar venous plexus into chilled SST tubes at baseline and 60 min after gavage to measure the systemic TBAs.

Eight weeks after the surgery, the rats were euthanized immediately after blood collection. Intestine segments of 0.5 cm length were excised from the descending and horizontal duodenum separately without rinsing. TBAs in the duodenum lumen were extracted by mixing the duodenal segments with 1 mL of 50% tert-butyl alcohol for 1 h at 37 °C. After centrifugation, the supernatant was collected and stored at -80 °C until analysis. BAs were measured with an automatic biochemistry analyzer (Roche Cobas 8000 system) using an enzyme cycling method.

Cell culture

Rat small intestine epithelial IEC-6 cells were purchased from Fuheng Biology (Shanghai, China), and cultured in Dulbecco's Modified Eagle Medium (Gibco, CA, United States) supplemented with 10% fetal bovine serum (Gibco, CA, United States), and maintained under standard culture conditions (in incubators at 37 °C in a 5% CO_2/95% air atmosphere). To investigate the effects of FXR and TGR5 activation on SIRT1, AMPK, and phosphorylated AMPK (p-AMPK) expression, IEC-6 cells were treated with GW4064 (5 μM, 24 h) and INT-777 (10 μM, 1 h) respectively, and the control groups were treated with an equal volume of dimethyl sulfoxide. At the end of the study, cells were harvested for protein and gene expression analyses.

Real-time quantitative polymerase chain reaction

Total mRNA of the duodenal mucosa and IEC-6 cells were extracted using TRIzol Reagent (Cwbio, China). The total mRNA was then reverse-transcribed into cDNA using a HiFiScript cDNA Synthesis Kit (Cwbio, China) according to the manufacturer's instructions. The cDNA was subjected to real-time quantitative polymerase chain reaction (RT-qPCR) quantitation with UltraSYBR Mixture (Cwbio, China) on a RT-qPCR system (Hehui biotech, China). GAPDH was used as an internal control. Primers used in this study are listed in Table 1.

Enzyme-linked immunosorbent assay

The duodenal mucosa was immediately flash-frozen in liquid nitrogen after the rats were euthanized. The cyclic adenosine 3′, 5′-monophosphate (cAMP) concentration in the duodenal mucosa was measured using an enzyme-linked immunosorbent assay kit according to the manufacturer's instructions (Sigma-Aldrich, United States).

Western blotting

Total proteins of the duodenal mucosa and IEC-6 cells were extracted with RIPA lysis buffer (Beyotime, China) and analyzed using a BCA protein assay kit (Beyotime, China). The primary antibodies used in western blotting were SIRT1 (Cell Signaling Technology, United States), AMPK (Cell Signaling Technology, United States), p-AMPK (Cell Signaling Technology, United States), and GAPDH (Proteintech, China). The protein bands were visualized using ECL solution (Millipore, United States), and band densitometry was assessed with ImageJ software.

Statistical analysis

Quantitative data were expressed as mean ± SD. The intergroups differences were evaluated by the Student's *t*-test except for blood glucose levels in the OGTT and ipPTT studies, which were analyzed by two-way repeated measures ANOVA (mixed model ANOVA) followed by Bonferroni's multiple comparison test. All analyses were performed using SPSS (Version 26). The criterion for statistical significance was set at $P < 0.05$.

Table 1 Primer sequence

Gene	Forward (5'-3')	Reverse (5'-3')
SIRT1	GGGAACCTCTGCCTCATCTACAT	CGCCACCTAACCTATGACACAA
AMPK	GAAGATCGGACACTACGTGCT	ACTGCCACTTTATGGCCTGTC
FXR	CATTACAACGCGCTCACCTG	CCCATCTCTCTGCACTTCCT
TGR5	TACTCACAGGGTTGGCACTG	CAAAAGTTGGGGGCCAAGTG
SHP	TCCGGTCCCCAGCATACTTA	GAAAGACTCCAGGCAGTGCT
GAPDH	GATTTGGCCGTATCGGAC	GAAGACGCCAGTAGACTC

FXR: Farnesoid X receptor; SHP: Small heterodimer partner; TGR5: Takeda G-protein-coupled receptor 5.

RESULTS

Effects of DJB on body weight and food intake

Body weight and food intake were comparable between the two groups before operation. Due to surgical stress, unrestored gastrointestinal function, and decreased food intake, the body weight of both groups fell to a minimum point in the first week after surgery. As food intake increased, the body weight of both groups gradually recovered to preoperative levels approximately 4 wk after operation. As a nonrestrictive surgery, the DJB group exhibited similar body weight and food intake as the sham group at all measured time points postoperatively (Figures 1A and B).

DJB rapidly improved glucose homeostasis in diabetic rats

There were no significant differences in FBG levels between the two groups preoperatively. The FBG of the DJB group rapidly and significantly declined as early as one week postoperatively and was maintained at a relatively stable level. While the FBG of the sham group was not alleviated after operation and showed a tendency to deteriorate over time. Compared to the sham group, the DJB group exhibited lower FBG at all postoperative time points (Figure 1C).

Consistent with rapidly reduced FBG, the DJB group showed significantly lower blood glucose excursion and AUC_{OGTT} during the OGTT studies at 2 and 8 wk postoperatively (Figures 1D-F), indicating improved glucose tolerance and increased systemic glucose disposal after DJB. To evaluate the impact of DJB on hepatic gluconeogenic capacity, ipPTT was conducted at 2 and 8 wk postoperatively. As shown in Figures 1G-I, the DJB group exhibited reduced glucose excursion and AUC_{ipPTT} in response to intraperitoneal pyruvate challenge, implying that DJB improved hepatic insulin sensitivity and decreased hepatic glucose output in diabetic rats early after surgery.

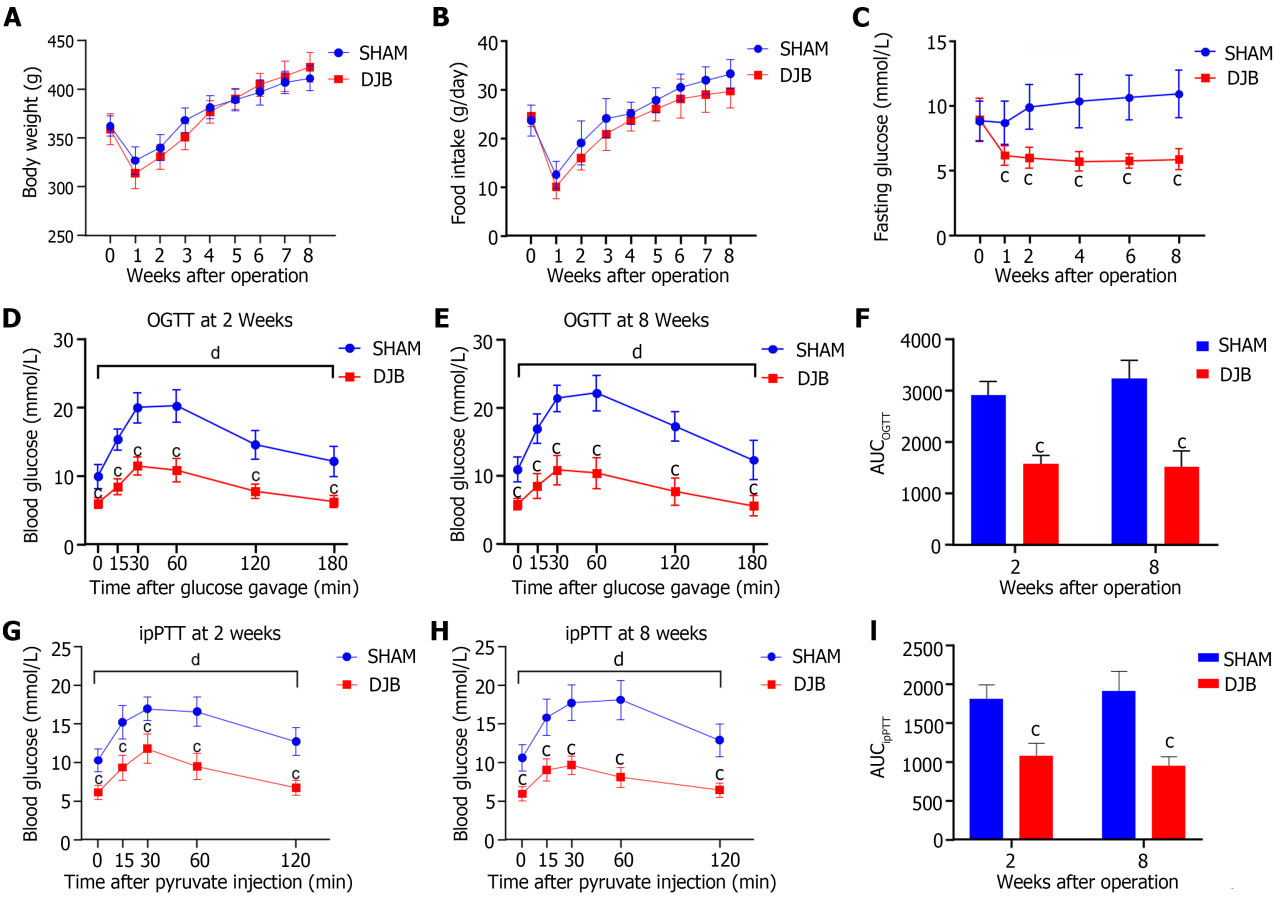
DJB increased systemic and intraduodenal TBAs, and activated duodenal BA signaling

Compared with the sham group, the DJB-operated rats exhibited elevated fasting and postprandial serum TBAs at 2 and 8 wk postoperatively (Figure 2A). Altered food and digestive juice flow in the gastrointestinal tract also affected luminal TBAs after DJB. As shown in Figure 2B, the DJB group displayed elevated intraluminal TBAs in both the descending and horizontal duodenum 8 wk postoperatively.

To determine the effects of increased intraduodenal TBAs on duodenal BA signaling, the mRNA levels of FXR, TGR5, and small heterodimer partner (SHP) in the duodenal mucosa were evaluated by RT-qPCR eight weeks after surgery. The mRNA expression of FXR and its target gene SHP were concurrently increased in the duodenal mucosa of the DJB group (Figures 2C and D), indicating that the BAs-FXR-SHP pathway was activated. As a membrane bound receptor, TGR5 activation leads to cAMP accumulation in cells. Although DJB did not enhance TGR5 gene expression in the duodenal mucosa (Figures 2C and D), it increased the cAMP content in the horizontal duodenum (Figure 2E). cAMP also tended to increase in the descending duodenum of the DJB group despite no statistical significance (Figure 2E). These results suggest that the duodenal TGR5 receptor may also be activated after DJB.

DJB increased SIRT1 expression and promoted phosphorylation of AMPK in the duodenal mucosa

The ipPTT studies suggested that hepatic gluconeogenesis was reduced after DJB. Elevated duodenal SIRT1 and p-AMPK are associated with suppressed hepatic glucose output *via* the gut-brain-liver neural loop[13,14]. Therefore, to elucidate the underlying mechanism of improved hepatic insulin sensitivity and glucose homeostasis after DJB, duodenal SIRT1 and p-AMPK expression were investigated by western blotting eight weeks after surgery. As shown in Figure 3, DJB increased SIRT1 expression and promoted phosphorylation of AMPK in both the descending and horizontal parts of the duodenum.



DOI: 10.3748/wjg.v28.i31.4338 **Copyright** ©The Author(s) 2022.

Figure 1 Effects of duodenal-jejunal bypass on metabolic parameters. A: Body weight of rats; B: Food intake of rats; C: Fasting blood glucose of rats; D: Oral glucose tolerance test (OGTT) at 2 wk after operation; E: OGTT at 8 wk after operation; F: Area under the curve (AUC) of OGTT at 2 and 8 wk after operation; G: Intraperitoneal pyruvate tolerance test (ipPTT) at 2 wk after operation; H: ipPTT at 8 wk after operation; I: AUC_{ipPTT} at 2 and 8 wk after operation. $^{c}P < 0.001$ duodenal-jejunal bypass (DJB) *vs* sham group by the Student's *t*-test or *post-hoc* Bonferroni's multiple comparison test. $^{d}P < 0.001$, DJB *vs* sham group by mixed model ANOVA. AUC_{OGTT}: Area under the curve of oral glucose tolerance test; AUC_{ipPTT}: Area under the curve of intraperitoneal pyruvate tolerance test; OGTT: Oral glucose tolerance test; ipPTT: Intraperitoneal pyruvate tolerance test; DJB: Duodenal-jejunal bypass.

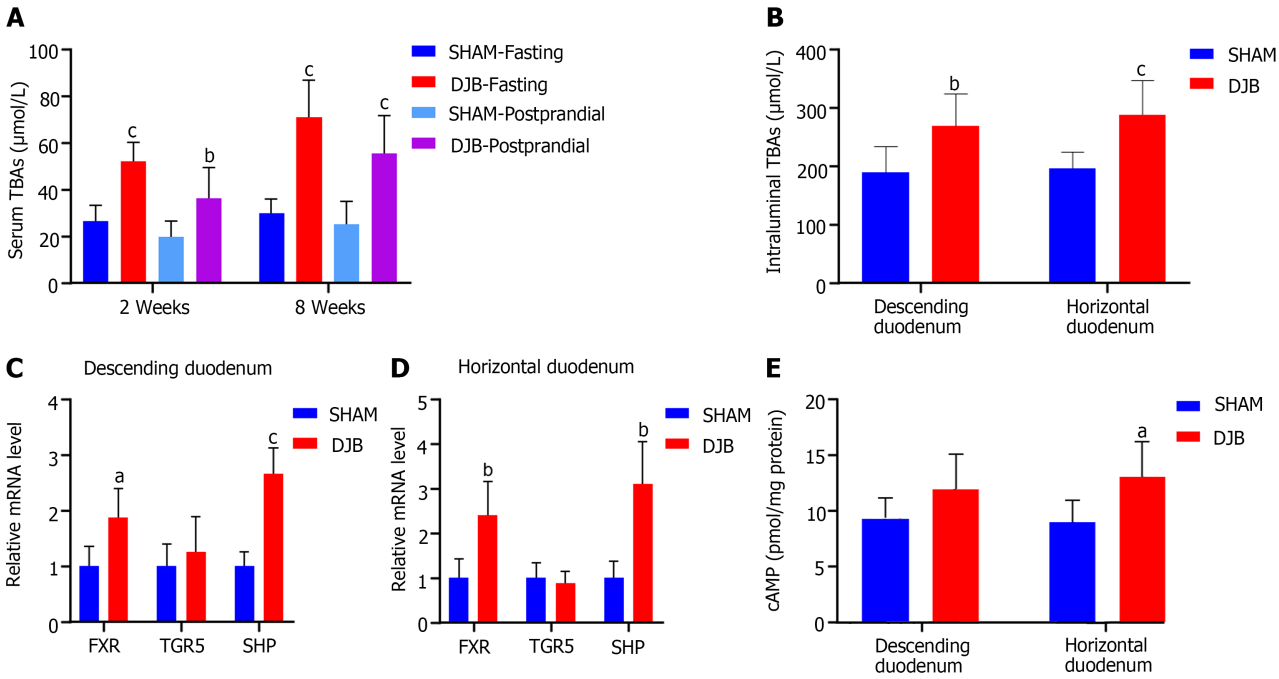
FXR and TGR5 activation increased SIRT1 expression and promoted phosphorylation of AMPK in IEC-6 cells

To verify whether increased SIRT1 and p-AMPK could be attributed to activated BA signaling in the duodenal mucosa, we treated rat small intestine epithelial IEC-6 cells with FXR and TGR5 agonists, respectively. Upon FXR activation by GW4064, the mRNA expression of FXR, SHP, and SIRT1 were all dramatically upregulated in IEC-6 cells (Figure 4A). Although INT-777 stimulation did not induce TGR5 transcription, it promoted the mRNA expression of SIRT1 (Figure 4B). In line with the increased mRNA expression, the protein levels of SIRT1 were also significantly elevated upon the activation of both BAs receptors (Figures 4C, D, F and G). Although FXR and TGR5 agonists did not increase the gene and protein expression of AMPK, they both promoted AMPK phosphorylation in IEC-6 cells (Figures 4C, E, F and H). These results indicate that the activated BA signaling pathway contributes to the upregulation of SIRT1 and the phosphorylation of AMPK.

DISCUSSION

In this study, we performed DJB and sham surgeries on diabetic rats induced by HFD and STZ, and demonstrated that DJB elevated intraduodenal TBAs, activated the BA signaling pathway and upregulated SIRT1 expression in the duodenal mucosa. By using specific BA receptor agonists, we proved that FXR and TGR5 activation increased SIRT1 expression and promoted phosphorylation of AMPK in rat small intestine epithelial cells, indicating that increased intraluminal BAs and activation of BA receptors contributed to the increased duodenal SIRT1 after DJB.

SIRT1 is an evolutionarily conserved NAD+-dependent deacetylase that belongs to the Sirtuins family (SIRT1-SIRT7)[22]. SIRT1 acts as a key metabolic sensor in the liver, skeletal muscles, adipose tissues, pancreatic islets, and other metabolic tissues. It plays an important role in various aging-related



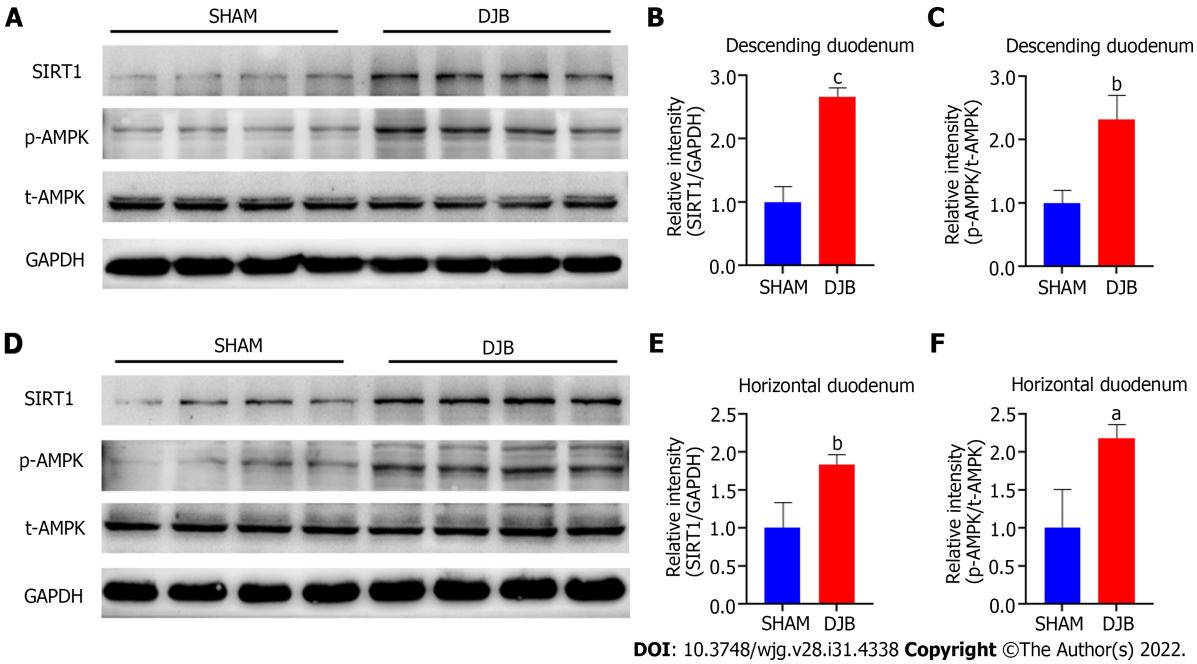
DOI: 10.3748/wjg.v28.i31.4338 **Copyright** ©The Author(s) 2022.

Figure 2 Duodenal-jejunal bypass increased serum and intraduodenal total bile acids and activated bile acids signaling in the duodenal mucosa. A: Fasting and postprandial serum total bile acids (TBAs) at 2 and 8 wk after operation; B: Intraluminal TBAs in the descending and horizontal duodenum at 8 wk after operation; C and D: Expression of key genes involved in BA signaling pathway in the mucosa of descending and horizontal duodenum; E: Cyclic adenosine 3',5'-monophosphate concentration in the duodenal mucosa. $^{a}P < 0.05$, $^{b}P < 0.01$, $^{c}P < 0.001$ duodenal-jejunal bypass *vs* sham group. DJB: Duodenal-jejunal bypass; TBAs: Total bile acids; FXR: Farnesoid X receptor; SHP: Small heterodimer partner; TGR5: Takeda G-protein-coupled receptor 5; cAMP: Cyclic adenosine 3',5'-monophosphate.

diseases, including insulin resistance, diabetes, obesity, hepatic steatosis, and cardiovascular diseases [22,23]. Liver-specific deletion of SIRT1 impairs hepatic and systemic insulin sensitivity in mice[24]. Muscular SIRT1 levels are decreased in patients with T2DM and HFD-induced insulin-resistant rats, and overexpression of SIRT1 in skeletal muscle improves muscular insulin sensitivity[25,26]. Adipose tissue-specific ablation of SIRT1 results in increased fat deposition, impaired glucose tolerance and insulin sensitivity in mice[27]. SIRT1 activation protects the function and morphology of residual pancreatic β-cells and induces β-cell regeneration from progenitor cells, thus improving glucose homeostasis[28].

Sleeve gastrectomy (SG) upregulates hepatic SIRT1 and dramatically ameliorates hepatic steatosis in HFD-fed obese mice[29]. RYGB activates the AMPK/SIRT1/PGC-1α pathway in the skeletal muscle of diabetic Zucker fatty rats, which contributes to diabetes remission[30]. Laparoscopic bariatric surgery increases SIRT1 levels in the peripheral blood of patients with obesity and T2DM, which is higher in the effective than in the ineffective group[31]. The effects of bariatric surgeries on duodenal SIRT1 expression have not been investigated previously. Duodenal SIRT1 is a novel therapeutic target for insulin resistance and diabetes. HFD-fed insulin-resistant rats exhibit significantly downregulated SIRT1 in the duodenal mucosa, and duodenum-specific knockdown of SIRT1 is sufficient to induce hepatic insulin resistance in normal chow-fed rats[14]. Our study is the first to demonstrate that DJB promotes SIRT1 expression in the duodenal mucosa. As duodenal SIRT1 activation further inhibits HGP and improves hepatic insulin sensitivity by triggering the gut-hypothalamus-liver neural network[14], we postulate that increased duodenal SIRT1 at least partly accounts for the improved hepatic insulin resistance and glucose homeostasis after DJB.

As an indispensable energy sensor, SIRT1 expression is closely related to energy status and environmental stress[32]. The SIRT1 transcription is usually activated during fasting, which transforms the metabolic status from gluconeogenesis to fat mobilization and fatty acid oxidation[32]. Chen *et al*[33] demonstrated that calorie restriction (CR) increased both pancreatic and hepatic SIRT1 expression in rats. Additionally, Civitarese *et al*[34] reported that CR for 6 mo promoted muscular SIRT1 expression in healthy overweight individuals. In mammalian cells, acute nutrient deprivation increases SIRT1 transcription by activating the Forkhead transcription factor Foxo3a[35]. Although food intake is not reduced after DJB, the duodenum is hindered from contact with ingested food, which might result in a duodenum-specific CR status, thus further inducing duodenal SIRT1 expression. Furthermore, gastric acids are not expelled into the duodenum after DJB, which increases the pH of duodenal content. The deacetylation activity of SIRT1 is pH-dependent, and higher pH attenuates the inhibition of SIRT1 by nicotinamide[36].



DOI: 10.3748/wjg.v28.i31.4338 **Copyright** ©The Author(s) 2022.

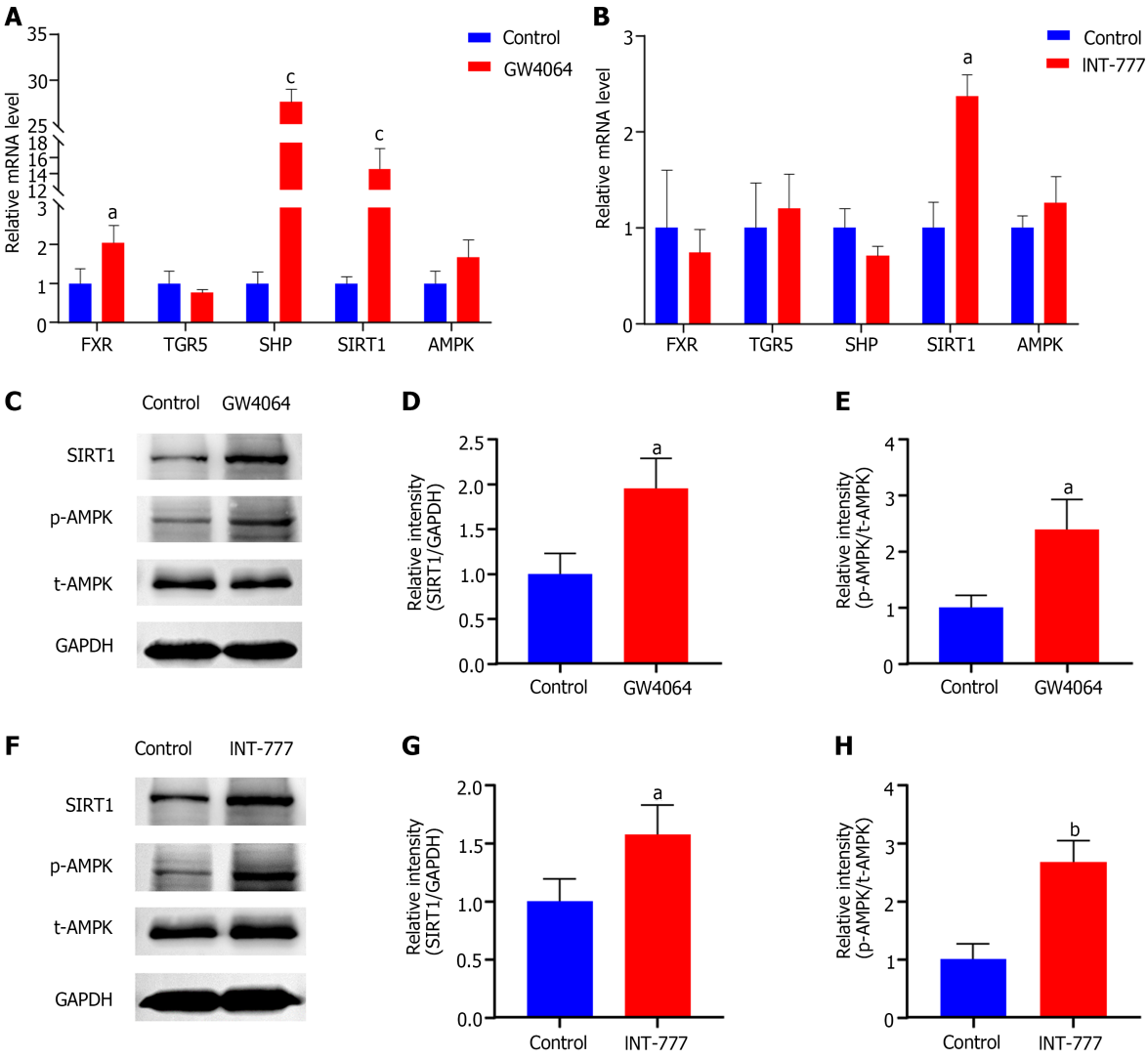
Figure 3 Duodenal-jejunal bypass increased SIRT1 expression and promoted phosphorylation of AMPK in the duodenal mucosa. A: Western blot images of SIRT1, phosphorylated AMPK (p-AMPK), and total AMPK (t-AMPK) in the descending duodenum; B and C: The relative intensity of SIRT1 and p-AMPK/t-AMPK in the descending duodenum; D: Western blot images of SIRT1, p-AMPK, and t-AMPK in the horizontal duodenum; E and F: The relative intensity of SIRT1 and p-AMPK/t-AMPK in the horizontal duodenum. $^{a}P < 0.05$, $^{b}P < 0.01$, $^{c}P < 0.001$ duodenal-jejunal bypass *vs* sham group. p-AMPK: Phosphorylated AMPK; t-AMPK: Total AMPK; DJB: Duodenal-jejunal bypass.

Increased intraduodenal BAs might be another key contributor to elevated duodenal SIRT1 after DJB. It is well documented that circulating BAs are increased after numerous metabolic surgeries, including DJB, SG, and RYGB[3,37,38]. By using genetically modified animal models, it has been proven that both FXR and TGR5 are required for the metabolic benefits of SG[39,40]. As demonstrated by our study, DJB not only elevated serum TBAs, but also significantly increased intraduodenal TBAs. Similarly, Ueno *et al* [41] demonstrated that DJB increased conjugated BAs in the bypassed jejunum just distal to the ligament of Treitz. Furthermore, we observed higher SHP mRNA and cAMP concentrations in the duodenal mucosa of DJB-operated rats, indicating that FXR and TGR5 signaling were activated after DJB. Whether causality exists between activated BA signaling and increased SIRT1 in enterocytes has not been investigated.

Numerous studies have suggested that BAs serve as upstream signaling molecules for SIRT1 in various tissues. FXR activation upregulates SIRT1 expression by promoting the transcription of SHP and repressing the transcription of p53 and miR34a in the livers of normal mice[19]. In diabetic *db/db* mice, TGR5 activation increases both the mRNA and protein levels of SIRT1 in the kidneys[42]. Similarly, TGR5 activation upregulates SIRT1 expression in the brains of Sprague Dawley rats[20]. These studies suggest that activation of duodenal FXR and/or TGR5 might account for the increased duodenal SIRT1 after DJB. To verify our hypothesis, we used GW4064 and INT-777 to activate FXR and TGR5 in IEC-6 cells and showed that both agonists increased SIRT1 expression in enterocytes. We also found that GW4064 increased FXR gene expression in IEC-6 cells in accordance with the elevated FXR mRNA in the duodenal mucosa after DJB. Similar changes in FXR mRNA were also observed in mouse mesangial cells after GW4064 stimulation[43].

In addition, we demonstrated that DJB promoted phosphorylation of AMPK in the duodenal mucosa, which might also contribute to improved glucose homeostasis after DJB, as duodenal AMPK activation improves hepatic insulin sensitivity and inhibits hepatic glucose output *via* the gut-hypothalamus-liver neural axis[13]. Jiao *et al*[4] reported that DJB promoted phosphorylation of AMPK in both the liver and skeletal muscle, which contributed to the restoration of normoglycemia after surgery. Likewise, SG enhances AMPK phosphorylation in both the liver and monocytes[44]. Similarly, RYGB exhibits anti-diabetic properties *via* AMPK activation in the liver and Kupffer cells[45]. Actually, as two important energy sensors in cells, AMPK and SIRT1 mutually regulate each other, share many common target molecules, and have similar effects on diverse processes such as glucose and energy metabolism[46]. Our study suggests that activated duodenal AMPK might also be attributed to elevated duodenal BAs because both FXR and TGR5 activation promoted phosphorylation of AMPK in IEC-6 cells.

There are some limitations in our study. First, we only investigated changes in TBAs in the duodenum after DJB. There are numerous components in the BA pool, and different components may exert different metabolic effects. Second, our study did not provide sufficient information on whether



DOI: 10.3748/wjg.v28.i31.4338 **Copyright** ©The Author(s) 2022.

Figure 4 Activation of farnesoid X receptor and Takeda G-protein-coupled receptor 5 increased SIRT1 and promoted phosphorylation of AMPK in rat small intestine epithelial IEC-6 cells. A and B: Effects of farnesoid X receptor (FXR) and Takeda G-protein-coupled receptor 5 (TGR5) activation on SIRT1, AMPK, and key genes involved in BA signaling pathway; C: Western blot images of SIRT1, phosphorylated AMPK (p-AMPK), and total AMPK (t-AMPK) in IEC-6 cells after FXR activation; D and E: The relative intensity of SIRT1 and p-AMPK/t-AMPK in IEC-6 cells after FXR activation. F: Western blot images of SIRT1, p-AMPK, and t-AMPK in IEC-6 cells after TGR5 activation; G and H: The relative intensity of SIRT1 and p-AMPK/t-AMPK in IEC-6 cells after TGR5 activation. $^{a}P < 0.05$, $^{b}P < 0.01$, $^{c}P < 0.001$ GW4064 or INT-777 *vs* control group. p-AMPK: Phosphorylated AMPK; t-AMPK: Total AMPK; FXR: Farnesoid X receptor; SHP: Small heterodimer partner; TGR5: Takeda G-protein-coupled receptor 5.

duodenal SIRT1 is indispensable for DJB-induced diabetic control, therefore, duodenum-specific SIRT1 loss- and gain-of-function animal models would be necessary for future studies.

CONCLUSION

DJB upregulates SIRT1 expression in the duodenal mucosa, which may partly account for surgery-induced diabetic control. Increased intraduodenal TBA levels and activated duodenal BA signaling pathway may contribute to the upregulation of duodenal SIRT1 after DJB.

ARTICLE HIGHLIGHTS

Research background

Duodenal-jejunal bypass (DJB) induces rapid and significant amelioration of type 2 diabetes mellitus in various diabetic rat models, while the mechanisms have not been fully elucidated. Duodenal SIRT1

regulates hepatic glucose production and hepatic insulin sensitivity through a gut-brain-liver axis, and activation of bile acid (BA) receptors promotes SIRT1 expression in many tissues. This study aimed at uncovering the roles of duodenal BAs and SIRT1 in the diabetic control after DJB.

Research motivation

To expand and deepen our understanding on the mechanisms underlying diabetes control after DJB, and to provide new ideas and targets for the non-surgical treatment of diabetes in the future.

Research objectives

To investigate the effects of DJB on the duodenal BA signaling pathway and SIRT1 expression in a diabetic rat model, and further reveal the roles of BAs in modulating SIRT1 expression in enterocytes.

Research methods

DJB and sham surgeries were performed on rats with diabetes induced by high-fat diet and low-dose streptozotocin. The effects of surgeries on metabolic parameters were compared accordingly. The intraduodenal BA concentration, the key genes of BA signaling pathway and SIRT1 in the duodenal mucosa were evaluated 8 wk postoperatively. Rat small intestine epithelial IEC-6 cells were treated with GW4064 and INT-777 to verify the effects of BA receptor activation on SIRT1 expression in enterocytes.

Research results

DJB rapidly and dramatically improved glucose homeostasis in the diabetic rats independently of body weight and food intake. DJB increased both systemic and intraduodenal total BAs, activated the BA signaling pathway and promoted SIRT1 expression in the duodenum mucosa. Activation of BA receptors including farnesoid X receptor and Takeda G-protein-coupled receptor 5 increased the mRNA and protein expression of SIRT1 in IEC-6 cells.

Research conclusions

DJB increases intraduodenal BA levels and activates the duodenal BA signaling pathway, which may further contribute to the improved hepatic insulin resistance and glucose homeostasis by upregulating SIRT1 expression in the duodenal mucosa.

Research perspectives

Our findings provide evidence that BA-mediated upregulation of SIRT1 in the duodenum contributes to the diabetic control after DJB. This study also implicates that duodenal BAs and SIRT1 might be potential targets for improving hepatic insulin sensitivity and systemic glucose homeostasis, which lays the groundwork for developing duodenal BA and SIRT1-specific treatments to alleviate diabetes.

ACKNOWLEDGEMENTS

The authors would like to acknowledge Sun M and Liu XM for their skillful technical assistance.

FOOTNOTES

Author contributions: Han HF and Yu WB conceived of the experiments; Liu SZ and Yu WB designed the experiments; Han HF, Zhang X, Wei M, and Huang X carried out the experiments, performed the statistical analyses and wrote the manuscript; and all authors have commented on the initial and final drafts of the manuscript and approved the final version of the article.

Supported by the National Natural Science Foundation of China, No. 81600617, 81700708, 81702647 and 82100853; and the Natural Science Foundation of Shandong Province, No. ZR2020MH246, ZR2021LZL003 and ZR2021QH028.

Institutional animal care and use committee statement: All procedures involving animals were reviewed and approved by the Institutional Animal Care Committee of Cheeloo College of Medicine, Shandong University, (Protocol No. 19085).

Conflict-of-interest statement: All the authors report no relevant conflicts of interest for this article.

Data sharing statement: No additional data are available.

ARRIVE guidelines statement: The authors have read the ARRIVE guidelines, and the manuscript was prepared and revised according to the ARRIVE guidelines.

Open-Access: This article is an open-access article that was selected by an in-house editor and fully peer-reviewed by

external reviewers. It is distributed in accordance with the Creative Commons Attribution NonCommercial (CC BY-NC 4.0) license, which permits others to distribute, remix, adapt, build upon this work non-commercially, and license their derivative works on different terms, provided the original work is properly cited and the use is non-commercial. See: https://creativecommons.org/Licenses/by-nc/4.0/

Country/Territory of origin: China

ORCID number: Hai-Feng Han 0000-0002-1417-9350; Shao-Zhuang Liu 0000-0003-2052-0516; Xiang Zhang 0000-0001-7417-6082; Meng Wei 0000-0002-0402-5083; Xin Huang 0000-0002-6208-4751; Wen-Bin Yu 0000-0001-7111-3780.

S-Editor: Wang JJ
L-Editor: A
P-Editor: Cai YX

REFERENCES

1 **Sun H**, Saeedi P, Karuranga S, Pinkepank M, Ogurtsova K, Duncan BB, Stein C, Basit A, Chan JCN, Mbanya JC, Pavkov ME, Ramachandaran A, Wild SH, James S, Herman WH, Zhang P, Bommer C, Kuo S, Boyko EJ, Magliano DJ. IDF Diabetes Atlas: Global, regional and country-level diabetes prevalence estimates for 2021 and projections for 2045. *Diabetes Res Clin Pract* 2022; **183**: 109119 [PMID: 34879977 DOI: 10.1016/j.diabres.2021.109119]

2 **Khorgami Z**, Shoar S, Saber AA, Howard CA, Danaei G, Sclabas GM. Outcomes of Bariatric Surgery Versus Medical Management for Type 2 Diabetes Mellitus: a Meta-Analysis of Randomized Controlled Trials. *Obes Surg* 2019; **29**: 964-974 [PMID: 30402804 DOI: 10.1007/s11695-018-3552-x]

3 **Zhang X**, Wang Y, Zhong M, Liu T, Han H, Zhang G, Liu S, Wei M, Wu Q, Hu S. Duodenal-Jejunal Bypass Preferentially Elevates Serum Taurine-Conjugated Bile Acids and Alters Gut Microbiota in a Diabetic Rat Model. *Obes Surg* 2016; **26**: 1890-1899 [PMID: 26715331 DOI: 10.1007/s11695-015-2031-x]

4 **Jiao J**, Bae EJ, Bandyopadhyay G, Oliver J, Marathe C, Chen M, Hsu JY, Chen Y, Tian H, Olefsky JM, Saberi M. Restoration of euglycemia after duodenal bypass surgery is reliant on central and peripheral inputs in Zucker fa/fa rats. *Diabetes* 2013; **62**: 1074-1083 [PMID: 23248171 DOI: 10.2337/db12-0681]

5 **Klein S**, Fabbrini E, Patterson BW, Polonsky KS, Schiavon CA, Correa JL, Salles JE, Wajchenberg BL, Cohen R. Moderate effect of duodenal-jejunal bypass surgery on glucose homeostasis in patients with type 2 diabetes. *Obesity (Silver Spring)* 2012; **20**: 1266-1272 [PMID: 22262157 DOI: 10.1038/oby.2011.377]

6 **de Jonge C**, Rensen SS, Verdam FJ, Vincent RP, Bloom SR, Buurman WA, le Roux CW, Schaper NC, Bouvy ND, Greve JW. Endoscopic duodenal-jejunal bypass liner rapidly improves type 2 diabetes. *Obes Surg* 2013; **23**: 1354-1360 [PMID: 23526068 DOI: 10.1007/s11695-013-0921-3]

7 **van Baar ACG**, Holleman F, Crenier L, Haidry R, Magee C, Hopkins D, Rodriguez Grunert L, Galvao Neto M, Vignolo P, Hayee B, Mertens A, Bisschops R, Tijssen J, Nieuwdorp M, Guidone C, Costamagna G, Devière J, Bergman JJGHM. Endoscopic duodenal mucosal resurfacing for the treatment of type 2 diabetes mellitus: one year results from the first international, open-label, prospective, multicentre study. *Gut* 2020; **69**: 295-303 [PMID: 31331994 DOI: 10.1136/gutjnl-2019-318349]

8 **van Baar ACG**, Nieuwdorp M, Holleman F, Soeters MR, Groen AK, Bergman JJGHM. The Duodenum harbors a Broad Untapped Therapeutic Potential. *Gastroenterology* 2018; **154**: 773-777 [PMID: 29428335 DOI: 10.1053/j.gastro.2018.02.010]

9 **Akiba Y**, Kaunitz JD. Duodenal chemosensing and mucosal defenses. *Digestion* 2011; **83** Suppl 1: 25-31 [PMID: 21389725 DOI: 10.1159/000323401]

10 **Rønnestad I**, Akiba Y, Kaji I, Kaunitz JD. Duodenal luminal nutrient sensing. *Curr Opin Pharmacol* 2014; **19**: 67-75 [PMID: 25113991 DOI: 10.1016/j.coph.2014.07.010]

11 **Lam TK**. Neuronal regulation of homeostasis by nutrient sensing. *Nat Med* 2010; **16**: 392-395 [PMID: 20376051 DOI: 10.1038/nm0410-392]

12 **Wang PY**, Caspi L, Lam CK, Chari M, Li X, Light PE, Gutierrez-Juarez R, Ang M, Schwartz GJ, Lam TK. Upper intestinal lipids trigger a gut-brain-liver axis to regulate glucose production. *Nature* 2008; **452**: 1012-1016 [PMID: 18401341 DOI: 10.1038/nature06852]

13 **Duca FA**, Côté CD, Rasmussen BA, Zadeh-Tahmasebi M, Rutter GA, Filippi BM, Lam TK. Metformin activates a duodenal Ampk-dependent pathway to lower hepatic glucose production in rats. *Nat Med* 2015; **21**: 506-511 [PMID: 25849133 DOI: 10.1038/nm.3787]

14 **Côté CD**, Rasmussen BA, Duca FA, Zadeh-Tahmasebi M, Baur JA, Daljeet M, Breen DM, Filippi BM, Lam TK. Resveratrol activates duodenal Sirt1 to reverse insulin resistance in rats through a neuronal network. *Nat Med* 2015; **21**: 498-505 [PMID: 25849131 DOI: 10.1038/nm.3821]

15 **Cao Y**, Jiang X, Ma H, Wang Y, Xue P, Liu Y. SIRT1 and insulin resistance. *J Diabetes Complications* 2016; **30**: 178-183 [PMID: 26422395 DOI: 10.1016/j.jdiacomp.2015.08.022]

16 **Li X**. SIRT1 and energy metabolism. *Acta Biochim Biophys Sin (Shanghai)* 2013; **45**: 51-60 [PMID: 23257294 DOI: 10.1093/abbs/gms108]

17 **Molinaro A**, Wahlström A, Marschall HU. Role of Bile Acids in Metabolic Control. *Trends Endocrinol Metab* 2018; **29**: 31-41 [PMID: 29195686 DOI: 10.1016/j.tem.2017.11.002]

18 **Ahmad TR**, Haeusler RA. Bile acids in glucose metabolism and insulin signalling - mechanisms and research needs. *Nat Rev Endocrinol* 2019; **15**: 701-712 [PMID: 31616073 DOI: 10.1038/s41574-019-0266-7]

19 **Lee J**, Padhye A, Sharma A, Song G, Miao J, Mo YY, Wang L, Kemper JK. A pathway involving farnesoid X receptor and small heterodimer partner positively regulates hepatic sirtuin 1 Levels *via* microRNA-34a inhibition. *J Biol Chem* 2010; **285**: 12604-12611 [PMID: 20185821 DOI: 10.1074/jbc.M109.094524]

20 **Liang H**, Matei N, McBride DW, Xu Y, Tang J, Luo B, Zhang JH. Activation of TGR5 protects blood brain barrier *via* the BRCA1/Sirt1 pathway after middle cerebral artery occlusion in rats. *J Biomed Sci* 2020; **27**: 61 [PMID: 32381096 DOI: 10.1186/s12929-020-00656-9]

21 **Liu S**, Zhang G, Wang L, Sun D, Chen W, Yan Z, Sun Y, Hu S. The entire small intestine mediates the changes in glucose homeostasis after intestinal surgery in Goto-Kakizaki rats. *Ann Surg* 2012; **256**: 1049-1058 [PMID: 23001083 DOI: 10.1097/SLA.0b013e31826c3866]

22 **Zhou S**, Tang X, Chen HZ. Sirtuins and Insulin Resistance. *Front Endocrinol (Lausanne)* 2018; **9**: 748 [PMID: 30574122 DOI: 10.3389/fendo.2018.00748]

23 **Morris BJ**. Seven sirtuins for seven deadly diseases of aging. *Free Radic Biol Med* 2013; **56**: 133-171 [PMID: 23104101 DOI: 10.1016/j.freeradbiomed.2012.10.525]

24 **Wang RH**, Kim HS, Xiao C, Xu X, Gavrilova O, Deng CX. Hepatic Sirt1 deficiency in mice impairs mTorc2/Akt signaling and results in hyperglycemia, oxidative damage, and insulin resistance. *J Clin Invest* 2011; **121**: 4477-4490 [PMID: 21965330 DOI: 10.1172/JCI46243]

25 **Fröjdö S**, Durand C, Molin L, Carey AL, El-Osta A, Kingwell BA, Febbraio MA, Solari F, Vidal H, Pirola L. Phosphoinositide 3-kinase as a novel functional target for the regulation of the insulin signaling pathway by SIRT1. *Mol Cell Endocrinol* 2011; **335**: 166-176 [PMID: 21241768 DOI: 10.1016/j.mce.2011.01.008]

26 **Zhang HH**, Qin GJ, Li XL, Zhang YH, Du PJ, Zhang PY, Zhao YY, Wu J. SIRT1 overexpression in skeletal muscle *in vivo* induces increased insulin sensitivity and enhanced complex I but not complex II-V functions in individual subsarcolemmal and intermyofibrillar mitochondria. *J Physiol Biochem* 2015; **71**: 177-190 [PMID: 25782776 DOI: 10.1007/s13105-015-0396-x]

27 **Li F**, Li H, Jin X, Zhang Y, Kang X, Zhang Z, Xu M, Qian Z, Ma Z, Gao X, Zhao L, Wu S, Sun H. Adipose-specific knockdown of *Sirt1* results in obesity and insulin resistance by promoting exosomes release. *Cell Cycle* 2019; **18**: 2067-2082 [PMID: 31296102 DOI: 10.1080/15384101.2019.1638694]

28 **Wu SY**, Liang J, Yang BC, Leung PS. SIRT1 Activation Promotes β-Cell Regeneration by Activating Endocrine Progenitor Cells *via* AMPK Signaling-Mediated Fatty Acid Oxidation. *Stem Cells* 2019; **37**: 1416-1428 [PMID: 31400234 DOI: 10.1002/stem.3073]

29 **Hua R**, Wang GZ, Shen QW, Yang YP, Wang M, Wu M, Shao YK, He M, Zang Y, Yao QY, Zhang ZY. Sleeve gastrectomy ameliorated high-fat diet (HFD)-induced non-alcoholic fatty liver disease and upregulated the nicotinamide adenine dinucleotide +/ Sirtuin-1 pathway in mice. *Asian J Surg* 2021; **44**: 213-220 [PMID: 32712045 DOI: 10.1016/j.asjsur.2020.05.030]

30 **Huang H**, Aminian A, Hassan M, Dan O, Axelrod CL, Schauer PR, Brethauer SA, Kirwan JP. Gastric Bypass Surgery Improves the Skeletal Muscle Ceramide/S1P Ratio and Upregulates the AMPK/ SIRT1/ PGC-1α Pathway in Zucker Diabetic Fatty Rats. *Obes Surg* 2019; **29**: 2158-2165 [PMID: 30809769 DOI: 10.1007/s11695-019-03800-z]

31 **Wang Y**, Wang DS, Cheng YS, Jia BL, Yu G, Yin XQ, Wang Y. Expression of MicroRNA-448 and SIRT1 and Prognosis of Obese Type 2 Diabetic Mellitus Patients After Laparoscopic Bariatric Surgery. *Cell Physiol Biochem* 2018; **45**: 935-950 [PMID: 29428938 DOI: 10.1159/000487287]

32 **Pardo PS**, Boriek AM. SIRT1 Regulation in Ageing and Obesity. *Mech Ageing Dev* 2020; **188**: 111249 [PMID: 32320732 DOI: 10.1016/j.mad.2020.111249]

33 **Chen YR**, Fang SR, Fu YC, Zhou XH, Xu MY, Xu WC. Calorie restriction on insulin resistance and expression of SIRT1 and SIRT4 in rats. *Biochem Cell Biol* 2010; **88**: 715-722 [PMID: 20651844 DOI: 10.1139/O10-010]

34 **Civitarese AE**, Carling S, Heilbronn LK, Hulver MH, Ukropcova B, Deutsch WA, Smith SR, Ravussin E; CALERIE Pennington Team. Calorie restriction increases muscle mitochondrial biogenesis in healthy humans. *PLoS Med* 2007; **4**: e76 [PMID: 17341128 DOI: 10.1371/journal.pmed.0040076]

35 **Nemoto S**, Fergusson MM, Finkel T. Nutrient availability regulates SIRT1 through a forkhead-dependent pathway. *Science* 2004; **306**: 2105-2108 [PMID: 15604409 DOI: 10.1126/science.1101731]

36 **Rymarchyk S**, Kang W, Cen Y. Substrate-Dependent Sensitivity of SIRT1 to Nicotinamide Inhibition. *Biomolecules* 2021; **11** [PMID: 33670751 DOI: 10.3390/biom11020312]

37 **Wu Q**, Zhang X, Zhong M, Han H, Liu S, Liu T, Wei M, Guo W, Xie H, Hu S, Zhang G. Effects of Bariatric Surgery on Serum Bile Acid Composition and Conjugation in a Diabetic Rat Model. *Obes Surg* 2016; **26**: 2384-2392 [PMID: 26843082 DOI: 10.1007/s11695-016-2087-2]

38 **Patti ME**, Houten SM, Bianco AC, Bernier R, Larsen PR, Holst JJ, Badman MK, Maratos-Flier E, Mun EC, Pihlajamaki J, Auwerx J, Goldfine AB. Serum bile acids are higher in humans with prior gastric bypass: potential contribution to improved glucose and lipid metabolism. *Obesity (Silver Spring)* 2009; **17**: 1671-1677 [PMID: 19360006 DOI: 10.1038/oby.2009.102]

39 **Ryan KK**, Tremaroli V, Clemmensen C, Kovatcheva-Datchary P, Myronovych A, Karns R, Wilson-Pérez HE, Sandoval DA, Kohli R, Bäckhed F, Seeley RJ. FXR is a molecular target for the effects of vertical sleeve gastrectomy. *Nature* 2014; **509**: 183-188 [PMID: 24670636 DOI: 10.1038/nature13135]

40 **Ding L**, Sousa KM, Jin L, Dong B, Kim BW, Ramirez R, Xiao Z, Gu Y, Yang Q, Wang J, Yu D, Pigazzi A, Schones D, Yang L, Moore D, Wang Z, Huang W. Vertical sleeve gastrectomy activates GPBAR-1/TGR5 to sustain weight loss, improve fatty liver, and remit insulin resistance in mice. *Hepatology* 2016; **64**: 760-773 [PMID: 27312543 DOI: 10.1002/hep.28689]

41 **Ueno T**, Tanaka N, Imoto H, Maekawa M, Kohyama A, Watanabe K, Motoi F, Kamei T, Unno M, Naitoh T. Mechanism of Bile Acid Reabsorption in the Biliopancreatic Limb After Duodenal-Jejunal Bypass in Rats. *Obes Surg* 2020; **30**: 2528-2537 [PMID: 32291708 DOI: 10.1007/s11695-020-04506-3]

42 **Wang XX**, Edelstein MH, Gafter U, Qiu L, Luo Y, Dobrinskikh E, Lucia S, Adorini L, D'Agati VD, Levi J, Rosenberg A, Kopp JB, Gius DR, Saleem MA, Levi M. G Protein-Coupled Bile Acid Receptor TGR5 Activation Inhibits Kidney Disease

in Obesity and Diabetes. *J Am Soc Nephrol* 2016; **27**: 1362-1378 [PMID: 26424786 DOI: 10.1681/ASN.2014121271]

43 **Jiang T**, Wang XX, Scherzer P, Wilson P, Tallman J, Takahashi H, Li J, Iwahashi M, Sutherland E, Arend L, Levi M. Farnesoid X receptor modulates renal lipid metabolism, fibrosis, and diabetic nephropathy. *Diabetes* 2007; **56**: 2485-2493 [PMID: 17660268 DOI: 10.2337/db06-1642]

44 **Angelini G**, Castagneto Gissey L, Del Corpo G, Giordano C, Cerbelli B, Severino A, Manco M, Basso N, Birkenfeld AL, Bornstein SR, Genco A, Mingrone G, Casella G. New insight into the mechanisms of ectopic fat deposition improvement after bariatric surgery. *Sci Rep* 2019; **9**: 17315 [PMID: 31754142 DOI: 10.1038/s41598-019-53702-4]

45 **Peng Y**, Li JZ, You M, Murr MM. Roux-en-Y gastric bypass improves glucose homeostasis, reduces oxidative stress and inflammation in livers of obese rats and in Kupffer cells *via* an AMPK-dependent pathway. *Surgery* 2017; **162**: 59-67 [PMID: 28291540 DOI: 10.1016/j.surg.2017.01.012]

46 **Ruderman NB**, Xu XJ, Nelson L, Cacicedo JM, Saha AK, Lan F, Ido Y. AMPK and SIRT1: a long-standing partnership? *Am J Physiol Endocrinol Metab* 2010; **298**: E751-E760 [PMID: 20103737 DOI: 10.1152/ajpendo.00745.2009]

World Journal of Gastroenterology

Submit a Manuscript: https://www.f6publishing.com

World J Gastroenterol 2022 August 21; 28(31): 4351-4362

DOI: 10.3748/wjg.v28.i31.4351

ISSN 1007-9327 (print) ISSN 2219-2840 (online)

ORIGINAL ARTICLE

Retrospective Study

Approaches to reconstruction of inferior vena cava by *ex vivo* liver resection and autotransplantation in 114 patients with hepatic alveolar echinococcosis

Yusufukadier Maimaitinijiati, Tuerganaili AJi, Tie-Min Jiang, Bo Ran, Ying-Mei Shao, Rui-Qing Zhang, Qiang Guo, Mao-Lin Wang, Hao Wen

Specialty type: Gastroenterology and hepatology

Provenance and peer review: Unsolicited article; Externally peer reviewed.

Peer-review model: Single blind

Peer-review report's scientific quality classification

Grade A (Excellent): 0
Grade B (Very good): B, B
Grade C (Good): 0
Grade D (Fair): 0
Grade E (Poor): 0

P-Reviewer: Sánchez JIA, Colombia; Singh N, United States

Received: February 11, 2022
Peer-review started: February 11, 2022
First decision: May 29, 2022
Revised: June 10, 2022
Accepted: July 25, 2022
Article in press: July 25, 2022
Published online: August 21, 2022

Yusufukadier Maimaitinijiati, Tie-Min Jiang, Hao Wen, State Key Laboratory on Pathogenesis, Prevention and Treatment of High Incidence Diseases in Central Asia, The First Clinical College, Xinjiang Medical University, Urumqi 830011, Xinjiang Uygur Autonomous Region, China

Yusufukadier Maimaitinijiati, Tuerganaili AJi, Tie-Min Jiang, Bo Ran, Ying-Mei Shao, Rui-Qing Zhang, Qiang Guo, Mao-Lin Wang, Department of Hepatobiliary Surgery, The First Affiliated Hospital of Xinjiang Medical University, Urumqi 830011, Xinjiang Uygur Autonomous Region, China

Ying-Mei Shao, Hao Wen, Xinjiang Organ Transplant Institution, The First Affiliated Hospital of Xinjiang Medical University, Urumqi 830011, Xinjiang Uygur Autonomous Region, China

Corresponding author: Hao Wen, MD, PhD, Chief Doctor, Professor, State Key Laboratory on Pathogenesis, Prevention and Treatment of High Incidence Diseases in Central Asia, The First Clinical College, Xinjiang Medical University, No. 8 Liyushan South Road, Xinshi District, Xinjiang Uygur Autonomous Region 830011, Xinjiang, China. surgeon0309@126.com

Abstract

BACKGROUND

Hepatic alveolar echinococcosis (AE) is most commonly found in retrohepatic inferior vena cava (RHIVC). *Ex vivo* liver resection and autotransplantation (ELRA) can better realize the radical resection of end-stage hepatic AE with severely compromised hepatocaval confluences, and reconstruction of the affected vessels. Currently, there is a scarcity of information regarding RHIVC reconstruction in ELRA.

AIM

To propose reasonable RHICV reconstruction strategies for *ex vivo* liver resection and autotransplantation.

METHODS

We retrospectively summarized the clinical data of 114 patients diagnosed with hepatic AE who treated by ELRA in our department. A total of 114 patients were

divided into three groups according to the different reconstruction methods of RHIVC: Group A with original RHIVC being repaired and reconstructed (n = 64), group B with RHIVC being replaced (n = 43), and group C with RHIVC being resected without reconstruction (n = 7). The clinical data of patients, including the operation time, anhepatic phase, intraoperative blood loss, complications and postoperative hospital stay, were analyzed and the patients were routinely followed up. The normally distributed continuous variables were expressed as means ± SD, whereas the abnormally distributed ones were expressed as median and analyzed by analysis of variance. Survival curve was plotted by the Kaplan-Meier method.

RESULTS

All patients were routinely followed up for a median duration of 52 (range, 12-125) mo. The 30 d mortality rate was 7.0% (8/114) and 7 patients died within 90 d. Among all subjects, the inferior vena cava (IVC)-related complication rates were 17.5% (11/63) in group A and 16.3% (7/43) in group B. IVC stenosis was found in 12 patients (10.5%), whereas thrombus was formed in 6 patients (5.3%). Twenty-two patients had grade III or higher complications, with the complication rates being 17.2%, 16.3%, and 57.1% in the three groups. The average postoperative hospital stay in the three groups was 32.3 ± 19.8, 26.7 ± 18.2, and 51.3 ± 29.4 d (P = 0.03), respectively.

CONCLUSION

ELRA can be considered a safe and feasible option for end-stage hepatic AE patients with RHIVC infiltration. The RHIVC reconstruction methods should be selected appropriately depending on the defect degree of AE lesions in IVC lumen. The RHIVC resection without any reconstruction method should be considered with caution.

Key Words: *Ex vivo* liver resection; Alveolar echinococcosis; Inferior vena cava; Vascular reconstruction; Liver transplantation; Artificial vessel

©The Author(s) 2022. Published by Baishideng Publishing Group Inc. All rights reserved.

Core Tip: We retrospectively summarized and analyzed the clinical data of 114 patients diagnosed with hepatic alveolar echinococcosis (AE) treated by *ex vivo* liver resection and autotransplantation (ELRA) in our department between August 2010 and December 2020. This study is the first and largest cohort to specifically compare the different inferior vena cava (IVC) reconstruction methods in ELRA. We present a more quantitative IVC reconstruction strategy for end-stage hepatic AE patients with retrohepatic IVC infiltration based on the outcomes of this study and our experience.

Citation: Maimaitinijiati Y, AJi T, Jiang TM, Ran B, Shao YM, Zhang RQ, Guo Q, Wang ML, Wen H. Approaches to reconstruction of inferior vena cava by *ex vivo* liver resection and autotransplantation in 114 patients with hepatic alveolar echinococcosis. *World J Gastroenterol* 2022; 28(31): 4351-4362
URL: https://www.wjgnet.com/1007-9327/full/v28/i31/4351.htm
DOI: https://dx.doi.org/10.3748/wjg.v28.i31.4351

INTRODUCTION

Echinococcosis is an infectious zoonotic parasitic disease[1,2]. Notably, 90% of the global burden of this disease occurs in China, and echinococcosis has been a major public health problem in the Northwestern area of China[3,4]. Hepatic alveolar echinococcosis (AE) has been considered invasive growth and systematic metastasis[5,6], but its insidious onset and slow progression usually contribute to the delayed diagnosis. The mortality rate within 10 years after diagnosis is over 90% if the lesion is inadequately or not treated[7-9]. To date, radical surgery combined with albendazole treatment has been considered the best option for AE patients[10,11]. However, it is difficult to perform radical hepatectomy *in vivo* when AE lesion invades the hepatocaval confluence[12]. Generally, only 35%-40% of patients can be treated with conventional radical resection[7]. Fortunately, *ex vivo* liver resection and autotransplantation (ELRA) can better realize the radical resection of end-stage hepatic AE with severely compromised outflow tract, and reconstruction of the affected vessels[13].

Retrohepatic inferior vena cava (RHIVC) is often severely invaded by AE lesions, and resection of the invaded duct segment often presents a variety of irregular shapes, resulting in different inferior vena cava (IVC) reconstruction methods and the complex process. Proper RHIVC reconstruction may simplify graft liver implantation, which is a key element to postoperative recovery. To the best of our

knowledge, there have been few studies on the reconstruction of IVC in ELRA worldwide[14,15], and no clear consensus has been reached on the optimal strategy. This research reported our experience with 114 hepatic AE patients using different IVC reconstruction methods in ELRA. This is the study with the largest sample size to date, which provides a quantitative strategy of IVC reconstruction for end-stage hepatic AE patients with RHIVC infiltration.

MATERIALS AND METHODS

Patients

A total of 114 patients with end-stage hepatic AE who received ELRA at the First Affiliated Hospital of Xinjiang Medical University between August 2010 and December 2020 were retrospectively analyzed. All patients were divided into three groups: Group A was the repaired and reconstructed group (n = 64) that sought reconstruction of the original RHIVC by self-suture or vascular patch, group B was the RHIVC replacement group (n = 43) that completely replaced the RHIVC with substitute vessels, and group C was the RHIVC resection without reconstruction group (n = 7) that excised the invaded RHIVC segment without reconstruction (Table 1).

Medical ethical approval

This study was approved by the Ethics Committee of First Affiliated Hospital of Xinjiang Medical University and conducted in accordance with the Helsinki Declaration[16]. Written and signed informed consent was obtained from all patients or their legal custodians.

Preoperative assessment

All subjects underwent comprehensive preoperative evaluation, including abdominal computed tomography angiography (CTA) and hepatic magnetic resonance imaging, to assess the location of the lesion, the extent of vessel and bile duct involvement. For patients whose CTA results suggested RHIVC severe stenosis or occlusion, IVC digital subtraction angiography was also performed. The predicted autograft liver mass (GLM) was detected by a three-dimensional reconstruction system.

Surgical procedures

More details of the ELRA procedures are reported in our previous study[13]. Here, we focused on the reconstruction of IVC. First, we ligated and resected the IVC between the upward side of the confluence of three hepatic veins and the site at 1 cm above the confluence of renal vein, and removed it together with the liver. Then the RHIVC was reconstructed *in vitro* individually depending on the defect of lumen wall after radical resection of AE lesion. When the defect was less than 120° of the lumen circumference, it was considered that directly suturing the defect of wall did not affect vascular tension or patency, and thus self-suture repair was performed. When the defect was more than 120° of the circumference, we repaired the lumen defect with vascular patches such as ligamentum teres hepatis and internal jugular veins, because direct suturing might lead to stenosis in this case. Moreover, the RHIVC was replaced in patients with extensive defect and being unable to obtain adequate vascular patches. The hepatic veins of autograft liver were anastomosed with an alternative vessel. In this case, the position and angle of anastomosis were relatively freely controlled, which facilitated the increased reflux of hepatic outflow and further improved the recovery of autograft liver function (Figure 1).

Uniquely, for some patients in this study, the preoperative CTA and IVC venography showed that the RHIVC segment was completely occluded, and suitably compensated by the collateral branches. During the operation, we further verified whether the RHIVC was completely occluded and whether the collateral circulation was sufficient. Finally, for the 7 patients, the AE infiltrated segment of IVC was resected without any reconstruction, the proximal end of IVC was anastomosed with autogenous hepatic vein, and the distal end was closed directly (Figure 1).

Postoperative management and follow-up

After surgery, all patients received systemic anticoagulant therapy. Low-molecular-weight heparin was used in the 1st week, and prothrombin time (PT) and international normalized ratio (INR) were closely observed. In the 2nd week, oral tablets were substituted, and patients in group A and group C were recommended to withdraw these drugs 1 mo later when the PT and INR returned to normal levels. Patients in group B, however, needed to continue the medication for a long term and closely observe the coagulation index regularly. Each patient was regularly followed up, and serological tests, liver function tests and CTA scans were performed every 3-6 mo after discharge. Postoperative complications were assessed according to the Clavein-Dindo classification system[17]. All patients were administered with albendazole (10 mg/kg/d) routinely for 2 years[18].

Statistical analyses

The statistical software IBM SPSS 22.0 (IBM Corp, Armonk, NY, United States) was used for data

Table 1 Clinical data of 114 alveolar echinococcosis patients treated by *ex vivo* liver resection and autotransplantation

Characteristics	Group A, *n* = 64	Group B, *n* = 43	Group C, *n* = 7	Total, *n* = 114	*P* value
Sex					0.12
Male	24	21	5	50	
Female	40	22	2	64	
Age in yr	36.9 ± 12.3	36.9 ± 10.5	30.8 ± 14.1	36.2 ± 11.8	0.29
Hepatitis B (+)	3	3	1	7	0.37
Intervention history					0.84
No	30	27	5	62	
Hepatectomy	11	9	1	21	
PTCD or ERCP	17	7	1	25	
Albendazole history	16	11	0	27	0.31
Extrahepatic lesion					0.44
No	51	30	6	87	
Lung	10	9	1	20	
Kidney	1	1	1	3	
Atrium	0	1	0	1	
Brain	4	2	0	6	
Bone	0	1	0	1	

ERCP: Endoscopic retrograde cholangio-pancreatography; PTCD: Percutaneous transhepatic cholangial drainage.

analysis. The normally distributed continuous variables were expressed as means ± SD, whereas the abnormally distributed ones were expressed as medians and analyzed by analysis of variance. Survival curve was plotted by the Kaplan–Meier method. $P < 0.05$ was considered statistically significant.

RESULTS

Patient characteristics

Altogether 114 patients were treated by ELRA, including 50 males (43.9%) and 64 females (56.1%), with an average age of 36.2 ± 11.8 (range, 15-64) years. Preoperative PTCD or ERCP was performed in 25 patients to reduce the bilirubin levels and biliary obstructions. There were 21 patients with a previous history of hepatectomy. Albendazole therapy was administered to 27 patients. The average GLM was 828.3 ± 250.8 g. There were no significant differences in basic clinical data among the three groups ($P > 0.05$; Table 1).

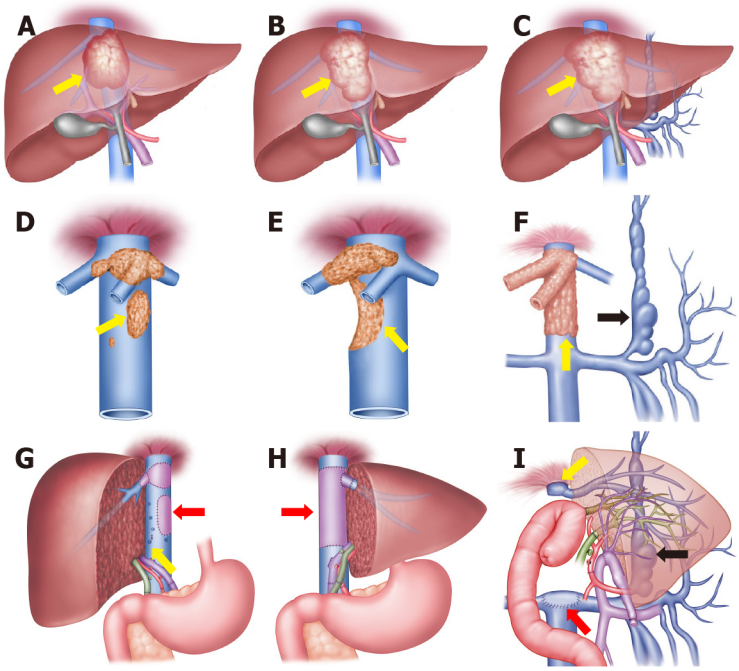
Intraoperative outcomes

Intraoperative reassessment confirmed that AE lesions invaded the RHIVC in all patients, and RHIVC repair or reconstruction was needed. Among them, the self-suture repairing was performed in 52 patients with a defective RHIVC lumen less than 120° of circumference after R0 resection. The lumen defect was repaired with autologous vascular patches in 12 patients whose defect was 120°-180° of wall circumference. Meanwhile, 43 patients had defect exceeding 180° of circumference with extensive range and difficulty in reestablishing with autogenous patches. For these cases, the RHIVC was replaced with artificial vascular grafts ($n = 38$) or allogeneic vascular ($n = 5$). In another 7 patients, preoperative imaging examination indicated that the RHIVC segment was occluded and a collateral circulation network was formed. During the operation, stable systemic hemodynamics with no obvious intestinal congestion was found after the IVC was ligated. Finally, the RHIVC was resected without reconstruction (Figure 2). The average operation time was 16.7 ± 2.9 h for group A, 15.5 ± 3.1 h for group B, and 16.9 ± 4.1 h for group C ($P = 0.56$), and the average anhepatic phase was 418.4 ± 108.3, 383.9 ± 117.0, and 337.4 ± 108.7 min in groups A, B and C ($P = 0.41$; Table 2).

Table 2 Intraoperative outcomes for 114 alveolar echinococcosis patients

	Group A, *n* = 64	Group B, *n* = 43	Group C, *n* = 7	Total, *n* = 114	*P* value
Operative time in h	16.7 ± 2.9	15.5 ± 3.2	16.9 ± 4.2	16.3 ± 3.1	0.56
Anhepatic phase in min	418.4 ± 108.3	383.9 ± 117.0	337.4 ± 108.7	394.0 ± 114.5	0.41
Blood loss in mL	1100 (400-15000)	1000 (400-8000)	2400 (800-14000)	1000 (400-15000)	0.07
Blood transfusion in U	5.8 ± 4.3	5.9 ± 3.9	14.8 ± 9.9	6.4 ± 6.2	0.90
Postoperative hospital stays in d	32.3 ± 19.8	26.7 ± 18.2	51.3 ± 29.4	36.4 ± 21.7	0.03
GLM in g	783.9 ± 233.5	908.6 ± 262.0	740.0 ± 235.6	828.3 ± 250.8	0.14
GLM/SLM, %	65.5 ± 18.9	74.1 ± 20.5	64.1 ± 17.8	68.6 ± 19.8	0.25
Materials (*n*)	Self-suture (52); Ligamentum teres hepatis (11); Internal jugular vein (1)	Artificial vascular (38); Allogeneic vascular (5)	Without reconstruction		

GLM: Graft liver mass; SLM: Standard liver mass.



DOI: 10.3748/wjg.v28.i31.4351 **Copyright** ©The Author(s) 2022.

Figure 1 Schematic diagrams of retrohepatic inferior vena cava reconstruction methods. A-C: Hepatic alveolar echinococcosis (AE) lesion invades the hepatocaval confluence; D: Retrohepatic inferior vena cava (RHIVC) is invaded by the AE lesion (yellow arrow); E: RHIVC is extensive invaded (yellow arrow); F: RHIVC completely occluded (yellow arrow), and compensation by the collateral branches (black arrow); G: Self-repairing reconstruction method, showed vascular patch repair (red arrow) and self-suture repair (yellow arrow); H: RHIVC replacement method, showed the RHIVC after replacement (red arrow); I: RHIVC resection without reconstruction method, showed IVC anastomoses with graft liver hepatic vein (yellow arrow) and adrenal vein (red arrow), the collateral circulation branches after operation (black arrow).

Postoperative and follow-up outcomes

All patients were followed up with a median duration of 52 (range, 12-125) mo, except for 1 patient who was lost to follow-up at 6 mo after the operation. No intraoperative death occurred. The 30 d mortality rate was 7.0% (8/114) and another 7 patients died within 90 d (15/114). Among all subjects, the IVC-related complication rates were 17.5% (11/63) in group A and 16.3% (7/43) in group B. IVC stenosis was found in 12 patients (10.5%), and thrombus was formed in 6 patients (5.3%). Twenty-two patients experienced grade III or higher complications according to the Clavin-Dindo classification system, and the complication rates were 17.2%, 16.3% and 57.1%, in the three groups (Table 3). The average

Table 3 Follow-up outcomes for 114 alveolar echinococcosis patients treated by *ex vivo* liver resection and autotransplantation

	Group A, *n* = 64	Group B, *n* = 43	Group C, *n* = 7	Total
Complications				
Clavien-Dindo Grade IIb or lower	27 (42.2%)	19 (44.2%)	3 (42.9%)	49 (43.0%)
Clavien-Dindo Grade IIIa or higher	11 (17.2%)	7 (16.3%)	4 (57.1%)	22 (19.3%)
IVC related complications				
IVC thrombosis	1 (1.6%)	5 (11.6%)	0	6 (5.3%)
IVC stenosis	10 (15.6%)	2 (4.7%)	0	12 (10.5%)
Liver related complications				
Biliary leakage	9 (14.1%)	7(16.3%)	3 (42.9%)	19 (16.7%)
Budd-chiari syndrome	1(1.6%)	1(2.33%)	0	2 (1.8%)
Hepatic dysfunction	8 (12.5%)	3(7.0%)	1 (14.3%)	12 (10.5%)
Pleural effusion	19	10	0	29
Ascites	8	6	3	17
Renal failure	3	0	0	3
Bone marrow suppression	0	0	1	1
Abdominal infection	2	2	1	5

IVC: Inferior vena cava.

postoperative hospital stay was 32.3 ± 19.8 d for group A, 26.7 ± 18.2 d for group B and 51.3 ± 29.4 d for group C (P = 0.03). Obviously, patients in group B obviously required a shorter postoperative hospital stay than the other two groups.

Kaplan-Meier survival analysis curve and log-rank test were used to observe the postoperative survival for the three groups based on the follow-up results. The survival rates of group A and group B were quite close, whereas that of group C was lower, but the differences were not statistically significant (P = 0.81). The early periods after surgery, especially in the 1st month, witnessed the high mortality rate (Figure 3).

DISCUSSION

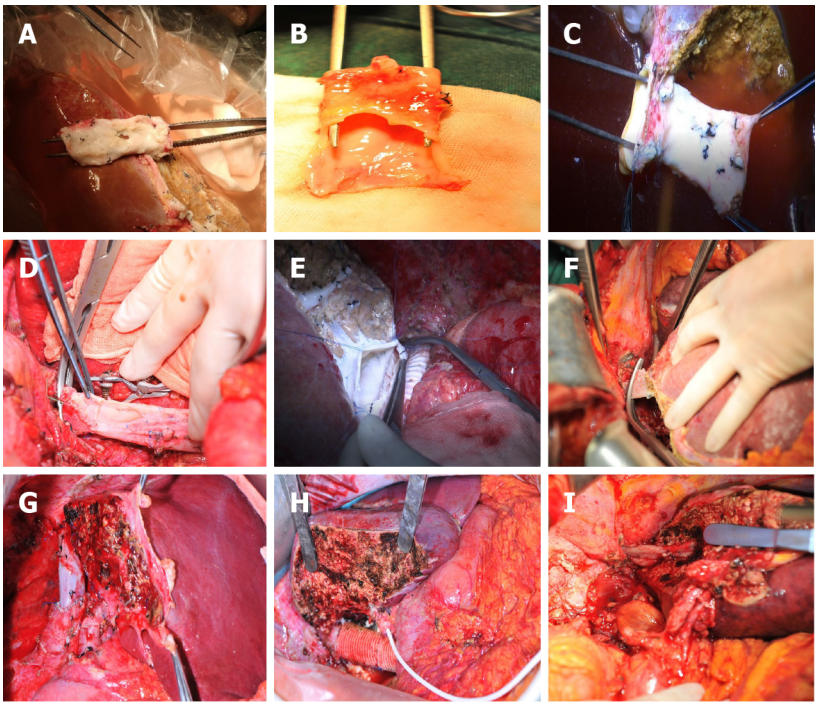
Hepatic AE is also known as "parasitic cancer," which is ascribed to its tumor-like characteristics with infiltration of vessels or biliary structures and distant metastasis[19]. The insidious onset and slow progression of AE usually contribute to the delayed diagnosis, and hepatic veins and RHIVC are often invaded by the time when treatment is sought in more than half of the patients, thus depriving them of the opportunity for traditional surgical resection[20,21]. In 1986, the Liver Transplantation Center of Bezancon Hospital in France was the first to report allogeneic liver transplantation (ALT) for an end-stage hepatic AE patient[22]. Since then, more successful clinical cases and treatment experience with liver transplantation for end-stage hepatic AE have been reported worldwide[23-26]. However, a shortage of donor livers and a significant recurrence rate have limited the further development of ALT for hepatic AE[24,27]. In 2010, our center first applied ELRA to manage a patient with end-stage hepatic AE[28]. Compared with ALT, this technique requires no graft donor or immunosuppressive treatment, and is more affordable[29,30]. In particular, it is more suitable for patients with severe invasion of RHIVC and intrahepatic veins whose are unresectable by traditional surgical methods. Notably, the corresponding reconstruction of autograft liver RHIVC remains the most challenging step in the ELRA procedures, since no uniform fixed pattern is available and individual design is required. To date, very few studies have investigated the reconstruction of IVC in ELRA worldwide (Table 4), and no clear consensus has been reached on the optimal reconstruction strategy. In this study, we analyzed the largest series of end-stage hepatic AE cases with seriously infringed RHIVC who received ELRA treatment, and discussed the safety and effectiveness of three different IVC reconstruction methods.

Reconstruction options for the RHIVC are assessed individually from preoperative evaluation and intraoperative reassessment of vascular defect. In our center, the repairing and reconstruction method was used when the defect in the RHIVC was less than 180° of the lumen circumference after radical resection of the lesion. The average operation time and anhepatic phase of this pattern were relatively

Table 4 Literature summary of inferior vena cava reconstruction in *ex vivo* liver resection and autotransplantation

Ref.	Number of cases	IVC reconstructed	Reconstructed type	Follow up time in mo	Effect of reconstruction
Wen *et al*[28], 2011	1	No	-	-	-
Hwang *et al*[34], 2012	6	No	-	-	-
Lei *et al*[15], 2015	1	Yes	III	12	Satisfied
Wen *et al*[29], 2016	15	No	-	-	-
Shen *et al*[14], 2018	45	Yes	I and II	22	Satisfied
Aji *et al*[13], 2018	69	No	-	-	-
Du *et al*[37], 2019	8	Yes	III	23	Satisfied
Ran *et al*[32], 2019	1	Yes	III	-	-
Kong *et al*[38], 2019	2	No	-	-	-
Yang *et al*[39], 2020	5	Yes	III	18	Unsatisfied
Zhang *et al*[40], 2020	1	Yes	II	6	Satisfied
Ran *et al*[41], 2021	7	Yes	III	64	Unsatisfied
Jiang *et al*[33], 2021	6	Yes	I	17.5	Satisfied

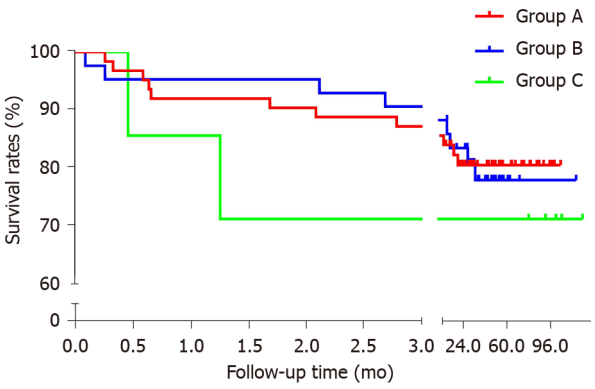
IVC: Inferior vena cava. Reconstructed type: I: Retrohepatic inferior vena cava (RHIVC) self-repairing reconstruction; II: RHIVC replacement; III: RHIVC resection without reconstruction; -: There is no related description.



DOI: 10.3748/wjg.v28.i31.4351 **Copyright** ©The Author(s) 2022.

Figure 2 Intraoperative procedures. A: The infiltrated retrohepatic inferior vena cava (RHIVC); B: The large defect of RHIVC after radical resection; C: The RHIVC with self-suture repairing; D: The original RHIVC anastomoses with hepatic vein; E: The artificial blood vessel anastomoses with graft liver hepatic vein; F: The suprahepatic IVC anastomoses with left hepatic vein; G: The autologous RHIVC after reconstruction; H: Artificial RHIVC; I: Anastomotic stoma of suprahepatic IVC and hepatic vein.

longer than the other two methods, which was attributed to the diversity and complexity of this approach. RHIVC stenosis occurred in 10 patients, but only 1 developed lower limb edema, and the symptoms disappeared after balloon dilation. Meanwhile, no clinical symptoms were found in the other 9 patients. It seemed that IVC stenosis after surgery might be related to the longer cold ischemia time and tunica intimal injury during the reconstruction process. In this regard, strict management of the



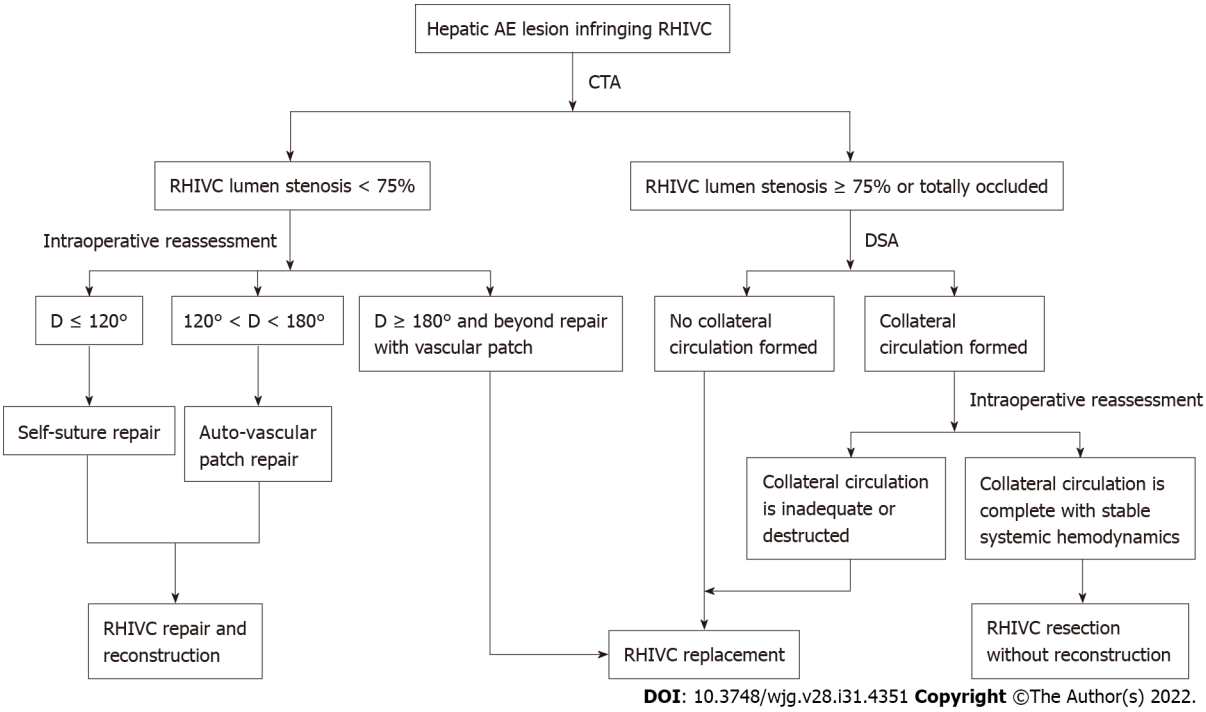
DOI: 10.3748/wjg.v28.i31.4351 **Copyright** ©The Author(s) 2022.

Figure 3 Kaplan-Meier survival analysis curve.

reconstruction time and shortening the cold ischemia phase as much as possible are the key factors for preventing IVC stenosis[31]. Based on previous reports[32,33] and our experience, the ligamentum teres hepatis is applied most often as a vascular patch, due to its convenience and strong plasticity. Postoperative patency and prognosis of these patients are satisfactory, suggesting that reconstruction with autogenous materials may be the optimal choice for RHIVC, although the process is complex and demanding.

Generally, replacement of the RHIVC is indicated for patients those with a large defect after resection that cannot be repaired by suture or patch. In the present study, 38 patients had the RHIVC replaced with artificial vessels, and 5 were treated with the cryopreserved allogeneic vascular donated after citizen death (DCD). Due to the shortage of resources, rejection, high preservation requirements and time restrictions, DCD vessels are not the first choice for substitute material. In our center, the expanded polytetrafluoroethylene artificial vessel (Sokang Corp, Shanghai, China)[34] is generally preferred. RHIVC replacement with artificial vascular is not only convenient, but also effectively shortens the anhepatic phase and operation time. On the other hand, artificial vessels are associated with potential risk, including venous thrombosis, artificial vascular malformation, and distortion or stenosis of anastomoses caused by postoperative liver hyperplasia. In our research, thrombosis of artificial vessels occurred in 5 patients, among them, 2 died of liver failure due to simultaneous thrombosis of the IVC and portal vein. Another 3 patients developed lower limb or scrotal edema, and the symptoms recovered after symptomatic treatments, including thrombolysis and anticoagulation. In addition, stenosis of anastomoses was found in 2 patients. As there may not be any clinical means for decreasing the incidence of graft thrombosis and stenosis apart from anti-coagulation and anti-infective treatment, we recommend that replacement of RHIVC with artificial materials should be avoided when it can be reestablished with autogenous materials.

Hepatic AE behaves like a slow-growing "warm cancer," and occlusion and severe stenosis of the IVC is a chronic process, which provides sufficient time for the establishment of collateral circulation. The obstructed blood flow can induce expansion of lumbar vein plexus, azygos vein and hemiazygos vein on both sides of the spine, as well as the formation of a functional collateral circulation network[32] Although the extent of vascular invasion is a vital indicator for the choice of reconstruction method, it remains controversial whether the IVC should be reconstructed for patients with adequate collateral circulation. Blair *et al*[35] proposed that, for low-grade retroperitoneal sarcoma, resection without reconstruction was performed after the establishment of collateral circulation. In addition, Hardwigse *et al*[36] also reported IVC resection without reconstruction in 6 patients with hepatic carcinoma. Unlike malignant tumors, the parasite grows relatively slow, which provides enough time for the organism to form collateral circulation. Among our subjects, 7 received RHIVC resection without reconstruction, since a sufficient collateral path was formed, but the outcomes were unsatisfactory. To be specific, postoperative complications occurred in all 7 patients, and their survival rate was only 71.1%. One patient died of liver failure on the 14th day after operation, and another one died of multiple organ failure caused by severe abdominal infection on the 38th day after operation. There is little previous information available concerning resection without reconstruction of the RHIVC in ELRA (Table 4). Before this study, Du *et al*[37] reported 8 patients receiving IVC resection without reconstruction, thus supporting this approach from the most reported cases at that time. In their subjects, 1 patient died of upper gastrointestinal bleeding, and 3 developed lower extremity or scrotal edema. Comparatively, the complication rate and postoperative hospital stay in our study were relatively high, which might be related to the immature collateral circulation or pathway destruction by excessive traction of diaphragm. It cannot be determined whether these poor outcomes are related to not providing reconstruction, and more studies are needed for further elucidation. To be sure, a comprehensive preoperative evaluation system and a meticulous intraoperative procedure are essential to the success of this method.



DOI: 10.3748/wjg.v28.i31.4351 **Copyright** ©The Author(s) 2022.

Figure 4 Strategy for retrohepatic inferior vena cava reconstruction in *ex vivo* liver resection and autotransplantation. CTA: Computed tomography angiography; D represents the defect of retrohepatic inferior vena cava lumen after resection; DSA: Digital subtraction angiography; RHIVC: Retrohepatic inferior vena cava.

Surgical planning based on a reasonable strategy can improve the success rate of operation and reduce related complications. In this study, although adverse outcomes were not entirely avoided, the postoperative complications and prognosis were acceptable, showing that our approaches were relatively safe and effective on end-stage hepatic AE with infiltrating outflow vessels of the liver. Based on the outcome of the present study and our experience, the following strategies are recommended for IVC reconstruction in hepatic AE patients treated by ELRA: (1) When the wall defect of the IVC after radical resection is less than 120° of the lumen circumference, the self-suture method can be used; (2) If the defect is 120°-180° of circumference, repair with autogenous vascular patches is the optimal choice; (3) When the defect has exceeded 180° of circumference and is difficult to repair by autologous patches, the RHIVC should be replaced. However, the strict anticoagulation therapy must be provided postoperatively; and (4) The RHIVC resection without reconstruction approaches are suitable when the IVC is completely blocked and the collateral circulation is fully formed (Figure 4). Although this study reports a retrospective single-center experience, it is also the largest cohort to specifically compare the different IVC reconstruction methods in ELRA, which can serve as a reference for IVC reconstruction in liver transplantation.

CONCLUSION

In short, ELRA can be considered a safe and feasible option for the end-stage hepatic AE patients with RHIVC infiltration. The RHIVC reconstruction approaches should be selected appropriately according to the lumen defect degree after radical resection. It should be emphasized that RHIVC resection without reconstruction should be considered with caution, and RHIVC reestablishment may be more beneficial for patients with poor compensation. Regrettably, the strategy does not consider the length of the wall defect, since it is related to the location, angle, elasticity and tension of the vessel, all of which are hard to be quantified without a larger dataset of cases. Therefore, prospective, multicenter studies with long-term follow-up are necessary to further evaluate and improve the strategy presented here.

ARTICLE HIGHLIGHTS

Research background

Ex vivo liver resection and auto-transplantation (ELRA) can better realize the radical resection of end-stage hepatic alveolar echinococcosis (AE) with severely compromised hepatocaval confluences, and the

reconstruction of the affected vessels.

Research motivation

There are no clear consensus has been reached on the strategy for retrohepatic inferior vena cava (RHIVC) reconstruction in ELRA.

Research objectives

To provide a strategy of RHIVC reconstruction for end-stage hepatic AE patients with hepatocaval confluence infiltration.

Research methods

The clinical data of 114 patients, including the operation time, anhepatic phase, intraoperative blood loss, complications and postoperative hospital stay, were analyzed and the patients were routinely followed up.

Research results

We found a lower survival rate in group C (resection without reconstruction method) than in groups A (self-suture repairing method) and B (replacement method). Also, the complications rate was higher in group C.

Research conclusions

The RHIVC reconstruction methods should be selected appropriately depending on the defect degree of AE lesions in IVC lumen.

Research perspectives

Our strategies can serve as a reference for IVC reconstruction in liver transplantation.

FOOTNOTES

Author contributions: Maimaitinijiati Y contributed to the conception and design, and drafting of the article; Maimaitinijiati Y and Ran B contributed to the acquisition of data, analysis, and interpretation of data; Jiang TM, Tuerganaili A, and Wen H contributed to the conception and design, and provision of study material; Jiang TM, Zhang RQ, Guo Q, and Wang ML contributed to the data collection; Shao YM did provision of study material; Zhang RQ analyzed the data; Wen H did final approval of the version to be submitted.

Institutional review board statement: The study was approved by the Human Ethics Committee of the First Affiliated Hospital of Xinjiang Medical University and conducted in accordance with the Declaration of Helsinki. All data were analyzed anonymously.

Informed consent statement: Informed written consent was obtained from the patient for publication of this report and any accompanying images.

Conflict-of-interest statement: The authors have no conflicts of interest to declare.

Data sharing statement: The datasets used and analyzed during the current study are available from the corresponding author on reasonable request.

Open-Access: This article is an open-access article that was selected by an in-house editor and fully peer-reviewed by external reviewers. It is distributed in accordance with the Creative Commons Attribution NonCommercial (CC BY-NC 4.0) license, which permits others to distribute, remix, adapt, build upon this work non-commercially, and license their derivative works on different terms, provided the original work is properly cited and the use is non-commercial. See: https://creativecommons.org/Licenses/by-nc/4.0/

Country/Territory of origin: China

ORCID number: Yusufukadier Maimaitinijiati 0000-0003-2069-9202; AJi Tuerganaili 0000-0001-6737-8874; Tie-Min Jiang 0000-0002-6100-1870; Bo Ran 0000-0002-0241-3410; Rui-Qing Zhang 0000-0003-3022-2555; Ying-Mei Shao 0000-0001-5154-345X; Qiang Guo 0000-0002-5943-4255; Mao-Lin Wang 0000-0001-8944-0894; Hao Wen 0000-0002-6431-9382.

S-Editor: Zhang H
L-Editor: Filipodia
P-Editor: Zhang H

REFERENCES

1 **McManus DP**, Zhang W, Li J, Bartley PB. Echinococcosis. *Lancet* 2003; **362**: 1295-1304 [PMID: 14575976 DOI: 10.1016/S0140-6736(03)14573-4]

2 **Eckert J**, Deplazes P. Biological, epidemiological, and clinical aspects of echinococcosis, a zoonosis of increasing concern. *Clin Microbiol Rev* 2004; **17**: 107-135 [PMID: 14726458 DOI: 10.1128/cmr.17.1.107-135.2004]

3 **Torgerson PR**, Keller K, Magnotta M, Ragland N. The global burden of alveolar echinococcosis. *PLoS Negl Trop Dis* 2010; **4**: e722 [PMID: 20582310 DOI: 10.1371/journal.pntd.0000722]

4 **Piarroux M**, Piarroux R, Giorgi R, Knapp J, Bardonnet K, Sudre B, Watelet J, Dumortier J, Gérard A, Beytout J, Abergel A, Mantion G, Vuitton DA, Bresson-Hadni S. Clinical features and evolution of alveolar echinococcosis in France from 1982 to 2007: results of a survey in 387 patients. *J Hepatol* 2011; **55**: 1025-1033 [PMID: 21354448 DOI: 10.1016/j.jhep.2011.02.018]

5 **Kern P**, Menezes da Silva A, Akhan O, Müllhaupt B, Vizcaychipi KA, Budke C, Vuitton DA. The Echinococcoses: Diagnosis, Clinical Management and Burden of Disease. *Adv Parasitol* 2017; **96**: 259-369 [PMID: 28212790 DOI: 10.1016/bs.apar.2016.09.006]

6 **Vuitton D**. Alveolar echinococcosis of the liver: a parasitic disease in search of a treatment. *Hepatology* 1990; **12**: 617-618 [PMID: 2401464 DOI: 10.1002/hep.1840120329]

7 **Bresson-Hadni S**, Vuitton DA, Bartholomot B, Heyd B, Godart D, Meyer JP, Hrusovsky S, Becker MC, Mantion G, Lenys D, Miguet JP. A twenty-year history of alveolar echinococcosis: analysis of a series of 117 patients from eastern France. *Eur J Gastroenterol Hepatol* 2000; **12**: 327-336 [PMID: 10750654 DOI: 10.1097/00042737-200012030-00011]

8 **Vuitton DA**, Azizi A, Richou C, Vuitton L, Blagosklonov O, Delabrousse E, Mantion GA, Bresson-Hadni S. Current interventional strategy for the treatment of hepatic alveolar echinococcosis. *Expert Rev Anti Infect Ther* 2016; **14**: 1179-1194 [PMID: 27686694 DOI: 10.1080/14787210.2016.1240030]

9 **Brunetti E**, Kern P, Vuitton DA; Writing Panel for the WHO-IWGE. Expert consensus for the diagnosis and treatment of cystic and alveolar echinococcosis in humans. *Acta Trop* 2010; **114**: 1-16 [PMID: 19931502 DOI: 10.1016/j.actatropica.2009.11.001]

10 **Filippou D**, Tselepis D, Filippou G, Papadopoulos V. Advances in liver echinococcosis: diagnosis and treatment. *Clin Gastroenterol Hepatol* 2007; **5**: 152-159 [PMID: 17157079 DOI: 10.1016/j.cgh.2006.08.017]

11 **Vuitton D A**, Bresson-Hadni S. Alveolar echinococcosis: evaluation of therapeutic strategies. *Expert Opin Orphan D* 2014; **67** [DOI: 10.1517/21678707.2014.870033]

12 **Qiu Y**, Yang X, Shen S, Huang B, Wang W. Vascular infiltration-based surgical planning in treating end-stage hepatic alveolar echinococcosis with ex vivo liver resection and autotransplantation. *Surgery* 2019; **165**: 889-896 [PMID: 30591376 DOI: 10.1016/j.surg.2018.11.007]

13 **Aji T**, Dong JH, Shao YM, Zhao JM, Li T, Tuxun T, Shalayiadang P, Ran B, Jiang TM, Zhang RQ, He YB, Huang JF, Wen H. Ex vivo liver resection and autotransplantation as alternative to allotransplantation for end-stage hepatic alveolar echinococcosis. *J Hepatol* 2018; **69**: 1037-1046 [PMID: 30031886 DOI: 10.1016/j.jhep.2018.07.006]

14 **Shen S**, Kong J, Zhao J, Wang W. Outcomes of different surgical resection techniques for end-stage hepatic alveolar echinococcosis with inferior vena cava invasion. *HPB (Oxford)* 2019; **21**: 1219-1229 [PMID: 30782476 DOI: 10.1016/j.hpb.2018.10.023]

15 **Lei JY**, Hao JC, Wang WT, Yan LN, Zhao JC, Huang B, Yuan D. Ex vivo liver resection followed by autotransplantation to a patient with advanced alveolar echinococcosis with a replacement of the retrohepatic inferior vena cava using autogenous vein grafting: a case report and literature review. *Medicine (Baltimore)* 2015; **94**: e514 [PMID: 25700312 DOI: 10.1097/MD.0000000000000514]

16 **World Medical Association**. World Medical Association Declaration of Helsinki: ethical principles for medical research involving human subjects. *JAMA* 2013; **310**: 2191-2194 [PMID: 24141714 DOI: 10.1001/jama.2013.281053]

17 **Dindo D**, Demartines N, Clavien PA. Classification of surgical complications: a new proposal with evaluation in a cohort of 6336 patients and results of a survey. *Ann Surg* 2004; **240**: 205-213 [PMID: 15273542 DOI: 10.1097/01.sla.0000133083.54934.ae]

18 **Wen H**, Vuitton L, Tuxun T, Li J, Vuitton DA, Zhang W, McManus DP. Echinococcosis: Advances in the 21st Century. *Clin Microbiol Rev* 2019; **32** [PMID: 30760475 DOI: 10.1128/cmr.00075-18]

19 **Conraths FJ**, Probst C, Possenti A, Boufana B, Saulle R, La Torre G, Busani L, Casulli A. Potential risk factors associated with human alveolar echinococcosis: Systematic review and meta-analysis. *PLoS Negl Trop Dis* 2017; **11**: e0005801 [PMID: 28715408 DOI: 10.1371/journal.pntd.0005801]

20 **Qian MB**, Abela-Ridder B, Wu WP, Zhou XN. Combating echinococcosis in China: strengthening the research and development. *Infect Dis Poverty* 2017; **6**: 161 [PMID: 29157312 DOI: 10.1186/s40249-017-0374-3]

21 **Bresson-Hadni S**, Koch S, Miguet JP, Gillet M, Mantion GA, Heyd B, Vuitton DA; European group of clinicians. Indications and results of liver transplantation for Echinococcus alveolar infection: an overview. *Langenbecks Arch Surg* 2003; **388**: 231-238 [PMID: 12905036 DOI: 10.1007/s00423-003-0394-2]

22 **Geering K**. Lipase and unspecific esterase activity in the fat body of Aedes aegypti L. *Acta Trop* 1975; **32**: 273-276 [PMID: 1988]

23 **Rajcáni J**, Krobová J, Málková D. Distribution of Lednice (Yaba 1) virus in the chick embryo. *Acta Virol* 1975; **19**: 467-472 [PMID: 1991]

24 **Koch S**, Bresson-Hadni S, Miguet JP, Crumbach JP, Gillet M, Mantion GA, Heyd B, Vuitton DA, Minello A, Kurtz S; European Collaborating Clinicians. Experience of liver transplantation for incurable alveolar echinococcosis: a 45-case European collaborative report. *Transplantation* 2003; **75**: 856-863 [PMID: 12660515 DOI: 10.1097/01.tp.0000054230.63568.79]

25 **Pan GD**, Yan LN, Li B, Lu SC, Zeng Y, Wen TF, Zhao JC, Cheng NS, Ma YK, Wang WT, Yang JY, Li ZH. Liver transplantation for patients with hepatic alveolar echinococcosis in late stage. *Hepatobiliary Pancreat Dis Int* 2004; **3**: 499-503 [PMID: 15567732]

26 **Li F**, Yang M, Li B, Yan L, Zen Y, Wen T, Zao J. Initial clinical results of orthotopic liver transplantation for hepatic alveolar echinococcosis. *Liver Transpl* 2007; **13**: 924-926 [PMID: 17538987 DOI: 10.1002/lt.21187]

27 **Bresson-Hadni S**, Blagosklonov O, Knapp J, Grenouillet F, Sako Y, Delabrousse E, Brientini MP, Richou C, Minello A, Antonino AT, Gillet M, Ito A, Mantion GA, Vuitton DA. Should possible recurrence of disease contraindicate liver transplantation in patients with end-stage alveolar echinococcosis? *Liver Transpl* 2011; **17**: 855-865 [PMID: 21455928 DOI: 10.1002/lt.22299]

28 **Wen H**, Dong JH, Zhang JH, Zhao JM, Shao YM, Duan WD, Liang YR, Ji XW, Tai QW, Aji T, Li T. Ex vivo liver resection followed by autotransplantation for end-stage hepatic alveolar echinococcosis. *Chin Med J (Engl)* 2011; **124**: 2813-2817 [PMID: 22040485]

29 **Wen H**, Dong JH, Zhang JH, Duan WD, Zhao JM, Liang YR, Shao YM, Ji XW, Tai QW, Li T, Gu H, Tuxun T, He YB, Huang JF. Ex Vivo Liver Resection and Autotransplantation for End-Stage Alveolar Echinococcosis: A Case Series. *Am J Transplant* 2016; **16**: 615-624 [PMID: 26460900 DOI: 10.1111/ajt.13465]

30 **Yang X**, Qiu Y, Huang B, Wang W, Shen S, Feng X, Wei Y, Lei J, Zhao J, Li B, Wen T, Yan L. Novel techniques and preliminary results of ex vivo liver resection and autotransplantation for end-stage hepatic alveolar echinococcosis: A study of 31 cases. *Am J Transplant* 2018; **18**: 1668-1679 [PMID: 29232038 DOI: 10.1111/ajt.14621]

31 **Rodrigues MG**, Castro PMV, Almeida TC, Danziere FR, Sergi Filho FA, Zeballos Sempertegui BE, Branez JR, Mota LT, Perosa de Miranda M, Gomes Dos Santos R, Genzini T. Impact of Cold Ischemia Time on the Function of Liver Grafts Preserved With Custodiol. *Transplant Proc* 2021; **53**: 661-664 [PMID: 33139037 DOI: 10.1016/j.transproceed.2020.03.002]

32 **Ran B**, Shao YM, Jiang TM, Zhang RQ, Guo Q, Abulizi A, Yimiti Y, Wen H, Aji T. Resection of retrohepatic inferior vena cava without reconstruction for hepatic alveolar echinococcosis. *Chin Med J (Engl)* 2019; **132**: 1623-1624 [PMID: 31205076 DOI: 10.1097/CM9.0000000000000297]

33 **Jiang T**, Ran B, Guo Q, Zhang R, Duan S, Zhong K, Wen H, Shao Y, Aji T. Use of the ligamentum teres hepatis for outflow reconstruction during ex vivo liver resection and autotransplantation in patients with hepatic alveolar echinococcosis: A case series of 24 patients. *Surgery* 2021; **170**: 822-830 [PMID: 33994007 DOI: 10.1016/j.surg.2021.03.040]

34 **Hwang S**, Jung DH, Ha TY, Ahn CS, Moon DB, Kim KH, Song GW, Park GC, Jung SW, Yoon SY, Namgoong JM, Park CS, Park YH, Park HW, Lee HJ, Lee SG. Usability of ringed polytetrafluoroethylene grafts for middle hepatic vein reconstruction during living donor liver transplantation. *Liver Transpl* 2012; **18**: 955-965 [PMID: 22511404 DOI: 10.1002/lt.23456]

35 **Blair AB**, Reames BN, Singh J, Gani F, Overton HN, Beaulieu RJ, Lum YW, Black JH 3rd, Johnston FM, Ahuja N. Resection of retroperitoneal sarcoma en-bloc with inferior vena cava: 20 year outcomes of a single institution. *J Surg Oncol* 2018; **118**: 127-137 [PMID: 29878363 DOI: 10.1002/jso.25096]

36 **Hardwigsen J**, Baqué P, Crespy B, Moutardier V, Delpero JR, Le Treut YP. Resection of the inferior vena cava for neoplasms with or without prosthetic replacement: a 14-patient series. *Ann Surg* 2001; **233**: 242-249 [PMID: 11176131 DOI: 10.1097/00000658-200102000-00014]

37 **Du Q**, Wang Y, Zhang M, Chen Y, Mei X, Li Y, Zhou Y, Fan H. A new treatment strategy for end-stage hepatic alveolar echinococcosis: IVC resection without reconstruction. *Sci Rep* 2019; **9**: 9419 [PMID: 31263143 DOI: 10.1038/s41598-019-45968-5]

38 **Kong J**, Shen S, Yang X, Wang W. Transhepatic-intrahepatic branches of the portal vein catheterization for ex vivo liver resection and autotransplantation: Two case reports of novel approach to perfuse the liver. *Medicine (Baltimore)* 2019; **98**: e14706 [PMID: 30882634 DOI: 10.1097/MD.0000000000014706]

39 **Yang X**, Wang T, Kong J, Huang B, Wang W. Resection of retrohepatic inferior vena cava without reconstruction in ex vivo liver resection and autotransplantation: a retrospective study. *BMC Surg* 2020; **20**: 56 [PMID: 32209078 DOI: 10.1186/s12893-020-00720]

40 **Zhang Y**, Xie P, Yang C, Yang H, Liu J, Zhou G, Deng S, Lau WY. Percutaneous stenting of left hepatic vein followed by Ex vivo Liver Resection and Autotransplantation in a patient with hepatic alveolar echinococcosis with Budd-Chiari syndrome. *Int J Surg Case Rep* 2020; **68**: 251-256 [PMID: 32199250 DOI: 10.1016/j.ijscr.2020.03.004]

41 **Ran B**, Maimaitinijiati Y, Yasen A, Jiang T, Zhang R, Guo Q, Shao Y, Wen H, Aji T. Feasibility of Retrohepatic Inferior Vena Cava Resection Without Reconstruction for Hepatic Alveolar Echinococcosis. *Am Surg* 2021; **87**: 443-449 [PMID: 33026233 DOI: 10.1177/0003134820951457]

World Journal of Gastroenterology

Submit a Manuscript: https://www.f6publishing.com

World J Gastroenterol 2022 August 21; 28(31): 4363-4375

DOI: 10.3748/wjg.v28.i31.4363

ISSN 1007-9327 (print) ISSN 2219-2840 (online)

ORIGINAL ARTICLE

Retrospective Study

Application of computed tomography-based radiomics in differential diagnosis of adenocarcinoma and squamous cell carcinoma at the esophagogastric junction

Ke-Pu Du, Wen-Peng Huang, Si-Yun Liu, Yun-Jin Chen, Li-Ming Li, Xiao-Nan Liu, Yi-Jing Han, Yue Zhou, Chen-Chen Liu, Jian-Bo Gao

Specialty type: Radiology, nuclear medicine and medical imaging

Provenance and peer review: Unsolicited article; Externally peer reviewed.

Peer-review model: Single blind

Peer-review report's scientific quality classification

Grade A (Excellent): A
Grade B (Very good): B, B
Grade C (Good): C
Grade D (Fair): 0
Grade E (Poor): 0

P-Reviewer: Ferreira GSA, Brazil; Ghoneim S, United States; Okasha H, Egypt; Sato H, Japan

Received: March 16, 2022
Peer-review started: March 16, 2022
First decision: June 11, 2022
Revised: June 11, 2022
Accepted: July 25, 2022
Article in press: July 25, 2022
Published online: August 21, 2022

Ke-Pu Du, Wen-Peng Huang, Yun-Jin Chen, Li-Ming Li, Yi-Jing Han, Yue Zhou, Chen-Chen Liu, Jian-Bo Gao, Department of Radiology, The First Affiliated Hospital of Zhengzhou University, Zhengzhou 450052, Henan Province, China

Si-Yun Liu, Department of Pharmaceutical Diagnostics, General Electric Company Healthcare, Beijing 100176, China

Xiao-Nan Liu, Department of Pathology, The First Affiliated Hospital of Zhengzhou University, Zhengzhou 450052, Henan Province, China

Corresponding author: Jian-Bo Gao, PhD, Academic Research, Chairman, Chief Doctor, Instructor, Department of Radiology, The First Affiliated Hospital of Zhengzhou University, No. 1 East Jianshe Road, Zhengzhou 450052, Henan Province, China.
jianbogaochina@163.com

Abstract

BACKGROUND

The biological behavior of carcinoma of the esophagogastric junction (CEGJ) is different from that of gastric or esophageal cancer. Differentiating squamous cell carcinoma of the esophagogastric junction (SCCEG) from adenocarcinoma of the esophagogastric junction (AEG) can indicate Siewert stage and whether the surgical route for patients with CEGJ is transthoracic or transabdominal, as well as aid in determining the extent of lymph node dissection. With the development of neoadjuvant therapy, preoperative determination of pathological type can help in the selection of neoadjuvant radiotherapy and chemotherapy regimens.

AIM

To establish and evaluate computed tomography (CT)-based multiscale and multiphase radiomics models to distinguish SCCEG and AEG preoperatively.

METHODS

We retrospectively analyzed the preoperative contrasted-enhanced CT imaging data of single-center patients with pathologically confirmed SCCEG (n = 130) and AEG (n = 130). The data were divided into either a training (n = 182) or a test group (n = 78) at a ratio of 7:3. A total of 1409 radiomics features were separately

extracted from two dimensional (2D) or three dimensional (3D) regions of interest in arterial and venous phases. Intra-/inter-observer consistency analysis, correlation analysis, univariate analysis, least absolute shrinkage and selection operator regression, and backward stepwise logical regression were applied for feature selection. Totally, six logistic regression models were established based on 2D and 3D multi-phase features. The receiver operating characteristic curve analysis, the continuous net reclassification improvement (NRI), and the integrated discrimination improvement (IDI) were used for assessing model discrimination performance. Calibration and decision curves were used to assess the calibration and clinical usefulness of the model, respectively.

RESULTS

The 2D-venous model (5 features, AUC: 0.849) performed better than 2D-arterial (5 features, AUC: 0.808). The 2D-arterial-venous combined model could further enhance the performance (AUC: 0.869). The 3D-venous model (7 features, AUC: 0.877) performed better than 3D-arterial (10 features, AUC: 0.876). And the 3D-arterial-venous combined model (AUC: 0.904) outperformed other single-phase-based models. The venous model showed a positive improvement compared with the arterial model (NRI > 0, IDI > 0), and the 3D-venous and combined models showed a significant positive improvement compared with the 2D-venous and combined models ($P < 0.05$). Decision curve analysis showed that combined 3D-arterial-venous model and 3D-venous model had a higher net clinical benefit within the same threshold probability range in the test group.

CONCLUSION

The combined arterial-venous CT radiomics model based on 3D segmentation can improve the performance in differentiating EGJ squamous cell carcinoma from adenocarcinoma.

Key Words: Esophagogastric junction; Squamous cell carcinoma; Adenocarcinoma; X-ray computed tomography; Radiomics

©The Author(s) 2022. Published by Baishideng Publishing Group Inc. All rights reserved.

Core Tip: In this study, multiscale and multiphase computed tomography (CT)-based radiomics models were constructed and evaluated to discriminate squamous cell carcinoma and adenocarcinoma of the esophagogastric junction (CEGJ) before operation. The results demonstrated that the combination of multiphase 3D CT radiomics features could improve the differentiation performance than 2D CT radiomics or single-phase-based radiomics. Therefore, radiomics method could help open up a new field for noninvasive diagnosis and personalized management of CEGJ.

Citation: Du KP, Huang WP, Liu SY, Chen YJ, Li LM, Liu XN, Han YJ, Zhou Y, Liu CC, Gao JB. Application of computed tomography-based radiomics in differential diagnosis of adenocarcinoma and squamous cell carcinoma at the esophagogastric junction. *World J Gastroenterol* 2022; 28(31): 4363-4375
URL: https://www.wjgnet.com/1007-9327/full/v28/i31/4363.htm
DOI: https://dx.doi.org/10.3748/wjg.v28.i31.4363

INTRODUCTION

Carcinoma of the esophagogastric junction (CEGJ) is defined as a carcinoma whose center is located within 5 cm above and below the esophagogastric anatomical junction and crosses the esophagogastric junction (EGJ). Due to the short and narrow EGJ site and the up-and-down invasive nature of the CEGJ, its biological behavior is different from that of gastric or esophageal cancer[1-3]. The Siewert staging, which is widely accepted in academia, classifies CEGJ into types I, II, and III based on the distance between the tumor center and the EGJ[4]. Because of the infiltrative growth pattern of the tumor, the distance between the tumor center and the EGJ in CEGJ is difficult to measure accurately, and Siewert staging is often not easy to determine directly. Squamous cell carcinoma of the esophagogastric junction (SCCEG) has different clinicopathological features from adenocarcinoma of the esophagogastric junction (AEG). Based on the results from previous research, mediastinal lymph node metastases are more likely to occur in SCCEG above the EGJ, whereas metastases from the AEG under the EGJ probably appear in the abdomen[5,6]. Differentiating SCCEG from AEG can indicate Siewert stage and whether the surgical route for patients with CEGJ is transthoracic or transabdominal, as well as aid in determining the extent of lymph node dissection. With the development of neoadjuvant therapy,

preoperative determination of pathological type can help in the selection of neoadjuvant radiotherapy and chemotherapy regimens.

Clinically, medical imaging plays a supporting role in pathological classification and tumor staging. Conventional computed tomography (CT), magnetic resonance imaging, and positron emission tomography rely primarily on the visual assessment of the imaging physician and have limitations in early identification of the pathological type of CEGJ. Although histological biopsies are commonly used in clinical practice, some patients have contraindications or low tolerance, and the biopsy sample is limited to the mucosal surface, which may provide an inadequate assessment of the entire tumor status [7]. Therefore, it is important to explore a reliable, practical, and non-invasive preoperative histological staging method for CEGJ, which is clinically important for neoadjuvant radiotherapy, surgical approach selection, and lymph node dissection in CEGJ patients. Radiomics technique uses a combined medical-industrial approach to transform traditional images into digital quantitative features, which has potential for digging the potential biological characteristics and heterogeneity of tumor images and has been widely and non-invasively used in the diagnosis, differential diagnosis, and disease evaluation[8-12]. Radiomics technique has also been studied in the differential diagnosis of squamous lung cancer and adenocarcinoma[13,14]. However, it is still unclear whether radiomics features extracted from CT images would be useful in predicting pathological type in patients with CEGJ.

Both of two-dimensional (2D) cross section or three-dimensional (3D) volume in CT images could be delineated for radiomics feature extraction. The reported radiomics-based gastric cancer studies have either utilized 2D or 3D segmentation[12,15]. However, it remains unclear whether to apply 2D or 3D regions of interest (ROIs) for pathological typing. The selection of 2D or 3D ROIs for outlining can influence radiomics feature values, feature stability, feature screening, and discriminative model performance[16-18]. And the controversy still exists for the performance of diagnosis or prognosis between 2D and 3D radiomics in tumor[16-18].

Therefore, in the current study, we aimed to construct and evaluate the multiscale and multiphase CT-based radiomics to discriminate SCCEG and AEG. The developed CT-based models might provide assistance in the personalized and precise treatment of clinical CEGJ patients, especially in the selection of surgical approach and determination of the extent of lymph node dissection.

MATERIALS AND METHODS

Patient selection

With institutional review board approval (ethical approval number: 2021-ky-1070-002) and waiver of the written informed consent, we retrospectively collected patients with SCCEG confirmed by gastroscopy and surgical pathology at the First Affiliated Hospital of Zhengzhou University from January 2010 to June 2021. The patient enrollment criteria included: (1) CT-enhanced abdominal examination within 30 d before surgery; (2) Complete clinicopathological data available; (3) The lesion covers at least 3 slices on CT cross section, and the maximum plane diameter is not less than 2 cm; and (4) No neoadjuvant chemoradiotherapy prior to CT examination. The exclusion criteria included: (1) Patient's history of other malignant tumors in combination; (2) Poor CT image quality or lack of raw DICOM data; and (3) Combined heart, lung, and other important organ dysfunction which could not allow CT examination to be performed. Finally, 130 patients with SCCEG were included, including 87 males and 43 females, aged 38-89 (65.72 ± 8.84) years, with a disease duration of 5 d to 4 years and main symptoms of dysphagia, obstructive sensation of eating, and abdominal pain. Another 130 patients with AEG who were matched with the SCCEG patients were also recruited, including 93 males and 37 females, aged 31-83 (62.95 ± 9.91) years.

CT image acquisition

Informed consent forms were signed before all patients underwent contrast-enhanced CT scans. CT scans were acquired using a 64-row CT scanner (GE Healthcare, Discovery CT 750 HD, United States) or 256-row CT scanner (GE Healthcare, Revolution CT, United States). Preparation for the examination: fasting for more than 8 h before the examination, intramuscular injection of scopolamine 10-20 mg 15-20 min before the examination to reduce gastrointestinal motility (Hangzhou Minsheng Pharmaceutical PG Roup Co., Ltd. Specifications: 10 mg/mL), and perform breath-holding exercises. Drink 800-1 000 mL of warm water 10 to 15 min before the examination. Scanning parameters: tube voltage 120 kV, tube current using automatic milliampere second technology, pitch 1.375/1.1; field of view (FOV) of 500 mm; 512 mm x 512 mm matrix, scan thickness 0.625mm to 5 mm, scan spacing 0.625mm to 5mm. Scan area: at least encompasses the lower esophagus to the lower border of both kidneys. Enhancement scan: 90-100 mL of non-ionic contrast agent was injected through the elbow vein using a high-pressure syringe (GE Medical Systems, iopromide, 370 mg/mL).

Image processing and segmentation

The arterial- and venous-phase CT images were isotropically resampled with a voxel size of 1 mm × 1 mm × 1 mm by using the trilinear interpolation in the Artificial Intelligence Kit software (A.K, version:

3.3.0.R, GE Healthcare, United States), in order to minimize the effect of different scanning protocols or equipment on quantitative inhomogeneity of histological features[19]. 2D ROIs were outlined along the largest cross-sectional area in the axial plane of CT images. After delineating the tumor cross-sectional area slice-by- slice in the axial plane, 3D ROIs were finally merged into volume of interest (VOI) (Figures 1 and 2). Care should be taken to avoid the gastric cavity and stomach contents, fatty tissue around the stomach wall, and blood vessels when segmenting. The 2D ROI or 3D VOI delineation was conducted by a radiologist (Chen YJ, 6 years of experience in imaging diagnosis). In order to ensure the reliability and reproducibility of the radiomics features, 30 patients were randomly selected to be segmented in a 2D and 3D manner. For inter-observer agreement analysis, when the radiologist (Chen YJ) conducted the first-time whole-dataset segmentation, another radiologist (Huang WP, 7 years of experience in imaging diagnosis) delineated the selected 30 patients at the same period. For intra-observer agreement analysis, the radiologist (Chen YJ) repeatedly conducted the segmentation 1 mo after the first-time delineation.

Radiomics feature extraction

The 2D or 3D radiomics features were extracted with open-source Python package Pyradiomics[20]. There were respectively 1409 radiomics features extracted from 2D or 3D ROIs in the arterial or venous phase. The original images and the transformed images based on different filters were mainly used for feature extraction. A total of 107 features were extracted from the original images, including 18 intensity statistical and 14 shape-based features. There were 75 textural features extracted from Gray Level Cooccurrence Matrix (GLCM), Gray Level Run Length Matrix (GLRLM), Gray Level Size Zone Matrix (GLSZM), Gray Level Dependence Matrix (GLDM), and Neighboring Gray Tone Difference Matrix (NGTDM). In addition, the same number of first-order grayscale statistical features and texture features were extracted based on different transformed images. A total of 744 features were extracted based on wavelet decomposition images with eight filter channels, 279 features were extracted based on Laplacian of Gaussian (LoG) transform images (sigma parameters selected as 1.0 mm, 3.0 mm, and 5.0 mm), and 279 features were extracted based on Local Binary Pattern (LBP) filtered images (2^{nd} order spherical harmonic function, spherical neighborhood operator with radius 1.0 and fine fraction 1)[20]. The features were extracted by discretizing the CT values within the ROIs based on a fixed interval width (bin width = 25 HU). The 2D and 3D radiomics features extracted from the randomly selected patients were used to calculate the intra-/inter-class correlation coefficients (ICCs). 2D or 3D features with intra- and inter-observer ICC values simultaneously greater than 0.75 were retained, which meant that the features with good repeatability were involved in the further analysis[18,21].

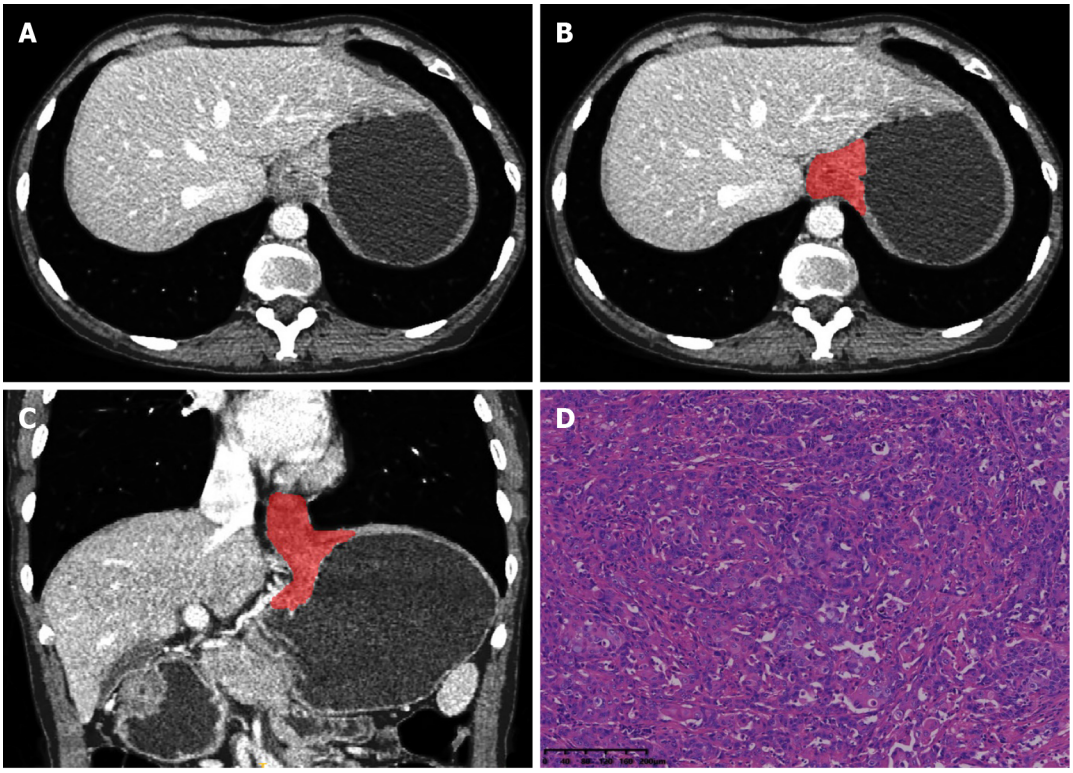
Feature selection and model construction

The 260 cases of data were divided into a training group and an internal test group by randomly stratified sampling at a ratio of 7:3. The training group was mainly used for preprocessing parameter determination, and feature screening and modeling, and the same treatment process, parameters, and model were applied to the test group for internal test. The same method was used for feature preprocessing and feature screening in the arterial and venous phase training samples, and independent arterial and venous radiomics models were established. The feature selection and final modeling procedure were performed as follows. The features were first preprocessed by excluding features with variance < 1.0, filling missing values with the median and *Z*-score normalization, and excluding collinear features with a cut-off value of correlation coefficients larger than 0.7. Then the Mann-Whitney *U*-test or *t*-test was used to select features with a significant difference between two classes ($P < 0.05$). The least absolute shrinkage and selection operator (LASSO) logistic regression (minimum binomial deviance) with 10-fold cross validation was conducted to avoid overfitting and the features with non-zero coefficients were retained[22]. Finally, the retained features were inputted into backward stepwise logistic regression with the minimum Akaike Information Criterion (AIC) to develop the regression radiomics model. The "Radscore" of each patient was calculated according to the formula (Radscore = $\beta_0 + \sum\beta_i x_i$, β_0 is a constant term and βi is the regression coefficient of the feature *x*i).

Four independent radiomics models were constructed, including: 2D arterial-phase model ($Radscore^{AP_2D}$), 2D venous-phase model ($Radscore^{VP_2D}$), 3D arterial-phase model ($Radscore^{AP_3D}$), and 3D venous-phase model ($Radscore^{VP_3D}$). Two combined models were derived based on the established independent model Radscore according to the regression formula (Radscore = $\beta_0 + \sum\beta_i x_i$, β_0 is a constant term and βi is the logistic regression coefficient of the model score *x*i). And the 2D arterial-venous combined model 3 ($Radscore^{AP_VP_2D}$) and 3D arterial-venous combined model ($Radscore^{AP_VP_3D}$) were established.

Evaluation of model predictive performance

The performance of the models was evaluated by using receiver operating characteristic curve (ROC) analysis to obtain the area under the ROC curve (AUC). The sensitivity, accuracy, negative predictive value, and positive predictive value were calculated based on the cut-off values corresponding to the maximum Youden index to evaluate the discrimination performance of the models. The cut-off values of the training group were applied to the test group to obtain their corresponding ROC parameters in



DOI: 10.3748/wjg.v28.i31.4363 **Copyright** ©The Author(s) 2022.

Figure 1 A 43-year-old man with squamous cell carcinoma of the esophagogastric junction. A: Axial computed tomography image in venous phase; B: Schematic diagram of 2D region of interest (ROI) segmentation on ITK-SNAP software; C: Schematic diagram of 3D ROI segmentation on ITK-SNAP software; D: Postoperative pathological image confirming squamous cell carcinoma of the esophagogastric junction (HE staining, × 200).

the test group. The calibration curve analysis and the Hosmer-Lemeshow test were used for evaluating model calibration and the goodness of fit ($P > 0.05$ indicates a good model fit). Delong's test was used to compare the AUC between paired models. Continuous net reclassification improvement (NRI) and integrated discrimination improvement (IDI) were used to assess ability of the models in improving the classification effectiveness[18]. The decision curve analysis (DCA) was used to assess the net clinical benefit or clinical utility of each model at different threshold probabilities.

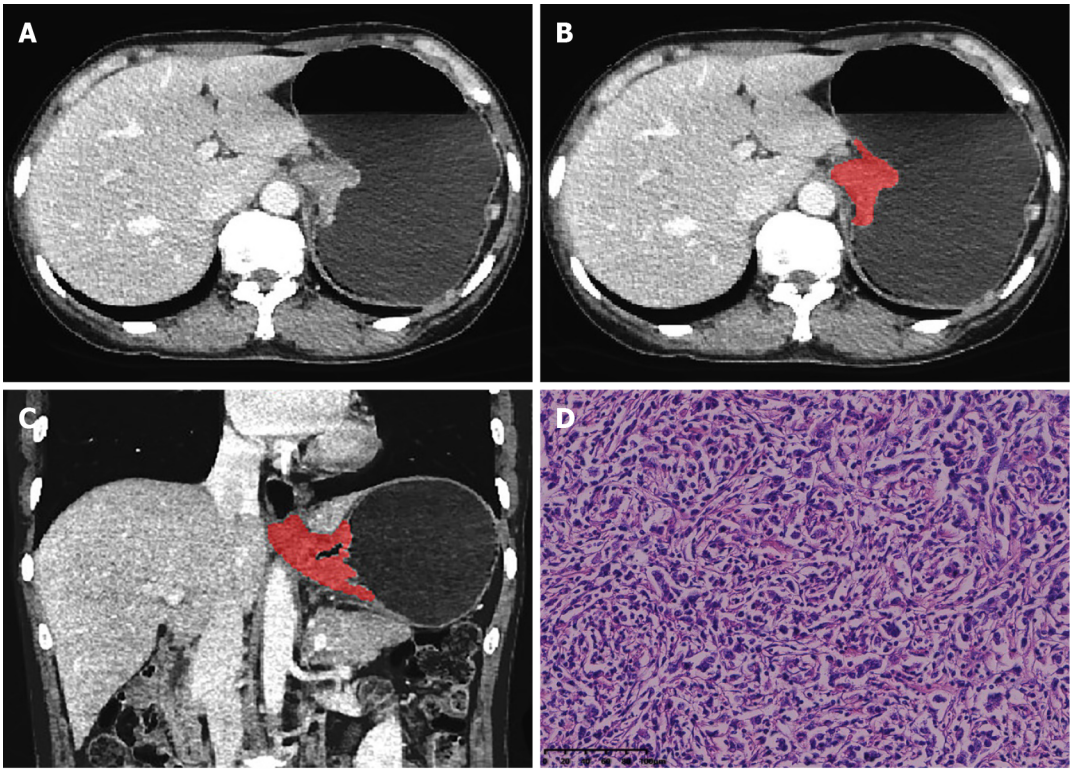
Statistical analysis

R software (version 3.6.3, http://www.r-project.org) was applied for statistical analyses in the current study. Radiomics features and Radscore are continuous variables, and data normality was tested using kurtosis and skewness values, and comparisons between two groups were made using independent samples *t*-test (for data with a normal distribution) or Mann-Whitney *U* test (for data not following a normal distribution). Categorical variables were tested by chi-square test or Fisher's exact test. A two-sided $P < 0.05$ was considered statistically significant. The optimism of the prediction accuracy of the model was validated using 1000-times Bootstrap in the training group. The following R packages were applied: "icc" for intra-/inter-class correlation coefficient; "glmnet" for logistic regression; "pROC" for ROC analysis; "rmda" for DCA; calibration function in the "rms" package for calibration analysis, and the "PredictABEL" package for NRI and IDI analysis.

RESULTS

Feature screening and model construction

Arterial phase model based on 2D ROI: A total of 175 radiomics features (ICCs > 0.75) were retained among 1409 features. There were 61 and 6 features retained rafter variance and correlation analysis, respectively. Among 6 features screened by univariate analysis and 10-fold cross validation LASSO regression (Figure 3A and B), 5 were further selected by stepwise logistic regression analysis. The Radscore^{AP_2D} is summarized in Supplementary Figure 1. The results of ICCs for individual features are shown in Supplementary Table 1 and the multivariable logistic regression results of features involved in the model are summarized in Supplementary Table 2. ROC curves for single 2D arterial features to identify SCCEG and AEG are shown in Supplementary Figure 2A and The 2D arterial model radiomics



DOI: 10.3748/wjg.v28.i31.4363 **Copyright** ©The Author(s) 2022.

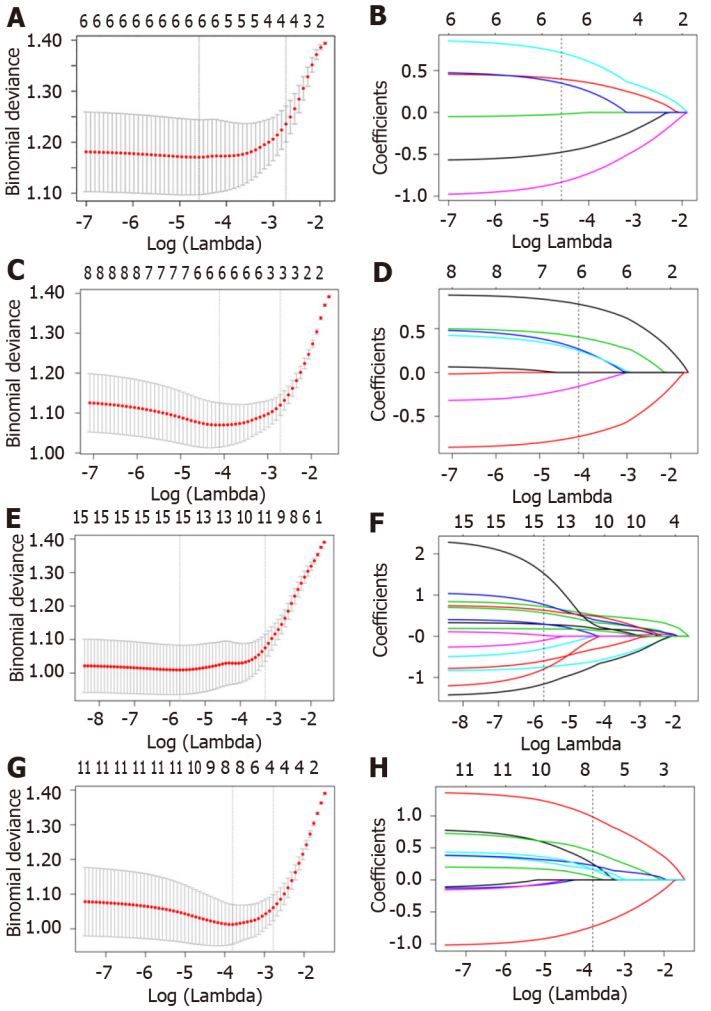
Figure 2 A 56-year-old man with adenocarcinoma of the esophagogastric junction. A: Axial computed tomography image in venous phase; B: Schematic diagram of 2D region of interest (ROI) segmentation on ITK-SNAP software; C: Schematic diagram of 3D ROI segmentation on ITK-SNAP software; D: Postoperative pathological image confirming adenocarcinoma of the esophagogastric junction (HE staining, × 200).

features and the differences of Rad-score^{AP_2D} in the training and test groups are shown in Supplementary Table 3.

Venous phase model based on 2D ROI: A total of 275 radiomics features (ICCs > 0.75) were retained among 1409 features. There were 124 and 12 features kept after variance and correlation analysis, respectively. Among 6 features screened by univariate analysis and 10-fold cross validation LASSO regression (Figure 3C and D), 5 were kept by stepwise logistic regression analysis. The Radscore^{VP_2D} is summarized in Supplementary Figure 3. The results of ICCs for individual features are shown in Supplementary Table 4 and the multivariable logistic regression results of features involved in the model are summarized in Supplementary Table 5. ROC curves for single 2D venous features to identify SCCEG and AEG are illustrated in Supplementary Figure 2C and The 2D venous model radiomics features and the differences of Rad-score^{VP_2D} in the training and test groups are shown in Supplementary Table 6.

Arterial phase model based on 3D ROI: A total of 714 radiomics features (ICCs > 0.75) were retained among 1409 features. There were 358 and 27 features kept after variance and correlation analysis, respectively. Among 15 features screened by univariate analysis and 10-fold cross validation LASSO regression (Figure 3E and F), 10 were kept by stepwise logistic regression analysis. The Radscore^{AP_3D} is summarized in Supplementary Figure 4. The ICCs for individual features are shown in Supplementary Table 7 and the multivariable logistic regression results of features involved in the model are summarized in Supplementary Table 8. ROC curves for single 3D arterial features to identify SCCEG and AEG are shown in Supplementary Figure 2E and the 3D arterial model radiomics features and the differences of Rad-score^{AP_3D} in the training and test groups are summarized in Supple-mentary Table 9.

Venous phase model based on 3D ROI: A total of 774 radiomics features (ICCs>0.75) were retained among 1409 features. There were 355 and 23 features kept after variance and correlation analysis, respectively. Among 8 features screened by univariate analysis and 10-fold cross validation LASSO regression (Figure 3G and H), 7 were kept by stepwise logistic regression analysis, and the Radscore^{VP_3D} is summarized in Supplementary Figure 5. The ICCs result for individual features are shown in Supplementary Table 10 and the multivariable logistic regression results of features involved in the model are summarized in Supplementary Table 11. ROC curves for single 3D venous features to identify SCCEG and AEG are shown in Supplementary Figure 2G and The 3D venous model radiomics features and the differences of Rad-score^{VP_3D} in the training and test groups are summarized in



DOI: 10.3748/wjg.v28.i31.4363 **Copyright** ©The Author(s) 2022.

Figure 3 Least absolute shrinkage and selection operator logistic regression feature screening graphs. The radiomics feature screening using the least absolute shrinkage and selection operator regression was performed to select the optimal model parameter λ using 10-fold cross-validation. A, C, E, and G: Graphs of binomial deviation of 2D-arterial model, 2D-venous model, 3D-arterial model, and 3D-venous model with parameter λ, respectively. The dashed lines indicate the selected optimal log(λ) values and the location of one standard error; B, D, F, and H: Graphs of variation of the radiomics characteristic coefficients with log(λ) for 2D-arterial model, 2D-venous model, 3D-arterial model, and 3D-venous model, respectively. The dotted line indicates the location of the selected optimal log(λ) value.

Supplementary Table 12.

2D arterial-venous combined model

By combining Radscore^{AP_2D} and Radscore^{VP_2D}, the 2D arterial-venous combined model was derived and the Radscor^{AP_VP_2D} is described in Supplementary Figure 6.

3D arterial-venous combined model

By combining Radscore^{AP_3D} and Radscore^{VP_3D}, the 3D arterial-venous combined model was derived and the Radscor^{AP_VP_3D} is summarized in Supplementary Figure 7.

In this study, a total of 10 candidate radiomics feature parameters were screened out in 2D arterial and venous phase images, mostly first-order features and texture features extracted based on Log transformed or wavelet transformed images, and the main categories included 4 first-order features, 2 GLRLM features, 2 GLSZM features, 1 GLDM feature, and 1 NGTDM feature. More features were screened out in the 3D arterial phase and venous phase images—17 in total, and the main categories included 6 first-order features, 4 GLDM features, 4 NGTDM features, 1 GLRLM feature, 1 GLSZM feature, and 1 GLCM feature.

Radiomics model performance

The AUC, specificity, sensitivity, accuracy, positive predictive value, and negative predictive value of the 6 models developed in this study to discriminate SCCEG from AEG in the training and test groups

are summarized in Table 1, and the ROC curves are shown in Figure 4. The model optimism was assessed by 1000-times bootstrap as shown in Table 2. It indicated that the 2D-arterial, 2D-venous, 3D-arterial, and 3D-venous model presented a degree of optimism less than 0.1 during repeated sampling. The Delong test results in the training and test groups are shown in Supplementary Table 13. All the 2D models had an AUC greater than 0.800 in the test group, except for the arterial model, which had an AUC of 0.752 in the test group. The AUC values of the venous model were higher than those of the arterial model (0.849 *vs* 0.808 and 0.831 *vs* 0.752) in both the training and test groups. All the 3D models had a higher AUC in the venous model than in the arterial model. In the combined models, both the 3D and 2D models were higher than their independent phase model both in the training and test groups. When comparing the performance between 2D and 3D models, the results showed that no matter for the independent phase model or the multi-phase-combined model, 3D models performed with a higher AUC than 2D models. Among all the models, the 3D-arterial-venous combined model had the highest AUC values of 0.904 and 0.901 in the training and test groups, respectively. As some statistical significance was not obvious during the Delong test, continuous NRI and IDI analyses were performed to evaluate the ability of each model for improving the classification and the results are shown in Supplementary Table 14. In both the training and test groups, the venous model demonstrated a positive improvement in discrimination over the arterial model (NRI > 0, IDI > 0), the 3D-venous model demonstrated a significant positive improvement in discrimination over the 2D-venous model (P < 0.05), both in the 3D model and in the 2D model, the combined model demonstrated a significant positive improvement in discrimination over the arterial model (P < 0.05); the 3D combined model reflected a significant positive improvement in discrimination compared with the 2D combined model (P < 0.05). In addition, the calibration curve (Figure 5) and the results of the Hosmer-Lemeshow test (Supplementary Table 15) indicate that the six models had good calibration. The clinical utility of the model was confirmed by the decision curve (Figure 6), in which the 3D-arterial-venous combined model and the 3D-venous model had higher net benefits in the test group within a threshold probability interval of 0.3-1.

DISCUSSION

In the current study, the multiscale and multiphase CT-based radiomics method was used to preoperatively discriminate SCCEG and AEG. The results showed that the combination of multiphase 3D CT radiomics features could improve the differentiation performance. Therefore, radiomics method could help open up a new field for noninvasive diagnosis and personalized management of CEGJ. Histopathology biopsy is a commonly used clinical method, and these radiomics features are considered to be complementary to histology biopsy but not a complete substitute for histopathology at this time. Repeat biopsy or endoscopic ultrasound deeper biopsies should be recommended if upper endoscopic biopsies are inconclusive or if it conflicts with the results suggested by radiomics features. Radiomics can provide an adequate reference if the patient has contraindications and low tolerance to endoscopic biopsy.

Previous studies have focused on the quantitative parameters of spectral CT. Zhou *et al*[23] found that the normalized iodine concentration, the $K_{40\text{-}70\ keV}$, and the effective atomic number in the arterial phase could identify SCCEG and AEG; the AUC values were 0.720, 0.730, and 0.706, respectively. Radiomics uses mathematically describable imaging features to comprehensively analyze tumor heterogeneity[24], and has not been validated for identifying SCCEG from AEG. Therefore, we tried to use radiomics features to identify the pathological type of CEGJ by comprehensively considering the effectiveness of different phases and segmentation method. In this study, more features were screened out in the 3D models of different phases than in the 2D models, which is related to the fact that the 3D ROIs contain the lesion as a whole and the extracted features have a larger distribution. The results showed that the efficacy of the venous features was higher than that of the arterial features in identifying SCCEG from AEG. Pathologically, squamous carcinoma grows faster and tends to grow in a swelling superposition with denser tissue structure, while adenocarcinoma mostly grows in an appendicular pattern with looser tissue structure[25]. With the prolongation of scanning time, the contrast agent continuously penetrates into the interstitial space of tumor cells, and more textural features appear in the venous phase, which better reflects the heterogeneous characteristics of squamous carcinoma. Tumor vascularization is a kind of biological behavior that reconstructs nutrition connection and promotes tumor development. Pathologic types, tumor origin, and structure of the microvasculature affect the enhancement pattern and radiomics-based parameters.

We found that among the features retained in the venous model, Dependence variance (GLDM) and Large dependence high gray level emphasis (GLDM) had larger weight in the 3D and 2D models, respectively. GLDM mainly describes the degree of dependence between voxel gray levels, and the SCCEG group reflects the high "Dependence variance" of 3D gray levels and the "Large dependence high gray level emphasis" of 2D gray levels, which reflects the large gray level heterogeneity of squamous cancer tissue in 3D features and the high gray level distribution in 2D features from texture features. The uneven distribution of tumor vessels in squamous carcinoma lesions is prone to tumor cell

Table 1 Model performance for differentiating squamous cell carcinoma of the esophagogastric junction and adenocarcinoma of the esophagogastric junction in the training and validation groups

	2D-ROI models			3D-ROI models		
Model	**Artery**	**Venous**	**Artery + venous**	**Artery**	**Venous**	**Artery + venous**
Training group						
AUC	0.808	0.849	0.869	0.876	0.877	0.904
95%CI	0.744-0.872	0.792-0.905	0.818-0.920	0.827-0.926	0.827-0.927	0.861-0.947
Threshold	0.095	-0.101	-0.370	-0.149	-0.352	0.043
Specificity	0.802	0.758	0.681	0.813	0.780	0.879
Sensitivity	0.736	0.802	0.890	0.824	0.857	0.802
Accuracy	0.769	0.780	0.786	0.819	0.819	0.841
NPV	0.753	0.793	0.861	0.822	0.845	0.816
PPV	0.788	0.768	0.736	0.815	0.796	0.869
Validation group						
AUC	0.752	0.831	0.845	0.824	0.879	0.901
95%CI	0.640-0.864	0.742-0.921	0.763-0.928	0.732-0.917	0.798-0.960	0.830-0.973
Threshold	0.095	-0.101	-0.370	-0.149	-0.352	0.043
Specificity	0.795	0.692	0.718	0.769	0.667	0.821
Sensitivity	0.641	0.769	0.769	0.744	0.872	0.795
Accuracy	0.718	0.731	0.744	0.756	0.769	0.808
NPV	0.689	0.750	0.757	0.750	0.839	0.800
PPV	0.758	0.714	0.732	0.763	0.723	0.816

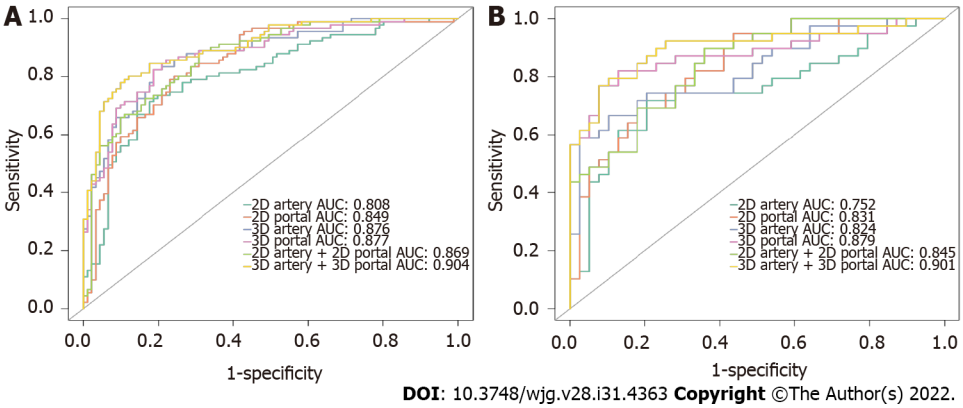
ROI: Region of interest; AUC: Area under the curve; NPV: Negative predictive value; PPV: Positive predictive value.

Table 2 Model optimism estimation by 1000-times bootstrap in the training group

Index	Model	Apparent AUC[1]	AUC Bootstrap-test[2] (mean, 95%CI)	Optimism
1	2D-arterial model	0.808	0.770 (0.767-0.772)	0.050
2	2D-venous model	0.849	0.820 (0.817-0.822)	0.036
3	3D-arterial model	0.876	0.815 (0.812-0.880)	0.080
4	3D-venous model	0.877	0.833 (0.830-0.835)	0.056

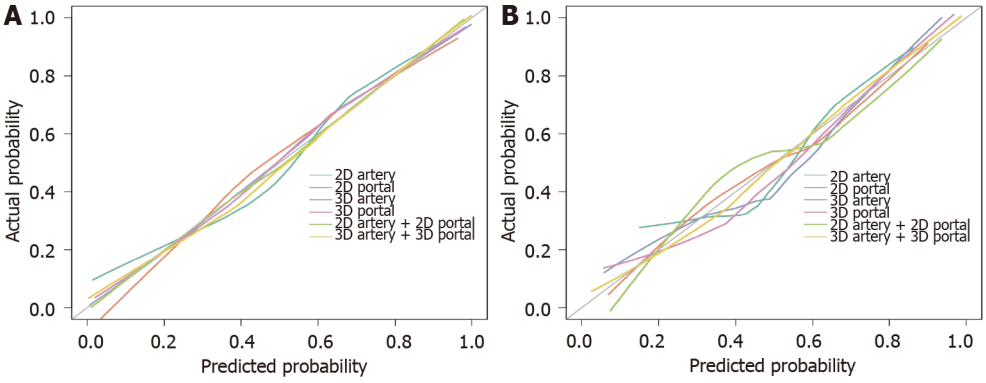
[1]The area under the curve of predictive model developed in the whole training dataset.
[2]The averaged model performance in the "out-of-bag" test set after 1000-times bootstrap. AUC: Area under the curve.

degeneration and necrosis, and it is speculated that the grayscale distribution of squamous carcinoma lesions has some complexity in different transformed images. In addition, features prevalent in the arterial and venous models are Busyness (NGTDM), Dependence variance (GLDM), first order grayscale features. NGTDM features can also represent a certain degree of grayscale distribution inhomogeneity. NGTDM describes the difference between adjacent grayscale values and average grayscale values within the quantized distance of the adjacent grayscale difference matrix, and the squamous carcinoma exhibits a high "Busyness", representing rapid intensity changes between pixels and their neighbors and reflecting the heterogeneous nature of the tissue. In addition, the first-order statistical gray value features calculated based on different dimensions and different phases of images were selected into each model simultaneously, indicating that the images of the SCCEG group in different phases and dimensions have lower gray values, which may be attributed to the histopathological inhomogeneity of microvessels within squamous carcinoma, less blood supply than adenocarcinoma, and lower gray statistical values in squamous carcinoma than adenocarcinoma.



DOI: 10.3748/wjg.v28.i31.4363 **Copyright** ©The Author(s) 2022.

Figure 4 Receiver operating characteristic curves of different models to identify squamous cell carcinoma and adenocarcinoma of the esophagogastric junction. A: Training group; B: Test group.



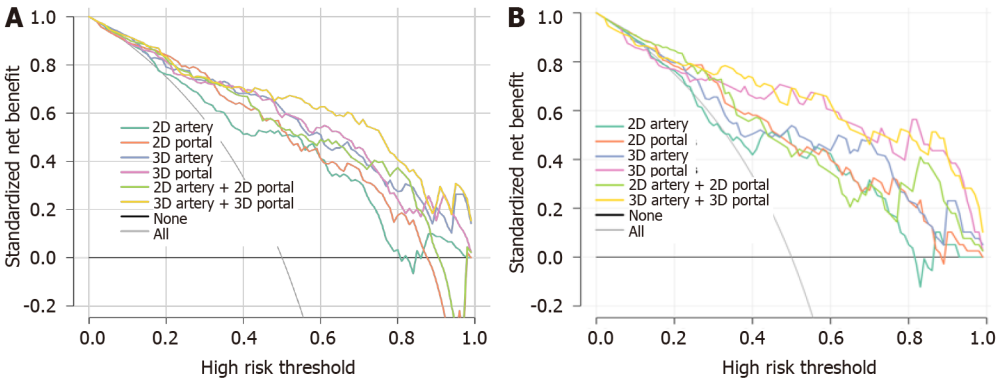
DOI: 10.3748/wjg.v28.i31.4363 **Copyright** ©The Author(s) 2022.

Figure 5 Calibration curves of 2D-arterial model, 2D-venous model, 3D-arterial model, 3D-venous model, 2D arterial-venous combined model, and 3D arterial-venous combined model to identify squamous cell carcinoma of the esophagogastric junction and adenocarcinoma of the esophagogastric junction. A: Training group; B: Test group.

For both of 2D and 3D models, the AUC difference was statistically significant between the arterial-venous combined model and the independent arterial model, while not significant between the arterial-venous combined model and the independent venous model. It suggested that the venous phase might contribute more predictive information compared with the arterial phase. Combining the NRI and IDI index results, the venous model showed a positive improvement in discrimination compared to the arterial model, and the 3D model showed a significant positive improvement in discrimination compared to the 2D model as well.

Most previous radiomics studies varied in the utilization of 2D or 3D segmentation. However, different delineation methods may result in different feature values and predictive performance. The study of different dimensional outlining approaches and the corresponding model performance can guide radiomics practice in related disease areas. Zhao *et al*[15] developed a dual-energy CT–based nomogram for noninvasive identification of the status of HER2 expression in gastric cancer, and both 2D and 3D radiomics nomograms performed well. Huang *et al*[18] found that the efficacy of the 3D model was superior to the 2D model when they developed 2D and 3D radiomics models to predict the aggressiveness of pancreatic solid pseudopapillary tumors. This study showed that in the discrimination of SCCEG and AEG, the use of 3D radiomics-based on CT images will be beneficial to improve the discrimination, but the time required for 3D segmentation was significantly longer than that of 2D, so it is also necessary to consider the improvement and optimization of automatic 3D lesion segmentation.

This study still has some limitations. First, the lesion morphology of CEGJ is not fixed, and manual segmentation methods are required. While the lesion travels along the gastric and esophageal walls in a tortuous manner, the consistency and stability of the annotation will affect the efficacy of the model. In this study, features with ICCs > 0.75 were used for subsequent analysis, which ensured the robustness of the radiomics features to some extent. More candidate semi-automatic or automatic segmentation algorithms would be welcomed to improve clinical efficiency. Second, our study was previously reported to include data on squamous cell carcinoma of the cardia or distal esophagus, but it is still a single-center retrospective study with a small sample size, especially for SCCEG, which inevitably



DOI: 10.3748/wjg.v28.i31.4363 **Copyright** ©The Author(s) 2022.

Figure 6 Decision curves for 2D-arterial model, 2D venous model, 3D-arterial model, 3D venous model, 2D arterial-venous combined model, and 3D arterial-venous combined model. A: Training group; B: Test group. The black horizontal line indicates no lesions as squamous cell carcinoma (NONE) and the grey line indicates all lesions as squamous cell carcinoma (ALL). The colored lines of each model respectively illustrate the net benefit brought to each patient. The closer the decision curves to the black and gray curves, the similar the clinical decision net benefit of the model compared with "treat ALL" or "treat NONE" decision. When comparing different models, the higher the model curve within the same threshold probability, the higher the clinical net benefit resulting from the model.

generates selectivity bias when paired with a larger number of AEGs. Future multicenter, prospective, large sample studies are needed to further improve and validate the diagnostic efficacy and generalization ability of the model. In addition, the main purpose of the current study was to evaluate the usefulness of 2D- or 3D-based radiomics methods and clinical data or laboratory test indicators were not included. There is much room for improvement of model reliability, which will be further collected in future studies in order to obtain a more comprehensive understanding.

CONCLUSION

In conclusion, multi-scale and multi-phase radiomics models based on CT imaging data were developed and validated for differentiating SCCEG from AEG before the operation in our study. The 3D radiomics model combining arterial and venous phase images showed encouraging performance than the corresponding 2D model. These models require further validation as decision support tools to guide clinical practice and develop individualized treatment plans for CEGJ patients. Currently, histopathological biopsy is still the common method of diagnosis.

ARTICLE HIGHLIGHTS

Research background

Differentiating squamous cell carcinoma of the esophagogastric junction (SCCEG) from adenocarcinoma of the esophagogastric junction (AEG) can indicate Siewert stage and whether the surgical route for patients with carcinoma of the esophagogastric junction (CEGJ) is transthoracic or transabdominal, as well as aid in determining the extent of lymph node dissection. With the development of neoadjuvant therapy, preoperative determination of pathological type can help in the selection of neoadjuvant radiotherapy and chemotherapy regimens.

Research motivation

Radiomics technique uses a combined medical-industrial approach to transform traditional images into digital quantitative features, which has potential for digging the potential biological characteristics and heterogeneity of tumor images and has been widely and non-invasively used in the diagnosis, differential diagnosis, and disease evaluation. However, to the best of our knowledge, there is no literature that has evaluated whether a radiomics signature derived from computed tomography (CT) images would be useful in predicting pathological type in patients with CEGJ.

Research objectives

In the current study, we proposed a CT radiomics-based classification method by considering the performance of 3D or 2D segmentation and multiple CT imaging phases to discriminate SCCEG and AEG.

Research methods

We retrospectively analyzed the preoperative contrasted-enhanced CT imaging data of single-center patients with pathologically confirmed SCCEG (n = 130) and AEG (n = 130). One thousand four hundred and nine radiomics features were separately extracted from 2D or 3D regions of interest in arterial and venous phases. Totally, 6 logistic regression models were established based on 2D and 3D multi-phase features.

Research results

The venous model showed a positive improvement compared with the arterial model (NRI > 0, IDI > 0), and the 3D-venous and combined models showed a significant positive improvement compared with the 2D-venous and combined models (P < 0.05). Decision curve analysis showed that the combined 3D-arterial-venous model and 3D-venous model had a higher net clinical benefit within the same threshold probability range in the test group.

Research conclusions

The combined arterial-venous CT radiomics model based on 3D segmentation can improve the performance in differentiating EGJ squamous cell carcinoma from adenocarcinoma.

Research perspectives

These models require further validation as decision support tools to guide clinical practice and develop individualized treatment plans for CEGJ patients.

FOOTNOTES

Author contributions: Du KP and Huang WP designed the research; Liu SY and Li LM performed the research; Chen YJ, Han YJ, Zhou Y, and Liu CC collected the data; Du KP and Huang WP analyzed the data and wrote the paper; Gao JB reviewed the paper; and all authors have read and approved the final manuscript.

Institutional review board statement: The study was approved by the Institutional Review Board at the First Affiliated Hospital of Zhengzhou University (No. 2021-ky-1070-002).

Conflict-of-interest statement: The authors declare that they have no competing interests to disclose.

Data sharing statement: All data generated or analyzed during this study are included in this published article.

Open-Access: This article is an open-access article that was selected by an in-house editor and fully peer-reviewed by external reviewers. It is distributed in accordance with the Creative Commons Attribution NonCommercial (CC BY-NC 4.0) license, which permits others to distribute, remix, adapt, build upon this work non-commercially, and license their derivative works on different terms, provided the original work is properly cited and the use is non-commercial. See: https://creativecommons.org/Licenses/by-nc/4.0/

Country/Territory of origin: China

ORCID number: Ke-Pu Du 0000-0002-3870-7656; Wen-Peng Huang 0000-0002-9104-1494; Si-Yun Liu 0000-0001-5611-382X; Yun-Jin Chen 0000-0002-2147-0912; Li-Ming Li 0000-0002-2910-9742; Yi-Jing Han 0000-0001-7358-0139; Yue Zhou 0000-0001-7781-7228; Chen-Chen Liu 0000-0001-5026-3288; Jian-Bo Gao 0000-0003-2621-3701.

S-Editor: Ma YJ
L-Editor: Wang TQ
P-Editor: Ma YJ

REFERENCES

1 **Sun X**, Wang G, Liu C, Xiong R, Wu H, Xie M, Xu S. Comparison of short-term outcomes following minimally invasive versus open Sweet esophagectomy for Siewert type II adenocarcinoma of the esophagogastric junction. *Thorac Cancer* 2020; **11**: 1487-1494 [PMID: 32239662 DOI: 10.1111/1759-7714.13415]
2 **Wang T**, Wu Y, Zhou H, Wu C, Zhang X, Chen Y, Zhao D. Development and validation of a novel competing risk model for predicting survival of esophagogastric junction adenocarcinoma: a SEER population-based study and external validation. *BMC Gastroenterol* 2021; **21**: 38 [PMID: 33499821 DOI: 10.1186/s12876-021-01618-7]
3 **Xu H**, Zhang L, Miao J, Liu S, Liu H, Jia T, Zhang Q. Patterns of recurrence in adenocarcinoma of the esophagogastric junction: a retrospective study. *World J Surg Oncol* 2020; **18**: 144 [PMID: 32593312 DOI: 10.1186/s12957-020-01917-5]
4 **Ito H**, Inoue H, Odaka N, Satodate H, Suzuki M, Mukai S, Takehara Y, Kida H, Kudo SE. Clinicopathological characteristics and optimal management for esophagogastric junctional cancer; a single center retrospective cohort study. *J*

Exp Clin Cancer Res 2013; **32**: 2 [PMID: 23289488 DOI: 10.1186/1756-9966-32-2]

5 **Huang Q**. Carcinoma of the gastroesophageal junction in Chinese patients. *World J Gastroenterol* 2012; **18**: 7134-7140 [PMID: 23326117 DOI: 10.3748/wjg.v18.i48.7134]

6 **Giganti F**, Ambrosi A, Petrone MC, Canevari C, Chiari D, Salerno A, Arcidiacono PG, Nicoletti R, Albarello L, Mazza E, Gallivanone F, Gianolli L, Orsenigo E, Esposito A, Staudacher C, Del Maschio A, De Cobelli F. Prospective comparison of MR with diffusion-weighted imaging, endoscopic ultrasound, MDCT and positron emission tomography-CT in the pre-operative staging of oesophageal cancer: results from a pilot study. *Br J Radiol* 2016; **89**: 20160087 [PMID: 27767330 DOI: 10.1259/bjr.20160087]

7 **Soo TM**, Bernstein M, Provias J, Tasker R, Lozano A, Guha A. Failed stereotactic biopsy in a series of 518 cases. *Stereotact Funct Neurosurg* 1995; **64**: 183-196 [PMID: 8817805 DOI: 10.1159/000098747]

8 **Bhandari A**, Ibrahim M, Sharma C, Liong R, Gustafson S, Prior M. CT-based radiomics for differentiating renal tumours: a systematic review. *Abdom Radiol (NY)* 2021; **46**: 2052-2063 [PMID: 33136182 DOI: 10.1007/s00261-020-02832-9]

9 **Reginelli A**, Nardone V, Giacobbe G, Belfiore MP, Grassi R, Schettino F, Del Canto M, Cappabianca S. Radiomics as a New Frontier of Imaging for Cancer Prognosis: A Narrative Review. *Diagnostics (Basel)* 2021; **11** [PMID: 34679494 DOI: 10.3390/diagnostics11101796]

10 **Ibrahim A**, Primakov S, Beuque M, Woodruff HC, Halilaj I, Wu G, Refaee T, Granzier R, Widaatalla Y, Hustinx R, Mottaghy FM, Lambin P. Radiomics for precision medicine: Current challenges, future prospects, and the proposal of a new framework. *Methods* 2021; **188**: 20-29 [PMID: 32504782 DOI: 10.1016/j.ymeth.2020.05.022]

11 **Lambin P**, Leijenaar RTH, Deist TM, Peerlings J, de Jong EEC, van Timmeren J, Sanduleanu S, Larue RTHM, Even AJG, Jochems A, van Wijk Y, Woodruff H, van Soest J, Lustberg T, Roelofs E, van Elmpt W, Dekker A, Mottaghy FM, Wildberger JE, Walsh S. Radiomics: the bridge between medical imaging and personalized medicine. *Nat Rev Clin Oncol* 2017; **14**: 749-762 [PMID: 28975929 DOI: 10.1038/nrclinonc.2017.141]

12 **Scapicchio C**, Gabelloni M, Barucci A, Cioni D, Saba L, Neri E. A deep look into radiomics. *Radiol Med* 2021; **126**: 1296-1311 [PMID: 34213702 DOI: 10.1007/s11547-021-01389-x]

13 **Ren C**, Zhang J, Qi M, Zhang Y, Song S, Sun Y, Cheng J. Correction to: Machine learning based on clinico-biological features integrated 18F-FDG PET/CT radiomics for distinguishing squamous cell carcinoma from adenocarcinoma of lung. *Eur J Nucl Med Mol Imaging* 2021; **48**: 1696 [PMID: 33532911 DOI: 10.1007/s00259-021-05226-1]

14 **Tomori Y**, Yamashiro T, Tomita H, Tsubakimoto M, Ishigami K, Atsumi E, Murayama S. CT radiomics analysis of lung cancers: Differentiation of squamous cell carcinoma from adenocarcinoma, a correlative study with FDG uptake. *Eur J Radiol* 2020; **128**: 109032 [PMID: 32361604 DOI: 10.1016/j.ejrad.2020.109032]

15 **Zhao H**, Li W, Huang W, Yang Y, Shen W, Liang P, Gao J. Dual-Energy CT-Based Nomogram for Decoding HER2 Status in Patients With Gastric Cancer. *AJR Am J Roentgenol* 2021; **216**: 1539-1548 [PMID: 33852330 DOI: 10.2214/AJR.20.23528]

16 **Xu L**, Yang P, Yen EA, Wan Y, Jiang Y, Cao Z, Shen X, Wu Y, Wang J, Luo C, Niu T. A multi-organ cancer study of the classification performance using 2D and 3D image features in radiomics analysis. *Phys Med Biol* 2019; **64**: 215009 [PMID: 31561245 DOI: 10.1088/1361-6560/ab489f]

17 **Meng L**, Dong D, Chen X, Fang M, Wang R, Li J, Liu Z, Tian J. 2D and 3D CT Radiomic Features Performance Comparison in Characterization of Gastric Cancer: A Multi-Center Study. *IEEE J Biomed Health Inform* 2021; **25**: 755-763 [PMID: 32750940 DOI: 10.1109/JBHI.2020.3002805]

18 **Huang WP**, Liu SY, Han YJ, Li LM, Liang P, Gao JB. Development of CT-Based Imaging Signature for Preoperative Prediction of Invasive Behavior in Pancreatic Solid Pseudopapillary Neoplasm. *Front Oncol* 2021; **11**: 677814 [PMID: 34079766 DOI: 10.3389/fonc.2021.677814]

19 **Mackin D**, Fave X, Zhang L, Yang J, Jones AK, Ng CS, Court L. Harmonizing the pixel size in retrospective computed tomography radiomics studies. *PLoS One* 2017; **12**: e0178524 [PMID: 28934225 DOI: 10.1371/journal.pone.0178524]

20 **van Griethuysen JJM**, Fedorov A, Parmar C, Hosny A, Aucoin N, Narayan V, Beets-Tan RGH, Fillion-Robin JC, Pieper S, Aerts HJWL. Computational Radiomics System to Decode the Radiographic Phenotype. *Cancer Res* 2017; **77**: e104-e107 [PMID: 29092951 DOI: 10.1158/0008-5472.CAN-17-0339]

21 **Koo TK**, Li MY. A Guideline of Selecting and Reporting Intraclass Correlation Coefficients for Reliability Research. *J Chiropr Med* 2016; **15**: 155-163 [PMID: 27330520 DOI: 10.1016/j.jcm.2016.02.012]

22 **Daghir-Wojtkowiak E**, Wiczling P, Bocian S, Kubik Ł, Kośliński P, Buszewski B, Kaliszan R, Markuszewski MJ. Least absolute shrinkage and selection operator and dimensionality reduction techniques in quantitative structure retention relationship modeling of retention in hydrophilic interaction liquid chromatography. *J Chromatogr A* 2015; **1403**: 54-62 [PMID: 26037317 DOI: 10.1016/j.chroma.2015.05.025]

23 **Zhou Y**, Hou P, Zha K, Liu D, Wang F, Zhou K, Gao J. Spectral Computed Tomography for the Quantitative Assessment of Patients With Carcinoma of the Gastroesophageal Junction: Initial Differentiation Between a Diagnosis of Squamous Cell Carcinoma and Adenocarcinoma. *J Comput Assist Tomogr* 2019; **43**: 187-193 [PMID: 30371624 DOI: 10.1097/RCT.0000000000000826]

24 **Gao X**, Ma T, Cui J, Zhang Y, Wang L, Li H, Ye Z. A CT-based Radiomics Model for Prediction of Lymph Node Metastasis in Early Stage Gastric Cancer. *Acad Radiol* 2021; **28**: e155-e164 [PMID: 32507613 DOI: 10.1016/j.acra.2020.03.045]

25 **Qiang JW**, Zhou KR, Lu G, Wang Q, Ye XG, Xu ST, Tan LJ. The relationship between solitary pulmonary nodules and bronchi: multi-slice CT-pathological correlation. *Clin Radiol* 2004; **59**: 1121-1127 [PMID: 15556595 DOI: 10.1016/j.crad.2004.02.018]

World Journal of Gastroenterology

Submit a Manuscript: https://www.f6publishing.com

World J Gastroenterol 2022 August 21; 28(31): 4376-4389

DOI: 10.3748/wjg.v28.i31.4376

ISSN 1007-9327 (print) ISSN 2219-2840 (online)

ORIGINAL ARTICLE

Retrospective Study

Preoperative contrast-enhanced computed tomography-based radiomics model for overall survival prediction in hepatocellular carcinoma

Peng-Zhan Deng, Bi-Geng Zhao, Xian-Hui Huang, Ting-Feng Xu, Zi-Jun Chen, Qiu-Feng Wei, Xiao-Yi Liu, Yu-Qi Guo, Sheng-Guang Yuan, Wei-Jia Liao

Specialty type: Gastroenterology and hepatology

Provenance and peer review: Unsolicited article; Externally peer reviewed.

Peer-review model: Single blind

Peer-review report's scientific quality classification

Grade A (Excellent): 0
Grade B (Very good): B, B
Grade C (Good): 0
Grade D (Fair): 0
Grade E (Poor): 0

P-Reviewer: Gupta T, India; Hu X, China

Received: April 20, 2022
Peer-review started: April 20, 2022
First decision: June 2, 2022
Revised: June 14, 2022
Accepted: July 20, 2022
Article in press: July 20, 2022
Published online: August 21, 2022

Peng-Zhan Deng, Bi-Geng Zhao, Xian-Hui Huang, Ting-Feng Xu, Zi-Jun Chen, Qiu-Feng Wei, Xiao-Yi Liu, Yu-Qi Guo, Sheng-Guang Yuan, Wei-Jia Liao, Laboratory of Hepatobiliary and Pancreatic Surgery, Affiliated Hospital of Guilin Medical University, Guilin 541001, Guangxi Zhuang Autonomous Region, China

Corresponding author: Wei-Jia Liao, MD, Chief Doctor, Professor, Laboratory of Hepatobiliary and Pancreatic Surgery, Affiliated Hospital of Guilin Medical University, No. 15 Lequn Road, Xiufeng District, Guilin 541001, Guangxi Zhuang Autonomous Region, China.
liaoweijia288@163.com

Abstract

BACKGROUND

Hepatocellular carcinoma (HCC) is the most common primary liver malignancy with a rising incidence worldwide. The prognosis of HCC patients after radical resection remains poor. Radiomics is a novel machine learning method that extracts quantitative features from medical images and provides predictive information of cancer, which can assist with cancer diagnosis, therapeutic decision-making and prognosis improvement.

AIM

To develop and validate a contrast-enhanced computed tomography-based radiomics model for predicting the overall survival (OS) of HCC patients after radical hepatectomy.

METHODS

A total of 150 HCC patients were randomly divided into a training cohort (n = 107) and a validation cohort (n = 43). Radiomics features were extracted from the entire tumour lesion. The least absolute shrinkage and selection operator algorithm was applied for the selection of radiomics features and the construction of the radiomics signature. Univariate and multivariate Cox regression analyses were used to identify the independent prognostic factors and develop the predictive nomogram, incorporating clinicopathological characteristics and the radiomics signature. The accuracy of the nomogram was assessed with the concordance index, receiver operating characteristic (ROC) curve and calibration

curve. The clinical utility was evaluated by decision curve analysis (DCA). Kaplan–Meier methodology was used to compare the survival between the low- and high-risk subgroups.

RESULTS

In total, seven radiomics features were selected to construct the radiomics signature. According to the results of univariate and multivariate Cox regression analyses, alpha-fetoprotein (AFP), neutrophil-to-lymphocyte ratio (NLR) and radiomics signature were included to build the nomogram. The C-indices of the nomogram in the training and validation cohorts were 0.736 and 0.774, respectively. ROC curve analysis for predicting 1-, 3-, and 5-year OS confirmed satisfactory accuracy [training cohort, area under the curve (AUC) = 0.850, 0.791 and 0.823, respectively; validation cohort, AUC = 0.905, 0.884 and 0.911, respectively]. The calibration curve analysis indicated a good agreement between the nomogram-prediction and actual survival. DCA curves suggested that the nomogram had more benefit than traditional staging system models. Kaplan–Meier survival analysis indicated that patients in the low-risk group had longer OS and disease-free survival (all $P < 0.0001$).

CONCLUSION

The nomogram containing the radiomics signature, NLR and AFP is a reliable tool for predicting the OS of HCC patients.

Key Words: Hepatocellular carcinoma; Radiomics; Contrast-enhanced computed tomography; Survival prediction

©The Author(s) 2022. Published by Baishideng Publishing Group Inc. All rights reserved.

Core Tip: The prognosis of hepatocellular carcinoma (HCC) patients remains poor even after radical resection. Therefore, a precise and reliable tool to predict the prognosis of HCC patients is urgently needed. We established a predictive model incorporating radiomics features extracted from preoperative contrast-enhanced computed tomography images, alpha-fetoprotein and neutrophil-to-lymphocyte ratio to predict the overall survival of patients with HCC, and the model was visualized *via* a nomogram. The nomogram showed good accuracy for survival prediction.

Citation: Deng PZ, Zhao BG, Huang XH, Xu TF, Chen ZJ, Wei QF, Liu XY, Guo YQ, Yuan SG, Liao WJ. Preoperative contrast-enhanced computed tomography-based radiomics model for overall survival prediction in hepatocellular carcinoma. *World J Gastroenterol* 2022; 28(31): 4376-4389
URL: https://www.wjgnet.com/1007-9327/full/v28/i31/4376.htm
DOI: https://dx.doi.org/10.3748/wjg.v28.i31.4376

INTRODUCTION

Primary liver cancer is the sixth most common malignancy and the third leading cause of cancer-related mortality in the world. Hepatocellular carcinoma (HCC) accounts for 75%-85% of primary liver cancers [1]. Presently, the main therapies for HCC include surgical resection, local ablation, interventional embolization and liver transplantation. For HCC patients with early-stage disease, hepatectomy and liver transplantation are the mainstay curative treatments. Due to the insidious onset and lack of evident clinical symptoms in the early stage, patients with HCC are often diagnosed at an advanced stage. Even after surgical resection, the prognosis of HCC patients remains poor due to postoperative recurrence and metastasis. It has been reported that the recurrence rate within 5 years reaches 60%[2].

Alpha-fetoprotein (AFP) has been widely applied as a biomarker of HCC for diagnosis, monitoring treatment response, assessing prognosis and detecting early recurrence. However, the specificity of AFP for diagnosing HCC is 99%-100%, but the sensitivity is only 20% to 45%[3]. Moreover, nearly 31% of patients with HCC are AFP negative[4]. Therefore, AFP still has limitations as a biomarker of HCC. It has been reported that the tumour microenvironment is closely related to the initiation and progression of HCC[5]. Recent studies have shown that a high density of tumour-infiltrating lymphocytes is associated with favourable outcomes[6]. The neutrophil-to-lymphocyte ratio (NLR) was reported to be an independent prognostic factor for patients with HCC[7,8].

Radiomics is a new method of medical image analysis that uses a series of data-mining algorithms or statistical analysis tools for the high-throughput extraction of quantitative metric features[9,10] to obtain prognostic and predictive information for clinical decision support. It has been recognized that

intratumor heterogeneity is often associated with tumour subtyping and can significantly impact prognosis and response to treatment[11,12]. Traditional radiological analysis is mainly based on naked-eye observation, which primarily focuses on tumour size and anatomical location but ignores intratumor heterogeneity. Radiomics features are able to provide a comprehensive overview of intratumor heterogeneity in a noninvasive manner[13]. Several recent studies indicate that radiomics features may potentially be a useful diagnostic and prognostic biomarker in liver cancer and other tumour types[14-16].

Due to the insufficiency of accurateness and objectiveness for prognostic markers in the prognostic evaluation of HCC patients, a precise and reliable tool to predict the prognosis of HCC patients is urgently needed. In the present study, we aimed to develop and validate a model based on contrast-enhanced computed tomography (CECT) images and clinical-pathologic characteristics to predict the overall survival (OS) of HCC patients.

MATERIALS AND METHODS

This study was composed of the following steps: (1) Patient recruitment and data collection; (2) CECT image acquisition, tumour segmentation, region of interest (ROI) selection, radiomics feature extraction and radiomics signature construction; (3) The radiomics signature and clinical-pathologic characteristics were combined to build a predictive model and visualized *via* a nomogram; and (4) Evaluation of the predictive model using receiver operating characteristic (ROC) curves, calibration curves, decision curve analysis (DCA) and Kaplan–Meier curves.

Patients

This retrospective study was approved by the research ethics committee of the Affiliated Hospital of Guilin Medical University and conducted in accordance with the Declaration of Helsinki. Informed consent was obtained from all patients.

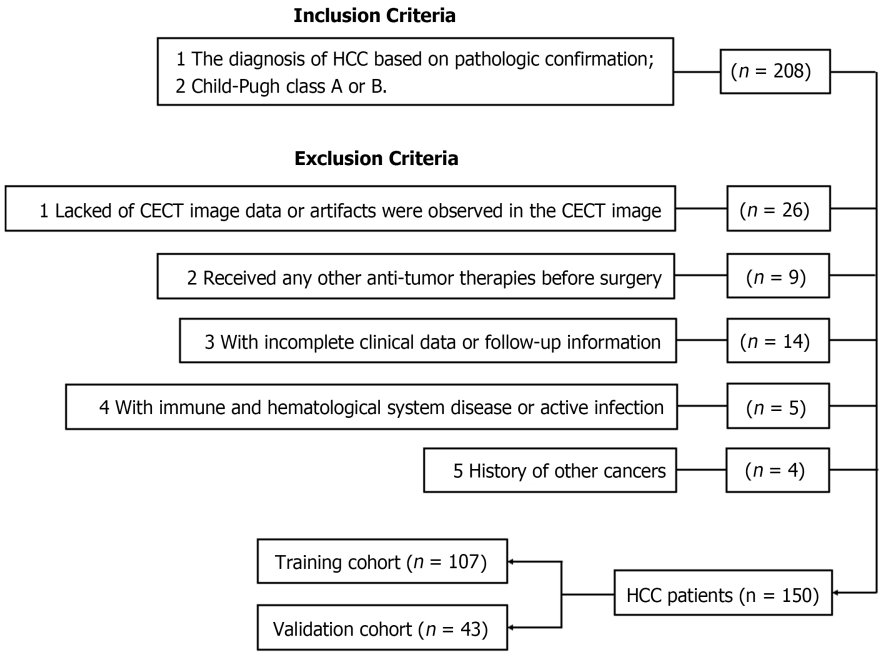
A total of 208 HCC patients who underwent radical resection at the Affiliated Hospital of Guilin Medical University with pathologically confirmed HCC were recruited from January 2014 to September 2017. Among them, 150 individuals fulfilled the inclusion and exclusion criteria (Figure 1). Radical resection was defined as a completed resection of the tumour mass with pathologically confirmed negative margins and no residual tumour or new lesion observed in two observations at an interval of no less than 4 wk. All tumour tissue samples were diagnosed by at least two experienced pathologists independently. All patients underwent CECT scans and haematological examinations before surgery. The 150 enrolled HCC patients were randomly divided into a training cohort (n = 107) and a validation cohort (n = 43) at a ratio of 2.5:1. Demographic and clinical-pathologic data were collected from medical records, including age, sex, alanine aminotransferase, AFP, American Joint Committee on Cancer tumor, node and metastasis (TNM) stage, Barcelona clinic liver cancer (BCLC) stage, hepatitis B surface antigen (HBsAg) and NLR.

Each patient was followed up *via* outpatient review. Routine postoperative examinations, including routine blood tests, liver function tests, renal function tests, serum AFP levels and abdominal ultrasonography, were performed every 2 mo after surgery within 2 years and then every 6 mo thereafter. A CECT scan was recommended if the examination results were abnormal or tumour recurrence was suspected. For patients who did not attend the follow-up visit, follow-up information was obtained by phone. OS was defined as the time from surgery to death or the last follow-up date, while disease-free survival (DFS) was defined as the time from surgery to tumour first intrahepatic and/or extrahepatic recurrence, death, or the last follow-up date.

CECT scan protocols and image preprocessing

Abdominal CECT scans were performed with two scanners: A Lightspeed VCT XT (GE Healthcare, United States) and an Optima CT660 (GE Healthcare, United States). The scanner was operated in cine mode, and the parameters were as follows: tube voltage of 120 kV, automatic tube current modulation with noise index of 8, tube rotation speed of 600 ms, pitch of 0.985:1, collimator of 0.625 mm. Iopromide (Ultravist 300, Bayer-Schering Pharma, Germany) was given intravenously in a volume of 1.5 mL/kg at a rate of 4 mL/s *via* the antecubital vein. The slice thickness and interval of the arterial and portal venous phase images was 5 mm. All images were reconstructed into images with a 1.25 mm slice thickness and 1.25 mm interval. All data were transferred to an advanced workstation (AW 4.7).

All CECT images in this study met the criteria delineated by the American Association for the Study of Liver Disease guidelines[17]. CECT images were exported in digital imaging and communication in medicine (DICOM) format from the picture archiving and communication system database. All DICOM images were converted to neuroimaging informatics technology initiative format by the SimpleITK package (version 1.2.0) of Python software (version 3.7).



DOI: 10.3748/wjg.v28.i31.4376 **Copyright** ©The Author(s) 2022.

Figure 1 Flowchart of the patient selection process. HCC: Hepatocellular carcinoma; CECT: Contrast-enhanced computed tomography.

Radiomics analysis and radiomics signature construction

Tumour segmentation was performed by 3D Slicer software (version 4.11.20210226). ROIs were drawn on each layer of the tumour in the horizontal plane from the upper boundary to the lower boundary. Tumour lesions were semiautomatically outlined on all arterial phase and portal venous phase images, and manual corrections were implemented whenever necessary. The images were reviewed independently by two blinded radiologists with 7 and 8 years of experience, and a third radiologist resolved any discrepancies. For patients with multiple tumours, only the largest tumour was selected.

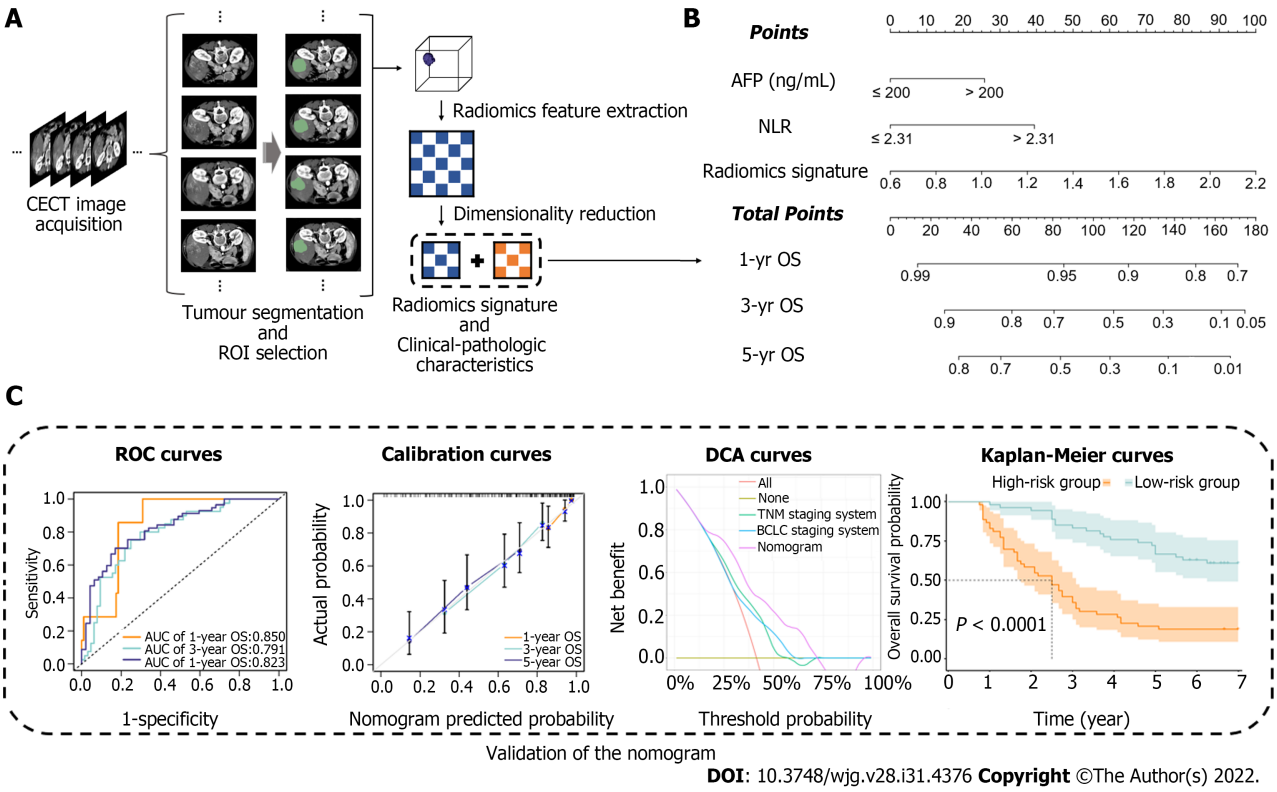
CECT image normalization and radiomics feature extraction were conducted by the Pyradiomics package (version 3.0.3) of Python software. The radiomics features extracted from ROIs included first order features, shape features (2D and 3D), gray level co-occurrence matrix features, gray level size zone matrix features, gray level run length matrix features, gray level dependence matrix features and neighbouring gray tone difference matrix features. Due to the large number of features, dimensionality reduction was essential. The least absolute shrinkage and selection operator (LASSO) algorithm with a 10-fold cross-validation approach was used to reduce the data dimension in the training cohort. Afterwards, the radiomics score, which was defined as the radiomics signature, was generated by linearly combining the selected radiomics features and their weighted coefficients. The workflow of radiomics analysis and radiomics signature construction is shown in Figure 2A. Afterwards, the concordance index (C-index) and ROC curve analysis were used to estimate the predictive value of the radiomics signature for 1-, 3- and 5-year OS.

Selection of the optimal cut-off value for NLR

According to our previous study[18], the optimal cut-off value for NLR in predicting the prognosis of HCC patients after curative resection was 2.31, which had both maximum sensitivity and specificity [area under the curve (AUC) = 0.723, 95%CI: 0.664–0.777].

Statistical analysis

Normality of distributions was tested by the Shapiro–Wilk test. Clinical-pathologic characteristics were compared by Student's *t* test and are presented as the mean ± SD for continuous variables conforming to a normal distribution. Nonnormally distributed continuous variables were compared using the Wilcoxon signed rank test and are presented as the median with interquartile range. Categorical variables were compared using the Pearson χ^2 test. Univariate and multivariate regression analyses were performed in the training cohort using the Cox proportional hazards model to identify the independent predictors for nomogram construction. The rms and regplot packages were used to establish a nomogram and calibration curve. The ROC curve analysis was performed using the timeROC package. The C-index, ROC curve and calibration curve were used to assess the accuracy of the nomogram. The Kaplan–Meier method and log-rank test were conducted to compare the different survival rates between the low- and high-risk subgroups in different cohorts. We built two predictive models based on BCLC and TNM staging systems. Patients were categorized into stage 0, stage A, stage



DOI: 10.3748/wjg.v28.i31.4376 **Copyright** ©The Author(s) 2022.

Figure 2 Workflow of model construction and validation. A: Contrast-enhanced computed tomography image acquisition, tumour segmentation, region of interest selection, radiomics feature extraction and radiomics signature construction; B: Combination of the radiomics signature and clinical-pathologic characteristics to build the predictive model, the model was visualized *via* nomogram; C: Evaluation of the predictive model by using receiver operating characteristic curves, calibration curves, decision curve analysis curves and Kaplan–Meier curves. CECT: Contrast-enhanced computed tomography; ROI: Region of interest; AFP: Alpha fetoprotein; NLR: Neutrophil-to-lymphocyte ratio; OS: Overall survival; ROC: Receiver operating characteristic; AUC: Area under the curve; DCA: Decision curve analysis; BCLC: Barcelona Clinic Liver Cancer.

B and stage C according to BCLC staging system; grade I, grade II, grade III and grade IV according to TNM staging system. DCA was conducted to compare the abovementioned two traditional staging systems with the nomogram. All statistical analyses were performed using SPSS software (version 24.0) or R software (version 4.1.2) and accepted as significant at $P < 0.05$.

RESULTS

Demographic and clinicopathological characteristics

A total of 150 HCC patients were enrolled in this study according to inclusion and exclusion criteria, with an average age of 49.9 years (range, 20-75 years), and 130 patients were male. A total of 136 patients were diagnosed with cirrhosis, while 137 patients were classified as Child–Pugh class A. A total of 124 patients were positive for HBsAg. Patients were randomly divided into a training cohort (n = 107) and a validation cohort (n = 43). The demographic and clinical-pathologic characteristics are summarized in Table 1. There were no significant differences in variables between the two cohorts.

Radiomics signature construction

In total, 1926 radiomics features were extracted from the ROIs. Based on the training cohort, radiomics features were reduced to 7 survival-related features by using the LASSO algorithm. The name of the selected features and the formula of the radiomics score are shown in Supplementary Table 1. The C-indices of the radiomics signature for predicting OS in the training and validation cohorts were 0.689 (95%CI: 0.626–0.751) and 0.746 (95%CI: 0.650–0.842), respectively. The ROC curves of the radiomics signature for predicting 1-, 3- and 5-year OS are shown in Figure 3 (AUC = 0.648, 0.753 and 0.807, respectively, in the training cohort; AUC = 0.921, 0.840 and 0.891, respectively, in the validation cohort).

Development and validation of the predictive nomogram

Based on the univariate regression analysis (Table 2), four variables with $P < 0.05$ were enrolled in the multivariate regression analysis. The results of multivariate regression analysis are displayed as forest plots (Figure 4). AFP [hazard ratio (HR), 1.8; 95%CI: 1.06–3.1, P = 0.03], NLR (HR, 2.5; 95%CI: 1.45–4.3, P

Table 1 The demographic and clinical-pathologic characteristics of patients

Variables	Training cohort (*n* = 107)	Validation cohort (*n* = 43)	*P* value
Age, yr (mean ± SD)	49.77 ± 10.57	50.35 ± 11.43	0.766
Sex (male/female)	94/13	36/7	0.501
Alcohol abuse (present/absent)	44/63	19/24	0.731
Tumor number (multiple/single)	22/85	10/33	0.716
Tumor diameter, cm (> 5/≤ 5)	69/38	24/19	0.322
MVI (present/absent)	46/61	17/26	0.698
Cirrhosis (present/absent)	100/7	36/7	0.123
TNM stage (I-II/III-IV)	54/53	18/25	0.340
BCLC stage (0-A/B-C)	61/46	20/23	0.243
WBC, × 10^9/L (median, IQR)	6.05 (5.00-7.3)	6.11 (5.04-8.04)	0.290
Platelets, × 10^9/L (mean ± SD)	190.75 ± 71.91	202.02 ± 79.32	0.401
LYMPH, × 10^9/L (median, IQR)	1.63 (1.19-1.94)	1.74 (1.35-2.04)	0.229
NEUT, × 10^9/L (median, IQR)	3.75 (2.68-4.07)	3.90 (2.85-5.17)	0.385
DB, μmol/L (median, IQR)	5.20 (4.20-5.81)	4.85 (3.68-5.56)	0.077
TB, μmol/L (median, IQR)	12.50 (9.43-15.91)	13.38 (8.93-17.11)	0.840
ALB, g/L (mean ± SD)	38.42 ± 4.30	36.87 ± 5.49	0.069
GLB, g/L (median, IQR)	31.80 (28.80-35.28)	32.22 (29.80-35.44)	0.480
GGT, U/L (mean ± SD)	115.26 ± 136.68	105.49 ± 82.44	0.662
ALT, U/L (median, IQR)	31.00 (21.24-44.14)	27.60 (17.46-42.88)	0.306
AST, U/L (median, IQR)	34.50 (26.55-51.51)	35.40 (25.55-46.02)	0.891
AFP, ng/mL (> 200/≤ 200)	50/57	23/20	0.454
HBsAg (positive/negative)	91/16	33/10	0.225
NLR (> 2.31/≤ 2.31)	50/57	21/22	0.815

IQR: Interquartile range; MVI: Microvascular invasion; TNM: Tumor, node and metastasis; BCLC: Barcelona clinic liver cancer; WBC: White blood cell count; LYMPH: Lymphocyte count; NEUT: Neutrophil count; DB: Direct bilirubin; TB: Total bilirubin; ALB: Albumin; GLB: Globulin; GGT: Gamma-glutamyl transpeptidase; ALT: Alanine transaminase; AST: Aspartate transaminase; AFP: Alpha fetoprotein; HBsAg: Hepatitis B surface antigen; NLR: Neutrophil-to-lymphocyte ratio.

< 0.001) and radiomics signature (HR, 3.7; 95%CI: 1.25–10.7, P = 0.018) were identified as independent predictors of OS. The abovementioned three variables were included to develop the predictive model and visualized *via* a nomogram (Figure 2B). The C-indices of the nomogram in the training and validation cohorts were 0.736 (95%CI: 0.681–0.791) and 0.774 (95%CI: 0.697–0.851), respectively. The AUC values of 1-, 3-, and 5-year OS were 0.850, 0.791 and 0.823, respectively, in the training cohort (Figure 5A) and 0.905, 0.884 and 0.911, respectively, in the validation cohort (Figure 5B). The calibration curves of the nomogram demonstrated good agreement between the predicted and actual survival probabilities (Figure 5C and D).

Evaluation of clinical practicality and risk stratification ability

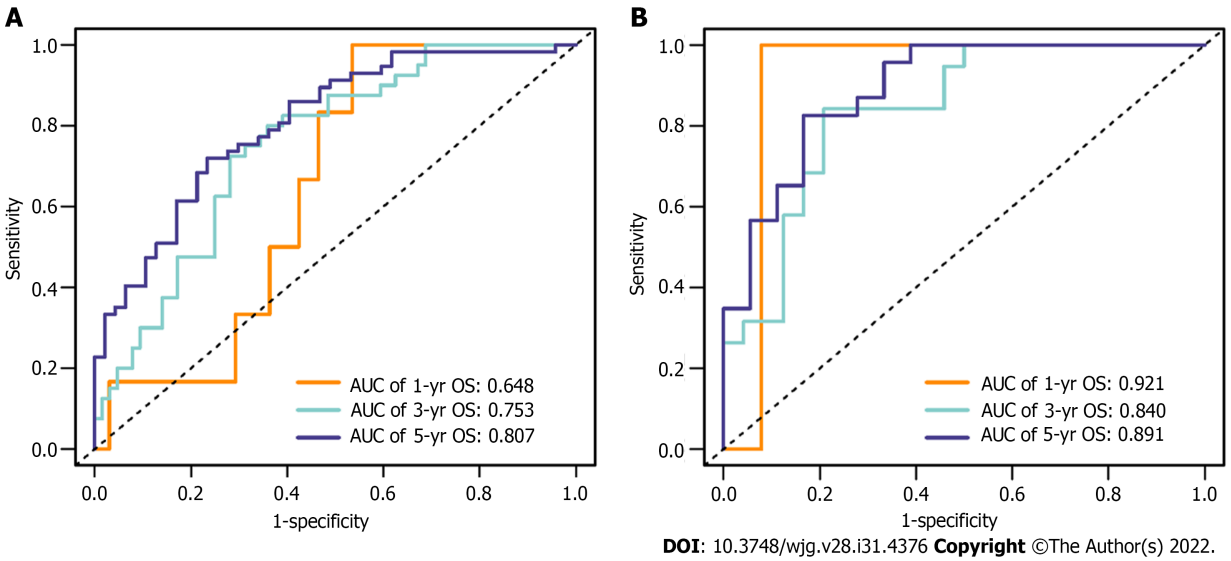
DCA curves showed that the nomogram received more net benefit than the BCLC staging system model and TNM staging system model in predicting 3- and 5-year OS at reasonable threshold probability (Figure 6).

To further explore the risk stratification ability of the nomogram, we calculated the total points of the nomogram for each patient. The total points conformed to a normal distribution in the training and validation cohorts. Patients were categorized into low- and high-risk subgroups based on whether the total points of the patient were lower (training cohort ≤ 89.8; validation cohort ≤ 66.0) or higher (training cohort > 89.8; validation cohort > 66.0) than the median points of each cohort. Kaplan–Meier curves indicated that patients in the low-risk subgroup had significantly longer OS and DFS, with all P < 0.001 (Figure 7).

Table 2 Univariate Cox regression analysis in the training cohort

Variables	Univariate Cox regression analysis		
	HR	95%CI	*P* value
Age, yr	0.993	0.971-1.016	0.545
Sex (male *vs* female)	0.789	0.376-1.657	0.532
Alcohol abuse (present *vs* absent)	1.133	0.692-1.854	0.620
Tumor number (multiple *vs* single)	1.060	0.594-1.892	0.843
Tumor diameter, cm (> 5 *vs* ≤ 5)	1.147	0.681-1.934	0.606
MVI (present *vs* absent)	1.506	0.921-2.461	0.102
Cirrhosis (present *vs* absent)	1.112	0.404-3.063	0.837
DB, μmol/L (> 6.8 *vs* ≤ 6.8)	1.551	0.766-3.140	0.223
ALB, g/L (> 35 *vs* ≤ 35)	0.677	0.388-1.181	0.169
GGT, U/L (> 50 *vs* ≤ 50)	1.482	0.879-2.499	0.140
ALT, U/L (> 40 *vs* ≤ 40)	1.671	1.002-2.787	0.049
AFP, ng/mL (> 200 *vs* ≤ 200)	2.202	1.340-3.619	0.002
HBsAg (positive *vs* negative)	1.013	0.516-1.991	0.969
NLR (> 2.31 *vs* ≤ 2.31)	3.160	1.901-5.251	< 0.001
Radiomics signature	10.315	3.829-27.786	< 0.001

HR: Hazard ratio; MVI: Microvascular invasion; DB: Direct bilirubin; ALB: Albumin; GGT: Gamma-glutamyl transpeptidase; ALT: Alanine transaminase; AFP: Alpha fetoprotein; HBsAg: Hepatitis B surface antigen; NLR: Neutrophil-to-lymphocyte ratio.

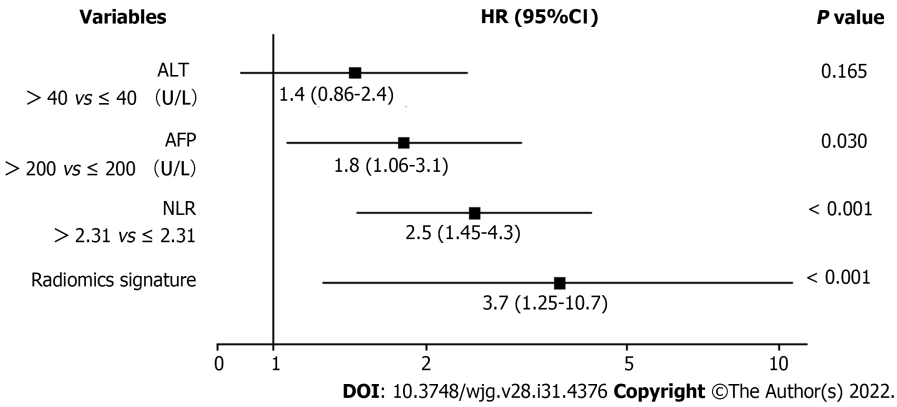


DOI: 10.3748/wjg.v28.i31.4376 **Copyright** ©The Author(s) 2022.

Figure 3 Receiver operating characteristic curves of the radiomics signature for predicting 1-, 3- and 5-year overall survival in the training and validation cohorts. A: Training cohort; B: Validation cohort. OS: Overall survival; AUC: Area under the curve.

DISCUSSION

In this study, we developed a nomogram for predicting the survival of HCC patients after radical hepatectomy. Seven radiomics features were selected from 1926 radiomics features, and then integrated into a single radiomics signature to comprehensively estimate CECT images. We included AFP, NLR and radiomics signature to build the predictive nomogram. The C-indices of the nomogram in the training cohort and validation cohort were 0.736 and 0.774, respectively. The AUCs and the calibration curve indicated satisfactory accuracy in both the training and validation cohorts (AUC of 1-, 3- and 5-year survival = 0.850, 0.791, 0.823 and 0.905, 0.884, 0.911, respectively). The high AUCs of the nomogram



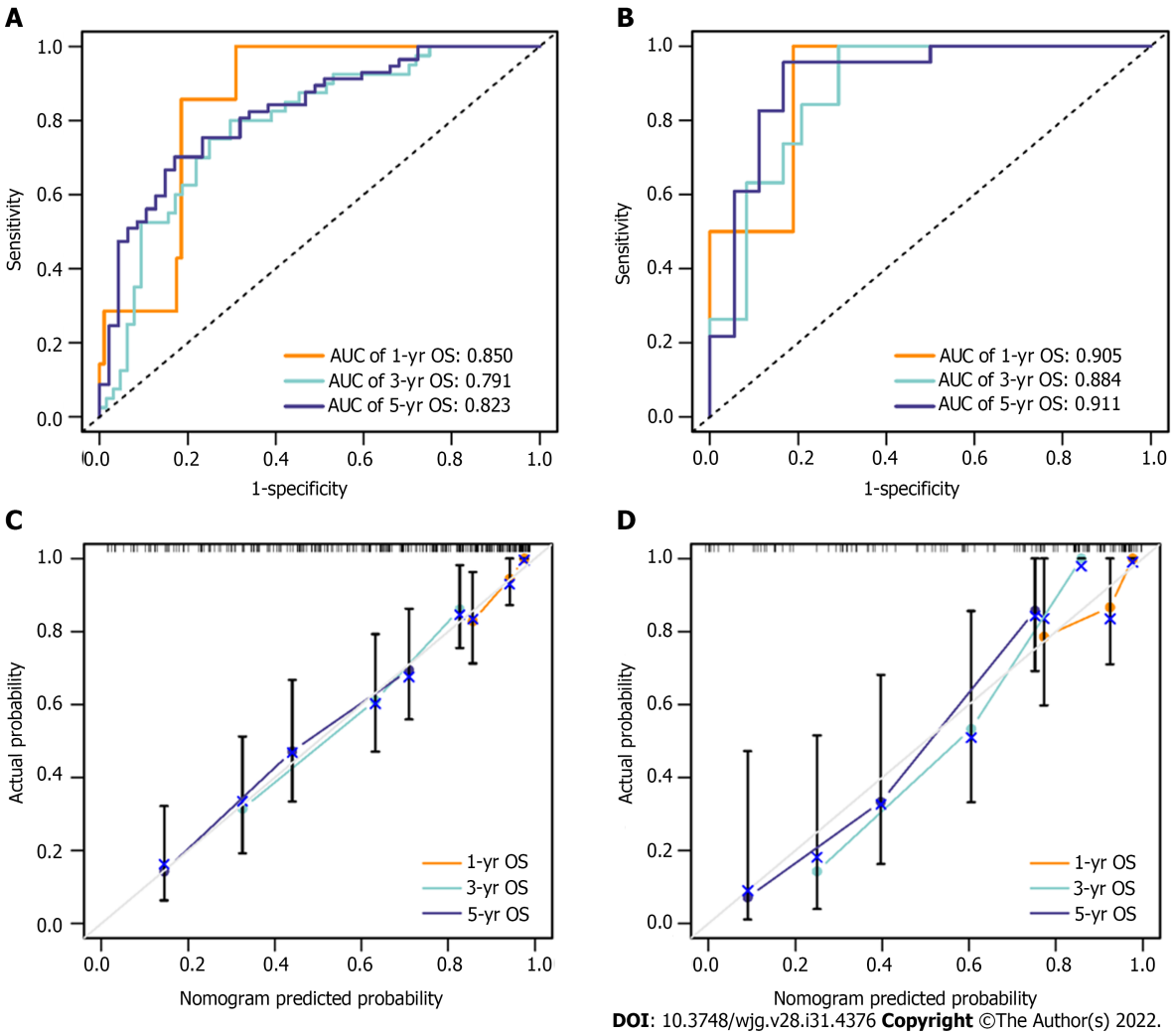
DOI: 10.3748/wjg.v28.i31.4376 **Copyright** ©The Author(s) 2022.

Figure 4 Forest plot of variables with multivariate regression analysis in the training cohort. Variables with a *P* value < 0.05 were considered significantly associated with the overall survival of hepatocellular carcinoma patients. ALT: Alanine transaminase; AFP: Alpha fetoprotein; NLR: Neutrophil-to-lymphocyte ratio; HR: Hazard ratio.

indicate a high accuracy in predicting OS. In DCA, comparing the traditional staging system with our nomogram with respect to predictive ability and clinical practicality, the predictive nomogram was superior to the traditional staging system (BCLC and TNM staging system) in predicting 3- and 5-year survival.

To our knowledge, our radiomics-based model that contains NLR and AFP to predict survival in patients with HCC is entirely novel. A few previous studies[19,20] have investigated the capability of radiomics analysis in predicting the prognosis of HCC patients, and these studies analysed the largest cross-sectional area, whereas entire-tumour analysis was conducted in this study, which can provide more comprehensive information and more effective evaluation of the tumour. Thus, compared with previous studies, radiomics analysis in this study may achieve better performance. Various models combining radiomics features with clinical-pathologic factors to predict prognosis have been developed. Nevertheless, very few studies have enrolled radiomics features and NLR as variables to build a prognostic prediction model for HCC patients. Wang *et al*[21] established an magnetic resonance imaging-based radiomics model incorporating a few clinical factors for predicting the 5-year survival of patients with HCC after radical surgery. The mean AUC in the validation cohort was 0.7578 (95%CI: 0.7056–0.8100).

As precision medicine has developed, accurate prediction of patient prognosis is the principal component of individualized therapy and improving patient prognosis. It has been reported that intratumor heterogeneity is common in a variety of tumours and correlated with clinical outcomes[22]. However, information about intratumor heterogeneity obtained from routine clinical examinations is limited. Radiomics analysis refers to computer-aided data mining of quantitative high-throughput imaging features extracted from medical images[9,10], and it has been reported that radiomics features have potential prognostic value in liver cancer[14], lung cancer[15] and breast cancer[16]. Compared with the interpretation of traditional radiology, radiomics could provide comprehensive information regarding intratumor heterogeneity that may be unable to be obtained by the naked eye of radiologists. To a certain extent, radiomics overcomes these limitations of traditional radiology. As a biomarker associated with HCC, AFP has been widely used for early diagnosis and monitoring of HCC. AFP was considered an independent risk factor for postoperative survival; moreover, patients with low serum AFP levels had longer OS after radical resection. However, AFP still has some limitations in the prognosis prediction of HCC. Prior studies have reported that AFP has no ability to predict prognosis in small HCC (diameter ≤ 3 cm)[23]. Immune cells such as neutrophils, macrophages and lymphocytes within the tumour microenvironment have been confirmed to affect tumour development and progression[24]. There is evidence suggesting that lymphocytes can inhibit tumour proliferation, invasion, and metastasis by enhancing immune surveillance[25]. Moreover, tumour-infiltrating lymphocytes were associated with better outcomes in a variety of tumours, probably linked to tumour infiltration, antitumor activity, lymphocyte induction and inhibition of angiogenesis[26]. One study indicated that neutrophils promote tumour invasion[27]. Neutrophils can inhibit the proliferation of lymphocytes and induce lymphocyte apoptosis[28]. Patients with an elevated NLR level have relative neutrophilia and lymphocytopenia. Therefore, a high NLR indicates a poor prognosis, and this has been confirmed in numerous cancers, including gastric cancer[29], colorectal cancer[30] and pancreatic cancer [31]. To date, there is growing attention to the potential of NLR to be a prognostic biomarker in patients with HCC[32,33]. The NLR is a modality of measuring systemic inflammation that is relatively inexpensive and conveniently obtained from routine preoperative blood tests. In our previous study, the optimal cut-off value of NLR was determined to be 2.31 for predicting the prognosis of patients with HCC, and this was confirmed by not only our previous retrospective trial but also other prospective clinical trials[32]. In summary, NLR is a potential independent predictor for HCC.



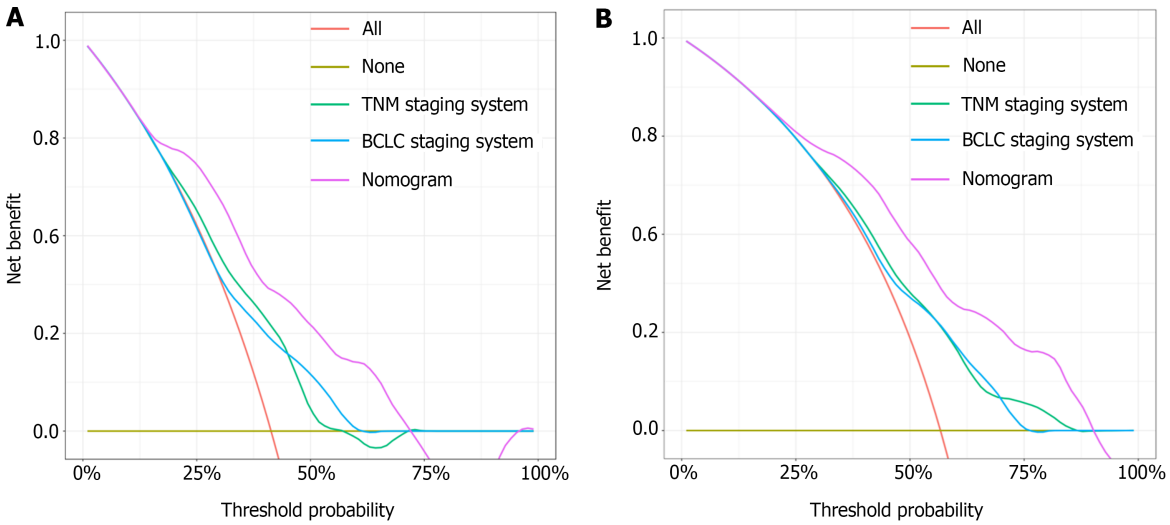
DOI: 10.3748/wjg.v28.i31.4376 **Copyright** ©The Author(s) 2022.

Figure 5 Accuracy of the nomogram for predicting 1-, 3- and 5-year OS in the training and validation cohorts was evaluated by receiver operating characteristic curves and calibration curves. A and B: Receiver operating characteristic curves of the nomogram in the training cohort (A) and validation cohort (B); C and D: Calibration curves of the nomogram in the training cohort (C) and validation cohort (D). In the calibration curve, the nomogram-predicted survival probability is represented on the x-axis, and the actual outcome of overall survival is represented on the y-axis. A closer fit of the coloured lines to the ideal grey line indicates better accuracy in predicting OS. OS: Overall survival; AUC: Area under the curve.

As a standardized and noninvasive imaging modality, CECT is widely utilized for diagnosis, staging, clinical decision-making and treatment response monitoring across numerous cancer types. An advantage of radiomics analysis is that it was performed on existing CECT images as a routine preoperative examination for patients with malignant tumours. Moreover, the variables included in this nomogram were easily acquired from routine blood examinations.

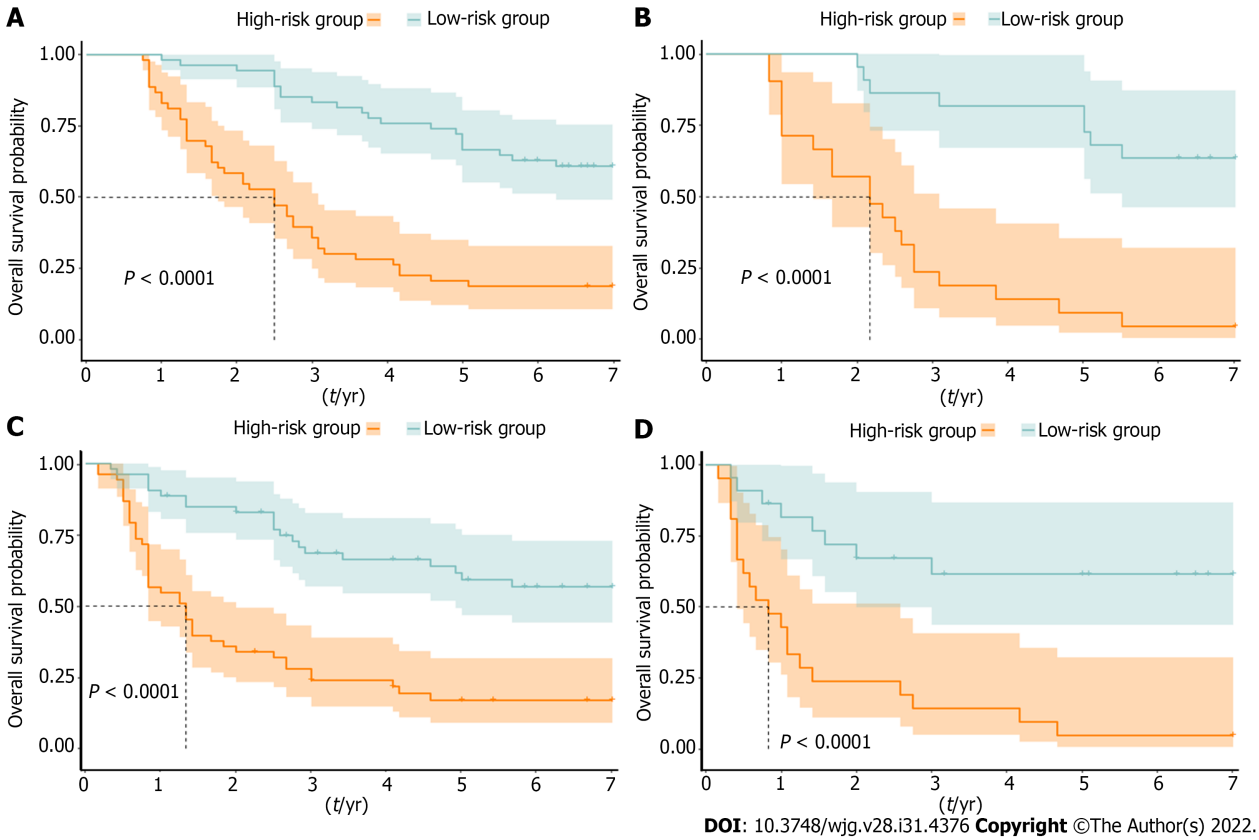
All CECT images were reconstructed with a slice thickness of 1.25 mm, and a previous report showed that slice thickness does not considerably influence the stability of the parameters[34].

The current study has several limitations. First, this study was a single-centre retrospective study. Insufficient data heterogeneity could be a major limitation of single-centre studies. Therefore, more patients from other centres are needed to further validate the reliability and clinical applicability of this prognostic model. Second, HCC is considered to be related to various aetiological factors, including alcohol, aflatoxin, hepatitis B virus and hepatitis C virus. Different aetiologies might result in different outcomes in HCC. Hepatitis B virus was the main aetiology of HCC in the present study. Thus, future studies are required to validate the efficacy and accuracy of this predictive model in HCC with different aetiologies. Third, the different contrast agents or the different injection speeds may affect the quantification of radiomic features[35] and thus affect the accuracy of the model. To overcome this limitation, multi-institutional validation and cross-validation are required in the future. Fourth, regions of interest were outlined semiautomatically and corrected manually when necessary. Hence, a certain degree of selection bias of the ROIs might be created by the different observers. This is a challenging problem for radiomics analysis to eliminate or reduce biases. Fifth, the correlation between radiomics features and biological behaviour remains unknown. Recently, radio-genomics has become an emerging area that integrates radiomics and genomics. Radio-genomics is the discipline that studies the relationship



DOI: 10.3748/wjg.v28.i31.4376 **Copyright** ©The Author(s) 2022.

Figure 6 Decision curve analysis was performed in all hepatocellular carcinoma patients to evaluate the clinical practicality of the nomogram for predicting 3- and 5-year overall survival compared with the Barcelona clinic liver cancer staging system model and tumor, node and metastasis staging system model. A and B: Decision curve analysis of the nomogram, Barcelona clinic liver cancer staging system model and tumor, node and metastasis staging system model in predicting 3- (A) and 5-year (B) OS. In the decision curve, the threshold probability is represented on the x-axis, and the net benefit is represented on the y-axis. A higher curve indicates a greater net benefit at any given threshold probability. The decision curve showed that the nomogram adds more net benefit than traditional staging system models. BCLC: Barcelona clinic liver cancer; TNM: Tumor, node and metastasis.



DOI: 10.3748/wjg.v28.i31.4376 **Copyright** ©The Author(s) 2022.

Figure 7 Risk stratification ability of the nomogram was estimated by the Kaplan–Meier method and log-rank test in the training and validation cohorts. A and B: Kaplan–Meier curves between the low- and high-risk subgroups of overall survival in the training cohort (A) and validation cohort (B); C and D: Kaplan–Meier curves between the low- and high-risk subgroups of disease-free survival in the training cohort (C) and validation cohort (D). Patients with hepatocellular carcinoma in the training and validation cohorts were divided into low- and high-risk subgroups according to whether the total points of each patient were lower or higher than the median points of each cohort.

between image phenotypes and genomics, which may contribute to precision medicine development [36]. Further research is still required to determine the potential correlation between radiomics and genomics in HCC. In future studies, we will incorporate genomic characteristics associated with HCC prognosis to construct a more comprehensive radio-genomics predictive model.

CONCLUSION

In conclusion, the nomogram combining the radiomics signature, NLR and AFP may contribute to postoperative outcome prediction and clinical treatment decision-making for HCC patients.

ARTICLE HIGHLIGHTS

Research background

Hepatocellular carcinoma (HCC) is the most common primary liver malignancy. The prognosis of HCC patients remains poor. Radiomics is an artificial intelligent-based method for obtaining prognostic and predictive information which may contribute to clinical outcomes improvement.

Research motivation

Currently, a few studies have analysed the largest cross-sectional area of HCC tumour. In this study, we have analysed the entire-tumour to build a more comprehensive prognostic prediction model with clinical characteristics. We aimed to develop a radiomics model for predicting the overall survival of HCC patients after hepatectomy.

Research objectives

In this study, we aimed to develop a radiomics model based on contrast-enhanced computed tomography (CECT) images for predicting the overall survival of HCC patients after radical hepatectomy.

Research methods

A total of 150 HCC patients were enrolled and randomly divided into a training cohort (n = 107) and a validation cohort (n = 43) at ratio 2.5:1. Radiomics features were extracted from the CECT images. In training cohort, the least absolute shrinkage and selection operator algorithm was applied for radiomics features selection and radiomics signature construction. Univariate and multivariate Cox regression analyses were used to develop the predictive model. The accuracy of the model was assessed with the concordance index, receiver operating characteristic curve and calibration curve. The clinical practicality was evaluated by decision curve analysis. The survival between the low- and high-risk subgroups was compared using Kaplan–Meier methodology.

Research results

In total, seven radiomics features were selected to construct the radiomics signature. Alpha-fetoprotein, neutrophil-to-lymphocyte ratio and radiomics signature were identified as independent risk predictors to build the predictive model. The C-indices of the model in the training and validation cohorts were 0.736 and 0.774, respectively. In receiver operating characteristic curve for predicting 1-, 3-, and 5-year overall survival, area under the curve (AUC) = 0.850, 0.791 and 0.823, respectively in training cohort; AUC = 0.905, 0.884 and 0.911, respectively in validation cohort. The calibration curve analysis indicated a good agreement between the model-prediction and actual survival. Decision curve analysis suggested that the predictive model had more benefit than traditional staging system models. In Kaplan–Meier survival analysis, patients in the low-risk group had longer overall survival and disease-free survival.

Research conclusions

The predictive model is a reliable tool for predicting the overall survival of HCC patients after radical hepatectomy.

Research perspectives

More precise and reliable tool to predict the prognosis of HCC patients is urgently needed. Radiomics is a new method for obtaining prognostic and predictive information. In this study, we aimed to develop a predictive model based on CECT images and clinical-pathologic characteristics to predict the overall survival of HCC patients.

FOOTNOTES

Author contributions: Deng PZ, Zhao BG and Huang XH contributed equally to this work; Liao WJ was the guarantor and designed the study; Deng PZ, Zhao BG, Xu TF, Chen ZJ, Wei QF, and Liu XY participated in the acquisition, analysis, and interpretation of the data; Deng PZ and Huang XH drafted the initial manuscript; Guo YQ, Yuan SG, and Liao WJ revised the article critically for important intellectual content.

Supported by the National Natural Science Foundation of China, No. 81372163; the Science and Technology Planning Project of Guilin, No. 20190218-1; the Openin Project of Key laboratory of High-Incidence-Tumor Prevention & Treatment (Guangxi Medical University), Ministry of Education, No. GKE-KF202101; the Program of Guangxi Zhuang Autonomous Region health and Family Planning Commission, No. Z20210706; and the Innovation and Entrepreneurship Project of University Students in Guangxi, No. 202110601002.

Institutional review board statement: The study was reviewed and approved by the research ethics committee of Affiliated Hospital of Guilin Medical University (Approval NO. 2021WJWZC14).

Informed consent statement: Informed consent was obtained from all patients.

Conflict-of-interest statement: There are no conflicts of interest to report.

Data sharing statement: No additional data are available.

Open-Access: This article is an open-access article that was selected by an in-house editor and fully peer-reviewed by external reviewers. It is distributed in accordance with the Creative Commons Attribution NonCommercial (CC BY-NC 4.0) license, which permits others to distribute, remix, adapt, build upon this work non-commercially, and license their derivative works on different terms, provided the original work is properly cited and the use is non-commercial. See: https://creativecommons.org/Licenses/by-nc/4.0/

Country/Territory of origin: China

ORCID number: Peng-Zhan Deng 0000-0003-1221-7664; Bi-Geng Zhao 0000-0001-6203-4159; Xian-Hui Huang 0000-0002-4306-1327; Ting-Feng Xu 0000-0003-0303-5471; Zi-Jun Chen 0000-0002-2488-8038; Qiu-Feng Wei 0000-0001-9355-2098; Xiao-Yi Liu 0000-0001-5563-7488; Yu-Qi Guo 0000-0002-6687-6828; Sheng-Guang Yuan 0000-0003-4846-0543; Wei-Jia Liao 0000-0002-8906-8612.

S-Editor: Zhang H
L-Editor: A
P-Editor: Cai YX

REFERENCES

1 **Sung H**, Ferlay J, Siegel RL, Laversanne M, Soerjomataram I, Jemal A, Bray F. Global Cancer Statistics 2020: GLOBOCAN Estimates of Incidence and Mortality Worldwide for 36 Cancers in 185 Countries. *CA Cancer J Clin* 2021; **71**: 209-249 [PMID: 33538338 DOI: 10.3322/caac.21660]
2 **Poon RT**, Fan ST, Lo CM, Liu CL, Wong J. Long-term survival and pattern of recurrence after resection of small hepatocellular carcinoma in patients with preserved liver function: implications for a strategy of salvage transplantation. *Ann Surg* 2002; **235**: 373-382 [PMID: 11882759 DOI: 10.1097/00000658-200203000-00009]
3 **Gupta S**, Bent S, Kohlwes J. Test characteristics of alpha-fetoprotein for detecting hepatocellular carcinoma in patients with hepatitis C. A systematic review and critical analysis. *Ann Intern Med* 2003; **139**: 46-50 [PMID: 12834318 DOI: 10.7326/0003-4819-139-1-200307010-00012]
4 **Zong J**, Fan Z, Zhang Y. Serum Tumor Markers for Early Diagnosis of Primary Hepatocellular Carcinoma. *J Hepatocell Carcinoma* 2020; **7**: 413-422 [PMID: 33376710 DOI: 10.2147/JHC.S272762]
5 **Leonardi GC**, Candido S, Cervello M, Nicolosi D, Raiti F, Travali S, Spandidos DA, Libra M. The tumor microenvironment in hepatocellular carcinoma (review). *Int J Oncol* 2012; **40**: 1733-1747 [PMID: 22447316 DOI: 10.3892/ijo.2012.1408]
6 **Nakagawa S**, Umezaki N, Yamao T, Kaida T, Okabe H, Mima K, Imai K, Hashimoto D, Yamashita YI, Ishiko T, Chikamoto A, Baba H. Survival impact of lymphocyte infiltration into the tumor of hepatocellular carcinoma in hepatitis B virus-positive or non-B non-C patients who underwent curative resection. *Hepatol Res* 2018; **48**: E126-E132 [PMID: 28696046 DOI: 10.1111/hepr.12936]
7 **Liao R**, Tang ZW, Li DW, Luo SQ, Huang P, Du CY. Preoperative neutrophil-to-lymphocyte ratio predicts recurrence of patients with single-nodule small hepatocellular carcinoma following curative resection: a retrospective report. *World J Surg Oncol* 2015; **13**: 265 [PMID: 26328917 DOI: 10.1186/s12957-015-0670-y]
8 **Motomura T**, Shirabe K, Mano Y, Muto J, Toshima T, Umemoto Y, Fukuhara T, Uchiyama H, Ikegami T, Yoshizumi T, Soejima Y, Maehara Y. Neutrophil-lymphocyte ratio reflects hepatocellular carcinoma recurrence after liver transplantation *via* inflammatory microenvironment. *J Hepatol* 2013; **58**: 58-64 [PMID: 22925812 DOI: 10.1016/j.jhep.2012.08.017]
9 **Gillies RJ**, Kinahan PE, Hricak H. Radiomics: Images Are More than Pictures, They Are Data. *Radiology* 2016; **278**: 563-

577 [PMID: 26579733 DOI: 10.1148/radiol.2015151169]
10 **Lambin P**, Rios-Velazquez E, Leijenaar R, Carvalho S, van Stiphout RG, Granton P, Zegers CM, Gillies R, Boellard R, Dekker A, Aerts HJ. Radiomics: extracting more information from medical images using advanced feature analysis. *Eur J Cancer* 2012; **48**: 441-446 [PMID: 22257792 DOI: 10.1016/j.ejca.2011.11.036]
11 **Gerlinger M**, Rowan AJ, Horswell S, Math M, Larkin J, Endesfelder D, Gronroos E, Martinez P, Matthews N, Stewart A, Tarpey P, Varela I, Phillimore B, Begum S, McDonald NQ, Butler A, Jones D, Raine K, Latimer C, Santos CR, Nohadani M, Eklund AC, Spencer-Dene B, Clark G, Pickering L, Stamp G, Gore M, Szallasi Z, Downward J, Futreal PA, Swanton C. Intratumor heterogeneity and branched evolution revealed by multiregion sequencing. *N Engl J Med* 2012; **366**: 883-892 [PMID: 22397650 DOI: 10.1056/NEJMoa1113205]
12 **Tu SM**, Bilen MA, Hess KR, Broaddus RR, Kopetz S, Wei C, Pagliaro LC, Karam JA, Ward JF, Wood CG, Rao P, Tu ZH, General R, Chen AH, Nieto YL, Yeung SC, Lin SH, Logothetis CJ, Pisters LL. Intratumoral heterogeneity: Role of differentiation in a potentially lethal phenotype of testicular cancer. *Cancer* 2016; **122**: 1836-1843 [PMID: 27018785 DOI: 10.1002/cncr.29996]
13 **Aerts HJ**, Velazquez ER, Leijenaar RT, Parmar C, Grossmann P, Carvalho S, Bussink J, Monshouwer R, Haibe-Kains B, Rietveld D, Hoebers F, Rietbergen MM, Leemans CR, Dekker A, Quackenbush J, Gillies RJ, Lambin P. Decoding tumour phenotype by noninvasive imaging using a quantitative radiomics approach. *Nat Commun* 2014; **5**: 4006 [PMID: 24892406 DOI: 10.1038/ncomms5006]
14 **Zheng BH**, Liu LZ, Zhang ZZ, Shi JY, Dong LQ, Tian LY, Ding ZB, Ji Y, Rao SX, Zhou J, Fan J, Wang XY, Gao Q. Radiomics score: a potential prognostic imaging feature for postoperative survival of solitary HCC patients. *BMC Cancer* 2018; **18**: 1148 [PMID: 30463529 DOI: 10.1186/s12885-018-5024-z]
15 **Huang Y**, Liu Z, He L, Chen X, Pan D, Ma Z, Liang C, Tian J. Radiomics Signature: A Potential Biomarker for the Prediction of Disease-Free Survival in Early-Stage (I or II) Non-Small Cell Lung Cancer. *Radiology* 2016; **281**: 947-957 [PMID: 27347764 DOI: 10.1148/radiol.2016152234]
16 **Li H**, Zhu Y, Burnside ES, Drukker K, Hoadley KA, Fan C, Conzen SD, Whitman GJ, Sutton EJ, Net JM, Ganott M, Huang E, Morris EA, Perou CM, Ji Y, Giger ML. MR Imaging Radiomics Signatures for Predicting the Risk of Breast Cancer Recurrence as Given by Research Versions of MammaPrint, Oncotype DX, and PAM50 Gene Assays. *Radiology* 2016; **281**: 382-391 [PMID: 27144536 DOI: 10.1148/radiol.2016152110]
17 **Heimbach JK**, Kulik LM, Finn RS, Sirlin CB, Abecassis MM, Roberts LR, Zhu AX, Murad MH, Marrero JA. AASLD guidelines for the treatment of hepatocellular carcinoma. *Hepatology* 2018; **67**: 358-380 [PMID: 28130846 DOI: 10.1002/hep.29086]
18 **Liao W**, Zhang J, Zhu Q, Qin L, Yao W, Lei B, Shi W, Yuan S, Tahir SA, Jin J, He S. Preoperative Neutrophil-to-Lymphocyte Ratio as a New Prognostic Marker in Hepatocellular Carcinoma after Curative Resection. *Transl Oncol* 2014; **7**: 248-255 [PMID: 24704092 DOI: 10.1016/j.tranon.2014.02.011]
19 **Ahn SJ**, Kim JH, Park SJ, Kim ST, Han JK. Hepatocellular carcinoma: preoperative gadoxetic acid-enhanced MR imaging can predict early recurrence after curative resection using image features and texture analysis. *Abdom Radiol (NY)* 2019; **44**: 539-548 [PMID: 30229421 DOI: 10.1007/s00261-018-1768-9]
20 **Zhou Y**, He L, Huang Y, Chen S, Wu P, Ye W, Liu Z, Liang C. CT-based radiomics signature: a potential biomarker for preoperative prediction of early recurrence in hepatocellular carcinoma. *Abdom Radiol (NY)* 2017; **42**: 1695-1704 [PMID: 28180924 DOI: 10.1007/s00261-017-1072-0]
21 **Wang XH**, Long LH, Cui Y, Jia AY, Zhu XG, Wang HZ, Wang Z, Zhan CM, Wang ZH, Wang WH. MRI-based radiomics model for preoperative prediction of 5-year survival in patients with hepatocellular carcinoma. *Br J Cancer* 2020; **122**: 978-985 [PMID: 31937925 DOI: 10.1038/s41416-019-0706-0]
22 **O'Connor JP**, Rose CJ, Waterton JC, Carano RA, Parker GJ, Jackson A. Imaging intratumor heterogeneity: role in therapy response, resistance, and clinical outcome. *Clin Cancer Res* 2015; **21**: 249-257 [PMID: 25421725 DOI: 10.1158/1078-0432.CCR-14-0990]
23 **Giannini EG**, Marenco S, Borgonovo G, Savarino V, Farinati F, Del Poggio P, Rapaccini GL, Anna Di Nolfo M, Benvegnù L, Zoli M, Borzio F, Caturelli E, Chiaramonte M, Trevisani F; Italian Liver Cancer (ITA. LI.CA) group. Alpha-fetoprotein has no prognostic role in small hepatocellular carcinoma identified during surveillance in compensated cirrhosis. *Hepatology* 2012; **56**: 1371-1379 [PMID: 22535689 DOI: 10.1002/hep.25814]
24 **Joyce JA**, Pollard JW. Microenvironmental regulation of metastasis. *Nat Rev Cancer* 2009; **9**: 239-252 [PMID: 19279573 DOI: 10.1038/nrc2618]
25 **Dunn GP**, Old LJ, Schreiber RD. The immunobiology of cancer immunosurveillance and immunoediting. *Immunity* 2004; **21**: 137-148 [PMID: 15308095 DOI: 10.1016/j.immuni.2004.07.017]
26 **Azimi F**, Scolyer RA, Rumcheva P, Moncrieff M, Murali R, McCarthy SW, Saw RP, Thompson JF. Tumor-infiltrating lymphocyte grade is an independent predictor of sentinel lymph node status and survival in patients with cutaneous melanoma. *J Clin Oncol* 2012; **30**: 2678-2683 [PMID: 22711850 DOI: 10.1200/JCO.2011.37.8539]
27 **Imai Y**, Kubota Y, Yamamoto S, Tsuji K, Shimatani M, Shibatani N, Takamido S, Matsushita M, Okazaki K. Neutrophils enhance invasion activity of human cholangiocellular carcinoma and hepatocellular carcinoma cells: an *in vitro* study. *J Gastroenterol Hepatol* 2005; **20**: 287-293 [PMID: 15683434 DOI: 10.1111/j.1440-1746.2004.03575.x]
28 **Ohtani H**. Focus on TILs: prognostic significance of tumor infiltrating lymphocytes in human colorectal cancer. *Cancer Immun* 2007; **7**: 4 [PMID: 17311363]
29 **Ishizuka M**, Oyama Y, Abe A, Kubota K. Combination of platelet count and neutrophil to lymphocyte ratio is a useful predictor of postoperative survival in patients undergoing surgery for gastric cancer. *J Surg Oncol* 2014; **110**: 935-941 [PMID: 25146385 DOI: 10.1002/jso.23753]
30 **Walsh SR**, Cook EJ, Goulder F, Justin TA, Keeling NJ. Neutrophil-lymphocyte ratio as a prognostic factor in colorectal cancer. *J Surg Oncol* 2005; **91**: 181-184 [PMID: 16118772 DOI: 10.1002/jso.20329]
31 **Stotz M**, Gerger A, Eisner F, Szkandera J, Loibner H, Ress AL, Kornprat P, AlZoughbi W, Seggewies FS, Lackner C, Stojakovic T, Samonigg H, Hoefler G, Pichler M. Increased neutrophil-lymphocyte ratio is a poor prognostic factor in patients with primary operable and inoperable pancreatic cancer. *Br J Cancer* 2013; **109**: 416-421 [PMID: 23799847 DOI:

10.1038/bjc.2013.332]

32 **Oh BS**, Jang JW, Kwon JH, You CR, Chung KW, Kay CS, Jung HS, Lee S. Prognostic value of C-reactive protein and neutrophil-to-lymphocyte ratio in patients with hepatocellular carcinoma. *BMC Cancer* 2013; **13**: 78 [PMID: 23409924 DOI: 10.1186/1471-2407-13-78]

33 **Shiraki T**, Ishizuka M, Kubota K, Kato M, Matsumoto T, Mori S, Shimizu T, Aoki T. An elevated neutrophil-to-lymphocyte ratio predicts a poor postoperative survival in primary hepatocellular carcinoma patients with a normal preoperative serum level of alpha-fetoprotein. *Surg Today* 2019; **49**: 661-669 [PMID: 30806789 DOI: 10.1007/s00595-019-01781-1]

34 **Duda D**, Kretowski M, Bezy-Wendling J. Effect of Slice Thickness on Texture-Based Classification of Liver Dynamic CT Scans. In: Saeed K, Chaki R, Cortesi A, Wierzchoń S, editors. Computer Information Systems and Industrial Management. CISIM 2013: Proceedings of the 12th IFIP TC8 International Conference on Computer Information Systems and Industrial Management. Berlin: Springer, 2013: 96-107 [DOI: 10.1007/978-3-642-40925-7_10]

35 **Kakino R**, Nakamura M, Mitsuyoshi T, Shintani T, Hirashima H, Matsuo Y, Mizowaki T. Comparison of radiomic features in diagnostic CT images with and without contrast enhancement in the delayed phase for NSCLC patients. *Phys Med* 2020; **69**: 176-182 [PMID: 31918370 DOI: 10.1016/j.ejmp.2019.12.019]

36 **Gopal N**, Yazdian Anari P, Turkbey E, Jones EC, Malayeri AA. The Next Paradigm Shift in the Management of Clear Cell Renal Cancer: Radiogenomics-Definition, Current Advances, and Future Directions. *Cancers (Basel)* 2022; **14** [PMID: 35159060 DOI: 10.3390/cancers14030793]

World Journal of Gastroenterology

Submit a Manuscript: https://www.f6publishing.com

World J Gastroenterol 2022 August 21; 28(31): 4390-4398

DOI: 10.3748/wjg.v28.i31.4390

ISSN 1007-9327 (print) ISSN 2219-2840 (online)

ORIGINAL ARTICLE

Retrospective Study

Nationwide retrospective study of hepatitis B virological response and liver stiffness improvement in 465 patients on nucleos(t)ide analogue

Alnoor Ramji, Karen Doucette, Curtis Cooper, Gerald Yosel Minuk, Mang Ma, Alexander Wong, David Wong, Edward Tam, Brian Conway, David Truong, Philip Wong, Lisa Barrett, Hin Hin Ko, Sarah Haylock-Jacobs, Nishi Patel, Gilaad G Kaplan, Scott Fung, Carla S Coffin

Specialty type: Gastroenterology and hepatology

Provenance and peer review: Unsolicited article; Externally peer reviewed.

Peer-review model: Single blind

P-Reviewer: Ferraioli G, Italy; Hua J, China

Received: April 22, 2022
Peer-review started: April 22, 2022
First decision: May 9, 2022
Revised: May 22, 2022
Accepted: July 25, 2022
Article in press: July 25, 2022
Published online: August 21, 2022

Alnoor Ramji, Hin Hin Ko, Department of Medicine, University of British Columbia, Vancouver V6T 1Z3, Canada

Karen Doucette, Mang Ma, Department of Medicine, University of Alberta, Edmonton T6G 2R7, Canada

Curtis Cooper, Department of Medicine, The Ottawa Hospital Research Institute, University of Ottawa, Ottawa ON K1H 8L6, Canada

Gerald Yosel Minuk, Department of Medicine, University of Manitoba, Winnipeg R3E 3J7, Canada

Alexander Wong, Department of Medicine, University of Saskatchewan, Saskatoon S7N 5E5, Canada

David Wong, Scott Fung, Department of Medicine,University Health Network, Toronto M5G 2C4, Canada

Edward Tam, Pacific Gastroenterology Associates, Vancouver V6Z 2K5, Canada

Brian Conway, David Truong, Vancouver Infectious Disease Centre, Vancouver V6Z 2C7, Canada

Philip Wong, Department of Medicine, McGill University, Montreal H3A 0G4, Canada

Lisa Barrett, Department of Microbiology and Immunology, Dalhousie University, Halifax B3H 4R2, Canada

Sarah Haylock-Jacobs, Nishi Patel, Gilaad G Kaplan, Carla S Coffin, Cumming School of Medicine, University of Calgary, Calgary T2N 1N4, Canada

Corresponding author: Alnoor Ramji, MD, Associate Professor, Department of Medicine, University of British Columbia, 2775 Laurel Str, Gordon and Leslie Diamond Health Care, Vancouver V6T 1Z3, Canada. ramji_a@hotmail.com

Abstract

BACKGROUND

Hepatitis B virus (HBV) nucleos(t)ide analog (NA) therapy reduces liver disease but requires prolonged therapy to achieve hepatitis B surface antigen (HBsAg) loss. There is limited North American real-world data using non-invasive tools for fibrosis assessment and few have compared 1st generation NA or lamivudine (LAM) to tenofovir disoproxil fumarate (TDF).

AIM

To assess impact of NA on virological response and fibrosis regression using liver stiffness measurement (LSM) (*i.e.*, FibroScan®).

METHODS

Retrospective, observational cohort study from the Canadian HBV Network. Data collected included demographics, NA, HBV DNA, alanine aminotransferase (ALT), and LSM. Patients were HBV monoinfected patients, treatment naïve, and received 1 NA with minimum 1 year follow-up.

RESULTS

In 465 (median 49 years, 37% female, 35% hepatitis B e antigen+ at baseline, 84% Asian, 6% White, and 9% Black). Percentage of 64 (n = 299) received TDF and 166 were LAM-treated with similar median duration of 3.9 and 3.7 years, respectively. The mean baseline LSM was 11.2 kPa (TDF) *vs* 8.3 kPa (LAM) (P = 0.003). At 5-year follow-up, the mean LSM was 7.0 kPa in TDF *vs* 6.7 kPa in LAM (P = 0.83). There was a significant difference in fibrosis regression between groups (*i.e.*, mean -4.2 kPa change in TDF and -1.6 kPa in LAM, P < 0.05). The last available data on treatment showed that all had normal ALT, but more TDF patients were virologically suppressed (< 10 IU/mL) (n = 170/190, 89%) *vs* LAM-treated (n = 35/58, 60%) (P < 0.05). None cleared HBsAg.

CONCLUSION

In this real-world North American study, approximately 5 years of NA achieves liver fibrosis regression rarely leads to HBsAg loss.

Key Words: Nucleos(t)ide analog therapy; Functional cure; Hepatitis B virus surface antigen loss; Fibrosis regression; Liver stiffness measurement; Transient elastography

©The Author(s) 2022. Published by Baishideng Publishing Group Inc. All rights reserved.

Core Tip: In summary in this real-world diverse cohort study of chronic hepatitis B patients in Canada, long-term nucleo(s)ide analog (either 1st or 2nd generation) therapy suppresses hepatitis B virus DNA and improves hepatic inflammation and liver fibrosis, as determined by non-invasive testing (*i.e.*, transient elastography). In patients treated for up to 5 years, none achieved hepatitis B surface antigen loss (functional cure), highlighting the need for improved therapeutic strategies to reduce the life-long burden of antiviral therapy.

Citation: Ramji A, Doucette K, Cooper C, Minuk GY, Ma M, Wong A, Wong D, Tam E, Conway B, Truong D, Wong P, Barrett L, Ko HH, Haylock-Jacobs S, Patel N, Kaplan GG, Fung S, Coffin CS. Nationwide retrospective study of hepatitis B virological response and liver stiffness improvement in 465 patients on nucleos(t)ide analogue. *World J Gastroenterol* 2022; 28(31): 4390-4398

URL: https://www.wjgnet.com/1007-9327/full/v28/i31/4390.htm

DOI: https://dx.doi.org/10.3748/wjg.v28.i31.4390

INTRODUCTION

Hepatitis B virus (HBV) nucleos(t)ide analog (NA) therapy is associated with fibrosis regression, reduced risk of hepatocellular carcinoma (HCC) and improved clinical outcomes[1]. The ultimate goal of HBV therapy is hepatitis B surface antigen (HBsAg) loss and considered a functional cure enabling treatment cessation, but rarely achieved with current NA. Without HBsAg clearance, stopping treatment may lead to severe viral and biochemical flares. Studies of European patients reported HBsAg loss in 20% patients after stopping long-term NA therapy. HBsAg loss among Asian virally suppressed patients was very low (< 5%) suggesting there are important differences among different groups of patients in terms of off-treatment response[2,3]. The approved 2nd generation NA, *i.e.*, entecavir (ETV),

tenofovir disoproxil fumarate (TDF) and tenofovir alafenamide (TAF) potently reduce serum viral load (HBV DNA) but they rarely achieve a functional cure despite prolonged therapy[4]. Studies in large Asian cohorts have compared the effect of NA with a low genetic barrier to drug resistance (*i.e.*, lamivudine, LAM) to higher potency (*i.e.*, ETV, TDF/TAF) NA on liver fibrosis regression and viral response[5]. A single centre Asian study of 124 patients treated with anti-HBV NA documented HBV DNA suppression but all had persistently detectable HBsAg, and none achieved intrahepatic viral marker reduction (*i.e.*, HBV covalently closed circular (ccc) DNA)[5]. A large retrospective Korean study showed lower risk of death or transplantation with ETV compared to LAM but no difference in HCC risk[6]. A recent global study involving 299 centers in 24 countries investigated outcomes after 10 years of follow-up of clinical trial patients treated with ETV or alternative NA[2]. The data revealed that 5305 Chinese ETV recipients maintained virological response with lower risk of HBV-related serious adverse events including HCC. However, approximately 17% of the cohort, and similar rate in other cohorts, continued to identify HBV-related liver disease progression[5,7]. Liver disease complications have also been reported in a Korean study of 440 cirrhotic patients (mostly genotype C) after 5 years of ETV therapy, with a 15% rate of liver disease decompensation in those with > 90% treatment adherence and 41% decompensation in patients with < 90% adherence[8].

There is limited real-world data evaluating the clinical impact of 1st *vs* 2nd generation long-term NA therapy in North American chronic hepatitis B (CHB) patients. These patients maybe characterised by greater diversity and genotype heterogeneity based on a diverse regions of origin. Disparities in access to HBV NA is a global issue. Similarly, in Canada, NA reimbursement criteria vary by provincial or territorial jurisdiction[9]. Until recently, antivirals with a high barrier to resistance such as TDF and ETV were not funded as first line therapies for CHB in two large population provincial health jurisdictions [*i.e.*, British Columbia (BC) and Ontario (ON)][9]. In particular, there were historic differences in reimbursement criteria with LAM utilized as first line in BC and ON, and TDF historically (before 2018) only reimbursed for persons with advanced fibrosis and/or decompensated cirrhosis. In BC and ON, HBV patients could access TDF if they failed LAM, developed resistance or very rarely, had intolerance to LAM. In this retrospective, multi-centre cohort study of 465 CHB patients followed in 8 provinces across Canada, we aim to assess HBV viral response, biochemical remission, liver fibrosis regression and HBsAg sero-clearance after treatment with median 4 years of either a 1st or 2nd line NA therapy.

MATERIALS AND METHODS

This was a retrospective observational cohort study, utilizing the Canadian Hepatitis B Network cohort data from January 1st, 2012-December 1st, 2019. Participating clinics provided data from electronic and/or paper charts. De-identified information was entered into a registry REDCap® database housed at the University of Calgary (U of C) under an approved U of C Conjoint Ethics Research Board (CHREB) protocol (Ethics ID # REB16-0041), and appropriate legal data sharing agreements[10]. Study subjects provided written informed consent to participate, or were included with a waiver of consent, according to local REB approval. Data extracted included demographics (age, sex, ethnicity), antiviral regimens, HBV DNA, hepatitis B e antigen (HBeAg), alanine aminotransferase (ALT) and liver stiffness measurement (LSM) prior to and during therapy. Inclusion: Adult patients >18 years, with known chronic HBV (*i.e.*, HBsAg persistence > 6 mo duration), HBV monoinfected, treatment naïve at baseline, and were on only a single antiviral agent for the study duration. Exclusion: Participants were excluded if they had received previous HBV therapy, had a liver transplant or were co-infected with other hepatotropic viruses (*e.g.*, HCV and HDV) or with HIV. ETV treated patients were also excluded for direct comparison of only two antiviral drugs. Persons who had their antiviral regiment switched (includes LAM-resistant patients switching to TDF) were also excluded. All patients had a minimum of 12 mo follow-up from treatment initiation, with at least annual HBV DNA evaluation using commercial assays (*i.e.*, sensitivity 20 IU/mL or 50 copies/mL, Abbott and/or < 20 IU/mL, Roche) and serial LSM performed using FibroScan® (Echosens, Paris, Fr). Liver fibrosis, based on Metavir staging, was classified as F0-F1 (< 7.3 kPa), F2-F3 (7.3-9.5 kPa) and F4 or cirrhosis (> 9.5 kPa)[11]. CHB management and treatment monitoring was directed by the center physician(s) and based on the Canadian consensus guidelines[12].

Statistical analyses

For all analyses, patients with missing data were excluded. Continuous data were summarized with the mean, 95% confidence interval (CI) and count (n). For comparisons between treatment groups (LAM *vs* TDF) at a given time point, two-tailed *t* test was used. Repeated measures analysis of variance (ANOVA) with post hoc test was used to compare continuous variables at different time points for each treatment group. Categorical data were summarized as proportion using mean % (n/n known). Fisher's exact test was used for comparison between dichotomous data. A linear mixed model was used to identify change over time in a multivariable linear mixed regression analysis. A *P* value of less than 0.05 was considered to be statistically significant. Statistical analyses were performed using SAS/STAT® software, IBM SPSS Statistics 27.0.1.0 and/or GraphPad Prism 9.0.

RESULTS

Characteristics of the study population

The study population included 465 patients who were treatment naïve at baseline. The mean age was 49 (SD 12.9) years, 37% were female, and 35% were HBeAg (+) at baseline. Most were Asian (84%, *n* = 345) (albeit from different East and/or South-East Asian) countries, 9% Black (*n* = 37), and 6% White (*n* = 25). Patients either received TDF (*n* = 299, 65%) or LAM (*n* = 166, 35%) therapies with similar median treatment duration of 3.9 and 3.7 years, respectively. There was no difference between treatment groups in sex or ethnicity. However, TDF treated individuals were more likely to be HBeAg positive (Table 1). Historically, patients from one provincial health jurisdiction (*i.e.*, British Columbia), only had access to TDF as first line therapy if they had cirrhosis. Thus, a greater proportion of persons in the TDF group also had advanced fibrosis (> stage F3/4) at baseline, compared to LAM (Table 1).

Summary of follow-up evaluation and outcomes

The mean baseline LSM prior to treatment was greater in TDF treated recipients (11.2 kPa, 95%CI: 9.9-12.4) than in those receiving LAM (8.3 kPa, 95%CI: 7.2-9.5) (Table 1). At baseline, serum HBV DNA and ALT levels were similar in both groups (Table 1). Compared to baseline, only TDF treated group achieved significant HBV DNA decline at 5 years follow up (p=0.0011) compared to LAM treated group (*P* = 0.37) (Figure 1A).

By year 5, 194/299 (64.9%) TDF patients had undetectable HBV DNA (< 10 IU/mL) than 88/166 (53.0%) LAM patients (*P* = 0.012, Chi-square test, Supplementary Table 1). Furthermore, a higher proportion of TDF treated patients had suppressed HBV DNA (< 10 IU/mL) (*n* = 170/190, 89%) *vs* LAM-treated (*n* = 35/58, 60%) (*P* < 0.05), but none achieved functional cure (HBsAg loss) at the end of the study period.

Both treatment groups had decline in ALT from baseline to 5-year follow-up (*P* = 0.014 for LAM and *P* < 0.0001 for TDF) (Figure 1B). As well, ALT normalization was achieved for both treatment groups by 1-year follow-up. More specifically, by year 5, 167/299 (55.9%) TDF patients achieved ALT normalization compared to 74/166 (44.6%) LAM patients (*P* = 0.020, Chi square test, Supplementary Table 2).

In patients with available serial long-term LSM data, NA treatment also led to improvement in liver inflammation and fibrosis regression with lower mean LSM at 5-year follow-up (7.0 kPa, 95%CI:5.8-8.2 for TDF and 6.7 kPa, 95%CI: 4.9-8.6 for LAM treated patients). Multivariable linear mixed regression with a linear mixed model showed a significant difference in fibrosis regression between antiviral treatment groups. Mean fibrosis regression was greater in TDF treated patients with -4.2 kPa change compared to -1.6 kPa in LAM recipients from baseline, *P* < 0.05 (Figure 2).

As well, by 4-year follow-up, LSM improved by ≥ 1 stage in 92/299 (20.8%) TDF patients compared to 29/166 (17.5%) LAM patients (*P* = 0.002, Chi square test).

Of the 26 HBeAg positive patients that received LAM treatment, 6 patients became HBeAg negative (23.1%). Of the 99 HBeAg positive patients that received TDF treatment, 27 patients (27.3%) achieved HBeAg loss. No data was available on LAM resistance however all patients enrolled in the study were on a single NA agent. It is standard clinical practice to switch to TDF in individuals who developed LAM resistance (and criteria for public formulary drug reimbursement in some provinces). Genotype data was not available in most patients.

DISCUSSION

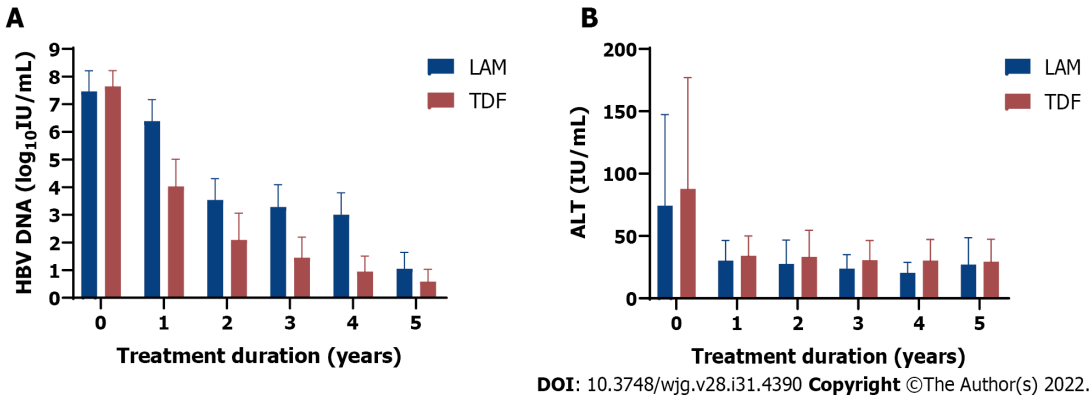
In this multi-centre, retrospective real-world Canadian study, we assessed clinical outcomes in CHB patients receiving long-term NA therapy. Both 1st generation (LAM) and higher potency antivirals (TDF) reduces HBV DNA and improves liver inflammation and fibrosis based on serial LSM evaluation even after ALT normalization. This study highlights the effectiveness of both antiviral drugs in inducing fibrosis regression in a diverse HBV patient cohort. However, up to 5-year follow-up period no CHB patients achieved HBsAg loss or functional cure. A clinically relevant proportion of patients continued to show low-level viremia, especially if treated with LAM. Persons with LAM- resistance switched to TDF were not included to avoid bias of 2 different regimens. Data on antiviral resistance testing is not available, and it is likely these patients would have been switched to TDF in both BC and ON pharmacare reimbursement criteria. The clinical implications of low-level viremia, especially association with residual HCC risk is unclear and requires further study[13,14].

Many studies including randomized clinical trials, observational cohorts and meta-analyses demonstrate that NA treatment improves clinical outcomes for persons living with chronic hepatitis B [1]. Observational studies from clinical databases also reflect real-world practice and complement clinical trials[15,16]. Single centre real-world Canadian studies have observed reduced HCC risk[17]. The majority of observational studies conducted on long-term NA therapy outcomes were done in HBV-endemic countries with a particular focus on Asia. Canada is non-endemic for HBV but due to high rates of immigration from many endemic regions, CHB remains an important health issue and affects a diverse, multi-ethnic population as persons have from multiple regions and encompasses 40 countries

Table 1 Summary of baseline characteristics of 465 study patients who were treated with either lamivudine or tenofovir disoproxil fumurate enrolled in the Canadian hepatitis B virus network

	LAM treated (*n* = 166)	TDF treated (*n* = 299)	*P* value
Age (yr)	51.6 (49.7-53.6)	47.2 (45.7-48.6)	< 0.001[c]
Male sex	58.4% (97/166)	64.9% (194/299)	0.194
Ethnicity (LAM 88%, *n* = 147/166 known, TDF, 88% *n* = 266/299 known)			
Asian	85.0% (125/147)	82.7% (220/266)	0.582
Black/African/Caribbean	5.4% (8/147)	10.9% (29/266)	0.072
White	6.8% (10/147)	5.6% (15/266)	0.669
Other	2.7% (4/147)	0.4% (1/266)	0.056
Laboratory			
HBeAg positive	24.1% (26/108)	39.9% (99/248)	0.004[b]
HBV DNA (log_{10} IU/mL)	7.5 (6.7-7.7) *n* = 149	7.6 (7.5-7.8) *n* = 269	0.260
ALT (IU/mL)	74.3 (62.0-86.7) *n* = 139	87.8 (76.8-98.7) *n* = 264	0.225
Mean ALT × ULN	2.7 (2.1-3.3) *n* = 139	3.7 (2.9-4.4) *n* = 264	0.077
Fibrosis (baseline)			
Mean Baseline Fibrosis (kPa)	8.3 (7.2-9.5) *n* = 100	11.2 (9.9-12.4) *n* = 184	0.003[b]
F0-F1 Fibrosis (< 7.3 kPa)	53% (53/100)	37.5% (69/184)	0.013[a]
F2-F3 Fibrosis (7.3-9.5 kPa)	25% (25/100)	16.9% (31/184)	0.119
F4 Fibrosis (> 9.5 kPa)	22% (22/100)	45.7% (84/184)	< 0.001[c]

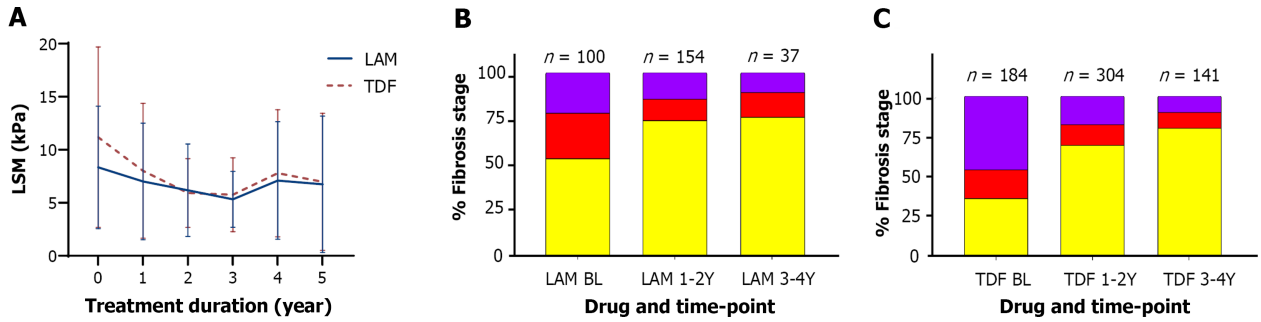
[a]*P* < 0.05.
[b]*P* < 0.01.
[c]*P* < 0.001.
Continuous data are shown as mean (95% CI, n known). Categorical data are shown as mean % (n/n known). For continuous data, a two-tailed *t* test was used. Whereas Fisher's exact test was used for categorical data. LAM: Lamivudine; TDF: Tenofovir disoproxil fumarate; HBV: Hepatitis B virus; ALT: Alanine aminotransferase; HBeAg: Hepatitis B e antigen; ULN: Upper limit of normal.



DOI: 10.3748/wjg.v28.i31.4390 **Copyright** ©The Author(s) 2022.

Figure 1 Comparison of clinical outcomes in 465 chronic hepatitis B patients receiving 1st generation (lamivudine or LAM, solid bar) *vs* 2nd generation (tenofovir disoproxil fumarate or TDF, dotted bar) hepatitis B virus nucleos(t)ide analog therapy from baseline (pre-treatment) followed for up to 5 years. A: Hepatitis B virus DNA decline (log_{10} IU/mL); B: Mean alanine aminotransferase (IU/mL) decline from baseline after starting lamivudine or tenofovir disoproxil fumarate. Mean with error bars representing standard deviation is plotted. LAM: Lamivudine; TDF: Tenofovir disoproxil fumarate; HBV: Hepatitis B virus; ALT: Alanine aminotransferase.

as based on Canadian HBV Network Data. Compared to other published real-world studies, the data is also relevant/applicable in a single-payer universal health care system with equal access care albeit differences in medication re-imbursement providing for the unique aspect of this study. The Canadian health care system does provide some financial assistance to cover the cost of antiviral therapy, and other associated costs (*i.e.*, physician visits, hospitalization, laboratory monitoring, diagnostic imaging



DOI: 10.3748/wjg.v28.i31.4390 **Copyright** ©The Author(s) 2022.

Figure 2 Comparison of lamivudine *vs* tenofovir disoproxil fumarate on liver stiffness measurement over time. A: Liver stiffness measurement change from baseline (before treatment) and while on treatment; mean with error bars representing standard deviation is plotted; B and C: Comparison of fibrosis severity at baseline, 1-2 years, and 3-4 years post-treatment for lamivudine (B) and for tenofovir disoproxil fumarate (C). F0-F1 (yellow), F2-F3 (red), and F4 (purple). LSM: Liver stiffness measurement; LAM: Lamivudine; TDF: Tenofovir disoproxil fumarate.

etc.) is reimbursed by provincial health care plans.

Our study is similar to previous published work that highlights the benefits of antiviral treatment in improving liver fibrosis. A systemic review and meta-analysis including 34 published studies of treated and untreated CHB patients also found low rates of NA-induced HBsAg seroclearance, highlighting the need for improved curative therapies[18]. In fact, HBsAg seroclearance generally occurred in untreated individuals with less active disease[18], and is consistent with retrospective data from the Canadian HBV Network of CHB patients comparing outcomes in individuals that remained HBsAg positive *vs* those with HBsAg loss[19].

The current study is limited by retrospective data and missing data at all defined time-points, including serial lab and LSMs, and highlights the limitation of real-world studies (*i.e.*, missed appointments, adherence and incomplete clinician documentation or reporting). We also excluded patients treated with the other approved 2nd generation NA (*i.e.*, ETV) for purposes of the study analysis to compare a single 1st *vs* 2nd generation NA therapy. Moreover, although our cohort was multi-ethnic most patients were Asian, albeit individuals were born in many different east and south-east Asian countries. Additionally, there was missing ethnicity data on 52 patients (11%). Overall, this data represents immigration from up to 40 countries, based on Canadian HBV Network Data. The 2016 Canadian census reported the top Asian countries of birth for recent immigrants are Philippines, India, China, Iran, Pakistan, Syria and South Korea and Syria (www.statcan.gc.ca). There is increasing data on LSM for assessment of liver inflammation and HBV-related fibrosis, although transient elastography is not widely available in resource limited countries compared to other non-invasive fibrosis markers such as aspartate aminotransferase to platelet ratio index (APRI) and Fibrosis4 (FIB4) calculator[20]. It is noteworthy that our analysis represents the largest North American study conducted to date on long-term follow-up with NA therapy utilizing this novel technology.

CONCLUSION

In summary in this real-world diverse cohort study of chronic hepatitis B patients in Canada, long-term nucleo(s)ide analog (either 1st or 2nd generation) therapy suppresses HBV DNA and improves hepatic inflammation and liver fibrosis, as determined by non-invasive testing (*i.e.*, transient elastography). In patients treated for up to 5 years, none achieved HBsAg loss (functional cure), highlighting the need for improved therapeutic strategies to reduce the life-long burden of antiviral therapy.

ARTICLE HIGHLIGHTS

Research background

Therapy of hepatitis B virus (HBV) with nucleos(t)ide analogues (NA) can be associated with fibrosis regression. There are both low and high potency agents approved for therapy and access to these therapies maybe variable. There is limited real-world data comparing these agents on their effect to result in fibrosis regression and long term outcomes.

Research motivation

Although high-potency agents are considered the standard of care, there has been variable access to these agents and indeed ongoing use of these agents in 1st world countries to include Canada. It is thus

important to provide evidence in outcomes to include fibrosis regression between the high and low potency NA's. This study may impact the use of these agents in the future, and allow consideration for switching from low to high potency agents if possible.

Research objectives

To assess HBV viral response, biochemical remission, liver fibrosis regression and hepatitis B surface antigen (HBsAg) sero-clearance after treatment with either a 1st or 2nd line NA therapy. These objectives were realized and the future impact would be the consideration of utilizing 1st *vs* 2nd line NA's. Further, other outcome measure to include HBsAg loss and development of hepatocellular carcinoma (HCC) may be considered.

Research methods

We performed a retrospective observational cohort study utilizing a National network in HBV. Novel aspects that allowed this study is the utilization of a National Network which was able to capture differences in NA utilization based on regional differences of reimbursement. The strength of this study lies in the diversity that the Canadian HBV Network provides. The utilization of liver stiffness by transient elastography in a North American cohort for this objective is also unique.

Research results

As per differences in utilization, a larger proportion of patients with advanced fibrosis were initiated with tenofovir disoproxil fumarate (TDF) compared to LAM. At the end of the study period there were similar stages of fibrosis between the 2 groups. There was an increased fibrosis regression in those treated with a high potency compared to a low-potency NA. More patients in the TDF group also achieved virological suppression, though alanine amino transferase (ALT) normalization was similar.

Research conclusions

In this diverse cohort treatment with low and high potency NA's achieves high rates of viral suppression, ALT normalization and a large proportion achieve fibrosis regression. The strength of national collaboration within a network is exemplified in this study in particular taking advantages of diversity within an overall similar medical system. These differences within a Network can be a powerful tool to answer research questions and can reduce a number of biases inherent when comparing populations/studies between countries or regions.

Research perspectives

The future direction would include potential for long-term outcomes with differential NA usage to include HBsAg loss or seroconversion and any differences in development of HCC albeit in a population with differences in stage of fibrosis at baseline. This study population and Network provides a unique perspective to answer this question.

FOOTNOTES

Author contributions: Ramji A contributed to study design, data contribution, and manuscript draft; Coffin CS contributed to manuscript draft, data contribution, data analysis, and resource support; Haylock-Jacobs S contributed to data analysis and manuscript draft; Patel N and Kaplan GG contributed to data analysis; all other authors contributed to data contribution, manuscript review and feedback.

Institutional review board statement: The study was reviewed and approved by the Conjoint Health Research Ethics Board, No. REB17-2321_REN4.

Conflict-of-interest statement: Dr. Alnoor Ramji and Dr. Carla S Coffin didn't receive at any time payment from a third party for any aspect for the submitted work; there are no relevant conflict of interest; there are no patents related to this work; Dr. Alnoor Ramji and Dr. Carla S Coffin have nothing to disclosure.

Data sharing statement: No data sharing is approved by the institutional ethics board.

Open-Access: This article is an open-access article that was selected by an in-house editor and fully peer-reviewed by external reviewers. It is distributed in accordance with the Creative Commons Attribution NonCommercial (CC BY-NC 4.0) license, which permits others to distribute, remix, adapt, build upon this work non-commercially, and license their derivative works on different terms, provided the original work is properly cited and the use is non-commercial. See: https://creativecommons.org/Licenses/by-nc/4.0/

Country/Territory of origin: Canada

ORCID number: Alnoor Ramji 0000-0003-4059-8767; Karen Doucette 0000-0002-1660-9166; Gerald Yosel Minuk 0000-0002-

2687-940X; Mang Ma 0000-0003-2587-1788; Alexander Wong 0000-0002-5984-3083; David Wong 0000-0002-1145-1611; Edward Tam 0000-0002-8306-3968; Brian Conway 0000-0001-6821-7829; David Truong 0000-0002-3190-784X; Philip Wong 0000-0002-3446-4116; Hin Hin Ko 0000-0002-2740-2486; Gilaad G Kaplan 0000-0003-2719-0556; Scott Fung 0000-0003-0501-8800; Carla S Coffin 0000-0002-1472-0901.

S-Editor: Chen YL
L-Editor: A
P-Editor: Chen YL

REFERENCES

1 **Lok AS**, McMahon BJ, Brown RS Jr, Wong JB, Ahmed AT, Farah W, Almasri J, Alahdab F, Benkhadra K, Mouchli MA, Singh S, Mohamed EA, Abu Dabrh AM, Prokop LJ, Wang Z, Murad MH, Mohammed K. Antiviral therapy for chronic hepatitis B viral infection in adults: A systematic review and meta-analysis. *Hepatology* 2016; **63**: 284-306 [PMID: 26566246 DOI: 10.1002/hep.28280]
2 **Hou JL**, Zhao W, Lee C, Hann HW, Peng CY, Tanwandee T, Morozov V, Klinker H, Sollano JD, Streinu-Cercel A, Cheinquer H, Xie Q, Wang YM, Wei L, Jia JD, Gong G, Han KH, Cao W, Cheng M, Tang X, Tan D, Ren H, Duan Z, Tang H, Gao Z, Chen S, Lin S, Sheng J, Chen C, Shang J, Han T, Ji Y, Niu J, Sun J, Chen Y, Cooney EL, Lim SG. Outcomes of Long-term Treatment of Chronic HBV Infection With Entecavir or Other Agents From a Randomized Trial in 24 Countries. *Clin Gastroenterol Hepatol* 2020; **18**: 457-467.e21 [PMID: 31306800 DOI: 10.1016/j.cgh.2019.07.010]
3 **Liaw YF**. Undesirable Long-Term Outcome of Entecavir Therapy in Chronic Hepatitis B With Cirrhosis. *Clin Gastroenterol Hepatol* 2020; **18**: 2146-2147 [PMID: 32088301 DOI: 10.1016/j.cgh.2020.02.028]
4 **Liem KS**, Fung S, Wong DK, Yim C, Noureldin S, Chen J, Feld JJ, Hansen BE, Janssen HLA. Limited sustained response after stopping nucleos(t)ide analogues in patients with chronic hepatitis B: results from a randomised controlled trial (Toronto STOP study). *Gut* 2019; **68**: 2206-2213 [PMID: 31462554 DOI: 10.1136/gutjnl-2019-318981]
5 **Wong DK**, Seto WK, Fung J, Ip P, Huang FY, Lai CL, Yuen MF. Reduction of hepatitis B surface antigen and covalently closed circular DNA by nucleos(t)ide analogues of different potency. *Clin Gastroenterol Hepatol* 2013; **11**: 1004-10.e1 [PMID: 23376799 DOI: 10.1016/j.cgh.2013.01.026]
6 **Lim YS**, Han S, Heo NY, Shim JH, Lee HC, Suh DJ. Mortality, liver transplantation, and hepatocellular carcinoma among patients with chronic hepatitis B treated with entecavir vs lamivudine. *Gastroenterology* 2014; **147**: 152-161 [PMID: 24583062 DOI: 10.1053/j.gastro.2014.02.033]
7 **Fan R**, Hou J. Reply. *Clin Gastroenterol Hepatol* 2020; **18**: 2147-2148 [PMID: 32684317 DOI: 10.1016/j.cgh.2020.03.024]
8 **Shin JW**, Jung SW, Lee SB, Lee BU, Park BR, Park EJ, Park NH. Medication Nonadherence Increases Hepatocellular Carcinoma, Cirrhotic Complications, and Mortality in Chronic Hepatitis B Patients Treated With Entecavir. *Am J Gastroenterol* 2018; **113**: 998-1008 [PMID: 29880971 DOI: 10.1038/s41395-018-0093-9]
9 **Congly SE**, Brahmania M. Variable access to antiviral treatment of chronic hepatitis B in Canada: a descriptive study. *CMAJ Open* 2019; **7**: E182-E189 [PMID: 30926602 DOI: 10.9778/cmajo.20180108]
10 **Coffin CS**, Ramji A, Cooper CL, Miles D, Doucette KE, Wong P, Tam E, Wong DK, Wong A, Ukabam S, Bailey RJ, Tsoi K, Conway B, Barrett L, Michalak TI, Congly SE, Minuk G, Kaita K, Kelly E, Ko HH, Janssen HLA, Uhanova J, Lethebe BC, Haylock-Jacobs S, Ma MM, Osiowy C, Fung SK; Canadian HBV Network. Epidemiologic and clinical features of chronic hepatitis B virus infection in 8 Canadian provinces: a descriptive study by the Canadian HBV Network. *CMAJ Open* 2019; **7**: E610-E617 [PMID: 31641059 DOI: 10.9778/cmajo.20190103]
11 **de Lédinghen V**, Vergniol J. Transient elastography (FibroScan). *Gastroenterol Clin Biol* 2008; **32**: 58-67 [PMID: 18973847 DOI: 10.1016/S0399-8320(08)73994-0]
12 **Coffin C**, Fung S, Alvarez F. Management of Hepatitis B Virus Infection: 2018 Guidelines from the Canadian Association for the Study of Liver Disease and Association of Medical Microbiology and Infectious Disease Canada. *Canadian Liver J* 2018; **1**: 156-217 [DOI: 10.3138/canlivj.2018-0008]
13 **Kim JH**, Sinn DH, Kang W, Gwak GY, Paik YH, Choi MS, Lee JH, Koh KC, Paik SW. Low-level viremia and the increased risk of hepatocellular carcinoma in patients receiving entecavir treatment. *Hepatology* 2017; **66**: 335-343 [PMID: 28012257 DOI: 10.1002/hep.28916]
14 **Kim TS**, Sinn DH, Kang W, Gwak GY, Paik YH, Choi MS, Lee JH, Koh KC, Paik SW. Hepatitis B virus DNA levels and overall survival in hepatitis B-related hepatocellular carcinoma patients with low-level viremia. *J Gastroenterol Hepatol* 2019; **34**: 2028-2035 [PMID: 31157456 DOI: 10.1111/jgh.14750]
15 **Kim WR**, Loomba R, Berg T, Aguilar Schall RE, Yee LJ, Dinh PV, Flaherty JF, Martins EB, Therneau TM, Jacobson I, Fung S, Gurel S, Buti M, Marcellin P. Impact of long-term tenofovir disoproxil fumarate on incidence of hepatocellular carcinoma in patients with chronic hepatitis B. *Cancer* 2015; **121**: 3631-3638 [PMID: 26177866 DOI: 10.1002/cncr.29537]
16 **Chon YE**, Park JY, Myoung SM, Jung KS, Kim BK, Kim SU, Kim DY, Ahn SH, Han KH. Improvement of Liver Fibrosis after Long-Term Antiviral Therapy Assessed by Fibroscan in Chronic Hepatitis B Patients With Advanced Fibrosis. *Am J Gastroenterol* 2017; **112**: 882-891 [PMID: 28374814 DOI: 10.1038/ajg.2017.93]
17 **Coffin CS**, Rezaeeaval M, Pang JX, Alcantara L, Klein P, Burak KW, Myers RP. The incidence of hepatocellular carcinoma is reduced in patients with chronic hepatitis B on long-term nucleos(t)ide analogue therapy. *Aliment Pharmacol Ther* 2014; **40**: 1262-1269 [PMID: 25312649 DOI: 10.1111/apt.12990]
18 **Yeo YH**, Ho HJ, Yang HI, Tseng TC, Hosaka T, Trinh HN, Kwak MS, Park YM, Fung JYY, Buti M, Rodríguez M, Treeprasertsuk S, Preda CM, Ungtrakul T, Charatcharoenwitthaya P, Li X, Li J, Zhang J, Le MH, Wei B, Zou B, Le A, Jeong D, Chien N, Kam L, Lee CC, Riveiro-Barciela M, Istratescu D, Sriprayoon T, Chong Y, Tanwandee T, Kobayashi

M, Suzuki F, Yuen MF, Lee HS, Kao JH, Lok AS, Wu CY, Nguyen MH. Factors Associated With Rates of HBsAg Seroclearance in Adults With Chronic HBV Infection: A Systematic Review and Meta-analysis. *Gastroenterology* 2019; **156**: 635-646.e9 [PMID: 30342034 DOI: 10.1053/j.gastro.2018.10.027]

19 **Coffin C**, Haylock-Jacobs S, Doucette K. Association between quantitative hepatitis B surface antigen levels (qHBsAg) and clinical outcomes of ethnically diverse Canadian chronic hepatitis B (CHB) patients: REtrospective and prospectiVe rEAL world evidence study of CHB in Canada (REVEAL- CANADA). The Liver Meeting, Annual Meeting American Association for the Study of Liver Disease; 2021; Canada. Digital Online, 2021 [DOI: 10.15406/jlrdt.2015.01.00007]

20 **Gane EJ**, Charlton MR, Mohamed R, Sollano JD, Tun KS, Pham TTT, Payawal DA, Gani RA, Muljono DH, Acharya SK, Zhuang H, Shukla A, Madan K, Saraf N, Tyagi S, Singh KR, Cua IHY, Jargalsaikhan G, Duger D, Sukeepaisarnjaroen W, Purnomo HD, Hasan I, Lesmana LA, Lesmana CRA, Kyi KP, Naing W, Ravishankar AC, Hadigal S. Asian consensus recommendations on optimizing the diagnosis and initiation of treatment of hepatitis B virus infection in resource-limited settings. *J Viral Hepat* 2020; **27**: 466-475 [PMID: 31785182 DOI: 10.1111/jvh.13244]

World Journal of Gastroenterology

Submit a Manuscript: https://www.f6publishing.com

World J Gastroenterol 2022 August 21; 28(31): 4399-4416

DOI: 10.3748/wjg.v28.i31.4399

ISSN 1007-9327 (print) ISSN 2219-2840 (online)

ORIGINAL ARTICLE

Observational Study

Radiomics and nomogram of magnetic resonance imaging for preoperative prediction of microvascular invasion in small hepatocellular carcinoma

Yi-Di Chen, Ling Zhang, Zhi-Peng Zhou, Bin Lin, Zi-Jian Jiang, Cheng Tang, Yi-Wu Dang, Yu-Wei Xia, Bin Song, Li-Ling Long

Specialty type: Gastroenterology and hepatology

Provenance and peer review: Unsolicited article; Externally peer reviewed.

Peer-review model: Single blind

Peer-review report's scientific quality classification

Grade A (Excellent): A
Grade B (Very good): 0
Grade C (Good): C
Grade D (Fair): 0
Grade E (Poor): 0

P-Reviewer: Granito A, Italy; Hussein R, Egypt

Received: December 14, 2021
Peer-review started: December 14, 2021
First decision: January 27, 2022
Revised: February 5, 2022
Accepted: July 24, 2022
Article in press: July 24, 2022
Published online: August 21, 2022

Yi-Di Chen, Ling Zhang, Zi-Jian Jiang, Cheng Tang, Li-Ling Long, Department of Radiology, The First Affiliated Hospital of Guangxi Medical University, Nanning 530021, Guangxi Zhuang Autonomous Region, China

Zhi-Peng Zhou, Bin Lin, Department of Radiology, Affiliated Hospital of Guilin Medical University, Guilin 541001, Guangxi Zhuang Autonomous Region, China

Yi-Wu Dang, Department of Pathology, The First Affiliated Hospital of Guangxi Medical University, Nanning 5350021, Guangxi Zhuang Autonomous Region, China

Yu-Wei Xia, Department of Technology, Huiying Medical Technology (Beijing), Beijing 100192, China

Bin Song, Department of Radiology, West China Hospital, Sichuan University, Chengdu 610041, Sichuan Province, China

Li-Ling Long, Key Laboratory of Early Prevention and Treatment for Regional High Frequency Tumor, Ministry of Education, Guangxi Medical University, Nanning 530021, Guangxi Zhuang Autonomous Region, China

Li-Ling Long, Guangxi Key Laboratory of Immunology and Metabolism for Liver Diseases, First Affiliated Hospital of Guangxi Medical University, Nanning 530021, Guangxi Zhuang Autonomous Region, China

Corresponding author: Li-Ling Long, MD, Chairman, Chief Doctor, Professor, Department of Radiology, The First Affiliated Hospital of Guangxi Medical University, No. 6 Shuangyong Road, Nanning 530021, Guangxi Zhuang Autonomous Region, China.
cjr.longliling@vip.163.com

Abstract

BACKGROUND

Microvascular invasion (MVI) of small hepatocellular carcinoma (sHCC) (≤ 3.0 cm) is an independent prognostic factor for poor progression-free and overall survival. Radiomics can help extract imaging information associated with tumor pathophysiology.

AIM

To develop and validate radiomics scores and a nomogram of gadolinium ethoxybenzyl-diethyl-enetriamine pentaacetic acid (Gd-EOB-DTPA)-enhanced magnetic resonance imaging (MRI) for preoperative prediction of MVI in sHCC.

METHODS

In total, 415 patients were diagnosed with sHCC by postoperative pathology. A total of 221 patients were retrospectively included from our hospital. In addition, we recruited 94 and 100 participants as independent external validation sets from two other hospitals. Radiomics models of Gd-EOB-DTPA-enhanced MRI and diffusion-weighted imaging (DWI) were constructed and validated using machine learning. As presented in the radiomics nomogram, a prediction model was developed using multivariable logistic regression analysis, which included radiomics scores, radiologic features, and clinical features, such as the alpha-fetoprotein (AFP) level. The calibration, decision-making curve, and clinical usefulness of the radiomics nomogram were analyzed. The radiomic nomogram was validated using independent external cohort data. The areas under the receiver operating curve (AUC) were used to assess the predictive capability.

RESULTS

Pathological examination confirmed MVI in 64 (28.9%), 22 (23.4%), and 16 (16.0%) of the 221, 94, and 100 patients, respectively. AFP, tumor size, non-smooth tumor margin, incomplete capsule, and peritumoral hypointensity in hepatobiliary phase (HBP) images had poor diagnostic value for MVI of sHCC. Quantitative radiomic features (1409) of MRI scans) were extracted. The classifier of logistic regression (LR) was the best machine learning method, and the radiomics scores of HBP and DWI had great diagnostic efficiency for the prediction of MVI in both the testing set (hospital A) and validation set (hospital B, C). The AUC of HBP was 0.979, 0.970, and 0.803, respectively, and the AUC of DWI was 0.971, 0.816, and 0.801 ($P < 0.05$), respectively. Good calibration and discrimination of the radiomics and clinical combined nomogram model were exhibited in the testing and two external validation cohorts (C-index of HBP and DWI were 0.971, 0.912, 0.808, and 0.970, 0.843, 0.869, respectively). The clinical usefulness of the nomogram was further confirmed using decision curve analysis.

CONCLUSION

AFP and conventional Gd-EOB-DTPA-enhanced MRI features have poor diagnostic accuracies for MVI in patients with sHCC. Machine learning with an LR classifier yielded the best radiomics score for HBP and DWI. The radiomics nomogram developed as a noninvasive preoperative prediction method showed favorable predictive accuracy for evaluating MVI in sHCC.

Key Words: Magnetic resonance imaging; Hepatocellular carcinoma; Radiomics; Nomogram

©The Author(s) 2022. Published by Baishideng Publishing Group Inc. All rights reserved.

Core Tip: Microvascular invasion (MVI) accounts for approximately 20% of small hepatocellular carcinoma (sHCC) (≤ 3.0 cm) and is a poor independent prognostic factor for progression-free survival and overall survival. However, no studies have been published on the preoperative prediction of the MVI of sHCC. This multi-center study was developed and validated radiomics scores and nomogram of gadoxetic acid-enhanced magnetic resonance imaging (EOB-MRI) for the preoperative prediction of MVI in sHCC. The results demonstrated that AFP and conventional EOB-MRI features have poor diagnostic accuracy for MVI in patients with sHCC. The radiomics scores of HBP and diffusion-weighted imaging can improve the ability to predict MVI. As a noninvasive preoperative prediction method, the radiomics nomogram presented in this study showed a favorable predictive accuracy in evaluating MVI of sHCC, which may help reassess the clinical therapeutic regimen for patients with sHCC.

Citation: Chen YD, Zhang L, Zhou ZP, Lin B, Jiang ZJ, Tang C, Dang YW, Xia YW, Song B, Long LL. Radiomics and nomogram of magnetic resonance imaging for preoperative prediction of microvascular invasion in small hepatocellular carcinoma. *World J Gastroenterol* 2022; 28(31): 4399-4416

URL: https://www.wjgnet.com/1007-9327/full/v28/i31/4399.htm

DOI: https://dx.doi.org/10.3748/wjg.v28.i31.4399

INTRODUCTION

Hepatocellular carcinoma (HCC) is the fourth most common cause of cancer-related death and ranks sixth in terms of incident cases worldwide[1]. HCC is an important public health problem worldwide, and the death rate has increased over the past few years[2,3]. The cut-off size to define small HCC (sHCC) has been adopted as 3.0 cm[4]. Although the prognosis of sHCC is better than other types of HCC, the higher postoperative recurrence rate results in poor long-term outcomes after resection of sHCC[5]. Previous studies have confirmed that tumor size, higher tumor stage, worse histological differentiation, and the presence of microvascular invasion (MVI) are significant risk factors for short-term recurrence of HCC[6-8]. In particular, the incidence of MVI, which is an independent poor prognostic factor for progression-free survival and overall survival of patients with sHCC, is generally about 20% in sHCC[9]. The presence or absence of MVI also suggests the need for different therapeutic options for HCC. Research has indicated that transcatheter arterial chemoembolization combined with intensity-modulated radiotherapy and sorafenib showed obvious clinical benefits in HCC patients with MVI[10]. Enlarged hepatectomy may be necessary for patients with sHCC and MVI.

Pathological examination of postoperative specimens is the gold standard for the diagnosis of MVI [11]. However, postoperative specimens exhibit hysteresis, which is not ideal for guiding treatment. In addition to being an invasive method, biopsy carries some risks of bleeding or tumor seeding[12]. Gadolinium ethoxybenzyl-diethylenetriamine pentaacetic acid (Gd-EOB-DTPA) contrast-enhanced liver magnetic resonance imaging (MRI) is a noninvasive examination used to diagnose a variety of liver diseases[13] and can be used to assess liver function in patients with various stages of liver disease[14]. Gd-EOB-DTPA MRI has been used to predict MVI based on tumor size, non-smooth tumor margin, incomplete capsule, and peritumoral hypointensity in the hepatobiliary phase[15-18]. However, sHCC has a small size, regular margin, complete capsule (or no capsule), and is usually free of peritumoral hypointensity. Therefore, it is difficult to predict the MVI of sHCC using traditional GD-EOB-DTPA MRI features.

Radiomics is an emerging field that attempts to quantify tumor heterogeneity related to the tumor parenchyma and microenvironment, including cellularity, extracellular matrix deposition, angiogenesis, necrosis, and fibrosis[19,20]. Machine learning is a scientific method of algorithms and statistical models that uses computers to interpret or predict patterns and inferences[21]. In many medical situations, medical imaging can be analyzed by machine learning through a series of processes, such as image registration, image segmentation, object detection, classification, and outcome prediction[22,23]. Automated computer algorithms can be used for quantitative image analysis, which can objectively quantify the heterogeneity of an image by measuring the spatial variation in the pixel intensity[24]. Radiomics with quantitative analysis provides a potential method for the diagnosis and prognosis of cancers[25,26]. Although a few studies have explored the feasibility of using radiomics based on computed tomography (CT) or MRI features to predict MVI in HCC[27-29], to our knowledge, previous studies have not investigated the prediction of MVI in sHCC. Therefore, this study aimed to explore the diagnostic value of liver Gd-EOB-DTPA MRI features in MVI of sHCC and to construct and validate the predictive efficacy of radiomics signatures and a nomogram for MVI in sHCC. This study also aimed to confirm the best modeling sequences, including images of T1 weighted imaging (T1WI), T2 weighted imaging (T2WI), diffusion-weighted imaging (DWI), and post-Gd-EOB-DTPA enhancement images of the arterial phase (AP), portal vein phase (PVP), and hepatobiliary phase (HBP), for extracting radiomics signatures by machine learning.

MATERIALS AND METHODS

Study cohort

The ethical review board of our institution approved this multi-center and external validation study (No. 2019 KY-E-134). This study adhered to the principles of the Declaration of Helsinki and the requirement for informed consent was waived. First, we retrospectively searched our institution's (Guangxi Medical University First Affiliated Hospital, Hospital A) departmental electronic database for patients with consecutive hospital visits who had undergone upper-abdomen MRI between January 2016 and June 2020. A total of 221 patients were enrolled who met the following inclusion criteria: (1) Patients received Gd-EOB-DTPA enhanced upper-abdomen MRI and small HCC (tumor size ≤ 3.0 cm) were diagnosed; (2) no macrovascular tumor invasion on MRI *(i.e.*, no tumor thrombus in the hepatic or portal veins); (3) primary HCC were diagnosed by histopathologic examination within two weeks after the MRI examination; and (4) MR images were of sufficient image quality. The exclusion criteria of this study were: (1) Patients who had undergone previous hepatobiliary surgery or liver-directed therapy (*i.e.*, transarterial chemoembolization or ablation); and (2) the lesions were diagnosed other than primary HCC. Second, we continuously recruited 94 and 100 participants as independent external validation sets from two other hospitals (Affiliated Hospital of Guilin Medical University and West China Hospital, Hospital B and C) between July 2020 and August 2021 using the same inclusion and exclusion criteria. All patients underwent hepatectomy and pathologic assessment within two weeks of the MRI

examination. The alpha fetal protein (AFP), Child-Pugh grades (grade A to C), and model for end-stage liver disease (MELD) scores were also analyzed and calculated for all patients (Figure 1).

Histopathologic analysis

Two experienced pathologists performed all the histological analyses in our central pathology laboratory. The Edmondson-Steiner classification was used to identify the major histological grades of HCC. When a tumor within a vascular space was lined by the endothelium, MVI was confirmed to be visible only microscopically, and the sites of positive MVI were documented. All disagreements were resolved by consensus.

MRI examination

All patients underwent 3.0 T MRI with six sequences of Gd-EOB-DTPA enhancement and DWI (Discovery MR750, GE Healthcare, Waukesha, WI, United States; Prisma and MAGNETOM Verio, Siemens Healthcare, Erlangen, Germany), including T1WI, T2WI, DWI, and post-injection phases of EOB as AP, PVP, and HBP. Detailed descriptions of the imaging acquisition protocols are summarized in Supplementary Table 1. For advanced DWI image quality, respiratory triggering, propeller, and resolve technical proposals were adopted.

Conventional radiological features analysis

Conventional radiological features were carefully evaluated based on the Liver Imaging Reporting and Data System (LI-RADS v2018), which included the tumor size, AP hyperenhancement, blood products in mass, capsule, corona enhancement, delayed central enhancement, diffusion restriction, fat or iron in mass more than the adjacent liver, fat or iron sparing in a solid mass, mosaic appearance, hepatobiliary phase hypointensity, hepatobiliary phase isointensity, and nodule-in-nodule appearance. The following MRI features were selected in this study: (1) Tumor size; the maximum diameter was measured on HBP axial images; (2) non-smooth tumor margin, which was defined as nodular with extranodular growth or multinodular confluence; (3) incomplete capsule, the region where the tumor border with liver tissue has no or incomplete capsule on portal venous phase or delayed phase; and (4) peritumoral hypointensity on HBP, wedge-shaped hypointense located outside of the tumor margin on HBP. After independent evaluation by three senior radiologists, discussions were conducted to reach a consensus wherever discrepancies occurred.

RADIOMICS SIGNATURES AND REPRODUCIBILITY ANALYSIS

Segmentation of the volume of interests

The Digital Imaging and Communications in Medicine images were transferred to the Big Data Intelligent Analysis Cloud Platform (Huiying Medical Technology Co., Ltd., Beijing, China). Two experts in liver MRI (senior radiologists with 15 and 25 years of experience) reviewed all images, and a radiologist manually segmented all target lesions who were blinded to the clinical information, creating a segmented volume of interest (VOI). After completion of the VOIs by a junior radiologist, the VOIs were reviewed by a senior radiologist for validation. To minimize the intensity variations caused by different scanning equipment and scanning parameters, these MR images were normalized by the standard deviation (μ-3σ, μ + 3σ) before feature extraction, and all delineated VOIs were automatically analyzed (Figure 2).

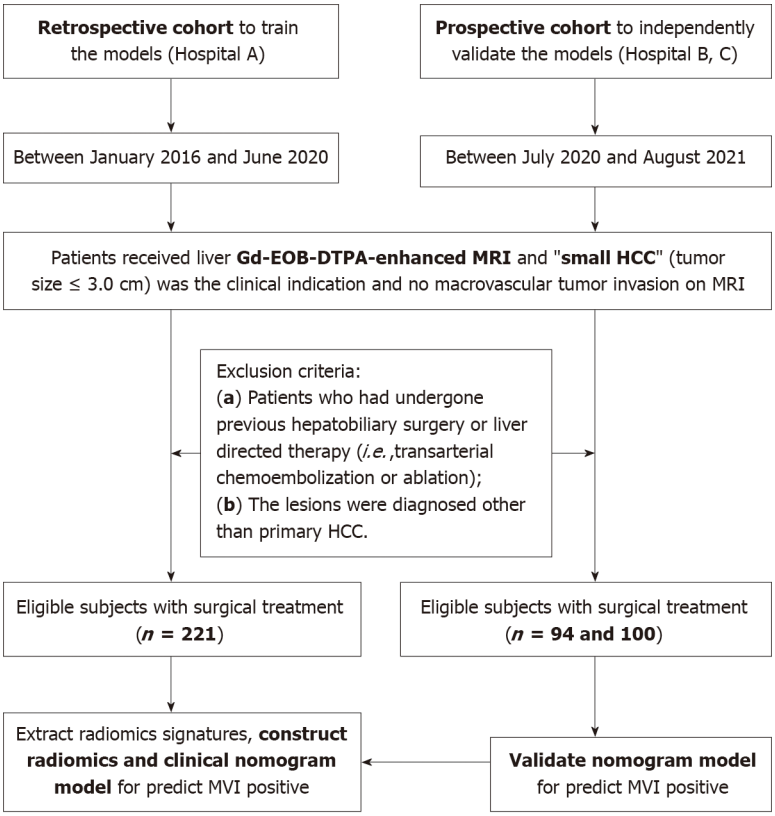
As two radiologists measured the radiomics features to assess reproducibility, we calculated the intraclass correlation coefficient (ICC). When the ICC was > 0.80, consistency was considered excellent.

Features extraction

We extracted 1409 quantitative imaging features from VOIs using the cloud platform big data intelligent analysis (http://radcloud.cn/). The features were categorized into four groups. The first-order statistical features were considered as group 1 (including a total of 18 descriptors), which delineated the distribution of voxel intensities in the MR images through common and basic metrics. Group 2 included shape- and size-based features (containing 14 three-dimensional features) that reflected the shape and size of the lesion areas. Group 3 included features of two-order texture, gray-level co-occurrence, and gray-level run-length texture matrices that were used to calculate those features, and 75 texture features were extracted to quantify the heterogeneity of lesions. The higher-order filter features such as group 4, Laplacian, wavelet, logarithmic, and exponential filters were applied to medical images, and then the first-order statistics and texture features were extracted based on the filtered image (1302 filter features).

Features selection

The least absolute shrinkage and selection operator (LASSO) was used to decrease irrelevance and redundancy. We performed a 10-fold cross-validation to select the optimal feature subset in LASSO regression, which was based on binomial deviance minimization criteria from the training cohort with a



DOI: 10.3748/wjg.v28.i31.4399 **Copyright** ©The Author(s) 2022.

Figure 1 Flow diagram of the study cohort. A total of 415 participants were included in this multi-center study.

maximum iteration of 2000. A variance threshold of 0.8 was used for the selected eigenvalues of the variance.

Model development and validation

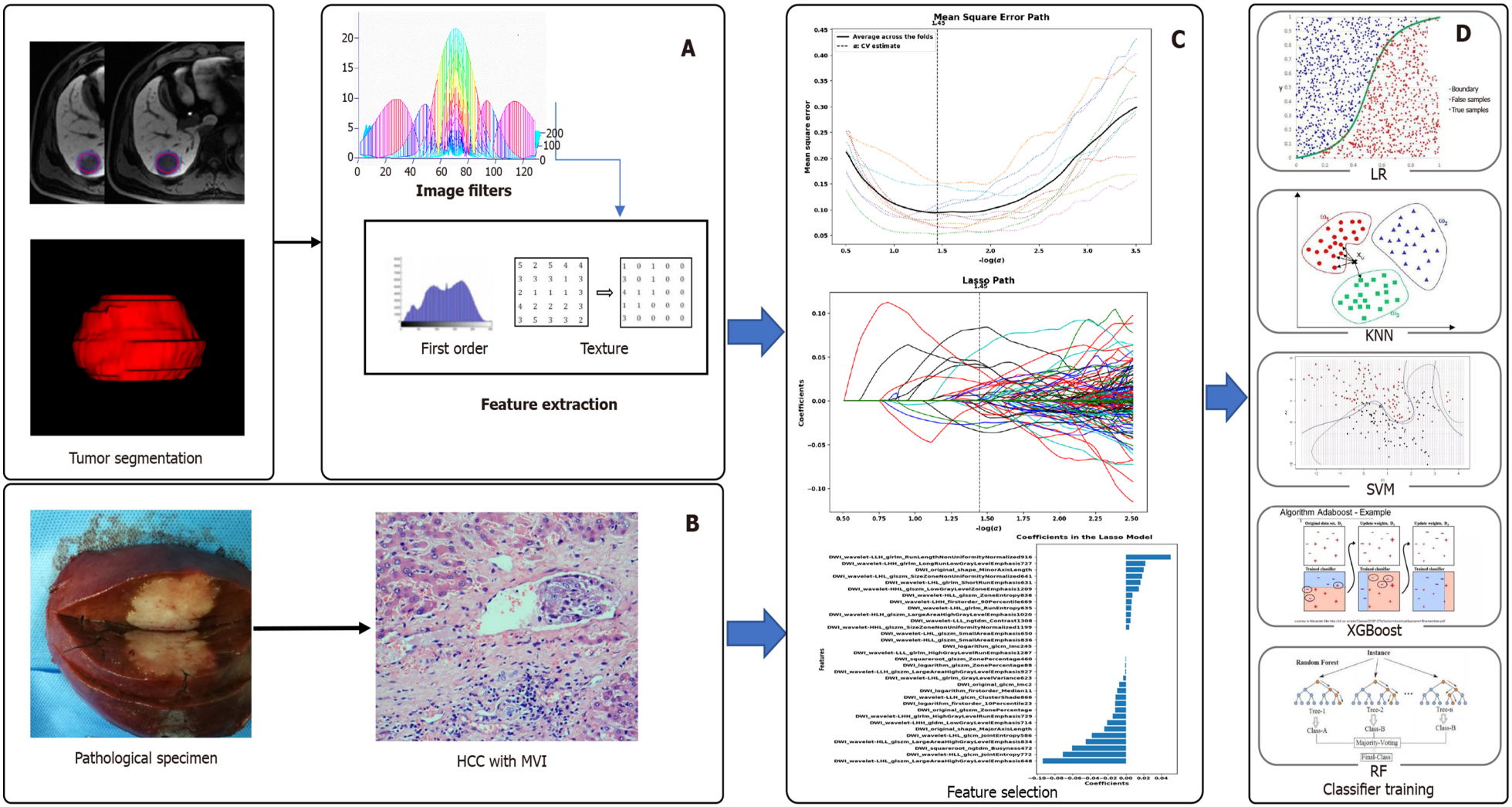
The retrospective data (Hospital A) were separated from the training and testing datasets using a random method with a ratio of 7:3, and external data (Hospitals B and C) as the independent validation sets. After feature qualification, based on the selected features, several machine learning classifiers can be used for classification analysis, creating models that can separate or predict MVI-positive data. In this study, radiomics-based LASSO models (machine learning) were constructed using T1WI, T2WI, DWI, AP, PVP, and HBP. We selected K-nearest neighbor (KNN), support vector machine (SVM), extreme gradient boosting (XGBoost), random forest (RF), logistic regression (LR), and decision tree (DT) as the machine learning classifiers, and the effectiveness of the model was improved using the validation method (Figure 2).

Confirmation of radiomics nomogram

R package (version 3.0, http://www.r-project.org/) was used to analyze the radiomics nomogram. Multivariate logistic regression analysis was performed to develop a model for predicting MVI, and all variables associated with MVI at a significant level were candidates for stepwise multivariate analysis. A nomogram was constructed based on the results of the multivariate logistic regression analysis. The receiver operating characteristic (ROC) curve was used to calculate the discrimination performance of the established models, and the values of the area under the curve (AUC) were compared using the Delong non-parametric approach. The calibration of the radiomics model was assessed using calibration curves. External data from the independent validation sets (hospitals B and C) were used to test the performance of the radiomics model. Finally, we constructed decision curves by calculating the net benefits for a range of threshold probabilities.

Statistical analyses

MedCalc 16.2.1 (Ostend, Belgium) and SPSS (version 22.0; Armonk, NY, United States) were used for the statistical analyses. The Kolmogorov-Smirnov method was used to identify the normal distribution of continuous variables. The differences in categorical and continuous variables were compared using the χ^2 test, Fisher's exact test, two-sample *t*-test, or Mann-Whitney *U* test, respectively. ROC analyses were performed to evaluate the predictive performance of MVI for sHCC. The Youden index was used for determining the cut-off values. Then, the AUC, sensitivity, and specificity were calculated, and a *Z*



DOI: 10.3748/wjg.v28.i31.4399 **Copyright** ©The Author(s) 2022.

Figure 2 Flow diagram for the radiomics of machine learning. A: Construct radiomics models, the volume of interest was delineated by experienced radiologists and three-dimensional images were formed, extracting quantitative features by software; B: Pathologic examination, firstly obtaining specimens of small hepatocellular carcinoma tissue, and then taking pathologic diagnosis for microvascular invasion; C: Data cleaning and dimensions reduction; D: Establishing the model for predicting microvascular invasion by machine learning. LR: Logistic regression; KNN: K-Nearest neighbor; SVM: Support vector machine; RF: Random forest.

test was used to compare the differences between the AUCs. Statistical significance was set at $P < 0.05$.

RESULTS

Patients and serological examinations

A total of 415 patients with qualified sHCC were enrolled in the final study (Figure 1). In hospitals A, B, and C, the mean participant age was 51.2 ± 10.9 (range 29-78) years, 53.04 ± 10.59 (range 28-77) years, and 54.01 ± 10.82 (range 28-85) years, respectively. Histological examination confirmed MVI in 64 (28.9%), 22 (23.4%), and 16 (16.0%) patients. The number of patients with hepatitis B, C and alcoholic hepatitis were 162 (73.3%), 21 (9.5%), 29 (13.1%); 71 (75.6%), 10 (10.6%), 8 (8.5%); and 82 (82.0%), 6 (6.0%), 2 (2.0%), respectively. The numbers of patients with cirrhosis were 173 (78.3%), 69 (73.4%), and 70 (70%), respectively. The median serum AFP levels were 26.10 (range 0.98-25451.00) ng/mL, 9.34 (range 1.09-6740.42) ng/mL, and 31.070 (range 0.713-4587.000) ng/mL, respectively. The median serum total bilirubin levels were 12.5 (range 2.9-64.6) μmol/L, 17.4 (range 3.6-446.9) μmol/L and 13.2 (range 4.4-47.2) μmol/L, respectively. The median direct bilirubin levels were 3.9 (range 1.0-17.0) μmol/L, 4.5 (range 1.0-218.9) μmol/L and 5.50 (range 1.50-26.84) μmol/L, respectively. The MELD scores were 13.9 ± 4.8 (range 7.0-26.9), 13.8 ± 5.8 (range 6.0-35.5) and 11.8 ± 4.5 (range 5.2-25.6). The number of Child-Pugh classes A, B, and C were 205 (93.2%), 13 (5.9%), 2 (0.9%), 81 (86.2%), 12 (12.8%), 1 (1.1%), 86 (86.0%), 13 (13.0%), and 1 (1.0%), respectively. There were 32 (14.5%), 142 (64.3%), 47 (21.2%); 12 (12.8%), 68 (72.3%), 14 (14.9%) and 8 (8.0%), 71 (71.0%), 21 (21.0%) cases that were histological grades I, II, and III, respectively (Table 1).

Conventional radiological features

In the group comparison of MVI-positive and negative, the AFP and tumor size were 33.91 (range 1.4-25451.0) and 22.52 (range 0.98-18929.00) (ng/mL) ($P = 0.026$), 2.34 ± 0.56 and 1.92 ± 0.67 (cm) ($P = 0.036$) in hospital A; 38.97 (range 1.90-6740.40) and 5.43 (range 1.10-2018.79) (ng/mL) ($P = 0.01$), 2.43 ± 0.57 and 2.11 ± 0.66 (cm) ($P = 0.047$) in hospital B; 109.72 (range 0.80-2278.00) and 24.41 (range 0.71-4587.00) (ng/mL) ($P = 0.032$), 2.47 ± 0.43 and 2.21 ± 0.64 (cm) ($P = 0.054$) in hospital C. In the MVI-positive group, the proportion of patients with non-smooth tumor margin, incomplete capsule, and peritumoral hypointensity was 39.7% (27/68) ($P = 0.019$), 40.3% (25/62) ($P = 0.02$), and 51.5% (17/33) ($P = 0.002$) in hospital A; 52.9% (9/17) ($P = 0.003$), 59.5% (25/42) ($P = 0.062$), and 35.7% (5/14) ($P = 0.304$) in hospital B; and 31.3% (10/32) ($P = 0.004$), 14.6% (6/41) ($P = 0.759$), and 63.6% (14/22) ($P = 0.002$) in hospital C (Table 2).

For discriminating MVI-positive, in hospital A, B and C the AUC of AFP was 0.597 [95% confidence interval (CI):0.528-0.662], 0.683 (95%CI):0.528-0.662] and 0.669 (95%CI:0.568-0.760), respectively; the AUC of tumor size was 0.675 (95%CI:0.609-0.736), 0.639 (95%CI:0.553-0.735) and 0.576 (95%CI:0.473-0.675), respectively; the AUC of non-smooth tumor margin was 0.580 (95%CI:0.512-0.646), 0.649 (95%CI:0.544-0.745) and 0.682 (95%CI:0.581-0.771), respectively; the AUC of incomplete capsule was 0.577 (95%CI:0.509-0.643), 0.595 (95%CI:0.489-0.695) and 0.521 (95%CI:0.419-0.622), respectively; the AUC of peritumoral hypointensity on HBP was 0.582 (95%CI:0.514-0.648), 0.551 (95%CI:0.445-0.654) and 0.667 (95%CI:0.565-0.758), respectively (Table 3).

Radiomics signatures

There were 155 and 66 patients with sHCC in the training and test datasets, respectively. The proportions of MVI-positive patients were 27.1% and 29%, respectively. There were no significant differences in patient characteristics between the training and testing cohorts ($P > 0.05$). Among the 1409 radiomics features in each T1WI, T2WI, DWI, AP, PVP, and HBP model, 443, 483, 467, 554, 462, and 453 features were selected based on a variance threshold of over 0.80. After LASSO analysis, five, 22, 33, four, eight, and 30 features were selected for T1WI, T2WI, DWI, AP, PVP, and HBP, respectively.

Robustness analysis results

We found that 70.5% (993/1409) of the features extracted from T1WI images had excellent consistency (ICC > 0.8), and all five features selected for modeling had excellent consistency (ICC median, 0.969; minimum, 0.877; maximum, 1.000). The features of 51.9% (731/1409) extracted from T2WI images had excellent consistency (ICC > 0.8), and most of the 22 features selected for modeling had good consistency (ICC median, 0.701; minimum, 0.41; maximum, 0.94). The features of 60.04% (846/1409) extracted from DWI images had excellent consistency (ICC > 0.8), and most of the 33 features selected for modeling had excellent consistency (ICC median, 0.869; minimum, 0.41; maximum, 0.98). The features of 67.8% (956/1409) extracted from AP images had excellent consistency (ICC > 0.8), and the ICC of the four features selected for modeling were 0.902, 0.884, 0.734, and 0.891. The features of 62.1% (875/1409) extracted from PVP images had excellent consistency (ICC > 0.8), and most of the eight features selected for modeling had excellent consistency (ICC median = 0.844, minimum = 0.500, maximum = 1.000). The features of 82.5% (1163/1409) extracted from HBP images had excellent consistency (ICC > 0.8), and most of the 30 features selected for modeling had excellent consistency (ICC

Table 1 Demographics, alpha fetal protein, bilirubin, tumor characteristics, and microvascular infiltration of the patients with small hepatocellular carcinoma in data sets of three hospitals

Characteristics	Hospital A (*n* = 221)	Hospital B (*n* = 94)	Hospital C (*n* = 100)
Age (yr)	mean ± SD: 51.2 ± 10.9 (range 29-78)	mean ± SD: 53.04 ± 10.59 (range 28-77)	mean ± SD: 54.01 ± 10.82 (range 28-85)
Male/female	189 (85.5%)/32 (14.5%)	84 (89.4%)/10 (10.6%)	85 (85.5%)/15 (15.0%)
Causes of liver disease			
Hepatitis B	162 (73.3%)	71 (75.6%)	82 (82.0%)
Hepatitis C	21 (9.5%)	10 (10.6%)	6 (6.0%)
Alcoholic hepatitis	29 (13.1%)	8 (8.5%)	2 (2.0%)
Others	9 (4.1%)	5 (5.3%)	10 (10.0%)
Cirrhosis			
Present	173 (78.3%)	69 (73.4%)	70 (70%)
Absent	48 (21.7%)	25 (26.6%)	30 (30%)
AFP (ng/mL)	Median: 26.10 (range 0.98-25451.00)	Median: 9.34 (range 1.09-6740.42)	Median: 31.070 (range 0.713- 4587.000)
TBiL (μmol/L)	Median: 12.5 (range 2.9-64.6)	Median: 17.4 (range 3.6-446.9)	Median: 13.2 (range 4.4-47.2)
DBiL (μmol/L)	Median: 3.9 (range 1.0-17.0)	Median: 4.5 (range 1.0-218.9)	Median: 5.50 (range 1.50-26.84)
MELD scores	mean ± SD: 13.9 ± 4.8 (range 7.0-26.9)	mean ± SD: 13.8 ± 5.8 (range 6.0-35.5)	mean ± SD: 11.8 ± 4.5 (range 5.2-25.6)
Child-Pugh classes			
A	205 (93.2%)	81 (86.2%)	86 (86.0%)
B	13 (5.9%)	12 (12.8%)	13 (13.0%)
C	2 (0.9%)	1 (1.1%)	1 (1.0%)
Edmondson-steiner grade			
Grade I	32 (14.5%)	12 (12.8%)	8 (8.0%)
Grade II	142 (64.3%)	68 (72.3%)	71 (71.0%)
Grade III	47 (21.2%)	14 (14.9%)	21 (21.0%)
Tumor size (cm)	mean ± SD: 2.04 ± 0.67 (range 0.60-3.00)	mean ± SD: 2.17 ± 0.42 (range 0.80-3.00)	mean ± SD: 2.20 ± 0.41 (range 0.90-3.00)
MVI			
Positive	64 (28.9%)	22 (23.4%)	16 (16.0%)
Negative	157 (71.1%)	72 (76.6%)	84 (84.0%)

TBiL: Total bilirubin; DBiL: Direct bilirubin; MELD: Model for end-stage liver disease; AFP: Alpha-fetoprotein; MVI: Microvascular infiltration.

median, 0.917; minimum, 0.690; maximum, 1.000).

Predictive performance of the machine learning classifiers

The machine learning classifiers used in this study were KNN, LR, MLP, RF, SVM, and DT. In general, all classifiers achieved satisfactory performance, with LR being the best machine learning method. To predict MVI, T1WI, T2WI, DWI, AP, PVP, and HBP radiomics models were constructed and validated. In the testing set, the AUCs were 0.776 (95%CI: 0.611-0.895), 0.813 (95%CI: 0.651-0.922), 0.971 (95%CI: 0.858-0.999), 0.788 (95%CI: 0.642-0.894), 0.790 (95%CI: 0.630-0.904) and 0.979 (95%CI: 0.911-1.000). In validation hospital B, the AUCs were 0.834 (95%CI: 0.742-0.904), 0.825 (95%CI: 0.732-0.896), 0.816 (95%CI: 0.678-0.876), 0.810 (95%CI: 0.715-0.884), 0.847 (95%CI: 0.758-0.913) and 0.970 (95%CI: 0.912-0.994). In validation hospital C, the AUCs were 0.766 (95%CI: 0.672-0.844), 0.761 (95%CI: 0.669-0.839), 0.801 (95%CI: 0.710-0.871), 0.824 (95%CI: 0.737-0.892), 0.833 (95%CI: 0.748-0.898) and 0.803 (95%CI: 0.680-0.834) (Figure 3, Table 4).

Development and validation of MVI predicting nomogram

The C-indexes of the radiomics and clinic combined nomogram with the model of T1WI, T2WI, DWI, AP, PVP and HBP were 0.771 (95%CI: 0.695-0.836), 0.895 (95%CI: 0.834-0.940), 0.990 (95%CI: 0.957-0.999), 0.774 (95%CI: 0.706-0.833), 0.746 (95%CI: 0.668-0.814) and 0.990 (95%CI: 0.944-0.993) in the training set,

Table 2 Age, gender, alpha-fetoprotein and radiologic features of patients with small hepatocellular carcinoma and relationship with microvascular infiltration

	Hospital A (*n* = 221)			Hospital B (*n* = 94)			Hospital C (*n* = 100)		
	Positive	Negative	*P* value	Positive	Negative	*P* value	Positive	Negative	*P* value
Age (yr)	50.9 ± 10.7	51.3 ± 10.9	0.840	51.7 ± 12.3	53.1 ± 10.1	0.597	53.5 ± 9.1	53.7 ± 11.0	0.958
Gender			0.593			0.443			0.259
Female	8	24		1	9		1	14	
Male	56	133		21	63		15	70	
AFP (ng/mL)	33.91 (range 1.40-25451.00)	22.52 (range 1-18929)	0.026	38.97 (range 1.90-6740.40)	5.43 (range 1.10-2018.79)	0.010	109.72 (range 0.80-2278.00)	24.41 (range 0.71-4587.00)	0.032
Size (cm)	2.34 ± 0.56	1.92 ± 0.67	0.036	2.43 ± 0.57	2.11 ± 0.66	0.047	2.47 ± 0.43	2.21 ± 0.64	0.054
Nonsmooth tumor margin			0.019			0.003			0.004
Absent	37	116		13	64		6	62	
Present	27	41		9	8		10	22	
Capsule			0.020			0.062			0.756
Absent	39	120		21	55		10	49	
Present	25	37		25	17		6	35	
Peritumoral hypointensity			0.002			0.304			0.007
Absent	47	141		17	63		70	8	
Present	17	16		5	9		14	8	

Size: Large tumor size; AFP: Alpha-fetoprotein; MVI: Microvascular infiltration.

respectively; 0.846 (95%CI: 0.594-0.883), 0.917 (95%CI: 0.640-0.915), 0.970 (95%CI: 0.843-0.997), 0.794 (95%CI: 0.615-0.876), 0.831 (95%CI: 0.650-0.916) and 0.971 (95%CI: 0.892-0.999) in the testing set, respectively; 0.895 (95%CI: 0.775-0.925), 0.886 (95%CI: 0.746-0.906), 0.843 (95%CI: 0.685-0.881), 0.886 (95%CI: 0.695-0.899), 0.918 (95%CI: 0.791-0.934) and 0.912 (95%CI: 0.918-0.996) in validation hospital B, respectively; 0.830 (95%CI: 0.667-0.850), 0.808 (95%CI: 0.654-0.867), 0.869 (95%CI: 0.694-0.899), 0.874 (95%CI: 0.674-0.884), 0.870 (95%CI: 0.732-0.887) and 0.808 (95%CI: 0.635-0.892) in validation hospital C, respectively (Figure 4, Table 5).

Decision curve analysis showed adequate performance for radiomics nomogram models for predicting MVI in sHCC. The proposed radiomics model to predict MVI showed a greater advantage than the "clinicoradiological" scheme ($P < 0.05$). There was no significant difference in predictive efficacy between the combination nomogram model and the single radiomics model ($P > 0.05$) (Figure 5).

DISCUSSION

In this multi-center study, we analyzed the clinical and imaging data of 415 patients with sHCC who underwent DWI, Gd-EOB-DTPA-enhanced MRI, and hepatectomy. We used a machine learning approach to construct radiomics signatures and nomogram models for preoperative prediction of MVI and then independently validated the machine learning and nomogram models. Our data showed that clinical and common MRI radiological features, including AFP, tumor size, non-smooth tumor margin, incomplete capsule, and HBP peritumoral hypointensity, have limited diagnostic value for MVI of sHCC. The LR classifier was the best machine learning method, and the radiomics scores of HBP and DWI had great diagnostic efficiency for predicting MVI of sHCC. The nomogram model of combined radiomics scores, APF, and common MRI features exhibited good calibration and discrimination in the training, testing, and independent external validation cohorts.

Gd-EOB-DTPA with a pendant ethoxybenzyl group covalently attached to gadopentetate dimeglumine is a hepatocyte-specific MRI contrast agent that can be taken up by hepatocytes *via* the organic anion transporting polypeptides[30]. Gd-EOB-DTPA, which has dual extracellular and hepatobiliary

Table 3 Diagnostic performance of alpha-fetoprotein and radiologic features for assessing microvascular infiltration of small hepatocellular carcinoma by receiver operating characteristic curve analysis

	AFP	Tumor size	Nonsmooth tumor margin	Incomplete capsule	Peritumoral hypointensity
Hospital A					
AUC	0.597	0.675	0.580	0.577	0.582
95%CI	0.528-0.662	0.609-0.736	0.512-0.646	0.509-0.643	0.514-0.648
P value	0.024	< 0.001	0.024	0.027	0.007
Sensitivity	34.92	70.31	42.19	39.06	26.56
Specificity	81.82	61.15	73.89	76.43	89.81
Hospital B					
AUC	0.683	0.639	0.649	0.595	0.551
95%CI	0.577-0.777	0.553-0.735	0.544-0.745	0.489-0.695	0.445-0.654
P value	0.006	0.035	0.008	0.005	0.304
Sensitivity	63.64	81.82	71.43	95.45	22.73
Specificity	72.06	44.44	88.89	23.61	87.50
Hospital C					
AUC	0.669	0.576	0.682	0.521	0.667
95%CI	0.568-0.760	0.473-0.675	0.581-0.771	0.419-0.622	0.565-0.758
P value	0.016	0.213	0.007	0.759	0.014
Sensitivity	87.50	68.75	62.50	62.50	50.00
Specificity	52.38	54.76	73.81	41.67	83.33

DeLong test for comparison of receiver operating characteristic curve. AFP: Alpha-fetoprotein; AUC: Area under the curve; 95%CI: 95% confidence interval.

properties that provide structural and functional information on liver lesions, can also provide information on nonspecific gadolinium chelates during dynamic enhancement[31,32]. Granito *et al*[33] reported that Gd-EOB-DTPA-enhanced MRI may improve the sensitivity of noninvasive diagnosis of small HCC nodules in patients with cirrhosis, and the double hypointensity in the portal/venous and HBP can be regarded as an MRI pattern, which is highly suggestive of hypovascular hepatocellular carcinoma. This previous study revealed that large tumor size, incomplete capsule, non-smooth tumor margin, peritumoral enhancement on AP, and peritumoral hypointensity on HBP could achieve predictive AUCs of up to 0.85 for MVI of HCC[34]. However, for small HCC (large tumor size ≤ 3 cm), the common MRI radiologic features are smooth tumor margin, complete capsule (or no capsule), and no peritumoral hypointensity in HBP. In this study, the results from three hospitals showed that these conventional MRI radiologic features had limited value in evaluating MVI for sHCC.

Based on these characteristics, we established a Gd-EOB-DTPA MRI radiomics model using machine learning to construct and validate radiomics models for predicting MVI of sHCC. Machine learning has demonstrated capabilities to learn and even master complex tasks, making it useful for computer-aided diagnosis and decision support systems[21]. Radiomics refers to a technique of high-throughput extraction of quantitative imaging features or textures to decode histology and create a high-dimensional dataset[35]. However, it was thought that the parameters of the MRI scanner would not have an obvious influence on the results of radiomics analysis after the images were standardized when a previous multi-center study[36] did not demand the same MRI scanners and parameters. However, to minimize the possible influence of other factors, a unified MRI scanner and image standardization process were used in our study. Furthermore, whole-tumor volume analysis was used to decrease sampling bias.

Although previous studies have verified that the radiomics features of CT imaging could predict MVI status in patients with HCC preoperatively, it has high diagnostic efficiency, and the AUC can reach approximately 0.85[27,37]. In addition, Feng *et al*[38] evaluated Gd-EOB-DTPA-enhanced MRI quantitative features of peri- and intratumoral regions, providing a radiomics model for MVI prediction in patients with HCC. In the validation cohort, the AUC, sensitivity, and specificity were 0.83%, 90.00%, and 75.00%, respectively. However, none of these studies predicted the MVI for sHCC or provided a clinical nomogram. In this study, we extracted radiomics signatures from images of Gd-EOB-DTPA-

Table 4 Receiver operator characteristic curve analysis of radiomics scores with different sequences of magnetic resonance imaging for predict microvascular infiltration of small hepatocellular carcinoma

	T1WI	T2WI	DWI	AP	PVP	HBP
Training set						
AUC	0.740	0.878	0.991	0.763	0.739	0.976
95%CI	0.661-0.808	0.814-0.926	0.958-0.999	0.695-0.823	0.661-0.807	0.940-0.991
P value	< 0.001	< 0.001	< 0.001	< 0.001	< 0.001	< 0.001
Sensitivity	77.08	82.98	95.74	71.43	56.25	89.83
Specificity	68.00	82.00	96.04	79.37	78.22	99.27
Testing set						
AUC	0.776	0.813	0.971	0.788	0.790	0.979
95%CI	0.611-0.895	0.651-0.922	0.858-0.999	0.642-0.894	0.630-0.904	0.911-1.000
P value	0.0004	< 0.001	< 0.001	0.0014	0.0001	< 0.001
Sensitivity	91.67	58.33	100.00	64.29	84.62	100.00
Specificity	57.69	92.00	84.62	93.75	73.08	91.43
Validation Hospital B						
AUC	0.834	0.825	0.816	0.810	0.847	0.970
95%CI	0.742-0.904	0.732-0.896	0.678-0.876	0.715-0.884	0.758-0.913	0.912-0.994
P value	< 0.001	< 0.001	0.0002	< 0.001	< 0.001	< 0.001
Sensitivity	63.64	95.45	71.43	57.14	54.55	95.45
Specificity	94.29	57.75	88.89	88.89	98.61	98.57
Validation Hospital C						
AUC	0.766	0.761	0.801	0.824	0.833	0.803
95%CI	0.672-0.844	0.669-0.839	0.710-0.871	0.737-0.892	0.748-0.898	0.680-0.834
P value	0.0001	0.0003	< 0.001	< 0.001	< 0.001	0.007
Sensitivity	80.00	60.00	90.00	86.67	85.71	83.33
Specificity	70.45	89.01	68.89	68.54	72.83	77.67

T1WI: T1 weighted imaging; T2WI: T2 weighted imaging; DWI: Diffusion weighted imaging; AP: Arterial phase; PVP: Portal vein phase; HBP: Hepatobiliary phase; AUC: Area under the curve; 95%CI: 95% confidence interval.

enhanced MRI and then built the model using T1WI, T2WI, AP, PVP, and HBP. The results illustrated that radiomics has the best modeling in HBP and DWI when the LR and classifier of machine learning are utilized, producing great diagnostic efficiency for predicting MVI. Furthermore, the independent external validation results confirmed this efficiency. This may be because the post-Gd-EOB-DTPA contrast enhancement images provide structural and functional information on HBP lesions. The LR algorithm is used to establish a cost function for a classification or regression problem and then solve the optimal model iteratively through the optimization method.

Our results also demonstrate that the radiomics characteristics of DWI images can accurately predict the MVI of sHCC. DWI is an MRI technology that can reflect the motion of water molecules *in vivo* and can be used to assess tumor cellularity[39]. HCC with MVI is more likely to have higher cellularity and poor differentiation than HCC without MVI[40]. Okamura *et al*[41] suggested that the apparent diffusion coefficient (ADC) value is a valuable predictor of poor differentiation and MVI and is significantly related to tumor recurrence. Kim *et al*[42] illustrated that the tumor-to-liver ADC ratio was a significant independent parameter for the MVI of sHCC and the degree of lymphocyte infiltration. Our research further extracted the radiomics characteristics of the tumor, which were based on DWI images that confirmed that the quantitative characteristics of the radiomics had good performance for predicting the MVI of sHCC.

A nomogram was built in our study, which converted each regression coefficient proportionally in multivariate logistic regression to a 0- to 100-point scale. The effect of features with the absolute value of the highest β coefficient was assigned 100 points. The total points of the independent variables were

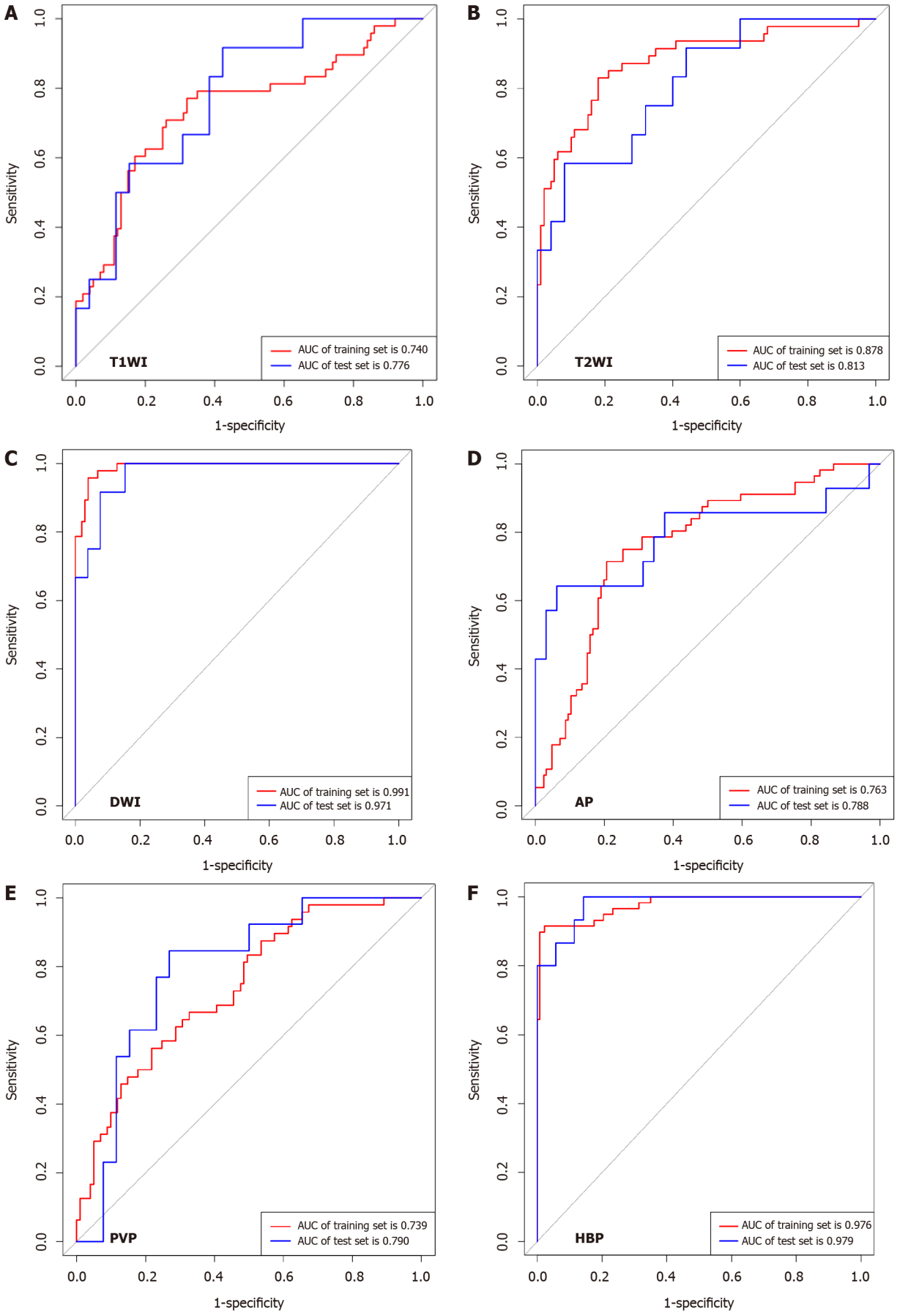
Table 5 Predictive performance of the nomogram prediction model for estimating the risk of microvascular infiltration presence in patients with small hepatocellular carcinoma

	Training set	Testing set	Validation Hospital B	Validation Hospital C
T1WI				
C-index	0.771	0.846	0.895	0.830
95%CI	0.695-0.836	0.594-0.883	0.775-0.925	0.667-0.850
P value	< 0.001	0.0014	< 0.001	0.0001
T2WI				
C-index	0.895	0.917	0.886	0.808
95%CI	0.834-0.940	0.640-0.915	0.746-0.906	0.654-0.867
P value	< 0.001	0.0001	< 0.001	0.0015
DWI				
C-index	0.990	0.970	0.843	0.869
95%CI	0.957-0.999	0.843-0.997	0.685-0.881	0.694-0.899
P value	< 0.001	< 0.001	0.0001	< 0.001
AP				
C-index	0.774	0.794	0.886	0.874
95%CI	0.706-0.833	0.615-0.876	0.695-0.899	0.674-0.884
P value	< 0.001	0.0025	< 0.001	< 0.001
PVP				
C-index	0.746	0.831	0.918	0.870
95%CI	0.668-0.814	0.650-0.916	0.791-0.934	0.732-0.887
P value	< 0.001	< 0.001	< 0.001	< 0.001
HBP				
C-index	0.990	0.971	0.912	0.808
95%CI	0.944-0.993	0.892-0.999	0.918-0.996	0.635-0.892
P value	< 0.001	< 0.001	< 0.001	0.0081

T1WI: T1 weighted imaging; T2WI: T2 weighted imaging; DWI: Diffusion weighted imaging; AP: Arterial phase; PVP: Portal vein phase; HBP: Hepatobiliary phase; 95%CI, 95% confidence interval; C-index: Concordance index.

converted to the predicted probabilities. The concordance index (C-index) was used to predict the performance of the nomogram and calibration with 1000 bootstrap samples to decrease the overfitting bias[43]. Our study incorporated six factors: radiomics signatures, APF, tumor size, non-smooth tumor margin, incomplete capsule, and peritumoral hypointensity. Radiomics combined with the clinico-radiological factors nomogram model achieved good concordance indices in predicting MVI in the training and validation cohorts. In particular, the nomogram with HBP and DWI radiomics model showed excellent predictive efficiency in the two external validation datasets, and decision curve analysis further confirmed the clinical usefulness of the nomogram.

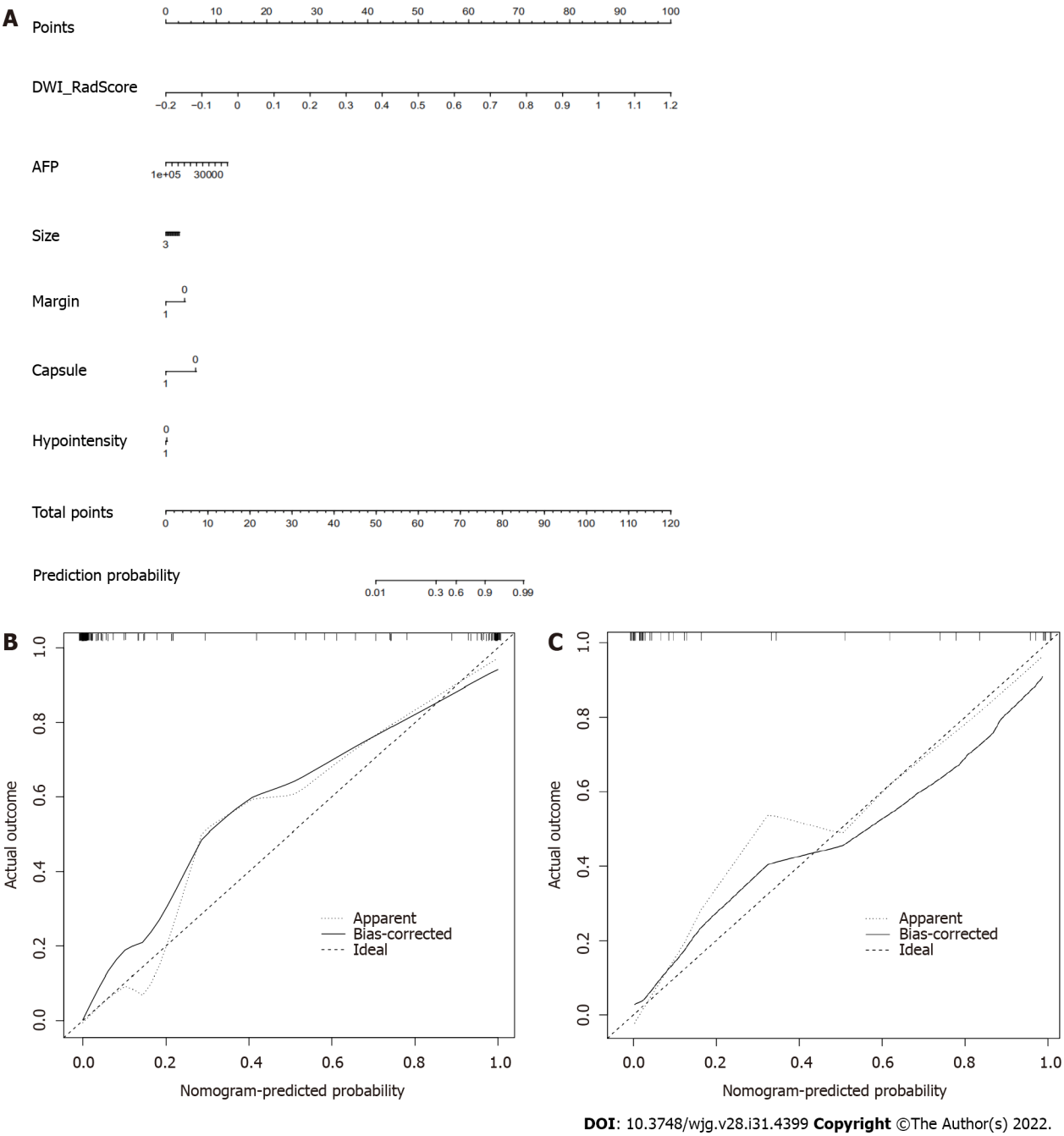
Nonetheless, this study had several limitations. First, the included patient population in this study had an inevitable bias in the inter-center distribution, although the application of radiomics and clinical nomogram was ensured by the multi-center nature of this study. To investigate the impact factors of bias on the baseline, we analyzed the age, AFP levels, liver function, and tumor size. Further larger-scale studies with more balanced subjects are needed to validate our results. Second, given the difficulty of collecting scalable medical imaging data for small HCC, many patients with small HCC who underwent transarterial chemoembolization or ablation could not be enrolled in the model of radiomics signatures and clinical nomogram to predict MVI. Given larger medical imaging datasets, deep networks are expected to improve prediction accuracy. Third, due to the lack of prognostic analysis in this study, we analyzed the different prognoses of sHCC patients with positive and negative MVI, which were predicted using a radiomics nomogram.



DOI: 10.3748/wjg.v28.i31.4399 **Copyright** ©The Author(s) 2022.

Figure 3 Receiver operating characteristic curve of different radiomics models for diagnosis microvascular invasion in small hepato-

cellular carcinoma (testing set). A: T1 weighted imaging [area under curve (AUC) was 0.776; 95% confidence interval (CI): 0.611-0.895]; B: T2 weighted imaging [AUC, 0.813; 95% confidence interval (CI): 0.651-0.922]; C: Diffusion weighted imaging (AUC, 0.971; 95%CI: 0.858-0.999); D: Arterial phase (AUC, 0.788; 95%CI: 0.642-0.894); E: Portal vein phase (AUC, 0.790; 95%CI: 0.630-0.904); F: Hepatobiliary phase (AUC, 0.990; 95%CI: 0.911-1.000). T1W1: T1 weighted imaging; T2W2: T2 weighted imaging; AUC: Area under curve; DWI: Diffusion weighted imaging; AP: Arterial phase; PVP: Portal vein phase; HBP: Hepatobiliary phase.

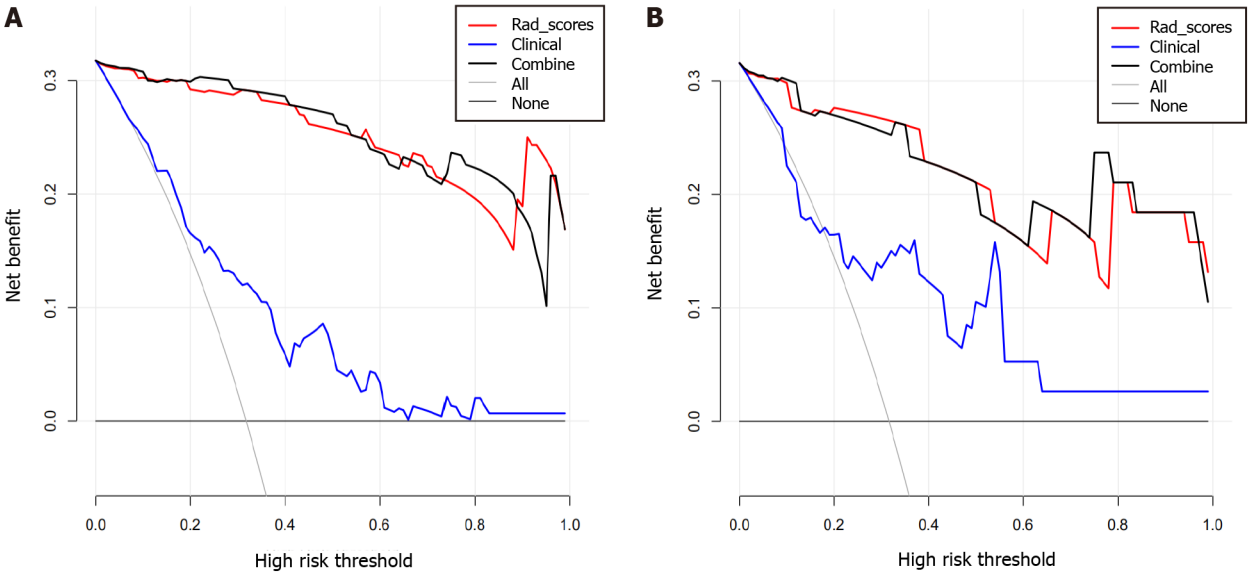


DOI: 10.3748/wjg.v28.i31.4399 **Copyright** ©The Author(s) 2022.

Figure 4 Nomogram of diffusion weighted imaging radiomics model to predict microvascular invasion in patients with small hepatocellular carcinoma. A: The nomogram was developed with radiomics signature and clinicoradiological factors. A vertical line was drawn according to the value of radiomics scores to determine the corresponding value of points. Similarly, the points of tumor markers were determined. The total points were the sum of the two points above. Finally, a vertical line was made according to the value of the total points to determine the probability of microvascular invasion (MVI); B: Validity of the predictive performance of the nomogram in estimating the risk of MVI presence in the training cohort; C: Validity of the predictive performance of the nomogram in estimating the risk of MVI presence in the validation cohort. AFP: Alpha-fetoprotein; DWI: Diffusion weighted imaging; Rad_score: Radiomics signatures score.

CONCLUSION

In conclusion, our study revealed that AFP and conventional Gd-EOB-DTPA-enhanced MRI features



DOI: 10.3748/wjg.v28.i31.4399 **Copyright** ©The Author(s) 2022.

Figure 5 Decision curve analysis. A and B: Decision curve analysis of the prediction model for training (A) and testing (B) cohort. Y-axis represents the net benefit, which is calculated by gaining true positives and deleting false positives. The X-axis is the probability threshold. The curve of the radiomics and combined nomogram over the clinical features that integrated AFP and radiological signatures showed the greatest benefit. AFP: Alpha-fetoprotein; Rad_score: Radiomics signatures score.

have poor diagnostic accuracies for MVI in sHCC. The radiomic signatures of HBP and DWI can further improve the ability to predict MVI. Furthermore, as a noninvasive preoperative prediction method, the radiomics nomogram showed favorable predictive accuracy for evaluating MVI in sHCC, which may help reassess the clinical therapeutic regimen for patients with sHCC.

ARTICLE HIGHLIGHTS

Research background

Microvascular invasion (MVI) of hepatocellular carcinoma (HCC) is an independent poor prognostic factor.

Research motivation

It is difficult to determine MVI of small hepatocellular carcinoma (HCC) (≤ 3.0 cm) by preoperative MRI conventional features.

Research objectives

To develop and validate radiomics scores and nomogram of gadolinium ethoxybenzyl diethylenetriamine pentaacetic acid (Gd-EOB-DTPA)-enhanced magnetic resonance imaging (MRI) for preoperative prediction of MVI in sHCC.

Research methods

Radiomics models of Gd-EOB-DTPA enhanced MRI and diffusion weighted images were constructed and validated by machine learning from data sets of three hospitals. A nomogram prediction model was developed using multivariable logistic regression analysis which included the radiomics scores, radiologic features, and alpha-fetoprotein (AFP) level.

Research results

AFP and MRI conventional features had poor diagnostic value for MVI of small HCC. The nomogram model (combined radiomics and clinic features) exhibited good calibration and discrimination in the testing and two external validation cohorts (in the two external validation cohorts, C-index was 0.912 and 0.808, respectively).

Research conclusions

As a noninvasive preoperative prediction method, the MRI radiomics nomogram shows favorable predictive accuracy for evaluate MVI in sHCC.

Research perspectives

This clinical prediction model may help in the selection of treatment options for small HCC.

ACKNOWLEDGEMENTS

The authors would like to thank Yingying Ezell for the language recheck and editing, Fuling Huang for his technical support, and Huiting Zhang (Siemens Healthineers, Wuhan, Hubei Province, China) for her constructive suggestions during the MRI scanning.

FOOTNOTES

Author contributions: Chen YD and Zhang L contributed equally to this work; Chen YD and Long LL was the guarantor and designed the study; Zhang L, Lin B, Jiang ZJ, Tang C, Dang YW, and Xia YW participated in the acquisition, analysis, interpretation of the data, and drafted the initial manuscript; Zhou ZP and Song B revised the article critically for important intellectual content.

Supported by the National Natural Science Foundation of China, No. 82060310; and Science and Technology Support Program of Sichuan Province, No. 2022YFS0071.

Institutional review board statement: The study was reviewed and approved by The First Affiliated Hospital of Guangxi Medical University Ethical Review Committee, No. 2019 KY-E-65.

Informed consent statement: All study participants, or their legal guardian, provided informed written consent prior to study enrollment.

Conflict-of-interest statement: There are no conflicts of interest to report.

Data sharing statement: The data that support the findings of this study are available in the Baidu Netdisk or our AI Scientific Research Platform (https://mics.radcloud.cn/). Further enquiries can be directed to the corresponding author.

STROBE statement: The authors have read the STROBE Statement—checklist of items, and the manuscript was prepared and revised according to the STROBE Statement—checklist of items.

Open-Access: This article is an open-access article that was selected by an in-house editor and fully peer-reviewed by external reviewers. It is distributed in accordance with the Creative Commons Attribution NonCommercial (CC BY-NC 4.0) license, which permits others to distribute, remix, adapt, build upon this work non-commercially, and license their derivative works on different terms, provided the original work is properly cited and the use is non-commercial. See: https://creativecommons.org/Licenses/by-nc/4.0/

Country/Territory of origin: China

ORCID number: Yi-Di Chen 0000-0001-6293-4624; Ling Zhang 0000-0001-7270-3555; Yi-Wu Dang 0000-0002-7793-1239; Bin Song 0000-0002-7269-2101; Li-Ling Long 0000-0003-3369-8532.

S-Editor: Chen YL
L-Editor: Filipodia
P-Editor: Yuan YY

REFERENCES

1 **Ghouri YA**, Mian I, Rowe JH. Review of hepatocellular carcinoma: Epidemiology, etiology, and carcinogenesis. *J Carcinog* 2017; **16**: 1 [PMID: 28694740 DOI: 10.4103/jcar.JCar_9_16]
2 **Xu J**. Trends in Liver Cancer Mortality Among Adults Aged 25 and Over in the United States, 2000-2016. *NCHS Data Brief* 2018; 1-8 [PMID: 30044212]
3 **Omata M**, Cheng AL, Kokudo N, Kudo M, Lee JM, Jia J, Tateishi R, Han KH, Chawla YK, Shiina S, Jafri W, Payawal DA, Ohki T, Ogasawara S, Chen PJ, Lesmana CRA, Lesmana LA, Gani RA, Obi S, Dokmeci AK, Sarin SK. Asia-Pacific clinical practice guidelines on the management of hepatocellular carcinoma: a 2017 update. *Hepatol Int* 2017; **11**: 317-370 [PMID: 28620797 DOI: 10.1007/s12072-017-9799-9]
4 **Viganò L**, Laurenzi A, Solbiati L, Procopio F, Cherqui D, Torzilli G. Open Liver Resection, Laparoscopic Liver Resection, and Percutaneous Thermal Ablation for Patients with Solitary Small Hepatocellular Carcinoma (≤ 30 mm): Review of the Literature and Proposal for a Therapeutic Strategy. *Dig Surg* 2018; **35**: 359-371 [PMID: 29890512 DOI:

10.1159/000489836]
5 **Hong YJ**, Kim SH, Choi GH, Kim KS, Choi JS. Long-term outcome after liver resection and clinicopathological features in patients with small hepatocellular carcinoma. *Korean J Hepatobiliary Pancreat Surg* 2011; **15**: 199-205 [PMID: 26421040 DOI: 10.14701/kjhbps.2011.15.4.199]
6 **Chen ZH**, Zhang XP, Wang H, Chai ZT, Sun JX, Guo WX, Shi J, Cheng SQ. Effect of microvascular invasion on the postoperative long-term prognosis of solitary small HCC: a systematic review and meta-analysis. *HPB (Oxford)* 2019; **21**: 935-944 [PMID: 30871805 DOI: 10.1016/j.hpb.2019.02.003]
7 **Lim KC**, Chow PK, Allen JC, Chia GS, Lim M, Cheow PC, Chung AY, Ooi LL, Tan SB. Microvascular invasion is a better predictor of tumor recurrence and overall survival following surgical resection for hepatocellular carcinoma compared to the Milan criteria. *Ann Surg* 2011; **254**: 108-113 [PMID: 21527845 DOI: 10.1097/SLA.0b013e31821ad884]
8 **Choi KK**, Kim SH, Choi SB, Lim JH, Choi GH, Choi JS, Kim KS. Portal venous invasion: the single most independent risk factor for immediate postoperative recurrence of hepatocellular carcinoma. *J Gastroenterol Hepatol* 2011; **26**: 1646-1651 [PMID: 21592228 DOI: 10.1111/j.1440-1746.2011.06780.x]
9 **Du M**, Chen L, Zhao J, Tian F, Zeng H, Tan Y, Sun H, Zhou J, Ji Y. Microvascular invasion (MVI) is a poorer prognostic predictor for small hepatocellular carcinoma. *BMC Cancer* 2014; **14**: 38 [PMID: 24460749 DOI: 10.1186/1471-2407-14-38]
10 **Zhao Y**, Zhu X, Wang H, Dong D, Gao S, Wang W. Safety and Efficacy of Transcatheter Arterial Chemoembolization Plus Radiotherapy Combined With Sorafenib in Hepatocellular Carcinoma Showing Macrovascular Invasion. *Front Oncol* 2019; **9**: 1065 [PMID: 31681599 DOI: 10.3389/fonc.2019.01065]
11 **Renzulli M**, Brocchi S, Cucchetti A, Mazzotti F, Mosconi C, Sportoletti C, Brandi G, Pinna AD, Golfieri R. Can Current Preoperative Imaging Be Used to Detect Microvascular Invasion of Hepatocellular Carcinoma? *Radiology* 2016; **279**: 432-442 [PMID: 26653683 DOI: 10.1148/radiol.2015150998]
12 **Rodríguez-Perálvarez M**, Luong TV, Andreana L, Meyer T, Dhillon AP, Burroughs AK. A systematic review of microvascular invasion in hepatocellular carcinoma: diagnostic and prognostic variability. *Ann Surg Oncol* 2013; **20**: 325-339 [PMID: 23149850 DOI: 10.1245/s10434-012-2513-1]
13 **Golfieri R**, Renzulli M, Lucidi V, Corcioni B, Trevisani F, Bolondi L. Contribution of the hepatobiliary phase of Gd-EOB-DTPA-enhanced MRI to Dynamic MRI in the detection of hypovascular small (≤ 2 cm) HCC in cirrhosis. *Eur Radiol* 2011; **21**: 1233-1242 [PMID: 21293864 DOI: 10.1007/s00330-010-2030-1]
14 **Verloh N**, Utpatel K, Zeman F, Fellner C, Schlitt HJ, Müller M, Stroszczynski C, Evert M, Wiggermann P, Haimerl M. Diagnostic performance of Gd-EOB-DTPA-enhanced MRI for evaluation of liver dysfunction: a multivariable analysis of 3T MRI sequences. *Oncotarget* 2018; **9**: 36371-36378 [PMID: 30555635 DOI: 10.18632/oncotarget.26368]
15 **Huang M**, Liao B, Xu P, Cai H, Huang K, Dong Z, Xu L, Peng Z, Luo Y, Zheng K, Peng B, Li ZP, Feng ST. Prediction of Microvascular Invasion in Hepatocellular Carcinoma: Preoperative Gd-EOB-DTPA-Dynamic Enhanced MRI and Histopathological Correlation. *Contrast Media Mol Imaging* 2018; **2018**: 9674565 [PMID: 29606926 DOI: 10.1155/2018/9674565]
16 **Lei Z**, Li J, Wu D, Xia Y, Wang Q, Si A, Wang K, Wan X, Lau WY, Wu M, Shen F. Nomogram for Preoperative Estimation of Microvascular Invasion Risk in Hepatitis B Virus-Related Hepatocellular Carcinoma Within the Milan Criteria. *JAMA Surg* 2016; **151**: 356-363 [PMID: 26579636 DOI: 10.1001/jamasurg.2015.4257]
17 **Kaibori M**, Ishizaki M, Matsui K, Kwon AH. Predictors of microvascular invasion before hepatectomy for hepatocellular carcinoma. *J Surg Oncol* 2010; **102**: 462-468 [PMID: 20872949 DOI: 10.1002/jso.21631]
18 **Suh YJ**, Kim MJ, Choi JY, Park MS, Kim KW. Preoperative prediction of the microvascular invasion of hepatocellular carcinoma with diffusion-weighted imaging. *Liver Transpl* 2012; **18**: 1171-1178 [PMID: 22767394 DOI: 10.1002/lt.23502]
19 **Davnall F**, Yip CS, Ljungqvist G, Selmi M, Ng F, Sanghera B, Ganeshan B, Miles KA, Cook GJ, Goh V. Assessment of tumor heterogeneity: an emerging imaging tool for clinical practice? *Insights Imaging* 2012; **3**: 573-589 [PMID: 23093486 DOI: 10.1007/s13244-012-0196-6]
20 **Aerts HJ**, Velazquez ER, Leijenaar RT, Parmar C, Grossmann P, Carvalho S, Bussink J, Monshouwer R, Haibe-Kains B, Rietveld D, Hoebers F, Rietbergen MM, Leemans CR, Dekker A, Quackenbush J, Gillies RJ, Lambin P. Decoding tumour phenotype by noninvasive imaging using a quantitative radiomics approach. *Nat Commun* 2014; **5**: 4006 [PMID: 24892406 DOI: 10.1038/ncomms5006]
21 **Erickson BJ**, Korfiatis P, Akkus Z, Kline TL. Machine Learning for Medical Imaging. *Radiographics* 2017; **37**: 505-515 [PMID: 28212054 DOI: 10.1148/rg.2017160130]
22 **Litjens G**, Kooi T, Bejnordi BE, Setio AAA, Ciompi F, Ghafoorian M, van der Laak JAWM, van Ginneken B, Sánchez CI. A survey on deep learning in medical image analysis. *Med Image Anal* 2017; **42**: 60-88 [PMID: 28778026 DOI: 10.1016/j.media.2017.07.005]
23 **Tao Q**, Lelieveldt BPF, van der Geest RJ. Deep Learning for Quantitative Cardiac MRI. *AJR Am J Roentgenol* 2020; **214**: 529-535 [PMID: 31670597 DOI: 10.2214/AJR.19.21927]
24 **Simpson AL**, Adams LB, Allen PJ, D'Angelica MI, DeMatteo RP, Fong Y, Kingham TP, Leung U, Miga MI, Parada EP, Jarnagin WR, Do RK. Texture analysis of preoperative CT images for prediction of postoperative hepatic insufficiency: a preliminary study. *J Am Coll Surg* 2015; **220**: 339-346 [PMID: 25537305 DOI: 10.1016/j.jamcollsurg.2014.11.027]
25 **Li M**, Fu S, Zhu Y, Liu Z, Chen S, Lu L, Liang C. Computed tomography texture analysis to facilitate therapeutic decision making in hepatocellular carcinoma. *Oncotarget* 2016; **7**: 13248-13259 [PMID: 26910890 DOI: 10.18632/oncotarget.7467]
26 **Gillies RJ**, Kinahan PE, Hricak H. Radiomics: Images Are More than Pictures, They Are Data. *Radiology* 2016; **278**: 563-577 [PMID: 26579733 DOI: 10.1148/radiol.2015151169]
27 **Xu X**, Zhang HL, Liu QP, Sun SW, Zhang J, Zhu FP, Yang G, Yan X, Zhang YD, Liu XS. Radiomic analysis of contrast-enhanced CT predicts microvascular invasion and outcome in hepatocellular carcinoma. *J Hepatol* 2019; **70**: 1133-1144 [PMID: 30876945 DOI: 10.1016/j.jhep.2019.02.023]
28 **Bakr S**, Echegaray S, Shah R, Kamaya A, Louie J, Napel S, Kothary N, Gevaert O. Noninvasive radiomics signature based on quantitative analysis of computed tomography images as a surrogate for microvascular invasion in hepatocellular carcinoma: a pilot study. *J Med Imaging (Bellingham)* 2017; **4**: 041303 [PMID: 28840174 DOI: 10.1117/1.JMI.4.4.041303]

29 **Chen Y**, Xia Y, Tolat PP, Long L, Jiang Z, Huang Z, Tang Q. Comparison of Conventional Gadoxetate Disodium-Enhanced MRI Features and Radiomics Signatures With Machine Learning for Diagnosing Microvascular Invasion. *AJR Am J Roentgenol* 2021; **216**: 1510-1520 [PMID: 33826360 DOI: 10.2214/AJR.20.23255]

30 **Kim SH**, Jeong WK, Kim Y, Kim MY, Kim J, Pyo JY, Oh YH. Hepatocellular carcinoma composed of two different histologic types: imaging features on gadoxetic acid-enhanced liver MRI. *Clin Mol Hepatol* 2013; **19**: 92-96 [PMID: 23593616 DOI: 10.3350/cmh.2013.19.1.92]

31 **Lee NK**, Kim S, Kim GH, Heo J, Seo HI, Kim TU, Kang DH. Significance of the "delayed hyperintense portal vein sign" in the hepatobiliary phase MRI obtained with Gd-EOB-DTPA. *J Magn Reson Imaging* 2012; **36**: 678-685 [PMID: 22649000 DOI: 10.1002/jmri.23700]

32 **van Kessel CS**, Veldhuis WB, van den Bosch MA, van Leeuwen MS. MR liver imaging with Gd-EOB-DTPA: a delay time of 10 minutes is sufficient for lesion characterisation. *Eur Radiol* 2012; **22**: 2153-2160 [PMID: 22645040 DOI: 10.1007/s00330-012-2486-2]

33 **Granito A**, Galassi M, Piscaglia F, Romanini L, Lucidi V, Renzulli M, Borghi A, Grazioli L, Golfieri R, Bolondi L. Impact of gadoxetic acid (Gd-EOB-DTPA)-enhanced magnetic resonance on the non-invasive diagnosis of small hepatocellular carcinoma: a prospective study. *Aliment Pharmacol Ther* 2013; **37**: 355-363 [PMID: 23199022 DOI: 10.1111/apt.12166]

34 **Lee S**, Kim SH, Lee JE, Sinn DH, Park CK. Preoperative gadoxetic acid-enhanced MRI for predicting microvascular invasion in patients with single hepatocellular carcinoma. *J Hepatol* 2017; **67**: 526-534 [PMID: 28483680 DOI: 10.1016/j.jhep.2017.04.024]

35 **Lambin P**, Leijenaar RTH, Deist TM, Peerlings J, de Jong EEC, van Timmeren J, Sanduleanu S, Larue RTHM, Even AJG, Jochems A, van Wijk Y, Woodruff H, van Soest J, Lustberg T, Roelofs E, van Elmpt W, Dekker A, Mottaghy FM, Wildberger JE, Walsh S. Radiomics: the bridge between medical imaging and personalized medicine. *Nat Rev Clin Oncol* 2017; **14**: 749-762 [PMID: 28975929 DOI: 10.1038/nrclinonc.2017.141]

36 **Hamerla G**, Meyer HJ, Schob S, Ginat DT, Altman A, Lim T, Gihr GA, Horvath-Rizea D, Hoffmann KT, Surov A. Comparison of machine learning classifiers for differentiation of grade 1 from higher gradings in meningioma: A multicenter radiomics study. *Magn Reson Imaging* 2019; **63**: 244-249 [PMID: 31425811 DOI: 10.1016/j.mri.2019.08.011]

37 **Peng J**, Zhang J, Zhang Q, Xu Y, Zhou J, Liu L. A radiomics nomogram for preoperative prediction of microvascular invasion risk in hepatitis B virus-related hepatocellular carcinoma. *Diagn Interv Radiol* 2018; **24**: 121-127 [PMID: 29770763 DOI: 10.5152/dir.2018.17467]

38 **Feng ST**, Jia Y, Liao B, Huang B, Zhou Q, Li X, Wei K, Chen L, Li B, Wang W, Chen S, He X, Wang H, Peng S, Chen ZB, Tang M, Chen Z, Hou Y, Peng Z, Kuang M. Preoperative prediction of microvascular invasion in hepatocellular cancer: a radiomics model using Gd-EOB-DTPA-enhanced MRI. *Eur Radiol* 2019; **29**: 4648-4659 [PMID: 30689032 DOI: 10.1007/s00330-018-5935-8]

39 **Taouli B**, Koh DM. Diffusion-weighted MR imaging of the liver. *Radiology* 2010; **254**: 47-66 [PMID: 20032142 DOI: 10.1148/radiol.09090021]

40 **Pawlik TM**, Delman KA, Vauthey JN, Nagorney DM, Ng IO, Ikai I, Yamaoka Y, Belghiti J, Lauwers GY, Poon RT, Abdalla EK. Tumor size predicts vascular invasion and histologic grade: Implications for selection of surgical treatment for hepatocellular carcinoma. *Liver Transpl* 2005; **11**: 1086-1092 [PMID: 16123959 DOI: 10.1002/Lt.20472]

41 **Okamura S**, Sumie S, Tonan T, Nakano M, Satani M, Shimose S, Shirono T, Iwamoto H, Aino H, Niizeki T, Tajiri N, Kuromatsu R, Okuda K, Nakashima O, Torimura T. Diffusion-weighted magnetic resonance imaging predicts malignant potential in small hepatocellular carcinoma. *Dig Liver Dis* 2016; **48**: 945-952 [PMID: 27338850 DOI: 10.1016/j.dld.2016.05.020]

42 **Kim JG**, Jang KM, Min GS, Kang TW, Cha DI, Ahn SH. Questionable correlation of the apparent diffusion coefficient with the histological grade and microvascular invasion in small hepatocellular carcinoma. *Clin Radiol* 2019; **74**: 406.e19-406.e27 [PMID: 30826002 DOI: 10.1016/j.crad.2019.01.019]

43 **Steyerberg EW**, Vergouwe Y. Towards better clinical prediction models: seven steps for development and an ABCD for validation. *Eur Heart J* 2014; **35**: 1925-1931 [PMID: 24898551 DOI: 10.1093/eurheartj/ehu207]

World Journal of Gastroenterology

Submit a Manuscript: https://www.f6publishing.com

World J Gastroenterol 2022 August 21; 28(31): 4417-4430

DOI: 10.3748/wjg.v28.i31.4417

ISSN 1007-9327 (print) ISSN 2219-2840 (online)

ORIGINAL ARTICLE

Observational Study

Prevalence and clinical characteristics of autoimmune liver disease in hospitalized patients with cirrhosis and acute decompensation in China

Zi-Xuan Shen, Dan-Dan Wu, Jie Xia, Xian-Bo Wang, Xin Zheng, Yan Huang, Bei-Ling Li, Zhong-Ji Meng, Yan-Hang Gao, Zhi-Ping Qian, Feng Liu, Xiao-Bo Lu, Jia Shang, Hua-Dong Yan, Yu-Bao Zheng, Wen-Yi Gu, Yan Zhang, Jian-Yi Wei, Wen-Ting Tan, Yi-Xin Hou, Qun Zhang, Yan Xiong, Cong-Cong Zou, Jun Chen, Ze-Bing Huang, Xiu-Hua Jiang, Sen Luo, Yuan-Yuan Chen, Na Gao, Chun-Yan Liu, Wei Yuan, Xue Mei, Jing Li, Tao Li, Xin-Yi Zhou, Guo-Hong Deng, Jin-Jun Chen, Xiong Ma, Hai Li

Specialty type: Gastroenterology and hepatology

Provenance and peer review: Unsolicited article; Externally peer reviewed.

Peer-review model: Single blind

Peer-review report's scientific quality classification

Grade A (Excellent): A
Grade B (Very good): B, B
Grade C (Good): 0
Grade D (Fair): 0
Grade E (Poor): 0

P-Reviewer: Haile D, Ethiopia; Hayat U, United States

Received: March 3, 2022
Peer-review started: March 3, 2022
First decision: April 25, 2022
Revised: May 19, 2022
Accepted: July 25, 2022
Article in press: July 25, 2022
Published online: August 21, 2022

Zi-Xuan Shen, Dan-Dan Wu, Wen-Yi Gu, Yan Zhang, Jian-Yi Wei, Xiong Ma, Hai Li, Department of Gastroenterology, Renji Hospital, School of Medicine, Shanghai Jiao Tong University, Shanghai 200127, China

Zi-Xuan Shen, Dan-Dan Wu, Wen-Yi Gu, Yan Zhang, Jian-Yi Wei, Xiong Ma, Hai Li, Shanghai Institute of Digestive Disease, Key Laboratory of Gastroenterology and Hepatology, Chinese Ministry of Health, Shanghai Jiao Tong University, Shanghai 200001, China

Jie Xia, Wen-Ting Tan, Guo-Hong Deng, Department of Infectious Diseases, Southwest Hospital, The Third Military Medical University (Army Medical University), Chongqing 400038, China

Xian-Bo Wang, Yi-Xin Hou, Qun Zhang, Center of Integrative Medicine, Beijing Ditan Hospital, Capital Medical University, Beijing 100102, China

Xin Zheng, Yan Xiong, Cong-Cong Zou, Department of Infectious Diseases, Institute of Infection and Immunology, Union Hospital, Tongji Medical College, Huazhong University of Science and Technology, Wuhan 430022, Hubei Province, China

Yan Huang, Jun Chen, Ze-Bing Huang, Department of Infectious Diseases, Hunan Key Laboratory of Viral Hepatitis, Xiangya Hospital, Central South University, Changsha 410008, Hunan Province, China

Bei-Ling Li, Jun Chen, Xiu-Hua Jiang, Jin-Jun Chen, Hepatology Unit, Department of Infectious Diseases, Nanfang Hospital, Southern Medical University, Guangzhou 510515, Guangdong Province, China

Zhong-Ji Meng, Sen Luo, Yuan-Yuan Chen, Department of Infectious Disease, Taihe Hospital, Hubei University of Medicine, Shiyan 430418, Hubei Province, China

Yan-Hang Gao, Na Gao, Chun-Yan Liu, Department of Hepatology, The First Hospital of Jilin University, Changchun 130031, Jilin Province, China

Zhi-Ping Qian, Wei Yuan, Xue Mei, Department of Liver Intensive Care Unit, Shanghai Public

Health Clinical Centre, Fudan University, Shanghai 201508, China

Feng Liu, Tianjin Institute of Hepatology, Nankai University Second People's Hospital, Tianjin 300102, China

Feng Liu, Jing Li, Tao Li, Department of Infectious Diseases and Hepatology, The Second Hospital of Shandong University, Jinan 250033, Shandong Province, China

Xiao-Bo Lu, Xin-Yi Zhou, Infectious Disease Center, The First Affiliated Hospital of Xinjiang Medical University, Urumqi 830054, Xinjiang, China

Jia Shang, Department of Infectious Diseases, Henan Provincial People's Hospital, Zhengzhou 450003, Henan Province, China

Hua-Dong Yan, Department of Infectious Diseases, Hwamei Hospital, The Second Hospital of Ningbo, University of Chinese Academy of Sciences, Ningbo 315153, Zhejiang Province, China

Yu-Bao Zheng, Department of Infectious Diseases, The Third Affiliated Hospital of Sun Yat-sen University, Guangzhou 510630, Guangdong Province, China

Corresponding author: Hai Li, MD, Professor, Department of Gastroenterology, Renji Hospital, School of Medicine, Shanghai Jiao Tong University, No. 1630 Dongfang Road, Shanghai 200127, China. hai_17@126.com

Abstract

BACKGROUND

Autoimmune liver disease (AILD) has been considered a relatively uncommon disease in China, epidemiological data for AILD in patients with cirrhosis and acute decompensation (AD) is sparse.

AIM

To investigate the prevalence, outcome and risk factors for AILD in cirrhotic patients complicated with AD in China.

METHODS

We collected data from patients with cirrhosis and AD from two prospective, multicenter cohorts in hepatitis B virus endemic areas. Patients were regularly followed up at the end of 28-d, 90-d and 365-d, or until death or liver transplantation (LT). The primary outcome in this study was 90-d LT-free mortality. Acute-on-chronic liver failure (ACLF) was assessed on admission and during 28-d hospitalization, according to the diagnostic criteria of the European Association for the Study of the Liver (EASL). Risk factors for death were analyzed with logistic regression model.

RESULTS

In patients with cirrhosis and AD, the overall prevalence of AILD was 9.3% (242/2597). Prevalence of ACLF was significantly lower in AILD cases (14%) than those with all etiology groups with cirrhosis and AD (22.8%) ($P < 0.001$). Among 242 enrolled AILD patients, the prevalence rates of primary biliary cirrhosis (PBC), autoimmune hepatitis (AIH) and PBC-AIH overlap syndrome (PBC/AIH) were 50.8%, 28.5% and 12.0%, respectively. In ACLF patients, the proportions of PBC, AIH and PBC/AIH were 41.2%, 29.4% and 20.6%. 28-d and 90-d mortality were 43.8% and 80.0% in AILD-related ACLF. The etiology of AILD had no significant impact on 28-d, 90-d or 365-d LT-free mortality in patients with cirrhosis and AD in both univariate and multivariate analysis. Total bilirubin (TB), hepatic encephalopathy (HE) and blood urea nitrogen (BUN) were independent risk factors for 90-d LT-free mortality in multivariate analysis. The development of ACLF during hospitalization only independently correlated to TB and international normalized ratio.

CONCLUSION

AILD was not rare in hospitalized patients with cirrhosis and AD in China, among which PBC was the most common etiology. 90-d LT-free mortality were independently associated with TB, HE and BUN.

Key Words: Prevalence; Autoimmune liver disease; Cirrhosis and acute decompensation; Mortality; Acute-on-chronic liver failure

©The Author(s) 2022. Published by Baishideng Publishing Group Inc. All rights reserved.

Core Tip: Autoimmune liver disease (AILD) has been regarded as a relatively rare disease in China. Our study reported that the overall prevalence of AILD was 9.3% hospitalized patients with cirrhosis and acute decompensation, among which primary biliary cirrhosis was the most prevalent type. In AILD patients with cirrhosis and acute decompensation, the etiology types of AILD had no significant effect on short-term mortality, total bilirubin, hepatic encephalopathy (HE) and blood urea nitrogen were independently associated with 90-d mortality in multivariate analysis. Strategies are needed to prevent presence of HE and closely monitor the changes of liver and renal function in clinical practice. These data will be a crucial complement to the public epidemiology research on AILD in Asian-Pacific regions.

Citation: Shen ZX, Wu DD, Xia J, Wang XB, Zheng X, Huang Y, Li BL, Meng ZJ, Gao YH, Qian ZP, Liu F, Lu XB, Shang J, Yan HD, Zheng YB, Gu WY, Zhang Y, Wei JY, Tan WT, Hou YX, Zhang Q, Xiong Y, Zou CC, Chen J, Huang ZB, Jiang XH, Luo S, Chen YY, Gao N, Liu CY, Yuan W, Mei X, Li J, Li T, Zhou XY, Deng GH, Chen JJ, Ma X, Li H. Prevalence and clinical characteristics of autoimmune liver disease in hospitalized patients with cirrhosis and acute decompensation in China. *World J Gastroenterol* 2022; 28(31): 4417-4430
URL: https://www.wjgnet.com/1007-9327/full/v28/i31/4417.htm
DOI: https://dx.doi.org/10.3748/wjg.v28.i31.4417

INTRODUCTION

Autoimmune liver disease (AILD) includes primary biliary cirrhosis (PBC), autoimmune hepatitis (AIH), primary sclerosing cholangitis (PSC) and immunoglobulin G 4-related diseases (IgG4-RD)[1-3]. Some patients display clinical manifestations of two different entities based on clinical and histological features, which is described as "overlap syndrome", among which PBC-AIH overlap syndrome (PBC/AIH) is the most common[4]. AILD has been considered to be a relatively rare etiology of chronic liver disease (CLD) in China where viral hepatitis has a high prevalence. However, recent findings indicated that the prevalence of AILD is increasing in the Asia-Pacific region. In Japan, AIH prevalence increased from 8.7 to 23.9 per 100000 population from 2004 to 2016[5]. In a city in northern China, PBC prevalence rose from 0.5 to 8.0 per 100000 population in the past 10 years[6]. Several studies have illustrated the prevalence and clinical characteristics of AILD in general population[7-9]. Few studies have been conducted to investigate the nature history of AILD, especially in the late stage of CLD-cirrhosis and acute decompensation (AD).

The Chinese Acute on Chronic Liver Failure (CATCH-LIFE) study consisted of two prospective, multicenter cohorts that enrolled hospitalized patients with CLD of various etiologies, most of whom had cirrhosis and complicated with AD. It is nationally representative of hospitalized CLD patients in China. In this study, we used the data from the CATCH-LIFE study to investigate the following: (1) The prevalence and short-term outcome of AILD in patients with cirrhosis and AD; (2) The impact of AILD etiology on mortality; and (3) Risk factors for 90-d mortality in AILD patients with cirrhosis and AD.

MATERIALS AND METHODS

Patients

Data were collected from 2 prospective, observational cohorts of the CATCH-LIFE study which enrolled hospitalized patients with CLD and acute events, from January 2015 to December 2016 and July 2018 to January 2019, respectively. The rationale and design of the cohorts have been described elsewhere[10, 11]. The medical ethics boards of the Shanghai Renji Hospital, approved the study. Written informed consent were obtained from every participant or his or her legal surrogates before enrollment.

Cirrhosis was diagnosed according to a computed tomography/magnetic resonance imaging scan, clinical symptoms, laboratory tests and medical history[12]. AD was defined as ascites, variceal hemorrhage, hepatic encephalopathy (HE), infection and jaundice within 1 mo[13]. The diagnosis of AILD was exclusionary. The following patients were excluded: Coinfections with other viruses [hepatitis A virus, hepatitis B virus (HBV), hepatitis C virus and hepatitis E virus], alcoholic liver disease, nonalcoholic fatty liver disease, schistosomiasis, metabolic liver diseases, chronic drug-induced liver disease, and cryptogenic liver disease.

PBC was defined according to the American Association for the Study of Liver Diseases clinical guidance in 2008[14], with at least 2 of the following: (1) Elevated serum alkaline phosphatase (ALP) [> 1.5 folds the upper limit of normal (ULN)] or gamma glutamyl transpeptidase (GGT) (> 3 ULN); (2) Positive test for antimitochondrial antibodies (AMA) (titer > 1:40); and (3) Compatible liver biopsy suggestive of suppurative destructive cholangitis (ductopenia, cholestasis, fibrosis and portal inflammation). AIH was defined based on simplified criteria (score > 6) proposed by the International

Autoimmune Hepatitis Group in 2008[15]. PBC/AIH overlap syndrome was strictly diagnosed according to the Paris Criteria proposed by Chazouillères *et al*[16] in 1998, which associated PBC and AIH either synchronously or consecutively. Presence of at least 2 of the 3 criteria was required. PBC criteria were the following: (1) ALP > 2 ULN or GGT > 5 ULN; (2) A positive serology for AMA; and (3) A liver biopsy specimen indicating florid bile duct lesions. AIH criteria were the following: (1) Serum alanine transaminase (ALT) > 5 ULN; (2) IgG > 2 ULN or a positive serology for anti-smooth muscle antibodies; and (3) A liver biopsy indicating moderate to severe periportal or periseptal lymphocytic piecemeal interface hepatitis.

Some uncommon etiologies of AILD in this study, such as PSC, PBC-PSC overlap syndrome, AIH-PSC overlap syndrome and IgG4-RD were categorized into a "others" group, as the number of cases of "others" was quite small to allow robust statistical analysis. Acute-on-chronic liver failure (ACLF) was diagnosed based on the European Association for the Study of the Liver (EASL) criteria[17]. Just as follows: (1) ACLF grade 1: Single kidney failure or single cerebral failure with renal dysfunction (1.5 mg/dL < creatinine < 1.9 mg/dL) or other single organ failure [serum bilirubin ≥ 12 mg/dL for liver; (international normalized ratio) INR = 2.5 for coagulation; vasopressors to maintain arterial pressure for circulation; $PaO_2/FiO_2 \leq 200$ or $SpO_2/FiO_2 \leq 214$ for respiration] with renal dysfunction and/or mild HE; (2) ACLF grade 2: The presence of 2 organ failures; and (3) ACLF grade 3: The failure no less than 3 organs.

Data collection

Demographics, medical history, imagological examination and laboratory parameters were obtained from every participant on admission. Participants were regularly followed up for 28 d, 90 d and 365 d until death or liver transplantation (LT). Development of ACLF was assessed on admission and during hospitalization within 28 d, respectively. The primary outcome of this study was 90-d LT-free mortality. The secondary outcome was ACLF development during 28-d hospitalization.

Statistical analysis

Continuous variables were summarized as mean (SD) or median (interquartile range) according to their distribution, while categorical variables were summarized as frequency (proportion). Comparisons between four groups were performed using Kruskal-Wallis test for continuous variables, Chi-square test or Fisher's exact test for categorical variables. The impact of the etiology of AILD on short-term mortality were analyzed using a multivariable logistic regression model, adjusting for potential confounders, including demographics (age, sex) and AD events (HE, gastrointestinal bleeding, infection and ascites). Logistic regression was also used to determine the risk factors for 90-d mortality and ACLF development during hospitalization. Variables with P values less than 0.1 were included in the multivariate logistic regression model[18,19]. All continuous variables were log2 transformed before entering the model. Two-tailed P values of 0.05 were considered statistically significant. Statistical analysis was conducted using R 3.6.2 and SPSS 19.0.

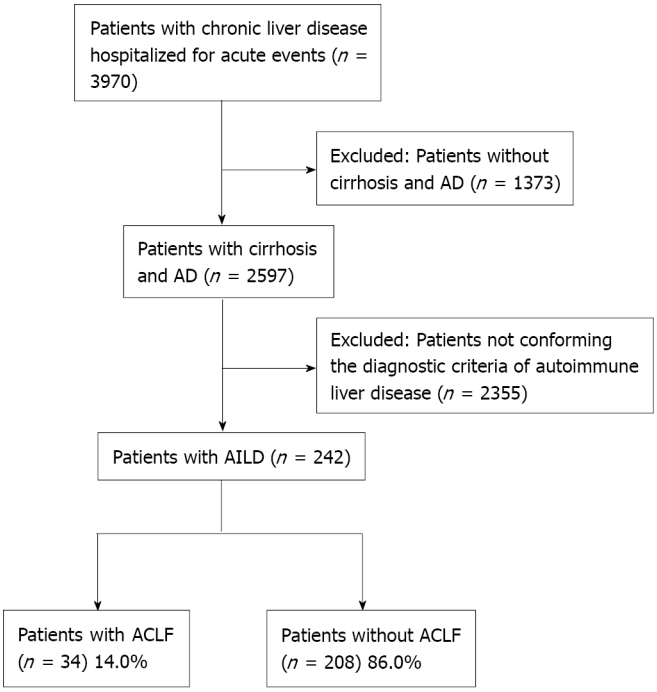
RESULTS

Prevalence of AILD and ACLF in patients with cirrhosis and AD

A total of 3970 patients from CATCH-LIFE study were screened, 2597 of whom had cirrhosis and AD. Eventually, 242 patients conforming the diagnostic criteria of AILD were finally enrolled (Figure 1). In patients with cirrhosis and AD, the overall prevalence of AILD was 9.3% (242/2597). Prevalence of ACLF was significantly lower in AILD cases (14%) than those with all etiology groups with cirrhosis and AD (22.8%) ($P < 0.001$). Distribution of participating centers in this study and number of AILD patients enrolled from each center were displayed in Figures 2A and 2B, respectively. Among the 242 enrolled AILD patients, 234 (96.6%) are from eastern China, where 94% of Chinese population resides; 8 (3.4%) are from western China, where 6% of Chinese population resides. Due to Renji Hospital accounted for 60.3% (146/242) of the total enrolled patients, we further analyzed district distribution of patients enrolled from Renji Hospital. Actually, these patients were from 20 different district all over the country (Figure 2C), the number of patients from each district was shown in Figure 2D. Distribution of patients enrolled from Renji Hospital were also consistent with population density distribution (divided by Hu Line) in China.

Baseline characteristics and outcomes among different etiologies in AILD patients

Baseline characteristics of 242 AILD patients with cirrhosis and AD categorized by etiology are depicted in Table 1. 123 (50.8%) patients showed PBC, 69 (28.5%) displayed AIH, 29 (12.0%) had AIH-PBC overlap syndrome (AIH/PBC) and 21 (8.7%) patients manifested other uncommon etiologies of AILD. Most patients were female (81.0%) and their mean age was 56.04 years. Patients with PBC/AIH had higher white blood cell ($P < 0.001$) and neutrophil-lymphocyte (NL) ratio ($P < 0.001$) levels than patients with PBC, AIH or others. ALT ($P < 0.001$) and AST ($P = 0.04$) levels were higher in the AIH/PBC group.



DOI: 10.3748/wjg.v28.i31.4417 **Copyright** ©The Author(s) 2022.

Figure 1 Flow chart of the study. AD: Acute decompensation; AILD: Autoimmune liver disease; ACLF: Acute-on-chronic liver failure.

In addition, the PBC group tended to have lower hemoglobin (P = 0.003) and higher ALP (P < 0.001) levels than other AILD etiologies.

Baseline characteristics of 34 ACLF patients categorized by etiology are shown in Table 2. PBC (41.2%) was still the most common etiology among ACLF patients with AILD, followed by AIH (29.4%), AIH/PBC overlap syndrome (20.6%) and others (8.8%). However, as the number of patients in some subgroups was small, the results may not be robust and require further validation in a larger population. At the end of 28-d and 90-d, no patients were lost to follow up. At the end of 365-d, 3 (1.2%) patients were lost to follow-up. Short-term (28-d, 90-d and 365-d) LT-free mortality of AILD patients with cirrhosis and AD are presented in Figure 3. Generally, among AILD patients with cirrhosis and AD, 90-d LT-free mortality were 17%. AIH/PBC had higher 28-d, 90-d and 365-d mortality, although the results were not statistically significant. Among patients with AILD-related ACLF, 28-d and 90-d mortality were 43.8% and 80.0%, respectively.

The impact of etiology on mortality

To investigate the effect of etiology on short-term (28-d, 90-d and 365-d) LT-free mortality in AILD patients with cirrhosis and AD, we constructed 3 models to gradually control other potential confounding factors (Table 3). Both univariate (unadjusted) and multivariate (adjusted I and adjusted II) analyses showed that compared to PBC, AIH patients were at lower risk for death at 90-d and 365-d, whereas PBC/AIH patients were at higher risk for death at all time periods. However, none of the associations were statistically significant. Subgroup analysis was conducted according to Child Turcotte Pugh and model for end-stage liver disease (MELD) score, there was no heterogeneity in the impact of etiology types on 90-d LT-free mortality in different AILD subgroups, as was shown in Supplementary Figure 1.

Risk factors of short-term mortality in AILD patients with cirrhosis and AD

Logistic regression model was conducted to assess the risk factors for 90-d LT-free mortality. Univariable analysis identified 10 variables on admission correlated with 90-d prognosis: Bacterial infection, HE, total bilirubin (TB), INR, blood urea nitrogen (BUN), albumin, ALT, white blood cell, NL-ratio and sodium (Supplementary Table 1). Variables with P < 0.1 were selected into multivariable model for further analysis. Only HE, TB and BUN were found to be independently associated with 90-d mortality in AILD patients with cirrhosis and AD (Figure 4). We also investigated risk factors for ACLF development during hospitalization (Table 4). 21 ACLF patients diagnosed on admission were excluded from analysis. Multivariable analysis revealed that only TB (P = 0.046) and INR (P = 0.048) independently correlated with ACLF development.

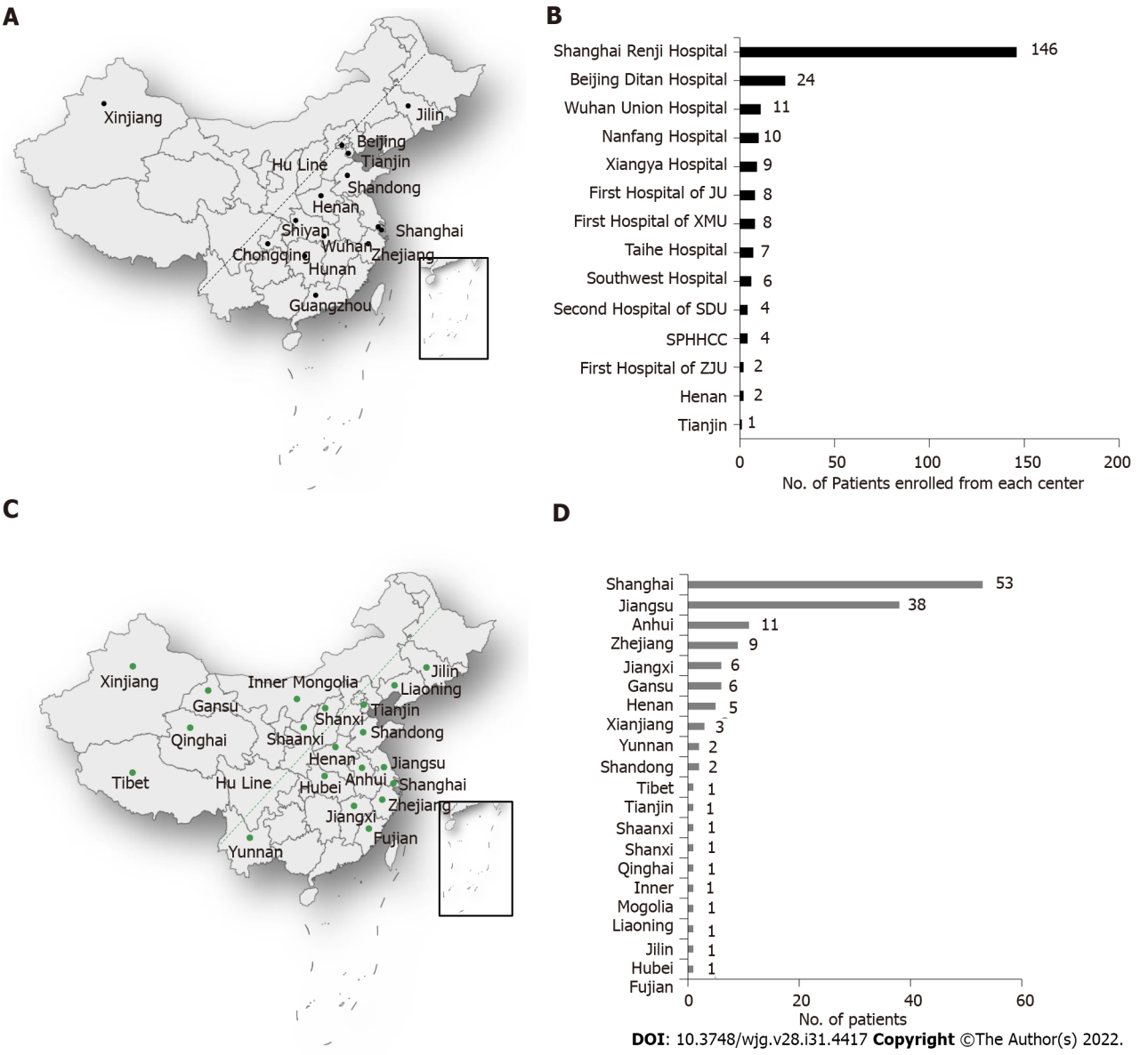
Table 1 Characteristics of autoimmune liver disease patients with cirrhosis and acute decompensation among different etiologies

	PBC	AIH	PBC/AIH	Others	*P* value
	n = 123	*n* = 69	*n* = 29	*n* = 21	
Demographics					
Age	56.00 (48.02, 63.83)	57.47 (49.33, 65.34)	52.62 (45.53, 60.85)	52.94 (41.15, 62.48)	0.28
Male, no. (%)	25 (20.3)	11 (15.9)	4 (13.8)	6 (28.6)	0.51
AD, no. (%)					
Bacterial infection	34 (27.6)	21 (30.4)	13 (44.8)	8 (38.1)	0.30
Ascites	82 (66.7)	42 (60.9)	17 (58.6)	14 (66.7)	0.77
Gastrointestinal bleeding	27 (22.0)	11 (15.9)	4 (13.8)	2 (9.5)	0.42
Hepatic encephalopathy	10 (8.1)	4 (5.8)	6 (20.7)	3 (14.3)	0.11
Jaundice	61 (49.6)	35 (50.7)	19 (65.5)	9 (42.9)	0.38
Laboratory results, median (IQR)					
TB, mg/dL	4.88 (1.60, 10.82)	5.15 (1.86, 11.14)	7.31 (3.04, 23.60)	4.88 (2.05, 11.72)	0.17
INR	1.29 (1.13, 1.52)	1.39 (1.23, 1.64)	1.39 (1.16, 1.49)	1.24 (1.15, 1.44)	0.044
Creatinine, mg/dL	0.65 (0.50, 0.88)	0.64 (0.51, 0.76)	0.67 (0.53, 0.79)	0.67 (0.45, 0.73)	0.51
Blood urea nitrogen, mmol/L	5.38 (3.70, 8.27)	4.73 (3.63, 5.95)	5.37 (3.90, 7.20)	4.50 (3.37, 6.60)	0.26
White blood cell, 10^9/L	4.39 (2.75, 6.34)	4.01 (2.81, 5.78)	6.85 (4.56, 11.76)	3.82 (3.10, 5.72)	0.001
Neutrophil-lymphocyte ratio	2.80 (1.73, 4.29)	2.00 (1.25, 3.25)	3.61 (3.01, 5.67)	2.89 (2.35, 4.86)	< 0.001
Platelet, 10^9/L	0.17 (0.11, 0.30)	0.15 (0.11, 0.25)	0.32 (0.14, 0.45)	0.12 (0.08, 0.30)	0.11
Albumin, g/L	30.30 (25.70, 33.70)	28.50 (25.70, 32.55)	29.90 (26.10, 33.80)	30.40 (28.45, 34.92)	0.262
ALT, IU/L	48.00 (24.50, 80.50)	59.00 (37.00, 116.00)	81.00 (61.00, 148.00)	57.90 (39.00, 85.40)	< 0.001
AST, IU/L	79.60 (48.40, 124.50)	87.00 (52.90, 187.00)	120.70 (79.00, 153.00)	90.00 (39.00, 148.00)	0.037
Hemoglobin, g/L	90.00 (68.00, 110.00)	99.00 (87.00, 119.00)	99.00 (85.00, 115.00)	98.00 (89.00, 112.00)	0.003
ALP, IU/L	208.50 (136.25, 313.00)	143.00 (105.74, 181.70)	175.50 (128.50, 243.00)	202.50 (133.50, 298.85)	< 0.001
GGT, IU/L	105.00 (51.23, 192.50)	86.63 (37.00, 126.00)	106.20 (58.70, 235.25)	122.70 (32.92, 220.22)	0.19
Pre-albumin, mg/L	78.30 (46.80, 113.90)	63.20 (40.93, 83.25)	77.30 (57.75, 97.80)	68.65 (54.75, 88.90)	0.25
Score, median (IQR)					
Child Turcotte Pugh	9.00 (8.00, 10.00)	9.00 (8.00, 10.25)	10.00 (8.00, 11.00)	9.00 (8.00, 11.00)	0.58
MELD	11.00 (7.00, 17.00)	15.00 (11.00, 21.00)	18.00 (14.00, 23.00)	12.00 (10.00, 16.00)	< 0.001
MELD Na	14.00 (7.75, 19.00)	17.00 (12.00, 23.00)	20.50 (15.75, 25.00)	13.00 (10.00, 19.00)	< 0.001
CLIF SOFA	5.00 (3.00, 6.00)	5.00 (3.00, 6.00)	6.00 (3.00, 7.00)	5.00 (4.00, 6.00)	0.44

PBC: Primary biliary cirrhosis; AIH: Autoimmune hepatitis; PBC/AIH: Primary biliary cirrhosis-autoimmune hepatitis overlap syndrome; AD: Acute decompensation; IQR: Interquartile range; TB: Total bilirubin; INR: International normalized ratio; ALT: Alanine transaminase; AST: Aspartate transaminase; ALP: Alkaline phosphatase; GGT: Gamma glutamyl transpeptidase; MELD: Model for end-stage liver disease; CLIF-SOFA: Chronic liver failure-sequential organ failure assessment.

DISCUSSION

The current study is the first nationwide investigation of the prevalence and short-term outcome of end-stage AILD in China, which is a traditional HBV high endemic area. Our study showed that the overall prevalence of AILD was 9.3% in tertiary hospitalized patients with cirrhosis and AD. PBC was responsible for half of AILD cases. The prevalence of ACLF was significantly lower in AILD patients than those with all etiology groups with cirrhosis and AD. Short-term mortality were extremely high in AILD-related ACLF.



DOI: 10.3748/wjg.v28.i31.4417 **Copyright** ©The Author(s) 2022.

Figure 2 Distribution and the number of autoimmune liver disease patients enrolled from each of center and from Renji Hospital. A: District distribution of each enrolled center; B: The number of patients enrolled from center; C: Population distribution of patients from Renji Hospital; D: The number of patients enrolled from each of the 20 districts. Approximately 94% of the total Chinse population resides east of the dividing line (Hu Line) in the figure, and 6% resides west of the line; 13 centers lie in eastern China, and 1 lies in western China.

EASL-CLIF study reported that the prevalence of ACLF was 30.9% in alcohol-related cirrhosis and AD, whereas COSSH study showed that the prevalence of ACLF reached up to 26.2% in patients with HBV-related cirrhosis and AD[17,20]. However, in this study, among 242 AILD patients with cirrhosis and AD, only 34 (14%) had ACLF, the prevalence was significantly lower than that of patients with other etiology types. One plausible explanation may be that AILD patients have distinct clinical characteristics (higher severity, higher prevalence of infection and lower prevalence of organ failures) that differ distinctly from those of patients with other etiologies, which led to lower prevalence of ACLF but higher short-term mortality.

Despite having higher levels of inflammation and liver injury, PBC/AIH had similar short-term mortality rates compared to PBC individually after adjusting for confounding factors. Neuhauser *et al* [21] and Yang *et al*[22] showed that a more aggressive clinical course and worse clinical consequences were observed in patients with PBC/AIH than patients with pure PBC. Based on these results, some experts suggested that PBC/AIH should be identified and aggressively treated. Notably, these studies only evaluate the univariate prognostic value of etiology and did not take confounders into consideration. It is, therefore, likely that they fail to objectively reveal the independent impact of etiology on the prognosis of AILD. PBC, AIH and PBC/AIH are all complex disorders but result in significant morbidity and mortality. Once progressed to liver failure, no effective treatment is clinically available. Herein, our results clearly showed that presence of HE, higher TB and BUN levels, rather than liver disease etiologies, were independently associated with short-term mortality in AILD patients with

Table 2 Characteristics of autoimmune liver disease patients with acute-on-chronic liver failure according to etiology

Variable	PBC	AIH	PBC/AIH	Others	*P* value
	n = 14	*n* = 10	*n* = 7	*n* = 3	
Demographics					
Age, median (IQR)	55.34 (48.88, 58.96)	55.94 (50.00, 64.01)	53.46 (47.97, 63.46)	50.85 (46.87, 58.00)	0.88
Male, no. (%)	6 (42.9)	1 (10.0)	0 (0.0)	2 (66.7)	0.04
AD, no. (%)					
Bacterial infection	7 (50.0)	3 (30.0)	6 (85.7)	2 (66.7)	0.14
Ascites	9 (64.3)	6 (60.0)	5 (71.4)	3 (100.0)	0.61
Gastrointestinal bleeding	1 (7.1)	1 (10.0)	0 (0.0)	1 (33.3)	0.39
Hepatic encephalopathy	4 (28.6)	3 (30.0)	4 (57.1)	2 (66.7)	0.40
Jaundice	10 (71.4)	9 (90.0)	6 (85.7)	2 (66.7)	0.64
Laboratory results, median (IQR)					
TB, mg/dL	16.78 (4.79, 27.10)	12.56 (8.94, 17.64)	23.60 (14.64, 27.52)	14.56 (8.94, 19.29)	0.71
INR	1.57 (1.34, 1.77)	2.64 (1.67, 2.80)	1.49 (1.44, 2.31)	1.50 (1.47, 1.97)	0.35
Creatinine, mg/dL	0.83 (0.79, 2.01)	0.58 (0.50, 0.74)	0.79 (0.75, 0.84)	0.68 (0.36, 1.46)	0.08
Blood urea nitrogen, mmol/L	12.05 (6.04, 20.65)	5.40 (2.74, 8.12)	7.70 (7.20, 9.25)	8.73 (6.92, 21.00)	0.09
White blood cell, 10^9/L	5.55 (3.62, 10.19)	4.57 (3.13, 5.34)	8.82 (6.55, 16.27)	6.71 (4.91, 9.37)	0.08
Neutrophil-lymphocyte ratio	4.55 (3.78, 5.84)	1.80 (1.06, 4.40)	7.64 (5.66, 12.77)	5.40 (4.86, 6.30)	0.05
Albumin, g/L	28.90 (26.75, 33.72)	27.80 (25.38, 31.48)	27.20 (25.05, 28.60)	27.40 (25.00, 31.15)	0.60
ALT, IU/L	105.15 (33.30, 186.90)	59.05 (38.65, 99.47)	113.90 (102.60, 204.10)	69.90 (57.55, 146.65)	0.37
AST, IU/L	121.50 (62.72, 182.23)	99.45 (61.10, 172.75)	153.00 (111.65, 238.05)	34.20 (30.30, 85.15)	0.33
Hemoglobin, g/L	88.00 (40.75, 138.00)	64.00 (33.00, 116.00)	65.00 (46.00, 77.50)	57.00 (55.20, 74.50)	0.89
ALP, IU/L	76.00 (69.00, 96.25)	86.50 (82.00, 90.75)	108.00 (89.00, 127.50)	91.40 (65.80, 102.90)	0.29
GGT, IU/L	187.00 (111.25, 252.80)	149.00 (125.65, 195.00)	153.00 (109.00, 365.00)	NA (NA, NA)	0.76
Pre-albumin, mg/L	89.00 (52.00, 119.57)	106.50 (45.25, 116.50)	63.00 (58.70, 258.60)	NA (NA, NA)	0.85
Albumin, g/L	66.50 (54.60, 115.00)	33.40 (23.55, 60.40)	87.65 (60.35, 91.55)	NA (NA, NA)	0.13
Score, median (IQR)					
Child Turcotte Pugh	9.50 (8.25, 10.75)	12.00 (10.00, 12.75)	11.00 (10.50, 12.50)	11.00 (11.00, 12.50)	0.04
MELD	20.00 (18.00, 22.75)	27.50 (18.50, 28.75)	24.00 (22.00, 28.00)	21.00 (20.50, 23.00)	0.17
MELD Na	21.00 (19.00, 25.00)	26.50 (23.00, 28.75)	29.00 (23.00, 32.00)	41.00 (39.00, 41.50)	0.12
CLIF SOFA	7.00 (6.25, 8.00)	7.00 (7.00, 8.00)	8.00 (6.50, 9.00)	9.00 (8.00, 10.00)	0.32

PBC: Primary biliary cirrhosis; AIH: Autoimmune hepatitis; PBC/AIH: Primary biliary cirrhosis-autoimmune hepatitis overlap syndrome; AD: Acute decompensation; IQR: Interquartile range; TB: Total bilirubin; INR: International normalized ratio; ALT: Alanine transaminase; AST: Aspartate transaminase; ALP: Alkaline phosphatase; GGT: Gamma glutamyl transpeptidase; MELD: Model for end-stage liver disease; CLIF-SOFA: Chronic liver failure-sequential organ failure assessment; NA: Not available.

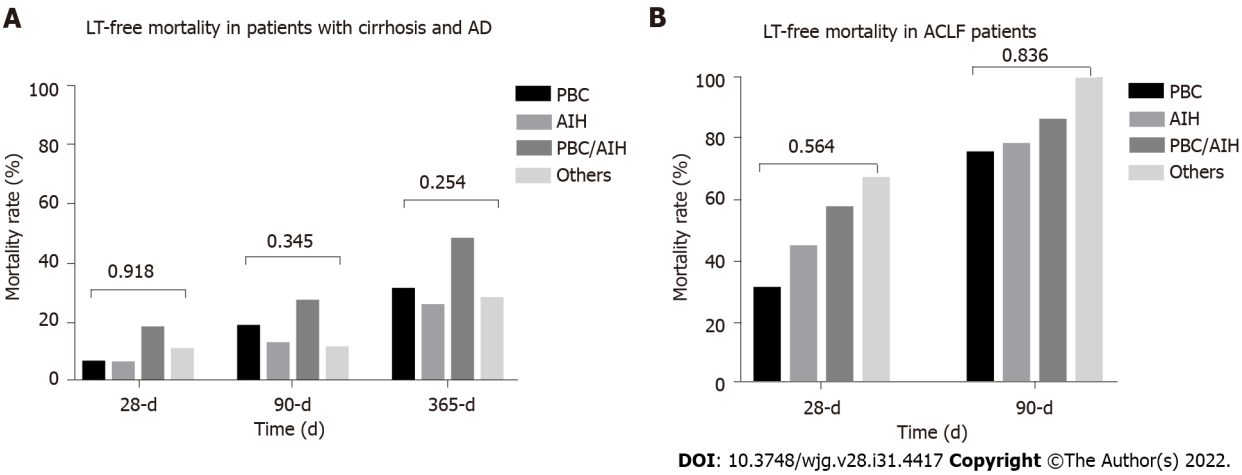
cirrhosis and AD. Therefore, in clinical management of AILD, physicians are supposed to pay more attention to the presence of HE and closely monitor the changes of liver and renal function.

This study had several strengths. With national samples, our multicenter data provided an overview of epidemiological features of end-stage AILD in China, where it is considered uncommon. Thus, we presented a national view of the disease. Indeed, most of the studies in this field originated from single center or other geographic areas[7,23-25]. We focused on the role of the etiology on short-term mortality. Moreover, we clarified that HE, TB and BUN were significant risk factors of short-term mortality in AILD patients with cirrhosis and AD. These data will be an important complement to the public epidemiological data of AILDs in Asian-Pacific regions.

Table 3 The impact of etiology on liver transplantation-free mortality in acute-on-chronic liver failure patients with cirrhosis and acute decompensation (primary biliary cirrhosis as a reference)

	n	Num of death (percentage)	Unadjusted OR (95%CI), *P* value	Adjusted I[1], OR (95%CI), *P* value	Adjusted II[2], OR (95%CI), *P* value
28-d LT-free mortality					
PBC	111	7 (6.3)	1.0	1.0	1.0
AIH	67	4 (6.0)	0.94 (0.24-3.25), 0.93	0.94 (0.24-3.24), 0.92	1.26 (0.3-4.85), 0.74
PBC/AIH	28	5 (17.9)	3.23 (0.89-11.05), 0.06	3.43 (0.93-11.93), 0.05	2.61 (0.63-10.21), 0.17
Others	19	2 (10.5)	1.75 (0.25-7.99), 0.51	1.75 (0.24-8.13), 0.51	1.46 (0.17-8.28), 0.70
90-d LT-free mortality					
PBC	103	19 (18.4)	1.0	1.0	1.0
AIH	64	8 (12.5)	0.63 (0.25-1.50), 0.31	0.64 (0.25-1.53), 0.33	0.74 (0.27-1.88), 0.54
PBC/AIH	26	7 (26.9)	1.63 (0.57-4.31), 0.34	1.70 (0.59-4.56), 0.30	1.18 (0.36-3.56), 0.77
Others	18	2 (11.1)	0.55 (0.08-2.17), 0.45	0.51 (0.08-2.02), 0.40	0.44 (0.05-2.08), 0.36
365-d LT-free mortality					
PBC	97	30 (30.9)	1.0	1.0	1.0
AIH	63	16 (25.4)	0.76 (0.37-1.54), 0.45	0.76 (0.36-1.53), 0.44	0.81 (0.38-1.68), 0.58
PBC/AIH	23	11 (47.8)	2.05 (0.9-5.20), 0.13	2.06 (0.81-5.24), 0.13	1.72 (0.63-4.61), 0.28
Others	18	5 (27.8)	0.86 (0.26-2.51), 0.79	0.89 (0.26-2.62), 0.84	0.82 (0.24-2.49), 0.74

[1]Adjusted age, gender.
[2]Adjusted age, gender, hepatic encephalopathy, ascites, infection and gastrointestinal bleeding.
OR: Odds ratio; CI: Confidence interval; PBC: Primary biliary cirrhosis; AIH: Autoimmune hepatitis; PBC/AIH: Primary biliary cirrhosis-autoimmune hepatitis overlap syndrome; LT: Liver transplantation.



DOI: 10.3748/wjg.v28.i31.4417 **Copyright** ©The Author(s) 2022.

Figure 3 Outcomes of autoimmune liver disease patients with acute decompensated cirrhosis and acute-on-chronic liver failure. A: Liver transplantation (LT)-free mortality in patients with cirrhosis and acute decompensation; B: LT-free mortality in patients with acute-on-chronic liver failure. LT: Liver transplantation; PBC: Primary biliary cirrhosis; AIH: Autoimmune hepatitis; PBC/AIH: Primary biliary cirrhosis-autoimmune hepatitis overlap syndrome; AD: Acute decompensation; ACLF: Acute-on-chronic liver failure.

There were still several limitations in our study. First, since AILD is a relatively rare disease, the number of patients recruited in our study was not quite large, especially ACLF patients. The limited sample size could also slightly reduce the accuracy of the results of risk factor analysis. Second, one of our centers, Renji hospital, is a nationwide center of AILD. Thus, some degree of selection bias could be present in the prevalence rates of AILD due to the participation of this center. However, our further

Table 4 Association of risk factors with acute-on-chronic liver failure development during hospitalization using logistic regression in univariate and multivariate analysis

	OR	95%CI	*P* value
Univariable logistic regression			
Demographic data			
Age	0.96	0.21-6.18	0.96
Male	2.89	0.83-9.17	0.08
Etiology	0.90	0.43-1.70	0.76
Acute decompensation events			
Overt ascites	0.92	0.3-3.14	0.89
Gastrointestinal bleeding	0.74	0.11-2.9	0.7
Bacterial infection	2.22	0.69-6.95	0.17
Hepatic encephalopathy	3.6	0.51-15.95	0.13
Laboratory data			
Total bilirubin	1.68	1.14-2.61	0.012
International normalized ratio	6.53	1.9-28.55	0.006
Creatinine	0.85	0.51-1.87	0.6
Blood urea nitrogen	1.52	0.84-2.63	0.12
Albumin	0.44	0.07-3.19	0.4
ALT	1.25	0.85-1.82	0.24
AST	1.14	0.73-1.75	0.55
White blood cells	0.88	0.45-1.75	0.72
Hemoglobin	0.39	0.11-1.5	0.16
K	1.53	0.13-18.28	0.74
Sodium	0	0-288.55	0.29
Neutrophil-lymphocyte ratio	1.37	0.84-2.23	0.21
ALP	1.15	0.59-2.27	0.7
GGT	0.86	0.54-1.34	0.52
Multivariable logistic regression			
Male	3.24	0.84-11.63	0.07
TB	1.56	1.03-2.47	0.046
INR	4.31	1.15-21.70	0.048

Variables with $P < 0.1$ in univariate analysis were selected into multivariate analysis. Acute-on-chronic liver failure diagnosed on admission was excluded from the analysis. Continuous variables were log transformed before entering the model (base 2). ALT: Alanine transaminase; AST: Aspartate transaminase; ALP: Alkaline phosphatase; GGT: Gamma glutamyl transpeptidase; OR: Odds ratio; CI: Confidence interval; TB: Total bilirubin; INR: International normalized ratio.

analysis showed that patients recruited from Renji Hospital were from 20 different districts all over the country, the population distribution of these patients were also consistent with that of Chinese population density.

CONCLUSION

In conclusion, our study showed that AILD was not rare in China. The etiology of AILD had no significant impact on short-term mortality in AILD patients with cirrhosis and AD. HE, elevated levels of TB and BUN were significantly associated with high 90-d mortality in these patients. Strategies are

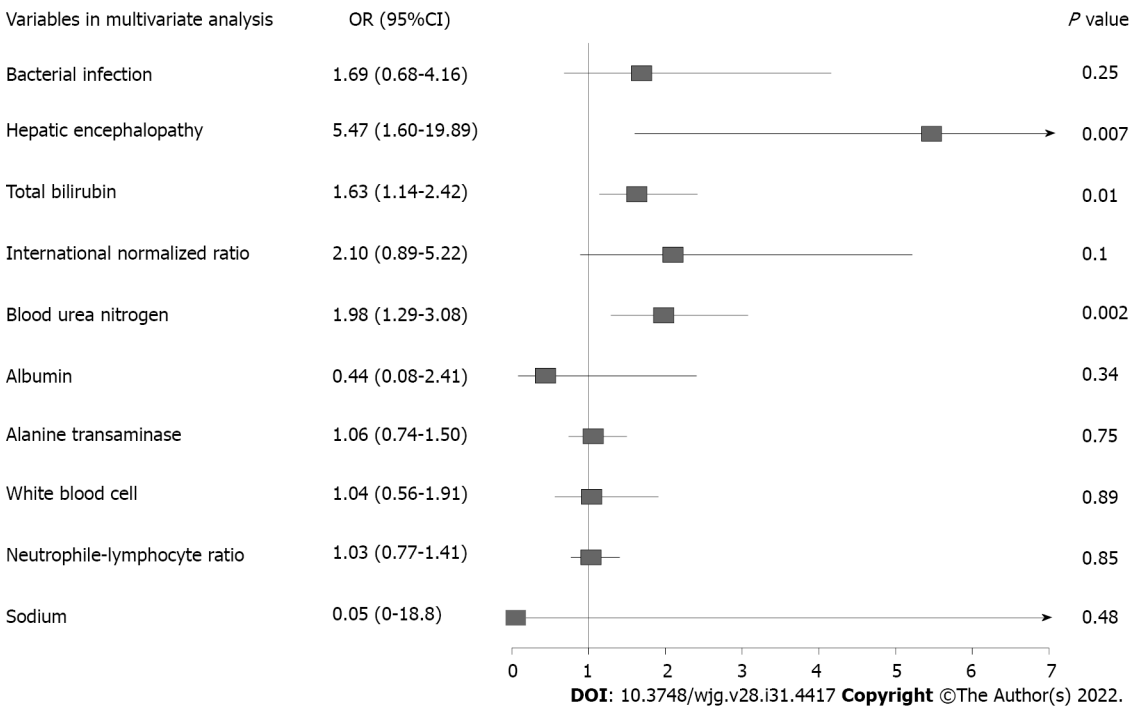


Figure 4 Multivariate analysis of 90-d liver transplantation free mortality in autoimmune liver disease patients with cirrhosis and acute decompensation. OR: Odds ratio; CI: Confidence interval.

needed to the presence of HE and closely monitor the changes of liver and renal function in clinical practice. These data will be a crucial complement to the public epidemiology of AILD in Asian-Pacific regions.

ARTICLE HIGHLIGHTS

Research background

Epidemiological research on autoimmune liver disease (AILD) in patients with end-stage liver disease is sparse in Asian-pacific areas.

Research motivation

This study aimed to provide a national view of epidemiological features of end-stage AILD in China.

Research objectives

To investigate the disease burden and risk factor of short-term mortality in AILD patients with cirrhosis and acute decompensation (AD), and thus provide clues on clinical management.

Research methods

Data were collected from two prospective, multicenter cohorts which enrolled patients with chronic liver disease and acute exacerbation from China. Logistic regression model was conducted to analyze risk factors.

Research results

The overall prevalence of AILD was 9.3% (242/2597) in patients with cirrhosis and AD, among which primary biliary cirrhosis was the most prevalent type. The etiology of AILD had no significant impact on short-term mortality in patients with cirrhosis and AD in univariate and multivariate analysis. Total bilirubin, hepatic encephalopathy (HE) and blood urea nitrogen independently correlated with 90-d LT-free mortality in multivariate analysis.

Research conclusions

AILD was not rare in hospitalized patients with cirrhosis and AD in China. 90-d mortality was independently associated with severity of the disease.

Research perspectives

In clinical management of AILD, strategies are needed to prevent presence of HE and closely monitor the changes of liver and renal function.

ACKNOWLEDGEMENTS

We acknowledge the following Chinese (Acute on) Chronic Liver Failure Consortium members and participants for their hard work. Department of Gastroenterology, Renji Hospital, School of Medicine, Shanghai Jiao Tong University - Shi-Jin Wang, Wen-Yi Gu, Liang Qiao, Yan Zhang; Clinical Research Institute, Shanghai Jiao Tong University School of Medicine, Shanghai, China, Zhang Wei-Tuo; Centre of Integrative Medicine, Beijing Ditan Hospital, Capital Medical University - Qun Zhang, Yi-Xin Hou, Yu-Xin Li, Yun-Yi Huang; Department of Infectious Diseases, Southwest Hospital, Third Military Medical University (Army Medical University) - Jie Xia; Yi Zhou; Bao-Yan Xu; Shu-Ning Sun, Yun-Jie Dan, Wen-Ting Tan; Department of Infectious Disease, Hunan Key Laboratory of Viral Hepatitis, Xiangya Hospital, Central South University - Jun Chen, Ruo-Chan Chen, Xiao-Xiao Liu; Department of Infectious Diseases, Institute of Infection and Immunology, Union Hospital, Tongji Medical College, Huazhong University of Science and Technology - Jing Liu, Ling Xu, Shue Xiong; Hepatology Unit, Department of Infectious Diseases, Nan-fang Hospital, Southern Medical University - Xiu-Hua Jiang, Bei-Ling Li, Cong-Yan Zhu; Department of Hepatology, First Hospital of Jilin University - Chang Jiang, Xiao-Yu Wen, Na Gao, Chun-Yan Liu; Department of Infectious Disease, Taihe Hospital, Hubei University of Medicine - Yuan-Yuan Chen, Sen Luo, Qing Lei; Department of Liver Intensive Care Unit, Shanghai Public Health Clinical Centre, Fudan University - Xue Mei, Liu-Juan Ji, Jie-Fei Wang; Department of Infectious Diseases and Hepatology, Second Hospital of Shandong University - Tao Li, Xuan-Qiong Fang, Zi-Yu Wang; Liver Disease Centre, First Affiliated Hospital of Xinjiang Medical University - Rong-Jiu Zheng, Nan Li; Department of Infectious Disease, Henan Provincial People's Hospital - Hui-Ming Jin; Affiliated Hospital of Logistics University of People's Armed Police Force - Hai Li, Qing Zhang, Xue-Qun Zheng; Department of Infectious Diseases, Affiliated Hospital of Logistics University of People's Armed Police Force - Shao-Yang Wang. We thank all the patients participated in the study.

FOOTNOTES

Author contributions: Shen ZX, Wu DD, Xia J, Wang XB, Zheng X, Huang Y and Li BL contributed equally to this work; Ma X and Li H contributed equally to this work; Li H generated the concept and designed the research; all authors acquired the data; Shen ZX, Wu DD performed statistical analysis; Shen ZX, Wu DD, Xia J, Wang XB generated the results; Shen ZX, Wu DD, Zheng X, Huang Y and Li BL interpreted the results; Shen ZX and Wu DD drafted the manuscript which was revised by Ma X and Li H for important intellectual content; Ma X made important contribution patient recruitment; Li H was responsible for administrative, technical, or material support and study supervision; and all authors have access to the data, approved this final version of the manuscript and are accountable for all aspects.

Supported by Shanghai Hospital Development Commission, No. SHDC2020CR1037B; the National Key R&D Program of China, No. 2017YFC0908100; the National Science and Technology Major Project, No. 2018ZX10302206, 2018ZX10723203 and 2017ZX10202202; Shanghai Municipal Education Commission-Guofeng Clinical Medicine Grant, No. 20152213; the National Natural Science Foundation of China, No. 82170629, 81930061, 81900579, 81970550, 82070613, 82070650, and 81972265; Chongqing Natural Science Foundation, No. CSTC2019jcyj-zdxmX0004; Beijing Municipal Science & Technology Commission, No. Z191100006619033; Local Innovative and Research Teams Project of Guangdong Pearl River Talents Program, No. 2017BT01S131; the Foundation for Innovative Research Groups of Hubei Provincial Natural Science Foundation, No. 2018CFA031; and Guangdong Basic and Applied Basic Research Foundation, No. 2020A1515010052.

Institutional review board statement: The study was conducted in accordance with the Declaration of Helsinki. The Medical Ethics Board of Shanghai Renji Hospital, Shanghai, China, approved the studies (ethics codes: [2014]148k and [2016]142k).

Informed consent statement: Informed consent was obtained from all patients for being included in the study.

Conflict-of-interest statement: All authors declare that they have no conflict of interest in this manuscript.

Data sharing statement: Data are available within 1 year after publication upon reasonable request *via* email: aclf_group@163.com.

STROBE statement: The authors have read the STROBE Statement-checklist of items, and the manuscript was

prepared and revised according to the STROBE Statement-checklist of items.

Open-Access: This article is an open-access article that was selected by an in-house editor and fully peer-reviewed by external reviewers. It is distributed in accordance with the Creative Commons Attribution NonCommercial (CC BY-NC 4.0) license, which permits others to distribute, remix, adapt, build upon this work non-commercially, and license their derivative works on different terms, provided the original work is properly cited and the use is non-commercial. See: https://creativecommons.org/Licenses/by-nc/4.0/

Country/Territory of origin: China

ORCID number: Zi-Xuan Shen 0000-0003-0122-3954; Dan-Dan Wu 0000-0002-0453-008X; Jie Xia 0000-0002-9580-7186; Xian-Bo Wang 0000-0002-3593-5741; Xin Zheng 0000-0001-6564-7807; Yan Huang 0000-0002-4747-3740; Bei-Ling Li 0000-0002-0633-5632; Zhong-Ji Meng 0000-0003-0401-535X; Yan-Hang Gao 0000-0002-6836-0614; Zhi-Ping Qian 0000-0003-4641-3348; Feng Liu 0000-0001-7060-3710; Xiao-Bo Lu 0000-0001-5532-7551; Jia Shang 0000-0001-9197-8773; Hua-Dong Yan 0000-0003-2792-7490; Yu-Bao Zheng 0000-0002-2630-2563; Wen-Yi Gu 0000-0002-1615-6064; Yan Zhang 0000-0003-0159-9062; Jian-Yi Wei 0000-0003-3897-6896; Wen-Ting Tan 0000-0002-2884-071X; Yi-Xin Hou 0000-0001-8233-7210; Qun Zhang 0000-0002-6365-0030; Yan Xiong 0000-0001-9356-4777; Cong-Cong Zou 0000-0002-9197-055X; Jun Chen 0000-0001-8320-636X; Ze-Bing Huang 0000-0003-0485-1294; Xiu-Hua Jiang 0000-0002-4646-6186; Sen Luo 0000-0001-5846-6717; Yuan-Yuan Chen 0000-0003-3587-7711; Na Gao 0000-0002-8622-9273; Jing Li 0000-0001-5878-6964; Tao Li 0000-0002-2548-5476; Guo-Hong Deng 0000-0003-1263-7220; Jin-Jun Chen 0000-0003-4275-9149; Xiong Ma 0000-0001-9616-4672; Hai Li 0000-0002-3645-6232.

S-Editor: Wang JJ
L-Editor: A
P-Editor: Wang JJ

REFERENCES

1 **Carbone M**, Neuberger JM. Autoimmune liver disease, autoimmunity and liver transplantation. *J Hepatol* 2014; **60**: 210-223 [PMID: 24084655 DOI: 10.1016/j.jhep.2013.09.020]
2 **Floreani A**, De Martin S, Secchi MF, Cazzagon N. Extrahepatic autoimmunity in autoimmune liver disease. *Eur J Intern Med* 2019; **59**: 1-7 [PMID: 30360943 DOI: 10.1016/j.ejim.2018.10.014]
3 **Chang C**, Tanaka A, Bowlus C, Gershwin ME. The use of biologics in the treatment of autoimmune liver disease. *Expert Opin Investig Drugs* 2020; **29**: 385-398 [PMID: 32102572 DOI: 10.1080/13543784.2020.1733527]
4 **Zhang H**, Yang J, Zhu R, Zheng Y, Zhou Y, Dai W, Wang F, Chen K, Li J, Wang C, Li S, Liu T, Abudumijiti H, Zhou Z, Wang J, Lu W, Xia Y, Lu J, Guo C. Combination therapy of ursodeoxycholic acid and budesonide for PBC-AIH overlap syndrome: a meta-analysis. *Drug Des Devel Ther* 2015; **9**: 567-574 [PMID: 25632224 DOI: 10.2147/DDDT.S74515]
5 **Katsumi T**, Ueno Y. Epidemiology and surveillance of autoimmune hepatitis in Asia. *Liver Int* 2022 [PMID: 34990076 DOI: 10.1111/liv.15155]
6 **Zhang L**, Bai SS. Epidemiological survey of hospitalized patients with primary biliary cirrhosis in urban areas of Hohhot. *World Latest Med Information* 2016; **16**: 6-7
7 **Jeong SH**. Current epidemiology and clinical characteristics of autoimmune liver diseases in South Korea. *Clin Mol Hepatol* 2018; **24**: 10-19 [PMID: 29307132 DOI: 10.3350/cmh.2017.0066]
8 **Abe M**, Mashiba T, Zeniya M, Yamamoto K, Onji M, Tsubouchi H; Autoimmune Hepatitis Study Group-Subgroup of the Intractable Hepato-Biliary Disease Study Group in Japan. Present status of autoimmune hepatitis in Japan: a nationwide survey. *J Gastroenterol* 2011; **46**: 1136-1141 [PMID: 21597932 DOI: 10.1007/s00535-011-0421-y]
9 **Lv T**, Chen S, Li M, Zhang D, Kong Y, Jia J. Regional variation and temporal trend of primary biliary cholangitis epidemiology: A systematic review and meta-analysis. *J Gastroenterol Hepatol* 2021; **36**: 1423-1434 [PMID: 33141955 DOI: 10.1111/jgh.15329]
10 **Gu WY**, Xu BY, Zheng X, Chen J, Wang XB, Huang Y, Gao YH, Meng ZJ, Qian ZP, Liu F, Lu XB, Shang J, Li H, Wang SY, Sun X. Acute-on-Chronic Liver Failure in China: Rationale for Developing a Patient Registry and Baseline Characteristics. *Am J Epidemiol* 2018; **187**: 1829-1839 [PMID: 29762630 DOI: 10.1093/aje/kwy083]
11 **Qiao L**, Wang X, Deng G, Huang Y, Chen J, Meng Z, Zheng X, Shi Y, Qian Z, Liu F, Gao Y, Lu X, Liu J, Gu W, Zhang Y, Wang T, Wu D, Dong F, Sun X, Li H. Cohort profile: a multicentre prospective validation cohort of the Chinese Acute-on-Chronic Liver Failure (CATCH-LIFE) study. *BMJ Open* 2021; **11**: e037793 [PMID: 33419900 DOI: 10.1136/bmjopen-2020-037793]
12 **Tsochatzis EA**, Bosch J, Burroughs AK. Liver cirrhosis. *Lancet* 2014; **383**: 1749-1761 [PMID: 24480518 DOI: 10.1016/S0140-6736(14)60121-5]
13 **Zhang Y**, Xu BY, Wang XB, Zheng X, Huang Y, Chen J, Meng ZJ, Gao YH, Qian ZP, Liu F, Lu XB, Shi Y, Shang J, Li H, Wang SY, Yin S, Sun SN, Hou YX, Xiong Y, Li BL, Lei Q, Gao N, Ji LJ, Li J, Jie FR, Zhao RH, Liu JP, Lin TF, Chen LY, Tan WT, Zhang Q, Zou CC, Huang ZB, Jiang XH, Luo S, Liu CY, Zhang YY, Li T, Ren HT, Wang SJ, Deng GH, Xiong SE, Liu XX, Wang C, Yuan W, Gu WY, Qiao L, Wang TY, Wu DD, Dong FC, Hua J. Prevalence and Clinical Significance of Portal Vein Thrombosis in Patients With Cirrhosis and Acute Decompensation. *Clin Gastroenterol Hepatol* 2020; **18**: 2564-2572.e1 [PMID: 32109631 DOI: 10.1016/j.cgh.2020.02.037]
14 **Lindor KD**, Gershwin ME, Poupon R, Kaplan M, Bergasa NV, Heathcote EJ; American Association for Study of Liver Diseases. Primary biliary cirrhosis. *Hepatology* 2009; **50**: 291-308 [PMID: 19554543 DOI: 10.1002/hep.22906]

15 **Hennes EM**, Zeniya M, Czaja AJ, Parés A, Dalekos GN, Krawitt EL, Bittencourt PL, Porta G, Boberg KM, Hofer H, Bianchi FB, Shibata M, Schramm C, Eisenmann de Torres B, Galle PR, McFarlane I, Dienes HP, Lohse AW; International Autoimmune Hepatitis Group. Simplified criteria for the diagnosis of autoimmune hepatitis. *Hepatology* 2008; **48**: 169-176 [PMID: 18537184 DOI: 10.1002/hep.22322]

16 **Chazouillères O**, Wendum D, Serfaty L, Montembault S, Rosmorduc O, Poupon R. Primary biliary cirrhosis-autoimmune hepatitis overlap syndrome: clinical features and response to therapy. *Hepatology* 1998; **28**: 296-301 [PMID: 9695990 DOI: 10.1002/hep.510280203]

17 **Moreau R**, Jalan R, Gines P, Pavesi M, Angeli P, Cordoba J, Durand F, Gustot T, Saliba F, Domenicali M, Gerbes A, Wendon J, Alessandria C, Laleman W, Zeuzem S, Trebicka J, Bernardi M, Arroyo V; CANONIC Study Investigators of the EASL–CLIF Consortium. Acute-on-chronic liver failure is a distinct syndrome that develops in patients with acute decompensation of cirrhosis. *Gastroenterology* 2013; **144**: 1426-1437, 1437.e1 [PMID: 23474284 DOI: 10.1053/j.gastro.2013.02.042]

18 **Jalan R**, Stadlbauer V, Sen S, Cheshire L, Chang YM, Mookerjee RP. Role of predisposition, injury, response and organ failure in the prognosis of patients with acute-on-chronic liver failure: a prospective cohort study. *Crit Care* 2012; **16**: R227 [PMID: 23186071 DOI: 10.1186/cc11882]

19 **Montalvo M**, Mistry E, Chang AD, Yakhkind A, Dakay K, Azher I, Kaushal A, Mistry A, Chitale R, Cutting S, Burton T, Mac Grory B, Reznik M, Mahta A, Thompson BB, Ishida K, Frontera J, Riina HA, Gordon D, Parella D, Scher E, Farkas J, McTaggart R, Khatri P, Furie KL, Jayaraman M, Yaghi S. Predicting symptomatic intracranial haemorrhage after mechanical thrombectomy: the TAG score. *J Neurol Neurosurg Psychiatry* 2019; **90**: 1370-1374 [PMID: 31427365 DOI: 10.1136/jnnp-2019-321184]

20 **Wu T**, Li J, Shao L, Xin J, Jiang L, Zhou Q, Shi D, Jiang J, Sun S, Jin L, Ye P, Yang L, Lu Y, Li T, Huang J, Xu X, Chen J, Hao S, Chen Y, Xin S, Gao Z, Duan Z, Han T, Wang Y, Gan J, Feng T, Pan C, Li H, Huang Y, Xie Q, Lin S, Li L; Chinese Group on the Study of Severe Hepatitis B (COSSH). Development of diagnostic criteria and a prognostic score for hepatitis B virus-related acute-on-chronic liver failure. *Gut* 2018; **67**: 2181-2191 [PMID: 28928275 DOI: 10.1136/gutjnl-2017-314641]

21 **Neuhauser M**, Bjornsson E, Treeprasertsuk S, Enders F, Silveira M, Talwalkar J, Lindor K. Autoimmune hepatitis-PBC overlap syndrome: a simplified scoring system may assist in the diagnosis. *Am J Gastroenterol* 2010; **105**: 345-353 [PMID: 19888204 DOI: 10.1038/ajg.2009.616]

22 **Yang F**, Wang Q, Wang Z, Miao Q, Xiao X, Tang R, Chen X, Bian Z, Zhang H, Yang Y, Sheng L, Fang J, Qiu D, Krawitt EL, Gershwin ME, Ma X. The Natural History and Prognosis of Primary Biliary Cirrhosis with Clinical Features of Autoimmune Hepatitis. *Clin Rev Allergy Immunol* 2016; **50**: 114-123 [PMID: 26411425 DOI: 10.1007/s12016-015-8516-5]

23 **Zhang X**, Chen P, Gao H, Hao S, Yang M, Zhao H, Hu J, Ma W, Li L. Bacterial Infection and Predictors of Mortality in Patients with Autoimmune Liver Disease-Associated Acute-On-Chronic Liver Failure. *Can J Gastroenterol Hepatol* 2018; **2018**: 5108781 [PMID: 29623264 DOI: 10.1155/2018/5108781]

24 **Grønbæk L**, Vilstrup H, Jepsen P. Autoimmune hepatitis in Denmark: incidence, prevalence, prognosis, and causes of death. A nationwide registry-based cohort study. *J Hepatol* 2014; **60**: 612-617 [PMID: 24326217 DOI: 10.1016/j.jhep.2013.10.020]

25 **Choudhuri G**, Somani SK, Baba CS, Alexander G. Autoimmune hepatitis in India: profile of an uncommon disease. *BMC Gastroenterol* 2005; **5**: 27 [PMID: 16098234 DOI: 10.1186/1471-230X-5-27]

World Journal of Gastroenterology

Submit a Manuscript: https://www.f6publishing.com

World J Gastroenterol 2022 August 21; 28(31): 4431-4441

DOI: 10.3748/wjg.v28.i31.4431

ISSN 1007-9327 (print) ISSN 2219-2840 (online)

ORIGINAL ARTICLE

Observational Study

Simple cholecystectomy is an adequate treatment for grade I T1bN0M0 gallbladder carcinoma: Evidence from 528 patients

Jun Shao, Hong-Cheng Lu, Lin-Quan Wu, Jun Lei, Rong-Fa Yuan, Jiang-Hua Shao

Specialty type: Gastroenterology and hepatology

Provenance and peer review: Unsolicited article; Externally peer reviewed.

Peer-review model: Single blind

Peer-review report's scientific quality classification

Grade A (Excellent): A
Grade B (Very good): B
Grade C (Good): 0
Grade D (Fair): 0
Grade E (Poor): 0

P-Reviewer: Mishra TS, India; Sahin TT, Turkey

Received: April 21, 2022
Peer-review started: April 21, 2022
First decision: May 30, 2022
Revised: June 12, 2022
Accepted: July 25, 2022
Article in press: July 25, 2022
Published online: August 21, 2022

Jun Shao, Hong-Cheng Lu, Lin-Quan Wu, Jun Lei, Rong-Fa Yuan, Jiang-Hua Shao, Department of Hepatobiliary Surgery, The Second Affiliated Hospital of Nanchang University, Nanchang 330006, Jiangxi Province, China

Corresponding author: Jiang-Hua Shao, MD, PhD, Chief Doctor, Full Professor, Department of Hepatobiliary Surgery, The Second Affiliated Hospital of Nanchang University, No. 1 Minde Road, Nanchang 330006, Jiangxi Province, China. shao5022@163.com

Abstract

BACKGROUND

T1b gallbladder carcinoma (GBC) is defined as a tumor that invades the perimuscular connective tissue without extension beyond the serosa or into the liver. However, controversy still exists over whether patients with T1b GBC should undergo cholecystectomy alone or radical GBC resection.

AIM

To explore the optimal surgical approach in patients with T1b gallbladder cancer of different pathological grades.

METHODS

Patients with T1bN0M0 GBC who underwent surgical treatment between 2000 and 2017 were included in the Surveillance, Epidemiology, and End Results database. The Kaplan-Meier method and log-rank test were used to analyze the overall survival (OS) and disease-specific survival (DSS) of patients with T1b GBC of different pathological grades. Cox regression analysis was used to identify independent predictors of mortality and explore the selection of surgical methods in patients with T1b GBC of different pathological grades and their relationship with prognosis.

RESULTS

Of the 528 patients diagnosed with T1bN0M0 GBC, 346 underwent simple cholecystectomy (SC) (65.5%), 131 underwent SC with lymph node resection (SC + LN) (24.8%), and 51 underwent radical cholecystectomy (RC) (9.7%). Without considering the pathological grade, both the OS ($P < 0.001$) and DSS ($P = 0.003$) of T1b GBC patients who underwent SC (10-year OS: 27.8%, 10-year DSS: 55.1%) alone were significantly lower than those of patients who underwent SC + LN (10-year OS: 35.5%, 10-year DSS: 66.3%) or RC (10-year OS: 50.3%, 10-year DSS: 75.9%). Analysis of T1b GBC according to pathological classification revealed no

significant difference in OS and DSS between different types of procedures in patients with grade I T1b GBC. In patients with grade II T1b GBC, obvious survival improvement was observed in the OS (P = 0.002) and DSS (P = 0.039) of those who underwent SC + LN (10-year OS: 34.6%, 10-year DSS: 61.3%) or RC (10-year OS: 50.5%, 10-year DSS: 78.8%) compared with those who received SC (10-year OS: 28.1%, 10-year DSS: 58.3%). Among patients with grade III or IV T1b GBC, SC + LN (10-year OS: 48.5%, 10-year DSS: 72.2%), and RC (10-year OS: 80%, 10-year DSS: 80%) benefited OS (P = 0.005) and DSS (P = 0.009) far more than SC (10-year OS: 20.1%, 10-year DSS: 38.1%) alone.

CONCLUSION

Simple cholecystectomy may be an adequate treatment for grade I T1b GBC, whereas more extensive surgery is optimal for grades II-IV T1b GBC.

Key Words: Gallbladder carcinoma; Tumor-node-metastasis; Survival analysis; Tumor grade; Surgical treatment

©The Author(s) 2022. Published by Baishideng Publishing Group Inc. All rights reserved.

Core Tip: T1b gallbladder carcinoma (GBC) is defined as a tumor that invades the perimuscular connective tissue without extension beyond the serosa or into the liver. However, controversy still exists over whether patients with T1b GBC should undergo cholecystectomy alone or radical GBC resection. In this study, we included patients with different histological grades of T1b GBC and compared the survival time of patients who underwent simple cholecystectomy, cholecystectomy with lymph node resection, or radical cholecystectomy to explore the optimal surgical approach for these patients.

Citation: Shao J, Lu HC, Wu LQ, Lei J, Yuan RF, Shao JH. Simple cholecystectomy is an adequate treatment for grade I T1bN0M0 gallbladder carcinoma: Evidence from 528 patients. *World J Gastroenterol* 2022; 28(31): 4431-4441

URL: https://www.wjgnet.com/1007-9327/full/v28/i31/4431.htm

DOI: https://dx.doi.org/10.3748/wjg.v28.i31.4431

INTRODUCTION

Gallbladder carcinoma (GBC) is the most common malignant tumor of the biliary tract, accounting for 80%-95% of malignant tumors of the biliary tract. The overall average survival of patients with GBC is only 6 mo, and the 5-year survival rate is < 5%[1,2]. According to global cancer statistics from 2020, 115949 people have been diagnosed with GBC worldwide and 84965 have died from this condition[3]. The treatment effect of adjuvant therapy, chemotherapy, radiotherapy, and targeted therapy on GBC remains unsatisfactory despite recent improvements in diagnosis and treatment methodology, and surgical resection remains the first choice for the treatment of GBC.

Different surgical resection methods are used to treat GBC, based on staging. According to the current tumor-node-metastasis (TNM) staging system of the American Joint Committee on Cancer (AJCC) guidelines, simple cholecystectomy (SC, gallbladder removal alone) is the appropriate treatment for patients with Tis or T1a GBC, radical cholecystectomy (RC, including cholecystectomy, lymph node (LN) dissection, and liver wedge resection) or expanded radical resection of GBC is recommended for patients with T1b-T3 GBC, and surgery is not recommended for T4 GBC[4-6]. However, whether patients with T1b GBC undergo SC or RC had remained controversial for a long time. A previous study found that the long-term survival rate of patients with T1b GBC after SC was equivalent to that after RC [7]. Some studies have also found that the prognosis of patients with T1b who underwent RC of GBC is significantly improved compared to that of patients who underwent cholecystectomy alone[8,9]. Therefore, whether patients with T1b GBC undergo SC or RC remains a clinical problem that surgeons must address.

Recent studies have found that, in addition to TNM staging, tumor pathological grading plays an important role in tumor prognosis and surgical selection. Studies have pointed out that low-grade tumors in the tongue[10], breast[11], and thyroid[12] have a significantly worse prognosis than high-grade tumors in the same locations. Furthermore, studies have pointed out that the median survival of patients with grade I GBC is significantly better than that of patients with grade II-IV GBC, indicating that tumor grade is also an extremely important indicator of the prognosis of GBC[13]. However, a question worthy of discussion is whether pathological classification can be used as the basis for the selection of surgery (SC or RC) in T1b patients.

In the present study, we obtained the treatment and survival data of patients with T1b GBC from the Surveillance, Epidemiology, and End Results (SEER) database[14], analyzed the survival of patients with different histological grades of T1b GBC, and compared the survival of patients who underwent SC, cholecystectomy with LN resection, and RC to assess the optimal surgical approach.

MATERIALS AND METHODS

Data source

The SEER database was established by the National Cancer Institute and contains follow-up information from patients with cancer. We used the SEER-18 database, derived from 18 regional registries representing approximately one-third of the US population, to collect data on patients with GBC between 2000 and 2017, including patient age, sex, histological codes, tumor histology, TNM stage (6th AJCC TNM staging system), tumor grade, surgical information, and patient survival.

Study population

Tumor histology and site codes were used to identify patients in the SEER database with GBC between 2000 and 2017. A total of 15671 patients were included in this study. Patients were excluded from our study for the following reasons: patients did not undergo surgery, patients with GBC other than T1bN0M0, incomplete follow-up data, unknown surgical resection range, tumor grade, or histological data. According to the 6th edition of the AJCC staging system, all T1b patients were staged according to clinical classification based on physical examination, imaging, endoscopy, biopsy, surgical exploration, and other relevant examinations; 528 patients with T1bN0M0 GBC were included (Figure 1). According to the surgical treatment information in the SEER database, patients who underwent SC without LN resection in our study were categorized as SC, those who underwent cholecystectomy with LN resection were categorized as SC + LN, and patients who underwent cholecystectomy and any type of liver resection with extensive LN dissection were categorized as RC. The major outcomes of this study were overall survival (OS) and disease-specific survival (DSS).

Statistical analysis

Both continuous and categorical variables (such as age and sex, tumor grade, tumor histological type, surgical approach, *etc.*) are presented as numbers (n) and percentages (%). Kaplan-Meier survival curves were generated to analyze the OS and DSS between the different groups, and the *P* values for the survival curves were determined using the log-rank test. A multivariate Cox proportional hazards model was built to verify the independent role of prognostic factors, and variables with a *P* value of < 0.1 on the log-rank test were incorporated into the model. The final model was built using a stepwise selection method, and the results were presented as adjusted hazard ratios (HRs) with corresponding 95% confidence intervals (CIs) and *P* values. All *P* values were two-sided, and values of $P < 0.05$ were considered statistically significant. Statistical analyses were performed using the statistical software Statistical Product and Service Solutions (SPSS) IBM (version 19.0).

RESULTS

General characteristics of patients with T1b GBC

In this retrospective study, 528 patients had pathologically confirmed T1bN0M0 GBC between 2000 and 2017. Of these, 385 (72.9%) were women, and 143 (27.1%) were men. The histological types were adenocarcinoma (73.3%), papillary adenocarcinoma (15%), and other tissue types (11.7%). The tumor pathological classification was grade I (30.5%), grade II (50.9%), and grades III and IV (18.6%). Therefore, grade III and grade IV GBC were combined into the same subgroup for analysis in the present study as few patients had grade IV GBC. Among the 528 patients with GBC, 346 underwent SC (65.5%), 131 underwent SC + LN (24.8%), and 51 underwent RC (9.7%) (Table 1).

Univariate analysis performed using the log-rank test revealed that the histological type ($P = 0.059$) and tumor grade ($P = 0.056$) did not significantly affect the 10-year OS of patients with T1b GBC. Younger age ($P < 0.001$) and female sex ($P = 0.007$) were associated with better OS, and patients who underwent RC (50.3%) or SC + LN (35.5%) achieved better OS than those who underwent SC (27.8%) ($P < 0.001$). The 10-year DSS was not significantly affected by histological type ($P = 0.058$), similar to the OS, and DSS rates were significantly higher in younger ($P = 0.023$) and female patients ($P = 0.016$). The DSS was also significantly affected by the extent of surgery, and the 10-year DSS of patients who underwent RC (75.9%) or SC + LN (66.3%) was higher than that of patients who underwent SC (55.1%) ($P = 0.002$). Although tumor grade had no significant effect on the 10-year OS of patients with T1b GBC, we found that the 10-year DSS of patients with grade III and IV tumors (48.9%) was significantly lower than that of patients with grade I (64.7%) or II tumors (62.1%) ($P = 0.002$) (Table 1).

Table 1 General characteristics and survival data for 528 patients with T1b gallbladder cancer

Characteristics	*n* = 528, *n* (%)	10-year survival	
		OS, %	DSS, %
Age, yr			
< 70	220 (41.7)	46.4%	62.7%
≥ 70	308 (58.3)	21.9%	58.9%
		P < 0.001	*P* = 0.023
Gender			
Male	143 (27.1)	13.7	47.5
Female	385 (72.9)	37.8	64
		P = 0.007	*P* = 0.016
Grade			
Grade I	161 (30.5)	33.1	64.7
Grade II	269 (50.9)	32.6	62.1
Grade III, IV	98 (18.6)	28.6	48.9
		P = 0.056	*P* = 0.002
Histological type			
Adenocarcinoma	387 (73.3)	30.5	61.6
Papillary	79 (15.0)	40.2	61.8
Other	62 (11.7)	29	51
		P = 0.059	*P* = 0.058
Surgery			
SC	346 (65.5)	27.8	55.1
SC + LN	131 (24.8)	35.5	66.3
RC	51 (9.7)	50.3	75.9
		P < 0.001	*P* = 0.002

OS: Overall survival; DSS: Disease-specific survival; SC: Simple cholecystectomy; LN: Lymph node resection; RC: Radical cholecystectomy; N: Number.

The impact of different surgical methods on the OS and DSS of patients with T1b GBC, regardless of pathological grade

Kaplan-Meier survival curves were generated for different types of surgery in patients with T1b GBC. The 10-year OS of patients who underwent more extensive surgery, including SC + LN (35.5%) and RC (50.3%), was significantly better than that of patients who underwent SC alone (27.8%) ($P < 0.001$) (Figure 2A). Consistent with OS, we found that the 10-year DSS of patients who underwent SC + LN (66.3%) or RC (75.9%) was significantly higher than that of patients who underwent SC (55.1%) ($P = 0.003$) (Figure 2B).

Using multivariate Cox regression analysis incorporating age, sex, tumor grade, tumor histological type, and surgery type, we confirmed that age, sex, and surgery type were independently associated with OS in patients with T1b GBC. Patients who underwent SC + LN (HR: 0.71, 95%CI: 0.53-0.95, $P = 0.020$) or RC (HR: 0.54, 95%CI: 0.32-0.89, $P = 0.015$) experienced a significant OS benefit compared to patients who underwent SC alone. Independent factors affecting DSS were sex, tumor grade, and surgery type, consistent with OS, and patients who underwent SC + LN (HR: 0.56, 95%CI: 0.37-0.83, $P = 0.020$) or RC (HR: 0.49, 95%CI: 0.27-0.92, $P = 0.015$) had improved DSS compared with patients who underwent SC. Table 2 shows the results of the multivariate Cox regression analysis of patients with T1b GBC based on the 10-year OS and DSS. Based on the above results, we concluded that patients with T1b GBC who underwent RC or SC + LN treatment had better OS and DSS than those who underwent SC, regardless of the pathological grade (Table 2).

Table 2 Multivariate Cox proportional hazards model for 10-year overall survival and disease-specific survival in 528 patients with T1b gallbladder cancer

Variable	10-year overall survival		10-year disease-specific survival	
	HR (95%CI)	*P* value	HR (95%CI)	*P* value
Age, yr				
< 70	Referent		Referent	
≥ 70	2.03 (1.57-2.63)	< 0.001	NA	NA
Gender				
Male	Referent		Referent	
Female	0.71 (0.55-0.91)	0.007	0.62 (0.45-0.87)	0.005
Grade				
Grade I	Referent		Referent	
Grade II	NA	NA	1.21 (0.83-1.76)	0.321
Grade III, IV	NA	NA	2.20 (1.43-3.38)	< 0.001
Histological type				
Adenocarcinoma	Referent		Referent	
Papillary	NA	NA	NA	NA
Other	NA	NA	NA	NA
Surgery				
SC	Referent		Referent	
SC + LN	0.71 (0.53-0.95)	0.020	0.56 (0.37-0.83)	0.004
RC	0.54 (0.32-0.89)	0.015	0.49 (0.27-0.92)	0.025

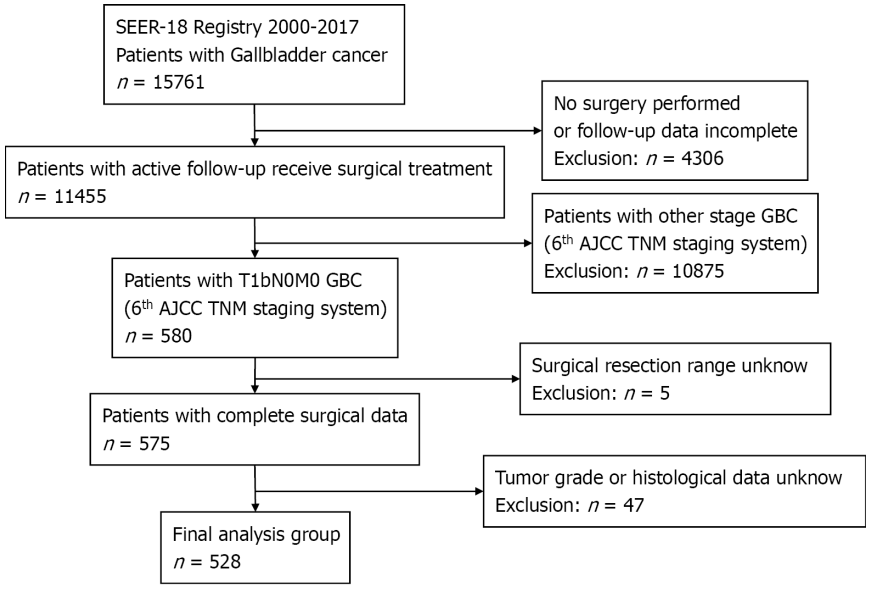
SC: Simple cholecystectomy; LN: Lymph node resection; RC: Radical cholecystectomy; N: Number; HR: Hazard ratio; CI: Confidence interval; NA: Not available.

The influence of operation methods on OS and DSS in patients with T1b GBC of different pathological grades

To verify the role of tumor grading in choosing the surgical approach for patients with T1b GBC, we divided the 528 patients with GBC into three subgroups based on tumor grade and analyzed the impact of different surgical approaches in each subgroup on 10-year OS and DSS. The type of surgery varied slightly between the different tumor grades, and Figure 2C shows the proportion of different surgical approaches in each subgroup. Of the 161 patients with grade I T1b GBC, 105 underwent SC (65%), 40 underwent SC + LN (25%), and 16 underwent RC (10%); of the 269 patients with grade II T1b GBC, 173 underwent SC (64%), 64 underwent SC + LN (24%), and 32 underwent RC (12%). Of the 98 patients with grade III or IV T1b GBC, 68 underwent SC (69%), 25 underwent SC + LN (26%), and 5 underwent RC (5%) (Figure 2C). Interestingly, no statistically significant differences were observed in OS (P = 0.734) and DSS (P = 0.953) between the different surgical types in patients with grade I T1b GBC (Figure 3A and B). However, an obvious improvement in the OS of patients with grade II T1b GBC who underwent SC + LN (34.6%) or RC (50.5%) was observed compared to that of patients who underwent SC (28.1%) (P = 0.002). The DSS of patients who underwent SC + LN (61.3%) or RC (78.8%) was also much higher than that of patients who underwent SC (58.3%) (P = 0.039) (Figure 3C and D). Moreover, the OS and DSS of patients with grade III and IV T1b GBC were both significantly affected by the type of surgery, and SC + LN (48.5%) or RC (80%) had a far more beneficial effect on OS than SC (20.1%; P = 0.005). Similar to OS, the DSS in patients who underwent SC + LN (72.2%) or RC (80%) was also much higher than that of patients who underwent SC (38.1%) (P = 0.009) (Figure 3E and F). These results show that patients with grade I T1b GBC who undergo SC can attain a survival benefit equivalent to that associated with SC + LN or RC.

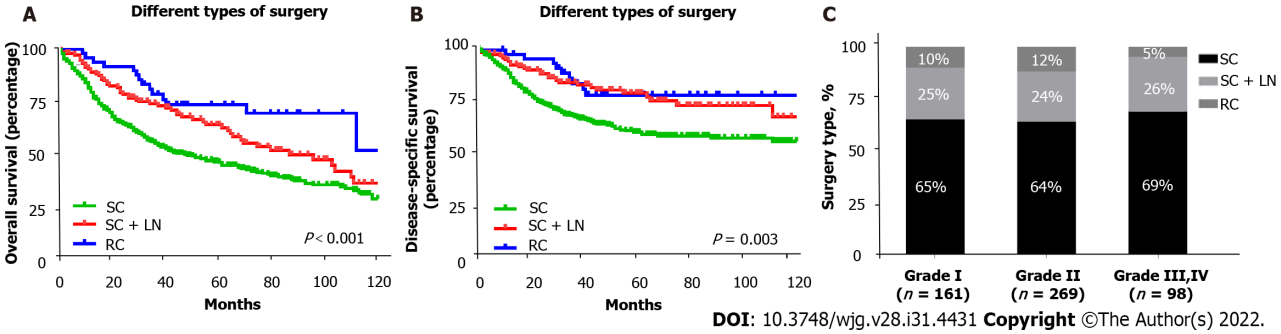
The influence of surgical methods on OS and DSS in patients with grade I T1b GBC

To further verify that surgery type did not significantly affect OS and DSS in patients with grade I T1b GBC, we conducted a univariate analysis of 161 patients with grade I T1b GBC. Using the log-rank test, we found that age (P = 0.022) and sex (P = 0.030) significantly affected the OS of patients with grade I



DOI: 10.3748/wjg.v28.i31.4431 **Copyright** ©The Author(s) 2022.

Figure 1 Flow diagram of the study population. A total of 528 patients with T1bN0M0 gallbladder cancer were included in this study.SEER: Surveillance, Epidemiology, and End Results database; AJCC: American Joint Committee on Cancer; TNM: Tumor-node-metastasis; GBC: Gallbladder cancer; N: Number.



DOI: 10.3748/wjg.v28.i31.4431 **Copyright** ©The Author(s) 2022.

Figure 2 Overall survival and disease-specific survival of 528 patients with T1b gallbladder cancer who received different surgical treatment assessed using Kaplan-Meier analysis, and the proportions of different surgical approaches. A: Overall survival of patients with T1b gallbladder cancer (GBC) received simple cholecystectomy (SC), SC with lymph node resection (SC + LN), or radical cholecystectomy (RC) ($P < 0.001$); B: Disease-specific survival of patients with T1b GBC who received SC, SC + LN, or RC ($P = 0.003$); C: The proportions of different surgical approaches in patients with different pathological grades of gallbladder cancer. SC: Simple cholecystectomy; LN: Lymph node resection; RC: Radical cholecystectomy.

T1b GBC, whereas the histological type of the tumor ($P = 0.799$) and surgical method ($P = 0.734$) had no significant effect on OS. Age ($P = 0.431$), sex ($P = 0.071$), tumor histological type ($P = 0.562$), and surgical method ($P = 0.953$) did not significantly affect DSS in patients with grade I T1b GBC (Table 3).

Subsequently, we performed multivariate Cox regression analysis based on age, sex, tumor grade, tumor histological type, and surgery type and found that age and sex were independent influencing factors for OS in patients with grade I T1b GBC; older age was associated with poor OS (HR: 1.67, 95%CI: 1.07-2.59, $P = 0.023$), and women had better OS (HR: 0.62, 95%CI: 0.40-0.96, $P = 0.031$). The histological type of the tumor and surgical method were not independent factors for OS in patients with grade I T1b GBC. Age, sex, histological tumor type, and surgical method were not independent risk factors for DSS in patients with grade I T1b GBC. Lastly, we verified that the type of surgery did not affect the OS and DSS of 161 patients with grade I T1b GBC (Table 4).

DISCUSSION

The current staging of GBC follows the TNM staging system of the AJCC guidelines, in which primary tumor invasion (T) is a crucial factor in the AJCC staging criteria that determines the surgical approach for GBC[15]. The goal of surgical intervention for GBC is to achieve R0 resection, which is the most important factor in predicting long-term survival. According to the staging system of the AJCC

Table 3 General characteristics and survival data for 161 patients with grade I T1b gallbladder cancer

Characteristics	*n* = 161, *n* (%)	10-year survival	
		OS, %	DSS, %
Age, yr			
< 70	72 (41.7)	65.8	70.6
≥ 70	89 (58.3)	58.0	79.1
		$P = 0.022$[1]	$P = 0.431$
Gender			
Male	49 (27.1)	54.6	72.6
Female	112 (72.9)	63.6	75.9
		$P = 0.030$[1]	$P = 0.071$
Histological type			
Adenocarcinoma	116 (73.3)	62.8	76.2
Papillary	32 (15.0)	60.1	74.6
Other	13 (11.7)	46.2	60.6
		$P = 0.799$	$P = 0.562$
Surgery			
SC	105 (65.5)	60.1	76.1
SC + LN	41 (24.8)	65.2	75.3
RC	15 (9.7)	56.6	67.0
		$P = 0.734$	$P = 0.953$

[1]$P < 0.05$.

OS: Overall survival; DSS: Disease-specific survival; SC: Simple cholecystectomy; LN: Lymph node resection; RC: Radical cholecystectomy; N: Number.

guidelines, Tis refers to the tumor in situ, T1a lesions invade the lamina propria, T1b lesions invade the muscular layer, T2 Lesions invade the connective tissue around the gallbladder muscle without extending to the serosal membrane or liver, T3 tumors perforate the gallbladder serosa or penetrate the liver or one other adjacent organ, and T4 tumors are defined as those that invade the main portal vein, hepatic artery, or two or more adjacent organs[16]. According to the recommendations of the National Comprehensive Cancer Network (NCCN) diagnosis and treatment guidelines, surgical treatment for Tis and T1a GBC should be SC, and RC is the first choice for the treatment of GBC with T1b-T3, whereas surgery is not recommended for T4[17]. Nevertheless, previous studies have also pointed out the controversy in the treatment of T1b, and some studies still reported long-term survival after SC for patients with T1b GBC that is comparable to that after radical resection and did not recommend extended cholecystectomy or radical resection for T1b GBC[18,19]. Therefore, controversy about the surgical treatment of T1b GBC has existed in clinical practice for many years. For example: (1) Should patients with GBC diagnosed as T1b by pathology undergo radical resection; (2) incidental CBC (IGBC) is defined as cholecystectomy for benign gallbladder lesions, but the postoperative pathological diagnosis is GBC[20,21]; and (3) should patients with T1b IGBC undergo another surgical procedure so that RC can be performed?

Tumor grade was categorized as well-differentiated (grade I), moderately differentiated (grade II), poorly differentiated (grade III), or undifferentiated (grade IV), depending on the pathological morphology of the tumor. As an important tumor index, pathological grading plays a crucial role in the prognosis and treatment of many tumors. For example, patients with differentiated T1N0M0 thyroid cancer should undergo total thyroidectomy, whereas patients with undifferentiated T1N0M0 thyroid cancer require total thyroidectomy and LN dissection[22]. However, to our knowledge, the role of tumor grade in the selection of surgical treatment for T1b GBC has not yet been explored. In our study, 528 cases of T1bN0M0 GBC were grouped according to the pathological grade. By analyzing the survival of patients with various pathological grades of GBC following different surgical methods, we found that both DSS and OS of patients with grade II-IV T1b GBC who underwent extensive surgery improved markedly compared to those who underwent SC. However, SC had a comparable survival benefit for both OS and DSS in patients with grade I T1b GBC compared to patients who underwent SC + LN or RC. Using Cox regression analysis, we also found that surgery type was not an independent

Table 4 Multivariate Cox proportional hazards model for 10-year overall survival and disease-specific survival in 161 patients with grade I T1b gallbladder cancer

Variable	10-year overall survival		10-year disease-specific survival	
	HR (95%CI)	*P* value	HR (95%CI)	*P* value
Age, yr				
< 70	Referent		Referent	
≥ 70	1.67 (1.07-2.59)	0.023	NA	NA
Gender				
Male	Referent		Referent	
Female	0.62 (0.40-0.96)	0.031	NA	NA
Histological type				
Adenocarcinoma	Referent		Referent	
Papillary	NA	NA	NA	NA
Other	NA	NA	NA	NA
Surgery				
SC	Referent		Referent	
SC + LN	NA	NA	NA	NA
RC	NA	NA	NA	NA

SC: Simple cholecystectomy; LN: Lymph node resection; RC: Radical cholecystectomy; N: Number; HR: Hazard ratio; CI: Confidence interval; NA: Not available.

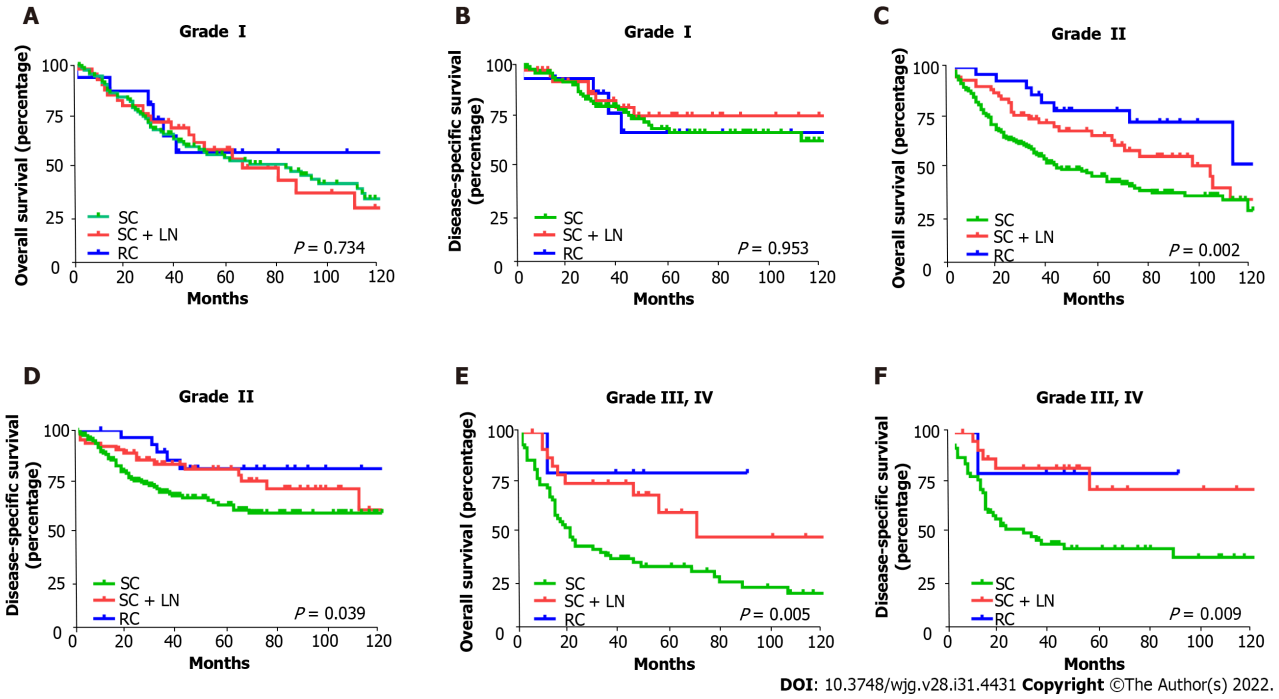
factor associated with survival in patients with grade I T1b GBC. These results indicate that the surgery type does not significantly affect OS or DSS in patients with grade I T1b GBC. Patients with grade I T1b GBC who undergo SC alone could obtain a similar survival benefit compared with those treated with SC + LN or RC, and more extensive surgery is the optimal treatment for T1b patients with grade II-IV tumors.

Thus, according to the NCCN guidelines and our research results, we propose the following answers to the two questions given above: (1) For GBC found during the operation, if perioperative frozen pathological examination reveals the TNM stage to be T1b, tumor histopathology should continue to be graded. If the pathological grade is confirmed to be grade I T1b GBC, SC should be performed, and patients with grade II-IV T1b GBC should undergo RC; and (2) for patients with T1b IGBC, the finding should be combined with the pathological grade to decide whether to perform surgery again; patients with grade II-IV T1b IGBC should undergo a second operation and radical resection of GBC to obtain survival benefits. Patients with grade I T1b IGBC do not need to undergo reoperation, which prevents the pain caused by the second operation and saves the patient money in terms of medical expenses.

To the best of our knowledge, this study is the first to use the SEER database, one of the largest population databases, to evaluate the role of tumor grading in choosing surgical approaches for patients with T1b GBC. However, our findings have some unavoidable limitations. First, this study is a retrospective analysis, and the SEER database lists only initial surgical treatment, so patients who underwent subsequent treatment may be included in our study. Furthermore, information on tumor recurrence, metastasis, or progression was also not available in the SEER database. Hence, prospective and multi-center studies of patients with T1b GBC are needed to further verify the impact of surgical methods on the prognosis of T1b patients with different pathological grades to provide a more appropriate, evidence-based rationale for determining the optimal surgical method for patients with T1b GBC of different pathological grades, and patients with grade I T1b GBC who underwent SC should be monitored for tumor recurrence, metastasis, or progression to validate the findings of our study.

CONCLUSION

We demonstrated a comparable survival benefit for patients with grade I T1b GBC who underwent SC, SC + LN or RC, whereas patients with grade II-IV T1b GBC benefit from SC + LN or RC, suggesting that SC may be a suitable treatment for patients with grade I T1b GBC, whereas RC or expanded radical resection is more suitable for those with grade II-IV T1b GBC.



DOI: 10.3748/wjg.v28.i31.4431 **Copyright** ©The Author(s) 2022.

Figure 3 The overall survival and disease-specific survival of patients with T1b gallbladder cancer stratified by pathological grades and surgical treatment using Kaplan-Meier analysis. A: Overall survival (OS) of patients with grade I T1b gallbladder cancer (GBC) by type of surgery (P = 0.734); B: Disease-specific survival (DSS) of patients with grade I T1b GBC by type of surgery (P = 0.953); C: OS of patients with grade II T1b GBC by type of surgery (P = 0.002); D: DSS of patients with grade II T1b GBC by type of surgery (P = 0.039); E: OS of patients with grade III, IV T1b GBC by type of surgery (P = 0.005); F: DSS of patients with grade III, IV T1b GBC by type of surgery (P = 0.009). SC: Simple cholecystectomy; LN: Lymph node resection; RC: Radical cholecystectomy.

ARTICLE HIGHLIGHTS

Research background

The surgical treatment of T1b gallbladder cancer has been controversial.

Research motivation

To solve the problem of choosing the surgical treatment for T1b gallbladder cancer.

Research objectives

To explore the optimal surgical approach in patients with T1b gallbladder cancer of different pathological grades.

Research methods

Analysis of survival differences in patients with different pathological grades of T1b gallbladder cancer who received different surgical treatment methods.

Research results

Patients with grade I T1b gallbladder cancer who underwent simple cholecystectomy attained a survival benefit equivalent to that of simple cholecystectomy with lymph node resection or radical cholecystectomy.

Research conclusions

Simple cholecystectomy is an adequate treatment for grade I T1b gallbladder carcinoma (GBC), whereas expanded radical resection is more suitable for grade II-IV T1b GBC.

Research perspectives

Simple cholecystectomy is a suitable treatment for patients with grade I T1b GBC.

ACKNOWLEDGEMENTS

The authors acknowledge the efforts of the SEER Program tumor registries in providing high-quality open resources for research.

FOOTNOTES

Author contributions: Shao J and Lu HC contributed equally to this work; Shao J, Shao JH, and Lu HC were involved in study concept and design, drafting of the manuscript and study supervision; Wu LQ contributed to collect data; Lei J and Yuan RF contributed to analyze the data; Shao JH, Shao J, and Lu HC critically revise the manuscript; all authors have read and approve the final manuscript.

Supported by the National Natural Science Foundation of China, No. 81773126, No. 81560475, and No. 82160486.

Institutional review board statement: The study was reviewed and approved by the Second Affiliated Hospital of Nanchang University Institutional Review Board, No. 74.

Informed consent statement: Patients from the Surveillance, Epidemiology, and End Results (SEER) database consented to participate in any scientific research worldwide.

Conflict-of-interest statement: There are no conflicts of interest to report.

Data sharing statement: The datasets used or analyzed in this study are available from the corresponding author at shao5022@163.com. Patients from the Surveillance, Epidemiology, and End Results (SEER) database consented to participate in any scientific research worldwide.

STROBE statement: The authors have read the STROBE Statement—checklist of items, and the manuscript was prepared and revised according to the STROBE Statement—checklist of items.

Open-Access: This article is an open-access article that was selected by an in-house editor and fully peer-reviewed by external reviewers. It is distributed in accordance with the Creative Commons Attribution NonCommercial (CC BY-NC 4.0) license, which permits others to distribute, remix, adapt, build upon this work non-commercially, and license their derivative works on different terms, provided the original work is properly cited and the use is non-commercial. See: https://creativecommons.org/Licenses/by-nc/4.0/

Country/Territory of origin: China

ORCID number: Hong-Cheng Lu 0000-0002-7053-6068; Jun Lei 0000-0002-8338-4972; Jiang-Hua Shao 0000-0002-1490-4102.

S-Editor: Chen YL
L-Editor: A
P-Editor: Chen YL

REFERENCES

1 **Lai CH**, Lau WY. Gallbladder cancer--a comprehensive review. *Surgeon* 2008; **6**: 101-110 [PMID: 18488776 DOI: 10.1016/s1479-666x(08)80073-x]
2 **Duffy A**, Capanu M, Abou-Alfa GK, Huitzil D, Jarnagin W, Fong Y, D'Angelica M, Dematteo RP, Blumgart LH, O'Reilly EM. Gallbladder cancer (GBC): 10-year experience at Memorial Sloan-Kettering Cancer Centre (MSKCC). *J Surg Oncol* 2008; **98**: 485-489 [PMID: 18802958 DOI: 10.1002/jso.21141]
3 **Sung H**, Ferlay J, Siegel RL, Laversanne M, Soerjomataram I, Jemal A, Bray F. Global Cancer Statistics 2020: GLOBOCAN Estimates of Incidence and Mortality Worldwide for 36 Cancers in 185 Countries. *CA Cancer J Clin* 2021; **71**: 209-249 [PMID: 33538338 DOI: 10.3322/caac.21660]
4 **Misra MC**, Guleria S. Management of cancer gallbladder found as a surprise on a resected gallbladder specimen. *J Surg Oncol* 2006; **93**: 690-698 [PMID: 16724357 DOI: 10.1002/jso.20537]
5 **Reid KM**, Ramos-De la Medina A, Donohue JH. Diagnosis and surgical management of gallbladder cancer: a review. *J Gastrointest Surg* 2007; **11**: 671-681 [PMID: 17468929 DOI: 10.1007/s11605-006-0075-x]
6 **Kanthan R**, Senger JL, Ahmed S, Kanthan SC. Gallbladder Cancer in the 21st Century. *J Oncol* 2015; **2015**: 967472 [PMID: 26421012 DOI: 10.1155/2015/967472]
7 **Benson AB 3rd**, Abrams TA, Ben-Josef E, Bloomston PM, Botha JF, Clary BM, Covey A, Curley SA, D'Angelica MI, Davila R, Ensminger WD, Gibbs JF, Laheru D, Malafa MP, Marrero J, Meranze SG, Mulvihill SJ, Park JO, Posey JA, Sachdev J, Salem R, Sigurdson ER, Sofocleous C, Vauthey JN, Venook AP, Goff LW, Yen Y, Zhu AX. NCCN clinical practice guidelines in oncology: hepatobiliary cancers. *J Natl Compr Canc Netw* 2009; **7**: 350-391 [PMID: 19406039 DOI: 10.6004/jnccn.2009.0027]

8 **Wagholikar GD**, Behari A, Krishnani N, Kumar A, Sikora SS, Saxena R, Kapoor VK. Early gallbladder cancer. *J Am Coll Surg* 2002; **194**: 137-141 [PMID: 11848630 DOI: 10.1016/s1072-7515(01)01136-x]

9 **Cucinotta E**, Lorenzini C, Melita G, Iapichino G, Currò G. Incidental gall bladder carcinoma: does the surgical approach influence the outcome? *ANZ J Surg* 2005; **75**: 795-798 [PMID: 16173995 DOI: 10.1111/j.1445-2197.2005.03528.x]

10 **Chuang ST**, Chen CC, Yang SF, Chan LP, Kao YH, Huang MY, Tang JY, Huang CM, Huang CJ. Tumor histologic grade as a risk factor for neck recurrence in patients with T1-2N0 early tongue cancer. *Oral Oncol* 2020; **106**: 104706 [PMID: 32330684 DOI: 10.1016/j.oraloncology.2020.104706]

11 **Metzger-Filho O**, Ferreira AR, Jeselsohn R, Barry WT, Dillon DA, Brock JE, Vaz-Luis I, Hughes ME, Winer EP, Lin NU. Mixed Invasive Ductal and Lobular Carcinoma of the Breast: Prognosis and the Importance of Histologic Grade. *Oncologist* 2019; **24**: e441-e449 [PMID: 30518616 DOI: 10.1634/theoncologist.2018-0363]

12 **Ho AS**, Luu M, Barrios L, Balzer BL, Bose S, Fan X, Walgama E, Mallen-St Clair J, Alam U, Shafqat I, Lin DC, Chen Y, Van Eyk JE, Maghami EG, Braunstein GD, Sacks WL, Zumsteg ZS. Prognostic Impact of Histologic Grade for Papillary Thyroid Carcinoma. *Ann Surg Oncol* 2021; **28**: 1731-1739 [PMID: 32808161 DOI: 10.1245/s10434-020-09023-2]

13 **Shibata K**, Uchida H, Iwaki K, Kai S, Ohta M, Kitano S. Lymphatic invasion: an important prognostic factor for stages T1b-T3 gallbladder cancer and an indication for additional radical resection of incidental gallbladder cancer. *World J Surg* 2009; **33**: 1035-1041 [PMID: 19225832 DOI: 10.1007/s00268-009-9950-4]

14 **Doll KM**, Rademaker A, Sosa JA. Practical Guide to Surgical Data Sets: Surveillance, Epidemiology, and End Results (SEER) Database. *JAMA Surg* 2018; **153**: 588-589 [PMID: 29617544 DOI: 10.1001/jamasurg.2018.0501]

15 **Giannis D**, Cerullo M, Moris D, Shah KN, Herbert G, Zani S, Blazer DG 3rd, Allen PJ, Lidsky ME. Validation of the 8th Edition American Joint Commission on Cancer (AJCC) Gallbladder Cancer Staging System: Prognostic Discrimination and Identification of Key Predictive Factors. *Cancers (Basel)* 2021; **13** [PMID: 33535552 DOI: 10.3390/cancers13030547]

16 **Liao X**, Zhang D. The 8th Edition American Joint Committee on Cancer Staging for Hepato-pancreato-biliary Cancer: A Review and Update. *Arch Pathol Lab Med* 2021; **145**: 543-553 [PMID: 32223559 DOI: 10.5858/arpa.2020-0032-RA]

17 **Benson AB 3rd**, D'Angelica MI, Abbott DE, Abrams TA, Alberts SR, Saenz DA, Are C, Brown DB, Chang DT, Covey AM, Hawkins W, Iyer R, Jacob R, Karachristos A, Kelley RK, Kim R, Palta M, Park JO, Sahai V, Schefter T, Schmidt C, Sicklick JK, Singh G, Sohal D, Stein S, Tian GG, Vauthey JN, Venook AP, Zhu AX, Hoffmann KG, Darlow S. NCCN Guidelines Insights: Hepatobiliary Cancers, Version 1.2017. *J Natl Compr Canc Netw* 2017; **15**: 563-573 [PMID: 28476736 DOI: 10.6004/jnccn.2017.0059]

18 **Lee H**, Kwon W, Han Y, Kim JR, Kim SW, Jang JY. Optimal extent of surgery for early gallbladder cancer with regard to long-term survival: a meta-analysis. *J Hepatobiliary Pancreat Sci* 2018; **25**: 131-141 [PMID: 29117469 DOI: 10.1002/jhbp.521]

19 **Kim HS**, Park JW, Kim H, Han Y, Kwon W, Kim SW, Hwang YJ, Kim SG, Kwon HJ, Vinuela E, Járufe N, Roa JC, Han IW, Heo JS, Choi SH, Choi DW, Ahn KS, Kang KJ, Lee W, Jeong CY, Hong SC, Troncoso A, Losada H, Han SS, Park SJ, Yanagimoto H, Endo I, Kubota K, Wakai T, Ajiki T, Adsay NV, Jang JY. Optimal surgical treatment in patients with T1b gallbladder cancer: An international multicenter study. *J Hepatobiliary Pancreat Sci* 2018; **25**: 533-543 [PMID: 30562839 DOI: 10.1002/jhbp.593]

20 **Hickman L**, Contreras C. Gallbladder Cancer: Diagnosis, Surgical Management, and Adjuvant Therapies. *Surg Clin North Am* 2019; **99**: 337-355 [PMID: 30846038 DOI: 10.1016/j.suc.2018.12.008]

21 **Varshney S**, Butturini G, Gupta R. Incidental carcinoma of the gallbladder. *Eur J Surg Oncol* 2002; **28**: 4-10 [PMID: 11869005 DOI: 10.1053/ejso.2001.1175]

22 **Perrier ND**, Brierley JD, Tuttle RM. Differentiated and anaplastic thyroid carcinoma: Major changes in the American Joint Committee on Cancer eighth edition cancer staging manual. *CA Cancer J Clin* 2018; **68**: 55-63 [PMID: 29092098 DOI: 10.3322/caac.21439]

World Journal of Gastroenterology

Submit a Manuscript: https://www.f6publishing.com

World J Gastroenterol 2022 August 21; 28(31): 4442-4455

DOI: 10.3748/wjg.v28.i31.4442

ISSN 1007-9327 (print) ISSN 2219-2840 (online)

META-ANALYSIS

Current standard values of health utility scores for evaluating cost-effectiveness in liver disease: A meta-analysis

Tomohiro Ishinuki, Shigenori Ota, Kohei Harada, Masaki Kawamoto, Makoto Meguro, Goro Kutomi, Hiroomi Tatsumi, Keisuke Harada, Koji Miyanishi, Toru Kato, Toshio Ohyanagi, Thomas T Hui, Toru Mizuguchi

Specialty type: Gastroenterology and hepatology

Provenance and peer review: Invited article; Externally peer reviewed.

Peer-review model: Single blind

Peer-review report's scientific quality classification

Grade A (Excellent): 0
Grade B (Very good): B
Grade C (Good): C
Grade D (Fair): D
Grade E (Poor): 0

P-Reviewer: Jin X, China; Jing X, China; Yeo W, China
A-Editor: Yao QG, China

Received: January 13, 2022
Peer-review started: January 13, 2022
First decision: April 16, 2022
Revised: April 26, 2022
Accepted: July 24, 2022
Article in press: July 24, 2022
Published online: August 21, 2022

Tomohiro Ishinuki, Toru Mizuguchi, Department of Nursing, Surgical Sciences, Sapporo Medical University, Sapporo 0608556, Japan

Shigenori Ota, Goro Kutomi, Toru Kato, Departments of Surgery, Surgical Science and Oncology, Sapporo Medical University, Sapporo 0608543, Japan

Kohei Harada, Department of Radiology, Sapporo Medical University, Sapporo 0608543, Japan

Masaki Kawamoto, Departments of Surgery, Nemuro City Hospital, Nemuro 0870008, Japan

Makoto Meguro, Departments of Surgery, Sapporo Satozuka Hospital, Sapporo 0040811, Japan

Hiroomi Tatsumi, Department of Intensive Care Medicine, Sapporo Medical University, Sapporo 0608543, Japan

Keisuke Harada, Department of Emergency Medicine, Sapporo Medical University, Sapporo 0608543, Japan

Koji Miyanishi, Department of Medical Oncology, Sapporo Medical University, Sapporo 0608543, Japan

Toshio Ohyanagi, Department of Liberal Arts and Sciences, Center for Medical Education, Sapporo Medical University, Sapporo 0608556, Japan

Thomas T Hui, Departments of Surgery, Stanford University School of Medicine, Stanford, 94598, United States

Corresponding author: Toru Mizuguchi, MD, PhD, Professor, Department of Nursing, Surgical Sciences, Sapporo Medical University, S1, W17, Chuo-ku, Sapporo 0608556, Japan.
tmizu@sapmed.ac.jp

Abstract

BACKGROUND

Health utility assessments have been developed for various conditions, including chronic liver disease. Health utility scores are required for socio-economic evaluations, which can aid the distribution of national budgets. However, the standard health utility assessment scores for specific health conditions are largely unknown.

AIM
To summarize the health utility scores, including the EuroQOL 5-dimensions 5-levels (EQ-5D-5L), EuroQol-visual analogue scale, short from-36 (SF-36), RAND-36, and Health Utilities Index (HUI)-Mark2/Mark3 scores, for the normal population and chronic liver disease patients.

METHODS
A systematic literature search of PubMed and MEDLINE, including the Cochrane Library, was performed. Meta-analysis was performed using the RevMan software. Multiple means and standard deviations were combined using the StatsToDo online web program.

RESULTS
The EQ-5D-5L and SF-36 can be used for health utility evaluations during antiviral therapy for hepatitis C. HUI-Mark2/Mark3 indicated that the health utility scores of hepatitis B patients are roughly 30% better than those of hepatitis C patients.

CONCLUSION
The EQ-5D-5L is the most popular questionnaire for health utility assessments. Health assessments that allow free registration would be useful for evaluating health utility in patients with liver disease.

Key Words: Quality of life; EuroQOL 5-dimensions 5-levels; Short from-36; RAND-36; Health Utilities Index-Mark

©The Author(s) 2022. Published by Baishideng Publishing Group Inc. All rights reserved.

Core Tip: This study summarized current knowledge about health utility assessments, including the EuroQOL 5-dimensions 5-levels (EQ-5D-5L), EuroQol-visual analogue scale, short from-36, RAND-36, and Health Utilities Index-Mark2/Mark3. The EQ-5D-5L is the most popular questionnaire for health utility assessments. Health utility assessments need to be used widely and routinely.

Citation: Ishinuki T, Ota S, Harada K, Kawamoto M, Meguro M, Kutomi G, Tatsumi H, Harada K, Miyanishi K, Kato T, Ohyanagi T, Hui TT, Mizuguchi T. Current standard values of health utility scores for evaluating cost-effectiveness in liver disease: A meta-analysis. *World J Gastroenterol* 2022; 28(31): 4442-4455
URL: https://www.wjgnet.com/1007-9327/full/v28/i31/4442.htm
DOI: https://dx.doi.org/10.3748/wjg.v28.i31.4442

INTRODUCTION

The quality of health is an important factor when assessing medical management rather than simple survival periods[1,2]. Health utility is an important factor in medical assessments and socio-economic politics[3]. National health budgets have risen steadily in various countries, and governments need to deeply consider the need to maintain a socio-economic balance[4]. Therefore, health benefits should be compared with social costs to avoid national financial collapse.

It is difficult to quantify health quality at regular intervals[5]. We are developing wearable devices that can automatically obtain health data, including data regarding mental health. Some health utility assessments require the use of questionnaires, which are associated with low compliance and involve bothersome calculations[2,6,7]. Before launching our novel health utility assessment tool, we performed this meta-analysis in order to summarize the currently available health utility assessment tools. The most useful questionnaire for evaluating health status depending on liver disease status or sex is unclear. In addition, no universal health utility assessment values for specific liver diseases or the normal population have been reported. Therefore, we conducted a meta-analysis to estimate health utility assessment values for specific populations.

The EuroQOL 5-dimensions 5-levels (EQ-5D-5L) is the simplest instrument for evaluating health utility and has been widely translated into various languages with high reliability and validity[6,8-10]. It only involves five questions and five answering levels. The health utility scores produced by the EQ-5D-5L can be used to calculate quality-adjusted life year (QALY) values[8]. The Health Utilities Index Mark 2/Mark 3 is another instrument for evaluating health utility scores and can also be used to obtain QALY values[11]. However, the Health Utilities Index is complicated, as it involves 45 questions, which take a long time to answer. The short-form 36-item (SF-36) is also widely used to evaluate health quality, although it does not directly involve QALY evaluations[9,12,13].

There are two types of SF-36, and the copyrights to these tools belong to The RAND Corporation (Santa Monica, CA, United States)[14] and QualityMetric (Johnston, RI, United States), respectively[15]. However, most researchers do not actively consider which version they use[12]. Therefore, the exact method and results of such assessments are not always described in the literature (Table 1).

In this meta-analysis, we describe the scores obtained with various health utility indexes (HUIs) in normal healthy populations or patients with different types of liver disease (Table 2)[16-32].

MATERIALS AND METHODS

Literature search

The PICOS scheme was used to set appropriate inclusion criteria. A systematic literature search of PubMed and MEDLINE, including the Cochrane Library, was performed independently by two authors (Ishunuki T and Ota S). The search was limited to human studies whose findings were reported in English. No restrictions were placed on the type of publication, the publication date, or publication status. The search strategy was based on different combinations of words for each database. For the PubMed database, the following combination was used: (("liver"[MeSH Terms] OR "liver"[All Fields] OR "livers"[All Fields] OR "liver s"[All Fields]) AND "qol"[All Fields]) AND (1990/1/1: 3000/12/12[pdat]). For the MEDLINE database, the following combination was used: [quality of life (QOL) and Liver].

Study selection

The two independent authors screened the titles and abstracts of the primary studies identified in the database search. Duplicate studies were excluded. The following inclusion criteria were employed for the meta-analysis: (1) Studies that compared QOL in patients who had liver disease; (2) Studies that compared QOL between male and female patients with liver disease; (3) Studies that reported at least one QOL outcome; and (4) If the same institute reported more than one study, only the most recent or the highest-level study was included.

Data extraction

The same two authors extracted the following primary data: (1) The questionnaires used for each QOL evaluation; (2) The first author, year of publication, and type of study; (3) The etiology of the disease and the number of times each intervention was performed; and (4) The timing of the evaluations.

Statistical analysis

Meta-analyses were performed using the RevMan software (version 5.3.; The Cochrane Collaboration). The mean differences (MD) between groups were calculated for continuous variables. The interquartile ranges of the data were transformed by dividing them by 1.35 to produce alternative standard deviation values. Multiple means and standard deviations were combined using the StatsToDo online web program (https://www.statstodo.com/index.php).

The chi-square test was used to evaluate heterogeneity, and the Cochran Q and I^2 statistics were reported. The I^2 value describes the percentage variation between studies in degrees of freedom. P values of <0.05 were considered significant.

RESULTS

EQ-5D-5L

The EQ-5D-5L has been widely investigated as a tool for evaluating general health in normal populations and patients with different stages of liver disease (Table 3)[17,18,22,25-27,30,32]. Health utility indices should be affected by age, sex, ethics, religion, and geography. However, the EQ-5D-5L produced similar utility indices for groups with different health statuses (Table 3), such as normal healthy individuals (0.8413 ± 0.1905) and hepatitis C virus (HCV)-infected patients with compensated or decompensated cirrhosis (0.8113 ± 0.2261 and 0.7903 ± 0.2182), HCV-infected patients exhibiting a sustained virologic response (SVR) (0.846 ± 0.1816), and patients with hepatocellular carcinoma 0.8127 ± 0.2084).

In general, the EQ-5D-5L produces significantly higher scores in males than in females (Figure 1A) (0.8267 ± 0.229 *vs* 0.7922 ± 0.239; $P < 0.001$). The mean total EuroQol-visual analogue scale score for the general population was found to be 79.796 ± 17.614 in two independent studies (Table 4)[26,30].

SF-36

The SF-36 consists of eight scales, including physical functioning (85.07 ± 15.40); role limitations due to physical health problems (RP)(82.50 ± 25.15); bodily pain (BP) (77.62 ± 17.55); general health perceptions

Table 1 Current health-related outcome for liver disease

Questionnaire	Total	Permission	Company/Organization
EQ-5D-5L	Five questions	Registration required	The EuroQol Research Foundation.
Health Utilities Index Mark 2 or 3	45 questions	Purchase required	Health Utilities Inc.
36-Item Short Form Survey	36 questions	Purchase required	QualityMetric
	36 questions	Free	The RAND Corporation

EQ-5D-5L: EuroQol 5-dimensions 5-levels.

Table 2 List of previous studies and health utility assessments

Ref.	Subjects and countries	EQ-5D-5L	EQ-VAS	HUI-mark	SF-36	Type of SF-36	Others
Jenkinson *et al*[16]	Normal population from United Kingdom				O	RAND®	
Ratcliffe *et al*[17]	Normal population/Liver transplantation patients from United Kingdom	Δ	Δ		O	Not described[1]	
Chong *et al*[18]	Normal population from Canada	O	Δ	Δ	Δ[1]		
Grieve *et al*[19]	Population from United Kingdom	O					
Bondini *et al*[20]	Population from United States			O	Δ[1]		CLDQ
Dan *et al*[21]	Population from United States			O			SF-6D
Björnsson *et al*[22]	Population from Sweden	O			O	Not described[1]	
Hsu *et al*[23]	Population from Vancouver				O	v2	HQLQv2
McDonald *et al*[24]	Population from United Kingdom	O					
Scalone *et al*[25]	Population from United Kingdom	O	Δ				
Vahidnia *et al*[26]	Population from United States	Δ	O				
Kaishima *et al*[27]	Population from Japan	O					
Blanco *et al*[28]	Population from Spain	Δ	O				
Kesen *et al*[29]	HCV patients from Turkey				O	Not described[1]	HADS
Cortesi *et al*[30]	Population from Italy	O	O				
Karimi Sari *et al*[31]	HCV patients from Iran				O	Not described[1]	
Zanone *et al*[32]	HCV patients from Italy	O					

[1]Modified scale excluding from the analyses.

O: The eligible study including the analyses; Δ: The excluding outcomes due to different conditions; EQ-5D-5L: EuroQol 5-dimensions 5-levels; EQ-VAS: EuroQol-visual analogue scale; HUI-mark: Health utility index mark; SF-36: Short from-36; CLDQ: Chronic liver disease questionnaire; SF-6D: Short form 6-dimensions; HQLQv2: Hepatitis Quality of Life® survey version 2; HADS: Hospital anxiety and depression scale; HCV: Hepatitis C virus.

(GH) (63.37 ± 14.16); vitality, energy, or fatigue (VT) (63.37 ± 14.16); social functioning (SF) (86.97 ± 15.13); role limitations due to emotional problems (RE) (83.94 ± 23.57); and general mental health (63.37 ± 14.16). Although the eligible healthy controls differed among countries and age groups, the health utility scores produced by each scale were similar (Table 5)[16,17,22,23].

Compensated liver cirrhosis vs sustained virologic response

Patients with hepatitis C had achieved an SVR exhibited significantly better health utility scores for each SF-36 scale (Figure 2)[22,29,31] and the EQ-5D-5L (Figure 1B)[18,19,22,32] than those with compensated liver cirrhosis (Table 6)[18,19,22,29,31,32]. In particular, significant differences in the scores for RP (61.5 ± 31.6 *vs* 73.3 ± 27.3), GH (64.8 ± 20.9 *vs* 74.8 ± 18.5), VT (70.5 ± 24.0 *vs* 78.1 ± 18.4), RE (56.8 ± 32.0 *vs* 68.1 ± 27.3), and the EQ-5D-5L (0.6863 ± 0.3065 *vs* 0.846 ± 0.1816) were seen between these groups. These results indicate that health utility indices improve by 10%-20% after patients with hepatitis C achieve an SVR.

Table 3 EuroQol 5-dimensions 5-levels

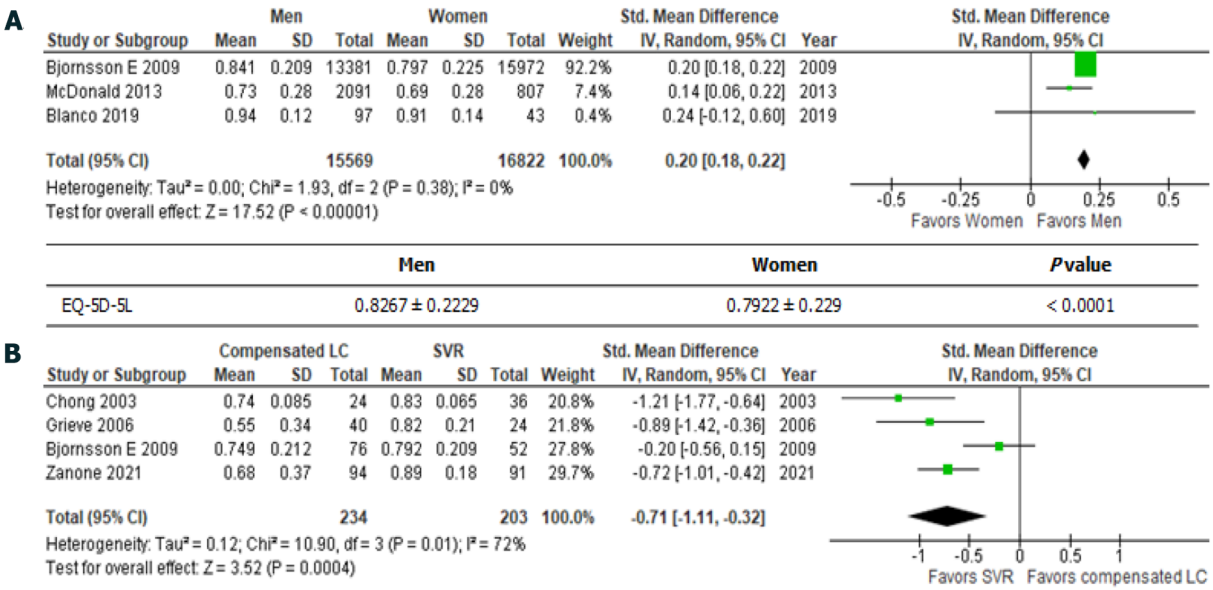
Ref.	Total	Mean	SD
Normal healthy individuals			
Ratcliffe *et al*[17]	3386	0.85	0.03
Chong *et al*[18]	1518	0.821	0.011
Björnsson *et al*[22]	29353	0.819	0.217
Vahidnia *et al*[26]	1565	0.94	0.1
Cortesi *et al*[30]	6800	0.915	0.107
Total	42622	0.8413	0.1905
Compensated cirrhosis with hepatitis C			
Chong *et al*[18]	24	0.74	0.085
Grieve *et al*[19]	40	0.55	0.34
Björnsson *et al*[22]	76	0.749	0.212
Scalone *et al*[25]	222	0.736	0.259
Kaishima *et al*[27]	20	0.824	0.106
Cortesi *et al*[30]	574	0.891	0.119
Zanone *et al*[32]	94	0.68	0.37
Total	1050	0.8113	0.2261
Decompensated cirrhosis with hepatitis C			
Chong *et al*[18]	9	0.66	0.2
Grieve *et al*[19]	64	0.45	0.24
Björnsson *et al*[22]	53	0.565	0.266
Kaishima *et al*[27]	4	0.524	0.25
Cortesi *et al*[30]	523	0.859	0.14
Total	653	0.7903	0.2182
Sustained virologic response			
Chong *et al*[18]	36	0.83	0.065
Grieve *et al*[19]	24	0.82	0.21
Björnsson *et al*[22]	52	0.792	0.209
Zanone *et al*[32]	91	0.89	0.18
Total	203	0.846	0.1816
Hepatocellular carcinoma			
Chong *et al*[18]	15	0.65	0.21
Grieve *et al*[19]	64	0.45	0.24
Scalone *et al*[25]	85	0.777	0.241
Kaishima *et al*[27]	14	0.75	0.057
Cortesi *et al*[30]	545	0.867	0.146
Total	723	0.8127	0.2084

HUI Mark-2/Mark-3

Hepatitis B and C are the main causes of viral-associated chronic liver disease (Figure 3)[20,21]. The health utility scores of hepatitis B patients were significantly better than those of hepatitis C patients (0.6312 ± 0.2867 *vs* 0.8186 ± 0.1886); *i.e.*, there was a roughly 30% difference between the scores of these patients.

Table 4 EuroQol-visual analogue scale in normal healthy individuals

Ref.	Total	Mean	SD
Vahidnia *et al*[26]	1565	87.6	10.6
Cortesi *et al*[30]	6800	78	18.4
Total	8365	79.796	17.614



DOI: 10.3748/wjg.v28.i31.4442 **Copyright** ©The Author(s) 2022.

Figure 1 EuroQOL 5-dimensions 5-levels. A: Men *vs* women; B: Compensated liver cirrhosis *vs* sustained virologic response. EQ-5D-5L: EuroQol 5-dimensions 5-levels.

DISCUSSION

Which HUI should be used for normal populations or patients with chronic liver disease?

In this meta-analysis, we summarized the findings of previous studies examining health utility evaluations in patients with chronic liver disease. Various questionnaires have been used to evaluate health utility in different populations/at different times. The EQ-5D-5L is the most popular of the questionnaires used to examine health utility scores internationally[17].

One of the concerns regarding the application of health utility scores is their sensitivity[33]. For example, the health utility scores produced by the EQ-5D-5L for patients with compensated cirrhosis and decompensated cirrhosis did not differ significantly (Table 3). On the other hand, the health utility scores for hepatitis C patients with compensated liver cirrhosis and those who achieved an SVR differed significantly according to both the SF-36 and EQ-5D-5L (Table 6). This indicated that both questionnaires are suitable for evaluating health utility in hepatitis C patients after viral elimination. Although the health utility scores derived from the EQ-5D-5L were calculated from 5 questions, the score range of the EQ-5D-5L (123.3%) was greater than that of the SF-36 (105.8%-119.2%). Therefore, the EQ-5D-5L could be suitable for evaluating health utility scores in this specific disease state. On the other hand, EQ-5D-5L-derived health utility scores are based on only five personal factors, mobility, self-care, usual activities, pain/discomfort, and anxiety/depression. Therefore, their sensitivity and any ceiling effects should be validated in each language and ethnic group.

It is well known that the prevailing subtype of viral hepatitis differs depending on the geographic region[34]. Hepatitis B is the prevailing subtype in East Asia[13], whereas hepatitis C is the most common in Western countries[35]. Both types of hepatitis can be controlled by nucleic acid analogs[36]. In this meta-analysis, the HUI scores of hepatitis C patients were roughly 30% lower than those of hepatitis B patients. The differences between hepatitis B and hepatitis C need to be investigated using the EQ-5D-5L and SF-36 in future.

The second concern regarding the use of questionnaires for health assessments relates to the number of questions in each questionnaire. The EQ-5D-5L consists of only five questions[8], whereas the other tools consist of 36[14-16] or 45[11] questions. The number of questions affects study compliance, especially in the elderly[37]. If possible, the number of questions should be minimized.

Table 5 Short from-36: Healthy controls

Ref.	Total	Mean	SD
Physical function			
Björnsson *et al*[22]	339	87	19
Jenkinson *et al*[16] M 60	681	80	22.1
Jenkinson *et al*[16] W 60	684	74.8	23.5
Ratcliffe *et al*[17]	8883	85.4	2.55
Hsu *et al*[23]	9367	85.8	20
Total	19954	85.07	15.40
Role physical			
Björnsson *et al*[22]	339	82	32
Jenkinson *et al*[16] M 60	717	78.8	36.1
Jenkinson *et al*[16] W 60	757	76.8	36.9
Ratcliffe *et al*[17]	9151	83.7	4.4
Hsu *et al*[23]	9367	82.1	33.2
Total	20331	82.50	25.15
Body pain			
Björnsson *et al*[22]	339	72	27
Jenkinson *et al*[16] M 60	724	78.8	23.6
Jenkinson *et al*[16] W 60	779	75	25.1
Ratcliffe *et al*[17]	9214	80	3.05
Hsu *et al*[23]	9367	75.6	23
Total	20423	77.62	17.55
General health			
Björnsson *et al*[22]	339	68	24
Jenkinson *et al*[16] M 60	707	62.9	20.3
Jenkinson *et al*[16] W 60	763	59	21.4
Ratcliffe *et al*[17]	9089	61.1	2.75
Hsu *et al*[23]	9367	65.8	18
Total	20265	63.37	14.16
Vitality, energy, fatigue			
Björnsson *et al*[22]	339	68	24
Jenkinson *et al*[16] M 60	707	62.9	20.3
Jenkinson *et al*[16] W 60	763	59	21.4
Ratcliffe *et al*[17]	9089	61.1	2.75
Hsu *et al*[23]	9367	65.8	18
Total	20265	63.37	14.16
Social function			
Björnsson *et al*[22]	339	88	21
Jenkinson *et al*[16] M 60	729	86.9	22.6
Jenkinson *et al*[16] W 60	783	85.9	22.6
Ratcliffe *et al*[17]	9219	87.8	2.8
Hsu *et al*[23]	9367	86.2	19.8

Total	20437	86.97	15.13
Role emotional			
Björnsson *et al*[22]	339	86	29
Jenkinson *et al*[16] M 60	714	85.8	29.5
Jenkinson *et al*[16] W 60	756	83.3	32.5
Ratcliffe *et al*[17]	9159	83.7	4.4
Hsu *et al*[23]	9367	84	31.7
Total	20335	83.94	23.57
Mental health, emotional, well-being			
Björnsson *et al*[22]	339	50	10
Jenkinson *et al*[16] M 60	697	78	17.5
Jenkinson *et al*[16] W 60	742	74.4	18.5
Ratcliffe *et al*[17]	9014	74.6	2.35
Hsu *et al*[23]	9367	77.5	15.3
Total	20159	75.64	12.23

Table 6 Compensated liver cirrhosis *vs* sustained virologic response

Questionnare	Compensated LC	SVR	*P* value	% improvement
SF-36: Physical function	79.3 ± 19.3	83.9 ± 17.8	0.07	105.8
SF-36: Role physical	61.5 ± 31.6	73.3 ± 27.3	0.004	119.2
SF-36: Body pain	80.8 ± 23.1	85.4 ± 21.3	0.09	105.7
SF-36: General health	64.8 ± 20.9	74.8 ± 18.5	< 0.001	115.4
SF-36: Vitality	70.5 ± 24.0	78.1 ± 18.4	0.002	110.8
SF-36: Social function	77.0 ± 19.0	83.3 ± 15.6	0.05	108.2
SF-36: Role emotional	56.8 ± 32.0	68.1 ± 27.3	< 0.001	119.9
SF-36: Mental health	77.2 ± 16.8	81.3 ± 15.2	0.12	105.3
EQ-5D-5L	0.6863 ± 0.3065	0.846 ± 0.1816	< 0.001	123.3

LC: Liver cirrhosis; SVR: Sustained virologic response; SF-36: Short from-36; EQ-5D-5L: EuroQol 5-dimensions 5-levels.

The last concern is about gaining permission to use such questionnaires for health utility assessments. It takes great effort to develop a questionnaire. However, health utility assessments need to be repeated continuously. In certain human health emergencies, the use of some vaccines has been allowed without patent royalties having to be paid[38]. Commercial companies that own the rights to health assessments should reconsider their policies regarding their use.

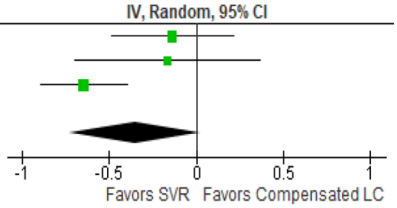
CONCLUSION

Health assessments that allow free registration would be useful for evaluating health utility in patients with liver disease. Alternatively, a portable QOL tracker could be used to perform QOL evaluations of any patient-reported outcome, and we are currently developing such a tracker.

A

Study or Subgroup	Compensated LC Mean	SD	Total	SVR Mean	SD	Total	Weight	Std. Mean Difference IV, Random, 95% CI	Year
Bjornsson E 2009	79	22	76	82	21	52	34.6%	-0.14 [-0.49, 0.22]	2009
Kesen 2019	58.51	31.25	27	63.51	28.27	27	24.9%	-0.17 [-0.70, 0.37]	2019
Karimi Sari 2020	83.96	8.49	127	89.08	7.22	127	40.6%	-0.65 [-0.90, -0.40]	2020
Total (95% CI)			230			206	100.0%	-0.35 [-0.73, 0.03]	

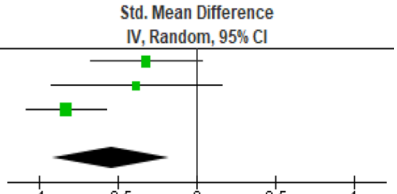
Heterogeneity: Tau² = 0.08; Chi² = 6.42, df = 2 (P = 0.04); I² = 69%
Test for overall effect: Z = 1.82 (P = 0.07)



B

Study or Subgroup	Compensated LC Mean	SD	Total	SVR Mean	SD	Total	Weight	Std. Mean Difference IV, Random, 95% CI	Year
Bjornsson E 2009	58	43	76	71	37	52	34.6%	-0.32 [-0.67, 0.04]	2009
Kesen 2019	36.11	42.36	27	52.77	44.03	27	24.4%	-0.38 [-0.92, 0.16]	2019
Karimi Sari 2020	68.54	12.34	127	78.54	11.82	127	40.9%	-0.83 [-1.08, -0.57]	2020
Total (95% CI)			230			206	100.0%	-0.54 [-0.91, -0.17]	

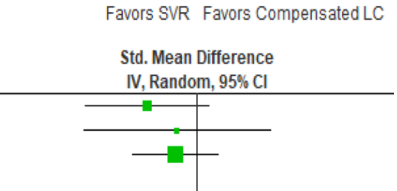
Heterogeneity: Tau² = 0.07; Chi² = 6.01, df = 2 (P = 0.05); I² = 67%
Test for overall effect: Z = 2.88 (P = 0.004)



C

Study or Subgroup	Compensated LC Mean	SD	Total	SVR Mean	SD	Total	Weight	Std. Mean Difference IV, Random, 95% CI	Year
Bjornsson E 2009	64	27	76	72	30	52	28.5%	-0.28 [-0.64, 0.07]	2009
Kesen 2019	64.51	19.06	27	66.7	20.21	27	12.5%	-0.11 [-0.64, 0.42]	2019
Karimi Sari 2020	94.27	7.23	127	95.1	6.74	127	59.0%	-0.12 [-0.36, 0.13]	2020
Total (95% CI)			230			206	100.0%	-0.16 [-0.35, 0.03]	

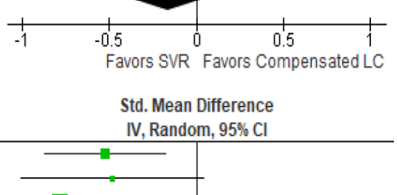
Heterogeneity: Tau² = 0.00; Chi² = 0.59, df = 2 (P = 0.74); I² = 0%
Test for overall effect: Z = 1.70 (P = 0.09)



D

Study or Subgroup	Compensated LC Mean	SD	Total	SVR Mean	SD	Total	Weight	Std. Mean Difference IV, Random, 95% CI	Year
Bjornsson E 2009	54	24	76	67	24	52	29.4%	-0.54 [-0.90, -0.18]	2009
Kesen 2019	43.59	19.92	27	53.92	20.84	27	12.9%	-0.50 [-1.04, 0.04]	2019
Karimi Sari 2020	75.73	8.89	127	82.45	7.66	127	57.8%	-0.81 [-1.06, -0.55]	2020
Total (95% CI)			230			206	100.0%	-0.69 [-0.88, -0.49]	

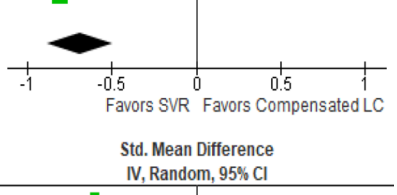
Heterogeneity: Tau² = 0.00; Chi² = 1.97, df = 2 (P = 0.37); I² = 0%
Test for overall effect: Z = 6.94 (P < 0.00001)



E

Study or Subgroup	Compensated LC Mean	SD	Total	SVR Mean	SD	Total	Weight	Std. Mean Difference IV, Random, 95% CI	Year
Bjornsson E 2009	52	28	76	67	24	52	30.2%	-0.56 [-0.92, -0.20]	2009
Kesen 2019	56.11	19.13	27	60.55	19.38	27	14.9%	-0.23 [-0.76, 0.31]	2019
Karimi Sari 2020	84.6	7.34	127	86.33	7.47	127	54.9%	-0.23 [-0.48, 0.01]	2020
Total (95% CI)			230			206	100.0%	-0.33 [-0.55, -0.12]	

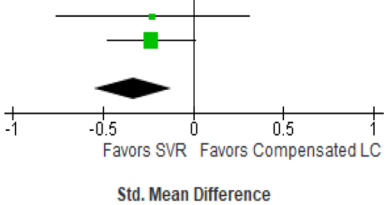
Heterogeneity: Tau² = 0.01; Chi² = 2.35, df = 2 (P = 0.31); I² = 15%
Test for overall effect: Z = 3.03 (P = 0.002)



F

Study or Subgroup	Compensated LC Mean	SD	Total	SVR Mean	SD	Total	Weight	Std. Mean Difference IV, Random, 95% CI	Year
Bjornsson E 2009	79	24	76	83	22	52	34.6%	-0.17 [-0.52, 0.18]	2009
Kesen 2019	66.66	26.62	27	73.14	22.91	27	26.5%	-0.26 [-0.79, 0.28]	2019
Karimi Sari 2020	77.92	11.76	127	85.62	7.88	127	38.9%	-0.77 [-1.02, -0.51]	2020
Total (95% CI)			230			206	100.0%	-0.43 [-0.86, 0.00]	

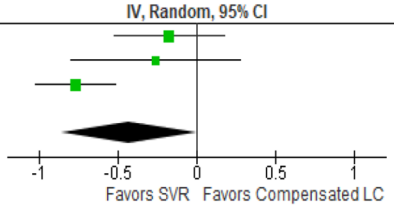
Heterogeneity: Tau² = 0.11; Chi² = 8.27, df = 2 (P = 0.02); I² = 76%
Test for overall effect: Z = 1.94 (P = 0.05)



G

Study or Subgroup	Compensated LC Mean	SD	Total	SVR Mean	SD	Total	Weight	Std. Mean Difference IV, Random, 95% CI	Year
Bjornsson E 2009	66	42	76	77	35	52	31.4%	-0.28 [-0.63, 0.08]	2009
Kesen 2019	33.33	41.36	27	58.02	43.94	27	14.6%	-0.57 [-1.12, -0.03]	2019
Karimi Sari 2020	56.33	17.16	127	66.61	16.18	127	54.0%	-0.61 [-0.87, -0.36]	2020
Total (95% CI)			230			206	100.0%	-0.50 [-0.72, -0.29]	

Heterogeneity: Tau² = 0.01; Chi² = 2.35, df = 2 (P = 0.31); I² = 15%
Test for overall effect: Z = 4.55 (P < 0.00001)



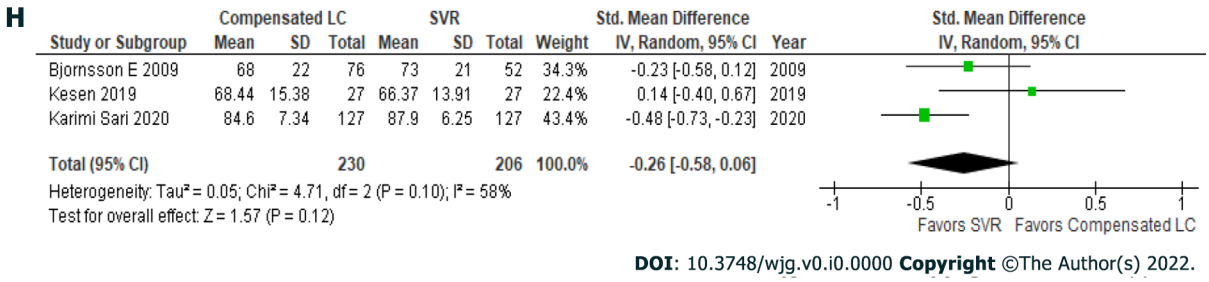
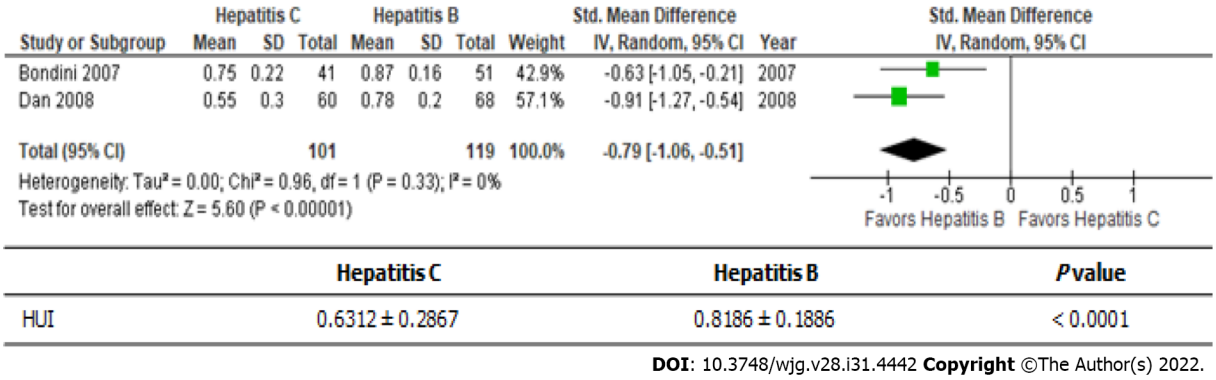


Figure 2 Short from-36: Compensated liver cirrhosis *vs* sustained virologic response. A: Physical function; B: Role physical; C: Body pain; D: General health; E: Vitality; F: Social function; G: Role emotional; H: Mental health.



	Hepatitis C	Hepatitis B	*P* value
HUI	0.6312 ± 0.2867	0.8186 ± 0.1886	< 0.0001

DOI: 10.3748/wjg.v28.i31.4442 **Copyright** ©The Author(s) 2022.

Figure 3 Health Utilities Index-Mark2 or 3: Hepatitis C *vs* hepatitis B. HUI: Health Utilities Index.

ARTICLE HIGHLIGHTS

Research background

The most useful questionnaire for evaluating health status depending on liver disease status or sex is unclear.

Research motivation

No universal health utility assessment values for specific liver diseases or the normal population have been reported.

Research objectives

The objective of this study was to conduct a meta-analysis to estimate health utility assessment values for specific populations in the liver disease.

Research methods

A systematic literature search was performed using PubMed and MEDLINE, including the Cochrane Library.

Research results

The short from-36 and EuroQOL 5-dimensions 5-levels (EQ-5D-5L) can be used for health utility evaluations during antiviral therapy for hepatitis C.

Research conclusions

The EQ-5D-5L is the most popular questionnaire for health utility assessments. Health assessments that allow free registration would be useful for evaluating health utility in patients with liver disease.

Research perspectives

Alternatively, a portable quality of life (QOL) tracker could be used to perform QOL evaluations of any patient-reported outcome in future.

ACKNOWLEDGEMENTS

We thank Sandy Tan and Miyako Nara for their valuable discussions and help in preparing this manuscript.

FOOTNOTES

Author contributions: Ishinuki T and Ota S conceptualized and designed the review; Ishinuki T, Harada K, Kawamoto M, and Meguro M searched for and screened the articles; Kutomi G, Tatsumi H, Harada K, and Kato T assessed the articles for eligibility; Miyanishi K and Ohyanagi T carried out the statistical analyses; Hui TT and Mizuguchi T drafted the initial manuscript; Mizuguchi T finalized the manuscript; and all of the authors reviewed and approved the final manuscript as submitted.

Supported by Grants-in-Aid from JSPS KAKENHI, No. JP 20K10404 (to Mizuguchi T) and No. JP 21K10715 (to Ishinuki T); the Hokkaido Hepatitis B Litigation Orange Fund, No. 2059198 (to Mizuguchi T) and No. 2136589 (to Harada K); Terumo Life Science Foundation, No. 2000666; Pfizer Health Research Foundation, No. 2000777; the Viral Hepatitis Research Foundation of Japan, No. 3039838; Project Mirai Cancer Research Grants, No. 202110251; Takahashi Industrial and Economic Research Foundation, No. 12-003-106; Daiichi Sankyo Company, No. 2109540; Shionogi and Co., No. 2109493; MSD, No. 2099412; Takeda Pharmaceutical Company, No. 2000555; Sapporo Doto Hospital, No. 2039118; Noguchi Hospital, No. 2029083; Doki-kai Tomakomai Hospital, No. 2059203; Tsuchida Hospital, No. 2000092; Shinyu-kai Noguchi Hospital, No. 2029083 (to Mizuguchi T); and the Yasuda Medical Foundation, No. 28-1 (to Ishinuki T).

Conflict-of-interest statement: All authors have nothing to disclose.

PRISMA 2009 Checklist statement: The authors have read the PRISMA 2009 Checklist statement, and the manuscript was prepared and revised according to the PRISMA 2009 Checklist statement.

Open-Access: This article is an open-access article that was selected by an in-house editor and fully peer-reviewed by external reviewers. It is distributed in accordance with the Creative Commons Attribution NonCommercial (CC BY-NC 4.0) license, which permits others to distribute, remix, adapt, build upon this work non-commercially, and license their derivative works on different terms, provided the original work is properly cited and the use is non-commercial. See: https://creativecommons.org/Licenses/by-nc/4.0/

Country/Territory of origin: Japan

ORCID number: Tomohiro Ishinuki 0000-0003-3225-9781; Shigenori Ota 0000-0003-3123-9172; Kohei Harada 0000-0002-3245-6980; Masaki Kawamoto 0000-0002-2800-6207; Makoto Meguro 0000-0002-9170-6919; Goro Kutomi 0000-0003-4557-5126; Hiroomi Tatsumi 0000-0002-9688-6154; Keisuke Harada 0000-0002-7497-6191; Koji Miyanishi 0000-0002-6466-3458; Toru Kato 0000-0002-8520-1949; Toshio Ohyanagi 0000-0001-8335-3087; Thomas T Hui 0000-0003-2717-3983; Toru Mizuguchi 0000-0002-8225-7461.

Corresponding Author's Membership in Professional Societies: The Japanese Society of Gastroenterology.

S-Editor: Ma YJ
L-Editor: A
P-Editor: Ma YJ

REFERENCES

1 **Donabedian A**. Evaluating the quality of medical care. 1966. *Milbank Q* 2005; **83**: 691-729 [PMID: 16279964 DOI: 10.1111/j.1468-0009.2005.00397.x]
2 **Hazawa Y**, Kutomi G, Shima H, Honma T, Ohmura T, Wada A, Mikami T, Hotta M, Narumi M, Ishinuki T, Kuno Y, Meguro M, Takemasa I, Okazaki M, Masuoka H, Asaishi K, Ohyanagi T, Hui TT, Mizuguchi T. The Unique Mental Impacts of Breast-Conserving Surgery and Mastectomy According to a Multi-Centered Cross Sectional Survey Conducted in Japan. *Arch Breast Cancer* 2020; **7**: 119-126 [DOI: 10.32768/abc.202073119-126]
3 **Whitehead SJ**, Ali S. Health outcomes in economic evaluation: the QALY and utilities. *Br Med Bull* 2010; **96**: 5-21 [PMID: 21037243 DOI: 10.1093/bmb/ldq033]
4 **Global Burden of Disease Cancer Collaboration**, Fitzmaurice C, Abate D, Abbasi N, Abbastabar H, Abd-Allah F, Abdel-Rahman O, Abdelalim A, Abdoli A, Abdollahpour I, Abdulle ASM, Abebe ND, Abraha HN, Abu-Raddad LJ, Abualhasan A, Adedeji IA, Advani SM, Afarideh M, Afshari M, Aghaali M, Agius D, Agrawal S, Ahmadi A, Ahmadian E, Ahmadpour E, Ahmed MB, Akbari ME, Akinyemiju T, Al-Aly Z, AlAbdulKader AM, Alahdab F, Alam T, Alamene GM, Alemnew BTT, Alene KA, Alinia C, Alipour V, Aljunid SM, Bakeshei FA, Almadi MAH, Almasi-Hashiani A, Alsharif U, Alsowaidi S, Alvis-Guzman N, Amini E, Amini S, Amoako YA, Anbari Z, Anber NH, Andrei CL, Anjomshoa M, Ansari F, Ansariadi

A, Appiah SCY, Arab-Zozani M, Arabloo J, Arefi Z, Aremu O, Areri HA, Artaman A, Asayesh H, Asfaw ET, Ashagre AF, Assadi R, Ataeinia B, Atalay HT, Ataro Z, Atique S, Ausloos M, Avila-Burgos L, Avokpaho EFGA, Awasthi A, Awoke N, Ayala Quintanilla BP, Ayanore MA, Ayele HT, Babaee E, Bacha U, Badawi A, Bagherzadeh M, Bagli E, Balakrishnan S, Balouchi A, Bärnighausen TW, Battista RJ, Behzadifar M, Bekele BB, Belay YB, Belayneh YM, Berfield KKS, Berhane A, Bernabe E, Beuran M, Bhakta N, Bhattacharyya K, Biadgo B, Bijani A, Bin Sayeed MS, Birungi C, Bisignano C, Bitew H, Bjørge T, Bleyer A, Bogale KA, Bojia HA, Borzì AM, Bosetti C, Bou-Orm IR, Brenner H, Brewer JD, Briko AN, Briko NI, Bustamante-Teixeira MT, Butt ZA, Carreras G, Carrero JJ, Carvalho F, Castro C, Castro F, Catalá-López F, Cerin E, Chaiah Y, Chanie WF, Chattu VK, Chaturvedi P, Chauhan NS, Chehrazi M, Chiang PP, Chichiabellu TY, Chido-Amajuoyi OG, Chimed-Ochir O, Choi JJ, Christopher DJ, Chu DT, Constantin MM, Costa VM, Crocetti E, Crowe CS, Curado MP, Dahlawi SMA, Damiani G, Darwish AH, Daryani A, das Neves J, Demeke FM, Demis AB, Demissie BW, Demoz GT, Denova-Gutiérrez E, Derakhshani A, Deribe KS, Desai R, Desalegn BB, Desta M, Dey S, Dharmaratne SD, Dhimal M, Diaz D, Dinberu MTT, Djalalinia S, Doku DT, Drake TM, Dubey M, Dubljanin E, Duken EE, Ebrahimi H, Effiong A, Eftekhari A, El Sayed I, Zaki MES, El-Jaafary SI, El-Khatib Z, Elemineh DA, Elkout H, Ellenbogen RG, Elsharkawy A, Emamian MH, Endalew DA, Endries AY, Eshrati B, Fadhil I, Fallah Omrani V, Faramarzi M, Farhangi MA, Farioli A, Farzadfar F, Fentahun N, Fernandes E, Feyissa GT, Filip I, Fischer F, Fisher JL, Force LM, Foroutan M, Freitas M, Fukumoto T, Futran ND, Gallus S, Gankpe FG, Gayesa RT, Gebrehiwot TT, Gebremeskel GG, Gedefaw GA, Gelaw BK, Geta B, Getachew S, Gezae KE, Ghafourifard M, Ghajar A, Ghashghaee A, Gholamian A, Gill PS, Ginindza TTG, Girmay A, Gizaw M, Gomez RS, Gopalani SV, Gorini G, Goulart BNG, Grada A, Ribeiro Guerra M, Guimaraes ALS, Gupta PC, Gupta R, Hadkhale K, Haj-Mirzaian A, Hamadeh RR, Hamidi S, Hanfore LK, Haro JM, Hasankhani M, Hasanzadeh A, Hassen HY, Hay RJ, Hay SI, Henok A, Henry NJ, Herteliu C, Hidru HD, Hoang CL, Hole MK, Hoogar P, Horita N, Hosgood HD, Hosseini M, Hosseinzadeh M, Hostiuc M, Hostiuc S, Househ M, Hussen MM, Ileanu B, Ilic MD, Innos K, Irvani SSN, Iseh KR, Islam SMS, Islami F, Jafari Balalami N, Jafarinia M, Jahangiry L, Jahani MA, Jahanmehr N, Jakovljevic M, James SL, Javanbakht M, Jayaraman S, Jee SH, Jenabi E, Jha RP, Jonas JB, Jonnagaddala J, Joo T, Jungari SB, Jürisson M, Kabir A, Kamangar F, Karch A, Karimi N, Karimian A, Kasaeian A, Kasahun GG, Kassa B, Kassa TD, Kassaw MW, Kaul A, Keiyoro PN, Kelbore AG, Kerbo AA, Khader YS, Khalilarjmandi M, Khan EA, Khan G, Khang YH, Khatab K, Khater A, Khayamzadeh M, Khazaee-Pool M, Khazaei S, Khoja AT, Khosravi MH, Khubchandani J, Kianipour N, Kim D, Kim YJ, Kisa A, Kisa S, Kissimova-Skarbek K, Komaki H, Koyanagi A, Krohn KJ, Bicer BK, Kugbey N, Kumar V, Kuupiel D, La Vecchia C, Lad DP, Lake EA, Lakew AM, Lal DK, Lami FH, Lan Q, Lasrado S, Lauriola P, Lazarus JV, Leigh J, Leshargie CT, Liao Y, Limenih MA, Listl S, Lopez AD, Lopukhov PD, Lunevicius R, Madadin M, Magdeldin S, El Razek HMA, Majeed A, Maleki A, Malekzadeh R, Manafi A, Manafi N, Manamo WA, Mansourian M, Mansournia MA, Mantovani LG, Maroufizadeh S, Martini SMS, Mashamba-Thompson TP, Massenburg BB, Maswabi MT, Mathur MR, McAlinden C, McKee M, Meheretu HAA, Mehrotra R, Mehta V, Meier T, Melaku YA, Meles GG, Meles HG, Melese A, Melku M, Memiah PTN, Mendoza W, Menezes RG, Merat S, Meretoja TJ, Mestrovic T, Miazgowski B, Miazgowski T, Mihretie KMM, Miller TR, Mills EJ, Mir SM, Mirzaei H, Mirzaei HR, Mishra R, Moazen B, Mohammad DK, Mohammad KA, Mohammad Y, Darwesh AM, Mohammadbeigi A, Mohammadi H, Mohammadi M, Mohammadian M, Mohammadian-Hafshejani A, Mohammadoo-Khorasani M, Mohammadpourhodki R, Mohammed AS, Mohammed JA, Mohammed S, Mohebi F, Mokdad AH, Monasta L, Moodley Y, Moosazadeh M, Moossavi M, Moradi G, Moradi-Joo M, Moradi-Lakeh M, Moradpour F, Morawska L, Morgado-da-Costa J, Morisaki N, Morrison SD, Mosapour A, Mousavi SM, Muche AA, Muhammed OSS, Musa J, Nabhan AF, Naderi M, Nagarajan AJ, Nagel G, Nahvijou A, Naik G, Najafi F, Naldi L, Nam HS, Nasiri N, Nazari J, Negoi I, Neupane S, Newcomb PA, Nggada HA, Ngunjiri JW, Nguyen CT, Nikniaz L, Ningrum DNA, Nirayo YL, Nixon MR, Nnaji CA, Nojomi M, Nosratnejad S, Shiadeh MN, Obsa MS, Ofori-Asenso R, Ogbo FA, Oh IH, Olagunju AT, Olagunju TO, Oluwasanu MM, Omonisi AE, Onwujekwe OE, Oommen AM, Oren E, Ortega-Altamirano DDV, Ota E, Otstavnov SS, Owolabi MO, P A M, Padubidri JR, Pakhale S, Pakpour AH, Pana A, Park EK, Parsian H, Pashaei T, Patel S, Patil ST, Pennini A, Pereira DM, Piccinelli C, Pillay JD, Pirestani M, Pishgar F, Postma MJ, Pourjafar H, Pourmalek F, Pourshams A, Prakash S, Prasad N, Qorbani M, Rabiee M, Rabiee N, Radfar A, Rafiei A, Rahim F, Rahimi M, Rahman MA, Rajati F, Rana SM, Raoofi S, Rath GK, Rawaf DL, Rawaf S, Reiner RC, Renzaho AMN, Rezaei N, Rezapour A, Ribeiro AI, Ribeiro D, Ronfani L, Roro EM, Roshandel G, Rostami A, Saad RS, Sabbagh P, Sabour S, Saddik B, Safiri S, Sahebkar A, Salahshoor MR, Salehi F, Salem H, Salem MR, Salimzadeh H, Salomon JA, Samy AM, Sanabria J, Santric Milicevic MM, Sartorius B, Sarveazad A, Sathian B, Satpathy M, Savic M, Sawhney M, Sayyah M, Schneider IJC, Schöttker B, Sekerija M, Sepanlou SG, Sepehrimanesh M, Seyedmousavi S, Shaahmadi F, Shabaninejad H, Shahbaz M, Shaikh MA, Shamshirian A, Shamsizadeh M, Sharafi H, Sharafi Z, Sharif M, Sharifi A, Sharifi H, Sharma R, Sheikh A, Shirkoohi R, Shukla SR, Si S, Siabani S, Silva DAS, Silveira DGA, Singh A, Singh JA, Sisay S, Sitas F, Sobngwi E, Soofi M, Soriano JB, Stathopoulou V, Sufiyan MB, Tabarés-Seisdedos R, Tabuchi T, Takahashi K, Tamtaji OR, Tarawneh MR, Tassew SG, Taymoori P, Tehrani-Banihashemi A, Temsah MH, Temsah O, Tesfay BE, Tesfay FH, Teshale MY, Tessema GA, Thapa S, Tlaye KG, Topor-Madry R, Tovani-Palone MR, Traini E, Tran BX, Tran KB, Tsadik AG, Ullah I, Uthman OA, Vacante M, Vaezi M, Varona Pérez P, Veisani Y, Vidale S, Violante FS, Vlassov V, Vollset SE, Vos T, Vosoughi K, Vu GT, Vujcic IS, Wabinga H, Wachamo TM, Wagnew FS, Waheed Y, Weldegebreal F, Weldesamuel GT, Wijeratne T, Wondafrash DZ, Wonde TE, Wondmieneh AB, Workie HM, Yadav R, Yadegar A, Yadollahpour A, Yaseri M, Yazdi-Feyzabadi V, Yeshaneh A, Yimam MA, Yimer EM, Yisma E, Yonemoto N, Younis MZ, Yousefi B, Yousefifard M, Yu C, Zabeh E, Zadnik V, Moghadam TZ, Zaidi Z, Zamani M, Zandian H, Zangeneh A, Zaki L, Zendehdel K, Zenebe ZM, Zewale TA, Ziapour A, Zodpey S, Murray CJL. Global, Regional, and National Cancer Incidence, Mortality, Years of Life Lost, Years Lived With Disability, and Disability-Adjusted Life-Years for 29 Cancer Groups, 1990 to 2017: A Systematic Analysis for the Global Burden of Disease Study. *JAMA Oncol* 2019; **5**: 1749-1768 [PMID: 31560378 DOI: 10.1001/jamaoncol.2019.2996]

5 **Carr AJ**, Gibson B, Robinson PG. Measuring quality of life: Is quality of life determined by expectations or experience? *BMJ* 2001; **322**: 1240-1243 [PMID: 11358783 DOI: 10.1136/bmj.322.7296.1240]

6 **Koide R**, Kikuchi A, Miyajima M, Mishina T, Takahashi Y, Okawa M, Sawada I, Nakajima J, Watanabe A, Mizuguchi T. Quality assessment using EQ-5D-5L after lung surgery for non-small cell lung cancer (NSCLC) patients. *Gen Thorac Cardiovasc Surg* 2019; **67**: 1056-1061 [PMID: 31098867 DOI: 10.1007/s11748-019-01136-0]

7 **Kikuchi A**, Koide R, Iwasaki M, Teramoto M, Satohisa S, Tamate M, Horiguchi M, Niwa N, Saito T, Mizuguchi T. Assessing quality of life using the brief cancer-related worry inventory for gynecological surgery. *World J Obstet Gynecol* 2019; **8**: 1-7 [DOI: 10.5317/wjog.v8.i1.1]

8 **Rabin R**, de Charro F. EQ-5D: a measure of health status from the EuroQol Group. *Ann Med* 2001; **33**: 337-343 [PMID: 11491192 DOI: 10.3109/07853890109002087]

9 **Ishinuki T**, Ota S, Harada K, Tatsumi H, Miyanishi K, Nagayama M, Takemasa I, Ohyanagi T, Hui TT, Mizuguchi T. Health-related quality of life in patients that have undergone liver resection: A systematic review and meta-analysis. *World J Meta-Anal* 2021; **9**: 88-100 [DOI: 10.13105/wjma.v9.i1.88]

10 **Shiroiwa T**, Fukuda T, Ikeda S, Igarashi A, Noto S, Saito S, Shimozuma K. Japanese population norms for preference-based measures: EQ-5D-3L, EQ-5D-5L, and SF-6D. *Qual Life Res* 2016; **25**: 707-719 [PMID: 26303761 DOI: 10.1007/s11136-015-1108-2]

11 **Younossi ZM**, Boparai N, McCormick M, Price LL, Guyatt G. Assessment of utilities and health-related quality of life in patients with chronic liver disease. *Am J Gastroenterol* 2001; **96**: 579-583 [PMID: 11232711 DOI: 10.1111/j.1572-0241.2001.03537.x]

12 **Whitehurst DG**, Engel L, Bryan S. Short Form health surveys and related variants in spinal cord injury research: a systematic review. *J Spinal Cord Med* 2014; **37**: 128-138 [PMID: 24559417 DOI: 10.1179/2045772313Y.0000000159]

13 **de Medeiros MMD**, Carletti TM, Magno MB, Maia LC, Cavalcanti YW, Rodrigues-Garcia RCM. Does the institutionalization influence elderly's quality of life? *BMC Geriatr* 2020; **20**: 44 [PMID: 32024479 DOI: 10.1186/s12877-020-1452-0]

14 **Hays RD**, Sherbourne CD, Mazel RM. The RAND 36-Item Health Survey 1.0. *Health Econ* 1993; **2**: 217-227 [PMID: 8275167 DOI: 10.1002/hec.4730020305]

15 **Ware JE**, Sherbourne CD. The MOS 36-item short-form health survey (SF-36). I. Conceptual framework and item selection. *Med Care* 1992; **30**: 473-483 [PMID: 1593914]

16 **Jenkinson C**, Coulter A, Wright L. Short form 36 (SF36) health survey questionnaire: normative data for adults of working age. *BMJ* 1993; **306**: 1437-1440 [PMID: 8518639 DOI: 10.1136/bmj.306.6890.1437]

17 **Ratcliffe J**, Longworth L, Young T, Bryan S, Burroughs A, Buxton M; Cost-Effectiveness of Liver Transplantation Team. Assessing health-related quality of life pre- and post-liver transplantation: a prospective multicenter study. *Liver Transpl* 2002; **8**: 263-270 [PMID: 11910572 DOI: 10.1053/jlts.2002.31345]

18 **Chong CA**, Gulamhussein A, Heathcote EJ, Lilly L, Sherman M, Naglie G, Krahn M. Health-state utilities and quality of life in hepatitis C patients. *Am J Gastroenterol* 2003; **98**: 630-638 [PMID: 12650799 DOI: 10.1111/j.1572-0241.2003.07332.x]

19 **Grieve R**, Roberts J, Wright M, Sweeting M, DeAngelis D, Rosenberg W, Bassendine M, Main J, Thomas H. Cost effectiveness of interferon alpha or peginterferon alpha with ribavirin for histologically mild chronic hepatitis C. *Gut* 2006; **55**: 1332-1338 [PMID: 15994216 DOI: 10.1136/gut.2005.064774]

20 **Bondini S**, Kallman J, Dan A, Younoszai Z, Ramsey L, Nader F, Younossi ZM. Health-related quality of life in patients with chronic hepatitis B. *Liver Int* 2007; **27**: 1119-1125 [PMID: 17845541 DOI: 10.1111/j.1478-3231.2007.01558.x]

21 **Dan AA**, Kallman JB, Srivastava R, Younoszai Z, Kim A, Younossi ZM. Impact of chronic liver disease and cirrhosis on health utilities using SF-6D and the health utility index. *Liver Transpl* 2008; **14**: 321-326 [PMID: 18306356 DOI: 10.1002/lt.21376]

22 **Björnsson E**, Verbaan H, Oksanen A, Frydén A, Johansson J, Friberg S, Dalgård O, Kalaitzakis E. Health-related quality of life in patients with different stages of liver disease induced by hepatitis C. *Scand J Gastroenterol* 2009; **44**: 878-887 [PMID: 19437190 DOI: 10.1080/00365520902898135]

23 **Hsu PC**, Krajden M, Yoshida EM, Anderson FH, Tomlinson GA, Krahn MD. Does cirrhosis affect quality of life in hepatitis C virus-infected patients? *Liver Int* 2009; **29**: 449-458 [PMID: 19267865 DOI: 10.1111/j.1478-3231.2008.01865.x]

24 **McDonald SA**, Hutchinson SJ, Palmateer NE, Allen E, Cameron SO, Goldberg DJ, Taylor A. Decrease in health-related quality of life associated with awareness of hepatitis C virus infection among people who inject drugs in Scotland. *J Hepatol* 2013; **58**: 460-466 [PMID: 23149064 DOI: 10.1016/j.jhep.2012.11.004]

25 **Scalone L**, Ciampichini R, Fagiuoli S, Gardini I, Fusco F, Gaeta L, Del Prete A, Cesana G, Mantovani LG. Comparing the performance of the standard EQ-5D 3L with the new version EQ-5D 5L in patients with chronic hepatic diseases. *Qual Life Res* 2013; **22**: 1707-1716 [PMID: 23192232 DOI: 10.1007/s11136-012-0318-0]

26 **Vahidnia F**, Stramer SL, Kessler D, Shaz B, Leparc G, Krysztof DE, Glynn SA, Custer B. Recent viral infection in US blood donors and health-related quality of life (HRQOL). *Qual Life Res* 2017; **26**: 349-357 [PMID: 27534773 DOI: 10.1007/s11136-016-1392-5]

27 **Kaishima T**, Akita T, Ohisa M, Sakamune K, Kurisu A, Sugiyama A, Aikata H, Chayama K, Tanaka J. Cost-effectiveness analyses of anti-hepatitis C virus treatments using quality of life scoring among patients with chronic liver disease in Hiroshima prefecture, Japan. *Hepatol Res* 2018; **48**: 509-520 [PMID: 29316059 DOI: 10.1111/hepr.13053]

28 **Blanco JR**, Barrio I, Ramalle-Gómara E, Beltran MI, Ibarra V, Metola L, Sanz M, Oteo JA, Melús E, Antón L. Gender differences for frailty in HIV-infected patients on stable antiretroviral therapy and with an undetectable viral load. *PLoS One* 2019; **14**: e0215764 [PMID: 31071105 DOI: 10.1371/journal.pone.0215764]

29 **Kesen O**, Kani HT, Yanartaş Ö, Aykut UE, Gök B, Gündüz F, Yılmaz Y, Özdoğan OC, Özen Alahdab Y. Evaluation of depression, anxiety and quality of life in hepatitis C patients who treated with direct acting antiviral agents. *Turk J Gastroenterol* 2019; **30**: 801-806 [PMID: 31530524 DOI: 10.5152/tjg.2019.18679]

30 **Cortesi PA**, Conti S, Scalone L, Jaffe A, Ciaccio A, Okolicsanyi S, Rota M, Fabris L, Colledan M, Fagiuoli S, Belli LS, Cesana G, Strazzabosco M, Mantovani LG. Health related quality of life in chronic liver diseases. *Liver Int* 2020; **40**: 2630-2642 [PMID: 32851764 DOI: 10.1111/liv.14647]

31 **Karimi-Sari H**, Hosseini MA, Nikjoo N, Bagheri Baghdasht MS, Alavian SM. Patient-reported outcomes of sleep, mood and quality of life after treatment of chronic hepatitis C infection using direct-acting antiviral agents. *Clin Microbiol Infect* 2020; **26**: 1093.e5-1093.e8 [PMID: 32353413 DOI: 10.1016/j.cmi.2020.04.029]

32 **Zanone MM**, Marinucci C, Ciancio A, Cocito D, Zardo F, Spagone E, Ferrero B, Cerruti C, Charrier L, Cavallo F, Saracco GM, Porta M. Peripheral neuropathy after viral eradication with direct-acting antivirals in chronic HCV hepatitis: A prospective study. *Liver Int* 2021; **41**: 2611-2621 [PMID: 34219359 DOI: 10.1111/liv.15002]

33 **Feng YS**, Kohlmann T, Janssen MF, Buchholz I. Psychometric properties of the EQ-5D-5L: a systematic review of the literature. *Qual Life Res* 2021; **30**: 647-673 [PMID: 33284428 DOI: 10.1007/s11136-020-02688-y]

34 **Jefferies M**, Rauff B, Rashid H, Lam T, Rafiq S. Update on global epidemiology of viral hepatitis and preventive strategies. *World J Clin Cases* 2018; **6**: 589-599 [PMID: 30430114 DOI: 10.12998/wjcc.v6.i13.589]

35 **Nainan OV**, Alter MJ, Kruszon-Moran D, Gao FX, Xia G, McQuillan G, Margolis HS. Hepatitis C virus genotypes and viral concentrations in participants of a general population survey in the United States. *Gastroenterology* 2006; **131**: 478-484 [PMID: 16890602 DOI: 10.1053/j.gastro.2006.06.007]

36 **Holmes JA**, Rutledge SM, Chung RT. Direct-acting antiviral treatment for hepatitis C. *Lancet* 2019; **393**: 1392-1394 [PMID: 30765125 DOI: 10.1016/S0140-6736(18)32326-2]

37 **Uchmanowicz B**, Chudiak A, Mazur G. The influence of quality of life on the level of adherence to therapeutic recommendations among elderly hypertensive patients. *Patient Prefer Adherence* 2018; **12**: 2593-2603 [PMID: 30584283 DOI: 10.2147/PPA.S182172]

38 **Davis BG**. Could You Patent the Sun? *ACS Cent Sci* 2021; **7**: 508-509 [PMID: 34056081 DOI: 10.1021/acscentsci.1c00377]

World Journal of Gastroenterology

Submit a Manuscript: https://www.f6publishing.com

World J Gastroenterol 2022 August 21; 28(31): 4456-4462

DOI: 10.3748/wjg.v28.i31.4456

ISSN 1007-9327 (print) ISSN 2219-2840 (online)

CASE REPORT

Low-grade myofibroblastic sarcoma of the liver misdiagnosed as cystadenoma: A case report

Jie Li, Xin-Yue Huang, Bo Zhang

Specialty type: Gastroenterology and hepatology

Provenance and peer review: Unsolicited article; Externally peer reviewed.

Peer-review model: Single blind

Peer-review report's scientific quality classification

Grade A (Excellent): A
Grade B (Very good): B
Grade C (Good): 0
Grade D (Fair): 0
Grade E (Poor): 0

P-Reviewer: El-Gendy HA, Egypt; Samizadeh B, Iran

Received: May 16, 2022
Peer-review started: May 16, 2022
First decision: June 6, 2022
Revised: June 10, 2022
Accepted: July 25, 2022
Article in press: July 25, 2022
Published online: August 21, 2022

Jie Li, Xin-Yue Huang, Bo Zhang, Department of Ultrasonic Imaging, Xiangya Hospital, Central South University, Changsha 410008, Hunan Province, China

Corresponding author: Bo Zhang, MD, Associate Chief Physician, Deputy Director, Department of Ultrasonic Imaging, Xiangya Hospital, Central South University, No. 87 Xiangya Road, Changsha 410008, Hunan Province, China. zhangbo8095@csu.edu.cn

Abstract

BACKGROUND

Low-grade myofibroblastic sarcoma (LGMS) is a rare malignant tumor. It has no specific clinical manifestations and commonly occurs in the head and neck, extremities and other body parts, with the liver not as its predisposing site.

CASE SUMMARY

We report a case report of a 58-year-old man with right upper abdominal pain for 11 d. Contrast-enhanced computed tomography (CECT), CE magnetic resonance imaging and CE ultrasound (US) all showed a cystic-solid mass in the right liver. As the initial clinical diagnosis was hepatic cystadenoma, surgical resection was performed, and the postoperative pathology indicated hepatic LGMS. The 3-mo follow-up showed favorable recovery of the patient. However, at 7-mo follow-up, two-dimensional US and CECT showed a suspected metastatic lesion in the right-middle abdomen.

CONCLUSION

Hepatic MS is particularly rare and easily misdiagnosed, more cases will contribute to the understanding and the diagnosis accuracy.

Key Words: Myofibroblastic sarcoma; Liver; Cystic-solid mass; Imaging; Diagnosis; Case report

©The Author(s) 2022. Published by Baishideng Publishing Group Inc. All rights reserved.

Core Tip: Myofibroblastic sarcoma (MS) is a rare malignant spindle-shaped cell tumor derived from mesenchymal tissue, and it is particularly rare in the liver. Pathological examination is the gold standard for the diagnosis of hepatic MS. There are different biological characteristics of different lesions and protocols for surgical treatment; therefore, we should pay attention to more information conducive to differential diagnosis in order to improve the preoperative diagnosis, and to choose an appropriate surgical approach.

Citation: Li J, Huang XY, Zhang B. Low-grade myofibroblastic sarcoma of the liver misdiagnosed as cystadenoma: A case report. *World J Gastroenterol* 2022; 28(31): 4456-4462
URL: https://www.wjgnet.com/1007-9327/full/v28/i31/4456.htm
DOI: https://dx.doi.org/10.3748/wjg.v28.i31.4456

INTRODUCTION

Myofibroblastic sarcoma (MS) is a rare mesenchymal spindle-shaped cell tumor, first discovered by Mentzel *et al*[1] in 1998. According to the differential degree of myofibroblasts, it can be divided into low, intermediate and high grade. The first two are collectively called low-grade MS (LGMS)[2]. MS is common in the head and neck, limbs and trunk, but it is extremely rare in the liver. So far, there are only four English language reports available. Here, we present a case of LGMS of the liver.

CASE PRESENTATION

Chief complaints

Right upper abdominal pain for 11 d.

History of present illness

A 58-year-old Chinese man presented with right upper abdominal pain without obvious predisposing factors 11 d prior to the visit. The symptom was not associated with eating and body position. He experienced no nausea or vomiting, no chills or fever, and no significant weight loss.

History of past illness

Right inguinal hernia surgery had been performed at another hospital 3 years prior to the present visit.

Personal and family history

No history of hepatitis and family or genetic history was claimed.

Physical examination

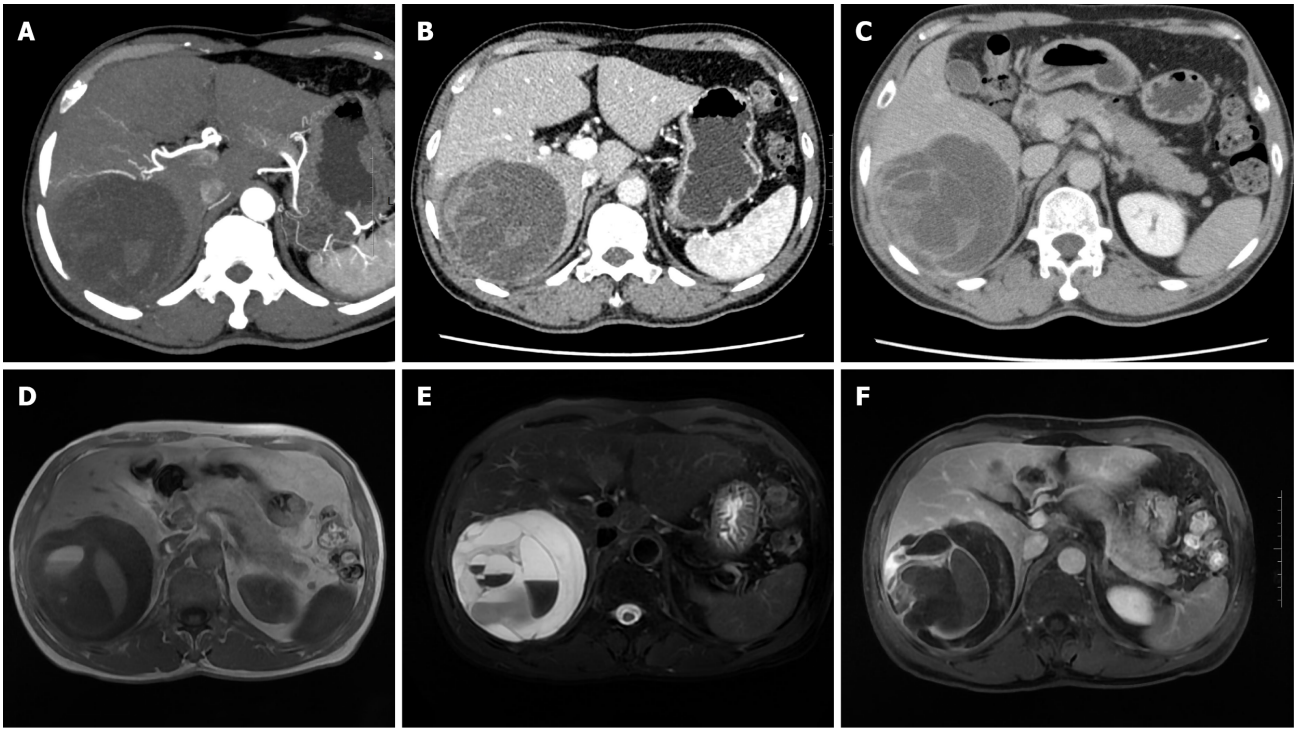
Physical examination showed a flat and soft abdomen without tenderness and rebound pain, and no palpable mass was found. The rest of the physical examination showed no abnormalities.

Laboratory examinations

Cholesterol (5.3 mmol/L) and low density lipoprotein (3.78 mmol/L) were elevated. Routine blood, liver function, renal function and prothrombin tests were normal. Complete quantitative detection of hepatitis B was negative. Alpha-fetoprotein (AFP), carcinoembryonic antigen (CEA) and carbohydrate antigen 19-9 (CA19-9) were normal.

Imaging examinations

Abdominal contrast-enhanced computed tomography (CECT) and hepatic vascular imaging showed that there was a cystic-solid hypodense mass with a size of approximate 99 mm × 92 mm in the right liver. Septa, which were slightly enhanced along with the solid parenchyma, were visible in the mass. The right hepatic vein was displaced due to the compression of the mass supplied by the right hepatic artery (Figure 1A-C). Abdominal CE-magnetic resonance imaging and diffusion-weighted imaging (DWI) showed: (1) A cystic-solid mass with low signal on T1-weighted imaging and high signal on T2-weighted imaging in the right liver, about 101 mm × 98 mm in size; (2) multiple uneven septa and fluid-fluid levels in the lesion; (3) DWI and apparent diffusion coefficient showed high signal and high B value, respectively; and (4) after enhancement, solid components and internal septa of the tumor were significantly enhanced accompanied by unenhanced cystic components (Figure 1D-F).



DOI: 10.3748/wjg.v28.i31.4456 **Copyright** ©The Author(s) 2022.

Figure 1 Abdominal contrast-enhanced computed tomography and hepatic vascular imaging examination, and magnetic resonance imaging examination. A: The right hepatic cystic-solid mass was supplied by the right hepatic artery, and the twisting of the supplying artery was seen; B and C: The portal phase and delayed phase, respectively; the solid portion and the septum were enhanced, and the intracapsular septum was clearly displayed; D and E: The lesions were low signal on T1-weighted imaging and high signal on T2-weighted imaging, with multiple septa of uneven thickness and fluid-fluid levels; F: After enhancement, the solid components and septa of the mass were significantly enhanced, but the cystic components were not.

Ultrasound (US) examination showed a 123 mm × 98 mm mixed-echo mass with regular shape and clear boundary in the right liver. The anechoic dark area was the main portion of the mass. The parenchymatous septa with uneven thickness were visible in the mass in which no obvious parasitic body sonogram was found. Color Doppler flow imaging showed punctate blood flow signals in the mass. CEUS showed that the peripheral and internal septa of the tumor were hyper-enhanced in the arterial phase, iso-enhanced in the portal and delayed phases, and unenhanced in the anechoic area in these three phases (Figure 2). Based on the above-mentioned examination, the mass was preliminarily identified as hepatic cystadenoma.

FINAL DIAGNOSIS

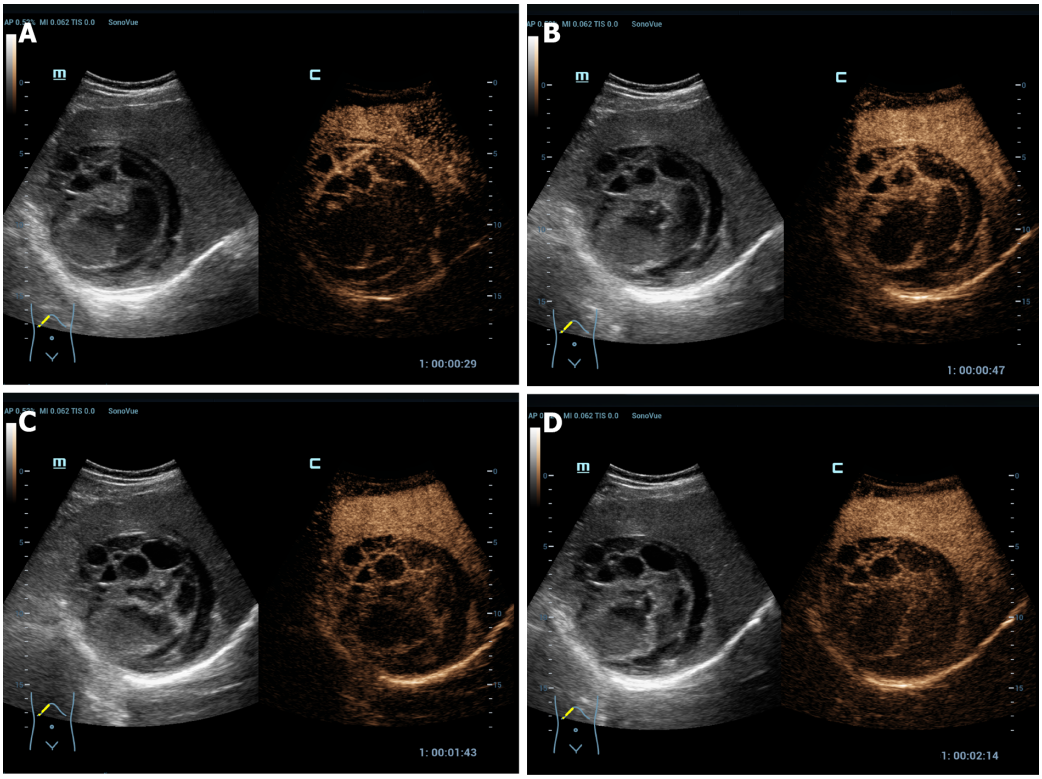
The postoperative pathology diagnosis of the presented case is LGMS of right liver (Figure 3).

TREATMENT

The patient underwent laparoscopic right hepatectomy under general anesthesia after preoperative investigations were completed.

OUTCOME AND FOLLOW-UP

The patient recovered well after the operation with the surgical incision healed uneventfully. No apparent event was observed at the postoperative 3-mo follow-up. However, at the 7-mo follow-up, two-dimensional ultrasound and CECT showed a 100 mm × 40 mm cystic-solid lesion occurring in the right middle abdomen, which showed similar properties to a liver lesion. The mass wall was enhanced after enhancement (Figure 4). The patient refused further surgery although the clinician initially believed that metastasis had probably occurred.



DOI: 10.3748/wjg.v28.i31.4456 **Copyright** ©The Author(s) 2022.

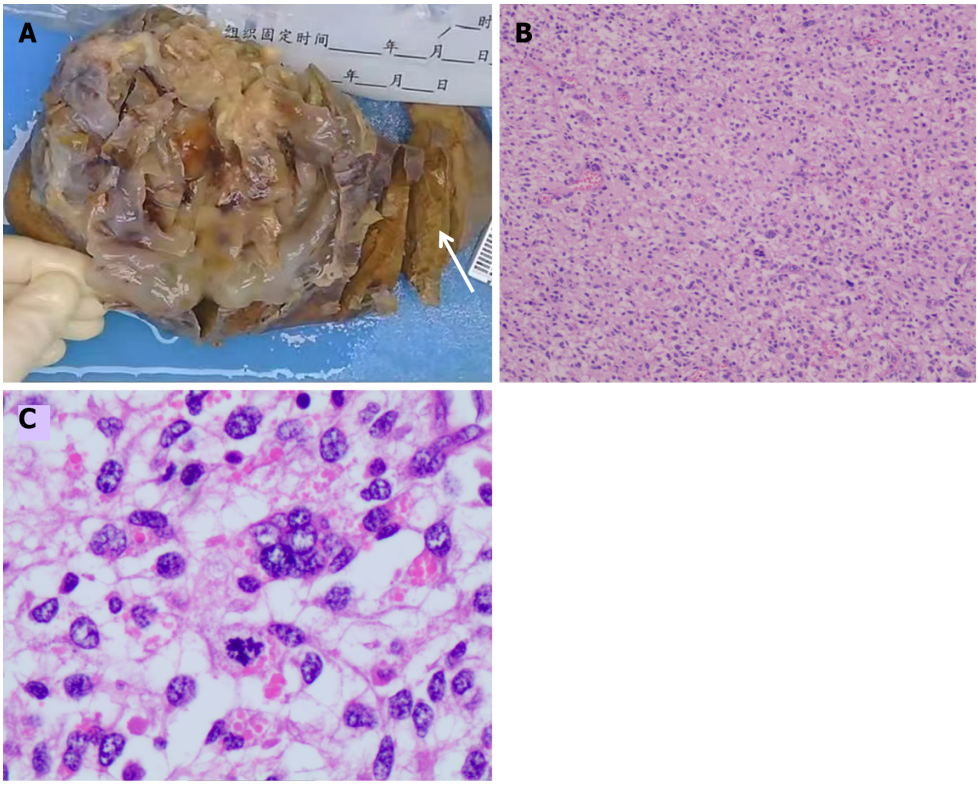
Figure 2 Contrast-enhanced ultrasound examination. The peripheral parenchyma and internal septa of the mixed-echo mass showed hyper-enhancement in the arterial phase, and iso-enhancement in the portal and delayed phases. A: Arterial phase; B: Early portal phase; C: Late portal phase; D: Delayed phase.

DISCUSSION

MS is a rare histological type of hepatic sarcoma. Given its rarity, the etiology is not clear, and most of the relevant reports are case reports or case series. Only seven relevant case reports[3-9] were obtained after a comprehensive literature search was conducted by us in CNKI, PubMed and Web of Science databases, involving seven patients (four men, three women; aged 25–38 years, n = 5; > 60 years, n = 2). As described in the WHO classification, males are slightly more predisposed for this disease than females; thus, not surprisingly, the present case was male. Most of the MSs were identified due to the swelling lesion detected or during physical examination. In the literature reports, five of the seven patients presented with abdominal distension and pain, and another two were asymptomatic. As for the present patient, the complaint was right upper abdominal pain. He had no history of hepatitis, although two of the seven patients reported previously had a history of hepatitis B. Serological examination, such as routine blood, liver function, renal function, and AFP and other tumor markers such as CEA, CA19-9 (all of which were in the normal range), was available for six of the seven patients reported previously and for the patient reported here. The remaining patient reported previously had impaired liver function. The lesions reported were mostly located in the right liver, and cystic-solid tumor was found in five cases, but no relevant data were available for the other two cases. For the present case, a cystic-solid tumor located in the right liver was also observed. Among the seven cases reported previously, five were misdiagnosed as liver cancer or hydatid disease as their preliminary clinical diagnosis, while the present case was misdiagnosed as hepatic cystadenoma. Surgical resection was performed in six of the seven patients, and liver lesions were found and biopsy was performed at 3 mo after surgery for the remaining patient initially diagnosed with retroperitoneal inflammatory myofibroblastic tumor. The pathological diagnosis for the current patient was LGMS infiltrated in the liver. Currently, surgical resection of MS is the preferred treatment, although primary treatment, prognosis and follow-up treatment are not clear. More data are needed to obtain reliable conclusions about the role of follow-up treatment such as radiotherapy and chemotherapy.

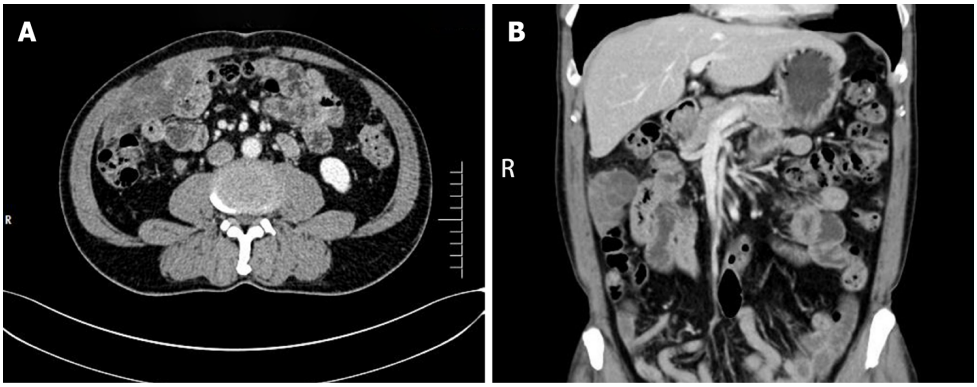
No specific clinical signs and symptoms were established currently due to the low incidence of hepatic MS, which was generally manifested as abdominal distension or discomfort and/or abnormal liver function, sometimes accompanied by sweating and weight loss. Although there was no clear report on tumor recurrence and metastasis, most hepatic MSs were observed as cystic-solid masses, showing infiltrative and destructive growth.

At present, hepatic MS is mainly diagnosed by histopathology and immunohistochemistry. Under light microscopy, the tumor tissue of the present case was mainly composed of spindle-shaped cells



DOI: 10.3748/wjg.v28.i31.4456 **Copyright** ©The Author(s) 2022.

Figure 3 Gross pathology specimen and pathological microscopy. A: A cystic-solid mass was seen with the naked eye, with soft texture and inconspicuous tumor capsule; its cut surface was polycystic, with yellowish jelly-like substances inside the cysts, and the cyst wall thickness was 1 mm-12 mm; no cirrhotic changes were observed in the peripheral liver tissue (arrow); B and C: Spindle-shaped cells are arranged in fascicles under light microscope, eosinophilic cytoplasm with atypia and mitotic figures were seen.



DOI: 10.3748/wjg.v28.i31.4456 **Copyright** ©The Author(s) 2022.

Figure 4 Abdominal contrast-enhanced computed tomography examination at 7-mo follow-up. A and B: The right middle abdomen of the patient in contrast-enhanced computed tomography showed a cystic-solid lesion, with the similar property as a liver lesion. After enhancement, the mass wall was enhanced.

with a diffuse infiltrative distribution. The cytoplasm was eosinophilic and the nucleus was polymorphic. Abnormal mitotic figures were present. The histopathological findings of this case are consistent with those previously reported. In the immunohistochemical study of the cases reported previously, expression of vimentin, smooth muscle actin (SMA) and desmin was commonly observed, along with partially positive actin. No hepatocyte markers, epithelial markers, S100, CD117, CD34, myogenin, pan-cytokeratin (CK-Pan) and h-caldesmon were not found in the tissue[10]. In the of the case reported here, immunohistochemical study was positive for vimentin, SMA and desmin, and negative for HePar-1, Glypican-3, CK-Pan, myogenin, Ard-1, MYOD1, SOX10 and CD31, with an approximately 10% Ki-67 index. As can be seen, the present case is mostly similar to those reported previously for this profile.

To date, due to lack of specific manifestations in imaging examinations, hepatic MS is easily misdiagnosed as liver cancer, hepatic hydatid disease, cystadenoma and other space-occupying lesions, and it is difficult to make a diagnosis in clinical practice as well. The hepatic MS reported here was mainly observed as a cystic-solid mass with well-defined borders and regular morphology. The cystic components within the mass were separated by septa of varying thickness, with a partially visible fluid-fluid levels. After enhancement, the solid portion and septa of the mass were enhanced to different degrees, with inconspicuous regression for the degree and velocity.

CEUS of this case showed that the peripheral and internal septa of the tumor were hyper-enhanced in the arterial phase, isoenhanced in the portal and delayed phases, while in two of the seven cases reported in the literature, the portal and delayed phases were hypo-enhanced. Hence, the CEUS features of hepatic MS require more case data.

Hepatic MS needs to be differentiated from liver cancer (particularly with liquefaction and necrosis), hepatic hydatid disease, and cystadenoma. When liver cancer is accompanied by liquefaction and necrosis, three-phase non-enhanced areas in the lesions may also be found, but most of them are patchy or irregular. Moreover, the substantial portion of the mass shows high enhancement in the arterial phase, and low enhancement in the portal and delayed phases. The process behaves in a fast-in and fast-out mode. In contrast, the non-enhancing area of hepatic MS lesions was separated by the internal septa of the mass, and the parenchyma and internal septa of the mass were not significantly regressed after enhancement. Patients with liver hydatid disease generally have a history of living in pastoral areas or exposure to pathogens. The typical imaging manifestations are mainly cystic masses, showing the mother and daughter sporocysts, with varying degrees of eggshell-like cyst wall calcification, intracystic streamer sign, lily sign, and cyst-within-cyst. Liver cystadenomas are cystic-solid masses with predominantly cystic components, along with mural nodules (papillary-solid components protruding into the cystic cavity on the cyst wall) as specific signs. Mural nodules show nodular enhancement in the portal phase and can continue to enhance in the delayed phase. Imaging examination can clearly show the size, location, border, number, blood supply, and internal and surrounding adjacent tissues of the tumor. However, there is currently no characteristic diagnostic basis for the imaging manifestations of hepatic MS.

The presented case was misdiagnosed for several reasons. First, the patient had no specific clinical history, presentation and abnormal laboratory indexes. Second, the preoperative imaging images were similar to those of cystadenoma. The internal separation of the mass was uniform, the blood flow of the mass was not abundant, and there was no washout after enhancement. Therefore, imaging diagnosis was limited to benign lesions, and malignant behavior was not considered.

In summary, MS of the liver has no characteristic manifestations in clinical performance, serological indicators and imaging findings. Therefore, there is a need to accumulate a large number of cases with complete data to provide meaningful research data for the diagnosis and treatment strategies of MS of the liver.

CONCLUSION

Due to the rarity of hepatic MS, more clinical data and in-depth research are needed to further analyze its pathological mechanism, biomarkers, and imaging manifestations. Improving the understanding of the imaging manifestations of hepatic MS will help improve the preoperative diagnosis rate and assist clinicians in performing precise surgical resection and follow-up treatment.

ACKNOWLEDGEMENTS

We are very grateful to Dr. Jiang Jia-Rui (Department of Pathology, Xiangya Hospital, Central South University) for providing professional guidance to the pathological analysis.

FOOTNOTES

Author contributions: Li J wrote and edited the original draft, reviewed the literature, contributed to data collection and analysis; Huang XY contributed to assist with the patient's CEUS; Zhang B performed the patient's US and CEUS, supervised the report, provided clinical advice, reviewed, and approved the final manuscript.

Informed consent statement: Informed written consent was obtained from the patients for the publication of this report and any accompanying images.

Conflict-of-interest statement: The authors declare that they have no conflict of interest.

CARE Checklist (2016) statement: The authors have read the CARE Checklist (2016), and the manuscript was

prepared and revised according to the CARE Checklist (2016).

Open-Access: This article is an open-access article that was selected by an in-house editor and fully peer-reviewed by external reviewers. It is distributed in accordance with the Creative Commons Attribution NonCommercial (CC BY-NC 4.0) license, which permits others to distribute, remix, adapt, build upon this work non-commercially, and license their derivative works on different terms, provided the original work is properly cited and the use is non-commercial. See: https://creativecommons.org/Licenses/by-nc/4.0/

Country/Territory of origin: China

ORCID number: Jie Li 0000-0001-8511-8005; Xin-Yue Huang 0000-0001-6546-7427; Bo Zhang 0000-0001-8012-0560.

S-Editor: Chen YL
L-Editor: Kerr C
P-Editor: Chen YL

REFERENCES

1 **Mentzel T**, Dry S, Katenkamp D, Fletcher CD. Low-grade myofibroblastic sarcoma: analysis of 18 cases in the spectrum of myofibroblastic tumors. *Am J Surg Pathol* 1998; **22**: 1228-1238 [PMID: 9777985 DOI: 10.1097/00000478-199810000-00008]
2 **Montgomery E**, Fisher C. Myofibroblastic differentiation in malignant fibrous histiocytoma (pleomorphic myofibrosarcoma): a clinicopathological study. *Histopathology* 2001; **38**: 499-509 [PMID: 11422493 DOI: 10.1046/j.1365-2559.2001.01152.x]
3 **Fang Y**, Yan T, Bi X, Zhang H, Zhou J, Huang Z, Xie Y, Zhang L, Zhao P, Cai J. Clinicopathological and immunohistochemical study of low-grade myofibroblastic sarcoma of the liver-One case report. *Zhongliu Yanjiu Yu Linchuang* 2011; **8**: 250-253 [DOI: 10.1007/s11805-011-0590-8]
4 **Pan Y**, Wu X, Liu J, Muheremu A. Abnormal liver function induced by myofibroblastic sarcoma infiltrating the liver: A case report. *Oncol Lett* 2015; **9**: 798-800 [PMID: 25621053 DOI: 10.3892/ol.2014.2740]
5 **Yi X**, Xiao D, Long X. Myofibroblastic sarcoma in liver: a case report. *Int J Clin Exp Pathol* 2015; **8**: 1073-1076 [PMID: 25755822]
6 **Wen J**, Zhao W, Li C, Shen JY, Wen TF. High-grade myofibroblastic sarcoma in the liver: A case report. *World J Gastroenterol* 2017; **23**: 7054-7058 [PMID: 29097878 DOI: 10.3748/wjg.v23.i38.7054]
7 **Yan T**, Bi X Y, Zhang H T, Zhao J J, Zhang L, Huang Z, Zhou H T, Li C, Cai J Q. A case of malignant myofibroblastic sarcoma of the liver. *Zhongguo Zhongliu Zazhi* 2011; **33**: 477-478 [DOI: 10.1007/s11805-011-0590-8]
8 **Zhang J Y**, Luo Y. Contrast-enhanced ultrasonographic manifestations of hepatic myofibroblastic sarcoma: a case report. *Linchuang Chaosheng Yixue Zazhi* 2021; **23**: 80 [DOI: 10.11152/mu.2013.2066.163.2hhs]
9 **Chen L G**, Li J. A case of spontaneous rupture of liver myofibroblastic sarcoma. *Zhongguo Gandan Waike Zazhi* 2021; **27**: 218-219 [DOI: 10.21037/hbsn-21-102]
10 **Jo VY**, Fletcher CD. WHO classification of soft tissue tumours: an update based on the 2013 (4th) edition. *Pathology* 2014; **46**: 95-104 [PMID: 24378391 DOI: 10.1097/PAT.0000000000000050]

World Journal of Gastroenterology

Submit a Manuscript: https://www.f6publishing.com

World J Gastroenterol 2022 August 21; 28(31): 4463-4466

DOI: 10.3748/wjg.v28.i31.4463

ISSN 1007-9327 (print) ISSN 2219-2840 (online)

LETTER TO THE EDITOR

Evidence-based considerations on bowel preparation for colonoscopy

Konstantinos Argyriou, Adolfo Parra-Blanco

Specialty type: Gastroenterology and hepatology

Provenance and peer review: Unsolicited article; Externally peer reviewed

Peer-review model: Single blind

Peer-review report's scientific quality classification

Grade A (Excellent): 0
Grade B (Very good): B, B, B
Grade C (Good): 0
Grade D (Fair): 0
Grade E (Poor): 0

P-Reviewer: Basson MD, United States; Kobayashi N, Japan; Okasha H, Egypt

Received: December 20, 2021
Peer-review started: December 20, 2021
First decision: March 10, 2022
Revised: March 26, 2022
Accepted: July 24, 2022
Article in press: July 24, 2022
Published online: August 21, 2022

Konstantinos Argyriou, Department of Gastroenterology, University Hospital of Larisa, Larisa GR41334, Greece

Adolfo Parra-Blanco, Department of Gastroenterology, Nottingham University Hospitals NHS Trust, Nottingham NG51PB, United Kingdom

Corresponding author: Konstantinos Argyriou, MD, MSc, PhD, Academic Research, Consultant Physician-Scientist, Department of Gastroenterology, University Hospital of Larisa, Mezourlo, Larisa GR41334, Greece. kosnar2@doctors.org.uk

Abstract

We recently read with interest the article, "Novel frontiers of agents for bowel cleansing for colonoscopy". This is a practical narrative review, which could be of particular importance to clinicians in order to improve their current practice. Although we appreciate the venture of our colleagues, based on our in-depth analysis, we came across several minor issues in the article; hence, we present our comments in this letter. If the authors consider these comments further in their relevant research, we believe that their contribution would be of considerable importance for future studies.

Key Words: Colonoscopy; Bowel preparation; Polyethylene glycol; Post-polypectomy syndrome; Post-polypectomy complications

©The Author(s) 2022. Published by Baishideng Publishing Group Inc. All rights reserved.

Core Tip: Colonoscopy is the gold standard investigation for the detection and treatment of colorectal neoplasia. The effectiveness and safety of the procedure mainly depends on the quality of bowel preparation (BP). Although international guidelines underline methods to ensure adequate BP, inadequate BP occurs in approximately one-third of the colonoscopies. The search for an ideal regimen to improve BP remains. The article by the authors addressed this issue successfully, but we detected several minor issues. Therefore, we would like to share our views and opinions on this interesting review.

Citation: Argyriou K, Parra-Blanco A. Evidence-based considerations on bowel preparation for colonoscopy. *World J Gastroenterol* 2022; 28(31): 4463-4466
URL: https://www.wjgnet.com/1007-9327/full/v28/i31/4463.htm
DOI: https://dx.doi.org/10.3748/wjg.v28.i31.4463

TO THE EDITOR

We read with great interest the frontier article, "Novel frontiers of agents for bowel cleansing for colonoscopy"[1]. Although the authors follow the infrastructure of the updated version of the European Society of Gastrointestinal Endoscopy Guideline on bowel preparation (BP) for the main part of their article, they do not make absolutely clear to the reader the way they selected the studies included in their own updated review[2]. Despite this shortcoming, in general the authors summarize the major findings of several reference studies successfully. The salient highlight of this article is that Di Leo *et al* [1] address the issue of BP holistically, from cleansing agents to the multifaceted outcomes of the currently followed BP strategies in specific populations, such as those with congestive heart failure or chronic renal failure, disclosing areas that need to be further investigated. However, we believe that the most striking point of this article is the introduction of the novel term "post colonoscopy syndrome," which sums up all the minor complications that an individual could develop post colonoscopy, worsening his/her quality of life. Therefore, this research has a strong reference and practical value for future studies, overcoming limitations. Nevertheless, through our in-depth reading, we found several shortcomings and anticipate a discussion with the authors.

Initially, we agree with the authors that the assessment of the quality of BP is of utmost importance. Adequate BP is crucial, not only to the efficacy and safety of colonoscopies but also for awarding privileges to the endoscopists[3]. However, there are no universally accepted criteria that endoscopists can use for the assessment of the quality of BP. As a result, at least five quality assessment scales have been currently fully or partially validated and used in daily practice for the assessment of the quality of BP, inducing significant heterogeneity when quality results are compared among different studies. The unanimous approval of a single scale is expected to resolve this issue but is still awaited[3]. By comparing the specific characteristics of all available scales, the authors can disclose areas that need to be further investigated, facilitating endoscopists to reach consensus. However, in this article, the authors only refer to the Ottawa Bowel Preparation Quality Scale, Boston Bowel Preparation Scale and the partially validated Aronchick Scale, excluding other validated scales, such as the Harefield Cleansing Scale, which was the first scale to be developed[3]. This limitation leaves an initial critical step underdiscussed in this review, perpetuating confusion.

In their summary of current evidence, the authors focus on high and low volume polyethylene glycol (PEG)-based preparations, leaving non-PEG-based solutions that have been found to be of equal efficacy to PEG-based formulas under-reviewed. The reason behind this exclusion is not mentioned. However, it constitutes an omission. For example, in this article, the authors do not discuss lactulose, a semi-synthetic derivative of lactose that after fermentation stimulates intestinal motility and increases osmotic pressure within the colon. Accumulated evidence from clinical trials suggest that lactulose has similar efficacy to PEG-based solutions with acceptable safety when used for BP not only in individuals undergoing ambulatory colonoscopy but also in those undergoing colonoscopy for lower gastrointestinal bleeding[4-6]. These results expand the armamentarium of our available solutions for BP; hence, all the relevant information should be supplemented in this review.

In addition to the under-discussed non-PEG based solutions, the authors provided sparse data regarding the safety of using non-PEG based and PEG-based preparations in specific populations. Although the authors quote evidence on the effectiveness and safety of these agents in various patient populations included in this review, their efficacy and safety in patients with liver cirrhosis are not examined. The reason behind this exclusion is not mentioned by the authors, leaving a critical step under-discussed in this review. Patients with cirrhosis demonstrate alterations in physiology and hemodynamics that make them vulnerable to develop electrolyte imbalances during BP[7]. Osmotically balanced solutions have been shown to be effective and safe for the management of hepatic encephalopathy in this patient population[8]. However, little is known regarding their safety when used for BP as patients with liver cirrhosis are often excluded from randomized controlled trials comparing different bowel cleansing agents. In a recent study that examined the safety and efficacy of low volume and high volume PEG based solutions in 166 patients with liver cirrhosis, it was shown that both formulations can be effectively and safely used for BP with low volume formulations showing better acceptability and compliance[9]. Considering the absence of an established BP protocol in patients with liver cirrhosis, we believe that all the relevant information should be included in this review, allowing the reader to acquire a detailed overview of the subject.

Another shortcoming lies at the reference of the agents intended to improve patient experience. More specifically, the authors suggest that the menthol candy drops improve BP in the candy drops-added group compared to controls, with no benefit in side effects. However, in the reference trial, other than

the efficacy, the trial authors state that menthol drops improved nausea (24.5% drops *vs* 4% controls; P = 0.04). Since this finding is important, this detail should be clarified[10].

Finally, the authors attempted to shed light on the pathophysiology of minor post colonoscopy complications that mainly included the symptoms of pain, discomfort and bloating, defined as post colonoscopy syndrome (PCS). We agree that the post BP changes in microbiota composition contribute to the occurrence of PCS. However, we believe that this is the tip of the iceberg. In order to understand the pathophysiology of PCS accurately, researchers should look into the complex mechanisms of abdominal pain and study the impact of BP in all of them[11]. Previous evidence suggested that mucosal changes occurring secondary to colonic over-distension during colonoscopy as well as stress, inflammation, ischemia, pH, bacterial products, immune mediators and neurotransmitters can all be related to visceral pain[12-16]. However, whether BP can have a negative impact is unknown. Future studies should aim to investigate these complex relationships and unravel the exact role of BP in the pathophysiology of PCS, as their results may allow clinicians to mitigate the negative effects and increase the individual acceptance of colonoscopy.

In summary, this review can be a valuable reference study, guiding clinicians in their daily practice. We offer our evidence-based considerations on the shortcomings of this review in an effort to further increase the value of the review and direct more comprehensive future studies. But, whether BP can have a negative impact is unknown. Future studies should aim to investigate these complex relationships and unravel the exact role of BP in the pathophysiology of PCS, as their results may allow clinicians to mitigate the negative effects and increase the individual acceptance of colonoscopy. In summary, this review can be a valuable reference study, guiding clinicians in their daily practice. We offer our evidence-based considerations on the shortcomings of this review in an effort to further increase the value of the review and direct more comprehensive future studies.

FOOTNOTES

Author contributions: Argyriou K and Parra-Blanco A designed and performed the research; Argyriou K wrote this comment; Parra-Blanco A revised the manuscript.

Conflict-of-interest statement: All the authors report no relevant conflicts of interest for this article.

Open-Access: This article is an open-access article that was selected by an in-house editor and fully peer-reviewed by external reviewers. It is distributed in accordance with the Creative Commons Attribution NonCommercial (CC BY-NC 4.0) license, which permits others to distribute, remix, adapt, build upon this work non-commercially, and license their derivative works on different terms, provided the original work is properly cited and the use is non-commercial. See: https://creativecommons.org/Licenses/by-nc/4.0/

Country/Territory of origin: Greece

ORCID number: Konstantinos Argyriou 0000-0002-2026-9678; Adolfo Parra-Blanco 0030226.

S-Editor: Wang JJ
L-Editor: Filipodia
P-Editor: Wang JJ

REFERENCES

1 **Di Leo M**, Iannone A, Arena M, Losurdo G, Palamara MA, Iabichino G, Consolo P, Rendina M, Luigiano C, Di Leo A. Novel frontiers of agents for bowel cleansing for colonoscopy. *World J Gastroenterol* 2021; **27**: 7748-7770 [PMID: 34963739 DOI: 10.3748/wjg.v27.i45.7748]

2 **Hassan C**, East J, Radaelli F, Spada C, Benamouzig R, Bisschops R, Bretthauer M, Dekker E, Dinis-Ribeiro M, Ferlitsch M, Fuccio L, Awadie H, Gralnek I, Jover R, Kaminski MF, Pellisé M, Triantafyllou K, Vanella G, Mangas-Sanjuan C, Frazzoni L, Van Hooft JE, Dumonceau JM. Bowel preparation for colonoscopy: European Society of Gastrointestinal Endoscopy (ESGE) Guideline - Update 2019. *Endoscopy* 2019; **51**: 775-794 [PMID: 31295746 DOI: 10.1055/a-0959-0505]

3 **Kastenberg D**, Bertiger G, Brogadir S. Bowel preparation quality scales for colonoscopy. *World J Gastroenterol* 2018; **24**: 2833-2843 [PMID: 30018478 DOI: 10.3748/wjg.v24.i26.2833]

4 **Jagdeep J**, Sawant G, Lal P, Bains L. Oral Lactulose vs. Polyethylene Glycol for Bowel Preparation in Colonoscopy: A Randomized Controlled Study. *Cureus* 2021; **13**: e14363 [PMID: 33972914 DOI: 10.7759/cureus.14363]

5 **Menacho AM**, Reimann A, Hirata LM, Ganzerella C, Ivano FH, Sugisawa R. Double-blind prospective randomized study comparing polyethylene glycol to lactulose for bowel preparation in colonoscopy. *Arq Bras Cir Dig* 2014; **27**: 9-12 [PMID: 24676290 DOI: 10.1590/s0102-67202014000100003]

6 **Li CX**, Guo Y, Zhu YJ, Zhu JR, Xiao QS, Chen DF, Lan CH. Comparison of Polyethylene Glycol versus Lactulose Oral Solution for Bowel Preparation prior to Colonoscopy. *Gastroenterol Res Pract* 2019; **2019**: 2651450 [PMID: 31097959 DOI: 10.1155/2019/2651450]

7 **Belsey J**, Epstein O, Heresbach D. Systematic review: oral bowel preparation for colonoscopy. *Aliment Pharmacol Ther* 2007; **25**: 373-384 [PMID: 17269992 DOI: 10.1111/j.1365-2036.2006.03212.x]

8 **Pontone S**, Angelini R, Standoli M, Patrizi G, Culasso F, Pontone P, Redler A. Low-volume plus ascorbic acid *vs* high-volume plus simethicone bowel preparation before colonoscopy. *World J Gastroenterol* 2011; **17**: 4689-4695 [PMID: 22180711 DOI: 10.3748/wjg.v17.i42.4689]

9 **Lee JM**, Lee JH, Kim ES, Lee JM, Yoo IK, Kim SH, Choi HS, Keum B, Seo YS, Jeen YT, Lee HS, Chun HJ, Um SH, Kim CD. The safety and effectiveness of 2-liter polyethylene glycol plus ascorbic acid in patients with liver cirrhosis: A retrospective observational study. *Medicine (Baltimore)* 2017; **96**: e9011 [PMID: 29390432 DOI: 10.1097/MD.0000000000009011]

10 **Sharara AI**, El-Halabi MM, Abou Fadel CG, Sarkis FS. Sugar-free menthol candy drops improve the palatability and bowel cleansing effect of polyethylene glycol electrolyte solution. *Gastrointest Endosc* 2013; **78**: 886-891 [PMID: 23769143 DOI: 10.1016/j.gie.2013.05.015]

11 **Pusceddu MM**, Gareau MG. Visceral pain: gut microbiota, a new hope? *J Biomed Sci* 2018; **25**: 73 [PMID: 30309367 DOI: 10.1186/s12929-018-0476-7]

12 **Sengupta JN**. Visceral pain: the neurophysiological mechanism. *Handb Exp Pharmacol* 2009; 31-74 [PMID: 19655104 DOI: 10.1007/978-3-540-79090-7_2]

13 **Million M**, Wang L, Wang Y, Adelson DW, Yuan PQ, Maillot C, Coutinho SV, Mcroberts JA, Bayati A, Mattsson H, Wu V, Wei JY, Rivier J, Vale W, Mayer EA, Taché Y. CRF2 receptor activation prevents colorectal distension induced visceral pain and spinal ERK1/2 phosphorylation in rats. *Gut* 2006; **55**: 172-181 [PMID: 15985561 DOI: 10.1136/gut.2004.051391]

14 **Ochoa-Cortes F**, Guerrero-Alba R, Valdez-Morales EE, Spreadbury I, Barajas-Lopez C, Castro M, Bertrand J, Cenac N, Vergnolle N, Vanner SJ. Chronic stress mediators act synergistically on colonic nociceptive mouse dorsal root ganglia neurons to increase excitability. *Neurogastroenterol Motil* 2014; **26**: 334-345 [PMID: 24286174 DOI: 10.1111/nmo.12268]

15 **Vanner S**, Greenwood-Van Meerveld B, Mawe G, Shea-Donohue T, Verdu EF, Wood J, Grundy D. Fundamentals of Neurogastroenterology: Basic Science. *Gastroenterology* 2016 [PMID: 27144618 DOI: 10.1053/j.gastro.2016.02.018]

16 **Gayer CP**, Basson MD. The effects of mechanical forces on intestinal physiology and pathology. *Cell Signal* 2009; **21**: 1237-1244 [PMID: 19249356 DOI: 10.1016/j.cellsig.2009.02.011]

World Journal of Gastroenterology

Submit a Manuscript: https://www.f6publishing.com

World J Gastroenterol 2022 August 21; 28(31): 4467-4470

DOI: 10.3748/wjg.v28.i31.4467

ISSN 1007-9327 (print) ISSN 2219-2840 (online)

LETTER TO THE EDITOR

Influence of different portal vein branches on hepatic encephalopathy during intrahepatic portal shunt *via* jugular vein

Xin Yao, Sheng He, Meng Wei, Jian-Ping Qin

Specialty type: Gastroenterology and hepatology

Provenance and peer review: Unsolicited article; Externally peer reviewed.

Peer-review model: Single blind

Peer-review report's scientific quality classification

Grade A (Excellent): A
Grade B (Very good): B
Grade C (Good): C
Grade D (Fair): 0
Grade E (Poor): 0

P-Reviewer: De Gregorio MA, Spain; Kordzaia D, Georgia; Wondmagegn H, Ethiopia

Received: February 11, 2022
Peer-review started: February 11, 2022
First decision: April 5, 2022
Revised: April 7, 2022
Accepted: July 22, 2022
Article in press: July 22, 2022
Published online: August 21, 2022

Xin Yao, Sheng He, Meng Wei, Jian-Ping Qin, Department of Gastroenterology, General Hospital of Western Theater Command, Chengdu 610083, Sichuan Province, China

Corresponding author: Jian-Ping Qin, MD, Chief Doctor, Doctor, Department of Gastroenterology, General Hospital of Western Theater Command, No. 270 Rongdu Road, Chengdu 610083, Sichuan Province, China. jpqqing@163.com

Abstract

This letter is regarding the study titled 'Targeted puncture of left branch of intrahepatic portal vein in transjugular intrahepatic portosystemic shunt (TIPS) to reduce hepatic encephalopathy'. Prior to the approval of TIPS dedicated stents (Viatorr stents) in China in October 2015, Fluency covered stents were typically used. As Fluency covered stents have a strong support force and axial elastic tension, a 'cap' may form if the stent is located too low at the end of the hepatic vein or too short at the end of the portal vein during surgery, leading to stent dysfunction. Since the blood shunted by the stent is from the main trunk of the portal vein, the correlation between the incidence of postoperative hepatic encephalopathy and the location of the puncture target (left or right portal vein branch) is worth discussion. Notably, no studies in China or foreign countries have proven the occurrence of left and right blood stratification after the accumulation of splenic vein and mesenteric blood flow in the main trunk of the portal vein in patients with cirrhotic portal hypertension.

Key Words: Viatorr stent; Portosystemic shunt; Transjugular intrahepatic; Hypertension; portal; Left and right portal vein branches

©The Author(s) 2022. Published by Baishideng Publishing Group Inc. All rights reserved.

Core Tip: This Letter to the Editor aims to analyse the effect of establishing a shunt in the left or right portal vein branch in transjugular intrahepatic portosystemic shunt on the incidence of postoperative hepatic encephalopathy in patients with cirrhotic portal hypertension. Based on preliminary clinical experience, it is thought that there is no difference in the incidence of hepatic encephalopathy among patients regardless of the use of a COOK bare stent or Viatorr stent with an inner diameter of 8 mm if a shunt is established in the left or right portal vein branch.

Citation: Yao X, He S, Wei M, Qin JP. Influence of different portal vein branches on hepatic encephalopathy during intrahepatic portal shunt *via* jugular vein. *World J Gastroenterol* 2022; 28(31): 4467-4470
URL: https://www.wjgnet.com/1007-9327/full/v28/i31/4467.htm
DOI: https://dx.doi.org/10.3748/wjg.v28.i31.4467

TO THE EDITOR

We read the article of Luo *et al*[1] titled "Targeted puncture of left branch of intrahepatic portal vein in transjugular intrahepatic portosystemic shunt (TIPS) to reduce hepatic encephalopathy" and are very interested in its conclusions. We think that therapy by "targeted puncture of the left branch of the intrahepatic portal vein in TIPS to reduce hepatic encephalopathy" is worthy of discussion.

First, Luo *et al*[1] performed a retrospective analysis of portal hypertension patients receiving TIPS from January 2000 to January 2013. During this period, a shunt was established using a Fluency stent (BARD, Voisins le Bretonneux, France) or Viatorr stent (W.L. Gore & Associates, Flagstaff, AZ, United States). However, the shunts were established in TIPS mainly using Fluency covered stents in China before the approval of TIPS dedicated stents (Viatorr stents) in China in October 2015. As Fluency covered stents have a strong support force and axial elastic tension, a 'cap' may form if the stent is located too low at the end of the hepatic vein or too short at the end of the portal vein during the operation, thereby leading to stent dysfunction. Since the blood shunted by the stent is from the main trunk of the portal vein, as shown in Figure 2 of Luo *et al*'s paper (the stent is inserted into the main trunk of the portal vein at the end of the portal vein for shunts in both the left and right portal vein branches), the correlation between the incidence of postoperative hepatic encephalopathy and the location of the puncture target (left or right portal vein branch) is worthy of discussion.

As pointed out by Luo *et al*[1], prior studies have reported that the backflow blood from the splenic and superior mesenteric veins is not thoroughly mixed but rather enters the left and right portal vein branches separately, *i.e.*, the blood from the superior mesenteric vein mainly flows into the right branch, while the blood from the splenic vein mainly flows into the left branch[2-3]. In a study on corrosion casting of the portal vein and hepatic artery ramifications in dogs, this study focused on explaining the anatomical features of the hepatic portal vein and hepatic artery in animals instead of the blood flow features of the portal vein system[2]. The author team believes that a substantial difference between animals and humans. In a study using carbon dioxide angiography, iodinated contrast medium was used to replace traditional angiography[3]. This study included chronic liver disease patients receiving percutaneous transhepatic puncture of the portal vein with the tube inserted into the splenic vein; a mechanical injection system was used to inject a total volume of 30 mL of contrast medium at a speed of 5 mL/s. Notably, a difference was observed in blood mixing at the left and right sides of the main trunk of the portal vein. An early study conducted in United States of America found that an increase in the pressure in the portal vein was followed by a decrease in hepatic blood inflow and blood flow rate and grading of liver function due to hepatic sinusoidal obstruction, perisinusoidal fibrosis and portal vein obstruction in cirrhosis was related to the portal blood flow rate; furthermore, portal hypertensive liver function damage was obvious, and the portal blood flow rate was low[4]. In the hyperdynamic splanchnic circulatory state, the progressive decrease in the portal blood flow rate suggests aggravation of hepatic parenchymal lesions and increased portal blood flow resistance. The author team believes that the blood flow rate decreased after splenic vein and mesenteric blood flows accumulated in the main trunk of the portal vein in cirrhotic portal hypertension patients, and so it was necessary to define the presence of different blood flow rates after the blood flows accumulated in the main trunk of the portal vein so as to achieve left and right blood stratification in the natural state. However, it is controversial at home and abroad whether there is difference between splenic vein blood flow velocity and mesenteric blood flow velocity in cirrhotic patients with portal hypertension after the accumulation of the main portal vein in the natural state. In a study conducted in 2020 in China, 15 patients with liver cirrhosis and upper gastrointestinal haemorrhage received TIPS, and blood samples were collected from the left branch, right branch and main trunk of the portal vein during the operation[5]. In these patients, the plasma ammonia concentration (μmol/L) was 96.4 ± 17.6 for the left branch *vs* 113.5 ± 18.4 for the right branch *vs* 106.9 ± 38.7 for the main trunk, without any statistically significant differences ($P > 0.05$). This study provides important evidence for the comparison of blood bacterial metabolites in the left and right branches of the cirrhotic portal vein.

TIPS dedicated stents (Viatorr stents) have been adopted for surgery at the Center since March 2016. In previous studies, COOK bare stents with an inner diameter of 8 mm were used to establish a shunt[6-7]. Although such a stent should be long enough at the end of the portal vein, the shunted blood was from the portal vein branches, so whether a shunt was established in the left or right portal vein branch had no significant effect on the incidence of hepatic encephalopathy. In a study conducted in China in 2020, 120 cirrhotic portal hypertension patients received TIPS using Viatorr stents. Intraoperative portal vein angiography showed that a shunt was established in the left portal vein branch for 52 patients and in the right portal vein branch for 68 patients[8]. There was no statistically significant difference in the

incidence of postoperative hepatic encephalopathy (χ^2 = 0.159, P = 0.69) between the left portal vein and right portal vein branch shunting groups. A recent study reported that the incidence of hepatic encephalopathy decreased significantly by controlling the inner diameter of the stent, *i.e.*, using a Viatorr stent with an inner diameter of 8 mm[9]. The bare area of a Viatorr stent may guarantee a smooth blood flow in the portal vein and prevent more blood not metabolised by the liver from directly entering the systemic circulation.

There is no information in the TIPS guidelines circulated in North America regarding differences in the incidence of postoperative hepatic encephalopathy when shunts are established in different portal vein branches[10-11]. We believe that there are no differences in the incidence of hepatic encephalopathy among postoperative patients when using a Viatorr stent with an inner diameter of 8 mm when the shunt is established in the left or right portal vein branch. As the postoperative medium and long-term efficacy of TIPS are related to clinical procedures, postoperative management of patients and other factors, future studies with larger sample sizes and multicentre randomised controlled trials are warranted.

FOOTNOTES

Author contributions: All authors wrote and edited the manuscript.

Conflict-of-interest statement: The authors declare no competing interests for this manuscript.

Open-Access: This article is an open-access article that was selected by an in-house editor and fully peer-reviewed by external reviewers. It is distributed in accordance with the Creative Commons Attribution NonCommercial (CC BY-NC 4.0) license, which permits others to distribute, remix, adapt, build upon this work non-commercially, and license their derivative works on different terms, provided the original work is properly cited and the use is non-commercial. See: https://creativecommons.org/Licenses/by-nc/4.0/

Country/Territory of origin: China

ORCID number: Xin Yao 0000-0002-9977-6153; Sheng He 0000-0002-4468-0728; Meng Wei 0000-0001-6197-9812; Jian-Ping Qin 0000-0001-7834-8830.

S-Editor: Chang KL
L-Editor: A
P-Editor: Chang KL

REFERENCES

1 **Luo SH**, Chu JG, Huang H, Zhao GR, Yao KC. Targeted puncture of left branch of intrahepatic portal vein in transjugular intrahepatic portosystemic shunt to reduce hepatic encephalopathy. *World J Gastroenterol* 2019; **25**: 1088-1099 [PMID: 30862997 DOI: 10.3748/wjg.v25.i9.1088]

2 **Ursic M**, Ravnik D, Hribernik M, Pecar J, Butinar J, Fazarinc G. Gross anatomy of the portal vein and hepatic artery ramifications in dogs: corrosion cast study. *Anat Histol Embryol* 2007; **36**: 83-87 [PMID: 17371378 DOI: 10.1111/j.1439-0264.2006.00719.x]

3 **Maruyama H**, Okugawa H, Ishibashi H, Takahashi M, Kobayashi S, Yoshizumi H, Yokosuka O. Carbon dioxide-based portography: an alternative to conventional imaging with the use of iodinated contrast medium. *J Gastroenterol Hepatol* 2010; **25**: 1111-1116 [PMID: 20594227 DOI: 10.1111/j.1440-1746.2010.06248.x]

4 **Ljubicić N**, Duvnjak M, Rotkvić I, Kopjar B. Influence of the degree of liver failure on portal blood flow in patients with liver cirrhosis. *Scand J Gastroenterol* 1990; **25**: 395-400 [PMID: 2186474 DOI: 10.3109/00365529009095505]

5 **Deng LYY**, Chen Y, Ye P, Liao HF, Zhen QL, Xie ZG, Zhao GR, Yao KC. Preliminary analysis of liver-related blood components in portal system *via* TIPS approach. *J Intervent Radiol* 2020; **29**: 608-661 [DOI: 10.3969/j.issn.1008-794X.2020.06.018]

6 **Qin JP**, Jiang MD, Tang W, Wu XL, Yao X, Zeng WZ, Xu H, He QW, Gu M. Clinical effects and complications of TIPS for portal hypertension due to cirrhosis: a single center. *World J Gastroenterol* 2013; **19**: 8085-8092 [PMID: 24307804 DOI: 10.3748/wjg.v19.i44.8085]

7 **Qin JP**, Tang SH, Jiang MD, He QW, Chen HB, Yao X, Zeng WZ, Gu M. Contrast enhanced computed tomography and reconstruction of hepatic vascular system for transjugular intrahepatic portal systemic shunt puncture path planning. *World J Gastroenterol* 2015; **21**: 9623-9629 [PMID: 26327770 DOI: 10.3748/wjg.v21.i32.9623]

8 **Yao X**, Zhou H, Tang SH, Huang S, Chen XL, Qin JP. Effect of intraoperative Viatorr stent implantation for shunting of blood flow in the left or right branch of the portal vein and its effect on clinical outcome in patients with cirrhotic portal hypertension undergoing transjugular intrahepatic portosystemic shunt. *J Clin Hepatol* 2020; **36**: 1970-1974 [DOI: 10.3969/j.issn.1001-5256.2020.09.012]

9 **Yao X**, Zhou H, Huang S, Tang SH, Qin JP. Effects of transjugular intrahepatic portosystemic shunt using the Viatorr stent on hepatic reserve function in patients with cirrhosis. *World J Clin Cases* 2021; **9**: 1532-1542 [PMID: 33728297 DOI:

10.12998/wjcc.v9.i7.1532]

10 **Boyer TD**, Haskal ZJ; American Association for the Study of Liver Diseases. The Role of Transjugular Intrahepatic Portosystemic Shunt (TIPS) in the Management of Portal Hypertension: update 2009. *Hepatology* 2010; **51**: 306 [PMID: 19902484 DOI: 10.1002/hep.23383]

11 **Boike JR**, Thornburg BG, Asrani SK, Fallon MB, Fortune BE, Izzy MJ, Verna EC, Abraldes JG, Allegretti AS, Bajaj JS, Biggins SW, Darcy MD, Farr MA, Farsad K, Garcia-Tsao G, Hall SA, Jadlowiec CC, Krowka MJ, Laberge J, Lee EW, Mulligan DC, Nadim MK, Northup PG, Salem R, Shatzel JJ, Shaw CJ, Simonetto DA, Susman J, Kolli KP, VanWagner LB; Advancing Liver Therapeutic Approaches (ALTA) Consortium. North American Practice-Based Recommendations for Transjugular Intrahepatic Portosystemic Shunts in Portal Hypertension. *Clin Gastroenterol Hepatol* 2021 [PMID: 34274511 DOI: 10.1016/j.cgh.2021.07.018]

World Journal of Gastroenterology

Submit a Manuscript: https://www.f6publishing.com

World J Gastroenterol 2022 August 21; 28(31): 4471-4474

DOI: 10.3748/wjg.v28.i31.4471

ISSN 1007-9327 (print) ISSN 2219-2840 (online)

LETTER TO THE EDITOR

Promising role of D-amino acids in irritable bowel syndrome

Yuka Ikeda, Kurumi Taniguchi, Haruka Sawamura, Ai Tsuji, Satoru Matsuda

Specialty type: Gastroenterology and hepatology

Provenance and peer review: Invited article; Externally peer reviewed.

Peer-review model: Single blind

Peer-review report's scientific quality classification

Grade A (Excellent): 0
Grade B (Very good): B, B
Grade C (Good): C
Grade D (Fair): 0
Grade E (Poor): 0

P-Reviewer: Gobin I; Ji G, China; Mamieva Z, Russia

Received: April 4, 2022
Peer-review started: April 4, 2022
First decision: May 29, 2022
Revised: June 14, 2022
Accepted: July 20, 2022
Article in press: July 20, 2022
Published online: August 21, 2022

Yuka Ikeda, Kurumi Taniguchi, Haruka Sawamura, Ai Tsuji, Satoru Matsuda, Department of Food Science and Nutrition, Nara Women's University, Nara 630-8506, Japan

Corresponding author: Satoru Matsuda, MD, PhD, Professor, Department of Food Science and Nutrition, Nara Women's University, Kita-Uoya Nishimachi, Nara 630-8506, Japan. smatsuda@cc.nara-wu.ac.jp

Abstract

Irritable bowel syndrome (IBS) is an important health care concern. Alterations in the microbiota of the gut-brain axis may be linked to the pathophysiology of IBS. Some dietary intake could contribute to produce various metabolites including D-amino acids by the fermentation by the gut microbiota. D-amino acids are the enantiomeric counterparts of L-amino acids, in general, which could play key roles in cellular physiological processes against various oxidative stresses. Therefore, the presence of D-amino acids has been shown to be linked to the protection of several organs in the body. In particular, the gut microbiota could play significant roles in the stability of emotion *via* the action of D-amino acids. Here, we would like to shed light on the roles of D-amino acids, which could be used for the treatment of IBS.

Key Words: Irritable bowel syndrome; D-amino acid; Gut microbiota; Colitis; Probiotics; Fecal microbiota transplantation

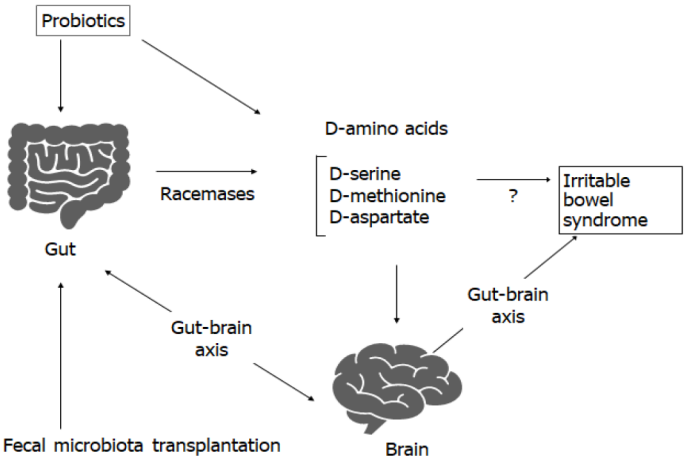
©The Author(s) 2022. Published by Baishideng Publishing Group Inc. All rights reserved.

Core Tip: The potential efficacy of D-amino acids for the treatment of irritable bowel syndrome is shown here.

Citation: Ikeda Y, Taniguchi K, Sawamura H, Tsuji A, Matsuda S. Promising role of D-amino acids in irritable bowel syndrome. *World J Gastroenterol* 2022; 28(31): 4471-4474
URL: https://www.wjgnet.com/1007-9327/full/v28/i31/4471.htm
DOI: https://dx.doi.org/10.3748/wjg.v28.i31.4471

TO THE EDITOR

With great interest, we have read the article by Mamieva *et al*[1]. As irritable bowel



DOI: 10.3748/wjg.v28.i31.4471 **Copyright** ©The Author(s) 2022.

Figure 1 Gut microbiota could contribute to the production of D-amino acids, which might play key roles in irritable bowel syndrome *via* direct action on the gut and/or indirect action through the gut-brain axis with emotional stability. Fecal microbiota transplantation consists of fecal microbiota infusion from a healthy donor into a recipient subject, which has been also shown to be a promising therapy for irritable bowel syndrome. Arrowheads mean stimulation and/or augmentation whereas hammerheads represent inhibition. Note that some critical events such as reactive oxygen species production, immune activation, and/or cytokine-induction have been omitted for clarity.

syndrome (IBS) could exacerbate the patients' quality of life, it is a considerable health care concern. Although the underlying pathophysiological mechanisms are not clear, the role of low-grade inflammation and mucosal immune activation appears to be obvious in the signs of IBS. IBS is a functional gastrointestinal disorder, and some probiotic supplementation may reduce the symptoms[2]. In addition, fecal microbiota transplantation expects recommendations for the treatment of IBS, suggesting that alterations in the gut microbiota-brain axis are linked to the pathophysiology of IBS (Figure 1). It has been revealed that some cytokines and neurotransmitters as well as several microbial metabolites including short chain fatty acids (SCFAs) such as acetate, lactate, butyrate, and propionate produced by the bacteria in the gut could modulate the integrity of brain function[1]. The bidirectional communication between the gut microbiota and the brain is well-known as the gut-brain axis, which could play an important role in the stability of emotion[3]. As shown in the article by Mamieva *et al*[1], the microbiota could influence the pathogenetic factors of IBS through the production of several microbial metabolites. Here, we would like to add the efficacy of D-amino acids for the alteration of IBS condition.

Mice treated with D-serine prior to the induction of colitis exhibited a reduction in the colonic inflammation that was not seen in mice fed L-serine[4]. In addition, D-serine efficiently suppressed the progression of chronic colitis. Therefore, D-serine might have effective properties as a preventive strategy and/or a treatment for colitis[4]. In addition, several studies have shown the significance of D-amino acids in clinical usage[5]. For example, D-methionine protects against the intestinal damage through anti-oxidative and anti-inflammatory effects, which could improve the gut microbiome imbalance by enhancing the growth of beneficial bacteria[6]. Protective effects of low-dose D-serine have been also shown to suppress the renal damage, which may promote the proliferation of kidney epithelial cells[7]. In addition, D-cysteine administration could defend the kidney from ischemia-reperfusion injury, which may be beneficial for the treatment of several renal diseases[8]. Gastroprotective effect with D-cysteine but not with L-cysteine has been shown *via* the effects of decreasing cellular damage, edema, and epithelium loss[9]. Treatment with D-aspartate may bring positive effects in the nervous system[10]. Furthermore, D-cycloserine is a glutamatergic N-methyl-D-aspartate receptor agonist which has been revealed to support the stability of emotion[11]. Furthermore, the activity of ovarian development with D-tryptophan is more effective than that with L-tryptophan[12]. These data suggest that D-amino acids could have beneficial and/or protective effects on various tissues, which might be favorable to the treatment of IBS (Figure 1). In particular, the emotional stability *via* the action of D-amino acids seems to be important[13], because it has been shown that different types of physiological and/or psychological stressors are known to contribute to the development, maintenance, and exacerbation of IBS[14].

The gut microbiota has a large genetic capacity to produce D-amino acids which are utilized as nutrients to support bacterial growth[15]. D-amino acids are essential elements of peptidoglycans in the cell wall of bacteria. Hence, higher levels of D-amino acids have been basically related to the mass of the gut microbiota[16]. Many bacterial species encode specific racemases that can convert L-amino acids to D-amino acids, which are frequently present in the peptidoglycan-containing bacteria in the gut microbiota[17]. Accordingly, the lumen of the gastro-intestinal tract in mammals may be rich in free D-amino acids that might be derived from such bacteria or fermented foods. Probably, the source of D-

amino acids in mammals may mostly be from their gut microbiota. For example, D-alanine production is linked to the relative abundance of bacterial species such as *Enterococcus* and *Lactobacillus* in the gut microbiota[18]. Therefore, the metabolism of D-amino acids in the body might be modified by the alteration of gut bacterial communities affecting the host health and/or homeostasis[19]. Reduction of the amount of several D-amino acids may promote senescence through the increase of reactive oxygen species production[20,21].

FOOTNOTES

Author contributions: Ikeda Y and Matsuda S contributed equally to this work; Ikeda Y, Taniguchi K, Sawamura H, Tsuji A, and Matsuda S designed the research study and wrote the manuscript; and all authors have read and approved the final manuscript.

Conflict-of-interest statement: All authors report no relevant conflicts of interest for this article.

Open-Access: This article is an open-access article that was selected by an in-house editor and fully peer-reviewed by external reviewers. It is distributed in accordance with the Creative Commons Attribution NonCommercial (CC BY-NC 4.0) license, which permits others to distribute, remix, adapt, build upon this work non-commercially, and license their derivative works on different terms, provided the original work is properly cited and the use is non-commercial. See: https://creativecommons.org/Licenses/by-nc/4.0/

Country/Territory of origin: Japan

ORCID number: Yuka Ikeda 0000-0003-4805-1758; Ai Tsuji 0000-0003-1619-7592; Satoru Matsuda 0000-0003-4274-5345.

S-Editor: Ma YJ
L-Editor: Wang TQ
P-Editor: Ma YJ

REFERENCES

1 **Mamieva Z**, Poluektova E, Svistushkin V, Sobolev V, Shifrin O, Guarner F, Ivashkin V. Antibiotics, gut microbiota, and irritable bowel syndrome: What are the relations? *World J Gastroenterol* 2022; **28**: 1204-1219 [PMID: 35431513 DOI: 10.3748/wjg.v28.i12.1204]
2 **Lee J**, Park SB, Kim HW, Lee HS, Jee SR, Lee JH, Kim TO. Clinical Efficacy of Probiotic Therapy on Bowel-Related Symptoms in Patients with Ulcerative Colitis during Endoscopic Remission: An Observational Study. *Gastroenterol Res Pract* 2022; **2022**: 9872230 [PMID: 35082846 DOI: 10.1155/2022/9872230]
3 **Barberio B**, Zamani M, Black CJ, Savarino EV, Ford AC. Prevalence of symptoms of anxiety and depression in patients with inflammatory bowel disease: a systematic review and meta-analysis. *Lancet Gastroenterol Hepatol* 2021; **6**: 359-370 [PMID: 33721557 DOI: 10.1016/S2468-1253(21)00014-5]
4 **Asakawa T**, Onizawa M, Saito C, Hikichi R, Yamada D, Minamidate A, Mochimaru T, Asahara SI, Kido Y, Oshima S, Nagaishi T, Tsuchiya K, Ohira H, Okamoto R, Watanabe M. Oral administration of D-serine prevents the onset and progression of colitis in mice. *J Gastroenterol* 2021; **56**: 732-745 [PMID: 34148144 DOI: 10.1007/s00535-021-01792-1]
5 **Müller C**, Fonseca JR, Rock TM, Krauss-Etschmann S, Schmitt-Kopplin P. Enantioseparation and selective detection of D-amino acids by ultra-high-performance liquid chromatography/mass spectrometry in analysis of complex biological samples. *J Chromatogr A* 2014; **1324**: 109-114 [PMID: 24315356 DOI: 10.1016/j.chroma.2013.11.026]
6 **Wu CH**, Ko JL, Liao JM, Huang SS, Lin MY, Lee LH, Chang LY, Ou CC. D-methionine alleviates cisplatin-induced mucositis by restoring the gut microbiota structure and improving intestinal inflammation. *Ther Adv Med Oncol* 2019; **11**: 1758835918821021 [PMID: 30792823 DOI: 10.1177/1758835918821021]
7 **Nakade Y**, Iwata Y, Furuichi K, Mita M, Hamase K, Konno R, Miyake T, Sakai N, Kitajima S, Toyama T, Shinozaki Y, Sagara A, Miyagawa T, Hara A, Shimizu M, Kamikawa Y, Sato K, Oshima M, Yoneda-Nakagawa S, Yamamura Y, Kaneko S, Miyamoto T, Katane M, Homma H, Morita H, Suda W, Hattori M, Wada T. Gut microbiota-derived D-serine protects against acute kidney injury. *JCI Insight* 2018; **3** [PMID: 30333299 DOI: 10.1172/jci.insight.97957]
8 **Kimura H**. The physiological role of hydrogen sulfide and beyond. *Nitric Oxide* 2014; **41**: 4-10 [PMID: 24491257 DOI: 10.1016/j.niox.2014.01.002]
9 **Souza LK**, Araújo TS, Sousa NA, Sousa FB, Nogueira KM, Nicolau LA, Medeiros JV. Evidence that d-cysteine protects mice from gastric damage *via* hydrogen sulfide produced by d-amino acid oxidase. *Nitric Oxide* 2017; **64**: 1-6 [PMID: 28137610 DOI: 10.1016/j.niox.2017.01.010]
10 **de Rosa V**, Secondo A, Pannaccione A, Ciccone R, Formisano L, Guida N, Crispino R, Fico A, Polishchuk R, D'Aniello A, Annunziato L, Boscia F. D-Aspartate treatment attenuates myelin damage and stimulates myelin repair. *EMBO Mol Med* 2019; **11** [PMID: 30559305 DOI: 10.15252/emmm.201809278]
11 **Levinson CA**, Rodebaugh TL, Fewell L, Kass AE, Riley EN, Stark L, McCallum K, Lenze EJ. D-Cycloserine facilitation of exposure therapy improves weight regain in patients with anorexia nervosa: a pilot randomized controlled trial. *J Clin Psychiatry* 2015; **76**: e787-e793 [PMID: 26132687 DOI: 10.4088/JCP.14m09299]
12 **Kobayashi K**, Maezawa T, Tanaka H, Onuki H, Horiguchi Y, Hirota H, Ishida T, Horiike K, Agata Y, Aoki M, Hoshi M,

Matsumoto M. The identification of D-tryptophan as a bioactive substance for postembryonic ovarian development in the planarian Dugesia ryukyuensis. *Sci Rep* 2017; **7**: 45175 [PMID: 28338057 DOI: 10.1038/srep45175]

13 **Taniguchi K**, Sawamura H, Ikeda Y, Tsuji A, Kitagishi Y, Matsuda S. D-Amino Acids as a Biomarker in Schizophrenia. *Diseases* 2022; **10** [PMID: 35225861 DOI: 10.3390/diseases10010009]

14 **Raskov H**, Burcharth J, Pommergaard HC, Rosenberg J. Irritable bowel syndrome, the microbiota and the gut-brain axis. *Gut Microbes* 2016; **7**: 365-383 [PMID: 27472486 DOI: 10.1080/19490976.2016.1218585]

15 **Macfarlane GT**, Macfarlane S. Bacteria, colonic fermentation, and gastrointestinal health. *J AOAC Int* 2012; **95**: 50-60 [PMID: 22468341 DOI: 10.5740/jaoacint.sge_macfarlane]

16 **Sasabe J**, Miyoshi Y, Rakoff-Nahoum S, Zhang T, Mita M, Davis BM, Hamase K, Waldor MK. Interplay between microbial D-amino acids and host D-amino acid oxidase modifies murine mucosal defence and gut microbiota. *Nat Microbiol* 2016; **1**: 16125 [PMID: 27670111 DOI: 10.1038/nmicrobiol.2016.125]

17 **Cava F**, Lam H, de Pedro MA, Waldor MK. Emerging knowledge of regulatory roles of D-amino acids in bacteria. *Cell Mol Life Sci* 2011; **68**: 817-831 [PMID: 21161322 DOI: 10.1007/s00018-010-0571-8]

18 **Gilmore MS**, Skaugen M, Nes I. Enterococcus faecalis cytolysin and lactocin S of Lactobacillus sake. *Antonie Van Leeuwenhoek* 1996; **69**: 129-138 [PMID: 8775973 DOI: 10.1007/BF00399418]

19 **Kawase T**, Nagasawa M, Ikeda H, Yasuo S, Koga Y, Furuse M. Gut microbiota of mice putatively modifies amino acid metabolism in the host brain. *Br J Nutr* 2017; **117**: 775-783 [PMID: 28393748 DOI: 10.1017/S0007114517000678]

20 **Nagano T**, Yamao S, Terachi A, Yarimizu H, Itoh H, Katasho R, Kawai K, Nakashima A, Iwasaki T, Kikkawa U, Kamada S. D-amino acid oxidase promotes cellular senescence *via* the production of reactive oxygen species. *Life Sci Alliance* 2019; **2** [PMID: 30659069 DOI: 10.26508/lsa.201800045]

21 **Canteros MG**. D-Arginine as a neuroprotective amino acid: promising outcomes for neurological diseases. *Drug Discov Today* 2014; **19**: 627-636 [PMID: 24252866 DOI: 10.1016/j.drudis.2013.11.010]



Published by **Baishideng Publishing Group Inc**
7041 Koll Center Parkway, Suite 160, Pleasanton, CA 94566, USA
Telephone: +1-925-3991568
E-mail: bpgoffice@wjgnet.com
Help Desk: https://www.f6publishing.com/helpdesk
https://www.wjgnet.com



© 2022 Baishideng Publishing Group Inc. All rights reserved.

ISSN 1007-9327 (print)
ISSN 2219-2840 (online)

World Journal of *Gastroenterology*

World J Gastroenterol 2022 August 28; 28(32): 4475-4743



Published by Baishideng Publishing Group Inc

World Journal of Gastroenterology

Contents

Weekly Volume 28 Number 32 August 28, 2022

REVIEW

4475 Colon mucus in colorectal neoplasia and beyond

Loktionov A

MINIREVIEWS

4493 Who to screen and how to screen for celiac disease

Singh P, Singh AD, Ahuja V, Makharia GK

4508 Assessment of physical stress during the perioperative period of endoscopic submucosal dissection

Chinda D, Shimoyama T

4516 Expanding beyond endoscopy: A review of non-invasive modalities in Barrett's esophagus screening and surveillance

Shahsavari D, Kudaravalli P, Yap JEL, Vega KJ

4527 Impact of microbiota-immunity axis in pancreatic cancer management

Bartolini I, Nannini G, Risaliti M, Matarazzo F, Moraldi L, Ringressi MN, Taddei A, Amedei A

4540 Liver Imaging Reporting and Data System criteria for the diagnosis of hepatocellular carcinoma in clinical practice: A pictorial minireview

Liava C, Sinakos E, Papadopoulou E, Giannakopoulou L, Potsi S, Moumtzouoglou A, Chatziioannou A, Stergioulas L, Kalogeropoulou L, Dedes I, Akriviadis E, Chourmouzi D

4557 Liver regeneration as treatment target for severe alcoholic hepatitis

Virovic-Jukic L, Ljubas D, Stojsavljevic-Shapeski S, Ljubičić N, Filipec Kanizaj T, Mikolasevic I, Grgurevic I

ORIGINAL ARTICLE

Basic Study

4574 Wumei pills attenuates 5-fluorouracil-induced intestinal mucositis through Toll-like receptor 4/myeloid differentiation factor 88/nuclear factor-κB pathway and microbiota regulation

Lu DX, Liu F, Wu H, Liu HX, Chen BY, Yan J, Lu Y, Sun ZG

4600 Sirolimus increases the anti-cancer effect of Huai Er by regulating hypoxia inducible factor-1α-mediated glycolysis in hepatocellular carcinoma

Zhou L, Zhao Y, Pan LC, Wang J, Shi XJ, Du GS, He Q

4620 Anti-tumour activity and toxicological studies of combination treatment of *Orthosiphon stamineus* and gemcitabine on pancreatic xenograft model

Yehya AHS, Subramaniam AV, Asif M, Kaur G, Abdul Majid AMS, Oon CE

World Journal of Gastroenterology

Weekly Volume 28 Number 32 August 28, 2022

Contents

4635 The mechanism of Yinchenhao decoction in treating obstructive-jaundice-induced liver injury based on Nrf2 signaling pathway

Liu JJ, Xu Y, Chen S, Hao CF, Liang J, Li ZL

4649 Anoctamin 5 regulates the cell cycle and affects prognosis in gastric cancer

Fukami T, Shiozaki A, Kosuga T, Kudou M, Shimizu H, Ohashi T, Arita T, Konishi H, Komatsu S, Kubota T, Fujiwara H, Okamoto K, Kishimoto M, Morinaga Y, Konishi E, Otsuji E

4668 Effects of Granule Dendrobii on chronic atrophic gastritis induced by N-methyl-N'-nitro-N-nitrosoguanidine in rats

Wu Y, Li Y, Jin XM, Dai GH, Chen X, Tong YL, Ren ZM, Chen Y, Xue XM, Wu RZ

Retrospective Study

4681 Machine learning predicts portal vein thrombosis after splenectomy in patients with portal hypertension: Comparative analysis of three practical models

Li J, Wu QQ, Zhu RH, Lv X, Wang WQ, Wang JL, Liang BY, Huang ZY, Zhang EL

Observational Study

4698 International patterns in incidence and mortality trends of pancreatic cancer in the last three decades: A joinpoint regression analysis

Ilic I, Ilic M

Prospective Study

4716 Differential diagnosis of different types of solid focal liver lesions using two-dimensional shear wave elastography

Guo J, Jiang D, Qian Y, Yu J, Gu YJ, Zhou YQ, Zhang HP

META-ANALYSIS

4726 Use of shear wave elastography for the diagnosis and follow-up of biliary atresia: A meta-analysis

Wagner ES, Abdelgawad HAH, Landry M, Asfour B, Slidell MB, Azzam R

LETTER TO THE EDITOR

4741 Is endoscopic mucosal ablation a valid option for treating colon polyps?

Liu XY, Ren RR, Wu C, Wang LY, Zhu ML

ABOUT COVER

Editorial Board Member of *World Journal of Gastroenterology*, PhD, MD, Associate Professor in Infectious Diseases, Department of Mental Health and Public Medicine, University of Campania "Luigi Vanvitelli", Naples 80130, Italy. caterina.sagnelli@unicampania.it

AIMS AND SCOPE

The primary aim of *World Journal of Gastroenterology* (*WJG*, *World J Gastroenterol*) is to provide scholars and readers from various fields of gastroenterology and hepatology with a platform to publish high-quality basic and clinical research articles and communicate their research findings online. *WJG* mainly publishes articles reporting research results and findings obtained in the field of gastroenterology and hepatology and covering a wide range of topics including gastroenterology, hepatology, gastrointestinal endoscopy, gastrointestinal surgery, gastrointestinal oncology, and pediatric gastroenterology.

INDEXING/ABSTRACTING

The *WJG* is now abstracted and indexed in Science Citation Index Expanded (SCIE, also known as SciSearch®), Current Contents/Clinical Medicine, Journal Citation Reports, Index Medicus, MEDLINE, PubMed, PubMed Central, Scopus, Reference Citation Analysis, China National Knowledge Infrastructure, China Science and Technology Journal Database, and Superstar Journals Database. The 2022 edition of Journal Citation Reports® cites the 2021 impact factor (IF) for *WJG* as 5.374; IF without journal self cites: 5.187; 5-year IF: 5.715; Journal Citation Indicator: 0.84; Ranking: 31 among 93 journals in gastroenterology and hepatology; and Quartile category: Q2. The *WJG*'s CiteScore for 2021 is 8.1 and Scopus CiteScore rank 2021: Gastroenterology is 18/149.

RESPONSIBLE EDITORS FOR THIS ISSUE

Production Editor: *Yu-Xi Chen*; **Production Department Director:** *Xu Guo*; **Editorial Office Director:** *Jia-Ru Fan*.

NAME OF JOURNAL
World Journal of Gastroenterology

ISSN
ISSN 1007-9327 (print) ISSN 2219-2840 (online)

LAUNCH DATE
October 1, 1995

FREQUENCY
Weekly

EDITORS-IN-CHIEF
Andrzej S Tarnawski

EDITORIAL BOARD MEMBERS
http://www.wjgnet.com/1007-9327/editorialboard.htm

PUBLICATION DATE
August 28, 2022

COPYRIGHT
© 2022 Baishideng Publishing Group Inc

INSTRUCTIONS TO AUTHORS
https://www.wjgnet.com/bpg/gerinfo/204

GUIDELINES FOR ETHICS DOCUMENTS
https://www.wjgnet.com/bpg/GerInfo/287

GUIDELINES FOR NON-NATIVE SPEAKERS OF ENGLISH
https://www.wjgnet.com/bpg/gerinfo/240

PUBLICATION ETHICS
https://www.wjgnet.com/bpg/GerInfo/288

PUBLICATION MISCONDUCT
https://www.wjgnet.com/bpg/gerinfo/208

ARTICLE PROCESSING CHARGE
https://www.wjgnet.com/bpg/gerinfo/242

STEPS FOR SUBMITTING MANUSCRIPTS
https://www.wjgnet.com/bpg/GerInfo/239

ONLINE SUBMISSION
https://www.f6publishing.com

© 2022 Baishideng Publishing Group Inc. All rights reserved. 7041 Koll Center Parkway, Suite 160, Pleasanton, CA 94566, USA
E-mail: bpgoffice@wjgnet.com https://www.wjgnet.com

World Journal of Gastroenterology

Submit a Manuscript: https://www.f6publishing.com

World J Gastroenterol 2022 August 28; 28(32): 4475-4492

DOI: 10.3748/wjg.v28.i32.4475

ISSN 1007-9327 (print) ISSN 2219-2840 (online)

REVIEW

Colon mucus in colorectal neoplasia and beyond

Alexandre Loktionov

Specialty type: Gastroenterology and hepatology

Provenance and peer review: Invited article; Externally peer reviewed.

Peer-review model: Single blind

Peer-review report's scientific quality classification

Grade A (Excellent): 0
Grade B (Very good): B
Grade C (Good): C
Grade D (Fair): 0
Grade E (Poor): 0

P-Reviewer: Almeida C, Portugal; M'Koma AE, United States

Received: January 27, 2022
Peer-review started: January 27, 2022
First decision: April 10, 2022
Revised: April 23, 2022
Accepted: August 6, 2022
Article in press: August 6, 2022
Published online: August 28, 2022

Alexandre Loktionov, DiagNodus Ltd, Cambridge CB4 0WS, United Kingdom

Corresponding author: Alexandre Loktionov, MD, PhD, Director, DiagNodus Ltd, St John's Innovation Centre, Cowley Road, Cambridge CB4 0WS, United Kingdom.
alex.loktionov@diagnodus.com

Abstract

Little was known about mammalian colon mucus (CM) until the beginning of the 21st century. Since that time considerable progress has been made in basic research addressing CM structure and functions. Human CM is formed by two distinct layers composed of gel-forming glycosylated mucins that are permanently secreted by goblet cells of the colonic epithelium. The inner layer is dense and impenetrable for bacteria, whereas the loose outer layer provides a habitat for abundant commensal microbiota. Mucus barrier integrity is essential for preventing bacterial contact with the mucosal epithelium and maintaining homeostasis in the gut, but it can be impaired by a variety of factors, including CM-damaging switch of commensal bacteria to mucin glycan consumption due to dietary fiber deficiency. It is proven that impairments in CM structure and function can lead to colonic barrier deterioration that opens direct bacterial access to the epithelium. Bacteria-induced damage dysregulates epithelial proliferation and causes mucosal inflammatory responses that may expand to the loosened CM and eventually result in severe disorders, including colitis and neoplastic growth. Recently described formation of bacterial biofilms within the inner CM layer was shown to be associated with both inflammation and cancer. Although obvious gaps in our knowledge of human CM remain, its importance for the pathogenesis of major colorectal diseases, comprising inflammatory bowel disease and colorectal cancer, is already recognized. Continuing progress in CM exploration is likely to result in the development of a range of new useful clinical applications addressing colorectal disease diagnosis, prevention and therapy.

Key Words: Colon; Colon mucus; Mucins; Goblet cells; Gut microbiota; Inflammatory bowel disease; Colorectal cancer

©The Author(s) 2022. Published by Baishideng Publishing Group Inc. All rights reserved.

Core Tip: Until recently colon mucus (CM) importance was largely ignored because its structure and functions were obscure. It is now known that human CM comprises a dense inner layer impenetrable for bacteria and a loose outer layer providing a habitat for abundant commensal microbiota. Mucus barrier integrity is essential for maintaining homeostatic balance between colonic mucosa and gut microbiota, and its impairment opens direct bacterial access to the epithelium, which induces inflammation and can cause severe disorders, including inflammatory bowel disease and colorectal cancer. Recent advances in colorectal mucus exploration and emerging new clinical applications based on this knowledge are discussed.

Citation: Loktionov A. Colon mucus in colorectal neoplasia and beyond. *World J Gastroenterol* 2022; 28(32): 4475-4492
URL: https://www.wjgnet.com/1007-9327/full/v28/i32/4475.htm
DOI: https://dx.doi.org/10.3748/wjg.v28.i32.4475

INTRODUCTION

The latest estimates of global cancer incidence and mortality provided for 2020 show that colorectal cancer (CRC) ranks third in terms of incidence and second in terms of mortality[1]. More than 1.9 million new CRC cases and over 935000 deaths caused by this disease were registered worldwide by GLOBOCAN in 2020[1]. Being the most prevalent type of gastrointestinal (GI) neoplasia, CRC is also the most preventable due to its association with modifiable life-style factors[2]. Besides, colorectal tumors are often curable as they grow slowly and can be detected and treated early if effective screening is applied[2,3]. One important biological feature of CRC is its origination from the colonic epithelium, enormous surface of which constitutes the interface between the human body and potentially carcinogenic gut content. Indeed, the intestinal lumen is inhabited by billions of diverse microorganisms forming a unique microbial ecosystem within the host's organism[4]. Microbial density inside the human colon reaches 10^{12} bacterial cells per gram of predominantly anaerobic colonic content that is, nevertheless, indispensable for host development and physiology[5]. This complex and sometimes aggressive ecosystem permanently interacts with the single layer of intestinal epithelial cells that are highly active, being involved in various absorption and secretion processes.

The immense surface of the intestinal mucosa defines the utmost importance of the continuous interplay between its epithelium and gut microbiota. Until the first decade of the XXI century bacteria were presumed to directly contact the epithelial cells[6]. Only in 2008 a research group from Gothenburg (Sweden) convincingly demonstrated the existence of a well-structured system of protective mucus that effectively separates the epithelium from gut content[7]. That seminal study was followed by impressively productive exploration of the gut mucus and its functional significance in health and disease. This review is focused on recent developments in this field, particularly highlighting the emerging evidence of the importance of colon mucus (CM) for the pathogenesis of inflammatory bowel disease (IBD) and colorectal tumors, as well as associated problems of colorectal disease diagnosis, prevention and treatment.

CM COMPOSITION AND STRUCTURAL CHARACTERISTICS

It is now well established that all surfaces of the columnar epithelia lining inner cavities of the human body are overlayed by mucus, which can be generally defined as a complex viscoelastic substance usually secreted by goblet or mucous cells and protecting the underlying epithelium[6,8]. Distinct mucus types naturally adapted for organ-specific functions are described for the GI tract, the respiratory system, the reproductive organs and the ocular surface[6,8,9]. Although mucus composition is organ-specific, its constituents always comprise water (90%-95%), electrolytes, lipids and various proteins[8]. The high water content makes normal CM transparent, which could be one of the reasons of the late discovery of its structure[6,7] schematically presented in Figure 1.

The review is focused on the colon, therefore further discussion is largely devoted to the CM, properties of which are determined by its specific proteins, mucins, defining structural and functional characteristics of this substance[10]. All GI tract mucins are densely decorated with complex carbohydrates or glycans[11]. It is important to stress that the high degree of mucin O-glycosylation protects the peptide bonds, hence rendering these proteins inert to the proteolytic action of the host's proteases[11,12]. There are 22 genes encoding mucins, the presence of phosphotransferase system (PTS)-rich sequences [tandem repeat units rich in proline, threonine (Thr) and serine (Ser)] being their characteristic feature[8-10]. In these proteins a large proportion of the Ser and Thr residues are O-glycosylated with the creation of a "bottle brush" configuration important for high water-binding capacity and gel-

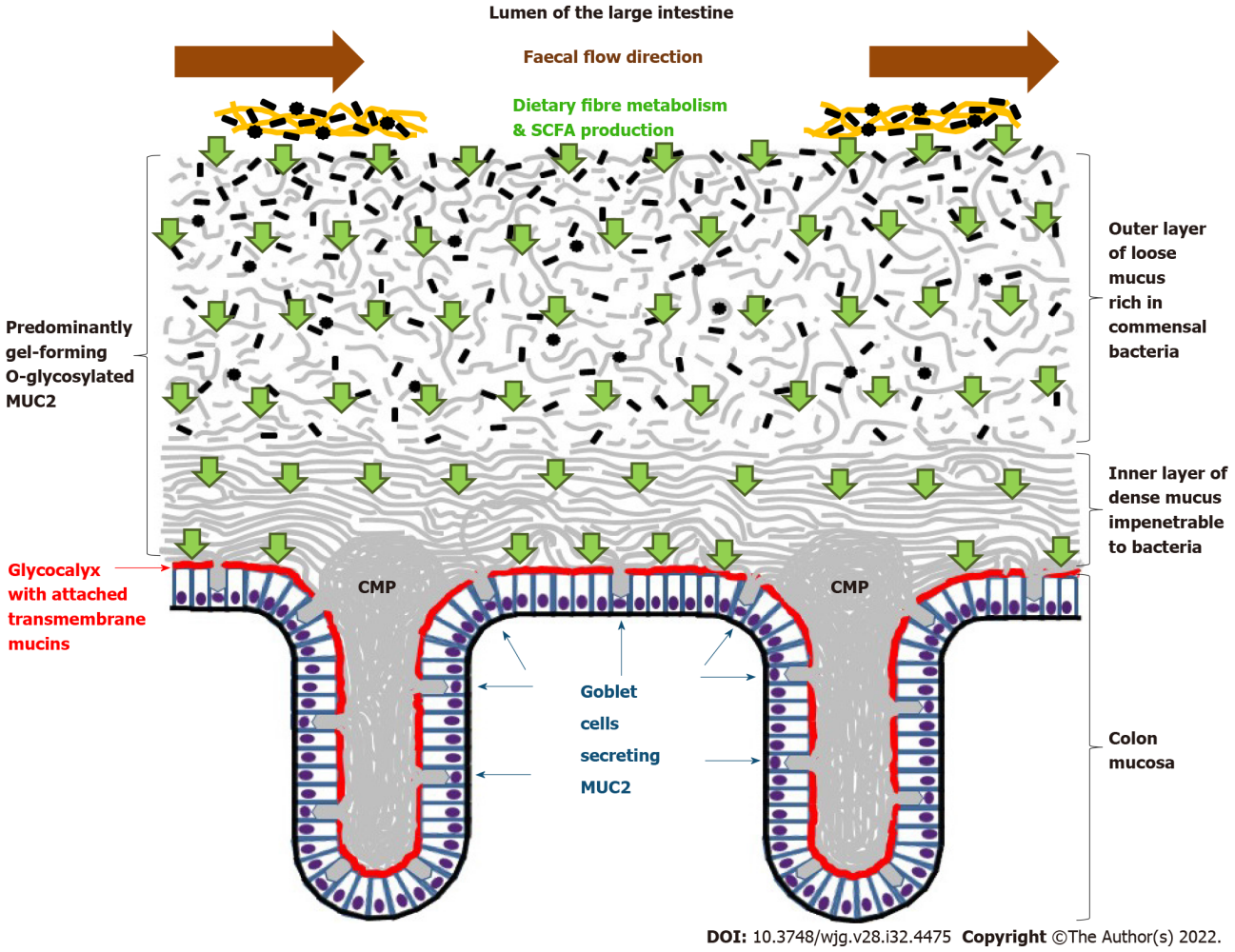


Figure 1 Schematic representation of normal human colonic mucosa and overlaying mucus layers. Small green arrows show short-chain fatty acid transport through colon mucus layers. Small black shapes show bacteria. CMP: Colon mucus plumes; MUC2: Mucins 2; SCFA: Short-chain fatty acids.

forming properties[8-10,13,14]. GI tract mucins can be subdivided into two classes comprising: (1) Transmembrane mucins that have a transmembrane domain enabling them to be anchored in the apical cell membrane; and (2) Gel-forming mucins that are synthesised and secreted by the goblet cells (GCs), thus being the key CM components[8,10,13,14].

Transmembrane mucins

The transmembrane mucins of epithelial cells are a family of large and extended glycoproteins that are attached to the apical cell membrane through a single-pass transmembrane domain involved in intracellular signaling. This family includes MUC1, MUC3, MUC4, MUC12, MUC13, MUC15, MUC16, MUC17, MUC 21 and MUC22 that vary in length and the presence of several specific domains[14,15]. All transmembrane mucins have PTS domains, which are heavily O-glycosylated, but glycosylation patterns along the GI tract vary, also being different in health and disease[15]. The transmembrane mucins MUC3, MUC12 and MUC17 cover the apical cell membrane of enterocytes and colonocytes, forming the attached protective glycan-rich diffusion barrier, called glycocalyx (Figure 1). It was reported that MUC3 is expressed throughout the whole intestine, MUC12 appears to be colon-specific, and MUC17 is abundant in the small intestine but is also found in the transverse colon[11,13,14]. The transmembrane mucins do not belong to the CM, and their precise role in health and disease remains to be fully elucidated. Detailed discussion on this subject can be found in a recent review by Pelaseyed and Hansson[15].

Gel-forming mucins

The gel-forming mucins of the GI tract are synthesised and secreted by the mucosal GCs. The most abundant and best characterized of the secreted mucins is MUC2, the main element of the mucus overlaying mucosal surfaces of the small intestine and colon. Other gel-forming mucins of the GI tract are MUC5AC (expressed in the stomach), MUC5B (weakly expressed in the colon) and MUC6 (expressed in the stomach and duodenum)[13,14]. The structural organization of the GI mucus was initially determined in rodents, and it was shown that mouse stomach and colon have two distinct

layers of dense (inner) and loose (outer) mucus, whereas this pattern is absent in the small intestine, where only a single layer of loose mucus is present[7,11,16]. It is now known that in the human colon the thickness of the dense inner mucus layer is about 200-300 μm, and the loose outer layer is at least twice as thick[6,10,11]. Figure 1 schematically shows the structure of the human CM. It should be stressed that, despite almost identical protein profiles dominated by MUC2, the two CM layers are essentially different[16]. In the normal conditions the dense inner layer is permanently renewed by colonic GCs producing MUC2, which remains anchored to the GCs and attached to the epithelium[10]. Remarkably, the high density of the inner CM layer appears to make it devoid of bacteria[7,11,16]. At a certain distance from the epithelial surface (over 200 μm in humans), the inner mucus is abruptly replaced by the loose outer CM layer, where commensal bacteria live and thrive[16]. The two mucus layers form a sharp border separating them. According to the current paradigm, the dense inner layer is converted into the loose outer mucus by endogenous (host's) proteases, however it is impossible to exclude that gut bacteria populating the outer layer also contribute to the conversion[7,10,11,16]. It is also worth noting that alongside the mammalian colon there are longitudinal differences in both microbiota composition and MUC2 O-glycan pattern distribution in the CM. It the mouse CM was generally characterized by the abundance of highly charged fucosylated glycans, but glycan sulfation level was higher in the distal colon, whereas sialic acid was more common in the proximal colon[17]. It was suggested that the observed differences in mucin glycan structures might be involved in the bacterial selection process by bacterial adhesin - mucin glycan interactions[17]. All these important basic findings are further discussed below in relation to interactions between gut microbiome, CM and colonic epithelium.

GOBLET CELLS AND THEIR ROLE IN CM FORMATION AND MAINTENANCE

Mucus production

Intestinal GCs are responsible for the continuous synthesis and secretion of gut mucus. The details of the complex process of MUC2 synthesis in the GCs are described in recent reviews[8,12,14], but it is useful to note that MUC2 monomers form C-terminal dimers and N-terminal trimers in the endoplasmic reticulum, and the extensive O-glycosylation of the large PTS domain of MUC2 occurs in the Golgi apparatus. The MUC2 polymer is then densely packed in the secretory granules of the GCs under conditions of the low pH and high calcium concentration[11,14,18]. It is believed that the formation of secretory granules occurs during the maturation of GCs coinciding with their migration from the crypt bottom towards the luminal surface[10]. Finally, the secretory granules undergo exocytosis by fusion with the apical membrane, thus releasing their content to the surface of the epithelium. Upon its release, which is accompanied by an increase in pH and a decrease in calcium concentration, the densely packed mucin expands over than 1000-fold[6,10]. The secreted MUC2 immediately unfolds into large net-like planar sheets that are then assembled in porous lamellar networks forming the dense inner CM layer[12,19,20]. The stability of the inner mucus layer is further increased by the formation of isopeptide bond crosslinks catalyzed by transglutaminase 3 produced by GCs and neighbouring colonocytes[21].

The process of permanent mucus renewal is very intense, inner layer renewal time in the mouse colon being only about 1 h[22]. It was also observed that GCs of the luminal surface epithelium produce mucus faster than their counterparts located in the crypt epithelium[22], and it has later been shown that the properties of mucus generated by GCs of the colonic surface epithelium (intercrypt GCs) differ from those of mucus secreted by crypt-resident GCs. Intercrypt GCs have a specific transcript profile and produce less dense and more penetrable mucus compared to the mucus "plumes" synthesised by crypt-resident GCs and possessing more stringent barrier properties[23] (Figure 1). Single GC analysis revealed that within the colonic epithelium there are several different GC clusters, all originating from stem cells at the bottom of the crypt but forming two distinct "differentiation trajectories". One of them, termed "canonical" GCs, is characterized by the expression of typical GC markers, whereas the other one expresses enterocyte-associated genes and was designated as "noncanonical"[23]. The intercrypt GC population appears to be predominantly composed of the most differentiated "canonical" GCs continuously secreting mucus at baseline. In contrast, "noncanonical" GCs, which are more abundant in the crypts and contribute to mucus "plume" secretion, are likely to be more responsive to external stimulation[23]. These results are in agreement with the identification of at least five clusters of GCs with distinct gene expression profiles in the human colon[24].

The discovery of colonic GC diversity inevitably leads to questions on functional differences between GC subpopulations and alternative regulatory mechanisms governing CM production in health and disease. The emerging evidence of GC participation in controlling immune responses in the gut is especially important in this context[25]. In 2012, McDole *et al*[26] reported that small intestinal GCs could endocytose low molecular weight soluble antigens from the gut lumen, being capable of delivering them through GC-associated antigen passages (GAPs) to underlying $CD103^+$ dendritic cells of the intestinal *Lamina propria*. Further studies of this group revealed the existence of this antigen-presenting phenomenon in the colon as well, when acetylcholine-induced GAP formation in colonic GCs was observed[27]. These GAPs could even translocate live commensal bacteria across the

epithelium following antibiotic treatment[28]. It is also believed that GAP formation may be associated with compound exocytosis by GCs, but not primary exocytosis[29]. Hence, the process of GAP formation involves both endocytosis and exocytosis, the two interlinked pathways closely related to autophagy[30], and it was not surprising that autophagy proteins were found to control mucin granule accumulation in colonic GCs[31]. Among autophagy-related factors associated with intestinal GCs, the NOD-like receptor family pyrin domain containing 6 (NLRP6) inflammasome has recently attracted considerable interest[32]. Wlodarska *et al*[33] first demonstrated that the NLRP6 inflammasome acts as a major orchestrator of mucin granule exocytosis in the colon. This theme was further developed by the identification of sentinel GCs localized at the colonic crypt entrance and capable of endocytosing microbe-derived ligands of toll-like receptors (TLRs) from the lumen. This, in turn, triggers the TLR pathway stimulation and leads to the activation of NLRP6 inflammasome. The response provokes compound exocytosis of MUC2 from the sentinel GCs, entailing their death and inducing enhanced mucus production from adjacent GCs through intercellular gap junction signaling[34]. Nevertheless, the described NLRP6 inflammasome involvement does not seem to be important for either CM formation or its function at baseline[35]. Taken together, these results suggest that NLRP6 modulates GC function and CM secretion only in response to interactions with TLR agonists, being inactive in the normal conditions[33]. The role of GCs in monitoring extracellular environment, interacting with the gut microbiota and communicating with the immune cells of the *Lamina propria*, is being actively studied and discussed[25,29,36], but further research is required for its comprehensive clarification.

Other products of goblet cells and protective properties of the CM

Although MUC2 is the main product of the GCs in the colon, mucin granules of these cells also contain other mucus components, such as Fc fragment of immunoglobulin (Ig) G-binding protein, calcium-activated chloride channel regulator 1, zymogen granule protein 16 (ZG16), anterior gradient 2, and trefoil factor 3[11,12]. Some of these proteins possess antibacterial properties. In particular, the lectin-like protein ZG16 prevents bacterial penetration into the inner CM layer[37]. Likewise, proteins resistin-like molecule beta, predominantly synthesised by colon GCs[38], and cathelin-related antimicrobial peptide, which is produced by both epithelial cells in colonic crypts and mucosal macrophages[39], were demonstrated to be bactericidal. Moreover, the loose outer mucus layer in the colon is likely to be intermixed with distally moving loose mucus generated in the small intestine and rich in antimicrobial peptides (AMPs) secreted by Paneth cells located in the mucosa of the small intestine[40]. Besides, the process of mucus barrier formation appears to be even more complex as it has recently been shown that in mice mucus abundantly produced in the proximal colon and encapsulating the faecal material considerably differs from that secreted in the distal colon for secondary strengthening the encapsulation process[41]. However, given numerous species-specific differences, direct extrapolation of these results to humans remains impossible until the matter is comprehensively investigated[42]. In any case, the presence of a range of AMPs probably produced at different sites throughout the GI tract was clearly demonstrated in human rectal mucus samples[43]. It can be added that secretory IgA antibodies produced by plasma cells residing in the intestinal *Lamina propria* were shown to be transported to the mucus by transcytosis[44], and IgA in the colon is concentrated in the outer mucus layer[45]. Finally, it should be mentioned that the steep oxygen gradient keeping the inner CM layer relatively well oxygenated also prevents anaerobic luminal pathogens from reaching the epithelium[46]. The presence of all these factors and the permanent distal movement of the outer CM with the peristaltic waves[10,47], contribute to the protection of the inner CM layer from bacterial invasion.

INTERACTIONS BETWEEN CM AND GUT MICROBIOTA

The human gut harbors a highly diverse community of commensal bacteria usually referred as microbiota, which exhibits both longitudinal and cross-sectional variation in both location and density [48,49]. Microbiota composition in the normal human colon is dominated by Bacteroidetes and Firmicutes phyla, with the presence of members of a few other phyla and strong variability between individuals[48,50]. Notably, dietary fiber digestion is one of the most important functions of the gut microbiota as these plant polysaccharides are largely indigestible by human glycoside hydrolases[51]. The anaerobic fermentation of fiber-derived sugars by gut lumen bacteria produces short-chain fatty acids (SCFAs), including butyrate, acetate and propionate. These SCFAs obviously pass through the intestinal mucus (Figure 1) before being taken up and utilized by the epithelium (butyrate provides up to 70% of colonocyte energy supply). SCFAs are indispensable for both intestinal homeostasis and a variety of effects on tissues and organs beyond the gut (see review by van der Hee and Wells[52]). Remarkably, abundantly glycosylated mucins of the CM can also be targeted by gut bacteria as nutrient sources[50]. Hence, mucin-decorating glycans are thought to constitute a critical resource utilized by commensals to enable them to thrive when diet-derived glycans are limited[53]. This suggestion was experimentally proven by the observations of gut microbiota switch to consuming host-secreted mucus glycoproteins during chronic or intermittent dietary fiber deficiency in mice[54]. The diet-induced microbiota behavior change was, however, unfavorable for the host, leading to CM barrier degradation

and lethal colitis development[54].

The described observations demonstrate that both the loose mucus of the small intestine and the loose outer CM layer serve as both energy sources and habitats for human gut microbiota[50]. In the colon of experimental animals (information regarding human microbiota is scarce) the outer mucus layer harbors a mixed population of commensals with the typical presence of *Akkermansia muciniphila* and bacteria of *Bacteroides* genus (*e.g.*, *Bacteroides thetaiotaomicron*, *Bacteroides fragilis*, *Bacteroides vulgatus*)[48-50]. Outer CM layer also contains *Rumminococcus gnavus*, *Rumminococcus torques*, and *Desulfovibrio desulfuricans*, as well as probiotic *Lactobacillus reuteri*, *Lactobacillus rhamnosus*, *Lactobacillus johnsonii*, *Bifidobacterium breve* and *Bifidobacterium longum*[55]. In addition, bacteria of relatively aerotolerant phyla (Proteobacteria, Actinobacteria) were reported to be occasionally present even closer to the mucosal surface[48,49].

It has been hypothesised that in health CM not only constitutes a physical barrier between bacteria and the epithelium but provides a bioactive environment selectively favorable for beneficial commensals and hostile for intruding pathogens[56]. As mentioned above, mucin glycoproteins provide nutrition for mucus-dwelling bacteria that are able to degrade them, like *Akkermansia muciniphila*, *Bacteroides fragilis* and *Rumminococcus gnavus*[50,53,56]. However, mucin glycans may not be the preferred carbon sources for some host commensals, including *Bacteroides thetaiotaomicron*[57]. Interestingly, this human gut symbiont was recently shown to possess a unique ability to initiate degradation of the complex sulphated O-glycans of the distal colon[58]. The activities of 12 sulfatases produced by this species were collectively sufficient for degrading all known sulphate linkages in mucin O-glycans, but only a single key sulfatase was disproportionally important for the utilization of sulphated O-glycans[58]. This example illustrates the challenging complexity of mucin degradation pathways that may become relevant for the development of future therapeutic applications.

CM is also responsible for the spatial organization of mucus-dwelling bacteria. Mucin-based networks with varying pore size and adhesiveness provide three-dimensional scaffolds for bacterial settlement, thus governing the process of bacterial colonisation[56]. Adhesiveness modulation by the host can also be employed as a mechanism altering microbiota composition[59]. Heterogenous glycan patterns of mucins affect bacterial motility and aggregation and prevent certain pathogens from aggregating and forming biofilms[56]. In addition, CM is believed to control the traffic of small signaling molecules, thereby regulating microbial behavior, and in some circumstances mucin glycans probably exert signaling functions themselves[56].

The diversity of mucin-decorating glycans constitutes a highly variable element of human CM and influences both gut microbiota behavior and host susceptibility to infectious and metabolic diseases[53,60]. Its importance for microbial community composition can be illustrated by the dependence of the latter on the presence of a functional copy of the galactoside 2-alpha-L-fucosyltransferase 2 (*FUT2*) gene encoding FUT2 that facilitates the attachment of the L-fucose monosaccharide to O-glycans, producing α (1,2)-fucosylated glycans[61]. The *FUT2* is one of the genes responsible for the expression of ABO histo-blood group antigen precursors in gut mucus[53,60-62]. Individuals with at least one functional *FUT2* allele are termed "secretors", although the gene does not actually regulate the secretion of proteins bearing α(1,2)-fucosylated glycans[60]. The homozygosity for the loss-of-function *FUT2* mutations (found in about 20% of Caucasians) defines "non-secretors"[53,60,62]. Interestingly, considerable differences in CM bacterial profiles were repeatedly detected between "secretors" and "non-secretors". Rausch *et al*[62] found that in healthy "secretors" the probiotic *Lactobacillus* genus was more prominent, whereas a clear association of the "non-secretor" status with the genus *Prevotella* was observed. Other *FUT2* genotype-associated phylotype changes, including the decrease of *Roseburia* and *Faecalibacterium* in endoscopic lavage samples from "non-secretors" or probiotic *Bifidobacterium* decrease in faeces from "non-secretors" were also reported[63,64]. In contrast, a few relatively large studies failed to detect any associations between *FUT2* genotype and gut microbiome shifts[65-67]. However, an even larger genome-wide association study (GWAS) comprising 8956 German individuals from five independent cohorts confirmed the previously identified associations of ABO histo-blood groups and FUT2 secretor status with *Bacteroides* and *Faecalibacterium* species[68]. These discrepancies are not surprising since GWAS studies assessing gut microbiome changes are usually based upon using homogenised stool samples. The use of this crude approach means that it is impossible to find out which bacteria are where, how their gene expression and functions are related to the local environment and how their spatial organization changes in disease[48]. It can be argued that samples obtained by mucosal biopsy, colonic lavage or CM collection are much more reliable and informative for analysing the microbiota populating CM. However, it is obvious that O-glycans associated with MUC2 strongly influence the composition of the commensal microbial population confined to the outer mucus layer in the colon.

It was already stated before that there are longitudinal differences in both microbiota composition and MUC2 O-glycan pattern distribution in the mammalian gut[17]. The distribution of O-glycosyl-transferases produced by the epithelial cells along the colon correlated well with the pattern of O-glycans[69]. These regional-specific characteristics of the gut glycan pattern are certainly acquired after birth, as neither sialic acid nor fucose gradients exist along the foetal intestine[70]. The differences developing in the postnatal life are thought to be related to the establishment of luminal microbiota acting as a potent environmental factor that provokes dramatic gene expression shifts in the host epithelium[70]. This view is supported by mouse experiments demonstrating that commensal

colonisation promotes structural and physiological adaptations of mucus barrier properties, thus contributing to intestinal homeostasis[71,72]. The complex interplay between gut microbiota and colonic mucosa continues into the maturity of the host and becomes even more important during ageing. In mice ageing causes a progressive decrease of CM thickness that is accompanied by considerable changes in faecal microbiota composition and more frequent contacts of luminal bacteria with the epithelium [73]. A similar reduction of CM layer thickness, primarily attributed to the reduced number of GCs, was observed in ageing rats[74]. Interestingly, a recent report shows that indoles produced by commensal bacteria can act *via* the aryl hydrocarbon receptor and interleukin 10 to restore the depleted population of colonic GCs in aged animals, hence supporting homeostasis[75]. Although age-related changes in the human CM system are poorly studied, it is notable that the intestinal microbiota composition in elderly subjects substantially differed from that in young adults, with a greater proportion of *Bacteroides* species and distinct abundance of *Clostridium* groups in the elderly[76].

To conclude this section of the review it is important to clarify that the gut mucus barrier, albeit essential, is just an element of the complex mechanism responsible for protecting the host's organism from unwanted risks. The immune system is the key driving force of this mechanism playing a central role in shaping the composition of the microbiota and defining its spatial distribution in close proximity to host tissues. Nevertheless, resident microorganisms interact with the immune system and influence the development of immune responses. Disruption of this complex and dynamic cross-talk can have deleterious consequences for host health contributing to the pathogenesis of many diseases including IBD and cancer[77].

CONSEQUENCES OF GUT MUCUS DETERIORATION EXPOSING COLONIC EPITHELIUM

CM and underlying epithelium: Host cells are released into mucus in the normal physiological conditions

It is well established that the intestinal epithelium is renewed every 4-5 d[78], and, before the discovery of CM structure and recognition of its importance[6], it was presumed that terminally differentiated enterocytes or colonocytes undergo spontaneous apoptosis and are finally "shed into the gut lumen" [78]. This simplistic notion needed to be revised, given the complexity of the two-layered CM structure and high density of the inner mucus layer[6,10,11]. Our group previously demonstrated that in healthy individuals exfoliated colonocytes are rarely found in CM samples collected either from the surface of the rectal mucosa or non-invasively[79,80]. Similarly, only small numbers of normal exfoliated colonocytes in mucus-containing surface washes of stool samples obtained from healthy volunteers were observed in earlier studies[81-83]. In view of the proven existence of the two-layered CM structure (Figure 1), an immediate question emerges: How exfoliated colonocytes and occasional neutrophils released from the epithelial surface manage to penetrate the dense inner mucus layer impenetrable for much smaller bacteria? No satisfactory answer has hitherto been found, but it was previously assumed that shed cells could be "trapped in the mucus" and degraded there[7].

Remarkably, well-preserved colonocytes were identified in all quoted studies that analysed CM[47, 79-83]. One could argue that intrarectal mucus collection might mechanically detach epithelial cells from the mucosa[79], however this explanation is not valid when CM is obtained non-invasively or from the surface of freshly excreted stool[80-83]. Although it is possible to hypothesise that the transport of the released cells might be assisted by the rapid CM layer renewal[22], or that focal partial cleavage of MUC2 may occur at sites of colonocyte exfoliation or neutrophil migration[16], mechanisms of this phenomenon remain obscure. In contrast, abundant presence of both exfoliated colonocytes and migrating inflammatory cells in CM samples obtained from patients with IBD and CRC is easy to explain by the structural damage of the CM barrier observed during these conditions and considered below. Despite the existing uncertainties on the mechanisms involved in cell accumulation in the mucus, it is indisputable that this easily accessible substance presents a highly informative material for multiple diagnostic applications.

CM barrier damage and its consequences in gut inflammation predisposing to CRC

CM presents the first defensive barrier against the luminal microbiota, its dense inner layer making bacterial contact with the colonic epithelium hardly possible in the healthy gut[7]. Although loose mucus of the small intestine contains commensal bacteria, it is rich in antimicrobial substances, and its permanent production by GCs in the normal conditions creates a continuous mucus flow preventing bacteria from reaching the epithelium[11,84]. Therefore, only severe CM impairment can lead to exposing the epithelial surface to direct contacts with the microbiota. The unique importance of MUC2-rich mucus for colonic epithelium protection was graphically demonstrated by the development of spontaneous colitis in *MUC2*-knockout mice unable to produce MUC2[85]. Likewise, microbiota-induced mucus layer defects were observed in genetically obese mice[86]. Experimentally modelled dietary fiber deficiency also led to CM barrier degradation, bacterial invasion of the mucosa and lethal colitis development[54]. The composition of intestinal microbiota is now recognised as a key factor for defining properties of the inner mucus layer[71,72], and it was clearly demonstrated that dysbiosis in

the mucus preceded experimental colitis development[87]. Results of all these experimental studies clearly demonstrate that the loss of CM barrier integrity combined with dysbiosis usually results in opportunistic invasion of the colonic mucosa by resident bacteria, inevitably leading to inflammation [77].

In patients with IBD, comprising ulcerative colitis (UC) and Crohn's disease (CD), CM deterioration and the abundance of mucolytic bacteria were observed[88,89]. Aforementioned mucus microbiota shifts related to *FUT2* "non-secretor" genotype entailed an increased risk of developing CD[62]. The gut bacteria in IBD patients are often confined to mucosa-adhering biofilms that can be defined as matrix-enclosed multispecies bacterial communities forming higher-order structures[90,91]. Mucosal biofilms were frequently found in IBD patients and patients with irritable bowel syndrome (IBS), and, sometimes, in clinically healthy individuals[88,91,92]. These findings indicate that bacterial biofilm formation does not immediately lead to inflammation development, being, at least to some extent, compatible with the preservation of homeostasis control by the immune system. Probable involvement of biofilms in IBS pathogenesis may open new ways for devising diagnostic approaches and therapeutic strategies addressing this highly prevalent condition[92].

Patterns of alterations in the colonic mucosa, its mucus layers and gut microbiota composition tend to differ between CD and UC[84]. For example, it was shown that a global expression of mucin genes was reduced in CD patients[93], whereas it was elevated in patients with UC[94]. Conversely, UC was also found to be associated with decreased numbers of mucosal GCs[95,96], as well as signs of CM layer reduced thickness and disruption[95,97,98]. In addition, the secretory response of colonic GCs to microbial challenge in active UC seems to be impaired, with the number of sentinel GCs significantly reduced and protective mucin sulphation decreased[99,100]. Intestinal mucosa dysfunction in IBD was further confirmed by signs of transcriptomic dysregulation of some key genes involved in colonic barrier maintenance, especially those encoding transmembrane mucins MUC1, MUC4 and MUC22 [101]. Consequently, the inner mucus layer of UC patients could be easily penetrated by luminal bacteria[98]. The observed dysregulation of transmembrane mucin synthesis might also indicate possible alterations of colonocyte glycocalyx[101].

The extreme complexity of IBD pathogenesis is generally admitted[102], and this fascinating subject is beyond the scope of this review. Nevertheless, a few more points related to IBD need to be addressed here, especially given the clearly elevated probability of CRC development in IBD patients[103]. In particular, modern Western diet characterized by limited dietary fiber intake is now regarded as a major risk factor for both IBD and CRC[104-106]. Consequently, diet correction may constitute an effective approach to disease prevention. Experimental studies demonstrate that fiber addition to the diet and administration of probiotic microbiota, especially *Bifidobacterium* species, can restore CM layer functionality and provide anti-inflammatory effects[107,108]. Likewise, tea polyphenols and citrus flavonoids were shown to protect CM integrity[109,110]. These findings look promising, however further research is required for designing dietary interventions targeting CM and suitable for treating IBD patients and preventing CRC development in this risk group.

Another consequence of CM barrier deterioration in IBD patients is related to the phenomenon of massive inflammatory cell migration from the *Lamina propria* of colonic mucosa to the impaired CM layer. Neutrophil and eosinophil biomarkers are abundantly present in stool samples from IBD patients, and stool calprotectin quantification is widely used for diagnosing UC and CD[111,112]. However, the scale of inflammatory cell migration towards the gut lumen became evident only recently. We were able to demonstrate that numerous immune cells can be found in CM samples obtained from IBD patients either intrarectally[79,113], or using non-invasive collection from the anal area following defaecation[80, 114,115]. Cytological analysis of the collected CM revealed that neutrophils were the most abundant cell type, but macrophages, eosinophils (especially in UC patients), plasma cells and lymphocytes were frequently detected as well[114]. The collected cells were very well preserved and looked viable, as phagocytosis and erythrophagocytosis by neutrophils and macrophages could be seen[114]. It was also hypothesised that neutrophils and eosinophils migrating to the loosened CM of IBD patients can easily undergo extracellular DNA trap formation (ET-osis), cell death producing the formation of antibacterial "extracellular traps" composed of released DNA and globular proteins [also called ET-osis exerted by neutrophils (NET-osis)][116]. This hypothesis, also assuming that CM in IBD serves as a supporting milieu for immune responses expanding from the mucosa, is discussed in detail elsewhere[116]. Taken together, recent advances in CM research suggest that even partial loss of this protective barrier compromises its function at different levels, including impaired control of the relationship between gut microbiota and mucus, dysregulation of CM layer maintenance by the epithelium and immune cells of the *Lamina propria*, insufficient production of AMPs and defects in the process of autophagy[117,118]. Initial signs of intestinal barrier impairment may precede the onset of clinical IBD manifestations by years[119], this interval probably constituting a good window of opportunity for applying preventive interventions and early therapeutic measures.

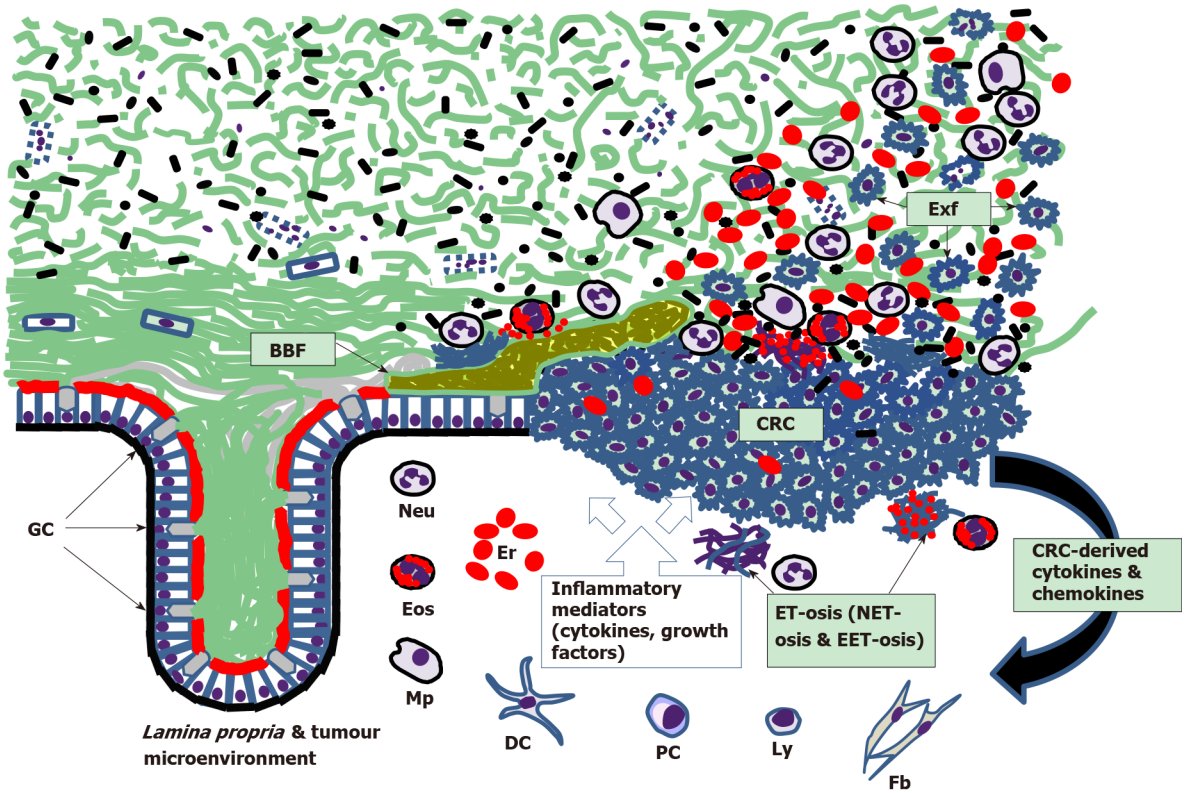
CM CHANGES ASSOCIATED WITH COLORECTAL NEOPLASIA

Although inflammation-related changes involving CM can contribute to colorectal tumor development [120], sporadic CRC grows slowly, early stages of this neoplasia being confined exclusively to colorectal mucosa[3]. However, it is evident that, like in active IBD, CM from CRC patients is very rich in cells shed from tumor surface (Figure 2). It is well established that numerous CRC markers can be detected in stool samples obtained from CRC patients[121,122], and the presence of cancer cells on the stool surface is well documented[79-81,123-125]. CM overlaying tumor surface, which was initially defined as "mucocellular layer"[126], serves as a medium accepting and preserving all cells and biomolecules released by the neoplastic tissue. This diagnostically informative material could be obtained from CRC patients by intrarectal collection with an inflatable device designed for this purpose[79]. Human DNA measurements in the mucus collected from tumor surface and at equal distances proximally and distally from tumor margins (resected colon segments were examined) revealed significantly higher DNA levels in the samples collected distally, hence confirming distal movement of the CM[79]. The latter finding of our group resulted in devising a completely non-invasive technique for CM sampling by swabbing the anal area immediately following defaecation[80]. The new method has recently been successfully applied for non-invasive CRC detection[127,128]. These findings confirm that CM constitutes a uniquely informative biological material possessing an enormous diagnostic potential owing to abundant presence of various biomarkers, comprising a wide range of proteins and nucleic acids[116,127,128]. While the described diagnostic importance of CM for CRC detection becomes obvious, this biological substance also emerges among major pathogenetic factors contributing to colorectal carcinogenesis. The key mechanisms of CM involvement in this process are probably related to the loss of homeostatic balance between CM layers and gut microbiota, which exposes the mucosa to both commensal and pathogenic bacteria and triggers cascades of unfavorable host responses that may eventually lead to neoplastic growth[120,129-131]. CM depletion effect was graphically demonstrated experimentally, when mice genetically deficient in the MUC2 were shown to develop colorectal tumors[132,133]. Furthermore, colon tumor development was observed in mice with colon-specific loss of *Atonal homolog 1* gene, which determines normal differentiation of secretory cells, comprising GCs[134]. GC depletion during 1,2-dimethylhydrazine-induced colon carcinogenesis in rats was reported as well[135]. In human colorectal tumors, MUC2 expression was decreased, and the degree of expression inhibition correlated with the progression from adenomas to advanced carcinomas[136]. In terms of prognostic significance, reduced MUC2 expression in CRC patients corresponded to poorer prognosis[137,138]. However, different types of CRC display different mucin expression patterns, as several mucin-encoding genes are overexpressed in mucinous carcinomas[139-141]. Mucus synthesis in the colonic GCs involves MUC2 O-glycosylation, and this process was found to be impaired in genetically modified mice predisposed to colitis-associated carcinogenesis[142,143]. Likewise, aberrant O-glycosylation was observed in malignant tumors removed from CRC patients[144]. All these findings indicate that CRC-associated changes in colon mucin gene expression and protein synthesis may occur either because of intrinsic genetic and immune disturbances or due to interactions of the preneoplastic or neoplastic epithelium with the microbial populations of the gut, impact of which needs to be considered as well.

It is now recognized that colorectal tumor development strongly depends on compositional and ecological changes of the microbiota[145]. Recent metagenomic studies revealed differences between gut bacterial communities in CRC patients and healthy individuals, the latter category being characterized by a lower abundance of potentially protective taxa (*e.g.*, *Roseburia*) combined with an increased presence of pro-carcinogenic taxa, such as *Bacteroides*, *Escherichia*, *Fusobacterium*, and *Porphyromonas*[145-147]. However, the existing body of evidence on CRC-related gut microbiome alterations was generated mostly by molecular analyses of faecal material that may not reliably reflect changes in CM-dwelling bacteria. For this reason, this theme will not be further discussed here, and a comprehensive review by Wong and Yu[145] can be recommended to interested readers.

In contrast, recent reports suggesting that bacterial biofilms formed on the surface of the colonic epithelium may be implicated in carcinogenesis deserve close attention[90,148]. This association is especially intriguing since bacterial biofilms can be easily identified endoscopically[92], thus potentially presenting a very good early indicator of neoplastic transformation risk. Biofilms in the colon of CRC patients are typically confined to the CM overlaying tumor surface or margins and seem to replace the inner mucus layer[148-150], which is apparently damaged during tumor growth. There is no clarity regarding mechanisms of biofilm carcinogenicity, but it was suggested that certain individuals are predisposed to form these bacterial structures, which may be capable of driving neoplastic transformation[149,151]. Proximal CRC and, especially, mucinous carcinomas were strongly associated with the presence of bacterial biofilms, whereas they were observed relatively rarely in distal CRC cases [149,150,152]. This pattern suggests that biofilms tend to specifically contribute to the serrated pathway of colorectal carcinogenesis[153].

The analysis of biofilm bacterial composition in CRC patients has revealed that human gut commensal *Bacteroides fragilis* capable of generating enterotoxigenic strains[154], as well as oral pathogens *Fusobacterium nucleatum*, *Parvimonas micra* and *Peptostreptococcus stomatis* were the main species detected in these biofilms[150]. Further work of the same group demonstrated the presence of patchy bacterial biofilms dominated by enterotoxigenic *Bacteroides fragilis* and colibactin-expressing



DOI: 10.3748/wjg.v28.i32.4475 Copyright ©The Author(s) 2022.

Figure 2 Scheme of colorectal mucus-associated events involved in colorectal cancer development. BBF: Bacterial biofilm; Exf: Exfoliated malignant cells of colorectal cancer; GC: Goblet cells; Neu: Neutrophils; Eos: Eosinophils; Mp: Macrophages; Er: Erythrocytes; DC: Dendritic cells; PC: Plasma cells; Ly: Lymphocytes; Fb: Fibroblasts; ET-osis: Extracellular DNA trap formation; NET-osis: ET-osis exerted by neutrophils; EET-osis: ET-osis exerted by eosinophils. Small black shapes show bacteria; CRC: Colorectal cancer.

Escherichia coli on the surface of the colonic mucosa of patients with familial adenomatous polyposis [155]. In these patients the biofilms were not confined to polyp surface, and no association with proximal tumor location could be observed[155]. Interestingly, co-colonisation of tumor-prone mice with the bacterial strains of these biofilms caused DNA damage in the colonic epithelium of the animals and accelerated carcinogenesis[155]. These findings were later confirmed in three murine models, where bacterial biofilm homogenates obtained from either CRC patients or healthy individuals manifestly promoted colon carcinogenesis[156]. Notably, *Fusobacterium nucleatum* did not seem to be required for carcinogenesis in these experiments, which might indicate that it is possibly involved at later stages of CRC development[156]. Overall, these results strongly suggest that polymicrobial biofilms may now be regarded as a colon carcinogen.

The reviewed advances in defining CM role in CRC development highlight a previously obscure area of pathogenetically important interplay between multiple elements. These elements include CM, gut microbiota (both mucus-dwelling and luminal), colonic epithelial cells (normal, malignant and especially mucus-producing GCs) and immune cells (both belonging to the tumor microenvironment or adjacent *Lamina propria* and actively migrating to CM through the epithelium). Figure 2 schematically depicts some of these interactions. Progressive CM deterioration results in its loosening that initially exposes colonic epithelium to occasional contacts with gut commensals and can later lead to possible pathogen invasion to the mucosa. CM deficiency probably triggers: (1) Epithelial homeostasis dysregulation accompanied by the loss of control over cell renewal process; and (2) Cascades of inflammatory responses exerted by both immune cells of the tumor microenvironment and adjacent *Lamina propria* and free immune cells migrating through colonic epithelium to the loosened CM. Although these events may potentially be reversible, one needs to be aware of less favorable scenarios, such as the development of IBS, IBD and colorectal tumors. The reported formation of bacterial biofilms in healthy individuals and patients with IBD, polyps and CRC illustrates this range of scenarios[92,149,155]. However, biofilm formation may depend on the genetic background of the host[153], and appears to be just one of at least a few possible pathways eventually leading to CRC.

Of course, there is no chance to properly discuss here multiple molecular pathways of CRC development[120], or complex impacts of immune responses affecting this process[157]. Nevertheless, a few more points directly related to the CM deserve to be addressed at the end. One of them concerns the process of antibacterial extracellular DNA trap formation or ET-osis by effector immune cells (termed NET-osis when exerted by neutrophils) that massively migrate to the loosened CM in both IBD and

CRC[116]. It is apparent that this process basically constitutes an element of a protective inflammatory response aiming to eliminate bacteria contacting colonic epithelium, but arriving neutrophils and eosinophils inevitably undergo degranulation and ET-osis, thus releasing cytotoxic factors (Figure 2) that damage host cells and probably induce poorly regulated compensatory proliferation of normal or malignant epithelial cells, which can stimulate neoplastic growth. The role of the ET-osis in CRC is being discussed but remains largely obscure and needs further exploration[116,158]. The other important point is related to possible ways of preserving CM integrity and avoiding its deterioration in view of CRC prevention. This goal can be achieved by establishing proper communication between the host and gut microbiota *via* balanced dietary patterns preventing dysbiosis development[131]. Indeed, diet is a major determinant of CRC risk, with red meat consumption increasing the risk and fiber uptake being protective[159]. Interestingly, both effects can be mediated by the CM. SCFAs (especially butyrate) produced by luminal microbiota during dietary fiber fermentation stimulates MUC2 expression in the colon and promotes proliferation of normal colonocytes[160], whereas cancer cell proliferation tends to be inhibited by butyrate because of the low differentiation of these cells[161]. There is no doubt that fiber-rich diets and SCFAs are beneficial for CM preservation and CRC prevention, but additional investigations are indispensable for designing effective dietary intervention schemes. On the other hand, it was shown that CM damage inflicted by sulphide-producing and mucin-degrading bacteria can faciliate epithelial hyperproliferation in the colon induced by heme-rich diet modelling high red meat consumption[162]. In that experimental model antibiotic treatment allowed normalizing gut microbiota composition, reinforcing the mucus barrier and eliminating the abnormal proliferation[162]. These examples demonstrate that both dietary corrections and drug therapy can be considered for CM protection and restoration with the purpose of preventing CRC.

The on-going progress in exploring the role of the CM in the pathogenesis of major colorectal diseases, especially CRC, is impressive, however many important points remain obscure. Therefore, thoroughly designed further studies are needed for elucidating fine mechanisms governing structural and functional CM changes in disease. It can be expected that numerous innovative practical applications addressing colorectal disease diagnosis, prevention and treatment will be developed once this challenging goal is achieved.

CONCLUSION

The presented analysis of the existing information regarding mammalian and human CM shows that this area was actively explored only since the beginning of the 21st century. Considerable progress has been made in basic research of CM structure and function, especially in experimental models. It is now evident that in the normal mammalian colon the CM is formed by two distinct layers composed of gel-forming glycosylated mucins that are permanently secreted by goblet cells of the colonic epithelium. The inner layer is dense and impenetrable for bacteria, whereas the loose outer layer provides a habitat for abundant commensal microbiota. Mucus barrier integrity is essential for preventing bacterial contact with the mucosal epithelium and maintaining homeostasis within the GI tract, but it can be impaired by a variety of factors, including CM-damaging switch of commensal bacteria to mucin glycan consumption due to dietary fiber deficiency. It is already proven that impairments in CM structure and function can lead to colonic barrier deterioration that opens direct bacterial access to the epithelium. Bacteria-induced damage dysregulates epithelial proliferation and causes inflammatory responses that may expand to the loosened CM and eventually result in severe disorders, including colitis and colorectal neoplasia. Recently described formation of bacterial biofilms within the inner CM layer was shown to be associated with both inflammation and cancer. Although obvious gaps in our knowledge of human CM remain, its importance for the pathogenesis of major colorectal diseases, comprising IBD and CRC, is generally recognized. Continuing progress in the field of CM exploration promises considerable future achievements and is likely to result in the development of a range of new useful clinical applications addressing colorectal disease diagnosis, prevention and therapy.

FOOTNOTES

Author contributions: Loktionov A is responsible for all work related to the preparation of this review paper; Loktionov A has designed paper structure, performed literature search, contributed figures, analysed literature data and wrote the paper.

Conflict-of-interest statement: The author reports no relevant conflicts of interest for this article.

Open-Access: This article is an open-access article that was selected by an in-house editor and fully peer-reviewed by external reviewers. It is distributed in accordance with the Creative Commons Attribution NonCommercial (CC BY-NC 4.0) license, which permits others to distribute, remix, adapt, build upon this work non-commercially, and license their derivative works on different terms, provided the original work is properly cited and the use is non-

commercial. See: https://creativecommons.org/Licenses/by-nc/4.0/

Country/Territory of origin: United Kingdom

ORCID number: Alexandre Loktionov 0000-0001-7836-3838.

S-Editor: Wang JJ
L-Editor: A
P-Editor: Wang JJ

REFERENCES

1 **Sung H**, Ferlay J, Siegel RL, Laversanne M, Soerjomataram I, Jemal A, Bray F. Global Cancer Statistics 2020: GLOBOCAN Estimates of Incidence and Mortality Worldwide for 36 Cancers in 185 Countries. *CA Cancer J Clin* 2021; **71**: 209-249 [PMID: 33538338 DOI: 10.3322/caac.21660]
2 **Brenner H**, Chen C. The colorectal cancer epidemic: challenges and opportunities for primary, secondary and tertiary prevention. *Br J Cancer* 2018; **119**: 785-792 [PMID: 30287914 DOI: 10.1038/s41416-018-0264-x]
3 **Grady WM**, Markowitz SD. The molecular pathogenesis of colorectal cancer and its potential application to colorectal cancer screening. *Dig Dis Sci* 2015; **60**: 762-772 [PMID: 25492499 DOI: 10.1007/s10620-014-3444-4]
4 **Relman DA**. The human microbiome: ecosystem resilience and health. *Nutr Rev* 2012; **70** Suppl 1: S2-S9 [PMID: 22861804 DOI: 10.1111/j.1753-4887.2012.00489.x]
5 **Sommer F**, Bäckhed F. The gut microbiota--masters of host development and physiology. *Nat Rev Microbiol* 2013; **11**: 227-238 [PMID: 23435359 DOI: 10.1038/nrmicro2974]
6 **Hansson GC**. Mucus and mucins in diseases of the intestinal and respiratory tracts. *J Intern Med* 2019; **285**: 479-490 [PMID: 30963635 DOI: 10.1111/joim.12910]
7 **Johansson ME**, Phillipson M, Petersson J, Velcich A, Holm L, Hansson GC. The inner of the two Muc2 mucin-dependent mucus layers in colon is devoid of bacteria. *Proc Natl Acad Sci U S A* 2008; **105**: 15064-15069 [PMID: 18806221 DOI: 10.1073/pnas.0803124105]
8 **Bansil R**, Turner BS. The biology of mucus: Composition, synthesis and organization. *Adv Drug Deliv Rev* 2018; **124**: 3-15 [PMID: 28970050 DOI: 10.1016/j.addr.2017.09.023]
9 **Taherali F**, Varum F, Basit AW. A slippery slope: On the origin, role and physiology of mucus. *Adv Drug Deliv Rev* 2018; **124**: 16-33 [PMID: 29108861 DOI: 10.1016/j.addr.2017.10.014]
10 **Paone P**, Cani PD. Mucus barrier, mucins and gut microbiota: the expected slimy partners? *Gut* 2020; **69**: 2232-2243 [PMID: 32917747 DOI: 10.1136/gutjnl-2020-322260]
11 **Pelaseyed T**, Bergström JH, Gustafsson JK, Ermund A, Birchenough GM, Schütte A, van der Post S, Svensson F, Rodríguez-Piñeiro AM, Nyström EE, Wising C, Johansson ME, Hansson GC. The mucus and mucins of the goblet cells and enterocytes provide the first defense line of the gastrointestinal tract and interact with the immune system. *Immunol Rev* 2014; **260**: 8-20 [PMID: 24942678 DOI: 10.1111/imr.12182]
12 **Birchenough GM**, Johansson ME, Gustafsson JK, Bergström JH, Hansson GC. New developments in goblet cell mucus secretion and function. *Mucosal Immunol* 2015; **8**: 712-719 [PMID: 25872481 DOI: 10.1038/mi.2015.32]
13 **Johansson ME**, Sjövall H, Hansson GC. The gastrointestinal mucus system in health and disease. *Nat Rev Gastroenterol Hepatol* 2013; **10**: 352-361 [PMID: 23478383 DOI: 10.1038/nrgastro.2013.35]
14 **Johansson ME**, Hansson GC. Immunological aspects of intestinal mucus and mucins. *Nat Rev Immunol* 2016; **16**: 639-649 [PMID: 27498766 DOI: 10.1038/nri.2016.88]
15 **Pelaseyed T**, Hansson GC. Membrane mucins of the intestine at a glance. *J Cell Sci* 2020; **133** [PMID: 32169835 DOI: 10.1242/jcs.240929]
16 **Johansson ME**, Larsson JM, Hansson GC. The two mucus layers of colon are organized by the MUC2 mucin, whereas the outer layer is a legislator of host-microbial interactions. *Proc Natl Acad Sci U S A* 2011; **108** Suppl 1: 4659-4665 [PMID: 20615996 DOI: 10.1073/pnas.1006451107]
17 **Holmén Larsson JM**, Thomsson KA, Rodríguez-Piñeiro AM, Karlsson H, Hansson GC. Studies of mucus in mouse stomach, small intestine, and colon. III. Gastrointestinal Muc5ac and Muc2 mucin O-glycan patterns reveal a regiospecific distribution. *Am J Physiol Gastrointest Liver Physiol* 2013; **305**: G357-G363 [PMID: 23832516 DOI: 10.1152/ajpgi.00048.2013]
18 **Ambort D**, Johansson ME, Gustafsson JK, Nilsson HE, Ermund A, Johansson BR, Koeck PJ, Hebert H, Hansson GC. Calcium and pH-dependent packing and release of the gel-forming MUC2 mucin. *Proc Natl Acad Sci U S A* 2012; **109**: 5645-5650 [PMID: 22451922 DOI: 10.1073/pnas.1120269109]
19 **Johansson ME**, Ambort D, Pelaseyed T, Schütte A, Gustafsson JK, Ermund A, Subramani DB, Holmén-Larsson JM, Thomsson KA, Bergström JH, van der Post S, Rodriguez-Piñeiro AM, Sjövall H, Bäckström M, Hansson GC. Composition and functional role of the mucus layers in the intestine. *Cell Mol Life Sci* 2011; **68**: 3635-3641 [PMID: 21947475 DOI: 10.1007/s00018-011-0822-3]
20 **Round AN**, Rigby NM, Garcia de la Torre A, Macierzanka A, Mills EN, Mackie AR. Lamellar structures of MUC2-rich mucin: a potential role in governing the barrier and lubricating functions of intestinal mucus. *Biomacromolecules* 2012; **13**: 3253-3261 [PMID: 22978827 DOI: 10.1021/bm301024x]
21 **Sharpen JDA**, Dolan B, Nyström EEL, Birchenough GMH, Arike L, Martinez-Abad B, Johansson MEV, Hansson GC, Recktenwald CV. Transglutaminase 3 crosslinks the secreted gel-forming mucus component Mucin-2 and stabilizes the colonic mucus layer. *Nat Commun* 2022; **13**: 45 [PMID: 35017479 DOI: 10.1038/s41467-021-27743-1]

22 **Johansson ME**. Fast renewal of the distal colonic mucus layers by the surface goblet cells as measured by *in vivo* labeling of mucin glycoproteins. *PLoS One* 2012; **7**: e41009 [PMID: 22815896 DOI: 10.1371/journal.pone.0041009]

23 **Nyström EEL**, Martinez-Abad B, Arike L, Birchenough GMH, Nonnecke EB, Castillo PA, Svensson F, Bevins CL, Hansson GC, Johansson MEV. An intercrypt subpopulation of goblet cells is essential for colonic mucus barrier function. *Science* 2021; **372** [PMID: 33859001 DOI: 10.1126/science.abb1590]

24 **Parikh K**, Antanaviciute A, Fawkner-Corbett D, Jagielowicz M, Aulicino A, Lagerholm C, Davis S, Kinchen J, Chen HH, Alham NK, Ashley N, Johnson E, Hublitz P, Bao L, Lukomska J, Andev RS, Björklund E, Kessler BM, Fischer R, Goldin R, Koohy H, Simmons A. Colonic epithelial cell diversity in health and inflammatory bowel disease. *Nature* 2019; **567**: 49-55 [PMID: 30814735 DOI: 10.1038/s41586-019-0992-y]

25 **Johansson ME**, Hansson GC. Is the intestinal goblet cell a major immune cell? *Cell Host Microbe* 2014; **15**: 251-252 [PMID: 24629330 DOI: 10.1016/j.chom.2014.02.014]

26 **McDole JR**, Wheeler LW, McDonald KG, Wang B, Konjufca V, Knoop KA, Newberry RD, Miller MJ. Goblet cells deliver luminal antigen to CD103+ dendritic cells in the small intestine. *Nature* 2012; **483**: 345-349 [PMID: 22422267 DOI: 10.1038/nature10863]

27 **Knoop KA**, McDonald KG, McCrate S, McDole JR, Newberry RD. Microbial sensing by goblet cells controls immune surveillance of luminal antigens in the colon. *Mucosal Immunol* 2015; **8**: 198-210 [PMID: 25005358 DOI: 10.1038/mi.2014.58]

28 **Knoop KA**, Gustafsson JK, McDonald KG, Kulkarni DH, Kassel R, Newberry RD. Antibiotics promote the sampling of luminal antigens and bacteria *via* colonic goblet cell associated antigen passages. *Gut Microbes* 2017; **8**: 400-411 [PMID: 28267403 DOI: 10.1080/19490976.2017.1299846]

29 **Knoop KA**, Newberry RD. Goblet cells: multifaceted players in immunity at mucosal surfaces. *Mucosal Immunol* 2018; **11**: 1551-1557 [PMID: 29867079 DOI: 10.1038/s41385-018-0039-y]

30 **Papandreou ME**, Tavernarakis N. Autophagy and the endo/exosomal pathways in health and disease. *Biotechnol J* 2017; **12** [PMID: 27976834 DOI: 10.1002/biot.201600175]

31 **Patel KK**, Miyoshi H, Beatty WL, Head RD, Malvin NP, Cadwell K, Guan JL, Saitoh T, Akira S, Seglen PO, Dinauer MC, Virgin HW, Stappenbeck TS. Autophagy proteins control goblet cell function by potentiating reactive oxygen species production. *EMBO J* 2013; **32**: 3130-3144 [PMID: 24185898 DOI: 10.1038/emboj.2013.233]

32 **Ghimire L**, Paudel S, Jin L, Jeyaseelan S. The NLRP6 inflammasome in health and disease. *Mucosal Immunol* 2020; **13**: 388-398 [PMID: 31988468 DOI: 10.1038/s41385-020-0256-z]

33 **Wlodarska M**, Thaiss CA, Nowarski R, Henao-Mejia J, Zhang JP, Brown EM, Frankel G, Levy M, Katz MN, Philbrick WM, Elinav E, Finlay BB, Flavell RA. NLRP6 inflammasome orchestrates the colonic host-microbial interface by regulating goblet cell mucus secretion. *Cell* 2014; **156**: 1045-1059 [PMID: 24581500 DOI: 10.1016/j.cell.2014.01.026]

34 **Birchenough GM**, Nyström EE, Johansson ME, Hansson GC. A sentinel goblet cell guards the colonic crypt by triggering Nlrp6-dependent Muc2 secretion. *Science* 2016; **352**: 1535-1542 [PMID: 27339979 DOI: 10.1126/science.aaf7419]

35 **Volk JK**, Nyström EEL, van der Post S, Abad BM, Schroeder BO, Johansson Å, Svensson F, Jäverfelt S, Johansson MEV, Hansson GC, Birchenough GMH. The Nlrp6 inflammasome is not required for baseline colonic inner mucus layer formation or function. *J Exp Med* 2019; **216**: 2602-2618 [PMID: 31420376 DOI: 10.1084/jem.20190679]

36 **McGuckin MA**, Hasnain SZ. Goblet cells as mucosal sentinels for immunity. *Mucosal Immunol* 2017; **10**: 1118-1121 [PMID: 28120847 DOI: 10.1038/mi.2016.132]

37 **Bergström JH**, Birchenough GM, Katona G, Schroeder BO, Schütte A, Ermund A, Johansson ME, Hansson GC. Gram-positive bacteria are held at a distance in the colon mucus by the lectin-like protein ZG16. *Proc Natl Acad Sci U S A* 2016; **113**: 13833-13838 [PMID: 27849619 DOI: 10.1073/pnas.1611400113]

38 **Propheter DC**, Chara AL, Harris TA, Ruhn KA, Hooper LV. Resistin-like molecule β is a bactericidal protein that promotes spatial segregation of the microbiota and the colonic epithelium. *Proc Natl Acad Sci U S A* 2017; **114**: 11027-11033 [PMID: 28973871 DOI: 10.1073/pnas.1711395114]

39 **Chen K**, Yoshimura T, Yao X, Gong W, Huang J, Dzutsev AK, McCulloch J, O'hUigin C, Bian XW, Trinchieri G, Wang JM. Distinct contributions of cathelin-related antimicrobial peptide (CRAMP) derived from epithelial cells and macrophages to colon mucosal homeostasis. *J Pathol* 2021; **253**: 339-350 [PMID: 33104252 DOI: 10.1002/path.5572]

40 **Gassler N**. Paneth cells in intestinal physiology and pathophysiology. *World J Gastrointest Pathophysiol* 2017; **8**: 150-160 [PMID: 29184701 DOI: 10.4291/wjgp.v8.i4.150]

41 **Bergstrom K**, Shan X, Casero D, Batushansky A, Lagishetty V, Jacobs JP, Hoover C, Kondo Y, Shao B, Gao L, Zandberg W, Noyovitz B, McDaniel JM, Gibson DL, Pakpour S, Kazemian N, McGee S, Houchen CW, Rao CV, Griffin TM, Sonnenburg JL, McEver RP, Braun J, Xia L. Proximal colon-derived O-glycosylated mucus encapsulates and modulates the microbiota. *Science* 2020; **370**: 467-472 [PMID: 33093110 DOI: 10.1126/science.aay7367]

42 **Birchenough GMH**, Johansson MEV. Forming a mucus barrier along the colon. *Science* 2020; **370**: 402-403 [PMID: 33093095 DOI: 10.1126/science.abe7194]

43 **Antoni L**, Nuding S, Weller D, Gersemann M, Ott G, Wehkamp J, Stange EF. Human colonic mucus is a reservoir for antimicrobial peptides. *J Crohns Colitis* 2013; **7**: e652-e664 [PMID: 23787054 DOI: 10.1016/j.crohns.2013.05.006]

44 **Johansen FE**, Kaetzel CS. Regulation of the polymeric immunoglobulin receptor and IgA transport: new advances in environmental factors that stimulate pIgR expression and its role in mucosal immunity. *Mucosal Immunol* 2011; **4**: 598-602 [PMID: 21956244 DOI: 10.1038/mi.2011.37]

45 **Rogier EW**, Frantz AL, Bruno ME, Kaetzel CS. Secretory IgA is Concentrated in the Outer Layer of Colonic Mucus along with Gut Bacteria. *Pathogens* 2014; **3**: 390-403 [PMID: 25437806 DOI: 10.3390/pathogens3020390]

46 **Espey MG**. Role of oxygen gradients in shaping redox relationships between the human intestine and its microbiota. *Free Radic Biol Med* 2013; **55**: 130-140 [PMID: 23127782 DOI: 10.1016/j.freeradbiomed.2012.10.554]

47 **Loktionov A**. Cell exfoliation in the human colon: myth, reality and implications for colorectal cancer screening. *Int J Cancer* 2007; **120**: 2281-2289 [PMID: 17351899 DOI: 10.1002/ijc.22647]

48 **Tropini C**, Earle KA, Huang KC, Sonnenburg JL. The Gut Microbiome: Connecting Spatial Organization to Function. *Cell Host Microbe* 2017; **21**: 433-442 [PMID: 28407481 DOI: 10.1016/j.chom.2017.03.010]

49 **Miller BM**, Liou MJ, Lee JY, Bäumler AJ. The longitudinal and cross-sectional heterogeneity of the intestinal microbiota. *Curr Opin Microbiol* 2021; **63**: 221-230 [PMID: 34428628 DOI: 10.1016/j.mib.2021.08.004]

50 **Martens EC**, Neumann M, Desai MS. Interactions of commensal and pathogenic microorganisms with the intestinal mucosal barrier. *Nat Rev Microbiol* 2018; **16**: 457-470 [PMID: 29904082 DOI: 10.1038/s41579-018-0036-x]

51 **El Kaoutari A**, Armougom F, Gordon JI, Raoult D, Henrissat B. The abundance and variety of carbohydrate-active enzymes in the human gut microbiota. *Nat Rev Microbiol* 2013; **11**: 497-504 [PMID: 23748339 DOI: 10.1038/nrmicro3050]

52 **van der Hee B**, Wells JM. Microbial Regulation of Host Physiology by Short-chain Fatty Acids. *Trends Microbiol* 2021; **29**: 700-712 [PMID: 33674141 DOI: 10.1016/j.tim.2021.02.001]

53 **Bergstrom KS**, Xia L. Mucin-type O-glycans and their roles in intestinal homeostasis. *Glycobiology* 2013; **23**: 1026-1037 [PMID: 23752712 DOI: 10.1093/glycob/cwt045]

54 **Desai MS**, Seekatz AM, Koropatkin NM, Kamada N, Hickey CA, Wolter M, Pudlo NA, Kitamoto S, Terrapon N, Muller A, Young VB, Henrissat B, Wilmes P, Stappenbeck TS, Núñez G, Martens EC. A Dietary Fiber-Deprived Gut Microbiota Degrades the Colonic Mucus Barrier and Enhances Pathogen Susceptibility. *Cell* 2016; **167**: 1339-1353.e21 [PMID: 27863247 DOI: 10.1016/j.cell.2016.10.043]

55 **Lennon G**, Balfe A, Earley H, Devane LA, Lavelle A, Winter DC, Coffey JC, O'Connell PR. Influences of the colonic microbiome on the mucous gel layer in ulcerative colitis. *Gut Microbes* 2014; **5**: 277-285 [PMID: 24714392 DOI: 10.4161/gmic.28793]

56 **Wang BX**, Wu CM, Ribbeck K. Home, sweet home: how mucus accommodates our microbiota. *FEBS J* 2021; **288**: 1789-1799 [PMID: 32755014 DOI: 10.1111/febs.15504]

57 **Schwalm ND 3rd**, Townsend GE 2nd, Groisman EA. Prioritization of polysaccharide utilization and control of regulator activation in Bacteroides thetaiotaomicron. *Mol Microbiol* 2017; **104**: 32-45 [PMID: 28009067 DOI: 10.1111/mmi.13609]

58 **Luis AS**, Jin C, Pereira GV, Glowacki RWP, Gugel SR, Singh S, Byrne DP, Pudlo NA, London JA, Baslé A, Reihill M, Oscarson S, Eyers PA, Czjzek M, Michel G, Barbeyron T, Yates EA, Hansson GC, Karlsson NG, Cartmell A, Martens EC. A single sulfatase is required to access colonic mucin by a gut bacterium. *Nature* 2021; **598**: 332-337 [PMID: 34616040 DOI: 10.1038/s41586-021-03967-5]

59 **McLoughlin K**, Schluter J, Rakoff-Nahoum S, Smith AL, Foster KR. Host Selection of Microbiota *via* Differential Adhesion. *Cell Host Microbe* 2016; **19**: 550-559 [PMID: 27053168 DOI: 10.1016/j.chom.2016.02.021]

60 **Taylor SL**, McGuckin MA, Wesselingh S, Rogers GB. Infection's Sweet Tooth: How Glycans Mediate Infection and Disease Susceptibility. *Trends Microbiol* 2018; **26**: 92-101 [PMID: 29079498 DOI: 10.1016/j.tim.2017.09.011]

61 **Dotz V**, Wuhrer M. Histo-blood group glycans in the context of personalized medicine. *Biochim Biophys Acta* 2016; **1860**: 1596-1607 [PMID: 26748235 DOI: 10.1016/j.bbagen.2015.12.026]

62 **Rausch P**, Rehman A, Künzel S, Häsler R, Ott SJ, Schreiber S, Rosenstiel P, Franke A, Baines JF. Colonic mucosa-associated microbiota is influenced by an interaction of Crohn disease and FUT2 (Secretor) genotype. *Proc Natl Acad Sci U S A* 2011; **108**: 19030-19035 [PMID: 22068912 DOI: 10.1073/pnas.1106408108]

63 **Tong M**, McHardy I, Ruegger P, Goudarzi M, Kashyap PC, Haritunians T, Li X, Graeber TG, Schwager E, Huttenhower C, Fornace AJ Jr, Sonnenburg JL, McGovern DP, Borneman J, Braun J. Reprograming of gut microbiome energy metabolism by the FUT2 Crohn's disease risk polymorphism. *ISME J* 2014; **8**: 2193-2206 [PMID: 24781901 DOI: 10.1038/ismej.2014.64]

64 **Wacklin P**, Mäkivuokko H, Alakulppi N, Nikkilä J, Tenkanen H, Räbinä J, Partanen J, Aranko K, Mättö J. Secretor genotype (FUT2 gene) is strongly associated with the composition of Bifidobacteria in the human intestine. *PLoS One* 2011; **6**: e20113 [PMID: 21625510 DOI: 10.1371/journal.pone.0020113]

65 **Davenport ER**, Goodrich JK, Bell JT, Spector TD, Ley RE, Clark AG. ABO antigen and secretor statuses are not associated with gut microbiota composition in 1,500 twins. *BMC Genomics* 2016; **17**: 941 [PMID: 27871240 DOI: 10.1186/s12864-016-3290-1]

66 **Turpin W**, Bedrani L, Espin-Garcia O, Xu W, Silverberg MS, Smith MI, Guttman DS, Griffiths A, Moayyedi P, Panaccione R, Huynh H, Steinhart H, Aumais G, Shestopaloff K, Dieleman LA, Turner D, Paterson AD, Croitoru K. FUT2 genotype and secretory status are not associated with fecal microbial composition and inferred function in healthy subjects. *Gut Microbes* 2018; **9**: 357-368 [PMID: 29533703 DOI: 10.1080/19490976.2018.1445956]

67 **Wang J**, Thingholm LB, Skiecevičienė J, Rausch P, Kummen M, Hov JR, Degenhardt F, Heinsen FA, Rühlemann MC, Szymczak S, Holm K, Esko T, Sun J, Pricop-Jeckstadt M, Al-Dury S, Bohov P, Bethune J, Sommer F, Ellinghaus D, Berge RK, Hübenthal M, Koch M, Schwarz K, Rimbach G, Hübbe P, Pan WH, Sheibani-Tezerji R, Häsler R, Rosenstiel P, D'Amato M, Cloppenborg-Schmidt K, Künzel S, Laudes M, Marschall HU, Lieb W, Nöthlings U, Karlsen TH, Baines JF, Franke A. Genome-wide association analysis identifies variation in vitamin D receptor and other host factors influencing the gut microbiota. *Nat Genet* 2016; **48**: 1396-1406 [PMID: 27723756 DOI: 10.1038/ng.3695]

68 **Rühlemann MC**, Hermes BM, Bang C, Doms S, Moitinho-Silva L, Thingholm LB, Frost F, Degenhardt F, Wittig M, Kässens J, Weiss FU, Peters A, Neuhaus K, Völker U, Völzke H, Homuth G, Weiss S, Grallert H, Laudes M, Lieb W, Haller D, Lerch MM, Baines JF, Franke A. Genome-wide association study in 8,956 German individuals identifies influence of ABO histo-blood groups on gut microbiome. *Nat Genet* 2021; **53**: 147-155 [PMID: 33462482 DOI: 10.1038/s41588-020-00747-1]

69 **Arike L**, Holmén-Larsson J, Hansson GC. Intestinal Muc2 mucin O-glycosylation is affected by microbiota and regulated by differential expression of glycosyltranferases. *Glycobiology* 2017; **27**: 318-328 [PMID: 28122822 DOI: 10.1093/glycob/cww134]

70 **Rokhsefat S**, Lin A, Comelli EM. Mucin-Microbiota Interaction During Postnatal Maturation of the Intestinal Ecosystem: Clinical Implications. *Dig Dis Sci* 2016; **61**: 1473-1486 [PMID: 26792279 DOI: 10.1007/s10620-016-4032-6]

71 **Jakobsson HE**, Rodríguez-Piñeiro AM, Schütte A, Ermund A, Boysen P, Bemark M, Sommer F, Bäckhed F, Hansson GC, Johansson ME. The composition of the gut microbiota shapes the colon mucus barrier. *EMBO Rep* 2015; **16**: 164-177

[PMID: 25525071 DOI: 10.15252/embr.201439263]
72 **Hayes CL**, Dong J, Galipeau HJ, Jury J, McCarville J, Huang X, Wang XY, Naidoo A, Anbazhagan AN, Libertucci J, Sheridan C, Dudeja PK, Bowdish DME, Surette MG, Verdu EF. Commensal microbiota induces colonic barrier structure and functions that contribute to homeostasis. *Sci Rep* 2018; **8**: 14184 [PMID: 30242285 DOI: 10.1038/s41598-018-32366-6]
73 **Sovran B**, Hugenholtz F, Elderman M, Van Beek AA, Graversen K, Huijskes M, Boekschoten MV, Savelkoul HFJ, De Vos P, Dekker J, Wells JM. Age-associated Impairment of the Mucus Barrier Function is Associated with Profound Changes in Microbiota and Immunity. *Sci Rep* 2019; **9**: 1437 [PMID: 30723224 DOI: 10.1038/s41598-018-35228-3]
74 **Merchant HA**, Rabbie SC, Varum FJ, Afonso-Pereira F, Basit AW. Influence of ageing on the gastrointestinal environment of the rat and its implications for drug delivery. *Eur J Pharm Sci* 2014; **62**: 76-85 [PMID: 24834990 DOI: 10.1016/j.ejps.2014.05.004]
75 **Powell DN**, Swimm A, Sonowal R, Bretin A, Gewirtz AT, Jones RM, Kalman D. Indoles from the commensal microbiota act *via* the AHR and IL-10 to tune the cellular composition of the colonic epithelium during aging. *Proc Natl Acad Sci U S A* 2020; **117**: 21519-21526 [PMID: 32817517 DOI: 10.1073/pnas.2003004117]
76 **Claesson MJ**, Cusack S, O'Sullivan O, Greene-Diniz R, de Weerd H, Flannery E, Marchesi JR, Falush D, Dinan T, Fitzgerald G, Stanton C, van Sinderen D, O'Connor M, Harnedy N, O'Connor K, Henry C, O'Mahony D, Fitzgerald AP, Shanahan F, Twomey C, Hill C, Ross RP, O'Toole PW. Composition, variability, and temporal stability of the intestinal microbiota of the elderly. *Proc Natl Acad Sci U S A* 2011; **108** Suppl 1: 4586-4591 [PMID: 20571116 DOI: 10.1073/pnas.1000097107]
77 **Hooper LV**, Littman DR, Macpherson AJ. Interactions between the microbiota and the immune system. *Science* 2012; **336**: 1268-1273 [PMID: 22674334 DOI: 10.1126/science.1223490]
78 **van der Flier LG**, Clevers H. Stem cells, self-renewal, and differentiation in the intestinal epithelium. *Annu Rev Physiol* 2009; **71**: 241-260 [PMID: 18808327 DOI: 10.1146/annurev.physiol.010908.163145]
79 **Loktionov A**, Bandaletova T, Llewelyn AH, Dion C, Lywood HG, Lywood RC, Rockall TA, Stebbing JF, Broughton M, Caffarey S, Marks CG. Colorectal cancer detection by measuring DNA from exfoliated colonocytes obtained by direct contact with rectal mucosa. *Int J Oncol* 2009; **34**: 301-311 [PMID: 19148463]
80 **Loktionov A**, Chhaya V, Bandaletova T, Poullis A. Assessment of cytology and mucin 2 in colorectal mucus collected from patients with inflammatory bowel disease: Results of a pilot trial. *J Gastroenterol Hepatol* 2016; **31**: 326-333 [PMID: 26248500 DOI: 10.1111/jgh.13083]
81 **Loktionov A**, O'Neill IK, Silvester KR, Cummings JH, Middleton SJ, Miller R. Quantitation of DNA from exfoliated colonocytes isolated from human stool surface as a novel noninvasive screening test for colorectal cancer. *Clin Cancer Res* 1998; **4**: 337-342 [PMID: 9516920]
82 **Bandaletova T**, Bailey N, Bingham SA, Loktionov A. Isolation of exfoliated colonocytes from human stool as a new technique for colonic cytology. *APMIS* 2002; **110**: 239-246 [PMID: 12076277 DOI: 10.1034/j.1600-0463.2002.100306.x]
83 **Davies RJ**, Freeman A, Morris LS, Bingham S, Dilworth S, Scott I, Laskey RA, Miller R, Coleman N. Analysis of minichromosome maintenance proteins as a novel method for detection of colorectal cancer in stool. *Lancet* 2002; **359**: 1917-1919 [PMID: 12057556 DOI: 10.1016/S0140-6736(02)08739-1]
84 **Johansson ME**. Mucus layers in inflammatory bowel disease. *Inflamm Bowel Dis* 2014; **20**: 2124-2131 [PMID: 25025717 DOI: 10.1097/MIB.0000000000000117]
85 **Van der Sluis M**, De Koning BA, De Bruijn AC, Velcich A, Meijerink JP, Van Goudoever JB, Büller HA, Dekker J, Van Seuningen I, Renes IB, Einerhand AW. Muc2-deficient mice spontaneously develop colitis, indicating that MUC2 is critical for colonic protection. *Gastroenterology* 2006; **131**: 117-129 [PMID: 16831596 DOI: 10.1053/j.gastro.2006.04.020]
86 **Schroeder BO**, Birchenough GMH, Pradhan M, Nyström EEL, Henricsson M, Hansson GC, Bäckhed F. Obesity-associated microbiota contributes to mucus layer defects in genetically obese mice. *J Biol Chem* 2020; **295**: 15712-15726 [PMID: 32900852 DOI: 10.1074/jbc.RA120.015771]
87 **Glymenaki M**, Singh G, Brass A, Warhurst G, McBain AJ, Else KJ, Cruickshank SM. Compositional Changes in the Gut Mucus Microbiota Precede the Onset of Colitis-Induced Inflammation. *Inflamm Bowel Dis* 2017; **23**: 912-922 [PMID: 28498157 DOI: 10.1097/MIB.0000000000001118]
88 **Swidsinski A**, Weber J, Loening-Baucke V, Hale LP, Lochs H. Spatial organization and composition of the mucosal flora in patients with inflammatory bowel disease. *J Clin Microbiol* 2005; **43**: 3380-3389 [PMID: 16000463 DOI: 10.1128/JCM.43.7.3380-3389.2005]
89 **Png CW**, Lindén SK, Gilshenan KS, Zoetendal EG, McSweeney CS, Sly LI, McGuckin MA, Florin TH. Mucolytic bacteria with increased prevalence in IBD mucosa augment *in vitro* utilization of mucin by other bacteria. *Am J Gastroenterol* 2010; **105**: 2420-2428 [PMID: 20648002 DOI: 10.1038/ajg.2010.281]
90 **Tytgat HLP**, Nobrega FL, van der Oost J, de Vos WM. Bowel Biofilms: Tipping Points between a Healthy and Compromised Gut? *Trends Microbiol* 2019; **27**: 17-25 [PMID: 30219265 DOI: 10.1016/j.tim.2018.08.009]
91 **Domingue JC**, Drewes JL, Merlo CA, Housseau F, Sears CL. Host responses to mucosal biofilms in the lung and gut. *Mucosal Immunol* 2020; **13**: 413-422 [PMID: 32112046 DOI: 10.1038/s41385-020-0270-1]
92 **Baumgartner M**, Lang M, Holley H, Crepaz D, Hausmann B, Pjevac P, Moser D, Haller F, Hof F, Beer A, Orgler E, Frick A, Khare V, Evstatiev R, Strohmaier S, Primas C, Dolak W, Köcher T, Klavins K, Rath T, Neurath MF, Berry D, Makristathis A, Muttenthaler M, Gasche C. Mucosal Biofilms Are an Endoscopic Feature of Irritable Bowel Syndrome and Ulcerative Colitis. *Gastroenterology* 2021; **161**: 1245-1256.e20 [PMID: 34146566 DOI: 10.1053/j.gastro.2021.06.024]
93 **Niv Y**. Mucin Genes Expression in the Intestine of Crohn's Disease Patients: a Systematic Review and Meta-analysis. *J Gastrointestin Liver Dis* 2016; **25**: 351-357 [PMID: 27689200 DOI: 10.15403/jgld.2014.1121.253.niv]
94 **Niv Y**. Mucin gene expression in the intestine of ulcerative colitis patients: a systematic review and meta-analysis. *Eur J Gastroenterol Hepatol* 2016; **28**: 1241-1245 [PMID: 27442499 DOI: 10.1097/MEG.0000000000000707]
95 **Strugala V**, Dettmar PW, Pearson JP. Thickness and continuity of the adherent colonic mucus barrier in active and

quiescent ulcerative colitis and Crohn's disease. *Int J Clin Pract* 2008; **62**: 762-769 [PMID: 18194279 DOI: 10.1111/j.1742-1241.2007.01665.x]

96 **Gersemann M**, Becker S, Kübler I, Koslowski M, Wang G, Herrlinger KR, Griger J, Fritz P, Fellermann K, Schwab M, Wehkamp J, Stange EF. Differences in goblet cell differentiation between Crohn's disease and ulcerative colitis. *Differentiation* 2009; **77**: 84-94 [PMID: 19281767 DOI: 10.1016/j.diff.2008.09.008]

97 **Swidsinski A**, Loening-Baucke V, Theissig F, Engelhardt H, Bengmark S, Koch S, Lochs H, Dörffel Y. Comparative study of the intestinal mucus barrier in normal and inflamed colon. *Gut* 2007; **56**: 343-350 [PMID: 16908512 DOI: 10.1136/gut.2006.098160]

98 **Johansson ME**, Gustafsson JK, Holmén-Larsson J, Jabbar KS, Xia L, Xu H, Ghishan FK, Carvalho FA, Gewirtz AT, Sjövall H, Hansson GC. Bacteria penetrate the normally impenetrable inner colon mucus layer in both murine colitis models and patients with ulcerative colitis. *Gut* 2014; **63**: 281-291 [PMID: 23426893 DOI: 10.1136/gutjnl-2012-303207]

99 **van der Post S**, Jabbar KS, Birchenough G, Arike L, Akhtar N, Sjovall H, Johansson MEV, Hansson GC. Structural weakening of the colonic mucus barrier is an early event in ulcerative colitis pathogenesis. *Gut* 2019; **68**: 2142-2151 [PMID: 30914450 DOI: 10.1136/gutjnl-2018-317571]

100 **Lennon G**, Balfe Á, Bambury N, Lavelle A, Maguire A, Docherty NG, Coffey JC, Winter DC, Sheahan K, O'Connell PR. Correlations between colonic crypt mucin chemotype, inflammatory grade and Desulfovibrio species in ulcerative colitis. *Colorectal Dis* 2014; **16**: O161-O169 [PMID: 24345279 DOI: 10.1111/codi.12503]

101 **Vancamelbeke M**, Vanuytsel T, Farré R, Verstockt S, Ferrante M, Van Assche G, Rutgeerts P, Schuit F, Vermeire S, Arijs I, Cleynen I. Genetic and Transcriptomic Bases of Intestinal Epithelial Barrier Dysfunction in Inflammatory Bowel Disease. *Inflamm Bowel Dis* 2017; **23**: 1718-1729 [PMID: 28885228 DOI: 10.1097/MIB.0000000000001246]

102 **Pizarro TT**, Stappenbeck TS, Rieder F, Rosen MJ, Colombel JF, Donowitz M, Towne J, Mazmanian SK, Faith JJ, Hodin RA, Garrett WS, Fichera A, Poritz LS, Cortes CJ, Shtraizent N, Honig G, Snapper SB, Hurtado-Lorenzo A, Salzman NH, Chang EB. Challenges in IBD Research: Preclinical Human IBD Mechanisms. *Inflamm Bowel Dis* 2019; **25**: S5-S12 [PMID: 31095706 DOI: 10.1093/ibd/izz075]

103 **Fantini MC**, Guadagni I. From inflammation to colitis-associated colorectal cancer in inflammatory bowel disease: Pathogenesis and impact of current therapies. *Dig Liver Dis* 2021; **53**: 558-565 [PMID: 33541800 DOI: 10.1016/j.dld.2021.01.012]

104 **Kaplan GG**, Ng SC. Understanding and Preventing the Global Increase of Inflammatory Bowel Disease. *Gastroenterology* 2017; **152**: 313-321.e2 [PMID: 27793607 DOI: 10.1053/j.gastro.2016.10.020]

105 **Birchenough G**, Schroeder BO, Bäckhed F, Hansson GC. Dietary destabilisation of the balance between the microbiota and the colonic mucus barrier. *Gut Microbes* 2019; **10**: 246-250 [PMID: 30252606 DOI: 10.1080/19490976.2018.1513765]

106 **Wang K**, Song M. Personalized nutrition for colorectal cancer. *Adv Cancer Res* 2021; **151**: 109-136 [PMID: 34148612 DOI: 10.1016/bs.acr.2021.02.004]

107 **Schroeder BO**, Birchenough GMH, Ståhlman M, Arike L, Johansson MEV, Hansson GC, Bäckhed F. Bifidobacteria or Fiber Protects against Diet-Induced Microbiota-Mediated Colonic Mucus Deterioration. *Cell Host Microbe* 2018; **23**: 27-40.e7 [PMID: 29276171 DOI: 10.1016/j.chom.2017.11.004]

108 **Kumar M**, Kissoon-Singh V, Coria AL, Moreau F, Chadee K. Probiotic mixture VSL#3 reduces colonic inflammation and improves intestinal barrier function in Muc2 mucin-deficient mice. *Am J Physiol Gastrointest Liver Physiol* 2017; **312**: G34-G45 [PMID: 27856417 DOI: 10.1152/ajpgi.00298.2016]

109 **D'Agostino EM**, Rossetti D, Atkins D, Ferdinando D, Yakubov GE. Interaction of tea polyphenols and food constituents with model gut epithelia: the protective role of the mucus gel layer. *J Agric Food Chem* 2012; **60**: 3318-3328 [PMID: 22364573 DOI: 10.1021/jf205111k]

110 **He W**, Liu M, Li Y, Yu H, Wang D, Chen Q, Chen Y, Zhang Y, Wang T. Flavonoids from Citrus aurantium ameliorate TNBS-induced ulcerative colitis through protecting colonic mucus layer integrity. *Eur J Pharmacol* 2019; **857**: 172456 [PMID: 31220438 DOI: 10.1016/j.ejphar.2019.172456]

111 **Sands BE**. Biomarkers of Inflammation in Inflammatory Bowel Disease. *Gastroenterology* 2015; **149**: 1275-1285.e2 [PMID: 26166315 DOI: 10.1053/j.gastro.2015.07.003]

112 **Gonczi L**, Bessissow T, Lakatos PL. Disease monitoring strategies in inflammatory bowel diseases: What do we mean by "tight control"? *World J Gastroenterol* 2019; **25**: 6172-6189 [PMID: 31749591 DOI: 10.3748/wjg.v25.i41.6172]

113 **Anderson N**, Suliman I, Bandaletova T, Obichere A, Lywood R, Loktionov A. Protein biomarkers in exfoliated cells collected from the human rectal mucosa: implications for colorectal disease detection and monitoring. *Int J Colorectal Dis* 2011; **26**: 1287-1297 [PMID: 21698353 DOI: 10.1007/s00384-011-1263-z]

114 **Bandaletova T**, Chhaya V, Poullis A, Loktionov A. Colorectal mucus non-invasively collected from patients with inflammatory bowel disease and its suitability for diagnostic cytology. *APMIS* 2016; **124**: 160-168 [PMID: 26589885 DOI: 10.1111/apm.12479]

115 **Loktionov A**, Chhaya V, Bandaletova T, Poullis A. Inflammatory bowel disease detection and monitoring by measuring biomarkers in non-invasively collected colorectal mucus. *J Gastroenterol Hepatol* 2017; **32**: 992-1002 [PMID: 27787913 DOI: 10.1111/jgh.13627]

116 **Loktionov A**. Eosinophils in the gastrointestinal tract and their role in the pathogenesis of major colorectal disorders. *World J Gastroenterol* 2019; **25**: 3503-3526 [PMID: 31367153 DOI: 10.3748/wjg.v25.i27.3503]

117 **McGuckin MA**, Eri R, Simms LA, Florin TH, Radford-Smith G. Intestinal barrier dysfunction in inflammatory bowel diseases. *Inflamm Bowel Dis* 2009; **15**: 100-113 [PMID: 18623167 DOI: 10.1002/ibd.20539]

118 **Antoni L**, Nuding S, Wehkamp J, Stange EF. Intestinal barrier in inflammatory bowel disease. *World J Gastroenterol* 2014; **20**: 1165-1179 [PMID: 24574793 DOI: 10.3748/wjg.v20.i5.1165]

119 **Mehandru S**, Colombel JF. The intestinal barrier, an arbitrator turned provocateur in IBD. *Nat Rev Gastroenterol Hepatol* 2021; **18**: 83-84 [PMID: 33318680 DOI: 10.1038/s41575-020-00399-w]

120 **Schmitt M**, Greten FR. The inflammatory pathogenesis of colorectal cancer. *Nat Rev Immunol* 2021; **21**: 653-667 [PMID: 33911231 DOI: 10.1038/s41577-021-00534-x]

121 **Carethers JM**. Fecal DNA Testing for Colorectal Cancer Screening. *Annu Rev Med* 2020; **71**: 59-69 [PMID: 31451044 DOI: 10.1146/annurev-med-103018-123125]

122 **Loktionov A**. Biomarkers for detecting colorectal cancer non-invasively: DNA, RNA or proteins? *World J Gastrointest Oncol* 2020; **12**: 124-148 [PMID: 32104546 DOI: 10.4251/wjgo.v12.i2.124]

123 **Matsushita H**, Matsumura Y, Moriya Y, Akasu T, Fujita S, Yamamoto S, Onouchi S, Saito N, Sugito M, Ito M, Kozu T, Minowa T, Nomura S, Tsunoda H, Kakizoe T. A new method for isolating colonocytes from naturally evacuated feces and its clinical application to colorectal cancer diagnosis. *Gastroenterology* 2005; **129**: 1918-1927 [PMID: 16344060 DOI: 10.1053/j.gastro.2005.10.007]

124 **Onouchi S**, Matsushita H, Moriya Y, Akasu T, Fujita S, Yamamoto S, Hasegawa H, Kitagawa Y, Matsumura Y. New method for colorectal cancer diagnosis based on SSCP analysis of DNA from exfoliated colonocytes in naturally evacuated feces. *Anticancer Res* 2008; **28**: 145-150 [PMID: 18383838]

125 **White V**, Scarpini C, Barbosa-Morais NL, Ikelle E, Carter S, Laskey RA, Miller R, Coleman N. Isolation of stool-derived mucus provides a high yield of colonocytes suitable for early detection of colorectal carcinoma. *Cancer Epidemiol Biomarkers Prev* 2009; **18**: 2006-2013 [PMID: 19589912 DOI: 10.1158/1055-9965.EPI-08-1145]

126 **Ahlquist DA**, Harrington JJ, Burgart LJ, Roche PC. Morphometric analysis of the "mucocellular layer" overlying colorectal cancer and normal mucosa: relevance to exfoliation and stool screening. *Hum Pathol* 2000; **31**: 51-57 [PMID: 10665913 DOI: 10.1016/s0046-8177(00)80198-7]

127 **Loktionov A**, Soubieres A, Bandaletova T, Mathur J, Poullis A. Colorectal cancer detection by biomarker quantification in noninvasively collected colorectal mucus: preliminary comparison of 24 protein biomarkers. *Eur J Gastroenterol Hepatol* 2019; **31**: 1220-1227 [PMID: 31498281 DOI: 10.1097/MEG.0000000000001535]

128 **Loktionov A**, Soubieres A, Bandaletova T, Francis N, Allison J, Sturt J, Mathur J, Poullis A. Biomarker measurement in non-invasively sampled colorectal mucus as a novel approach to colorectal cancer detection: screening and triage implications. *Br J Cancer* 2020; **123**: 252-260 [PMID: 32398859 DOI: 10.1038/s41416-020-0893-8]

129 **Biragyn A**, Ferrucci L. Gut dysbiosis: a potential link between increased cancer risk in ageing and inflammaging. *Lancet Oncol* 2018; **19**: e295-e304 [PMID: 29893261 DOI: 10.1016/S1470-2045(18)30095-0]

130 **Coleman OI**, Haller D. Microbe-Mucus Interface in the Pathogenesis of Colorectal Cancer. *Cancers (Basel)* 2021; **13** [PMID: 33557139 DOI: 10.3390/cancers13040616]

131 **Pothuraju R**, Chaudhary S, Rachagani S, Kaur S, Roy HK, Bouvet M, Batra SK. Mucins, gut microbiota, and postbiotics role in colorectal cancer. *Gut Microbes* 2021; **13**: 1974795 [PMID: 34586012 DOI: 10.1080/19490976.2021.1974795]

132 **Velcich A**, Yang W, Heyer J, Fragale A, Nicholas C, Viani S, Kucherlapati R, Lipkin M, Yang K, Augenlicht L. Colorectal cancer in mice genetically deficient in the mucin Muc2. *Science* 2002; **295**: 1726-1729 [PMID: 11872843 DOI: 10.1126/science.1069094]

133 **Yang K**, Popova NV, Yang WC, Lozonschi I, Tadesse S, Kent S, Bancroft L, Matise I, Cormier RT, Scherer SJ, Edelmann W, Lipkin M, Augenlicht L, Velcich A. Interaction of Muc2 and Apc on Wnt signaling and in intestinal tumorigenesis: potential role of chronic inflammation. *Cancer Res* 2008; **68**: 7313-7322 [PMID: 18794118 DOI: 10.1158/0008-5472.CAN-08-0598]

134 **Bossuyt W**, Kazanjian A, De Geest N, Van Kelst S, De Hertogh G, Geboes K, Boivin GP, Luciani J, Fuks F, Chuah M, VandenDriessche T, Marynen P, Cools J, Shroyer NF, Hassan BA. Atonal homolog 1 is a tumor suppressor gene. *PLoS Biol* 2009; **7**: e39 [PMID: 19243219 DOI: 10.1371/journal.pbio.1000039]

135 **Novaes RD**, Sequetto PL, Vilela Gonçalves R, Cupertino MC, Santos EC, Mello VJ, Araújo MR, Silva E, Oliveira TT. Depletion of enteroendocrine and mucus-secreting cells is associated with colorectal carcinogenesis severity and impaired intestinal motility in rats. *Microsc Res Tech* 2016; **79**: 3-13 [PMID: 26208280 DOI: 10.1002/jemt.22534]

136 **Mizoshita T**, Tsukamoto T, Inada KI, Hirano N, Tajika M, Nakamura T, Ban H, Tatematsu M. Loss of MUC2 expression correlates with progression along the adenoma-carcinoma sequence pathway as well as de novo carcinogenesis in the colon. *Histol Histopathol* 2007; **22**: 251-260 [PMID: 17163399 DOI: 10.14670/HH-22.251]

137 **Betge J**, Schneider NI, Harbaum L, Pollheimer MJ, Lindtner RA, Kornprat P, Ebert MP, Langner C. MUC1, MUC2, MUC5AC, and MUC6 in colorectal cancer: expression profiles and clinical significance. *Virchows Arch* 2016; **469**: 255-265 [PMID: 27298226 DOI: 10.1007/s00428-016-1970-5]

138 **Kasprzak A**, Siodła E, Andrzejewska M, Szmeja J, Seraszek-Jaros A, Cofta S, Szaflarski W. Differential expression of mucin 1 and mucin 2 in colorectal cancer. *World J Gastroenterol* 2018; **24**: 4164-4177 [PMID: 30271081 DOI: 10.3748/wjg.v24.i36.4164]

139 **Tozawa E**, Ajioka Y, Watanabe H, Nishikura K, Mukai G, Suda T, Kanoh T, Hatakeyama K. Mucin expression, p53 overexpression, and peritumoral lymphocytic infiltration of advanced colorectal carcinoma with mucus component: is mucinous carcinoma a distinct histological entity? *Pathol Res Pract* 2007; **203**: 567-574 [PMID: 17679024 DOI: 10.1016/j.prp.2007.04.013]

140 **Walsh MD**, Clendenning M, Williamson E, Pearson SA, Walters RJ, Nagler B, Packenas D, Win AK, Hopper JL, Jenkins MA, Haydon AM, Rosty C, English DR, Giles GG, McGuckin MA, Young JP, Buchanan DD. Expression of MUC2, MUC5AC, MUC5B, and MUC6 mucins in colorectal cancers and their association with the CpG island methylator phenotype. *Mod Pathol* 2013; **26**: 1642-1656 [PMID: 23807779 DOI: 10.1038/modpathol.2013.101]

141 **Li G**, Yang S, Shen P, Wu B, Sun T, Sun H, Ji F, Zhou D. SCF/c-KIT signaling promotes mucus secretion of colonic goblet cells and development of mucinous colorectal adenocarcinoma. *Am J Cancer Res* 2018; **8**: 1064-1073 [PMID: 30034943]

142 **An G**, Wei B, Xia B, McDaniel JM, Ju T, Cummings RD, Braun J, Xia L. Increased susceptibility to colitis and colorectal tumors in mice lacking core 3-derived O-glycans. *J Exp Med* 2007; **204**: 1417-1429 [PMID: 17517967 DOI: 10.1084/jem.20061929]

143 **Bergstrom K**, Liu X, Zhao Y, Gao N, Wu Q, Song K, Cui Y, Li Y, McDaniel JM, McGee S, Chen W, Huycke MM, Houchen CW, Zenewicz LA, West CM, Chen H, Braun J, Fu J, Xia L. Defective Intestinal Mucin-Type O-Glycosylation Causes Spontaneous Colitis-Associated Cancer in Mice. *Gastroenterology* 2016; **151**: 152-164.e11 [PMID: 27059389 DOI: 10.1053/j.gastro.2016.03.039]

144 **Jiang Y**, Liu Z, Xu F, Dong X, Cheng Y, Hu Y, Gao T, Liu J, Yang L, Jia X, Qian H, Wen T, An G. Aberrant O-glycosylation contributes to tumorigenesis in human colorectal cancer. *J Cell Mol Med* 2018; **22**: 4875-4885 [PMID: 29999571 DOI: 10.1111/jcmm.13752]

145 **Wong SH**, Yu J. Gut microbiota in colorectal cancer: mechanisms of action and clinical applications. *Nat Rev Gastroenterol Hepatol* 2019; **16**: 690-704 [PMID: 31554963 DOI: 10.1038/s41575-019-0209-8]

146 **Feng Q**, Liang S, Jia H, Stadlmayr A, Tang L, Lan Z, Zhang D, Xia H, Xu X, Jie Z, Su L, Li X, Li J, Xiao L, Huber-Schönauer U, Niederseer D, Al-Aama JY, Yang H, Wang J, Kristiansen K, Arumugam M, Tilg H, Datz C. Gut microbiome development along the colorectal adenoma-carcinoma sequence. *Nat Commun* 2015; **6**: 6528 [PMID: 25758642 DOI: 10.1038/ncomms7528]

147 **Yu J**, Feng Q, Wong SH, Zhang D, Liang QY, Qin Y, Tang L, Zhao H, Stenvang J, Li Y, Wang X, Xu X, Chen N, Wu WK, Al-Aama J, Nielsen HJ, Kiilerich P, Jensen BA, Yau TO, Lan Z, Jia H, Li J, Xiao L, Lam TY, Ng SC, Cheng AS, Wong VW, Chan FK, Yang H, Madsen L, Datz C, Tilg H, Wang J, Brünner N, Kristiansen K, Arumugam M, Sung JJ. Metagenomic analysis of faecal microbiome as a tool towards targeted non-invasive biomarkers for colorectal cancer. *Gut* 2017; **66**: 70-78 [PMID: 26408641 DOI: 10.1136/gutjnl-2015-309800]

148 **Li S**, Konstantinov SR, Smits R, Peppelenbosch MP. Bacterial Biofilms in Colorectal Cancer Initiation and Progression. *Trends Mol Med* 2017; **23**: 18-30 [PMID: 27986421 DOI: 10.1016/j.molmed.2016.11.004]

149 **Dejea CM**, Wick EC, Hechenbleikner EM, White JR, Mark Welch JL, Rossetti BJ, Peterson SN, Snesrud EC, Borisy GG, Lazarev M, Stein E, Vadivelu J, Roslani AC, Malik AA, Wanyiri JW, Goh KL, Thevambiga I, Fu K, Wan F, Llosa N, Housseau F, Romans K, Wu X, McAllister FM, Wu S, Vogelstein B, Kinzler KW, Pardoll DM, Sears CL. Microbiota organization is a distinct feature of proximal colorectal cancers. *Proc Natl Acad Sci U S A* 2014; **111**: 18321-18326 [PMID: 25489084 DOI: 10.1073/pnas.1406199111]

150 **Drewes JL**, White JR, Dejea CM, Fathi P, Iyadorai T, Vadivelu J, Roslani AC, Wick EC, Mongodin EF, Loke MF, Thulasi K, Gan HM, Goh KL, Chong HY, Kumar S, Wanyiri JW, Sears CL. High-resolution bacterial 16S rRNA gene profile meta-analysis and biofilm status reveal common colorectal cancer consortia. *NPJ Biofilms Microbiomes* 2017; **3**: 34 [PMID: 29214046 DOI: 10.1038/s41522-017-0040-3]

151 **Hold GL**, Garrett WS. Gut microbiota. Microbiota organization--a key to understanding CRC development. *Nat Rev Gastroenterol Hepatol* 2015; **12**: 128-129 [PMID: 25688055 DOI: 10.1038/nrgastro.2015.25]

152 **Li S**, Peppelenbosch MP, Smits R. Bacterial biofilms as a potential contributor to mucinous colorectal cancer formation. *Biochim Biophys Acta Rev Cancer* 2019; **1872**: 74-79 [PMID: 31201828 DOI: 10.1016/j.bbcan.2019.05.009]

153 **DeDecker L**, Coppedge B, Avelar-Barragan J, Karnes W, Whiteson K. Microbiome distinctions between the CRC carcinogenic pathways. *Gut Microbes* 2021; **13**: 1854641 [PMID: 33446008 DOI: 10.1080/19490976.2020.1854641]

154 **Sears CL**. Enterotoxigenic Bacteroides fragilis: a rogue among symbiotes. *Clin Microbiol Rev* 2009; **22**: 349-369, Table of Contents [PMID: 19366918 DOI: 10.1128/CMR.00053-08]

155 **Dejea CM**, Fathi P, Craig JM, Boleij A, Taddese R, Geis AL, Wu X, DeStefano Shields CE, Hechenbleikner EM, Huso DL, Anders RA, Giardiello FM, Wick EC, Wang H, Wu S, Pardoll DM, Housseau F, Sears CL. Patients with familial adenomatous polyposis harbor colonic biofilms containing tumorigenic bacteria. *Science* 2018; **359**: 592-597 [PMID: 29420293 DOI: 10.1126/science.aah3648]

156 **Tomkovich S**, Dejea CM, Winglee K, Drewes JL, Chung L, Housseau F, Pope JL, Gauthier J, Sun X, Mühlbauer M, Liu X, Fathi P, Anders RA, Besharati S, Perez-Chanona E, Yang Y, Ding H, Wu X, Wu S, White JR, Gharaibeh RZ, Fodor AA, Wang H, Pardoll DM, Jobin C, Sears CL. Human colon mucosal biofilms from healthy or colon cancer hosts are carcinogenic. *J Clin Invest* 2019; **129**: 1699-1712 [PMID: 30855275 DOI: 10.1172/JCI124196]

157 **Dienstmann R**, Vermeulen L, Guinney J, Kopetz S, Tejpar S, Tabernero J. Consensus molecular subtypes and the evolution of precision medicine in colorectal cancer. *Nat Rev Cancer* 2017; **17**: 79-92 [PMID: 28050011 DOI: 10.1038/nrc.2016.126]

158 **Khan U**, Chowdhury S, Billah MM, Islam KMD, Thorlacius H, Rahman M. Neutrophil Extracellular Traps in Colorectal Cancer Progression and Metastasis. *Int J Mol Sci* 2021; **22** [PMID: 34298878 DOI: 10.3390/ijms22147260]

159 **O'Keefe SJ**. Diet, microorganisms and their metabolites, and colon cancer. *Nat Rev Gastroenterol Hepatol* 2016; **13**: 691-706 [PMID: 27848961 DOI: 10.1038/nrgastro.2016.165]

160 **Hajjar R**, Richard CS, Santos MM. The role of butyrate in surgical and oncological outcomes in colorectal cancer. *Am J Physiol Gastrointest Liver Physiol* 2021; **320**: G601-G608 [PMID: 33404375 DOI: 10.1152/ajpgi.00316.2020]

161 **Ryu SH**, Kaiko GE, Stappenbeck TS. Cellular differentiation: Potential insight into butyrate paradox? *Mol Cell Oncol* 2018; **5**: e1212685 [PMID: 30250879 DOI: 10.1080/23723556.2016.1212685]

162 **Ijssennagger N**, Belzer C, Hooiveld GJ, Dekker J, van Mil SW, Müller M, Kleerebezem M, van der Meer R. Gut microbiota facilitates dietary heme-induced epithelial hyperproliferation by opening the mucus barrier in colon. *Proc Natl Acad Sci U S A* 2015; **112**: 10038-10043 [PMID: 26216954 DOI: 10.1073/pnas.1507645112]

World Journal of Gastroenterology

Submit a Manuscript: https://www.f6publishing.com

World J Gastroenterol 2022 August 28; 28(32): 4493-4507

DOI: 10.3748/wjg.v28.i32.4493

ISSN 1007-9327 (print) ISSN 2219-2840 (online)

MINIREVIEWS

Who to screen and how to screen for celiac disease

Prashant Singh, Achintya Dinesh Singh, Vineet Ahuja, Govind K Makharia

Specialty type: Gastroenterology and hepatology

Provenance and peer review: Invited article; Externally peer reviewed.

Peer-review model: Single blind

Peer-review report's scientific quality classification

Grade A (Excellent): 0
Grade B (Very good): B
Grade C (Good): C
Grade D (Fair): D
Grade E (Poor): 0

P-Reviewer: Deng K, China; Liu C, China

Received: December 31, 2021
Peer-review started: December 31, 2021
First decision: January 27, 2022
Revised: March 3, 2022
Accepted: June 16, 2022
Article in press: June 16, 2022
Published online: August 28, 2022

Prashant Singh, Department of Gastroenterology, University of Michigan, Ann Arbor, MI 48109, United States

Achintya Dinesh Singh, Department of Medicine, Cleveland Clinic, Cleveland, OH 44195, United States

Vineet Ahuja, Govind K Makharia, Department of Gastroenterology and Human Nutrition, All India Institute of Medical Sciences, New Delhi 110029, India

Corresponding author: Govind K Makharia, MBBS, MD, DM, Professor, Department of Gastroenterology and Human Nutrition, All India Institute of Medical Sciences, Ansari Nagar, New Delhi 110029, India. govindmakharia@gmail.com

Abstract

Celiac disease (CeD) is a chronic gluten-induced enteropathy with plethoric manifestations. The typical manifestations of CeD such as chronic diarrhea and malabsorption are widely recognized, however, many patients have atypical manifestations like iron deficiency anemia, idiopathic short stature, hypertransaminesemia or infertility, *etc.* These patients often present to the primary care physicians and/or non-gastrointestinal specialties. However, due to a lack of awareness among the healthcare professionals about the various atypical manifestations, many patients are not screened for CeD. In this review, we have summarized the available literature about the prevalence of CeD in various gastrointestinal (chronic diarrhea) and non-gastrointestinal conditions (iron deficiency anemia, short stature, cryptogenic hypertransaminesemia, cryptogenic cirrhosis or idiopathic ataxia *etc.*) where the diagnosis of CeD should be considered. In addition, we also discuss special scenarios where screening for CeD should be considered even in absence of symptoms such as patients with type 1 diabetes, Down's syndrome, and first-degree relatives of patients with CeD. Further, we discuss the diagnostic performance and limitations of various screening tests for CeD such as IgA anti-tissue transglutaminase antibodies, anti-endomysial antibodies and anti-deamidated gliadin antibodies. Based on the current recommendations, we propose a diagnostic algorithm for patients with suspected CeD.

Key Words: Screening; Diagnosis; Serology; High-risk group; Small intestine; Enteropathy

©The Author(s) 2022. Published by Baishideng Publishing Group Inc. All rights reserved.

Core Tip: In this review article, we have summarized the available literature about the prevalence of celiac disease (CeD) in various gastrointestinal (chronic diarrhea) and non-gastrointestinal conditions (such as iron deficiency anemia, short stature, cryptogenic hypertransaminesemia, cryptogenic cirrhosis or idiopathic ataxia *etc.*).We thereby share the various clinical indications for screening for CeD. Also, we elucidate the diagnostic performance of various serological assays along with their limitations and propose an algorithm to diagnose patients with suspected CeD.

Citation: Singh P, Singh AD, Ahuja V, Makharia GK. Who to screen and how to screen for celiac disease. *World J Gastroenterol* 2022; 28(32): 4493-4507
URL: https://www.wjgnet.com/1007-9327/full/v28/i32/4493.htm
DOI: https://dx.doi.org/10.3748/wjg.v28.i32.4493

INTRODUCTION

Celiac disease (CeD) is an immune-mediated enteropathy that affects approximately 0.7% of the world population[1]. The disease is related to a complex interplay between genetic, environmental and host immunity-related factors. It is triggered by ingestion of gluten, a protein present in cereals such as wheat, barley, and rye in genetically-predisposed individuals. The phenotypic expression of CeD is variable. It ranges from being clinically asymptomatic to severely symptomatic disease[2,3]. Also, CeD once thought to affect only small intestines, is now considered a multi-system disorder. While there are convincing clinical and epidemiological evidence of involvement of extra-small intestinal organs, the exact pathogenesis of their involvement remains unexplored. It is likely that the human leukocyte antigen (HLA)-DQ2 restricted gliadin peptide induced T-cells which originate in the small intestine, circulate in peripheral blood and home in other organs leading to organ specific cell injury[4,5].

The clinical manifestations of CeD may be related to the gastrointestinal tract, called "classical CeD" seen in 50%-60% of all cases or non-gastrointestinal symptoms called "non-classical CeD" accounting for 40%-50% of cases[6,7]. The non-classic symptoms like short stature anemia, dyspepsia, infertility or hypertransaminesemia could be the sole manifestations of CeD making the clinical diagnosis more elusive. Additionally, CeD can co-exist with type 1 diabetes or other autoimmune diseases and its clinical manifestations may remain submerged with the manifestations of primary disease or it may remain clinically silent[8,9].

Because of its diverse manifestations, patients with CeD may present to healthcare professionals other than gastroenterologists or pediatricians such as hematologists with anemia, endocrinologists for short stature or type 1 diabetes, or gynecologists with infertility. The lack of typical manifestations combined with unfamiliarity with the disease lowers the index of suspicion for CeD in such clinical settings. This results in the missed diagnosis of CeD and about 85%-90% of the patients with CeD remain undiagnosed[10-12]. A delay in the diagnosis and institution of appropriate treatment adds to significant morbidity and even mortality in these patients[13].

Over past two decades, certain group of patients with conditions like short stature, iron deficiency anemia, type 1 diabetes, first-degree relatives have been reported to have a much higher prevalence of CeD compared to the general population[2,14]. Assiduous screening in these conditions can improve the detection of CeD compared to population-based screening for CeD. However, while most gastrointestinal societies agree that there is not enough evidence to recommend screening for CeD in the general population, they offer varying recommendations about which at-risk groups should be routinely screened for CeD[15,16].

In the present review, we summarize the present literature regarding the prevalence of CeD in many conditions to facilitate identification of high-risk groups who could benefit from screening for CeD. We have sub-grouped the indications for screening as definitive (when the data to support the screening is robust), probable (when the data to support screening exists but heterogenous) and possible (when there is a biological plausibility, but the evidence is insufficient). Later, we also highlight about the screening strategy for CeD once a decision for screening has been made based on clinical indication.

REVIEW METHODOLOGY

Relevant studies were searched utilizing MEDLINE, EMBASE and Scopus databases. Also, additional studies were cross-referenced from the various articles. Studies were identified with the medical subject heading terms and keywords–"celiac disease", "celiac", "coeliac disease", "tissue transglutaminase antibody", "endomysial antibody", "anti-endomysium antibody". They were combined using the set operator AND with keywords for relevant medical condition/risk factor (type 1 diabetes mellitus, irritable bowel syndrome, first degree relatives *etc.*). Studies from all languages were reviewed for

appropriateness to the clinical question and potentially relevant papers were assessed in detail.

Terms, definitions and analysis

For the purpose of this manuscript, CeD is defined as: (1) Villous abnormalities of modified marsh grade 2 on duodenal biopsies along with positive celiac-specific serology [anti-tissue transglutaminase antibody (anti-tTG Ab), anti-endomysial antibody (AEA), anti-deamidated gliadin peptide or antigliadin antibody (anti-DGP Ab)]; and (2) presence of at least modified marsh 2 lesion on duodenal histology along with unequivocal clinical and/or histological response to a gluten free diet (GFD). Seroprevalence of CeD is defined as the prevalence of positive anti-tTG Ab and/or AEA and/or anti-DGP Ab. Pooled prevalence of CeD in the manuscript refers to pooled prevalence of biopsy-proven CeD.

DEFINITE INDICATIONS FOR SCREENING FOR CED

Patients with chronic diarrhea

The classical gastrointestinal symptoms of CeD include chronic or intermittent diarrhea, steatorrhea, abdominal bloating, flatulence, and weight loss[7]. A proportion of patients with CeD may have mild gastrointestinal manifestations such as bowel dysmotility, abdominal pain/discomfort, and bloating, and with this symptom complex, they are can be labelled as having functional gastrointestinal diseases including irritable bowel syndrome (IBS).

One of the classic manifestations of CeD, both in the children and adults, is chronic diarrhea which occurs secondary to diffuse enteropathy and malabsorption. Chronic diarrhea in children is often associated with failure to thrive, irritability and distension of the abdomen. Chronic diarrhea is a predominant manifestation in 43%-85% of patients with newly diagnosed CeD. Conversely, the prevalence of CeD in patients referred to secondary care with chronic diarrhea has been reported to range from 3% to 12.2%[17,18]. Given the high occurrence of CeD in patients with chronic diarrhea and the delay in diagnosis of CeD, several gastroenterology societies such as American Gastroenterological Association, and British Society of Gastroenterology has recommended screening for CeD as first line investigation in patients with chronic diarrhea[17,19]. Therefore, all patients presenting with chronic diarrhea should be screened for CeD.

Patients with iron deficiency anemia

Anemia affects approximately 12%-69% patients in the western countries and 85%-90% of Indian patients with CeD[20-25]. Iron deficiency anemia (IDA) could be an isolated manifestation of CeD even in the absence of GI symptoms. Iron deficiency is the commonest form of anemia in CeD[20,26,27].

In a review including 2998 patients from 18 studies, Mahadev *et al*[14] have reported prevalence of CeD in patients presenting with iron deficiency anemia. Of 2998 patients with IDA included in this meta-analysis, the estimated pooled prevalence of CeD was reported to be 3.2% (95%CI: 2.6-3.9). Thus, approximately 1 in 31 patients with IDA have CeD. The authors did not find any relationship between the age and gender of the participant and the prevalence of CeD in patients with IDA. However, the prevalence of CeD in them vary significantly with geographic region. The prevalence of CeD in iron deficiency anemia is significantly higher in Asian countries (4.1% in Turkey and 6.4% in Iran) compared to that in the European countries (2.4%). It is important to note that the prevalence of iron deficiency anemia could vary based on the geographical region and according to the socio economic strata of the society[28]. They also found that smaller studies were more likely to report higher prevalence of CeD compared to studies with larger sample size. However, even in larger studies (those including > 200 patients), the pooled prevalence of CeD in patients with IDA was still significantly higher (2.7%) than that in the general population. Thus, the prevalence of CeD in patients with IDA is at-least 2-3 times higher prevalence of CeD than in the general population. Considering the overall high prevalence, all patients with iron deficiency anemia should be screened for CeD.

Patients with short stature

The manifestations of CeD start in childhood and hence growth failure/restriction is an important manifestation of CeD. Short stature is more frequent in those diagnosed during childhood/adolescence than patients diagnosed in adulthood. Importantly, institution of GFD in these patients can result in early catch-up growth for the initial 2-3 years[2,29,30]. Early diagnosis and compliance with GFD in patients with CeD result in rapid recovery and patients may achieve normal adult height.

Several studies have estimated the prevalence of CeD in children with idiopathic short stature. We systematically reviewed and meta-analyzed 17 studies and 3759 patients (1582 with all-cause short stature and 2177 with idiopathic short stature), and found that the pooled seroprevalence of CeD based on positive anti-tTG Ab and AEA is 11.2% (95%CI: 4.0-21.2) and 9.7% (95%CI: 2.7-20.2) for all-cause and idiopathic short stature, respectively. Similarly, pooled prevalence of biopsy-confirmed CeD is 7.4% (95%CI: 4.7-10.6) and 11.6% (95%CI: 4.1-22.2), for all-cause and idiopathic short stature, respectively[31].

In summary, approximately 1 in 14 patients with all-cause short stature and 1 in 9 patients with idiopathic short stature has biopsy-confirmed CeD. Therefore, all patients with CeD should be screened for CeD.

Patients with type 1 diabetes

Because of sharing of genetic susceptibility, especially HLA, type 1 diabetes is often associated with CeD [3,6]. In a systematic review and meta-analysis by Elfström *et al*[32] of 27 studies including 26605 patients with type 1 diabetes, the pooled prevalence of CeD was 6% (95%CI: 5-6.9) of CeD. Thus, more than 1 in 18 patients with type 1 diabetes mellitus have biopsy-proven CeD. The prevalence of CeD in children patients with type 1 diabetes is much higher (6.2%, 95%CI: 6.1- 6.3) than those with adult patients with type 1 diabetes (2.7%, 95%CI: 2.1-2.3) ($P < 0.001$). There is no geographical variation and almost a similar prevalence of CeD is reported in type 1 diabetes from all over the world. Therefore, all patients with type 1 diabetes should be screened for CeD[32].

First-degree relatives of patients with CeD

Because of sharing of genetic susceptibility, first-degree relatives (FDRs) of patients with CeD are at a higher risk of developing CeD in comparison to the general population. The prevalence of CeD in FDRs of patients with CeD has been extensively investigated and it ranges widely in the literature from 1.6% to 38%[33-35]. Singh *et al*[36] in a systematic review and meta-analysis including 41 studies, has reported 708 CeD patients amongst 10252 FDRs suggesting a pooled prevalence of CeD of 7.5% (95%CI: 6.3-8.8) in them. Among the FDRs, the risk of having CeD is highest amongst siblings, followed by offspring and the least in the parents. Daughters and sisters of the CeD patients are at the highest risk (1 in 7 and 1 in 8, respectively) of developing CeD. The risk of developing CeD is 1 in 13 in sons, 1 in 16 in brothers, 1 in 32 in mothers and 1 in 33 in fathers[36]. Majority of studies reporting prevalence of CeD in FDRs have been cross-sectional and there is a lack of longitudinal studies for assessment of risk of developing CeD over time or over lifetime. It is still unclear if there is role for repeat screening every few years after an initial negative screening or repeat screening should be reserved for FDRs who develop symptoms. Based on the abovementioned high-quality data, all FDRs of index patients with CeD should be screened for CeD.

The data on the prevalence of CeD in second-degree relatives (SDRs) of patients with CeD is sparse [37,38]. In a meta-analysis of two eligible studies including 641 SDRs, Weinstein *et al*[39] observed a pooled prevalence of CeD in SDRs to be 2.3% (95%CI: 1.3-3.8). The current literature on this topic has several limitations including availability of few studies, small sample size, and high risk of bias. Given these limitations, the magnitude of risk of CeD in SDRs is not clear. Therefore, in view of insufficient data, screening of SDRs of patients with CeD for CeD is not justifiable at the present time.

Patients with dermatitis herpetiformis

Dermatitis herpetiformis is among the most common manifestations of CeD and could be the first extra-intestinal manifestations to be clinically recognized. It presents as a cluster of intensely pruritic papules and/or vesicles, followed by erosions and excoriations. The most common sites are elbows, knees, scalp, and buttocks, typically along the extensor surface of the upper and lower extremities.

The extent of skin lesions may vary from small area to more diffuse involving many sites at one time [40,41]. Furthermore, these lesions may appear intermittently and may be absent at the time of examination.

The pathognomonic histology with immunohistochemistry or immunofluorescence shows granular IgA deposits and neutrophil infiltrates in the papillary dermis. Almost 85% of these patients with a Caucasian ethnicity carry HLA-DQ2 mutations while the remaining have HLA-DQ8[42]. Typically, only two-third patients with DH have villous abnormalities and one third of them have no enteropathy[43]. A survey of 1138 biopsy-confirmed patients with CeD, found a 9.8% prevalence of DH in patients with CeD[44].

A study from Finland have also shown that 17% of patients with CeD have DH[45]. Therefore, all patients with a diagnosis of DH should be screened for CeD, even in the absence of intestinal manifestations.

Patients with Down's syndrome

The prevalence of CeD in patients with Down's syndrome has been extensively investigated. Based on data from 31 studies including 4383 patients with Down syndrome, a recent meta-analysis reported a pooled prevalence of CeD in them to be 5.8% (95%CI: 4.7-7.2)[46]. Prevalence of CeD was higher in the studies including only children with Down syndrome than in those including both adults and children with Down's syndrome. The higher prevalence of CeD in Down syndrome is independent of the geographical location as studies from Europe, America and Asia have all shown higher prevalence of CeD among patients with Down syndrome. Based on this high-quality evidence, all patients with Down syndrome should be screened for CeD.

PROBABLE INDICATIONS FOR SCREENING FOR CED

Patients with liver diseases

Patients with CeD can have a variety of liver related manifestations that ranges from elevation of serum transaminases to cirrhosis. Elevated transaminases can be seen in 27% (95%CI: 13-44) of newly diagnosed patients with CeD and they normalize in 63% to 90% of patients within 1 year of GFD[47].

Cryptogenic hypertransaminesemia

Sainsbury *et al*[47] in a systematic review including six studies has reported a pooled prevalence of biopsy-proven CeD of 3.6% amongst patients with cryptogenic hypertransaminesemia. In a study of 463 adults with CeD[48], 40.6% patients had elevated AST/ALT levels at the time of diagnosis compared to 24.2% CeD patients after initiation of GFD. The quality of evidence has been considered high due to very large effect size without any significant imprecision. Given the high prevalence of CeD in patients with cryptogenic hypertransaminesemia, and a potential for reversal of serum transaminases level with GFD, it is justifiable to screen patients with cryptogenic hypertransaminesemia for CeD.

Cryptogenic cirrhosis

Undetected CeD can lead to persistent liver injury progressing from elevated liver biochemistries to cirrhosis of the liver[49-53]. In one of the earlyreports, Kaukinen *et al*[52] found a reversal in the hepatic dysfunction after initiation of GFD in four patients awaiting liver transplantation and eventually three of them were remitted from liver transplantation list. In a recent prospective study by Wakim-Fleming *et al*[54], of 204 consecutive biopsy proven patients with liver cirrhosis, CeD was reported in 2.5% of the patients. There was improvement in liver function tests with initiation of GFD in these patients.

However, these studies had serious limitations including small sample size (all subjects with less than 100 subjects), selection bias, imprecision and inconsistent results. Given these limitations, the quality of evidence is poor to suggest a true estimate of prevalence of CeD in cryptogenic cirrhosis. In view of the data of improvement in liver functions with GFD, it may be worthwhile to screen the patients with cryptogenic cirrhosis for CeD.

Patients with auto-immune hepatitis

Recently, in a systematic review of eight eligible studies, the prevalence of biopsy-proven CeD was 3.5% (95%CI: 1.6-5.3) amongst 567 individuals with autoimmune hepatitis, which is clearly higher than that in the general populations[55]. However, these studies had serious limitations including small sample size, selection bias, imprecision and inconsistent results. Despite these limitations, we suggest screening for CeD in all patients with autoimmune hepatitis because of the relatively higher pooled prevalence of CeD in these subjects compared to the general population.

Patients with irritable bowel syndrome

Patients with CeD may have minor gastrointestinal infection including diarrhea, abdominal pain, bloating sensation without any definitive manifestations for malabsorption. Such patients are often diagnosed as irritable bowel syndrome in general clinical practice, unless screened for CeD. In a study by Irvine *et al*[56] including 22 studies with 6991 patients with IBS, the reported pooled prevalence of CeD was 3.3% (95%CI: 2.3-4.5) in them.

The pooled prevalence of CeD in patients with IBS varies significantly with the IBS subtype and their geographical location. The prevalence of CeD is higher in patients with diarrhea-predominant IBS (pooled prevalence 5.4%, 95%CI: 3.3-7.8) compared to those with constipation-predominant IBS [1.8% (95%CI: 0.9-3.0)] and mixed form of IBS [3.1% (95%CI: 1.7-5.1)].

Interestingly in the above meta-analysis, all but one study was from secondary or tertiary care referral centers. Furthermore, 20 of the 22 studies were from Europe and Asia with pooled prevalence of CeD in patients with IBS in them was 3.9% (95%CI: 2.1-6.3) and 3.7% (95%CI: 2.2-5.6), respectively. The only study from North America, which also evaluated celiac serology positive individuals with IBS further with duodenal biopsies, did not find an increased prevalence of CeD in patients with IBS. A recent study from Iraq found a prevalence of 5% among 100 patients with IBS[57].

Thus, the utility to screening for CeD in individuals with IBS in primary care settings or the general population remains unclear. Based on available evidence, it may be justifiable to screen patients with diarrhea predominant-IBS and mixed IBS presenting to secondary or tertiary care centers for CeD in Europe and Asia.

Patients with osteoporosis

Patients with CeD are at an increased risk for developing varying degrees of osteopenia and osteoporosis. Patients with untreated CeD have low bone mineral density agnostic to the clinical presentation[58,59]. The reported pooled prevalence of osteoporosis and osteopenia is 14.4% (95%CI: 9-20.5) and 39.6% (95%CI: 31.1-48.8), respectively in 563 pre-menopausal women and men with CeD[60]. Along with osteoporosis, patients with CeD are also at a higher risk of developing bone fractures. A comparative meta-analysis of 20995 patients with CeD and 97777 controls from eight studies published

between 2000 and 2007, found that patients with CeD have a 43% higher risk for developing non-traumatic fracture compared with controls[61]. Also a recent study found that patients with newly diagnosed CeD have low bone marrow density and this improves after initiation of GFD[62].

Laszkowska *et al*[63] performed a systematic review and meta-analysis to estimate the prevalence of CeD in patients with osteoporosis. They pooled data on 3188 patients with osteoporosis from eight studies and reported a weighted pooled prevalence of CeD to be 1.6% (95%CI: 1.1-2.0). The authors observed a positive correlation between underlying prevalence of CeD in the general population and the prevalence of CeD in osteoporosis suggesting the prevalence of CeD in patients with osteoporosis is higher in the areas with higher prevalence of CeD in the general population. Therefore, the prevalence of CeD does not appear to be significantly higher in patients presenting with osteoporosis than that in the general population. Given these findings, while all individuals with new diagnosis of osteoporosis may not need screening for CeD, however patients with osteoporosis having additional symptoms of CeD such as iron deficiency anemia, chronic diarrhea should be screened for CeD.

POSSIBLE CONDITIONS FOR SCREENING FOR CED

Patients with dyspepsia

In a systematic review and meta-analysis, we pooled the data from 19 studies involving 9711 patients with dyspepsia in whom initial screening for CeD was performed either by using celiac serological test (anti-tTG ab or AEA) followed by duodenal mucosal biopsy in seropositive patients or the duodenal mucosal biopsy alone in all eligible patients[64]. The pooled prevalence of CeD has been found to be 1.4% (95%CI: 0.9-1.8) in patients with dyspepsia. Another meta-analysis including ten studies also reported the prevalence of CeD to be 1% in patients with dyspepsia[65]. As the prevalence of CeD in patients with dyspepsia is almost like that in the general population, patients with dyspepsia may not be a higher risk of having CeD. It is, however, still unclear if patients with refractory dyspeptic symptoms are at higher risk of having CeD.

Women with infertility

The patients with CeD can delayed menarche, early menopause, recurrent abortions, infertility, intrauterine growth retardation, and low birth weight (preterm and small for gestational age babies)[66,67]. Additionally, reports have suggested that women with infertility have conceived after initiation of GFD with a diagnosis of CeD[68,69]. Furthermore, there are multiple studies reporting the prevalence of CeD in women with infertility in women who had been investigated for the causes of infertility earlier (unexplained or idiopathic infertility) and those women with infertility who were never investigated for infertility (all cause infertility).

Women with unexplained or idiopathic infertility

Based on case-control studies, two previous meta-analyses have reported that women with unexplained infertility have 5-6 times increased odds of having CeD compared to the general population[70,71]. However, a recent meta-analysis did not find an increased prevalence of CeD in women with unexplained infertility[72]. They reported a pooled prevalence of 0.6% for biopsy-proven CeD in women with unexplained infertility which is very close to the prevalence of CeD in the general population. Of note, a common limitation of all three meta-analyses is the small sample size of primary studies. Based on the current evidence, it is not clear if all women with unexplained infertility should be screened for CeD or not and more research is needed in this area.

Women with "all-cause infertility"

In a systematic review and meta-analysis, Glimberg *et al*[72] pooled the data from 11 eligible studies including 1617 women with "all-cause" infertility and found a prevalence of 0.7% (95%CI: 0.2-1.2) for biopsy-proven CeD. Based on abovementioned data, screening women with all-cause infertility for CeD, may not be justified. However, as above, more studies are needed to further explore the prevalence of CeD in women with infertility.

Patients with idiopathic cardiomyopathy

There are only a few studies which have systematically explored the prevalence of CeD in patients with idiopathic cardiomyopathy[73-77]. The prevalence of CeD in these studies have ranged from 0% to 5.7%. Most of these studies have limitations including a high risk of bias, small sample size and heterogenous patient population included in these studies. Given these serious limitations in the quality of evidence, the present level of evidence does not support screening of patients with idiopathic cardiomyopathy for CeD. Future studies with better study design, larger sample size and various geographic regions should be undertaken for estimation of risk of CeD in patients with cardiomyopathy.

Patients with autoimmune thyroid diseases

In a recent systematic review and meta-analysis, Roy *et al*[78] estimated the pooled prevalence of CeD to be 1.6% (1.3%-1.9%) among 6024 patients with autoimmune thyroid diseases from 15 studies. The review has included even those studies where patients having villous abnormalities of modified marsh grade 1 and 2 have been included as CeD. When the analysis was restricted to those with villous abnormalities of modified Marsh 3, a pooled prevalence of CeD declined to 1.4% (95%CI: 1-1.8) in them. The prevalence of CeD is lower in patients with hypothyroidism (1.4%, 95%CI: 1-1.9) than patietns with hyperthyroidism (2.6%, 95%CI: 0.7-4.4). The available data do not support that routine screening for CeD will likely not be of benefit for majority of patients with autoimmune thyroid diseases. However, larger studies with rigorous methodology are needed in this area.

Patients with idiopathic epilepsy

Several studies have evaluated the prevalence of CeD in patients with idiopathic epilepsy[79-81]. In a systematic review, a pooled prevalence of CeD in patients with idiopathic epilepsy is 2.1% (95%CI: 1.6-2.6, n = 3389) has been reported[80]. The quality of the studies included in this review have major limitations including high overall risk of bias (which decreases our confidence in the estimate), inconsistency (several studies showing no increased risk while others showing increased risk), and imprecision. Based on the presently available data, screening of patient with idiopathic epilepsy for CeD cannot be recommended. There is a need for multicentric studies including larger sample size for better estimation of risk of CeD in patients with idiopathic epilepsy.

Patients with idiopathic cerebellar ataxia

The neurological manifestations of CeD and gluten-related disorders are broad, conditions like ataxia and peripheral neuropathy are well recognized, others such as migraine, epilepsy, dementia, cognitive impairment and depression have also been reported[82-85]. Patients with idiopathic sporadic ataxia and a positive anti-gliadin antibodies AGA) (either IgG or IgA or both) with or without presence of enteropathy are diagnosed as gluten ataxia[83].

Gluten ataxia commonly presents as a sporadic ataxia and most patients do not have associated enteropathy. A systematic review and meta-analysis have found higher odds of anti-gliadin antibodies positive in patients with idiopathic cerebellar ataxia (OR 4.2, 95%CI: 3.1-5.9) as compared to controls [86]. The odds of a positive AGA have not been found to be higher in patients with hereditary ataxia (OR 1.41, 95%CI: 0.82-2.44). Most of the studies included in the review are cross-sectional, and the results show significant imprecision or inconsistency. Considering that treatment response in gluten ataxia would depend on the duration of the ataxia and that GFD may positively impact the ataxia, patients with idiopathic or undiagnosed ataxia should be screened for gluten ataxia using IgG and IgA anti-gliadin antibody[87,88].

A very few studies have evaluated presence of CeD in patients in patients presenting with ataxia. In a study by Hadjivassiliou *et al*[89], reported that 24% patients with gluten sensitivity ataxia had CeD. While Pellecchia *et al*[90] found all 3 patients with a positive IgG anti-gliadin Ab to behave CeD. Bushara *et al*[91] biopsied seven of the nine patients with gluten sensitivity ataxia and none were diagnosed to have CeD. Small number of patients, high risk of bias and heterogenous results of these studies limit drawing of a robust conclusion. Therefore, based on the available data, no definitive recommendation can be made to screen patients with sporadic and idiopathic ataxia for CeD.

Patients with dental enamel defects

Only 2 studies have examined the occurrence of CeD in patients with dental enamel defects[92,93] and in them the prevalence of CeD ranged between 7.7%-17.8%. In one of these studies, one year of GFD resulted in significantly higher reversal of enamel changes in CeD patients compared to those without CeD (48% *vs* 3.4% patients, $P < 0.001$), suggestive of a causal association[92] Despite the relatively higher prevalence estimate of CeD seen in these studies, there is likelihood of some publication bias and these studies had very small sample size.

In two recent case-control studies, patients with CeD had higher dental enamel defects and other oral manifestations like aphthous ulcers were much higher compared to controls[94,95]. For these reasons, large-scale community-based studies across different socio-cultural and geographical populations need to be undertaken to ensure accounting for confounding factors that influence oral health as well as generalizability of the results. Until such time, screening of adults or children with dental enamel defects for CeD is not clear.

We have summarized the reported prevalence of CeD in the various clinical conditions based on the organ systems in Figure 1 and based on the indication in Table 1.

HOW TO SCREEN FOR CED?

While there is significant heterogeneity among clinicians in selecting the medical conditions where they

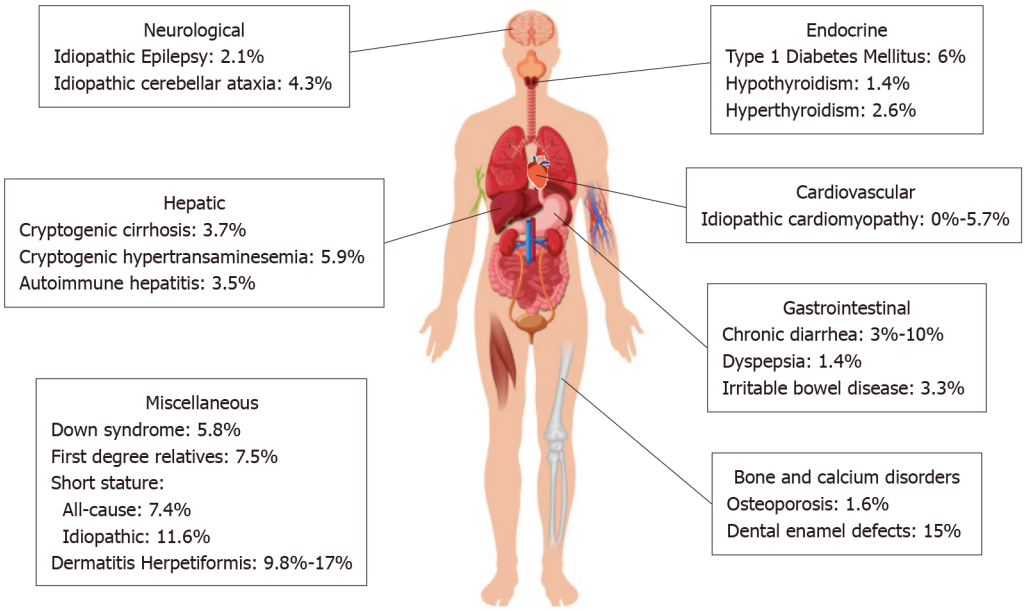
Table 1 The pooled prevalence of celiac disease in various conditions

Condition	Pooled prevalence (%)	95%CI
Definite indications		
Chronic diarrhea[18][a]	3-10	NA
Iron deficiency anemia[14]	3.2	2.6-3.9
Short stature[32]		
All-cause	7.4	4.7-10.6
Idiopathic	11.6	4.1-22.2
Type 1 diabetes[33]	6	5-6.9
Pediatric age group	6.2	6.1-6.3
Adults	2.7	2.1-2.3
First-degree relatives[37]	7.5	6.3-8.8
Dermatitis herpetiformis[45,46][a]	9.8-17	NA
Down syndrome[47]	5.8	4.7-7.2
Probable indications		
Cryptogenic hypertransaminesemia[48]	5.9	3.1-9.34
Autoimmune hepatitis[56]	3.5	1.6-5.3
Irritable bowel syndrome[57]	3.3	2.3-4.5
Diarrhea predominant IBS	5.4	3.3-7.8
Constipation predominant IBS	1.8	0.9-3.0
Mixed-IBS	3.1	1.7-5.1
Osteoporosis[64]	1.6	1.1-2.0
Possible indications		
Dyspepsia[65]	1.4	0.9-1.8
Women with infertility[73]		
All-cause infertility	0.7	0.2-1.2
Idiopathic infertility	0.6	0.0-1.6
Idiopathic cardiomyopathy[74-78][a]	0-5.7	
Autoimmune thyroid disease[79]	1.6	1.3-1.9
Hypothyroidism	1.4	1-1.9
Hyperthyroidism	2.6	0.7-4.4
Idiopathic epilepsy[81]	2.1	1.6-2.6
Idiopathic cerebellar ataxia[87]	4.3	3.1-5.9
Dental enamel defects[93,94]	15	11-21

[a]Expressed as a range.
NA: Not available.

screen patients for CeD; there also exists significant variation in selecting the screening tool for CeD. Currently, celiac specific serological tests are the first-line investigations for screening for CeD. Duodenal biopsies showing villous atrophy, crypt hyperplasia and increase in intra-epithelial lymphocytes on a gluten-containing diet continues to be 'gold standard' for patients with CeD. Given the invasive nature of upper GI endoscopy, limited availability in resource limited countries and associated cost, this 'gold-standard' can however not be applied to all patients who need to be screened for CeD.

The specific celiac serological tests include IgA anti-tTG Ab, IgA AEA, and IgG anti-DGP Ab. While IgA/IgG AGA had been used screening for CeD in the past, however, given their poor specificity and



DOI: 10.3748/wjg.v28.i32.4493 **Copyright** ©The Author(s) 2022.

Figure 1 Summary of the prevalence of celiac disease in various associated conditions based on the various systems. The reported prevalence per the present literature, the studies may be limited by the number and quality of studies available.

sensitivity they are no longer recommended to be used for screening for CeD. In the section below, we briefly discuss the utility of three commonly used celiac-specific serological tests for screening for CeD.

IgA anti-tTG Ab

Given its widespread availability, ease of performance and lower costs compared to other celiac specific serological tests, IgA anti-tTG Ab is the most used serological test for screening for CeD. Recent systematic review has shown that pooled sensitivity and specificity of anti-tTG Ab for CeD are 92.8% (95%CI: 90.3-94.8) and 97.9% (95%CI: 96.4-98.8), respectively. IgA anti-tTG Ab testing should be combined with total serum IgA levels to rule out IgA deficiency which is 10-15 times more common in patients with CeD compared to general population[96]. In patients with IgA deficiency, duodenal biopsies or further serologic testing such as IgG- based anti-deamidated gliadin peptide antibodies (anti-DGP Ab) should be pursued.

Despite their widespread use and high sensitivity, these anti-tTG Ab assays have high inter-assay variability in their diagnostic performance[97,98]. Although anti-tTG Ab assays are the first-line investigation to screen for CeD, healthcare providers should realize that false-negative rate of a single IgA anti-tTG Ab assay can be over 20% suggesting a single negative IgA anti-tTG Ab assay cannot be relied upon as a sole test to rule out CeD especially if clinical suspicion for CeD is high[97]. In these cases, a negative IgA anti-tTG Ab assay must be followed with duodenal biopsies.

Moreover, the issue of diagnostic performance of these assays is further complicated by the fact that there is significant intra-assay variation in the performance of IgA anti-tTG Ab assays in racially and geographically distinct population[98]. Majority of the studies of diagnostic performance of IgA anti-tTG Ab assays (including the manufacturer provided validation studies) are performed in Caucasian studies and unfortunately, these results cannot be extrapolated to other ethnic populations. However, sensitivity of these assays can be improved without significantly compromising the specificity if receiver operator curve-based cut-offs can be developed for each population. Thus, multi-institutional collaborative workshops at national and international levels using coded and blinded standardized sera from well-defined patients with CeD (with varying levels of titers) and healthy controls are necessary to identify and validate population-specific cut-off values as well as the best performing IgA anti-tTG Ab assays for each population. Till then, diagnostic performance of commonly available anti-tTG Ab assays should be studied at each center performing anti-tTG Ab testing.

Finally, recent guidelines now allow for a diagnosis of CeD to be established without duodenal biopsy in a subset of patients with CeD; on the basis of high levels of anti-tTG Ab [× 10 fold upper limit of normal (ULN)] and positive AEA in a second sample[99]. However, these guidelines are often not interpreted correctly and many healthcare providers interpret low level titers as diagnostic of CeD. Even with anti-tTG Ab titers as high as 10-fold ULN, a confirmatory AEA testing on a second sample might not be obtained given either due to inappropriate interpretation of the guidelines or the lack of availability of AEA testing. This can lead to 'overdiagnosis' of CeD as anti-tTG Ab at low titers have poor positive predictive value for CeD. Therefore, there is urgent need for widespread dissemination of diagnostic algorithms and guidelines among primary care physicians, gastroenterologists, and non-

Table 2 The sensitivity and specificity of the screening tests for celiac disease

Test	Sensitivity	Specificity
Anti-tissue transglutaminase antibody[97]	92.8% (95%CI: 90.3-94.8)	97.9% (95%CI: 96.4- 98.8)
Anti-endomysial antibody[97]	73% (95%CI: 61-83)	99.0% (95%CI 98.0-99.0)
Deamidated gliadin peptide antibodies[97]	87.8% (95%CI: 85.6-89.9)	94.1% (95%CI: 92.5-95.5)
Point-of care tests (107)		
Anti-anti-tissue transglutaminase antibody + Anti-gliadin antibody	94.0% (95%CI: 89.9-96.5)	94.4% (95%CI: 90.9-96.5)
IgA anti-tissue transglutaminase antibody	90.5% (95%CI: 82.3-95.1)	94.8% (95%CI: 92.5-96.4)

gastroenterology specialists.

AEA

AEA is an indirect immunofluorescence-based testing requiring rhesus monkey esophagus or human umbilical cord as substrates. Therefore, it can only be performed in specialized laboratories and is much more labor intensive compared to ELISA based assays. Moreover, the results are based on subjective interpretation of the results. Based on a recent systematic review, the pooled sensitivity and specificity of AEA for the diagnosis of AEA were 73.0% (95%CI: 61.0-83.0) and 99.0% (95%CI: 98.0-99.0), respectively[96]. Given the limitations of the testing described above, AEA is not an ideal screening test for CeD outside of referral centers. Although a positive AEA testing is very highly suggestive of CeD (given specificity approaching 100%), a negative AEA should not be relied upon to rule out CeD.

IgG anti-DGP Ab

IgG anti-DGP Ab are the latest serologic assays for CeD and have been shown to have pooled sensitivity of 87.8% (95%CI: 85.6-89.9) and pooled specificity of 94.1% (95%CI: 92.5-95.5)[96]. Although pooled sensitivity of IgG anti-DGP Ab assays is high, it is still lower than pooled sensitivity of IgA anti-tTG Ab assay. Furthermore, several studies have shown that isolated IgG anti-DGP Ab in patients with normal serum IgA levels do not increase the yield of the diagnosis of CeD. Therefore, currently IgG anti-DGP Ab cannot be used to replace IgA anti-tTG Ab as the first line strategy to screen for CeD. Its role in CeD diagnosis is as a complementary assay to be used in patients with IgA deficiency (where IgA anti-tTG Ab assays cannot be relied upon).

Point of care tests

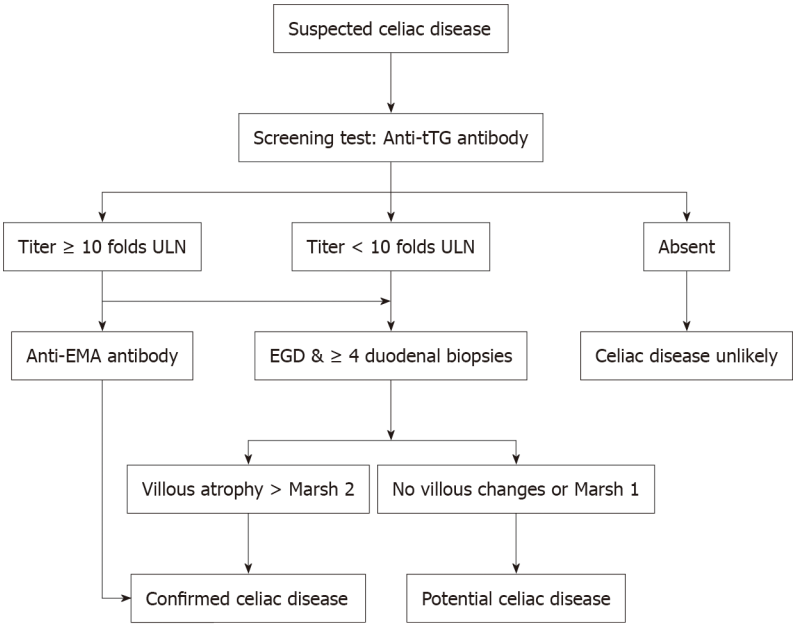
Recently, point of care tests (POCTs) for CeD are commercially available in Europe. Studies have reported significant variability in their sensitivity (70% to 100%) and specificity (85% to 100%). The pooled sensitivity and specificity of all POCTs (based on anti-tTG Ab or anti-DGP Ab or anti-tTG Ab + Anti-gliadin antibodies) for diagnosing CeD has been reported to be 94.0% (95%CI: 89.9-96.5) and 94.4% (95%CI: 90.9-96.5), respectively[100]. The pooled positive and negative likelihood ratios for POCTs are 16.7 and 0.06, respectively. The pooled sensitivity and specificity for IgA anti-tTGAb based POCTs are 90.5% (95%CI: 82.3-95.1) and 94.8% (95%CI: 92.5-96.4), respectively. However, this pooled sensitivity appears to be lower compared to standard ELISA based IgA anti-tTG Ab assay. Therefore, wherever available anti-tTG Ab should be used as first line screening test. However, POCTs can be an excellent alternative in areas with limited access to laboratory-based testing. All the above tests are summarized in Table 2.

Further testing

Once the screening test is positive in an individual suspected to have CeD, the health-care professional should follow the suggested guidelines by many Gastroenterology professional Societies for further evaluation[15,19]. We have suggested a testing schematic for the various indications for suspected CeD in Figure 2.

CONCLUSION

There is good evidence to suggest screening of patients with chronic diarrhea, iron deficiency anemia, short stature, dermatitis herpetiformis, type 1 diabetes, Down's syndrome, as well as first-degree relatives of CeD. The possible indications for screening of CeD include cryptogenic elevated transaminases, cryptogenic cirrhosis autoimmune hepatitis, IBS, autoimmune thyroid disease, and osteoporosis/osteoporosis. There is need for systematic studies for many conditions such as rheumatological diseases, psoriasis, cardiomyopathy, neurological diseases, and liver diseases for the prevalence



DOI: 10.3748/wjg.v28.i32.4493 **Copyright** ©The Author(s) 2022.

Figure 2 A screening algorithm for patients with suspected celiac disease. EGD: Esophagogastroduodenoscopy; ULN: Upper limit of normal.

of CeD in them. Screening for CeD is a well standardized, simple, and relatively inexpensive process and it provides an opportunity for early detection of CeD in them.

ACKNOWLEDGEMENTS

We acknowledge the support of Department of Biotechnology, Government of India, for creation of Indian Consortium on Celiac Disease and National Celiac Disease Biorepository. We do appreciate the support from Research Section of our institution for facilitating the research on Celiac disease.

FOOTNOTES

Author contributions: Singh P and Makharia GK were involved in review concept and the article structure; Singh P, Singh AD were involved in data collection and writing the first draft of the manuscript; All the authors contributed in reviewing and editing the final draft of the manuscript.

Conflict-of-interest statement: There are no conflicts of interest.

Open-Access: This article is an open-access article that was selected by an in-house editor and fully peer-reviewed by external reviewers. It is distributed in accordance with the Creative Commons Attribution NonCommercial (CC BY-NC 4.0) license, which permits others to distribute, remix, adapt, build upon this work non-commercially, and license their derivative works on different terms, provided the original work is properly cited and the use is non-commercial. See: https://creativecommons.org/Licenses/by-nc/4.0/

Country/Territory of origin: India

ORCID number: Prashant Singh 0000-0002-3796-2372; Achintya Dinesh Singh 0000-0001-9094-1071; Vineet Ahuja 0000-0002-5474-9709; Govind K Makharia 0000-0002-2474-2194.

S-Editor: Zhang H
L-Editor: A
P-Editor: Zhang H

REFERENCES

1 **Singh P**, Arora A, Strand TA, Leffler DA, Catassi C, Green PH, Kelly CP, Ahuja V, Makharia GK. Global Prevalence of

Celiac Disease: Systematic Review and Meta-analysis. *Clin Gastroenterol Hepatol* 2018; **16**: 823-836.e2 [PMID: 29551598 DOI: 10.1016/j.cgh.2017.06.037]
2 **Nardecchia S**, Auricchio R, Discepolo V, Troncone R. Extra-Intestinal Manifestations of Coeliac Disease in Children: Clinical Features and Mechanisms. *Front Pediatr* 2019; **7**: 56 [PMID: 30891436 DOI: 10.3389/fped.2019.00056]
3 **Jericho H**, Guandalini S. Extra-Intestinal Manifestation of Celiac Disease in Children. *Nutrients* 2018; **10** [PMID: 29895731 DOI: 10.3390/nu10060755]
4 **Lindfors K**, Ciacci C, Kurppa K, Lundin KEA, Makharia GK, Mearin ML, Murray JA, Verdu EF, Kaukinen K. Coeliac disease. *Nat Rev Dis Primers* 2019; **5**: 3 [PMID: 30631077 DOI: 10.1038/s41572-018-0054-z]
5 **Al-Bawardy B**, Codipilly DC, Rubio-Tapia A, Bruining DH, Hansel SL, Murray JA. Celiac disease: a clinical review. *Abdom Radiol (NY)* 2017; **42**: 351-360 [PMID: 28078381 DOI: 10.1007/s00261-016-1034-y]
6 **Lebwohl B**, Sanders DS, Green PHR. Coeliac disease. *Lancet* 2018; **391**: 70-81 [PMID: 28760445 DOI: 10.1016/S0140-6736(17)31796-8]
7 **Ludvigsson JF**, Leffler DA, Bai JC, Biagi F, Fasano A, Green PH, Hadjivassiliou M, Kaukinen K, Kelly CP, Leonard JN, Lundin KE, Murray JA, Sanders DS, Walker MM, Zingone F, Ciacci C. The Oslo definitions for coeliac disease and related terms. *Gut* 2013; **62**: 43-52 [PMID: 22345659 DOI: 10.1136/gutjnl-2011-301346]
8 **Lundin KE**, Wijmenga C. Coeliac disease and autoimmune disease-genetic overlap and screening. *Nat Rev Gastroenterol Hepatol* 2015; **12**: 507-515 [PMID: 26303674 DOI: 10.1038/nrgastro.2015.136]
9 **Medical Advisory Secretariat**. Clinical utility of serologic testing for celiac disease in asymptomatic patients: an evidence-based analysis. *Ont Health Technol Assess Ser* 2011; **11**: 1-63 [PMID: 23074415]
10 **Choung RS**, Larson SA, Khaleghi S, Rubio-Tapia A, Ovsyannikova IG, King KS, Larson JJ, Lahr BD, Poland GA, Camilleri MJ, Murray JA. Prevalence and Morbidity of Undiagnosed Celiac Disease From a Community-Based Study. *Gastroenterology* 2017; **152**: 830-839.e5 [PMID: 27916669 DOI: 10.1053/j.gastro.2016.11.043]
11 **Riznik P**, De Leo L, Dolinsek J, Gyimesi J, Klemenak M, Koletzko B, Koletzko S, Korponay-Szabó IR, Krencnik T, Not T, Palcevski G, Sblattero D, Vogrincic M, Werkstetter KJ. Diagnostic Delays in Children With Coeliac Disease in the Central European Region. *J Pediatr Gastroenterol Nutr* 2019; **69**: 443-448 [PMID: 31219933 DOI: 10.1097/MPG.0000000000002424]
12 **Catassi C**, Gatti S, Fasano A. The new epidemiology of celiac disease. *J Pediatr Gastroenterol Nutr* 2014; **59** Suppl 1: S7-S9 [PMID: 24979197 DOI: 10.1097/01.mpg.0000450393.23156.59]
13 **Lebwohl B**, Green PHR, Söderling J, Roelstraete B, Ludvigsson JF. Association Between Celiac Disease and Mortality Risk in a Swedish Population. *JAMA* 2020; **323**: 1277-1285 [PMID: 32259229 DOI: 10.1001/jama.2020.1943]
14 **Mahadev S**, Laszkowska M, Sundström J, Björkholm M, Lebwohl B, Green PHR, Ludvigsson JF. Prevalence of Celiac Disease in Patients With Iron Deficiency Anemia-A Systematic Review With Meta-analysis. *Gastroenterology* 2018; **155**: 374-382.e1 [PMID: 29689265 DOI: 10.1053/j.gastro.2018.04.016]
15 **Rubio-Tapia A**, Hill ID, Kelly CP, Calderwood AH, Murray JA; American College of Gastroenterology. ACG clinical guidelines: diagnosis and management of celiac disease. *Am J Gastroenterol* 2013; **108**: 656-76; quiz 677 [PMID: 23609613 DOI: 10.1038/ajg.2013.79]
16 **Al-Toma A**, Volta U, Auricchio R, Castillejo G, Sanders DS, Cellier C, Mulder CJ, Lundin KEA. European Society for the Study of Coeliac Disease (ESsCD) guideline for coeliac disease and other gluten-related disorders. *United European Gastroenterol J* 2019; **7**: 583-613 [PMID: 31210940 DOI: 10.1177/2050640619844125]
17 **Arasaradnam RP**, Brown S, Forbes A, Fox MR, Hungin P, Kelman L, Major G, O'Connor M, Sanders DS, Sinha R, Smith SC, Thomas P, Walters JRF. Guidelines for the investigation of chronic diarrhoea in adults: British Society of Gastroenterology, 3rd edition. *Gut* 2018; **67**: 1380-1399 [PMID: 29653941 DOI: 10.1136/gutjnl-2017-315909]
18 **Panezai MS**, Ullah A, Ballur K, Gilstrap L, Khan J, Tareen B, Kakar M, Rasheed A, Waheed A, Ghleilib I, White J, Cason FD. Frequency of Celiac Disease in Patients With Chronic Diarrhea. *Cureus* 2021; **13**: e20495 [PMID: 35047307 DOI: 10.7759/cureus.20495]
19 **Husby S**, Murray JA, Katzka DA. AGA Clinical Practice Update on Diagnosis and Monitoring of Celiac Disease-Changing Utility of Serology and Histologic Measures: Expert Review. *Gastroenterology* 2019; **156**: 885-889 [PMID: 30578783 DOI: 10.1053/j.gastro.2018.12.010]
20 **Harper JW**, Holleran SF, Ramakrishnan R, Bhagat G, Green PH. Anemia in celiac disease is multifactorial in etiology. *Am J Hematol* 2007; **82**: 996-1000 [PMID: 17636474 DOI: 10.1002/ajh.20996]
21 **Halfdanarson TR**, Litzow MR, Murray JA. Hematologic manifestations of celiac disease. *Blood* 2007; **109**: 412-421 [PMID: 16973955 DOI: 10.1182/blood-2006-07-031104]
22 **Haapalahti M**, Kulmala P, Karttunen TJ, Paajanen L, Laurila K, Mäki M, Mykkänen H, Kokkonen J. Nutritional status in adolescents and young adults with screen-detected celiac disease. *J Pediatr Gastroenterol Nutr* 2005; **40**: 566-570 [PMID: 15861017 DOI: 10.1097/01.mpg.0000154658.16618.f9]
23 **Howard MR**, Turnbull AJ, Morley P, Hollier P, Webb R, Clarke A. A prospective study of the prevalence of undiagnosed coeliac disease in laboratory defined iron and folate deficiency. *J Clin Pathol* 2002; **55**: 754-757 [PMID: 12354801 DOI: 10.1136/jcp.55.10.754]
24 **Singh P**, Arora S, Makharia GK. Presence of anemia in patients with celiac disease suggests more severe disease. *Indian J Gastroenterol* 2014; **33**: 161-164 [PMID: 24243078 DOI: 10.1007/s12664-013-0423-1]
25 **Dahele A**, Ghosh S. Vitamin B12 deficiency in untreated celiac disease. *Am J Gastroenterol* 2001; **96**: 745-750 [PMID: 11280545 DOI: 10.1111/j.1572-0241.2001.03616.x]
26 **Bodé S**, Gudmand-Høyer E. Symptoms and haematologic features in consecutive adult coeliac patients. *Scand J Gastroenterol* 1996; **31**: 54-60 [PMID: 8927941 DOI: 10.3109/00365529609031627]
27 **Jansson-Knodell CL**, Rubio-Tapia A. Case Finding for the Pale Celiac Patient: New Iron Deficiency Anemia Guidelines Missing Many Anemic Celiacs? *Gastroenterology* 2021; **160**: 2617-2618 [PMID: 33387513 DOI: 10.1053/j.gastro.2020.10.063]
28 **Kassebaum NJ**, Jasrasaria R, Naghavi M, Wulf SK, Johns N, Lozano R, Regan M, Weatherall D, Chou DP, Eisele TP,

Flaxman SR, Pullan RL, Brooker SJ, Murray CJ. A systematic analysis of global anemia burden from 1990 to 2010. *Blood* 2014; **123**: 615-624 [PMID: 24297872 DOI: 10.1182/blood-2013-06-508325]

29 **Boersma B**, Houwen RH, Blum WF, van Doorn J, Wit JM. Catch-up growth and endocrine changes in childhood celiac disease. Endocrine changes during catch-up growth. *Horm Res* 2002; **58** Suppl 1: 57-65 [PMID: 12373016 DOI: 10.1159/000064771]

30 **Luciano A**, Bolognani M, Di Falco A, Trabucchi C, Bonetti P, Castellarin A. [Catch-up growth and final height in celiac disease]. *Pediatr Med Chir* 2002; **24**: 9-12 [PMID: 11938689]

31 **Singh AD**, Singh P, Farooqui N, Strand T, Ahuja V, Makharia GK. Prevalence of celiac disease in patients with short stature: A systematic review and meta-analysis. *J Gastroenterol Hepatol* 2021; **36**: 44-54 [PMID: 32621396 DOI: 10.1111/jgh.15167]

32 **Elfström P**, Sundström J, Ludvigsson JF. Systematic review with meta-analysis: associations between coeliac disease and type 1 diabetes. *Aliment Pharmacol Ther* 2014; **40**: 1123-1132 [PMID: 25270960 DOI: 10.1111/apt.12973]

33 **Rubio-Tapia A**, Van Dyke CT, Lahr BD, Zinsmeister AR, El-Youssef M, Moore SB, Bowman M, Burgart LJ, Melton LJ 3rd, Murray JA. Predictors of family risk for celiac disease: a population-based study. *Clin Gastroenterol Hepatol* 2008; **6**: 983-987 [PMID: 18585974 DOI: 10.1016/j.cgh.2008.04.008]

34 **Bonamico M**, Ferri M, Mariani P, Nenna R, Thanasi E, Luparia RP, Picarelli A, Magliocca FM, Mora B, Bardella MT, Verrienti A, Fiore B, Uccini S, Megiorni F, Mazzilli MC, Tiberti C. Serologic and genetic markers of celiac disease: a sequential study in the screening of first degree relatives. *J Pediatr Gastroenterol Nutr* 2006; **42**: 150-154 [PMID: 16456406 DOI: 10.1097/01.mpg.0000189337.08139.83]

35 **Högberg L**, Fälth-Magnusson K, Grodzinsky E, Stenhammar L. Familial prevalence of coeliac disease: a twenty-year follow-up study. *Scand J Gastroenterol* 2003; **38**: 61-65 [PMID: 12608466 DOI: 10.1080/00365520310000456]

36 **Singh P**, Arora S, Lal S, Strand TA, Makharia GK. Risk of Celiac Disease in the First- and Second-Degree Relatives of Patients With Celiac Disease: A Systematic Review and Meta-Analysis. *Am J Gastroenterol* 2015; **110**: 1539-1548 [PMID: 26416192 DOI: 10.1038/ajg.2015.296]

37 **Kurppa K**, Salminiemi J, Ukkola A, Saavalainen P, Löytynoja K, Laurila K, Collin P, Mäki M, Kaukinen K. Utility of the new ESPGHAN criteria for the diagnosis of celiac disease in at-risk groups. *J Pediatr Gastroenterol Nutr* 2012; **54**: 387-391 [PMID: 22094901 DOI: 10.1097/MPG.0b013e3182407c6b]

38 **Kotze LM**, Brambila Rodrigues AP, Kotze LR, Nisihara RM. A Brazilian experience of the self transglutaminase-based test for celiac disease case finding and diet monitoring. *World J Gastroenterol* 2009; **15**: 4423-4428 [PMID: 19764094 DOI: 10.3748/wjg.15.4423]

39 **Weinstein WM**, Brow JR, Parker F, Rubin CE. The small intestinal mucosa in dermatitis herpetiformis. II. Relationship of the small intestinal lesion to gluten. *Gastroenterology* 1971; **60**: 362-369 [PMID: 5554078]

40 **Brow JR**, Parker F, Weinstein WM, Rubin CE. The small intestinal mucosa in dermatitis herpetiformis. I. Severity and distribution of the small intestinal lesion and associated malabsorption. *Gastroenterology* 1971; **60**: 355-361 [PMID: 5554077]

41 **Reunala T**, Hervonen K, Salmi T. Dermatitis Herpetiformis: An Update on Diagnosis and Management. *Am J Clin Dermatol* 2021; **22**: 329-338 [PMID: 33432477 DOI: 10.1007/s40257-020-00584-2]

42 **Persechino F**, Galli G, Persechino S, Valitutti F, Zenzeri L, Mauro A, Corleto VD, Parisi P, Ziparo C, Evangelisti M, Quatrale G, Di Nardo G. Skin Manifestations and Coeliac Disease in Paediatric Population. *Nutrients* 2021; **13** [PMID: 34684612 DOI: 10.3390/nu13103611]

43 **Mansikka E**, Hervonen K, Kaukinen K, Collin P, Huhtala H, Reunala T, Salmi T. Prognosis of Dermatitis Herpetiformis Patients with and without Villous Atrophy at Diagnosis. *Nutrients* 2018; **10** [PMID: 29783727 DOI: 10.3390/nu10050641]

44 **Green PHR**, Stavropoulos SN, Panagi SG, Goldstein SL, Mcmahon DJ, Absan H, Neugut AI. Characteristics of adult celiac disease in the USA: results of a national survey. *Am J Gastroenterol* 2001; **96**: 126-131 [PMID: 11197241 DOI: 10.1111/j.1572-0241.2001.03462.x]

45 **Collin P**, Huhtala H, Virta L, Kekkonen L, Reunala T. Diagnosis of celiac disease in clinical practice: physician's alertness to the condition essential. *J Clin Gastroenterol* 2007; **41**: 152-156 [PMID: 17245213 DOI: 10.1097/01.mcg.0000212618.12455.a8]

46 **Du Y**, Shan LF, Cao ZZ, Feng JC, Cheng Y. Prevalence of celiac disease in patients with Down syndrome: a meta-analysis. *Oncotarget* 2018; **9**: 5387-5396 [PMID: 29435186 DOI: 10.18632/oncotarget.23624]

47 **Sainsbury A**, Sanders DS, Ford AC. Meta-analysis: Coeliac disease and hypertransaminasaemia. *Aliment Pharmacol Ther* 2011; **34**: 33-40 [PMID: 21545472 DOI: 10.1111/j.1365-2036.2011.04685.x]

48 **Castillo NE**, Vanga RR, Theethira TG, Rubio-Tapia A, Murray JA, Villafuerte J, Bonder A, Mukherjee R, Hansen J, Dennis M, Kelly CP, Leffler DA. Prevalence of abnormal liver function tests in celiac disease and the effect of a gluten-free diet in the US population. *Am J Gastroenterol* 2015; **110**: 1216-1222 [PMID: 26150087 DOI: 10.1038/ajg.2015.192]

49 **Singh P**, Agnihotri A, Jindal G, Sharma PK, Sharma M, Das P, Gupta D, Makharia GK. Celiac disease and chronic liver disease: is there a relationship? *Indian J Gastroenterol* 2013; **32**: 404-408 [PMID: 23918040 DOI: 10.1007/s12664-013-0352-z]

50 **Ludvigsson JF**, Elfström P, Broomé U, Ekbom A, Montgomery SM. Celiac disease and risk of liver disease: a general population-based study. *Clin Gastroenterol Hepatol* 2007; **5**: 63-69.e1 [PMID: 17161656 DOI: 10.1016/j.cgh.2006.09.034]

51 **Lindgren S**, Sjöberg K, Eriksson S. Unsuspected coeliac disease in chronic 'cryptogenic' liver disease. *Scand J Gastroenterol* 1994; **29**: 661-664 [PMID: 7939405 DOI: 10.3109/00365529409092489]

52 **Kaukinen K**, Halme L, Collin P, Färkkilä M, Mäki M, Vehmanen P, Partanen J, Höckerstedt K. Celiac disease in patients with severe liver disease: gluten-free diet may reverse hepatic failure. *Gastroenterology* 2002; **122**: 881-888 [PMID: 11910339 DOI: 10.1053/gast.2002.32416]

53 **Ratziu V**, Nourani M, Poynard T. Discussion on celiac disease in patients with severe liver disease: gluten-free diet may reverse hepatic failure. *Gastroenterology* 2002; **123**: 2158-9; author reply 2159 [PMID: 12454882 DOI:

10.1053/gast.2002.37302]
54 **Wakim-Fleming J**, Pagadala MR, McCullough AJ, Lopez R, Bennett AE, Barnes DS, Carey WD. Prevalence of celiac disease in cirrhosis and outcome of cirrhosis on a gluten free diet: a prospective study. *J Hepatol* 2014; **61**: 558-563 [PMID: 24842303 DOI: 10.1016/j.jhep.2014.05.020]
55 **Haggård L**, Glimberg I, Lebwohl B, Sharma R, Verna EC, Green PHR, Ludvigsson JF. High prevalence of celiac disease in autoimmune hepatitis: Systematic review and meta-analysis. *Liver Int* 2021; **41**: 2693-2702 [PMID: 34219350 DOI: 10.1111/liv.15000]
56 **Irvine AJ**, Chey WD, Ford AC. Screening for Celiac Disease in Irritable Bowel Syndrome: An Updated Systematic Review and Meta-analysis. *Am J Gastroenterol* 2017; **112**: 65-76 [PMID: 27753436 DOI: 10.1038/ajg.2016.466]
57 **Al-Abachi KT**. Screening for Celiac Disease in Patients with Irritable Bowel Syndrome Fulfilling Rome III Criteria. J Coloproctology 2022; 42: 20-24 [DOI: 10.1055/s-0041-1736645]
58 **Mazure R**, Vazquez H, Gonzalez D, Mautalen C, Pedreira S, Boerr L, Bai JC. Bone mineral affection in asymptomatic adult patients with celiac disease. *Am J Gastroenterol* 1994; **89**: 2130-2134 [PMID: 7977227]
59 **Kemppainen T**, Kröger H, Janatuinen E, Arnala I, Kosma VM, Pikkarainen P, Julkunen R, Jurvelin J, Alhava E, Uusitupa M. Osteoporosis in adult patients with celiac disease. *Bone* 1999; **24**: 249-255 [PMID: 10071918 DOI: 10.1016/s8756-3282(98)00178-1]
60 **Ganji R**, Moghbeli M, Sadeghi R, Bayat G, Ganji A. Prevalence of osteoporosis and osteopenia in men and premenopausal women with celiac disease: a systematic review. *Nutr J* 2019; **18**: 9 [PMID: 30732599 DOI: 10.1186/s12937-019-0434-6]
61 **Olmos M**, Antelo M, Vazquez H, Smecuol E, Mauriño E, Bai JC. Systematic review and meta-analysis of observational studies on the prevalence of fractures in coeliac disease. *Dig Liver Dis* 2008; **40**: 46-53 [PMID: 18006396 DOI: 10.1016/j.dld.2007.09.006]
62 **Mosca C**, Thorsteinsdottir F, Abrahamsen B, Rumessen JJ, Händel MN. Newly Diagnosed Celiac Disease and Bone Health in Young Adults: A Systematic Literature Review. *Calcif Tissue Int* 2022; **110**: 641-648 [PMID: 34978602 DOI: 10.1007/s00223-021-00938-w]
63 **Laszkowska M**, Mahadev S, Sundström J, Lebwohl B, Green PHR, Michaelsson K, Ludvigsson JF. Systematic review with meta-analysis: the prevalence of coeliac disease in patients with osteoporosis. *Aliment Pharmacol Ther* 2018; **48**: 590-597 [PMID: 29984519 DOI: 10.1111/apt.14911]
64 **Singh AD**, Ellias S, Singh P, Ahuja V, Makharia GK. The Prevalence of the Celiac Disease in Patients with Dyspepsia: A Systematic Review and Meta-Analysis. *Dig Dis Sci* 2021; Epub ahead of print [PMID: 34268659 DOI: 10.1007/s10620-021-07142-8]
65 **Ford AC**, Ching E, Moayyedi P. Meta-analysis: yield of diagnostic tests for coeliac disease in dyspepsia. *Aliment Pharmacol Ther* 2009; **30**: 28-36 [PMID: 19416130 DOI: 10.1111/j.1365-2036.2009.04008.x]
66 **Eliakim R**, Sherer DM. Celiac disease: fertility and pregnancy. *Gynecol Obstet Invest* 2001; **51**: 3-7 [PMID: 11150866 DOI: 10.1159/000052881]
67 **Gasbarrini A**, Torre ES, Trivellini C, De Carolis S, Caruso A, Gasbarrini G. Recurrent spontaneous abortion and intrauterine fetal growth retardation as symptoms of coeliac disease. *Lancet* 2000; **356**: 399-400 [PMID: 10972376 DOI: 10.1016/S0140-6736(00)02535-6]
68 **Bennett SI**, Gupta A. Successful Pregnancy on a Gluten-Free Diet in a Woman with Seven Miscarriages and Nonceliac Gluten Sensitivity. AACE Clin Case Rep 2018; 4: e443-e446 [DOI: 10.4158/ACCR-2018-0095]
69 **Alecsandru D**, López-Palacios N, Castaño M, Aparicio P, García-Velasco JA, Núñez C. Exploring undiagnosed celiac disease in women with recurrent reproductive failure: The gluten-free diet could improve reproductive outcomes. *Am J Reprod Immunol* 2020; **83**: e13209 [PMID: 31709662 DOI: 10.1111/aji.13209]
70 **Singh P**, Arora S, Lal S, Strand TA, Makharia GK. Celiac Disease in Women With Infertility: A Meta-Analysis. *J Clin Gastroenterol* 2016; **50**: 33-39 [PMID: 25564410 DOI: 10.1097/MCG.0000000000000285]
71 **Tersigni C**, Castellani R, de Waure C, Fattorossi A, De Spirito M, Gasbarrini A, Scambia G, Di Simone N. Celiac disease and reproductive disorders: meta-analysis of epidemiologic associations and potential pathogenic mechanisms. *Hum Reprod Update* 2014; **20**: 582-593 [PMID: 24619876 DOI: 10.1093/humupd/dmu007]
72 **Glimberg I**, Haggård L, Lebwohl B, Green PHR, Ludvigsson JF. The prevalence of celiac disease in women with infertility-A systematic review with meta-analysis. *Reprod Med Biol* 2021; **20**: 224-233 [PMID: 33850456 DOI: 10.1002/rmb2.12374]
73 **Curione M**, Barbato M, De Biase L, Viola F, Lo Russo L, Cardi E. Prevalence of coeliac disease in idiopathic dilated cardiomyopathy. *Lancet* 1999; **354**: 222-223 [PMID: 10421311 DOI: 10.1016/s0140-6736(99)01501-9]
74 **De Bem RS**, Da Ro Sa Utiyama SR, Nisihara RM, Fortunato JA, Tondo JA, Carmes ER, Souza RA, Pisani JC, Amarante HM. Celiac disease prevalence in Brazilian dilated cardiomyopathy patients. *Dig Dis Sci* 2006; **51**: 1016-1019 [PMID: 16758314 DOI: 10.1007/s10620-006-9337-4]
75 **Menezes TM**, Motta ME. Celiac disease prevalence in children and adolescents with myocarditis and dilated cardiomiopathy. *J Pediatr (Rio J)* 2012; **88**: 439-442 [PMID: 23093320 DOI: 10.2223/JPED.2219]
76 **Vizzardi E**, Lanzarotto F, Carabellese N, Mora A, Bertolazzi S, Benini F, Nodari S, Dei Cas L, Lanzini A. Lack of association of coeliac disease with idiopathic and ischaemic dilated cardiomyopathies. *Scand J Clin Lab Invest* 2008; **68**: 692-695 [PMID: 18609114 DOI: 10.1080/00365510802085370]
77 **Zahmatkeshan M**, Fallahpoor M, Amoozgar H. Prevalence of celiac disease in children with idiopathic dilated cardiomyopathy. *Iran J Pediatr* 2014; **24**: 587-592 [PMID: 25793066]
78 **Roy A**, Laszkowska M, Sundström J, Lebwohl B, Green PH, Kämpe O, Ludvigsson JF. Prevalence of Celiac Disease in Patients with Autoimmune Thyroid Disease: A Meta-Analysis. *Thyroid* 2016; **26**: 880-890 [PMID: 27256300 DOI: 10.1089/thy.2016.0108]
79 **Işıkay S**, Kocamaz H. Prevalence of celiac disease in children with idiopathic epilepsy in southeast Turkey. *Pediatr Neurol* 2014; **50**: 479-481 [PMID: 24656466 DOI: 10.1016/j.pediatrneurol.2014.01.021]
80 **Julian T**, Hadjivassiliou M, Zis P. Gluten sensitivity and epilepsy: a systematic review. *J Neurol* 2019; **266**: 1557-1565

[PMID: 30167878 DOI: 10.1007/s00415-018-9025-2]
81 **Vieira C**, Jatobá I, Matos M, Diniz-Santos D, Silva LR. Prevalence of celiac disease in children with epilepsy. *Arq Gastroenterol* 2013; **50**: 290-296 [PMID: 24474232 DOI: 10.1590/S0004-28032013000400010]
82 **Bürk K**, Farecki ML, Lamprecht G, Roth G, Decker P, Weller M, Rammensee HG, Oertel W. Neurological symptoms in patients with biopsy proven celiac disease. *Mov Disord* 2009; **24**: 2358-2362 [PMID: 19845007 DOI: 10.1002/mds.22821]
83 **Hadjivassiliou M**, Duker AP, Sanders DS. Gluten-related neurologic dysfunction. *Handb Clin Neurol* 2014; **120**: 607-619 [PMID: 24365341 DOI: 10.1016/B978-0-7020-4087-0.00041-3]
84 **Hadjivassiliou M**, Aeschlimann P, Sanders DS, Mäki M, Kaukinen K, Grünewald RA, Bandmann O, Woodroofe N, Haddock G, Aeschlimann DP. Transglutaminase 6 antibodies in the diagnosis of gluten ataxia. *Neurology* 2013; **80**: 1740-1745 [PMID: 23576621 DOI: 10.1212/WNL.0b013e3182919070]
85 **Fousekis FS**, Beka ET, Mitselos IV, Milionis H, Christodoulou DK. Thromboembolic complications and cardiovascular events associated with celiac disease. *Ir J Med Sci* 2021; **190**: 133-141 [PMID: 32691305 DOI: 10.1007/s11845-020-02315-2]
86 **Lin CY**, Wang MJ, Tse W, Pinotti R, Alaedini A, Green PHR, Kuo SH. Serum antigliadin antibodies in cerebellar ataxias: a systematic review and meta-analysis. *J Neurol Neurosurg Psychiatry* 2018; **89**: 1174-1180 [PMID: 29866704 DOI: 10.1136/jnnp-2018-318215]
87 **Hadjivassiliou M**, Davies-Jones GA, Sanders DS, Grünewald RA. Dietary treatment of gluten ataxia. *J Neurol Neurosurg Psychiatry* 2003; **74**: 1221-1224 [PMID: 12933922 DOI: 10.1136/jnnp.74.9.1221]
88 **Hadjivassiliou M**, Sanders DD, Aeschlimann DP. Gluten-related disorders: gluten ataxia. *Dig Dis* 2015; **33**: 264-268 [PMID: 25925933 DOI: 10.1159/000369509]
89 **Hadjivassiliou M**, Grünewald R, Sharrack B, Sanders D, Lobo A, Williamson C, Woodroofe N, Wood N, Davies-Jones A. Gluten ataxia in perspective: epidemiology, genetic susceptibility and clinical characteristics. *Brain* 2003; **126**: 685-691 [PMID: 12566288 DOI: 10.1093/brain/awg050]
90 **Pellecchia MT**, Scala R, Filla A, De Michele G, Ciacci C, Barone P. Idiopathic cerebellar ataxia associated with celiac disease: lack of distinctive neurological features. *J Neurol Neurosurg Psychiatry* 1999; **66**: 32-35 [PMID: 9886447 DOI: 10.1136/jnnp.66.1.32]
91 **Bushara KO**, Goebel SU, Shill H, Goldfarb LG, Hallett M. Gluten sensitivity in sporadic and hereditary cerebellar ataxia. *Ann Neurol* 2001; **49**: 540-543 [PMID: 11310636]
92 **El-Hodhod MA**, El-Agouza IA, Abdel-Al H, Kabil NS, Bayomi KA. Screening for celiac disease in children with dental enamel defects. *ISRN Pediatr* 2012; **2012**: 763783 [PMID: 22720168 DOI: 10.5402/2012/763783]
93 **Martelossi S**, Zanatta E, Del Santo E, Clarich P, Radovich P, Ventura A. Dental enamel defects and screening for coeliac disease. *Acta Paediatr Suppl* 1996; **412**: 47-48 [PMID: 8783757 DOI: 10.1111/j.1651-2227.1996.tb14249.x]
94 **Alsadat FA**, Alamoudi NM, El-Housseiny AA, Felemban OM, Dardeer FM, Saadah OI. Oral and dental manifestations of celiac disease in children: a case-control study. *BMC Oral Health* 2021; **21**: 669 [PMID: 34965875 DOI: 10.1186/s12903-021-01976-4]
95 **Zoumpoulakis M**, Fotoulaki M, Topitsoglou V, Lazidou P, Zouloumis L, Kotsanos N. Prevalence of Dental Enamel Defects, Aphthous-Like Ulcers and Other Oral Manifestations in Celiac Children and Adolescents: A Comparative Study. *J Clin Pediatr Dent* 2019; **43**: 274-280 [PMID: 31283894 DOI: 10.17796/1053-4625-43.4.9]
96 **Chou R**, Bougatsos C, Blazina I, Mackey K, Grusing S, Selph S. Screening for Celiac Disease: Evidence Report and Systematic Review for the US Preventive Services Task Force. *JAMA* 2017; **317**: 1258-1268 [PMID: 28350935 DOI: 10.1001/jama.2016.10395]
97 **Singh P**, Singh A, Silvester JA, Sachdeva V, Chen X, Xu H, Leffler DA, Ahuja V, Duerksen DR, Kelly CP, Makharia GK. Inter- and Intra-assay Variation in the Diagnostic Performance of Assays for Anti-tissue Transglutaminase in 2 Populations. *Clin Gastroenterol Hepatol* 2020; **18**: 2628-2630 [PMID: 31546060 DOI: 10.1016/j.cgh.2019.09.018]
98 **Naiyer AJ**, Hernandez L, Ciaccio EJ, Papadakis K, Manavalan JS, Bhagat G, Green PH. Comparison of commercially available serologic kits for the detection of celiac disease. *J Clin Gastroenterol* 2009; **43**: 225-232 [PMID: 18724250 DOI: 10.1097/MCG.0b013e31816200e5]
99 **Husby S**, Koletzko S, Korponay-Szabó I, Kurppa K, Mearin ML, Ribes-Koninckx C, Shamir R, Troncone R, Auricchio R, Castillejo G, Christensen R, Dolinsek J, Gillett P, Hróbjartsson A, Koltai T, Maki M, Nielsen SM, Popp A, Størdal K, Werkstetter K, Wessels M. European Society Paediatric Gastroenterology, Hepatology and Nutrition Guidelines for Diagnosing Coeliac Disease 2020. *J Pediatr Gastroenterol Nutr* 2020; **70**: 141-156 [PMID: 31568151 DOI: 10.1097/MPG.0000000000002497]
100 **Singh P**, Arora A, Strand TA, Leffler DA, Mäki M, Kelly CP, Ahuja V, Makharia GK. Diagnostic Accuracy of Point of Care Tests for Diagnosing Celiac Disease: A Systematic Review and Meta-Analysis. *J Clin Gastroenterol* 2019; **53**: 535-542 [PMID: 29912751 DOI: 10.1097/MCG.0000000000001081]

World Journal of Gastroenterology

Submit a Manuscript: https://www.f6publishing.com

World J Gastroenterol 2022 August 28; 28(32): 4508-4515

DOI: 10.3748/wjg.v28.i32.4508

ISSN 1007-9327 (print) ISSN 2219-2840 (online)

MINIREVIEWS

Assessment of physical stress during the perioperative period of endoscopic submucosal dissection

Daisuke Chinda, Tadashi Shimoyama

Specialty type: Gastroenterology and hepatology

Provenance and peer review: Invited article; Externally peer reviewed.

Peer-review model: Single blind

Peer-review report's scientific quality classification

Grade A (Excellent): 0
Grade B (Very good): B, B, B
Grade C (Good): 0
Grade D (Fair): D
Grade E (Poor): 0

P-Reviewer: Feng JB, China; He CY, China; Li XB, China; Linghu EQ, China

Received: January 14, 2022
Peer-review started: January 14, 2022
First decision: April 16, 2022
Revised: April 28, 2022
Accepted: July 31, 2022
Article in press: July 31, 2022
Published online: August 28, 2022

Daisuke Chinda, Tadashi Shimoyama, Department of Gastroenterology, Hirosaki University Graduate School of Medicine, Hirosaki 036-8562, Japan

Daisuke Chinda, Division of Endoscopy, Hirosaki University Hospital, Hirosaki 036-8563, Japan

Tadashi Shimoyama, Department of Internal Medicine, Aomori General Health Examination Center, Aomori 030-0962, Japan

Corresponding author: Tadashi Shimoyama, FACG, MD, PhD, Director, Department of Internal Medicine, Aomori General Health Examination Center, 2-12-19 Tsukuda, Aomori 030-0962, Japan. tsimo@hirosaki-u.ac.jp

Abstract

The advantage of endoscopic submucosal dissection (ESD) is that it is less invasive than surgery. ESD is one of the best treatments for older patients as surgery in this age group of patients is difficult. However, it is unclear how much lower the physical stress of ESD is compared with that of surgery. Thus, objective methods are required to assess physical stress in patients who have undergone ESD. The current review of ESD aimed to summarize the recent advancements in the assessment of physical stress during the perioperative period, focusing on changes in energy metabolism and serum opsonic activity (SOA). Based on metabolic changes, resting energy expenditure (REE) was measured using an indirect calorimeter. The stress factor calculated from the REE and the basal energy expenditure computed using the Harris-Benedict equation can be used to assess physical stress. SOA was assessed using the chemiluminescence method, wherein the use of chemiluminescent probes (*i.e.*, lucigenin and luminol) allowed quantification of reactive oxygen species generated by neutrophils. Using an auto luminescence analyzer, the results were evaluated based on the maximum light emission and area under the emission curve. These quantifiable results revealed the minimal invasiveness of ESD.

Key Words: Physical stress; Endoscopic submucosal dissection; Indirect calorimeter; Resting energy expenditure; Chemiluminescence; Serum opsonic activity

©The Author(s) 2022. Published by Baishideng Publishing Group Inc. All rights reserved.

Core Tip: Concerning the degree of physical invasiveness of patients before and after endoscopic submucosal dissection (ESD), assessment methods based on changes in energy metabolism using an indirect calorimeter and serum opsonic activity (SOA) measured by lucigenin- and luminol-dependent chemiluminescence are useful and easy to measure. During the perioperative period of ESD, the increase in resting energy expenditure and stress factor were lower than those reported for surgery, and SOA changes involved a minor increase in the production of lower-toxicity reactive oxygen species. These assessment methods demonstrated that the physical stress of ESD is less invasive than that of surgery.

Citation: Chinda D, Shimoyama T. Assessment of physical stress during the perioperative period of endoscopic submucosal dissection. *World J Gastroenterol* 2022; 28(32): 4508-4515
URL: https://www.wjgnet.com/1007-9327/full/v28/i32/4508.htm
DOI: https://dx.doi.org/10.3748/wjg.v28.i32.4508

INTRODUCTION

Endoscopic treatment for early-stage cancer is indicated when there is a very low probability of lymph node metastasis and when curative en bloc resection is possible[1-3]. Endoscopic submucosal dissection (ESD) is widely used for early gastrointestinal cancer because it is a safe and effective treatment that can preserve function[4-7]. In addition, ESD has a higher rate of en bloc curative resection than endoscopic mucosal resection[8]. Therefore, ESD enables a more precise histopathological diagnosis. ESD is also performed on early gastrointestinal cancer lesions, where surgery was previously common, and often results in a curative resection[9,10]. The most significant advantage for patients is that the physical stress associated with ESD is less than that associated with surgery. From the above, ESD is one of the best treatment options for older patients who are considered difficult to operate on[11-14]. However, it is unclear how much lower the physical stress of ESD is than that of surgery; thus, objective methods are required to assess the physical stress of patients who have undergone ESD. With the increase in the number of older people, the number of patients undergoing ESD for early intestinal cancer is increasing. With advances in endoscopic diagnosis, intestinal cancer will be detected at an earlier stage, and more patients will be treated with ESD. Therefore, it is desirable to develop a method that can evaluate physical stress, even in older patients who are subjected to ESD.

Moreover, ESD is an endoscopic surgery performed on various gastrointestinal tracts, and it is expected that physical stress will differ depending on the organ involved. There is a difference between gastric and colorectal ESD in terms of both technical difficulty and perioperative management. In our facility, because gastric ESD is performed orally, patients fasted after dinner the night before ESD and underwent ESD with pethidine hydrochloride and midazolam or diazepam. In contrast, colorectal ESD requires bowel cleansing prior to colonoscopy. During fasting for ESD, patients are supplied with a drip transfusion and undergo whole bowel irrigation the previous evening and the day of ESD. As patients may need to change their posture to make the ESD procedure easier, colorectal ESD is performed in the awakened state with the analgesic pethidine hydrochloride. Thus, it can be presumed that physical stress in the perioperative period of gastric ESD differs from that of colorectal ESD. Therefore, an assessment method that can compare the physical stress of ESD procedures for different organs is needed.

The current review aimed to summarize the recent advances in physical stress assessment during the perioperative period of ESD, focusing on the changes in energy metabolism and serum opsonic activity (SOA). Additionally, the physical stresses during the perioperative period of gastric and colorectal ESD in comparison to surgery are discussed.

EARLY INVESTIGATIONS

Serum levels of interleukin (IL)-6, IL-8, tumor necrosis factor-α, and C-reactive protein fluctuate during the perioperative period[15-18]. Myre *et al*[19] reported that high and low doses of remifentanil affect the release of catecholamines (norepinephrine and epinephrine) differently during laparoscopic fundoplication. However, there have been no effective blood tests to assess physical invasiveness to date.

A report on ESD in the early stages of gastric cancer points out that increased salivary amylase activity in patients may indicate intraoperative stress[20]. However, this change is a hyperacute reaction of the endocrine system, and it is not possible to assess the physical invasion of ESD throughout the perioperative period.

ASSESSMENT OF PHYSICAL STRESS BY ENERGY METABOLISM

Surgical invasion alters metabolism, and the increased physical stress causes an increase in the patient's energy requirements[21-23]. The patient is subject to two principal metabolic responses: The responses to starvation and stress[24-26]. In addition, the energy requirements are associated with a degree of physical invasiveness[27].

Therefore, changes in resting energy expenditure (REE) measured using an indirect calorimeter can be used to evaluate physical stress. An indirect calorimeter measures the amount of oxygen consumed and the amount of carbon dioxide produced during metabolism and the energy consumption[21]. On the other hand, basal energy expenditure (BEE) is calculated using the Harris-Benedict equation based on the patient's height and body weight. It reflects the energy requirements of each patient[28]. Previous studies have compared BEE during the surgical perioperative period[29-32], but there are few reports using REE measurements. It is presumed that the measurement of REE is more complicated than that of BEE, and few facilities have the calorimeter required for the measurement. On the other hand, the greatest advantage of this method is acceptability for the patients. Because these methods require only exhalation, the patient can rest on the bed, and the measurement time is approximately 5 min each time.

The stress factor (SF) can be done by measured energy expenditure divided by the predicted energy expenditure using the Harris-Benedict equation and the active factor and assess the perioperative physical stress of ESD, even in older patients. According to Long's method[28], the total energy expenditure is defined as the product of BEE, SF, and the activity factor, and it is theoretically the same as the REE measured at rest. Since the activity factor on the day of ESD is the same as that on postoperative day (POD) 1, the SF on POD 1 can be calculated by setting SF on the day to be 1.0[33,34]. From the above, SF is a marker indicating the degree of hypermetabolic state[33,34]. The values of SFs are recognized as 1.1 for low invasiveness, 1.2 for medium invasiveness, and 1.8 for high invasiveness [28], and these values are used as indicators to determine perioperative energy management.

As shown in Table 1, the changes in the perioperative REE and SFs differed between gastric and colorectal ESD[33,34]. Regarding gastric ESD, the REE and REE/BEE increased significantly from the day of gastric ESD to POD 1. The SF for gastric ESD on POD 1 was calculated as 1.07, setting the SF on the day to 1.0[33]. There was no significant difference in REE on the day of ESD and POD 1 for colorectal ESD. However, REE/BEE was significantly higher on POD 1 than on the day of ESD. The SF for colorectal ESD on POD 1 was calculated as 1.06[34].

Regarding the perioperative REEs in surgery for gastric and colorectal cancer, Fredrix *et al*[26] reported that REE on the 7th and 8th PODs was 1.069% compared to the preoperative value. With respect to the SF on the third day after the surgery, Inoue *et al*[35] reported it was 1.4 for moderate invasive surgery such as subtotal gastrectomy or colectomy, and 1.6 for highly invasive surgery such as total gastrectomy. In our previous studies, REEs and SFs were evaluated on POD 1 when the patient was presumed to have the highest degree of physical and psychological stress; however, they remained low compared to those for surgeries[33,34].

ASSESSMENT OF PHYSICAL STRESS BY SOA

Opsonization is a humoral immune response involving the complement system that facilitates the capture and uptake of foreign substances by neutrophils and other phagocytes. An increase in SOA causes neutrophil activation and stimulates the secretion of reactive oxygen species (ROS)[36,37], which is associated with physical stress[38-40]. Among ROS, superoxide anions (O^{2-}) and hydrogen peroxide (H_2O_2) induce DNA fragmentation in cells, causing inflammation and tissue damage[37]. In sports medicine, there have been many reports that physical stress is evaluated by changes in SOA, an index of the immune capacity of non-specific neutrophils[39-41].

The chemiluminescence method is easy to perform, requiring only a blood sample and enabling the quantification of ROS produced by neutrophils[38-40]. This method is useful because the collected biological samples can be measured simultaneously under the same conditions. It detects ROS using chemiluminescent probes (*i.e.*, lucigenin and luminol).

O^{2-} is produced by neutrophils. Its formation is mediated by NADPH oxidase, which is activated by phagocytosis, and converted to H_2O_2 by superoxide dismutase[36,37]. Furthermore, each ROS has a different oxidation potential. When neutrophils release azurophilic granules containing myeloperoxidase (MPO), H_2O_2 reacts with Cl^- to produce hypochlorous acid (HOCl), which is a more powerful oxidant than H_2O_2[36,37]. Lucigenin is associated with the detection of O^{2-}, whereas luminol reflects the total amount of ROS produced by MPO, including HOCl[36,37]. Thus, the oxidative stress measured by luminol-dependent chemiluminescence is generally considered more toxic as it reflects all types of ROS in a sample.

To measure SOA in the peripheral blood, zymosan, an activator of the alternative complement pathway found in *Saccharomyces cerevisiae*, was opsonized in serum samples of patients who underwent ESD. Lucigenin- and luminol-dependent chemiluminescence were used to detect and quantify the ROS secreted by the neutrophils of a healthy volunteer against these opsonized zymosan molecules[36,37,

Table 1 Perioperative changes in resting energy expenditure, resting energy expenditure/basal energy expenditure, and stress factors by endoscopic submucosal dissection

	ESD preoperative state	ESD postoperative state
Gastric cancer		
REE (kcal)	1170.3 ± 209.0	1238.4 ± 235.5[c]
REE/BEE	0.96 ± 0.11	1.03 ± 0.14[c]
Stress factor		1.07
Colorectal cancer		
REE (kcal)	1107.0 ± 204.4	1139.9 ± 185.2[c]
REE/BEE	0.96 ± 0.12	1.00 ± 0.13[c]
Stress factor		1.06

[c]$P < 0.001$ *vs* endoscopic submucosal dissection (ESD) preoperative state.

Data are presented as mean ± SD. The stress factor on ESD in the postoperative state was computed by setting the stress factor on the day of ESD to be 1.0. ESD: Endoscopic submucosal dissection; REE: Resting energy expenditure; BEE: Basal energy expenditure.

42]. The emission curve measured by the chemiluminescence method was evaluated using an autoluminescence analyzer, focusing on the peak height and the area under the curve. For each measurement, the serum of a healthy volunteer was used as the standard value for ROS production. The results of the chemiluminescence method were calculated as a percentage compared to standard serum levels[36,37,42]. Changes in SOA, measured by the chemiluminescence method, are valuable in assessing the physical stress associated with endoscopic treatment of early-stage cancer[42].

As shown in Table 2, a significant increase in the peak height and area under the curve of lucigenin-dependent chemiluminescence was observed for gastric ESD on POD 1 and 4. Both of these percentages tended to decrease on POD 4 compared with those on POD 1. However, there was no significant increase in these parameters for luminol-dependent chemiluminescence on POD 1 and 4. In contrast, for colorectal cancer, the peak height and area under the curve of lucigenin-dependent chemiluminescence showed no significant difference in POD 1 but a significant increase in POD 4 compared with those on the day of ESD. Furthermore, no significant changes in these parameters were noted on luminol-dependent chemiluminescence during the perioperative period, similar to gastric ESD[42]. In contrast, previous studies on patients undergoing gastrointestinal surgery with different degrees of surgical stress found higher SOA measured by luminol-dependent chemiluminescence[43,44]. The difference in SOA between ESD and surgery suggests that ESD is less invasive.

Based on the results of the chemiluminescence method, changes in SOA during the perioperative period of ESD were associated with a slight increase in the production of less toxic ROS. The difference in the peak height of SOA between gastric and colorectal ESD, measured by lucigenin-dependent chemiluminescence, may be related to the difference in stimulation to post-ESD ulcers. Both gastric and colorectal ESD patients started eating meals 2 d after the procedure. Post-gastric ESD ulcers are immediately stimulated by gastric acid and oral bacteria. In cases of colorectal ESD, feces are defecated by intestinal tract-cleaning compositions, and the population of gut microbiota is markedly reduced before ESD. Therefore, SOA may have increased significantly on POD 4 because the post-ESD ulcer is stimulated by feces after resuming meals.

CONCLUSION

The current review summarizes the methods to assess the physical invasiveness of ESD in patients based on changes in REE measured using an indirect calorimeter and SOA measured by the chemiluminescence method. These methods are easy to perform and non-invasive, even in older patients. In addition, the results showed that changes in perioperative physical stress differed between gastric and colorectal ESD. The increases in perioperative REE and SF after ESD were lower than those reported for surgery. The perioperative changes in SOA after ESD were associated with slight increases in the production of less toxic ROS. These findings suggest that ESD does not cause significant physical stress.

In recent years, laparoscopic and less-invasive surgeries have become widespread. Further multicenter studies are needed to compare the changes in REE and SFs between ESD and less-invasive surgeries. There are also new procedures for endoscopic therapies, such as peroral endoscopic myotomy (POEM) and laparoscopic endoscopic cooperative surgery (LECS). In the future, it will be important to evaluate the physical stress of these procedures as well.

Table 2 Endoscopic submucosal dissection perioperative changes in serum opsonic activity measured by lucigenin- and luminol-dependent chemiluminescence

	The day of ESD	POD1	POD4
Gastric cancer			
Lucigenin			
Peak height (%)	100.6	106.3[b]	105.9[b]
	(71.4-178.5)	(78.5-282.4)	(77.6-214.4)
Area under the curve (%)	98.4	105.6[b]	103.5[b]
	(48.7-184.7)	(64.8-265.3)	(66.0-222.8)
Luminol			
Peak height (%)	98.4	100.1	99.6
	(62.7-168.3)	(63.6-199.2)	(69.7-186.6)
Area under the curve (%)	99.7	102.6	101.8
	(68.2-155.7)	(68.0-182.9)	(73.2-170.7)
Colorectal cancer			
Lucigenin			
Peak height (%)	102.3	105.2	105.3[a]
	(71.4-132.7)	(61.8-137.4)	(65.7-137.1)
Area under the curve (%)	99.4	101.9	102.6[a]
	(68.2-134.3)	(60.9-140.0)	(64.0-139.7)
Luminol			
Peak height (%)	97.3	100.2	99.9
	(70.9-132.5)	(76.6-132.0)	(74.9-134.7)
Area under the curve (%)	99.1	102.1	102.3
	(75.8-131.4)	(78.3-128.6)	(77.4-134.3)

[a]$P < 0.05$, [b]$P < 0.01$ *vs* the day of endoscopic submucosal dissection.
Data are expressed as median with interquartile range in parenthesis. ESD: Endoscopic submucosal dissection; POD: Postoperative day.

FOOTNOTES

Author contributions: Chinda D and Shimoyama T designed the review; Chinda D interpreted the data and drafted the manuscript; Shimoyama T critically revised the paper.

Supported by the Karoji Memorial Fund for Medical Research.

Conflict-of-interest statement: There are no conflicts of interest to report.

Open-Access: This article is an open-access article that was selected by an in-house editor and fully peer-reviewed by external reviewers. It is distributed in accordance with the Creative Commons Attribution NonCommercial (CC BY-NC 4.0) license, which permits others to distribute, remix, adapt, build upon this work non-commercially, and license their derivative works on different terms, provided the original work is properly cited and the use is non-commercial. See: https://creativecommons.org/Licenses/by-nc/4.0/

Country/Territory of origin: Japan

ORCID number: Daisuke Chinda 0000-0003-1690-5923; Tadashi Shimoyama 0000-0001-9615-0000.

Corresponding Author's Membership in Professional Societies: American Gastroenterological Association, No. 186311; American College of Gastroenterology, FACG.

S-Editor: Chen YL
L-Editor: A

P-Editor: Chen YL

REFERENCES

1 **Tanaka S**, Kashida H, Saito Y, Yahagi N, Yamano H, Saito S, Hisabe T, Yao T, Watanabe M, Yoshida M, Saitoh Y, Tsuruta O, Sugihara KI, Igarashi M, Toyonaga T, Ajioka Y, Kusunoki M, Koike K, Fujimoto K, Tajiri H. Japan Gastroenterological Endoscopy Society guidelines for colorectal endoscopic submucosal dissection/endoscopic mucosal resection. *Dig Endosc* 2020; **32**: 219-239 [PMID: 31566804 DOI: 10.1111/den.13545]

2 **Hashiguchi Y**, Muro K, Saito Y, Ito Y, Ajioka Y, Hamaguchi T, Hasegawa K, Hotta K, Ishida H, Ishiguro M, Ishihara S, Kanemitsu Y, Kinugasa Y, Murofushi K, Nakajima TE, Oka S, Tanaka T, Taniguchi H, Tsuji A, Uehara K, Ueno H, Yamanaka T, Yamazaki K, Yoshida M, Yoshino T, Itabashi M, Sakamaki K, Sano K, Shimada Y, Tanaka S, Uetake H, Yamaguchi S, Yamaguchi N, Kobayashi H, Matsuda K, Kotake K, Sugihara K; Japanese Society for Cancer of the Colon and Rectum. Japanese Society for Cancer of the Colon and Rectum (JSCCR) guidelines 2019 for the treatment of colorectal cancer. *Int J Clin Oncol* 2020; **25**: 1-42 [PMID: 31203527 DOI: 10.1007/s10147-019-01485-z]

3 **Ono H**, Yao K, Fujishiro M, Oda I, Uedo N, Nimura S, Yahagi N, Iishi H, Oka M, Ajioka Y, Fujimoto K. Guidelines for endoscopic submucosal dissection and endoscopic mucosal resection for early gastric cancer (second edition). *Dig Endosc* 2021; **33**: 4-20 [PMID: 33107115 DOI: 10.1111/den.13883]

4 **Tanoue K**, Fukunaga S, Nagami Y, Sakai T, Maruyama H, Ominami M, Otani K, Hosomi S, Tanaka F, Taira K, Kamata N, Yamagami H, Tanigawa T, Shiba M, Watanabe T, Fujiwara Y. Long-term outcome of endoscopic submucosal dissection for early gastric cancer in patients with severe comorbidities: a comparative propensity score analysis. *Gastric Cancer* 2019; **22**: 558-566 [PMID: 30382467 DOI: 10.1007/s10120-018-0889-8]

5 **Ryu SJ**, Kim BW, Kim BG, Kim JH, Kim JS, Kim JI, Park JM, Oh JH, Kim TH, Kim JJ, Park SM, Park CH, Song KY, Lee JH, Kim SG, Kim DJ, Kim W. Endoscopic submucosal dissection *vs* surgical resection for early gastric cancer: a retrospective multicenter study on immediate and long-term outcome over 5 years. *Surg Endosc* 2016; **30**: 5283-5289 [PMID: 27338583 DOI: 10.1007/s00464-016-4877-y]

6 **Dumoulin FL**, Hildenbrand R. Endoscopic resection techniques for colorectal neoplasia: Current developments. *World J Gastroenterol* 2019; **25**: 300-307 [PMID: 30686899 DOI: 10.3748/wjg.v25.i3.300]

7 **Kondo A**, de Moura EG, Bernardo WM, Yagi OK, de Moura DT, de Moura ET, Bravo JG, Yamazaki K, Sakai P. Endoscopy *vs* surgery in the treatment of early gastric cancer: Systematic review. *World J Gastroenterol* 2015; **21**: 13177-13187 [PMID: 26675093 DOI: 10.3748/wjg.v21.i46.13177]

8 **Xu X**, Wang T, Zheng Z, Chen X, Liu W, Sun C, Wang B. Endoscopic submucosal dissection for large colorectal epithelial neoplasms: A single center experience in north China. *Medicine (Baltimore)* 2017; **96**: e7967 [PMID: 28885349 DOI: 10.1097/MD.0000000000007967]

9 **Kim SG**, Ji SM, Lee NR, Park SH, You JH, Choi IJ, Lee WS, Park SJ, Lee JH, Seol SY, Kim JH, Lim CH, Cho JY, Kim GH, Chun HJ, Lee YC, Jung HY, Kim JJ. Quality of Life after Endoscopic Submucosal Dissection for Early Gastric Cancer: A Prospective Multicenter Cohort Study. *Gut Liver* 2017; **11**: 87-92 [PMID: 27282267 DOI: 10.5009/gnl15549]

10 **Kim YI**, Kim YA, Kim CG, Ryu KW, Kim YW, Sim JA, Yun YH, Choi IJ. Serial intermediate-term quality of life comparison after endoscopic submucosal dissection *vs* surgery in early gastric cancer patients. *Surg Endosc* 2018; **32**: 2114-2122 [PMID: 29067581 DOI: 10.1007/s00464-017-5909-y]

11 **Hirasaki S**, Tanimizu M, Nasu J, Shinji T, Koide N. Treatment of elderly patients with early gastric cancer by endoscopic submucosal dissection using an insulated-tip diathermic knife. *Intern Med* 2005; **44**: 1033-1038 [PMID: 16293912 DOI: 10.2169/internalmedicine.44.1033]

12 **Isomoto H**, Ohnita K, Yamaguchi N, Fukuda E, Ikeda K, Nishiyama H, Akiyama M, Ozawa E, Nakao K, Kohno S, Shikuwa S. Clinical outcomes of endoscopic submucosal dissection in elderly patients with early gastric cancer. *Eur J Gastroenterol Hepatol* 2010; **22**: 311-317 [PMID: 19494784 DOI: 10.1097/MEG.0b013e32832c61d7]

13 **Chang JW**, Jung DH, Park JC, Shin SK, Lee SK, Lee YC. Long-Term Outcomes and Prognostic Factors of Endoscopic Submucosal Dissection for Early Gastric Cancer in Patients Aged ≥75 Years. *Cancers (Basel)* 2020; **12** [PMID: 33142928 DOI: 10.3390/cancers12113222]

14 **Kim GH**, Choi KD, Ko Y, Park T, Kim KW, Park SY, Na HK, Ahn JY, Lee JH, Jung KW, Kim DH, Song HJ, Lee GH, Jung HY. Impact of Comorbidities, Sarcopenia, and Nutritional Status on the Long-Term Outcomes after Endoscopic Submucosal Dissection for Early Gastric Cancer in Elderly Patients Aged ≥ 80 Years. *Cancers (Basel)* 2021; **13** [PMID: 34298811 DOI: 10.3390/cancers13143598]

15 **Nishiguchi K**, Okuda J, Toyoda M, Tanaka K, Tanigawa N. Comparative evaluation of surgical stress of laparoscopic and open surgeries for colorectal carcinoma. *Dis Colon Rectum* 2001; **44**: 223-230 [PMID: 11227939 DOI: 10.1007/BF02234297]

16 **Wang G**, Jiang Z, Zhao K, Li G, Liu F, Pan H, Li J. Immunologic response after laparoscopic colon cancer operation within an enhanced recovery program. *J Gastrointest Surg* 2012; **16**: 1379-1388 [PMID: 22585532 DOI: 10.1007/s11605-012-1880-z]

17 **Benoit O**, Faron M, Margot N, Creavin B, Debove C, Tiret E, Parc Y, Lefevre JH. C-Reactive Protein Values After Colorectal Resection: Can We Discharge a Patient With a C-Reactive Protein Value >100? *Dis Colon Rectum* 2019; **62**: 88-96 [PMID: 30451748 DOI: 10.1097/DCR.0000000000001216]

18 **Ding S**, Ma H, Wang G, Yu Z, Li K, Huang A. Effect of Remifentanil Combined Anesthesia on Cytokines and Oxidative Stress in Patients undergoing Laparoscopic Surgery for Colon Cancer. *J Coll Physicians Surg Pak* 2019; **29**: 8-11 [PMID: 30630560 DOI: 10.29271/jcpsp.2019.01.8]

19 **Myre K**, Raeder J, Rostrup M, Buanes T, Stokland O. Catecholamine release during laparoscopic fundoplication with high and low doses of remifentanil. *Acta Anaesthesiol Scand* 2003; **47**: 267-273 [PMID: 12648191 DOI:

10.1034/j.1399-6576.2003.00073.x]

20 **Uesato M**, Nabeya Y, Akai T, Inoue M, Watanabe Y, Kawahira H, Mamiya T, Ohta Y, Motojima R, Kagaya A, Muto Y, Hayashi H, Matsubara H. Salivary amylase activity is useful for assessing perioperative stress in response to pain in patients undergoing endoscopic submucosal dissection of gastric tumors under deep sedation. *Gastric Cancer* 2010; **13**: 84-89 [PMID: 20602194 DOI: 10.1007/s10120-009-0541-8]

21 **Yatabe T**, Kitagawa H, Yamashita K, Hanazaki K, Yokoyama M. Energy expenditure measured using indirect calorimeter after minimally invasive esophagectomy in ventilated postoperative patients. *Asia Pac J Clin Nutr* 2014; **23**: 555-559 [PMID: 25516312 DOI: 10.6133/apjcn.2014.23.4.20]

22 **Kalnins D**, Pencharz PB, Grasemann H, Solomon M. Energy expenditure and nutritional status in pediatric patients before and after lung transplantation. *J Pediatr* 2013; **163**: 1500-1502 [PMID: 23870785 DOI: 10.1016/j.jpeds.2013.05.063]

23 **Ferreira LG**, Santos LF, Anastácio LR, Lima AS, Correia MI. Resting energy expenditure, body composition, and dietary intake: a longitudinal study before and after liver transplantation. *Transplantation* 2013; **96**: 579-585 [PMID: 23851933 DOI: 10.1097/TP.0b013e31829d924e]

24 **Kawakami M**, Liu M, Wada A, Otsuka T, Nishimura A. Resting Energy Expenditure in Patients with Stroke during the Subacute Phases - Relationships with Stroke Types, Location, Severity of Paresis, and Activities of Daily Living. *Cerebrovasc Dis* 2015; **39**: 170-175 [PMID: 25720382 DOI: 10.1159/000375155]

25 **Powell-Tuck J**. Nutritional interventions in critical illness. *Proc Nutr Soc* 2007; **66**: 16-24 [PMID: 17343768 DOI: 10.1017/S0029665107005253]

26 **Fredrix EW**, Soeters PB, von Meyenfeldt MF, Saris WH. Resting energy expenditure in cancer patients before and after gastrointestinal surgery. *JPEN J Parenter Enteral Nutr* 1991; **15**: 604-607 [PMID: 1766048 DOI: 10.1177/0148607191015006604]

27 **Lobo DN**, Gianotti L, Adiamah A, Barazzoni R, Deutz NEP, Dhatariya K, Greenhaff PL, Hiesmayr M, Hjort Jakobsen D, Klek S, Krznaric Z, Ljungqvist O, McMillan DC, Rollins KE, Panisic Sekeljic M, Skipworth RJE, Stanga Z, Stockley A, Stockley R, Weimann A. Perioperative nutrition: Recommendations from the ESPEN expert group. *Clin Nutr* 2020; **39**: 3211-3227 [PMID: 32362485 DOI: 10.1016/j.clnu.2020.03.038]

28 **Long CL**, Schaffel N, Geiger JW, Schiller WR, Blakemore WS. Metabolic response to injury and illness: estimation of energy and protein needs from indirect calorimetry and nitrogen balance. *JPEN J Parenter Enteral Nutr* 1979; **3**: 452-456 [PMID: 575168 DOI: 10.1177/014860717900300609]

29 **Bendavid I**, Lobo DN, Barazzoni R, Cederholm T, Coëffier M, de van der Schueren M, Fontaine E, Hiesmayr M, Laviano A, Pichard C, Singer P. The centenary of the Harris-Benedict equations: How to assess energy requirements best? *Clin Nutr* 2021; **40**: 690-701 [PMID: 33279311 DOI: 10.1016/j.clnu.2020.11.012]

30 **Tignanelli CJ**, Andrews AG, Sieloff KM, Pleva MR, Reichert HA, Wooley JA, Napolitano LM, Cherry-Bukowiec JR. Are Predictive Energy Expenditure Equations in Ventilated Surgery Patients Accurate? *J Intensive Care Med* 2019; **34**: 426-431 [PMID: 28382850 DOI: 10.1177/0885066617702077]

31 **Donadon M**, Mimmo A, Costa G, Cimino M, Viganò L, Palmisano A, Torzilli G. Measurement of Total Liver Volume Using the Energy Expenditure: A New Formula. *World J Surg* 2018; **42**: 3350-3356 [PMID: 29691622 DOI: 10.1007/s00268-018-4632-8]

32 **Fredrix EW**, Soeters PB, Wouters EF, Deerenberg IM, von Meyenfeldt MF, Saris WH. Effect of different tumor types on resting energy expenditure. *Cancer Res* 1991; **51**: 6138-6141 [PMID: 1657379]

33 **Chinda D**, Shimoyama T, Hayamizu S, Miyazawa K, Arai T, Yanagimachi M, Tsukamoto T, Mikami T, Fukuda S. Energy metabolism during the perioperative period of gastric endoscopic submucosal dissection. *J Clin Biochem Nutr* 2017; **61**: 153-157 [PMID: 28955134 DOI: 10.3164/jcbn.17-16]

34 **Chinda D**, Shimoyama T, Miyazawa K, Arai T, Hayamizu S, Yanagimachi M, Tsukamoto T, Akitaya K, Tatsuta T, Kawaguchi S, Kikuchi H, Hiraga H, Sawaya M, Sakuraba H, Mikami T, Fukuda S. Estimation of perioperative invasiveness of colorectal endoscopic submucosal dissection evaluated by energy metabolism. *J Clin Biochem Nutr* 2018; **63**: 164-167 [PMID: 30279629 DOI: 10.3164/jcbn.18-12]

35 **Inoue Y**. Estimation of energy need -Should stress factor and activity factor be considered? JSPEN 2010; 25: 573-579

36 **Suzuki K**, Sato H, Kikuchi T, Abe T, Nakaji S, Sugawara K, Totsuka M, Sato K, Yamaya K. Capacity of circulating neutrophils to produce reactive oxygen species after exhaustive exercise. *J Appl Physiol (1985)* 1996; **81**: 1213-1222 [PMID: 8889756 DOI: 10.1152/jappl.1996.81.3.1213]

37 **Hasegawa H**, Suzuki K, Nakaji S, Sugawara K. Analysis and assessment of the capacity of neutrophils to produce reactive oxygen species in a 96-well microplate format using lucigenin- and luminol-dependent chemiluminescence. *J Immunol Methods* 1997; **210**: 1-10 [PMID: 9502580 DOI: 10.1016/s0022-1759(97)00159-2]

38 **Lee S**, Takahashi I, Matsuzaka M, Yamai K, Danjo K, Kumagai T, Umeda T, Itai K, Nakaji S. The relationship between serum selenium concentration and neutrophil function in peripheral blood. *Biol Trace Elem Res* 2011; **144**: 396-406 [PMID: 21691799 DOI: 10.1007/s12011-011-9108-8]

39 **Mikami M**, Takahashi I, Matsuzaka M, Danjo K, Yamai K, Inoue R, Iwane K, Umeda T, Nakaji S. The relationship between exhaled carbon monoxide and human neutrophil function in the Japanese general population. *Luminescence* 2011; **26**: 162-166 [PMID: 21681908 DOI: 10.1002/bio.1199]

40 **Suzuki K**, Nakaji S, Yamada M, Liu Q, Kurakake S, Okamura N, Kumae T, Umeda T, Sugawara K. Impact of a competitive marathon race on systemic cytokine and neutrophil responses. *Med Sci Sports Exerc* 2003; **35**: 348-355 [PMID: 12569227 DOI: 10.1249/01.MSS.0000048861.57899.04]

41 **Miura M**, Umeda T, Nakaji S, Liu Q, Tanabe M, Kojima A, Yamamoto Y, Sugawara K. Effect of 6 mo' training on the reactive oxygen species production capacity of neutrophils and serum opsonic activity in judoists. *Luminescence* 2005; **20**: 1-7 [PMID: 15586397 DOI: 10.1002/bio.777]

42 **Chinda D**, Shimoyama T, Arai T, Sawada K, Akitaya K, Kudo S, Yasuda K, Miyazawa K, Akimoto N, Sato S, Hayamizu S, Tatsuta T, Kikuchi H, Hiraga H, Sawaya M, Sakuraba H, Mikami T, Nakaji S, Fukuda S. Usefulness of serum opsonic activity measured by chemiluminescence method to assess the invasiveness of colorectal endoscopic mucosal dissection. *Free Radic Res* 2020; **54**: 810-817 [PMID: 31615273 DOI: 10.1080/10715762.2019.1681590]

43 **Yokota K**, Nishihira T, Shineha R, Sayama J, Nitta Y, Kimura M, Mori S. Association between elevated plasma granulocyte colony-stimulating factor and the degree of surgical stress in patients undergoing gastrointestinal surgery. *Surg Today* 1995; **25**: 579-584 [PMID: 7549267 DOI: 10.1007/BF00311429]
44 **Yokota K**, Shineha R, Nishihira T, Mori S. Perioperative alterations in polymorphonuclear leukocyte function of gastrointestinal surgery. *Tohoku J Exp Med* 1993; **169**: 103-112 [PMID: 8236241 DOI: 10.1620/tjem.169.103]

World Journal of Gastroenterology

Submit a Manuscript: https://www.f6publishing.com

World J Gastroenterol 2022 August 28; 28(32): 4516-4526

DOI: 10.3748/wjg.v28.i32.4516

ISSN 1007-9327 (print) ISSN 2219-2840 (online)

MINIREVIEWS

Expanding beyond endoscopy: A review of non-invasive modalities in Barrett's esophagus screening and surveillance

Dariush Shahsavari, Praneeth Kudaravalli, John Erikson L Yap, Kenneth J Vega

Specialty type: Gastroenterology and hepatology

Provenance and peer review: Invited article; Externally peer reviewed.

Peer-review model: Single blind

Peer-review report's scientific quality classification

Grade A (Excellent): 0
Grade B (Very good): B, B
Grade C (Good): 0
Grade D (Fair): 0
Grade E (Poor): E

P-Reviewer: Deng K, China; Okasha H, Egypt; Spadaccini M, Italy

Received: January 14, 2022
Peer-review started: January 14, 2022
First decision: April 12, 2022
Revised: May 14, 2022
Accepted: July 26, 2022
Article in press: July 26, 2022
Published online: August 28, 2022

Dariush Shahsavari, Praneeth Kudaravalli, John Erikson L Yap, Kenneth J Vega, Division of Gastroenterology and Hepatology, Augusta University-Medical College of Georgia, Augusta, GA 30912, United States

Corresponding author: Kenneth J Vega, AGAF, FACG, FACP, MD, Professor, Division of Gastroenterology and Hepatology, Augusta University-Medical College of Georgia, 1120 15th Street AD 2226, Augusta, GA 30912, United States. kvega@augusta.edu

Abstract

Barrett's esophagus (BE) is a condition that results from replacement of the damaged normal squamous esophageal mucosa to intestinal columnar mucosa and is the most significant predisposing factor for development of esophageal adenocarcinoma. Current guidelines recommend endoscopic evaluation for screening and surveillance based on various risk factors which has limitations such as invasiveness, availability of a trained specialist, patient logistics and cost. Trans-nasal endoscopy is a less invasive modality but still has similar limitations such as limited availability of trained specialist and costs. Non-endoscopic modalities, in comparison, require minimal intervention, can be done in an office visit and has the potential to be a more ideal choice for mass public screening and surveillance, particularly in patents at low risk for BE. These include newer generations of esophageal capsule endoscopy which provides direct visualization of BE, and tethered capsule endomicroscopy which can obtain high-resolution images of the esophagus. Various cell collection devices coupled with biomarkers have been used for BE screening. Cytosponge, in combination with TFF3, as well as EsophaCap and EsoCheck have shown promising results in various studies when used with various biomarkers. Other modalities including circulatory microRNAs and volatile organic compounds that have demonstrated favorable outcomes. Use of these cell collection methods for BE surveillance is a potential area of future research.

Key Words: Barrett's esophagus; Screening; Surveillance; Non-endoscopic; Cytosponge; Esophacap; Esocheck

©The Author(s) 2022. Published by Baishideng Publishing Group Inc. All rights reserved.

Core Tip: This review summarizes the non-endoscopic modalities available for the screening and surveillance of Barrett's esophagus which include esophageal imaging devices (trans-nasal endoscopy, esophageal capsule, tethered capsule endomicroscopy), cell collection devices (Cytosponge, Esophacap, Esocheck), circulatory micro-RNAs and volatile organic compounds. There is promise using some of the noninvasive modalities for mass screening in BE and a role in surveillance is yet to be determined.

Citation: Shahsavari D, Kudaravalli P, Yap JEL, Vega KJ. Expanding beyond endoscopy: A review of non-invasive modalities in Barrett's esophagus screening and surveillance. *World J Gastroenterol* 2022; 28(32): 4516-4526
URL: https://www.wjgnet.com/1007-9327/full/v28/i32/4516.htm
DOI: https://dx.doi.org/10.3748/wjg.v28.i32.4516

INTRODUCTION

The esophagus is normally lined by stratified squamous epithelium. The mucosa of the esophagus is regularly exposed to gastric acid and bile through reflux from the stomach which can result in mucosal damage. The injury is usually repaired by regeneration of the squamous mucosa. However, in some patients, the mucosal damage is repaired resulting in a metaplastic columnar epithelium with gastric and intestinal features. The condition is termed Barrett's esophagus (BE) and is recognized as the major risk factor for the development of esophageal adenocarcinoma (EAC)[1]. It is estimated that as many as 5.6% of United States adults have BE based on modeling using EAC rates[2]. Of note, endoscopic prevalence is widely variable based on geographic location of the population studied[3-6]. Current estimates are likely an underrepresentation given that upper endoscopy is required for diagnosis. Mean age at BE identification is approximately 55 years and is two to threefold more common in men than in women[7,8]. Among patients undergoing upper endoscopy, compared to Caucasians, African Americans have a significantly lower BE prevalence[9,10]. Accepted BE risk factors besides Caucasian race include age > 50, male, chronic (> 5 years) or frequent (> once weekly) gastroesophageal reflux disease (GERD), smoking, obesity (Body mass index > 35), and family history of BE or EAC (first degree relative)[11].

Endoscopy is currently the mainstay for BE diagnosis and management. An endoscopic approach is inappropriate for mass screening as it is not cost effective resulting in missed opportunities to discover patients with undiagnosed BE. Current screening guidelines target individuals with GERD and multiple risk factors for endoscopy to detect BE then enroll those with it into a surveillance program. However, this approach does not take into consideration that most EAC cases do not have a diagnosis of BE prior [12]. This provides an excellent opportunity for non-endoscopic techniques to be used as a public health tool for screening (identification of disease) and surveillance. Individuals belonging to the low risk BE strata are best suited for non-endoscopic modalities as they require minimal intervention whereas the high risk BE group would require more precise but also more invasive endoscopic based technologies [13]. Non-endoscopic techniques provide cost-effective, less invasive screening tools and more importantly increase the ease of accessibility to screening opportunities.

WHO DO WE SCREEN

Screening for BE is recommended in patients with multiple known risk factors including chronic or frequent GERD, age greater than 50 years, male sex, Caucasian race, smoking, obesity along with family history of a 1st degree relative with BE or EAC. Currently, screening the general population with only GERD symptoms is not recommended per society guidelines[14,15].

ESOPHAGEAL IMAGING DEVICES

Currently, high-definition white light endoscopy is the mainstay of BE screening and surveillance. Despite being safe and well-tolerated, it is invasive and associated with higher costs and side effects [16]. Trans-nasal endoscopy (TNE, Figure 1) has been proposed as a less invasive alternative to screen for BE. TNE is an ultra-thin endoscope (diameter < 6 mm) used in the outpatient setting to directly visualize the distal esophagus. This has occurred in primary care offices[17,18] and mobile vans for community BE screening[19]. Drawbacks of TNE are limited availability, cost, decontamination facility for reuse, and need for trained operators.



Figure 1 Trans-nasal endoscopy. Courtesy: Image obtained from public domain.

ESOPHAGEAL CAPSULE ENDOSCOPY

Esophageal capsule endoscopy (ECE), similar to small bowel capsule endoscopy, consists of a wireless capsule containing a camera, battery, and radio transmitter. Images are transmitted to a digital receiver and transferred to a computer for analysis[20]. A meta-analysis of 9 studies comprising of 618 patients showed a pooled sensitivity of 78% and specificity of 86% (EGD as the reference had sensitivity and specificity of 78% and 90% respectively)[21]. The suboptimal diagnostic accuracy is contributed to rapid esophageal transit time. Newer versions of ECE have been developed to overcome this issue and allow prolonged imaging. PillCam ESO (Medtronic Inc, Minneapolis, MN) was initially approved by Food and Drug Administration in 2004 and a second-generation device (PillCam ESO2, Figure 2A) with cameras at both ends of the capsule. The second-generation device captures images (PillCam ESO2, Figure 2B) at a rate of 18 frames per seconds (fps)[22]. A third-generation capsule (PillCam UGI) with a wider angle of view (174°) and higher recording rate (35 fps) is under investigation with pilot data suggesting inferiority to standard endoscopy regarding BE detection[23]. Another solution for the rapid esophageal transit issue is the detachable string magnetically controlled capsule endoscopy (also known as wireless magnetically controlled capsule endoscopy or WMCCE) which has been shown to be feasible and well tolerated in various studies[24-26]. A recent prospective multicenter study showed sensitivity of 92% and specificity of 80% for high-risk esophageal varices[27]. With regards to cost-effectiveness of ECE compared to traditional endoscopy, the results have been equivocal[28-30]. More studies are needed to determine of this modality is viable and cost-effective for BE screening.

TETHERED CAPSULE ENDOMICROSCOPY

Another variant of ECE is optical coherence tomography tethered capsule endomicroscopy (OTC-TCE, Figure 3) which uses optical-frequency domain imaging technology that rapidly acquires high-resolution, 3-dimensional, cross-sectional images of the entire esophagus[31,32]. In a proof-of-concept study of 13 subjects (7 normal volunteers and 6 with known BE), no complications were reported, and 12/13 patients reported preference of this method over conventional endoscopy[33]. The feasibility and safety of this method was further demonstrated in a recent multi-center study of 147 patients with known BE, and a blinded comparison of maximum extent of BE measured by OTC-TCE and EGD showed a strong correlation (r = 0.77-0.79, P < 0.05)[34]. In this study, high-quality microscopic images of the entire esophageal wall were obtained in the majority of the cases (93.7%). Larger prospective studies are needed to assess diagnostic yield and cost-effectiveness in the general population setting.

CELL COLLECTION DEVICES WITH BIOMARKERS

Various devices have been designed for esophageal cell collection. These samples can be analyzed cytologically and coupled with various biomarkers.

Cytosponge™—Trefoil Factor Family Protein 3

The Cytosponge (Medtronic, Minneapolis, MN, Figure 4) is a 30 mm polyurethane sponge, compressed withing a gelatin capsule and attached to a string[13]. Once patient swallows the capsule and it reaches the stomach, the capsule opens up and reveals the sponge. As the string is pulled back, the Cytosponge collects cells from the lining of the entire esophagus and oropharynx. Although several biomarkers have

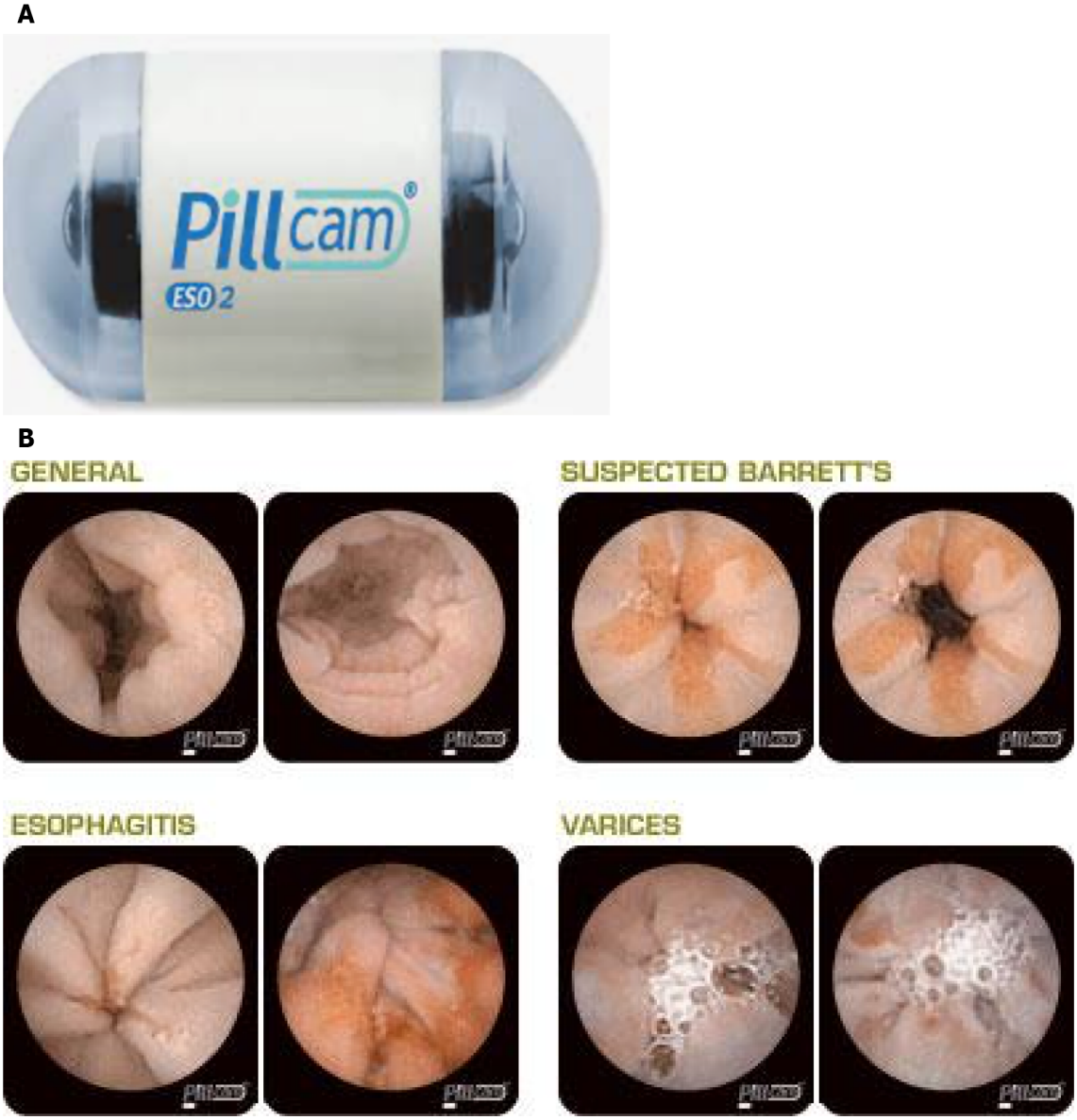


Figure 2 PillCam ESO2 and image. A: PillCam ESO2; B: PillCam ESO2 images showing normal, esophagitis, suspected Barrett's and varices. Courtesy: Image obtained from public domain.

been used with Cytosponge including a multi-gene next-generation sequencing panel, differentially methylated genes, and microRNAs, the most well-established biomarker used with Cytosponge has been trefoil factor family protein 3 (TFF3) immunohistochemical staining[35-37].

In a multicenter case-control study of 11 United Kingdom hospitals (total subjects = 1,110; 463 dyspepsia controls and 647 BE patients), Cytosponge-TFF3 was performed prior to endoscopy[38]. BE was diagnosed with specificity of 92.4% and sensitivity of 79.9% (87.2% in patients with larger circumferential BE than 3 cm). Fitzgerald *et al*[39] in the BEST3 trial, a multicenter RCT study in 109 United Kingdom general practice clinics, demonstrated in patients with GERD symptoms, Cytosponge-TTF3 results in improved detection of BE, treatable dysplasia, and early cancer. In a systematic review of 13 studies, this method was shown to be cost-effective and well-tolerated through multiple patient populations[40]. Another patient-level review of 5 prospective trials assessing Cytosponge performance in patients with reflux disease, BE and eosinophilic esophagitis, also showed tolerability and safety of this device [41].

The advantage of Cytosponge is that it is not operator-dependent, it is quick, and does not require specialized equipment or extensive training, so it could easily be applied to a primary care setting[40].

EsophaCap™

EsophaCap (CapNostics, Concord, NC, Figure 5) is a sponge on string device similar to Cytosponge, albeit smaller and softer[42]. EsophaCap has been used in a pilot trial using a panel of 2 methylated DNA markers (MDM), 3-VAV2 and zinc finger protein 682-ZNF682, on whole esophageal brushings (49

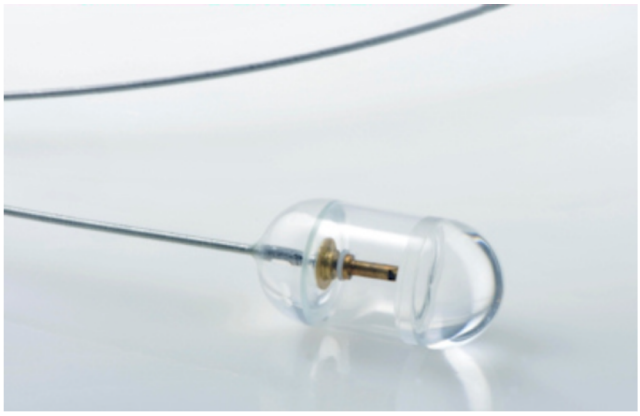


Figure 3 Tethered capsule endomicroscopy. Courtesy: Image obtained from public domain.



Figure 4 Cytosponge (Medtronic, Minneapolis, MN). Courtesy: Image obtained from public domain.

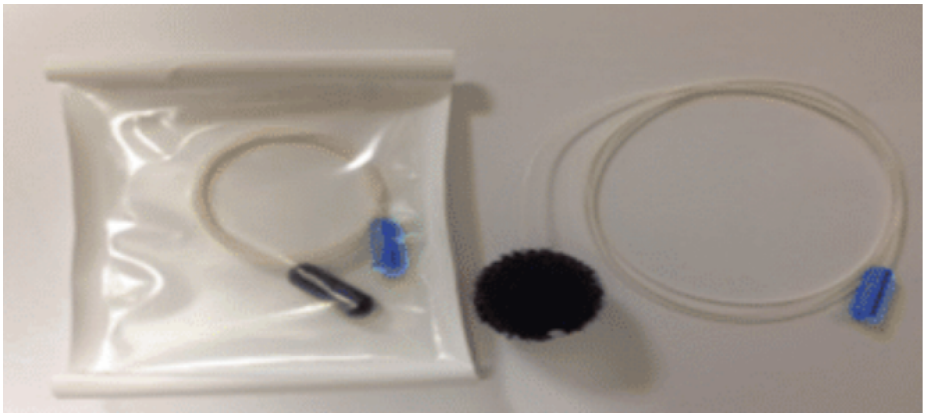


Figure 5 EsophaCap (CapNostics, Concord, NC). Courtesy: Image obtained from public domain.

BE case and 36 controls), and in 40 subjects (20 BE cases and 20 controls) randomly assigned to swallow EsophaCap[42]. Overall, 80% of MDM candidates showed high accuracy for BE (AUCs 0.84-0.94) with sensitivity and specificity of 100%. The EsophCap was swallowed and withdrawn in 98% of subjects with no reported major complications, and 32% had minimal abrasions. More recently, in the same group conducted a multi-center case-cohort study of 268 subjects swallowed the capsule, but 201 met the inclusion criteria (112 cases and 89 controls) using the two previously mentioned MDMs and included 3 additional markers (NDRG4, FER1L4, and ZNF568)[43]. Cross-validated sensitivity and specificity were 92% and 94% respectively. EsophaCap was well tolerated in most patients (performed mostly by non-physicians) and 95% preferred the device over endoscopy. Currently a case-control trial is ongoing to identify potential biomarkers for the early detection of BE, esophageal carcinoma (both adenocarcinoma and squamous cell carcinoma) using EsophaCap (ClinicalTrial.gov ID: NCT04214119).

EsoCheck™

EsoCheck (Lucid Diagnostics, New York, NY, Figure 6) is a balloon-based sampling device which consists of a collapsible balloon attached to thin silicone catheter connected to a syringe[13]. Once EsoCheck is swallowed and is in the stomach, the balloon is inflated by injecting air into the catheter and withdrawn through the distal 3-6 cm of the esophagus, collecting epithelial cells. After sampling the area described above, the balloon is deflated which leads to its retraction into to the capsule, thereby protecting the sample from bio-contamination from the mid or proximal esophagus as well as oropharynx.

Several biomarkers including MDMs have been used with EsoCheck. In a pilot study, Moinova *et al* [44] performed a genome-wide screening and identified high-frequency methylation within the CCNA1 DNA locus. They tested CCNA1 and VIM DNA methylation (already an established BE biomarker) using EsoCheck in 173 individuals with or without BE and showed an AUC = 0.95 for discriminating metaplasia and neoplasia *vs* normal individuals for both, and with both biomarkers combined, the panel had a sensitivity of 95% and specificity of 91%. The results were replicated in an independent validation cohort of 149 subjects. The device was generally well-tolerated but 28 (18%) of subjects could not swallow the pill and 9% had poor DNA yield.

A new multi-center, single-arm trial is underway to study of the screening efficacy of a new generation EsoCheck device in combination with EsoGuard (2-marker MDM panel) in at risk population (ClinicalTrial.gov ID: NCT042293458).

OTHER METHODS

Circulatory MicroRNAs

MicroRNAs (miRNAs) are short (approximately 18-25 nucleotides in length) non-coding RNAs which regulate gene expression by binding to mRNAs to inhibit their translation or facilitate their degradation [45]. miRNAs play role in cell growth, differentiation and migration and can be dysregulated in malignancy[46]. Several miRNAs have been shown to be differently expressed in patients with BE. In a quantitative real-time PCR analysis of 60 disease/normal-paired tissues from 30 patients with esophagitis or BE, miR-143, miR-145, miR-194, and miR-215 were significantly higher, while miR-203 and miR-205 were lower in BE tissues[47]. Analysis on circulating miRNA levels confirmed that miR-194 and miR-215 were significantly upregulated in BE patients. Additionally, serum miR-130a was also shown to be elevated in BE and EAC patients[48]. Pavlov *et al*[49] in a study of 69 patients showed serum miR-320e and miR-199a-3p to be significantly lower in BE compared to patients with normal epithelium. Investigators have recently reported miR-4485-5p as a novel biomarker of esophageal dysplasia worthy of continued investigation[50]. These markers provide a non-invasive method, requiring only a patient's peripheral blood sample and likely increasing acceptability and tolerability, but validation studies are needed in larger cohorts to demonstrate adequate sensitivity as well as specificity for widespread use.

Volatile Organic Compounds

Detection of cancer through exhaled breath using volatile organic compounds (VOC) has shown promising results for various cancers[51,52]. Two techniques have been used in patients with BE or esophageal cancer, which are gas chromatography-mass spectrometry and electronic nose (E-nose) apparatus[53-56]. The gas chromatography method was used to analyze exhaled breath samples from 81 patients (including 48 esophageal cancer patients) and 129 controls (including 16 patients with BE), and although this method was able to discriminate esophageal cancer from controls (AUC = 0.97), it was not able to identify patients with BE[56]. The drawback of this method is that it is costly and labor-intensive. The electronic nose apparatus, which consists of an array of 3 metal oxide sensors, uses a chemical to electrical interface to measure VOC profiles associated with various diseases and can be combined with machine learning[57]. In cross-sectional study of 122 patients with dysplastic BE, breath samples while in a fasting state were analyzed in real-time using the e-nose device[54]. Subjects were at various stages of treatment or surveillance. The data was introduced into an artificial neuronal network to discriminate differences in subjects stratified by the presence or absence of BE on biopsies. The test showed the ability to detect BE with a sensitivity of 82%, specificity of 80%, and accuracy of 81% (AUC = 0.79). In another proof-of-concept study of 402 patients (129 patients with BE and 141 patients with GERD symptoms), 5-minute breath samples were collected, and the test was able to identify BE patients with a sensitivity of 91% and specificity of 74%[53]. Other advantages of E-nose compared to the gas chromatography-mass spectrometry is cost and portability. More validation studies at the general population level are needed for use as a potential BE screening method.



Figure 6 EsoCheck (Lucid Diagnostics, New York, NY). Courtesy: Image obtained from public domain.

FUTURE TRENDS

Circulatory tumor DNA (CtDNA), miniscule amounts of fragmented DNA originating from tumor cells, has been proposed as a part of multi-cancer early detection (MCED) project. The Circulating Cell-free Genome Atlas trial in a prospective, case-controlled observational study showed that a blood-based MCED test using CtDNA in combination with machine learning could detect cancer signals for multiple cancer types and predict cancer signal origin with promising accuracy[58]. Most recently, a large multi-center MCED trial called PATHFINDER study began recruiting participants across 31 United States sites to examine DNA methylation patterns in blood samples to detect various cancers including esophageal cancers[59]. Since BE is a pre-malignant condition, more specific studies need to be conducted in the future to assess feasibility.

SURVEILLANCE

Patients with BE are currently recommended to enter a surveillance endoscopic program based on histological findings and degree of dysplasia[14,60]. This has been associated with a significant mental burden on these patients, presenting as various forms of anxiety and stress related to thoughts of disease progression as well as potential implications of the test, with many finding the program physically burdensome and intrusive[61]. This opens up opportunity for non-invasive surveillance options, which could even be performed in the setting of regular outpatient clinic visits. These modalities can potentially facilitate access to care for a larger population of patients and increase compliance similar to non-invasive tests for colorectal cancer screening programs[62]. As such, non-endoscopic cell collection methods have the potential for use in BE surveillance but so far, no studies have compared their use with conventional endoscopy for the purpose of BE surveillance, leaving this important area ripe for future investigation.

CONCLUSION

Despite advances in screening and surveillance programs for BE, their lack of efficiency is demonstrated by the fact that only one in ten cases of EAC is diagnosed within a surveillance program. Upper endoscopy remains the gold standard but barriers exist to function as an effective screening tool which include high cost, invasiveness, possible complications, need for a trained specialist, and patient desirability. Screening guidelines have been published by several societies that are based on risk factors and do not include the general population. Less invasive modalities have been proposed for BE screening (Table 1). TNE has been used in outpatient settings including offices and mobile medical vans with some success. ECE has shown promising results, and newer generations have attempted to circumvent the issue of rapid esophageal transit with higher frame rates, wider angle view, and magnetic control. OTC-TCE is capable in acquiring high-resolution, 3-dimensional cross-sectional esophageal images with safety and feasibility been demonstrated in multi-center studies. Various cell collection devices coupled with biomarkers have been used for BE screening. Cytosponge, in combination with TFF3, is a cost-effective and well-tolerated method. Similar devices including EsophaCap and EsoCheck have shown promising results when used with various biomarkers and multi-center large-scale trials are currently underway. Circulatory MicroRNAs have been proposed for BE screening as they are expressed differently in this population. VOC using gas chromatography-mass

Table 1 Non-endoscopic methods for detection of Barrett's esophagus

Device name	Application	Detection method	Company	FDA approved	Commercially available
Esophageal capsule endoscopy (ECE)	Swallowed	Direct visualization	Given imaging	Yes (First generation: 2004)	Three generations (SB1, SB2, SB3)
Tethered capsule endomicroscopy (OTC-TCE)	Swallowed	Direct visualization	N/A	No	No
Cytosponge	Swallowed	Cell collection	Medtronic	Yes (2018)	Yes
Esophacap	Swallowed	Cell collection	PAVmed (previously CapNostics)	Yes (2021)	No
EsoCheck	Swallowed	Cell collection	PAVmed (Lucid Diagnostics)	Yes (2019)	Yes
Circulatory microRNAs	Blood sample	miRNA collection	N/A	No	No
Volatile organic compounds (VOC)	Breath sample	VOC collection	Aeonose (Netherlands)	No	No

spectrometry and electronic nose have been used to identify BE or EAC with varying success. Finally, CtDNA is now being used as a part of "multi-cancer early detection" campaign which may play a role in detection of pre-cancer states such as BE. Using these non-invasive methods could also play a role as a surveillance tool once patients are identified with BE. Large future studies are desired to demonstrate the efficacy and feasibility for the BE surveillance population.

FOOTNOTES

Author contributions: Shahsavari D performed the majority of the writing and prepared tables, Kudaravalli P contributed to writing and prepared figures; Yap JEL provided input in writing the paper; Vega KJ designed the outline, coordinated the writing of the paper, edited the paper for intellectual content and is the guarantor.

Conflict-of-interest statement: No conflict of interest exists for any author of this manuscript.

Open-Access: This article is an open-access article that was selected by an in-house editor and fully peer-reviewed by external reviewers. It is distributed in accordance with the Creative Commons Attribution NonCommercial (CC BY-NC 4.0) license, which permits others to distribute, remix, adapt, build upon this work non-commercially, and license their derivative works on different terms, provided the original work is properly cited and the use is non-commercial. See: https://creativecommons.org/Licenses/by-nc/4.0/

Country/Territory of origin: United States

ORCID number: Dariush Shahsavari 0000-0002-4514-6973; Praneeth Kudaravalli 0000-0001-8242-8729; John Erikson L Yap 0000-0002-0441-3211; Kenneth J Vega 0000-0002-2432-6123.

Corresponding Author's Membership in Professional Societies: American Gastroenterological Association; American College of Gastroenterology; American Society for Gastrointestinal Endoscopy.

S-Editor: Chang KL
L-Editor: A
P-Editor: Chang KL

REFERENCES

1 **Que J**, Garman KS, Souza RF, Spechler SJ. Pathogenesis and Cells of Origin of Barrett's Esophagus. *Gastroenterology* 2019; **157**: 349-364.e1 [PMID: 31082367 DOI: 10.1053/j.gastro.2019.03.072]
2 **Hayeck TJ**, Kong CY, Spechler SJ, Gazelle GS, Hur C. The prevalence of Barrett's esophagus in the US: estimates from a simulation model confirmed by SEER data. *Dis Esophagus* 2010; **23**: 451-457 [PMID: 20353441 DOI: 10.1111/j.1442-2050.2010.01054.x]
3 **Hirota WK**, Loughney TM, Lazas DJ, Maydonovitch CL, Rholl V, Wong RK. Specialized intestinal metaplasia, dysplasia, and cancer of the esophagus and esophagogastric junction: prevalence and clinical data. *Gastroenterology* 1999; **116**: 277-285 [PMID: 9922307 DOI: 10.1016/s0016-5085(99)70123-x]

4 **Cameron AJ**, Zinsmeister AR, Ballard DJ, Carney JA. Prevalence of columnar-lined (Barrett's) esophagus. Comparison of population-based clinical and autopsy findings. *Gastroenterology* 1990; **99**: 918-922 [PMID: 2394347 DOI: 10.1016/0016-5085(90)90607-3]

5 **Gerson LB**, Shetler K, Triadafilopoulos G. Prevalence of Barrett's esophagus in asymptomatic individuals. *Gastroenterology* 2002; **123**: 461-467 [PMID: 12145799 DOI: 10.1053/gast.2002.34748]

6 **Ormsby AH**, Kilgore SP, Goldblum JR, Richter JE, Rice TW, Gramlich TL. The location and frequency of intestinal metaplasia at the esophagogastric junction in 223 consecutive autopsies: implications for patient treatment and preventive strategies in Barrett's esophagus. *Mod Pathol* 2000; **13**: 614-620 [PMID: 10874664 DOI: 10.1038/modpathol.3880106]

7 **Spechler SJ**. Barrett's esophagus. *Semin Gastrointest Dis* 1996; **7**: 51-60 [PMID: 8705259]

8 **Cook MB**, Wild CP, Forman D. A systematic review and meta-analysis of the sex ratio for Barrett's esophagus, erosive reflux disease, and nonerosive reflux disease. *Am J Epidemiol* 2005; **162**: 1050-1061 [PMID: 16221805 DOI: 10.1093/aje/kwi325]

9 **Abrams JA**, Fields S, Lightdale CJ, Neugut AI. Racial and ethnic disparities in the prevalence of Barrett's esophagus among patients who undergo upper endoscopy. *Clin Gastroenterol Hepatol* 2008; **6**: 30-34 [PMID: 18063419 DOI: 10.1016/j.cgh.2007.10.006]

10 **Khoury JE**, Chisholm S, Jamal MM, Palacio C, Pudhota S, Vega KJ. African Americans with Barrett's esophagus are less likely to have dysplasia at biopsy. *Dig Dis Sci* 2012; **57**: 419-423 [PMID: 21909989 DOI: 10.1007/s10620-011-1900-y]

11 **Qumseya BJ**, Bukannan A, Gendy S, Ahemd Y, Sultan S, Bain P, Gross SA, Iyer P, Wani S. Systematic review and meta-analysis of prevalence and risk factors for Barrett's esophagus. *Gastrointest Endosc* 2019; **90**: 707-717.e1 [PMID: 31152737 DOI: 10.1016/j.gie.2019.05.030]

12 **Wenker TN**, Tan MC, Liu Y, El-Serag HB, Thrift AP. Prior Diagnosis of Barrett's Esophagus Is Infrequent, but Associated with Improved Esophageal Adenocarcinoma Survival. *Dig Dis Sci* 2018; **63**: 3112-3119 [PMID: 30109579 DOI: 10.1007/s10620-018-5241-y]

13 **Yusuf A**, Fitzgerald RC. Screening for Barrett's Oesophagus: Are We Ready for it? *Curr Treat Options Gastroenterol* 2021; 1-16 [PMID: 33746508 DOI: 10.1007/s11938-021-00342-1]

14 **Shaheen NJ**, Falk GW, Iyer PG, Gerson LB; American College of Gastroenterology. ACG Clinical Guideline: Diagnosis and Management of Barrett's Esophagus. *Am J Gastroenterol* 2016; **111**: 30-50; quiz 51 [PMID: 26526079 DOI: 10.1038/ajg.2015.322]

15 **American Gastroenterological Association**, Spechler SJ, Sharma P, Souza RF, Inadomi JM, Shaheen NJ. American Gastroenterological Association medical position statement on the management of Barrett's esophagus. *Gastroenterology* 2011; **140**: 1084-1091 [PMID: 21376940 DOI: 10.1053/j.gastro.2011.01.030]

16 **Levy I**, Gralnek IM. Complications of diagnostic colonoscopy, upper endoscopy, and enteroscopy. *Best Pract Res Clin Gastroenterol* 2016; **30**: 705-718 [PMID: 27931631 DOI: 10.1016/j.bpg.2016.09.005]

17 **Wilkins T**, Gillies RA. Office-based ultrathin esophagogastroduodenoscopy in a primary care setting. *J Am Board Fam Pract* 2004; **17**: 438-442 [PMID: 15575035 DOI: 10.3122/jabfm.17.6.438]

18 **Cho S**, Arya N, Swan K, Cirocco M, Kandel G, Kortan P, Marcon N. Unsedated transnasal endoscopy: a Canadian experience in daily practice. *Can J Gastroenterol* 2008; **22**: 243-246 [PMID: 18354752 DOI: 10.1155/2008/514297]

19 **Sami SS**, Dunagan KT, Johnson ML, Schleck CD, Shah ND, Zinsmeister AR, Wongkeesong LM, Wang KK, Katzka DA, Ragunath K, Iyer PG. A randomized comparative effectiveness trial of novel endoscopic techniques and approaches for Barrett's esophagus screening in the community. *Am J Gastroenterol* 2015; **110**: 148-158 [PMID: 25488897 DOI: 10.1038/ajg.2014.362]

20 **Fernandez-Urien I**, Carretero C, Armendariz R, Muñoz-Navas M. Esophageal capsule endoscopy. *World J Gastroenterol* 2008; **14**: 5254-5260 [PMID: 18785275 DOI: 10.3748/wjg.14.5254]

21 **Bhardwaj A**, Hollenbeak CS, Pooran N, Mathew A. A meta-analysis of the diagnostic accuracy of esophageal capsule endoscopy for Barrett's esophagus in patients with gastroesophageal reflux disease. *Am J Gastroenterol* 2009; **104**: 1533-1539 [PMID: 19491867 DOI: 10.1038/ajg.2009.86]

22 **Park J**, Cho YK, Kim JH. Current and Future Use of Esophageal Capsule Endoscopy. *Clin Endosc* 2018; **51**: 317-322 [PMID: 30078304 DOI: 10.5946/ce.2018.101]

23 **Duvvuri A**, Desai M, Vennelaganti S, Higbee A, Gorrepati VS, Dasari C, Chandrasekar VT, Vennalaganti P, Kohli D, Sathyamurthy A, Rai T, Sharma P. Diagnostic accuracy of a novel third generation esophageal capsule as a non-invasive detection method for Barrett's esophagus: A pilot study. *J Gastroenterol Hepatol* 2021; **36**: 1222-1225 [PMID: 32996655 DOI: 10.1111/jgh.15283]

24 **Xiu H**, Lu Y, Liu X, Liu F, Zhang L, Zhao C, Sun X. Detachable string magnetically controlled capsule endoscopy for complete observation of the upper gastrointestinal tract. *Eur J Gastroenterol Hepatol* 2021; **33**: 508-513 [PMID: 32956183 DOI: 10.1097/MEG.0000000000001939]

25 **Song J**, Bai T, Zhang L, Xiang XL, Xie XP, Hou XH. Better view by detachable string magnetically controlled capsule endoscopy for esophageal observation: a retrospective comparative study. *Dis Esophagus* 2020; **33** [PMID: 32008045 DOI: 10.1093/dote/doz104]

26 **Chen YZ**, Pan J, Luo YY, Jiang X, Zou WB, Qian YY, Zhou W, Liu X, Li ZS, Liao Z. Detachable string magnetically controlled capsule endoscopy for complete viewing of the esophagus and stomach. *Endoscopy* 2019; **51**: 360-364 [PMID: 30822803 DOI: 10.1055/a-0856-6845]

27 **Wang S**, Huang Y, Hu W, Mao H, McAlindon ME, Liu Y, Yang L, Zhang C, Xu M, He C, Dang T, Wu B, Ji D, Zhang L, Mao X, Liu C, Xu D, Li Y, Li G, Han J, Lv F, Liang X, Jin S, Zhang S, Tai FWD, Xu Q, Yang C, Wang G, Wang L, Li B, Yang H, Xie P, Deng L, Ren L, Chang Z, Wang X, Wang S, Gao X, Li J, Zhu L, Wang F, Zhang G, Jiang X, Pan J, Meng W, Li X, Hou J, Dray X, Liao Z, Qi X. Detachable string magnetically controlled capsule endoscopy for detecting high-risk varices in compensated advanced chronic liver disease (CHESS1801): A prospective multicenter study. *Lancet Reg Health West Pac* 2021; **6**: 100072 [PMID: 34327406 DOI: 10.1016/j.lanwpc.2020.100072]

28 **Gerson L**, Lin OS. Cost-benefit analysis of capsule endoscopy compared with standard upper endoscopy for the detection of Barrett's esophagus. *Clin Gastroenterol Hepatol* 2007; **5**: 319-325 [PMID: 17368231 DOI: 10.1016/j.cgh.2006.12.022]

29 **Rubenstein JH**, Inadomi JM, Brill JV, Eisen GM. Cost utility of screening for Barrett's esophagus with esophageal capsule endoscopy *vs* conventional upper endoscopy. *Clin Gastroenterol Hepatol* 2007; **5**: 312-318 [PMID: 17368230 DOI: 10.1016/j.cgh.2006.12.008]

30 **Lin OS**, Schembre DB, Mergener K, Spaulding W, Lomah N, Ayub K, Brandabur JJ, Bredfeldt J, Drennan F, Gluck M, Jiranek GC, McCormick SE, Patterson D, Kozarek RA. Blinded comparison of esophageal capsule endoscopy *vs* conventional endoscopy for a diagnosis of Barrett's esophagus in patients with chronic gastroesophageal reflux. *Gastrointest Endosc* 2007; **65**: 577-583 [PMID: 17324414 DOI: 10.1016/j.gie.2006.06.035]

31 **Yun SH**, Tearney GJ, Vakoc BJ, Shishkov M, Oh WY, Desjardins AE, Suter MJ, Chan RC, Evans JA, Jang IK, Nishioka NS, de Boer JF, Bouma BE. Comprehensive volumetric optical microscopy in vivo. *Nat Med* 2006; **12**: 1429-1433 [PMID: 17115049 DOI: 10.1038/nm1450]

32 **Gora MJ**, Quénéhervé L, Carruth RW, Lu W, Rosenberg M, Sauk JS, Fasano A, Lauwers GY, Nishioka NS, Tearney GJ. Tethered capsule endomicroscopy for microscopic imaging of the esophagus, stomach, and duodenum without sedation in humans (with video). *Gastrointest Endosc* 2018; **88**: 830-840.e3 [PMID: 30031805 DOI: 10.1016/j.gie.2018.07.009]

33 **Gora MJ**, Sauk JS, Carruth RW, Gallagher KA, Suter MJ, Nishioka NS, Kava LE, Rosenberg M, Bouma BE, Tearney GJ. Tethered capsule endomicroscopy enables less invasive imaging of gastrointestinal tract microstructure. *Nat Med* 2013; **19**: 238-240 [PMID: 23314056 DOI: 10.1038/nm.3052]

34 **Dong J**, Grant C, Vuong B, Nishioka N, Gao AH, Beatty M, Baldwin G, Baillargeon A, Bablouzian A, Grahmann P, Bhat N, Ryan E, Barrios A, Giddings S, Ford T, Beaulieu-Ouellet E, Hosseiny SH, Lerman I, Trasischker W, Reddy R, Singh K, Gora M, Hyun D, Quénéhervé L, Wallace M, Wolfsen H, Sharma P, Wang KK, Leggett CL, Poneros J, Abrams JA, Lightdale C, Leeds S, Rosenberg M, Tearney GJ. Feasibility and Safety of Tethered Capsule Endomicroscopy in Patients With Barrett's Esophagus in a Multi-Center Study. *Clin Gastroenterol Hepatol* 2022; **20**: 756-765.e3 [PMID: 33549871 DOI: 10.1016/j.cgh.2021.02.008]

35 **Katz-Summercorn A**, Anand S, Ingledew S, Huang Y, Roberts T, Galeano-Dalmau N, O'Donovan M, Liu H, Fitzgerald RC. Application of a multi-gene next-generation sequencing panel to a non-invasive oesophageal cell-sampling device to diagnose dysplastic Barrett's oesophagus. *J Pathol Clin Res* 2017; **3**: 258-267 [PMID: 29085666 DOI: 10.1002/cjp2.80]

36 **Chettouh H**, Mowforth O, Galeano-Dalmau N, Bezawada N, Ross-Innes C, MacRae S, Debiram-Beecham I, O'Donovan M, Fitzgerald RC. Methylation panel is a diagnostic biomarker for Barrett's oesophagus in endoscopic biopsies and non-endoscopic cytology specimens. *Gut* 2018; **67**: 1942-1949 [PMID: 29084829 DOI: 10.1136/gutjnl-2017-314026]

37 **Li X**, Kleeman S, Coburn SB, Fumagalli C, Perner J, Jammula S, Pfeiffer RM, Orzolek L, Hao H, Taylor PR, Miremadi A, Galeano-Dalmau N, Lao-Sirieix P, Tennyson M, MacRae S, Cook MB, Fitzgerald RC. Selection and Application of Tissue microRNAs for Nonendoscopic Diagnosis of Barrett's Esophagus. *Gastroenterology* 2018; **155**: 771-783.e3 [PMID: 29906417 DOI: 10.1053/j.gastro.2018.05.050]

38 **Ross-Innes CS**, Debiram-Beecham I, O'Donovan M, Walker E, Varghese S, Lao-Sirieix P, Lovat L, Griffin M, Ragunath K, Haidry R, Sami SS, Kaye P, Novelli M, Disep B, Ostler R, Aigret B, North BV, Bhandari P, Haycock A, Morris D, Attwood S, Dhar A, Rees C, Rutter MD, Sasieni PD, Fitzgerald RC; BEST2 Study Group. Evaluation of a minimally invasive cell sampling device coupled with assessment of trefoil factor 3 expression for diagnosing Barrett's esophagus: a multi-center case-control study. *PLoS Med* 2015; **12**: e1001780 [PMID: 25634542 DOI: 10.1371/journal.pmed.1001780]

39 **Fitzgerald RC**, di Pietro M, O'Donovan M, Maroni R, Muldrew B, Debiram-Beecham I, Gehrung M, Offman J, Tripathi M, Smith SG, Aigret B, Walter FM, Rubin G; BEST3 Trial team, Sasieni P. Cytosponge-trefoil factor 3 *vs* usual care to identify Barrett's oesophagus in a primary care setting: a multicentre, pragmatic, randomised controlled trial. *Lancet* 2020; **396**: 333-344 [PMID: 32738955 DOI: 10.1016/S0140-6736(20)31099-0]

40 **Iqbal U**, Siddique O, Ovalle A, Anwar H, Moss SF. Safety and efficacy of a minimally invasive cell sampling device ('Cytosponge') in the diagnosis of esophageal pathology: a systematic review. *Eur J Gastroenterol Hepatol* 2018; **30**: 1261-1269 [PMID: 30044236 DOI: 10.1097/MEG.0000000000001210]

41 **Januszewicz W**, Tan WK, Lehovsky K, Debiram-Beecham I, Nuckcheddy T, Moist S, Kadri S, di Pietro M, Boussioutas A, Shaheen NJ, Katzka DA, Dellon ES, Fitzgerald RC; BEST1 and BEST2 study investigators. Safety and Acceptability of Esophageal Cytosponge Cell Collection Device in a Pooled Analysis of Data From Individual Patients. *Clin Gastroenterol Hepatol* 2019; **17**: 647-656.e1 [PMID: 30099104 DOI: 10.1016/j.cgh.2018.07.043]

42 **Iyer PG**, Taylor WR, Johnson ML, Lansing RL, Maixner KA, Yab TC, Simonson JA, Devens ME, Slettedahl SW, Mahoney DW, Berger CK, Foote PH, Smyrk TC, Wang KK, Wolfsen HC, Ahlquist DA. Highly Discriminant Methylated DNA Markers for the Non-endoscopic Detection of Barrett's Esophagus. *Am J Gastroenterol* 2018; **113**: 1156-1166 [PMID: 29891853 DOI: 10.1038/s41395-018-0107-7]

43 **Iyer PG**, Taylor WR, Johnson ML, Lansing RL, Maixner KA, Hemminger LL, Cayer FK, Yab TC, Devens ME, Slettedahl SW, Broderick BT, Mahoney DW, McGlinch MC, Berger CK, Foote PH, Giakomopoulos M, Allawi H, Smyrk TC, Wang KK, Katzka DA, Wolfsen HC, Burke JA, Ahlquist DA, Kisiel JB. Accurate Nonendoscopic Detection of Barrett's Esophagus by Methylated DNA Markers: A Multisite Case Control Study. *Am J Gastroenterol* 2020; **115**: 1201-1209 [PMID: 32558685 DOI: 10.14309/ajg.0000000000000656]

44 **Moinova HR**, LaFramboise T, Lutterbaugh JD, Chandar AK, Dumot J, Faulx A, Brock W, De la Cruz Cabrera O, Guda K, Barnholtz-Sloan JS, Iyer PG, Canto MI, Wang JS, Shaheen NJ, Thota PN, Willis JE, Chak A, Markowitz SD. Identifying DNA methylation biomarkers for non-endoscopic detection of Barrett's esophagus. *Sci Transl Med* 2018; **10** [PMID: 29343623 DOI: 10.1126/scitranslmed.aao5848]

45 **Bartel DP**. MicroRNAs: genomics, biogenesis, mechanism, and function. *Cell* 2004; **116**: 281-297 [PMID: 14744438 DOI: 10.1016/s0092-8674(04)00045-5]

46 **Clark RJ**, Craig MP, Agrawal S, Kadakia M. microRNA involvement in the onset and progression of Barrett's esophagus: a systematic review. *Oncotarget* 2018; **9**: 8179-8196 [PMID: 29487725 DOI: 10.18632/oncotarget.24145]

47 **Cabibi D**, Caruso S, Bazan V, Castiglia M, Bronte G, Ingrao S, Fanale D, Cangemi A, Calò V, Listì A, Incorvaia L, Galvano A, Pantuso G, Fiorentino E, Castorina S, Russo A. Analysis of tissue and circulating microRNA expression during metaplastic transformation of the esophagus. *Oncotarget* 2016; **7**: 47821-47830 [PMID: 27374102 DOI: 10.18632/oncotarget.10291]

48 **Wang L**, Ji F, Liu G, Wang W, Li Z, Yue Y, Wang Z. Upregulation of circulating miR130a is correlated with development of Barrett's esophagus and esophageal adenocarcinoma. *Onco Targets Ther* 2019; **12**: 1-7 [PMID: 30588024 DOI: 10.2147/OTT.S162603]

49 **Pavlov K**, Kluiver J, Meijer C, Boersma-van Ek W, Kruyt FAE, Karrenbeld A, Kleibeuker JH, Peters FTM, van den Berg A. Circulating miRNAs in patients with Barrett's esophagus, high-grade dysplasia and esophageal adenocarcinoma. *J Gastrointest Oncol* 2018; **9**: 1150-1156 [PMID: 30603135 DOI: 10.21037/jgo.2018.08.01]

50 **Craig MP**, Rajakaruna S, Paliy O, Sajjad M, Madhavan S, Reddy N, Zhang J, Bottomley M, Agrawal S, Kadakia MP. Differential MicroRNA Signatures in the Pathogenesis of Barrett's Esophagus. *Clin Transl Gastroenterol* 2020; **11**: e00125 [PMID: 31934893 DOI: 10.14309/ctg.0000000000000125]

51 **Hanna GB**, Boshier PR, Markar SR, Romano A. Accuracy and Methodologic Challenges of Volatile Organic Compound-Based Exhaled Breath Tests for Cancer Diagnosis: A Systematic Review and Meta-analysis. *JAMA Oncol* 2019; **5**: e182815 [PMID: 30128487 DOI: 10.1001/jamaoncol.2018.2815]

52 **Krilaviciute A**, Heiss JA, Leja M, Kupcinskas J, Haick H, Brenner H. Detection of cancer through exhaled breath: a systematic review. *Oncotarget* 2015; **6**: 38643-38657 [PMID: 26440312 DOI: 10.18632/oncotarget.5938]

53 **Peters Y**, Schrauwen RWM, Tan AC, Bogers SK, de Jong B, Siersema PD. Detection of Barrett's oesophagus through exhaled breath using an electronic nose device. *Gut* 2020; **69**: 1169-1172 [PMID: 32098798 DOI: 10.1136/gutjnl-2019-320273]

54 **Chan DK**, Zakko L, Visrodia KH, Leggett CL, Lutzke LS, Clemens MA, Allen JD, Anderson MA, Wang KK. Breath Testing for Barrett's Esophagus Using Exhaled Volatile Organic Compound Profiling With an Electronic Nose Device. *Gastroenterology* 2017; **152**: 24-26 [PMID: 27825962 DOI: 10.1053/j.gastro.2016.11.001]

55 **Markar SR**, Wiggins T, Antonowicz S, Chin ST, Romano A, Nikolic K, Evans B, Cunningham D, Mughal M, Lagergren J, Hanna GB. Assessment of a Noninvasive Exhaled Breath Test for the Diagnosis of Oesophagogastric Cancer. *JAMA Oncol* 2018; **4**: 970-976 [PMID: 29799976 DOI: 10.1001/jamaoncol.2018.0991]

56 **Kumar S**, Huang J, Abbassi-Ghadi N, Mackenzie HA, Veselkov KA, Hoare JM, Lovat LB, Španěl P, Smith D, Hanna GB. Mass Spectrometric Analysis of Exhaled Breath for the Identification of Volatile Organic Compound Biomarkers in Esophageal and Gastric Adenocarcinoma. *Ann Surg* 2015; **262**: 981-990 [PMID: 25575255 DOI: 10.1097/SLA.0000000000001101]

57 **Chan DK**, Leggett CL, Wang KK. Diagnosing gastrointestinal illnesses using fecal headspace volatile organic compounds. *World J Gastroenterol* 2016; **22**: 1639-1649 [PMID: 26819529 DOI: 10.3748/wjg.v22.i4.1639]

58 **Klein EA**, Richards D, Cohn A, Tummala M, Lapham R, Cosgrove D, Chung G, Clement J, Gao J, Hunkapiller N, Jamshidi A, Kurtzman KN, Seiden MV, Swanton C, Liu MC. Clinical validation of a targeted methylation-based multi-cancer early detection test using an independent validation set. *Ann Oncol* 2021; **32**: 1167-1177 [PMID: 34176681 DOI: 10.1016/j.annonc.2021.05.806]

59 **Nadauld LD**, McDonnell CH 3rd, Beer TM, Liu MC, Klein EA, Hudnut A, Whittington RA, Taylor B, Oxnard GR, Lipson J, Lopatin M, Shaknovich R, Chung KC, Fung ET, Schrag D, Marinac CR. The PATHFINDER Study: Assessment of the Implementation of an Investigational Multi-Cancer Early Detection Test into Clinical Practice. *Cancers (Basel)* 2021; **13** [PMID: 34298717 DOI: 10.3390/cancers13143501]

60 **ASGE Standards of Practice Committee**, Qumseya B, Sultan S, Bain P, Jamil L, Jacobson B, Anandasabapathy S, Agrawal D, Buxbaum JL, Fishman DS, Gurudu SR, Jue TL, Kripalani S, Lee JK, Khashab MA, Naveed M, Thosani NC, Yang J, DeWitt J, Wani S; ASGE Standards of Practice Committee Chair. ASGE guideline on screening and surveillance of Barrett's esophagus. *Gastrointest Endosc* 2019; **90**: 335-359.e2 [PMID: 31439127 DOI: 10.1016/j.gie.2019.05.012]

61 **Britton J**, Hamdy S, McLaughlin J, Horne M, Ang Y. Barrett's oesophagus: A qualitative study of patient burden, care delivery experience and follow-up needs. *Health Expect* 2019; **22**: 21-33 [PMID: 30430714 DOI: 10.1111/hex.12817]

62 **Adler A**, Geiger S, Keil A, Bias H, Schatz P, deVos T, Dhein J, Zimmermann M, Tauber R, Wiedenmann B. Improving compliance to colorectal cancer screening using blood and stool based tests in patients refusing screening colonoscopy in Germany. *BMC Gastroenterol* 2014; **14**: 183 [PMID: 25326034 DOI: 10.1186/1471-230X-14-183]

World Journal of Gastroenterology

Submit a Manuscript: https://www.f6publishing.com

World J Gastroenterol 2022 August 28; 28(32): 4527-4539

DOI: 10.3748/wjg.v28.i32.4527

ISSN 1007-9327 (print) ISSN 2219-2840 (online)

MINIREVIEWS

Impact of microbiota-immunity axis in pancreatic cancer management

Ilenia Bartolini, Giulia Nannini, Matteo Risaliti, Francesco Matarazzo, Luca Moraldi, Maria Novella Ringressi, Antonio Taddei, Amedeo Amedei

Specialty type: Gastroenterology and hepatology

Provenance and peer review: Invited article; Externally peer reviewed.

Peer-review model: Single blind

Peer-review report's scientific quality classification

Grade A (Excellent): 0
Grade B (Very good): B, B
Grade C (Good): C, C, C
Grade D (Fair): D
Grade E (Poor): 0

P-Reviewer: Jiang M, China; Leowattana W, Thailand; Li HL, China; Luo ZW, China; Uhlmann D, Germany; Volynets GV, Russia

Received: January 19, 2022
Peer-review started: January 19, 2022
First decision: May 29, 2022
Revised: June 28, 2022
Accepted: July 27, 2022
Article in press: July 27, 2022
Published online: August 28, 2022

Ilenia Bartolini, Matteo Risaliti, Francesco Matarazzo, Maria Novella Ringressi, Antonio Taddei, Department of Experimental and Clinical Medicine, HPB Surgery Unit, Azienda Ospedaliero-Universitaria Careggi, Florence 50134, Italy

Giulia Nannini, Amedeo Amedei, Department of Experimental and Clinical Medicine, SOD of Interdisciplinary Internal Medicine, Azienda Ospedaliera-Universitaria Careggi, Florence 50134, Italy

Luca Moraldi, Division of Oncologic Surgery, Department of Oncology, Careggi University Hospital, Firenze 50134, Italy

Corresponding author: Amedeo Amedei, PhD, Professor, Department of Experimental and Clinical Medicine, SOD of Interdisciplinary Internal Medicine, Azienda Ospedaliera-Universitaria Careggi, Largo Brambilla 3, Florence 50134, Italy. amedeo.amedei@unifi.it

Abstract

The microbiota impact on human diseases is well-known, and a growing body of literature is providing evidence about the complex interplay between microbiota-immune system-human physiology/pathology, including cancers. Together with the defined risk factors (*e.g.*, smoke habits, diet, diabetes, and obesity), the oral, gut, biliary, and intrapancreatic microbiota contribute to pancreatic cancer development through different pathways including the interaction with the immune system. Unfortunately, a great majority of the pancreatic cancer patients received a diagnosis in advanced stages not amenable to be radically treated and potentially cured. Given the poor pancreatic cancer prognosis, complete knowledge of these complicated relationships could help researchers better understand the disease pathogenesis and thus provide early potential non-invasive biomarkers, new therapeutic targets, and tools for risk stratification that might result in greater therapeutic possibilities and eventually in a better and longer patient survival.

Key Words: Gastrointestinal tumors; Hepatopancreatobiliary tumors; Pancreatic cancer; Gut microbiota; Dysbiosis; Cancer development; Carcinogenesis

©The Author(s) 2022. Published by Baishideng Publishing Group Inc. All rights reserved.

Core Tip: Despite improvements in traditional patient treatment, pancreatic cancer remains a tumor with an increasing incidence and a poor prognosis, often diagnosed in late stages. The oral, gut, biliary, and intrapancreatic microbiota might contribute to pancreatic cancer through different pathways including a complex interplay with the immune system. Comprehending these complicated relationships could help researchers better understand the pathogenesis of pancreatic cancer, thus providing new promising options for early diagnosis, therapeutic targets, and risk stratification hoping that could translate into better and longer patient survival.

Citation: Bartolini I, Nannini G, Risaliti M, Matarazzo F, Moraldi L, Ringressi MN, Taddei A, Amedei A. Impact of microbiota-immunity axis in pancreatic cancer management. *World J Gastroenterol* 2022; 28(32): 4527-4539
URL: https://www.wjgnet.com/1007-9327/full/v28/i32/4527.htm
DOI: https://dx.doi.org/10.3748/wjg.v28.i32.4527

INTRODUCTION

Pancreatic cancer (PanCa), with its most common subtype ductal adenocarcinoma, is a relatively uncommon but highly lethal neoplasm. Despite years of research, the PanCa patients are often diagnosed in advanced stages having less than a 30% chance of being alive 1 year after diagnosis and less than a 10% 5-year survival rate[1-3].

The human body is colonized by a huge number of microorganisms, which include bacteria, archaea, viruses, and fungi. This articulate community with the environment and the microorganism metabolites is known as microbiota. Usually, the commensal community lives in equilibrium with the host in a condition defined as "eubiosis;" however, if for some reason the equilibrium is broken, a condition called dysbiosis occurs[4]. A growing body of the literature reported the complex interplay of the microbiota with the immune system and the intestinal barrier in a bidirectional influence that plays a key role in health and disease, including cancer[5-7].

Evidence about the potential causal role of microbiota on PanCa development is still scarce, but it is gaining great attention over the last few years[8,9]. The oral, gut, biliary, and intrapancreatic microbiota seem to contribute to PanCa initiation and development. Furthermore, microbiota both act through a direct effect or indirectly through the interaction with the immune system or through the production of circulating toxins. Understanding these complicated relationships could help researchers better define the causes of different pathologies, including PanCa, and thus provide new therapeutic targets and tools for risk stratification[10].

Finally, given the diagnosis frequently made in advanced stages and the poor prognosis of this tumor together with the lack of markers able to detect an early PanCa, the chance to use the gut microbiota as an early non-invasive biomarker might result in greater therapeutic possibilities and, eventually, in a better and longer patient survival[11].

This review aims to provide the current state of the microbiota immunity axis impact in every step of PanCa, trying to highlight potential promising new therapeutic options.

CANCER DEVELOPMENT

Although often no identifiable risk factors can be found, genetic factors, lifestyle, and chronic pancreatitis are well-recognized[12]. It is notable that most of them cause dysbiosis too[1,12].

Because an estimated 70% of the bacteria in the human body have not been grown yet, studying the human microbiota is a difficult endeavor[13]. A breakthrough in DNA sequencing occurred in the mid-2000s thanks to next-generation sequencing[14]. Through gene sequencing, metagenomics, metatranscriptomics, metaproteomics, and metabolomics (the recently introduced "meta-omics" techniques) analysis of strain composition, production of metabolites, and other bacterial activities can be performed [15,16]. Consequently, the significant microbiota impact on human physiology and pathology has been increasingly acknowledged over the years. Although the evidence is still in its infancy, being a small part of more complex mechanisms, the potential role of the microbiome itself and microbiome-immune system interplay on PanCa onset and development has been recently advocated.

Different microbial compositions in healthy people and disease

Although whether changes in the balance between microbial species could be a cause or an effect of disease onset and development is difficult to state[17], microbial composition analyses have been performed in different districts including the oral cavity, duodenum, gut, bile, and pancreatic tissue. Conflicting results can be found in analyzing the studies, but the influence of other risk factors (for

example, smoking habit) may create bias and at least, partially explain some differences.

Association between periodontal disease or oral dysbiosis and several kinds of cancers (oral, hematological, digestive tract, prostate, uterus, lung, and breast) has been reported with different strengths of association[18]. In analyzing this relationship, PanCa has been one of the most studied cancers[16,18]. *Porphyromonas gingivalis, Fusobacterium,* and *Aggregatibacter actinomycetemcomitans* in the oral microbiota were related to a higher risk of developing PanCa[17,19,20]. Similarly, analyzing the saliva, the presence of *Streptococcus* and *Leptotrichia* was associated with a higher risk of human PanCa, and *Granulicatella adiacens* was found to be increased in these patients. On the contrary, the presence of *Veillonella* and *Neisseria* was associated with a lower risk of PanCa, and *Streptococcus mitis* appeared to be reduced in these patients[21-23]. Higher representation of *Prevotella* and *Vaillonella* was more frequently found in patients with jaundice[22].

Fusobacterium, Rothia, Actinomyces, Corynebacterium, Atopobium, Peptostreptococcus, Catonella, Oribacterium, Filifactor, Campylobacter, Moraxella, and *Tannerella* were more abundant in the PanCa patients' tongue coatings, while *Haemophilus, Porphyromonas,* and *Paraprevotella* were more abundant in healthy people. *Haemophilus* and *Porphyromonas* or *Leptotrichia* and *Fusobacterium* represented unique signatures able to identify healthy people or patients with PanCa[24].

Helicobacter pylori (*H. pylori*) is a well-known pathogenetic agent in gastric cancer, and its role in colorectal cancer development has also been suggested[25]. Being more represented in the stomach and duodenum of the PanCa patients than in controls, *H. pylori* could also have a role in the development of this cancer. It elicits chronic mucosal inflammation and alters the gut microbiota causing bacterial translocation[3,26]. However, this relationship is particularly argued due to the frequent associations with several other known risk factors thus precluding definitive conclusions[9].

Association between gut dysbiosis and several kinds of cancers (breast, lung, digestive tract, and above all colorectal) has been reported. Lower gut microbial biodiversity was found in stool samples of PanCa patients[27]. Furthermore, significantly higher levels of mucus-degrader Verrucomicrobia and Bacteroidetes including the Gram-negative bacteria lipopolysaccharide (LPS) producers *Prevotella* and *Hallella* together with other LPS producers *Veillonella*, *Klebsiella*, *Selenomonas*, and *Enterobacter* have been found in the gut microbiota of PanCa patients compared to healthy people. In parallel, lower levels of other Firmicutes, notably the butyrate-producers *Coprococcus* and *Anaerostipes*, have been found[2,27,28]. However, the exact clinical correlation is still unknown, and further studies are needed. Finally, higher levels of *Bifidobacterium pseudolongum* were documented in both gut and tumor specimens[28].

The pancreas is considered a sterile organ because of its alkaline pH and the presence of digestive enzymes that make bacterial proliferation difficult[29]. However, some potential ways through which microbes could reach it have been recently proposed even if definitive conclusions cannot be drawn. They include colonization from the duodenum or the biliary tract following reflux and colonization through the lymphatic and/or portal system[28]. Finally, the potential tissue contamination during sample collection and processing is another way of colonization. The majority of the human PanCa tissues were found to be colonized, mainly by *Gammaproteobacteria*[30-33], and a greater abundance of bacteria and fungi have been found in PanCa tissue of both human and animal models[28,30,31].

Acinetobacter, Enterobacter, Pseudomonas, Delftia, Enterococcus, Streptococcus, Corynebacterium, Propionibacterium, Sphingomonas, and *Staphylococcus* with a significant *Klebsiella* predominance were found in the human PanCa group compared to the healthy control (samples from organ donations)[32]. In addition, higher levels of *Malassezia* species in cancer tissue were related to PanCa progression, while *Candida, Aspergillus,* or *Saccharomyces* species did not cause cancer development after repopulation following mycobiome ablation[34]. In animal models, a relatively higher abundance of *Lactobacillus* was found in the pancreatic tissue of the control group, while a relatively higher abundance of *Fusobacterium* species and Proteobacteria were found in the pancreatic tissue of the cancer group[17,33]. Furthermore, significant differences have been discovered in microbiota composition found in different PanCa stages [28].

Finally, bile contamination, mainly related to biliary stenting and endoscopic procedures, was significantly found in patients affected by PanCa. The more represented species in bile samples (collected during endoscopic procedures or surgery) were *Escherichia coli* (*E. coli*) and different species of *Pseudomonas*, *Enterobacter*, and *Enterococcus*[34-37].

The main microbiota modifications are summarized in Table 1.

Pathogenetic PanCa models

The pathogenetic relationship between microbiota and PanCa is far from being completely understood, and the proposed potential pathogenetic mechanisms are derived mainly from animal models[17]. The microbiota promotes carcinogenesis in direct or indirect ways. Indirect action could be elicited through the production of circulating toxins or harmful metabolites or through the interaction with the immune system. Both innate and adaptive immune responses are active in fighting human cancers[38]. The anticancer immunological mechanisms include the cytotoxic CD 8+ T cells, T helper (Th) cells, mature dendritic cells, macrophages, and natural killer cells. Myeloid-derived suppressor cells (MDSCs) are immature myeloid cells able to suppress both innate and adaptive immunity with different mechanisms, promoting regulatory T cell development and simultaneously inhibiting the effector T cells and natural killer cells[39].

Table 1 Different microbial compositions in patients affected by pancreatic cancer

Anatomical district	Microbiota	Implications
Oral		
	Higher microbial biodiversity	Confer higher risk of developing PanCa[17,19,20,23]
	Porphyromonas gingivalis, Fusobacterium	
	Aggregatibacter actinomycetemcomitans	
	Streptococcus, Leptotrichia, Neisseria elongata	
	Granulicatella adiacens	More abundant in PanCa than control[23]
	Fusobacterium, Rothia, Actinomyces	
	Corynebacterium, Atopobium	
	Peptostreptococcus, Catonella	
	Oribacterium, Filifactor	
	Campylobacter, Moraxella, Tannerella	
	Fungi:	
	Candida	
Gut		
	Bacteroidetes	More abundant in PanCa than control[27,28]
	Prevotella, Hallella	
	Proteobacteria	
	Klebsiella, Enterobacter	
	Verrucomicrobia	
	Bifidobacterium pseudolongum	
	Veillonella	
	Firmicutes	Less abundant in PanCa than control[27]
	Coprococcus, Anaerostipes	
Pancreas		
	Proteobacteria	More abundant in PanCa than control[17,28,30-33]
	Gammaproteobacteria	
	Pseudomonas, Acinetobacter, Enterobacter	
	Delftia, Klebsiella, Sphingomonas	
	Firmicutes	
	Enterococcus, Streptococcus, Staphylococcus	
	Fusobacteria	
	Fusobacterium species	
	Acinetobacteria	
	Bifidobacterium pseudolongum	
	Corynebacterium, Propionibacterium	
	Lactobacillus	Less abundant in PanCa than control[17,33]
	Fungi	Confer higher risk of PanCa progression[31]
	Malassezia	

PanCa: Pancreatic cancer.

Most of these models have also been reported in other cancer types.

A direct carcinogenic effect of *Porphyromonas gingivalis* is related to the apoptosis inhibition of the epithelial cells, the activation of the *p53* gene, and the induction of *KRAS* mutation, the latter two through the production of the enzyme peptidyl-arginine deiminase[40]. *KRAS* mutation can be found in almost all PanCa. Interestingly, germ-free *KRAS*-mutated mice demonstrated slower PanCa progression suggesting that gene mutation itself is not sufficient to cause cancer development[28,29]. Intestinal microbiota has a direct long-distance effect on PanCa development through up/downregulation of pro/anti-cancer pathways[32]. *Pseudomonas aeruginosa* is related to higher levels of the anti-apoptotic and pro-proliferative proteins Bel-XL, Mcl-1, survivin, c-Myc, and cyclin DI[41]. The hepatotropic viruses that cause hepatitis B or C can contribute to PanCa development through the modulation of the PI3K/AKT signaling pathway and tissue inflammation[22].

One of the most common bacterial components related to cancer development is LPS, which is a direct cause of *KRAS* gene mutation and can stimulate nuclear factor-κB that further increases *KRAS* mutation risk. Furthermore, LPS is an activator of the toll-like receptor (TLR) signaling pathway thus enhancing pancreatic inflammation[21,29]. *H. pylori* is an LPS producer[29]. Deoxycholic acid, a bacterial metabolite of cholic acid, promotes carcinogenesis through the activation of the epidermal growth factor and STAT3 signaling pathway[2]. *Desulfovibrio vulgaris* and other sulfate-reducing bacteria produce genotoxic hydrogen sulfide when the diet is enriched in proteins and fats[42]. Other carcinogenic bacterial metabolites from proteolytic fermentation include phenols, ammonia, and other nitrogen-rich products. *Candida* induces PanCa through the production of the carcinogen nitrosamines or acetaldehyde[10,43].

Finally, many studies highlighted the role of the immune system on PanCa[44-46]. The activation of the immune system by the microbiota of different districts can cause local and/or systemic inflammation that worsen dysbiosis sustaining a vicious circle. For example, *H. pylori* presence in the stomach is related to reduced production of acid/achlorhydria that might trigger dysbiosis[9]. Gut dysbiosis induces chronic pancreatic inflammation. Pancreatic microbiota can further elicit an inflammatory response interacting with both innate and specific immune systems. The immunosuppressive cells, regulatory T cells and MDSC, are predominant at the expense of cytotoxic T lymphocytes, indicating that the phenotype is immunosuppressive[32,44,47]. This aspect implies that the immune system is faulty, most likely due to cancer itself, which causes local and systemic immunological dysfunction escaping the immune system's detection[48,49].

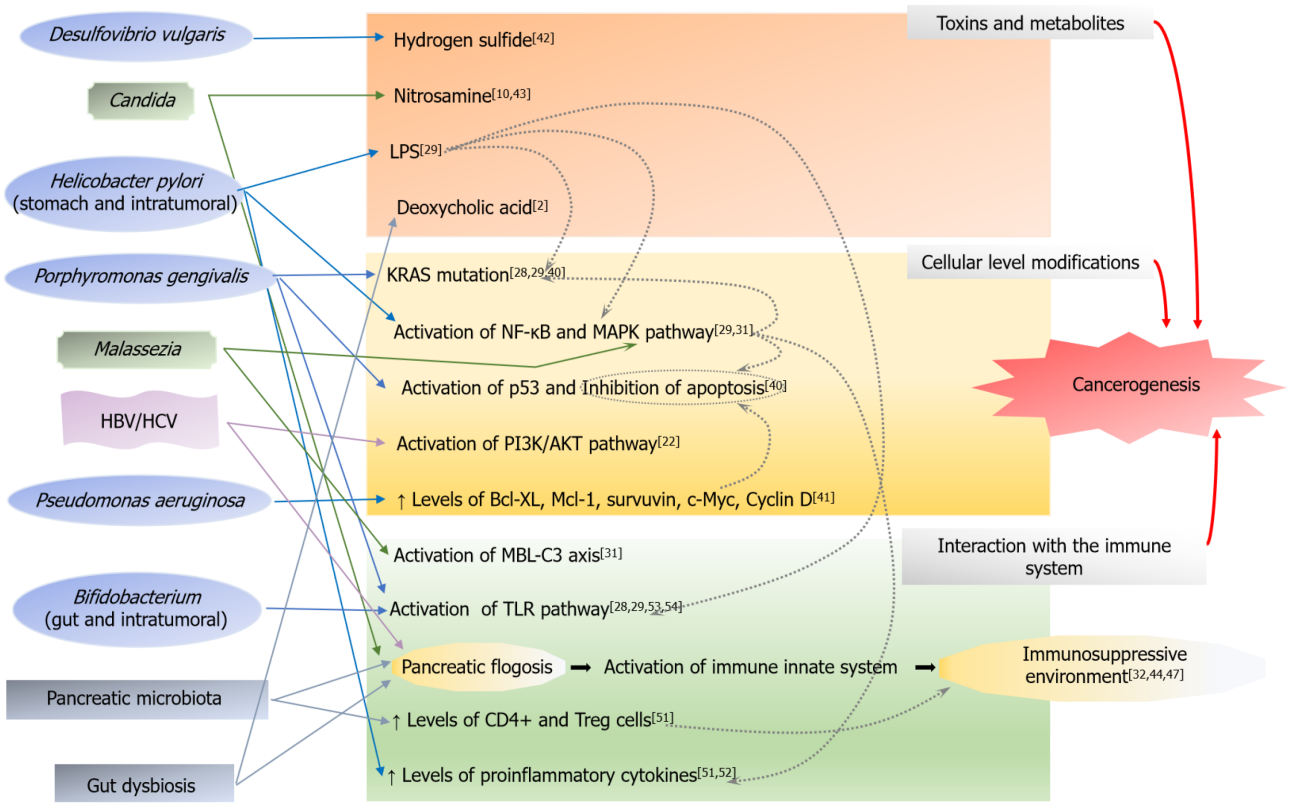
Furthermore, the tumor microenvironment contributes to the development of PanCa promoting a Th2 polarization with the production of higher levels of interleukin (IL)-17 and IL-10 and reduced production of interferon-γ, which promotes cancer progression[28,50]. The presence of this microenvironment kind and a dense stroma represents a unique PanCa peculiarity[51]. Interestingly, smoke habits impact microbiota inducing immunosuppression with reduced levels of IgG and the making of biofilms, hence possibly promoting the proliferation of harmful bacteria[30]. In an experimental setting, Pushalkar *et al*[28] demonstrated that germ-free mice did not show PanCa progression, while fecal microbiota transplantation received from sick mice hampered Th1 differentiation of CD4+ and activation of CD8+ T cells hence causing cancer progression.

In humans, *Citrobacter freundii* was found to be associated with immunosuppression and the activation of several oncogenic pathways. Furthermore, the enrichment of nine microbes including *Acidovorax ebreus* and *Shigella sonnei* was related to the downregulation of tumor-suppressive pathways and immune dysregulation with reduced levels of M2 macrophages, activated memory, and CD8+ T cells[51]. *H. pylori* infection of human PanCa tissue was reported to be associated with higher levels of IL-8 and vascular endothelial growth factor and with the proliferation of several factors including nuclear factor-κB, activator protein 1, and serum response element[52].

Malassezia can interact with the MAPK pathway causing the production of high levels of proinflammatory cytokines, including IL-6, and can activate mast cells[31]. Similarly, *Trichosporon* can increase the level of IL-6, tumor necrosis factor-α, and interferon-γ[8]. *Candida* triggers inflammatory response (Th17-mediated), activating the MDSCs[10,43]. *Porphyromonas gingivalis* and *Aggregatibacter* activate, similarly to *Bifidobacterium pseudolongum*[53], the TLR signaling pathway increasing the risk of PanCa development in both animal models and humans[28,54]. Different studies documented that mice deficient in pattern recognition receptors signaling, including TLR 4, TLR7, TLR9, and mincle, show less PanCa progression[53,55,56].

In this scenario, another critical pattern recognition receptors is the mannose-binding lectin (MBL). The complement cascade is triggered when MBL binds to the glycans of the fungal wall, for example, *Malassezia*. The MBL-C3 axis might be involved in cancer development given that extratumoral suppression of MBL or C3 was associated with a lower risk of PanCa onset and MBL- or C3-deficient mice showed greater defense against PanCa progression[31].

Each component of the microbiota might be implicated in PanCa through different pathogenetic mechanisms and the role of fungal dysbiosis is still far from being completely explored and understood. Figure 1 summarizes this complex relationship.



DOI: 10.3748/wjg.v28.i32.4527 **Copyright** ©The Author(s) 2022.

Figure 1 Pathogenetic models. This figure aims at simplifying the complex interplay between microbiota in different anatomical districts and the immune system in carcinogenesis. Each component of the microbiota might be implicated in pancreatic cancer through different pathogenetic mechanisms. LPS: Lipopolysaccharide; NF-kB: Nuclear Factor kB; HBV/HCV: Hepatitis B/C virus; MBL: Mannose-binding lectin; TLR: Toll-like receptor; Treg: T regulatory.

CURRENT TREATMENTS FOR PanCa

Impact of microbiota in surgical treatment

Whenever technically feasible and oncologically appropriate, surgical treatment is the best chance of cure that could be offered to the patients.

In a small prospective study, both pre- and postoperative gut microbiota was found to be enriched in *Akkermansia, Aeromonas, Enterobacteriaceae, Bacteroidales* and decreased in *Lachnospiraceae, Prevotella,* and *Faecatitalea*. Furthermore, *Bacteroides* were more frequently associated with higher postoperative morbidity, longer hospital stays, and longer intensive care unit stay[57].

When patients present with severe jaundice, a biliary drain is required before surgery. On the one hand, biliary drain could cause bile contamination; on the other hand, it could restore physiologic bile flow permitting the maintenance of gut eubiosis. The percentage of bile contamination in stented patients was reported to be up to 92% of the samples collected during surgery, while fungal presence was found in 25% of the patients. Fungal presence was directly related to the longer period between biliary drain positioning and surgery[58]. A frequent presence of at least one bacterial species showing antibiotic resistance was also reported, and these patients presented with significantly higher rates of postoperative morbidity[37]. In a large retrospective analysis of 1964 patients undergoing pancreatoduodenectomy and receiving preoperative biliary drain, 30.8% of them presented biliary contamination with the most common contaminants being *Enterococcus, Klebsiella*, and *Enterobacter*.

Postoperative pancreatic fistula (POPF) is the main postoperative complication following pancreatic surgery, and it is related to higher morbidity rates. Bile contamination was an independent risk factor for POPF grade B/C with an odds ratio of 1.33. Furthermore, bile contamination was associated with wound and catheter infections[36]. Similar data were reported in successively published papers[59]. Coppola *et al*[60] found in the bile different microbes related to different complications: *E. coli*, *Klebsiella pneumoniae (K. pneumoniae)*, and *Enterococcus faecalis* were prevalent in surgical site infections; *E. coli*, *K. pneumoniae*, *Enterococcus faecalis*, and *Enterococcus faecium* were more abundant in POPF; and *E. coli*, *Enterococcus faecalis* and *Enterococcus faecium* were found in delayed empty gastric syndrome. Abe *et al*[61] analyzed the cultures of drainage fluid from patients undergoing pancreatic surgery. They found that the presence of *Enterobacter* species, *Enterococcus* species, and *Candida* species was significantly associated with clinically relevant POPF. Furthermore, the presence of *Candida* species resulted in being an independent factor for POPF C and POPF-related hemorrhages[61,62]. On the contrary, in other

studies (with a restricted number of patients), bactobilia or fungal bile contamination were not reported to be associated with higher POPF rates or different global morbidity and mortality rates[58,63]. Different population samples and geographic bias in defining POPF or in sample collection and analysis could at least partially explain the differences.

Impact of microbiota in chemotherapy response

In the setting of advanced stages, traditional chemotherapy, mainly based on the FOLFIRINOX regimen (5-fluorouracil, oxaliplatin, and irinotecan) or gemcitabine with or without cisplatin or nab-paclitaxel, has a pivotal role. Chemoresistance is one of the most challenging aspects of systemic treatment.

Microbiota affects gemcitabine response thus influencing patients' prognoses. Most of the PanCa-associated abundant bacteria, including *K. pneumoniae* and other species from the *Gammaproteobacteria*, are cytidine deaminase producers. The production of this enzyme results in higher gemcitabine degradation and consequent chemoresistance[30]. Consistently, quinolone administration in patients infected with *K. pneumoniae* allowed for a better prognosis[64]. Nevertheless, gemcitabine use can alter the gut microbiota composition being a potential cause of PanCa progression[65], and the use of antibiotics increases side effects[66]. Adding *Lactobacillus paracasei* improved gemcitabine response in mouse models[67]. Similarly, *Lactobacillus spp*. reduced diarrhea, which is one of the most common side effects of chemotherapy based on irinotecan[42].

Although evidence is still scarce, the use of oncolytic viruses, mostly adenovirus, in combination with gemcitabine may improve its efficacy through different mechanisms including an antitumor immunity booster activity[68].

Other relations between microbiota and response to chemotherapy have been tested for other kinds of solid cancer, and specific data on PanCa are still needed[42].

Impact of microbiota in immunotherapy

Immunotherapy resulted in a game-changer in the treatment of several solid malignancies in the recent decade, and the inhibition of immunological checkpoints has been the most explored strategy for eliciting an antitumor immune response[69,70]. The immune checkpoint inhibitors are monoclonal antibodies targeting molecules, such as the programmed cell death protein 1/programmed death-ligand 1 or cytotoxic T-lymphocyte antigen 4 expressed by tumor or immune cells.

PanCa is one of the cancers for which no immunotherapeutic drugs have been licensed since many clinical trials have failed to show a benefit in terms of response rate and survival[42]. The weak success of the immune checkpoint inhibitor treatment is due to the immunologically "cold" phenotype characterized by the low mutation load and limited expression of neoantigens in PanCa in addition to the immunosuppressive action of the resident stromal cells. Although the fine mechanism of interaction between the microbiota and the immune system in PanCa needs to be examined in-depth, the combination of immune checkpoint inhibitors and chemotherapy could produce promising results. For example, specific polymeric nanoformulations of oxaliplatin and doxorubicin can upregulate the damage-associated molecular patterns expression in PanCa models, activating dendritic cell maturation and adaptive immune response[71]. These two nanoformulations act both by preventing tumor growth and by showing a prophylactic action through inoculation in Pan02 mouse models.

Vaccines are the most effective way to overcome the PanCa hypoimmunogenicity, and nanotechnologies can enhance their immunostimulatory effects[72].

Recent studies have highlighted the importance of stromal macrophages demonstrating the possibility to restore antitumor immunity. The employment of TLR agonists and kinase inhibitors can induce an M1-like polarization. Different PanCa models have been treated with nanoformulations with the ability to reprogram the macrophages phenotype, showing excellent results[73,74].

OTHER IMPLICATIONS OF MICROBIOTA ALTERATIONS AND OTHER FUTURE PERSPECTIVES

Modifying microbiota composition to reduce the risk of PanCa development

As previously reported, several modifiable risk factors have been recognized including smoking habits, alcohol abuse, and diet (high meat intake and low fruit consumption). It is expected that about a quarter of PanCa could be avoided by acting on these factors[9,75]. Since most of them are strictly connected with the microbiota, the possibility to modulate its composition or function could be a promising tool against cancer. There is an ongoing phase II randomized clinical trial (NCT04631445) analyzing the effect of a ketogenic diet in metastatic patients receiving chemotherapy, but unluckily the microbiota evaluation is not included.

A growing number of studies are analyzing the potential role of the so-called "next-generation probiotics" or "live biotherapeutics" that includes short-chain fatty acids producers. These microbes are implied in maintaining the intestinal barrier integrity with the reduction of bacterial translocation and in the reduction of fungal overgrowth[2]. But, to date, specific results of the effects on PanCa are lacking.

In animal models, the 4-wk oral administration of the probiotics *Lactobacillus paracasei* and *Lactobacillus reuteri* alone or combined with an intraperitoneal injection of gentamicin was related to a lower chance of developing precursors of PanCa. Furthermore, they allowed a lower increase of liver enzymes caused by gemcitabine[76]. Similarly, oral administration of the probiotic *Aspergillus oryzae* showed an antitumoral activity. The heptelidic acid was the involved bacterial-produced molecule able to pass the intestinal barrier, reach other organs, and induce apoptosis through the p38 MAPK signaling pathway [77].

In experimental studies with xenografts, Sethi *et al*[50] found that administration of oral antibiotics causing bacterial depletion achieved an antitumor effect through a switch from Th2 immune phenotype toward a Th1 differentiation of CD4+ T cells, with the activation of CD8+ T cells, lower levels of MDSCs, and finally an increase in M1 macrophage differentiation together with lower levels of the protumor IL-17a and IL-10 in the tumor microenvironment. Furthermore, these changes were not seen in T and B cells-deprived animals. Similarly, the administration of oral antibiotics to wild-type mice caused a reduction of the PanCa size by 50% through the reversing of the immunosuppressive tumor microenvironment[28].

Further research about microbial engineering strategies that could allow on-site recruitment of CD8+ T cells *via* interferon-γ production or interaction with the complement cascade is strongly warranted[2].

Despite few specific studies being available, the fecal microbiota transplant through modifying the entire gut microbiota ecology, could represent a great opportunity in PanCa treatment. Experiments in fecal microbiota transplantation animal models confirmed the responsibility of gut microbiota in the modulation of the intratumoral microbiome[78].

Drug delivery systems are bio-responsive elements able to change and thus release drugs in a particular microenvironment (*e.g.*, low level of pH, hypoxia, or presence of specific enzymes). Consequently, the drug delivery systems have been recently proposed as a promising instrument for microbiota modulation through the delivery of pre/probiotics with the capability of depleting protumoral bacteria and eliminating their toxins[79].

However, specific studies are needed to introduce this promising tool in routine clinical practice.

Microbiota as a biomarker of PanCa

Since complete PanCa prevention is not expected, an early diagnosis would be of great help in widening the chance to cure the patients.

Within the species found to be increased/decreased in the saliva of the affected patients compared to the control group, *Neisseria elongata* and *Streptococcus mitis* resulted in a distinguishing signature of PanCa with a sensitivity of 96.4% and a specificity of 82.1% representing a potential biomarker for early cancer detection[23]. In the saliva of the PanCa patients, the ratio of *Leptotrichia* and *Porphyromonas* was reported to be significantly higher compared with the control group[53]. The presence of a high level of serum antibodies against *Porphyromonas gingivalis* was found to be associated with a two-fold higher risk of developing PanCa within 5 years, while high levels of anti-commensal microbe antibodies seemed related to a reduced risk of PanCa[11].

Kim *et al*[80] found that altered human microbiota composition evaluated with microbial extracellular vesicles from blood samples could represent a novel biomarker. Six species, *Ruminococcaceae UCG-014, Lachnospiraceae NK4A136 group, Akkermansia, Turicibacter, Ruminiclostridium,* and *Lachnospiraceae UCG-001*, were more abundant, while four species, *Stenotrophomonas, Sphingomonas, Propionibacterium*, and *Corynebacterium*, were less represented in PanCa patients. With these findings, a prediction model for PanCa was built, and the related area under the receiver operating characteristic curve was 1.000[80].

Furthermore, experiments with spontaneous PanCa in animal models demonstrated that the polyamine metabolism of some gut bacteria including *Lactobacillus* was significantly dysregulated in the very early stages of PanCa[1].

Unfortunately, none of the presented potential biomarkers is available in clinical practice[21]. So, further studies are strongly warranted to validate new diagnostic tools.

Prognostic value of changes in the microbiota of the PanCa patients

One of the most frequently asked questions by patients affected by cancers is about their prognosis. The finding of further prognostic markers, other than the well-known staging systems, could help doctors answer this patient concern.

Riquelme *et al*[78] compared the disparity in microbiota composition of the PanCa tissue of the patients with different prognoses using 16S rRNA gene sequencing. Long-term survivors (alive 5 years after surgery) showed the highest alpha-diversity and a particular signature composed of *Pseudoxanthomonas, Streptomyces, Saccharopolyspora,* and *Bacillus clausii* with an area under the curve of 97.5%. Furthermore, this group of bacteria was associated with greater activation of CD8+ T cells. Furthermore, gut microbiome from short-term survival could induce PanCa onset in a mouse model through the establishment of an immunosuppressive environment suggesting the role of both intrapancreatic and gut microbiome[28,78]. Tumors showing a lower immunosuppressive environment (more neoantigens MUC16 - CA 125 - and CD8+ T cells) confer longer survival rates[81].

Using data from The Cancer Genome Atlas, Chakladar *et al*[51] found that only *Acidovorax ebreus* was linked to a high tumor grade. A significantly higher microbial biodiversity in metastatic and short-survival patients with a predominant percentage of Proteobacteria, particularly *Acidovorax ebreus* and members of the *Gammaproteobacteria*, was also reported. *Citrobacter freundii* and *Shigella sonnei* were associated with the dysregulation of cancer-associated pathways. Furthermore, they found different microbes associated with survival and metastasis. Analyzing The Cancer Genome Atlas database, a prognostic score was proposed by other authors. The high tumor score was associated with p53 mutation, higher tumor mutational burden, and unfavorable and immunosuppressive tumor microenvironment. This high score was found to be related to increased cell proliferation and a higher chance of achieving a positive margin following surgery[82].

In a study with almost 300 PanCa patients, the presence of *Fusobacterium* species was found to be an independent factor of higher mortality[83]. Similarly, the presence of *Pseudomonas aeruginosa* was found to be a negative prognostic biomarker[41].

CONCLUSION

The complex interplay between microbiota and the immune system at different anatomical districts (mostly gut and pancreas/intratumor) might have a role in both the onset and progression of PanCa. Due to the poor prognosis of this tumor despite global advances in surgery and perioperative management, every effort to find new potential targets is welcome. Modifications in microbial composition related to cancer onset could be both a promising target for microbiota shaping and cancer treatment and a potential biomarker for early cancer detection. With the progressive advances in microbiota knowledge, new possibilities for treatment and patient stratification could be expected in the coming years with an improved prognosis for patients with PanCa.

FOOTNOTES

Author contributions: Bartolini I, Nannini G, and Risaliti M contributed to writing—original draft preparation; all the authors contributed to conceptualization and design of the study, critical revision of the article, and final approval of the version of the paper; Taddei A and Amedei A supervised this study.

Conflict-of-interest statement: All the authors report no relevant conflicts of interest for this article.

Open-Access: This article is an open-access article that was selected by an in-house editor and fully peer-reviewed by external reviewers. It is distributed in accordance with the Creative Commons Attribution NonCommercial (CC BY-NC 4.0) license, which permits others to distribute, remix, adapt, build upon this work non-commercially, and license their derivative works on different terms, provided the original work is properly cited and the use is non-commercial. See: https://creativecommons.org/Licenses/by-nc/4.0/

Country/Territory of origin: Italy

ORCID number: Ilenia Bartolini 0000-0003-0387-2042; Giulia Nannini 0000-0002-6481-6864; Matteo Risaliti 0000-0001-8476-2536; Francesco Matarazzo 0000-0002-8241-1772; Luca Moraldi 0000-0002-6481-4172; Maria Novella Ringressi 0000-0002-1644-0583; Antonio Taddei 0000-0003-2963-4085; Amedeo Amedei 0000-0002-6797-9343.

S-Editor: Gong ZM
L-Editor: Filipodia
P-Editor: Gong ZM

REFERENCES

1 **Mendez R**, Kesh K, Arora N, Di Martino L, McAllister F, Merchant N, Banerjee S. Microbial dysbiosis and polyamine metabolism as predictive markers for early detection of pancreatic cancer. *Carcinogenesis* 2020; **41**: 561-570 [PMID: 31369062 DOI: 10.1093/carcin/bgz116]

2 **Brandi G**, Turroni S, McAllister F, Frega G. The Human Microbiomes in Pancreatic Cancer: Towards Evidence-Based Manipulation Strategies? *Int J Mol Sci* 2021; **22** [PMID: 34576078 DOI: 10.3390/ijms22189914]

3 **Wang Y**, Yang G, You L, Yang J, Feng M, Qiu J, Zhao F, Liu Y, Cao Z, Zheng L, Zhang T, Zhao Y. Role of the microbiome in occurrence, development and treatment of pancreatic cancer. *Mol Cancer* 2019; **18**: 173 [PMID: 31785619 DOI: 10.1186/s12943-019-1103-2]

4 **Iebba V**, Totino V, Gagliardi A, Santangelo F, Cacciotti F, Trancassini M, Mancini C, Cicerone C, Corazziari E, Pantanella F, Schippa S. Eubiosis and dysbiosis: the two sides of the microbiota. *New Microbiol* 2016; **39**: 1-12 [PMID: 26922981]

5 **Pagliari D**, Piccirillo CA, Larbi A, Cianci R. The Interactions between Innate Immunity and Microbiota in Gastrointestinal

Diseases. *J Immunol Res* 2015; **2015**: 898297 [PMID: 26078983 DOI: 10.1155/2015/898297]
6 **Russo E**, Giudici F, Ricci F, Scaringi S, Nannini G, Ficari F, Luceri C, Niccolai E, Baldi S, D'Ambrosio M, Ramazzotti M, Amedei A. Diving into Inflammation: A Pilot Study Exploring the Dynamics of the Immune-Microbiota Axis in Ileal Tissue Layers of Patients with Crohn's Disease. *J Crohns Colitis* 2021; **15**: 1500-1516 [PMID: 33611347 DOI: 10.1093/ecco-jcc/jjab034]
7 **Niccolai E**, Russo E, Baldi S, Ricci F, Nannini G, Pedone M, Stingo FC, Taddei A, Ringressi MN, Bechi P, Mengoni A, Fani R, Bacci G, Fagorzi C, Chiellini C, Prisco D, Ramazzotti M, Amedei A. Significant and Conflicting Correlation of IL-9 With *Prevotella* and *Bacteroides* in Human Colorectal Cancer. *Front Immunol* 2020; **11**: 573158 [PMID: 33488574 DOI: 10.3389/fimmu.2020.573158]
8 **Kaźmierczak-Siedlecka K**, Dvořák A, Folwarski M, Daca A, Przewłócka K, Makarewicz W. Fungal Gut Microbiota Dysbiosis and Its Role in Colorectal, Oral, and Pancreatic Carcinogenesis. *Cancers (Basel)* 2020; **12** [PMID: 32455985 DOI: 10.3390/cancers12051326]
9 **Archibugi L**, Signoretti M, Capurso G. The Microbiome and Pancreatic Cancer: An Evidence-based Association? *J Clin Gastroenterol* 2018; **52** Suppl 1: S82-S85 [PMID: 30001289 DOI: 10.1097/MCG.0000000000001092]
10 **Kaźmierczak-Siedlecka K**, Stachowska E, Folwarski M, Przewłócka K, Makarewicz W, Bryl E. The potential of gut microbiome as a non-invasive predictive biomarker for early detection of pancreatic cancer and hepatocellular carcinoma. *Eur Rev Med Pharmacol Sci* 2021; **25**: 7275-7284 [PMID: 34919227 DOI: 10.26355/eurrev_202112_27421]
11 **Michaud DS**, Izard J, Wilhelm-Benartzi CS, You DH, Grote VA, Tjønneland A, Dahm CC, Overvad K, Jenab M, Fedirko V, Boutron-Ruault MC, Clavel-Chapelon F, Racine A, Kaaks R, Boeing H, Foerster J, Trichopoulou A, Lagiou P, Trichopoulos D, Sacerdote C, Sieri S, Palli D, Tumino R, Panico S, Siersema PD, Peeters PH, Lund E, Barricarte A, Huerta JM, Molina-Montes E, Dorronsoro M, Quirós JR, Duell EJ, Ye W, Sund M, Lindkvist B, Johansen D, Khaw KT, Wareham N, Travis RC, Vineis P, Bueno-de-Mesquita HB, Riboli E. Plasma antibodies to oral bacteria and risk of pancreatic cancer in a large European prospective cohort study. *Gut* 2013; **62**: 1764-1770 [PMID: 22990306 DOI: 10.1136/gutjnl-2012-303006]
12 **Yadav D**, Lowenfels AB. The epidemiology of pancreatitis and pancreatic cancer. *Gastroenterology* 2013; **144**: 1252-1261 [PMID: 23622135 DOI: 10.1053/j.gastro.2013.01.068]
13 **Lagier JC**, Khelaifia S, Alou MT, Ndongo S, Dione N, Hugon P, Caputo A, Cadoret F, Traore SI, Seck EH, Dubourg G, Durand G, Mourembou G, Guilhot E, Togo A, Bellali S, Bachar D, Cassir N, Bittar F, Delerce J, Mailhe M, Ricaboni D, Bilen M, Dangui Nieko NP, Dia Badiane NM, Valles C, Mouelhi D, Diop K, Million M, Musso D, Abrahão J, Azhar EI, Bibi F, Yasir M, Diallo A, Sokhna C, Djossou F, Vitton V, Robert C, Rolain JM, La Scola B, Fournier PE, Levasseur A, Raoult D. Culture of previously uncultured members of the human gut microbiota by culturomics. *Nat Microbiol* 2016; **1**: 16203 [PMID: 27819657 DOI: 10.1038/nmicrobiol.2016.203]
14 **Szychowiak P**, Villageois-Tran K, Patrier J, Timsit JF, Ruppé É. The role of the microbiota in the management of intensive care patients. *Ann Intensive Care* 2022; **12**: 3 [PMID: 34985651 DOI: 10.1186/s13613-021-00976-5]
15 **Zhang X**, Li L, Butcher J, Stintzi A, Figeys D. Advancing functional and translational microbiome research using meta-omics approaches. *Microbiome* 2019; **7**: 154 [PMID: 31810497 DOI: 10.1186/s40168-019-0767-6]
16 **Herremans KM**, Riner AN, Cameron ME, McKinley KL, Triplett EW, Hughes SJ, Trevino JG. The oral microbiome, pancreatic cancer and human diversity in the age of precision medicine. *Microbiome* 2022; **10**: 93 [PMID: 35701831 DOI: 10.1186/s40168-022-01262-7]
17 **Akshintala VS**, Talukdar R, Singh VK, Goggins M. The Gut Microbiome in Pancreatic Disease. *Clin Gastroenterol Hepatol* 2019; **17**: 290-295 [PMID: 30144522 DOI: 10.1016/j.cgh.2018.08.045]
18 **Irfan M**, Delgado RZR, Frias-Lopez J. The Oral Microbiome and Cancer. *Front Immunol* 2020; **11**: 591088 [PMID: 33193429 DOI: 10.3389/fimmu.2020.591088]
19 **Michaud DS**. Role of bacterial infections in pancreatic cancer. *Carcinogenesis* 2013; **34**: 2193-2197 [PMID: 23843038 DOI: 10.1093/carcin/bgt249]
20 **Fan X**, Alekseyenko AV, Wu J, Peters BA, Jacobs EJ, Gapstur SM, Purdue MP, Abnet CC, Stolzenberg-Solomon R, Miller G, Ravel J, Hayes RB, Ahn J. Human oral microbiome and prospective risk for pancreatic cancer: a population-based nested case-control study. *Gut* 2018; **67**: 120-127 [PMID: 27742762 DOI: 10.1136/gutjnl-2016-312580]
21 **Amara S**, Yang LV, Tiriveedhi V, Muzaffar M. Complex Role of Microbiome in Pancreatic Tumorigenesis: Potential Therapeutic Implications. *Cells* 2022; **11** [PMID: 35741028 DOI: 10.3390/cells11121900]
22 **Wei MY**, Shi S, Liang C, Meng QC, Hua J, Zhang YY, Liu J, Zhang B, Xu J, Yu XJ. The microbiota and microbiome in pancreatic cancer: more influential than expected. *Mol Cancer* 2019; **18**: 97 [PMID: 31109338 DOI: 10.1186/s12943-019-1008-0]
23 **Farrell JJ**, Zhang L, Zhou H, Chia D, Elashoff D, Akin D, Paster BJ, Joshipura K, Wong DT. Variations of oral microbiota are associated with pancreatic diseases including pancreatic cancer. *Gut* 2012; **61**: 582-588 [PMID: 21994333 DOI: 10.1136/gutjnl-2011-300784]
24 **Lu H**, Ren Z, Li A, Li J, Xu S, Zhang H, Jiang J, Yang J, Luo Q, Zhou K, Zheng S, Li L. Tongue coating microbiome data distinguish patients with pancreatic head cancer from healthy controls. *J Oral Microbiol* 2019; **11**: 1563409 [PMID: 30728915 DOI: 10.1080/20002297.2018.1563409]
25 **Butt J**, Jenab M, Pawlita M, Tjønneland A, Kyrø C, Boutron-Ruault MC, Carbonnel F, Dong C, Kaaks R, Kühn T, Boeing H, Schulze MB, Trichopoulou A, Karakatsani A, La Vecchia C, Palli D, Agnoli C, Tumino R, Sacerdote C, Panico S, Bueno-de-Mesquita B, Vermeulen R, Gram IT, Weiderpass E, Borch KB, Quirós JR, Agudo A, Rodríguez-Barranco M, Santiuste C, Ardanaz E, Van Guelpen B, Harlid S, Imaz L, Perez-Cornago A, Gunter MJ, Zouiouich S, Park JY, Riboli E, Cross AJ, Heath AK, Waterboer T, Hughes DJ. Antibody Responses to *Helicobacter pylori* and Risk of Developing Colorectal Cancer in a European Cohort. *Cancer Epidemiol Biomarkers Prev* 2020; **29**: 1475-1481 [PMID: 32332031 DOI: 10.1158/1055-9965.EPI-19-1545]
26 **Mei QX**, Huang CL, Luo SZ, Zhang XM, Zeng Y, Lu YY. Characterization of the duodenal bacterial microbiota in patients with pancreatic head cancer vs. healthy controls. *Pancreatology* 2018; **18**: 438-445 [PMID: 29653723 DOI: 10.1016/j.pan.2018.03.005]

27 **Ren Z**, Li A, Jiang J, Zhou L, Yu Z, Lu H, Xie H, Chen X, Shao L, Zhang R, Xu S, Zhang H, Cui G, Sun R, Wen H, Lerut JP, Kan Q, Li L, Zheng S. Gut microbiome analysis as a tool towards targeted non-invasive biomarkers for early hepatocellular carcinoma. *Gut* 2019; **68**: 1014-1023 [PMID: 30045880 DOI: 10.1136/gutjnl-2017-315084]

28 **Pushalkar S**, Hundeyin M, Daley D, Zambirinis CP, Kurz E, Mishra A, Mohan N, Aykut B, Usyk M, Torres LE, Werba G, Zhang K, Guo Y, Li Q, Akkad N, Lall S, Wadowski B, Gutierrez J, Kochen Rossi JA, Herzog JW, Diskin B, Torres-Hernandez A, Leinwand J, Wang W, Taunk PS, Savadkar S, Janal M, Saxena A, Li X, Cohen D, Sartor RB, Saxena D, Miller G. The Pancreatic Cancer Microbiome Promotes Oncogenesis by Induction of Innate and Adaptive Immune Suppression. *Cancer Discov* 2018; **8**: 403-416 [PMID: 29567829 DOI: 10.1158/2159-8290.CD-17-1134]

29 **Daniluk J**, Daniluk U, Rogalski P, Dabrowski A, Swidnicka-Siergiejko A. Microbiome-Friend or Foe of Pancreatic Cancer? *J Clin Med* 2021; **10** [PMID: 34884327 DOI: 10.3390/jcm10235624]

30 **Geller LT**, Barzily-Rokni M, Danino T, Jonas OH, Shental N, Nejman D, Gavert N, Zwang Y, Cooper ZA, Shee K, Thaiss CA, Reuben A, Livny J, Avraham R, Frederick DT, Ligorio M, Chatman K, Johnston SE, Mosher CM, Brandis A, Fuks G, Gurbatri C, Gopalakrishnan V, Kim M, Hurd MW, Katz M, Fleming J, Maitra A, Smith DA, Skalak M, Bu J, Michaud M, Trauger SA, Barshack I, Golan T, Sandbank J, Flaherty KT, Mandinova A, Garrett WS, Thayer SP, Ferrone CR, Huttenhower C, Bhatia SN, Gevers D, Wargo JA, Golub TR, Straussman R. Potential role of intratumor bacteria in mediating tumor resistance to the chemotherapeutic drug gemcitabine. *Science* 2017; **357**: 1156-1160 [PMID: 28912244 DOI: 10.1126/science.aah5043]

31 **Aykut B**, Pushalkar S, Chen R, Li Q, Abengozar R, Kim JI, Shadaloey SA, Wu D, Preiss P, Verma N, Guo Y, Saxena A, Vardhan M, Diskin B, Wang W, Leinwand J, Kurz E, Kochen Rossi JA, Hundeyin M, Zambrinis C, Li X, Saxena D, Miller G. The fungal mycobiome promotes pancreatic oncogenesis *via* activation of MBL. *Nature* 2019; **574**: 264-267 [PMID: 31578522 DOI: 10.1038/s41586-019-1608-2]

32 **Thomas RM**, Gharaibeh RZ, Gauthier J, Beveridge M, Pope JL, Guijarro MV, Yu Q, He Z, Ohland C, Newsome R, Trevino J, Hughes SJ, Reinhard M, Winglee K, Fodor AA, Zajac-Kaye M, Jobin C. Intestinal microbiota enhances pancreatic carcinogenesis in preclinical models. *Carcinogenesis* 2018; **39**: 1068-1078 [PMID: 29846515 DOI: 10.1093/carcin/bgy073]

33 **Del Castillo E**, Meier R, Chung M, Koestler DC, Chen T, Paster BJ, Charpentier KP, Kelsey KT, Izard J, Michaud DS. The Microbiomes of Pancreatic and Duodenum Tissue Overlap and Are Highly Subject Specific but Differ between Pancreatic Cancer and Noncancer Subjects. *Cancer Epidemiol Biomarkers Prev* 2019; **28**: 370-383 [PMID: 30373903 DOI: 10.1158/1055-9965.EPI-18-0542]

34 **Shrader HR**, Miller AM, Tomanek-Chalkley A, McCarthy A, Coleman KL, Ear PH, Mangalam AK, Salem AK, Chan CHF. Effect of bacterial contamination in bile on pancreatic cancer cell survival. *Surgery* 2021; **169**: 617-622 [PMID: 33268071 DOI: 10.1016/j.surg.2020.09.029]

35 **Serra N**, Di Carlo P, Gulotta G, d' Arpa F, Giammanco A, Colomba C, Melfa G, Fasciana T, Sergi C. Bactibilia in women affected with diseases of the biliary tract and pancreas. A STROBE guidelines-adherent cross-sectional study in Southern Italy. *J Med Microbiol* 2018; **67**: 1090-1095 [PMID: 29975626 DOI: 10.1099/jmm.0.000787]

36 **Okano K**, Suzuki Y. Influence of bile contamination for patients who undergo pancreaticoduodenectomy after biliary drainage. *World J Gastroenterol* 2019; **25**: 6847-6856 [PMID: 31885425 DOI: 10.3748/wjg.v25.i47.6847]

37 **Stecca T**, Nistri C, Pauletti B, Greco A, Di Giacomo A, Caratozzolo E, Bonariol L, Massani M. Bacteriobilia resistance to antibiotic prophylaxis increases morbidity after pancreaticoduodenectomy: a monocentric retrospective study of 128 patients. *Updates Surg* 2020; **72**: 1073-1080 [PMID: 32314259 DOI: 10.1007/s13304-020-00772-z]

38 **Balkwill FR**, Mantovani A. Cancer-related inflammation: common themes and therapeutic opportunities. *Semin Cancer Biol* 2012; **22**: 33-40 [PMID: 22210179 DOI: 10.1016/j.semcancer.2011.12.005]

39 **Ostrand-Rosenberg S**. Myeloid-derived suppressor cells: more mechanisms for inhibiting antitumor immunity. *Cancer Immunol Immunother* 2010; **59**: 1593-1600 [PMID: 20414655 DOI: 10.1007/s00262-010-0855-8]

40 **Zhou Y**, Luo GH. *Porphyromonas gingivalis* and digestive system cancers. *World J Clin Cases* 2019; **7**: 819-829 [PMID: 31024953 DOI: 10.12998/wjcc.v7.i7.819]

41 **Joukar F**, Mavaddati S, Mansour-Ghanaei F, Samadani AA. Gut Microbiota as a Positive Potential Therapeutic Factor in Carcinogenesis: an Overview of Microbiota-Targeted Therapy. *J Gastrointest Cancer* 2020; **51**: 363-378 [PMID: 31025167 DOI: 10.1007/s12029-019-00237-6]

42 **Abdul Rahman R**, Lamarca A, Hubner RA, Valle JW, McNamara MG. The Microbiome as a Potential Target for Therapeutic Manipulation in Pancreatic Cancer. *Cancers (Basel)* 2021; **13** [PMID: 34359684 DOI: 10.3390/cancers13153779]

43 **Chung LM**, Liang JA, Lin CL, Sun LM, Kao CH. Cancer risk in patients with candidiasis: a nationwide population-based cohort study. *Oncotarget* 2017; **8**: 63562-63573 [PMID: 28969011 DOI: 10.18632/oncotarget.18855]

44 **Amedei A**, Niccolai E, Benagiano M, Della Bella C, Cianchi F, Bechi P, Taddei A, Bencini L, Farsi M, Cappello P, Prisco D, Novelli F, D'Elios MM. Ex vivo analysis of pancreatic cancer-infiltrating T lymphocytes reveals that ENO-specific Tregs accumulate in tumor tissue and inhibit Th1/Th17 effector cell functions. *Cancer Immunol Immunother* 2013; **62**: 1249-1260 [PMID: 23640603 DOI: 10.1007/s00262-013-1429-3]

45 **Niccolai E**, Cappello P, Taddei A, Ricci F, D'Elios MM, Benagiano M, Bechi P, Bencini L, Ringressi MN, Coratti A, Cianchi F, Bonello L, Di Celle PF, Prisco D, Novelli F, Amedei A. Peripheral ENO1-specific T cells mirror the intratumoral immune response and their presence is a potential prognostic factor for pancreatic adenocarcinoma. *Int J Oncol* 2016; **49**: 393-401 [PMID: 27210467 DOI: 10.3892/ijo.2016.3524]

46 **Niccolai E**, Taddei A, Ricci F, Rolla S, D'Elios MM, Benagiano M, Bechi P, Bencini L, Ringressi MN, Pini A, Castiglione F, Giordano D, Satolli MA, Coratti A, Cianchi F, Bani D, Prisco D, Novelli F, Amedei A. Intra-tumoral IFN-γ-producing Th22 cells correlate with TNM staging and the worst outcomes in pancreatic cancer. *Clin Sci (Lond)* 2016; **130**: 247-258 [PMID: 26590104 DOI: 10.1042/CS20150437]

47 **Feig C**, Gopinathan A, Neesse A, Chan DS, Cook N, Tuveson DA. The pancreas cancer microenvironment. *Clin Cancer Res* 2012; **18**: 4266-4276 [PMID: 22896693 DOI: 10.1158/1078-0432.CCR-11-3114]

48 **Inman KS**, Francis AA, Murray NR. Complex role for the immune system in initiation and progression of pancreatic

cancer. *World J Gastroenterol* 2014; **20**: 11160-11181 [PMID: 25170202 DOI: 10.3748/wjg.v20.i32.11160]

49 **Zou W**. Immunosuppressive networks in the tumour environment and their therapeutic relevance. *Nat Rev Cancer* 2005; **5**: 263-274 [PMID: 15776005 DOI: 10.1038/nrc1586]

50 **Sethi V**, Kurtom S, Tarique M, Lavania S, Malchiodi Z, Hellmund L, Zhang L, Sharma U, Giri B, Garg B, Ferrantella A, Vickers SM, Banerjee S, Dawra R, Roy S, Ramakrishnan S, Saluja A, Dudeja V. Gut Microbiota Promotes Tumor Growth in Mice by Modulating Immune Response. *Gastroenterology* 2018; **155**: 33-37.e6 [PMID: 29630898 DOI: 10.1053/j.gastro.2018.04.001]

51 **Chakladar J**, Kuo SZ, Castaneda G, Li WT, Gnanasekar A, Yu MA, Chang EY, Wang XQ, Ongkeko WM. The Pancreatic Microbiome is Associated with Carcinogenesis and Worse Prognosis in Males and Smokers. *Cancers (Basel)* 2020; **12** [PMID: 32962112 DOI: 10.3390/cancers12092672]

52 **Takayama S**, Takahashi H, Matsuo Y, Okada Y, Manabe T. Effects of Helicobacter pylori infection on human pancreatic cancer cell line. *Hepatogastroenterology* 2007; **54**: 2387-2391 [PMID: 18265671]

53 **Zambirinis CP**, Levie E, Nguy S, Avanzi A, Barilla R, Xu Y, Seifert L, Daley D, Greco SH, Deutsch M, Jonnadula S, Torres-Hernandez A, Tippens D, Pushalkar S, Eisenthal A, Saxena D, Ahn J, Hajdu C, Engle DD, Tuveson D, Miller G. TLR9 ligation in pancreatic stellate cells promotes tumorigenesis. *J Exp Med* 2015; **212**: 2077-2094 [PMID: 26481685 DOI: 10.1084/jem.20142162]

54 **Olsen I**, Lambris JD, Hajishengallis G. *Porphyromonas gingivalis* disturbs host-commensal homeostasis by changing complement function. *J Oral Microbiol* 2017; **9**: 1340085 [PMID: 28748042 DOI: 10.1080/20002297.2017.1340085]

55 **Seifert L**, Werba G, Tiwari S, Ly NNG, Alothman S, Alqunaibit D, Avanzi A, Barilla R, Daley D, Greco SH, Torres-Hernandez A, Pergamo M, Ochi A, Zambirinis CP, Pansari M, Rendon M, Tippens D, Hundeyin M, Mani VR, Hajdu C, Engle D, Miller G. Author Correction: The necrosome promotes pancreatic oncogenesis *via* CXCL1 and Mincle-induced immune suppression. *Nature* 2021; **591**: E28 [PMID: 33707632 DOI: 10.1038/s41586-021-03322-8]

56 **Ochi A**, Nguyen AH, Bedrosian AS, Mushlin HM, Zarbakhsh S, Barilla R, Zambirinis CP, Fallon NC, Rehman A, Pylayeva-Gupta Y, Badar S, Hajdu CH, Frey AB, Bar-Sagi D, Miller G. MyD88 inhibition amplifies dendritic cell capacity to promote pancreatic carcinogenesis *via* Th2 cells. *J Exp Med* 2012; **209**: 1671-1687 [PMID: 22908323 DOI: 10.1084/jem.20111706]

57 **Schmitt FCF**, Brenner T, Uhle F, Loesch S, Hackert T, Ulrich A, Hofer S, Dalpke AH, Weigand MA, Boutin S. Gut microbiome patterns correlate with higher postoperative complication rates after pancreatic surgery. *BMC Microbiol* 2019; **19**: 42 [PMID: 30777006 DOI: 10.1186/s12866-019-1399-5]

58 **Tortajada P**, Sauvanet A, Truant S, Regenet N, Souche R, Benoist S, Muscari F, Regimbeau JM, Gaujoux S, Cunha AS, Schwarz L; French-Achbt Working Group. Does Fungal Biliary Contamination after Preoperative Biliary Drainage Increase Postoperative Complications after Pancreaticoduodenectomy? *Cancers (Basel)* 2020; **12** [PMID: 33007843 DOI: 10.3390/cancers12102814]

59 **Parapini ML**, Skipworth JRA, Mah A, Desai S, Chung S, Scudamore CH, Segedi M, Vasilyeva E, Li J, Kim PT. The association between bacterobilia and the risk of postoperative complications following pancreaticoduodenectomy. *HPB (Oxford)* 2022; **24**: 277-285 [PMID: 34301475 DOI: 10.1016/j.hpb.2021.06.428]

60 **Coppola A**, La Vaccara V, Farolfi T, Fiore M, Cascone C, Ramella S, Spoto S, Ciccozzi M, Angeletti S, Coppola R, Caputo D. Different Biliary Microbial Flora Influence Type of Complications after Pancreaticoduodenectomy: A Single Center Retrospective Analysis. *J Clin Med* 2021; **10** [PMID: 34070003 DOI: 10.3390/jcm10102180]

61 **Abe K**, Kitago M, Shinoda M, Yagi H, Abe Y, Oshima G, Hori S, Yokose T, Endo Y, Kitagawa Y. High risk pathogens and risk factors for postoperative pancreatic fistula after pancreatectomy; a retrospective case-controlled study. *Int J Surg* 2020; **82**: 136-142 [PMID: 32861892 DOI: 10.1016/j.ijsu.2020.08.035]

62 **Sato A**, Masui T, Nakano K, Sankoda N, Anazawa T, Takaori K, Kawaguchi Y, Uemoto S. Abdominal contamination with Candida albicans after pancreaticoduodenectomy is related to hemorrhage associated with pancreatic fistulas. *Pancreatology* 2017; **17**: 484-489 [PMID: 28336225 DOI: 10.1016/j.pan.2017.03.007]

63 **Müssle B**, Hempel S, Kahlert C, Distler M, Weitz J, Welsch T. Prognostic Impact of Bacterobilia on Morbidity and Postoperative Management After Pancreatoduodenectomy: A Systematic Review and Meta-analysis. *World J Surg* 2018; **42**: 2951-2962 [PMID: 29464345 DOI: 10.1007/s00268-018-4546-5]

64 **Weniger M**, Hank T, Qadan M, Ciprani D, Michelakos T, Niess H, Heiliger C, Ilmer M, D'Haese JG, Ferrone CR, Warshaw AL, Lillemoe KD, Werner J, Liss A, Fernández-Del Castillo C. Influence of Klebsiella pneumoniae and quinolone treatment on prognosis in patients with pancreatic cancer. *Br J Surg* 2021; **108**: 709-716 [PMID: 34157083 DOI: 10.1002/bjs.12003]

65 **Panebianco C**, Adamberg K, Jaagura M, Copetti M, Fontana A, Adamberg S, Kolk K, Vilu R, Andriulli A, Pazienza V. Influence of gemcitabine chemotherapy on the microbiota of pancreatic cancer xenografted mice. *Cancer Chemother Pharmacol* 2018; **81**: 773-782 [PMID: 29473096 DOI: 10.1007/s00280-018-3549-0]

66 **Corty RW**, Langworthy BW, Fine JP, Buse JB, Sanoff HK, Lund JL. Antibacterial Use Is Associated with an Increased Risk of Hematologic and Gastrointestinal Adverse Events in Patients Treated with Gemcitabine for Stage IV Pancreatic Cancer. *Oncologist* 2020; **25**: 579-584 [PMID: 32181968 DOI: 10.1634/theoncologist.2019-0570]

67 **Chen SM**, Chieng WW, Huang SW, Hsu LJ, Jan MS. The synergistic tumor growth-inhibitory effect of probiotic Lactobacillus on transgenic mouse model of pancreatic cancer treated with gemcitabine. *Sci Rep* 2020; **10**: 20319 [PMID: 33230218 DOI: 10.1038/s41598-020-77322-5]

68 **Lu SY**, Hua J, Xu J, Wei MY, Liang C, Meng QC, Liu J, Zhang B, Wang W, Yu XJ, Shi S. Microorganisms in chemotherapy for pancreatic cancer: An overview of current research and future directions. *Int J Biol Sci* 2021; **17**: 2666-2682 [PMID: 34326701 DOI: 10.7150/ijbs.59117]

69 **Ciardiello D**, Vitiello PP, Cardone C, Martini G, Troiani T, Martinelli E, Ciardiello F. Immunotherapy of colorectal cancer: Challenges for therapeutic efficacy. *Cancer Treat Rev* 2019; **76**: 22-32 [PMID: 31079031 DOI: 10.1016/j.ctrv.2019.04.003]

70 **Postow MA**, Callahan MK, Wolchok JD. Immune Checkpoint Blockade in Cancer Therapy. *J Clin Oncol* 2015; **33**: 1974-1982 [PMID: 25605845 DOI: 10.1200/JCO.2014.59.4358]

71 **Zhao X**, Yang K, Zhao R, Ji T, Wang X, Yang X, Zhang Y, Cheng K, Liu S, Hao J, Ren H, Leong KW, Nie G. Inducing enhanced immunogenic cell death with nanocarrier-based drug delivery systems for pancreatic cancer therapy. *Biomaterials* 2016; **102**: 187-197 [PMID: 27343466 DOI: 10.1016/j.biomaterials.2016.06.032]

72 **Liu L**, Kshirsagar P, Christiansen J, Gautam SK, Aithal A, Gulati M, Kumar S, Solheim JC, Batra SK, Jain M, Wannemuehler MJ, Narasimhan B. Polyanhydride nanoparticles stabilize pancreatic cancer antigen MUC4β. *J Biomed Mater Res A* 2021; **109**: 893-902 [PMID: 32776461 DOI: 10.1002/jbm.a.37080]

73 **Zhou W**, Zhou Y, Chen X, Ning T, Chen H, Guo Q, Zhang Y, Liu P, Li C, Chu Y, Sun T, Jiang C. Pancreatic cancer-targeting exosomes for enhancing immunotherapy and reprogramming tumor microenvironment. *Biomaterials* 2021; **268**: 120546 [PMID: 33253966 DOI: 10.1016/j.biomaterials.2020.120546]

74 **Zhang F**, Parayath NN, Ene CI, Stephan SB, Koehne AL, Coon ME, Holland EC, Stephan MT. Genetic programming of macrophages to perform anti-tumor functions using targeted mRNA nanocarriers. *Nat Commun* 2019; **10**: 3974 [PMID: 31481662 DOI: 10.1038/s41467-019-11911-5]

75 **Capurso G**, Lahner E. The interaction between smoking, alcohol and the gut microbiome. *Best Pract Res Clin Gastroenterol* 2017; **31**: 579-588 [PMID: 29195678 DOI: 10.1016/j.bpg.2017.10.006]

76 **Chen SM**, Hsu LJ, Lee HL, Lin CP, Huang SW, Lai CJ, Lin CW, Chen WT, Chen YJ, Lin YC, Yang CC, Jan MS. Lactobacillus Attenuate the Progression of Pancreatic Cancer Promoted by Porphyromonas Gingivalis in *K-rasG12D* Transgenic Mice. *Cancers (Basel)* 2020; **12** [PMID: 33255941 DOI: 10.3390/cancers12123522]

77 **Konishi H**, Isozaki S, Kashima S, Moriichi K, Ichikawa S, Yamamoto K, Yamamura C, Ando K, Ueno N, Akutsu H, Ogawa N, Fujiya M. Probiotic Aspergillus oryzae produces anti-tumor mediator and exerts anti-tumor effects in pancreatic cancer through the p38 MAPK signaling pathway. *Sci Rep* 2021; **11**: 11070 [PMID: 34040123 DOI: 10.1038/s41598-021-90707-4]

78 **Riquelme E**, Zhang Y, Zhang L, Montiel M, Zoltan M, Dong W, Quesada P, Sahin I, Chandra V, San Lucas A, Scheet P, Xu H, Hanash SM, Feng L, Burks JK, Do KA, Peterson CB, Nejman D, Tzeng CD, Kim MP, Sears CL, Ajami N, Petrosino J, Wood LD, Maitra A, Straussman R, Katz M, White JR, Jenq R, Wargo J, McAllister F. Tumor Microbiome Diversity and Composition Influence Pancreatic Cancer Outcomes. *Cell* 2019; **178**: 795-806.e12 [PMID: 31398337 DOI: 10.1016/j.cell.2019.07.008]

79 **Zhu R**, Lang T, Yan W, Zhu X, Huang X, Yin Q, Li Y. Gut Microbiota: Influence on Carcinogenesis and Modulation Strategies by Drug Delivery Systems to Improve Cancer Therapy. *Adv Sci (Weinh)* 2021; **8**: 2003542 [PMID: 34026439 DOI: 10.1002/advs.202003542]

80 **Kim JR**, Han K, Han Y, Kang N, Shin TS, Park HJ, Kim H, Kwon W, Lee S, Kim YK, Park T, Jang JY. Microbiome Markers of Pancreatic Cancer Based on Bacteria-Derived Extracellular Vesicles Acquired from Blood Samples: A Retrospective Propensity Score Matching Analysis. *Biology (Basel)* 2021; **10** [PMID: 33805810 DOI: 10.3390/biology10030219]

81 **Balachandran VP**, Łuksza M, Zhao JN, Makarov V, Moral JA, Remark R, Herbst B, Askan G, Bhanot U, Senbabaoglu Y, Wells DK, Cary CIO, Grbovic-Huezo O, Attiyeh M, Medina B, Zhang J, Loo J, Saglimbeni J, Abu-Akeel M, Zappasodi R, Riaz N, Smoragiewicz M, Kelley ZL, Basturk O; Australian Pancreatic Cancer Genome Initiative; Garvan Institute of Medical Research; Prince of Wales Hospital; Royal North Shore Hospital; University of Glasgow; St Vincent's Hospital; QIMR Berghofer Medical Research Institute; University of Melbourne, Centre for Cancer Research; University of Queensland, Institute for Molecular Bioscience; Bankstown Hospital; Liverpool Hospital; Royal Prince Alfred Hospital, Chris O'Brien Lifehouse; Westmead Hospital; Fremantle Hospital; St John of God Healthcare; Royal Adelaide Hospital; Flinders Medical Centre; Envoi Pathology; Princess Alexandria Hospital; Austin Hospital; Johns Hopkins Medical Institutes; ARC-Net Centre for Applied Research on Cancer, Gönen M, Levine AJ, Allen PJ, Fearon DT, Merad M, Gnjatic S, Iacobuzio-Donahue CA, Wolchok JD, DeMatteo RP, Chan TA, Greenbaum BD, Merghoub T, Leach SD. Identification of unique neoantigen qualities in long-term survivors of pancreatic cancer. *Nature* 2017; **551**: 512-516 [PMID: 29132146 DOI: 10.1038/nature24462]

82 **Katsuta E**, Huyser M, Yan L, Takabe K. A prognostic score based on long-term survivor unique transcriptomic signatures predicts patient survival in pancreatic ductal adenocarcinoma. *Am J Cancer Res* 2021; **11**: 4294-4307 [PMID: 34659888]

83 **Mitsuhashi K**, Nosho K, Sukawa Y, Matsunaga Y, Ito M, Kurihara H, Kanno S, Igarashi H, Naito T, Adachi Y, Tachibana M, Tanuma T, Maguchi H, Shinohara T, Hasegawa T, Imamura M, Kimura Y, Hirata K, Maruyama R, Suzuki H, Imai K, Yamamoto H, Shinomura Y. Association of Fusobacterium species in pancreatic cancer tissues with molecular features and prognosis. *Oncotarget* 2015; **6**: 7209-7220 [PMID: 25797243 DOI: 10.18632/oncotarget.3109]

World Journal of Gastroenterology

Submit a Manuscript: https://www.f6publishing.com

World J Gastroenterol 2022 August 28; 28(32): 4540-4556

DOI: 10.3748/wjg.v28.i32.4540

ISSN 1007-9327 (print) ISSN 2219-2840 (online)

MINIREVIEWS

Liver Imaging Reporting and Data System criteria for the diagnosis of hepatocellular carcinoma in clinical practice: A pictorial minireview

Christina Liava, Emmanouil Sinakos, Elissavet Papadopoulou, Lamprini Giannakopoulou, Stamatia Potsi, Anestis Moumtzouoglou, Anthi Chatziioannou, Loukas Stergioulas, Lydia Kalogeropoulou, Ioannis Dedes, Evangelos Akriviadis, Danai Chourmouzi

Specialty type: Gastroenterology and hepatology

Provenance and peer review: Invited article; Externally peer reviewed.

Peer-review model: Single blind

Peer-review report's scientific quality classification

Grade A (Excellent): 0
Grade B (Very good): B, B, B
Grade C (Good): 0
Grade D (Fair): 0
Grade E (Poor): 0

P-Reviewer: Ishikawa T, Japan; Kumar SKY, India; Tamori A, Japan

Received: January 31, 2022
Peer-review started: January 31, 2022
First decision: February 24, 2022
Revised: March 10, 2022
Accepted: July 27, 2022
Article in press: July 27, 2022
Published online: August 28, 2022

Christina Liava, Emmanouil Sinakos, Anthi Chatziioannou, Evangelos Akriviadis, 4th Department of Internal Medicine, Hippokratio Hospital, Aristotle University of Thessaloniki, Thessaloniki 54642, Greece

Elissavet Papadopoulou, Lamprini Giannakopoulou, Stamatia Potsi, Anestis Moumtzouoglou, Loukas Stergioulas, Lydia Kalogeropoulou, Ioannis Dedes, Danai Chourmouzi, Department of Radiology, Interbalkan Medical Center, Thessaloniki 57001, Greece

Corresponding author: Emmanouil Sinakos, MD, PhD, Associate Professor, 4th Department of Internal Medicine, Hippokratio Hospital, Aristotle University of Thessaloniki, 49 Konstantinoupoleos Str, Thessaloniki 54642, Greece. em_sinakos@yahoo.com

Abstract

Hepatocellular carcinoma (HCC) is the sixth most common cancer. The main risk factors associated with HCC development include hepatitis B virus, hepatitis C virus, alcohol consumption, aflatoxin B1, and nonalcoholic fatty liver disease. However, hepatocarcinogenesis is a complex multistep process. Various factors lead to hepatocyte malignant transformation and HCC development. Diagnosis and surveillance of HCC can be made with the use of liver ultrasound (US) every 6 mo. However, the sensitivity of this imaging method to detect HCC in a cirrhotic liver is limited, due to the abnormal liver parenchyma. Computed tomography (CT) and magnetic resonance imaging (MRI) are considered to be most useful tools for at-risk patients or patients with inadequate US. Liver biopsy is still used for diagnosis and prognosis of HCC in specific nodules that cannot be definitely characterized as HCC by imaging. Recently the American College of Radiology designed the Liver Imaging Reporting and Data System (LI-RADS), which is a comprehensive system for standardized interpretation of CT and MRI liver examinations that was first proposed in 2011. In 2018, it was integrated into the American Association for the Study of Liver Diseases guidance statement for HCC. LI-RADS is designed to ensure high sensitivity, precise categorization, and high positive predictive value for the diagnosis of HCC and is applied to "high-risk populations" according to specific criteria. Most importantly LI-RADS criteria achieved international collaboration and consensus among liver experts around

the world on the best practices for caring for patients with or at risk for HCC.

Key Words: Hepatocellular carcinoma; Hepatocarcinogenesis; Computed tomography; Magnetic resonance imaging; Liver Imaging Reporting and Data System

©The Author(s) 2022. Published by Baishideng Publishing Group Inc. All rights reserved.

Core Tip: Worldwide, hepatocellular carcinoma (HCC) is the sixth most common malignancy and fourth cause of cancer-related death. Progress on the diagnosis and treatment possibilities of HCC has been made over the past decades. We herein review the available knowledge on the carcinogenesis, surveillance of HCC, and relevant data with the Liver Imaging Reporting and Data System (LI-RADS) algorithm that was recently integrated into the American Association for the Study of Liver Diseases clinical practice guidelines. LI-RADS aims to avoid false-positive examinations and ensure high sensitivity and positive predictive value in high-risk populations with simultaneous achievement of probabilistic categorization of the tumor.

Citation: Liava C, Sinakos E, Papadopoulou E, Giannakopoulou L, Potsi S, Moumtzouoglou A, Chatziioannou A, Stergioulas L, Kalogeropoulou L, Dedes I, Akriviadis E, Chourmouzi D. Liver Imaging Reporting and Data System criteria for the diagnosis of hepatocellular carcinoma in clinical practice: A pictorial minireview. *World J Gastroenterol* 2022; 28(32): 4540-4556
URL: https://www.wjgnet.com/1007-9327/full/v28/i32/4540.htm
DOI: https://dx.doi.org/10.3748/wjg.v28.i32.4540

INTRODUCTION

Hepatocellular carcinoma (HCC) is the sixth most common cancer and the third leading cause of cancer-related death worldwide[1]. Up to 90% of HCC cases arise on the background of established liver cirrhosis or advanced fibrosis, which has been developed due to a known etiology[2]. The most predominant risk factors for HCC worldwide are hepatitis B virus (HBV), hepatitis C virus (HCV), alcohol consumption, and nonalcoholic fatty liver disease[3].

The prognosis of HCC is significantly influenced by the disease stage at the time of diagnosis. Patients with HCC detection at an early stage can be treated with potentially curative therapies[4]. Imaging plays an important role in the early diagnosis of HCC, both in the context of surveillance strategies of at-risk populations and in the phase of confirmatory studies for a new liver nodule. Most importantly, imaging studies for the diagnosis of HCC, usually performed with computed tomography (CT) or magnetic resonance imaging (MRI), have approximately 100% specificity. Therefore, HCC is among the few malignancies for which management can be established on the basis of noninvasive imaging, without histologic confirmation[5].

CT and MRI are extensively used in clinical practice for the diagnosis of HCC. However, their diagnostic accuracy is decreased when strong criteria are not applied. In addition, the variable algorithms and recommendations from different scientific societies have created some degree of confusion in the interpretation of the radiological findings. To standardize the performance of liver imaging in patients with risk factors for developing HCC, the American College of Radiology (ACR) introduced in 2011 the first version of the Liver Imaging Reporting and Data System (LI-RADS)[6]. The LI-RADS criteria were created to standardize the terminology used for HCC imaging, allow probabilistic categorization, and provide personalized medical care[7]. It has been updated in 2013, 2014, 2017, and 2018 and is considered a dynamic document, which can be expanded and refined in response to new knowledge and user feedback[8].

In this pictorial review, we analyze the rational for the radiological diagnosis of HCC, present the LI-RADS criteria and associate them with characteristic images per category in order to enhance the familiarization of clinicians with the use of this system in clinical practice.

HEPATOCARCINOGENESIS AND IMAGING CORRELATES

Hepatocarcinogenesis is a complex multistep process characterized by alterations at several levels (molecular, cellular, and histologic levels). Chronic liver inflammation can lead to continuous cycles of persistent cell injury, death, and regeneration, causing subsequent genetic damage and epigenetic alterations of hepatocytes[9]. Various factors lead to hepatocyte malignant transformation and HCC

development, such as genetic susceptibility, mutual interplays between viral and non-viral risk factors, cellular microenvironment, immune cells, and the severity of the underlying chronic liver disease. An altered microenvironment plays a significant role in all stages of neoplastic growth, from the early mutation stage, through to invasion, and eventually, to metastatic stage[10,11].

The molecular pathogenesis of HCC varies according to the distinct etiologies[10]. HBV and HCV are the two main viruses, which can be implicated in the development of HCC[12]. HBV genome integration can target cancer-relevant genes, and protein x can alter the expression of growth-control genes and inactivate the tumor suppressor p53 leading to HCC development[12,13]. On the other hand, HCV infection is not characterized by oncogenic effects; however mutations can result from oxidative stress caused by chronic inflammation[12]. Alcohol-induced hepatocarcinogenesis is another risk factor for developing HCC. Chronic alcohol intake is associated with proinflammatory cytokine production and oxidative stress, which can lead to the development of fibrosis, cirrhosis, and ultimately HCC[14]. Aflatoxin-B1 also plays a role in hepatocarcinogenesis. This fungal toxin is associated with a specific *p53* mutation and activation of oncogenes such as the Human Harvey-ras proto-oncogene[15,16].

Irrespective of etiology, cirrhosis is the main underlying cause for most HCC cases. During cirrhosis, regenerating nodules are developed, which provide an appropriate microenvironment for the development of normal hepatocytes to dysplastic hepatocytes to neoplastic lesions and culminating in HCC through the subsequent agglomeration of multiple DNA alterations[17]. Histologically, abnormal precursor hepatic lesions including cirrhotic nodules, low-grade dysplastic nodules, and high-grade dysplastic nodules dedifferentiate and progressively develop to form early and eventually advanced HCCs[5]. This continuum biologic procedure may happen simultaneously at various rates in different parts of the liver.

During hepatocarcinogenesis, the vascular supply of the nodules modifies together with malignant progression and the number of intranodular portal tracts diminishes progressively, while the number of unpaired arteries increases. Eventually, HCC is supplied mainly by the abnormal hepatic artery system *via* neoangiogenic unpaired arteries[18]. It is important for both clinicians and radiologists to understand these hemodynamic changes during hepatocarcinogenesis as these are correlated with the enhancing pattern precursor hepatic lesions and finally of HCCs on imaging studies. Arterial phase hyperenhancement and portal venous and/or delayed phases wash-out relative to the background liver on contrast enhanced multiphasic CT and MRI are the most important imaging features of HCC and are correlated with the blood supply of the nodules with malignant transformation.

Features during hepatocarcinogenesis also include tumor capsule and fibrous septa formation and fat accumulation within hepatocytes during the early phases (dysplasia and early HCC), while fat usually regresses with the progression to overt HCC.

Iron may also accumulate within hepatocytes during the dysplastic phases of hepatocarcinogenesis and usually also regresses with progression to HCC. Finally organic anionic transporting polypeptides expression declines during hepatocarcinogenesis (organic anion transporting polypeptide 8 expression levels decrease during hepatocarcinogenesis prior to reduction in portal tracts and increases in unpaired arteries). It is worth noting that abnormal venous drainage of HCCs occurs during hepatocarcinogenesis from hepatic veins to sinusoids and then to portal veins, which may explain why HCC has a tendency to spread through the portal venous system rather than hepatic veins[5].

HCC DIAGNOSIS

Early diagnosis of HCC is enhanced by the use of surveillance strategies in certain populations that are at risk of developing HCC. Typically these patients include cirrhotic patients with Child-Pugh stage A and B as well as cirrhotic patients with Child-Pugh stage C awaiting liver transplantation[19,20]. Regarding patients with chronic hepatitis B, the use of risk scores (especially PAGE-B) is recommended to prioritize patients for surveillance[21]. Finally, it is recommended that patients with severe fibrosis enter surveillance programs on an individual basis after careful assessment of their risk[19,20]. Regarding tools that should be used for surveillance, most international societies recommend only the use of abdominal ultrasound (US) every 6 mo, as the use of alpha-fetoprotein is still controversial[19,20]. CT or MRI may be utilized for surveillance in selected patients with inadequate US visualization or at high risk for inadequate US[20].

Once a new nodule is discovered in the liver of a cirrhotic patient, further imaging work-up with either CT or MRI is recommended[19,20]. These modalities are also the gold standard for HCC diagnosis outside the use of surveillance programs. The peculiar vascular derangement that occurs during hepatic carcinogenesis, as previously described, correlate with imaging phases and have led to the implementation of accurate non-invasive criteria for HCC diagnosis. Integration of LI-RADS version 2018 into the American Association for the Study of Liver Diseases (AASLD) HCC clinical practice guidelines, was a major step. As a result, the AASLD management suggestions are directly associated with the LI-RADS categories[20].

The routine use of liver biopsy is not suggested for the diagnosis of HCC[20]. Biopsy shortcomings include risks associated with the procedure. Another important issue is that small lesions < 2 cm are

often difficult to target in a cirrhotic liver leading to high false negatives. However, the role of tumor tissue analysis in HCC is essential in cases of a cirrhotic patient that lacks typical imaging characteristics or in cases where molecular profiling is needed to determine systemic therapy options[22]. It should also be noted that the diagnosis should be confirmed with pathology in non-cirrhotic patients[19]. In all of these cases, the pathological diagnosis of HCC should be based on International Consensus recommendations using appropriate histopathological analyses and immunohistochemistry[23,24].

DESCRIPTION OF LIRADS

LI-RADS has provided a standardized guidance, which contributes to a universal language for liver imaging findings. All LI-RADS diagnostic tables can be found for free at the ACR website (https://www.acr.org/ClinicalResources/Reporting-and-Data-Systems/LI-RADS). By philosophy, LI-RADS diagnostic algorithm is developed to ensure high specificity and positive predictive value (PPV) for HCC diagnosis to avoid false-positive examinations. To obtain a high PPV, LI-RADS should be used only to populations at high risk for developing HCC[25]. This "high-risk population" includes adult patients with liver cirrhosis (except for vascular causes of cirrhosis), chronic HBV infection with or without cirrhosis, and patients diagnosed with current or prior HCC (Figures 1 and 2)[26].

Determining patients who meet the at-risk criteria is not always easy. Cirrhotic patients are usually diagnosed based only on clinical signs, symptoms, and diagnostic markers with or without histological confirmation.

Measurement of liver stiffness using FibroScan could be a useful predictor of HCC appearance in patients with chronic hepatitis B and/or C[26]. If the patient is considered with a high pre-test probability of HCC, LI-RADS may be used with a recommendation that the referring physician confirms the patient's risk status (Figure 3).

Although HCC may develop in patients with non-alcoholic fatty liver disease/steatohepatitis without cirrhosis, sufficient data are lacking to support that LI-RADS would provide an adequately high PPV for HCC in this sub-cirrhotic population group[27]. LI-RADS does not apply to patients < 18-years-old and patients with liver cirrhosis due to vascular diseases (*e.g.*, cardiac hepatopathy, Budd-Chiari syndrome), because the above-mentioned diseases are characterized by hypervascular benign liver lesions in liver imaging, which raise the probability of false positive results and reduce the PPV for HCC diagnosis[17].

LI-RADS CATEGORIES

LI-RADS CT/MRI Diagnostic Algorithm version 2018 (v2018) is characterized by eight diagnostic categories, which are used for individual liver lesions with increasing probability of HCC and malignancy with higher categories. The several LI-RADS categories do not have an exact association to the histologic categories but instead reflect the probability of individual liver lesions being benign, HCC, or non-HCC malignancy. The LI-RADS CT/MRI algorithm is used in a stepwise manner starting with LR-not categorizable (NC). It is followed by LR-tumor in vein (TIV), LR-1, LR-2, and LR-M. Once the above categories are excluded, the CT/MRI diagnostic table is used to determine an observation LR-3, LR-4, or LR-5 category (Figure 4). LI-RADS criteria uses the term observation to generically refer to an area with an imaging appearance that is distinctive from the rest of the liver. Such an area may be a true lesion or a pseudolesion.

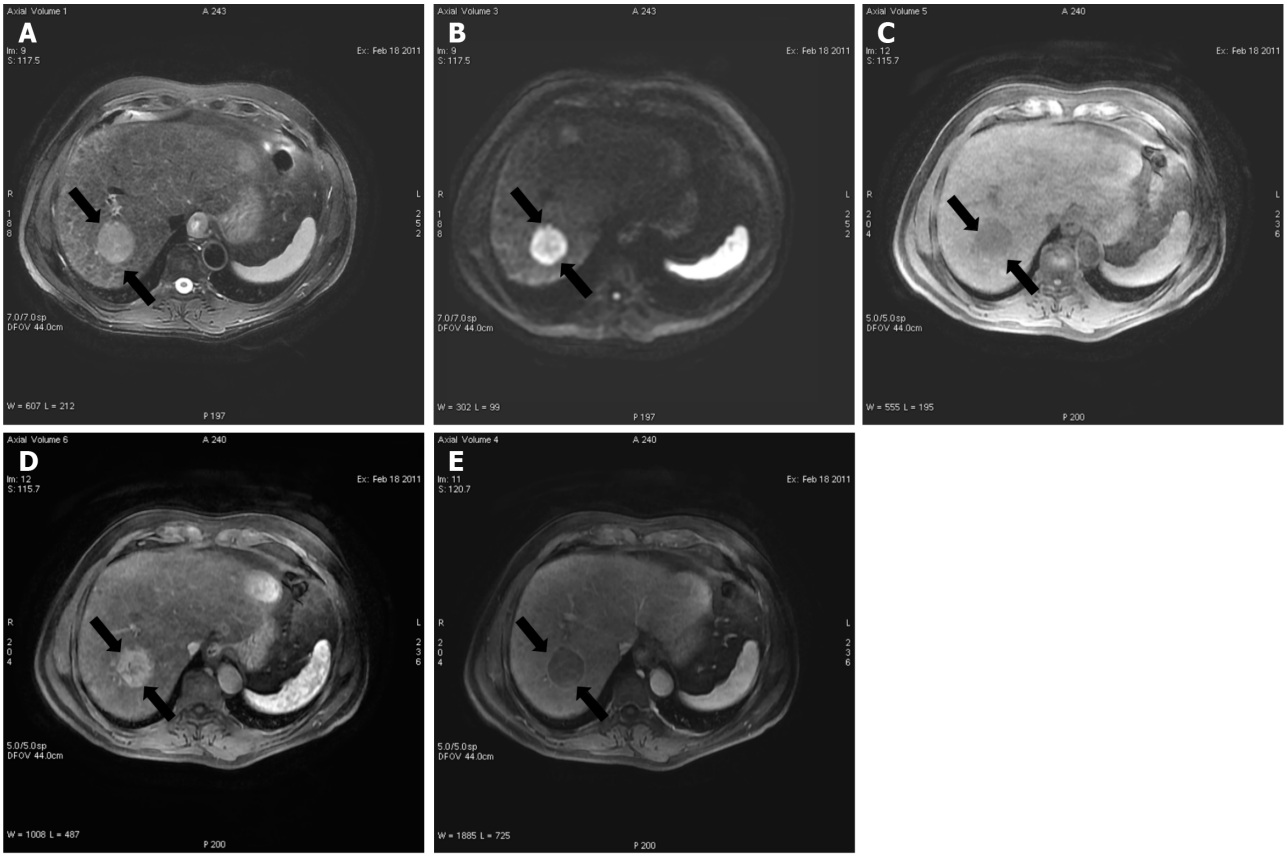
LR-NC

CT and MRI need to meet minimal technical requirements to yield the desired diagnostic accuracy. For CT, multidetector CT (≥ 8 detectors) is requisite, whereas for MRI, 1.5 or 3 T magnets are required according to LI-RADS guidance. Administration of intravenous contrast and acquisition of a multiphase liver protocol including images before contrast, late hepatic arterial phase, portal venous phase, and delayed phase images is required to allow for diagnosis of HCC[20]. The most important characteristic is the acquisition of a technically adequate and well-timed arterial phase.

LI-RADS guidance strongly suggests that imaging should be performed during the late arterial phase, *i.e.* when the hepatic artery and portal vein are both enhanced, as this correlates with the time when arterialized tumor tissue is maximally enhanced relative to background liver (Figure 5). If an observation cannot be categorized due to image degradation or omission, then radiologists may choose to assign an LR-NC category (Figure 6). LI-RADS currently does not provide guidance on scoring the severity of artifact. In these cases, radiologists should use their judgment in suggesting either repeat or alternative imaging within 3 mo to better characterize the liver lesion.

LR-TIV

The presence of TIV should be ruled out. LR-TIV category is defined by definite enhancing tissue with a vein, indicating the presence of TIV. Whenever is possible the most likely etiology of TIV should be



DOI: 10.3748/wjg.v28.i32.4540 **Copyright** ©The Author(s) 2022.

Figure 1 A 52-year-old male with hepatocellular carcinoma and chronic hepatitis B. A: A segment VII mass showed a high signal on the short tau inversion recovery image; B: High on diffusion-weighted imaging; C: Low on unenhanced volumetric interpolated breath-hold examination image; D: Non-rim arterial phase hyperenhancement on arterial phase; E: Washout and enhancing capsule on portal phase. Lesion showed typical imaging findings of hepatocellular carcinoma categorized as LR-5 according to Liver Imaging Reporting and Data System criteria.

assigned (due to HCC or non HCC malignancy) (Figures 7 and 8).

LR-1 definitely benign

LR-1 is applied to observations that are benign. Management should be returned to routine surveillance at 6 mo intervals.

LR-2 probably benign

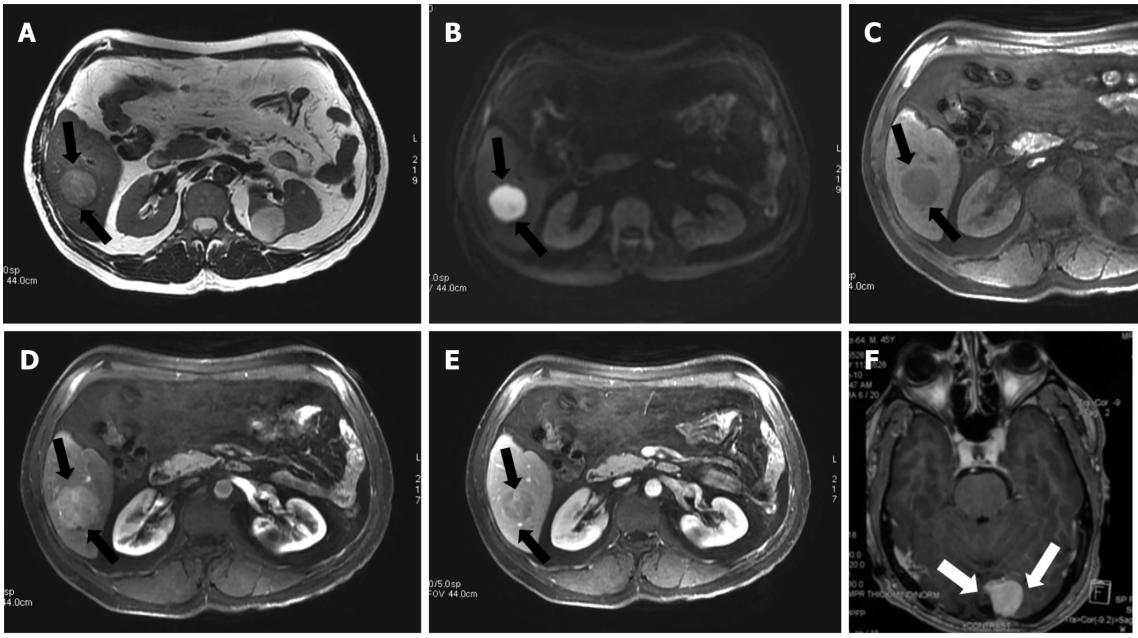
LR-2 is applied to observations that are probably benign. Management should be returned to routine surveillance at 6 mo intervals (Figure 9).

LR-M

LR-M for HCC observations display imaging characteristics of malignancy but not features that are specific. The LR-M category was created to maintain the specificity of the LI-RADS guidance for diagnosis of HCC while not losing sensitivity for liver malignancies. LR-M features include a targetoid or non-targetoid mass with infiltrative appearance, marked diffusion restriction, necrosis, or other characteristics suggestive of non-HCC malignancy[28]. Targetoid mass is defined by rim enhancement in the arterial phase, peripheral washout, and progressive central enhancement on delayed phases. Although any liver malignancy can appear with characteristics of LR-M, the most common entities in patients at increased risk for developing HCC are intrahepatic cholangiocarcinoma (CCA), combined tumors (CCA-HCC), and atypical HCC. LR-M observations are commonly biopsied to propose the appropriate treatment (Figure 10).

LI-RADS diagnostic table

If the above categories (LR-TIV, LR-M, LR-1, and LR-2) are considered and excluded, the radiologist should use the LI-RADS diagnostic criteria based on combinations of major imaging features. The diagnostic table includes the predominant imaging characteristics of HCC in order to generate categories ranging from intermediate probability to definite HCC (LR-3, LR-4, LR-5). For CT and MRI, the LI-RADS predominant characteristics consist of the following: (1) Size; (2) The presence of non-rim



DOI: 10.3748/wjg.v28.i32.4540 **Copyright** ©The Author(s) 2022.

Figure 2 A 45-year-old man with a segment VI lesion. A: The lesion demonstrated a high signal on T2 weighted image; B: High on diffusion-weighted imaging; C: Low on volumetric interpolated breath-hold examination; D: Non-rim arterial-phase hyper-enhancement on arterial-phase image; E: Washout on portal phase. If we applied Liver Imaging Reporting and Data System (LI-RADS) criteria, the erroneous diagnosis of hepatocellular carcinoma could be made. However, the patient did not meet the at-risk criteria to apply LI-RADS. Histologic examination of the lesion demonstrated metastatic hemangiopericytoma; F: Magnetic resonance imaging of the brain, axial post-contrast T1-weighted image showed an extra-axial lobulated, occipital enhancing mass corresponding to recurrence of hemangiopericytoma 12 mo after total surgical excision.

arterial phase hyperenhancement (APHE), which is defined by the appearance of enhancement that is unequivocally significantly than that of the background liver[29]. On MRI the enhancing portion must have higher intensity and on CT higher attenuation than background liver in the arterial phase; (3) Non-peripheral washout, which is defined as a visually assessed temporal decrease in enhancement in whole or at least in part relative to composite liver tissue from earlier to later phase leading to hypoenhancement; and (4) Enhancing capsule, which is defined as a smooth, uniform, and sharply outlined area of enhancement around a liver lesion which is either thicker or more conspicuous than fibrotic tissue detected in chronic liver disease.

It is worth mentioning that no single major imaging characteristic in the algorithm is specific enough to categorize a liver lesion as LR-5, and that LI-RADS liver lesions less than 10 mm in diameter cannot be categorized as LR-5.

LR-3 intermediate probability of malignancy

Liver lesions categorized as LR-3 have intermediate probability of being considered HCC, and the recommendation is to undergo short follow-up imaging in 3 to 6 mo (Figures 11 and 12).

LR-4 probably HCC

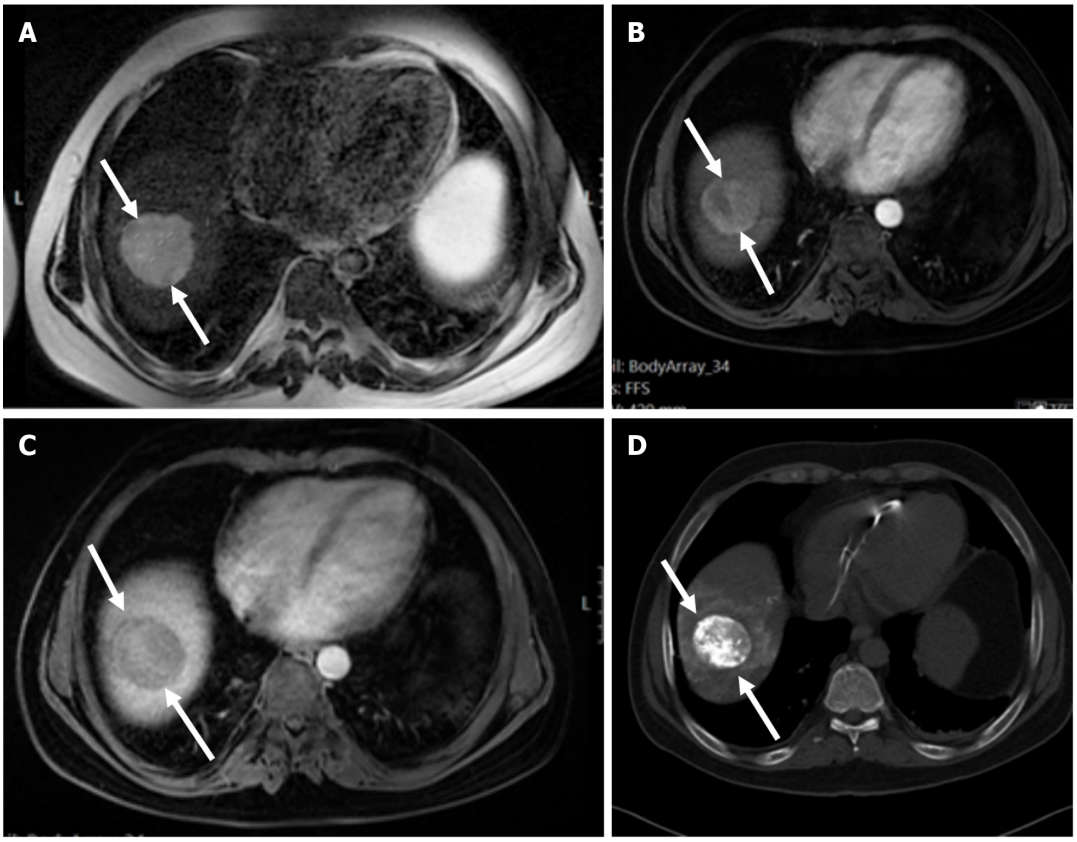
Observations categorized as LR-4 have a high probability of being considered definite HCC, and the suggestion is for an individualized multidisciplinary approach that may comprise biopsy, probable treatment, or follow-up (Figure 13).

LR-5 definitely HCC

It is worth noting that for LR-5 categorization, non-rim APHE must be present. The criteria for LR-5 category has a PPV approaching 100% in patients at high risk for developing HCC. Liver lesions categorized as LR-5 are considered definite HCC and therefore staging and treatment is suggested without biopsy (Figures 14-17).

Ancillary features

Ancillary features (AFs) can be used at the radiologist's discretion to adapt the category and to enhance the ability for reaching the final diagnosis. Although AFs are an important component of LI-RADS, their impact may be small (Figure 13). Various AFs likely can be taken out from LI-RADS criteria without compromising diagnostic performance[30].



DOI: 10.3748/wjg.v28.i32.4540 **Copyright** ©The Author(s) 2022.

Figure 3 A 47 mm liver mass was incidentally found, in a 40-year-old man with beta thalassemia, during cardiac magnetic resonance investigation for myocardial iron overload. A-C: On abdominal magnetic resonance imaging, the lesion demonstrated high signal intensity on T2 weighted image (A), arterial phase hyperenhancement on post-contrast arterial phase (B), and washout on portal phase (C). Although there are no current evidence-based guidelines for patients with beta thalassemia without cirrhosis, the hepatologist confirmed the patient's risk status and proposed that Liver Imaging Reporting and Data System (LI-RADS) should be applied. According to the LI-RADS criteria, the lesion was categorized as LR-5 (definite hepatocellular carcinoma); D: Unenhanced computed tomography scan after transarterial chemoembolization showed accumulation of iodized oil (arrow) within the tumor.

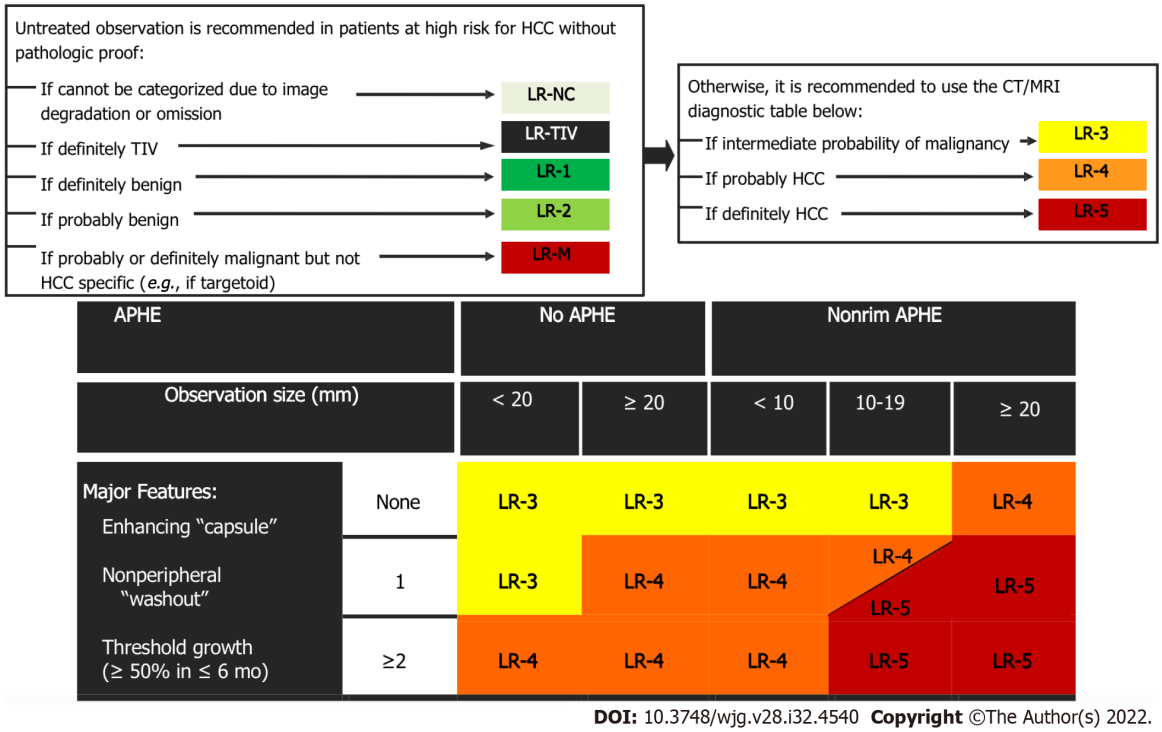
Treatment response algorithm (LI-RADS)

LI-RADS treatment response guidance (LR-TR) offers imaging criteria for evaluation of the success rate of locoregional therapy (Figures 17, 18, and 19). However, the guidance is not created for evaluating the response to systemic therapy, which is often at the patient-level rather than a lesion-level evaluation.

LI-RADS IN CLINICAL PRACTICE

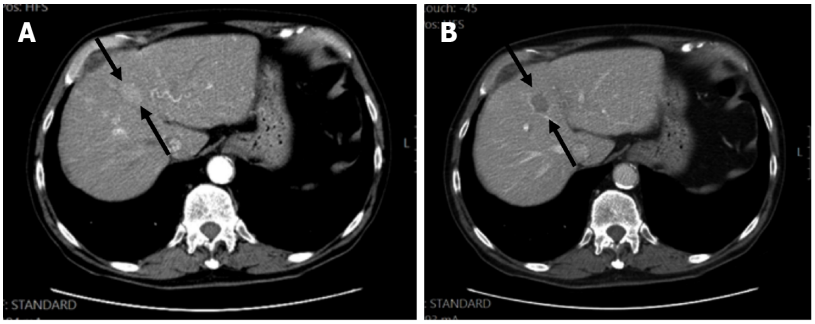
The LI-RADS "lexicon" provide strict diagnostic criteria and reporting guidelines in order to enhance the consistency and clarity of radiologist interpretation and reporting. Subsequently, the communication between radiologists and clinicians has been improved. The adoption of a universal liver imaging lexicon is of great importance. This lexicon was designed to standardize the terminology used to describe liver imaging findings and is suggested for use in various patient settings including patients with cirrhosis, chronic HBV infection, current or prior HCC and following loco-regional therapy to assess tumor response[31,32]. In this sense, the integration of LI-RADS into the AASLD HCC clinical practice guidelines was a major achievement. However, global unification of diagnostic algorithms of HCC is still an unmet need.

Variability in terminology and definitions creates confusion between clinicians and challenges the significance of the published literature. For example, multiple terms have been used to describe nodules without APHE that are hypointense in the hepatobiliary phase of a gadoxetate-enhanced MRI examination[33]. The LI-RADS Hepatobiliary Agent Working Group suggests standardized terminology for these nodules: "hepatobiliary phase hypointense nodules without APHE." A single term with a uniform definition enhances the ability of scientific investigators to define and pool data associated with these nodules and assists radiologists and referring clinicians in interpreting their clinical significance [31]. However, there are still areas of uncertainty. Non-cirrhotic patients at increased risk for developing HCC, such as those with chronic HCV infection or nonalcoholic steatohepatitis with advanced fibrosis,



DOI: 10.3748/wjg.v28.i32.4540 **Copyright** ©The Author(s) 2022.

Figure 4 Diagnostic algorithm of liver lesions in computed tomography/magnetic resonance imaging (Liver Imaging Reporting and Data System v2018 CORE). Observations in the cell LR-4 and LR-5 are categorized based on one additional major feature: LR-4 if enhancing "capsule" and LR-5 if nonperipheral "washout" or threshold growth. APHE: Arterial phase hyperenhancement; CT: Computed tomography; HCC: Hepatocellular carcinoma; MRI: Magnetic resonance imaging; TIV: Tumor in vein.



DOI: 10.3748/wjg.v28.i32.4540 **Copyright** ©The Author(s) 2022.

Figure 5 Hepatocellular carcinoma in a 60-year-old man with hepatitis C. A: Computed tomography scan, late arterial phase were the hepatic artery and portal vein are both enhanced, showed a segment VIII lesion measuring 27 mm with non-rim arterial phase hyper-enhancement; B: In the portal phase, washout was seen.

do not meet criteria for diagnosis of HCC with the use of LI-RADS. This is an example of an important gap in the generalized implementation of the LI-RADS criteria which necessitates further research.

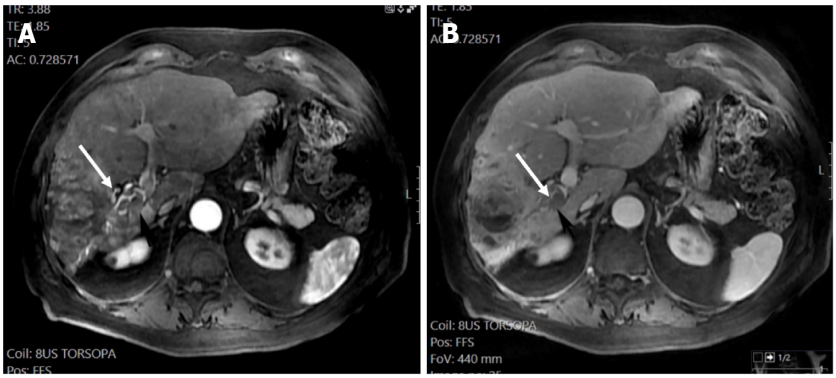
CONCLUSION

The diagnosis of HCC in clinical practice is based on imaging, using mainly CT and MRI. As the early diagnosis of HCC is associated with the overall prognosis, accurate identification of potential malignant liver lesions using these modalities is essential. LI-RADS is a comprehensive guidance that provides standardized interpretation and reporting of CT and MR liver imaging. LI-RADS is suggested to be used only to patients at high risk for developing HCC in a step-wise fashion that analyzes all the relevant radiologic characteristics according to a pre-defined manner. Clinicians that care for patients with liver disease must be familiar with the characterization of liver lesions using the LI-RADS criteria as this offers correct assessment of liver lesions and truthful communication between specialties.



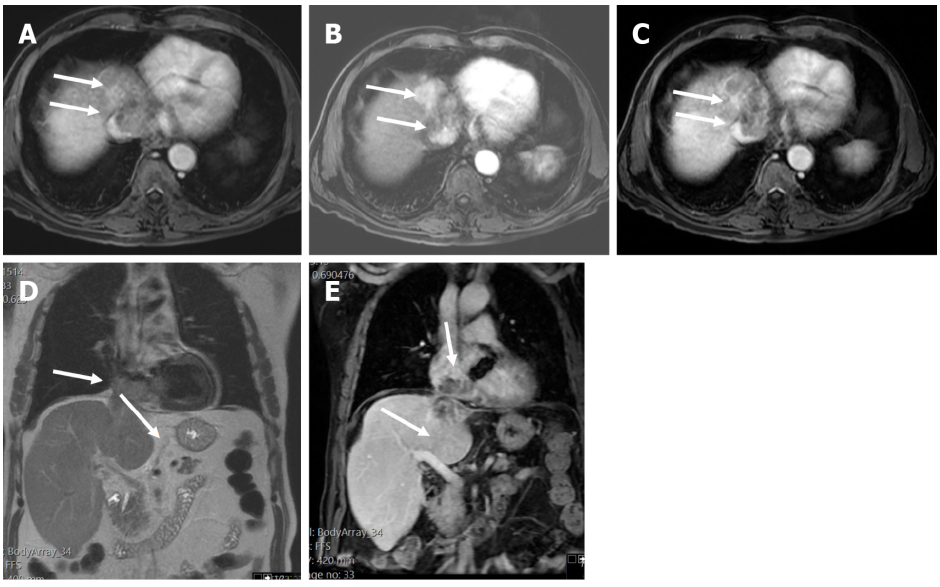
DOI: 10.3748/wjg.v28.i32.4540 **Copyright** ©The Author(s) 2022.

Figure 6 LR-non-categorizable category. Magnetic resonance imaging in a 74-year-old man with hepatitis C. A: Axial short tau inversion recovery shows an observation in segment VIII with high signal intensity (arrow) within a nodular liver consistent with cirrhosis; On arterial post-contrast image (B) and on portal phase (C) (arrows) the observation shows low signal intensity. However the arterial phase is early to characterize a possible arterialized lesion (LR-NC category).



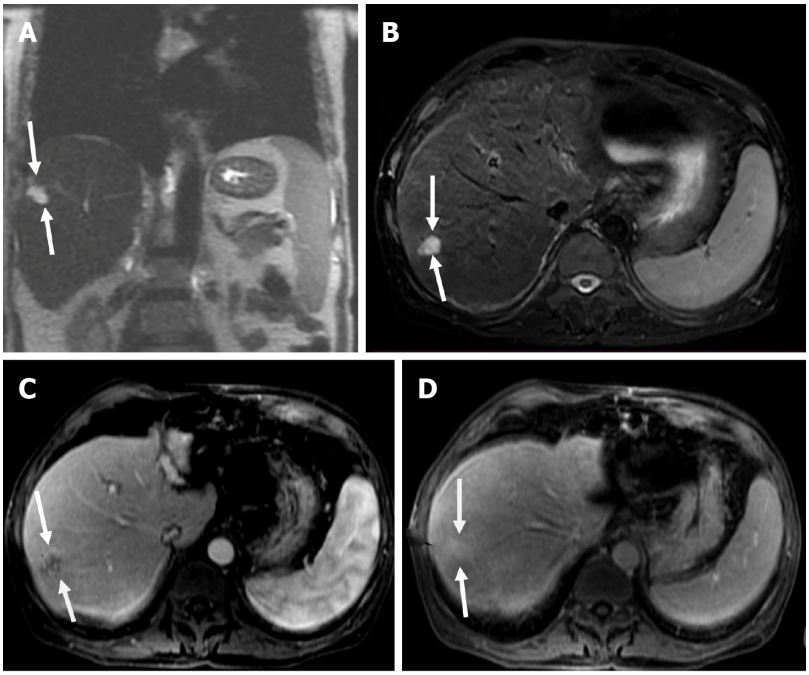
DOI: 10.3748/wjg.v28.i32.4540 **Copyright** ©The Author(s) 2022.

Figure 7 LR-tumor in vein (definite tumor in vein) in a 70-year-old man with alcoholic liver cirrhosis. Magnetic resonance imaging arterial phase and portal venous phase demonstrated a large inhomogeneous enhancing mass with definite enhancing soft tissue extending to the right portal vein (arrows). A: Magnetic resonance imaging arterial phase; B: Portal venous phase.



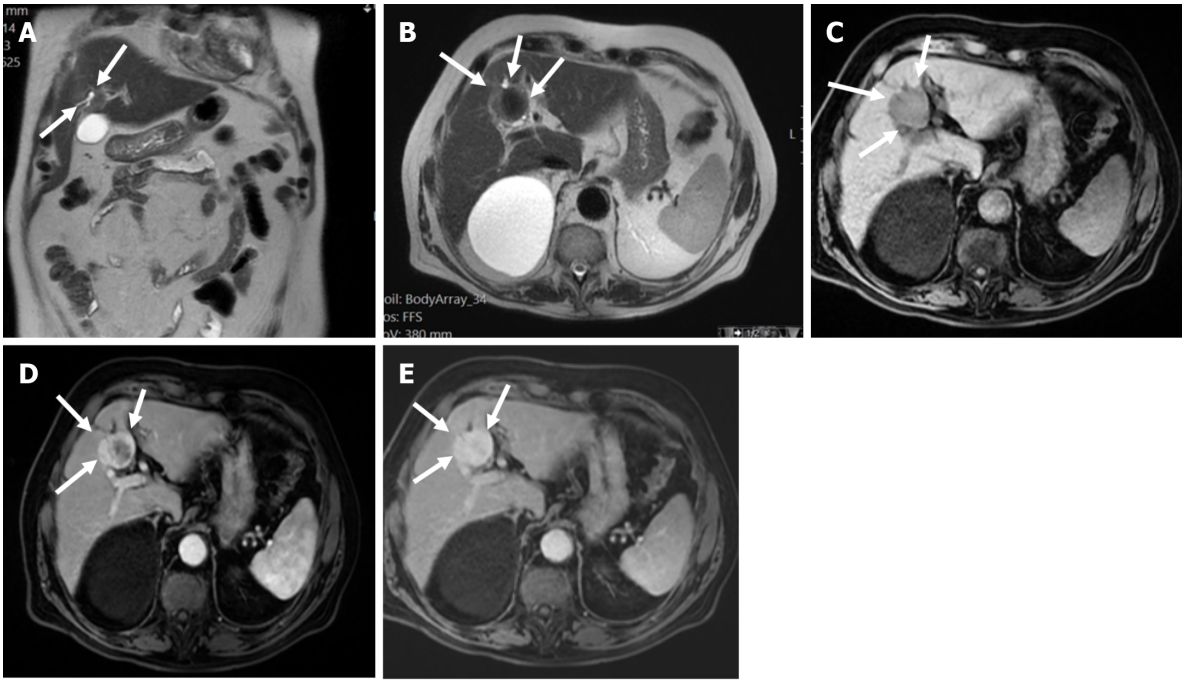
DOI: 10.3748/wjg.v28.i32.4540 **Copyright** ©The Author(s) 2022.

Figure 8 Two-dimensional transthoracic echocardiogram revealed a mobile right atrial mass protruding from the inferior vena cava, in a patient with chronic hepatitis B and cirrhosis. A-C: Axial T1 weighted image (T1WI) (A), arterial post-contrast (B) and portal phase (C) showed direct right atrial extension of hepatic segment VIII-IVA tumor through the inferior vena cava, categorized as LR-tumor in vein (arrows); D and E: Coronal T2 weighted image (D) and coronal post-contrast T1WI (E) showed better craniocaudal tumor extension (arrows).



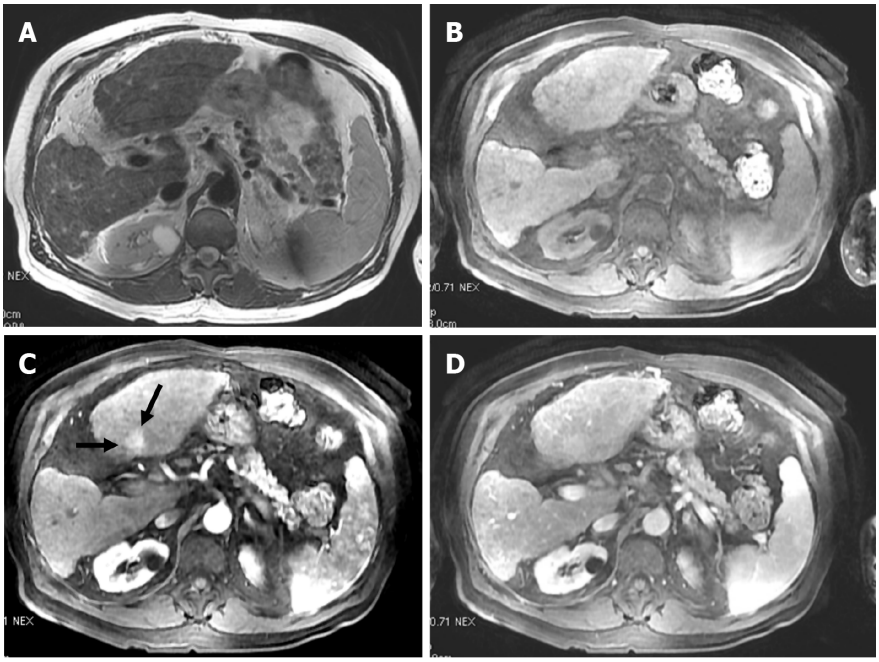
DOI: 10.3748/wjg.v28.i32.4540 **Copyright** ©The Author(s) 2022.

Figure 9 Coronal T2 weighted image and axial short tau inversion recovery image. A and B: Coronal T2 weighted image (T2WI) (A) and axial short tau inversion recovery image (B) showed a 2 cm lesion in segment VII with high signal intensity (bright) within a nodular liver consistent with cirrhosis; C: Post-contrast image showed nodular peripheral enhancement; D: On delay image, the lesion showed progressive filling. In progressive cirrhosis, hemangiomas are likely to decrease in size, become more fibrotic, and are difficult to diagnose radiologically. However, the bright signal on T2WI and the enhancement pattern was pathognomonic for hemangioma of the liver consistent with LR-2.



DOI: 10.3748/wjg.v28.i32.4540 **Copyright** ©The Author(s) 2022.

Figure 10 T1 weighted image and T2 weighted image. A and B: Coronal (A) and axial (B) T2 weighted images showed a low signal segment V mass in a patient with chronic hepatitis B (arrows); C: The mass showed low signal intensity (arrows) on T1 weighted image; D and E: In the arterial phase (D), there was peripheral enhancement (arrows) and progressive filling (arrows) in the portal phase (E) categorized as LR-M. Histologic examination confirmed the diagnosis of cholangiocarcinoma and not hepatocellular carcinoma.



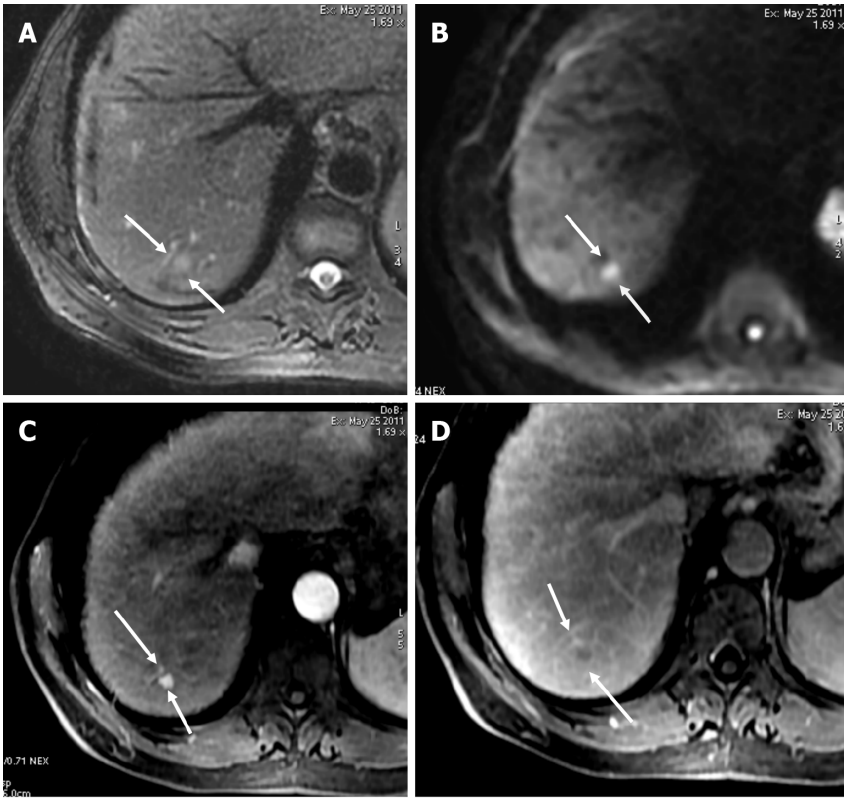
DOI: 10.3748/wjg.v28.i32.4540 **Copyright** ©The Author(s) 2022.

Figure 11 T2 weighted image and volumetric interpolated breath-hold examination. A and B: Axial T2 weighted image (A) and volumetric interpolated breath-hold examination (VIBE) (B) showed a shrunken and nodular liver that was consistent with cirrhosis; C and D: On post-contrast VIBE arterial-phase image (C), a 1.6 cm lesion in segment IVb demonstrated hyperenhancement (arrows) without washout on portal venous phase image (D). According to Liver Imaging Reporting and Data System criteria, the lesion was categorized as LR-3.



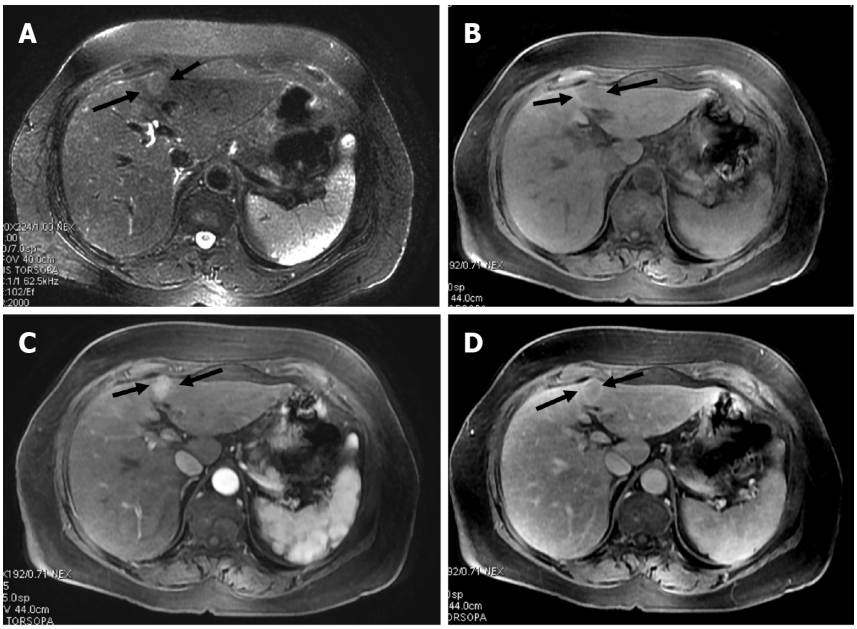
DOI: 10.3748/wjg.v28.i32.4540 **Copyright** ©The Author(s) 2022.

Figure 12 Axial short tau inversion recovery image. A and B: A IVa segment observation with low signal intensity (arrows) measuring > 20 mm (A) and high signal intensity on pre-contrast image (arrows on B); C and D: On arterial (C) and portal (D) phase there was no arterial phase hyperenhancement or washout and the lesion was categorized as LR-3.



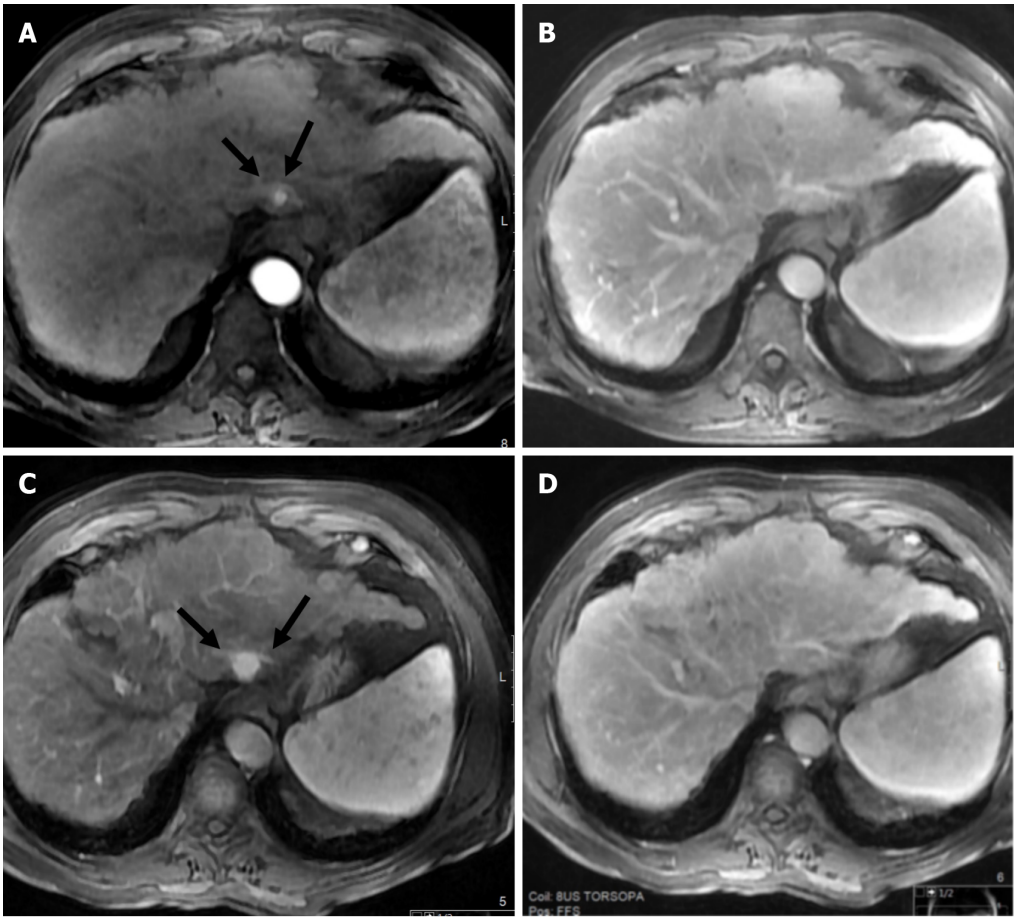
DOI: 10.3748/wjg.v28.i32.4540 **Copyright** ©The Author(s) 2022.

Figure 13 Axial short tau inversion recovery and diffusion-weighted imaging. A and B: Axial short tau inversion recovery (A) and diffusion-weighted imaging (DWI) (B) images showed a < 10 mm segment VII observation with high signal intensity; C and D: In the arterial phase (C), arterial phase hyperenhancement was seen with washout in the portal phase (D) categorized as LR-4. Restriction on DWI does not allow to upgrade from LR-4 to LR-5, because ancillary features lack sufficient specificity for hepatocellular carcinoma to allow for an LR-5 upgrade.



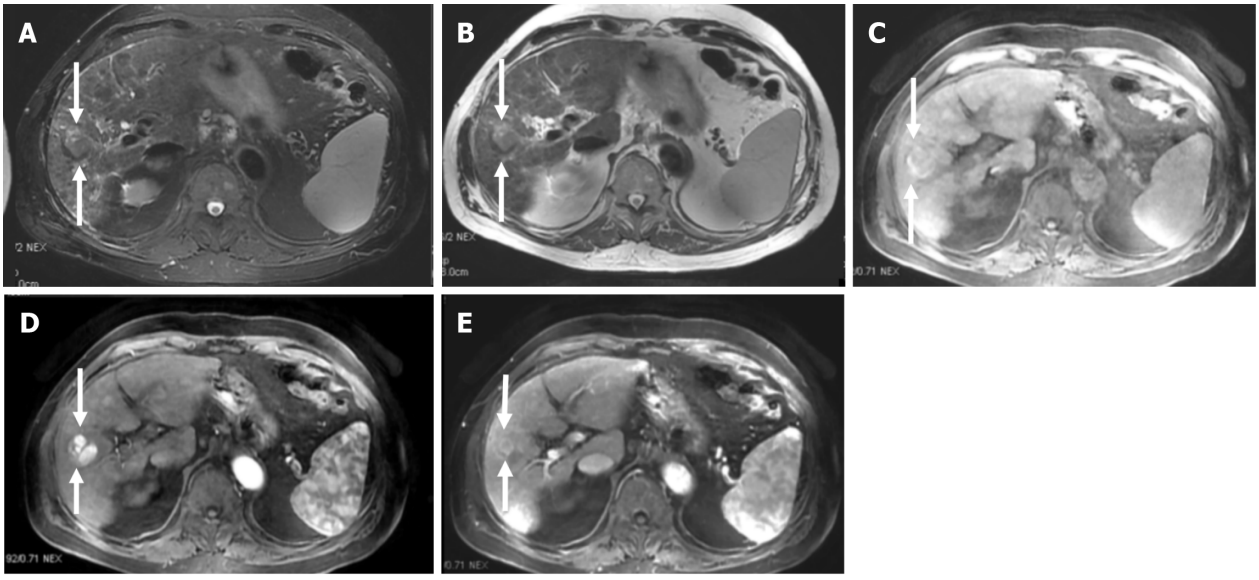
DOI: 10.3748/wjg.v28.i32.4540 **Copyright** ©The Author(s) 2022.

Figure 14 A 62-year-old female with chronic hepatitis C. A: On axial short tau inversion recovery image, a 21 mm IVb segment observation with relative high signal intensity is seen (arrows); B: On axial volumetric interpolated breath-hold examination image the observation shows low signal intensity (arrows); C and D: On post-contrast images, major features of hepatocellular carcinoma (HCC), arterial phase hyperenhancement (arrows) on arterial phase (C), washout and enhancing capsule (arrows) on portal (D) were seen, indicating LR-5 (definitely HCC).



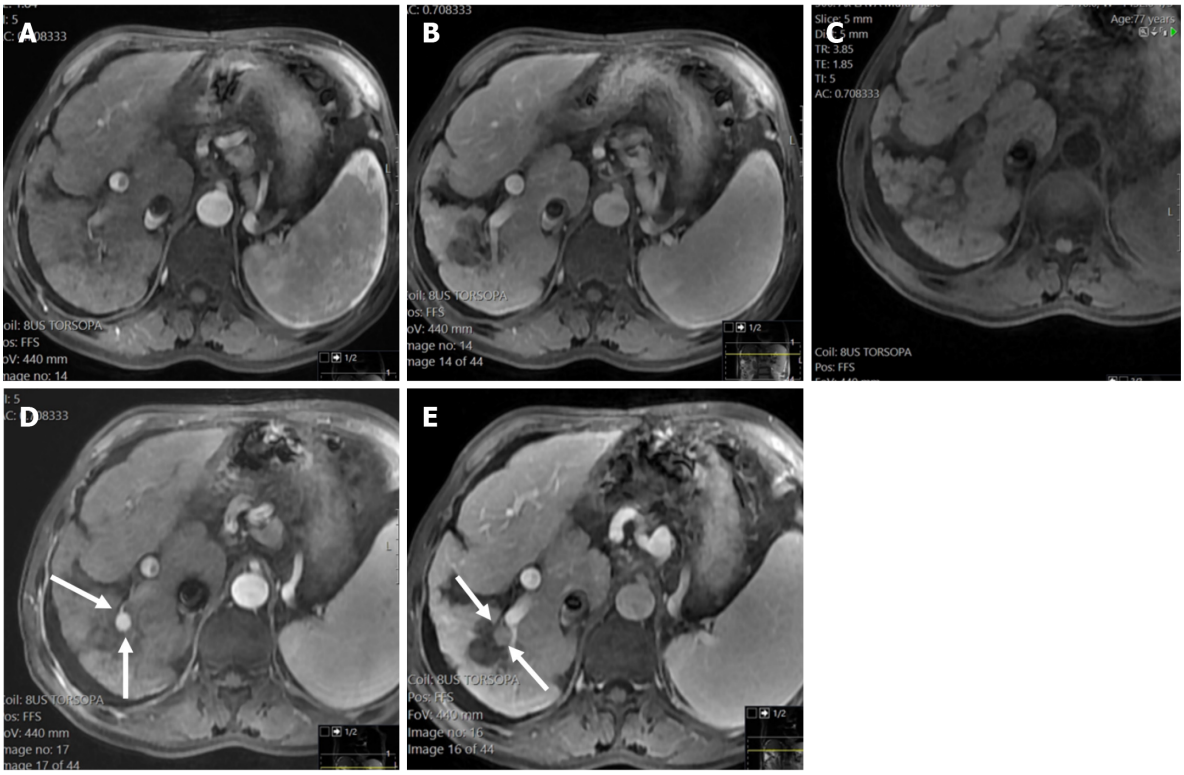
DOI: 10.3748/wjg.v28.i32.4540 **Copyright** ©The Author(s) 2022.

Figure 15 A 60-year-old male with hepatitis B and cirrhosis. A and B: A < 10 mm segment II observation demonstrated arterial phase hyperenhancement (APHE) (arrows) on arterial post-contrast images (A) without washout (B), categorized as LR-3 observation; C and D: 1-year later, the observation measured 18 mm, showed APHE (arrows) in the arterial phase (C) without definite washout in the portal phase (D). However due to threshold growth, it was categorized as LR-5.



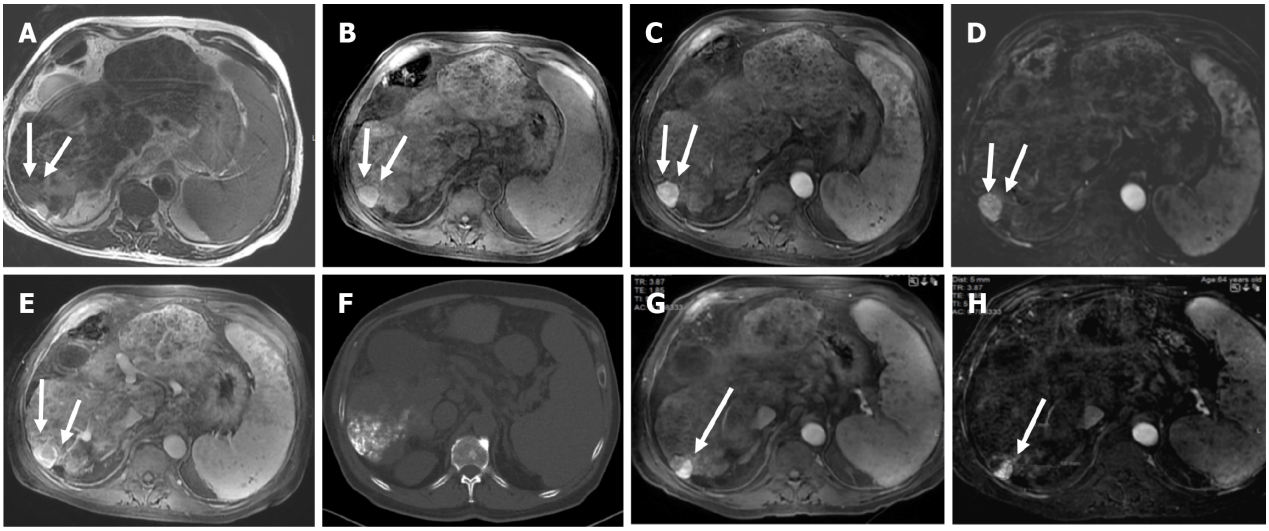
DOI: 10.3748/wjg.v28.i32.4540 **Copyright** ©The Author(s) 2022.

Figure 16 LR-5 observation. A and B: Axial short tau inversion recovery (A) and T2 weighted (B) showed a segment VI observation with relative high signal intensity (arrows); C: On pre-contrast volumetric interpolated breath-hold examination image, peripherally high signal was seen; D: In the arterial phase, multiple hyperenhanced nodules within nodule were seen (arrows); E: In the portal phase, segmental washout was seen (arrows) categorized as LR-5.



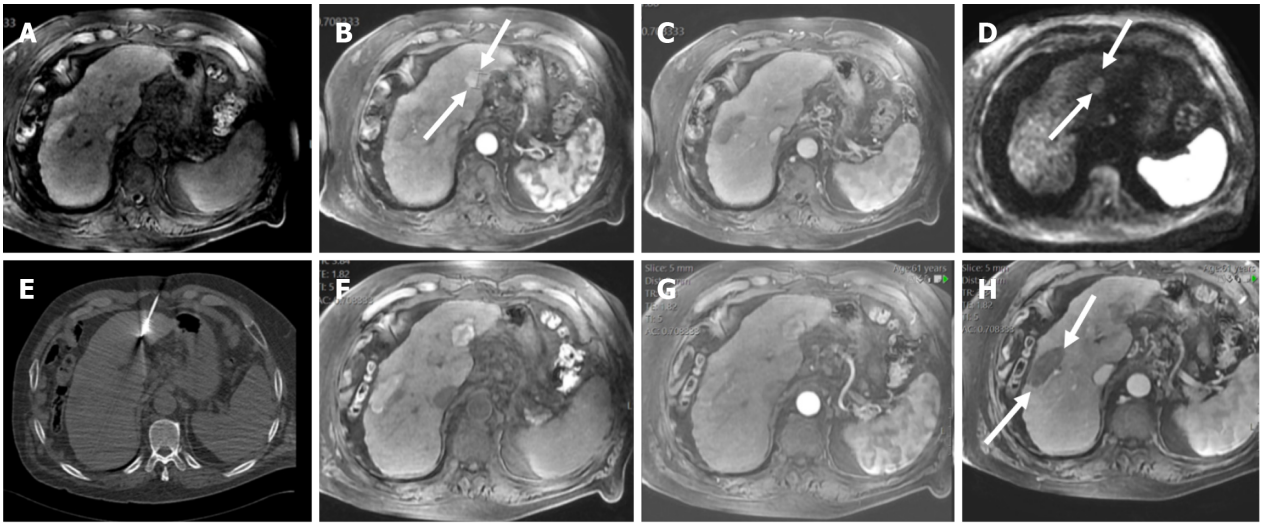
DOI: 10.3748/wjg.v28.i32.4540 **Copyright** ©The Author(s) 2022.

Figure 17 LR-5 observation. A and B: Axial post-contrast images arterial (A) and portal phase (B) showed an ablation defect in segment VI without residual areas of arterial enhancement or washout. This was classified as LR-treatment response non-viable; C-E: Later pre-contrast (C) arterial (D) and portal (E) phase showed a new nodule (arrows) measuring 12 mm with strong arterial enhancement and washout categorized as LR-5. If a new tumor arises within or adjacent to a treated lesion, this observation should be assigned a new non-treated LI-RADS category.



DOI: 10.3748/wjg.v28.i32.4540 **Copyright** ©The Author(s) 2022.

Figure 18 LR-5 observation. A and B: Axial T2 weighted (A) and volumetric interpolated breath-hold examination (B) show a segment VI observation with high signal intensity (arrows); C and D: On arterial phase (C) strong enhancement is seen, better depicted on subtracted image (D); E: On portal phase washout is seen categorized as LR-5; F: Unenhanced computed tomography scan after TACE shows accumulation of iodized oil (arrow) within the tumor; G and H: However on post-contrast follow up magnetic resonance imaging on arterial phase (G) there is residual nodular enhancement within a lesion clearly depicted on subtracted image (H) categorized as LR-treatment response viable.



DOI: 10.3748/wjg.v28.i32.4540 **Copyright** ©The Author(s) 2022.

Figure 19 Axial volumetric interpolated breath-hold examination, arterial phase. A-C: Axial volumetric interpolated breath-hold examination (A), arterial phase (B) showed an observation measuring almost 20 mm with arterial phase hyperenhancement (arrows) without washout on portal image (C) categorized as LR-4; D and E: On diffusion-weighted imaging (D), the observation showed high signal intensity (arrows) but the ancillary features lacked sufficient specificity for hepatocellular carcinoma to allow for an LR-5 upgrade. After multidisciplinary discussion, ablation was performed (E); F-H: On follow-up, an ablation defect was seen without residual areas of arterial enhancement or washout. This was classified as LR-treatment response non-viable. Note a previous ablation defect in the right lobe (arrows).

FOOTNOTES

Author contributions: Liava C, Sinakos E, Danai C, Chatziioannou A, and Akriviadis E drafted the article; Papadopoulou E, Giannakopoulou L, Potsi S, Moumtzouoglou A, Stergioulas L, Kalogeropoulou L, Dedes I, and Chourmouzi D provided the computed tomography and magnetic resonance imaging images and drafted the figure legends; Sinakos E made critical revisions related to important intellectual content and approved the final version of the manuscript.

Conflict-of-interest statement: The authors have no conflicts of interest to declare.

Open-Access: This article is an open-access article that was selected by an in-house editor and fully peer-reviewed by external reviewers. It is distributed in accordance with the Creative Commons Attribution NonCommercial (CC BY-NC 4.0) license, which permits others to distribute, remix, adapt, build upon this work non-commercially, and license their derivative works on different terms, provided the original work is properly cited and the use is non-commercial. See: https://creativecommons.org/Licenses/by-nc/4.0/

Country/Territory of origin: Greece

ORCID number: Christina Liava 0000-0001-9523-5694; Emmanouil Sinakos 0000-0003-0923-050X; Elissavet Papadopoulou 0000-0001-6475-0415; Lamprini Giannakopoulou 0000-0002-9697-6125; Stamatia Potsi 0000-0001-6266-9875; Anestis Moumtzouoglou 0000-0001-6517-6371; Anthi Chatziioannou 0000-0002-8931-6786; Loukas Stergioulas 0000-0002-8109-2298; Lydia Kalogeropoulou 0000-0001-5461-5885; Ioannis Dedes 0000-0001-7265-4765; Evangelos Akriviadis 0000-0002-7906-6445; Danai Chourmouzi 0000-0001-6918-5160.

S-Editor: Fan JR
L-Editor: Filipodia
P-Editor: Chen YX

REFERENCES

1 **World Health organization**. International Agency for Research on Cancer, Global Cancer Observatory Cancer Today 2020–IARC. [cited 10 January 2022]. Available from: https://gco.iarc.fr/today/fact-sheets-cancers
2 **Forner A**, Llovet JM, Bruix J. Hepatocellular carcinoma. *Lancet* 2012; **379**: 1245-1255 [PMID: 22353262 DOI: 10.1016/S0140-6736(11)61347-0]
3 **Dimitroulis D**, Damaskos C, Valsami S, Davakis S, Garmpis N, Spartalis E, Athanasiou A, Moris D, Sakellariou S, Kykalos S, Tsourouflis G, Garmpi A, Delladetsima I, Kontzoglou K, Kouraklis G. From diagnosis to treatment of hepatocellular carcinoma: An epidemic problem for both developed and developing world. *World J Gastroenterol* 2017; **23**: 5282-5294 [PMID: 28839428 DOI: 10.3748/wjg.v23.i29.5282]

4 **Reig M**, Forner A, Rimola J, Ferrer-Fàbrega J, Burrel M, Garcia-Criado Á, Kelley RK, Galle PR, Mazzaferro V, Salem R, Sangro B, Singal AG, Vogel A, Fuster J, Ayuso C, Bruix J. BCLC strategy for prognosis prediction and treatment recommendation: The 2022 update. *J Hepatol* 2022; **76**: 681-693 [PMID: 34801630 DOI: 10.1016/j.jhep.2021.11.018]

5 **Choi JY**, Lee JM, Sirlin CB. CT and MR imaging diagnosis and staging of hepatocellular carcinoma: part I. Development, growth, and spread: key pathologic and imaging aspects. *Radiology* 2014; **272**: 635-654 [PMID: 25153274 DOI: 10.1148/radiol.14132361]

6 **Cunha GM**, Sirlin CB, Fowler KJ. Imaging diagnosis of hepatocellular carcinoma: LI-RADS. *Chin Clin Oncol* 2021; **10**: 3 [PMID: 32527115 DOI: 10.21037/cco-20-107]

7 **Santillan CS**, Tang A, Cruite I, Shah A, Sirlin CB. Understanding LI-RADS: a primer for practical use. *Magn Reson Imaging Clin N Am* 2014; **22**: 337-352 [PMID: 25086933 DOI: 10.1016/j.mric.2014.04.007]

8 **Moura Cunha G**, Chernyak V, Fowler KJ, Sirlin CB. Up-to-Date Role of CT/MRI LI-RADS in Hepatocellular Carcinoma. *J Hepatocell Carcinoma* 2021; **8**: 513-527 [PMID: 34104640 DOI: 10.2147/JHC.S268288]

9 **Alqahtani A**, Khan Z, Alloghbi A, Said Ahmed TS, Ashraf M, Hammouda DM. Hepatocellular Carcinoma: Molecular Mechanisms and Targeted Therapies. *Medicina (Kaunas)* 2019; **55** [PMID: 31450841 DOI: 10.3390/medicina55090526]

10 **Llovet JM**, Kelley RK, Villanueva A, Singal AG, Pikarsky E, Roayaie S, Lencioni R, Koike K, Zucman-Rossi J, Finn RS. Hepatocellular carcinoma. *Nat Rev Dis Primers* 2021; **7**: 6 [PMID: 33479224 DOI: 10.1038/s41572-020-00240-3]

11 **Villanueva A**. Hepatocellular Carcinoma. *N Engl J Med* 2019; **380**: 1450-1462 [PMID: 30970190 DOI: 10.1056/NEJMra1713263]

12 **Farazi PA**, DePinho RA. Hepatocellular carcinoma pathogenesis: from genes to environment. *Nat Rev Cancer* 2006; **6**: 674-687 [PMID: 16929323 DOI: 10.1038/nrc1934]

13 **Tokino T**, Tamura H, Hori N, Matsubara K. Chromosome deletions associated with hepatitis B virus integration. *Virology* 1991; **185**: 879-882 [PMID: 1962459 DOI: 10.1016/0042-6822(91)90564-r]

14 **McClain CJ**, Hill DB, Song Z, Deaciuc I, Barve S. Monocyte activation in alcoholic liver disease. *Alcohol* 2002; **27**: 53-61 [PMID: 12062638 DOI: 10.1016/s0741-8329(02)00212-4]

15 **Ozturk M**. p53 mutation in hepatocellular carcinoma after aflatoxin exposure. *Lancet* 1991; **338**: 1356-1359 [PMID: 1682737 DOI: 10.1016/0140-6736(91)92236-u]

16 **Riley J**, Mandel HG, Sinha S, Judah DJ, Neal GE. In vitro activation of the human Harvey-ras proto-oncogene by aflatoxin B1. *Carcinogenesis* 1997; **18**: 905-910 [PMID: 9163674 DOI: 10.1093/carcin/18.5.905]

17 **Ramakrishna G**, Rastogi A, Trehanpati N, Sen B, Khosla R, Sarin SK. From cirrhosis to hepatocellular carcinoma: new molecular insights on inflammation and cellular senescence. *Liver Cancer* 2013; **2**: 367-383 [PMID: 24400224 DOI: 10.1159/000343852]

18 **Jiang HY**, Chen J, Xia CC, Cao LK, Duan T, Song B. Noninvasive imaging of hepatocellular carcinoma: From diagnosis to prognosis. *World J Gastroenterol* 2018; **24**: 2348-2362 [PMID: 29904242 DOI: 10.3748/wjg.v24.i22.2348]

19 **European Association for the Study of the Liver**. EASL Clinical Practice Guidelines: Management of hepatocellular carcinoma. *J Hepatol* 2018; **69**: 182-236 [PMID: 29628281 DOI: 10.1016/j.jhep.2018.03.019]

20 **Marrero JA**, Kulik LM, Sirlin CB, Zhu AX, Finn RS, Abecassis MM, Roberts LR, Heimbach JK. Diagnosis, Staging, and Management of Hepatocellular Carcinoma: 2018 Practice Guidance by the American Association for the Study of Liver Diseases. *Hepatology* 2018; **68**: 723-750 [PMID: 29624699 DOI: 10.1002/hep.29913]

21 **Papatheodoridis G**, Dalekos G, Sypsa V, Yurdaydin C, Buti M, Goulis J, Calleja JL, Chi H, Manolakopoulos S, Mangia G, Gatselis N, Keskin O, Savvidou S, de la Revilla J, Hansen BE, Vlachogiannakos I, Galanis K, Idilman R, Colombo M, Esteban R, Janssen HL, Lampertico P. PAGE-B predicts the risk of developing hepatocellular carcinoma in Caucasians with chronic hepatitis B on 5-year antiviral therapy. *J Hepatol* 2016; **64**: 800-806 [PMID: 26678008 DOI: 10.1016/j.jhep.2015.11.035]

22 **Rastogi A**. Changing role of histopathology in the diagnosis and management of hepatocellular carcinoma. *World J Gastroenterol* 2018; **24**: 4000-4013 [PMID: 30254404 DOI: 10.3748/wjg.v24.i35.4000]

23 **International Consensus Group for Hepatocellular NeoplasiaThe International Consensus Group for Hepatocellular Neoplasia**. Pathologic diagnosis of early hepatocellular carcinoma: a report of the international consensus group for hepatocellular neoplasia. *Hepatology* 2009; **49**: 658-664 [PMID: 19177576 DOI: 10.1002/hep.22709]

24 **Bosman FT**, Carneiro F, Hruban RH, Theise ND. WHO Classification of Tumours of the Digestive System. 4th ed. IARC press, 2010

25 **Franette C**. Hepatocellular Carcinoma: Moving into the 21st Cenury, An Issue of Clinics in Liver Disease. 1st ed. Elsevier press, 2020

26 **Tatsumi A**, Maekawa S, Sato M, Komatsu N, Miura M, Amemiya F, Nakayama Y, Inoue T, Sakamoto M, Enomoto N. Liver stiffness measurement for risk assessment of hepatocellular carcinoma. *Hepatol Res* 2015; **45**: 523-532 [PMID: 24961848 DOI: 10.1111/hepr.12377]

27 **Piscaglia F**, Svegliati-Baroni G, Barchetti A, Pecorelli A, Marinelli S, Tiribelli C, Bellentani S; HCC-NAFLD Italian Study Group. Clinical patterns of hepatocellular carcinoma in nonalcoholic fatty liver disease: A multicenter prospective study. *Hepatology* 2016; **63**: 827-838 [PMID: 26599351 DOI: 10.1002/hep.28368]

28 **Chernyak V**, Fowler KJ, Kamaya A, Kielar AZ, Elsayes KM, Bashir MR, Kono Y, Do RK, Mitchell DG, Singal AG, Tang A, Sirlin CB. Liver Imaging Reporting and Data System (LI-RADS) Version 2018: Imaging of Hepatocellular Carcinoma in At-Risk Patients. *Radiology* 2018; **289**: 816-830 [PMID: 30251931 DOI: 10.1148/radiol.2018181494]

29 **Kielar AZ**, Chernyak V, Bashir MR, Do RK, Fowler KJ, Mitchell DG, Cerny M, Elsayes KM, Santillan C, Kamaya A, Kono Y, Sirlin CB, Tang A. LI-RADS 2017: An update. *J Magn Reson Imaging* 2018; **47**: 1459-1474 [PMID: 29626376 DOI: 10.1002/jmri.26027]

30 **van der Pol CB**, Dhindsa K, Shergill R, Zha N, Ferri M, Kagoma YK, Lee SY, Satkunasingham J, Wat J, Tsai S. MRI LI-RADS Version 2018: Impact of and Reduction in Ancillary Features. *AJR Am J Roentgenol* 2021; **216**: 935-942 [PMID: 33534620 DOI: 10.2214/AJR.20.23031]

31 **Marks RM**, Masch WR, Chernyak V. LI-RADS: Past, Present, and Future, From the *AJR* Special Series on Radiology

Reporting and Data Systems. *AJR Am J Roentgenol* 2021; **216**: 295-304 [PMID: 33052720 DOI: 10.2214/AJR.20.24272]

32 **Elsayes KM**, Kielar AZ, Chernyak V, Morshid A, Furlan A, Masch WR, Marks RM, Kamaya A, Do RKG, Kono Y, Fowler KJ, Tang A, Bashir MR, Hecht EM, Jambhekar K, Lyshchik A, Rodgers SK, Heiken JP, Kohli M, Fetzer DT, Wilson SR, Kassam Z, Mendiratta-Lala M, Singal AG, Lim CS, Cruite I, Lee J, Ash R, Mitchell DG, McInnes MDF, Sirlin CB. LI-RADS: a conceptual and historical review from its beginning to its recent integration into AASLD clinical practice guidance. *J Hepatocell Carcinoma* 2019; **6**: 49-69 [PMID: 30788336 DOI: 10.2147/JHC.S186239]

33 **Motosugi U**, Murakami T, Lee JM, Fowler KJ, Heiken JP, Sirlin CB; LI-RADS HBA Working Group. Recommendation for terminology: Nodules without arterial phase hyperenhancement and with hepatobiliary phase hypointensity in chronic liver disease. *J Magn Reson Imaging* 2018; **48**: 1169-1171 [PMID: 30347132 DOI: 10.1002/jmri.26515]

World Journal of Gastroenterology

Submit a Manuscript: https://www.f6publishing.com

World J Gastroenterol 2022 August 28; 28(32): 4557-4573

DOI: 10.3748/wjg.v28.i32.4557

ISSN 1007-9327 (print) ISSN 2219-2840 (online)

MINIREVIEWS

Liver regeneration as treatment target for severe alcoholic hepatitis

Lucija Virovic-Jukic, Dominik Ljubas, Sanja Stojsavljevic-Shapeski, Neven Ljubičić, Tajana Filipec Kanizaj, Ivana Mikolasevic, Ivica Grgurevic

Specialty type: Gastroenterology and hepatology

Provenance and peer review: Invited article; Externally peer reviewed.

Peer-review model: Single blind

Peer-review report's scientific quality classification

Grade A (Excellent): 0
Grade B (Very good): B
Grade C (Good): C
Grade D (Fair): 0
Grade E (Poor): 0

P-Reviewer: Spahr L, Switzerland; Tyson LD, United Kingdom

Received: February 26, 2022
Peer-review started: February 26, 2022
First decision: May 9, 2022
Revised: May 30, 2022
Accepted: June 16, 2022
Article in press: June 16, 2022
Published online: August 28, 2022

Lucija Virovic-Jukic, Sanja Stojsavljevic-Shapeski, Neven Ljubičić, Department of Gastroenterology and Hepatology, Sisters of Charity University Hospital Center, Zagreb 10000, Croatia

Lucija Virovic-Jukic, Dominik Ljubas, Neven Ljubičić, Tajana Filipec Kanizaj, Ivica Grgurevic, Department of Internal Medicine, University of Zagreb School of Medicine, Zagreb 10000, Croatia

Neven Ljubičić, Department of Internal Medicine, University of Zagreb School of Dental Medicine, Zagreb 10000, Croatia

Tajana Filipec Kanizaj, Department of Gastroenterology, Merkur University Hospital, Zagreb 10000, Croatia

Ivana Mikolasevic, Department of Gastroenterology, Rijeka University Hospital Center, Rijeka 51000, Croatia

Ivana Mikolasevic, Department of Internal Medicine, University of Rijeka School of Medicine, Rijeka 10000, Croatia

Ivica Grgurevic, Department of Gastroenterology, Hepatology and Clinical Nutrition, Dubrava University Hospital, Zagreb 10000, Croatia

Corresponding author: Lucija Virovic-Jukic, Doctor, MD, PhD, Associate Professor, Department of Gastroenterology and Hepatology, Sisters of Charity University Hospital Center, Vinogradska cesta 29, Zagreb 10000, Croatia. lucija.virovic.jukic@kbcsm.hr

Abstract

Severe alcoholic hepatitis (AH) is a distinct entity in the spectrum of alcohol-related liver disease, with limited treatment options and high mortality. Supportive medical care with corticosteroids in selected patients is the only currently available treatment option, often with poor outcomes. Based on the insights into the pathogenetic mechanisms of AH, which are mostly obtained from animal studies, several new treatment options are being explored. Studies have implicated impaired and deranged liver regeneration processes as one of the culprit mechanisms and a potential therapeutic target. Acknowledging evidence for the beneficial effects of granulocyte colony-stimulating factor (G-CSF) on liver regeneration and immunomodulation in animal models, several human studies investigated its role in the treatment of advanced alcohol-related liver disease and AH. Contrary to the previously published studies suggesting benefits of G-CSF in

the outcomes of patients with severe AH, these effects were not confirmed by a recently published multicenter randomized trial, suggesting that other options should rather be pursued. Stem cell transplantation represents another option for improving liver regeneration, but evidence for its efficacy in patients with severe AH and advanced alcohol-related liver disease is still very scarce and unconvincing, with established lack of efficacy in patients with compensated cirrhosis. In this review, we summarize the current knowledge on the pathogenesis and experimental therapies targeting liver regeneration. The lack of high-quality studies and evidence is a major obstacle in further treatment development. New insights into the pathogenesis of not only liver injury, but also liver regeneration processes are mandatory for the development of new treatment options. A reliable experimental model of the pathogenesis of AH and processes involved in liver recovery is still missing, and data obtained from animal studies are essential for future research.

Key Words: Severe alcoholic hepatitis; Alcohol-related liver disease; Treatment; Liver regeneration; Granulocyte colony-stimulating factor; Stem cell transplantation

©The Author(s) 2022. Published by Baishideng Publishing Group Inc. All rights reserved.

Core Tip: Current treatment options for patients with severe alcoholic hepatitis (AH) are unsatisfactory, resulting in high mortality rates. Liver regeneration is impaired in patients with severe AH and represents an appealing therapeutic target. Granulocyte-colony stimulating factor, alone or in combination with stem cell therapy represents a promising therapeutic option for severe AH. Contrary to animal and several small human studies, evidence from recent studies failed to show benefit of these liver regeneration therapies in patients with advanced alcohol related liver disease.

Citation: Virovic-Jukic L, Ljubas D, Stojsavljevic-Shapeski S, Ljubičić N, Filipec Kanizaj T, Mikolasevic I, Grgurevic I. Liver regeneration as treatment target for severe alcoholic hepatitis. *World J Gastroenterol* 2022; 28(32): 4557-4573
URL: https://www.wjgnet.com/1007-9327/full/v28/i32/4557.htm
DOI: https://dx.doi.org/10.3748/wjg.v28.i32.4557

INTRODUCTION

The harmful use of alcohol is responsible for more than 3 million deaths every year (5.3% of all-cause mortality) and is one of the most common causes of liver disease worldwide[1,2]. Excessive alcohol consumption can cause a spectrum of partially overlapping liver injuries, including steatosis, steatohepatitis, fibrosis and cirrhosis. All these histological changes with accompanying clinical manifestations are collectively termed alcohol-related liver disease (ALD).

Alcoholic hepatitis (AH) is a distinct clinical manifestation of ALD, characterized by jaundice and sometimes accompanied with other signs of hepatic decompensation and liver failure such as ascites or encephalopathy, which occurs in patients with excessive alcohol consumption[3]. Underlying this clinical condition are histological changes including steatosis, hepatocyte injury with ballooning degeneration and lobular neutrophil infiltration, which are characteristic of alcoholic steatohepatitis, and which usually occur in the presence of advanced fibrosis or cirrhosis[3]. The prognosis of AH is generally dismal but significantly dependent on the severity of the disease. Patients with severe forms of AH (defined by Maddrey's Discriminant Function ≥ 32) have a significantly worse prognosis with mortality rates reported between 20% and 30% after 1 mo, and 30% to 40% after 6 mo from presentation [4]. Although patients with a non-severe form of AH have a < 10% risk of mortality after 1 mo and survival of patients with severe AH seems to have improved over the last decades, the condition still carries a poor prognosis[3].

CURRENT TREATMENT OPTIONS FOR SEVERE AH

Patient stratification based on the disease severity and prognosis is necessary for treatment decisions in AH. A Maddrey's Discriminant Function ≥ 32, Model for End-Stage Liver Disease (MELD) score ≥ 21, and/or Glasgow Alcoholic Hepatitis score ≥ 9 are models most commonly used to identify patients with severe disease.

Alcohol abstinence and appropriate nutrition are the cornerstone of treatment of AH, regardless of disease severity[3,5,6]. Energy intake of 30-40 kcal/kg per day and protein intake of 1.2-1.5 g/kg per day are currently recommended by most treatment guidelines. Treatment of alcohol withdrawal symptoms, hepatic encephalopathy, ascites and other comorbidities with vitamin B supplementation also represent general measures required in many patients.

For many years, corticosteroids have been used in the treatment of patients with severe forms of AH, with varying results. A large, multicenter randomized trial comparing steroids with pentoxifylline (STOPAH) showed modest reduction in mortality after 28 d of treatment with prednisolone compared to pentoxifylline, but no improvement in long-term outcomes was observed after 90 d and 1 year[7]. These findings were also confirmed by a recent meta-analysis[8]. Wide use of corticosteroids is limited not only by scarcity of data on its efficacy, but also by safety concerns, especially regarding infections and risk of gastrointestinal bleeding. However, corticosteroids are considered the only treatment option for severe AH with proven or likely benefit[3,5,6].

Patients with severe AH who fail to respond to standard supportive care and corticosteroids may require liver transplantation. However, since the diagnosis of AH implies recent alcohol abuse, these patients are not readily accepted for liver transplantation by most transplant centers because of inadequate abstinence period. Nonetheless, an increasing number of centers are considering and performing liver transplantation in highly selected patients with severe AH[9,10]. The survival benefit for transplanted patients with severe AH has been demonstrated in several trials and a model study, and concern of alcohol abuse relapse after early transplantation has been addressed in several small studies, which showed similar relapse rates to those recorded in patients with 6-mo abstinence period in highly selected groups of patients[11,12]. Still, liver transplantation is not an option for the majority of patients with severe AH.

PATHOPHYSIOLOGY OF LIVER INJURY AND LIVER REGENERATION

The spectrum of alcohol related liver damage results from an interplay of several interrelated pathophysiological mechanisms caused by continuous excessive alcohol consumption. Direct injury to hepatocytes and inflammation cause a series of consecutive events resulting in histological changes characteristic for ALD[13,14]. Ethanol metabolites, namely acetaldehyde, can cause direct damage to hepatocytes through oxidative stress, lipid peroxidation, mitochondrial dysfunction and alterations in lipid metabolism, resulting in steatosis. Consequently, damaged hepatocytes activate apoptosis and necrosis pathways, which result in the release of damage-associated molecular patterns (DAMPs), cell derived molecules that trigger the immune system, which causes further damage. Another mechanism involved in the pathogenesis of ALD results from a deranged gut-liver axis[15]. Increased gut permeability and dysbiosis caused by alcohol consumption allow for translocation of lipopolysaccharides and other bacterial products, collectively termed pathogen-associated molecular patterns (PAMPs), through splanchnic vasculature into the liver. Stimulation of resident macrophages in the liver (Kupffer cells) by PAMPs and DAMPs through activation of toll-like receptors enhances nuclear factor kappa-B (NFkB) signaling and results in expression of proinflammatory cytokines, such as tumor necrosis factor-α (TNF-α), interleukin (IL)-1β and IL-6[16]. These proinflammatory cytokines together with chemokines released by Kupffer and other liver cells recruit neutrophils and other immune cells that infiltrate liver parenchyma and contribute to secondary liver injury. Chemokine receptors also promote inflammation through NFkB signaling. All these triggers that activate Kupffer cells and other inflammatory cells also stimulate the release of platelet-derived growth factor and transforming growth factor-β (TGF-β). These profibrotic cytokines stimulate hepatic stellate cells and myofibroblasts to produce collagens, thus promoting fibrosis with consequent distortion in the liver architecture, which is a hallmark of cirrhosis. Activated immune cells induce hepatic injury by formation of reactive oxygen species, which are responsible for oxidative stress. Ethanol metabolism also changes the redox state of hepatocytes and increases their vulnerability to free radicals by depletion of antioxidant storage.

At the same time when hepatic injury causes hepatocyte apoptosis and necrosis, it also stimulates liver regeneration. The liver is an organ with unique regenerative capacity and employs multiple mechanisms for regeneration in order to restore functional tissue following insults such as toxic injury or partial hepatectomy[17]. The knowledge on the pathophysiology of liver damage in AH and insights into the liver regeneration processes mostly come from animal studies[17,18]. However, the existing animal models do not reproduce the main histological features of poor prognosis in patients with severe AH, such as severe fibrosis and bilirubinostasis, which are necessary to understand the processes occurring in such a milieu[19].

It is presumed that damaged hepatocytes release signals which trigger liver regeneration processes in order to restore functional liver parenchyma[20]. Multiple extracellular signals regulating hepatocyte proliferation during liver regeneration have been identified[17]. Among them, hepatocyte growth factor (HGF) and its receptor, ligands of the epidermal growth factor receptor and TGF-α seem to have a major role. Other signaling pathways include TNF-α and its receptor, IL-6, vascular endothelial growth factor (VEGF) and its receptors, several complex signaling pathways such as Hedgehog pathway, Wnt and β-

catenin, Hippo and Yap pathway, as well as several other hormones and signaling molecules[17]. In their absence, the regeneration process will be impaired and delayed but not completely inhibited. In animal models, the first intracellular signaling pathways activated following partial hepatectomy include β-catenin and Notch pathways, followed by activation of signal transducer and activator of transcription 3 (STAT3) and NFκB, which are regulated by IL-6 and TNF-α[17]. Although different mechanisms may activate these pathways, the exact triggers have not been clearly established.

It seems that local, paracrine signals between proliferating hepatocytes and other cell types such as hepatic stellate cells and liver sinusoidal endothelial cells are also important for regeneration. Thus, hepatocytes are at the center of orchestrated liver regeneration processes aimed to restore histologically complete liver tissue, and all liver cell types are able to proliferate during the process. VEGF and angiopoietins are mitogenic for liver sinusoidal endothelial cells, TGFα for sinusoidal endothelial and hepatic stellate cells, fibroblast growth factor 1 and 2 for stellate cells and sinusoidal endothelial cells, and granulocyte-macrophage colony-stimulating factor for Kupffer cells. For sinusoidal endothelial and Kupffer cells, there is evidence that precursor cells migrating from the bone marrow may also be involved in the regeneration process, in addition to local cell proliferation[17].

Normal hepatocyte proliferation and liver regeneration processes, however, seem to be less effective in ALD. Chronic ethanol exposure impairs liver regeneration by interfering with normal microRNA signaling and DNA synthesis, thus inhibiting mature hepatocyte proliferation[14].

The lack of a reliable experimental model with abnormal liver regeneration makes it difficult to understand how these processes affect alcohol-injured livers. It has been proposed that in severe injury, hepatocytes might be unable to initiate the regeneration and tissue healing by themselves, which is then stimulated by liver progenitor or oval cells that become activated and give rise to hepatocytes and other non-parenchymal liver cells[21]. Furthermore, some data suggest that under conditions where normal regeneration processes are impaired by alcohol exposure, liver progenitor cells may accumulate in damaged livers, but are unable to differentiate into mature hepatocytes, which might explain why some patients with severe AH fail to improve. This hypothesis has been corroborated by the results of a human study on tissue samples obtained from explanted livers of patients with severe AH having undergone salvage liver transplantation[22]. The authors showed that patients with severe AH who were unresponsive to medical treatment had decreased expression of TNF-α and IL-6, the cytokines shown to be involved in liver regeneration, as well as an aberrant regeneration process in which accumulated hepatic progenitor cells showed predominantly cholangiocyte differentiation and failed to produce mature hepatocytes[22].

All these pathophysiological mechanisms responsible for liver damage and ineffective regeneration associated with ALD are the potential treatment targets in AH. A number of molecules and treatments have been investigated in the attempts to stop and reverse deleterious effects of alcohol in the development and progression of changes associated with ALD[23].

EXPERIMENTAL OPTIONS TARGETING LIVER REGENERATION FOR THE TREATMENT OF SEVERE AH

Liver regeneration represents one of the key targets for the development of new treatments for severe AH. Hepatocyte damage and death in AH should be counterbalanced by liver regeneration, in order to restore normal liver structure and function. However, ineffective liver regeneration has been proposed as the culprit for progressive liver failure in patients with severe AH. Recognizing complex mechanisms involved in liver regeneration processes, a number of treatment targets are currently being explored and developed.

Granulocyte colony-stimulating factor

Granulocyte colony-stimulating factor (G-CSF) stimulates bone marrow to produce neutrophils and stem cells (SCs), which are consequently released into the blood. In animal models of toxic liver injury, G-CSF administration was shown to mobilize hematopoietic SCs, ameliorate liver injury, promote liver regeneration, and improve liver function and survival.

In a murine model of acute and chronic liver injury, G-CSF accelerated liver regeneration predominantly by promoting proliferation of endogenous hepatocytes, and the process was to a smaller degree mediated by bone marrow originating SCs[24]. In a recently published study in mice exposed to alcohol and irradiation, pretreatment with G-CSF was associated with enhanced macrophage infiltration, preserved tissue structure and function, and improved survival. G-CSF pretreatment stimulated liver regeneration, as shown by immunofluorescence staining for liver SCs. Interestingly, higher expression of hepatic progenitor cells was observed in the injured but untreated control group. This could confirm previous findings that progenitor cells accumulate in response to injury, but are unable to restore normal tissue and function without stimulation[25]. Moreover, G-CSF treatment in mice may mitigate radiation induced fibrosis[26]. Although not based on disease models fully consistent with AH, these animal studies underpin G-CSF as a potential therapeutic strategy in the treatment of liver disease.

In human studies, G-CSF was used as an induction agent for SC recruitment, or as therapy for liver failure by itself, for its other beneficial effects not attributable to SC mobilization, such as improved liver regeneration and neutrophil function. The most important human studies using G-CSF in order to improve liver regeneration and outcomes in ALD are summarized in Table 1.

In a small randomized trial in patients with alcoholic cirrhosis and biopsy-proven AH, G-CSF showed increased CD34+ SC mobilization, increased HGF, and proliferation of hepatic progenitor cells compared to control group, but liver histology, neutrophils and levels of proinflammatory cytokines (IL-6, TNF-α) remained similar[27].

In a randomized controlled trial in patients with acute-on-chronic liver failure (ACLF), G-CSF increased the numbers of CD34+ cells in the livers of treated patients, improved clinical outcomes including reduced Child-Turcotte-Pugh (CTP) and MELD scores, and showed lower rates of hepatorenal syndrome, hepatic encephalopathy or sepsis in treated patients compared to control group [28]. Similar effects were confirmed in a randomized open-label study from India in patients with severe AH, where treatment with G-CSF showed increased counts of CD34+ cells in peripheral blood and ameliorated both CTP and MELD scores, as well as Maddrey's Discriminant Function values after 1, 2 and 3 mo. More importantly, G-CSF therapy increased the 90-day survival rate of patients with severe AH, compared to standard treatment[29]. Five-day dosing regimen of G-CSF has been most widely used, but multiple cycle G-CSF therapy seems appealing, as it may extend the bridging period to transplantation. Only one trial assessed the effects of multiple cycle therapy compared to standard medical therapy in patients with decompensated alcoholic cirrhosis. Repeated treatment cycles were not associated with serious adverse events, but significantly reduced the risk of infections, improved ascites control, and had a positive effect on the patients' quality of life[30].

Consequent studies explored the possible synergistic effects of G-CSF in combination with other immunostimulants such as erythropoietin or plerixafor. In mice, treatment with G-CSF, plerixafor or a combination of G-CSF with plerixafor showed increased circulating hematopoietic SCs with various liver engrafting potential for tested agents, but reduced degree of fibrosis in all treatment groups. However, bone marrow derived hepatocytes and SCs were detected with low frequencies, suggesting alternative mechanisms in liver regeneration[31]. Results of a study investigating combination therapy with G-CSF and plerixafor in patients with end-stage liver disease are unknown[32].

In a randomized controlled trial in patients with decompensated cirrhosis treated with G-CSF and erythropoietin compared to G-CSF alone, combination therapy showed significant improvements in CTP and MELD scores, as well as a reduced incidence of renal injury, encephalopathy and ascites episodes. In addition, combination therapy altered both cellular and protein expression patterns in liver tissue, leading to higher Ki67+ proliferation index, macrophage infiltration rates, and decreased markers of fibrosis progression[33]. However, some clinical trials, as well as animal studies, suggest that these improvements are not solely related to effective cell proliferation.

Apart from its direct effects on liver regeneration, G-CSF is a readily used agent for stimulating SC mobilization and grafting. The mechanisms affecting SC mobilization are thought to be multifaceted and dependent on the interplay between changes in the liver tissue and bone marrow settings. In bone marrow, SC receptors and anchoring mediators are responsible for keeping them nested and quiet. Since cell mobilization can be sufficient in mice without G-CSF receptors expressed on their hematopoietic SCs, G-CSF impact might be achieved indirectly by altering the stromal bone marrow environment as well[34]. End-stage liver disease might undermine mobilization effects of G-CSF due to spleen enlargement and bone marrow dysfunction as a concomitant feature of end-stage liver disease. A case-control study in patients with AH showed weaker response in CD34+ cell recruitment in comparison to healthy controls[27]. Examination of bone marrow specimens of patients with liver cirrhosis revealed altered SC function, which might be the cause of lower mobilization rates, especially when combined with increased levels of proinflammatory cytokines[35].

SC therapy

SCs and tissue engineering have become an attractive field of medical research. Current insights into molecular aspects of hepatic injury of various etiologies bolster SCs as a novel and promising strategy for the treatment and restoration of damaged liver. Traits of liver progenitor cells, often called oval cells, were described in animal toxicity studies investigating hepatocyte reaction in the course of carbon tetrachloride, galactosamine and N-nitrosomorpholine exposure[40]. Increase in α-fetoprotein (AFP) and thymidine tracing of immature hepatocytes suggested that regenerated cells were derived from oval cells, which have a pivotal role in the rat liver tissue response to injury[41]. In humans, those cells correspond to intermediate hepatobiliary cells presumably residing in canals of Hering, and were proven to have capacity for differentiating into both hepatocytes and bile duct cells. They are frequently found in structures called ductular reactions in cirrhotic liver[42,43]. They are usually called liver progenitor cells or intrinsic progenitor cells to distinguish them from non-hepatic SCs derived from bone marrow or other tissues. Human liver progenitor cells exhibit markers during immunophenotyping, which are different from those in oval cells in rats, while simultaneously failing to express AFP, a marker commonly used in animal studies to assess the hepatocyte repair rate. AFP is classified as an oncofetal protein in humans and is produced during embryonic development by the liver and the yolk sac, from which hematopoietic cell lineage derives[44]. Moreover, partial hepatectomy and exposure to

Table 1 Summary of human studies with granulocyte colony-stimulating factor treatment in patients with alcohol-related liver disease

Study population	Methods	Outcomes	Ref.
RCT included 24 pts with ALC and biopsy proven ASH[1]	Group A (13 pts) received SMT + G-CSF and group B (11 pts) received SMT only	Higher increase in CD34+ cell count, HGF, proliferating HPCs and Ki67+/cytokeratin 7+ staining in group A	Spahr *et al* [27], 2008
RCT included 27 pts with ALC presenting with ACLF[1]	Group A (15 pts) received G-CSF + SMT, and group B (12 pts) received placebo + SMT	Group A had higher median leukocyte and neutrophil counts after 1 w and higher CD34+ cell count after 1 mo, together with improvement in 60-day survival, reduced CTP, MELD and SOFA scores	Garg *et al* [28], 2012
RCT included 46 pts with severe AH[1]	Group A (23 pts) received G-CSF, while group B (23 pts) received SMT	In group A, higher CD34+ count was observed together with marked CTP, MELD and mDF score improvements after 1, 2 and 3 mo and higher survival rate at 90 d	Singh *et al* [29], 2014
RCT included 38 pts with ALC[1]	Group A (14 pts) received SMT + GH qd for 12 mo + initial G-CSF 5-d treatment and then 4 G-CSF cycles every 3 mo; group B (15 pts) received initial G-CSF 5-d treatment and then 4 G-CSF cycles every 3 mo, and group C received SMT only	Groups A and B had better TFS after 12 mo and higher QOL scores, as well as higher CD34+ mobilization rate at day 6, with lower incidence of sepsis and SBP	Verma *et al* [36], 2018
RCT included 35 pts with ALC[1]	Group A (19 pts) received G-CSF + EPO and group B (16 pts) received G-CSF only	Group A had higher improvement of CTP and MELD score, together with lower incidence of AKI, HE and ascites; histologically number of CD163+ macrophages and KI67+ index were increased	Anand *et al* [33], 2019
RCT included 57 pts with severe AH[1]	Group A (18 pts) received SMT + G-CSF, group B (19 pts) received SMT + G-CSF + NAC, and group C (20 pts) received SMT alone	Pts in group A and B had higher 90-d survival rate; in group A, improvement in mDF was observed at mo 1, 2 and 3, together with reduction in MELD score after 3 mo	Singh *et al* [37], 2018
RCT included 28 pts with severe AH[1]	Group A (14 pts) received G-CSF and group B (14 pts) received placebo	Group A had better MELD score, lower incidence of infections as well as lower 90-d mortality	Shasthry *et al* [38], 2019
RCT included 48 pts with ALC[1]	Group A (25 pts) was treated with 4 cycles of 5-d G-CSF therapy and group B (23 pts) was treated with SMT only	Group A had higher CD34+ and neutrophil count at day 6; higher 1-year survival, amelioration in CTP and MELD scores together with better ascites control and lower infection risk were observed after 12 mo	De *et al*[30], 2021
RCT included 176 pts with ACLF precipitated by alcohol consumption[1]	Group A (88 pts) was treated with G-CSF + SMT, and group B (88 pts) was treated with SMT	There were no statistically significant differences in respect of TFS, 90-d and 360-d survival rates and infection incidence	Engelmann *et al*[39], 2021

[1]Patient(s) has/have dropped-out, underwent deceased donor liver transplant, or death outcome occurred.

ACLF: Acute-on-chronic liver failure; AKI: Acute kidney injury; ALC: Alcoholic liver cirrhosis; ASH: Alcoholic steatohepatitis; GH: Growth hormone; HE: Hepatic encephalopathy; HPC: Hepatocyte progenitor cell; mDF: Maddrey's Discriminant Function for alcoholic hepatitis; NAC: N-acetyl-cysteine; pt(s): Patient(s); qd: Quaque die; QOL: Quality of life; SBP: Spontaneous bacterial peritonitis; SMT: Standard medical treatment; SOFA score: Sequential Organ Failure Assessment score; TFS: Transplant-free survival.

carcinogens enhance SC factor production by oval cells, indicating genetic similarity between them and hematopoietic SCs[45]. Although some authors, based on animal studies, dispute the role of hepatic progenitor cells in liver regeneration, most studies suggest that they become important in severe liver injury, as occurs in AH[17]. Indeed, it has been demonstrated that the origin of hepatocytes during liver regeneration varies in different models, and that although hepatocytes are the main drivers for regeneration under normal conditions, an alternative regeneration process may be initiated by liver progenitor cells[46].

Using SCs for liver regeneration has several advantages; they are easily obtained from the patient, can be cryopreserved, self-renewed and are plentiful, and therefore, they represent a safe and inexpensive treatment option that can be easily repeated and is not related to ethical concerns frequently seen in orthotopic liver transplantation. Cell-based therapy relies mostly on stem or progenitor cells because mature hepatocytes are scarce and are unable to engraft successfully[47]. Although hepatocyte transplantations have been performed, mostly using cell grafts isolated from livers unsuitable for liver transplantation, and despite many advantages, the shortage of high-quality grafts, histological incompatibility, the need for immunosuppression and unproven long-term benefits are major drawbacks that prevent their clinical use and impose search for other alternatives.

In humans, stem and progenitor cells involved in the liver regeneration process are classified as hepatic and non-hepatic. Liver progenitor cells, as previously mentioned, correspond to oval cells described in rats. Non-hepatic progenitor cells represent a wide range of cells arising from different tissues. Mesenchymal SCs and hematopoietic SCs found in bone marrow represent the most frequently used SCs[46].

Animal and *in vitro* studies are the cornerstone for investigating beneficial effects of SCs in liver injury. The proposed mechanisms for alleviating liver injury include hepatocyte growth stimulation and cell differentiation, paracrine impact on neighboring cells, reduction in inflammatory cytokine production, and counteracting fibrosis by metalloproteinase expression[48,49]. Cell stemness has been noted in several cell types, *e.g.*, hepatoblasts, liver progenitor cells, hematopoietic and mesenchymal SCs. *In vitro* expanding and harvesting of hepatoblasts in mice, as a counterpart to human liver progenitor cells, is not promising[50]. On the other hand, induced pluripotent SCs were able to produce hepatocytes similar both structurally and functionally to the ones seen in wild type mice[51].

Sepsis-related injury in mice can be reduced by using bone marrow derived mesenchymal SCs, which restore liver function and architecture and enhance immunosuppressive cytokine production, thus increasing the levels of transcription factors important in the oxidative stress cascade[52]. In animal studies, endothelial progenitor cells in combination with hematopoietic SCs have also been used to reduce sinusoidal endothelial cell injury, which was not described in human studies[53]. In mice, amelioration of small-for-size graft injury was achieved by adipocyte derived SCs owing to their ability to enhance VEGF production[54].

In the fibrosis model caused by carbon-tetrachloride, mesenchymal SC application led to decrease in apoptosis, fibrosis and immune cell tissue infiltration, especially macrophages, which was also proven in animal studies of AH[55,56].

Current trials in humans report using therapeutic strategies based on mesenchymal SCs (mostly from bone marrow and adipose tissue) and hematopoietic SCs. The summary and key findings of clinical studies using SCs in the treatment of ALD are summarized in Table 2.

Hematopoietic SCs

Hematopoietic SCs were the first one used in liver tissue engineering owing to their ability of homing in liver tissue. Efficient *in vitro* differentiation of hematopoietic SCs to hepatocytes in a period of several days supported this theory[74]. Engrafted in the livers of mice, hematopoietic SCs demonstrated great ability to repopulate, indicating that hematopoietic SCs may be used as cell reconstruction therapy beyond the scope of hematologic malignancy treatment[75]. After anchoring in the liver tissue, hematopoietic SCs showed a potential to transdifferentiate to hepatocytes, as well as to fuse with tissue host cells, thus changing the cell genetic properties[76]. HGF is an important paracrine regulator of cell growth, embryologic development, as well as cell regeneration process. In hepatocytes, it renders antiapoptotic effects. Correlations between IL-1, IL-6, and HGF levels and CTP scoring system imply that HGF secretion might be counteracting inflammatory response in liver tissue[77]. Molecular interaction between hematopoietic SCs and HGF has also been observed. HGF receptors show wide tissue distribution, but their distribution among hematopoietic SCs and reticuloendothelial cells attracts most attention. Together with G-CSF receptors, these receptors promote hematopoietic SC growth under *in vitro* conditions and are responsible for determining tissue macrophage function in acute liver injury by affecting their IL-6 and IL-10 production[78,79]. The aforementioned theoretical and molecular knowledge along with the success achieved in mice seemed to be reasonable enough to justify the use of hematopoietic SCs for liver regeneration, but further research refuted this theory. Attempts at transplanting hematopoietic SCs into mice suffering from liver injury yielded poor results indicating an insufficient repopulation rate for appropriate tissue repair[80]. Genetic engineering of hematopoietic SCs could overcome the challenge of low tissue homing rates. Indeed, using genetically modified mesenchymal SCs expressing higher rates of HGF improves cell engraftment in liver injury[81].

In patients with AH treated by SC therapy (CD34+ and mesenchymal SCs, collected after mobilization with G-CSF), no significant improvement of liver function assessed by MELD score or proliferation of hepatic progenitor cells was noted in comparison to the control group[66]. Analysis of the liver tissue samples from patients with AH treated by SC therapy failed to show a difference in hepatocyte proliferative activity compared to the control group. However, the study showed expansion of macrophages together with an upregulated expression of genes involved in inflammation and regenerative pathways[67].

In view of the above, better understanding of the hematopoietic SC kinetics and genetic properties is needed to popularize their utilization in ALD.

Mesenchymal SCs

Albeit being present in various tissues, mesenchymal SCs are mostly acquired from bone marrow, which embraces several different stem lineages. The most commonly used cell population is CD34+ endowed with potential to differentiate to hepatocytes, myocardial cells, pancreatic cells, *etc.*[58]. The plasticity of mesenchymal SCs appears to play a secondary role, since their immunomodulatory, anti-fibrotic and anti-oxidative properties spark more interest. In ethanol exposed mice, a simultaneous decline in IL-6 and TNF-α, and an increase in IL-10 and glutathione lays out their immunosuppressive effect[56]. In a murine model of colitis, adipocyte derived mesenchymal SCs administered intravenously counterbalanced the decline in glutathione levels and superoxide-dismutase activity, thus preventing tissue injury caused by reactive oxygen species, which is seen in ALD as well[82].

Table 2 Summary of human studies using stem cells in patients with alcohol-related liver disease

Study population	Methods	Outcomes	Ref.
5 pts with ALC	G-CSF mobilized mononuclear CD34+ PBSCs collected by leukapheresis and injected *via* PV (the dose not stated)	Higher mobilization rate was associated with higher CTP and MELD score amelioration	Gaia *et al*[57], 2006
4 pts with ALC (2 also had HCV, 1 had HBV)[1]	Between 1 × 10^6 and 2 × 10^8 G-CSF mobilized mononuclear CD34+ PBSCs collected by leukapheresis and injected *via* PV (3 pts) or HA (2 pts)	3/4 pts had improvement in bilirubin and albumin levels after 2 mo[58]; At 12 mo 2/3 pts had and albumin and bilirubin levels lower than the baseline values[59]	Gordon *et al*[58], 2006; Laxman *et al*[59], 1993
2 pts with ALC	> 2 × 10^6 G-CSF mobilized CD34+ PBSCs collected by leukapheresis and injected *via* PV	2/2 pts had no cirrhosis related hospital admissions afterwards up to 30/34 m, CTP and MELD improved and reached plateau at 12 mo, IL-6 and TNF-□ transiently decreased	Yannaki *et al*[60], 2006
5 pts with ALC (2 of which had HCV infection)	1.6-5.2 × 10^8mononuclear CD34+ BMCs were aspirated from BM and injected *via* HA	At 4 mo CTP score improved, and relative mean change (%) from baseline values of bilirubin, albumin and INR were -24, 7 and -3, respectively	Lyra *et al*[61], 2007
9 pts with ALC	38.7-349.9 × 10^6 G-CSF mobilized mononuclear CD34+ PBSCs collected by leukapheresis and injected *via* HA after cultivation *in vitro* for 7 d	7/9 patients had improvements in CTP score, 5/9 had resolution of ascites, significant decrease in mean bilirubin levels and insignificant decrease in albumin levels, AST and ALT	Pai *et al*[62], 2008
1 pt with ALC	MSC taken by BM aspiration were cultured and differentiation into hepatocyte-like cells was induced. Afterwards 3-5 × 10^7 cells were injected *via* PV	Reduced MELD score, reduced serum creatinine, increase in serum albumin, better life quality and reduced hospitalization rate	Kharaziha *et al*[63], 2009
4 pts with ALC (2 of which had HCV)[1]	2-15 × 10^8 MN-BMSCs were collected by BM aspiration and injected *via* HA	After 12 mo, albumin and bilirubin levels were improved (but not significantly) and mean values of CTP and MELD score were unchanged	Couto *et al*[64], 2011
A case-control study with 5 pts with ALC	8 ± 7.3 × 10^9 mononuclear CD34+, CD44+, CD45+, CD117+ BMCs were isolated after BM aspiration and injected *via* cubital vein	Improvement of serum albumin levels, prothrombin time, total protein and average CTP score (from 6.8 ± 1.3 to 5.8 ± 0.8)	Saito *et al*[65], 2011
RCT included 58 pts with ALC[1]	Group A (30 pts) received SMT and group B received 0.47 ± 0.15 × 10^8/kg G-CSF mobilized mononuclear BMCs collected by BM aspiration and injected *via* HA	Both groups had reduction in steatosis at 4w and improved MELD scores at 12w[66], but higher CD68+ macrophage infiltration was seen in group B at 4w[67]	Spahr *et al*[66], 2013; Lanthier *et al*[67], 2017
12 pts with ALC[1]	5 × 10^7 BM-MSCs were collected by BM aspiration, amplified for 1 mo and administered twice *via* HA	Fibrosis score, CTP and MELD score and albumin levels improved	Jang *et al*[68], 2014
17 patients involved; 5 pts (29.4%) with ASH[1]	0.05-0.4 × 10^6 G-CSF mobilized CD133+ PBSCs were collected by leukapheresis and injected *via* HA, followed by additional G-CSF administration	In CTP class C patients, MELD score worsened during G-CSF application, but at 2 mo overall MELD score improved and at 3 mo INR values were lower and albumin levels higher	Andreone *et al*[69], 2015
RCT involving 25 patients; 11 pts with ALC (5 in group A, 6 in group B)[1]	Group A (23 pts) received SMT and group B (22 pts) received G-CSF mobilized CD34+ PBSCs were collected by leukapheresis and injected *via* HA	At 1 mo albumin levels were improved (P = 0.001) but were not sustained at 3 mo, when creatinine levels and MELD score were significantly improved, and AST and INR improved marginally	Sharma *et al*[70], 2015
RCT involving 55 pts with ALC (18 in group A and B, and 19 in group C)[1]	Group A received SMT, group B (once) and group C (twice) received 5 × 10^7 BM-MSCs collected by BM aspiration, cultured for 1 mo and injected afterwards *via* HA	At 6 mo fibrosis reduced in both groups in comparison to control, CTP scores also improved in comparison to baseline	Suk *et al*[71], 2016
RCT involving 4 pts with ALC (2 in group 1, 1 in group 2 and 1 in group 3)	Group 1 received SMT, group 2 received G-CSF alone, and group 3 received 1.67 × 10^9-2 × 10^{10}/50 mL G-CSF mobilized CD34+ CD133+ mononuclear PBSCs injected *via* HV	Group 3 showed improvement in median CTP score	Yu *et al*[72], 2017
6 pts with ALC[1]	1 × 10^8 AD-MSCs obtained from abdominal fat tissue and expanded *in vitro* were injected *via* HA	2/5 pts had fibrosis score improvement (METAVIR), 1/5 pt had activity score improvement (METAVIR), 5/5 pts improved in CTP scores and MELD score improved in 4/5 pts, while in 1 pt it increased	Huang *et al*[73], 2019

[1]Patient(s) dropped-out, underwent deceased donor liver transplant, or death outcome occurred.

AD-MSC: Adipose derived-mesenchymal stem cell; ALC: Alcoholic liver cirrhosis; AH: Alcoholic hepatitis; BM: Bone marrow; BMC: Bone marrow cell; BM-MSC: Bone marrow mesenchymal stem cell; CTP: Child-Turcotte-Pugh; DDLT: Deceased donor liver transplant; HA: Hepatic artery; HBV: Hepatitis B virus; HCV: Hepatitis C virus; HGF: Hepatocyte growth factor; HPC: Hepatic progenitor cell; MELD: Model for End-Stage Liver Disease; MN-BMSC: Mononuclear bone marrow stem cell; pt(s): Patient(s); PV: Portal vein; RCT: Randomized controlled trial; SMT: Standard medical therapy.

Mesenchymal SCs orchestrate the overall inflammatory response of cells through complex alterations of cytokine networks, resulting in anti-inflammatory set up. While executive cells and their functions in the liver are various, probably the best course of events during injury can be seen by looking at macrophage polarization, a feature that encompasses liver tissue damage. M1 macrophage lineage is held responsible for triggering inflammation, while M2 Lineage contributes to down-regulation of inflammation and hepatocyte proliferation. M2 type macrophages secrete IL-10, VEGF, matrix metalloproteinases and TGF-β1, which are engaged in the resolution phase of liver damage. Although TGF-β1 is considered a proliferative agent, its long-term secretion during chronic liver disease restrains proliferation of hepatocytes together with IL-1 and interferon-γ secreted by M1 macrophages[83,84]. Apart from HGF, the impact on macrophage bipolar differentiation can also be listed as a key effect of mesenchymal SCs. At the cellular level, mesenchymal SC application hampers M1 macrophage and Th17 mediated inflammatory response, subsequently reducing the expression of TGF-β1 and fibrosis markers in carbon-tetrachloride induced liver fibrosis *in vivo*[55,85].

IL-22

Several T-lymphocyte populations participate in the events occurring during ALD development. At the onset, a cascade of inflammatory events initiated by previously mentioned PAMPs and DAMPs is governed by Th1 lymphocytes. In later stages, immune response becomes dichotomous. Th17 lymphocytes represent the main subfamily associated with down-regulation of proinflammatory response and prevention of excessive tissue damage. Antagonistic effect of the Th17 subfamily is mediated by IL-22. IL-22 can bind to both IL-22 and IL-10 receptors through which it sets off the STAT3 signaling pathway response. STAT3 pathway is also a target of IL-1 and IL-6; therefore, especially in chronic settings, this pathway can have both ameliorating and detrimental effects[86]. Moreover, the production of counteracting cytokines (IL-17 and IL-22) by the same lymphocyte type (Th17) shows the complexity of immune response during liver damage. In chronic conditions, Th17 lymphocytes are located in parenchymal and extra-parenchymal tissue compartments and their count correlates with disease severity in humans[87]. On the other hand, in IL-22 knockout mice, hepatitis induced higher levels of liver enzymes indicating greater tissue damage in comparison to mice with normal IL-22 secretion[88]. Furthermore, IL-22 administration in a mouse model of ALD showed marked improvement in liver enzymes with reduction of liver steatosis. Notably, these hepatoprotective effects were abolished in STAT3 deficient mice[89]. In a murine model of ACLF, a shift from the pro-regenerative IL-6/STAT3 pathway to anti-regenerative IFN-γ/STAT1 pathway was noticed, with consequently impaired liver regeneration[90]. Treatment with IL-22 reversed this shift and improved outcomes by reprogramming impaired regenerative pathways[90].

All these studies implicated IL-22 as a possible therapeutic option for ALD, owing to its antioxidant, proliferative and antimicrobial effects, offering improvement of liver function with potentially few side effects. However, human studies on the use of IL-22 are still sparse. A study investigating an IL-22 analog, F-625, in the treatment of AH included 18 patients, divided in three groups according to the dose administered (10 μg/kg, 30 μg/kg, and 45 μg/kg). Significant amelioration of MELD score values, reduction in inflammatory cytokine concentrations, and better survival rates were observed after a 42-day follow-up period. More importantly, no serious adverse events were documented, showing IL-22 analogs as an attractive treatment modality that needs to be further investigated[91].

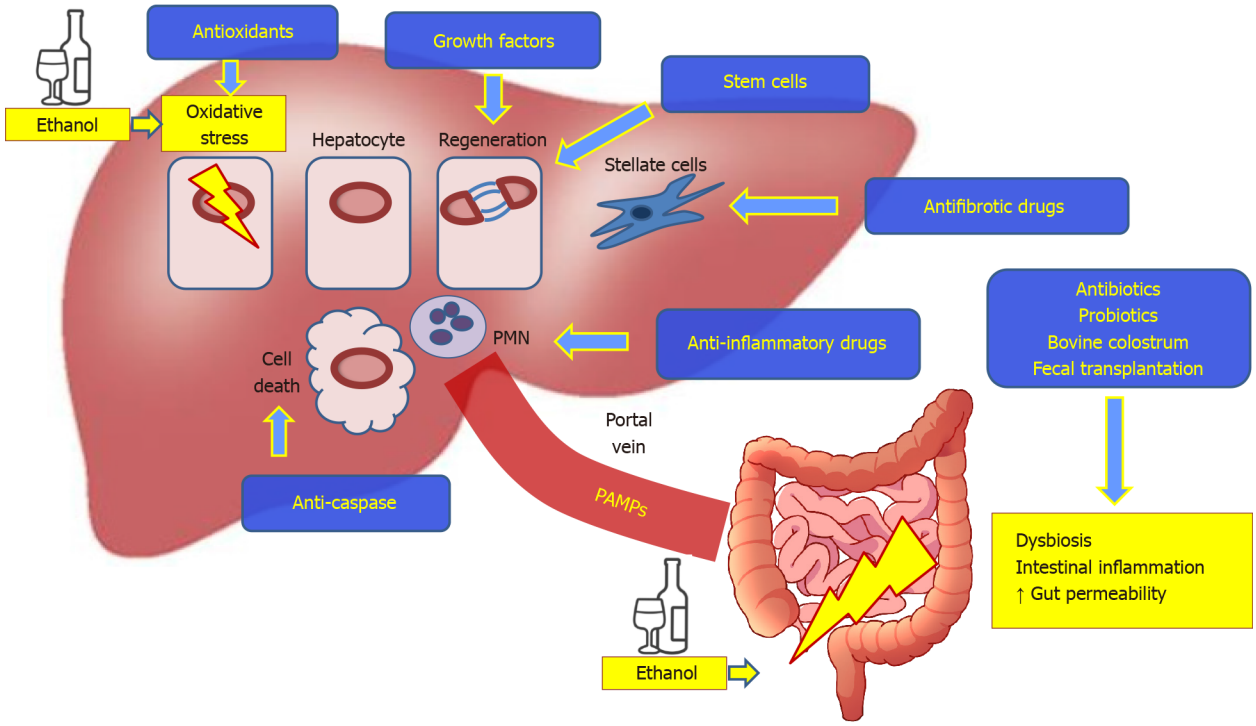
OTHER EXPERIMENTAL APPROACHES AND THERAPEUTICS WITH POTENTIAL BENEFIT IN THE TREATMENT OF SEVERE AH

Since treatment options for severe AH are limited, a number of other experimental approaches have been developed, based on the proposed mechanisms involved in the pathophysiology of AH[14,23]. Treatment targets of the potential experimental therapies are shown in Figure 1.

Anti-inflammatory agents

Considering AH as a severe inflammatory condition involving multiple mechanisms, cells and signaling pathways, anti-inflammatory agents represent an attractive treatment option.

Pentoxifylline is a phosphodiesterase inhibitor that has been used in the treatment of severe AH for its ability to inhibit TNF-α production. Although the initial randomized study showed improved short-term survival compared to placebo, these findings were not confirmed by subsequent studies, including the previously mentioned STOPAH trial[7,92]. Although it seems that pentoxifylline reduced the incidence of hepatorenal syndrome, the drug is considered unlikely to provide benefit and is not recommended for the treatment of severe AH by the European Association for the Study of the Liver and the guidelines issued by the American Association for the Study of Liver Diseases, while the American College of Gastroenterology classifies pentoxifylline as a therapy with a potential benefit[3,5,6].



DOI: 10.3748/wjg.v28.i32.4557 **Copyright** ©The Author(s) 2022.

Figure 1 Treatment targets of the potential experimental therapies for severe alcoholic hepatitis. PAMPs: Pathogen-associated molecular patterns; PMN: Polymorphonuclear leukocyte.

Treatment of severe AH with anti-TNF-α agents such as infliximab and etanercept seemed to be a desirable option, given their efficacy in the treatment of autoimmune diseases. Unfortunately, despite expectations, both drugs failed to show benefit in clinical trials for severe AH[14,23]. On the contrary, the use of TNF-α inhibitors was associated with an increased risk of severe infections and mortality, and therefore are not considered as a treatment option for severe AH by current guidelines[3,5,6]. The lack of their efficacy in AH may be explained by profound immunosuppression caused by TNF blockage, but also by suppression of liver regeneration, which is also mediated by TNF-α and is necessary to restore liver function.

Other inflammatory cytokines have also been studied as therapeutic targets for severe AH, including IL-1 receptor antagonist anakinra, and a C-C chemokine receptor 2 and 5 antagonist cenicriviroc, but data are still insufficient.

Antioxidants

Since increasing evidence suggests oxidative stress as one of the key mechanisms responsible for cellular injury in severe AH, the use of antioxidants has generated much interest.

N-acetylcysteine (NAC) is an antioxidant thought to restore glutathione stores and has been tested in several studies in the treatment of AH. However, the drug failed to show improvement in liver injury or survival. A combination of NAC with prednisolone showed greater early improvement in liver function, lower incidence of hepatorenal syndrome and infections, and improved short-term survival compared to prednisolone alone, but this effect was not sustained after 3 mo[93]. Further studies are awaited to confirm the efficacy of this combination[3,5,6].

Metadoxine is another antioxidant used in several small open-label studies, also in combination with a corticosteroid or pentoxifylline, where it showed improved survival. Along with some other beneficial effects and a favorable safety profile, metadoxine is an attractive option for the treatment of severe AH, but larger studies are expected to confirm these findings.

Gut dysbiosis and gut-liver axis

Gut-liver axis dysfunction with increased gut permeability and dysbiosis associated with alcohol drinking has been recognized as an important trigger for inflammation in AH. Consequently, a number of agents targeting gut barrier function and dysbiosis have emerged as treatment options for AH. These include bovine colostrum and hyperimmune bovine colostrum, antibiotics (rifaximin, amoxicillin-clavulanic acid, ciprofloxacin, gentamicin, vancomycin, meropenem), probiotics (VSL#3, *Lactobacillus rhamnosus*) and fecal transplantation. Some of these treatments have shown very promising preliminary results, and further studies are eagerly awaited.

Apoptosis

Alcohol induces hepatocyte death *via* necrosis and apoptosis processes, the latter including a number of pathways, which have been investigated as treatment targets in AH. Emricasan is a caspase inhibitor that showed promising results in early phase trials, but further studies were stopped because of concerns about liver toxicity. Selonsertib is another oral inhibitor of apoptosis with better safety profile, but its efficacy has not been established compared to corticosteroids.

Obeticholic acid

Cholestasis is one of the characteristic features of AH. Obeticholic acid is a farnesoid X receptor ligand that protects hepatocytes against bile toxicity. Favorable results in the treatment of cholestatic liver disease offer promises for obeticholic acid in the treatment of AH, pending results of ongoing studies.

DISCUSSION

Severe AH still represents a life-threatening condition with high short-term mortality. A lack of effective treatments with proven benefit and good safety profile imposes the need for new therapeutic approaches. Several pathways are being explored, targeting different mechanisms involved in the pathogenesis of AH. Stimulation of liver regeneration together with other beneficial effects suggest G-CSF and SC transplantation as possible therapeutic targets.

In animal models of toxic liver injury, G-CSF demonstrated evidence for increased mobilization of hematopoietic SCs, ameliorating liver injury, promoting liver regeneration, improved liver function and survival. These beneficial effects encouraged human studies, and the first results were promising, showing mobilization of SCs and proliferation of hepatic progenitor cells that were considered proof of efficacy[27]. Enhanced cell proliferation might not be crucial for the regeneration process as immunohistochemical staining using Ki67/CK+, chief markers of mitosis, showed diverse results[27,67]. Subsequent randomized trials from India investigating the role of G-CSF treatment in patients with ACLF and AH demonstrated not only increased mobilization of SCs, but also improved clinical outcomes, measured by reduction in liver function scores, as well as improved survival[28,29]. Other positive outcomes included improved immune dysfunction with lower rates of complications, including hepatic encephalopathy, ascites, kidney injury, and infections[30,33,36,38].

However, in a large multicenter randomized study from Germany that enrolled 176 patients with ACLF, treatment with G-CSF did not improve liver function scores, occurrence of infections, or transplant-free or overall survival. Severe adverse reactions associated with the treatment, together with the lack of efficacy, led to premature termination of the study[39]. Discrepancies in the findings between this and previous smaller single-center studies (Table 1) are not completely understood. Several possible reasons for such conflicting results between Asian and European studies, including a selection bias or study design could not completely explain these differences[94]. Another possible explanation might be a large rate of infections in the German study that triggered an excessive inflammatory response, which could have counteracted the beneficial effects of G-CSF. However, the substantiated evidence from this trial strongly discourages the use of G-CSF in the treatment of ACLF. Still, it is important to note that the results of G-CSF for the treatment of ACLF cannot be directly extrapolated to AH due to great heterogeneity of ACLF cohorts regarding the cause of the underlying liver disease and the precipitating event for ACLF. In the previously mentioned German (GRAFT) study, alcohol abuse was the precipitating event in approximately half of the patients in both treatment groups, while bacterial infections and gastrointestinal bleeding were triggers for ACLF in the majority of the remaining cases[39]. However, the authors did not prove benefit of G-CSF over standard medical treatment in a cohort of patients with alcohol-related ACLF, which probably comprised mostly patients with AH.

SC transplantation offers another possibility for improved liver regeneration. In recent years, a number of studies investigated the outcomes of SC treatment in patients with liver disease of various etiology. However, studies focusing on patients with ALD are still sparse and recruited small numbers of patients; therefore, outcomes of each study are often insufficient to draw definitive conclusions. The majority of studies were actually phase I/II clinical trials, focused on the feasibility, safety and short-term outcomes of the procedure. One case-control study and five randomized controlled trials compared the effects of SC therapy to standard medical therapy alone (Table 2). The heterogeneity of the findings could be explained by several reasons.

Studies differed according to the SC population and terminology used, including peripheral blood SCs, mononuclear bone marrow SCs, mesenchymal SCs or hematopoietic SCs. Hematopoietic SCs are mononuclear cells typically collected by leukapheresis, and are often described as peripheral blood SCs. In studies where bone marrow aspiration was performed, mononuclear bone marrow SCs represent a combination of several SC types including mesenchymal cells that build up the stromal compartment of bone marrow. Except for mesenchymal SCs, the hallmark of the aforementioned cells is expression of transmembrane phosphoglycoprotein, CD34. In a small study, two CD34+ cell populations were differentiated based on their *in vitro* property of adherence. Adherent CD34+ cells expressed genes important for hepatic tissue differentiation; therefore, SCs with specific phenotype could be pivotal for gaining

therapeutic effect, although they were encountered in a relatively small fraction after mobilization[58]. Promising results were obtained in a small study using G-CSF mobilized mononuclear CD34+ peripheral blood SCs collected by leukapheresis and injected *via* hepatic artery after *in vitro* cultivation for 7 d[62]. It could be assumed that a 5-fold increase in cell count obtained by *in vitro* cultivation could yield better results.

Except for small and heterogeneous patient groups with different conditions (alcoholic cirrhosis, AH, and some with multifactorial origin of liver disease), studies used different G-CSF dosing regimens and SC administration routes (*via* hepatic artery or portal vein), number of SC infusions, outcomes measures, and follow-up period.

In the study including 10 patients, 4 of them with AH, having undergone bone derived mononuclear cell transplantation, serum bilirubin and INR levels decreased and albumin levels increased after 4-mo follow-up[61]. In another study including two patients with AH, histological analysis did not reveal changes in fibrosis stage; however, improvement of both CTP and MELD scores was achieved[60]. In a controlled trial, patients with decompensated ALD treated with G-CSF mobilized mononuclear bone marrow cells had reduction in steatosis and improved MELD scores after 12-wk follow-up, but similar to patients treated by standard medical therapy[66]. There was no difference between the SC treated and control groups according to hepatocyte proliferation. However, a more pronounced macrophage infiltration of the liver was observed in the treatment group, together with higher expression of the genes involved in regenerative processes[66,67]. Another small study involving two patients with AH also assessed CTP and MELD scores after hematopoietic SC aspiration and administration, but without G-CSF stimulation[64]. At the end of a 12-mo follow-up period, no significant differences in serum albumin and bilirubin levels or mean CTP and MELD scores were noticed. Using scintigraphy in this study, the authors managed to document a high percentage of SC retention in liver tissue (41% and 32% after 3 and 24 h, respectively). This research is valuable in terms of assessing cell tropism and dissemination, but also reported several major adverse events, raising concerns about the safety of the procedure[64]. The effects of SC treatment on liver fibrosis were also investigated in several studies, but benefits were shown in only one of them[71]. Probably the most discouraging results were obtained in a randomized multicenter study from the United Kingdom, investigating the efficacy of G-CSF treatment alone or in combination with CD133+ hematopoietic SC infusion obtained by leukapheresis, and compared to standard medical treatment in patients with compensated liver cirrhosis[95]. No improvement of liver dysfunction as assessed by MELD score or fibrosis was observed in either treatment group when compared to standard medical care. However, treatment with G-CSF alone or in combination with SC therapy was associated with an increased frequency of adverse events[95].

The explanation of this paradox and lack of evidence for clinical efficacy of SC therapy for the treatment of AH is still not completely understood. One of the possible explanations might be a relapse of alcohol use in the follow-up period, which is common in clinical practice. In the STOPAH trial, only 45% of patients with AH abstained from alcohol at 6 mo and 37% at 12 mo, meaning that relapse of alcohol use occurred in two thirds of patients surviving an episode of AH after a one-year follow-up period[7]. In a study from Barcelona investigating alcohol abstinence in patients surviving an episode of AH, the investigators also report complete abstinence in only 39% of patients after a median follow-up period of 55 mo, and showed that it had positive impact on long-term survival[96]. Similar results were obtained in a study from the United Kingdom, where 65% of patients surviving an episode of AH experienced alcohol relapse, and abstinence was shown to be the only predictor of long-term survival in these patients[97]. Indeed, in a previously mentioned randomized study investigating bone marrow mononuclear cell transplantation with G-CSF in patients with decompensated ALD, 81% of whom met the histological criteria for AH, alcohol abstinence was achieved in 67% of patients during 12-wk follow-up period, while almost one-third returned to moderate alcohol drinking[66]. The study failed to show benefit of such therapy compared to standard medical treatment, and alcohol relapse in 31% of study patients might be one possible explanation for such results. Another possible explanation is that the effects of SC and other treatments aimed to stimulate liver regeneration depend on the etiology of the liver disease. It has been shown that in ALD related cirrhosis, acute and chronic exposure to alcohol interferes with liver regeneration capacity and may actually impair hepatic progenitor cell response to injury, as mentioned previously, resulting in poor outcomes[14,23,98,99].

CONCLUSION

Ineffective liver regeneration is probably one of the key contributors to liver failure in patients with severe AH. Many cytokines, including TNF-α, IL-6 and IL-22, and STAT3 and NFκB pathways have been shown as potent activators of hepatic regeneration. However, an altered differentiation process seems to cause repopulation of the liver parenchyma by immature hepatocytes that fail to differentiate into mature hepatocytes, which could explain why some patients with severe forms of AH fail to recover. Novel treatment options that would help overcome this obstacle and improve liver regeneration seem intriguing, but so far, the evidence for their efficacy is unconvincing.

The lack of a reliable animal model that could represent the whole spectrum of liver changes associated with ALD in humans still is one of the major obstacles in the research of ALD. Development of an experimental model including not only steatosis and mild inflammation, but also fibrosis, severe inflammation and bilirubinostasis with an altered regeneration process, which are the hallmarks of severe AH in humans, represents an imperative for future research and development of new treatment options.

Better understanding of the molecular mechanisms behind ALD has given us apprehension of the multifaceted nature of the disease revealing novel treatment targets. In the light of evidence from recently published studies, G-CSF therapy does not seem like a feasible treatment option in the near future. Succeeding studies on SC therapy should aim to investigate long-term effects and define precise SC recruitment protocols providing clinicians with clear guidelines on both the G-CSF application regimen and SC administration routes. Until further insights, future research on liver reconstitution remains a challenge.

FOOTNOTES

Author contributions: Virovic-Jukic L designed the study, performed literature search, outlined the manuscript and revised it; Ljubas D performed literature search and writing; Stojsavljevic-Shapeski S designed the study and outlined the manuscript; Ljubičić N, Filipec Kanizaj T, Mikolasevic I and Grgurevic I revised the manuscript for important intellectual content.

Conflict-of-interest statement: All the authors report no relevant conflicts of interest for this article.

Open-Access: This article is an open-access article that was selected by an in-house editor and fully peer-reviewed by external reviewers. It is distributed in accordance with the Creative Commons Attribution NonCommercial (CC BY-NC 4.0) license, which permits others to distribute, remix, adapt, build upon this work non-commercially, and license their derivative works on different terms, provided the original work is properly cited and the use is non-commercial. See: https://creativecommons.org/Licenses/by-nc/4.0/

Country/Territory of origin: Croatia

ORCID number: Lucija Virovic-Jukic 0000-0002-6350-317X; Dominik Ljubas 0000-0001-5115-2141; Sanja Stojsavljevic-Shapeski 0000-0002-1626-3003; Neven Ljubičić 0000-0002-5207-4357; Tajana Filipec Kanizaj 0000-0002-9828-8916; Ivana Mikolasevic 0000-0001-9676-0642; Ivica Grgurevic 0000-0003-0520-3483.

Corresponding Author's Membership in Professional Societies: European Association for the Study of the Liver, No. 13346; Croatian Society of Gastroenterology; Croatian Medical Chamber.

S-Editor: Gao CC
L-Editor: A
P-Editor: Gao CC

REFERENCES

1 **World Health Organization**. Global status report on alcohol and health 2018. [cited 15 February 2022]. In: World Health Organization [Internet]. Available from: https://apps.who.int/iris/bitstream/handle/10665/274603/9789241565639-eng.pdf?ua=1
2 **GBD 2016 Alcohol Collaborators**. Alcohol use and burden for 195 countries and territories, 1990-2016: a systematic analysis for the Global Burden of Disease Study 2016. *Lancet* 2018; **392**: 1015-1035 [PMID: 30146330 DOI: 10.1016/S0140-6736(18)31310-2]
3 **European Association for the Study of the Liver**. EASL Clinical Practice Guidelines: Management of alcohol-related liver disease. *J Hepatol* 2018; **69**: 154-181 [PMID: 29628280 DOI: 10.1016/j.jhep.2018.03.018]
4 **Maddrey WC**, Boitnott JK, Bedine MS, Weber FL Jr, Mezey E, White RI Jr. Corticosteroid therapy of alcoholic hepatitis. *Gastroenterology* 1978; **75**: 193-199 [PMID: 352788 DOI: 10.1016/0016-5085(78)90401-8]
5 **Singal AK**, Bataller R, Ahn J, Kamath PS, Shah VH. ACG Clinical Guideline: Alcoholic Liver Disease. *Am J Gastroenterol* 2018; **113**: 175-194 [PMID: 29336434 DOI: 10.1038/ajg.2017.469]
6 **Crabb DW**, Im GY, Szabo G, Mellinger JL, Lucey MR. Diagnosis and Treatment of Alcohol-Associated Liver Diseases: 2019 Practice Guidance From the American Association for the Study of Liver Diseases. *Hepatology* 2020; **71**: 306-333 [PMID: 31314133 DOI: 10.1002/hep.30866]
7 **Thursz MR**, Richardson P, Allison M, Austin A, Bowers M, Day CP, Downs N, Gleeson D, MacGilchrist A, Grant A, Hood S, Masson S, McCune A, Mellor J, O'Grady J, Patch D, Ratcliffe I, Roderick P, Stanton L, Vergis N, Wright M, Ryder S, Forrest EH; STOPAH Trial. Prednisolone or pentoxifylline for alcoholic hepatitis. *N Engl J Med* 2015; **372**: 1619-1628 [PMID: 25901427 DOI: 10.1056/NEJMoa1412278]
8 **Louvet A**, Thursz MR, Kim DJ, Labreuche J, Atkinson SR, Sidhu SS, O'Grady JG, Akriviadis E, Sinakos E, Carithers RL

Jr, Ramond MJ, Maddrey WC, Morgan TR, Duhamel A, Mathurin P. Corticosteroids Reduce Risk of Death Within 28 Days for Patients With Severe Alcoholic Hepatitis, Compared With Pentoxifylline or Placebo-a Meta-analysis of Individual Data From Controlled Trials. *Gastroenterology* 2018; **155**: 458-468.e8 [PMID: 29738698 DOI: 10.1053/j.gastro.2018.05.011]

9 **Mathurin P**, Moreno C, Samuel D, Dumortier J, Salleron J, Durand F, Castel H, Duhamel A, Pageaux GP, Leroy V, Dharancy S, Louvet A, Boleslawski E, Lucidi V, Gustot T, Francoz C, Letoublon C, Castaing D, Belghiti J, Donckier V, Pruvot FR, Duclos-Vallée JC. Early liver transplantation for severe alcoholic hepatitis. *N Engl J Med* 2011; **365**: 1790-1800 [PMID: 22070476 DOI: 10.1056/NEJMoa1105703]

10 **Im GY**, Kim-Schluger L, Shenoy A, Schubert E, Goel A, Friedman SL, Florman S, Schiano TD. Early Liver Transplantation for Severe Alcoholic Hepatitis in the United States--A Single-Center Experience. *Am J Transplant* 2016; **16**: 841-849 [PMID: 26710309 DOI: 10.1111/ajt.13586]

11 **Lee BP**, Samur S, Dalgic OO, Bethea ED, Lucey MR, Weinberg E, Hsu C, Rinella ME, Im GY, Fix OK, Therapondos G, Han H, Victor DW, Voigt MD, Eswaran S, Terrault NA, Chhatwal J. Model to Calculate Harms and Benefits of Early *vs* Delayed Liver Transplantation for Patients With Alcohol-Associated Hepatitis. *Gastroenterology* 2019; **157**: 472-480.e5 [PMID: 30998988 DOI: 10.1053/j.gastro.2019.04.012]

12 **Lee BP**, Chen PH, Haugen C, Hernaez R, Gurakar A, Philosophe B, Dagher N, Moore SA, Li Z, Cameron AM. Three-year Results of a Pilot Program in Early Liver Transplantation for Severe Alcoholic Hepatitis. *Ann Surg* 2017; **265**: 20-29 [PMID: 27280501 DOI: 10.1097/SLA.0000000000001831]

13 **Stickel F**, Datz C, Hampe J, Bataller R. Pathophysiology and Management of Alcoholic Liver Disease: Update 2016. *Gut Liver* 2017; **11**: 173-188 [PMID: 28274107 DOI: 10.5009/gnl16477]

14 **Louvet A**, Mathurin P. Alcoholic liver disease: mechanisms of injury and targeted treatment. *Nat Rev Gastroenterol Hepatol* 2015; **12**: 231-242 [PMID: 25782093 DOI: 10.1038/nrgastro.2015.35]

15 **Szabo G**, Bala S. Alcoholic liver disease and the gut-liver axis. *World J Gastroenterol* 2010; **16**: 1321-1329 [PMID: 20238398 DOI: 10.3748/wjg.v16.i11.1321]

16 **Hosseini N**, Shor J, Szabo G. Alcoholic Hepatitis: A Review. *Alcohol Alcohol* 2019; **54**: 408-416 [PMID: 31219169 DOI: 10.1093/alcalc/agz036]

17 **Michalopoulos GK**, Bhushan B. Liver regeneration: biological and pathological mechanisms and implications. *Nat Rev Gastroenterol Hepatol* 2021; **18**: 40-55 [PMID: 32764740 DOI: 10.1038/s41575-020-0342-4]

18 **Diehl AM**. Developmental Morphogens & Recovery from Alcoholic Liver Disease. *Adv Exp Med Biol* 2018; **1032**: 145-151 [PMID: 30362097 DOI: 10.1007/978-3-319-98788-0_11]

19 **Altamirano J**, Miquel R, Katoonizadeh A, Abraldes JG, Duarte-Rojo A, Louvet A, Augustin S, Mookerjee RP, Michelena J, Smyrk TC, Buob D, Leteurtre E, Rincón D, Ruiz P, García-Pagán JC, Guerrero-Marquez C, Jones PD, Barritt AS 4th, Arroyo V, Bruguera M, Bañares R, Ginès P, Caballería J, Roskams T, Nevens F, Jalan R, Mathurin P, Shah VH, Bataller R. A histologic scoring system for prognosis of patients with alcoholic hepatitis. *Gastroenterology* 2014; **146**: 1231-9.e1 [PMID: 24440674 DOI: 10.1053/j.gastro.2014.01.018]

20 **Jung Y**, Witek RP, Syn WK, Choi SS, Omenetti A, Premont R, Guy CD, Diehl AM. Signals from dying hepatocytes trigger growth of liver progenitors. *Gut* 2010; **59**: 655-665 [PMID: 20427400 DOI: 10.1136/gut.2009.204354]

21 **Piscaglia AC**, Shupe TD, Oh SH, Gasbarrini A, Petersen BE. Granulocyte-colony stimulating factor promotes liver repair and induces oval cell migration and proliferation in rats. *Gastroenterology* 2007; **133**: 619-631 [PMID: 17681181 DOI: 10.1053/j.gastro.2007.05.018]

22 **Dubuquoy L**, Louvet A, Lassailly G, Truant S, Boleslawski E, Artru F, Maggiotto F, Gantier E, Buob D, Leteurtre E, Cannesson A, Dharancy S, Moreno C, Pruvot FR, Bataller R, Mathurin P. Progenitor cell expansion and impaired hepatocyte regeneration in explanted livers from alcoholic hepatitis. *Gut* 2015; **64**: 1949-1960 [PMID: 25731872 DOI: 10.1136/gutjnl-2014-308410]

23 **Sehrawat TS**, Liu M, Shah VH. The knowns and unknowns of treatment for alcoholic hepatitis. *Lancet Gastroenterol Hepatol* 2020; **5**: 494-506 [PMID: 32277902 DOI: 10.1016/S2468-1253(19)30326-7]

24 **Yannaki E**, Athanasiou E, Xagorari A, Constantinou V, Batsis I, Kaloyannidis P, Proya E, Anagnostopoulos A, Fassas A. G-CSF-primed hematopoietic stem cells or G-CSF per se accelerate recovery and improve survival after liver injury, predominantly by promoting endogenous repair programs. *Exp Hematol* 2005; **33**: 108-119 [PMID: 15661404 DOI: 10.1016/j.exphem.2004.09.005]

25 **Ramos IPR**, Dias ML, Nunes De Moraes AC, Meireles Ferreira FG, Souza SAL, Gutfilen B, Barboza T, Ferreira Pimentel C, Paz Batista CM, Kasai-Brunswick TH, Fortes FDSA, De Andrade CBV, Goldenberg RCDS. Granulocyte Colony-Stimulating Factor Treatment Before Radiotherapy Protects Against Radiation-Induced Liver Disease in Mice. *Front Pharmacol* 2021; **12**: 725084 [PMID: 34867327 DOI: 10.3389/fphar.2021.725084]

26 **Li N**, Zhang L, Li H, Fang B. Administration of granulocyte colony-stimulating factor ameliorates radiation-induced hepatic fibrosis in mice. *Transplant Proc* 2010; **42**: 3833-3839 [PMID: 21094866 DOI: 10.1016/j.transproceed.2010.09.010]

27 **Spahr L**, Lambert JF, Rubbia-Brandt L, Chalandon Y, Frossard JL, Giostra E, Hadengue A. Granulocyte-colony stimulating factor induces proliferation of hepatic progenitors in alcoholic steatohepatitis: a randomized trial. *Hepatology* 2008; **48**: 221-229 [PMID: 18537187 DOI: 10.1002/hep.22317]

28 **Garg V**, Garg H, Khan A, Trehanpati N, Kumar A, Sharma BC, Sakhuja P, Sarin SK. Granulocyte colony-stimulating factor mobilizes CD34(+) cells and improves survival of patients with acute-on-chronic liver failure. *Gastroenterology* 2012; **142**: 505-512.e1 [PMID: 22119930 DOI: 10.1053/j.gastro.2011.11.027]

29 **Singh V**, Sharma AK, Narasimhan RL, Bhalla A, Sharma N, Sharma R. Granulocyte colony-stimulating factor in severe alcoholic hepatitis: a randomized pilot study. *Am J Gastroenterol* 2014; **109**: 1417-1423 [PMID: 24935272 DOI: 10.1038/ajg.2014.154]

30 **De A**, Kumari S, Singh A, Kaur A, Sharma R, Bhalla A, Sharma N, Kalra N, Singh V. Multiple Cycles of Granulocyte Colony-Stimulating Factor Increase Survival Times of Patients With Decompensated Cirrhosis in a Randomized Trial. *Clin Gastroenterol Hepatol* 2021; **19**: 375-383.e5 [PMID: 32088302 DOI: 10.1016/j.cgh.2020.02.022]

31 **Tsolaki E**, Athanasiou E, Gounari E, Zogas N, Siotou E, Yiangou M, Anagnostopoulos A, Yannaki E. Hematopoietic stem

cells and liver regeneration: differentially acting hematopoietic stem cell mobilization agents reverse induced chronic liver injury. *Blood Cells Mol Dis* 2014; **53**: 124-132 [PMID: 24923531 DOI: 10.1016/j.bcmd.2014.05.003]

32 **Koneru B**. Mobilization of Stem Cells With G-CSF and Mozobil in Patients With End Stage Liver Disease. [accessed 2021 Feb 18]. In: ClinicalTrials.gov [Internet]. Bethesda (MD): U.S. National Library of Medicine. Available from: https://www.clinicaltrials.gov/ct2/show/NCT01711073 ClinicalTrials.gov Identifier: NCT01711073

33 **Anand L**, Bihari C, Kedarisetty CK, Rooge SB, Kumar D, Shubham S, Kumar G, Sahney A, Sharma MK, Maiwall R, Kumar A, Sarin SK. Early cirrhosis and a preserved bone marrow niche favour regenerative response to growth factors in decompensated cirrhosis. *Liver Int* 2019; **39**: 115-126 [PMID: 29962032 DOI: 10.1111/liv.13923]

34 **Schuettpelz LG**, Borgerding JN, Christopher MJ, Gopalan PK, Romine MP, Herman AC, Woloszynek JR, Greenbaum AM, Link DC. G-CSF regulates hematopoietic stem cell activity, in part, through activation of Toll-like receptor signaling. *Leukemia* 2014; **28**: 1851-1860 [PMID: 24518205 DOI: 10.1038/leu.2014.68]

35 **Bihari C**, Anand L, Rooge S, Kumar D, Saxena P, Shubham S, Sukriti, Trehanpati N, Kumar G, Pamecha V, Sharma S, Rastogi A, Kumar A, Sarin SK. Bone marrow stem cells and their niche components are adversely affected in advanced cirrhosis of the liver. *Hepatology* 2016; **64**: 1273-1288 [PMID: 27486864 DOI: 10.1002/hep.28754]

36 **Verma N**, Kaur A, Sharma R, Bhalla A, Sharma N, De A, Singh V. Outcomes after multiple courses of granulocyte colony-stimulating factor and growth hormone in decompensated cirrhosis: A randomized trial. *Hepatology* 2018; **68**: 1559-1573 [PMID: 29278428 DOI: 10.1002/hep.29763]

37 **Singh V**, Keisham A, Bhalla A, Sharma N, Agarwal R, Sharma R, Singh A. Efficacy of Granulocyte Colony-Stimulating Factor and N-Acetylcysteine Therapies in Patients With Severe Alcoholic Hepatitis. *Clin Gastroenterol Hepatol* 2018; **16**: 1650-1656.e2 [PMID: 29391265 DOI: 10.1016/j.cgh.2018.01.040]

38 **Shasthry SM**, Sharma MK, Shasthry V, Pande A, Sarin SK. Efficacy of Granulocyte Colony-stimulating Factor in the Management of Steroid-Nonresponsive Severe Alcoholic Hepatitis: A Double-Blind Randomized Controlled Trial. *Hepatology* 2019; **70**: 802-811 [PMID: 30664267 DOI: 10.1002/hep.30516]

39 **Engelmann C**, Herber A, Franke A, Bruns T, Reuken P, Schiefke I, Zipprich A, Zeuzem S, Goeser T, Canbay A, Berg C, Trebicka J, Uschner FE, Chang J, Mueller T, Aehling N, Schmelzle M, Splith K, Lammert F, Lange CM, Sarrazin C, Trautwein C, Manns M, Häussinger D, Pfeiffenberger J, Galle PR, Schmiedeknecht A, Berg T. Granulocyte-colony stimulating factor (G-CSF) to treat acute-on-chronic liver failure: A multicenter randomized trial (GRAFT study). *J Hepatol* 2021; **75**: 1346-1354 [PMID: 34364917 DOI: 10.1016/j.jhep.2021.07.033]

40 **Kuhlmann WD**, Peschke P. Hepatic progenitor cells, stem cells, and AFP expression in models of liver injury. *Int J Exp Pathol* 2006; **87**: 343-359 [PMID: 16965562 DOI: 10.1111/j.1365-2613.2006.00485.x]

41 **Lowes KN**, Croager EJ, Olynyk JK, Abraham LJ, Yeoh GC. Oval cell-mediated liver regeneration: Role of cytokines and growth factors. *J Gastroenterol Hepatol* 2003; **18**: 4-12 [PMID: 12519217 DOI: 10.1046/j.1440-1746.2003.02906.x]

42 **Zhou H**, Rogler LE, Teperman L, Morgan G, Rogler CE. Identification of hepatocytic and bile ductular cell lineages and candidate stem cells in bipolar ductular reactions in cirrhotic human liver. *Hepatology* 2007; **45**: 716-724 [PMID: 17326146 DOI: 10.1002/hep.21557]

43 **Duncan AW**, Dorrell C, Grompe M. Stem cells and liver regeneration. *Gastroenterology* 2009; **137**: 466-481 [PMID: 19470389 DOI: 10.1053/j.gastro.2009.05.044]

44 **Sell S**, Becker FF, Leffert HL, Watabe L. Expression of an oncodevelopmental gene product (alpha-fetoprotein) during fetal development and adult oncogenesis. *Cancer Res* 1976; **36**: 4239-4249 [PMID: 61804]

45 **Fujio K**, Evarts RP, Hu Z, Marsden ER, Thorgeirsson SS. Expression of stem cell factor and its receptor, c-kit, during liver regeneration from putative stem cells in adult rat. *Lab Invest* 1994; **70**: 511-516 [PMID: 7513770]

46 **Li Y**, Lu L, Cai X. Liver Regeneration and Cell Transplantation for End-Stage Liver Disease. *Biomolecules* 2021; **11** [PMID: 34944550 DOI: 10.3390/biom11121907]

47 **Berardis S**, Dwisthi Sattwika P, Najimi M, Sokal EM. Use of mesenchymal stem cells to treat liver fibrosis: current situation and future prospects. *World J Gastroenterol* 2015; **21**: 742-758 [PMID: 25624709 DOI: 10.3748/wjg.v21.i3.742]

48 **Lv Y**, So KF, Xiao J. Liver regeneration and alcoholic liver disease. *Ann Transl Med* 2020; **8**: 567 [PMID: 32775368 DOI: 10.21037/atm.2020.02.168]

49 **Watanabe Y**, Tsuchiya A, Seino S, Kawata Y, Kojima Y, Ikarashi S, Starkey Lewis PJ, Lu WY, Kikuta J, Kawai H, Yamagiwa S, Forbes SJ, Ishii M, Terai S. Mesenchymal Stem Cells and Induced Bone Marrow-Derived Macrophages Synergistically Improve Liver Fibrosis in Mice. *Stem Cells Transl Med* 2019; **8**: 271-284 [PMID: 30394698 DOI: 10.1002/sctm.18-0105]

50 **Miyajima A**, Tanaka M, Itoh T. Stem/progenitor cells in liver development, homeostasis, regeneration, and reprogramming. *Cell Stem Cell* 2014; **14**: 561-574 [PMID: 24792114 DOI: 10.1016/j.stem.2014.04.010]

51 **Si-Tayeb K**, Noto FK, Nagaoka M, Li J, Battle MA, Duris C, North PE, Dalton S, Duncan SA. Highly efficient generation of human hepatocyte-like cells from induced pluripotent stem cells. *Hepatology* 2010; **51**: 297-305 [PMID: 19998274 DOI: 10.1002/hep.23354]

52 **Selim SA**, El-Baset SAA, Kattaia AAA, Askar EM, Elkader EA. Bone marrow-derived mesenchymal stem cells ameliorate liver injury in a rat model of sepsis by activating Nrf2 signaling. *Histochem Cell Biol* 2019; **151**: 249-262 [PMID: 30250973 DOI: 10.1007/s00418-018-1731-4]

53 **Qiao J**, Qi K, Chu P, Mi H, Yang N, Yao H, Xia Y, Li Z, Xu K, Zeng L. Infusion of endothelial progenitor cells ameliorates liver injury in mice after haematopoietic stem cell transplantation. *Liver Int* 2015; **35**: 2611-2620 [PMID: 25872801 DOI: 10.1111/liv.12849]

54 **Ma T**, Liu H, Chen W, Xia X, Bai X, Liang L, Zhang Y, Liang T. Implanted adipose-derived stem cells attenuate small-for-size liver graft injury by secretion of VEGF in rats. *Am J Transplant* 2012; **12**: 620-629 [PMID: 22151301 DOI: 10.1111/j.1600-6143.2011.03870.x]

55 **Huang B**, Cheng X, Wang H, Huang W, la Ga Hu Z, Wang D, Zhang K, Zhang H, Xue Z, Da Y, Zhang N, Hu Y, Yao Z, Qiao L, Gao F, Zhang R. Mesenchymal stem cells and their secreted molecules predominantly ameliorate fulminant hepatic failure and chronic liver fibrosis in mice respectively. *J Transl Med* 2016; **14**: 45 [PMID: 26861623 DOI: 10.1186/s12967-016-0792-1]

56 **Wan YM**, Li ZQ, Zhou Q, Liu C, Wang MJ, Wu HX, Mu YZ, He YF, Zhang Y, Wu XN, Li YH, Xu ZY, Wu HM, Xu Y, Yang JH, Wang XF. Mesenchymal stem cells alleviate liver injury induced by chronic-binge ethanol feeding in mice *via* release of TSG6 and suppression of STAT3 activation. *Stem Cell Res Ther* 2020; **11**: 24 [PMID: 31931878 DOI: 10.1186/s13287-019-1547-8]

57 **Gaia S**, Smedile A, Omedè P, Olivero A, Sanavio F, Balzola F, Ottobrelli A, Abate ML, Marzano A, Rizzetto M, Tarella C. Feasibility and safety of G-CSF administration to induce bone marrow-derived cells mobilization in patients with end stage liver disease. *J Hepatol* 2006; **45**: 13-19 [PMID: 16635534 DOI: 10.1016/j.jhep.2006.02.018]

58 **Gordon MY**, Levicar N, Pai M, Bachellier P, Dimarakis I, Al-Allaf F, M'Hamdi H, Thalji T, Welsh JP, Marley SB, Davies J, Dazzi F, Marelli-Berg F, Tait P, Playford R, Jiao L, Jensen S, Nicholls JP, Ayav A, Nohandani M, Farzaneh F, Gaken J, Dodge R, Alison M, Apperley JF, Lechler R, Habib NA. Characterization and clinical application of human CD34+ stem/progenitor cell populations mobilized into the blood by granulocyte colony-stimulating factor. *Stem Cells* 2006; **24**: 1822-1830 [PMID: 16556705 DOI: 10.1634/stemcells.2005-0629]

59 **Laxman RS**, Srinivasan MC. Actinomycetes as resource pools for industrially useful enzymes: an overview. *Hindustan Antibiot Bull* 1993; **35**: 23-32 [PMID: 8181952 DOI: 10.1111/j.1365-2184.2008.00491.x]

60 **Yannaki E**, Anagnostopoulos A, Kapetanos D, Xagorari A, Iordanidis F, Batsis I, Kaloyannidis P, Athanasiou E, Dourvas G, Kitis G, Fassas A. Lasting amelioration in the clinical course of decompensated alcoholic cirrhosis with boost infusions of mobilized peripheral blood stem cells. *Exp Hematol* 2006; **34**: 1583-1587 [PMID: 17046578 DOI: 10.1016/j.exphem.2006.06.012]

61 **Lyra AC**, Soares MB, da Silva LF, Fortes MF, Silva AG, Mota AC, Oliveira SA, Braga EL, de Carvalho WA, Genser B, dos Santos RR, Lyra LG. Feasibility and safety of autologous bone marrow mononuclear cell transplantation in patients with advanced chronic liver disease. *World J Gastroenterol* 2007; **13**: 1067-1073 [PMID: 17373741 DOI: 10.3748/wjg.v13.i7.1067]

62 **Pai M**, Zacharoulis D, Milicevic MN, Helmy S, Jiao LR, Levicar N, Tait P, Scott M, Marley SB, Jestice K, Glibetic M, Bansi D, Khan SA, Kyriakou D, Rountas C, Thillainayagam A, Nicholls JP, Jensen S, Apperley JF, Gordon MY, Habib NA. Autologous infusion of expanded mobilized adult bone marrow-derived CD34+ cells into patients with alcoholic liver cirrhosis. *Am J Gastroenterol* 2008; **103**: 1952-1958 [PMID: 18637092 DOI: 10.1111/j.1572-0241.2008.01993.x]

63 **Kharaziha P**, Hellström PM, Noorinayer B, Farzaneh F, Aghajani K, Jafari F, Telkabadi M, Atashi A, Honardoost M, Zali MR, Soleimani M. Improvement of liver function in liver cirrhosis patients after autologous mesenchymal stem cell injection: a phase I-II clinical trial. *Eur J Gastroenterol Hepatol* 2009; **21**: 1199-1205 [PMID: 19455046 DOI: 10.1097/MEG.0b013e32832a1f6c]

64 **Couto BG**, Goldenberg RC, da Fonseca LM, Thomas J, Gutfilen B, Resende CM, Azevedo F, Mercante DR, Torres AL, Coelho HS, Maiolino A, Alves AL, Dias JV, Moreira MC, Sampaio AL, Sousa MA, Kasai-Brunswick TH, Souza SA, Campos-de-Carvalho AC, Rezende GF. Bone marrow mononuclear cell therapy for patients with cirrhosis: a Phase 1 study. *Liver Int* 2011; **31**: 391-400 [PMID: 21281433 DOI: 10.1111/j.1478-3231.2010.02424.x]

65 **Saito T**, Okumoto K, Haga H, Nishise Y, Ishii R, Sato C, Watanabe H, Okada A, Ikeda M, Togashi H, Ishikawa T, Terai S, Sakaida I, Kawata S. Potential therapeutic application of intravenous autologous bone marrow infusion in patients with alcoholic liver cirrhosis. *Stem Cells Dev* 2011; **20**: 1503-1510 [PMID: 21417817 DOI: 10.1089/scd.2011.0074]

66 **Spahr L**, Chalandon Y, Terraz S, Kindler V, Rubbia-Brandt L, Frossard JL, Breguet R, Lanthier N, Farina A, Passweg J, Becker CD, Hadengue A. Autologous bone marrow mononuclear cell transplantation in patients with decompensated alcoholic liver disease: a randomized controlled trial. *PLoS One* 2013; **8**: e53719 [PMID: 23341981 DOI: 10.1371/journal.pone.0053719]

67 **Lanthier N**, Lin-Marq N, Rubbia-Brandt L, Clément S, Goossens N, Spahr L. Autologous bone marrow-derived cell transplantation in decompensated alcoholic liver disease: what is the impact on liver histology and gene expression patterns? *Stem Cell Res Ther* 2017; **8**: 88 [PMID: 28420441 DOI: 10.1186/s13287-017-0541-2]

68 **Jang YO**, Kim YJ, Baik SK, Kim MY, Eom YW, Cho MY, Park HJ, Park SY, Kim BR, Kim JW, Soo Kim H, Kwon SO, Choi EH, Kim YM. Histological improvement following administration of autologous bone marrow-derived mesenchymal stem cells for alcoholic cirrhosis: a pilot study. *Liver Int* 2014; **34**: 33-41 [PMID: 23782511 DOI: 10.1111/liv.12218]

69 **Andreone P**, Catani L, Margini C, Brodosi L, Lorenzini S, Sollazzo D, Nicolini B, Giordano R, Montemurro T, Rizzi S, Dan E, Giudice V, Viganò M, Casadei A, Foschi FG, Malvi D, Bernardi M, Conti F, Lemoli RM. Reinfusion of highly purified CD133+ bone marrow-derived stem/progenitor cells in patients with end-stage liver disease: A phase I clinical trial. *Dig Liver Dis* 2015; **47**: 1059-1066 [PMID: 26427587 DOI: 10.1016/j.dld.2015.08.018]

70 **Sharma M**, Rao PN, Sasikala M, Kuncharam MR, Reddy C, Gokak V, Raju B, Singh JR, Nag P, Nageshwar Reddy D. Autologous mobilized peripheral blood CD34(+) cell infusion in non-viral decompensated liver cirrhosis. *World J Gastroenterol* 2015; **21**: 7264-7271 [PMID: 26109814 DOI: 10.3748/wjg.v21.i23.7264]

71 **Suk KT**, Yoon JH, Kim MY, Kim CW, Kim JK, Park H, Hwang SG, Kim DJ, Lee BS, Lee SH, Kim HS, Jang JY, Lee CH, Kim BS, Jang YO, Cho MY, Jung ES, Kim YM, Bae SH, Baik SK. Transplantation with autologous bone marrow-derived mesenchymal stem cells for alcoholic cirrhosis: Phase 2 trial. *Hepatology* 2016; **64**: 2185-2197 [PMID: 27339398 DOI: 10.1002/hep.28693]

72 **Yu SJ**, Yoon JH, Kim W, Lee JM, Lee YB, Cho Y, Lee DH, Lee M, Yoo JJ, Cho EJ, Lee JH, Kim YJ, Kim CY. Ultrasound-guided percutaneous portal transplantation of peripheral blood monocytes in patients with liver cirrhosis. *Korean J Intern Med* 2017; **32**: 261-268 [PMID: 27044856 DOI: 10.3904/kjim.2015.267]

73 **Huang KC**, Chuang MH, Lin ZS, Lin YC, Chen CH, Chang CL, Huang PC, Syu WS, Chiou TW, Hong ZH, Tsai YC, Harn HJ, Lin PC, Lin SZ. Transplantation with GXHPC1 for Liver Cirrhosis: Phase 1 Trial. *Cell Transplant* 2019; **28**: 100S-111S [PMID: 31722556 DOI: 10.1177/0963689719884885]

74 **Jang YY**, Collector MI, Baylin SB, Diehl AM, Sharkis SJ. Hematopoietic stem cells convert into liver cells within days without fusion. *Nat Cell Biol* 2004; **6**: 532-539 [PMID: 15133469 DOI: 10.1038/ncb1132]

75 **Lagasse E**, Connors H, Al-Dhalimy M, Reitsma M, Dohse M, Osborne L, Wang X, Finegold M, Weissman IL, Grompe M. Purified hematopoietic stem cells can differentiate into hepatocytes in vivo. *Nat Med* 2000; **6**: 1229-1234 [PMID: 11062533 DOI: 10.1038/81326]

76 **Willenbring H**, Wang X, Akkari Y, Torimaru Y, Foster M, Al-Dhalimy M, Lavilette D, Kabat D, Lagasse E, Finegold M, Olson S, Grompe M. In Vivo Cell Fusion: A New Way To Treat Genetic Liver Disease. *Mol Ther* 2003; **7** Suppl 5: S455 [DOI: 10.1016/S1525-0016(16)41619-9]

77 **Prystupa A**, Kiciński P, Sak J, Boguszewska-Czubara A, Toruń-Jurkowska A, Załuska W. Proinflammatory Cytokines (IL-1α, IL-6) and Hepatocyte Growth Factor in Patients with Alcoholic Liver Cirrhosis. *Gastroenterol Res Pract* 2015; **2015**: 532615 [PMID: 26448742 DOI: 10.1155/2015/532615]

78 **Zarnegar R**, Michalopoulos GK. The many faces of hepatocyte growth factor: from hepatopoiesis to hematopoiesis. *J Cell Biol* 1995; **129**: 1177-1180 [PMID: 7775566 DOI: 10.1083/jcb.129.5.1177]

79 **Kamimoto M**, Mizuno S, Nakamura T. Reciprocal regulation of IL-6 and IL-10 balance by HGF *via* recruitment of heme oxygenase-1 in macrophages for attenuation of liver injury in a mouse model of endotoxemia. *Int J Mol Med* 2009; **24**: 161-170 [PMID: 19578789 DOI: 10.3892/ijmm_00000219]

80 **Fausto N**. Liver regeneration and repair: hepatocytes, progenitor cells, and stem cells. *Hepatology* 2004; **39**: 1477-1487 [PMID: 15185286 DOI: 10.1002/hep.20214]

81 **Zhang Y**, Li R, Rong W, Han M, Cui C, Feng Z, Sun X, Jin S. Therapeutic effect of hepatocyte growth factor-overexpressing bone marrow-derived mesenchymal stem cells on CCl_4-induced hepatocirrhosis. *Cell Death Dis* 2018; **9**: 1186 [PMID: 30538216 DOI: 10.1038/s41419-018-1239-9]

82 **da Costa Gonçalves F**, Grings M, Nunes NS, Pinto FO, Garcez TN, Visioli F, Leipnitz G, Paz AH. Antioxidant properties of mesenchymal stem cells against oxidative stress in a murine model of colitis. *Biotechnol Lett* 2017; **39**: 613-622 [PMID: 28032203 DOI: 10.1007/s10529-016-2272-3]

83 **Ju C**, Mandrekar P. Macrophages and Alcohol-Related Liver Inflammation. *Alcohol Res* 2015; **37**: 251-262 [PMID: 26717583]

84 **Fabregat I**, Moreno-Càceres J, Sánchez A, Dooley S, Dewidar B, Giannelli G, Ten Dijke P; IT-LIVER Consortium. TGF-β signalling and liver disease. *FEBS J* 2016; **283**: 2219-2232 [PMID: 26807763 DOI: 10.1111/febs.13665]

85 **Zhang L**, Zhou D, Li J, Yan X, Zhu J, Xiao P, Chen T, Xie X. Effects of Bone Marrow-Derived Mesenchymal Stem Cells on Hypoxia and the Transforming Growth Factor beta 1 (TGFβ-1) and SMADs Pathway in a Mouse Model of Cirrhosis. *Med Sci Monit* 2019; **25**: 7182-7190 [PMID: 31550244 DOI: 10.12659/MSM.916428]

86 **Zhao J**, Qi YF, Yu YR. STAT3: A key regulator in liver fibrosis. *Ann Hepatol* 2021; **21**: 100224 [PMID: 32702499 DOI: 10.1016/j.aohep.2020.06.010]

87 **Lafdil F**, Miller AM, Ki SH, Gao B. Th17 cells and their associated cytokines in liver diseases. *Cell Mol Immunol* 2010; **7**: 250-254 [PMID: 20305686 DOI: 10.1038/cmi.2010.5]

88 **Zenewicz LA**, Yancopoulos GD, Valenzuela DM, Murphy AJ, Karow M, Flavell RA. Interleukin-22 but not interleukin-17 provides protection to hepatocytes during acute liver inflammation. *Immunity* 2007; **27**: 647-659 [PMID: 17919941 DOI: 10.1016/j.immuni.2007.07.023]

89 **Ki SH**, Park O, Zheng M, Morales-Ibanez O, Kolls JK, Bataller R, Gao B. Interleukin-22 treatment ameliorates alcoholic liver injury in a murine model of chronic-binge ethanol feeding: role of signal transducer and activator of transcription 3. *Hepatology* 2010; **52**: 1291-1300 [PMID: 20842630 DOI: 10.1002/hep.23837]

90 **Xiang X**, Feng D, Hwang S, Ren T, Wang X, Trojnar E, Matyas C, Mo R, Shang D, He Y, Seo W, Shah VH, Pacher P, Xie Q, Gao B. Interleukin-22 ameliorates acute-on-chronic liver failure by reprogramming impaired regeneration pathways in mice. *J Hepatol* 2020; **72**: 736-745 [PMID: 31786256 DOI: 10.1016/j.jhep.2019.11.013]

91 **Arab JP**, Sehrawat TS, Simonetto DA, Verma VK, Feng D, Tang T, Dreyer K, Yan X, Daley WL, Sanyal A, Chalasani N, Radaeva S, Yang L, Vargas H, Ibacache M, Gao B, Gores GJ, Malhi H, Kamath PS, Shah VH. An Open-Label, Dose-Escalation Study to Assess the Safety and Efficacy of IL-22 Agonist F-652 in Patients With Alcohol-associated Hepatitis. *Hepatology* 2020; **72**: 441-453 [PMID: 31774566 DOI: 10.1002/hep.31046]

92 **Akriviadis E**, Botla R, Briggs W, Han S, Reynolds T, Shakil O. Pentoxifylline improves short-term survival in severe acute alcoholic hepatitis: a double-blind, placebo-controlled trial. *Gastroenterology* 2000; **119**: 1637-1648 [PMID: 11113085 DOI: 10.1053/gast.2000.20189]

93 **Nguyen-Khac E**, Thevenot T, Piquet MA, Benferhat S, Goria O, Chatelain D, Tramier B, Dewaele F, Ghrib S, Rudler M, Carbonell N, Tossou H, Bental A, Bernard-Chabert B, Dupas JL; AAH-NAC Study Group. Glucocorticoids plus N-acetylcysteine in severe alcoholic hepatitis. *N Engl J Med* 2011; **365**: 1781-1789 [PMID: 22070475 DOI: 10.1056/NEJMoa1101214]

94 **Marot A**, Singal AK, Moreno C, Deltenre P. Granulocyte colony-stimulating factor for alcoholic hepatitis: A systematic review and meta-analysis of randomised controlled trials. *JHEP Rep* 2020; **2**: 100139 [PMID: 32775975 DOI: 10.1016/j.jhepr.2020.100139]

95 **Newsome PN**, Fox R, King AL, Barton D, Than NN, Moore J, Corbett C, Townsend S, Thomas J, Guo K, Hull D, Beard HA, Thompson J, Atkinson A, Bienek C, McGowan N, Guha N, Campbell J, Hollyman D, Stocken D, Yap C, Forbes SJ. Granulocyte colony-stimulating factor and autologous CD133-positive stem-cell therapy in liver cirrhosis (REALISTIC): an open-label, randomised, controlled phase 2 trial. *Lancet Gastroenterol Hepatol* 2018; **3**: 25-36 [PMID: 29127060 DOI: 10.1016/S2468-1253(17)30326-6]

96 **Altamirano J**, López-Pelayo H, Michelena J, Jones PD, Ortega L, Ginès P, Caballería J, Gual A, Bataller R, Lligoña A. Alcohol abstinence in patients surviving an episode of alcoholic hepatitis: Prediction and impact on long-term survival. *Hepatology* 2017; **66**: 1842-1853 [PMID: 28646515 DOI: 10.1002/hep.29338]

97 **Potts JR**, Goubet S, Heneghan MA, Verma S. Determinants of long-term outcome in severe alcoholic hepatitis. *Aliment Pharmacol Ther* 2013; **38**: 584-595 [PMID: 23879720 DOI: 10.1111/apt.12427]

98 **Horiguchi N**, Ishac EJ, Gao B. Liver regeneration is suppressed in alcoholic cirrhosis: correlation with decreased STAT3 activation. *Alcohol* 2007; **41**: 271-280 [PMID: 17630087 DOI: 10.1016/j.alcohol.2007.04.008]

99 **Chen J**, Ishac EJ, Dent P, Kunos G, Gao B. Effects of ethanol on mitogen-activated protein kinase and stress-activated protein kinase cascades in normal and regenerating liver. *Biochem J* 1998; **334** (Pt 3): 669-676 [PMID: 9729476 DOI: 10.1042/bj3340669]

World Journal of Gastroenterology

Submit a Manuscript: https://www.f6publishing.com

World J Gastroenterol 2022 August 28; 28(32): 4574-4599

DOI: 10.3748/wjg.v28.i32.4574

ISSN 1007-9327 (print) ISSN 2219-2840 (online)

ORIGINAL ARTICLE

Basic Study

Wumei pills attenuates 5-fluorouracil-induced intestinal mucositis through Toll-like receptor 4/myeloid differentiation factor 88/nuclear factor-κB pathway and microbiota regulation

Dong-Xue Lu, Feng Liu, Hua Wu, Hai-Xia Liu, Bing-Yu Chen, Jing Yan, Yin Lu, Zhi-Guang Sun

Specialty type: Gastroenterology and hepatology

Provenance and peer review: Unsolicited article; Externally peer reviewed.

Peer-review model: Single blind

Peer-review report's scientific quality classification

Grade A (Excellent): 0
Grade B (Very good): B
Grade C (Good): 0
Grade D (Fair): 0
Grade E (Poor): 0

P-Reviewer: Vorobjova T, Estonia

Received: September 14, 2021
Peer-review started: September 14, 2021
First decision: December 27, 2021
Revised: January 5, 2022
Accepted: July 18, 2022
Article in press: July 18, 2022
Published online: August 28, 2022

Dong-Xue Lu, Hua Wu, Department of Nutrition, Acupuncture and Moxibustion and Massage College & Health Preservation and Rehabilitation College, Nanjing University of Chinese Medicine, Nanjing 210023, Jiangsu Province, China

Feng Liu, Department of Orthopaedics, Nanjing Pukou District Chinese Medicine Hospital, Nanjing 210000, Jiangsu Province, China

Hai-Xia Liu, Department of Oncology, Affiliated Hospital of Nanjing University of Chinese Medicine, Nanjing 210000, Jiangsu Province, China

Bing-Yu Chen, Department of Geriatrics, The First Affiliated Hospital of Henan University of Traditional Chinese Medicine, Zhengzhou 451150, Henan Province, China

Jing Yan, Key Laboratory for Metabolic Diseases in Chinese Medicine, The First Clinical Medical College, Nanjing University of Chinese Medicine, Nanjing 210023, Jiangsu Province, China

Yin Lu, Key Pharmacology Laboratory of Jiangsu Province, Nanjing University of Chinese Medicine, Nanjing 210023, Jiangsu Province, China

Zhi-Guang Sun, The First Clinical Medical College, Nanjing University of Chinese Medicine, Nanjing 210023, Jiangsu Province, China

Corresponding author: Zhi-Guang Sun, PhD, Chief Doctor, Professor, The First Clinical Medical College, Nanjing University of Chinese Medicine, No. 138, Xianlin Avenue, Qixia District, Nanjing 210023, Jiangsu Province, China. 110399@njucm.edu.cn

Abstract

BACKGROUND

Radiotherapy and chemotherapy can kill tumor cells and improve the survival rate of cancer patients. However, they can also damage normal cells and cause serious intestinal toxicity, leading to gastrointestinal mucositis[1]. Traditional Chinese medicine is effective in improving the side effects of chemotherapy. Wumei pills (WMP) was originally documented in the Treatise on Exogenous Febrile Diseases. It has a significant effect on chronic diarrhea and other gastrointestinal diseases, but it is not clear whether it affects chemotherapy-

induced intestinal mucositis (CIM).

AIM

To explore the potential mechanism of WMP in the treatment of CIM through experimental research.

METHODS

We used an intraperitoneal injection of 5-fluorouracil (5-Fu) to establish a CIM mouse model and an oral gavage of WMP decoction (11325 and 22650 mg/kg) to evaluate the efficacy of WMP in CIM. We evaluated the effect of WMP on CIM by observing the general conditions of the mice (body weight, food intake, spleen weight, diarrhea score, and hematoxylin and eosin stained tissues). The expression of tumor necrosis factor-α (TNF-α), interleukin-6 (IL-6), IL-1β, and myeloperoxidase (MPO), as well as the Toll-like receptor 4/myeloid differentiation factor 88/nuclear factor-κB (TLR4/MyD88/NF-κB) signaling pathway proteins and tight junction proteins (zonula occludens-1, claudin-1, E-cadherin, and mucin-2) was determined. Furthermore, intestinal permeability, intestinal flora, and the levels of short-chain fatty acids (SCFA) were also assessed.

RESULTS

WMP effectively improved the body weight, spleen weight, food intake, diarrhea score, and inflammatory status of the mice with intestinal mucositis, which preliminarily confirmed the efficacy of WMP in CIM. Further experiments showed that in addition to reducing the levels of TNF-α, IL-1β, IL-6, and MPO and inhibiting the expression of the TLR4/MyD88/NF-κB pathway proteins, WMP also repaired the integrity of the mucosal barrier of mice, regulated the intestinal flora, and increased the levels of SCFA (such as butyric acid).

CONCLUSION

WMP can play a therapeutic role in CIM by alleviating inflammation, restoring the mucosal barrier, and regulating gut microbiota.

Key Words: Wumei pills; Gut flora; Intestinal mucosal inflammation; Mucosal barrier; Short-chain fatty acids; Intestinal permeability

©The Author(s) 2022. Published by Baishideng Publishing Group Inc. All rights reserved.

Core Tip: In this study, the compound Wumei pills was selected as the representative of the traditional Chinese medicine compound, and it was clarified that the compatibility of the compound medicines may also regulate the intestinal flora, which is instructive for the study of the onset mode and mechanism of the Chinese medicine compound. The results obtained will provide a scientific basis for finding clinical potential treatment and intervention strategies for chemotherapy-induced intestinal mucositis.

Citation: Lu DX, Liu F, Wu H, Liu HX, Chen BY, Yan J, Lu Y, Sun ZG. Wumei pills attenuates 5-fluorouracil-induced intestinal mucositis through Toll-like receptor 4/myeloid differentiation factor 88/nuclear factor-κB pathway and microbiota regulation. *World J Gastroenterol* 2022; 28(32): 4574-4599
URL: https://www.wjgnet.com/1007-9327/full/v28/i32/4574.htm
DOI: https://dx.doi.org/10.3748/wjg.v28.i32.4574

INTRODUCTION

Chemotherapy plays an important role in the comprehensive treatment of malignant tumors and can greatly improve the survival rate of patients with cancer. Although chemotherapy kills tumor cells, it also damages normal cells and induces serious gastrointestinal toxicity; this results in gastrointestinal mucositis, which has been associated with bone marrow suppression, nausea and vomiting, and diarrhea[1]. The gastrointestinal toxicity of chemotherapy seriously affects the treatment process and prognosis of cancer patients[2,3]. Chemotherapy-induced intestinal mucositis (CIM) is more common in patients receiving 5-fluorouracil (5-Fu), irinotecan, methotrexate, cisplatin, and cytarabine[4,5]. It has been reported that the incidence of mucositis is 40% after conventional chemotherapy and can increase up to 80% with high-dose or continuous chemotherapy. Villus atrophy, crypt goblet cell reduction, intestinal epithelial cell hypoplasia, and mucosal barrier dysfunction are the main pathological changes associated with intestinal mucositis[6,7]. Some studies have confirmed that an imbalance in the

intestinal flora can be seen in CIM[8-10]. Therefore, regulating the intestinal flora may be a new therapeutic target for alleviating intestinal mucositis. The treatment of CIM in modern medicine is mainly through combating inflammation and oxidative stress, but the clinical effect of these strategies is not so satisfactory. Thence, there is an urgent need to identify drugs that can effectively treat intestinal mucositis. Increasing evidence shows that traditional Chinese medicine has a significant effect in improving the side effects of chemotherapy, especially with regard to gastrointestinal reactions[11-13].

Wumei pills (WMP) was originally documented in the Treatise on Exogenous Febrile Disease (200-210, AD), and it comprises ten herbs: *Fructus* Mume [*Prunus mume* (Sieb.) Sieb. et Zuce, WM], *Angelicae sinensis* Radix [*Angelica sinensis* (Oliv.) Diels, DG], Asari Radix Et Rhizoma (*Asarum sieboldii Miq*, XX), Aconiti Lateralis Radix Praeparata (*Aconitum carmichaelii Debx*, FZ), Phellodendri chinensis cortex (*Phellodendron chinense Schneid.*, HB), Zanthoxyli Pericarpium (*Zanthoxylum bungeanum Maxim*, HJ), Cinnamomi Ramulus (*Cinnamomum cassia* Presl, GZ), Radix Ginseng (*Panax ginseng C. A. Meyer*, RS), Rhizoma Coptidis (*Coptis chinensis Franch.*, HL), and Rhizoma Zingiberis (*Zingiber oj-jicinale Rosc.*, GJ). It is a classically prescribed traditional Chinese medicine for the treatment of a variety of digestive system diseases and significantly treats diarrhea, upper abdominal pain, and loss of appetite[14,15]. Preliminary clinical studies have shown that WMP has a significant effect on chemotherapy-induced diarrhea[16,17]. It has been reported that WMP is a safe and effective formula. Moreover, WMP has shown significant clinical benefits for digestive diseases, such as ulcerative colitis[18], immune colitis, and irritable bowel syndrome[19-21]. It can also exert an anti-hyperglycemic effect by adjusting the intestinal flora, improving the inflammatory response, and increasing the levels of short-chain fatty acids (SCFA)[22]. However, there is little information on the effects of WMP on CIM. As inflammation and microbiota play significant roles in intestinal mucositis, we hypothesized that WMP might affect CIM in mice. Therefore, we examined the effect of WMP on intestinal mucositis, intestinal mucosal barrier, and intestinal flora in a CIM mouse model. The results of this study may provide new treatment strategies of using traditional Chinese preparations for the treatment of CIM.

MATERIALS AND METHODS

Materials

WMP (WM 24 g, DG 6 g, XX 9 g, FZ 9 g, HB 9 g, HJ 6 g, GZ 9 g, RS 15 g, HL 24 g, and GJ 15 g) was purchased from the Chinese Pharmacy of Jiangsu Provincial Hospital of Traditional Chinese Medicine (Nanjing, China). 5-Fu was obtained from Shanghai Yuanye Bio-Technology Co., Ltd. (CAS: 51-21-8, Shanghai, China, Lot #: N09M10W82518) and FITC-dextran (FD4, 250 mg) was purchased from Sigma-Aldrich Co. LLC (Shanghai, China, Lot #: BCCC2153). Primary antibodies against rabbit Toll-like receptor 4 (TLR-4) (A5258), zonula occludens-1 (ZO-1) (21773-1-AP), mucin-2 (F-2) (sc-515032), GAPDH (AP0063), myeloid differentiation factor 88 (MyD88) (4283S), and nuclear factor-κB (NF-κB) p65 (8242S) were purchased from Abclonal (United States), Proteintech (United States), Santa Cruz Biotechnology (United States), and Bioworld (China). Primary antibodies against mouse claudin-1 (71-7800) and E-cadherin (14472s) were purchased from Invitrogen (United States) and Cell Signaling Technology (Danvers, MA/CST, United States). Goat anti-mouse immunoglobulin G (IgG) (H&L ab6708) and goat anti-rabbit IgG (H&L ab6717) were obtained from Shanghai Abcam Co., Ltd. (Shanghai, China). The primers used to amplify the interleukin-6 (*IL-6*) (forward: Lot No: 1922401831; reverse: Lot No: 1922401832), *IL-1β* (forward: Lot No:1922401835; reverse: Lot No:1922401836), tumor necrosis factor-α (*TNF-α*) (forward: Lot No: 1922401833; reverse: Lot No: 1922401834), and myeloperoxidase (*MPO*) (forward: Lot No: 1922401837; reverse: Lot No: 1922401838) were purchased from Sangon Biotech Co., Ltd. (Shanghai, China). The TRIzol® Reagent (No. 15596018) was obtained from Thermo Fisher Scientific Co., Ltd. (Shanghai, China); the HiScript II Q RT SuperMix for qPCR (+gDNA wiper) (No. R22) was purchased from Vazyme Biotech Co., Ltd. (Nanjing, China); and the iQTM RT SYBR® Green Supermix for qPCR (No. 170-8880AP) was purchased from BIO-RAD Co., Ltd. (Shanghai, China). All the reagents and chemicals were used for study only.

Animals

BABL/C mice (aged 6-8 wk, weighing 18 ± 2 g, male) were obtained from the Shanghai SLAC Laboratory Animal Co., Ltd. (Production License: SCXK: 2017-0005, Shanghai, China). Mice were kept under specific pathogen-free conditions (12 h light/12 h dark cycle, 45%-55% relative humidity, and temperature of 26-28 °C) with free access to food and clean water. The study protocols were approved by the Animal Experimental Ethics Committee of Nanjing University of Chinese Medicine (No. 202006A022) and carried out on the basis of the animal ethics standards of the Nanjing University of Chinese Medicine Laboratory Animal Ethics Committee. The animal certificate number is 20170005027187. All reasonable efforts were made to minimize animal suffering.

Experimental design

After 7 d of adaptive feeding, the BALB/C mice were divided randomly into four groups (n = 10 per group): Control group, 5-Fu group (40 mg/kg), and WMP treatment groups (WMP-11.325, 11325

mg/kg; WMP-22.650, 22650 mg/kg). Except for the control mice, 5-Fu was administered to the mice through intraperitoneal injection once daily for the first 5 d. In addition, the vehicle or different doses of WMP were intragastrically administered to the mice during the experiment. After the treatment, the mice were fasted for 12 h, and they were anesthetized and sacrificed *via* cervical dislocation. The experimental process is illustrated in Figure 1.

Assessment of mucositis and sample collection

Indicators of disease severity, including body weight, food intake, and diarrhea severity, were evaluated daily for the assessment of mucositis. Diarrhea severity was classified into five grades according to stool consistency[23]: (1) 0, normal; (2) 1, slightly wet; (3) 2, moderate wet; (4) 3, loose; and (5) 4, watery stool. Jejunal and colonic tissues were removed quickly and douched with clean cold saline, and then the length of the colon was measured. The samples (1 cm × 1 cm) were immersed in 4 % paraformaldehyde for 24 h and embedded in paraffin for histopathological, immunohistochemical, and immunofluorescence analyses and Alcian blue staining. Blood samples were collected and centrifuged at 12000 rpm for 10 min at 4 °C. The residual intestinal tissue samples were stored at -80 °C and used for biochemical analysis. The feces were also collected from the colon/rectum of the mice to perform a microbiota analysis.

Histopathological assessment

The sections (3.0-μm thick) cut from paraffin blocks and stained with hematoxylin and eosin (H&E) were used for measuring the intestinal mucosal damage and inflammatory cell infiltration with a light microscope. Histopathological scores were calculated on the basis of a previous study[24].

Immunohistochemical analysis

The paraffin sections were dewaxed with xylene and absolute ethanol, washed with phosphate-buffered saline (PBS, pH 7.4), and blocked with 5% bovine serum albumin. Then, the paraffin sections were incubated with an anti-TLR4 antibody (1:600), anti-MyD88 antibody (1:600), or anti-NF-κB p65 antibody (1:600) overnight at -4 °C and incubated with an anti-rabbit secondary antibody the next day. The slides were stained with 3,3-diaminobenzidine (DAB) and counterstained with hematoxylin. The sections were observed with a light microscope.

Intestinal permeability

The toxic effects of chemotherapy may weaken the intestinal epithelial barrier, allowing the contents of the lumen to pass through the paracellular space into the blood. The animals were subjected to fasting from 9 pm on the first day and denied access to water for 12 h. On the second day, FITC-dextran (50 mg/mL) was orally administered to the animals according to their body weight (0.1 mL/10 g). After 3 h, isoflurane anesthesia was administered and the mice were investigated using IVIS Luminaseries II in Living Imaging (480 nm excitation wavelength, 520 nm emission wavelength). After the mice woke up, blood was obtained from the orbit and the serum was separated. A microplate reader was used to measure the serum fluorescence value (480 nm excitation wavelength, 520 nm emission wavelength) and FITC-dextran standards were used to prepare a standard curve for the leakage of FITC in the serum.

Alcian blue staining

The paraffin sections were dewaxed with xylene and absolute ethanol and oxidized with 0.5% periodate solution, followed by incubation with Alcian blue acidification solution for 3 min and staining solution for 30 min. Next, the sections were washed with running water for 5 min, and the slides were stained with nuclear fast red staining solution. The sections were observed under a light microscope and photographed.

Immunofluorescence

Paraffin sections dewaxed with xylene and absolute ethanol were used for antigen retrieval. They were incubated with anti-mucin-2 antibody (1:500), anti-ZO-1 antibody (1:500), anti-claudin-1 antibody (1:500), and anti-rabbit secondary antibody (FITC-labeled, 1:200). The slides were stained with 4′,6-diamidino-2-phenylindole in the dark for 10 min. The sections were observed under a light microscope.

Total RNA extraction and quantitative real-time polymerase chain reaction

Total RNA was extracted from the jejunum and colon/rectum and reverse transcribed into cDNA using the HiScript II Q RT SuperMix according to the manufacturer's instructions. Quantitative real-time polymerase chain reaction (qRT-PCR) was conducted by using the ChamQ Universal SYBR qPCR Master Mix in an Applied Biosystems Step-One Fast Real-Time PCR system. The reaction program was as follows: Pre-denaturation at 95 °C for 30 s, 40 cycles at 95 °C for 10 s and 60 °C for 30 s, followed by annealing at 95 °C for 15 s, 60 °C for 60 s, and 95 °C for 15 s. The primer sequences used for amplifying the genes encoding the target inflammatory factors IL-1β, IL-6, TNF-α, and MPO are listed in Table 1. The relative quantification of the target genes was carried out by the $2^{-\Delta\Delta Ct}$ method, and GAPDH was

Table 1 Primer sequences

Gene		Primer sequences (5' - 3')
IL-6	Forward	CCAAGAGGTGAGTGCTTCCC
	Reverse	CTGTTGTTCAGACTCTCTCCCT
IL-1β	Forward	GCAACTGTTCCTGAACTCAACT
	Reverse	ATCTTTTGGGGTCCGTCAACT
TNF-α	Forward	TGTGGAAACATCGCAAGAAG
	Reverse	CCAACCTTTCAGAGGTCCAA
MPO	Forward	AGCTGCAGTACGTCAAGCAGGA
	Reverse	TTTGCAAACTGTATTTCGCTCTGG

TNF-α: Tumor necrosis factor-α; IL-6: Interleukin-6; IL-1β: Interleukin-1β; MPO: Myeloperoxidase.

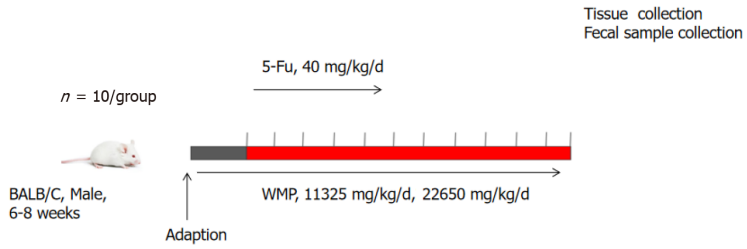


Figure 1 Flow chart of modeling and drug delivery. WMP: Wumei pills; 5-Fu: 5-fluorouracil.

used as the internal control.

Western blot analysis

The total proteins of the intestinal tissue were extracted with a protein extraction kit. Briefly, 100 mg of tissue was grinded with prepared protein lysis solution (RIPA lysis solution:Phosphatase inhibitor:1% PMSF = 100:1:1), and centrifuged at 12000 rmp for 10 min at 4 °C, and 10 μL of supernatant was used for protein quantification with the NanoDropTM One/OneC and the other used for western blot analysis. Protein samples were separated on 6% to 12% sodium dodecyl sulfate-polyacrylamide gels and transferred to polyvinylidene difluoride (PVDF) membranes. The protein-loaded PVDF membranes were blocked for 2 h in 5% skim milk and incubated with primary antibodies overnight at 4 °C and then with secondary antibodies for 1.5 h according to the manufacturer's instructions. Protein expression was detected using a western blot enhanced chemiluminescence substrate, and the results were compared using the ImageJ software. The working dilutions of the antibodies against the following proteins were prepared: TLR4, 1:600; MyD88 1:600; NF-kB, 1:1000; ZO-1, 1:1000; claudin-1, 1:1000; E-cadherin, 1:1000; and GAPDH, 1:20000. A GAPDH antibody was used for verifying the equal loading of the samples of different groups.

16S ribosomal DNA gene sequence analysis

To perform 16S rRNA sequencing, we pooled the feces from six mice in each group (control, 5-Fu, 5-Fu + WMP 11325, and 5-Fu + WMP 22650 groups). Microbial DNA was extracted from 24 samples using the E.Z.N.A.® soil DNA Kit (Omega Bio-tek, Norcross, GA, United States) according to the manufacturer's protocols. The final DNA concentration and purification were determined using a NanoDrop 2000 UV-VIS spectrophotometer (Thermo Scientific, Wilmington, United States), and DNA quality was checked through 1% agarose gel electrophoresis. The V3-V4 hypervariable regions of the bacterial 16S rRNA gene were amplified with the primers 338F (5'-ACTCCTACGGGAGGCAGCAG-3') and 806R (5'-GGACTACHVGGGTWTCTAAT-3') using a thermocycler PCR system (GeneAmp 9700, ABI, United States). The resulting PCR products were extracted from a 2% agarose gel and further purified using the AxyPrep DNA Gel Extraction Kit (Axygen Biosciences, Union City, CA, United States). The products were quantified using QuantiFluor™-ST (Promega, United States) according to the manufacturer's protocol, and purified amplicons were pooled in equimolar amounts and subjected to paired-end sequencing (2 × 300) on an Illumina MiSeq platform (Illumina, San Diego, United States) according to the standard protocols of Majorbio Bio-Pharm Technology Co. Ltd. (Shanghai, China).

Quantification of SCFA

The fecal content (50 mg) of each mouse was placed into a 2-mL centrifuge tube, followed by the addition of 1.0 mL NaOH. The solution was homogenized for 10 min and centrifuged at 13000 rpm for 10 min. Next, 600 μL of supernatant was added to a centrifuge tube with 10 μL of caproic acid-d3, and the mixture was vortexed. The mixture (500 μL) was added to a 10-mL centrifuge tube, followed by the addition of 300 μL of ultrapure water; the mixture was then vortexed. Next, 500 μL of 1-propanol: Pyridine (3:2, v/v) and 100 μL of propyl chloroformate were added; the mixture was vortexed for 30 s and sonicated for 1 min. After derivatization, 300 μL of *n*-hexane was added to extract the derivatized material, followed by vortexing for 1 min and centrifugation at 2000 rpm for 10 min. The upper layer of the solution (200 μL) was placed in a 1.5-mL centrifuge tube and 200 μL of *n*-hexane was added to the centrifuge tube, vortexed for 1 min, and centrifuged at 2000 rpm for 10 min. The upper layer solution (200 μL) from the previous step was vortexed twice. After centrifugation at 18000 rpm for 10 min, the supernatant was filtered through a 0.22 μm membrane filter. SCFAs were quantified using gas chromatography-mass spectrometry (GCMS-QP2010, Shimadzu, Japan) equipped with an Rtx-5MS capillary column (30 m × 0.25 mm × 0.25 μm). For mass spectroscopy, an electron bombardment ionization source, a full scan, and a scanning mode were adopted. The electron energy was 70 eV.

Statistical analysis

Raw data related to intestinal flora were analyzed on the free online platform of Majorbio Cloud Platform (www.majorbio.com). Data are presented as the mean ± SDE of the mean. Differences between two groups were analyzed with GraphPad Prism 8.3. One-way analysis of variance was used for the comparison of more than two groups. The metabolites were filtered by variable influence on projection (VIP) selection from the PLS-DA and the filtering conditions were VIP > 1 and $P < 0.05$. In all cases, statistical significance was set at $P < 0.05$ ($^{a}P < 0.05$, $^{b}P < 0.01$, $^{c}P < 0.001$ and $^{d}P < 0.0001$, compared with the normal group; $^{e}P < 0.05$, $^{f}P < 0.01$, $^{g}P < 0.001$, and $^{h}P < 0.0001$, compared with the 5-Fu group).

RESULTS

Effect of 5-Fu

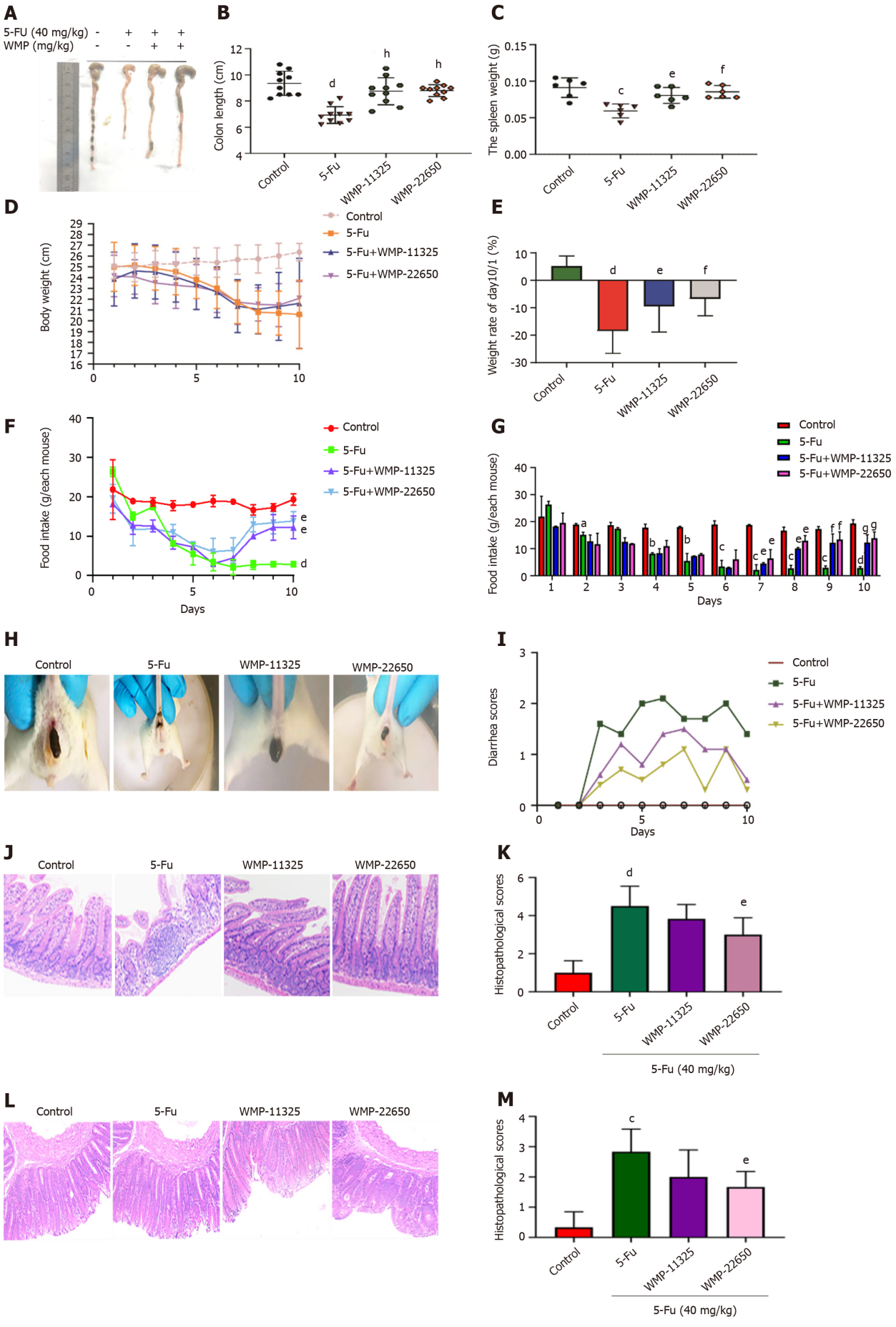
After intraperitoneal injections of 5-Fu, the mice exhibited mild to severe diarrheal symptoms including wet and watery stools, reduced movement, weight loss, and reduced appetite. The changes in colon length, spleen weight, body weight, and appetite, as well as the incidence of diarrhea were regarded as preliminary indices[25], and these changes are shown in Figures 2A-I. The colon length was significantly shortened, and the spleen weight was remarkedly decreased in the mouse models. At the beginning of the experiment, all the mice had similar body weights and appetites, with no diarrhea. In the experiment period, there was no diarrhea and the body weight and food intake gradually increased in the control group mice. However, for the mice that received 5-Fu, the colon length was significantly shortened, the spleen weight markedly decreased, the appetite reduced, and the body weight continuously declined. Serious diarrhea was observed in the mouse models after day 3. WMP increased the colon length of mice in the WMP-11325 mg/kg and WMP-22650 mg/kg groups in a dose-dependent manner. The mice showed increased appetites, and their body weights recovered after day 7. Notably, the diarrhea scores of the mice in the WMP-11325 mg/kg and WMP-22650 mg/kg groups began to decrease by day 8, although they still had severe diarrhea.

Histopathological assessment of the colon and jejunum

Morphological changes in the colon and jejunum were observed, as shown in Figures 2J-M. H&E staining showed that 5-Fu damaged the intestinal epithelium to different degrees, and the most significant epithelial damage was observed in the jejunal tissue (Figures 2L-M). There were no histological abnormalities in the control group, whereas huge ulcers with inflammatory cell infiltration, atrophied glands, and shortened villus length were observed in the jejunal epithelial tissues of the model group mice. The damage was milder in the colon mucosa (Figures 2J-K), which manifested as a small number of inflammatory cells infiltrating the mucosal layer, accompanied by shortened villus length. This condition was alleviated after WMP treatment. WMP effectively accelerated the recovery of injury in a dose-dependent manner. Model mice in the 22650 mg/kg WMP group presented well-ordered glands, increased villus length, and a few impairments like those observed in the control mice.

Effect of WMP on inflammatory cytokines

To evaluate the effects of WMP on inflammation, the mRNA levels of the inflammatory cytokines *TNF-α*, *IL-1β*, *IL-6*, and *MPO* in colonic and jejunal tissues were investigated using qRT-PCR (Figures 2N-O). In both tissues, the mRNA levels of the inflammatory cytokines were significantly elevated ($P < 0.05$) in the 5-Fu group. This condition was alleviated by WMP treatment. WMP effectively decreased the mRNA levels of inflammatory cytokines in a dose-dependent manner. Mice in the 22650 mg/kg WMP group showed lower mRNA levels of inflammatory cytokines ($P < 0.05$) than those in the 5-Fu group.


A
5-FU (40 mg/kg) - + + +
WMP (mg/kg) - - + +
B
Colon length (cm)
Control
5-Fu
WMP-11325
WMP-22650
C
The spleen weight (g)
D
Body weight (cm)
Control
5-Fu
5-Fu+WMP-11325
5-Fu+WMP-22650
E
Weight rate of day10/1 (%)
F
Food intake (g/each mouse)
Days
G
Food intake (g/each mouse)
Days
H
Control
5-Fu
WMP-11325
WMP-22650
I
Diarrhea scores
Days
J
Control
5-Fu
WMP-11325
WMP-22650
K
Histopathological scores
5-Fu (40 mg/kg)
L
Control
5-Fu
WMP-11325
WMP-22650
M
Histopathological scores
5-Fu (40 mg/kg)

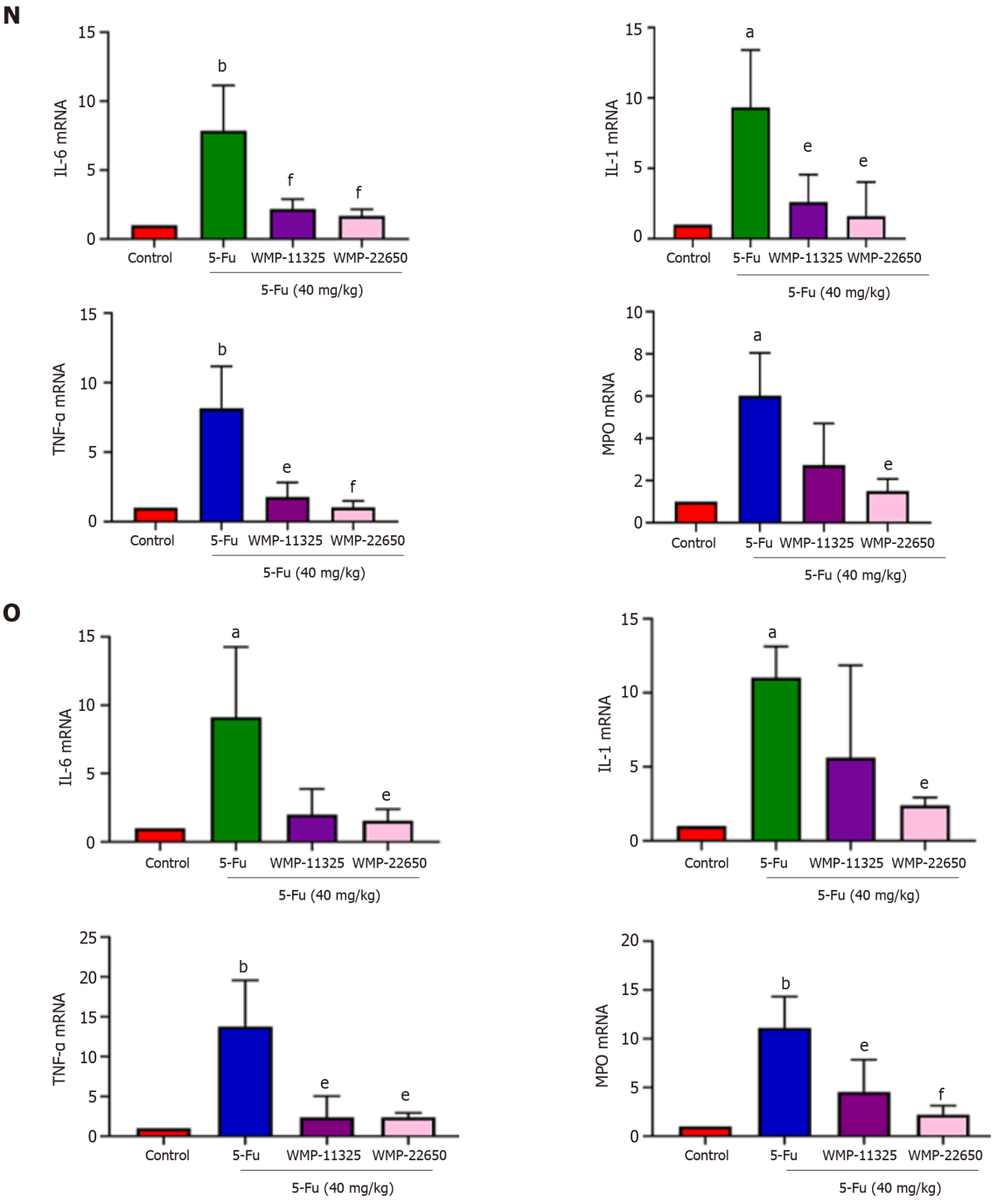


Figure 2 Effect of Wumei pills on routine observation, histopathological assessment (*n* = 10, 200 ×), and inflammatory cytokines on intestinal mucositis in mice. A and B: Colon length; C: Spleen weight; D and E: Body weight; F and G: Food intake; H and I: Diarrhea scores; J and K: Histopathological assessment of the jejunum; L and M: Histopathological assessment of the colon; N: Levels of tumor necrosis factor-α (*TNF-α*), interleukin-1β (*IL-1β*), *IL-6*, *IL-10*, and myeloperoxidase (*MPO*) in the jejunum; O: Levels of *TNF-α*, *IL-1β*, *IL-6*, *IL-10*, and *MPO* in the colon. Values represent the mean ± SEM. $^{a}P < 0.05$, $^{b}P < 0.01$ *vs* control group and $^{e}P < 0.05$, $^{f}P < 0.01$ *vs* 5-fluorouracil group. WMP: Wumei pills; TNF-α: Tumor necrosis factor-α; IL-6: Interleukin-6; IL-1β: Interleukin-1β; MPO: Myeloperoxidase; 5-Fu: 5-fluorouracil.

Effect of WMP on inflammatory proteins

The western blot analysis of the changes in the TLR4/MyD88/NF-κB pathway proteins following WMP administration (Figures 3A-D) showed that 5-Fu administration significantly increased the expression of the TLR4, MyD88, and NF-κB proteins. Although 11325 mg/kg WMP administration had a mild effect, 22650 mg/kg WMP markedly decreased the levels of TLR4, MyD88, and NF-κB proteins to almost normal levels. To further investigate the effect of WMP on the expression of TLR4/MyD88/NF-κB, immunohistochemical analysis was performed to detect protein expression (Figures 3E and 3F). Compared to that in the normal group, the 5-Fu group had significantly higher levels of TLR4/MyD88/NF-κB ($P < 0.01$). In contrast, the expression of TLR4/MyD88/NF-κB in the WMP group decreased in a dose-dependent manner.

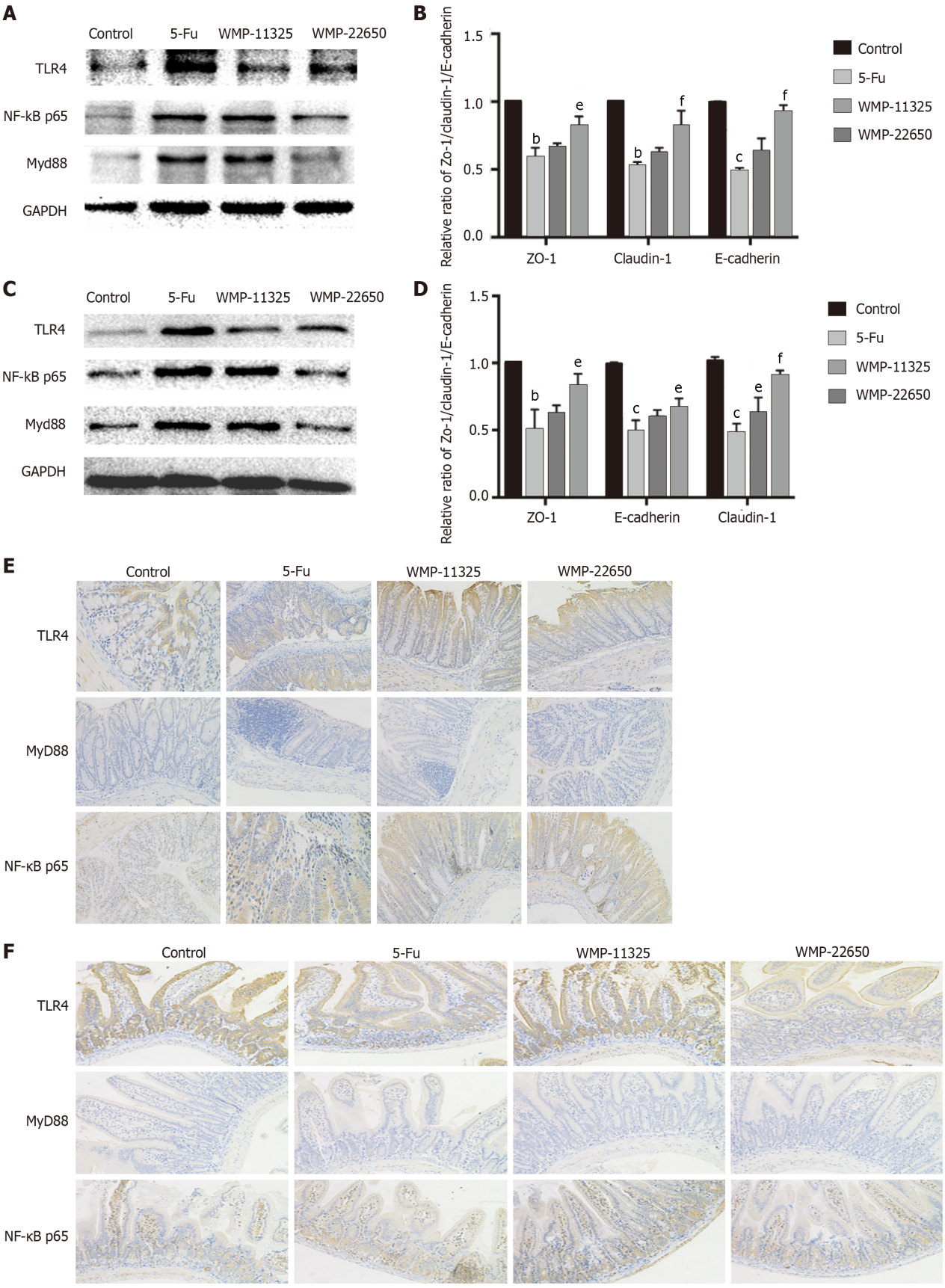


Figure 3 Effect of Wumei pills on expression of Toll-like receptor 4/myeloid differentiation factor 88/nuclear factor-κB pathway proteins as demonstrated by western blot and immunohistochemistry staining. A and B: Expression of Toll-like receptor 4 (TLR4), myeloid differentiation factor 88 (MyD88), and nuclear factor-κB (NF-κB) proteins in the jejunum; C and D: Expression of TLR4, MyD88, and NF-κB proteins in the colon; E: Expression of TLR4, MyD88, and NF-κB proteins in the colon; F: Expression of TLR4, MyD88, and NF-κB proteins in the jejunum. WMP: Wumei pills; TLR4: Toll-like receptor4; MyD88: Myeloid differentiation factor 88; NF-κB: Nuclear factor-κB; 5-Fu: 5-fluorouracil.

Effect of WMP on intestinal mucosal barrier

To evaluate the effects of WMP on the integrity of the intestinal mucosal barrier, we performed a FITC-dextran leakage experiment (Figures 4A and 4B). Dextran leakage was significantly greater in the 5-Fu group than in the control group ($P < 0.05$). WMP effectively prevented dextran leakage. The serum FITC-dextran concentration decreased in the WMP group, while the model group had significantly higher FITC-dextran concentration than the control group.

Effect of WMP on intestinal mucosal barrier proteins

Western blot analysis of the changes in tight junction proteins (ZO-1, claudin-1, and E-cadherin) after WMP administration (Figures 4C-F) showed that 5-Fu administration significantly decreased the expression of the ZO-1, Claudin-1, and E-cadherin proteins ($P < 0.05$, *vs* control group), which was reversed by the administration of 11325 mg/kg and 22650 mg/kg WMP. To further estimate the effect of WMP on tight junction proteins, their expression levels were assessed using immunofluorescence (Figures 4G-J). The results showed that 5-Fu significantly reduced the expression of ZO-1, claudin-1, and E-cadherin; however, WMP treatment significantly increased the expression of these proteins to levels similar to those in the normal group.

Effect of WMP on the synthesis and secretion of mucin-2

To determine whether WMP affects the synthesis of mucin-2 in the model mice, Alcian blue staining and mucin fluorescent staining were conducted, and the number of goblet cells (Figures 4K-N) was determined. The thickness of the mucus layer (concentration of mucin-2) in the 5-Fu group was lower than that in the control mice ($P < 0.01$), suggesting that the goblet cells of the mice in the 5-Fu group were severely damaged. However, there was a significant increase in the mucus layer thickness ($P < 0.05$, *vs* 5-Fu group) after treatment with 11325 mg/kg WMP and 22650 mg/kg WMP.

Changes in microbial composition and diversity

We next assessed the richness and diversity of the microbiota by alpha diversity analysis (Figures 5A and 5B). Four indices were used to analyze microbial diversity, including the Shannon, Ace, Chao, and Simpson indices. The 5-Fu group mice had the lowest Ace, Chao, and Shannon indexes, but with a higher Simpson index; the results also revealed that the richness and diversity of the microbiota community in mice of the 5-Fu group were remarkably reduced compared with those in the control group. These adverse effects were ameliorated after WMP administration. The Ace, Chao, and Shannon indices increased while the Simpson index decreased in the WMP groups.

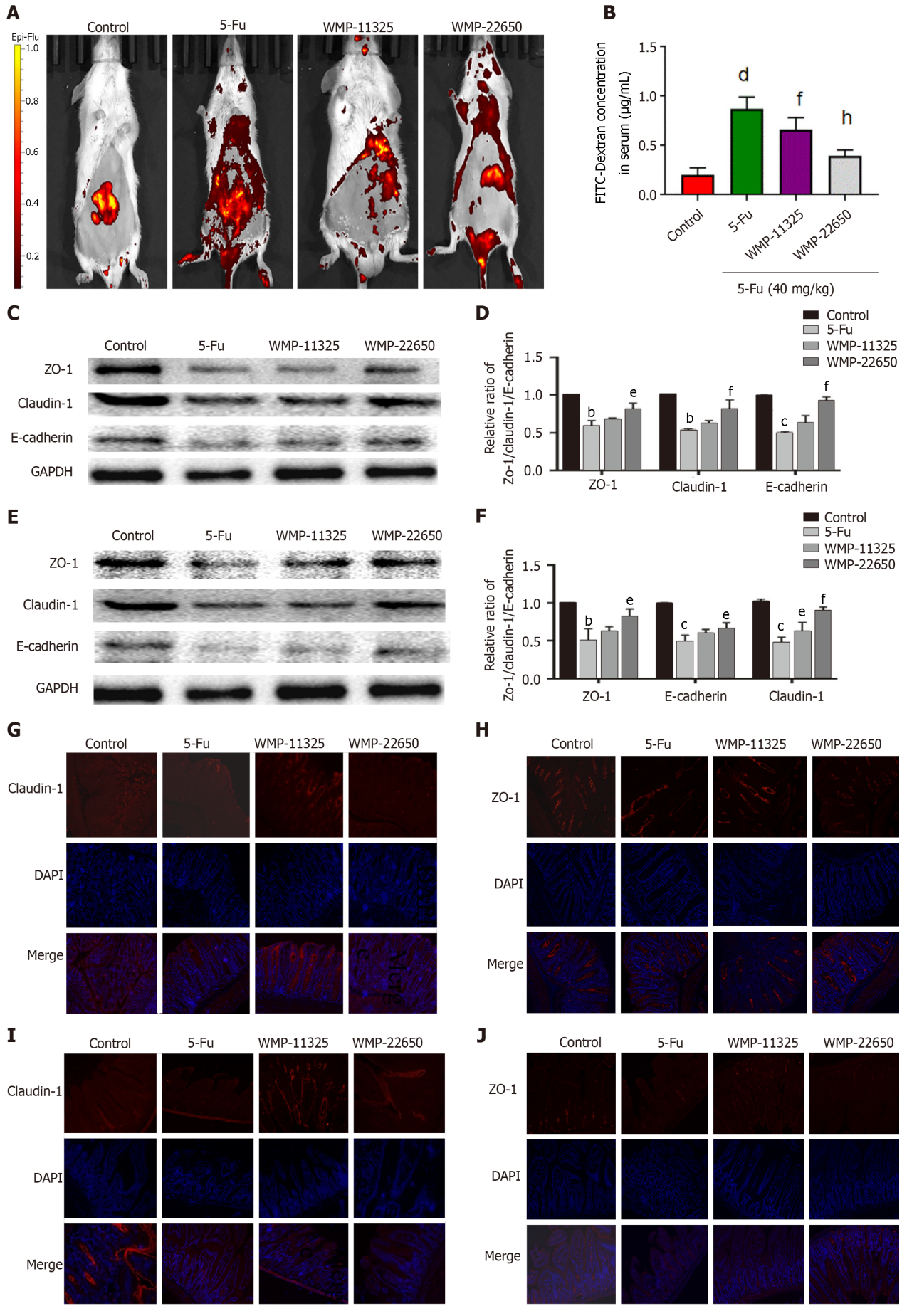
To evaluate the structure of the gut microbiota of each group, beta diversity analysis was performed and the results are presented in Figure 5C. Principal component analysis showed that compared to the other three groups, the structure of the gut microbial community in the 5-Fu group showed the highest diversity, whereas in the WMP groups, the diversity was reduced, and the values between those of the 5-Fu group and the 22650 mg/kg WMP group were much closer to those between the control group and the 11325 mg/kg group. These results indicate that WMP can increase microbial diversity and stabilize the microbial community.

Taxonomic analysis of microbiota community

The relative abundance of the classification units of the microbiota community is presented as a stacking histogram (Figures 5D-I). The Kruskal-Wallis test was used to analyze the difference in the microbial communities of the groups at different levels, and the results showed that at the phylum level, all samples contained *Bacteroidetes*, *Proteobacteria*, *Firmicutes*, *Verrucomicrobia*, *Campilobacterota*, *Patescibacteria*, *Desulfobacterota*, and *Actinobacteria*. The most abundant phyla were *Proteobacteria*, *Bacteroidetes*, and *Firmicutes*. 5-Fu led to a marked increase in the relative abundance of *Bacteroidetes* and *Campilobacterota*, but a decrease in that of *Firmicutes*. The abundance of *Firmicutes* increased and that of *Bacteroidetes* decreased in the 22650 mg/kg WMP group compared with the 5-Fu group (Figure 6A).

The data showed that *Bacilli*, *Bacteroidia*, and *Clostridia* were the major classes in the control mice, whereas the abundance of *Bacilli* was significantly decreased and those of *Bacteroidia* and *Clostridia* were increased in the 5-Fu group (Figure 6B). After WMP treatment, the number of *Bacilli* in the 11325 mg/kg WMP group was not significantly different, whereas in the 22650 mg/kg WMP group, a significant decrease was observed. *Bacteroidia* and *Clostridia* were decreased in the WMP group, but compared with the model group, *Bacteroidia* were decreased more significantly in the 22650 mg/kg WMP group, and *Clostridia* were decreased more significantly in the 11325 mg/kg WMP group.

At the order level, *Lactobacillales*, *Bacteroidales*, and *Lachnospirales* were the most abundant in the control mice, while *Staphylococci* were the most abundant in the 5-Fu mice (Figure 6C). At the family level, *Lactobacillaceae* and *Bacteroidaceae* were significantly decreased, and *Staphylococcales* and *Muribaculaceae* were increased after 5-Fu treatment. WMP administration effectively increased the abundance of *Lactobacillaceae* and *Bacteroidaceae* in the model mice and decreased the abundance of *Staphylococcales* and *Muribaculaceae* (Figure 6D). WMP increased the abundance of *Lactobacillaceae* in a dose-dependent manner. In the 11325 mg/kg WMP group, the abundance of *Bacteroidaceae* was significantly increased. A total of 20 genera were detected in all the samples (Figure 6E). We found that *Helicobacter* was the


A
Control
5-Fu
WMP-11325
WMP-22650
Epi-Flu
1.0
0.8
0.6
0.4
0.2
B
FITC-Dextran concentration in serum (μg/mL)
1.5
1.0
0.5
0.0
d
f
h
Control
5-Fu
WMP-11325
WMP-22650
5-Fu (40 mg/kg)
C
Control
5-Fu
WMP-11325
WMP-22650
ZO-1
Claudin-1
E-cadherin
GAPDH
D
Control
5-Fu
WMP-11325
WMP-22650
Relative ratio of Zo-1/claudin-1/E-cadherin
1.5
1.0
0.5
0.0
b
e
b
f
c
f
ZO-1
Claudin-1
E-cadherin
E
Control
5-Fu
WMP-11325
WMP-22650
ZO-1
Claudin-1
E-cadherin
GAPDH
F
Control
5-Fu
WMP-11325
WMP-22650
Relative ratio of Zo-1/claudin-1/E-cadherin
1.5
1.0
0.5
0.0
b
e
c
e
c
e
f
ZO-1
E-cadherin
Claudin-1
G
Control
5-Fu
WMP-11325
WMP-22650
Claudin-1
DAPI
Merge
H
Control
5-Fu
WMP-11325
WMP-22650
ZO-1
DAPI
Merge
I
Control
5-Fu
WMP-11325
WMP-22650
Claudin-1
DAPI
Merge
J
Control
5-Fu
WMP-11325
WMP-22650
ZO-1
DAPI
Merge

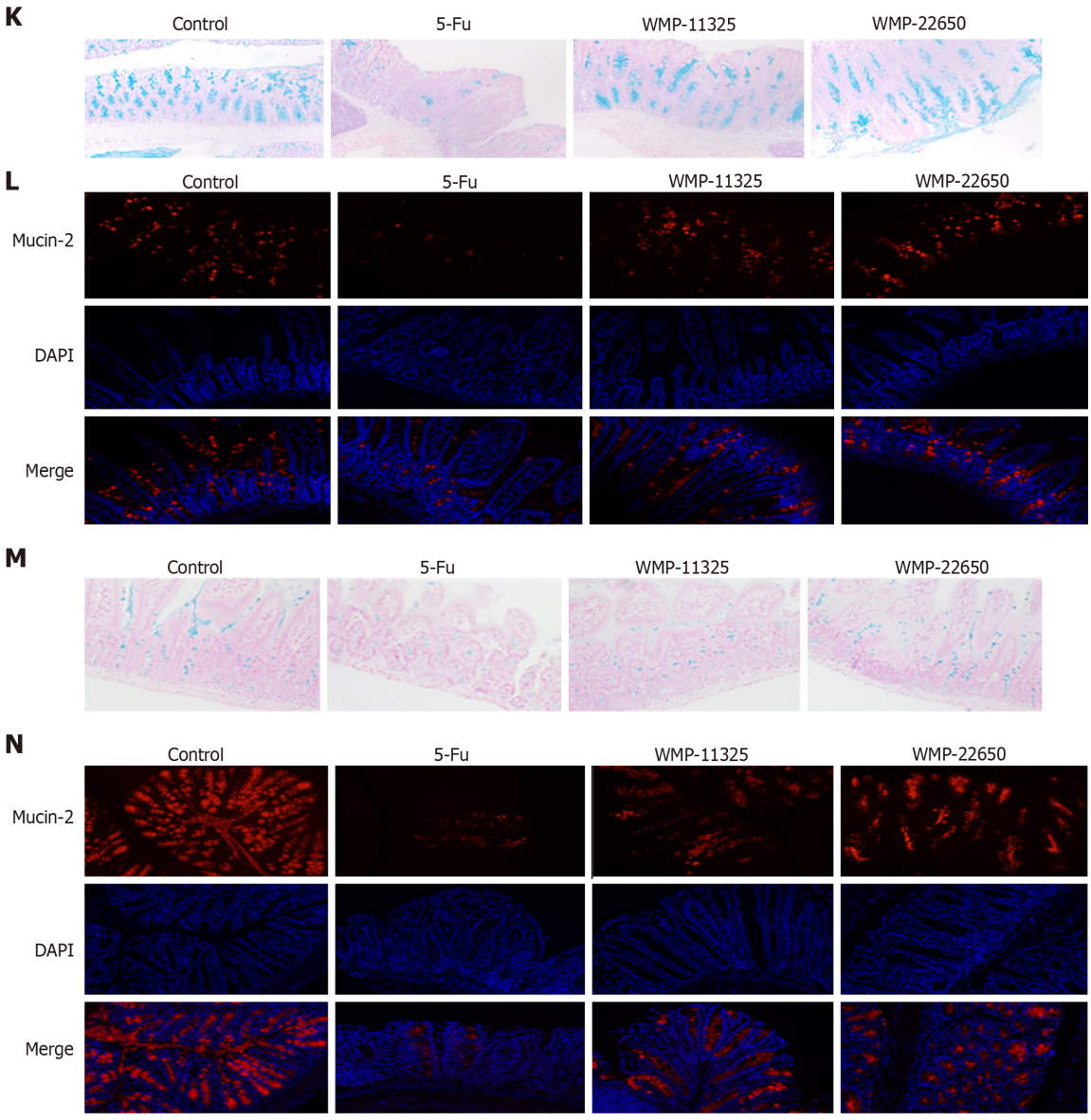
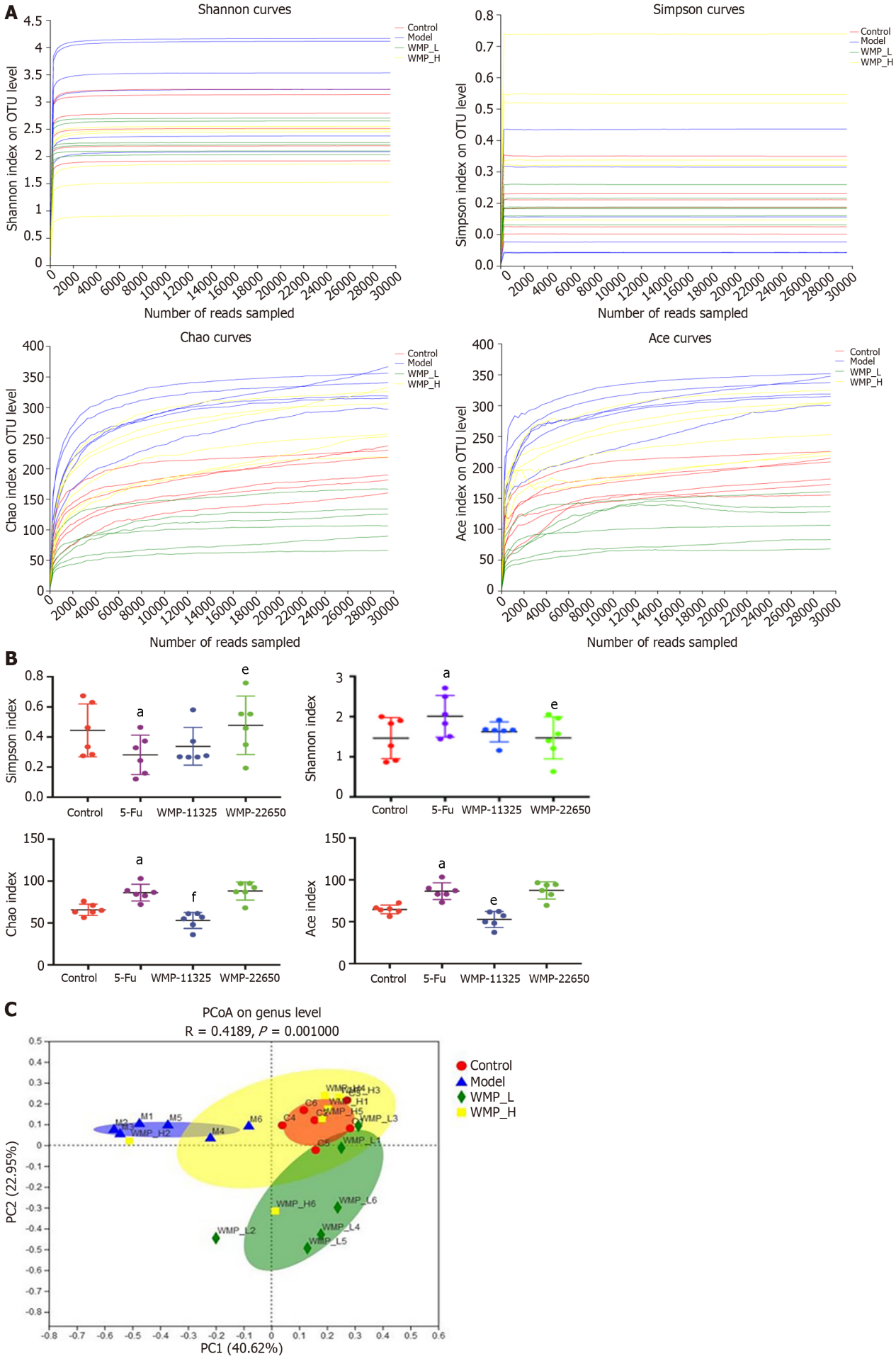


Figure 4 Effect of Wumei pills on intestinal leakage and expression of mucosal barrier proteins. A: Representative fluorescent images of mice assessed by IVIS. Excitation: 480 nm; emission: 520 nm; B: Concentration of dextran measured by mean fluorescence intensity of FITC in serum; C and D: Expression of zonula occludens-1 (ZO-1), E-cadherin, and claudin-1 proteins in the jejunum; E and F: Expression of ZO-1, E-cadherin, and claudin-1 proteins in the colon; G and H: Expression of ZO-1 and claudin-1 proteins in the jejunum; I and J: Expression of ZO-1 and claudin-1 proteins in the colon; K and L: Alcian blue staining and immunofluorescence staining for mucin-2 in the jejunum; M and N: Alcian blue staining and immunofluorescence staining for mucin-2 in the jejunum. Values represent the mean ± SEM. $^{b}P < 0.01$, $^{c}P < 0.001$, $^{d}P < 0.0001$ *vs* control group and $^{e}P < 0.05$, $^{f}P < 0.01$, $^{h}P < 0.0001$ *vs* 5-fluorouracil group. WMP: Wumei pills; ZO-1: Zonula occludens-1; 5-Fu: 5-fluorouracil.

characteristic bacterium in the 5-Fu group. In addition, mice in the 5-Fu group showed higher relative abundances of *Staphylococcales*, *Muribaculaceae*, and *Lachnospiraceae* than the control mice (Figure 6F).

LEfse and microbiota-cytokine correlation analysis

We used LEfse analysis to test the specific bacteria present in all groups. In view of the cladogram (Figure 6G), some specific bacteria were selected (Figure 6H) at the phylum level. Each group was tested for several specific bacteria. In general, *Lactobacillus*, *Verrucomicrobiota*, and *Akkermansia* were the three major genera associated with the control group, while *Helicobacter*, *Muribaculaceae*, and *Campilobacterota* were the major genera associated with the 5-Fu group. *Firmicutes* was significantly increased in the 22650 mg/kg WMP group due to the alleviation of intestinal mucositis in this group. However, in the 11325 mg/kg WMP group, *Bacteroidetes* was the main genus, which may be related to the LDA threshold or the concentration of WMP. In addition, Spearman analysis was used to analyze the association between microbiota and inflammatory cytokines (Figure 6I). The results indicated that the abundance of *Lactobacillus*, *Akkermansia*, *Escherichia coli*, and *Rumbutzia* negatively correlated with the expression of inflammatory cytokines, whereas *Prevotella*, *Isovaleribacter*, and *Helicobacter pylori* positively correlated with the expression of inflammatory cytokines.


A
Shannon curves
Shannon index on OTU level
Number of reads sampled
Control
Model
WMP_L
WMP_H
Simpson curves
Simpson index on OTU level
Chao curves
Chao index on OTU level
Ace curves
Ace index on OTU level
B
Simpson index
Shannon index
Chao index
Ace index
Control
5-Fu
WMP-11325
WMP-22650
C
PCoA on genus level
R = 0.4189, P = 0.001000
PC1 (40.62%)
PC2 (22.95%)

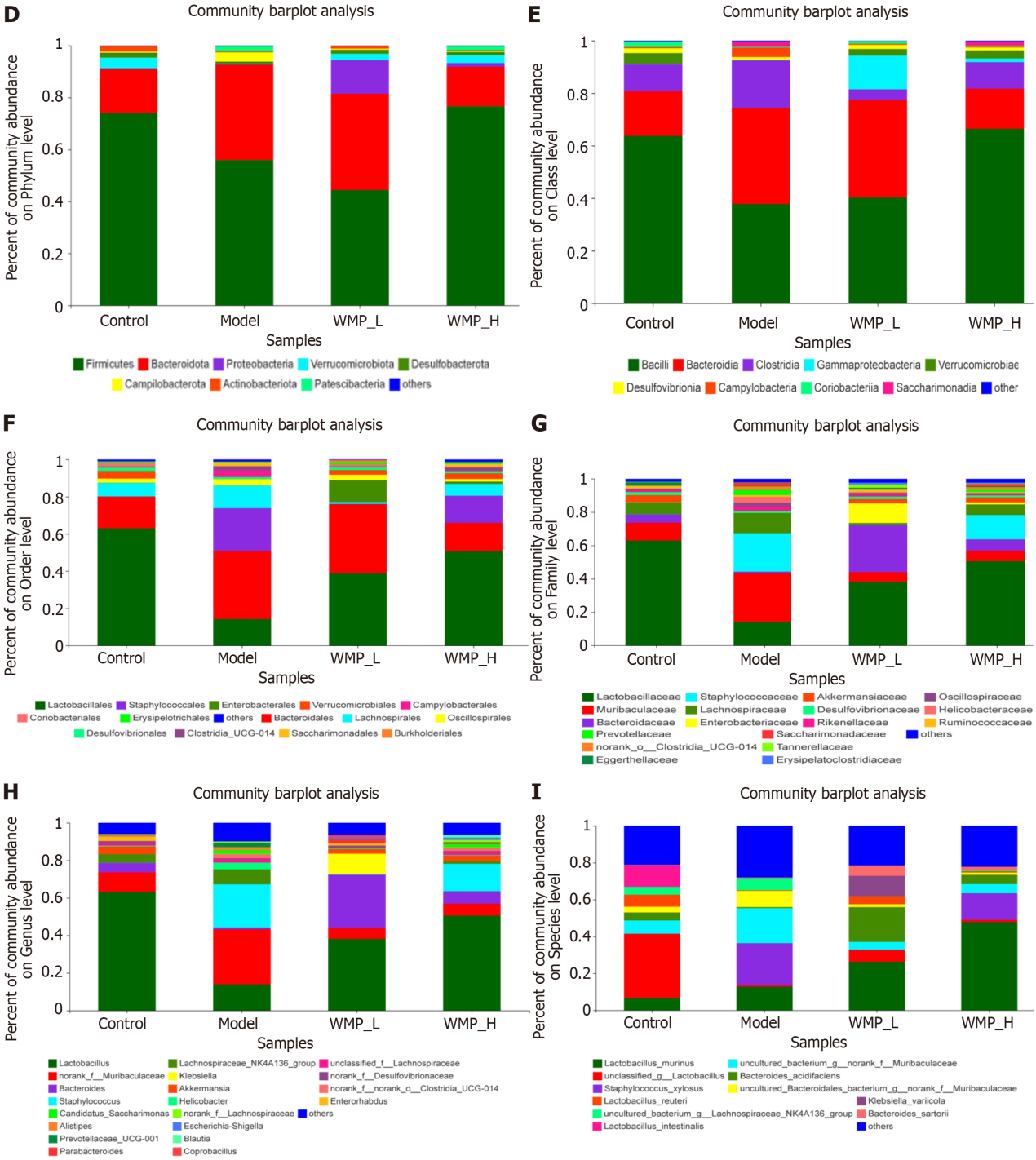
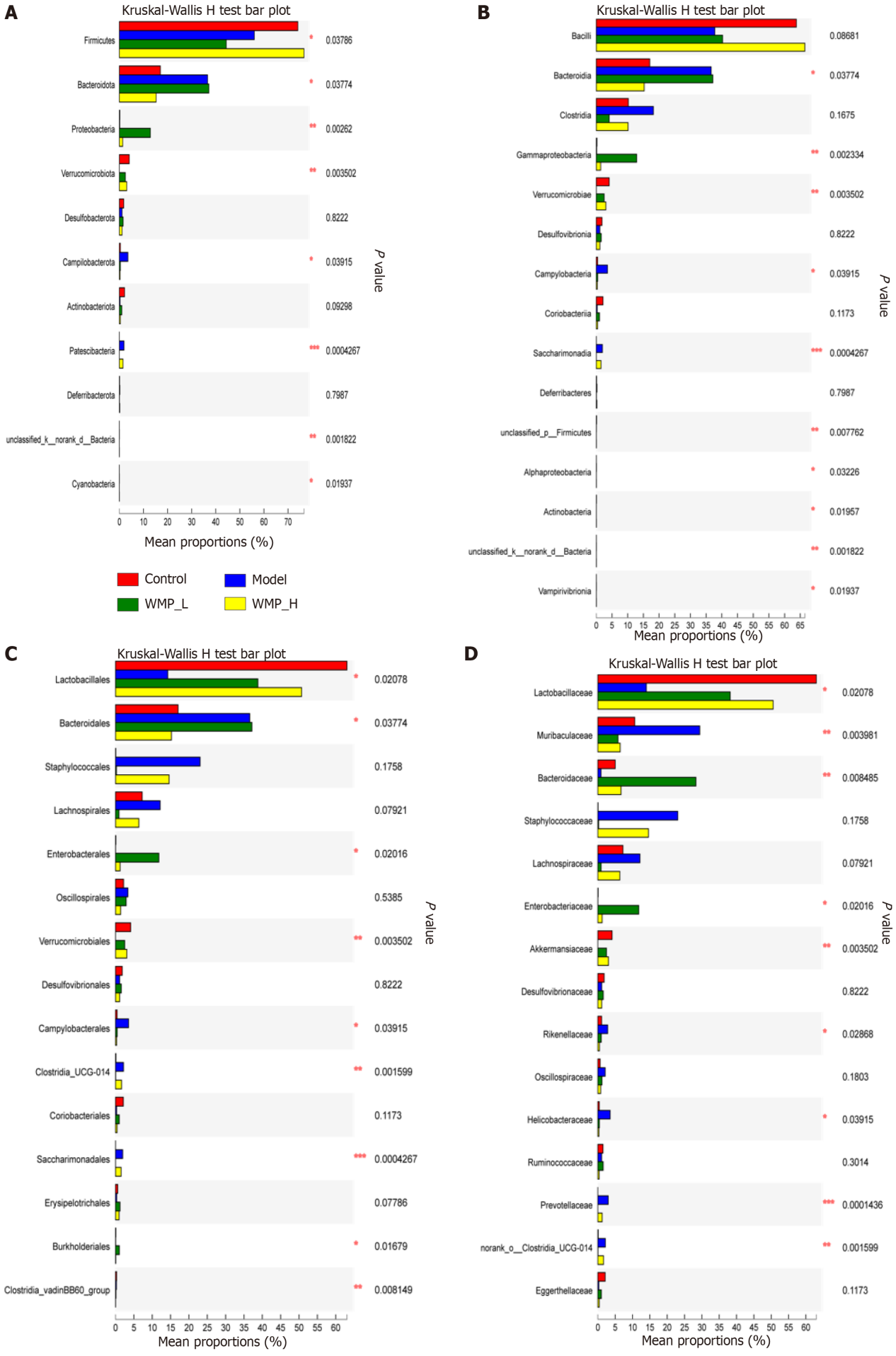


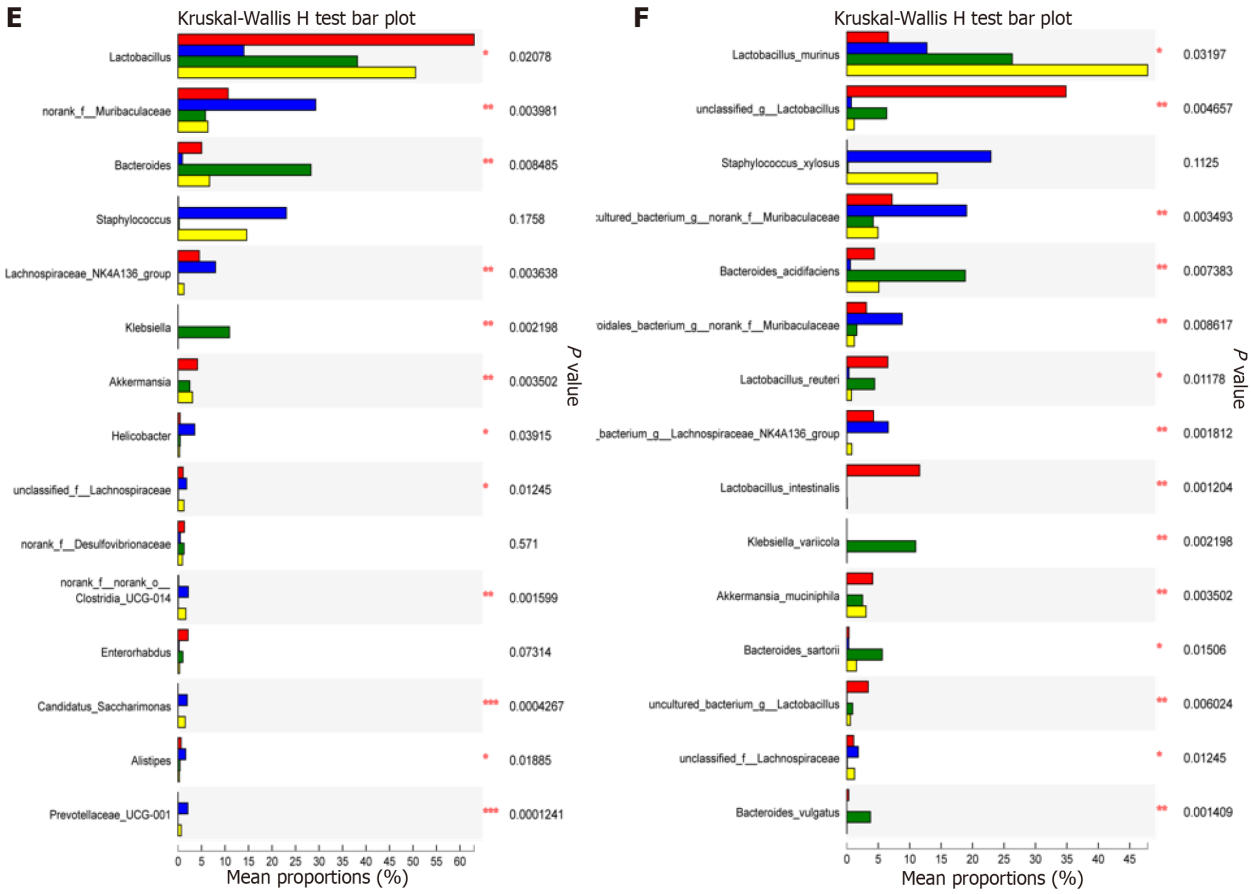
Figure 5 Microbial alpha, beta diversity, and taxonomy analysis. A: Dilution curve analysis; B: Alpha diversity (Shannon index, Simpson index, Ace index, and Chao index); C: Beta diversity; D-I: Taxonomy analysis of microbiota community. Values represent the mean ± SEM. $^{a}P < 0.05$ *vs* control group and $^{e}P < 0.05$, $^{f}P < 0.01$ *vs* 5-Fu group. WMP: Wumei pills; 5-Fu: 5-fluorouracil.

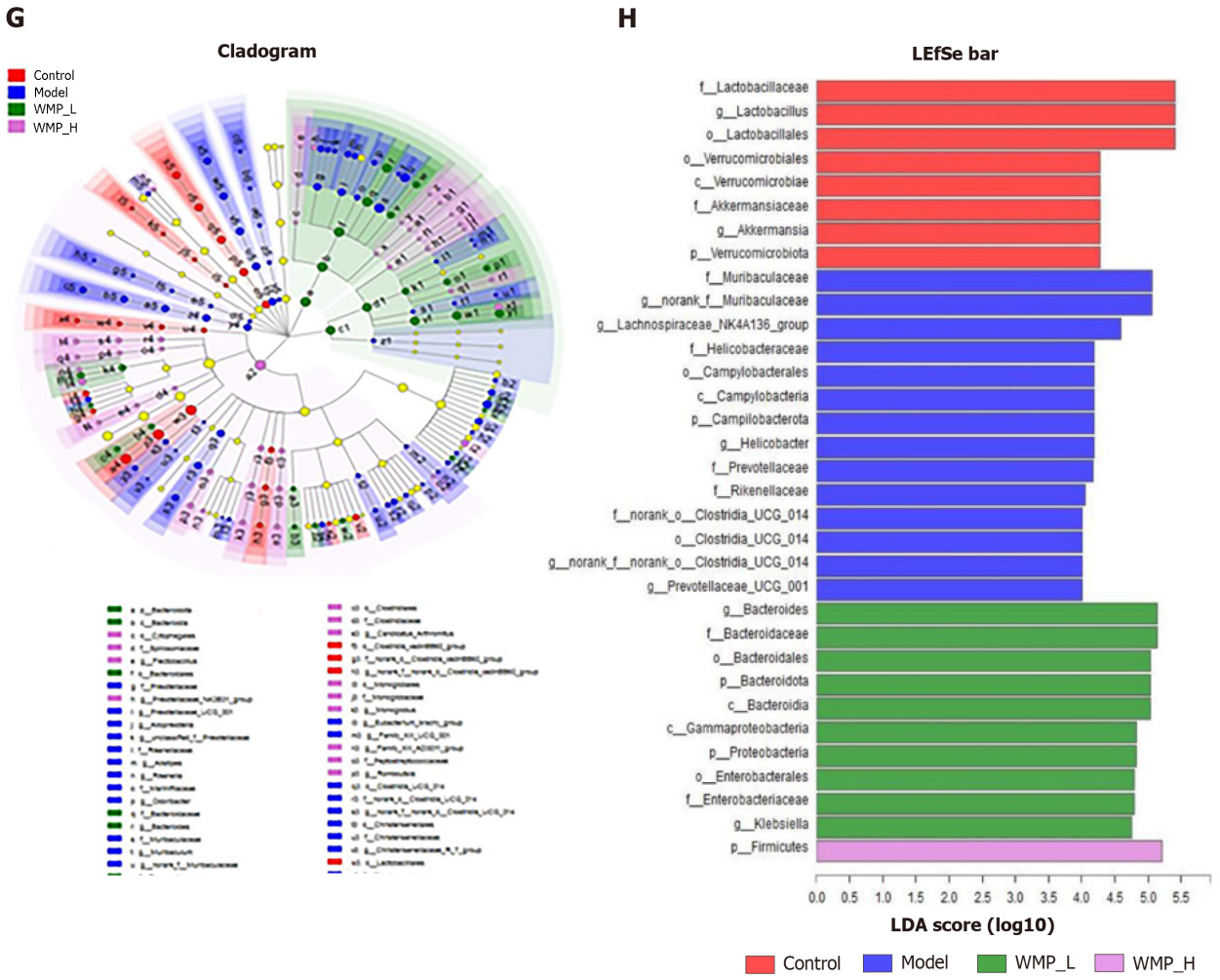
Taxonomic analysis was used to detect specific genera in all the samples (Figures 7A and 7B), which showed that the relative abundance of the probiotics *Lactobacillus* was reduced in the 5-Fu group compared with that in the control group. The abundance of pathogenic bacteria, such as *Muribaculaceae* and *Staphylococcales*, increased following the 5-Fu injection. WMP administration both increased the relative abundance of *Lactobacillus* and decreased the relative abundance of *Muribaculaceae* and *Staphylococcales*.

SCFAs in fecal samples

The levels of SCFA are closely related to the barrier function of the intestinal epithelium. To assess the effect of 5-Fu and WMP treatments on microbial metabolites, the levels of SCFAs, such as acetate, propionate, butyrate, isobutyrate, isobutyrate, 2-methyl-butyrate, and valerate, in the feces were determined (Figure 7C). The levels of acetate, propionate, butyrate, 2-methyl-butyrate, and valerate


A
Kruskal-Wallis H test bar plot
Firmicutes
Bacteroidota
Proteobacteria
Verrucomicrobiota
Desulfobacterota
Campilobacterota
Actinobacteriota
Patescibacteria
Deferribacterota
unclassified_k__norank_d__Bacteria
Cyanobacteria
0.03786
0.03774
0.00262
0.003502
0.8222
0.03915
0.09298
0.0004267
0.7987
0.001822
0.01937
P value
0 10 20 30 40 50 60 70
Mean proportions (%)
Control
Model
WMP_L
WMP_H
B
Kruskal-Wallis H test bar plot
Bacilli
Bacteroidia
Clostridia
Gammaproteobacteria
Verrucomicrobiae
Desulfovibrionia
Campylobacteria
Coriobacteriia
Saccharimonadia
Deferribacteres
unclassified_p__Firmicutes
Alphaproteobacteria
Actinobacteria
unclassified_k__norank_d__Bacteria
Vampirivibrionia
0.08681
0.03774
0.1675
0.002334
0.003502
0.8222
0.03915
0.1173
0.0004267
0.7987
0.007762
0.03226
0.01957
0.001822
0.01937
P value
0 5 10 15 20 25 30 35 40 45 50 55 60 65
Mean proportions (%)
C
Kruskal-Wallis H test bar plot
Lactobacillales
Bacteroidales
Staphylococcales
Lachnospirales
Enterobacterales
Oscillospirales
Verrucomicrobiales
Desulfovibrionales
Campylobacterales
Clostridia_UCG-014
Coriobacteriales
Saccharimonadales
Erysipelotrichales
Burkholderiales
Clostridia_vadinBB60_group
0.02078
0.03774
0.1758
0.07921
0.02016
0.5385
0.003502
0.8222
0.03915
0.001599
0.1173
0.0004267
0.07786
0.01679
0.008149
P value
0 5 10 15 20 25 30 35 40 45 50 55 60
Mean proportions (%)
D
Kruskal-Wallis H test bar plot
Lactobacillaceae
Muribaculaceae
Bacteroidaceae
Staphylococcaceae
Lachnospiraceae
Enterobacteriaceae
Akkermansiaceae
Desulfovibrionaceae
Rikenellaceae
Oscillospiraceae
Helicobacteraceae
Ruminococcaceae
Prevotellaceae
norank_o__Clostridia_UCG-014
Eggerthellaceae
0.02078
0.003981
0.008485
0.1758
0.07921
0.02016
0.003502
0.8222
0.02868
0.1803
0.03915
0.3014
0.0001436
0.001599
0.1173
P value
0 5 10 15 20 25 30 35 40 45 50 55 60
Mean proportions (%)


E
Kruskal-Wallis H test bar plot
Lactobacillus
norank_f__Muribaculaceae
Bacteroides
Staphylococcus
Lachnospiraceae_NK4A136_group
Klebsiella
Akkermansia
Helicobacter
unclassified_f__Lachnospiraceae
norank_f__Desulfovibrionaceae
norank_f__norank_o__Clostridia_UCG-014
Enterorhabdus
Candidatus_Saccharimonas
Alistipes
Prevotellaceae_UCG-001
0.02078
0.003981
0.008485
0.1758
0.003638
0.002198
0.003502
0.03915
0.01245
0.571
0.001599
0.07314
0.0004267
0.01885
0.0001241
P value
Mean proportions (%)
F
Kruskal-Wallis H test bar plot
Lactobacillus_murinus
unclassified_g__Lactobacillus
Staphylococcus_xylosus
Bacteroides_acidifaciens
Lactobacillus_reuteri
Lactobacillus_intestinalis
Klebsiella_variicola
Akkermansia_muciniphila
Bacteroides_sartorii
uncultured_bacterium_g__Lactobacillus
unclassified_f__Lachnospiraceae
Bacteroides_vulgatus
0.03197
0.004657
0.1125
0.003493
0.007383
0.008617
0.01178
0.001812
0.001204
0.002198
0.003502
0.01506
0.006024
0.01245
0.001409
P value
Mean proportions (%)


G
Cladogram
Control
Model
WMP_L
WMP_H
H
LEfSe bar
f__Lactobacillaceae
g__Lactobacillus
o__Lactobacillales
o__Verrucomicrobiales
c__Verrucomicrobiae
f__Akkermansiaceae
g__Akkermansia
p__Verrucomicrobiota
f__Muribaculaceae
g__norank_f__Muribaculaceae
g__Lachnospiraceae_NK4A136_group
f__Helicobacteraceae
o__Campylobacterales
c__Campylobacteria
p__Campilobacterota
g__Helicobacter
f__Prevotellaceae
f__Rikenellaceae
f__norank_o__Clostridia_UCG_014
o__Clostridia_UCG_014
g__norank_f__norank_o__Clostridia_UCG_014
g__Prevotellaceae_UCG_001
g__Bacteroides
f__Bacteroidaceae
o__Bacteroidales
p__Bacteroidota
c__Bacteroidia
c__Gammaproteobacteria
p__Proteobacteria
o__Enterobacterales
f__Enterobacteriaceae
g__Klebsiella
p__Firmicutes
LDA score (log10)
Control
Model
WMP_L
WMP_H

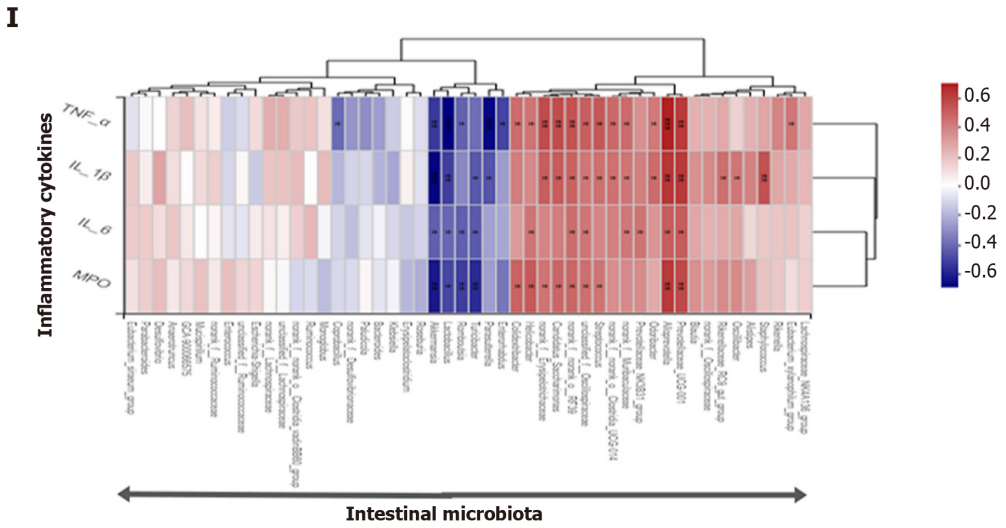


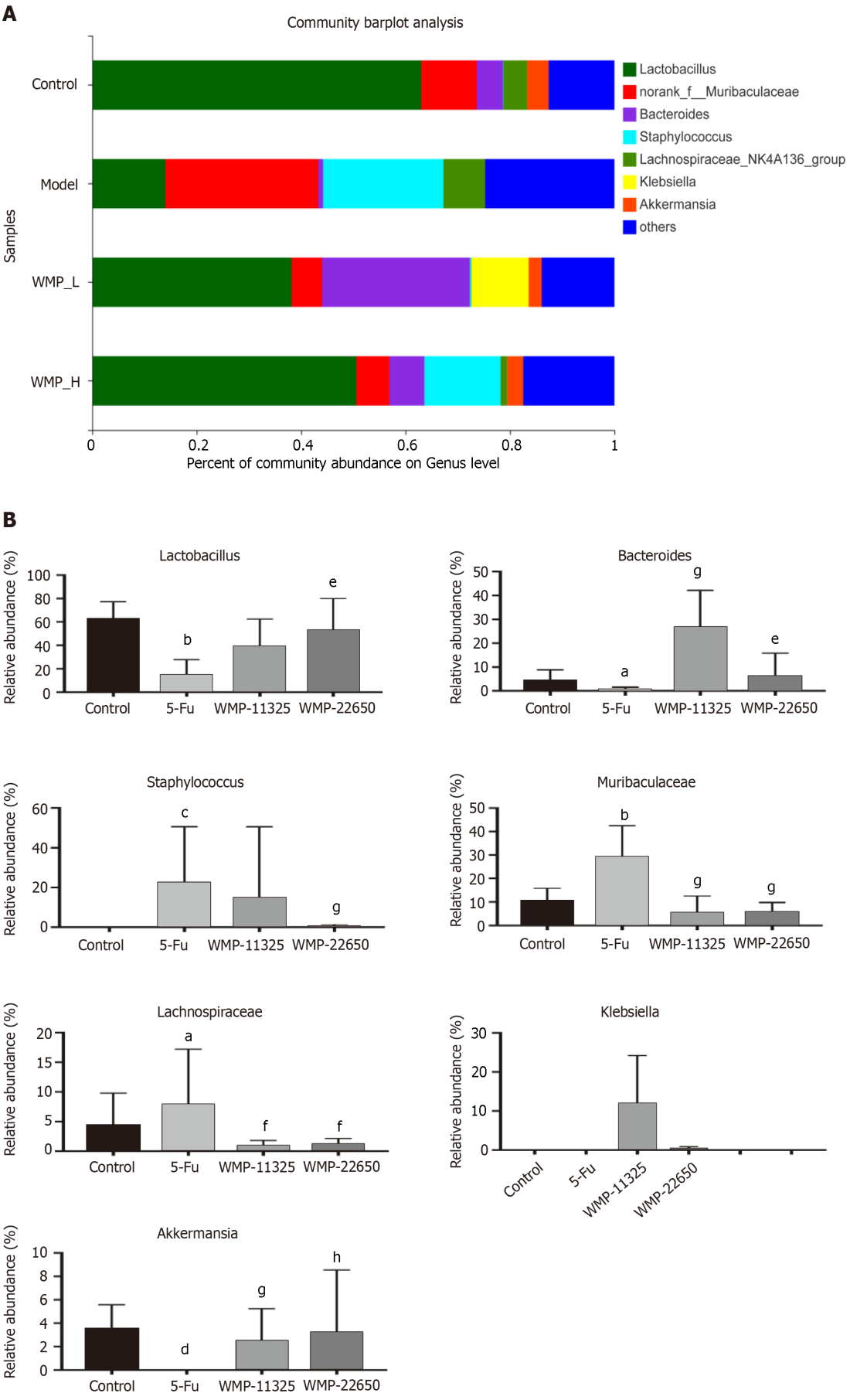
Figure 6 Kruskal-Wallis analysis of different bacterial groups, LEfse analysis, and microbiota-cytokine correlation. A: Phylum level; B: Class level; C: Order level; D: Family level; E: Genus level; F: Species level; G: Overall exhibition of LEfse analysis by cladogram; H: LDA scores of the specific enriched genera in each group; I: Spearman analysis of microbiota-cytokine correlation. WMP: Wumei pills; TNF-α: Tumor necrosis factor-α; IL-6: Interleukin-6; IL-1β: Interleukin-1β; MPO: Myeloperoxidase.

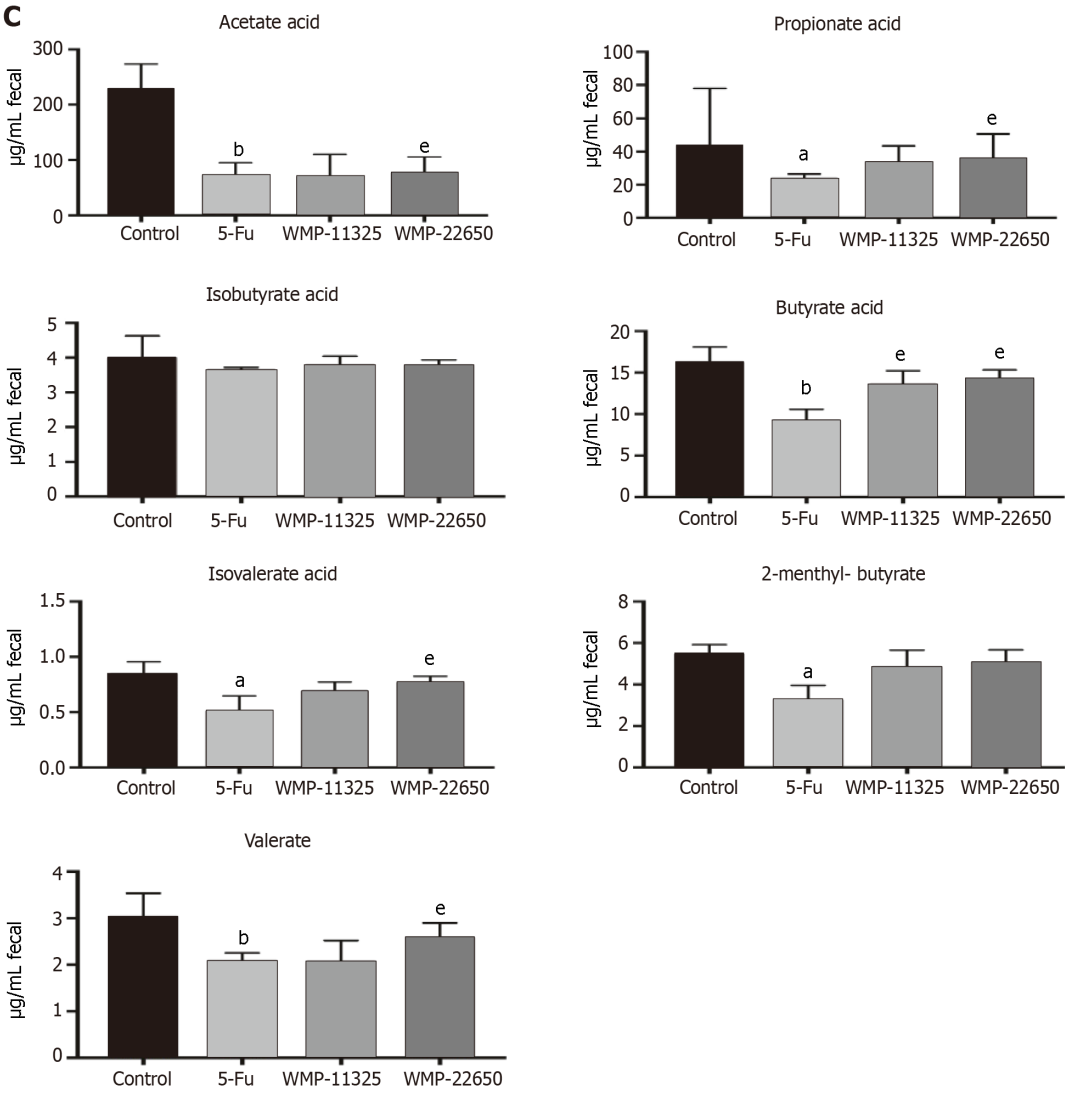
markedly decreased in the feces of mice treated with 5-Fu, compared with those in the feces of the control mice ($P < 0.05$). WMP treatment significantly increased the levels of acetate, propionate, and butyrate, but had no significant effect on the levels of isobutyrate and isovalerate. In addition, the results showed that WMP restored the abundance of *Lactobacillaceae*, which is the main family that produces SCFA (Figure 7D).

DISCUSSION

Traditional Chinese medicine prescriptions are an important source of new drugs for the prevention and treatment of gastrointestinal toxicity caused by chemotherapy drugs[25]. Drug interaction is considered to play a vital role in the combination of traditional Chinese medicine and modern medicine [26]. WMP originated from the Treatise on Exogenous Febrile Disease (200-210 AD), comprising ten herbs: WM, DG, XX, GZ, FZ, HB, HJ, RS, GJ, and HL. According to previous reports, WMP has various pharmacological effects on gastrointestinal tract diseases, such as ulcerative colitis, immune enteritis, and irritable bowel syndrome[19-21]. In this study, we found that WMP effectively improved the weight, food intake, spleen weight, and diarrhea scores of mice with intestinal mucositis. In addition, WMP significantly reduced 5-Fu-induced morphological damage to the jejunum and colon, which manifested as the shortening of villi height, destruction of crypts, and inflammatory cell infiltration. This study explored the protective effect of WMP and its associated mechanism on intestinal mucosal damage caused by 5-Fu.

The mechanism of the pathogenesis of intestinal mucositis is complicated. Inflammation, intestinal barrier dysfunction, and imbalance of the intestinal flora can cause mucosal damage[27-29]. Inflammation is involved in intestinal mucositis, and TLRs play a key role in regulating the intestinal epithelial barrier and innate immunity. TLR4 induces NF-κB activation, thereby controlling the expression of inflammatory cytokine genes through the Toll/IL-1R domain with the specific adaptor protein, MyD88 [30-32]. NF-κB is a key regulator of innate and adaptive immune responses, and is involved in the regulation of inflammation and cell cycle[33]. After the treatment with 5-Fu, the NF-κB pathway was activated, leading to the release of inflammatory factors. Moreover, the secretion of pro-inflammatory cytokines (such as TNF-α) increased and caused the infiltration of granulocytes and promoted intestinal barrier damage. In addition, it has been demonstrated that MPO, a marker of neutrophil infiltration, participates in the inflammatory process by causing oxidation in the inflammatory area[34]. Changes in the levels of inflammatory cytokines have been reported to be regulated by NF-κB p65[35]. NF-κB is a universal transcription factor involved in the inflammatory response, and studies have confirmed that it plays an important role in the pathological mechanism of CIM[36,37]. Therefore, the inhibition of the NF-κB signaling pathway may be an important factor in reducing intestinal mucosal damage. IL-1β, IL-6, and TNF-α are vital pro-inflammatory cytokines that widely affect the inflammatory process[38-40]. IL-1β and TNF-α have been reported to exhibit a synergistic effect on the activation of the NF-κB pathway and inflammation[41]. IL-6 exhibits a range of biological effects, especially those related to the pathogenesis of inflammatory diseases[42]. In addition, under inflammatory conditions, the protein


A
Community barplot analysis
Control
Model
WMP_L
WMP_H
Samples
Lactobacillus
norank_f__Muribaculaceae
Bacteroides
Staphylococcus
Lachnospiraceae_NK4A136_group
Klebsiella
Akkermansia
others
0
0.2
0.4
0.6
0.8
1
Percent of community abundance on Genus level
B
Lactobacillus
Bacteroides
Staphylococcus
Muribaculaceae
Lachnospiraceae
Klebsiella
Akkermansia
Relative abundance (%)
Control
5-Fu
WMP-11325
WMP-22650



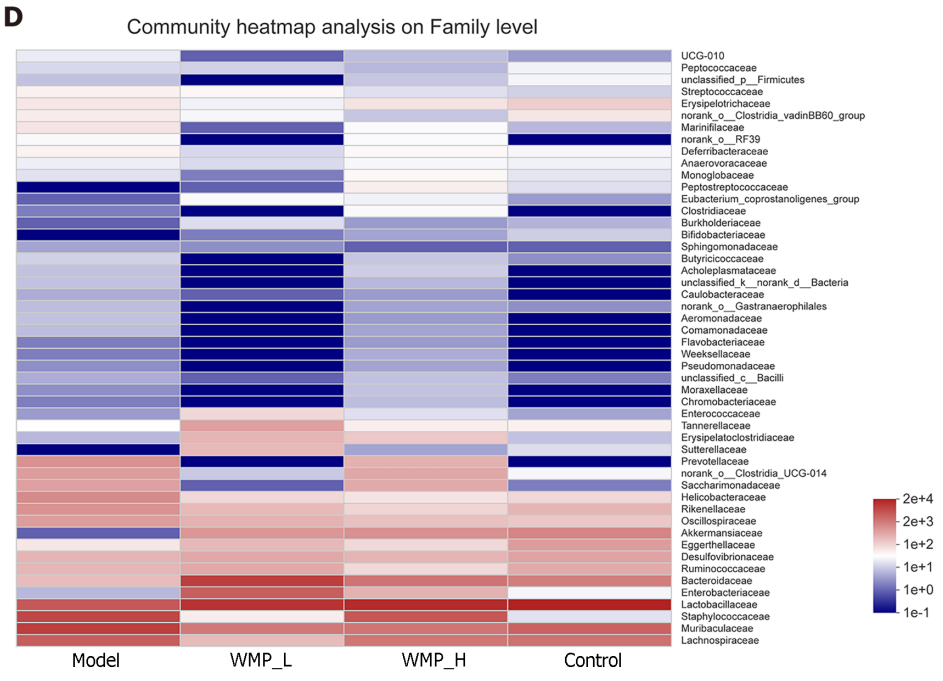


Figure 7 Effect of Wumei pills on taxonomy analysis of specific genera, the contents of short-chain fatty acids in feces, and heatmap of gut microbiota. A: Relative abundance of specific genera at each sample; B: Relative abundance of *Lactobacillus*, *Bacteroides*, *Staphylococcus*, *Muribaculaceae*,

Lachnospiraceae, *Klebslella*, and *Akkermansla* in each group; C: Effect of Wumei pills on the contents of short-chain fatty acids in feces; D: Heatmap of gut microbiota (family level). Values represent the mean ± SEM. [a]*P* < 0.05, [b]*P* < 0.01, [c]*P* < 0.001 and [d]*P* < 0.0001, compared with the normal group; [e]*P* < 0.05, [f]*P* < 0.01, [g]*P* < 0.001, and [h]*P* < 0.0001, compared with the 5-Fu group. WMP: Wumei pills; 5-Fu: 5-fluorouracil.

level and activity of MPO increase[43]. The results of this study also revealed that 5-Fu induced an increase in the expression of proteins associated with the TLR4-MyD88 signaling pathway and inflammatory cytokines, which was significantly inhibited by WMP. WMP significantly decreased the expression levels of TNF-α, IL-1β, IL-6, and MPO in mice with intestinal mucositis and inhibited the increase in TLR4 levels induced by 5-Fu. The expression of the downstream proteins, including MyD88 and NF-κB, was also significantly downregulated. The inhibitory effect of WMP on the TLR4-MyD88 signaling pathway suggests that this pathway may be involved in the alleviation of intestinal mucositis by WMP.

In addition to inflammation, damage to the intestinal epithelial barrier is one of the mechanisms of CIM. The dysfunction of the integrity of the intestinal mucosal barrier (mainly the tight junctions, mucus layer, and intestinal epithelial cells) plays an significant role in the pathogenesis of chemotherapy-induced intestinal toxicity and related diarrhea[44]. Tight junctions maintain the structure and function of the intestinal mucosal barrier by sealing the paracellular space of the intestinal epithelium; this is destroyed under inflammatory conditions[45,46]. Tight junctions comprise core proteins, which are the most adhesive junction complexes in mammalian epithelial cells. The lack of tight junction increases intestinal permeability and contributes to the development of intestinal inflammation[47,48]. Therefore, through the FITC-dextran leakage experiment, we found that WMP reduced intestinal penetration in mice treated with 5-Fu. Furthermore, through western blot and immunofluorescence, we found that the tight junction protein (ZO-1, claudin-1, and E-cadherin) expression levels in the 5-Fu group were significantly reduced and that WMP was able to reverse these changes and increase the expression levels of the tight junction proteins. This effect was more significant in the 22650 mg/kg WMP group than in the 11325 mg/kg group.

In addition to the epithelial barrier, a mucus barrier is also present. The mucus barrier is composed of a hydrated gel covering the surface of the epithelial mucosa, which is formed by the mucin synthesized and secreted by special epithelial cells (such as intestinal goblet cells). This forms a barrier that prevents the direct contact between the large particles (including most bacteria) and the epithelial cell layer[49]. For instance, unlike normal mice, mucin-2-knockout mice developed severe colitis following exposure to harmful stimuli[49,50]. In addition, these mice developed colitis at the same time, and the microbiota was detected in the deep sterile intestinal crypts. By using Alcian blue staining and immunofluorescence to analyze the synthesis and secretion of mucin-2 in goblet cells, we found that the level of mucin-2 synthesis or secretion in goblet cells in the 5-Fu group was lower, indicating that 5-Fu had no serious damage to goblet cells. After the intragastric administration of WMP, we observed a gradual recovery of the biological function of goblet cells, an increase in the synthesis of mucin-2, and an improvement of the intestinal mucosal barrier.

An increasing number of studies have shown that the intestinal flora plays a key role in intestinal inflammation-related diseases, such as antibiotic-related diarrhea, irritable bowel syndrome, radiotherapy, and chemotherapy-related diarrhea[51-54]. The dynamic balance of the intestinal flora is a key factor affecting gastrointestinal health, and gastrointestinal diseases disrupt the dynamic balance of the intestinal flora. Some studies have shown that WMP or its active ingredients can affect the inflammatory response by regulating the intestinal flora[3,22,55]. However, there is no direct evidence proving that WMP can relieve 5-Fu-induced intestinal mucositis by influencing the intestinal flora. Therefore, we used 16S rDNA amplification sequencing to analyze the composition and abundance of the intestinal flora in stool samples. According to the analysis of microbial diversity, the intestinal flora of mice in the 5-Fu group changed significantly. After WMP treatment, the intestinal flora of mice in the 5-Fu group gradually tended towards healthy intestinal microbes, and the abundance of lactobacilli was significantly increased. The 22650 mg/kg WMP group had a better effect. In addition, the intestinal flora can regulate the changes in inflammatory cytokines[56], which is consistent with our results. The composition of the intestinal flora in the WMP group negatively correlated with inflammatory factors, while that in the 5-Fu group showed the opposite trend.

Bacteroides, *Lactobacillus*, *Staphylococcus*, *Muribculaceae*, *Helicobacter pylori*, and *Parabacteria* play an important role in the development of intestinal mucositis. *Lactobacillus* can enhance TJ protein expression, inhibit NF-κB activation, and reduce intestinal permeability[57-60]. *Bacteroides*, *Staphylococcus*, *Muribculaceae*, *Helicobacter pylori*, and *Parabacteria* are generally considered pathogenic or conditional pathogens. For instance, elevated levels of *Parabacteria* and *Bacteroides* can induce colitis in mice[61], and *Helicobacter pylori* infection can cause peptic ulcer disease and gastric cancer[62]. Methicillin-resistant *Staphylococcus aureus* often colonizes the rectum and is associated with necrotizing enterocolitis[63,64]. Bacteroides S24-7 (*Muribaculaceae*) is the dominant bacterial family of Bacteroides, and its increase is closely related to inflammatory enteritis[65]. In this study, 5-Fu administration activated NF-κB, inhibited tight junction protein expression, and increased inflammatory cytokines and intestinal permeability. The relative abundance of *Lactobacilli* in the 5-Fu group markedly dropped.

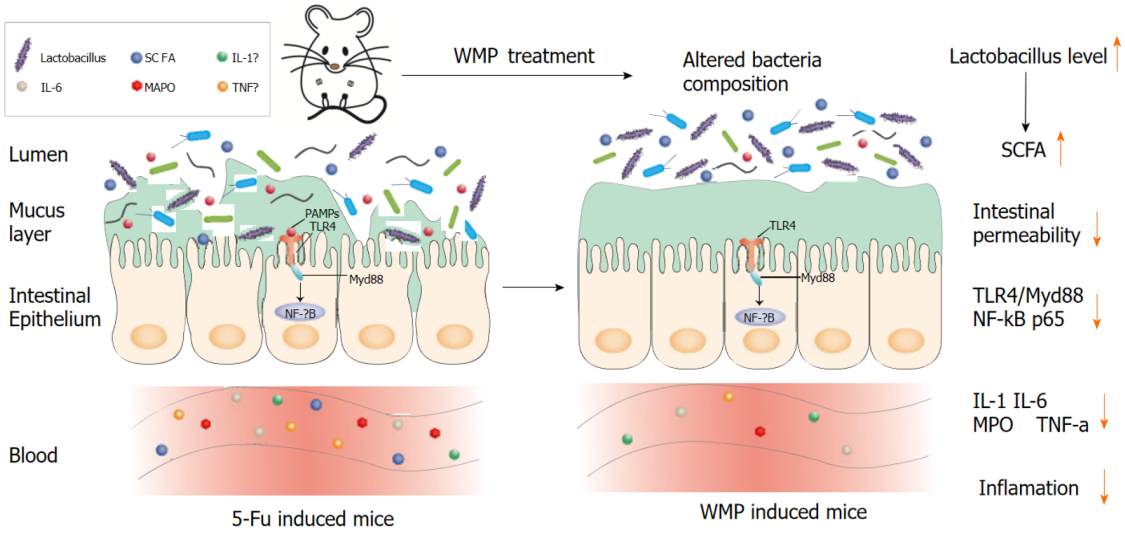


Figure 8 Schematic illustration of mechanisms for Wumei pills treatment in 5-fluorouracil-induced intestinal mucositis. WMP: Wumei pills; TNF-α: Tumor necrosis factor-α; IL-6: Interleukin-6; IL-1β: Interleukin-1β; MPO: Myeloperoxidase; SCFAs: Short-chain fatty acids; TLR4: Toll-like receptor 4; MyD88: Myeloid differentiation factor 88; NF-κB: Nuclear factor-κB; 5-Fu: 5-fluorouracil.

However, 22650 mg/kg WMP exerted a stronger effect than 11325 mg/kg WMP on the relative abundance of *Lactobacilli*. SCFA-producing bacteria have beneficial effects on the host by inhibiting inflammation, providing nutrition for colon cells, and protecting the intestinal mucosa[66]. As an SCFA-producing bacterium, *Lactobacillus* can lower the pH of the host colonic cells and inhibit the growth of pathogenic bacteria[67]. Therefore, this study preliminarily confirmed that WMP can change the composition and abundance of the intestinal flora and exert anti-inflammatory effects.

The functions of the intestinal microflora, including immune regulation, nutritional support of the colonic epithelium, and maintenance of stable barrier function, are closely related to SCFA. A previous study reported the involvement of metabolites in the development of intestinal mucositis[68]. It has been reported that SCFA protect the intestinal mucosa by reducing the level of inflammation[69]. SCFA can be absorbed by fluids that cause sodium decomposition through a process independent of circulating AMP. Therefore, the reduction in SCFA is related to diarrhea[70]. Butyrate reduces diarrhea by enhancing intestinal permeability[71]. In 5-Fu-induced diarrhea, the production of SCFAs was significantly reduced. Previous studies have found that WMP can significantly increase the abundance of butyric acid-producing bacteria (*Firmicutes*) in 5-Fu treated mice. Therefore, the results of this study were consistent with those of previous studies. WMP significantly changed the fecal SCFA content in 5-Fu treated mice. It increased the concentrations of acetic acid, propionic acid, and butyric acid, indicating that WMP can improve the production of SCFA and inhibit the progression of chemotherapy-induced intestinal mucosal inflammation.

CONCLUSION

In summary, our results demonstrate the beneficial effects and the associated mechanisms of WMP against CIM in mice (Figure 8). WMP activates the NF-κB pathway by restraining p65 translocation from the cytoplasm to the nucleus and inhibiting the expression of TLR4/MyD88/NF-κB proteins, resulting in the downregulation of expression of the inflammatory factors IL-1β, IL-6, MPO, and TNF-α, and increased expression of tight junction proteins (ZO-1, claudin-1, E-cadherin, and mucin-2). Moreover, WMP restores the diversity and abundance of the intestinal flora. WMP increases the relative abundance of *Lactobacilli* but decreases that of *Bacteroides*, *Helicobacter*, and *Parabacteroides*. Although further fecal bacterial transplantation or the downstream-mediated potential mechanisms of specific bacteria are worth exploring, WMP has potential therapeutic effects against CIM.

ARTICLE HIGHLIGHTS

Research background

Radiotherapy and chemotherapy can kill tumor cells and improve the survival rate of cancer patients. However, they can also damage normal cells and cause serious intestinal toxicity, leading to gastrointestinal mucositis. Traditional Chinese medicine is effective in improving the side effects of

chemotherapy. Wumei pills (WMP) is a classic prescription in Treatise on Febrile Diseases. It has a significant effect on chronic diarrhea and other gastrointestinal diseases, but it is not clear if it has an effect on chemotherapy-induced intestinal mucositis (CIM).

Research motivation

To explore the potential mechanism of WMP in the treatment of CIM using experimental research.

Research objectives

Exploring the mechanism of WMP to alleviate chemotherapy-induced intestinal mucosal inflammation may be to regulate the intestinal flora, thereby inhibiting the activation of downstream inflammatory signaling pathways and exerting anti-inflammatory effects.

Research methods

We used an intraperitoneal injection of 5-fluorouracil (5-Fu) to establish a mouse model of CIM and oral gavage of WMP decoction (11325 and 22650 mg/kg) to evaluate the efficacy of WMP in CIM. We evaluated the effect of WMP on CIM by observing the general conditions of mice (body weight, food intake, spleen weight, diarrhea score, and hematoxylin and eosin staining). To explore the potential mechanism of WMP in CIM, the expression of the inflammatory factors tumor necrosis factor-α (TNF-α), interleukin- 6 (IL-6), IL-1β, and myeloperoxidase (MPO), Toll-like receptor 4/myeloid differentiation-factor 88/nuclear factor-κB (TLR4/MyD88/NF-κB) signaling pathway proteins, and tight junction proteins [zonula occludens-1 (ZO-1), claudin-1, E-cadherin, and mucin-2] was determined. Furthermore, intestinal permeability, intestinal flora, and the levels of short-chain fatty acids (SCFA) were also assessed in the mice.

Research results

WMP effectively improved the body weight, spleen weight, food intake, diarrhea score, and inflammatory pathological status of mice with intestinal mucositis, which preliminarily confirmed the efficacy of WMP in CIM. Further experiments showed that WMP did not only reduce the levels of TNF-α, IL-1β, IL-6, and MPO, and inhibited the expression of TLR4/MyD88/NF-κB, but also repaired the integrity of the mucosal barrier of mice, regulated the intestinal flora, and increased the levels of SCFA (such as butyric acid).

Research conclusions

In summary, our results demonstrate the beneficial effects of WMP against CIM in mice and the associated mechanisms. WMP activates the NF-κB pathway by restraining p65 translocation from the cytoplasm to the nucleus and inhibiting the expression of TLR4/MyD88/NF-κB proteins, resulting in the downregulated expression of inflammatory factors (IL-1β, IL-6, MPO, and TNF-α) and increased expression of tight junction proteins (ZO-1, claudin-1, E-cadherin, and mucin-2). Moreover, WMP restores the diversity and abundance of the intestinal flora. In particular, WMP increases the relative abundance of *Lactobacilli* but decreases the relative abundance of *Bacteroides*, *Helicobacter*, and *Parabacteroides*.

Research perspectives

WMP has potential therapeutic effects against CIM, and further fecal bacterial transplantation or the downstream-mediated potential mechanisms of specific bacteria are worth exploring.

ACKNOWLEDGEMENTS

We would like to thank all the team members for their assistance during data collection and compiling the manuscript. We are also grateful to all the members of the faculty and staff of the College of Foreign Languages who have supported and guided us throughout this study.

FOOTNOTES

Author contributions: Lu DX and Liu F contributed to the study design, data analysis and interpretation, and writing of the manuscript; Yan J contributed to the study design, data analysis, and drafting of the manuscript; Lu Y, Chen BY, Liu HX, and Wu H were responsible for data collection and analysis.

Supported by the National Natural Science Foundation of China, No. 81673795.

Institutional animal care and use committee statement: All animal experiments were approved by Animal Experimental Ethics Committee of Nanjing University of Chinese Medicine (No. 202006A022).

Conflict-of-interest statement: All the authors report no relevant conflicts of interest for this article.

Data sharing statement: No additional data are available.

ARRIVE guidelines statement: The authors have read the ARRIVE guidelines, and the manuscript was prepared and revised according to the ARRIVE guidelines.

Open-Access: This article is an open-access article that was selected by an in-house editor and fully peer-reviewed by external reviewers. It is distributed in accordance with the Creative Commons Attribution NonCommercial (CC BY-NC 4.0) license, which permits others to distribute, remix, adapt, build upon this work non-commercially, and license their derivative works on different terms, provided the original work is properly cited and the use is non-commercial. See: https://creativecommons.org/Licenses/by-nc/4.0/

Country/Territory of origin: China

ORCID number: Dong-Xue Lu 0000-0002-8206-2509; Feng Liu 0000-0003-0331-4067; Hua Wu 0000-0002-6377-5810; Hai-Xia Liu 0000-0003-4541-3469; Bing-Yu Chen 0000-0002-0105-3978; Jing Yan 0000-0003-3616-072X; Yin Lu 0000-0003-2603-8485; Zhi-Guang Sun 0000-0002-1641-8888.

S-Editor: Wang JJ
L-Editor: Wang TQ
P-Editor: Guo X

REFERENCES

1 **Keefe DM**, Brealey J, Goland GJ, Cummins AG. Chemotherapy for cancer causes apoptosis that precedes hypoplasia in crypts of the small intestine in humans. *Gut* 2000; **47**: 632-637 [PMID: 11034578 DOI: 10.1136/gut.47.5.632]
2 **Lee YH**, Hong J, Kim I, Choi Y, Park HK. Prospective evaluation of clinical symptoms of chemotherapy-induced oral mucositis in adult patients with acute leukemia: A preliminary study. *Clin Exp Dent Res* 2020; **6**: 90-99 [PMID: 32067405 DOI: 10.1002/cre2.253]
3 **Chen H**, Zhang F, Li R, Liu Y, Wang X, Zhang X, Xu C, Li Y, Guo Y, Yao Q. Berberine regulates fecal metabolites to ameliorate 5-fluorouracil induced intestinal mucositis through modulating gut microbiota. *Biomed Pharmacother* 2020; **124**: 109829 [PMID: 31958765 DOI: 10.1016/j.biopha.2020.109829]
4 **Saadeh CE**. Chemotherapy- and radiotherapy-induced oral mucositis: review of preventive strategies and treatment. *Pharmacotherapy* 2005; **25**: 540-554 [PMID: 15977916 DOI: 10.1592/phco.25.4.540.61035]
5 **Hecht JR**. Gastrointestinal toxicity or irinotecan. *Oncology (Williston Park)* 1998; **12**: 72-78 [PMID: 9726096]
6 **Martens EC**, Neumann M, Desai MS. Interactions of commensal and pathogenic microorganisms with the intestinal mucosal barrier. *Nat Rev Microbiol* 2018; **16**: 457-470 [PMID: 29904082 DOI: 10.1038/s41579-018-0036-x]
7 **Zhang W**, Gan D, Jian J, Huang C, Luo F, Wan S, Jiang M, Wan Y, Wang A, Li B, Zhu X. Protective Effect of Ursolic Acid on the Intestinal Mucosal Barrier in a Rat Model of Liver Fibrosis. *Front Physiol* 2019; **10**: 956 [PMID: 31417419 DOI: 10.3389/fphys.2019.00956]
8 **Al-Qadami G**, Van Sebille Y, Le H, Bowen J. Gut microbiota: implications for radiotherapy response and radiotherapy-induced mucositis. *Expert Rev Gastroenterol Hepatol* 2019; **13**: 485-496 [PMID: 30907164 DOI: 10.1080/17474124.2019.1595586]
9 **Niu M**, Li Q, Zhang J, Wen F, Dang W, Duan G, Li H, Ruan W, Yang P, Guan C, Tian H, Gao X, Zhang S, Yuan F, Han Y. Characterization of Intestinal Microbiota and Probiotics Treatment in Children With Autism Spectrum Disorders in China. *Front Neurol* 2019; **10**: 1084 [PMID: 31749754 DOI: 10.3389/fneur.2019.01084]
10 **Zhou C**, Xu P, Huang C, Liu G, Chen S, Hu G, Li G, Liu P, Guo X. Effects of subchronic exposure of mercuric chloride on intestinal histology and microbiota in the cecum of chicken. *Ecotoxicol Environ Saf* 2020; **188**: 109920 [PMID: 31733937 DOI: 10.1016/j.ecoenv.2019.109920]
11 **Liu Y**, Pan T, Zou W, Sun Y, Cai Y, Wang R, Han P, Zhang Z, He Q, Ye F. Relationship between traditional Chinese medicine constitutional types with chemotherapy-induced nausea and vomiting in patients with breast cancer: an observational study. *BMC Complement Altern Med* 2016; **16**: 451 [PMID: 27829423 DOI: 10.1186/s12906-016-1415-3]
12 **Pan L**, Zheng QH, Rui XM, Wu ZJ, Ye BY, Chen KY, Meng XL. Clinical study of Jianpi Shugan Decoction on reducing adverse reaction of dose-intensive chemotherapy for breast cancer. *China J Tradit Chinese Med Pharm***35**: 2149-2152
13 **Liu CT**, Chen YH, Huang YC, Chen SY, Tsai MY. Chemotherapy in conjunction with traditional Chinese medicine for survival of patients with early female breast cancer: protocol for a non-randomized, single center prospective cohort study. *Trials* 2019; **20**: 741 [PMID: 31847861 DOI: 10.1186/s13063-019-3848-8]
14 **Tao M**, Wang X, Wang A, Gao N, Pan J, Liu X. Effect of jiaweiwumel decoction on regulatory T cells and interleukin-10 in a rat model of ulcerative colitis. *J Tradit Chin Med* 2015; **35**: 312-315 [PMID: 26237836 DOI: 10.1016/s0254-6272(15)30103-5]
15 **Ma NX**, Sun W, Wu J, Liu SL, Weng L, Liu YQ, Pu WX, Wu TT, Ding XL, Huang NG, Zheng PQ, Zou X. Compound Wumei Powder Inhibits the Invasion and Metastasis of Gastric Cancer *via* Cox-2/PGE2-PI3K/AKT/GSK3*β*/*β*-Catenin Signaling Pathway. *Evid Based Complement Alternat Med* 2017; **2017**: 3039450 [PMID: 29358963 DOI: 10.1155/2017/3039450]

16 **Gong SD**, Shi Y. Experience of Professor ZHOU Zhongying Using Wumei Pill in Treating Chemotherapy Related Diarrhea of Esophageal Cancer. *Zhejiang Zhongyiyao Daxue Xuebao* 2018; **42**: 287-289

17 **Yin YJ**. A Clinical Study on the Treatment and Prevention of 76 Cases of Chemotherapy-related Diarrhea with Fengsui Wumei Decoction. *Jiangsu Zhongyi Zazhi* 2014; **46**: 34-35

18 **Cui YH**, Xie JC, Xu DQ, Tang Y, Tang MW. Analysis of Clinical Effect of Modified Wumei Pills in Treating Cold-heat Complicated Syndrome of Ulcerative Colitis. *Elect J Clin Med Literature* 2020; **38**: 12+14

19 **Shen Y**, Zhao H, Pan YM, Lyu P, Zeng ZH, Li Y, Hou L. Effect of Wumei Pills on NF-κB and IL-10 in Mice with Immunotherapy-Induced Colitis. *Shijie Zhongyiyao* 2019; **14**: 3188-3192

20 **Zhao H**, Lyu P, Hou L, Zeng ZH, Li Y, Fan QY, Shen Y. Effects of Wumei Wan on interleukin-1β, phosphorylase nuclear factor-κB and forkhead transcription factor 3 in rats with immune colitis. *Beijing Zhongyiyao Daxue Xuebao* 2019; **42**: 947-953

21 **Su LW**, Zheng H, Huang MY, Huang SG. Meta-analysis of Wumei Decoction on Diarrhea- predominant Irritable Bowel Syndrome. *J Emerg Tradit Chin Med***28**: 1554-1558

22 **Chen J**, Zhou GZ. Effect of Modified Wumei Pill Combined with Azintamide and Probiotics on Stool Property and Intestinal Mucosal Barrier Function for Patients with Diarrhea after LC. *J Sichuan Traditional Chinese Medicine* 2020; **38**: 117-120

23 **Bowen JM**, Stringer AM, Gibson RJ, Yeoh AS, Hannam S, Keefe DM. VSL#3 probiotic treatment reduces chemotherapy-induced diarrhea and weight loss. *Cancer Biol Ther* 2007; **6**: 1449-1454 [PMID: 17881902 DOI: 10.4161/cbt.6.9.4622]

24 **Sann H**, Erichsen Jv, Hessmann M, Pahl A, Hoffmeyer A. Efficacy of drugs used in the treatment of IBD and combinations thereof in acute DSS-induced colitis in mice. *Life Sci* 2013; **92**: 708-718 [PMID: 23399699 DOI: 10.1016/j.lfs.2013.01.028]

25 **Liu SH**, Cheng YC. Old formula, new Rx: the journey of PHY906 as cancer adjuvant therapy. *J Ethnopharmacol* 2012; **140**: 614-623 [PMID: 22326673 DOI: 10.1016/j.jep.2012.01.047]

26 **Bjornsson TD**, Callaghan JT, Einolf HJ, Fischer V, Gan L, Grimm S, Kao J, King SP, Miwa G, Ni L, Kumar G, McLeod J, Obach SR, Roberts S, Roe A, Shah A, Snikeris F, Sullivan JT, Tweedie D, Vega JM, Walsh J, Wrighton SA; Pharmaceutical Research and Manufacturers of America Drug Metabolism/Clinical Pharmacology Technical Working Groups. The conduct of in vitro and in vivo drug-drug interaction studies: a PhRMA perspective. *J Clin Pharmacol* 2003; **43**: 443-469 [PMID: 12751267]

27 **van Vliet MJ**, Harmsen HJ, de Bont ES, Tissing WJ. The role of intestinal microbiota in the development and severity of chemotherapy-induced mucositis. *PLoS Pathog* 2010; **6**: e1000879 [PMID: 20523891 DOI: 10.1371/journal.ppat.1000879]

28 **Odenwald MA**, Turner JR. The intestinal epithelial barrier: a therapeutic target? *Nat Rev Gastroenterol Hepatol* 2017; **14**: 9-21 [PMID: 27848962 DOI: 10.1038/nrgastro.2016.169]

29 **Li HL**, Lu L, Wang XS, Qin LY, Wang P, Qiu SP, Wu H, Huang F, Zhang BB, Shi HL, Wu XJ. Alteration of Gut Microbiota and Inflammatory Cytokine/Chemokine Profiles in 5-Fluorouracil Induced Intestinal Mucositis. *Front Cell Infect Microbiol* 2017; **7**: 455 [PMID: 29124041 DOI: 10.3389/fcimb.2017.00455]

30 **Cario E**, Gerken G, Podolsky DK. Toll-like receptor 2 controls mucosal inflammation by regulating epithelial barrier function. *Gastroenterology* 2007; **132**: 1359-1374 [PMID: 17408640 DOI: 10.1053/j.gastro.2007.02.056]

31 **Kawai T**, Akira S. TLR signaling. *Semin Immunol* 2007; **19**: 24-32 [PMID: 17275323 DOI: 10.1016/j.smim.2006.12.004]

32 **Thorpe DW**, Stringer AM, Gibson RJ. Chemotherapy-induced mucositis: the role of the gastrointestinal microbiome and toll-like receptors. *Exp Biol Med (Maywood)* 2013; **238**: 1-6 [PMID: 23479757 DOI: 10.1258/ebm.2012.012260]

33 **Wu JT**, Kral JG. The NF-kappaB/IkappaB signaling system: a molecular target in breast cancer therapy. *J Surg Res* 2005; **123**: 158-169 [PMID: 15652965 DOI: 10.1016/j.jss.2004.06.006]

34 **Chami B**, Martin NJJ, Dennis JM, Witting PK. Myeloperoxidase in the inflamed colon: A novel target for treating inflammatory bowel disease. *Arch Biochem Biophys* 2018; **645**: 61-71 [PMID: 29548776 DOI: 10.1016/j.abb.2018.03.012]

35 **Huang QH**, Wu X, Chen XH, Wu JZ, Su ZR, Liang JL, Li YC, Lai XP, Chen JN, Liu YH. Patchouli oil isolated from the leaves of Pogostemon cablin ameliorates ethanol-induced acute liver injury in rats *via* inhibition of oxidative stress and lipid accumulation. *RSC Adv* 2018; **8**: 24399-24410 [PMID: 35539211 DOI: 10.1039/c8ra02422g]

36 **Zhang T**, Lu SH, Bi Q, Liang L, Wang YF, Yang XX, Gu W, Yu J. Volatile Oil from Amomi Fructus Attenuates 5-Fluorouracil-Induced Intestinal Mucositis. *Front Pharmacol* 2017; **8**: 786 [PMID: 29170638 DOI: 10.3389/fphar.2017.00786]

37 **Zhai Z**, Boquete JP, Lemaitre B. Cell-Specific Imd-NF-κB Responses Enable Simultaneous Antibacterial Immunity and Intestinal Epithelial Cell Shedding upon Bacterial Infection. *Immunity* 2018; **48**: 897-910.e7 [PMID: 29752064 DOI: 10.1016/j.immuni.2018.04.010]

38 **Young RS**, Wiles BM, McGee DW. IL-22 Enhances TNF-α- and IL-1-Induced CXCL8 Responses by Intestinal Epithelial Cell Lines. *Inflammation* 2017; **40**: 1726-1734 [PMID: 28656529 DOI: 10.1007/s10753-017-0614-5]

39 **Pott J**, Kabat AM, Maloy KJ. Intestinal Epithelial Cell Autophagy Is Required to Protect against TNF-Induced Apoptosis during Chronic Colitis in Mice. *Cell Host Microbe* 2018; **23**: 191-202.e4 [PMID: 29358084 DOI: 10.1016/j.chom.2017.12.017]

40 **Wang C**, Li W, Wang H, Ma Y, Zhao X, Zhang X, Yang H, Qian J, Li J. Saccharomyces boulardii alleviates ulcerative colitis carcinogenesis in mice by reducing TNF-α and IL-6 levels and functions and by rebalancing intestinal microbiota. *BMC Microbiol* 2019; **19**: 246 [PMID: 31694526 DOI: 10.1186/s12866-019-1610-8]

41 **Dinarello CA**. Proinflammatory cytokines. *Chest* 2000; **118**: 503-508 [PMID: 10936147 DOI: 10.1378/chest.118.2.503]

42 **Zhang S**, Xu W, Wang H, Cao M, Li M, Zhao J, Hu Y, Wang Y, Li S, Xie Y, Chen G, Liu R, Cheng Y, Xu Z, Zou K, Gong S, Geng L. Inhibition of CREB-mediated ZO-1 and activation of NF-κB-induced IL-6 by colonic epithelial MCT4 destroys intestinal barrier function. *Cell Prolif* 2019; **52**: e12673 [PMID: 31418947 DOI: 10.1111/cpr.12673]

43 **Bajic JE**, Eden GL, Lampton LS, Cheah KY, Lymn KA, Pei JV, Yool AJ, Howarth GS. Rhubarb extract partially improves mucosal integrity in chemotherapy-induced intestinal mucositis. *World J Gastroenterol* 2016; **22**: 8322-8333 [PMID: 27729739 DOI: 10.3748/wjg.v22.i37.8322]

44 **Wardill HR**, Bowen JM. Chemotherapy-induced mucosal barrier dysfunction: an updated review on the role of intestinal

tight junctions. *Curr Opin Support Palliat Care* 2013; **7**: 155-161 [PMID: 23492816 DOI: 10.1097/SPC.0b013e32835f3e8c]
45 **Capaldo CT**, Powell DN, Kalman D. Layered defense: how mucus and tight junctions seal the intestinal barrier. *J Mol Med (Berl)* 2017; **95**: 927-934 [PMID: 28707083 DOI: 10.1007/s00109-017-1557-x]
46 **France MM**, Turner JR. The mucosal barrier at a glance. *J Cell Sci* 2017; **130**: 307-314 [PMID: 28062847 DOI: 10.1242/jcs.193482]
47 **Turner JR**. Intestinal mucosal barrier function in health and disease. *Nat Rev Immunol* 2009; **9**: 799-809 [PMID: 19855405 DOI: 10.1038/nri2653]
48 **Arrieta MC**, Madsen K, Doyle J, Meddings J. Reducing small intestinal permeability attenuates colitis in the IL10 gene-deficient mouse. *Gut* 2009; **58**: 41-48 [PMID: 18829978 DOI: 10.1136/gut.2008.150888]
49 **Johansson ME**, Phillipson M, Petersson J, Velcich A, Holm L, Hansson GC. The inner of the two Muc2 mucin-dependent mucus layers in colon is devoid of bacteria. *Proc Natl Acad Sci U S A* 2008; **105**: 15064-15069 [PMID: 18806221 DOI: 10.1073/pnas.0803124105]
50 **Van der Sluis M**, De Koning BA, De Bruijn AC, Velcich A, Meijerink JP, Van Goudoever JB, Büller HA, Dekker J, Van Seuningen I, Renes IB, Einerhand AW. Muc2-deficient mice spontaneously develop colitis, indicating that MUC2 is critical for colonic protection. *Gastroenterology* 2006; **131**: 117-129 [PMID: 16831596 DOI: 10.1053/j.gastro.2006.04.020]
51 **Kim HJ**, Lee SH, Hong SJ. Antibiotics-Induced Dysbiosis of Intestinal Microbiota Aggravates Atopic Dermatitis in Mice by Altered Short-Chain Fatty Acids. *Allergy Asthma Immunol Res* 2020; **12**: 137-148 [PMID: 31743970 DOI: 10.4168/aair.2020.12.1.137]
52 **Harris LA**, Baffy N. Modulation of the gut microbiota: a focus on treatments for irritable bowel syndrome. *Postgrad Med* 2017; **129**: 872-888 [PMID: 28936910 DOI: 10.1080/00325481.2017.1383819]
53 **Wang J**, Feng W, Zhang S, Chen L, Tang F, Sheng Y, Ao H, Peng C. Gut microbial modulation in the treatment of chemotherapy-induced diarrhea with Shenzhu Capsule. *BMC Complement Altern Med* 2019; **19**: 126 [PMID: 31185967 DOI: 10.1186/s12906-019-2548-y]
54 **Li S**, Qi Y, Chen L, Qu D, Li Z, Gao K, Chen J, Sun Y. Effects of Panax ginseng polysaccharides on the gut microbiota in mice with antibiotic-associated diarrhea. *Int J Biol Macromol* 2019; **124**: 931-937 [PMID: 30503788 DOI: 10.1016/j.ijbiomac.2018.11.271]
55 **Wang J**, Feng W, Zhang S, Chen L, Sheng Y, Tang F, He J, Xu X, Ao H, Peng C. Ameliorative effect of Atractylodes macrocephala essential oil combined with Panax ginseng total saponins on 5-fluorouracil induced diarrhea is associated with gut microbial modulation. *J Ethnopharmacol* 2019; **238**: 111887 [PMID: 31004726 DOI: 10.1016/j.jep.2019.111887]
56 **Lin CH**, Chen CC, Chiang HL, Liou JM, Chang CM, Lu TP, Chuang EY, Tai YC, Cheng C, Lin HY, Wu MS. Altered gut microbiota and inflammatory cytokine responses in patients with Parkinson's disease. *J Neuroinflammation* 2019; **16**: 129 [PMID: 31248424 DOI: 10.1186/s12974-019-1528-y]
57 **Rocha-Ramírez LM**, Pérez-Solano RA, Castañón-Alonso SL, Moreno Guerrero SS, Ramírez Pacheco A, García Garibay M, Eslava C. Probiotic *Lactobacillus* Strains Stimulate the Inflammatory Response and Activate Human Macrophages. *J Immunol Res* 2017; **2017**: 4607491 [PMID: 28758133 DOI: 10.1155/2017/4607491]
58 **Tulyeu J**, Kumagai H, Jimbo E, Watanabe S, Yokoyama K, Cui L, Osaka H, Mieno M, Yamagata T. Probiotics Prevents Sensitization to Oral Antigen and Subsequent Increases in Intestinal Tight Junction Permeability in Juvenile-Young Adult Rats. *Microorganisms* 2019; **7** [PMID: 31623229 DOI: 10.3390/microorganisms7100463]
59 **Shen ZH**, Zhu CX, Quan YS, Yang ZY, Wu S, Luo WW, Tan B, Wang XY. Relationship between intestinal microbiota and ulcerative colitis: Mechanisms and clinical application of probiotics and fecal microbiota transplantation. *World J Gastroenterol* 2018; **24**: 5-14 [PMID: 29358877 DOI: 10.3748/wjg.v24.i1.5]
60 **Gao Y**, Han T, Han C, Sun H, Yang X, Zhang D, Ni X. Propofol Regulates the TLR4/NF-κB Pathway Through miRNA-155 to Protect Colorectal Cancer Intestinal Barrier. *Inflammation* 2021; **44**: 2078-2090 [PMID: 34081253 DOI: 10.1007/s10753-021-01485-0]
61 **Dziarski R**, Park SY, Kashyap DR, Dowd SE, Gupta D. Pglyrp-Regulated Gut Microflora Prevotella falsenii, Parabacteroides distasonis and Bacteroides eggerthii Enhance and Alistipes finegoldii Attenuates Colitis in Mice. *PLoS One* 2016; **11**: e0146162 [PMID: 26727498 DOI: 10.1371/journal.pone.0146162]
62 **Lahner E**, Carabotti M, Annibale B. Treatment of *Helicobacter pylori* infection in atrophic gastritis. *World J Gastroenterol* 2018; **24**: 2373-2380 [PMID: 29904244 DOI: 10.3748/wjg.v24.i22.2373]
63 **Argemi X**, Hansmann Y, Prola K, Prévost G. Coagulase-Negative Staphylococci Pathogenomics. *Int J Mol Sci* 2019; **20** [PMID: 30862021 DOI: 10.3390/ijms20051215]
64 **Romano-Keeler J**, Shilts MH, Tovchigrechko A, Wang C, Brucker RM, Moore DJ, Fonnesbeck C, Meng S, Correa H, Lovvorn HN 3rd, Tang YW, Hooper L, Bordenstein SR, Das SR, Weitkamp JH. Distinct mucosal microbial communities in infants with surgical necrotizing enterocolitis correlate with age and antibiotic exposure. *PLoS One* 2018; **13**: e0206366 [PMID: 30365522 DOI: 10.1371/journal.pone.0206366]
65 **Lagkouvardos I**, Lesker TR, Hitch TCA, Gálvez EJC, Smit N, Neuhaus K, Wang J, Baines JF, Abt B, Stecher B, Overmann J, Strowig T, Clavel T. Sequence and cultivation study of Muribaculaceae reveals novel species, host preference, and functional potential of this yet undescribed family. *Microbiome* 2019; **7**: 28 [PMID: 30782206 DOI: 10.1186/s40168-019-0637-2]
66 **Zhang X**, Zhao Y, Xu J, Xue Z, Zhang M, Pang X, Zhang X, Zhao L. Modulation of gut microbiota by berberine and metformin during the treatment of high-fat diet-induced obesity in rats. *Sci Rep* 2015; **5**: 14405 [PMID: 26396057 DOI: 10.1038/srep14405]
67 **Faubion WA**, Sandborn WJ. Probiotic therapy with E. coli for ulcerative colitis: take the good with the bad. *Gastroenterology* 2000; **118**: 630-631 [PMID: 10702217 DOI: 10.1016/s0016-5085(00)70272-1]
68 **Weng YJ**, Gan HY, Li X, Huang Y, Li ZC, Deng HM, Chen SZ, Zhou Y, Wang LS, Han YP, Tan YF, Song YJ, Du ZM, Liu YY, Wang Y, Qin N, Bai Y, Yang RF, Bi YJ, Zhi FC. Correlation of diet, microbiota and metabolite networks in inflammatory bowel disease. *J Dig Dis* 2019; **20**: 447-459 [PMID: 31240835 DOI: 10.1111/1751-2980.12795]
69 **Parada Venegas D**, De la Fuente MK, Landskron G, González MJ, Quera R, Dijkstra G, Harmsen HJM, Faber KN,

Hermoso MA. Short Chain Fatty Acids (SCFAs)-Mediated Gut Epithelial and Immune Regulation and Its Relevance for Inflammatory Bowel Diseases. *Front Immunol* 2019; **10**: 277 [PMID: 30915065 DOI: 10.3389/fimmu.2019.00277]

70 **Lu Y**, Fan C, Li P, Lu Y, Chang X, Qi K. Short Chain Fatty Acids Prevent High-fat-diet-induced Obesity in Mice by Regulating G Protein-coupled Receptors and Gut Microbiota. *Sci Rep* 2016; **6**: 37589 [PMID: 27892486 DOI: 10.1038/srep37589]

71 **Rivière A**, Selak M, Lantin D, Leroy F, De Vuyst L. Bifidobacteria and Butyrate-Producing Colon Bacteria: Importance and Strategies for Their Stimulation in the Human Gut. *Front Microbiol* 2016; **7**: 979 [PMID: 27446020 DOI: 10.3389/fmicb.2016.00979]

World Journal of Gastroenterology

Submit a Manuscript: https://www.f6publishing.com

World J Gastroenterol 2022 August 28; 28(32): 4600-4619

DOI: 10.3748/wjg.v28.i32.4600

ISSN 1007-9327 (print) ISSN 2219-2840 (online)

ORIGINAL ARTICLE

Basic Study

Sirolimus increases the anti-cancer effect of Huai Er by regulating hypoxia inducible factor-1α-mediated glycolysis in hepatocellular carcinoma

Lin Zhou, Yang Zhao, Li-Chao Pan, Jing Wang, Xian-Jie Shi, Guo-Sheng Du, Qiang He

Specialty type: Gastroenterology and hepatology

Provenance and peer review: Invited article; Externally peer reviewed.

Peer-review model: Single blind

Peer-review report's scientific quality classification

Grade A (Excellent): 0
Grade B (Very good): B
Grade C (Good): C
Grade D (Fair): 0
Grade E (Poor): 0

P-Reviewer: Lashen SA, Egypt; Zaghloul MS, Egypt

Received: November 10, 2021
Peer-review started: November 10, 2021
First decision: January 9, 2022
Revised: January 11, 2022
Accepted: July 16, 2022
Article in press: July 16, 2022
Published online: August 28, 2022

Lin Zhou, Yang Zhao, Jing Wang, Qiang He, Department of Hepatobiliary and Pancreaticosplenic Surgery, Beijing ChaoYang Hospital, Capital Medical University, Beijing 100020, China

Li-Chao Pan, Xian-Jie Shi, Guo-Sheng Du, Faculty of Hepato-Pancreato-Biliary Surgery, Chinese PLA General Hospital, Beijing 100853, China

Corresponding author: Guo-Sheng Du, MD, Professor, Faculty of Hepato-Pancreato-Biliary Surgery, Chinese PLA General Hospital, No. 28 Fuxing Road, Haidian District, Beijing 100853, China. duguosheng309@126.com

Abstract

BACKGROUND

Glycolysis caused by hypoxia-induced abnormal activation of hypoxia inducible factor-1α (HIF-1α) in the immune microenvironment promotes the progression of hepatocellular carcinoma (HCC), leading to enhanced drug resistance in cancer cells. Therefore, altering the immunosuppressive microenvironment by improving the hypoxic state is a new goal in improving cancer treatment.

AIM

To analyse the role of HIF-1α, which is closely related to tumour proliferation, invasion, metastasis, and angiogenesis, in the proliferation and invasion of liver cancer, and to explore the HIF-1α pathway-mediated anti-cancer mechanism of sirolimus (SRL) combined with Huai Er.

METHODS

Previous studies on HCC tissues identified the importance of HIF-1α, glucose transporter 1 (GLUT1), and lactate dehydrogenase A (LDHA) expression. In this study, HepG2 and Huh7 cell lines were treated, under hypoxic and normoxic conditions, with a combination of SRL and Huai Er. The effects on proliferation, invasion, cell cycle, and apoptosis were analysed. Proteomics and genomics techniques were used to analyze the HIF-1α-related signalling pathway during SRL combined with Huai Er treatment and its inhibition of the proliferation of HCC cells.

RESULTS

High levels of HIF-1α, LDHA, and GLUT-1 were found in poorly differentiated

HCC, with lower patient survival rates. Hypoxia promoted the proliferation of HepG2 and Huh7 cells and weakened the apoptosis and cell cycle blocking effects of the SRL/Huai Er treatment. This was achieved by activation of HIF-1α and glycolysis in HCC, leading to the upregulation of LDHA, GLUT-1, Akt/mammalian target of rapamycin (mTOR), vascular endothelial growth factor (VEGF), and Forkhead box P3 and downregulation of phosphatase and tensin homolog deleted on chromosome ten (PTEN) and p27. The hypoxia-induced activation of HIF-1α showed the greatest attenuation in the SRL/Huai Er (S50 + H8) group compared to the drug treatments alone (P < 0.001). The S50 + H8 treatment significantly downregulated the expression of mTOR and HIF-1α, and significantly reduced the expression of VEGF mRNA. Meanwhile, the combined blocking of mTOR and HIF-1α enhanced the downregulation of *Akt/mTOR*, *HIF-1α*, *LDHA*, and *GLUT-1* mRNA and resulted in the downregulation of *PTEN*, *p27*, and *VEGF* mRNA (P < 0.001).

CONCLUSION

SRL increases the anti-cancer effect of Huai Er, which reduces the promotion of hypoxia-induced HIF-1α on the Warburg effect by inhibition of the PI3K/Akt/mTOR-HIF-1α and HIF-1α-PTEN signalling pathways in HCC.

Key Words: Hepatocellular carcinoma; Sirolimus; Huai Er; Warburg effect; Hypoxia inducible factor-1α

©The Author(s) 2022. Published by Baishideng Publishing Group Inc. All rights reserved.

Core Tip: Hypoxia-mediated glycolysis is associated with poorly differentiated hepatocellular carcinoma (HCC) and a poor prognosis. Hypoxia inducible factor-1α (HIF-1α), induced by hypoxia, promotes the growth of HepG2 and Huh7 cells and weakens the anti-cancer effect of sirolimus (SRL) and Huai Er. SRL increased the anti-cancer effect of Huai Er, which reduced the promotion of hypoxia-induced HIF-1α on the Warburg effect by inhibiting the PI3K/Akt/mammalian target of rapamycin-HIF-1α and HIF-1α-phosphatase and tensin homolog deleted on chromosome ten signalling pathways in HCC.

Citation: Zhou L, Zhao Y, Pan LC, Wang J, Shi XJ, Du GS, He Q. Sirolimus increases the anti-cancer effect of Huai Er by regulating hypoxia inducible factor-1α-mediated glycolysis in hepatocellular carcinoma. *World J Gastroenterol* 2022; 28(32): 4600-4619

URL: https://www.wjgnet.com/1007-9327/full/v28/i32/4600.htm

DOI: https://dx.doi.org/10.3748/wjg.v28.i32.4600

INTRODUCTION

Hepatocellular carcinoma (HCC) is the third leading cause of cancer-related death worldwide. Its incidence and mortality are increasing annually, particularly in the younger age groups[1]. More than half of the cases are in China, with more than 90% being related to hepatitis B[1]. Therefore, cancer death is the primary cause of death in China, with liver cancer ranking second with 390000 cases[1,2]. Immunosuppressive cells of Forkhead box P3$^+$ (Foxp3$^+$) Tregs, neutrophils, MDSC, and others infiltrate the tumour[3,4]. Hypoxia-induced hypoxia inducible factor-1α (HIF-1α)-mediated glycolysis, infiltration of extracellular matrix, and accumulation of lactic acid in the anoxic microenvironment promote abnormal metabolism of cancer cells. This, combined with abnormal tumour immunity, leads to downregulation of immune surveillance, increased immune escape, and promotion of proliferation, invasion, and metastasis[4].

Hanahan proposed "abnormal energy metabolism" as the seventh feature of cancer[5], in which the metabolism of tumour cells, mainly represented by abnormal glucose metabolism (Warburg effect) and abnormal lipid metabolism, is closely related to tumour occurrence and metastasis. Recent studies have suggested that abnormal glucose metabolism in cancer is not only related to metabolic enzymes, metabolic pathways, and other related signal transduction pathways, but also to the immune status and local microenvironment of tumour tissues[6-8].

The anoxic environment induces the activation and upregulation of HIF-1α expression which promotes glycolysis, increases glucose transporter 1 (GLUT1) expression, and accelerates tumour cell metabolism[9]. It has been confirmed that HIF-1α can upregulate the activity of glycolytic enzymes by 90%[10] and produce a large amount of lactic acid through metabolism. Lactic acid is transported out of the cells and forms a high lactic acid environment in cancer tissue, leading to metabolic competition with T cells. This further inhibits the function, proliferation, and activation of infiltrated lymphocytes; destroys the killing effect and anti-tumour function; and promotes tumour immune escape[9-12].

However, cancer cells can efficiently use circulating lactic acid to produce glucose by anaerobic glycolysis, and a large number of electrons produced by metabolism adhere to lactic acid to compensate for the voltage instability inside and outside the cell caused by the high-speed electron movement of cancer cells, while ensuring the steady-state demand for energy and microenvironment for rapid growth and proliferation[10-12].

HIF-1α induction by Akt/mammalian target of rapamycin (mTOR)-mediated growth factors only involves the translation of mRNA under normoxia[13]; however, the regulatory mechanism of PI3K/Akt/mTOR on HIF-1α and the activation mechanism of PI3K are not clear under hypoxia. There may be alternative regulated signalling pathways because our results showed that the PI3K/Akt inhibitor, LY294002, cannot completely inhibit the expression of HIF-1α. Inhibiting the expression of HIF-lα and blocking the transmission of oxygen deficiency signals have become a new target for tumour therapy. Huai Er, also known as Trametes robiniophila Murr, is a traditional Chinese medicine. Various studies have demonstrated that Huai Er inhibits cancer progression and improves patient prognosis[14, 15]. The purpose of this study was to explore the regulatory mechanism of sirolimus (SRL) and Huai Er on HepG2 cell proliferation caused by abnormal activation of the HIF-1α pathway induced by hypoxia and to provide a theoretical basis for new clinical treatments for liver cancer.

MATERIALS AND METHODS

Regent and ethics approval

The hepatoma cell lines, HepG2 and Huh 7, were purchased from the Institute of Basic Medicine, Chinese Academy of Medical Sciences. Liver tissue was obtained from the pathological laboratory with written informed consent obtained in accordance with the Declaration of Helsinki of the World Medical Association. The study complied with the Institutional Guidelines for the Care and Use of Laboratory Animals and was approved by the Ethics Committee of Beijing Chaoyang Hospital (No. 2021-1-19-3) and PLA General Hospital (S2108-013-01). The experimental flowchart is shown in Supplementary Figure 1.

Cell proliferation experiment

HepG2 and Huh 7 cells were cultured at a density of 1 × 10^3/well with 100 μL complete medium (10% fetal bovine serum + RMPI-1640, Gibco, United States) overnight for 24 h, then treated with SRL, Huai Er, Ly294002 (Ly), and KC7F2 (KC7) for 24-48 h, and a mixture of 50 μL 1 × PBS and 20 μL MTS (Promega, United States) was added and co-cultured for 2-4 h. The OD value at 490 nm was used to calculate the IC_{50} values of the drugs and blockers.

Cell scratch assay

HepG2 and Huh7 cells were cultured at a density of 1 × 10^6/well for 24 h before scratching with a "cross" and culturing with 2 mL of treatment solution. Imaging identified the clear position of scratches, and images were acquired at 0 h, 24 h, and 48 h, the position of the scratch was marked, and the scratch images were analysed using Image J[16]. The treatment groups were as follows: Huai Er (H) (Gaitianli Co.), SRL (S) (Sigma, United States), Ly294002 (Ly) (TargetMol, United States), KC7F2 (KC7) (TargetMol, United States), H + S, H + Ly, H + KC7, S + Ly, S + KC7, Ly + KC7, and S + H + Ly + KC7.

Plate clone formation assay

HepG2 and Huh7 cells at a density of 500/well were cultured for 24 h, the culture medium was then changed before the addition of SRL, Huai Er, hypoxia (simulated by 200 μM $CoCl_2$, Sigma, United States), and SRL + Huai Er, and the cells were cultured for 10 d. After washing with 1 × PBS, the cells were fixed with 1% paraformaldehyde, stained with crystal violet, and photographed to observe the size of colonies.

Cell cycle and apoptosis assays

Preparation of single-cell suspension: A single-cell suspension was prepared using 0.25 % non-EDTA trypsin (Gibco, United States) to digest the cultured cells treated with Huai Er, SRL, and Huai Er + SRL.

Apoptosis detection: The prepared single-cell suspension was co-incubated with 5 μL of fluorescein isothiocyanate labelled Annexin V antibody and 2.5 μL of phycoerythrin-labelled PI antibody (BD, United States) for 15 min in a dark room at room temperature, washed with 1 ml precooled 1 × Binding Buffer, and centrifuged at 1200 rpm/min for 5 min, and the supernatant was discarded. The apoptosis rates of HepG2 and Huh 7 cells were determined by flow cytometry.

Cell cycle detection: The prepared single-cell suspension was fixed with 1 mL of 70% precooled ethanol at 4 °C for 12 h. After centrifugation at 1000 *g* for 5 min, the supernatant was discarded and the cell pellet was washed with 1 mL of precooled 1 × PBS, with 500 μL of PI/RNase staining buffer (BD Biosciences, United States) added for 10^6-10^7 cells to re-suspend cells for detection.

Immunohistochemistry

Paraffin-embedded tissues were sliced into thin tissue sections of 5 μm and heated at 60 °C for 30 min. The sections then underwent a dewaxing step, 3% hydrogen peroxide inactivation, antigen retrieval in a microwave at 100 °C for 20 min, and blocking for 30 min. Next, the cells were incubated with primary antibodies against HIF-1α, lactate dehydrogenase A (LDHA), and GLUT-1 (1:100) (Proteintech, United States) overnight. The cells were then incubated with the secondary antibody from PV-9000 kits (OriGene Technologies, United States) for 60 min, before staining with the DAB kit (Vector, United States) under a Nikon microscope system.

Protein isolation and Western blot analysis

Cultured cancer cells were lysed by trypsinisation at 4 °C and the total protein was extracted. Protein purity was determined using a bicinchoninic acid assay, according to the manufacturer's instructions and Western blot analysis was performed.

Reverse transcription-polymerase chain reaction gene detection

Total RNA was extracted using the TRIzol reagent (Life Technologies, Carlsbad, CA, United States), and the OD value was determined using a spectrophotometer. Primers were designed using the NCBI online primer design software Primer-BLAST and synthesised by Beijing Jingke Xinye Biotechnology Co., Ltd (China). The names of the primers and the corresponding sequence information are listed in Supplementary Table 1. Then, 24 μL of the reaction system was prepared for cDNA synthesis and stored at -20 °C for later use. After that, a 20 μL reaction system was prepared, and then instantaneous centrifugation was performed in the fluorescence quantitative polymerase chain reaction (PCR) instrument to carry out the reverse transcription (RT)-PCR reaction according to the manufacturer's protocol (Life Technologies, United States).

Statistical analysis

Images from an optical microscope were captured and stored, and the results of flow cytometry were analysed using FlowJo10.0 software. The data were analysed using SPSS 22.0. Each index is expressed as the mean ± SD, and the difference between two groups was tested using the *t*-test. Statistical significance was set at $P < 0.05$. Single-factor ANOVA was used to determine statistical differences among different experimental groups. Differences were considered significant at $P < 0.05$.

RESULTS

High level of HIF-1α and the Warburg effect indicate a poor survival benefit

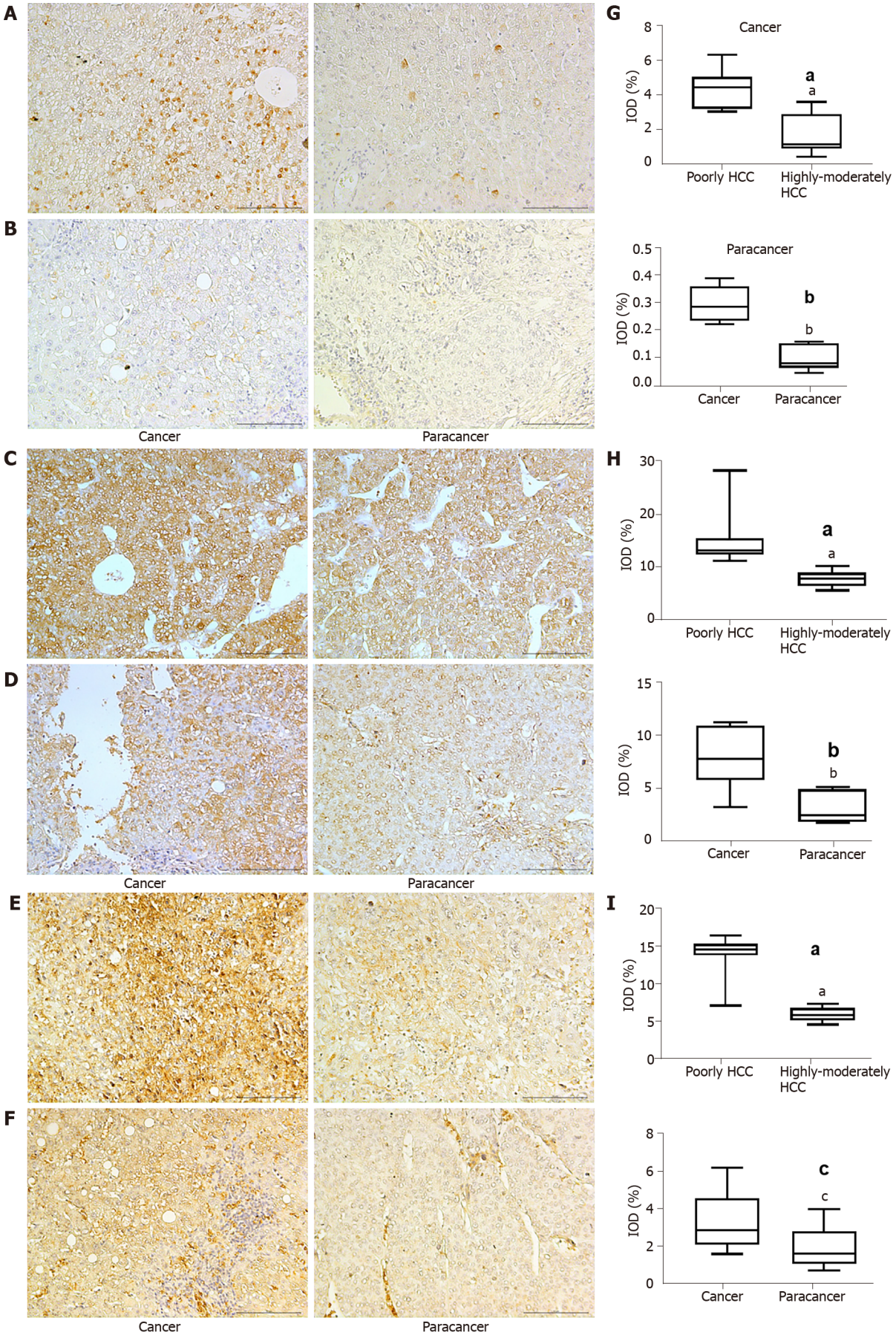
We identified high expression levels of HIF-1α in patients with poorly differentiated HCC, with expression being higher in the cancer tissue than in para-carcinoma tissue (Figure 1A, B and G) ($P < 0.001$). Higher levels of GLUT-1 ($P < 0.05$) and LDHA ($P < 0.001$) were identified in cancer tissues compared to para-carcinoma tissues, indicating an enhanced glycolytic effect (Warburg effect); these higher levels of expression were also observed in patients with poorly differentiated HCC compared to those with moderately differentiated HCC (Figure 1C-F, H and I) ($P < 0.001$). The high levels of HIF-1α, GLUT-1, and LDHA were all associated with poorer survival outcomes ($P < 0.01$). Based on these results and our previous research on the effect of Huai Er and SRL on HCC in a rat model[15], we explored the effect of Huai Er combined with SRL on the glucose metabolism pathway in HepG2 and Huh7 cell lines, to determine the synergistic mechanism of tumour growth inhibition.

Optimal inhibitory concentrations of SRL, Huai Er, Ly294002, and KC7F2 on HepG2 cells

The suppression of proliferation of HepG2 and Huh7 cells increased gradually with the administration of SRL at concentrations ranging from 0.1 nM to 1000 nM. A gradual increase was also observed on the administration of Huai Er at concentrations ranging from 4 mg/mL to 8 mg/mL. The optimal inhibitory concentration was identified as 50 nM for SRL (S50) and 8 mg/mL for Huai Er (H8), using IC_{50} curve calculation. An optimal inhibitory concentration of 25 μM was calculated for Ly294002 (a specific inhibitor of PI3K) (Ly25) and 20 μM for KC7F2 (a selective inhibitor of HIF-1α) (KC7). These optimal concentrations were used in the following study with S50, H8, Ly25, and KC7 groups.

Huai Er displays a greater inhibitory effect than SRL on the invasion of HepG2 and Huh7 cells

The scratch test results showed that H8 treatment significantly inhibited the invasion of HepG2 and Huh 7 cells compared to S50 treated cells and the control group (Figure 2A and B). The addition of S50 enhanced the inhibitory effect of the H8 treatment, showing a greater inhibitory effect on invasion compared to the monotherapies (Figure 2C and E).



DOI: 10.3748/wjg.v28.i32.4600 **Copyright** ©The Author(s) 2022.

Figure 1 Expression of hypoxia inducible factor-1α, lactate dehydrogenase A, and glucose transporter 1 in hepatocellular carcinoma. A

and B: Expression of hypoxia inducible factor-1 (HIF-1α) in poorly (A) and highly-moderately differentiated hepatocellular carcinoma (HCC) (B); C and D: Expression of lactate dehydrogenase A (LDHA) in poorly (C) and highly-moderately differentiated HCC (D); E and F: Expression of glucose transporter 1 (GLUT1) in poorly (E) and highly-moderately differentiated HCC (F); F: Expression of GLUT1 in high-moderately HCC, (Magnification: 200 ×, scale bar 10 μm); G-I: Comparison of HIF-1α (G), LDHA (H), and GLUT1 (I) in different groups by *t* test. Magnification: 200 ×, scale bar = 10 μm. [a]*P* < 0.001 *vs* poorly differentiated HCC; [b]*P* < 0.001 *vs* cancer; [c]*P* < 0.05 *vs* cancer.

Huai Er plus SRL treatment shows a greater inhibitory effect on invasion than other combined applications

Compared with the control group, the combination of any two drugs, Huai Er, SRL, Ly25, or KC7, significantly inhibited the invasion of cancer cells ($P < 0.001$) (Figure 2A, B, D and F). Huai Er application combined with S50, Ly25, or KC7 revealed a stronger inhibitory effect on the invasion of HepG2 and Huh 7 cells than other combined applications, with the strongest effect being noted in the H8 + S50 treatment group ($P < 0.001$) (Figure 2A, B, D and F).

Hypoxia promotes the proliferation of HepG2 and Huh7 cells

High proliferation of HepG2 and Huh7 cells was observed when maintained in a hypoxic environment at an appropriate concentration of $CoCl_2$, compared to when maintained under normoxic conditions (Figure 2G and H). The inhibitory effect of H8 + S50 on the proliferation of these cells was weakened after culturing under hypoxia (Figure 2G and H).

Promotion of cell apoptosis in both HepG2 and Huh7 cells after SRL and Huai Er treatment

SRL and Huai Er promote the apoptosis of HepG2 and Huh7 cells under normoxia: The apoptosis rate of HepG2 (Figure 3A-H) and Huh7 (Figure 3I-P) cells increased gradually 24 h to 48 h after treatment with S50 and H8 ($P < 0.001$) (Figure 3A, B, G, I, J and O). The combination of S50 + H8 caused the highest promotion of apoptosis in this time period, compared to the single-drug treatments ($P < 0.001$) (Figure 3E, G, M and O). These results indicate that Huai Er may enhance the pro-apoptotic effect of S50 on HCC cells.

Hypoxia reduces the apoptosis effect of SRL and Huai Er on HepG2 and Huh7 cells: Despite the longer treatment time under hypoxia, the increased apoptosis rate of HepG2 and Huh7 cells (Figure 3C, D, H, K, L and P), observed with treatment under normoxia, was significantly reduced ($P < 0.05$, Figure 3). There was also a decrease in apoptosis levels after S50 + H8 treatment under hypoxia (Figure 3E, F, H, M, N and P) in both HepG2 and Huh7 cells.

SRL and Huai Er treatment blocks cell cycle processes of HepG2 and Huh7 cells

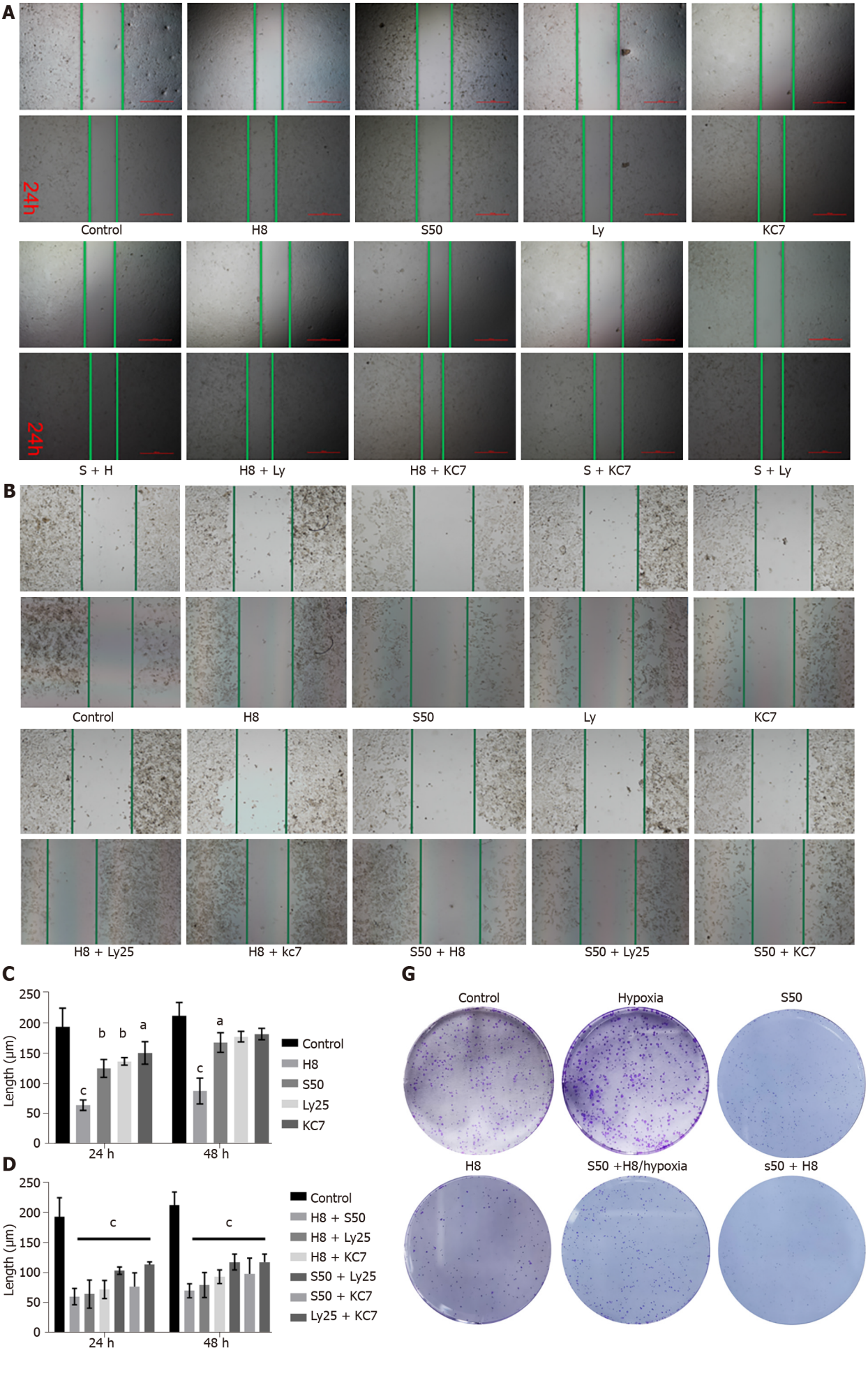
Hypoxia weakens the blocking effect of SRL and Huai Er on the cell cycle: Treatment with S50 and H8 showed a significant blocking effect, in the form of mitotic stagnation in the G2 phase. Increased proportions of S and G2 phase HepG2 cells were observed (Figure 4A-H), while Huh 7 cells showed an increased proportion in the G2 phase (Figure 4I-P). Both cell types had a decreased proportion in the G1 phase ($P < 0.01$) (Figure 4A-D and I-L). The blocking effect occurred gradually over time (Figure 4A-D and I-L) ($P < 0.01$). When cultured under hypoxia, the blocking effect of SRL and Huai Er on HepG2 and Huh7 cells was weakened, and there was no significant difference in the S50 treatment group, compared with the hypoxia group after treatment at either time point, ($P > 0.05$) (Figure 4E, F, H, M, N and P); however, the difference in H8 remained statistically significant ($P < 0.001$).

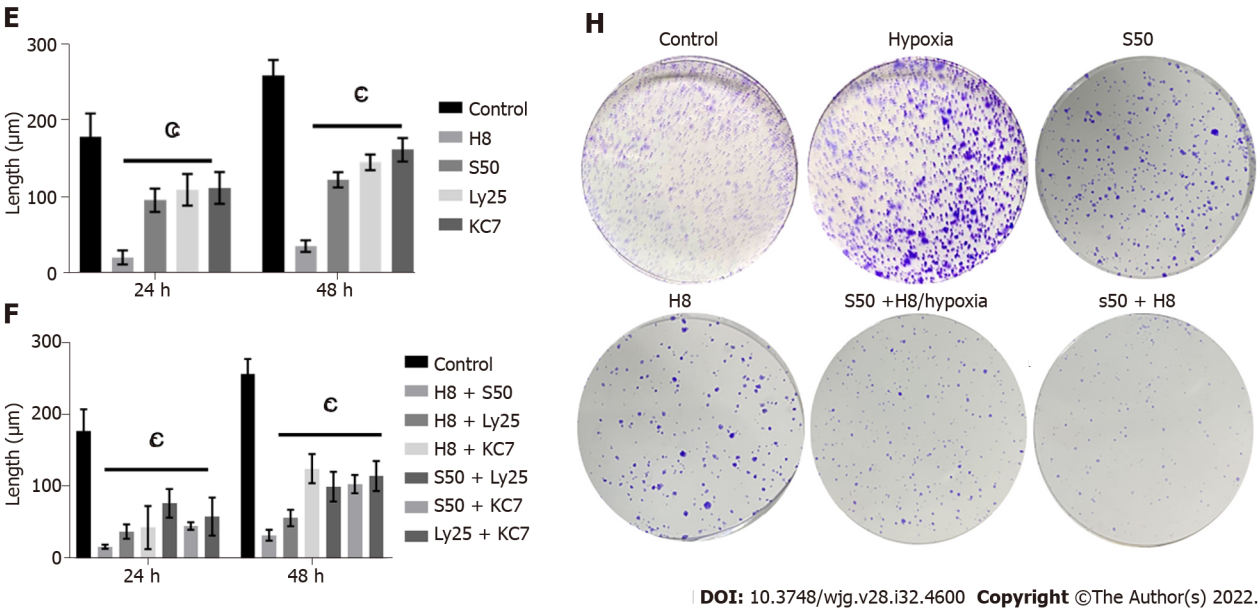
SRL application with Huai Er has a synergistic effect in blocking the cell mitotic cycle: S50 + H8 treatment significantly inhibited the cell division of HepG2 cells in the S phase under normoxia, while the ratio of G1 phase to G2 phase cells decreased both at 24 h and 48 h (Supplementary Figure 2A-C) ($P < 0.05$) (Supplementary Figure 2C). This ratio was significantly higher than that observed for the single drug treatments ($P < 0.01$) (Supplementary Figure 2E and F), suggesting that SRL and Huai Er may have synergistic inhibitory effects. Hypoxia attenuated the synergistic inhibitory effect of S50 + H8 on the cell cycle of HepG2 (Supplementary Figure 2A-D), decreasing the proportion of S-phase cells ($P < 0.01$). The ratio of G1 phase to G2 phase cells after S50 + H8 treatment was significantly higher than that of the S50 group ($P < 0.01$), but not significantly different from that in the H8 group (Supplementary Figure 2G and H), at both timepoints.

Thus, we believe that the combined SRL and Huai Er treatment can significantly arrest the cell cycle of HepG2 and Huh7 cells; therefore, protein and gene-level analyses were mainly focused on HepG2 cells.

SRL combined with Huai Er significantly decreases the expression of mTOR and HIF-1α

To further explore the molecular mechanism of SRL combined with Huai Er, Western blot was used to analyse the expression levels of the key proteins in the PI3K signalling pathway (mTOR) and in hypoxia-induced factor-mediated glycolysis (HIF-1α). Compared with the control and the monotherapy


A
24h
Control
H8
S50
Ly
KC7
24h
S + H
H8 + Ly
H8 + KC7
S + KC7
S + Ly
B
Control
H8
S50
Ly
KC7
H8 + Ly25
H8 + kc7
S50 + H8
S50 + Ly25
S50 + KC7
C
Length (μm)
250
200
150
100
50
0
b
b
a
c
a
c
24 h
48 h
Control
H8
S50
Ly25
KC7
D
Length (μm)
250
200
150
100
50
0
c
c
24 h
48 h
Control
H8 + S50
H8 + Ly25
H8 + KC7
S50 + Ly25
S50 + KC7
Ly25 + KC7
G
Control
Hypoxia
S50
H8
S50 +H8/hypoxia
s50 + H8



DOI: 10.3748/wjg.v28.i32.4600 **Copyright** ©The Author(s) 2022.

Figure 2 Inhibitory effect of different drugs on HepG2 and Huh 7 cell invasion and proliferation as demonstrated by scratch and plate clone formation assays. A and B: Scratch images of HepG2 (A) and Huh7 cells (B) treated with different drugs; C and D: Effect of single drug treatment (C) and combination treatment (D) on HepG2 invasion; E and F: Effect of single drug treatment (E) and combination treatment (F) on Huh 7 invasion; G and H: Clonal size of HepG2 (G) and Huh 7 cells (H) treated with different drugs. $^{a}P < 0.05$ *vs* control; $^{b}P < 0.01$ *vs* control; $^{c}P < 0.001$ *vs* control. H8: 8 mg/mL for Huai Er; S50: 50 nM for sirolimus; Ly25: Ly294002; KC7: 20 μM for KC7F2.

treatments, S50 + H8 significantly reduced the expression levels of mTOR and HIF-1α (Supplementary Figure 3A-C).

Hypoxia-induced HIF-1α promotes HepG2 cell proliferation by enhancing the Warburg effect

Hypoxia can significantly upregulate the expression of *HIF-1α* mRNA, while increasing the expression of *LDHA* and *GLUT-1* mRNA in anaerobic glycolysis, leading to the promotion of vascular endothelial growth factor (*VEGF*) mRNA expression (Supplementary Figure 3D and E). Hypoxia also downregulated the mRNA expression of *FoxP3*, *p27*, and Phosphatase and tensin homolog deleted on chromosome ten phosphatase and tensin homolog deleted on chromosome ten (*PTEN*). Although there was an increase in the expression of Akt and mTOR, no significant difference was observed (Supplementary Figure 3D and E). These results suggest that hypoxia-induced HIF-1α upregulation can mediate downstream activation, leading to an enhancement of HepG2 cell proliferation by upregulating the expression of LDHA and GLUT-1.

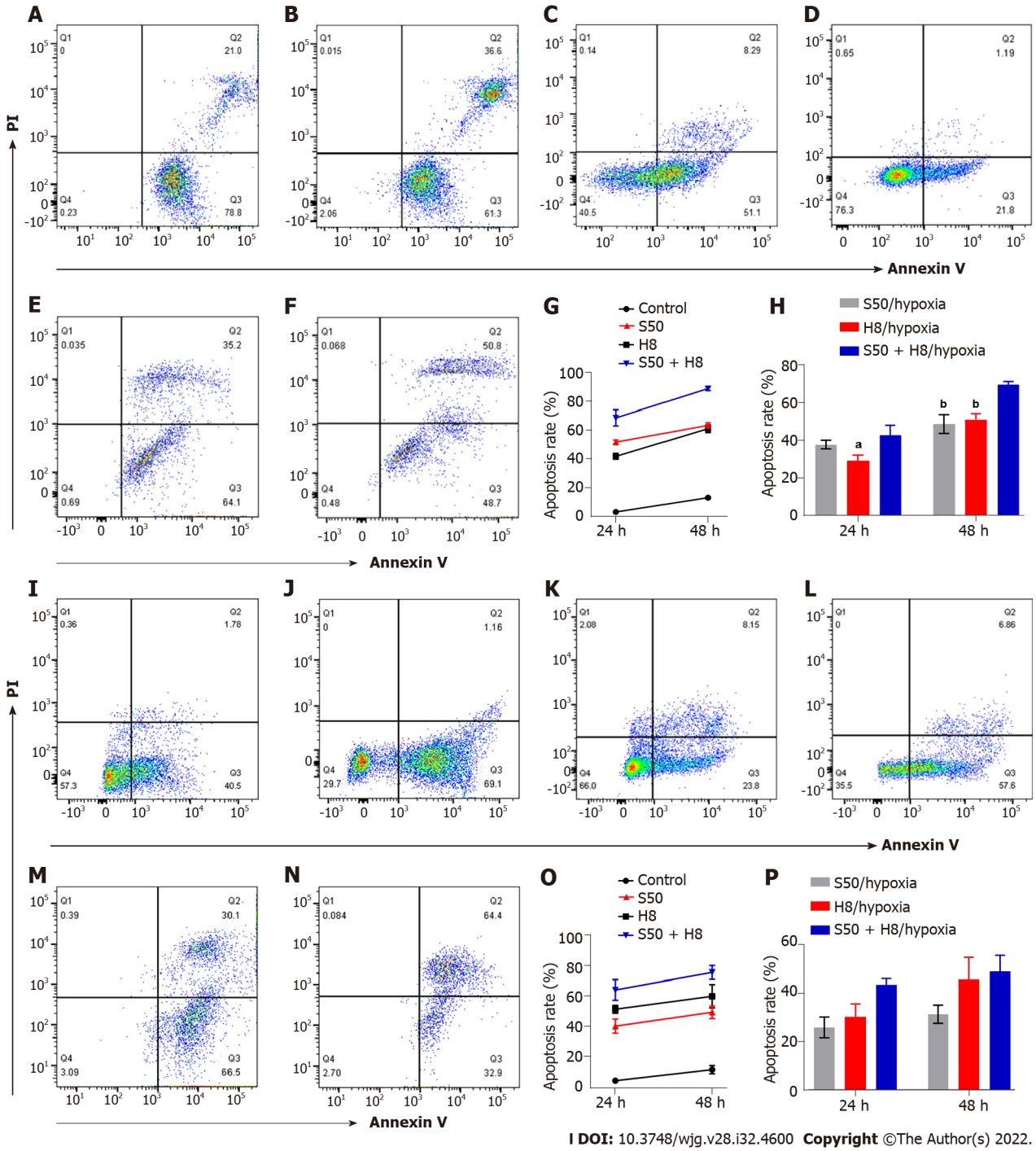
Effect of SRL and Huai Er on expression of target gene mRNA under normoxia

SRL promotes the mRNA expression of *Akt*, *p27*, and *PTEN*, and decreases the mRNA expression of *FoxP3* and *VEGF*: Compared to the control group, the expression of *mTOR* mRNA showed no significant expression changes. However, SRL significantly upregulated the mRNA expression of *Akt*, *p27*, and *PTEN*; this upregulation changed significantly over time (Figure 5A). In addition, SRL treatment significantly downregulated the mRNA expression of *FoxP3* and *VEGF* over the same timeperiod (Figure 5A).

Effect of Huai Er on the mRNA expression of *Akt*, *mTOR*, *FoxP3*, and *VEGF*: Compared with the control group, Huai Er treatment significantly downregulated the mRNA expression of *Akt*, *mTOR*, *FoxP3*, and *VEGF*; this downregulation was significantly increased over time (Figure 5B). The mRNA levels of *p27* ($P_{24\,h} = 0.0066$, $P_{48\,h} = 0.0038$) and *PTEN* ($P_{24\,h} = 0.003$, $P_{48\,h} = 0.0007$) were increased at both time points. *Akt* and *mTOR* expression showed the most significant downregulation after treatment, leading to a reduction in *FoxP3* and *VEGF* mRNA levels from 24 h to 48 h.

SRL and Huai Er downregulate the expression of HIF-1α induced by hypoxia

SRL treatment blocked the downstream amplification effect caused by the expression of mTOR *mRNA* under hypoxia, which significantly downregulated the enhancement effect of hypoxia on *HIF-1α* mRNA expression ($P < 0.01$) (Figure 5C). The treatment also decreased the mRNA expression levels of *VEGF*, *LDHA*, and *GLUT-1* ($P < 0.01$), and simultaneously upregulated the mRNA expression of *p27*, *PTEN*, and *FoxP3* ($P < 0.001$) (Figure 5C). Compared with the hypoxia group, the Huai Er treatment attenuated the hypoxia-induced enhanced mRNA expression of *HIF-1α* and downregulated the mRNA expression of *Akt*, *mTOR*, *VEGF*, and *FoxP3* ($P < 0.01$) (Figure 5C). It also significantly decreased the mRNA



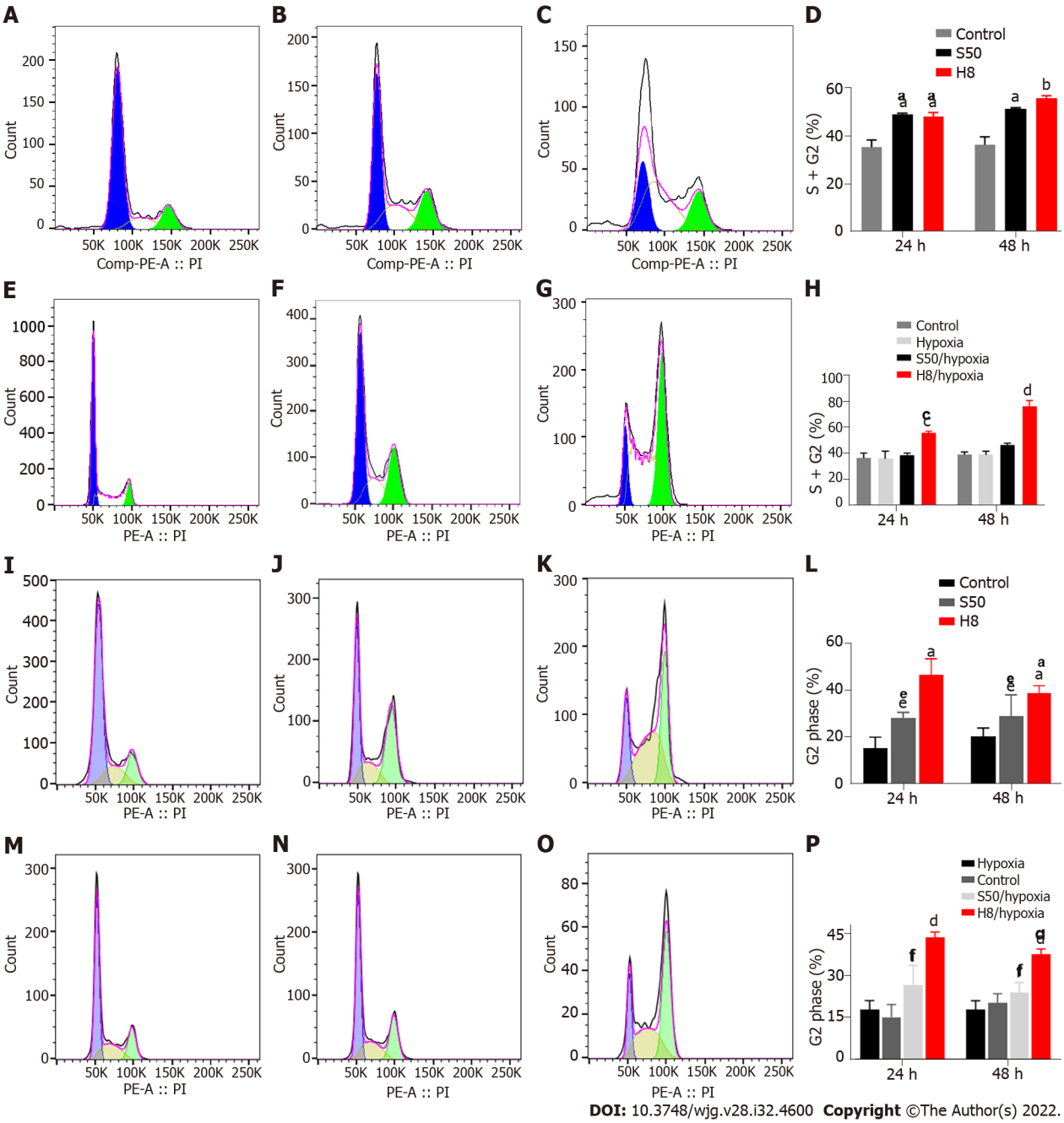
I DOI: 10.3748/wjg.v28.i32.4600 **Copyright** ©The Author(s) 2022.

Figure 3 Effects of sirolimus and Huai Er on apoptosis of HepG2 and Huh 7 cells under normoxic and hypoxic conditions. A-F: Scatter diagrams of apoptosis of HepG2 cells intervened with sirolimus (SRL) (A), with Huai Er (B), with SRL under hypoxia (C), with Huai Er under hypoxia (D), with S50 + H8 under normoxia (E), and with S50 + H8 under hypoxia (F); G and H: Apoptosis rates of HepG2 cell at 24 h and 48 h under normoxia (G) and under hypoxia (H); I-N: Scatter diagrams of apoptosis of Huh 7 cells intervened with SRL (I), with Huai Er (J), with SRL under hypoxia (K), with Huai Er under hypoxia (L), with S50 + H8 under normoxia (M), and with S50 + H8 under hypoxia (N); O and P: Apoptosis rates of Huh 7 cells at 24 h and 48 h under normoxia (O) and under hypoxia (P). $^{a}P < 0.01$ *vs* H8 + S50/hypoxia; $^{b}P < 0.001$ *vs* H8 + S50/hypoxia; $^{c}P < 0.05$ *vs* H8 + S50/hypoxia. H8: 8 mg/mL for Huai Er; S50: 50 nM for SRL.

expression levels of *LDHA* and *GLUT-1* ($P < 0.001$) and upregulated the mRNA expression of *p27* and *PTEN* ($P < 0.001$) (Figure 5C).

LY294002 treatment downregulates hypoxia-induced HIF-1α expression and weakens its mediated glycolytic effect

LY294002 specifically inhibits PI3K, leading to a downstream blocking effect. Ly25 treatment significantly downregulated the mRNA expression of *Akt* and *mTOR* and caused a reduction in *VEGF* and *FoxP3* mRNA expression. Downregulation of mRNA expression of *HIF-1 α, LDHA*, and *GLUT-1*, and upregulation of *p27* and *PTEN* (Figure 6A) were also observed. When compared with the control



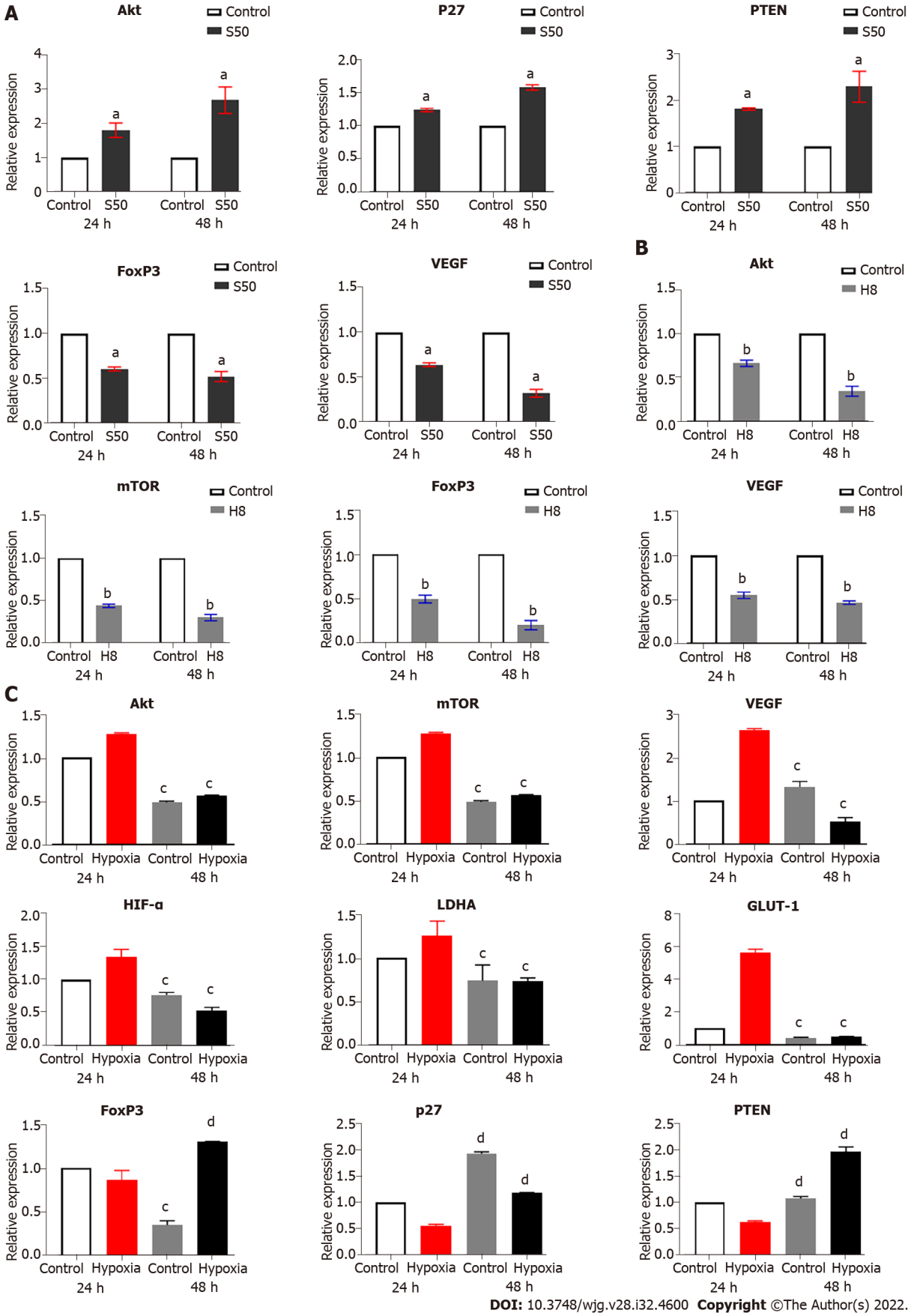
DOI: 10.3748/wjg.v28.i32.4600 **Copyright** ©The Author(s) 2022.

Figure 4 Effects of sirolimus and Huai Er on cell cycle progression of HepG2 and Huh 7 cells under normoxic and hypoxic conditions. A-C: Peak graphs of apoptosis of control HepG2 cells (A) and those treated with sirolimus (SRL) (B) and Huai Er (C) under normoxia; D: HepG2 cell cycle distribution at 24 h and 48 h under normoxia; E-G: Peak graphs of apoptosis of control HepG2 cells (E) and those treated with SRL (F) and Huai Er (G) under hypoxia; H: HepG2 cell cycle distribution at 24 h and 48 h under hypoxia; I-K: Peak graphs of apoptosis of control Huh 7 cells (I) and those treated with SRL (J) and Huai Er (K) under normoxia; L: Huh 7 cell cycle distribution at 24 h and 48 h under normoxia; M-O: Peak graphs of apoptosis of control Huh 7 cells (M) and those treated with SRL (N) and Huai Er (O) under hypoxia; P: Huh 7 cell cycle distribution at 24 h and 48 h under hypoxia. $^{a}P < 0.01$ *vs* control; $^{b}P < 0.001$ *vs* control; $^{c}P < 0.01$ *vs* hypoxia; $^{d}P < 0.001$ *vs* hypoxia; $^{e}P < 0.05$ *vs* control; $^{f}P < 0.05$ *vs* hypoxia. H8: 8 mg/mL for Huai Er; S50: 50 nM for SRL.

group, only the expression of *Akt* mRNA was significantly downregulated at 24 h ($P < 0.05$) (Figure 6); significant differences among the other groups only became apparent after 48 h ($P < 0.05$) (Figure 6A). Except for *FoxP3*, there were significant differences between 48 h and 24 h in the other groups ($P < 0.05$) (Figure 6A).

KC7F2 blocks HIF-1α and results in decreased mRNA expression of LDHA and GLUT-1

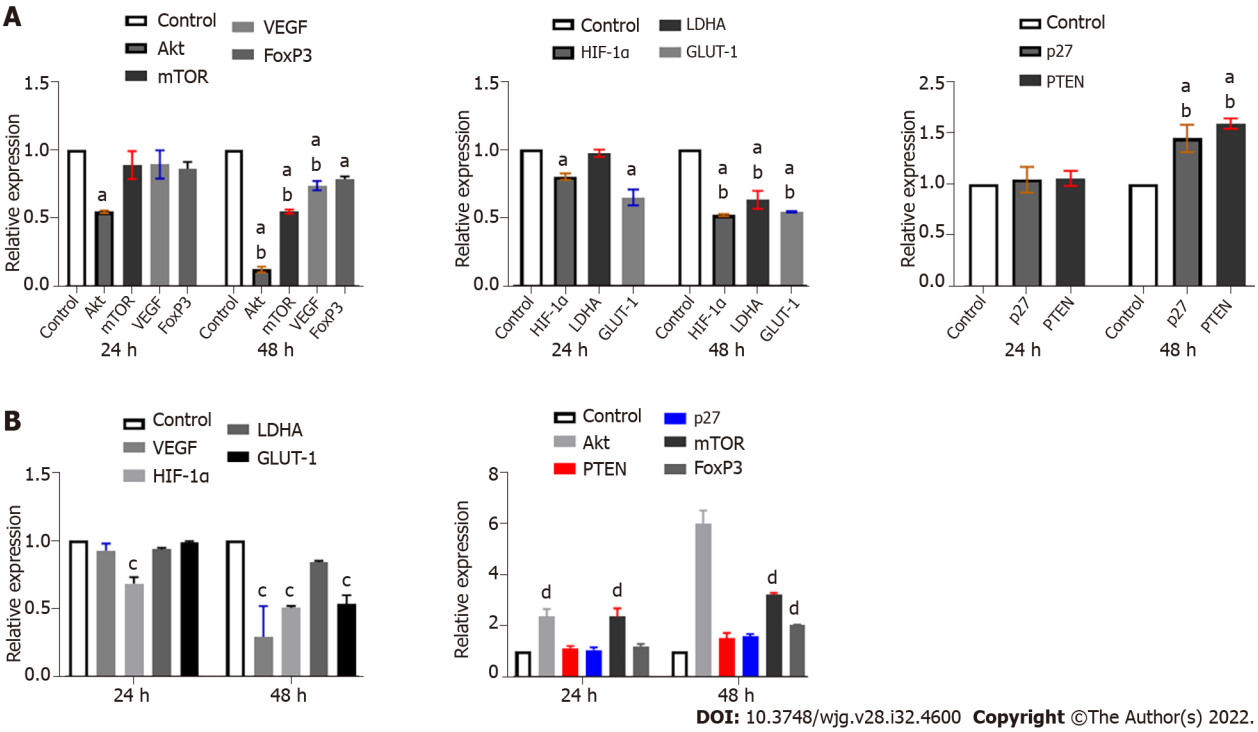
Under normoxia, HIF-1α in tissues was quickly degraded by the intracellular, oxygen-dependent, ubiquitin protease degradation pathway, and its stable expression was weak. Therefore, we used the KC7F2-specific blockade of HIF-1α as a reference. Upon treatment with KC7F2, the mRNA expression of *Akt*, *mTOR*, *PTEN*, and *p27* was upregulated, while the mRNA expression of *VEGF*, *HIF-1α*, *LDHA*, and *GLUT-1* was downregulated (Figure 6B).



DOI: 10.3748/wjg.v28.i32.4600 **Copyright** ©The Author(s) 2022.

Figure 5 Effects of sirolimus & Huai Er on expression of target genes under under normoxic and hypoxic conditions. A: The mRNA levels of *Akt*, *p27*, *PTEN*, *FOXP3*, and *VEGF* in cells treated with sirolimus (SRL) under normoxic condiction at 24 h and 48 h; B: The mRNA levels of *Akt*, *mTOR*, *FOXP3*, and *VEGF* in cells treated with Huai Er under normoxic condiction at 24 h and 48 h; C: The mRNA level of *Akt*, *mTOR*, *VEGF*, *HIF-1α*, *LDHA*, *GLUT-1*, *FOXP3*, *p27*, and *PTEN* in cells treated with SRL and Huai Er under hypoxia at 24 h and 48 h. $^{a}P < 0.05$ *vs* control; $^{b}P < 0.05$ *vs* control; $^{c}P < 0.01$ *vs* hypoxia; $^{d}P < 0.001$ *vs* hypoxia.

PTEN: Phosphatase and tensin homolog deleted on chromosome ten; FoxP3: Forkhead box P3; VEGF: Vascular endothlial growth factor; mTOR: Mammalian target of rapamycin; HIF-1α: Hypoxia inducible factor-1α; LDHA: Lactate dehydrogenase A; GLUT-1: Glucose transporter 1.



DOI: 10.3748/wjg.v28.i32.4600 **Copyright** ©The Author(s) 2022.

Figure 6 Effect of intervention with LY49002 and KC7F2 on mRNA expression of target genes. A: Effect of LY294002 intervention on expression of different genes under normoxic condition; B: Effect of KC7F2 intervention on expression of different genes under normoxic condition. $^{a}P < 0.05$ *vs* control; $^{b}P < 0.05$ *vs* 24 h; $^{c}P < 0.05$ *vs* control; $^{d}P < 0.01$ *vs* control. mTOR: Mammalian target of rapamycin; VEGF: Vascular endothlial growth factor; FoxP3: Forkhead box P3; HIF-1α : Hypoxia inducible factor-1α; LDHA: Lactate dehydrogenase A; GLUT-1: Glucose transporter 1; PTEN: Phosphatase and tensin homolog deleted on chromosome ten.

Ly25 and KC7 treatment weakens the promotion of anaerobic glycolysis mediated by hypoxia-induced HIF-1α accumulation

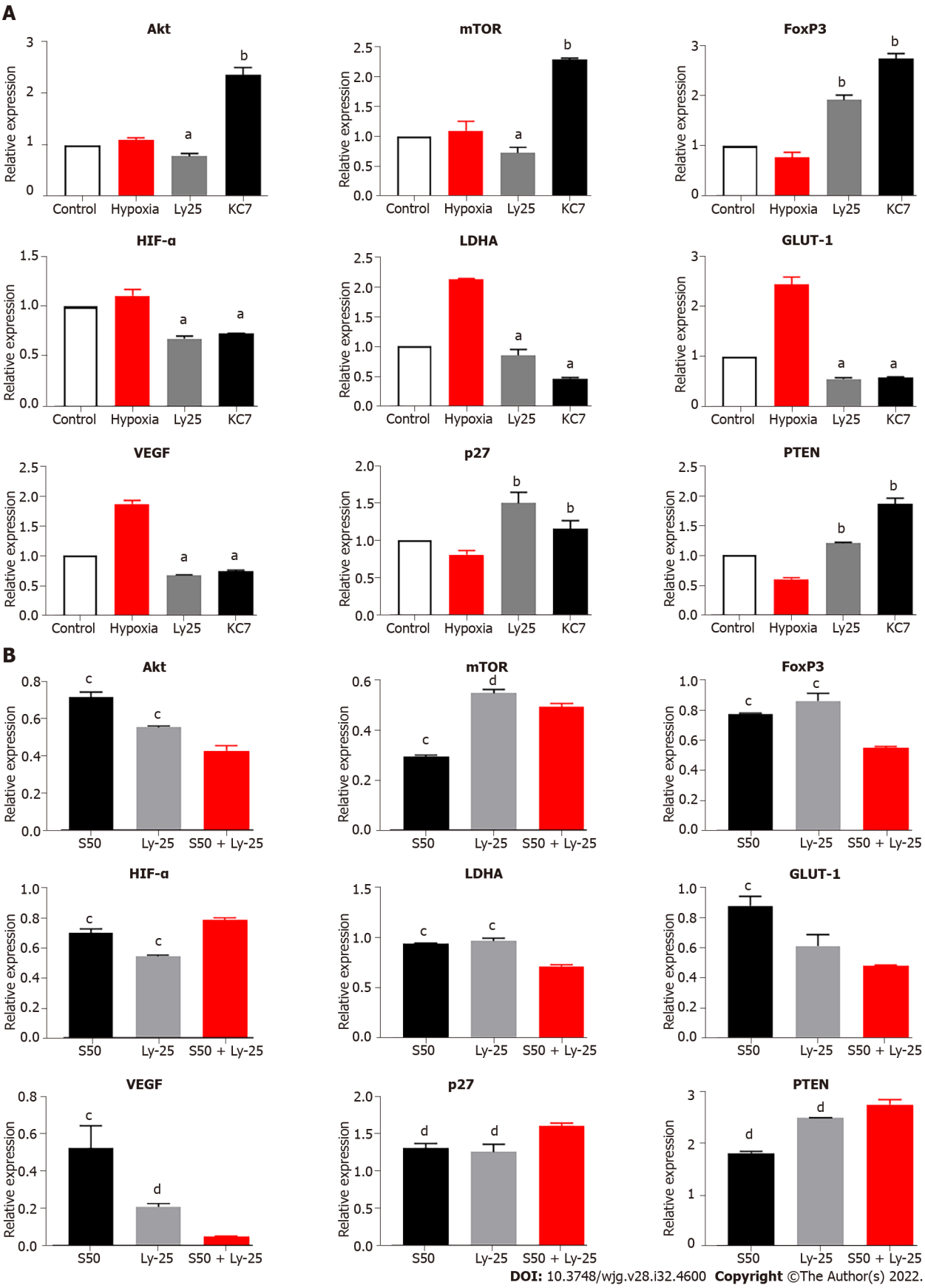
The mRNA expression of *Akt, mTOR, VEGF, HIF-1α, LDHA*, and *GLUT-1* was decreased after treatment with Ly25 ($P < 0.05$) (Figure 7A), while the mRNA expression of *p27, PTEN*, and *FoxP3* was upregulated ($P < 0.05$) (Figure 7A). KC7F2 specifically inhibited the expression of HIF-1α, which downregulated the hypoxia-induced *HIF-1α* mRNA expression ($P < 0.05$). There was also a significant downregulation of *LDHA, GLUT-1*, and *VEGF* mRNA expression ($P < 0.05$) (Figure 7A), while upregulation of *p27* and *PTEN* mRNA expression was observed. However, blocking with KC7 did not inhibit the Akt/mTOR signalling pathway ($P < 0.05$) (Figure 7A), indicating that other regulatory pathways may be involved.

Combined treatment of SRL with Huai Er significantly downregulates the expression of Akt/mTOR

The S50 + H8 combined treatment significantly downregulated the mRNA levels of *Akt* and *mTOR* to a greater extent than the downregulation observed with the H8 treatment alone. In contrast, individual S50 treatment resulted in an upregulation (Figure 8A). The downregulation of *Akt* and *mTOR* mRNA expression resulted in a significant downregulation of *VEGF* ($P < 0.01$) and *FoxP3* mRNA expression ($P < 0.05$) (Figure 8A), and an upregulation of *p27* ($P < 0.01$) and *PTEN* mRNA expression ($P < 0.05$) (Figure 8A).

SRL combined with Ly25 enhances the inhibition of anaerobic glycolysis

Compared with S50 and Ly25 individual treatments, the S50 + Ly25 combination significantly reduced the mRNA expression of *VEGF* and *FoxP3* ($P < 0.05$) (Figure 7B), and significantly upregulated the mRNA expression of *PTEN* and *p27*; there was a significant difference in *p27* mRNA between the two groups ($P < 0.05$). PTEN expression only showed a significant difference between the S50 and S50 + Ly25 groups ($P < 0.05$) (Figure 7B). Downregulation of *Akt, LDHA*, and *GLUT-1* mRNA expression was observed in the S50 + Ly25 group and was more significant than that in the hypoxia group; the difference between groups was significant ($P < 0.01$) (Figure 7B).



DOI: 10.3748/wjg.v28.i32.4600 **Copyright** ©The Author(s) 2022.

Figure 7 Effect of single or combined drug intervention on target gene mRNA expression. A: Effects of LY294002 and KC7F2 on expression of different genes under hypoxia; B: Effect of S50 combined with Ly25 on expression of different genes. [a]*P* < 0.05 *vs* hypoxia; [b]*P* < 0.05 *vs* hypoxia; [c]*P* < 0.05 *vs* S50 + Ly25; [d]*P* < 0.01 *vs* S50 + Ly25. mTOR: Mammalian target of rapamycin; VEGF: Vascular endothlial growth factor; FoxP3: Forkhead box P3; HIF-1α: Hypoxia inducible factor-1α; LDHA: Lactate dehydrogenase A; GLUT-1: Glucose transporter 1; PTEN: Phosphatase and tensin homolog deleted on chromosome ten.

SRL combined with KC7F2 enhances the inhibition of the Akt/mTOR signalling pathway

Compared with the S50 and KC7F2 groups, the combined treatment of S50 + KC7F2 significantly downregulated the mRNA expression of *VEGF* ($P < 0.01$) (Figure 8B) and upregulated the mRNA expression of *p27* ($P < 0.05$) and *PTEN* ($P < 0.01$) (Figure 8B). S50 + KC7F2 treatment also significantly downregulated the mRNA levels of *Akt* and *mTOR* ($P < 0.01$) (Figure 8B), and neutralised the downregulation of *FoxP3* mRNA expression by S50 and upregulation of *FoxP3* mRNA expression by KC7F2 (Figure 8B).

DISCUSSION

A large number of infiltrated lymphocytes, fibroblasts, macrophages, neutrophils, myeloid-derived suppressor cells (MDSCs), and other immune cells result in local immunosuppression and a hypoxic environment which activates HIF-1α[4]. The highly acidic microenvironment caused by the abnormal metabolism of cancer cells and local microvascular infiltration plays an important role in tumor recurrence, proliferation, and invasion[4]. In this study, we indirectly confirmed that high expression of HIF-1α, LHDA, and GLUT-1 in poorly differentiated HCC indicates active glycolysis.

The anoxic and hyperacidic environment of local cancer tissue leads to the inhibition of immune cell function and downregulation of immune cell activity. Cancer cells can constantly adapt to this microenvironment, absorb circulating lactic acid for energy supply, and thus compete with infiltrating immune cell metabolism. This results in a lack of nutrition for T cells in local tissues, low anti-tumour effect, and resultant immune escape of tumour cells[7,12].

It has been confirmed that highly infiltrated regulatory T cells and neutrophils in the local microenvironment are negatively correlated with tumour pathological differentiation and prognosis. In addition, the increase in $FoxP3^+$ Tregs and neutrophil-to-lymphocyte ratio in peripheral blood before surgery is related to a poor prognosis after surgery[17,18]. We confirmed the relationship between $FoxP3^+$ Tregs and recurrence of liver cancer and its inhibitory effect on T cells[15,17]. We found that SRL combined with Huai Er and Thymalfaxin could reduce the level of $FoxP3^+$ Tregs in peripheral blood, delaying the time to tumour recurrence after liver transplantation[19]. However, the specific mechanism of action of $FoxP3^+$ Tregs remains unclear. The present study aimed to explore whether SRL application in combination with Huai Er can achieve antitumour effects by affecting the glycolytic pathway.

Mechanism analysis of proliferation inhibition by SRL combined with Huai Er

Due to the immunosuppressive microenvironment of hypoxia and lactic acid accumulation, most of the $CD8^+$ T lymphocytes infiltrating HCC were in a non-functional state and had a low immune response [10,20]. The cytokine TGF-β and chemokines CXCR4 and CXCR7 produced during tumour proliferation tend to recruit circulating neutrophils and Tregs to the local microenvironment; tumour-related neutrophils can recruit Tregs in cancer tissues through the role of chemokines[3,21]. This interaction between neutrophils and Tregs may enhance the inhibitory properties of the tumour microenvironment. Our previous studies confirmed that $FoxP3^+$ Tregs and $PD\text{-}L1^+$ neutrophils are highly expressed in HCC patients, with or without recurrence[17]. The levels of IL-10 and TGF-β in peripheral blood are significantly higher in patients with cancer than in normal individuals, which is consistent with published results[15,17]. $FoxP3^+$ Tregs inhibit $CD8^+$ T cells to promote tumour growth by secreting IL-10 and TGF-β, which may be a target for the anticancer mechanism of Huai Er. In this study, the cell proliferation assay confirmed that SRL and Huai Er inhibited the growth and proliferation of HepG2 and Huh 7 cell lines in a time- and dose-dependent manner. Treatment with SRL at 50 nM and Huai Er at 8 mg/mL showed the greatest inhibition.

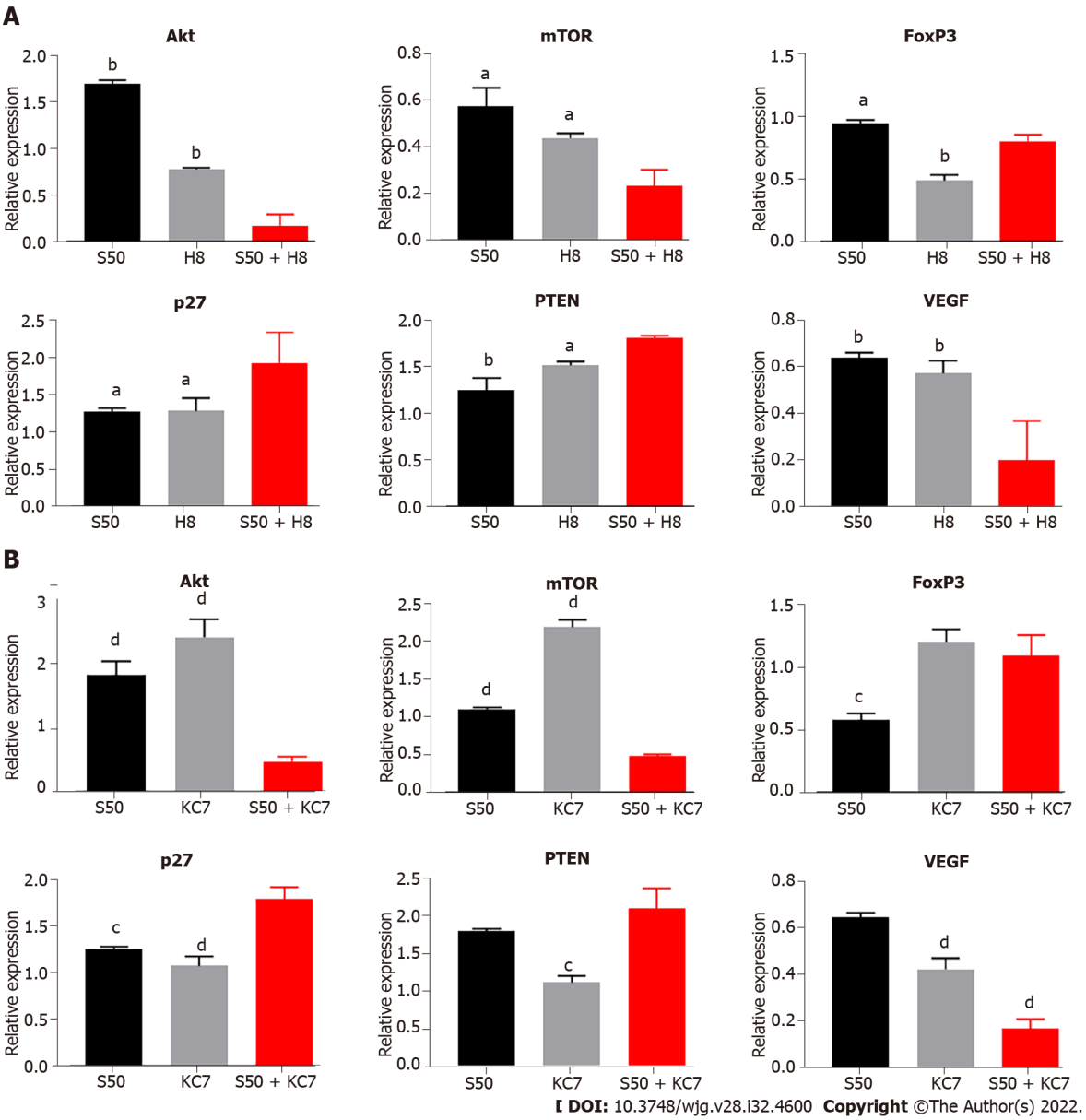
The inhibitory effect of SRL combined with Huai Er was significantly better than that of either of them alone and that of SRL or Huai Er combined with LY294002 and KC7F2 when observing cell invasion by cell scratch assay. This suggested a synergistic effect in inhibiting the invasion of HepG2 and Huh 7 cells. Furthermore, SRL combined with Huai Er displayed high inhibition of the proliferation of cancer cell colonies. These results indicate that Huai Er and SRL inhibited the proliferation and invasion of HepG2 and Huh 7 cells in a concentration- and time-dependent manner.

We confirmed that the apoptosis-promoting effects of SRL and HuaiEr on HepG2 and Huh 7 cells affected mainly early apoptosis, with the combined treatment having a greater effect. Furthermore, SRL and Huai Er significantly increased the proportion of cells in the S + G2 or G2 phase, and this proportion was higher in the combined treatment group compared to the monotherapy groups.

We believe that the inhibitory effect of SRL combined with Huai Er on HepG2 and Huh 7 cell proliferation is achieved mainly by inducing cell cycle arrest in the G2 phase and promoting apoptosis.

Effects of hypoxia and HIF-1α on the anti-tumour effect of Huai Er and SRL

Hypoxia is a common pathophysiological change during the development of most solid tumours[22]. The expression of HIF-1α is first activated by hypoxia in tissue cells, which induces $CD4^+$ T cells to differentiate into $FoxP3^+$ Tregs[23] and plays a role in the regulation of FoxP3 expression[24,25]. Hypoxia can induce the expression of PD-L1 (CD274) on the surface of immune cells (macrophages,



DOI: 10.3748/wjg.v28.i32.4600 Copyright ©The Author(s) 2022.

Figure 8 Effect of S50 combined H8 or KC7 intervention on target gene mRNA expression. A: Regulatory effect of S50 + H8 on expression of different genes under hypoxia condition; B: Effect of S50 + KC7 on expression of different genes. [a]*P* < 0.05 *vs* S50 + H8; [b]*P* < 0.01 *vs* S50 + H8; [c]*P* < 0.05 *vs* S50 + KC7; [d]*P* < 0.01 *vs* S50 + KC7. mTOR: Mammalian target of rapamycin; VEGF: Vascular endothlial growth factor; FoxP3: Forkhead box P3; PTEN: Phosphatase and tensin homolog deleted on chromosome ten.

neutrophils, dendritic cells, MDSCs, *etc.*) and cancer cells[26], which competitively binds to PD-1 receptors on the surface of T cells, resulting in impaired T cell activation function[27,28]. In this study, hypoxia promoted the formation and growth of cancer cell colonies, resulting in a significant increase in the number of cancer cell colonies in the S50 + H8 group. In addition, hypoxia increased the survival rate of HepG2 and Huh 7 cells, whereas Huai Er and SRL promoted their apoptosis.

Although the apoptotic effect increased gradually over time, the maximum apoptotic effect under normoxic conditions was significantly lower than that under hypoxic conditions in both the single drug and S50 + H8 groups. Although hypoxia could significantly downregulate the blocking effect of SRL on the S + G2 phase of HepG2 cells and G2 phase of Huh7 cells, it had less effect on the cell cycle stagnation caused by H8 treatment. Under hypoxic conditions, the S50 + H8 group still had an increased proportion of cells in the S + G2 phase although this proportion was lower than that observed in normoxia. This may be because Huai Er is involved in multiple signalling pathways rather than acts within a single cell signalling pathway which is blocked during hypoxia.

Under normoxic conditions, SRL and Huai Er can act synergistically to inhibit tumour proliferation, but this effect is weakened under hypoxic conditions, possibly due to downstream effects activated by HIF-1α. This indicates that removing the hypoxic environment of tumours may be the key to increasing the efficacy of anti-cancer drugs.

Analysis of HIF-1α regulated tumour growth induced by the hypoxic environment

When cultured under hypoxia, the promotion of HepG2 and Huh 7 cell proliferation and the decrease in apoptosis and cell cycle progression by S50 + H8 treatment indicated that hypoxia plays an important role in HCC. Under hypoxic conditions, *HIF-1α* and *mTOR* in HCC cell lines were shown to be upregulated; in addition, *LDHA, GLUT-1*, and *VEGF* mRNA expression was upregulated and *PTEN* and *p27* mRNA expression was inhibited. The mRNA expression levels of Akt and mTOR were upregulated in the hypoxic environment, although this was not statistically significant. The relative decrease in *Akt* and *mTOR* mRNA expression over time may be related to the activation of the HIF-1α-PTEN-Akt pathway by hypoxia, thereby increasing the glucose metabolism mediated by HIF-1α.

Molecular mechanism of HIF-1α regulated by Huai Er and SRL

The decrease in *HIF-1α* and *mTOR* levels in the S50, H8, and S50 + H8 treatment groups may indicate a potential target pathway for S50 + H8 application in the treatment of HCC. With the intervention of SRL, the mRNA expression of *VEGF* and *FoxP3* was downregulated, while the mRNA expression of *Akt, PTEN*, and *p27* was upregulated. With the intervention of Huai Er, the mRNA expression of *Akt, mTOR, VEGF*, and *FoxP3* was downregulated, while the mRNA expression of *PTEN* and *p27* was upregulated. The combined effects of downregulation of *VEGF, Akt*, and *mTOR* mRNA expression and upregulation of *p27* and *PTEN* were observed more significantly in the S50 + H8 group than in the individual treatment groups. The downregulation of *FoxP3* mRNA was lower than that in the H8 treatment group; this may be associated with the immunomodulatory function of SRL.

Under hypoxic conditions, the accumulation of *HIF-1α* mRNA after treatment with SRL and Huai Er was downregulated. In addition, the mRNA expression of *Akt, mTOR, VEGF, LDHA*, and *GLUT-1* was downregulated, and *PTEN* and *P27* were upregulated. However, the effect of Huai Er combined with SRL was enhanced compared with that of monotherapies, which further confirmed that SRL combined with Huai Er exerted anti-tumour effects through the PI3K-Akt-mTOR-HIF-1α pathway. Previous studies have reported that hypoxia-induced cumulative activation of HIF-1 α can downregulate the mRNA expression of *PTEN* and *P27*, enhance the glycolytic function of tumour cells, and promote the growth and proliferation of tumour cells by upregulating *LDHA* and *GLUT-1* mRNA expression[29]. There have been debates in the literature regarding the mechanism by which[30] hypoxia decreases the expression of FoxP3, with some saying that this is not HIF-1 dependent[31]. In our study, the expression changes of FoxP3 were not consistent with HIF-1 α under hypoxic conditions; this requires further research on co-culture with T cells. The final effect of a significant reduction in *VEGF* mRNA expression was observed, and therefore, we believe that there exists a co-effect of the HIF-1α-PTEN-Akt /mTOR pathway.

Most anticancer drugs decrease the downstream activation effect by reducing the activity of the PI3K-Akt-mTOR pathway[32,33]. PTEN negatively regulates PI3K/Akt signalling and is a well-known tumour suppressor[34]. Studies have demonstrated a strong correlation between alterations in the PTEN/PI3K/Akt cascades and the carcinogenesis of human tumours, including HCC, therefore making it a promising therapeutic target for HCC[34-36]. It has been proved that an increase in PTEN can inhibit the expression of PI3K/pAkt[37]. The upregulation of PTEN can indirectly increase p27 by secreting signal factors[38,39], while the increased PTEN acts on the PI3K-Akt-mTOR pathway and downregulates the expression of pAkt[40,41], further weakening the downstream activation effect. We believe that in this study, the intervention of SRL and Huai Er played a role by downregulating the activity of the Akt/mTOR pathway and increasing the expression of PTEN. SRL can increase the sensitivity of HepG2 cells to Huai Er and exert an anticancer effect through the PI3K-Akt-mTOR-PTEN and PTEN-Akt/mTOR-FoxP3 regulation pathways.

To further investigate the regulatory effect of the above-mentioned effector drugs on HIF-1α, LY294002 and KC7F2 blockers were selected to interfere with the expression of Akt and HIF-1α in the cell pathway. LY294002 inhibits downstream activation and the results showed that LY294002 could significantly reduce the hypoxia-induced upregulation of *HIF-1α* mRNA and attenuate the hypoxia-mediated upregulation of *LDHA, GLUT-1*, and *VEGF* mRNA expression. We observed that the mRNA expression of *PTEN* and *p27* was significantly upregulated, while *Akt* and *mTOR* were downregulated, further confirming the existence of the HIF-1α-PTEN-Akt/mTOR intervention pathway. In addition, the expression of FoxP3 was significantly upregulated, confirming that the regulation of FoxP3 by hypoxia did not completely depend on changes in HIF-1α. We also blocked HIF-1α, using KC7F2 inhibitor, and found that the expression of HIF-1α, LDHA, GLUT-1, and VEGF was significantly downregulated, especially LHDA. The enhancement effect on PTEN and FoxP3 was higher than that with LY294002 treatment, which further confirmed that the effect of hypoxia on FoxP3 was independent of the change in HIF-1α and the existence of the HIF-1α-PTEN effect. The combined treatment of SRL + Ly and SRL + KC7 showed that the regulation of PTEN, p27, and the mRNA expression of *VEGF* and *FoxP3* was consistent with the trend seen during single drug intervention. Based on the above discussion, we further summarize the functional pathways of this study (Supplementary Figure 4).

Thus, we believe that hypoxia can induce the accumulation of HIF-1α and enhance its mediated downstream promoting effect, thereby promoting the growth of tumour cells. SRL can enhance the hypoxia-induced HIF-1α downregulation by Huai Er and attenuate the enhanced effect of glucose

metabolism, mediated by HIF-1α, thus exerting an antitumour effect through the PI3K-Akt-mTOR-HIF-1α and HIF-1α-PTEN-Akt/mTOR pathways.

The overexpression of HIF-1α, the role of FoxP3 in regulating transcription, and the combined intervention of both on the expression of post-transcriptional proteins require further study. In addition, the co-culture of cells affected by T-cell killing function to determine changes in gene and protein levels will be the next research direction of this study.

CONCLUSION

SRL increases the anti-cancer effect of Huai Er, which reduces the promotion of hypoxia-induced HIF-1α on the Warburg effect by inhibiting the PI3K/Akt/mTOR-HIF-1α and HIF-1α-PTEN signalling pathways in HCC.

ARTICLE HIGHLIGHTS

Research background

Hypoxic and high lactate environment further aggravates the aerobic glycolytic effect of cancer and promotes the proliferation and metastasis of liver cancer. Hypoxia-inducible factor 1α plays an important role in the Warburg effect.

Research motivation

We found in clinical practice that the combination of sirolimus (SRL) and Huai Er granules can prolong the survival time of liver transplant patients and delay tumor recurrence. The mechanism of such combination therapy is unclear.

Research objectives

To clarify the regulatory mechanism of SRL combined with Huaier intervention on the Warburg effect.

Research methods

In order to solve the scientific problems raised in this study, immunohistochemistry, cell culture, cell scratch and clone formation assays, and flow cytometry were used to analyze the changes of cell levels.

Research results

Hypoxia-mediated glycolysis was associated with poorly differentiation HCC and a lower prognosis. Hypoxic-induced HIF-1α promoted the growth of HepG2 and Huh7 cells, which was weakened with the treatment of SRL and Huai Er. SRL increased the anti-cancer effect of Huai Er, which reduced the promotion of hypoxia-induced HIF-1α on the Warburg effect by inhibiting the PI3K/Akt/mammalian target of rapamycin (mTOR)-HIF-1α and HIF-1α-phosphatase and tensin homolog deleted on chromosome ten (PTEN) signaling pathways in HCC.

Research conclusions

SRL increases the anti-cancer effect of Huai Er, which reduces the promotion of hypoxia-induced HIF-1α on the Warburg effect by inhibiting the PI3K/Akt/mTOR-HIF-1α and HIF-1α-PTEN signaling pathways in HCC.

Research perspectives

This study confirmed that SRL combined with Huai Er can downregulate the Warburg effect mediated by HIF-1α, laying a foundation for the combined treatment of HCC with traditional Chinese and western medicine.

FOOTNOTES

Author contributions: Zhou L, Zhao Y, and Pan LC contributed equally to this work; Zhou L, Shi XJ, and He Q contributed to conception and design; Du GS, Shi XJ, and He Q contributed to administrative support; He Q and Du GS contributed to provision of study materials; Zhou L, Pan LC, and Wang J contributed to experimental manipulation; Zhao Y, Wang J, and Zhou L contributed to collection and assembly of data; Wang J and Zhao Y contributed to data analysis and interpretation; all authors contributed to manuscript writing and final approval.

Supported by the Natural Science Foundation of Capital Medical University, No. PYZ20014 and No. PYZ21074.

Institutional review board statement: The study was reviewed and approved by the Ethics Committee of Beijing Chaoyang Hospital, No. 2021-1-19-3; and PLA General Hospital, No. S2108-013-01.

Informed consent statement: All study participants, or their legal guardians, provided written informed consent for personal and medical data collection prior to study enrolment.

Conflict-of-interest statement: The authors have no conflicts of interest to declare.

Data sharing statement: The data used and analysed in this study are included in the article or are available from the corresponding and first authors upon reasonable request.

ARRIVE guidelines statement: The authors have read the ARRIVE guidelines, and the manuscript was prepared and revised according to the ARRIVE guidelines.

Open-Access: This article is an open-access article that was selected by an in-house editor and fully peer-reviewed by external reviewers. It is distributed in accordance with the Creative Commons Attribution Non Commercial (CC BY-NC 4.0) license, which permits others to distribute, remix, adapt, build upon this work non-commercially, and license their derivative works on different terms, provided the original work is properly cited and the use is non-commercial. See: https://creativecommons.org/Licenses/by-nc/4.0/

Country/Territory of origin: China

ORCID number: Lin Zhou 0000-0001-8055-4203; Yang Zhao 0000-0003-4901-2216; Li-Chao Pan 0000-0003-4384-8522; Jing Wang 0000-0001-7199-4784; Xian-Jie Shi 0000-0001-7712-2258; Guo-Sheng Du 0000-0002-0732-031X; Qiang He 0000-0002-8900-1688.

S-Editor: Chen YL
L-Editor: Wang TQ
P-Editor: Yu HG

REFERENCES

1 **Siegel RL**, Miller KD, Jemal A. Cancer statistics, 2020. *CA Cancer J Clin* 2020; **70**: 7-30 [PMID: 31912902 DOI: 10.3322/caac.21590]
2 **Forner A**, Reig M, Bruix J. Hepatocellular carcinoma. *Lancet* 2018; **391**: 1301-1314 [PMID: 29307467 DOI: 10.1016/S0140-6736(18)30010-2]
3 **Zhou SL**, Zhou ZJ, Hu ZQ, Huang XW, Wang Z, Chen EB, Fan J, Cao Y, Dai Z, Zhou J. Tumor-Associated Neutrophils Recruit Macrophages and T-Regulatory Cells to Promote Progression of Hepatocellular Carcinoma and Resistance to Sorafenib. *Gastroenterology* 2016; **150**: 1646-1658.e17 [PMID: 26924089 DOI: 10.1053/j.gastro.2016.02.040]
4 **Cheng SC**, Quintin J, Cramer RA, Shepardson KM, Saeed S, Kumar V, Giamarellos-Bourboulis EJ, Martens JH, Rao NA, Aghajanirefah A, Manjeri GR, Li Y, Ifrim DC, Arts RJ, van der Veer BM, Deen PM, Logie C, O'Neill LA, Willems P, van de Veerdonk FL, van der Meer JW, Ng A, Joosten LA, Wijmenga C, Stunnenberg HG, Xavier RJ, Netea MG. mTOR- and HIF-1α-mediated aerobic glycolysis as metabolic basis for trained immunity. *Science* 2014; **345**: 1250684 [PMID: 25258083 DOI: 10.1126/science.1250684]
5 **Hanahan D**, Weinberg RA. Hallmarks of cancer: the next generation. *Cell* 2011; **144**: 646-674 [PMID: 21376230 DOI: 10.1016/j.cell.2011.02.013]
6 **Amann T**, Hellerbrand C. GLUT1 as a therapeutic target in hepatocellular carcinoma. *Expert Opin Ther Targets* 2009; **13**: 1411-1427 [PMID: 19874261 DOI: 10.1517/14728220903307509]
7 **Amann T**, Maegdefrau U, Hartmann A, Agaimy A, Marienhagen J, Weiss TS, Stoeltzing O, Warnecke C, Schölmerich J, Oefner PJ, Kreutz M, Bosserhoff AK, Hellerbrand C. GLUT1 expression is increased in hepatocellular carcinoma and promotes tumorigenesis. *Am J Pathol* 2009; **174**: 1544-1552 [PMID: 19286567 DOI: 10.2353/ajpath.2009.080596]
8 **He G**, Jiang Y, Zhang B, Wu G. The effect of HIF-1α on glucose metabolism, growth and apoptosis of pancreatic cancerous cells. *Asia Pac J Clin Nutr* 2014; **23**: 174-180 [PMID: 24561986 DOI: 10.6133/apjcn.2014.23.1.14]
9 **Kakudo N**, Morimoto N, Ogawa T, Taketani S, Kusumoto K. Hypoxia Enhances Proliferation of Human Adipose-Derived Stem Cells *via* HIF-1α Activation. *PLoS One* 2015; **10**: e0139890 [PMID: 26465938 DOI: 10.1371/journal.pone.0139890]
10 **Weljie AM**, Jirik FR. Hypoxia-induced metabolic shifts in cancer cells: moving beyond the Warburg effect. *Int J Biochem Cell Biol* 2011; **43**: 981-989 [PMID: 20797448 DOI: 10.1016/j.biocel.2010.08.009]
11 **Hui S**, Ghergurovich JM, Morscher RJ, Jang C, Teng X, Lu W, Esparza LA, Reya T, Le Zhan, Yanxiang Guo J, White E, Rabinowitz JD. Glucose feeds the TCA cycle *via* circulating lactate. *Nature* 2017; **551**: 115-118 [PMID: 29045397 DOI: 10.1038/nature24057]
12 **Chen YJ**, Mahieu NG, Huang X, Singh M, Crawford PA, Johnson SL, Gross RW, Schaefer J, Patti GJ. Lactate metabolism is associated with mammalian mitochondria. *Nat Chem Biol* 2016; **12**: 937-943 [PMID: 27618187 DOI: 10.1038/nchembio.2172]
13 **Masoud GN**, Li W. HIF-1α pathway: role, regulation and intervention for cancer therapy. *Acta Pharm Sin B* 2015; **5**: 378-389 [PMID: 26579469 DOI: 10.1016/j.apsb.2015.05.007]

14 **Chen Q**, Shu C, Laurence AD, Chen Y, Peng BG, Zhen ZJ, Cai JQ, Ding YT, Li LQ, Zhang YB, Zheng QC, Xu GL, Li B, Zhou WP, Cai SW, Wang XY, Wen H, Peng XY, Zhang XW, Dai CL, Bie P, Xing BC, Fu ZR, Liu LX, Mu Y, Zhang L, Zhang QS, Jiang B, Qian HX, Wang YJ, Liu JF, Qin XH, Li Q, Yin P, Zhang ZW, Chen XP. Effect of Huaier granule on recurrence after curative resection of HCC: a multicentre, randomised clinical trial. *Gut* 2018; **67**: 2006-2016 [PMID: 29802174 DOI: 10.1136/gutjnl-2018-315983]

15 **Zhou L**, Pan LC, Zheng YG, Zhang XX, Liu ZJ, Meng X, Shi HD, Du GS, He Q. Reduction of FoxP3$^+$ Tregs by an immunosuppressive protocol of rapamycin plus Thymalfasin and Huaier extract predicts positive survival benefits in a rat model of hepatocellular carcinoma. *Ann Transl Med* 2020; **8**: 472 [PMID: 32395516 DOI: 10.21037/atm.2020.03.129]

16 **Schneider CA**, Rasband WS, Eliceiri KW. NIH Image to ImageJ: 25 years of image analysis. *Nat Methods* 2012; **9**: 671-675 [PMID: 22930834 DOI: 10.1038/nmeth.2089]

17 **Zhou L**, Wang J, Lyu SC, Pan LC, Shi XJ, Du GS, He Q. PD-L1$^+$ NEUT, Foxp3$^+$ Treg, and NLR as New Prognostic Marker with Low Survival Benefits Value in Hepatocellular Carcinoma. *Technol Cancer Res Treat* 2021; **20**: 15330338211045820 [PMID: 34605709 DOI: 10.1177/15330338211045820]

18 **Zhou L**, Wang J, Zhang XX, Lyu SC, Pan LC, Du GS, Lang R, He Q. Prognostic Value of Preoperative NLR and Vascular Reconstructive Technology in Patients With Pancreatic Cancer of Portal System Invasion: A Real World Study. *Front Oncol* 2021; **11**: 682928 [PMID: 34604028 DOI: 10.3389/fonc.2021.682928]

19 **Zhou L**, Pan LC, Zheng YG, Du GS, Fu XQ, Zhu ZD, Song JY, Liu ZJ, Su XZ, Chen W, Zheng DH, Suo LL, Yang SZ. Novel strategy of sirolimus plus thymalfasin and huaier granule on tumor recurrence of hepatocellular carcinoma beyond the UCSF criteria following liver transplantation: A single center experience. *Oncol Lett* 2018; **16**: 4407-4417 [PMID: 30214575 DOI: 10.3892/ol.2018.9226]

20 **Vaupel P**, Mayer A. Hypoxia-Driven Adenosine Accumulation: A Crucial Microenvironmental Factor Promoting Tumor Progression. *Adv Exp Med Biol* 2016; **876**: 177-183 [PMID: 26782210 DOI: 10.1007/978-1-4939-3023-4_22]

21 **Mishalian I**, Bayuh R, Eruslanov E, Michaeli J, Levy L, Zolotarov L, Singhal S, Albelda SM, Granot Z, Fridlender ZG. Neutrophils recruit regulatory T-cells into tumors *via* secretion of CCL17--a new mechanism of impaired antitumor immunity. *Int J Cancer* 2014; **135**: 1178-1186 [PMID: 24501019 DOI: 10.1002/ijc.28770]

22 **Hayashi Y**, Yokota A, Harada H, Huang G. Hypoxia/pseudohypoxia-mediated activation of hypoxia-inducible factor-1α in cancer. *Cancer Sci* 2019; **110**: 1510-1517 [PMID: 30844107 DOI: 10.1111/cas.13990]

23 **Lee JH**, Elly C, Park Y, Liu YC. E3 Ubiquitin Ligase VHL Regulates Hypoxia-Inducible Factor-1α to Maintain Regulatory T Cell Stability and Suppressive Capacity. *Immunity* 2015; **42**: 1062-1074 [PMID: 26084024 DOI: 10.1016/j.immuni.2015.05.016]

24 **Lequeux A**, Noman MZ, Xiao M, Van Moer K, Hasmim M, Benoit A, Bosseler M, Viry E, Arakelian T, Berchem G, Chouaib S, Janji B. Targeting HIF-1 alpha transcriptional activity drives cytotoxic immune effector cells into melanoma and improves combination immunotherapy. *Oncogene* 2021; **40**: 4725-4735 [PMID: 34155342 DOI: 10.1038/s41388-021-01846-x]

25 **Noman MZ**, Desantis G, Janji B, Hasmim M, Karray S, Dessen P, Bronte V, Chouaib S. PD-L1 is a novel direct target of HIF-1α, and its blockade under hypoxia enhanced MDSC-mediated T cell activation. *J Exp Med* 2014; **211**: 781-790 [PMID: 24778419 DOI: 10.1084/jem.20131916]

26 **Shalapour S**, Lin XJ, Bastian IN, Brain J, Burt AD, Aksenov AA, Vrbanac AF, Li W, Perkins A, Matsutani T, Zhong Z, Dhar D, Navas-Molina JA, Xu J, Loomba R, Downes M, Yu RT, Evans RM, Dorrestein PC, Knight R, Benner C, Anstee QM, Karin M. Erratum: Inflammation-induced IgA$^+$ cells dismantle anti-liver cancer immunity. *Nature* 2017; **552**: 430 [PMID: 29168501 DOI: 10.1038/nature25028]

27 **Taube JM**, Klein A, Brahmer JR, Xu H, Pan X, Kim JH, Chen L, Pardoll DM, Topalian SL, Anders RA. Association of PD-1, PD-1 ligands, and other features of the tumor immune microenvironment with response to anti-PD-1 therapy. *Clin Cancer Res* 2014; **20**: 5064-5074 [PMID: 24714771 DOI: 10.1158/1078-0432.CCR-13-3271]

28 **Schultz L**, Chaux A, Albadine R, Hicks J, Kim JJ, De Marzo AM, Allaf ME, Carducci MA, Rodriguez R, Hammers HJ, Argani P, Reuter VE, Netto GJ. Immunoexpression status and prognostic value of mTOR and hypoxia-induced pathway members in primary and metastatic clear cell renal cell carcinomas. *Am J Surg Pathol* 2011; **35**: 1549-1556 [PMID: 21881486 DOI: 10.1097/PAS.0b013e31822895e5]

29 **Hsu TS**, Lai MZ. Hypoxia-inducible factor 1α plays a predominantly negative role in regulatory T cell functions. *J Leukoc Biol* 2018; **104**: 911-918 [PMID: 29901858 DOI: 10.1002/JLB.MR1217-481R]

30 **Wang XD**, Liu CX, Wu YL, Chen J. [Hypoxia and its simulant CoCl(2) down-regulates Foxp3 expression independent from HIF-1alpha]. *Zhongguo Shi Yan Xue Ye Xue Za Zhi* 2009; **17**: 533-536 [PMID: 19549358]

31 **Tang H**, Li RP, Liang P, Zhou YL, Wang GW. miR-125a inhibits the migration and invasion of liver cancer cells *via* suppression of the PI3K/AKT/mTOR signaling pathway. *Oncol Lett* 2015; **10**: 681-686 [PMID: 26622553 DOI: 10.3892/ol.2015.3264]

32 **Yulyana Y**, Ho IA, Sia KC, Newman JP, Toh XY, Endaya BB, Chan JK, Gnecchi M, Huynh H, Chung AY, Lim KH, Leong HS, Iyer NG, Hui KM, Lam PY. Paracrine factors of human fetal MSCs inhibit liver cancer growth through reduced activation of IGF-1R/PI3K/Akt signaling. *Mol Ther* 2015; **23**: 746-756 [PMID: 25619723 DOI: 10.1038/mt.2015.13]

33 **Maehama T**, Dixon JE. The tumor suppressor, PTEN/MMAC1, dephosphorylates the lipid second messenger, phosphatidylinositol 3,4,5-trisphosphate. *J Biol Chem* 1998; **273**: 13375-13378 [PMID: 9593664 DOI: 10.1074/jbc.273.22.13375.]

34 **Liu F**, He Y, Liang Y, Wen L, Zhu Y, Wu Y, Zhao L, Li Y, Mao X, Liu H. PI3-kinase inhibition synergistically promoted the anti-tumor effect of lupeol in hepatocellular carcinoma. *Cancer Cell Int* 2013; **13**: 108 [PMID: 24176221 DOI: 10.1186/1475-2867-13-108]

35 **Fresno Vara JA**, Casado E, de Castro J, Cejas P, Belda-Iniesta C, González-Barón M. PI3K/Akt signalling pathway and cancer. *Cancer Treat Rev* 2004; **30**: 193-204 [PMID: 15023437 DOI: 10.1016/j.ctrv.2003.07.007]

36 **Zhu L**, Sun Y, Zhang S, Wang L. Rap2B knockdown suppresses malignant progression of hepatocellular carcinoma by inactivating the PTEN/PI3K/Akt and ERK1/2 pathways. *Mol Cell Biochem* 2020; **466**: 55-63 [PMID: 32052247 DOI: 10.1007/s11010-020-03687-w]

37 **Wang DD**, Yang SJ, Chen X, Shen HY, Luo LJ, Zhang XH, Zhong SL, Zhao JH, Tang JH. miR-222 induces Adriamycin resistance in breast cancer through PTEN/Akt/$p27^{kip1}$ pathway. *Tumour Biol* 2016; **37**: 15315-15324 [PMID: 27699665 DOI: 10.1007/s13277-016-5341-2]

38 **Hackenbeck T**, Knaup KX, Schietke R, Schödel J, Willam C, Wu X, Warnecke C, Eckardt KU, Wiesener MS. HIF-1 or HIF-2 induction is sufficient to achieve cell cycle arrest in NIH3T3 mouse fibroblasts independent from hypoxia. *Cell Cycle* 2009; **8**: 1386-1395 [PMID: 19342889 DOI: 10.4161/cc.8.9.8306]

39 **Fu X**, Wen H, Jing L, Yang Y, Wang W, Liang X, Nan K, Yao Y, Tian T. MicroRNA-155-5p promotes hepatocellular carcinoma progression by suppressing PTEN through the PI3K/Akt pathway. *Cancer Sci* 2017; **108**: 620-631 [PMID: 28132399 DOI: 10.1111/cas.13177]

40 **Semenza GL**. HIF-1 mediates metabolic responses to intratumoral hypoxia and oncogenic mutations. *J Clin Invest* 2013; **123**: 3664-3671 [PMID: 23999440 DOI: 10.1172/JCI67230]

41 **Rasmussen KD**, Helin K. Role of TET enzymes in DNA methylation, development, and cancer. *Genes Dev* 2016; **30**: 733-750 [PMID: 27036965 DOI: 10.1101/gad.276568.115]

World Journal of Gastroenterology

Submit a Manuscript: https://www.f6publishing.com

World J Gastroenterol 2022 August 28; 28(32): 4620-4634

DOI: 10.3748/wjg.v28.i32.4620

ISSN 1007-9327 (print) ISSN 2219-2840 (online)

ORIGINAL ARTICLE

Basic Study

Anti-tumour activity and toxicological studies of combination treatment of *Orthosiphon stamineus* and gemcitabine on pancreatic xenograft model

Ashwaq Hamid Salem Yehya, Ayappa V Subramaniam, Muhammad Asif, Gurjeet Kaur, Amin M S Abdul Majid, Chern Ein Oon

Specialty type: Integrative and complementary medicine

Provenance and peer review: Invited article; Externally peer reviewed.

Peer-review model: Single blind

Peer-review report's scientific quality classification

Grade A (Excellent): A
Grade B (Very good): 0
Grade C (Good): 0
Grade D (Fair): D
Grade E (Poor): 0

P-Reviewer: Hamaya Y, Japan; Matsumoto T, Japan

Received: January 10, 2022
Peer-review started: January 10, 2022
First decision: April 16, 2022
Revised: April 26, 2022
Accepted: June 26, 2022
Article in press: June 26, 2022
Published online: August 28, 2022

Ashwaq Hamid Salem Yehya, Ayappa V Subramaniam, Gurjeet Kaur, Chern Ein Oon, Institute for Research in Molecular Medicine, Universiti Sains Malaysia, Penang 11800, Malaysia

Ashwaq Hamid Salem Yehya, Cancer Research, Eman Biodiscoveries, Kedah 08000, Malaysia

Muhammad Asif, Department of Pharmacology, Faculty of Pharmacy, The Islamia University of Bahawalpur, Punjab 63100, Pakistan

Amin M S Abdul Majid, Department of Cancer Biology and Therapeutics, The John Curtin School of Medical Research, Australia 2601, Australia

Corresponding author: Chern Ein Oon, PhD, Associate Professor, Institute for Research in Molecular Medicine, Universiti Sains Malaysia, Chancellory II, Penang 11800, Malaysia. chern.oon@usm.my

Abstract

BACKGROUND

Pancreatic cancer is the most aggressive cancer type. Gemcitabine is the first line chemo-drug used for pancreatic cancer but exerts a broad spectrum of organ toxicities and adverse effects in patients.

AIM

To evaluate the anti-tumour activity and toxicological effects of *Orthosiphon stamineus* extract formulation (ID: C5EOSEW5050ESA trademarked as Nuvastatic™), and gemcitabine combination on pancreatic xenograft model.

METHODS

Mice were randomly divided into six groups of 6 mice each (n = 6) and given different treatments for 28 d. The study design consisted of a 2 x 3 factorial treatment structure, with gemcitabine (yes/no) by oral (at 1200 and 400 mg/kg per day). Human pancreatic cancer cells were injected subcutaneously into the flanks of athymic nude mice. C5EOSEW5050ESA (200 or 400 mg/kg per day) was administered orally, while gemcitabine (10 mg/kg per 3 d) was given intraperitoneally either alone or in combination treatment. Histopathological analyses of vital organs, tumour tissues, and incidence of lethality were analysed. Analyses of

tumour necrosis and proliferation were determined by haematoxylin-eosin staining and immunohistochemistry for Ki-67, respectively.

RESULTS

No signs of toxicity or damage to vital organs were observed in all treatment groups compared to the untreated group. C5EOSEW5050ESA at 200 mg/kg and gemcitabine combination had no additive antitumor effects compared to a single treatment. Remarkably, a comparably greater response in a reduction in tumour growth, Ki-67 protein expression, and necrosis was demonstrated by 400 mg/kg of C5EOSEW5050ESA and gemcitabine combination than that of the individual agents.

CONCLUSION

These results highlighted the synergistic activity of C5EOSEW5050ESA with gemcitabine to reduce pancreatic tumour growth in mice compared to a single treatment. Thus, this study provides valuable insights into using C5EOSEW5050ESA as a complementary treatment with gemcitabine for pancreatic cancer.

Key Words: Pancreatic cancer; *Orthosiphon stamineus*; C5EOSEW5050ESA; Gemcitabine; Complementary medicine

©The Author(s) 2022. Published by Baishideng Publishing Group Inc. All rights reserved.

Core Tip: The combination of C5EOSEW5050ESA at 400 mg/kg and gemcitabine synergistically reduced tumour growth compared to either drug alone by reducing Ki-67 cell proliferation marker and tumour necrosis. In addition, no signs of toxicity or damage to vital organs in single C5EOSEW5050ESA or gemcitabine and chemo-herbal combinations treated animals compared to the untreated group, indicating the safety and efficacy of the combination treatment in a short term study. Findings from this study may provide the basis for product formulation and manufacturing of botanical drugs to be used as complementary medicine for the treatment of cancer.

Citation: Yehya AHS, Subramaniam AV, Asif M, Kaur G, Abdul Majid AMS, Oon CE. Anti-tumour activity and toxicological studies of combination treatment of *Orthosiphon stamineus* and gemcitabine on pancreatic xenograft model. *World J Gastroenterol* 2022; 28(32): 4620-4634

URL: https://www.wjgnet.com/1007-9327/full/v28/i32/4620.htm

DOI: https://dx.doi.org/10.3748/wjg.v28.i32.4620

INTRODUCTION

Pancreatic cancer is one of the deadliest cancers globally and has the most unfavourable survival rate of any cancer[1]. Chemotherapy, radiation, surgery, and molecular targeting agents are common strategies to treat pancreatic cancer. However, the majority of these systemic treatments are associated with severe side effects[1]. Gemcitabine, a nucleoside analogue of cytidine, is the first line of treatment used to treat pancreatic cancer[2]. However, its overall success rates are poor. In addition, combination treatments of gemcitabine with other chemo-drugs, such as capecitabine, irinotecan, oxaliplatin, and cisplatin, may cause multiple adverse reactions and drug resistance, leading to a reduction of drug efficacy[3].

Herbal products have been traditionally used to treat many diseases in Asian countries[4]. Data from pre-clinical and clinical studies have also highlighted that these natural herbs, when combined with conventional radio- or chemotherapies, can sensitise tumour cells to treatments to improve cancer patients' survival and quality of life[5,6]. Nevertheless, this is not always the case, as studies have also shown that herbal medicines, when combined with chemotherapies, may instead enhance the toxicity potential of chemo drugs, leading to increased incidences of severe side effects[7].

Therefore, understanding the interactions of herbal-chemo drugs is necessary for the appropriate use of these combinations to prevent the emergence of toxicity and therapeutic failure in cancer patients. *Orthosiphon stamineus* (*O.s*) is a traditional Asian herbal medicine used to treat various diseases, including cancers[8]. The safety profile of *O.s* has already been established globally by numerous research groups using *in vivo* and *in vitro* models[3,9]. Our research group has already established the antitumor efficacy of *O.s* against colon cancer[9,10]. C5OSEW5050ESA (Nuvastatic™) is a proprietary extract of *O.s* that completed a phase 2/3 clinical study for cancer fatigue in cancer patients with solid tumours receiving chemotherapy[11]. However, no study has reported the toxicity profile of C5OSEW5050ESA in a pancreatic cancer xenograft model as a stand-alone or in combination with

Table 1 Treatment conditions for 28 d

No.	Group	The route of treatment and dose
1	Group I (untreated group- distilled water)	Oral (1 mg/kg per day)
2	Group II (chemodrug-gemcitabine)	Intraperitoneal (10 mg/kg per 3 d)
3	Group III (low dose of *O.s*)	Oral (200 mg/kg per day)
4	Group IV (low dose of *O.s* -gemcitabine combination)	Oral (200 mg/kg per day) + Intraperitoneal (10 mg/kg per 3 d)
5	Group V (high dose of *O.s*)	Oral (400 mg/kg per day)
6	Group VI (high dose of *O.s*-gemcitabine combination)	Oral (400 mg/kg per day) + Intraperitoneal (10 mg/kg per 3 d)

O.s: *Orthosiphon stamineus*.

gemcitabine. We have previously reported that the combination treatment of *O.s* and gemcitabine showed no toxicity in mice, either as a stand-alone or in combination[3]. Furthermore, *O.s* significantly sensitised Panc-1 towards gemcitabine *in vitro*[4]. Consequently, the present study was designed to evaluate the toxicological effects of Nuvastatic™ and gemcitabine either alone or in combination using the pancreatic cancer nude mice model.

MATERIALS AND METHODS

Plant materials and chemicals

Orthosiphon stamineus extract (C5EOSEW5050ESA) was purchased from NatureCeutical Sdn Bhd, Malaysia. Gemcitabine (Catalogue No. S1149) was obtained from Selleckchem, Houston, TX, United States. C5EOSEW5050ESA was dissolved in sterile distilled water and filtered by a membrane filter unit (0.22 μm). C5EOSEW5050ESA was administered orally to mice, while gemcitabine was given *via* intraperitoneal injection after being dissolved in phosphate buffer saline (PBS).

Animals

Male athymic nude mice (procured from iDNA, Malaysia) were kept in filter-top cages under controlled atmospheric conditions at the EMAN Testing and Research laboratory, School of Pharmaceutical Sciences, USM. Autoclaved food, water, and bedding of cages were changed every 48 h. The animal study was approved and conducted under strict guidelines according to USM Animal Ethics Committee (Reference #: USM/Animal Ethics Approval/2016/(97) (746).

Cell lines

Panc-1, a pancreatic cancer cell line, was purchased from American Type Culture Collection (ATCC). The cells were maintained in Dulbecco's Modified Eagle Medium (DMEM) (Thermo Scientific, United States) supplemented with 10% fetal bovine serum (Biowest, United States) and 100 units/mL penicillin-streptomycin (Nacalai Tesque, United States). Cells were kept at 37 °C in a humidified incubator with 5% CO_2 atmosphere.

***In vivo* assessment of tumour growth in a nude mouse xenograft model:** Panc-1 cells (20×10^6 cells suspended in 200 μL of a mixture of DMEM and matrigel in a 1:1 ratio) were injected subcutaneously on the dorsal side of each mouse. Treatment with gemcitabine and *Et. O.s* in different combinations or as a stand-alone was initiated when at least three of the tumours in any group reached 100 mm^3.

Experimental treatment design

Mice were randomly divided into six groups of 6 mice each ($n = 6$) and given different treatments for 28 d, as mentioned in Table 1. The body weight of all mice and tumour size was measured every 3rd day. At the end of the study, all the mice were euthanised with a combination of ketamine and xylazine when the tumour volumes from the untreated group reached 1000 mm^3. The blood samples were collected for haematological and serum biochemical tests. Organs (liver, kidney, and spleen) were harvested and weighed to observe the changes in the organ weights of treated animals compared to the untreated group. Tumour tissues and organs were collected and fixed with 10% buffered formalin. Paraffin blocks were prepared, and sections of 5 μm were stained with haematoxylin and eosin (HE). Ten microscopic fields per slide were examined at × 20 and × 40 magnification, and photomicrographic images were captured using a digital camera.

Blood parameters and biochemical tests

Blood samples were used to measure different haematological parameters, including haemoglobin (Hb) levels, total blood count, differential counting of white blood cells, packed cell volume (PCV), mean cell volume (MCV), mean cell haemoglobin (MCH), mean cell haemoglobin concentration (MCHC), red cell distribution width (RDW), creatinine, urea, uric acid, aspartate aminotransferase (AST), alanine aminotransferase (ALT), alkaline phosphatase (ALP), gamma-glutamyl transferase (GGT), total bilirubin, cholesterol (low and high-density cholesterol), triglycerides, total protein, albumin, globulin, albumin/globulin ratio, and minerals (sodium, potassium, and chloride).

Histopathological examination

Key organs (liver, kidney, and spleen) were harvested and fixed in a 10% buffered formaldehyde solution. An automated tissue processing machine then processed the fixed tissues and embedded them in paraffin wax to prepare sample blocks.

Haematoxylin and eosin staining

Tissue sections of 5 mm thickness were cut and prepared at 60 °C. The slides were dewaxed in xylene and rehydrated through graded alcohol. Slides were rinsed and incubated with haematoxylin for 4 min. After rinsing, eosin was added to the slides for 1 min. Next, slides were rinsed in tap water and briefly air-dried at room temperature. Slides were then mounted with glycerol (Sigma, United States). Stained slides were examined and scored for the percentage of necrosis within the tumour areas by a pathologist (GK) under a light microscope.

Immunohistochemistry staining

The formalin-fixed-paraffin-embedded (FFPE) tissue sections were prepared at 60 °C, dewaxed in xylene, and rehydrated through graded alcohol. Antigens were retrieved using Dako's antigen retrieval buffer (1 ×, pH 9.0) and then microwaved on high for 15 min. Slides were cooled, washed and then blocked with hydrogen peroxidase and BSA. Then slides were treated with primary antibody Ki67 (Dako, Glostrup, Denmark) and left to incubate at 4 °C overnight at 1:50 dilution. The next day, slides were treated with secondary antibody goat anti-mouse (Dako, Glostrup, Denmark) for 1 h at 1:500 dilution. Later, avidin-biotin complex (Vector Laboratories, United States) was added to tissues for 1 h. After that, Dab stain (Dako, Glostrup, Denmark) and haematoxylin were added to the slides. Finally, slides were air-dried at room temperature and mounted with glycerol (Sigma, United States). Using ImageJ, the Ki-67 score was determined as the percentage of tumour cells that showed brown nuclear staining over the total number of nuclei from five random fields per tumour section.

Statistical analysis

Graphing software Excel (Microsoft, United States) and Prism (GraphPad, United States) were used for statistical analysis. Data were presented as mean ± SD whereas the parametric data analysis was performed using a one-way analysis of variance (ANOVA). Two-way ANOVA was used to understand if there is an interaction between the two independent variables on the dependent variable. The Tukey's honest significant difference (HSD) post hoc test was used to assess the significant differences among all groups. Analysis for non-parametric data was performed using Kruskal-Wallis ANOVA. A value of $P < 0.05$ was considered significant when compared to values in the respective untreated group.

RESULTS

Effect of treatment on mouse body weight and key organs

C5EOSEW5050ESA demonstrated no toxicity in mice: The average body weight within the untreated group increased compared to other treatment groups (Table 2). However, there was no notable difference in body weight between untreated groups and other treatment groups (Table 2). In addition, the weight of vital organs, including the kidney, liver, and spleen, remained unchanged post-treatment with either C5EOSEW5050ESA and/or gemcitabine (Table 3).

Haematological-biochemical parameters and electrolyte profiles: No significant changes were observed in the Hb level, total blood cells count, or differential counting of WBC, PCV, MCV, MCH, MCHC, and RDW when compared with the corresponding parameters in the untreated group (Table 4). No significant changes were noted in serum parameters, *i.e.* creatinine, urea, uric acid, AST, ALT, ALP, GGT, total bilirubin, total protein, albumin, globulin, and albumin/globulin ratio, which were observed in animal groups treated with C5EOSEW5050ESA at (200 or 400 mg/kg per day) alone or in combination with gemcitabine (10 mg/kg per 3 d) after 28 d treatment when compared to the untreated group (Table 5). Normal ALT, ALP, and AST levels in the serum indicate that there is no damage in hepatocytes. Similarly, urea and total bilirubin levels were also within the normal range, indicating the lack of toxicity in the kidneys when treated with C5EOSEW5050ESA and gemcitabine either alone or in

Table 2 Effect of C5EOSEW5050ESA and gemcitabine alone or in combination on mouse body weight

No.	Group	Days										*P* value
		0	2	5	8	11	14	17	20	23	26	28	
1	Untreated	24.2 ± 0.8	24.5 ± 1.0	24.7 ± 0.6	24.7 ± 0.9	24.6 ± 1.1	24.8 ± 0.9	25.0 ± 0.3	24.8 ± 0.6	24.6 ± 0.7	24.5 ± 1.1	24.5 ± 0.9	-
2	Gemcitabine (10 mg/kg per 3 d)	24.2 ± 0.7	24.3 ± 1.5	24.1 ± 1.2	23.9 ± 1.7	24.1 ± 1.3	24.0 ± 1.3	24.2 ± 0.5	24.5 ± 0.9	24.6 0 ± .5	24.3 ± 0.7	24.0 ± 0.9	NS
3	*O.s* (200 mg/kg per day)	23.6 ± 0.6	23.9 ± 0.7	24.9 ± 0.9	23.9 ± 1.1	24.1 ± 1.2	23.8 ± 1.1	24.0 ± 0.7	23.9 ± 9.0	23.8 ± 1.2	24.0 ± 1.5	23.8 ± 0.5	NS
4	*O.s* (200 mg/kg per day) and gemcitabine (10 mg/kg per 3 d) combination	24.0 ± 0.8	24.0 ± 1.2	23.9 ± 1.0	24.0 ± 1.1	23.4 ± 1.3	23.9 ± 1.5	24.1 ± 0.7	24.2 ± 0.7	23.9 ± 1.3	23.7 ± 1.1	23.5 ± 1.1	NS
5	*O.s* (400 mg/kg per day)	24.2 ± 0.7	24.4 ± 0.8	24.3 ± 1.0	24.5 ± 1.3	24.1 ± 1.0	24.3 ± 1.0	24.2 ± 1.0	24.4 ± 1.3	24.1 ± 1.4	24.0 ± 1.5	23.8 ± 1.2	NS
6	*O.s* (400 mg/kg per day) and gemcitabine (10 mg/kg per 3 d) combination	23.9 ± 0.7	24.0 ± 0.2	23.4 ± 0.7	23.4 ± 0.7	23.4 ± 0.5	23.4 ± 0.4	23.3 ± 0.5	23.5 ± 0.5	23.3 ± 0.8	23.3 ± 0.5	23.3 ± 0.3	NS

Each group contains 6 mice. The results showed no significant difference in the reduction of body weight of mice compared to the untreated group. Data are represented as mean ± SD. (NS: Not significant compared to the untreated group, $P > 0.05$). No statistical difference was also observed among all treatment groups using Two-way ANOVA and Tukey's honest significant difference posthoc test. *O.s*: *Orthosiphon stamineus*.

Table 3 Effect of C5EOSEW5050ESA and gemcitabine alone or in combination on mouse key organ weight

No.	Group	Organ weight, g			*P* value
		Liver	Kidney	Spleen	
1	Untreated	1.7 ± 0.22	0.47 ± 0.06	0.11 ± 0.03	-
2	Gemcitabine (10 mg/kg per 3 d)	1.7 ± 0.23	0.46 ± 0.06	0.10 ± 0.03	NS
3	*O.s* (200 mg/kg per day)	1.67 ± 0.23	0.47 ± 0.06	0.11 ± 0.03	NS
4	*O.s* (200 mg/kg per day) and gemcitabine (10 mg/kg per 3 d) combination	1.31 ± 0.25	0.41 ± 0.08	0.07 ± 0.03	NS
5	*O.s* (400 mg/kg per day)	1.37 ± 0.35	0.41 ± 0.09	0.24 ± 0.02	NS
6	*O.s* (400 mg/kg per day) and gemcitabine (10 mg/kg per 3 d) combination	1.43 ± 0.19	0.43 ± 0.09	0.08 ± 0.02	NS

Data are presented as mean ± SD ($n = 6$) (NS: Not significant compared to the untreated group, $P > 0.05$). No statistical difference was also observed among all treatment groups using two-way ANOVA and Tukey's honest significant difference posthoc test. *O.s*: *Orthosiphon stamineus*.

combination treatment (Table 5). Electrolytes were within the normal ranges in all the groups, with no significant changes observed compared to the untreated group (Table 5).

Histopathology analysis: Histopathological examination of formalin-fixed paraffin-embedded tissues of the spleen (Figure 1), kidney (Figure 2), and liver (Figure 3) of all treatment groups, as well as the untreated group, revealed normal histology without pathological evidence of inflammation or necrosis. In addition, the liver did not exhibit an accumulation of neutral fats or triglycerides within the liver cells. However, the liver cells demonstrated mild swelling in all groups except for C5EOSEW5050ESA (200 mg/kg per day) treatment group (Figure 3).

C5EOSEW5050ESA and gemcitabine combination synergistically inhibited pancreatic tumour growth in the xenograft model

Single treatments with gemcitabine at 10 mg/kg and C5EO-SEW5050ESA at 200 mg/kg or 400 mg/kg inhibited tumour growth and reduced tumour weight compared to the vehicle untreated group (Figures 4A and B). However, compared to a single treatment, no additive effect in inhibiting tumour growth and tumour weight was obtained with 200 mg/kg C5EOSE-W5050ESA combined with gemcitabine

Table 4 Haematological parameters in different treatment groups

No.	Group	Hb,g/L	Total RBC as 10^{12}/L	PCV, L/L	MCV, fL	MCH, pg	MCHC, g/L	RDW, %	Total WBC as 10^9/L	N, %	L, %	M, %	E, %	B, %	Plts as 10^9 /L
1	Untreated	121 ± 1.0	7.91 ± 0.9	0.36 ± 0.0	46 ± 1.5	15 ± 0.7	332 ± 1.1	20.6 ± 1.0	5.8 ± 1.3	37 ± 1.0	55 ± 1.1	5 ± 0.8	2 ± 0.1	1 ± 0.0	790 ± 1.2
2	Gemcitabine (10 mg/kg per 3 d)	118 ± 1.4	7.60 ± 1.1	0.38 ± 0.0	50.0 ± 1.8	16.0 ± 0.6	313 ± 1.8	22.1 ± 0.7	6.0 ± 1.2	33.0 ± 1.2	60.0 ± 0.7	6.0 ± 1.3	1.0 ± 0.1	0.0 ± 0.1	720 ± 1.4
3	*O.s* (200 mg/kg per day)	118 ± 1.5	8.0 ± 0.8	0.38 ± 0.0	48.0 ± 2.0	15.0 ± 1.1	307 ± 0.9	22.3 ± 1.6	6.10 ± 0.7	35.0 ± 0.8	53.0 ± 0.6	9.0 ± 1.0	1.0 ± 0.1	2.0 ± 0.0	801 ± 0.8
4	*O.s* (200 mg/kg per day) and gemcitabine (10 mg/kg per 3 d) combination	115 ± 1.7	7.1 ± 1.4	0.35 ± 0.0	50.0 ± 1.6	16.0 ± 0.7	321 ± 1.5	21.5 ± 0.8	5.70 ± 1.5	32.0 ± 0.9	60.0 ± 1.1	5.0 ± 0.7	2.0 ± 0.1	1.0 ± 0.1	760 ± 0.9
5	*O.s* (400 mg/kg per day)	123 ± 1.6	7.9 ± 0.7	0.36 ± 0.0	46.0 ± 1.5	16.0 ± 1.6	335 ± 2.0	21.0 ± 0.9	5.70 ± 1.8	33.0 ± 1.2	61.0 ± 1.2	4.0 ± 0.6	2.0 ± 0.1	0.0 ± 0.0	740 ± 1.0
6	*O.s* (400 mg/kg per day) and gemcitabine (10 mg/kg per 3 d) combination	123 ± 1.1	7.70 ± 0.9	0.36 ± 0.0	47.0 ± 1.2	16.0 ± 0.4	331 ± 1.2	22.6 ± 1.3	6.0 ± 1.5	30.0 ± 0.9	60.0 ± 1.1	8.0 ± 1.3	1.0 ± 0.1	1.0 ± 0.0	810 ± 1.3

Results are expressed as mean ± SD (n = 6). The P values in all treated groups were insignificant compared to the untreated group. No statistical difference was also observed among all treatment groups using two-way ANOVA and Tukey's honest significant difference posthoc test. B: Basophile; E: Eosinophile; Hb: Haemoglobin; L: Lymphocyte; M: Monocyte; MCH: Mean cell haemoglobin; MCHC: Mean cell haemoglobin concentration; MCV: Mean cell volume; N: Neutrophile; *O.s*: *Orthosiphon stamineus;* PCV: Packed cell volume; Plts: Platelets; RBC: Red blood cells; RDW: Red cell distribution width; WBC: White blood cells.

(Figure 4A and B). However, C5EOSEW5050ESA at 400 mg/kg combined with gemcitabine significantly reduced tumour growth and tumour weight compared to individual treatment groups (Figures 4A and B).

C5EOSEW5050ESA and gemcitabine combination synergistically inhibited pancreatic tumour necrosis in the xenograft model: A single treatment with gemcitabine at 10 mg/kg and C5EOSEW5050ESA at 200 mg/kg or 400 mg/kg reduced tumour necrosis compared to untreated tumour cells (Figure 5). No additive effect in reducing tumour necrosis was obtained with C5EOSEW5050ESA at 200 mg/kg and gemcitabine combination compared to a single treatment (Figure 5D). However, C5EOSEW5050ESA at 400 mg/kg and gemcitabine combination significantly reduced tumour necrosis compared to single treatment groups of the respective doses (Figure 5).

C5EOSEW5050ESA combined with gemcitabine synergistically inhibited Ki67 protein expression in pancreatic tumour tissue: Ki67 proliferative marker protein was highly expressed in the untreated group compared to all treatment groups (Figure 6). Compared to a single treatment, no additive effect in reducing Ki67 protein expression was obtained with 200 mg/kg C5EOSEW5050ESA and gemcitabine combination (Figure 6). However, 400 mg/kg C5EOSEW5050ESA and gemcitabine combination synergistically inhibited the expression of Ki67 protein compared to single treatment and other treatment groups (Figure 6).

Table 5 Blood biochemical parameters and electrolyte profiles in different treatment groups

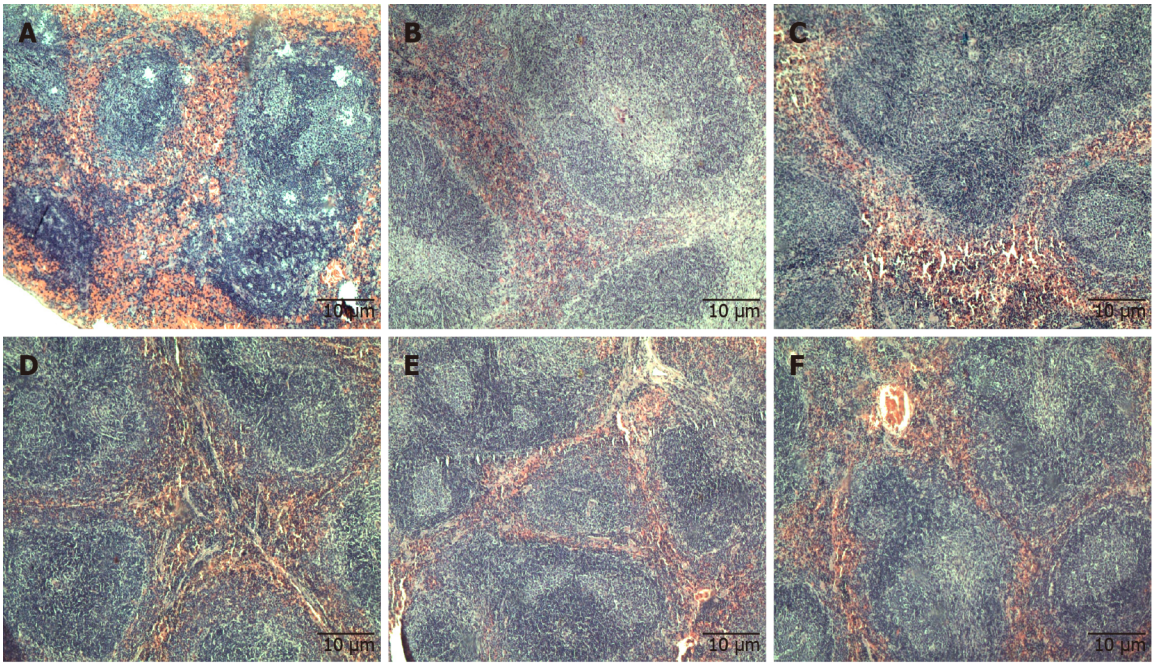
No.	Group	Creatinine, mmol/L	Urea,mmol/L	Uric acid, mmol/L	AKT, U/L	AST, U/L	ALT, U/L	GGT, U/L	Total protein, g/L	Albumin, g/L	Globulin, g/L	Albumin/ Globulin ratio	Total Bilirubin, μmol/L	Na	K	CL
1	Untreated	28.1 ± 1.5	8.80 ± 0.9	0.20 ± 0.0	96.0 ± 0.5	195 ± 0.7	73.0 ± 0.7	< 3.0 ± 0.0	50.0 ± 0.5	30.0 ± 1.1	23.0 ± 0.5	1.40 ± 0.3	< 2.0 ± 0.0	178 ± 0.3	8.00 ± 0.7	124 ± 1.1
2	Gemcitabine (10 mg/kg per 3 d)	28.0 ± 1.9	9.00 ± 1.1	0.16 ± 0.1	93.0 ± 1.1	190 ± 0.9	72.0 ± 0.9	< 3.0 ± 0.0	52.0 ± 1.2	32.0 ± 0.7	24.0 ± 0.7	1.40 ± 0.2	< 2.0 ± 0.0	173 ± 0.5	9.30 ± 0.4	123 ± 0.2
3	*O.s* (200 mg/kg per day)	29.0 ± 1.5	9.20 ± 1.3	0.19 ± 0.0	98.0 ± 1.2	201 ± 1.1	80.0 ± 1.1	< 3.0 ± 0.0	50.5 ± 0.7	33.0 ± 0.3	23.0 ± 0.7	1.30 ± 0.3	< 2.0 ± 0.0	174 ± 0.8	9.00 ± 0.8	128 ± 0.9
4	*O.s* (200 mg/kg per day) and gemcitabine (10 mg/kg per 3 d) combination	27.5 ± 1.1	9.50 ± 0.9	0.21 ± 0.1	101 ± 0.9	210 ± 0.7	77.0 ± 0.7	< 3.0 ± 0.0	51.3 ± 1.1	29.9 ± 0.9	22.5 ± 0.9	1.30 ± 0.2	< 2.0 ± 0.0	186 ± 0.9	8.60 ± 0.6	130 ± 1.1
5	*O.s* (400 mg/kg per day)	28.5 ± 0.9	8.80 ± 0.7	0.22 ± 0.1	101 ± 0.7	199 ± 0.9	66.0 ± 0.5	< 3.0 ± 0.0	51.9 ± 0.5	32.4 ± 0.8	25.0 ± 0.9	1.40 ± 0.2	< 2.0 ± 0.0	190 ± 0.4	10.0 ± 0.5	133 ± 0.9
6	*O.s* (400 mg/kg per day) and gemcitabine (10 mg/kg per 3 d) combination	27.0 ± 0.8	8.50 ± 1.3	0.21 ± 0.0	103 ± 0.8	190 ± 0.7	70.0 ± 0.9	< 3.0 ± 0.0	52.0 ± 0.7	30.5 ± 0.6	24.0 ± 0.7	1.40 ± 0.1	< 2.0 ± 0.0	185 ± 0.6	9.80 ± 0.9	123 ± 0.5

Results are expressed as the mean ± SD (n = 6). The P values in all treated groups were insignificant compared to the untreated group. No statistical difference was also observed among all treatment groups using two-way ANOVA and Tukey's honest significant difference posthoc test. AKT: Alkaline phosphatase; ALT: Alanine aminotransferase; AST: Aspartate aminotransferase; CL: Chloride; GGT: Gamma-glutamyl transferase; K: Potassium; Na: Sodium; *O.s*: *Orthosiphon stamineus*.

DISCUSSION

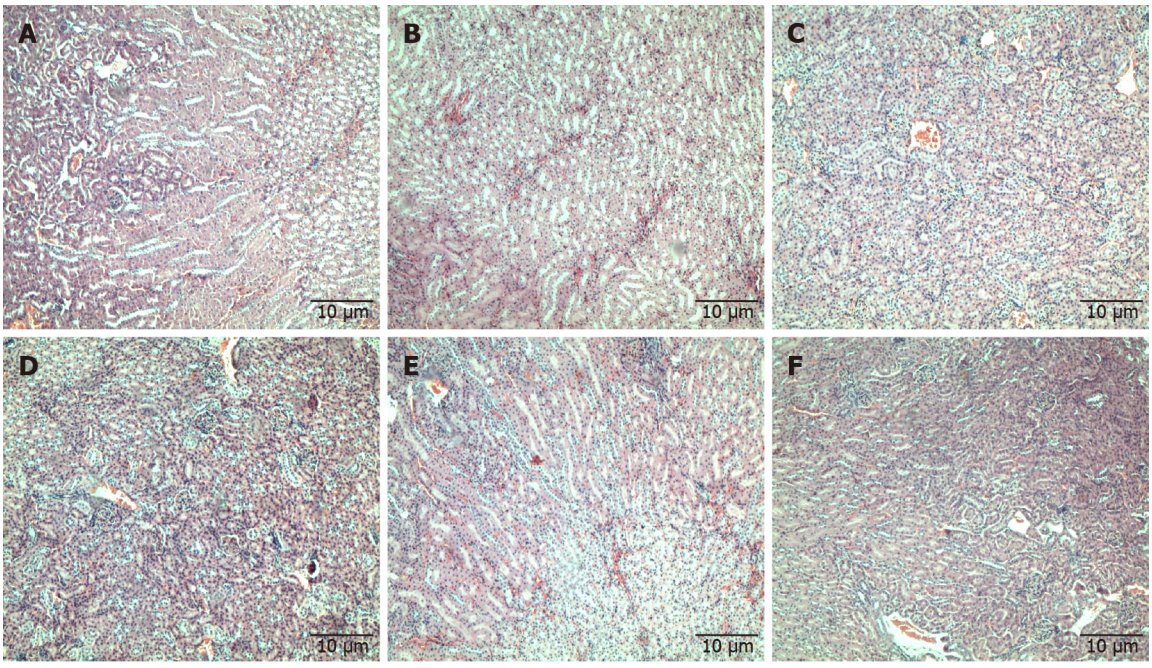
Studies have shown that therapeutic combinations containing low-dose marketed drugs and plant extracts/isolated compounds or essential oils may improve the safety profile of marketed drugs and produce synergistic actions[12,13]. The safety profile of C5EOSEW5050ESA has previously been established[14,15], with its LD_{50} values reported to be greater than 5000 mg/kg[15]. Chemo-herbal combinations are one of the possible therapeutic options which can be employed to improve the efficacy of a drug, reduce adverse drug effects and increase disease-free intervals and overall survival rates in cancer patients. The majority of chemotherapeutic drugs destroy tumours and retard cancer growth but may also damage healthy tissues. Thus, new chemo-herbal combinations are anticipated to play an essential role in developing more effective and safer strategies to inhibit cancer progress with minimal side effects[4].

We have previously shown the synergistic anti-cancer effects of combined C5EOSEW5050ESA and gemcitabine treatment on Panc-1 and MiaPaCa-2 pancreatic cancer cell lines[3]. Moreover, no toxicity was observed in mice in an acute toxicity study[3]. In the current study, the combination treatment in a pancreatic tumour xenograft model revealed no abnormal signs in any of the treatment groups (Figures 1-3). Moreover, no significant difference in organ weight change was noted when compared to the



DOI: 10.3748/wjg.v28.i32.4620 **Copyright** ©The Author(s) 2022.

Figure 1 Tissue sections of mice spleen stained with haematoxylin and eosin. Tissue sections from untreated and treated groups showed normal spleen architecture. A: Untreated; B: Gemcitabine (10 mg/kg per 3 d); C: C5EOSEW5050ESA (200 mg/kg per day); D: C5EOSEW5050ESA (200 mg/kg per day) and gemcitabine (10 mg/kg per 3 d) combination; E: C5EOSEW5050ESA (400 mg/kg per day); F: C5EOSEW5050ESA (400 mg/kg per day) and gemcitabine (10 mg/kg per 3 d) combination.

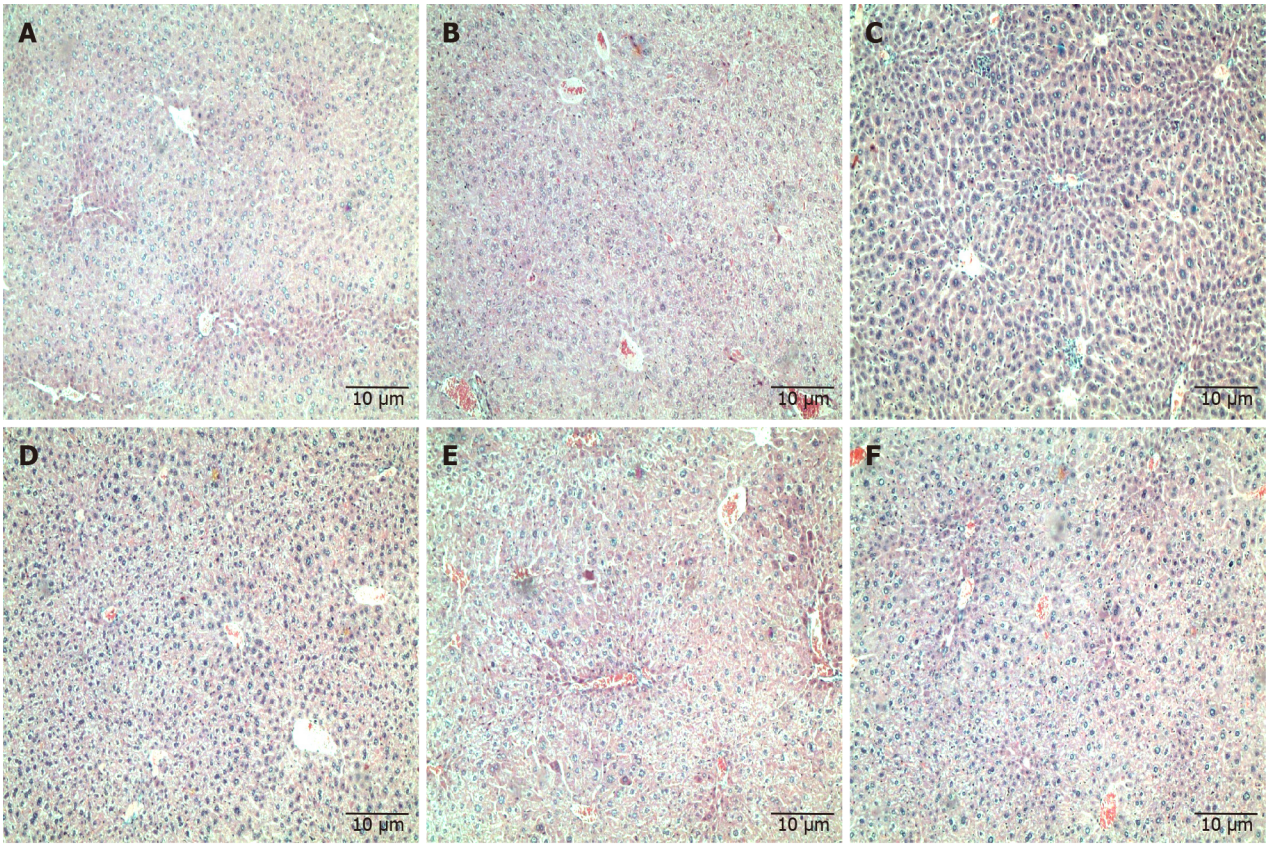


DOI: 10.3748/wjg.v28.i32.4620 **Copyright** ©The Author(s) 2022.

Figure 2 Tissue sections of mice kidneys stained with haematoxylin and eosin. Tissue sections showed normal glomeruli and tubules in all treated groups and untreated. A: Untreated; B: Gemcitabine (10 mg/kg per 3 d); C: C5EOSEW5050ESA (200 mg/kg per day); D: C5EOSEW5050ESA (200 mg/kg per day) and gemcitabine (10 mg/kg per 3 d) combination; E: C5EOSEW5050ESA (400 mg/kg per day); F: C5EOSEW5050ESA (400 mg/kg per day) and gemcitabine (10 mg/kg per 3 d) combination.

untreated group, supporting the relatively safe nature of selected chemo-herbal combinations (Table 3).

Clinical biochemistry and haematological analyses play a significant role in evaluating the signs of toxicity induced by drugs[16]. No significant alterations in haematological parameters were observed in the animal blood samples treated with C5EOSEW5050ESA and gemcitabine combination, indicating



DOI: 10.3748/wjg.v28.i32.4620 **Copyright** ©The Author(s) 2022.

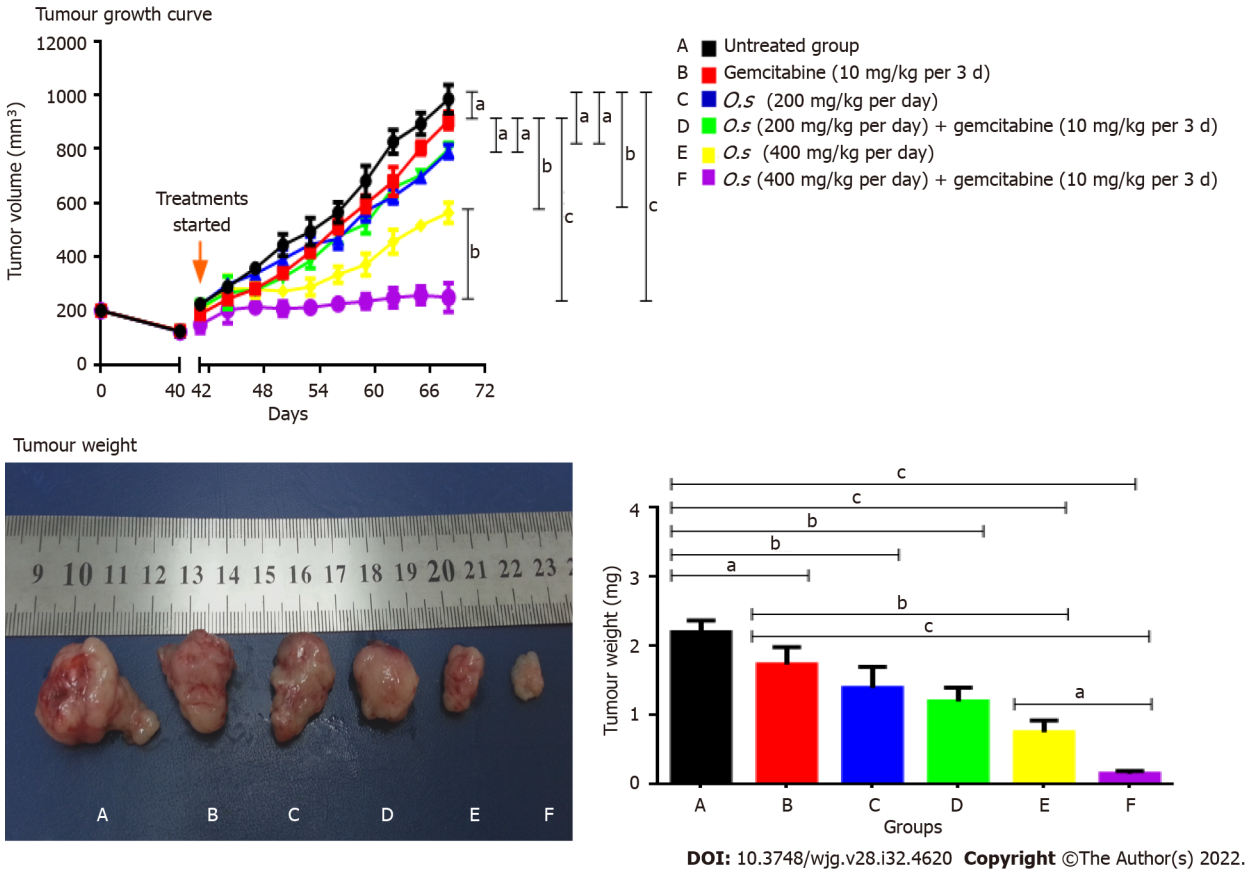
Figure 3 Tissue sections of mice liver stained with haematoxylin and eosin. Liver sections showed normal architecture with distinct hepatic cells, sinusoidal spaces, and a central vein in all treatment groups and untreated; mild hepatocellular swelling is seen in all groups except the C5EOSEW5050ESA (200 mg/kg per day) group where no swelling is present. A: Untreated; B: Gemcitabine (10 mg/kg per 3 d); C: C5EOSEW5050ESA (200 mg/kg per day); D: C5EOSEW5050ESA (200 mg/kg per day) and gemcitabine (10 mg/kg per 3 d) combination; E: C5EOSEW5050ESA (400 mg/kg per day); F: C5EOSEW5050ESA (400 mg/kg per day) and gemcitabine (10 mg/kg per 3 d) combination.

that these combinations did not damage the blood cells (Table 4). Increased serum bilirubin concentration and occurrence of tissue haemolysis are commonly seen when the liver is impaired[17]. The absence of these observations in the current study demonstrated the non-toxic effects of the C5EOSEW5050ESA gemcitabine combination on haemoglobin metabolic pathways (Table 4). A slight drop in white blood count and platelets and mild myelosuppression have been reported with extended treatment duration and high doses of gemcitabine[18]. In 2013, the MPACT phase III trial, which included over 800 patients, showed a significant overall survival benefit with the combination of nanomolecular albumin-bound (nab)-paclitaxel and gemcitabine (nabPGem) over gemcitabine monotherapy, with acceptable toxicity. The overall toxicity of nabPGem is lower than in the triple chemotherapy 5-FU, leucovorin, irinotecan and oxaliplatin, especially haematotoxicity and rates of neutropenic fever[19,20]. However, the current study and our previous toxicity study revealed no reduction in white blood cells and platelets (Table 4)[3]. In fact, C5EOSEW5050ESA and gemcitabine combination at the higher dose enhanced its efficacy at reducing tumour growth without causing any side effects, at least in this short term study.

Kidneys are particularly vulnerable to high doses of drugs as they eradicate many drugs and their metabolites. Therefore, renal function tests measure various substances, including serum urea, serum creatinine, and albumin, to determine the current health of the kidneys[21]. In the present study, there was no nephrotoxicity observed, indicating the safe nature of chemo-herbal combinations. The results showed normal level concentrations of urea, creatinine, and albumin and were supported by the typical renal architecture of kidney sections (Figure 2).

Liver function tests, for such markers as ALT, AST, ALP, and GGT, are used to measure hepatocellular damage during illnesses[22]. There were no significant changes in the serum levels of AST, ALT, ALP, and GGT in all treatment groups (Table 5). In addition, the hepatocellular architecture appeared normal in all treatment groups (Figure 3).

As a single treatment, gemcitabine at 10 mg/kg and C5EOSEW5050ESA at 200 mg/kg or 400 mg/kg inhibited tumour growth compared to untreated mice (Figure 4). Compared to a single treatment, no additive inhibition of tumour growth was obtained with 200 mg/kg C5EOSEW5050ESA and gemcitabine combination (Figure 4). However, C5EOSEW5050ESA at 400 mg/kg and gemcitabine

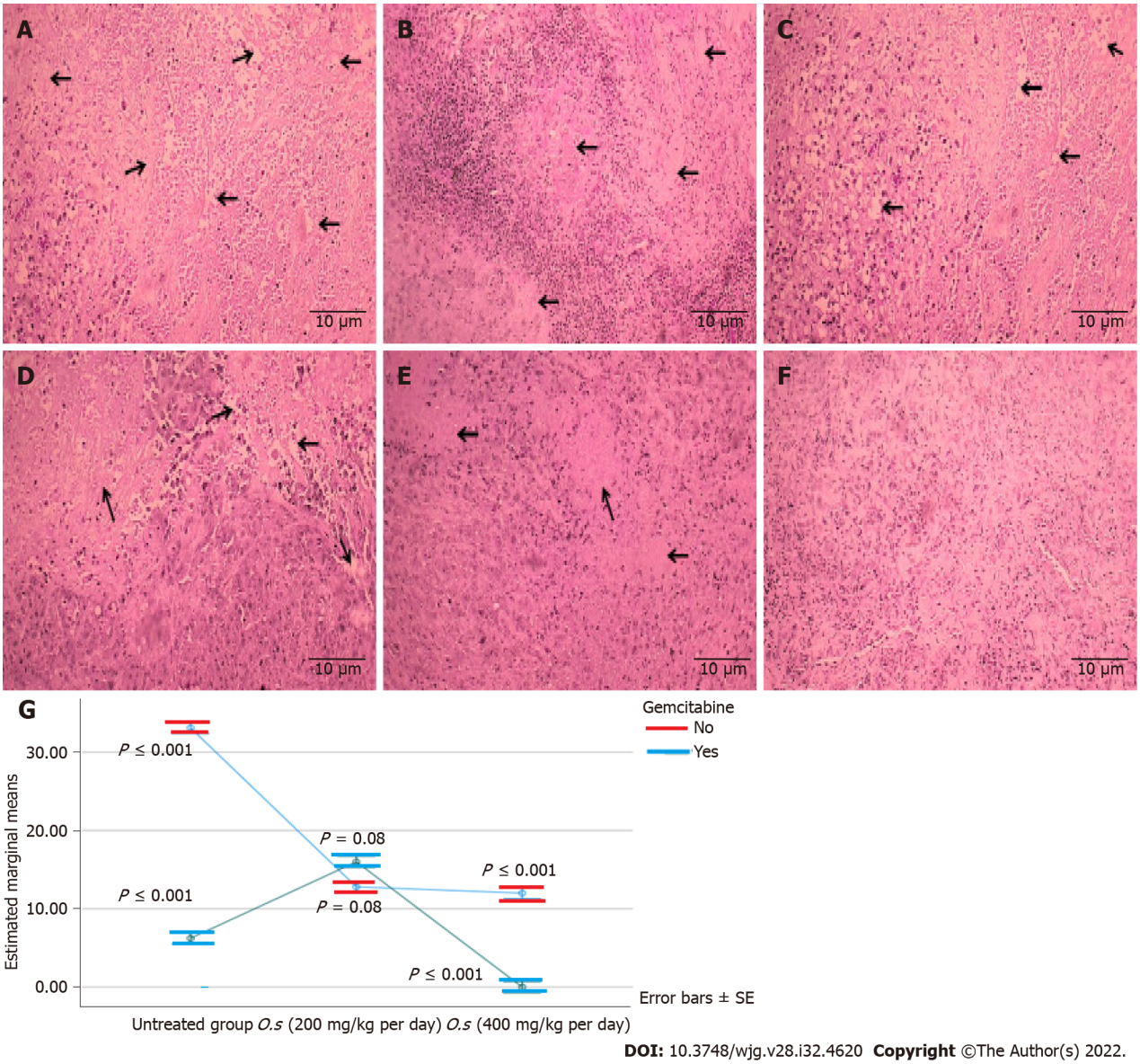


DOI: 10.3748/wjg.v28.i32.4620 **Copyright** ©The Author(s) 2022.

Figure 4 Tumour growth curve of Panc-1 cells in subcutaneous pancreatic tumour growth in nude mice and tumour weight. Treatments were given when the tumours reached 100 mm^3. A: Untreated; B: Gemcitabine (10 mg/kg per 3 d); C: C5EOSEW5050ESA (200 mg/kg per day); D: C5EOSEW5050ESA (200 mg/kg per day) and gemcitabine (10 mg/kg per 3 d) combination; E: C5EOSEW5050ESA (400 mg/kg per day); F: C5EOSEW5050ESA (400 mg/kg per day) and gemcitabine (10 mg/kg per 3 d) combination. Combination treatment of 400 mg/kg C5EOSEW5050ESA and gemcitabine (F) synergistically reduced the tumour growth compared to a single treatment. The combination treatment of 400 mg/kg C5EOSEW5050ESA and gemcitabine (F) significantly reduced tumour weight compared to a single treatment. Error bars represent standard deviations. Statistics analysis ($^aP < 0.05$; $^bP < 0.01$; $^cP < 0.001$, two-way ANOVA for tumour growth, one-way ANOVA with Tukey's HSD posthoc test for tumour weight, $n = 6$ animals per group) using SPSS and GraphPad Prism 6.0 software.

combination significantly reduced tumour growth compared to the single treatment groups of the respective doses (Figure 4). Further studies investigating how combination treatment affects pancreatic cancer cell proliferation and apoptosis or necrosis will shed light on their mode of action. In our previous study, C5EOSEW5050ESA and gemcitabine combination inhibited the survival and proliferation of Panc-1 cells *in vitro*[23]. Also, the combination of C5EOSEW5050ESA and gemcitabine-induced apoptosis and reduced EMT markers and multidrug-resistant genes (*MDR-1*, *MRP-4*, and *MRP-5*), and the Notch signalling pathway[24]. In the current study, the tumour necrosis percentage was estimated in tissue sections stained by HE. Single treatment of gemcitabine and C5EOSEW5050ESA either at low or high dose reduced the tumour percentage compared to untreated (Figure 5). There were no additional effects in the reduction of tumour necrosis post-treatment with a low dose of C5EOSEW5050ESA and gemcitabine combination compared to a single treatment (Figure 5). However, the high dose of C5EOSEW5050ESA and gemcitabine combination reduced tumour necrosis compared to a single treatment (Figure 5).

The combination treatment of C5EOSEW5050ESA at a high dose and gemcitabine significantly reduced Ki67 protein expression in tumour cells compared to a single treatment (Figure 6), indicating reduced cell proliferation in the former group. The epigallocatechin-3-*O*-gallate (EGCG) polyphenol is enriched in C5EOSEW5050ESA extract. Others have reported EGCG to inhibit tumour growth and induce apoptosis in mice implanted with head, neck, and lung cancers by decreasing the Ki67 expression in tissues from the xenograft model and downregulating caspase-3, caspase-8, caspase-9, and Bax in mouse vascular smooth muscle cells[25,26]. Another study showed that resveratrol inhibited Ki67 expression in pancreatic cancer cells *in vitro* and *in vivo* by sensitising pancreatic cancer cells to gemcitabine treatment[25]. It is postulated that the polyphenols in C5EOSEW5050ESA may act synergistically with gemcitabine in the pancreatic tumour xenograft model. C5EOSEW5050ESA worked in synergy with gemcitabine to reduce pancreatic tumour growth and tumour necrosis in mice compared to a single treatment of either C5EOSEW5050ESA or gemcitabine. Thus, based on current findings, it is proposed that 50% ethanol extract of *O.s* has the potential to be used in combination with



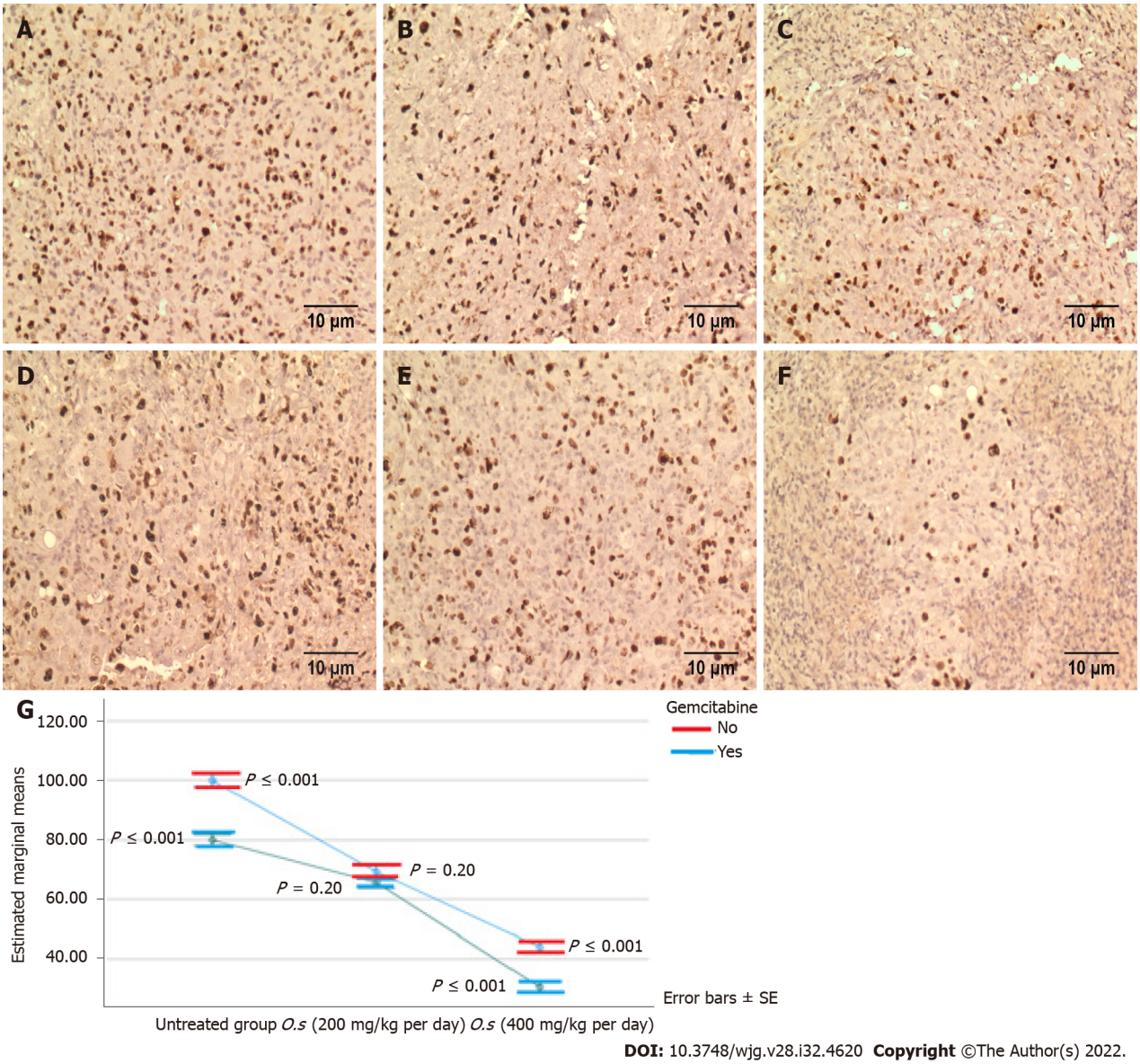
DOI: 10.3748/wjg.v28.i32.4620 **Copyright** ©The Author(s) 2022.

Figure 5 Tumour necrosis percentage in tumour tissues stained with haematoxylin and eosin. A: Untreated group; B: Gemcitabine (10 mg/kg per 3 d); C: *Orthosiphon stamineus* (*O.s*) (200 mg/kg per day); D: *O.s* (200 mg/kg per day) + gemcitabine (10 mg/kg per 3 d); E: *O.s* (400 mg/kg per day); F: *O.s* (400 mg/kg per day) + gemcitabine (10 mg/kg per 3 d); G: Estimated marginal means of necrosis. Combination treatment of 400 mg/kg C5EOSEW5050ESA with gemcitabine synergistically inhibited tumour necrosis compared to a single treatment. Arrows indicate the necrotic area in tumour sections. Error bars represent standard deviations. Statistics analysis (two-way ANOVA, *n* = 6 animals per group) using SPSS software. *O.s*: *Orthosiphon stamineus*.

gemcitabine to treat pancreatic cancer.

CONCLUSION

This study provides preliminary scientific evidence about the safety profile of *O.s* derived extract C5EOSEW5050ESA present in Nuvastatic™ in combination with gemcitabine in an athymic nude mice model. Furthermore, this work demonstrated that C5EOSEW5050ESA extract in combination with gemcitabine is relatively safe in the acute toxicity study. Furthermore, the clinical efficacy and safety of Nuvastatic™ in cancer asthenia have been evaluated in phase III clinical trials (ClinicalTrials.gov, Identifier: NCT04546607). Therefore, Nuvastatic™ has the potential to be employed as a complementary treatment with gemcitabine to treat pancreatic cancer.



DOI: 10.3748/wjg.v28.i32.4620 **Copyright** ©The Author(s) 2022.

Figure 6 Ki67 proliferation protein expression in treated and untreated groups. A: Untreated group; B: *Orthosiphon stamineus* (*O.s*) (200 mg/kg per day); C: *O.s* (400 mg/kg per day); D: Gemcitabine (10 mg/kg per 3 d); E: *O.s* (200 mg/kg per day) + gemcitabine (10 mg/kg per 3 d); F: *O.s* (400 mg/kg per day) + gemcitabine (10 mg/kg per 3 d); G: Estimated marginal means of Ki67. Single treatment either by C5EOSEW5050ESA or gemcitabine significantly reduced the Ki67 protein expression in tumour tissues compared to the untreated group. No significant reduction of Ki67 protein expression was noted between the groups treated by C5EOSEW5050ESA 200 mg/kg per day and the gemcitabine combination. Combination treatment of C5EOSEW5050ESA 400 mg/kg per day and gemcitabine synergistically reduced Ki67 protein expression in tumour tissue compared to a single treatment. Error bars represent standard deviations. Statistics analysis (Two-way ANOVA, *n* = 6 animals per group) using SPSS software. *O.s*: *Orthosiphon stamineus*.

ARTICLE HIGHLIGHTS

Research background

Gemcitabine is the cornerstone for pancreatic cancer but demonstrates adverse effects in patients. *Orthosiphon stamineus* (*O.s*) has been traditionally used to treat various diseases. C5OSEW5050ESA (Nuvastatic™) is a proprietary extract of *O.s* that completed a phase 2/3 clinical study for cancer fatigue in cancer patients with solid tumours receiving chemotherapy.

Research motivation

No study has reported the toxicity profile of C5OSEW5050ESA in a pancreatic tumour animal model either as a stand-alone or in combination with gemcitabine.

Research objectives

To determine the anti-tumour activity and potential toxicity of Nuvastatic™ and gemcitabine combination on pancreatic xenograft model.

Research methods

Human pancreatic cancer cells were injected subcutaneously into athymic nude mice. C5EOSEW5050ESA (200 or 400 mg/kg per day) was administered orally, while gemcitabine (10 mg/kg/3 d) was given intraperitoneally either alone or in combination treatment. Histopathological analyses of key organs, tumour tissues, and incidence of lethality were determined.

Research results

C5EOSEW5050ESA at 200 mg/kg and gemcitabine combination had no additive antitumor effects compared to a single treatment. A comparably greater response in a reduction in tumour growth *via* a reduction of Ki-67 protein expression, and a decrease in necrosis was also demonstrated by 400 mg/kg of C5EOSEW5050ESA and gemcitabine combination compared to that of individual agents. No signs of organ toxicities were observed in any treatment group.

Research conclusions

The combination of C5EOSEW5050ESA with gemcitabine significantly reduced the pancreatic tumour growth in mice compared to a single treatment. This study provides valuable insights into using C5EOSEW5050ESA as a complementary treatment to gemcitabine for pancreatic cancer.

Research perspectives

Findings from this study may provide the basis for product formulation and manufacturing of botanical drugs (Nuvastatic™) to be used as complementary medicine for the treatment of pancreatic cancer patients.

ACKNOWLEDGEMENTS

Ashwaq Yehya was supported by TWAS-USM (The Academy of Sciences for the Developing World, Italy-Universiti Sains Malaysia).

FOOTNOTES

Author contributions: Yehya AHS and Subramaniam AV carried out the experiments; Yehya AHS drafted the manuscript; Yehya AHS, Asif M, and Kaur G analysed the data; Abdul Majid AMS conceived and planned the experiments; Oon CE designed the experiments, derived the model, and supervised the project; All authors have read and approved the final manuscript.

Supported by the NKEA Research Grant Scheme (NRGS) by the Ministry of Agriculture Malaysia, No. 304/CIPPM/650736/k123.

Institutional animal care and use committee statement: The animal study was approved and conducted under strict guidelines according to USM Animal Ethics Committee (Reference #: USM/Animal Ethics Approval/2016/(97)(746).

Conflict-of-interest statement: Amin Malik Shah Abdul Majid has a commercial interest in C5EOSEW5050ESA *O.s* extract of Nuvastatic™. All the other authors declare no financial and non-financial competing interests.

Data sharing statement: No additional data are available.

ARRIVE guidelines statement: The authors have read the ARRIVE guidelines, and the manuscript was prepared and revised according to the ARRIVE guidelines.

Open-Access: This article is an open-access article that was selected by an in-house editor and fully peer-reviewed by external reviewers. It is distributed in accordance with the Creative Commons Attribution NonCommercial (CC BY-NC 4.0) license, which permits others to distribute, remix, adapt, build upon this work non-commercially, and license their derivative works on different terms, provided the original work is properly cited and the use is non-commercial. See: https://creativecommons.org/Licenses/by-nc/4.0/

Country/Territory of origin: Malaysia

ORCID number: Ashwaq Hamid Salem Yehya 0000-0001-7464-1618; Ayappa V Subramaniam 0000-0002-3302-6704; Muhammad Asif 0000-0001-8989-9945; Gurjeet Kaur 0000-0002-6232-5703; Amin MS Abdul Majid 0000-0001-7499-2258; Chern Ein Oon 0000-0002-4685-6408.

S-Editor: Ma YJ

L-Editor: Filipodia
P-Editor: Ma YJ

REFERENCES

1 **Looi CK**, Chung FF, Leong CO, Wong SF, Rosli R, Mai CW. Therapeutic challenges and current immunomodulatory strategies in targeting the immunosuppressive pancreatic tumor microenvironment. *J Exp Clin Cancer Res* 2019; **38**: 162 [PMID: 30987642 DOI: 10.1186/s13046-019-1153-8]
2 **Shukla SK**, Purohit V, Mehla K, Gunda V, Chaika NV, Vernucci E, King RJ, Abrego J, Goode GD, Dasgupta A, Illies AL, Gebregiworgis T, Dai B, Augustine JJ, Murthy D, Attri KS, Mashadova O, Grandgenett PM, Powers R, Ly QP, Lazenby AJ, Grem JL, Yu F, Matés JM, Asara JM, Kim JW, Hankins JH, Weekes C, Hollingsworth MA, Serkova NJ, Sasson AR, Fleming JB, Oliveto JM, Lyssiotis CA, Cantley LC, Berim L, Singh PK. MUC1 and HIF-1alpha Signaling Crosstalk Induces Anabolic Glucose Metabolism to Impart Gemcitabine Resistance to Pancreatic Cancer. *Cancer Cell* 2017; **32**: 71-87.e7 [PMID: 28697344 DOI: 10.1016/j.ccell.2017.06.004]
3 **Yehya AHS**, Asif M, Kaur G, Hassan LEA, Al-Suede FSR, Abdul Majid AMS, Oon CE. Toxicological studies of *Orthosiphon stamineus* (Misai Kucing) standardized ethanol extract in combination with gemcitabine in athymic nude mice model. *J Adv Res* 2019; **15**: 59-68 [PMID: 30581613 DOI: 10.1016/j.jare.2018.05.006]
4 **Yehya AH**, Asif M, Tan YJ, Sasidharan S, Majid AMA, Oon CE. Broad spectrum targeting of tumor vasculature by medicinal plants: An updated review. *J Herb Med* 2017; **169**: 13 [DOI: 10.1016/j.hermed.2017.03.003]
5 **Dhar D**. Pancreatic cancer chemoprevention and intervention strategies employing a natural agent-bitter melon juice. University of Colorado at Denver, Anschutz Medical Campus. Strauss Health, 2018. Available from: https://digitalcollections.cuanschutz.edu/work/ns/46f7586e-f98e-459f-ab65-95fdd3a0bad5
6 **Qi F**, Zhao L, Zhou A, Zhang B, Li A, Wang Z, Han J. The advantages of using traditional Chinese medicine as an adjunctive therapy in the whole course of cancer treatment instead of only terminal stage of cancer. *Biosci Trends* 2015; **9**: 16-34 [PMID: 25787906 DOI: 10.5582/bst.2015.01019]
7 **Alissa EM**. Medicinal herbs and therapeutic drugs interactions. *Ther Drug Monit* 2014; **36**: 413-422 [PMID: 24452064 DOI: 10.1097/FTD.0000000000000035]
8 **Tabana YM**, Al-Suede FS, Ahamed MB, Dahham SS, Hassan LE, Khalilpour S, Taleb-Agha M, Sandai D, Majid AS, Majid AM. Cat's whiskers (Orthosiphon stamineus) tea modulates arthritis pathogenesis *via* the angiogenesis and inflammatory cascade. *BMC Complement Altern Med* 2016; **16**: 480 [PMID: 27881135 DOI: 10.1186/s12906-016-1467-4]
9 **Ahamed MB**, Aisha AF, Nassar ZD, Siddiqui JM, Ismail Z, Omari SM, Parish CR, Majid AM. Cat's whiskers tea (Orthosiphon stamineus) extract inhibits growth of colon tumor in nude mice and angiogenesis in endothelial cells *via* suppressing VEGFR phosphorylation. *Nutr Cancer* 2012; **64**: 89-99 [PMID: 22136553 DOI: 10.1080/01635581.2012.630160]
10 **Yehya AHS**, Asif M, Petersen SH, Subramaniam AV, Kono K, Majid AMSA, Oon CE. Angiogenesis: Managing the Culprits behind Tumorigenesis and Metastasis. *Medicina (Kaunas)* 2018; **54** [PMID: 30344239 DOI: 10.3390/medicina54010008]
11 **Xue R**, Fang Z, Zhang M, Yi Z, Wen C, Shi T. TCMID: Traditional Chinese Medicine integrative database for herb molecular mechanism analysis. *Nucleic Acids Res* 2013; **41**: D1089-D1095 [PMID: 23203875 DOI: 10.1093/nar/gks1100]
12 **Mahmood H**, Khan IU, Asif M, Khan RU, Asghar S, Khalid I, Khalid SH, Irfan M, Rehman F, Shahzad Y, Yousaf AM, Younus A, Niazi ZR, Asim M. In vitro and in vivo evaluation of gellan gum hydrogel films: Assessing the co impact of therapeutic oils and ofloxacin on wound healing. *Int J Biol Macromol* 2021; **166**: 483-495 [PMID: 33130262 DOI: 10.1016/j.ijbiomac.2020.10.206]
13 **Tanzeem MU**, Asghar S, Khalid SH, Asif M, Ullah MS, Khan IU, Khalid I, Faran SA, Rehman A, Gohar UF, Hussain T. Clove oil based co-surfactant free microemulsion of flurbiprofen: Improved solubility with ameliorated drug-induced gastritis. *Pak J Pharm Sci* 2019; **32**: 2787-2793 [PMID: 32024615]
14 **Mohamed EA**, Lim CP, Ebrika OS, Asmawi MZ, Sadikun A, Yam MF. Toxicity evaluation of a standardised 50% ethanol extract of Orthosiphon stamineus. *J Ethnopharmacol* 2011; **133**: 358-363 [PMID: 20937371 DOI: 10.1016/j.jep.2010.10.008]
15 **Shafaei A**, Esmailli K, Farsi E, Aisha AF, Abul Majid AM, Ismail Z. Genotoxicity, acute and subchronic toxicity studies of nano liposomes of Orthosiphon stamineus ethanolic extract in Sprague Dawley rats. *BMC Complement Altern Med* 2015; **15**: 360 [PMID: 26467526 DOI: 10.1186/s12906-015-0885-z]
16 **Féres CA**, Madalosso RC, Rocha OA, Leite JP, Guimarães TM, Toledo VP, Tagliati CA. Acute and chronic toxicological studies of Dimorphandra mollis in experimental animals. *J Ethnopharmacol* 2006; **108**: 450-456 [PMID: 16872769 DOI: 10.1016/j.jep.2006.06.002]
17 **Doig K**. Introduction to increased destruction of erythrocytes. Rodak's Hematology-E-Book: Clinical Principles and Applications, 2015: 348
18 **Ou XM**, Li WC, Liu DS, Li YP, Wen FQ, Feng YL, Zhang SF, Huang XY, Wang T, Wang K, Wang X, Chen L. VEGFR-2 antagonist SU5416 attenuates bleomycin-induced pulmonary fibrosis in mice. *Int Immunopharmacol* 2009; **9**: 70-79 [PMID: 18976720 DOI: 10.1016/j.intimp.2008.10.002]
19 **Von Hoff DD**, Ervin T, Arena FP, Chiorean EG, Infante J, Moore M, Seay T, Tjulandin SA, Ma WW, Saleh MN, Harris M, Reni M, Dowden S, Laheru D, Bahary N, Ramanathan RK, Tabernero J, Hidalgo M, Goldstein D, Van Cutsem E, Wei X, Iglesias J, Renschler MF. Increased survival in pancreatic cancer with nab-paclitaxel plus gemcitabine. *N Engl J Med* 2013; **369**: 1691-1703 [PMID: 24131140 DOI: 10.1056/NEJMoa1304369]
20 **Vogl UM**, Andalibi H, Klaus A, Vormittag L, Schima W, Heinrich B, Kafka A, Winkler T, Öhler L. Nab-paclitaxel and gemcitabine or FOLFIRINOX as first-line treatment in patients with unresectable adenocarcinoma of the pancreas: does

sequence matter? *BMC Cancer* 2019; **19**: 28 [PMID: 30621630 DOI: 10.1186/s12885-018-5240-6]

21 **Ashley C**, Dunleavy A. The renal drug handbook: the ultimate prescribing guide for renal practitioners: CRC Press, 2017

22 **Ekstedt M**, Hagström H, Nasr P, Fredrikson M, Stål P, Kechagias S, Hultcrantz R. Fibrosis stage is the strongest predictor for disease-specific mortality in NAFLD after up to 33 years of follow-up. *Hepatology* 2015; **61**: 1547-1554 [PMID: 25125077 DOI: 10.1002/hep.27368]

23 **Yehya AHS**, Asif M, Abdul Majid AMS, Oon CE. Complementary effects of Orthosiphon stamineus standardized ethanolic extract and rosmarinic acid in combination with gemcitabine on pancreatic cancer. *Biomed J* 2021; **44**: 694-708 [PMID: 35166208 DOI: 10.1016/j.bj.2020.05.015]

24 **Hoster E**, Rosenwald A, Berger F, Bernd HW, Hartmann S, Loddenkemper C, Barth TF, Brousse N, Pileri S, Rymkiewicz G, Kodet R, Stilgenbauer S, Forstpointner R, Thieblemont C, Hallek M, Coiffier B, Vehling-Kaiser U, Bouabdallah R, Kanz L, Pfreundschuh M, Schmidt C, Ribrag V, Hiddemann W, Unterhalt M, Kluin-Nelemans JC, Hermine O, Dreyling MH, Klapper W. Prognostic Value of Ki-67 Index, Cytology, and Growth Pattern in Mantle-Cell Lymphoma: Results From Randomized Trials of the European Mantle Cell Lymphoma Network. *J Clin Oncol* 2016; **34**: 1386-1394 [PMID: 26926679 DOI: 10.1200/JCO.2015.63.8387]

25 **Fantini M**, Benvenuto M, Masuelli L, Frajese GV, Tresoldi I, Modesti A, Bei R. In vitro and in vivo antitumoral effects of combinations of polyphenols, or polyphenols and anticancer drugs: perspectives on cancer treatment. *Int J Mol Sci* 2015; **16**: 9236-9282 [PMID: 25918934 DOI: 10.3390/ijms16059236]

26 **Yan X**, Li Y, Yu H, Wang W, Wu C, Yang Y, Hu Y, Shi X, Li J. Epigallocatechin-3-gallate inhibits H_2O_2-induced apoptosis in Mouse Vascular Smooth Muscle Cells *via* 67kD Laminin Receptor. *Sci Rep* 2017; **7**: 7774 [PMID: 28798484 DOI: 10.1038/s41598-017-08301-6]

World Journal of Gastroenterology

Submit a Manuscript: https://www.f6publishing.com

World J Gastroenterol 2022 August 28; 28(32): 4635-4648

DOI: 10.3748/wjg.v28.i32.4635

ISSN 1007-9327 (print) ISSN 2219-2840 (online)

ORIGINAL ARTICLE

Basic Study

The mechanism of Yinchenhao decoction in treating obstructive-jaundice-induced liver injury based on Nrf2 signaling pathway

Jun-Jian Liu, Yan Xu, Shuai Chen, Cheng-Fei Hao, Jing Liang, Zhong-Lian Li

Specialty type: Gastroenterology and hepatology

Provenance and peer review: Unsolicited article; Externally peer reviewed.

Peer-review model: Single blind

Peer-review report's scientific quality classification

Grade A (Excellent): 0
Grade B (Very good): B, B
Grade C (Good): 0
Grade D (Fair): 0
Grade E (Poor): 0

P-Reviewer: Aoki H, Japan; Cengiz M, Turkey

Received: March 24, 2022
Peer-review started: March 24, 2022
First decision: May 30, 2022
Revised: June 8, 2022
Accepted: June 24, 2022
Article in press: June 24, 2022
Published online: August 28, 2022

Jun-Jian Liu, Cheng-Fei Hao, Zhong-Lian Li, The Second Department of Hepatobiliary and Pancreatic Surgery, Tianjin Medical University NanKai Hospital, Tianjin 300102, China

Yan Xu, Graduate School, Tianjin Medical University, Tianjin 3000070, China

Shuai Chen, Department of Thoracic Surgery, Xuzhou City Hospital of Traditional Chinese Medicine, Xuzhou 221000, Jiangsu Province, China

Jing Liang, School of Foreign Languages, Chengdu University of Traditional Chinese Medicine, Chengdu 610000, Sichuan Province, China

Corresponding author: Zhong-Lian Li, MD, PhD, Chief Doctor, Doctor, Professor, Surgeon, The Second Department of Hepatobiliary and Pancreatic Surgery, Tianjin Medical University NanKai Hospital, No. 6 Changjiang Street, Nankai District, Tianjin 300102, China. nkyylzl@163.com

Abstract

BACKGROUND

Obstructive jaundice (OJ) is caused by bile excretion disorder after partial or complete bile duct obstruction. It may cause liver injury through various mechanisms. Traditional Chinese medicine (TCM) has a lot of advantages in treating OJ. The recovery of liver function can be accelerated by combining Chinese medicine treatment with existing clinical practice. Yinchenhao decoction (YCHD), a TCM formula, has been used to treat jaundice. Although much progress has been made in recent years in understanding the mechanism of YCHD in treating OJ-induced liver injury, it is still not clear.

AIM

To investigate chemical components of YCHD that are effective in the treatment of OJ and predict the mechanism of YCHD.

METHODS

The active components and putative targets of YCHD were predicted using a network pharmacology approach. Gene Ontology biological process and Kyoto Encyclopedia of Genes and Genomes path enrichment analysis were carried out by cluster profile. We predicted the biological processes, possible targets, and associated signaling pathways that YCHD may involve in the treatment of OJ. Thirty male Sprague–Dawley rats were randomly divided into three groups, each

consisting of 10 rats: the sham group (Group S), the OJ model group (Group M), and the YCHD-treated group (Group Y). The sham group only received laparotomy. The OJ model was established by ligating the common bile duct twice in Groups M and Y. For 1 wk, rats in Group Y were given a gavage of YCHD (3.6 mL/kg) twice daily, whereas rats in Groups S and M were given the same amount of physiological saline after intragastric administration daily. After 7 d, all rats were killed, and the liver and blood samples were collected for histopathological and biochemical examinations. Total bilirubin (TBIL), direct bilirubin (DBIL), alanine aminotransferase (ALT), and aspartate transaminase (AST) levels in the blood samples were detected. The gene expression levels of inducible nitric oxide synthase (iNOS) and endothelial nitric oxide synthase (eNOS), and the nucleus positive rate of NF-E2 related factor 2 (Nrf2) protein were measured. Western blot analyses were used to detect the protein and gene expression levels of Nrf2, Kelch-like ECH-associated protein 1, NAD(P)H quinone dehydrogenase 1 (NQO1), and glutathione-S-transferase (GST) in the liver tissues. One-way analysis of variance was used to evaluate the statistical differences using the statistical package for the social sciences 23.0 software. Intergroup comparisons were followed by the least significant difference test and Dunnett's test.

RESULTS

The effects of YCHD on OJ involve biological processes such as DNA transcription factor binding, RNA polymerase II specific regulation, DNA binding transcriptional activator activity, and nuclear receptor activity. The protective effects of YCHD against OJ were closely related to 20 pathways, including the hepatitis-B, the mitogen-activated protein kinase, the phosphatidylinositol 3-kinase/protein kinase B, and tumor necrosis factor signaling pathways. YCHD alleviated the swelling and necrosis of hepatocytes. Following YCHD treatment, the serum levels of TBIL (176.39 ± 17.03 μmol/L *vs* 132.23 ± 13.88 μmol/L, $P < 0.01$), DBIL (141.41 ± 14.66 μmol/L *vs* 106.43 ± 10.88 μmol/L, $P < 0.01$), ALT (332.07 ± 34.34 U/L *vs* 269.97 ± 24.78 U/L, $P < 0.05$), and AST (411.44 ± 47.64 U/L *vs* 305.47 ± 29.36 U/L, $P < 0.01$) decreased. YCHD promoted the translocation of Nrf2 into the nucleus (12.78 ± 0.99 % *vs* 60.77 ± 1.90 %, $P < 0.001$). After YCHD treatment, we found a decrease in iNOS (0.30 ± 0.02 *vs* 0.20 ± 0.02, $P < 0.001$) and an increase in eNOS (0.18 ± 0.02 vs 0.32 ± 0.02, $P < 0.001$). Meanwhile, in OJ rats, YCHD increased the expressions of Nrf2 (0.57 ± 0.03 *vs* 1.18 ± 0.10, $P < 0.001$), NQO1 (0.13 ± 0.09 *vs* 1.19 ± 0.07, $P < 0.001$), and GST (0.12 ± 0.02 *vs* 0.50 ± 0.05, $P < 0.001$), implying that the potential mechanism of YCHD against OJ-induced liver injury was the upregulation of the Nrf2 signaling pathway.

CONCLUSION

OJ-induced liver injury is associated with the Nrf2 signaling pathway. YCHD can reduce liver injury and oxidative damage by upregulating the Nrf2 pathway.

Key Words: Yinchenhao decoction; Obstructive jaundice; Network pharmacology; Liver injury; Animal models; Oxidative stress

©The Author(s) 2022. Published by Baishideng Publishing Group Inc. All rights reserved.

Core tip: Obstructive Jaundice (OJ) may cause liver injury through various mechanisms. Traditional Chinese medicine has lots of advantages in treating OJ. The mechanism of Yinchenhao decoction (YCHD) for treating OJ-induced liver injury has made significant progress in recent years, but it is still unclear. We used the network pharmacology approach to predict the active components and putative targets of YCHD. We created the OJ rat models and through randomized controlled trials, concluded that YCHD could alleviate liver injury and oxidative damage, thereby promoting the translocation of NF-E2 related factor 2 (Nrf2) to the nucleus, and upregulating the Nrf2 signaling pathway.

Citation: Liu JJ, Xu Y, Chen S, Hao CF, Liang J, Li ZL. The mechanism of Yinchenhao decoction in treating obstructive-jaundice-induced liver injury based on Nrf2 signaling pathway. *World J Gastroenterol* 2022; 28(32): 4635-4648

URL: https://www.wjgnet.com/1007-9327/full/v28/i32/4635.htm

DOI: https://dx.doi.org/10.3748/wjg.v28.i32.4635

INTRODUCTION

Obstructive jaundice (OJ), a common disease in clinical practice, is caused by biliary stones or tumors blocking the bile ducts, causing bile not to flow smoothly into the duodenum, causing elevated bilirubin levels in the blood, yellow-stained sclera and skin, urine yellowing, and other relevant symptoms. OJ can cause liver injury, inflammation, intestinal barrier dysfunction, endotoxemia, coagulation dysfunction, decreased immune function, and malnutrition[1,2]. Therefore, understanding the mechanism of OJ is crucial. Although progress has been made in recent years, it remains unclear. The mechanism of liver damage caused by OJ is mainly related to cholestasis, endotoxemia, inflammatory factors, and oxidative stress[3,4]. Numerous endotoxins activate Kupffer cells during OJ, producing reactive oxygen species (ROS) and reactive nitrogen free radicals (RNS)[5], both of which are important in the body's metabolism.

Oxidative stress is an important pathological mechanism of OJ-induced liver injury. It is present throughout the OJ process[6]. Under normal circumstances, the body's oxidation and antioxidation systems are in a state of dynamic balance. The production and clearance of active molecules such as ROS and RNS are increased as a result of OJ. The balance between oxidation and antioxidation is disrupted, resulting in oxidative stress. Protective actions against ROS are performed by several enzymes, such as superoxide dismutase, catalase, and glutathione peroxidase, as well as nonenzymatic compounds such as glutathione, tocopherol, ascorbate and vitamin E[7-9]. Bile acid has been shown to reduce hepatocyte mitochondrial oxidative phosphorylation activity, directly damage mitochondrial energy metabolism, and produce excess ROS[10], while antioxidants can reduce bile acid-induced oxidative stress injury.

NF-E2 related factor 2 (Nrf2) is a key regulator of antioxidant reduction in tissues and cells. Kelch-like ECH-associated protein 1 (Keap1) is a cytoskeletal anchoring protein that acts as a specific inhibitor of Nrf2. Under normal circumstances, Nrf2 is bound to Keap1 in the cytoplasm, which can be rapidly degraded *via* the ubiquitin-proteasome pathway[11,12]. When the body is stimulated by oxidative stress, Nrf2 is released from sequestration and translocated to the nucleus, where it promotes the transcription of antioxidant and cytoprotective genes. Phase 2 detoxification enzyme genes, such as NAD(P)H quinone dehydrogenase 1 (NQO1), and glutathione-S-transferase (GST) and antioxidant genes, such as heme oxygenase-1 (HO-1) and γ-glutamylcysteine synthetase (γ-GCS) are among the cytoprotective genes[13]. Yinchenhao decoction (YCHD) is a classic traditional Chinese medicine (TCM) formula from the Treatise on Exogenous Febrile Disease. It consists of Yinchen (Artemisiae Scopariae Herba), Zhizi (Gardenia jasminoides Ellis, Gardeniae Fructus), and Dahuang (Radix Rhei et Rhizoma), which is a common prescription for the treatment of damp-heat jaundice. Studies have shown that YCHD has a positive effect on a variety of stagnant damp-heat diseases of the liver meridian not only on enzymes and proteins in the liver and blood, regulating bile acid, bilirubin, lipid, and glucose metabolism but also on pathological processes such as liver fibrosis, inflammation, and hepatocyte apoptosis directly through liver Kupffer cells, hepatic stellate cells, and other cells. Additionally, it can also regulate intestinal flora and protect the liver.

MATERIALS AND METHODS

Active ingredients of YCHD

We used keywords Yinchen, Zhizi, and Dahuang to search the TCM systems pharmacology database and analysis platform (TCMSP) database. According to the standard of oral bioavailability ≥ 30% and drug likeness ≥ 0.18, 13, 16 and 15 active ingredients were obtained. β-Sitosterol is a common component of Yinchen, Zhizi and Dahuang. Yinchen and Zhizi both contain quercetin. After removing the duplicates, YCHD contained 41 active chemical components.

OJ targets

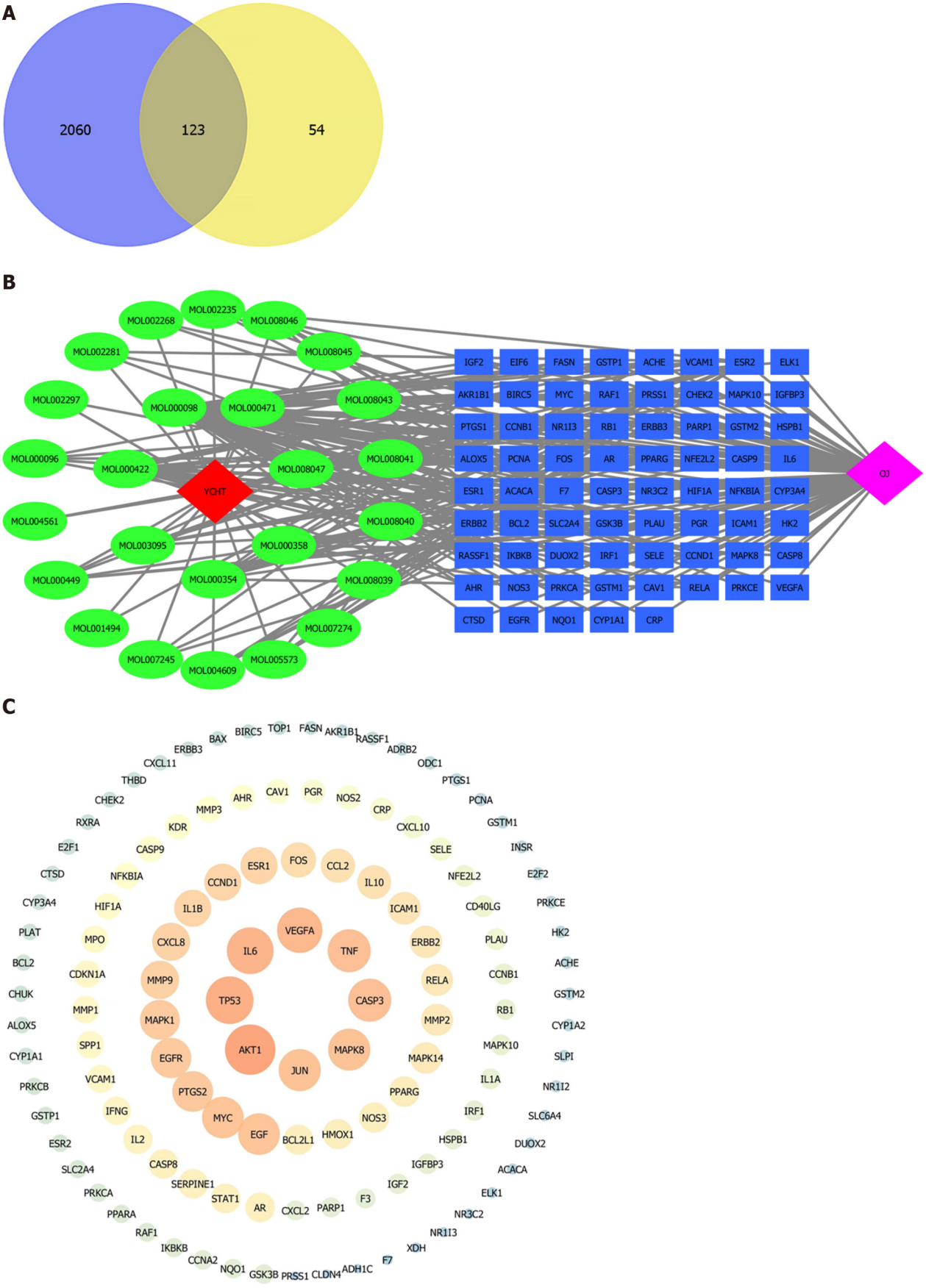
The related targets of OJ were found using the GeneCards database (https://www.genecards.org/). A total of 2183 disease targets were obtained.

Intersection targets of YCHD and OJ

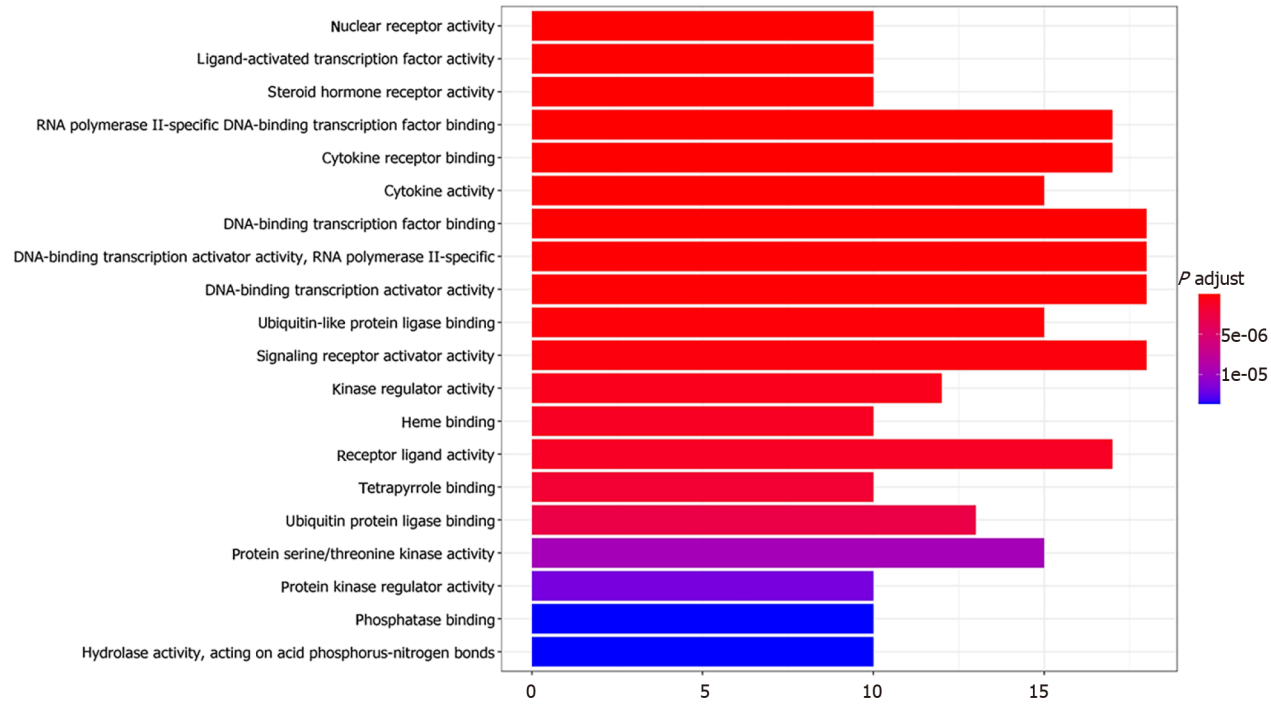
The intersection targets of YCHD and OJ were discovered using R4.0.2 software to analyze the action targets of the main chemical components of YCHD and the targets of OJ. Figure 1A shows the Venn diagram of 123 intersection target genes, or the targets of YCHD acting on OJ. The chemical composition and intersection target of YCHD were entered into the Cytoscape software to construct a Component-Target network of YCHD for treating OJ. The network consists of 153 nodes and 463 edges (Figure 1B).

Protein–protein interaction network

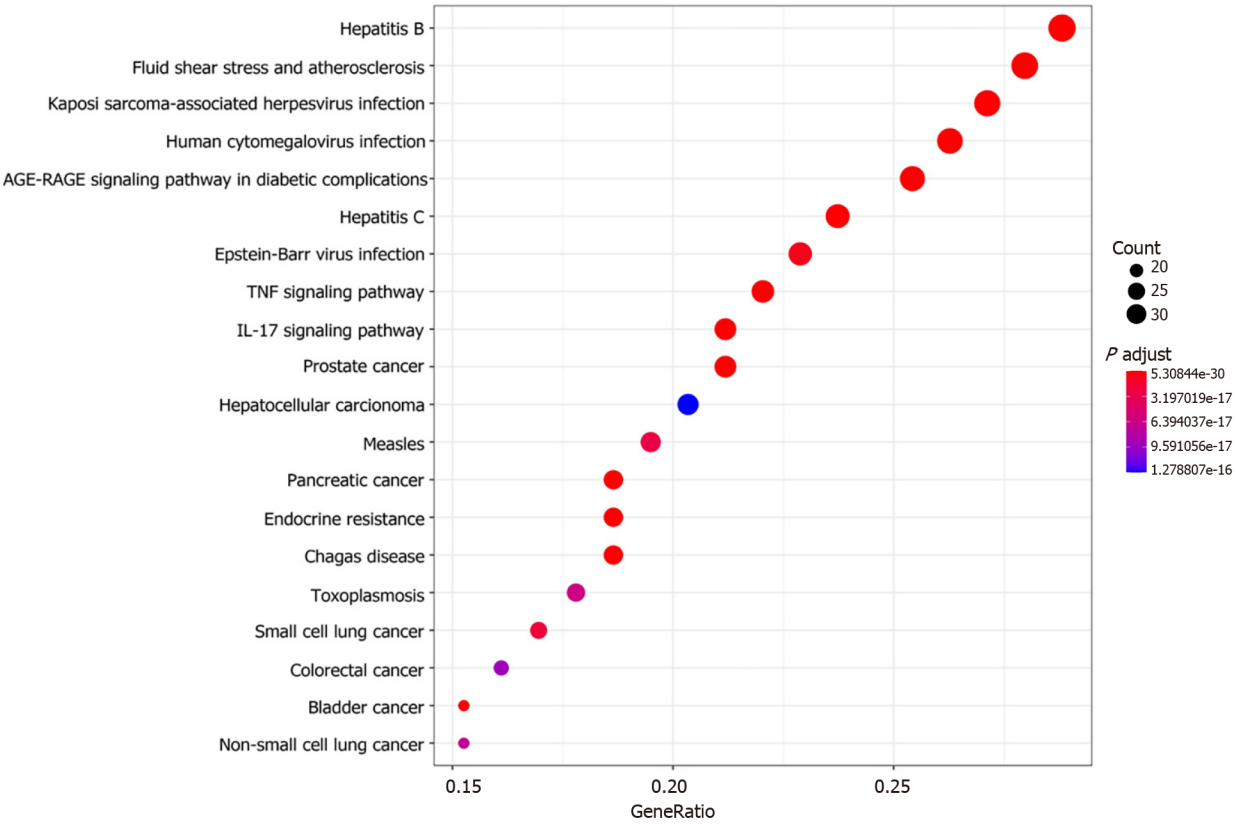
The protein–protein interaction (PPI) data came from the search tool for the retrieval of interacting genes/proteins database (https://string-db.org), which provides information on predicted and experi-

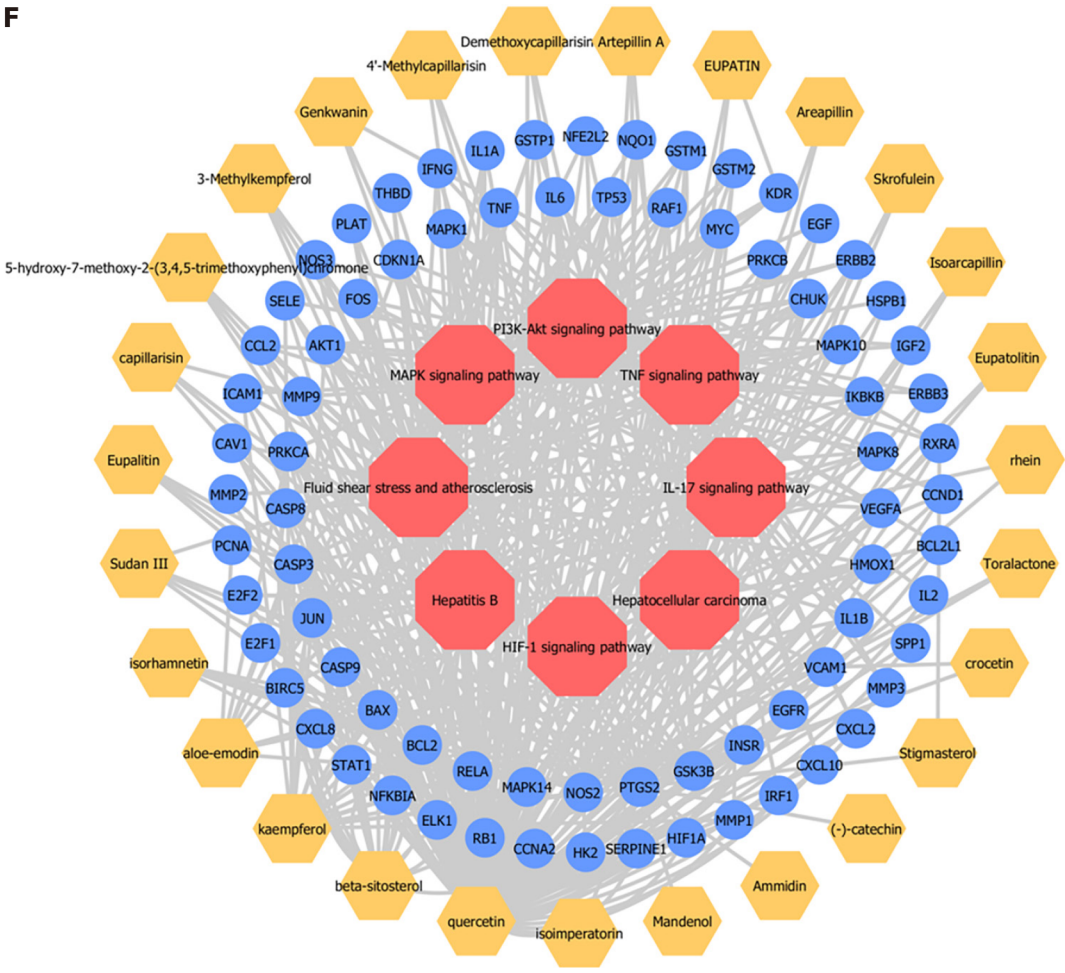

A
2060
123
54
B
MOL002235
MOL002268
MOL008046
MOL002281
MOL008045
MOL002297
MOL000098
MOL000471
MOL008043
MOL000096
MOL000422
YCHT
MOL008047
MOL008041
MOL004561
MOL008040
MOL003095
MOL000358
MOL000449
MOL000354
MOL008039
MOL001494
MOL007274
MOL007245
MOL004609
MOL005573
IGF2
EIF6
FASN
GSTP1
ACHE
VCAM1
ESR2
ELK1
AKR1B1
BIRC5
MYC
RAF1
PRSS1
CHEK2
MAPK10
IGFBP3
PTGS1
CCNB1
NR1I3
RB1
ERBB3
PARP1
GSTM2
HSPB1
ALOX5
PCNA
FOS
AR
PPARG
NFE2L2
CASP9
IL6
ESR1
ACACA
F7
CASP3
NR3C2
HIF1A
NFKBIA
CYP3A4
ERBB2
BCL2
SLC2A4
GSK3B
PLAU
PGR
ICAM1
HK2
RASSF1
IKBKB
DUOX2
IRF1
SELE
CCND1
MAPK8
CASP8
AHR
NOS3
PRKCA
GSTM1
CAV1
RELA
PRKCE
VEGFA
CTSD
EGFR
NQO1
CYP1A1
CRP
OJ
C
BAX
BIRC5
TOP1
FASN
AKR1B1
RASSF1
ADRB2
ERBB3
CXCL11
ODC1
THBD
PTGS1
CHEK2
AHR
CAV1
PGR
NOS2
PCNA
MMP3
CRP
RXRA
KDR
CXCL10
GSTM1
E2F1
CASP9
SELE
INSR
CTSD
NFKBIA
ESR1
FOS
CCL2
CCND1
IL10
NFE2L2
E2F2
CYP3A4
HIF1A
IL1B
ICAM1
CD40LG
PRKCE
PLAT
MPO
CXCL8
VEGFA
IL6
TNF
ERBB2
PLAU
HK2
BCL2
CDKN1A
MMP9
RELA
CCNB1
ACHE
CHUK
TP53
CASP3
GSTM2
MMP1
MAPK1
MMP2
RB1
ALOX5
CYP1A2
SPP1
AKT1
MAPK8
MAPK10
CYP1A1
EGFR
MAPK14
SLPI
VCAM1
JUN
IL1A
PRKCB
PTGS2
PPARG
NR1I2
GSTP1
IFNG
MYC
NOS3
IRF1
SLC6A4
EGF
BCL2L1
HMOX1
ESR2
IL2
HSPB1
DUOX2
SLC2A4
CASP8
IGFBP3
ACACA
SERPINE1
IGF2
PRKCA
STAT1
AR
CXCL2
PARP1
F3
ELK1
PPARA
NR3C2
RAF1
NR1I3
IKBKB
XDH
CCNA2
F7
NQO1
GSK3B
PRSS1
CLDN4
ADH1C

D


Nuclear receptor activity
Ligand-activated transcription factor activity
Steroid hormone receptor activity
RNA polymerase II-specific DNA-binding transcription factor binding
Cytokine receptor binding
Cytokine activity
DNA-binding transcription factor binding
DNA-binding transcription activator activity, RNA polymerase II-specific
DNA-binding transcription activator activity
Ubiquitin-like protein ligase binding
Signaling receptor activator activity
Kinase regulator activity
Heme binding
Receptor ligand activity
Tetrapyrrole binding
Ubiquitin protein ligase binding
Protein serine/threonine kinase activity
Protein kinase regulator activity
Phosphatase binding
Hydrolase activity, acting on acid phosphorus-nitrogen bonds
0
5
10
15
P adjust
5e-06
1e-05

E


Hepatitis B
Fluid shear stress and atherosclerosis
Kaposi sarcoma-associated herpesvirus infection
Human cytomegalovirus infection
AGE-RAGE signaling pathway in diabetic complications
Hepatitis C
Epstein-Barr virus infection
TNF signaling pathway
IL-17 signaling pathway
Prostate cancer
Hepatocellular carcinoma
Measles
Pancreatic cancer
Endocrine resistance
Chagas disease
Toxoplasmosis
Small cell lung cancer
Colorectal cancer
Bladder cancer
Non-small cell lung cancer
0.15
0.20
0.25
GeneRatio
Count
20
25
30
P adjust
5.30844e-30
3.197019e-17
6.394037e-17
9.591056e-17
1.278807e-16



DOI: 10.3748/wjg.v28.i32.4635 **Copyright** ©The Author(s) 2022.

Figure 1 Network construction. A: Venn diagram of the candidate targets in Yinchenhao decoction (YCHD) and obstructive jaundice (OJ); B: The Component-Target network. The blue circles refer to 123 putative targets of YCHD for the treatment of OJ. The red and purple diamonds represent YCHD and OJ, respectively. The green oval represents the chemical composition. The blue rectangle represents the target protein. The degree indicates the number of routes connected to this node in the network; C: The protein–protein interaction network. The size of the set node is proportional to the degree, and the larger the degree, the redder the color, indicating that the target interaction is higher. The key targets are protein kinase B, tumor protein 53, interleukin 6, vascular endothelial growth factor A, and caspase-3. They are the core targets of YCHD in treating OJ; D: The Gene Ontology enrichment analysis of involved biological processes; E: The Kyoto Encyclopedia of Genes and Genomics pathway enrichment analysis of putative targets; F: Component-target-signaling pathway network. The red hexagon represents the signaling pathway; the yellow hexagon represents the component; and the blue circle represents the target.

mental protein interactions. The intersection target's protein interaction relationship was then obtained. However, one protein was not involved in the interaction. The protein interaction information was then entered into the Cytoscape software to construct and analyze the protein interaction network, yielding the PPI network of the YCHD and OJ intersection target. The network consists of 122 nodes. Protein kinase B (PKB/Akt) 1, tumor protein 53 (TP53), interleukin 6 (IL-6), vascular endothelial growth factor A (VEGFA), caspase-3 (CASP3), and so on can be seen in the picture. They are the core targets of YCHD in the treatment of OJ (Figure 1C).

GO and KEGG pathway enrichment analysis

The R software was used to import data from the Bioconductor database (https://www.bioconductor.org/). The protein in network construction was analyzed for Gene Ontology (GO) and Kyoto Encyclopedia of Genes and Genomics (KEGG) enrichment. A total of 135 GO entries and 162 KEGG pathways were identified, and the first 20 target enrichment GO entries and KEGG pathways were plotted onto a bar chart and a bubble chart. The results indicated that the effects of YCHD on OJ involved biological processes such as DNA transcription factor binding, RNA polymerase II specific, DNA-binding transcription activator activity, and nuclear receptor activity (Figure 1D). The protective effects of YCHD against OJ were closely related to 20 pathways, including the hepatitis-B, mitogen-activated protein kinase (MAPK), phosphatidylinositol 3-kinase (PI3K)/Akt , and tumor necrosis factor (TNF) signaling pathways (Figure 1E). the Component-Target-signaling pathway network was created using the Cytoscape software (Figure 1F).

Reagents

Yinchen, Zhizi, and Dahuang were provided by the particle pharmacy of Tianjin Medical University NanKai Hospital. Serum total bilirubin (TBIL) kits, direct bilirubin (DBIL) kits, alanine transaminase (ALT) kits, and aspartate aminotransferase (AST) kits were purchased from the National Institute of Biochemistry. Thermo Fisher Scientific (Shanghai, China) provided the Nrf2 antibody (PA5-27882), Keap1 antibody (PA5-99434), and protein marker (26617. Anti-NQO1 antibody (ab80588) and Anti-GST3/GST antibody (ab138491) were purchased from Abcam (Shanghai, China). β-Actin (66009-1-Ig) was purchased from Proteintech Group (Wuhan, China). Goat anti-rabbit immunoglobulin G (IgG) (ZB-2301) and anti-mouse IgG (ZB-2305) were purchased from Beijing Zhongshan Gold Bridge Biotechnology (Beijing, China). Poly (vinylidene fluoride) membrane (IPHV00010), electrochemiluminescence (ECL) kit (WBKLS0×500), and radioimmunoprecipitation assay buffer (RIPA) lysis buffer (20-188) were provided by Millipore Corporation (Shanghai, China). 4% paraformaldehyde solution, poly-L-lysine, antigen retrieval solution, goat serum, NOS3 (A-9; sc-376751), NOS2 (A-9; sc-7271), S-A/HRP, DAB kit, and hematoxylin and eosin staining kit were purchased from Santa Cruz Biotechnology (Beijing, China). Bicinchoninic acid (BCA) protein assay kit was provided by Beijing Solarbio Science & Technology (Beijing, China).

YCHD preparation

According to Shanghan Lun, a dose of YCHD contains Yinchen (82.5 g), Zhizi (14 g), and Dahuang (27.5 g). We boiled it twice after soaking it for 30 min. Then, we concentrated two boiling mixtures to 124 mL each. The final liquid contained 1 g/mL of the crude drug.

Animals

Thirty-two healthy SPF-rated Sprague–Dawley rats (200–230 g) were purchased from Beijing HFK Bioscience (license No. SCXK Jin 2020-0008). The experimental protocol was approved by the Animal Research Committee of Tianjin Medical University NanKai Hospital (approval no. NKYY-DWLL-2021-102). All the animals were reared in the Laboratory Animal Center of Tianjin Medical University Nankai Hospital. We strictly followed the rules of the experimental animal center. The rats were fed and acclimatized to laboratory conditions (22–24°C, 12 h/12 h light/dark, 60%–65% humidity, *ad libitum* access to food and water) for 2 wk prior to experimentation.

Experiments

Thirty healthy rats were divided into three groups, each with 10 rats: the sham group (Group S), obstructive jaundice model group (Group M), and YCHD-treated group (Group Y). We created OJ models in Groups M and Y by ligating the common bile duct twice and transecting between the sutures. The successful establishment of the bile duct OJ model was demonstrated by the yellowing of the rats' skin after 3 d. In Group S, the common bile ducts were not clamped and served as a control. From then on, rats in Group Y were given a gavage of YCHD (3.6 mL/kg) twice daily for 1 wk, whereas rats in Groups S and M were given the same amount of physiological saline after intragastric administration daily. Intragastric gavage administration was carried out with conscious animals. All rats were killed on d 10 after the operation, and the liver and blood samples were collected for further research. Every effort was made to alleviate animal suffering. Animal experiments followed were strictly complied with the Guide for the Care and Use of Laboratory Animals.

Serum biochemistry analysis

The blood samples were centrifuged at 3000 r/min for 10 min to obtain the upper serum specimens. The serum levels of TBIL, DBIL, ALT and AST were measured.

Histological analysis

The liver tissue was fixed in 4% paraformaldehyde. The samples were sliced into 4–5-μm thick slices and stained with H&E to observe the changes in histology under the microscope after decalcification, dehydration, permeation, and paraffin encapsulation.

Immunohistochemical analysis

Antigen repair, blocking of endogenous peroxidase, incubation of primary and secondary antibodies, DAB staining, restaining of the nucleus, and sealing was performed on dewaxed liver tissue sections. As a result, the nucleus was blue, while the positive DAB expression was brown. The visual field was randomly selected. The levels of inducible nitric oxide synthase (iNOS) and endothelial nitric oxide synthase (eNOS) gene expression, and the nucleus positive rate of Nrf2 protein, were measured.

Western blotting

Liver tissue samples were lysed with RIPA lysis buffer and centrifuged to prepare protein solution. A BCA protein assay kit was used to determine the protein content. Sample feeding, electrophoresis, membrane transfer, and sealing were carried out in order. The specimens were then incubated with the

following primary antibodies, anti-Nrf2 (1:500), anti-Keap1 (1:500), anti-NQO1 (1:10000), anti-GST3/GST (1:1000), and β-actin (1:5000). After washing three times with tris buffered saline-Tween 20 (TBST), the membranes were incubated with rabbit horseradish peroxidase (HRP)-conjugated secondary antibody at 4C for 1 h. Electrochemiluminescence was used to detect the proteins, and ImageJ software was used to calculate the average optical density (AOD). The relative content of Nrf2, Keap1, NQO1 and GST in rat liver tissue was calculated by dividing the AOD value of the target protein in the sample by the AOD value of β-actin.

Statistical analyses

All data were presented as mean ± SD. One-way analysis of variance was used to assess statistical differences using SPSS 23.0 software (SPSS Inc., Chicago, IL, USA). For homogeneity of variance, the least significant difference test was used for homogeneity of variance, and Dunnett's test was used for nonhomogeneity of variance. The *post hoc* test above was used to determine the significance of the statistical results. $P < 0.05$ was considered statistically significant.

RESULTS

Effects of YCHD on biochemical indicators

Biochemical markers of liver function include AST, ALT, TBIL and DBIL. The serum levels of TBIL, DBIL, ALT and AST in Groups M and Y were significantly higher than in Group S (Figure 2A). When compared to Group M, serum levels of TBIL, DBIL, ALT and AST decreased after 1 wk of YCHD intervention in Group Y. The liver function of OJ rats was improved after YCDH treatment.

Histopathological effects

Hepatocytes in Group M were swollen, necrotic, and had neutrophil infiltration and erythrocyte accumulation in the sinusoids, compared with Group S. Group M showed obvious signs of liver injury. The swelling and necrosis of hepatocytes were alleviated in Group Y compared to Group M. After YCHD treatment, the degree of liver injury was significantly reduced (Figure 2B).

Nrf2 translocation

The nucleus positive rate of Nrf2 protein was lower in Group M than in Group S. Compared with Group M, the positive rate in Group Y was significantly higher, suggesting that after the intervention of YCHD, Nrf2 protein was transferred from the cytoplasm to the nucleus, potentially reducing the oxidative damage to OJ liver tissue by regulating the nuclear translocation of Nrf2 (Figure 3).

Effects of YCHD on expression of NOS3 (eNOS) and NOS2 (iNOS)

The AOD of eNOS in Group M decreased when compared to Group S, while that of iNOS increased (Figure 3). Compared with Group M, the AOD of eNOS in Group Y increased, while that of iNOS decreased.

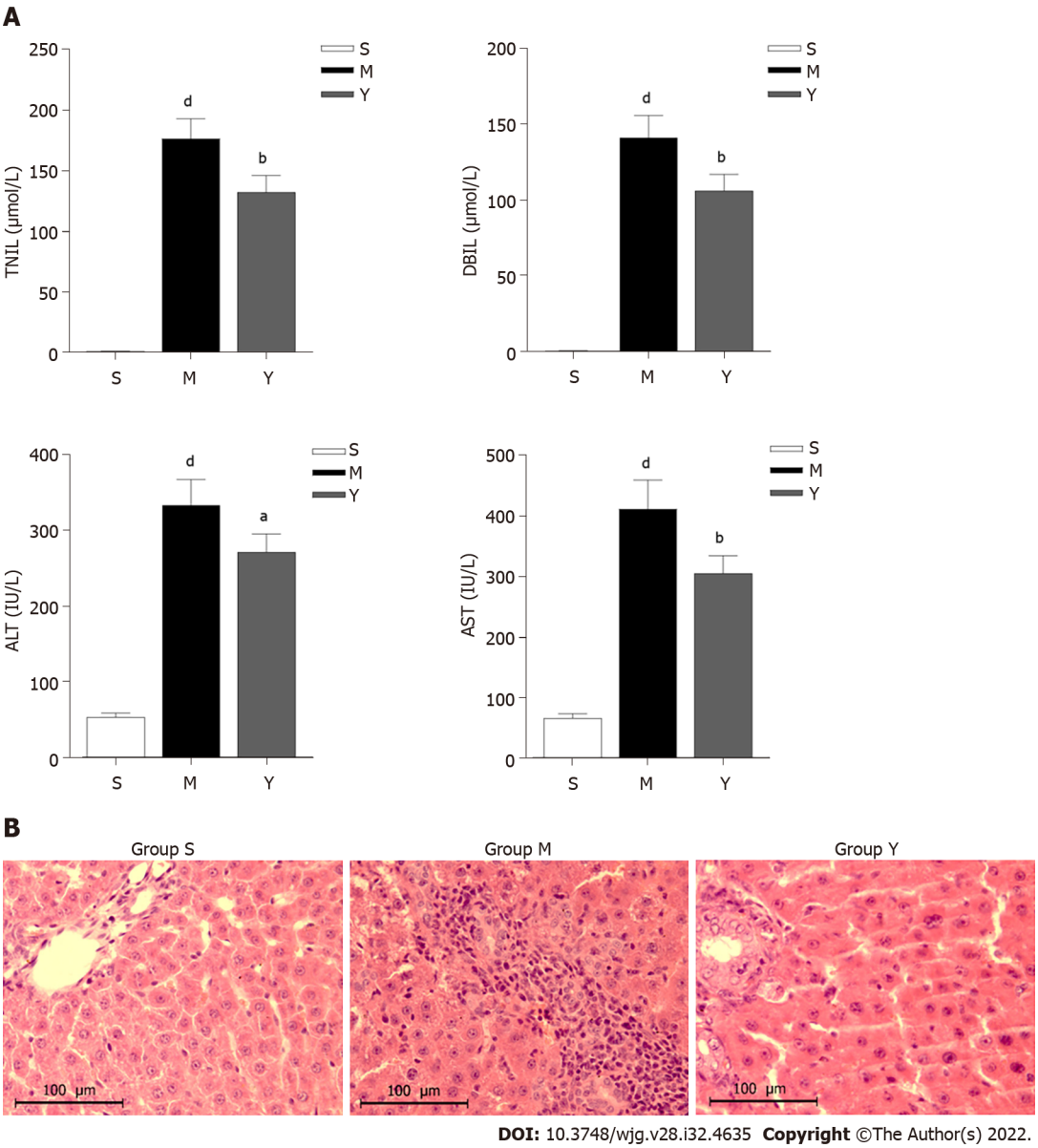
Effects of YCHD on expression of proteins related to the Nrf2 signaling pathway

The expression levels of Nrf2, Keap1 and NQO1 in Group M decreased when compared to Group S. Compared with Group M, the expression levels of Nrf2, NQO1 and GST increased in Group Y, but there was no significant difference in the expression of Keap1 between these two groups (Figure 3).

DISCUSSION

OJ is caused by bile excretion disorder after partial or complete bile duct obstruction. The metabolism of total bile acid (TBA) is disrupted, resulting in an increase in TBA in the blood of up to 60 times the normal amount. Bile buildup causes harmful substances to clump together. Damage in the reticuloendothelial system function causes spillover of bacteria and endotoxin into the systemic circulation[14]. OJ can cause liver damage, inflammation, decreased bowel barrier function, endotoxemia, clotting dysfunction, decreased immune function, and malnutrition. It can cause liver injury through various mechanisms, such as inflammation, endotoxemia and oxidative stress[15]. OJ leads to an increase in the production and clearance of active molecules, such as ROS and RNS. Increased lipid peroxidation and the balance between the hepatic oxidative and antioxidant systems worsen liver injury[16]. OJ causes liver damage and hepatocyte apoptosis by suppressing the protein kinase RNA-like endoplasmic reticulum kinase-induced pathway[17].

YCHD is one of the classic prescriptions for treating liver diseases. The chemical components of YCHD mainly include flavonoids, volatile oils and coumarin, among which the common flavonoids are quercetin, isorhamnetin and cirsimaritin, which belong to a class of compounds with antioxidant, anti-



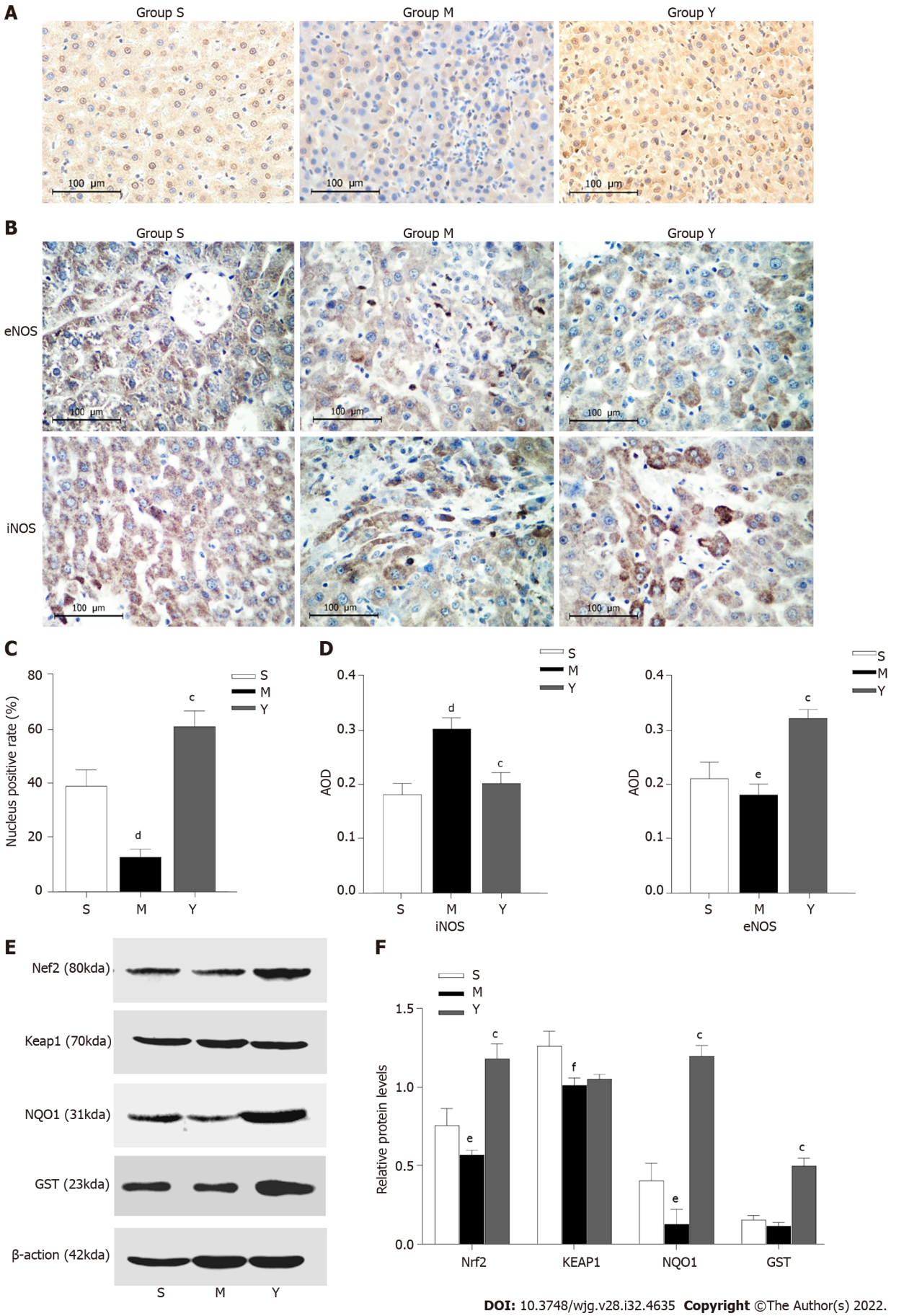
DOI: 10.3748/wjg.v28.i32.4635 **Copyright** ©The Author(s) 2022.

Figure 2 Yinchenhao decoction relieves the hepatic injury induced by obstructive jaundice. A: Yinchenhao decoction (YCHD) treatment improved the liver function of obstructive jaundice (OJ) rats. The concentrations of total bilirubin, direct bilirubin, aspartate transaminase, and alanine aminotransferase in the serum of rats; B: Histological changes of liver tissue (hematoxylin and eosin staining ×400, scale bar 100 μm). Group S: Sham group; Group M: OJ model group; Group Y: YCHD-treated group. $^{a}P < 0.05$, $^{b}P < 0.01$, $^{c}P < 0.001$ *vs* Group M; and $^{d}P < 0.001$ *vs* Group S. TBIL: Total bilirubin; DBIL: Direct bilirubin; ALT: Alanine aminotransferase; AST: Aspartate transaminase.

inflammatory, antitumor and other effects. Recent studies have shown that YCHD increases bile acid reabsorption and restore the balance of bile acid excretion, thereby reducing the impact of toxic bile acids on liver injury in rats[18]. YCHD alleviates lithogenic-diet-induced cholelithiasis and improves biliary cholesterol supersaturation to restore biliary cholesterol homeostasis[19]. YCHD could alleviate liver damage by reducing the levels of important cytokines such as TNF-α, myeloid differentiation primary response 88 (MyD88), and nuclear factor B in the Toll-like receptor 4 signaling pathway. YCHD may reduce liver fibrosis by regulating targets in the apoptosis-related TNF, PI3K-Akt and MAPK signaling pathways, promoting hematopoietic stem cell apoptosis while decreasing hematopoietic progenitor cell apoptosis[20]. YCHD showed therapeutic effects on cholangiocarcinoma by regulating related target protein, inhibiting cell proliferation, and increasing the rate of apoptosis[21].

In our study, we demonstrated that YCHD alleviated the swelling and necrosis of hepatocytes, while also regulating serum levels of ALT, AST, TBIL and DBIL. These findings suggest that YCHD can effectively reduce OJ-induced liver injury and improve liver function.

NO plays a dual role in liver damage. NO is still maintained at a physiological level in the early stages of the disease, which can dilate blood vessels, inhibit platelet aggregation, and improve liver blood flow. RNS is an active group whose derivatives revolve around NO. In the physiological state, iNOS is inactive, but in a physiological state, iNOS is activated and expressed, causing it to catalyze L-



DOI: 10.3748/wjg.v28.i32.4635 **Copyright** ©The Author(s) 2022.

Figure 3 Effects of Yinchenhao decoction on the proteins related to the NF-E2 related factor 2 signaling pathway. A: Effect of Yinchenhao

decoction (YCHD) on NF-E2 related factor 2 (Nrf2) translocation. Nrf2 nucleus localization was measured by immunohistochemistry (DAB staining × 400, scale bar 100 μm). The nucleus is blue and the positive expression of DAB is brown; B: Expression of inducible nitric oxide synthase (iNOS) and endothelial nitric oxide synthase (eNOS) in each group (scale bar 100 μm); C: The nucleus positive rate of Nrf2; D: Relative expression levels of iNOS and eNOS; E: Validation of the potential targets using western blotting. Representative western blotting images of the protein kinase of Nrf2, Kelch-like ECH-associated protein 1 (Keap1), NAD(P)H quinone dehydrogenase 1 (NQO1), and glutathione-S-transferase (GST); F: The bar chart displays the relative levels of Nrf2, Keap1, NQO1 and GST. Group S: Sham group; Group M: Obstructive jaundice model group; Group Y: YCHD-treated group. $^{a}P < 0.05$, $^{b}P < 0.01$, $^{c}P < 0.001$ *vs* Group M; $^{d}P < 0.001$, $^{e}P < 0.05$, $^{f}P < 0.01$ *vs* Group S.

arginine to produce a large amount of NO[22]. NO can easily interact with O2 to produce free radicals and nitro compounds such as ONOO and its proton form HOONO. Recent studies have shown that with the aggravation of cholestasis, various stimulating factors such as endotoxin and inflammation activate the expression of iNOS in liver tissue, resulting in a large amount of NO, which is cytotoxic and causes liver injury[23]. We found expression of NOS3 (eNOS) and NOS2 (iNOS) in the liver tissue of rats. When OJ occurred, the expression of eNOS decreased, while that of iNOS increased. However, after YCHD intervention, the amount of iNOS decreased, suggesting that YCHD can reduce overexpression of NO by adjusting eNOS and iNOS and keeping it at a physiological level to reduce oxidative damage and improve liver microcirculation.

Nrf2 is an important nuclear transcription factor. Under normal circumstances, Nrf2 is bound to Keap1 in the cytoplasm, where it will be rapidly degraded *via* the ubiquitin–proteasome pathway. When the body is stimulated by oxidative stress, Nrf2 dissociates from Keap1. A heterodimer is formed when free Nrf2 combines with one of the small Maf (musculoaponeurotic fibrosarcoma oncogene homolog) proteins. Then, it binds to the antioxidant response elements (AREs), which are enhancer sequences in the regulatory regions, to promote the transcription of genes that encode redox balancing factors, detoxifying enzymes, and stress response proteins, such as GSH, GST, NQO1, HO-1 and glutathione cysteine ligase catalytic subunit[13]. Expression of HO-1 and NQO1 reduces oxidative stress by facilitating removal of ROS[24]. p53 induction and apoptosis were reduced in NQO1-deficient mice, and chemically induced tumors susceptibility was increased[25]. The Nrf2/ARE signaling pathway has been shown to effectively remove excessive ROS from the body, inhibiting oxidation and inflammatory reactions and reducing hepatocellular apoptosis. Increased ROS and oxidative stress injury could lead to gastric mucosal damage and malignancies[26,27]. Overexpression of HO-1 increases the production of CO, which protects cardiomyocytes from apoptosis by generating H_2O_2 in the mitochondria and producing PKB/Akt [28]. The expression of Nrf2 mRNA in silenced neurons for the frataxin gene decreased, and the cells may be more sensitive to oxidative stress[29]. Sulforaphane, an Nrf2 activator, enhances running capacity in rats by upregulating Nrf2 signaling and reduces muscle fatigue by reducing oxidative stress caused by exhaustive exercise[30]. As a result, Nrf2 plays an important role in the response to oxidative stress. Following the intervention of YCHD, the positive rate of Nrf2 in nucleus was significantly increased, suggesting that Nrf2 protein was transferred from the cytoplasm to the nucleus. Nrf2 can only function in the nucleus, forming the Nrf2–Maf heterodimer and binding to ARE to activate antioxidant and metabolic genes. Therefore, YCHD may be able to reduce oxidative damage to OJ liver tissue by regulating the nuclear translocation of Nrf2. As a result, the ability of antioxidant stress is enhanced. We assessed the Nrf2 signaling pathway, which is an important ARE signaling pathway. Expression of Nrf2 was decreased in OJ rats, but significantly increased with YCHD treatment. GSH and NQO1 are the downstream antioxidant factors of the Nrf2 signaling pathway. In the YCHD group, their expression was higher. It was discovered that YCHD protects against OJ-induced oxidative stress by activating the Nrf2 signaling pathway.

CONCLUSION

We found through network pharmacology research that YCHD has multicomponent, multitarget, and multipathway function characteristics. The mechanism could be related to many biological processes, such as anti-inflammatory activity, inhibition of liver fibrosis, antioxidant activity, and apoptosis. This provides the theoretical basis for further research into the molecular mechanism of action of YCHD in the treatment of OJ. In a future study, the chemical composition of YCHD and its associated targets can be studied accurately using the results predicted by network pharmacology. Measurements of ROS accumulation, antioxidant factors (GSH and NQO1), and iNOS were used to assess the status of oxidative stress caused by OJ. We have demonstrated that YCHD can increase the expression of Nrf2, promote translocation of Nrf2 to the nucleus, reduce overexpression of NO by adjusting eNOS and iNOS, and activate downstream GSH and NQO1expression; all of which would protect liver tissue from oxidative damage. Besides, it can also alleviate liver injury and oxidative damage, promote the translocation of Nrf2 to the nucleus, and upregulate the Nrf2 signaling pathway. In a nutshell, the present study looked into the protective effects of YCHD against OJ-induced liver injury. The Nrf2 signaling was upregulated as a potential mechanism. Although many mechanisms are involved in the occurrence

and progression of OJ, we report here for the first time that YCHD can promote the translocation of Nrf2 to the nucleus and upregulate the Nrf2 signaling pathway, which could be a new way to look at antioxidation mechanisms. OJ can be effectively treated using a combination of TCM and modern medicine.

ACKNOWLEDGMENTS

We would like to acknowledge Zhong-Lian Li for his skillful technical assistance and Jing Liang from Chengdu University of traditional Chinese medicine, for her English language proofreading to improve the content of the manuscript.

ARTICLE HIGHLIGHTS

Research background

Obstructive jaundice (OJ) may lead to liver injury through various mechanisms. Oxidative stress is an important pathological mechanism of OJ-induced liver injury. It is present throughout the OJ process. Yinchenhao decoction (YCHD), a traditional Chinese medicine (TCM) formula, has been widely used for treating jaundice in clinical practice. Recent studies have confirmed that YCHD can effectively alleviate liver injury. However, the mechanism of YCHD treating OJ-induced liver injury has not yet been fully clarified.

Research motivation

To provide much more scientific evidence for the clinical application of YCHD and promote the combination of TCM and modern medicine to treat diseases more effectively.

Research objectives

We aimed to investigate the effective chemical components of YCHD and predict the mechanism of YCHD in the treatment of OJ-induced liver injury and oxidative damage.

Research methods

By the network pharmacology approach, we predicted the chemical composition of YCHD and its associated targets. Measurements of inducible nitric oxide synthase (iNOS), endothelial nitric oxide synthase (eNOS), the nucleus positive rate of NF-E2 related factor 2 (Nrf2) protein, and the protein expression levels of Nrf2, Kelch-like ECH-associated protein 1, NAD(P)H quinone dehydrogenase 1 (NQO1) and glutathione-S-transferase (GST) were used to assess the status of oxidative stress caused by OJ.

Research results

Network pharmacology research showed that YCHD had multicomponent, multitarget, and multipathway function characteristics. YCHD increased expression of Nrf2, promoted translocation of Nrf2 to the nucleus, reduced overexpression of NO by adjusting eNOS and iNOS, and activated expression of GST and NQO1; all of which protect liver tissue from oxidative damage.

Research conclusions

YCHD can alleviate liver injury and reduce oxidative damage. Although various mechanisms are involved in the occurrence and development of OJ, we report that YCHD can promote the translocation of Nrf2 to the nucleus, and upregulate the Nrf2 signaling pathway, which may provide a new perspective for the study of the mechanism of antioxidation. This provides the theoretical basis for further research into the molecular mechanism of action of YCHD in the treatment of OJ.

Research perspectives

TCM formulas like YCHD have been widely used for thousands of years. In the near future, more in-depth research on the molecular mechanism of TCM can guide clinical treatment more effectively.

FOOTNOTES

Author contributions: Liu JJ, Xu Y, and Li ZL designed and coordinated the study; Liu JJ, Xu Y, and Chen S performed the experiments and acquired the data; Xu Y, Chen S, and Hao CF analyzed the data; Liu JJ, and Xu Y wrote the manuscript; Liang J proofread the manuscript; and All authors approved the final version of the article.

Supported by the Scientific and Technological Project in Key Areas of Traditional Chinese Medicine of Tianjin

Municipal Health and Health Committee, China, No. 2019003; and the Integrated Traditional Chinese and Western Medicine Project of Tianjin Municipal Health and Health Committee, China, No. 2021042.

Institutional review board statement: The study was reviewed and approved by the Institutional Review Board of Tianjin Medical University Nankai Hospital.

Institutional animal care and use committee statement: All animal experiments conformed to the internationally accepted principles for the care and use of laboratory animals (license No. SCXK Jin 2020-0008). The experimental protocol was approved by the Animal Research Committee of Tianjin Medical University Nankai Hospital (approval No. NKYY-DWLL-2021-102).

Conflict-of-interest statement: The authors declare that they have no conflicts of interest.

Data sharing statement: No additional data are available.

ARRIVE guidelines statement: The authors have read the ARRIVE guidelines, and the manuscript was prepared and revised according to the ARRIVE guidelines.

Open-Access: This article is an open-access article that was selected by an in-house editor and fully peer-reviewed by external reviewers. It is distributed in accordance with the Creative Commons Attribution NonCommercial (CC BY-NC 4.0) license, which permits others to distribute, remix, adapt, build upon this work non-commercially, and license their derivative works on different terms, provided the original work is properly cited and the use is non-commercial. See: https://creativecommons.org/Licenses/by-nc/4.0/

Country/Territory of origin: China

ORCID number: Jun-Jian Liu 0000-0002-2754-8602; Yan Xu 0000-0003-4350-8413; Shuai Chen 0000-0003-0134-8300; Cheng-Fei Hao 0000-0002-2491-411X; Jing Liang 0000-0001-8484-3547; Zhong-Lian Li 0000-0001-5211-7612.

S-Editor: Ma YJ
L-Editor: Kerr C
P-Editor: Yu HG

REFERENCES

1 **Atalay E**, Ozdemir MT, Tur BK, Erdogdu HI, Sisman P. The effect of alphalipoic acid on oxidative parameters and liver injury in rats with obstructive jaundice. *Bratisl Lek Listy* 2019; **120**: 843-848 [PMID: 31747765 DOI: 10.4149/BLL_2019_140]
2 **Unal Y**, Tuncal S, Kosmaz K, Kucuk B, Kismet K, Cavusoglu T, Celepli P, Senes M, Yildiz S, Hucumenoglu S. The Effect of Calcium Dobesilate on Liver Damage in Experimental Obstructive Jaundice. *J Invest Surg* 2019; **32**: 238-244 [PMID: 29589984 DOI: 10.1080/08941939.2018.1451936]
3 **Yang R**, Zhu S, Pischke SE, Haugaa H, Zou X, Tonnessen TI. Bile and circulating HMGB1 contributes to systemic inflammation in obstructive jaundice. *J Surg Res* 2018; **228**: 14-19 [PMID: 29907203 DOI: 10.1016/j.jss.2018.02.049]
4 **Cichoż-Lach H**, Michalak A. Oxidative stress as a crucial factor in liver diseases. *World J Gastroenterol* 2014; **20**: 8082-8091 [PMID: 25009380 DOI: 10.3748/wjg.v20.i25.8082]
5 **Keshavarzian A**, Choudhary S, Holmes EW, Yong S, Banan A, Jakate S, Fields JZ. Preventing gut leakiness by oats supplementation ameliorates alcohol-induced liver damage in rats. *J Pharmacol Exp Ther* 2001; **299**: 442-448 [PMID: 11602653]
6 **Silina EV**, Stupin VA, Abramov IS, Bolevich SB, Deshpande G, Achar RR, Sinelnikova TG. Oxidative Stress and Free Radical Processes in Tumor and Non-Tumor Obstructive Jaundice: Influence of Disease Duration, Severity and Surgical Treatment on Outcomes. *Pathophysiology* 2022; **29**: 32-51 [PMID: 35366288 DOI: 10.3390/pathophysiology29010005]
7 **Majima HJ**, Indo HP, Suenaga S, Matsui H, Yen HC, Ozawa T. Mitochondria as possible pharmaceutical targets for the effects of vitamin E and its homologues in oxidative stress-related diseases. *Curr Pharm Des* 2011; **17**: 2190-2195 [PMID: 21774784 DOI: 10.2174/138161211796957490]
8 **Mao G**, Kraus GA, Kim I, Spurlock ME, Bailey TB, Beitz DC. Effect of a mitochondria-targeted vitamin E derivative on mitochondrial alteration and systemic oxidative stress in mice. *Br J Nutr* 2011; **106**: 87-95 [PMID: 21324214 DOI: 10.1017/S0007114510005830]
9 **Mao G**, Kraus GA, Kim I, Spurlock ME, Bailey TB, Zhang Q, Beitz DC. A mitochondria-targeted vitamin E derivative decreases hepatic oxidative stress and inhibits fat deposition in mice. *J Nutr* 2010; **140**: 1425-1431 [PMID: 20554905 DOI: 10.3945/jn.110.121715]
10 **Sinha K**, Das J, Pal PB, Sil PC. Oxidative stress: the mitochondria-dependent and mitochondria-independent pathways of apoptosis. *Arch Toxicol* 2013; **87**: 1157-1180 [PMID: 23543009 DOI: 10.1007/s00204-013-1034-4]
11 **Turpaev KT**. Keap1-Nrf2 signaling pathway: mechanisms of regulation and role in protection of cells against toxicity caused by xenobiotics and electrophiles. *Biochemistry (Mosc)* 2013; **78**: 111-126 [PMID: 23581983 DOI: 10.1134/S0006297913020016]

12 **Taguchi K**, Yamamoto M. The KEAP1-NRF2 System as a Molecular Target of Cancer Treatment. *Cancers (Basel)* 2020; **13** [PMID: 33375248 DOI: 10.3390/cancers13010046]

13 **Yang L**, Palliyaguru DL, Kensler TW. Frugal chemoprevention: targeting Nrf2 with foods rich in sulforaphane. *Semin Oncol* 2016; **43**: 146-153 [PMID: 26970133 DOI: 10.1053/j.seminoncol.2015.09.013]

14 **Margaritis VG**, Filos KS, Michalaki MA, Scopa CD, Spiliopoulou I, Nikolopoulou VN, Vagianos CE. Effect of oral glutamine administration on bacterial tanslocation, endotoxemia, liver and ileal morphology, and apoptosis in rats with obstructive jaundice. *World J Surg* 2005; **29**: 1329-1334 [PMID: 16136290 DOI: 10.1007/s00268-005-7721-4]

15 **Assimakopoulos SF**, Thomopoulos KC, Patsoukis N, Georgiou CD, Scopa CD, Nikolopoulou VN, Vagianos CE. Evidence for intestinal oxidative stress in patients with obstructive jaundice. *Eur J Clin Invest* 2006; **36**: 181-187 [PMID: 16506963 DOI: 10.1111/j.1365-2362.2006.01616.x]

16 **Galicia-Moreno M**, Rodríguez-Rivera A, Reyes-Gordillo K, Segovia J, Shibayama M, Tsutsumi V, Vergara P, Moreno MG, Muriel P. N-acetylcysteine prevents carbon tetrachloride-induced liver cirrhosis: role of liver transforming growth factor-beta and oxidative stress. *Eur J Gastroenterol Hepatol* 2009; **21**: 908-914 [PMID: 19398917 DOI: 10.1097/MEG.0b013e32831f1f3a]

17 **Wu YL**, Li ZL, Zhang XB, Liu H. Yinchenhao decoction attenuates obstructive jaundice-induced liver injury and hepatocyte apoptosis by suppressing protein kinase RNA-like endoplasmic reticulum kinase-induced pathway. *World J Gastroenterol* 2019; **25**: 6205-6221 [PMID: 31749592 DOI: 10.3748/wjg.v25.i41.6205]

18 **Cai FF**, Wu R, Song YN, Xiong AZ, Chen XL, Yang MD, Yang L, Hu Y, Sun MY, Su SB. Yinchenhao Decoction Alleviates Liver Fibrosis by Regulating Bile Acid Metabolism and TGF-β/Smad/ERK Signalling Pathway. *Sci Rep* 2018; **8**: 15367 [PMID: 30337590 DOI: 10.1038/s41598-018-33669-4]

19 **Zhou Q**, Hu H, Zhao G, Liu P, Wang Y, Zhang H. Effect and related mechanism of Yinchenhao decoction on mice with lithogenic diet-induced cholelithiasis. *Exp Ther Med* 2021; **21**: 316 [PMID: 33717259 DOI: 10.3892/etm.2021.9747]

20 **Cai FF**, Bian YQ, Wu R, Sun Y, Chen XL, Yang MD, Zhang QR, Hu Y, Sun MY, Su SB. Yinchenhao decoction suppresses rat liver fibrosis involved in an apoptosis regulation mechanism based on network pharmacology and transcriptomic analysis. *Biomed Pharmacother* 2019; **114**: 108863 [PMID: 30991286 DOI: 10.1016/j.biopha.2019.108863]

21 **Chen Z**, Lin T, Liao X, Li Z, Lin R, Qi X, Chen G, Sun L, Lin L. Network pharmacology based research into the effect and mechanism of Yinchenhao Decoction against Cholangiocarcinoma. *Chin Med* 2021; **16**: 13 [PMID: 33478536 DOI: 10.1186/s13020-021-00423-4]

22 **Tsuchihashi S**, Kaldas F, Chida N, Sudo Y, Tamura K, Zhai Y, Qiao B, Busuttil RW, Kupiec-Weglinski JW. FK330, a novel inducible nitric oxide synthase inhibitor, prevents ischemia and reperfusion injury in rat liver transplantation. *Am J Transplant* 2006; **6**: 2013-2022 [PMID: 16796718 DOI: 10.1111/j.1600-6143.2006.01435.x]

23 **Picón-Pagès P**, Garcia-Buendia J, Muñoz FJ. Functions and dysfunctions of nitric oxide in brain. *Biochim Biophys Acta Mol Basis Dis* 2019; **1865**: 1949-1967 [PMID: 30500433 DOI: 10.1016/j.bbadis.2018.11.007]

24 **Sekine H**, Okazaki K, Ota N, Shima H, Katoh Y, Suzuki N, Igarashi K, Ito M, Motohashi H, Yamamoto M. The Mediator Subunit MED16 Transduces NRF2-Activating Signals into Antioxidant Gene Expression. *Mol Cell Biol* 2016; **36**: 407-420 [PMID: 26572828 DOI: 10.1128/MCB.00785-15]

25 **Iskander K**, Gaikwad A, Paquet M, Long DJ 2nd, Brayton C, Barrios R, Jaiswal AK. Lower induction of p53 and decreased apoptosis in NQO1-null mice lead to increased sensitivity to chemical-induced skin carcinogenesis. *Cancer Res* 2005; **65**: 2054-2058 [PMID: 15781611 DOI: 10.1158/0008-5472.CAN-04-3157]

26 **Borrego S**, Vazquez A, Dasí F, Cerdá C, Iradi A, Tormos C, Sánchez JM, Bagán L, Boix J, Zaragoza C, Camps J, Sáez G. Oxidative Stress and DNA Damage in Human Gastric Carcinoma: 8-Oxo-7'8-dihydro-2'-deoxyguanosine (8-oxo-dG) as a Possible Tumor Marker. *Int J Mol Sci* 2013; **14**: 3467-3486 [PMID: 23389043 DOI: 10.3390/ijms14023467]

27 **Ma Y**, Zhang L, Rong S, Qu H, Zhang Y, Chang D, Pan H, Wang W. Relation between gastric cancer and protein oxidation, DNA damage, and lipid peroxidation. *Oxid Med Cell Longev* 2013; **2013**: 543760 [PMID: 24454985 DOI: 10.1155/2013/543760]

28 **Piantadosi CA**, Carraway MS, Babiker A, Suliman HB. Heme oxygenase-1 regulates cardiac mitochondrial biogenesis *via* Nrf2-mediated transcriptional control of nuclear respiratory factor-1. *Circ Res* 2008; **103**: 1232-1240 [PMID: 18845810 DOI: 10.1161/01.RES.0000338597.71702.ad]

29 **D'Oria V**, Petrini S, Travaglini L, Priori C, Piermarini E, Petrillo S, Carletti B, Bertini E, Piemonte F. Frataxin deficiency leads to reduced expression and impaired translocation of NF-E2-related factor (Nrf2) in cultured motor neurons. *Int J Mol Sci* 2013; **14**: 7853-7865 [PMID: 23574943 DOI: 10.3390/ijms14047853]

30 **Oh S**, Komine S, Warabi E, Akiyama K, Ishii A, Ishige K, Mizokami Y, Kuga K, Horie M, Miwa Y, Iwawaki T, Yamamoto M, Shoda J. Nuclear factor (erythroid derived 2)-like 2 activation increases exercise endurance capacity *via* redox modulation in skeletal muscles. *Sci Rep* 2017; **7**: 12902 [PMID: 29018242 DOI: 10.1038/s41598-017-12926-y]

World Journal of Gastroenterology

Submit a Manuscript: https://www.f6publishing.com

World J Gastroenterol 2022 August 28; 28(32): 4649-4667

DOI: 10.3748/wjg.v28.i32.4649

ISSN 1007-9327 (print) ISSN 2219-2840 (online)

ORIGINAL ARTICLE

Basic Study

Anoctamin 5 regulates the cell cycle and affects prognosis in gastric cancer

Tomoyuki Fukami, Atsushi Shiozaki, Toshiyuki Kosuga, Michihiro Kudou, Hiroki Shimizu, Takuma Ohashi, Tomohiro Arita, Hirotaka Konishi, Shuhei Komatsu, Takeshi Kubota, Hitoshi Fujiwara, Kazuma Okamoto, Mitsuo Kishimoto, Yukiko Morinaga, Eiichi Konishi, Eigo Otsuji

Specialty type: Gastroenterology and hepatology

Provenance and peer review: Unsolicited article; Externally peer reviewed.

Peer-review model: Single blind

Peer-review report's scientific quality classification
Grade A (Excellent): 0
Grade B (Very good): B
Grade C (Good): C, C
Grade D (Fair): 0
Grade E (Poor): 0

P-Reviewer: Gao W, China; Gao JP, China; Zhu Z, China

Received: February 28, 2022
Peer-review started: February 28, 2022
First decision: May 9, 2022
Revised: June 10, 2022
Accepted: July 27, 2022
Article in press: July 27, 2022
Published online: August 28, 2022

Tomoyuki Fukami, Atsushi Shiozaki, Toshiyuki Kosuga, Michihiro Kudou, Hiroki Shimizu, Takuma Ohashi, Tomohiro Arita, Hirotaka Konishi, Shuhei Komatsu, Takeshi Kubota, Hitoshi Fujiwara, Kazuma Okamoto, Eigo Otsuji, Division of Digestive Surgery, Department of Surgery, Kyoto Prefectural University of Medicine, Kyoto 602-8566, Japan

Mitsuo Kishimoto, Department of Pathology, Kyoto City Hospital, Kyoto 604-8845, Japan

Yukiko Morinaga, Eiichi Konishi, Department of Pathology, Kyoto Prefectural University of Medicine, Kyoto 602-8566, Japan

Corresponding author: Atsushi Shiozaki, MD, PhD, Assistant Professor, Division of Digestive Surgery, Department of Surgery, Kyoto Prefectural University of Medicine, 465 Kajii-cho, Kamigyo-ku, Kyoto 602-8566, Japan. shiozaki@koto.kpu-m.ac.jp

Abstract

BACKGROUND

Anoctamin 5 (ANO5)/transmembrane protein 16E belongs to the ANO/ transmembrane protein 16 anion channel family. ANOs comprise a family of plasma membrane proteins that mediate ion transport and phospholipid scrambling and regulate other membrane proteins in numerous cell types. Previous studies have elucidated the roles and mechanisms of ANO5 activation in various cancer types. However, it remains unclear whether ANO5 acts as a plasma membrane chloride channel, and its expression and functions in gastric cancer (GC) have not been investigated.

AIM

To examine the role of ANO5 in the regulation of tumor progression and clinicopathological significance of its expression in GC.

METHODS

Knockdown experiments using ANO5 small interfering RNA were conducted in human GC cell lines, and changes in cell proliferation, cell cycle progression, apoptosis, and cellular movement were assessed. The gene expression profiles of GC cells were investigated following ANO5 silencing by microarray analysis. Immunohistochemical staining of ANO5 was performed on 195 primary tumor

samples obtained from patients with GC who underwent curative gastrectomy between 2011 and 2013 at our department.

RESULTS

Reverse transcription-quantitative polymerase chain reaction (PCR) and western blotting demonstrated high ANO5 mRNA and protein expression, respectively, in NUGC4 and MKN45 cells. In these cells, ANO5 silencing inhibited cell proliferation and induced apoptosis. In addition, the knockdown of ANO5 inhibited G_1-S phase progression, invasion, and migration. The results of the microarray analysis revealed changes in the expression levels of several cyclin-associated genes, such as *CDKN1A*, *CDK2/4/6*, *CCNE2*, and *E2F1*, in ANO5-depleted NUGC4 cells. The expression of these genes was verified using reverse transcription-quantitative PCR. Immunohistochemical staining revealed that high ANO5 expression levels were associated with a poor prognosis. Multivariate analysis identified high ANO5 expression as an independent prognostic factor for 5-year survival in patients with GC (P = 0.0457).

CONCLUSION

ANO5 regulates the cell cycle progression by regulating the expression of cyclin-associated genes and affects the prognosis of patients with GC. These results may provide insights into the role of ANO5 as a key mediator in tumor progression and/or promising prognostic biomarker for GC.

Key Words: Anoctamin 5; Gastric cancer; Cell cycle; G1/S checkpoint; Cell proliferation

©The Author(s) 2022. Published by Baishideng Publishing Group Inc. All rights reserved.

Core Tip: The present study aimed to investigate the role of anoctamin 5 (ANO5) in the regulation of tumor progression and the clinicopathological significance of its expression in gastric cancer. Immunohistochemical staining revealed that high ANO5 expression levels were associated with a poor prognosis in patients with gastric cancer. Microarray analysis results suggest that ANO5 regulates cell cycle progression by regulating the expression of cyclin-associated genes. Our results provide insights into the role of ANO5 as a mediator of and/or biomarker for gastric cancer.

Citation: Fukami T, Shiozaki A, Kosuga T, Kudou M, Shimizu H, Ohashi T, Arita T, Konishi H, Komatsu S, Kubota T, Fujiwara H, Okamoto K, Kishimoto M, Morinaga Y, Konishi E, Otsuji E. Anoctamin 5 regulates the cell cycle and affects prognosis in gastric cancer. *World J Gastroenterol* 2022; 28(32): 4649-4667
URL: https://www.wjgnet.com/1007-9327/full/v28/i32/4649.htm
DOI: https://dx.doi.org/10.3748/wjg.v28.i32.4649

INTRODUCTION

The anoctamin (ANO)/transmembrane protein 16 (TMEM16) family is present in numerous eukaryotes, and ten ANO paralogs, ANO1-ANO10 (TMEM16A-H, TMEM16J and K), have been identified in vertebrates[1]. Of these, several function as calcium-activated chloride channels. ANOs comprise a family of plasma membrane proteins that mediate ion transport, phospholipid scrambling, and other membrane protein regulation in numerous cell types[2-6]. Their expression has been detected in both epithelial and non-epithelial tissues types[4]. Although the regulation of ANOs has been extensively examined, the mechanisms by which increased intracellular calcium concentration activates chloride or cation conductance have not been elucidated.

Recent molecular and biochemical studies reported a role for ANOs in human carcinogenesis. For instance, the expression of ANO proteins is upregulated in cancer and associated with a poor patient prognosis[7]. A relationship has been demonstrated between ANO1 and patient prognosis in various cancer types, including gastric, esophageal, breast, lung, and head and neck cancer[8-12]. The upregulation of the genes encoding ANO1 and ANO3 has been associated with several cancer types, specifically gastrointestinal stromal tumors, breast cancer, and squamous cell carcinoma[12,13]. Furthermore, ANO6 has been strongly implicated in the metastatic potential of breast cancer[14]. The expression levels of other members of the ANO family are also associated with cell proliferation and cancer development[15-17].

In our previous studies, we identified a crucial role for several chloride ion channels and transporters in patients with gastric cancer (GC); intracellular chloride regulates proliferation and cell cycle progression[18,19], whereas furosemide, a potent inhibitor of the $Na^+/K^+/2Cl^-$ cotransporter, induces G_0/G_1 arrest[20]. Furthermore, leucine rich repeat containing 8 VRAC subunit A regulate the proliferation,

apoptosis, migration, and invasion of GC cells[21].

ANO5 has recently been implicated in various cancers, such as thyroid[22] and pancreatic cancer[23]; however, limited information is presently available on its involvement in tumor progression in patients with GC or the clinical significance of its expression. Therefore, in the present study, we investigated whether ANO5 contributes to the regulation of cancer growth and evaluated its clinicopathological significance in GC.

MATERIALS AND METHODS

Cell lines, antibodies

MKN7, MKN45, MKN74, HGC27, and NUGC4 human GC cell lines were purchased from the Riken Cell Bank (Tsukuba, Japan). Cells were cultured in RPMI-1640 (Nacalai Tesque, Kyoto, Japan) containing 100 μg/mL of streptomycin, 100 U/mL penicillin, and 10% FBS at 37 °C in a 5% CO_2 incubator. Rabbit polyclonal anti-ANO5 antibody was obtained from Funakoshi (GTX81161) for immunohistochemical (IHC) analysis and western blotting. Mouse monoclonal anti-β-actin antibody was provided by Sigma-Aldrich (St. Louis, MO, United States) and HRP-conjugated anti-rabbit and mouse secondary antibodies by Cell Signaling Technology (Beverly, MA, United States).

Reverse transcription-quantitative polymerase chain reaction

RNA was extracted from cancer cells using an RNeasy kit (Qiagen, Valencia, CA, United States). The Step One plus™ Real-Time polymerase chain reaction (PCR) System (Applied Biosystems, Foster City, CA, United States) and TaqMan Gene Expression Assays (Applied Biosystems) were employed for reverse transcription-quantitative PCR analysis using the following PCR thermocycling conditions: initial denaturation step at 95 °C for 10 min, followed by 40 cycles at 95 °C for 15 s and 60 °C for 1 min. The expression levels of the following genes were assessed: *ANO5* (Hs01381106_m1), *CDKN1A* (Hs00355782_m1), *CDK2* (Hs00608082_m1), *CDK4* (Hs00175935_m1), *CDK6* (Hs00608037_m1), cyclin E2 (CCNE2; Hs00180319_m1), and *E2F1* (Hs00153451_m1) (all from Applied Biosystems). The expression of each gene was normalized using the housekeeping gene β-actin (Hs01060665_g1; Applied Biosystems). All assays were performed in triplicates.

Western blotting

The cells were washed twice with ice-cold PBS and harvested in M-PER lysis buffer (Pierce, Rockford, IL, United States) supplemented with protease inhibitors (Pierce Biotechnology). Protein concentrations were measured using a modified Bradford assay (Bio-Rad, Hercules, CA, United States). Cell lysates containing equal amounts of total protein (10 mg/lane) were resolved using 10% SDS-PAGE and subsequently transferred to polyvinylidene fluoride membranes (GE Healthcare, Piscataway, NJ, United States). Membranes were incubated with antibodies for 24 h at 4 °C. Band densities were quantified using ImageJ (version 1.52; National Institutes of Health).

Small interfering RNA transfection

All small interfering RNA (siRNA) reverse transfection procedures were performed using Lipofectamine® RNAiMAX reagent (Invitrogen, Carlsbad, CA, United States) with a final siRNA concentration of 20 nmol/L, according to the manufacturer's instructions. ANO5 siRNA (Stealth RNAi siRNA; HSS137119, Stealth RNAi siRNA; HSS137120) and control siRNA (Stealth RNAiTM siRNA Negative Control) were obtained from Invitrogen.

Overexpression study

Control-HaloTag^R plasmid (Promega, G6591) and ANO5-HaloTag^R plasmid (pFN21AE5809) were transfected using P3000TM (Invitrogen) and lipofectamine 3000 (Invitrogen) following the manufacturer's instructions. After passaging, ANO5-expressing cells were used for the cell proliferation assay.

Cell proliferation assay

NUGC4 and MKN45 cells were seeded at densities of 1.0 and 2.0 × 10^5 cells/well, respectively, on six-well plates and incubated at 37 °C in a 5% CO_2 incubator. The siRNA was transfected 24 h after seeding. The cells were detached from the plates with trypsin-EDTA 48 h and 72 h after siRNA transfection and counted using a hemocytometer.

Cell proliferation activity was measured using the water-soluble tetrazolium salts-8 assay with Cell Count Reagent SF (Nacalai Tesque). NUGC4, MKN45, and MKN7 cells were seeded at a density of 1.0 × 10^4, 1.0 × 10^4, and 1.5 × 10^4 cells/well, respectively, in 24-well plates and were incubated at 37 °C in a 5% CO_2 incubator. The siRNA was transfected 24 h after seeding. Cell proliferation was evaluated every 24 h by measuring the absorbance at 450 nm using a Thermo Scientific Multiskan FC (Thermo Fisher Scientific).

Cell cycle assay

Cell cycle progression was assessed 48 h after siRNA transfection by flow cytometry. Cells were detached from the plates using trypsin-EDTA and subsequently treated with 0.2% Triton X-100 and stained with propidium iodide with RNase staining buffer (BD Biosciences, San Jose, CA, United States). Flow cytometry data were acquired using a BD Accuri C6 plus flow cytometer (BD Biosciences) to assess DNA content in at least 10000 cells.

Apoptosis assay

Cells were evaluated 72 h after transfection and stained using the ANNEXIN V-FITC Kit (Beckman Coulter, Brea, CA, United States). The frequencies of early and late apoptotic cells among at least 10000 cells were assessed using a BD Accuri C6 plus flow cytometer.

Migration and invasion assays

Migration assays were performed using 24-well cell culture inserts with 8-μm pores (BD Biosciences), whereas invasion assays were performed using Biocoat Matrigel® (BD Biosciences). At 48 h post-transfection, NUGC4 and MKN45 cells were seeded at a density of 3.0 × 10^5 cells/well in serum-free RPMI-1640 in the upper chamber, whereas the lower chamber contained RPMI-1640 with 10% FBS. Matrigel and the cells remaining in the upper chamber after a 48-h incubation were removed. Diff-Quick staining reagents (Sysmex) were used to stain migrated or invaded cells, which were counted in four independent fields of view. Both assays were conducted thrice.

Microarray analysis

NUGC4 and MKN45 cells were transfected with either control or ANO5 siRNA. At 48 h after siRNA transfection, total RNA was extracted using RNeasy kit. Cyanine 3 (Cy3)-labeled cRNA was prepared from 0.1 μg total RNA using the Low Input Quick Amp Labeling Kit (Agilent Technologies, CA, United States) and then subjected to RNeasy column purification (Qiagen). Dye incorporation and cRNA yields were assessed using a NanoDrop 2000 Spectrophotometer (Thermo Fisher Scientific). Subsequently, 0.6 μg Cy3-labeled cRNA was fragmented in a 25 μL reaction volume containing 1 × Agilent fragmentation buffer and 2 × Agilent blocking agent at 60 °C for 30 min. The 2 × Agilent hybridization buffer (25 μL) was then added, and hybridization to SurePrint G3 Human GE 8 × 60K Microarray Ver3.0 (Agilent Technologies) was conducted at 65 °C for 17 h in a rotating Agilent hybridization oven. The microarrays were then washed with GE Wash Buffer 1 (Agilent Technologies) at room temperature for 1 min, followed by GE Wash buffer 2 (Agilent Technologies) at 37 °C for 1 min.

Microarray data processing

Slides were scanned using the Agilent SureScan Microarray Scanner (G2600D) with the one color scan setting for 8 × 60k array slides. The scanned images were analyzed with Feature Extraction Software (Agilent Technologies) using the default parameters to obtain background-subtracted and spatially detrended processed signal intensities. Microarray data were analyzed using ingenuity pathway analysis software (Ingenuity Systems, Redwood City, CA).

Patients and primary tissue samples

Histologically proven primary GC tumor samples were obtained from 195 consecutive patients who underwent curative gastrectomy between 2011 and 2013 at Kyoto Prefectural University of Medicine, Japan. For mRNA analysis, frozen tissue samples of normal stomach and tumors were collected from surgical specimens and stored at -80 °C. Written informed consent was obtained from all patients prior to enrollment. Patients with noncurative resection or preoperative chemotherapy were excluded from the study. Tumor staging was conducted according to the International Union Against Cancer/TNM Classification of Malignant Tumors (8^{th} edition)[24]. The present study was approved by the Institutional Review Board of the Kyoto Prefectural University of Medicine (ERB-C-1195).

IHC

The Vectastain avidin-biotinylated peroxidase complex Elite Kit (Vector Laboratories, Burlingame, CA, United States) was employed for IHC staining using the avidin-biotinylated peroxidase complex method. After deparaffinization in xylene, sections were rehydrated in a graded series of ethanol solutions. The sections were then incubated in 0.3% H_2O_2 for 30 min to block endogenous peroxidase activity. Endogenous biotin, biotin receptors, and avidin-binding sites were also blocked using an Avidin/Biotin Blocking Kit (Vector laboratories). Sections were incubated with ANO5 antibody diluted 1:100 at 37 °C for 1 h and then at 4 °C overnight. Cells were visualized using the standard avidin-biotinylated peroxidase complex method, with hematoxylin as the counterstain.

ANO5 expression levels in immunohistochemically stained samples were semi-quantitatively graded based on the staining intensity and proportion of cytoplasm in the stained cancer cells. The staining intensity was scored as 0 (no staining), 1 (weak staining), 2 (moderate staining), or 3 (strong staining). The proportion of stained tumor cells as a percentage of the stained area in the cancer area was scored

from 0 to 1.0. IHC scores were calculated as the maximum multiplied product of intensity and proportion scores (0-3.0). IHC diagnosis was based on tumor ANO5 expression assessment, and other IHC parameters were performed by at least two physicians, including an experienced pathologist.

Quantification of intracellular chloride concentration and low chloride stimulation

MQAE reagent, a chloride-sensitive fluorescence probe (Dojindo Laboratories, Kumamoto, Japan) was used to assess intracellular chloride concentrations. NUGC4 and MKN45 cells were seeded in 24-well plates at a density of 3.0×10^4 cells/well and then incubated in normal medium at 37 °C with 5% CO_2. The medium was then replaced with standard and low-chloride medium in which MQAE was dissolved, and cells were incubated at 37 °C in a CO_2 incubator for a further 12 h. Following washing with PBS five times, the fluorescence intensity of MQAE was evaluated under a fluorescence microscope (BZ-X800; Keyence, Osaka, Japan). Three fields of view were analyzed *per* sample at × 100 magnification. Quantification was performed using a BZ-X800 analyzer and accompanying software (BZ-H4C, v.1.1.1.8; Keyence).

A low chloride stimulation experiment was conducted to examine the effects of changes in intracellular chloride concentrations on GC cells. A low-chloride medium supplemented with 10% FBS was prepared in chloride-free RPMI-1640 (chloride replaced with NO_3^-) (Nacalai Tesque).

c-Jun N-terminal kinase signaling pathway inhibitor treatment

To block the c-Jun N-terminal kinase (JNK) signaling pathway, NUGC4 and MKN45 cells were incubated with the JNK inhibitor SP600125 (10μm, ab120065, Abcam) according to manufacturer's instructions. The cells were divided into 3 groups: control, ANO5 siRNA, and JNK inhibitor (ANO5 siRNA + SP600125). Cell proliferation was detected every 24 h after ANO5 silencing.

Statistical analysis

Statistical analysis was performed using the Mann-Whitney *U* test for two-group comparisons. Categorical data were analyzed using Fisher's exact test. The Kaplan–Meier method was used to construct survival curves, and differences in survival were examined using the log-rank test for equality. Prognostic factors were identified using the Cox proportional hazard model. These analyses were performed using the JMP statistical software (version 15; SAS Institute, Cary, NC, United States). Data are presented in the graphs as the mean ± standard error of the mean. $P < 0.05$ was considered a statistically significant difference.

RESULTS

ANO5 expression in GC cells

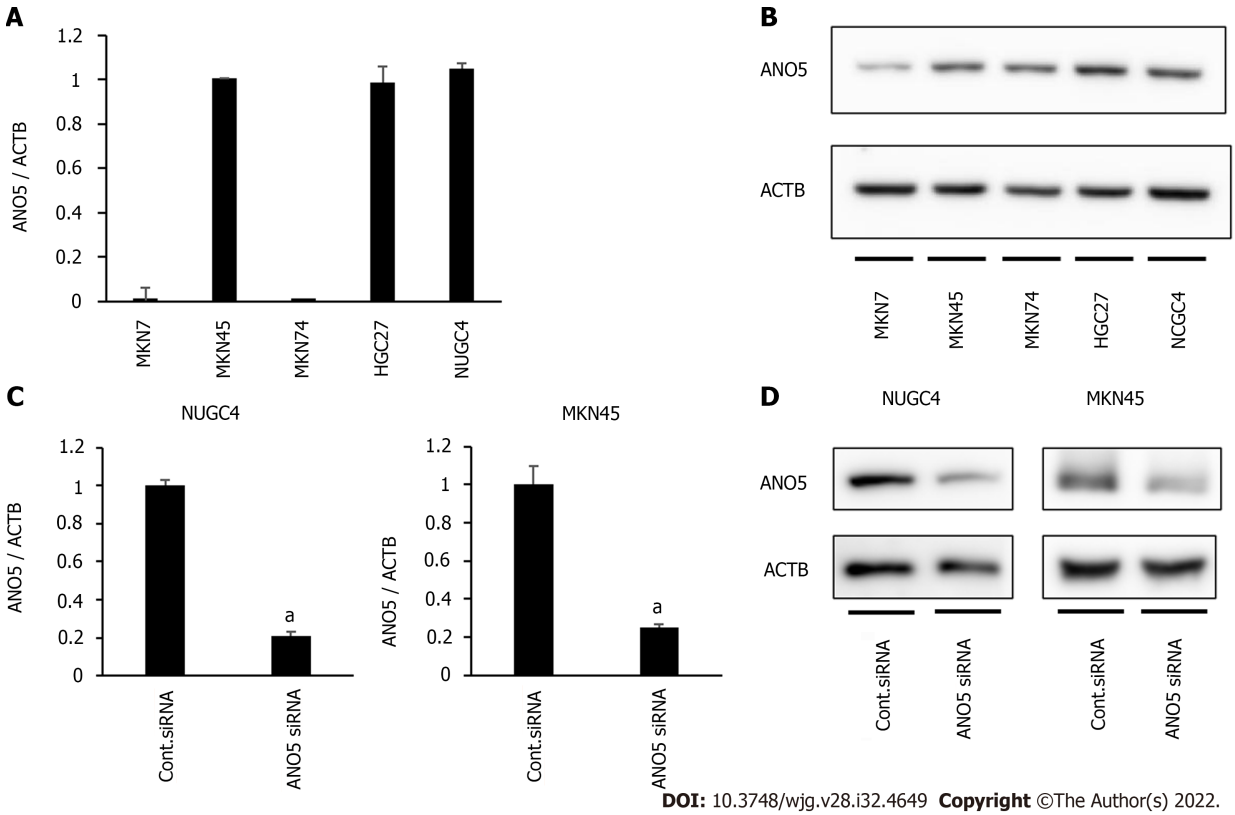
ANO5 gene and protein expression were first examined in five human GC cell lines, MKN7, MKN45, MKN74, HGC27, and NUGC4, by reverse transcription-quantitative PCR and western blotting. ANO5 expression was detected in several cells in the five GC cell lines (Figure 1A and B). Compared to paired adjacent normal tissue, ANO5 expression was significantly upregulated in GC tissue ($P = 0.004$; $n = 12$; Supplementary Figure 1).

ANO5 expression was knocked down using siRNA in NUGC4 and MKN45 cells, and its effects on tumor progression were assessed. *ANO5* mRNA (Figure 1C) and protein levels (Figure 1D) were downregulated in NUGC4 and MKN45 cells. We also conducted an overexpression study in MKN7 cells. The ANO5 plasmid increased *ANO5* mRNA levels (Supplementary Figure 2A, left panel).

ANO5 regulates cell growth and survival in GC cells

The effect of ANO5 siRNA transfection on the proliferation and cell cycle progression of NUGC4 and MKN45 cells were subsequently examined. Compared with the control siRNA, the number of NUGC4 and MKN45 cells was significantly reduced at 48 h and 72 h after the transfection with ANO5 siRNA (Figure 2A, left panel). The results of the cell proliferation assay showed that the relative absorbance of GC cells transfected with the control siRNA (NUGC4 and MKN45) was significantly lower than that of GC cells transfected with ANO5 siRNA (HSS137119) (NUGC4 and MKN45) (Figure 2A, right panel). Whereas, ANO5 plasmid increased the relative absorbance of MKN7 cell (Supplementary Figure 2B). Moreover, ANO5 silencing increased the numbers of NUGC4 and MKN45 cells in the G_0/G_1 phase (Figure 2B). These results indicated that ANO5 regulated the proliferation and cell cycle of GC cells.

To further clarify the role of ANO5, apoptosis assays were performed in NUGC4 and MKN45 cells. ANO5 silencing significantly increased the frequency of early and late apoptotic NUGC4 cells and the frequency of early apoptotic MKN45 cells 72 h after siRNA transfection (Figure 3A). These results indicated that the apoptosis in NUGC4 and MKN45 cells was regulated by ANO5 expression. Another ANO5 siRNA (HSS137120) was used to assess its impact on cell growth and survival, with results similar to those of HSS137119 (Supplementary Figure 3).



DOI: 10.3748/wjg.v28.i32.4649 **Copyright** ©The Author(s) 2022.

Figure 1 Anoctamin 5 expression in gastric cancer cells. A: Real-time quantitative reverse transcription-quantitative polymerase chain reaction (PCR) showed the expression of anoctamin 5 (*ANO5*) in various cell lines in gastric cancer; B: Western blotting showed the expression of ANO5 in various cell lines in GC; C: Real-time quantitative PCR revealed that ANO5 small interfering RNA (siRNA) effectively reduced *ANO5* mRNA levels in NUGC4 and MKN45 cells; D: Western blotting revealed that ANO5 siRNA effectively reduced ANO5 protein levels in NUGC4 and MKN45 cells. n = 3, mean ± standard error of the mean. $^{a}P < 0.05$ (significantly different from control siRNA). ANO5: Anoctamin 5; ACTB: β-actin; siRNA: Small interfering RNA.

ANO5 promotes the migration and invasion

The effects of the ANO5 silencing on NUGC4 and MKN45 cell migration and invasion were examined using a Boyden chamber assay. The results demonstrated that ANO5 knockdown in NUGC4 and MKN45 cells significantly reduced their migration and invasion (Figure 3B).

Gene expression profiling in ANO5 siRNA-transfected NUGC4 cells

To elucidate the molecular mechanisms underlying the regulation of cellular functions by ANO5, the gene expression profiles of NUGC4 cells transfected with ANO5 siRNA were investigated using microarray. The results revealed that the expression levels of 3491 genes in NUGC4 cells following ANO5 knockdown exhibited fold-changes > 1.8 compared with those in the negative control. Among these, the expression levels of 1802 genes were upregulated, whereas those of 1689 genes were downregulated in NUGC4 cells following ANO5 knockdown. The top 20 genes with significant changes in expression in the ANO5-depleted NUGC4 cells are listed in Tables 1 and 2. Ingenuity pathway analysis showed that 'Cancer' was the top-ranked disease and disorder, while 'DNA Replication, Recombination, and Repair' and 'Cell Cycle' were the two top-ranking molecular and cellular functions (Table 3).

Validation of gene and protein expression

The microarray analysis identified 'Cell Cycle: G1/S Checkpoint Regulation' as one of the top-ranking canonical pathways in ANO5-depleted NUGC4 cells (Figure 4A). To confirm these results, seven genes were selected (*CDK2*, *CDK4*, *CDK6*, *CDKN1A/p21*, *CCNE2*, *E2F1*, and *Rb*). These genes were included in 'Cell Cycle: G1/S Checkpoint Regulation,' and *CDK2* and *CDK6* were the two top-ranking downregulated genes in NUGC4 cells following ANO5 knockdown (Table 2). Reverse transcription-quantitative PCR was used to confirm the expression levels of six genes. NUGC4 and MKN45 cells transfected with ANO5 siRNA had significantly lower *CDK2*, *CDK4*, *CDK6*, *CDKN1A*, *CCNE2*, and *E2F1* expression levels and significantly higher *CDKN1A* expression levels than cells transfected with the control siRNA (Figure 4B). Furthermore, ANO5 plasmid decreased *CDKN1A/p21* mRNA levels (Supplementary Figure 2A, right panel). Western blotting revealed that phosphorylated Rb was inhibited following ANO5 knockdown in NUGC4 and MKN45 cells (Figure 4C). Since the *CDK2* gene is located upstream of Rb and downstream of p21 in the cell cycle transition from G_1 phase to S phase, the downregulation of

Table 1 The 20 upregulated genes that displayed the greatest changes in their expression in anoctamin 5-depleted NUGC4 cells

Gene symbol	Gene name	Gene ID	Fold change
PLCXD1	*Phosphatidylinositol-specific phospholipase C X domain containing 1*	TC0X00006433.hg.1	31.97
NDRG4	*NDRG family member 4*	TC1600008034.hg.1	29.88
CYP3A5	*Cytochrome P450 family 3 subfamily A member 5*	TC0700011953.hg.1	24.81
PLCXD1	*Phosphatidylinositol-specific phospholipase C X domain containing 1*	TC0Y00006433.hg.1	23.44
REG4	*Regenerating family member 4*	TC0100015477.hg.1	19.70
*CIDE**B***	*Cell death-inducing DFFA-like effector b*	TC1400008752.hg.1	17.86
DHRS9	*Dehydrogenase/reductase 9*	TC0200009905.hg.1	17.02
CIDEC	*Cell death-inducing DFFA-like effector c*	TC0300010217.hg.1	16.73
SPRR1A	*Small proline rich protein 1A*	TC0100010017.hg.1	16.66
APOD	*Apolipoprotein D*	TC0300013645.hg.1	16.57
SEMA7A	*Semaphorin 7A*	TC1500010018.hg.1	16.09
C11orf86	*Chromosome 11 open reading frame 86*	TC1100008109.hg.1	15.57
BNIPL	*BCL2 interacting protein like*	TC0100009936.hg.1	15.52
SUSD2	*Sushi domain containing 2*	TC2200006883.hg.1	15.25
MAPRE3	*Microtubule-associated protein RP/EB family member 3*	TC0200007048.hg.1	14.99
CYP1A1	*Cytochrome P450 family 1 subfamily A member 1*	TC1500010042.hg.1	14.69
GOLT1A	*Golgi transport 1A*	TC0100017022.hg.1	13.79
CNN2	*Calponin 2*	TC1900006507.hg.1	13.74
ANTXR2	*ANTXR cell adhesion molecule 2*	TC0400011144.hg.1	13.54
APOBEC1	*Apolipoprotein B mRNA editing enzyme catalytic subunit 1*	TC1200009789.hg.1	12.19

Table 2 The 20 downregulated genes that displayed the greatest changes in their expression in anoctamin 5-depleted NUGC4 cells

Gene symbol	Gene name	Gene ID	Fold change
CDK2	*Cyclin-dependent kinase 2*	TC1200007819.hg.1	-53.84
DTL	*Denticleless E3 ubiquitin ligase homolog*	TC0100011512.hg.1	-27.60
RABL3	*RAB, member of RAS oncogene family like 3*	TC0300012157.hg.1	-20.16
CKS1B	*CDC28 protein kinase regulatory submit 1B*	TC0100010100.hg.1	-19.34
LMNB1	*Lamin B1*	TC0500008544.hg.1	-19.18
IFRD2	*Interferon-related developmental regulator 2*	TC0300013981.hg.1	-18.61
PLK1	*Polo like kinase 1*	TC1600007235.hg.1	-17.89
GINS1	*GINS complex subunit 1*	TC2000007016.hg.1	-17.87
CDK6	*Cyclin-dependent kinase 6*	TC0700011785.hg.1	-17.08
XRCC2	*X-ray repair cross complementing 2*	TC0700013119.hg.1	-14.77
POGLUT3	*Protein O-glucosyltransferase 3*	TC1100012229.hg.1	-14.47
DSG2	*Desmoglein 2*	TC1800007014.hg.1	-14.37
NEMP1	*Nuclear envelope integral membrane protein 1*	TC1200010946.hg.1	-14.31
CBX5	*Chromobox 5*	TC1200010833.hg.1	-14.20
ANKRD52	*Ankyrin repeat domain 52*	TC1200010902.hg.1	-14.20
ITGB1	*Integrin subunit beta 1*	TC1000010265.hg.1	-14.16
H2BC14	*H2B clustered histone 14*	TC0600007377.hg.1	-13.25

SCAMP2	*Secretory carrier membrane protein 2*	TC1500010047.hg.1	-13.05
CMTM7	*CKLF like MARVEL transmembrane domain containing 7*	TC0300006968.hg.1	-13.02
GINS4	*GINS complex subunit 4*	TC0800007416.hg.1	-12.66

ANO5 in GC cells appears to affect the transition from the G1 phase to the S phase by regulating the expression of p21 and its downstream genes in signal pathways.

In addition, the gene expression profile of MKN45 cells transfected with ANO5 siRNA was investigated by microarray. Changes in gene expression in ANO5-depleted NUGC4 and MKN45 cells are depicted in Supplementary Figure 4. Among the 21440 genes, 7246 genes were upregulated and 6622 genes were downregulated in both cell lines, for a total of 13868 genes (64.7%) with identical expression direction in NUGC4 and MKN45 cells. The direction of gene expression changes of gene related to 'Cell Cycle: G_1/S Checkpoint Regulation' was consistent in both cell lines (Supplementary Table 1). Furthermore, all 40 genes displayed in Tables 1 and 2 showed the identical expression patterns in ANO5-depleted MKN45 cells (Supplementary Table 2). These results supported that ANO5 affected the cell cycle through similar mechanisms in both NUGC4 and MKN45 cell lines.

ANO5 inhibits the JNK pathway

Activation of the JNK and p38 MAPK classes of protein kinases mediates cellular responses such as apoptosis and the maturation of some cell types. JNK stabilizes p21 protein through phosphorylation [25]. To elucidate the regulatory role of ANO5 in the JNK signaling pathway in GC cells, we examined the phosphorylation of the JNK protein. ANO5 silencing significantly increased JNK phosphorylation levels in NUGC4 and MKN45 cells (Figure 4D). Furthermore, the increase of *CDKN1A/p21* mRNA expression induced by ANO5 silencing in NUGC4 and MKN45 cells was suppressed by JNK inhibition (Supplementary Figure 5, lower panel). Whereas, treatment with JNK inhibitors did not affect ANO5 mRNA expression (Supplementary Figure 5, upper panel). These results indicated that ANO5 expression regulated the cell cycle by upregulating p21 *via* JNK cascade activation in GC cells.

Effects of low-chloride conditions

To elucidate the molecular mechanisms through which ANO5 affects the cell cycle transition from G_1 to S phase, changes in the intracellular ion environment were examined. A previous study has reported that intracellular chloride affects cancer growth through the phosphorylation of several key molecules in signal transduction pathways[20]. We previously reported that the culturing in a Cl^--replaced medium (replacement of Cl^- by NO_3^-) decreased the intracellular chloride concentration [$(Cl^-)_i$] and inhibited cell growth in GC cells[19]. Our previous study also demonstrated that JNK activation under low-chloride conditions inhibited GC cell growth by upregulating p21 expression[18]. Intracellular chloride concentrations in the cells were measured based on the fluorescence intensity of MQAE, a chloride-sensitive fluorescence probe. The results revealed an increases in the fluorescence intensity of MQAE in NUGC4 and MKN45 cells following ANO5 knockdown (Figure 5). Therefore, ANO5 knockdown altered intracellular chloride concentrations in GC cells. Furthermore, low-chloride conditions effectively increased JNK phosphorylation and reduced Rb phosphorylation (Supplementary Figure 6). These results indicated that ANO5 regulated the cell cycle *via* JNK signaling by controlling intracellular chloride levels.

IHC analysis of ANO5 expression in human GC tissue

IHC detected the expression of ANO5 in non-cancerous gastric (Figure 6A) and cancerous epithelia (Figure 6B). ANO5 was observed to be expressed in the cell membranes and cytoplasm of GC tissue. The criteria for the staining intensity score were defined as 0 (no staining; Figure 6C), 1 (weak staining; Figure 6D), 2 (moderate staining; Figure 6E), or 3 (strong staining; Figure 6F). The median and mean scores for ANO5 expression were 0.9 (range, 0-2.1) and 0.97 (standard deviation = 0.53), respectively. A cut-off value of 1.3 was used to obtain the smallest *P* value in comparison of 5-year overall survival (OS) rates[26]. The 5-year OS rates for each cut-off value are presented in Table 4.

Patients with GC were divided into low- (ANO5 scores < 1.3, n = 137) and high-ANO5 (ANO5 scores ≥ 1.3, n = 58) expression groups based on a cut-off value of 1.3 (Figure 6G). Analysis of the clinicopathological features revealed that ANO5 expression levels were not associated with any of the variables (Table 5). To evaluate the prognostic significance of ANO5 after surgery, the following ten variables were compared: sex, age, tumor location, tumor length, histological type, lymphatic invasion, venous invasion, the pathological T stage, pathological N stage, and ANO5 IHC scores. Univariate analysis showed that patient prognosis was correlated with tumor length, lymphatic invasion, venous invasion, pathological T stage, pathological N stage, and ANO5 IHC scores (P = 0.0020, 0.0002, 0.0126, < 0.0001, < 0.0001, and 0.0104, respectively). Multivariate analysis identified high ANO5 expression (≥ 1.3) as an independent prognostic factor (P = 0.0457) (Table 6). Furthermore, the 5-year OS rate was significantly lower in the high expression group (73.9%) than in the low expression group (89.6%). Data obtained from the Kaplan-Meier plotter database also indicated that high ANO5 expression correlates with poor

Table 3 Ingenuity pathway analysis of anoctamin 5-depleted NUGC4 cells

Category	Name	Molecules	*P* value (range)
Disease and Disorders	Cancer	3136	1.54×10^{-3}–2.23×10^{-15}
	Neurological Disease	76	1.27×10^{-3}–2.23×10^{-15}
	Organismal Injury and Abnormalities	3147	1.54×10^{-3}–2.23×10^{-15}
	Cardiovascular Disease	138	1.43×10^{-3}–4.07×10^{-14}
	Reproductive System Disease	1942	1.54×10^{-3}–1.09×10^{-10}
Molecular and Cellular Functions	DNA Replication, Recombination, and Repair	460	1.54×10^{-3}–9.69×10^{-22}
	Cell Cycle	650	1.54×10^{-3}–1.98×10^{-20}
	Cellular Assembly and Organization	533	1.57×10^{-3}–9.22×10^{-16}
	Cellular Development	691	1.59×10^{-3}–2.66×10^{-14}
	Cellular Growth and Proliferation	677	1.40×10^{-3}–2.66×10^{-14}
Physiological System Development and Function	Connective Tissue Development and Function	60	1.14×10^{-3}–8.83×10^{-6}
	Tissue Development	164	1.57×10^{-3}–1.11×10^{-4}
	Embryonic Development	80	1.21×10^{-3}–2.07×10^{-4}
	Hair and Skin Development and Function	55	6.37×10^{-4}–2.07×10^{-4}
	Organ Development	69	6.37×10^{-4}–2.07×10^{-4}

Table 4 Five-year overall survival rates with cut-off values for anoctamin 5 expression scores

Cut-off value	5-yr OS rate		*P* value
	Low group	High group	
1.0	87.0% (n = 101)	83.7% (n = 94)	0.5136
1.1	87.7% (n = 115)	81.9% (n = 80)	0.2890
1.2	88.8% (n = 127)	78.6% (n = 68)	0.0759
1.3	89.6% (n = 137)	73.9% (n = 58)	0.0104[a]
1.4	88.1% (n = 142)	78.6% (n = 53)	0.0380[a]
1.5	87.4% (n = 152)	78.5% (n = 43)	0.0751

[a]$P < 0.05$: Log-rank test.
OS: Overall survival.

prognosis in GC (Supplementary Figure 7), which was consistent with the present results.

DISCUSSION

The ANO family of membrane proteins, also known as TMEM16, play key roles in several physiological functions, including ion transport to phospholipid scrambling[27] and ion channel regulation[28]. While the roles of ANO1 (TMEM16A) and ANO2 (TMEM16B) as calcium-activated chloride channels have been firmly established[29-32], the functions of other family members remain unclear.

Previous studies have evaluated the expression and role of ANO5 during tumor development in various cancer types. Song *et al*[33] demonstrated that ANO5 (TMEM16E) was widely expressed in the epithelial cells of the human gastrointestinal tract. ANO5 is also expressed in human pancreatic cancer tissues but not in normal pancreatic tissue[23]. Chang *et al*[22] reported that ANO5 expression was downregulated in thyroid cancer, which promoted thyroid cancer cell migration and invasion. However, the expression of ANO5 in human GC tissue and the pathophysiological role of its expression in GC cells have not been demonstrated.

The present study revealed that ANO5 downregulation in GC cells regulates the cell cycle and induces apoptosis, while inhibiting proliferation, migration, and invasion. These results highlight the

Table 5 Relationships between clinicopathological factors of gastric cancer patients and anoctamin 5 expression

Variables		N	IHC score		*P* value
			High group (1.3)	Low group (< 1.3)	
Total		195	58	137	
Sex	Male	128	35	93	0.3262
	Female	67	23	44	
Age	< 65	77	25	52	0.5246
	65	118	33	85	
Tumor location	U	41	15	26	0.3367
	M, L	154	43	111	
Tumor length (mm)	< 30	63	22	41	0.3158
	30	132	36	96	
Histological type	tub1, tub2, pap	96	35	61	0.0596
	por, sig, muc	99	23	76	
Lymphatic invasion	Negative	110	34	76	0.7529
	Positive	85	24	61	
Venous invasion	Negative	131	38	93	0.7419
	Positive	64	20	44	
pT	pT1-2	137	37	100	0.2312
	pT3-4	58	21	37	
pN	pN0	139	40	99	0.7294
	pN1-3	56	18	38	

IHC: Immunohistochemical; L: Lower; M: Middle; pap: muc: Mucinous adenocarcinoma; Papillary adenocarcinoma; pN: pathological N stage; por: Poorly differentiated adenocarcinoma; pT: pathological T stage; sig: Signet-ring cell carcinoma;tub: Tubular adenocarcinoma; U: Upper.

potential of ANO5 inhibitors as therapeutic agents for the treatment of GC or other cancer types with high ANO5 expression levels. The present study also indicates that ANO5 plays a key role in the proliferation of GC cells. Cell cycle analysis showed that the number of cells remaining in the G_0/G_1 phase was significantly increased, whereas the number of cells in the S or G_2/M phase was decreased in ANO5-depleted NUGC4 and MKN45 cells, suggesting that ANO5 downregulation inhibits GC cell proliferation *via* cell cycle arrest at the G_0/G_1 phase.

The induction of p21 is dependent on the tumor suppressor protein, p53. However, chloride ions have been shown to play important roles in cell cycle progression by regulating the expression of p21 through a p53-independent pathway in GC cells[19]. It has also been demonstrated that a decrease in chloride induced G_0/G_1 phase arrest by downregulating CDK2 and phosphorylated Rb expression through p21 upregulation. Furthermore, p38 and JNK activation under low-chloride conditions inhibits GC cell viability by upregulating p21 expression[18].

Moreover, ANO5 expression in GC cells affects the transition from the G_1 to the S phase of the cell cycle by regulating the expression of p21 and its downstream genes through the activation of JNK signaling. To the best of our knowledge, the chloride channel activity of ANO5 has not been confirmed to date. To elucidate the molecular mechanisms underlying the effects of ANO5, we evaluated the changes in the intracellular chloride ion environment in this study. A quantitative analysis of intracellular chloride ion concentrations was conducted based on the fluorescence intensity of MQAE. Immunofluorescent analysis showed that the fluorescence intensity of MQAE increased following ANO5 silencing, indicating a decrease in intracellular chloride concentration. These results suggest that the downregulation of ANO5 induces G_0/G_1 phase arrest by altering the expression of G_1/S checkpoint-related genes through the intracellular chloride environment of GC cells. Furthermore, since ANO5 functioned as a chloride channel, it may have the potential to inhibit tumor growth by regulating intracellular chloride concentrations in therapeutic settings.

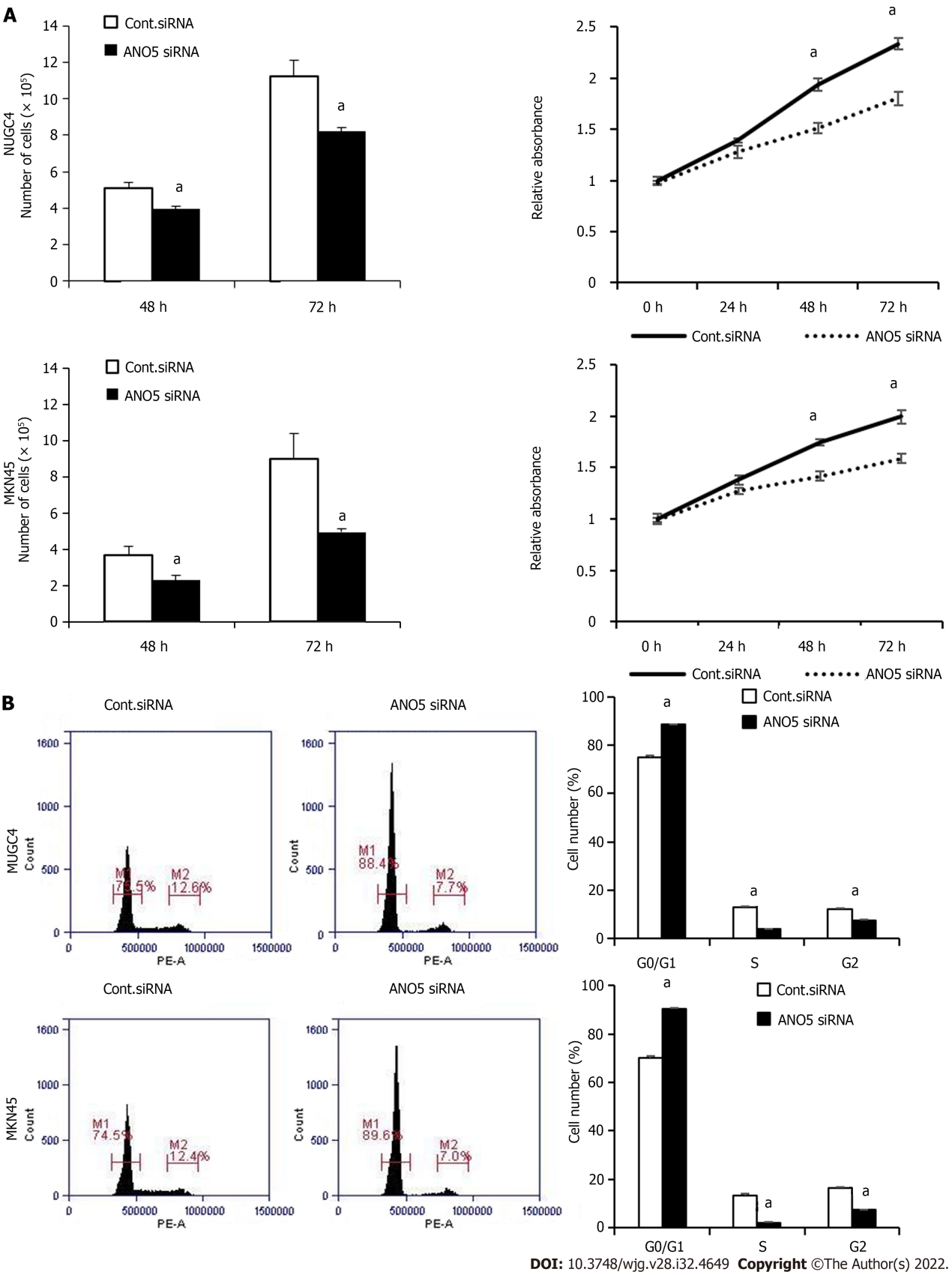
Although ANO5 was recently implicated in various cancers, its role in tumor progression in patients with GC remains unclear. To demonstrate the clinical significance of ANO5 expression, the survival rate of 195 patients who underwent curative resection for primary GC was investigated. IHC analysis

Table 6 Univariate and multivariate analyses of prognostic factors associated with 5-year overall survival

Variables	N	Univariate		Multivariate	
		5-yr OS rate (%)	*P* value	HR (95%CI)	*P* value
Total	195				
Sex					
Male	128	87.9	0.3274		
Female	67	85.3			
Age					
< 65	77	89.7	0.4113		
65	118	85.2			
Location					
U	41	80.9	0.2629		
M, L	154	88.6			
Tumor length (mm)					
< 30	63	97.8	0.0020[a]	3.010 (0.347-26.12)	0.3176
30	132	80.1			
Histological type					
tub1, tub2, pap	96	88.3	0.4544		
por, sig, muc	99	85.6			
Lymphatic invasion					
Negative	110	96.1	0.0002[a]	1.872 (0.549-6.384)	0.3166
Positive	85	75.7			
Venous invasion					
Negative	131	90.6	0.0126[a]	1.085 (0.476-2.472)	0.8469
Positive	64	79.3			
pT					
pT1-2	137	95.9	< 0.0001[a]	5.240 (1.807-15.20)	0.0023[c]
pT3-4	58	65.5			
pN					
pN0	139	94.1	< 0.0001[a]	2.148 (0.695-6.643)	0.1844
pN1-3	56	67.6			
IHC score					
< 1.3	137	89.6	0.0104[a]	2.318 (1.016-5.288)	0.0457[c]
1.3	58	73.9			

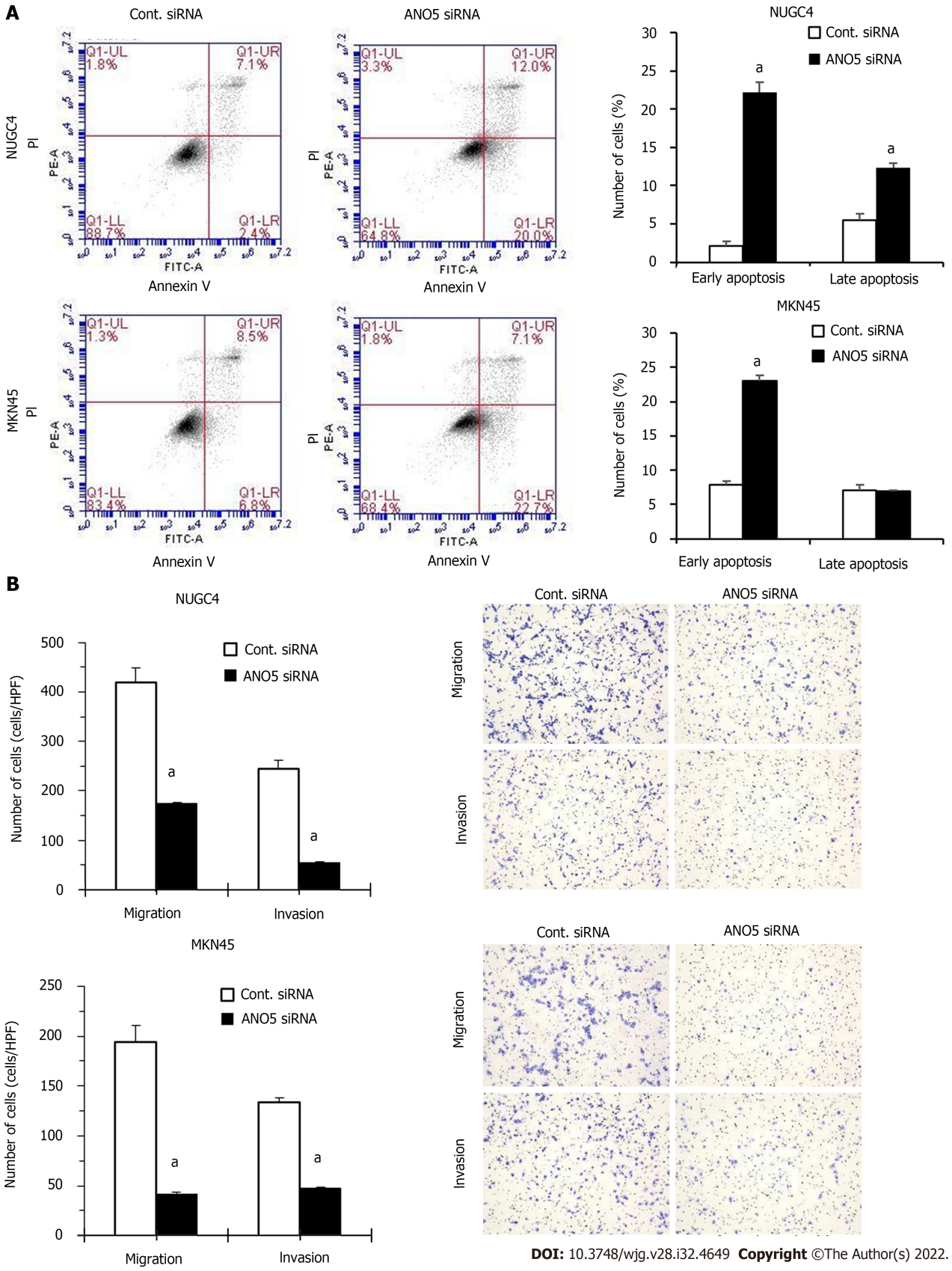
[a]*P* < 0.05: Log-rank test.
[c]*P* < 0.05: Cox hazard regression analysis.
CI: Confidence interval; HR: Hazard ratio; IHC: Immunohistochemical; L: Lower; M: Middle; muc: Mucinous adenocarcinoma; OS: Overall survival; pap: Papillary adenocarcinoma; pN: Pathological N stage; por: Poorly differentiated adenocarcinoma; pT: Pathological T stage; sig: Signet-ring cell carcinoma; tub: Tubular adenocarcinoma; U: Upper.

revealed that high ANO5 expression levels were a poor prognostic factor in patients with GC. Under low-chloride conditions, ANO5 appeared to function as a chloride channel in GC cells. Previous findings showed that various ion transporters function as biomarkers and therapeutic targets[34,35]. Targeting ion channels that are activated in cancer cells may be an important strategy for cancer therapy. To the best of our knowledge, the present study is the first to report a relationship between ANO5 expression and the prognosis of patients with GC. Additional functional studies are needed to provide insights into the role of ANO5 in GC progression.



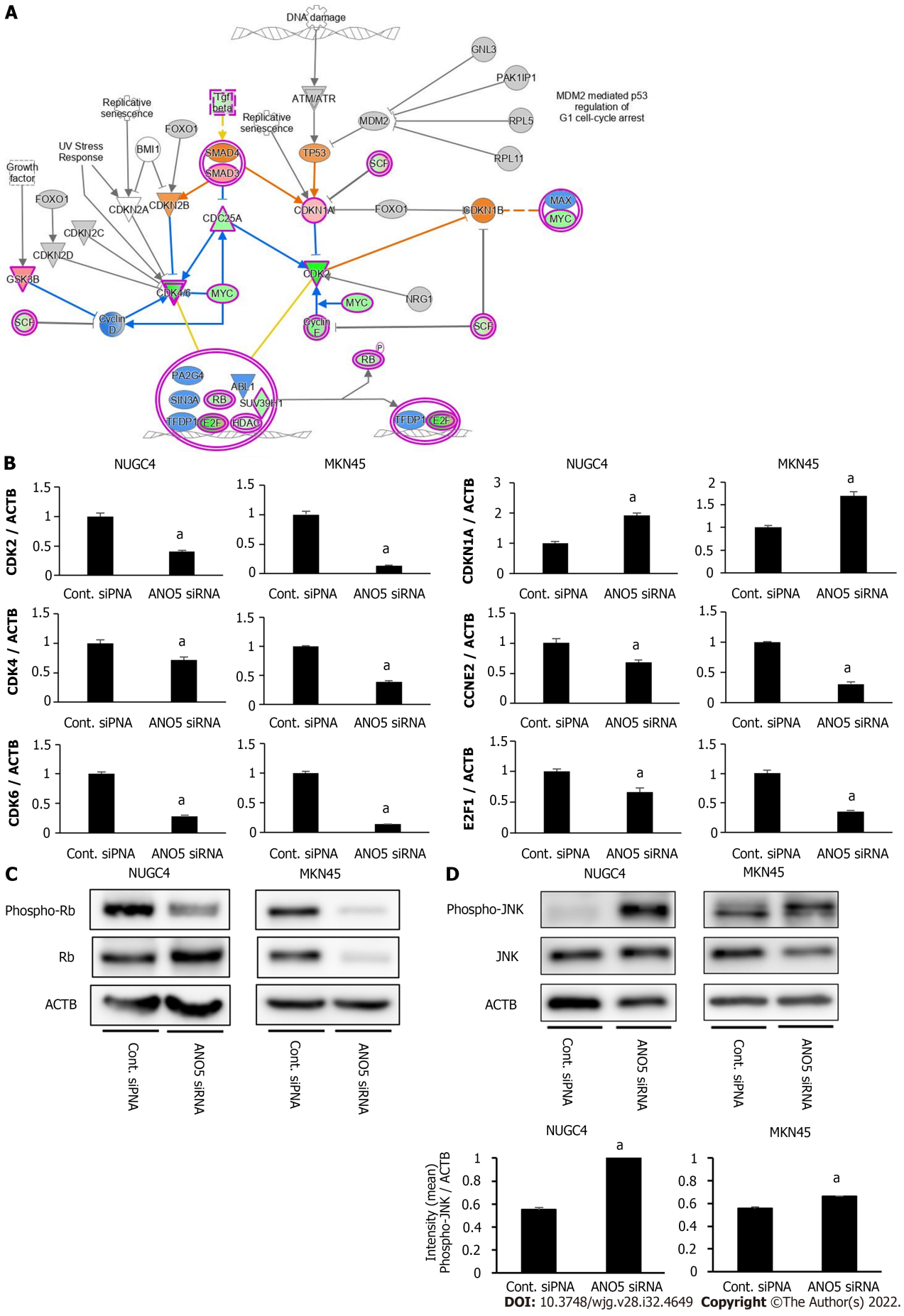
DOI: 10.3748/wjg.v28.i32.4649 **Copyright** ©The Author(s) 2022.

Figure 2 Anoctamin 5 controlled the proliferation and the cell cycle in gastric cancer cells. A: The downregulation of anoctamin 5 (ANO5) inhibited the proliferation of NUGC4 and MKN45 cells. Cell numbers were counted 48 h and 72 h after small interfering RNA transfection (left panel). The proliferative ability of NUGC4 and MKN45 cells was significantly suppressed following ANO5 downregulation (right panel); B: The downregulation of ANO5 increased the number of cells in the G_0/G_1 phase in NUGC4 and MKN45 cells. Cells transfected with control or ANO5 small interfering RNA were stained with propidium iodide and analyzed by flow cytometry. n = 3, mean ± standard error of the mean. $^aP < 0.05$ (significantly different from control small interfering RNA). ANO5: Anoctamin 5; siRNA: Small interfering RNA; Cont.: Control.



DOI: 10.3748/wjg.v28.i32.4649 **Copyright** ©The Author(s) 2022.

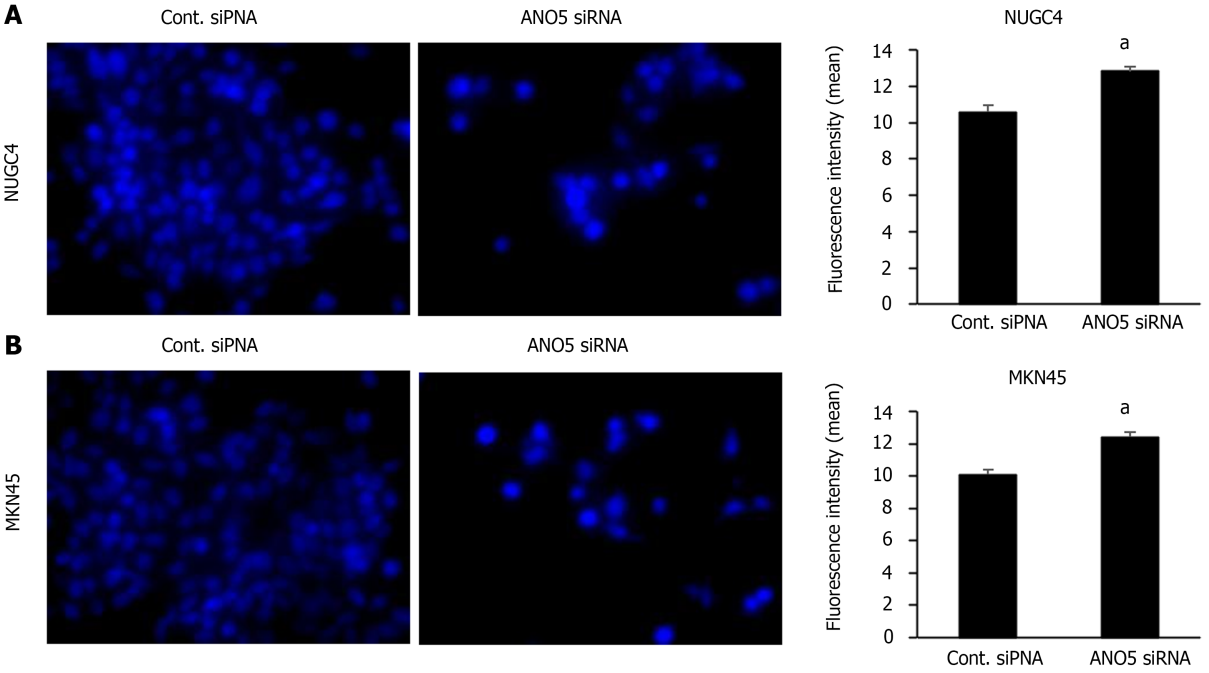
Figure 3 Anoctamin 5 controlled apoptosis, migration, and invasion in gastric cancer cells. A: The downregulation of anoctamin 5 (ANO5) increased the early and late apoptotic cell proportions of NUGC4 and MKN45 cells. Control or ANO5 small interfering RNA-transfected cells were stained with propidium iodide and annexin V and subjected to flow cytometry; B: The downregulation of ANO5 significantly decreased NUGC4 and MKN45 cell migration and invasion, which were evaluated using a Boyden chamber assay. Magnification: × 40. n = 3, mean ± standard error of the mean. $^{a}P < 0.05$ (significantly different from control small interfering RNA). ANO5: Anoctamin 5; PI: Propidium iodide; siRNA: Small interfering RNA; Cont.: Control.



DOI: 10.3748/wjg.v28.i32.4649 **Copyright** ©The Author(s) 2022.

Figure 4 Network analyses by microarray analysis and ingenuity pathway analysis. A: The signaling map of "Cell Cycle: G_1/S Checkpoint

Regulation," one of the top-ranked canonical pathways related to the depletion of anoctamin 5 (ANO5) according to ingenuity pathway analysis. Red and green colors indicate genes with expression levels that were higher or lower, respectively, than reference RNA levels; B: To verify gene expression profiling data, *CDK2*, *CDK4*, *CDK6*, *CDKN1A*, *CCNE2*, and *E2F1* were examined by real-time reverse transcription-quantitative polymerase chain reaction. The downregulation of ANO5 effectively reduced *CDK2*, *CDK4*, *CDK6*, *CCNE2*, and *E2F1* mRNA levels and increased *CDKN1A/p21* mRNA levels in NUGC4 and MKN45 cells; C: The downregulation of ANO5 effectively reduced the phosphorylation levels of Rb protein in NUGC4 and MKN45 cells; D: The downregulation of ANO5 increased the phosphorylation of the c-Jun N-terminal kinase protein in NUGC4 and MKN45 cells. n = 3, mean ± standard error of the mean. $^{a}P < 0.05$ (significantly different from control small interfering RNA). ANO5: Anoctamin 5; siRNA: Small interfering RNA; Cont.: Control; JNK: c-Jun N-terminal kinase; ACTB: β-actin.



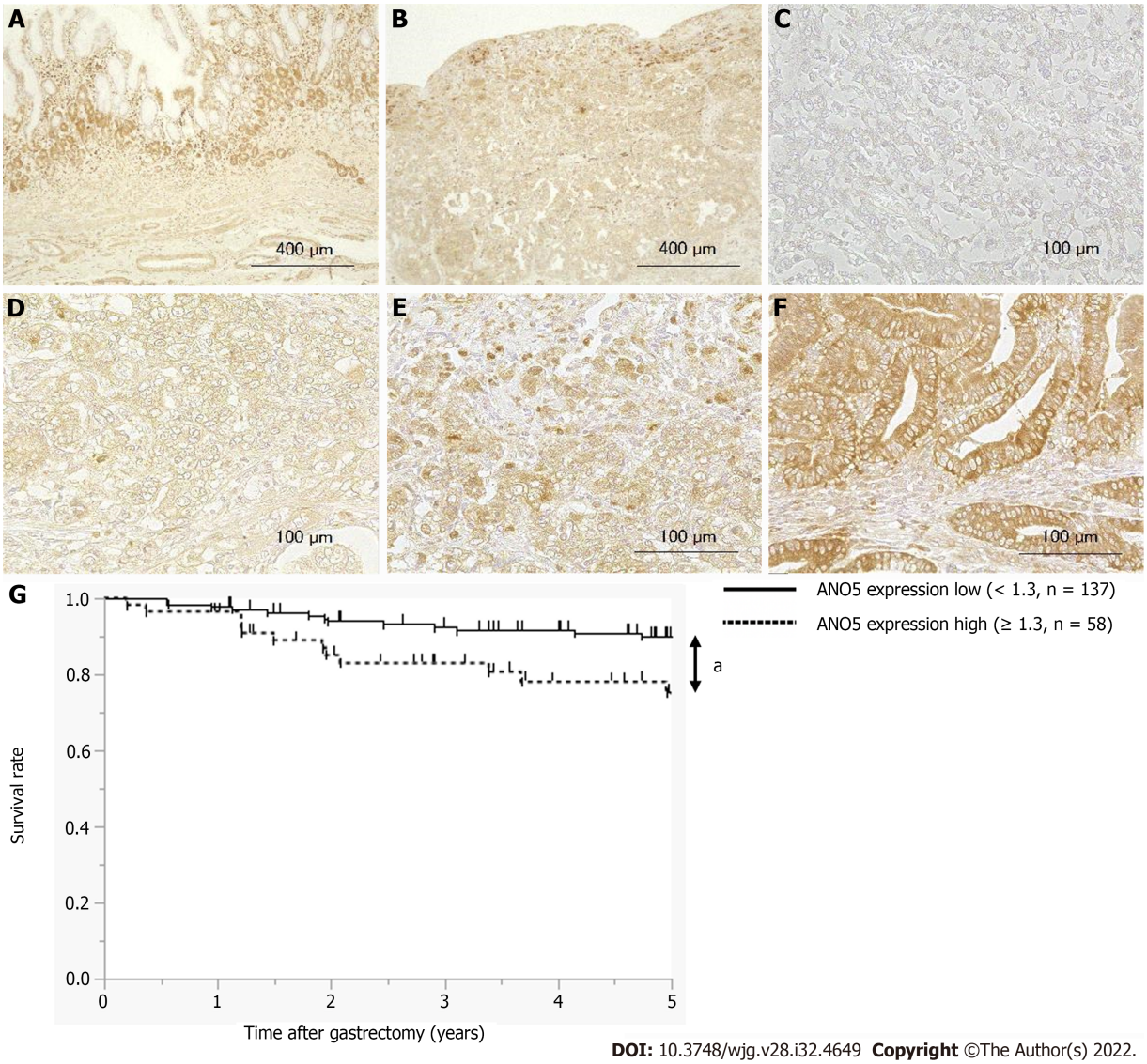
DOI: 10.3748/wjg.v28.i32.4649 **Copyright** ©The Author(s) 2022.

Figure 5 Immunofluorescent analysis of intracellular chloride concentration using MQAE reagent, a chloride-sensitive fluorescence probe. The downregulation of anoctamin 5 increased the fluorescence intensity of MQAE in NUGC4 and MKN45 cells. A: NUGC4 cell; B: MKN45 cell. n = 3, mean ± standard error of the mean. $^{a}P < 0.05$ (significantly different from control small interfering RNA). ANO5: Anoctamin 5; siRNA: Small interfering RNA; Cont.: Control.

This study has some limitations that must be addressed. First, it was a retrospective study. Due to the limited sample size, the pathological N stage classification factors were not correlated with the 5-year OS rate. Therefore, further studies are required to confirm our results. Second, in the selection of GC cell lines, we selected five cell lines; however, only three were used in the study.

CONCLUSION

The present study revealed that ANO5 plays a significant role in cell cycle progression in human GC cells. The results of microarray analysis showed the impact of ANO5 on the expression of G_1/S checkpoint-related genes. Furthermore, ANO5 expression significantly affected JNK signaling. Collectively, these results indicate that ANO5 plays an important role in cell cycle progression by regulating the expression of p21 through JNK signaling in human GC cells. The results of the IHC analysis also suggest that high ANO5 expression levels are a poor prognostic factor in patients with GC. The present study may contribute to the identification of ANO5 as a key mediator of tumor progression, with it ultimately being a promising prognostic biomarker or a novel therapeutic target for GC.



DOI: 10.3748/wjg.v28.i32.4649 **Copyright** ©The Author(s) 2022.

Figure 6 Anoctamin 5 protein expression levels in human gastric cancer tissues and a survival analysis based on anoctamin 5 expression. A: Non-cancerous gastric epithelia were immunohistochemically stained using an anti-anoctamin 5 (ANO5) antibody. Magnification: × 100; B: Primary human gastric cancer samples were immunohistochemically stained using an anti-ANO5 antibody. Magnification: × 100; C: The immunohistochemical staining results of ANO5 are shown as intensity 0. Magnification: × 400; D: Intensity 1. Magnification: × 400; E: Intensity 2. Magnification: × 400; F: Intensity 3. Magnification: × 400; G: Gastric cancer patients were classified into two groups based on ANO5 expression: A low ANO5 expression group (< 1.3, *n* = 137) and high ANO5 expression group (≥ 1.3, *n* = 58). [a]*P* < 0.05 (significant difference). ANO5: Anoctamin 5.

ARTICLE HIGHLIGHTS

Research background

Anoctamin 5 (ANO5) is a member of a family of calcium-activated chloride channels containing 10 members, also known as transmembrane proteins, and has been reported to be associated with various cancers.

Research motivation

The role of ANO5 in gastric cancer (GC) remains poorly understood. In the present study, we analyzed the relationship between ANO5 expression and tumor progression in GC.

Research objectives

The objectives of the present study were to investigate whether ANO5 contributes to the regulation of cancer growth and to clarify its clinicopathological significance in GC.

Research methods

Knockdown experiments were performed by transfecting human GC cell lines with ANO5 small

interfering RNA. Gene expression was then assessed using microarray analysis. Samples from 195 patients with GC were subjected to immunohistochemistry for ANO5, and its relationship with clinicopathological factors and prognosis were examined.

Research results

ANO5 knockdown suppressed the proliferation, migration, and invasion of cells and enhanced apoptosis. Cell cycle analysis showed that ANO5 knockdown suppressed the progression of G1-S phase. The results of microarray analysis showed up- or downregulated expression of genes related to "Cell Cycle: G1/S Checkpoint Regulation" in ANO5 knockdown NUGC4 cells. Survival analysis showed significantly poorer 5-year survival in the ANO5 high expression group (high *vs* low; 73.9 *vs* 89.6%, P = 0.0104). Immunohistochemistry multivariate analysis identified the high expression of ANO5 as an independent prognostic factor for 5-year survival in GC patients (P = 0.0457).

Research conclusions

ANO5 plays a significant role in cell cycle progression in human GC cells. The results of the immunohistochemistry analysis suggest that high ANO5 expression levels are a poor prognostic factor in patients with GC.

Research perspectives

The present study may contribute to the identification of ANO5 as a key mediator in tumor progression, with it ultimately being a promising prognostic biomarker or a novel therapeutic target of GC.

FOOTNOTES

Author contributions: Fukami T and Shiozaki A contributed equally to this work; All authors read and approved the final manuscript and agreed to be accountable for all aspects of the report.

Supported by Japan Society for the Promotion of Science, No. 21K08689, No. 21K16456, No. 20K09016, No. 20K09084, No. 19K09202 and No. 19K09182.

Institutional review board statement: The study was reviewed and approved by the Kyoto Prefectural University of Medicine Institutional Review Board, No. ERB-C-1195.

Informed consent statement: Informed consent to be included in the study, or the equivalent, was obtained from all patients.

Conflict-of-interest statement: All the authors report no relevant conflicts of interest for this article.

Data sharing statement: Technical appendix, statistical code, and dataset available from the corresponding author at shiozaki@koto.kpu-m.ac.jp. Participants gave informed consent for data sharing.

Open-Access: This article is an open-access article that was selected by an in-house editor and fully peer-reviewed by external reviewers. It is distributed in accordance with the Creative Commons Attribution NonCommercial (CC BY-NC 4.0) license, which permits others to distribute, remix, adapt, build upon this work non-commercially, and license their derivative works on different terms, provided the original work is properly cited and the use is non-commercial. See: https://creativecommons.org/Licenses/by-nc/4.0/

Country/Territory of origin: Japan

ORCID number: Tomoyuki Fukami 0000-0002-2585-3611; Atsushi Shiozaki 0000-0003-3739-160X; Toshiyuki Kosuga 0000-0002-1657-7272; Michihiro Kudou 0000-0003-3518-528X; Hiroki Shimizu 0000-0002-6463-8498; Takuma Ohashi 0000-0003-0939-3739; Tomohiro Arita 0000-0001-7127-6504; Hirotaka Konishi 0000-0002-4899-8944; Shuhei Komatsu 0000-0001-6074-7614; Takeshi Kubota 0000-0002-2246-3028; Hitoshi Fujiwara 0000-0002-6507-4313; Kazuma Okamoto 0000-0002-8270-4217; Mitsuo Kishimoto 0000-0002-7407-9044; Yukiko Morinaga 0000-0003-2311-1830; Eiichi Konishi 0000-0002-7122-2271; Eigo Otsuji 0000-0002-3260-8155.

S-Editor: Fan JR
L-Editor: Filipodia
P-Editor: Cai YX

REFERENCES

1 **Pang C**, Yuan H, Ren S, Chen Y, An H, Zhan Y. TMEM16A/B associated CaCC: structural and functional insights.

Protein Pept Lett 2014; **21**: 94-99 [PMID: 24151904 DOI: 10.2174/09298665113206660098]
2 **Pedemonte N**, Galietta LJ. Structure and function of TMEM16 proteins (anoctamins). *Physiol Rev* 2014; **94**: 419-459 [PMID: 24692353 DOI: 10.1152/physrev.00039.2011]
3 **Whitlock JM**, Hartzell HC. Anoctamins/TMEM16 Proteins: Chloride Channels Flirting with Lipids and Extracellular Vesicles. *Annu Rev Physiol* 2017; **79**: 119-143 [PMID: 27860832 DOI: 10.1146/annurev-physiol-022516-034031]
4 **Schreiber R**, Uliyakina I, Kongsuphol P, Warth R, Mirza M, Martins JR, Kunzelmann K. Expression and function of epithelial anoctamins. *J Biol Chem* 2010; **285**: 7838-7845 [PMID: 20056604 DOI: 10.1074/jbc.M109.065367]
5 **Kunzelmann K**. TMEM16, LRRC8A, bestrophin: chloride channels controlled by Ca(2+) and cell volume. *Trends Biochem Sci* 2015; **40**: 535-543 [PMID: 26254230 DOI: 10.1016/j.tibs.2015.07.005]
6 **Wanitchakool P**, Wolf L, Koehl GE, Sirianant L, Schreiber R, Kulkarni S, Duvvuri U, Kunzelmann K. Role of anoctamins in cancer and apoptosis. *Philos Trans R Soc Lond B Biol Sci* 2014; **369**: 20130096 [PMID: 24493744 DOI: 10.1098/rstb.2013.0096]
7 **Miettinen M**. Immunohistochemistry of soft tissue tumours - review with emphasis on 10 markers. *Histopathology* 2014; **64**: 101-118 [PMID: 24111893 DOI: 10.1111/his.12298]
8 **Lu G**, Shi W, Zheng H. Inhibition of STAT6/Anoctamin-1 Activation Suppresses Proliferation and Invasion of Gastric Cancer Cells. *Cancer Biother Radiopharm* 2018; **33**: 3-7 [PMID: 29466035 DOI: 10.1089/cbr.2017.2287]
9 **Shang L**, Hao JJ, Zhao XK, He JZ, Shi ZZ, Liu HJ, Wu LF, Jiang YY, Shi F, Yang H, Zhang Y, Liu YZ, Zhang TT, Xu X, Cai Y, Jia XM, Li M, Zhan QM, Li EM, Wang LD, Wei WQ, Wang MR. ANO1 protein as a potential biomarker for esophageal cancer prognosis and precancerous lesion development prediction. *Oncotarget* 2016; **7**: 24374-24382 [PMID: 27016410 DOI: 10.18632/oncotarget.8223]
10 **Jia L**, Liu W, Guan L, Lu M, Wang K. Inhibition of Calcium-Activated Chloride Channel ANO1/TMEM16A Suppresses Tumor Growth and Invasion in Human Lung Cancer. *PLoS One* 2015; **10**: e0136584 [PMID: 26305547 DOI: 10.1371/journal.pone.0136584]
11 **Bill A**, Gutierrez A, Kulkarni S, Kemp C, Bonenfant D, Voshol H, Duvvuri U, Gaither LA. ANO1/TMEM16A interacts with EGFR and correlates with sensitivity to EGFR-targeting therapy in head and neck cancer. *Oncotarget* 2015; **6**: 9173-9188 [PMID: 25823819 DOI: 10.18632/oncotarget.3277]
12 **Britschgi A**, Bill A, Brinkhaus H, Rothwell C, Clay I, Duss S, Rebhan M, Raman P, Guy CT, Wetzel K, George E, Popa MO, Lilley S, Choudhury H, Gosling M, Wang L, Fitzgerald S, Borawski J, Baffoe J, Labow M, Gaither LA, Bentires-Alj M. Calcium-activated chloride channel ANO1 promotes breast cancer progression by activating EGFR and CAMK signaling. *Proc Natl Acad Sci U S A* 2013; **110**: E1026-E1034 [PMID: 23431153 DOI: 10.1073/pnas.1217072110]
13 **Duran C**, Hartzell HC. Physiological roles and diseases of Tmem16/Anoctamin proteins: are they all chloride channels? *Acta Pharmacol Sin* 2011; **32**: 685-692 [PMID: 21642943 DOI: 10.1038/aps.2011.48]
14 **Dutertre M**, Lacroix-Triki M, Driouch K, de la Grange P, Gratadou L, Beck S, Millevoi S, Tazi J, Lidereau R, Vagner S, Auboeuf D. Exon-based clustering of murine breast tumor transcriptomes reveals alternative exons whose expression is associated with metastasis. *Cancer Res* 2010; **70**: 896-905 [PMID: 20103641 DOI: 10.1158/0008-5472.CAN-09-2703]
15 **Li Y**, Wang X, Vural S, Mishra NK, Cowan KH, Guda C. Exome analysis reveals differentially mutated gene signatures of stage, grade and subtype in breast cancers. *PLoS One* 2015; **10**: e0119383 [PMID: 25803781 DOI: 10.1371/journal.pone.0119383]
16 **Jun I**, Park HS, Piao H, Han JW, An MJ, Yun BG, Zhang X, Cha YH, Shin YK, Yook JI, Jung J, Gee HY, Park JS, Yoon DS, Jeung HC, Lee MG. ANO9/TMEM16J promotes tumourigenesis *via* EGFR and is a novel therapeutic target for pancreatic cancer. *Br J Cancer* 2017; **117**: 1798-1809 [PMID: 29024940 DOI: 10.1038/bjc.2017.355]
17 **Li C**, Cai S, Wang X, Jiang Z. Identification and characterization of ANO9 in stage II and III colorectal carcinoma. *Oncotarget* 2015; **6**: 29324-29334 [PMID: 26317553 DOI: 10.18632/oncotarget.4979]
18 **Shiozaki A**, Otsuji E, Marunaka Y. Intracellular chloride regulates the G(1)/S cell cycle progression in gastric cancer cells. *World J Gastrointest Oncol* 2011; **3**: 119-122 [PMID: 22007274 DOI: 10.4251/wjgo.v3.i8.119]
19 **Miyazaki H**, Shiozaki A, Niisato N, Ohsawa R, Itoi H, Ueda Y, Otsuji E, Yamagishi H, Iwasaki Y, Nakano T, Nakahari T, Marunaka Y. Chloride ions control the G1/S cell-cycle checkpoint by regulating the expression of p21 through a p53-independent pathway in human gastric cancer cells. *Biochem Biophys Res Commun* 2008; **366**: 506-512 [PMID: 18067855 DOI: 10.1016/j.bbrc.2007.11.144]
20 **Shiozaki A**, Miyazaki H, Niisato N, Nakahari T, Iwasaki Y, Itoi H, Ueda Y, Yamagishi H, Marunaka Y. Furosemide, a blocker of Na+/K+/2Cl- cotransporter, diminishes proliferation of poorly differentiated human gastric cancer cells by affecting G0/G1 state. *J Physiol Sci* 2006; **56**: 401-406 [PMID: 17052386 DOI: 10.2170/physiolsci.RP010806]
21 **Kurashima K**, Shiozaki A, Kudou M, Shimizu H, Arita T, Kosuga T, Konishi H, Komatsu S, Kubota T, Fujiwara H, Okamoto K, Kishimoto M, Konishi E, Otsuji E. LRRC8A influences the growth of gastric cancer cells *via* the p53 signaling pathway. *Gastric Cancer* 2021; **24**: 1063-1075 [PMID: 33864161 DOI: 10.1007/s10120-021-01187-4]
22 **Chang Z**, Cai C, Han D, Gao Y, Li Q, Feng L, Zhang W, Zheng J, Jin J, Zhang H, Wei Q. Anoctamin5 regulates cell migration and invasion in thyroid cancer. *Int J Oncol* 2017; **51**: 1311-1319 [PMID: 28902351 DOI: 10.3892/ijo.2017.4113]
23 **Song HY**, Zhou L, Hou XF, Lian H. Anoctamin 5 regulates cell proliferation and migration in pancreatic cancer. *Int J Clin Exp Pathol* 2019; **12**: 4263-4270 [PMID: 31933826]
24 **James DB**, Mary KG, Christian W. International Union Against Cancer (UICC) TNM classification of malignant tumors. 8th edition. Wiley: New York, 2017
25 **Kim GY**, Mercer SE, Ewton DZ, Yan Z, Jin K, Friedman E. The stress-activated protein kinases p38 alpha and JNK1 stabilize p21(Cip1) by phosphorylation. *J Biol Chem* 2002; **277**: 29792-29802 [PMID: 12058028 DOI: 10.1074/jbc.M201299200]
26 **Mazumdar M**, Glassman JR. Categorizing a prognostic variable: review of methods, code for easy implementation and applications to decision-making about cancer treatments. *Stat Med* 2000; **19**: 113-132 [PMID: 10623917 DOI: 10.1002/(sici)1097-0258(20000115)19:1<113::aid-sim245>3.0.co;2-o]
27 **Suzuki J**, Umeda M, Sims PJ, Nagata S. Calcium-dependent phospholipid scrambling by TMEM16F. *Nature* 2010; **468**: 834-838 [PMID: 21107324 DOI: 10.1038/nature09583]

28 **Huang F**, Wang X, Ostertag EM, Nuwal T, Huang B, Jan YN, Basbaum AI, Jan LY. TMEM16C facilitates Na(+)-activated K+ currents in rat sensory neurons and regulates pain processing. *Nat Neurosci* 2013; **16**: 1284-1290 [PMID: 23872594 DOI: 10.1038/nn.3468]

29 **Caputo A**, Caci E, Ferrera L, Pedemonte N, Barsanti C, Sondo E, Pfeffer U, Ravazzolo R, Zegarra-Moran O, Galietta LJ. TMEM16A, a membrane protein associated with calcium-dependent chloride channel activity. *Science* 2008; **322**: 590-594 [PMID: 18772398 DOI: 10.1126/science.1163518]

30 **Schroeder BC**, Cheng T, Jan YN, Jan LY. Expression cloning of TMEM16A as a calcium-activated chloride channel subunit. *Cell* 2008; **134**: 1019-1029 [PMID: 18805094 DOI: 10.1016/j.cell.2008.09.003]

31 **Yang YD**, Cho H, Koo JY, Tak MH, Cho Y, Shim WS, Park SP, Lee J, Lee B, Kim BM, Raouf R, Shin YK, Oh U. TMEM16A confers receptor-activated calcium-dependent chloride conductance. *Nature* 2008; **455**: 1210-1215 [PMID: 18724360 DOI: 10.1038/nature07313]

32 **Terashima H**, Picollo A, Accardi A. Purified TMEM16A is sufficient to form Ca2+-activated Cl- channels. *Proc Natl Acad Sci U S A* 2013; **110**: 19354-19359 [PMID: 24167264 DOI: 10.1073/pnas.1312014110]

33 **Song HY**, Tian YM, Zhang YM, Zhou L, Lian H, Zhu JX. A novel finding of anoctamin 5 expression in the rodent gastrointestinal tract. *Biochem Biophys Res Commun* 2014; **451**: 258-262 [PMID: 25094048 DOI: 10.1016/j.bbrc.2014.07.121]

34 **Siveen KS**, Nizamuddin PB, Uddin S, Al-Thani M, Frenneaux MP, Janahi IA, Steinhoff M, Azizi F. TRPV2: A Cancer Biomarker and Potential Therapeutic Target. *Dis Markers* 2020; **2020**: 8892312 [PMID: 33376561 DOI: 10.1155/2020/8892312]

35 **Xu R**, Wang X, Shi C. Volume-regulated anion channel as a novel cancer therapeutic target. *Int J Biol Macromol* 2020; **159**: 570-576 [PMID: 32442571 DOI: 10.1016/j.ijbiomac.2020.05.137]

World Journal of Gastroenterology

Submit a Manuscript: https://www.f6publishing.com

World J Gastroenterol 2022 August 28; 28(32): 4668-4680

DOI: 10.3748/wjg.v28.i32.4668

ISSN 1007-9327 (print) ISSN 2219-2840 (online)

ORIGINAL ARTICLE

Basic Study

Effects of Granule Dendrobii on chronic atrophic gastritis induced by N-methyl-N'-nitro-N-nitrosoguanidine in rats

Yue Wu, Yu Li, Xiao-Ming Jin, Guan-Hai Dai, Xuan Chen, Ye-Ling Tong, Ze-Ming Ren, Yu Chen, Xiao-Min Xue, Ren-Zhao Wu

Specialty type: Medicine, research and experimental

Provenance and peer review: Unsolicited article; Externally peer reviewed.

Peer-review model: Single blind

Peer-review report's scientific quality classification

Grade A (Excellent): 0
Grade B (Very good): B, B
Grade C (Good): C
Grade D (Fair): D
Grade E (Poor): 0

P-Reviewer: Herold Z, Hungary; Nakajima N, Japan; Sahin Y, Turkey

Received: March 13, 2022
Peer-review started: March 13, 2022
First decision: June 11, 2022
Revised: June 23, 2022
Accepted: August 5, 2022
Article in press: August 5, 2022
Published online: August 28, 2022

Yue Wu, First College of Clinical Medicine, Zhejiang Chinese Medical University, Hangzhou 310052, Zhejiang Province, China

Yue Wu, Yu Li, Guan-Hai Dai, Xuan Chen, Ye-Ling Tong, Ze-Ming Ren, Xiao-Min Xue, Ren-Zhao Wu, Institute of Basic Medicine, Zhejiang Academy of Traditional Chinese Medicine, Hangzhou 310007, Zhejiang Province, China

Yu Li, College of Basic Medicine, Zhejiang Chinese Medical University, Hangzhou 310052, Zhejiang Province, China

Xiao-Ming Jin, Stark Neuroscience Research Institute & Department of Anatomy, Cell Biology and Physiology, Indiana University School of Medicine, Indianapolis, IN 46202, United States

Yu Chen, Department of Experimental Animals, Zhejiang Academy of Traditional Chinese Medicine, Hangzhou 310007, Zhejiang Province, China

Corresponding author: Ren-Zhao Wu, MD, Chief Physician, Professor, Institute of Basic Medicine, Zhejiang Academy of Traditional Chinese Medicine, No. 132 Tianmushan Road, Xihu District, Hangzhou 310007, Zhejiang Province, China. wufeng03@126.com

Abstract

BACKGROUND

Dendrobium officinale is an herb of Traditional Chinese Medicine (TCM) commonly used for treating stomach diseases. One formula of Granule Dendrobii (GD) consists of *Dendrobium officinale* and American Ginseng (*Radix Panacis quinquefolii*), and is a potent TCM product in China. Whether treatment with GD can promote gastric acid secretion and alleviate gastric gland atrophy in chronic atrophic gastritis (CAG) requires verification.

AIM

To determine the effect of GD treatment on CAG and its potential cellular mechanism.

METHODS

A CAG model was induced by feeding rats N-methyl-N'-nitro-N-nitroso-guanidine (MNNG) for 12 wk. After oral administration of low, moderate, and high doses of GD in CAG rats for 8 wk, its effects on body weight, gastric mucosa

histology, mucosal atrophy, intestinal metaplasia, immunohistochemical staining of proliferating cell nuclear antigen (PCNA) and B-cell lymphoma-2, and hemoglobin and red blood cells were examined.

RESULTS

The body weights of MNNG-induced CAG model rats before treatment (143.5 ± 14.26 g) were significantly lower than that of healthy rats (220.2 ± 31.20 g, $P < 0.01$). At the 8th week of treatment, the body weights of rats in the low-, moderate-, and high-dose groups of GD (220.1 ± 36.62 g) were significantly higher than those in the untreated group (173.3 ± 28.09 g, all $P < 0.01$). The level of inflammation in gastric tissue of the high-dose group (1.68 ± 0.54) was significantly reduced ($P < 0.01$) compared with that of the untreated group (3.00 ± 0.00, $P < 0.05$). The number and thickness of gastric glands in the high-dose group (31.50 ± 6.07/mm, 306.4 ± 49.32 μm) were significantly higher than those in the untreated group (26.86 ± 6.41/mm, 244.3 ± 51.82 μm, respectively, $P < 0.01$ and $P < 0.05$), indicating improved atrophy of gastric mucosa. The areas of intestinal metaplasia were significantly lower in the high-dose group (1.74% ± 1.13%), medium-dose group (1.81% ± 0.66%) and low-dose group (2.36% ± 1.08%) than in the untreated group (3.91% ± 0.96%, all $P < 0.01$). The expression of PCNA in high-dose group was significantly reduced compared with that in untreated group ($P < 0.01$). Hemoglobin level in the high-dose group (145.3 ± 5.90 g/L), medium-dose group (139.3 ± 5.71 g/L) and low-dose group (137.5 ± 7.56 g/L) was markedly increased compared with the untreated group (132.1 ± 7.76 g/L; $P < 0.01$ or $P < 0.05$).

CONCLUSION

Treatment with GD for 8 wk demonstrate that GD is effective in the treatment of CAG in the MNNG model by improving the histopathology of gastric mucosa, reversing gastric atrophy and intestinal metaplasia, and alleviating gastric inflammation.

Key Words: Chronic atrophic gastritis; Granule Dendrobii; N-methyl-N'-nitro-N-nitrosoguanidine; Intestinal metaplasia

©The Author(s) 2022. Published by Baishideng Publishing Group Inc. All rights reserved.

Core Tip: Symptomatic treatment is mainly adopted for chronic atrophic gastritis (CAG) in modern medicine, and no drugs are available to promote gastric acid secretion and alleviate gastric gland atrophy. Our study shows that treatment with Granule Dendrobii (GD) for 8 wk was effective in reducing weight loss, gastric mucosal inflammation, atrophy and intestinal metaplasia, and loss of hemoglobin and erythrocytes in a rat model of CAG induced by N-methyl-N'-nitro-N-nitrosoguanidine. GD also alleviated the overexpression of PCNA and B-cell lymphoma-2 in CAG rats. These results provide new evidence on the use of GD not only for improving clinical symptoms but also for normalizing the abnormal histological changes of CAG.

Citation: Wu Y, Li Y, Jin XM, Dai GH, Chen X, Tong YL, Ren ZM, Chen Y, Xue XM, Wu RZ. Effects of Granule Dendrobii on chronic atrophic gastritis induced by N-methyl-N'-nitro-N-nitrosoguanidine in rats. *World J Gastroenterol* 2022; 28(32): 4668-4680

URL: https://www.wjgnet.com/1007-9327/full/v28/i32/4668.htm

DOI: https://dx.doi.org/10.3748/wjg.v28.i32.4668

INTRODUCTION

Chronic atrophic gastritis (CAG), characterized by thinning mucosal layer and loss or atrophy of gastric mucosal glands, is considered a premalignant change of gastric cancer (GC)[1]. It has been reported that the prevalence of CAG and intestinal metaplasia (IM) is 16% and 13%, respectively, and increases to 27% in countries with a high GC incidence[2]. The incidence of GC in patients with CAG or IM is 0.004%-0.3% per person each year, indicating that these patients have a higher risk of GC[3]. At present, the treatment of CAG in modern medicine mainly focuses on symptomatic treatment, and no drugs are available to promote gastric acid secretion and alleviate gastric gland atrophy. Therefore, it is essential to look for alternative therapies to reduce symptoms in CAG patients and improve their quality of life [4]. Traditional Chinese medicine (TCM) is often used for the treatment of CAG and has shown efficacy. However, there is a lack of scientific research on the effect of TCM in improving gastric mucosa atrophy and IM.

Dendrobium officinale is an herb of TCM commonly used for treating stomach diseases. The TCM literature states that it has the following functions: "thickening the stomach and intestines" (improving stomach function) and "smoothing stomach qi" (enhancing gastric motility and accelerating gastric emptying). One formula of Granule Dendrobii (GD) consisting of *Dendrobium officinale* and American Ginseng (*Radix Panacis quinquefolii*) is a potent TCM product in China. An earlier clinical study found that GD treatment of CAG reversed gastric mucosa atrophy and improved gastric mucosa and IM[5]. To provide scientific evidence for the clinical application of this product, we studied the effect of GD on gastric mucosa atrophy and IM reversal, as well as changes in proliferating cell nuclear antigen (PCNA) and B-cell lymphoma-2 (Bcl-2) in a CAG model induced by N-methyl-N'-nitro-N-nitrosoguanidine (MNNG) in rats.

MATERIALS AND METHODS

Herbal products and drugs

Herbal product under investigation: Granule Dendrobii (GD, Li Zuan Brand, Zhejiang Tian Huang Pharmaceutical Co., Ltd, China) 3 g per bag, contained 0.5g of crude *Dendrobium Officinale* and 0.4 g of American Ginseng (*Radix Panacis Quinquefolii*). Based on the theory of TCM, this formula has the functions of enhancing energy metabolism of the stomach and restoring its nutrient supply to improve the production of body fluid, which makes it suitable for treating the type of CAG that has lower levels of energy production and nutrient supply. The dosage for clinical treatment was 18 g/d (equivalent to 5.4 g herbs/d).

Herbal product as control: Yangweishu Granule (YWS, prodeuced by Shenlu Shuanghe Pharmaceutical Co., Ltd, Hefei, China) 10 g per bag contained dang*shen* (*Radix Codonopsis*), chenpi (*Pericarpium Citri Reticulatae*), huangjing (*Polygonatum sibiricum*), shanyao (*Rhizoma Dioscoreae*), xuanshen (*Radix Scrophulariae*), wumei (*Fructus Mume*), shanzha (*Fructus Crataegi*), beishashen (*Glehnia littoralis*), ganjiang (*Rhizoma Zingiberis*), tusizi (*Cuscuta Chinensis*), baizhu (*Rhizoma Atractylodis Macrocephalae*), dextrin and saccharose. The dosage for clinical treatment was 20 g/d.

Animals

All experiments were performed on Wistar rats (50% male) obtained from the Shanghai Slack Laboratory Animal Co., Ltd. All the animals were kept in a temperature (25 ± 2 ℃)- and humidity-controlled animal facility on a 12-h light/dark cycle, with food and water supplied *ad libitum*. The protocol was designed to minimize pain or discomfort to the animals. All procedures were approved by the Animal Care and Use Committee of the Institutional Guide for the Care and Use of Laboratory Animals at Zhejiang Institute of Traditional Chinese Medicine.

MNNG-induced CAG model in rats

MNNG (Tokyo Chemical Industry, Japan) was added to the drinking water for six-week-old Wistar rats (50% male). The MNNG stock solution was made every week by mixing MNNG with distilled water to a concentration of 1 g/L and kept in a refrigerator in the dark. For daily use, the stock solution was diluted to 167 μg/mL with distilled water and stored in 200 mL opaque water bottles for the rats to drink freely. The bottles were changed daily. As earlier studies established the development of CAG in 2 to 3 mo, with pathological changes from initial erosive and inflammation of the gastric mucosa in several weeks to gradual atrophy and dysplasia, the rats were provided with MNNG for a period of 12 wk for model generation.

Experimental grouping and histological methods

To confirm the development of CAG in this model, 4 MNNG model animals and 4 normal animals were sacrificed for gastric histopathological examination at the end of model generation. The rats were then randomly divided into the following five groups. Three treatment groups were fed with 0.6 g, 1.2 g, and 2.4 g/kg body weight/day of GD as the low (12 rats), medium (12 rats) and high (14 rats) dosage groups, respectively. The fourth group was fed with physiological saline at the same volume as the untreated model group (14 rats), and the last group was fed with YWS (12 rats) granule 4.0 g/kg/d as a positive control group. In addition, 14 normal rats were given physiological saline at the same volume as the normal control group. Two rats were reserved for the high-dose group, the normal control group and the untreated model group in order to sacrifice the animals for pathological pre-examination to determine the termination point of the course when the treatment was almost finished. Each group was given its corresponding treatment daily for 8 wk.

The day after the last administration, all the rats were anesthetized and blood was taken from the abdominal aorta. The stomach was quickly removed and fixed in formalin. The longitudinal length and full layer of the anterior stomach to the duodenum was collected. A strip of tissue from the lateral wall was taken as the standard pathological sample. After paraffin embedding, the tissue was sliced into 4 μm sections and stained with Hematoxylin-Eosin (HE)[6], Alcian Blue (AB)[7], and immunohisto-

chemistry against PCNA (antibody against gastric epithelial cell proliferating cell nuclear antigen, NeoMarkers, United States) and Bcl-2 (anti-Bcl-2 antibody, Millipore, United States).

PCNA and Bcl-2 staining: After dewaxing, the sections were incubated with 3% H_2O_2 deionized water for 10 min, followed by incubation with primary antibodies at room temperature or 37 ℃ for 1 to 2 h. After rinsing in PBS, secondary antibodies were added and incubated at room temperature or 37 ℃ for 20 min. The sections were rinsed in PBS, and processed for color rendering dehydration, transparency and sealing.

Histological evaluation of gastric mucosa

Gastric mucosal inflammation: The effect of treatment on gastric mucosal inflammation induced by MNNG in CAG rats was evaluated using a semi-quantitative method. Specifically, after the entire gastric mucosa was observed under the microscope low power view, 10 fields of view in the gastric antrum were selected to determine inflammation. According to the diagnostic criteria for gastritis proposed by Houston in 1994[8,9], the degree of inflammatory cell infiltration is divided into seven grades from 0 to 3. Grade 0: no inflammation; Grade 0.5: inflammation between 0 to 1 observed under a microscope; Grade 1: multiple chronic inflammatory cell infiltrations seen in the pit of the stomach or the bottom of the inherent gland; Grade 1.5: inflammation between Grade 1 to 2 observed under a microscope; Grade 2: more inflammatory cells in the gastric mucosa from the fovea to the myometrium; Grade 2.5: inflammation between Grade 2 to 3 observed under a microscope; Grade 3: numerous inflammatory cells seen in the gastric mucosa.

Changes in gland thickness and gland number on gastric mucosa: Five fields of gastric antrum mucosa were obtained from each section, and the gland thickness in each field was measured with a micrometer. The average value of the five fields in each section was determined (μm). At 100X power, the total number of proper glands in the gastric antrum between 0.2-1.2 mm of the pyloric ring in rats were counted and expressed as "units/mm".

The number of gastric primary cells and parietal cells: At 400× power, the mean numbers of gastric primary cells and parietal cells from 5 fields in the gastric body mucosa starting from 1.0 mm below the border between the anterior stomach and the gastric body were counted from each section.

Intestinal metaplasia: Intestinal metaplasia was evaluated by analyzing images from AB stained sections. Five photos of gastric mucosa in the gastric antrum were randomly obtained from each section using a Nikon ECLIPSE Ti microfilming system at a magnification of 400×. Each group was imaged under the same conditions. A Leica QWin color<RG> image analysis system was used for analysis. Under the same conditions, the proportion (%) of the total positively stained area over the total analyzed area of each photo was calculated. An average proportion was calculated from 5 photos in each rat and used for statistical comparisons among all the experimental groups.

Immunohistochemistry of PCNA and Bcl-2

As pathological changes in CAG are correlated with proliferation and apoptosis of the gastric mucosa, we examined the expression of PCNA and Bcl-2 proteins in gastric mucosa. PCNA is an intraconuclear protein that is expressed in a small amount during the quiescence phase of DNA synthesis. It is an important indicator of cell proliferation because its changes are consistent with intracellular DNA replication. Bcl-2 is a gene that inhibits apoptosis. Its overexpression can inhibit cell apoptosis and is indicative of a favorable precondition for the transformation of malignant cells. Positive staining of PCNA was located in the nucleus, while positive staining of Bcl-2 was located in the cytoplasm and was occasionally accompanied by nuclear staining. Based on previous studies[10-14], we used a semi-quantitative grading method to quantify positive cells. Proportions of positive cells were calculated by counting the numbers of positive cells and total cells in five fields randomly observed under a high-power view (400 ×). A score was assigned according to the percentage of positive cells: 0 for 5%, 1 point for 6%-25%, 2 points for 26%-50%, and 3 points for > 50%. Then the intensity of staining of positive cells was scored: 0 for non-staining, 1 point for light yellow, 2 points for brownish yellow, and 3 points for brown. Finally, these points were added together. 0 was negative "-", 1-2 points were weakly positive "+", 3-4 points were moderately positive "++", and 5-6 points were strongly positive "+++".

Detection of hemoglobin and erythrocytes

As reduced iron absorption and utilization due to gastric mucosal atrophy in CAG often lead to decreases in hemoglobin and erythrocyte count in rats, we examined whether treatment with GD would also improve these parameters in CAG rats. After the rats were anesthetized with pentobarbital, blood was collected from the abdominal aorta. Whole blood was placed in a disposable vacuum blood collection anticoagulant tube and routine blood tests were carried out using an XT-1800iv five-classification hemocyte analyzer (Hisen Meikang Co., Japan). Reports of the analysis were automatically generated.

Statistical analysis

Statistical analyses were performed using SPSS software 17.0 (SPSS Inc., Chicago, United States). Quantitative data were expressed as the mean ± SD. Differences among multiple groups were compared by one-way ANOVA, and pairwise comparisons between groups were followed by the least significant difference if the variances were homogeneous, and the Dunnett T3 method was used otherwise. Numerical data were analyzed with the χ^2 test.

RESULTS

Effects of Granule Dendrobii on weight loss in rats with MNNG-induced CAG

The mean body weight of rats with MNNG-induced CAG before treatment was 143.5 ± 14.3 g, which was significantly lower than that of the normal rats (Figure 1, 220.2 ± 31.2 g, $P < 0.01$). On completion of model generation, there were no significant differences in body weight among all the treatment groups (Figure 1, $P > 0.05$).

At the end of treatment, the body weights of all the treatment groups (except YWS) had significantly recover when compared with those of the untreated group (Figure 1, $P < 0.05$). At the 8th wk of treatment, the mean body weights of groups treated with high (220.1 ± 36.6 g, $P < 0.01$), medium (198.1 ± 13.5 g, $P < 0.05$), and low doses (197.6 ± 27.3 g, $P < 0.05$) of GD were significantly higher than that of the untreated group (173.3 ± 28.1 g). The results at 8 wk after treatment indicated that GD treatment had the effect of reducing weight loss in the MNNG model of CAG.

Pathological changes in gastric mucosa after treatment

In normal rats, the gastric mucosal glands were relatively thick and numerous, and the epithelial cells were neatly arranged without defect or exfoliation. The glands were regular in shape and basically the same in size. AB staining showed a small amount of blue staining in the deep mucosa without IM. In the CAG group, the gastric mucosa was atrophic and thinned with reduced glands. There was edema and surface exfoliation. The infiltration of many acute and chronic inflammatory cells was visible in the interstitium. Hyperemia and thickening of the mucosal myometrium were observed. Atypical hyperplasia was seen, with cells of irregular size and shape and a disordered arrangement. AB staining revealed that the entire mucosa was stained blue in the presence of IM. In the CAG rats treated with high-dose GD, the pathological changes were reduced and atrophy was improved. The epithelial cells were well arranged without defect or exfoliation. The shapes of the glands were regular with similar size and shape. AB staining showed a very light blue color in the deep part of the gastric antrum mucosa, suggesting almost no IM (Figure 2A). In the CAG rats treated with medium-dose GD, the pathological changes were similar to those in the high-dose group with significant improvement. Such changes could be classified as mild to moderate superficial gastritis. AB staining showed a normal staining pattern with no IM, and was similar to that in the high-dose group (Figure 2A). In the CAG rats treated with low-dose GD, the pathological changes as shown by HE staining were slightly alleviated with improvements in atrophy compared with the untreated group, but inflammatory cell infiltration was observed in the mucosal layer. These changes were classified as mild to moderate superficial gastritis. On AB staining, there was a small amount of blue staining in the deep mucosa with IM (Figure 2A).

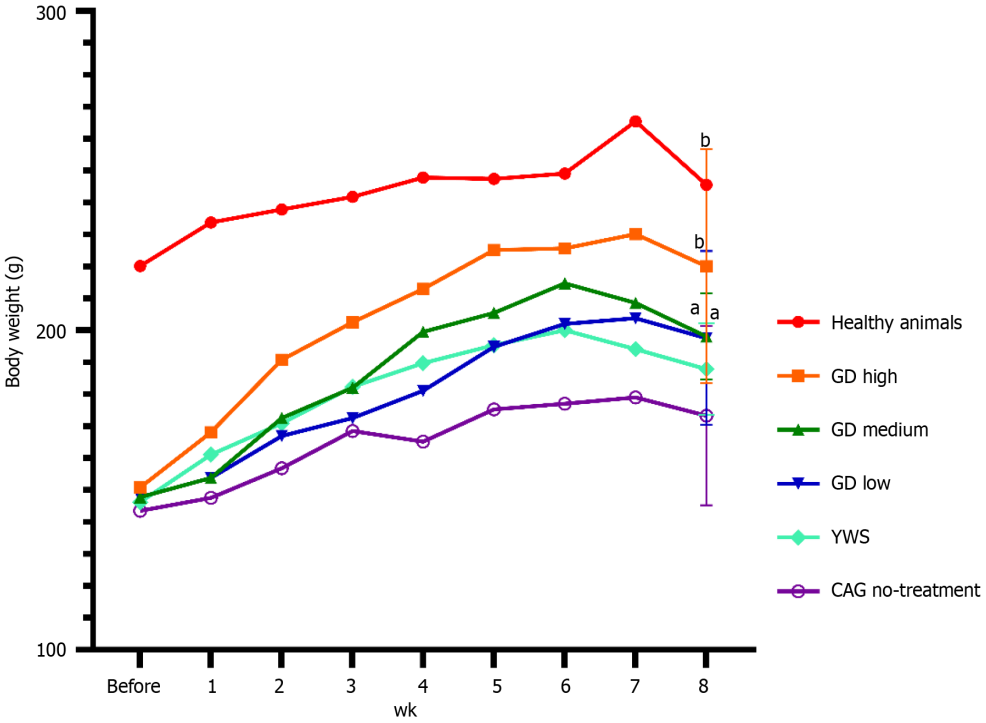
After 8 wk of GD treatment in CAG rats, the levels of gastric mucosal inflammation in the high-dose (1.68 ± 0.54) and medium-dose (2.08 ± 0.42) groups were significantly lower than those in the low-dose, no-treatment, and YWS groups (Figure 2B, $P < 0.01$ for all comparisons).

Treatment with Granule Dendrobii improved the thickness and gland numbers of gastric mucosa in rats with CAG

At 8 wk after CAG generation, significant decreases in the thickness and number of glands in the gastric mucosa were observed. The number (31.50 ± 6.07 unit/mm) and thickness (306.4 ± 49.32 μm) of glands in gastric tissue of the high-dose group were significantly higher than those of the no-treatment group (26.86 ± 6.41 unit/mm, 244.3 ± 51.82 μm, respectively), indicating a significant reduction in the atrophy of gastric mucosa in the treatment group (Figure 2C and D, $P < 0.01$ or $P < 0.05$). The glandular thickness of gastric tissue in the medium- and low-dose groups was also significantly improved compared with that in the no-treatment group (Figure 2C, $P < 0.01$ or $P < 0.05$).

Treatment with GD increased the numbers of chief cells and parietal cells in the gastric mucosa of CAG rats

At 8 wk after model preparation, there was a significant decrease in the number of chief cells in the CAG group when compared with the healthy animal group ($P < 0.05$). After 8 wk of treatment, the numbers of chief cells (165.5 ± 12.65 unit/field) and parietal cells (425.4 ± 16.0 unit/field) in gastric mucosa in the high-dose group were significantly higher than those in no-treatment group (chief cells: 148.7 ± 6.38 unit/field; parietal cells: 407.2 ± 18.6 unit/field), indicating a protective effect of GD



DOI: 10.3748/wjg.v28.i32.4668 **Copyright** ©The Author(s) 2022.

Figure 1 Changes in body weight of chronic atrophic gastritis rats during the 8-wk treatment period. Data were evaluated for statistical significance by one-way ANOVA, least significant difference test and Dunnett T3 test, and are presented as follows: $^{a}P < 0.05$ and $^{b}P < 0.01$ *vs* chronic atrophic gastritis with no-treatment group. GD High: Chronic atrophic gastritis rats treated with a high dosage of Granule Dendrobii; GD Medium: Chronic atrophic gastritis rats treated with a medium dosage of Granule Dendrobii; GD Low: Chronic atrophic gastritis rats treated with a low dosage of Granule Dendrobii; YWS: Chronic atrophic gastritis rats treated with Yangweishu; CAG: Chronic atrophic gastritis.

treatment on chief cells and parietal cells in gastric mucosa. The number of chief cells in gastric mucosa of the medium- and low-dose groups was also significantly higher than the no-treatment group (Figure 2E, $P < 0.01$ and $P < 0.05$, respectively); but the number of parietal cells in gastric mucosa of the medium- and low-dose groups was not significantly higher than that in the no-treatment group (Figure 2F, $P > 0.05$).

Treatment with GD improved intestinal metaplasia of gastric mucosa in CAG rats

At 8 wk after model preparation, quantitative analysis of gastric mucosa in the CAG rats showed that the percentage of IM increased significantly (0.95 ± 0.72% and 3.91 ± 0.96% in the healthy animal and CAG groups, respectively, $P < 0.05$). After treatment with GD for 8 wk, the areas of IM in the high-dose (1.74 ± 1.13%), medium-dose (1.81 ± 0.66%), and low-dose (2.36 ± 1.08%) groups were significantly lower than that in the no-treatment group ($P < 0.01$ for all), suggesting a significant improvement in IM after treatment with GD (Figure 2G).

Treatment with GD decreased the expression of PCNA and Bcl-2 in gastric mucosa of CAG rats

In healthy rats, the number of PCNA expressing cells in gastric mucosa was low and mainly located in the proliferation zone, with regular distribution and weak staining. In the CAG rats without treatment, the number of PCNA expressing cells in gastric mucosa was increased and distributed in nearly all layers with deeper staining. In the high dose group, the expression and distribution of PCNA were similar to that of the healthy animal group, with less PCNA expressing cells mainly located in the proliferation zone than the CAG with no-treatment group (Figure 3).

Table 1 shows a summary of the expression of PCNA and Bcl-2 in gastric mucosa. PCNA expression in the CAG group was significantly higher than that in the healthy animal group ($P < 0.01$), while its expressions in the high-dose and low-dose groups was significantly lower than that in the CAG group ($P < 0.01$). Similarly, the expression of Bcl-2 was significantly higher in the CAG group than in the healthy animals group ($P < 0.01$). The expression of Bcl-2 in the high-dose, medium-dose, and low-dose groups was lower than that of the no-treatment group, but without statistical significance ($P > 0.05$).

Treatment with GD improved hemoglobin and erythrocyte count in CAG rats

As shown in Figure 4A, hemoglobin in the CAG group (132.1 ± 7.76) was significantly reduced compared with that in the healthy animal group (145.6 ± 6.26, $P < 0.01$). In the high-dose (145.3 ± 5.90),

Table 1 Expression of proliferating cell nuclear antigen and B-cell lymphoma-2 in gastric tissues of different groups of rats

Grouping	PCNA						Bcl-2					
	+++	++	+	-	*n*	*P* value	+++	++	+	-	*n*	*P* value
GD high	1	3	10	0	14	< 0.01	3	4	7	0	14	> 0.05
GD medium	5	4	3	0	12	> 0.05	2	8	2	0	12	> 0.05
GD low	3	2	7	0	12	< 0.01	1	6	5	0	12	> 0.05
YWS	4	3	5	0	12	< 0.05	2	7	3	0	12	> 0.05
Healthy animals	0	0	14	0	14	< 0.01	0	3	11	0	14	< 0.01
CAG no-treatment	9	5	0	0	14	-	5	7	2	0	14	-
6 groups of χ^2-test	χ^2 value	38.96					20.97					
	P value	$P < 0.01$					$P < 0.05$					

Data were evaluated for statistical significance by one-way ANOVA, least significant difference test and Dunnett T3 test. The *P* value in the table is the χ^2 test of each group compared to the group with chronic atrophic gastritis without treatment. The χ^2 value in the table is the χ^2 test of multi-group row lists with 6 groups. GD high: Chronic atrophic gastritis rats treated with a high dosage of Granule Dendrobii; GD medium: Chronic atrophic gastritis rats treated with a medium dosage of Granule Dendrobii; GD low: Chronic atrophic gastritis rats treated with low dosage of Granule Dendrobii; YWS: Chronic atrophic gastritis rats treated with Yangweishu; PCNA: Proliferating cell nuclear antigen; Bcl-2: B-cell lymphoma-2; CAG: Chronic atrophic gastritis.

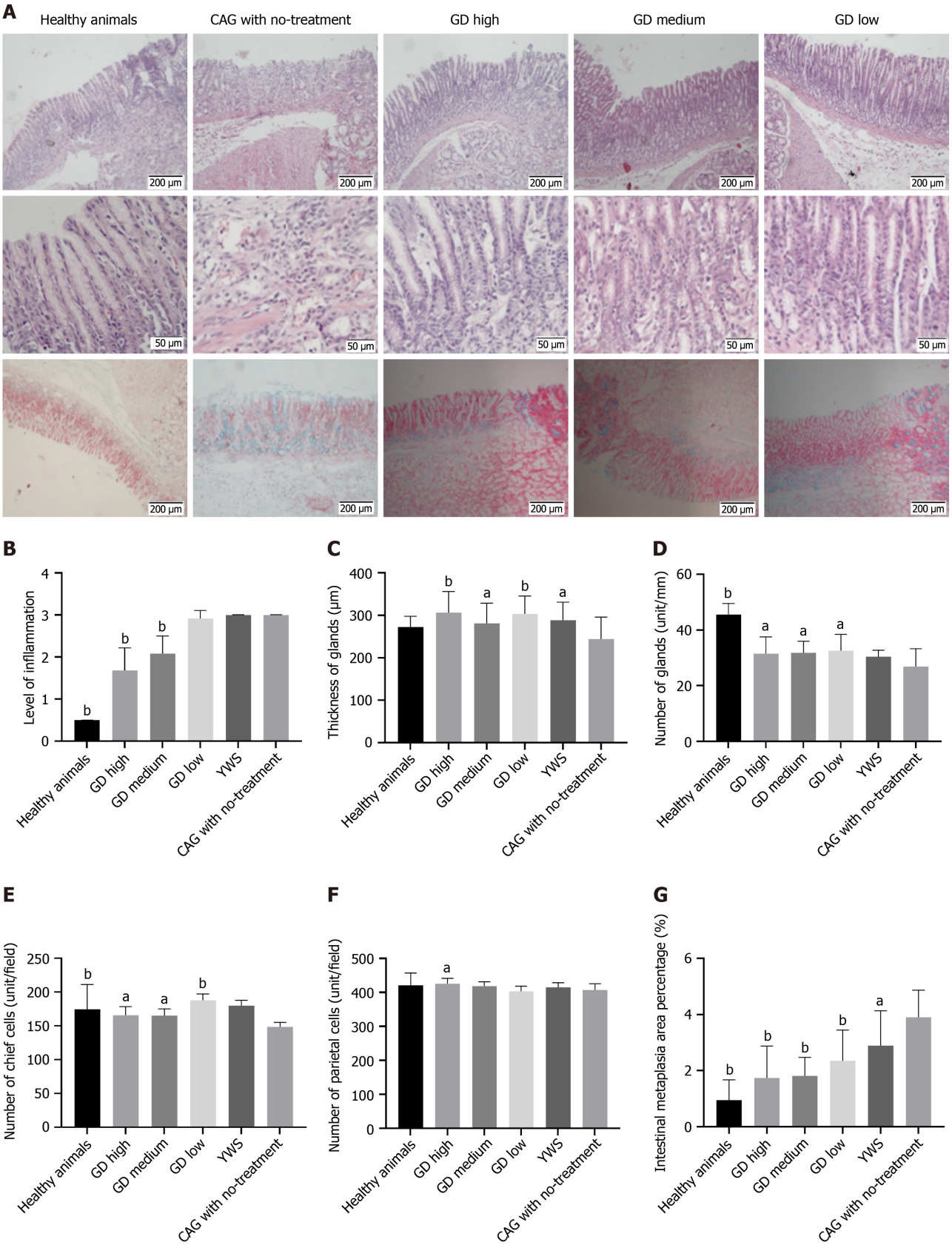
medium-dose (139.3 ± 5.71) and low-dose groups (137.5 ± 7.56) of GD after 8 wk of treatment, hemoglobin was significantly higher than that in the no-treatment group ($P < 0.01$ or $P < 0.05$). In addition, there was a dose-dependent relationship between the increase in hemoglobin and the dose of GD used. The increase in hemoglobin level in the high-dose group was significantly greater than that in the medium and low-dose group (Figure 4A, $P < 0.05$). Erythrocyte count in the untreated group was lower than that in the healthy animal group, but the difference was not statistically significant (Figure 4B, $P > 0.05$). After 8 wk of treatment, the high-dose group and the medium-dose group had significant increases in erythrocyte counts compared with the no-treatment group ($P < 0.01$). In addition, there was a dose-dependent relationship between the increase in erythrocyte count and dose of GD used. The increase in erythrocyte count in the high dose group was significantly greater than that in the low dose group (Figure 4B, $P < 0.05$). These results suggest that treatment with GD for 8 wk increased hemoglobin and erythrocytes in CAG rats.

DISCUSSION

Treatment with GD for 8 wk resulted in significant improvements in body weight, gastric mucosal inflammation, atrophy, and intestinal metaplasia in rats with MNNG-induced CAG. GD also increased the reduced levels of hemoglobin and erythrocytes in CAG rats. Furthermore, GD improved gastric mucosal lesions and improved the secondary pathological changes of CAG including reduced hemoglobin and red blood cell count, and overall body condition. It was observed that GD alleviated the overexpression of PCNA and Bcl-2 in model rats, which maybe one of the therapeutic mechanisms related to the reduction of gastric mucosal inflammation and mucosal damage.

Rodent models of CAG can be induced by chemical stimulation (ethanol, ammonia water, sodium deoxycholate, *etc.*), autoimmunity against gastric mucosa homogenization, *Helicobacter pylori* and MNNG. Among these, the carcinogen (MNNG) induction method is widely used to generating a CAG model[15-17], with lesion severity being adjustable according to the length of induction time. Specifically, mild atrophy of gastric mucosa generally develops within 25 wk in rats, the CAG model with IM established within 35 wk[18], while early GC develops in 7-9 mo. As the CAG rat model induced by MNNG is stable, relatively severe, and resistant to natural recovery, it is credible for testing the efficacy of therapeutic treatment.

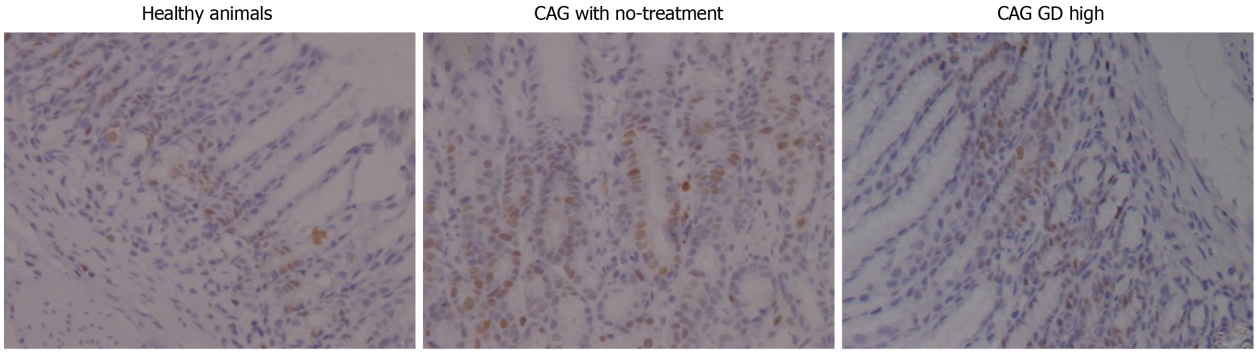
Dendrobium officinale extraction has been shown to effectively reduce the incidence of GC in rats and may be valuable in the prevention of GC[19]. *Dendrobium officinale* polysaccharide, the main active ingredient of *Dendrobium officinale*, can effectively inhibit the progression of premalignant gastric lesions induced by MNNG[20]. The formula of GD is mild. The combination of *Dendrobium candidum* and American ginseng has the functions of tonifying Qi, and Yin, and nourishing the stomach to promote the production of body fluid, making it suitable for the treatment and recovery of digestive diseases. Such functions are also in line with records in relevant traditional literature. Treating CAG with TCM is relatively safe and feasible during long-term use, while the effect is holistic and comprehensive, and research in this direction has significant prospects[21].



DOI: 10.3748/wjg.v28.i32.4668 **Copyright** ©The Author(s) 2022.

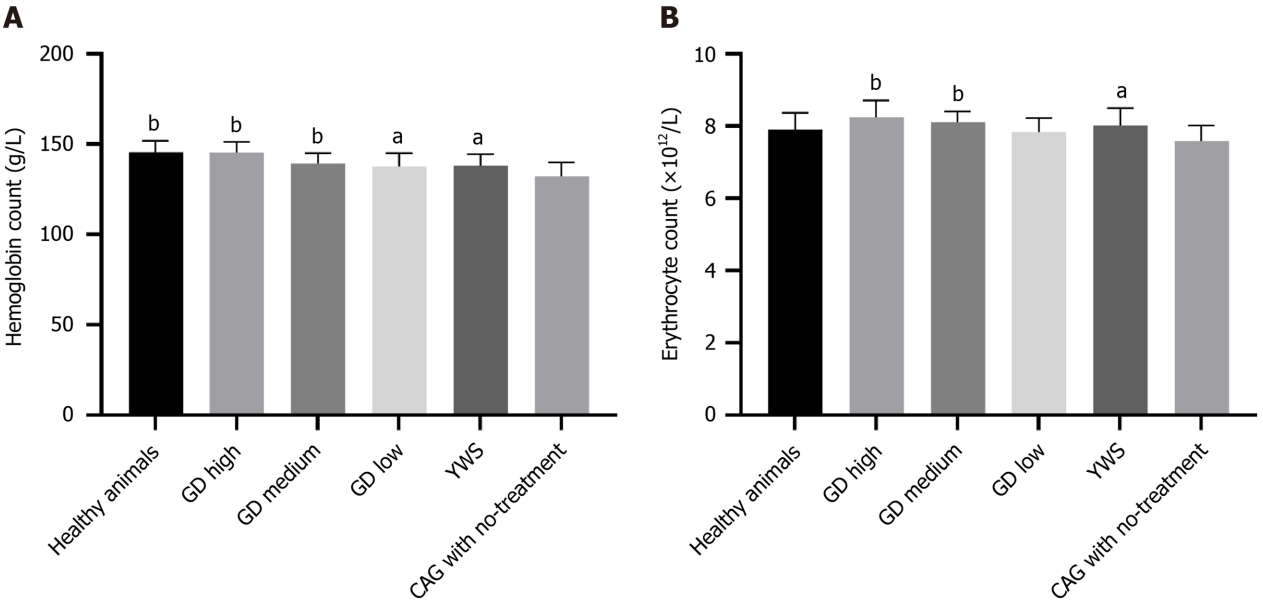
Figure 2 Pathological changes of gastric mucosa after treatment. A: Improved histopathology of gastric mucosa; B: Reduced inflammation of gastric mucosa; C and D: Treatment with Granule Dendrobii improved the thickness and gland number of gastric mucosa in rats with chronic atrophic gastritis; E and F: Treatment with Granule Dendrobii increased the number of chief cells and parietal cells in gastric mucosa in rats with chronic atrophic gastritis; G: Treatment with Granule Dendrobii improved intestinal metaplasia of gastric mucosa in rats with chronic atrophic gastritis. Data were evaluated for statistical significance by one-way

ANOVA, least significant difference test and Dunnett T3 test, and are represented as follows: $^{a}P < 0.05$ and $^{b}P < 0.01$ *vs* chronic atrophic gastritis with no-treatment group. GD High: Chronic atrophic gastritis rats treated with a high dosage of Granule Dendrobii; GD Medium: Chronic atrophic gastritis rats treated with a medium dosage of Granule Dendrobii; GD Low: Chronic atrophic gastritis rats treated with a low dosage of Granule Dendrobii; YWS: Chronic atrophic gastritis rats treated with Yangweishu; CAG: Chronic atrophic gastritis.



DOI: 10.3748/wjg.v28.i32.4668 **Copyright** ©The Author(s) 2022.

Figure 3 Treatment with Granule Dendrobii decreased the expression of PCNA in gastric mucosa of chronic atrophic gastritis rats. A summary of the expression of PCNA and B-cell lymphoma-2 in gastric mucosa is indicated in Table 1. GD high: Chronic atrophic gastritis rats treated with a high dosage of Granule Dendrobii; CAG: Chronic atrophic gastritis.



DOI: 10.3748/wjg.v28.i32.4668 **Copyright** ©The Author(s) 2022.

Figure 4 Treatment with Granule Dendrobii improved hemoglobin and erythrocyte count in chronic atrophic gastritis rats. A: Hemoglobin count; B. Erythrocyte count. Data were evaluated for statistical significance by one-way ANOVA, least significant difference test and Dunnett T3 test, and are presented as follows: $^{a}P < 0.05$ and $^{b}P < 0.01$ *vs* chronic atrophic gastritis with no-treatment group. GD high: Chronic atrophic gastritis rats treated with a high dosage of Granule Dendrobii; GD medium: Chronic atrophic gastritis rats treated with a medium dosage of Granule Dendrobii; GD low: Chronic atrophic gastritis rats treated with a low dosage of Granule Dendrobii; YWS: Chronic atrophic gastritis rats treated with Yangweishu; CAG: Chronic atrophic gastritis.

In recent years, treatment with traditional Chinese herbal medicine has been reported to improve CAG gastric mucosal atrophy and IM. In *Helicobacter pylori* positive CAG, a TCM herbal formula was shown to improve clinical symptoms and efficacy rate, and reverse atrophy in gastric mucosa in CAG patients[22]. Fuzi Lizhong decoction can reverse IM due to CAG to a certain extent through a mechanism related to the regulation of shh gene expression of the diseased gastric mucosa[23]. Recent research reported that notoginsenoside R1, an ingredient of *Panax notoginseng*, can improve CAG by increasing Bcl-2 expression and decreasing Bax expression in gastric tissue of rats with CAG induced by MNNG combined with an irregular diet[24]. Morroniside, an extract from *Cornus officinalis*, was shown to relieve gastric mucosa injury due to CAG by preventing inflammation[25]. Modified Sijunzi

Decoction (MSD) relieved the symptoms of CAG, improved the pathologic changes in CAG including fatigue and tiredness symptoms in CAG patients[26]. Berberine, an isoquinoline alkaloid from *Rhizoma coptidis*, has an inhibitory effect on gastritis[27] and GC cells[28], and significantly improves the pathological characteristics of gastric tissue, and alleviated serum biochemical indices[29]. These studies show that in addition to the formula we used in this study (*Dendrobium officinale* and *American ginseng*), fuzi Lizhong Decoction, notoginsenoside R1, morroniside, MSD, berberine, or TCM treatment aimed at invigorating spleen, soothing the liver, promoting blood circulation and detoxification, also have varying degrees of anti-inflammatory effects and reverse gastric mucosal atrophy and IM.

Some researchers believe that it is difficult to achieve the effect of reversing gastric mucosal atrophy and IM in CAG or they doubt the reported efficacy. For example, clinical studies have shown that eradication of *Helicobacter pylori* can improve chronic gastritis. Although some studies have shown certain improvement in gastric atrophy, IM seems reversible[30]. Some people also think that advanced atrophic gastritis may be irreversible[31]. As the conclusions by different authors vary widely, further long-term prospective studies in different ethnic and geographical environments are needed to provide more reliable evidence on the reversibility of gastric atrophy and IM[32].

As discussed above, it is believed that it is difficult to reverse gastric mucosal atrophy and gastric mucosal IM in CAG. However, as this conclusion is mainly based on observations of gastric mucosal atrophy and gastric mucosal IM following eradication of *Helicobactor pylori*, the question of whether a different treatment (*i.e.*, TCM) will be effective in reversing gastric atrophy and IM remains to be answered.

Our histological data support that treatment with GD for 8 wk was effective in reversing gastric mucosa atrophy and IM. Whether this effect can be duplicated in human CAG patients requires confirmation in clinical studies with large sample sizes, and strict control and rigorous experimental design. The results will provide new evidence on the use of GD not only for improving clinical symptoms but also for normalizing abnormal histological changes in CAG.

CONCLUSION

This study shows that treatment with GD for 8 wk was effective in reducing weight loss, gastric mucosal inflammation and atrophy, and intestinal metaplasia in a rat model of CAG induced by MNNG. GD also reduced the decreases in hemoglobin level and erythrocytopenia in this model. The treatment resulted in alleviation of the overexpression of PCNA and Bcl-2 in the model rats which may be an underlying mechanism that contributes to the reduction in gastric mucosal inflammation and mucosal damage.

ARTICLE HIGHLIGHTS

Research background

Dendrobium officinale is often used to treat stomach diseases. One formula of Granule Dendrobii (GD) consisting of *Dendrobium officinale* and American ginseng (*Radix Panacis quinquefolii*) is a potent Traditional Chinese Medicine product in China for chronic atrophic gastritis (CAG) as it reverses gastric mucosa atrophy and improves gastric mucosa intestinal metaplasia (IM).

Research motivation

This study determined the effect of GD treatment on CAG and its potential cellular mechanism to provide a reference for future treatment.

Research objectives

To study the effect and cellular mechanism of GD in the treatment of CAG, and to provide scientific evidence for the clinical application of GD.

Research methods

A rat model of CAG induced by N-methyl-N'-nitro-N-nitrosoguanidine (MNNG) was established, and treatment with GD resulted in weight loss, gastric mucosa atrophy and intestinal metaplasia reversal, as well as changes in PCNA and B-cell lymphoma-2 (Bcl-2) after 8 wk of treatment.

Research results

Treatment with GD for 8 wk resulted in significant improvements in body weight, gastric mucosal inflammation, atrophy, and IM in rats with CAG induced by MNNG. GD also increased the reduced levels of hemoglobin and erythrocytes in CAG rats.

Research conclusions

GD improved gastric mucosal lesions and the secondary pathological changes of CAG including hemoglobin and red blood cell reductions, and overall body condition. GD also alleviated the overexpression of PCNA and Bcl-2 in model rats, which maybe one of the therapeutic mechanisms related to the reduction in gastric mucosal inflammation and mucosal damage.

Research perspectives

Our research group will continue to confirm whether the effect of GD can be duplicated in CAG patients by clinical studies with large sample sizes, strict control and rigorous experimental design, and further study the molecular and cellular mechanism of GD.

ACKNOWLEDGEMENTS

The authors would like to acknowledge Dr. Chun-Li Zhang and Dr. Min Yang from Tongde Hospital of Zhejiang Province for their professional advice on pathological work, as well as Peng Ren from Jiangsu Yanchang Science and Technology Co., Ltd for statistical analysis assistance.

FOOTNOTES

Author contributions: Wu RZ, Wu Y, Dai GH and Ren ZM designed the research; Wu Y, Li Y, Chen Y and Xue XM performed the research and acquired the data; Dai GH, Jin XM, Chen X and Tong YL analyzed and interpreted the data; Wu Y, Wu RZ and Jin XM wrote the manuscript; Wu Y and Jin XM extensively revised the manuscript for clarity and grammar; all authors have read and approve the final manuscript.

Supported by the Science and Technology Department of Zhejiang Province, No. LGF19H280008; and the Provincial Natural Science Foundation of Zhejiang Province, No. LY15H280011.

Institutional review board statement: The Institutional Review Board approval is not applicable in this study because it did not involve human beings.

Institutional animal care and use committee statement: All procedures involving animals were reviewed and approved by Zhejiang Academy of Traditional Chinese Medicine Research Ethics Committee.

Conflict-of-interest statement: All the authors report no relevant conflicts of interest for this article.

Data sharing statement: All data generated or analyzed during this study are included in this paper, and further inquiries can be directed to the corresponding author (E-mail: wufeng03@126.com).

ARRIVE guidelines statement: The authors have read the ARRIVE guidelines, and the manuscript was prepared and revised according to the ARRIVE guidelines.

Open-Access: This article is an open-access article that was selected by an in-house editor and fully peer-reviewed by external reviewers. It is distributed in accordance with the Creative Commons Attribution NonCommercial (CC BY-NC 4.0) license, which permits others to distribute, remix, adapt, build upon this work non-commercially, and license their derivative works on different terms, provided the original work is properly cited and the use is non-commercial. See: https://creativecommons.org/Licenses/by-nc/4.0/

Country/Territory of origin: China

ORCID number: Yue Wu 0000-0003-4628-7628; Xiao-Ming Jin 0000-1234-2436-6523; Yu Chen 0000-0003-4179-0259; Ren-Zhao Wu 0000-0002-4140-9887.

S-Editor: Gong ZM
L-Editor: A
P-Editor: Gong ZM

REFERENCES

1 **Park YH**, Kim N. Review of atrophic gastritis and intestinal metaplasia as a premalignant lesion of gastric cancer. *J Cancer Prev* 2015; **20**: 25-40 [PMID: 25853101 DOI: 10.15430/JCP.2015.20.1.25]
2 **Marques-Silva L**, Areia M, Elvas L, Dinis-Ribeiro M. Prevalence of gastric precancerous conditions: a systematic review and meta-analysis. *Eur J Gastroenterol Hepatol* 2014; **26**: 378-387 [PMID: 24569821 DOI:

10.1097/MEG.0000000000000065]
3 **Zhang L**, Liu Y, You P, Feng G. Occurrence of gastric cancer in patients with atrophic gastritis during long-term follow-up. *Scand J Gastroenterol* 2018; **53**: 843-848 [PMID: 29911441 DOI: 10.1080/00365521.2018.1477987]
4 **Li Y**, Zhang Y, Meng H, Liao M, Su Z, Zhai M, Jiang L, Li P, Ding X. Efficacy and safety of acupuncture therapy for chronic atrophic gastritis: A meta-analysis and trial sequential analysis protocol. *Medicine (Baltimore)* 2019; **98**: e17003 [PMID: 31464956 DOI: 10.1097/MD.0000000000017003]
5 **Wu RZ**, Chen JX, Xia L, Xu H, Yao LY, Fu HZ, Chen XL, Xie K. Clinical study on Tiepi Fengdou Granules (Capsules) in treating chronic atrophic gastritis with deficiency of qi and yin. *Shanghai Zhongyiyao Zazhi* 2004; **38**: 28-29 [DOI: 10.16305/j.1007-1334.2004.10.012]
6 **Jiang JY**, Liu DJ, Liu MX. The protective effect of NF-κB signaling pathway inhibitor PDTC on mice with chronic atrophic gastritis. *Scand J Gastroenterol* 2021; **56**: 1131-1139 [PMID: 34310252 DOI: 10.1080/00365521.2021.1953130]
7 **Qin R**, Wang NN, Chu J, Wang X. Expression and significance of homeodomain protein Cdx2 in gastric carcinoma and precancerous lesions. *World J Gastroenterol* 2012; **18**: 3296-3302 [PMID: 22783055 DOI: 10.3748/wjg.v18.i25.3296]
8 **Dixon MF**, Genta RM, Yardley JH, Correa P. Classification and grading of gastritis. The updated Sydney System. International Workshop on the Histopathology of Gastritis, Houston 1994. *Am J Surg Pathol* 1996; **20**: 1161-1181 [PMID: 8827022 DOI: 10.1097/00000478-199610000-00001]
9 **Khakoo SI**, Lobo AJ, Shepherd NA, Wilkinson SP. Histological assessment of the Sydney classification of endoscopic gastritis. *Gut* 1994; **35**: 1172-1175 [PMID: 7959220 DOI: 10.1136/gut.35.9.1172]
10 **Qi SN**, Xu S, Chen J, Lv NH. Lesion mutants of p53, MDM2 and PCNA protein expression in gastric mucosal and the relationship with helicobacter pylori infection. *Shandong Yiyao* 2009; **49**: 1-4
11 **Meng J**, Yang JX, Lu XF, Dai X, Fang J. Xiao Pi granules on the expression of Bcl-2 and bax in gastric mucosa of rats with Chronic atrophic gastritis and atypical hyperplasia. *Zhongguo Zhongxiyi Jiehe Xiaohua Zazhi* 2007; **15**: 214-217
12 **Meng J**, Yang JX, Lu XF, Dai X, Fang J. Xiao pi Granules on the expression of PCNA in rats with chronic atrophic gastritis with atypical hyperplasia. *Liaoning Zhongyi Zazhi* 2007; **33**: 369-371
13 **He XL**, Peng CF, Huang ZM, Guo LJ. The effect of Cynanchum auriculatum Royle ex Wight on the expression of p53 and PCNA protein in rats induced by chronic atrophic gastritis with atypical hyperplasia. *Shizhen Guoyi Guoyao* 2010; **21**: 2090-2391
14 **Jiang XY**, Qian LP, Zheng XJ, Xia YY, Jiang YB, Sun DY. Effect of Ginkgo biloba extract on proto-oncogene expression in rats with gastric mucosal precancerous lesions. *Weichangbingxue He Ganbingxue Zazhi* 2010; **19**: 982-984
15 **Zhu X**, Liu S, Zhou J, Wang H, Fu R, Wu X, Wang J, Lu F. Effect of Astragalus polysaccharides on chronic atrophic gastritis induced by N-methyl-N'-nitro-N-nitrosoguanidine in rats. *Drug Res (Stuttg)* 2013; **63**: 597-602 [PMID: 24026959 DOI: 10.1055/s-0033-1341518]
16 **Zhang J**, Huang K, Zhong G, Huang Y, Li S, Qu S, Zhang J. Acupuncture Decreases NF-κB p65, miR-155, and miR-21 and Increases miR-146a Expression in Chronic Atrophic Gastritis Rats. *Evid Based Complement Alternat Med* 2016; **2016**: 9404629 [PMID: 27293468 DOI: 10.1155/2016/9404629]
17 **Kubo Y**, Matsui H, Ninomiya T, Mizukami Y, Onji M. Non-invasive approach for diagnosing atrophic gastritis using the 13C-bicarbonate breath test. *Int J Mol Med* 2001; **7**: 381-384 [PMID: 11254877 DOI: 10.3892/ijmm.7.4.381]
18 **Yin J**, Yi J, Yang C, Xu B, Lin J, Hu H, Wu X, Shi H, Fei X. Chronic atrophic gastritis and intestinal metaplasia induced by high-salt and N-methyl-N'-nitro-N-nitrosoguanidine intake in rats. *Exp Ther Med* 2021; **21**: 315 [PMID: 33717258 DOI: 10.3892/etm.2021.9746]
19 **Zhao Y**, Liu Y, Lan XM, Xu GL, Sun YZ, Li F, Liu HN. Effect of *Dendrobium officinale* Extraction on Gastric Carcinogenesis in Rats. *Evid Based Complement Alternat Med* 2016; **2016**: 1213090 [PMID: 28119756 DOI: 10.1155/2016/1213090]
20 **Zhao Y**, Li B, Wang G, Ge S, Lan X, Xu G, Liu H. *Dendrobium officinale* Polysaccharides Inhibit 1-Methyl-2-Nitro-1-Nitrosoguanidine Induced Precancerous Lesions of Gastric Cancer in Rats through Regulating Wnt/β-Catenin Pathway and Altering Serum Endogenous Metabolites. *Molecules* 2019; **24** [PMID: 31340453 DOI: 10.3390/molecules24142660]
21 **Ding PJ**, Liu HY. Research progress of TCM treatment for Chronic Atrophic Gastritis. *Shiyong Zhongyi Neike Zazhi* 2010; **24**: 6-8
22 **Zeng J**, Ge Y, Guo H, Xia SJ. Treatment of pylori pyrolytic gastritis with the method of invigorating the spleen, soothing blood circulation and activating blood. *Jilin Zhongyiyao* 2017; **37**: 907-911 [DOI: 10.13463/j.cnki.jlzyy.2017.09.013]
23 **Liu XY**, Liu XM, Yang ZB. Clinical efficacy and mechanism of Fuzilizhong Decoction in the treatment of chronic atrophic gastritis intestinal metaplasia. *Yunnan Zhongyi Xueyuan Xuebao* 2016; **39**: 54-57
24 **Luo C**, Sun Z, Li Z, Zheng L, Zhu X. Notoginsenoside R1 (NGR1) Attenuates Chronic Atrophic Gastritis in Rats. *Med Sci Monit* 2019; **25**: 1177-1186 [PMID: 30757999 DOI: 10.12659/MSM.911512]
25 **Zhang J**, Wang H. Morroniside protects against chronic atrophic gastritis in rat *via* inhibiting inflammation and apoptosis. *Am J Transl Res* 2019; **11**: 6016-6023 [PMID: 31632569]
26 **Tian G**, Wu C, Li J, Liang B, Zhang F, Fan X, Li Z, Wang Y, Liu D, Lai-Han Leung E, Chen J. Network pharmacology based investigation into the effect and mechanism of Modified Sijunzi Decoction against the subtypes of chronic atrophic gastritis. *Pharmacol Res* 2019; **144**: 158-166 [PMID: 30991106 DOI: 10.1016/j.phrs.2019.04.012]
27 **Wu X**, Li X, Dang Z, Jia Y. Berberine demonstrates anti-inflammatory properties in Helicobacter pylori-infected mice with chronic gastritis by attenuating the Th17 response triggered by the B cell-activating factor. *J Cell Biochem* 2018; **119**: 5373-5381 [PMID: 29345340 DOI: 10.1002/jcb.26681]
28 **Hu Q**, Li L, Zou X, Xu L, Yi P. Berberine Attenuated Proliferation, Invasion and Migration by Targeting the AMPK/HNF4α/WNT5A Pathway in Gastric Carcinoma. *Front Pharmacol* 2018; **9**: 1150 [PMID: 30405404 DOI: 10.3389/fphar.2018.01150]
29 **Tong Y**, Zhao X, Wang R, Li R, Zou W, Zhao Y. Therapeutic effect of berberine on chronic atrophic gastritis based on plasma and urine metabolisms. *Eur J Pharmacol* 2021; **908**: 174335 [PMID: 34265298 DOI: 10.1016/j.ejphar.2021.174335]
30 **Zivny J**, Wang TC, Yantiss R, Kim KH, Houghton J. Role of therapy or monitoring in preventing progression to gastric

cancer. *J Clin Gastroenterol* 2003; **36**: S50-60; discussion S61 [PMID: 12702966 DOI: 10.1097/00004836-200305001-00009]

31 **Genta RM**, Graham DY. Intestinal metaplasia, not atrophy or achlorhydria, creates a hostile environment for Helicobacter pylori. *Scand J Gastroenterol* 1993; **28**: 924-928 [PMID: 8266024 DOI: 10.3109/00365529309103137]

32 **Genta RM**. Atrophy, metaplasia and dysplasia: are they reversible? *Ital J Gastroenterol Hepatol* 1998; **30** Suppl 3: S324-S325 [PMID: 10077766]

World Journal of Gastroenterology

Submit a Manuscript: https://www.f6publishing.com

World J Gastroenterol 2022 August 28; 28(32): 4681-4697

DOI: 10.3748/wjg.v28.i32.4681

ISSN 1007-9327 (print) ISSN 2219-2840 (online)

ORIGINAL ARTICLE

Retrospective Study

Machine learning predicts portal vein thrombosis after splenectomy in patients with portal hypertension: Comparative analysis of three practical models

Jian Li, Qi-Qi Wu, Rong-Hua Zhu, Xing Lv, Wen-Qiang Wang, Jin-Lin Wang, Bin-Yong Liang, Zhi-Yong Huang, Er-Lei Zhang

Specialty type: Gastroenterology and hepatology

Provenance and peer review: Unsolicited article; Externally peer reviewed.

Peer-review model: Single blind

Peer-review report's scientific quality classification

Grade A (Excellent): A
Grade B (Very good): B
Grade C (Good): C
Grade D (Fair): 0
Grade E (Poor): 0

P-Reviewer: Balakrishnan DS, India; El-Nakeep S, Egypt

Received: April 16, 2022
Peer-review started: April 16, 2022
First decision: May 12, 2022
Revised: May 25, 2022
Accepted: July 31, 2022
Article in press: July 31, 2022
Published online: August 28, 2022

Jian Li, Rong-Hua Zhu, Xing Lv, Wen-Qiang Wang, Jin-Lin Wang, Bin-Yong Liang, Zhi-Yong Huang, Er-Lei Zhang, Hepatic Surgery Center, Tongji Hospital, Tongji Medical College, Huazhong University of Science and Technology, Wuhan 430030, Hubei Province, China

Qi-Qi Wu, Department of Trauma Surgery, Tongji Hospital, Tongji Medical College, Huazhong University of Science and Technology, Wuhan 430030, Hubei Province, China

Corresponding author: Er-Lei Zhang, MD, Doctor, Department of Hepatic Surgery Center, Tongji Hospital, Tongji Medical College, Huazhong University of Science and Technology, No. 1095 Jiefang Avenue, Qiaokou District, Wuhan 430030, Hubei Province, China.
baiyu19861104@163.com

Abstract

BACKGROUND

For patients with portal hypertension (PH), portal vein thrombosis (PVT) is a fatal complication after splenectomy. Postoperative platelet elevation is considered the foremost reason for PVT. However, the value of postoperative platelet elevation rate (PPER) in predicting PVT has never been studied.

AIM

To investigate the predictive value of PPER for PVT and establish PPER-based prediction models to early identify individuals at high risk of PVT after splenectomy.

METHODS

We retrospectively reviewed 483 patients with PH related to hepatitis B virus who underwent splenectomy between July 2011 and September 2018, and they were randomized into either a training (n = 338) or a validation (n = 145) cohort. The generalized linear (GL) method, least absolute shrinkage and selection operator (LASSO), and random forest (RF) were used to construct models. The receiver operating characteristic curves (ROC), calibration curve, decision curve analysis (DCA), and clinical impact curve (CIC) were used to evaluate the robustness and clinical practicability of the GL model (GLM), LASSO model (LSM), and RF model (RFM).

RESULTS

Multivariate analysis exhibited that the first and third days for PPER (PPER1, PPER3) were strongly associated with PVT [odds ratio (OR): 1.78, 95% confidence interval (CI): 1.24-2.62, P = 0.002; OR: 1.43, 95%CI: 1.16-1.77, P < 0.001, respectively]. The areas under the ROC curves of the GLM, LSM, and RFM in the training cohort were 0.83 (95%CI: 0.79-0.88), 0.84 (95%CI: 0.79-0.88), and 0.84 (95%CI: 0.79-0.88), respectively; and were 0.77 (95%CI: 0.69-0.85), 0.83 (95%CI: 0.76-0.90), and 0.78 (95%CI: 0.70-0.85) in the validation cohort, respectively. The calibration curves showed satisfactory agreement between prediction by models and actual observation. DCA and CIC indicated that all models conferred high clinical net benefits.

CONCLUSION

PPER1 and PPER3 are effective indicators for postoperative prediction of PVT. We have successfully developed PPER-based practical models to accurately predict PVT, which would conveniently help clinicians rapidly differentiate individuals at high risk of PVT, and thus guide the adoption of timely interventions.

Key Words: Portal hypertension; Splenectomy; Portal vein thrombosis; Postoperative platelet elevation rate; Practical model; Machine learning

©The Author(s) 2022. Published by Baishideng Publishing Group Inc. All rights reserved.

Core Tip: For patients with portal hypertension related to hepatitis B virus, postoperative platelet elevation rate (PPER) is an important predictor of the formation of portal vein thrombosis (PVT) after splenectomy. This study was the first to construct PPER-based practical models for predicting PVT, which would be helpful for clinicians to recognize individuals at high risk of PVT as soon as possible.

Citation: Li J, Wu QQ, Zhu RH, Lv X, Wang WQ, Wang JL, Liang BY, Huang ZY, Zhang EL. Machine learning predicts portal vein thrombosis after splenectomy in patients with portal hypertension: Comparative analysis of three practical models. *World J Gastroenterol* 2022; 28(32): 4681-4697
URL: https://www.wjgnet.com/1007-9327/full/v28/i32/4681.htm
DOI: https://dx.doi.org/10.3748/wjg.v28.i32.4681

INTRODUCTION

Liver cirrhosis is recognized as an extremely important and rapidly increasing disease burden in the world[1]. In the progressive stage of liver cirrhosis, the complications caused by portal hypertension (PH), including esophagogastric variceal bleeding and hypersplenism, pose a great threat to the patients' life and health[2,3]. Liver transplantation is currently recommended as a curative treatment for liver cirrhosis combined with PH; however, due to the shortage of liver sources and high transplantation cost, its clinical practicability is limited[4,5]. Transjugular intrahepatic portosystemic shunt seems to be a gospel for PH, but unfortunately, restenosis or/and hepatic encephalopathy will occur in more than 60% of patients[6,7]. In Asia, splenectomy (or combined with devascularization) has been widely adopted as an effective treatment for hypersplenism or esophageal and gastric variceal bleeding caused by PH[8,9].

Portal vein thrombosis (PVT) is often defined as thrombosis within the portal vein trunk or intrahepatic portal branches, with or without the splenic vein or superior mesenteric vein involvement [10,11]. PVT is considered a dreaded complication after splenectomy for patients with PH[12], and the probability of PVT has been reported to be 4.8%-51.5%[13-15]. For patients with acute PVT and PVT resulting in superior mesenteric vein thrombosis, it has been reported that PVT may be closely associated with acute liver failure and could influence mortality[16]. Hence, strategies are needed to prevent PVT in patients who underwent splenectomy. In clinical practice, anticoagulation is a critical method for the prevention and treatment of PVT in patients after splenectomy. However, when the anticoagulation therapy should be started remains controversial. Early anticoagulation may result in life-threatening bleeding events for patients with liver cirrhosis. Whether anticoagulant therapy should be prescribed to all patients after splenectomy deserves careful consideration. In addition, the majority of patients with PVT are asymptomatic and only a few experience abdominal discomfort[12]. Therefore, there is an urgent requirement to find effective diagnostic methods to early and rapidly identify individuals with high risk of PVT after splenectomy, and then further guide clinicians to take intervention measures. Color Doppler ultrasonography and/or contrast-enhanced computed

tomography (CT) is commonly applied for the final diagnosis of PVT[17]; however, they seem to be useless for screening out the high-risk individuals who are vulnerable to PVT. Given this, many scholars attempted to investigate the risk factors closely related to the occurrence of PVT after splenectomy[8,18-21]. Several investigators paid attention to the fact that preoperative low platelet count (PLT) and postoperative high PLT may be crucial predictors of the risk of PVT postoperatively[19,22].

Generally speaking, patients with PH will experience rebounding rises in PLT after splenectomy[23], combined with hemodynamic changes in the portal venous system, and thus these patients are highly prone to developing PVT[24]. However, the effect of the amplitude of sharp postoperative rises in PLT on PVT has received little attention. We speculated that the postoperative platelet elevation rate (PPER) should be an important predictor of PVT. To the best of our knowledge, there are no reports on the relationship between PPER and PVT.

In recent years, to meet the urgent demand of finding effective methods to predict PVT after splenectomy, several studies have attempted to construct predictive models for PVT after splenectomy in patients with cirrhosis using multivariate regression analysis[25,26]. However, there are few clinical variables included in the analysis and the accuracy of these prediction models is still unsatisfactory. Therefore, there is an urgent need for an efficient and accurate visualization model.

Nowadays, novel machine learning algorithms based on more clinical features have shown great potential in various aspects of medical research, especially in the construction of predictive models, and the features screened for model construction are clinically interpretable[27-29]. Gao *et al*[28] constructed four machine learning models based on 53 raw clinical features of coronavirus disease 2019 patients to distinguish individuals at high risk for mortality, with an area under the receiver operating characteristics (ROC) curve (AUC) of 0.976. Kawakami *et al*[29] developed seven supervised machine learning classifiers based on 32 clinical parameters, among which the random forest (RF) model showed the best performance in distinguishing epithelial ovarian cancer from benign ovarian tumors with an AUC of 0.968. The wide range of applications of machine learning methods has surpassed conventional statistical analysis due to their higher accuracy, which might enable machine learning to be increasingly applied in the field of medical research[30-32]. Although compared with traditional multivariate analysis methods, machine learning algorithms have overwhelming advantages in constructing clinical prediction models, so far, only Wang *et al*[33] have tried to construct a prediction model of PVT after splenectomy in cirrhotic patients with PH using machine learning algorithms. The model that they constructed has greatly improved the prediction efficiency compared with the traditional models. However, the clinical parameters involved in the construction of the model are extremely complex, which limits its clinical use.

Therefore, the purpose of this study was to evaluate the predictive value of PPER for the risk of PVT after splenectomy for patients with PH. In addition, we sought to build simple, efficient, and accurate practical models for predicting PVT with machine learning algorithms to facilitate assisting clinicians in the early identification of individuals at high risk of PVT after splenectomy and taking intervention measures in time. We present the following article in accordance with the TRIPOD reporting checklist.

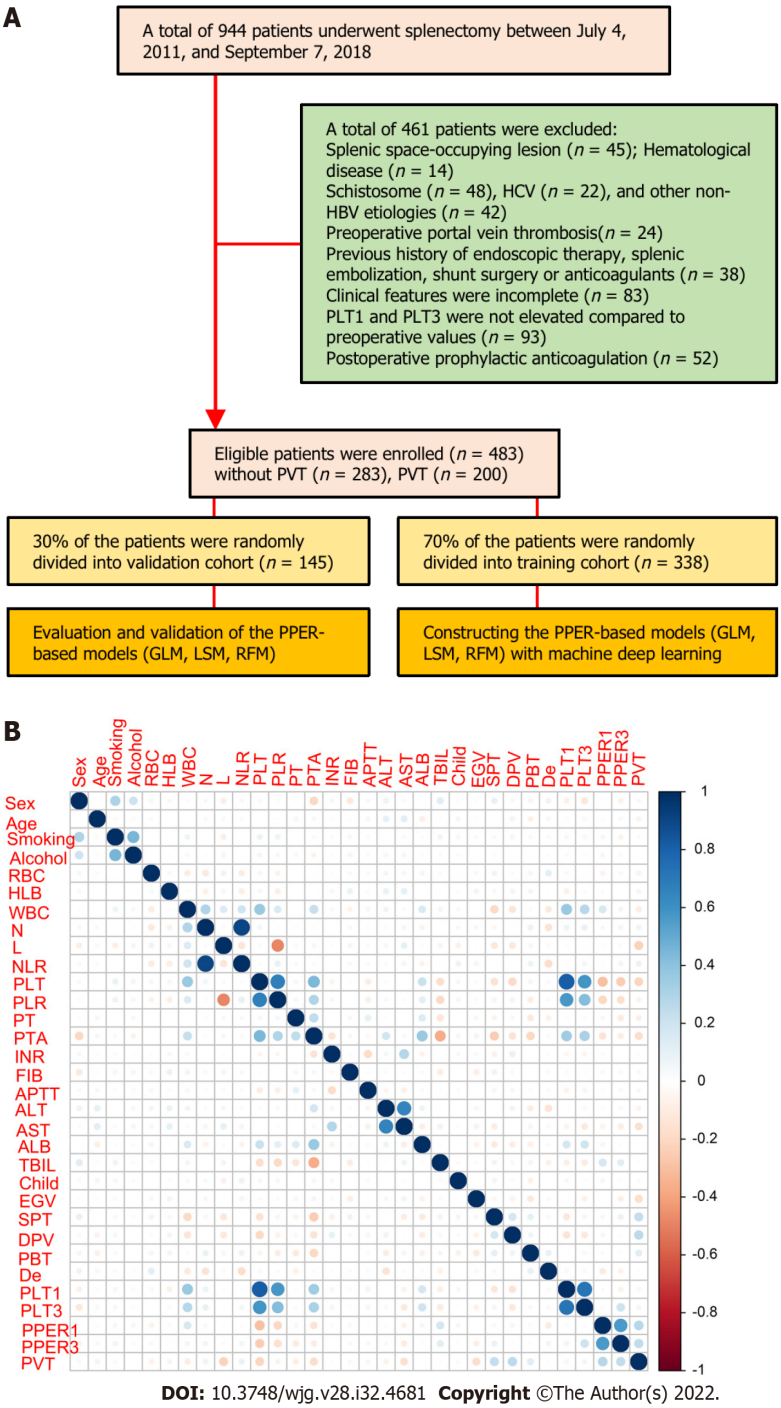
MATERIALS AND METHODS

Study population

We retrospectively recruited 944 consecutive patients aged no less than 18 years who underwent splenectomy at our institution between July 4, 2011 and September 7, 2018. The patients with the following conditions were excluded: (1) Splenic space-occupying lesion; (2) Hematological disease; (3) PH caused by non-hepatitis B virus (HBV) related etiologies, such as schistosome, hepatitis C virus, or other unknown causes; (4) Presence of PVT confirmed by preoperative imaging; (5) Previous history of endoscopic therapy, splenic embolization, shunt surgery, or anticoagulants; (6) Incomplete clinical features; (7) Unelevated PLT on the first (PLT1) and third day (PLT3) after the operation compared to the preoperative values; and (8) Receiving prophylactic anti-coagulant therapy after splenectomy. Finally, a total of 483 patients with PH interrelated to HBV were included in this study. The flow diagram of patient selection and study design is shown in Figure 1A. The study was approved by the Medical Ethics Committee of Tongji Medical College, Huazhong University of Science and Technology. Owing to the retrospective nature of this study, written informed consent was waived.

Data collection

All the patients' clinical features were acquired from the electronic medical record system in our institution, which mainly included sex, age, smoking and drinking history, previous treatment history, etiologies, blood biochemical parameters, and imaging information. The blood biochemical parameters included routine blood tests [red blood cells (RBC), reference interval: 4.30-5.80 × 10^{12}/L; hemoglobin, reference interval: 130.0-175.0 g/L; white blood cells (WBC), reference interval: 3.50-9.50 × 10^{9}/L; neutrophil count (N), reference interval: 1.80-6.30 × 10^{9}/L; lymphocyte count (L), reference interval: 1.10-3.20 × 10^{9}/L; neutrophil to lymphocyte ratio (NLR); PLT, reference interval: 125.0-350.0 × 10^{9}/L; platelet to lymphocyte ratio], coagulation function [prothrombin time, reference interval: 11.5-14.5 s;



DOI: 10.3748/wjg.v28.i32.4681 **Copyright** ©The Author(s) 2022.

Figure 1 Flow chart and correlation chart. A: Flow diagram of patient selection and study design; B: Correlation matrix between candidate variables. The size and color of the circle in the matrix reflect the correlation between the corresponding variables. The darker the blue, the stronger the positive correlation between variables, and the darker the red, the stronger the negative correlation between variables. HCV: Hepatitis C virus; HBV: Hepatitis B virus; PLT1 and PLT3: Platelet counts on the first and third days after operation; PVT: Portal vein thrombosis; GLM: Generalized linear model; LSM: Least absolute shrinkage and selection operator model; RFM: Random forest model; RBC: Red blood cells; HLB: Hemoglobin; WBC: White blood cells; N: Neutrophil count; L: Lymphocyte count; NLR: Neutrophil to lymphocyte ratio; PLT: Platelet count; PLR: Platelet to lymphocyte ratio; PT: Prothrombin time; PTA: Prothrombin activity; INR: International normalized ratio; FIB: Fibrinogen; APTT: Activated partial thromboplastin time; ALT: Alanine aminotransaminase; AST: Aspartate aminotransaminase; ALB: Serum albumin; TBIL: Total serum bilirubin; Child: Child-Pugh grade; EGV: Esophageal and gastric varices; SPT: Spleen thickness; DPV: Diameter of the portal vein; PBT: Preoperative blood transfusion; De: Devascularization; PPER1: Platelet elevation rate at postoperative day 1; PPER3: Platelet elevation rate at postoperative day 3.

prothrombin activity (PTA), reference interval: 75.0%-125.0%; international normalized ratio, reference interval: 0.80-1.20; fibrinogen, reference interval: 2.00-4.00 g/L; activated partial thromboplastin time, reference interval: 29.0-42.0 s], and liver function [alanine aminotransaminase (ALT), reference interval: ≤ 41 U/L; aspartate aminotransaminase (AST), reference interval: ≤ 40 U/L; serum albumin, reference interval: 35.0-52.0 g/L; serum total bilirubin, reference interval: ≤ 26 μmol/L] within 7 d before surgery, as well as PLT1 and PLT3. The preoperative Child-Pugh grade was divided into three levels of A, B, and

C[34], with grade C excluded. Information on the esophageal and gastric varices (EGV), spleen thickness (SPT), diameter of the portal vein (DPV), and preoperative blood transfusion (PBT) within 7 d before the operation was also collected.

Definition of variables

We diagnosed PVT by color Doppler ultrasound examination[35] and contrast-enhanced CT would be applied as an auxiliary examination when its diagnosis was questioned[36]. In this study, abdominal ultrasound and contrast-enhanced CT examinations were routinely performed within 7 d before the operation. Routine ultrasonography was performed on the 7th day after the operation[19,20], or at any time when there were suspected clinical symptoms of PVT such as fever, severe abdominal pain, vomiting, abnormal liver function, and leukocytosis[12].

According to the definition of varices[8], EGV was divided into EGV without varices and EGV with varices in this study. SPT was defined as the vertical distance between the splenic hilum and the cut point of the lateral margin, and DPV was measured as the largest anteroposterior diameter at the point of intersection with the hepatic artery, during the patient's breath holding[37].

The PPER was calculated from the preoperative PLT and postoperative PLT. For example, PPER1 (at the first day) was calculated as (PLT1 - PLT)/ PLT × 100%, and PPER3 (at the third day) was calculated as (PLT3 - PLT)/ PLT × 100%.

Development of models

All candidates were randomly divided into two parts by using the "caret" package, of which 70% were assigned to a training cohort and 30% were assigned to a validation cohort. All model building was performed in the training cohort. Multivariate forward stepwise logistic regression analysis was used to select valuable variables to construct the generalized linear model (GLM). The least absolute shrinkage and selection operator (LASSO) was a well-established shrinkage method that can effectively screen meaningful variables from a large set of variables with potential multicollinearity to develop the LASSO model (LSM)[38], which was implemented by using the "glmnet" package. RF was composed of a great number of individual decision trees running as a whole[39]. These multifarious decision tree models were applied for the construction of the RF model (RFM)[40]. The importance of candidate variables was reflected by the mean decreased Gini (MDG) score.

Evaluation of models

The robustness and clinical practicability of models were assessed using the ROC curve, calibration curve, decision curve analysis (DCA), and clinical impact curve (CIC). The AUC were used to estimate the discernment of each model by using "rms" packages. The calibration curves were applied to examine the calibration ability of each model and calibrated with 1000 bootstrap samples to reduce overfitting bias. The clinical applicability of each model was informed by DCA and CIC using "rms" and "rmda" packages.

Statistical analysis

Statistical analyses were performed with R Statistical Software (version 4.1.2, https://www.r-project.org/). Continuous variables were tested for normality. Those with normality are described as the mean ± SD, while those without normality are described as the median and interquartile range. Continuous variables were compared using the student's *t*-test or non-parametric rank-sum test (Kruskal-Wallis test) as appropriate. Categorical variables are described as numbers (percentage) and were compared using the Chi-square test or Fisher exact test as appropriate. Correlations between candidate variables were determined by Spearman's correlation coefficient. All statistical tests were two-tailed, and $P < 0.05$ was considered significant.

RESULTS

Patient demographics and characteristics

The detailed clinical characteristics of 483 patients with PH are summarized in Table 1. All participants were randomly and automatically divided into a training cohort (n = 338, 70%) and a validation cohort (n = 145, 30%). The presence of PVT was diagnosed in 200 (41.4%) cases, 135 (39.9%) cases, and 65 (44.8%) cases in the overall cohort, training cohort, and verification cohort, respectively. Consistent with the results of the intergroup comparison, among the 31 candidate variables included, 14 were associated with PVT, including RBC, WBC, L, NLR, PLT, PTA, ALT, AST, EGV, SPT, DPV, PBT, PPER1, and PPER3 (Figure 1B and Supplementary Table 1), which indicated that PPER1 and PPER3 were highly likely to be potential predictors of PVT.

Logistic regression analysis

Univariate and multivariate logistic regression analyses for risk factors associated with PVT in the

Table 1 Detailed clinical characteristics of 483 patients with portal hypertension

Variable	Training cohort			Validation cohort		
	Without PVT (*n* = 203)	PVT (*n* =135)	*P* value	Without PVT (*n* = 80)	PVT (*n* = 65)	*P* value
Sex, *n* (%)			0.312			0.86
Female	69 (34.0)	38 (28.1)		20 (25.0)	18 (27.7)	
Male	134 (66.0)	97 (71.9)		60 (75.0)	47 (72.3)	
Age, *n* (%)			0.179			0.999
< 60 yr	165 (81.3)	118 (87.4%)		71 (88.8)	58 (89.2)	
≥ 60 yr	38 (18.7)	17 (12.6%)		9 (11.2)	7 (10.8)	
Smoking, *n* (%)			0.703			0.983
No	167 (82.3)	108 (80.0)		64 (80.0)	51 (78.5)	
Yes	36 (17.7)	27 (20.0)		16 (20.0)	14 (21.5)	
Alcohol, *n* (%)			0.577			0.587
No	167 (82.3)	115 (85.2)		69 (86.2)	53 (81.5)	
Yes	36 (17.7)	20 (14.8)		11 (13.8)	12 (18.5)	
RBC[1] (× 10^{12}/L)	3.59 (3.20-3.93)	3.57 (3.21-3.90)	0.69	3.74 (3.49-4.02)	3.55 (3.22-3.93)	0.044
HLB[1] (g/L)	89.3 (78.1-103)	93.2 (82.1-104)	0.093	89.5 (79.5-107)	91.1 (82.8-101)	0.965
WBC[1] (× 10^{9}/L)	2.51 (1.83-3.40)	2.18 (1.48-2.87)	0.007	2.46 (1.95-3.21)	2.09 (1.58-2.92)	0.06
N[1] (× 10^{9}/L)	1.35 (0.98-2.09)	1.27 (0.85-2.00)	0.177	1.38 (1.06-1.98)	1.15 (0.87-1.77)	0.147
L[1] (× 10^{9}/L)	0.79 (0.56-1.14)	0.50 (0.38-0.79)	< 0.001	0.78 (0.51-1.11)	0.63 (0.45-0.91)	0.045
NLR[1]	1.78 (1.18-2.99)	2.43 (1.42-4.18)	0.003	1.90 (1.23-3.08)	2.16 (1.39-3.16)	0.559
PLT[1] (× 10^{9}/L)	48.0 (36.0-64.5)	33.8 (26.0-47.9)	< 0.001	46.0 (32.1-57.0)	35.0 (27.0-48.0)	0.012
PLR[1]	60.6 (43.4-97.0)	72.5 (35.0-99.7)	0.779	55.6 (37.9-91.3)	58.8 (31.8-86.8)	0.692
PT[1] (s)	15.5 (14.1-16.6)	15.3 (12.9-16.4)	0.221	15.7 (14.4-16.3)	15.3 (13.9-16.2)	0.294
PTA[1] (%)	64.0 (57.0-73.5)	60.0 (50.0-69.0)	< 0.001	67.0 (57.0-73.0)	63.0 (54.0-72.0)	0.269
INR[1]	1.34 (1.23-1.47)	1.42 (1.29-1.62)	< 0.001	1.32 (1.23-1.50)	1.36 (1.23-1.50)	0.519
FIB[1] (g/L)	2.35 (1.62-3.86)	2.52 (1.82-3.78)	0.269	2.29 (1.74-4.14)	2.57 (1.83-3.62)	0.764
APTT[1] (s)	40.7 (37.5-44.8)	40.6 (36.9-44.9)	0.787	41.3 (37.9-44.3)	41.0 (38.5-44.1)	0.822
ALT[1] (U/L)	22.0 (16.0-30.5)	21.0 (15.0-28.0)	0.578	25.5 (17.8-40.0)	18.0 (15.0-27.0)	0.007
AST[1] (U/L)	29.0 (22.0-40.0)	25.0 (22.0-35.0)	0.021	30.5 (24.8-43.5)	25.0 (21.0-34.0)	0.009
ALB[1] (g/L)	35.9 (32.7-39.5)	35.8 (32.6-39.5)	0.881	35.7 (33.1-38.3)	36.4 (33.7-39.6)	0.551
TBIL[1] (μmol/L)	18.1 (12.4-24.6)	18.8 (12.4-27.0)	0.671	18.8 (13.6-24.6)	18.0 (14.4-26.1)	0.796
Child-Pugh grade, *n* (%)			0.644			0.999
A	146 (71.9)	101 (74.8)		58 (72.5)	48 (73.8)	
B	57 (28.1)	34 (25.2)		22 (27.5)	17 (26.2)	
EGV, *n* (%)			0.023			0.001
No	67 (33.0)	62 (45.9)		17 (21.2)	32 (49.2)	
Yes	136 (67.0)	73 (54.1)		63 (78.8)	33 (50.8)	
SPT[1] (cm)	5.50 (4.60-6.40)	6.40 (5.40-7.55)	< 0.001	5.70 (4.45-6.70)	6.30 (5.30-7.30)	0.034
DPV[1] (cm)	1.30 (1.10-1.40)	1.50 (1.25-1.70)	< 0.001	1.30 (1.10-1.50)	1.40 (1.20-1.60)	0.088
PBT, *n* (%)			0.126			0.023

No	159 (78.3)	95 (70.4)		67 (83.8)	43 (66.2)	
Yes	44 (21.7)	40 (29.6)		13 (16.2)	22 (33.8)	
De, *n* (%)			0.457			0.344
No	16 (7.88)	7 (5.19)		4 (5.00)	6 (9.23)	
Yes	187 (92.1)	128 (94.8)		76 (95.0)	59 (90.8)	
PLT1[1] (× 10^9/L)	79.0 (61.0-106)	79.0 (64.0-102)	0.866	74.0 (57.7-93.8)	77.0 (61.0-102)	0.418
PLT3[1] (× 10^9/L)	103 (78.5-158)	117 (85.0-164)	0.131	98.5 (75.5-140)	112 (81.0-156)	0.122
PPER1[1] (%)	0.59 (0.34-0.88)	1.18 (0.57-2.31)	< 0.001	0.70 (0.36-1.11)	0.87 (0.64-2.03)	0.002
PPER3[1] (%)	1.15 (0.62-2.02)	2.38 (1.52-3.87)	< 0.001	1.32 (0.79-2.04)	2.29 (1.36-3.54)	< 0.001

[1]Continuous variables are presented as the median and interquartile range (IQR).

PH: Portal hypertension; PVT: Portal vein thrombosis; RBC: Red blood cells; HLB: Hemoglobin; WBC: White blood cells; N: Neutrophil count; L: Lymphocyte count; NLR: Neutrophil to lymphocyte ratio; PLT: Platelet count; PLR: Platelet to lymphocyte ratio; PT: Prothrombin time; PTA: Prothrombin activity; INR: International normalized ratio; FIB: Fibrinogen; APTT: Activated partial thromboplastin time; ALT: Alanine aminotransaminase; AST: Aspartate aminotransaminase; ALB: Serum albumin; TBIL: Total serum bilirubin; EGV: Esophageal and gastric varices; SPT: Spleen thickness; DPV: Diameter of the portal vein; PBT: Preoperative blood transfusion; De: Devascularization; PLT1: Platelet count at postoperative day 1; PLT3: Platelet count at postoperative day 3; PPER1: Platelet elevation rate at postoperative day 1; PPER3: Platelet elevation rate at postoperative day 3.

overall cohort are presented in Table 2. In the univariate analysis, a total of 11 variables with $P < 0.05$ were included in the further multivariate analysis. Finally, the following six variables were revealed to be closely associated with the occurrence of PVT: L [odds ratio (OR): 0.28, 95% confidence interval (CI): 0.14-0.54, $P < 0.001$], EGV (OR: 0.51, 95%CI: 0.32-0.79, $P = 0.003$), SPT (OR: 1.22, 95%CI: 1.06-1.40, $P = 0.005$), DPV (OR: 3.57, 95%CI: 1.86-7.03, $P < 0.001$), PPER1 (OR: 1.78, 95%CI: 1.24-2.62, $P = 0.002$), and PPER3 (OR: 1.43, 95%CI: 1.16-1.77, $P < 0.001$). This result demonstrated that PPER1 and PPER3 were independent risk factors for the occurrence of PVT.

Establishment of PPER-based models

As shown in Supplementary Table 2, the following five variables strongly associated with PVT were chosen to construct the GLM: L (OR: 0.34, 95%CI: 0.14-0.77, $P = 0.01$), SPT (OR: 1.21, 95%CI: 1.02-1.44, $P = 0.02$), DPV (OR: 5.85, 95%CI: 2.57-14.05, $P < 0.001$), PPER1 (OR: 1.77, 95%CI: 1.13-2.82, $P = 0.01$), and PPER3 (OR: 1.42, 95%CI: 1.12-1.84, $P = 0.005$). The optimal LSM was obtained when all 31 candidate variables were shrunk to 10 through the LASSO (Figure 2A and B), which included L, NLR, PLT, PTA, AST, EGV, SPT, DPV, PPER1, and PPER3. In the RF, the total sample group had the smallest error of 24.56%, when the number of random trees was 133 (Figure 2C). A total of 133 random trees were set and passed through five iterations, and the importance scores of the candidate variables are presented in Figure 2D. Ultimately, nine variables with higher MDG scores were selected to construct the RFM.

Assessment and verification of PPER-based models

The ROC curves of the GLM, LSM, and RFM in the training cohort are shown in Figure 3A, and their AUCs were 0.83 (95%CI: 0.79-0.88), 0.84 (95%CI: 0.79-0.88), and 0.84 (95%CI: 0.79-0.88), respectively. All models had excellent calibration ability in the training cohort (Figure 3B). DCA and CIC revealed that they both conferred high clinical net benefits (Figures 3C and 4A-C).

In the validation cohort, the ROC curves of all models are presented in Figure 3D, and their AUC were 0.77 (95%CI: 0.69-0.85), 0.83 (95%CI: 0.76-0.90), and 0.78 (95%CI: 0.70-0.85), respectively. All models demonstrated highly satisfactory calibration capability and clinical functionality (Figures 3E and F and 4D-F).

Importance of PPER for models

As shown in Figure 5A, the nomogram for GLM recruited a total of five variables, including L, SPT, DPV, PPER1, and PPER3, which happened to be the intersection variables of the GLM, LSM, and RFM (Figure 5B). From this, it appeared that the aforementioned variables were significant predictors of the occurrence of PVT and they produced remarkable effects on the construction of the models. Moreover, the present study revealed that among these variables shared by the GLM, LSM, and RFM, the order of weight from high to low was DPV, PPER1, PPER3, SPT, and L (Figure 5C), which fully promulgated the predictive value of the PPER (PPER1 and PPER3) for PVT in all models.

Comparative analysis of PPER-based models

The performance of three PPER-based models in predicting PVT in different cohorts is shown in Table 3. In the overall cohort, the accuracy of the GLM, LSM, and RFM was 76.2%, 77.4%, and 77.4% respectively. In the training cohort, the accuracy of the GLM, LSM, and RFM was 79.6%, 79.0%, and

Table 2 Univariate and multivariate logistic regression analyses for risk factors associated with portal vein thrombosis in the overall cohort

Variable	Univariate		Multivariate[1]	
	OR (95%CI)	*P* value	OR (95%CI)	*P* value
Sex (female *vs* male)	1.18 (0.79-1.76)	0.42		
Age (< *vs* ≥ 60 yr)	0.68 (0.40-1.16)	0.16		
Smoking (no *vs* yes)	1.15 (0.73-1.81)	0.56		
Alcohol (no *vs* yes)	0.96 (0.59-1.56)	0.86		
RBC[2] (× 10^{12}/L)	0.71 (0.44-1.14)	0.16		
HLB[2] (g/L)	1.01 (0.99-1.02)	0.22		
WBC[2] (× 10^9/L)	0.87 (0.76-1.00)	0.05		
N[2] (× 10^9/L)	1.05 (0.98-1.12)	0.20		
L[2] (× 10^9/L)	0.27 (0.16-0.45)	< 0.001	0.28 (0.14-0.54)	< 0.001
NLR[2]	1.07 (1.01-1.14)	0.03	1.03 (0.98-1.11)	0.42
PLT[2] (× 10^9/L)	0.98 (0.97-0.99)	< 0.001	0.99 (0.98-1.01)	0.98
PLR[2]	1.00 (1.00-1.00)	0.18		
PT[2] (s)	0.94 (0.89-1.00)	0.07		
PTA[2] (%)	0.97 (0.96-0.99)	< 0.001	0.99 (0.98-1.02)	0.73
INR[2]	0.98 (0.88-1.09)	0.74		
FIB[2] (g/L)	1.06 (0.93-1.21)	0.42		
APTT[2] (s)	0.99 (0.96-1.01)	0.38		
ALT[2] (U/L)	0.99 (0.98-1.00)	0.16		
AST[2] (U/L)	0.98 (0.97-0.99)	< 0.001	0.99 (0.98-1.00)	0.14
ALB[2] (g/L)	1.00 (0.97-1.04)	0.97		
TBIL[2] (μmol/L)	1.00 (0.99-1.02)	0.78		
Child-Pugh (A *vs* B)	0.88 (0.59-1.33)	0.56		
EGV (no *vs* yes)	0.48 (0.33-0.69)	< 0.001	0.51 (0.32-0.79)	0.003
SPT[2] (cm)	1.34 (1.19-1.50)	< 0.001	1.22 (1.06-1.40)	0.005
DPV[2] (cm)	4.72 (2.69-8.29)	< 0.001	3.57 (1.86-7.03)	< 0.001
PBT (no *vs* yes)	1.78 (1.17-2.70)	0.01	1.33 (0.79-2.26)	0.28
De (no *vs* yes)	1.09 (0.53-2.25)	0.81		
PLT1[2] (× 10^9/L)	1.00 (0.99-1.00)	0.32		
PLT3[2] (× 10^9/L)	1.00 (1.00-1.00)	0.25		
PPER[2] (%)	2.77 (2.1-3.66)	< 0.001	1.78 (1.24-2.62)	0.002
PPER3[2] (%)	1.86 (1.58-2.19)	< 0.001	1.43 (1.16-1.77)	< 0.001

[1]Forward stepwise analysis.
[2]Continuous variables.
PVT: Portal vein thrombosis; OR: Odds ratio; CI: Confidence interval; RBC: Red blood cells; HLB: Hemoglobin; WBC: White blood cells; N: Neutrophil count; L: Lymphocyte count; NLR: Neutrophil to lymphocyte ratio; PLT: Platelet count; PLR: Platelet to lymphocyte ratio; PT: Prothrombin time; PTA: Prothrombin activity; INR: International normalized ratio; FIB: Fibrinogen; APTT: Activated partial thromboplastin time; ALT: Alanine aminotransaminase; AST: Aspartate aminotransaminase; ALB: Serum albumin; TBIL: Total serum bilirubin; EGV: Esophageal and gastric varices; SPT: Spleen thickness; DPV: Diameter of the portal vein; PBT: Preoperative blood transfusion; De: Devascularization; PLT1: Platelet count at postoperative day 1; PLT3: Platelet count at postoperative day 3; PPER1: Platelet elevation rate at postoperative day 1; PPER3: Platelet elevation rate at postoperative day 3.

78.7% respectively. In the validation cohort, the accuracy of the GLM, LSM, and RFM was 74.5%, 79.3%, and 76.6% respectively. When other metrics of the models, such as AUC, sensitivity, specificity, positive predictive value, negative predictive value, kappa values, and Brier scores, were comprehensively

Table 3 Performance of models for portal vein thrombosis risk prediction in different cohorts

	AUC (95%CI)	Sensitivity (95%CI)	Specificity (95%CI)	PPV (95%CI)	NPV (95%CI)	Accuracy (%)	F1	Kappa	Brier
Overall cohort									
GLM	0.812 (0.773-0.851)	0.710 (0.642-0.772)	0.799 (0.747-0.844)	0.714 (0.650-0.775)	0.796 (0.740-0.841)	76.2	0.712	0.509	0.169
LSM	0.822 (0.784-0.861)	0.640 (0.569-0.706)	0.869 (0.824-0.906)	0.776 (0.709-0.824)	0.774 (0.718-0.832)	77.4	0.701	0.522	0.163
RFM	0.814 (0.775-0.854)	0.665 (0.595-0.730)	0.852 (0.805-0.891)	0.760 (0.695-0.812)	0.782 (0.727-0.837)	77.4	0.709	0.526	0.168
Training cohort									
GLM	0.833 (0.787-0.879)	0.674 (0.588-0.752)	0.877 (0.824-0.919)	0.784 (0.705-0.842)	0.802 (0.736-0.865)	79.6	0.725	0.564	0.157
LSM	0.839 (0.794-0.884)	0.733 (0.650-0.806)	0.828 (0.768-0.877)	0.739 (0.662-0.810)	0.824 (0.759-0.874)	79.0	0.736	0.562	0.153
RFM	0.838 (0.793-0.883)	0.756 (0.674-0.825)	0.808 (0.747-0.860)	0.723 (0.647-0.800)	0.832 (0.769-0.879)	78.7	0.739	0.559	0.154
Validation cohort									
GLM	0.769 (0.691-0.846)	0.646 (0.518-0.761)	0.825 (0.724-0.901)	0.750 (0.625-0.839)	0.742 (0.628-0.847)	74.5	0.694	0.477	0.190
LSM	0.826 (0.755-0.897)	0.708 (0.582-0.814)	0.863 (0.767-0.929)	0.807 (0.687-0.883)	0.784 (0.676-0.884)	79.3	0.754	0.577	0.163
RFM	0.777 (0.700-0.853)	0.631 (0.502-0.747)	0.875 (0.782-0.938)	0.804 (0.678-0.876)	0.745 (0.632-0.864)	76.6	0.707	0.516	0.187

AUC: Area under the receiver operating characteristics curve; CI: Confidence interval; PPV: Positive predictive value; NPV: Negative predictive value; GLM: Generalized linear model; LSM: Least absolute shrinkage and selection operator model; RFM: Random forest model.

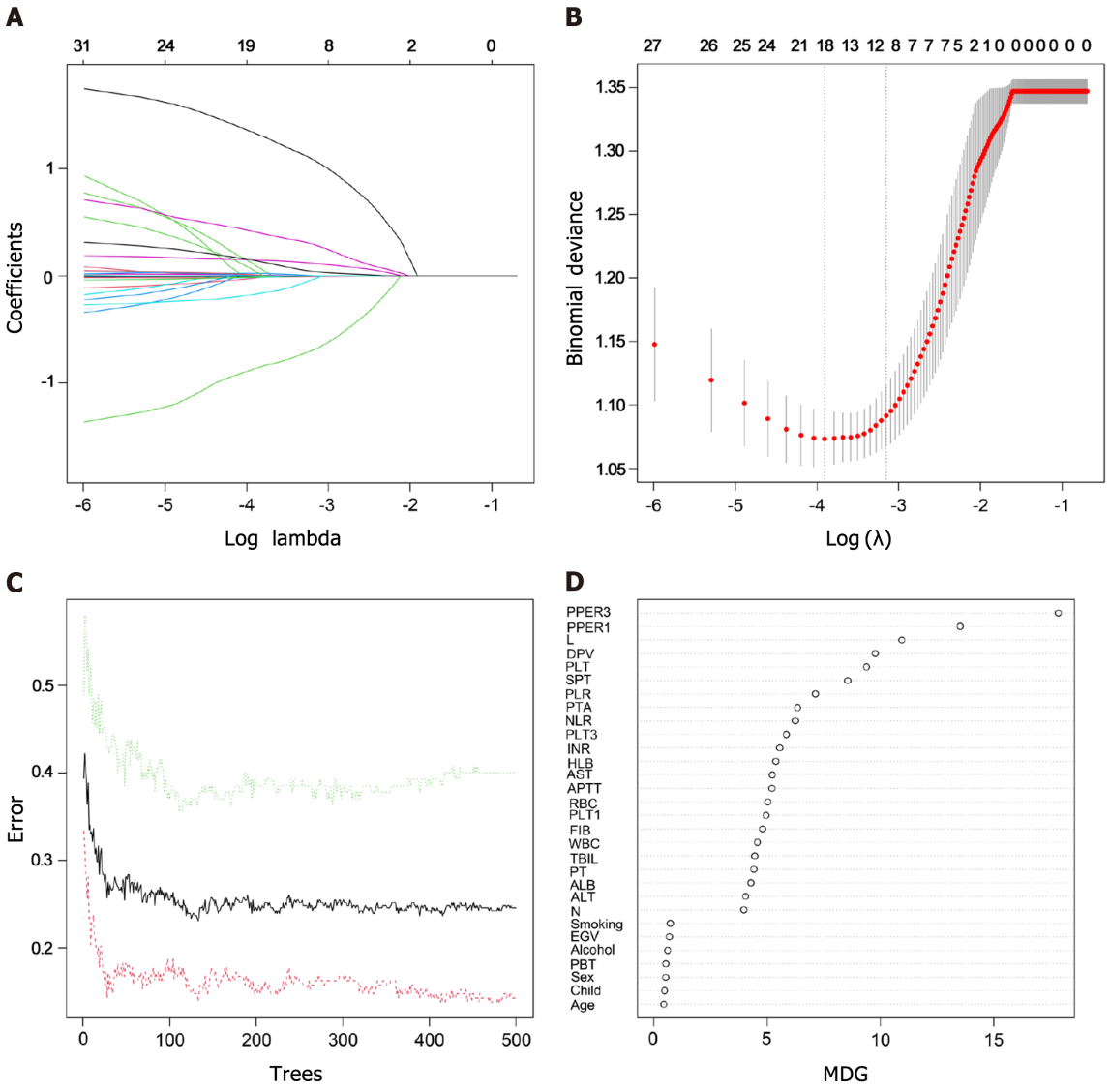
considered, the LSM and RFM appeared to be slightly superior to the GLM.

DISCUSSION

Undoubtedly, PVT is a lethal complication after splenectomy in cirrhotic patients with PH[12]. Once PVT exists, there will be elevated portal venous pressure, ischemic bowel necrosis, progressive impairment of liver function, and even liver failure, which can eventually be life-threatening[41,42]. Therefore, research on the optimization of early detection of individuals at high risk of PVT after splenectomy is urgently needed. In this study, we successfully constructed the PPER-based models for predicting PVT by machine/deep learning, which would be conducive to early identifying the population at high risk of PVT.

In the present study, conventional generalized linear (CGL) method and machine/deep learning (including the LASSO and RF) were applied separately to screen out the variables that greatly affected the PVT prediction. The CGL method is characterized by strong interpretability, especially when the multifactorial forward stepwise regression method is used, and therefore, it has been widely applied as the traditional method to construct a predictive model[43]. However, with the rapid progress of artificial intelligence technology, a novel prediction model based on machine/deep learning has emerged with a higher probability of accuracy, which has led some clinicians to question the value of the CGL model in the clinical application of individualized patients[44]. Coincidentally, our research results proclaimed that the performance of the LSM and RFM seemed to be slightly better than the GLM.

Interestingly, the PPER-based models contained the following five intersecting factors, namely, SPT, DPV, L, PPER1, and PPER3, which sufficiently illustrated that these were the main contributors to the higher incidence of PVT. Previous studies found that preoperative SPT and DPV were important predictors of the formation of PVT after splenectomy in patients with PH[8,45], which was highly consistent with our findings. A very reasonable explanation is that a wide preoperative DPV and SPT will lead to slow portal vein blood flow, which is closely related to postoperative thrombosis[45,46].

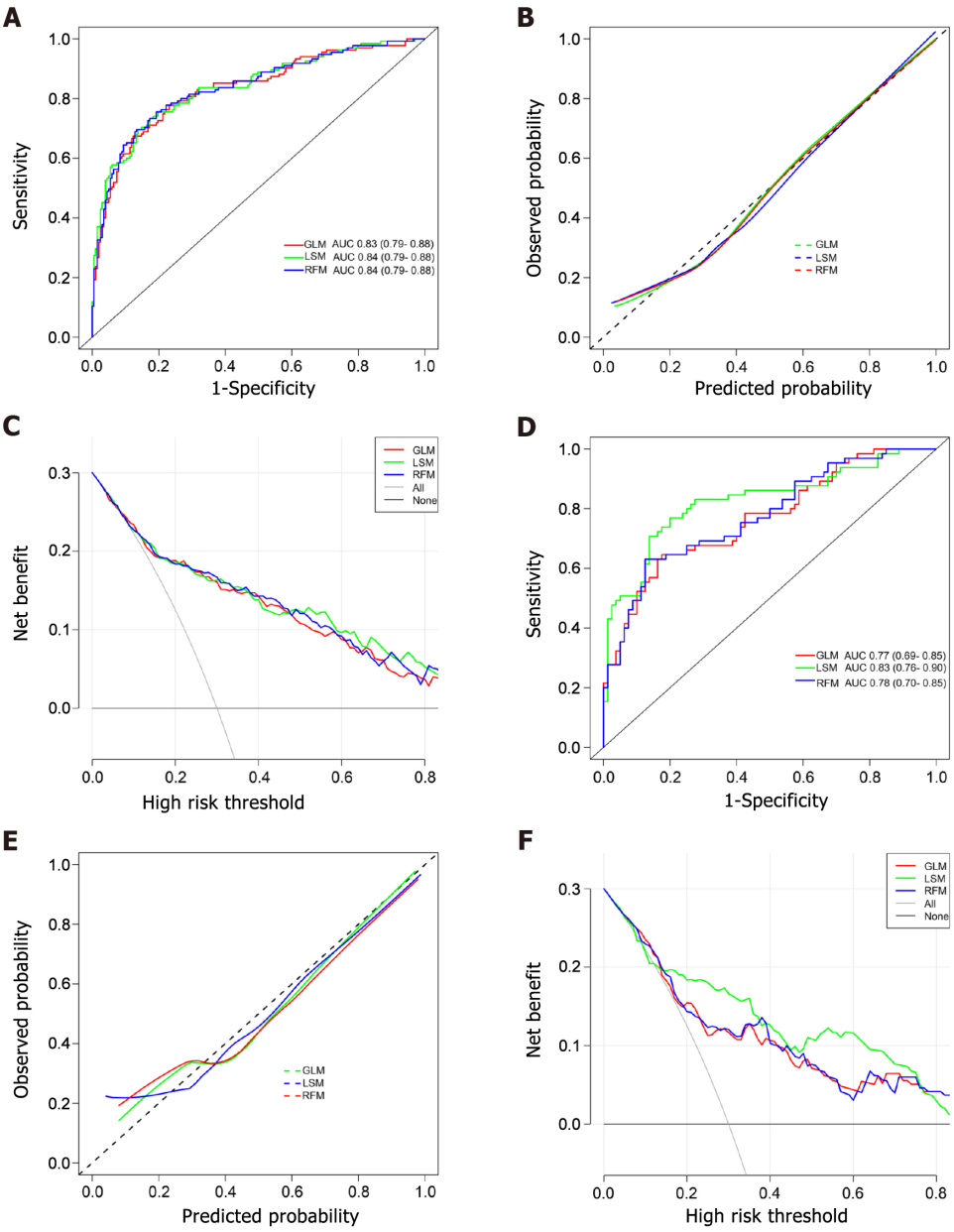


DOI: 10.3748/wjg.v28.i32.4681 **Copyright** ©The Author(s) 2022.

Figure 2 Features selection. A: Least absolute shrinkage and selection operator variable trace profiles of the 31 features. The 3-fold cross-validation was employed; B: Mean square error (MSE) plots of models under different lambda. The lambda corresponding to one MSE away from the minimum MSE was the optimal lambda value of 0.043, and the target variables shrunk to 10; C: Relationships between the error and number of trees. There are three lines, green representing error in the positive event group, red representing error in the negative event group, and black representing error in the total sample group; D: Importance scores of the candidate features. RBC: Red blood cells; HLB: Hemoglobin; WBC: White blood cells; N: Neutrophil count; L: Lymphocyte count; NLR: Neutrophil to lymphocyte ratio; PLT: Platelet count; PLR: Platelet to lymphocyte ratio; PT: Prothrombin time; PTA: Prothrombin activity; INR: International normalized ratio; FIB: Fibrinogen; APTT: Activated partial thromboplastin time; ALT: Alanine aminotransaminase; AST: Aspartate aminotransaminase; ALB: Serum albumin; TBIL: Total serum bilirubin; Child: Child-Pugh grade; EGV: Esophageal and gastric varices; SPT: Spleen thickness; DPV: Diameter of the portal vein; PBT: Preoperative blood transfusion; PLT1: Platelet count at postoperative day 1; PLT3: Platelet count at postoperative day 3; PPER1: Platelet elevation rate at postoperative day 1; PPER3: Platelet elevation rate at postoperative day 3; MDG: Mean decreased Gini.

In most cases, platelet, erythrocyte, and leukocyte counts rose dramatically over a short time after splenectomy in patients with PH, and the blood was hypercoagulable[8]. Therefore, previous studies suggested that preoperative low platelet and leukocyte counts were founders of the formation of PVT postoperatively[47]. This study revealed that preoperative L was an influential factor in PVT postoperatively, which coincided with the above view. Of note, the present study employed the PPER to reflect the magnitude of dynamic changes in preoperative and postoperative PLT. Subsequently, it was found that the PPER had high predictive value for the risk of PVT postoperatively, which was not addressed previously.

Stamou *et al*[48] reported that the median time to the formation of PVT after splenectomy in patients with PH was the 6th day (range, 3-11). Lu *et al*[8] concluded that 49.19% of patients developed PVT within 7 d after splenectomy. Therefore, scholars routinely applied ultrasonography examination to diagnose the PVT on the 7th day after splenectomy[8,19,20]. In this study, combined with the preoperative predictors and PPER, the PPER-based models that we constructed can effectively discriminate individuals with high risk of PVT as early as the first 3 d after the operation, which was



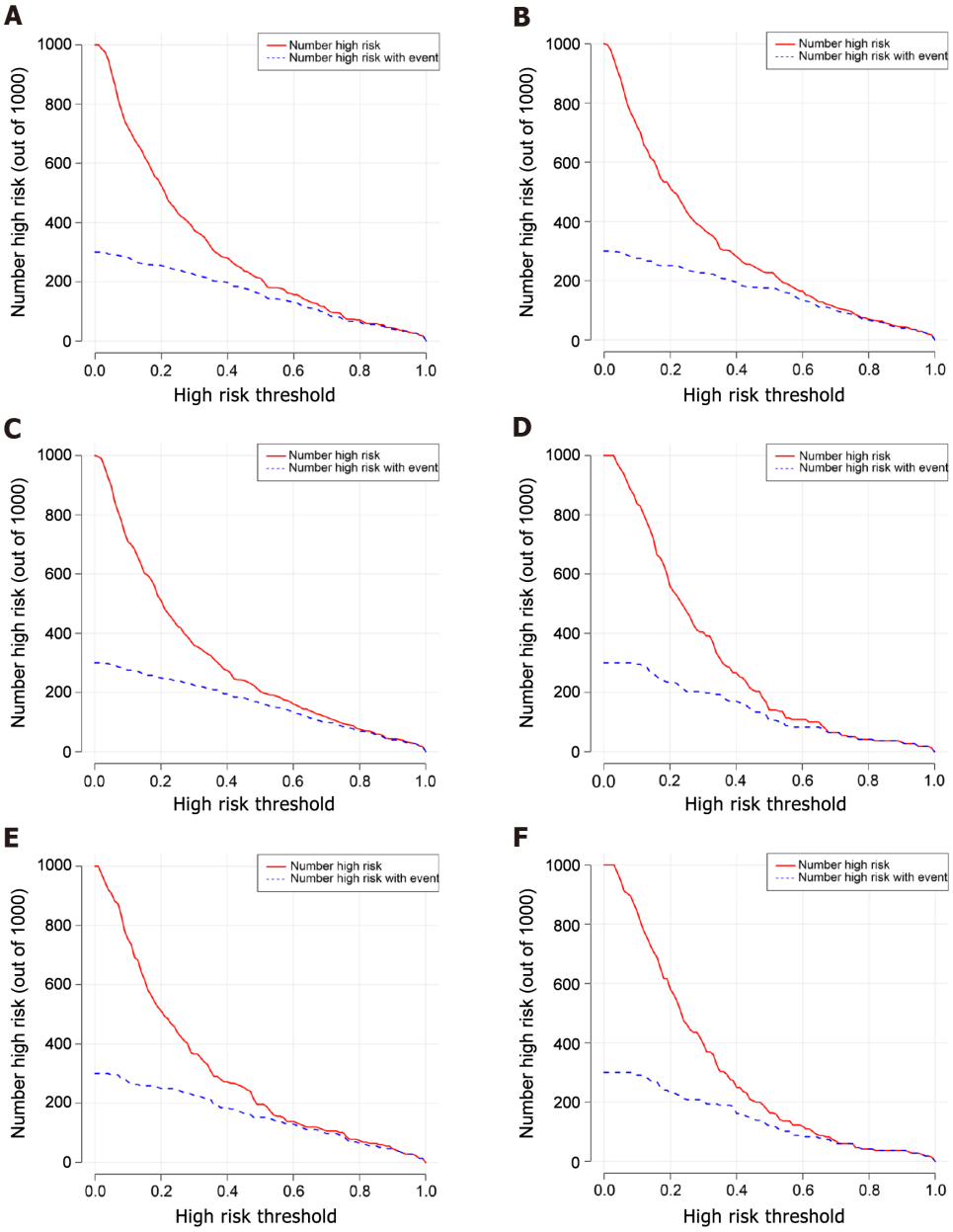
DOI: 10.3748/wjg.v28.i32.4681 **Copyright** ©The Author(s) 2022.

Figure 3 Evaluation and validation of the postoperative platelet elevation rate-based models in the training cohort and validation cohort. A and D: The receiver operating characteristic curves of the postoperative platelet elevation rate (PPER)-based models; B and E: The calibration curves of the PPER-based models; C and F: The decision curve analysis of the PPER-based models. GLM: Generalized linear model; LSM: Least absolute shrinkage and selection operator model; RFM: Random forest model; AUC: Area under the receiver operating characteristic curve.

extremely critical for guiding clinicians' treatment strategies.

Currently, there is no standard preventive regimen for PVT after splenectomy in cirrhotic patients with PH[49]. Most scholars have recently advocated that the prophylactic anticoagulant therapy is administered earlier postoperatively, which will be more helpful in reducing the incidence of PVT[50,51]. However, it should be cautiously chosen because in patients with liver cirrhosis, it cannot avoid the risk of bleeding[51]. In addition, if the preventive regimens are routinely adopted for all individuals with PH after splenectomy, it is bound to raise the suspicion of overtreatment. Excitingly, in the present study, the accuracy of the PPER-based models in predicting PVT was up to 80%, which can distinguish individuals at high risk of PVT with high efficiency, and thus guide clinicians to take targeted individualized preventive measures in time.

The present study has some limitations. First, due to the retrospective nature of the study, selection bias cannot be eliminated. Second, the uncommon preoperative factors that may influence the formation of PVT, such as splenic vein diameter, spleen volume, and portal vein flow velocity[8,19], were not routinely measured in our institution and thus failed to be included in the present study. However, the SPT and DPV in this study can indirectly reflect these indicators to a certain extent[45,46]. Third, this was a monocentric study design. Although the PPER-based models demonstrated excellent performance



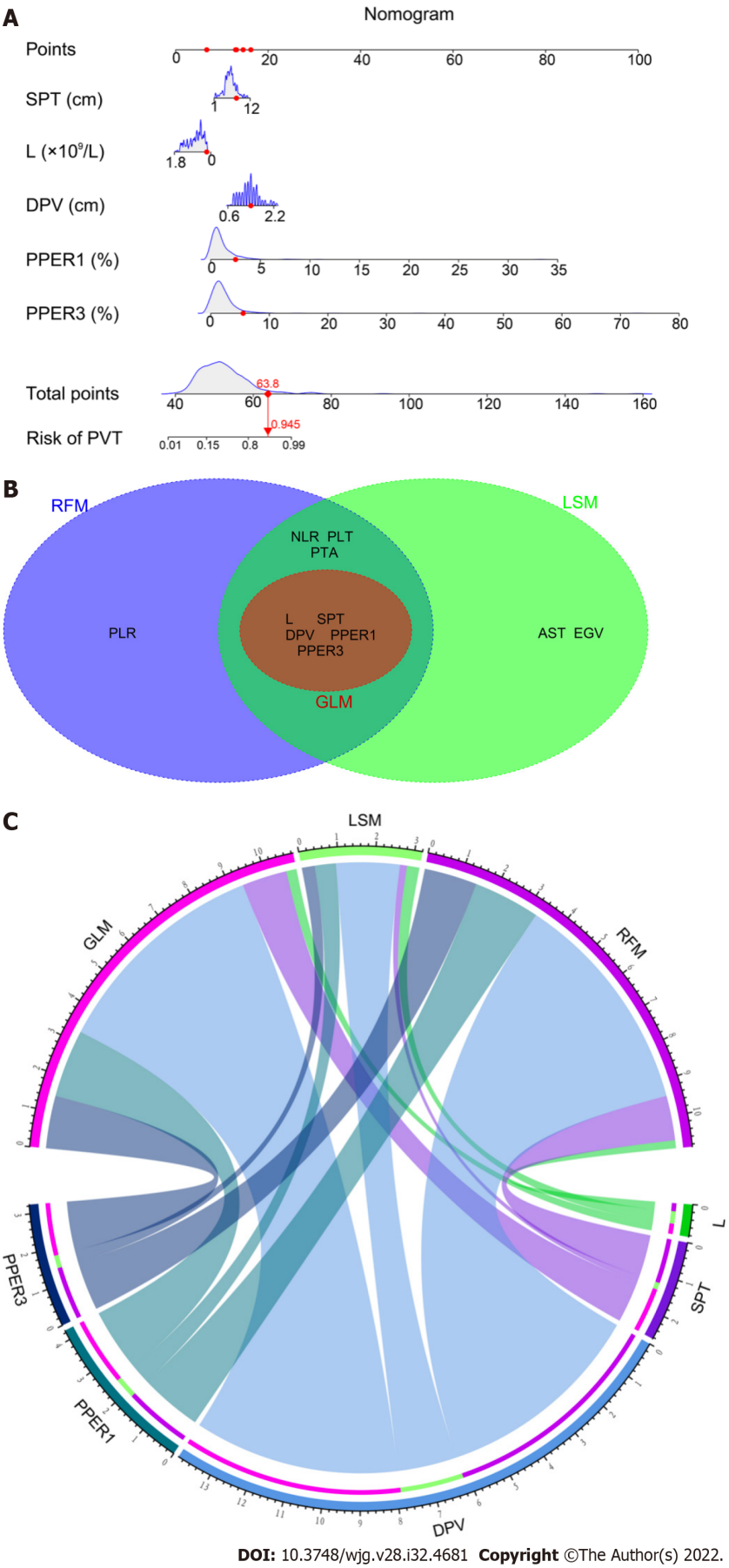
DOI: 10.3748/wjg.v28.i32.4681 **Copyright** ©The Author(s) 2022.

Figure 4 Clinical impact curves of the postoperative platelet elevation rate-based models in the training cohort and validation cohort. A and D: Clinical impact curves for the generalized linear model; B and E: Clinical impact curves for the least absolute shrinkage and selection operator model; C and F: Clinical impact curves for the random forest model.

for predicting PVT, they still lacked the verification of external cohorts. Therefore, large-scale prospective multicenter studies are warranted, which are beneficial to the popularity and application of the PPER-based models.

CONCLUSION

PPER1 and PPER3 are effective indicators for postoperative prediction of PVT. We have successfully developed the PPER-based practical models for predicting PVT, which could help clinicians identify individuals at high risk for PVT early and efficiently, and thus guide the timely intervention measures.



DOI: 10.3748/wjg.v28.i32.4681 **Copyright** ©The Author(s) 2022.

Figure 5 Nomogram for the generalized linear model and weighting of variables. A: Nomogram for the generalized linear model (GLM); B: Intersection variables among the GLM, least absolute shrinkage and selection operator model (LSM), and random forest model (RFM); C: Weights of the intersection

variables in the GLM, LSM, and RFM, respectively. SPT: Spleen thickness; L: Lymphocyte count; DPV: Diameter of portal vein; PPER1 and PPER3: The first and third days for postoperative platelet elevation rate; PVT: Portal vein thrombosis; PLR: Platelet to lymphocyte ratio; NLR: Neutrophil to lymphocyte ratio; PLT: Platelet count; PTA: Prothrombin activity; EGV: Esophageal and gastric varices; AST: Aspartate aminotransaminase.

ARTICLE HIGHLIGHTS

Research background

Patients with portal hypertension (PH) often experience rebounding rises in platelets following splenectomy. However, the value of postoperative platelet elevation rate (PPER) in predicting portal vein thrombosis (PVT) is unknown.

Research motivation

PVT is a potentially fatal complication after splenectomy for patients with PH, and the probability of PVT has been reported to be nearly 50%. Therefore, there is an imperious demand for effective diagnostic methods to early and rapidly identify individuals at high risk of PVT after splenectomy to further help clinicians take intervention measures as soon as possible.

Research objectives

We aimed to investigate the predictive value of PPER for PVT and establish PPER-based practical prediction models to early identify individuals at high risk of PVT after splenectomy.

Research methods

We retrospectively reviewed 483 patients with PH related to hepatitis B virus who underwent splenectomy between July 2011 and September 2018, and they were randomized into either a training (n = 338) or a validation (n = 145) cohort. The generalized linear (GL) method, least absolute shrinkage and selection operator (LASSO), and random forest (RF) were used to construct models. The receiver operating characteristic (ROC) curves, calibration curve, decision curve analysis (DCA), and clinical impact curve (CIC) were used to evaluate the robustness and clinical practicability of the GL model (GLM), LASSO model (LSM), and RF model (RFM).

Research results

PPER at the first (PPER1) and third (PPER3) days were strongly associated with PVT [odds ratio (OR): 1.78, 95% confidence interval (CI): 1.24-2.62, P = 0.002; OR: 1.43, 95%CI: 1.16-1.77, P < 0.001, respectively] in the multivariate logistic regression analysis. The areas under ROC curves of the GLM, LSM, and RFM in the training cohort were 0.83 (95%CI: 0.79-0.88), 0.84 (95%CI: 0.79-0.88), and 0.84 (95%CI: 0.79-0.88), respectively; and were 0.77 (95%CI: 0.69-0.85), 0.83 (95%CI: 0.76-0.90), and 0.78 (95%CI: 0.70-0.85) in the validation cohort, respectively. The calibration curves showed satisfactory agreement between prediction by models and actual observation. DCA and CIC indicated that all models conferred high clinical net benefit.

Research conclusions

PPER1 and PPER3 are effective indicators for predicting PVT. We have successfully developed the PPER-based practical models to accurately predict PVT, which could conveniently help clinicians rapidly differentiate individuals at high risk of PVT, and further guide the adoption of timely interventions.

Research perspectives

According to our experience, patients with a more remarkable increase in platelet count in the first 3 d after operation have a higher probability of PVT, which should be prioritized for prophylactic anticoagulation.

FOOTNOTES

Author contributions: All authors contributed to the study; Li J wrote the manuscript, and collected and analysed the data; Wu QQ collected the data, and contributed to the follow-up results; Zhu RH, Lv X, and Wang WQ collected the data and performed the analysis; Wang JL contributed to the data; Liang BY and Huang ZY provided the resources and supervision; Zhang EL contributed to writing the manuscript, and drafting the conception and design; all authors read and approved the final manuscript.

Supported by National Natural Science Foundation of China, No. 81902839; and Hubei Provincial Special Grants for Scientific and Technical Innovation, No. 2021BCA115.

Institutional review board statement: The study was approved by the Medical Ethics Committee of Tongji Medical College, Huazhong University of Science and Technology (No. 2022-LSZ (S066)).

Informed consent statement: Written informed consent from the patients was waived due to the retrospective nature of this study.

Conflict-of-interest statement: All authors declare no conflicts of interest related to this article.

Data sharing statement: No additional data are available.

Open-Access: This article is an open-access article that was selected by an in-house editor and fully peer-reviewed by external reviewers. It is distributed in accordance with the Creative Commons Attribution NonCommercial (CC BY-NC 4.0) license, which permits others to distribute, remix, adapt, build upon this work non-commercially, and license their derivative works on different terms, provided the original work is properly cited and the use is non-commercial. See: https://creativecommons.org/Licenses/by-nc/4.0/

Country/Territory of origin: China

ORCID number: Jian Li 0000-0001-9025-4968; Qi-Qi Wu 0000-0002-5556-4394; Rong-Hua Zhu 0000-0002-8588-7493; Xing Lv 0000-0002-8363-6383; Wen-Qiang Wang 0000-0002-9648-5481; Jin-Lin Wang 0000-0003-0073-4197; Zhi-Yong Huang 0000-0002-2239-0674; Er-Lei Zhang 0000-0002-7251-0275.

S-Editor: Fan JR
L-Editor: Wang TQ
P-Editor: Chen YX

REFERENCES

1 **GBD 2017 Cirrhosis Collaborators**. The global, regional, and national burden of cirrhosis by cause in 195 countries and territories, 1990-2017: a systematic analysis for the Global Burden of Disease Study 2017. *Lancet Gastroenterol Hepatol* 2020; **5**: 245-266 [PMID: 31981519 DOI: 10.1016/S2468-1253(19)30349-8]
2 **Wright AS**, Rikkers LF. Current management of portal hypertension. *J Gastrointest Surg* 2005; **9**: 992-1005 [PMID: 16137597 DOI: 10.1016/j.gassur.2004.09.028]
3 **Bancu S**, Borz C, Popescu G, Torok A, Mureşan A, Bancu L, Turcu M. [Spleno-renal distal and proximal shunts for hypersplenism due to hepatic cirrhosis]. *Chirurgia (Bucur)* 2007; **102**: 665-668 [PMID: 18323228]
4 **Adam R**, Karam V, Delvart V, O'Grady J, Mirza D, Klempnauer J, Castaing D, Neuhaus P, Jamieson N, Salizzoni M, Pollard S, Lerut J, Paul A, Garcia-Valdecasas JC, Rodríguez FS, Burroughs A; All contributing centers (www. eltr.org); European Liver and Intestine Transplant Association (ELITA). Evolution of indications and results of liver transplantation in Europe. A report from the European Liver Transplant Registry (ELTR). *J Hepatol* 2012; **57**: 675-688 [PMID: 22609307 DOI: 10.1016/j.jhep.2012.04.015]
5 **Bodzin AS**, Baker TB. Liver Transplantation Today: Where We Are Now and Where We Are Going. *Liver Transpl* 2018; **24**: 1470-1475 [PMID: 30080954 DOI: 10.1002/lt.25320]
6 **Narahara Y**, Kanazawa H, Fukuda T, Matsushita Y, Harimoto H, Kidokoro H, Katakura T, Atsukawa M, Taki Y, Kimura Y, Nakatsuka K, Sakamoto C. Transjugular intrahepatic portosystemic shunt versus paracentesis plus albumin in patients with refractory ascites who have good hepatic and renal function: a prospective randomized trial. *J Gastroenterol* 2011; **46**: 78-85 [PMID: 20632194 DOI: 10.1007/s00535-010-0282-9]
7 **Salerno F**, Merli M, Riggio O, Cazzaniga M, Valeriano V, Pozzi M, Nicolini A, Salvatori F. Randomized controlled study of TIPS versus paracentesis plus albumin in cirrhosis with severe ascites. *Hepatology* 2004; **40**: 629-635 [PMID: 15349901 DOI: 10.1002/hep.20364]
8 **Lu S**, Hu G, Chen S, Wang J. Risk Factors of Portal Vein Thrombosis after Devascularization Treatment in Patients with Liver Cirrhosis: A Nested Case-Control Study. *Biomed Res Int* 2020; **2020**: 9583706 [PMID: 32908928 DOI: 10.1155/2020/9583706]
9 **de Cleva R**, Herman P, D'albuquerque LA, Pugliese V, Santarem OL, Saad WA. Pre- and postoperative systemic hemodynamic evaluation in patients subjected to esophagogastric devascularization plus splenectomy and distal splenorenal shunt: a comparative study in schistomomal portal hypertension. *World J Gastroenterol* 2007; **13**: 5471-5475 [PMID: 17907290 DOI: 10.3748/wjg.v13.i41.5471]
10 **Parikh S**, Shah R, Kapoor P. Portal vein thrombosis. *Am J Med* 2010; **123**: 111-119 [PMID: 20103016 DOI: 10.1016/j.amjmed.2009.05.023]
11 **Hepatobiliary Disease Study Group**, Chinese Society of Gastroenterology; Chinese Medical Association. [Consensus for management of portal vein thrombosis in liver cirrhosis (2020, Shanghai)]. *Zhonghua Gan Zang Bing Za Zhi* 2020; **28**: 999-1007 [PMID: 34865346 DOI: 10.3760/cma.j.cn501113-20201112-00612]
12 **van't Riet M**, Burger JW, van Muiswinkel JM, Kazemier G, Schipperus MR, Bonjer HJ. Diagnosis and treatment of portal vein thrombosis following splenectomy. *Br J Surg* 2000; **87**: 1229-1233 [PMID: 10971433 DOI: 10.1046/j.1365-2168.2000.01514.x]
13 **Ikeda M**, Sekimoto M, Takiguchi S, Kubota M, Ikenaga M, Yamamoto H, Fujiwara Y, Ohue M, Yasuda T, Imamura H, Tatsuta M, Yano M, Furukawa H, Monden M. High incidence of thrombosis of the portal venous system after laparoscopic

splenectomy: a prospective study with contrast-enhanced CT scan. *Ann Surg* 2005; **241**: 208-216 [PMID: 15650628 DOI: 10.1097/01.sla.0000151794.28392.a6]

14 **Krauth MT**, Lechner K, Neugebauer EA, Pabinger I. The postoperative splenic/portal vein thrombosis after splenectomy and its prevention--an unresolved issue. *Haematologica* 2008; **93**: 1227-1232 [PMID: 18556406 DOI: 10.3324/haematol.12682]

15 **Qi X**, Bai M, Guo X, Fan D. Pharmacologic prophylaxis of portal venous system thrombosis after splenectomy: a meta-analysis. *Gastroenterol Res Pract* 2014; **2014**: 292689 [PMID: 25243008 DOI: 10.1155/2014/292689]

16 **Zhang Y**, Xu BY, Wang XB, Zheng X, Huang Y, Chen J, Meng ZJ, Gao YH, Qian ZP, Liu F, Lu XB, Shi Y, Shang J, Li H, Wang SY, Yin S, Sun SN, Hou YX, Xiong Y, Li BL, Lei Q, Gao N, Ji LJ, Li J, Jie FR, Zhao RH, Liu JP, Lin TF, Chen LY, Tan WT, Zhang Q, Zou CC, Huang ZB, Jiang XH, Luo S, Liu CY, Zhang YY, Li T, Ren HT, Wang SJ, Deng GH, Xiong SE, Liu XX, Wang C, Yuan W, Gu WY, Qiao L, Wang TY, Wu DD, Dong FC, Hua J. Prevalence and Clinical Significance of Portal Vein Thrombosis in Patients With Cirrhosis and Acute Decompensation. *Clin Gastroenterol Hepatol* 2020; **18**: 2564-2572.e1 [PMID: 32109631 DOI: 10.1016/j.cgh.2020.02.037]

17 **Rossi S**, Ghittoni G, Ravetta V, Torello Viera F, Rosa L, Serassi M, Scabini M, Vercelli A, Tinelli C, Dal Bello B, Burns PN, Calliada F. Contrast-enhanced ultrasonography and spiral computed tomography in the detection and characterization of portal vein thrombosis complicating hepatocellular carcinoma. *Eur Radiol* 2008; **18**: 1749-1756 [PMID: 18369630 DOI: 10.1007/s00330-008-0931-z]

18 **Wang L**, Liu GJ, Chen YX, Dong HP, Zhang YQ, Wang LX. Combined use of D-dimer and P-selectin for the diagnosis of splenic or portal vein thrombosis following splenectomy. *Thromb Res* 2010; **125**: e206-e209 [PMID: 20079524 DOI: 10.1016/j.thromres.2009.12.012]

19 **Wu S**, Wu Z, Zhang X, Wang R, Bai J. The incidence and risk factors of portal vein system thrombosis after splenectomy and pericardial devascularization. *Turk J Gastroenterol* 2015; **26**: 423-428 [PMID: 26350689 DOI: 10.5152/tjg.2015.0063]

20 **Zhang Y**, Wen TF, Yan LN, Yang HJ, Deng XF, Li C, Wang C, Liang GL. Preoperative predictors of portal vein thrombosis after splenectomy with periesophagogastric devascularization. *World J Gastroenterol* 2012; **18**: 1834-1839 [PMID: 22553410 DOI: 10.3748/wjg.v18.i15.1834]

21 **Wu LF**, Bai DS, Shi L, Jin SJ, Zhou BH, Jiang GQ. Predictors of portal vein thrombosis after laparoscopic splenectomy and azygoportal disconnection in hepatitis B cirrhosis: a prospective study. *Surg Endosc* 2022; **36**: 4090-4098 [PMID: 34518951 DOI: 10.1007/s00464-021-08730-5]

22 **Matsui T**, Usui M, Wada H, Iizawa Y, Kato H, Tanemura A, Murata Y, Kuriyama N, Kishiwada M, Mizuno S, Sakurai H, Isaji S. Platelet Activation Assessed by Glycoprotein VI/Platelet Ratio Is Associated With Portal Vein Thrombosis After Hepatectomy and Splenectomy in Patients With Liver Cirrhosis. *Clin Appl Thromb Hemost* 2018; **24**: 254-262 [PMID: 29050501 DOI: 10.1177/1076029617725600]

23 **Ushitora Y**, Tashiro H, Takahashi S, Amano H, Oshita A, Kobayashi T, Chayama K, Ohdan H. Splenectomy in chronic hepatic disorders: portal vein thrombosis and improvement of liver function. *Dig Surg* 2011; **28**: 9-14 [PMID: 21293126 DOI: 10.1159/000321886]

24 **Zhang Y**, Wen T, Yan L, Chen Z, Yang H, Deng X, Liang G, Li G, Zhang X, Ran S, Liao Z. The changes of hepatic hemodynamics and functional hepatic reserve after splenectomy with periesophagogastric devascularization. *Hepatogastroenterology* 2009; **56**: 835-839 [PMID: 19621712]

25 **Xu W**, Cheng Y, Tu B. [Construction and validation of a nomogram for predicting the risk of portal vein thrombosis after splenectomy in patients with hepatitis B cirrhosis]. *Nan Fang Yi Ke Da Xue Xue Bao* 2020; **40**: 1265-1272 [PMID: 32990234 DOI: 10.12122/j.issn.1673-4254.2020.09.07]

26 **Yuan HL**, Wang M, Chu WW, Li FX, Lu JJ, Li Y. Nomogram Model for Prediction of Portal Vein Thrombosis in Patients with Liver Cirrhosis After Splenectomy: A Retrospective Analysis of 2 Independent Cohorts. *Med Sci Monit* 2021; **27**: e929844 [PMID: 34075015 DOI: 10.12659/MSM.929844]

27 **Dong Z**, Lin Y, Lin F, Luo X, Lin Z, Zhang Y, Li L, Li ZP, Feng ST, Cai H, Peng Z. Prediction of Early Treatment Response to Initial Conventional Transarterial Chemoembolization Therapy for Hepatocellular Carcinoma by Machine-Learning Model Based on Computed Tomography. *J Hepatocell Carcinoma* 2021; **8**: 1473-1484 [PMID: 34877267 DOI: 10.2147/JHC.S334674]

28 **Gao Y**, Cai GY, Fang W, Li HY, Wang SY, Chen L, Yu Y, Liu D, Xu S, Cui PF, Zeng SQ, Feng XX, Yu RD, Wang Y, Yuan Y, Jiao XF, Chi JH, Liu JH, Li RY, Zheng X, Song CY, Jin N, Gong WJ, Liu XY, Huang L, Tian X, Li L, Xing H, Ma D, Li CR, Ye F, Gao QL. Machine learning based early warning system enables accurate mortality risk prediction for COVID-19. *Nat Commun* 2020; **11**: 5033 [PMID: 33024092 DOI: 10.1038/s41467-020-18684-2]

29 **Kawakami E**, Tabata J, Yanaihara N, Ishikawa T, Koseki K, Iida Y, Saito M, Komazaki H, Shapiro JS, Goto C, Akiyama Y, Saito R, Takano H, Yamada K, Okamoto A. Application of Artificial Intelligence for Preoperative Diagnostic and Prognostic Prediction in Epithelial Ovarian Cancer Based on Blood Biomarkers. *Clin Cancer Res* 2019; **25**: 3006-3015 [PMID: 30979733 DOI: 10.1158/1078-0432.CCR-18-3378]

30 **Ganggayah MD**, Taib NA, Har YC, Lio P, Dhillon SK. Predicting factors for survival of breast cancer patients using machine learning techniques. *BMC Med Inform Decis Mak* 2019; **19**: 48 [PMID: 30902088 DOI: 10.1186/s12911-019-0801-4]

31 **Heo J**, Yoon JG, Park H, Kim YD, Nam HS, Heo JH. Machine Learning-Based Model for Prediction of Outcomes in Acute Stroke. *Stroke* 2019; **50**: 1263-1265 [PMID: 30890116 DOI: 10.1161/STROKEAHA.118.024293]

32 **Churpek MM**, Yuen TC, Winslow C, Meltzer DO, Kattan MW, Edelson DP. Multicenter Comparison of Machine Learning Methods and Conventional Regression for Predicting Clinical Deterioration on the Wards. *Crit Care Med* 2016; **44**: 368-374 [PMID: 26771782 DOI: 10.1097/CCM.0000000000001571]

33 **Wang M**, Ding L, Xu M, Xie J, Wu S, Xu S, Yao Y, Liu Q. A novel method detecting the key clinic factors of portal vein system thrombosis of splenectomy & cardia devascularization patients for cirrhosis & portal hypertension. *BMC Bioinformatics* 2019; **20**: 720 [PMID: 31888439 DOI: 10.1186/s12859-019-3233-3]

34 **Pugh RN**, Murray-Lyon IM, Dawson JL, Pietroni MC, Williams R. Transection of the oesophagus for bleeding oesophageal varices. *Br J Surg* 1973; **60**: 646-649 [PMID: 4541913 DOI: 10.1002/bjs.1800600817]

35 **Tran T**, Demyttenaere SV, Polyhronopoulos G, Séguin C, Artho GP, Kaneva P, Fried GM, Feldman LS. Recommended timing for surveillance ultrasonography to diagnose portal splenic vein thrombosis after laparoscopic splenectomy. *Surg Endosc* 2010; **24**: 1670-1678 [PMID: 20039066 DOI: 10.1007/s00464-009-0828-1]

36 **Anton A**, Campreciós G, Pérez-Campuzano V, Orts L, García-Pagán JC, Hernández-Gea V. The Pathophysiology of Portal Vein Thrombosis in Cirrhosis: Getting Deeper into Virchow's Triad. *J Clin Med* 2022; **11** [PMID: 35160251 DOI: 10.3390/jcm11030800]

37 **Gaiani S**, Gramantieri L, Venturoli N, Piscaglia F, Siringo S, D'Errico A, Zironi G, Grigioni W, Bolondi L. What is the criterion for differentiating chronic hepatitis from compensated cirrhosis? *J Hepatol* 1997; **27**: 979-985 [PMID: 9453422 DOI: 10.1016/s0168-8278(97)80140-7]

38 **McEligot AJ**, Poynor V, Sharma R, Panangadan A. Logistic LASSO Regression for Dietary Intakes and Breast Cancer. *Nutrients* 2020; **12** [PMID: 32878103 DOI: 10.3390/nu12092652]

39 **Majhi R**, Thangeda R, Sugasi RP, Kumar N. Analysis and prediction of COVID-19 trajectory: A machine learning approach. *J Public Aff* 2020; e2537 [PMID: 33349741 DOI: 10.1002/pa.2537]

40 **Strobl C**, Boulesteix AL, Zeileis A, Hothorn T. Bias in random forest variable importance measures: illustrations, sources and a solution. *BMC Bioinformatics* 2007; **8**: 25 [PMID: 17254353 DOI: 10.1186/1471-2105-8-25]

41 **Anstee QM**, Dhar A, Thursz MR. The role of hypercoagulability in liver fibrogenesis. *Clin Res Hepatol Gastroenterol* 2011; **35**: 526-533 [PMID: 21570930 DOI: 10.1016/j.clinre.2011.03.011]

42 **D'Amico G**, De Franchis R; Cooperative Study Group. Upper digestive bleeding in cirrhosis. Post-therapeutic outcome and prognostic indicators. *Hepatology* 2003; **38**: 599-612 [PMID: 12939586 DOI: 10.1053/jhep.2003.50385]

43 **Song L**, Langfelder P, Horvath S. Random generalized linear model: a highly accurate and interpretable ensemble predictor. *BMC Bioinformatics* 2013; **14**: 5 [PMID: 23323760 DOI: 10.1186/1471-2105-14-5]

44 **Amin MB**, Greene FL, Edge SB, Compton CC, Gershenwald JE, Brookland RK, Meyer L, Gress DM, Byrd DR, Winchester DP. The Eighth Edition AJCC Cancer Staging Manual: Continuing to build a bridge from a population-based to a more "personalized" approach to cancer staging. *CA Cancer J Clin* 2017; **67**: 93-99 [PMID: 28094848 DOI: 10.3322/caac.21388]

45 **Chen H**, Trilok G, Wang F, Qi X, Xiao J, Yang C. A single hospital study on portal vein thrombosis in cirrhotic patients - clinical characteristics & risk factors. *Indian J Med Res* 2014; **139**: 260-266 [PMID: 24718401]

46 **Li MX**, Zhang XF, Liu ZW, Lv Y. Risk factors and clinical characteristics of portal vein thrombosis after splenectomy in patients with liver cirrhosis. *Hepatobiliary Pancreat Dis Int* 2013; **12**: 512-519 [PMID: 24103282 DOI: 10.1016/s1499-3872(13)60081-8]

47 **Kinjo N**, Kawanaka H, Akahoshi T, Tomikawa M, Yamashita N, Konishi K, Tanoue K, Shirabe K, Hashizume M, Maehara Y. Risk factors for portal venous thrombosis after splenectomy in patients with cirrhosis and portal hypertension. *Br J Surg* 2010; **97**: 910-916 [PMID: 20474001 DOI: 10.1002/bjs.7002]

48 **Stamou KM**, Toutouzas KG, Kekis PB, Nakos S, Gafou A, Manouras A, Krespis E, Katsaragakis S, Bramis J. Prospective study of the incidence and risk factors of postsplenectomy thrombosis of the portal, mesenteric, and splenic veins. *Arch Surg* 2006; **141**: 663-669 [PMID: 16847237 DOI: 10.1001/archsurg.141.7.663]

49 **Kawanaka H**, Akahoshi T, Kinjo N, Konishi K, Yoshida D, Anegawa G, Yamaguchi S, Uehara H, Hashimoto N, Tsutsumi N, Tomikawa M, Maehara Y. Impact of antithrombin III concentrates on portal vein thrombosis after splenectomy in patients with liver cirrhosis and hypersplenism. *Ann Surg* 2010; **251**: 76-83 [PMID: 19864937 DOI: 10.1097/SLA.0b013e3181bdf8ad]

50 **Yao W**, Feng Y, Liu T, Li W, Zhang M, Yao Y, Wu S. Rivaroxaban versus low-molecular weight heparin plus warfarin prevents portal vein system thrombosis after splenectomy and pericardial devascularization: A randomized clinical trial. *EXCLI J* 2021; **20**: 537-549 [PMID: 33883982 DOI: 10.17179/excli2020-3120]

51 **Ding H**, Zhang Y, Zhao L, Wu S, Liu J, Wang C, Pei T, Su Y. What intervention regimen is most effective prevention for Portal venous system thrombosis after splenectomy in cirrhotics patients with Portal hypertension? *Pharmacol Res* 2020; **157**: 104825 [PMID: 32330553 DOI: 10.1016/j.phrs.2020.104825]

World Journal of Gastroenterology

Submit a Manuscript: https://www.f6publishing.com

World J Gastroenterol 2022 August 28; 28(32): 4698-4715

DOI: 10.3748/wjg.v28.i32.4698

ISSN 1007-9327 (print) ISSN 2219-2840 (online)

ORIGINAL ARTICLE

Observational Study

International patterns in incidence and mortality trends of pancreatic cancer in the last three decades: A joinpoint regression analysis

Irena Ilic, Milena Ilic

Specialty type: Gastroenterology and hepatology

Provenance and peer review: Invited article; Externally peer reviewed.

Peer-review model: Single blind

Peer-review report's scientific quality classification

Grade A (Excellent): 0
Grade B (Very good): B
Grade C (Good): C, C
Grade D (Fair): 0
Grade E (Poor): 0

P-Reviewer: Dhamnetiya D, India; Zimmitti G, Italy

Received: March 2, 2022
Peer-review started: March 2, 2022
First decision: April 12, 2022
Revised: May 5, 2022
Accepted: June 20, 2022
Article in press: June 20, 2022
Published online: August 28, 2022

Irena Ilic, Faculty of Medicine, University of Belgrade, Belgrade 11000, Serbia

Milena Ilic, Department of Epidemiology, Faculty of Medical Sciences, University of Kragujevac, Kragujevac 34000, Serbia

Corresponding author: Milena Ilic, MD, PhD, Professor, Department of Epidemiology, Faculty of Medical Sciences, University of Kragujevac, S. Markovica 69, Kragujevac 34000, Serbia. drmilenailic@yahoo.com

Abstract

BACKGROUND

Pancreatic cancer, as the one of most fatal malignancies, remains a critical issue in the global burden of disease.

AIM

To estimate trends in pancreatic cancer incidence and mortality worldwide in the last three decades.

METHODS

A descriptive epidemiological study was done. Pancreatic cancer incidence and mortality data were obtained from the database of the World Health Organization. Analysis of pancreatic cancer incidence and mortality during 2020 was performed. The age-standardized rates (ASRs, expressed *per* 100000) were presented. To estimate trends of incidence and mortality of pancreatic cancer, joinpoint regression analysis was used: the average annual percent change (AAPC) with the corresponding 95% confidence interval (95%CI) was calculated. Additionally, analysis was performed by sex and age. In this paper, the trend analysis included only countries with high and medium data quality.

RESULTS

A total of 495773 (262865 male and 232908 female) new cases and 466003 (246840 male and 219163 female) deaths from pancreatic cancer were reported worldwide in 2020. In both sexes, most of the new cases (191348; 38.6% of the total) and deaths (182074; 39.1% of the total) occurred in the Western Pacific Region. In both sexes, the highest ASRs were found in the European Region, while the lowest rates were reported in the South-East Asia Region. The general pattern of rising pancreatic cancer incidence and mortality was seen across countries worldwide in observed period. Out of all countries with an increase in pancreatic cancer

incidence, females in France and India showed the most marked rise in incidence rates (AAPC = +3.9% and AAPC = +3.7%, respectively). Decreasing incidence trends for pancreatic cancer were observed in some countries, but without significance. Out of all countries with an increase in pancreatic cancer mortality rates, Turkmenistan showed the most marked rise both in males (AAPC = +10.0%, 95%CI: 7.4–12.5) and females (AAPC = +6.4%, 95%CI: 3.5–9.5). The mortality trends of pancreatic cancer were decreasing in both sexes only in Canada and Mexico.

CONCLUSION
Further research is needed to explain the cause of large international differences in incidence and mortality trends of pancreatic cancer in last three decades.

Key Words: Pancreatic cancer; Incidence; Mortality; Joinpoint analysis; International pattern

©The Author(s) 2022. Published by Baishideng Publishing Group Inc. All rights reserved.

Core tip: Pancreatic cancer, as one of the most fatal malignancies, remains a critical issue in global burden of disease. About 500000 new cases and 470000 deaths from pancreatic cancer were recorded in 2020 across the world. Globally, the rate of pancreatic cancer incidence in 2020 was 4.9 *per* 100000 for both sexes together, while mortality rate was 4.5 *per* 100000. Increasing trends in both incidence and mortality of pancreatic cancer were observed in most countries across the world. Further efforts to explore the reasons for differences in international pattern in pancreatic cancer incidence and mortality could be critical for global cancer control.

Citation: Ilic I, Ilic M. International patterns in incidence and mortality trends of pancreatic cancer in the last three decades: A joinpoint regression analysis. *World J Gastroenterol* 2022; 28(32): 4698-4715
URL: https://www.wjgnet.com/1007-9327/full/v28/i32/4698.htm
DOI: https://dx.doi.org/10.3748/wjg.v28.i32.4698

INTRODUCTION

Pancreatic cancer is one of the most lethal cancers, with insidious onset, aggressive nature and poor prognosis[1-3]. The 5-year overall survival rate of pancreatic cancer is low (~10%), since more than half of the cases are confirmed at an advanced stage[3,4]. Based on GLOBOCAN 2020 estimates, pancreatic cancer remains a large part of the global burden of disease, and ranks as the 12th most common malignancy (2.6% of all cancers) and the 7th leading cause of cancer mortality (4.7% of all cancers)[1,2]. Age-standardized incidence and mortality rates are about fivefold higher in countries with high/very high Human Development Index than in low/medium countries[2].

World Health Organization (WHO) estimated pancreatic cancer as the third leading cancer-related cause of death in people of all ages for both sexes in the USA, Germany, Italy, Austria, Czechia, Finland, Hungary, Malta, Spain and Switzerland in 2020[2]. In four countries (Finland, Qatar, Benin and Guadeloupe), pancreatic cancer was the second leading cause of death of all cancers in 2020 in females aged ≥ 70 years[2]. The Global Burden of Disease (GBD) Study ranked pancreatic cancer as the seventh top cause of absolute years of life lost (YLLs) among all cancers in both sexes in 2017, while it ranked ninth in 2007 among the top causes for YLLs worldwide[5]. Also, the GBD study showed that the disability adjusted life years caused by pancreatic cancer have more than doubled from 1990 to 2017 globally[6].

The age patterns were similar for both incidence and mortality of pancreatic cancer, with the rates increasing with increasing age; the burden moderately grew after 30 years of age and came to peak after 80 years of age, with similar trend in males and females[3,5-7]. In 27 countries of the EU and in the UK, between 1990 and 2019, incidence and mortality from pancreatic cancer significantly increased by 0.65% and 0.55% per year, respectively[8].

WHO and the United Nations Sustainable Development Goals, published in 2015, target to reduce premature mortality rate attributed to cancer by one third by 2030[9]. However, according to Ferlay *et al* [10], by 2025 there will be more deaths annually from pancreatic cancer in the EU countries than deaths from breast cancer, and it will become the third most important cause of cancer death in the EU after lung and colorectal cancer. In addition, a particularly important issue is how the COVID-19 pandemic will affect the management of patients with pancreatic cancer that can be disrupted or delayed, particularly in the context of treatment selection and postoperative care to reduce the risk of SARS-CoV-2-associated morbidity and mortality[11,12].

Recent estimates suggest that pancreatic cancer is becoming a critical public health challenge and a growing health service issue both in developed and developing countries[1,10,13]. The aim of this manuscript was to assess international patterns in incidence and mortality of pancreatic cancer.

MATERIALS AND METHODS

Study design

This descriptive epidemiological study comprised the annual underlying cause of disease and death data to describe trends in incidence and mortality from pancreatic cancer in the world in last three decades.

Data source

Data of pancreatic cancer incidence and mortality were extracted from the WHO databases[2], *i.e.* the GLOBOCAN estimates of cancer incidence and mortality generated by the International Agency for Research on Cancer. Pancreatic cancer estimates included site code C25, based on the 10th revision of the International Classification of Diseases and Related Health Problems to classify cause of disease and death (ICD-10)[14].

The WHO databases provide a comprehensive and comparable assessment of incidence and mortality of pancreatic cancer[2]. These databases provide high-quality statistics based on national vital registries worldwide. The methods used to compile the GLOBOCAN 2020 estimates involved predictions, modeling of incidence-to-mortality ratios, and approximation from neighboring countries. For pancreatic cancer, we extracted all incidence and mortality data available from WHO databases in all years available since 1991. The WHO estimates comprise only national mortality data series that meet the minimal inclusion criteria according to the WHO-defined medium data quality level, based on degree of population coverage, completeness and accuracy[15]. Level of data quality was classified using criteria described by WHO[14]: data of high quality (ICD-9 or ICD-10 coding is used and completeness is > 90% and ill-defined codes appear on < 10% of registrations), medium quality (completeness is 70%–90% OR ill-defined codes appear on 10%–20% of registrations OR non-ICD codes used although completeness is > 90% and ill-defined codes appear on < 10% of registrations) and low quality (completeness < 70% OR ill-defined codes appear on > 20% of registrations).

This study presented the incidence and mortality figures for 185 WHO Member States, as well as for six WHO regions (Africa, Americas, South-East Asia, Europe, Eastern Mediterranean, and Western Pacific). First analysis of incidence and mortality for pancreatic cancer was for 2020. The trends analyses included only countries with data for pancreatic cancer incidence/mortality available in the observed period (from 1991 or later) continuously, provided that there were data for at least 15 years in a row continuously. Countries with missing values in any year of trend analysis were excluded from the analysis. Specifics about the availability of incidence and mortality data of pancreatic cancer since 1991, as well as the quality classification of data for different countries by years in observed period are defined in Supplementary Table 1. In this study, the trend analysis included only countries with high/medium data quality.

For pancreatic cancer incidence and mortality, all figures were adjusted by age and presented as age-standardized rates (ASRs, *per* 100000 persons) calculated by the direct method of standardization by age and sex, using the World standard population according to the Segi–Doll World reference population [2].

Statistical analysis

Trends in pancreatic cancer incidence and mortality rates were calculated using Joinpoint regression analysis software version 4.9.0.0 (National Cancer Institute, Bethesda, MD, USA – March 2021, available through the Surveillance Research Program of the US National Cancer Institute), proposed by Kim *et al* [16]. The joinpoint regression analysis was used to assess the magnitude and direction of temporal trends in incidence and mortality of pancreatic cancer. The joinpoint regression analysis detected points, the so-called joinpoints, at which there was a significant change in trend in rates of pancreatic cancer, using the calendar year as a regression variable. The ASR was used as the dependent variable, while the by-variables were sex and age group. A Monte Carlo permutation test for multiple comparisons was used and 4499 randomly selected data sets, which finds the best fit line for each segment[16]. The analysis started with a minimum of zero joinpoints (*i.e.*, a straight line) and tested whether a change in the trend was significant by testing more joinpoints up to the maximum of four (five segments)[16]. The resulting regression equation was: $y = a + bx$, where $y = ln(rate)$ and x = calendar year, with slope a and y intercept b, whereby average annual percent change (AAPC) was estimated as $100 \times (eb\ \ 1)$. The Grid Search method was selected[17]. The trend of pancreatic cancer incidence and mortality in each country was presented with a straight line in the whole period, even if there were changes in trends in the observed period. The AAPC over the entire study period with the corresponding 95% confidence interval (95%CI) was determined[18]. In describing the direction of temporal trends, the terms significant increase or significant decrease were used, in order to signify that the slope of the trend was

statistically significant ($P < 0.05$, on the basis of the statistical significance of the AAPC compared to zero). Additionally, analysis was performed by sex and age (30–49, 50–69, ≥ 70 years) in selected countries. Trends were not evaluated separately among persons aged < 30 years due to the small number of pancreatic cancer cases in this age group. A line diagram of joinpoint analysis for individual countries provided information about the number of the joinpoints for the trends in incidence and mortality of pancreatic cancer by sex, by describing of annual percent change and the corresponding 95%CI.

Ethics statement

This study was approved by the Ethics Committee of the Faculty of Medical Sciences, University of Kragujevac (No. 01-14321).

RESULTS

Pancreatic cancer incidence and mortality: 2020 results

Globally, the total number of new pancreatic cancer cases was 495 773 in 2020: it was diagnosed in 262 865 (53%) males and 232 908 (47%) females (Figure 1). The total number of pancreatic cancer deaths was 466 003 (246 840 males and 219 163 females). Male to female ratio was: 1.1:1 both for incidence and mortality. In both sexes, most new cases (191 348; 38.6% of the total) and deaths (182 074; 39.1% of the total) occurred in the Western Pacific Region. In males, the least number of pancreatic cancer new cases (6062; 2.3% of total) and deaths (5920; 2.4% of total) was recorded in the African region. In females, the least number of pancreatic cancer new cases (5048; 2.2% of total) and deaths (4924; 2.2% of total) was recorded in the Eastern Mediterranean Region.

The global ASR of incidence of pancreatic cancer was 4.9 *per* 100000 population in both sexes (5.7 in males *vs* 4.1 in females), and ASR of mortality was 4.5 (5.3 in males *vs* 3.8 in females) (Figure 2). In both sexes, the highest incidence ASRs was found in the European Region (9.3 in males *vs* 6.2 in females), while the lowest rates were in the South-East Asia Region (1.6 in males *vs* 1.0 in females). Also in both sexes, the highest mortality ASRs were found in the European Region (8.7 in males *vs* 5.7 in females), while the lowest rates were in the South-East Asia Region (1.6 in males *vs* 1.0 in females).

There were significant international variations in incidence and mortality of pancreatic cancer in 2020 (Figures 3 and 4). The highest ASRs of incidence and mortality of pancreatic cancer in both sexes in 2020 were in Hungary (11.2 and 10.2, respectively). The highest incidence ASRs in males and females were in Hungary (13.7 and 9.2 *per* 100000), followed by Uruguay (12.8 and 8.9), while the lowest rates (equally about 0.5) were reported in Botswana, Eswatini and Malawi in males, and in India, Sri Lanka and Pakistan in females. The highest mortality ASR in males was in Hungary (12.6) and in females in Uruguay (8.5), while the lowest rate was in Malawi in males (0.46) and in Pakistan in females (0.30). In comparison to males, the incidence and mortality ASRs were lower in females in countries across the world in 2020: The only exceptions were for females in Bahrain, Belize, Brunei, Burkina Faso, Cabo Verde, Eswatini, Gabon, Ghana, Kenya, Libya, Malawi, Nepal, New Zealand, Peru, Qatar, Gambia, Uganda and United Arab Emirates where rates higher than in males were recorded.

Patterns in pancreatic cancer incidence trends

Most of the countries showed a meaningful increase in pancreatic cancer incidence in both males and females, but the magnitude of increasing incidence trends for pancreatic cancer was higher in females than in males in almost all countries (Figure 5). Out of all countries with an increase in pancreatic cancer incidence, females in France and India showed the most marked rise in incidence rates (AAPC = +3.9% and AAPC = +3.7%, respectively). In males in Kuwait and Turkey the most marked rise in incidence rates was recorded (both equally by AAPC = +3.6%). In some countries, pancreatic cancer incidence trends were significantly increasing in females (Czechia, Germany, India, Latvia, Lithuania, Malta, Netherlands, Norway and Switzerland), in contrast to males. Decreasing trends of pancreatic cancer incidence were observed in some countries but without significance. In some of the most developed countries (such as the UK and Sweden), in both sexes significantly increasing trends in pancreatic cancer incidence rates were observed in the last decade, which followed a previous period characterized by a declining incidence trend (Supplementary Figure 1). In contrast to that, two decades of continuous growth, a downward trend of pancreatic cancer incidence rates in both sexes happened in the more recent decade in Denmark.

Pattern in pancreatic cancer mortality trends

The majority of analyzed countries showed a significant increase in pancreatic cancer mortality in both males and females, but the magnitude of mortality increasing trends for pancreatic cancer was higher in females than in males in almost all countries since 1991 (Figure 6). Out of all countries with an increase in pancreatic cancer mortality rates, Turkmenistan showed the most marked rise both in males (AAPC = +10.0%, 95%CI: 7.4–12.5) and females (AAPC = +6.4%, 95%CI: 3.5–9.5). In some countries, pancreatic

New cases

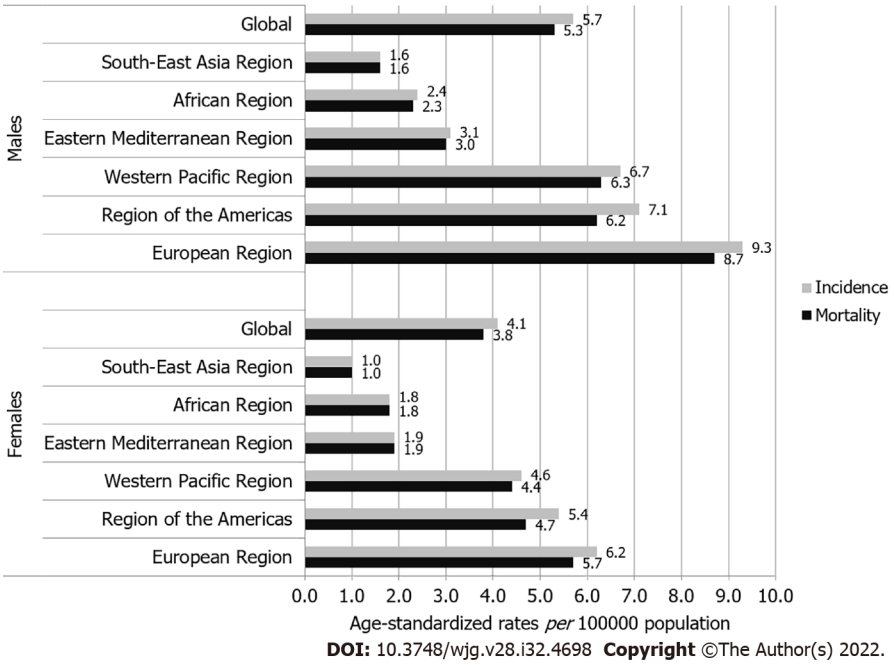
	Males			Females	
	Number	%		Number	%
Western Pacific Region	103678	39.5	Western Pacific Region	87670	37.6
European Region	77571	29.5	European Region	75755	32.5
Region of the Americas	51415	19.6	Region of the Americas	48580	20.9
South-East Asia Region	15855	6.0	South-East Asia Region	10345	4.4
Eastern Mediterranean Region	8211	3.1	African Region	5464	2.3
African Region	6062	2.3	Eastern Mediterranean Region	5048	2.2
Global	262865	100.0	Global	232908	100.0

Deaths

	Males			Females	
	Number	%		Number	%
Western Pacific Region	97911	39.7	Western Pacific Region	84163	38.4
European Region	73872	29.9	European Region	71138	32.5
Region of the Americas	45785	18.6	Region of the Americas	43522	19.9
South-East Asia Region	15411	6.2	South-East Asia Region	10045	4.6
Eastern Mediterranean Region	7874	3.2	African Region	5326	2.4
African Region	5920	2.4	Eastern Mediterranean Region	4924	2.2
Global	246840	100.0	Global	219163	100.0

DOI: 10.3748/wjg.v28.i32.4698 **Copyright** ©The Author(s) 2022.

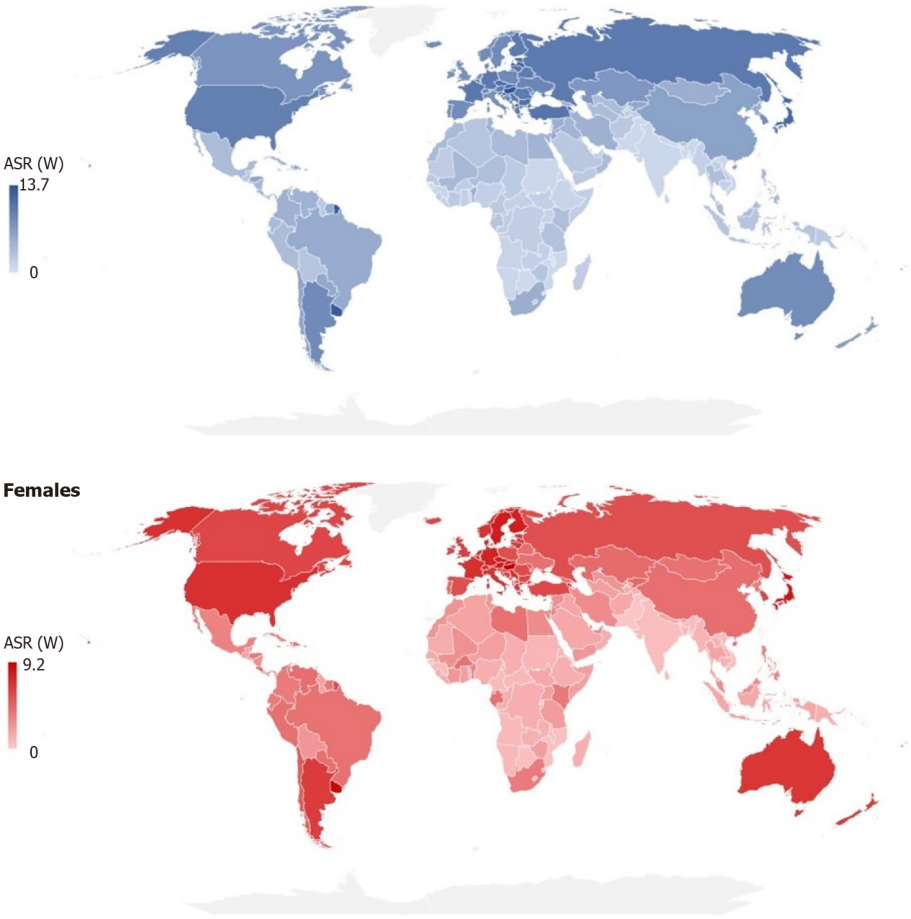
Figure 1 Number of new cases and deaths of pancreatic cancer, by World Health Organization regions and sex, 2020.



DOI: 10.3748/wjg.v28.i32.4698 **Copyright** ©The Author(s) 2022.

Figure 2 Incidence and mortality of pancreatic cancer (global and by World Health Organization regions), by sex, 2020.

cancer mortality trends were significantly increasing in males (Colombia, Kyrgyzstan and Mauritius), in contrast to females. Our results suggested that there were only two countries where significant decreasing pancreatic cancer mortality trends were observed in both sexes: Canada (by 0.4% per year in males and by 0.2% per year in females) and Mexico (by 0.7% in males and 0.8% in females). However, there were only two countries where decreasing pancreatic cancer mortality trends were observed in males only: Czechia (by 0.4% per year) and Ireland (by 0.7%). In some of the most developed countries (such as the USA, UK and Germany) significantly increasing trends in pancreatic cancer mortality rates were observed since the 1990s (Supplementary Figure 2).



DOI: 10.3748/wjg.v28.i32.4698 **Copyright** ©The Author(s) 2022.

Figure 3 Estimated age-standardized incidence rates of pancreatic cancer in 2020. ASR (W): Age-standardized rate (using World standard population, *per* 100000).

Pattern in pancreatic cancer trends according to age classes, by sexes

The greatest increase in pancreatic cancer incidence was noted in people aged ≥ 70 years in France in both males (by +4.2% per year) and females (by +4.9%) (Table 1). An increase was observed in most of the countries in both sexes for persons aged ≥ 50 years. A decreasing trend in incidence of pancreatic cancer was recorded only in females aged ≥ 70 years in Canada (by 0.3% per year). Also, a decreasing trend in pancreatic cancer incidence in males aged ≥ 70 years was noted only in Canada (by 0.4% per year). In males aged 30–49 years, incidence rates decreased mainly in transitional countries (Czechia by 1.9%, Estonia 2.1%, Latvia 2.2%, Lithuania 2.2% and Slovakia 1.5%). In almost all countries a significantly increasing trend in mortality of pancreatic cancer was recorded both in males and females aged ≥ 70 years. A similar pattern was observed in people aged 50–69 years. The greatest increase in pancreatic cancer mortality was in people aged ≥ 70 years in Turkmenistan in both males (by +12.8%) and females (by +11.4%). Large disparities were observed in changes of rates among the young age group, where mortality rates decreased over the study period for most countries. The favorable change was higher in transitional countries (Czechia by 3.3% in males, 2.7% in females; Latvia by 2.7% in males, 4.7% in females).

DISCUSSION

In 2020, the highest incidence and mortality rates of pancreatic cancer were reported in developed countries. The pattern of rising pancreatic cancer incidence and mortality was seen across countries worldwide in the last three decades, in both developed and transitioned populations. Increasing trend was most pronounced among persons aged ≥ 50 years, similarly among males and females. However, it is promising that pancreatic cancer mortality rates were declining in some countries such as Canada and Mexico.

In both sexes together, the highest incidence and mortality rates of pancreatic cancer in 2020 were reported in the European region (7.6 cases and 7.1 deaths *per* 100000 persons, respectively) and the Americas region (6.2 cases and 5.4 deaths *per* 100000 persons, respectively), while the lowest were

Table 1 Joinpoint analysis for pancreatic cancer incidence and mortality trends[1], by country/sex/age, since 1991 (as per data availability)

Countries[2]	Incidence						Mortality					
	Males			Females			Males			Females		
	30-49	50-69	70+	30-49	50-69	70+	30-49	50-69	70+	30-49	50-69	70+
Australia	+1.8[1]	+0.8[1]	+0.7[1]	+1.7[1]	+1.3[1]	+0.8[1]	0.2	-0.1	+0.4[1]	-0.2	-0.0	+0.8[1]
Austria[2]							-0.3	-0.2	-0.0	0.4	0.3	+0.3[1]
Belarus[2]	0.7	-0.1	-0.2	0.7	0.2	0.5						
Belgium[2]							-1.2[1]	-0.2	0.2	0.6	+0.6[1]	+0.6[1]
Brazil	2.5	+4.2[1]	1.3	-	2.5	-0.0	+0.5[1]	+1.4[1]	+1.6[1]	+2.0[1]	+1.6[1]	+1.6[1]
Bulgaria	0.2	+2.9[1]	+2.5[1]	+2.9[1]	+2.8[1]	+3.1[1]	-1.2[1]	+1.5[1]	+2.1[1]	1.1	+1.8[1]	+2.6[1]
Canada	0.2	-0.2	-0.4[1]	0.7	0.3	-0.3[1]	-0.3	-0.8[1]	-0.1	0.0	-0.6[1]	+0.3[1]
Chile	-	4.0	-1.3	-	0.3	-0.8	+2.2[1]	0.4	+1.1[1]	0.6	+0.8[1]	+1.2[1]
China[3]	0.6	+0.8[1]	+1.0[1]	-0.3	0.4	+1.6[1]	+2.0[1]	0.5	+1.1[1]	-	0.4	+1.8[1]
Colombia	-	0.2	-1.7	-0.1	-0.9	-0.8	0.9	0.3	0.3	0.6	-0.5	+0.7[1]
Costa Rica	-0.7	-1.8[1]	-0.3	-0.3	-0.9	-0.5	0.2	-1.4	-0.9	-1.8	0.4	-1.7[1]
Croatia	-1.0	+0.7[1]	0.7	0.6	+1.8[1]	+0.8[1]	-1.2	+0.8[1]	+1.7[1]	0.1	+1.3[1]	+2.1[1]
Cuba[2]							1.3	-0.1	-0.8[1]	0.4	0.3	-0.3
Czechia	-1.9[1]	+0.3[1]	+0.6[1]	0.4	+1.1[1]	+0.7[1]	-3.3[1]	-0.2	+0.4[1]	-2.7[1]	+0.5[1]	+0.4[1]
Denmark	-0.7	+1.1[1]	+1.0[1]	0.8	+0.7[1]	+0.9[1]	-1.9[1]	+0.5[1]	0.5	-1.6	0.2	+0.7[1]
El Salvador[2]							+5.8[1]	+2.9[1]	+4.7[1]	-1.1	+4.2[1]	+3.0[1]
Estonia	-2.1[1]	0.1	+1.7[1]	-1.5	0.7	1.3	-3.2[1]	-1.0[1]	-1.6[1]	-	0.4	+3.3[1]
Finland	-1.4[1]	+0.9[1]	0.3	-0.4	+1.3[1]	+0.5[1]	-2.5[1]	+0.7[1]	+0.5[1]	-2.5[1]	+0.9[1]	+0.6[1]
France	+1.7[1]	+2.9[1]	+4.2[1]	+2.8[1]	+3.5[1]	+4.9[1]	-0.5[1]	+0.3[1]	+0.4[1]	+1.6[1]	+1.3[1]	+1.1[1]
Germany	-1.2	1.1	+1.2[1]	0.9	1.4	0.7	-0.2	0.2	+0.6[1]	+0.7[1]	+0.8[1]	+0.8[1]
Guatemala[2]							-4.1[1]	0.4	0.7	-1.6	0.3	-0.5
Hungary[2]							-2.0[1]	+0.6[1]	+0.5[1]	-0.5	+1.0[1]	+0.9[1]
Iceland	-	-0.1	0.4	-	-0.1	-0.3	-	-1.4	0.8		-1.2	-0.1
India[2,3]	0.1	0.9	2.4	3.7	+4.0[1]	+4.5[1]						
Ireland	0.9	+1.3[1]	-0.0	1.5	0.3	+0.7[1]	-1.2	-1.1[1]	-0.0	-2.1	-0.9[1]	+0.9[1]
Israel	1.3	+1.2[1]	+1.6[1]	+4.2[1]	+1.8[1]	+1.2[1]	-1.0	0.2	+1.0[1]	0.7	0.6	+1.0[1]
Italy	1.4	+0.9[1]	+1.4[1]	+4.5[1]	+1.8[1]	+2.1[1]	-0.4	0.0	+0.7[1]	0.5	+0.6[1]	+1.3[1]
Japan	-1.2	+0.7[1]	+0.5[1]	0.8	+1.6[1]	+1.0[1]	-1.4[1]	+1.0[1]	+0.7[1]	-1.0[1]	+1.7[1]	+1.5[1]
Kuwait	-	3.1	6.6	-0.0	-1.6	-	-	1.3	-1.9	-	2.7	2.1
Kyrgyzstan[2]							-0.1	0.2	+5.7[1]	3.1	0.6	+3.2[1]
Latvia	-2.2[1]	0.0	-0.4	-2.3	+1.4[1]	0.7	-2.7[1]	-0.2	-0.2	-4.7[1]	-0.1	+2.0[1]
Lithuania	-2.2[1]	-0.1	-0.1	1.5	0.1	+1.3[1]	-0.7	-0.5[1]	0.2	1.0	0.0	+1.3
Luxembourg[2]							-	-0.2	1.0	-	0.5	1.2
Malta	-	1.2	0.2	-	3.0	+2.3[1]	-	1.4	-0.7	-	+2.0[1]	+1.8[1]
Mauritius[2]							-1.4	+1.4[1]	+2.5[1]	-	0.4	0.4
Mexico[2]							0.5	-0.8[1]	-0.7[1]	-0.6	-1.5[1]	-0.0
Netherlands	0.5	+0.6[1]	0.5	0.6	+1.6[1]	+1.0[1]	-0.5	-0.5[1]	0.3	0.6	+1.0[1]	+0.7[1]
New Zealand	2.0	-0.3	0.4	0.8	0.1	0.9	1.0	-0.9	0.3	1.2	-0.5	+1.2[1]

North Macedonia[2]							0.2	+1.2[1]	+2.1[1]	1.3	+1.6[1]	+1.9[1]
Norway	-0.8	0.4	0.2	0.2	+1.3[1]	0.3	-0.4	-0.1	0.3	-1.8	0.2	+0.5[1]
Panama[2]							-	-0.1	0.4	0.3	0.5	-0.5
Republic of Korea	-						-0.5[1]	-0.3	+2.7[1]	0.4	0.1	+4.5[1]
Republic of Moldova[2]							-0.1	0.3	0.6	-2.2	-0.3	+1.7[1]
Romania[2]							-0.8	+1.4[1]	+2.2[1]	-0.1	+1.5[1]	+3.0[1]
Russian Federation[2]							-1.6[1]	0.0	+1.3[1]	-0.2	-0.0	+2.1[1]
Serbia[2]							-0.6	+1.0[1]	+2.1[1]	0.5	+1.1[1]	+2.8[1]
Singapore[2]							0.6	0.8	+2.1[1]	-	0.5	+2.1[1]
Slovakia	-1.5[1]	+1.0[1]	+1.6[1]	0.7	+1.5[1]	+2.3[1]	-2.2[1]	0.1	+0.9[1]	-0.2	+0.9[1]	+1.9[1]
Slovenia	0.6	+1.2[1]	+1.4[1]	2.8	+1.9[1]	+1.8[1]	-1.5	+0.7[1]	+1.1[1]	0.8	0.4	+1.1[1]
Spain	0.2	+1.3[1]	0.3	2.0	+2.4[1]	+0.9[1]	-0.3	+0.7[1]	+1.2[1]	+1.5[1]	+1.4[1]	+1.5[1]
Sweden	-0.4	0.0	-0.4	0.2	0.1	0.0	-2.2[1]	0.0	+0.4[1]	-1.8[1]	-0.2	+0.6[1]
Switzerland	1.2	0.9	-1.0	1.1	0.6	+1.9[1]	-0.7	0.2	-0.2	0.7	0.1	+0.8[1]
Turkey[2]	2.3	+3.4[1]	+4.5[1]	1.6	+3.6[1]	+2.3[1]						
Turkmenistan[2]							-	+8.1[1]	+12.8[1]		3.2	+11.4[1]
United Kingdom	0.3	+0.4[1]	+0.4[1]	+1.1[1]	+0.7[1]	+0.9[1]	-0.6[1]	-0.2	0.2	-0.3	-0.0	+0.7[1]
United States	0.3	+0.6[1]	+0.5[1]	+1.6[1]	+0.7[1]	+0.4[1]	-0.0	-0.0	+0.4[1]	+0.7[1]	-0.1	+0.5[1]
Uruguay[2]							-2.3	+1.6[1]	+1.3[1]	2.4	+1.0[1]	+1.8[1]
Venezuela[2]							-1.8[1]	0.8	0.3	-0.1	0.5	0.4

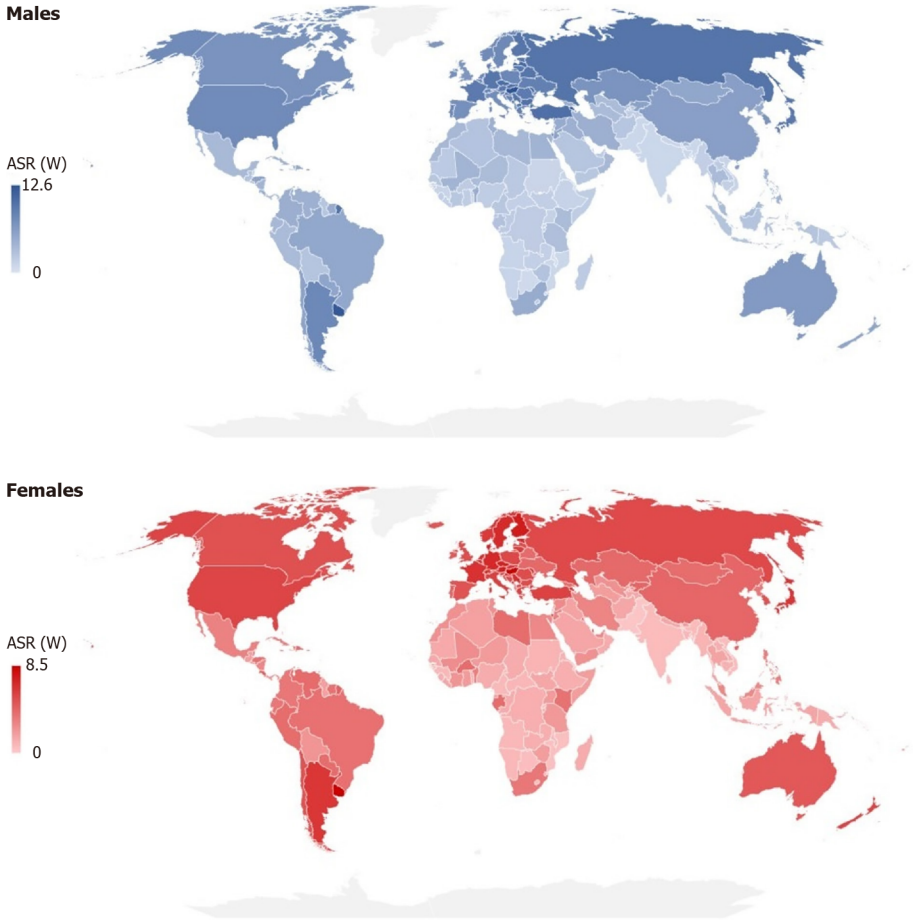
Source: GLOBOCAN 2020 estimates[2].

[1]Statistically significant trend ($P < 0.05$), for full period presented.

[2]Joinpoint results are not shown for incidence/mortality in some countries, because there were no data for pancreatic cancer in the whole observed period continuously. For the trend analysis, we presented all incidence/mortality data available from 1991 onwards, provided that there were data for at least 15 years in a row continuously.

[3]These countries have sample vital registration systems (although coverage is low, the sample provides population-representative information)[14].

recorded in South-East Asia (equally 1.3 cases and deaths *per* 100000 persons). Since due to delayed disease detection and limited effectiveness of therapies the survival for pancreatic cancer remains poor [3,4,19], its mortality is still largely determined by its incidence. Besides, the overall survival rates vary little between developed and developing countries[20]. Since the risk of pancreatic cancer occurrence increases linearly with age and the average age at the time of diagnosis of pancreatic cancer is 70 years [2-6], significant geographic differences in pancreatic cancer incidence and mortality rates could be explained by differences in life expectancy at birth by region. Although improving continuously in all regions in the past decades, life expectancy at birth in 2019 was the highest in countries in Northern America and Europe, and the lowest in South Asia and Africa[21]. Also, the GBD study showed the association of age-standardized incidence and mortality rates for pancreatic cancer with development status at the national level (measured by the Socio-demographic Index, that composes the total fertility rate among women under the age of 25 years, mean education for individuals aged ≥ 15 years, and income per capita) in 2017[6]. Based on the current evidence, international variations in incidence rates of pancreatic cancer are mainly attributed to exposure to environmental factors, particularly tobacco smoking, obesity, diabetes mellitus, alcohol consumption[6,22,23]. Additionally, the migrant effect among Japanese in Hawaii[24] and the discrepancies in pancreatic cancer incidence in Chinese populations[25], which share a similar genetics, but have lived in different regions, indicate that cancer development was mainly determined by environmental factors. Based on the WHO 2015 estimates, the prevalence of tobacco smoking was the highest in countries in the European Region (35% in Greece, equally 33% in the Russian Federation and Serbia), intermediate (~20%) in Western Pacific and Eastern Mediterranean Regions, and lowest (~10%) in Africa and the Americas[26]. Based on the results of the GBD Study, pancreatic cancer deaths worldwide were primarily attributable to smoking (25.9% in males, 16.1% in females), high fasting plasma glucose (9.3% in males, 8.6% in females), and high body mass index (5.0% in males, 7.4% in females) in 2017[6]. In both sexes together in 2017, fraction of pancreatic cancer age-standardized deaths attributable to smoking was the highest in central Europe (28.2% of all pancreatic cancer deaths), while the highest fraction attributable to high fasting plasma

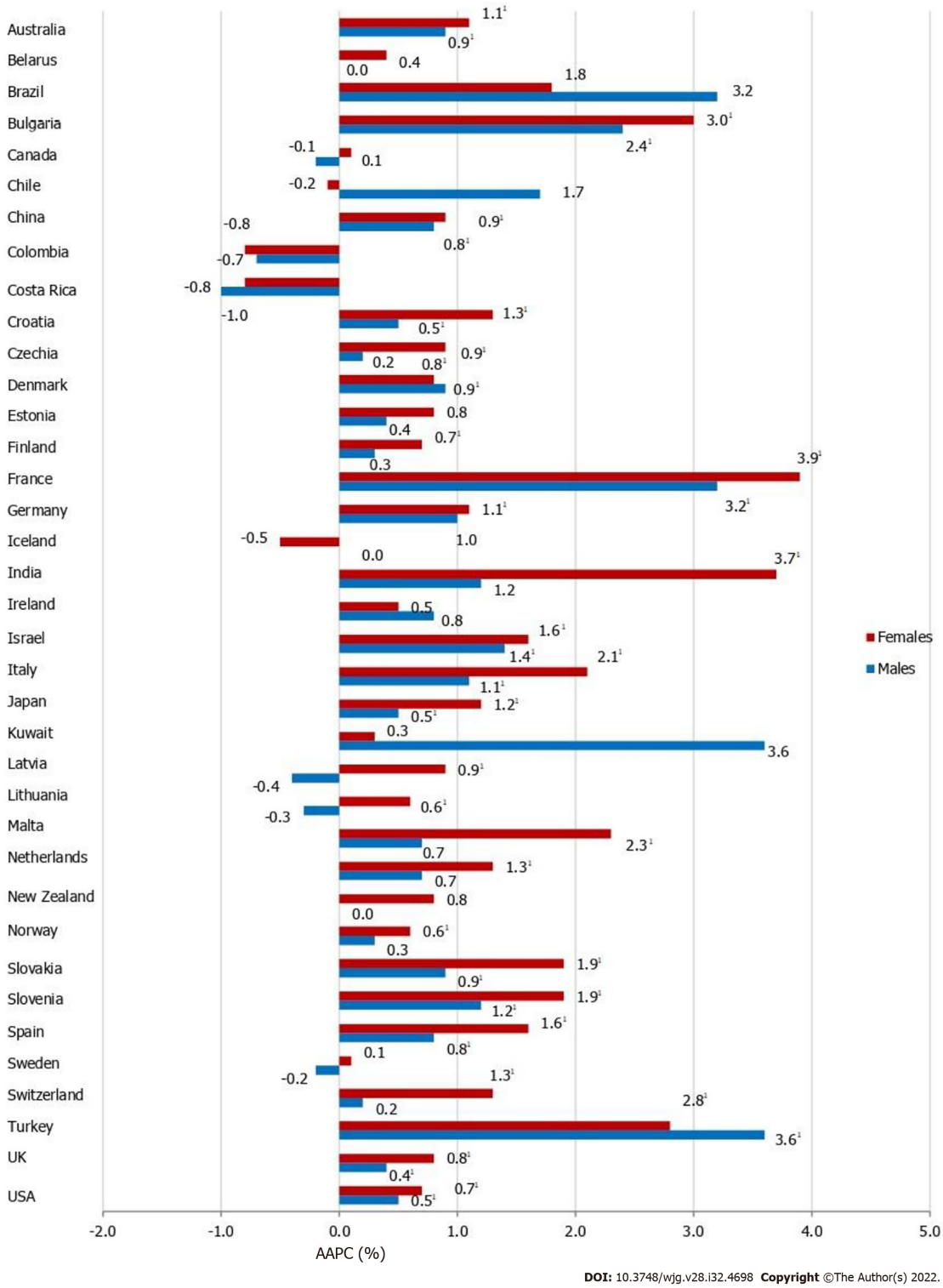


DOI: 10.3748/wjg.v28.i32.4698 **Copyright** ©The Author(s) 2022.

Figure 4 Estimated age-standardized mortality rates of pancreatic cancer in 2020. ASR (W): Age-standardized rate (using World standard population, *per* 100000).

glucose was observed in Oceania (16.6%), and the highest fraction attributable to high body mass index was observed in high-income North America (10.2%)[6]. Similarly, the correlation analysis of risk factors for pancreatic cancer for 48 countries showed that higher incidence and mortality rates among men were significantly associated with higher prevalence of smoking, alcohol drinking, physical inactivity, obesity and high cholesterol levels[27]. At the same time, pancreatic cancer rates among women were linked with higher prevalence of smoking, alcohol consumption and high cholesterol. In contrast, the correlation analysis indicated absence of association between the prevalence of diabetes mellitus and the incidence and mortality for pancreatic cancer. A recent meta-analysis involving 23 cohort studies indicated that diabetes mellitus was associated with a 52% excess risk for pancreatic cancer[28]. However, the issue of the validity of a cancer certificate always exists and the impact of variations in data quality on incidence rate cannot be ruled out, especially for pancreatic and other cancers with poorer prognosis and in older age groups[29,30]. Pancreatic cancer incidence rates in the world in 2020 indicate the possibility that there is an underestimation of the incidence rates in many countries, mainly in developing countries[2]. Many countries reported an incidence rate that was equal to the mortality rate of pancreatic cancer in 2020, while in a few countries, the mortality rate was higher than the incidence rate[2]. Besides, in many countries, cancer registries were not populational, but sometimes reported data only from urban/metropolitan area.

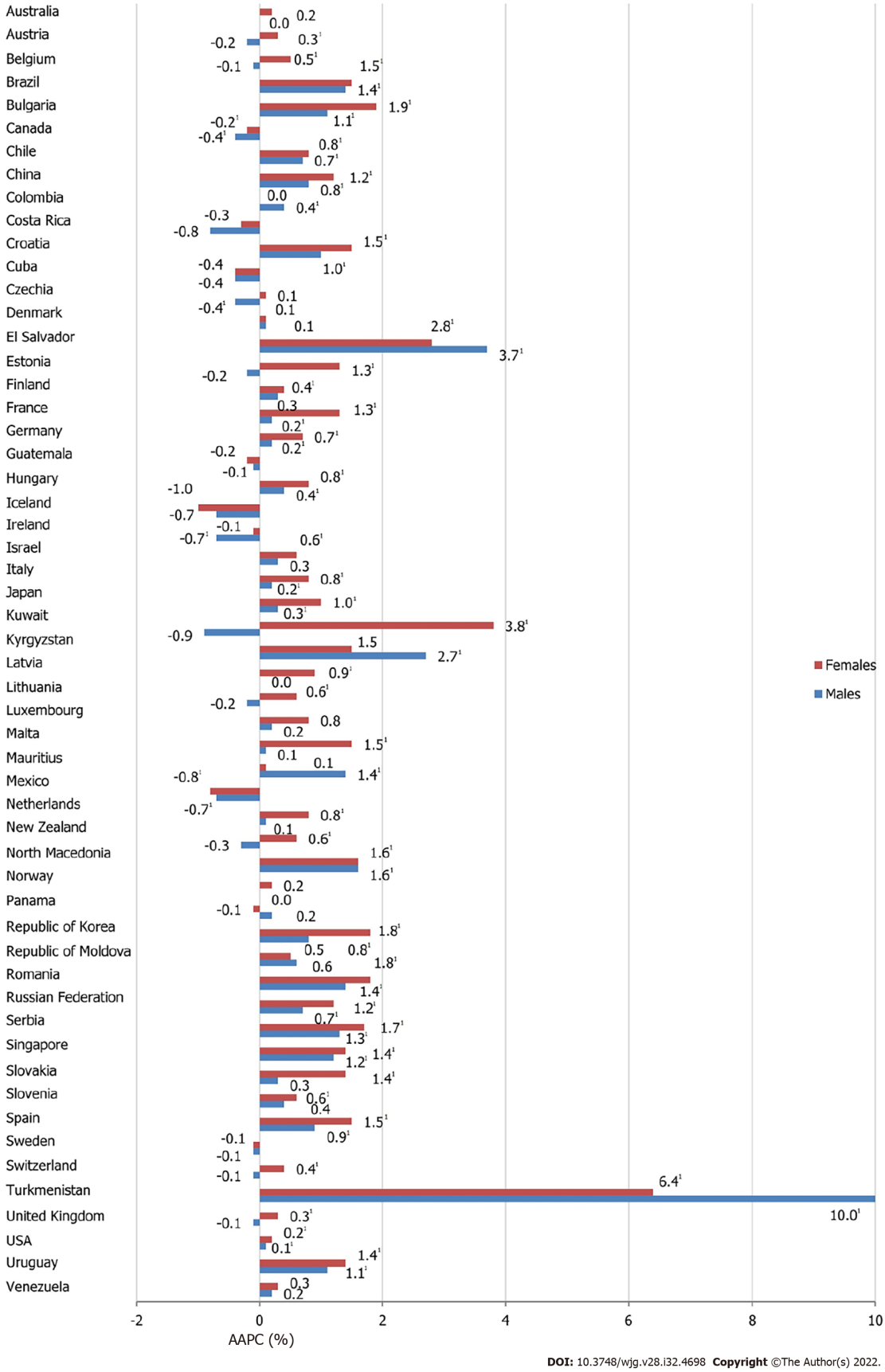
Our study showed unfavorable trends in pancreatic cancer incidence rates in both males and females in many countries in the world in the last three decades. The incidence was noticeably increasing throughout European countries, USA, Australia and Japan, while stable trends in incidence were noted in Canada, Sweden and Ireland. One previous study showed that pancreatic cancer incidence rates gradually increased in males and females among all ages in the USA, Canada, the Netherlands, Australia and New Zealand from the mid-1990s until 2014[31]. In the same study, a decreasing trend of pancreatic cancer incidence in males was noticed only in Iceland and Croatia, while in women there was a significant increasing trend in the incidence of pancreatic cancer in most of the countries from the 1990s onwards[31]. The pancreatic cancer incidence in both sexes in China increased continuously from 1990 to 2019[32]. The observed increasing trends in pancreatic cancer incidence could be attributed to population growth and aging, as well as changes in the prevalence of risk factors for cancer[6,33,34]. The GBD study demonstrated that there was a link between increasing trends in incidence for pancreatic



DOI: 10.3748/wjg.v28.i32.4698 **Copyright** ©The Author(s) 2022.

Figure 5 Pancreatic cancer incidence trends, by country and sex: a joinpoint analysis. [1]Statistically significant trend ($P < 0.05$). Joinpoint results are not shown for incidence in some countries, because there were no data for pancreatic cancer in the whole observed period continuously. For the trend analysis, we presented all incidence data available from 1991 onwards, provided that there were data for at least 15 years in a row continuously. AAPC: Average annual percent change.

cancer and increases in development status at the national level in period 1990–2017[6]. Also, one previous study indicated that increasing trends in pancreatic cancer incidence in both sexes were correlated with socioeconomic development (measured by Human Development Index and Gross Domestic Product per capita)[35]. In the 1980s, a rapid social and economic transition from the lifestyle that characterized socialistic countries (such as countries of the former Eastern Bloc, *etc*.) to an industrialized westernized lifestyle took place[36-38]. It is hypothesized that, with a lag phase, undergoing different states of social and economic transition has contributed to the sharply increasing trends of pancreatic cancer incidence that have been observed in eastern and southern European countries, China



DOI: 10.3748/wjg.v28.i32.4698 **Copyright** ©The Author(s) 2022.

Figure 6 Pancreatic cancer mortality trends, by country and sex: a joinpoint analysis. [1]Statistically significant trend ($P < 0.05$). Joinpoint results are not shown for mortality in some countries, because there were no data for pancreatic cancer in the whole observed period continuously. For the trend analysis, we presented all mortality data available from 1991 onwards, provided that there were data for at least 15 years in a row continuously. AAPC: Average annual percent change.

and Brazil since the 2000s. Based the results of the Czech MONICA and post-MONICA studies, cigarette smoking prevalence declined significantly only in males (from 45.0% in 1985 to 23.9% in 2016/17), while there was no change in the prevalence of smoking in females (from 20.9% to 25.9%) over the analyzed period[38]. Throughout the entire 30-year survey period, for both sexes significantly decreased prevalence of dyslipidemia and the consumption of meat and fat was observed, with increase in vegetable oil intake and fresh fruit and vegetables, whereas a significant increase in body mass index was observed in males only[38]. Both the incidence and mortality trends of pancreatic cancer significantly increased in China during the last decades, which could be due to the rise of the prevalence of overweight to 28.1%, diabetes to 11.2%, and smoking to 28.1% of adults: namely, China consumes about 40% of the world's total cigarettes, and that predominantly among men, with a large increase in consumption over the past few decades[32,39]. A large-scale nationwide cohort study in the Republic of Korea, which included 9 514 171 adults during a median follow-up period of 7.3 years, indicated that diabetes and alcohol consumption were associated with an increased risk of pancreatic cancer[40]. The influence of the improvement of medical imaging on the diagnosis of pancreatic cancer, that is, on the increasing trends of the incidence of pancreatic cancer during the last few decades cannot be ruled out [41].

Pancreatic cancer mortality rates across the countries showed an increasing trend in both sexes. A decreasing trend, however, was found in both sexes only in Canada and Mexico, and a level-off was observed in Denmark, Norway, Sweden, Panama, Moldova and Venezuela. With the exception of some developing countries (Latvia, Kyrgyzstan, Mauritius, Turkmenistan, Nicaragua and Colombia), in all other populations the magnitude of the increase in mortality from pancreatic cancer was higher in women. While the increased trends of pancreatic cancer mortality have long been observed in developed countries (such as the USA, Japan, Germany, France, Italy and Spain)[33], in recent years, a precipitous increase has also been reported in developing countries (such as Kyrgyzstan, Turkmenistan, Bulgaria and Serbia)[42,43]. Some of these changes have been associated with western lifestyle and environmental factors that are linked to an increased risk of pancreatic cancer occurrence (including smoking, diabetes, alcohol consumption, obesity, physical inactivity, and high-energy food intake)[8,22, 23,27,35,38,44]. International patterns in incidence and mortality trends of pancreatic cancer in the last three decades mostly reflect different phases of the smoking epidemic across countries, and among males and females[26]. In support of that, our study indicated that mortality rates from pancreatic cancer showed a slower rise among women and a drop among men in China in the last decade (from 1998 to 2012), which could be affected by reduced prevalence of tobacco consumption[44,45]. Also, significantly decreasing trends in pancreatic cancer mortality in both sexes in Mexico (especially since 2008) can partially be attributed to changes in smoking patterns which are resulting from new tobacco tax/laws which were implemented in Mexico in 2007/2008[46]. Unfortunately, due to the silent nature of disease, late diagnosis, and limited treatment options, and the metastatic potential of pancreatic cancer cells, and its poor prognosis, most pancreatic cancers are diagnosed at an advanced stage, which is not amenable to treatment[42,43]. Differences in the international patterns in incidence and mortality trends of pancreatic cancer in the last three decades could be pertinent to impel continuous efforts to identify novel risk factors (particularly the modifiable risk factors) and implement policies for more effective pancreatic cancer control[34]. Global inequalities in standard medical practices (prevention/diagnosis/therapy) and their impact on pancreatic cancer mortality have not yet been systematically explored[47].

In our study, significantly lower favorable pancreatic cancer incidence trends in the young age group (30–49 years) were observed in women compared to men in all countries. Both older age groups (50–69 and ≥ 70 years), for both men and women, generally showed similar trends in the incidence of pancreatic cancer. Other studies have reported similar results[29,30]. Similar to incidence, significantly less favorable trends in mortality of pancreatic cancer in the young age group (30–49 years) were observed in women compared to men in all countries. In both older age groups (50–69 and ≥ 70 years), both men and women generally showed similarly increasing trends in the mortality of pancreatic cancer. It is particularly promising that in males aged 30–49 years, pancreatic cancer mortality trends were falling in most of the countries. Some studies also reported an increasing trend in mortality for pancreatic cancer in the past decade, especially among women and those aged ≥ 50 years in some countries[24,28]. Although in countries where there is a significant trend in increasing incidence of pancreatic cancer, this increase was recorded at the age of ≥ 50 years. Of particular concern is the significant trend in increasing incidence of pancreatic cancer in the youngest group (30–49 years), which is registered in our study mainly in developed countries (UK, USA, Australia, France, Israel, Italy and Bulgaria). Also, although the trend in increasing mortality from pancreatic cancer was recorded at the age of ≥ 50 years, the significant trend in increasing mortality from pancreatic cancer among the youngest group (30–49 years) in women is particularly worrying (mainly in developed countries such as the USA, France, Germany, Spain and Brazil) and in males in Chile, China, Brazil and El Salvador. Although there is no unified definition, some authors defined the onset of pancreatic cancer at an age of ≤ 50 years as early onset[48,49]. Similar to our results, one study found a significantly increasing trend in incidence of pancreatic cancer among persons younger than 40 years only in women in four high-income countries (Canada, UK, France and the Netherlands)[27]. Despite the fact that some studies suggest an association with cigarette smoking, genetic factors, obesity and metabolic disorders, the

reasons for the increasing trends in incidence and mortality of early-onset pancreatic cancer are still not well understood[50-52]. Population data on tobacco use from 12 European countries revealed that in both men and women, smoking prevalence was the highest among young adults aged 25–44 years, and decreased with increasing age[50]. Results of two prospective US cohort studies indicated that established risk factors were more strongly associated with earlier-onset pancreatic cancer (*i.e.*, among those aged ≤ 60 years), while association attenuated among older people[51]. The question of whether the frequency of performing diagnostic and therapeutic procedures, as well as autopsies at a younger age has an impact on the trend in incidence and mortality from earlier-onset pancreatic cancer should also be clarified in future research[53].

However, certain comparisons of trends may not be feasible due to the unavailability or incompleteness of data in the registries from some countries. Additionally, some factors may contribute to difficulties in international comparisons, including differences in quality of data (such as variations in medical certification, the coding process, accuracy, coverage and completeness of death certification, frequency and registry of autopsies)[2]. However, the observed disparities in trends for pancreatic cancer incidence and mortality across the countries can help generate hypotheses of pancreatic cancer etiology, enable the identification of unknown risk factors, and evaluate preventive/therapy measures. Therefore, the assessment of the patterns in trends in incidence and mortality for pancreatic cancer worldwide based on available data from registries that did not cover all countries (primarily without all African and many Asian countries) is difficult, does not allow for accurate interpretation or valid generalization.

Along with either increasing or stable current incidence and mortality trends of pancreatic cancer in many countries, with the aging population and the increase in prevalence of certain risk factors (cigarette smoking, overweight/obesity, diabetes and alcohol consumption), and taking into consideration that screening for pancreatic cancer is currently not recommended, it would be difficult to expect that the UN Sustainable Development Goal of reducing mortality from cancers (hence pancreatic cancer) by one-third by 2030 can be achieved[8]. Additionally, pancreatic cancer survival is still consistently low [20]. Since the COVID-19 pandemic began there has been concern regarding the possible delay in the diagnosis/treatment of pancreatic cancer, as indicated by a recent study in Portugal[54] about the pancreatic cancer having been diagnosed at a later stage during the pandemic, which is a matter that should be elucidated in future research. In summary, the marked international differences in rates and trends in incidence and mortality of pancreatic cancer indicate the need for introducing a more effective public health approach to prevention and improvements in diagnostic and treatment practices worldwide.

This study analyzed both incidence and mortality figures of pancreatic cancer for 185 WHO member states for 2020. Our study analyzed international patterns in trends of incidence and mortality of pancreatic cancer in the last three decades by sex and age groups. One of the major strengths of our study was the use of the GLOBOCAN database and the large population-based datasets, whereby the trends analysis was conducted only for countries with quality of data that was classified as high or medium. Finally, the described international patterns and trends in pancreatic cancer incidence and mortality over time may be useful in generating hypotheses about risk factors for pancreatic cancer.

However, several possible limitations in this study should be considered. First, there is always a question of reliability and validity of cancer certificates. Also, the quality of data varied significantly from country to country. Additionally, comparison between some countries could be difficult because statistical data quality might change and differ over time. An issue of under-reporting of pancreatic cancer, particularly in developing countries, could introduce bias in the assessment of incidence and mortality trends. Availability of data for the incidence/mortality of pancreatic cancer for each country is different, and in some countries limited. Not all of the data are available for all of the years in the analyzed period (since 1991). Therefore, the data of incidence and mortality are taken for different intervals for some countries, which makes it difficult to compare trends across countries. Besides, our trend analysis did not cover countries with statistical data classified as low quality, which therefore did not allow comparisons for a number of countries. In addition, for some countries, data on pancreatic cancer were available for incidence or mortality only, so greater caution in the inference about trends is recommended. Finally, an epidemiological fallacy was an inherent limitation of this study. Possible modes of mitigation for the above-mentioned limitations include greater diagnostic accuracy of pancreatic cancer, better quality of death certification, implementation of mandatory population-based cancer registry, further reduction of the proportion of uncertain causes of death, introduction of registration of autopsies (*e.g.*, part of pancreatic cancer cases diagnosed at autopsy was missing on the death certificates), provision of survival data for pancreatic cancer patients, as well as the improvements and availability of pancreatic cancer treatment across countries[55-57]. Based on accurate assessment of epidemiological characteristics of pancreatic cancer, policy-makers could provide a better planning for funding, access to more effective treatment and care strategies, scientific and clinical advances in development of effective screening tests, improving early diagnosis and improving survival[55]. Despite these limitations, this study can help assess the international patterns in incidence and mortality trends of pancreatic cancer, which still need to be elucidated in analytical epidemiological studies in the future.

CONCLUSION

Increasing trends in pancreatic cancer incidence and mortality were observed in the last three decades in many countries, in both sexes and most age groups. Further efforts to explore the reasons of differences in international pattern of pancreatic cancer incidence and mortality could be critical for global disease control.

ARTICLE HIGHLIGHTS

Research background

Pancreatic cancer, as the one of most fatal malignancies, remains a critical issue in the global burden of disease.

Research motivation

The main motivation of this study was to describe the international patterns in incidence and mortality trends of pancreatic cancer in the last three decades. Accurate assessment of pancreatic cancer burden is crucial for more effective disease control.

Research objectives

The aim of this study was to estimate trends in incidence and mortality due to pancreatic cancer in the world in the last three decades.

Research methods

A descriptive epidemiological study was done. Pancreatic cancer incidence and mortality data were obtained from the World Health Organization database. The age-standardized rates (expressed *per* 100000) were presented. To estimate trends of incidence and mortality of pancreatic cancer, joinpoint regression analysis was used: the average annual percent change (AAPC) with the corresponding 95% confidence interval (95%CI) was calculated.

Research results

The general pattern of rising pancreatic cancer incidence and mortality was seen across countries worldwide. Out of all countries with an increase in pancreatic cancer incidence, females in France and India showed the most marked rise in incidence rates (AAPC = +3.9% and AAPC = +3.7%, respectively). Decreasing pancreatic cancer incidence trends have been observed in some countries but without significance. Out of all countries with an increase in pancreatic cancer mortality rates, Turkmenistan showed the most marked rise both in males (AAPC = +10.0%, 95%CI: 7.4%–12.5%) and females (AAPC = +6.4%, 95%CI: 3.5%–9.5%). The mortality trends of pancreatic cancer were decreasing in both sexes only in Canada and Mexico.

Research conclusions

The increasing trends in incidence and mortality from pancreatic cancer were observed across the world, particularly in developed countries. The favorable pattern in trends in incidence and mortality of pancreatic cancer was reported in only a few countries.

Research perspectives

Further research is needed to explain the cause of large international differences in incidence and mortality trends of pancreatic cancer.

FOOTNOTES

Author contributions: All authors equally contributed to this paper with conception and design of the study, data acquisition and analysis, interpretation of data, searched the literature, drafting and critical revision and editing, and approval of the final version.

Supported by Ministry of Education, Science and Technological development, Republic of Serbia, 2011-2020, No. 175042.

Institutional review board statement: This study was approved by the Ethics Committee of the Faculty of Medical Sciences, University of Kragujevac (No. 01-14321).

Informed consent statement: The study was conducted using publicly available data. No patient approvals were

sought nor required for this study. The data used for inputs and analysis were derived from public sources (such as websites, primarily). Our research question about the international trends in incidence and mortality of pancreatic cancer in last three decades was based on the number of pancreatic cancer cases and deaths in the world in last three decades. Therefore, as our model-based analysis used aggregated (not individually identifiable) data from publicly available sources, patients were not involved in the design, or conduct, or reporting or dissemination plans of the research.

Conflict-of-interest statement: All the authors report no relevant conflicts of interest for this article.

Data sharing statement: No additional data are available.

STROBE statement: The authors have read the STROBE Statement-checklist of items, and the manuscript was prepared and revised according to the STROBE Statement-checklist of items.

Open-Access: This article is an open-access article that was selected by an in-house editor and fully peer-reviewed by external reviewers. It is distributed in accordance with the Creative Commons Attribution NonCommercial (CC BY-NC 4.0) license, which permits others to distribute, remix, adapt, build upon this work non-commercially, and license their derivative works on different terms, provided the original work is properly cited and the use is non-commercial. See: https://creativecommons.org/Licenses/by-nc/4.0/

Country/Territory of origin: Serbia

ORCID number: Irena Ilic 0000-0001-5347-3264; Milena Ilic 0000-0003-3229-4990.

S-Editor: Gao CC
L-Editor: Kerr C
P-Editor: Li X

REFERENCES

1 **Sung H**, Ferlay J, Siegel RL, Laversanne M, Soerjomataram I, Jemal A, Bray F. Global Cancer Statistics 2020: GLOBOCAN Estimates of Incidence and Mortality Worldwide for 36 Cancers in 185 Countries. *CA Cancer J Clin* 2021; **71**: 209-249 [PMID: 33538338 DOI: 10.3322/caac.21660]

2 **Ferlay J**, Colombet M and Bray F. Cancer Incidence in Five Continents, CI5plus: IARC CancerBase No. 9. [cited 7 Feb 2022]. In: International Agency for Research on Cancer [Internet]. Available from: http://ci5.iarc.fr

3 **Howlader N**, Noone AM, Krapcho M, Miller D, Brest A, Yu M, Ruhl J, Tatalovich Z, Mariotto A, Lewis DR, Chen HS, Feuer EJ, Cronin KA. SEER Cancer Statistics Review, 1975-2018. [cited 22 Feb 2022]. In: National Cancer Institute [Internet]. Available from: https://seer.cancer.gov/csr/1975_2018/

4 **Wang H**, Liu J, Xia G, Lei S, Huang X. Survival of pancreatic cancer patients is negatively correlated with age at diagnosis: a population-based retrospective study. *Sci Rep* 2020; **10**: 7048 [PMID: 32341400 DOI: 10.1038/s41598-020-64068-3]

5 **Global Burden of Disease Cancer Collaboration**, Fitzmaurice C, Abate D, Abbasi N, Abbastabar H, Abd-Allah F, Abdel-Rahman O, Abdelalim A, Abdoli A, Abdollahpour I, Abdulle ASM, Abebe ND, Abraha HN, Abu-Raddad LJ, Abualhasan A, Adedeji IA, Advani SM, Afarideh M, Afshari M, Aghaali M, Agius D, Agrawal S, Ahmadi A, Ahmadian E, Ahmadpour E, Ahmed MB, Akbari ME, Akinyemiju T, Al-Aly Z, AlAbdulKader AM, Alahdab F, Alam T, Alamene GM, Alemnew BTT, Alene KA, Alinia C, Alipour V, Aljunid SM, Bakeshei FA, Almadi MAH, Almasi-Hashiani A, Alsharif U, Alsowaidi S, Alvis-Guzman N, Amini E, Amini S, Amoako YA, Anbari Z, Anber NH, Andrei CL, Anjomshoa M, Ansari F, Ansariadi A, Appiah SCY, Arab-Zozani M, Arabloo J, Arefi Z, Aremu O, Areri HA, Artaman A, Asayesh H, Asfaw ET, Ashagre AF, Assadi R, Ataeinia B, Atalay HT, Ataro Z, Atique S, Ausloos M, Avila-Burgos L, Avokpaho EFGA, Awasthi A, Awoke N, Ayala Quintanilla BP, Ayanore MA, Ayele HT, Babaee E, Bacha U, Badawi A, Bagherzadeh M, Bagli E, Balakrishnan S, Balouchi A, Bärnighausen TW, Battista RJ, Behzadifar M, Bekele BB, Belay YB, Belayneh YM, Berfield KKS, Berhane A, Bernabe E, Beuran M, Bhakta N, Bhattacharyya K, Biadgo B, Bijani A, Bin Sayeed MS, Birungi C, Bisignano C, Bitew H, Bjørge T, Bleyer A, Bogale KA, Bojia HA, Borzì AM, Bosetti C, Bou-Orm IR, Brenner H, Brewer JD, Briko AN, Briko NI, Bustamante-Teixeira MT, Butt ZA, Carreras G, Carrero JJ, Carvalho F, Castro C, Castro F, Catalá-López F, Cerin E, Chaiah Y, Chanie WF, Chattu VK, Chaturvedi P, Chauhan NS, Chehrazi M, Chiang PP, Chichiabellu TY, Chido-Amajuoyi OG, Chimed-Ochir O, Choi JJ, Christopher DJ, Chu DT, Constantin MM, Costa VM, Crocetti E, Crowe CS, Curado MP, Dahlawi SMA, Damiani G, Darwish AH, Daryani A, das Neves J, Demeke FM, Demis AB, Demissie BW, Demoz GT, Denova-Gutiérrez E, Derakhshani A, Deribe KS, Desai R, Desalegn BB, Desta M, Dey S, Dharmaratne SD, Dhimal M, Diaz D, Dinberu MTT, Djalalinia S, Doku DT, Drake TM, Dubey M, Dubljanin E, Duken EE, Ebrahimi H, Effiong A, Eftekhari A, El Sayed I, Zaki MES, El-Jaafary SI, El-Khatib Z, Elemineh DA, Elkout H, Ellenbogen RG, Elsharkawy A, Emamian MH, Endalew DA, Endries AY, Eshrati B, Fadhil I, Fallah Omrani V, Faramarzi M, Farhangi MA, Farioli A, Farzadfar F, Fentahun N, Fernandes E, Feyissa GT, Filip I, Fischer F, Fisher JL, Force LM, Foroutan M, Freitas M, Fukumoto T, Futran ND, Gallus S, Gankpe FG, Gayesa RT, Gebrehiwot TT, Gebremeskel GG, Gedefaw GA, Gelaw BK, Geta B, Getachew S, Gezae KE, Ghafourifard M, Ghajar A, Ghashghaee A, Gholamian A, Gill PS, Ginindza TTG, Girmay A, Gizaw M, Gomez RS, Gopalani SV, Gorini G, Goulart BNG, Grada A, Ribeiro Guerra M, Guimaraes ALS, Gupta PC,

Gupta R, Hadkhale K, Haj-Mirzaian A, Hamadeh RR, Hamidi S, Hanfore LK, Haro JM, Hasankhani M, Hasanzadeh A, Hassen HY, Hay RJ, Hay SI, Henok A, Henry NJ, Herteliu C, Hidru HD, Hoang CL, Hole MK, Hoogar P, Horita N, Hosgood HD, Hosseini M, Hosseinzadeh M, Hostiuc M, Hostiuc S, Househ M, Hussen MM, Ileanu B, Ilic MD, Innos K, Irvani SSN, Iseh KR, Islam SMS, Islami F, Jafari Balalami N, Jafarinia M, Jahangiry L, Jahani MA, Jahanmehr N, Jakovljevic M, James SL, Javanbakht M, Jayaraman S, Jee SH, Jenabi E, Jha RP, Jonas JB, Jonnagaddala J, Joo T, Jungari SB, Jürisson M, Kabir A, Kamangar F, Karch A, Karimi N, Karimian A, Kasaeian A, Kasahun GG, Kassa B, Kassa TD, Kassaw MW, Kaul A, Keiyoro PN, Kelbore AG, Kerbo AA, Khader YS, Khalilarjmandi M, Khan EA, Khan G, Khang YH, Khatab K, Khater A, Khayamzadeh M, Khazaee-Pool M, Khazaei S, Khoja AT, Khosravi MH, Khubchandani J, Kianipour N, Kim D, Kim YJ, Kisa A, Kisa S, Kissimova-Skarbek K, Komaki H, Koyanagi A, Krohn KJ, Bicer BK, Kugbey N, Kumar V, Kuupiel D, La Vecchia C, Lad DP, Lake EA, Lakew AM, Lal DK, Lami FH, Lan Q, Lasrado S, Lauriola P, Lazarus JV, Leigh J, Leshargie CT, Liao Y, Limenih MA, Listl S, Lopez AD, Lopukhov PD, Lunevicius R, Madadin M, Magdeldin S, El Razek HMA, Majeed A, Maleki A, Malekzadeh R, Manafi A, Manafi N, Manamo WA, Mansourian M, Mansournia MA, Mantovani LG, Maroufizadeh S, Martini SMS, Mashamba-Thompson TP, Massenburg BB, Maswabi MT, Mathur MR, McAlinden C, McKee M, Meheretu HAA, Mehrotra R, Mehta V, Meier T, Melaku YA, Meles GG, Meles HG, Melese A, Melku M, Memiah PTN, Mendoza W, Menezes RG, Merat S, Meretoja TJ, Mestrovic T, Miazgowski B, Miazgowski T, Mihretie KMM, Miller TR, Mills EJ, Mir SM, Mirzaei H, Mirzaei HR, Mishra R, Moazen B, Mohammad DK, Mohammad KA, Mohammad Y, Darwesh AM, Mohammadbeigi A, Mohammadi H, Mohammadi M, Mohammadian M, Mohammadian-Hafshejani A, Mohammadoo-Khorasani M, Mohammadpourhodki R, Mohammed AS, Mohammed JA, Mohammed S, Mohebi F, Mokdad AH, Monasta L, Moodley Y, Moosazadeh M, Moossavi M, Moradi G, Moradi-Joo M, Moradi-Lakeh M, Moradpour F, Morawska L, Morgado-da-Costa J, Morisaki N, Morrison SD, Mosapour A, Mousavi SM, Muche AA, Muhammed OSS, Musa J, Nabhan AF, Naderi M, Nagarajan AJ, Nagel G, Nahvijou A, Naik G, Najafi F, Naldi L, Nam HS, Nasiri N, Nazari J, Negoi I, Neupane S, Newcomb PA, Nggada HA, Ngunjiri JW, Nguyen CT, Nikniaz L, Ningrum DNA, Nirayo YL, Nixon MR, Nnaji CA, Nojomi M, Nosratnejad S, Shiadeh MN, Obsa MS, Ofori-Asenso R, Ogbo FA, Oh IH, Olagunju AT, Olagunju TO, Oluwasanu MM, Omonisi AE, Onwujekwe OE, Oommen AM, Oren E, Ortega-Altamirano DDV, Ota E, Otstavnov SS, Owolabi MO, P A M, Padubidri JR, Pakhale S, Pakpour AH, Pana A, Park EK, Parsian H, Pashaei T, Patel S, Patil ST, Pennini A, Pereira DM, Piccinelli C, Pillay JD, Pirestani M, Pishgar F, Postma MJ, Pourjafar H, Pourmalek F, Pourshams A, Prakash S, Prasad N, Qorbani M, Rabiee M, Rabiee N, Radfar A, Rafiei A, Rahim F, Rahimi M, Rahman MA, Rajati F, Rana SM, Raoofi S, Rath GK, Rawaf DL, Rawaf S, Reiner RC, Renzaho AMN, Rezaei N, Rezapour A, Ribeiro AI, Ribeiro D, Ronfani L, Roro EM, Roshandel G, Rostami A, Saad RS, Sabbagh P, Sabour S, Saddik B, Safiri S, Sahebkar A, Salahshoor MR, Salehi F, Salem H, Salem MR, Salimzadeh H, Salomon JA, Samy AM, Sanabria J, Santric Milicevic MM, Sartorius B, Sarveazad A, Sathian B, Satpathy M, Savic M, Sawhney M, Sayyah M, Schneider IJC, Schöttker B, Sekerija M, Sepanlou SG, Sepehrimanesh M, Seyedmousavi S, Shaahmadi F, Shabaninejad H, Shahbaz M, Shaikh MA, Shamshirian A, Shamsizadeh M, Sharafi H, Sharafi Z, Sharif M, Sharifi A, Sharifi H, Sharma R, Sheikh A, Shirkoohi R, Shukla SR, Si S, Siabani S, Silva DAS, Silveira DGA, Singh A, Singh JA, Sisay S, Sitas F, Sobngwi E, Soofi M, Soriano JB, Stathopoulou V, Sufiyan MB, Tabarés-Seisdedos R, Tabuchi T, Takahashi K, Tamtaji OR, Tarawneh MR, Tassew SG, Taymoori P, Tehrani-Banihashemi A, Temsah MH, Temsah O, Tesfay BE, Tesfay FH, Teshale MY, Tessema GA, Thapa S, Tlaye KG, Topor-Madry R, Tovani-Palone MR, Traini E, Tran BX, Tran KB, Tsadik AG, Ullah I, Uthman OA, Vacante M, Vaezi M, Varona Pérez P, Veisani Y, Vidale S, Violante FS, Vlassov V, Vollset SE, Vos T, Vosoughi K, Vu GT, Vujcic IS, Wabinga H, Wachamo TM, Wagnew FS, Waheed Y, Weldegebreal F, Weldesamuel GT, Wijeratne T, Wondafrash DZ, Wonde TE, Wondmieneh AB, Workie HM, Yadav R, Yadegar A, Yadollahpour A, Yaseri M, Yazdi-Feyzabadi V, Yeshaneh A, Yimam MA, Yimer EM, Yisma E, Yonemoto N, Younis MZ, Yousefi B, Yousefifard M, Yu C, Zabeh E, Zadnik V, Moghadam TZ, Zaidi Z, Zamani M, Zandian H, Zangeneh A, Zaki L, Zendehdel K, Zenebe ZM, Zewale TA, Ziapour A, Zodpey S, Murray CJL. Global, Regional, and National Cancer Incidence, Mortality, Years of Life Lost, Years Lived With Disability, and Disability-Adjusted Life-Years for 29 Cancer Groups, 1990 to 2017: A Systematic Analysis for the Global Burden of Disease Study. *JAMA Oncol* 2019; **5**: 1749-1768 [PMID: 31560378 DOI: 10.1001/jamaoncol.2019.2996]

6 **GBD 2017 Pancreatic Cancer Collaborators**. The global, regional, and national burden of pancreatic cancer and its attributable risk factors in 195 countries and territories, 1990-2017: a systematic analysis for the Global Burden of Disease Study 2017. *Lancet Gastroenterol Hepatol* 2019; **4**: 934-947 [PMID: 31648972 DOI: 10.1016/S2468-1253(19)30347-4]

7 **Lippi G**, Mattiuzzi C. The global burden of pancreatic cancer. *Arch Med Sci* 2020; **16**: 820-824 [PMID: 32542083 DOI: 10.5114/aoms.2020.94845]

8 **Yu J**, Yang X, He W, Ye W. Burden of pancreatic cancer along with attributable risk factors in Europe between 1990 and 2019, and projections until 2039. *Int J Cancer* 2021; **149**: 993-1001 [PMID: 33937984 DOI: 10.1002/ijc.33617]

9 **UN General Assembly**. Transforming our world: the 2030 Agenda for Sustainable Development, 21 October 2015, A/RES/70/1. [cited 7 Feb 2022]. In: UN General Assembly [Internet]. Available from http://www.refworld.org/docid/57b6e3e44.html

10 **Ferlay J**, Partensky C, Bray F. More deaths from pancreatic cancer than breast cancer in the EU by 2017. *Acta Oncol* 2016; **55**: 1158-1160 [PMID: 27551890 DOI: 10.1080/0284186X.2016.1197419]

11 **Pergolini I**, Demir IE, Stöss C, Emmanuel K, Rosenberg R, Friess H, Novotny A. Effects of COVID-19 Pandemic on the Treatment of Pancreatic Cancer: A Perspective from Central Europe. *Dig Surg* 2021; **38**: 158-165 [PMID: 33640885 DOI: 10.1159/000513157]

12 **McKay SC**, Pathak S, Wilkin RJW, Kamarajah SK, Wigmore SJ, Rees J, Dunne DFJ, Garcea G, Ahmad J, de Liguori Carino N, Sultana A, Silva M, Lykoudis P, Nasralla D, Milburn J, Shah N, Kocher HM, Bhogal R, Baron RD, Navarro A, Halle-Smith J, Al-Sarireh B, Sen G, Jamieson NB, Briggs C, Stell D, Aroori S, Bowles M, Kanwar A, Harper S, Menon K, Prachalias A, Srinivasan P, Frampton AE, Jones C, Arshad A, Tait I, Spalding D, Young AL, Durkin D, Ghods-Ghorbani M, Sutcliffe RP, Roberts KJ. Impact of SARS-CoV-2 pandemic on pancreatic cancer services and treatment pathways: United Kingdom experience. *HPB (Oxford)* 2021; **23**: 1656-1665 [PMID: 34544628 DOI: 10.1016/j.hpb.2021.03.003]

13 **Klein AP**. Pancreatic cancer: a growing burden. *Lancet Gastroenterol Hepatol* 2019; **4**: 895-896 [PMID: 31648975 DOI: 10.1016/S2468-1253(19)30323-1]

14 **World Health Organization**. International classification of disease and related health problems: 10th revision. [cited 7 Feb 2022]. In: World Health Organization [Internet]. Available from: https://www.who.int/standards/classifications/classification-of-diseases

15 **Mathers CD**, Fat DM, Inoue M, Rao C, Lopez AD. Counting the dead and what they died from: an assessment of the global status of cause of death data. *Bull World Health Organ* 2005; **83**: 171-177 [PMID: 15798840]

16 **Kim HJ**, Fay MP, Feuer EJ, Midthune DN. Permutation tests for joinpoint regression with applications to cancer rates. *Stat Med* 2000; **19**: 335-351 [PMID: 10649300 DOI: 10.1002/(sici)1097-0258(20000215)19:3<335::aid-sim336>3.0.co;2-z]

17 **Lerman PM**. Fitting segmented regression models by grid search. *Appl Stat* 1980; **29**: 77-84 [DOI: 10.2307/2346413]

18 **Clegg LX**, Hankey BF, Tiwari R, Feuer EJ, Edwards BK. Estimating average annual per cent change in trend analysis. *Stat Med* 2009; **28**: 3670-3682 [PMID: 19856324 DOI: 10.1002/sim.3733]

19 **Grossberg AJ**, Chu LC, Deig CR, Fishman EK, Hwang WL, Maitra A, Marks DL, Mehta A, Nabavizadeh N, Simeone DM, Weekes CD, Thomas CR Jr. Multidisciplinary standards of care and recent progress in pancreatic ductal adenocarcinoma. *CA Cancer J Clin* 2020; **70**: 375-403 [PMID: 32683683 DOI: 10.3322/caac.21626]

20 **Allemani C**, Matsuda T, Di Carlo V, Harewood R, Matz M, Nikšić M, Bonaventure A, Valkov M, Johnson CJ, Estève J, Ogunbiyi OJ, Azevedo E Silva G, Chen WQ, Eser S, Engholm G, Stiller CA, Monnereau A, Woods RR, Visser O, Lim GH, Aitken J, Weir HK, Coleman MP; CONCORD Working Group. Global surveillance of trends in cancer survival 2000-14 (CONCORD-3): analysis of individual records for 37 513 025 patients diagnosed with one of 18 cancers from 322 population-based registries in 71 countries. *Lancet* 2018; **391**: 1023-1075 [PMID: 29395269 DOI: 10.1016/S0140-6736(17)33326-3]

21 **GBD 2019 Demographics Collaborators**. Global age-sex-specific fertility, mortality, healthy life expectancy (HALE), and population estimates in 204 countries and territories, 1950-2019: a comprehensive demographic analysis for the Global Burden of Disease Study 2019. *Lancet* 2020; **396**: 1160-1203 [PMID: 33069325 DOI: 10.1016/S0140-6736(20)30977-6]

22 **Lugo A**, Peveri G, Bosetti C, Bagnardi V, Crippa A, Orsini N, Rota M, Gallus S. Strong excess risk of pancreatic cancer for low frequency and duration of cigarette smoking: A comprehensive review and meta-analysis. *Eur J Cancer* 2018; **104**: 117-126 [PMID: 30347287 DOI: 10.1016/j.ejca.2018.09.007]

23 **Maisonneuve P**, Lowenfels AB. Risk factors for pancreatic cancer: a summary review of meta-analytical studies. *Int J Epidemiol* 2015; **44**: 186-198 [PMID: 25502106 DOI: 10.1093/ije/dyu240]

24 **Maskarinec G**, Noh JJ. The effect of migration on cancer incidence among Japanese in Hawaii. *Ethn Dis* 2004; **14**: 431-439 [PMID: 15328946]

25 **Liu Z**, Shi O, Cai N, Jiang Y, Zhang K, Zhu Z, Yuan H, Fang Q, Suo C, Franceschi S, Zhang T, Chen X. Disparities in Cancer Incidence among Chinese Population *vs* Migrants to Developed Regions: A Population-Based Comparative Study. *Cancer Epidemiol Biomarkers Prev* 2019; **28**: 890-899 [PMID: 30944147 DOI: 10.1158/1055-9965.EPI-18-0827]

26 **World Health Organization**. WHO report on the global tobacco epidemic, 2015: raising taxes on tobacco. [cited 7 Feb 2022]. In: World Health Organization [Internet]. Available from: https://apps.who.int/iris/handle/10665/178574

27 **Huang J**, Lok V, Ngai CH, Zhang L, Yuan J, Lao XQ, Ng K, Chong C, Zheng ZJ, Wong MCS. Worldwide Burden of, Risk Factors for, and Trends in Pancreatic Cancer. *Gastroenterology* 2021; **160**: 744-754 [PMID: 33058868 DOI: 10.1053/j.gastro.2020.10.007]

28 **Pang Y**, Kartsonaki C, Guo Y, Bragg F, Yang L, Bian Z, Chen Y, Iona A, Millwood IY, Lv J, Yu C, Chen J, Li L, Holmes MV, Chen Z. Diabetes, plasma glucose and incidence of pancreatic cancer: A prospective study of 0.5 million Chinese adults and a meta-analysis of 22 cohort studies. *Int J Cancer* 2017; **140**: 1781-1788 [PMID: 28063165 DOI: 10.1002/ijc.30599]

29 **Møller B**, Jerm MB, Larønningen S, Johannesen TB, Seglem AH, Larsen IK, Myklebust TÅ. The validity of cancer information on death certificates in Norway and the impact of death certificate initiated cases on cancer incidence and survival. *Cancer Epidemiol* 2021; **75**: 102023 [PMID: 34560362 DOI: 10.1016/j.canep.2021.102023]

30 **Rahu K**, McKee M, Mägi M, Rahu M. The fall and rise of cancer registration in Estonia: The dangers of overzealous application of data protection. *Cancer Epidemiol* 2020; **66**: 101708 [PMID: 32446217 DOI: 10.1016/j.canep.2020.101708]

31 **Luo G**, Zhang Y, Guo P, Ji H, Xiao Y, Li K. Global Patterns and Trends in Pancreatic Cancer Incidence: Age, Period, and Birth Cohort Analysis. *Pancreas* 2019; **48**: 199-208 [PMID: 30589831 DOI: 10.1097/MPA.0000000000001230]

32 **Zhu B**, Wu X, Guo T, Guan N, Liu Y. Epidemiological Characteristics of Pancreatic Cancer in China From 1990 to 2019. *Cancer Control* 2021; **28**: 10732748211051536 [PMID: 34713730 DOI: 10.1177/10732748211051536]

33 **Lucas AL**, Malvezzi M, Carioli G, Negri E, La Vecchia C, Boffetta P, Bosetti C. Global Trends in Pancreatic Cancer Mortality From 1980 Through 2013 and Predictions for 2017. *Clin Gastroenterol Hepatol* 2016; **14**: 1452-1462.e4 [PMID: 27266982 DOI: 10.1016/j.cgh.2016.05.034]

34 **Tsai HJ**, Chang JS. Environmental Risk Factors of Pancreatic Cancer. *J Clin Med* 2019; **8** [PMID: 31510046 DOI: 10.3390/jcm8091427]

35 **Wong MCS**, Jiang JY, Liang M, Fang Y, Yeung MS, Sung JJY. Global temporal patterns of pancreatic cancer and association with socioeconomic development. *Sci Rep* 2017; **7**: 3165 [PMID: 28600530 DOI: 10.1038/s41598-017-02997-2]

36 **Shkolnikov VM**, Churilova E, Jdanov DA, Shalnova SA, Nilssen O, Kudryavtsev A, Cook S, Malyutina S, McKee M, Leon DA. Time trends in smoking in Russia in the light of recent tobacco control measures: synthesis of evidence from multiple sources. *BMC Public Health* 2020; **20**: 378 [PMID: 32293365 DOI: 10.1186/s12889-020-08464-4]

37 **Psota M**, Bandosz P, Gonçalvesová E, Avdičová M, Bucek Pšenková M, Studenčan M, Pekarčíková J, Capewell S, O'Flaherty M. Explaining the decline in coronary heart disease mortality rates in the Slovak Republic between 1993-2008. *PLoS One* 2018; **13**: e0190090 [PMID: 29320517 DOI: 10.1371/journal.pone.0190090]

38 **Cífková R**, Bruthans J, Wohlfahrt P, Krajčoviechová A, Šulc P, Jozífová M, Eremiášová L, Pudil J, Linhart A, Widimský J Jr, Filipovský J, Mayer O Jr, Škodová Z, Poledne R, Stávek P, Lánská V. 30-year trends in major cardiovascular risk factors in the Czech population, Czech MONICA and Czech post-MONICA, 1985 - 2016/17. *PLoS One* 2020; **15**: e0232845 [PMID: 32392239 DOI: 10.1371/journal.pone.0232845]

39 **Liu S**, Zhang M, Yang L, Li Y, Wang L, Huang Z, Chen Z, Zhou M. Prevalence and patterns of tobacco smoking among

Chinese adult men and women: findings of the 2010 national smoking survey. *J Epidemiol Community Health* 2017; **71**: 154-161 [PMID: 27660401 DOI: 10.1136/jech-2016-207805]

40 **Park JH**, Han K, Hong JY, Park YS, Park JO. Association between alcohol consumption and pancreatic cancer risk differs by glycaemic status: A nationwide cohort study. *Eur J Cancer* 2022; **163**: 119-127 [PMID: 35065369 DOI: 10.1016/j.ejca.2021.12.027]

41 **Defossez G**, Uhry Z, Delafosse P, Dantony E, d'Almeida T, Plouvier S, Bossard N, Bouvier AM, Molinié F, Woronoff AS, Colonna M, Grosclaude P, Remontet L, Monnereau A; French Network of Cancer Registries (FRANCIM). Cancer incidence and mortality trends in France over 1990-2018 for solid tumors: the sex gap is narrowing. *BMC Cancer* 2021; **21**: 726 [PMID: 34167516 DOI: 10.1186/s12885-021-08261-1]

42 **Saad AM**, Turk T, Al-Husseini MJ, Abdel-Rahman O. Trends in pancreatic adenocarcinoma incidence and mortality in the United States in the last four decades; a SEER-based study. *BMC Cancer* 2018; **18**: 688 [PMID: 29940910 DOI: 10.1186/s12885-018-4610-4]

43 **Seoane-Mato D**, Nuñez O, Fernández-de-Larrea N, Pérez-Gómez B, Pollán M, López-Abente G, Aragonés N. Long-term trends in pancreatic cancer mortality in Spain (1952-2012). *BMC Cancer* 2018; **18**: 625 [PMID: 29866063 DOI: 10.1186/s12885-018-4494-3]

44 **GBD 2019 Risk Factors Collaborators**. Global burden of 87 risk factors in 204 countries and territories, 1990-2019: a systematic analysis for the Global Burden of Disease Study 2019. *Lancet* 2020; **396**: 1223-1249 [PMID: 33069327 DOI: 10.1016/S0140-6736(20)30752-2]

45 **Zhang K**, Tartarone A, Pérez-Ríos M, Novello S, Mariniello A, Roviello G, Zhang J. Smoking burden, MPOWER, future tobacco control and real-world challenges in China: reflections on the WHO report on the global tobacco epidemic 2021. *Transl Lung Cancer Res* 2022; **11**: 117-121 [PMID: 35242633 DOI: 10.21037/tlcr-22-27]

46 **Hernández-Garduño E**. The impact of tobacco tax/law implementation on pancreatic cancer mortality in Mexico, 1999-2015. *Ecancermedicalscience* 2018; **12**: ed85 [PMID: 30483361 DOI: 10.3332/ecancer.2018.ed85]

47 **Noel M**, Fiscella K. Disparities in Pancreatic Cancer Treatment and Outcomes. *Health Equity* 2019; **3**: 532-540 [PMID: 31663065 DOI: 10.1089/heq.2019.0057]

48 **Raimondi S**, Maisonneuve P, Löhr JM, Lowenfels AB. Early onset pancreatic cancer: evidence of a major role for smoking and genetic factors. *Cancer Epidemiol Biomarkers Prev* 2007; **16**: 1894-1897 [PMID: 17855711 DOI: 10.1158/1055-9965.EPI-07-0341]

49 **Piciucchi M**, Capurso G, Valente R, Larghi A, Archibugi L, Signoretti M, Stigliano S, Zerboni G, Barucca V, La Torre M, Cavallini M, Costamagna G, Marchetti P, Ziparo V, Delle Fave G. Early onset pancreatic cancer: risk factors, presentation and outcome. *Pancreatology* 2015; **15**: 151-155 [PMID: 25708929 DOI: 10.1016/j.pan.2015.01.013]

50 **Gallus S**, Lugo A, Liu X, Behrakis P, Boffi R, Bosetti C, Carreras G, Chatenoud L, Clancy L, Continente X, Dobson R, Effertz T, Filippidis FT, Fu M, Geshanova G, Gorini G, Keogan S, Ivanov H, Lopez MJ, Lopez-Nicolas A, Precioso J, Przewozniak K, Radu-Loghin C, Ruprecht A, Semple S, Soriano JB, Starchenko P, Trapero-Bertran M, Tigova O, Tzortzi AS, Vardavas C, Vyzikidou VK, Colombo P, Fernandez E; TackSHS Project Investigators. Who Smokes in Europe? *J Epidemiol* 2021; **31**: 145-151 [PMID: 32249267 DOI: 10.2188/jea.JE20190344]

51 **Yuan C**, Kim J, Wang QL, Lee AA, Babic A; PanScan/PanC4 I-III Consortium, Amundadottir LT, Klein AP, Li D, McCullough ML, Petersen GM, Risch HA, Stolzenberg-Solomon RZ, Perez K, Ng K, Giovannucci EL, Stampfer MJ, Kraft P, Wolpin BM. The age-dependent association of risk factors with pancreatic cancer. *Ann Oncol* 2022; **33**: 693-701 [PMID: 35398288 DOI: 10.1016/j.annonc.2022.03.276]

52 **McWilliams RR**, Maisonneuve P, Bamlet WR, Petersen GM, Li D, Risch HA, Yu H, Fontham ET, Luckett B, Bosetti C, Negri E, La Vecchia C, Talamini R, Bueno de Mesquita HB, Bracci P, Gallinger S, Neale RE, Lowenfels AB. Risk Factors for Early-Onset and Very-Early-Onset Pancreatic Adenocarcinoma: A Pancreatic Cancer Case-Control Consortium (PanC4) Analysis. *Pancreas* 2016; **45**: 311-316 [PMID: 26646264 DOI: 10.1097/MPA.0000000000000392]

53 **LaPelusa M**, Shen C, Arhin ND, Cardin D, Tan M, Idrees K, Geevarghese S, Chakravarthy B, Berlin J, Eng C. Trends in the Incidence and Treatment of Early-Onset Pancreatic Cancer. *Cancers (Basel)* 2022; **14** [PMID: 35053447 DOI: 10.3390/cancers14020283]

54 **Brito M**, Laranjo A, Sabino J, Oliveira C, Mocanu I, Fonseca J. Digestive Oncology in the COVID-19 Pandemic Era. *GE Port J Gastroenterol* 2021; **579**: 1-8 [PMID: 34192128 DOI: 10.1159/000514784]

55 **Laugesen K**, Ludvigsson JF, Schmidt M, Gissler M, Valdimarsdottir UA, Lunde A, Sørensen HT. Nordic Health Registry-Based Research: A Review of Health Care Systems and Key Registries. *Clin Epidemiol* 2021; **13**: 533-554 [PMID: 34321928 DOI: 10.2147/CLEP.S314959]

56 **Gupta N**, Yelamanchi R. Pancreatic adenocarcinoma: A review of recent paradigms and advances in epidemiology, clinical diagnosis and management. *World J Gastroenterol* 2021; **27**: 3158-3181 [PMID: 34163104 DOI: 10.3748/wjg.v27.i23.3158]

57 **Fest J**, Ruiter R, van Rooij FJ, van der Geest LG, Lemmens VE, Ikram MA, Coebergh JW, Stricker BH, van Eijck CH. Underestimation of pancreatic cancer in the national cancer registry - Reconsidering the incidence and survival rates. *Eur J Cancer* 2017; **72**: 186-191 [PMID: 28033529 DOI: 10.1016/j.ejca.2016.11.026]

World Journal of Gastroenterology

Submit a Manuscript: https://www.f6publishing.com

World J Gastroenterol 2022 August 28; 28(32): 4716-4725

DOI: 10.3748/wjg.v28.i32.4716

ISSN 1007-9327 (print) ISSN 2219-2840 (online)

ORIGINAL ARTICLE

Prospective Study

Differential diagnosis of different types of solid focal liver lesions using two-dimensional shear wave elastography

Jia Guo, Dong Jiang, Yi Qian, Jiao Yu, Yi-Jun Gu, Yu-Qing Zhou, Hui-Ping Zhang

Specialty type: Radiology, nuclear medicine and medical imaging

Provenance and peer review: Unsolicited article; Externally peer reviewed.

Peer-review model: Single blind

Peer-review report's scientific quality classification

Grade A (Excellent): A
Grade B (Very good): B
Grade C (Good): 0
Grade D (Fair): 0
Grade E (Poor): 0

P-Reviewer: Corvino A, Italy; Giacomelli L, Italy

Received: April 6, 2022
Peer-review started: April 6, 2022
First decision: June 27, 2022
Revised: July 15, 2022
Accepted: July 31, 2022
Article in press: July 31, 2022
Published online: August 28, 2022

Jia Guo, Department of Ultrasound, Shuguang Hospital Affiliated to Shanghai University of Traditional Chinese Medicine, Shanghai 201203, China

Dong Jiang, Yi Qian, Yi-Jun Gu, Department of Ultrasound, Eastern Hepatobiliary Surgery Hospital Affiliated to Naval Medical University, Shanghai 200433, China

Jiao Yu, Department of Infectious Diseases, Eastern Hepatobiliary Surgery Hospital Affiliated to Naval Medical University, Shanghai 200433, China

Yu-Qing Zhou, Hui-Ping Zhang, Department of Ultrasound, Shanghai Changning Maternity and Infant Health Hospital, East China Normal University, Shanghai 200050, China

Corresponding author: Hui-Ping Zhang, MD, PhD, Associate Chief Physician, Department of Ultrasound, Shanghai Changning Maternity and Infant Health Hospital, East China Normal University, No. 786 Yuyuan Road, Shanghai 200050, China. zhanggirldan@163.com

Abstract

BACKGROUND

The clinical management and prognosis differ between benign and malignant solid focal liver lesions (FLLs), as well as among different pathological types of malignant FLLs. Accurate diagnosis of the possible types of solid FLLs is important. Our previous study confirmed the value of shear wave elastography (SWE) using maximal elasticity (Emax) as the parameter in the differential diagnosis between benign and malignant FLLs. However, the value of SWE in the differential diagnosis among different pathological types of malignant FLLs has not been proved.

AIM

To explore the value of two-dimensional SWE (2D-SWE) using Emax in the differential diagnosis of FLLs, especially among different pathological types of malignant FLLs.

METHODS

All the patients enrolled in this study were diagnosed as benign, malignant or undetermined FLLs by conventional ultrasound. Emax of FLLs and the periphery of FLLs was measured using 2D-SWE and compared between benign and malignant FLLs or among different pathological types of malignant FLLs.

RESULTS

The study included 32 benign FLLs in 31 patients and 100 malignant FLLs in 96 patients, including 16 cholangiocellular carcinomas (CCCs), 72 hepatocellular carcinomas (HCCs) and 12 liver metastases. Thirty-five FLLs were diagnosed as undetermined by conventional ultrasound. There were significant differences between Emax of malignant (2.21 ± 0.57 m/s) and benign (1.59 ± 0.37 m/s) FLLs (P = 0.000), and between Emax of the periphery of malignant (1.52 ± 0.39 m/s) and benign (1.36 ± 0.44 m/s) FLLs (P = 0.040). Emax of liver metastases (2.73 ± 0.99 m/s) was significantly higher than that of CCCs (2.14 ± 0.34 m/s) and HCCs (2.14 ± 0.46 m/s) (P = 0.002). The sensitivity, specificity and accuracy were 71.00%, 84.38% and 74.24% respectively, using Emax > 1.905 m/s (AUC 0.843) to diagnose as malignant and 23 of 35 (65.74%) FLLs with undetermined diagnosis by conventional ultrasound were diagnosed correctly.

CONCLUSION

Malignant FLLs were stiffer than benign ones and liver metastases were stiffer than primary liver carcinomas. 2D-SWE with Emax was a useful complement to conventional ultrasound for the differential diagnosis of FLLs.

Key Words: Focal liver lesions; Conventional ultrasound; Two-dimensional shear wave elastography; Differential diagnosis

©The Author(s) 2022. Published by Baishideng Publishing Group Inc. All rights reserved.

Core Tip: Two-dimensional shear wave elastography (2D-SWE) could address the limitations of point SWE and provide overall elastic information in tumors and locate the stiffest part of the tumors. We used 2D-SWE with maximal elasticity to measure the stiffness of focal liver lesions (FLLs) and to explore the value of 2D-SWE in the differential diagnosis of FLLs, especially among different pathological types of malignant FLLs. Our results showed malignant FLLs were stiffer than benign ones and liver metastases were stiffer than primary liver carcinomas. 2D-SWE with Emax was useful complement to conventional ultrasound for the differential diagnosis of FLLs.

Citation: Guo J, Jiang D, Qian Y, Yu J, Gu YJ, Zhou YQ, Zhang HP. Differential diagnosis of different types of solid focal liver lesions using two-dimensional shear wave elastography. *World J Gastroenterol* 2022; 28(32): 4716-4725

URL: https://www.wjgnet.com/1007-9327/full/v28/i32/4716.htm

DOI: https://dx.doi.org/10.3748/wjg.v28.i32.4716

INTRODUCTION

The clinical management and prognosis differ between benign and malignant solid focal liver lesions (FLLs), and among different pathological types of malignant FLLs[1-3]. Accurate diagnosis of solid FLLs, not only as benign or malignant FLLs, but also the possible types of malignant FLLs, is important [4-6].

Ultrasound elastography, especially two-dimensional shear wave elastography (2D-SWE) which provides quantitative information about tissue stiffness, is a useful tool to differentiate malignant from benign FLLs[7,8]. Our previous study confirmed the value of SWE in the differential diagnosis between benign and malignant FLLs[9].

However, the value of SWE in the differential diagnosis among different pathological types of malignant FLLs has not been proved. Park *et al*[10] showed that cholangiocellular carcinoma (CCC) had the lowest shear wave velocity, followed by liver metastases, and hepatocellular carcinoma (HCC) had the highest shear wave velocity; whereas Gerber *et al*[11] showed that CCC had the highest stiffness and liver metastases had the lowest.

Considering the inhomogeneity of tumor stiffness (especially malignant tumors), we used maximal elasticity (Emax) as the parameter to evaluate the stiffness of FLLs and obtained promising results[9]. In the present study, we used 2D-SWE with Emax as the parameter to measure the stiffness of FLLs and to explore the value of SWE with Emax in the differential diagnosis of FLLs, especially among different pathological types of malignant FLLs.

MATERIALS AND METHODS

Study design

This was a prospective study that was approved by the institutional ethical review board of our hospital. All patients provided written informed consent before ultrasound examination.

Patients

Inpatients in the department of Hepatobiliary Surgery between November 2021 and January 2022 who met the following criteria were included: (1) One or more solid FLLs shown on conventional ultrasound with a maximal lesion depth < 8 cm; and (2) The targeted FLL showed as green on quality mode, indicating good quality of SWE. The exclusion criteria were: (1) Patients refused to join the study; and (2) No definite final diagnosis; malignant tumors except for liver metastases had to be diagnosed pathologically after surgery; benign tumors or liver metastases could be diagnosed pathologically or by contrast-enhanced ultrasound (CEUS) together with contrast-enhanced computed tomography (CT) or contrast-enhanced magnetic resonance imaging (MRI) 1 wk before or after 2D-SWE. We included 132 solid FLLs in 127 patients. The gender, age and history of malignancy were recorded.

Conventional ultrasound examination

An Acuson Sequoia diagnostic ultrasound machine (Siemens Medical Solutions, Mountain View, CA, United States) and a transabdominal 5C1 probe were used for conventional ultrasound examination. Before the examinations, all patients fasted for at least 8 h.

One ultrasound physician with > 15 years' experience in conventional ultrasound performed the hepatic ultrasound scan to detect FLLs. The length and width of every lesion were measured to calculate the volume according to the formula[12]: $V = 0.5\ LW^2$ (V: Volume; L: Length; W: Width). A diagnosis as benign, malignant or undetermined was made for each lesion by the ultrasound physician according to the ultrasound features including the number, size, shape, boundary, echogenicity and blood flow of the lesion and surrounding hepatic echogenicity.

2D-SWE examination

After conventional ultrasound examination, another ultrasound physician who was well trained in ultrasound elastography performed all the 2D-SWE examinations using the same ultrasound equipment and probe, putting no pressure on the skin through the probe. The patients were asked to lie flat on the examination bed. The targeted FLL was shown clearly on the screen and the 2D-SWE mode was activated. A region of interest (ROI) was drawn including the whole or partial tumor and some surrounding liver tissue. If the tumor showed green on quality mode (Figure 1A), it meant that the quality of the 2D-SWE image was up to standard. In velocity mode, we set the speed bar at 0.5-4.0 m/s (Figure 1B); drew two circular ROIs (with 3 mm diameter) to be placed at the stiffest site in the tumor and at the periphery of the tumor (Figure 1C). The maximum values of the two ROIs were recorded (Figure 1D) as Emax for further analysis.

Statistical analysis

SPSS version 13.0 (IBM Corporation, Chicago, IL, United States) was used for statistical analysis. $P < 0.05$ was considered statistically significant. Normal distribution using the Kolmogorov-Smirnov test was used first for measurement data. Independent sample *t* test, one way analysis of variance and least significant difference were used for data with normal distribution and the data were reported as mean ± SD. Otherwise, the Mann-Whitney or Kruskal-Wallis test was used and the data were reported as interquartile range. The cut-off point of Emax was calculated by a receiver operating characteristic curve. The enumerative data were presented as numbers and percentage and Pearson's chi-square test and Fisher's exact test were used for statistical analysis.

RESULTS

Patients and final diagnosis

There were 132 solid FLLs in 127 patients (80 men and 47 women; aged 24-77 years; mean age 54.23 ± 12.04 years) in this study, including 32 benign FLLs in 31 patients (6 focal nodular hyperplasia, 15 hemangioma and 11 diagnosed definitely as benign but without pathological results) and 100 malignant FLLs in 96 patients (16 CCCs, 72 HCCs and 12 liver metastases). The differences in age, gender and history of malignancy between the malignant and benign groups are shown in Table 1. Compared with patients with benign FLLs, patients with malignant FLLs were older and more often male. The history of malignancy had no significant difference between the two groups. The differences in age, gender and history of malignancy among three types of malignancy are shown in Table 2. The age and gender had no significant differences among the three groups, although the age of patients with liver metastases was significantly higher than that of patients with HCC. Patients with liver metastases were more often

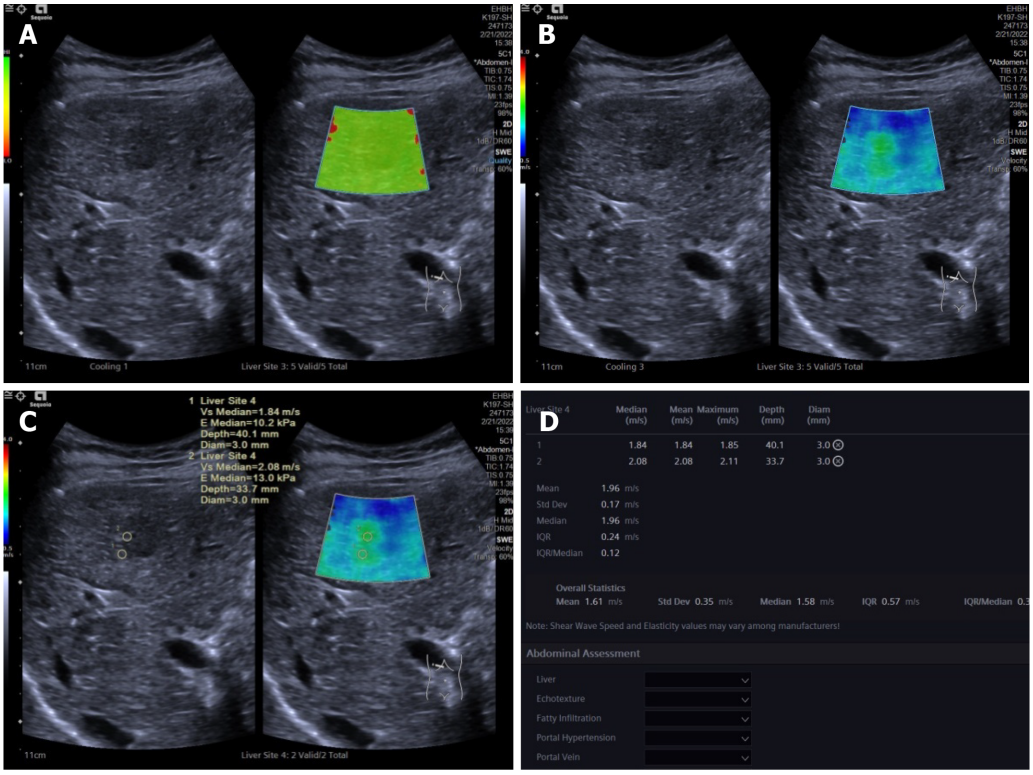
Table 1 Differences in age, gender and history of malignancy between malignant and benign groups

	Age (yr)	Gender		History of malignancy	
		Male	Female	Yes	No
Malignant (n = 96)	44.68 ± 12.30	73	23	11	85
Benign (n = 31)	57.31 ± 10.36	7	24	1	30
t/χ^2	5.633	28.729		1.856	
P value	0.000	0.000		0.291	

Table 2 Differences in age, gender and history of malignancy among three types of malignancy

	Age (yr)	Gender		History of malignancy	
		Male	Female	Yes	No
CCCs (n = 16)	58.63 ± 10.37	11	5	1	15
HCCs (n = 69)	56.07 ± 10.51[a]	54	15	5	64
Liver metastasis (n = 11)	63.18 ± 7.55	8	3	5	6
F/χ^2	2.460	0.720		14.165	
P value	0.091	0.698		0.001	

[a]P = 0.035 *vs* liver metastases. CCCs: Cholangiocellular carcinomas; HCCs: Hepatocellular carcinomas.



DOI: 10.3748/wjg.v28.i32.4716 **Copyright** ©The Author(s) 2022.

Figure 1 Two-dimensional shear wave elastography images in patients with focal liver lesions. A: Tumor shown on quality mode as green indicated that the quality of two-dimensional shear wave elastography image was up to standard; B: Tumor shown in velocity mode, speed bar set at 0.5-4.0 m/s; C: Two circular regions of interest (ROIs, with 3 mm diameter) placed at the stiffest site in the tumor and at the periphery of tumor; D: Maximum values of the two ROIs recorded as maximal elasticity.

had a history of malignancy, compared with patients with primary liver cancer, including HCC and CCC.

Conventional ultrasound results

Volume of benign FLLs (20.73-113.69 cm^3) and malignant FLLs (30.56-79.62 cm^3) had no significant difference ($Z = 0.263$, $P = 0.793$). Volume of CCCs (39.58-120.22 cm^3), HCCs (26.34-75.69 cm^3) and liver metastases (32.76-41.67 cm^3) had no significant difference ($\chi^2 = 1.869$, $P = 0.393$). For 32 benign FLLs, 12 were diagnosed as benign, 18 as undetermined and two were misdiagnosed as malignant. For 100 malignant FLLs, 81 (12 CCCs, 59 HCCs and 10 metastases) were diagnosed correctly as malignant, 17 were undetermined (4 CCCs, 11 HCCs and 2 liver metastases) and 2 were misdiagnosed as benign (both HCCs). The undetermined rate of conventional ultrasound was 26.52% (35/132). For the FLLs with definite diagnosis by conventional ultrasound, the sensitivity, specificity and accuracy were 85.71%, 97.59% and 95.88%, respectively.

2D SWE results

Comparisons between benign and malignant FLLs: The differences in 2D-SWE results between benign and malignant FLLs are shown in Table 3. Emax of malignant FLLs were significantly higher than those of benign FLLs. Emax of the periphery of malignant FLLs were significantly higher than those of benign FLLs. The cut-off point of Emax of the tumors was 1.905 with AUC 0.843 (Figure 2). The sensitivity, specificity and accuracy were 71.00%, 84.38% and 74.24% respectively using Emax > 1.905 m/s for diagnosis as malignant (Figure 3). For 35 FLLs with undetermined diagnosis by conventional ultrasound, 23 (65.71%) FLLs including 14 of 18 benign and nine of 17 malignant FLLs were diagnosed correctly.

Comparisons among different types of malignant FLLs: The differences in 2D-SWE results among different types of malignant FLLs are shown in Table 4. There were significant differences among Emax of CCCs, HCCs and liver metastases. Emax of liver metastases was significantly higher than that of CCCs and HCCs. There were no significant differences among Emax values of the periphery of CCCs, HCCs and liver metastases.

DISCUSSION

In this study, we explored the value of 2D-SWE using Emax as the quantitative parameter in the differential diagnosis of FLLs, especially among different pathological types of malignant FLLs. Our results showed that malignant FLLs were stiffer than benign ones and liver metastases were stiffer than primary liver carcinomas. 2D-SWE with Emax was a useful complement to conventional ultrasound for the differential diagnosis of FLLs.

The comparison of patients' basic information showed that compared with patients with benign FLLs, patients with malignant FLLs tended to be older, male and have a history of malignancy. Among three different types of malignant FLLs, the distribution of patients' age and gender had no significant difference, while patients with liver metastases were more likely to have a history of malignancy. These results were similar to those in previous studies[13].

Conventional ultrasound is well recognized as the first imaging choice for the screening and diagnosis of FLLs[14]. However, the diagnostic efficiency of conventional ultrasound for the differential diagnosis of benign and malignant FLLs or among different pathological types of malignant FLLs was not good enough. For some FLLs, the diagnosis using conventional ultrasound alone is difficult[15]. That is one of the reasons for the development of new ultrasound technologies, including CEUS and ultrasound elastography. In this study, we diagnosed FLLs as benign, malignant and undetermined by conventional ultrasound and 35 of 132 (26.52%) were diagnosed as undetermined. Further diagnosis using other imaging methods was necessary.

CEUS could provide similar or better diagnostic performance for the differential diagnosis of FLLs without radiation and iodine allergy, compared with contrast enhanced CT[16]. CEUS has particularly high value for the differential diagnosis of complex cystic and cysticlike FLLs[17,18]. In this study, for some benign tumors or liver metastases without pathological diagnosis, the combined results of CEUS together with contrast enhanced CT or contrast enhanced MRI were as final. Compared with CEUS, ultrasound elastography has the advantages of being less expensive and less time-consuming[19].

Our previous study using virtual touch tissue quantification imaging with Emax has proven its value in the differential diagnosis between benign and malignant FLLs[9]. 2D-SWE is one of the most advanced elastography techniques and could provide overall elastic information in tumors and locate the stiffest part[20]. In this study, the cutoff point of Emax was 1.905, which was similar to our previous result[9]. Twenty-three of 35 (65.71%) FLLs with undetermined diagnosis by conventional ultrasound were diagnosed accurately using 2D-SWE with Emax. If FLLs could be diagnosed confidently using conventional ultrasound, no further examination was needed; otherwise, 2D-SWE with Emax could be a useful complement to conventional ultrasound and improve the diagnostic efficiency.

Table 3 Differences in two-dimensional shear wave elastography results between benign and malignant focal liver lesions

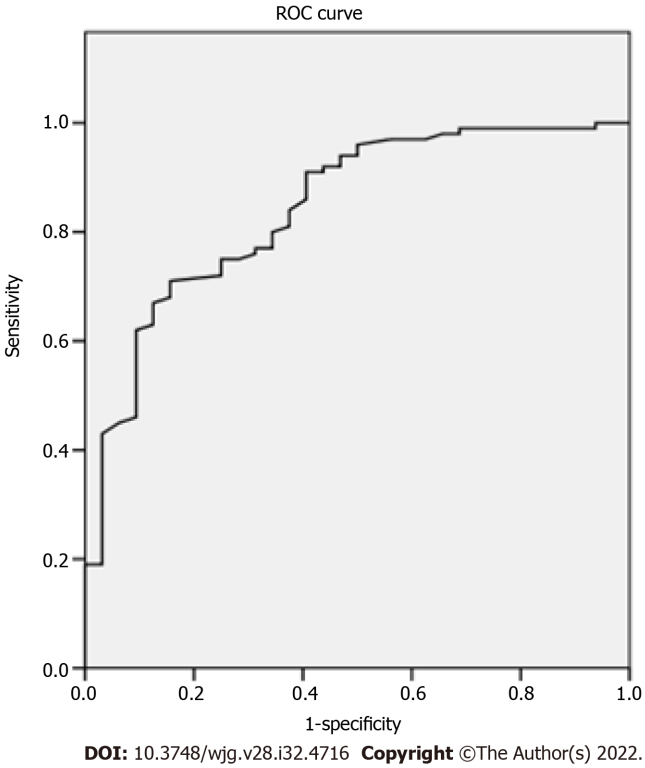
	Emax of tumors (m/s)	Emax of periphery of tumors (m/s)
Malignant (n = 100)	2.21 ± 0.57	1.52 ± 0.39
Benign (n = 32)	1.59 ± 0.37	1.36 ± 0.44
t	5.781	2.073
P value	0.000	0.040

Emax: Maximal elasticity.

Table 4 Differences of two-dimensional shear wave elastography results among different types of malignant focal liver lesions

	Emax of the tumors (m/s)	Emax of the periphery of tumors (m/s)
CCCs (n = 16)	2.14 ± 0.34[a]	1.56 ± 0.39
HCCs (n = 72)	2.14 ± 0.46[b]	1.54 ± 0.37
Liver metastases (n = 12)	2.73 ± 0.99	1.36 ± 0.46
F	6.418	1.299
P value	0.002	0.277

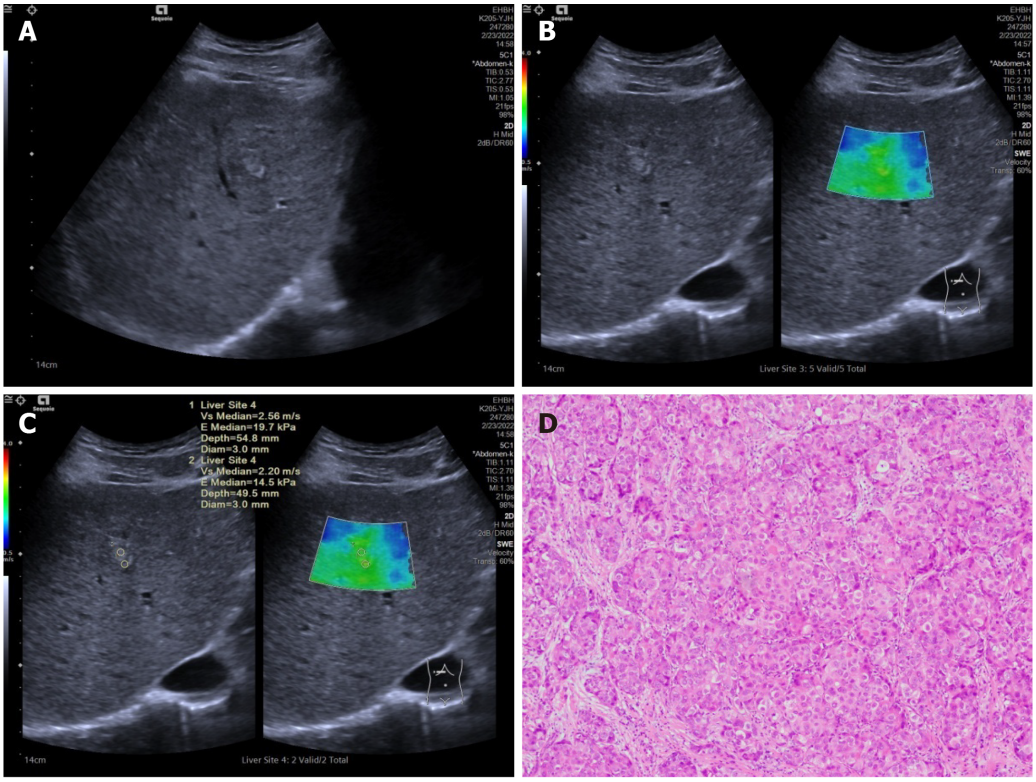
[a]P = 0.005 *vs* liver metastases.
[b]P = 0.001 *vs* liver metastases.
Emax: Maximal elasticity; CCCs: Cholangiocellular carcinomas; HCCs: Hepatocellular carcinomas.



DOI: 10.3748/wjg.v28.i32.4716 **Copyright** ©The Author(s) 2022.

Figure 2 Receiver operating characteristic curve of maximum elasticity for malignant and benign focal liver lesions.

The elastic differences among different types of malignant FLLs are still uncertain. Our results showed that the stiffness of liver metastases was significantly higher than that of primary liver tumors, including CCCs and HCCs, while the stiffness of CCCs and HCCs had no significant differences. This was similar to the study of Park *et al*[21], which showed that the stiffness of HCCs was significantly lower than that of liver metastases. However, some other studies had the opposite results[10,11]. One



DOI: 10.3748/wjg.v28.i32.4716 **Copyright** ©The Author(s) 2022.

Figure 3 Ultrasound and pathologic images in a 51-year old male patients with hepatocellular carcinomas. A: A tumor shown on conventional ultrasound were diagnosed as undetermined; B: Tumor shown as stiffer, compared with surrounding liver tissue in two-dimensional shear wave elastography velocity mode; C: Maximal elasticity of the tumor was higher than 1.905 m/s and the tumor was diagnosed as malignant; D: Pathological examination confirmed the tumor as hepatocellular carcinomas (HE, × 200).

study reported that CCCs had the lowest stiffness and HCCs the highest stiffness[10]. Another study found that CCCs had the highest stiffness and liver metastases the lowest[11]. One important reason for the conflicting results is that the sample number in every study was not large enough, and it is necessary to carry out further studies with large samples to confirm our results.

There were some limitations to our study. First, as mentioned above, only a few cases of CCCs and liver metastases were included. Second, no pathological methods were used to confirm the stiffness of the tumors and explain the differences among different pathological types of malignant FLLs.

CONCLUSION

In conclusion, malignant FLLs were stiffer than benign FLLs and liver metastases were stiffer than primary liver carcinomas. 2D-SWE with Emax was a useful complement to conventional ultrasound for the differential diagnosis of FLLs.

ARTICLE HIGHLIGHTS

Research background

Conventional ultrasound is the first imaging choice for liver diseases with the diagnostic efficiency not good enough, which promotes the development of new ultrasound technologies, such as contrast enhanced ultrasound and ultrasound elastography. Two dimensional shear wave elastography (2D-SWE) is convenient, less time-consuming and inexpensive. SWE plays an important role in the assessment of liver fibrosis and in the differential diagnosis of benign and malignant focal liver lesions (FLLs). However, its value for the differential diagnosis among different types of malignant FLLs has not been proved.

Research motivation

Though the value of SWE for the differential diagnosis between malignant and benign FLLs was not

widely recognized, our previous study showed promising results using maximal elasticity (Emax) as the parameter to differentiate malignant FLLs from benign ones. As the clinical management and prognosis of different pathological types of malignant FLLs are different, it is important to diagnose accurately of the possible pathological types. So, it was necessary to explore the value of 2D-SWE with Emax in differential diagnosis of different pathological types of malignant FLLs.

Research objectives

We aim to explore the value of 2D-SWE using Emax in the differential diagnosis of FLLs, especially among different pathological types of malignant FLLs.

Research methods

In this study, we diagnosed all FLLs as benign, malignant and undetermined using conventional ultrasound. And the stiffness of FLLs and the periphery of FLLs were evaluated using 2D-SWE and the quantitative parameter Emax. Emax of FLLs and the periphery of FLLs were compared between benign and malignant FLLs or among different pathological types of malignant FLLs.

Research results

There were totally 132 FFLs in 127 patients enrolled in the study, including 32 benign FLLs, 16 cholangiocellular carcinomas (CCCs), 72 hepatocellular carcinomas (HCCs) and 12 liver metastases. Thirty-five FLLs were diagnosed as undermined by conventional ultrasound. Emax of malignant FLLs (2.21 ± 0.57 m/s) were significantly higher than those of benign FLLs (1.59 ± 0.37 m/s) (P = 0.000). Emax of the periphery of malignant FLLs (1.52 ± 0.39 m/s) were significantly higher than those of benign FLLs (1.36 ± 0.44 m/s) (P = 0.040). The cut-off point of Emax of the tumors was 1.905 with AUC 0.843. The sensitivity, specificity and accuracy were 71.00%, 84.38% and 74.24% respectively using Emax > 1.905 m/s for diagnosis as malignant and 23 of 35 (65.74%) FLLs with undetermined diagnosis by conventional ultrasound were diagnosed correctly. Emax of liver metastases (2.73 ± 0.99 m/s) was significantly higher than that of primary liver carcinomas, including CCCs (2.14 ± 0.34 m/s) and HCCs (2.14 ± 0.46 m/s) (P = 0.002).

Research conclusions

Malignant FLLs were stiffer than benign ones and liver metastases were stiffer than primary liver carcinomas. 2D-SEW with Emax was a useful complement to conventional ultrasound for the differential diagnosis of FLLs.

Research perspectives

In this study, we demonstrated the differences of 2D-SWE with Emax between benign and malignant FLLs and among different pathological types of malignant FLLs. Prospective study to explore the value of 2D-SWE with Emax in the evaluatation the different stiffness of liver metastases from different sources or the different stiffness of HCC with different microvascular invasion grade will be necessary.

FOOTNOTES

Author contributions: Guo J and Jiang D contributed equally to this work; Guo J, Jiang D, Yu J and Zhang HP designed the study; Guo J, Jiang D, Qian Y and Gu YJ performed the research and collected data; Zhang HP and Zhou YQ performed statistical analysis; Guo J and Jiang D wrote the manuscript; all authors have read and approved the final manuscript.

Supported by Natural Science Foundation of Shanghai of China, No. 19ZR1441500, No. 22ZR1458200; Science Research Foundation of Shanghai Municipal Health Commission, No. 202140378; and Key Program of Science and Technology Commission Foundation of Changning, Shanghai, China, No. CNKW2020Z04.

Institutional review board statement: The study was approved by the Institutional Ethical Review Board of Eastern Hepatobiliary Surgery Hospital Affiliated to Naval Medical University (Approval No. EHBHKY2021-K-017).

Clinical trial registration statement: This study is registered at clinical hospital center 'Eastern Hepatobiliary Surgery Hospital, Naval Medical University' trial registry. The registration identification number is ChiCTR2100049831.

Informed consent statement: All patients provided written informed consent prior to study enrollment before ultrasound examinations.

Conflict-of-interest statement: All the authors report no relevant conflicts of interest for this article.

Data sharing statement: No additional data are available.

CONSORT 2010 statement: The authors have read the CONSORT 2010 statement, and the manuscript was prepared and revised according to the CONSORT 2010 statement.

Open-Access: This article is an open-access article that was selected by an in-house editor and fully peer-reviewed by external reviewers. It is distributed in accordance with the Creative Commons Attribution NonCommercial (CC BY-NC 4.0) license, which permits others to distribute, remix, adapt, build upon this work non-commercially, and license their derivative works on different terms, provided the original work is properly cited and the use is non-commercial. See: https://creativecommons.org/Licenses/by-nc/4.0/

Country/Territory of origin: China

ORCID number: Yu-Qing Zhou 0001-0002-0001-0002; Hui-Ping Zhang 0000-0002-3890-6436.

S-Editor: Gong ZM
L-Editor: A
P-Editor: Gong ZM

REFERENCES

1 **Yao J**, Liang X, Liu Y, Li S, Zheng M. Trends in Incidence and Prognostic Factors of Two Subtypes of Primary Liver Cancers: A Surveillance, Epidemiology, and End Results-Based Population Study. *Cancer Control* 2022; **29**: 10732748211051548 [PMID: 35147456 DOI: 10.1177/10732748211051548]
2 **Macias RIR**, Banales JM, Sangro B, Muntané J, Avila MA, Lozano E, Perugorria MJ, Padillo FJ, Bujanda L, Marin JJG. The search for novel diagnostic and prognostic biomarkers in cholangiocarcinoma. *Biochim Biophys Acta Mol Basis Dis* 2018; **1864**: 1468-1477 [PMID: 28782657 DOI: 10.1016/j.bbadis.2017.08.002]
3 **Lang SA**, Bednarsch J, Czigany Z, Joechle K, Kroh A, Amygdalos I, Strnad P, Bruns T, Heise D, Ulmer F, Neumann UP. Liver transplantation in malignant disease. *World J Clin Oncol* 2021; **12**: 623-645 [PMID: 34513597 DOI: 10.5306/wjco.v12.i8.623]
4 **Stollmayer R**, Budai BK, Tóth A, Kalina I, Hartmann E, Szoldán P, Bérczi V, Maurovich-Horvat P, Kaposi PN. Diagnosis of focal liver lesions with deep learning-based multi-channel analysis of hepatocyte-specific contrast-enhanced magnetic resonance imaging. *World J Gastroenterol* 2021; **27**: 5978-5988 [PMID: 34629814 DOI: 10.3748/wjg.v27.i35.5978]
5 **Cao SE**, Zhang LQ, Kuang SC, Shi WQ, Hu B, Xie SD, Chen YN, Liu H, Chen SM, Jiang T, Ye M, Zhang HX, Wang J. Multiphase convolutional dense network for the classification of focal liver lesions on dynamic contrast-enhanced computed tomography. *World J Gastroenterol* 2020; **26**: 3660-3672 [PMID: 32742134 DOI: 10.3748/wjg.v26.i25.3660]
6 **Huf S**, Platz Batista da Silva N, Wiesinger I, Hornung M, Scherer MN, Lang S, Stroszczynski C, Fischer T, Jung EM. Analysis of Liver Tumors Using Preoperative and Intraoperative Contrast-Enhanced Ultrasound (CEUS/IOCEUS) by Radiologists in Comparison to Magnetic Resonance Imaging and Histopathology. *Rofo* 2017; **189**: 431-440 [PMID: 28449169 DOI: 10.1055/s-0042-124347]
7 **da Silva NPB**, Hornung M, Beyer LP, Hackl C, Brunner S, Schlitt HJ, Wiggermann P, Jung EM. Intraoperative Shear Wave Elastography vs. Contrast-Enhanced Ultrasound for the Characterization and Differentiation of Focal Liver Lesions to Optimize Liver Tumor Surgery. *Ultraschall Med* 2019; **40**: 205-211 [PMID: 30340245 DOI: 10.1055/a-0649-1000]
8 **Wang W**, Zhang JC, Tian WS, Chen LD, Zheng Q, Hu HT, Wu SS, Guo Y, Xie XY, Lu MD, Kuang M, Liu LZ, Ruan SM. Shear wave elastography-based ultrasomics: differentiating malignant from benign focal liver lesions. *Abdom Radiol (NY)* 2021; **46**: 237-248 [PMID: 32564210 DOI: 10.1007/s00261-020-02614-3]
9 **Zhang HP**, Gu JY, Bai M, Li F, Zhou YQ, Du LF. Value of shear wave elastography with maximal elasticity in differentiating benign and malignant solid focal liver lesions. *World J Gastroenterol* 2020; **26**: 7416-7424 [PMID: 33362393 DOI: 10.3748/wjg.v26.i46.7416]
10 **Park H**, Park JY, Kim DY, Ahn SH, Chon CY, Han KH, Kim SU. Characterization of focal liver masses using acoustic radiation force impulse elastography. *World J Gastroenterol* 2013; **19**: 219-226 [PMID: 23345944 DOI: 10.3748/wjg.v19.i2.219]
11 **Gerber L**, Fitting D, Srikantharajah K, Weiler N, Kyriakidou G, Bojunga J, Schulze F, Bon D, Zeuzem S, Friedrich-Rust M. Evaluation of 2D- Shear Wave Elastography for Characterisation of Focal Liver Lesions. *J Gastrointestin Liver Dis* 2017; **26**: 283-290 [PMID: 28922441 DOI: 10.15403/jgld.2014.1121.263.dsh]
12 **Tomayko MM**, Reynolds CP. Determination of subcutaneous tumor size in athymic (nude) mice. *Cancer Chemother Pharmacol* 1989; **24**: 148-154 [PMID: 2544306 DOI: 10.1007/BF00300234]
13 **Lin L**, Yan L, Liu Y, Qu C, Ni J, Li H. The Burden and Trends of Primary Liver Cancer Caused by Specific Etiologies from 1990 to 2017 at the Global, Regional, National, Age, and Sex Level Results from the Global Burden of Disease Study 2017. *Liver Cancer* 2020; **9**: 563-582 [PMID: 33083281 DOI: 10.1159/000508568]
14 **Osho A**, Rich NE, Singal AG. Role of imaging in management of hepatocellular carcinoma: surveillance, diagnosis, and treatment response. *Hepatoma Res* 2020; **6** [PMID: 32944652 DOI: 10.20517/2394-5079.2020.42]
15 **Bartolotta TV**, Taibbi A, Midiri M, Matranga D, Solbiati L, Lagalla R. Indeterminate focal liver lesions incidentally discovered at gray-scale US: role of contrast-enhanced sonography. *Invest Radiol* 2011; **46**: 106-115 [PMID: 20938345 DOI: 10.1097/RLI.0b013e3181f44184]
16 **Kim TK**, Noh SY, Wilson SR, Kono Y, Piscaglia F, Jang HJ, Lyshchik A, Dietrich CF, Willmann JK, Vezeridis A, Sirlin CB. Contrast-enhanced ultrasound (CEUS) liver imaging reporting and data system (LI-RADS) 2017 - a review of

important differences compared to the CT/MRI system. *Clin Mol Hepatol* 2017; **23**: 280-289 [PMID: 28911220 DOI: 10.3350/cmh.2017.0037]

17 **Corvino A**, Catalano O, Corvino F, Sandomenico F, Petrillo A. Diagnostic Performance and Confidence of Contrast-Enhanced Ultrasound in the Differential Diagnosis of Cystic and Cysticlike Liver Lesions. *AJR Am J Roentgenol* 2017; **209**: W119-W127 [PMID: 28639831 DOI: 10.2214/AJR.16.17062]

18 **Corvino A**, Catalano O, Setola SV, Sandomenico F, Corvino F, Petrillo A. Contrast-enhanced ultrasound in the characterization of complex cystic focal liver lesions. *Ultrasound Med Biol* 2015; **41**: 1301-1310 [PMID: 25666723 DOI: 10.1016/j.ultrasmedbio.2014.12.667]

19 **Platz Batista da Silva N**, Schauer M, Hornung M, Lang S, Beyer LP, Wiesinger I, Stroszczynski C, Jung EM. Intrasurgical dignity assessment of hepatic tumors using semi-quantitative strain elastography and contrast-enhanced ultrasound for optimisation of liver tumor surgery. *Clin Hemorheol Microcirc* 2016; **64**: 735-745 [PMID: 27767982 DOI: 10.3233/CH-168029]

20 **Kayadibi Y**, Ucar N, Kaya MF, Yildirim E, Bektas S. Characterization of Suspicious Microcalcifications on Mammography Using 2D Shear-Wave Elastography. *Ultrasound Med Biol* 2021; **47**: 2532-2542 [PMID: 34127332 DOI: 10.1016/j.ultrasmedbio.2021.05.008]

21 **Park HS**, Kim YJ, Yu MH, Jung SI, Jeon HJ. Shear Wave Elastography of Focal Liver Lesion: Intraobserver Reproducibility and Elasticity Characterization. *Ultrasound Q* 2015; **31**: 262-271 [PMID: 26086459 DOI: 10.1097/RUQ.0000000000000175]

World Journal of Gastroenterology

Submit a Manuscript: https://www.f6publishing.com

World J Gastroenterol 2022 August 28; 28(32): 4726-4740

DOI: 10.3748/wjg.v28.i32.4726

ISSN 1007-9327 (print) ISSN 2219-2840 (online)

META-ANALYSIS

Use of shear wave elastography for the diagnosis and follow-up of biliary atresia: A meta-analysis

Ellen S Wagner, Hussien Ahmed H Abdelgawad, Meghan Landry, Belal Asfour, Mark B Slidell, Ruba Azzam

Specialty type: Gastroenterology and hepatology

Provenance and peer review: Unsolicited article; Externally peer reviewed.

Peer-review model: Single blind

Peer-review report's scientific quality classification

Grade A (Excellent): A, A
Grade B (Very good): 0
Grade C (Good): C
Grade D (Fair): 0
Grade E (Poor): 0

P-Reviewer: El-Karaksy H, Egypt; Pop TL, Romania; Redkar RG, India

Received: May 1, 2022
Peer-review started: May 1, 2022
First decision: June 19, 2022
Revised: July 10, 2022
Accepted: July 31, 2022
Article in press: July 31, 2022
Published online: August 28, 2022

Ellen S Wagner, Ruba Azzam, Pediatric Gastroenterology, Hepatology, and Nutrition, The University of Chicago Medicine, Comer Children' s Hospital, Chicago, IL 60637, United States

Hussien Ahmed H Abdelgawad, Department of Medicine, Zagazig University, Zagazig 44511, Egypt, Egypt

Meghan Landry, Department of Pediatrics, The University of Chicago Medicine, Comer Children' s Hospital, Chicago, IL 60637, United States

Belal Asfour, Graduate School of Professional Education-Biomedical Informatics, University of Chicago, Chicago, IL 60637, United States

Mark B Slidell, Department of Surgery, The University of Chicago Medicine, Comer Children' s Hospital, Chicago, IL 60637, United States

Corresponding author: Ruba Azzam, MD, MPH, Associate Professor, Pediatric Gastroenterology, Hepatology, and Nutrition, The University of Chicago Medicine, Comer Children' s Hospital, 5841 S Maryland Ave MC 4065, Chicago, IL 60637, United States.
razzam@peds.bsd.uchicago.edu

Abstract

BACKGROUND

Timely differentiation of biliary atresia (BA) from other infantile cholestatic diseases can impact patient outcomes. Additionally, non-invasive staging of fibrosis after Kasai hepatoportoenterostomy has not been widely standardized. Shear wave elastography is an ultrasound modality that detects changes in tissue stiffness. The authors propose that the utility of elastography in BA can be elucidated through meta-analysis of existing studies.

AIM

To assess the utility of elastography in: (1) BA diagnosis, and (2) post-Kasai fibrosis surveillance.

METHODS

A literature search identified articles that evaluated elastography for BA diagnosis and for post-Kasai follow-up. Twenty studies met criteria for meta-analysis: Eleven for diagnosis and nine for follow-up post-Kasai. Estimated diagnostic odds ratio (DOR), sensitivity, and specificity of elastography were calculated through a random-effects model using Meta-DiSc software.

RESULTS
Mean liver stiffness in BA infants at diagnosis was significantly higher than in non-BA, with overall DOR 24.61, sensitivity 83%, and specificity 79%. Post-Kasai, mean liver stiffness was significantly higher in BA patients with varices than in patients without, with DOR 16.36, sensitivity 85%, and specificity 76%. Elastography differentiated stage F4 fibrosis from F0-F3 with DOR of 70.03, sensitivity 96%, and specificity 89%. Elastography also differentiated F3-F4 fibrosis from F0-F2 with DOR of 24.68, sensitivity 85%, and specificity 81%.

CONCLUSION
Elastography has potential as a non-invasive modality for BA diagnosis and surveillance post-Kasai. This paper's limitations include inter-study method heterogeneity and small sample sizes. Future, standardized, multi-center studies are recommended.

Key Words: Biliary atresia; Cholestasis; Hepatic portoenterostomy; Fibrosis; Esophageal and gastric varices; Elasticity imaging techniques

©The Author(s) 2022. Published by Baishideng Publishing Group Inc. All rights reserved.

Core Tip: Ultrasound elastography is an emerging, non-invasive imaging modality to detect organ stiffness. It may be a useful tool in biliary atresia (BA) diagnosis and post-Kasai fibrosis surveillance. In a meta-analysis of twenty existing studies (eleven for diagnosis and nine for follow-up), this paper shows that mean liver stiffness is significantly higher in BA patients compared to non-BA patients at time of diagnosis. Post-Kasai, elastography can differentiate between early and advanced fibrosis as well as help to discern the presence or absence of varices. While there are limitations to this analysis, elastography shows great promise for its utility as a non-invasive modality for BA patients.

Citation: Wagner ES, Abdelgawad HAH, Landry M, Asfour B, Slidell MB, Azzam R. Use of shear wave elastography for the diagnosis and follow-up of biliary atresia: A meta-analysis. *World J Gastroenterol* 2022; 28(32): 4726-4740
URL: https://www.wjgnet.com/1007-9327/full/v28/i32/4726.htm
DOI: https://dx.doi.org/10.3748/wjg.v28.i32.4726

INTRODUCTION

Biliary atresia (BA) is a progressive, fibroinflammatory disease of the biliary system that exclusively affects infants. It accounts for about 30% of all cases of prolonged cholestasis in the first three months of life[1]. Its incidence is estimated to be approximately 1:10000-19000 live births, with increased prevalence in East Asian countries to up to 1:2700[2]. The initial clinical manifestations include progressive jaundice, deep-colored urine, light colored stools, and an increase in conjugated serum bilirubin levels. The similarity in clinical presentation and blood biochemistry results between patients with BA and those with other infantile cholestatic liver diseases represents a great challenge to clinicians in accurately establishing a final diagnosis in a timely fashion. Early identification of BA in an infant with cholestatic jaundice is crucial, as the Kasai portoenterostomy (KPE) procedure may help restore bile flow and prevent the otherwise rapid progression to biliary cirrhosis. A BA outcomes meta-analysis by Jimenez-Rivera *et al*[2] included fourteen studies that focused on native liver survival (NLS), all of which reported improved NLS when KPE was performed at an earlier age. Given its progressive nature, BA is the most common indication for liver transplantation in the pediatric population, with NLS ranging from 24.0% to 52.8% at ten years post-KPE[2]. Patients with BA who have undergone KPE need close clinical monitoring to assess for signs of chronic liver disease progression, particularly as they approach potential need for liver transplant. Currently, there are no widely accepted, validated non-invasive tests to pre-operatively diagnose BA nor to evaluate for progressive fibrosis after KPE.

While ultrasound findings, such as absence of a contractile gall bladder after feeding or the presence of a triangular cord sign, can be suggestive of BA, ultrasound alone is not diagnostic[3]. In order to diagnose BA, a liver biopsy is performed to assess for the histopathologic signs of biliary obstruction, portal edema, and fibrosis[4]. When performed at age 60 d or less, liver biopsy is 96.4% sensitive for the diagnosis of BA[3]. The progressive nature of the disease makes it imperative that a diagnosis is made as early as possible. The gold standard test to confirm BA is a formal cholangiogram. Assessment for progression of chronic liver disease post-KPE is usually achieved by the constellation of findings on laboratory and radiologic testing as well as consideration for repeat liver biopsy and/or upper

gastrointestinal endoscopy, with no standardized guidelines for non-invasive staging of hepatic fibrosis nor timing for endoscopic evaluation for potential variceal evolution. Invasive procedures carry risks, both procedural as well as those related to sedation or anesthesia[4]. Delays at each juncture, both in diagnosis and in post-KPE surveillance, can have a potentially detrimental impact on patient outcome.

Ultrasound elastography (UE) is an emerging imaging modality that uses applied force *via* ultrasound probe to measure the elastic properties of tissue[5,6]. UE can be classified into strain imaging and shear wave imaging. Strain imaging relies on a normal external force (push) or intrinsic forces (*i.e.*, respiration or cardiovascular movement) within the body. For this reason, strain imaging is difficult to quantify and reproduce, particularly in deeper organs, leading to limited applicability in the liver. As a result, strain imaging was not the focus of this analysis[7,8].

Shear wave imaging, also called shear wave elastography (SWE) utilizes a dynamic stress and can be further classified into transient elastography (TE), point shear wave elastography (pSWE; also called VTQ or Virtual Touch Quantification on some platforms), and two-dimensional shear wave elastography (2D-SWE; also called VTIQ or Virtual Touch IQ on some platforms)[8,9]. TE, which is performed using the FibroScan (Echosens, Paris, France) system, utilizes a mechanical punch to generate forces and measure unidirectional pressure waves[5]. pSWE and 2D-SWE differ from TE in that they utilize B mode ultrasound imaging guidance, which enables direct visualization of tissue, as well as an acoustic radiation force impulse (ARFI) in order to measure tissue stress. pSWE enables the measurement of average shear wave speed within a region of interest while 2D-SWE uses multiple foci of tissue displacement along an axis to generate a quantitative map of shear wave speed[5].

SWE has been studied extensively in adult liver literature with studies in pediatric liver disease emerging only recently[6]. And yet, while multiple authors have addressed the utility of SWE for diagnosis and management in BA, there have been no large-scale studies nor meta-analyses on this modality. The aim of this meta-analysis is to evaluate the utility of SWE in: (1) the differentiation of BA from other cholestatic liver diseases of infancy, and (2) the assessment of fibrosis progression in post-KPE follow-up.

MATERIALS AND METHODS

This review was conducted in strict accordance with the Cochrane handbook of systematic reviews of interventions[10]. We followed the Preferred Reporting Items for Systematic Review and Meta-Analysis of Diagnostic Test Accuracy studies (PRISMA-DTA statement)[11]. The review was publicly registered with the Open Science Framework (OSF). The statistical analysis was performed by co-authors H.A., who has over four years as a biostatistician in a clinical research organization, and M.L., who is a clinical research coordinator employed by the University of Chicago.

Search strategy and eligibility criteria

PubMed, Scopus, Web of Science, EBSCO, and Cochrane Central were searched for English language studies with information on BA and elastography from 2010 to 2021. Two of the authors performed the literature search using the keywords: “Elastography” AND “biliary atresia”.

Full texts were reviewed to select eligible studies for meta-analysis. Studies were included if the following criteria were met: (1) The study used SWE to differentiate BA from other cholestatic liver diseases of infancy; (2) the study used SWE in the follow-up of patients with BA for the development of fibrosis/cirrhosis post-KPE; and (3) the study assessed the accuracy of SWE for the diagnosis or follow-up of liver fibrosis based on the cut-off point for liver stiffness and/or spleen stiffness values.

Exclusion criteria were as follows: (1) Full text article was not available and/or abstract and article were not available in English; (2) the study was not specific to BA and/or did not utilize SWE (3) the study evaluated the accuracy of SWE combined with other diagnostic methods; (4) the study used SWE as a reference test to study novel biomarkers; and (5) the study was a review article, letter to the editor, case report, editorial, case series, or consensus statement. Only studies with reliable data for extraction and analysis were included in the meta-analysis.

Data extraction

Two authors independently reviewed and extracted the data from each included study. Data were extracted for study characteristics (*e.g.*, first author and year of publication, study period, study setting, study design, and sample size), baseline characteristics of the included patients (*e.g.*, age of patients, laboratory date, age at diagnosis), and diagnostic data (*e.g.*, sensitivity, specificity, predictive values).

Risk of bias assessment

Two researchers assessed the risk of bias of studies included using version 2 of the Quality Assessment of Diagnostic Test Accuracy Studies (QUADAS-2) tool[12]. QUADAS-2 examines seven items on the representation of patient spectrum, selection criteria, reference standard, verification bias, timing, and study withdrawals. Both reviewers scored the tool independently; all disagreements were discussed and consensus was reached.

Data analysis

Heterogeneity was assessed by visual inspection of the forest plots and measured by I-square and Chi-Square tests. In case of significant heterogeneity ($P < 0.1$), a random effect model was used. Continuous data were pooled as standardized mean difference (SMD) in a meta-analysis model using inverse variance method with the respective 95% confidence intervals. We used Comprehensive Meta Analysis (CMA, United States) software version 3.3.070 for windows. Methods described in reference[13] were utilized to compute missing standard deviations. The diagnostic accuracy indicators of each test were pooled as sensitivity, specificity, and diagnostic odds ratio (DOR) with the corresponding 95% confidence intervals by the DerSimonian-Laird random effect model using MetaDiSc Beta-1.4 software. In addition, the Summary Receiver Operating Characteristic (SROC) curve was used for the evaluation of diagnostic tests and represents the relationship between true positive and negative rates considering the varying diagnostic thresholds among studies. The summary of the test performance was represented with an AUC of 1.0 (100%) indicating perfect discriminatory ability to distinguish BA from non-BA.

Seven studies used SWE machinery that reported results in units of m/s as opposed to kPa, with four being evaluated for diagnostic test accuracy[14-18] and two for utility of SWE for follow-up[19,20]. Values reported in m/s were converted to kPa as per reference[8] (Supplementary material).

RESULTS

Electronic search yielded 243 studies with 42 identified as potentially meeting inclusion criteria (Figure 1). Full text articles were retrieved and assessed for final eligibility. After the review of all full text articles, 22 were excluded due to study design and unreliable data for extraction, the use of SWE as an adjunct to the primary study of a novel biomarker, and subject comparison to healthy controls (as opposed to other cholestatic infants). Eleven studies on the utility of SWE in accurately differentiating BA from other cholestatic liver diseases of infancy met criteria for inclusion, as well as nine studies that evaluated the utility of SWE in assessing and monitoring the development of hepatic fibrosis/cirrhosis post-KPE. The studies included were mostly single center, retrospective analyses conducted in infants and children (age 0-18 years) and published in peer-reviewed journals between 2010 and 2021. Detailed individual study characteristics are presented in Table 1.

The overall quality of the included studies assessed by the QUADAS-2 (Figure 2), was moderate to high. All analyzed studies were found to have low risk of bias in five or more of the seven items, with the exception of[21], which showed unclear risk of bias in two of seven items and high risk of bias in patient selection. Unclear risk of bias was reported in patient selection due to lack of clear selection criteria in several studies. Potential risk of bias in the index test was recorded in several studies due to lack of reporting on blinding relative to reference standard results. Potential bias in reference standards emerged due to the use of multiple different reference standards (surgical exploration, intraoperative cholangiography, liver biopsy) with possibility for incorrect classification of BA. Finally, bias in the flow and timing was primarily due to a lack of reported details in some of the included studies.

SWE for the diagnosis of BA

Data on SWE for distinguishing BA from other cholestatic neonatal liver diseases were collected from 11 studies with 1307 total patients (560 with BA and 747 without BA). The mean liver stiffness value was significantly higher in the BA group compared to the non-BA group (overall SMD = 2.30 kPa, 95%CI: 1.69, 2.90, $P < 0.0001$). Pooled studies were heterogeneous ($P < 0.01$, $I^2 = 94\%$) (Figure 3). Of the 11 studies included, five reported on performing diagnostic test analysis using liver biopsy as the reference test, one study[22] used surgical exploration or cholangiography, and the reference was not specified in another[16].

The forest plot of sensitivity and specificity for the diagnostic performance of the liver stiffness value measured by SWE for differentiating BA from other etiologies of neonatal cholestasis is shown in Figure 4A. The pooled sensitivity was 83% (95%CI: 80%, 86%) and specificity was 79%, (95%CI: 76%, 82%). The SROC curves of SWE for the diagnosis of BA are illustrated in Figure 4B. The SROC curve was symmetric, and the AUC was 0.91, Q was 0.84 (SE = 0.02). The DOR was 24.61, (95%CI: 12.74, 47.53, $I^2 = 72.4\%$) as shown in Figure 4C. Two of the 11 articles did not report a cut-off value for differentiating between BA and non-BA[14,15] and were excluded from this analysis.

SWE for the follow-up of patients with BA

Data on SWE to assess liver disease progression in post-KPE follow-up were collected from nine studies including 327 total patients [101 patients with varices, 124 patients without varices, 41 patients with fibrosis (F0-F2), and 61 patients with fibrosis (F3-F4)]. Fibrosis stage is reported *via* METAVIR standards, a scale from F0 to F4 where F0 shows no signs of histologic fibrosis, F2 represents moderate fibrosis with few bridges/septa, F3 is numerous septa without cirrhosis, and F4 signifies cirrhosis.

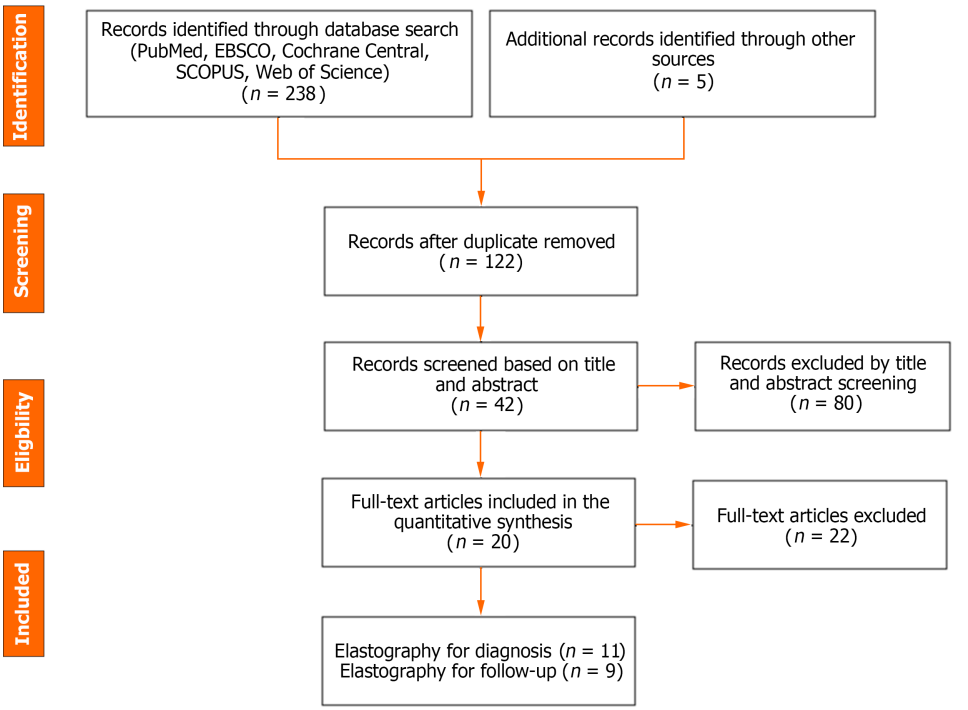
The mean liver stiffness value was significantly higher in patients with varices in comparison to patients without varices (overall SMD 1.38 kPa, 95%CI: 1.02, 1.74, $P < 0.00001$). Pooled studies were homogenous ($P = 0.29$, $I^2 = 19\%$) (Figure 5A). Only three studies reported data on the diagnostic

Table 1 Main characteristics of studies included in the meta-analysis

Ref.	Country	Study design	Elastography Method; machine; probe, if specified	Reference standard	Sample size	Type of patient	Main finding
Diagnosis							
Hanquinet *et al* [14], *Pediatric Radiology*, 2015	Switzerland	Single center retrospective analysis	pSWE (VTQ); Acuson S2000 or S3000 (Siemens Healthcare, Erlangen, Germany)	Liver biopsy; Cholangiogram	20	Cholestatic infants; mean age 52.1 d	Utilizing SWE in addition to standard abdominal ultrasound can provide useful information on liver fibrosis to aid in the diagnosis of BA
Leschied *et al* [15], *Pediatric Radiology*, 2015	USA	Prospective cohort	pSWE (VTQ) and 2D-SWE (VTIQ), Acuson S3000 (Siemens Healthcare, Erlangen, Germany); 9L4 Transducer	Liver biopsy; Cholangiogram	11	Infants with suspected liver disease; mean age 3.8 mo	Shear wave speeds were significantly higher in children with BA than those without
Wang *et al*[31], *Journal of Ultrasound Medicine*, 2016	China	Single center case control	pSWE; Aixplorer (SuperSonic Imagine SA, Aix-en-Provence, France); L15-4 linear probe	KPE	38	Cholestatic infants age 16 to 140 d	Mean shear wave speeds were higher for BA patients than non-BA cholestatic patients and control patients
Zhou *et al* [22], *European Radiology*, 2017	China	Single center prospective analysis	pSWE; Aixplorer (SuperSonic Imagine SA, Aix-en-Provence, France); SL15-4 linear array transducer	Liver biopsy; Cholangiogram; surgical exploration	172	Cholestatic infants, age 2 to 140 d	SWE is useful to differentiate BA from non-BA; its performance does not outperform grey scale ultrasound
Wu *et al*[32], *Hepatology*, 2018	Taiwan	Single center prospective analysis	TE; FibroScan 502 Touch (Echosens, Paris, France); S1 probe	Liver biopsy; cholangiogram	48	Cholestatic infants, age 35 to 61 d	Liver stiffness assessment during the work up of cholestatic infants may facilitate diagnosis of BA
Dillman *et al*[16], *Journal of Pediatrics*, 2019	USA	Multiple center prospective analysis	2D-SWE (VTIQ) and pSWE (VTQ); Acuson S2000 or S3000 (Siemens Healthcare, Erlangen, Germany); 9L4 linear transducer probe	Not specified	41	Cholestatic infants, age 24 to 52 d	SWE and GGT can help discriminate BA from other causes of cholestasis
Duan *et al*[33], *BioMed Research International*, 2019	China	Single center case control	2D-SWE; TUS-Aplio 500 (Canon Medical Systems, Tokyo, Japan); 14L5 linear array probe	Liver biopsy; KPE	138	Cholestatic infants, age 5-90 d	SWE can help distinguish BA from other cholestatic diseases; the diagnostic specificity increases when combined with grey-scale ultrasound
Chen *et al*[17], *European Radiology*, 2020	China	Single center multiple method (prospective and retrospective) analysis	pSWE (VTQ); Acuson S2000 (Siemens Healthcare, Erlangen, Germany); 4-9MHz linear transducer	Liver biopsy; cholangiogram	308 in subgroup 1; 187 in subgroup 2	Cholestatic infants, age under 100 d	Shear wave speed, coupled with presence of triangular cord sign, provided moderate-to-high accuracy for BA diagnosis. This study also found high diagnostic performance in a risk stratification model built on five predictors (shear wave speed, triangular cord sign, GGT, abnormal gallbladder, clay-colored stool)
Liu *et al*[18], *International Journal of Clinical Practice*, 2020	China	Single center retrospective analysis	2D-SWE (VTIQ) and pSWE (VTQ); Acuson OXANA2 (Siemens Healthcare, Erlangen, Germany); 3-5.5 MHz-6C1 convex and 4-9MHz 9L4 linear array probe	Surgical exploration	59	Cholestatic infants, age 25 to 141 d	VTQ and VTIQ can help distinguish BA from non-BA in cholestatic infants; VTIQ has higher sensitivity and specificity than VTQ
Shen *et al*[34], *BMC Pediatrics*, 2020	China	Single center retrospective analysis	pSWE; Aixplorer (SuperSonic Imagine SA, Aix-en-	Not specified	282	Cholestatic infants, age under 120 d	Liver stiffness measurements and GGT values have the potential to decrease rates of BA

			Provence, France); L15-4 linear probe				misdiagnosis
Wang *et al*[35], *Academic Radiology*, 2020	China	Single center prospective analysis	2D-SWE; Aixplorer (SuperSonic Imagine SA, Aix-en-Provence, France); linear probe	Liver biopsy; Cholangiogram	294	Cholestatic infants, age under 70 d	Age, gallbladder morphology, and liver elasticity incorporated together into a nomogram shows an improved predictive value for BA diagnosis
Follow-up							
Chongsrisawat *et al*[36], *BMC Gastroenterology*, 2011	Thailand	Single center prospective analysis	TE; FibroScan 502 Touch (Echosens, Paris, France)	Endoscopy	73	BA patients after KPE, mean age 9.11 yr	TE is useful for predicting the presence of EV/GV in BA patients post-KPE
Colecchia *et al* [37], *Digestive and Liver Disease*, 2011	Italy	Single center prospective analysis	TE; FibroScan (Echosens, Paris, France)	Endoscopy	31	BA patients after KPE, age 4 to 25 yr	Non-invasive studies, such as liver stiffness measurement, can predict the presence of EV in BA patients post-KPE
Shin *et al*[38], *Journal of Ultrasound Medicine*, 2014	South Korea	Single center retrospective analysis	TE; FibroScan 502 Touch (Echosens, Paris, France); S or M probe	Liver biopsy	47	BA patients, mean age 60 d	TE may be a useful, non-invasive method for diagnosing severe fibrosis and cirrhosis; may predict outcomes before surgery or liver biopsy in infants with BA
Shen *et al*[39], *World Journal of Gastroenterology*, 2015	China	Single center retrospective analysis	TE; FibroScan (Echosens, Paris, France); S probe	Liver biopsy	31	BA patients, age 34 to 121 d	TE can be a useful, non-invasive technique to assess liver fibrosis in children with BA. The cut-off value of 15.15 kPa can distinguish cirrhotic from non-cirrhotic patients
Chen *et al*[40], *Nature Scientific Reports*, 2016	China	Single center retrospective analysis	2D-SWE; Aixplorer (SuperSonic Imagine SA, Aix-en-Provence, France); SC-1 curvilinear probe	Liver biopsy	24	BA patients after KPE, mean age 6.6 yr	2D-SWE has more promise as a means of assessing liver fibrosis in BA patients than APRI or FIB-4 scoring
Tomita *et al*[20], *Pediatric Radiology* , 2016	Japan	Single center prospective analysis	pSWE (VTQ); Acuson S2000 (Siemens Healthcare, Erlangen, Germany); 4C1 probe	Liver biopsy; endoscopy	28	BA patients, age 0.1 to 33.6 yr	Liver and spleen stiffness measured *via* ARFI has potential as a non-invasive marker of liver fibrosis and esophageal varices in BA patients
Sintusek *et al*[41], *Journal of Pediatric Gastroenterology and Nutrition*, 2019	Thailand	Single center prospective analysis	TE; FibroScan Compact 530 (Echosens, Paris, France); S or M probe	Endoscopy	51	BA patients after KPE, mean age 10.63 yr	Spleen stiffness can predict the presence of esophageal varices in children with BA; combination of spleen and liver stiffness measurements to diagnose varices increases diagnostic yield
Yokoyama *et al* [19], *Hepatology Research*, 2019	Japan	Single center prospective study	2D-SWE; Aplio i900 (Canon Medical Systems, Tokyo, Japan); i8CX1 transducer	Endoscopy	34	BA patients after KPE, age 1034 to 3940 d	Spleen stiffness (measured *via* 2D-SWE) is the most accurate predictor of high risk esophageal/gastric varices in BA patients
Srisuwan *et al* [21], *Siriraj Medical Journal*, 2021	Thailand	Single center cross-sectional study	TE; FibroScan 502 Touch (Echosens, Paris, France); S or M probe	Endoscopy	20	BA patients after KPE, age 2.3 to 21.0 yr	There is correlation between liver stiffness measurement and clinical/radiological evidence of portal hypertension. TE can predict presence of esophageal varices with high sensitivity

Point SW: Point shear wave elastography; 2D SW: Two-dimensional shear wave elastography; VTIQ: Virtual Touch IQ, alternative nomenclature for two-dimensional shear wave elastography; VTQ: Virtual touch quantification, alternative nomenclature for point Shear Wave Elastography; TE: Transient elastography; KPE: Kasai hepatoportoenterostomy; BA: Biliary atresia; EV: Esophageal varices; GV: Gastric varices; ARFI: Acoustic radiation force impulse.



DOI: 10.3748/wjg.v28.i32.4726 **Copyright** ©The Author(s) 2022.

Figure 1 Preferred Reporting Items for Systematic Review and Meta-Analysis flow diagram of the meta-analysis.

performance of spleen stiffness measured by SWE for predicting the presence of varices in patients with BA post-KPE. The mean spleen stiffness value was significantly higher in patients with varices when compared to patients without varices (overall SMD 1.66 kPa, 95%CI: 1.19, 2.14, $P < 0.00001$). Pooled studies were homogenous ($P = 0.42$, $I^2 = 0\%$) (Figure 5B).

The forest plot of the sensitivity and specificity for the diagnostic performance of liver stiffness value measured by SWE to predict the presence of varices is shown in Figure 6A. The pooled sensitivity was 85% (95%CI: 77%, 91%), while the specificity was 76%, 95%CI (67%, 83%). Illustrated in Figure 6B, the SROC curve was symmetric and the AUC was 0.86 with Q value of 0.80 (SE = 0.05). The DOR was 16.36, 95%CI (8.18, 32.70), $I^2 = 0\%$, showing no heterogeneity among the pooled studies (Figure 6C).

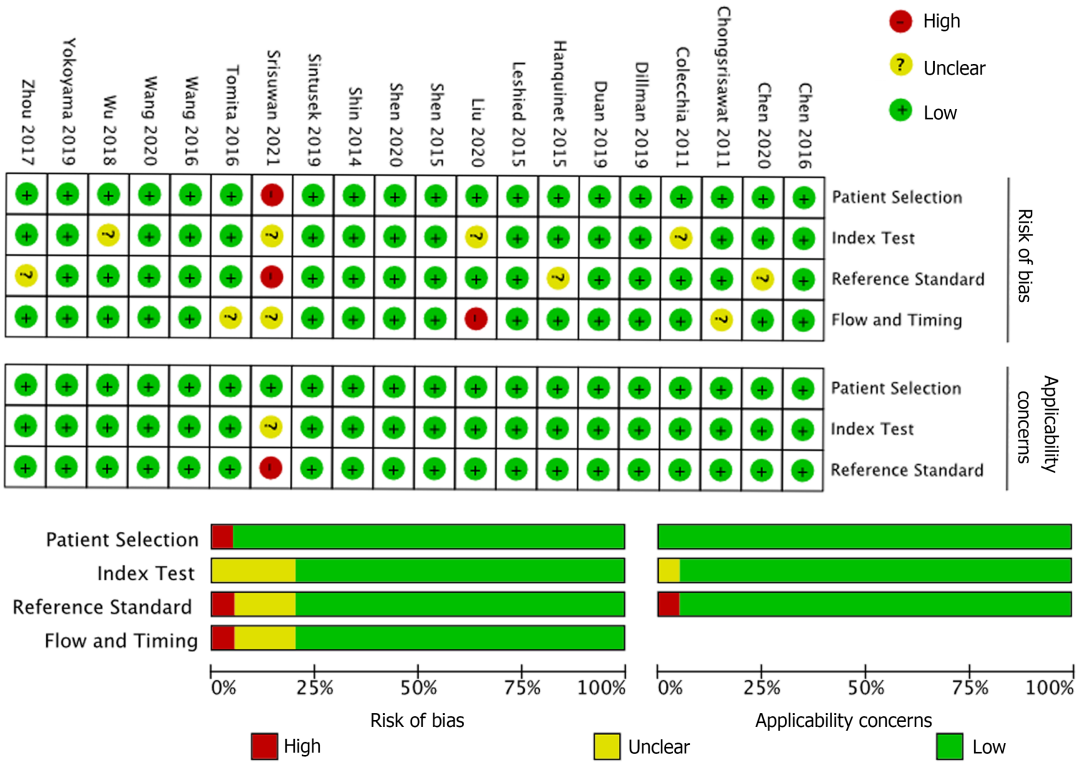
Three studies utilized spleen stiffness measured by SWE to predict the presence of varices with endoscopy as a reference test. The pooled sensitivity was 84% (95%CI: 69%, 94%), while the specificity was 84%, 95%CI (73%, 92%). The AUC of the SROC curve was 0.91, with Q value of 0.85 (SE = 0.403). The DOR was 28.93, 95%CI (8.99, 93.14), $I^2 = 0\%$, showing no heterogeneity among the pooled studies (Supplementary Figure 1).

Four studies used liver stiffness value measured by SWE to predict the presence of liver fibrosis F4 (vs F0-3) when liver biopsy was the reference test. The forest plot for the sensitivity and specificity of the diagnostic performance of liver stiffness value measured by SWE to predict the presence of liver fibrosis F4 is shown in Figure 7A. The pooled sensitivity was 96% (95%CI: 79%, 100%), while the specificity was 89%, (95%CI: 81%, 94%). The SROC curves of liver stiffness value measured by SWE are illustrated in Figure 7B. The AUC of the SROC curve was 0.95, with Q value of 0.89 (SE = 0.04). The DOR was 70.04, (95%CI: 16.06, 305.40), $I^2 = 0\%$, showing no heterogeneity among the pooled studies (Figure 7C).

Three studies used the liver stiffness value measured by SWE to predict the presence of liver fibrosis F3-4 (*vs* F0-2) when liver biopsy was the reference test. The pooled sensitivity was 85% (95%CI: 71%, 94%), and specificity 81%, 95%CI (67%, 91%). The AUC of the SROC curve was 0.91, with Q value of 0.84 (SE = 0.04). The DOR was 24.68, 95%CI (7.43, 82.01), $I^2 = 0\%$, showing no heterogeneity among the pooled studies (Supplementary Figure 2).

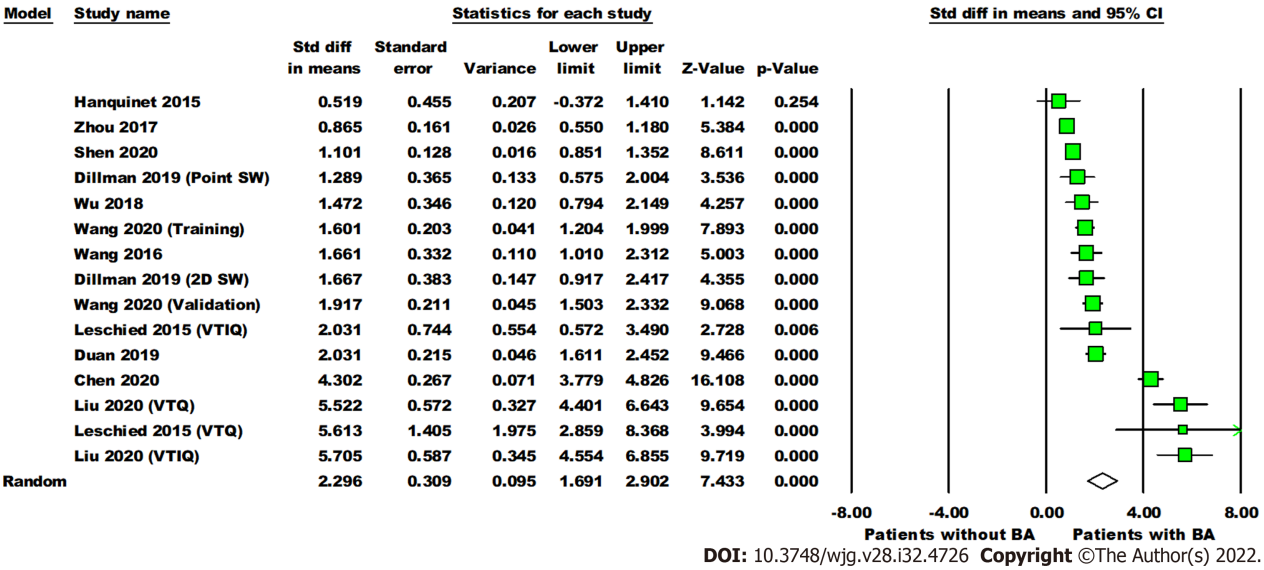
DISCUSSION

Early diagnosis of BA is crucial to patient outcomes. At present, diagnosis depends on invasive liver biopsy and intraoperative cholangiogram. The present meta-analysis is the first to our knowledge to assess the potential utility of preoperative SWE in establishing the diagnosis of BA. In our meta-analysis, we observed that liver stiffness value measured by SWE had high diagnostic accuracy for differentiating BA from other neonatal cholestasis (AUC = 0.91) with high summary sensitivity of 83% as well as summary specificity of 79% and DOR of 24.61. Notably, several of the studies used different



DOI: 10.3748/wjg.v28.i32.4726 **Copyright** ©The Author(s) 2022.

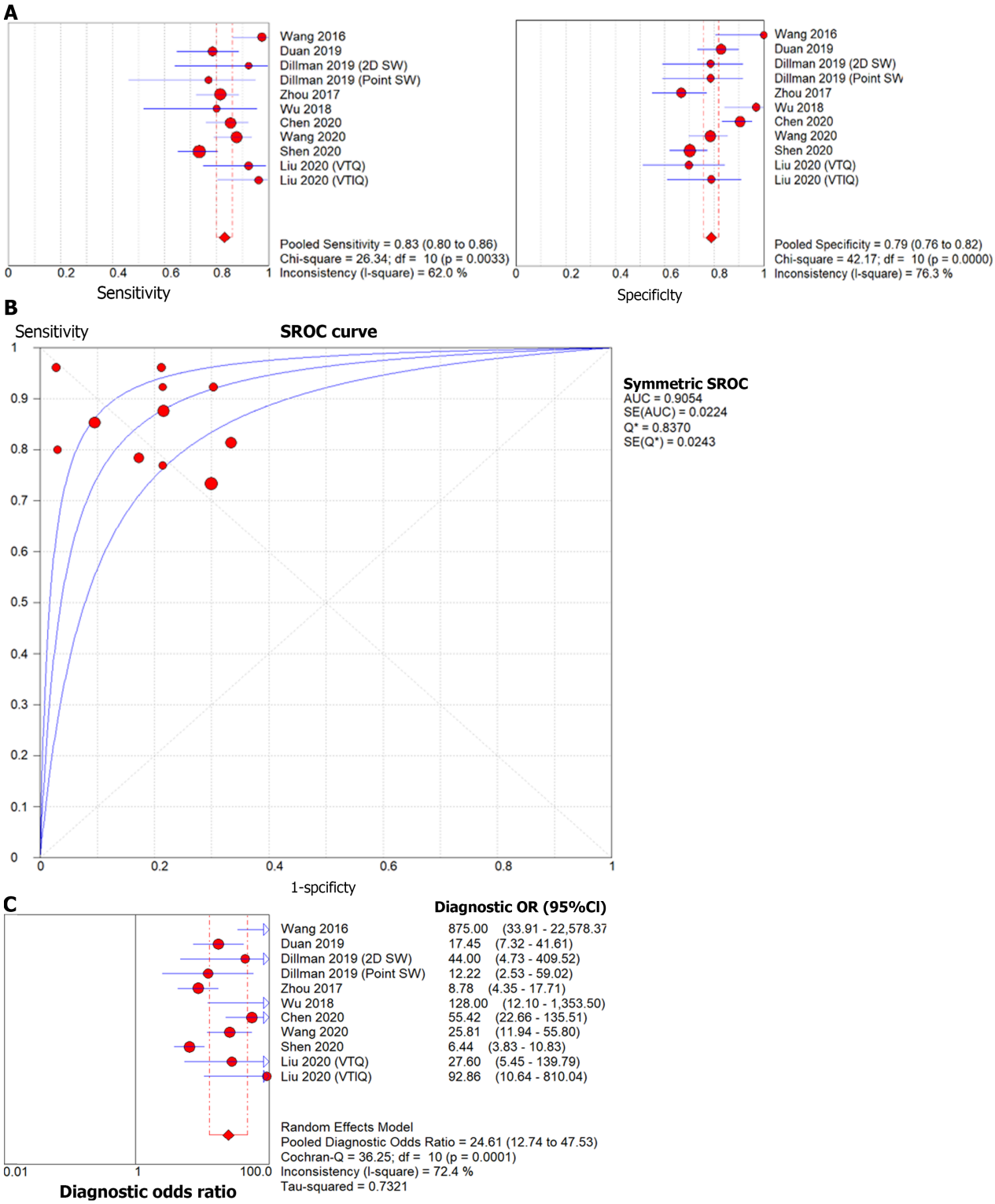
Figure 2 Quality assessment by Quality Assessment of Diagnostic Test Accuracy Studies (QUADAS-2) of the included studies.



Model	Study name	Std diff in means	Standard error	Variance	Lower limit	Upper limit	Z-Value	p-Value
	Hanquinet 2015	0.519	0.455	0.207	-0.372	1.410	1.142	0.254
	Zhou 2017	0.865	0.161	0.026	0.550	1.180	5.384	0.000
	Shen 2020	1.101	0.128	0.016	0.851	1.352	8.611	0.000
	Dillman 2019 (Point SW)	1.289	0.365	0.133	0.575	2.004	3.536	0.000
	Wu 2018	1.472	0.346	0.120	0.794	2.149	4.257	0.000
	Wang 2020 (Training)	1.601	0.203	0.041	1.204	1.999	7.893	0.000
	Wang 2016	1.661	0.332	0.110	1.010	2.312	5.003	0.000
	Dillman 2019 (2D SW)	1.667	0.383	0.147	0.917	2.417	4.355	0.000
	Wang 2020 (Validation)	1.917	0.211	0.045	1.503	2.332	9.068	0.000
	Leschied 2015 (VTIQ)	2.031	0.744	0.554	0.572	3.490	2.728	0.006
	Duan 2019	2.031	0.215	0.046	1.611	2.452	9.466	0.000
	Chen 2020	4.302	0.267	0.071	3.779	4.826	16.108	0.000
	Liu 2020 (VTQ)	5.522	0.572	0.327	4.401	6.643	9.654	0.000
	Leschied 2015 (VTQ)	5.613	1.405	1.975	2.859	8.368	3.994	0.000
	Liu 2020 (VTIQ)	5.705	0.587	0.345	4.554	6.855	9.719	0.000
Random		2.296	0.309	0.095	1.691	2.902	7.433	0.000

DOI: 10.3748/wjg.v28.i32.4726 **Copyright** ©The Author(s) 2022.

Figure 3 Forest plot comparing the liver stiffness value (Kpa) between the patients with and without biliary atresia. Dillman, Wang (2020), Leschied, and Liu each have multiple analyses due to different shear wave elastography modes and/or phases of study (training, validation). Point SW: Point shear wave elastography; 2D SW: Two-dimensional shear wave elastography; VTIQ: Virtual touch IQ, alternative nomenclature for two-dimensional shear wave elastography; VTQ: Virtual touch quantification, alternative nomenclature for point shear wave elastography.

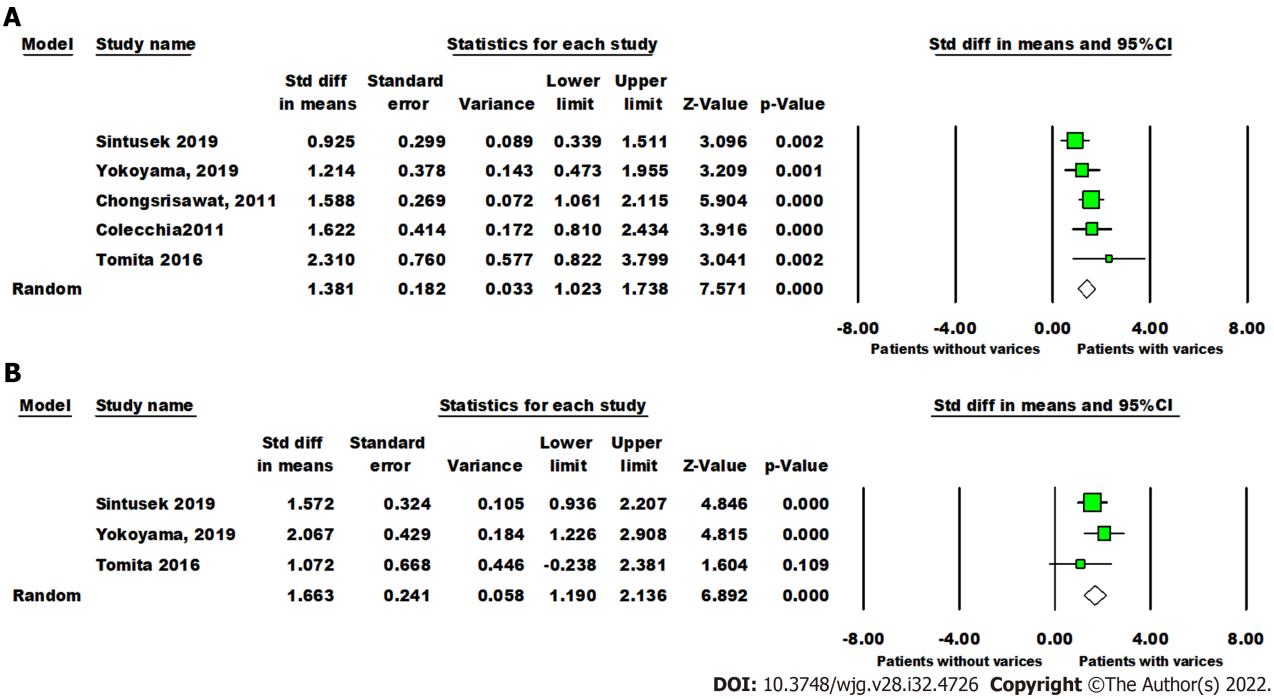


DOI: 10.3748/wjg.v28.i32.4726 **Copyright** ©The Author(s) 2022.

Figure 4 Forest plot of liver stiffness value measured by shear wave elastography to differentiate biliary atresia from other neonatal cholestasis. A: Diagnostic sensitivity and specificity; B: Summary receiver operating characteristic curve; C: Diagnostic odds ratio. Point SW: Point shear wave elastography; 2D SW: Two-dimensional shear wave elastography; VTIQ: Virtual touch IQ, alternative nomenclature for two-dimensional shear wave elastography; VTQ: Virtual touch quantification, alternative nomenclature for point shear wave elastography.

reference standards (five utilized liver biopsy, one utilized surgical exploration or cholangiography, and one did not specify its reference standard). When interpreted within the context of pathophysiology of BA, with fibrosis beginning at bile duct obliteration, in comparison to non-BA cholestasis which has variable degrees of fibrosis, these results reflect the potential for SWE to aid in the diagnostic process.

Post-KPE, a significant number of patients develop persistent cholestasis, portal hypertension, and progressive fibrosis. Risk stratification for these patients continues to be a clinical challenge for hepato-



DOI: 10.3748/wjg.v28.i32.4726 **Copyright** ©The Author(s) 2022.

Figure 5 Forest plot comparing liver and spleen stiffness value between post-Kasai patients with or without varices. A: The liver stiffness value (Kpa); B: Spleen stiffness value (Kpa).

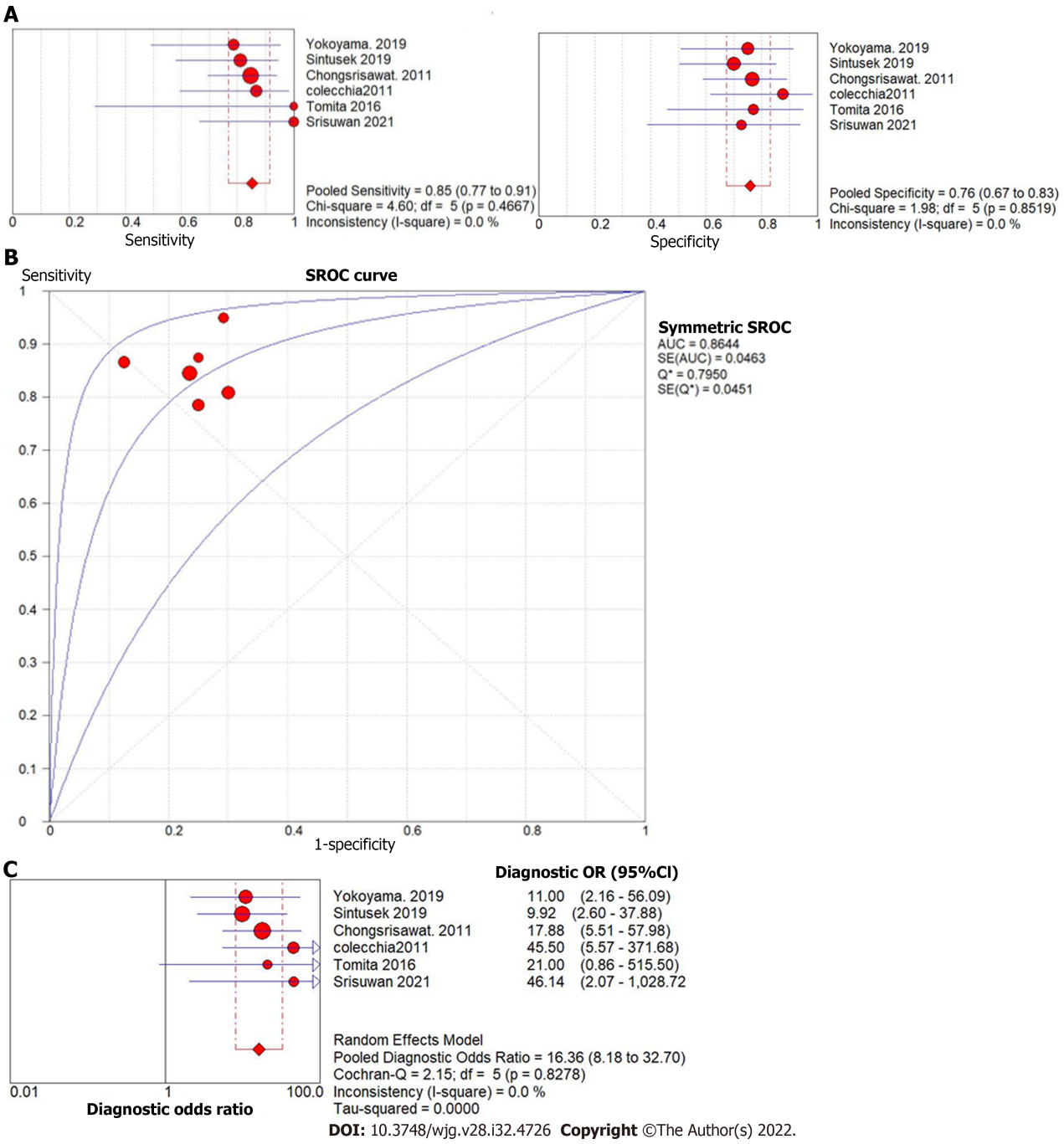
logists. The second portion of this analysis explored the potential utility of SWE for accurately assessing the progression of hepatic fibrosis post-KPE. We observed significant differences in liver and spleen stiffness in patients with varices. The diagnostic accuracy of liver stiffness value measured by SWE was similar to spleen stiffness value to predict the presence of varices post-KPE (AUC = 0.86 and 0.92, respectively). The pooled sensitivity was comparable between liver stiffness and spleen stiffness (85% *vs* 84%), but the pooled specificity of spleen stiffness was higher than liver stiffness (84% *vs* 76%). Notably, only three studies investigated spleen stiffness and five investigated liver stiffness to predict the presence of post-KPE varices.

This analysis also demonstrated significant predictive efficacy for the presence and severity of biopsy-proven liver fibrosis in four studies. Liver stiffness value measured by SWE to determine advanced liver fibrosis (F4 *vs* F0-3) has high diagnostic accuracy (AUC = 0.95), sensitivity (96%) and specificity (89%). Liver stiffness value measured by SWE to differentiate between F3-4 and F0-2 fibrosis has a lower diagnostic accuracy (AUC = 0.91), with sensitivity (85%) and specificity (81%). This is in line with studies in the adult literature, which have found increased accuracy of SWE for high grade (stage F3-4) fibrosis in comparison to F0-F2[23].

Although the findings from this meta-analysis are compelling, there are notable limitations to the analysis. The studies included in this analysis were mostly small and single-center, which limits generalizability across large, non-homogenous populations. Furthermore, each study analyzed for BA diagnosis was performed on infants of different average age (with ranges from two to 140 d of life); given the rapid evolution of fibrosis in BA, the variety of ages analyzed may influence the results.

In addition to the use of different reference standards (liver biopsy *vs* surgical exploration or cholangiogram), there were notable differences in methodology from study to study, in particular regarding patients' fasting status and sedation, sonographer characteristics (blinded *vs* non-blinded, level of expertise, *etc.*), number of measurements obtained, and measurement quality standards. Previous analyses of SWE technology have highlighted significant differences in results obtained depending on sedation and fasting status, operator dependence, and probe choice[5,24-27]. This demonstrates the importance of methodological unity in comparison between data sets. While our results are promising, this is an important implication in terms of broad applicability of our meta-analysis and the need for further, well-designed trials to address the potential utility of SWE in BA.

Patient factors aside, several study centers utilized different SWE platforms (TE *vs* pSWE *vs* 2D-SWE) and machines (detailed in Table 1), each of which reported results in either kPa or m/s. As such, analysis relied upon interconversion of results from Young's modulus to shear modulus (kPa to m/s) [7]. While there is a well-documented mathematical proof enabling this interconversion, the proof relies upon assumptions about tissue characteristics, notably that the tissue has constant density and homogeneity, displays isotropic and elastic characteristics, and is linear under compressible stress (Supplementary material)[7,8]. The inherent characteristics of an inflamed, potentially fibrotic liver do not fit well into this description, which is important to mention given an analysis that relies heavily on



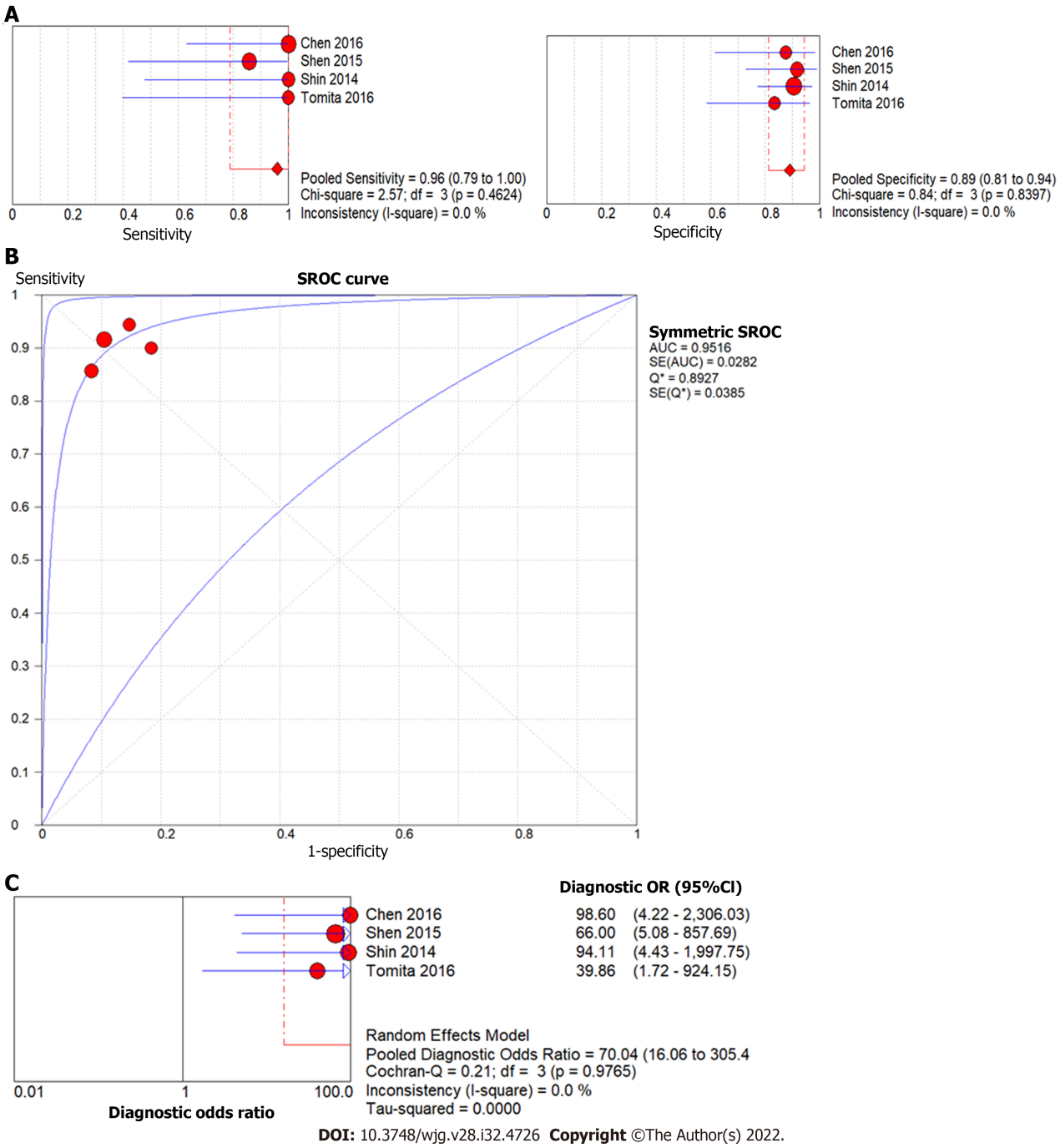
DOI: 10.3748/wjg.v28.i32.4726 **Copyright** ©The Author(s) 2022.

Figure 6 Forest plot of liver stiffness value measured by shear wave elastography to predict the presence of varices in post-Kasai patients. A: Diagnostic sensitivity and specificity; B: Summary receiver operating characteristic curve; C: Diagnostic odds ratio.

interconversion between results[28,29]. In a similar vein, a recent study by Darweesh *et al*[30] found that cholestasis itself can increase liver stiffness measurements in adult patients, separate to histologic findings of fibrosis; future studies must take this potential confounder into account. This meta-analysis must be interpreted within the context of these limitations, with future studies taking important steps to address potential limitations and barriers to interpretation during the study design, data collection and analysis phases of work.

CONCLUSION

Despite non-standardized methodology across analyzed articles as well as reliance upon data interconversion, this meta-analysis highlights the potential of SWE as a non-invasive method to assist in both the diagnosis as well as post-KPE follow-up of BA. Further standardized, multi-center studies are needed in order to better elucidate this potential. By applying uniform methods, machinery, and data reporting (in



DOI: 10.3748/wjg.v28.i32.4726 **Copyright** ©The Author(s) 2022.

Figure 7 Forest plot of liver stiffness value measured by shear wave elastography to predict the presence of liver fibrosis F4 (vs F0-3) in post-Kasai patients. A: Diagnostic sensitivity and specificity; B: Summary receiver operating characteristic curve; C: Diagnostic odds ratio.

either kPa or m/s), further studies may be able to identify SWE as a non-invasive tool with utility both in diagnosis of BA as well as post-KPE prediction of outcomes.

ARTICLE HIGHLIGHTS

Research background

Biliary atresia (BA) is a progressive infantile cholestatic disease. Diagnosis is confirmed by intra-operative cholangiogram; any delays to diagnosis and palliating Kasai hepatoportoenterostomy can increase the odds of needing liver transplant. Following Kasai, patients will need surveillance for progression of liver disease, which often requires liver biopsy.

Research motivation

Because the diagnosis and surveillance of BA both involve invasive procedures, there are risks for delay and/or adverse outcomes at each stage. By using non-invasive shear wave elastography (SWE), which measures changes in tissue stiffness, to identify liver stiffness thresholds for BA diagnosis and evolution of fibrosis post-Kasai, clinicians may be able to accurately diagnose and surveil BA without invasive procedures.

Research objectives

The authors performed a meta-analysis on studies into the utility of SWE for BA diagnosis and post-Kasai surveillance in order to determine whether existing literature could help identify liver stiffness thresholds for BA diagnosis and development of fibrosis post-Kasai.

Research methods

A literature search yielded twenty studies, eleven for diagnosis and nine for follow-up post-Kasai. Diagnostic odds ratio (DOR), sensitivity, and specificity of elastography were calculated through a random-effects model.

Research results

Mean liver stiffness in BA infants was higher than in cholestatic infants without BA with DOR 24.61, sensitivity 83%, specificity 79%. Mean liver stiffness post-Kasai was significantly higher in patients with varices than those without (DOR 16.36, sensitivity 85%, specificity 76%). SWE differentiated METAVIR F4 fibrosis from F0-F3 (DOR 70.03, sensitivity 96%, specificity 89%) as well as F3-F4 fibrosis from F0-F2 (DOR 24.68, sensitivity 85%, specificity 81%).

Research conclusions

SWE may be a useful, non-invasive modality for the diagnosis and post-Kasai surveillance in BA. The analysis is limited by methodological heterogeneity between studies as well as small sample sizes.

Research perspectives

In order for SWE to be useful for future BA cases, larger, standardized, multi-center studies are recommended to establish appropriate protocols.

FOOTNOTES

Author contributions: Wagner ES performed literature search, data acquisition and interpretation, manuscript drafting, and final approval; Abdelgawad HAH performed data acquisition, statistical analysis and interpretation, manuscript structure, drafting, and revisions; Landry M performed statistical analysis and interpretation, manuscript structure and revisions; Asfour B performed figure compilation and manuscript revisions; Slidell MB performed manuscript compilation, revisions, and final approval; Azzam R performed project structure, data acquisition and interpretation, manuscript revisions, and final approval.

Conflict-of-interest statement: There are no conflicts of interest to report.

PRISMA 2009 Checklist statement: The authors have read the PRISMA 2009 Checklist, and the manuscript was prepared and revised according to the PRISMA 2009 Checklist.

Open-Access: This article is an open-access article that was selected by an in-house editor and fully peer-reviewed by external reviewers. It is distributed in accordance with the Creative Commons Attribution NonCommercial (CC BY-NC 4.0) license, which permits others to distribute, remix, adapt, build upon this work non-commercially, and license their derivative works on different terms, provided the original work is properly cited and the use is non-commercial. See: https://creativecommons.org/Licenses/by-nc/4.0/

Country/Territory of origin: United States

ORCID number: Ellen S Wagner 0000-0003-2013-5255; Hussien Ahmed H Abdelgawad 0000-0001-7101-837X; Meghan Landry 0000-0001-9822-5117; Belal Asfour 0000-0002-6562-6229; Mark B Slidell 0000-0002-9551-5888; Ruba Azzam 0000-0003-0151-2123.

S-Editor: Chen YL
L-Editor: A
P-Editor: Cai YX

REFERENCES

1 **Fischler B**, Lamireau T. Cholestasis in the newborn and infant. *Clin Res Hepatol Gastroenterol* 2014; **38**: 263-267 [PMID: 24746684 DOI: 10.1016/j.clinre.2014.03.010]

2 **Jimenez-Rivera C**, Jolin-Dahel KS, Fortinsky KJ, Gozdyra P, Benchimol EI. International incidence and outcomes of biliary atresia. *J Pediatr Gastroenterol Nutr* 2013; **56**: 344-354 [PMID: 23263590 DOI: 10.1097/MPG.0b013e318282a913]

3 **Lee JY**, Sullivan K, El Demellawy D, Nasr A. The value of preoperative liver biopsy in the diagnosis of extrahepatic biliary atresia: A systematic review and meta-analysis. *J Pediatr Surg* 2016; **51**: 753-761 [PMID: 26932252 DOI: 10.1016/j.jpedsurg.2016.02.016]

4 **Dezsőfi A**, Baumann U, Dhawan A, Durmaz O, Fischler B, Hadzic N, Hierro L, Lacaille F, McLin VA, Nobili V, Socha P, Vajro P, Knisely AS; ESPGHAN Hepatology Committee. Liver biopsy in children: position paper of the ESPGHAN Hepatology Committee. *J Pediatr Gastroenterol Nutr* 2015; **60**: 408-420 [PMID: 25383787 DOI: 10.1097/MPG.0000000000000632]

5 **Bamber J**, Cosgrove D, Dietrich CF, Fromageau J, Bojunga J, Calliada F, Cantisani V, Correas JM, D'Onofrio M, Drakonaki EE, Fink M, Friedrich-Rust M, Gilja OH, Havre RF, Jenssen C, Klauser AS, Ohlinger R, Saftoiu A, Schaefer F, Sporea I, Piscaglia F. EFSUMB guidelines and recommendations on the clinical use of ultrasound elastography. Part 1: Basic principles and technology. *Ultraschall Med* 2013; **34**: 169-184 [PMID: 23558397 DOI: 10.1055/s-0033-1335205]

6 **Thumar V**, Squires JH, Spicer PJ, Robinson AL, Chan SS. Ultrasound Elastography Applications in Pediatrics. *Ultrasound Q* 2018; **34**: 199-205 [PMID: 30169493 DOI: 10.1097/RUQ.0000000000000379]

7 **Shiina T**, Nightingale KR, Palmeri ML, Hall TJ, Bamber JC, Barr RG, Castera L, Choi BI, Chou YH, Cosgrove D, Dietrich CF, Ding H, Amy D, Farrokh A, Ferraioli G, Filice C, Friedrich-Rust M, Nakashima K, Schafer F, Sporea I, Suzuki S, Wilson S, Kudo M. WFUMB guidelines and recommendations for clinical use of ultrasound elastography: Part 1: basic principles and terminology. *Ultrasound Med Biol* 2015; **41**: 1126-1147 [PMID: 25805059 DOI: 10.1016/j.ultrasmedbio.2015.03.009]

8 **Sigrist RMS**, Liau J, Kaffas AE, Chammas MC, Willmann JK. Ultrasound Elastography: Review of Techniques and Clinical Applications. *Theranostics* 2017; **7**: 1303-1329 [PMID: 28435467 DOI: 10.7150/thno.18650]

9 **Ozturk A**, Grajo JR, Dhyani M, Anthony BW, Samir AE. Principles of ultrasound elastography. *Abdom Radiol (NY)* 2018; **43**: 773-785 [PMID: 29487968 DOI: 10.1007/s00261-018-1475-6]

10 **Ferrari J**, Higgins JP, Williams RL. Interventions for treating hallux valgus (abductovalgus) and bunions. *Cochrane Database Syst Rev* 2000; CD000964 [PMID: 10796404 DOI: 10.1002/14651858.CD000964]

11 **McInnes MDF**, Moher D, Thombs BD, McGrath TA, Bossuyt PM; and the PRISMA-DTA Group, Clifford T, Cohen JF, Deeks JJ, Gatsonis C, Hooft L, Hunt HA, Hyde CJ, Korevaar DA, Leeflang MMG, Macaskill P, Reitsma JB, Rodin R, Rutjes AWS, Salameh JP, Stevens A, Takwoingi Y, Tonelli M, Weeks L, Whiting P, Willis BH. Preferred Reporting Items for a Systematic Review and Meta-analysis of Diagnostic Test Accuracy Studies: The PRISMA-DTA Statement. *JAMA* 2018; **319**: 388-396 [PMID: 29362800 DOI: 10.1001/jama.2017.19163]

12 **Whiting PF**, Rutjes AW, Westwood ME, Mallett S, Deeks JJ, Reitsma JB, Leeflang MM, Sterne JA, Bossuyt PM; QUADAS-2 Group. QUADAS-2: a revised tool for the quality assessment of diagnostic accuracy studies. *Ann Intern Med* 2011; **155**: 529-536 [PMID: 22007046 DOI: 10.7326/0003-4819-155-8-201110180-00009]

13 **Wan X**, Wang W, Liu J, Tong T. Estimating the sample mean and standard deviation from the sample size, median, range and/or interquartile range. *BMC Med Res Methodol* 2014; **14**: 135 [PMID: 25524443 DOI: 10.1186/1471-2288-14-135]

14 **Hanquinet S**, Courvoisier DS, Rougemont AL, Dhouib A, Rubbia-Brandt L, Wildhaber BE, Merlini L, McLin VA, Anooshiravani M. Contribution of acoustic radiation force impulse (ARFI) elastography to the ultrasound diagnosis of biliary atresia. *Pediatr Radiol* 2015; **45**: 1489-1495 [PMID: 25943691 DOI: 10.1007/s00247-015-3352-6]

15 **Leschied JR**, Dillman JR, Bilhartz J, Heider A, Smith EA, Lopez MJ. Shear wave elastography helps differentiate biliary atresia from other neonatal/infantile liver diseases. *Pediatr Radiol* 2015; **45**: 366-375 [PMID: 25238807 DOI: 10.1007/s00247-014-3149-z]

16 **Dillman JR**, DiPaola FW, Smith SJ, Barth RA, Asai A, Lam S, Campbell KM, Bezerra JA, Tiao GM, Trout AT. Prospective Assessment of Ultrasound Shear Wave Elastography for Discriminating Biliary Atresia from other Causes of Neonatal Cholestasis. *J Pediatr* 2019; **212**: 60-65.e3 [PMID: 31253405 DOI: 10.1016/j.jpeds.2019.05.048]

17 **Chen Y**, Zhao D, Gu S, Li Y, Pan W, Zhang Y. Three-color risk stratification for improving the diagnostic accuracy for biliary atresia. *Eur Radiol* 2020; **30**: 3852-3861 [PMID: 32162000 DOI: 10.1007/s00330-020-06751-7]

18 **Liu YF**, Ni XW, Pan Y, Luo HX. Comparison of the diagnostic value of virtual touch tissue quantification and virtual touch tissue imaging quantification in infants with biliary atresia. *Int J Clin Pract* 2021; **75**: e13860 [PMID: 33236451 DOI: 10.1111/ijcp.13860]

19 **Yokoyama S**, Ishigami M, Honda T, Kuzuya T, Ishizu Y, Ito T, Hirooka Y, Tanaka Y, Tainaka T, Shirota C, Chiba K, Uchida H, Fujishiro M. Spleen stiffness by 2-D shear wave elastography is the most accurate predictor of high-risk esophagogastric varices in children with biliary atresia. *Hepatol Res* 2019; **49**: 1162-1168 [PMID: 31132304 DOI: 10.1111/hepr.13381]

20 **Tomita H**, Ohkuma K, Masugi Y, Hosoe N, Hoshino K, Fuchimoto Y, Fujino A, Shimizu T, Kato M, Fujimura T, Ishihama H, Takahashi N, Tanami Y, Ebinuma H, Saito H, Sakamoto M, Nakano M, Kuroda T. Diagnosing native liver fibrosis and esophageal varices using liver and spleen stiffness measurements in biliary atresia: a pilot study. *Pediatr Radiol* 2016; **46**: 1409-1417 [PMID: 27300741 DOI: 10.1007/s00247-016-3637-4]

21 **Srisuwan W**, Laochareonsuk W, Wetwittayakhlang P, Kritsaneepaiboon S, Sangkhathat S. Correlation of Transient Elastography and Biliary Cirrhosis in Longterm Survivors of Biliary Atresia. *Siriraj Med J* 2021; **73**: 32-37 [DOI: 10.33192/smj.2021.05]

22 **Zhou LY**, Jiang H, Shan QY, Chen D, Lin XN, Liu BX, Xie XY. Liver stiffness measurements with supersonic shear wave elastography in the diagnosis of biliary atresia: a comparative study with grey-scale US. *Eur Radiol* 2017; **27**: 3474-3484 [PMID: 28083694 DOI: 10.1007/s00330-016-4710-y]

23 **Gharibvand MM**, Asare M, Motamedfar A, Alavinejad P, Momeni M. Ultrasound shear wave elastography and liver

biopsy to determine liver fibrosis in adult patients. *J Family Med Prim Care* 2020; **9**: 943-949 [PMID: 32318450 DOI: 10.4103/jfmpc.jfmpc_828_19]

24 **Andersen ES**, Christensen PB, Weis N. Transient elastography for liver fibrosis diagnosis. *Eur J Intern Med* 2009; **20**: 339-342 [PMID: 19524169 DOI: 10.1016/j.ejim.2008.09.020]

25 **Goldschmidt I**, Streckenbach C, Dingemann C, Pfister ED, di Nanni A, Zapf A, Baumann U. Application and limitations of transient liver elastography in children. *J Pediatr Gastroenterol Nutr* 2013; **57**: 109-113 [PMID: 23539048 DOI: 10.1097/MPG.0b013e31829206a0]

26 **de Lédinghen V**, Le Bail B, Rebouissoux L, Fournier C, Foucher J, Miette V, Castéra L, Sandrin L, Merrouche W, Lavrand F, Lamireau T. Liver stiffness measurement in children using FibroScan: feasibility study and comparison with Fibrotest, aspartate transaminase to platelets ratio index, and liver biopsy. *J Pediatr Gastroenterol Nutr* 2007; **45**: 443-450 [PMID: 18030211 DOI: 10.1097/MPG.0b013e31812e56ff]

27 **Franchi-Abella S**, Corno L, Gonzales E, Antoni G, Fabre M, Ducot B, Pariente D, Gennisson JL, Tanter M, Corréas JM. Feasibility and Diagnostic Accuracy of Supersonic Shear-Wave Elastography for the Assessment of Liver Stiffness and Liver Fibrosis in Children: A Pilot Study of 96 Patients. *Radiology* 2016; **278**: 554-562 [PMID: 26305193 DOI: 10.1148/radiol.2015142815]

28 **Barr RG**. Shear wave liver elastography. *Abdom Radiol (NY)* 2018; **43**: 800-807 [PMID: 29116341 DOI: 10.1007/s00261-017-1375-1]

29 **Friedrich-Rust M**, Romen D, Vermehren J, Kriener S, Sadet D, Herrmann E, Zeuzem S, Bojunga J. Acoustic radiation force impulse-imaging and transient elastography for non-invasive assessment of liver fibrosis and steatosis in NAFLD. *Eur J Radiol* 2012; **81**: e325-e331 [PMID: 22119555 DOI: 10.1016/j.ejrad.2011.10.029]

30 **Darweesh SK**, Zayed N, Atef M, Ramzy E, Yousry A, Musa S. Increased liver stiffness by transient elastography and acoustic radiation force impulse imaging in patients with extrahepatic cholestasis. *Eur J Gastroenterol Hepatol* 2021; **33**: 1097-1103 [PMID: 32804844 DOI: 10.1097/MEG.0000000000001881]

31 **Wang X**, Qian L, Jia L, Bellah R, Wang N, Xin Y, Liu Q. Utility of Shear Wave Elastography for Differentiating Biliary Atresia From Infantile Hepatitis Syndrome. *J Ultrasound Med* 2016; **35**: 1475-1479 [PMID: 27229132 DOI: 10.7863/ultra.15.08031]

32 **Wu JF**, Lee CS, Lin WH, Jeng YM, Chen HL, Ni YH, Hsu HY, Chang MH. Transient elastography is useful in diagnosing biliary atresia and predicting prognosis after hepatoportoenterostomy. *Hepatology* 2018; **68**: 616-624 [PMID: 29486516 DOI: 10.1002/hep.29856]

33 **Duan X**, Peng Y, Liu W, Yang L, Zhang J. Does Supersonic Shear Wave Elastography Help Differentiate Biliary Atresia from Other Causes of Cholestatic Hepatitis in Infants Less than 90 Days Old? *Biomed Res Int* 2019; **2019**: 9036362 [PMID: 31275991 DOI: 10.1155/2019/9036362]

34 **Shen Q**, Tan SS, Wang Z, Cai S, Pang W, Peng C, Chen Y. Combination of gamma-glutamyl transferase and liver stiffness measurement for biliary atresia screening at different ages: a retrospective analysis of 282 infants. *BMC Pediatr* 2020; **20**: 276 [PMID: 32498678 DOI: 10.1186/s12887-020-02172-z]

35 **Wang Y**, Jia LQ, Hu YX, Xin Y, Yang X, Wang XM. Development and Validation of a Nomogram Incorporating Ultrasonic and Elastic Findings for the Preoperative Diagnosis of Biliary Atresia. *Acad Radiol* 2021; **28** Suppl 1: S55-S63 [PMID: 32972841 DOI: 10.1016/j.acra.2020.08.035]

36 **Chongsrisawat V**, Vejapipat P, Siripon N, Poovorawan Y. Transient elastography for predicting esophageal/gastric varices in children with biliary atresia. *BMC Gastroenterol* 2011; **11**: 41 [PMID: 21501480 DOI: 10.1186/1471-230X-11-41]

37 **Colecchia A**, Di Biase AR, Scaioli E, Predieri B, Iughetti L, Reggiani ML, Montrone L, Ceccarelli PL, Vestito A, Viola L, Paolucci P, Festi D. Non-invasive methods can predict oesophageal varices in patients with biliary atresia after a Kasai procedure. *Dig Liver Dis* 2011; **43**: 659-663 [PMID: 21596631 DOI: 10.1016/j.dld.2011.04.006]

38 **Shin NY**, Kim MJ, Lee MJ, Han SJ, Koh H, Namgung R, Park YN. Transient elastography and sonography for prediction of liver fibrosis in infants with biliary atresia. *J Ultrasound Med* 2014; **33**: 853-864 [PMID: 24764341 DOI: 10.7863/ultra.33.5.853]

39 **Shen QL**, Chen YJ, Wang ZM, Zhang TC, Pang WB, Shu J, Peng CH. Assessment of liver fibrosis by Fibroscan as compared to liver biopsy in biliary atresia. *World J Gastroenterol* 2015; **21**: 6931-6936 [PMID: 26078570 DOI: 10.3748/wjg.v21.i22.6931]

40 **Chen S**, Liao B, Zhong Z, Zheng Y, Liu B, Shan Q, Xie X, Zhou L. Supersonic shearwave elastography in the assessment of liver fibrosis for postoperative patients with biliary atresia. *Sci Rep* 2016; **6**: 31057 [PMID: 27511435 DOI: 10.1038/srep31057]

41 **Sintusek P**, Siriporn N, Punpanich D, Chongsrisawat V, Poovorawan Y. Spleen and Liver Stiffness to Detect Esophageal Varices in Children with Biliary Atresia. *J Pediatr Gastroenterol Nutr* 2019; **69**: 411-415 [PMID: 31348121 DOI: 10.1097/MPG.0000000000002430]

World Journal of Gastroenterology

Submit a Manuscript: https://www.f6publishing.com

World J Gastroenterol 2022 August 28; 28(32): 4741-4743

DOI: 10.3748/wjg.v28.i32.4741

ISSN 1007-9327 (print) ISSN 2219-2840 (online)

LETTER TO THE EDITOR

Is endoscopic mucosal ablation a valid option for treating colon polyps?

Xiang-Yu Liu, Ran-Ran Ren, Chen Wu, Ling-Yun Wang, Mei-Lin Zhu

Specialty type: Gastroenterology and hepatology

Provenance and peer review: Unsolicited article; Externally peer reviewed.

Peer-review model: Single blind

Peer-review report's scientific quality classification

Grade A (Excellent): A
Grade B (Very good): B
Grade C (Good): 0
Grade D (Fair): 0
Grade E (Poor): 0

P-Reviewer: Nakaji K, Japan; Trna J, Czech Republic

Received: May 3, 2022
Peer-review started: May 3, 2022
First decision: June 19, 2022
Revised: June 24, 2022
Accepted: July 25, 2022
Article in press: July 25, 2022
Published online: August 28, 2022

Xiang-Yu Liu, Ran-Ran Ren, Chen Wu, Ling-Yun Wang, Department of Gastroenterology, Jining No. 1 People's Hospital, Jining 272000, Shandong Province, China

Chen Wu, College of Clinical Medicine, Jining Medical University, Jining 272013, Shandong Province, China

Mei-Lin Zhu, Department of Geriatrics, Jining No. 1 People's Hospital, Jining 272000, Shandong Province, China

Corresponding author: Mei-Lin Zhu, MD, Attending Doctor, Department of Geriatrics, Jining No. 1 People's Hospital, No. 6 Jiankang Road, Jining 272000, Shandong Province, China.
yibeinaica@126.com

Abstract

The present letter to editor is related to endoscopic mucosal ablation (EMA). EMA is safe and effective in the treatment of colonic polyps when endoscopic resection is not possible or available, but the indication of EMA should be determined for a further large number of studies. EMA should be used with caution for larger lesions.

Key Words: Endoscopy; Mucosal ablation; Colon polyp; Endoscopic mucosal ablation

©The Author(s) 2022. Published by Baishideng Publishing Group Inc. All rights reserved.

Core Tip: Endoscopic mucosal ablation (EMA) is safe and effective in the treatment of colonic polyps when endoscopic resection is not possible or available, but we think EMA should be more cautious with caution for larger lesions.

Citation: Liu XY, Ren RR, Wu C, Wang LY, Zhu ML. Is endoscopic mucosal ablation a valid option for treating colon polyps? *World J Gastroenterol* 2022; 28(32): 4741-4743
URL: https://www.wjgnet.com/1007-9327/full/v28/i32/4741.htm
DOI: https://dx.doi.org/10.3748/wjg.v28.i32.4741

TO THE EDITOR

We were pleased to read the excellent article published by Mendoza Ladd *et al*[1]. Their report showed a new and safe method for treating colon polyps. Patients were followed up for 1 year and showed no polyp recurrence. However, this study still has issues that we would like to discuss with the authors.

We want to know the indications for the endoscopic mucosal ablation (EMA) method, such as the size of the lesion and the type of preoperative pathology. Argon plasma coagulation is often used for benign diseases or small polyps or as a supplement when there is residual tumor or recurrence after endoscopic mucosal resection[2-5] or endoscopic submucosal dissection[6,7]. For large lesions of the colon, especially laterally spreading tumors, lesions often become high-grade intraepithelial neoplasias or even cancers[8]. Chemical staining, image enhancement endoscopy (such as narrow band imaging and blue laser imaging), magnifying endoscopy or confocal laser endomicroscopy[9] is needed to help make a diagnosis. If the lesion is high-grade internal neoplasia or cancer, the presurgery computed tomography examination needs to be improved to detect lymph node metastasis. During surgery, how to judge the integrity of the lesion and its marginal treatment needs to be further explored.

The main drawback of EMA is that it cannot produce complete specimens for pathological analysis. The pathology of the preoperative lesion biopsy may not reflect the entire lesion condition. We cannot know whether the lesion has high-grade intraepithelial neoplasia or carcinoma, nor can we determine whether the patient needs additional surgical treatment. Although the review of colonoscopy and biopsy after 1 year did not reveal lesion recurrence, lesions can take longer to recur.

In summary, the indication of EMA should be determined from a large number of studies. EMA should be used with caution for larger lesions.

FOOTNOTES

Author contributions: Liu XY and Ren RR contributed equally to this work; Liu XY, Wu C and Ren RR wrote the manuscript; Zhu ML, Wang LY and Ren RR searched the relevant literature; Liu XY and Zhu ML revised the manuscript; all authors have read and approve the final manuscript.

Conflict-of-interest statement: All the authors report no relevant conflicts of interest for this article.

Open-Access: This article is an open-access article that was selected by an in-house editor and fully peer-reviewed by external reviewers. It is distributed in accordance with the Creative Commons Attribution NonCommercial (CC BY-NC 4.0) license, which permits others to distribute, remix, adapt, build upon this work non-commercially, and license their derivative works on different terms, provided the original work is properly cited and the use is non-commercial. See: https://creativecommons.org/Licenses/by-nc/4.0/

Country/Territory of origin: China

ORCID number: Xiang-Yu Liu 0000-0003-4702-976X; Ran-Ran Ren 0000-0002-2287-373X; Chen Wu 0000-0003-1352-8931; Ling-Yun Wang 0000-0003-4514-7498; Mei-Lin Zhu 0000-0003-3830-5494.

S-Editor: Fan JR
L-Editor: A
P-Editor: Fan JR

REFERENCES

1 **Mendoza Ladd A**, Espinoza J, Garcia C. Endoscopic mucosal ablation - an alternative treatment for colonic polyps: Three case reports. *World J Gastroenterol* 2020; **26**: 7258-7262 [PMID: 33362381 DOI: 10.3748/wjg.v26.i45.7258]
2 **Estifan E**, Cavanagh Y, Grossman MA. Hybrid Argon Plasma Coagulation for Treatment of Gastric Intestinal Metaplasia. *Cureus* 2020; **12**: e7427 [PMID: 32337147 DOI: 10.7759/cureus.7427]
3 **Fujishiro M**, Yahagi N, Kakushima N, Kodashima S, Muraki Y, Ono S, Kobayashi K, Hashimoto T, Yamamichi N, Tateishi A, Shimizu Y, Oka M, Ogura K, Kawabe T, Ichinose M, Omata M. Successful nonsurgical management of perforation complicating endoscopic submucosal dissection of gastrointestinal epithelial neoplasms. *Endoscopy* 2006; **38**: 1001-1006 [PMID: 17058165 DOI: 10.1055/s-2006-944775]
4 **Regula J**, Wronska E, Nasierowska A, Polkowski M, Pachlewski J, Butruk E. Endoscopic argon plasma coagulation (APC) after piecemeal polypectomy of colorectal adenomas two-years follow-up study. *Gastrointest Endosc* 1997; **45**: AB37 [DOI: 10.1016/s0016-5107(97)80050-8]
5 **Zlatanic J**, Waye JD, Kim PS, Baiocco PJ, Gleim GW. Large sessile colonic adenomas: use of argon plasma coagulator to supplement piecemeal snare polypectomy. *Gastrointest Endosc* 1999; **49**: 731-735 [PMID: 10343218 DOI: 10.1016/s0016-5107(99)70291-9]
6 **Tsiamoulos ZP**, Bourikas LA, Saunders BP. Endoscopic mucosal ablation: a new argon plasma coagulation/injection technique to assist complete resection of recurrent, fibrotic colon polyps (with video). *Gastrointest Endosc* 2012; **75**: 400-

404 [PMID: 22154411 DOI: 10.1016/j.gie.2011.09.003]
7 **Muñoz-Largacha JA**, Litle VR. Endoscopic mucosal ablation and resection of Barrett's esophagus and related diseases. *J Vis Surg* 2017; **3**: 128 [PMID: 29078688 DOI: 10.21037/jovs.2017.07.10]
8 **Saito T**, Kobayashi K, Sada M, Matsumoto Y, Mukae M, Kawagishi K, Yokoyama K, Koizumi W, Saegusa M, Murakami Y. Comparison of the histopathological characteristics of large colorectal laterally spreading tumors according to growth pattern. *J Anus Rectum Colon* 2019; **3**: 152-159 [PMID: 31768465 DOI: 10.23922/jarc.2018-036]
9 **Tang BF**, Nian YY, Dang T. Advances of confocal laser endomicroscope in digestive diseases. *Zhonguo Xiaohua Neijing Zazhi* 2022; **39**: 164-168 [DOI: 10.3760/cma.j.cn321463-20210301-00057]



Published by **Baishideng Publishing Group Inc**
7041 Koll Center Parkway, Suite 160, Pleasanton, CA 94566, USA
Telephone: +1-925-3991568
E-mail: bpgoffice@wjgnet.com
Help Desk: https://www.f6publishing.com/helpdesk
https://www.wjgnet.com



© 2022 Baishideng Publishing Group Inc. All rights reserved.